

Towards a higher international standard - *World Journal of Gastroenterology* will be published semimonthly in 2004

Lian-Sheng Ma, Bo-Rong Pan, Jing-Yun Ma, Jia-Yu Xu, Xie-Ning Wu, Xian-Lin Wang, Han-Ming Lu, Harry Hua-Xiang Xia, Hong-Xiang Liu, Jian-Zhong Zhang, Qin Su, Shi-Yan Ren, Li Zhu, Li-Hong Zhu, You-Yong Lu

Lian-Sheng Ma, Bo-Rong Pan, Jing-Yun Ma, Jia-Yu Xu, Xie-Ning Wu, Xian-Lin Wang, Han-Ming Lu, Harry Hua-Xiang Xia, Hong-Xiang Liu, Jian-Zhong Zhang, Qin Su, Shi-Yan Ren, Li Zhu, Li-Hong Zhu, You-Yong Lu, The WJG Press, PO Box 2345, Beijing 100023, China

Correspondence to: Lian-Sheng Ma, M.D., The WJG Press, PO Box 2345, Beijing 100023, China. wjg@wjgnet.com
Telephone: +86-10-85381901 **Fax:** +86-10-85381893
Received: 2003-12-10 **Accepted:** 2003-12-11

Ma LS, Pan BR, Ma JY, Xu JY, Wu XN, Wang XL, Lu HM, Xia HHX, Liu HX, Zhang JZ, Su Q, Ren SY, Zhu L, Zhu LH, Lu YY. Towards a higher international standard - *World Journal of Gastroenterology* will be published semimonthly in 2004. *World J Gastroenterol* 2004; 10(1): 1-4

<http://www.wjgnet.com/1007-9327/10/1.asp>

INTRODUCTION

World Journal of Gastroenterology (WJG) is an international academic journal in digestology published in China. The WJG was established in 1995 under the name of *China National Journal of New Gastroenterology*, and adapted its present title in 1998. The WJG (ISSN 1007-9327), now published monthly by the WJG Press, is a 210×297 mm-sized journal with 256 pages in each issue. The Journal is distributed by the Beijing Newspaper and Periodical Subscription and Distribution Bureau (Postal Issuance Code 82-261). In response to continuing growth in both basic and clinical studies on digestive diseases and the increasing demands for the international exchange in science and technology, the WJG journal will be published twice monthly from January 2004, with 160 pages in each issue. The publication dates are on the 1st and 15th of each month.

MISSION

The WJG seeks to publish high-quality, original and innovative papers and short communications on basic and clinical studies in gastroenterology and hepatology. The editors accept manuscripts that report important findings in esophageal cancer, gastric cancer, liver cancer, intestinal cancer, viral hepatitis, *Helicobacter pylori* infection, as well as Chinese medicine and integrated Chinese and Western medicine in the treatment of digestive diseases. The Journal gives a higher priority to review articles that are based mainly on the own work of the authors. Thus, the WJG establishes itself as a window for the international academic exchange, and provides a bridge to the world for local medical researchers and professionals.

EDITORIAL BOARDS

The WJG Editorial Board consists of 179 members, representing a team of worldwide experts in gastroenterology and hepatology. They are from 53 countries including: Albania (1), Algeria (1), Argentina (2), Austria (1), Belarus (1), Belgium (1), Brazil (1),

Bulgaria (1), Canada (1), China (41), Costa Rica (1), Croatia (1), Denmark (1), Egypt (1), Finland (1), France (2), Germany (7), Greece (1), Hungary (2), Iceland (1), India (2), Iran (1), Ireland (2), Israel (2), Italy (2), Japan (4), Latvia (1), Lithuania (1), Macedonia (1), Malaysia (2), Monaco (1), Netherlands (3), New Zealand (1), Pakistan (1), Philippines (1), Poland (2), Portugal (1), Romania (1), Russia (3), Singapore (1), Slovakia (1), Slovenia (2), South Africa (1), South Korea (2), Spain (1), Sri Lanka (1), Sweden (2), Switzerland (2), Thailand (1), Turkey (1), United Kingdom (6), United States (56), and Yugoslavia (1).

The WJG has a group of young and middle-aged experts who have made outstanding achievements in both medical research and clinical practice. The duties of WJG editorial members are to evaluate the originality, innovation, scientific standards and readability of the papers, provide constructive comments, suggestions and advice for further revision and improve English writing for papers written by non-English speaking authors. Acceptance of a submitted paper is based on the overall assessment of the title, introduction, materials and methods, findings, and discussion sections, and whether the paper reflects a high standard of clinical or basic study on digestive diseases. There has been a considerable variation in the quality of papers submitted to the journal over the past years. Major problems include the scientific standards and readability. To overcome these problems and improve the quality of the journal, the WJG has established its evaluation criteria.

EVALUATION

According to the evaluation of editorial members, submitted papers are classified as "high priority", "ready for publication", "publication after revision", "re-evaluation after revision" and "rejection". To ensure the academic standards of published papers, WJG defines the following evaluation criteria:

Title should accurately reflect the scientific nature of the study, and should be concise and innovative.

Abstract should clearly present the research background and objectives, the materials and methods, the findings (including important data) and the conclusion. The innovative and focal points of study should be consistent with the objectives, the materials and methods, the findings (including important data), and the conclusion.

Introduction should include research objectives and other study related matters.

Materials and methods should include material characteristics, e.g., randomization of large samples, safety and efficiency, double-blind and double-simulation, comparisons between multi-center parallel control groups in contrast to clinical experiments, special cases, and cell or tissue samples. Test methods and techniques should be standard, innovative, or systematic. Improved or innovative methods should be repeatable and verifiable by others. The design of comparative studies should be rational and reliable, and statistical methods should be appropriate.

Results should have a well-defined scientific conclusion based on the experimental evidence. Attention should be paid to the

sample size and statistical analysis when evaluating a clinical study. **Discussion** should include logistic and systematic theoretical analyses and valuable scientific conclusions.

Bibliography Studies quoted should be proper and sufficient, especially for the latest literature.

General evaluation The originality, scientific standard, innovation and readability of the paper should reflect the advances in clinical and basic studies in gastroenterology and hepatology.

EDITING

Excellent papers as assessed by the editorial board may be published without revision. The authors will be advised to revise their papers according to the comments/suggestions made by the editorial members and in consistent with the journal format. The revised papers will be subjected to the first and second language processing. Format-revised papers will then be put into layout. Thereafter, laid out draft will be sent to the editor-in-charge for the proofreading and finally for printing once there are no grammatical and spelling mistakes. In order to ensure the editing quality of published papers, WJG defines the following editorial criteria.

Title should be concise and unique. The following words should be avoided: evaluation, study, analysis, observation, investigation, exploration, the article “the” and abbreviations that are not commonly used. For further information, please refer to “*Writing English Title for Scientific Papers*” <http://www.wjgnet.com/1009-3079/new/26.asp>.

Abstract should be in a structural format. Objectives should be directly pointed to the topic, e.g. “To investigate the...”. A summary of the background or current development in the topic may be provided. Methods (including materials) and findings (including important data) should be stated in the past tense, and conclusion should be stated in the present tense. Personal address and voice should be natural, avoiding using “the dangling participles”. First sentence of the abstract should not be a repetition of the title, it should be more specific. For further information, please see “*Writing English Abstract for Scientific Papers*” <http://www.wjgnet.com/1009-3079/new/25.asp>.

Text (1) *Short sentences*: Short sentences are preferred. As much as possible, multiple subordinate clauses should be avoided. The spelling and tenses should be correct, and tenses should be consistent. The past tense should be generally used in the Methods and Results sections. In the Discussion, the past tense should be used when a specific study is cited and present tense should be used when a conclusive statement is made based on previous studies. Tenses used in the main and subordinate clauses should be consistent with the tenses and implications of the paragraph. For Chinese authors, the Chinese version of the paper should be referred to in order to accurately express the original meanings. When using the participial phrases to express the adverb and attribute, attention should be paid to the proper voice usage for proper correspondence. Word comparisons should be consistent, and the same term should be used to refer to the same thing. Basic data and their percentages should be checked during editing. Editing checks should include accurate use of symbols and Latin terms (singular and plural forms). (2) *Numerals*: Numerals appearing at the beginning of the sentence should be stated in words, e.g. Sixteen cases...or A total number of 16 cases. No Arabic numerals, e.g. 16 cases, 100 patients, should be used to start a sentence. (3) *Abbreviations*: When an *abbreviation is used* for the first time in the text, the entire term should be spelt out, followed by the *abbreviation* in parenthesis. (4) *Italics*: The following should be italicized: Latin terms of bacteria, virus, plants and animals, statistical symbols, genetic symbols, END for endonucleases (first three characters), measurement

symbols, Latin terms, e.g. *in vivo*, *in situ*, *et al*, and titles of publications stated in the bibliography. (5) *Graphs*: The same graph should be used only once, data expressed in graphs should not be expressed in table again, or *vice versa*. Data shown in tables and graphs should be the same as those in the text. Annotation of the graph or table data should be stated in the present tense, e.g. the data are shown in Table 1. Graphs and tables should be included in the body text, first letter of the notation/definition should be capitalized, the rest should be in small letters.

References should be indicated in the order appeared in the text. Authors and titles should be consistent with those shown in the first page of the paper. The same is true for journals, year, volume number, pages (beginning and last pages), and PMID codes.

Others (1) The manuscript should be printed in double-space. (2) Formal language should be used. Informal and non-standard abbreviations or contractions, e.g., isn't, aren't, hasn't, hadn't, haven't, don't, can't, wouldn't, a lot of, a bit, too (also), thru (through), exam (examination), lab (laboratory), *etc.* should be avoided. (3) Methods and results should be objectively presented, statements should be simple and unexaggerated. Emotional or advertising promotional terms should be avoided. (4) The verb form is preferable, the gerund or noun form of verb should be avoided. (5) Proper use of articles is required, countable nouns should be expressed in the plural form as much as possible. (6) A prepositional phrase or a hyphen should be used to break off a noun phrase, and a long series of adjectives or nouns to modify nouns should be avoided. (7) As much as possible, sentences begin with important facts, not with phrases or subordinate clauses. (8) When referring to the work or research outcome of other investigators, the authors should state full name of the investigators, in the case of more than two investigators, the term “*et al*” should be used. For further information, please see “*Writing Scientific Paper in English*” <http://www.wjgnet.com/1009-3079/new/31.asp>.

COLUMNS

WJG consists of the following columns.

Review papers come from experts who are specialized in the fields.

Special topics include esophageal cancer, gastric cancer, liver cancer, viral hepatitis, Chinese medicine, integrated Chinese and Western medicine, and pioneering papers with Chinese characteristics or first-class international standards.

Basic research Studies should have complete experiment data, high academic values, and innovative and original findings.

Clinical research Studies should demonstrate randomization of large samples, safety and efficiency, double-blind and double-simulation, comparison between multi-center control groups and clinical experiments.

Brief reports should present innovative and original phase outcomes.

Case reports should have some instructional significance to clinical practitioners.

MANUSCRIPT MANAGEMENT

In an effort to speed up the computerization and electronization of WJG manuscript management, improve the journal quality, standardize editing procedures, and increase the work efficiency, the WJG Publishing Manuscript Management System was successfully established on April 15, 2003. It enables the automation and electronization of submission registration, submission acknowledgment, preliminary evaluation, second evaluation, evaluation results, final decision, acceptance/rejection notification, editing processing, data

exchange, and Internet submission inquiry. Authors can follow-up the status of their submitted papers at the WJG website, by typing in user name (first author's name) and password (manuscript number). Information regarding serial number, journal name, title, author, date of receipt, editing date, acceptance/rejection date, official invoice number, date of publication, issue (volume) and pages will be provided.

PUBLICATION FREQUENCY

From January 2004, the journal will be published twice monthly. Thus, the submission-publication lag period is expected to be controlled as short as between 1 to 4 months. This journal has been included in the famous international search systems such as the Science Citation Index-Expanded and *Index Medicus*/MEDLINE, in the hope of demonstrating the world leading position of Chinese researchers in gastroenterology. For instance, the paper "Different approaches to caudate lobectomy with "curettag and aspiration" technique using a special instrument PMID: A report of 76 cases" written by Shu-You Peng, Jiang-Tao Li, Yi-Ping Mou, Ying-Bin Liu, Yu-Lian Wu, He-Qing Fang, Li-Ping Cao, Li Chen, Xiu-Jun Cai, Cheng-Hong Peng, Department of Surgery, 2nd Affiliated Hospital, School of Medicine, Zhejiang University and published in volume 10 of 2003 is of international standards. The submission-publication lag time of this paper was only 45 days.

TYPESETTING AND PRINTING

The WJG uses a uniform font and format from the top margin of book, column, title, author, position of authors, fund and grants, contact address, e-mail address, telephone numbers, fax numbers, date of receipt, acceptance date, abstract, reference format, class 1 heading font, class 2 heading font, graph, chart, to references. No subsequent papers are followed after the end of each paper, thus, papers can be used in the abstract database, ASP, SML, or PDF format. WJG uses the PageMaker publishing software, hence files can be automatically converted to ASP, XML or PDF format.

The printing films for WJG are imported films. Heidelberg color printing is used for the monochrome and color printing. In addition, the three-sided knife is used for trimming. Actual printing work is contracted by the Beijing KH Printing Company. The printing service covers the full-length production work from filming, design drafting, pre-binding sample, to full delivery to the magazine office for approval. Printing follows after every aspect has been approved.

ELECTRONIC VERSION

WJG website (<http://www.wjgnet.com/1007-9327/index.asp>) went online on April 15, 2003, and as of December 21, 2003, the site has been visited 678 857 times. The electronic version of the WJG has the following seven columns.

Journal introduces Editorial Board, Board member briefs, indexing services by which the WJG is abstracted, and current impact factor.

Published gives information about the publisher, copyright and subscription.

Submission includes instructions to authors and details for preparing review, original manuscript, brief report and case report.

News lists journals indexed in *Index Medicus* (IM) and impact factors by Journal Citation Reports (JCR).

Submission search allows authors to enter user name and password to obtain full information (up to 28 features) on their submissions.

E-journal allows search for current and previous issues (1995-2003). The WJG E-journal offers options such as HTM or PDF

files, abstracts, related studies, citation frequency, visiting times, download counts, and comments.

Reference links WJG proofreads the entire reference and first page to ensure accuracy of the author, title, year, volume, page number, and PMID. Reference is also linked with the PubMed and <http://www.wjgnet.com/1007-9327/index.asp> abstracts and documents for citation accuracy, thus providing readers with an access to the citation material and abstract.

CIRCULATION

In 2003, 973 WJG journals were circulated, that is 168 local post office subscriptions within 27 Chinese administrative regions, 105 international subscriptions from 56 countries and regions, and 700 complimentary issues mailed to the investigators in charge of National Project No. 973 and No. 863, as well as the project coordinators of China National Natural Science Foundation. We are providing with complimentary copies of the e-journal to the members of the American College of Gastroenterology, the American Association for the Study of Liver Diseases, and the American Association for Cancer Research, hoping that more international experts in gastroenterology read the papers published in the WJG. Currently, circulation volume of the e-journal has reached 21 200 copies.

SUBMISSION SOURCES AND GRANT STATUS FOR PUBLISHED PAPERS

The upgrade of our national scientific research standards has gradually increased the quality of scientific papers. A higher growth rate was noticed in the volume of papers coming from the famous universities, research facilities (especially laboratories with excellent scientific records), subject groups and scientists. During the period from April 01 to October 01, 2003, we received a total of 618 papers: 501 (81.06%) from China, and 117 (18.93%) from the overseas. A total of 521 papers (21 reviews, 27 esophageal cancer, 54 gastric cancer, 65 liver cancer, 39 intestinal cancer, 46 viral hepatitis, 20 *Helicobacter pylori*, 115 basic studies, 62 clinical studies, 62 brief reports, 8 case reports, and 2 letters from readers) were published in issues 1 to 10 in 2003, 450 (86.37%) were from Chinese institutions, and 71 (13.62%) from the overseas. There were 2 949 authors with 14.41% being from the overseas. The authors were from 34 nations and regions including Argentina, Australia, Pakistan, Brazil, Belgium, Poland, Denmark, Germany, France, Finland, Korea, the Netherlands, Canada, Croatia, United States, South Africa, Yugoslavia, Japan, Sweden, Switzerland, Saudi Arabia, Thailand, Turkey, Spain, Greece, Singapore, Hungary, Iran, Italy, India, United Kingdom, the Mainland of China, Taiwan and Hong Kong. Grant-funded papers accounted for 292 (56.04%) of the published papers. Grant-funded case study papers accounted for 440 (84.45%) papers, which were composed of 25 (4.79%) international grant-funded, 180 (34.54%) National Project No. 973 and No. 863, and National Science Council funded, and 235 (45.10%) government (ministry or provincial office) funded papers. In 2002, the WJG published 226 papers from 26 regions, 93.36% from China, and 6.63% from the overseas, and 60.61% were grant-funded papers. In 2001, the WJG published 173 papers from 20 regions and 112 institutions, 35% were from the overseas and 55% were grant-funded. In 2000, the WJG published 205 papers, and 50% were grant-funded. In 1999, the WJG published 144 papers from 20 regions and 100 institutions, 23% were from overseas and 50% were grant-funded. In 1998, the WJG published 183 papers from 11 regions, 9.84% were from the overseas and 59.56% were grant-funded.

VISITING NUMBER AND DOWNLOAD COUNT

The WJG started producing dynamic web pages from issues 4 to 9 in 2003 e-journal. Visiting number and download count of the papers were recorded. A total of 322 papers were published from issues 4 to 9, and 265 (82.29%) papers were visited and downloaded. During the period from April 13 to October 13, 2003, these 265 papers were visited 35 745 times, or an average of 134.89 times per paper. The highest visiting number was 1 918 and the lowest one was 11. Of these papers 131 (49.43%) had visiting times exceeding 100, 123 (46.41%) had 30-99 times and 11 (4.15%) had 11-29 times. The highest download count was 1 087 and the lowest was 10. For instance, in the review paper "RNA interference: Antiviral weapon and beyond. World J Gastroenterol 2003; 9(8): 1657-1661" written by Quan-Chu Wang, Qing-He Nie, Zhi-Hua Feng, The Center of Diagnosis and Treatment for Infectious Diseases of Chinese PLA, Tangdu Hospital, Fourth Military Medical University was visited 1 918 times and downloaded 1 087 times.

IMPACT FACTORS

Impact factor is an international journal evaluation index. It is a general quantification index reflecting the importance of a journal. Usually a greater impact factor would mean that a journal has a greater academic impact and effect. The total journal citation frequency refers to the total number that the entire paper content of a journal has been abstracted from the time the issue was published in the yearly statistics. It is a highly objective and practical evaluation index capable of showing the usage and degree of attention paid to the journal, as well as its effects and status in the science community. In the Journal Citation Reports (JCR) of the Institute for Scientific Information (ISI), the impact factor of the WJG in 2002 was rated 2.532 with a citation frequency of 1 535, which was ranked thirteenth among 45 journals in the international gastroenterology and liver disease fields, and ranked 797th among the 5 876 international science journals registered in the SCI. The impact factor of the WJG in 2001 and 2000 was 1.445 and 0.993, respectively, with a citation frequency of 722 and 327, respectively. The complete electronic version (ASP, PDF) of the papers published since 1998 has been linked to the PubMed digest, hence worldwide readers can have a free access to the papers published in the WJG using the PubMed search engine. Authors of the journal are thus given worldwide and immediate exposure. As a result, the impact factor of the journal has shown an annual growth, and more importantly, the international influence of the journal continues to expand.

AWARDS FOR PUBLISHED PAPERS

A total of 15 papers won the National, Ministerial, or Provincial Science and Technology Progress Awards during the 1998-

2002 period. For example, the paper "Pharmacokinetics of traditional Chinese syndrome and recipe: A hypothesis and its verification (I). World J Gastroenterol 2000; 6(3): 384-391" written by Huang X, Ren P, Wen AD, Wang LL, Zhang L, Gao F, won the second prize of the National Science & Technology Progress Award.

COLLECTIONS OF INTERNATIONAL SEARCH SYSTEMS

Science Citation Index[®]-Expanded (SCI-E) of the ISI is a comprehensive search engine that collects over 5 876 authoritative scientific journals from different parts of the world. It has a stringent journal selection standard, and is an internationally recognized principal scientific statistics and evaluation engine, thus making it an important citation in the assessment of the value of a journal and the academic standards of its papers. The special citing and cited relations between the author-to-author and paper-to-paper for SCI-E make SCI-E become the most authoritative assessment system for scientific research results internationally. The frequency of scientific journals and papers that are collected or cited by SCI-E in one country or region, will be considered as an index of assessing the scientific research standards for that country or region. Since 1998, the WJG has been successively collected by (SCI-E, Research Alert[®], Current Contents/Clinical Medicine[®], Journal Citation Reports[®], Clinical Medicine Citation Index[®]), *Index Medicus*/MEDLINE (US), Chemical Abstracts, CA (US), EMBASE/Excerpta Medica, EM (Netherlands), Abstract Journals, AJ (Russia).

HONORS

The WJG is nationally recognized as a core journal in national natural science and an outstanding journal in science and technology, with an honor of the 2nd National Journal Award, and was listed as one of the 100 most important journals in China. In 2001, it was selected into the China Journal Square consisting of "200" journals. It was awarded a specific project grant for the key academic journals by the National Natural Science Foundation in 2002 (project grant no.: 30224801).

Overall, the WJG has already developed to a value-oriented (quality and quantity) journal and functions pursuant to the international standard requirements. In addition, the journal has also completed the management marketation from manuscript submission to publication. Fair and scientific evaluation is applied to make acceptance/rejection decision for each paper submitted. In terms of academic standards and editorial quality, the WJG aims to become one of the best international journals. With the strong support of the authorities, authors, readers, the entire editorial board and the community, the WJG will become one of the most influential international academic journals of its field.

Edited by Xia HHX, Liu HX and Wang XL

Primary gastric lymphoma

Ahmad M. Al-Akwaa, Neelam Siddiqui, Ibrahim A. Al-Mofleh

Ahmad M. Al-Akwaa, Neelam Siddiqui, Ibrahim A. Al-Mofleh, Gastroenterology Division, Neelam Siddiqui, Oncology Division, Department of Medicine, College of Medicine and King Khalid University Hospital, King Saud University, Riyadh, Saudi Arabia

Correspondence to: Professor Ibrahim A. Al-Mofleh, MD, Department of Medicine, Gastroenterology Division (59), College of Medicine & KKHU, P. O. Box 2925, Riyadh 11461, Saudi Arabia. iamofleh@yahoo.com

Telephone: +966-1-4671215 **Fax:** +966-1-4671217

Received: 2003-08-08 **Accepted:** 2003-10-08

Abstract

AIM: The purpose of this review is to describe the various aspects of primary gastric lymphoma and the treatment options currently available.

METHODS: After a systematic search of Pubmed, Medscape and MDconsult, we reviewed and retrieved literature regarding gastric lymphoma.

RESULTS: Primary gastric lymphoma is rare however, the incidence of this malignancy is increasing. Chronic gastritis secondary to *Helicobacter pylori* (*H pylori*) infection has been considered a major predisposing factor for MALT lymphoma. Immune histochemical marker studies and molecular biology utilizing polymerase chain reaction have facilitated appropriate diagnosis and abolished the need for diagnostic surgical resection. Advances in imaging techniques including Magnetic Resonance Imaging (MRI) and Endoscopic Ultrasonography (EUS) have helped evaluation of tumor extension and invasion. The clinical course and prognosis of this disease is dependent on histopathological sub-type and stage at the time of diagnosis. Controversy remains regarding the best treatment for early stages of this disease. Chemotherapy, surgery and combination have been studied and shared almost comparable results with survival rate of 70-90%. However, chemotherapy possesses the advantage of preserving gastric anatomy. Radiotherapy alone has been tried and showed good results. Stage III E, IVE disease treatment is solely by chemotherapy and surgical resection has been a remote consideration.

CONCLUSION: We conclude that methods of diagnosis and staging of the primary gastric lymphoma have dramatically improved. The modalities of treatment are many and probably chemotherapy is superior because of high success rate, preservation of stomach and tolerable complications.

Al-Akwaa AM, Siddiqui N, Al-Mofleh IA. Primary gastric lymphoma. *World J Gastroenterol* 2004; 10(1): 5-11
<http://www.wjgnet.com/1007-9327/10/5.asp>

INTRODUCTION

Primary gastric lymphoma is a rare tumor, accounting for less than 5% of primary gastric neoplasms^[1-5]. However it is the most common extranodal lymphoma, representing 4-20% of all extranodal lymphomas^[6,7]. In the Middle East, stomach is the most common gastrointestinal site, with an incidence rate

similar to that reported in the western literature^[8-11]. However Turkish and Indian series suggested that intestinal lymphomas have been more predominant than gastric lymphoma in those regions^[12,13].

Gastric lymphomas are prevalent in patients aged more than 50 years, however it still has been reported in the second decade of life^[14,15]. Reported median age is 60-65 years and males are 2-3 times more affected than females^[16-18]. Recently, several studies have shown an increase in the incidence among HIV infected and AIDS patients, affecting increasingly younger age groups^[19-21].

PATHOLOGY

Malignant lymphomas affect the stomach as a primary tumor or as part of more wide spread disease process. Stomach is the most common site with secondary lymphoma^[22,23]. Generally lymphomas are considered as "primary" in the gastrointestinal tract when the initial symptoms of the disease are in the abdomen indicating a disturbance of the gastrointestinal function, or when the bulk of the disease is in the stomach.

Most gastric lymphomas are thought to arise in the mucosa or submucosa from the so-called mucosa-associated lymphoid tissues (MALT), which usually develop after chronic inflammation induced by *H pylori* infection^[23-26]. Histologically and immunohistochemically MALT lymphomas are of the B-cell non-Hodgkins type (NHLs) and share many features in common, therefore they are denoted as malignant lymphomas of MALT. The association between *H pylori* chronic gastritis and MALT lymphoma has been confirmed in large population based studies where immunological evidence of *H pylori* infection has been shown to be more in patients with gastric lymphomas than in matched controls^[24-26]. Other forms of gastric lymphomas are non-MALT type, although many may be initially MALT tumors. Rare tumors may be T cell in origin^[27-30].

The histological classification may vary from low to high grade. Grading has been classified into low, intermediate and high grade. Other terminology of primary and secondary high-grade lymphomas has been adopted^[24]. In the histology of secondary high-grade lymphomas, there is evidence of low-grade component. Various systems (Rappaport, Working formulation and Modified Kiel) have frequently been utilized for histological classification, Combination of two or three classification systems have also been commonly used^[17,23,30,31].

A majority of primary gastric lymphomas are histologically of the diffuse histiocytic or large cell type^[15,32,33]. Reports from Saudi Arabia have shown a predominance of diffuse large B-cell type^[14,33]. Gastric maltoma represents up to one half of primary gastric lymphoma. In the last few years, the Revised European American Lymphoma (REAL) classification of lymphoid neoplasms has been widely used with the advantage of high reproducibility and clinical relevance (Tables 1,2)^[32,34].

Microscopically, low-grade lymphomas may not easily be distinguished from pseudolymphomas, a term used to describe the lymphocytic infiltration of the gastric mucosa, which may occur with chronic gastritis and peptic ulceration. Pseudolymphomas may mimic clinically and endoscopically gastric adenocarcinomas or lymphomas. Pathologists can differentiate between pseudolymphomas and lymphomas based on several histological characteristics which indicate malignant

changes, like prominent lymphoepithelial lesions (lymphoid infiltration of glands or crypts with partial destruction), Dutcher bodies and moderate cytologic atypia^[35]. In cases which can not be diagnosed with histological differentiation, immunohistochemical marker studies or molecular biology utilizing polymerase chain reaction (PCR) may facilitate establishing an accurate diagnosis^[36,37]. However, recent studies have indicated that the great majority of pseudolymphomas are in fact true lymphomas of low-grade malignancy using markers of clonality, and this term preferably has to be abandoned^[37].

Table 1 The REAL classification of non-Hodgkin's Lymphomas

B-cell lymphomas	
Precursor B-cell lymphomas:	B-lymphoblastic
Mature B-cell lymphomas:	B-cell CLL/small lymphocytic
	Follicular
	Marginal-zone-nodal
	Extranodal marginal-zone (MALT)
	Splenic marginal-zone
	Lymphoplasmacytic
	Mantle-cell
	Diffuse large B-cell
	Primary mediastinal large B-cell
	Burkitt's like
	Burkitt's
T-cell lymphomas	
Precursor T-cell lymphomas:	T-lymphoblastic
Mature T-cell lymphomas:	Mycosis fungoides/sezary syndrome
	Peripheral T-cell (many subtypes)
	Anaplastic large T/null cell
	Adult T-cell leukemia/lymphoma

Table 2 Histologic classification of gastrointestinal lymphomas

B-cell	
Mucosa-associated lymphoid tissue (MALT)-type (extranodal marginal-zone lymphoma):	Low-grade
	High-grade, with or without a low-grade component
Immunoproliferative small intestinal disease (IPSID):	Low-grade
	High-grade, with or without a low-grade component
Lymphomatous polyposis (mantle-cell lymphoma)	
Burkitt's and Burkitt's-like	
Other types of low- or high-grade lymphoma corresponding to lymph node equivalents	
T-cell	
Enteropathy-associated T-cell lymphoma (EATCL)	
Other types not associated with enteropathy	

Macroscopically, gastric lymphomas may appear as ulcerated (single, multiple or diffuse), polypoid, granulonodular or infiltrative lesions^[13,24,33]. Ulcerative type alone or combined with other lesions has been the most frequent endoscopic presentation of primary tumors. The lesion may vary from fine nodularity or normally looking mucosa to very advanced large fungating ulcerated mass^[13]. Endoscopically, the differentiation between lymphomas and adenocarcinomas may not be easy, however early lymphomas tend to produce larger tumors than adenocarcinomas and may be multifocal as well^[15]. Gastric lymphomas involve more frequently the antrum and corpus^[33]. In a series, 46% of lesions are located at gastric body^[24]. Entire

gastric involvement has also been reported^[18,24]. In advanced diseases tumors may spread to extraintestinal sites like central nervous system, bone, liver, kidneys, ovary and lungs^[24].

CLINICAL PRESENTATION

The initial symptoms of upper abdominal pain and early satiety may be vague and nonspecific, leading to a delayed establishment of diagnosis up to several years^[39]. Symptoms and signs may mimic that of other abdominal pathologies including peptic ulcer disease, gall bladder, pancreatic or functional disorders as well as other gastric neoplasms^[15]. Other common symptoms included weight loss, nausea, vomiting, abdominal fullness and indigestion^[30,31,33]. Weakness, night sweat, jaundice, fever and dysphagia occur less frequently^[13,23,30]. Many patients came down late with advanced disease and complications may develop before diagnosis^[38]. Twenty to thirty percent may present with bleeding in the form of hematemesis or melena while, gastric obstruction and perforation are less common^[37,38]. Physical examination could be normal in 55%-60%^[30]. Common signs include epigastric tenderness and palpable mass. The tenderness is encountered in 20%-35% and masses in 17%-25%^[15,23,31]. Other uncommon findings included fever, hepatomegaly, splenomegaly, jaundice and lymphadenopathy. In one series, lymphadenopathy is found in 12%^[24,30,31]. Signs of malnutrition may also appear in advanced disease^[39].

DIAGNOSIS

Clinical presentation and radiological features are often nonspecific. Esophagogastroduodenoscopy (EGD) and biopsy are primary methods for diagnosis^[15,40]. The diagnosis of low-grade MALT lymphoma by forceps biopsy is often difficult in early disease and repeated endoscopies and biopsies may be required before final diagnosis is achieved^[25].

Multiple and step biopsies are required because endoscopic findings may vary from subtle mucosal changes to gross lesions. These may include mucosal edema, friability, patchy redness, irregular patchy gray or whitish granularity, contact bleeding, superficial irregular erosions and ulcerations^[33]. Repeated endoscopic biopsies are mandatory in case of clinical suspicion and negative or inconclusive histology. Furthermore, endoscopic mucosal resection enhances the histological yield^[41]. Occasionally, rapid diagnosis by endoscopy can be made by detection of monoclonality in immunoglobulin heavy chain rearrangement of the lymphoproliferative disease by PCR^[42]. It is recommended that biopsy specimens should undergo histological, immunohistochemical and genotyping studies to make the diagnosis.

Radiological examinations can help establish diagnosis and determine the extent of the lesions. Gastric wall thickening, atypical ulcer deformities, obstruction and mass effect are enhanced features suggestive, but not specific for gastric lymphoma^[30,31,38]. CT scan of the abdomen can identify the gastric wall thickening or mass lesions in 85% of cases. Sometimes it may show typical imaging features of more homogenous and pronounced mural thickening that can help differentiate lymphomas from adenocarcinomas^[42,43]. On CT scan, three quarters of cases of low grade MALT lymphomas may present with infiltrative form and polypoid form in the remainder. Lymphadenopathy is detected in only 50%^[43]. Conventional sonographic examination can be of value in identification of gastrointestinal involvement as well as abdominal lymph node enlargement in lymphoma staging. The MRI features include irregularly thickened mucosal folds, irregular submucosal infiltration, annular constricting lesion, exophytic tumor growth, mesenteric masses and mesenteric/retroperitoneal lymphadenopathy^[44]. EUS is a valuable

technique in assessing the extent and invasion of the lesion. By EUS, infiltrative carcinomas tend to show a vertical growth in the gastric wall, while lymphomas tend to show mainly a horizontal extension^[45,46]. It is highly accurate in determining the depth of lymphomatous infiltration and the presence of perigastric lymph nodes, thus providing additional information for therapeutic planning. It can differentiate between lymphomas and carcinomas in early stages, but in advanced stages both have similar appearances. With the development of the above diagnostic methods, open surgery is rarely needed to confirm the diagnosis.

STAGING

After establishing the diagnosis of primary gastric lymphoma, staging is essential for planning treatment. It is also important to rule out systemic lymphoma with secondary involvement of the stomach. The staging process starts with endoscopy and step biopsy to rule out microscopic infiltration of nearby structures like the duodenum. Chest radiography may show gross lesions in the lungs and mediastinum. CT scan of chest, abdomen and pelvis permits assessment of nodal involvement above and below the diaphragm, and extension of the tumor outside the stomach. EUS may be employed for accurate estimation of both the depth of invasion and involvement of regional lymph nodes^[45,46]. It is superior to CT scan in false negative cases. Bone marrow examination helps determine presence or absence of tumor spread. Indirect laryngoscopy is also helpful for excluding Waldeyer's ring involvement, which is reported to be associated with gastric lymphoma^[32].

Table 3 Staging classification according to Musshoff's criteria

Stage	Definition
IE	Lymphoma limited to the stomach
IIE ₁	Involvement of stomach and contiguous lymph nodes
IIE ₂	Involvement of stomach and noncontiguous subdiaphragmatic lymph nodes
III	Involvement of stomach and lymph nodes on both sides of diaphragm
IV	Hematogenous spread (stomach and one or more extralymphatic organs or tissues)

The following subscripts may be added E=extranodal, S=splenic, A=asymptomatic, B=symptomatic.

Table 4 Modified Blackledge staging system for gastrointestinal lymphomas

Stage I	Tumor confined to gastrointestinal tract without serosal penetration: Single primary site Multiple, non-contiguous lesions
Stage II	Tumor extending into abdomen from primary site: Nodal involvement II ₁ Local (gastric/mesenteric) II ₂ Distant (para-aortic/paracaval)
Stage II_E	Penetration of serosa to involve adjacent 'structures': Enumerate actual site of involvement, e.g. stage II _E (pancreas), stage II _E (large intestine), stage II _E (post-abdominal wall) Perforation/peritonitis
Stage IV	Disseminated extranodal involvement or a gastrointestinal-tract lesion with supradiaphragmatic nodal involvement

Various staging systems have been used. The Ann Arbor staging for primary lymphomas has been modified by

Musshoff, and utilized by several authors for staging gastric lymphomas (Table 3)^[18,47,48]. Several alternative staging systems have been proposed, and the revised version of the Blackledge staging system has been recommended for general use (Table 4)^[49,34]. Several authors have suggested that such staging modification may be of prognostic significance^[50,51,53].

TREATMENT

The modalities of treatment for gastric lymphomas have been a controversial subject, and the best regimen has not been standardized. However, options of treatment depend on the histologic classification and stage of the disease. Some centers adopt surgery alone, while others advocate non-surgical treatment with radiation, chemotherapy or both.

SURGERY

Traditionally, aggressive surgical resection has been the main stay of treatment because it can collect definitive tissues for pathologic examination, allow exploration of the abdomen, reduce tumor burden and obviate the concern that gastric hemorrhage or perforation would complicate medical treatment of lymphomas. More recently, radical gastrectomy is disputed and considered unnecessary. Lesser procedures are now accepted where resection of the gross disease and involved lymph nodes will provide adequate results^[39,52,53]. Several reports have shown a superior outcome when surgical resection is undertaken in the early stages of the disease with a 5-year survival rate of 80%-93%^[54,55].

Kazaya *et al* advocated wide resection of early gastric tumor and extensive lymph node dissection^[15]. Other authors also found surgery alone to be an adequate treatment for stage IE or pure MALT lymphomas with a survival rate of >95%, provided staging is performed after radical gastrectomy^[56]. In a large series of patients treated according to *H pylori* status, tumor grade and stage, surgical resection remained the treatment of choice in patients with stage IIE, low-grade lymphoma and non-responders of stage IE treated by eradication for *H pylori*, however the author advised further studies to compare surgical with conservative treatment^[57].

A prospective study from France, has found that in stages IE and IIE, the complete response, survival rate and disease free survival rates were similar to those who underwent complete resection, partial or no surgery prior to administration of chemotherapy. The survival rates of 60% with surgery alone compared to 85% if adjuvant chemotherapy was given, were reported^[40]. In a retrospective study of 92 patients from Italy in different stages who underwent surgical resection when it was feasible, the ten-year actuarial survival rates were 100% and 80% for stage IE and IIE respectively compared with 21% and 0 for stage IIIE and IVE^[58].

Surgical resection with clear margins is advised in order to maximize the chance of cure^[39,55,59]. On the contrary, other reports have found no difference in survival, whether the margin of resection was clear or not, as long as post-operative chemotherapy had been given^[60,61].

The mortality and morbidity related to surgery were similar if not more than those related to non-surgical treatment for stage I and II. Therefore, aggressive surgery is not indicated due to increased morbidity which is outweighing the benefit gained in terms of survival^[60-62] and gastrointestinal organ preservation may provide substantial advantage for the quality of life in these patients^[39]. Resectability rates ranged from 60%-88%, and the 5-year survival ranged from 50%-87%^[55,60]. Debulking of advanced disease was associated with the high morbidity and mortality and low response rates of 6%-40%^[63]. Operative mortality was between 3%-25% with higher rates

for palliative procedures which were performed for symptomatic relief, removal of tumor mass and avoidance of hemorrhage or perforation related to other mode of therapy^[63]. In a prospective study of 208 patients, there was no difference in therapeutic outcome in surgically or conservatively treated patients, even after complete resection, the authors concluded that surgery favored by most authors in treatment of primary gastric lymphoma should be reassessed^[64].

CHEMOTHERAPY

The effect of chemotherapy alone as a sole treatment for gastric lymphomas is still debatable. The needs behind trying chemotherapy were the considerable morbidity and mortality associated with resection^[63]. Stomach conservation, and avoidance of postoperative complications such as myocardial infarction, gastrointestinal bleeding, enterocutaneous fistula and malabsorption syndrome were important factors that obviated the choice of chemotherapy. Initial trial in a small number of patients in stage I E and II E has shown excellent results by combination of chemotherapy and radiotherapy with a survival rate of 70% and few complications^[52]. Salvgnol *et al* reported a survival rate of 71% in patients treated by chemotherapy^[55]. Another recent study on aggressive gastrointestinal lymphoma found primary chemotherapy with or without radiotherapy useful and induced a complete response in 81% of patients, with fewer complications compared with surgery including less risk of perforation or bleeding^[65]. Other reports showed no apparent difference in survival between patients treated by chemotherapy or surgery and chemotherapy with survival rates of 67% and 60%, respectively. There has been no report of serious adverse effects such as bleeding or perforation in chemotherapy-treated patients of intermediate and high grade non-Hodgkin lymphomas^[60]. In a report from Italy, 17 patients with resectable large cell lymphoma treated primarily by chemotherapy with or without consolidation radiotherapy, only two failed in the first line therapy and 15 were free of disease at 6 years^[66]. Consolidation radiotherapy might improve the efficacy of chemotherapy. None of the patients experienced acute treatment related morbidity or mortality from local complications^[68]. In three recent trials with variable chemotherapy regimens, the survival rates of 82%-88% in stage IE and IIE, high grade lymphoma with only few and manageable complications were found^[65,67,68].

In other series, chemotherapy alone compared with surgical resection alone, has shown no significant difference in the matter of survival. The overall 2-year survival was 67% and 81%^[69-71].

In patients with comorbid factors and increased risk of surgery-related morbidity and mortality, chemotherapy offered an effective or equally effective mode of treatment to surgical resection 57% vs 58%^[71].

The fear of chemotherapy-related complications, for instance, bleeding and perforation, has been disputed, and less significant compared with surgical resection^[65,67-69]. Some authors reported the incidence of chemotherapy-related bleeding between zero and three percent and no perforation^[60,72]. Therefore, chemotherapy has been suggested and adopted as a primary mode of treatment. Combined chemotherapy comprising cyclophosphamide, doxorubicin, vincristine and prednisolone (CHOP), has been the preferable and the most effective regimen for all tumor stages^[31,65]. Several other regimens have also been used with almost similar efficacy and comparable toxicity^[75]. While cyclophosphamide, vincristine and prednisolone (COP) were adopted for low grade lymphomas, high grade tumors were treated with doxorubicin, teniposide, cyclophosphamide and prednisolone (AVmCP). The latter two regimens combined with surgical resection have shown the survival rates of 80% and 100%, respectively^[73].

COMBINED THERAPY

Multimodal therapy, combining resection with chemotherapy and occasionally radiotherapy have been commonly and widely accepted in many centers. It has significantly improved the 5-year survival^[10,27,55,59,60,74]. Combination of radical surgery followed by chemotherapy has been associated with a significantly improved outcome in comparison with chemotherapy alone^[73]. Lin *et al* have compared surgery, surgery with adjuvant chemotherapy and chemotherapy alone and found the 5-year survival rates of 57%, 76% and 58% compared with 0% in the untreated group. They recommended surgery when feasible with adjuvant chemotherapy as the mainstay of treatment for gastric lymphoma^[71]. A Chinese study has suggested that chemotherapy plays a role in improving survival rates post-surgical resection^[53]. A prospective study from France in 1990 reported a 100% survival in patients with high-grade tumors who underwent resection and adjuvant chemotherapy. A recent series has shown the superiority of combined surgery and chemotherapy to single mode with survival rates between 86%-94% for stages IE and IIE^[53,59,66]. In these series the survival rates were higher for those who had complete resection, resection was the most important variable and major determinant of prolonged complete remission^[59,60]. Survival was higher in low-grade lymphomas, although the initial response might be superior in high grade lymphomas^[59]. Combined radical surgery and chemotherapy depending on the histologic grading were also associated with prolonged remission^[73].

Resection of the tumor with clear margins is thought to have a better prognosis than with diseased margins^[52,74,75]. However, other authors have found insignificant difference between the two procedures as long as post-operative chemotherapy was administered, and the extent of the disease at time of surgery, full thickness disease and lymph node involvement were important determining factors^[39].

On the contrary, other studies reported no significant difference in outcome in groups treated with single or combined mode of treatment^[57,62,70,72].

The stage and histologic grade of the disease play a role in the selection of the treatment modality, in addition to the comorbid disease and age of the patients.

Early stages of the disease regardless of the histological grade may be controlled by chemotherapy or chemotherapy and radiotherapy with the advantage of gastric conservation and avoidance of post-operative mortality and morbidity^[54,62,65-67,69,74]. On the other hand, surgery is advocated as the first option with adequate control of the disease^[57-59, 61], and occasionally with the necessity of wide resection and extensive lymph node dissection^[15,78], however, adjuvant chemotherapy is indicated to control the local and distant disease if any^[75,78].

In advanced stages of gastric lymphoma (stage III E, IV E) the behaviour of the tumor has the same manner as other advanced non-Hodgkin lymphomas, therefore combined chemotherapy is considered the treatment of choice for locally advanced or disseminated aggressive disease. In a prospective study of 700 patients with aggressive lymphoma treated with intensive chemotherapy, no difference in outcome was observed between patients with an advanced aggressive nodal lymphoma and the subset of patients (15%) in which the lymphoma was deemed to occur in the gastrointestinal tract^[40].

MALT lymphomas have aroused special interest because regression of the tumor has been reported after *H pylori* eradication. Standardization of therapy is not yet available and is still a subject of controversies. The initial results were shown in five of six patients with low grade MALT lymphomas who had regression of the tumor after eradication of *H pylori*^[77]. Thiede and associates studied a total of 120 patients with early gastric MALT lymphomas treated with amoxicillin and

omeprazole, a complete remission rate of 81% was achieved with partial response in 9%^[78]. Zucca and colleagues, in a large multinational cooperative study, treated 233 patients with antibiotics and randomized them to observation alone or maintenance with chlorambucil. Complete remission was documented in 62% and partial response in 12% with a 6-month median time to lymphoma regression. At a 40-month follow-up, a total of 15 (13%) cases had relapse^[79]. Manfred reported regression of reactive lymphoid infiltrates after *H pylori* eradication, without endoscopic or histological regression in MALT lymphomas^[26]. It is not yet known which stages of MALT lymphomas respond to *H pylori* eradication. Although it seems that eradication therapy is an adequate option of treatment taking into consideration the utility of endosonography in determining the invasion of the disease^[80].

Surgical resection, radiotherapy or chemotherapy and their combination have proven to be effective treatment modalities. Radiotherapy was tried as a local form of treatment in a small number of patients, resulting in a survival rate of 93%. Surgery, radiotherapy and antibiotics were compared and similar results were found^[81].

Radiotherapy

In most instances, radiotherapy is used as an adjuvant to surgery, chemotherapy or both. It has rarely been tried as a single mode of therapy^[31,81]. However, limited trials have suggested that radiotherapy can be utilized as a primary mode of treatment with reasonable outcome^[78,81].

Radiotherapy has been studied in comparison with other treatment modalities for stage IE and IIE with comparable outcome of 80%-89% survival^[13,31,68]. Higher survival rates (93%) have been reported in early stages of MALT lymphomas not responding to antibiotics^[83]. Radiation was used post-operatively in high- and low-grade lymphomas, for any residual tumors in stages I and II to improve the disease free survival^[9,57]. Combined chemotherapy might improve the chance of stomach conservation which may approach 100%^[72]. Total gastrectomy has not improved the survival in patients in whom radiotherapy has been utilized as the primary mode of therapy with a survival rate of 84%. Contradictory studies have found the combined radiotherapy with either resection or chemotherapy to be of no significant difference in both modalities with a survival rate of 82%-88%^[9,68,81].

PROGNOSIS

The prognostic factors in early stages were evaluated and defined in several studies. Good prognosis was associated with low grade disease, age below 65 years, free surgical margins in cases of resection, and achievement of initial complete remission^[49,50,53]. In advanced diseases, good prognosis was found in low-grade histology, initial complete response, and in general the prognosis is the same as non-gastrointestinal lymphoma^[50]. The grade of the disease also plays an important role in prognosis with better survival in low-grade disease rather than primary or secondary high-grade taking into consideration the stage^[17]. Five-year survival rates were reported to be 91% for low-grade, 73% for secondary high-grade and 56% for primary high-grade tumors^[17]. Debulking of the disease has not significantly altered the prognosis^[50,53,61,64].

CONCLUSION

Due to the rarity of primary gastric lymphoma, many aspects of this neoplasm are still controversial. The incidence of the disease is increasing and HIV-infected people are more vulnerable. Universally, gastric lymphoma is the commonest gastrointestinal lymphoma except in a few countries where

small intestinal lymphoma has been reported to be more common. On many occasions, patients present late, however with the availability of sophisticated diagnostic tools, the diagnosis can be made early and the classification and staging can be assessed accurately. The REAL classification despite being complex, has met a general agreement among pathologists and facilitated reproducibility. Most of the gastric lymphomas are primarily MALT type in origin. The best treatment for primary gastric lymphoma has not yet been exactly identified. It seems that for advanced disease, i.e., stage III and IV, combined chemotherapy and radiotherapy is superior since surgery is associated with failure of complete resection and significant morbidity and mortality. Most recent reports have advocated conservative treatment for early stages IE and IIE with the advantage of stomach conservation. On the other hand, many centers are still considering tumor resection as a better option. *H pylori* eradication with close observation has been considered adequate to treat early MALT lymphoma. Randomized trials are still needed to clarify whether conservative, surgical or combined treatment is more appropriate for treatment of localized gastric lymphoma.

REFERENCES

- 1 **Loehr WJ**, Mujahed Z, Zahn FD, Gray GR, Thorbjarnarson B. Primary lymphoma of the gastrointestinal tract: a review of 100 cases. *Ann Surg* 1969; **170**: 232-238
- 2 **Sandler RS**. Has primary gastric lymphoma become more common? *J Clin Gastroenterol* 1984; **6**: 101-107
- 3 **Aozasa K**, Tsujimoto M, Inoue A, Nakagawa K, Hanai J, Nosaka J. Primary gastrointestinal lymphoma. A clinicopathologic study of 102 patients. *Oncology* 1985; **42**: 97-103
- 4 **Laajam MA**, Al Mofleh IA, Al Faleh FZ, Al Aska AI, Jessen K, Hussain J, Al Rashed RS. Upper Gastrointestinal Endoscopy in Saudi Arabia: Analysis of 6386 procedures. *Quarterly J Med* 1988; **249**: 21-25
- 5 **Al Mofleh IA**. Endoscopic features of primary upper gastrointestinal lymphoma. *J Clin Gastroenterol* 1994; **19**: 69-74
- 6 **Aisenberg AC**. Coherent view of non-Hodgkin's lymphoma. *J Clin Oncol* 1995; **13**: 2656-2675
- 7 **ReMine SG**. Abdominal lymphoma. Role of surgery. *Surg Clin North Am* 1985; **65**: 301-313
- 8 **Salem P**, Anaissie E, Allam C, Geha S, Hashimi L, Ibrahim N, Jabbour J, Habboubi N, Khalyf M. Non-Hodgkin's lymphomas in the Middle East. A study of 417 patients with emphasis on special features. *Cancer* 1986; **58**: 1162-1166
- 9 **Almasri NM**, Al Abbadi M, Rewaily E, Abulkhalil A, Tarawneh MS. Primary gastrointestinal lymphomas in Jordan are similar to those in Western countries. *Mod Pathology* 1997; **10**: 137-141
- 10 **Gray GM**, Rosenberg SA, Cooper AD, Gregory PB, Stein DT, Herzenberg H. Lymphomas involving the gastrointestinal tract. *Gastroenterology* 1982; **82**: 143-152
- 11 **Willich NA**, Reinartz G, Horst EJ, Delker G, Reers B, Hiddemann W, Tiemann M, Parwaresch R, Grothaus-Pinke B, Kocik J, Koch P. Operative and conservative management of primary gastric lymphoma: interim results of a German multicenter study. *Int J Radiat Oncol Biol Phys* 2000; **46**: 895-901
- 12 **Dincol D**, Icli F, Erekel S, Gunel N, Karaoguz H, Demirkazik A. Primary gastrointestinal lymphomas in Turkey: A retrospective analysis of clinical features and results of treatment. *J Surg Oncol* 1992; **51**: 270-273
- 13 **Chandran RR**, Raj EH, Chaturvedi HK. Primary gastrointestinal lymphoma: 30 year experience at the cancer institute, Madras, India. *J Surg Oncol* 1995; **60**: 41-49
- 14 **Kyriacou C**, Loewen RD, Gibbon K, Hafeez M, Stuart AE, Whorton G, Al-Faleh FZ, Al-Mofleh I, Jessen K, Mass RE, El-Saghir N, Al-Khudairy N, Rifai MM, Qteishat W. Pathology and clinical features of gastro-intestinal lymphoma in Saudi Arabia. *Scottish Med J* 1991; **36**: 68-74
- 15 **Kitamura K**, Yamaguchi T, Okamoto K, Ichikawa D, Hoshima M, Taniguchi H, Takahashi T. Early gastric lymphoma; a clinicopathologic study of ten patients, literature review, and compari-

- son with early gastric adenocarcinoma. *Cancer* 1996; **77**: 850-857
- 16 **Shimm DS**, Dosoretz DE, Anderson T, Linggood RM, Harris NL, Wang CC. Primary gastric lymphoma; an analysis with emphasis on prognostic factors and radiation therapy. *Cancer* 1983; **52**: 2044-2048
- 17 **Cogliatti SB**, Schmid U, Schumacher URS, Eckert F, Hansmann ML, Hedderich J, Takahashi H, Lennert K. Primary B-cell gastric lymphoma: A clinicopathological study of 145 patients. *Gastroenterology* 1991; **101**: 1159-1170
- 18 **Weingrad DN**, Decosse JJ, Sherlock P, Straus D, Lieberman PH, Filippa DA. Primary gastrointestinal lymphoma: A 30-year review. *Cancer* 1982; **49**: 1258-1265
- 19 **Hayes J**, Dunn E. Has the incidence of primary gastric lymphoma increased? *Cancer* 1989; **63**: 2073-2076
- 20 **Powitz F**, Bogner JR, Sandor P, Zietz C, Goebel FD, Zoller WG. Gastrointestinal lymphomas in patients with AIDS. *Z Gastroenterol* 1997; **35**: 179-185
- 21 **Imrie KR**, Sawka CA, Kutas G, Brandwein J, Warner E, Burkes R, Quirt I, McGeer A, Shepherd FA. HIV-associated lymphoma of the gastrointestinal tract: The University of Toronto AIDS-Lymphoma Study Group experience. *Leuklymphoma* 1995; **16**: 343-349
- 22 **Dragosics B**, Bauer P, Radzskiewicz T. Primary gastrointestinal non-Hodgkin's lymphoma. A retrospective clinicopathological study of 150 cases. *Cancer* 1985; **55**: 1060-1073
- 23 **Radzskiewicz T**, Dragosics B, Bauer P. Gastrointestinal malignant lymphomas of the mucosa-associated lymphoid tissue: Factors relevant to prognosis. *Gastroenterology* 1992; **102**: 1628-1638
- 24 **Parsonnet J**, Hansen S, Rodriguez L, Gelb AB, Warnke RA, Jellum E, Orentreich N, Vogelman JH, Friedman GD. *Helicobacter pylori* infection and gastric lymphoma. *N Engl J Med* 1994; **330**: 1267-1271
- 25 **Stolte M**. *Helicobacter pylori* gastritis and gastric MALT-lymphoma. *Lancet* 1992; **339**: 745-746
- 26 **Isaacson P**, Wright DH. Extranodal malignant lymphoma arising from mucosa associated lymphoid tissue. *Cancer* 1984; **53**: 2515-2524
- 27 **Muller AF**, Maloney A, Jenkins D, Dowling F, Smith P, Bessell EM, Toghil PJ. Primary gastric lymphoma in clinical practice 1973-1992. *Gut* 1995; **36**: 679-683
- 28 **Kanavaros P**, Lavergne A, Galian A, Houdart R, Bernard JF. Primary gastric peripheral T-cell malignant lymphoma with helper/inducer phenotype. First case with a complete histological, ultrastructural, and immunochemical study. *Cancer* 1988; **61**: 1602-1610
- 29 **Moubayed P**, Kaiserling E, Stein H. T-cell lymphoma of the stomach, morphologic and immunological studies characterizing two cases of T-cell lymphoma. *Virchows Arch A Pathol Anat Histopathol* 1987; **411**: 523-529
- 30 **Brooks JJ**, Enterline HT. Primary gastric lymphomas: a clinicopathologic study of 58 cases with long-term follow-up and literature review. *Cancer* 1983; **51**: 701-711
- 31 **Sutherland AG**, Kennedy M, Anderson DN, Park KGM, Keenan RA, Davidson AI. Gastric lymphoma in Grampian region: presentation, treatment and outcome. *J R Coll Surg Edinb* 1996; **41**: 143-147
- 32 **Harris NL**, Jaffe ES, Stein H, Banks PM, Chan JK, Cleary ML, Delsol G, De Wolf-Peters C, Falini B, Gatter KC. A revised European-American classification of lymphoid neoplasms: a proposal from the international lymphoma study group. *Blood* 1994; **84**: 1361-1392
- 33 **El Saghir NS**, Jessen K, Al-Mofleh IA, Ajarim DS, Fawzy E, Al-Faleh FZ, Dahaba N, Qteishat W. Primary gastrointestinal lymphoma in the Middle East: Analysis of 23 cases from Riyadh, Saudi Arabia. *Saudi Med J* 1990; **11**: 95-98
- 34 **Armitage JO**, Cavalli F, Longo DL. Text atlas of lymphomas, 1st ed. London. *Martin Dunitz Ltd* 1999; **2**: 133-152
- 35 **Wotherspoon AC**, Ortiz-Hidalgo C, Falzon MR, Isaacson PG. *Helicobacter pylori*-associated gastritis and primary B-cell gastric lymphoma. *Lancet* 1991; **338**: 1175-1176
- 36 **Ono H**, Kondo H, Saito D, Yoshida S, Shiroa K, Yamaguchi H, Yokota T, Hosokawa K, Fukuda H, Hayashi S. Rapid diagnosis of gastric malignant lymphoma from biopsy specimens: Detection of immunoglobulin heavy chain reaction. *Jpn J Cancer Res* 1993; **84**: 813-817
- 37 **Isaacson PG**. Recent developments in our understanding of gastric lymphomas. *Am J Surg Pathol* 1996; **20**(Suppl 1): S1-S7
- 38 **Al-Mofleh IA**. Complications of primary upper gastrointestinal lymphoma. *Ann Saudi Med* 1992; **12**: 297-299
- 39 **Rackner VL**, Thirlby RC, Ryan JA. Role of surgery in multimodality therapy for gastrointestinal lymphoma. *Am J Surg* 1991; **161**: 570-575
- 40 **Salles G**, Herbrecht R, Tilly H, Berger F, Brousse N, Gisselbrecht C, Coiffier B. Aggressive primary gastrointestinal lymphomas: review of 91 patients treated with LNH-84 regimen. *Am J Med* 1991; **90**: 77-84
- 41 **Suekane H**, Iida M, Kuwano Y, Kohroggi N, Yao T, Iwashita A, Fujishima M. Diagnosis of primary early gastric lymphoma. Usefulness of endoscopic mucosal resection for histologic evaluation. *Cancer* 1993; **71**: 1207-1213
- 42 **Park SH**, Han JK, Kim TK, Lee JW, Kim SH, Kim YI, Choi BI, Yeon KM, Han MC. Unusual gastric tumors: radiologic-pathologic correlation. *Radiographics* 1999; **19**: 1435-1446
- 43 **Brown JA**, Carson BW, Gascayne RD, Cooperberg PL, Connors JM, Mason AC. Low grade gastric MALT lymphoma: radiographic findings. *Clin Radiol* 2000; **55**: 384-389
- 44 **Chou CK**, Chen LT, Sheu RS, Yang CW, Wang ML, Jaw TS, Liu GC. MRI manifestations of gastrointestinal lymphoma. *Abdom Imaging* 1994; **19**: 495-500
- 45 **Yucl C**, Ozdemir H, Isik S. Role of endosonography in the evaluation of gastric malignancy. *J Ultrasound Med* 1999; **18**: 283-288
- 46 **Caletti G**, Fusaroli P, Togliani T, Bocu P, Roda E. Endosonography in gastric lymphoma and large gastric folds. *Eur J Ultrasound* 2000; **11**: 31-40
- 47 **Musshoff K**. Clinical staging classification of non-Hodgkin's lymphomas. *Strahlentherapie* 1977; **153**: 218-221
- 48 **Carbone PP**, Kaplan HS, Musshoff K, Smithes DW, Tubiana M. Report of the committee on Hodgkin disease staging procedures. *Cancer Res* 1971; **31**: 1860-1861
- 49 **Rohatiner A**, d' Amore F, Coiffier B, Crowther D, Gospodarowicz M, Isaacson P, Lister TA, Norton A, Salem P, Shipp M. Report on a workshop convened to discuss the pathological and staging of GI tract lymphomas. *Ann Oncol* 1994; **5**: 397-400
- 50 **Azab MB**, Henry-Amar M, Rougier P, Bognel C, Theodore C, Carde P, Lasser P, Cosset JM, Caillou B, Oroz JP, Marcel H. Prognostic factors in primary gastrointestinal non-Hodgkin lymphoma. *Cancer* 1989; **64**: 1208-1217
- 51 **Weingrad DN**, Decosse JJ, Sherlock P, Straus D, Lieberman PH, Filippa DA. Primary gastrointestinal lymphoma: a 30-year review. *Cancer* 1982; **49**: 1258-1265
- 52 **Maor MH**, Velasquez WS, Fuller LM, Silvermintz KB. Stomach conservation in stage IE and IIE gastric non-Hodgkin's lymphoma. *J Clin Oncol* 1990; **8**: 266-271
- 53 **Liang R**, Todd D, Chan TK, Chiu E, Lie A, Kwong YL, Choy D, Ho FC. Prognostic factors for primary gastrointestinal lymphoma. *Hematol Oncol* 1995; **13**: 153-163
- 54 **Fung CY**, Grossbard ML, Linggood RM, Younger J, Flieder A, Harris NL, Graeme-Cook F. Mucosa-associated lymphoid tissue lymphoma of the stomach: long term outcome after local treatment. *Cancer* 1999; **85**: 9-17
- 55 **Salvagno L**, Soraru M, Busetto M, Puccetti C, Sava C, Endrizzi L, Giusto M, Aversa S, Chiarion Sileni V, Polico R, Bianco A, Rupolo M, Nitti D, Doglioni C, Lise M. Gastric non-Hodgkin's lymphoma: analysis of 252 patients from a multicenter study. *Tumori* 1999; **85**: 113-121
- 56 **Kodera Y**, Yamamura Y, Nakamura S, Shimizu Y, Torii A, Hirai T, Yasui K, Morimoto T, Kato T, Kito T. The role of radical gastrectomy with systematic lymphadenectomy for the diagnosis and treatment of primary gastric lymphoma. *Ann Surg* 1998; **227**: 45-50
- 57 **Fischbach W**, Dragosics B, Kolve-Goebler ME, Ohmann C, Greiner A, Yang Q, Bohm S, Verreet P, Horstmann O, Busch M, Duhmke E, Muller-Hermelink HK, Wilms K, Allingers S, Bauer P, Bauer S, Bender A, Brandstatter G, Chott A, Dittrich C, Erhart K, Eysselt D, Ellersdorfer H, Ferlitsch A, Fridrik MA, Gartner A, Hausmaninger M, Hinterberger W, Hugel K, Ilsinger P, Jonaus K, Judmaier G, Karner J, Kerstan E, Knoflach P, Lenz K, Kandutsch A, Lobmeyer M, Michlmeier H, Mach H, Marosi C, Ohlinger W, Oprean H, Pointer H, Pont J, Salabon H, Samec HJ, Ulsperger A, Wimmer A, Wewalka F. Primary gastric B-cell lymphoma: results of a prospective multicenter study. *Gastroenterology* 2000; **119**: 1191-1202
- 58 **Lucandri G**, Stipa F, Mingazzini PL, Ferri M, Sapienza P, Stipa S.

- The role of surgery in the treatment of primary gastric lymphoma. *Anticancer Res* 1998; **18**: 2089-2094
- 59 **Vaillant JC**, Ruskone-Fourmestreaux A, Aegerter P, Gayet B, Rambaud JC, Valleur P, Parc R. Management and long-term results of surgery for localized gastric lymphomas. *Am J Surg* 2000; **179**: 216-222
- 60 **Popescu RA**, Wotherspoon AC, Cunningham D, Norman A, Prendiville J, Hill ME. Surgery plus chemotherapy or chemotherapy alone for primary intermediate and high-grade gastric non-Hodgkin's lymphoma: The Royal Marsden Hospital experience. *Eur J Cancer* 1999; **35**: 928-934
- 61 **Ong CL**, Ti TK, Rauff A. Primary gastric lymphoma. *Singapore Med J* 1993; **34**: 442-444
- 62 **Cooper DI**, Doria R, Salloum E. Primary gastrointestinal lymphomas. *Gastroenterologist* 1996; **4**: 54-64
- 63 **Law MM**, Willimas SB, Wong JH. Role of surgery in the management of primary lymphoma of the gastrointestinal tract. *J Surg Oncol* 1996; **61**: 199-204
- 64 **Koch P**, del Valle F, Berdel WE, Willich NA, Reers B, Hiddemann W, Grothaus-Pinke B, Reinartz G, Brockmann J, Temmensfeld A, Schmitz R, Rube C, Probst A, Jaenke G, Bodenstern H, Junker A, Pott C, Schultz J, Heinecke A, Parwaresch R, Tiemann M. Primary gastrointestinal non-Hodgkin's lymphoma: II. Combined surgical and conservative or conservative management only in localized gastric lymphoma - results of the prospective German multicenter study. The German Multicenter Study Group on GIT-NHL. *J Clin Oncol* 2001; **19**: 3874-3883
- 65 **Raderer M**, Valencak J, Osterreicher C, Drach J, Hejna M, Kornek G, Scheithauer W, Brodowicz ZT, Chott A, Dragosics B. Chemotherapy for the treatment of patients with primary high grade gastric B-cell lymphoma of modified Ann Arbor stages IE and IIE. *Cancer* 2000; **88**: 1979-1985
- 66 **Tondini C**, Balzarotti M, Santoro A, Zanini M, Fornier M, Giardini R, Di Felice G, Bozzetti F, Bonadonna G. Initial chemotherapy of primary resectable large-cell lymphoma of the stomach. *Ann Oncol* 1997; **8**: 497-499
- 67 **Liu HT**, Hsu C, Chen CL, Chiang IP, Chen LT, Chen YC, Cheng AL. Chemotherapy alone versus surgery followed by chemotherapy for stage I/II large-cell lymphoma of the stomach. *Am J Hematol* 2000; **64**: 175-179
- 68 **Ferreri AJ**, Cordio S, Paro S, Ponzoni M, Freschi M, Veglia F, Villa E. Therapeutic management of stage I-II high-grade primary gastric lymphomas. *Oncology* 1999; **56**: 274-282
- 69 **Thieblemont C**, Dumontet C, Bouafia F, Hequet O, Arnaud P, Espinouse D, Felman P, Berger F, Salles G, Coiffier B. Outcome in relation to treatment mortalities in 38 patients with localized gastric lymphoma: A retrospective study of patients treated during 1976-2001. *Leuk Lymphoma* 2003; **44**: 257-262
- 70 **Au E**, Ang PT, Tan P, Sng I, Fong CM, Chua EJ, Ong YW. Gastrointestinal lymphoma-a review of 54 patients in Singapore. *Ann Acad Med Singapore* 1997; **26**: 758-761
- 71 **Lin KM**, Penney DG, Mahmoud A, Chae W, Kolachalam RB, Young SC. Advantage of surgery and adjuvant chemotherapy in the treatment of primary gastrointestinal lymphoma. *J Surg Oncol* 1997; **64**: 237-241
- 72 **Ferreri AJ**, Cordio S, Ponzoni M, Villa E. Non-surgical treatment with primary chemotherapy, with and without radiation therapy of stage I-II high-grade lymphoma. *Leuk Lymphoma* 1999; **33**: 531-541
- 73 **Ruskone-Fourmestreaux A**, Aegerter P, Delmer A, Brousse N, Galian A, Rambaud JC. Primary digestive tract lymphoma: a prospective multicentric study of 91 patients. *Gastroenterology* 1993; **105**: 1662-1671
- 74 **Thirlby RC**. Gastrointestinal lymphoma: a surgical perspective. *Oncology (Huntingt)* 1993; **7**: 29-32,34
- 75 **Thomas CR Jr**, Share R. Gastrointestinal lymphoma. *Med Pediatr Oncol* 1991; **19**: 48-60
- 76 **Tedeschi L**, Romanelli A, Dallavalle G, Tavani E, Arnoldi E, Vinci M, Mortara G, Bedoni P, Labianca R, Luporini G. Stages I and II non-Hodgkin's lymphoma of the gastrointestinal tract. Retrospective analysis of 79 patients and review of the literature. *J Clin Gastroenterol* 1994; **18**: 99-104
- 77 **Wotherspoon AC**, Doglioni C, Diss TC, Pan L, Moschini A, de Boni M, Isaacson PG. Regression of primary low-grade B-cell gastric lymphoma of mucosa-associated lymphoid tissue type after eradication of *Helicobacter pylori*. *Lancet* 1993; **342**: 575-577
- 78 **Pinotti G**, Zucca E, Roggero E, Pascarella A, Bertoni F, Savio A, Savio E, Capella C, Pedrinis E, Saletti P, Morandi E, Santandrea G, Cavalli F. Clinical features, treatment and outcome in a series of 93 patients with low-grade gastric MALT lymphoma. *Leuk Lymphoma* 1997; **26**: 527-537
- 79 **Bertoni F**, Conconi A, Capella C, Motta T, Giardini R, Ponzoni M, Pedrinis E, Novero D, Rinaldi P, Cazzaniga G, Biondi A, Wotherspoon A, Hancock BW, Smith P, Souhami R, Cotter FE, Cavalli F, Zucca E. International extranodal lymphoma study group: United Kingdom lymphoma group. Molecular follow-up in gastric mucosa-associated lymphoid tissue lymphoma: early analysis of the LY03 cooperative trial. *Blood* 2002; **99**: 2541-2544
- 80 **Fischbach W**. Primary gastric lymphoma of MALT: considerations of pathogenesis, diagnosis and therapy. *Can J Gastroenterol* 2000; **14**(Suppl D): 44D-50D
- 81 **Kocher M**, Muller RP, Ross D, Hoederath A, Sack H. Radiotherapy for treatment of localized non-Hodgkin's lymphoma. *Radiother Oncol* 1997; **42**: 37-41

Safety of interferon b treatment for chronic HCV hepatitis

D Festi, L Sandri, G Mazzella, E Roda, T Sacco, T Staniscia, S Capodicasa, A Vestito, A Colecchia

D Festi, L Sandri, G Mazzella, E Roda, A Colecchia, Department of Internal Medicine and Gastroenterology, University of Bologna, Bologna, Italy

T Sacco, T Staniscia, S Capodicasa, A Vestito, Department of Medicine and Aging, University G.d' Annunzio, Chieti, Italy

Correspondence to: Davide Festi, MD Dipartimento di Medicina Interna e Gastroenterologia, Policlinico S.Orsola-Malpighi, Via Massarenti 9, 40126 Bologna, Italy. festi@med.unibo.it

Telephone: +39-051-6364123 **Fax:** +39-051-6364123

Received: 2003-07-12 **Accepted:** 2003-10-23

Abstract

Hepatitis C is a major cause of liver-related morbidity and mortality worldwide. In fact, chronic hepatitis C is considered as one of the primary causes of chronic liver disease, cirrhosis and hepatocellular carcinoma, and is the most common reason for liver transplantation. The primary objectives for the treatment of HCV-related chronic hepatitis is to eradicate infection and prevent progression of the disease. The treatment has evolved from the use of α -interferon (IFN α) alone to the combination of IFN α plus ribavirin, with a significant improvement in the overall efficacy, and to the newer PEG-IFNs which have further increased the virological response, used either alone or in combination with ribavirin. Despite these positive results, in terms of efficacy, concerns are related to the safety and adverse events. Many patients must reduce the dose of PEG-IFN or ribavirin, others must stop the treatment and a variable percentage of subjects are not suitable owing to intolerance toward drugs. IFN β represents a potential therapeutic alternative for the treatment of chronic viral hepatitis and in some countries it plays an important role in therapeutic protocols. Aim of the present paper was to review available data on the safety of IFN β treatment in HCV-related chronic hepatitis.

The rates of treatment discontinuation and/or dose modification due to the appearance of severe side effects during IFN β are generally low and in several clinical studies no requirements for treatment discontinuation and/or dose modifications have been reported. The most frequent side effects experienced during IFN β treatment are flu-like syndromes, fever, fatigue and injection-site reactions. No differences in terms of side-effect frequency and severity between responders and non-responders have been reported. A more recent study, performed to compare IFN β alone or in combination with ribavirin, confirmed the good safety profile of both treatments. Similar trends of adverse event frequency have been observed in subpopulations such as patients with genotype-1b HCV hepatitis unresponsive to IFN α treatment or with HCV-related cirrhosis and patients with acute viral hepatitis. If further studies will confirm the efficacy of combined IFN β and ribavirin treatment, this regimen could represent a safe and alternative therapeutic option in selected patients.

Festi D, Sandri L, Mazzella G, Roda E, Sacco T, Staniscia T, Capodicasa S, Vestito A, Colecchia A. Safety of interferon β treatment for chronic HCV hepatitis. *World J Gastroenterol* 2004; 10(1): 12-16

<http://www.wjgnet.com/1007-9327/10/12.asp>

INTRODUCTION

Hepatitis C is a major cause of liver-related morbidity and mortality worldwide and represents a significant public health problem^[1]. In fact, chronic hepatitis C is considered as one of the primary causes of chronic liver disease, cirrhosis and hepatocellular carcinoma, and is the most common reason for liver transplantation^[2]. Based on the increased knowledge surrounding the natural history of the disease, the primary objectives for the treatment of hepatitis C virus (HCV)-related chronic hepatitis are to eradicate infection and prevent progression to cirrhosis and thereby preventing complications associated with end-stage liver disease^[3,4]. The treatment of HCV has evolved from the use of a single agent - mainly interferon alpha (IFN α) to the combination of IFN α and ribavirin treatment. Combination therapy can significantly improve the overall treatment efficacy compared to monotherapy (i.e., from 10%-15% of sustained viral clearance to 30%-40%) and now represents the standard treatment for chronic hepatitis.

Recently, new IFN preparations, such as pegylated IFNs (PEG-IFNs), have been introduced in clinical practice. Results obtained from large, multicenter studies of combined PEG-IFN and ribavirin treatment have shown a further increase in treatment efficacy. In fact, HCV infection was eradicated in 47%-54% of patients treated with PEG-IFN α -2b^[5]. Similar results have been found with PEG-IFN α -2a treatment^[6]. However, despite these positive results, several clinical problems remain. Of primary significance is the large number of patients treated with PEG-IFN (both α -2a and α -2b) and ribavirin who discontinue treatment due to the occurrence of adverse events associated with therapy. In fact, it has been reported that 34%-42% of patients treated with PEG-IFN α -2b (high and low doses, respectively) required dose reductions due to the appearance of adverse events and 13% stopped treatment for safety reasons^[5]. In another trial concerning the efficacy of PEG-IFN α -2a, dose modifications due to adverse events were required in 8% of patients and treatment discontinuation was required in 19%^[6]. In a pivotal trial of IFN α -2b and ribavirin performed by McHutchison *et al.*^[7], dose reductions due to adverse events were needed in 13% and 17% of patients treated for 24 and 48 weeks, respectively. Treatment discontinuation rates were 8% and 21% in patients treated for 24 and 48 weeks, respectively. Furthermore, it has been recently documented that, due primarily to safety issues, the number of HCV patients eligible for current treatments and the rate of treatment completion were much lower in clinical practice than in clinical trials^[8]. These concerns are particularly relevant considering that the primary goals of HCV treatment are viral eradication and the slowing of disease progression^[9,10].

Since IFNs are a family of glycoproteins with a broad range of antiviral effects, IFN beta (IFN β) represents a potential therapeutic alternative for the treatment of chronic viral hepatitis. In fact, in some countries, mainly in Japan, IFN β already plays a central role in therapeutic protocols. Differences have been reported between the physicochemical, biological and pharmacological properties of IFN α and IFN β ^[11,12]. Three forms of human IFN β are available:^[13] 1) Natural human IFN β (nIFN β) which is produced using human fibroblasts and is currently used in Japan for the treatment of chronic hepatitis C. 2) Recombinant human IFN β -1a (rhIFN β -1a), which is

procured from mammalian cells and is identical to IFN β that occurs naturally in humans. 3) *Escherichia coli*-produced recombinant human IFN β (IFN β -1b) which contains an altered amino acid sequence with a serine substitution for the cysteine at position 17. rhIFN β -1a appears to have advantages over the other two formulations and, in particular, is less immunogenic and more potent^[14]. The aim of the present paper was to review available data on the safety of IFN β for the treatment of chronic hepatitis C. Since IFN β has been widely used for the treatment of multiple sclerosis (MS), studies referring to the safety of IFN β in MS are reviewed briefly before discussing the results of this treatment in HCV-related chronic hepatitis.

IFN β in multiple sclerosis

Recombinant IFN β is currently the gold standard for the treatment of relapsing-remitting MS (RRMS). In MS, IFN β treatment lasts several years and regimens require high doses and frequent administration. Therefore, safety data on IFN β therapy recorded in MS studies and clinical practice could be useful for providing an overview of the drug's safety characteristics.

In the PRISMS (prevention of relapses and disability by interferon beta-1a subcutaneously in multiple sclerosis) study^[15], 560 patients with RRMS received 2.2 μ g or 4.4 μ g IFN β or placebo subcutaneously (s c) thrice weekly (t.i.w.) for 2 years (PRISMS-2) and then, the subjects completing treatment ($n=503$) or study ($n=533$) were re-randomized to receive either 2.2 μ g or 4.4 μ g IFN β s c, t.i.w., for an additional 2 years (PRISMS-4)^[16]. The adverse events reported during the PRISMS-4 study were similar to those observed in the PRISMS-2 trial and, in general, most adverse events were mild. During the 4-year period of observation, the most frequent events reported were injection-site inflammation, flu-like symptoms, headache and fatigue, with similar rates in both active treatment groups. In the 2.2- and 4.4 μ g groups, respectively, less frequent adverse events included laboratory abnormalities such as lymphopenia (27% and 35%), elevated ALT levels (24% and 30%), elevated AST levels (11% and 20%) and thrombocytopenia (3% and 8%). All cases of thrombocytopenia were mild and only one patient over the 4 years (in the 4.4 μ g group) stopped treatment due to lymphopenia. In two other patients, treatment was discontinued as a result of elevated liver enzymes. In the SPECTRIMS (secondary progressive efficacy trial of rebif [interferon beta-1a] in multiple sclerosis) study^[17] conducted in secondary progressive MS (SPMS) patients using a treatment schedule similar to that used in the PRISMS-2 study, the type, frequency and severity of adverse events with IFN β -1a were similar to those reported in the PRISMS study. Overall, IFN β -1a was well tolerated. Of the 618 patients enrolled, 3 receiving placebo, 8 receiving 2.2 μ g IFN β -1a and 7 receiving 4.4 μ g IFN β -1a discontinued treatment permanently. In general, liver function test abnormalities were mild or moderate and either resolved with treatment interruption or no treatment modification whatsoever. The recent EVIDENCE (The evidence for interferon dose-response: European North American comparative efficacy) study^[18] compared the safety and efficacy of IFN β -1a, 4.4 μ g, s c, t.i.w., to IFN β -1b, 3.0 μ g, once weekly by intramuscular (i m) injection, in 677 patients with RRMS over 24 weeks. The most common adverse events recorded were injection-site disorders, flu-like symptoms, headaches, rhinitis and fatigue. The higher frequency of injection-site disorders in the IFN β -1a group was related to the more frequent administration of this agent. However, injection-site disorders were mild and no skin necrosis was observed in over 20 000 s c injections. Hepatic and hematologic laboratory abnormalities were also more common on IFN β -1a but again, these abnormalities were generally mild and responsive to dose

reductions (if required). In both treatment groups, severe laboratory abnormalities were rare (<1%).

IFN β pharmacokinetics

IFN β can be administered intravenously (i v), intramuscularly (i m) and subcutaneously (s c). Pharmacokinetic and pharmacodynamic studies^[19-21] have shown that the extent and duration of the clinical and biologic effects of IFN β are independent of the route of administration. Furthermore, studies evaluating the most efficacious IFN β dosing regimen^[22-25] have shown that, in general, the highest doses have the greatest efficacy. However, these higher doses are also associated with a greater incidence of side effects (see below).

Evaluation of IFN β safety

Similar to the adverse events associated with IFN α therapy^[26,27], the side effects of IFN β can be separated into different categories, namely: a) common side effects (these range from mild-to-severe in nature and do not require dose modification), b) mild-to-moderate side effects which occur less frequently (i.e., less than 10% of treated patients) and may or may not require dose modification, and c) severe or life-threatening side effects. Thus far, no severe or life-threatening side effects have been reported with IFN β use. Clinical IFN β data are based on the results of clinical studies involving 1096 patients^[23-25,28-52]. Studies have been performed on treatment-naïve patients as well as patients who did not respond to previous treatment (generally with IFN α), two other studies were performed in special populations (i.e., cirrhotic patients and patients with renal failure)^[46,54].

Discontinuation and dose modification during IFN β treatment

The rates of treatment discontinuation and/or dose modification due to the appearance of severe side effects during IFN β are generally low (Table 1). Furthermore, several clinical studies reported no requirements for treatment discontinuation and/or dose modifications. Kiyosawa *et al*^[28] found that in naïve patients treated with i v IFN β , dose modifications due to leukocyte counts below $1 \times 10^9/L$ were required in only 4.2% of patients (1 of 12 patients). In a study by Villa *et al*^[29] 5.3% of patients (1 of 19) did not complete the trial. Reasons for discontinuation were not specified. A comparison study of i v recombinant IFN β and IFN α -2b plus ribavirin in patients who did not respond to previous IFN α treatment found that 12% of patients in the IFN α -2b plus ribavirin group (12 of 100) withdrew from treatment due to side effects such as flu-like symptoms. In the IFN β group, the corresponding frequency was 9% (9 of 100 patients)^[30].

Table 1 Frequency of treatment discontinuation and dose modifications during therapy with IFN β

	Number of cases	References
Discontinuation		
Adverse events	14	25,28,29,30
Laboratory abnormalities	2	31
Dose modifications		
Adverse events	-	
Laboratory abnormalities	1	43

In a comparative study of two different doses (9 MU and 12 MU) of rhIFN β produced using Chinese hamster ovaries, Habersetzer *et al*^[25] observed a treatment discontinuation rate of 18.2% (2 of 11 patients in the lower dose group) in naïve patients due to the occurrence of side effects such as mild depression and cutaneous ulcers at the injection site. A treatment discontinuation rate of 18.2% (2 of 11 patients) was also found in a study^[31] comparing the effects of different IFN β

administration regimens (i v 6 MU once daily versus 3 MU twice daily), two patients who discontinued treatment were using IFN β twice daily. Liver enzyme alterations (serum ALT/AST levels >700 IU/l) and severe proteinuria (urinary protein excretion >40 g/L and serum albumin level <30 g/L) were the causes of discontinuation. In conclusion, the frequency of treatment discontinuation and dose modifications that occur during IFN β therapy is low.

Frequency of side effects during IFN β treatment

The frequency of side effects experienced during IFN β treatment is reported in Table 2.

Table 2 Frequency of side effects with IFN β therapy

Side effects	Frequency (range) (%)	References
Flu-like syndrome	10-100	25,30,32,33,35, 36, 37, 39, 46
Fever	67-100	28,43,40
Fatigue	16-74	24, 33, 39,46
Local reactions (at the injection site)	43-76	25,34, 37
Headaches	8-47	33, 39, 46
Malaise	50	39
Arthro-myalgias	21-42	39,40,46
Weight loss	6-42	39,40
Gastrointestinal symptoms	20-26	25,37, 38
Anxiety, insomnia, irritability	10-25	32, 39, 38
Depression	10-21	25, 38,46
Alopecia	8-16	33, 39
Proteinuria	46-73	22, 51
Reduced platelet count	13-44	22, 32,51
Reduced white-cell count	13-20	32,38

Flu-like syndromes, fever, fatigue and injection-site reactions are the most frequently observed side effects of IFN β therapy. No differences in terms of the frequency and severity of side effects between therapeutic responders and non-responders have been reported. In order to better evaluate the clinical significance of these side effects, results have been analysed with reference to the type of study.

Clinical studies evaluating the safety of IFN β

In a study of 8 naïve patients, Chemello *et al*^[32] found that treatment with i v natural human fibroblast IFN β was well tolerated, the predominant side effect was a mild form of a flu-like syndrome, which lasted between 3 and 23 days after the initiation of therapy. No hematologic toxicity was observed and reductions in white-blood-cell and platelet counts occurred in only one patient. A low side-effect rate was also observed in a study of 90 naïve patients treated with i m IFN β for 6 months^[33]. In fact, mild flu-like syndromes appeared in less than 10% of treated patients and asthenia in 16% of patients. The frequency of other side effects was less than 10%. The same investigators^[34] obtained similar results in another study of naïve patients treated with s c IFN β . A good safety profile with mild, transient flu-like syndromes as the predominant side effect was documented in two Italian studies^[35,36] performed in patients previously unresponsive to IFN α and subsequently treated with i v IFN β . Pellicano *et al*^[37] treated 30 patients who did not respond to a standard course of IFN α therapy with rhIFN β -1a (12 MU s.c., t.i.w.) for 3 months. The observed rate of flu-like symptoms, inflammation at the injection site, abdominal symptoms and psychiatric disturbances were 63%, 43%, 26% and 13%, respectively.

Clinical studies comparing different doses of IFN β

In a study of 92 naïve patients, Fesce *et al*^[24] compared two

different doses of i m natural human fibroblast IFN β : 3 MU and 6 MU t.i.w. for 12 months. Compared to the low-dose group, an increased frequency of flu-like syndromes (17% vs 9%), weakness (73% vs 57%), headache (48% vs 30%) and irritability (23% vs 11%) was documented in the high-dose group. However, these differences were not statistically significant. Habersetzer *et al*^[25] compared two different doses of recombinant IFN β -1a administered s c for 24 weeks in 21 naïve patients: 9 MU t.i.w. and 12 MU t.i.w. No differences were found between the two groups with regards to individual side effects. In a study aimed at comparing i v IFN β 3 MU twice daily vs 6 MU once daily in genotype-1b HCV-infected patients with high virus titres^[23], side effects were found to be more prevalent in the 3-MU group, particularly proteinuria (56% vs 30%) and thrombocytopenia (44% vs 20%).

Clinical studies comparing the safety of IFN β to IFN α

Several studies comparing the safety of IFN β and IFN α have been performed^[29,30,38-42].

Frosi *et al*^[38] compared IFN α and IFN β in 20 naïve patients treated for 6 months and did not observe any significant differences between the two treatment groups in terms of the frequency of adverse events. In another study^[39], flu-like syndromes and hair loss were less frequent in the IFN β group (16% and 16%, respectively) compared to the IFN α group (86% and 57%, respectively), the frequency of other adverse events were similar between the two groups. Cecere *et al*^[40] evaluated the efficacy and tolerability of the following types of IFN in 150 patients: lymphoblastoid IFN α , leukocytic IFN α and natural IFN β . The frequency of side effects was lower in the IFN β group than in the other treatment groups. In the IFN β , the frequency of lymphoblastoid IFN α and leukocytic IFN α , respectively, fever was present in 66.8%, 83.9% and 73.4%, the frequency of bone and muscle pains in 33%, 72.5% and 46.3%, fatigue in 21%, 52% and 31%, and the frequency of weight loss in 6%, 21% and 15%. Barbaro *et al*^[30] found no significant differences in the rates of side effects and treatment discontinuation between IFN β -treated and recombinant IFN α -2b plus ribavirin-treated patients ($n=200$) who were non-responders to previous IFN α -2b therapy.

Clinical studies evaluating combination therapy (IFN β plus ribavirin)

Kakumu *et al*^[43] compared the efficacy of ribavirin alone, IFN β alone and combined ribavirin/IFN β therapy. The combined therapy was found to significantly reduce red-blood-cell count and hemoglobin concentrations. A significant reduction in white-blood-cell count was documented in the IFN β and combined treatment groups. Despite these findings, all enrolled patients completed the study. More recently, a multicenter, randomised and controlled study has been performed^[44] to compare rhIFN β alone or in combination with ribavirin. One hundred and two naïve patients with chronic hepatitis C were randomized to receive either rhIFN β -1a alone (6 MU, s.c., everyday) or in combination with ribavirin for 6 weeks. All patients in the IFN β -alone group completed the study, while 3 of 51 patients in the combined treatment group stopped therapy due to adverse events. Overall, both treatment regimens were well tolerated, hematological and hematochemical parameters remained unchanged by the end of the study period (except for a significant decrease in hemoglobin levels in the combined treatment group).

Clinical studies in sub-populations of patients

Vezzoli *et al*^[45] evaluated the efficacy and safety of IFN β in 10 patients with genotype-1b HCV hepatitis who were

unresponsive to a previous cycle of IFN α treatment, no reference to side effects was reported. Bernardinello *et al*^[46] examined the safety and tolerability of natural i m IFN β in 61 patients with HCV-related cirrhosis and found that the treatment was well tolerated, the most frequent side effects were fatigue (24%), irritability or depression (21%), arthromyalgias (21%), headache (21%) and flu-like symptoms (16%). The frequency of these adverse events are similar to those found in chronic hepatitis patients without cirrhosis using IFN β . Interestingly, in this study, the probability of developing clinically significant liver-related events during the follow-up period was not significantly different in untreated *versus* treated patients (the cumulative probability of decompensation at 60 months was 24% in treated patients and 35% in untreated ones). Although a recent Cochrane review^[47] states that there is no definitive conclusion about the safety of IFN β in acute hepatitis, IFN β has been used in patients with acute hepatitis without causing significant side effects^[48-50]. Takano *et al*^[49] studied the effects of six different IFN β treatment schedules in 97 patients with acute non-A, non-B hepatitis. The authors did not report data regarding the safety of IFN β , however, all enrolled patients completed the study. A pharmacokinetic study^[54] has been performed in patients with end-stage renal failure, i v infusion of natural human IFN β was found to be safe.

CONCLUSION

HCV infection is a major health problem and efforts have been made to identify drugs able to eradicate the disease and, thereby reducing HCV-related morbidity and mortality. According to recent consensus conference reports^[55,56], treatment of IFN α in combination with ribavirin represents the standard therapy for HCV-related chronic hepatitis. However, the use of high treatment doses for long periods, which is often required in subgroups of patients (i.e., those with genotype 1 disease) to reach acceptable levels of efficacy, increases the risk of side effects and as a result, can reduce patient compliance to treatment. In these cases, the search for further treatment strategies could be useful. IFN β has been proposed as a possible therapy for chronic hepatitis. Studies examining the use of IFN β in hepatitis originated in Japan^[57] but, in recent years, studies have also been performed in Europe^[25,29,30,32-38,40,44-46,53]. According to the available data, the treatment of chronic hepatitis C with IFN β is associated with a good safety and tolerability profile. In fact, in most clinical studies, the frequency of side effects is lower, or at least similar, to that reported with IFN α therapy. Furthermore, the rate of dropouts in controlled clinical studies as well as the need for dose reductions or treatment discontinuation are very low. IFN β has also been shown to be well tolerated and has an excellent safety profile in special patient populations, such as those with acute hepatitis^[48-50], cirrhosis^[46], and renal insufficiency^[54].

The goals of treatment strategies for HCV-related chronic hepatitis are to eradicate HCV infection and to reduce disease progression. The availability of different therapeutic choices is critical in achieving these goals, particularly in patients unresponsive to a standard course of antiviral therapy. Due to its good safety profile, IFN β may represent a possible second-line therapy if additional clinical studies can confirm this drug's efficacy, mainly in combination with ribavirin.

The eradication of HCV and the prevention or slowing of disease progression are clinical challenges that require a careful cost/benefit analysis. In order to expand the population of patients eligible for therapy and to treat subjects who cannot tolerate first-line treatments, new therapeutic options should be evaluated. If further studies will confirm the efficacy of combined IFN β and ribavirin treatment, this regimen can represent a safe, alternative therapeutic option.

REFERENCES

- 1 **Ray Kim W.** The burden of hepatitis C in the United States. *Hepatology* 2002; **36**: S30-S34
- 2 **Alberti A,** Chemello L, Benvegna', L. Natural history of hepatitis C. *J Hepatol* 1999; **31** (Suppl 1): 17-24
- 3 **Alberti A,** Benvegna' L. Management of hepatitis C. *J Hepatol* 2003; **38**: S104-S118
- 4 **Mazzella G,** Accogli E, Sottili S, Festi D, Orsini M, Salzetta A, Novelli V, Cipolla A, Fabbri C, Pezzoli A, Roda E. Alpha interferon may prevent hepatocellular carcinoma in HCV-related liver cirrhosis. *J Hepatol* 1996; **24**: 141-147
- 5 **Manns MP,** McHutchinson JG, Gordon SC, Rustgi VK, Shiffman M, Reindollar R, Goodman ZD, Koury K, Ling M, Albrecht JK. Peginterferon alfa-2b plus ribavirin compared with interferon alfa-2b plus ribavirin for initial treatment of chronic hepatitis C: a randomized trial. *Lancet* 2001; **358**: 958-965
- 6 **Zeuzem S,** Feinman SV, Rasenack J, Heathcote EJ, Lai MY, Gane E, O' Grady J, Reichen J, Diago M, Lin A, Hoffman J, Brunda MJ. Peginterferon alfa-2a in patients with chronic hepatitis C. *N Engl J Med* 2000; **343**: 1666-1672
- 7 **McHutchinson JG,** Gordon SC, Schiff ER, Shiffmann ML, Lee WM, Rustgi VK, Goodman ZD, Ling MH, Cort S, Albrecht JK. Interferon alfa-2b alone or in combination with ribavirin as initial treatment for chronic hepatitis. Hepatitis Interventional Therapy Group. *N Engl J Med* 1998; **339**: 1485-1492
- 8 **Falck-Ytter Y,** Kale H, Mullen K, Sarbah S, Sorescu L, McCullough A. Surprisingly small effect of antiviral treatment in patients with hepatitis C. *Ann Intern Med* 2002 **136**: 288-292
- 9 **Poynard T,** McHutchinson J, Davis GL, Esteban-Mur R, Goodman Z, Bedossa P, Albrecht J. Impact of interferon alfa-2b and ribavirin on progression of liver fibrosis in patients with chronic hepatitis C. *Hepatology* 2000; **32**: 1131-1137
- 10 **Yoshida H,** Arakawa Y, Sata M, Nishiguchi S, Yano M, Fujiyama S, Yamada G, Yokosuka O, Shiratori Y, Omata M. Interferon therapy prolonged life expectancy among chronic hepatitis C patients. *Gastroenterology* 2002; **123**: 483-491
- 11 **Petska S,** Langer JA, Zoon KC, Samuel CE. Interferons and their actions. *Ann Rev Biochem* 1987; **56**: 727-777
- 12 **Bocci V.** Physicochemical and biological properties of interferons and their potential uses in drug delivery systems. *Crit Rev Drug Carrier Syst* 1992; **9**: 91-133
- 13 **Alam JJ.** Interferon- β treatment of human disease. *Curr Opin Biotechnol* 1995; **6**: 688-691
- 14 **Salmon P,** Le Cottonnec JY, Galazka A, Abdul-Ahad A, Darragh A. Pharmacokinetics and pharmacodynamics of recombinant human interferon- β in healthy male volunteers. *J Interferon Cytokine Res* 1996; **16**: 759-764
- 15 **PRISMS Study Group.** Randomized double-blind placebo-controlled study of interferon-beta-1a in relapsing/remitting multiple sclerosis. *Lancet* 1998; **352**: 1498-1504
- 16 **PRISMS Study Group.** PRISMS-4: long-term efficacy of interferon-beta-1a in relapsing MS. *Neurology* 2001; **56**: 1628-1636
- 17 **SPECTRIMS Study Group.** Randomized controlled trial of interferon-beta-1a in secondary progressive MS. *Neurology* 2001; **56**: 1496-1504
- 18 **Panitch H,** Goodin DS, Francis G, Chang P, Coyle PK, O' Connor P, Monaghan E, Li D, Weinshenker B. Randomized, comparative study of interferon beta-1a treatment regimens in MS: The EVIDENCE Trial. *Neurology* 2002; **59**: 1496-1506
- 19 **Munafa A,** Trincharad-Lugan I, Nguyen TXQ, Buraglio M. Comparative pharmacokinetics and pharmacodynamics of recombinant human interferon beta-1a after intramuscular and subcutaneous administration. *Eur J Neurol* 1998; **5**: 187-193
- 20 **Matsuyama S,** Henmi S, Ichihara N, Sone S, Kikuchi T, Ariga T, Taguchi F. Protective effects of murine recombinant interferon b administered by intravenous, intramuscular or subcutaneous route on mouse hepatitis virus infection. *Antiviral Res* 2000; **47**: 131-137
- 21 **Scagnolari C,** Bellomi F, Turriziani O, Bagnato F, Tomassini V, Lavalpe V, Ruggieri M, Bruschi F, Meucci G, Dicuonzo G, Antonelli G. Neutralizing and binding antibodies to IFN-beta: relative frequency in relapsing-remitting multiple sclerosis patients treated with different IFN β preparations. *J Interferon Cytokine Res* 2002; **22**: 207-213

- 22 **Shiratori Y**, Perelson AS, Weinberger L, Imazeki F, Yokosuka O, Nakata R, Ihori M, Hirota K, Ono N, Motojima T, Nishigaki M, Omata M. Different turnover rate of hepatitis C virus clearance by different treatment regimens using interferon-beta. *J Hepatol* 2000; **33**: 313-322
- 23 **Suzuki F**, Chayama K, Tsubota A, Akuta N, Someya T, Kobayashi M, Suzuki Y, Saitoh S, Arase Y, Ikeda K, Kumada H. Twice-daily administration of interferon-beta for chronic hepatitis C is not superior to a once-daily regimen. *J Gastroenterol* 2001; **36**: 242-247
- 24 **Fesce E**, Airolidi A, Mondazzi L, Maggi G, Gubertini G, Bernasconi G, Del Poggio P, Bozzetti F, Ideo G. Intramuscular beta interferon for chronic hepatitis C: is it worth trying? *Ital J Gastroenterol Hepatol* 1998; **30**: 185-188
- 25 **Habersetzer F**, Boyer N, Marcellin P, Bailly F, Ahmed SN, Alam J, Benhamou JP, Trepo C. A pilot study of recombinant interferon beta-1a for the treatment of chronic hepatitis C. *Liver* 2000; **20**: 437-441
- 26 **Dusheiko G**. Side effects of alpha interferon in chronic hepatitis C. *Hepatology* 1997; **26**: 112S-121S
- 27 **Fried MW**. Side effects of therapy of hepatitis C and their management. *Hepatology* 2002; **36**: 237S-244S
- 28 **Kiyosawa K**, Sodeyama T, Nakano Y, Yoda H, Tanaka E, Hayata T, Tsuchiya K, Yousuf M, Furuta S. Treatment of chronic non-A non-B hepatitis with human interferon beta: a preliminary study. *Antiviral Res* 1989; **12**: 151-161
- 29 **Villa E**, Trande P, Grottola A, Buttafoco P, Rebecchi AM, Stroffolini T, Callea F, Merighi A, Camellini L, Zoboli P, Cosenza R, Miglioli L, Loria P, Iori R, Carulli N, Manenti F. Alpha but not beta interferon is useful in chronic active hepatitis due to hepatitis C virus. A prospective, double-blind, randomized study. *Dig Dis Sci* 1996; **41**: 1241-1247
- 30 **Barbaro G**, Di Lorenzo G, Soldini M, Giancaspro G, Pellicelli A, Grisorio B, Barbarini G. Intravenous recombinant interferon-beta versus interferon-alpha-2b and ribavirin in combination for short-term treatment of chronic hepatitis C patients not responding to interferon-alpha. *Scand J Gastroenterol* 1999; **34**: 928-933
- 31 **Shiratori Y**, Nakata R, Shimizu N, Katada H, Hisamitsu S, Yasuda E, Matsumura M, Narita T, Kawada K, Omata M. High viral eradication with a daily 12-week natural interferon β treatment regimen in chronic hepatitis C patients with low viral load. *Dig Dis Sci* 2000; **45**: 2414-2421
- 32 **Chemello L**, Silvestri E, Cavalletto L, Bernardinello E, Pontisso P, Belassi F, Alberti A. Pilot study on the efficacy of intravenous natural b interferon therapy in Italian patients with chronic hepatitis C and relation to the HCV genotype. *Int Hepat Comm* 1995; **3**: 237-243
- 33 **Castro A**, Suarez D, Inglada L, Carballo E, Dominguez A, Diago M, Such J, Del Olmo JA, Perez-Mota A, Pedreira J, Quiroga JA, Carreno V. Multicenter randomized, controlled study of intramuscular administration of interferon β for the treatment of chronic hepatitis C. *J Interferon Cytokine Res* 1997; **17**: 27-30
- 34 **Castro A**, Carballo E, Dominguez A, Diago M, Suarez D, Quiroga JA, Carreno V. Tolerance and efficacy of subcutaneous interferon β administered for treatment of chronic hepatitis C. *J Interferon Cytokine Res* 1997; **17**: 65-67
- 35 **Mazzoran L**, Grassi G, Giacca M, Gerini U, Baracetti S, Fannicanelles M, Zorat F, Pozzato G. Pilot study on the safety and efficacy of intravenous natural beta-interferon therapy in patients with chronic hepatitis C unresponsive to alpha-interferon. *Ital J Gastroenterol Hepatol* 1997; **29**: 338-342
- 36 **Montalto G**, Tripi S, Cartabellotta A, Fulco M, Soresi M, Di Gaetano G, Carroccio A, Levvero M. Intravenous natural β interferon in white patients with chronic hepatitis C who are nonresponders to a interferon. *Am J Gastroenterol* 1998; **93**: 950-953
- 37 **Pellicano R**, Palmas F, Cariti G, Tappero G, Boero M, Tabone M, Suriani R, Pontisso P, Pitaro M, Rizzetto M. Re-treatment with interferon-beta of patients with chronic hepatitis C virus infection. *Eur J Gastroenterol Hepatol* 2002; **14**: 1377-1382
- 38 **Frosi A**, Sgorbati C, Bosio Bestetti M, Lodeville D, Vezzoli S, Vezzoli F. Interferon a and b in chronic hepatitis C: efficacy and tolerability. *Clin Drug Invest* 1995; **9**: 226-231
- 39 **Perez R**, Pravia R, Artimez ML, Giganto F, Rodriguez M, Lombrana JL, Rodrigo L. Clinical efficacy of intramuscular human interferon b vs interferon-a2 for the treatment of chronic hepatitis C. *J Viral Hepatitis* 1995; **2**: 103-106
- 40 **Cecere A**, Romano C, Caiazzo R, Lucariello A, Tancredi L, Gattoni A. Lymphoblastoid a interferon, leukocytic α -IFN and natural β -IFN in the treatment of chronic hepatitis C: a clinical comparison of 150 cases. *Hepato Res* 1999; **15**: 225-237
- 41 **Furusyo N**, Hayashi J, Ohmiya M, Sawayama Y, Kawakami Y, Ariyama I, Kinukawa N, Kashiwagi S. Differences between interferon-a and -b treatment for patients with chronic hepatitis C virus infection. *Dig Dis Sci* 1999; **44**: 608-617
- 42 **Asahina Y**, Izumi N, Uchihara M, Noguchi O, Tsuchiya K, Hamano K, Kanazawa N, Itakura J, Miyake S, Sakai T. A potent antiviral effect on hepatitis C viral dynamics in serum and peripheral blood mononuclear cells during combination therapy with high-dose daily interferon alfa plus ribavirin and intravenous twice-daily treatment with interferon beta. *Hepatology* 2001; **34**: 377-384
- 43 **Kakumu S**, Yoshioka K, Wakita T, Ishikawa T, Takayanagi M, Higashi Y. A pilot study of ribavirin and interferon beta for the treatment of chronic hepatitis C. A pilot study of ribavirin and interferon beta for the treatment of chronic hepatitis C. *Gastroenterology* 1993; **105**: 507-512
- 44 **Rizzetto M**, Alberti A, Craxi A, Ideo G, Demelia L, Pitaro M, Picciotto A. for the IBIS Study Group. Open, multicenter, randomized, controlled trial to compare safety and efficacy of r-hIFN beta 1a alone or in combination with ribavirin in HCV naïve patients. *Dig Liver Dis* 2003; **35** (Suppl 1): A14
- 45 **Vezzoli M**, Girola S, Fossati G, Mazzucchelli I, Gritti D, Mazzone A. Beta-interferon therapy of chronic hepatitis HCV+, 1b genotype. *Recenti Prog Med* 1998; **89**: 235-240
- 46 **Bernardinello E**, Cavalletto L, Chemello L, Mezzocollini I, Donada C, Benvegno L, Merkel C, Gatta A, Alberti A. Long-term clinical outcome after β -interferon therapy in cirrhotic patients with chronic hepatitis C. *Hepatogastroenterol* 1999; **46**: 3216-3222
- 47 **Poynard T**, Regimbeau C, Myers RP, Thevenot T, Leroy V, Mathurin P, Opolon P, Zarski JP. Interferon for acute hepatitis C. *Cochrane Database Syst Rev* 2002; **1**: CD000369
- 48 **Omata M**, Uokosuka O, Takano S. Resolution of acute C hepatitis after therapy with natural beta interferon. *Lancet* 1991; **338**: 914-915
- 49 **Takano S**, Satomura Y, Omata M. Effects of interferon beta on non-A, non-B acute hepatitis: a prospective, randomized, controlled-dose study. *Gastroenterology* 1994; **107**: 805-811
- 50 **Oketani M**, Higashi T, Yamasaki N, Shinmyozu K, Osame M, Arima T. Complete response to twice-a-day interferon-beta with standard interferon-alpha therapy in acute hepatitis C after a needle-stick. *J Clin Gastroenterol* 1999; **28**: 49-51
- 51 **Fukutomi T**, Fukutomi M, Iwao M, Watanabe H, Tanabe Y, Hiroshige K, Kinukawa N, Nakamura M, Nawata H. Predictors of the efficacy of intravenous natural interferon-beta treatment in chronic hepatitis C. *Med Sci Monit* 2000; **6**: 692-698
- 52 **Fujiwara K**, Mochida S, Matsuo S. Randomized control trial of interferon-beta injections at 12-h intervals as a therapy for chronic hepatitis C. *Hepatology Res* 1998; **12**: 240-251
- 53 **Barbarini G**, Calderon W, Bottari G. Beta-interferon therapy of chronic C hepatitis in 85 patients: results after one year of treatment. *Med J Infect Paras Dis* 1994; **9**: 25-28
- 54 **Nakayama H**, Shiotani S, Akiyama S, Gotoh H, Tani M, Akine Y. Pharmacokinetic study of human beta-interferon in patients with end-stage renal failure. *Clin Nephrol* 2001; **56**: 382-386
- 55 **Anonymous**. EASL International Consensus Conference on Hepatitis C. *J Hepatol* 1999; **31** (Suppl 1): 1-264
- 56 **Anonymous**. National Institute of Health Consensus Development Conference: Management of Hepatitis C: 2002. *Hepatology* 2002; **36** (Suppl 1): S1-S252
- 57 **Kobayashi Y**, Watanabe S, Konishi M, Yokoi M, Kakehashi R, Kaito M, Kondo M, Hayashi Y, Jomori T, Suzuki S. Quantitation and typing of serum hepatitis C virus RNA in patients with chronic hepatitis C treated with interferon-beta. *Hepatology* 1993; **18**: 1319-1325

Differences in proximal (cardia) versus distal (antral) gastric carcinogenesis via retinoblastoma pathway

Christian Gulmann, Helen Hegarty, Antoinette Grace, Mary Leader, Stephen Patchett, Elaine Kay

Christian Gulmann, Helen Hegarty, Antoinette Grace, Mary Leader, Elaine Kay, Department of Pathology, Beaumont Hospital and Royal College of Surgeons in Ireland, Dublin, Ireland

Stephen Patchett, Department of Gastroenterology, Beaumont Hospital, Dublin, Ireland

Supported by The Research Committee of the Royal College of Surgeons in Ireland

Correspondence to: Christian Gulmann, Department of Pathology, Royal College of Surgeons in Ireland, Beaumont Hospital, Dublin 9, Ireland. cgulmann@rcsi.ie

Telephone: +353-1-809 3701 **Fax:** +353-1-809 3720

Received: 2003-08-11 **Accepted:** 2003-10-25

Abstract

AIM: Disruption of cell cycle regulation is a critical event in carcinogenesis, and alteration of the retinoblastoma (pRb) tumour suppressor pathway is frequent. The aim of this study was to compare alterations in this pathway in proximal and distal gastric carcinogenesis in an effort to explain the observed striking epidemiological differences.

METHODS: Immunohistochemistry was performed to investigate expression of p16 and pRb in the following groups of both proximal (cardia) and distal (antral) tissue samples: (a) biopsies showing normal mucosa, (b) biopsies showing intestinal metaplasia and, (c) gastric cancer resection specimens including uninvolved mucosa and tumour.

RESULTS: In the antrum there were highly significant trends for increased p16 expression with concomitant (and in the group of carcinomas inversely proportional) decreased pRb expression from normal mucosa to intestinal metaplasia to uninvolved mucosa (from cancer resections) to carcinoma. In the cardia, there were no differences in p16 expression between the various types of tissue samples whereas pRb expression was higher in normal mucosa compared with intestinal metaplasia and tissue from cancer resections.

CONCLUSION: Alterations in the pRb pathway appear to play a more significant role in distal gastric carcinogenesis. It may be an early event in the former location since the trend towards p16 overexpression with concomitant pRb underexpression was seen as early as between normal mucosa and intestinal metaplasia. Importantly, the marked differences in expression of pRb and p16 between the cardia and antrum strongly support the hypothesis that tumours of the two locations are genetically different which may account for some of the observed epidemiological differences.

Gulmann C, Hegarty H, Grace A, Leader M, Patchett S, Kay E. Differences in proximal (cardia) versus distal (antral) gastric carcinogenesis via retinoblastoma pathway. *World J Gastroenterol* 2004; 10(1): 17-21

<http://www.wjgnet.com/1007-9327/10/17.asp>

INTRODUCTION

In the last decades the pattern of incidence of gastric cancer in the Western world has changed. Distal (corpus and antrum) cancers have decreased slightly whereas proximal (cardia/gastro-oesophageal) cancers have increased more than any other cancer^[1,2]. The tumours are morphologically indistinguishable and intestinal metaplasia (IM) appears to be an important step in carcinogenesis in both sites^[3,4]. The observed epidemiological differences are likely to be due to differences in the genetic pathways of carcinogenesis. However, so far they are poorly evaluated^[4-6].

Abnormal regulation of the cell cycle is a feature of many neoplasms^[7]. Regulation of the G1/S checkpoint is critical and is controlled by the retinoblastoma protein (pRb). Phosphorylated pRb releases E2F transcription factors which activate genes involved in DNA synthesis and cause G1/S transition. Phosphorylation of pRb is stimulated by the cyclin dependent kinase (CDK) 4-cyclin D complex. p16 specifically binds CDK4 which displaces it from cyclin D and thus acts to maintain pRb in an underphosphorylated state which causes G1 arrest^[8]. Disruption of this so-called 'Rb pathway' is a critical event in many tumours. It is resulted from primary inactivation of Rb function, by overexpression of CDKs, or through loss of p16^[7] which has a similar effect of G1/S progression. Several studies have shown a reciprocal expression of p16 and pRb^[9,10]. The role of the pRb pathway in gastric carcinogenesis is the subject of many papers. In distal gastric cancers it may be that disruption of p16 is an early event^[11] and a recent immunohistochemical study^[12] has shown a progressive decrease in expression from gastritis to atrophy and dysplasia. Less information is available on the role of pRb expression.

The aim of the present study was to compare the role of the pRb pathway in proximal and distal gastric cancers. p16 and pRb immunoexpression was investigated in the following groups of both proximal (cardia) and distal (antral) tissue samples: (a) biopsies showing normal mucosa, (b) biopsies showing intestinal metaplasia and, (c) gastric cancer resection specimens including uninvolved mucosa and tumour.

MATERIALS AND METHODS

Patient and specimen data

Six groups were included in this cross sectional study on archival, paraffin embedded tissues. The material was retrieved from the files in Beaumont Hospital, Dublin, Ireland and the local ethics committee approved the study. Tissue samples from the gastric cardia included endoscopic biopsies showing histologically normal mucosa ($n=56$) or IM ($n=49$) and material from gastric cancer resection specimens ($n=39$). Non-involved mucosa as well as tumour were investigated in the latter specimens. Tissue samples from the gastric antrum included the same groups: Normal ($n=52$), IM ($n=50$) as well as non-involved mucosa and tumour from cancer resections ($n=78$). All patients were Caucasians. Clinical details are shown in Table 1.

Endoscopic biopsy material was obtained from patients who had presented to the endoscopy service with a variety of upper gastrointestinal symptoms. Biopsies of the cardia were

Table 1 Clinical data

	Proximal			Distal		
	Biopsies normal	Biopsies IM	Cancer resections	Biopsies normal	Biopsies IM	Cancer resections
Number of subjects	56	49	39	52	50	78
Gender[F/M]	28/28	22/27	13/26	30/22	29/21	34/44
Age, years	50 (16)	58 (16) _A	67 (11) _B	52 (18)	59 (14) _C	69 (10) _D
Mean and (SD)						
Tumour type			30 Intestinal 9 Diffuse			42 Intestinal 36 Diffuse
TNM-stage, mean and (SD)			T 3.1 (0.6) N 1.0 (0.8)			T 3.0 (1.1) N 1.0 (0.8)

There was a significant stepwise increase in patient age between patients with biopsies showing normal mucosa to patients with biopsies showing IM to patients with gastric cancer resections in both proximal and distal locations. A-D, $P < 0.0001$. SD=Standard deviation.

only included when clearly labelled as such on the original request form without any endoscopic suspicion of Barrett's oesophagus or any prior or subsequent oesophageal biopsies showing Barrett's metaplasia. The distinction between proximal and distal gastric cancers was made on the basis of the clinical data as well as macroscopic description of the resection specimens on the pathology report. A case was labelled as proximal gastric cancer if it straddled the gastro-oesophageal junction with approximately equal amounts in the oesophagus and stomach and no histological evidence of Barrett's mucosa in the oesophagus. Distal gastric cancers were labelled as such when the tumour was clinically, macroscopically and histologically (i.e. at no point adjacent to squamous mucosa) confined to the more distal stomach. Tumours were classified according to the Lauren classification^[13] as diffuse or intestinal.

Methods

Initially, 4 μ m sections were cut from all blocks and stained with haematoxylin and eosin. Tissue microarrays (TMAs) were constructed^[14]. The technique involves taking cylindrical core biopsies from 'donor' blocks with subsequent precise arraying into a new 'recipient' paraffin block using a precision instrument (Beecher Instruments, Silver Spring, MD, USA)^[14,15]. Two different types of TMAs were constructed. Endoscopic biopsy fragments from wax blocks were arrayed using 2 mm punches. This size punch covers most endoscopic fragments in toto and all individual fragments from a donor wax block were sampled in separate cores (in this study 1-8 cores per donor block). Therefore, all the tissue from an original donor block containing endoscopic biopsy material was arrayed into the TMA block. Each 'biopsy-TMA' could hold up to 40 2 mm cores (i.e. up to 40 donor blocks depending on numbers of tissue fragments per original donor block). In the cancer resection specimens a different type of TMA was constructed due to the large size of tissue pieces in each block. The whole-section glass-slides were evaluated and areas of tumour as well as uninvolved mucosa were marked on the glass slides and identified in the corresponding wax blocks. Four 0.6 mm core biopsies were taken from each area. In 31 cases tumour and uninvolved mucosa were not present in the same wax block and two separate blocks were used. In this fashion, a total of 8 cores were taken per case (4 from tumour and 4 from uninvolved mucosa) with 35-40 cases (a total of 280-320 cores) fitted on to each TMA-block. Using TMAs the total number of TMA-blocks constructed was twenty-one.

Immunohistochemistry

Monoclonal mouse antibodies directed against p16 (1:100. Clone G175-405, PharMingen, USA) and pRb (1:300. Clone M7131, DAKO, Denmark) were used. Immunostaining was

performed using standard procedures. Heat mediated antigen retrieval using a pressure cooker was required to unmask the antigen sites. Antibody binding was detected using the Vectastain universal elite ABC-peroxidase kit (Vector Laboratories Inc., Burlingame, CA, USA). The positive p16 control was a case of severe uterine cervical dysplasia which strongly expressed p16 in dysplastic foci. The positive control for pRb was a multi-tissue block including tonsil.

Immunohistochemical interpretation

p16 Positive staining was defined as nuclear staining whereas cytoplasmic staining was considered non-specific and ignored. Extent was scored semi-quantitatively as negative (0) if <5% of cells stained, 1 if 5-25% of cells stained, 2 if 26-50% of cells stained and 3 if >50% cells stained. In cancer resections the average score was calculated from each of the four 0.6 mm TMA cores of either carcinoma or non-involved mucosa. The average score of each of the four decided the overall positivity/negativity.

pRb Nuclear staining was considered positive. Extent was scored semi-quantitatively as negative (0) if <5% of cells stained, 1 if 5-25% of cells stained, 2 if 26-50% of cells stained and 3 if >50% cells stained. In cancer resections the average score was calculated from each of the four 0.6 mm TMA cores of either carcinoma or non-involved mucosa. The average score of each of the four decided the overall positivity/negativity.

Statistical analysis

Statistical significance was defined as $P < 0.05$. Chi-square test was used for comparison between groups. Logistic regression analysis on the actual numbers of positive cases was used to test trends between tissue types within the proximal and distal groups.

RESULTS

Comparisons of p16 expression between different histological subsets within proximal and distal locations

In mucosa from biopsies (i.e. not associated with carcinoma) with and without intestinal metaplasia there was a low level of expression in both proximal and distal locations, mainly within the neck regions of the glands and absent in superficial epithelium. In distal tissue samples there was a statistically significant stepwise increase from normal mucosa to intestinal metaplasia to non-involved mucosa from cancer resections to carcinoma ($P < 0.0001$, Table 2). In proximal tissue samples no such trend was noted and there were no differences between the different tissue samples (Figure 4). No differences in p16 expression were noted between tumour types in either of the two locations and there were no correlations between p16 expression and stage of tumour or any clinical parameters.

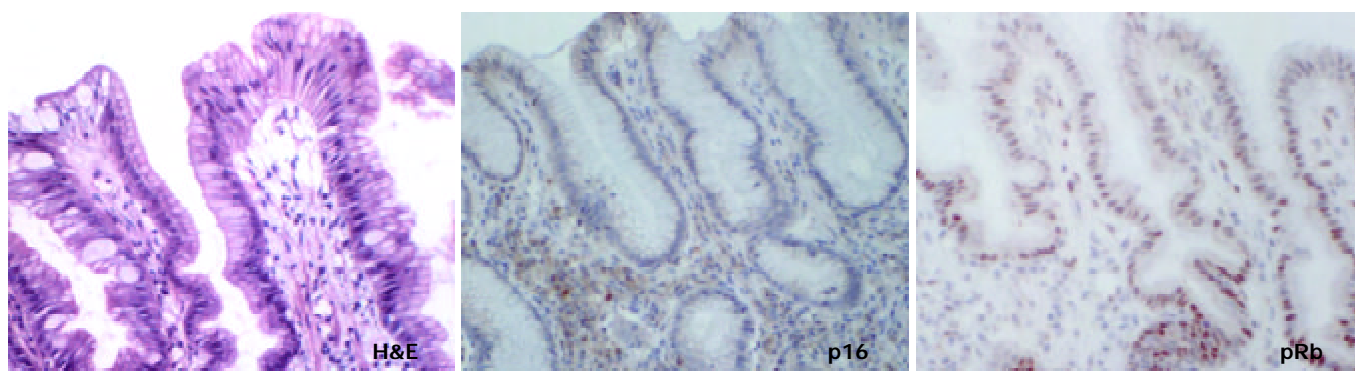


Figure 1 Antral biopsy showing focal intestinal metaplasia. This composite figure shows the H&E appearance, negative p16 staining (with some positive inflammatory cells in the background) and positive pRb staining limited to the neck region of the glands. Original magnification 200×.

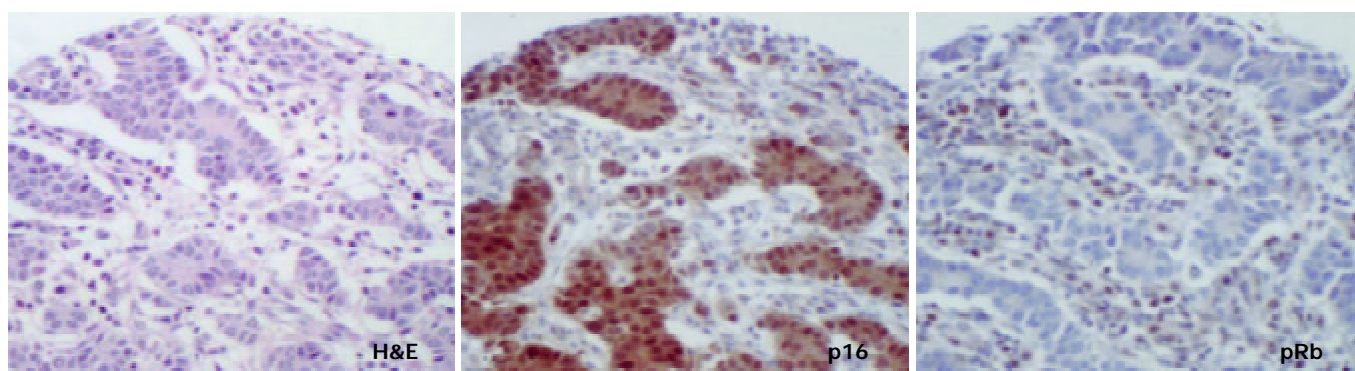


Figure 2 Gastric antral carcinoma of intestinal type. The same 0.6 mm TMA core is shown stained with H&E, p16 and pRb. The latter is negative whereas p16 shows strong nuclear and cytoplasmic staining. The cytoplasmic staining was ignored for the scoring. Original magnification 200×.

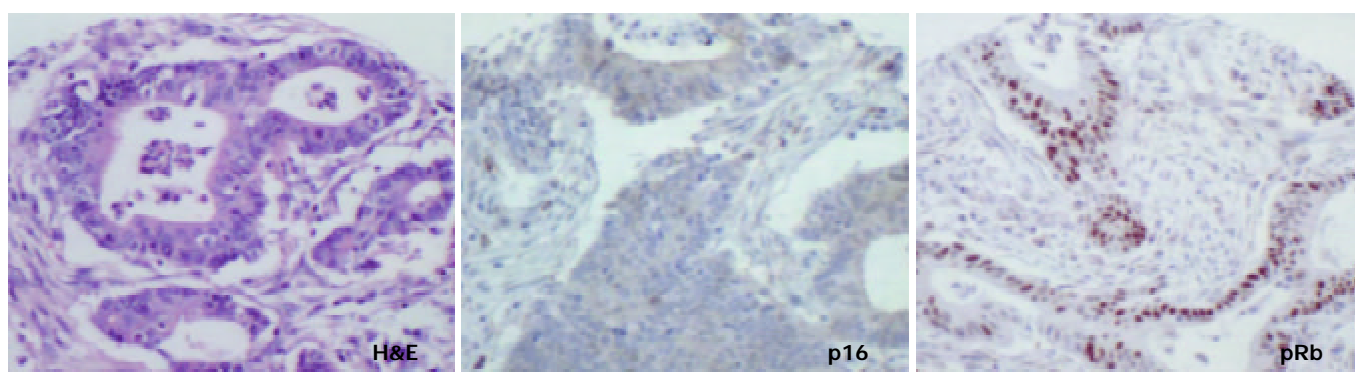


Figure 3 Gastric antral carcinoma of intestinal type. The same 0.6 mm TMA core is shown stained with H&E, p16 and pRb. The latter shows strong and crisp nuclear staining whereas p16 is negative. Original magnification 200×.

Table 2 Percentage of cases staining for and extent scores of p16 and pRb

	Proximal				Distal			
	Biopsies normal	Biopsies IM	Resections UM	Resections cancer	Biopsies normal	Biopsies IM	Resections UM	Resections cancer
Number and (%) of cases positive for p16	12 (21%)	13 (27%)	8 (21%)	13 (33%)	4 (8%)	13 (26%)	37 (47%)	42 (54%)
Mean (and SD) of extent scores for p16	0.21 (0.41)	0.27 (0.45)	0.23 (0.48)	0.41 (0.68)	0.077 (0.27)	0.26 (0.44)	0.49 (0.53)	0.69 (0.79)
Number and (%) of cases positive for pRb	52 (93%)	37 (76%)	31 (80%)	30 (77%)	46 (88%)	35 (70%)	51 (65%)	38 (49%)
Mean (and SD) of extent scores for pRb	0.41 (0.5)	0.34 (0.48)	0.33 (0.48)	0.5 (0.51)	0.42 (0.5)	0.24 (0.43)	0.17 (0.38)	0.28 (0.45)

SD: Standard deviation. UM: Uninvolved mucosa from cancer resections.

Comparisons of pRb expression between different histological subsets within proximal and distal locations

pRb was highly expressed in normal epithelium and intestinal metaplasia, mainly in the more proliferative areas, i.e. the neck region within the glandular epithelium. In both proximal and distal stomach there was a statistically significant trend for decreased pRb expression from normal mucosa to intestinal metaplasia to non-involved mucosa from cancer resections to carcinoma. It was more pronounced in the distal tissue samples ($P < 0.0001$) than in the proximal tissue samples ($P = 0.035$) and in the latter location it was mainly a function of the high expression in normal mucosa compared with the other histological subsets which showed very similar expression rates (Figure 5). No differences in pRb expression were noted between tumour types in the two locations and there were no correlations between pRb expression and stage of tumour or any clinical parameters.

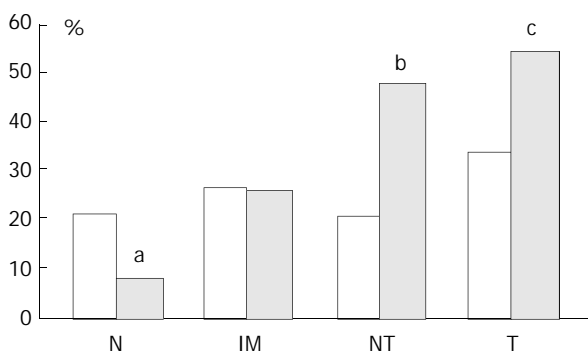


Figure 4 Graph showing percentage of p16 positive cases as pairs of proximal (empty columns, left hand sides) and distal (black columns, right hand sides) tissue samples. N: Biopsies showing normal mucosa, IM: Biopsies showing intestinal metaplasia, NT: Non-involved mucosa from gastric cancer resection specimens, T: Tumour from gastric cancer resection specimens. There was a significant stepwise increase in expression from normal mucosa → intestinal metaplasia → non-involved mucosa from cancer resections → carcinoma in the distal stomach only. ^aThere was a significantly lower p16 expression in distal normal mucosa than in proximal normal mucosa, $P = 0.0045$. ^b and ^c: There was a significantly higher p16 expression in both non-involved as well as carcinoma from cancer resections from distal compared with proximal stomach, ^b $P = 0.0048$ and ^c $P = 0.036$.

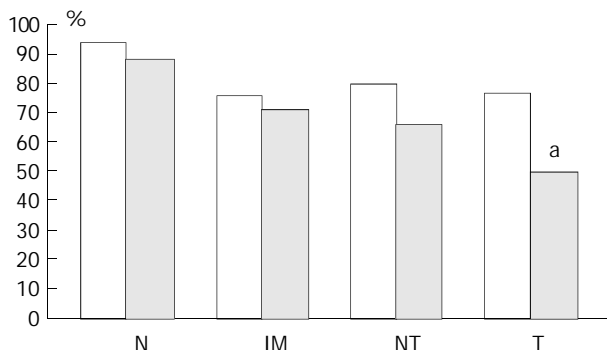


Figure 5 Graph showing percentage of pRb positive cases as pairs of proximal (empty columns, left hand side) and distal (black columns, right hand side) tissue samples. N: Biopsies showing normal mucosa, IM: Biopsies showing intestinal metaplasia, NT: Non-involved mucosa from gastric cancer resection specimens, T: Tumour from gastric cancer resection specimens. There was a significant stepwise decrease in expression from normal mucosa → intestinal metaplasia → non-involved mucosa from cancer resections → carcinoma in both the

distal and proximal stomach although in the latter location it was most likely due to the high expression in normal mucosa compared with the other types of tissues. ^aThere was a significantly lower pRb expression in distal than in proximal carcinomas, $P = 0.0047$.

Comparison of p16 and pRb expressions between similar histological subsets in proximal versus distal location

In cancer resection specimens there was a significantly lower expression of p16 in proximal than distal location, both in uninvolved mucosa ($P = 0.0048$) and carcinoma ($P = 0.0036$) whereas the opposite was seen in normal mucosa ($P = 0.0045$) (Figure 4). pRb expression was significantly higher in proximal carcinomas ($P = 0.0047$) (Figure 5).

Correlations between pRb and p16

In distal carcinomas there was a significantly negative association between expressions of the two molecules ($P = 0.043$) (Table 3).

Table 3 p16 versus pRb staining in distal gastric carcinomas

		pRb	
		+	-
p16	+	16	26
	-	22	14

This distribution was significant, $P = 0.043$.

DISCUSSION

Disruption of cell cycle regulation is a critical event in carcinogenesis. Alteration of the retinoblastoma (pRb) tumour suppressor pathway, which controls the G1/S checkpoint, is a common event in many neoplasms and typically implicates abnormal expression of both pRb and p16 although other molecules may be involved.

The current study aimed to compare alterations in this pathway in proximal and distal gastric carcinogenesis in an effort to explain the observed epidemiological differences between the two sites. Immunohistochemistry was performed to investigate expression of p16 and pRb in various histological stages from normal mucosa to carcinoma in both proximal (cardia) and distal (antral) tissue samples.

The results of this study showed highly significant trends for increase in p16 expression with a concomitant decrease in pRb expression in distal tissue samples from normal mucosa to intestinal metaplasia to uninvolved mucosa from cancer resections to carcinoma. This suggests that the pRb pathway plays a definite role in distal gastric carcinogenesis. It may be an early event since the trend towards p16 overexpression and pRb underexpression was seen even between normal mucosa and intestinal metaplasia. In the proximal stomach no differences in p16 expression were seen between the various stages whereas pRb expression decreased slightly from normal mucosa to carcinoma. This seemed to be mainly an effect of a higher expression of pRb in normal mucosa compared with any of the other tissue samples. Furthermore, the trend for decreasing pRb was not matched by an increase in p16 expression and there was no inverse relationship between the two molecules in the group of carcinomas. Taken together this argues against the pRb pathway as important in proximal gastric carcinogenesis.

Other studies on (distal) gastric carcinogenesis have shown a similar p16 'overexpression' in gastric carcinomas^[16,17] with weak staining in non-involved mucosa. However, a recent immunohistochemical study found a progressive p16 decrease and a pRb increase from gastritis to dysplasia^[12] in samples from the cardia. This is surprising in view of the *opposite* trend

in distal gastric samples seen here and also by others^[17]. The reason for this discrepancy is uncertain. In the above-mentioned study patients were from an area in China with a high incidence of gastric carcinoma and compared with the current study, different entities (chronic gastritis, dysplasia) were investigated. Also, racial differences may play a role since all the patients in this study were Caucasians.

A study on p16 expression in normal tissues^[18] showed some staining in gastric antral glands. The following scenario is therefore likely: p16 is expressed with a low frequency in the normal state, which may be related to a relatively low proliferative status. In support of this is the limited expression in glandular (proliferative area) rather than surface epithelium (quiescent area) seen here and also noted by others^[17,18]. In tumours there may be loss of negative feedback through decrease in pRb expression which causes p16 overexpression and other studies have also shown an inverse relationship between expression of the two molecules^[9,10]. The current study showed mainly cases of distal gastric cancer resections with gain of p16 expression in cancers compared with non-involved mucosa. However, loss of p16 expression in cancers compared with uninvolved mucosa was also seen in some cases and it is entirely possible that, whereas most cancers lose pRb function/expression, some preferentially lose p16 expression.

This study did not entirely rule out a role for the pRb pathway in proximal gastric carcinogenesis since other molecules participate in this complex cell cycle control mechanism. It is unlikely, however, since altered expression of p16 and pRb would be expected if abnormal feedback from other molecules in this pathway existed.

In conclusion this study strongly suggests that alterations in the pRb pathway are significant in distal, but not proximal, gastric carcinogenesis. In the former location it may be an early event. Importantly, this study therefore supports the hypothesis that tumours of the two locations are genetically different which may account for some of the observed epidemiological differences.

ACKNOWLEDGEMENTS

Mr. Ronan Conroy is thanked for his help with the statistical analysis.

REFERENCES

- 1 **Blot WJ**, Devesa SS, Kneller RW, Fraumeni JF Jr. Rising incidence of adenocarcinoma of the esophagus and gastric cardia. *JAMA* 1991; **265**: 1287-1289
- 2 **Devesa SS**, Blot WJ, Fraumeni JF Jr. Changing patterns in the incidence of esophageal and gastric carcinoma in the United States. *Cancer* 1998; **83**: 2049-2053

- 3 **Jass JR**. Role of intestinal metaplasia in the histogenesis of gastric carcinoma. *J Clin Pathol* 1980; **33**: 801-810
- 4 **Ruol A**, Parenti A, Zaninotto G, Merigliano S, Costantini M, Cagol M, Alfieri R, Bonavina L, Peracchia A, Ancona E. Intestinal metaplasia is the probable common precursor of adenocarcinoma in Barrett esophagus and adenocarcinoma of the gastric cardia. *Cancer* 2000; **88**: 2520-2528
- 5 **Morales TG**, Camargo E, Bhattacharyya A, Sampliner RE. Long-term follow-up of intestinal metaplasia of the gastric cardia. *Am J Gastroenterol* 2000; **95**: 1677-1680
- 6 **Sipponen P**. Intestinal metaplasia and gastric carcinoma. *Ann Clin Res* 1981; **13**: 139-143
- 7 **Sherr CJ**. The Pezcoller lecture: cancer cell cycles revisited. *Cancer Res* 2000; **60**: 3689-3695
- 8 **Liggett WH Jr**, Sidransky D. Role of the p16 tumor suppressor gene in cancer. *J Clin Oncol* 1998; **16**: 1197-1206
- 9 **Yang G**, Zhang Z, Liao J, Seril D, Wang L, Goldstein S, Yang CS. Immunohistochemical studies on Waf1p21, p16, pRb and p53 in human esophageal carcinomas and neighboring epithelia from a high-risk area in northern China. *Int J Cancer* 1997; **72**: 746-751
- 10 **Lee WA**, Woo DK, Kim YI, Kim WH. p53, p16 and Rb expression in adenosquamous and squamous cell carcinomas of the stomach. *Pathol Res Pract* 1999; **195**: 747-752
- 11 **Jang TJ**, Kim DI, Shin YM, Chang HK, Yang CH. p16(INK4a) Promoter hypermethylation of non-tumorous tissue adjacent to gastric cancer is correlated with glandular atrophy and chronic inflammation. *Int J Cancer* 2001; **93**: 629-634
- 12 **Zhou Y**, Gao SS, Li YX, Fan ZM, Zhao X, Qi YJ, Wei JP, Zou JX, Liu G, Jiao LH, Bai YM, Wang LD. Tumor suppressor gene p16 and Rb expression in gastric cardia precancerous lesions from subjects at a high incidence area in northern China. *World J Gastroenterol* 2002; **8**: 423-425
- 13 **Lauren P**. The two histologic main types of gastric carcinoma: diffuse and so-called intestinal-type carcinoma. *APMIS* 1965; **64**: 31-49
- 14 **Kononen J**, Bubendorf L, Kallioniemi A, Barlund M, Schraml P, Leighton S, Torhorst J, Mihatsch MJ, Sauter G, Kallioniemi OP. Tissue microarrays for high-throughput molecular profiling of tumor specimens. *Nat Med* 1998; **4**: 844-847
- 15 **Moch H**, Kononen T, Kallioniemi OP, Sauter G. Tissue microarrays: what will they bring to molecular and anatomic pathology? *Adv Anat Pathol* 2001; **8**: 14-20
- 16 **Rocco A**, Schandl L, Nardone G, Tulassay Z, Staibano S, Malfertheiner P, Ebert MP. Loss of expression of tumor suppressor p16(INK4) protein in human primary gastric cancer is related to the grade of differentiation. *Dig Dis* 2002; **20**: 102-105
- 17 **Tsujie M**, Yamamoto H, Tomita N, Sugita Y, Ohue M, Sakita I, Tamaki Y, Sekimoto M, Doki Y, Inoue M, Matsuura N, Monden T, Shiozaki H, Monden M. Expression of tumor suppressor gene p16(INK4) products in primary gastric cancer. *Oncology* 2000; **58**: 126-136
- 18 **Nielsen GP**, Stemmer-Rachamimov AO, Shaw J, Roy JE, Koh J, Louis DN. Immunohistochemical survey of p16INK4A expression in normal human adult and infant tissues. *Lab Invest* 1999; **79**: 1137-1143

Edited by Wang XL

Effect of NF- κ B, survivin, Bcl-2 and Caspase3 on apoptosis of gastric cancer cells induced by tumor necrosis factor related apoptosis inducing ligand

Liu-Qin Yang, Dian-Chun Fang, Rong-Quan Wang, Shi-Ming Yang

Liu-Qin Yang, Dian-Chun Fang, Rong-Quan Wang, Shi-Ming Yang, Department of Gastroenterology, Southwest Hospital, Third Military Medical University, Chongqing 400038, China

Supported by the Scientific Research Foundation of Chinese PLA, during the 10th-Five-Year Plan Period, No. 01MA172

Correspondence to: Dian-Chun Fang, M.D., Ph.D. Southwest Hospital, Third Military Medical University, Chongqing 400038, China. fangdianchun@hotmail.com

Telephone: +86-23-68754624 or +86-23-68754124

Fax: +86-23-68754124

Received: 2003-05-11 **Accepted:** 2003-08-16

Abstract

AIM: To study the effect of NF- κ B, survivin, Bcl-2 and Caspase3 on tumor necrosis factors related apoptosis inducing ligand (TRAIL) induced apoptosis of gastric cancer cells.

METHODS: Gastric cancer cells of SGC-7901, MKN28, MKN45 and AGS lines were cultured in PRMI-1640 medium and the apoptosis rates of the cells of 4 lines were observed after treatment of tumor necrosis factors related apoptosis inducing ligand (TRAIL) with a flow cytometer. The expression of NF- κ B, survivin, Bcl-2 and Caspase3 in gastric cancer cells of 4 lines was analyzed with Western blot.

RESULTS: After the gastric cancer cells were exposed to TRAIL 300 ng/ml for 24 hours, the apoptosis rate was 36.05%, 20.27%, 16.50% and 11.80% in MKN28, MKN45, AGS and SGC-7901 cells respectively. Western blot revealed that the expressions of NF- κ B and survivin were lower in MKN28 cells than in MKN45, AGS and SGC-7901 cells. In contrast, the expression of Caspase3 was higher in MKN28 cells than in MKN45, AGS and SGC-7901 cells.

CONCLUSION: There is a selectivity of TRAIL potency to induce apoptosis in gastric cancer cells of different cell lines. The anticancer potency of TRAIL is associated with the decreased expression of NF- κ B and survivin and increased expression of Caspase3 of gastric cancer cells.

Yang LQ, Fang DC, Wang RQ, Yang SM. Effect of NF- κ B, survivin, Bcl-2 and Caspase3 on apoptosis of gastric cancer cells induced by tumor necrosis factor related apoptosis inducing ligand. *World J Gastroenterol* 2004; 10(1): 22-25

<http://www.wjgnet.com/1007-9327/10/22.asp>

INTRODUCTION

Tumor necrosis factors related apoptosis inducing ligand (TRAIL) is one of the members of TNF family. TRAIL, also known as APO-2L^[1,2], is highly homologous to FasL. TRAIL is capable of inducing apoptosis of many kinds of cancer cells but nontoxic to normal cells^[3-13]. It has been found that cells of different cancers and even different types of cells of a cancer

exhibit significantly different sensitivity to TRAIL^[14-17].

Nuclear transcript factor (NF- κ B), survivin and Bcl-2 are apoptosis inhibitors and play a key role in the mechanism of anti-apoptosis of tumors^[18-29]. If the activity of these factors is suppressed, tumor cells can undergo apoptosis and stop growing^[30,31]. Various modulation elements of cell apoptosis exert their action through Caspase enzyme system. Among them, Caspase 3 (also known as CPP32, YAMA, or apopain) is probably the one that so far best correlates with apoptosis^[32,33]. Furthermore, Caspase 3 expression could be detected in several human malignancies such as non-small cell lung carcinoma^[34], esophageal squamous cell carcinoma^[35] and gastric cancer^[36]. The inhibition of cell apoptosis is closely related to the onset, development and sensitivity to chemotherapy of malignant tumors. Consequently, we studied the relationship of the sensitivity of the cells of 4 gastric cancer cell lines to TRAIL with the expression of NF- κ B, survivin, Bcl-2 and Caspase3 in order to clarify why and how gastric cancer cells were resistant to TRAIL.

MATERIALS AND METHODS

SGC-7901 line of gastric cancer cells was preserved in our laboratory. MKN28, MKN45 and AGS cell lines were donated by our colleagues of the Fourth Military Medical University. NC membrane and mouse antihuman survivin monoclonal antibody were bought from Santa Cruz Biotech Company. Mouse antihuman NF- κ B (p65) monoclonal antibody, mouse antihuman Bcl-2 monoclonal antibody, mouse antihuman Caspase3 monoclonal antibody and peroxidase-conjugated rabbit anti-mouse IgG were from the Zhongshan Company in Beijing, and ECL chemofluorescent agent kit was from DingguoBiotech Center in Beijing. TRAIL protein was prepared by ourselves^[37].

Gastric cancer cells of SGC-7901, MKN28, MKN45 and AGS lines were incubated in PRMI-1640 medium and 10% inactivated calf serum. Penicillin and streptomycin were added to a final concentration of 100 u/ml. Generation transition of the cells was achieved every 3 to 5 days through the adoption of 0.25% pancreatic enzyme and 0.02% EDTA.

Gastric cancer cells in the logarithmic proliferation stage were studied. The culture medium of every cell line was distributed into 5 bottles (100 ml in each). TRAIL was added to the 5 bottles of every cell line with a final concentration of 0 ng/ml, 50 ng/ml, 100 ng/ml, 200 ng/ml and 300 ng/ml respectively. All the bottles were incubated under 37 °C, 5%CO₂ and saturated humidity for 24 hours.

The apoptosis rate of gastric cancer cells was determined with a flow cytometer. All the cells were collected, digested and washed twice in PBS, and the floating cells were precipitated with 0.1 ml PBS. After the cells were fixed in 70% precooled ethanol for 24 hours, they were stained with PI and examined.

Western blot was used to determine the expression of NF- κ B, survivin, Bcl-2 and Caspase3. The gastric cancer cells were

ruptured with lysozyme and protein concentration of cells was measured with Lowry method. The protein concentration was unified with PBS. In order to denature the protein, the samples were heated with middle molecular weight protein Marker to 100 °C for 3 minutes. The protein, after being separated with SDS-PAGE electrophoresis, was transferred to a piece of nitrocellulose membrane with moisture transfer technique at 100v for 2 hours. The membrane was stained with ponceau-S to confirm whether the protein transfer was successful. Five percent of defat milk powder-PBS solution was used to block the unspecific antibody binding site for one hour. Then the membrane was washed 3 times in PBS-T solution, 15 minutes each time. Monoclonal antibody solution (1:1 000) of mouse antihuman NF- κ B, survivin, Bcl-2 and Caspase3 was incubated with the membrane for 1 hour respectively. Again, each piece of membrane was washed 3 times in PBS-T solution, 15 minutes each time. Then, all the membranes were incubated with rabbit antimouse IgG solution (1:1 000) for one hour. The membranes were washed 3 times in PBS-T solution, 15 minutes each time. Eventually, the membranes were incubated with chemofluorescent agent for 5 minutes, and then were exposed to X-ray films in a dark room. The X-ray films were developed and examined.

SPSS statistic soft package was used to undergo single factor Chi square analysis and *t* test. $P < 0.05$ was considered as significant.

RESULTS

TRAIL exerted a considerable apoptosis-inducing effect on the 4 line gastric cancer cells and the effect was in a dosage dependent manner. Figure 1 shows that the gastric cancer cells of the 4 lines had a different sensitivity to TRAIL. After the action of 300 ng/ml TRAIL for 24 hours, the apoptosis rate was 36.05% in MKN28, 20.27% in MKN45, 16.50% in AGS and 11.80% in SGC-7901 lines. The apoptosis rate was significantly higher in MKN28 than in other 3 kinds of cells ($P < 0.05$), but there was no significant difference among the other 3 lines of gastric cancer cells. SGC-7901 cells were resistant to TRAIL.

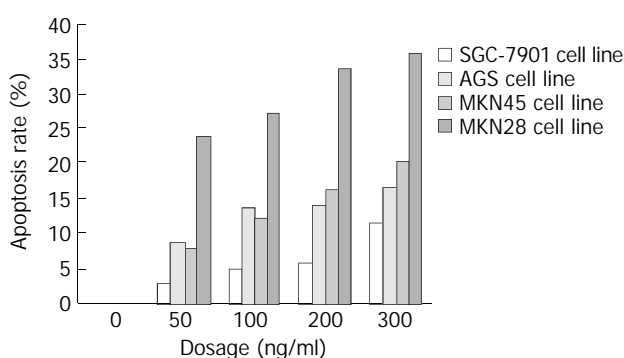


Figure 1 Changes of apoptosis rate in 4 gastric cancer cell lines after 24 hours action of different dosage of TRAIL.

The expression of NF- κ B (p65) in the 4 lines of gastric cancer cells is shown in Figure 2. NF- κ B expression was lower in MKN28 than in SGC-7901 cells, but no significant difference was found between MKN45 and AGS cells.

Before administration of TRAIL, Western blot revealed that the expression of survivin was significantly lower in MKN28 than in SGC-7901 cells, and no significant difference was found between MKN45 and AGS cells (Figure 3).

Before administration of TRAIL, Western blot revealed that the expression of Bcl-2 had no significant difference in the 4 line gastric cancer cells (Figure 4).

Before administration of TRAIL, Western blot showed that the expression of Caspase 3 was lower in SGC-7901 and highest in MKN28 cells. The expression in AGS and MKN45 cells was in the middle range (Figure 5).

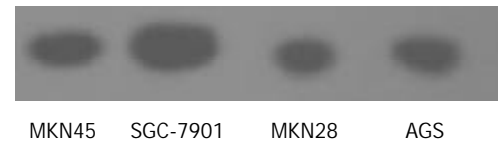


Figure 2 Expression of NF- κ B in 4 lines of gastric cancer cells.

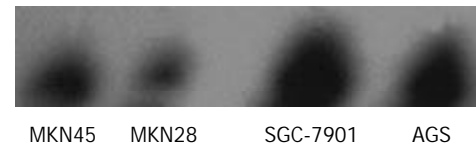


Figure 3 Expression of survivin in 4 lines of gastric cancer cells.

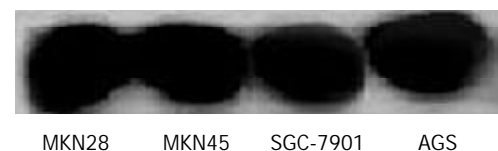


Figure 4 Expression of Bcl-2 in 4 lines of gastric cancer cells.

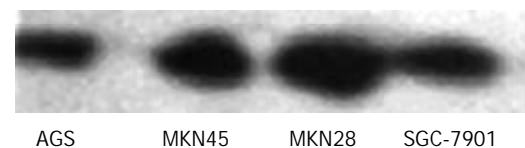


Figure 5 Expression of Caspase 3 in 4 lines of gastric cancer cells.

DISCUSSION

TRAIL is a recently discovered apoptosis inducing molecule. It has aroused great interest in the medical circle because it can selectively induce cancer cells, transform cells and virus-infected cells to undergo apoptosis with no toxicity to normal cells. In this study, anticancer effect of TRAIL on the 4 lines of gastric cancer cells was observed. We found that TRAIL exerted a certain degree of apoptosis inducing action on the gastric cancer cells and the action potency was dosage dependent. Twenty-four hours after administration of 300 ng/ml TRAIL, the apoptosis rate was 36.05% in MKN28, 20.27% in MKN45, 16.50% in AGS and 11.80% in SGC-7901 cells. This implies that the sensitivity to apoptosis inducing action of TRAIL varied among the 4 lines of gastric cancer cells.

Apoptosis is a cellular suicidal action. This process is under the combined modulation of apoptosis promoting factors including p53, Fas and others and apoptosis inhibiting factors including Bcl-2, CIAP, survivin and others. Survivin is an inhibitor of apoptosis protein (IAP), which has been found to be crucial for mitosis and cell cycle progression^[38]. Survivin could act directly on Caspases and mainly suppress the activity of Caspase 3 and Caspase 7^[39]. Disruption of survivin-microtubule interactions could result in loss of survivin's anti-apoptosis function and increase caspase-3 activity, a mechanism involved in cell death during mitosis^[40]. In addition, it has been found that deficiency of survivin in transgenic mice could exacerbate Fas-induced apoptosis via mitochondrial pathways^[41]. In the present study, we found that the difference of sensitivity to TRAIL among the 4 lines of gastric cancer

cells was related to the expression of survivin and Caspase of the cells. SGC-7901 cells with high expression of survivin and low expression of Caspase 3 were resistant to TRAIL, but MKN28 cells with low expression of survivin and high expression of Caspase 3 were sensitive to TRAIL. So, the determination of the expression level of survivin and Caspase 3 in gastric cancer cells is helpful to determine whether the cells are sensitive to TRAIL. To suppress the expression of survivin and increase the expression of Caspase 3 could strengthen the sensitivity of gastric cancer cells to TRAIL^[42].

The transcription factor NF- κ B is a key regulator of immune responses and inflammation operating through the induction of numerous genes, including those coding for cytokines, chemokines and adhesion molecules^[43-45]. NF- κ B suppresses apoptosis by inducing expression of a number of genes whose products inhibit apoptosis, including inhibitors of apoptosis (IAPs), Caspase 8-FADD-like IL-1 β -converting enzyme (Caspase 8-FLICE) inhibitory protein (cFLIP), A1 (also known as Bfl1), TNF receptor associated factor 1 (TRAF1) and TRAF2. These anti-apoptotic proteins have been found to work in a coordinated fashion to block apoptosis at multiple steps along the apoptotic cascade or to regulate other pro- or anti-apoptotic pathways^[46]. NF- κ B could also regulate the expression of several members of the Bcl-2 family^[47]. In this study, we found that the sensitivity of the 4 line gastric cancer cells to TRAIL was related to the expression of NF- κ B. SGC-7901 cells showed a relatively high expression of NF- κ B and were resistant to TRAIL. On the contrary, MKN28 cells with a low expression of NF- κ B were sensitive to TRAIL. It is considered that suppression of the expression of NF- κ B in gastric cancer cells can increase their sensitivity to TRAIL.

Bcl-2 is a proto-oncogene and can suppress apoptosis. Bcl-2 has been found to be closely related to the onset and drug resistance of many kinds of malignant tumors^[48-52]. Previous studies have confirmed that overexpression of Bcl-2 in the cells of various malignant tumors could result in resistance against cell apoptosis induced by chemotherapeutic agents such as cisplatin^[53,54] and arsenic trioxide^[55]. If Bcl-2 expression is suppressed, tumors are impelled to undergo apoptosis. We found that the sensitivity difference among the 4 lines of gastric cancer cells was not related with Bcl-2 expression, but the sensitivity difference to TRAIL did occur among them. This finding was in agreement with the recently published data on breast cancer^[56].

To sum up, TRAIL possesses the characteristics of selectively inducing apoptosis of tumor cells. TRAIL-resistant tumor cells may be related to the expression of apoptosis-inhibitor survivin and NF- κ B. Suppression of the expression of survivin and NF- κ B, and reinforcement of Caspase 3 expression would increase the sensitivity of gastric cancer cells to TRAIL. Further study is imperative to clarify the mechanism of the apoptosis-inducing action of TRAIL.

REFERENCES

- Pitti RM**, Marsters SA, Ruppert S, Donahue CJ, Moore A, Ashkenazi A. Induction of apoptosis by Apo-2 ligand, a new member of the tumor necrosis factor cytokine family. *J Biol Chem* 1996; **271**: 12687-12690
- LeBlanc HN**, Ashkenazi A. Apo2L/TRAIL and its death and decoy receptors. *Cell Death Differ* 2003; **10**: 66-75
- Walczak H**, Miller RE, Ariail K, Gliniak B, Griffith TS, Kubin M, Chin W, Jones J, Woodward A, Le T, Smith C, Smolak P, Goodwin RG, Rauch CT, Schuh JC, Lynch DH. Tumoricidal activity of tumor necrosis factor-related apoptosis-inducing ligand *in vivo*. *Nat Med* 1999; **5**: 157-163
- Silvestris F**, Cafforio P, Tucci M, Dammacco F. Negative regulation of erythroblast maturation by Fas-L(+)/TRAIL(+) highly malignant plasma cells: a major pathogenetic mechanism of anemia in multiple myeloma. *Blood* 2002; **99**: 1305-1313
- Odoux C**, Albers A, Amoscato AA, Lotze MT, Wong MK. TRAIL, FasL and a blocking anti-DR5 antibody augment paclitaxel-induced apoptosis in human non-small-cell lung cancer. *Int J Cancer* 2002; **97**: 458-465
- Seki N**, Hayakawa Y, Brooks AD, Wine J, Wiltout RH, Yagita H, Tanner JE, Smyth MJ, Sayers TJ. Tumor necrosis factor-related apoptosis-inducing ligand-mediated apoptosis is an important endogenous mechanism for resistance to liver metastases in murine renal cancer. *Cancer Res* 2003; **63**: 207-213
- Kim DM**, Koo SY, Jeon K, Kim MH, Lee J, Hong CY, Jeong S. Rapid induction of apoptosis by combination of flavopiridol and tumor necrosis factor (TNF)-alpha or TNF-related apoptosis-inducing ligand in human cancer cell lines. *Cancer Res* 2003; **63**: 621-626
- Smyth MJ**, Takeda K, Hayakawa Y, Peschon JJ, van den Brink MR, Yagita H. Nature's TRAIL-on a path to cancer immunotherapy. *Immunity* 2003; **18**: 1-6
- Guillemet J**, Saint-Laurent N, Rochaix P, Cuvillier O, Levade T, Schally AV, Pradayrol L, Buscail L, Susini C, Bousquet C. Somatostatin receptor subtype 2 sensitizes human pancreatic cancer cells to death ligand-induced apoptosis. *Proc Natl Acad Sci U S A* 2003; **100**: 155-160
- Naka T**, Sugamura K, Hylander BL, Widmer MB, Rustum YM, Repasky EA. Effects of tumor necrosis factor-related apoptosis-inducing ligand alone and in combination with chemotherapeutic agents on patients' colon tumors grown in SCID mice. *Cancer Res* 2002; **62**: 5800-5806
- Wajant H**, Pfizenmaier K, Scheurich P. TNF-related apoptosis inducing ligand (TRAIL) and its receptors in tumor surveillance and cancer therapy. *Apoptosis* 2002; **7**: 449-459
- Inoue H**, Shiraki K, Yamanaka T, Ohmori S, Sakai T, Deguchi M, Okano H, Murata K, Sugimoto K, Nakano T. Functional expression of tumor necrosis factor-related apoptosis-inducing ligand in human colonic adenocarcinoma cells. *Lab Invest* 2002; **82**: 1111-1119
- Wei XC**, Wang XJ, Chen K, Zhang L, Liang Y, Lin XL. Killing effect of TNF-related apoptosis inducing ligand regulated by tetracycline on gastric cancer cell line NCI-N87. *World J Gastroenterol* 2001; **7**: 559-562
- MacFarlane M**, Harper N, Snowden RT, Dyer MJ, Barnett GA, Pringle JH, Cohen GM. Mechanisms of resistance to TRAIL-induced apoptosis in primary B cell chronic lymphocytic leukaemia. *Oncogene* 2002; **21**: 6809-6818
- Held J**, Schulze-Osthoff K. Potential and caveats of TRAIL in cancer therapy. *Drug Resist Updat* 2001; **4**: 243-252
- de Almodovar CR**, Ruiz-Ruiz C, Munoz-Pinedo C, Robledo G, Lopez-Rivas A. The differential sensitivity of Bcl-2-overexpressing human breast tumor cells to TRAIL or doxorubicin-induced apoptosis is dependent on Bcl-2 protein levels. *Oncogene* 2001; **20**: 7128-7133
- Ibrahim SM**, Ringel J, Schmidt C, Ringel B, Muller P, Koczan D, Thiesen HJ, Lohr M. Pancreatic adenocarcinoma cell lines show variable susceptibility to TRAIL-mediated cell death. *Pancreas* 2001; **23**: 72-79
- Ohshima K**, Sugihara M, Haraoka S, Suzumiya J, Kanda M, Kawasaki C, Shimazaki K, Kikuchi M. Possible immortalization of Hodgkin and Reed-Sternberg cells: telomerase expression, lengthening of telomere, and inhibition of apoptosis by NF-kappaB expression. *Leuk Lymphoma* 2001; **41**: 367-376
- Wall NR**, O'Connor DS, Plescia J, Pommier Y, Altieri DC. Suppression of survivin phosphorylation on Thr34 by flavopiridol enhances tumor cell apoptosis. *Cancer Res* 2003; **63**: 230-235
- Hussein MR**, Haemel AK, Wood GS. Apoptosis and melanoma: molecular mechanisms. *J Pathol* 2003; **199**: 275-288
- Kim IK**, Jung YK, Noh DY, Song YS, Choi CH, Oh BH, Masuda ES, Jung YK. Functional screening of genes suppressing TRAIL-induced apoptosis: distinct inhibitory activities of Bcl-X(L) and Bcl-2. *Br J Cancer* 2003; **88**: 910-917
- Fulda S**, Meyer E, Debatin KM. Inhibition of TRAIL-induced apoptosis by Bcl-2 overexpression. *Oncogene* 2002; **21**: 2283-2294
- Zhou HB**, Zhu JR. Paclitaxel induces apoptosis in human gastric carcinoma cells. *World J Gastroenterol* 2003; **9**: 442-445
- Guo XZ**, Shao XD, Liu MP, Xu JH, Ren LN, Zhao JJ, Li HY, Wang D. Effect of bax, bcl-2 and bcl-xL on regulating apoptosis in tis-

- sues of normal liver and hepatocellular carcinoma. *World J Gastroenterol* 2002; **8**: 1059-1062
- 25 **Li HL**, Chen DD, Li XH, Zhang HW, Lü YQ, Ye CL, Ren XD. Changes of NF- κ B, p53, Bcl-2 and caspase in apoptosis induced by JTE-522 in human gastric adenocarcinoma cell line AGS cells: role of reactive oxygen species. *World J Gastroenterol* 2002; **8**: 431-435
- 26 **Xu AG**, Li SG, Liu JH, Gan AH. Function of apoptosis and expression of the proteins Bcl-2, p53 and C-myc in the development of gastric cancer. *World J Gastroenterol* 2001; **7**: 403-406
- 27 **Wang LD**, Zhou Q, Wei JP, Yang WC, Zhao X, Wang LX, Zou JX, Gao SS, Li YX, Yang CS. Apoptosis and its relationship with cell proliferation, p53, Waf1p21, bcl-2 and c-myc in esophageal carcinogenesis studied with a high-risk population in northern China. *World J Gastroenterol* 1998; **4**: 287-293
- 28 **Liu HF**, Liu WW, Fang DC, Men RP. Expression of bcl-2 protein in gastric carcinoma and its significance. *World J Gastroenterol* 1998; **4**: 228-230
- 29 **Zhou HB**, Yan Y, Sun YN, Zhu JR. Resveratrol induces apoptosis in human esophageal carcinoma cells. *World J Gastroenterol* 2003; **9**: 408-411
- 30 **Dalen H**, Neuzil J. alpha-Tocopheryl succinate sensitises a T lymphoma cell line to TRAIL-induced apoptosis by suppressing NF-kappa B activation. *Br J Cancer* 2003; **88**: 153-158
- 31 **Biswas DK**, Martin KJ, McAlister C, Cruz AP, Graner E, Dai SC, Pardee AB. Apoptosis Caused by Chemotherapeutic Inhibition of Nuclear Factor-kappaB Activation. *Cancer Res* 2003; **63**: 290-295
- 32 **Nicholson DW**, Ali A, Thornberry NA, Vaillancourt JP, Ding CK, Gallant M, Gareau Y, Griffin PR, Labelle M, Lazebnik YA. Identification and inhibition of the ICE/CED-3 protease necessary for mammalian apoptosis. *Nature* 1995; **376**: 37-43
- 33 **Fernandes-Alnemri T**, Litwack G, Alnemri ES. CPP32, a novel human apoptotic protein with homology to Caenorhabditis elegans cell death protein Ced-3 and mammalian interleukin-1 beta-converting enzyme. *J Biol Chem* 1994; **269**: 30761-30764
- 34 **Tormanen-Napankangas U**, Soini Y, Kahlos K, Kinnula V, Paakko P. Expression of caspases-3, -6 and -8 and their relation to apoptosis in non-small cell lung carcinoma. *Int J Cancer* 2001; **93**: 192-198
- 35 **Hsia JY**, Chen CY, Chen JT, Hsu CP, Shai SE, Yang SS, Chuang CY, Wang PY, Miaw J. Prognostic significance of caspase-3 expression in primary resected esophageal squamous cell carcinoma. *Eur J Surg Oncol* 2003; **29**: 44-48
- 36 **Kania J**, Konturek SJ, Marlicz K, Hahn EG, Konturek PC. Expression of survivin and caspase-3 in gastric cancer. *Dig Dis Sci* 2003; **48**: 266-271
- 37 **Li XA**, Fang DC, Yang SM, Luo YH. The expression, purification and anticancer activity of TRAIL. *Acta Acad Med Milit Tert* 2002; **23**: 1058-1060
- 38 **Suzuki A**, Hayashida M, Ito T, Kawano H, Nakano T, Miura M, Akahane K, Shiraki K. Survivin initiates cell cycle entry by the competitive interaction with Cdk4/p16(INK4a) and Cdk2/cyclin E complex activation. *Oncogene* 2000; **19**: 3225-3234
- 39 **Shin S**, Sung BJ, Cho YS, Kim HJ, Ha NC, Hwang JI, Chung CW, Jung YK, Oh BH. An anti-apoptotic protein human survivin is a direct inhibitor of caspase-3 and -7. *Biochemistry* 2001; **40**: 1117-1123
- 40 **Li F**, Ambrosini G, Chu EY, Plescia J, Tognin S, Marchisio PC, Altieri DC. Control of apoptosis and mitotic spindle checkpoint by survivin. *Nature* 1998; **396**: 580-584
- 41 **Conway EM**, Pollefeyt S, Steiner-Mosonyi M. Deficiency of survivin in transgenic mice exacerbates Fas-induced apoptosis via mitochondrial pathways. *Gastroenterology* 2002; **123**: 619-631
- 42 **Wall NR**, O' Connor DS, Plescia J, Pommier Y, Altieri DC. Suppression of survivin phosphorylation on Thr34 by flavopiridol enhances tumor cell apoptosis. *Cancer Res* 2003; **63**: 230-235
- 43 **Gong JP**, Liu CA, Wu CX, Li SW, Shi YJ, Li XH. Nuclear factor kB activity in patients with acute severe cholangitis. *World J Gastroenterol* 2002; **8**: 346-349
- 44 **Rossi A**, Kapahi P, Natoli G, Takahashi T, Chen Y, Karin M, Santoro MG. Anti-inflammatory cyclopentenone prostaglandins are direct inhibitors of IkappaB kinase. *Nature* 2000; **403**: 103-108
- 45 **Ghosh S**, Karin M. Missing pieces in the NF-kB puzzle. *Cell* 2002; **109** (Suppl): S81-S96
- 46 **Lin A**, Karin M. NF-kappaB in cancer: a marked target. *Semin Cancer Biol* 2003; **13**: 107-114
- 47 **Wang CY**, Guttridge DC, Mayo MW. NF-kappaB induces expression of the Bcl-2 homologue A1/Bfl-1 to preferentially suppress chemotherapy-induced apoptosis. *Mol Cell Biol* 1999; **19**: 5923-5929
- 48 **Sosic D**, Richardson JA, Yu K. Twist regulates cytokine gene expression through a negative feedback loop that represses NF-kappaB activity. *Cell* 2003; **112**: 169-180
- 49 **Zhou HB**, Zhu JR. Paclitaxel induces apoptosis in human gastric carcinoma cells. *World J Gastroenterol* 2003; **9**: 442-445
- 50 **Liu JR**, Chen BQ, Yang YM, Wang XL, Xue YB, Zheng YM, Liu RH. Effect of apoptosis on gastric adenocarcinoma cell line SGC-7901 induced by cis-9, trans-11-conjugated linoleic acid. *World J Gastroenterol* 2002; **8**: 999-1004
- 51 **Zhao AG**, Zhao HL, Jin XJ, Yang JK, Tang LD. Effects of Chinese Jianpi herbs on cell apoptosis and related gene expression in human gastric cancer grafted onto nude mice. *World J Gastroenterol* 2002; **8**: 792-796
- 52 **Wu YL**, Sun B, Zhang XJ, Wang SN, He HY, Qiao MM, Zhong J, Xu JY. Growth inhibition and apoptosis induction of Sulindac on Human gastric cancer cells. *World J Gastroenterol* 2001; **7**: 796-800
- 53 **Siervo-Sassi RR**, Marrangoni AM, Feng X, Naoumova N, Winans M, Edwards RP, Lokshin A. Physiological and molecular effects of Apo2L/TRAIL and cisplatin in ovarian carcinoma cell lines. *Cancer Lett* 2003; **190**: 61-72
- 54 **Rudin CM**, Yang Z, Schumaker LM, VanderWeele DJ, Newkirk K, Egorin MJ, Zuhowski EG, Cullen KJ. Inhibition of glutathione synthesis reverses Bcl-2-mediated cisplatin resistance. *Cancer Res* 2003; **63**: 312-318
- 55 **Xu HY**, Yang YL, Gao YY, Wu QL, Gao GQ. Effect of arsenic trioxide on human hepatoma cell line BEL-7402 cultured *in vitro*. *World J Gastroenterol* 2000; **6**: 681-687
- 56 **Kim IK**, Jung YK, Noh DY, Song YS, Choi CH, Oh BH, Masuda ES, Jung YK. Functional screening of genes suppressing TRAIL-induced apoptosis: distinct inhibitory activities of Bcl-X(L) and Bcl-2. *Br J Cancer* 2003; **88**: 910-917

Edited by Xu JY and Wang XL

Construction and identification of recombinant vectors carrying herpes simplex virus thymidine kinase and cytokine genes expressed in gastric carcinoma cell line SGC7901

Jian-Hua Zhang, Ming-Xi Wan, Jia-Ying Yuan, Bo-Rong Pan

Jian-Hua Zhang, Ming-Xi Wan, Department of Biomedical Engineering, School of Life Science and Technology, Xi'an Jiaotong University, 28 West Xianning Road, Xi'an 710049, Shaanxi Province, China

Jia-Ying Yuan, Department of Ultrasonic Diagnosis, Xijing Hospital, Fourth Military Medical University, 127 West Changle Road, Xi'an 710033, Shaanxi Province, China

Bo-Rong Pan, Department of Oncology, Xijing Hospital, Fourth Military Medical University, 127 West Changle Road, Xi'an 710033, Shaanxi Province, China

Supported by Doctoral Foundation of Xi'an Jiaotong University, No.69925101 and National Natural Science Foundation of China, No.30270404

Correspondence to: Dr. Ming-Xi Wan, Department of Biomedical Engineering, School of Life Science and Technology, Xi'an Jiaotong University, 28 West Xianning Road, Xi'an 710049, Shaanxi Province, China. wanmingxi@yahoo.com.cn

Telephone: +86-29-2667924

Received: 2002-12-07 **Accepted:** 2003-03-18

Abstract

AIM: To construct and identify the recombinant vectors carrying herpes simplex virus thymidine kinase (HSV-TK) and tumor necrosis factor alpha (TNF- α) or interleukin-2 (IL-2) genes expressed in gastric carcinoma cell line SGC7901.

METHODS: The fragments of HSV-TK, internal ribosome entry sites (IRES) and TNF- α or IL-2 genes were inserted in a TK-IRES-TNF- α or TK-IRES-IL-2 order into pEGFP-N₃ and pLXSN to generate the therapeutic vectors pEGFP-TT, pEGFP-TI, pL(TT)SN and pL(TI)SN respectively, which were structurally confirmed by the digestion analysis of restriction endonuclease. The former two plasmids were used for the transient expression of recombinant proteins in the target cells while pL(TT)SN and pL(TI)SN were transfected into SGC7901 cells by lipofectamine for the stable expression of objective genes through G418 selection. The protein products expressed transiently and stably in SGC7901 cells by the constructed vectors were confirmed by fluorescent microscopy and Western blot respectively.

RESULTS: The inserted fragments in all constructed plasmids were structurally confirmed to be consistent with that of the published data. In the transient expression, both pEGFP-TT and pEGFP-TI were shown expressed in nearly 50% of the transfected SGC7901 cells. Similarly, the G418 selected vectors PL(TT)SN and PL(TI)SN were confirmed to be successful in the stable expression of the objective proteins in the target cells.

CONCLUSION: The constructed recombinant vectors in the present study that can express the suicide gene TK in combination with cytokines genes may serve as the potential tools to perform more effective investigations in future for the gene therapy of gastric carcinoma.

Zhang JH, Wan MX, Yuan JY, Pan BR. Construction and identification of recombinant vectors carrying herpes simplex virus thymidine kinase and cytokine genes expressed in gastric carcinoma cell line SGC7901. *World J Gastroenterol* 2004; 10(1): 26-30

<http://www.wjgnet.com/1007-9327/10/26.asp>

INTRODUCTION

Gastric cancer is one of the most common malignancies both in China and abroad^[1-7]. Despite the improvements in surgical techniques, radiation and chemotherapeutic regimens, the disease remains a great challenge. Most patients still die finally of their disease, even after apparent "curative resection". In recent years, the promising conception of gene therapy has been advocated in a hope to deal with the malignant diseases more effectively. One of the landmark discoveries for this therapeutic strategy is the transfer of suicide genes, such as HSV-TK, into the tumor cells, which has been shown to exert antitumor efficacy on a variety of cancer cells^[8-11]. The expressed HSV-TK/ganciclovir (GCV) system can not only inhibit the DNA synthesis of the target cells but also produce a bystander effect against tumors^[12-16]. However, these effects have been found to be unstable in some of the transfected cells, which may result in a decreased efficiency in the treatment of malignancies. The use of tissue-specific vectors to deliver genes and combination of TK with cytokine genes may improve the efficacy of the antitumor effects^[17-20]. In the present study, therefore, we tried to construct and identify the recombinant vectors containing HSV-TK, IRES in combination with cytokine genes, TNF- α or IL-2, in an attempt to establish more effective recombinants for the gene therapy of gastric malignancies.

MATERIALS AND METHODS

Materials

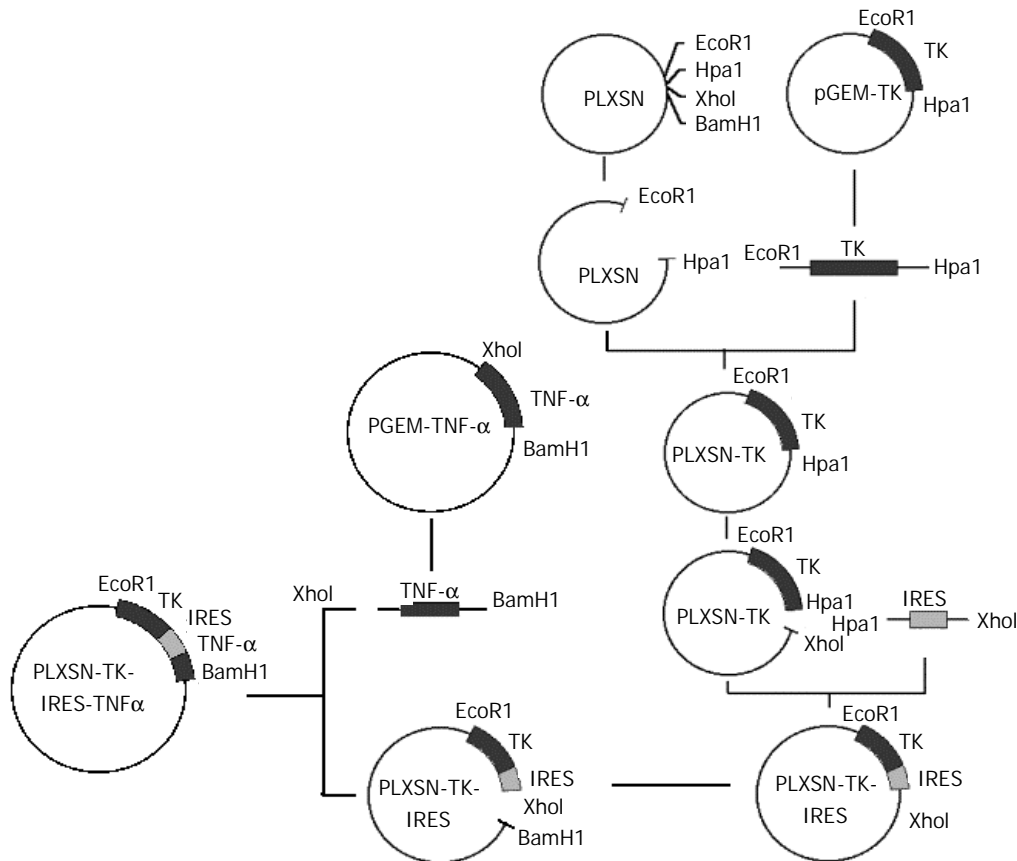
Reagents Restriction enzymes (*EcoR* I, *Hpa* I, *Xho* I and *Bam*HI), T₄ DNA ligase and *Taq* DNA polymerase were purchased from Gibco Co., USA. Lipofectamine was supplied by Boeringer Mannheim Co., Mannheim, Germany. Monoclonal antibodies of mouse anti-IL-2 and anti-TNF- α proteins and horseradish peroxidase-conjugated antimouse immunoglobulin were purchased from Zhongshan Co., Shanghai, China.

PCR primers The primer sequences used in the study were designed according to that of the individual genes (Table 1) with the modification of adding the recognition site sequences for the corresponding restriction enzymes (*EcoR* I, *Hpa* I, *Xho* I and *Bam*HI), and synthesized by Shanghai GeneCore Bio Technologies Co.

Plasmids and cell lines Plasmid pBluescript-TK was provided by Shanghai Institute of Biochemistry. pIRZA1neo with 585 bp IRES sequence^[21,22] was purchased from Invitrogen Co., USA. The plasmid PT₇-TNF- α , pEGFP-N₃ carrying green fluorescent protein (GFP) gene, pGEM-T-Easy vector and *E.coli* JM109 were provided by Orthopedic Oncology Institute of PLA,

Table 1 Primer sequences of amplified genes

Genes	Primer sequences	Fragment length
TK	Forward: 5' -GC GAA TTC ATG GCT TCG TAC CCC TGC CAT C-3' Reverse: 5' -GC GTT AAC TTA AGC CTC CCC CAT CTC CCG G-3'	1 128 bp
IL-2	Forward: 5' -GC CTC GAG ATG TAC AGG ATG CAA CTC CTG-3' Reverse: 5' -GC GGA TTC TTA AGT CAG TGT TGA GAT GAT GC-3'	456 bp
TNF- α	Forward: 5' -GC CTC GAG ATG GTC AGA TCA TCT TCT CGA AC -3' Reverse: 5' -GC GGA TCC TTA CAG GGC AAT GAT CCC AAA -G-3'	474 bp
IRES	Forward: 5' -GC GTT AAC AAT TCC GCC CCT CTC CCT CCC CC-3' Reverse: 5' -GC CTC GAG AAT AGT AGC ACA AAA AGT TTC C-3'	585 bp

**Figure 1** Diagram of the construction of the expression vector PL(TT)SN.

Xi' an, China. The retroviral expressing vector pLXSN was provided by Dr. Yu Bing from Fourth Military Medical University, Xi' an, China. IL-2 cDNA was made from human peripheral blood by RT-PCR.

The gastric carcinoma cell line SGC7901 was provided by Shanghai Institute of Biochemistry. Virus packaging cell PA317 and NIH3T3 cell lines were provided by Dr. Yu Bing. Cells were maintained in RPMI 1640 medium supplemented with 10% FBS (Hangzhou, Sijiqing Biotech Company), 2 mM L-glutamine, 100 units/ml penicillin and 100 μ g/ml streptomycin. The PA317 was used as the packaging cell and the NIH 3T3 cells were used to assay the virus titre. The cell cultures were maintained at 37 °C in a humidified atmosphere with 5% CO₂.

Methods

Construction of the recombinant vectors The recombinant vectors were constructed with routine molecular cloning techniques^[23-25]. The DNA fragments of HSV-TK, IRES, TNF- α and IL-2 were obtained by PCR amplification with specific primers from their corresponding templates. For the transient

expression of the recombinant genes, the fragments of HSV-TK, IRES, TNF- α and the fragments of HSV-TK, IRES, IL-2 were cloned into pEGFP-N₃ to generate pEGFP-TT and pEGFP-TI respectively. Similarly, those fragments were separately inserted into pLXSN to generate plasmid PL (TT) SN and PL (TI) SN as shown in Figure 1 for the selection of the stable expression vectors. The structure of all these constructed vectors was confirmed by the digestion analysis of restriction endonuclease.

Transient expression The transient expression of recombinants was performed according to the literature^[26]. The constructed vectors pEGFP-TT and pEGFP-TI, and the control plasmid were transfected into SGC7901 cells with a routine protocol by lipofectamine. Twenty hours after the transfection, cells were harvested and the expressed marker protein GFP fused with the objective genes were detected under a fluorescent microscope.

Stable expression The plasmids pL(TT)SN, pL(TI)SN and pL(TK)SN were transfected respectively into PA317 cells with lipofectamine (Gibco) according to the manufacturer's

instruction. After 48 h of transfection, G418 (Promega) was added to the culture media at a concentration of $500 \text{ mg} \cdot \text{L}^{-1}$ to select G418-resistant colonies. After 2-weeks' culture with the changing of the G418-containing media every 3 days, the supernatant of G418-resistant colony was collected and diluted to different concentrations to infect NIH3T3 cells, which was further undergone the G418 selection for 2w when the G418-resistant NIH3T3 colonies were counted for the determination of viral titre. The viral titer of pL(TT)SN, pL(TI)SN, pL(TK)SN and empty plasmid pLXSN were $5 \times 10^8 \text{ CFU/L}$, $6 \times 10^8 \text{ CFU/L}$, $1 \times 10^9 \text{ CFU/L}$ and $1 \times 10^9 \text{ CFU/L}$ respectively.

For the stable expression of recombinants, a total number of 5×10^5 SGC7901 cells were incubated in a 6-well plate for 24 h, then rinsed with serum-free RPMI 1640 medium twice and incubated with $100 \mu\text{l}$ supermatant of G418-resistant PA317 colony for 3 h. After 4-weeks' cultivation, the G418-resistant colonies designated as SGC/TK-TNF- α , SGC/TK-IL-2, SGC/TK and SGC/0 respectively were used to confirm the objective gene expression by Western blot analysis.

Western blotting analysis The SGC/TT and SGC/TI cells were incubated respectively in the six-well plates at a density of 2.5×10^5 cells/well for 24 h, followed by a further cultivation of 48 h with the culture medium replaced with 1 ml of serum-free RPMI 1640. Then the serum-free medium was totally collected, concentrated in a microconcentrator to $20 \mu\text{l}$ and subjected to electrophoresis on a $120 \text{ g} \cdot \text{L}^{-1}$ SDS/PAGE gel. Proteins were transferred to a nitrocellulose membrane and incubated overnight in $50 \text{ ml} \cdot \text{L}^{-1}$ fat free milk in PBS at 4°C . After washed in $10 \text{ ml} \cdot \text{L}^{-1}$ fat free milk, the membrane was incubated with monoclonal antibody of mouse anti-rhIL-2 or anti-TNF- α , followed by incubation with horseradish peroxidase-conjugated antimouse immunoglobulin. Proteins were detected by using the ECL kit according to the manufacturer's protocol (Amersham).

RESULTS

Identification of constructed vectors

The segment analysis by restriction endonuclease digestion confirmed that the inserted gene sequences in all of the constructed plasmids were structurally consistent with that of the published data. The inserted fragments in pEGFP-TI and pEGFP-TT were identified as shown in Figure 2.

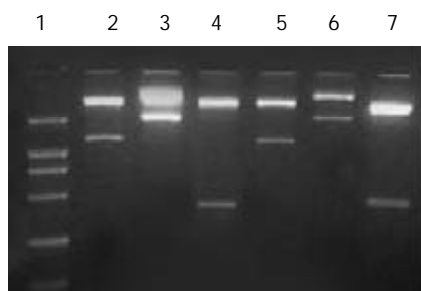


Figure 2 Segment analyses of pEGFP-TI and pEGFP-TT by restriction endonuclease digestion. Lane 1: DNA marker (from top to bottom: 1 543, 994, 697, 515 and 337 bp); Lane 2: pEGFP-TI/*EcoRI* and *HpaI* (TK gene 128 bp); Lane 3: pEGFP-TI/*EcoRI* and *XhoI* (TK+IRES 1.71kb); Lane 4: pEGFP-TI/*XhoI* and *BamHI* (IL-2 gene 456 bp); Lane 5: pEGFP-TT/*EcoRI* and *HpaI* (TK gene 128 bp); Lane 6: pEGFP-TT/*EcoRI* and *XhoI* (TK+IRES 1.71 kb); Lane 7: pEGFP-TT/*XhoI* and *BamHI* (TNF- α gene 474 bp).

Transient expressions of GFP-TT and GFP-TI protein

Twenty hours after the transfection, the GFP fluorescence was detected under fluorescent microscope in nearly 50% of the

total cells transfected with pEGFP-TT or pEGFP-TI. The fluorescence was gradually increased with time and peaked at 72 h, which indicated that the TK-IRES-IL-2 and TK-IRES-TNF- α were transiently expressed in SGC7901 cells (Figure 3 A and B).

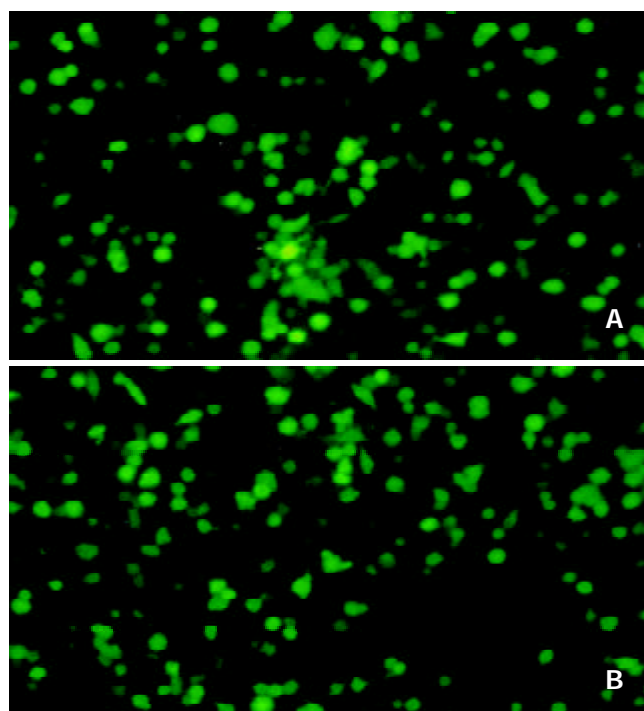


Figure 3 Transient expression of the recombinant genes in SGC7901 cells. A: Transient expression of pEGFP-TT in SGC7901 cells $\times 100$. B: Transient expression of pEGFP-TI in SGC7901 cells $\times 100$.

Expressions of stable transfectants

The stable expression of recombinant proteins in SGC7901 cells was confirmed by Western blotting, in which two distinct bands of 15ku and 17ku were observed on the nitrocellulose membrane, corresponding to the fragment sizes of IL-2 and TNF- α respectively (Figure 4).

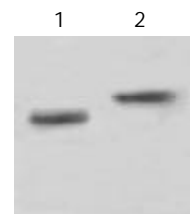


Figure 4 Stably expressed recombinant protein in transduced SGC7901 cells confirmed by Western blot. Lane 1: IL-2 (15ku) expressed in SGC/TI cells; Lane 2: TNF- α (17ku) expressed in SGC/TT cells.

DISCUSSION

Gene therapy has become a promising strategy for the treatment of gastric cancer^[27-31], in which the transfer of suicide genes into tumor cells has emerged as an attractive modality for the selective elimination of cancer cells^[14-16,30,31]. The suicide genes encode non-mammalian enzymes that can convert nontoxic prodrugs into cellular toxic metabolites. The most widely used suicide gene is the HSV-TK/ganciclovir (GCV) system that can convert prodrug GCV into GCV monophosphate. The latter is further phosphorylated by cellular kinase to form GCV

triphosphate, a toxic substance that can inhibit cellular DNA synthesis and lead to cell death. Besides, the “bystander effect” induced by TK gene can also enhance the tumor-killing capacity of the HSV-TK/GCV system^[16-20,32]. Because of the antitumor properties exerted by certain cytokines such as IL-2 and TNF- α , it is believed that the gene therapy combining cytokine with TK suicide gene would be more beneficial and effective for the treatment of cancers, which has been strongly supported by some of the recently published literatures^[33]. However, there are fewer reports of this therapeutic strategy applied to the antitumor study of gastric malignancy.

Construction of a bicistronic retroviral vector with an internal ribosome entry site (IRES)^[34,35] allows the simultaneous expression of two genes from a single transcript, which has been demonstrated to be efficient. However, the expressive levels of the objective protein are found lower in some circumstance. Five different genes, including human IL-2, IL-4, granulocyte macrophage stimulating factor, HSV-TK and hepatitis C virus core gene, have been tested using the modified vector for the gene transfer^[36,37]. The new bicistronic vector, modified by abolishing the functional viral gag initiation codon and keeping it before the 5' end to the first initiation codon of the transduced gene, has made the protein expression greatly increased compared with the original vector. As the RNA levels and splicing patterns of these two vectors remain similar, the improvement was most likely at the translation level. Thus, the incorporation of the internal ribosome entry site sequence into a proper location of the retroviral vector for gene therapy represents a promising strategy to facilitate the simultaneous and efficient expression of several genes from the same promoter^[21,22].

In the present study, we employed the strategy to construct our expression vectors, in which the IRES gene was cloned in TK-IRES-TNF- α or TK-IRES-IL-2 order and the recombinants were constructed in combination with TK and cytokine genes. In the transient expression, the constructed vectors pEGFP-TT and pEGFP-TI were shown to be effectively expressed *in vitro* as demonstrated by the appearance of the fusing fluorescent protein GFP^[26,38] in nearly 50% of the transfected SGC7901 cells. Similarly, in the experiment of stable expression, the G418 selected vectors PL(TT)SN and PL(TD)SN were also confirmed to be successful in both of the transfection into the target cells and the expression of the objective proteins. All of these results indicate that the expressive vectors constructed in the present study may serve as the potential tools to perform more effective investigations for the gene therapy of gastric carcinoma in future. Further studies are therefore needed to elucidate and characterize the antitumor effects of these constructed vectors on the transfected SGC7901 cells.

REFERENCES

- Xu CT**, Huang LT, Pan BR. Current gene therapy for stomach carcinoma. *World J Gastroenterol* 2001; **7**: 752-759
- Song ZJ**, Gong P, Wu YE. Relationship between the expression of iNOS, VEGF, tumor angiogenesis and gastric cancer. *World J Gastroenterol* 2002; **8**: 591-595
- Tao HQ**, Zou SC. Effect of preoperative regional artery chemotherapy on proliferation and apoptosis of gastric carcinoma cells. *World J Gastroenterol* 2002; **8**: 451-454
- Han Y**, Han ZY, Zhou XM, Shi R, Zheng Y, Shi YQ, Miao JY, Pan BR, Fan DM. Expression and function of classical protein kinase C isoenzymes in gastric cancer cell line and its drug-resistant sublines. *World J Gastroenterol* 2002; **8**: 441-445
- Wang X**, Lan M, Shi YQ, Lu J, Zhong YX, Wu HP, Zai HH, Ding J, Wu KC, Pan BR, Jin JP, Fan DM. Differential display of vincristine-resistance-related genes in gastric cancer SGC7901 cell. *World J Gastroenterol* 2002; **8**: 54-59
- Shen LZ**, Wu WX, Xu DH, Zheng ZC, Liu XY, Ding Q, Hua YB, Yao K. Specific CEA-producing colorectal carcinoma cell killing with recombinant adenoviral vector containing cytosine deaminase gene. *World J Gastroenterol* 2002; **8**: 270-275
- Thomas AL**, Steward WP. Recent advances in the nonsurgical treatment of upper gastrointestinal tract tumors. *Expert Rev Anticancer Ther* 2001; **1**: 258-268
- Narita M**, Bahar R, Hatano M, Kang MM, Tokuhisa T, Goto S, Saisho H, Sakiyama S, Tagawa M. Tissue-specific expression of a suicide gene for selective killing of neuroblastoma cells using a promoter region of the NCX gene. *Cancer Gene Ther* 2001; **8**: 997-1002
- Van Dillen IJ**, Mulder NH, Vaalburg W, de Vries EF, Hospers GA. Influence of the bystander effect on HSV-tk/GCV gene therapy. A review. *Curr Gene Ther* 2002; **2**: 307-322
- Nowak AK**, Lake RA, Kindler HL, Robinson BW. New approaches for mesothelioma: biologics, vaccines, gene therapy, and other novel agents. *Semin Oncol* 2002; **29**: 82-96
- Qiao J**, Doubrovin M, Sauter BV, Huang Y, Guo ZS, Balatoni J, Akhurst T, Blasberg RG, Tjuvahev JG, Chen SH, Woo SL. Tumor-specific transcriptional targeting of suicide gene therapy. *Gene Ther* 2002; **9**: 168-175
- Engelmann C**, Heslan JM, Fabre M, Lagarde JP, Klatzmann D, Panis Y. Importance, mechanisms and limitations of the distant bystander effect in cancer gene therapy of experimental liver tumors. *Cancer Lett* 2002; **179**: 59-69
- Adachi Y**, Matsubara S, Muramatsu T, Curiel DT, Reynolds PN. Midkine promoter-based adenoviral suicide gene therapy to midkine-positive pediatric tumor. *J Pediatr Surg* 2002; **37**: 588-592
- Pulkkanen KJ**, Laukkanen JM, Fuxe J, Kettunen MI, Rehn M, Kannasto JM, Parkkinen JJ, Kauppinen RA, pettersson RF, Yla-Herttuala S. The combination of HSV-tk and endostatin gene therapy eradicates orthotopic human renal cell carcinomas in nude mice. *Cancer Gene Ther* 2002; **9**: 908-916
- Floeth FW**, Shand N, Bohar H, Prisack HB, Felsberg J, Neuen-Jacob E, Aulich A, Burger KJ, Bock WJ, Weber F. Local inflammation and devascularization-*in vivo* mechanisms of the “bystander effect” in VPC-mediated HSV-Tk/GCV gene therapy for human malignant glioma. *Cancer Gene Ther* 2001; **8**: 843-851
- Warren P**, Song W, Holle E, Holmes L, Wei Y, Li J, Wagner T, Yu X. Combined HSV-TK/GCV and secondary lymphoid tissue chemokine gene therapy inhibits tumor growth and elicits potent antitumor CTL response in tumor-bearing mice. *Anticancer Res* 2002; **22**: 599-604
- Guan J**, Ma L, Wei L. Characteristics of ovarian cancer cells transduced by the bicistronic retroviral vector containing GM-CSF and HSV-TK genes. *Chin Med J* 2001; **114**: 147-151
- Hall SJ**, Canfield SE, Yan Y, Hassen W, Selleck WA, Chen SH. A novel bystander effect involving tumor cell-derived Fas and FasL interactions following Ad.HSV-tk and Ad.mIL-12 gene therapies in experimental prostate cancer. *Gene Ther* 2002; **9**: 511-517
- Boucher PD**, Ostruszka LJ, Murphy PJ, Shewach DS. Hydroxyurea significantly enhances tumor growth delay *in vivo* with herpes simplex virus thymidine kinase/ganciclovir gene therapy. *Gene Ther* 2002; **9**: 1023-1030
- Hayashi K**, Hayashi T, Sun HD, Takeda Y. Contribution of a combination of ponocidin and acyclovir/ganciclovir to the anti-tumor efficacy of the herpes simplex virus thymidine kinase gene therapy system. *Hum Gene Ther* 2002; **10**: 415-423
- Ulrich-Vinther M**, Carmidy EE, Goater JJ, S balle K, O' Keefe RJ, Schwarz EM. Recombinant adeno-associated virus-mediated osteoprotegerin gene therapy inhibits wear debris-induced osteolysis. *J Bone Joint Surg Am* 2002; **84A**: 1405-1412
- Wong ET**, Ngoi SM, Lee CG. Improved co-expression of multiple genes in vectors containing internal ribosome entry sites (IRESes) from human genes. *Gene Ther* 2002; **9**: 337-344
- Cao MM**, Pan W, Chen QL, Ma ZC, Ni ZJ, Wu XL, Wu WB, Pan X, Cao GW, Qi ZT. Construction of the eukaryotic expression vector expressing the fusion protein of human endostatin protein and IL3 signal peptide. *Shijie Huaren Xiaohua Zazhi* 2001; **9**: 43-46
- Pan X**, Ke CW, Pan W, Wu WB, Zhang B, He X, Cao GW, Qi ZT. Construction of eukaryotic expression vector carrying IFN- β gene under control of human HBV promoter. *Shijie Huaren Xiaohua Zazhi* 2000; **8**: 520-523

- 25 **Zhang J**, Liu YF, Yang SJ, Sun ZW, Qiao Q, Zhang SZ. Construction and expression of mouse/humanized scFv and their fusion to humanized mutant TNF α against hepatocellular carcinoma. *Shijie Huaren Xiaohua Zazhi* 2000; **8**: 616-620
- 26 **Cheng H**, Liu YF, Zhang HZ, Shen WA, Zhang SZ. Construction and expression of anti-HCC immunotoxin of sFv-TNF- α and GFP fusion proteins. *Shijie Huaren Xiaohua Zazhi* 2001; **9**: 640-644
- 27 **Chen JP**, Lin C, Xu CP, Zhang XY, Wu M. The therapeutic effects of recombinant adenovirus RA538 on human gastric carcinoma cells *in vitro* and *in vivo*. *World J Gastroenterol* 2000; **6**: 855-860
- 28 **Feng RH**, Zhu ZG, Li JF, Liu BY, Yan M, Yin HR, Lin YZ. Inhibition of human telomerase in MKN-45 cell line by antisense hTR expression vector induces cell apoptosis and growth arrest. *World J Gastroenterol* 2002; **8**: 436-440
- 29 **Yu ZC**, Ding J, Pan BR, Fan DM, Zhang XY. Expression and bio-activity identification of soluble MG₇ scFv. *World J Gastroenterol* 2002; **8**: 99-102
- 30 **Guo SY**, Gu QL, Liu BY, Zhu ZG, Yin HR, Lin YZ. Experimental study on the treatment of gastric cancer by TK gene combined with mIL-2 gene. *Shijie Huaren Xiaohua Zazhi* 2000; **8**: 974-978
- 31 **Huang H**, Wang A. The adenovirus-mediated HSV-TK/GCV suicide gene system in the treatment of tongue carcinoma cell line. *Zhonghua Kouqiang Yiyue Zazhi* 2001; **36**: 457-460
- 32 **Gao G**, Huang T, Chen S. *In vitro* and *in vivo* bystander effect of adenovirus-mediated transfer of the herpes simplex virus thymidine kinase gene. *Zhonghua Waike Zazhi* 2002; **40**: 301-303
- 33 **Majumdar AS**, Zolotorey A, Samuel S, Tran K, Vertin B, Hall-Meier M, Antoni BA, Adeline E, Philip M, Philip R. Efficacy of herpes simplex virus thymidine kinase in combination with cytokine gene therapy in an experimental metastatic breast cancer model. *Cancer Gene Ther* 2000; **7**: 1086-1099
- 34 **Kobayashi T**, Kida Y, Kaneko T, Pastan I, Kobayashi K. Efficient ablation by immunotoxin-mediated cell targeting of the cell types that express human interleukin-2 receptor depending on the internal ribosome entry site. *J Gene Med* 2001; **3**: 505-510
- 35 **Royal RE**, Kershaw MH, Reeves ME, Wang G, Daly T, Treisman J, Lam J, Hwu P. Increased functional expression of transgene in primary human lymphocytes using retroviral vectors modified with IRES and splicing motifs. *Gene Ther* 2002; **9**: 1085-1092
- 36 **Wang SI**, Mukhtar H. A high-efficiency translational control element with potential for cancer gene therapy. *Int J Oncol* 2002; **20**: 1269-1274
- 37 **Qiao J**, Roy V, Girard MH, Caruso M. High translation efficiency is mediated by the encephalomyocarditis virus internal ribosomal entry sites if the natural sequence surrounding the eleventh AUG is retained. *Hum Gene Ther* 2002; **13**: 881-887
- 38 **Zhang X**, Wu J, Li X, Fu L, Gao D, Bai H, Liu X. Effects of recombinant human bone morphogenic protein-2 and hyaluronic acid on invasion of brain glioma *in vivo*. *Zhonghua Yixue Zazhi* 2002; **82**: 90-93

Edited by Zhu LH

Does surgical resection of hepatocellular carcinoma accelerate cancer dissemination?

I-Shyan Sheen, Kuo-Shyang Jeng, Shou-Chuan Shih, Po-Chuan Wang, Wen-Hsiung Chang, Horng-Yuan Wang, Li-Rung Shyung, Shee-Chan Lin, Chin-Roa Kao, Yi-Chun Tsai, Tsu-Yen Wu

I-Shyan Sheen, Divisions of Hepatogastroenterology, Chang Gung Memorial Hospital, Taipei, Taiwan, China

Kuo-Shyang Jeng, Departments of Surgery, Mackay Memorial Hospital, Taipei, Taiwan, China

Shou-Chuan Shih, Po-Chuan Wang, Wen-Hsiung Chang, Horng-Yuan Wang, Li-Rung Shyung, Shee-Chan Lin, Chin-Roa Kao, Department of Internal Medicine, Mackay Memorial Hospital, Taipei, Taiwan, China

Yi-Chun Tsai, Tsu-Yen Wu, Medical Research, Mackay Memorial Hospital, Taipei, Taiwan, China

Kuo-Shyang Jeng, Mackay Junior School of Nursing, Taipei, Taiwan, China

Supported by the grants from the Department of Health, National Science Council, Executive Yuan, Taiwan (Dr. Jeng) (NSC 86-2314-B-95-001)

Correspondence to: Kuo-Shyang Jeng, M.D., F.A.C.S. Department of Surgery, Mackay Memorial Hospital, No. 92, Sec 2, Chung-San North Road, Taipei, Taiwan, China. issheen.jks@msa.hinet.net

Telephone: +886-2-25433535 **Fax:** +886-2-27065704

Received: 2003-08-30 **Accepted:** 2003-10-01

Abstract

AIM: This study was to investigate whether surgery could increase cancer dissemination and postoperative recurrence in patients with hepatocellular carcinoma (HCC) by detection of human α -fetoprotein messenger RNA (hAFP mRNA). hAFP mRNA in the peripheral blood of patients with HCC has been considered as a surrogate marker for circulating tumor cells.

METHODS: Eighty-one consecutive patients who underwent curative resection for HCC entered this prospective cohort study. We examined hAFP mRNA from the peripheral blood obtained preoperatively, perioperatively, and postoperatively to correlate the prognosis after curative resections from HCC patients and from the control subjects. Detection of hAFP mRNA by reverse transcriptase and polymerase chain reaction amplification (RT-PCR) was performed with primers specifically. The relations between the clinical variables (age, sex, associated liver cirrhosis, hepatitis B virus infection, hepatitis C virus infection, serum α -fetoprotein and Child-Pugh class), the histological variables (size, capsule, vascular permeation, grade of differentiation, and daughter nodules), hAFP mRNA in peripheral blood of 3 different sessions, and postoperative course (recurrence, and recurrence related death) were analysed.

RESULTS: No hAFP mRNA was detected in control group subjects. Twenty-two (27%), 24 (30%) and 19 (23%) of 81 HCC patients had hAFP mRNA positivity in the preoperative, perioperative and postoperative peripheral blood. The preoperative presence did not influence the risk of HCC recurrence (55% vs 41%, $P=0.280$). In contrast, patients with postoperative presence had a significantly higher recurrence (90% vs 31%, $P<0.001$; odds ratio 19.2; 95% confidence interval: 4.0-91.7). In the multivariate analysis by COX proportional hazards model, postoperative positivity

had a significant influence on recurrence ($P=0.067$) and recurrence related mortality ($P=0.017$). Whereas, the perioperative positivity of hAFP mRNA did not increase HCC recurrence (58% vs. 39%, $P=0.093$). The correlation between perioperative hAFP mRNA positivity and recurrence related mortality had no statistical significance ($P=0.836$).

CONCLUSION: From our study, perioperative detection of hAFP mRNA in peripheral blood of patients has no clinical relevance and significant role in the prediction of HCC recurrence. Surgical resection itself may not accelerate cancer dissemination and does not increase postoperative recurrence significantly either.

Sheen IS, Jeng KS, Shih SC, Wang PC, Chang WH, Wang HY, Shyung LR, Lin SC, Kao CR, Tsai YC, Wu TY. Does surgical resection of hepatocellular carcinoma accelerate cancer dissemination? *World J Gastroenterol* 2004; 10(1): 31-36
<http://www.wjgnet.com/1007-9327/10/31.asp>

INTRODUCTION

Hepatocellular carcinoma (HCC) is the leading malignancy with a poor prognosis in areas of high hepatitis B and C prevalence^[1-4]. After curative resections of HCC, a large proportion of patients develop tumor recurrence within the first 3 years. Whether intraoperative manipulation contributes to cancer dissemination remains a debating subject.

How to detect these disseminated cancer cells in the perioperative period is a problem. The isolation and identification of tumor cells in a small blood sample by conventional methods is very difficult because the number of malignant cells in the circulation may be extremely small^[5-8]. Recently, it has become possible and sensitive to identify tumor-specific gene transcripts (messenger RNA/circular DNA) by means of polymerase chain reaction (PCR). With the use of PCR-based method which permits detection of 1 tumor cell among 10^7 normal peripheral, mononuclear blood cells, the blood-borne dispersion of tumor cells during surgical manipulation has been reported in humans with prostatic carcinoma, melanoma, breast carcinoma and pancreatic carcinoma^[9-12].

For detecting HCC cells in circulation, reverse transcriptase (RT) PCR targeting human α -fetoprotein (hAFP) messenger RNA (mRNA) or human albumin mRNA has been proposed^[13-22]. Lack of the specificity of albumin mRNA has been emphasized^[21,22]. Human AFP mRNA has been accepted as a liver specific and cancer-specific marker^[23,24]. Many clinical studies have suggested that hAFP mRNA in peripheral blood can be used as a surrogate marker of circulating HCC cells and as a prognostic indicator in patients treated with ethanol injection and/or arterial embolization^[18].

In an attempt to elucidate whether surgical resection of HCC accelerated cancer dissemination, we designed this prospective study.

MATERIALS AND METHODS

Study population

From August 1995 to July 1999, 81 consecutive patients [42 men and 39 women, with a mean age of 52±13 years (range: 16 to 79 years)] with HCC undergoing curative hepatic resection at Mackay Memorial Hospital, Taipei, Taiwan, China, were enrolled in this prospective study (Table 1). Patients who had previously or simultaneously other malignant disorders, and who had previously received hepatectomy, intraoperative blood transfusion, preoperative and postoperative hepatic arterial chemoembolization (TACE) or neoadjuvant ethanol injection were all excluded.

Table 1 Demographic data including clinical and tumor variables of patients with HCC undergoing curative resection (n=81)

Variables	No. of patients (%)
Age (mean, years)	52±13
Male	42 (52)
Cirrhosis	56 (69)
Child- Pugh' s class A	70 (86)
HBsAg (+)	62 (77)
Anti-HCV (+)	31 (38)
Serum AFP <20 ng/ml	29 (36)
20-10 ³ ng/ml	29 (36)
>10 ³ ng/ml	23 (28)
Size of HCC < 3 cm	25 (30)
3-10 cm	28 (35)
> 10 cm	28 (35)
Complete capsule	28 (35)
Daughter nodules	32 (40)
Vascular permeation	37 (46)
Edmondson-Steiner' s grade I	6 (7)
grade II	36 (44)
grade III	26 (32)
grade IV	13 (16)

AFP: serum alpha fetoprotein, HBsAg(+): positive hepatitis B surface antigen, Anti-HCV(+): positive hepatitis C virus antibody, Edmondson and Steiner grade: differentiation grades I, II, III, and IV.

The hepatectomy procedure was selected according to the patient' s liver function and cancer location. Prior to resection, intraoperative ultrasonography to scan the entire hepatic field was performed in every patient. Surgery was defined as curative when all gross lesions were removed with an over 1 cm free resection margin which was proven tumor-free histologically. The surgical procedures included 62 major resections (6 extended right lobectomies, 18 right lobectomies, 14 left lobectomies, and 24 double segmentectomies) and 19 minor resections (11 segmentectomies, 5 subsegmentectomies, and 3 wedge resections).

Peripheral blood samples for detection of hAFP mRNA were obtained from all study patients from forearm one day prior to surgery (preoperation), immediately (i.e., within 12 hours) after liver resection (perioperation), and 90 days after surgery (postoperation) from all 81 patients.

After discharge, all the patients were followed up at our outpatient clinic and received regular clinical assessments to detect tumor recurrence including periodic abdominal ultrasonography (every 2-3 months during the first 5 years, then every 4-6 months thereafter), and serum AFP and liver biochemistry (every 2 months during the first 2 years, then every 4 months during the following 3 years, and every 6 months thereafter). Abdominal computed tomography scans (CT) were also done (every 6 months during the first 5 years, then every year). Hepatic arteriography was obtained if there was a suspicion of cancer recurrence from ultrasonography or

CT scan, or serum AFP. Chest X ray to detect pulmonary metastasis was done every 6 months. Bone scan to detect osseous metastasis was undertaken every 6 months. Detection of tumor on any imaging studies was defined as "clinical recurrence".

Parameters analyzed for recurrence included sex (male vs. female), age, the presence of liver cirrhosis, Child-Pugh class of liver functional reserve (A vs. B), hepatitis B virus infection (hepatitis B surface antigen), hepatitis C virus infection (anti-hepatitis C virus antibody), serum AFP level (<20 ng/ml vs. 20-1 000 ng/ml vs. >1 000 ng/ml), tumor size (<3 cm vs. 3-10 cm vs. >10 cm), tumor encapsulation (complete vs. incomplete or absent), presence of daughter nodules, and vascular permeation (including vascular invasion and/or tumor thrombi, in either the portal vein or hepatic vein), and cell differentiation (Edmondson and Steiner grades I, II, III and IV)(Table1).

A control group included 30 healthy volunteers without liver disease and 20 patients with chronic liver disease without evidence of HCC. They also received hAFP mRNA detection from peripheral blood.

Detection of hAFP mRNA

We used human hepatocytes to determine the sensitivity of the assay. Using tetradecyltrimethyl- ammonium bromide, nucleated cells were isolated from peripheral blood. Total RNA was extracted from cryopreserved liver tissues. The sequences of the sense primers were 5' -ACT GAA TCC AGA ACA CTG CAT AG-3' (external-sense) and 5' -TGC AGT CAA TGC ATC TTT CAC CA-3' (internal-sense) and those of the antisense primers 5' -TGG AAT AGC TTC CAT ATT GGA TTC- 3' (external-antisense) and 5' -AAG TGG CTT CTT GAA CAA ACT GG- 3' (internal-antisense). The sizes of the amplified products of hAFP mRNA were 176 and 101 base pairs by external and internal primer pairs, respectively.

A Hep G2 (hepatoblastoma) cell line served as positive control for hAFP mRNA expression. For negative controls, we used EDTA treated water (filtered and vaporized). With cDNA derived from Hep G2, specific bands for hAFP (101 bp) were observed. In contrast, the cell lines that served as negative controls did not yield these bands. It was also impossible to detect free RNA extracted from 5 ml aliquots of control blood, in which Hep G2 cells were suspended. The sensitivity of our assay, determined in a dilution experiment using freshly isolated human hepatocytes (10⁵ to 10¹) in 1 ml whole blood before RNA extraction, was approximately 1 hepatocyte for every 10⁵ peripheral mononuclear cells.

Ethylendiamine tetraacetic acid (EDTA)-treated whole blood was centrifuged and the plasma fraction was removed. The cellular fraction was enriched for mononuclear cells (MNC) or possible tumor cells according to the method described by Oppenheim. Total cellular RNA was then extracted with PUREscript RNA isolation kits TRI-Zol (Life Technologies Inc., Gaithersburg, USA), from 5 µg of which cDNA was synthesized. The reverse transcription reaction solution contained 6 µl of 5×first strand buffer, 10 mM dithiothreitol, 125 mM each of dCTP, dATP, dGTP and dTTP, 0.3 µg of random hexamers, and 200 units of superscriptase II moloney murine leukemia virus reverse transcriptase (Life Technologies Inc.). The RNA solution was incubated at 95 °C for 10 minutes, quickly chilled on ice, then mixed with the reverse transcription reaction solution (total volume 20 µl), and incubated at 37 °C for 60 minutes. The first PCR reaction solution contained 5 µl of the synthesized cDNA solution, 10 µl of 10X polymerase reaction buffer, 500 µM each of dCTP, dATP, dGTP and dTTP, 15 pmol of each external primer (EX-sense and EX-antisense), 4 units of Thermus Brockiamus Prozyme DNA polymerase (PROtech Technology Ent. Co., Ltd. Taipei, Taiwan, China), and water. The PCR cycles were: denaturing at 94 °C for 1 minute, annealing at 52 °C for 1 minute,

and primer extension at 72 °C for 1 minute. The cycles were repeated 40 times. The PCR product was reamplified with internal primers for nested PCR to obtain a higher sensitivity. The first and second PCR components were the same, but for the primer pairs (IN-sense and IN-antisense), the final product was electrophoresed on 2 % agarose gel and stained with ethidium bromide for the specific band of 101 base pairs.

Statistical analysis

A statistical software (SPSS for Windows, version 8.0, Chicago, Illinois) was used, with Student's *t*-test for continuous variables, χ^2 test or Fisher's exact test for categorical variables. Stepwise logistic regression and COX proportional hazards model were used for multivariate stepwise analysis to identify independently significant factors in predicting recurrence and mortality. A *P* value <0.05 was defined as significant.

RESULTS

No hAFP mRNA was detected in peripheral blood of all patients in control group

In patients with HCC, hAFP mRNA in peripheral blood was detected in 27% (22/81), 30% (24/81), and 23% (19/81) preoperatively, perioperatively and postoperatively, respectively. According to hAFP mRNA status, we classified patients into 8 groups. For example, in group 1, hAFP mRNA was consistently positive preoperatively, perioperatively, and postoperatively; in group 2, positive preoperatively and perioperatively but negative postoperatively; and in group 8, consistently negative preoperatively, perioperatively, and postoperatively, *etc* (Table 2).

Thirty-six patients (44.4%) had clinically detectable recurrence during the follow-up period (median 3 years, range 2-5 years), of whom 25 died. The presence of hAFP mRNA preoperatively did not correlate with the risk of recurrence (55% *vs.* 41%, *P*=0.280) and recurrence related mortality (*P*=0.7283) (Tables 3 and 4). In contrast, patients with postoperative hAFP mRNA had a significantly higher recurrence rate (90% *vs.* 31%, *P*<0.001), with an odds ratio of 19.2 (95% confidence interval [CI]: 4.0-91.7), which was also significantly associated with recurrence related mortality (*P*=0.017) (in the multivariate analysis by COX proportional hazards model) (Tables 3 and 4). The presence of hAFP mRNA perioperatively did not significantly correlate with the risk of recurrence (58% *vs.* 39%, *P*=0.093) and the recurrence related mortality (*P*=0.836) (Tables 3 and 4).

On multivariate analysis, the significant predictors of recurrence included vascular premeation (*P*=0.023), grade of cellular differentiation (*P*=0.007) and postoperative hAFP mRNA positivity (*P*<0.001 by univariate; *P*=0.067 by multivariate, weak significance) (Table 3). The significant parameters correlating with mortality after recurrence consisted of grade of cellular differentiation (*P*=0.057, weak significance) and postoperative hAFP mRNA (*P*=0.017) (Table 4).

Table 3 Predictors of HCC recurrence

Variables	<i>P</i> values	
	UV	MV
Sex	0.274	-
Age	0.842	-
Liver cirrhosis	0.019	-
HBsAg (+)	0.505	-
Anti-HCV (+)	0.622	-
Serum AFP	<0.001	-
Child-Pugh class	0.087	-
Size (<3 cm, >10 cm)	0.140	-
Capsule	<0.001	n.s.
Daughter nodules	<0.001	n.s.
Vascular permeation	<0.001	0.023
Edmondson Steiner grade	<0.001	0.007
Preoperative hAFP mRNA(+)	0.280	-
Preoperative hAFP mRNA(+)	0.093	-
Postoperative hAFP mRNA(+)	<0.001	0.067

UV: univariate analysis, MV: multivariate analysis, AFP: serum alpha fetoprotein, HBsAg(+): positive hepatitis B surface antigen, Anti-HCV(+): positive hepatitis C virus antibody, Edmondson and Steiner grade: differentiation grades I, II *vs.* III, IV, n.s.: not significant.

Table 4 Correlation between variables and recurrence related mortality

Variables	<i>P</i> values	
	UV	MV
Sex	0.815	-
Age	0.930	-
Liver cirrhosis	0.039	n.s.
HBsAg (+)	0.835	-
Anti-HCV (+)	0.548	-
Serum AFP	<0.000	-
Child-Pugh class	0.092	-
Size (<3 cm, >10 cm)	0.274	-
Capsule	0.004	n.s.
Daughter nodules	0.004	n.s.
Vascular permeation	<0.001	n.s.
Edmondson Steiner grade	<0.001	0.057
Preoperative hAFP mRNA (+)	0.728	-
Perioperative hAFP mRNA (+)	0.835	-
Postoperative hAFP mRNA (+)	<0.001	0.017

UV: univariate analysis, MV: multivariate analysis, AFP: serum alpha fetoprotein, HBsAg (+): positive hepatitis B surface antigen, Anti-HCV(+): positive hepatitis C virus antibody, Edmondson Steiner grade: differentiation grades I, II *vs.* III, IV, n.s. :not significant.

Table 2 Correlation among timing of blood sample collection and circulating tumor cell status and postoperative recurrence

Group	Preoperation (baseline)	Perioperation (within 12 hours after surgery)	Postoperation (90 days after surgery)	Number of patients	Patient number of recurrence (%)
1.	Positive	Positive	Positive	9	8 (88.9)
2.	Positive	Positive	Negative	3	2 (66.7)
3.	Positive	Negative	Positive	2	2 (100)
4.	Positive	Negative	Negative	8	0 (0)
5.	Negative	Positive	Positive	5	4 (80)
6.	Negative	Positive	Negative	7	0 (0)
7.	Negative	Negative	Positive	3	3 (100)
8.	Negative	Negative	Negative	44	17 (38.6)
Overall				81	36 (44.4)

DISCUSSION

Surgical dissemination of tumor cells has been observed in various solid cancers and manipulation *per se* has been regarded as the main cause. According to Nishizaki, using inoculation of VX2 carcinoma into rabbit liver, manual manipulation of a tumor might well enhance metastasis^[25]. According to Liotta, tumor massage resulted in at least a 10-fold rise over the initial concentration of tumor cells, as well as a higher proportion of large clumps^[26]. Yamanaka *et al.* demonstrated a large quantity of HCC cells in the portal vein during hepatic resection^[27]. In our series, 30% of patients had the presence of hAFP mRNA perioperatively. The detection rate seemed higher than that of preoperation (27%), and postoperation (23%), but the difference had no statistical significance among them. In addition, this increase did not correlate with postresection recurrence. Further more, from individual group point of view, we found the alteration from preoperative negativity to perioperative positivity in groups 5 and 6 (Table 2). Whereas the postoperative recurrence varied greatly (80% vs 0%) between them. Statistically, perioperative detection did not contribute to cancer dissemination (Table 3).

The interpretation of detection of hAFP mRNA remains controversial. From our study, among 3 different sessions of blood sampling, only postoperative detection of hAFP mRNA correlated significantly with postresection recurrence related mortality. We proposed that some possible factors contributed to the different significance among the three different blood sampling times.

The detection before surgery may be attributed to the cells released spontaneously from primary tumor *in situ*. HCC tissue is surrounded by a vascular space analogous to the hepatic sinusoids. Because of this anatomic structure, tumor cells might easily be released into the sinusoids spontaneously. Thereafter, they might migrate into the portal or hepatic vein and finally enter the systemic circulation. However, from our study, these preoperative circulating HCC cells had no prognostic significance.

Molecular methods now permit us to detect a small number of cancer cells in the blood by use of RT-PCR targeting a cell-specific gene. Studies in animal models have indicated that at least 10^4 circulating tumor cells are required for metastasis to develop. To date, however, the absolute number of cells required for metastasis in the human circulation is unclear and even if cancer cells are detected in the circulation, their potential to develop metastatic foci is unknown. When malignant cells were released into the circulation, a variety of host and tumor cell factors could determine their distribution and fate^[28-33]. Most circulating HCC cells may rapidly die in the blood by various host immune and non-immune defenses, and are destroyed by mechanical forces, including turbulence and the trauma associated with vascular adhesion and transcapillary passage, or lysed by lymphocytes, monocytes, and natural killer (NK) cells. Some tumor cells are nonspecifically trapped or specifically arrested in the first capillary bed encountered. Circulating tumor cells trapped in a given location could then recirculate and arrest at other locations, then grow into tumor colonies^[29-33].

Okuda *et al.*^[34] and Komeda *et al.*^[14] could not detect any hAFP gene transcripts in patients with liver metastases or in healthy persons. Ijichi *et al.* considered this RT-PCR assay targeting hAFP mRNA as a sensitive and specific method for detecting HCC cells in the circulation *in vivo* and *in vitro* experiments, and no positivity was found in any healthy controls^[35]. From our study, hAFP mRNA could not be detected from all the 50 controls. However, some authors suggested that AFP gene was not hepatoma-specific, but rather a liver-specific marker^[13,15,17,18,36,37].

Surgery itself may increase the release of liver cells, not only HCC cells but also normal hepatocytes. Both kinds of cells may contribute to the positivity of hAFP mRNA. According to Louha M, not only liver surgery but also nonsurgical invasive managements such as needle liver biopsy or intervention therapies such as TACE, chemotherapy and ethanol ablation therapy, the increased shedding of either HCC cells or normal hepatocytes into circulation might contribute to the increase of detection rate of hAFP mRNA^[38]. This was also the reason why we excluded those who had received these intervention therapies from the current study.

It has become a fact that RT-PCR based tests lose its specificity for HCC cell detection when they are performed on samples obtained immediately after surgical or nonsurgical invasive procedures. This pitfall may also account for the gap between the frequency of cell detection after surgery and the expected tumor recurrence rate. A consensus existed that hAFP mRNA might not be regarded as specific markers of HCC cells if blood samples were taken during liver surgery^[39].

Secondly, the different site of blood sampling might contribute to the discrepancy. Central venous blood in Kienle's study was drawn before it passed through any capillary bed, with only a short distance after leaving the liver, the cells expressing hAFP might not undergo apoptosis or were not filtered out in capillary beds, therefore possibly accounting for the high detection rate (46%) during surgery^[37]. Another factor influencing the detection of hAFP mRNA in intraoperative central venous blood samples might be by a "dilution effect" following intraoperative blood transfusion^[37]. This was the reason why we excluded those receiving transfusion from our study.

Thirdly, the different blood sampling time might contribute to the discrepancy. Similarly, from the literature, in intraoperative detection of other tumors, this factor also existed. Brown *et al.* sampled blood at the time of maximum tumor manipulation and postoperative 24 hours in those with breast cancer^[11]. Eschwege P obtained blood samples 5 minutes after prostate carcinoma removal^[9]. Warr RP obtained blood samples at 2 different sessions and 24 hours postoperatively in those with malignant melanoma^[10]. According to Hayashi N, the blood samples were obtained through a catheter in the portal vein before, during, and after manipulation of colorectal cancer^[40].

Lemoni obtained peripheral blood samples at two different intervals: the first, during the exploratory phase and the second, after hepatectomy was completed^[41]. Witzigmann obtained blood samples before and during the operation (after mobilization of the liver), and on the second postoperative day^[39]. Louha obtained peripheral blood samples before treatment, 1 hour and 24 hours after percutaneous ethanol injection or TACE treatment^[38]. Witzigmann obtained blood samples on the second day after TACE^[39].

Louha found unexpectedly that liver cells began spreading at an early stage during surgery, i.e., after liver mobilization and rotation, before liver parenchyma transection. This was probably related to the sponge-like structure of the liver and to the stretching and compression of the organ during liver mobilization^[42]. Surgery-related liver cell spreading also occurred more frequently, compared with that induced by needle liver biopsy. This difference of cell number was probably related to the different degree of manipulation on the liver between resection and biopsy.

In the present study, we selected the sampling time within the first 12 hours after hepatectomy because of two reasons. First, the so-called "maximal manipulation" during surgery was usually difficult to define. The degrees of manipulation among the mobilization of the liver, or the division of important vessels and ducts of the segment or lobe, and the dissection of

hepatic parenchyma, were difficult to quantitate. In addition, the detailed procedure among individual patients varied. Second, we believed that within 12 hours after resection, the released cells, if present, might still remain. Funaki, Okuda, and Ijichi thought destruction of circulating HCC cells transiently liberated during surgery needed 7 days^[15,34,35].

From prognostic point of view, in literature, whether the shedding of cancer cells during intraoperative manipulation contributed to cancer dissemination and postoperative recurrence has remained debatable^[33].

Witzigmann^[39] and Lemonie^[41] did not find any correlation between postresection recurrence of HCC and the presence of hAFP mRNA irrespective of whether it was measured before, during, or after surgery. Lemonie mentioned that his result concurred with other experimental and clinical data, suggesting that release of abnormal cells in the circulation, either spontaneously or secondary to surgical manipulation, was an intermittent and transient phenomenon^[41]. Okuda found that most patients whose hAFP mRNA was not detected in peripheral blood perioperatively were diagnosed as free of intrahepatic recurrence or distant metastasis within 9 months after the operation^[34].

In contrast, Ijichi *et al.* suggested that surgical dissemination might actually cause HCC recurrence within a short period^[35]. The fact that alteration from negative to positive hAFP mRNA throughout the perioperative time might indicate a high risk of recurrence has been emphasized by Okuda^[34]. Funaki *et al.* reported that hAFP mRNA positive 2-3 days after the operation might be thought of as a high risk indicator of recurrence^[15]. Ferris found HCC recurred in 28% of patients with HCC after orthotopic liver transplantation^[43]. Ferris inferred that circulating HCC cells were present in the peripheral blood even after removal of the diseased liver, and that these residual tumor cells formed intra- and extra-hepatic metastatic foci after transplantation. To decrease cancer dissemination, we suggest that forceful mobilization or manipulation of the liver has to be avoided.

In addition, some studies have proposed anesthesia and unrelated surgery promote the spread of malignant disease^[44]. It is another challenging issue whether surgery *per se*, or general anesthesia *per se*, or both, may change the immune system of the host perioperatively and increase the opportunity of postoperative cancer spread.

Based on Salo's animal studies, during an operation, operative trauma was generally considered to have a greater role than anaesthesia in altering immune responses. The immune responses to major surgery, and operative complications resulting in massive mediator release might place the patient at risk^[44].

Recent investigations have suggested that general anesthesia may cause an unregulated activation of the process of apoptosis leading to lymphocytopenia and immune suppression resulting in different response in B-lymphocytes (but not in T-lymphocytes), natural killer cell activity or antibody-dependent cellular cytotoxicity 3-4 days after surgery^[44,45]. The true trigger mechanisms are still unclear. However, lymphocytopenia was not found in our patients, and it might not have significant contribution to recurrence. The association between transfusion-induced immunosuppression and poorer prognosis in patients with cancer has also been mentioned^[46]. It was also the reason why we excluded those receiving intraoperative transfusion from this study.

The postoperative presence of circulating HCC cells may therefore represent surviving malignancy that can continue the metastatic process. The possible explanations are as follows. A proportion of cancer cells released from the resected tumor (s) survive in the circulation for a long time without being destroyed, or the presence of unresected occult metastases are undetectable at the time of surgery, or a newly developing

malignant focus is too small to be detected by conventional follow-up studies.

Perioperative detection of hAFP mRNA has no relevant and significant role in the prediction of prognosis. We suggest surgical resection itself accelerate cancer dissemination and does not increase postoperative recurrence significantly either.

REFERENCES

- Anonymous.** Primary liver cancer in Japan. Clinicopathologic features and results of surgical treatment. Liver Cancer Study Group of Japan. *Ann Surg* 1990; **211**: 277-287
- Lee CS, Hwang LY, Beasley RP, Hsu HC, Lee HS, Lin TY.** Prognostic significance of histologic findings in resected small hepatocellular carcinoma. *Acta Chir Scand* 1988; **154**: 199-203
- Lai EC, Ng IO, Ng MM, Lok AS, Tam PC, Fan ST, Choi TK, Wong J.** Long term results of resection for large hepatocellular carcinoma: A multivariate analysis of clinicopathological features. *Hepatology* 1990; **11**: 815-818
- Jeng KS, Chen BF, Lin HJ.** En bloc resection for extensive hepatocellular carcinoma: Is it advisable? *World J Surg* 1994; **18**: 834-839
- Goldblatt SA, Nadel EM.** Cancer cells in the circulating blood: a critical review. *Acta Cytol* 1965; **305**: 6-20
- Glaves D.** Correlation between circulation cancer cells and incidence of metastases. *Br J Cancer* 1983; **48**: 665-673
- Fidler IJ.** The biology of human cancer metastasis. 7th Jan Waldenstrom lecture. *Acta Oncol* 1991; **30**: 668-675
- Raper SR.** Answering questions on a microscopic scale: the detection of circulation cancer cells. *Surgery* 1999; **126**: 827-828
- Eschwege P, Dumas F, Blanchet P, Le Maire V, Benoit G, Jardin A, Lacour B, Loric S.** Haematogenous dissemination of poststatic epithelium cells during radical prostatectomy. *Lancet* 1995; **346**: 1528-1530
- Warr RP, Zebedee Z, Kenealy J, Rigby H, Kemshead JT.** Detection of melanoma seeding during surgical procedures - an RT-PCR based model. *Eur J Surg Oncol* 2002; **28**: 832-837
- Brown DC, Purushotham AD, Birnie GD, George WD.** Detection of intraoperative tumor cell dissemination in patients with breast cancer by use of reverse transcription and polymerase chain reaction. *Surgery* 1995; **117**: 96-101
- Miyazono F, Takao S, Natsugoe S, Uchikura K, Kijima F, Aridome K, Shinchi H, Aikou T.** Molecular detection of circulating cancer cells during surgery in patients with biliary-pancreatic cancer. *Am J Surg* 1999; **77**: 475-479
- Matsumura M, Niwa Y, Hikiba Y, Okano K, Kato N, Shiina S, Shirator Y, Omata M.** Sensitive assay for detection of hepatocellular carcinoma associated gene transcription (Alpha-fetoprotein mRNA) in blood. *Biol and Biophys Communi* 1995; **2**: 813-815
- Komeda T, Fukuda Y, Sando T, Kita R, Furudawa M, Nishida N, Amenomri M, Nakao K.** Sensitive detection of circulating hepatocellular carcinoma cells in peripheral venous blood. *Cancer* 1995; **75**: 2214-2219
- Funaki NO, Tanaka J, Seto S, Kasamatsu T, Kaido T, Imamura M.** Hematogenous spreading of hepatocellular carcinoma cells: possible participation in recurrence in the liver. *Hepatology* 1997; **25**: 564-568
- Jiang SY, Shyu RY, Huang MF, Tang HS, Young TH, Roffler SR, Chiou YS, Yeh MY.** Detection of alphafetoprotein-expressing cells in the blood of patients with hepatoma and hepatitis. *Br J Cancer* 1997; **75**: 928-933
- Wong IHN, Lau WY, Leung T, Johnson PJ.** Quantitative comparison of alpha-fetoprotein and albumin mRNA levels in hepatocellular carcinoma/adenoma, non-tumor liver and blood: implications in cancer detection and monitoring. *Cancer Lett* 2000; **156**: 141-149
- Matsumura M, Niwa Y, Kato N, Komatsu Y, Shiina S, Kawabe T, Kawase T, Toyoshima H, Ihori M, Shiratori Y.** Detection of α -fetoprotein mRNA, an indicator of hematogenous spreading hepatocellular carcinoma, in the hepatocellular carcinoma, in the circulation: A possible predictor of metastatic hepatocellular carcinoma. *Hepatology* 1994; **20**: 1418-1425
- Barbu V, Bonnand AM, Hillaire S, Coste T, Chazouilleres O, Gugenheim J, Boucher E, Poupon R, Poupon RE.** Circulating al-

- bumin messenger RNA in hepatocellular carcinoma: results of a multicenter prospective study. *Hepatology* 1997; **26**: 1171-1175
- 20 **Hillaire S**, Barbu V, Boucher E, Moukhtar M, Poipon R. Albumin messenger RNA as a marker of circulating hepatocytes in hepatocellular carcinoma. *Gastroenterology* 1994; **106**: 239-242
- 21 **Chou HC**, Sheu JC, Huang GT, Wang JT, Chen DS. Albumin messenger RNA is not specific for circulating hepatoma cells. *Gastroenterology* 1994; **2**: 630
- 22 **Muller C**, Petermann D, Pfeffel F, Osterreicher C, Fugger R. Lack of specificity of albumin-mRNA-positive cells as a marker of circulating hepatoma cells. *Hepatology* 1997; **25**: 896-899
- 23 **Niwa Y**, Matsumura M, Shiratori Y, Imamura M, Kato N, Shiina S, Okudaira T, Ikeda Y, Inoue T, Omata M. Quantitation of α -fetoprotein and albumin messenger RNAs in human hepatocellular carcinoma. *Hepatology* 1996; **23**: 1384-1392
- 24 **Di Bisceglie AM**, Dusheiko GM, Paterson AC, Alexander J, Shouval D, Lee CS, Beasley RP, Kew MC. Detection of alphafetoprotein messenger RNA in human hepatocellular carcinoma and hepatoblastoma tissue. *Br J Cancer* 1986; **54**: 779-785
- 25 **Nishizaki T**, Matsumata T, Kanematsu T, Yasunaga C, Sugimachi K. Surgical manipulation of VX2 carcinoma in the rabbit liver evokes enhancement of metastases. *J Surg Res* 1990; **49**: 92-97
- 26 **Liotta LA**, Kleinerman J, Saidel GM. Quantitative relationships of intravascular tumor cells, tumor vessels and pulmonary metastasis following tumor implantation. *Cancer Res* 1974; **34**: 997-1004
- 27 **Yamanaka N**, Okamoto E, Fujihara S, Kato T, Fujimoto J, Oriyama T, Mitsunobu M, Toyosaka A, Uematsu K, Yamamoto K. Do the tumor cells of hepatocellular carcinomas dislodge into the portal venous stream during hepatic resection? *Cancer* 1992; **70**: 2263-2267
- 28 **Hermanek P**, Hutter RVP, Sobin LH, Wittekind C. International Union Against Cancer. Classification of isolated tumor cells and micrometastasis. *Cancer* 1999; **86**: 2668-2673
- 29 **Glaves D**. Metastasis: reticuloendothelial system and organ retention of disseminated malignant cells. *Int J Cancer* 1980; **26**: 115-122
- 30 **Fidler I**, Gersten D, Riggs C. Relationship of host immune status to tumor cell arrest, distribution, and survival in experimental metastasis. *Cancer* 1977; **40**: 46-55
- 31 **Mayhew E**, Glaves D. Quantitation of tumorigenic disseminating and arrested cancer cells. *Br J Cancer* 1984; **50**: 159-166
- 32 **Romsdahl MM**, Mcgrath RG, Hoppe E, McGrew EA. Experimental model for the study of tumor cells in the blood. *Acta Cytol* 1965; **9**: 141-145
- 33 **Mori M**, Mimori K, Ueo H, Karimine N, Barnard GF, Sugimachi K, Akiyoshi T. Molecular detection of circulating solid carcinoma cells in the peripheral blood: the concept of early systemic disease. *Int J Cancer* 1996; **68**: 739-743
- 34 **Okuda N**, Nakao A, Takeda S, Oshima K, Kanazumi N, Nonami T, Kurokawa T, Takagi H. Clinical significance of alpha-fetoprotein mRNA during perioperative period in HCC. *Hepatogastroenterology* 1999; **46**: 381-386
- 35 **Ijichi M**, Takayama T, Matsumura M, Shiratori Y, Omata M, Makuuchi M. alpha-Fetoprotein mRNA in the circulation as a predictor of postsurgical recurrence of hepatocellular carcinoma: a prospective study. *Hepatology* 2002; **35**: 853-860
- 36 **Ishikawa T**, Kashiwagi H, Iwakami Y, Hirai M, Kawamura T, Aiyoshi Y, Yashiro T, Ami Y, Uchida K, Miwa M. Expression of alpha-fetoprotein and prostate-specific antigen genes in several tissues and detection of mRNAs in normal circulating blood by reverse transcriptase-polymerase chain reaction. *Jpn J Clin Oncol* 1998; **28**: 723-728
- 37 **Kienle P**, Weitz J, Klaes R, Koch M, Benner A, Lehnert T, Herfarth C, von Knebel Doeberitz M. Detection of isolated disseminated tumor cells in bone marrow and blood samples of patients with hepatocellular carcinoma. *Arch Surg* 2000; **135**: 213-218
- 38 **Louha M**, Poussin K, Ganne N, Zylberberg H, Nalpas B, Nicolet J, Capron F, Soubrane O, Vons C, Pol S, Beaugrand M, Berthelot P, Franco D, Trinchet JC, Brechot C, Paterlini P. Spontaneous and iatrogenic spreading of liver-derived cells into peripheral blood of patients with primary liver cancer. *Hepatology* 1997; **26**: 43-50
- 39 **Witzigmann H**, Geibler F, Benedix F, Thiery J, Uhlmann D, Tannapfel A, Wittekind C, Hauss J. Prospective evaluation of circulating hepatocytes by α -fetoprotein messenger RNA in patients with hepatocellular carcinoma. *Surgery* 2002; **131**: 34-43
- 40 **Hayashi N**, Egami H, Kai M, Kurusu Y, Takano S, Ogawa M. No-touch isolation technique reduces intraoperative shedding of tumor cells into the portal vein during resection of colorectal cancer. *Surgery* 1999; **125**: 369-374
- 41 **Lemonie A**, Bricon TL, Salvucci M, Azoulay D, Pham P, Raccuia J, Bismuth H, Debuire B. Prospective evaluation of circulating hepatocytes by alpha-fetoprotein mRNA in humans during liver surgery. *Ann Surg* 1997; **226**: 43-50
- 42 **Louha M**, Nicolet J, Zylberberg H, Sabile A, Vons C, Vona G, Poussin K, Tournebize M, Capron F, Pol S, Franco D, Lacour B, Brechot C, Paterlini-Brechot P. Liver resection and needle liver biopsy cause hematogenous dissemination of liver cells. *Hepatology* 1999; **29**: 879-882
- 43 **Ferris JV**, Baron RL, Marsh JW, Oliver JH, Carr BI, Dodd III GD. Recurrent hepatocellular carcinoma after liver transplantation: spectrum of CT findings and recurrence patterns. *Radiology* 1996; **198**: 233-238
- 44 **Salo M**. Effects of anaesthesia and surgery on the immune response. *Acta Anaesthesiol Scand* 1992; **36**: 201-220
- 45 **Delogu G**, Mortti S, Famularo G, Marce;ono S, Santini G, Antonucci A, Marandola M, Signore L. Mitochondria perturbations and oxidant stress in lymphocytes from patients undergoing surgery and general anesthesia. *Arch Surg* 2001; **136**: 1190-1196
- 46 **Yamamoto J**, Kosuge T, Takayama T, Shimada K, Yamasaki S, Ozaki H, Yamaguchi N, Mizuno S, Makuuchi M. Perioperative blood transfusion promotes recurrence of hepatocellular carcinoma after hepatectomy. *Surgery* 1994; **115**: 303-309

Effects of *Ginkgo biloba* extract on cell proliferation and cytotoxicity in human hepatocellular carcinoma cells

Jane CJ Chao, Chia Chou Chu

Jane CJ Chao, Chia Chou Chu, School of Nutrition and Health Sciences, Taipei Medical University, Taipei 110, Taiwan, China

Supported by Taipei Medical University, No. TMU90-Y05-A112

Correspondence to: Jane CJ Chao, School of Nutrition and Health Sciences, Taipei Medical University, Taipei 110, Taiwan, China. chenju@tmu.edu.tw

Telephone: +86-2-2736-1661 #6551~6556 Ext. 117

Fax: +886-2-2737-3112

Received: 2003-08-23 **Accepted:** 2003-10-12

Abstract

AIM: To study the effect of *Ginkgo biloba* extract (EGb 761) containing 22-27% flavonoids (ginkgo-flavone glycosides) and 5-7% terpenoids (ginkgolides and bilobalides) on cell proliferation and cytotoxicity in human hepatocellular carcinoma (HCC) cells.

METHODS: Human HCC cell lines (HepG2 and Hep3B) were incubated with various concentrations (0-1 000 mg/L) of EGb 761 solution. After 24 h incubation, cell proliferation and cytotoxicity were determined by 3-(4,5-dimethylthiazol-2-yl)-5-(3-carboxymethoxyphenyl)-2-(4-sulfophenyl)-2H-tetrazolium (MTS) assay and lactate dehydrogenase (LDH) release, respectively. After 48 h incubation, the expression of proliferating cell nuclear antigen (PCNA) and p53 protein was measured by Western blotting.

RESULTS: The results showed that EGb 761 (50-1 000 mg/L) significantly suppressed cell proliferation and increased LDH release ($P < 0.05$) in HepG2 and Hep3B cells compared with the control group. The cell proliferation of HepG2 and Hep3B cells treated with EGb 761 (1 000 mg/L) was 45% and 39% of the control group ($P < 0.05$), respectively. LDH release of HepG2 cells without and with EGb 761 (1 000 mg/L) treatment was 6.7% and 37.7%, respectively, and that of Hep3B cells without and with EGb 761 (1 000 mg/L) treatment was 7.2% and 40.3%, respectively. The expression of PCNA and p53 protein in HepG2 cells treated with EGb 761 (1 000 mg/L) was 85% and 174% of the control group, respectively.

CONCLUSION: *Ginkgo biloba* extract significantly can suppress proliferation and increase cytotoxicity in HepG2 and Hep3B cells. Additionally, *Ginkgo biloba* extract can decrease PCNA and increase p53 expression in HepG2 cells.

Chao JCJ, Chu CC. Effects of *Ginkgo biloba* extract on cell proliferation and cytotoxicity in human hepatocellular carcinoma cells. *World J Gastroenterol* 2004; 10(1): 37-41
<http://www.wjgnet.com/1007-9327/10/37.asp>

INTRODUCTION

Extract from the leaves of *Ginkgo biloba* (maidenhair tree) has been used therapeutically in China and Western countries for centuries. The liquid extract was made from dried leaves with an extraction ratio of 1:50^[1]. Standard *Ginkgo biloba*

extract, EGb 761 (commercial name), contains 22-27% flavonoids (ginkgo-flavone glycosides) and 5-7% terpenoids (ginkgolides and bilobalides), which are the most important active substances in the extract. The most important flavonoids are glycosides of kaempferol, quercetin, and isorhamnetin with glucose or rhamnose. Ginkgolides, not found in any other living species and only present in *Ginkgo biloba* extract, can be divided into types A, B, C, and a very small quantity of J, which are only different in the number and position of hydroxyl groups.

Ginkgo biloba extract has been mentioned in the traditional Chinese pharmacopoeia, and used for the treatment of asthma and bronchitis^[1]. *Ginkgo biloba* extract is well known for its antioxidant property, which may result from its ability to scavenge free radicals^[2], and to neutralize ferryl ion-induced peroxidation^[3]. Several studies have reported that the antioxidant activity of *Ginkgo biloba* extract could be helpful in the prevention and therapy of diseases and degenerative processes associated with oxidative stress^[4-8]. However, there have been very limited studies on the anti-proliferative activity of *Ginkgo biloba* extract. Ginkgetin or isoginkgetin, a biflavonoid from *Ginkgo biloba* extract, at 10 $\mu\text{mol/L}$ showed a suppressive activity against lymphocyte proliferation induced by concanavalin A (ConA) or lipopolysaccharides (LPS)^[9]. Additionally, Su *et al.*^[10] found that ginkgetin selectively inhibited the proliferation of human ovarian carcinoma OVCAR-3 cells via the induction of apoptosis in a dose-dependent manner. So far, no study has investigated the effect of *Ginkgo biloba* extract on hepatocellular carcinoma (HCC), which is the most common malignant tumor occurred in men in Taiwan. It is reasonably hypothesized that *Ginkgo biloba* extract may be helpful for the therapy of HCC through regulating cell proliferation and/or cell death. Therefore, the purpose of this study was to investigate the cytotoxic effect of *Ginkgo biloba* extract on HCC.

MATERIALS AND METHODS

Cell culture and treatments

Human hepatocellular carcinoma cell lines, HepG2 (BCRC No. 60025) and Hep3B2.1-7 (Hep3B, BCRC No. 60434) were purchased from the Bioresources Collection and Research Center (BCRC) of the Food Industry Research and Development Institute (Hsinchu, Taiwan). Cells were grown in 900 mL/L minimum essential medium (MEM, GIBCO™, Invitrogen Corp., Carlsbad, CA) containing 100 mL/L fetal bovine serum (GIBCO™) at 37 °C in a humidified atmosphere of 950 mL/L air and 50 mL/L CO₂. Prior to addition of the treatment, the cells were grown to 80-90% confluency and synchronized by incubating in the basal medium (100% MEM) for 24 h. The cells were then incubated with various concentrations (0-1 000 mg/L) of standard *Ginkgo biloba* extract solution (EGb 761, Cerenin®, Dr. Willmar Schwabe GmbH and Co., Karlsruhe, Germany) for 24 or 48 h. *Ginkgo biloba* extract contained 22-27% flavonoids and 5-7% terpenoids in 10 mL/L ethanol and 10 mL/L sorbitol solution. Cells without addition of *Ginkgo biloba* extract as the control group were incubated with 10 mL/L ethanol and 10 mL/L sorbitol solution. The cells and medium were collected. Protein contents in cells and medium were

measured by the modified method of Lowry *et al.*^[11] using a Bio-Rad DC protein kit (Bio-Rad Laboratories, Hercules, CA).

Cell proliferation assay

Cell viability was colorimetrically determined at 490 nm using a commercial proliferation assay kit (CellTiter 96[®] AQ_{ueous}, Promega Corp., Madison, WI). After incubation with various concentrations of EGb 761 for 24 h, the cells ($n=8$) in a 96-well plate were incubated with 333 mg/L 3-(4,5-dimethylthiazol-2-yl)-5-(3-carboxymethoxyphenyl)-2-(4-sulfophenyl)-2H-tetrazolium (MTS) and 25 $\mu\text{mol/L}$ phenazine methosulfate solution for 3 h at 37 °C in a humidified, 50 mL/L CO₂ atmosphere^[12]. The absorbance of soluble formazan produced by cellular reduction of MTS was measured at 490 nm using an ELISA reader (Multiskan RC, Labsystems, Helsinki, Finland).

Cell cytotoxicity assay

Lactate dehydrogenase (LDH) release from cells was determined as an index of cytotoxicity or necrosis. The quantity of LDH released by the cells into the medium was measured by the decrease in the absorbance at 340 nm for NADH disappearance within 5 min^[13]. After incubation with various concentrations of EGb 761 for 24 h, the cell culture supernatant and medium (100 μL) were mixed with 900 μL of modified Krebs-Henseleit buffer (118 mmol/L NaCl, 4.8 mmol/L KCl, 1 mmol/L KH₂PO₄, 24 mmol/L NaHCO₃, 3 mmol/L CaCl₂, 0.8 mmol/L MgPO₄, pH 7.4), 0.2 mmol/L NADH, 1.36 mmol/L sodium pyruvate, and 20 mg/L bovine serum albumin (BSA). Percentage of LDH release ($n=3$) was equal to LDH activity in medium divided by that in both cell culture supernatant and medium $\times 100\%$.

Analysis of proliferating cell nuclear antigen (PCNA) and p53 protein

After incubation with various concentrations of EGb 761 for 48 h, cell suspension (15 μg and 50 μg protein for PCNA and p53) pooled from 6 independent experiments ($n=6$) was mixed with an equal volume of 2 \times SDS-PAGE sample buffer (0.125 mol/L Tris-HCl, pH 6.8/40 mg/L SDS/200 mL/L glycerol/100 mL/L 2-mercaptoethanol)^[14], denatured at 100 °C for 3 min, and applied to SDS-PAGE (Bio-Rad Mini-PROTEAN 3 Cell, Bio-Rad Laboratories). Proteins were separated by 12.5% resolving gel, with 4% stacking gel in the running buffer (25 mmol/L Tris, pH 8.3/192 mmol/L glycine/1 mg/L SDS) at 100 V for 1.5 h. After that, the proteins were transferred onto nitrocellulose membrane (0.45 μm) using a semi-dry transfer unit (Hoefer Semiphor TE 70, Amersham Biosciences Corp., San Francisco, CA) in Towbin buffer (25 mmol/L Tris/192 mmol/L glycine/1.3 mmol/L SDS/100 mL/L methanol) at 200 mA for 1.5 h^[15]. The membrane was washed briefly with PBS, and incubated with a blocking buffer (50 mg/L skim milk/1 mL/L Tween-20 in PBS) for 1 h. Then the membrane was incubated with 0.4 mg/L mouse anti-human PCNA (PC-10, 0.2 mg/L), p53 (DO-1, 0.4 mg/L), or α -tubulin (TU-02, 1 mg/L) mAb (Santa Cruz Biotechnology, Inc., Santa Cruz, CA) at room temperature for 1 h. Alpha-tubulin was as an internal control. The membrane was washed 3 times with the wash buffer (1 mL/L Tween-20 in PBS), and incubated with 0.2 mg/L goat anti-mouse IgG-horseradish peroxidase conjugate (Santa Cruz Biotechnology, Inc.) for 1.5 h. The blot was washed 3 times again with the wash buffer, incubated with luminol reagent (Santa Cruz Biotechnology, Inc.) for 1 min, and exposed to an X-ray film (Eastman Kodak Co., Rochester, NY) for 5-10 s. The bands were quantitated by an image analysis system (Gel analysis system, EverGene Biotechnology, Taipei, Taiwan) and Phoretix 1D Lite software (version 4.0, Phoretix International Ltd., Newcastle upon Tyne, UK).

Statistical analysis

Data are expressed as $\bar{x}\pm s$. Data were analyzed by one-way ANOVA to determine the treatment effect using SAS (version 8.2, SAS Institute Inc., Cary, NC). Fisher's least significant difference test was used to make *post-hoc* comparisons if the treatment effect was demonstrated. Differences were considered significant when $P<0.05$.

RESULTS

Cell proliferation assay

After 24 h incubation, EGb 761 (25-1 000 mg/L) significantly inhibited cell growth ($P<0.05$) in HepG2 cells compared with the control group in a dose-dependent manner determined by MTS assay (Figure 1). EGb 761 at 750 and 1 000 mg/L inhibited cell growth to 50% and 45% of the control, respectively, in HepG2 cells. Similarly, EGb 761 (50-1 000 mg/L) dose-dependently inhibited cell growth ($P<0.05$) in Hep3B cells compared with the control group. EGb 761 at 750 and 1 000 mg/L inhibited cell growth to 48% and 39% of the control, respectively, in Hep3B cells.

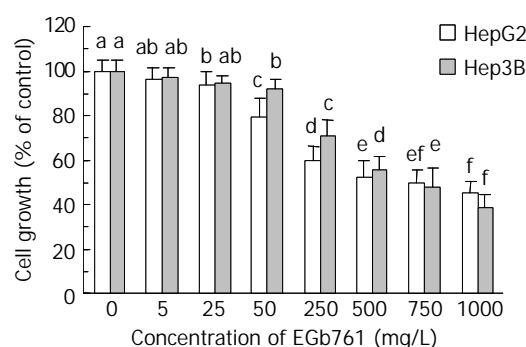


Figure 1 Effects of EGb 761 on cell growth in HepG2 and Hep3B cells measured by MTS assay. Data are expressed as $\bar{x}\pm s$ ($n=8$). Values not sharing the same letter differed significantly ($P<0.05$) in the same cell line by Fisher's least significant difference test.

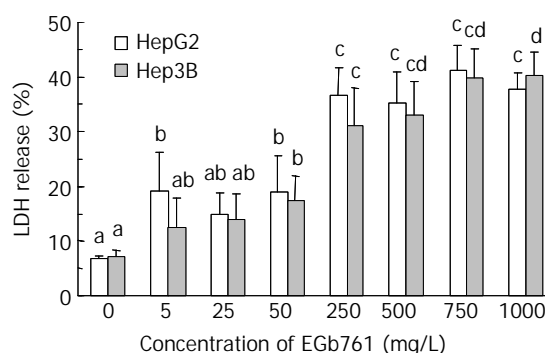


Figure 2 Effects of EGb 761 on cell cytotoxicity in HepG2 and Hep3B cells determined by lactate dehydrogenase (LDH) release. Data are expressed as $\bar{x}\pm s$ ($n=3$). Values not sharing the same letter differed significantly ($P<0.05$) in the same cell line by Fisher's least significant difference test.

Cell cytotoxicity assay

Cell cytotoxicity was directly measured by LDH release. After 24 h incubation, EGb 761 (50-1 000 mg/L) significantly increased cell cytotoxicity ($P<0.05$) in both HepG2 and Hep3B cells compared with the control group (6.7% and 7.2% in HepG2 and Hep3B cells) (Figure 2). EGb 761 at a dose of 250 mg/L significantly increased LDH release to 36.6% and 31.2% ($P<0.05$), respectively, in HepG2 and Hep3B cells compared with EGb 761 at a dose of 50 mg/L (18.9% and

17.5% in HepG2 and Hep3B cells). However, EGb 761 at the dose of 250-1 000 mg/L did not dose-dependently increase cell cytotoxicity in both HepG2 (35.2-41.3% LDH release) and Hep3B (31.2-40.3% LDH release) cells.

Analysis of proliferating cell nuclear antigen (PCNA) and p53 protein

After 48 h incubation with EGb 761, the expression of PCNA and p53 protein in HepG2 cells was analyzed by SDS-PAGE and Western blotting. EGb 761 at the dose of 500, 750, and 1 000 mg/L decreased PCNA expression to 90%, 84%, and 85% of the control, respectively (Figure 3). However, EGb 761 at the dose of 500, 750, and 1 000 mg/L increased p53 expression to 135%, 152%, and 174% of the control, respectively (Figure 4).

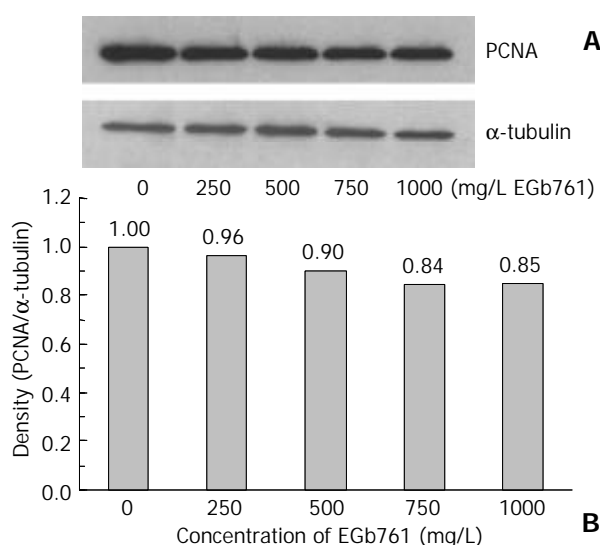


Figure 3 Expression of proliferating cell nuclear antigen (PCNA) with the molecular weight of 36 kDa which was visualized by Western blotting (A) and quantitated by an image analysis system (B) after HepG2 cells were incubated with 0-1 000 mg/L EGb 761 for 48 h. Samples were pooled from 6 independent experiments ($n = 6$). Alpha-tubulin (55 kDa) was as an internal control.

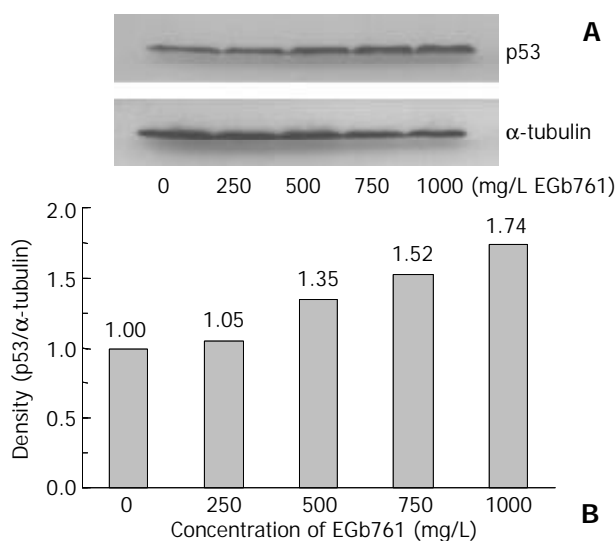


Figure 4 Expression of p53 protein with the molecular weight of 53 kDa which was visualized by Western blotting (A) and quantitated by an image analysis system (B) after HepG2 cells were incubated with 0-1 000 mg/L EGb 761 for 48 h. Samples were pooled from 6 independent experiments ($n=6$). Alpha-tubulin (55 kDa) was as an internal control.

DISCUSSION

Ginkgo biloba extract (EGb 761) at the dose of 50-1 000 mg/L significantly decreased cell proliferation measured by MTS assay in a dose-dependent manner in both HepG2 and Hep3B cells with 50% inhibition at approximately 750 mg/L. Similarly, EGb 761 and ginkgolide B were found to inhibit cell proliferation in highly aggressive human breast cancer MDA-231 cells in a dose-dependent manner^[16]. Another *Ginkgo biloba* extract, IPS200 devoid of proanthocyanidins, at 200 mg/L decreased cell proliferation of Hep3B cells^[17]. EGb 761 also showed an inhibitory effect on cell proliferation of cultured vascular smooth muscle cells in a dose-dependent pattern *in vitro* and significantly decreased the percentage of proliferating cells in the balloon-injured abdominal aorta of cholesterol-fed rabbits *in vivo*^[18]. Additionally, EGb 761 given orally at 50 or 100 mg/kg·d or superoxide dismutase injected intravenously at 15 000 U/kg·d inhibited preretinal proliferation in pigmented rabbits, suggesting that antioxidants might efficiently prevent preretinal proliferation^[19]. The biflavonoids of *Ginkgo biloba* extract, ginkgetin and isoginkgetin at 10 μmol/L, inhibited lymphocyte proliferation induced by Con A or LPS^[9]. Ginkgetin was also found to dose-dependently inhibit the growth of human ovarian adenocarcinoma OVCAR-3 cells with 50% inhibition at 1.8 mg/L^[20]. Quercetin, an important flavonoid of *Ginkgo biloba* extract, significantly inhibited cell proliferation of HCC cell lines BEL-7402, HuH-7, and HLE with a peak inhibition at 50 μmol/L^[21]. The inhibitory effect of EGb 761 on cell proliferation may be attributed to its antioxidation capacity, however, other constituents of EGb 761 may contribute to its cytotoxic action. Recently, *Ginkgo biloba* extract has been reported to affect gene expression related to cell growth^[17]. EGb 761 dramatically reduced, in a consistent manner, the expression of α-fetoprotein in Hep3B cells using fluorescence and membrane DNA microarrays, in which protein is present at very low concentration in adults but is increased in hepatoma patients. Moreover, IPS200 inhibited 40-50% mRNA levels of peripheral-type benzodiazepine receptor, positively correlated with cell proliferation and metastasis in MDA-231, Hep3B, and U87 (human glioblastoma) cells using quantitative RT-PCR and Northern blot analysis. In contrast to our study, a previous study demonstrated that the components of *Ginkgo biloba* extract, such as quercetin, kaempferol, sciadopitysin, ginkgetin, and isoginkgetin, enhanced cell proliferation of normal human skin fibroblasts *in vitro*^[22]. The various effects of *Ginkgo biloba* extract on cell proliferation may result from different cell lines, cell morphology (normal vs malignant), and the dosage of *Ginkgo biloba* extract or the individual constituents.

Besides the inhibitory effect of EGb 761 on cell proliferation, EGb 761 at higher doses (50-1 000 mg/L) significantly increased cytotoxicity determined by LDH release in both HepG2 and Hep3B cells. However, the cytotoxic effect of EGb 761 reached the plateau at the dose over 250 mg/L. The cytotoxic effect of EGb 761 could be attributed to necrosis and/or apoptosis. Our result revealed increased LDH release as an index of necrosis in EGb 761-treated cells, indicating that EGb 761 could enhance necrosis. Although we did not directly measure apoptosis, the expression of p53 protein, as an inducer of apoptosis in human HCC cells^[23], was increased in EGb 761-treated groups. There may exist the possibility that apoptosis contributes to the cytotoxic effect of EGb 761. The cytotoxic activity of EGb 761 has been suspected to derive from ginkgolic acids^[24,25] and ginkgetin^[10] through their induction of apoptosis. Ginkgolic acids restricted in EGb 761 at less than 5 μg/g have been recognized as hazardous compounds with suspected cytotoxic, allergenic, mutagenic, and carcinogenic properties^[24,25]. Ginkgolic acids caused death

of cultured chick embryonic neurons in a dose-dependent manner, and ginkgolide acid-induced death showed both signs of apoptosis and necrosis possibly via the mediation of protein phosphatase 2C^[24]. Additionally, increased apoptotic cells from 6% (control) to nearly 80% were found in human keratinocyte cell line HaCaT incubated with ginkgolide acids at the concentration of more than 30 mg/L, which was primarily regulated by transformation of mitochondria probably induced by uncoupling of oxidative phosphorylation^[25]. Ginkgetin (5 mg/L) increased intracellular levels of hydrogen peroxide and induced apoptosis in OVCAR-3 cells, which was mediated mainly through the activation of caspase (s) by the generation of hydrogen peroxide perhaps through autooxidation of ginkgetin^[10]. However, some constituents of EGb 761 have been reported to possess anti-apoptotic capacity^[26,27]. EGb 761 (100 mg/L), ginkgolide J (100 μmol/L), and ginkgolide B (10 μmol/L) reduced apoptosis from 74% in staurosporine-induced apoptotic chick embryonic neurons to 24%, 62%, and 31%, respectively^[26]. Furthermore, EGb 761 (100 mg/L) and bilobalide (100 μmol/L) rescued rat neurons from apoptosis induced by serum deprivation. A previous study also found that the total flavonoids of EGb 761, two pure flavonoid components (rutin and quercetin), and a mixture of flavonoids and terpenes protected cerebellar granule cells from oxidative stress and apoptosis induced by hydroxyl radicals^[27]. However, total terpenes of EGb 761 neither protected against apoptosis nor had a synergistic effect, suggesting that terpenes did not scavenge hydroxyl radicals directly to suppress apoptosis. The apoptosis-stimulatory and anti-apoptotic properties of EGb 761 might depend on the target cells, the dosage, and its constituents.

Both cell proliferation and apoptosis were involved in HCC^[27]. The expression of PCNA and p53 proteins has been regarded as cell proliferation and apoptosis biomarkers, respectively, for the malignant phenotype of HCC, and was associated with prognosis and therapeutic outcome^[28-31]. Cell proliferation was increased as HCC progressed to become more poorly differentiated^[29,30]. Apoptotic HCC cancer cells were consistently negative for PCNA, and p53-positive cancer cells showed apoptosis^[28]. Consistent with the result of MTS assay that EGb 761 suppressed cell proliferation of HCC cells, EGb 761 at the dose of 500-1 000 mg/L decreased the expression of PCNA by 10-16%. Additionally, the expression of p53 protein, measured in HepG2 cells expressing endogenous p53, while not in Hep3B cells lacking endogenous p53 expression^[32], was increased by 35-74% in EGb 761-treated groups (500-1 000 mg/L). It suggested that EGb 761 might be potentially useful for the prevention of HCC progression. *Ginkgo biloba* extract or its constituent has been considered as an anti-cancer agent. A previous study showed that EGb 761 ameliorated the deleterious effects on the forestomach and liver in mice with benzo(a)pyrene-induced gastric carcinoma^[33]. Furthermore, combined quercetin and a recombinant adenovirus vector expressing human p53, granulocyte-macrophage colony-stimulating factor (GM-CSF), and B7-1 (CD80) genes, as a combined anti-cancer agent, synergistically inhibited cell proliferation and induced apoptosis of HCC cells^[21].

In conclusion, *Ginkgo biloba* extract at the concentration above 50 mg/L can significantly suppress cell proliferation and increase cell cytotoxicity in human hepatocellular carcinoma cell lines. Additionally, *Ginkgo biloba* extract can decrease PCNA and increase p53 protein expression in HepG2 cells, suggesting that *Ginkgo biloba* extract may regulate not only cell proliferation but also apoptosis of HCC cells. Therefore, *Ginkgo biloba* extract may have therapeutic potential for HCC.

REFERENCES

- Kleijnen J**, Knipschild P. *Ginkgo biloba*. *Lancet* 1992; **340**: 1136-1139
- Gardès-Albert M**, Ferradini C, Sekaki A, Droy-Lefaix MT. Oxygen-centered free radicals and their interactions with EGb 761 or CP 202. In: Ferradini C, Droy-Lefaix MT, Christen Y, eds. *Advances in Ginkgo biloba extract research: Ginkgo biloba extract (EGb 761) as a free-radical scavenger*. New York: Elsevier Science 1993: 1-11
- Deby C**, Deby-Dupont G, Dister M, Pincemail J. Efficiency of *Ginkgo biloba* Extract (EGb 761) in neutralizing ferryl ion-induced peroxidations: therapeutic implication. In: Ferradini C, Droy-Lefaix MT, Christen Y, eds. *Advances in Ginkgo biloba extract research: Ginkgo biloba extract (EGb 761) as a free-radical scavenger*. New York: Elsevier Science 1993: 13-26
- Tosaki A**, Droy-Lefaix MT. Effects of free-radical scavengers, superoxide dismutase, catalase and *Ginkgo biloba* extract (EGb 761) on reperfusion-induced arrhythmias in isolated hearts. In: Ferradini C, Droy-Lefaix MT, Christen Y, eds. *Advances in Ginkgo biloba extract research: Ginkgo biloba extract (EGb 761) as a free-radical scavenger*. New York: Elsevier Science 1993: 141-152
- Šrám RJ**, Binková B, Stejskalová J, Topinka J. Effect of EGb 761 on lipid peroxidation, DNA repair and antioxidant activity. In: Ferradini C, Droy-Lefaix MT, Christen Y, eds. *Advances in Ginkgo biloba extract research: Ginkgo biloba extract (EGb 761) as a free-radical scavenger*. New York: Elsevier Science 1993: 27-38
- Szabo ME**, Droy-Lefaix MT, Doly M. Reduction of reperfusion-induced ionic imbalance by superoxide dismutase, vitamin E and *Ginkgo biloba* extract 761 in spontaneously hypertensive rat retina. In: Ferradini C, Droy-Lefaix MT, Christen Y, eds. *Advances in Ginkgo biloba extract research: Ginkgo biloba extract (EGb 761) as a free-radical scavenger*. New York: Elsevier Science 1993: 93-106
- Oken BS**, Storzbach DM, Kaye JA. The efficacy of *Ginkgo biloba* extract on cognitive function in Alzheimer disease. *Arch Neurol* 1998; **55**: 1409-1415
- Onen A**, Deveci E, Inaloz SS, Isik B, Kilinc M. Histopathological assessment of the prophylactic effect of *ginkgo-biloba* extract on intestinal ischemia-reperfusion injury. *Acta Gastroenterol Belg* 1999; **62**: 386-389
- Lee SJ**, Choi JH, Son KH, Chang HW, Kang SS, Kim HP. Suppression of mouse lymphocyte proliferation in vitro by naturally-occurring biflavonoids. *Life Sci* 1995; **57**: 551-558
- Su Y**, Sun CM, Chuang HH, Chang PT. Studies on the cytotoxic mechanisms of ginkgetin in a human ovarian adenocarcinoma cell line. *Naunyn Schmiedebergs Arch Pharmacol* 2000; **362**: 82-90
- Lowry OH**, Rosebrough NJ, Farr A, Randall RJ. Protein measurement with the Folin phenol reagent. *J Biol Chem* 1951; **193**: 265-275
- Dunigan DD**, Waters SB, Owen TC. Aqueous soluble tetrazolium/formazan MTS as an indicator of NADH- and NADPH-dependent dehydrogenase activity. *Biotechniques* 1995; **19**: 640-649
- Arechabala B**, Coiffard C, Rivalland P, Coiffard LJ, de Roeck-Holtzauer Y. Comparison of cytotoxicity of various surfactants tested on normal human fibroblast cultures using the neutral red test, MTT assay and LDH release. *J Appl Toxicol* 1999; **19**: 163-165
- Laemmli UK**. Cleavage of structural proteins during the assembly of the head of bacteriophage T4. *Nature* 1970; **227**: 680-685
- Towbin H**, Staehelin T, Gordon J. Electrophoretic transfer of proteins from polyacrylamide gels to nitrocellulose sheets: procedure and some applications. *Proc Natl Acad Sci U S A* 1979; **76**: 4350-4354
- Papadopoulos V**, Kapsis A, Li H, Amri H, Hardwick M, Culty M, Kasprzyk PG, Carlson M, Moreau JP, Drieu K. Drug-induced inhibition of the peripheral-type benzodiazepine receptor expression and cell proliferation in human breast cancer cells. *Anticancer Res* 2000; **20**: 2835-2847
- Li W**, Pretner E, Shen L, Drieu K, Papadopoulos V. Common gene targets of *Ginkgo biloba* extract (EGb 761) in human tumor cells: relation to cell growth. *Cell Mol Biol* 2002; **48**: 655-662
- Lin SJ**, Yang TH, Chen YH, Chen JW, Kwok CF, Shiao MS, Chen YL. Effects of *Ginkgo biloba* extract on the proliferation of vascular smooth muscle cells *in vitro* and on intimal thickening and interleukin-1beta expression after balloon injury in cholesterol-fed rabbits *in vivo*. *J Cell Biochem* 2002; **85**: 572-582
- Baudouin C**, Ettaiche M, Imbert F, Droy-Lefaix MT, Gastaud P, Lapalus P. Inhibition of preretinal proliferation by free radical scavengers in an experimental model of tractional retinal detachment. *Exp Eye Res* 1994; **59**: 697-706
- Sun CM**, Syu WJ, Huang YT, Chen CC, Ou JC. Selective cyto-

- toxicity of ginkgetin from *Selaginella moellendorffii*. *J Nat Prod* 1997; **60**: 382-384
- 21 **Shi M**, Wang FS, Wu ZZ. Synergetic anticancer effect of combined quercetin and recombinant adenoviral vector expressing human wild-type p53, GM-CSF and B7-1 genes on hepatocellular carcinoma cells *in vitro*. *World J Gastroenterol* 2003; **9**: 73-78
- 22 **Kim SJ**, Lim MH, Chun IK, Won YH. Effects of flavonoids of *Ginkgo biloba* on proliferation of human skin fibroblast. *Skin Pharmacol* 1997; **10**: 200-205
- 23 **Lee KH**, Kim KC, Jung YJ, Ham YH, Jang JJ, Kwon H, Sung YC, Kim SH, Han SK, Kim CM. Induction of apoptosis in p53-deficient human hepatoma cell line by wild-type p53 gene transduction: inhibition by antioxidant. *Mol Cells* 2001; **12**: 17-24
- 24 **Ahlemeyer B**, Selke D, Schaper C, Klumpp S, Krieglstein J. Ginkgolic acids induce neuronal death and activate protein phosphatase type-2C. *Eur J Pharmacol* 2001; **430**: 1-7
- 25 **Hecker H**, Johannisson R, Koch E, Siegers CP. *In vitro* evaluation of the cytotoxic potential of alkylphenols from *Ginkgo biloba* L. *Toxicology* 2002; **177**: 167-177
- 26 **Ahlemeyer B**, Mowes A, Krieglstein J. Inhibition of serum deprivation- and staurosporine-induced neuronal apoptosis by *Ginkgo biloba* extract and some of its constituents. *Eur J Pharmacol* 1999; **367**: 423-430
- 27 **Chen C**, Wei T, Gao Z, Zhao B, Hou J, Xu H, Xin W, Packer L. Different effects of the constituents of EGb 761 on apoptosis in rat cerebellar granule cells induced by hydroxyl radicals. *Biochem Mol Biol Int* 1999; **47**: 397-405
- 28 **Terada T**, Nakanuma Y. Expression of apoptosis, proliferating cell nuclear antigen, and apoptosis-related antigens (bcl-2, c-myc, Fas, Lewis(y) and p53) in human cholangiocarcinomas and hepatocellular carcinomas. *Pathol Int* 1996; **46**: 764-770
- 29 **Mise K**, Tashiro S, Yogita S, Wada D, Harada M, Fukuda Y, Miyake H, Isikawa M, Izumi K, Sano N. Assessment of the biological malignancy of hepatocellular carcinoma: relationship to clinicopathological factors and prognosis. *Clin Cancer Res* 1998; **4**: 1475-1482
- 30 **Nakano A**, Watanabe N, Nishizaki Y, Takashimizu S, Matsuzaki S. Immunohistochemical studies on the expression of P-glycoprotein and p53 in relation to histological differentiation and cell proliferation in hepatocellular carcinoma. *Hepatol Res* 2003; **25**: 158-165
- 31 **Qin LX**, Tang ZY. The prognostic molecular markers in hepatocellular carcinoma. *World J Gastroenterol* 2002; **8**: 385-392
- 32 **Lee KH**, Kim KC, Jung YJ, Ham YH, Jang JJ, Kwon H, Sung YC, Kim SH, Han SK, Kim CM. Induction of apoptosis in p53-deficient human hepatoma cell line by wild-type p53 gene transduction: inhibition by antioxidant. *Mol Cells* 2001; **12**: 17-24
- 33 **Agha AM**, El-Fattah AA, Al-Zuhair HH, Al-Rikabi AC. Chemopreventive effect of *Ginkgo biloba* extract against benzo(a)pyrene-induced forestomach carcinogenesis in mice: amelioration of doxorubicin cardiotoxicity. *J Exp Clin Cancer Res* 2001; **20**: 39-50

Edited by Zhu LH and Wang XL

Increased nociceptin/orphanin FQ plasma levels in hepatocellular carcinoma

Ferenc Szalay, Mónika B Hantos, Andrea Horvath, Peter L. Lakatos, Aniko Folhoffer, Kinga Dunkel, Dalma Hegedus, Kornélia Tekes

Ferenc Szalay, Andrea Horvath, Peter L. Lakatos, Aniko Folhoffer, Kinga Dunkel, Dalma Hegedus, 1st Department of Medicine of Semmelweis University, Budapest, Hungary

Kornélia Tekes, Department of Pharmacodynamics of Semmelweis University, Budapest, Hungary

Mónika B Hantos, Neurochemical Research Unit of Hungarian Academy of Sciences, Budapest, Hungary

Correspondence to: Professor Ferenc Szalay, MD., PhD, 1st Department of Medicine Semmelweis University, Koranyi S u. 2/A, Budapest, H-1083 Hungary. szalay@bell.sote.hu

Telephone: +36-1-210 1007 **Fax:** +36-1-210 1007

Received: 2003-10-08 **Accepted:** 2003-11-16

Abstract

AIM: The heptadecapeptide nociceptin alias orphanin FQ is the endogenous agonist of opioid receptor-like 1 receptor. It is involved in modulation of pain and cognition. High blood level was reported in patients with acute and chronic pain, and in Wilson disease. An accidental observation led us to investigate nociceptin in hepatocellular carcinoma.

METHODS: Plasma nociceptin level was measured by radioimmunoassay, aprotinin was used as protease inhibitor. Hepatocellular carcinoma was diagnosed by laboratory, ultrasound, other imaging, and confirmed by fine needle biopsy. Results were compared to healthy controls and patients with other chronic liver diseases.

RESULTS: Although nociceptin levels were elevated in patients with Wilson disease (14.0 ± 2.7 pg/mL, $n=26$), primary biliary cirrhosis (12.1 ± 3.2 pg/mL, $n=21$) and liver cirrhosis (12.8 ± 4.0 pg/mL, $n=15$) compared to the healthy controls (9.2 ± 1.8 pg/mL, $n=29$, $P < 0.001$ for each), in patients with hepatocellular carcinoma a ten-fold increase was found (105.9 ± 14.4 pg/mL, $n=29$, $P < 0.0001$). High plasma levels were found in each hepatocellular carcinoma patient including those with normal alpha fetoprotein and those with pain (104.9 ± 14.9 pg/mL, $n=12$) and without (107.7 ± 14.5 pg/mL, $n=6$).

CONCLUSION: A very high nociceptin plasma level seems to be an indicator for hepatocellular carcinoma. Further research is needed to clarify the mechanism and clinical significance of this novel finding.

Szalay F, Hantos MB, Horvath A, Lakatos PL, Folhoffer A, Dunkel K, Hegedus D, Tekes K. Increased nociceptin/orphanin FQ plasma levels in hepatocellular carcinoma. *World J Gastroenterol* 2004; 10(1): 42-45

<http://www.wjgnet.com/1007-9327/10/42.asp>

INTRODUCTION

The heptadecapeptide nociceptin (N/OFQ), alias orphanin FQ, is the endogenous agonist ligand of a G-protein-coupled,

naloxon insensitive opioid receptor-like 1 receptor (ORL1), recently named as NOP^[1]. Although N/OFQ is structurally related to opioid peptides, especially to dynorphin A, it does not interact with μ , δ and κ receptors. The nociceptin/NOP system represents a new peptide-based signalling pathway. Nociceptin is involved in a number of pharmacological actions in the central nervous system (CNS), including modulation of pain and cognition. However, numerous studies investigating the functional role of nociceptin in physiology have failed to provide coherent view, and its exact physiological role remains to be determined^[2,3]. Although N/OFQ is produced by some brain structure and peripheral neurons, it is present in the liquor and blood^[4], and recent data prove that nociceptin transcripts are expressed in human immune cells as well^[5]. NOP mRNA is expressed not only in nervous system, but in immune cells and other organs including the liver^[6-8]. High nociceptin blood level was shown in patients with acute and chronic pains^[9], and Wilson disease^[10].

An accidental observation led us to investigate plasma nociceptin level in patients with hepatocellular carcinoma (HCC). While measuring plasma nociceptin in patients with Wilson disease, we noticed that in one patient the nociceptin level was extremely high compared both with the controls and other Wilson patients. This patient had liver cirrhosis and primary hepatocellular carcinoma without any pain. This observation prompted us to study N/OFQ in patients with hepatocellular carcinoma and other liver diseases. Striking differences were found.

MATERIALS AND METHODS

Patients

Plasma nociceptin level was measured in 26 patients with Wilson disease (aged from 14-55 years, 11 with hepatic, and 15 with neurological symptoms, each D-penicillamine treated), 21 patients with primary biliary cirrhosis (age ranged from 36-72 years; each woman with AMA M2 positive, histologically proven and treated with ursodeoxycholic acid; mean disease duration: 9.4 years), 18 patients with chronic hepatitis (14 HCV positive, 1 HBV positive and 3 autoimmune, each proved by liver biopsy), 15 patients with liver cirrhosis (9 alcoholic, 6 HCV positive), and 18 patients with primary hepatocellular carcinoma (8 with alcoholic cirrhosis, 6 HCV cirrhosis, 1 HBV cirrhosis, 1 Wilson disease, 1 PBC, and 1 patient without any underlying liver disease) from the Hepatological Unit, the 1st Department of Medicine, the Semmelweis University, Budapest. The diagnosis of HCC was based on clinical laboratory tests, US, CT, MRI findings and was confirmed by fine needle aspiration cytology, and histology, in which 3 cases underwent surgery, and one case by autopsy. Serum alpha fetoprotein (AFP) was elevated in 11 out of 18 HCC patients. The size of the tumour ranged from 2.5 cm to 12 cm in diameter. It was smaller than 5 cm in 5 patients, and larger than 5 cm in 13 patients. No metastasis was found outside the liver. In the HCC group 12 patients had temporary pain treated with non-opioid analgetics and 6

patients were without any pain.

Two scoring systems were used for characterisation of patients with HCC. The distribution of patients according to the Barcelona Clinic Liver Cancer (BCLC) classification^[11], which includes the performance status, single or multifocal appearance of the tumor, vascular invasion, portal hypertension, Okuda stage and Child-Pugh classification: Stage A1 ($n=5$), stage A4 ($n=6$), stage B ($n=3$) and stage D ($n=4$). Ranking of patients according to the Cancer of the Liver Italian Program group (CLIP) criteria^[12,13], which includes Child-Pugh stage, tumor morphology and extent, presence of portal vein thrombosis and serum level of alpha fetoprotein: CLIP 0 ($n=2$), CLIP 1 ($n=5$), CLIP 2 ($n=5$), CLIP 3 ($n=4$), CLIP 4 ($n=1$), CLIP 5 ($n=1$). Demographics, clinical data and ranking of HCC patients according to the BCLC and CLIP classification are shown in Table 1.

Twenty-nine healthy persons including blood donors and members of the medical staff served as control group. The study was approved by the Local Regional Committee of Science and Research Ethics. Written informed consent was obtained.

Methods

Blood drawn from fasting subjects between 08:00 and 10:00 AM was collected in vacutainer tubes containing K-EDTA as anticoagulant. Aprotinin was added immediately as protease inhibitor. Plasma samples were stored at minus 80 °C. Nociceptin was measured by radioimmunoassay (¹²⁵I-Nociceptin kit, Phoenix Pharmaceuticals, Phoenix, CA, USA) with minimum sensitivity of 1 pg/mL, as described before^[9]. Comparison of the plasma N/OFQ concentration in groups was made using Mann-Whitney U Test. Correlation between N/OFQ level and liver function test results was evaluated by Spearman RO correlation.

RESULTS

Results are shown in Figure 1. Although nociceptin levels were elevated in patients with Wilson disease (14.0 ± 2.7 pg/mL), in patients with PBC (12.1 ± 3.2 pg/mL) and liver cirrhosis (12.8 ± 4.0 pg/mL) compared to the healthy controls (9.2 ± 1.8

pg/mL, $P<0.001$ for each), more than ten-fold higher values were found (105.9 ± 14.4 pg/mL, $P<0.0001$) in patients with HCC. In patients with chronic hepatitis the N/OFQ level was 10.2 ± 3.6 , but the difference was not significant compared to the healthy controls. The clinical data, chemical laboratory findings, AFP and N/OFQ levels of patients with HCC are individually indicated in Table 1.

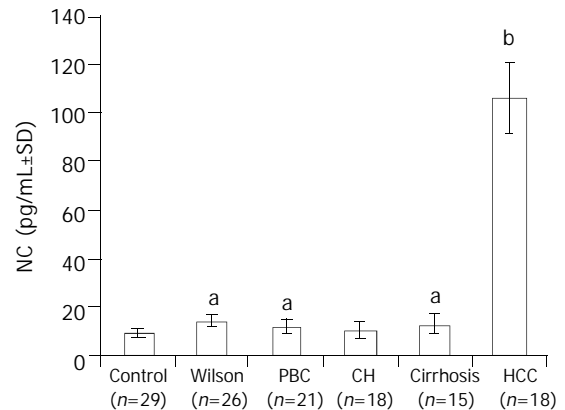


Figure 1 Plasma nociceptin level (pg/mL±SD) in healthy controls (Control) and in patients with Wilson disease (Wilson), primary biliary cirrhosis (PBC), chronic hepatitis (CH), cirrhosis and hepatocellular carcinoma (HCC). * $P<0.001$ vs control, ^b $P<0.0001$ vs control and each other group.

We did not find any correlation between nociceptin level and liver chemical laboratory tests including AFP in any group of patients with liver disease. Nociceptin was elevated in each HCC patient including those with normal AFP. The N/OFQ level did not show correlation with the presence and severity of the pain. High levels were found in subgroups of patients with pain (104.9 ± 14.9 pg/mL, $n=12$) and without pain (107.7 ± 14.5 pg/mL, $n=6$). There was no difference in nociceptin level between groups with tumor size smaller than 5 cm and larger than 5 cm (109.4 ± 16.5 , $n=5$ and 115.2 ± 12.7 , $n=13$,

Table 1 Profile of patients with HCC and plasma N/OFQ levels

	Age	Gender	Aetiology	AFP (ng/mL)	Tumor size in UH	Uni-nod.	Multi-nod.	BCLC st.cl.	CLIP cl.	Bi (mg/dL)	ALP (U/L)	GGT (U/L)	Ascites	C-P	N/OFQ (pg/mL)
1	80	M	Alcoholic	937	15×11 cm	+		A 4	3	1.72	306	102	-	A	108.39
2	64	M	Alcoholic	1 385.9	5×7×6 cm	+		A 1	1	1.92	242	107	-	A	95.02
3	60	M	Alcoholic	89	5 -15 mm and 3 cm		+	B	2	1.07	2 169	1 000	-	B	96.05
4	62	M	Alcoholic	91	1-1.5 cm and 3.5 cm		+	B	2	1.12	2 038	995	-	B	104.17
5	80	M	Alcoholic	937	15×11 cm	+		A 1	3	1.71	306	102	-	A	111.59
6	70	M	Alcoholic	459	7×6 cm	+		A 1	2	0.78	192	68	-	A	111.51
7	59	M	Alcoholic	7.7	23 mm	+		D	2	8.32	44.3	97	-	C	128
8	66	M	Alcoholic	2	1.5 cm	+		A 1	0	1.25	192	24	-	A	81.6
9	48	F	HCV	15	6×6 cm	+		A 4	1	5.75	1 766	253	-	B	90.41
10	66	M	HCV	171	two, 2×2 cm lesion		+	A 4	1	2.55	460	232	-	A	89.81
11	76	M	HCV	9	6×7 cm + 5×4 cm		+	D	4	13.91	834	276	+	C	114.65
12	78	M	HCV	350	5×6 cm	+		A 1	0	0.68	270	37	-	A	114.7
13	48	F	HCV	13	21×20 mm and 16×21 mm		+	B	1	1.36	474	1 060	-	A	128
14	81	M	HCV	1 050	8×10 cm	+		A 4	3	3	569	517	-	A	98.31
15	66	M	HBV	6	4×4.5 cm	+		D	2	3.35	442	199	+	C	106.03
16	45	F	WD	5	60×46 mm	+		A 4	1	0.42	910	212	+	B	128
17	68	F	PBC	3 480	11×7.5 cm	+		D	5	4.79	1 856	960	+	C	172.2
18	32	F	Unknown	1 050	100×85×180 mm	+		A 4	3	0.34	233	24	-	-	85.5

AFP=alpha fetoprotein, BCLC st. cl.=Barcelona Clinic Liver Cancer (BCLC) staging classification, CLIP cl.=Cancer of the Liver Italian Program Group (CLIP) scoring system, Bi=Serum total bilirubin, ALP=alkaline phosphatase, GGT=gamma glutamyl transferase, C-P=Child-Pugh score, N/OFQ=nociceptin/orphanin FQ.

respectively) or between single nodular and multinodular HCC groups, and even symptomatic or asymptomatic tumors. No difference was found in the N/OFQ level between any subgroup of patients with different BCLC and CLIP score values.

Repeated nociceptin measurements were done in one patient before and after non-surgical ablation treatment of HCC. The high nociceptin level did not decrease significantly at least within 10 days following ethanol injection treatment of the tumor, since values were 116 pg/mL before, and 110, 108, 112, 103 pg/mL after treatment at 1, 3, 7, and 10 days, respectively.

However, progressive and significant elevation in plasma nociceptin level parallel with the increase of AFP was observed in a PBC patient with HCC during the follow up. This 67 year old patient was monitored and treated with ursodeoxycholic acid throughout 18 years when her liver tumor was detected by yearly regular ultrasound check up. Fine needle aspiration cytology proved HCC, and she died within two years. Nociceptin was measured in blood samples collected from other reason. The AFP level was normal throughout the years, but elevated at the time of the diagnosis of HCC (426 ng/mL) and rose up to 3 480 ng/mL. The plasma nociceptin (10.6 pg/mL) was within the normal range (9.2 ± 1.8 pg/mL) in the tumor free stage, ten-fold higher (103.7 pg/mL) when the tumor was diagnosed and reached 172.2 pg/mL before the death. Sixteen-fold higher nociceptin content was measured in the tumor tissue (0.16 pg/mg) compared to the tumor-free liver tissue sample (0.01 pg/mg) taken during the autopsy. Detailed presentation of this case is published in this issue of World Journal of Gastroenterology (Horvath *et al* World J Gastroenterol 2004; 10: 152-154)

DISCUSSION

Shortly after cloning of the three known opioid receptors a fourth member of the subfamily of G protein-coupled receptors was identified. In a search for additional opioid receptor subtypes, a sequence of an opioid-like receptor, termed ORL1 was found, which, however, did not bind any of the known natural opioid ligands. Therefore ORL1 represented an "orphan" receptor. Later two working groups simultaneously reported the isolation of the natural ligand for ORL1, a 17 aminoacid polypeptide and named it orphanin FQ or nociceptin^[14,15].

Anatomic studies have revealed high levels of expression of N/OFQ messenger RNS in brain structures involved in sensory, emotional and cognitive processing. Like all other neuropeptides, the heptadecapeptid N/OFQ is synthesized as a part of a larger precursor named prepro-nociceptin, a 176 aminoacid polypeptide in human, from which N/OFQ and nocistatin are cleaved in brain cells and peripheral neurons^[16,17]. Although nociceptin is present in the brain, the liquor and blood, human immune cells and polymorphonuclear cells, the gastrointestinal tract and other organs, there are no data on N/OFQ or its receptor in malignant diseases with exception of human neuroblastoma cell lines^[18,19]. This is the first report focusing on nociceptin in hepatocellular carcinoma and other liver diseases.

The novel finding of this study is the striking elevation in plasma N/OFQ level in patients with hepatocellular carcinoma. Although nociceptin was elevated in patients with Wilson disease, primary biliary cirrhosis and liver cirrhosis, very high levels over ten-fold increase compared with healthy controls was found in HCC. Since nociceptin level was extremely high in each patient with HCC, and the difference among HCC patients and groups of patients with other liver diseases was highly significant ($P < 0.0001$), the very high plasma level of nociceptin seems to be an indicator for HCC. It is remarkable that nociceptin level was very high in even those patients with normal level of alpha-fetoprotein^[20]. The size of HCC is an

important element of prognostic assessment^[21]. However, nociceptin level was equally very high in patients with tumor size smaller and larger than 5 cm in diameter.

Further research is needed to clarify the mechanism and clinical significance of the highly elevated nociceptin level in HCC. Increased production or decreased catabolism of nociceptin may be the cause of elevation in plasma level. It is to be determined whether the tumor produces nociceptin or it gives signal for brain cells or peripheral neurons to increase the secretion of N/OFQ. We had the opportunity to determine the tissue nociceptin content in one PBC patient with HCC. Although more than 15-fold higher nociceptin content was measured in the carcinoma tissue than in the tumor-free liver tissue samples taken during autopsy, it did not necessarily mean that nociceptin was produced by the tumor. It is also possible that the tumor simply accumulates nociceptin via binding it by NOP receptors. This possibility could be supported by the fact that ORL1/NOP receptor mRNA has been detected in the liver^[22], although no study is yet available on nociceptin or its receptor mRNA expression in hepatocellular carcinoma tissue.

Nociceptin is involved in the processing of pain signals, and it modulates the pain perception^[23,24]. However, we did not find difference in N/OFQ level between patients with pain and without. There was no correlation between the plasma N/OFQ level and the severity of pain.

Whether a very high plasma N/OFQ level is a specific marker of HCC should be investigated and subjected to further study. Since nociceptin transcripts are expressed in immune cells^[5], it has also been shown that polymorphonuclear cells express nociceptin receptors and N/OFQ stimulates neutrophil chemotaxis and recruitment^[25]. The high nociceptin level could also be an indicator of altered reaction of the body including immunological, cytokine and other mechanisms. The bacterial endotoxin (LPS) and proinflammatory cytokines including TNF-alpha, commonly increased in malignancies, induce N/OFQ mRNAs in astrocytes. It may suggest a role for nociceptin in neural-glia communication and in inflammatory responses^[26].

In humans, the N/OFQ gene has been mapped to the chromosomal location 8p21^[27]. Transcription of this gene was shown to be enhanced by cytokines, neurotrophic factors^[26], also by estrogen^[28]. This cAMP-dependent transcription could be blocked by glucocorticoids^[19]. Our patients in this study have not received glucocorticoid treatment, and only one PBC patient used transdermal estrogen hormone replacement for osteoporosis prevention.

Elevated N/OFQ level might partly represent a compensatory mechanism in the nociceptin/NOP system to modulate pain perception in the central nervous system. That mechanism might explain why some patients with a very high plasma N/OFQ level did not have any pain despite advanced stage of the malignant liver tumor. It is remarkable that nociceptin in HCC patients was 3-fold higher than the highest values reported in patients with chronic pain without malignant diseases^[19]. We believe that our results could stimulate further investigation.

REFERENCES

- 1 **Calo' G**, Rizzi A, Bigoni R, Guerrini R, Salvadori S, Regoli D. Pharmacological profile of nociceptin/orphanin FQ receptors. *Clin Exp Pharmacol Physiol* 2002; **29**: 223-228
- 2 **Terenius L**, Sandin J, Sakurada T. Nociceptin/orphanin FQ metabolism and bioactive metabolites. *Peptides* 2000; **21**: 919
- 3 **Heinricher MM**. Orphanin FQ/nociceptin: from neural circuitry to behavior. *Life Sci* 2003; **73**: 813-822
- 4 **Brooks H**, Elton CD, Smart D, Rowbotham DJ, McKnight AT, Lambert DG. Identification of nociceptin in human cerebrospinal fluid: comparison of level in pain and non-pain states. *Pain* 1998; **78**: 71-73

- 5 **Arjomand J**, Cole S, Evans C. Novel orphanin FQ/nociceptin transcripts are expressed in human immune cells. *J Neuroimmunol* 2002; **130**: 100
- 6 **Peluso J**, Gaveriaux-Ruff C, Matthes HW, Filliol D, Kieffer BL. Orphanin FQ/nociceptin binds functionally coupled ORL1 receptors on human immune cell lines and alters peripheral blood mononuclear cell proliferation. *Brain Res Bull* 2001; **54**: 655-660
- 7 **Peluso J**, LaForge KS, Matthes HW, Kreek MJ, Kieffer BL, Gaveriaux-Ruff C. Distribution of nociceptin/orphanin FQ receptor transcript in human central nervous system and immune cells. *J Neuroimmunol* 1998; **81**: 184-192
- 8 **Reinscheid RK**, Nothacker HP, Civelli O. The orphanin FQ/nociceptin gene: structure, tissue distribution of expression and functional implications obtained from knockout mice. *Peptides* 2000; **21**: 901-906
- 9 **Ko MH**, Kim YH, Woo RS, Kim KW. Quantitative analysis of nociceptin in blood of patients with acute and chronic pain. *Neuroreport* 2002; **13**: 1631-1633
- 10 **Hantos MB**, Szalay F, Lakatos PL, Hegedüs D, Firneisz G, Reiczigel J, Torok T, Tekes K. Elevated plasma nociceptin level in patients with Wilson disease. *Brain Research Bulletin* 2002; **58**:311-313
- 11 **Llovet JM**, Bru C, Bruix J. Prognosis of hepatocellular carcinoma: the BCLC staging classification. *Semin Liver Dis* 1999; **19**: 329-337
- 12 **The Cancer of the Liver Italian Program (CLIP) Investigators.** A new prognostic system for hepatocellular carcinoma: a retrospective study of 435 patients. *Hepatology* 1998; **28**: 751-755
- 13 **Zhao WH**, Ma ZM, Zhou XR, Feng YZ, Fang BS. Prediction of recurrence and prognosis in patients with hepatocellular carcinoma after resection by use of CLIP score. *World J Gastroenterol* 2002; **8**: 237-242
- 14 **Reinscheid RK**, Nothacker HP, Bourson A, Ardati A, Henningsen RA, Bunzow JR, Grandy DK, Langen H, Monsma FJ Jr, Civelli O. Orphanin FQ: a neuropeptide that activates an opioidlike G protein-coupled receptor. *Science* 1995; **270**: 792-794
- 15 **Meunier JC**, Mollereau C, Toll L, Suandeu C, Moisan C, Alvineire P, Butour JL, Guillemot JC, Ferrara P, Monserrat B. Isolation and structure of the endogenous agonist of opioid receptor-like ORL-1 receptor. *Nature* 1995; **377**: 532-535
- 16 **Okuda-Ashitaka E**, Ito S. Nocistatin: a novel neuropeptide encoded by the gene for the nociceptin/orphanin FQ precursor. *Peptides* 2000; **21**: 1101-1109
- 17 **Okuda-Ashitaka E**, Minami T, Tachibana S, Yoshihara Y, Nishiuchi Y, Kimura T, Ito S. Nocistatin, a peptide that blocks nociceptin action in pain transmission. *Nature* 1998; **392**: 286-289
- 18 **Spampinato S**, Di Toro R, Qusem AR. Nociceptin-induced internalization of the ORL1 receptor in human neuroblastoma cells. *Neuroreport* 2001; **12**: 3159-3163
- 19 **Sirianni MJ**, Fujimoto KI, Nelson CS, Pellegrino MJ, Allen RG. Cyclic AMP analogs induce synthesis, processing and secretion of prepro nociceptin/orphanin FQ-derived peptides by NS20Y neuroblastoma cells. *DNA Cell Biol* 1999; **18**: 51-58
- 20 **Qin LX**, Tang ZY. The prognostic significance of clinical and pathological features in hepatocellular carcinoma. *World J Gastroenterol* 2002; **8**: 193-199
- 21 **Bruix J**, Llovet JM. Prognostic assessment and evaluation of the benefits of treatment. *J Clin Gastroenterol* 2002; **35**(Suppl 2): S138-142
- 22 **Wang JB**, Johnson PS, Imai Y, Persico AM, Ozenberger BA, Eppler CM, Uhl GR. cDNA cloning of an orphan opiate receptor gene family member and its splice variant. *FEBS Lett* 1994; **348**: 75-79
- 23 **Inoue M**, Kawashima T, Takeshima H, Calo G, Inoue A, Nakata Y, Ueda H. *In vivo* pain-inhibitory role of nociceptin/orphanin FQ in spinal cord. *J Pharmacol Exp Ther* 2003; **305**: 495-501
- 24 **Meunier JC**. Utilizing functional genomics to identify new pain treatments: the example of nociceptin. *Am J Pharmacog* 2003; **3**: 117-130
- 25 **Serhan CN**, Fierro IM, Chiang N, Pouliot M. Cutting edge: Nociceptin stimulates neutrophil chemotaxis and recruitment: inhibition by aspirin-triggered-15-epi-lipoxin A₄. *J Immunol* 2001; **166**: 3650-3654
- 26 **Buzas B**, Symes AJ, Cox BM. Regulation of nociceptin/orphanin FQ gene expression by neurotrophic cytokines and neurotrophic factors in neurons and astrocytes. *J Neurochem* 1999; **72**: 556-563
- 27 **Mollereau C**, Simons MJ, Soularue P, Liners F, Vassart G, Meunier JC, Parmentier M. Structure, tissue distribution and chromosomal localization of the prepronociceptin gene. *Proc Natl Acad Sci U S A* 1996; **93**: 8666-8670
- 28 **Xie GX**, Ito E, Maruyama K, Suzuki Y, Sugano S, Sharma M, Pietruck C, Palmer PP. The promoter region of the human prepronociceptin gene and its regulation by cyclic AMP and steroid hormones. *Gene* 1999; **238**: 427-436

Edited by Zhang JZ

Potential role of p53 mutation in chemical hepatocarcinogenesis of rats

Wei-Guo Deng, Yan Fu, Yu-Lin Li, Toshihiro Sugiyama

Wei-Guo Deng, Department of Nutrition and Food Hygiene, School of Public Health, Jilin University, Changchun 130021, Jilin Province, China

Yan Fu, Department of Obstetrics and Gynecology, First Hospital, Jilin University, Department of Pathology, School of Preclinical Medicine, Jilin University, Changchun 130021, Jilin Province, China

Yu-Lin Li, Department of Pathology, School of Preclinical Medicine, Jilin University, Changchun 130021, Jilin Province, China

Toshihiro Sugiyama, Department of Biochemistry, Akita University School of Medicine, 1-1-1 Hondo, Akita, 010-8543, Japan

Supported by Jilin University Excellent Young Teacher Foundation, No. 2001033

Correspondence to: Dr. Yan Fu, Department of Obstetrics and Gynecology, First Hospital, Jilin University, 1 Xinmin Street, Changchun 130021, Jilin Province, China

Telephone: +86-431-5612482

Received: 2003-06-05 **Accepted:** 2003-08-16

Abstract

AIM: Inactivation of p53 gene is one of the most frequent genetic alterations in carcinogenesis. The mutation status of p53 gene was analyzed, in order to understand the effect of p53 mutation on chemical hepatocarcinogenesis of rats.

METHODS: During hepatocarcinogenesis of rats induced by 3'-methyl-4-dimethylaminoazobenzene (3'-Me-DAB), prehepatocarcinoma and hepatocarcinoma foci were collected by laser capture microdissection (LCM), and quantitatively analyzed for levels of p53 mRNA by LightCycler™ real-time RT-PCR and for mutations in p53 gene exons 5-8 by direct sequencing.

RESULTS: Samples consisting of 44 precancerous foci and 24 cancerous foci were collected by LCM. A quantitative analysis of p53 mRNA showed that p53 mRNA peaked at an early stage (week 6) in the prehepatocarcinoma lesion, more than ten times that of adjacent normal tissue, and gradually decreased from week 6 to week 24. The expression of p53 mRNA in adjacent normal tissue was significantly lower than that in prehepatocarcinoma. Similar to prehepatocarcinoma, p53 mRNA in cancer was markedly higher than that in adjacent normal tissue at week 12, and was closer to normal at week 24. Direct p53 gene sequencing showed that 35.3% (24/68) (9 precancer, 15 cancer) LCM samples exhibited point mutations, 20.5% of prehepatocarcinoma LCM samples presented missense mutations at exon 6/7 or/and 8, and was markedly lower than 62.5% of hepatocarcinoma ones ($P < 0.01$). Mutation of p53 gene formed the mutant hot spots at 5 codons. Positive immunostaining for p53 protein could be seen in prehepatocarcinoma and hepatocarcinoma foci at 24 weeks.

CONCLUSION: p53 gene mutation is present in initial chemical hepatocarcinogenesis, and the mutation of p53 gene induced by 3'-Me-DAB is an important factor of hepatocarcinogenesis.

Deng WG, Fu Y, Li YL, Sugiyama T. Potential role of p53 mutation in chemical hepatocarcinogenesis of rats. *World J Gastroenterol* 2004; 10(1): 46-52

<http://www.wjgnet.com/1007-9327/10/46.asp>

INTRODUCTION

Abnormalities of some tumor suppressor genes and oncogenes play important roles in the development and progression of hepatoma^[1,2]. Gene abnormalities in precancerous liver lesions (adenomatous hyperplasia and atypical adenomatous hyperplasia) and early hepatocellular carcinoma have been reported^[3-5]. p53 tumor suppressor protein plays an important role in preventing malignant development, and p53 function is lost or compromised in most human cancers^[6-8]. One of the principal functions of p53 is to inhibit cell growth, and p53 shows a strong cell cycle arrest and apoptotic activities^[9,10]. As a result, cell proliferation is suppressed and/or programmed cell death is induced^[11,12]. In cells with DNA injury, p53 can stop the cell cycle through p21 protein and then promote DNA repair. When DNA is seriously damaged, p53 can induce the cell to undergo programmed cell death to maintain the stability of genome and cells. Loss of p53 function activates oncogenes and inactivates cancer suppressor genes, playing an essential role in multistage carcinogenesis^[13,14]. Some study has shown that mutation and loss of p53 gene are closely related to the conversion of adenoma to early colorectal cancer, and so are those in liver^[15]. When cancer cell differentiation is low and the tumor becomes large, p53 gene mutation frequently arises in hepatocarcinoma, making p53 gene most closely concerned with the progress of hepatocarcinoma^[16]. It is not yet clear which of these gene alterations is responsible for hepatocarcinogenesis, especially in a prehepatocarcinoma lesion.

3'-methyl-4-dimethylaminoazobenzene (3'-Me-DAB) could produce prehepatocarcinomatous lesions (altered focus and neoplastic nodules) in rats. Our study showed that mutation of p53 gene, in precancerous and cancerous foci of the F344 rat liver induced by 3'-Me-DAB, was successfully detected by integrating LCM, LightCycler RT-PCR with direct sequencing.

MATERIALS AND METHODS

Animals

Thirty-nine male F344 rats at 10 weeks of age were kept in a room with a 12h light and dark cycle and maintained at 22 °C. They were provided with a diet containing 0.06% 3'-Me-DAB^[17] and tap water *ad libitum* for 6 weeks, 12 weeks, and 24 weeks, respectively. After the last day of each experimental period, the animals were anesthetized with ether and hepatectomized. The cavum thoracis and abdominal cavity were opened immediately with a sterilized scalpel, and part of the liver was quickly dissected out, placed in a cryomold, covered with Tissue-Tek O. C. T compound before being frozen in liquid nitrogen, and preserved at -80 °C until use. The remaining liver was perfused with 30% PBS-buffered sucrose before being removed and fixed in 10% neutral formalin, and then embedded in paraffin.

LCM of sample

The liver preserved at -80°C was sequentially sliced into twenty $10\ \mu\text{m}$ thick sections, in a cryostat, which were mounted on clean microscope slides. The sections were stored at -80°C . Of the 10 successive slide sections, three were stained chemically with H&E and immunohistochemically with glutathione *S* transferase placenta (GST-P) and AFP polyclonal antibody using Elite ABC kit (Funakoshi Co. Ltd., Tokyo, Japan). Prehepatocarcinoma and hepatocarcinoma foci were diagnosed by Pathologists and their positions were identified on the slides. Other slide sections underwent quick H&E staining based on the LCM manufacturer's protocols, and were then cleaned in xylene for over 1 min. Once air-dried, slides were ready for LCM. Based on the position of GST-P (+) or AFP (+) foci from immunostained slide sections and the cancer pathology on the H&E section, a LCM cap was placed over the target area of the slide section^[18,19]. Target foci in the same position as GST-P (+) or AFP (+) foci were then microdissected.

Extraction of DNA of LCM samples

After microdissection, the LCM cap was inserted into an Eppendorf tube containing $50\ \mu\text{l}$ of digestion buffer of 0.04% proteinase K, 10 mM Tris-HCl pH 8.0, 1 mM EDTA, and 1% Tween-20. The tube was then placed upside down overnight at 37°C . Following ethanol precipitation, DNA was extracted by the phenol/chloroform/isopropanol method and used directly as a template for PCR.

Extraction of total RNA of LCM samples

After laser transfer, the LCM cap was gently placed on the Eppendorf tube containing $200\ \mu\text{l}$ of reaction mixture. The tube was inverted back and shaken several times for over two minutes to digest the tissue on the cap. The digestive solution was removed from the Eppendorf tube and placed into a 1.5 ml sturdy tube, extraction and purification of total RNA were conducted according to conventional methods. The pellet of total RNA was then resuspended in H_2O , and stored at -80°C .

Primers for RT-PCR, direct sequencing of p53

We designed upstream PCR primers P1, P2, and P3 in the region corresponding to introns 4, 5, and 7 (Figure 1 and Table 1). They were used in combination with downstream primers P4, P5, and P6 within the region corresponding to introns 5, 7 and 8 of p53 gene (Figure 1 and Table 1), to specifically amplify exons 5, 6/7, and 8 of the functional p53 gene without p53 pseudo-gene. The primers Pmu and Pmd for RT-PCR were located on exons 7 and 8 (Figure 1 and Table 1).

Quantitative analysis of mRNA

RNAs extracted from prehepatocarcinoma and hepatocarcinoma foci captured by LCM were reverse-transcribed into first strand cDNA at 42°C for 50 min and at 99°C for 5 min using Oligo-dT-adaptor-primer of an RNA PCR kit (Takara, Co. Ltd., Japan) as the primer. A $1\ \mu\text{l}$ aliquot of first-strand cDNA or H_2O (as a negative control) was put into LightCycler capillary, together with $1\ \mu\text{l}$ of 20 pM primer (Table 1) for target DNA and $18\ \mu\text{l}$ of mixture of LightCycler-DNA Master SYBR Green I mixture. Various concentrations of standard sample cDNA were also used to construct a standard curve. After instantaneous centrifugation, capillaries were loaded onto a LightCycler instrument. Quantitative analysis of mRNA was conducted under PCR conditions in Table 1. The standard curve was shown as a straight line of linear regression with cycle number *versus* log-concentration of standard samples. This standard curve, in turn, was used to estimate the concentration of each sample. Since the expression of β -actin mRNA is constant in all types of cells, it was used to calibrate the original concentration of mRNA, i.e., the concentration unit of mRNA in tissue was defined as the ratio of target mRNA copies *versus* β -actin mRNA copies^[20].

Mutation screening of p53 exons 5, 6/7, and 8

DNAs from the same LCM samples were amplified by PCR under the conditions in Table 1. PCR products were refined by a Microcon-100 kit (Takara, Co. Ltd., Japan). The sense strand

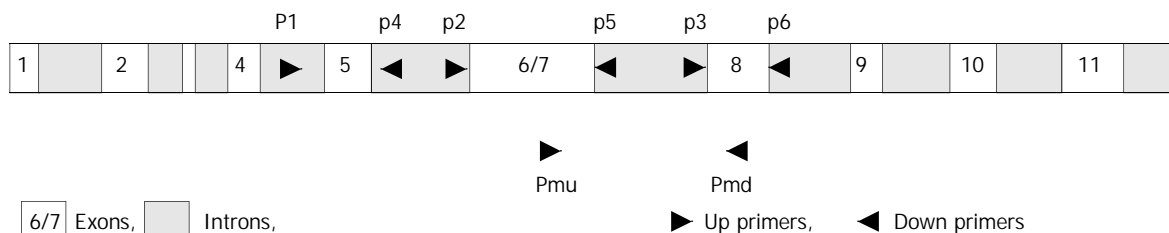


Figure 1 Strategy of primers. To avoid p53 pseudogene co-amplification, the upstream PCR primers P1, P2, and P3 in the region corresponding to introns 4, 5, and 7 were used in combination with downstream primers P4, P5, and P6 within the region corresponding to introns 5, 7, and 8 of p53 gene. Primers Pmu and Pmd for RT-PCR located in exons 7 and 8, respectively.

Table 1 Primer sequences and PCR conditions used in sequencing DNA of p53 gene and RT-PCR

Exons	Primer	Primer sequences of p53	Conditions
5	P1	GACCTTTGATTCTTTCTCCTCTCC	94°C , 3 min (94°C , 30 sec; 56°C , 30 sec; 72°C , 30 sec) $\times 30$
	P4	GGGAGACCCTGGACAACCAG	
6/7	P2	GCCTCTGACTTATTCTTGCTC	94°C , 3 min (94°C , 30 sec; 56°C , 30 sec; 72°C , 30 sec) $\times 30$
	P5	CCCAACCTGGCACACAGCTTC	
8	P3	CTGTGCCTCCTCTTGTCCTG	94°C , 3 min (94°C , 30 sec; 56°C , 30 sec; 72°C , 30 sec) $\times 30$
	P6	CCACCTTCTTTGTCTGCTG	
P53 mRNA	Pu	GTCGGCTCCGACTATAACCACTATC	95°C , 2 min (95°C , 0 sec; 56°C , 5 sec; 72°C , 11 sec) $\times 30$
	Pd	CTCTCTTTGCACTCCCTGGGGG	
GST-P mRNA	Pu	ATCGTCCACGCAGCTTTGA	95°C , 2 min (95°C , 0 sec; 57°C , 5 sec; 72°C , 13 sec) $\times 30$
	Pd	AGCCTCCTTCTGGTCTTTC	
β -actin mRNA	Pu	ACCACCATGTACCCAGGCAT	95°C , 2 min (95°C , 0 sec; 56°C , 5 sec; 72°C , 10 sec) $\times 30$
	Pd	CCGGACTCATCGTACTCCTG	

of PCR products was sequenced using a cycler sequencing ready reaction kit (ABI, Perkin-Elmer Corp., USA) and analyzed on an ABI Prism™ 310 genetic analyzer (ABI, Perkin-Elmer Corp., USA).

Immunohistochemical staining

Immunohistochemical staining was conducted using the avidin-biotin-peroxidase complex technique (Vectastain Elite ABC Kit, Funakoshi Co. Ltd., Tokyo, Japan)^[21]. Paraffin-embedded or frozen rat liver specimens were sectioned at 5 μ m and placed on a precleaned glass microscope slide. After deparaffination and blocking of endogenous biotin activity, the sections were incubated with primary antibodies (anti-GST-P IgG diluted at 1:500, anti-AFP IgG diluted at 1:200 (polyclonal antibody) and anti-p53 monoclonal antibody Ab1 (Oncogene Science, Inc., USA) diluted at 1:100) for 90 min at 30 °C, then incubated with biotinylated anti-rabbit (for polyclonal antibody) or anti-mouse (for monoclonal antibody) secondary antibody for 30 min at 30 °C. The slides were incubated for 30 min with avidin-peroxidase conjugates. Finally, the sections were reacted with 3' 3-diaminobenzidine tetrahydrochloride and hydrogen peroxide for 3 min followed by counter-staining with hematoxylin. For a negative control, pre-immune serum instead of primary antibody was used.

Statistical methods

Student-*t* test was used to identify the differences of mRNA concentration in normal tissue, precancerous and cancerous foci.

RESULTS

Hepatocarcinogenesis

Prehepatocarcinoma foci could be found in all (13) the livers of rats treated with 3'-Me-DAB for 12 weeks, which were intensely stained by GST-P (Figure 2, B). By H&E staining, the size of prehepatocarcinoma cells was similar to that of normal hepatocytes, but the cytoplasm of precancer cells

was clearer. Under low power magnification, the edge of prehepatocarcinoma focus was distinct and bright (Figure 2, A). Hepatocarcinoma foci were seen in 6 liver sections. By H&E staining, the sizes of nuclei were different, the cytoplasm was a little basophilic and a lot of fat vesicles were present in cytoplasm of hepatocarcinoma cells (Figure 2, C). Immunohistochemically staining for AFP was intensive in hepatocarcinoma foci. At week 24 (Figure 2, D), all (13) the livers exhibited hepatocarcinoma foci and some showed prehepatocarcinoma foci simultaneously. The diameter of precancerous foci was 0.5 mm-1.0 mm at week 6, 1.2 mm-1.5 mm at week 12 and >2.5 mm at week 23. Forty-four precancerous and 24 cancerous samples were obtained for DNA sequencing analysis and quantitative analysis of p53 mRNA.

Expression of p53 and GST-P mRNA

The time course of p53 gene expression showed that the mRNA levels peaked at week 6 in prehepatocarcinoma foci and at week 12 in hepatocarcinoma foci, although they declined significantly by week 24 ($P < 0.01$, Figure 3). The relative concentration of p53 mRNA in adjacent normal tissue remained significantly lower than in prehepatocarcinoma and hepatocarcinoma foci. In hepatocarcinoma foci, the relative concentration of p53 mRNA was 10 *odd* times higher than in adjacent normal tissue at week 6 of the experiment ($P = 5.6 \times 10^{-9}$) and 4 times as high at week 12 ($P = 4.8 \times 10^{-9}$). p53 mRNA concentration was also significantly higher in cancer than in adjacent normal tissue at week 12 ($P = 0.028$). However, at week 24, p53 mRNA of both prehepatocarcinoma and hepatocarcinoma foci was obviously elevated. Relative p53 mRNA concentration was the highest in prehepatocarcinoma foci and the lowest in adjacent normal tissue among the three tissues examined (Figure 3).

Moreover, the expression of GST-P mRNA was low in adjacent normal tissue from week 6 to week 24, and was significantly higher in prehepatocarcinoma foci than in adjacent normal tissue and hepatocarcinoma foci ($P < 0.001$),

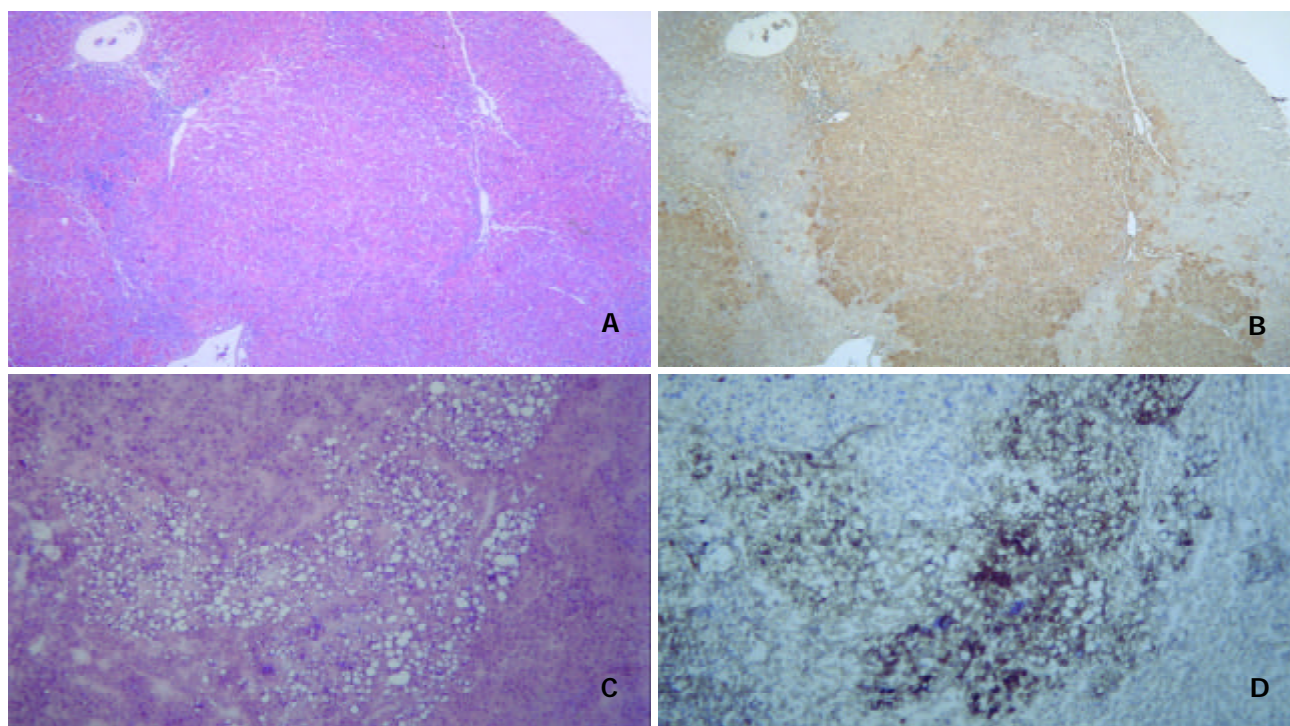


Figure 2 Hepatocarcinogenesis. A: Prehepatocarcinoma foci were stained by H&E, morphology of prehepatocarcinoma cells was similar to that of normal hepatocytes, and the edge of prehepatocarcinoma focus was distinct and bright. B: Prehepatocarcinoma focus was as intensely stained by GST-P as A. C: Hepatocarcinoma foci by H&E staining showed a lot of foam cells. D: Immunohistochemical staining for AFP was intense in hepatocarcinoma foci.

and higher in hepatocarcinoma foci than in adjacent normal tissue (Figure 4).

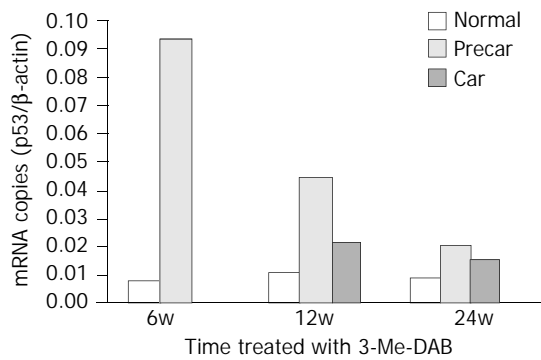


Figure 3 Quantitative analysis of p53 mRNA. After rats were treated with 3'-Me-DAB for 6, 12 and 24 weeks, the expressions of p53 mRNA were markedly higher in prehepatocarcinoma than in hepatocarcinoma and adjacent normal tissue, $P < 0.001$. The time course of p53 mRNA showed that mRNA levels peaked at week 6, and gradually decreased to minimum at week 24. Normal=adjacent normal tissue, Precar=prehepatocarcinoma, Car=hepatocarcinoma.

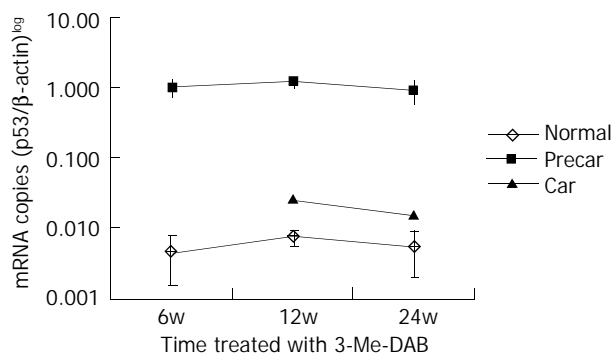


Figure 4 Quantitative analysis of GST-P mRNA. After rats were treated with 3'-Me-DAB for 6, 12 and 24 weeks, the expressions of GST-P mRNA were markedly higher in prehepatocarcinoma than that in hepatocarcinoma and adjacent normal tissue, $P < 0.001$, and also higher in hepatocarcinoma than that in adjacent normal tissue, $P < 0.001$. GST-P mRNA levels were expressed on a logarithmic scale. Normal=adjacent normal tissue, Precar=prehepatocarcinoma, Car=hepatocarcinoma.

Direct sequencing analysis of p53 mutation

Direct sequencing analysis of genomic DNA from 24 LCM samples showed 39 mutations at 18 codons of exons 6/7 and 8 in p53 gene (Figure 5, A, C, E). Of these 39 mutations, 10 transition mutations (1 A:T→G:C, 9 G:C→A:T) (Figure 5, A,C) and 29 transversion mutations (9 G:C→C:G, 9 G:C→T:A, 5 C:G→A:T, 2 C:G→G:C, 2 A:T→C:G, 1 T:A→A:T and 1 A:T→T:A) (Figure 5, E) were identified. A base inserting mutation following the first base substitution, G→TA, in codon 283 of exon 7 resulted in a putative substitution "end" for glutamic acid in p53 protein. Interestingly, four LCM samples had triple mutations and eight LCM samples had double mutations in exons 6/7 or/and 8 simultaneously. One LCM sample with triple mutations and 3 with double mutations were prehepatocarcinoma foci, and 3 other samples with triple mutations and 5 with double mutations were hepatocarcinoma foci.

In brief, 24/68 (35.3%) of LCM samples had mutations of p53 gene. No mutation in exon 5 was found by direct sequencing.

Incidence of p53 gene mutation in hepatocarcinogenesis

20.5% precancerous foci samples expressed point mutation or

inserting mutation in exons 6/7 and 8, and the incidence of mutation was markedly higher than that of cancerous samples ($\chi^2=12.02$, $P < 0.01$). At 12 weeks, the incidence of mutation was significantly higher in hepatocarcinoma samples than in prehepatocarcinoma samples, $P=0.034$ by Fisher's exact probabilities (Figure 6). At 24 weeks, the incidence of mutation was not different between prehepatocarcinoma and hepatocarcinoma foci samples.

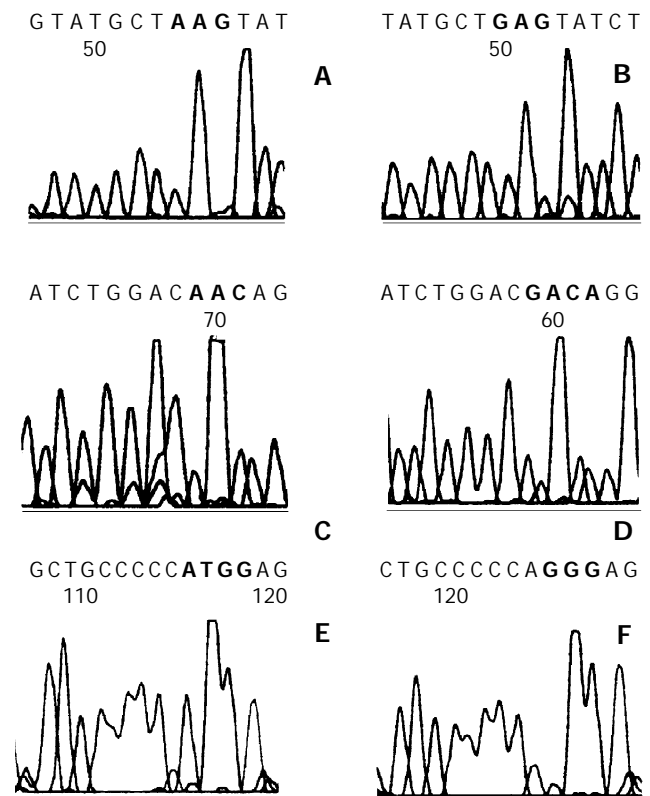


Figure 5 Direct sequencing of p53 exons 6/7 and 8. A: GAG to AAG transition mutation (red box) at codon 202 of exon 6/7 was seen in prehepatocarcinoma foci at 6 weeks. C: Four hepatocarcinoma foci with GAC to AAC transition mutation (red box) at codon 206 formed one of the mutation hot spots. E: GGG to TGG transversion mutation (red box) at codon 300 of exon 8 in hepatocarcinoma foci. B, D and F were normal sequence.

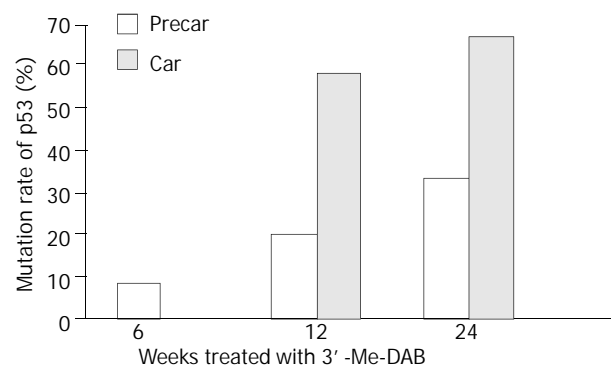


Figure 6 Mutation ratio of p53 exons 6/7 and 8 in prehepatocarcinoma (precar) and hepatocarcinoma foci (car).

Hot spot of mutation

Among the 34 mutation codons of p53 exons 6/7 and 8, 9 were at codon 233, 5 at codons 278 and 279, respectively, 4 at codon 206 (Figure 5,C), and 3 mutations were at codon 112. These mutational codons formed the mutational hot spots of precancerous and cancerous foci in this study, and were located in highly conservative DNA binding domain of p53 protein.

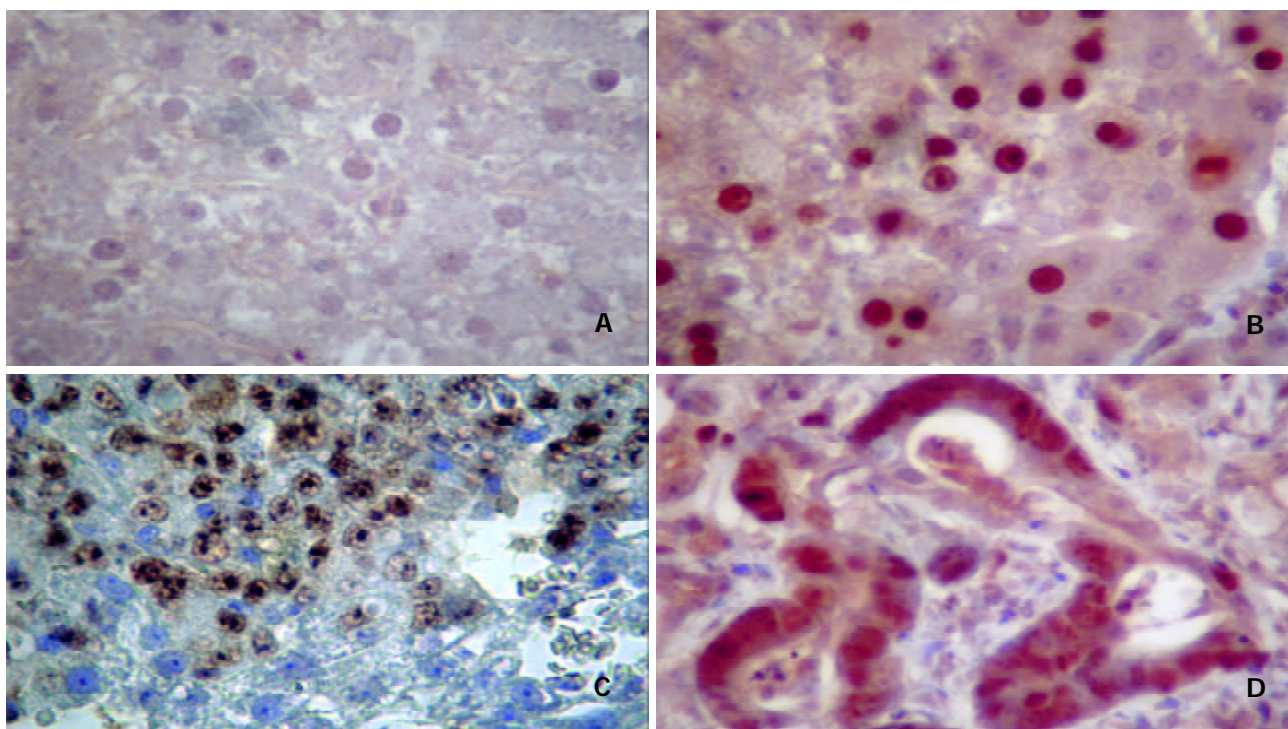


Figure 7 Mutant p53 protein expressions in prehepatocancer and hepatocancer. A: Normal tissue. B: Nuclei of prehepatocarcinoma cells immunostained by anti-p53 Ab1. C: Nuclei of hepatocellular carcinoma cells stained by anti-p53 Ab1. D: Nuclei of adenohepatoma cells stained by anti-p53 Ab1. Enlarged nuclei intensely stained for Ab1 were seen in cells. Original magnification 400 \times .

Expression of p53 protein in cells

As shown in Figure 7, paraffin-embedded or frozen liver sections from rats treated with 3'-Me-DAB for 24 weeks exhibited intensive immunostaining of p53 protein in at least 30% cells of prehepatocarcinoma (Figure 7B) and hepatocarcinoma foci (Figure 7, C, D). Staining was predominantly limited to enlarged nuclei with intensive staining for the anti-p53 antibody. In contrast, no liver sections from rats treated with 3'-Me-DAB for 6 or 12 weeks demonstrated immunostaining for p53 protein (Figure 7, A).

DISCUSSION

Researchers are used to studying human tumors by obtaining human hepatocarcinoma tissue after hepatectomy, but it is difficult to obtain pre-hepatocarcinoma foci in cases without clinical symptoms. We and other investigators were therefore constrained to using rats as the animal model for assessing the effects of p53 gene mutations on hepatocarcinogenesis^[22,23]. It has been found that rat p53 gene differs from human p53 gene, in that it processes pseudogenes in its genome^[24,25]. Pitfalls associated with p53 pseudogene co-amplification from genomic DNA could be avoided, however, by designing PCR primers based on the intron sequence^[24,26].

Carcinogenesis is a complex process characterized by the cumulative activation of various oncogenes and the inactivation of suppressor genes. About 30-40% of human hepatocarcinomas and 20-60% of rat experimental tumors demonstrated mutations of p53 gene^[2,27-30]. Chemically induced rat liver cancer proceeds through multiple, distinct initiation-promotion-progression stages and mutation of the suppressor p53 gene has been found in relatively early preneoplastic lesions in the rat liver.

We used quantification of p53 mRNA expression to detect genetic alterations at RNA level in the present study. The results showed that in precancerous foci of the rat liver, p53 mRNA rose quickly and peaked at week 6 of 3'-Me-DAB treatment. It then gradually decreased from week 12 and fell to a minimum

at week 24 of the experiment. Similar results were also seen in cancer foci. The time course of mRNA expression differed from that of p53 protein accumulation in nuclei. GST-P is one of the detoxification enzymes involved in the metabolism of 3'-Me-DAB as well as other carcinogens and plays a protective role during chemical hepatocarcinogenesis. It is considered as an early marker of preneoplastic lesion. When GST-P played a protective role, mRNA transcript increased coincidentally with positive GST-P immunostaining in prehepatocarcinoma foci of the rats at all experimental time points tested (data not shown). GST-P overexpression was not consistent with an aberration in p53 protein expression^[31].

In this paper, 20.5% of precancerous foci occurring after week 6, week 12, and week 24 exhibited missense mutations of p53 exons 6/7 or/and 8, with double or triple codon mutations found in the same sample by direct sequencing. Of the hepatocarcinoma foci, 58.3% and 66.7% had mutations in p53 gene at week 12 and week 24 of 3'-Me-DAB treatment, respectively. Mutations were distributed widely throughout exons 6/7 and 8, but not in exon 5. p53 mutation rate increased from week 6 to week 24, suggesting that p53 gene mutation is closely associated with hepatocarcinoma development and progression. It is possible that p53 mutation ran through the initiative, intermediate, and late stages of hepatocarcinogenesis, and was not an event occurring only at the advanced stage of liver cancer. Therefore, mutant p53 molecules have been thought to have some unique properties that are important in carcinogenesis in rats^[32].

A tetramer of p53 molecules has been assembled through carboxyterminal oligomerization domains. This allows the central domains to interact directly with a consensus DNA element. As a consequence, aminoterminal transactivation domains could interact with basal transcription factors, resulting in increased gene expression^[33,34]. Among the 39 mutation codons of p53 exons 6/7 and 8, 9 were at codon 233, 5 at codons 278 and 279, respectively, 4 at codon 206, and 3 mutations were at codon 212. These mutational codons formed

mutational hot spots of precancerous and cancerous foci in this study, and were located in the highly conservative DNA binding domain of p53 protein^[35].

Over 90% of mutations are missensed, causing the substitution of amino acids. It has been found that mutation hot spots were dispersed in three exons of p53 gene, and three hotspots fell within two evolutionarily highly conserved regions^[35,36], suggesting no single spot is responsible for maintaining p53 tumor suppressor function. In fact, a certain oncogenic agent could act on only one or more spots of the p53 gene DNA sequence. The effect of the hotspots is yet uncertain, because a certain oncogenic agent has made different mutational hotspots of p53 gene in different species^[37-40] and tissues^[28,39,40].

Amino acid residues 278 and 279 of the p53 protein have been found to be located in helix H₂ of loop-sheet-helix fitting in the major groove of DNA, allowing them to contact edges of the bases, and to play a central role in DNA recognition^[41], so mutation occurring in this area may cause p53 to lose its growth regulation.

Positive immunostaining of p53 was only found in sections of LCM samples treated with 3' -Me-DAB for 24 weeks, not in those treated for 6 or 12 weeks, demonstrating that p53 protein accumulates relatively late during hepatocarcinogenesis. Positive immunostaining of p53 was consistent with the increased half-life of mutant p53 protein compared to wild-type p53^[35,42,43]. As the half-life of wild-type p53 protein is short, it is usually too difficult to detect it in normal tissue with Western blotting or immunohistochemical staining. Mutant p53 protein could competitively inhibit the function of wild p53 protein, promoting hyperplasia of cells and leading to tumor development^[44,45]. A few studies have reported that accumulation of p53 protein in nuclei in late chemical hepatocarcinogenesis was not synchronized with the increased expression of p53 mRNA^[28,46,47]. The rise of p53 mRNA markedly preceded the rise of the expression quantity of p53 protein^[19,48].

We showed that mutation of p53 gene occurred in early precancerous and cancerous foci of F344 rats treated with 3' -Me-DAB and mutation increased progressively from week 6 to week 24, but the expression of p53 mRNA decreased progressively from week 6 to week 24. The detection of p53 gene mutation may benefit the early diagnosis of tumors^[49], and also may aid in understanding the mechanism behind hepatocarcinogenesis.

REFERENCES

- Teeguarden JG**, Newton MA, Dragan YP, Pitot HC. Genome-wide loss of heterozygosity analysis of chemically induced rat hepatocellular carcinomas reveals elevated frequency of allelic imbalances on chromosomes 1, 6, 8, 11, 15, 17, and 20. *Mol Carcinog* 2000; **28**: 51-61
- De Miglio MR**, Muroi MR, Simile MM, Viridis P, Asara G, Frau M, Calvisi DF, Seddaiu MA, Pascale RM, Feo F. Frequent loss of heterozygosity at the Hcr1 (hepatocarcinogenesis resistance) locus on chromosome 10 in primary hepatocellular carcinomas from LFF1 rat strain. *Hepatology* 2001; **33**: 1110-1117
- Kishimoto Y**, Shiota G, Kamisaki Y, Wada K, Nakamoto K, Yamawaki M, Kotani M, Itoh T, Kawasaki H. Loss of the tumor suppressor p53 gene at the liver cirrhosis stage in Japanese patients with hepatocellular carcinoma. *Oncology* 1997; **54**: 304-310
- Ashida K**, Kishimoto Y, Nakamoto K, Wada K, Shiota G, Hirooka Y, Kamisaki Y, Itoh T, Kawasaki H. Loss of heterozygosity of the retinoblastoma gene in liver cirrhosis accompanying hepatocellular carcinoma. *J Cancer Res Clin Oncol* 1997; **123**: 489-495
- Lu JP**, Mao JQ, Li MS, LU SL, Hu XQ, Zhu SN, Nomura S. *In situ* detection of TGF betas, TGF beta receptor II mRNA and telomerase activity in rat cholangiocarcinogenesis. *World J Gastroenterol* 2003; **9**: 590-594
- Ryan KM**, Phillips AC, Vousden KH. Regulation and function of the p53 tumor suppressor protein. *Curr Opin Cell Biol* 2001; **13**: 332-337
- Miller DP**, Liu G, De Vivo I, Lynch TJ, Wain JC, Su L, Christiani DC. Combinations of the variant genotypes of GSTP1, GSTM1, and p53 are associated with an increased lung cancer risk. *Cancer Res* 2002; **62**: 2819-2823
- Campling B**, El-Deiry W. Clinical Implication of p53 Mutation in Lung Cancer. *Mol Biotechnol* 2003; **24**: 141-156
- Vousden KH**. p53: death star. *Cell* 2000; **103**: 691-694
- Wilson DR**. Viral-mediated gene transfer for cancer treatment. *Curr Pharm Biotechnol* 2002; **3**: 151-164
- Vousden KH**. Switching from life to death: The Miz-ing link between Myc and p53. *Cancer Cell* 2002; **2**: 351-352
- Vousden KH**. Activation of the p53 tumor suppressor protein. *Biochim Biophys Acta* 2002; **1602**: 47-59
- Harris CC**. p53: at the crossroads of molecular carcinogenesis and risk assessment. *Science* 1993; **262**: 1980-1981
- Livingstone LR**, White A, Sprouse J, Livanos E, Jacks T, Tlsty TD. Altered cell cycle arrest and gene amplification potential accompany loss of wild-type p53. *Cell* 1992; **70**: 923-935
- Fearon ER**, Vogelstein B. A genetic model for colorectal tumorigenesis. *Cell* 1990; **61**: 759-767
- Oda T**, Tsuda H, Scarpa A, Sakamoto M, Hirohashi S. p53 gene mutation spectrum in hepatocellular carcinoma. *Cancer Res* 1992; **52**: 6358-6364
- Sugioka Y**, Fujii-Kuriyama Y, Kitagawa T, Muramatsu M. Changes in polypeptide pattern of rat liver cells during chemical hepatocarcinogenesis. *Cancer Res* 1985; **45**: 365-378
- Bonner RF**, Emmert-Buck M, Cole K, Pohida T, Chuaqui R, Goldstein S, Liotta LA. Laser capture microdissection: molecular analysis of tissue. *Science* 1997; **278**: 1481-1483
- Fu Y**, Deng WG, Li YL, Sugiyama T. Quantitative analysis of p53 and related genes mRNA in rat hepatocarcinogenesis induced by 3' -Me-DAB. *Ai Zheng* 2003; **22**: 35-41
- Wittwer CT**, Ririe KM, Andrew RV, David DA, Gundry RA, Balis, UJ. The LightCycler: a microvolume multisample fluorimeter with rapid temperature control. *Biotechniques* 1997; **22**: 176-181
- Lehman TA**, Haffty BG, Carbone CJ, Bishop LR, Gumbs AA, Krishnan S, Shields PG, Modali R, Turner BC. Elevated frequency and functional activity of a specific germ-line p53 intron mutation in familial breast cancer. *Cancer Res* 2000; **60**: 1062-1069
- Fukuda I**, Ogawa K. Alternatively-spliced p53 mRNA in the FAA-HTC1 rat hepatoma cell line without the splice site mutations. *Cell Struct Funct* 1992; **17**: 427-432
- Ohgaki H**, Hard GC, Hirota N, Maekawa A, Takahashi M, Kleihues P. Selective mutation of codons 204 and 213 of the p53 gene in rat tumors induced by alkylating N-nitroso compounds. *Cancer Res* 1992; **52**: 2995-2998
- Weghorst CM**, Buzard GS, Calvert RJ, Hulla JE, Rice JM. Cloning and sequence of a processed p53 pseudogene from rat: a potential source of false 'mutations' in PCR fragments of tumor DNA. *Gene* 1995; **166**: 317-322
- Lin Y**, Chan SH. Cloning and characterization of two processed p53 pseudogenes from the rat genome. *Gene* 1995; **156**: 183-189
- Hulla JE**, Schneider RP. Structure of the rat p53 tumor suppressor gene. *Nucleic Acids Res* 1993; **21**: 713-717
- Masui T**, Nakanishi H, Inada K, Imai T, Mizoguchi Y, Yada H, Futakuchi M, Shirai T, Tatematsu M. Highly metastatic hepatocellular carcinomas induced in male F344 rats treated with N-nitrosomorpholine in combination with other hepatocarcinogens show a high incidence of p53 gene mutations along with altered mRNA expression of tumor-related genes. *Cancer Lett* 1997; **112**: 33-45
- Bressac B**, Kew M, Wands J, Ozturk M. Selective G to T mutations of p53 gene in hepatocellular carcinoma from southern Africa. *Nature* 1991; **350**: 429-431
- Volkman M**, Hofmann WJ, Muller M, Rath U, Otto G, Zentgraf H, Galle PR. p53 overexpression is frequent in European hepatocellular carcinoma and largely independent of the codon 249 hot spot mutation. *Oncogene* 1994; **9**: 195-204
- Vancutsem PM**, Lazarus P, Williams GM. Frequent and specific mutations of the rat p53 gene in hepatocarcinomas induced by tamoxifen. *Cancer Res* 1994; **54**: 3864-3867

- 31 **Liu YP**, Lin Y, Ng ML. Immunochemical and genetic analysis of the p53 gene in liver preneoplastic nodules from aflatoxin-induced rats in one year. *Ann Acad Med Singapore* 1996; **25**: 31-36
- 32 **Haas MJ**, Pitot HC. Characterization of rare p53 mutants from carcinogen-treated albumin-simian virus 40 T-antigen transgenic rats. *Mol Carcinog* 1998; **21**: 128-134
- 33 **Vousden KH**, Lu X. Live or let die: the cell's response to p53. *Nat Rev Cancer* 2002; **2**: 594-604
- 34 **Vogelstein B**, Lane D, Levine AJ. Surfing the p53 network. *Nature* 2000; **408**: 307-310
- 35 **Hollstein M**, Sidransky D, Vogelstein B, Harris CC. p53 mutations in human cancers. *Science* 1991; **253**: 49-53
- 36 **Tam AS**, Foley JF, Devereux TR, Maronpot RR, Massey TE. High frequency and heterogeneous distribution of p53 mutations in aflatoxin B1-induced mouse lung tumors. *Cancer Res* 1999; **59**:3634-3640
- 37 **Denissenko MF**, Koudriakova TB, Smith L, O'Connor TR, Riggs AC, Pfeifer GP. The p53 codon 249 mutational hotspot in hepatocellular carcinoma is not related to selective formation or persistence of aflatoxin B1 adducts. *Oncogene* 1998; **17**: 3007-3014
- 38 **Hulla JE**, Chen ZY, Eaton DL. Aflatoxin B1-induced rat hepatic hyperplastic nodules do not exhibit a site-specific mutation within the p53 gene. *Cancer Res* 1993; **53**: 9-11
- 39 **Hsu IC**, Metcalf RA, Sun T, Welsh JA, Wang NJ, Harris CC. Mutational hotspot in the p53 gene in human hepatocellular carcinomas. *Nature* 1991; **350**: 427-428
- 40 **Makino H**, Ishizaka Y, Tsujimoto A, Nakamura T, Onda M, Sugimura T, Nagao M. Rat p53 gene mutations in primary zymbal gland tumors induced by 2-Amino-3-methylimidazo [4,5-f] quinoline, a food mutagen. *Proc Natl Acad Sci U S A* 1992; **89**: 4850-4854
- 41 **Cho Y**, Gorina S, Jeffrey PD, Pavletich NP. Crystal structure of a p53 tumor suppressor-DNA complex: understanding tumorigenic mutations. *Science* 1994; **265**: 346-355
- 42 **Oren M**, Maltzman W, Levine AJ. Post-translational regulation of the 54K cellular tumor antigen in normal and transformed cells. *Mol Cell Biol* 1981; **1**: 101-110
- 43 **Sturzbecher HW**, Chumakov P, Welch WJ, Jenkins JR. Mutant p53 proteins bind hsp 72/73 cellular heat shock-related proteins in SV40-transformed monkey cells. *Oncogene* 1987; **1**: 201-211
- 44 **Milner J**, Medcalf EA. Cotranslation of activated mutant p53 with wild type drives the wild-type p53 protein into the mutant conformation. *Cell* 1991; **65**: 765-774
- 45 **Michalovitz D**, Halevy O, Oren M. p53 mutations: Gains or losses? *J Cell Biochem* 1991; **45**: 22-29
- 46 **Hsu HC**, Tseng HJ, Lai PL, Lee PH, Peng SY. Expression of p53 gene in 184 unifocal hepatocellular carcinomas: association with tumor growth and invasiveness. *Cancer Res* 1993; **53**: 4691-4694
- 47 **Ng IO**, Srivastava G, Chung LP, Tsang SW, Ng MM. Overexpression and point mutations of p53 tumor suppressor gene in hepatocellular carcinomas in Hong Kong Chinese people. *Cancer* 1994; **74**: 30-37
- 48 **Mosner J**, Mummenbrauer T, Bauer C, Sczakiel G, Grosse F, Deppert W. Negative feedback regulation of wild-type p53 biosynthesis. *EMBO J* 1995; **14**: 4442-4449
- 49 **Ono K**, Tanaka T, Tsunoda T, Kitahara O, Kihara C, Okamoto A, Ochiai K, Takagi T, Nakamura Y. Identification by cDNA microarray of genes involved in ovarian carcinogenesis. *Cancer Res* 2000; **60**: 5007-5011

Edited by Zhu LH and Wang XL

Superantigen-SEA gene modified tumor vaccine for hepatocellular carcinoma: An *in vitro* study

Shao-Ying Lu, Yan-Fang Sui, Zeng-Shan Li, Jing Ye, Hai-Long Dong, Ping Qu, Xiu-Min Zhang, Wen-Yong Wang, Yu-Song Li

Shao-Ying Lu, Yan-Fang Sui, Zeng-Shan Li, Jing-Ye, Hai-Long Dong, Ping-Qu, Xiu-Min Zhang, Wen-Yong Wang, Yu-Song Li, Department of Pathology, Fourth Military Medical University, Xi'an 710032, Shaanxi Province, China

Shao-Ying Lu, Ph.D. Candidate of Xi'an Jiaotong University
Supported by National Natural Science Foundation of China, No. 30271474 and No. 39770827

Correspondence to: Professor Yan-Fang Sui, Department of Pathology, Fourth Military Medical University, Xi'an 710032, China. suiyanf@fmmu.edu.cn

Telephone: +86-29-3374541-211 **Fax:** +86-29-3374597

Received: 2003-05-13 **Accepted:** 2003-06-12

Abstract

AIM: To construct an eukaryotic superantigen gene expression vector containing the recombinant gene of SEA and CD80 molecule transmembrane region (CD80TM), and to express staphylococcus enterotoxin A (SEA) on the membrane of hepatocellular carcinoma (HCC) cell to form a superantigen gene modified tumor vaccine for HCC.

METHODS: SEA and linker-CD80TM gene were amplified through PCR from plasmid containing cDNA of SEA and CD80. Gene fragments were then subcloned into the multiple cloning sites of retroviral vector pLXSN. Recombinant plasmid was transferred into HepG2 cells mediated with lipofectamine, positive clones were selected in culture medium containing G418. RT-PCR and indirect immunofluorescence studies confirmed that SEA was expressed specifically on HCC cell membrane. INF- γ -ELISPOT study demonstrated that SEA protein was expressed on the membrane of HCC cells. Cytotoxicity of HepG2-SEA primed CTLs (SEA-T) was analyzed by ^{51}Cr release assay. T cells cultured with rhIL-2 (IL-2-T) were used as control.

RESULTS: Restriction digestion and sequence analyses confirmed the correctness of length, position and orientation of inserted fusion genes. SEA was expressed on the surface of HepG2 cells, HepG2-SEA had strong stimulating effect on production of HepG2 specific CTL ($P < 0.001$). SEA-T had enhanced cytotoxicity to HepG2 cells ($P < 0.05$).

CONCLUSION: Tumor cell membrane expressed superantigen can be used to reinforce the immune effect of tumor cell vaccine for HCC, which provides a new method of the enhanced active immunotherapy for HCC.

Lu SY, Sui YF, Li ZS, Ye J, Dong HL, Qu P, Zhang XM, Wang WY, Li YS. Superantigen-SEA gene modified tumor vaccine for hepatocellular carcinoma: An *in vitro* study. *World J Gastroenterol* 2004; 10(1): 53-57

<http://www.wjgnet.com/1007-9327/10/53.asp>

INTRODUCTION

Autologous and allogeneic tumor cells have been used as tumor

vaccines in clinic for a long time^[1,2]. The tumor cell-based vaccines possess the entire relevant tumor antigens recognized by the immune system and can be produced even without knowing the gene sequence of specific antigens. To identify the tumor specific antigen is time consuming, only few tumor specific antigens have been identified until now. But tumor cell-based immunization could not always elicit anti-tumor responses in sufficient magnitude to cause regression of established tumors due to scarcity of stimulatory surface molecules such as MHC-I, MHC-II or CD80^[3].

Superantigens are a family of bacterial and viral proteins that bind to MHC class II molecules as unprocessed proteins and activate a large number of T cells bearing T cell receptor variable region beta chain (TCR V β)^[4,5]. These T cells proliferate, and secrete cytokines (e.g. IFN- γ , TNF- α , IL-2, and IL-12), induce strong cytolytic activity, and mediate tumor regression^[6-12]. SEA is an important member of superantigen family. Anchoring SEA onto MHC-II negative tumor cells through monoclonal antibody has been demonstrated to direct T cell-mediated cytotoxicity against these tumors^[13,14]. Other studies suggested that artificially anchoring a recombinant superantigen-transmembrane region chimera (SAG-TM) onto a tumor cell surface could substitute for the effect of MHC-II presentation^[15].

In the present study we sought to construct an eukaryotic expression vector containing recombinant gene of SEA and transmembrane region sequence of CD80 molecule (CD80TM). Recombinant gene was transfected into HCC cells, chimera protein (SEA-CD80TM) was expressed on the membrane of living cells. SEA gene modified cells were irradiated and used as a superantigen enhanced tumor cell-based vaccine for HCC, which was capable of inducing antitumor immunity *in vitro*.

MATERIALS AND METHODS

Reagents

EX Taq DNA polymerase, T4 DNA ligation kit Ver.2.0, and restriction endonuclease were obtained from TakaRa Biotechnology (Dalian). DNA isolation and purification kit was purchased from Shanghai ShunHua Biotechnology. LipofectamineTM 2000 were from Invitrogen. IPTG, X-gal, DNA maker and FITC labeled sheep anti mouse IgG were from Sino-American Biotechnology. Dulbecco's modified Eagle media, Trizol and G418 were from GibcoBRL. Access RT-PCR system was from Promega. Human INF- γ ELISPOT assay kit was from Diaclone, Recombinant human interleukin-2 (rhIL-2) and BD TriTESTTM antibody CD4 FITC/ CD8 PE/ CD3 PerCP were from BD Biosciences. Mouse anti-SEA monoclonal antibody was provided by the Department of Immunology, Fourth Military Medical University, P. R. China.

Plasmids

PBluescript II KS (+) plasmids containing cDNA of SEA and CD80 were constructed by Li *et al*^[16]. Retroviral vector pLXSN was preserved in our laboratory.

Cell culture

Human HCC cell lines HepG2 and SMMC-7721 were cultured

in DMEM containing 10% heat-inactivated fetal calf serum, 100 units/ml penicillin, 100 µg/ml streptomycin, 0.292 mg/ml glutamine. The cell lines were incubated in a humidified 5% CO₂ incubator at 37 °C.

Polymerase chain reaction (PCR) and vector construction

The primers used for cloning SEA (774 bp) and CD80TM (147 bp) were as follows. SEA, forward: GCGAATTCGCATGAAAAAACAGCATTAC, reverse: CGGGATCCACTGTATATAAATATATATCAAT. CD80TM, forward1: GGTGGCTCTGGCGGTGGCGGATCGGATAACCTGCTCCCATCC, forward2: CGGGATCCGGTGGAGGCGGTTTCAGGCGGAGGTGGCTCTGGCGGT, reverse: CCGCTCGAGTTATACAGGGCGTACT. Linker (GGGSGGGSGGGSGGG) was introduced into the upstream of CD80TM using two forward primers. PCR was performed in a 50 µl reaction system consisting of 1 µM each primer, 200 µM each dNTP, 5 µL 10×polymerase reaction buffer, and 1.25U EX Taq DNA polymerase with 1 µL SEA or CD80 gene vector. Samples were heated to 94 °C for 5 min followed by 30 cycles at 94 °C for 30 s, at 50 °C for 50 s, and at 68 °C for 1 min. The final extension was done at 72 °C for 7 min. Then 10 µl of each PCR product was electrophoresed on 1 % agarose gel containing 0.5 µg/mL EB, and PCR products were then purified from agarose gel according to the protocol of DNA purification kit. DNA fragments of SEA (S) and linker-CD80TM (LC) were subcloned into pBluescript II ks(+). The positive clones were selected from the transfected DH5α by the method described by Sambrook *et al*^[17]. The constructed plasmids (designated as ks-S, ks-LC) were identified by restriction enzyme analysis. DNA sequences were verified in DNA sequencing core facility in Bioasia Biotechnology (Shanghai, China). Gene fragments were cut with *EcoRI-BamHI*, *BamHI-XhoI*, and inserted into the *EcoRI-XhoI* site of pLXSN to construct SAg gene expression vector pLXSN-SLC. The recombinant gene was verified by digestion with restriction endonuclease (Figure 1).

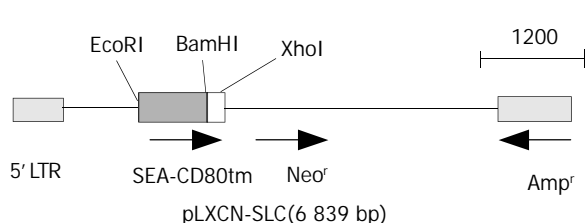


Figure 1 Gene map of expression vector.

In vitro transfection of pLXSN-SLC

pLXSN-SLC was transfected into HepG2 cells using Lipofectamine™ 2000 reagent according to the manufacturer's instructions. Briefly, 2×10⁵ HepG2 cells were seeded into 12-well culture plates and cultured for 18 hours until 90% to 95% confluence of the cells, transfection was performed with 1 µg of DNA per dish. Forty eight h after transfection, cells were passaged at 1:4 dilution into a fresh medium. The next day, G418 400 µg/mL was added into culture medium for the screening of stably transfected cells. The cells were then grown in G418 culture medium for 4 weeks and cloned by limiting dilution. Mock cell line transfected with empty pLXSN vector was selected in G418, and used as control (HepG2-pLXSN).

Detection of SEA expression in transfected cells

Expression of SEA in screened monoclonal cells was detected by RT-PCR. Total RNA was extracted from the tumor cells (HepG2 cells and SEA gene transfected or mock transfected HepG2 cells) using Trizol reagent. RNA (1.5 µg) was used to

synthesize cDNA in 20 µl reaction mixtures following standard protocol of Access RT-PCR system. PCR was carried out with 5 µl of RT products in 50 µl PCR reaction buffer containing *Tfi* polymerase, 1 mM MgCl₂, annealing temperature was 50 °C. SEA cDNA was used as positive control in PCR. Indirect immunofluorescence was performed to locate the expressed SEA. Briefly, 2×10⁵ SEA transfected HepG2 cells (HepG2-SEA) were plated into 12-well culture plates. At the bottom of each well a sterilized coverslip was placed in advance. HepG2 cells were plated as control. When the plated cells were 95-100% confluence, the coverslips were washed twice in cold PBS (0.01M) and fixed with 4% paraformaldehyde for 30 min at room temperature. Cells were stained following the standard protocol of indirect immunofluorescence. First antibody was 1:100 diluted mouse anti-SEA monoclonal antibody in PBS, irrelevant sheep anti-mouse IgG was used as control. Second antibody was 1:500 diluted FITC labeled sheep anti-mouse IgG in 0.1% Evans blue. Coverslips were then mounted directly onto a glass slide with a tiny drop of 50% glycerol in PBS (9.1 mM Na₂HPO₄/1.7 mM NaH₂PO₄/50 mM NaCl, pH 7.4). Fluorescent images were captured at 490 nm using a Nikon Eclipse E1000 microscope attached to a MicroMax camera (Princeton Instruments, Trenton, NJ).

Preparation of T cell lines

Human peripheral blood mononuclear cells (PBMC) were isolated from healthy volunteers by routine density centrifugation, and stimulated with HepG2-SEA to establish SEA-reactive T-cell line (SEA-T). The T cell line was stimulated repeatedly by exposure to irradiated (4 000 rad) HepG2-SEA and rhIL-2 (200 U/mL) in complete medium for 2 weeks, and then stored in frozen. These cells were thawed 1 week before use. T-cell lines stimulated by HepG2-pLXSN (pLXSN-T), HepG2 (HepG2-T) or just maintained with rhIL-2 (IL-2-T) were also prepared and used as control. Cell phenotypes of T cell lines were analyzed using BD TriTEST™ antibody by FACS.

Elispot assay

PVDF 96-well plates were incubated with 100 µl of 70% ethanol for 10 min at room temperature, and washed three times in 100 µl of PBS. Capture antibody was added and incubated at 4 °C overnight. After washed in 100 µl of PBS, each well was added 100 µl of 2% skimmed dry milk in PBS, and incubated for 2 hours at room temperature. Wells were emptied and tapped on absorbent paper, 5×10⁴ effector cells (including SEA-T, pLXSN-T, HepG2-T, IL-2-T) and 1×10⁴ target cells (irradiated HepG2) were seeded to each well and incubated for 20 h in RPMI-1640 medium without IL-2 and serum. Plates were then washed and incubated with detection antibody in PBS-1% BSA for 1 hour and 30 min at 37 °C, and with streptavidin-alkaline phosphatase for 1 h at 37 °C. After washed, substrate (5-bromo-4-chloro-3-indolyl phosphate/nitroblue tetrazolium) was added and incubated for 5-20 min. After the final washing, dark-violet spots on plate membranes were counted under microscope.

Cytotoxicity of HepG2-SEA stimulated T cell line

Cytotoxicity was measured in a standard 4-hour ⁵¹Cr-release assay and expressed in formula: (%) specific lysis = 100 × (experimental - background cpm / maximal background cpm). Target cells (HepG2, SMMC-7721) were labeled for 2 hours with Na₂⁵¹CrO₄ (⁵¹Cr, New England Nuclear, Boston, MA), 250 µCi/1×10⁶ cells. The cells were then washed twice and 5×10³ cells per well were seeded in triplicate in v-bottomed microtiter plates. Effector cells (SEA-T, HepG2-T and IL-2-T) were added at an effector-to-target (E:T) cell ratio of 40:1, 25:1, 10:1, 5:1 and 3:1, respectively. The plates were incubated

at 37 °C and 5% CO₂ for 4 h, supernatants were collected, and the released ⁵¹Cr was measured with a gamma counter (LKB-Wallac 1 282; Stockholm, Sweden). Spontaneous release was estimated by incubation of target cells in medium alone, and maximum release by resuspending the wells with 0.1% Tween 20. Spontaneous release was typically less than 30% of maximum release.

Statistical analysis

All experiments were performed in triplicate, data were presented as the mean ± SD and analyzed using Student's *t* test.

RESULTS

Insertion of SEA and linker-CD80TM into MCS of pLXSN

PCR products were subcloned into a pBluescript II ks (+) vector. DNA sequencing confirmed the correct sequence of both fragments. SEA gene was cloned into the *EcoR* I/*Xho* I site of pLXSN with linker-CD80TM. Recombinant gene SEA-linker-CD80TM was 1.0 kb with *EcoR* I and *Xho* I restriction site on each side, the size of pLXSN was 5.9 kb. Expressing vector pLXSN-SLC was digested by *EcoR* I/*Xho* I, 1.0 kb and 5.9 kb DNA fragments were appeared as expected (Figure 2).

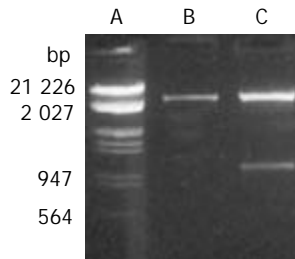


Figure 2 Enzyme digestion analysis of expression vector. A. Lambda DNA (*EcoR*I, *Hind*III); B. pLXSN (*EcoR*I, *xho*I); C. pLXSN-SLC (*EcoR*I, *xho*I).

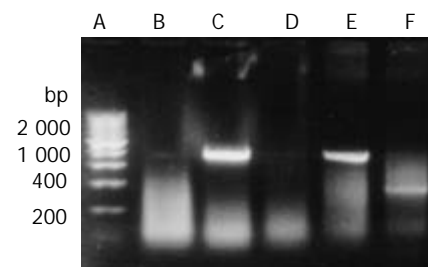


Figure 3 RT-PCR detected the transcription of SEA gene. A. 200 bp DNA marker; B. HepG2; C. HepG2 transfected with pLXSN-SLC; D. HepG2 transfected with pLXSN; E. Positive control; F. β -actin (RNA of C).

SEA expressed on the membrane of HepG2

HepG2 was transfected with plasmid pLXSN-SLC and empty pLXSN vector, respectively. The expression of SEA was detected in HepG2 cells transfected with pLXSN-SLC only by RT-PCR (Figure 3). Indirect immunofluorescence test confirmed that most of the expressed SEA appeared to be located on the HepG2 cells membrane (Figure 4). SEA expression was detected in 5-10 percent of cells screened with G418. Irradiated HepG2-SEA cells were used as T cell stimulator in following experiments.

Increased HepG2 reactive T cells with HepG2-SEA

Interferon- γ (IFN- γ) ELISPOT assay was used to detect the

specificity of HepG2 CD8⁺ T cells quantitatively. Cells tested included unstimulated PBMC (IL-2-T) and polyclonal T-lymphocyte lines stimulated by HepG2-SEA, HepG2-pLXSN or HepG2. After a short term of culture *in vitro*, the percentage of positive cells was more than 90% for CD3⁺, 80% to 90% for CD8⁺, and 5% to 10% for CD4⁺ (Figure 5). The number of HepG2 reactive CTL in the SEA-T cell line was much higher than that of HepG2-T (155.67±7.22 vs 38.03±8.18, *t*=18.67, *P*<0.0001), pLXSN-T (39.50±6.26, *t*=21.06, *P*<0.0001) or IL-2-T (32.00±4.26, *t*=25.56, *P*<0.0001) (Figure 6). Both the size and density of spots in SEA-T group were greater than those of controls (data not shown). The difference of spot number between HepG2-T and IL-2-T cell lines was not significant (*t*=-1.13, *P*=0.321).

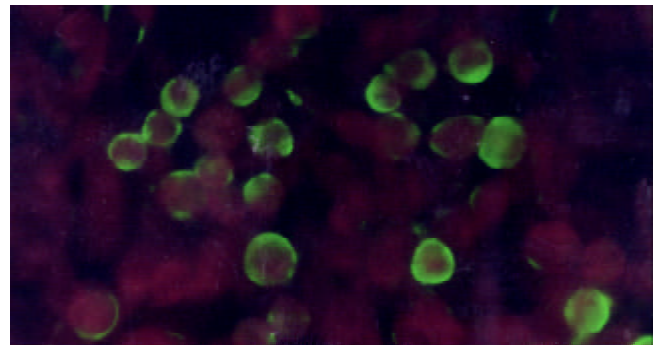


Figure 4 SEA expressed on the membrane of HepG2 (indirect immunofluorescence). HepG2-SEA cells were stained according to the standard protocol of indirect immunofluorescence. First antibody is mouse anti-SEA IgG and second antibody is FITC labeled sheep anti-mouse IgG diluted in 0.1% evan blue. Positive signal is green while the background is red. SEA was located on the membrane of HepG2. Untransfected HepG2 cells did not express SEA (data not show).

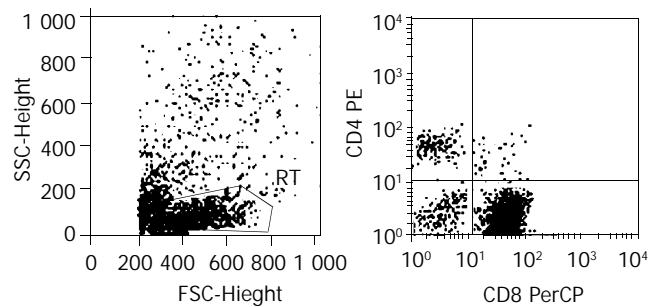


Figure 5 Lymphocyte phenotype analysis. 1×10^5 SEA-T cells were stained with BD TriTEST™ antibody CD4 FITC/CD8 PE/CD3 PerCP, and assayed by FACS. CD3⁺90.75%, CD8⁺84.46%, CD4⁺6.29%.

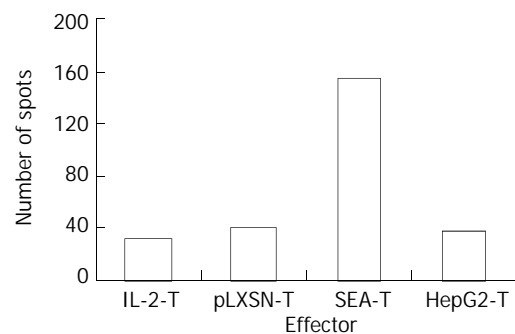


Figure 6 HepG2-SEA increased the number of hepG2 specific CTL in T lymphocyte line. Each bar represents average of spots in triplicate wells.

Enhanced cytotoxicity elicited by membrane expressed SEA

Cytotoxicity of the SEA-T effector cell line against HepG2, and SMMC-7721 target cells was measured (Figure 7). HepG2-T and IL-2-T cells were used as control. In contrast, SEA-T was highly efficient in directing specific lysis of HepG2 cells when compared with HepG2-T ($51.55 \pm 5.051\%$ vs 33.16 ± 4.54 , $t=4.47$, $P=0.011$). The two T cell lines had effective cytotoxicity to SMMC-7721 cells.

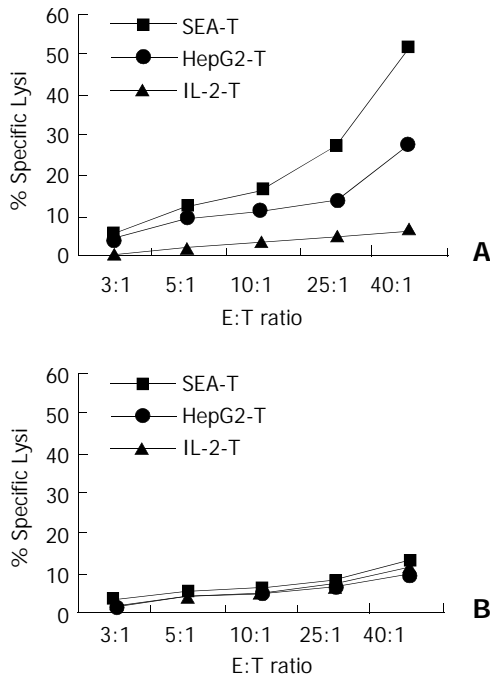


Figure 7 Membrane expressed SEA enhanced specific lysis on autologous tumor cells. Cytotoxicity was measured in a standard 4-hour ^{51}Cr -release assay. Target cells (HepG2, SMMC-7721) were seeded in triplicate in v-bottomed microtiter plates at a concentration of 5×10^3 cells per well. Effector cells were added at an effector-to-target (E:T) cell ratio of 40:1, 25:1, 10:1, 5:1 and 3:1 respectively. A: SEA-T was highly efficient in directing specific lysis of HepG2 cells (squares), HepG2-T has moderate cytotoxicity on HepG2 (cross) cells ($P < 0.001$). B: None of T cell line has killing effect on SMMC-7721 cells.

DISCUSSION

T cells have been found to possess various potent antitumor effects through releasing cytotoxic effector molecules such as perforin or growth-suppressive cytokines IFN- γ and TNF- α ^[18-21]. However, the frequency of tumor-specific T cells could be generally too low and insufficient to interfere with progressive tumor growth. The goal of this experiment was to examine the possibility of developing a new experimental vaccine from irradiated HepG2 cells that were transfected to express superantigen-SEA on membrane (designed as HepG2-SEA) to augment cellular and humoral anti-tumor immune responses. Superantigen is the most effective T cell activator. Upon stimulation by superantigens, naïve T cells could respond and then become quickly anergized and/or deleted, while mature T cells could not become anergized^[22-24]. Characteristics of superantigens can thus be exploited to enhance specific antigen responses. Because superantigens can cause anergy and/or deletion of potentially competing naïve T cells bearing the same V β element (s), thus there is less “competition” for cytokines and the desired specific immune response can be amplified.

HCC cells do not induce an effective immunological rejection process because of their weak antigenicity, the abnormal expression of MHC molecules as well as the

deletion or deficiency of costimulatory molecules. In the present study, the expressed superantigen-SEA on the membrane of HepG2 cells was confirmed by RT-PCR and indirect immunofluorescence assays. When HepG2-SEA cells were used as a vaccine, two stimulating signals would be present to T cells simultaneously, one was SEA, the other was tumor-associated antigens expressed on the surface of HepG2 cells, which facilitated the occurrence of specific anti-tumor immune reaction.

IFN- γ ELISPOT (enzyme-linked immunospot) assay was used for the quantitative detection of HepG2-specific CD8⁺ T cells. This technique could detect T cells that secrete a given cytokine (e.g., IFN- γ) in response to an antigenic stimulation^[25]. The size and density of spots represented the quantity of IFN- γ secreted by single CTL^[18]. The results showed that the number of HepG2 cell specific CTLs in repeatedly stimulated T cell line (SEA-T) with new vaccines was significantly increased than that of HepG2 cell-based vaccines ($P < 0.001$). Cytotoxic assay demonstrated that SEA-T was highly efficient in directing specific lysis of HepG2 cells other than SMMC-7721 cells. When compared with HepG2-T, the difference induced by new vaccines had statistical significance ($P = 0.011$). So we conclude that tumor cell membrane expressed SEA can stimulate the proliferation of tumor specific CTL and enhance the specific lysis on autologous tumor cells.

This superantigen modified tumor cell-based vaccine has an advantage over ordinary tumor cell-based vaccines in three aspects. First, this vaccine could make up for the disadvantage of low-level expression of class II MHC molecule on the surface of most tumor cells^[26]. It has been found that T cell activation by SEA superantigen could occur in the absence or presence of MHC class II^[14,27-29], and artificially anchoring a superantigen onto a cell surface through transmembrane protein could substitute for MHC-II presentation^[15]. Second, although most immunotherapeutic strategies have focused on activating tumor-specific CD8⁺ T cells, optimal antitumor activity could be achieved if both CD4⁺ and CD8⁺ tumor specific T cells were induced^[30,31]. Likewise, if tumor immunity plays a role in limiting the recurrence of primary tumor or the future onset of metastatic diseases, then CD4⁺ and CD8⁺ immunological memory should be optimized. Both CD4⁺ and CD8⁺ T cells can be activated by bacterial superantigens. Third, superantigens could preferentially direct cytotoxicity against MHC-II-positive cells^[32-34], *in vivo* administration of intact superantigens in sufficiently therapeutic amount could produce unwanted cytotoxicity to normal cells. Anchoring of superantigen and other TM fusion proteins on the surface of tumor cells would offer a novel strategy for the use of superantigens as immunostimulatory molecules. This method can confine the effect of SEA within the tumor, thus decreasing the side effects of treatment.

As presented above, irradiated HepG2-SEA cells could be used as an effective tumor cell-based vaccine *in vitro*. The superantigen enhanced vaccine is superior to tumor cell alone on the prime of tumor cell specific T cells, which provides a new strategy for the addition of superantigen as immunostimulatory molecules in tumor therapy. *In vivo* studies are currently under way to evaluate the effectiveness of these superantigen based vaccines for cancer therapy.

REFERENCES

- 1 Teshima T, Mach N, Hill GR, Pan L, Gillesen S, Dranoff G, Ferrara JL. Tumor cell vaccine elicits potent antitumor immunity after allogeneic T-cell-depleted bone marrow transplantation. *Cancer Res* 2001; **61**: 162-171
- 2 Nelson WG, Simons JW, Mikhak B, Chang JF, DeMarzo AM, Carducci MA, Kim M, Weber CE, Baccala AA, Goeman MA, Clift

- SM, Ando DG, Levitsky HI, Cohen LK, Sanda MG, Mulligan RC, Partin AW, Carter HB, Piantadosi S, Marshall FF. Cancer cells engineered to secrete granulocyte-macrophage colony-stimulating factor using *ex vivo* gene transfer as vaccines for the treatment of genitourinary malignancies. *Cancer Chemother Pharmacol* 2000; **46**(Suppl): S67-S72
- 3 **Antonia SJ**, Seigne J, Diaz J, Muro-Cacho C, Extermann M, Farmelo MJ, Friberg M, Alsarraj M, Mahany JJ, Pow-Sang J, Cantor A, Janssen W. Phase I trial of a B7-1 (CD80) gene modified autologous tumor cell vaccine in combination with systemic interleukin-2 in patients with metastatic renal cell carcinoma. *J Urol* 2002; **167**: 1995-2000
 - 4 **Marrack P**, Kappler J. The staphylococcal enterotoxins and their relatives. *Science* 1990; **248**: 705-711
 - 5 **Fraser JD**. High-affinity binding of staphylococcal enterotoxins A and B to HLA-DR. *Nature* 1989; **339**: 221-223
 - 6 **Kotzin BL**, Leung DY, Kappler J, Marrack P. Superantigens and their potential role in human disease. *Adv Immunol* 1993; **54**: 99-166
 - 7 **Leung DY**, Gately M, Trumble A, Ferguson-Darnell B, Schlievert PM, Picker LJ. Bacterial superantigens induce T cell expression of the skin-selective homing receptor, the cutaneous lymphocyte-associated antigen, via stimulation of interleukin 12 production. *J Exp Med* 1995; **181**: 747-753
 - 8 **Sriskandan S**, Evans TJ, Cohen J. Bacterial superantigen-induced human lymphocyte responses are nitric oxide dependent and mediated by IL-12 and IFN- γ . *J Immunol* 1996; **156**: 2430-2435
 - 9 **Lando PA**, Hedlund G, Dohlsten M, Kalland T. Bacterial superantigens as anti-tumour agents: induction of tumour cytotoxicity in human lymphocytes by staphylococcal enterotoxin A. *Cancer Immunol Immunother* 1991; **33**: 231-237
 - 10 **Ochi A**, Migita K, Xu J, Siminovitch K. *In vivo* tumor immunotherapy by a bacterial superantigen. *J Immunol* 1993; **151**: 3180-3186
 - 11 **Dow SW**, Elmslie RE, Willson AP, Roche L, Gorman C, Potter TA. *In vivo* tumor transfection with superantigen plus cytokine genes induces tumor regression and prolongs survival in dogs with malignant melanoma. *J Clin Invest* 1998; **101**: 2406-2414
 - 12 **Shu S**, Krinock RA, Matsumura T, Sussman JJ, Fox BA, Chang AE, Terman DS. Stimulation of tumor-draining lymph node cells with superantigenic staphylococcal toxins leads to the generation of tumor-specific effector T cells. *J Immunol* 1994; **152**: 1277-1288
 - 13 **Wang Q**, Yu H, Zhang L, Ju D, Pan J, Xia D, Yao H, Zhang W, Wang J, Cao X. Adenovirus-mediated intratumoral lymphotactin gene transfer potentiates the antibody-targeted superantigen therapy of cancer. *J Mol Med* 2002; **80**: 585-594
 - 14 **Ihle J**, Holzer U, Krull F, Dohlsten M, Kalland T, Niethammer D, Dannecker GE. Antibody-targeted superantigens induce lysis of major histocompatibility complex class II-negative T-cell leukemia lines. *Cancer Res* 1995; **55**: 623-628
 - 15 **Wahlsten JL**, Mills CD, Ramakrishnan S. Antitumor response elicited by a superantigen-transmembrane sequence fusion protein anchored onto tumor cells. *J Immunol* 1998; **161**: 6761-6767
 - 16 **Li Z**, Sui Y, Jiang Y, Lei Z, Shang J, Zheng Y. Reconstruction of SEA-B7.1 double signals on human hepatocellular carcinoma cells and analysis of its immunological effect. *Biochem Biophys Res Commun* 2001; **288**: 454-461
 - 17 **Sambrook J**, Fritsch EF, Maniatis T. *Molecular Cloning: A Laboratory Manual*, 2nd ed. New York: Cold Spring Harbor Laboratory Press 1989
 - 18 **Clay TM**, Hobeika AC, Mosca PJ, Lysterly HK, Morse MA. Assays for monitoring cellular immune responses to active immunotherapy of cancer. *Clin Cancer Res* 2001; **7**: 1127-1135
 - 19 **Street SE**, Cretney E, Smyth MJ. Perforin and interferon- γ activities independently control tumor initiation, growth, and metastasis. *Blood* 2001; **97**: 192-197
 - 20 **Masson D**, Tschopp J. Isolation of a lytic, pore-forming protein (perforin) from cytolytic T-lymphocytes. *J Biol Chem* 1985; **260**: 9069
 - 21 **Merger M**, Viney JL, Borojevic R, Steele-Norwood D, Zhou P, Clark DA, Riddell R, Maric R, Podack ER, Croitoru K. Defining the roles of perforin, Fas/FasL, and tumour necrosis factor alpha in T cell induced mucosal damage in the mouse intestine. *Gut* 2002; **51**: 155-163
 - 22 **Stohl W**, Elliott JE, Lynch DH, Kiener PA. CD95 (Fas)-based, superantigen-dependent, CD4+ T cell-mediated down-regulation of human *in vitro* immunoglobulin responses. *J Immunol* 1998; **160**: 5231-5238
 - 23 **Torres BA**, Perrin GQ, Mujtaba MG, Subramaniam PS, Anderson AK, Johnson HM. Superantigen enhancement of specific immunity: antibody production and signaling pathways. *J Immunol* 2002; **169**: 2907-2914
 - 24 **Mahlknecht U**, Herter M, Hoffmann MK, Niethammer D. The toxic shock syndrome toxin-1 induces anergy in human T cells *in vivo*. *Hum Immunol* 1996; **45**: 42-45
 - 25 **Herr W**, Schneider J, Lohse AW, Meyer zum Buschenfelde KH, Wolfel T. Detection and quantification of blood-derived CD8+ T lymphocytes secreting tumor necrosis factor alpha in response to HLA-A2.1-binding melanoma and viral peptide antigens. *J Immunol Methods* 1996; **191**: 131-142
 - 26 **Baskar S**. Gene-modified tumor cells as cellular vaccine. *Cancer Immunol Immunother* 1996; **43**: 165-173
 - 27 **Gidlof C**, Dohlsten M, Lando P, Kalland T, Sundstrom C, Totterman TH. A superantigen-antibody fusion protein for t-cell immunotherapy of human B-lineage malignancies. *Blood* 1997; **89**: 2089-2097
 - 28 **Lando PA**, Dohlsten M, Hedlund G, Akerblom E, Kalland T. T cell killing of human colon carcinomas by monoclonal-antibody-targeted superantigens. *Cancer Immunol Immunother* 1993; **36**: 223-228
 - 29 **Holzer U**, Bethge W, Krull F, Ihle J, Handgretinger R, Reisfeld RA, Dohlsten M, Kalland T, Niethammer D, Dannecker GE. Superantigen-staphylococcal-enterotoxin-A-dependent and antibody-targeted lysis of GD2-positive neuroblastoma cells. *Cancer Immunol Immunother* 1995; **41**: 129-136
 - 30 **Mortara L**, Gras-Masse H, Rommens C, Venet A, Guillet JG, Bourgault-Villada I. Type 1 CD4+ T-cell help is required for induction of antipeptide multispecific cytotoxic T lymphocytes by a lipopeptidic vaccine in rhesus macaques. *J Virol* 1999; **73**: 4447-4451
 - 31 **Yu Z**, Restifo NP. Cancer vaccines: progress reveals new complexities. *J Clin Invest* 2002; **110**: 289-294
 - 32 **Torres BA**, Kominsky S, Perrin GQ, Hobeika AC, Johnson HM. Superantigens: the good, the bad, and the ugly. *Exp Biol Med* 2001; **226**: 164-176
 - 33 **Herrmann T**, Maryanski JL, Romero P, Fleischer B, MacDonald HR. Activation of MHC class I-restricted CD8+ CTL by microbial T cell mitogens. Dependence upon MHC class II expression of the target cells and V beta usage of the responder T cells. *J Immunol* 1990; **144**: 1181-1186
 - 34 **Hansson J**, Ohlsson L, Persson R, Andersson G, Ilback NG, Litton MJ, Kalland T, Dohlsten M. Genetically engineered superantigens as tolerable antitumor agents. *Proc Natl Acad Sci U S A* 1997; **94**: 2489-2494

CT-guided percutaneous ethanol injection with disposable curved needle for treatment of malignant liver neoplasms and their metastases in retroperitoneal lymph nodes

Chang-Jing Zuo, Pei-Jun Wang, Cheng-Wei Shao, Min-Jie Wang, Jian-Ming Tian, Yi Xiao, Fang-Yuan Ren, Xi-Yan Hao, Min Yuan

Chang-Jing Zuo, Pei-Jun Wang, Cheng-Wei Shao, Min-Jie Wang, Jian-Ming Tian, Yi Xiao, Fang-Yuan Ren, Xi-Yan Hao, Min Yuan, Department of Radiology, Changhai Hospital, Second Military Medical University, Shanghai 200433, China

Supported by the National Natural Science Foundation of China, No. 30070233

Correspondence to: Chang-Jing Zuo, Department of Radiology, Changhai Hospital, the Second Military Medical University, Shanghai 200433, China. baobao66@sh163.net

Telephone: +86-21-25070575

Received: 2003-05-10 **Accepted:** 2003-06-12

Abstract

AIM: To explore the feasibility of computed tomography (CT)-guided percutaneous ethanol injection (PEI) using a disposable curved needle for treatment of malignant liver neoplasms and their metastases in retroperitoneal lymph nodes.

METHODS: CT-guided PEI was conducted using a disposable curved needle in 26 malignant liver tumors smaller than 5 cm in diameter and 5 lymph node metastases of liver cancer in the retroperitoneal space. The disposable curved needle was composed of a straight trocar (21G) and stylet, a disposable curved tip (25 G) and a fine stylet. For the tumors found in deep sites and difficult to reach, or for hepatic masses inaccessible to the injection using a straight needle because of portal vein and bile ducts, the straight trocar was used at first to reach the side of the tumor. Then, the disposable curved needle was used via the trocar. When the needle reached the tumor center, appropriate amount of ethanol was injected. For relatively large malignant liver tumors, multi-point injection was carried out for a better distribution of the ethanol injected throughout the masses. The curved needle was also used for treatment of the metastasis in retroperitoneal lymph nodes blocked by blood vessels and inaccessible by the straight needle.

RESULTS: All of the 26 liver tumors received 2 or more times of successful PEI, through which ethanol was distributed throughout the whole tumor mass. Effect of the treatment was monitored by contrast-enhanced multi-phase CT and magnetic resonance imaging (MRI) examinations three months later. Of the 18 lesions whose diameters were smaller than 3 cm, the necrotic change across the whole mass and that in most areas were observed in 15 and 3 tumors, respectively. Among the 8 tumors sizing up to 5 cm, 5 were completely necrotic and 3 largely necrotic. Levels of tumor seromarkers were significantly reduced in some of the cases. In 5 patients with metastases of liver cancer in retroperitoneal lymph nodes who received 1 to 3 times of PEI, all the foci treated were completely necrotic and smaller demonstrated by dynamic contrast-enhanced CT or MRI 3 months later.

CONCLUSION: CT-guided PEI using a disposable curved needle is effective, time-saving and convenient, providing an alternative therapy for the treatment of malignant liver tumors and their retroperitoneal lymph node metastases.

Zuo CJ, Wang PJ, Shao CW, Wang MJ, Tian JM, Xiao Y, Ren FY, Hao XY, Yuan M. CT-guided percutaneous ethanol injection with disposable curved needle for treatment of malignant liver neoplasms and their metastases in retroperitoneal lymph nodes. *World J Gastroenterol* 2004; 10(1): 58-61
<http://www.wjgnet.com/1007-9327/10/58.asp>

INTRODUCTION

Percutaneous ethanol injection (PEI) is a common procedure for the treatment of malignant liver neoplasms. But in the treatment of small or deep foci with CT-guided PEI, repeated punctures are necessary for the needle tip to reach an appropriate position. This may result in prolongation of the operation time and an increase of the risk for complications. This article reported our recent experience in PEI treatment of liver tumors using a disposable curved needle.

MATERIALS AND METHODS

Clinical data

Thirty-one patients (22 males, 9 females; 37 to 72 years old, mean 48.9 years) were included in this study. Of them, 19 had primary liver cancer and 7 had metastatic liver tumors, including a single focus in 15 patients and multiple foci (\geq two tumors) in 11 patients. Twenty-six foci in 26 patients were treated by PEI using a disposable curved needle, including 18 smaller than 3 cm in diameter and 8 sizing from 3 cm to 5 cm. Metastases in retroperitoneal lymph nodes were found in 5 patients, with a single node involved in 3, 2 nodes in one and 3 nodes in the other. All of the five patients received PEI treatment, one lesion for each. Every patient was informed of possible complications and the consent was obtained before operation. The procedure was approved by the Ethics Commission of the hospital.

Instruments

PQ 5000 V helical CT machine (Picker International INC, Cleveland, Ohio, USA) was used to guide the puncture. The disposable curved needle set (DCHNS, COOK, Bloomington, USA) is composed of a tip (25 G), a fine stylet, a straight trocar (21 G) and a trocar stylet. Volume Zoom multi-slice helical CT scanner (Siemens AG, Forchheim, Germany) and Symphony 1.5T MRI machine (Siemens AG, Munchen, Germany) were used to evaluate the post-operative lesions.

Procedures

The location, morphology and size of the focus were determined by enhanced CT or MRI. Prothrombin time, blood

routine, liver function and tumor markers were evaluated. The patients were fasted for four hours and notified of precautions before the procedure. Sedatives were administered for patients with mental stress.

An appropriate posture was selected and the skin surface was marked. The focal area was scanned by 5-10 mm thickness to determine the optimal puncture point, angle and depth. Local sterilization, draping and local anesthesia with 2% lidocaine were conducted. The patients were advised to hold breath at rest, when the needle was inserted into the focus according to the preplanned angle. The needle was adjusted under CT guidance in case of any deviation. The disposable curved needle was used in the following cases: 1) foci too small in size or too deep in location for the straight needle, 2) the way to the tumor center blocked by the portal vessel or bile duct, 3) large foci with multiple-site injections of ethanol by one puncture. When the straight trocar of the disposable curved needle reached the proximity of the tumor, stylet was withdrawn and the 25 G curved needle was inserted. The needle tip was 90° to the needle body in a natural state. When the tip traveled out of the trocar, it was bent by its own elasticity. The next step was to direct the tip to the focus and insert into it the tumor. Then, the stylet was removed and ethanol was injected. For the larger foci, the trocar was inserted, through which ethanol was injected from superficial to deeper areas. After that, the flexible needle was inserted, through which ethanol was injected into the areas around the trocar. Before injecting ethanol, a test withdrawal was done to make sure that the needle was not misled to the blood vessel or biliary duct. Ethanol injection should be sufficient to diffuse to all or most parts of the tumor. The total volume of ethanol injected each time should not exceed 40 ml. As absolute alcohol is of low density, it could be mixed with a small amount of contrast medium to increase its density so that the diffusion of ethanol could be more visible. A small amount of the anesthetic was administered while the needle was being withdrawn. When the needle was removed, a check-up was necessary to see whether the ethanol was well distributed within the tumor, whether there was ethanol reflux, or whether passage of the needle through the pulmonary region caused pneumothorax.

Postoperative treatment included fluid replacement, analgesic and liver protection therapies, and re-examination of liver function and tumor markers. A second treatment was given at an interval of 5 to 7 days.

Outcome evaluation

Multi-slice helical CT scan or contrast-enhanced MRI was done three months after PEI to evaluate the outcome by the necrotic area of the foci, changes of the tumor marker level and clinical manifestations.

RESULTS

All of the 26 tumors received 2 or more times of CT-guided PEI. Single-point or multi-point injections were performed for foci smaller than 3 cm, and multi-point injections for all of the foci larger than 3 cm in diameter. The ethanol distribution was found to cover the whole tumor areas in all these 26 cases (Figures 1-4). CT or MRI images showed that, of the 18 foci smaller than 3 cm, 15 were completely necrotic (Figure 5) and the remaining three were mostly necrotic. Of the 8 foci larger than 3 cm, 5 were completely necrotic and the other three were mostly necrotic. In four patients who were found to have residue nodules, CT-guided PEI was performed again, and AFP level declined markedly and the symptoms improved in some of these patients. Apart from abdominal pain of varying degrees during the procedure, no other severe complication was observed.

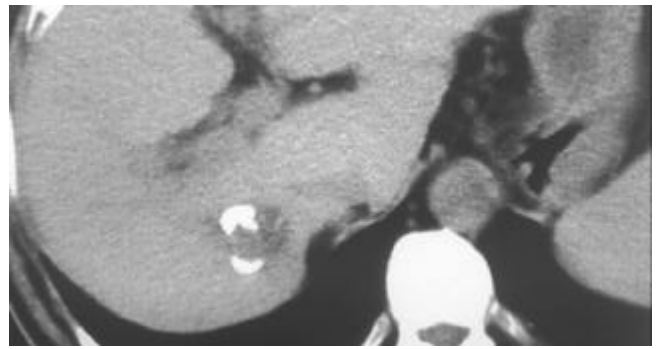


Figure 1 A tumor in the right lobe of liver (2.2 cm×2.0 cm). A small amount of high-density iodipin could be seen in some areas of the tumor receiving TACE.

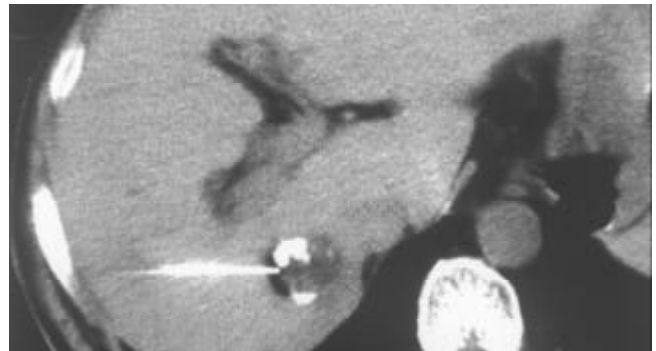


Figure 2 When a deeply embedded tumor is difficult for a straight needle to reach the appropriate point within it, a straight trocar (21G) is used to reach the tumor side.

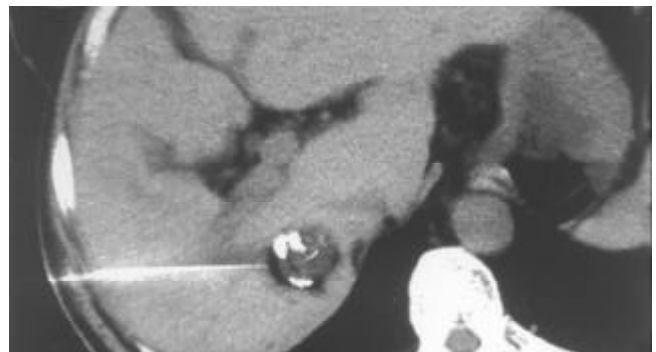


Figure 3 Insertion of the 25-G disposable curved needle into the tumor through the straight trocar. The tip position is adjusted to the target by changing the direction of the curved needle. Ethanol can be injected at multiple points within the tumor by changing the direction of the curved needle.

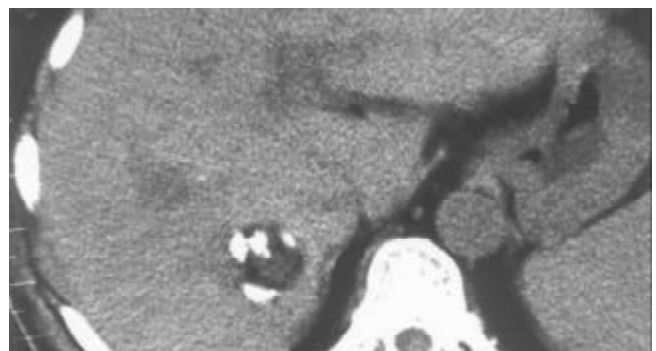


Figure 4 Distribution of ethanol in the whole tumor.

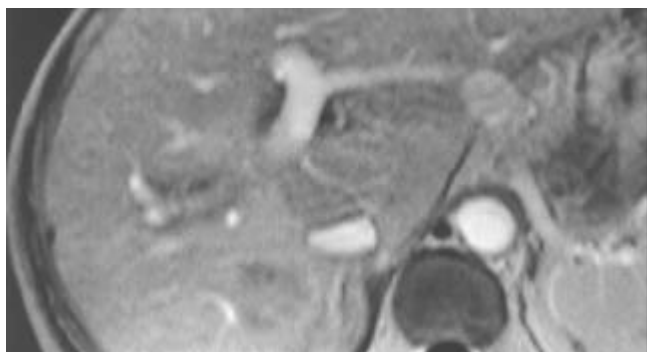


Figure 5 A complete necrotic change of the tumor found at enhanced MRI check-up three months after the PEI.

DISCUSSION

The common treatments for malignant liver tumors include surgery, transcatheter arterial chemoembolization (TACE), PEI, radiofrequency thermal ablation, microwave coagulation, laser thermal ablation therapy^[1-4]. Although surgery is the most radical treatment, it is not indicative for patients with severe cirrhosis or in cases where tumors are very close to the major vessels. Surgery was not usually preferable if there were multiple foci within the liver^[5]. TACE is a good alternative, but it causes severe damage to the liver. The outcome of TACE is usually poor for tumors with insufficient blood supply. PEI is a better alternative approach for treatment of malignant liver tumors, as it has proved to be effective and to cause minimal trauma^[6-10]. According to Ryu *et al.*, PEI was the choice of treatment for clinical stage II patients with tumors smaller than 3 cm. For clinical stage I patients with such small tumors, selective PEI or surgical resection should be considered^[11]. In these cases, the outcomes of PEI and surgery were similar but better than TACE. Therefore, PEI should be selected according to the conditions of individual patients^[12]. Combination of PEI and TACE and other treatment was sometimes used to achieve optimal outcomes^[13-18]. Moreover, PEI is more convenient and safer than radiofrequency thermal ablation and microwave coagulation therapy. PEI has become a preferable approach for lesions adjacent to main biliary ducts or to intestinal loops and for well-differentiated hepatocellular carcinoma^[19-21].

Chemotherapy, radiotherapy and surgery have become the routine treatments for retroperitoneal metastases of liver cancer and other malignant tumors^[22-28], but some of the lesions are not sensitive to radiotherapy and chemotherapy. In addition, radiotherapy and chemotherapy are more traumatic and expensive. Dissection of metastatic lymph nodes usually results in more traumas and complications. Some patients whose general conditions are poor can not tolerate chemotherapy, radiotherapy or surgery. While CT-guided PEI is more effective for the treatment of lymph node metastases in the retroperitoneal space and abdominal cavity with less trauma and lower cost. Following CT-guided PEI, appropriate chemotherapy and radiotherapy still can be considered.

Clear visualization of tumor location and ethanol distribution during CT-guided PEI for malignant liver tumors makes it possible to inject sufficient ethanol for a better outcome. It is especially suitable for foci that could be clearly detected on ultrasound^[29]. For the CT-guided PEI, it is a key step to insert the needle accurately into the target. Using the needle with a disposable curved tip, it is convenient to reach the foci and to avoid disadvantages of routine PEI procedure. What you need to do is to insert the trocar to the edge of the tumor and the disposable curved needle tip into the tumor through the trocar. It saves time and reduces complications. The disposable curved

tip can easily reach a deeply embedded tumor and avoid possible damages to the surrounding vessels or bile ducts. For tumors larger than 3 cm, multiple injections are necessary. By the procedure described here, a straight trocar is used at first to inject ethanol, and then the disposable curved needle tip is inserted through the trocar to inject ethanol into areas that the straight trocar cannot reach, so that ethanol can diffuse to the whole tumor. Retroperitoneal lymph nodes are usually deep and adjacent to abdominal aorta and inferior vena cava, PEI is usually done under CT guidance because CT guidance is accurate and the distribution of ethanol within the metastatic lymph node can be clearly visualized. The disposable curved needle can be used for metastatic lymph nodes in way to which is blocked by vessels. For larger metastatic lymph nodes, multiple-site injections of ethanol by one puncture can be done using a disposable curved needle and the procedure is more convenient than that using a routine straight needle.

As we know, this is the first report describing the use of a disposable curved puncture needle in CT-guided PEI for malignant liver tumors and retroperitoneal lymph node metastases. This procedure could also be used in CT-guided acetic acid injection for liver tumors^[30,31], ethanol injection for adrenal tumors^[32], and thymus ethanol injection for myasthenia gravis^[33].

REFERENCES

- 1 **Goldberg SN**, Ahmed M. Minimally invasive image-guided therapies for hepatocellular carcinoma. *J Clin Gastroenterol* 2002; **35**(5 Suppl 2): S115-129
- 2 **Livraghi T**. Radiofrequency ablation, PEIT, and TACE for hepatocellular carcinoma. *J Hepatobiliary Pancreat Surg* 2003; **10**: 67-76
- 3 **Seki T**, Tamai T, Nakagawa T, Imamura M, Nishimura A, Yamashiki N, Ikeda K, Inoue K. Combination therapy with transcatheter arterial chemoembolization and percutaneous microwave coagulation therapy for hepatocellular carcinoma. *Cancer* 2000; **89**: 1245-1251
- 4 **Pacella CM**, Bizzarri G, Cecconi P, Caspani B, Magnolfi F, Bianchini A, Anelli V, Pacella S, Rossi Z. Hepatocellular carcinoma: long-term results of combined treatment with laser thermal ablation and transcatheter arterial chemoembolization. *Radiology* 2001; **219**: 669-678
- 5 **Lau WY**, Leung TW, Yu SC, Ho SK. Percutaneous local ablative therapy for hepatocellular carcinoma: a review and look into the future. *Ann Surg* 2003; **237**: 171-179
- 6 **Livraghi T**. Percutaneous ethanol injection in the treatment of hepatocellular carcinoma in cirrhosis. *Hepato-gastroenterology* 2001; **48**: 20-24
- 7 **Livraghi T**, Giorgio A, Marin G, Salmi A, de Sio I, Bolondi L, Pompili M, Brunello F, Lazzaroni S, Torzilli G. Hepatocellular carcinoma and cirrhosis in 746 patients: long-term results of percutaneous ethanol injection. *Radiology* 1995; **197**: 101-108
- 8 **Lin SM**, Lin DY, Lin CJ. Percutaneous ethanol injection therapy in 47 cirrhotic patients with hepatocellular carcinoma 5 cm or less: a long-term result. *Int J Clin Pract* 1999; **53**: 257-262
- 9 **Livraghi T**, Benedini V, Lazzaroni S, Meloni F, Torzilli G, Vettori C. Long term results of single session percutaneous ethanol injection in patients with large hepatocellular carcinoma. *Cancer* 1998; **83**: 48-57
- 10 **Takayasu K**, Muramatsu Y, Asai S, Muramatsu Y, Kobayashi T. CT fluoroscopy-assisted needle puncture and ethanol injection for hepatocellular carcinoma: a preliminary study. *Am J Roentgenol* 1999; **173**: 1219-1224
- 11 **Ryu M**, Shimamura Y, Kinoshita T, Konishi M, Kawano N, Iwasaki M, Furuse J, Yoshino M, Moriyama N, Sugita M. Therapeutic results of resection, transcatheter arterial embolization and percutaneous transhepatic ethanol injection in 3225 patients with hepatocellular carcinoma: a retrospective multicenter study. *Jpn J Clin Oncol* 1997; **27**: 251-257
- 12 **Ueno S**, Tanabe G, Nuruki K, Oketani M, Komorizono Y, Hokotate H, Fukukura Y, Baba Y, Imamura Y, Aikou T. Prognosis of hepatocellular carcinoma associated with Child class B and

- C cirrhosis in relation to treatment: a multivariate analysis of 411 patients at a single center. *J Hepatobiliary Pancreat Surg* 2002; **9**: 469-477
- 13 **Tanaka K**, Nakamura S, Numata K, Kondo M, Morita K, Kitamura T, Saito S, Kiba T, Okazaki H, Sekihara H. The long term efficacy of combined transcatheter arterial embolization and percutaneous ethanol injection in the treatment of patients with large hepatocellular carcinoma and cirrhosis. *Cancer* 1998; **82**: 78-85
- 14 **Kirchhoff T**, Chavan A, Galanski M. Transarterial chemoembolization and percutaneous ethanol injection therapy in patients with hepatocellular carcinoma. *Eur J Gastroenterol Hepatol* 1998; **10**: 907-909
- 15 **Lencioni R**, Paolicchi A, Moretti M, Pinto F, Armillotta N, Di Giulio M, Cicorelli A, Donati F, Cioni D, Bartolozzi C. Combined transcatheter arterial chemoembolization and percutaneous ethanol injection for the treatment of large hepatocellular carcinoma: local therapeutic effect and long-term survival rate. *Eur Radiol* 1998; **8**: 439-444
- 16 **Koda M**, Murawaki Y, Mitsuda A, Oyama K, Okamoto K, Idobe Y, Suou T, Kawasaki H. Combination therapy with transcatheter arterial chemoembolization and percutaneous ethanol injection compared with percutaneous ethanol injection alone for patients with small hepatocellular carcinoma: a randomized control study. *Cancer* 2001; **92**: 1516-1524
- 17 **Kamada K**, Kitamoto M, Aikata H, Kawakami Y, Kono H, Imamura M, Nakanishi T, Chayama K. Combination of transcatheter arterial chemoembolization using cisplatin-lipiodol suspension and percutaneous ethanol injection for treatment of advanced small hepatocellular carcinoma. *Am J Surg* 2002; **184**: 284-290
- 18 **Guo WJ**, Yu EX, Liu LM, Li J, Chen Z, Lin JH, Meng ZQ, Feng Y. Comparison between chemoembolization combined with radiotherapy and chemoembolization alone for large hepatocellular carcinoma. *World J Gastroenterol* 2003; **9**: 1697-1701
- 19 **Livraghi T**, Goldberg SN, Lazzaroni S, Meloni F, Solbiati L, Gazelle GS. Small hepatocellular carcinoma: treatment with radiofrequency ablation versus ethanol injection. *Radiology* 1999; **210**: 655-661
- 20 **Livraghi T**, Lazzaroni S, Meloni F. Radiofrequency thermal ablation of hepatocellular carcinoma. *Eur J Ultrasound* 2001; **13**: 159-166
- 21 **Horigome H**, Nomura T, Saso K, Itoh M. Standards for selecting percutaneous ethanol injection therapy or percutaneous microwave coagulation therapy for solitary small hepatocellular carcinoma: consideration of local recurrence. *Am J Gastroenterol* 1999; **94**: 1914-1917
- 22 **Uenishi T**, Hirohashi K, Tanaka H, Yamamoto T, Kubo S, Kinoshita H. A surgically treated case of hepatocellular carcinoma with extensive lymph node metastases. *Hepatogastroenterology* 2000; **47**: 1714-1716
- 23 **Uenishi T**, Hirohashi K, Shuto T, Kubo S, Tanaka H, Sakata C, Ikebe T, Kinoshita H. The clinical significance of lymph node metastases in patients undergoing surgery for hepatocellular carcinoma. *Surg Today* 2000; **30**: 892-895
- 24 **Mosharafa AA**, Foster RS, Leibovich BC, Bihrl R, Johnson C, Donohue JP. Is post-chemotherapy resection of seminomatous elements associated with higher acute morbidity? *J Urol* 2003; **169**: 2126-2128
- 25 **Foster R**, Bihrl R. Current status of retroperitoneal lymph node dissection and testicular cancer: when to operate. *Cancer Control* 2002; **9**: 277-283
- 26 **Hendry WF**, Norman AR, Dearnaley DP, Fisher C, Nicholls J, Huddart RA, Horwich A. Metastatic nonseminomatous germ cell tumors of the testis: results of elective and salvage surgery for patients with residual retroperitoneal masses. *Cancer* 2002; **94**: 1668-1676
- 27 **Steyerberg EW**, Marshall PB, Keizer HJ, Habbema JD. Resection of small, residual retroperitoneal masses after chemotherapy for nonseminomatous testicular cancer: a decision analysis. *Cancer* 1999; **85**: 1331-1341
- 28 **Hermans BP**, Foster RS, Bihrl R, Little S, Sandler A, Einhorn LH, Donohue JP. Is retroperitoneal lymph node dissection necessary for adult paratesticular rhabdomyosarcoma? *J Urol* 1998; **160**(6 Pt 1): 2074-2077
- 29 **Lee MJ**, Mueller PR, Dawson SL, Gazelle SG, Hahn PF, Goldberg MA, Boland GW. Percutaneous ethanol injection for the treatment of hepatic tumors: indications, mechanism of action, technique, and efficacy. *Am J Roentgenol* 1995; **164**: 215-220
- 30 **Ohnishi K**, Yoshioka H, Ito S, Fujiwara K. Prospective randomized controlled trial comparing percutaneous acetic acid injection and percutaneous ethanol injection for small hepatocellular carcinoma. *Hepatology* 1998; **27**: 67-72
- 31 **Arrive L**, Rosmorduc O, Dahan H, Fartoux L, Monnier-Cholley L, Lewin M, Poupon R, Tubiana JM. Percutaneous acetic acid injection for hepatocellular carcinoma: using CT fluoroscopy to evaluate distribution of acetic acid mixed with an iodinated contrast agent. *Am J Roentgenol* 2003; **180**: 159-162
- 32 **Wang P**, Zuo C, Qian Z, Tian J, Ren F, Zhou D. Computerized tomography guided percutaneous ethanol injection for the treatment of hyperfunctioning pheochromocytoma. *J Urol* 2003; **170**(4Pt1): 1132-1134
- 33 **Wang P**, Zuo C, Tian J, Qian Z, Ren F, Shao C, Wang M, Lu T. CT-guided percutaneous ethanol injection of the thymus for treatment of myasthenia gravis. *Am J Roentgenol* 2003; **181**: 721-724

Edited by Su Q and Wang XL

Cooperative inhibitory effects of antisense oligonucleotide of cell adhesion molecules and cimetidine on cancer cell adhesion

Nan-Hong Tang, Yan-Ling Chen, Xiao-Qian Wang, Xiu-Jin Li, Feng-Zhi Yin, Xiao-Zhong Wang

Nan-Hong Tang, Yan-Ling Chen, Xiao-Qian Wang, Xiu-Jin Li, Feng-Zhi Yin, Hepato-Biliary Surgery Institute of Fujian Province, Union Hospital, Fujian Medical University, Fuzhou 350001, Fujian Province, China

Xiao-Zhong Wang, Gastroenterology Department, Union Hospital, Fujian Medical University, Fuzhou 350001, Fujian Province, China
Supported by the Foundation of Education Committee of Fujian Province, No. K99054

Correspondence to: Nan-Hong Tang, Hepato-Biliary Surgery Institute of Fujian Province, Union Hospital, 29 Xinquan Road, Fuzhou 350001, Fujian Province, China. fztjh@sina.com

Telephone: +86-591-3357896 Ext. 8373

Received: 2003-06-05 **Accepted:** 2003-08-16

Abstract

AIM: To explore the cooperative effects of antisense oligonucleotide (ASON) of cell adhesion molecules and cimetidine on the expression of E-selectin and ICAM-1 in endothelial cells and their adhesion to tumor cells.

METHODS: After treatment of endothelial cells with ASON and/or cimetidine and induction with TNF- α , the protein and mRNA changes of E-selectin and ICAM-1 in endothelial cells were examined by flow cytometry and RT-PCR, respectively. The adhesion rates of endothelial cells to tumor cells were measured by cell adhesion experiment.

RESULTS: In comparison with TNF- α inducing group, lipo-ASON and lipo-ASON/cimetidine could significantly decrease the protein and mRNA levels of E-selectin and ICAM-1 in endothelial cells, and lipo-ASON/cimetidine had most significant inhibitory effect on E-selectin expression (from $36.37 \pm 1.56\%$ to $14.23 \pm 1.07\%$, $P < 0.001$). Meanwhile, cimetidine alone could inhibit the expression of E-selectin ($36.37 \pm 1.56\%$ vs $27.2 \pm 1.31\%$, $P < 0.001$), but not ICAM-1 ($69.34 \pm 2.50\%$ vs $68.07 \pm 2.10\%$, $P > 0.05$) and the two kinds of mRNA, either. Compared with TNF- α inducing group, the rate of adhesion was markedly decreased in lipo-E-selectin ASON and lipo-E-selectin ASON/cimetidine treated groups ($P < 0.05$), and lipo-E-selectin ASON/cimetidine worked better than lipo-E-selectin ASON alone except for HepG2/ECV304 group ($P < 0.05$). However, the decrease of adhesion was not significant in lipo-ICAM-1 ASON and lipo-ICAM-1 ASON/cimetidine treated groups except for HepG2/ECV304 group ($P > 0.05$).

CONCLUSION: These data demonstrate that ASON in combination with cimetidine *in vitro* can significantly reduce the adhesion between endothelial cells and hepatic or colorectal cancer cells, which is stronger than ASON or cimetidine alone. This study provides some useful proofs for gene therapy of antiadhesion.

Tang NH, Chen YL, Wang XQ, Li XJ, Yin FZ, Wang XZ. Cooperative inhibitory effects of antisense oligonucleotide of cell adhesion molecules and cimetidine on cancer cell adhesion. *World J Gastroenterol* 2004; 10(1): 62-66

<http://www.wjgnet.com/1007-9327/10/62.asp>

INTRODUCTION

Previous researches have shown that recurrence and metastasis of cancer are closely related to the adhesion between tumor cells and endothelial cells. A variety of cell adhesion molecules (CAM) induced by cytokines such as IL- β and TNF- α released by tumor cells, promote the adhesion. Therefore, how to inhibit the adhesion is worth of study.

Antisense oligonucleotide (ASON) technique is a new alternative of gene therapy. ASOs are short synthetic oligonucleotides (10 to 25 bases in length) designed to hybridize to RNA (sense strand) that encodes the protein of interest. On binding to an mRNA, the oligonucleotide may inhibit the expression of target protein by multiple mechanisms^[1,2], exhibiting an important significance in antiviral and cancer treatment researches^[3,4]. Phosphorothioate oligonucleotides have a sulfur substituting for one of the nonbridging oxygens in the phosphate backbone, markedly enhancing the stability against cellular and serum nucleases^[5,6]. E-selectin, an early expressed CAM, and intercellular adhesion molecule-1 (ICAM-1), a late expressed CAM, are important proteins that mediate cell adhesion. Relevant studies on antiinflammation or antiadhesion using ASON have aroused increasing attention^[7-9].

Cimetidine, a kind of H2R antagonist, has been shown to improve the survival of patients with colorectal cancer, melanoma, and renal cell cancer. Other H2R antagonists including ranitidine and famotidine did not have such an effect^[10,11], indicating that cimetidine may exert its effect by enhancing the host immune response against tumor cells^[12] or by blocking the cell growth-promoting activity of histamine^[13], but not directly via histamine antagonism.

The key of anti-metastatic therapy lies in the complete inhibition of metastasis, because even if one metastatic colony is formed in an organ, it may result in death of the host eventually. Combined treatment may be an effective way to reach the goal. On the basis of previous work, we investigated the combined inhibitory effects of E-selectin or ICAM-1 ASON and cimetidine on tumor cell adhesion to provide data for further animal experiment and potential clinical application.

MATERIALS AND METHODS

Materials

Human endothelial cell line ECV304, hepatic cancer cell lines HepG2 and BEL7404 and colorectal cancer cell line Ls-174-t were purchased from the Cellular Biology Institute of Chinese Academy of Sciences and grown in DF medium (DMEM: Ham's F12=3:1) containing 100 mL · L⁻¹ fetal calf serum, penicillin 1 × 10⁵ U · L⁻¹ and streptomycin 100 mg · L⁻¹. Transfection kit TransFast™ liposome, Taq enzyme, RT-PCR kit and marker were from Promega. Mouse anti-human ICAM-1 mAb and E-selectin mAb were from Lab Vision. RNA extract (Trizol) was purchased from GIBCO BRL. Human recombinant TNF- α was purchased from Jingmei Biological Engineering Co., Shenzhen. ³H-TdR was purchased from the Atomic Energy Institute of Shanghai. Cimetidine was the product of Smithkline d Beecham Pharmaceutical Co., Germany.

ASON and primers

As previously described^[14,15], phosphorothioate oligoribonucleotides of ICAM-1, E-selectin and control ASON were synthesized by Sheng Gong Bio-Engineering Company, Shanghai. The sequences of ICAM-1, E-selectin and control ASON, and the primers for ICAM-1, E-selectin and β -actin are shown in Table 1.

Table 1 Sequences of ASON and primers

Name	Sequence	Length
ASON		
E-selectin	5'-TTCCCCAGATGCACCTGTTT-3'	
ICAM-1	5'-CCCCACCACTTCCCCTC-3'	
Control primer	5'-GCCGAGTCCATGTCGTACGC-3'	
E-selectin	Forward: 5'-AAAATGTTCAAGCCTGGCAGTTCC-3' Reverse: 5'-GTGGTGATGGGTGTTGCGGTTTCA-3'	509 bp
ICAM-1	Forward: 5'-CACAAGCCACGCCTCCCTGAACCTA-3' Reverse: 5'-TGTGGCCCTTTGTGTTTGTATGCTA-3'	458 bp
β -actin	Forward: 5'-CTGTCTGGCGGCACCACCAT-3' Reverse: 5'-GCAACTAAGTCATAGTCCGC-3'	250 bp

Methods

Preparation of lipo-ASON In order to improve the efficiency of ASON uptake of cells and prevent degradation in cultured cells and human serum, we used a commercial liposome that was comprised of synthetic cationic lipid and neutral lipid. It enhanced ASON's biofunction by improving its merging with cell membrane of eukaryotic cells and entering cell plasma to combine with mRNA^[16]. At a lower final concentration of 1/10 the nude ASON, lipo-ASON worked more effectively on inhibition in our previous report. According to the manufacturer's protocol of TransFast™ liposome, 200 μ l of serum-free medium per well should contain 3.6 μ l (1.5 μ g) ASON and 4.4 μ l liposome. So 10 minutes before the experiment, ASON was first mixed with serum-free medium, then liposome was added to make lipo-ASON medium (1 μ mol/L) at room temperature.

Treatment of endothelial cells A total of 5×10^4 ECV304 endothelial cells (3 to 6 generations) per well were put into a 24-well plate and incubated at 37 °C in 5 mL/L CO₂ humidified atmosphere for 48 hours, when cells grew to a confluence of 80%. E-selectin and ICAM-1 were divided into 5 groups according to the following different treatments, respectively. Group I (Basal): Treatment with TNF- α without lipo-ASON or cimetidine, and the cultivation time was identical to the other groups. Group II (TNF- α): After cultivation for 48 hours, the supernatants were discarded, endothelial cells were washed with PBS and replaced with 200 μ l of serum-free medium. Group III (cimetidine): After cultivation for 24 hours, 200 μ l of serum-free medium containing cimetidine (10^{-8} M) was added and cultured for another 24 hours, then the supernatants were discarded, cells were washed with PBS and replaced with 200 μ l of serum-free medium. Group IV (lipo-ASON): After cultivation for 48 hours, the supernatants were discarded, cells were washed with PBS and replaced with 200 μ l of serum-free medium containing lipo-ASON. Group V (lipo-ASON/cimetidine): After cultivation for 24 hours, 200 μ l of serum-free medium containing cimetidine (10^{-8} M) was added and cultured for another 24 hours, then the supernatants were discarded, cells were washed with PBS and replaced with 200 μ l of serum-free medium containing lipo-ASON.

Groups II to V were cultured for 4 hours at 37 °C. For E-selectin expression groups, the supernatants were discarded, 200 μ l medium containing 5 ng TNF- α was added and continuously cultured for 4 hours at 37 °C. For ICAM-1 expression groups, the supernatants were discarded, 200 μ l

medium was added and continuously cultured for 4 hours at 37 °C, then 5 ng TNF- α was added and cultured for 16 hours.

Flow cytometry Endothelial cells, treated with ASON or cimetidine and TNF- α as described above, were removed from the plate by brief trypsinization with 0.25% trypsin. Cells were washed with DME plus 10% FCS, stained with primary mAb (2 μ g/ μ l) diluted in D-PBS containing 2% BSA and 0.2% sodium azide, followed by fluorescein-conjugated goat anti-mouse IgG. Each step was performed at 4 °C. Cells were analyzed by flow cytometry using a Brite HSFACScan (BID-RAD, US).

RT-PCR 2.5×10^5 of ECV304 endothelial cells per well were placed into a 6-well plate and then performed as described above. Total cellular RNAs were extracted and quantitated by a spectrophotometer. 2 μ g of RNA was used to perform reverse transcription as recommended by the supplier. E-selectin gene was amplified 30 cycles by half-quantitation under the following conditions: denaturation at 94 °C for 5 min followed by 94 °C for 30 s, at 64 °C for 45 s and at 72 °C for 45 s, then extension at 72 °C for 7 min. ICAM-1 gene was amplified 30 cycles by half-quantitation under the following conditions: denaturation at 94 °C for 5 min followed by 94 °C for 30 s, at 60 °C for 45 s and at 72 °C for 45 s, then extension at 72 °C for 7 minutes. For analysis, 10 μ l of the amplified product was tested in 20 g/L agarose gel with ethidium bromide staining, then photographed and scan-analysed. The ratio of average integrated density value (IDV) of E-selectin and ICAM-1 to IDV of β -actin was expressed as the relative intensity of E-selectin and ICAM-1, respectively.

Monolayer cell adhesion assays 1×10^4 ECV304 endothelial cells per well were placed into a 96-well plate and then performed as described above. Human hepatic cancer cell lines HepG2 and BEL7404 and colorectal cancer cell line Ls-174-t were subcultured for 24 hours, then incubated with medium containing ³H-TdR (9 μ Ci/ml) for 12 hours at 37 °C. The three kinds of cells (2.5×10^5) were added to ECV304 monolayer in a final volume of 0.1 ml respectively, and incubated for 1 h at 37 °C. Nonadherent cells were removed from the plate by gentle washing with warm PBS. By brief trypsinization with 0.25% trypsin, the adherent cells were removed onto a piece of fiberglass paper (49#), washed with 5% trichloroacetic acid and dried at 80 °C. The number of adherent cells was determined by measuring flash value using a flash-detecting device (Tri-Carb 2300TR, Packard Co Lit).

Statistics analysis

Data were presented with $\bar{x} \pm s$, statistical analysis was performed using ANOVA. Differences were judged to be statistically significant when the *P* value was less than 0.05.

RESULTS

Effect of ASON and/or cimetidine on expression of E-selectin and ICAM-1

Using cytofluorometry, we examined the effect of lipo-ASON or cimetidine on the level of E-selectin and ICAM-1 protein in ECV304 cells stimulated by TNF- α (Figure 1). Maximum expression of E-selectin or ICAM-1 was observed in TNF- α inducing group with no other treatments. Compared with TNF- α inducing group, the expression of E-selectin in all treated groups was differently decreased ($P < 0.001$), most markedly in lipo-ASON/cimetidine treated group ($P < 0.001$, vs lipo-ASON alone group), showing that lipo-ASON in combination with cimetidine had a better inhibitory effect. Similarly, the expression of ICAM-1 in lipo-ASON and lipo-ASON/cimetidine treated groups decreased significantly ($P < 0.001$), but the change of ICAM-1 expression in cimetidine treated group was not significant ($P = 0.296$), suggesting that cimetidine did not affect ICAM-1 expression in endothelial cells.

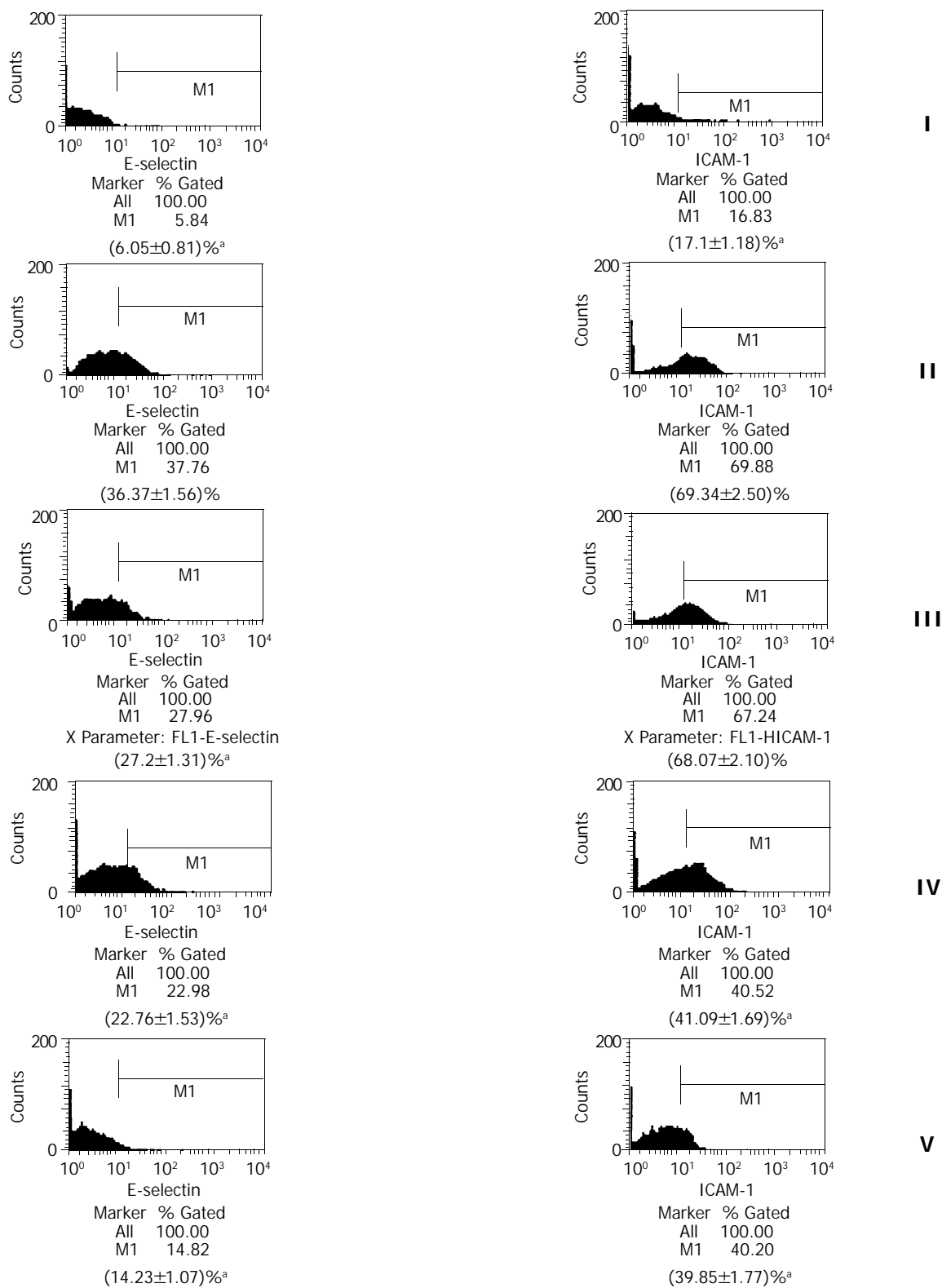


Figure 1 Effect of ASON on expression of E-selectin and ICAM-1 in endothelial cells (^a*P*<0.01, vs group II, *n*=5). I: Basal, II: TNF- α , III: cimetidine, IV: lipo-ASON, V: lipo-ASON/cimetidine.

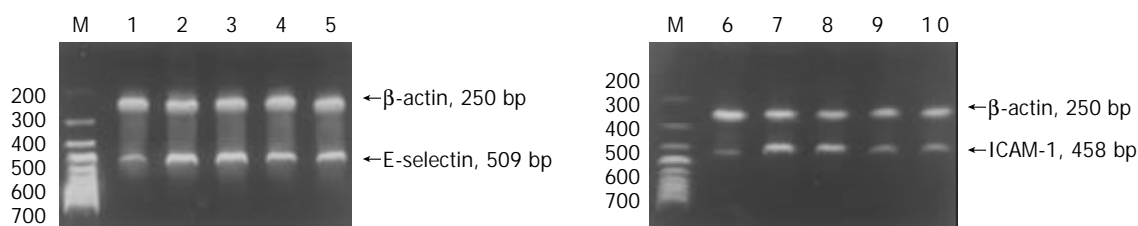


Figure 2 Agarose gel electrophoresis of RT-PCR products. M:Marker, 1: E/basal, 2: E/TNF- α , 3: E/cimetidine, 4: E/lipo-ASON, 5: E/lipo-ASON/cimetidine, 6: I/basal, 7: I/TNF- α , 8: I/cimetidine, 9: I/lipo-ASON, 10: I/cimetidine.

Agarose gel electrophoresis of RT-PCR products

To investigate the effects of lipo-ASON and/or cimetidine on the level of E-selectin and ICAM-1 mRNA, RT-PCR analysis was carried out. As shown in Figures 2 and 3, TNF- α could induce E-selectin and ICAM-1 gene expression. Lipo-ASON or lipo-ASON/cimetidine could significantly reduce the level of E-selectin and ICAM-1 mRNA, but cimetidine did not.

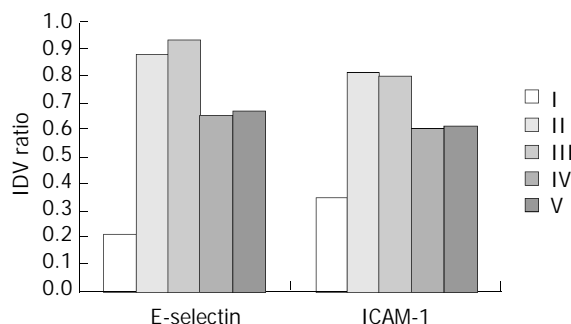


Figure 3 Relative expression value of ICAM-1 and E-selectin to β -actin by RT-PCR. I: Basal, II: TNF- α , III: Cimetidine, IV: Lipo-ASON, V: Lipo-ASON/Cimetidine.

Effect of ASON and/or cimetidine on adhesion

To examine the effects of lipo-ASON and/or cimetidine on the adhesion between tumor cells and ECV304 cells, a monolayer cell adhesion assay was carried out. As shown in Table 2, the adhesions of HepG2, BEL7404 and Ls-174-t cells to ECV304 cells were strongly induced by stimulation with TNF- α . Compared with TNF- α inducing group, the rate of adhesion was markedly decreased in lipo-E-selectin ASON and lipo-E-selectin ASON/cimetidine treated groups ($P < 0.05$), and lipo-E-selectin ASON/cimetidine worked better than lipo-E-selectin ASON alone except for HepG2/ECV304 group ($P < 0.05$). However, the decrease of adhesion was not significant in lipo-ICAM-1 ASON and lipo-ICAM-1 ASON/cimetidine treated groups except for HepG2/ECV304 group ($P > 0.05$).

Table 2 Adhesion rate of endothelial cells transfected by E-selectin and ICAM-1 ASON to tumor cells ($\bar{x} \pm s$)%

Group	I	II	III	IV	V
E-selectin/HepG2	17.7 \pm 0.9 ^a	80.4 \pm 6.2	58.9 \pm 2.7	38.0 \pm 5.0 ^a	24.1 \pm 1.5 ^a
E-selectin/BEL7404	8.1 \pm 1.0 ^a	75.9 \pm 0.6	52.2 \pm 2.4 ^a	26.7 \pm 1.6 ^a	17.4 \pm 1.1 ^{a,b}
E-selectin/Ls-174-t	16.0 \pm 1.6 ^a	77.9 \pm 5.7	53.9 \pm 2.6 ^a	43.1 \pm 1.7 ^a	29.5 \pm 2.6 ^{a,b}
ICAM-1/HepG2	5.0 \pm 1.3 ^a	71.0 \pm 2.4	68.6 \pm 1.8	69.0 \pm 1.4	67.3 \pm 2.2 ^a
ICAM-1/BEL7404	3.0 \pm 0.9 ^a	65.9 \pm 4.1	63.6 \pm 5.0	63.5 \pm 4.0	64.7 \pm 1.7
ICAM-1/Ls-174-t	5.8 \pm 0.8 ^a	63.0 \pm 2.0	63.4 \pm 1.2	64.5 \pm 1.8	62.8 \pm 1.3

(1) I: Basal, II: TNF- α , III: Cimetidine, IV: Lipo-ASON, V: Lipo-ASON/Cimetidine. (2) ^a $P < 0.05$, vs group II; ^b $P < 0.05$, group V vs group IV.

DISCUSSION

ICAM-1 cDNA with 2.98 Kb in length consists of 5' -untranslated region, 57 bp, a continuous open reading frame, 1 598 bp, and 3' -untranslated region, 1 330 bp. E-selectin cDNA with 3.85 Kb in length consists of 5' -untranslated region, 116 bp, a continuous open reading frame, 1 830 bp, and 3' -untranslated region, 1 898 bp. Bennett's research^[14] showed that among all the designed ASONs, ASONs hybridized to 3' -untranslated region were more potent than those hybridized to AUG transcription-initiation site or 5' -untranslated region. In our previous experiment, we found that each selected ASON of ICAM-1 and E-selectin hybridized to 3' -untranslated region

could reduce the expression of objective gene by nearly 40% respectively, demonstrating that their effects were sequence specific. This loss in mRNA might be due to the ASON targeted objective pre-mRNA in the nucleus, which resulted in activation of endogenous RNase H or a related enzyme and mediated hydrolysis of mRNA-ODN at the hybridization site^[17,18].

With the presence of cytokines such as IL-1 β and TNF- α secreted by tumor cells, vascular endothelial cells can produce different adhesive molecules at different times. After stimulation of cytokines, E-selectin shows its features in 4 to 5 hours, which mediate the early adhesion, and ICAM-1 shows its features in 12 to 48 hours, which mediate the late adhesion. In this article, through the treatment with E-selectin or ICAM-1 ASON before the induction by TNF- α , the expressions of objective molecules were blocked, but the adhesion between endothelial cells and tumor cells was only significantly inhibited by E-selectin ASON. The reasons were as follows: 1) Hepatic and colorectal cancer cells could highly express sle^x Ag^[19], the ligand of E-selectin. It is the major molecule that mediates the adhesion to endothelial cells directly. 2) ICAM-1 also appeared in the membrane of hepatic or colorectal cancer cells. The adhesion between cancer cells and vascular endothelial cells *in vitro* resorted to LFA-1^[20], the ligand of ICAM-1, which expresses on the membrane of white blood cells. However, there were no white blood cells to bridge *in vivo*. 3) Hepatic or colorectal cancer cells like HepG2 could also express affluent integrin $\alpha_2\beta_1$, which directly mediated the adhesion between tumor cells and endothelial cells^[19]. It is this kind of molecules that work in ICAM-1 ASON treated group.

Cimetidine, a kind of H2 receptor antagonist, has been used to inhibit the secretion of gastric acid in clinic. It has also been used to prolong the survival of patients with various forms of cancer in recent years^[21,22]. Even at the highest noncytotoxic concentration (10^{-4} M), cimetidine has been shown not to influence the expression of ICAM-1 protein, ICAM-1 mRNA and E-selectin mRNA, but could obviously reduce the expression of E-selectin protein^[22,23]. We proposed that cimetidine's inhibitory action on metastasis was due to blocking the adhesion between endothelial cells and tumor cells, especially colorectal cells with higher expression of sle^x Ag^[24]. Since other H2 receptor antagonists, such as ranitidine and famotidine, did not play the same role under the same experimental conditions^[22], it has become obvious that the mechanism of cimetidine's inhibiting function is involved in a step after transcription. p38 MAPK^[25], for instance, might be the regulatory molecule that activates the expression, of a number of genes at the level of posttranscription^[26-28].

Our research demonstrated that E-selectin played a primary role in initiating the adhesion of cancer cells to vascular endothelial cells through its interaction with its specific ligand, sialyl Lewis antigens^[29,30]. Lipo-E-selectin ASON in combination with cimetidine could inhibit the expression of E-selectin more effectively and reduce the adhesive rate of endothelial cells to tumor cells in early stage, reaching the goal of double benefits from outside and inside of cells. It not only guarantees the major aim of inhibiting adhesion, but also lowers the negative influence of cells subjected to drug *ab extra*. In short, this study provides some useful proofs for gene therapy of antiadhesion, which would become a new therapeutic alternative to inhibit high recurrence and metastasis of hepatic or colorectal cancer.

REFERENCES

- Giles RV. Antisense oligonucleotide technology: from EST to therapeutics. *Curr Opin Mol Ther* 2000; **2**: 238-252
- Capiati DA, Vazquez G, Tellez Inon MT, Boland RL. Antisense oligonucleotides targeted against protein kinase c alpha inhibit proliferation of cultured avian myoblasts. *Cell Prolif* 2000; **33**:

- 307-315
- 3 **Zhou S**, Wen SM, Zhang DF, Wang QL, Wang SQ, Ren H. Sequencing of PCR amplified HBV DNA pre-c and c regions in the 2.2.15 cells and antiviral action by targeted antisense oligonucleotide directed against sequence. *World J Gastroenterol* 1998; **4**: 434-436
 - 4 **Wang XW**, Yuan JH, Zhang RG, Guo LX, Xie Y, Xie H. Antihepatoma effect of alpha-fetoprotein antisense phosphorothioate oligodeoxyribonucleotides *in vitro* and in mice. *World J Gastroenterol* 2001; **7**: 345-351
 - 5 **Acosta R**, Montanez C, Gomez P, Cisneros B. Delivery of antisense oligonucleotides to PC12 cells. *Neurosci Res* 2002; **43**: 81-86
 - 6 **Agrawal S**, Kandimalla ER, Yu D, Hollister BA, Chen SF, Dexter DL, Alford TL, Hill B, Bailey KS, Bono CP, Knoerzer DL, Morton PA. Potentiation of antitumor activity of irinotecan by chemically modified oligonucleotides. *Int J Oncol* 2001; **18**: 1061-1069
 - 7 **Guo F**, Li Y, Wu S. Antisense IRAK-2 oligonucleotide blocks IL-1-stimulated NF-kappaB activation and ICAM-1 expression in cultured endothelial cells. *Inflammation* 1999; **23**: 535-543
 - 8 **Stepkowski SM**, Wang ME, Condon TP, Cheng-Flournoy S, Stecker K, Graham M, Qu X, Tian L, Chen W, Kahan BD, Bennett CF. Protection against allograft rejection with intercellular adhesion molecule-1 antisense oligodeoxynucleotides. *Transplantation* 1998; **66**: 699-707
 - 9 **Cheng Q**, Chen X, Ye Y. Antisense oligonucleotide attenuates renal tubulointerstitial injury in mice with unilateral ureteral obstruction. *Zhonghua Yixue Zazhi* 1999; **79**: 533-537
 - 10 **Lawson JA**, Adams WJ, Morris DL. Rantidine and cimetidine differ in their *in vitro* and *in vivo* effects on human colonic cancer growth. *Br J Cancer* 1996; **73**: 872-876
 - 11 **Hahm KB**, Kim WH, Lee SL, Kang JK, Park IS. Comparison of immunomodulative effects of the histamine-2 receptor antagonist cimetidine ranitidine, and famotidine on peripheral blood mononuclear cells in gastric cancer patients. *Scand J Gastroenterol* 1995; **30**: 265-271
 - 12 **Adams WJ**, Morris DL, Rose WR, Lubowski DZ, King DW. Cimetidine preserves non-specific immune function after colonic resection for cancer. *Aust N Z J Surg* 1994; **64**: 847-852
 - 13 **Adams WJ**, Lawson JA, Morris DL. Cimetidine inhibits *in vivo* growth of human colon cancer and reverses histamine stimulated *in vitro* and *in vivo* growth. *Gut* 1994; **35**: 1632-1636
 - 14 **Bennett CF**, Condon TP, Grimm S, Chan H, Chiang MY. Inhibition of endothelial cell adhesion molecule expression with antisense oligonucleotides. *J of Immunol* 1994; **152**: 3530-3540
 - 15 **Zhang XP**, Kelemen SE, Eisen HJ. Quantitative assessment of cell adhesion molecule gene expression in endomyocardial biopsy specimens from cardiac transplant recipients using competitive polymerase chain reaction. *Transplantation* 2000; **70**: 505-513
 - 16 **Gao X**, Huang L. Cationic liposome mediated gene transfer. *Gene Ther* 1995; **2**: 710-722
 - 17 **Condon TP**, Bennett CF. Altered mRNA splicing and inhibition of human E-selectin expression by an antisense oligonucleotide in human umbilical vein endothelial cells. *J Biol Chem* 1996; **271**: 30398-30403
 - 18 **Vickers TA**, Koo S, Bennett CF, Crooke ST, Dean NM, Baker BF. Efficient reduction of target RNAs by small interfering RNA and RNase H-dependent antisense agents. A comparative analysis. *J Biol Chem* 2003; **278**: 7108-7118
 - 19 **Kawakami-Kimura N**, Narita T, Ohmori K, Yoneda T, Matsumoto K, Nakamura T, Kannagi R. Involvement of hepatocyte growth factor in increased integrin expression on HepG2 cells triggered by adhesion to endothelial cells. *Br J Cancer* 1997; **75**: 47-53
 - 20 **Tanabe K**, Alexander JP, Steinbach F, Campbell S, Novick AC, Klein EA. Retroviral transduction of intercellular adhesion molecule-1 enhances endothelial attachment of bladder cancer. *Urol Res* 1997; **25**: 401-405
 - 21 **Matsumoto S**. Cimetidine and survival with colorectal cancer. *Lancet* 1995; **346**: 115
 - 22 **Kobayashi K**, Matsumoto S, Morishima T, Kawabe T, Okamoto T. Cimetidine inhibits cancer cell adhesion to endothelial cells and prevents metastasis by blocking E-selectin expression. *Cancer Res* 2000; **60**: 3978-3984
 - 23 **Leonardi A**, DeFranchis G, De Paoli M, Fregona I, Plebani M, Secchi A. Histamine-induced cytokine production and ICAM-1 expression in human conjunctival fibroblasts. *Curr Eye Res* 2002; **25**: 189-196
 - 24 **Matsumoto S**, Imaeda Y, Umemoto S, Kobayashi K, Suzuki H, Okamoto T. Cimetidine increases survival of colorectal cancer patients with high levels of sialyl Lewis-X and sialyl Lewis-A epitope expression on tumour cells. *Br J Cancer* 2002; **86**: 161-167
 - 25 **Read MA**, Whitley MZ, Gupta S, Pierce JW, Best J, Davis RJ, Collins T. Tumor necrosis factor α -induced E-selectin expression is activated by the nuclear factor- κ B and c-JUN N-terminal kinase/p38 mitogen-activated protein kinase pathways. *J Biol Chem* 1997; **272**: 2753-2761
 - 26 **Pietersma A**, Tilly BC, Gaestel M, de Jong N, Lee JC, Koster JF, Sluiter W. p38 mitogen activated protein kinase regulates endothelial VCAM-1 expression at the post-transcriptional level. *Biochem Biophys Res Commun* 1997; **230**: 44-48
 - 27 **Caivano M**. Role of MAP kinase cascades in inducing arginine transporters and nitric oxide synthetase in RAW264 macrophages. *FEBS Lett* 1998; **429**: 249-253
 - 28 **Miyazawa K**, Mori A, Miyata H, Akahane M, Ajisawa Y, Okudaira H. Regulation of interleukin-1 β -induced interleukin-6 gene expression in human fibroblast-like synoviocytes by p38 mitogen-activated protein kinase. *J Biol Chem* 1998; **273**: 24832-24838
 - 29 **Majuri ML**, Niemela R, Tiisala S, Renkonen O, Renkonen R. Expression and function of α 2,3-sialyl- and α 1,3/1,4-fucosyltransferases in colon adenocarcinoma cell lines: role in synthesis of E-selectin counter-receptors. *Int J Cancer* 1995; **63**: 551-559
 - 30 **Kunzendorf U**, Kruger-Krasagakes S, Notter M, Hock H, Walz G, Diamantstein T. A sialyl-Le(x)-negative melanoma cell line binds to E-selectin but not to P-selectin. *Cancer Res* 1994; **54**: 1109-1112

Edited by Zhu LH and Wang XL

Single-level dynamic spiral CT of hepatocellular carcinoma: Correlation between imaging features and density of tumor microvessels

Wei-Xia Chen, Peng-Qiu Min, Bin Song, Bong-Liang Xiao, Yan Liu, Ying-Hui Ge

Wei-Xia Chen, Peng-Qiu Min, Bin Song, Department of Radiology, West China Hospital, Sichuan University, Chengdu 610041, Sichuan Province, China

Bong-Liang Xiao, Department of Toxicology and Pathology, School of Public Health, Sichuan University, Chengdu 610041, Sichuan Province, China

Yan Liu, Department of Radiology, West China Hospital, Sichuan University, now working in Rijin Hospital, Shanghai, China

Ying-Hui Ge, Department of Radiology, West China Hospital, Sichuan University, now working in Henan Province Hospital, Henan Province, China

Correspondence to: Wei-Xia Chen, MD, Department of Radiology, West China Hospital, Sichuan University, Chengdu 610041, Sichuan Province, China. wxchen25@sohu.com

Telephone: +86-28-85422595 **Fax:** +86-28-85582944

Received: 2003-06-21 **Accepted:** 2003-07-30

Abstract

AIM: To investigate the correlation of enhancement features of hepatocellular carcinoma (HCC) revealed by single-level dynamic spiral CT scanning (DSCT) with tumor microvessel density (MVD), and to determine the validity of DSCT in assessing *in vivo* tumor angiogenic activity of HCC.

METHODS: Twenty six HCC patients were diagnosed histopathologically. DSCT was performed for all patients according to standard scanning protocol. Time-density curves were generated, relevant curve parameters were measured, and gross enhancement morphology was analyzed. Operation was performed to remove HCC lesions 1 to 2 weeks following CT scan. Histopathological slides were carefully prepared for the standard F₈RA immunohistochemical staining and tumor microvessel counting. Enhancement imaging features of HCC lesions were correlatively studied with tumor MVD and its intra-tumor distribution characteristics.

RESULTS: On DSCT images of HCC lesions, three patterns of time-density curve and three types of gross enhancement morphology were recognized. Histomorphologically, the distribution of positively stained tumor endothelial cells within tumor was categorized into 3 types. Curve parameters such as peak enhancement value and contrast enhancement ratio were significantly correlated with tumor tissue MVD ($r=0.508$ and $r=0.423$, $P<0.01$ and $P<0.05$ respectively). Both the pattern of time-density curve and the gross enhancement morphology of HCC lesions were also correlated with tumor MVD, and reflected the distributive features of tumor microvessels within HCC lesions. Correlation between the likelihood of intrahepatic metastasis of HCC lesions with densely enhanced pseudocapsules and rich pseudocapsular tumor MVD was found.

CONCLUSION: Enhancement imaging features of HCC lesions on DSCT scanning are correlated with tumor MVD, and reflect the intra-tumor distribution characteristics of

tumor microvessels. DSCT is valuable in assessing the angiogenic activity and tumor neovascularity of HCC patients *in vivo*.

Chen WX, Min PQ, Song B, Xiao BL, Liu Y, Ge YH. Single-level dynamic spiral CT of hepatocellular carcinoma: Correlation between imaging features and density of tumor microvessels. *World J Gastroenterol* 2004; 10(1): 67-72

<http://www.wjgnet.com/1007-9327/10/67.asp>

INTRODUCTION

Tumor angiogenesis plays a fundamental role in the pathogenesis of tumor growth and metastasis^[1-3], and significantly influences the biological behaviors of tumor and prognosis of patients^[3-6]. The inhibition or blockade of this angiogenic activity, on the other hand, can slow down the tumor growth rate and positively affect the outcome of patients^[7-9]. Although a single standardized and thoroughly validated method to evaluate the structure and function of tumor angiogenesis is not available, some histomorphological markers, such as microvessel density (MVD) and vascular endothelial growth factor, have been used as indicators of tumor angiogenic activity currently^[3,10-12]. However, these markers were studied immunohistochemically *in vitro* on biopsy or surgical tissues, and could not provide information of functional status of tumor angiogenesis, and were hardly to repeat for patients in follow-up. An ideal test should be non-invasive, fast, easy to perform, repeatable and reproducible, and most importantly, it should provide accurate and comprehensive information on the structure and biological characteristics of tumors *in vivo*.

Modern medical imaging modalities can depict the blood flow or reflect the hemodynamic changes. Recent studies using Doppler Sonography^[13-16] or MR^[17-28] or CT^[29,30] to assess tumor angiogenesis and neovascularity have yielded encouraging results in differential diagnosis and the correlation of aggressiveness and metastasis of tumor with the prognosis of patients. Correlation of enhanced imaging features of hepatocellular carcinoma (HCC) with tumor MVD was investigated to determine the validity of single-level dynamic spiral CT scanning (DSCT) *in vivo* for assessment of tumor angiogenic activity and neovascularity.

MATERIALS AND METHODS

Study subjects

From June 1997 to January 1999, 26 HCC patients were histopathologically proved and used for the study, and all the patients met the criteria for DSCT scanning and for histopathological specimen sampling and slides preparation. There were 23 males and 3 females with a mean age of 43.5 years (27 to 72 years). None of them had anti-tumor therapies prior to CT examination, and 1-2 weeks after CT, surgery was performed on all HCC patients to remove the lesions.

DSCT protocol

A Somatom Plus 4 VA spiral CT scanner (Siemens, Erlangen, Germany) was used for the study, 2 ml/kg of 65% angiografin or ultravist-300 (Schering, Germany) was used as intravenous contrast agent and injected via the antecubital route on the constant rate of 3 ml/sec. Before the start of CT scanning, the patients were educated and trained on how to cooperate for CT examination. The whole scanning procedure included 3 steps. First, all the liver was scanned without enhancement, then dynamic scanning at the selected target slice level (single-slice dynamic scanning) was followed, and finally the portal venous phase spiral CT acquisition of the entire liver was obtained. The target slice was selected based on the abnormal findings on the initial scanning. Only the central slice with the smallest area of tumor necrosis was chosen as the target for dynamic scanning. The dynamic scanning was performed 18 seconds after intravenous administration of contrast agent. For the dynamic scanning the sequence scan mode was employed with the cycle time of 2.3 seconds. A total of 18 slices were generated. The spiral scan mode was used for the initial scan and acquisition data on the final portal venous phase. Seven mm was used for calibration, table feed and slice thickness (pitch=1/1), and the scan delay time for the portal venous phase was 65 seconds.

Image data processing

Generation of time-density (T-D) curve Any visible blood vessel, necrotic foci and hypodense septum were avoided in selection of the region of interest (ROI) for HCC lesions. For the abdominal aorta, ROI was placed in its cross sectional center. The size of ROI was restricted to around 1 cm in diameter. With the built-in software program, the T-D curves of both HCC lesions and abdominal aorta were generated on the basis of the selected ROIs.

T-D curve parameters Several curve parameters were defined for the T-D curve of HCC lesions. (a) The peak enhancement value (PV) of the abdominal aorta was defined as the CT attenuation number at the junction between the up-slope portion with the steepest rise and the portion with gradual or flat rise. The corresponding time was referred to as the peak enhancement time (PT). (b) The PV for HCC lesion was the result of maximum enhancement CT attenuation number minus the baseline CT attenuation number on plain CT scan, and the time to reach the maximum CT attenuation number after enhancement was the PT. (c) The contrast enhancement ratio (CER) was defined as the percentage of the PV of HCC lesion divided by the PV of the abdominal aorta. Patterns of T-D curves were analyzed and the related curve parameters (PV, PT, and CER) were calculated.

Image interpretation All the CT images were jointly analyzed with standardized criteria by two senior radiologists experienced in liver imaging. Special attention was paid to the morphological enhancement patterns of HCC lesions and other associated imaging findings, such as pseudocapsules, daughter foci, and invasion of the portal venous system.

Histomorphological analysis of tissue specimen

Great care was taken to ensure that the matching of tissue sampling sites of surgically resected gross HCC tumor specimen with the correspondingly selected ROIs on DSCT images was on one-to-one basis. The obtained tissue specimens were processed by standard macro- and micro-slide techniques to verify the histomorphological tumor extension. Then slides of 5 μ m thickness were stained with the standard immunoperoxidase method using factor VIII-related antigen (F₈RA stain)^[2]. Criteria for positive stain and microvessel counting were those established by Weidner *et al*^[2-3]. Two

independent experienced pathologists counted each ROI separately, and consensus counting was done for dispute. The counting was first proceeded at 100 x magnification for "hot spot" representing the area of the highest microvessel density (MVD), then switched to 200 x magnification for clear depiction and better counting. For each slide three "hot spots" were counted, and the mean count represented the final MVD. The distribution of "hot spots" within tumor lesions was also recorded.

Statistical analysis

Pearson's correlation analysis and variance analysis were performed to test the strength of association between CT imaging features and the histomorphological marker, $P < 0.05$ was considered statistically significant.

RESULTS

Dynamic CT scan

Patterns of T-D curve Some distinctively different patterns of T-D curves of HCC lesions were observed and categorized into three types. Type I, the initial rise of T-D curve was very fast and steep, then abruptly changed to a more flat and steady gradual rise till the plateau phase. This curve pattern occurred in 7 patients. In type II curve, the up-rise of the curve slope was obvious, yet relatively smooth, no abrupt turn in the configuration of the curve up-slope. Thirteen patients demonstrated T-D curve pattern of type II. Type III curve in 6 patients was characterized by slow and flat rise of the initial curve up-slope with low amplitude. These three patterns of T-D curves of HCC lesions are depicted in Figure 1, and the calculated curve parameters are summarized in Table 1. PV and CER of type III patients were obviously lower than those of type I and type II patients, and the differences were statistically significant ($P < 0.05$). On the other hand, the differences of PV and CER between type I and type II patients were not statistically significant. There was a trend for PT to increase gradually from type I to type III, but the differences among the three types were not statistically significant.

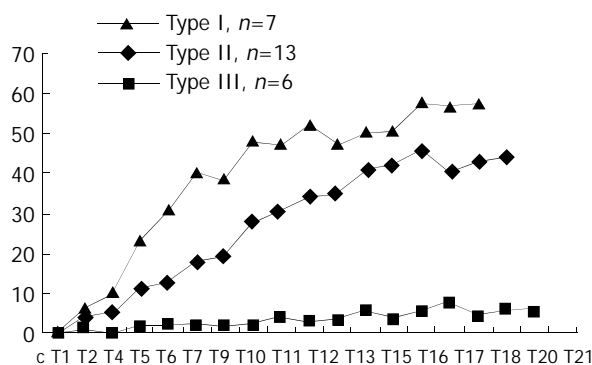


Figure 1 Three patterns (I, II, III) of time-density curve observed in HCC patients. The transverse axis represents the time and the Y-axis represents the peak enhancement value in Hounsfield units.

Table 1 HCC time-density curve patterns

Curve parameters	Type I	Type II	Type III
Number of patients	7	13	6
PV (Hu)	53.6 \pm 7.8	47.9 \pm 12.6	20.6 \pm 7.2 ^a
PT (Sec)	43.8 \pm 9.5	52.2 \pm 7.7	57.9 \pm 8.3
CER (%)	25.0 \pm 7.2	22.5 \pm 6.5	8.2 \pm 3.4 ^a

^aThe differences of PV and CER between type III and those of type I and II were statistically significant ($P < 0.05$).

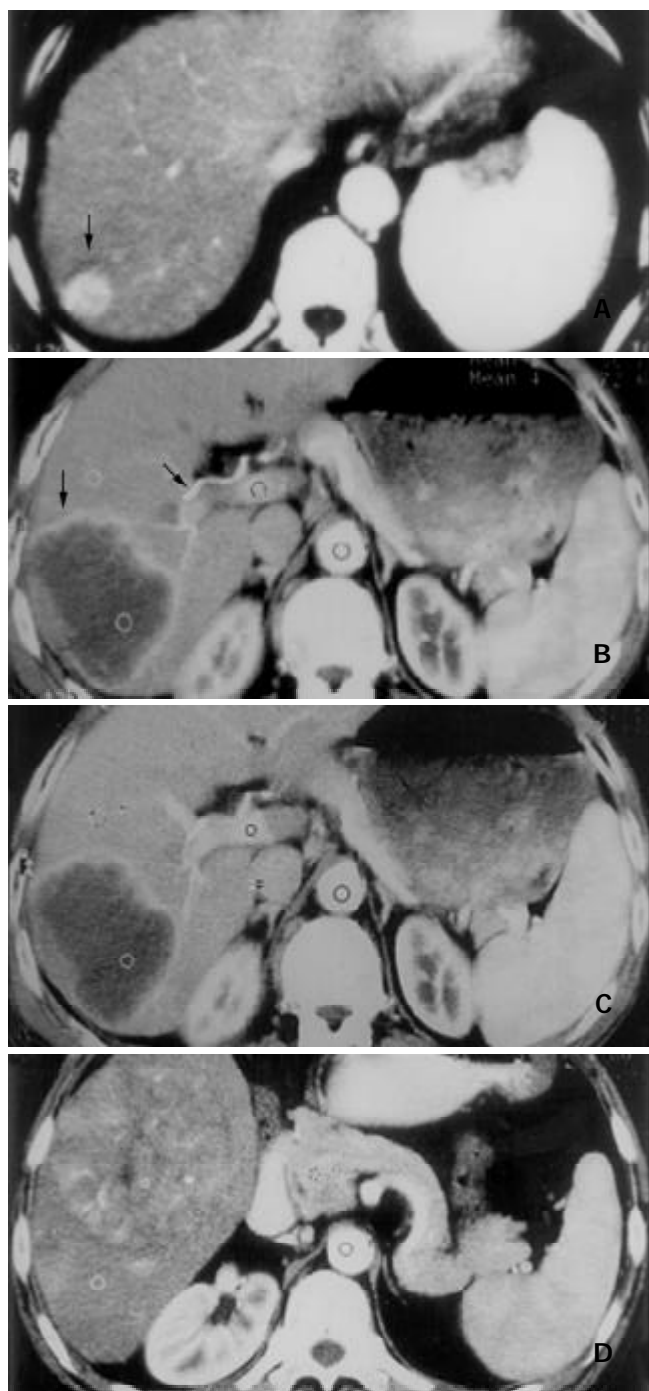


Figure 2 Three types of enhancement morphology depicted in HCC patients. A: Type A. Marked and homogeneous enhancement of the entire HCC lesion in the posterosuperior segment of right hepatic lobe (black arrow). B: Type B. Bright peripheral ring-like enhancement of HCC lesion on arterial phase image in the right posterosuperior segment (black arrow), and the dilated right hepatic artery (black arrow). C: Portal venous image at the same slice level as in (B). HCC lesion remained hypodense despite obvious enhancement of normal liver parenchyma elsewhere. D: Type C. Inhomogeneous patchy enhancement of HCC lesion in right lower hepatic lobe from arterial phase image. Bright dots and linear shadows represent enhanced tumor vessels within the lesion.

Morphological enhancement patterns of HCC The gross morphological enhancement manifestations of HCC lesions could also be grouped into 3 types (Figure 2). Type A was seen in 7 patients, the HCC lesions were densely enhanced in a homogeneous pattern (Figure 2A). The mean transverse diameter of lesions was 3.1 cm. Type B was in 5 patients, the

lesions demonstrated complete or partial rim-like peripheral enhancement, without or with only few dots of enhanced tumor vessels within the lesion center (Figure 2B, 2C). Mean diameter was 5.7 cm. Type C was seen in 14 patients, HCC lesions were inhomogeneously enhanced in a patchy fashion. Many small round-shaped, linear or reticular shadows representing enhanced tumor vessels were clearly visible, along with many hypodense necrotic foci and fibrous septa within the lesions (Figure 2D). The mean transverse diameter in this group of patients was 8.5 cm. The differences in the transverse diameter of tumor lesions among the three groups were statistically significant.

Immunohistochemical findings

F₈RA staining revealed a great variation in the distribution of positively stained tumor vascular endothelial cells within HCC lesions. Such a distribution variability in our patient could be roughly grouped into three patterns (Figure 3). (1) Twelve patients exhibited very rich blood sinusoids but scanty tumor microvessels in the interstitium. In 9 patients, positively stained sinusoidal endothelial cells were abundant and distributed inhomogeneously in a patchy fashion (Figure 3A). But in the rest 3 patients, sinusoidal endothelial cells had no positive staining. (2) Eleven patients had both rich sinusoids and interstitial microvessels, a large number of positively stained endothelial cells were distributed in both sinusoids and interstitium (Figure 3B). (3) Three patients had rich interstitium, with few interstitial microvessels and scanty sinusoids, and positively stained endothelial cells were very scarce (Figure 3C).

The MVD of HCC tumor tissue varied greatly from 6 to 91 among patients.

Correlation of DSCT features and tumor MVD

(1) T-D curve parameters and MVD A statistically significant positive correlation was demonstrated between tumor MVD and both PV and CER of corresponding HCC lesions. The correlation coefficients (*r*) were 0.508 (*P*<0.01) and 0.423 (*P*<0.05) respectively. However, MVD had no positive correlation with PT.

(2) Curve patterns, enhancement morphology and MVD The relationships between tumor MVD and T-D curve patterns and the three gross enhancement morphological types of HCC lesions are summarized in Table 2. The tumor MVDs of T-D curve type III and the gross enhancement morphology type B were significantly lower than those of curve type I and II (*P*<0.05), and gross morphology type A and C (*P*<0.05), respectively. The differences of MVDs between types I, II of T-D curve and the enhancement morphological patterns (type A, C) were not statistically significant.

Table 2 HCC time-density curve patterns, types of gross enhancement morphology and tumor MVD

	Type I	Type II	Type III	Type A	Type B	Type C
Patient No	7	13	6	7	5	14
MVD	41.8±16.7	48.0±18.2	23.0±7.4 ^a	49.7±14.2	15.6±5.7 ^b	44.0±19.7

^aThe differences of MVDs between type III and type I, type II were statistically significant (*P*<0.05). ^bThe differences of MVDs between types B, A, C were statistically significant (*P*<0.05).

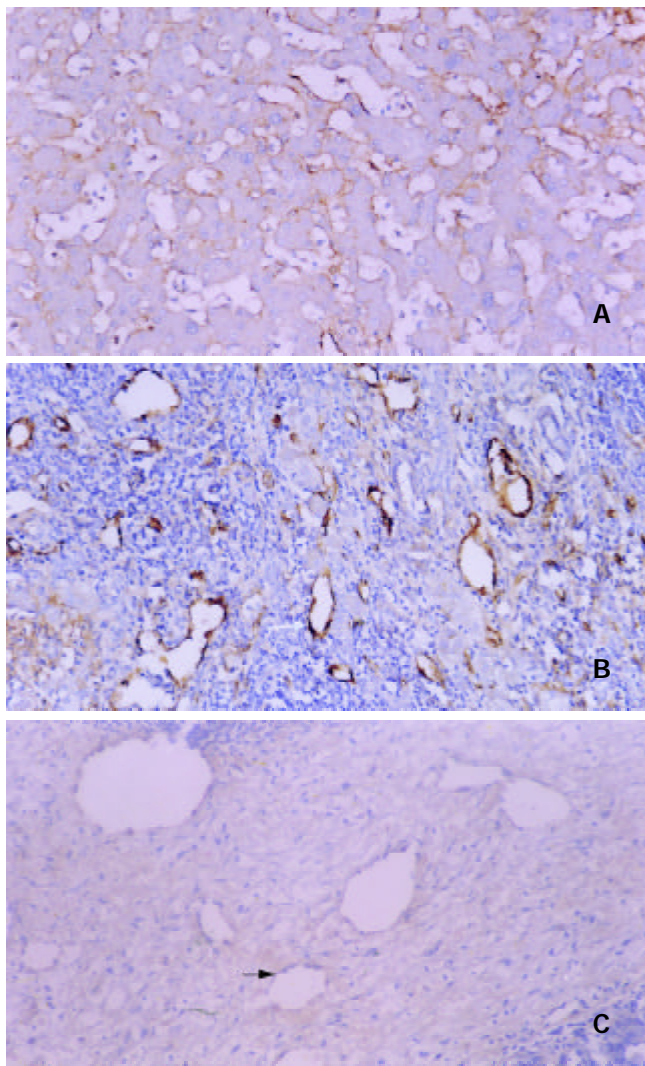
(3) Curve patterns, enhancement morphology and distribution of MVD The intratumoral distribution characteristics of tumor MVD and their relationships with T-D curve patterns and gross morphological enhancement types of HCC lesions are listed in Table 3.

Table 3 HCC time-density curve patterns, types of gross enhancement morphology and intratumoral MVD distribution

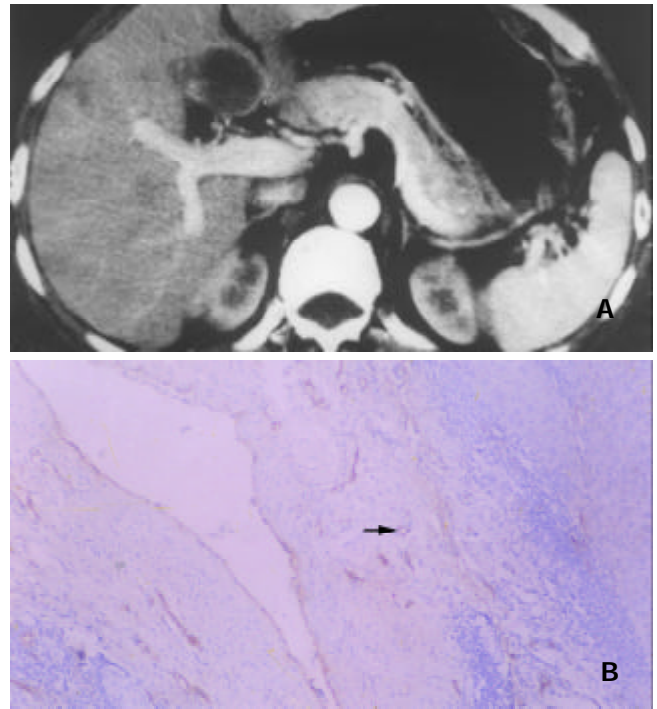
	Type I	Type II	Type III	Type A	Type B	Type C
Rich S	0	10	2	4	2	6
Rich S & I MVD	7	3	1	3	0	8
Scanty S & I MVD	0	0	3	0	3	0

S-tumor blood sinusoids, I-tumor interstitium.

(4) Other DSCT signs and related histomorphological changes Eleven patients demonstrated intrahepatic metastatic foci or daughter lesions. 7 of the 11 patients had prominent pseudocapsules that were hyperdense on DSCT images (Figure 4). In 1 patient the pseudocapsule remained to be hypodense throughout the entire scanning period, and no discrete pseudocapsule was discernible in the other 3 patients. Immunohistochemical F₈RA stain revealed abundant positively stained tumor endothelial cells in connective tissue of the tumor pseudocapsule in 8 patients. In the remaining 3 patients, judgement could not be made as whether or not the tumor pseudocapsule was present on the histopathological slides, due to improper tissue sampling, which missed the border region between HCC lesion and the neighboring normal liver tissue.

**Figure 3** Three patterns of intratumoral MVD distribution revealed by F₈RA immunohistochemical staining. A: Pattern I. Markedly dilated and abundant blood sinusoids with very rich positively stained sinusoidal endothelial cells and scanty tumor interstitium. B: Pattern II. Sinusoids and interstitium

abundant and rich in positively stained endothelial cells (black arrow). C: Pattern III. Rich tumor interstitium with few positively stained endothelial cells (white arrow) and scanty blood sinusoids.

**Figure 4** Enhancement of HCC pseudocapsules and pseudocapsular MVD. A: Marked enhancement of HCC pseudocapsule (hyperdensity) in the medial segment of left hepatic lobe shown by DSCT. Note the similar enhancement pattern of the satellite or daughter lesion in the anterior segment of right hepatic lobe. B: F₈RA staining Rich positively stained endothelial cells within tumor pseudocapsule (black arrow) revealed by F₈RA staining.

DISCUSSION

MVD, one of the histomorphological markers, is currently regarded as the best available means to represent tumor angiogenesis, and has been widely used to characterize tumor angiogenic activity *in vitro*. However, it may not be an ideal method for clinical purposes, as it is invasive and hard to perform and to repeat. Clearly, from the clinical perspective, it is of great clinical importance to look for a noninvasive method, which can provide *in vivo* overall functional information about tumor angiogenesis, besides accurate morphological information. We designed this dynamic spiral CT study to investigate the correlation of enhancement patterns of HCC lesions with the histomorphological marker of tumor angiogenesis – tumor MVD, and to determine the validity of DSCT in assessing angiogenic activity and neovascularity of HCC lesions.

Our study showed that the curve parameters generated from T-D curves of HCC lesions, such as PV and CER, were positively correlated to tumor MVD with statistical significance. As T-D curve parameters were representative of the hemodynamic characteristics of tumor microvasculature, this observation indicated that the degree of tumor enhancement on DSCT was affected by tumor MVD. The tumor enhancement degree could also truly reflect the distribution characteristics of tumor microvessels within a tumor mass, as the area with the greatest enhancement was often associated with the highest MVD. Higher tumor MVD was shown to be associated with worse degree of

malignancy and more potential of metastases^[4,10], thus it is possible to estimate the biological behaviors of HCC in terms of aggressiveness and metastasis by calculating the parameters of HCC T-D curve through dynamic spiral CT scanning.

The patterns of T-D curves of HCC lesions also provided *in vivo* clues to the histomorphological distribution characteristics of tumor microvessels within a tumor mass. Type I curve was often histologically associated with rich blood sinusoids and microvessels in the interstitium, both demonstrating abundant positively stained tumor vascular endothelial cells. Such a histomorphological feature of microvessel-rich tumor interstitium might well explain the early rapid rise of the up-slope and the high amplitude of this type of T-D curves observed in this subset of HCC patients. As more and more contrast agents reached the sinusoids where the rate of blood flow was sluggish, alteration of the rise pace resulted in an abrupt turn of the curve up-slope configuration. Abundant, often dilated and tortuous sinusoids with positively stained tumor endothelial cells resulted in type II curve. Sluggish blood flow with prolonged accumulation of contrast agent in sinusoids might cause the slow and steady rise of the up-slope of T-D curve in this group of HCC patients. However, in 3 patients with type II curve, both sinusoids and interstitium showed rich positively stained endothelial cells. Two reasons might be implicated for this discrepancy between T-D curve pattern and histomorphological marker. First, the hemodynamic effect of rich blood sinusoids might overrun that of microvessel-rich interstitium in these 3 HCC patients, causing the distribution of contrast-containing blood within the tumor mass to be relatively slower. Misrepresentation due to sampling error was another possible reason. As the selected area of ROI was 1 cm, much larger than what could be represented on a histological slide, it was possible that the selected ROIs might actually contain many more sinusoids than what was shown on the corresponding histological slides in these 3 HCC patients. Type III curve was histologically characterized either by rich interstitium but with scanty interstitial microvessels and scanty blood sinusoids, or by rich sinusoids which were devoid of positively stained endothelial cells. These tumor sinusoids had structural and functional resemblance to those of normal liver sinusoids, therefore, the rise of the up-slope in this type of T-D curve was quite slow and flat in the hepatic arterial phase. In the patient with type III curve, both rich sinusoids and interstitial microvessels with positively stained endothelial cells were observed. We speculated that the cause might be the mismatch of selected ROI with the sampling site for histomorphological measurement, and the variation in tumor angiogenic activity within a tumor lesion, which could lead to the misrepresentation by MVD.

The study also found that the gross enhancement morphology of HCC lesions was related to the distribution of tumor microvessels within a tumor mass. As shown in Table 3, type A enhancement morphology was mainly seen in relatively small HCC lesions, while type C enhancement morphology was found in larger lesions. However, both types were histomorphologically characterized by rich blood sinusoids or coexistence of microvessel-rich interstitium, both of which had abundant positively stained endothelial cells. Such findings might suggest that when a hypervascular HCC lesion was small, the distribution of tumor microvessels within it tended to be homogeneous, giving rise to the homogeneous enhancement appearance on DSCT scan. With the tumor became larger, intratumoral necrosis, fibrous septation and granulation formation occurred. The original homogeneity of tumor microvessels distribution was altered and distorted, so did the gross morphological enhancement patterns on CT images. Type B enhancement morphology showed that tumor interstitium was abundant in quantity, but either with scanty

interstitial microvessels and few sinusoids, or with rich sinusoids that were devoid of positively stained endothelial cells. In sharp contrast, tumor microvessels with positively stained endothelial cells were rich in pseudocapsules of this type of HCC patients. Thus the gross morphological enhancement pattern could well reflect the underlying histomorphological characteristics of tumor microvessels in this group of HCC patients. Therefore, by analyzing the enhancement morphology of HCC lesions on dynamic spiral CT scan, it was possible to estimate both the *in vivo* tumor angiogenic activity and the distribution characteristics of tumor neovascularity. Compared to the measurement of histomorphological markers, dynamic spiral CT was able to maximally avoid the possibility of sampling errors and offered a comprehensive overview of the gross enhancement morphology of HCC lesions.

Our another interesting finding was that most of HCC lesions with intrahepatic metastases or daughter foci demonstrated characteristic hyperdense pseudocapsules on dynamic CT images corresponding to hepatic arterial phase. These pseudocapsules were histomorphologically characterized by very rich positively stained endothelial cells diffusely distributed in the connective tissues of pseudocapsules. Such an association indicated that hypervascularized tumor pseudocapsules with abundant interstitial structurally defective tumor microvessels^[31] might facilitate intrahepatic metastasis or homogeneous spreading of HCC.

Though the close positive correlation of enhancement imaging features of HCC lesions revealed by DSCT with tumor MVD was demonstrated, several other factors, such as perfusion rate, microvessel permeability, and size or volume of extracellular space, might also influence the uptake rate of contrast agent by tumor tissue, thus affecting the configurations of T-D curve. Little has been known about major contributors for the difference in the contrast agent uptake rate^[11,32]. We suspect that the differences might depend on the type or even subtype of tumors, and further studies are required to clarify this issue.

In conclusion, the characteristics of T-D curve of HCC revealed by DSCT scanning are closely related to tumor MVD. The gross enhancement morphology of HCC lesions on DSCT images can reflect the features of histomorphological distribution of tumor microvessels within a tumor. DSCT is valid for the *in vivo* assessment of tumor angiogenic activity and neovascularity of HCC lesions, which is very important in making differential diagnosis, evaluating tumor malignancy and aggressiveness, monitoring therapeutic effects, and determining the final outcome of HCC patients.

ACKNOWLEDGEMENT

Our thanks go to Dr. Luinan Yan, MD, and Dr. Sheng He, MD, for their valuable assistance of this research work.

REFERENCES

- 1 **Folkman J**, Shing Y. Angiogenesis. *J Biol Chem* 1992; **267**: 10931-10934
- 2 **Weidner N**, Semple J, Welch W, Folkman J. Tumor angiogenesis and metastasis: correlation in invasive breast carcinoma. *N Engl J Med* 1991; **324**: 1-8
- 3 **Weidner N**. Intratumor microvessel density as a prognostic factor in cancer. *Am J Pathol* 1995; **147**: 9-19
- 4 **Jinno K**, Tanimizu M, Hyodo I, Nishikawa Y, Hosokawa Y, Doi T, Endo H, Yamashita T, Okada Y. Circulating vascular endothelial growth factor (VEGF) is a possible tumor marker for metastasis in human hepatocellular carcinoma. *J Gastroenterol* 1998; **33**: 376-382
- 5 **Weidner N**, Carroll PR, Flax J, Blumenfeld W, Folkman J. Tumor angiogenesis correlates with metastasis in invasive prostate carcinoma. *Am J Pathol* 1993; **143**: 401-409

- 6 **Poon RT**, Ng IO, Lau C, Yu WC, Yang ZF, Fan ST, Wong J. Tumor microvessel density as a predictor of recurrence after resection of hepatocellular carcinoma: a prospective study. *J Clin Oncol* 2002; **20**: 1775-1785
- 7 **Augustin HG**. Antiangiogenic tumor therapy: will it work? *Trends Pharmacol Sci* 1998; **19**: 216-222
- 8 **Hama Y**, Shimizu T, Hosaka S, Sugeno A, Usuda N. Therapeutic efficacy of the angiogenesis inhibitor O-(chloroacetyl-carbamoyl) fumagillol (TNP-470; AGM-1470) for human anaplastic thyroid carcinoma in nude mice. *Exp Toxicol Pathol* 1997; **49**: 239-247
- 9 **Kin M**, Torimura T, Ueno T, Nakamura T, Ogata R, Sakamoto M, Tamaki S, Sata M. Angiogenesis inhibitor TNP-470 suppresses the progression of experimentally-induced hepatocellular carcinoma in rats. *Int J Oncol* 2000; **16**: 375-382
- 10 **Tomisaki S**, Ohno S, Ichiyoshi Y, Kuwano H, Maehara Y, Sugimachi K. Microvessel quantification and its possible relation with liver metastasis in colorectal cancer. *Cancer* 1996; **77**(8 Suppl): 1722-1728
- 11 **Hawighorst H**, Knapstein PG, Knopp MV, Vaupel P, van Kaick G. Cervical carcinoma: standard and pharmacokinetic analysis of time-intensity curves for assessment of tumor angiogenesis and patient survival. *MAGMA* 1999; **8**: 55-62
- 12 **Wild R**, Ramakrishnan S, Sedgewick J, Griffioen AW. Quantitative assessment of angiogenesis and tumor vessel architecture by computer-assisted digital image analysis: effects of VEGF-toxin conjugate on tumor microvessel density. *Microvasc Res* 2000; **59**: 368-376
- 13 **Sahin Akyar G**, Sumer H. Color Doppler ultrasound and spectral analysis of tumor vessels in the differential diagnosis of solid breast masses. *Invest Radiol* 1996; **31**: 72-79
- 14 **Raza S**, Baum JK. Solid breast lesions: evaluation with power Doppler US. *Radiology* 1997; **203**: 164-168
- 15 **Louvar E**, Littrup PJ, Goldstein A, Yu L, Sakr W, Grignon D. Correlation of color Doppler flow in the prostate with tissue microvascularity. *Cancer* 1998; **83**: 135-140
- 16 **Peters-Engl G**, Medl M, Mirau M, Wanner C, Bilgi S, Sevela P, Obermair A. Color-coded and spectral Doppler flow in breast carcinoma-relationship with the tumor microvasculature. *Breast Cancer Res Treat* 1998; **47**: 83-89
- 17 **Stomper PC**, Winston JS, Herman S, Klippenstein DL, Arredondo MA, Blumenson LE. Angiogenesis and dynamic MR imaging gadolinium enhancement of malignant and benign breast lesions. *Breast Cancer Res Treat* 1997; **45**: 39-46
- 18 **Hawighorst H**, Knapstein PG, Weikel W, Knopp MV, Zuna I, Knof A, Brix G, Schaeffer U, Wilkens C, Schoenberg SO, Essig M, Vaupel P, van Kaick G. Angiogenesis of uterine cervical carcinoma: characterization by pharmacokinetic magnetic resonance parameters and histological microvessel density with correlation to lymphatic involvement. *Cancer Res* 1997; **57**: 4777-4786
- 19 **Pham CD**, Roberts TP, van Bruggen N, Melnyk O, Mann J, Ferrara N, Cohen RL, Brasch RC. Magnetic resonance imaging detects suppression of tumor vascular permeability after administration of antibody to vascular endothelial growth factor. *Cancer Invest* 1998; **16**: 225-230
- 20 **Hawighorst H**, Knapstein PG, Knopp MV, Weikel W, Brix G, Zuna I, Schonberg SO, Essig M, Vaupel P, van Kaick G. Uterine cervical carcinoma: comparison of standard and pharmacokinetic analysis of time-intensity curves for assessment of tumor angiogenesis and patient survival. *Cancer Res* 1998; **58**: 3598-3602
- 21 **Hawighorst H**, Schaeffer U, Knapstein PG, Knopp MV, Weikel W, Schonberg SO, Essig M, van Kaick G. Detection of angiogenesis-dependent parameters by functional MRI: correlation with histomorphology and evaluation of clinical relevance as prognostic factor using cervix carcinoma as an example. *Rofu Fortschr Geb Rontgenstr Neuen Bildgeb Verfahr* 1998; **169**: 499-504
- 22 **Hawighorst H**, Weikel W, Knapstein PG, Knopp MV, Zuna I, Schonberg SO, Vaupel P, van Kaick G. Angiogenic activity of cervical carcinoma: assessment by functional magnetic resonance imaging-based parameters and a histomorphological approach in correlation with disease outcome. *Clin Cancer Res* 1998; **4**: 2305-2312
- 23 **Mayr NA**, Hawighorst H, Yuh WT, Essig M, Magnotta VA, Knopp MV. MR microcirculation assessment in cervical cancer: correlations with histomorphological tumor markers and clinical outcome. *J Magn Reson Imaging* 1999; **10**: 267-276
- 24 **Miles KA**, Charnsangavej C, Lee FT, Fishman EK, Horton K, Lee TY. Application of CT in the investigation of angiogenesis in oncology. *Acad Radiol* 2000; **7**: 840-850
- 25 **Gossmann A**, Helbich TH, Mesiano S, Shames DM, Wendland MF, Roberts TP, Ferrara N, Jaffe RB, Brasch RC. Magnetic resonance imaging in an experimental model of human ovarian cancer demonstrating altered microvascular permeability after inhibition of vascular endothelial growth factor. *Am J Obstet Gynecol* 2000; **183**: 956-963
- 26 **Okuhata Y**, Brasch RC, Pham CD, Daldrup H, Wendland MF, Shames DM, Roberts TP. Tumor blood volume assays using contrast-enhanced magnetic resonance imaging: regional heterogeneity and postmortem artifacts. *J Magn Reson Imaging* 1999; **9**: 685-690
- 27 **Padhani AR**, Neeman M. Challenges for imaging angiogenesis. *Br J Radiol* 2001; **74**: 886-890
- 28 **Roberts HC**, Roberts TP, Brasch RC, Dillon WP. Quantitative measurement of microvascular permeability in human brain tumors achieved using dynamic contrast-enhanced MR imaging: correlation with histologic grade. *Am J Neuroradiol* 2000; **21**: 891-899
- 29 **Miles KA**. Tumour angiogenesis and its relation to contrast enhancement on computed tomography: a review. *Eur J Radiol* 1999; **30**: 198-205
- 30 **Kwak BK**, Shim HJ, Park ES, Kim SA, Choi D, Lim HK, Park CK, Chung JW, Park JH. Hepatocellular carcinoma: correlation between vascular endothelial growth factor level and degree of enhancement by multiphase contrast-enhanced computed tomography. *Invest Radiol* 2001; **36**: 487-492
- 31 **Less JR**, Skalak TC, Sevic EM, Jain RK. Microvascular architecture in a mammary carcinoma: branching patterns and vessel dimensions. *Cancer Res* 1991; **51**: 265-273
- 32 **Degani H**, Gusic V, Weinstein D, Fields S, Strano S. Mapping pathophysiological features of breast tumors by MRI at high spatial resolution. *Nat Med* 1997; **3**: 780-782

Protective effect of nitric oxide induced by ischemic preconditioning on reperfusion injury of rat liver graft

Jian-Ping Gong, Bing Tu, Wei Wang, Yong Peng, Shou-Bai Li, Lu-Nan Yan

Jian-Ping Gong, Wei Wang, Lu-Nan Yan, Department of General Surgery, Huaxi Hospital, Sichuan University, Chengdu 610041, Sichuan Province, China

Jian-Ping Gong, Bing Tu, Yong Peng, Shou-Bai Li, Department of General Surgery, the Second Affiliated Hospital of Chongqing Medical University, Chongqing 400010, China

Supported by the National Natural Science Foundation of China, No. 30200278, and China Postdoctoral Science Foundation, No. 2001-5

Correspondence to: Dr. Jian-Ping Gong, Department of General Surgery, the Second Affiliated Hospital of Chongqing Medical University, 74 Linjiang Road, Chongqing 400010, China. gongjianping11@hotmail.com

Telephone: +86-23-63766701 **Fax:** +86-23-63829191

Received: 2003-03-04 **Accepted:** 2003-04-03

Abstract

AIM: Ischemic preconditioning (IP) is a brief ischemic episode, which confers a state of protection against the subsequent long-term ischemia-reperfusion injuries. However, little is known regarding the use of IP before the sustained cold storage and liver transplantation. The present study was designed to evaluate the protective effect of IP on the long-term preservation of liver graft and the prolonged anhepatic-phase injury.

METHODS: Male Sprague-Dawley rats were used as donors and recipients of orthotopic liver transplantation. All livers underwent 10 min of ischemia followed by 10 min of reperfusion before harvest. Rat liver transplantation was performed with the portal vein clamped for 25 min. Tolerance of transplanted liver to the reperfusion injury and liver damage were investigated. The changes in adenosine concentration in hepatic tissue and those of nitric oxide (NO) and tumor necrosis factor (TNF) in serum were also assessed.

RESULTS: Recipients with IP significantly improved their one-week survival rate and liver function, they had increased levels of circulating NO and hepatic adenosine, and a reduced level of serum TNF, as compared to controls. Histological changes indicating hepatic injuries appeared improved in the IP group compared with those in control group. The protective effect of IP was also obtained by administration of adenosine, while blockage of the NO pathway using N ω -nitro-L-arginine methyl ester abolished the protective effect of IP.

CONCLUSION: IP appears to have a protective effect on the long-term preservation of liver graft and the prolonged anhepatic-phase injuries. NO may be involved in this process.

Gong JP, Tu B, Wang W, Peng Y, Li SB, Yan LN. Protective effect of nitric oxide induced by ischemic preconditioning on reperfusion injury of rat liver graft. *World J Gastroenterol* 2004; 10(1): 73-76

<http://www.wjgnet.com/1007-9327/10/73.asp>

INTRODUCTION

Liver transplantation is an accepted therapy for patients with

end-stage liver diseases^[1]. Hepatic ischemia-reperfusion (I/R) injury associated with liver transplantation is an unresolved problem in the clinical practice. Primary non-function of liver graft remains one of the most severe complications of liver transplantation, and poor initial graft function also occurs in one third of cases after liver transplantation. To deal with these complications, no effective treatment can be used but retransplantation^[2,3]. Evidently, approaches need to be established to handle or even to avoid these complications.

The underlying mechanisms of cold I/R injuries are still poorly understood. Long-term ischemia of liver graft leads to impairment of liver function and reduction in survival rate of the recipients^[4]. On the other hand, anhepatic phase is the most important parameter for orthotopic rat liver transplantation (ORLT), because prolonged anhepatic phase can be associated with an endotoxin-like syndrome caused by the warm intestinal ischemia and is not related to the cold ischemia injuries of the liver^[5]. The hepatic reticulo-endothelial system plays a key role in the elimination of endotoxins. The detoxification system is usually deficient in recipients due to liver failure and is completely absent during the anhepatic phase of transplantation. The endotoxin content has been proven to increase markedly in the portal circulation of cirrhotic patients compared to that in the peripheral blood^[6]. The hypothermia may affect the ability of Kupffer cells to eliminate endotoxins and to release cytokines, such as tumor-necrosis factor (TNF). It has been shown that TNF is partly responsible for initiation of the lethal toxicity of endotoxins^[7].

Ischemic preconditioning (IP) is a process by which a brief ischemic episode confers a state of protection against the subsequent more sustained ischemic insult^[8]. Recent studies have demonstrated that a brief ischemia treatment, followed by an episode of reperfusion, can reduce the sustained I/R injury^[9,10]. These observations suggest a potential application of IP in liver transplantation. In this study, the protective effect of IP on the long-term preservation of liver grafts and the prolonged anhepatic phase was observed.

MATERIALS AND METHODS

Materials

Male *Sprague-Dawley* rats weighing 200 to 230 g supplied by the Center of Experimental Animal in Sichuan University, were used as donors and recipients. Animals were bred in a controlled environment with a 12 hour light/dark cycle. Donor rats were fasted for 12 hours with free access to water before surgery, while the recipients had free access to normal rat chow and water before surgery. This study was approved by Sichuan Bioethics Committee, and the procedures were carried out according to the routine animal-care guidelines.

ORLT

Liver transplantation was performed according to Kamada's cuff-technique^[11] under anesthesia with ether inhalation. Briefly, the abdomen was opened through a midline incision and the liver was freed from its ligaments with minimal manipulation. The donor bile duct was transected, and a 0.4 cm

length of tube was inserted into the lumen of the bile duct and secured with a circumferential 5-0 silk suture. The animal was injected intravenously with 50 U of heparin. The liver was perfused through portal vein with an intravenous cannula connected with a syringe with 36 U of heparin in 6 ml of cold saline. The donor liver was placed in the saline bath at 4 °C for 100 min. The cuff preparation of portal vein and infrahepatic vena cava was performed also in the saline-ice bath. After the recipient liver was removed, the donor liver was implanted in the orthotopic position by connecting the suprahepatic vena cava with a running suture, inserting cuffs into the infrahepatic vena cava and the portal vein, and splint tube into the bile duct. The anhepatic phase was estimated to be 25 min for all recipients. ORLT was performed without artery reconstruction.

Experimental design

A total number of 128 rats were randomly divided into 4 groups, 32 for each. 1) Control group, the donor livers were flushed through the portal veins with physiological saline containing heparin only before harvested. 2) IP group, before the donor livers were harvested, the portal vein and hepatic artery were interrupted for 10 min, and the blood flow was restored for 10 min, then the liver was treated as control group. 3) Adenosine group, the donor livers were flushed through the portal vein with physiological saline containing heparin and adenosine (10 mmol/L) only before harvested. 4) N ω -nitro-L-arginine methyl ester (NAME) group, the donor livers were treated as IP group, but NAME (10 mmol/L), an NO synthesis inhibitor, was included in flushing solution. For each group, half of animals were used to investigate the one-week survival rate of recipients, and the remaining animals were for sample collection of blood from infrahepatic vena cava and hepatic tissue after 2 hours of reperfusion.

Determination of liver function and survival

Serum alanine transaminase (ALT) was measured using an automated analyzer (BECKMAN CX7, Beckman Instruments, Fullerton, CA). Survival of recipients was observed for 7 days after operation.

Determination of serum NO

Values of circulating nitrate and nitrite were determined to reflect serum NO level. Serum was separated by centrifugation and stored at -70 °C before use. Nitrite was measured after enzymatic conversion by nitrate reductase using the Griess reaction, as described by Schmidt^[12]. Values obtained represented the sum of serum nitrite and nitrate.

Determination of serum TNF

Serum was separated by centrifugation, and concentration of serum TNF was measured by radioimmunoassay. The TNF standard (100 μ l, Sigma, ST. Louis, MO, USA) and the serum samples (100 μ l) were added separately to appropriate tubes. Two hundred μ l of the 0 ng/ml TNF standard was added to each non-specific binding tube. All tubes were added 100 μ l of ¹²⁵I-TNF reagent (Sigma, ST. Louis, MO, USA). TNF antiserum (100 μ l) was also added to each tube, except the nonspecific binding tubes. Incubation was done at 4 °C for 24 hours following gentle agitation for 2-3 seconds. With 500 μ l of precipitating reagent added, the tubes were vortexed immediately, and incubated for 20 minutes at room temperature (-25 °C). All the tubes were centrifuged at 1500 \times g for 25 min, the suspension was dropped out. Radioactivity was read using a gamma counter (262 Factory, Xi'an, Shaanxi, China).

Assay for adenosine from hepatic tissue

Adenosine standard was purchased from Sigma (St. Louis, MO,

USA). High-performance liquid chromatography (HPLC) was performed using a Beckman Gold Nouveau system equipped with a 168 photo-diode-array detector (210 nm; 262 Factory, Xi'an, Shaanxi, China). Satisfactory separation of the marker substances was obtained with a reversed-phase column and eluted at a flow rate of 1 ml/min. Adenosine separation was allowed to precede in a phosphate-buffer solution (331 mmol/L KH₂PO₄, pH 6.24) containing 3.5% CH₃CN and 2.3 mmol/L *t*-butylamine (TBA). Lyophilized liver tissue was homogenized in 0.5 ml of 0.42 mol/L perchloric acid and incubated for 20 min at 4 °C. The supernatant was separated by centrifugation at 3 000 rpm for 10 min at 0.5 °C, and neutralized with 85 μ l/200 μ l NaOH. After 5 min of centrifugation at 3 000 rpm, 20 μ l of the supernatant was subjected to HPLC.

Histopathologic examination

Liver samples were fixed in 10% neutral buffered formalin, embedded in paraffin. Sections of 5 μ m in thickness were prepared, stained with hematoxylin and eosin, and observed under a light microscope.

Statistics

All statistical computations were performed using SPSS software (version 10.0 for Windows 98; SPSS, Inc., Chicago, Illinois). The *P* values less than 0.05 were considered statistically significant.

RESULTS

Animal survival

The survival rates of these four groups are shown in Figure 1. Most of the recipients died within 3 days after liver transplantation. The survival rate at day 7 was higher in IP group (87.5%, 7 of 8) and adenosine group (87.5%, 7 of 8) than that in control group (37.5%, 3 of 8) and NAME group (25%, 2 of 8, *P*<0.05, Figure 1).

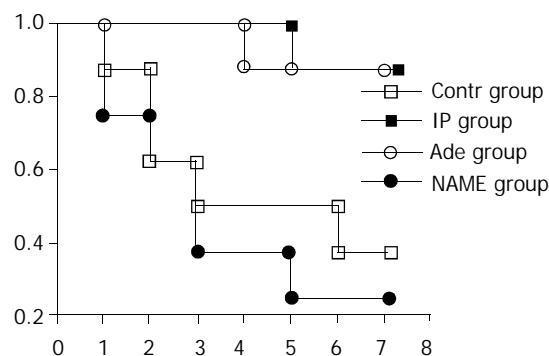


Figure 1 Survival of recipients in different groups. The donor livers were treated respectively as described in Materials and Methods, and the recipients were divided into control (Contr group), IP (IP group), adenosine (Ade group), and NAME-treated groups. The 7-day survival rate was 37.5% (3/8) and 25% (2/8), respectively, in the control group and NAME group, compared with 87.5% (7/8) in both the IP group and adenosine group (*P*<0.05). The survival curves were calculated using Kaplan-meier's methods.

Liver function

The serum ALT values in control group (588 \pm 58 U/L) were significantly higher as compared to those in IP group (287 \pm 82 U/L) (*P*<0.001). Meanwhile, administration of adenosine also reduced the level of serum ALT (357 \pm 93 U/L) as compared to that in control group (*P*<0.001). However, with administration of NAME, the response in ALT level to IP was abrogated (634 \pm 65 U/L, *P*>0.05, Figure 2).

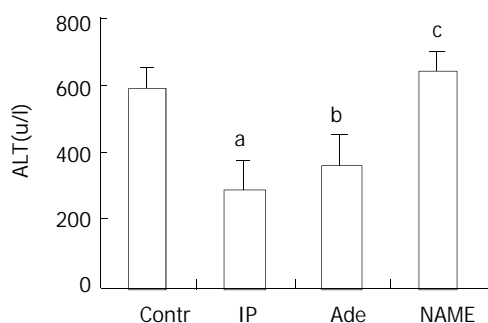


Figure 2 Values of serum ALT in different groups of recipients at 2 hours after ORLT. The ALT levels in control group and NAME group increased significantly compared with IP group and adenosine group. ^a P and ^b P <0.001, ^c P >0.05 vs. control group. The values were expressed as means \pm SD.

Serum TNF and NO level

TNF concentration in serum was measured 2 hours after ORLT as described previously^[5,6]. In IP group (1.15 \pm 0.23 ng/ml) and adenosine group (1.14 \pm 0.27 ng/ml), it was significantly lower compared to that in control group (1.59 \pm 0.35 ng/ml, P <0.01). The level in NAME group (1.71 \pm 0.23 ng/ml) was as high as that in control group (P >0.05, Figure 3).

Concentrations of NO were shown to be 32.96 \pm 6.10 μ mol/L, 29.14 \pm 6.49 μ mol/L in IP and adenosine groups, respectively, which were significantly higher than that in control group (15.44 \pm 2.99 μ mol/L, P <0.001). The value of the recipients in NAME group was 13.74 \pm 3.11 μ mol/L, which was similar to that in control group (P >0.05, Figure 4).

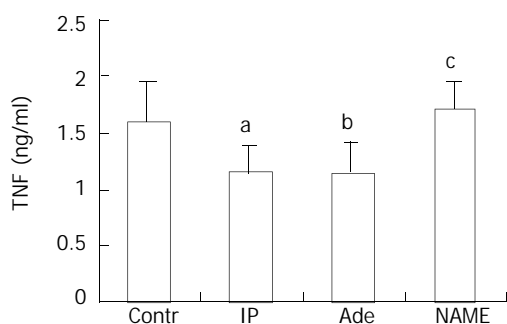


Figure 3 Serum TNF levels measured at 2 hours after ORLT in different recipient groups. In control and NAME groups, the concentrations of serum TNF were elevated significantly as compared to those in IP and adenosine groups. ^a P and ^b P <0.01, ^c P >0.05 vs. control group. Values were expressed as means \pm SD.

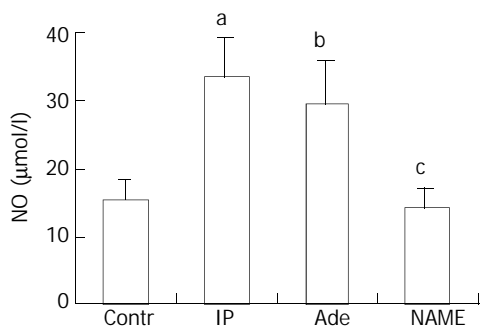


Figure 4 NO levels in serum at 2 hours after ORLT. When the donor livers were pretreated with IP or adenosine, the serum NO levels were elevated significantly. When IP-treatment followed by administration with NAME, the serum NO concentration was as low as that in control group. ^a P and ^b P <0.001, ^c P >0.05 vs. control group. Values were expressed as means \pm SD.

Adenosine in hepatic tissue

Figure 5 shows the levels of hepatic adenosine at 2 hours after ORLT in liver grafts. Concentrations of tissue adenosine were 7.22 \pm 1.83 mol/g, 5.68 \pm 1.32 mol/g, and 5.56 \pm 1.19 mol/g in liver grafts pretreated with IP, adenosine and IP+NAME, respectively, which were higher than that in the reference liver grafts (3.69 \pm 0.54 μ mol per gram of dry liver tissue, P <0.05). Animal survival and liver function were improved after adenosine administration. The protective effect of IP was abrogated in NAME group, though the content of adenosine in the tissue also increased.

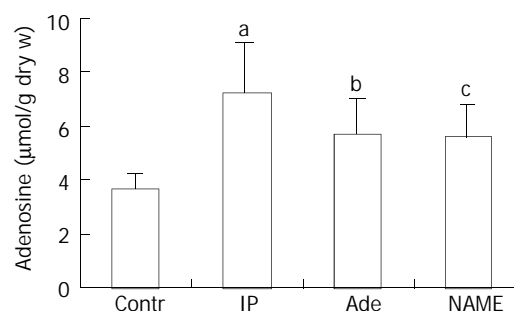


Figure 5 Adenosine concentrations in liver tissues at 2 hours after ORLT. When the donor livers were pretreated with IP or adenosine, or even the IP-treatment followed NAME, the adenosine levels in dry hepatic tissue were elevated as compared to that in control group. ^a P , ^b P and ^c P <0.05 vs. control group. Results were expressed as means \pm SD.

Histopathologic examination

Hepatocyte swelling and ballooning were observed in tissues from the control and NAME groups. No identifiable morphological alterations or only minor changes were found in IP and adenosine groups (data not shown).

DISCUSSION

The ORLT model, established in 1973 by Lee *et al.*^[13], has received wide acceptance in the study of liver transplantation. IP is a procedure originally described during heart transplantation. A brief ischemia treatment followed by reperfusion has been shown to be able to decrease infarct size after subsequent prolonged I/R^[8,14,15]. IP has been found to be protective during transplantation of several organs including brain, intestine and skeletal muscle^[16-18]. In liver, IP was found to reduce tissue damages and mortality after warm ischemia and cold ischemic storage^[5, 19].

In the present study, The harvested livers were preserved in saline for 100 min at 4 °C and the anhepatic phase was selected for 25 minutes, poor outcomes of recipients in control group were observed, and the survival rate 7 days after operation was 37.5% (3/8). In IP group, ALT level was reduced markedly and the survival rate was significantly elevated (87.5%, 7 of 8). The protective effect of IP was further indicated by the morphologic parameters presented.

The effects of a long anhepatic phase on the graft were associated with an endotoxin-like syndrome induced by the prolonged congestion of internal organs. Endotoxemia has been shown to be one of the processes causative for early graft dysfunction^[20,21]. This was most probably associated with Kupffer cell activation by splanchnic endotoxin accumulation and release during intestinal congestion/reperfusion^[22,23]. During the ORLT with a long anhepatic phase, Kupffer cells were shown to be directly responsible for overproduction of TNF, causing endotoxicosis-like syndrome^[24]. The cytotoxic effects of TNF are associated with activation of phospholipase

A₂, release of ceramide, formation of reactive oxygen intermediate (ROI) and promotion of cell apoptosis. However, it is not known whether the protective effect of IP in this study was associated with TNF.

The definite mechanism underlying IP is not clear, and there are several explanations about its protective effects. According to some authors, the protective effects were not attributed to blood flow alterations^[25,26]. However, the IP protective effect was associated to certain substances produced by ischemic tissue against injury^[4]. On the contrary, another study indicated that IP could improve blood flow, and decrease hepatic vascular resistance of liver grafts preserved in cold storage^[10], and this was probably related to some potential mediators such as NO and adenosine.

NO was reported to exert a protective effect through inhibiting endothelin synthesis^[27], and the upregulating effect of adenosine NO release in endothelial cells was also documented^[28]. During ischemia, adenosine is rapidly formed from adenosine triphosphate and reaches high concentrations. Enhanced adenosine level might in turn induce NO synthesis through the activation of adenosine A₂ receptors^[27]. The functions of the two mediators might lead to an improvement in graft blood flow and accordingly improve liver function. Since the ROIs are known to cause cell injury by promoting the peroxidation of lipids and proteins in cell membranes, it is possible that the antioxidant action of NO might also be involved in the protective effect of IP.

In the present study, the concentrations of NO in serum and adenosine in hepatic tissues of IP group were significantly higher than those in control group. In contrast, the level of serum TNF was greatly reduced after IP treatment. Furthermore, the protective effect of IP was also achieved by administration of adenosine before the donor livers were harvested. Our results showed NAME had negative effects on the protective effect of IP and suppressed NO synthesis, indicating that, in the absence of NO, adenosine was unable to develop protective effects. IP might exert its protective role by inducing the production of NO.

In summary, the data presented suggest that an elevated adenosine level can induce the generation of NO under IP, conferring protection to liver grafts and recipients. IP may be an important approach to reduce the transplantation risk resulted from preservation/reperfusion injuries. Further studies are needed for further understanding of the underlying mechanisms.

REFERENCES

- 1 Lemasters JJ, Thurman RG. Reperfusion injury after liver preservation for transplantation. *Annu Rev Pharmacol Toxicol* 1997; **37**: 327-338
- 2 Ploeg RJ, D' Alessandro AM, Knechtle SJ, Stegall MD, Pirsch JD, Hoffmann RM, Sasaki T, Sollinger HW, Belzer FO, Kalayoglu M. Risk factors for primary dysfunction after liver transplantation—a multivariate analysis. *Transplantation* 1993; **55**: 807-813
- 3 Strasberg SM, Howard TK, Molmenti EP, Hertl M. Selecting the donor liver: risk factors for poor function after orthotopic liver transplantation. *Hepatology* 1994; **20**(4Pt1): 829-838
- 4 Yin DP, Sankary HN, Chong AS, Ma LL, Shen J, Foster P, Williams JW. Protective effect of ischemic preconditioning on liver preservation-reperfusion injury in rats. *Transplantation* 1998; **66**: 152-157
- 5 Urata K, Nguyen B, Brault A, Lavoie J, Rocheleau B, Huet PM. Decreased survival in rat liver transplantation with extended cold preservation: role of portal vein clamping time. *Hepatology* 1998; **28**: 366-373
- 6 Lumsden AB, Henderson JM, Kutner MH. Endotoxin levels measured by a chromogenic assay in portal, hepatic and peripheral venous blood in patients with cirrhosis. *Hepatology* 1988; **8**: 232-236
- 7 Fernandez ED, Flohe S, Siemers F, Nau M, Ackermann M, Ruwe M, Schade FU. Endotoxin tolerance protects against local hepatic ischemia/reperfusion injury in the rat. *J Endotoxin Res* 2000; **6**: 321-328
- 8 Murry CE, Jennings RB, Reimer KA. Preconditioning with ischemia: a delay of lethal cell injury in ischemic myocardium. *Circulation* 1986; **74**: 1124-1136
- 9 Arai M, Thurman RG, Lemasters JJ. Contribution of adenosine A(2) receptors and cyclic adenosine monophosphate to protective ischemic preconditioning of sinusoidal endothelial cells against Storage/Reperfusion injury in rat livers. *Hepatology* 2000; **32**: 297-302
- 10 Ricciardi R, Schaffer BK, Kim RD, Shah SA, Donohue SE, Wheeler SM, Quarfordt SH, Callery MP, Meyers WC, Chari RS. Protective effects of ischemic preconditioning on the cold-preserved liver are tyrosine kinase dependent. *Transplantation* 2001; **72**: 406-412
- 11 Kamada N, Calne RY. A surgical experience with five hundred thirty liver transplants in the rat. *Surgery* 1983; **93**(1Pt1): 64-69
- 12 Moshage H, Kok B, Huizenga JR, Jansen PL. Nitrite and nitrate determinations in plasma: a critical evaluation. *Clin Chem* 1995; **41**(6Pt1): 892-896
- 13 Lee S, Charters AC, Chandler JG, Orloff MJ. A technique for orthotopic liver transplantation in the rat. *Transplantation* 1973; **16**: 664-669
- 14 Martin HB, Walter CL. Preconditioning: an endogenous defense against the insult of myocardial ischemia. *Anesth Analg* 1996; **83**: 639-645
- 15 Schwarz ER, Whyte WS, Kloner RA. Ischemic preconditioning. *Curr Opin Cardiol* 1997; **12**: 475-481
- 16 Heurteaux C, Lauritzen I, Widmann C, Lazdunski M. Essential role of adenosine, adenosine A1 receptors, and ATP-sensitive K⁺ channels in cerebral ischemic preconditioning. *Proc Natl Acad Sci U S A* 1995; **92**: 4666-4670
- 17 Schroeder CA Jr, Lee HT, Shah PM, Babu SC, Thompson CI, Belloni FL. Preconditioning with ischemia or adenosine protects skeletal muscle from ischemic tissue reperfusion injury. *J Surg Res* 1996; **63**: 29-34
- 18 Hotter G, Closa D, Prados M, Fernandez-Cruz L, Prats N, Gelpi E, Rosello-Catafau J. Intestinal preconditioning is mediated by a transient increase in nitric oxide. *Biochem Biophys Res Commun* 1996; **222**: 27-32
- 19 Arai M, Thurman RG, Lemasters JJ. Ischemic preconditioning of rat livers against cold storage-reperfusion injury: role of nonparenchymal cells and the phenomenon of heterologous preconditioning. *Liver Transpl* 2001; **7**: 292-299
- 20 Clavien PA, Harvey PR, Strasberg SM. Preservation and reperfusion injuries in liver allografts. An overview and synthesis of current studies. *Transplantation* 1992; **53**: 957-978
- 21 Zipfel A, Schenk M, You MS, Lauchart W, Bode C, Viebahn R. Endotoxemia in organ donors: graft function following liver transplantation. *Transpl Int* 2000; **13**(Suppl 1): S286-287
- 22 Maring JK, Klompaker IJ, Zwaveling JH, van Der Meer J, Limburg PC, Slooff MJ. Endotoxins and cytokines during liver transplantation: changes in plasma levels and effects on clinical outcome. *Liver Transpl* 2000; **6**: 480-488
- 23 Miyata T, Yokoyama I, Todo S, Tzakis A, Selby R, Starzl TE. Endotoxaemia, pulmonary complications, and thrombocytopenia in liver transplantation. *Lancet* 1989; **2**: 189-191
- 24 Urata K, Brault A, Rocheleau B, Huet PM. Role of Kupffer cells in the survival after rat liver transplantation with long portal vein clamping times. *Transpl Int* 2000; **13**: 420-427
- 25 Cohen MV, Liu GS, Downey JM. Preconditioning causes improved wall motion as well as smaller infarcts after transient coronary occlusion in rabbits. *Circulation* 1991; **84**: 341-349
- 26 Peralta C, Hotter G, Closa D, Gelpi E, Bulbena O, Rosello-Catafau J. Protective effect of preconditioning on the injury associated to hepatic ischemia-reperfusion in the rat: role of nitric oxide and adenosine. *Hepatology* 1997; **25**: 934-937
- 27 Peralta C, Hotter G, Closa D, Prats N, Xaus C, Gelpi E, Rosello-Catafau J. The protective role of adenosine in inducing nitric oxide synthesis in rat liver ischemia preconditioning is mediated by activation of adenosine A2 receptors. *Hepatology* 1999; **29**: 126-132
- 28 Smits P, Williams SB, Lipson DE, Banitt P, Rongen GA, Creager MA. Endothelial release of nitric oxide contributes to the vasodilator effect of adenosine in humans. *Circulation* 1995; **92**: 2135-2141

Effects of cytokines on carbon tetrachloride-induced hepatic fibrogenesis in rats

Li-Juan Zhang, Jie-Ping Yu, Dan Li, Yue-Hong Huang, Zhi-Xin Chen, Xiao-Zhong Wang

Li-Juan Zhang, Jie-Ping Yu, Department of Gastroenterology, Renmin Hospital, Wuhan University Medical School, Wuhan 430060, Hubei Province, China

Dan Li, Yue-Hong Huang, Zhi-Xin Chen, Xiao-Zhong Wang, Department of Gastroenterology, Union Hospital of Fujian Medical University, Fuzhou 350001, Fujian Province, China

Supported by Science and Technology fund of Fujian Province, No. 2003D05

Correspondence to: Xiao-Zhong Wang, Department of Gastroenterology, Union Hospital of Fujian Medical University, Fuzhou 350001, Fujian Province, China. drwangxz@pub6.fz.fj.cn

Telephone: +86-591-3357896-8482

Received: 2003-06-16 **Accepted:** 2003-07-24

Abstract

AIM: To observe the possible effects of transforming growth factor (TGF) β_1 , interleukin (IL)-6, tumor-necrosis factor (TNF) α and IL-10 on experimental rat hepatic fibrosis.

METHODS: One hundred SD rats were divided randomly into the three groups. Control group received intraperitoneal injection of saline (2 ml·kg⁻¹), twice a week. Fibrogenesis group was injected intraperitoneally with 50% carbon tetrachloride (CCl₄) (2 ml·kg⁻¹) twice a week. Fibrosis-intervention group was given IL-10 at a dose of 4 μ g·kg⁻¹ 20 minutes before CCl₄ administration from the third week. At the fifth, seventh, and ninth weeks, 7 to 10 rats in each group were sacrificed to collect serum. Levels of TGF- β_1 , TNF- α , IL-6 and IL-10 were determined by enzyme-linked immunosorbent assay (ELISA). The liver tissues were taken for routine histological examination.

RESULTS: Hepatic fibrosis was developed with the injection of CCl₄. Values of the circulating TGF β_1 , TNF α , IL-6 and IL-10 in the control group were 25.49±5.56 ng·L⁻¹, 15.18±3.83 ng·L⁻¹, 63.64±13.03 ng·L⁻¹ and 132.90±12.13 ng·L⁻¹, respectively. Their levels in the CCl₄-intoxication group were 31.13±6.41 ng·L⁻¹, 18.91±5.31 ng·L⁻¹, 89.08±25.39 ng·L⁻¹ and 57.63±18.88 ng·L⁻¹, respectively, and those in the IL-10-intervention group were 26.11±5.32 ng·L⁻¹, 13.99±1.86 ng·L⁻¹, 74.71±21.15 ng·L⁻¹ and 88.19±20.81 ng·L⁻¹, respectively. A gradual increase was observed in the levels of TGF β_1 , TNF α and IL-6 during hepatic fibrogenesis. These changes were partially reversed by simultaneous administration of IL-10. The histological parameters, characterized by CCl₄-intoxification, also seemed to be improved with IL-10 treatment, the collagen production was reduced at the ninth week and the histological activity index was decreased from 7.9±1.2 to 4.7±0.9.

CONCLUSION: TGF β_1 , TNF α and IL-6 may play important roles during CCl₄-induced hepatic fibrogenesis, and IL-10 may counterbalance their effects.

Zhang LJ, Yu JP, Li D, Huang YH, Chen ZX, Wang XZ. Effects of cytokines on carbon tetrachloride-induced hepatic fibrogenesis in rats. *World J Gastroenterol* 2004; 10(1): 77-81
<http://www.wjgnet.com/1007-9327/10/77.asp>

INTRODUCTION

Hepatic fibrosis is a common process of chronic liver injuries, characterized by increased deposition and altered composition of extracellular matrix (ECM)^[1-3]. Its final stage is cirrhosis, with the liver architecture distorted by collagen bands and formation of islands of regenerating parenchymal cells^[4,5]. Advanced fibrosis and cirrhosis are generally considered irreversible conditions. Many of the cellular mechanisms have been associated to hepatic fibrosis. Cytokines are soluble autocrine and paracrine mediators^[6]. Expression of several cytokines has been described in human liver diseases and experimental liver injuries. Carbon tetrachloride (CCl₄) is a hepatotoxin, causing liver necrosis, fibrosis and cirrhosis when administered sequentially. Hepatotoxicity is thought to involve two phases^[7]. First, CCl₄ is metabolized by cytochrome P450 in hepatocytes, giving rise to highly reactive trichloromethyl radicals. Second, inflammatory responses caused by CCl₄ play an important role. In the latter process, some hepatic cells, including Kupffer cells (KCs), hepatic stellate cells (HSCs) and sinusoidal endothelial cells (SECs), are activated to secrete cytokines which mediate the liver fibrogenesis. Several functions have been attributed to cytokines, including activation of HSCs, modulating expression and deposition of matrix proteins and regulating the regeneration of hepatocytes. Therefore, resolution of liver fibrosis could be associated with the downregulation of inflammatory responses mediated by cytokines^[8,9]. Among the cytokines, transforming growth factor (TGF) β_1 is associated to the activation of HSC and the following production of ECM^[10]. Tumor-necrosis factor (TNF) α and interleukin (IL)-6 are considered major hepatotoxicity mediators in several experimental models of liver injuries^[11]. IL-10 can modulate the inflammatory response and alleviate hepatotoxicity^[12]. In the present study, levels of circulating TGF β_1 , TNF- α , IL-6 and IL-10 were measured to investigate their possible roles during CCl₄-induced hepatic fibrogenesis in rats.

MATERIALS AND METHODS

Animals

One hundred SD rats, weighing 140 to 180 g, were divided randomly into control ($n=24$), fibrogenesis ($n=40$) and fibrosis-intervention groups ($n=36$). All rats were bred under routine conditions (room temperature, 22 °C±2 °C; humidity, 55%±5%; light, 12 hrs per day; drinking tap water and eating in any time; animal feed was provided by BK Company in Shanghai, China). The control rats were injected intraperitoneally with saline at a dose of 2 ml·kg⁻¹, twice a week. The rats in the other groups received intraperitoneal injection of 50% CCl₄ (2 ml·kg⁻¹), twice a week, as described previously^[13]. From the third week, the rats in intervention group were given intraperitoneally IL-10 (4 μ g·kg⁻¹, dissolved in saline) 20 minutes before CCl₄ administration, as proposed by Nelson *et al*^[14]. All injections were performed at Monday and Thursday, with their body weights determined before each injection. In the fifth week, 3 rats in the fibrogenesis group and 2 in the intervention group died. In the seventh week, 8 and 4 animals

in these two groups died. In the ninth week, 10 and 6 died. At this time point, 3 rats in the control group also died. In the fifth, seventh and ninth weeks, 7 to 10 rats in each group were sacrificed to collect plasma from the common carotid artery and their liver samples.

Histological examination

The formalin-fixed liver tissues were embedded in paraffin. Sections were stained with hematoxylin and eosin (HE) and examined under a light microscope independently by two pathologists. Stages of fibrosis were assessed using a semi-quantitative score method as described previously. Histological activity index (HAI) was evaluated using a numerical system proposed by Knodell *et al*^[15].

Enzyme-linked immunosorbent assay (ELISA)

Serum was collected by centrifugation at 4 °C and frozen till use. The levels of TGF- β_1 , TNF- α , IL-6 and IL-10 were measured by ELISA using the kits following the manufacture's instructions (Endogen Company, USA). Briefly, diluted serum samples were added in duplicate to 96-well plates coated with antibody and incubated at 37 °C for 2 hours. After each well was washed five times with washing buffer, peroxidase-labeled secondary antibody was added to each well and the plate was incubated at 37 °C for 1 hour. After each well was washed in a similar manner, the plate was incubated with tetramethylbenzidine at room temperature for 20 minutes. The reaction was stopped by adding 1 N sulfuric acid. Optical density was measured at 450 nm using a spectrophotometric reader. Sample concentration was accessed by a standard curve.

Statistical analysis

All data were expressed as $\bar{x} \pm s$, *t* test was used for comparison between groups. *P* values less than 0.05 were regarded as statistically significance.

RESULTS

Animal model

Liver fibrosis, as shown histologically, became remarkable during the treatment with CCl₄. In the fifth week, steatosis and ballooning degeneration were obvious. In the seventh week, the collagen fibers increased and began to extend to the parenchyma. In the ninth week, complete fibrous septa were seen and psedolobular structures were also present occasionally. In the IL-10-intervention group, the CCl₄-caused alterations as described above seemed to be markedly alleviated, with no evident changes observed in the fifth week, less profound steatosis and necrosis noted in the seventh week, and only early-stage fibrosis found in the ninth week. HAI decreased from 7.9 ± 1.2 in the fibrogenesis group to 4.7 ± 0.9 in the IL-10-intervention group ($P < 0.05$) (Figures 1-5).

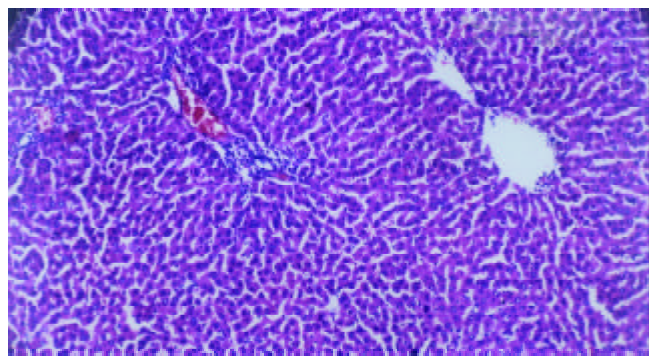


Figure 1 Liver of normal rat (H-E staining, $\times 100$).

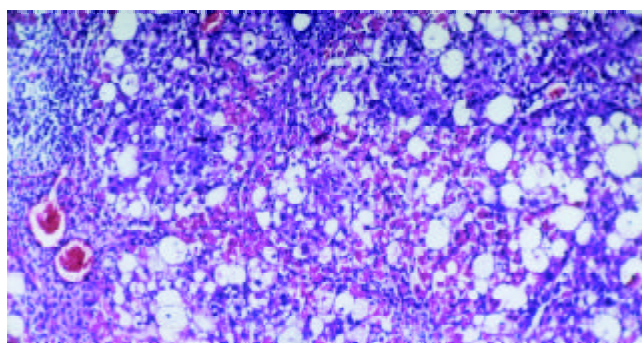


Figure 2 Liver of rats in group C (the fifth week, H-E staining, $\times 100$).

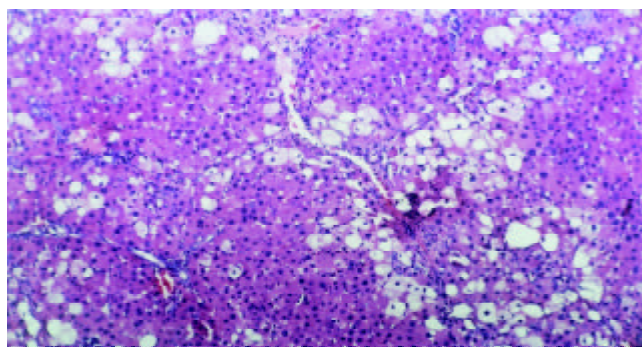


Figure 3 Liver of rats in group C (the seventh week, H-E staining, $\times 100$).

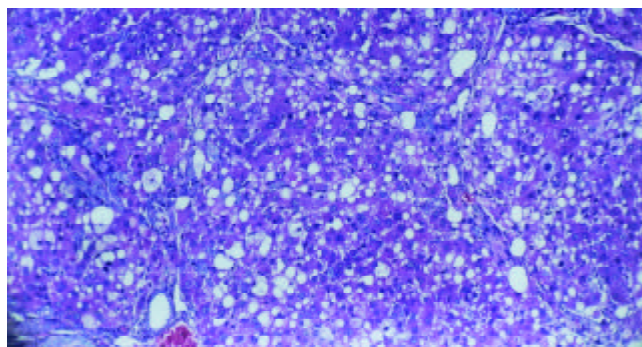


Figure 4 Liver of rats in group C (the ninth week, H-E staining, $\times 100$).

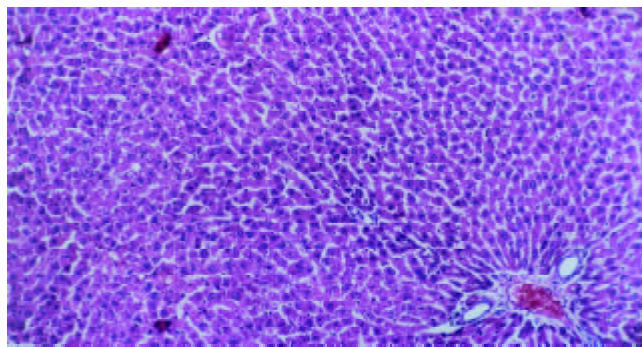


Figure 5 Liver of rats in group E (the ninth week, H-E staining, $\times 100$).

Serum levels of TGF β_1 , TNF- α , IL-6 and IL-10

As shown in Figure 6, the level of circulating IL-10 was lower in fibrogenesis group than in the control group ($P < 0.05$). The levels of TGF- β_1 , TNF- α and IL-6 in were higher in

fibrogenesis group than in the control group ($P < 0.05$). However, values of these three cytokines were significantly reduced after the intervention treatment with IL-10 ($P < 0.05$), being similar to the levels in the control group ($P > 0.05$). Therefore, serum concentrations of TGF- β_1 , IL-6 and TNF- α were increased during CCl₄-caused hepatic fibrogenesis.

Table 1 Concentrations of TGF- β_1 , TNF- α , IL-6 and IL-10 in sera from different groups (ng·L⁻¹)

Groups	Numbers of rats	TGF- β_1	TNF- α	IL-6	IL-10
Control (N)	21	25.49±5.56	15.18±3.83	63.64±13.03	132.90±12.13 ^{a,b}
Fibrogenesis (C)	30	31.13±6.41	18.91±5.31	89.08±25.39	57.63±18.88
IL-10-intervention (E)	30	26.11±5.32	13.99±1.86	74.71±21.15	88.19±20.81 ^c

^a $P < 0.05$ vs. C, ^b $P < 0.05$ vs. E, ^c $P > 0.05$ vs. C.

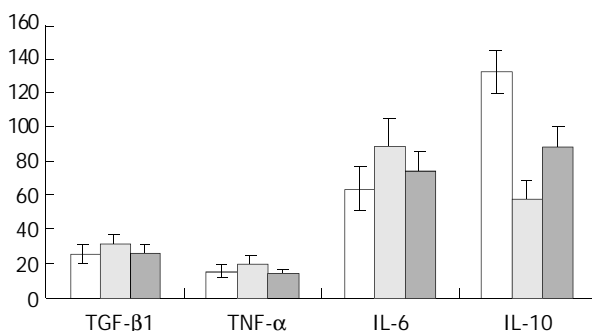


Figure 6 Levels of TGF- β_1 , TNF- α , IL-6 and IL-10 in serum from control, fibrogenesis and IL-10-intervention groups.

As shown in Figures 7-10, concentrations of TGF- β_1 , TNF- α and IL-6 were gradually increased along with CCl₄-intoxication ($P < 0.05$). These changes were partially reversed by the treatment with IL-10, particularly in the ninth week ($P < 0.05$).

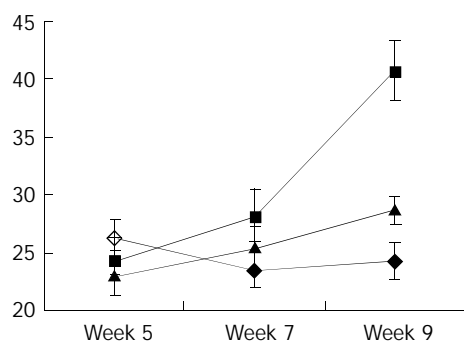


Figure 7 Levels of TGF- β_1 in serum from control (◆-), fibrogenesis (■-) and IL-10-intervention groups (▲-).

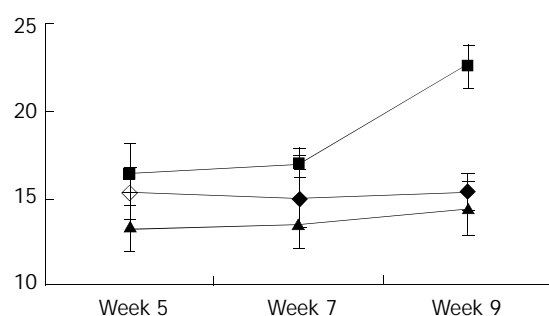


Figure 8 Levels of TNF- α in serum from control (◆-), fibrogenesis (■-) and IL-10-intervention groups (▲-).

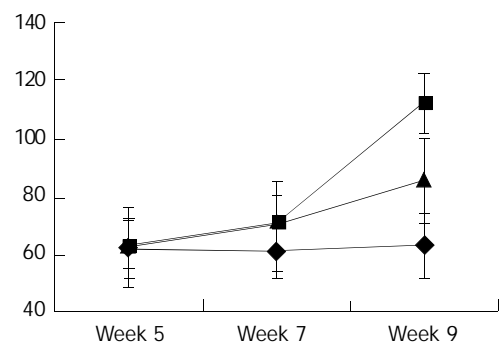


Figure 9 Levels of IL-6 in serum from control (◆-), fibrogenesis (■-) and IL-10-intervention groups (▲-).

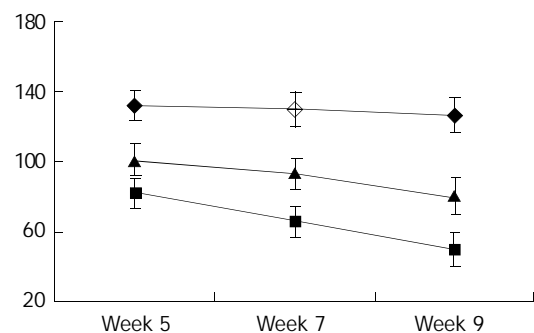


Figure 10 Levels of IL-10 in serum from control (◆-), fibrogenesis (■-) and IL-10-intervention groups (▲-).

DISCUSSION

Previous data have shown that rats chronically exposed to CCl₄ were resistant to cirrhosis. In rats, exposed to CCl₄ for 8 to 12 weeks could result in localized fibrosis^[16]. In the present study, fully developed hepatic fibrosis was observed in the rats after 9 weeks of CCl₄ intoxication. The contents of cytokines in serum were found to vary during the process. Cytokines constitute a complex network involved in the regulation of inflammatory responses and homeostasis of organ functions. Following liver injury, a wound healing process evolves, including proliferation of surrounding hepatocytes, proliferation and differentiation of stem cells, and conversion of parasinoidal cells into activated HSCs capable of driving the accumulation of ECM. If the injuries were persistent or the wound healing process was aberrant, the final phenotype might be a fibrotic, dysfunctional liver^[8]. A number of cytokines and growth factors could augment or inhibit the fibrotic response to injuries^[18]. Accumulating data indicate that HSCs are the major source of fibrillar and non-fibrillar matrix proteins during hepatic fibrogenesis. When activated, HSCs could proliferate and transform to a myofibroblast-like phenotype, expressing α -smooth muscle actin (α -SMA) and collagen types I, III and IV, fibronectin and proteoglycan^[19]. It has been found several cytokines play roles by acting on HSC, and among them, TGF- β_1 is one of the most important cytokines involved in the fibrotic and cirrhotic transformation of the liver^[20-23]. After a fibrogenic injury, expression of three forms of TGF- β is greatly upregulated in HSCs. It was reported that administration of TGF- β_1 *in vivo* induced an inflammatory reaction, and knock-out of TGF- β_1 gene resulted in widespread inflammatory diseases. Therefore, TGF- β_1 may have a pro-inflammatory effect.

TNF- α was originally identified as a circulating factor that resulted in remarkable hemorrhage and necrosis of tumors when administered to tumor-bearing mice. It has been implicated in a number of liver diseases and is an important mediator of

many physiological conditions. Several evidences suggest that TNF- α is among the most crucial components in the early signaling pathways leading to regeneration. However, there has been evidence that TNF- α is a primary endogenous factor mediating acute inflammatory conditions such as endotoxic shock. It appears that inhibition of the TNF- α effect might have a broader clinical application value than expected previously^[26]. In several animal models of immune-mediated liver injury or hepatotoxin sensitization, TNF- α administration could lead to hepatocyte apoptosis and liver failure^[27]. Besides its modulation effect on ECM production, TNF- α has been considered a mediator of cell injuries in liver caused by alcoholism, reperfusion, primary graft nonfunctional, graft rejection and endotoxic insult^[28,29]. TNF- α is expressed by both infiltrating inflammatory cells and hepatocytes in chronic liver injuries, and it has been proposed to play an important role during tissue damage^[30]. Our data provide a further evidence for the role during hepatic fibrosis.

The role of IL-6 during chronic liver injuries and fibrogenesis remains to be clarified. Some reports provided evidences for an important role of IL-6 in reducing CCl₄-induced acute and chronic liver injury and fibrosis^[31-33]. However, some other data showed that the serum level of IL-6 was associated with hepatic necroinflammatory activity in patients with chronic hepatitis and cirrhosis^[34,35]. Our results support the latter view. Animal experiments showed that IL-6 was associated to activated HSCs during acute and chronic injuries, indicating that IL-6 is a responsive element to liver injuries. Moreover, CCl₄-induced expression of TGF- β ₁ and hepatocyte growth factor in liver was shown to be associated with the serum level of IL-6. Thus, IL-6 might be vitally involved in fibrotic changes, partly by modulating intrahepatic expression of other cytokines^[36,37].

Recent studies have suggested a protective role of IL-10 during liver transplantation and experimental liver injuries induced by galactosamine and lipopolysaccharide^[38]. However, the mechanism of the protective effects is not fully understood. IL-10 is a potent anti-inflammatory cytokine that inhibits the synthesis of pro-inflammatory cytokines by T helper type 1 cells. It is produced locally in the liver and acts in an autocrine or a paracrine manner. Previous reports indicated that IL-10 had some role in remodeling ECM^[39,40]. IL-10 was shown to downregulate the synthesis of collagen type I and to upregulate expression of metalloproteinase. It could also play an antifibrogenic role by downregulating the profibrogenic cytokines including TGF- β ₁ and TNF- α ^[11,41]. Nelson *et al* treated 24 patients with chronic hepatitis C using IL-10, and found that IL-10 administration resulted in reduction of the serum ALT level, partial resolution of the hepatic inflammation and alleviation of the fibrosis^[14]. IL-10 may be useful in the treatment of chronic liver diseases regarding the prevention of advanced fibrosis and cirrhosis^[42].

REFERENCES

- 1 **Friedman SL.** Molecular mechanisms of hepatic fibrosis and principles of therapy. *J Gastroenterol* 1997; **32**: 424-430
- 2 **Du WD,** Zhang YE, Zhai WR, Zhou XM. Dynamic changes of type I, III and IV collagen synthesis and distribution of collagen-producing cells in carbon tetrachloride-induced rat liver fibrosis. *World J Gastroenterol* 1999; **5**: 397-403
- 3 **Wang JY,** Guo JS, Yang CQ. Expression of exogenous rat collagenase *in vitro* and in a rat model of liver fibrosis. *World J Gastroenterol* 2002; **8**: 901-907
- 4 **Friedman SL.** Seminars in medicine of the Beth Israel Hospital, Boston. The cellular basis of hepatic fibrosis: Mechanisms and treatment strategies. *N Engl J Med* 1993; **328**: 1828-1835
- 5 **Abdel-Aziz G,** Lebeau G, Rescan PY, Clement B, Rissel M, Deugnier Y, Campion JP, Guillouzo A. Reversibility of hepatic fibrosis in experimentally induced cholestasis in rat. *Am J Pathol* 1990; **137**: 1333-1342
- 6 **Nakamura T,** Sakata R, Ueno T, Sata M, Ueno H. Inhibition of transforming growth factor β prevents progression of liver fibrosis and enhances hepatocyte regeneration in dimethylnitrosamine-treated rats. *Hepatology* 2000; **32**: 247-255
- 7 **Shi J,** Aisaki K, Ikawa Y, Wake K. Evidence of hepatocyte apoptosis in rat liver after the administration of carbon tetrachloride. *Am J Pathol* 1998; **153**: 515-525
- 8 **Friedman SL.** Cytokines and fibrogenesis. *Semin Liver Dis* 1999; **19**: 129-140
- 9 **Koziel JK.** Cytokines in viral hepatitis. *Semin Liver Dis* 1999; **19**: 157-169
- 10 **Bissell DM,** Roulot D, George J. Transforming growth factor β and the liver. *Hepatology* 2001; **34**: 859-867
- 11 **Kovalovich K,** DeAngelis RA, Li W, Furth EE, Ciliberto G, Taub R. Increased toxin-induced liver injury and fibrosis in interleukin-6-deficient mice. *Hepatology* 2000; **31**: 149-159
- 12 **Yoshidome H,** Kato A, Edwards MJ, Lentsch AB. Interleukin-10 suppresses hepatic ischemia/reperfusion injury in mice: implications of a central role for nuclear factor κ B. *Hepatology* 1999; **30**: 203-208
- 13 **Morrow JD,** Awad JA, Kato T, Takahashi K, Badr KF, Robert LJ 2nd, Burk KF. Formation of novel non-cyclooxygenase-derived prostanoids (F2-isoprostanines) in carbon tetrachloride hepatotoxicity. An animal model of lipid peroxidation. *J Clin Invest* 1992; **90**: 2502-2507
- 14 **Nelson DR,** Lauwers GY, Lau JY, Davis G. Interleukin 10 treatment reduces fibrosis in patients with chronic hepatitis C: a pilot trial of interferon nonresponders. *Gastroenterology* 2000; **118**: 655-660
- 15 **Knodell RG,** Ishak KG, Black WC, Chen TS, Craig R, Kaplowitz N, Kiernan TW, Wollman J. Formulation and application of a numerical scoring system for assessing histological activity in asymptomatic chronic active hepatitis. *Hepatology* 1981; **1**: 431-435
- 16 **Tsukamoto H,** Matsuoka M, French SW. Experimental models of hepatic fibrosis: a review. *Semin Liver Dis* 1990; **10**: 56-65
- 17 **Missale G,** Ferrari C, Fiaccadori F. Cytokine mediators in acute inflammation and chronic course of viral hepatitis. *Ann Ital Med Int* 1995; **10**: 14-18
- 18 **Davis BH,** Kresina TF. Hepatic fibrogenesis. *Clin Lab Med* 1996; **16**: 361-375
- 19 **Iredale JP,** Benyon RC, Pickering J, McCullen M, Northrop M, Pawley S, Hovell C, Arthur MJ. Mechanisms of spontaneous resolution of rat liver fibrosis. Hepatic stellate cell apoptosis and reduced hepatic expression of metalloproteinase inhibitors. *J Clin Invest* 1998; **102**: 538-549
- 20 **Nakamura T,** Sakata R, Ueno T, Sata M, Ueno H. Inhibition of transforming growth factor β prevents progression of liver fibrosis and enhances hepatocyte regeneration in dimethylnitrosamine-treated rats. *Hepatology* 2000; **32**: 247-255
- 21 **Dooley S,** Delvoux B, Lahme B, Mangasser-Stephan K, Gressner AM. Modulation of transforming growth factor β response and signaling during transdifferentiation of rat hepatic stellate cells to myofibroblasts. *Hepatology* 2000; **31**: 1094-1106
- 22 **Garcia-Trevijano ER,** Irapuru MJ, Fontana L, Dominguez-Rosales JA, Auster A, Covarrubias-Pinedo A, Rojkind M. Transforming growth factor β 1 induces the expression of α 1 (I) procollagen mRNA by a hydrogen peroxide-C/EBP β -dependent mechanism in rat hepatic stellate cells. *Hepatology* 1999; **29**: 960-970
- 23 **Si XH,** Yang LJ. Extraction and purification of TGF β and its effect on the induction of apoptosis of hepatocytes. *World J Gastroenterol* 2001; **7**: 527-531
- 24 **Bissell DM,** Wang SS, Jarnagin WR, Roll FJ. Cell-specific expression of transforming growth factor-beta in rat liver. Evidence for autocrine regulation of hepatocyte proliferation. *J Clin Invest* 1995; **96**: 447-455
- 25 **Knittel T,** Janneck T, Muller T, Fellmer P, Ramadori G. Transforming growth factor beta 1-regulated gene expression of Ito cells. *Hepatology* 1996; **24**: 352-360
- 26 **Llorent L,** Richaud-Patin Y, Alcocer-Castillejos N, Ruiz-soto R, Mercado MA, Orozco H, Gamboa-Dominguez A, Alcocer-Varela J. Cytokine gene expression in cirrhotic and non-cirrhotic human liver. *J Hepatol* 1996; **24**: 555-563
- 27 **Zhang GL,** Wang YH, Teng HL, Lin ZB. Effects of aminoguanidine

- on nitric oxide production induced by inflammatory cytokines and endotoxin in cultured rat hepatocytes. *World J Gastroenterol* 2001; **7**: 331-334
- 28 **Roberts RA**, James NH, Cosulich SC. The role of protein kinase B and mitogen-activated protein kinase in epidermal growth factor and tumor necrosis factor α -mediated rat hepatocyte survival and apoptosis. *Hepatology* 2000; **31**: 420-427
- 29 **Crespo J**, Cayon A, Fernandez-Gil P, Hernandez-Guerra M, Mayorga M, Dominguez-Diez A, Fernandez-Escalante JC, Pons-Romero F. Gene expression of tumor necrosis factor α and TNF-receptors, p55 and p75, in nonalcoholic steatohepatitis patients. *Hepatology* 2001; **34**: 1158-1163
- 30 **Hernandez-munoz I**, de La Torre P, Sanchez-Alcazar JA, Garcia I, Santiago E, Munoz-Yague MT, Solis-Herruzo JA. Tumor necrosis factor α inhibits collagen $\alpha 1$ (I) gene expression in rat hepatic stellate cells through a G protein. *Gastroenterology* 1997; **113**: 625-640
- 31 **Selzner M**, Camargo CA, Clavien PA. Ischemia impairs liver regeneration after major tissue loss in rodents: protective effects of interleukin-6. *Hepatology* 1999; **30**: 469-475
- 32 **Sakamoto T**, Liu Z, Murase N, Ezure T, Yokomuro S, Poli V, Demetris AJ. Mitosis and apoptosis in the liver of interleukin-6-deficient mice after partial hepatectomy. *Hepatology* 1999; **29**: 403-411
- 33 **Peters M**, Blinn G, Jostock T, Schirmacher P, Meyer zum Buschenfelde KH, Galle PR, Rose-John S. Combined interleukin-6 and soluble interleukin-6 receptor accelerates murine liver regeneration. *Gastroenterol* 2000; **119**: 1663-1671
- 34 **Wang JY**, Wang XL, Lin P. Detection of serum TNF- α , IFN- γ , IL-6 and IL-8 in patients with hepatitis B. *World J Gastroenterol* 1999; **5**: 38-40
- 35 **Zhen Z**, Zhou JY, Liu JX, Hong ZJ, Pei X. Relationship between IL-6 and IL-6R and their pathogenicity in viral hepatitis. *Shijie Huaren Xiaohua Zazhi* 2000; **8**: 1434-1435
- 36 **Cressman DE**, Greenbaum LE, DeAngelis RA, Ciliberto G, Furth EE, Poli V, Taub R. Liver failure and defective hepatocyte regeneration in interleukin-6-deficient mice. *Science* 1996; **274**: 1379-1383
- 37 **Natsume M**, Tsuji H, Harada A, Akiyama M, Yano T, Ishikura H, Nakanishi I, Matsushima K, Kaneko S, Mukaid N. Attenuated liver fibrosis and depressed serum albumin levels in carbon tetrachloride-treated IL-6-deficient mice. *J Leukoc Biol* 1999; **66**: 601-608
- 38 **Louis H**, Le Moine O, Peny MO, Gulbis B, Nisol F, Goldman M, Deviere J. Hepatoprotective role of interleukin 10 in galactosamine/lipopolysaccharide mouse liver injury. *Gastroenterology* 1997; **112**: 935-942
- 39 **Reitamo S**, Remitz A, Tamai K, Uitto J. Interleukin-10 modulates type 1 collagen and matrix metalloprotease gene expression in cultured human skin fibroblasts. *J Clin Invest* 1994; **94**: 2489-2492
- 40 **Thompson K**, Maltby J, Fallowfield J, McAulay M, Millward-Sadler H, Sheron N. Interleukin-10 expression and function in experimental murine liver inflammation and fibrosis. *Hepatology* 1998; **28**: 1597-1606
- 41 **Louis H**, Van Laethem JL, Wu W, Quertinmont E, Degraef C, Van den Berg K, Demols A, Goldman M, Le Moine O, Geerts A, Deviere J. Interleukin-10 controls neutrophilic infiltration, hepatocyte proliferation, and liver fibrosis induced by carbon tetrachloride in mice. *Hepatology* 1998; **28**: 1607-1615
- 42 **Wang XZ**, Zhang LJ, Li D, Huang YH, Chen ZX, Li B. Effects of transmitters and interleukin-10 on rat hepatic fibrosis induced by CCl₄. *World J Gastroenterol* 2003; **9**: 539-543

Edited by Su Q and Wang XL

HBV cccDNA in patients' sera as an indicator for HBV reactivation and an early signal of liver damage

Ying Chen, Johnny Sze, Ming-Liang He

Ying Chen, Johnny Sze, Ming-Liang He, The Institute of Molecular Biology, The University of Hong Kong, Hong Kong, China

Supported by CRCG grant from the University of Hong Kong, CERG grant from University Grant Council of Hong Kong, and Research Fund from Science and Technology Commission of Shanghai, China

Correspondence to: Dr. Ming-Liang He, The Institute of Molecular Biology, The University of Hong Kong, Hong Kong, China. mlhe@hkucc.hku.hk

Telephone: +852-2299-0758 **Fax:** +852-2817-1006

Received: 2003-08-02 **Accepted:** 2003-10-22

Abstract

AIM: To evaluate the covalently closed circle DNA (cccDNA) level of hepatitis B virus (HBV) in patients' liver and sera.

METHODS: HBV DNA was isolated from patients' liver biopsies and sera. A sensitive real-time PCR method, which is capable of differentiation of HBV viral genomic DNA and cccDNA, was used to quantify the total HBV cccDNA. The total HBV viral DNA was quantitated by real-time PCR using a HBV diagnostic kit (PG Biotech, LTD, Shenzhen, China) described previously.

RESULTS: For the first time, we measured the level of HBV DNA and cccDNA isolated from ten HBV patients' liver biopsies and sera. In the liver biopsies, cccDNA was detected from all the biopsy samples. The copy number of cccDNA ranged from 0.03 to 173.1 per cell, the copy number of total HBV DNA ranged from 0.08 to 3 717 per cell. The ratio of total HBV DNA to cccDNA ranged from 1 to 3 406. In the sera, cccDNA was only detected from six samples whereas HBV viral DNA was detected from all ten samples. The ratio of cccDNA to total HBV DNA ranged from 0 to 1.77%. To further investigate the reason why cccDNA could only be detected in some patients' sera, we performed longitudinal studies. The cccDNA was detected from the patients' sera with HBV reactivation but not from the patients' sera without HBV reactivation. The level of cccDNA in the sera was correlated with ALT and viral load in the HBV reactivation patients.

CONCLUSION: HBV cccDNA is actively transcribed and replicated in some patients' hepatocytes, which is reflected by a high ratio of HBV total DNA vs cccDNA. Detection of cccDNA in the liver biopsy will provide an end-point for the anti-HBV therapy. The occurrence of cccDNA in the sera is an early signal of liver damage, which may be another important clinical parameter.

Chen Y, Sze J, He ML. HBV cccDNA in patients' sera as an indicator for HBV reactivation and an early signal of liver damage. *World J Gastroenterol* 2004; 10(1): 82-85
<http://www.wjgnet.com/1007-9327/10/82.asp>

INTRODUCTION

Chronic hepatitis B Virus (HBV) infection is one of the most

common diseases leading to a high morbidity and mortality due to the development of liver failure, liver cirrhosis (LC) and hepatocellular carcinomas (HCC)^[3-28]. There are over 300 million people suffering from HBV infection worldwide, and more than 10% of Chinese are HBV carriers^[3,5,14]. Infection by hepatitis B virus causes complicated biochemical, immunological and histological changes in host^[7-9,11,16,18,23,24,27]. Viral kinetic studies have shown that the viral load goes through a complex series of stages during anti-HBV chemotherapy^[21,22,29-31]. The HBV reactivation often occurs after cessation of anti-HBV treatment^[22,24,32], which is reflected by the increases of hepatitis B e antigen (HBeAg) and DNA levels in serum. Clinically, this may manifest as hepatitis, hepatic failure, and even death. Despite its clinical importance, there are few data on the incidence and risk factors of hepatitis due to HBV reactivation after chemotherapy. In particular, the relationship of various HBV virological parameters and HBV reactivation is unclear.

HBV covalently closed circular (ccc) DNA is a critical intracellular replicative intermediate, which acts as the template for transcription of viral RNAs serving either as viral pregenome RNAs, or as mRNAs coding for the multifunctional polymerase, core, X and envelope (S) proteins^[25,26]. All the HBV proteins play crucial roles in HBV gene transcription, replication, viral packaging and recycling. Due to lack of proofreading functions of polymerase, HBV goes through a fast mutagenesis and creates drug resistant strains^[13,17,19,24,26,29,32], which contributes to the viral cccDNA pool. Because cccDNA of HBV is resource of new HBV viruses and resistance to drug treatment, it is believed that cccDNA is the major reason for HBV reactivation after stopping the anti-HBV therapy^[21,24,25]. Monitoring of HBV viral load, antigens, mutations and cccDNA levels will therefore provide a direct indication of HBV activity in the body^[12,13,15,17-21, 28-32].

We previously developed a sensitive method to quantify HBV cccDNA, which has been successfully used to determine the amount of HBV cccDNA isolated from liver biopsy^[1]. Here we report that HBV cccDNA can be detected both in liver biopsy and in patients' sera. The sera cccDNA level is correlated with ALT and viral load in HBV reactivation patients, but cannot be detected in patients' sera without HBV reactivation. Our results indicate that the occurrence of cccDNA is an early signal of liver damage, which may be another important clinical parameter.

MATERIALS AND METHODS

cccDNA standard^{1,2]}

A plasmid containing Chinese HBV genome (pHBV-adr) was a gift from Professor Yuan Wang. The supercoiled plasmid (cccDNA) was isolated by CsCl purification. The cccDNA concentration was determined by measurement of OD260 and verified by agarose gel electrophoresis. The copy number was determined by its molecular weight.

HBV viral DNA preparation^[1]

HBV viral DNA was extracted from either 200 ul of patients' sera or weighed liver biopsies using a QIAamp DNA blood or

tissue mini kit (QIAGEN, Hilden, Germany) according to the manufacturer's instructions.

Quantification of HBV cccDNA using real-time PCR

HBV cccDNA quantification was performed as described previously^[1,2], with minor modifications. Briefly, a pair of primers (forward primer: 5'-ACTCTTGGACTCBCAGCAATG-3', reverse primer: 5'-CTTTATACGGGTCAATGTCCA-3'), which can specifically amplify a DNA fragment from HBV cccDNA but not viral genomic DNA by PCR, were used for real-time PCR. In a typical real-time PCR reaction, 250 nM of the probe (5'-FAM-CTTTTTCACCTCTGCCTAATCATCTCWTGTTCA-TAMRA-3') and 900 nM of the two PCR primers were used. For total HBV quantification, PCR amplification was performed with an HBV DNA diagnostic kit (PG Biotech. Ltd, China) using ABI 7900HT sequence detection system. The PCR program consisted of an initial denaturing step at 95 °C for 10 min, followed by 40 amplification cycles at 95 °C for 15 sec and at 61.5 °C for 1 min.

Patient samples

The patients were treated with chemotherapy at Queen Mary Hospital, Hong Kong, from January 2000 to May 2002. In accordance with the standard protocols, all the patients who received chemotherapy were screened for HBsAg, HBsAb, human immunodeficiency virus antibody (HIV Ab), and HBV DNA by PCR and hepatitis C antibody (anti-HCV), with commercially-available enzyme immunoassays (Abbott Laboratories, Chicago, IL, USA). HBcAb was tested by RIA (Corab; Abbott). For all HBsAg positive patients, further serological testing for hepatitis B e antigen (HBeAg), hepatitis B e antibody (HBeAb) and serum HBV DNA was performed by PCR, and chemotherapy was administered with lamivudine. All HbsAg-positive recipients were tested at 2-week intervals for liver function (including serum alanine aminotransferase, serum albumin and bilirubin) and serum HBV DNA during chemotherapy. Hepatitis serology (HBsAg, HBeAg, HBeAb, HBV DNA by PCR, and HCV RNA by RT-PCR) was performed on the serum collected preceding and during the events whenever there was any clinical suspicion of liver damage due to hepatitis B infection. The occurrences of hepatic events (acute hepatitis, chronic hepatitis, anicteric and icteric hepatitis, hepatic failure) were recorded. Hepatitis was defined as a more than three-fold elevation of serum aminotransferase above the upper limit of normal, on two consecutive determinations at least five days apart. HBV reactivation was defined to occur when preceded or accompanied by an elevation of serum HBV DNA to more

than ten times that of the pre-exacerbation baseline, or when the serum HBV DNA turned from negative to positive, or when the HBsAg became positive and remained so for two consecutive readings five days apart.

All serum and biopsy samples were stored at -70 °C. All patients who developed post-chemotherapy hepatitis due to HBV reactivation were treated with lamivudine 100 mg once daily.

RESULTS

HBV cccDNA existed in all patients' hepatocytes but only in a subset of patients' sera

To elucidate the cccDNA status in HBV patients, we quantified the cccDNA and total HBV DNA level in the liver biopsies. The total DNA was isolated from weighed liver biopsies and quantified with an HBV diagnostic kit by real-time PCR. The HBV cccDNA was also measured by real-time PCR. HBV cccDNA was detected in all the HBV patients' liver biopsies. The copy number of cccDNA in patients' hepatocytes ranged from 0.05 to 168 copies per cell, which is consistent with the estimates from Southern blot data^[10]. The copy number of total HBV DNA in patients' hepatocytes ranged from 0.08 to over 3 000 copies per cell. The ratio of cccDNA to total HBV DNA ranged from 1 to 3 406 (Table 1), indicating that cccDNA in patients' hepatocytes had active replication and relative silent status.

To investigate whether cccDNA could be released into sera due to liver inflammation and necrosis, viral DNA was isolated from patients' sera and quantified by real-time PCR. Interestingly, cccDNA could only be detected in a subset of patients' sera, while HBV DNA was detected in all the patients' sera. The copy number of viral load ranged from 5.4×10^5 to 1.8×10^{11} per ml while the copy number of cccDNA ranged from undetectable level (less than 1 000 copies/ml^[11]) to 3.1×10^7 per ml. The ratio of cccDNA to total viral DNA ranged from 0 to 1.77%. There was no correlation between the copy number of cccDNA and total viral DNA in the randomized patients (Table 1).

cccDNA is an early signal of liver damage

To investigate the medical significance of cccDNA in sera, longitudinal studies were performed. Patients with or without HBV reactivation during lamivudine treatment were chosen for this study. The patients' sera were collected every two weeks and HBV DNA was isolated for quantification of HBV cccDNA and total HBV DNA. According to our results, HBV cccDNA was not detectable by sensitive real-time PCR in patients without HBV reactivation (data not shown), but was detectable in patients with HBV reactivation (Figures

Table 1 HBV cccDNA in patients' hepatocytes and sera

Patients	HBV DNA in the Biopsies (copy/cell)			HBV DNA in the sera (copy/ml)		
	cccDNA	HBV DNA ^a	HBV/ccc ^b	cccDNA	HBV DNA ^c	ccc/HBV ^d
1	2.05	195.5	98.7	3.4×10^6	4.8×10^{10}	0.01%
2	0.03	0.17	5.8	UN	6.6×10^7	--
3	173.1	799.5	4.6	3.1×10^5	6.0×10^{10}	0.001%
4	0.16	8.13	51.7	UN	1.9×10^7	--
5	0.03	0.08	2.8	UN	5.4×10^5	--
6	16.02	17.4	1.1	2.4×10^6	5.3×10^8	0.46%
7	18.03	3717	206	3.1×10^7	1.8×10^{11}	0.02%
8	0.79	13.1	16.5	UN	2.4×10^{10}	--
9	0.05	153.3	3406	2.8×10^5	3.0×10^9	0.01%
10	2.06	16.4	8	2.7×10^6	7.5×10^8	1.77%

^aThe total HBV copies per cell in the patients' liver biopsies; ^bThe ratio of total HBV DNA to cccDNA in the patients' liver biopsy; ^cThe total HBV copies per ml of the patients' sera; ^dThe ratio of cccDNA to total HBV DNA in the patients' sera. UN, undetectable.

1A and 1B). The cccDNA level was correlated with viral load (Figures 1A and 1B), which occurred earlier than ALT. Before the ALT value increased, both the cccDNA level and viral load rose to a high level. Once the ALT value increased, the cccDNA level dropped rapidly. These results suggest that patients whose sera contain cccDNA are at a high risk of HBV reactivation, and that HBV cccDNA develops in the sera earlier than ALT elevation.

Our results suggest that serum cccDNA level may be an important parameter for anti-HBV treatment, and that a low level of cccDNA in hepatocytes should be an end point of anti-HBV treatment.

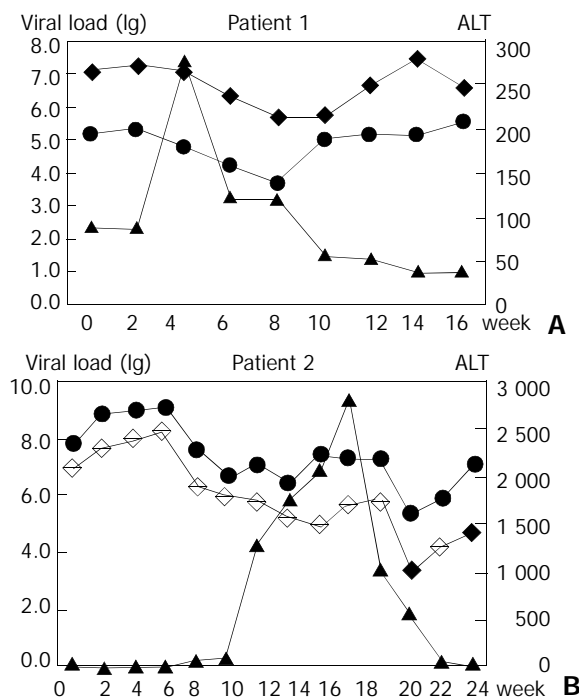


Figure 1 Kinetics of cccDNA in HBV reactivation patients. The copy numbers of total HBV and cccDNA were determined by real-time PCR. The cccDNA level was parallel to the total viral load both in the patients 1 and 2; the cccDNA level increased before ALT rose. Diamond: HBV viral load, dot: cccDNA, triangle: ALT.

DISCUSSION

Little information is available about HBV cccDNA and its activities *in vivo* due to the difficulty of differentiation of HBV cccDNA and viral genomic DNA, although a lot of work has been done on the HBV viral kinetics^[21,22,29-31]. In the hepatitis B virus life cycle, cccDNA serves as templates for viral gene transcription and replication in hepatocytes^[25,26]. It has been shown that cccDNA is the major reason for HBV reactivation after cessation of anti-HBV treatment^[24,25]. Therefore, quantification of HBV cccDNA will provide useful information for the end-point of anti-HBV therapy.

In this paper, we first report the quantitative data on HBV cccDNA in patients' liver biopsy and sera. We previously established a quantitative real-time PCR method which can specifically differentiate HBV viral genomic DNA and cccDNA^[1]. This sensitive method provided us an opportunity to investigate HBV cccDNA status in the liver biopsy and patients' sera. Our data indicated that cccDNA in the patients' liver might have two status: active and relative silent status. This was reflected by the ratio of viral total DNA to cccDNA. To our surprising, HBV cccDNA was also detected in a part of patients' sera. The release of cccDNA of hepatitis B virus to the sera might be the consequence of liver damages, such as

liver inflammation, necrosis. Longitudinal studies revealed that the release of cccDNA to the sera was an early signal of liver damage, which is correlated with ALT and viral load in HBV reactivated patients. Therefore, measurement of the cccDNA level in the liver may provide an end-point of anti-HBV therapy, and detection of the cccDNA level in the sera may provide a better guidance to protect patients from HBV reactivation.

Because this is the first time to provide the quantitative data on HBV cccDNA status, and the limitation of patient samples, more clinic studies on the cccDNA kinetics are required to better understand HBV biology and provide a better guidance for the anti-HBV treatment.

ACKNOWLEDGMENTS

We wish to thank Prof. Y. Wang (Inst. Of Biochemistry, Shanghai, China) for providing HBV genomic clone pHBV, and Dr. G. Lau (Queen Mary Hospital, Hong Kong) for the liver biopsies and sera.

REFERENCES

- 1 He ML, Wu J, Chen Y, Lin MC, Lau GK, Kung HF. A new and sensitive method for the quantification of HBV cccDNA by real-time PCR. *Biochem Biophys Res Commun* 2002; **295**: 1102-1107
- 2 Chen Y, Du Y, Wu Y, Chan CP, Tan YQ, Kung HF, He ML. Inhibition of hepatitis B virus (HBV) replication by stably-expressed shRNA. *Biochem Biophys Res Commun* 2003; **311**: 398-404
- 3 Wang FS. Current status and prospects of studies on human genetic alleles associated with hepatitis B virus infection. *World J Gastroenterol* 2003; **9**: 641-644
- 4 Tang ZY. Hepatocellular carcinoma-cause, treatment and metastasis. *World J Gastroenterol* 2001; **7**: 445-454
- 5 Cai RL, Meng W, Lu HY, Lin WY, Jiang F, Shen FM. Segregation analysis of hepatocellular carcinoma in a moderately high-incidence area of East China. *World J Gastroenterol* 2003; **9**: 2428-2432
- 6 Cao ZX, Chen XP, Wu ZD. Effects of splenectomy in patients with cirrhosis undergoing hepatic resection for hepatocellular carcinoma. *World J Gastroenterol* 2003; **9**: 2460-2463
- 7 Wang NS, Wu ZL, Zhang YE, Guo MY, Liao LT. Role of hepatitis B virus infection in pathogenesis of IgA nephropathy. *World J Gastroenterol* 2003; **9**: 2004-2008
- 8 Wang JY, Liu P. Abnormal immunity and gene mutation in patients with severe hepatitis-B. *World J Gastroenterol* 2003; **9**: 2009-2011
- 9 Wang KX, Peng JL, Wang XF, Tian Y, Wang J, Li CP. Detection of T lymphocyte subsets and mIL-2R on surface of PBMC in patients with hepatitis B. *World J Gastroenterol* 2003; **9**: 2017-2020
- 10 Li XM, Yang YB, Hou HY, Shi ZJ, Shen HM, Teng BQ, Li AM, Shi MF, Zou L. Interruption of HBV intrauterine transmission: A clinical study. *World J Gastroenterol* 2003; **9**: 1501-1503
- 11 Wu CH, Ouyang EC, Walton C, Promrat K, Forouhar F, Wu GY. Hepatitis B virus infection of transplanted human hepatocytes causes a biochemical and histological hepatitis in immunocompetent rats. *World J Gastroenterol* 2003; **9**: 978-983
- 12 Jaboli MF, Fabbri C, Liva S, Azzaroli F, Nigro G, Giovanelli S, Ferrara F, Miracolo A, Marchetto S, Montagnani M, Colecchia A, Festi D, Reggiani LB, Roda E, Mazzella G. Long-term alpha interferon and lamivudine combination therapy in non-responder patients with anti-HBe-positive chronic hepatitis B: Results of an open, controlled trial. *World J Gastroenterol* 2003; **9**: 1491-1495
- 13 Wang Y, Liu H, Zhou Q, Li X. Analysis of point mutation in site 1896 of HBV precore and its detection in the tissues and serum of HCC patients. *World J Gastroenterol* 2000; **6**: 395-397
- 14 Roussos A, Goritsas C, Pappas T, Spanaki M, Papadaki P, Ferti A. Prevalence of hepatitis B and C markers among refugees in Athens. *World J Gastroenterol* 2003; **9**: 993-995
- 15 Peng XM, Chen XJ, Li JG, Gu L, Huang YS, Gao ZL. Novel assay of competitively differentiated polymerase chain reaction for screening point mutation of hepatitis B virus. *World J Gastroenterol* 2003; **9**: 1743-1746
- 16 Song CZ, Bai ZL, Song CC, Wang QW. Aggregate formation of hepatitis B virus X protein affects cell cycle and apoptosis. *World*

- J Gastroenterol* 2003; **9**: 1521-1524
- 17 **Yang X**, Tang XP, Lei JH, Luo HY, Zhang YH. A novel stop codon mutation in HBsAg gene identified in a hepatitis B virus strain associated with cryptogenic cirrhosis. *World J Gastroenterol* 2003; **9**: 1516-1520
- 18 **Shen LJ**, Zhang HX, Zhang ZJ, Li JY, Chen MQ, Yang WB, Huang R. Detection of HBV, PCNA and GST-pi in hepatocellular carcinoma and chronic liver diseases. *World J Gastroenterol* 2003; **9**: 459-462
- 19 **Yang SS**, Hsu CT, Hu JT, Lai YC, Wu CH. Lamivudine does not increase the efficacy of interferon in the treatment of mutant type chronic viral hepatitis B. *World J Gastroenterol* 2002; **8**: 868-871
- 20 **Zhuang L**, You J, Tang BZ, Ding SY, Yan KH, Peng D, Zhang YM, Zhang L. Preliminary results of Thymosin- α 1 versus interferon- α -treatment in patients with HBeAg negative and serum HBV DNA positive chronic hepatitis B. *World J Gastroenterol* 2001; **7**: 407-410
- 21 **Lewin SR**, Ribeiro RM, Walters T, Lau GK, Bowden S, Locarnini S, Perelson AS. Analysis of hepatitis B viral load decline under potent therapy: complex decay profiles observed. *Hepatology* 2001; **34**: 1012-1020
- 22 **Lau GK**, He ML, Fong DY, Bartholomeusz A, Au WY, Lie AK, Locarnini S, Liang R. Preemptive use of lamivudine reduces hepatitis B exacerbation after allogeneic hematopoietic cell transplantation. *Hepatology* 2002; **36**: 702-709
- 23 **Hou CS**, Wang GQ, Lu SL, Yue B, Li MR, Wang XY, Yu JW. Role of activation-induced cell death in pathogenesis of patients with chronic hepatitis B. *World J Gastroenterol* 2003; **9**: 2356-2358
- 24 **Yokosuka O**, Omata M, Imazeki F, Okuda K, Summers J. Changes of hepatitis B virus DNA in liver and serum caused by recombinant leukocyte interferon treatment: analysis of intrahepatic replicative hepatitis B virus DNA. *Hepatology* 1985; **5**: 728-734
- 25 **Seeger C**, Mason WS. Hepatitis B Virus Biology. *Microb Molec Biol Review* 2000; **64**: 51-58
- 26 **Summers J**, Mason WS. Replication of the genome of a hepatitis B-like virus by reverse transcription of an RNA intermediate. *Cell* 1982; **29**: 403-415
- 27 **Jiang YG**, Wang YM, Liu TH, Liu J. Association between HLA class II gene and susceptibility or resistance to chronic hepatitis B. *World J Gastroenterol* 2003; **9**: 2221-2225
- 28 **Fan CL**, Wei L, Jiang D, Chen HS, Gao Y, Li RB, Wang Y. Spontaneous viral clearance after 6-21 years of hepatitis B and C viruses coinfection in high HBV endemic area. *World J Gastroenterol* 2003; **9**: 2012-2016
- 29 **Gaillard RK**, Barnard J, Lopez V, Hodges P, Bourne E, Johnson L, Allen MI, Condreay P, Miller WH, Condreay LD. Kinetic analysis of wild-type and YMDD mutant hepatitis B virus polymerases and effects of deoxyribonucleotide concentrations on polymerase activity. *Antimicrob Agents Chemother* 2002; **46**: 1005-1013
- 30 **Tsiang M**, Rooney JF, Toole JJ, Gibbs CS. Biphasic clearance kinetics of hepatitis B virus from patients during adefovir dipivoxil therapy. *Hepatology* 1999; **29**: 1863-1869
- 31 **Zeuzem S**, de Man RA, Honkoop P, Roth WK, Schalm SW, Schmidt JM. Dynamics of hepatitis B virus infection *in vivo*. *J Hepatol* 1997; **27**: 431-436
- 32 **Ni YH**, Chang MH, Hsu HY, Chen HL. Long-term follow-up study of core gene deletion mutants in children with chronic hepatitis B virus infection. *Hepatology* 2000; **32**: 124-128

Edited by Wang XL

Expression of TIMP-1 and TIMP-2 in rats with hepatic fibrosis

Qing-He Nie, Guo-Rong Duan, Xin-Dong Luo, Yu-Mei Xie, Hong Luo, Yong-Xing Zhou, Bo-Rong Pan

Qing-He Nie, Guo-Rong Duan, Xin-Dong Luo, Yu-Mei Xie, Hong Luo, Yong-Xing Zhou, Chinese PLA Centre of Diagnosis and Treatment for Infectious Diseases, Tangdu Hospital, Fourth Military Medical University, Xi'an 710038, Shaanxi Province, China
Bo-Rong Pan, Department of Oncology, Xijing Hospital, Fourth Military Medical University, Xi'an 710032, Shaanxi Province, China
Supported by the Postdoctoral Science Foundation of China, No. 1999-10

Correspondence to: Dr. Qing-He Nie, Chinese PLA Centre of Diagnosis and Treatment for Infectious Diseases, Tangdu Hospital, Fourth Military Medical University, Xi'an 710038, Shaanxi Province, China. nieqinghe@hotmail.com

Telephone: +86-29-3377852 **Fax:** +86-29-3537377

Received: 2003-05-13 **Accepted:** 2003-06-02

Abstract

AIM: To investigate the location and expression of TIMP-1 and TIMP-2 in the liver of normal and experimental hepatic fibrosis in rats.

METHODS: The rat models of experimental immunity hepatic fibrosis ($n=20$) were prepared by the means of immunologic attacking with human serum albumin (HSA), and normal rats ($n=10$) served as control group. Both immunohistochemistry and *in situ* hybridization methods were respectively used to detect the TIMP-1 and TIMP-2 mRNA and related antigens in liver. The liver tissue was detected to find out the gene expression of TIMP-1 and TIMP-2 with RT-PCR.

RESULTS: The TIMP-1 and TIMP-2 related antigens in livers of experimental group were expressed in myofibroblasts and fibroblasts (TIMP-1: 482 ± 65 vs 60 ± 20 ; TIMP-2: 336 ± 48 vs 50 ± 19 , $P<0.001$). This was the most obvious in portal area and fibrous septum. The positive signals were located in cytoplasm, not in nucleus. Such distribution and location were confirmed by *situ* hybridization (TIMP-1/*b-actin*: 1.86 ± 0.47 vs 0.36 ± 0.08 ; TIMP-2/*b-actin*: 1.06 ± 0.22 vs 0.36 ± 0.08 , $P<0.001$). The expression of TIMP-1 and TIMP-2 was seen in the liver of normal rats, but the expression level was very low. However, the expression of TIMP-1 and TIMP-2 in the liver of experimental group was obviously high.

CONCLUSION: In the process of hepatic fibrosis, fibroblasts and myofibroblasts are the major cells that express TIMPs. The more serious the hepatic fibrosis is in the injured liver, the higher the level of TIMP-1 and TIMP-2 gene expression.

Nie QH, Duan GR, Luo XD, Xie YM, Luo H, Zhou YX, Pan BR. Expression of TIMP-1 and TIMP-2 in rats with hepatic fibrosis. *World J Gastroenterol* 2004; 10(1): 86-90

<http://www.wjgnet.com/1007-9327/10/86.asp>

INTRODUCTION

Chronic viral hepatitis, alcoholism and schistosomiasis are the most common diseases in China^[1-9]. At present, two main strategies for the treatment of chronic liver diseases are anti-

viral therapies and anti-fibrotic therapies^[10-14]. Hepatic fibrosis is a main pathologic basis of chronic liver diseases, particularly caused by viral hepatitis, and cirrhosis as a severe outcome is the end stage of various chronic liver diseases with increased synthesis and/or inhibition of matrix degradation. Although important progress in hepatic fibrosis has been achieved in the last decades, its mechanism is still debated at present. The formation of hepatic fibrosis is a response to inflammation, but it is interesting that hepatic fibrosis is not found in acute liver injury. It has been proved by the experiment *in vitro* that apoptosis could not be found in inactive hepatic stellate cells (HSC). This may imply that the mechanism of hepatic fibrosis is complicated, and many questions are being explored^[15-23].

Hepatic fibrosis is a pathological process with the overlapped extracellular matrix (ECM) protein. The latest evidence suggests that the change of ECM mainly is regulated by metalloproteinases (MMPs). Hepatic fibrosis is formed because the specific tissue inhibitors of metalloproteinases (TIMPs) inhibit ECM degradation^[24-28]. Which cells can express and produce TIMPs? Until now, there still are different views on the involvement of TIMPs in normal liver tissue and experimental hepatic fibrosis rats. The expression and location of TIMPs antigens and TIMP mRNA are measured in rat livers with mAb and cDNA probes of TIMP-1 and TIMP-2 by immunohistochemical staining, and gene expression of TIMP-1 and TIMP-2 is observed by PCR technique.

MATERIALS AND METHODS

Animal experiments

Forty adult female Wistar rats, weighing 120-150 g (provided by Experimental Animal Centre of Fourth Military Medical University) were employed in the study. The rats were randomly divided into 2 groups. A rat model of hepatic fibrosis was produced by immunological attacking with human serum albumin (HSA), using the method introduced by Wang *et al*^[29]. Anti-mouse monoclonal antibody IgG was purchased from Coulter Co.(France). Twenty healthy female Wistar rats were regarded as control group. Animals survived from the experimental attack were randomly allocated as follows. All rats were injected with 0.5 mL HSA diluted with normal saline (0.5 mL equals to 4 mg HSA) and same quantity of an incomplete Freund's adjuvant (Sigma), once every 14 days for the first two times, then once every 10 days, 2 times. Ten days after the last injection, serum antibody was measured. Positive rats were chosen for experiment through coccygeal vein injection of HSA, twice a week, 2.5 mg for each at the first week, and then gradually 0.5 mg- increase once for each to 4.5 mg, and this dose was maintained for 2 months. All animals were sacrificed under narcosis, and their livers were immediately excised. Part of liver specimen was frozen in liquid nitrogen, part fixed in 40 g/L formaldehyde, the rest was fixed with glutaraldehyde, and investigated with electron microscope.

Immunohistochemical staining of TIMP-1 and TIMP-2

According to the methods previously described^[30-33], the serial paraffin sections of liver samples at 4 μ m thickness were performed for SP immune staining described by streptomycin

Table 1 Sequences of TIMP-1, TIMP-2 and β -actin primers

	Primer	Nucleic acid sections	Position (bp)
TIMP-1	Positive strand	5'-TTCGTGGGGACACCAGAAGTC-3'	482
	Antisense strand	5'-TATCTGGGACCGCAGGGACTG-3'	
β -actin	Positive strand	5'-GGAGAAGATGACCCAGATCA-3'	234
	Antisense strand	5'-GATCTTCATGAGGTAGTCAG-3'	
TIMP-2	Positive strand	5'-GTTTTGCAATGCAGATGTAG-3'	540
	Antisense strand	5'-ATGTCGAGAAACTCCTGCTT-3'	
β -actin	Positive strand	5'-ACCCCACTGAAAAA-3'	120
	Antisense strand	5'-ATCTTCAAACCTCCATGATG-3'	

avidin-peroxidase immunohistochemical kit (Maxim Biological Technology Company, USA). Anti-mouse monoclonal antibodies of TIMP-1 and TIMP-2 were also obtained from Maxim. The sections were deparaffinized and rehydrated. After retrieval of the antigens, nonspecific binding sites were blocked with 100 mL/L normal serum for 20 min. The sections were incubated with monoclonal antibody against TIMP-1 or TIMP-2 at 4 °C overnight, and then with secondary antibody at 37 °C for 30-40 min, avidin-peroxidase at 37 °C for 20 min, and finally with DAB to be colorated for 10 min, and counterstained with hematoxylin, dehydrated with ethanol, rinsed in xylene, and mounted with gum for microscopic examination and photography. To ensure the reliability of the experiment, rabbit serum and phosphate buffer were used instead of monoclonal antibody and secondary antibody, respectively. In addition, 10 healthy liver tissues were selected for control group. The background density of positive cells from 5 microscopic fields at random was measured, and its mean value was used for statistical analysis with SPSS 10.0.

In situ hybridization

The experiment was performed as previously described^[33,34] using *in situ* hybridization kit (Boshide Biological Technology Limited Company, Wuhan, China, No MK1549). Briefly, the serial paraffin sections (thickness 4 μ m) were dried at 80 °C, then deparaffinized by xylene and rehydrated in graded ethanol, acidified in 1 mol/L HCl for 30 min, and blocked in 30 ml/L H₂O₂ 3 mL for 10 min before digestion with proteinase K for 30 min, and then dehydrated with graded ethanol. After prehybridization at 37-40 °C for 2 h, the labeled cDNA probes were denatured at 95 °C for 10 min, then at -20 °C for 10 min, added onto liver tissue sections which had been prehybridized at 37 °C overnight. The sections were washed with 2 \times SSC, 1 \times SSC, and 0.2 \times SSC respectively. Buffer I was added, and then blocking solution was added at room temperature for 20 min, and then rabbit anti-digoxin at 37 °C for 60 min, biotinylated goat anti-rabbit at 37 °C for 30 min, SABC at 37 °C for 30 min, finally DAB was added to develop color. After several washings, the sections were counter-stained with hematoxylin, dehydrated with ethanol, rinsed in xylene, and mounted with gum for microscopic examination and photography. Blank control: TIMP-1 and TIMP-2 cDNA probes for positive hepatic tissues were replaced by prehybridization solution. Negative control: *in situ* hybridization was performed in 10 normal liver tissues. Semi-quantitative results were determined by *in situ* hybridization. (-) as no positive cells, (+) as positive cells <1/3 of all hepatic cells, (++) as positive cells between 1/3-2/3 of all hepatic cells, (+++) as positive cells >2/3 of all hepatic cells in a lobule.

PCR amplification

PCR primers of TIMP-1 were designed according to the whole TIMP-1 cDNA sequence of rats^[35]. The PCR primers of TIMP-1 and TIMP-2 are listed in Table 1.

Total RNA of the liver was extracted with an isolation system (Promega). PCR was performed in 20 μ L reaction volume containing 2 μ L cDNA, 2 μ L 10 \times buffer, 2 μ L (2 mmol/L) 4 \times dNTP, 10 mmol/L primer (2 μ L TIMP-1, 2 μ L β -actin and 2 μ L TIMP-1, 2 μ L β -actin, respectively) and 1U *Taq* DNA polymerase. The samples were subjected to 30 thermal cycles, each consisting of 2 min at 97 °C for pre-denaturation, 30 s at 94 °C for denaturing, 30 s at 56 °C for annealing, 50 s at 72 °C for extension and 7 min at 72 °C for final extension after the last cycle. Ten μ L sample of PCR product was subjected to electrophoresis in 20 g/L agarose gel with TAE buffer at 50 V for 1 h. After stained with ethidium bromide, quantitative analysis was performed. The ratios of TIMP-1/*b-actin* and TIMP-2/*b-actin* were regarded as the expression levels of TIMP-1 and TIMP-2.

Pathologic observation

Some liver sections were stained with hematoxylin and eosin, while other sections for Von Gieson and Masson special staining. The liver samples were also fixed with glutaraldehyde, and examined with electron microscope.

Statistical analysis

Was performed with SPSS 10.0.

RESULTS

Pathologic findings

In liver tissues from rats with hepatic fibrosis, hyperplasia of the lattice fibers and collagenous fibers was observed in portal area and extended outwards. Hyperplasia surrounding the central vein observed was distributed along hepatic sinus and connected each other. The hepatic lobules were encysted and separated by collagen bundles. The normal structure of lobules was destroyed, and pseudolobules formed. Infiltration of inflammatory cells was found around the portal area and central vein. The structure of liver tissues was normal in control.

Under electron microscopy, proliferation of activated hepatic stellate cells (HSC) surrounded by collagen fibers was found in early stage, in which abundant rough endoplasmic reticulum and lipids were present. Eventually, with the deposition of collagen bundles, myofibroblasts formed in portal area, and the deposition of collagens produced a wide compartment. Lots of collagen fibrils resided within the space of Disse. A vast amount of swelling mitochondria and some lipids were detectable in degenerative hepatocytes.

TIMP-1 and TIMP-2 expression and localization

TIMP-1 and TIMP-2 antigens in the liver from experimental rats were detected in myofibroblasts, fibroblasts and vascular endothelial cells predominantly in the portal area and fibrous septum. Expression of TIMP-1 and TIMP-2 exhibited as brown particles in cytoplasm. No positive expression was found in nucleus. There was only a mild positive expression in vascular

endothelial cells of the normal rat liver. Image pattern analysis showed that the expression in the experimental group was much stronger than that in the control group (Table 2, Figure 1), so did the *in situ* hybridization (Figure 2). In order to confirm the specificity of immunohistochemical experiment, the first antibody and second antibody were replaced by at serum and buffer, respectively. Negative results were found in controls, with specific confirming experiment *for in situ* hybridization, and no positive result was found.

Table 2 Expression of TIMP-1 and TIMP-2 related antigens in rat liver

Group	n	TIMP-1	TIMP-2
Experimental group	20	482.50±65.00	336.50±48.32
Normal group	10	59.8±20.31	49.86±18.54

$P < 0.001$.

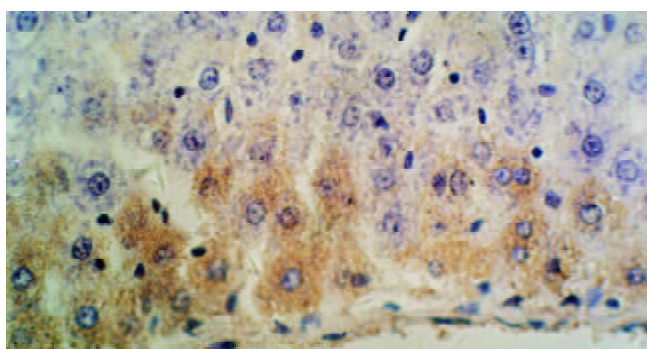


Figure 1 Expression of TIMP-1-related antigens in liver tissue from rats with experimental fibrosis (Immunohistochemical staining ×400).

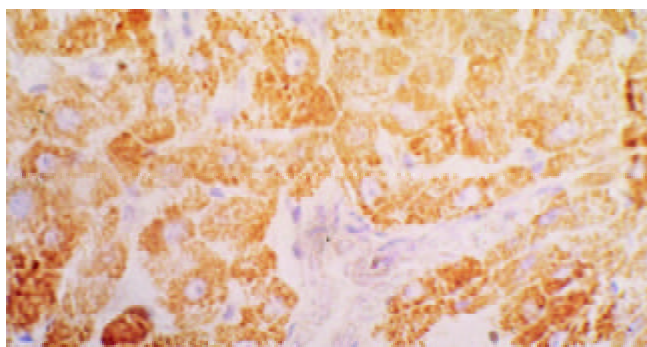


Figure 2 Expression of TIMP-1 mRNA in liver tissue from rats with experimental fibrosis (*in situ* hybridization ×400).

TIMP-1 and TIMP-2 gene expression

The expression of TIMP-1 in the liver of normal rats was strikingly low, while its expression in experimental group was significantly higher than that in the normal group (Table 3).

Table 3 Gene expression of TIMP-1 and TIMP-2 in rat liver

Group	n	TIMP-1/β-actin	TIMP-2/β-actin
Experimental group	20	1.86±0.47	1.06±0.22
Normal group	10	0.36±0.08	0.36±0.08

$P < 0.001$.

DISCUSSION

It is necessary to establish and develop an ideal animal model

of hepatic fibrosis, so as to investigate the etiology or pathogenesis, to explore the effective diagnosis or treatment and to select or evaluate anti-fibrotic medicines. An ideal animal model should be very similar to the characteristics of human disease, with distinct stages of disease and a low mortality. The model should be economically and easily established without difficulty to get the animals.

Researchers began to establish the hepatic fibrosis model of rats with carbon tetrachloride (CCL₄) in 1936, which was an early study on animal model of hepatic fibrosis and cirrhosis. Since it was repeatedly improved, the experimental model has been widely employed. People gradually established various models, such as rat model by bile duct ligation (Zimmermann, 1992), rabbit model with schistosomiasis (Dunn, 1994), rat model by thioacetamide (Okanoue, 1954), *etc.* However, these models with various characteristics are not very ideal to the animal experiment because of their common shortcomings that the hepatic fibrosis lasted shortly and was absorbed spontaneously soon.

In 1966, Paronetto and Popper^[36] have proved that an immune response could induce liver injury. The animals injected repeatedly with the globulin or swine albumin or the serum from swine, bovine or horse developed hepatic fibrosis after 5 weeks, and cirrhosis after 10 weeks. However, the model had a high mortality because of allergic reaction. We studied various models and improved the model developed by Wang *et al*^[29]. The survival rate of rats obviously increased and the fibrosis lasted for more than 363 days when the rats were injected with a small quantity of dexamethasone through its caudal vein soon after the first or secondary attack. The fibrosis was proved pathologically and the formation of fibrosis belonged to the type III allergic reaction induced by the immunocomplex of albumin. Under electron microscopy it was proved that the pathological process stimulated the proliferation of hepatic stellate cells (HSC), which would transform to the myofibroblasts and secrete a large amount of collagens.

At present, it was found that TIMP-1 in the injured liver increased early and obviously, and many researchers thought that TIMP-1 was a very important promoting factor in the process of hepatic fibrosis^[27,32,37], and that it could inhibit MMPs (such as MMP-1) to deposit ECM. Up to now, only TIMP-1 and TIMP-2 were found in liver and TIMP-1 increased more obviously than TIMP-2, and strong expression of TIMP-1 reflected the severity of hepatic fibrosis. With the method of immunohistochemistry, we found that TIMP-1 and TIMP-2 were expressed obviously only in myofibroblasts or fibroblasts of livers from experimental group, mostly in portal area and fibrous septum, while very mildly in vascular endothelial cells of livers from control group. Such a distribution was also shown in the results of *in situ* hybridization.

The results of *in situ* hybridization demonstrated that TIMP-1 mRNA was expressed in hepatocytes and in almost all mesenchymal cells, especially strong in lipocytes of inflammation area of the liver induced by CCL₄ or bile duct ligation model^[38]. Our results indicated that it was strongly expressed only in myofibroblasts, fibroblasts and vascular endothelial cells, mainly in portal area and fibrous septum. The results of immunohistochemistry were similar. Whether the expression difference is due to various models or other causes is still unknown.

From the gene expression levels of TIMP-1 and TIMP-2 we suggested that the more severe the hepatic fibrosis was, the higher the gene expression levels of TIMP-1 and TIMP-2 were, and that the strong expression of TIMP-1 inhibited the degeneration of collagen by MMP-1 and pro MMP-9, and that the expression of TIMP-2 inhibited MMP-2, MMP-9, *etc.* to promote the deposition of ECM. The continuous deposition of collagen fibers in the liver finally resulted in hepatic fibrosis.

The concentrations of TIMP-1 and TIMP-2 in peripheral blood indicated their gene expression levels. Iredale *et al.*^[39] isolated hepatocytes, HSC and Kupffer cells from the liver of experimental hepatic fibrosis model, but failed to find TIMP-1 mRNA in hepatocytes with Northern hybridization in 1997. We detected the expression of TIMP-1 in hepatocytes, HSC and Kupffer cells with PCR technique, and the expression of TIMP-1 was mild in normal rat liver, but strong in fibrotic rat liver. Therefore, further experiments might prove no expression of TIMP-1 in hepatocytes. The strong expression of TIMP-1 in fibroblasts and myofibroblasts of fibrotic liver probably resulted from the activation of HSC. In fact, hepatic fibrosis was essentially a “repair” reaction to chronic liver damage because of the cell-cell interaction mediated by cytokines and the activation of HSC induced by the interaction of mesenchymal cells. The persistence of HSC activation was induced by repeated liver damage. Thus, the activation of HSC was mainly in the pathologic process of hepatic fibrosis^[19,21].

Although TIMP-1 and TIMP-2 were closely related to hepatic fibrosis, study on TIMPs has just begun. Thus far, the mechanism of strong expression of TIMP-1 and TIMP-2 in fibrotic liver is still unknown, and other characteristics of TIMPs are being studied^[40-43]. To enhance the study on TIMPs has become very important for the diagnosis, treatment and pathogenesis of hepatic fibrosis^[44-47].

ACKNOWLEDGEMENT

We acknowledge the advice and help of Prof. Meng-Dong Li.

REFERENCES

- Nie QH, Li MD, Hu DR, Chen GZ. Study on the cause of human protective immunodeficiency after HCV infection. *Shijie Huaren Xiaohua Zazhi* 2000; **8**: 28-30
- Dai YM, Shou ZP, Ni CR, Wang NJ, Zhang SP. Localization of HCV RNA and capsid protein in human hepatocellular carcinoma. *World J Gastroenterol* 2000; **6**: 136-137
- Wang Y, Liu H, Zhou Q, Li X. Analysis of point mutation in site 1896 of HBV precore and its detection in the tissues and serum of HCC patients. *World J Gastroenterol* 2000; **6**: 395-397
- Hu YP, Yao YC, Li JX, Wang XM, Li H, Wang ZH, Lei ZH. The cloning of 3' truncated preS/2S gene from HBV genomic DNA and its expression in transgenic mice. *World J Gastroenterol* 2000; **6**: 734-737
- Wen SJ, Xiang KJ, Huang ZH, Zhou R, Qi XZ. Construction of HBV specific ribozyme and its recombinant with HDV and their cleavage activity *in vitro*. *World J Gastroenterol* 2000; **6**: 377-380
- Nie QH, Li L, Li MD, Hu DR, Zhu YH, Chen GZ. Clinical and immunopathological studies in GBV-B infection. *Shijie Huaren Xiaohua Zazhi* 2000; **8**: 775-781
- Wang FS, Wu ZZ. Current situation in studies of gene therapy for liver cirrhosis and liver fibrosis. *Shijie Huaren Xiaohua Zazhi* 2000; **8**: 371-373
- Wang GQ, Kong XT. Action of cell factor and Decorin in tissue fibrosis. *Shijie Huaren Xiaohua Zazhi* 2000; **8**: 458-460
- Liu F, Wang XM, Liu JX, Wei MX. Relationship between serum TGFβ1 of chronic hepatitis B and hepatic tissue pathology and hepatic fibrosis quantity. *Shijie Huaren Xiaohua Zazhi* 2000; **8**: 528-531
- Yao XX. Diagnosis and treatment of liver fibrosis. *Shijie Huaren Xiaohua Zazhi* 2000; **8**: 681-689
- Albanis E, Friedman SL. Hepatic fibrosis. Pathogenesis and principles of therapy. *Clin Liver Dis* 2001; **5**: 315-334
- Sherker AH, Senosier M, Kermack D. Treatment of transfusion-dependent thalassemic patients infected with hepatitis C virus with interferon alpha-2b and ribavirin. *Hepatology* 2003; **37**: 223
- Han HL, Lang ZW. Changes in serum and histology of patients with chronic hepatitis B after interferon alpha-2b treatment. *World J Gastroenterol* 2003; **9**: 117-121
- Wang XZ, Zhang LJ, Li D, Huang YH, Chen ZX, Li B. Effects of transmitters and interleukin-10 on rat hepatic fibrosis induced by CCl₄. *World J Gastroenterol* 2003; **9**: 539-543
- Jiang HQ, Zhang XL. Mechanism of liver fibrosis. *Shijie Huaren Xiaohua Zazhi* 2000; **8**: 687-689
- Schuppan D, Ruehl M, Somasundaram R, Hahn EG. Matrix as a modulator of hepatic fibrogenesis. *Semin Liver Dis* 2001; **21**: 351-372
- Vaillant B, Chiaramonte MG, Cheever AW, Soloway PD, Wynn TA. Regulation of hepatic fibrosis and extracellular matrix genes by the th response: new insight into the role of tissue inhibitors of matrix metalloproteinases. *J Immunol* 2001; **167**: 7017-7026
- Wei HS, Lu HM, Li DG, Zhan YT, Wang ZR, Huang X, Cheng JL, Xu QF. The regulatory role of AT 1 receptor on activated HSCs in hepatic fibrogenesis: effects of RAS inhibitors on hepatic fibrosis induced by CCl₄. *World J Gastroenterol* 2000; **6**: 824-828
- Schuppan D, Ruehl M, Somasundaram R, Hahn EG. Matrix as a modulator of hepatic fibrogenesis. *Semin Liver Dis* 2001; **21**: 351-372
- Lewindon PJ, Pereira TN, Hoskins AC, Bridle KR, Williamson RM, Shepherd RW, Ramm GA. The role of hepatic stellate cells and transforming growth factor-beta (1) in cystic fibrosis liver disease. *Am J Pathol* 2002; **160**: 1705-1715
- Benyon RC, Arthur MJ. Extracellular matrix degradation and the role of hepatic stellate cells. *Semin Liver Dis* 2001; **21**: 373-384
- Liu YK, Shen W. Effect of Cordyceps sinensis on hepatocytic proliferation of experimental hepatic fibrosis in rats. *Shijie Huaren Xiaohua Zazhi* 2002; **10**: 388-391
- Qin JP, Jiang MD. Phenotype and regulation of hepatic stellate cells and liver fibrosis. *Shijie Huaren Xiaohua Zazhi* 2001; **9**: 801-804
- Yoshiji H, Kuriyama S, Miyamoto Y, Thorgeirsson UP, Gomez DE, Kawata M, Yoshii J, Ikenaka Y, Noguchi R, Tsujinoue H, Nakatani T, Thorgeirsson SS, Fukui H. Tissue inhibitor of metalloproteinases-1 promotes liver fibrosis development in a transgenic mouse model. *Hepatology* 2000; **32**: 1248-1254
- Murphy FR, Issa R, Zhou X, Ratnarajah S, Nagase H, Arthur MJ, Benyon C, Iredale JP. Inhibition of apoptosis of activated hepatic stellate cells by tissue inhibitor of metalloproteinase-1 is mediated *via* effects on matrix metalloproteinase inhibition: implications for reversibility of liver fibrosis. *J Biol Chem* 2002; **277**: 11069-11076
- Dudas J, Kovalszky I, Gallai M, Nagy JO, Schaff Z, Knittel T, Mehde M, Neubauer K, Szalay F, Ramadori G. Expression of decorin, transforming growth factor-beta 1, tissue inhibitor metalloproteinase 1 and 2, and type IV collagenases in chronic hepatitis. *Am J Clin Pathol* 2001; **115**: 725-735
- Nie QH, Cheng YQ, Xie YM, Zhou YX, Bai XG, Cao YZ. Methodologic research on TIMP-1, TIMP-2 detection as a new diagnostic index for hepatic fibrosis and its significance. *World J Gastroenterol* 2002; **8**: 282-287
- Nie QH, Cheng YQ, Xie YM, Zhou YX, Cao YZ. Inhibiting effect of antisense oligonucleotides phosphorothioate on gene expression of TIMP-1 in rat liver fibrosis. *World J Gastroenterol* 2001; **7**: 363-369
- Wang BE, Wang ZF, Ying WY, Huang SF, Li JJ. The study on animal model of experimental liver fibrosis. *Zhonghua Yixue Zazhi* 1989; **69**: 503-505
- Nie QH, Hu DR, Li MD, Xie Q. The expression of HGV/GBV-C or HCV related antigens in the liver tissue of patients coinfecting with hepatitis C and G viruses. *Shijie Huaren Xiaohua Zazhi* 2000; **8**: 114-115
- Nie QH, Li MD, Hu DR, Li L. The expression of hepatitis G virus-related antigens in the liver tissues of with hepatitis patients. *Zhonghua Chuanranbing Zazhi* 2000; **18**: 173-175
- Nie QH, Zhou YX, Xie YM. Expression and significance of tissue inhibitors of metalloproteinase-1 and -2 in serum and liver tissue of patients with liver cirrhosis. *Zhonghua Yixue Zazhi* 2001; **81**: 805-807
- Xie YM, Nie QH, Zhou YX, Cheng YQ, Kang WZ, Zhao YL. Tissue inhibitors of metalloproteinase-1 and -2 (TIMP-1 and TIMP-2) mRNA and antigens location in the liver of patients with cirrhosis. *Zhonghua Chuanranbing Zazhi* 2001; **19**: 352-354
- Nie QH, Hu DR, Li MD, Li L, Zhu YH. Detection of hepatitis G virus RNA in liver tissue using digoxigenin labelled probe *in situ* hybridization. *Shijie Huaren Xiaohua Zazhi* 2000; **8**: 771-774
- Okada A, Garnier JM, Vicaire S, Basset P. Cloning of the cDNA encoding rat tissue inhibitor of metalloproteinase 1 (TIMP-1),

- amino acid comparison with other TIMPs, and gene expression in rat tissues. *Gene* 1994; **147**: 301-302
- 36 **Paronetto F**, Popper H. Chronic liver injury induced by immunologic reactions. Cirrhosis following immunization with heterologous sera. *Am J Pathol* 1966; **49**: 1087-1101
- 37 **Flisiak R**, Maxwell P, Prokopowicz D. Plasma tissue inhibitor of metalloproteinases-1 and transforming growth factor beta 1—possible non-invasive biomarkers of hepatic fibrosis in patients with chronic B and C hepatitis. *Hepatology* 2002; **49**: 1369-1372
- 38 **Roeb E**, Purucker E, Breuer B, Nguyen H, Heinrich PC, Rose-John S, Matern S. TIMP expression in toxic and cholestatic liver injury in rat. *J Hepatol* 1997; **27**: 535-544
- 39 **Iredale JP**, Benyon RC, Arthur MJ, Ferris WF, Alcolado R, Winwood PJ, Clark N, Murphy G. Tissue inhibitor of metalloproteinase-1 messenger RNA expression is enhanced relative to interstitial collagenase messenger RNA in experimental liver injury and fibrosis. *Hepatology* 1996; **24**: 176-184
- 40 **Benyon RC**, Arthur MJ. Extracellular matrix degradation and the role of hepatic stellate cells. *Semin Liver Dis* 2001; **21**: 373-384
- 41 **Lewindon PJ**, Pereira TN, Hoskins AC, Bridle KR, Williamson RM, Shepherd RW, Ramm GA. The role of hepatic stellate cells and transforming growth factor-beta (1) in cystic fibrosis liver disease. *Am J Pathol* 2002; **160**: 1705-1715
- 42 **Schnabl B**, Purbeck CA, Choi YH, Hagedorn CH, Brenner D. Replicative senescence of activated human hepatic stellate cells is accompanied by a pronounced inflammatory but less fibrogenic phenotype. *Hepatology* 2003; **37**: 653-664
- 43 **Liu YK**, Shen W. Inhibitive effect of cordyceps sinensis on experimental hepatic fibrosis and its possible mechanism. *World J Gastroenterol* 2003; **9**: 529-533
- 44 **Lamireau T**, Desmouliere A, Bioulac-Sage P, Rosenbaum J. Mechanisms of hepatic fibrogenesis. *Arch Pediatr* 2002; **9**: 392-405
- 45 **Brenner DA**, Waterboer T, Sung Kyu Choi, Lindquist JN, Stefanovic B, Burchardt E, Yamauchi M, Gillan A, Rippe RA. New aspects of hepatic fibrosis. *J Hepatol* 2000; **32**(Suppl 1): 32-38
- 46 **de Lorenzo MS**, Ripoll GV, Yoshiji H, Yamazaki M, Thorgeirsson UP, Alonso DF, Gomez DE. Altered tumor angiogenesis and metastasis of B16 melanoma in transgenic mice overexpressing tissue inhibitor of metalloproteinases-1. *In Vivo* 2003; **17**: 45-50
- 47 **Liu WB**, Yang CQ, Jiang W, Wang YQ, Guo JS, He BM, Wang JY. Inhibition on the production of collagen type I,III of activated hepatic stellate cells by antisense TIMP-1 recombinant plasmid. *World J Gastroenterol* 2003; **9**: 316-319

Edited by Zhang JZ and Wang XL

Protective role of metallothionein (I/II) against pathological damage and apoptosis induced by dimethylarsinic acid

Guang Jia, Yi-Qun Gu, Kung-Tung Chen, You-Yong Lu, Lei Yan, Jian-Ling Wang, Ya-Ping Su, J. C. Gaston Wu

Guang Jia, Lei Yan, Jian-Ling Wang, Department of Occupational and Environmental Health Sciences, School of Public Health, Peking University, Beijing 100083, China

Yi-Qun Gu, Department of Pathology, Hepingli Hospital, Beijing 100013, China

Kung-Tung Chen, Department of General Education, Ming-hsin University of Science and Technology, Taiwan, China

You-Yong Lu, School of Oncology, Peking University, Beijing 100034, China

Ya-Ping Su, J. C. Gaston Wu, Department of Chemistry, National Taiwan Normal University, Taiwan, China

Correspondence to: Dr. Guang Jia, Department of Occupational and Environmental Health Sciences, School of Public Health, Peking University, 38 Xue Yuan Road, Beijing 100083, China. jiaguangjia@yahoo.com.cn

Telephone: +86-10-82801523 **Fax:** +86-10-62015583

Received: 2003-07-04 **Accepted:** 2003-07-24

Abstract

AIM: To better clarify the main target organs of dimethylarsinic acid toxicity and the role of metallothionein (MTs) in modifying dimethylarsinic acid (DMAA) toxicity.

METHODS: MT-I/II null (MT^{-/-}) mice and the corresponding wild-type mice (MT^{+/+}), six in each group, were exposed to DMAA (0-750 mg/kg body weight) by a single oral injection. Twenty four hours later, the lungs, livers and kidneys were collected and undergone pathological analysis, induction of apoptotic cells as determined by TUNEL and MT concentration was detected by radio-immunoassay.

RESULTS: Remarkable pathological lesions were observed at the doses ranging from 350 to 750 mg/kg body weight in the lungs, livers and kidneys and MT^{+/+} mice exhibited a relatively slight destruction when compared with that in dose matched MT^{-/-} mice. The number of apoptotic cells was increased in a dose dependent manner in the lungs and livers in both types of mice. DMAA produced more necrotic cells rather than apoptotic cells at the highest dose of 750 mg/kg, however, no significant increase was observed in the kidney. Hepatic MT level in MT^{+/+} mice was significantly increased by DMAA in a dose-dependent manner and there was no detectable amount of hepatic MT in untreated MT^{-/-} mice.

CONCLUSION: DMAA treatment can lead to the induction of apoptosis and pathological damage in both types of mice. MT exhibits a protective effect against DMAA toxicity.

Jia G, Gu YQ, Chen KT, Lu YY, Yan L, Wang JL, Su YP, Wu JCG. Protective role of metallothionein (I/II) against pathological damage and apoptosis induced by dimethylarsinic acid. *World J Gastroenterol* 2003; 10(1): 91-95

<http://www.wjgnet.com/1007-9327/10/91.asp>

INTRODUCTION

Arsenic is a metalloid that naturally occurs in soil, water, and

air. Arsenicals are also non-biodegradable by-products during production of copper, lead, and other ores and coal consumption. Exposure to arsenic by food, drinking water, soil and air containing arsenic is widely existed in the world. Inorganic arsenicals are well known human carcinogens, specifically for the lung, liver, kidney, skin, bladder and other internal organs^[1,2]. Dimethylarsinic acid (DMAA) is a major form of organic arsenic in the environment and the main metabolite of ingested inorganic arsenicals in most mammals, including humans^[2-4]. DMAA itself can be used as herbicide and pesticide and also naturally exists in some seafood. Recent studies have revealed that DMAA is a genotoxic, multi-site promoter of carcinogenesis as well as a complete carcinogen in rodents^[5-7], which provides a novel clue to investigate the mechanism of arsenicals in carcinogenesis.

Arsenicals, including DMAA, are moderately effective inducers of MT in mice and rats^[8,9]. MTs, thiol-rich metal binding proteins, have been shown to be easily induced by oxidative stress and heavy metals and play an important role in homeostasis of essential metals, detoxication of heavy metals, scavenging reactive oxygen intermediates and preventing carcinogenesis as an endogenous defensive factor^[10-15]. Especially to be mentioned, its capacity of scavenging hydroxyl and superoxide radicals is much more efficient than GSH, an established antioxidant^[15]. Among the four major isoforms of identified MTs, MT-I and MT-II existing in all tissues examined, are the predominant forms in the livers. Recently Liu *et al*^[16] reported that MT-I/II null mice were more sensitive than wild type mice to hepatotoxic and nephrotoxic effects of oral or injected inorganic arsenicals. Sakurai *et al*^[17] reported that DMAA could induce apoptosis by reducing glutathione (GSH) *in vitro*. However, the effect of MT on induction of apoptosis and the main organic toxicity by DMAA *in vivo* remain elusive.

MT-I/II null (MT^{-/-}) mice have been proved to be a good tool for studying MT's normal function and the consequences of its deficiency^[18]. In the present study, MT-I/II null (MT^{-/-}) mice and the corresponding wild-type mice (MT^{+/+}) were exposed to DMAA by oral injection, we investigated the pathological lesions and apoptosis in main target organs including the liver, lung and kidney of the mice, to elucidate the toxicity of DMAA and the ability of MT to modify DMAA toxicity.

MATERIALS AND METHODS

Chemicals

Dimethylarsinic acid (purity 100 %) was purchased from Wako Pure Chemical Co. (Osaka, Japan). An *in situ* apoptosis detection kit (ApopTagTM) was purchased from Intergen Co. NY, USA.

Animals and treatment

MT null (MT^{-/-}) mice whose MT-I and II genes had null mutation and wild type (MT^{+/+}) mice provided kindly by Dr. A. Choo (Murdoch Institute for Research into Birth Defects, Royal Children's Hospital, Australia), were of a mixed genetic background of 129 Ola and C57BL/6 strains. F1

hybrid mice were mated with C57BL/6 mice, and their offsprings were back-crossed to C57BL/6 for six generations. MT^{-/-} and MT^{+/+} mice were obtained by mating of those heterozygous (MT^{+/-}) mice.

MT^{-/-} and MT^{+/+} mice were routinely bred in the vivarium of the National Institute for Environmental Studies (NIES, Japan). Microbiological and viral examinations were performed with regular quarantine procedures for more than one year, and we did not find either pathogenic infections or significant phenotypical abnormalities. Both strains of mice were housed in cages in ventilated animal rooms with a controlled temperature of 23±1 °C, a relative humidity of 55±10%, and a 12 h light/dark cycle. They were maintained on standard laboratory chow and tap water *ad lib*, and received humane care throughout the experiment according to the guidelines of the NIES. Eight-week-old female MT^{-/-} and MT^{+/+} mice were assigned randomly in equal numbers to all groups (six mice for each treatment group). Fresh DMAA solution was prepared by dissolving it in sterilized water. The mice were administered DMAA (0-750 mg/kg) by oral gavage.

Sample collection

At 24 h after administration of DMAA, the lung, liver and kidney were collected from each mouse under diethyl ether anesthesia. Portions of tissues were fixed in 10% neutral formalin, processed by the standard histological techniques, and stained with hematoxylin and eosin for light microscopic examination. For TUNEL staining, sections (5 µm) were placed on poly-L-lysine precoated slides.

TUNEL for apoptosis

Apoptotic cells were detected with an apoptosis detection kit according to the manufacturer's instructions. Briefly, the samples were incubated with digoxigenin-labeled dNTP in the presence of terminal deoxynucleotidyl transferase followed by peroxidase-conjugated anti-digoxigenin antibody. Nuclear staining of apoptotic cells was detected with 3', 3'-diaminobenzidine followed by counterstaining of nuclei with methyl green. An apoptosis index (AI) was obtained by dividing the number of positive cells in the area observed^[19].

MT Concentration

MT (MT-I and MT-II isoforms) concentration in the liver was measured by radioimmunoassay using sheep anti-rat MT-I antiserum^[20]. The detection limit of this method was 0.2 µg MT/g of tissue.

Statistical analysis

ANOVA with subsequent *post hoc*'s test was used as appropriate. All values were expressed as $\bar{x}\pm s$. Differences were considered significant at $P<0.05$.

RESULTS

Histopathological observation

In untreated MT^{-/-} mice and the corresponding MT^{+/+} mice, the lung, liver and kidney showed normal morphology. Significant lesions were observed at doses of DMAA ranging from 375 to 750 mg/kg body weight in both types of mice. However, the pathological lesions in MT^{-/-} mice were more severely widespread when compared to that in dose matched MT^{+/+} mice.

Changes including congestion, atelectasis and mild to moderate hemorrhages in the alveoli of the lungs were observed in MT^{-/-} mice. Adequate air space in the alveoli was observed more frequent in MT^{+/+} mice compared to that of MT^{-/-} mice. Pulmonary capillary congestion could affect alveolar space, resulting in severe acute impairment of respiratory function.

Capillary rupture led to leakage of red blood cells into the interstitium, as well as into the alveoli (Figure 1).

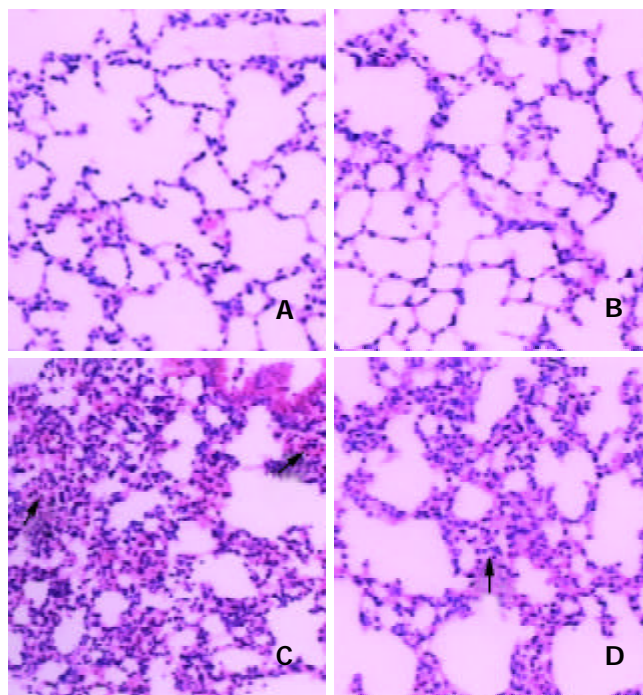


Figure 1 Typical HE staining. The bar is 100 µm. A, B: the lungs from control of MT^{-/-} and MT^{+/+} mice; C, D: the lungs from 750 mg/kg DMAA group of MT^{-/-} and MT^{+/+} mice. Arrows indicate atelectasis and hemorrhage.

At 24 h after DMAA treatment, severe liver damages characterized by cellular cloudy swelling, paleness of cell cytoplasm, vacuolization of hepatocytes and a few areas of focal necrosis were found in MT^{-/-} mice while a limited degree of changes was observed in dose matched MT^{+/+} mice livers (Figure 2).

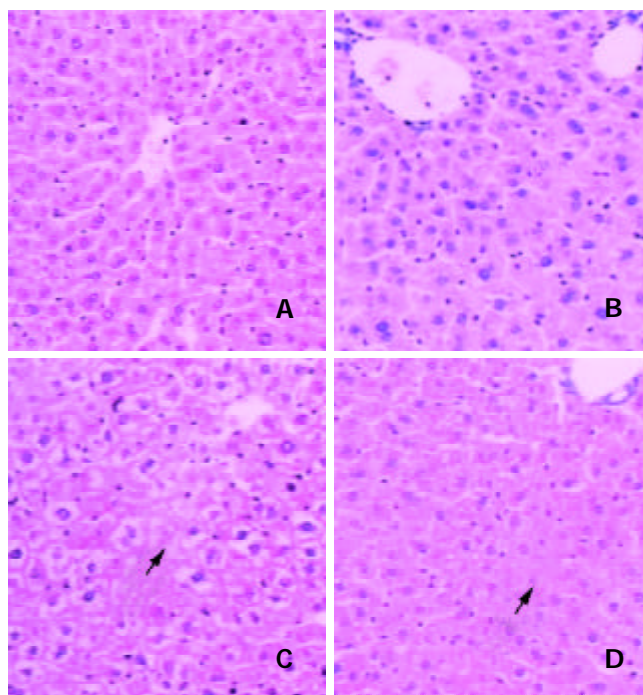


Figure 2 Typical HE staining. The bar is 100 µm. A, B: the livers from control of MT^{-/-} and MT^{+/+} mice; C, D: the livers from 750 mg/kg DMAA group of MT^{-/-} and MT^{+/+} mice. The arrows indicate necrosis.

Histological changes in the kidney are shown in Figure 3. Treatment with DMAA produced swelling of glomerulus and its surrounding tubular tissue and urinary space compression in both types of mice.

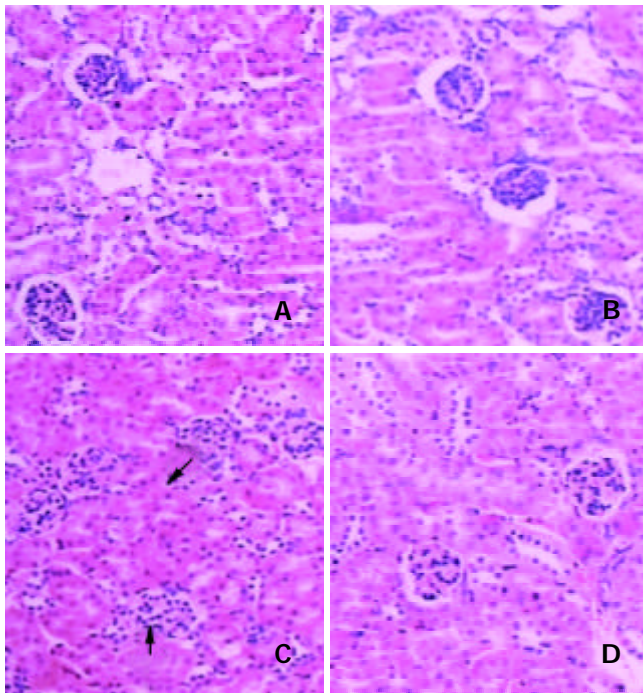


Figure 3 Typical HE staining. The bar is 100 μ m. A, B: the kidneys from control of MT^{-/-} and MT^{+/+} mice; C, D: the kidneys from 750 mg/kg DMAA group of MT^{-/-} and MT^{+/+} mice. The arrows indicate the swelling of glomerulus and the surrounding tubular tissue and urinary space compression.

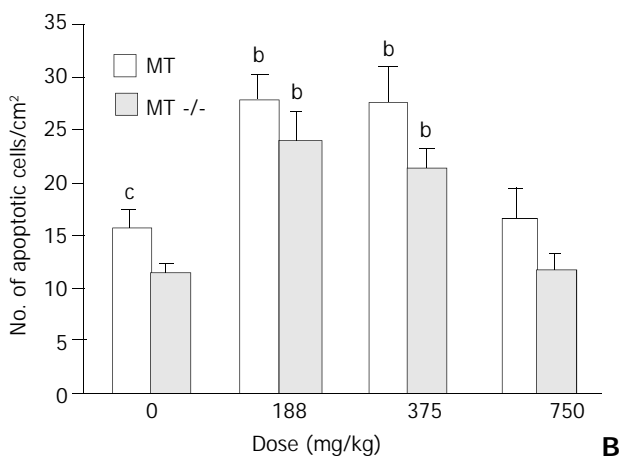
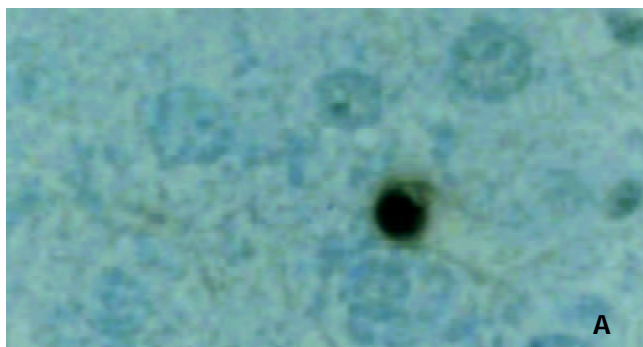


Figure 5 Apoptosis in livers of MT^{+/+} and MT^{-/-} mice detected by TUNEL twenty-four hours after oral DMAA treatment. A: Typical apoptotic cells in the liver of MT^{-/-} mice at a dose of

188 mg/kg body weight. Brown staining indicates apoptotic cells. The bar is 20 μ m. B: AI in the livers. All values were expressed as $\bar{x} \pm s$. ANOVA with subsequent *post hoc*'s test was performed for comparison of AI. ^{a,b}Significant difference at $P < 0.05$, $P < 0.01$ when compared with the corresponding control group. ^{c,d}Significant difference at $P < 0.05$, $P < 0.01$ when compared with the dose-matched MT^{-/-} mice group.

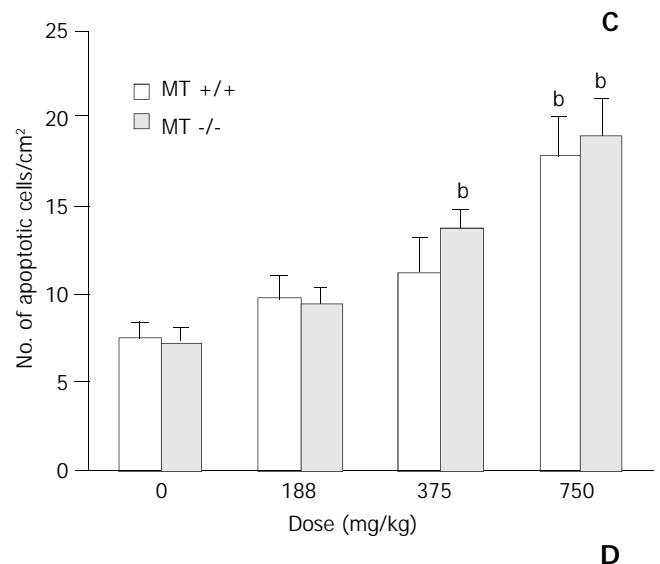
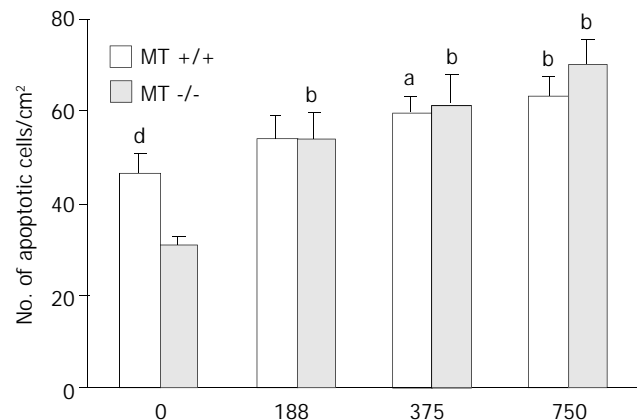
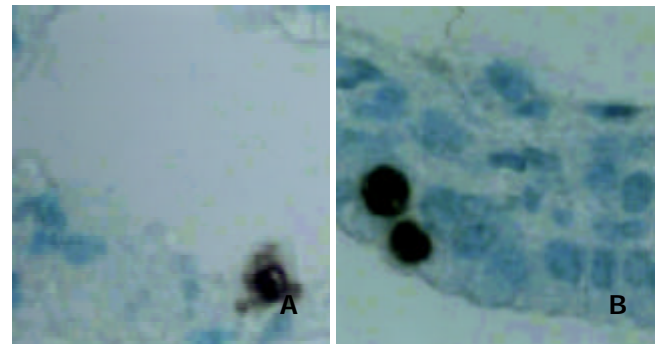


Figure 4 Apoptosis in lungs of MT^{+/+} and MT^{-/-} mice detected by TUNEL twenty-four hours after oral DMAA treatment. A: Typical apoptotic cells in alveolar area of MT^{-/-} mice at a dose of 188 mg/kg body weight. Brown staining indicates the apoptotic cells. The bar is 20 μ m. B: Typical apoptotic cells in bronchial area of MT^{-/-} mice at a dose of 188 mg/kg body weight. Brown staining indicates apoptotic cells. The bar is 20 μ m. C: AI in alveolar area. D: AI in bronchial area. All the values were expressed as $\bar{x} \pm s$. ANOVA with subsequent *post hoc*'s test was performed for comparison of AI. ^{a,b}Significant difference at $P < 0.05$, $P < 0.01$ when compared with the corresponding control group. ^{c,d}Significant difference at $P < 0.05$, $P < 0.01$ when compared with the dose-matched MT^{-/-} mice group.

Induction of apoptotic cells detected in lungs, livers and kidneys of $MT^{-/-}$ and $MT^{+/+}$ mice

High induction of apoptotic cells in bronchial epithelial cells was observed in $MT^{-/-}$ mice treated with DMAA at 375 mg/kg body weight, however, the same changes were not observed in dose matched $MT^{+/+}$ mice. At a high dose of 750 mg/kg body weight, the coincident increase of apoptotic cells was observed in both types of mice and no significant difference was observed between them.

In control group, the incidence of apoptotic cells in alveolar epithelial cells in $MT^{+/+}$ mice was significantly higher than that in $MT^{-/-}$ mice, implying that $MT^{+/+}$ mice might have a stronger ability to induce apoptosis than $MT^{-/-}$ mice. A significant increase of apoptotic cells occurred in $MT^{-/-}$ mice treated by 188 mg/kg DMAA, a relative low dose when compared with that in bronchial epithelial cells. However, no significant increase was observed in $MT^{+/+}$ mice at the same dose of 188 mg/kg DMAA. With the increase of dose, high induction of apoptotic cells was observed in both types of mice (Figure 4).

Figure 5 shows that in control group, the incidence of apoptotic cells in $MT^{+/+}$ mice was $156.33 \pm 41.041/\text{cm}^2$, significantly higher than that in $MT^{-/-}$ mice. The incidence of apoptotic cells in the livers rose with the increase of dose in both types of mice. However, at the highest dose of 750 mg/kg, DMAA produced more necrotic cells rather than apoptotic cells observed by HE staining (Figure 2).

DMAA failed to induce remarkable apoptotic cells in the kidneys from both types of mice (data not shown).

MT concentration in liver of $MT^{+/+}$ mice

MT concentration was determined in the liver of $MT^{+/+}$ mice and $MT^{-/-}$ mice treated with DMAA (Figure 6). Hepatic MT level in $MT^{+/+}$ mice was significantly increased by DMAA in a dose-dependent manner. However, there was no detectable amount of hepatic MT in untreated $MT^{-/-}$ mice, and it could not be induced by DMAA.

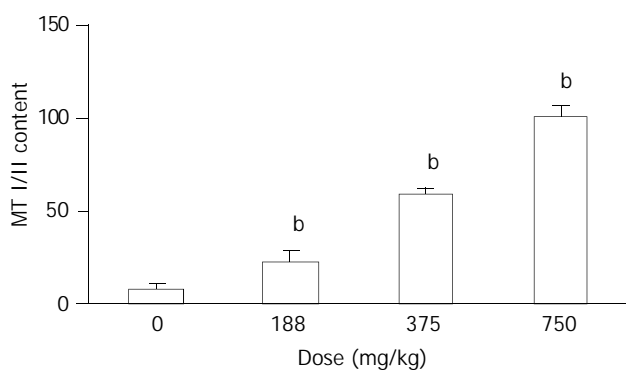


Figure 6 MT concentration in livers of $MT^{+/+}$ mice detected by radio-immunoassay. All the values were expressed as $\bar{x} \pm s$. ANOVA with subsequent *post hoc* 's test was performed for comparison of AI. ^bSignificant difference at $P < 0.01$ when compared with the corresponding control group.

DISCUSSION

The present study demonstrated that DMAA could produce pathological lesions in the lungs, livers and kidneys, and induce apoptosis in the lungs and livers. Most importantly, it is the first report to show that inability to produce MT-I/II in $MT^{-/-}$ mice caused an increased sensitivity to toxicity induced by DMAA.

Treatment with DMAA caused severe and wide spread lesions in $MT^{-/-}$ mice, whereas, these changes were much less severe in $MT^{+/+}$ mice. It indicates that $MT^{-/-}$ mice were more

sensitive to DMAA and MT played a protective role against the toxicities to main organs. Yamanaka^[7] reported that DMAA in mice could be further metabolized and converted into dimethylarsine radicals and dimethyl arsenic peroxy radicals. Marked formation of 8-oxod G was observed in the lung and liver, which are the target organs for arsenic carcinogenesis. No increase in 8-oxod G levels was observed in the kidney. Meanwhile, MT was capable of scavenging hydroxyl and superoxide radicals and its capability of scavenging them was much more efficient^[11,12,15]. In our study, the expression of MT (I/II) was induced by DMAA in a dose dependent manner in the livers of $MT^{+/+}$ mice, no MT(I/II) was observed in $MT^{-/-}$ mice. Thus the reduction of lesions induced by DMAA in the main target organs of $MT^{+/+}$ mice could be explained at least partly by MT reduction induced by DMAA, and the toxicity induced by DMAA could be explained partly by way of oxidative stress participation.

After a lethal damaging stimulation, two main structural routes of cell death might occur: apoptosis and necrosis. It has become apparent that the magnitude and type of injurious stimuli could determine whether a cell underwent death through apoptosis or necrosis. Severe damaging stimuli tended to result in necrosis, and lower grade damaged stimuli tended to cause apoptosis^[21-30].

Recently, Sakurai *et al* reported that DMAA could induce apoptosis by reducing glutathione (GSH) *in vitro*^[17]. However, the effect of MT on the induction of apoptosis by DMAA *in vivo* remains elusive. Furthermore, the perturbation of apoptosis has been thought to contribute to carcinogenesis either through enhanced initiation or progression^[29-38]. In this study, the induction of apoptosis was detected by TUNEL in the lungs, livers and kidneys from both types of mice. In the lungs, a significant increase of apoptosis was observed in alveolar cells of $MT^{-/-}$ mice at a relative low level compared with that in bronchial cells, suggesting that alveolar cells were more sensitive than bronchial cells and MT had some protective role against the induction of apoptosis induced by DMAA at a relative low level. With the increase of dose, DMAA induced high levels of apoptosis in both types of mice and at the highest dose of 750 mg/kg, necrotic cells predominated over apoptosis in the livers, revealing the serious toxicity of DMAA at this dose. Since the kidney is the major organ for arsenic elimination and most of arsenicals could be rapidly eliminated through the kidney^[1-3], renal cells are thus exposed to a major portion of the absorbed arsenical dose. However, the induction of apoptosis was not affected by DMAA, the underlying mechanism needs further investigations.

In conclusion, the present studies demonstrate that oral administration of DMAA can produce toxic response of the respiratory system, liver and kidney in both $MT^{-/-}$ and $MT^{+/+}$ mice. The pathological effects are clearly pronounced in $MT^{-/-}$ mice. Intracellular MT appears to play an important role in preventing the toxic effects of DMAA.

ACKNOWLEDGEMENT

We thank Dr. Sone Hideko and Masahiko Satoh (National Institute for Environmental Studies, Japan) for kindly providing the experiment materials. This work was supported in part by a Grant-in-aid for Scientific Research from the Ministry of Education, China and a grant from the Japan Science and Technology Agency, Japan.

REFERENCES

- Huff J, Chan P, Nyska A. Is the human carcinogen arsenic carcinogenic to laboratory animals? *Toxicol Sci* 2000; **55**: 17-23
- Kitchin KT. Recent advances in arsenic carcinogenesis: modes

- of action, animal model systems, and methylated arsenic metabolites. *Toxicol Appl Pharmacol* 2001; **172**: 249-261
- 3 **Goering PL**, Aposhian HV, Mass MJ, Cebrian M, Beck BD, Waalkes MP. The enigma of arsenic carcinogenesis: role of metabolism. *Toxicol Sci* 1999; **49**: 5-14
 - 4 **Braman RS**, Foreback CC. Methylated forms of arsenic in the environment. *Science* 1973; **182**: 1247-1249
 - 5 **Yamamoto S**, Wanibuchi H, Hori T, Yano Y, Matsui-Yuasa I, Otani S, Chen H, Yoshida K, Kuroda K, Endo G, Fukushima S. Possible carcinogenic potential of dimethylarsinic acid as assessed in rat *in vivo* models: a review. *Mutat Res* 1997; **386**: 353-361
 - 6 **Kenyon EM**, Hughes MF. A concise review of the toxicity and carcinogenicity of dimethylarsinic acid. *Toxicology* 2001; **160**: 227-236
 - 7 **Yamanaka K**, Takabayashi F, Mizoi M, An Y, Hasegawa A, Okada S. Oral exposure of dimethylarsinic acid, a main metabolite of inorganic arsenics, in mice leads to an increase in 8-Oxo-2'-deoxyguanosine level, specifically in the target organs for arsenic carcinogenesis. *Biochem Biophys Res Commun* 2001; **287**: 66-70
 - 8 **Kreppel H**, Bauman JW, Liu J, McKim JM Jr, Klaassen CD. Induction of metallothionein by arsenicals in mice. *Fundam Appl Toxicol* 1993; **20**: 184-189
 - 9 **Albores A**, Koropatnick J, Cherian MG, Zelazowski AJ. Arsenic induces and enhances rat hepatic metallothionein production *in vivo*. *Chem Biol Interact* 1992; **85**: 127-140
 - 10 **Cherian MG**, Howell SB, Imura N, Klaassen CD, Koropatnick J, Lazo JS, Waalkes MP. Role of metallothionein in carcinogenesis. *Toxicol Appl Pharmacol* 1994; **126**: 1-5
 - 11 **Andrews GK**. Regulation of metallothionein gene expression by oxidative stress and metal ions. *Biochem Pharmacol* 2000; **59**: 95-104
 - 12 **Viarengo A**, Burlando B, Ceratto N, Panfoli I. Antioxidant role of metallothioneins: a comparative overview. *Cell Mol Biol* 2000; **46**: 407-417
 - 13 **Cheng ML**, Wu J, Wang HQ, Xue LM, Tan YZ, Ping L, Li CX, Huang NH, Yao YM, Ren LZ, Ye L, Li L, Jia ML. Effect of Maotai liquor in inducing metallothioneins and on hepatic stellate cells. *World J Gastroenterol* 2002; **8**: 520-523
 - 14 **Huang GW**, Yang LY. Metallothionein expression in hepatocellular carcinoma. *World J Gastroenterol* 2002; **8**: 650-653
 - 15 **Deneke SM**. Thiol-based antioxidants. *Curr Top Cell Regul* 2000; **36**: 151-180
 - 16 **Liu J**, Liu Y, Goyer RA, Achanzar W, Waalkes MP. Metallothionein-I/II null mice are more sensitive than wild-type mice to the hepatotoxic and nephrotoxic effects of chronic oral or injected inorganic arsenicals. *Toxicol Sci* 2000; **55**: 460-467
 - 17 **Sakurai T**, Qu W, Sakurai MH, Waalkes MP. A major human arsenic metabolite, dimethylarsinic acid, requires reduced glutathione to induce apoptosis. *Chem Res Toxicol* 2002; **15**: 629-637
 - 18 **Michalska AE**, Choo KH. Targeting and germ-line transmission of a null mutation at the metallothionein I and II loci in mouse. *Proc Natl Acad Sci U S A* 1993; **90**: 8088-8092
 - 19 **Jia G**, Tohyama C, Sone H. DNA damage triggers imbalance of proliferation and apoptosis during development of preneoplastic foci in the liver of Long-Evans Cinnamon rats. *Int J Oncol* 2002; **21**: 755-761
 - 20 **Tohyama C**, Shaikh ZA. Metallothionein in plasma and urine of cadmium-exposed rats determined by a single-antibody radioimmunoassay. *Fundam Appl Toxicol* 1981; **1**: 1-7
 - 21 **Wu K**, Zhao Y, Liu BH, Li Y, Liu F, Guo J, Yu WP. RRR- α -tocopheryl succinate inhibits human gastric cancer SGC-7901 cell growth by inducing apoptosis and DNA synthesis arrest. *World J Gastroenterol* 2002; **8**: 26-30
 - 22 **Gao F**, Yi J, Shi GY, Li H, Shi XG, Tang XM. The sensitivity of digestive tract tumor cells to As₂O₃ is associated with the inherent cellular level of reactive oxygen species. *World J Gastroenterol* 2002; **8**: 36-39
 - 23 **Shen ZY**, Shen WY, Chen MH, Shen J, Cai WJ, Yi Z. Nitric oxide and calcium ions in apoptotic esophageal carcinoma cells induced by arsenite. *World J Gastroenterol* 2002; **8**: 40-43
 - 24 **Shan CM**, Li J. Study of apoptosis in human liver cancers. *World J Gastroenterol* 2002; **8**: 247-252
 - 25 **Liu JW**, Tang Y, Shen Y, Zhong XY. Synergistic effect of cell differential agent-II and arsenic trioxide on induction of cell cycle arrest and apoptosis in hepatoma cells. *World J Gastroenterol* 2003; **9**: 65-68
 - 26 **Gu QL**, Li NL, Zhu ZG, Yin HR, Lin YZ. A study on arsenic trioxide inducing *in vitro* apoptosis of gastric cancer cell lines. *World J Gastroenterol* 2000; **6**: 435-437
 - 27 **Tu SP**, Zhong J, Tan JH, Jiang XH, Qiao MM, Wu YX, Jiang SH. Induction of apoptosis by arsenic trioxide and hydroxy-camptothecin in gastric cancer cells *in vitro*. *World J Gastroenterol* 2000; **6**: 532-539
 - 28 **Shen ZY**, Shen J, Li QS, Chen CY, Chen JY, Yi Z. Morphological and functional changes of mitochondria in apoptotic esophageal carcinoma cells induced by arsenic trioxide. *World J Gastroenterol* 2002; **8**: 31-35
 - 29 **Evan GI**, Vousden KH. Proliferation, cell cycle and apoptosis in cancer. *Nature* 2001; **411**: 342-348
 - 30 **Waalkes MP**, Fox DA, States JC, Patierno SR, McCabe MJ Jr. Metals and disorders of cell accumulation: modulation of apoptosis and cell proliferation. *Toxicol Sci* 2000; **56**: 255-261
 - 31 **Manning FC**, Patierno SR. Apoptosis: Inhibitor or instigator of carcinogenesis? *Cancer Invest* 1996; **14**: 455-465
 - 32 **Chen YX**, Zhong XY, Qin YF, Bing W, He LZ. 15d-PGJ(2) inhibits cell growth and induces apoptosis of MCG-803 human gastric cancer cell line. *World J Gastroenterol* 2003; **9**: 2149-2153
 - 33 **Wang L**, Li J, Li Q, Zhang J, Duan XL. Morphological changes of cell proliferation and apoptosis in rat jejunal mucosa at different ages. *World J Gastroenterol* 2003; **9**: 2060-2064
 - 34 **Jiang YA**, Luo HS, Zhang YY, Fan LF, Jiang CQ, Chen WJ. Telomerase activity and cell apoptosis in colon cancer cell by human telomerase reverse transcriptase gene antisense oligodeoxynucleotide. *World J Gastroenterol* 2003; **9**: 1981-1984
 - 35 **Liu ZS**, Tang SL, Ai ZL. Effects of hydroxyapatite nanoparticles on proliferation and apoptosis of human hepatoma BEL-7402 cells. *World J Gastroenterol* 2003; **9**: 1968-1971
 - 36 **Li MY**, Deng H, Zhao JM, Dai D, Tan XY. Peroxisome proliferator-activated receptor gamma ligands inhibit cell growth and induce apoptosis in human liver cancer BEL-7402 cells. *World J Gastroenterol* 2003; **9**: 1683-1688
 - 37 **Li JY**, Wang XZ, Chen FL, Yu JP, Luo HS. Nimesulide inhibits proliferation via induction of apoptosis and cell cycle arrest in human gastric adenocarcinoma cell line. *World J Gastroenterol* 2003; **9**: 915-920
 - 38 **Cheng ML**, Wu J, Wang HQ, Xue LM, Tan YZ, Ping L, Li CX, Huang NH, Yao YM, Ren LZ, Ye L, Li L, Jia ML. Effect of Maotai liquor in inducing metallothioneins and on hepatic stellate cells. *World J Gastroenterol* 2002; **8**: 520-523

Edited by Zhu LH and Wang XL

Effect of Qingyitang on activity of intracellular Ca^{2+} - Mg^{2+} -ATPase in rats with acute pancreatitis

Ying Qiu, Yong-Yu Li, Shu-Guang Li, Bo-Gen Song, Gui-Fen Zhao

Ying Qiu, Bo-Gen Song, Gui-Fen Zhao, Department of Pathology, Medical School of Tongji University, Shanghai 200331, China

Yong-Yu Li, Department of Pathophysiology, Medical School of Tongji University, Shanghai 200331, China

Shu-Guang Li, Department of Prevention Medicine, Medical School of Tongji University, Shanghai 200331, China

Supported by National Natural Science Foundation of China, No. 30060031

Correspondence to: Yong-Yu Li, Department of Pathophysiology, Medical School of Tongji University, 500 Zhennan Road, Shanghai 200331, China. liyyu@163.net

Telephone: +86-21-68537254 **Fax:** +86-21-62846993

Received: 2003-03-03 **Accepted:** 2003-05-21

Abstract

AIM: To study the change of intracellular calcium-magnesium ATPase (Ca^{2+} - Mg^{2+} -ATPase) activity in pancreas, liver and kidney tissues of rats with acute pancreatitis (AP), and to investigate the effects of Qingyitang (QYT) (Decoction for clearing the pancreas) and tetrandrine (Tet) and vitamin E (VitE) on the activity of Ca^{2+} - Mg^{2+} -ATPase.

METHODS: One hundred and five Sprague-Dawley rats were randomly divided into: normal control group, AP group, treatment group with QYT (1 ml/100 g) or Tet (0.4 ml/100 g) or VitE (100 mg/kg). AP model was prepared by a retrograde injection of sodium taurocholate into the pancreatic duct. Tissues of pancreas, liver and kidney of the animals were taken at 1 h, 5 h, 10 h respectively after AP induction, and the activity of Ca^{2+} - Mg^{2+} -ATPase was studied using enzyme-histochemistry staining. Meanwhile, the expression of Ca^{2+} - Mg^{2+} -ATPase of the tissues was studied by RT-PCR.

RESULTS: The results showed that the positive rate of Ca^{2+} - Mg^{2+} -ATPase in AP group (8.3%, 25%, 29.2%) was lower than that in normal control group (100%) in all tissues ($P < 0.01$), the positive rate of Ca^{2+} - Mg^{2+} -ATPase in treatment group with QYT (58.3%, 83.3%, 83.3%), Tet (50.0%, 70.8%, 75.0%) and VitE (54.2%, 75.0%, 79.2%) was higher than that in AP group (8.3%, 25.0%, 29.2%) in all tissues ($P < 0.01$). RT-PCR results demonstrated that in treatment groups Ca^{2+} - Mg^{2+} -ATPase gene expression in pancreas tissue was higher than that in AP group at the observing time points, and the expression at 5 h was higher than that at 1 h. The expression of Ca^{2+} - Mg^{2+} -ATPase in liver tissue was positive, but without significant difference between different groups.

CONCLUSION: The activity and expression of intracellular Ca^{2+} - Mg^{2+} -ATPase decreased in rats with AP, suggesting that Ca^{2+} - Mg^{2+} -ATPase may contribute to the occurrence and development of cellular calcium overload in AP. QYT, Tet and VitE can increase the activity and expression of Ca^{2+} - Mg^{2+} -ATPase and may relieve intracellular calcium overload to protect the tissue and cells from injuries.

Qiu Y, Li YY, Li SG, Song BG, Zhao GF. Effect of Qingyitang on

activity of intracellular Ca^{2+} - Mg^{2+} -ATPase in rats with acute pancreatitis. *World J Gastroenterol* 2004; 10(1): 100-104
<http://www.wjgnet.com/1007-9327/10/100.asp>

INTRODUCTION

The pathogenesis of acute pancreatitis (AP) is complicated. A number of theories have been proposed. It is generally accepted that "calcium overload" plays a key role in the occurrence and progression of AP^[1-3]. However, the exact mechanism of intracellular calcium overload in acute pancreatitis is not clear yet. This study was designed to explore the mechanism of intracellular calcium overload by determining the activity of intracellular Ca^{2+} - Mg^{2+} ATPase in AP rats. The experiment also investigated the therapeutic mechanisms of some medicines, such as Chinese medicines Qingyitang (QYT) and tetrandrine (Tet), and Vitamin E (VitE) on AP in rats.

MATERIALS AND METHODS

Animals

One hundred and five Sprague-Dawley (SD) rats including male and female (1:1) were used. The animals, weighing 220-250 g, were provided by the Animal Center of Chinese Academy of Sciences, Shanghai, China.

Reagents

Sodium taurocholate from Sigma Co. was diluted with distilled water to make a 4% solution for use. QYT was from Zunyi Medical College, Tet from the Pharmaceutical Institute of the Second Military Medical University, VitE (emulsion, 2 ml/kg) from Xinan Pharmaceutical Factory, ATP disodium salt from Shanghai Institute of Biochemistry, Chinese Academy of Sciences. Trizol, reverse transcriptase Superscript II RNase H- were from Gib Co. (USA), hexamer from Promega (USA), and Taq DNA polymerase, dNTP, RNAase inhibitor from Takara Co. (Japan), diethyl pyrocarbonate (DEPC) from Serva Co. (USA). Primers for Ca^{2+} - Mg^{2+} -ATPase (upstream primer -5' GAACATCCTGCAGACGGACA-3', downstream primer -5' CAAAGCTATGGGAGTGGTGG-3') (790-1 241 bp) and primers for GAPDH (upper -5' ACCACAGTCCATGCCAT CAC-3', lower -5' TCCACCACCCTGTTGCTGTA-3') were purchased from Takara Co. (Japan).

Animal model preparation and grouping

The rats were randomly divided into normal control group ($n=9$), AP+ normal saline (NS) group ($n=24$), AP+QYT group ($n=24$), AP+Tet group ($n=24$), AP+VitE group ($n=24$). In normal control group the pancreas of rats were exposed. In the other groups, the pancreas of rats was exposed and sodium taurocholate was injected into the pancreatic duct to induce AP^[4]. In AP+NS group, rats were injected with NS (0.4 ml/100 g, ip) after AP induction. In AP+QYT group, rats were infused with QYT (1 ml/100 g) by a nose-gastric catheter, in AP+Tet group, rats were injected peritoneally

with Tet (0.4 ml/100 g), and in AP+VitE group, rats were given VitE (100 mg/kg) intravenously through mesenteric vein.

HE staining

At 1 h, 5 h or 10 h after operation, the tissue samples of pancreas, liver and kidney were taken and fixed with formalin solution. Some sections of the specimens were stained with HE, and then observed under a light microscope.

Enzyme histochemistry

Some of the tissue blocks were used for enzyme histochemistry staining. Four μm thick tissue slices were mounted to polylysine-coated slides with a cryotome. Wachstein-Meisid lead nitrate method^[5] was used to conduct enzyme histochemistry stain for intracellular Ca²⁺-Mg²⁺-ATPase. The slides were examined under a light microscope.

RT-PCR

Primers for Ca²⁺-Mg²⁺-ATPase gene were designed based on mRNA sequence of intracellular Ca²⁺-Mg²⁺-ATPase^[6]. GAPDH gene was used as internal housekeeping gene. Total RNA of pancreas and liver were taken for RT-PCR at 1 h and 5 h after AP was induced. Total RNA was extracted with Trizol reagents. Quantity and purity of RNA were determined with an ultraviolet spectrophotometer. RNA integrity was confirmed by agar gel electrophoresis. The reverse transcription system was 20 μl in volume, containing 2 μg total RNA, 1 μl reverse transcriptase, 1 μl dNTP (10 mmol/L), 2 μl (100 ng/1 μl) hexamer, 4 μl 5×buffer, 2 μl 0.1M DTT, 8 μl water. The mixture was incubated at 37 °C for 1 hour and then at 70 °C for 15 minutes to inactivate reverse transcriptase. cDNA was used as a template for subsequent PCR. PCR reaction was performed in a thermal cycler (PE480). PCR reaction solution contained 1 μl cDNA, 2 μl dNTP (2 mmol/L), 1 μl primers, 2.5 μl 10×buffer, 2U Taq polymerase, 18 μl water. PCR process was at 94 °C for 5 minutes, followed by 35 cycles at 94 °C for 1 min, at 57 °C for 1 min, and at 72 °C for 1 min. Final extension was at 72 °C for 10 minutes, 8 μl of PCR products was examined on 1% agar gel electrophoresis. The bands were observed and photographed under Ultraviolet light.

Statistical analysis

Data were analyzed by χ² test and P<0.01 was considered significant.

RESULTS

Pathological findings in pancreas, liver and kidney tissues of AP rats

Pancreas Large areas of hemorrhage were found in pancreatic tissue of AP+NS group. Acinar structure was obscure. There were large areas of necrosis. Some nuclei were lysed and disappeared. Apparently saponified spots were seen. A

number of inflammatory cell infiltrations were observed in the peri-necrotic tissues. In AP+QYT, AP+Tet or AP+VitE groups, the pancreas only slightly swelled with sporadic bleeding and necrosis, and mild inflammatory infiltration in the pancreatic tissue.

Liver In AP+NS group, degeneration and necrosis of the liver cells were found, and hepatocytes were disordered and some hepatic cords disappeared. In AP+QYT, AP+Tet or AP+VitE groups, hepatocytes were only degenerated and swelled with slight focal hemorrhagic necrosis.

Kidney In AP+NS group, epithelial cells in the proximal convoluted renal tubule were observed with degeneration and necrosis. Hyperemia, swelling and inflammatory cell infiltration were seen in renal glomeruli. Only edema was found in proximal convoluted renal tubular epithelial cells in AP+QYT, AP+Tet and AP+VitE groups (Figure 1).

Activity of intracellular Ca²⁺-Mg²⁺-ATPase in pancreas, liver and kidney tissues of AP rats

Positive stains were diffusely distributed in cellular membrane and cytoplasm of pancreatic acinar cells, hepatocytes, and proximal renal tubule epithelial cells. Positive rate of Ca²⁺-Mg²⁺-ATPase stain in tissues of normal group was significantly higher than that of other groups. The lowest positive rate was found in AP+NS group (P<0.01). There was no significant difference between groups of AP+QYT, AP+Tet, and AP+VitE (P>0.05) (Table 1, Figure 2).

Positive cells were defined as cells with uneven chocolate brown particles in cytoplasm under light microscope. The darker the staining color was, the higher the activity was. The cells were classified into 4 levels based on color intensity and number of positive cells. No staining or only a small number of light brown particles in cellular membrane and cytoplasm, and more than 25% of stained cells were negative (-); with a medium number of brown particles, and 25%-50% of stained cells were positive (+); with a large number of brown particles and more than 50% of stained cells were positive (++); more than 75% of stained cells were positive (+++).

Expression of Ca²⁺-Mg²⁺-ATPase in pancreas and liver tissues of AP rats

By RT-PCR technique, the expression of Ca²⁺-Mg²⁺-ATPase in pancreas and liver of all groups was measured respectively. The gene fragment of Ca²⁺-Mg²⁺-ATPase was 451 bp. The amplified fragment of internal housekeeping gene GAPDH was 450 bp. The results showed that the highest expression of Ca²⁺-Mg²⁺-ATPase was in normal group, the lowest was in AP+NS group, and moderate in AP+QYT, AP+Tet and AP+VitE groups. The expression decreased with time in AP+NS group, While in AP+QYT, AP+Tet and AP+VitE groups, the expression increased with time. The expression of Ca²⁺-Mg²⁺-ATPase in liver had no significant difference between groups (Figure 3).

Table 1 Positive rate of activity of intracellular Ca²⁺-Mg²⁺-ATPase in tissues of AP rats

Group	n	Pancreatic acinar cells				Hepatocytes				Renal epithelial cells			
		-	+	++~+++	Positive (%)	-	+	++~+++	Positive (%)	-	+	++~+++	Positive (%)
Normal group	9	0	5	4	100 ^a	0	3	6	100 ^a	0	5	6	100 ^a
AP+NS	24	22	2	0	8.3	18	5	1	25.0	17	5	2	29.2
AP+QYT	24	10	7	7	58.3 ^a	4	11	9	83.3 ^a	4	12	8	83.3 ^a
AP+Tet	24	12	9	3	50.0 ^a	7	9	8	70.8 ^a	6	10	8	75.0 ^a
AP+VitE	24	11	7	6	54.2 ^a	6	11	7	75.0 ^a	5	11	8	79.2 ^a

^aP<0.01 vs AP+NS.

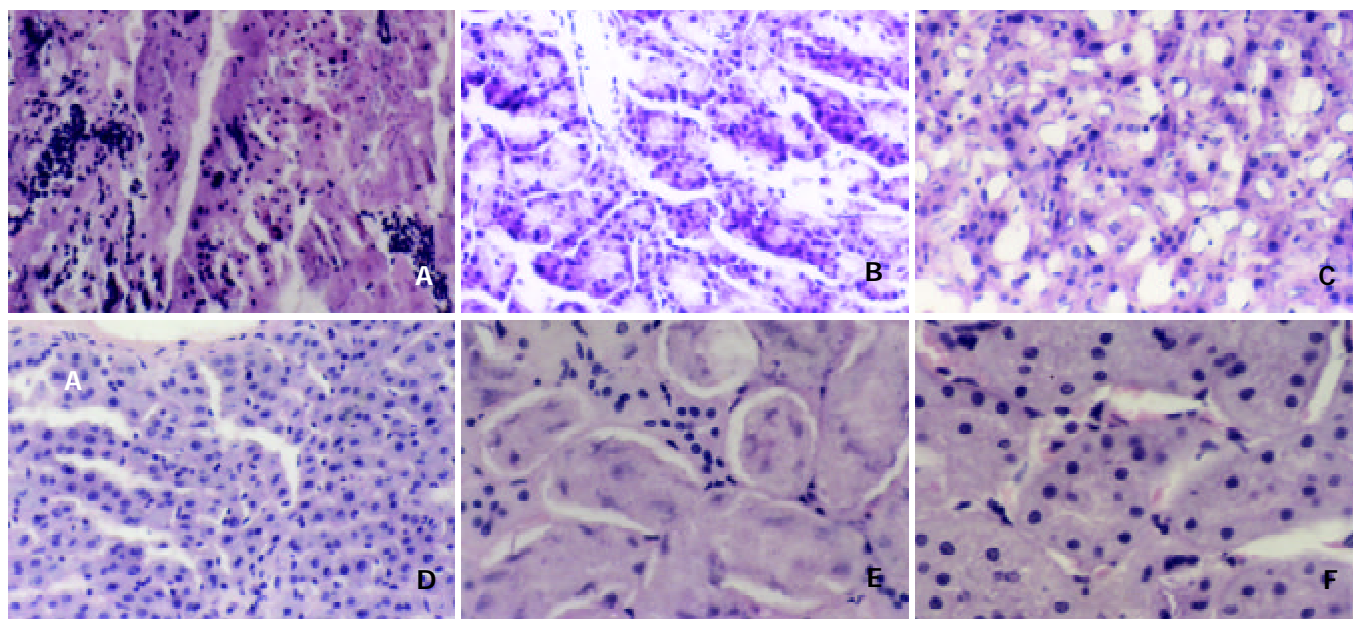


Figure 1 Histopathological findings in AP rats before and after treatment, HE stains. A: Morphological changes in pancreatic tissue of AP rats before treatment, $\times 200$. B: Morphological changes in pancreatic tissue of AP rats after treatment with QYT, $\times 200$. C: Morphological changes in hepatic tissue of AP rats before treatment, $\times 200$. D: Morphological changes in hepatic tissue of AP rats after treatment with VitE, $\times 200$. E: Morphological changes in renal tissue of AP rats before treatment, $\times 400$. F: Morphological changes in hepatic tissue of AP rats after treatment with Tet, $\times 400$.

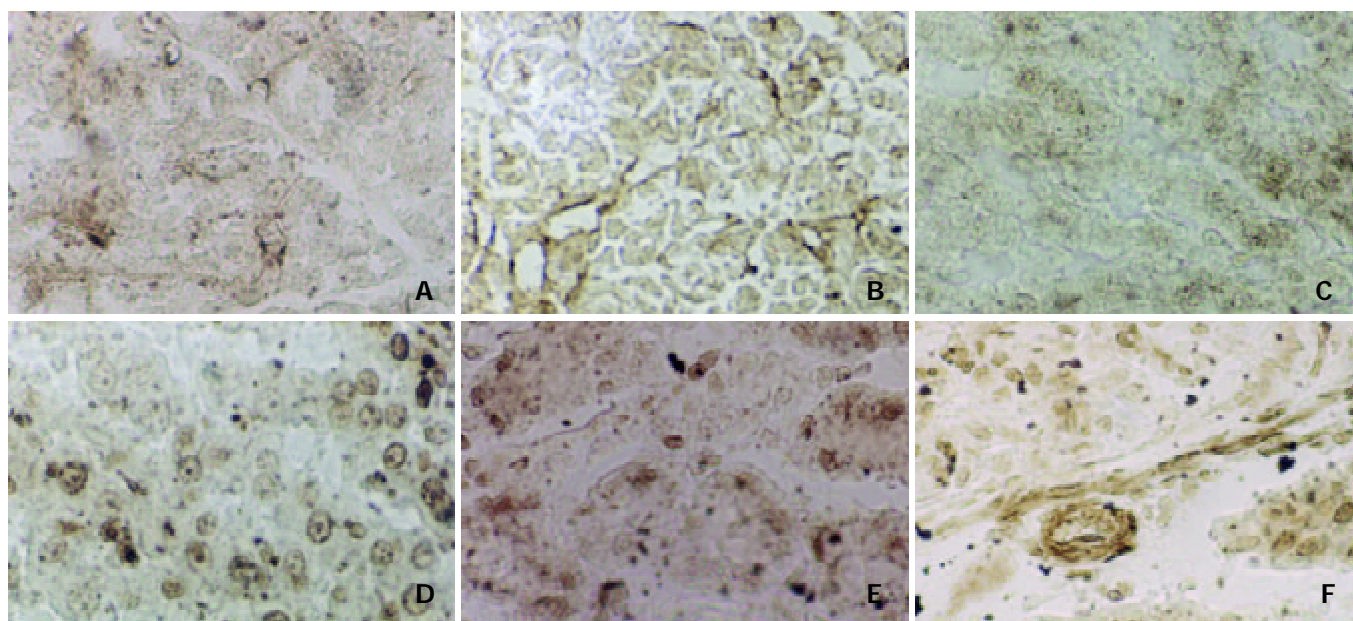


Figure 2 Enzyme histochemistry staining for intracellular Ca^{2+} - Mg^{2+} -ATPase in AP rats before and after treatment. A: Pancreatic tissue in AP rats before treatment, $\times 400$. B: Pancreatic tissue in AP rats after treatment with QYT, $\times 400$. C: Hepatic tissue in AP rats before treatment, $\times 200$. D: Hepatic tissue in AP rats after treatment with VitE, $\times 200$. E: Renal tissue in AP rats before treatment, $\times 400$. F: Renal tissue in AP rats after treatment with Tet, $\times 400$.

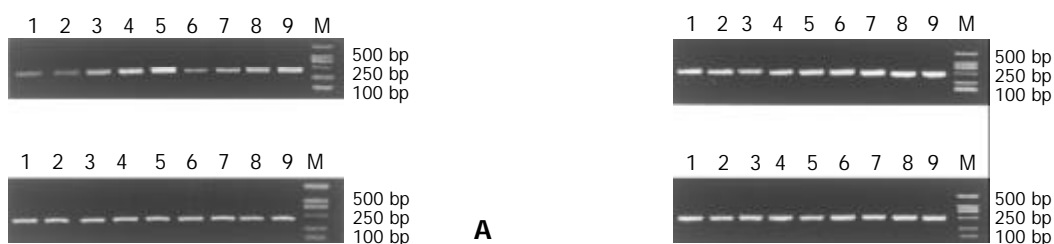


Figure 3 Expression of Ca^{2+} - Mg^{2+} -ATPase in AP rats before and after treatment analyzed by RT-PCR. A: Expression of Ca^{2+} - Mg^{2+} -ATPase mRNA in pancreatic tissue of different groups. B: Expression of Ca^{2+} - Mg^{2+} -ATPase mRNA in hepatic tissue of different groups. C: amplification product of GAPDH gene in pancreatic tissue of different groups. D: amplification product of GAPDH gene in hepatic tissue of different groups. Note: 1: AP 1 h, 2: AP 5 h, 3: QYT+AP 1 h, 4: QYT+AP 5 h, 5: Normal control group, 6: Tet+AP 1 h, 7: Tet+AP 5 h, 8: VitE+AP 1 h, 9: VitE+AP 5 h, M: PCR marker.

DISCUSSION

The level of intracellular free calcium (Ca²⁺) is not only dependent on the inflow of extracellular calcium through cell membrane and release from calcium reservoir inside the cell, but also on the function of Ca²⁺-Mg²⁺-ATPase on cell membrane and membrane of endoplasmic reticulum and mitochondria. By Ca²⁺-Mg²⁺-ATPase, Ca²⁺ could be pumped out of cell or into calcium reservoir. Thus Ca²⁺-Mg²⁺-ATPase could play an important role in intracellular calcium homeostasis^[7-9].

Activity and expression of intracellular Ca²⁺-Mg²⁺-ATPase in AP and its implication

Our experimental results showed that, in AP rats, the activity of Ca²⁺-Mg²⁺-ATPase in pancreatic, hepatic and renal tissues was decreased in AP rats. At the same time the pathological findings were aggravated. These results suggested that alteration of Ca²⁺-Mg²⁺-ATPase activity in AP might take part in the occurrence and progression of AP. It was reported that permeability of cell membrane was increased in AP. Ca²⁺ inflow might increase and lead to intracellular calcium overload. In the meantime, some stimulating factors could activate corresponding receptors on the surface of membrane to activate guanylate cyclation (GC). As a result, energy was released to cascade effector phospholipase C intracellular phosphatidylinositol diphosphate (PIP₂) into inositol triphosphate (IP₃) and diacylglycerol (DG). The IP₃ subsequently activated IP₃ receptors on endoplasmic reticulum to stimulate Ca²⁺ release from calcium reservoir. Consequently intracellular Ca²⁺ level increased abruptly. If the intracellular Ca²⁺-Mg²⁺-ATPase activity was decreased, Ca²⁺ could not be effectively pumped back into the reservoir or out of cells, which further aggravated intracellular calcium overload^[10,11]. Intracellular calcium overload further facilitated the release of pro-inflammatory mediators, which would cause strong contraction and thrombosis of microcirculation. Thus energy metabolism in tissues was disordered and ATP production was reduced^[12-16]. In addition, large quantities of free radicals produced during acute pancreatitis would cause phospholipids re-distribution in cell membrane. All of these factors might contribute to the inhibition of ATPase activity, which in turn would aggravate intracellular calcium overload. The vicious cycle occurred. Therefore, decrease of intracellular Ca²⁺-Mg²⁺-ATPase activity plays a key role in the development and aggravation of calcium overload.

In the present study, we found that activity of intracellular Ca²⁺-Mg²⁺-ATPase was decreased in hepatocyte of AP rat, but the expression of Ca²⁺-Mg²⁺-ATPase in the tissues did not change greatly. This finding suggested that intracellular Ca²⁺-Mg²⁺-ATPase activity was not only dependent on the level of its gene expression but also was affected by many other factors^[17-19].

Therapeutic effect and mechanism of QYT, Tet and VitE

Chinese medicine QYT is an effective compound in the treatment of AP. It has been proved to have bacteriostatic and anti-inflammatory effects, and to promote intestinal movement^[20,21]. Tet is a kind of bisbenzylisoquinoline alkaloid extracted from root tuber of *Stephania tetrandran*, a Chinese herbal medicine. It has been proved to be a natural non-selective calcium channel blocker^[22,23], and VitE has also been proved to be a scavenging agent of free radicals and blocker for lipid peroxidation^[24-27]. The present study found that in AP rats, intracellular Ca²⁺-Mg²⁺-ATPase activity in pancreatic, hepatic and renal tissues was increased after treatment with the above three medicines, and in pancreas the expression of Ca²⁺-Mg²⁺-ATPase was enhanced. Furthermore, pathological changes of hemorrhage and necrosis in the tissues were relieved. The complicating ascites and pleural effusion were improved^[28-34].

In summary, QYT, Tet and VitE have certain protecting effects on tissues and cells in AP, and the mechanisms are related with improved blood supply, increased intracellular Ca²⁺-Mg²⁺-ATPase activity and reduced intracellular calcium overload.

REFERENCES

- Weber H**, Roesner JP, Nebe B, Rychly J, Werner A, Schroder H, Jonas L, Leitzmann P, Schneider KP, Dummler W. Increased cytosolic Ca²⁺ amplifies oxygen radical induced alterations of the ultrastructure and the energy metabolism of isolated rat pancreatic acinar cells. *Digestion* 1998; **59**: 175-185
- Pu Q**, Yan L, Shen J. Effects of calcium overload in the conversion of acute edematous pancreatitis to necrotizing pancreatitis in rats. *Zhonghua Yixue Zazhi* 1999; **79**: 143-145
- Redondo Valdeolmillos M**, del Olmo Martinez ML, Almaraz Gomez A, Belmonte A, Coca MC, Caro-Paton Gomez A. The effects of an oral calcium overload on the rat exocrine pancreas. *Gastroenterol Hepatol* 1999; **22**: 211-217
- Rueda Chimento JC**, Ortega Medina L, Arguello de Andres JM, Landa Garcia JJ, Balibrea Cantero JL. Experimental acute pancreatitis in the rat. The quantification of pancreatic necrosis after the retrograde ductal injection of sodium taurocholate. *Rev Esp Enferm Dig* 1991; **80**: 178-182
- Tachibana T**, Nawa T. Ultrastructural localization of Ca(++)-ATPases in Meissner's corpuscle of the Mongolian gerbil. *Arch Histol Cytol* 1992; **55**: 375-379
- Gunteski-Hamblin AM**, Greeb J, Shull GE. A novel Ca²⁺ pump expressed in brain, kidney, and stomach is encoded by an alternative transcript of the slow-twitch muscle sarcoplasmic reticulum Ca-ATPase gene. Identification of cDNAs encoding Ca²⁺ and other cation-transporting ATPases using an oligonucleotide probe derived from the ATP-binding site. *J Biol Chem* 1988; **263**: 15032-15040
- Pariente JA**, Lajas AI, Pozo MJ, Camello PJ, Salido GM. Oxidizing effects of vanadate on calcium mobilization and amylase release in rat pancreatic acinar cells. *Biochem Pharmacol* 1999; **58**: 77-84
- Gorini A**, Villa RF. Effect of *in vivo* treatment of clonidine on ATP-ase's enzyme systems of synaptic plasma membranes from rat cerebral cortex. *Neurochem Res* 2001; **26**: 821-827
- Fu Y**, Wang S, Lu Z, Li H, Li S. Erythrocyte and plasma Ca²⁺, Mg²⁺ and cell membrane adenosine triphosphatase activity in patients with essential hypertension. *Chin Med J* 1998; **111**: 147-149
- Weber H**, Roesner JP, Nebe B, Rychly J, Werner A, Schroder H, Jonas L, Leitzmann P, Schneider KP, Dummler W. Increased cytosolic Ca²⁺ amplifies oxygen radical-induced alterations of the ultrastructure and the energy metabolism of isolated rat pancreatic acinar cells. *Digestion* 1998; **59**: 175-185
- Parkinson NA**, James AF, Hendry BM. Actions of endothelin-1 on calcium homeostasis in Madin-Darby canine kidney tubule cells. *Nephrol Dial Transplant* 1996; **11**: 1532-1537
- van Ooijen B**, Ouwendijk RJ, Kort WJ, Zijlstra FJ, Vincent JE, Wilson JH, Westbroek DL. Raised plasma thromboxane B2 levels in experimental acute necrotizing pancreatitis in rats. The effects of flunarizine, dazoxiben, and indomethacin. *Scand J Gastroenterol* 1988; **23**: 188-192
- Xu H**, Shi AY. Effect of magnesium on postischemic reperused myocardial mitochondria. *Shengli Xuebao* 1996; **48**: 303-306
- Bassani RA**, Bassani JW, Lipsius SL, Bers DM. Diastolic SR Ca efflux in atrial pacemaker cells and Ca-overloaded myocytes. *Am J Physiol* 1997; **273**(2 Pt 2): H886-892
- He ZJ**, Matikainen MP, Alho H, Harmoinen A, Ahola T, Nordback I. Extraprostatic organ impairment in caerulein induced pancreatitis. *Ann Chir Gynaecol* 1999; **88**: 112-117
- Jiang XC**, D' Armiento J, Mallampalli RK, Mar J, Yan SF, Lin M. Expression of plasma phospholipid transfer protein mRNA in normal and emphysematous lungs and regulation by hypoxia. *J Biol Chem* 1998; **273**: 15714-15718
- Yokomori H**, Oda M, Kamegaya Y, Ogi M, Tsukada N, Ishii H. Bile canalicular contraction and dilatation in primary culture of rat hepatocytes-possible involvement of two different types of plasma membrane Ca (2+)-Mg(2+)-ATPase and Ca(2+)-pump-

- ATPase. *Med Electron Microsc* 2001; **34**: 115-122
- 18 **Ding J**, Wu Z, Crider BP, Ma Y, Li X, Slaughter C, Gong L, Xie XS. Identification and functional expression of four isoforms of ATPase II, the putative aminophospholipid translocase. Effect of isoform variation on the ATPase activity and phospholipid specificity. *J Biol Chem* 2000; **275**: 23378-23386
- 19 **Hansson A**, Willows RD, Roberts TH, Hansson M. Three semi-dominant barley mutants with single amino acid substitutions in the smallest magnesium chelatase subunit form defective AAA+ hexamers. *Proc Natl Acad Sci U S A* 2002; **99**: 13944-13949
- 20 **Wu C**, Li Z, Xiong D. An experimental study on curative effect of Chinese medicine Qingyitang in acute necrotizing pancreatitis. *Zhongguo Zhongxiyi Jiehe Zazhi* 1998; **18**: 236-238
- 21 **Deng Q**, Wu C, Li Z, Xiong D, Liang Y, Lu L, Sun X. The prevention of infection complicating acute necrotizing pancreatitis: an experimental study. *Zhonghua Waike Zazhi* 2000; **38**: 625-629
- 22 **Xie QM**, Tang HF, Chen JQ, Bian RL. Pharmacological actions of tetrandrine in inflammatory pulmonary diseases. *Acta Pharmacol Sin* 2002; **23**: 1107-1113
- 23 **Wang B**, Xiao JG. Effect of tetrandrine on free intracellular calcium in cultured calf basilar artery smooth muscle cells. *Acta Pharmacol Sin* 2002; **23**: 1121-1126
- 24 **Christman JW**, Holden EP, Blackwell TS. Strategies for blocking the systemic effects of cytokines in the sepsis syndrome. *Crit Care Med* 1995; **23**: 955-963
- 25 **Jiang XC**, Tall AR, Qin S, Lin M, Schneider M, Lalanne F, Deckert V, Desrumaux C, Athias A, Witztum JL, Lagrost L. Phospholipid transfer protein deficiency protects circulating lipoproteins from oxidation due to the enhanced accumulation of vitamin E. *J Biol Chem* 2002; **277**: 31850-31856
- 26 **Prokop'eva NV**, Gulyaeva LF, Kolosova NG. Time course of malonic dialdehyde and alpha-tocopherol in rat pancreas during the first hours of acute pancreatitis. *Bull Exp Biol Med* 2000; **129**: 452-454
- 27 **Antosiewicz J**, Popinigis J, Ishiguro H, Hayakawa T, Wakabayashi T. Cerulein-induced acute pancreatitis diminished vitamin E concentration in plasma and increased in the pancreas. *Int J Pancreatol* 1995; **17**: 231-236
- 28 **Kempainen E**, Hietaranta A, Puolakkainen P, Sainio V, Halttunen J, Haapiainen R, Kivilaakso E, Nevalainen T. Bactericidal/permeability-increasing protein and group I and II phospholipase A2 during the induction phase of human acute pancreatitis. *Pancreas* 1999; **18**: 21-27
- 29 **Nevalainen TJ**, Gronroos JM, Kortesus PT. Pancreatic and synovial type phospholipases A2 in serum samples from patients with severe acute pancreatitis. *Gut* 1993; **34**: 1133-1136
- 30 **Smirnov DA**. Acute pancreatitis and biological antioxidants. *Khirurgiia* 1994; **3**: 30-32
- 31 **Li ZL**, Wu CT, Lu LR, Zhu XF, Xiong DX. Traditional Chinese medicine Qingyitang alleviates oxygen free radical injury in acute necrotizing pancreatitis. *World J Gastroenterol* 1998; **4**: 357-359
- 32 **Wu CT**, Li ZL, Xiong DX. Relationship between enteric microecologic dysbiosis and bacterial translocation in acute necrotizing pancreatitis. *World J Gastroenterol* 1998; **4**: 242-245
- 33 **Ai J**, Gao HH, He SZ, Wang L, Luo DL, Yang BF. Effects of matrine, artemisinin, tetrandrine on cytosolic [Ca²⁺]_i in guinea pig ventricular myocytes. *Acta Pharmacol Sin* 2001; **22**: 512-515
- 34 **Lai JH**. Immunomodulatory effects and mechanisms of plant alkaloid tetrandrine in autoimmune diseases. *Acta Pharmacol Sin* 2002; **23**: 1093-1101

Edited by Zhu LH and Wang XL

Red oil A5 inhibits proliferation and induces apoptosis in pancreatic cancer cells

Mi-Lian Dong, Xian-Zhong Ding, Thomas E. Adrian

Mi-Lian Dong, Affiliated Taizhou Hospital, Wenzhou Medical College, Linhai 317000, Zhejiang Province, China

Xian-Zhong Ding, Thomas E. Adrian, Northwestern University Medical School, Chicago, IL60611-3008, U.S.A

Supported by the National Cancer Institute of USA, No. CA72712, and Special Funds for Zhejiang 151 Talent Project of China, No. 98-2095

Correspondence to: Mi-Lian Dong, Taizhou Hospital of Wenzhou Medical College, 150 Ximen Street, Linhai 317000, Zhejiang Province, China. mdong2@hotmail.com

Telephone: +86-576-5315829 **Fax:** +86-576-5315829

Received: 2003-06-04 **Accepted:** 2003-08-16

Abstract

AIM: To study the effect of red oil A5 on pancreatic cancer cells and its possible mechanisms.

METHODS: Effect of different concentrations of red oil A5 on proliferation of three pancreatic cancer cell lines, AsPC-1, MiaPaCa-2 and S2013, was measured by ³H-methyl thymidine incorporation. Time-dependent effects of 1:32 000 red oil A5 on proliferation of three pancreatic cancer cell lines, were also measured by ³H-methyl thymidine incorporation, and Time-course effects of 1:32 000 red oil A5 on cell number. The cells were counted by Z1-Coulter Counter. Flow-cytometric analysis of cellular DNA content in the control and red oil A5 treated AsPC-1, MiaPaCa-2 and S2013 cells, were stained with propidium iodide. TUNEL assay of red oil A5-induced pancreatic cancer cell apoptosis was performed. Western blotting of the cytochrome c protein in AsPC-1, MiaPaCa-2 and S2013 cells treated 24 hours with 1:32 000 red oil A5 was performed. Proteins in cytosolic fraction and in mitochondria fraction were extracted. Proteins extracted from each sample were electrophoresed on SDS-PAGE gels and then were transferred to nitrocellulose membranes. Cytochrome c was identified using a monoclonal cytochrome c antibody. Western blotting of the caspase-3 protein in AsPC-1, MiaPaCa-2 and S2013 cells treated with 1:32 000 red oil A5 for 24 hours was carried out. Proteins in whole cellular lysates were electrophoresed on SDS-PAGE gels and then transferred to nitrocellulose membranes. Caspase-3 was identified using a specific antibody. Western blotting of poly-ADP ribose polymerase (PARP) protein in AsPC-1, MiaPaCa-2 and S2013 cells treated with 1:32 000 red oil A5 for 24 hours was performed. Proteins in whole cellular lysates were separated by electrophoresis on SDS-PAGE gels and then transferred to nitrocellulose membranes. PARP was identified by using a monoclonal antibody.

RESULTS: Red oil A5 caused dose- and time-dependent inhibition of pancreatic cancer cell proliferation. Propidium iodide DNA staining showed an increase of the sub-G0/G1 cell population. The DNA fragmentation induced by red oil A5 in these three cell lines was confirmed by the TUNEL assay. Furthermore, Western blotting analysis indicated that cytochrome c was released from mitochondria to cytosol during apoptosis, and caspase-3 was activated following red oil A5 treatment which was measured by procaspase-3 cleavage and PARP cleavage.

CONCLUSION: These findings show that red oil A5 has potent anti-proliferative effects on human pancreatic cancer cells with induction of apoptosis *in vitro*.

Dong ML, Ding XZ, Adrian TE. Red oil A5 inhibits proliferation and induces apoptosis in pancreatic cancer cells. *World J Gastroenterol* 2004; 10(1): 105-111

<http://www.wjgnet.com/1007-9327/10/105.asp>

INTRODUCTION

Pancreatic cancer is one of the most enigmatic and aggressive malignant diseases^[1-4]. It is now the fourth leading cause of cancer death in both men and women in the USA and the incidence of this disease shows no sign of decline^[1-3,5]. Pancreatic cancer is characterized by a poor prognosis and lack of effective response to conventional therapy^[6]. The 5-year survival rate is less than 4% and the median survival period after diagnosis is less than 6 months^[7,8]. At present, surgical resection is still the only effective treatment option, but only about 15% of carcinomas of the head of pancreas are resectable and there are few long-term survivors even after apparent curative resection^[7,8]. On the other hand, chemotherapy or radiation therapy provide only limited palliation, without meaningful improvement of survival in patients with non-resectable pancreatic cancer^[7-9]. Only new therapeutic strategies can improve this dismal situation^[10,11].

A series of prospective and case-control studies have shown an association between higher fish intake and reduced cancer incidence, and other benefits including inhibition of cancer cell proliferation, induction of apoptosis^[12-22]. Recent studies indicate that diets containing a high proportion of long-chain n-3 polyunsaturated fatty acids was associated with inhibition of growth and metastasis of human cancer including pancreatic cancer^[12,14,23,24]. Diets rich in linoleic acid (LA), an n-6 fatty acid, stimulate the progression of human cancer cell in athymic nude mice, whereas supplement of fish oil components, docosahexaenoic acid (DHA) and eicosapentaenoic acid (EPA) exerts suppressive effects. Fish oil has been shown to reduce the induction of different cancer in animal models by a mechanism which may involve suppression of mitosis, increase apoptosis through long-chain n-3 polyunsaturated fatty acid EPA^[12,14,25-27]. In parallel, dietary supplementation with DHA is accompanied by reduced levels of 12- and 15-hydroxyeicosatetraenoic acids (12- and 15-HETE), suggesting that changes in eicosanoid biosynthesis may have been responsible for the observed decrease in tumor growth^[14,16,28,29]. Previous studies also have shown that the anti-cancer effect of fish oil is accompanied by a decreased production of cyclooxygenase and lipoxygenase metabolites^[10,30,31]. The efficacy of fish oil which we have found exhibits particularly potent anticancer effects that appear to be related to its content of lipoxygenase inhibitors rather than its EPA or DHA contents. Red oil A5 is lipid isolates from the epithelial layer of the echinoderm. This oil is non-toxic and exerts a marked anti-inflammatory effect in laboratory animals. Red oil A5 almost totally inhibits pancreatic cancer cell proliferation at dilutions

of up to 1:32 000. The inhibition of proliferation induced by this fish oil is accompanied by marked induction of apoptosis. To date, no information is available regarding the effects of red oil A5 in pancreatic cancer. In the present study, the effects of red oil A5 on proliferation, apoptosis and cell cycle distribution were investigated in pancreatic cancer cells.

MATERIALS AND METHODS

Pancreatic cancer cell lines

The human pancreatic cancer cell lines (AsPC-1, MiaPaCa-2 and S2013) were purchased from the American Type Culture Collection (Rockville, MD, USA). These cell lines span the types of differentiation in human pancreatic adenocarcinomas. AsPC-1 and MiaPaCa-2 are poorly-differentiated, whereas S2013 is well-differentiated but heterogenous.

The cells were cultured in Dulbecco's Modified Eagle's Medium (DMEM) (obtained from Sigma, St. Louis, MO) supplemented with penicillin G (100 U/mL), streptomycin (100 U/mL) and 10% Fetal Bovine Serum (FBS) (purchased from Atlanta Biologicals, Atlanta, GA) in humidified air with 5% CO₂ at 37 °C. The cells were harvested by incubation in trypsin-EDTA (obtained from Sigma, St. Louis, MO) solution for 10-15 minutes. Then the cells were centrifuged at ×300 g for 5 minutes and the cell pellets suspended in fresh culture medium prior to seeding into culture flasks or plates.

Red oil A5

Red oil A5 (Coastside Research Chemical Co.) was dissolved in 1:2 DMEM as a stock solution. The stock solution was diluted to the appropriate concentrations with serum-free medium prior to the experiments.

Cell proliferation assay

Cell proliferation was analyzed by the ³H-methyl thymidine (from Amersham Inc., Arlington Heights, IL) incorporation and cell counting. Following treatment of pancreatic cancer cells with a series of concentrations of red oil A5 from 1:64 000 to 1:4 000 for 24 hours, and following treatment of pancreatic cancer cells with 1:32 000 red oil A5 for 6, 12 and 24 hours, cellular DNA synthesis was assayed by adding ³H-methyl thymidine 0.5 μCi/well. After a 2 hour incubation, the cells were washed twice with PBS, precipitated with 10% TCA for two hours and solubilized from each well with 0.5 ml of 0.4 N sodium hydroxide. Incorporation of ³H-methyl thymidine into DNA was measured by adding scintillation cocktail and counting in a scintillation counter (LSC1414 WinSpectral, Wallac, Turku, Finland). For cell counting, the cells were seeded in 12-well plates and cultured in serum-free medium for 24 hours prior to red oil A5 treatment and then switched to serum-free medium with or without 1:32 000 red oil A5 for the respective treatment times (24, 48, 72 and 96 hours). The cells were removed from the plates by trypsinization to produce a single cell suspension for cell counting. The cells were counted using Z1-Coulter Counter (Luton, UK).

Analysis of cellular DNA content by flow cytometry

The cells were grown at 50%-60% confluence in T75 flasks, serum-starved for 24 hours and then treated with 1:32 000 red oil A5 for 24 hours. At the end of the treatment, the cells were harvested with trypsin-EDTA solution to produce a single cell suspension. The cells were then pelleted by centrifugation and washed twice with PBS. Then the cell pellets were suspended in 0.5 ml PBS and fixed in 5 mL ice-cold 70 % ethanol at 4 °C. The fixed cells were centrifuged at 300×g for 10 minutes and the pellets were washed with PBS. After resuspension with 1 ml PBS, the cells were incubated with 10 μL of RNase I (10 mg/mL) and 100 μL of propidium iodide (400 μg/mL; Sigma) and

shaken for 1 hour at 37 °C in the dark. Samples were analyzed by flow cytometry. The red fluorescence of single events was recorded using a laser beam at 488 nm excitation λ with 610 nm as emission λ, to measure the DNA index.

Terminal deoxynucleotidyl transferase-mediated deoxyuridine triphosphate nick-end labeling (TUNEL) assay

TUNEL assay kits were purchased from Pharmingen and PARP antibody from BioMol. The assay was carried out for terminal incorporation of fluorescein 12-dUTP by terminal deoxynucleotidyl transferase into fragmented DNA, in pancreatic cells. Cells grown in T75 flasks were cultured in serum-free conditions for 24 hours and then treated with or without 1:32 000 red oil A5 for 24 hours. The cells were then trypsinized and fixed in 1% ethanol-free formaldehyde-PBS for 15 minutes. The cells were incubated with the enzyme substrate mixture with the addition of 20 mM EDTA and then counterstained with 5 μg/mL propidium iodide in PBS containing 0.5 mg/mL DNase-free RNase A, in the dark for 30 minutes. Laser flow cytometry was used to quantify the green fluorescence of fluorescein-12-dUDP incorporated against the red fluorescence of propidium iodide.

Preparation of cytosolic and mitochondrial extraction

Mitochondria/Cytosol Fractionation Kit was purchased from BioVision (Mountain View, CA94043, USA). Cells (5×10⁷) were collected by centrifugation at 600×g for 5 minutes at 4 °C from control and red oil A5-treated AsPC-1, MiaPaCa-2 and S2013 cells. Wash the cells with ice-cold PBS twice. Centrifuge at 600×g for 5 minutes at 4 °C. Remove the supernatant and resuspend the cells with 1.0 mL of 1×Cytosol Extraction Buffer Mix containing DTT and Protease Inhibitors. Incubate on ice for 10 minutes. Homogenize the cells in an ice-cold dounce tissue grinder (45 strokes) until 70-80% of the nuclei do not have the shiny ring. Transfer the homogenate to a 1.5 mL microcentrifuge tube, and centrifuge at 700×g for 10 minutes at 4 °C. Transfer the supernatant to a fresh 1.5 mL tube, and centrifuge at 10 000×g for 30 minutes at 4 °C. Collect the supernatant as cytosolic fraction. Resuspend the pellet in 0.1 mL Mitochondrial Extraction Buffer Mix containing DTT and Protease inhibitors, vortex for 10 seconds and save as Mitochondrial Fraction. Both cytosolic fraction and mitochondrial fraction were stored at -80 °C until ready for Western blot.

Western blot

Cells were seeded into flasks and grown to 50% to 60% confluence for 24 hours. The cells were then placed in serum-free medium with or without 1:32 000 red oil A5 for a period of 24 hours. In the end, the attached cells and floating cells were extracted in lysis buffer [20 mM Tris-HCl (pH 7.4), 2 mM sodium vanadate, 1.0 mM sodium fluoride, 100 mM NaCl, 2.0 mM phosphate substrate, 1% NP40, 0.5% sodium deoxycholate, 20 μg/mL each aprotinin and leupeptin, 25.0 μg/mL pepstatin, and 2.0 mM each EDTA and EGTA] for further analysis. Protein concentrations were determined using the bicinchoninic acid assay with BSA as standard. Western blot was carried out using standard techniques. Briefly, equal amounts of proteins in each sample were resolved in 10% sodium dodecyl sulfate polyacrylamide gel electrophoresis (SDS-PAGE) and the proteins transferred onto nitrocellulose membranes. After blocking with non-fat dried milk, the membranes were incubated with the appropriate dilution of primary antibody (Santa Cruz Biotech, Santa Cruz, CA, USA). The membranes were then incubated with a horseradish peroxidase-conjugated secondary antibody. The proteins were detected by an enhanced chemiluminescence detection system (Santa Cruz Biotech), and light emission was captured on

Kodak X-ray films (Eastman Kodak Company, Rochester, NY). The rabbit polyclonal antibody against cytochrome c and caspase-3, and the mouse monoclonal antibody against PARP were also purchased from Santa Cruz Biotech.

Statistical analysis

The data was analyzed by analysis of variance (ANOVA) with Bonferonni's or Dunnet's multiple comparison post-test for significance between each two groups. This analysis was performed with the Prism software package (GraphPad, San Diego, CA, USA). The data were expressed as mean \pm SEM and represented at least 3 different experiments.

RESULTS

Effect of red oil A5 on thymidine incorporation in pancreatic cancer cells

Red oil A5 caused marked, concentration-dependent inhibition of thymidine incorporation in AsPC-1, MiaPaCa-2 and S2013 cells, at concentrations ranging from 1:64 000 to 1:4 000 (ANOVA, AsPC-1: $F(5,23)=86.99$, $P<0.0001$; MiaPaCa-2: $F(5,23)=92.63$, $P<0.0001$; S2013: $F(5,23)=94.94$, $P<0.0001$ (Figure 1). The red oil A5-induced inhibition of proliferation was also time-dependent (ANOVA, AsPC-1: $F(3,11)=89.88$, $P<0.0001$; MiaPaCa-2: $F(3,11)=53.64$, $P<0.0001$; S2013: $F(3,11)=80.06$, $P<0.0001$ (Figure 2).

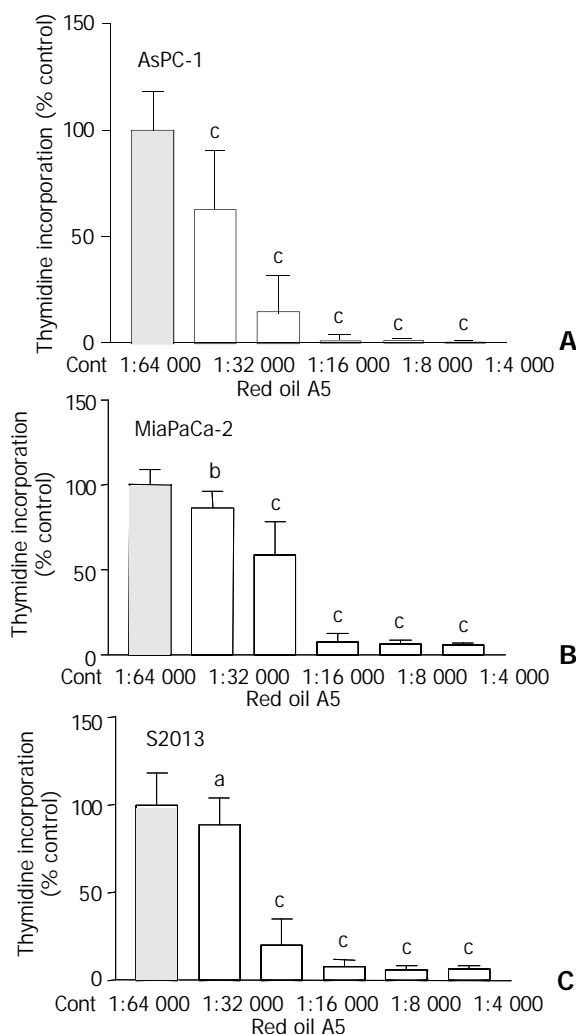


Figure 1 (A,B,C) Effect of different concentrations of red oil A5 on proliferation of three pancreatic cancer cell lines, AsPC-1, MiaPaCa-2 and S2013, as measured by ^3H -methyl thymidine incorporation. Results are expressed as % of control from three separate experiments. ^a $P<0.05$, ^b $P<0.01$, ^c $P<0.001$ vs control.

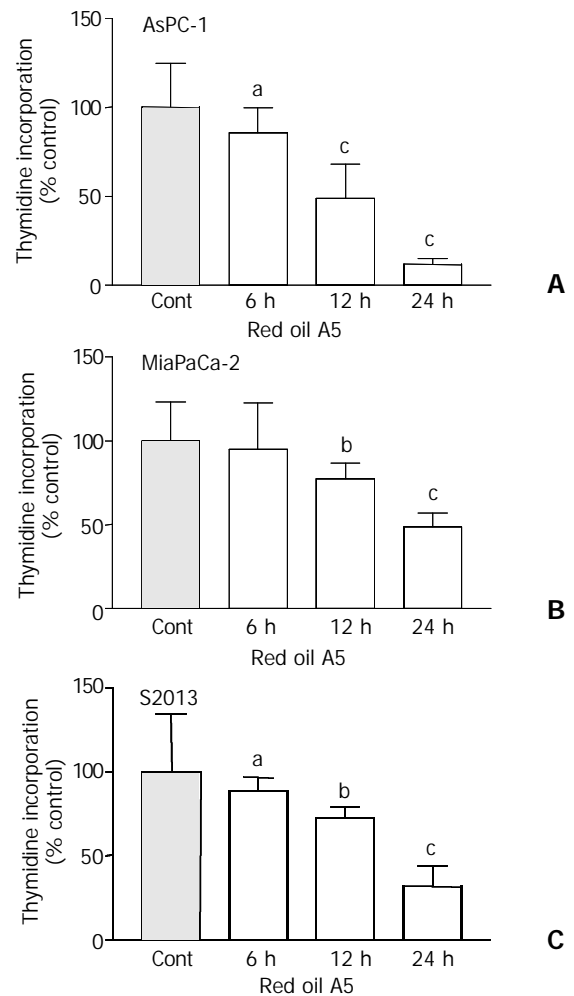


Figure 2 (A,B,C) Time-dependent effects of 1:32 000 red oil A5 on proliferation of three pancreatic cancer cell lines, AsPC-1, MiaPaCa-2 and S2013, as measured by ^3H -methyl thymidine incorporation at 6, 12 and 24 hours. The results are expressed as % of control from three separate experiments. ^a $P<0.05$, ^b $P<0.01$, ^c $P<0.001$ vs control.

Effect of red oil A5 on pancreatic cancer cell proliferation measured by cell counting

Red oil A5 induced significant time dependent inhibition of pancreatic cancer cell growth, as measured by the cell number in AsPC-1, MiaPaCa-2 and S2013 cells (two-way ANOVA, AsPC-1: $F(4,29)=49.54$, $P<0.0001$; MiaPaCa-2: $F(4,29)=43.48$, $P<0.0001$; S2013: $F(4,29)=39.25$, $P<0.0001$). During the first 24 hours, no obvious effects were seen compared to controls. At 48, 72, and 96 hours, red oil A5 resulted in a marked and progressive decrease in cell number compared to control (Figure 3).

Effect of red oil A5 on cell cycle phase distribution

To understand the mechanism of inhibition of cell proliferation, the distribution of cell cycle phases was analyzed following treatment with 1:32 000 red oil A5 for 24 hours. The cells were accumulated in the G2/M-phase in AsPC-1, MiaPaCa-2 and S2013 cell lines. The number of the cells in S-phase was increased also in all three cell lines when compared to control. A peak of the sub-G0/G1 cell population, a hallmark of apoptosis, was seen following 24 hours, exposure in all three cell lines (Figure 4).

Apoptosis of pancreatic cancer cells induced by red oil A5

To characterize the observed apoptosis, analysis of DNA fragmentation was carried out using the TUNEL assay. TUNEL staining of pancreatic cancer cells was markedly increased by 1:32 000 red oil A5 treatment for 24 hours (Figure 5).

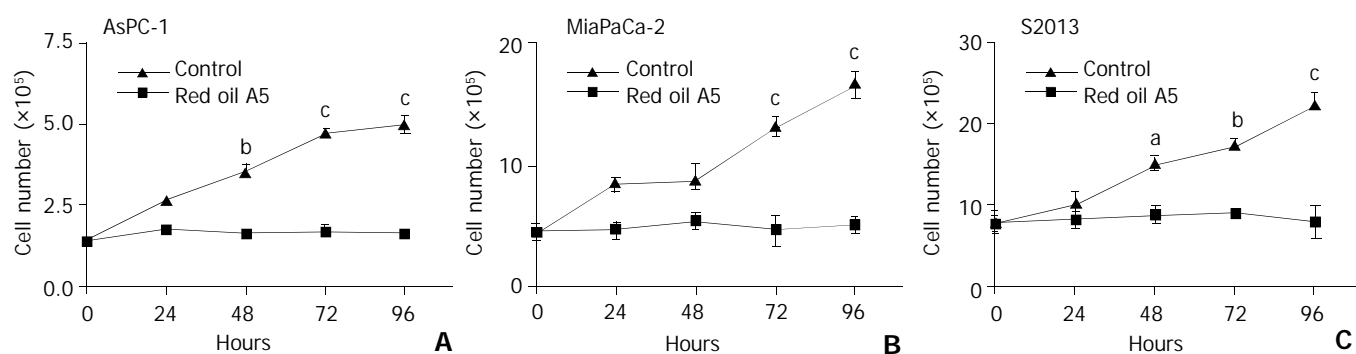


Figure 3 (A,B,C) Time-course effects of 1:32 000 red oil A5 on cell number in AsPC-1, MiaPaCa-2 and S2013 cells from 24 to 96 hours. The data represent mean \pm SEM of three separate experiments. ^a $P < 0.05$, ^b $P < 0.01$, ^c $P < 0.001$ vs control.

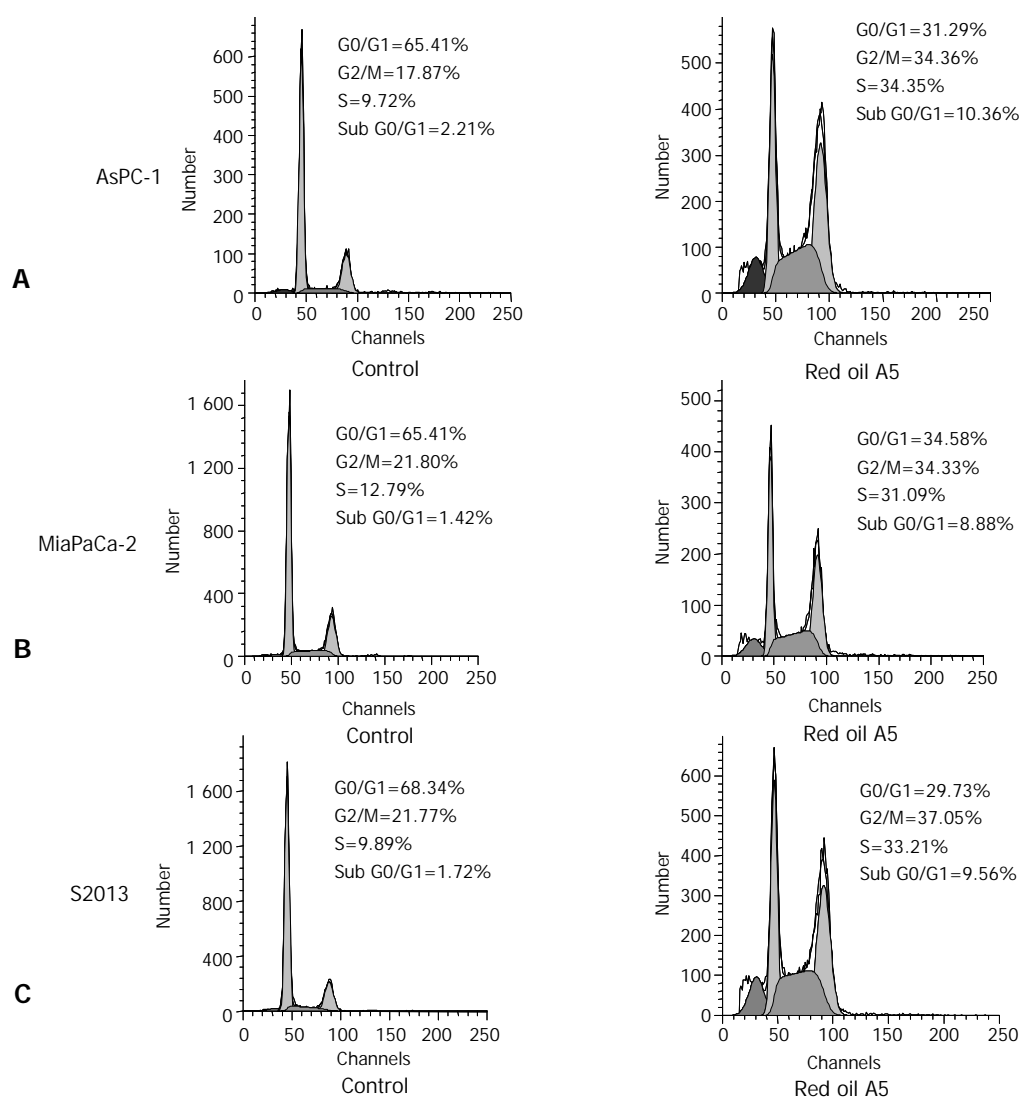


Figure 4 (A,B,C) Flow-cytometric analysis of cellular DNA content in control and red oil A5 treated AsPC-1, MiaPaCa-2 and S2013 cells, stained with propidium iodide. The cells were treated with 1:32000 red oil A5 in serum-free conditions for 24 hours. The distribution of cell cycle phases is expressed as % of total cells. Results were representative of three separate experiments.

Red oil A5 induced cytochrome C release

Cytochrome c is a mitochondrial protein that is released from the mitochondria to cytosol during apoptosis when mitochondrial membrane permeability is disrupted. An increase in the amount of cytochrome c in the cytosolic fraction was seen in all three cell lines, AsPC-1, MiaPaCa-2 and S2013 after red oil A5 treatment. Meanwhile, a decrease in the amount of cytochrome c in the mitochondrial fraction was seen in all three cell lines after red oil A5 treatment (Figure 6).

Effect of red oil A5 on activation of caspase-3 and cleavage of PARP

The expression and activation of caspase-3 by cleavage as well as the specific cleavage of its downstream substrate, PARP during apoptosis were observed by Western blotting. The 32 kDa procaspase-3 was cleaved into products of lower molecular weight, including a band corresponding to the 17 kDa active form. The uncleaved 116 kDa proform of PARP and its active 85 kDa cleaved fragment were detected. Both caspase-3

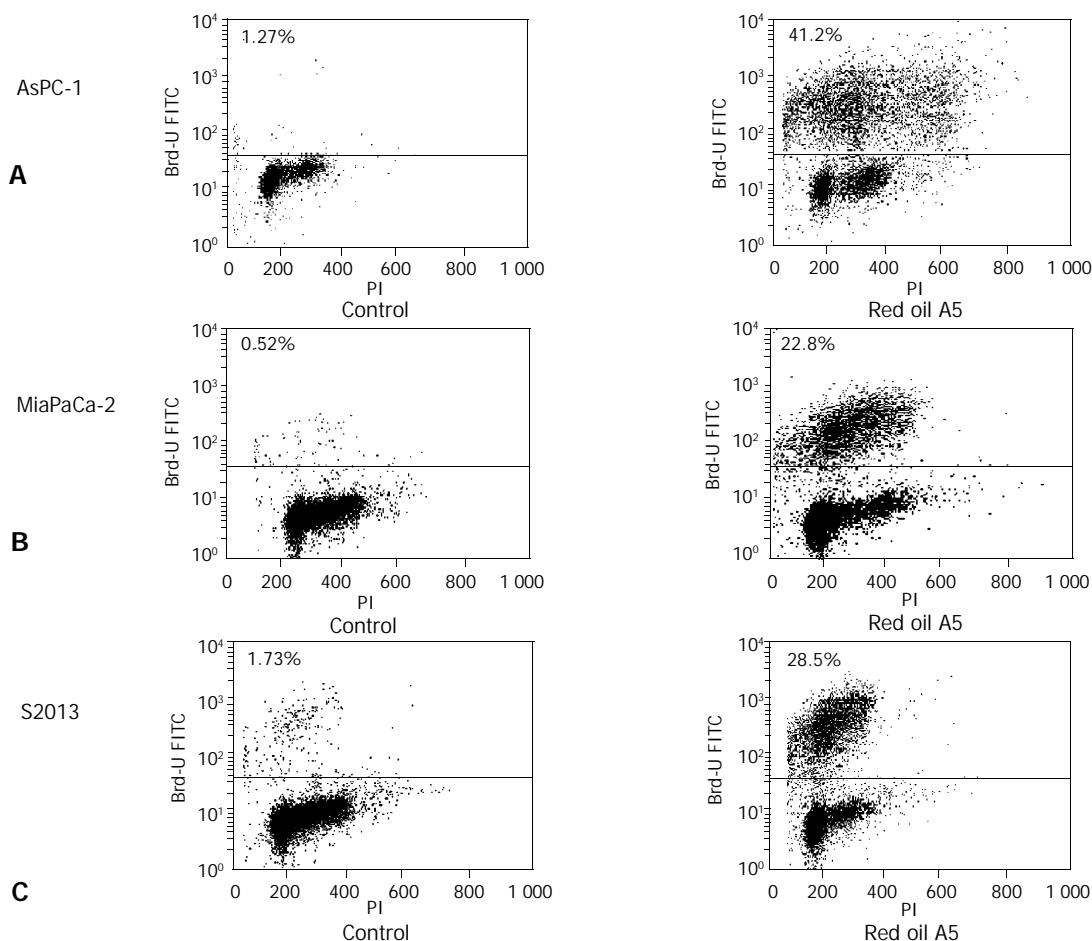


Figure 5 (A,B,C) TUNEL assay of red oil A5-induced pancreatic cancer cell apoptosis. Dot plot shows TdT-mediated dUTP nick-end labeling of control cells and cells treated with 1:32 000 red oil A5 which is expressed as % of total cells. The increases in fluorescence events in the upper panels are due to UTP labeling of fragmented DNA. The results are representative of three different experiments.

activation and PARP cleavage were induced and coincident with the induction of apoptosis (Figures 7, 8).

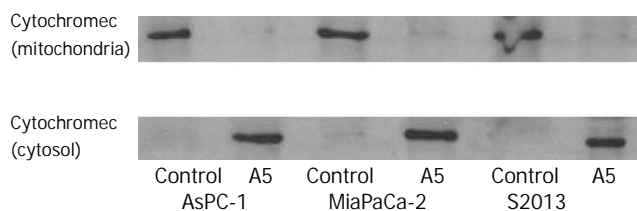


Figure 6 Western blot of the cytochrome c protein in AsPC-1, MiaPaCa-2 and S2013 cells treated with 1:32 000 red oil A5 for 24 hours. Proteins in cytosolic fraction and in mitochondrial fraction are extracted. Proteins extracted from each sample are electrophoresed on an SDS-PAGE gel and then are transferred to nitrocellulose membranes. Cytochrome c is identified using a monoclonal cytochrome c antibody. The results are representative of three different experiments.

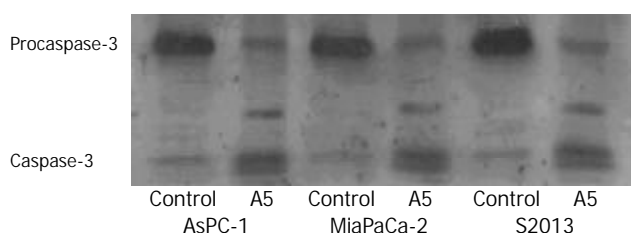


Figure 7 Western blot of the caspase-3 protein in AsPC-1, MiaPaCa-2 and S2013 cells are treated with 1:32 000 red oil A5

for 24 hours. Proteins in the whole cellular lysates are electrophoresed on an SDS-PAGE gel and then transferred to nitrocellulose membranes. Caspase-3 is identified using a specific antibody. The results are representative of three different experiments.

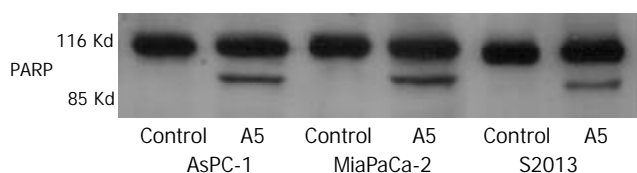


Figure 8 Western blot of poly-ADP ribose polymerase (PARP) protein in AsPC-1, MiaPaCa-2 and S2013 cells are treated with 1:32 000 red oil A5 for 24 hours. Proteins in whole cellular lysates are separated by electrophoresis on SDS-PAGE gels and then are transferred to nitrocellulose membranes. PARP is identified using a monoclonal antibody. The results are representative of three different experiments.

DISCUSSION

Because of its significant medical properties, fish oil has been used for many years. The experimental results in the present study indicate that red oil A5 inhibits proliferation and induces apoptosis in pancreatic cancer cells.

In preliminary experiments, we tested a series of concentrations of red oil A5 ranging from 1:64 000 to 1:4 000. At low concentrations, red oil A5 inhibited growth and induced apoptosis in a concentration-dependent and time-dependent manner in all three cell lines tested. Because 1:32 000 red oil

A5 inhibited ^3H -methyl thymidine incorporation into DNA by about 30%-50% in 24 hours, we tested this concentration on cell proliferation by cell counting over a longer time period (24 to 96 hours). The results revealed profound inhibition that was time-dependent.

To better understand the effect of red oil A5 on the proliferation of pancreatic cancer cells, flow cytometric analysis of propidium iodide-stained cells and TUNEL assay were carried out. Cytometric analysis showed that cells were accumulated in the G2/M-phase and S-phase in all three cell lines at 24 hours, compared to control. These cell cycle changes suggested that pancreatic cancer cells underwent an oxidative stress response to red oil A5, with DNA damage leading to apoptosis. Because the effects of red oil A5 persisted throughout the course of cell proliferation, cells with DNA damage increased progressively and developed apoptosis successively. Therefore, the sub-G0/G1 cell population typical of apoptosis was observed after 24-hour treatment with red oil A5. At the late stages of apoptosis, genomic DNA was cleaved in fragments following activation of endonucleases. The TUNEL assay used attachment of a fluorescent indicator to identify DNA fragments in apoptotic cells. The TUNEL assay results showed marked apoptosis in all the cell lines tested.

Red oil A5 induces cytochrome c release from the mitochondria to cytosol. Caspases are cysteine proteases produced as inactive forms and activated during apoptosis. Apoptosis in pancreatic cancer cells is mitochondria dependent as evidenced by release of cytochrome c into the cytosol^[32]. Caspases induce cytochrome c release from mitochondria by activating cytosolic factors^[33]. Once cytochrome c is released from the mitochondria, it complexes with apoptosis, apoptotic protease-activating factor 1 to activate caspase-3^[34-37]. Caspase-3 is the most important executor in the apoptotic process. Caspase-3 plays an important role in the apoptotic program of cells^[38-44]. The present experiment shows that caspase-3 is activated by cleavage of procaspase during apoptosis of pancreatic cancer cells induced by red oil A5. Furthermore red oil A5 also causes specific activation by cleavage of the caspase-3 substrate, PARP provides further evidence of apoptosis. PARP, a nuclear protein implicated in DNA repair, is one of the earliest proteins targeted for a specific cleavage to the signature 85-kDa fragment during apoptosis. PARP cleavage can serve as a sensitive parameter for identification of early apoptosis^[45,46].

Induction of cancer cell apoptosis, without affecting healthy cells or producing side-effects, is a major goal for development of new therapeutic agents. Our findings indicate that red oil A5 has a potent anti-proliferative effect on human pancreatic cancer cells with induction of apoptosis.

REFERENCES

- 1 **Blackstock AW**, Cox AD, Tepper JE. Treatment of pancreatic cancer: current limitations, future possibilities. *Oncology* 1996; **10**: 301-307
- 2 **Cameron JL**, Pitt HA, Yeo CJ, Lillemoe KD, Kaufman HS. One hundred and forty-five consecutive pancreaticoduodenotomies without mortality. *Ann Surg* 1993; **217**: 430-435
- 3 **Doll R**, Peto R. Mortality in relation to smoking: 20 years observations on male British doctors. *Br Med J* 1976; **2**: 1525-1536
- 4 **Abbruzzese JL**. Past and present treatment of pancreatic adenocarcinoma: chemotherapy as a standard treatment modality. *Semin Oncol* 2002; **29**(6 Suppl 20): 2-8
- 5 **Ozawa F**, Friess H, Tempia-Caliera A, Kleeff J, Buchler MW. Growth factors and their receptors in pancreatic cancer. *Teratog Carcinog Mutagen* 2001; **21**: 27-44
- 6 **Kleeff J**, Friess H, Berberat PO, Martignoni ME, Z' graggen K, Buchler MW. Pancreatic cancer—new aspects of molecular biology research. *Swiss Surg* 2000; **6**: 231-234
- 7 **Silverberg E**. Boring CC, Squires TS. Cancer Statistics, 1990. *CA Cancer J Clin* 1990; **40**: 9-26
- 8 **Hunstad DA**, Norton JA. Management of pancreatic carcinoma. *Surg Oncol* 1995; **4**: 61-74
- 9 **Neri B**, Cini G, Doni L, Fulignati C, Turrini M, Pantalone D, Mini E, De Luca Cardillo C, Fioretti LM, Ribecco AS, Moretti R, Scatizzi M, Zocchi G, Quattrone A. Weekly gemcitabine plus Epirubicin as effective chemotherapy for advanced pancreatic cancer: a multicenter phase II study. *Br J Cancer* 2002; **87**: 497-501
- 10 **Ding XZ**, Tong WG, Adrian TE. Cyclooxygenases and lipoxygenases as potential targets for treatment of pancreatic cancer. *Pancreatol* 2001; **1**: 291-299
- 11 **Su Z**, Lebedeva IV, Gopalkrishnan RV, Goldstein NI, Stein CA, Reed JC, Dent P, Fisher PB. A combinatorial approach for selectively inducing programmed cell death in human pancreatic cancer cells. *Proc Natl Acad Sci U S A* 2001; **98**: 10332-10337
- 12 **Fay MP**, Freedman LS, Clifford CK, Midthune DN. Effect of different types and amounts of fat on the development of mammary tumors in rodents: a review. *Cancer Res* 1997; **57**: 3979-3988
- 13 **Ravichandran D**, Cooper A, Johnson CD. Effect of lithium gamma-linolenate on the growth of experimental human pancreatic carcinoma. *Br J Surg* 1998; **85**: 1201-1205
- 14 **Hawkins RA**, Sangster K, Arends MJ. Apoptotic death of pancreatic cancer cells induced by polyunsaturated fatty acids varies with double bond number and involves an oxidative mechanism. *J Pathol* 1998; **185**: 61-70
- 15 **Ravichandran D**, Cooper A, Johnson CD. Growth inhibitory effect of lithium gammalinolenate on pancreatic cancer cell lines: the influence of albumin and iron. *Eur J Cancer* 1998; **34**: 188-192
- 16 **Falconer JS**, Ross JA, Fearon KC, Hankins RA, O' Riordain MG, Carter DC. Effect of eicosapentaenoic acid and other fatty acids on the growth *in vitro* of human pancreatic cancer cell lines. *Br J Cancer* 1994; **69**: 826-832
- 17 **Clerc P**, Bensaadi N, Pradel P, Estival A, Clemente F, Vaysse N. Lipid-dependent proliferation of pancreatic cancer cell lines. *Cancer Res* 1991; **51**: 3633-3638
- 18 **Tisdale MJ**. Inhibition of lipolysis and muscle protein degradation by EPA in cancer cachexia. *Nutrition* 1996; **12**(1 Suppl): S31-33
- 19 **Barber MD**, Ross JA, Voss AC, Tisdale MJ, Fearon KC. The effect of an oral nutritional supplement enriched with fish oil on weight-loss in patients with pancreatic cancer. *Br J Cancer* 1999; **81**: 80-86
- 20 **Von Hoff DD**, Bears D. New drugs for patients with pancreatic cancer. *Curr Opin Oncol* 2002; **14**: 621-627
- 21 **Barber MD**, Fearon KC, Tisdale MJ, McMillan DC, Ross JA. Effect of a fish oil-enriched nutritional supplement on metabolic mediators in patients with pancreatic cancer cachexia. *Nutr Cancer* 2001; **40**: 118-124
- 22 **Tang DG**, La E, Kern J, Kehrer JP. Fatty acid oxidation and signaling in apoptosis. *Biol Chem* 2002; **383**: 425-442
- 23 **Hawkins RA**, Sangster K, Arends MJ. Apoptotic death of pancreatic cancer cells induced by polyunsaturated fatty acids varies with double bond number and involves an oxidative mechanism. *J Pathol* 1998; **185**: 61-70
- 24 **Huang PL**, Zhu SN, Lu SL, Dai ZS, Jin YL. Inhibitor of fatty acid synthase induced apoptosis in human colonic cancer cells. *World J Gastroenterol* 2000; **6**: 295-297
- 25 **Calviello G**, Palozza P, Franceschelli P, Frattucci A, Piccioni E, Tessitore L, Bartoli GM. Eicosapentaenoic acid inhibits the growth of liver preneoplastic lesions and alters membrane phospholipid composition and peroxisomal beta-oxidation. *Nutr Cancer* 1999; **34**: 206-212
- 26 **Bartsch H**, Nair J, Owen RW. Dietary polyunsaturated fatty acids and cancers of the breast and colorectum: emerging evidence for their role as risk modifiers. *Carcinogenesis* 1999; **20**: 2209-2218
- 27 **Lai PB**, Ross JA, Fearon KC, Anderson JD, Carter DC. Cell cycle arrest and induction of apoptosis in pancreatic cancer cells exposed to eicosapentaenoic acid *in vitro*. *Br J Cancer* 1996; **74**: 1375-1383
- 28 **Karmali RA**, Donner A, Gobel S, Shimamura T. Effect of n-3 and n-6 fatty acids on 7, 12 dimethylbenz anthracene-induced mammary tumorigenesis. *Anticancer Res* 1989; **9**: 1161-1167
- 29 **Rose DP**, Connolly JM. Antiangiogenicity of docosahexaenoic acid and its role in the suppression of breast cancer cell growth in nude mice. *Int J Oncol* 1999; **15**: 1011-1015
- 30 **Larsen LN**, Hovik K, Bremer J, Holm KH, Myhren F, Borretzen B. Heneicosapentaenoate (21: 5n-3): its incorporation into lipids

- and its effects on arachidonic acid and eicosanoid synthesis. *Lipids* 1997; **32**: 707-714
- 31 **Noguchi M**, Earashi M, Minami M, Kinoshita K, Miyazaki I. Effects of eicosapentaenoic and docosahexaenoic acid on cell growth and prostaglandin E and Leukotriene B production by a human breast cancer cell line (MDA-MB-231). *Oncology* 1995; **52**: 458-464
- 32 **Qanungo S**, Basu A, Das M, Haldar S. 2-Methoxyestradiol induces mitochondria dependent apoptotic signaling in pancreatic cancer cells. *Oncogene* 2002; **21**: 4149-4157
- 33 **Bossy-Wetzel E**, Green DR. Caspases induce cytochrome c release from mitochondria by activating cytosolic factors. *J Biol Chem* 1999; **274**: 17484-17490
- 34 **Tong WG**, Ding XZ, Witt RC, Adrian TE. Lipoxygenase inhibitors attenuate growth of human pancreatic cancer xenografts and induce apoptosis through the mitochondrial pathway. *Mol Cancer Ther* 2002; **1**: 929-935
- 35 **Gerhard MC**, Schmid RM, Hacker G. Analysis of the cytochrome c-dependent apoptosis apparatus in cells from human pancreatic carcinoma. *Br J Cancer* 2002; **86**: 893-898
- 36 **Mouria M**, Gukovskaya AS, Jung Y, Buechler P, Hines OJ, Reber HA, Pandol SJ. Food-derived polyphenols inhibit pancreatic cancer growth through mitochondrial cytochrome C release and apoptosis. *Int J Cancer* 2002; **10**: 761-769
- 37 **Kluck RM**, Bossy-Wetzel E, Green DR, Newmeyer DD. The release of cytochrome c from mitochondria: a primary site for Bcl-2 regulation of apoptosis. *Science* 1997; **275**: 1132-1136
- 38 **Thornberry NA**, Lazebnik Y. Caspase: enemies within. *Science* 1998; **281**: 1312-1316
- 39 **Mancini M**, Nicholson DW, Roy S, Thornberry NA, Peterson EP, Casciola-Rosen LA, Rosen A. The caspase-3 precursor has a cytosolic and mitochondrial distribution: implications for apoptotic signaling. *J Cell Biol* 1998; **140**: 1485-1495
- 40 **Kothakota S**, Azuma T, Reinhard C, Klippel A, Tang J, Chu K, McGarry TJ, Kirschner MW, Kohts K, Kwiatkowski DJ, Williams LT. Caspase-3-generated fragment of gelsolin: effector of morphological change in apoptosis. *Science* 1997; **278**: 294-298
- 41 **Kobayashi D**, Sasaki M, Watanabe N. Caspase-3 activation downstream from reactive oxygen species in heat-induced apoptosis of pancreatic carcinoma cells carrying a mutant p53 gene. *Pancreas* 2001; **22**: 255-260
- 42 **Virkajarvi N**, Paakko P, Soini Y. Apoptotic index and apoptosis influencing proteins bcl-2, mcl-1, bax and caspases 3, 6 and 8 in pancreatic carcinoma. *Histopathology* 1998; **33**: 432-439
- 43 **Pirocanac EC**, Nassirpour R, Yang M, Wang J, Nardin SR, Gu J, Fang B, Moossa AR, Hoffman RM, Bouvet M. Bax-induction gene therapy of pancreatic cancer. *J Surg Res* 2002; **106**: 346-351
- 44 **Kirsch DG**, Doseff A, Chau BN, Lim DS, de Souza-Pinto NC, Hansford R, Kastan MB, Lazebnik YA, Hardwick JM. Caspase-3-dependent cleavage of Bcl-2 promotes release of cytochrome c. *J Biol Chem* 1999; **274**: 21155-21161
- 45 **Decker P**, Isenberg D, Muller S. Inhibition of caspase-3-mediated poly (ADP-ribose) polymerase (PARP) apoptotic cleavage by human PARP autoantibodies and effect on cells undergoing apoptosis. *J Biol Chem* 2000; **275**: 9043-9046
- 46 **Sellers WR**, Fisher DE. Apoptosis and cancer drug targeting. *J Clin Invest* 1999; **104**: 1655-1661

Edited by Wu XN

Transfection of mEpo gene to intestinal epithelium *in vivo* mediated by oral delivery of chitosan-DNA nanoparticles

Jing Chen, Wu-Li Yang, Ge Li, Ji Qian, Jing-Lun Xue, Shou-Kuan Fu, Da-Ru Lu

Jing Chen, Ge Li, Ji Qian, Jing-Lun Xue, Da-Ru Lu, State Key Laboratory of Genetic Engineering, Institute of Genetics, School of Life sciences, Fudan University, Shanghai 200433, China

Wu-Li Yang, Shou-Kuan Fu, The Key Laboratory of Molecular Engineering of Polymers under Ministry of Education, Department of Macromolecular Science, Fudan University, Shanghai, 200433, China
Supported by the State High Technology Development Program 863 (2001AA217181), the National Natural Science Foundation of China (No.50233030), Foundation of Doctor Degree Thesis from Ministry of Education (199925), Encourage Project of Teaching and Research of University Excellent Youth Teacher, and the Youth Foundation of Fudan University

Correspondence to: Dr. Da-Ru Lu, State Key Laboratory of Genetic Engineering, Institute of Genetics, School of Life Sciences, Fudan University, Shanghai 200433, China. drlu@fudan.edu.cn

Telephone: +86-21-65642424 **Fax:** +86-21-65642799

Received: 2003-05-12 **Accepted:** 2003-06-19

Abstract

AIM: To prepare the chitosan-pmEpo nanoparticles and to study their ability for transcellular and paracellular transport across intestinal epithelia by oral administration.

METHODS: ICR mice were fed with recombinant plasmid AAV-tetO-CMV-mEpo (containing mEpo gene) or pCMV β (containing LacZ gene), whether it was wrapped by chitosan or no. Its size and shape were observed by transmission electron microscopy. Agarose gel electrophoresis was used to assess the efficiency of encapsulation and stability against nuclease digestion. Before and after oral treatment, blood samples were collected by retro-orbital puncture, and hematocrits were used to show the physiological effect of mEpo.

RESULTS: Chitosan was able to successfully wrap the plasmid and to protect it from DNase degradation. Transmission electron microscopy showed that freshly prepared particles were approximately 70-150 nm in size and fairly spherical. Three days after fed the chitosan-pCMV β complex was fed, the mice were killed and most of the stomach and 30% of the small intestine were stained. Hematocrit was not modified in naive and 'naked' mEpo-fed mice, a rapid increase of hematocrit was observed during the first 4 days of treatment in chitosan-mEpo-fed animals, reaching $60.9 \pm 1.2\%$ ($P < 0.01$), and sustained for a week. The second feed (6 days after the first feed) was still able to promote a second hematocrit increase in chitosan-mEpo-fed animals, reaching $65.9 \pm 1.4\%$ ($P < 0.01$), while the second hematocrit increase did not appear in the 'naked' mEpo-second-fed mice.

CONCLUSION: Oral chitosan-DNA nanoparticles can efficiently deliver genes to enterocytes, and may be used as a useful tool for gene transfer.

Chen J, Yang WL, Li G, Qian J, Xue JL, Fu SK, Lu DR. Transfection of mEpo gene to intestinal epithelium *in vivo* mediated by oral delivery of chitosan-DNA nanoparticles. *World J Gastroenterol* 2004; 10(1): 112-116

<http://www.wjgnet.com/1007-9327/10/112.asp>

INTRODUCTION

The oral delivery of peptide, protein, vaccine and nucleic acid-based biotechnology products is the greatest challenge facing the drug delivery industry. Oral delivery is most attractive due to easy administration, leading to improved convenience and compliance to patients, thereby reducing the overall healthcare cost. Gene therapy will provide a huge new therapeutic opportunity, and has stimulated an interest in oral gene delivery. To date, various methods have been used for oral gene therapy, such as cationic lipids, recombinant viruses, recombinant live bacteria, polymers, and particle bombardment to buccal mucosa^[1-3].

Chitosan is a natural biodegradable mucoadhesive polysaccharide derived from crustacean shells, and a biocompatible polymer that has been widely used in controlled drug delivery^[4-9], and it may provide a less immunogenic and non-toxic carrier for successful oral delivery of plasmid DNA. Complex coacervates of DNA and chitosan could be used as a delivery vehicle in gene therapy and vaccine design^[10-12], and have been shown to increase transcellular and paracellular transport of macromolecules across intestinal epithelial monolayers^[13-15], further indicative of its potential in oral gene delivery.

Erythropoietin is a glycoprotein, which stimulates red blood cell production. It is produced in the kidney and stimulates the division and differentiation of committed erythroid progenitors in the bone marrow. When the kidney function decreases, anemia or low red blood cells are developed. Erythropoietin is used in patients with anemia associated with chronic renal failure, and in cancer patients for stimulation of erythropoiesis during autologous transfusion. Erythropoietin is also a good reporter gene in gene therapy study *in vivo*, because obvious biological effect can be observed even in a low dose of it. Hormones of therapeutic interest like growth hormone and erythropoietin require a tight adjustment of dose delivery to prevent adverse effects. Since most of the physiological regulatory processes are difficult to transfer to engineered cells, transgene expression must rely on artificial regulatory systems. Artificial inducible expression systems use transcriptional stimulation by chimeric transactivating factors, the activity of which can be controlled by drugs such as tetracycline derivatives^[16], mifepristone^[17], ecdysone^[18], or rapamycin^[19]. Heard observed that retrovirus-engineered myoblasts expressing rtTA and the chimeric transactivator conferring doxycycline-inducible gene expression, could be stably engrafted in mice, thus allowing the long-term control of Epo secretion *in vivo*^[20]. Here we reported the oral gene therapy using chitosan-DNA nanoparticles carrying murine Epo (mEpo driven by tetO-CMV and rtTA) and LacZ, and demonstrated their efficacy in delivering genes to enterocytes.

MATERIALS AND METHODS

Materials

Chitosan (molecular weight, about 300 000Da) was supplied by Shandong Luneng Chemical Company. Plasmid pCMV β was purchased from Clontech. mEpo was a gift from Jean

Michel Heard (MD, Laboratoire Re´trovirus et Transfert Ge´ne´tique, Institut Pasteur, Paris, France). A 630 bp DNA fragment containing the murine Epo coding sequence was inserted between tetO-CMV promoter and 5' end of the SV40 polyadenylation signal puHD10.3^[21]. An expression cassette for the reverse transactivator (rtTA) chimeric protein^[16] was inserted into the SV40 polyadenylation signal in reverse orientation. This cassette contains a 1 858 bp fragment of the MFG retroviral vector^[22] encompassing the 5' LTR and *gag* intronic sequences, followed by an 1 020 bp of the rtTA coding sequence.

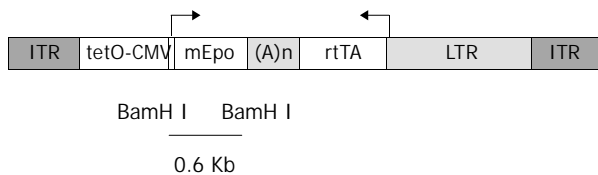


Figure 1 Structure of rAAV-ET vector. ITR: AAV-2 inverted terminal repeats, tetO-CMV: tetracycline-inducible promoter including seven repeats of the tetracycline operator inserted upstream of the CMV minimal promoter, mEpo: murine erythropoietin cDNA, (A)n: SV40 bidirectional polyadenylation signal, rtTA: coding sequences for the tetracycline reverse transactivator, LTR: long terminal repeat of the MFG retrovirus construct. The BamHI fragment used as an Epo-specific probe is indicated.

The construction was then constructed into the pSUB-201 AAV vector plasmid, giving rise to pAAV-ET, with a total length of 5 017 bp (Figure 1). Plasmid was purified by CsCl super centrifugation.

Nanoparticle formulation

Nanoparticles were made by complex coacervation of chitosan and DNA as reported^[12]. Plasmid (10 µg) was added to 100 µl of 50 mM sodium sulfate and heated to 55 °C. Chitosan (pH 5.7, 0.02% in a 25 mM sodium acetate-acetic acid buffer) was also heated to 55 °C and 100 µl of chitosan was added to the DNA–sodium sulfate solution while samples were vortexed at a high speed for 20 s. Complex particles were examined immediately and stored at room temperature.

Measurement of nanoparticle size and morphology

Transmission electron microscopy (TEM, Hitachi HU-11B) was used to determine the particle size and morphology. A drop of particle dispersion was placed on a carbon-coated copper grid, and the particle size was determined from the micrographs.

DNase degradation test

Agarose gel electrophoresis was performed in a 1% (w:v) gel, ethidium bromide included for visualization, for 2 h at 60V. To assess the efficiency of encapsulation and stability against nuclease digestion, uncomplexed plasmid DNA (1 µg) and chitosan-DNA complex (containing 1 µg plasmid) were incubated with 1 mU DNaseI per µg of DNA for 1 h at 37 °C. Adding EDTA stopped the reaction. Then the undegraded (1 µg) and degraded plasmid, undegraded and degraded chitosan-DNA complex, were subjected to agarose gel electrophoresis as described above.

Gene expression and animal experiments

ICR mice (4-week-old, purchased from BK Company, Shanghai) were fed with either chitosan–DNA nanoparticles containing the LacZ gene (pCMVβ, 50 µg/mice) or ‘naked’ plasmid DNA (pCMVβ), using animal feeding needles. Three

days later, the mice were killed, with their stomachs and small intestines surgically removed. The whole tissues were stained with 4-chloro-5-bromo-3-indolyl-β-galactoside (X-Gal) according to standard protocols. After stained overnight in a humidified chamber, the tissues were photographed by a digital camera (Nikon CoolPIX995). The pictures were transferred into a computer and adjusted for equal brightness and contrast using Adobe Photoshop.

ICR mice were fed every week with either chitosan–DNA nanoparticles containing the mEpo gene (50 µg/mice) or ‘naked’ plasmid DNA using animal feeding needles. Doxycycline-HCl (Sigma, Saint-Quentin Fallavier, France) was dissolved in drinking water to a final concentration of 200 µg/mL with 5% sucrose. No obvious side effect was observed in animals. Hematocrit was measured every two days by collecting 40 µL of blood via retro-orbital puncture before and after feeding.

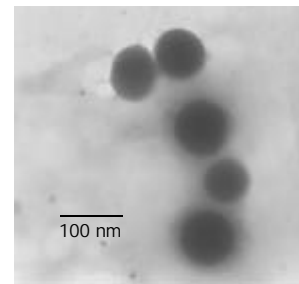


Figure 2 Measurement of microsphere size and morphology. Transmission electron micrographs of chitosan–DNA nanoparticles, and scale bar represents 100 nm.

Statistical analysis

Results of quantitative data in hematocrit analysis were expressed as mean ±SD, statistical differences between groups were tested with F-test, and the significant level was defined as a *P* < 0.01. The data were analyzed by SPSS statistical software.

RESULTS

Nanoparticle synthesis and characterization

We synthesized nanoparticles by complexing high-molecular-weight (about 300 000Da) chitosan with plasmid DNA, and obtained the particles by adding 0.02% chitosan, pH 5.7, at 55 °C to plasmid DNA (50 µg/ml in 50 mM sodium sulfate) during high-speed vortexing. Transmission electron microscopy showed that freshly prepared particles were approximately 70–150 nm in size and fairly spherical (Figure 2). The encapsulation efficiency was higher than 98 %, and the complex could efficiently protect the plasmid from DNase degradation (Figure 3).

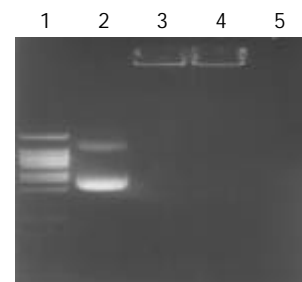


Figure 3 Determination of encapsulation efficiency, and DNase degradation test. Line 1. DNA ladder, Line 2. undegraded pCMVβ (1 µg), Line 3. undegraded chitosan-DNA complex (containing plasmid 1 µg), Line 4. degraded chitosan-DNA complex (containing plasmid 1 µg), Line 5. degraded plasmid (1 µg).

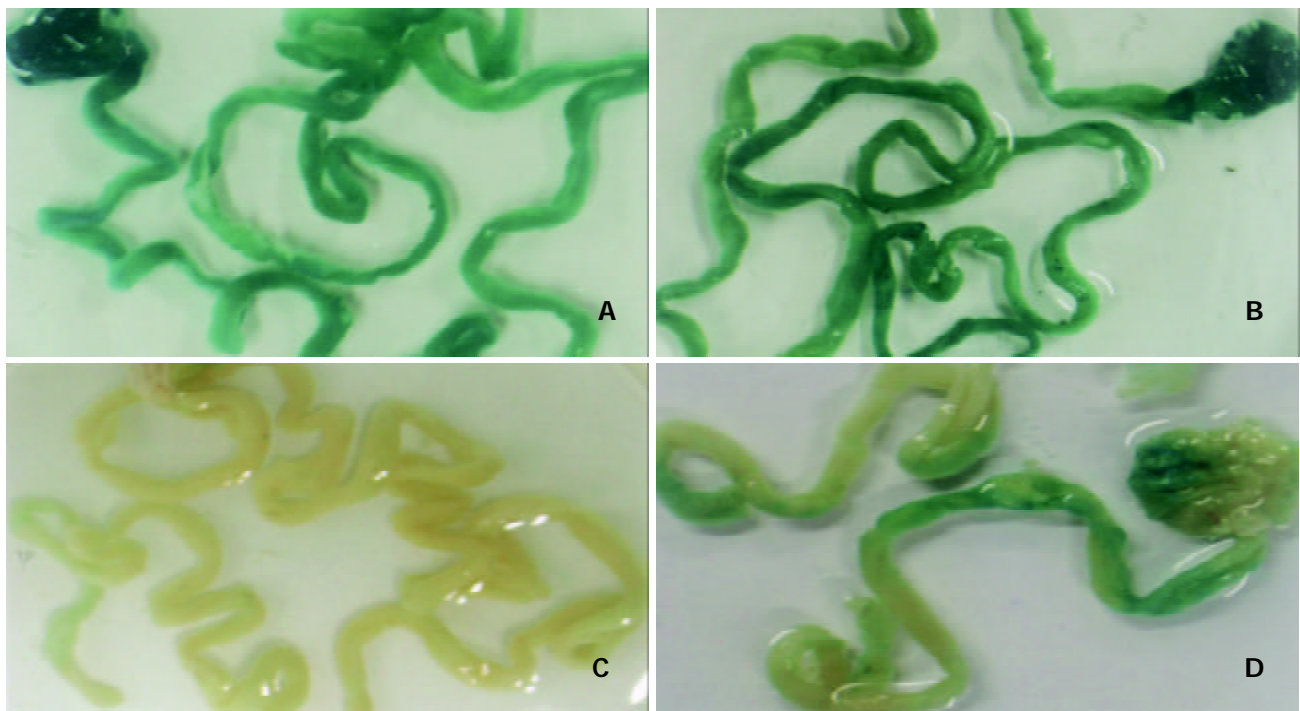


Figure 4 β -galactosidase expression in mouse stomach and small intestine 3 days after oral delivery of DNA nanoparticles. A-D: Whole tissue staining for LacZ, only stained sections are shown. The mice were fed with high-molecular-weight chitosan-pCMV β nanospheres at a dose of 50 μ g (A) or 100 μ g (B) per mouse, PBS (C) or 'naked' DNA (pCMV β , D).

Gene expression studies

To assess the expression and distribution of transduced genes after oral DNA delivery, we fed ICR mice with either chitosan-DNA nanoparticles containing the LacZ gene (pCMV β) or 'naked' plasmid DNA (pCMV β), and then determined the expression of bacterial β -galactosidase (LacZ) in the stomach and small intestine 3 days after oral administration of DNA (Figures 4A-D). Most of the whole small intestines and stomachs were stained. Although naive mice and those fed with 'naked' DNA showed some background staining, mice fed nanoparticles showed a higher level of gene expression both in stomachs and in small intestines.

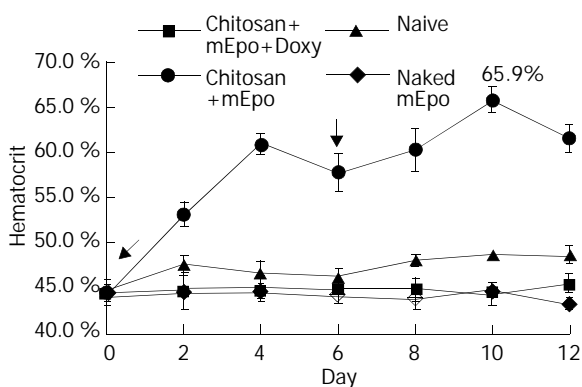


Figure 5 mEpo expression and its physiological effect test. Hematocrit was measured every two days in mice fed with (●) chitosan-mEpo and doxycycline (200 μ g/mL), $n=9$; (▲) chitosan-mEpo alone, $n=3$; (◆) doxycycline (200 μ g/mL) alone, $n=4$; (■) naked mEpo and doxycycline (200 μ g/mL), $n=5$. ↓ indicating the mice fed with 'naked' mEpo DNA or chitosan-Epo.

mEpo expression and its physiological effect

Hematocrit was measured every two days in mice that were fed with 'naked' mEpo DNA, chitosan-mEpo and doxycycline-HCl or not (Figure 5). To assess the basal Epo secretion level, three animals were fed with chitosan-mEpo and not treated

with doxycycline, and their hematocrit remained 45%-48%. Doxycycline (200 μ g/mL) was added to drinking water for naive ($n=4$), 'naked' mEpo-fed mice ($n=5$), and chitosan-mEpo-fed mice ($n=9$). Though hematocrit was not modified in naive and 'naked' mEpo-fed mice, a rapid increase was observed during the first 4 days of treatment in chitosan-mEpo-dox-fed animals, reaching $60.9 \pm 1.2\%$, and sustained for a week. The second feed (6 days after the first feed) seemed to promote a second hematocrit increase in chitosan-mEpo-dox-fed animals, reaching $65.9 \pm 1.4\%$, while the second hematocrit increase did not appear in the 'naked' mEpo-second-fed mice (Figure 5). Statistical analysis showed the hematocrit level in chitosan-mEpo-dox-fed group was significantly higher than that in other groups ($F=184.1$, $P<0.01$), while there were no significant difference between the 'naked' mEpo-fed group and naïve group ($F=0.3$, $P>0.01$). These results indicated that oral administration of chitosan-mEpo induced repetitively robust Epo secretion in doxycycline-treated mice.

DISCUSSION

In 1998, Heard *et al* transfected erythropoietin in mice by intramuscular injection of an adeno-associated vector, and they observed the long-term, high-level and controlled expression of erythropoietin in mice^[23]. Although viral gene delivery vectors yielded a high transfection efficiency over a wide range of cell targets^[24-26], they presented major drawbacks, such as virally induced inflammatory responses and oncogenic effects. To circumvent these obstacles, gene delivery research also aimed at the development of non-viral gene delivery vectors. To date, there have been many available methods that are able to deliver plasmids to cells *in vitro* and *in vivo*, such as liposomes^[27], cationic polymers^[28], electro-gene-transfer^[29], ultrasound^[30] and hydrodynamic^[31], but they have also many disadvantages, such as toxicity, relatively low transfection efficiency as compared to viral gene delivery vectors, tissue damage and difficulties of application in humans.

However, chitosan is a useful oral gene carrier because of its adhesive and transport properties in the gut, and has already

been available in a pill form as an alternative therapy to reduce dietary fat and cholesterol absorption^[32]. Recently, chitosan has been successfully used to deliver a reporter gene (encoding chloram-phenicol acetyl transferase) orally to enterocytes, Peyer's patches and mesenteric lymph nodes^[33]. Chitosan, when complexed with plasmid DNA, can form stable nanoparticles that are endocytosed by cells in the gastrointestinal tract. Further more, its safety and non-toxicity have been shown in animal models and humans^[12,34,35], indication that chitosan-DNA nanoparticles may be a useful tool for gene therapy by oral administration.

Ion concentration, temperature, pH and the ratio of chitosan to DNA (or N/P) were the four main factors that influenced the formulation of chitosan-DNA complex^[36]. The conditions we used above, could make the complex smaller, more stable, and easier to be absorbed. The zeta potential was approximately +10 mV at pH 5.7 and close to neutral at pH 7. Thus, the particles might be positively charged at gastric and early duodenal pH but neutral thereafter at more physiological or alkaline pH. Since pH influences the formulation and stability of the complex, the buffer that dilutes the complex is crucial in the test. The 25 mM sodium acetate-acetic acid buffer (pH 5.7) is able to partially neutralize the alkaline condition in small intestine, making the complex infect more enterocytes than other buffers (PBS, Ringer's, buffer saline). The long-term expression and the expression level still need to be improved, such as to increase the complex's absorptivity and to resist expression silence *etc.*

Further more, as chitosan is a mucoadhesive polymer^[37-39], such DNA nanoparticles might adhere to gastrointestinal epithelia, be transported across the mucosal boundary by M cells and transfect epithelial and/or immune cells in the gut associated lymphoid tissues either directly or through 'antigen transfer', indicating that it may generate protective mucosal immune responses.

ACKNOWLEDGEMENTS

We thank Dr. Jihua Yao, Dr. Huanzhang Zhu, Mrs. Qi Shen and Dr. Bin Lu for their help in this work.

REFERENCES

- 1 **Page DT**, Cudmore S. Innovations in oral gene delivery: challenges and potentials. *Drug Discov Today* 2001; **6**: 92-101
- 2 **Jung T**, Kamm W, Breitenbach A, Kaiserling E, Xiao JX, Kissel T. Biodegradable nanoparticles for oral delivery of peptides: is there a role for polymers to affect mucosal uptake? *Eur J Pharm Biopharm* 2000; **50**: 147-160
- 3 **Ren JM**, Zou QM, Wang FK, He Q, Chen W, Zen WK. PELA microspheres loaded *H pylori* lysates and their mucosal immune response. *World J Gastroenterol* 2002; **8**: 1098-1102
- 4 **Ko JA**, Park HJ, Hwang SJ, Park JB, Lee JS. Preparation and characterization of chitosan microparticles intended for controlled drug delivery. *Int J Pharm* 2002; **249**: 165-174
- 5 **Shimono N**, Takatori T, Ueda M, Mori M, Higashi Y, Nakamura Y. Chitosan dispersed system for colon-specific drug delivery. *Int J Pharm* 2002; **245**: 45-54
- 6 **Tozaki H**, Odoriba T, Okada N, Fujita T, Terabe A, Suzuki T, Okabe S, Muranishi S, Yamamoto A. Chitosan capsules for colon-specific drug delivery: enhanced localization of 5-aminosalicylic acid in the large intestine accelerates healing of TNBS-induced colitis in rats. *J Control Release* 2002; **82**: 51-61
- 7 **Lee JY**, Nam SH, Im SY, Park YJ, Lee YM, Seol YJ, Chung CP, Lee SJ. Enhanced bone formation by controlled growth factor delivery from chitosan-based biomaterials. *J Control Release* 2002; **78**: 187-197
- 8 **Vila A**, Sanchez A, Tobio M, Calvo P, Alonso MJ. Design of biodegradable particles for protein delivery. *J Control Release* 2002; **78**: 15-24
- 9 **Tozaki H**, Komoike J, Tada C, Maruyama T, Terabe A, Suzuki T, Yamamoto A, Muranishi S. Chitosan capsules for colon-specific drug delivery: improvement of insulin absorption from the rat colon. *J Pharm Sci* 1997; **86**: 1016-1021
- 10 **Leong KW**, Mao HQ, Truong-Le VL, Roy K, Walsh SM, August JT. DNA-polycation nanospheres as non-viral gene delivery vehicles. *J Control Release* 1998; **53**: 183-193
- 11 **Kumar M**, Behera AK, Lockey RF, Zhang J, Bhullar G, De La Cruz CP, Chen LC, Leong KW, Huang SK, Mohapatra SS. Intranasal gene transfer by chitosan-DNA nanospheres protects BALB/c mice against acute respiratory syncytial virus infection. *Hum Gene Ther* 2002; **13**: 1415-1425
- 12 **Roy K**, Mao HQ, Huang SK, Leong KW. Oral gene delivery with chitosan-DNA nanoparticles generates immunologic protection in a murine model of peanut allergy. *Nat Med* 1999; **5**: 387-391
- 13 **Artursson P**, Lindmark T, Davis SS, Illum L. Effect of chitosan on the permeability of monolayers of intestinal epithelial cells (Caco-2). *Pharm Res* 1994; **11**: 1358-1361
- 14 **Ranaldi G**, Marigliano I, Vespignani I, Perozzi G, Sambuy Y. The effect of chitosan and other polycations on tight junction permeability in the human intestinal Caco-2 cell line(1). *J Nutr Biochem* 2002; **13**: 157-167
- 15 **Dodane V**, Amin Khan M, Merwin JR. Effect of chitosan on epithelial permeability and structure. *Int J Pharm* 1999; **182**: 21-32
- 16 **Gossen M**, Freundlieb S, Bender G, Muller G, Hillen W, Bujard H. Transcriptional activation by tetracyclines in mammalian cells. *Science* 1995; **268**: 1766-1769
- 17 **Wang Y**, O' Malley BW Jr, Tasai SY, O' Malley BW. A regulatory system for use in gene transfer. *Proc Natl Acad Sci U S A* 1994; **91**: 8180-8184
- 18 **No D**, Yao TP, Evans RM. Ecdysone- inducible gene expression in mammalian cells and transgenic mice. *Proc Natl Acad Sci U S A* 1996; **93**: 3346-3351
- 19 **Rivera VM**, Clackson T, Natesan S, Pollock R, Amara JF, Keenan T, Magari SR, Phillips T, Courage NL, Cerasoli F Jr, Holt DA, Gilman M. A humanized system for pharmacologic control of gene expression. *Nat Med* 1996; **2**: 1028-1032
- 20 **Bohl D**, Naffakh N, Heard JM. Long-term control of erythropoietin secretion by doxycycline in mice transplanted with engineered primary myoblasts. *Nat Med* 1997; **3**: 299-305
- 21 **Gossen M**, Bujard H. Tight control of gene expression in mammalian cells by tetracycline-responsive promoters. *Proc Natl Acad Sci U S A* 1992; **89**: 5547-5551
- 22 **Dranoff G**, Jaffee E, Lazenby A, Golumbek P, Levitsky H, Brose K, Jackson V, Hamada H, Pardoll D, Mulligan RC. Vaccination with irradiated tumor cells engineered to secrete murine granulocyte-macrophage colony-stimulating factor stimulates potent, specific, and long-lasting anti-tumor immunity. *Proc Natl Acad Sci U S A* 1993; **90**: 3539-3543
- 23 **Bohl D**, Salvetti A, Moullier P, Heard JM. Control of erythropoietin delivery by doxycycline in mice after intramuscular injection of adeno-associated vector. *Blood* 1998; **92**: 1512-1517
- 24 **Ghazizadeh S**, Taichman LB. Virus-mediated gene transfer for cutaneous gene therapy. *Hum Gene Ther* 2000; **11**: 2247-2251
- 25 **May C**, Rivella S, Callegari J, Heller G, Gaensler KM, Luzzatto L, Sadelain M. Therapeutic haemoglobin synthesis in beta-thalassaemic mice expressing lentivirus-encoded human beta-globin. *Nature* 2000; **406**: 82-86
- 26 **Lee HC**, Kim SJ, Kim KS, Shin HC, Yoon JW. Remission in models of type 1 diabetes by gene therapy using a single-chain insulin analogue. *Nature* 2000; **408**: 483-488
- 27 **Cao YJ**, Shibata T, Rainov NG. Liposome-mediated transfer of the bcl-2 gene results in neuroprotection after *in vivo* transient focal cerebral ischemia in an animal model. *Gene Ther* 2002; **9**: 415-419
- 28 **Bragonzi A**, Boletta A, Biffi A, Muggia A, Sersale G, Cheng SH, Bordignon C, Assael BM, Conese M. Comparison between cationic polymers and lipids in mediating systemic gene delivery to the lungs. *Gene Ther* 1999; **6**: 1995-2004
- 29 **Lu QL**, Bou-Gharios G, Partridge TA. Non-viral gene delivery in skeletal muscle: a protein factory. *Gene Ther* 2003; **10**: 131-142
- 30 **Taniyama Y**, Tachibana K, Hiraoka K, Aoki M, Yamamoto S, Matsumoto K, Nakamura T, Ogihara T, Kaneda Y, Morishita R. Development of safe and efficient novel nonviral gene transfer

- using ultrasound: enhancement of transfection efficiency of naked plasmid DNA in skeletal muscle. *Gene Ther* 2002; **9**: 372-380
- 31 **Niidome T**, Huang L. Gene therapy progress and prospects: nonviral vectors. *Gene Ther* 2002; **9**: 1647-1652
- 32 **Gallaher CM**, Munion J, Hesslink R Jr, Wise J, Gallaher DD. Cholesterol reduction by glucomannan and chitosan is mediated by changes in cholesterol absorption and bile acid and fat excretion in rats. *J Nutr* 2000; **130**: 2753-2759
- 33 **MacLaughlin FC**, Mumper RJ, Wang J, Tagliaferri JM, Gill I, Hinchcliffe M, Rolland AP. Chitosan and depolymerized chitosan oligomers as condensing carriers for *in vivo* plasmid delivery. *J Control Release* 1998; **56**: 259-272
- 34 **Koping-Hoggard M**, Tubulekas I, Guan H, Edwards K, Nilsson M, Varum KM, Artursson P. Chitosan as a nonviral gene delivery system. Structure-property relationships and characteristics compared with polyethylenimine *in vitro* and after lung administration *in vivo*. *Gene Ther* 2001; **8**: 1108-1121
- 35 **Bokura H**, Kobayashi S. Chitosan decreases total cholesterol in women: a randomized, double-blind, placebo-controlled trial. *Eur J Clin Nutr* 2003; **57**: 721-725
- 36 **Borchard G**. Chitosans for gene delivery. *Adv Drug Deliv Rev* 2001; **52**: 145-150
- 37 **Takeuchi H**, Yamamoto H, Niwa T, Hino T, Kawashima Y. Mucoadhesion of polymer-coated liposomes to rat intestine *in vitro*. *Chem Pharm Bull* 1994; **42**: 1954-1956
- 38 **Bernkop-Schnurch A**, Krajicek ME. Mucoadhesive polymers as platforms for peroral peptide delivery and absorption: synthesis and evaluation of different chitosan- EDTA conjugates. *J Control Release* 1998; **50**: 215-223
- 39 **Ferrari F**, Rossi S, Bonferoni MC, Caramella C, Karlsen J. Characterization of rheological and mucoadhesive properties of three grades of chitosan hydrochloride. *Farmaco* 1997; **52**: 493-497

Edited by Zhang JZ and Wang XL

Ultrastructure of junction areas between neurons and astrocytes in rat supraoptic nuclei

Li Duan, Hua Yuan, Chang-Jun Su, Ying-Ying Liu, Zhi-Ren Rao

Li Duan, Hua Yuan, Ying-Ying Liu, Zhi-Ren Rao, Institute of Neurosciences, Fourth Military Medical University, Xi'an 710032, Shaanxi Province, China

Chang-Jun Su, Tangdu Hospital, Fourth Military Medical University, Xi'an 710032, Shaanxi Province, China

Supported by National Natural Science Foundation of China, No. 39770251 and The Fourth Military Medical University Foundation (CX01A024)

Correspondence to: Dr. Zhi-Ren Rao, Institute of Neurosciences, Fourth Military Medical University, Xi'an 710032, Shaanxi Province, China. zrrao@fmmu.edu.cn

Telephone: +86-29-83374505 **Fax:** +86-29-83246270

Received: 2003-05-11 **Accepted:** 2003-06-12

Abstract

AIM: To determine the ultrastructure of junction areas between neurons and astrocytes of supraoptic nuclei in rats orally administered 30 g/L NaCl solution for 5 days.

METHODS: The anti-connexin (CX) 43 and anti-CX32 double immunoelectromicroscopic labeled method, and anti-Fos or anti-glial fibrillary acidic protein (GFAP) immunohistochemistry were used to detect changes in the junctional area between neurons and astrocytes in supraoptic nuclei of 5 rats after 30 g/L NaCl solution was given for 5 days.

RESULTS: A heterotypic connexin32/connexin43 gap junction (HGJ) between neurons and astrocytes (AS) in rat supraoptic nuclei was observed, which was characterized by the thickening and dark staining of cytomembranes with a narrow cleft between them. The number of HGJs and Fos like immunoreactive (-LI) cells was significantly increased following hyperosmotic stimuli, that is, the rats were administered 30 g/L NaCl solution orally or 90 g/L NaCl solution intravenously. HGJs could be blocked with carbenoxolone (CBX), a gap junction blocker, and the number of Fos-LI neurons was significantly decreased compared with that in rats without CBX injection, while Fos-LI ASs were not affected.

CONCLUSION: HGJ may be a rapid adaptive signal structure between neurons and ASs in response to stimulation.

Duan L, Yuan H, Su CJ, Liu YY, Rao ZR. Ultrastructure of junction areas between neurons and astrocytes in rat supraoptic nuclei. *World J Gastroenterol* 2004; 10(1): 117-121

<http://www.wjgnet.com/1007-9327/10/117.asp>

INTRODUCTION

Human and animals normally maintain homeostasis of ion concentration, pH, body fluid and osmotic pressure. Homeostasis would markedly change, if human and animals drink excessive hypernatric fluids. Variations in osmotic pressure of extracellular fluid induce changes in cell volume that result in profound alteration of cell function and signal transduction between cells by modifying both extracellular and intercellular spatial arrangement and solute concentrations. Osmotic stimuli are

resulted from the integration of multiple sensory inputs including peripheral and central osmoreceptors^[1,2]. Peripheral osmoreceptors are mainly localized in mesenteric vasculature of the upper small intestine and hepatic portal vein^[3]. The osmotic, immune, and noxious information from these peripheral receptors would transmit to medullary nuclei (the medullary visceral zone-MVZ that includes nucleus of the tractus solitarius and ventrolateral medulla) via vagus^[4-8]. The effects of infusions of salt and water on the stomach can be mostly prevented by damage of the splanchnic or hepatic vagal nerves^[3]. The neurons in medullary nucleus relay information and reach the supraoptic nucleus (SON) and paraventricular nucleus (PVN) of hypothalamic neurosecretory cells^[4-6].

It is well known that the supraoptic nucleus (SON) plays a key role in regulation of osmotic pressure regulation. Increased Cx32 mRNA levels in rat supraoptic nuclei have been found in late pregnancy and during lactation^[2]. But the ultrastructural characteristics of the gap junctions (GJs) between neurons and astrocytes in SON following osmotic stimulation are unknown. In the present study, the characteristics of ultrastructure at junction areas between the neurons and astrocytes were examined in rat SON following hyperosmotic stimulation by using an immuno-electron-microscopic technique, and a heterotypic Cx32/Cx43 GJs at junction areas between neurons and astrocytes was observed.

It is well known that carbenoxolone (CBX), a drug to treat gastric ulcer, could block information transmitting *via* GJs, but whether CBX affects action of GJs between the neurons and astrocytes in SON is not clear. Thus, we studied the effect of CBX on GJs and found that CBX inhibited the activity of neurons in SON rather than the activity of astrocytes.

MATERIALS AND METHODS

Animal model

Ten adult male Sprague-Dawley rats (250-300 g) were provided by the Laboratory Animal Center, Fourth Military Medical University (FMMU, Xi'an, China) and divided into experimental group and control group. The protocols used in animal study were approved by the FMMU Committee of Animal Use for Research and Education. Adequate measures were taken to minimize pains or discomforts for all experimental animals. The experimental animals were fed with 30 g/L NaCl solution, the control animals with fresh water. After 5 days, the animals were anesthetized (ip) and transcardially perfused with 500 mL solution of 0.1 mol/L PB (pH 7.4) containing 40 g/L paraformaldehyde and 2 g/L saturated picric acid for 0.5 hour. Hypothalamus including SON was then removed immediately and placed in 0.05 mol/L PB containing 200 g/L sucrose at 4 °C overnight.

Tissue preparation

Hypothalamus including SON was cut into 50 µm thick frontal sections on a vibratome (Microslicer DTK-100; Dosaka, Kyoto, Japan) and placed into 0.01 mol/L KPBS for 60 minutes. Subsequently, the sections were frozen in liquid nitrogen for enhancement of penetration of antibody. Then the sections were placed in 0.01 mol/L KPBS and divided randomly into three groups.

The sections in the first group were incubated in rabbit polyclonal antibody against GFAP (1:3 000, Dako) for 48 hours at 4 °C, and then in secondary goat anti-rabbit IgG (1:500, Sigma) and in ABC complex (1:500, Sigma) at room temperature for 2 hours. Finally, the sections were visualized with glucose oxidase-DAB-nikel as a chromogen.

The sections in the second group were incubated in rabbit anti-Cx43 antibody (Chemicon, CA) for 48 hours at 4 °C, and then processed according to the methods mentioned above. After washed, the sections were again incubated with monoclonal antibody against Cx32 (Chemicon, CA) and labeled with 5nm gold particles.

The sections in the third group were used as control.

After washed with 0.01 mol/L PBS, the sections were post-fixed with 10 g/L OsO₄ in PB for 45 minutes, dehydrated through a graded ethanol and propylene oxide, flat-embedded with Epon 812. The sections were examined with a light microscope and the regions containing GFAP-like immunoreactive (-LI) cells or Cx-32- and Cx43- LI cells were investigated under an electron microscope. Small pieces from tissue were sampled from SON and re-embedded in beam capsules. Tissue samples from the selected regions were cut into sections on an ultramicrotome (Reichert – Nissei S; Leica, Vienna, Austria), and prepared for the study with electron microscope (H-7100; Hitachi, Tokyo, Japan).

CBX blockade

Twenty-one adult male SD rats were divided into three groups. The rats in control group ($n=5$) were intravenously injected with 9 g/L NaCl (1 mL). The rats in hyperosmotic group ($n=10$) were intravenously injected with 90 g/L NaCl (1 mL). The rats in the third group rats ($n=6$) were pre-injected with CBX (1.5 µg/g, 10 g/L) into the lateral ventricle and 2 hours latter, injected with 90g /L NaCl (1 mL) into the femoral vein. One hour after NaCl injection, all the rats in three groups were transcardially perfused. The brains were removed with the methods mentioned above. Then the hypothalamus including SON was cut into 30 µm thick frontal sections on a cryostat (Cryostat; Leitz, Wetzal, Germany).

The sections from each rat were randomly divided into three sets. Two sets were processed for anti-Fos and anti-glial fibrillary acidic protein (GFAP) immunohistochemical staining respectively. Briefly, the sections were incubated with rabbit polyclonal antibodies anti-Fos (1:3 000; Santa Cruz), and GFAP (1:3 000; Dako) at 4 °C for 48 hours, and then in goat anti-rabbit IgG (1:500, Sigma) and ABC complex (1:500, Sigma) at room temperature for 2 hours. Nickel-intensified DAB reaction was used to detect peroxidase. The other set group of sections was treated as control, and processed without primary antibodies and therefore no immunoreactivity was found.

RESULTS

The behaviors of control animals were normal, while experimental animals looked languid and emaciated.

Puncta electron dense areas at the membrane of junction areas between neurons and astrocytes within SON were found on control sections. This structure consisted of astrocytic process on one side and neurons (cell body or dendrite) on the other side. It was characterized by thickened and dark stained membrane with a 2nm-cleft between them (Figure1A).

We also observed anti-GFAP-like immunoreactive (-LI) processes located within astrocyte side of the junction area between neurons and astrocytes (Figure1B).

The results of anti-Cx32 and anti-Cx43 double immunoelectron-microscopic reaction indicated that Cx32-LI and Cx43-LI appeared in the neuron side and astrocyte side of the junction areas respectively (Figure1C). We concluded that

puncta electron dense areas at the junction areas might be the heterotypic Cx32/Cx43 gap junction that was called heterotypic gap junction (HGJ) in our study.

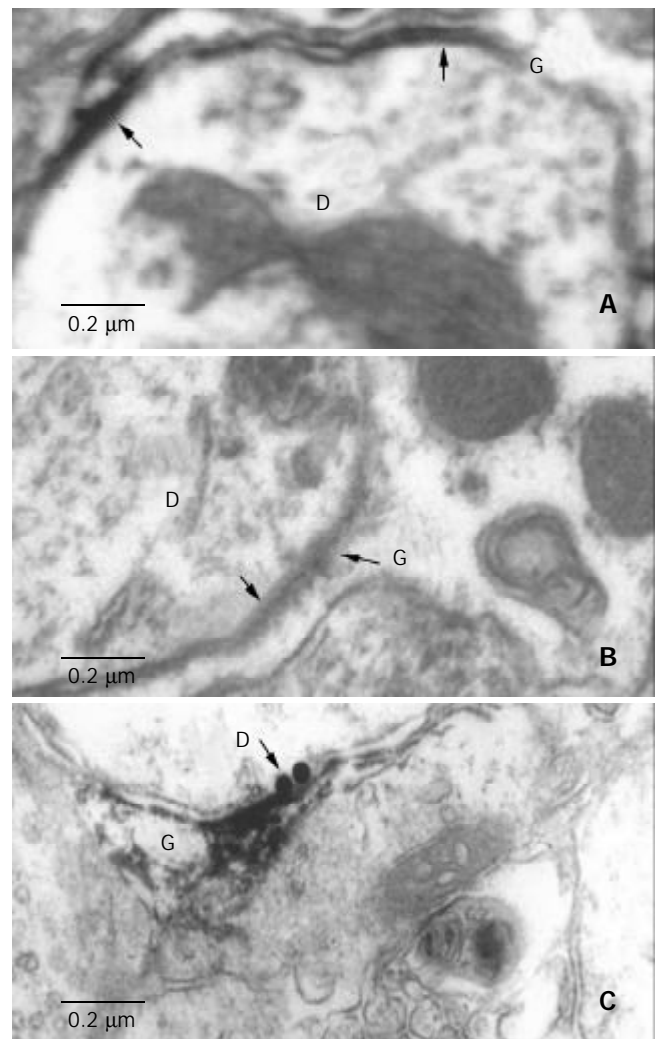


Figure 1 Electron microscopic observation of HGJ. A: A dendrite (D) contacts with the process of ASs (G), the arrow indicates the thickened and dark stained cell membrane, and there is a narrow cleft between them. B: Peroxidase labeling shows a dendrite (D) and a process of astrocyte (G). C: Located between the Cx32-LI dendrites (D) (5 nm black gold particles labeling, black arrow) and astrocytic process (G) (peroxidase labeling).

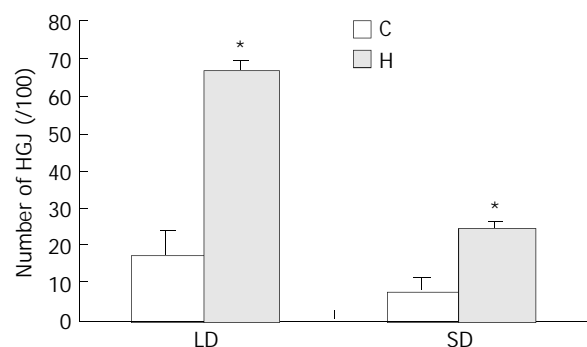


Figure 2 Histogram comparison between hyperosmotic group (H) and control group (C) demonstrating percentages of HGJ formed by processes of astrocytes with neuronal dendrites (LD: large dendrites, SD: small dendrites). The percentage indicated the ratio of positive LD or SD bearing HGJ in the total number of LD or SD, respectively. Significant difference was seen between the experimental group and control group ($P<0.001$).

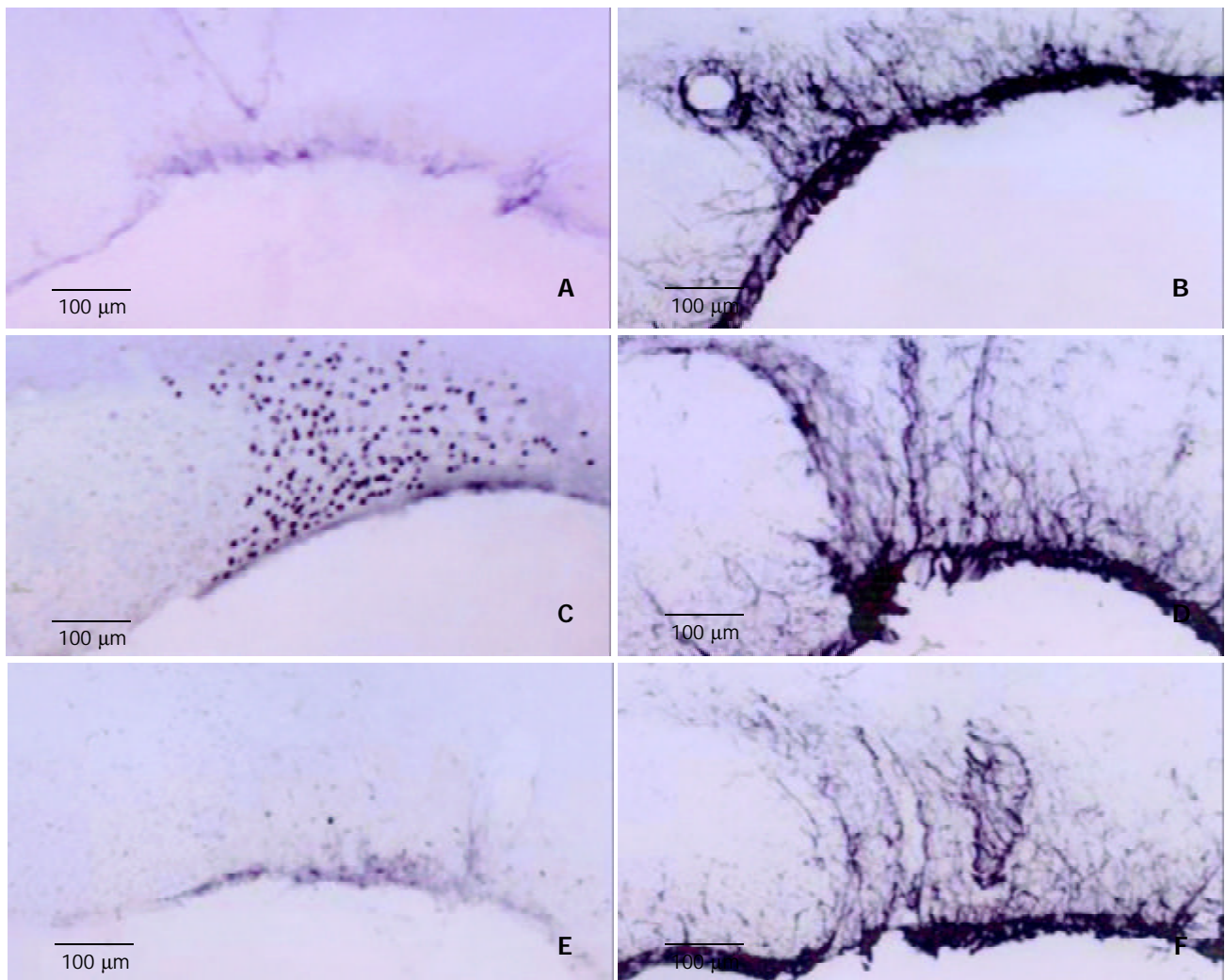


Figure 3 A,B: Expression of Fos-LI neurons and GFAP-LI ASs in SON of control group rats. C, D: Number of Fos-LI neurons and GFAP-LI ASs in hyperosmotic stimulation group compared to that of control group. E, F: Inhibited expression of Fos-LI neurons in CBX-injected rats, and uninhibited GFAP-LI ASs.

It is of interest to note that the number of HGJ in SON of the experimental group rats was significantly increased compared with that in control. We found that 17.43 per 100 large dendrites ($\geq 1 \mu\text{m}$) and 7.43 per 100 smaller dendrites ($< 1 \mu\text{m}$) had specialized areas in SON of normal control rats, while in SON of experimental group rats, 66.75 per 100 large dendrites ($\geq 1 \mu\text{m}$) and 24.35 per 100 smaller dendrites ($< 1 \mu\text{m}$) were found to bear HGJs. Statistical analysis suggested that there was a significant difference in the number of dendrites and axons bearing specialized areas between the control and experimental rats (Figure 2). It indicated that HGJs could sensitively respond to stimulation.

CBX inhibited expression of Fos-LI neurons. In control group, Fos-LI neurons in SON were not found and a few GFAP-LI astrocytes were observed. In hyperosmotic group, the number of Fos-LI neurons was significantly increased compared with that in control group. The number of GFAP-LI astrocytes was also slightly increased, and activated GFAP-LI astrocytes became hypertrophied and their processes became thickened. In the third group, the number of Fos-LI neurons in SON was decreased more significantly than that in hyperosmotic group, while GFAP-LI ASs did not differ remarkably (Figure 3).

DISCUSSION

It is well known that peripheral osmoreceptors are mainly localized in the mesenteric vasculature of the upper small

intestine and the hepatic portal vein^[3]. The osmotic, immune, and noxious information from these peripheral receptors could transmit to medullary nuclei (medullary visceral zone-MVZ that include nucleus of the tractus solitarius and ventrolateral medulla) *via* vagal nerve^[4-8]. The neurons in medullary nuclei could relay information and reach hypothalamic neurosecretory cells of the supraoptic nucleus (SON) and paraventricular nucleus (PVN)^[4-6].

Our study indicated that astrocytes, as well as neurons, could sensitively respond to hyperosmotic stimuli induced by administration of 30 g/L NaCl solution orally or 90 g/L NaCl solution intravenously. Activated astrocytes appeared to be GFAP-LI positive, and activated neurons exhibited Fos-LI nuclei. The activated astrocytes have been found to be generally marked with GFAP, and neurons with Fos^[9-12].

The discovery of intercommunication between neurons and astrocytes was an important advance in neurobiology in recent twenty years^[13]. It has been that gap junction is an important channel of intercellular communication and also a direct link of the interiors of cells^[14-16], and consists of connexins of the protein family^[17,18]. However, about 15 types of Cx (followed by molecular mass designation) have been identified in mammals including the nervous and non-nervous systems^[19,20]. At least 9 of the 15 types of Cx identified so far were expressed in CNS^[21]. The same Cx types could be expressed in different cells and more than one Cx type could be expressed by the same cell. Nagy and Rash^[18] reported that Cx30 was labeled by 5nm

gold particles and Cx43 was labeled with immunoperoxidase, which was observed at the same astrocytic GJ in rat brain. Neurons and oligodendrocytes expressed Cx32, astrocytes expressed Cx43, and ependyma and leptomeningeal cells expressed both Cx26 and Cx43.

It is well known that GJs may occur between the same cell types such as neurons and glia, they may also occur between different cell types such as neuron and astrocyte, neuron and oligodendrocyte, and astrocyte and oligodendrocyte. GJs consisting of the same Cx protein have been termed as homotypic GJs^[14-16], while that consisting of different Cxs at two sides of GJs in culture as heterotypic Cxs GJ^[17, 21]. It was reported that heterotypic Cx45/Cx43 GJs were observed in culture HeLa cells^[11, 22, 23] and the oligo-astrocyte GJs in white matter arose by pairing astrocytic Cx43 with oligodendrocytic Cx45^[24]. Whether there were GJs between the neurons and astrocytes, some studies suggested that astrocytes might play a direct role in neuromodulation through GJs-mediated interaction between astrocytes and neurons^[15, 17]; Meanwhile, on the basis of fracture replica immunogold labeling, no evidence has been found for GJs between glial cells and neurons in the adult brain^[19].

This study demonstrated that Cx32 and Cx43 appeared simultaneously at the neuronal side and astrocyte side, respectively, and formed the heterotypic Cx32/Cx43 gap junction. The special heterotypic Cx32/Cx43 gap junctions observed in this study had a narrow cleft (diameter: 2nm) between the neuronal and astrocytic membranes. This structure differed from the conventional gap junction, which has a seven-layer structure. It is of interest to note that the number of HGJs in SON of experimental group rats was significantly increased compared with that in control rats. In this study we also observed other types of ultrastructures, for example, synapses between neurons and astrocytes, tripartite synaptic structures and the gap junction between glial cells, but their number and structure did not show any significant change following stimulation (data not shown). It indicated that HGJs might be involved in signal communication of osmotic pressure regulation.

Results from this study indicated that the expression of Fos-LI neurons in experimental animals, which were injected CBX into the lateral ventricular, was markedly decreased compared with control animals. CBX, a glycyrrhetic acid, is used to treat gastric ulcer by blocking information transmitting via gap junction. It was reported that CX cloud block GJs between neurons, and delay induction of epileptiform activity and reduces established epileptiform activity^[25-27], and significantly decrease the spread of cell death induced by ischemia^[28]. CX could also blocks GJs between glia^[29, 30] or between neurons and glia^[15, 31].

There has been debate on direction of intercommunication between the neurons and astrocytes coupling. Nedergaard^[32] and Robinson *et al.*^[33] described that unidirectional dye coupling from astrocytes to neurons and from astrocytes to oligodendrocytes occurred in intact neural tissues. Alvarez-Maubecin *et al.*^[15] also suggested the existence of functional coupling between brainstem glia and noradrenergic neurons in slices taken from postnatal animals. But Rozental *et al.* and Carmignoto^[15, 34] considered that there was bidirectional signaling through gap junction between neurons and astrocytes. The results from the present research indicated that the expression of Fos-LI SON neurons induced by hyperosmotic stimulation could be inhibited with CBX, while the response of astrocytes to stimulation was not affected. It is suggested that the signaling via HGJs is unidirectional from astrocytes to neurons.

REFERENCES

- Bourque CW**, Oliet SH. Osmoreceptors in the central nervous system. *Annu Rev Physiol* 1997; **59**: 601-619
- Hussy N**, Deleuze C, Desarmenien MD, Moos FC. Osmotic regulation of neuronal activity: a new role for taurine and glial cells in a hypothalamic neuroendocrine structure. *Prog Neurobiol* 2000; **62**: 113-134
- Baertschi AJ**, Pence RA. Gut-brain signaling of water absorption inhibits vasopressin in rats. *Am J Physiol* 1995; **268**: R236-R247
- Bourque CW**, Oliet SH, Richard D. Osmoreceptors, osmoreception, and osmoregulation. *Front Neuroendocrinol* 1994; **15**: 231-274
- Dong YX**, Xiong KH, Rao ZR, Shi JW. Fos expression in catecholaminergic medullary neurons induced by chemical stimulation of stomach projecting to the paraventricular nucleus of hypothalamus in rats. *China Natl J New Gastroenterol* 1997; **3**: 72-74
- Yang ZJ**, Rao ZR, Ju G. Evidence for the medullary visceral zone as a neuronal station of neuroimmunomodulation. *Neurosci Res* 2000; **38**: 237-247
- Ge X**, Yang ZJ, Duan L, Rao ZR. Evidence for involvement of the neuronal pathway containing the peripheral vagus nerve, medullary visceral zone and central amygdaloid nucleus in neuroimmunomodulation. *Brain Res* 2001; **914**: 149-158
- Wang X**, Wang BR, Zhang XJ, Xu Z, Ding YQ, Ju G. Evidences for vagus nerve in maintenance of immune balance and transmission of immune information from gut to brain in STM-infected rats. *World J Gastroenterol* 2002; **8**: 540-545
- Colburn RW**, DeLeo JA. The effect of perineural colchicine on nerve injury-induced spinal glial activation and neuropathic pain behavior. *Brain Res Bull* 1999; **49**: 419-427
- Coyle DE**. Partial peripheral nerve injury leads to activation of astroglia and microglia which parallels the development of allodynic behavior. *Glia* 1998; **23**: 75-83
- Eliasson C**, Sahlgren C, Berthold CH, Stakeberg J, Celis JE, Betsholtz C, Eriksson JE, Pekny M. Intermediate filament protein partnership in astrocytes. *J Biol Chem* 1999; **274**: 3996-4006
- Hashizume H**, DeLeo JA, Colburn RW, Weinstein JN. Signal glial activation and cytokine expression after lumbar root injury in the rat. *Spine* 2000; **25**: 1206-1217
- Hermanson O**, Blomqvist A. Differential expression of the AP-1/CRE-binding proteins FOS and CREB in preproenkephalin mRNA-expressing neurons of the rat parabrachial nucleus after nociceptive stimulation. *Brain Res Mol Brain Res* 1997; **51**: 188-196
- Bezzi P**, Volterra A. A neuron-glia signalling network in the active brain. *Curr Opin Neurobiol* 2001; **11**: 387-394
- Alvarez-Maubecin V**, Garcia-Hernandez F, Williams JT, Van Nockstaele EJ. Functional coupling between neurons and glia. *J Neurosci* 2000; **20**: 4091-4098
- Rozental R**, Andrade-Rozental AF, Zheng X, Urban M, Spray DC, Chiu FC. Gap junction-mediated bidirectional signaling between human fetal hippocampal neurons and astrocytes. *Dev Neurosci* 2001; **23**: 420-431
- Froes MM**, Correia AH, Garcia-Abreu J, Spray DC, Campos de Carvalho AC, Neto MV. Gap-junctional coupling between neurons and astrocytes in primary central nervous system cultures. *Proc Natl Acad Sci U S A* 1999; **96**: 7541-7546
- Nagy JI**, Rash JE. Connexin and gap junctions of astrocytes and oligodendrocytes in the CNS. *Brain Res* 2000; **32**: 29-44
- Rash JE**, Yasumura T, Dudek FE, Nagy JI. Cell-specific expression of connexins and evidence of restricted gap junctional coupling between glial cells and between neurons. *J Neurosci* 2001; **21**: 1983-2000
- Ma XD**, Sui YF, Wang WL. Expression of gap junction genes connexin 32, connexin 43 and their proteins in hepatocellular carcinoma and normal liver tissues. *World J Gastroenterol* 2000; **6**: 66-69
- Rozental R**, Giaume C, Spray DC. Gap junctions in the nervous system. *Brain Res* 2000; **32**: 11-15
- Bukauskas FF**, Angele AB, Verselis VK, Bennett MV. Coupling asymmetry of heterotypic connexin 45/connexin43-EGFP gap junctions: properties of fast and slow gating mechanisms. *Proc Natl Acad Sci U S A* 2002; **99**: 7113-7118
- Bittman K**, Becker DL, Cicirata F, Parnavelas JG. Connexin expression in homotypic and heterotypic cell coupling in the developing cerebral cortex. *J Comp Neurol* 2002; **443**: 201-212
- Kunzelmann P**, Blumcke I, Traub O, Dermietzel R, Willecke K.

- Coexpression of connexin45 and -32 in oligodendrocytes of rat brain. *J Neurocytol* 1997; **26**: 17-22
- 25 **Jahromi SS**, Wentlandt K, Piran S, Carlen PL. Anticonvulsant actions of gap junctional blockers in an *in vitro* seizure model. *J Neurophysiol* 2002; **88**: 1893-1902
- 26 **Schmitz D**, Schuchmann S, Fisahn A, Draguhn A, Buhl EH, Petrasch-Parwez E, Dermietzel R, Heinemann U, Traub RD. Axo-axonal coupling. A novel mechanism for ultrafast neuronal communication. *Neuron* 2001; **31**: 831-840
- 27 **Traub RD**, Draguhn A, Whittington MA, Baldeweg T, Bibbig A, Buhl EH, Schmitz D. Axonal gap junctions between principal neurons: a novel source of network oscillations, and perhaps epileptogenesis. *Rev Neurosci* 2002; **13**: 1-30
- 28 **Frantseva MV**, Kokarotseva L, Perez Velazquez JL. Ischemia-induced brain damage depends on a specific gap-junctional coupling. *J Cereb Blood Flow Metab* 2002; **22**: 453-462
- 29 **Bani-Yaghoob M**, Underhill TM, Naus CC. Gap junction blockage interferes with neuronal and astroglial differentiation of mouse P19 embryonal carcinoma cells. *Dev Genet* 1999; **24**: 69-81
- 30 **Menezes JR**, Froes MM, Moura Neto V, Lent R. Gap junction-mediated coupling in the postnatal anterior subventricular zone. *Dev Neurosci* 2000; **22**: 34-43
- 31 **Ozog MA**, Siushansian R, Naus CC. Blocked gap junctional coupling increases glutamate-induced neurotoxicity in neuron-astrocyte co-cultures. *J Neuropathol Exp Neurol* 2002; **61**: 132-141
- 32 **Nedergaard M**. Direct signaling from astrocytes to neurons in cultures of mammalian brain cells. *Science* 1994; **263**: 1768-1771
- 33 **Robinson SR**, Hampson EC, Munro MN, Vanczy DI. Unidirectional coupling of gap junctions between neuroglia. *Science* 1993; **262**: 1072-1074
- 34 **Carmignoto G**. Reciprocal communication systems between astrocytes and neurons. *Progr Neurobiol* 2000; **62**: 561-581

Edited by Ren SY and Wang XL

Effects of exercise on lipid metabolism and musculoskeletal fitness in female athletes

Kung-Tung Chen, Rong-Sen Yang

Kung-Tung Chen, Department of General Education, Ming Hsin University of Science and Technology, Hsinchu 304, Taiwan, China
Rong-Sen Yang, Department of Orthopaedics, College of Medicine, National Taiwan University, Taipei 10043, Taiwan, China
Supported by the National Science Council of Taiwan, NSC91-2413-H-159-001

Correspondence to: Dr. Rong-Sen Yang, Department of Orthopaedics, National Taiwan University Hospital, No.7 Chung-Shan South Road, Taipei 10043, Taiwan, China. yang@ha.mc.ntu.edu.tw
Telephone: +886-2-2312-3456 Ext 3958 **Fax:** +886-2-23936577
Received: 2003-10-16 **Accepted:** 2003-11-20

Abstract

AIM: This study investigated the effects of intense training on lipid metabolism, bone metabolism and bone mineral density (BMD) in female athletes.

METHODS: Sixty-six female subjects participated in this study, age ranging from 18 to 55 years. The sample group included thirty-six athletic subjects and the control group comprised thirty non-athletic individuals. Five athletes competed with national level (5/36) and nine non-athletic subjects (9/30) were postmenopausal women. The assessment items included body composition, radius BMD, calcaneus BMD, lung function, muscular endurance, renal and liver function, bone marker assay and hormone status. All data were analysed, using SPSS 10.0 software, and were presented as mean rank statistical difference, using the Kurskal-Wallis (K-W) test. After that the non-parameter statistics were used. Either *K* value or *P* value below 0.05 was considered significant.

RESULTS: Urine deoxyypyridinoline/creatinine (Dpd/Cre) levels increased significantly (5.93 ± 2.31 vs 6.85 ± 1.43 , $K < 0.01$), sit-reach (29.30 ± 9.48 cm vs 41.31 ± 9.43 cm, $K < 0.001$, $P < 0.001$), 1 minute sit-ups with bended knees (1 min sit-ups) (17.60 ± 9.34 count vs 30.00 ± 10.38 count, $K < 0.001$, $P < 0.001$), and vertical jump (25.27 ± 6.63 cm vs 34.69 ± 7.99 cm, $K < 0.001$, $P < 0.001$) improved significantly in the athletes group. The athletes group also had a significantly increased level of estriol (E_3) (0.14 ± 0.13 pg/mL vs 0.07 ± 0.04 pg/mL, $K < 0.01$, $P < 0.01$), radius BMD (1.37 ± 0.49 gm/cm² vs 1.19 ± 0.40 gm/cm², $K < 0.05$) and calcaneus BMD (0.57 ± 0.17 gm/cm² vs -0.20 ± 0.17 gm/cm², $K < 0.01$, $P < 0.05$) compared with those of the controls. The high density lipoprotein (HDL) (65.00 ± 14.02 mg/dL vs 52.26 ± 4.84 mg/dL, $K < 0.05$, $P < 0.05$) was significantly lower in postmenopausal inactive athletes (5/36) than premenopausal active athletes (31/36). On the other hand, low-density lipoprotein (LDL) (98.35 ± 23.84 mg/dL vs 131.00 ± 21.63 mg/dL, $K < 0.05$, $P < 0.01$), cholesterol (CHO) (164.03 ± 27.01 mg/dL vs 193.00 ± 23.48 mg/dL, $K < 0.05$, $P < 0.05$), triglyceride (TG) (63.00 ± 26.39 mg/dL vs 147.00 ± 87.21 mg/dL, $K < 0.01$), body fat % (BF%) ($28.16 \pm 4.90\%$ vs $34.84 \pm 4.44\%$, $K < 0.05$, $P < 0.001$) and body mass index (BMI) (21.98 ± 2.98 kg/m² vs 26.42 ± 5.01 kg/m², $K < 0.05$, $P < 0.001$) were significantly higher in postmenopausal inactive athletes (5/36) than premenopausal active athletes (31/36). TG (90.22 ± 39.82 mg/dL vs 147.00 ± 87.21 mg/dL), CHO

(186.44 ± 24.90 mg/dL vs 193.00 ± 23.48 mg/dL) were higher, but the HDL was significantly lower (62.18 ± 10.68 mg/dL vs 52.26 ± 4.84 mg/dL, $P < 0.05$) in postmenopausal athletes (5/36) group than in postmenopausal control group (9/30).

CONCLUSION: Postmenopausal athletes (5/36) who no longer took competing exercises had reduced levels of physical activity, faced increased risk of cardiovascular disease compared to active athletes (31/36) and the postmenopausal controls (9/30). We may thus concluded that long term exercise effectively improves musculoskeletal fitness and prevents BMD loss in female athletes.

Chen KT, Yang RS. Effects of exercise on lipid metabolism and musculoskeletal fitness in female athletes. *World J Gastroenterol* 2004; 10(1): 122-126

<http://www.wjgnet.com/1007-9327/10/122.asp>

INTRODUCTION

Weightlessness or immobilization, as experienced by astronauts in space, is a well known cause of significant and rapid bone mineral loss^[1-24]. Furthermore sedentary individuals generally have a lower bone mass than physically active individuals, moderate exercise is known to increase skeletal mass^[3]. The above effect is most obvious in sports that place a significant stress on the skeleton. Investigations of athletes have identified physical activity as a major determinant of bone mass in the general population.

Physical fitness significantly influences quality of life. In Taiwan, medical care quality and public health environment have improved markedly over recent decades. The incidence of fatal infectious diseases thus has reduced significantly and the life span of Taiwanese has elongated. Simultaneously, the incidence of chronic diseases has increased, yet people remain ignorant of the importance of exercise^[1-5].

Exercising for 20-60 min per day, three days per week, at moderate intensity level of 3-6 Metabolic Equivalent units (METs) for most individuals derives at least some health-related benefits, including improved cardiorespiratory fitness, muscle strength and endurance, flexibility and body composition, as well as associated psychological benefits. Consequently, lifelong physical exercise is recommended to optimize health-related benefits^[2-8]. And the influence of physical activity and exercise training on BMD in females previously has been assessed in cross-sectional, retrospective longitudinal and controlled trial studies^[3-13].

Even though no relationship about growth hormone and BMD was found. But the effect of E_3 significantly improved BMD by inhibiting bone resorption, female athletes with low estradiol (E_2) level take a risk for increased lipid peroxidation following exercise^[11-15]. Thus hormone status and lipid metabolism may play an important role in the protection against cardiovascular disease, this physiological response has implications for risks of heart disease. Longitudinal information on associations between life style factors and age-related bone loss remains quite controversial. Some studies have found no relationship between bone loss and body composition or body weight, while others

have shown them to predict bone mass changes^[3-16].

Therefore, the purpose of this study was to explore the physiological function of female athletes, including BMD, renal function, liver function, hormone status, bone marker assay, lipid metabolism and muscle biology related to the effectiveness of exercise intervention for the health status of female athletes compared with controls.

MATERIALS AND METHODS

Subjects

Sixty-six female subjects participated in this investigation, with ages ranging between 18 and 55 yrs. The sample group was the athlete group ($n=36$), while the control group comprised non-athletic individuals ($n=30$). Inclusion criteria were that the female athletes had participated in high-intensity resistance or impact activities (e.g., basketball, dancing). Exclusion criteria for both the subjects and the controls were that the subjects had no major medical illnesses, including coronary artery disease which could influence lipid metabolism, and were free of other risk factors that are associated with influencing lipid metabolism, such as smoking or ethanol intake or treatment within the last two years with systemic glucocorticoids, anticonvulsants, bisphosphonates, oestrogen, or raloxifene. Five athletes competed with national level (5/36) and nine non-athletic subjects (9/30) were included in the analysis of postmenopausal women. The parameters to be measured included body composition, radius BMD and calcaneus BMD, lung function, muscular endurance, renal function, liver function and hormone status.

Anthropometric measurement of body composition

Anthropometric measurements were taken based on conventional criteria. The measurement procedures of body weight (Wt) and body height (Ht) were estimated to the nearest 0.1 kg and 0.5 cm, respectively. Finally BMI was calculated using the formula: $BMI (kg/m^2) = Wt (kg) / Ht (m)^2$.

Health related fitness

They were tested using a modified Guthrie R test^[6]. Health related fitness tests included vertical jump, 3 min steps, sit-reach, hand grip and 1 min sit-ups items.

Lung function

Respiratory muscle strength and pulmonary function were assessed by spirometry. The flow volume and respiratory muscle forces were measured using a Fukuda, microspiro HI-501 model spirometer.

Renal and liver function

Sixty-six blood samples per subject were drawn from an antecubital vein with the subjects in the seated position. Routine complete blood counts (CBC) were taken using a Sysmex-E9000 (TOA Electronic, Inc., Tokyo, Japan) and renal and liver function tests were performed using a Hitachi 7170 instrument (Hitachi Electronic, Inc., Tokyo, Japan) by clinical chemistry laboratory staff at Li-Shin Hospital, Taoyuan County, Taiwan.

Hormone status

E_2 , E_3 , triiodothyronine (T_3), thyroxine (T_4), thyroid stimulating hormone (TSH), parathyroid hormone (PTH), cortisol and human growth hormone (HGH) were assayed in basal conditions, using commercial radioimmunoassay (RIA) and enzymeimmunoassay (EIA) Kits.

Bone marker assay

Serum bone specific alkaline phosphatase (BAP) activity was

measured using an EIA kit obtained from Metra Biosystems (Monuntain View, CA, USA). Urine Dpd level was measured using enzyme immunoassay (Ciba-Corning ACS-180) kits purchased from Bayer international (Bayer Diagnostics, Tarrytown, NY, USA).

BMD determination

Calcaneus site BMD was measured via speed of sound (SOS) equipped for a bone mineral densitometry (Aloka Medical Ltd, modelAOS-100, Tokyo, Japan) and all BMD values were also expressed as a T-score, accurately reflecting the BMD. Distal site BMD was measured using the osmometer DTX-100 (SPA, Single Photon Absorptiometry, Osmometer, Rodovre, Denmark). The scanners were calibrated daily against the standard calibration block supplied by the manufacturer to control baseline drift.

Statistical analysis

All data were analysed, using SPSS 10.0 software, and were presented as mean rank statistical difference, using the Kurskal-Wallis (K-W) test. After that the non-parameter statistics were be used. The confidence interval was set at 95% and the significance level used was $K < 0.05$ (two sides). All statistical analyses were carried out with SPSS statistical package. The Kruskal-Wallis test does not use any information on the relative magnitude of each observation when compared with every other observation in the combined sample. This comparison is replaced in each observation by its rank in the pool sample. The smallest observation is replaced by its rank 1, the next smallest by rank 2, and so on, the largest by its rank n . Since the test is an extension of the Mann-Whitney-Wilcoxon (M-W-W) test. Either K value or P value below 0.05 is considered significant.

RESULTS

No difference in body composition

The thirty-six female athletes enrolled in this cross-sectional study did not differ significantly in terms of BF, BF%, BMI and resistance compared with the control group (Table 1).

Table 1 Body composition of two groups

Variables	66 females		K-Value
	Control group $n=30$	Athlete group $n=36$	
	mean rank		
Body fat	31.68	35.01	0.483
BF%	33.83	33.22	0.898
BMI	32.45	34.38	0.685
Resistance	34.95	32.29	0.575

Exercise improvements muscular endurance in female athletes

These two different groups did not differ significantly in muscular endurance. The hand grip (28.06 ± 6.14 kg vs 26.85 ± 5.73 kg), 3 min steps (55.32 ± 6.90 count/min vs 57.82 ± 7.21 count/min) and vital capacity (86.86 ± 15.98 L vs 88.23 ± 12.05 L) in athlete group were better than those in control group, but did differ significantly in terms of sit-reach (29.3 ± 9.48 cm vs 41.31 ± 9.43 cm, $K < 0.001$, $P < 0.001$), 1 min sit-ups (17.60 ± 9.34 count vs 30.00 ± 10.38 count, $K < 0.001$, $P < 0.001$) and vertical jump (25.27 ± 6.63 cm vs 34.69 ± 7.99 cm, $K < 0.001$, $P < 0.001$) as listed in Table 2.

Lipid metabolism

Table 3 shows that the results were not significantly different between both groups. But lipid metabolism including HDL (59.36 ± 12.23 mg/dL vs 63.23 ± 13.83 mg/dL) and Hb (12.95 ± 1.22 g/dL vs 13.43 ± 1.09 g/dL) in the athlete group was higher than

in the control group. However, LDL (105.93±30.76 mg/dL vs 102.89±25.92 mg/dL), TG (81.53±49.53 mg/dL vs 74.60±48.31 mg/dL) and CHO (170.20±32.20 mg/dL vs 168.06±28.13 mg/dL) were lower in the athlete group than those of the control group. Thus exercise could improve the lipid metabolism, and it is good for health.

Table 3 No significant differences in blood CHO and lipid variables between both groups

Group	n	HDL	LDL	CHO	TG	Hb
Control group (mean rank)	30	31.92	34.65	34.92	35.02	28.75
Athlete group (mean rank)	36	34.82	32.54	32.32	32.24	37.46

Table 2 Muscular strength and endurance assessment among controls and athlete groups

Group	n	Sit-reach	1 min sit-ups	Vertical jump	Hand grip	3 min steps	Vital capacity
Control group (mean rank)	30	22.18	22.05	22.23	31.27	29.60	30.58
Athlete group (mean rank)	36	42.93 ^{ab}	43.04 ^{ab}	42.89 ^{ab}	35.36	36.75	35.93

^aK<0.001 vs statistically significant when compared with control group. ^bP<0.001 vs statistically significant when compared with control group.

Table 5 BMD, urine electrolytes, blood electrolytes in two groups

Group	n	Urine-Cre	Blood-Ca	BMD/radius	BMD /calcaneus	Blood-Cl
Control group (mean rank)	30	26.87	42.42	28.38	26.23	45.90
Athletes group (mean rank)	36	39.03 ^{ad}	26.07 ^b	37.76 ^a	39.56 ^{bd}	23.17 ^c

^aK<0.05 vs statistically significant when compared with control group. ^bK<0.01 vs statistically significant when compared with control group. ^cK<0.001 vs statistically significant when compared with control group. ^dP<0.05 vs statistically significant when compared with control group.

Table 6 Hormonal findings in athletes with significance by non-parameter statistics test compared with controls

Group	n	Cortisol	E ₃	T ₃	T ₄	PTH	HGH
Control group (mean rank)	30	32.28	25.78	31.77	36.43	31.37	35.65
Athletes group (mean rank)	36	34.51	39.93 ^{ab}	34.94	31.06	35.28	31.71

^aK<0.01 vs statistically significant when compared with control group. ^bP<0.01 vs statistically significant when compared with control group.

Table 7 Biochemical bone turnover markers and BMD in athletes with significance by non-parameter statistics test as compared with controls

Group	n	Dpd	Urine-Cre (24 hrs)	Dpd/Cre	BAP	BMD/radius	BMD/Calcaneus
Control group (mean rank)	30	25.87	27.23	25.72	20.10	28.38	26.23
Athletes group (mean rank)	36	39.86 ^{be}	38.72 ^{ad}	39.99 ^b	43.83 ^{ef}	37.76 ^a	39.56 ^b

^aK<0.05 vs statistically significant when compared with control group. ^bK<0.01 vs statistically significant when compared with control group. ^cK<0.001 vs statistically significant when compared with control group. ^dP<0.05 vs statistically significant when compared with control group. ^eP<0.01 vs statistically significant when compared with control group. ^fP<0.001 vs statistically significant when compared with control group.

Table 8 Postmenopausal female athlete lipid metabolism compared to premenopausal active athletes

Athletes group	n	BF%	BMI	HDL	LDL	CHO	TG	Hb
Premenopausal (mean rank)	31	16.84	17.08	20.15	16.74	16.98	16.55	18.79
Postmenopausal (mean rank)	5	28.60 ^{ac}	27.30 ^{be}	8.30 ^{ac}	29.40 ^{ad}	27.90 ^{ac}	30.60 ^b	16.70

^aK<0.05 vs statistically significant when compared with premenopausal group. ^bK<0.01 vs statistically significant when compared with premenopausal group. ^cP<0.05 vs statistically significant when compared with premenopausal group. ^dP<0.01 vs statistically significant when compared with premenopausal group. ^eP<0.001 vs statistically significant when compared with premenopausal group.

Table 4 Serum enzyme activities related to renal and liver metabolism

Group	n	ALP	Cre	ALB	DBIL
Control group (mean rank)	30	27.07	27.88	27.77	27.65
Athlete group (mean rank)	36	38.86 ^{ac}	38.18 ^{ab}	38.28 ^a	38.38 ^a

^aK<0.05 vs statistically significant when compared with control group. ^bP<0.05 vs statistically significant when compared with control group. ^cP<0.01 vs statistically significant when compared with control group.

Renal and liver function

Table 4 shows that no difference between the data (data not shown here) of the two groups in terms of blood enzymes such

as glutamic oxalocetic transminase (GOT), glutamic pyruvic transminase (GPT), blood urea nitrogen (BUN), uric acid (UA), total protein (TP), globulin (GLO) and bilirubin (BIL). But the control group displayed significantly lower alkaline phosphatase (ALP) (61.03 ± 13.99 U/L vs 70.81 ± 15.23 U/L, $K < 0.05$, $P < 0.01$), ALB (4.52 ± 0.18 g/dL vs 4.62 ± 0.27 g/dL, $K < 0.05$), Cre (0.75 ± 0.09 mg/dL vs 0.81 ± 0.10 mg/dL, $P < 0.05$, $K < 0.05$) and direct bilirubin (DBIL) (0.25 ± 1.11 mg/dL vs 0.29 ± 0.8 mg/dL, $K < 0.05$) than the athlete group.

Electrolytes and BMD

According to non-parameter statistical tests, both the radius BMD (1.37 ± 0.49 gm/cm² vs 1.19 ± 0.40 gm/cm², $K < 0.05$) and calcaneus BMD (0.57 ± 0.17 gm/cm² vs -0.20 ± 0.17 gm/cm², $K < 0.01$, $P < 0.05$), increased significantly in the athlete group compared with those of the control group. Moreover, the athlete group's body electrolytes such as urine-Cre (132.22 ± 72.30 mg/dL vs 166.83 ± 62.52 mg/dL, $K < 0.05$, $P < 0.05$), blood calcium (Ca) (8.76 ± 0.32 mg/dL vs 8.43 ± 0.37 mg/dL, $K < 0.01$) and chloride (Cl) (99.94 ± 2.41 meq/L vs 102.83 ± 1.97 meq/L, $K < 0.001$) significantly decreased compared to the control group.

Hormone status

HGH and T₄ were lower in the athlete group than in the control group (8.95 ± 1.51 µg/dL vs 9.38 ± 1.51 µg/dL), but cortisol (11.39 ± 4.03 µg/dL vs 10.75 ± 3.42 µg/dL), E₂ (88.82 ± 66.42 pg/mL vs 80.56 ± 63.10 pg/mL), T₃ (112.07 ± 13.52 ng/dL vs 114.78 ± 17.16 ng/dL) and PTH (39.07 ± 16.97 pg/mL vs 34.70 ± 11.66 pg/mL) levels were higher. Notably, E₃ level (0.14 ± 0.13 pg/mL vs 0.07 ± 0.04 pg/mL, $K < 0.01$, $P < 0.01$) significantly increased in the athlete group compared to those of the control group.

Bone marker assay and BMD

All biochemical and bone turnover markers, for example, (67.97 ± 39.67 nmol/mmol vs 102.63 ± 46.97 nmol/mmol, $K < 0.01$, $P < 0.01$), Dpd/Cre ratio (5.93 ± 2.31 vs 6.85 ± 1.43 , $K < 0.01$), and BAP (14.04 ± 3.31 µg/L vs 20.93 ± 6.17 µg/L, $K < 0.001$, $P < 0.001$) significantly increased in the female athlete group compared to those of the control group. The athletes displayed positive correlation of regional radius BMD ($K < 0.05$) and calcaneus BMD ($K < 0.01$, $P < 0.05$) with these results (Table 7).

Lipid metabolism in postmenopausal athletes

Table 8 displays levels of LDL (98.35 ± 23.84 mg/dL vs 131.00 ± 21.63 mg/dL, $K < 0.05$, $P < 0.01$), CHO (164.03 ± 27.01 mg/dL vs 193.00 ± 23.48 mg/dL, $K < 0.05$, $P < 0.05$), TG (63.00 ± 26.39 mg/dL vs 147.00 ± 87.21 mg/dL, $K < 0.01$), BF% ($28.16 \pm 4.90\%$ vs $34.84 \pm 4.44\%$, $K < 0.05$, $P < 0.001$) and BMI (21.98 ± 2.98 kg/m² vs 26.42 ± 5.01 kg/m², $K < 0.05$, $P < 0.001$) increased in the postmenopausal (5/36) inactive athletes group compared to the premenopausal (31/36) active athletes. Then the level of HDL (65.00 ± 14.02 mg/dL vs 52.26 ± 4.84 mg/dL, $K < 0.05$, $P < 0.05$) markedly decreased in the postmenopausal (5/36) inactive athletes.

Table 9 Lipid metabolism of postmenopausal female athletes

Postmenopausal group	n	BMI	HDL	LDL	CHO	TG	Hb
Control group (mean rank)	9	6.56	9.00	7.11	7.06	6.44	7.61
Athletes group (mean rank)	5	9.20	4.80*	8.20	8.30	9.40	7.30

* $P < 0.05$ vs statistically significant when compared with postmenopausal control group.

Lipid metabolism in postmenopausal females

Results from this study show higher levels of TG (90.22 ± 39.82 mg/dL vs 147.00 ± 87.21 mg/dL), CHO (186.44 ± 24.90 mg/dL vs 193.00 ± 23.48 mg/dL), but lower levels of HDL (62.18 ± 10.68 mg/dL vs 52.26 ± 4.84 mg/dL, $P < 0.05$), Hb (13.82 ± 0.88 g/dL vs 13.52 ± 0.21 g/dL) in postmenopausal athletes (5/36) group compared with the postmenopausal control group (9/30). This implies that the effect is a cardiovascular disease risk for postmenopausal retired female athletes (Table 9).

DISCUSSION

The data in this study were expressed as mean $\bar{x} \pm s$. Statistical significance in the mean values was evaluated by the Student's *t* test. But in our study, only sixty-six female subjects participated in this investigation. Therefore, we use K-W test to analyze the results of all tests. The Kruskal-Wallis test does not use any information on the relative magnitude of each observation when compared with every other observation in the combined sample. This comparison is replaced in observation by its rank in the pool sample. The smallest observation is replaced by its rank 1, the next smallest by rank 2, and so on, the largest by its rank *n*. Since the test is an extension of the M-W-W test. Either *K* value or *P* value below 0.05 was considered significant.

Exercise is important for maintaining skeletal health. However, the ability of exercise to influence bone might not be entirely related to hormone status. This study has shown that hormones and exercise interact to influence bone adaptations, and thus raise E₃ level related to increased BMD following exercise in female athletes. For example, serum E₂, cortisol, PTH and T₃ levels in the athlete group were higher than those of the controls, and the major finding of this study was that increased radius BMD ($K < 0.05$) and calcaneus BMD ($K < 0.01$, $P < 0.05$) were significantly and positively related to serum E₃ ($K < 0.01$, $P < 0.01$) concentrations^[10-12]. Therefore, a clear understanding the interaction suggested by the present data between E₃ concentration and the adaptation of bone to exercise is important, and provides an interaction through which the estrogen receptors involved in the early response of bone cells might increase their responsiveness to loading^[11,12].

These results indicate that physical exercise positively affects the maintenance of radius BMD ($K < 0.05$), calcaneus BMD ($K < 0.01$, $P < 0.05$) in female athletes, thus increased E₃ level can prevent BMD loss and possible risk of osteoporosis^[12]. The athletes have higher levels of all the biomarkers than the controls, including Dpd ($K < 0.01$, $P < 0.01$), urine-Cre ($K < 0.05$, $P < 0.05$), Dpd/Cre ratio ($K < 0.005$), BAP ($K < 0.001$, $P < 0.001$) and lower levels of blood-Ca ($K < 0.01$), blood-Cl ($K < 0.001$) these results were associated with markedly increased radius BMD and calcaneus BMD^[13-22].

Further studies are required to examine a larger population, and also to consider the effects of BMD marker assay (for example insulin-like growth factors).

Physical inactivity has been designated by the American Heart Association as a major modifiable risk factor for cardiovascular disease. Numerous studies have examined individual morbidity and mortality from cardiovascular disease. The results presented here indicate that exercise can improve physiological characteristics, such the lowering levels of serum CHO and TG in female athletes, all of which may improve cardiovascular fitness and reduce morbidity and mortality from cardiovascular disease^[12-16,23-26].

But the findings regarding the renal function, liver function and lipid metabolism of retired female athletes were surprising. Enzyme activity indicates that this group (5/36) may not have the same health benefits from physical exercise as the control subjects. Specifically, this group displayed decreased HDL ($K < 0.05$, $P < 0.05$), Hb and increased LDL ($K < 0.05$, $P < 0.01$),

CHO ($K < 0.05$, $P < 0.05$), TG ($K < 0.01$) compared to the premenopausal active athletes (31/36). Postmenopausal retired female athletes (5/36) engaged in less physical activity than previously, displayed increase rates of liver and renal dysfunction, which require further investigation^[17,23-28].

An understanding of the dyslipidemia and ensuing atherosclerosis has implications for the pathophysiology of coronary heart disease (CHD). Risk of cardiac morbidity and mortality is directly related to concentration of plasma total CHO or LDL. Lipid lowering therapy has been shown to reduce the risk of cardiovascular events in both high risk individuals and patients with manifest CHD^[17-22,24-28]. The present study has found that postmenopausal retired female athletes (5/36) who were no longer engaged in strenuous physical activity, they had a significantly higher BF% ($K < 0.05$, $P < 0.001$) and BMI ($K < 0.05$, $P < 0.001$) compared to the active female athletes (31/36) group, specifically, in lipid dysfunction marker with the postmenopausal retired female athletes. Results from this study show higher levels of TG, CHO, but lower levels of HDL, Hb in athletes (5/36) group compared with the control group (9/30). Then, five postmenopausal athletes (5/36), who had retired from competition, and were engaged in less physical activity than previously, had significantly higher BF%, BMI and lipid dysfunction markers had a significantly decreased level of HDL ($P < 0.05$) compared to the controls (9/30). This suggest that the effect is a cardiovascular disease risk for postmenopausal retired female athletes.

Future studies should recruit more numbers of female athletes, who have retired from competition but still maintained high levels of physical activity, and then compare this group with the low physical activity group that serves as the control group. Lipid metabolism related apolipoprotein E (*ApoE*) genotypes with an allele specific oligonucleotide (ASO) based microarray system may interact with exercise training to affect their plasma lipid profiles. To clarify the atherogenic risk of different lipoprotein phenotypes, the relations among total CHO, LDL, HDL and CHD risk in older female athletes should be investigated.

ACKNOWLEDGEMENTS

We are grateful to Li-Shin Hospital in Taoyuan County, Taiwan that provided all laboratory tests in this study, which helped us to complete the research subjects.

REFERENCES

- Huuskonen J**, Vaisanen SB, Kroger H, Jurvelin JS, Alhava E, Rauramaa R. Regular physical exercise and bone mineral density: a four-year controlled randomized trial in middle-aged men. The DNASCO study. *Osteoporos Int* 2001; **12**: 349-355
- Humphries B**, Newton RU, Bronks R, Marshall S, McBride J, Triplett MT, Hakkinen K, Kraemer WJ, Humphries N. Effect of exercise intensity on bone density, strength, and calcium turnover in older women. *Med Sci Sports Exerc* 2000; **32**: 1043-1050
- Wolff I**, van Croonenborg JJ, Kemper HC, Kostense PJ, Twisk JW. The effect of exercise training programs on bone mass: a meta-analysis of published controlled trials in pre- and postmenopausal women. *Osteoporos Int* 1999; **9**: 1-12
- Karlsson MK**. Skeletal effects of exercise in men. *Calcif Tissue Int* 2001; **69**: 196-199
- Pettersson U**, Nordstrom P, Lorentzon R. A comparison of bone mineral density and muscle strength in young male adults with different exercise level. *Calcif Tissue Int* 1999; **64**: 490-498
- Guthrie R**. The use of medical examinations for employment purposes. *J Law Med* 2003; **11**: 93-102
- Kraemer WJ**, Ratamess NA, French DN. Resistance training for health and performance. *Curr Sports Med Rep* 2002; **1**: 165-171
- Hendriksen JJ**, Meeuwse T. The effect of intermittent training in hypobaric hypoxia on sea-level exercise: a cross-over study in humans. *Eur J Appl Physiol* 2003; **88**: 396-403
- Williams CD**, Dobridge JD, Meyer WR, Hackney AC. Effects of the route of estrogen administration and exercise on hormonal levels in postmenopausal women. *Fertil Steril* 2002; **77**: 1118-1124
- Leelawattana R**, Ziambaras K, Roodman WJ, Lyss C, Wagner D, Klug T, Armamento VR, Civitelli R. The oxidative metabolism of estradiol conditions postmenopausal bone density and bone loss. *J Bone Miner Res* 2000; **15**: 2513-2520
- Deschenes MR**, Kraemer WJ. Performance and physiologic adaptations to resistance training. *Am J Phys Med Rehabil* 2002; **81**: S3-16
- Hayashi T**, Ito I, Kano H, Endo H, Iguchi A. Estriol (E_3) replacement improves endothelial function and bone mineral density in very elderly women. *J Gerontol A Biol Sci Med Sci* 2000; **55**: 183-190
- Hou MF**, Lin SB, Yuan SS, Tsai LY, Tsai SM, Hsieh JS, Huang TJ. Diagnostic value of urine deoxyypyridinoline for detecting bone metastases in breast cancer patients. *Ann Clin Lab Sci* 2003; **33**: 55-61
- Miller CJ**, Dunn EV, Thomas EJ, Sankarankutty M. Urinary free deoxyypyridinoline excretion in lactating and non-lactating Arabic women of the United Arab Emirates. *Ann Clin Biochem* 2003; **40**: 394-397
- Ormarsdottir S**, Ljunggren O, Mallmin H, Olofsson H, Blum WF, Loof L. Circulating levels of insulin-like growth factors and their binding proteins in patients with chronic liver disease: Lack of correlation with bone mineral density. *Liver* 2001; **21**: 123-128
- Wu LY**, Yang TC, Kuo SW, Hsiao CF, Hung YJ, Hsieh CH, Tseng HC, Hsieh AT, Chen TW, Chang JB, Pei D. Correlation between bone mineral density and plasma lipids in Taiwan. *Endocrine Res* 2003; **29**: 317-319
- Huang TH**, Lin SC, Chang FL, Hsieh SS, Liu SH, Yang RS. Effects of different exercise modes on mineralization, structure, and biomechanical properties of growing bone. *J Appl Physiol* 2003; **95**: 300-307
- Tsauo JY**, Chien MY, Yang RS. Spinal performance and functional impairment in postmenopausal women with osteoporosis and osteopenia without vertebral fracture. *Osteoporos Int* 2002; **13**: 456-460
- Huang TH**, Yang RS, Hsieh SS, Liu SH. Effects of caffeine and exercise on the development of bone: a densitometric and histomorphometric study in young Wistar rats. *Bone* 2002; **30**: 293-299
- Hui SL**, Perkins AJ, Zhou L, Longcope C, Econs MJ, Peacock M, McClintock C, Johnston CC Jr. Bone loss at the femoral neck in premenopausal white women: effects of weight change and sex-hormone levels. *J Clin Endocrinol Metab* 2002; **87**: 1539-1543
- Prestwood KM**, Kenny AM, Kleppinger A, Kulldorff M. Ultralow-dose micronized 17beta-estradiol and bone density and bone metabolism in older women: a randomized controlled trial. *JAMA* 2003; **290**: 1042-1048
- van den Beld AW**, de Jong FH, Grobbee DE, Pols HA, Lamberts SW. Measures of bioavailable serum testosterone and estradiol and their relationships with muscle strength, bone density, and body composition in elderly men. *J Clin Endocrinol Metab* 2000; **85**: 3276-3282
- Guichelaar MM**, Malinchoc M, Sibonga J, Clarke BL, Hay JE. Bone metabolism in advanced cholestatic liver disease: analysis by bone histomorphometry. *Hepatology* 2002; **36**: 895-903
- Fan JG**, Zhong L, Xu ZJ, Tia LY, Ding XD, Li MS, Wang GL. Effects of low-calorie diet on steatohepatitis in rats with obesity and hyperlipidemia. *World J Gastroenterol* 2003; **9**: 2045-2049
- Lu LG**, Zeng MD, Li JQ, Hua J, Fan JG, Fan ZP, Qiu DK. Effects of lipid on proliferation and activation of rat hepatic stellate cells (I). *World J Gastroenterol* 1998; **4**: 497-499
- Wakatsuki A**, Okatani Y, Ikenoue N, Shinohara K, Watanabe K, Fukaya T. Effect of lower dose of oral conjugated equine estrogen on size and oxidative susceptibility of low-density lipoprotein particles in postmenopausal women. *Circulation* 2003; **108**: 808-813
- Tanko LB**, Bagger YZ, Nielsen SB, Christiansen C. Does serum cholesterol contribute to vertebral bone loss in postmenopausal women? *Bone* 2003; **32**: 8-14
- Chen BY**, Wei JG, Wang YC, Wang CM, Yu J, Yang XX. Effects of cholesterol on the phenotype of rabbit bile duct fibroblasts. *World J Gastroenterol* 2003; **9**: 351-355

Acute diarrhea during army field exercise in southern China

Yang Bai, Ying-Chun Dai, Jian-Dong Li, Jun Nie, Qing Chen, Hong Wang, Yong-Yu Rui, Ya-Li Zhang, Shou-Yi Yu

Yang Bai, Ya-Li Zhang, Nan Fang Hospital, The First Military Medical University, Guangzhou 510515, Guangdong Province, China
Ying-Chun Dai, Jian-Dong Li, Jun Nie, Qing Chen, Hong Wang, Yong-Yu Rui, Shou-Yi Yu, Department of Epidemiology, The First Military Medical University, Guangzhou 510515, Guangdong Province, China

Supported by the Key Program of Military Medical Science and Technique Foundation during the 9th-Five Year Plan Period

Correspondence to: Yang Bai, Department of Digestive Diseases, Nan Fang Hospital, The First Military Medical University, Guangzhou 510515, Guangdong Province, China. baiyang1030@hotmail.com

Telephone: +86-20-61641531

Received: 2003-03-05 **Accepted:** 2003-06-02

Abstract

AIM: During emergency period, infectious diseases can be a major threat to military forces. During field training in southern China, diarrhea is the main cause of nonbattle injury. To evaluate the causes of and risk factors for diarrhea in emergency period, we collected clinical and epidemiological data from the People's Liberation Army (PLA) during field training in southern China.

METHODS: From September 25 to October 2 1997, 2636 military personnel were investigated. Fecal sample cultures for lapactic pathogens were obtained from 103 military personnel with diarrhea. In addition, a questionnaire was administered to 103 cases and 206 controls to evaluate the association between illness and potential risk factors. At the same time, another questionnaire of 1:4 case-case control was administered to 22 severe cases (each severe case paired 4 mild cases).

RESULTS: The training troop's diarrhea incidence rate was significantly higher than that of garrison. The diarrhea incidence rate of officers was significantly lower than that of soldiers. A lapactic pathogen was identified in 63.1% (65/103) of the troops with diarrhea. *Enterotoxigenic Escherichia coli* (35.0%) and *pleiomona shigelloides* (16.5%) were the most common bacterial pathogens. All bacterial isolates were sensitive to norfloxacin and ceftazidime. However, almost all of them were resistant to sulfamethoxazole, trimethoprim-sulfamethoxazole, oxytetracycline, doxycycline, furazolidone, ampicillin and cloromycetin to a different degree. Risk factors associated with diarrhea included drinking raw water, eating outside, contacting diarrhea patients, lacking sanitation, depression, lacking sleep, which were established by multiple-factor logistic regression analysis. In addition, the unit incidence rate was associated with the density of flies and the average daily boiled water available by regression and discriminate analysis.

CONCLUSION: A series of risk factors are associated with the incidence rate of diarrhea. Our results may provide a useful basis for prevention and cure of diarrhea in emergency period of PLA.

Bai Y, Dai YC, Li JD, Nie J, Chen Q, Wang H, Rui YY, Zhang YL, Yu SY. Acute diarrhea during army field exercise in southern China. *World J Gastroenterol* 2004; 10(1): 127-131
<http://www.wjgnet.com/1007-9327/10/127.asp>

INTRODUCTION

Acute diarrhea (abbreviated diarrhea) is a common disease during peace and war period in the army^[1-4]. It has been shown that the year incidence rate of diarrhea varied from 49.5% to 64.0% in the stationed army in southern China and the main pathogens were *enterotoxigenic Escherichia coli* (ETEC) and *enteropathogenic Escherichia coli* (EPEC)^[5]. Diarrhea is also a serious problem for military forces during an emergency period usually including war, military maneuver, dealing with emergency and providing disaster relief, field training, *etc.* In addition, diarrhea is the major cause of nonbattle injury^[6,7]. The life style, sanitary system, and appliance of foreign armies are quite different from our army, therefore, the results from their study cannot be applied to our army^[8-13]. To probe into the epidemic features, pathogen spectrum and the main risk factors of diarrhea during an emergency period and to provide the basis for taking preventive and therapeutic measures, we carried out an initial study during an army exercising in a coastal training field in southern China.

At the training base in the west of Leizhou Peninsula, weeds and bushes are overgrown and tall trees are rare. There is no other inhabitant except the garrison. The weather is harsh, with constant high temperature, high humidity, and plenty of rain. Insects, such as flies and midges, are present everywhere. Along the coastline, camps, kitchens, reservoirs, simple toilets, garbage disposal facilities, and other life support facilities have been established. At the base, the whole sanitary standard is low and the living condition is hard. During exercises, villagers nearby provide fried dishes, cold dishes, fruits, and other seafood products. None of the food has hygiene certificates. The source of drinking water is from the wells with self-prepared covers. The water supply is limited, and no laboratory test has been carried out to check the quality of the water.

MATERIALS AND METHODS

Concerned definition

As was recommended by WHO, the definition of diarrhea is attacking acutely, having three or more motions with properties changed. Those whose interval between two diarrheas exceeded 7 days were recorded twice. According to the clinical manifestations, cases were divided into group of severe cases and group of mild cases. Severe cases were defined as those with diarrhea of more than 5 stools or accompanied by fever ($\geq 38^{\circ}\text{C}$).

Surveillance of disease

Our study lasted for 20 days, and was divided into transporting and assembling stage (8 days) and field training stage (12 days). At the first stage, diarrhea patients were investigated retrospectively by battalion medical officers because the army was on the move. We began formal surveillance at the second stage. Battalion medical officers and investigators registered all training soldiers and collected information about diarrhea attack twice a day (morning and evening). They also delivered fecal samples to laboratory for detection of pathogens before antibiotics were used.

Pathogen detection

The samples on LB were incubated in alkaline peptone solution

for 24 hours at 37 °C. Next day 1 ml of culture medium was taken out and put into glycerin and paraffin oil separately. Detection of pathogens was based on the diarrhea detection rules of WHO^[14]. ETEC was detected by a DNA probe, which was prepared by our department. The micro-biochemical tubes used to detect the germs of enterobacteriaceae, vibrio and serum of Shigella, Salmonella, EPEC and EIEC were bought from Lanzhou Institute of Biological Products.

The antibiotic susceptibility was performed by K-B method recommended by WHO^[15]. The antibiotics included norfloxacin, ceftazidime sulfamethoxazole, trimethoprim-sulfamethoxazole, oxytetracycline, doxycycline, furazolidone, ampicillin and cloromycetin. Standard strain coliform bacillus ATCC25923 and staphylococcus aureus ATCC25923 and pseudomonas ATCC27853 were used for quality control.

Epidemiologic survey

The diarrhea patients identified by surveillance were investigated using "The army acute diarrhea epidemiological case survey form" and "System distress checklist (SCL-90)" in 48 hours by 1:2 case-control study. Controls were chosen from soldiers without diarrhea within 7 days in the same company, with the same sex, the same rank. The differences of age and time of military service were within 1 year. The 129 investigated factors in 15 categories in these two survey forms were analyzed with conditional one-way and multiple logistic regression analysis. To explore the relationship between environmental hygiene and the unit diarrhea incidence, unit environmental hygiene questionnaire of field training troop was filled by surveillance group. In addition, 1:4 case-case control was administered to 22 severe cases (each severe case paired 4 mild cases) to study the main factors of severe clinical manifestations.

Quality control

(1) In order to reduce the failure of report and to increase the collection rate of specimens, we strengthened propaganda and organization and tried to make officers and soldiers fully understand the meaning and purpose of our study. (2) All investigators were trained. (3) To ensure the quality of survey, the screening results from one or two companies were checked randomly and about 10% of the forms in the same day were reinvestigated to identify potential mistakes. (4) The collected fecal specimens were sent in iceboxes and examined by a full-time laboratory technician.

Statistic methods

The data were recorded and checked using SPSS10.0/PC statistical package (SPSS, Chicago). Proportions were compared using the chi-square test with Fisher's exact test. Conditional multiple logistic regression analysis was performed using SAS. Logistic models were established by the maximum-likelihood method. Confidence intervals were calculated by the method of Woolf for univariate analysis and logistic-regression parameter estimates and their standard errors were used for multivariate analysis^[16]. A two-tailed *P* value of 0.05 was considered as statistically significant.

RESULTS

Diarrhea incidence rate

The personnel investigated consisted of 320 officers and 2 316 soldiers in the training troop, and 24 officers and 180 soldiers in the garrison. They were all males, with a mean age of 22 years (SD of 4 years, ranging from 18 to 48 years). There was no difference in constituent ratio in these two troops by statistic analysis ($\chi^2=0.025$, $P=0.874$). During the whole training

period, the diarrhea incidence rate was 7.32% (193/2 636). The diarrhea incidence rate at the second training stage was 4.10% (108/2 636), which was significantly higher than that of the permanent garrison in corresponding time (0.98%, 2/204). The incidence rate of each training company varied from 0.84% to 12.38%. There was also a significant difference among different companies in the same battalion ($\chi^2=11.105$, $P<0.001$), but no difference was found in the same company. The severe cases who could not work due to diarrhea accounted for 20.4% of the patients with diarrhea.

Pathogen detection

We surveyed 108 diarrhea patients and collected 103 samples (including 37 cotton swabs of anus). The collection rate was 95.4%. Most of the samples were watery and loose stools; few were mucus or pus and bloody stool.

The pathogens found in our study included 72 strains of 6 types of lapactic bacteria (Table 1). The positive detection rate was 63.1% (65/103). The most common pathogen was ETEC, followed by plesiomonas shigelloides. The rate of Shigella and Samonella infection was relatively high. There were 7 samples in which two types of pathogens were detected at the same time. Campylobacter and Yersinia were not found because of the limited conditions on the spot.

Table 1 Pathogen detection rate

Pathogen	Number of patients	Detection rate (%)
ETEC	36	35%
Plesiomonas shigelloides	17	16.5%
Salmonella	6	5.8%
Shigella	5	4.9%
EIEC	3	2.9%
Aeromonas schubertii	2	1.9%
Aeromonas hydrophila	1	1%
Vibrio metschnikovi	1	1%
Vibrio vulnificus	1	1%

The susceptibility of seventy-two strains of lapactic bacteria to nine types of antibiotics was examined. It showed that all these bacteria were sensitive to norfloxacin (95.8%) and ceftazidime (100%). All the lapactic bacteria were resistant to sulfamethoxazole, trimethoprim-sulfamethoxazole, oxytetracycline, doxycycline, furazolidone, ampicillin and cloromycetin to a different degree (Table 2)^[17,18].

Table 2 Resistance rate of pathogens to antibiotics

Antibiotics	ETEC <i>n</i> [*] =36	Vibrio <i>n</i> =22	Salmonnlla <i>n</i> =6	Shigella <i>n</i> =5	EIEC <i>n</i> =3	Overall <i>n</i> =72
Sulfamethoxazole	91.7	68.2	83.3	100.0	66.7	83.3
Trimethoprim-Sulfamethoxazole	91.7	59.1	83.3	80.0	66.7	79.2
Oxytetracycline	69.4	77.3	100.0	100.0	100.0	75.0
Doxycycline	61.1	72.7	100.0	100.0	100.0	69.4
Furazolidone	16.7	90.9	50.5	100.0	33.3	52.0
Ampicillin	30.6	36.4	50.0	40.0	33.3	34.7
Cloromycetin	25.0	4.5	0.0	40.0	33.3	18.1
Norfloxacin	5.6	0.0	0.0	20.0	0.0	4.2
Ceftazidime	0.0	0.0	0.0	0.0	0.0	0.0

**n* was the number of strains.

Sixty-eight environmental specimens (drinking water, flies, seafood, cooking utensils of the training troops and local vendors) were examined for lapactic pathogens^[19-22]. Forty-two strains of 10 types of lapactic pathogens were detected, including 14 strains of lapactic vibrio, 12 strains of aerobacter

cloacae, 8 strains of *Plesiomonas shigelloides*, 8 strains of *Aeromonas*, 7 strains of ETEC, 3 strains of *Shigella*, 2 strains of *Salmonella* and 1 strain of EIEC (Table 3). All the environmental specimens had lapactic pathogens to some extent, especially flies, seafood, and cooking utensils of the local vendors, which reached 87.5%, 80.0%, and 73.3%, respectively^[23].

Table 3 Detection rate of lapactic pathogens from environmental specimens

Source of specimen	Number	Detection rate (%)
Flies	8	87.5
Seafood	10	80.0
Cooking utensils of vendors	15	73.3
Drinking water	15	66.7
Cooking utensils of troops	10	40.0
Camping appliances	10	20.0
Total	68	61.8

Risk factors analysis

Analysis of individual risk factors of diarrhea Unconditional single factor logistic regression analysis was performed, and the result showed that 25 factors were in association with individual diarrhea. In order to control interactions and confounding factors, and to make the studied factors more actually significant in theory, the above-mentioned 25 factors were entered to the equation of conditional multivariate logistic regression following the significant level <0.05 , seven statistical significant variables were screened in the end (Table 4).

Analysis of unit risk factors of diarrhea Thirty-seven environmental sanitary questionnaires, which were checked to satisfy statistic requirements, were analyzed. Linear stepping regression was performed to determine the relationship between the 23 environmental factors with the incidence of field training troops. The result indicated that the density of flies in toilets, garbage disposal methods and daily average boiled water supply per person were the main factors. The regression equation was $\text{incidence} = -3.107 + 2.051 * \text{density of flies in toilets} + 1.601 * \text{garbage disposal methods} - 0.743 * \text{daily average boiled water supply per person}$. The standard regression coefficient was 0.544, 0.264, and 0.201, respectively. The R square was 0.784. The variance analysis showed that F value of the regression equation was 40.34 ($P < 0.001$).

To simplify the equation and improve the goodness of fit, ten curves estimation (quadratic, compound, growth, logarithmic, cubic, s, exponential, power, inverse and logistic) was used to fit the relation between the density of flies in toilets

and the diarrhea incidence. R square of 5 curves estimation (power, compound, growth, exponential and logistic) was larger than that of linear regression equation, of which power's R square reached 0.816 and the left four's R square was 0.798.

The diarrhea incidence rates were further divided into 3 groups: $\leq 3\%$, 3-6%, $\geq 6\%$. According to the field environmental sanitary questionnaire and the incidence, stepping discriminate function was used to establish the discriminate function. The discriminate function was composed of six variables (density of flies in toilets, toilet disinfection, density of flies in garbage dump, disposal method of garbage, density of flies near waste water and use of anti-fly cover) (Table 5). The false discriminate rate was 0%, 13.3% and 11.1%, respectively. The total false discriminate rate was 91.9%.

Table 5 Linear discriminant function coefficients

Factor	Linear discriminant	Function coefficient		
		$<3\%$	3%-6%	$\geq 6\%$
Disinfection of toilets	29.354	46.645	45.882	
Garbage disposal methods	-14.564	-34.839	-25.324	
Density of flies in toilets	9.127	7.143	19.911	
Density of flies in garbage dumps	8.753	16.595	16.056	
Density of flies near waste-water	15.855	38.361	27.858	
Use of anti-fly cover	21.243	34.128	32.386	
Constant	-46.378	-117.197	-133.264	

Analysis of case-case control study Twenty-two case-case control study questionnaires were collected, 20 of them had no missing data and were analyzed by single factor conditional logistic regression. The result showed that 30 possible risk factors had a relationship with severe symptoms. Drinking raw water within seven days, eating outside, not washing hand before eating, were then analyzed by conditional logistic multiple-regression (Table 6).

DISCUSSION

The diarrhea incidence rate during the training stage was 4.10%, which was significantly higher than that of the garrison at the corresponding time (0.98%) and much higher than the 10 day incidence rate (1.35%) of a stationed army in the same season^[5]. Because of the differences in duration, location and diagnostic standard in an emergency period, the rates could not be directly compared, however, the increase of diarrhea incidence rate was a common phenomenon during emergency. There must be some factors that contribute to the increased diarrhea incidence, and

Table 4 Multiple-factor conditional logistic- regression results of case-control study

Factor	Regression coefficient	Standard error	Odds ratio	95% Confidence interval	P value
Drinking raw water	3.1460	0.4638	23.2148	9.3641-57.6862	0.0000
Eating outside	3.1365	0.6055	23.0229	7.0273-75.4280	0.0000
Contacting with patients	2.9447	0.5707	19.0055	6.2104-58.1625	0.0000
Lack of hygiene knowledge	1.7776	0.5071	5.9155	2.1893-15.9833	0.0005
Depression	1.1654	0.3633	3.2071	1.5735-6.5364	0.0013
Not frequently cutting fingernails	1.0504	0.3888	2.8588	1.3341-6.1258	0.0069
Lack of sleep	0.6555	0.21264	1.9261	1.2360-3.0016	0.0038

Table 6 Multiple-factor conditional logistic regression results of case-case control study

Factors	Regression coefficient	Standard error	Odd ratio (OR)	95% confidence interval	P value
Drinking raw water	3.8610	1.1724	47.5119	4.7738-472.8718	0.0010
Eating outside	2.5711	0.7506	13.0802	3.0040-56.9537	0.0006
Not washing hand before eating	1.3445	0.6142	2.7487	1.1519-12.7877	0.0286

if we can find these factors and control them, we should be able to strengthen the fighting capacity of the army.

The incidence rate of officers was clearly lower than that of soldiers, which was not in accordance with the results from stationed army and other related researches^[24]. For example, a research of Hyams in "desert shield action" suggested the incidence rate was not affected by age and rank, while another study showed that the risk of officers was a little higher than that of soldiers. More data are still needed to confirm the real features of our army^[25]. According to our study, the possible explanation was that the training and working of soldiers were more intensive, meanwhile their hygiene habits were worse than officers. In addition, they drank raw water and eating outside more often than officers^[26].

From our research, the time distribution of diarrhea can be concluded as follow. The number of patients increased obviously in the early days of an action, then became stable after three or four days, and sustained at a certain rate^[27]. During this period the incidence rate in each unit of the army was different and small outbreak could be seen occasionally, which was similar to some conclusions from foreign armies. The possible reasons of the increased rate during the early time were as follows. Normal living pattern of soldiers was disrupted and physically weakened. During training, soldiers increased significantly their contact with environments and the chances of infection were also increased. Failure to adapt to a new environment and lack of immunity, and no sanitary and anti-epidemic measures were taken. These possible reasons still need to be further explored. To control the incidence peak at early stages, we should strengthen propaganda on hygiene and enhance soldiers' abilities to self-guard against diarrhea. In addition, antibiotics should be used to prevent special diarrheas (such as tourist diarrhea, soldier diarrhea with special task), but attention should be paid to selection and time limit of antibiotics^[28,29]. With the army's adapting to the environment and the perfection of preventive measures, the incidence rate maintained at a lower degree. However, because of the existence of many unhygienic temporary food stalls outside the camps and soldiers often eating outside, outbreak of different scales did take place^[30,31]. Apart from propaganda, we should strengthen the discipline and forbid soldiers to eat outside the camps.

In spite of the failure to detect *Campylobacter* and *Yersinia* due to limited condition on spot, 61.3% detection rate indicated that bacterial diarrhea was a main cause in Summer and Autumn during field training in coastal area in southern China. It was reported ETEC was the most common pathogen in stationed army^[32] and so was in our study, which was in accordance with some reports from American army^[8]. It suggested that ETEC was one of the focal points in diarrhea prevention in army, no matter Chinese or foreign^[8,33-35], stationed or training in field. We should enhance the basic clinical and preventive researches on diarrhea to guarantee fighting capacity. Moreover, we detected a relatively high rate of vibrio, especially that of *Vibrio cholerae* which was 16.5%, at the second place^[36]. This may be correlated with training at coastal area as water, food, and articles for daily use contain high counts of such pathogens (results not shown). Many studies showed that this germ had a relatively high detection rate in southeast coastal area.

It is important to evaluate hygiene standards of our army and develop related education to analyze individual risk factors of diarrhea. The incidence rate will decrease markedly if we can efficiently control these risk factors. As shown in Table 4, after multi variable analysis seven variables emerged as significant risk factors, which were drinking raw water, eating outside, lack of hygiene knowledge, not frequently trimming nails, contacting with diarrhea patients, having no enough sleep

and depression. Of these factors the first two were consistent with the results from stationed army, which indicates that the two risk factors are common in our military officers and soldiers. So it is necessary to strengthen sanitary education, to enforce administration, and to change unhealthy habits. During the survey, we found that none of the patients was separated from others and all the patients ate, slept and trained with the healthy personnel, which made contact transmission more easily.

For a long time, mental factors of diarrhea in an emergency period have been ignored. To explore the relationship between mental factors and diarrhea in an emergency period, we used "SCL-90" widely used in foreign countries, especially in mental health field. In a study, the mental condition of new recruits and the influence of each mental factor on injury in military training were analyzed by "SCL-90" in our army, and evaluation of the results was excellent. It indicated that using "SCL-90" to analyze the mental factors was feasible^[37-40]. In an emergency period, especially in modern warfare, intense danger and cruelty would cause a great pressure on servicemen's mentality. Therefore, mental factor may be a risk factor of diarrhea in an emergency period. In our study, 1:2 case-control study was performed to evaluate the relation between mental factor and diarrhea. The result of single-factor analysis suggested that the gross score and 9 factors (except paranoiac factor) were associated with diarrhea. In addition, the result of multiple-factor analysis suggested that depression was a risk factor of diarrhea, as only depression was entered to the aggressive equation. Whether this relation exists or not is still a problem worth further studying. The possible explanation is that mental factor, acting through the neuroendocrine system, can lead to enterocinesia and gastroenteric secretion disorder or weaken the immune functions, so the body is more susceptible to pathogens, resulting in diarrhea^[41,42].

Case-case control study has been used to analyze the risk factors of chronic infant diarrhea^[40] but not used to analyze that of diarrhea in a military emergency period. For the first time, we used it to analyze the risk factors of diarrhea in an emergency period. During the emergency period, it was critical to deal with the problems which influenced the fighting capacity due to limited human and material resources. Our study demonstrated that 20.4% of diarrhea patients could not work, because of the severe clinical manifestations. If these patients can be prevented from diarrhea, the fighting capacity will be greatly increased. In our study, the result indicated that three risk factors (drinking raw water 7 days before diarrhea, eating outside, not washing hand before eating) had a relation with severe clinical manifestations. Overall, the result indicated that preventive measures should be taken to control the three risk factors.

No report has been published on using unit incidence as risk factors to prevent diarrhea. In our study, the unit diarrhea incidence rate was different. To maintain the fighting capacity, decreasing the unit incidence rate is important. If we can find out the unit risk factors, measures can be taken to control them. The result of linear stepping regression showed that three (density of flies in toilets, garbage disposal methods and daily average boiled-water supply) out of 23 potential factors might be the cause of the increased unit incidence. From the standard regression coefficient, the density of flies in toilets had the major influence on diarrhea incidence rate. The higher the density of flies in toilets, the higher the diarrhea incidence rate. Fly is an important route of transmission, which has been confirmed before. The study of the Gulf War also demonstrated that persistent existence of flies was an important reason of low-epidemic diarrhea. Meanwhile, we thought the garbage disposal methods have a relation with the density of flies. Some troops buried garbage by the sanitary unit strictly, thus preventing the reproduction of flies.

ACKNOWLEDGEMENTS

We would like to thank all the military personnel participated in this study. We are also grateful to Professor Chen Pingyan in Department of Statistics, Professor Xie Yaning in Department of Psychology of the First Military Medical University, and Professor Wang Nengping in CDC of Nanfang Hospital, Professor Liu Qing in Department of Statistics of Sun yet-sen Medical University for their generous help in this study.

REFERENCES

- Sanchez JL**, Gelnett J, Petrucci BP, Defraites RF, Taylor DN. Diarrheal disease incidence and morbidity among United States military personnel during short-term missions overseas. *Am J Trop Med Hyg* 1998; **58**: 299-304
- Heggors JP**. Microbial invasion—the major ally of war (natural biological warfare). *Mil Med* 1978; **143**: 390-394
- Quin NE**. The impact of diseases on military operations in the Persian Gulf. *Mil Med* 1978; **147**: 728-734
- Pazzaglia Walker RI**. A retrospective survey of enteric infections in active duty Navy and Marine Corps personnel. *Mil Med* 1982; **147**: 27-33
- Nie J**, Yu SY, Chen YZ, Chen Q, Wu M, Meng FH. The epidemiological investigation on acute diarrhea in a certain unit of PLA in South China. *Zhongguo Gonggong Weisheng Zazhi* 1996; **12**: 249-250
- Hyams KC**, Riddle J, Trump DH, Graham JT. Endemic infectious diseases and biological warfare during the Gulf War: a decade of analysis and final concerns. *Am J Trop Med Hyg* 2001; **65**: 664-670
- Connor P**, Farthing MJ. Travellers' diarrhoea: a military problem? *J R Army Med Corps* 1999; **145**: 95-101
- Haberberger RL Jr**, Mikhail IA, Burans JP, Hyams KC, Glenn JC, Diniega BM, Sorgen S, Mansour N, Blacklow NR, Woody JN. Travelers' diarrhea among United States military personnel during joint American-Egyptian armed forces exercises in Cairo Egypt. *Mil Med* 1991; **156**: 27-30
- Pazzaglia G**, Walker RI. A retrospective survey of enteric infections in active duty Navy and Marine Corps personnel. *Mil Med* 1982; **147**: 27-33
- Echeverria P**, Ramirez G, Blacklow NR, Ksiazek T, Cukor G, Cross JH. Travelers' diarrhea among U.S. Army troops in South Korea. *J Infect Dis* 1979; **139**: 215-219
- Barrett KE**. New insights into the pathogenesis of intestinal dysfunction: secretory diarrhea and cystic fibrosis. *World J Gastroenterol* 2000; **6**: 470-474
- Oyfo BA**, el-Gendy A, Wasfy MO, el-Etr SH, Churilla A, Murphy J. A survey of enteropathogens among United States military personnel during Operation Bright Star '94, in Cairo, Egypt. *Mil Med* 1995; **160**: 331-334
- Oyfo BA**, Peruski LF, Ismail TF, el Etr SH, Churilla AM, Wasfy MO, Petrucci BP, Gabriel ME. Enteropathogens associated with diarrhea among military personnel during Operation Bright Star 96, in Alexandria, Egypt. *Mil Med* 1997; **162**: 396-400
- Oyfo BA**, Lesmana M, Subekti D, Tjaniadi P, Larasati W, Putri M, Simanjuntak CH, Punjabi NH, Santoso W, Muzahar, Sukarma, Sriwati, Sarumpaet S, Abdi M, Tjindi R, Ma'ani H, Sumardiati A, Handayani H, Campbell JR, Alexander WK, Beecham HJ 3rd, Corwin AL. Surveillance of bacterial pathogens of diarrhea disease in Indonesia. *Dia Microbiol Infect Dis* 2002; **44**: 227-234
- Tan TY**. Use of molecular techniques for the detection of antibiotic resistance in bacteria. *Exp Rev Mol Dia* 2003; **3**: 93-103
- Song J**, Swekla M, Colorado P, Reddy R, Hoffmann S, Fine S. Liver abscess and diarrhea as initial manifestations of ulcerative colitis: case report and review of the literature. *Dig Dis Sci* 2003; **48**: 417-421
- Ruskone-Fourmestreaux A**, Attar A, Chassard D, Coffin B, Bornet F, Bouhnik Y. A digestive tolerance study of maltitol after occasional and regular consumption in healthy humans. *Eur J Clin Nutr* 2003; **57**: 26-30
- Bhattacharya SK**. Therapeutic methods for diarrhoea in children. *World J Gastroenterol* 2000; **6**: 497-500
- Taylor WR**, Schell WL, Wells JG, Choi K, Kinnunen DE, Heiser PT, Helstad AG. A foodborne outbreak of enterotoxigenic *Escherichia coli* diarrhea. *N Engl J Med* 1982; **306**: 1093-1095
- Davis H**, Taylor JP, Perdue JN, Stelma GN Jr, Humphreys JM Jr, Rowntree R 3rd, Greene KD. A shigellosis outbreak traced to commercially distributed shredded lettuce. *Am J Epidemiol* 1988; **128**: 1312-1314
- Martin DL**, Gustafson TL, Pelosi JW, Suarez L, Pierce GV. Contaminated produce—a common source for two outbreaks of *Shigella* gastroenteritis. *Am J Epidemiol* 1986; **124**: 299-305
- Griffin MR**, Surowiec JJ, McCloskey DI, Capuano B, Pierzynski B, Quinn M, Wojnarski R, Parkin WE, Greenberg H, Gary GW. Foodborne Norwalk virus. *Am J Epidemiol* 1982; **115**: 178-184
- Binder HJ**. Pathophysiology of diarrhea. *Shijie Huaren Xiaohua Zazhi* 1997; **5**: 62
- Haberberger RL**, Scott DA, Thornton SA, Hyams KC. Diarrheal disease aboard a U.S. Navy ship after a brief port visit to a high risk area. *Mil Med* 1994; **159**: 445-448
- Hyams KC**, Bourgeois AL, Merrell BR, Rozmajzl P, Escamilla J, Thornton SA, Wasserman GM, Burke A, Echeverria P, Green KY. Diarrheal disease during Operation Desert Shield. *N Engl J Med* 1991; **325**: 1423-1428
- Wolfe M**. Acute diarrhea associated with travel. *Am J Med* 1990; **88**: 345-375
- Sharp TW**, Thornton SA, Wallace MR, Defraites RF, Sanchez JL, Batchelor RA, Rozmajzl PJ, Hanson RK, Echeverria P, Kapikian AZ. Diarrhea disease among military personnel during operation Restore Hope, Somalia, 1992-1993. *Am J Trop Med Hyg* 1995; **52**: 188-193
- Dupont H**. Prevention and treatment of traveler's diarrhea. *N Engl J Med* 1993; **328**: 1821-1827
- Xiong Q**. Microbial sensitivity tests result of Dysenteric Bacillus. *Shijie Huaren Xiaohua Zazhi* 1996; **4**: 536
- DeMaio J**, Bailey L, Hall K, Boyd R. A major outbreak of foodborne gastroenteritis among Air Force personnel during Operation Desert Storm. *Mil Med* 1993; **158**: 161-164
- Bruins J**, Bwire R, Slooman EJ, van Leusden AJ. Diarrhea morbidity among Dutch military service men in Goma, Zaire. *Mil Med* 1995; **160**: 446-448
- Huerta M**, Grotto I, Gdalevich M, Mimouni D, Gavrieli B, Yavzori M, Cohen D, Shpilberg O. A waterborne outbreak of gastroenteritis in the Golan Heights due to enterotoxigenic *Escherichia coli*. *Infection* 2000; **28**: 267-271
- Sack DA**, Kaminsky DC, Sack RB, Wamola IA, Orskov F, Orskov I, Slack RC, Arthur RR, Kapikian AZ. Enterotoxigenic *Escherichia coli* diarrhea of travelers: a prospective study of American Peace Corps volunteers. *Johns Hopkins Med J* 1977; **141**: 63-70
- Echeverria P**, Blacklow NR, Zipkin C, Vollet JJ, Olson JA, DuPont HL, Cross JH. Etiology of gastroenteritis among Americans living in the Philippines. *Am J Epidemiol* 1979; **109**: 493-501
- Steffen R**, Mathewson JJ, Ericsson CD, DuPont HL, Helminger A, Balm TK, Wolff K, Witassek F. Travelers' diarrhea in West Africa and Mexico: fecal transport systems and liquid bismuth subsalicylate for self-therapy. *J Infect Dis* 1988; **157**: 1008-1013
- Cohen D**, Sela T, Slepion R, Yavzori M, Ambar R, Orr N, Robin G, Shpielberg O, Eldad A, Green M. Prospective cohort studies of shigellosis during military field training. *Eur J Clin Microbiol Infect Dis* 2001; **20**: 123-126
- Zhang LX**. An investigation on new recruits' mental condition of army. *Jiefangjun Yufang Yixue Zazhi* 1997; **15**: 374-375
- Zhou H**, Li F, Zhang YG, Lei ZJ, Yang Y. Recruit training injure and psychology factors. *Renmin Junyi* 2000; **43**: 64-65
- Chui SF**, Liu XH, Yang XG, Liu YL, Jin BA, Zhang ZY. An investigation of singletons of new recruit's mental health. *Renmin Junyi* 1998; **41**: 64-65
- Xu NF**, Wu B, Yuan JA, Chen SQ. The case-control study on infant chronic diarrhea's risk factors. *Zhongguo Gonggong Weishen Xuebai* 1999; **14**: 41-43
- Ivashkin VT**, Lapina TL, Bondarenko OY, Sklanskaya OA, Grigoriev PY, Vasiliev YV, Yakovenko EP, Gulyaev PV, Fedchenko VI. Azithromycin in a triple therapy for *H pylori* eradication in active duodenal ulcer. *World J Gastroenterol* 2002; **8**: 879-882
- Qin XY**, Shen KT, Zhang X, Cheng ZH, Xu XR, Han ZG. Establishment of an artificial beta-cell line expressing insulin under the control of doxycycline. *World J Gastroenterol* 2002; **8**: 367-370

Alteration of somatostatin receptor subtype 2 gene expression in pancreatic tumor angiogenesis

Ren-Yi Qin, Ru-Liang Fang, Manoj Kumar Gupta, Zheng-Ren Liu, Da-Yu Wang, Qing Chang, Yi-Bei Chen

Ren-Yi Qin, Ru-Liang Fang, Manoj Kumar Gupta, Zheng-Ren Liu, Da-Yu Wang, Qing Chang, Yi-Bei Chen, Department of Surgery, Tongji Hospital, Tongji Medical College, Huazhong University of Science and Technology, Wuhan 430030, Hubei Province, China

Supported by National Natural Science Foundation of China, No. 30271473

Correspondence to: Professor Ren-Yi Qin, Department of Surgery, Tongji Hospital, Tongji Medical College, Huazhong University of Science and Technology, Wuhan 430030, Hubei, Province, China. ryqin@tjh.tjmu.edu.cn

Telephone: +86-27-83662389 **Fax:** +86-27-83662389

Received: 2003-06-04 **Accepted:** 2003-07-30

Abstract

AIM: To explore the difference of somatostatin receptor subtype 2 (SST2R) gene expression in pancreatic cancerous tissue and its adjacent tissue, and the relationship between the change of SST2R gene expression and pancreatic tumor angiogenesis related genes.

METHODS: The expressions of SST2R, DPC4, p53 and ras genes in cancer tissues of 40 patients with primary pancreatic cancer, and the expression of SST2R gene in its adjacent tissue were determined by immunohistochemical LSAB method and EnVision™ method. Chi-square test was used to analyze the difference in expression of SST2R in pancreatic cancer tissue and its adjacent tissue, and the correlation of SST2R gene expression with the expression of p53, ras and DPC4 genes.

RESULTS: Of the tissue specimens from 40 patients with primary pancreatic cancer, 35 (87.5%) cancer tissues showed a negative expression of SST2R gene, whereas 34 (85%) a positive expression of SST2R gene in its adjacent tissues. Five (12.5%) cancer tissues and its adjacent tissues simultaneously expressed SST2R. The expression of SST2R gene was markedly higher in pancreatic tissues adjacent to cancer than in pancreatic cancer tissues ($P < 0.05$). The expression rates of p53, ras and DPC4 genes were 50%, 60% and 72.5%, respectively. There was a significant negative correlation of SST2R with p53 and ras genes ($\chi^2 = 9.33$, $P < 0.01$), but no significant correlation with DPC4 gene ($\chi^2 = 2.08$, $P > 0.05$).

CONCLUSION: There was a significant difference of SST2R gene expression in pancreatic cancer tissues and its adjacent tissues, which might be one cause for the different therapeutic effects of somatostatin and its analogs on pancreatic cancer patients. There were abnormal expressions of SST2R, DPC4, p53 and ras genes in pancreatic carcinogenesis, and moreover, the loss or decrease of SST2R gene expression was significantly negatively correlated with the overexpression of tumor angiogenesis correlated p53 and ras genes, suggesting that SST2R gene together with p53 and ras genes may participate in pancreatic cancerous angiogenesis.

Qin RY, Fang RL, Gupta MK, Liu ZR, Wang DY, Chang Q, Chen YB. Alteration of somatostatin receptor subtype 2 gene expression in pancreatic tumor angiogenesis. *World J Gastroenterol* 2004; 10(1): 132-135

<http://www.wjgnet.com/1007-9327/10/132.asp>

INTRODUCTION

Recent studies have indicated that somatostatin and its analogs have obviously antiproliferative effects on various solid tumors, such as colon cancer, liver cancer, which are mediated through somatostatin receptors^[1-7], but a large number of clinical researches indicate that the therapeutic effects of somatostatin and its analogs on pancreatic cancer are different, the reason is not known^[8,9]. Moreover, studies have already reported that the change of SST2R gene expression in human pancreatic cancerous cells is related with tumor angiogenesis factors such as transforming growth factor beta (TGF- β), but the relationship between SST2R and tumor angiogenesis related genes such as DPC4, ras and p53 is still not clear^[10]. Our study aimed at exploring the cause for the different therapeutic effects of somatostatin and its analogs on human pancreatic cancer, and the relationship between the changes of SST2R gene expression and pancreatic tumor angiogenesis correlated genes.

MATERIALS AND METHODS

Tissue specimens

Tissue samples from 40 primary pancreatic cancer patients were obtained from the Department of Pathology in Tongji Hospital. The patients consisted of 26 males and 14 females aged from 33 to 71 years (means: 55.65 years). All lesions were diagnosed pathologically as pancreatic ductal adenocarcinoma, consisting of 23 pancreatic cancers in the head, and 17 pancreatic cancers in the body and tail of pancreas. All patients were staged according to UICC TNM classification, I-II in 14 patients, and III-IV in 26 patients. All the specimens of pancreatic cancer tissues and its adjacent tissues were fixed and dehydrated in 10% formalin, embedded in paraffin and cut into 4 μ m serial sections.

Reagents

Goat SST2R and DPC4 polyclonal antibodies were from Santa Cruz (USA). p53, ras monoclonal antibody and mouse anti-human ras monoclonal antibody were from Maixin Biotech Kaifa Company (Fuzhou, China). Secondary biotinylated rabbit anti-sheep IgG (ZB-2050) was from ZYMED (USA). EnVision™ mouse-anti reagent kit, EnVision™ rabbit-anti reagent kit and peroxidase conjugated streptavidin were from DAKO (Denmark).

Immunohistochemical staining

Three-step methods (LSAB) were used for DPC4 and SST2R staining, and two-step methods (EnVision™ system) were used for p53 and ras genes. Formalin-fixed, paraffin-embedded sections were dewaxed, rehydrated, and boiled in 0.01M-citrate buffer, pH 6.0 in a microwave oven for 10 minutes. Then primary antibody was added and incubated at 4 °C overnight. Biotinylated rabbit anti-sheep IgG (1:300 dilution) was added

and incubated at 37 °C for 1 hour, followed by incubation with peroxidase conjugated streptavidin (1:400 dilution) at 37 °C for 30 minutes. For p53 and ras staining, peroxidase conjugated streptavidin was replaced by EnVision. DAB chromogen was applied for 10 to 20 minutes and rinsed for visualization under microscope, followed by slight counterstaining with haematoxylin, dehydration, and finally cover slips were sealed with permount. Negative control was obtained by replacing the primary antibody with PBS.

Evaluation of immunohistochemical staining

Positive staining was located in cell membrane/cytoplasm for SST2R, and the cytoplasm for DPC4 and ras, and the nucleus for p53. At least 1000 cells were counted per 40 X 10 field. The expressions were graded, as follows. Negative (-) if <10% of the cancerous cells in a given specimen were positively stained. Weak positive (+) if 10% to 20% of the cancerous cells in a given specimen were positively stained. Positive (++) if 20% to 50% of the cancer cells in a given specimen were positively stained, and strongly positive (+++) if 75% of the cancer cells in a given specimen were positively stained.

Statistical analysis

Chi-square test was used to analyze the results. $P < 0.05$ was considered statistically significant.

RESULTS

Expression of SST2R gene in pancreatic cancer tissue and its adjacent tissue

The expression rate of SST2R gene was markedly higher in the adjacent non-cancerous tissue (85%) than in cancer tissue (12.5%) ($P < 0.05$). Twenty-nine patients (72.5%) expressed SST2R gene only in the adjacent non-cancerous tissue. For SST2R gene expression in pancreatic cancer tissue, strong positive was only 10%, weak positive 2.5%, and negative 87.5%, 12.5% pancreatic cancer tissue and its adjacent non-cancerous tissue expressed SST2R simultaneously (Table 1 and Figures 1, 2).

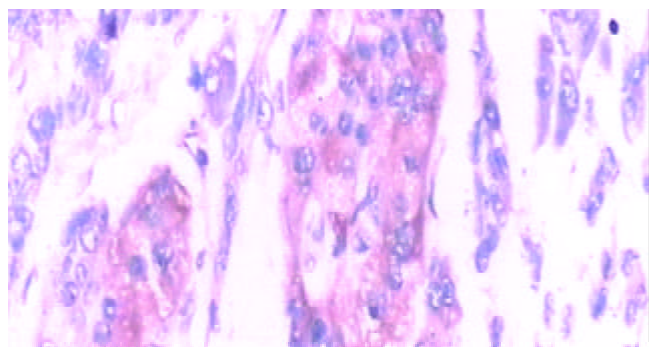


Figure 1 Ductal adenocarcinoma in pancreatic head (Immunohisto-chemistry LSAB method, $\times 400$). Brown yellow staining of SST2R gene expression in cell membrane/cytoplasm.

Expression of p53 gene in pancreatic cancer tissue

For p53 gene in pancreatic cancerous tissue, 19 patients (47.5%) had strong positive expression, 20 patients (50%) negative expression, and 1 patient (2.5%) weak positive expression. The SST2R gene expression in 17 patients with strong positive expression of p53 was negative. Three patients with strong positive expression of SST2R were negative for p53 gene expression. The SST2R and p53 gene expressions in 1 patient were strong positive. One patient with weak positive expression of p53 gene was negative for SST2R gene expression. The SST2R gene expression of 1 patient with strong positive expression of p53 gene was weak positive (Table 1 and Figure 3).

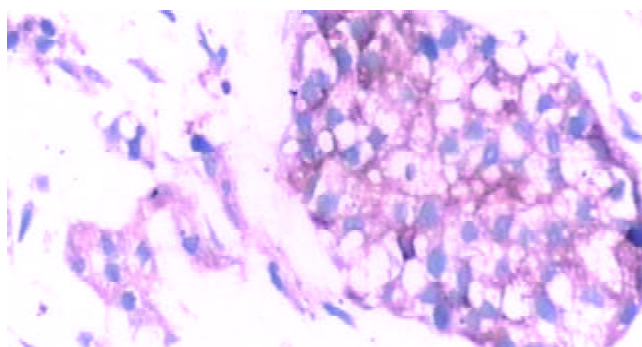


Figure 2 Pancreatic ductal adenocarcinoma in pancreatic body and tail (Immunohistochemistry LSAB method, $\times 400$). Brown yellow staining of SST2R gene expression in cell membrane/cytoplasm.

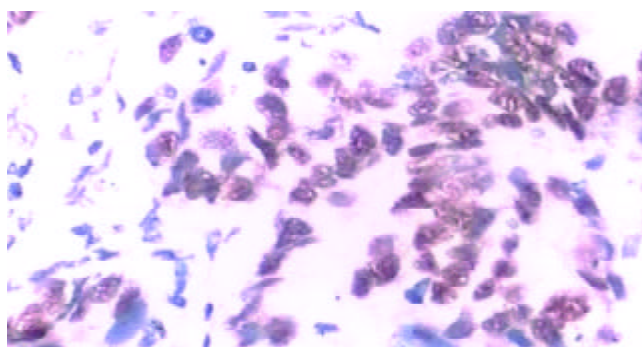


Figure 3 Ductal adenocarcinoma in pancreatic head (EnVision™ method, $\times 400$). Brown yellow staining of p53 gene expression in cell nucleus.

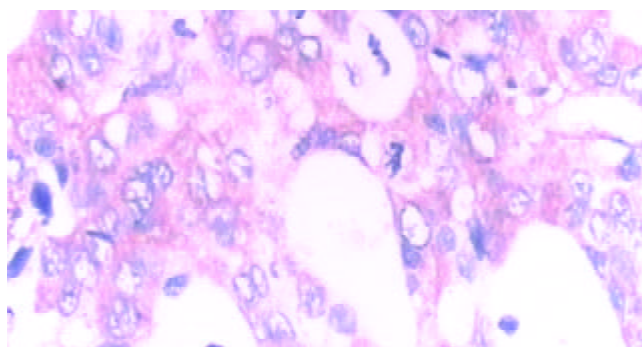


Figure 4 Ductal adenocarcinoma in pancreatic body and tail (EnVision™ method, $\times 400$). Brown yellow staining of ras gene expression located in cytoplasm.

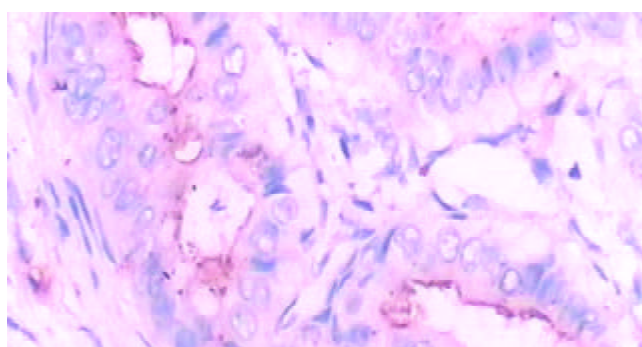


Figure 5 Ductal adenocarcinoma in pancreatic body and tail (EnVision™ method, $\times 400$). Brown yellow staining of DPC4 gene expression located in cytoplasm.

Expression of ras gene in pancreatic cancer tissue

For expression of ras gene, 14 patients (35%) were strong positive, 10 patients (25%) weak positive, and 16 patients (40%) negative. Eleven patients with strong positive expression of ras gene showed negative expression of SST2R gene, 1 patient with negative expression of ras gene showed strong positive expression of SST2R gene. The SST2R and ras genes in 4 patients showed positive expression of different grades correspondingly. The SST2R and ras gene expressions in 15 patients were negative. Nine patients with weak positive expression of ras gene were negative for SST2R gene expression (Table 1 and Figure 4).

Expression of DPC4 gene in pancreatic cancer tissue

Seven patients (17.5%) were positive, 4 patients (10%) weak positive, and 29 patients (72.5%) negative for DPC4 gene expression. Twenty-six patients (65%) had negative expression of both DPC4 and SST2R gene. Of the 9 patients with negative expression of SST2R gene, 5 patients were strong positive, and 4 patients weak positive for DPC4 gene expression. Both SST2R and DPC4 genes expression of 2 patients were strong positive. One patient with negative expression of DPC4 gene was weak positive for SST2R gene expression (Table 1 and Figure 5).

Statistical analysis indicated that SST2R was significantly negatively correlated with the expression of p53 or ras genes ($P < 0.01$), whereas not distinctly correlated with DPC4 gene ($P > 0.05$).

Table 1 Expressions of SST2R and ras, DPC4 and p53 genes in 40 primary pancreatic cancerous tissues

	Strong positive (+++ to +++) n (%)	Weak positive (+) n (%)	Negative (-) n (%)
SST2R	4.0 (10)	1.0 (2.5)	35.0 (87.5)
ras	14.0 (35)	10.0 (25)	16.0 (4)
DPC4	7.0 (17.5)	4.0 (10)	19.0 (47.5)
P53	19.0 (47.5)	1.0 (2.5)	20.0 (50)
Cancer adjacent SST2R	34.0 (85)	0.0	6.0 (15)

DISCUSSION

Somatostatin and its analogs can inhibit the growth of benign and malignant tumors, and it has been found that the inhibitory effects are directly correlated with the expression of SST2R on tumor tissues^[11-15]. The mechanisms of the inhibition are the combined interaction of somatostatin and its analogs with SST2R in tumor tissues, either directly inhibiting division and proliferation of tumor cells or inhibiting the activities of growth factors such as vascular endothelial growth factor (VEGF), insulin-like growth factor (IGF)^[16-21], and moreover, counteracting tumorigenesis and tissue proliferation^[22,23]. In addition, somatostatin and its analogs could arrest pancreatic cancer cell cycle at G₀-S₁ phase by up-regulating p27, and thus induced apoptosis^[24,25].

The expression of SST2R was decreased or lost in primary pancreatic cancerous tissue^[26-29], but there is no report on the expression of SST2R in pancreatic cancerous adjacent tissue. Our study showed that 5 of 40 primary pancreatic cancer tissues showed positive expression of SST2R gene, suggesting that most of pancreatic cancerous tissues lack the expression of SST2R, which may be the major reason why somatostatin and its analogs had no marked therapeutic effects on pancreatic cancer. Interestingly, expression of SST2R was higher in most of the pancreatic cancerous adjacent tissues, which may be beneficial for somatostatin and its analogs to inhibit fast outward infiltration and growth of tumor cells. Our study

indicated that if SST2R decreased in pancreatic cancerous tissue and its adjacent tissue, somatostatin and its analogs might not have therapeutic effect on pancreatic cancer. But when pancreatic cancerous tissue and its adjacent tissue obviously expressed SST2R, they had a definite therapeutic effect on patients with pancreatic cancer. Hence the differences in the expression of SST2R in pancreatic cancerous tissue and its adjacent tissue would certainly lead to different therapeutic effects. At present, this is the main possible cause for the different therapeutic effects of somatostatin and its analogs on pancreatic cancer. We consider that it is important to define the expression of SST2R in pancreatic cancerous tissue and its adjacent tissue before using somatostatin and its analogs. This will be beneficial to the ultimate definition of the exact therapeutic effects of somatostatin and its analogs on pancreatic cancer.

Mutations of DPC4, ras and p53 genes have been found to play crucial roles in tumor angiogenesis^[30-32]. The mutation rates of these genes are higher in pancreatic cancerous tissue, indicating that the similar mechanism of pancreatic tumorigenesis with other tumorigenesis involving mutation and abnormal expression of multiple genes. Our study indicated that the expression of SST2R gene was significantly negatively correlated with p53 and ras genes, suggesting that the decrease or loss of SST2R gene expression in pancreatic cancerous tissue participates in tumor angiogenesis through certain pathway, further investigation is required to probe into its the mechanism.

REFERENCES

- 1 **O'Byrne KJ**, Schally AV, Thomas A, Carney DN, Steward WP. Somatostatin, its receptors and analogs, in lung cancer. *Chemotherapy* 2001; **47**(Suppl): 78-108
- 2 **Kouroumalis E**, Skordilis P, Thermos K, Vasilaki A, Moschandrea J, Manousos ON. Treatment of hepatocellular carcinoma with octreotide: a randomised controlled study. *Gut* 1998; **42**: 442-447
- 3 **Wolff RA**. Chemoprevention for pancreatic cancer. *Int J Gastrointest Cancer* 2003; **33**: 27-41
- 4 **Samonakis DN**, Moschandreas J, Arnaoutis T, Skordilis P, Leontidis C, Vafiades I, Kouroumalis E. Treatment of hepatocellular carcinoma with long acting somatostatin analogues. *Oncol Rep* 2002; **9**: 903-907
- 5 **Hejna M**, Schmidinger M, Raderer M. The clinical role of somatostatin analogues as antineoplastic agents: much ado about nothing? *Ann Oncol* 2002; **13**: 653-668
- 6 **Hofslie E**. The somatostatin receptor family—a window against new diagnosis and therapy of cancer. *Tidsskr Nor Laegeforen* 2002; **122**: 487-491
- 7 **Vainas IG**. Octreotide in the management of hormone-refractory prostate cancer. *Chemotherapy* 2001; **47**(Suppl 2): 109-126
- 8 **Raderer M**, Kurtaran A, Scheithauer W, Fiebigler W, Weinlaender G, Oberhuber G. Different response to the long-acting somatostatin analogues lanreotide and octreotide in a patient with a malignant carcinoid. *Oncology* 2001; **60**: 141-145
- 9 **Raderer M**, Hamilton G, Kurtaran A, Valencak J, Haberl I, Hoffmann O, Kornek GV, Vorbeck F, Hejna MH, Virgolini I, Scheithauer W. Treatment of advanced pancreatic cancer with the long-acting somatostatin analogue lanreotide: *in vitro* and *in vivo* results. *Br J Cancer* 1999; **79**: 535-537
- 10 **Gupta MK**, Qin RY. Mechanism and its regulation of tumor-induced angiogenesis. *World J Gastroenterol* 2003; **9**: 1144-1155
- 11 **Rochaix P**, Delesque N, Esteve JP, Saint-Laurent N, Voight JJ, Vaysse N, Susini C, Buscail L. Gene therapy for pancreatic carcinoma: local and distant antitumor effects after somatostatin receptor sst2R gene transfer. *Hum Gene Ther* 1999; **10**: 995-1008
- 12 **Buscail L**, Saint-Laurent N, Chastre E, Vaillant JC, Gest Capella G, Kalthoff H, Lluís F, Vaysse N, Susini C. Loss of sst2 Somatostatin receptor gene expression in human pancreatic and colorectal cancer. *Cancer Res* 1996; **56**: 1823-1827
- 13 **Guillemet J**, Saint-Laurent N, Rochaix P, Cuvillier O, Levade T, Schally AV, Pradayrol L, Buscail L, Susini C, Bousquet C. Soma-

- rostatin receptor subtype 2 sensitizes human pancreatic cancer cells to death ligand-induced apoptosis. *Proc Natl Acad Sci U S A* 2003; **100**: 155-160
- 14 **Vernejoul F**, Faure P, Benali N, Calise D, Tiraby G, Pradayrol L, Susini C, Buscail L. Antitumor effect of *in vivo* somatostatin receptor subtype 2 gene transfer in primary and metastatic pancreatic cancer models. *Cancer Res* 2002; **62**: 6124-6131
- 15 **Faiss S**, Pape UF, Bohmig M, Dorffel Y, Mansmann U, Golder W, Riecken EO, Wiedenmann B. Prospective, randomized, multicenter trial on the antiproliferative effect of lanreotide, interferon alfa, and their combination for therapy of metastatic neuroendocrine gastroenteropancreatic tumors—the International Lanreotide and Interferon Alfa Study Group. *J Clin Oncol* 2003; **21**: 2689-2696
- 16 **Hortala M**, Ferjoux G, Estival A, Bertrand C, Schulz S, Pradayrol L, Susini C, Clemente F. Inhibitory role of the somatostatin receptor SST2 on the intracrine-regulated cell proliferation induced by the 210-amino acid fibroblast growth factor-2 isoform: implication of JAK2. *J Biol Chem* 2003; **278**: 20574-20581
- 17 **Pollak MN**, Schally AV. Mechanisms of antineoplastic action of somatostatin analogs. *Proc Soc Exp Biol Med* 1998; **217**: 143-152
- 18 **Buscail L**, Vernejoul F, Faure P, Torrisani J, Susini C. Regulation of cell proliferation by somatostatin. *Ann Endocrinol* 2002; **63**(2 Pt 3): 2S13-2S18
- 19 **Puente E**, Saint-Laurent N, Torrisani J, Furet C, Schally AV, Vaysse N, Buscail L, Susini C. Transcriptional activation of mouse sst2 somatostatin receptor promoter by transforming growth factor-beta. Involvement of Smad4. *J Biol Chem* 2001; **276**: 13461-13468
- 20 **Pages P**, Benali N, Saint-Laurent N, Esteve JP, Schally AV, Tkaczuk J, Vaysse N, Susini C, Buscail L. Sst2 somatostatin receptor mediates cell cycle arrest and induction of p27(Kip1). Evidence for the role of SHP-1. *J Biol Chem* 1999; **274**: 15186-15193
- 21 **Kikutsuji T**, Harada M, Tashiro S, Ii S, Moritani M, Yamaoka T, Itakura M. Expression of somatostatin receptor subtypes and growth inhibition in human exocrine pancreatic cancers. *J Hepatobiliary Pancreat Surg* 2000; **7**: 496-503
- 22 **Bousquet C**, Puente E, Buscail L, Vaysse N, Susini C. Antiproliferative effect of somatostatin and analogs. *Chemotherapy* 2001; **47**(Suppl 2): 30-39
- 23 **Ferjoux G**, Bousquet C, Cordelier P, Benali N, Lopez F, Rochemaix P, Buscail L, Susini C. Signal transduction of somatostatin receptors negatively controlling cell proliferation. *J Physiol Paris* 2000; **94**: 205-210
- 24 **Benali N**, Cordelier P, Calise D, Pages P, Rochemaix P, Nagy A, Esteve JP, Pour PM, Schally AV, Vaysse N, Susini C, Buscail L. Inhibition of growth and metastatic progression of pancreatic carcinoma in hamster after somatostatin receptor subtype 2 (sst2) gene expression and administration of cytotoxic somatostatin analog AN-238. *Proc Natl Acad Sci U S A* 2000; **97**: 9180-9185
- 25 **Fisher WE**, Wu Y, Amaya F, Berger DH. Somatostatin receptor subtype 2 gene therapy inhibits pancreatic cancer *in vitro*. *J Surg Res* 2002; **105**: 58-64
- 26 **Buscail L**, Saint-Laurent N, Chastre E, Vaillant JC, Gespach C, Capella G, Kalthoff H, Lluís F, Vaysse N, Susini C. Loss of sst2 somatostatin receptor gene expression in human pancreatic and colorectal cancer. *Cancer Res* 1996; **56**: 1823-1827
- 27 **Benali N**, Ferjoux G, Puente E, Buscail L, Susini C. Somatostatin receptors. *Digestion* 2000; **621**(Suppl 1): 27-32
- 28 **Fueger BJ**, Hamilton G, Raderer M, Pangerl T, Traub T, Angelberger P, Baumgartner G, Dudczak R, Virgolini I. Effects of chemotherapeutic agents on expression of somatostatin receptors in pancreatic tumor cells. *J Nucl Med* 2001; **42**: 1856-1862
- 29 **Qin RY**, Qiu FZ. SST2R and SST2R mRNA expression in rats with pancreatic cancer and the effect of octreotide. *Yixian Bingxue* 2002; **2**: 41-44
- 30 **Schwarte-Waldhoff I**, Volpert OV, Bouck NP, Sipos B, Hahn SA, Klein-Scory S, Luttes J, Kloppel G, Graeven U, Eilert-Micus C, Hintelmann A, Schmiegel W. Smad4/DPC4-mediated tumor suppression through suppression of angiogenesis. *Proc Natl Acad Sci U S A* 2000; **97**: 9624-9629
- 31 **Shu X**, Wu W, Mosteller RD, Broek D. Sphingosine kinase mediates vascular endothelial growth factor-induced activation of ras and mitogen-activated protein kinases. *Mol Cell Biol* 2002; **22**: 7758-7768
- 32 **Bacher M**, Schrader J, Thompson N, Kuschela K, Gemsa D, Waeber G, Schlegel J. Up-regulation of macrophage migration inhibitory factor gene and protein expression in glial tumor cells during hypoxic and hypoglycemic stress indicates a critical role for angiogenesis in glioblastoma multiforme. *Am J Pathol* 2003; **162**: 11-17

Edited by Ren SY and Wang XL

Perioperative cimetidine administration promotes peripheral blood lymphocytes and tumor infiltrating lymphocytes in patients with gastrointestinal cancer: Results of a randomized controlled clinical trial

Cong-Yao Lin, De-Jiao Bai, Hong-Yin Yuan, Kun Wang, Guo-Liang Yang, Ming-Bai Hu, Zhou-Qing Wu, Yan Li

Cong-Yao Lin, De-Jiao Bai, Hong-Yin Yuan, Kun Wang, Guo-Liang Yang, Ming-Bai Hu, Zhou-Qing Wu, Yan Li, Department of Oncology, Zhongnan Hospital of Wuhan University, Wuhan 430071, Hubei Province, China

Supported by the Science Progress Project of Hubei Province, No. 2001AA301C35

Co-correspondents: Cong-Yao Lin and Yan Li

Correspondence to: Professor Cong-Yao Lin, Department of Oncology, Zhongnan Hospital of Wuhan University, 169 Dong Hu Rd, Wuhan 430073, Hubei Province, China. liyansd@hotmail.com

Telephone: +86-27-87335585 **Fax:** +86-27-87307622

Received: 2003-06-16 **Accepted:** 2003-07-24

Abstract

AIM: To study the effects of perioperative administration of cimetidine (CIM) on peripheral blood lymphocytes, natural killer (NK) cells and tumor infiltrating lymphocytes (TIL) in patients with gastrointestinal (GI) cancer.

METHODS: Forty-nine GI cancer patients were randomized into treatment group, who took CIM in perioperative period, and control group, who did not take the drug. The treatment was initiated 7 days before operation and continued for 10 days after surgery. At baseline examination before operation, on the 2nd and 10th postoperative days, total T lymphocytes, T helper cells, T suppressor cells, and NK cells in peripheral blood were measured respectively by immunocytochemical method using mouse-anti human CD₃, CD₄, CD₈ and CD₅₇ monoclonal antibodies. Blood samples from 20 healthy volunteers were treated in the same way as normal controls. Surgical specimens were examined during routine histopathological evaluation for the presence of TIL in tumor margin. Immunohistochemical study was performed to measure the proportion of T and B lymphocytes in TIL population. T and B lymphocytes were detected respectively using mouse-anti-human CD₃ and CD₂₀ monoclonal antibodies.

RESULTS: In comparison with normal controls, both the treatment and control groups had decreased T cells, T helper cells and NK cells at baseline. In control group, total T cells, T helper cells and NK cells declined continuously with the disease progression and the decrease became more obvious after operation. From baseline to the 2nd postoperative day, the proportion of total T cells, T helper cells, and NK cells went down from 60.5±4.6% to 56.2±3.8%, 33.4±3.7% to 28.1±3.4%, and 15.0±2.8% to 14.2±2.2%, respectively. On the other hand, there were significant improvements in these parameters after CIM treatment. On the 10th postoperative day, the treatment group had significantly higher percentages of total T cells, T helper cells and NK cells than control group. Moreover, CIM treatment also boosted TIL response, as was reflected by findings that 68%

(17/25) of the patients in treatment group had significant TIL responses and only 25% (6/24) of the cases had discernible TIL responses ($P < 0.01$).

CONCLUSION: Perioperative application of CIM to GI cancer patients could help restore the diminished cellular immunity induced by tumor burden and surgical maneuver. The drug could also boost TIL responses to tumor. These effects suggest that the drug be used as an immunomodulator for GI cancer patients.

Lin CY, Bai DJ, Yuan HY, Wang K, Yang GL, Hu MB, Wu ZQ, Li Y. Perioperative cimetidine administration promotes peripheral blood lymphocytes and tumor infiltrating lymphocytes in patients with gastrointestinal cancer: Results of a randomized controlled clinical trial. *World J Gastroenterol* 2004; 10(1): 136-142
<http://www.wjgnet.com/1007-9327/10/136.asp>

INTRODUCTION

Gastric and colorectal cancers are the most common cancers in China, with their incidence ranking number one and number four respectively. Although surgery, chemotherapy and radiotherapy are major treatment options for GI cancer, the long-term survival is low. Treatment failure is mainly due to recurrence and metastasis. One major cause for such an adverse outcome is the patients' diminished immunity against residual tumor cells after surgery. Therefore, how to restore and improve the patients' immunity against cancer has been an area of active study.

There has been much progress in understanding the relationship between the immune system and GI cancer, which has led to the use of immunomodulatory therapy as an adjuvant and palliative treatment. Many non-specific immunomodulatory agents such as levamisole, CIM, alpha interferon, *n*-3 fatty acids, polysaccharide K (PSK), supplementary diet with glutamine, arginine and omega-3-fatty acids, and Bacillus Calmette-Guerin (BCG) have been tried^[1-4]. CIM is a type 2 histamine receptor antagonist widely used for the treatment of peptic ulcers. It also has important effects on immune system. Administration of CIM has been found to preserve, to some degree, the patients' perioperative immunity^[5,6], to improve the survival of patients with colorectal cancer, melanoma, and renal cell cancer^[7-15]. Although it is not clear whether this effect of CIM on cancer is direct or indirect, it has been proposed that CIM may act by enhancing the host immune response to tumor cells^[16,17] or by blocking the cell growth-promoting activity of histamine in cancer cell lines^[14,16-20].

In this study, we used CIM in the perioperative period as an adjuvant immunomodulatory agent, and studied its effects on peripheral blood lymphocytes, NK cells and TIL in a randomized controlled clinical trial in patients with GI cancer.

MATERIALS AND METHODS

Study design

This was a prospective, randomized clinical trial. The subjects included in this study were selected from patients with pathologically confirmed GI cancer who were admitted to the Department of Oncology, Zhongnan Hospital of Wuhan University, from Sept.1997 to May 1998. The entry criteria were: primary GI cancers indicative of surgery, no preoperative evidence of distant metastasis, no history of previous immunity-impairing chronic diseases such as diabetes mellitus, and no history of preoperative chemotherapy, radiotherapy or immunotherapy. From a total of 125 patients admitted during this period, 49 eligible patients were recruited and staged according to the International Union against Cancer Classification. After signing informed consent forms, the patients were randomized into treatment group ($n=25$) and control group ($n=24$). The clinico-pathological characteristics of the two groups were comparable and balanced. The patients in treatment group started oral CIM treatment (Tagamet, Tianjin Smith Kline and French Laboratories Ltd.) at the dose of 400 mg, tid, 7 days before operation until the operation day. During and after operation, they were given CIM at 600 mg, i.v. drip, bid, until the 10th postoperative day. The patients in control group received similar routine treatment except for perioperative CIM intervention. All the patients in both groups underwent curative resection of cancer.

Separation of peripheral blood mononuclear cells (PBMCs) and immunocytochemical staining

From all the patients in both groups, 2 ml of venous blood was taken and heparinized at admission, before operation, on the 2nd and the 10th postoperative days, respectively. PBMCs were obtained immediately by standard Ficoll-Hypaque gradient centrifugation at 2 000 rpm for 20 min at 4 °C and smeared onto slides, dried and fixed for immunocytochemical staining. The primary antibodies were mouse-anti-human CD₃, CD₄, CD₈ and CD₅₇ monoclonal antibodies (Sigma Chemical Company, St Louis, MO, USA) for the detection of total T lymphocytes, helper T lymphocytes, inhibitor T lymphocytes and natural killer (NK) cells, respectively. The primary antibody was visualized with avidin-biotin-peroxidase supersensitive kit (Wuhan Boster Bioengineering Co. Ltd., Wuhan, China). The slides were counterstained with methyl green. PBMCs from 20 healthy controls were processed in the same way as normal controls.

The slides were mounted and viewed under binocular microscope (Olympus, Japan) by an independent viewer. Positive cells were stained green in nuclei and yellow-brown in cytoplasm and cell membrane (Figure 1). A total of 200 cells were counted on each slide and positive cells were recorded. The immunocytochemical staining procedure was repeated 3 times and the percentage of each cell subpopulation was calculated and expressed as mean \pm standard deviation ($\bar{x}\pm s$).

Immunohistochemical study on TIL in surgical specimens

Immediately after resection, the specimens were cut open and washed clean. For each patient, three pieces of tumor samples were taken at different sites from the peripheral margin of the tumor, fixed in 10% neutral formalin and processed in standard histopathology procedure. For observation of TIL responses, conventional HE staining was performed on the 4 μ m thick tissue sections. Immunohistochemical staining on the sections was conducted for subpopulation study of TIL, with anti-CD₃ monoclonal antibody to recognize T lymphocytes and anti-CD₂₀ monoclonal antibody to recognize B lymphocytes (both from Sigma). The immunohistochemical staining procedure followed a standard protocol. The sections were

counterstained by hematoxylin, mounted and interpreted under microscope. The number of TIL was recorded in five high power (HP, 200 \times) view fields randomly chosen at the tumor border. The degree of TIL response was determined based on a modified grading system by Jass^[21]. Grade I (\pm): no TIL response, in which there were less than 10 infiltrating lymphocytes per HP view field; grade II (+): mild TIL response, in which there were 10-100 infiltrating lymphocytes per HP view field; grade III (++) : intermediate TIL response, in which there were 101-200 infiltrating lymphocytes per HP view field; and grade IV (+++) : prominent TIL response in which there were over 201 infiltrating lymphocytes per HP view field. Grades I and II TIL responses were defined as poor responses and grades III and IV lymphocyte responses as significant responses.

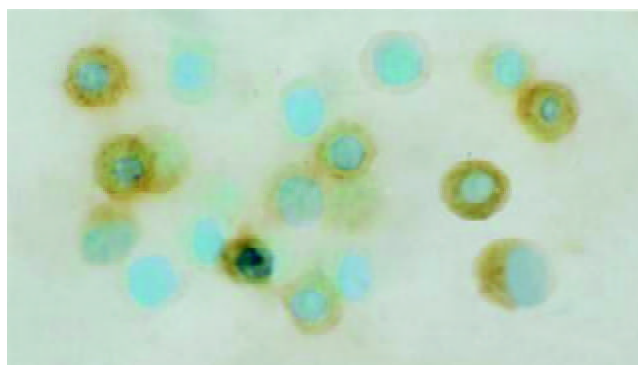


Figure 1 Immunocytochemical staining of PBMCs with monoclonal antibodies to CD₃, CD₄, CD₈ and CD₅₇. Positive cells were stained green in the nuclei and yellow-brown in cytoplasm and cell membrane. The microphoto showed CD₃ positive cells.

Statistical analysis

All data were expressed as mean \pm standard deviation ($\bar{x}\pm s$). Analysis of variance (ANOVA) was used to process the data within groups. Student's *t* test and *chi*-square test were used to evaluate the differences between groups. For the comparison in TIL response among different tumor TNM stages, Fisher's exact test was used. All the tests were two-tailed with a level of significance $P=0.05$.

RESULTS

Clinico-pathological characteristics of patients

A total of 49 eligible patients were enrolled in this study, 25 of whom were randomized into treatment group and 24 into control group. Their clinico-pathological characteristics are detailed in Table 1. There were no statistically significant differences in demographic and histopathologic variables between the two groups ($P>0.05$) (Table 1).

Percentages of lymphocyte subpopulations at baseline

At randomization, the percentages of CD₃⁺, CD₄⁺, CD₅₇⁺ cells and the CD₄⁺/CD₈⁺ ratio in both treatment and control groups were lower than those in normal control ($P<0.001$), and the percentage of CD₈⁺ cells was higher in treatment and control groups than in normal control ($P<0.05$) (Table 2). There were no statistically significant differences between the treatment and control groups in the percentages of the above parameters, implying that the patients were well balanced with regard to peripheral lymphocyte subpopulations at randomization. The results indicated that the cellular immunity was significantly decreased in patients with GI cancer in this study population.

Table 1 Clinico-pathological characteristics of 49 GI cancer patients

Parameters	Treatment group (n=25)	Control group (n=24)
Age (y)		
Mean (range)	50 (25-73)	53 (27-78)
Gender		
Male	13	16
Female	12	8
Tumor sites		
Stomach	6	5
Colon	3	3
Rectum	16	16
Pathological types		
Tubular adenocarcinoma	14	12
Papillary adenocarcinoma	3	3
Villous adenocarcinoma	2	1
Signet-ring-cell carcinoma	2	3
Mucous adenocarcinoma	4	5
TNM stages		
I	3	5
II	7	9
III	9	6
IV	6	4
Tumor differentiation		
Well differentiated	5	6
Moderately differentiated	8	7
Poorly differentiated	12	11

All the variables showed no statistically significant differences between the two groups ($P>0.05$).

Table 2 Baseline values of lymphocyte subpopulations in peripheral blood mononuclear cells of normal control, treatment and control groups (%; $\bar{x}\pm s$)

Groups	n	CD ₃ ⁺	CD ₄ ⁺	CD ₈ ⁺	CD ₅₇ ⁺	CD ₄ ⁺ /CD ₈ ⁺
Normal control	20	67.1±6.3	40.2±5.1	27.7±5.0	18.5±2.31	1.49/0.24
Treatment	25	60.8±6.3 ^b	33.6±4.2 ^b	30.6±5.2	14.8±4.4 ^a	1.15±0.34 ^b
Control	24	60.5±4.6 ^b	33.4±3.7 ^b	31.0±3.9 ^a	15.0±2.8 ^a	1.11±0.25 ^b

^a $P<0.05$ vs normal control, ^b $P<0.01$ vs normal control.

Changes in lymphocyte subpopulations in PBMCs during CIM treatment

During the perioperative period, dynamic changes in the percentages of peripheral blood lymphocyte subpopulations were observed in both treatment and control groups. Preoperative treatment with CIM for 1 wk had positive effects on the percentages of CD₃⁺, CD₄⁺ lymphocytes, and CD₄⁺/CD₈⁺ ratio. CD₃⁺ cells were increased from 60.8±6.3% at randomization to 63.0±4.9% after CIM treatment for 1 wk. After operation, CD₃⁺ cells were decreased to 60.3±5.4% on the 2nd postoperative day, and recovered gradually thereafter until it reached 64.2±3.9% on the 10th postoperative day, which was higher than the pretreatment level. In contrast, the percentage of CD₃⁺ cells in control group continued declining during the perioperative period, and became significantly lower than that in the treatment group on both the 2nd and 10th postoperative days. The changes in CD₄⁺ and CD₅₇⁺ cells followed a similar pattern (Table 3, Figures 2, 3, 4).

Effects of CIM treatment on TIL

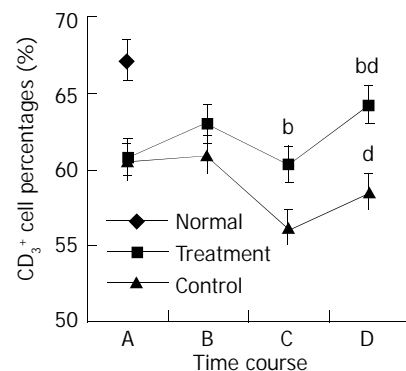
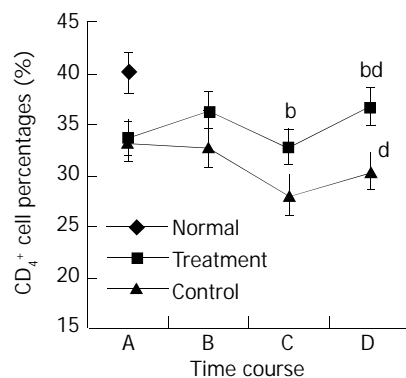
In addition to routine histopathological examinations of

resected specimens, all the tumor sections were reviewed for the presence of peritumor lymphocytes and TIL responses. Six out of 24 patients (25%) in control group had discernible lymphocyte infiltration in the peritumor area, whereas 17 out of 25 cases (68%) in CIM treatment group had obvious TIL responses ($P<0.01$) (Table 4).

Table 3 Changes of lymphocytes and NK cells in perioperative period (%; $\bar{x}\pm s$)

Items	Groups	Perioperative period			
		A	B	C	D
CD ₃ ⁺	Treatment	60.8±6.3	63.0±4.9 ^d	60.3±5.4 ^a	64.2±3.9 ^d
	Control	60.5±4.6	61.0±2.7	56.2±3.8 ^{bd}	58.6±4.0 ^{ab}
CD ₄ ⁺	Treatment	33.6±4.2	36.3±3.4 ^a	32.8±4.0 ^d	36.6±6.2 ^d
	Control	33.4±3.7	32.8±3.3 ^b	28.1±3.4 ^{bd}	30.4±3.3 ^{ab}
CD ₈ ⁺	Treatment	30.6±5.2	29.6±4.3	31.1±4.3	29.4±3.6
	Control	31.0±3.9	31.2±4.8	32.9±4.4 ^a	32.1±5.3
CD ₅₇ ⁺	Treatment	14.8±4.4	15.7±3.8	17.2±3.7	21.1±4.5 ^b
	Control	15.0±2.8	13.1±2.5	14.2±2.2 ^b	15.6±1.7 ^b
CD ₄ ⁺ / CD ₈ ⁺	Treatment	1.15±0.34	1.25±0.23 ^a	1.08±0.21 ^d	1.27±0.30 ^d
	Control	1.11±0.25	1.08±0.22 ^b	0.87±0.17 ^{bd}	0.98±0.24 ^{ab}

A: at admission, B: before operation, C: on the 2nd postoperative day, D: on the 10th postoperative day. ^a $P<0.05$, ^d $P<0.01$, B vs A, C vs B, D vs C; ^b $P<0.01$ vs treatment group.

**Figure 2** Changes in CD₃⁺ cell percentages in perioperative period. A: at randomization; B: before operation; C: on the 2nd postoperative day; and D: on the 10th postoperative day. The difference in CD₃⁺ percentages between treatment and control groups at time points C and D was statistically significant, ^b $P<0.01$. The difference in CD₃⁺ percentages on the 10th postoperative day and the randomization day was statistically significant for both treatment and control groups, ^d $P<0.01$.**Figure 3** Changes in CD₄⁺ cell percentages in perioperative period. A: at randomization; B: before operation; C: on the 2nd postoperative day; and D: on the 10th postoperative day. The difference in CD₄⁺ percentages between treatment and control

groups at time points C and D was statistically significant, ^b*P*<0.01. The differences in CD₄⁺ percentages on the 10th postoperative day and the randomization day was statistically significant for both treatment and control groups, ^d*P*<0.01.

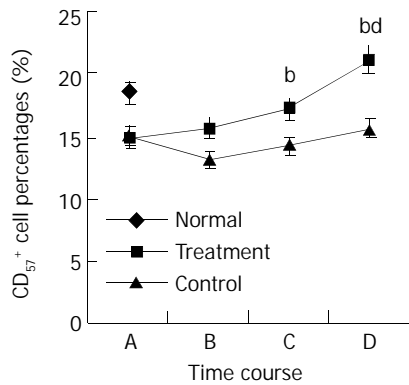


Figure 4 Changes in CD₅₇⁺ cell percentages in perioperative period. A: at randomization; B: before operation; C: on the 2nd postoperative day; and D: on the 10th postoperative day. The difference in CD₅₇⁺ percentages between treatment and control groups at time points C and D was statistically significant, ^b*P*<0.01. The differences in CD₅₇⁺ percentages between treatment group and normal control on the 10th postoperative day was statistically significant, ^d*P*<0.01.

Table 4 TIL responses in treatment and control groups

Groups	SR		PR		Total	Rate (%)
	+++	++	+	+		
Treatment	9	8	6	2	25	68 ^b
Control	2	4	9	9	24	25
Total	23		26		49	

SR=significant response, PR=poor response. ^b*P*<0.01 vs control group, *chi-square* test.

There was a negative correlation between TIL response and the clinico-pathological stages of the tumor (Table 5). In control group, TIL responses were mainly observed in TNM stages I and II cases, and there were very few peritumor lymphocyte responses in stages III and IV cases. In contrast, there were obvious TIL responses in 78% (7/9) of TNM stage III cases and 83% (5/6) of stage IV cases in CIM treatment group, both of which were significantly higher than those in control group (*P*<0.05 and *P*<0.01, respectively, Fisher's exact test) (Figure 4). Immunohistochemical studies of the specimens revealed that most of the TILs were CD₃⁺ T lymphocytes clustered around tumor tissues. There were few CD₂₀⁺ cells in TIL population.

Table 5 Comparison in TIL responses by TNM stages between control and treatment groups

TNM stages	Groups	Poor response	Significant response	Response rate (%)
I	Treatment	2	1	33
	Control	3	2	40
II	Treatment	3	4	57
	Control	6	3	33
III	Treatment	2	7	78 ^a
	Control	5	1	17
IV	Treatment	1	5	83 ^b
	Control	4	0	0

^a*P*<0.05, ^b*P*<0.01, vs control (Fisher's exact test).

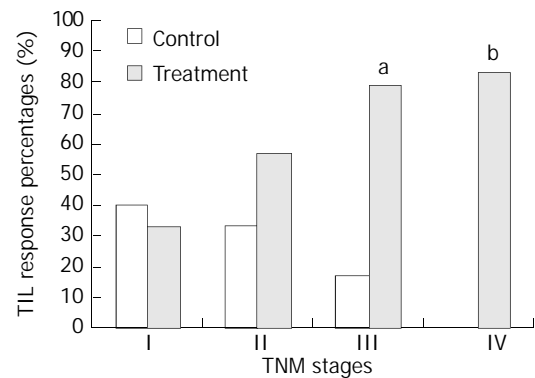


Figure 5 TIL responses in surgical specimens in treatment and control groups. In control group, there was a progressive decrease in TIL responses with increase of TNM staging. On the other hand, the treatment group showed a steady increase in TIL responses after CIM treatment for 1 wk. The differences in TIL response rates were statistically significant between treatment and control groups for TNM stages III and IV diseases (^a*P*<0.05 and ^b*P*<0.01, respectively, Fisher's exact test).

DISCUSSION

To date, surgical resection remains the only approach that can offer possible cure for GI cancer patients. However, operation itself is a double-edged sword to cancer patients in terms of tumor immunology. On the one hand, a successful operation can remove tumor burden which is immuno-suppressive. This will help bring about an improved clinical outcome for most patients. On the other hand, the operation itself is a major blow to the immune system. Lines of evidence suggest that surgical patients undergo a period of immunodepression immediately after operation, the length of which depends on many factors such as the general status of the patients, extent of the operation itself, pre-operative treatment. Previous studies demonstrated that T helper cells decreased and T suppressor cells increased significantly as early as 1 day after surgery.^[22-24] Many subsequent studies also confirmed that surgery for patients with lung cancer^[25], esophageal cancer^[26], gastric cancer^[27,28] and colorectal cancer^[29,30] induced immediate severe immunosuppression. For cancer patients, an important function adversely affected by this immunosuppression is the anti-tumor response itself. This immunosuppression might increase the chance of accelerated growth of residual tumors or micro-metastases already present at the time of surgical resection. As a result, postoperative immunosuppression maybe one of the major contributing factors for post-operative recurrence and metastases. Indeed our previous study found a local recurrent rate as high as 34.27% for rectal cancer 5 years after curative resection, most of which (89.04%) occurred 3 years after operation^[31]. Other studies also revealed that 7% to 65% of rectal cancer patients would develop local recurrence after curative surgery^[32-34]. Therefore, how to effectively improve peri-operative immunity of GI cancer patients remains a major challenge of significant clinical importance.

Many researches have been conducted to tackle this problem, and one approach is to use small molecular immunomodulator drugs such as CIM, a histamine H₂ receptor antagonist. It has long been observed that histamine was a growth factor for certain cancers and could, by itself, stimulate tumor cell proliferation^[18-20]. As one of the many important chemo-mediators involved in immune responses, histamine had inhibitory effects on immune response^[35-38] via its H₂ receptors^[39]. It was discovered that T suppressor cells, which are part of the regulatory arm of the immune system, could express histamine receptors on their surface^[40-42], and histamine was capable of suppressing the immune response by activating

these T suppressor cells^[43]. Many tumors, particularly colorectal cancer, secrete histamine resulting in elevated histamine levels within the tumor. Histamine is also often secreted in response to surgical resection of colorectal cancers. All these factors working together will create an immuno-suppressive environment both in the area of tumor growth and in the whole body, facilitating tumor growth.

Several clinical studies have shown that administration of CIM could help reduce the immuno-suppression due to increased histamine level in the tumor environment^[15,16,44-46]. *In vitro* studies also demonstrated that CIM could inhibit the adhesion of some breast cancer cells^[47], and the adhesion of human colon cancer cells to human umbilical cord cells^[48], a very important step in tumor growth and progression. *In vivo* experimental studies also showed that daily administration of CIM to a mouse model of colon cancer significantly retarded tumor growth by up-regulating the expression of tumor-suppressive cytokines^[49], and the use of CIM also retarded the growth of human melanoma in a nude mouse model and prolonged the survival of tumor bearing SCID mice by directly inhibiting the proliferation of tumor cells and indirectly promoting the infiltration of activated macrophages to tumor site^[50,51].

In line with previous findings, our study discovered the diminished cellular immunity in GI cancer patients. Compared with normal controls, the total T lymphocytes (CD₃⁺), T helper lymphocytes (CD₄⁺), and NK cells (CD₅₇⁺) were significantly decreased in GI cancer patients. This reflects the nature that GI tumor burden exerts inhibitory effects on immune system. Moreover, the percentages of these immune cells showed a continuously declining trend with the progression of the disease, as reflected by the finding that patients with advanced TNM stage tumors had a more profound decrease in these immune cells than those with early stage tumors. Surgery itself, while removing the tumor burden, did have a temporary negative impact on host cellular immunity, as reflected by the marked decline in total T lymphocytes, T helper cells and NK cells in the immediate post-operative period. This decline continued with a downhill course in control group, in which no immunity-boosting therapies were given besides conventional surgical treatment. It is noteworthy that total T cells, T helper cells and NK cells did not return to baseline level 10 days after curative resection. This again highlighted the fact that while most patients in control group were physically recovered from operation at this time, they were far from immunologically recovered, and some interventional measures should be warranted to facilitate the recovery of cellular immune functions.

In contrast to control group, patients in treatment group showed favorable responses to CIM therapy in terms of cellular immunity parameters. After CIM treatment for 1 wk, total T cells, T helper cells and NK cells showed a slow but steady increase, although the increments did not reach statistical significance for NK cells, they did reach statistical significance for both total T cells and T helper cells. However, their levels were still lower than those found in normal controls, implying that while GI cancer patients have reduced their cellular immunity, they were nevertheless responsive to immunity-boosting measures, although such measures alone could not efficiently restore the hosts' cellular immunity to the level of normal controls. The data demonstrated again that surgery itself reduced cellular immunity, but to a much less degree, as a result of CIM treatment. Moreover, such reductions were quickly addressed and a positive balance was reached 10 days after CIM treatment, as reflected by the fact that the total T cells, T helper cells and NK cells on the 10th postoperative day were significantly higher than the baseline level (at randomization). Although total T cells, T helper cells were not up to the level of normal controls, NK cells did exceed the

level of normal controls. If the cellular immunity parameters for both treatment and control groups on the 10th postoperative day were analyzed, it would be obvious that CIM treatment did exert remarkable boosting effects on cellular immunity parameters.

The current study also demonstrated that immunity-enhancing effects of CIM treatment were not limited to peripheral blood immune cells alone, it also enhanced TIL response at the tumor site, as was revealed by the findings that while 25% of the patients in the control group had discernible TIL responses in the peri-tumor area, as high as 68% of cases in the treatment group showed obvious TIL responses. As demonstrated by immunohistochemical studies, most of the TILs were T lymphocytes. TILs have been found to be the highly effective tumoricidal lymphocytes^[52-54], and TIL treatment could decrease the relapse rate and prolong the survival of stage III melanoma patients with one positive lymph node^[55,56], and the overall survival of stage IV gastric and colorectal cancers^[57,58], and induce regression of metastatic tumors in the lung, liver and lymph nodes in patients with advanced melanoma after lymphodepletion^[59]. The enhanced TIL response at the tumor site induced by CIM treatment, therefore, might help reduce tumor aggressiveness and promote local control.

In summary, the current randomized clinical trial demonstrated that perioperative administration of CIM to GI cancer patients helped accelerate the recovery of cellular immunity and boost TIL responses at the tumor sites. This has potential therapeutic implications. Since circulating T lymphocytes and NK cells are major defense mechanisms against tumor cells released into the circulation, and TIL is one of the most crucial factors restricting local tumor growth and progression, it is desirable to use it as an immunomodulator in the perioperative period. Moreover, since CIM has many other favorable effects besides immunomodulation on lymphocytes, such as activating macrophages, increasing tumor inhibitory cytokines^[49], enhancing the antigen presenting capacity of dendritic cells^[60], reducing tumor cell proliferation, inhibiting tumor cell metastasis via anti-adhesion mechanisms^[49] and increasing the overall survival of colorectal cancer patients with high levels of sialyl Lewis-X and sialyl Lewis-A epitope expression on tumor cells^[61], it is therefore advisable to use this low cost, convenient and almost nontoxic drug as a practical immunity-enhancing measure for GI cancer patients.

REFERENCES

- 1 **Yip D**, Strickland AH, Karapetis CS, Hawkins CA, Harper PG. Immunomodulation therapy in colorectal carcinoma. *Cancer Treat Rev* 2000; **26**: 169-190
- 2 **Weiss G**, Meyer F, Matthies B, Pross M, Koenig W, Lippert H. Immunomodulation by perioperative administration of n-3 fatty acids. *Br J Nutr* 2002; **87** (Suppl 1): S89-94
- 3 **Shibata M**, Nezu T, Kanou H, Nagata Y, Kimura T, Takekawa M, Ando K, Fukuzawa M. Immunomodulatory effects of low dose cis-Diaminedichloroplatinum (cisplatin) combined with UFT and PSK in patients with advanced colorectal cancer. *Cancer Invest* 2002; **20**: 166-173
- 4 **Wu GH**, Zhang YW, Wu ZH. Modulation of postoperative immune and inflammatory response by immune-enhancing enteral diet in gastrointestinal cancer patients. *World J Gastroenterol* 2001; **7**: 357-362
- 5 **Tayama E**, Hayashida N, Fukunaga S, Tayama K, Takaseya T, Hiratsuka R, Aoyagi S. High-dose cimetidine reduces proinflammatory reaction after cardiac surgery with cardiopulmonary bypass. *Ann Thorac Surg* 2001; **72**: 1945-1949
- 6 **Bai DJ**, Yang GL, Yuan HY, Li Y, Wang K. Effects of cimetidine on T lymphocyte subsets in perioperative gastrointestinal cancer patients. *Shijie Huaren Xiaohua Zazhi* 2000; **8**: 147-149
- 7 **Adams WJ**, Morris DL. Short-course cimetidine and survival with

- colorectal cancer. *Lancet* 1994; **344**: 1768-1769
- 8 **Matsumoto S.** Cimetidine and survival with colorectal cancer. *Lancet* 1995; **346**: 115
 - 9 **Svendson LB,** Ross C, Knigge U, Frederiksen HJ, Graversen P, Kjaergard J, Luke M, Stimpel H, Sparso BH. Cimetidine as an adjuvant treatment in colorectal cancer. A double-blind, randomized pilot study. *Dis Colon Rectum* 1995; **38**: 514-518
 - 10 **Hellstrand K,** Naredi P, Lindner P, Lundholm K, Rudenstam CM, Hermodsson S, Asztely M, Hafstrom L. Histamine in immunotherapy of advanced melanoma: a pilot study. *Cancer Immunol Immunother* 1994; **39**: 416-419
 - 11 **Creagan ET,** Ahmann DL, Green SJ, Long HJ, Frytak S, Itri LM. Phase II study of recombinant leukocyte A interferon (IFN- α) plus cimetidine in disseminated malignant melanoma. *J Clin Oncol* 1985; **3**: 977-981
 - 12 **Sagaster P,** Micksche M, Flamm J, Ludwig H. Randomised study using IFN- α versus IFN- α plus coumarin and cimetidine for treatment of advanced renal cell cancer. *Ann Oncol* 1995; **6**: 999-1003
 - 13 **Morris DL,** Adams WJ. Cimetidine and colorectal cancer-old drug, new use? *Nat Med* 1995; **1**: 1243-1244
 - 14 **Sasson AR,** Gamagami R, An Z, Wang X, Moossa AR, Hoffman RM. Cimetidine: an inhibitor or promoter of tumor growth? *Int J Cancer* 1999; **81**: 835-838
 - 15 **Kelly MD,** King J, Cherian M, Dwerryhouse SJ, Finlay IG, Adams WJ, King DW, Lubowski DZ, Morris DL. Randomized trial of preoperative cimetidine in patients with colorectal carcinoma with quantitative assessment of tumor-associated lymphocytes. *Cancer* 1999; **85**: 1658-1663
 - 16 **Hansbrough JF,** Zapata-Sirvent RL, Bender EM. Prevention of alterations in postoperative lymphocyte subpopulations by cimetidine and ibuprofen. *Am J Surg* 1986; **151**: 249-255
 - 17 **Adams WJ,** Morris DL, Ross WR, Lubowski DZ, King DW, Peters L. Cimetidine preserves non-specific immune function after colonic resection for cancer. *Aust N Z J Surg* 1994; **64**: 847-852
 - 18 **Adams WJ,** Lawson JA, Morris DL. Cimetidine inhibits *in vivo* growth of human colon cancer and reverses histamine stimulated *in vitro* and *in vivo* growth. *Gut* 1994; **35**: 1632-1636
 - 19 **Lawson JA,** Adams WJ, Morris DL. Ranitidine and cimetidine differ in their *in vitro* and *in vivo* effects on human colonic cancer growth. *Br J Cancer* 1996; **73**: 872-876
 - 20 **Reynolds JL,** Akhter J, Morris DL. *In vitro* effect of histamine and histamine H1 and H2 receptor antagonists on cellular proliferation of human malignant melanoma cell lines. *Melanoma Res* 1996; **6**: 95-99
 - 21 **Jass JR,** Ajioka Y, Allen JP, Chan YF, Cohen RJ, Nixon JM, Radjokovic M, Restall AP, Stables SR, Zwi LJ. Assessment of invasive growth pattern and lymphocytic infiltration in colorectal cancer. *Histopathology* 1996; **28**: 543-548
 - 22 **Hansbrough JF,** Bender EM, Zapata-Sirvent R, Anderson J. Altered helper and suppressor lymphocyte populations in surgical patients. A measure of postoperative immunosuppression. *Am J Surg* 1984; **148**: 303-307
 - 23 **Nichols PH,** Ramsden CW, Ward U, Sedman PC, Primrose JN. Perioperative immunotherapy with recombinant interleukin 2 in patients undergoing surgery for colorectal cancer. *Cancer Res* 1992; **52**: 5765-5769
 - 24 **Espi A,** Arenas J, Garcia-Granero E, Marti E, Lledo S. Relationship of curative surgery on natural killer cell activity in colorectal cancer. *Dis Colon Rectum* 1996; **39**: 429-434
 - 25 **Leaver HA,** Craig SR, Yap PL, Walker WS. Lymphocyte responses following open and minimally invasive thoracic surgery. *Eur J Clin Invest* 2000; **30**: 230-238
 - 26 **van Sandick JW,** Gisbertz SS, ten Berge JJ, Boermeester MA, van der Pouw Kraan TC, Out TA, Obertop H, van Lanschot JJ. Immune responses and prediction of major infection in patients undergoing transhiatal or transthoracic esophagectomy for cancer. *Ann Surg* 2003; **237**: 35-43
 - 27 **Sato N,** Endo S, Kimura Y, Ikeda K, Aoki K, Iwaya T, Akiyama Y, Noda Y, Saito K. Influence of a human protease inhibitor on surgical stress induced immunosuppression. *Dig Surg* 2002; **19**: 300-305
 - 28 **Yao XX,** Yin L, Sun ZC. The expression of hTERT mRNA and cellular immunity in gastric cancer and precancerosis. *World J Gastroenterol* 2002; **8**: 586-590
 - 29 **Braga M,** Vignali A, Zuliani W, Radaelli G, Gianotti L, Martani C, Toussoun G, Di Carlo V. Metabolic and functional results after laparoscopic colorectal surgery: a randomized, controlled trial. *Dis Colon Rectum* 2002; **45**: 1070-1077
 - 30 **Wang YX,** Ruan CP, Li L, Shi JH, Kong XT. Clinical significance of changes of perioperative T cell and expression of its activated antigen in colorectal cancer patients. *World J Gastroenterol* 1999; **5**: 181-182
 - 31 **Yuan HY,** Li Y, Yang GL, Bei DJ, Wang K. Study on the causes of local recurrence of rectal cancer after curative resection: analysis of 213 cases. *World J Gastroenterol* 1998; **4**: 527-529
 - 32 **Ballantyne GH,** Quin J. Surgical treatment of liver metastases in patients with colorectal cancer. *Cancer* 1993; **71**(12 Suppl): 4252-4266
 - 33 **Vaughn D,** Haller DG. Nonsurgical management of recurrent colorectal cancer. *Cancer* 1993; **71**: 4278-4292
 - 34 **Turk PS,** Wanebo HJ. Results of surgical treatment of nonhepatic recurrence of colorectal carcinoma. *Cancer* 1993; **71**(12 Suppl): 4267-4277
 - 35 **Beer DJ,** Rocklin RE. Histamine-induced suppressor-cell activity. *J Allergy Clin Immunol* 1984; **73**: 439-452
 - 36 **Lima M,** Rocklin RE. Histamine modulates *in vitro* IgG production by pokeweed mitogen-stimulated human mononuclear cells. *Cell Immunol* 1981; **64**: 324-336
 - 37 **Rocklin RE,** Blidy A, Kamal M. Physicochemical characterization of human histamine-induced suppressor factor. *Cell Immunol* 1983; **76**: 243-252
 - 38 **Uotila P.** Inhibition of prostaglandin E2 formation and histamine action in cancer immunotherapy. *Cancer Immunol Immunother* 1993; **37**: 251-254
 - 39 **Black JW,** Duncan WA, Durant CJ, Ganellin CR, Parsons EM. Definition and antagonism of histamine H2-receptors. *Nature* 1972; **236**: 385-390
 - 40 **Melmon KL,** Bourne HR, Weinstein J, Sela M. Receptors for histamine can be detected on the surface of selected leukocytes. *Science* 1972; **177**: 707-709
 - 41 **Osband M,** McCaffrey R. Solubilization, separation, and partial characterization of histamine H₁ and H₂ receptors from calf thymocyte membranes. *J Biol Chem* 1979; **254**: 9970-9972
 - 42 **Burtin C,** Scheinmann P, Salomon JC, Lespinats G, Canu P. Decrease in tumour growth by injections of histamine or serotonin in fibrosarcoma-bearing mice: Influence of H₁ and H₂ histamine receptors. *Br J Cancer* 1982; **45**: 54-60
 - 43 **Rocklin RE,** Greineder DK, Melmon KL. Histamine-induced suppressor factor (HSF): Further studies on the nature of the stimulus and the cell which produces it. *Cell Immunol* 1979; **44**: 404-415
 - 44 **Adams WJ,** Lawson JA, Nicholson SE, Cook TA, Morris DL. The growth of carcinogen-induced colon cancer in rats is inhibited by cimetidine. *Eur J Surg Oncol* 1993; **19**: 332-335
 - 45 **Nishiguchi S,** Tamori A, Shiomi S, Enomoto M, Tatsumi N, Koh N, Habu D, Sakaguchi H, Takeda T, Seki S, Nakamura K, Kubo S, Kinoshita H. Cimetidine reduces impairment of cellular immunity after transcatheter arterial embolization in patients with hepatocellular carcinoma. *Hepatogastroenterology* 2003; **50**: 460-462
 - 46 **Zhu Q,** Si F, Xu JY, Wu YL. Effect of Cimetidine against digestive tract tumors. *Huaren Xiaohua Zazhi* 1998; **6**: 68-69
 - 47 **Bobek V,** Boubelik M, Kovarik J, Taltyonov O. Inhibition of adhesion breast cancer cells by anticoagulant drugs and cimetidine. *Neoplasma* 2003; **50**: 148-151
 - 48 **Kobayashi K,** Matsumoto S, Morishima T, Kawabe T, Okamoto T. Cimetidine inhibits cancer cell adhesion to endothelial cells and prevents metastasis by blocking E-selectin expression. *Cancer Res* 2000; **60**: 3978-3984
 - 49 **Takahashi K,** Tanaka S, Ichikawa A. Effect of cimetidine on intratumoral cytokine expression in an experimental tumor. *Biochem Biophys Res Commun* 2001; **281**: 1113-1119
 - 50 **Szincsak N,** Hegyesi H, Hunyadi J, Falus A, Juhasz I. Different h2 receptor antihistamines dissimilarly retard the growth of xenografted human melanoma cells in immunodeficient mice. *Cell Biol Int* 2002; **26**: 833-836
 - 51 **Szincsak N,** Hegyesi H, Hunyadi J, Martin G, Lazar-Molnar E, Kovacs P, Rivera E, Falus A, Juhasz I. Cimetidine and a tamoxifen derivative reduce tumour formation in SCID mice xenotransplanted with a human melanoma cell line. *Melanoma Res* 2002; **12**: 231-240

- 52 **Rosenberg SA**, Spiess P, Lafreniere R. A new approach to the adoptive immunotherapy of cancer with tumor-infiltrating lymphocytes. *Science* 1986; **233**: 1318-1321
- 53 **Rosenberg SA**. Progress in human tumour immunology and immunotherapy. *Nature* 2001; **411**: 380-384
- 54 **Wang XZ**, Li B, Zheng XX, Qu YZ, Lin GZ, Tang NH, Chen ZX. Experimental and clinical study on tumor infiltrating lymphocytes in solid tumor. *Xin Xiaohuabingxue Zazhi* 1997; **5**: 481-482
- 55 **Dreno B**, Nguyen JM, Khammari A, Pandolfino MC, Tessier MH, Bercegeay S, Cassidanius A, Lemarre P, Billaudel S, Labarriere N, Jotereau F. Randomized trial of adoptive transfer of melanoma tumor-infiltrating lymphocytes as adjuvant therapy for stage III melanoma. *Cancer Immunol Immunother* 2002; **51**: 539-546
- 56 **Labarriere N**, Pandolfino MC, Gervois N, Khammari A, Tessier MH, Dreno B, Jotereau F. Therapeutic efficacy of melanoma-reactive TIL injected in stage III melanoma patients. *Cancer Immunol Immunother* 2002; **51**: 532-538
- 57 **Kono K**, Takahashi A, Ichihara F, Amemiya H, Iizuka H, Fujii H, Sekikawa T, Matsumoto Y. Prognostic significance of adoptive immunotherapy with tumor-associated lymphocytes in patients with advanced gastric cancer: a randomized trial. *Clin Cancer Res* 2002; **8**: 1767-1771
- 58 **Liu SC**, Yuan SZ. Relationship between infiltration of dendritic cells, pericancerous lymphocytic reaction and prognosis in colorectal carcinomas. *Xin Xiaohuabingxue Zazhi* 1997; **5**: 156-157
- 59 **Dudley ME**, Wunderlich JR, Robbins PF, Yang JC, Hwu P, Schwartzentruber DJ, Topalian SL, Sherry R, Restifo NP, Hubicki AM, Robinson MR, Raffeld M, Duray P, Seipp CA, Rogers-Freezer L, Morton KE, Mavroukakis SA, White DE, Rosenberg SA. Cancer regression and autoimmunity in patients after clonal repopulation with antitumor lymphocytes. *Science* 2002; **298**: 850-854
- 60 **Kubota T**, Fujiwara H, Ueda Y, Itoh T, Yamashita T, Yoshimura T, Okugawa K, Yamamoto Y, Yano Y, Yamagishi H. Cimetidine modulates the antigen presenting capacity of dendritic cells from colorectal cancer patients. *Br J Cancer* 2002; **86**: 1257-1261
- 61 **Matsumoto S**, Imaeda Y, Umemoto S, Kobayashi K, Suzuki H, Okamoto T. Cimetidine increases survival of colorectal cancer patients with high levels of sialyl Lewis-X and sialyl Lewis-A epitope expression on tumour cells. *Br J Cancer* 2002; **86**: 161-167

Edited by Zhu LH and Wang XL

Response of TT virus to IFN plus ribavirin treatment in patients with chronic hepatitis C

Javier Moreno, Gloria Moraleda, Rafael Barcena, Mluisa Mateos, Santos del Campo

Javier Moreno, Rafael Barcena, Santos del Campo, Gloria Moraleda, Department of Gastroenterology, Hospital Ramon y Cajal, Facultad de Medicina, Universidad de Alcala, Madrid, Spain
Mluisa Mateos, Department of Microbiology, Hospital Ramon y Cajal, Madrid, Spain

Supported by Fundacion Manchega de Investigacion y Docencia en Gastroenterologia and partially by Red Nacional en Investigación de Hepatología y Gastroenterología (RNIHG)

Javier Moreno and Gloria Moraleda contributed equally to this work

Correspondence to: Dr. Rafael Barcena Marugan, Department of Gastroenterology, Hospital Ramon y Cajal, Ctra. Colmenar, Km 9.1, 28034 Madrid, Spain. rbarcena@hrc.insalud.es

Telephone: +34-91-3368093 **Fax:** +34-91-7291456

Received: 2003-08-11 **Accepted:** 2003-10-22

Abstract

AIM: TT virus (TTV) is a newly described DNA virus related to posttransfusion hepatitis that produces persistent viremia in the absence of clinical manifestations. PEG-IFN plus ribavirin have been useful in the treatment of chronic hepatitis C infection. This study investigated the responses of TT virus (TTV) and hepatitis C virus (HCV) to PEG-IFN plus ribavirin therapy.

METHODS: Fifteen patients infected with HCV were treated with PEG-IFN (0.5 µg/body weight/week) and ribavirin (1 000 mg-1 200 mg/daily) for 48 weeks. Blood samples were drawn at the beginning and the end of the therapy. Serum TTV DNA and HCV RNA were quantified by real time PCR.

RESULTS: At the beginning of treatment, TTV infection was detected in 10/15 (66.6%) of HCV-infected patients. Loss of serum TTV DNA at the end of therapy occurred in 6/10 (60%) patients. Out of these 6 patients, 4 (67%) became positive for TTV DNA after 6 months of therapy. Regarding HCV viremia, 11/15 (73%) patients were negative for serum HCV RNA after 48 weeks of therapy, 7/11 (64%) of these cases also became negative for TTV DNA following the combined treatment. In the 3/4 (75%) patients who were positive for HCV RNA at the end of therapy, TTV DNA was detected as well. Sustained HCV response at 6 months after treatment was 53% (8/15).

CONCLUSION: No TTV sustained response can be achieved in any patient after PEG-IFN plus ribavirin administration.

Moreno J, Moraleda G, Barcena R, Mateos M, del Campo S. Response of TT virus to IFN plus ribavirin treatment in patients with chronic hepatitis C. *World J Gastroenterol* 2004; 10(1): 143-146
<http://www.wjgnet.com/1007-9327/10/143.asp>

INTRODUCTION

TT virus (TTV) has been recently identified in patients with elevated alanine aminotransferase (ALT) levels following transfusions^[1]. TTV presents an extreme diffusion of active

infection throughout the world^[2]. It is known that TTV may be highly contagious although its way of spread is poorly understood. However, its high prevalence rate among the people receiving or being in contact with blood products could indicate that TTV can be parenterally transmitted^[3]. Although it has been proposed that TT virus be responsible for the small proportion of acute and chronic forms of hepatitis that still remain unsolved, no other illness has yet been attributed to the virus. The TTV genome is a circular, single-stranded DNA of negative polarity, which shares similarities with members of the Circoviridae family and, in contrast to DNA viruses, TTV isolates exhibit a high level of genetic heterogeneity^[4,5].

Hepatitis C virus (HCV) is the major cause of chronic liver infection which may progress to cirrhosis and eventually to hepatocellular carcinoma (HCC)^[6]. Recently, pegylated interferon (PEG-IFN), initially alone and later in combination with ribavirin, a nucleoside analogue with a broad antiviral activity against a variety of DNA and RNA viruses, has provided new perspectives for the treatment of most patients with chronic HCV infection^[7,8]. Co-infection of TTV and HCV is commonly seen maybe because both viruses share the same transmission routes such as blood transfusion^[9]. In previous studies, IFN therapy was reported to be effective against TTV^[10,11], but the possible susceptibility of the virus to the combination of PEG-IFN plus ribavirin treatment has not yet been investigated. Thus, we investigated the response of TTV infection to PEG-IFN plus ribavirin therapy in patients with chronic hepatitis C and evaluated whether PEG-IFN plus ribavirin combined therapy on chronic hepatitis C was influenced by a TTV co-infection.

MATERIALS AND METHODS

Patients

We enrolled randomly in the study 15 patients (11 males and 4 females, mean age: 41.6 years, range: 30 to 57 years) with chronic HCV infection who had undergone PEG-IFN plus ribavirin therapy. The diagnosis of chronic hepatitis was made on histological (stage of fibrosis and grade of activity) and biochemical liver function tests. Five patients had a history of blood transfusion, 6 acquired HCV infection by parenteral route (intravenous drug abusers, tattoos..) and in 4 patients the transmission route was unknown. Biochemical and virological features of the patients are shown in Table 1.

PEG-IFN was administered intramuscularly at a dose of 0.5 µg/body weight/week, ribavirin was given orally at a dose of 1 000-1 200 mg/daily (weight adjusted) for 48 weeks. Blood samples were taken at the baseline time and when therapy was stopped. To evaluate the effects of PEG-IFN plus ribavirin, levels of ALT, TTV DNA and HCV RNA were evaluated at each time. TTV and HCV clearance was defined as the disappearance of serum TTV DNA and HCV RNA after 48 weeks of combined treatment. All patients gave written informed consent before enrollment in the study, which was approved by the Ethics Committee of the hospital.

Detection and quantification of TTV DNA

Total DNA was purified from 200 µl of serum using the high

pure viral nucleic acid kit (Roche Diagnostic, Mannheim, Germany) and eluted in 50 μ l distilled water. TTV DNA was subjected to nested PCR for qualitative analysis. First PCR was performed with primer pair NG054/NG132^[12] and nested PCR with primer pair T801/T935^[13]. In those positive samples for viral DNA, TTV DNA quantification was carried out with real time PCR by the SYBR Green approach using primers targeting a fragment of the untranslated region (UTR) of the viral genome as previously described by Garcia *et al*^[14].

HCV markers

HCV antibodies (anti-HCV) were determined by immunoassay (Ortho Diagnostic System, Raritan, NJ). Serum HCV RNA levels were measured using the Amplicor HCV monitor test (Roche). HCV genotyping was carried out using the Inno-Lipa HCV test (Innogenetics).

Statistical analysis

Statistical analyses were performed using Student's *t* test. Data were analyzed with the computer program SPSS (SPSS Inc., Chicago, IL, USA). A probability (*P*) value less than 0.05 was considered statistically significant.

RESULTS

Detection and response of TTV to PEG-IFN plus ribavirin therapy

Fifteen patients infected with HCV were monitored randomly for levels of TTV and HCV in serum, at the beginning and end of PEG-IFN plus ribavirin combined treatment. Of the 15 patients, serum TTV DNA could be detected in 10/15 (67%) by real time PCR at the beginning of therapy, with a TTV value that ranged from 1.3×10^3 to 1.7×10^5 genomes/ml of serum (mean: 3.4×10^4 genomes/ml). After 48 weeks of PEG-

IFN plus ribavirin therapy, 6/10 patients (60%) lost serum TTV DNA. Regarding the 4 patients who still had detectable serum TTV DNA, TTV value ranged from 10^3 to 4×10^4 genomes/ml of serum (mean: 1.4×10^4 genomes/ml). In 3/4 patients (75%) positive for TTV, circulating HCV RNA was detected simultaneously after completion of the combined therapy. With respect to these 4 positive TTV DNA patients, at the end of treatment and relative to baseline levels, 3 patients (75%) had a reduction of serum TTV load and 1 case (25%) presented an increase in the levels of serum TTV DNA. The latter patient presented a grade III fibrosis while the remaining 3 individuals presented a grade I fibrosis (Table 1).

When TTV DNA was analyzed at 6 months after stopping PEG-IFN plus ribavirin administration, four responders (67%) had a relapse of TTV viremia, in the 2 remaining cases no serum samples were available (Table 1). The 4 patients, who did not eliminate TTV DNA at the end of treatment, still maintained DNA during the follow-up period. With respect to the 5 TTV DNA negative patients at the beginning of therapy, 1 (20%) became positive for TTV after stopping combined therapy, 2 (40%) cases remained negative for TTV and in 2 individuals viral marker was not determined (Table 1).

Serum TTV DNA level with respect to HCV in non-responder and responder patients to PEG-IFN plus ribavirin treatment was also analyzed and no statistically significant differences were found when pretreatment serum samples were compared between both groups ($P=0.281$). However, we observed that those patients eliminating TTV at the end of therapy presented a lower basal HCV load when compared with the non-responder TTV patients (1.1×10^6 vs 2.1×10^6 genomes/ml, respectively $P=0.03$). Regarding the changes of ALT levels, no statistical differences were observed when they were analyzed between TTV responder and non-responder (Table 2). In contrast, serum ALT level was persistently maintained

Table 1 Features of patients in the study

Patient No.	HCV Genotype	Fibrosis	Before treatment			End of treatment			6 months after treatment		
			ALT	TTV	HCV	ALT	TTV	HCV	ALT	TTV	HCV
1	1a	I	51	1.7×10^5	5×10^5	26	-	-	83	+	ND
2	1a	III	139	1.5×10^3	9.4×10^5	35	-	-	19	ND	-
3	1a	III	102	1.7×10^3	8×10^5	30	-	-	11	+	-
4	1b	III	225	1.1×10^4	1.1×10^6	29	4×10^4	-	27	+	-
5	1a	II	82	1.4×10^3	9×10^5	30	-	-	168	+	1.9×10^6
6	1b	III	92	1.3×10^3	1.5×10^6	42	-	-	48	+	-
7	3a	II	117	1.8×10^4	2.4×10^6	9	-	-	23	ND	-
8	1b	III	102	-	1.5×10^6	59	-	-	39	-	-
9	1b	I	86	5.7×10^4	7×10^5	30	1.3×10^4	6×10^5	44	+	9.9×10^5
10	1b	I	183	-	9×10^4	26	-	-	17	+	-
11	1a	I	77	-	2.5×10^6	16	-	-	27	ND	-
12	1b	I	72	4.6×10^4	2×10^5	36	10^3	3.5×10^5	76	+	5×10^5
13	1a	III	101	-	2.3×10^5	47	-	3×10^4	153	ND	+
14	1b	I	68	-	5×10^5	29	-	-	56	-	2×10^5
15	1a	I	29	3.1×10^4	6.3×10^6	13	2.5×10^3	2.1×10^6	30	+	+

ALT level was expressed as IU/L. TTV and HCV loads were expressed as viral genomes/ml of serum.

Table 2 Changes of ALT levels in TTV and HCV responder and non-responder patients to PEG-IFN plus ribavirin therapy

	TTV		<i>P</i> ^a	HCV		<i>P</i> ^a
	Responders (<i>n</i> =6)	Non-responders (<i>n</i> =4)		Responders (<i>n</i> =11)	Non-responders (<i>n</i> =4)	
Before therapy	97.16 \pm 30.18	103.0 \pm 84.87	0.09	112.54 \pm 51.90	72.00 \pm 31.01	0.33
End of therapy	28.66 \pm 11.09	27.00 \pm 9.83	0.92	30.09 \pm 12.96	31.50 \pm 14.20	0.76

ALT level was expressed as IU/L. ^aStudent's *t*-test.

in the normal range before and after the combined therapy in one patient who did not eliminate TTV and HCV (Table 2, patient No. 15).

HCV response to PEG-IFN plus ribavirin treatment

Pretreatment serum HCV RNA values ranged between 9×10^4 and 6.3×10^6 genomes/ml of serum (mean: 1.36×10^6 genomes/ml). The decline of HCV viremia was clearly evident after therapy and the response rate was 73% (11/15). When serum HCV RNA pretreatment levels were compared between non-responder and responder patients, the difference was statistically significant (1.85×10^6 vs 1.15×10^6 genomes/ml, respectively; $P=0.005$). Sustained HCV response after 6 months of treatment was found in 8/15 (53%) patients, 2 patients (13%) became HCV RNA positive during the follow-up period and in one case no serum sample was available for the detection of HCV RNA (Table 1). Following combined therapy, baseline and final ALT levels between responder and non-responder patients were compared but the differences between both groups were not statistically significant (Table 2).

DISCUSSION

Many studies have been done trying to assess whether TTV could cause liver disease, but its molecular properties and its pathogenic potential are still poorly understood. Different epidemiological studies have clearly indicated that TTV is a transmissible blood-borne virus sharing common transmission routes with hepatitis viruses. Then, coinfection of TTV was frequently observed in patients with chronic hepatitis C^[9]. We found that 66.6% of our patients infected with HCV were TTV DNA-positive, which confirms previous studies showing that the prevalence of TTV infection varied between 30%-88%^[15,16].

It has been reported that TTV infection treated with IFN alone had a response rate of 62%-83% after monotherapy^[11,17]. Our data showed that 60% of the TTV-infected patients could eliminate TT virus at the end of PEG-IFN plus ribavirin combination treatment. By comparing our results with earlier published studies, the novel and interesting information obtained from our work is that the treatment of TTV infection with PEG-IFN plus ribavirin, for a period of 48 weeks, did not promote an additional and increased response to therapy. Then, ribavirin did not produce any effect on TTV replication because of the similar sensitivity of TTV to combined treatment or to standard IFN monotherapy. Moreover, in these published studies the sustained TTV response after 6 months of therapy was decreased to 32%-50%^[18]. In contrast, in our series no sustained clearance of TTV was achieved in any patient after 6 months of combined therapy. It is well known that TTV tended to last many years^[19] although spontaneously resolved viremias after short periods of time were described in the literature^[20]. That the majority of our TTV responder patients relapsed during the follow-up period could suggest the possibility that TTV could become temporarily latent, as a result of the sensitivity of TTV to PEG-IFN during its administration, and that a new reinfection of the virus occurred. In other words, it was possible that TTV could persist in other type cells such as peripheral blood mononuclear cells where TTV persistence could occur^[10]. Among other explanations, it could be possible that because of TTV high level of genetic diversity, viral genomes with different PEG-IFN sensitivities could arise over time. Finally, we suggest that TTV response to PEG-IFN may be affected by a combination of virus and host factors as observed in other viruses^[21].

With respect to the effect of PEG-IFN plus ribavirin administration for the treatment of chronic hepatitis C, this study confirms earlier reports in which HCV infection responded positively to the combined therapy with a high rate

of viral clearance and normalization of ALT levels during the treatment period. Both factors occurred in HCV/TTV-coinfected patients as well as in non-coinfected ones, so it could be suggested that the response of HCV to IFN-PEG plus ribavirin treatment was not affected by TTV coinfection. Moreover, in those patients without sustained TTV response ALT levels were normal in contrast with those who had a HCV relapse. Then, in agreement with other published studies, TTV might not have any clinical association with producing HCV hepatitis^[16,22]. Furthermore, another interesting result from our study was that PEG-IFN plus ribavirin therapy seemed to be specially efficacious in patients with more advanced liver diseases such as grade III fibrosis. Thus, in 45.5% of HCV responder patients with advanced fibrosis, only 25% of non-responder ones presented a minor grade fibrosis, which supported the beneficial effect of PEG-IFN on patients with difficult-to-treat diseases reported in previous studies^[23,24].

In conclusion, TTV has a similar response rate to PEG-IFN plus ribavirin combined treatment or to IFN monotherapy, suggesting that neither PEG-IFN nor ribavirin has any additional effect on TTV replication. Furthermore, TTV relapse was found in most of the responder patients after the combined therapy was stopped for 6 months, so it seems likely that TTV is not as sensitive to PEG-IFN as HCV.

REFERENCES

- 1 **Nishizawa T**, Okamoto H, Konishi K, Yoshizawa H, Miyakawa Y, Mayumi M. A novel DNA virus (TTV) associated with elevated transaminase levels in posttransfusion hepatitis of unknown etiology. *Biochem Biophys Res Commun* 1997; **241**: 92-97
- 2 **Abe K**, Inami T, Asano K, Miyoshi C, Masaki N, Hayashi S, Ishikawa K, Takebe Y, Win KM, El Zayadi AR, Han KH, Zhang DY. TT virus infection is widespread in the general populations from different geographic regions. *J Clin Microbiol* 1999; **37**: 2703-2705
- 3 **Matsumoto A**, Yeo AE, Shih JW, Tanaka E, Kiyosawa K, Alter HJ. Transfusion-associated TT virus infection and its relationship to liver disease. *Hepatology* 1999; **30**: 283-288
- 4 **Miyata H**, Tsunoda H, Kazi A, Yamada A, Khan MA, Murakami J, Kamahora T, Shiraki K, Hino S. Identification of a novel GC-rich 113-nucleotide region to complete the circular, single-stranded DNA genome of TT virus, the first human circovirus. *J Virol* 1999; **73**: 3582-3586
- 5 **Hijikata M**, Takahashi K, Mishiro S. Complete circular DNA genome of a TT virus variant (isolate name SANBAN) and 44 partial ORF2 sequences implicating a great degree of diversity beyond genotypes. *Virology* 1999; **260**: 17-22
- 6 **Levero M**, Tagger A, Balsano C, De Marzio E, Avantaggiati ML, Natoli G, Diop D, Villa E, Diodati G, Alberti A. Antibodies to hepatitis C virus in patients with hepatocellular carcinoma. *J Hepatol* 1991; **12**: 60-63
- 7 **Brillanti S**, Garson J, Foli M, Whitby K, Deaville R, Masci C, Miglioli M, Barbara L. A pilot study of combination therapy with ribavirin plus interferon alfa for interferon alfa-resistant chronic hepatitis C. *Gastroenterology* 1994; **107**: 812-817
- 8 **Hoofnagle JH**, Di Bisceglie AM. The treatment of chronic viral hepatitis. *N Engl J Med* 1997; **336**: 347-356
- 9 **Irving WL**, Ball JK, Berridge S, Curran R, Grabowska AM, Jameson CL, Neal KR, Ryder SD, Thomson BJ. TT virus infection in patients with hepatitis C: frequency, persistence, and sequence heterogeneity. *J Infect Dis* 1999; **180**: 27-34
- 10 **Maggi F**, Pistello M, Vatteroni M, Presciuttini S, Marchi S, Isola P, Fornai C, Fagnani S, Andreoli E, Antonelli G, Bendinelli M. Dynamics of persistent TT virus infection, as determined in patients treated with alpha interferon for concomitant hepatitis C virus infection. *J Virol* 2001; **75**: 11999-12004
- 11 **Nishizawa Y**, Tanaka E, Orii K, Rokuhara A, Ichijo T, Yoshizawa K, Kiyosawa K. Clinical impact of genotype 1 TT virus infection in patients with chronic hepatitis C and response of TT virus to alpha-interferon. *J Gastroenterol Hepatol* 2000; **15**: 1292-1297

- 12 **Okamoto H**, Takahashi M, Nishizawa T, Ukita M, Fukuda M, Tsuda F, Miyakawa Y, Mayumi M. Marked genomic heterogeneity and frequent mixed infection of TT virus demonstrated by PCR with primers from coding and noncoding regions. *Virology* 1999; **259**: 428-436
- 13 **Takahashi K**, Hoshino H, Ohta Y, Yoshida N, Mishiro S. Very high prevalence of TT virus (TTV) infection in general population of Japan revealed by a new set of PCR primers. *Hepatol Res* 1998; **12**: 233-239
- 14 **Garcia JM**, Marugan RB, Garcia GM, Lindeman MLM, Abete JF, del Terron SC. TT virus infection in patients with chronic hepatitis B and response of TTV to lamivudine. *World J Gastroenterol* 2003; **9**: 1261-1264
- 15 **Lai YC**, Hu RT, Yang SS, Wu CH. Coinfection of TT virus and response to interferon therapy in patients with chronic hepatitis B or C. *World J Gastroenterol* 2002; **8**: 567-570
- 16 **Meng XW**, Komatsu M, Goto T, Nakane K, Ohshima S, Yoneyama K, Lin JG, Watanabe S. Clinical significance of TT virus in chronic hepatitis C. *J Gastroenterol Hepatol* 2001; **16**: 202-208
- 17 **Dai CY**, Yu ML, Chuang WL, Hou NJ, Hou C, Chen SC, Lin ZY, Hsieh MY, Wang LY, Chang WY. The response of hepatitis C virus and TT virus to high dose and long duration interferon-alpha therapy in naive chronic hepatitis C patients. *Antiviral Res* 2002; **53**: 9-18
- 18 **Kawanaka M**, Niiyama G, Mahmood S, Ifukube S, Yoshida N, Onishi H, Hanano S, Ito T, Yamada G. Effect of TT virus co-infection on interferon response in chronic hepatitis C patients. *Liver* 2002; **22**: 351-355
- 19 **Matsumoto A**, Yeo AE, Shih JW, Tanaka E, Kiyosawa K, Alter HJ. Transfusion-associated TT virus infection and its relationship to liver disease. *Hepatology* 1999; **30**: 283-288
- 20 **Lefrere JJ**, Roudot-Thoraval F, Lefrere F, Kanfer A, Mariotti M, Lerable J, Thauvin M, Lefevre G, Rouger P, Girot R. Natural history of the TT virus infection through follow-up of TTV DNA-positive multiple-transfused patients. *Blood* 2000; **95**: 347-351
- 21 **Booth JC**, Foster GR, Kumar U, Galassini R, Goldin RD, Brown JL, Thomas HC. Chronic hepatitis C virus infections: predictive value of genotype and level of viraemia on disease progression and response to interferon alpha. *Gut* 1995; **36**: 427-432
- 22 **Watanabe H**, Saito T, Kawamata O, Shao L, Aoki M, Terui Y, Mitsuhashi H, Matsuo T, Takeda Y, Saito K, Togashi H, Shinzawa H, Takahashi T. Clinical implications of TT virus superinfection in patients with chronic hepatitis C. *Am J Gastroenterol* 2000; **95**: 1776-1780
- 23 **Pockros PJ**. Developments in the treatment of chronic hepatitis C. *Expert Opin Investig Drugs* 2002; **11**: 515-528
- 24 **Heathcote EJ**, Shiffman ML, Cooksley WG, Dusheiko GM, Lee SS, Balart L, Reindollar R, Reddy RK, Wright TL, Lin A, Hoffman J, De Pamphilis J. Peginterferon alfa-2a in patients with chronic hepatitis C and cirrhosis. *N Engl J Med* 2000; **343**: 1673-1680

Edited by Wang XL

Do there exist synergistic antitumor effects by coexpression of herpes simplex virus thymidine kinase with cytokine genes on human gastric cancer cell line SGC7901?

Jian-Hua Zhang, Ming-Xi Wan, Jia-Ying Yuan, Bo-Rong Pan

Jian-Hua Zhang, Ming-Xi Wan, Department of Biomedical Engineering, School of Life Science and Technology, Xi'an Jiaotong University, 28 West Xianning Road, Xi'an 710049, Shaanxi Province, China

Jia-Ying Yuan, Department of Ultrasonic Diagnosis, Xijing Hospital, Fourth Military Medical University, 127 West Changle Road, Xi'an 710033, Shaanxi Province, China

Bo-Rong Pan, Department of Oncology, Xijing Hospital, Fourth Military Medical University, 127 West Changle Road, Xi'an 710033, Shaanxi Province, China

Supported by Doctoral Foundation of Xi'an Jiaotong University, No.69925101 and National Natural Science Foundation of China, No.30270404

Correspondence to: Dr. Ming-Xi Wan, Department of Biomedical Engineering, School of Life Science and Technology, Xi'an Jiaotong University, 28 West Xianning Road, Xi'an 710049, Shaanxi Province, China. wanmingxi@yahoo.com.cn

Telephone: +86-29-2667924

Received: 2003-03-03 **Accepted:** 2003-04-01

Abstract

AIM: To evaluate the synergistic antitumor effects of herpes simplex virus thymidine kinase (HSV-TK) together with tumor necrosis factor alpha (TNF- α) or interleukin-2 (IL-2) gene expression on gastric cancer cell line SGC7901.

METHODS: Recombinant vectors pL(TT)SN and pL(TI)SN, which express TK-IRES-TNF- α and TK-IRES-IL-2 genes separately, as well as the control plasmids pL(TK)SN and pLXSN were employed to transfect PA317 cells respectively to generate the viruses that can stably express the objective genes through G418 selection. The gastric cancer cells were then transfected by the retroviral serum from the package cells and maintained in culture to determine the cell growth and apoptosis. The cytotoxic effects of HSV-TK together with TNF- α or IL-2 gene expression on the transfected cancer cells were evaluated by the cell viability and bystander effects in the presence of GCV supplemented in the cultural medium.

RESULTS: Expression of recombinant proteins including TNF- α and IL-2 by stable transfectants was confirmed by Western blotting. The percentage of cell apoptosis in the SGC/0, SGC/TK-TNF- α , SGC/TK-IL-2 and SGC/TK clone was 2.3%, 12.3%, 11.1% and 10.9% respectively at 24 h post-transfection. Cell growth status among all the experimental groups as judged by cell absorbance (A) at 570nm did not exhibit any significant difference ($P>0.05$); although it was noted to be slightly lower in the SGC/TT group. Cell survival rate in SGC/TI, SGC/TT and SGC/TK group was significantly decreased in a dose-dependent manner of GCV compared with that of the SGC/0 group ($P<0.05-0.01$). Among all studied cells, the SGC/TT was shown most sensitive to GCV with a half lethal dose of 0.5 mg·L⁻¹. In contrast, the survival rate of SGC/0 cells was not affected by the presence of GCV with the doses less than 10 mg·L⁻¹. The half lethal dose of

GCV for SGC/0 cells was more than 100 mg·L⁻¹. Marked bystander effect induced by SGC/TI, SGC/TT and SGC/TK cells was confirmed by the fact that 20% of these stable transfectants could kill 50% of the co-cultured cells, in which the most prominent bystander effect was found in the circumstance of SGC/TT presence. However, no significant difference of these variables was found among SGC/TI, SGC/TT and SGC/TK cells ($P>0.05$).

CONCLUSION: The synergistic antitumor effects produced by the co-expression of HSV-TK with TNF- α or IL-2 genes were not present in the transfected SGC7901 cells. The mechanism underlying these phenomena was not known.

Zhang JH, Wan MX, Yuan JY, Pan BR. Do there exist synergistic antitumor effects by coexpression of herpes simplex virus thymidine kinase with cytokine genes on human gastric cancer cell line SGC7901? *World J Gastroenterol* 2004; 10(1): 147-151 <http://www.wjgnet.com/1007-9327/10/147.asp>

INTRODUCTION

Gastric cancer is one of the most prevalent malignancies in China^[1]. Despite the recent progress in early diagnosis and treatment of the disease, aggressive surgical or chemotherapeutic interventions have not sufficiently prolonged the survival time of patients with distant metastases^[2]. Thus, searching for more effective therapeutic modalities, especially for the stage IV gastric cancer patients, has become an urgent task in our daily medical practice.

The transfer of suicide genes into tumor cells that is currently being studied as a method of treatment for various cancers has made the target cells become sensitive to the pharmacological agents. Suicide gene therapy with the herpes simplex virus thymidine kinase (HSV-TK) fragment, the most widely used strategy for the cancer therapeutic study^[3], has been shown to exert antitumor efficacy in various cancer models^[4-7]. However, its efficacy seems not to be fully developed to eliminate tumor cells in some of the investigations^[8-12]. Gene therapy with HSV-TK and cytokine genes together may produce a complementary effect, and has become a new insight for the treatment of malignancies^[13, 14].

Previously, we constructed two retroviral vectors, pL(TT)SN and pL(TI)SN, which have been confirmed to express TK-IRES-TNF- α and TK-IRES-IL-2 genes respectively in the gastric cancer cell line SGC7901^[15]. In the present study, the synergistic antitumor effects of these vectors on human gastric cancer cells were investigated in the presence of GCV to confirm their efficiency.

MATERIALS AND METHODS

Cell lines and vectors

The mouse fibroblast cell line NIH3T3 and the amphotropic retroviral packaging cells PA317 were the generous gifts from

Dr. Yu Bing (Fourth Military Medical University, Xi'an, China). The human gastric carcinoma cell lines SGC7901 were obtained from Shanghai Institute of Biochemistry. All of the cells were maintained in RPMI 1640 medium, supplemented with 10% FBS (Hangzhou, Sijiqing Biotech Company), 2 mM L-glutamine, 100 units/ml penicillin and 100 µg/ml streptomycin. The PA317 was used as the packaging cell and the NIH 3T3 cells were employed to assay the virus titre. The cell cultures were maintained at 37 °C in a humidified atmosphere with 5% CO₂.

The recombinant vectors pL(TT)SN and pL(TI)SN, which express TK-IRES-TNF-α and TK-IRES-IL-2 genes respectively, as well as the control plasmid pL(TK)SN carrying only TK fragment were constructed and identified in our previous study^[15]. The empty plasmid PLXSN used as another control vector was provided by Dr. Yu Bing (Fourth Military Medical University, Xi'an, China).

Establishment of stable transfectants

The retrovirus plasmids pL(TT)SN, pL(TI)SN, pL(TK)SN and pLXSN were transferred into PA317 cells respectively by lipofectamine (Gibco) according to the manual instructions^[16, 17]. After 48 h of transfection, G418 (Promega) was added to the culture medium at a concentration of 500 mg·L⁻¹ to select G418-resistant colonies. After 2-weeks' culture with the changing of the G418-containing medium every 3 days, the supernatant of G418-resistant colonies was collected and diluted to different concentrations to infect NIH3T3 cells, which were further undergone the G418 selection for 2w, then the G418-resistant NIH3T3 colonies were counted for the determination of viral titre^[18]. The viral titers of pL(TT)SN, pL(TI)SN, pL(TK)SN and empty plasmid pLXSN were 5×10⁸ CFU/L, 6×10⁸ CFU/L, 1×10⁹ CFU/L and 1×10⁹ CFU/L respectively.

A total number of 5×10⁵ SGC7901 cells were incubated in a 6-well plate for 24 h, then rinsed with serum-free RPMI 1640 medium twice and incubated with 100 µl supernatant of G418-resistant PA317 colony for 3 h. After 4-weeks' cultivation, the G418-resistant colonies designated as SGC/TK-TNF-α, SGC/TK-IL-2, SGC/TK and SGC/0 respectively according to the transfected vectors were collected and used both to confirm the objective gene expression by Western blot and to perform other determinations.

For Western blotting, the SGC/TT and SGC/TI cells were incubated respectively in the six-well plates at a density of 2.5×10⁵ cells/well for 24 h, followed by a further cultivation of 48 h with the culture medium replaced with 1 ml of serum-free RPMI 1640. Then the serum-free medium was totally collected, concentrated in a microconcentrator to 20 µl and subjected to electrophoresis on a 120 g·L⁻¹ SDS/PAGE gel. Proteins were transferred to a nitrocellulose membrane and incubated overnight in 50 ml·L⁻¹ fat free milk in PBS at 4 °C. After washed in 10 ml·L⁻¹ fat free milk, the membrane was incubated with monoclonal antibody of mouse anti-rhIL-2 or anti-TNF-α, followed by incubation with horseradish peroxidase-conjugated antimouse immunoglobulin. Proteins were detected by using the ECL kit according to the manufacturer's instruction (Amersham)^[19].

Determination of cell apoptosis

Cell apoptosis was quantitated by the protocol of flow cytometry. Briefly, 100 µl of the observed cells (2×10⁵) in binding buffer and 5 µl of FITC-conjugated annexin V/PI dual staining reagents (Annexin V-FITC kit, Pharmingen, USA) were transferred in turn into a 5 ml culture tube and incubated for 15 min at room temperature in the dark. After 400 µl of binding buffer was added into the culture tube, the flow cytometric analysis for apoptosis was performed as soon as possible within 12 h (FACScaliber; Becton, Dickinson, USA).

Cell growth assay

Cell growth was scaled in SGC/TI, SGC/TT, SGC/TK and SGC/0 cells as described in the references^[20, 21]. Cells were cultured in 24-well plate (Nuc, Co) at 37 °C in a humidified atmosphere with 5% CO₂ and adjusted to a density of 1.5×10⁴ cells/well at the time of determination. Cell absorbance (A) at 570nm was determined each day for 6 days. The figures obtained were used to draw a cell growth curve.

MTT assay

An MTT assay was conducted to determine the cell survival rate^[22, 23]. Following 24 h incubation, cells cultured in 96-well plates were treated with different concentrations of GCV (Roche Co.) and continued to be cultured for 6 d, when the MTT mixture was added to medium and the cells were incubated further for another 4 h. The absorbance of the cells was measured at a wavelength of 525nm with a microtiter plate reader. The survival rate was expressed as A/B×100%, where A was the absorbance value from the experimental cells and B was that from the control by SGC7901 cells.

Bystander effect observation

Twenty-four hours after tumor cells were infected with recombinant retrovirus, different proportions of transfected and untransfected cells that were adjusted to a density of 1×10⁵ cells/well were co-cultured on 4-well flat-bottom plates at 37 °C for 5 d in the presence of 5 mg·L⁻¹ GCV. The cell survival rate was measured by MTT method^[24].

Statistical analysis

Quantitative variables are described as mean ± standard error of the mean. Categorical variables are expressed as percentages. Comparisons between means were done with the Student's *t*-test. Comparison between percentages was performed with the χ^2 test. A *P* value <0.05 was taken as the criterion of statistical significance.

RESULTS

Expressions of stable transfectants

The stable expression of recombinant proteins in target cells was confirmed by Western blot, in which two distinct bands of 15ku and 17ku were observed on the nitrocellulose membrane, corresponding to the fragment sizes of IL-2 and TNF-α respectively (Figure 1).

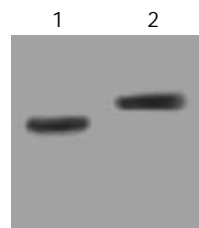


Figure 1 Stably expressed recombinant protein in transduced SGC7901 cells confirmed by Western blot. Lane 1: IL-2 (15ku) expressed in SGC/TI cells; Lane 2: TNF-α (17ku) expressed in SGC/TT cells.

Cell apoptosis

Cells in the early phase of apoptosis were labeled by single annexin V fluorescence. The percentage of cell apoptosis in the SGC/0, SGC/TK-TNF-α, SGC/TK-IL-2 and SGC/TK clone was 2.3%, 12.3%, 11.1% and 10.9% respectively at 24 h post-transfection, indicating a slightly higher percentage of apoptosis appeared in the SGC/TK-TNF-α, SGC/TNF-α

and SGC/TK clones compared with that in the SGC/0 clone ($P>0.05$, Figure 2).

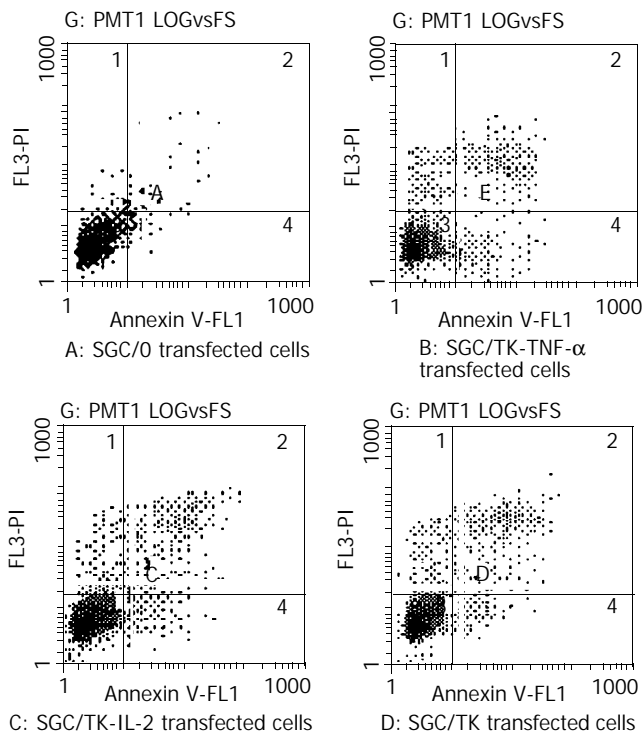


Figure 2 Percentage of early apoptotic cells in different groups of transfectants.

Cell growth status

The A value of cells among all experimental groups did not exhibit any significant difference ($P>0.05$), although it was slightly lower in the SGC/TT group (Figure 3). The result showed that the cell growth status was not severely influenced by the vector's variety used for the transfection in the present study.

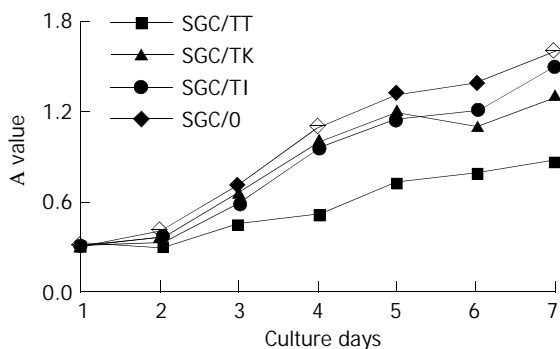


Figure 3 Cell growth status of the different transfectants.

Cell viability

Cell survival rate in SGC/TI, SGC/TT and SGC/TK group was significantly decreased in a dose-dependent manner of GCV compared with that of the SGC/0 group ($P<0.05-0.01$). Among all studied cells, the SGC/TT was shown most sensitive to GCV with a half lethal dose of $0.5 \text{ mg} \cdot \text{L}^{-1}$. In contrast, the survival rate of SGC/0 cells was not affected by the presence of GCV with the doses less than $10 \text{ mg} \cdot \text{L}^{-1}$. The half lethal dose of GCV for SGC/0 cells was more than $100 \text{ mg} \cdot \text{L}^{-1}$ (Figure 4).

Bystander effect

Marked bystander effect was shown by SGC/TI, SGC/TT and SGC/TK cells as manifested by the fact that 20% of these stable

transfectants could kill 50% of the co-cultured cells (Figure 5). However, the most prominent bystander effect was found in the circumstance of SGC/TT presence.

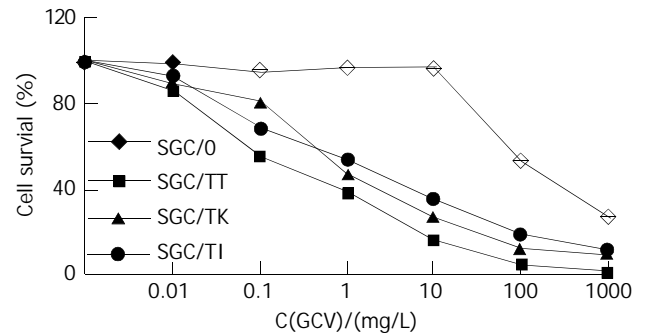


Figure 4 Cell survival rate in different experimental group treated with $5 \text{ mg} \cdot \text{L}^{-1}$ GCV for 6 d.

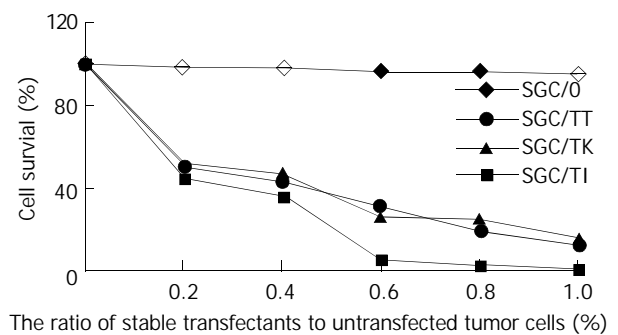


Figure 5 Bystander effect of different transfectants.

DISCUSSION

Transfer of suicide gene into tumor cells has emerged as an attractive strategy of gene therapy for the selective elimination of cancer cells, in which the suicide gene system alone or in combination with other immunological genes have been considered to be the favorable modalities for the treatment of malignancies^[25-27]. The suicide genes encode non-mammalian enzymes that can convert nontoxic prodrugs into cellular toxic metabolites. The most widely used suicide gene is the HSV-TK/GCV system that can convert prodrug GCV into phosphorylated GCV. The latter is further phosphorylated by the cellular kinase to form GCV triphosphate, a toxic substance that can inhibit cellular DNA synthesis and lead cell to death. Besides, the "bystander effect" induced by TK gene can also enhance the tumor-killing capacity of the HSV-TK/GCV system^[28-30]. However, it was found in some investigations that the antitumor efficiency of this system was limited by the lower rate of gene transfection and their insufficient induction of host immunity^[31-33].

Cytokine therapy is another strategy for the treatment of malignancies. It can not only directly kill tumor cells, inhibit tumorigenesis and tumor metastasis, but can also enhance these effects by the induction of antitumor immunity. Based on the antitumor properties of certain cytokines such as IL-2 and TNF- α , it is believed that the gene therapy combining cytokine with TK suicide gene would produce more beneficial and effective effects for the treatment of cancers, which has received strong supports from some of the recently published literatures. Majumdar and his associates^[33] have compared the therapeutic effect of IL-2 expression alone with that by the co-expression of IL-2 and TK genes on squamous cell carcinoma in nude mice, and found that the combined gene expression was most efficient for the gene therapy. In another study, Chen *et al.*^[34]

reported that cytokine gene IL-2 could act synergistically with the suicide gene to induce a systemic antitumor immunity. Unfortunately, there have been few reports up to the present about this therapeutic strategy in the antitumor study of gastric malignancy.

In the present study, we tried to observe the antitumor effects by the co-expression of suicide gene HSV-TK and cytokine gene TNF- α or IL-2 on gastric carcinoma cell lines SGC7901. It was found that the percentage of cell apoptosis in the SGC/0, SGC/TK-TNF- α , SGC/TK-IL-2 and SGC/TK clone was 2.3%, 12.3%, 11.1% and 10.9% respectively at 24 h post-transfection, and the cell growth status as judged by cell absorbance (A) at 570nm among all the experimental groups did not exhibit any significant difference ($P>0.05$), although they were noted to be slightly varied in the SGC/TT group. This indicated that the apoptosis and growth status of SGC7901 cells were not severely influenced by the vector's variety used in the study. Whereas the cell survival rate in SGC/0, SGC/TT and SGC/TK group was significantly decreased in a dose-dependent manner of GCV compared with that of the SGC/0 group ($P<0.05-0.01$) in the presence of GCV, in which the SGC/TT cells were shown to be most sensitive to GCV with a half lethal dose of 0.5 mg·L⁻¹. In contrast, the survival rate of SGC/0 cells was not affected by the presence of GCV with the doses less than 10 mg·L⁻¹. The half lethal dose of GCV for SGC/0 cells was more than 100 mg·L⁻¹. Marked bystander effect induced by SGC/0, SGC/TT and SGC/TK cells was also confirmed by the fact that 20% of these stable transfectants could kill 50% of the co-cultured cells and the most prominent bystander effect was found in the presence of SGC/TT. However, no significant difference of these variables was found among SGC/0, SGC/TT and SGC/TK cells, which meant that the synergistic antitumor effects produced by the co-expression of HSV-TK and TNF- α or IL-2 genes were not present in the transfected SGC7901 cells. Whether this was due to the speciality of the gastric cancer cell line is unknown. Further studies, therefore, are needed to elucidate the mechanisms underlying these phenomena in order to search for more efficient therapeutic modalities for the treatment of gastric malignancies.

REFERENCES

- Xu CT**, Huang LT, Pan BR. Current gene therapy for stomach carcinoma. *World J Gastroenterol* 2001; **7**: 752-759
- Ikeda Y**, Mori M, Adachi Y, Matsushima T, Sugimachi K, Saku M. Carcinoembryonic antigen (CEA) in stage IV gastric cancer as a risk factor for liver metastasis: a univariate and multivariate analysis. *J Surg Oncol* 1993; **53**: 235-238
- van der Eb MM**, Cramer SJ, Vergouwe Y, Schagen FH, van Krieken JH, van der Eb AJ, Rinkes IH, van de Velde CJ, Hoeben RC. Severe hepatic dysfunction after adenovirus-mediated transfer of the herpes simplex virus thymidine kinase gene and ganciclovir administration. *Gene Ther* 1998; **5**: 451-458
- Narita M**, Bahar R, Hatano M, Kang MM, Tokuhisa T, Goto S, Saisho H, Sakiyama S, Tagawa M. Tissue-specific expression of a suicide gene for selective killing of neuroblastoma cells using a promoter region of the NCX gene. *Cancer Gene Ther* 2001; **8**: 997-1002
- Van Dillen JJ**, Mulder NH, Vaalburg W, de Vries EF, Hospers GA. Influence of the bystander effect on HSV-tk/GCV gene therapy. A review. *Curr Gene Ther* 2002; **2**: 307-322
- Nowak AK**, Lake RA, Kindler HL, Robinson BW. New approaches for mesothelioma: biologics, vaccines, gene therapy, and other novel agents. *Semin Oncol* 2002; **29**: 82-96
- Qiao J**, Doubrovin M, Sauter BV, Huang Y, Guo ZS, Balatoni J, Akhurst T, Blasberg RG, Tjuvahev JG, Chen SH, Woo SL. Tumor-specific transcriptional targeting of suicide gene therapy. *Gene Ther* 2002; **9**: 168-175
- Engelmann C**, Heslan JM, Fabre M, Lagarde JP, Klatzmann D, Panis Y. Importance, mechanisms and limitations of the distant bystander effect in cancer gene therapy of experimental liver tumors. *Cancer Lett* 2002; **179**: 59-69
- Adachi Y**, Matsubara S, Muramatsu T, Curiel DT, Reynolds PN. Midkine promoter-based adenoviral suicide gene therapy to midkine-positive pediatric tumor. *J Pediatr Surg* 2002; **37**: 588-592
- Pulkkanen KJ**, Laukkanen JM, Fuxe J, Kettunen MI, Rehn M, Kannasto JM, Parkkinen JJ, Kauppinen RA, pettersson RF, Yla-Herttuala S. The combination of HSV-tk and endostatin gene therapy eradicates orthotopic human renal cell carcinomas in nude mice. *Cancer Gene Ther* 2002; **9**: 908-916
- Floeth FW**, Shand N, Bohar H, Prisack HB, Felsberg J, Neuen-Jacob E, Aulich A, Burger KJ, Bock WJ, Weber F. Local inflammation and devascularization-*in vivo* mechanisms of the "bystander effect" in VPC-mediated HSV-Tk/GCV gene therapy for human malignant glioma. *Cancer Gene Ther* 2001; **8**: 843-851
- Warren P**, Song W, Holle E, Holmes L, Wei Y, Li J, Wagner T, Yu X. Combined HSV-TK/GCV and secondary lymphoid tissue chemokine gene therapy inhibits tumor growth and elicits potent antitumor CTL response in tumor-bearing mice. *Anticancer Res* 2002; **22**: 599-604
- Niranjan A**, Moriuchi S, Lunsford LD, Kondziolka D, Flickinger JC, Fellows W, Rajendiran S, Tamura M, Cohen JB, Glorioso JC. Effective treatment of experimental glioblastoma by HSV vector-mediated TNF alpha and HSV-tk gene transfer in combination with radiosurgery and ganciclovir administration. *Mol Ther* 2000; **2**: 114-120
- Zhang R**, DeGroot LJ. An adenoviral vector expressing functional heterogeneous proteins herpes simplex viral thymidine kinase and human interleukin-2 has enhanced *in vivo* antitumor activity against medullary thyroid carcinoma. *Endocr Relat Cancer* 2001; **8**: 315-325
- Zhang JH**, Wan MX, Yuan JY, Pan BR. Construction and identification of the recombinant vectors carrying herpes simplex virus thymidine kinase and cytokine genes expressed in gastric carcinoma cell line SGC7901. *World J Gastroenterol* 2003; **9** (data to be published)
- Chen Y**, Wu Q, Song SY, Su WJ. Activation of JNK by TPA promotes apoptosis via PKC pathway in gastric cancer cells. *World J Gastroenterol* 2002; **8**: 1014-1018
- Shen ZY**, Xu LY, Chen MH, Shen J, Cai WJ, Zeng Y. Progressive transformation of immortalized esophageal epithelial cells. *World J Gastroenterol* 2002; **8**: 976-981
- Zhao LS**, Qin S, Zhou TY, Tang H, Liu L, Lei BJ. DNA-based vaccination induces humoral and cellular immune responses against hepatitis B virus surface antigen in mice without activation of C-myc. *World J Gastroenterol* 2000; **6**: 239-243
- Khurana VG**, Katusic ZS. Gene transfer for cerebrovascular disease. *Curr Cardiol Rep* 2001; **3**: 10-16
- Akyurek LM**, Nallamshetty S, Aoki K, San H, Yang ZY, Nabel GJ, Nabel EG. Coexpression of guanylate kinase with thymidine kinase enhances prodrug cell killing *in vitro* and suppresses vascular smooth muscle cell proliferation *in vivo*. *Mol Ther* 2001; **3**: 779-786
- Pulkkanen KJ**, Parkkinen JJ, Laukkanen JM, Kettunen MI, Tyynela K, Kauppinen RA, Ala-Opas MY, Yla-Herttuala S. HSV-tk gene therapy for human renal cell carcinoma in nude mice. *Cancer Gene Ther* 2001; **8**: 529-536
- Cao WX**, Ou JM, Fei XF, Zhu ZG, Yin HR, Yan M, Lin YZ. Methionine-dependence and combination chemotherapy on human gastric cancer cells *in vitro*. *World J Gastroenterol* 2002; **8**: 230-232
- Wei XC**, Wang XJ, Chen K, Zhang L, Liang Y, Lin XL. Killing effect of TNF-related apoptosis inducing ligand regulated by tetracycline on gastric cancer cell line NCI-N87. *World J Gastroenterol* 2001; **7**: 559-562
- Guo SY**, Gu QL, Liu BY, Zhu ZG, Yin HR, Lin YZ. Experimental study on the treatment of gastric cancer by TK gene combined with mL-2 gene. *Shijie Huaren Xiaohua Zazhi* 2000; **8**: 974-978
- Guan J**, Ma L, Wei L. Characteristics of ovarian cancer cells transduced by the bicistronic retroviral vector containing GM-CSF and HSV-tk genes. *Chin Med J* 2001; **114**: 147-151
- Balzarini J**, Ostrowski T, Goslinski T, De Clercq E, Golankiewicz

- B. Pronounced cytostatic activity and bystander effect of a novel series of fluorescent tricyclic acyclovir and ganciclovir derivatives in herpes simplex virus thymidine kinase gene-transduced tumor cell lines. *Gene Ther* 2002; **9**: 1173-1182
- 27 **Burrows FJ**, Gore M, Smiley WR, Kanemitsu MY, Jolly DJ, Read SB, Nicholas T, Kruse CA. Purified herpes simplex virus thymidine kinase retroviral particles: III. Characterization of bystander killing mechanisms in transfected tumor cells. *Cancer Gene Ther* 2002; **9**: 87-95
- 28 **Hall SJ**, Canfield SE, Yan Y, Hassen W, Selleck WA, Chen SH. A novel bystander effect involving tumor cell-derived Fas and FasL interactions following Ad.HSV-tk and Ad.mIL-12 gene therapies in experimental prostate cancer. *Gene Ther* 2002; **9**: 511-517
- 29 **Boucher PD**, Ostruszka LJ, Murphy PJ, Shewach DS. Hydroxyurea significantly enhances tumor growth delay *in vivo* with herpes simplex virus thymidine kinase/ganciclovir gene therapy. *Gene Ther* 2002; **9**: 1023-1030
- 30 **Hayashi K**, Hayashi T, Sun HD, Takeda Y. Contribution of a combination of ponocidin and acyclovir/ganciclovir to the anti-tumor efficacy of the herpes simplex virus thymidine kinase gene therapy system. *Hum Gene Ther* 2002; **10**: 415-423
- 31 **Huang H**, Wang A. The adenovirus-mediated HSV-tk/GCV suicide gene system in the treatment of tongue carcinoma cell line. *Zhonghua Kouqiang Yixue Zazhi* 2001; **36**: 457-460
- 32 **Gao G**, Huang T, Chen S. *In vitro* and *in vivo* bystander effect of adenovirus-mediated transfer of the herpes simplex virus thymidine kinase gene. *Zhonghua Waikexue Zazhi* 2002; **40**: 301-303
- 33 **Majumdar AS**, Zolotorey A, Samuel S, Tran K, Vertin B, Hall-Meier M, Antoni BA, Adeline E, Philip M, Philip R. Efficacy of herpes simplex virus thymidine kinase in combination with cytokine gene therapy in an experimental metastatic breast cancer model. *Cancer Gene Ther* 2000; **7**: 1086-1099
- 34 **Chen SH**, Kosai K, Xu B, Khiem PN, Contant C, Finegold MJ, Woo SL. Combined suicide and cytokine gene therapy for hepatic metastasis of colon carcinoma: sustained antitumor immunity prolongs animal survival. *Cancer Res* 1996; **56**: 3758-3762

Edited by Zhu LH

Rising plasma nociceptin level during development of HCC: A case report

Andrea Horvath, Aniko Folhoffer, Peter Laszlo Lakatos, Judit Halász, Gyorgy Illyés, Zsuzsa Schaff, Monika Beatrix Hantos, Kornelia Tekes, Ferenc Szalay

Andrea Horvath, Aniko Folhoffer, Peter Laszlo Lakatos, Ferenc Szalay, 1st Department of Medicine of Semmelweis University, Budapest, Hungary

Judit Halász, Gyorgy Illyés, Zsuzsa Schaff, 2nd Department of Pathology of Semmelweis University, Budapest, Hungary

Kornelia Tekes, Department of Pharmacodynamics of Semmelweis University, Budapest, Hungary

Monika Beatrix Hantos, Neurochemical Research Unit of Hungarian Academy of Sciences, Budapest, Hungary

Correspondence to: Szalay Ferenc, MD, PhD, 1st Department of Medicine, Semmelweis University, Korányi St. 2/A, H-1083 Budapest, Hungary. szalay@bell.sote.hu

Telephone: +36-1-210-1007 **Fax:** +36-1-210-1007

Received: 2003-09-23 **Accepted:** 2003-11-16

Abstract

AIM: Although liver cirrhosis is a predisposing factor for hepatocellular carcinoma (HCC), relatively few reports are available on HCC in primary biliary cirrhosis. High plasma nociceptin (N/OFQ) level has been shown in Wilson disease and in patients with acute and chronic pain.

METHODS: We report a follow-up case of HCC, which developed in a patient with primary biliary cirrhosis. The tumor appeared 18 years after the diagnosis of PBC and led to death within two years. Alfa fetoprotein and serum nociceptin levels were monitored before and during the development of HCC. Nociceptin content was also measured in the tumor tissue.

RESULTS: The importance and the curiosity of the presented case was the novel finding of the progressive elevation of plasma nociceptin level up to 17-fold (172 pg/mL) above the baseline (9.2±1.8 pg/mL), parallel with the elevation of alpha fetoprotein (from 13 ng/mL up to 3 480 ng/mL) during tumor development. Nociceptin content was more than 15-fold higher in the neoplastic tissue (0.16 pg/mg) than that in the tumor-free liver tissue samples (0.01 pg/mg) taken during the autopsy.

CONCLUSION: Results are in concordance with our previous observation that a very high plasma nociceptin level may be considered as an indicator for hepatocellular carcinoma.

Horvath A, Folhoffer A, Lakatos PL, Halász J, Illyés G, Schaff Z, Hantos MB, Tekes K, Szalay F. Rising plasma nociceptin level during development of HCC: A case report. *World J Gastroenterol* 2004; 10(1): 152-154

<http://www.wjgnet.com/1007-9327/10/152.asp>

INTRODUCTION

The incidence of hepatocellular carcinoma (HCC) in primary biliary cirrhosis (PBC) is reported to range from 0.5% to 4.2%, which is somewhat less frequent than that in liver cirrhosis from other etiologies^[1,2]. However, recent reports have shown an increasing trend. The incidence of HCC was found higher

in stage III/IV than in stage I/II patients^[1,3,4].

Relatively few prospective and comprehensive studies are available on HCC in PBC, and the number of case reports is also limited. Summarizing the data of the literature, 126 of 6 188 PBC patients (2.0%) were found to have HCC. Since HCC usually develops many years after the diagnosis of PBC, screening of HCC has clinical importance and offers best with hope for early detection. Serum AFP is a widely accepted marker of HCC^[5]; however, using the conventional cut-off value of 500 ng/mL, it has a sensitivity of about 50% and a specificity of more than 90% in detecting HCC in a patient with coexisting liver disease^[6]. The average survival of patients with HCC improved in the last decades^[7]. Female HCC patients often have a better prognosis than male patients^[8]. Because of the lack of sensitive markers of malignant hepatic tumors, HCC is usually recognized in the advanced stage.

We reported a follow-up case of HCC in a PBC patient. The importance of this case is the novel finding of progressive elevation in plasma nociceptin (N/OFQ, formerly named as orphanin FQ) up to 17-fold above the baseline, parallel with the elevation of alpha fetoprotein (AFP) during tumor development. Moreover, high nociceptin content was found in the tumor tissue as well.

Nociceptin, a newly discovered neuropeptide of 17 aminoacids, is the natural agonist of NOP receptor, earlier named opioid receptor-like 1 (ORL1) receptor. N/OFQ is a neuropeptide that is endowed with pronociceptive activity *in vivo*. Both the long and the short splice variants of the OP4 receptor mRNA were isolated in rat liver^[9]; however, there are no data about its physiological or pathophysiological role in liver function. To date only few clinical studies on nociceptin were reported, and only one of them dealt with liver disease.

Findings of the presented case are in concordance with our previous observation that a high plasma NC level may be an indicator of HCC.

CASE REPORT

A 47-year-old woman was admitted for fatigue, itching, hepatomegaly, high alkaline phosphatase and gamma-GT levels. Primary biliary cirrhosis was diagnosed based on the clinical symptoms, laboratory findings, AMA M2 positivity, normal US and ERCP pictures. Liver biopsy revealed stage II/III. There was no family history of liver disease or autoimmune disease, and all other confounding risk factors including alcohol, HBV and HCV infections were excluded. The patient was a heavy smoker. The past surgical history was significant only for an appendectomy and two caesarean sections. Her menopause started at the age of 38. Bone mineral density was slightly below the normal range at the time of diagnosis of PBC. Ursodeoxycholic acid (Ursofalk) treatment, calcium and vitamin D supplementation were introduced.

Severe progression of osteoporosis was observed during the following years. Five years after the diagnosis of PBC significantly decreased bone mineral density was shown both on the femoral neck (T-score: -5.12, Z score: -3.38) and on the lumbar vertebrae (T-score: -5.44, Z-score: -3.9). At the age of

57 despite the calcium, vitamin-D supplementation, calcitonin and bisphosphonate (Fosamax) treatment, the severe osteoporosis led to hip fracture and multiple vertebral collapses, which made the patient lifelong disabled.

Progression of PBC to stage IV occurred. She was monitored by yearly US, by regular laboratory tests and AFP every 3–4 months. For different reasons we collected blood samples for plasma nociceptin level determination as well. Sampling was done in conformity to accepted ethical standards and was approved by the regional ethical committee.

Hepatocellular carcinoma developed 18 years after the diagnosis of PBC. Regular follow-up US investigations revealed a focal lesion of 2.5 cm in diameter, which increased rapidly in segment V of the liver. Fine needle biopsy findings proved hepatocellular carcinoma. After the HCC diagnosis a continuous and rapid increase in the size of the tumor, an elevation of ALP, GGT, plasma nociceptin and AFP levels and clinical deterioration were observed.

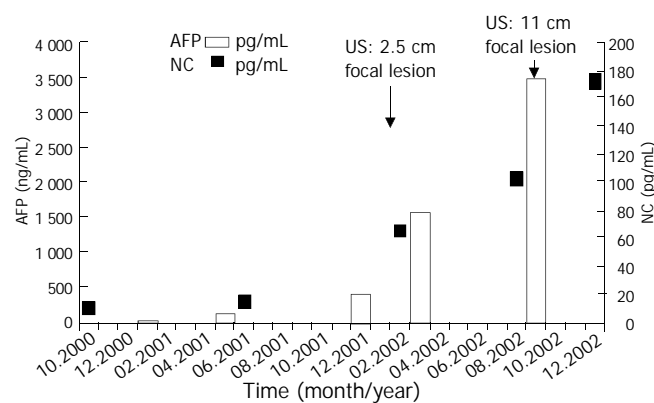


Figure 1 Serum alpha fetoprotein and plasma nociceptin levels before and during the development of hepatocellular carcinoma in the presented patient with primary biliary cirrhosis.

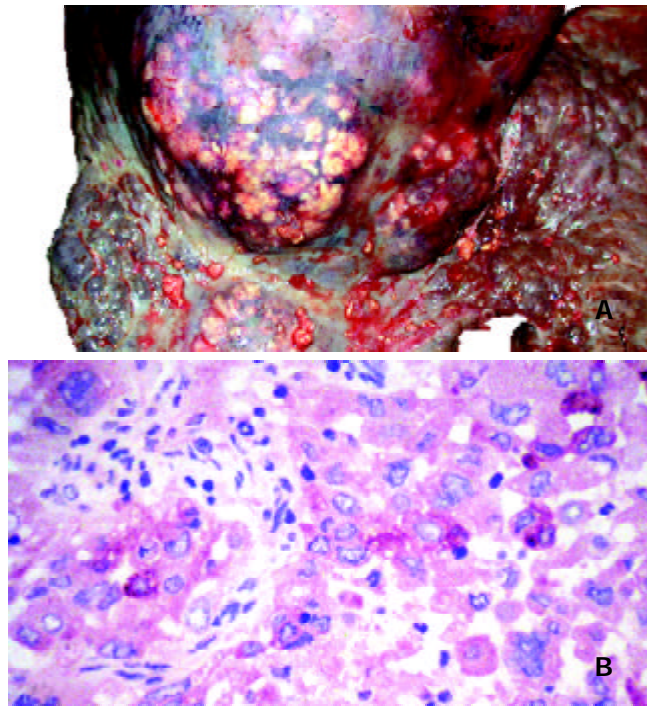


Figure 2 Hepatocellular carcinoma in the presented patient with primary biliary cirrhosis. A: Gross view of liver at autopsy. Grayish nodules of carcinoma protrude on the surface of the cirrhotic liver. Bar=1 cm. B: The focal red staining on the histologic picture of the hepatocellular carcinoma shows the immunohistochemical reaction of AFP. Original magnification 400 \times .

The AFP value had been within the normal range one year before the tumor was detected (13 ng/mL), but it was elevated at the time of the diagnosis of HCC (426 ng/mL) and rose up to 3480 ng/mL. The plasma nociceptin measured by radioimmunoassay ^{125}I -Nociceptin-kit, Phoenix Pharmaceuticals, Phoenix, CA, USA (10.6 pg/mL) was within the normal range (9.2 ± 1.8 pg/mL) in the tumor-free stage, while progressive elevation was detected during the tumor development (15.8, 65.8, 103.7, 128.0, 172.2 pg/mL), reaching the highest value before death (Figure 1). Higher nociceptin content was measured in the tumor tissue (0.16 pg/mg) compared to the tumor-free liver tissue sample (0.01 pg/mg) taken during the autopsy. The patient refused any surgical or other systemic or local tumor treatment. The size of the tumor increased up to 12 cm in diameter and involved segments V, VII, VIII and partly IV. No metastasis was detected, but necrosis developed in the central region of the tumor. The patient received supportive treatment, analgetics, and died of tumorous cachexia 19 months after the discovery of HCC. The autopsy confirmed both PBC stage IV and HCC. Focal presence of AFP was shown in the tumor by immunohistochemistry (Figures 2 A and B).

A nociceptin content in the HCC tissue (0.16 pg/mg) was 15-fold higher than that in the tumor free liver tissue sample (0.01 pg/mg) taken during the autopsy.

DISCUSSION

The presented case is a further example of the occurrence of HCC in PBC, and it supports previous observations that HCC usually develops in stage III/IV patients^[3]. The tumor developed 18 years after the diagnosis of PBC and led to the death of the patient within two years. Furthermore, severe osteoporosis is a common disorder in PBC, although recently it is considered as a non-specific complication^[10,11]. In our patient the early menopause together with PBC resulted in many bone fractures causing lifelong disability. The low serum osteocalcin level indicated a low turnover osteoporosis. High serum osteoprotegerin and low RANKL have been reported in PBC^[12], and we found the same alteration in this patient. Progression of bone loss was detected despite the serum osteoprotegerin was two-fold higher than normal, which suggested that inflammatory process in the liver could also contribute to the elevation of osteoprotegerin.

This is the first follow-up case in which progressive elevation of plasma nociceptin level was detected in parallel with the elevation of AFP during tumor development, and high N/OFQ content was found in the tumor tissue.

Nociceptin is the endogenous agonist of a G-protein coupled, naloxon insensitive opioid-like 1 receptor (ORL1) recently named as OP4. Although nociceptin is structurally related to opioid peptides, especially to dynorphin A, it does not interact with μ , δ and κ receptors. N/OFQ/OP4 system is a newly discovered peptide-based signalling pathway, involved in the modulation of pain and cognition. Opioid antagonists were successfully used for the treatment of pruritus in patients with PBC^[13]. These results together with the data that high plasma N/OFQ level has been reported in Wilson disease and in patients with chronic pain, led us to measure plasma nociceptin level in primary biliary cirrhosis^[14]. Our motivation was reinforced by an accidental observation that we found extremely high N/OFQ in a Wilson patient with advanced HCC.

The nociceptin levels in blood samples collected in the pre-tumor stage and during the tumor development period clearly showed that the elevation of N/OFQ was parallel with that of AFP and the clinical deterioration. When the tumor was first detected the N/OFQ level was 6-fold higher than that in healthy controls (65.8 versus 9.2 ± 1.8 pg/mL, $n=29$) and in other PBC patients without HCC (12.1 ± 3.2 pg/mL, $n=21$). When the tumor reached 11 cm the N/OFQ level was 17-fold

higher than normal. Since N/OFQ content was 15-fold higher in tumor tissue than in tumor free parts of the liver, the question arose whether nociceptin was produced by HCC tissue or it accumulated in the tumor by passive binding or via increased nociceptin receptor expression.

Further research is needed to clarify the mechanism and clinical significance of the highly elevated N/OFQ level in HCC. Since N/OFQ transcripts are expressed in immune cells^[15], the high N/OFQ level may also be an indicator of altered reaction of the body including immunological, cytokine and other mechanisms.

Elevated N/OFQ level might represent a compensatory mechanism in the N/OFQ/OP4 system to modulate pain perception in the central nervous system. This mechanism could explain why some patients with a very high plasma N/OFQ level did not have pain despite advanced stage of malignant liver tumor. It is remarkable that the N/OFQ was 3-fold higher in our patient than the highest values reported in patients with chronic pain without malignant disease^[16].

In conclusion, the novel finding of this study is that progressive elevation of plasma nociceptin was detected in parallel with the elevation of AFP during tumor development, as well as high N/OFQ content was found in the tumor tissue in a PBC patient with hepatocellular carcinoma. This is in concordance with our previous observation that high plasma N/OFQ level might be considered as an indicator of HCC.

REFERENCES

- 1 **Nakanuma Y**, Terada T, Doishita K, Miwa A. Hepatocellular carcinoma in primary biliary cirrhosis: an autopsy study. *Hepatology* 1990; **11**: 1010-1016
- 2 **Krasner N**, Johnson PJ, Portmann B, Watkinson G, Macsween RNM, Williams R. Hepatocellular carcinoma in primary biliary cirrhosis. *Gut* 1979; **20**: 255-258
- 3 **Jones D**, Metcalf J, Collier J, Bassendine M, James O. Hepatocellular carcinoma in primary biliary cirrhosis and its impact on outcomes. *Hepatology* 1997; **26**: 1138-1142
- 4 **Caballeria L**, Pares A, Castells A, Gines A, Bru C, Rodes J. Hepatocellular carcinoma in primary biliary cirrhosis: similar incidence to that in hepatitis C virus-related cirrhosis. *Am J Gastroenterol* 2001; **96**: 1160-1163
- 5 **Nguyen MH**, Keefe EB. Screening for hepatocellular carcinoma. *J Clin Gastroenterol* 2002; **35**(5 Suppl 2): S86-91
- 6 **Johnson PJ**. The role of serum alpha-fetoprotein estimation in the diagnosis and management of hepatocellular carcinoma. *Clin Liver Dis* 2001; **5**: 145-159
- 7 **Tang ZY**. Clinical research of hepatocellular carcinoma in the 21st century. *China Natl J Gastroenterol* 1995; **1**: 2-3
- 8 **Qin LX**, Tang ZY. The prognostic significance of clinical and pathological features in hepatocellular carcinoma. *World J Gastroenterol* 2002; **8**: 193-199
- 9 **Wang JB**, Johnson PS, Imai Y, Persico AM, Ozenberger BA, Eppler CM, Uhl GR. cDNA cloning of an orphan opiate receptor gene family member and its splice variant. *FEBS Lett* 1994; **348**: 75-79
- 10 **Newton J**, Francis R, Prince M, James O, Bassendine M, Rawlings D, Jones D. Osteoporosis in primary biliary cirrhosis revisited. *Gut* 2001; **49**: 282-287
- 11 **Floreani A**. Osteoporosis is not a specific complication of primary biliary cirrhosis (PBC). *Gut* 2002; **50**: 898; author reply 898-899
- 12 **Szalay F**, Hegedus D, Lakatos PL, Tornai I, Bajnok E, Dunkel K, Lakatos P. High serum osteoprotegerin and low RANKL in primary biliary cirrhosis. *J Hepatol* 2003; **38**: 395-400
- 13 **Neuberger J**, Jones EA. Liver transplantation for intractable pruritus is contraindicated before an adequate trial of opiate antagonist therapy. *Eur J Gastroenterol Hepatol* 2001; **13**: 1393-1394
- 14 **Hantos MB**, Szalay F, Lakatos PL, Hegedus D, Firneisz G, Reiczigel J, Torok T, Tekes K. Elevated plasma nociceptin level in patients with Wilson disease. *Brain Res Bull* 2002; **58**: 311-313
- 15 **Arjomand J**, Cole S, Evans C. Novel orphanin FQ/nociceptin transcripts are expressed in human immune cells. *J Neuroimmunol* 2002; **13**: 1631-1633
- 16 **Ko MH**, Kim YH, Woo RS, Kim KW. Quantitative analysis of nociceptin in blood of patients with acute and chronic pain. *Neuroreport* 2002; **13**: 1361-1363

Edited by Zhang JZ

ATM and ATR: Sensing DNA damage

Jun Yang, Zheng-Ping Xu, Yun Huang, Hope E. Hamrick, Penelope J. Duerksen-Hughes, Ying-Nian Yu

Jun Yang, Zheng-Ping Xu, Yun Huang, Ying-Nian Yu, Department of Pathology and Pathophysiology, and Department of Public Health, School of Medicine, Zhejiang University, Hangzhou, 310031, Zhejiang Province, China

Hope E. Hamrick, Department of Psychology, Wellesley College, Wellesley, MA, 02481, U S A

Penelope J. Duerksen-Hughes, Center for Molecular Biology and Gene Therapy, School of Medicine, Loma Linda University, Loma Linda, CA 92354, U S A

Supported by National Key Basic Research and Development Program No. 2002CB512901, China; National Natural Science Foundation No. 30300277, China; the Initial Funds for Returned Overseas Chinese Scholar from Zhejiang University and Ministry of Education, China

Correspondence to: Dr. Ying-Nian Yu, Department of Pathology and Pathophysiology, School of Medicine, Zhejiang University, 353 Yanan Road, Hangzhou, 310031, Zhejiang Province, China. ynyu@hznc.com

Telephone: +86-571-8721 7149 **Fax:** +86-571-8721 7149

Received: 2003-07-17 **Accepted:** 2003-08-18

Abstract

Cellular response to genotoxic stress is a very complex process, and it usually starts with the "sensing" or "detection" of the DNA damage, followed by a series of events that include signal transduction and activation of transcription factors. The activated transcription factors induce expressions of many genes which are involved in cellular functions such as DNA repair, cell cycle arrest, and cell death. There have been extensive studies from multiple disciplines exploring the mechanisms of cellular genotoxic responses, which have resulted in the identification of many cellular components involved in this process, including the mitogen-activated protein kinases (MAPKs) cascade. Although the initial activation of protein kinase cascade is not fully understood, human protein kinases ATM (ataxia-telangiectasia, mutated) and ATR (ATM and Rad3-related) are emerging as potential sensors of DNA damage. Current progresses in ATM/ATR research and related signaling pathways are discussed in this review, in an effort to facilitate a better understanding of genotoxic stress response.

Yang J, Xu ZP, Huang Y, Hamrick HE, Duerksen-Hughes PJ, Yu YN. ATM and ATR: Sensing DNA damage. *World J Gastroenterol* 2004; 10(2): 155-160

<http://www.wjgnet.com/1007-9327/10/155.asp>

INTRODUCTION

Cellular response to genotoxic stress is a very complex process. However, it can be "simply" envisioned as a signal transduction cascade in which DNA lesions act as the initial signal that is detected by sensors and passed down through transducers. Eventually the effectors receive the signal and execute various cellular functions (Figure 1). Much knowledge has been gained over the years concerning the signal transducers, and a large group of serine-threonine protein kinases, namely the mitogen-activated protein kinases (MAPKs), along with their upstream kinases, have been shown to play prominent roles in cellular

genotoxic responses^[1]. Three major classes of MAPKs, i.e., extracellular signal-regulated kinase (ERK), c-Jun N-terminal kinase/stress-activated protein kinase (JNK/SAPK), and p38 (also known as SAPK2, RK, CSBP, or Mxi2), could all be activated by various genotoxic stresses^[1-7]. Although the precise mechanism has not been fully understood, it is known that damage to cellular DNA somehow leads to the activation of a group of serine-threonine kinases called MAPK kinase kinases (MAPKKK, or MEKK, MEK kinase), which phosphorylate the downstream dual-specificity kinases called MAPK kinases (MAPKK, or MEK, MAPK/ERK kinase). These MAPKKs then phosphorylate the threonine and tyrosine residues in MAPKs. This three-component module could be assembled together by scaffold proteins that ensure the efficiency and specificity of each individual MAPK pathway^[8-10]. The activated MAPKs then translocate to the nucleus and phosphorylate scores of target proteins, including many transcription factors. Among these transcription factors is the tumor suppressor p53 protein, which plays such an important role in the genotoxic stress response that has earned the reputation as the "universal sensor for genotoxic stress"^[2,11,12].

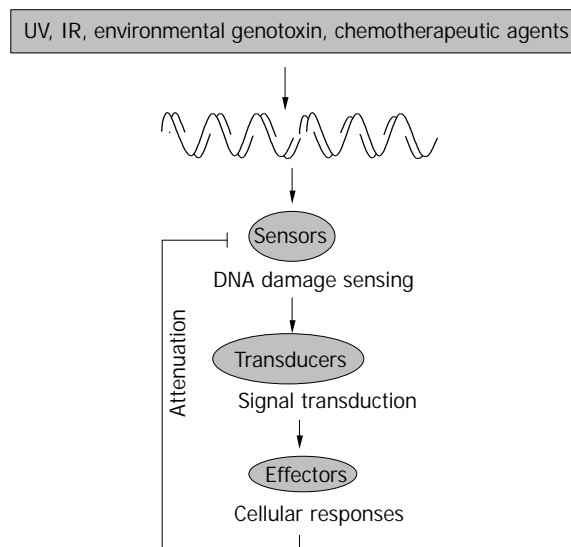


Figure 1 A general schematic representation of cellular responses to genotoxic stress. Ultraviolet (UV), ionizing radiation (IR), and various chemicals can induce DNA damage, such as double strand breaks (DSBs), which can be detected by "sensors". This generates some signal that can be transduced by the transducers to effector molecules. Finally, there is the presence of an attenuation mechanism to control the cellular response to genotoxic stress.

Although studies on MAPKs have provided a lot useful information about signal transducers, the initial sensors for DNA damage remain to be identified. Recently, it has been proposed that some multi-protein complexes that are involved in DNA maintenance or repair, such as the Rad family member Rad1, 9, 17, 26, and Hus1, might function as DNA damage sensors^[13-18]. Members of the phosphatidylinositol 3-kinase (PI-3) superfamily, which are activated at the very early stages of DNA damage response, could also serve as sensors, as

well as initiators, of the ensuing cellular genotoxic stress response, including ATM and ATR in humans^[19]. Although these proteins share the PI-3-like kinase domain, they could not function as lipid kinases, but rather as serine-threonine protein kinases^[14,20-25].

ATM AND ATR

Biochemistry of ATM and ATR

One distinguishing characteristic of the PI-3 family members is their unusually large size, which ranges from around 300 kDa to over 500 kDa. ATM is a 3 056 amino acid (aa) protein while ATR is a 2 644 aa protein, and both have a C-terminal catalytic domain (-300 aa) which is flanked by two loosely conserved domains. Although it has not been known how exactly these two kinases sense the DNA damage, it is clear that both kinases can be activated by DNA damage. However, it has been found that ATM responds primarily to double-strand breaks induced by ionizing irradiation (IR), while ATR also reacts to UV or stalled replication forks^[13,14,26-29].

Activation of ATM and ATR

Several mechanisms have been proposed for the activation of ATM and ATR by DNA damage: a) direct activation through interaction with damaged DNA, b) indirect activation through interaction with DNA repair or maintenance proteins, or c) a combination of both^[30]. Existing experimental data support the third mechanism, that they are activated both through interactions with DNA and members of the repair complexes. For example, ATM could bind directly to DNA. Furthermore, pre-treatment of DNA-cellulose matrix with IR or restriction enzymes could stimulate ATM binding, suggesting that ATM binds to DNA ends^[31,32]. ATR could also bind to DNA, with a higher affinity to UV-damaged than undamaged DNA. In addition, damaged DNA could stimulate the kinase activity of ATR to a significantly higher level than undamaged DNA^[33,34]. ATM and ATR also interact with many proteins that co-localize at the site of DNA damage. For example, ATM as a part of a super protein complex called BRCA1-associated genome surveillance complex (BASC), is involved in the recognition and repair of aberrant DNA structures. It has been found this complex contains several other proteins such as breast cancer gene 1 (BRCA1), mismatch-repair protein hRad50, and BLM helicase^[35]. ATM could bind to histone deacetylase HDAC1 both *in vitro* and *in vivo*, and the extent of this association was increased after exposure of MRC5CV1 human fibroblasts to IR^[36]. ATR was also able to bind to Rad17^[37] and BRCA1^[38], and associated with components of the nucleosome remodeling and deacetylating (NRD) complex such as chromodomain-helicase-DNA-binding protein 4 (CHD4) and histone-deacetylase-2 (HDAC2)^[39]. All these data support the model that multiple checkpoint protein complexes localize at the sites of DNA damage independently and interact to trigger the checkpoint-signaling cascade.

Interaction with c-Abl

c-Abl, a non-receptor tyrosine kinase that is ubiquitously expressed and localized in both nucleus and cytoplasm, could be up-regulated following exposure to IR or genotoxic chemicals such as cisplatin, methyl methane sulfonate (MMS), mitomycin-C, hydrogen peroxide, but not UV^[3,40-42]. IR-induced activation of c-Abl has been shown to require the involvement of ATM in some cases, with ATM phosphorylating serine residue 465 located within the kinase domain of c-Abl^[43-45]. However, other studies found that c-Abl was not essential for ATM function in chromosomal maintenance, suggesting that c-Abl and ATM are at least partially independent^[46].

An important effect which has been found following the activation of c-Abl, is the induction of cell cycle arrest in a p53-dependent manner, with the possible involvement of Rb, but not p21^{Cip}^[47,48]. c-Abl could directly interact with and phosphorylate p53, and regulate the level of p53 by preventing its nuclear export and ubiquitination-dependent degradation^[49,50]. It could also induce apoptosis in response to DNA damage^[51,52], although this activity involved collaboration with p73 more than p53^[53-55]. c-Abl binds to p73 through its Src-homology (SH3) domain to phosphorylate p73 at tyrosine residues, which in turn activates p73-dependent apoptosis pathway.

Regulation of the tumor suppressor p53 protein

Since p53 is such an important mediator in cellular response to genotoxic stress, it is no wonder that ATM/ATR can regulate p53 activity at multiple levels (Figure 2). The most straightforward way to manage p53 is through direct interaction, e.g., phosphorylation of p53. Both ATM and ATR have been shown to phosphorylate p53 protein at serine 15 to enhance its transactivating activity^[56-59]. ATM is also required for dephosphorylation of Ser 376, which can create a binding site for 14-3-3 protein. The association of p53 and 14-3-3 could increase the affinity of p53 for its specific DNA sequence, therefore enhancing its transcriptional activity^[60]. Other sites that could be phosphorylated by ATM on p53 include Ser 6, 9, 46, and Thr 18, which may be important for the apoptotic activity of p53 (Ser 46) or may enhance the acetylation of p53 (Ser 6, 9, Thr18)^[61]. In addition, ATM/ATR could regulate p53 through the action of other kinases. For example, ATM-activated c-Abl could phosphorylate p53 at Ser 20, which is important for the stabilization of p53 since this modification interferes with the binding between p53 and its regulator murine double minute 2 (Mdm2)^[49,62]. ATM-activated Chk2 could also phosphorylate p53 protein at Ser 20 and possibly at other sites, leading to the activation of p53^[63-65]. Furthermore, ATM has been found able to bind and phosphorylate Mdm2 and HDM2 (the human homologue of Mdm2), thus inhibiting p53 degradation and promoting its accumulation in cells^[66-68].

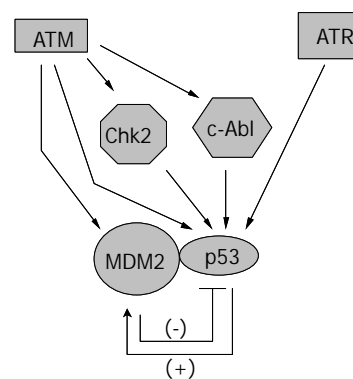


Figure 2 Regulation of p53 protein by ATM and ATR. ATM and ATR can influence the activity of p53 directly through phosphorylation or indirectly through the action of other kinases. Furthermore, ATM can regulate p53 through phosphorylation of Mdm2 molecule, the negative regulator of p53, which can be up-regulated by p53.

Activation of MAPKs

Accumulative data support the notion that the activation of MAPKs in response to genotoxic stress is ATM/ATR dependent. For example, DNA damaging stimuli, including etoposide (ETOP), adriamycin (ADR), IR, and UV could activate ERK1/2 in primary (MEF and IMR90), immortalized (NIH3T3) and transformed (MCF-7) cells. It has further been shown that ERK activation in response to ETOP could be

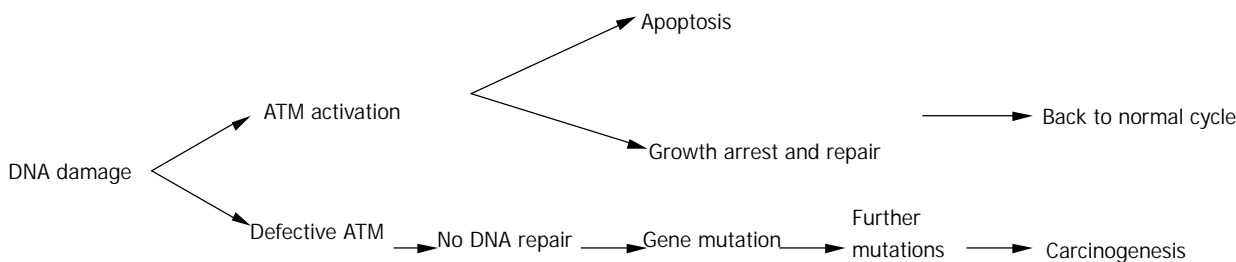


Figure 3 The relationship between ATM and carcinogenesis.

abolished in ATM^{-/-} fibroblasts (GM05823) independently of p53^[69]. UVA (320–400 nm) triggered ATM-dependent p53 phosphorylation and JNK activation that resulted in apoptosis, while ATR was required for UVC (200–290 nm)-mediated p53 phosphorylation and JNK activation^[70]. In addition, activation of ATM by gamma irradiation could lead to the activation of MKK6 and p38 γ isoform, and that activation of both MKK6 and p38 γ was essential for the proper regulation of G2 checkpoint in mammalian cells^[71].

Although the link between ATM/ATR and MAPKs has been established, it is still not clear how ATM/ATR activates MAPKs. In general, MAPK pathways are activated by extracellular signals or signals generated in the cytoplasm, and then the activated MAPKs transduce the specific “messages” to the nucleus. However, in response to genotoxic stress, the signal seems to flow from the nucleus to the cytoplasm to activate MAPKs. In this case, c-Abl kinase may provide an explanation. It has been found that c-Abl can activate p38 through MKK6^[72–74], and JNK by translocating from nucleus to cytoplasm to phosphorylate hematopoietic progenitor kinase (HPK1), an upstream kinase of JNK^[75]. Therefore, c-Abl may fulfill a role as the message carrier to transduce signals between subcellular locations. This may further explain why in response to genotoxic stress the activation of p38 was rather late (- 1 h) and prolonged^[71], while the cytokine activation of p38 was rapid and transient (maximum around 30–60 min)^[76].

In addition to their ability to activate MAPKs, ATM/ATR may also regulate these kinases through their negative regulators, the dual specificity of phosphatase MAPK and phosphatase family (MKP). One member of the MKP family, MKP-5, is known to dephosphorylate and inactivate the stress-activated JNK and p38. The phosphorylation-dephosphorylation cycle of JNK and p38 stimulated by radiomimetic chemical neocarzinostatin (NCS), which can induce double strand breaks (DSBs), could be attenuated in A-T cells^[77], further emphasizing the role of ATM as a master regulator in the cellular response to genotoxic stress.

Mutations in ATM in association with cancer

Homozygous mutations in the ATM gene can cause human genetic disorder ataxia-telangiectasia (A-T), which is characterized by cerebellar degeneration, immunodeficiency, cancer predisposition, and acute sensitivity to IR. The affected individual has been found to be prone to develop T cell prolymphocytic leukemia, B cell chronic lymphocytic leukemia, as well as sporadic colon cancer with microsatellite instability^[78]. ATM-deficient mice also showed a striking predisposition to lymphoid malignancies, particularly thymic lymphomas, to which they succumbed before the age of 1 year. However, much of the literature on ATM mutations and cancer was not about A-T patients, but was, instead, on heterozygous carriers of A-T mutations. For example, recent studies have found an unusually high occurrence of breast cancer in the relatives of A-T patients, and that loss of heterozygosity of ATM occurred frequently during the early stages of breast cancer development^[79].

Furthermore, heterozygous mice were more sensitive to radiation-induced cataracts than their wild-type counterparts^[80]. Spring *et al.*, established a knock-in mouse mutant in which an inframe deletion was previously found to cause A-T in humans was induced. Mice homozygous for this mutation could produce small amounts of inactive ATM and usually showed the hallmarks of the *Atm*-knockout phenotype. Notably, mice heterozygous for this mutation were predisposed to various cancers, unlike the animals that carry a single knockout allele that does not produce any protein^[81]. Therefore, ATM heterozygotes in human population might also be more radiosensitive, and have a higher risk for cancer^[82](Figure 3).

No human disease has been found to link to defects in ATR, although it was found that defects in ATR led to embryonic lethality in mice, suggesting that ATR is essential for development of ATR^[83,84]. Nonetheless, it is known that over-expressing the inactive form of ATR had a dominant negative effect, causing increased sensitivity to DNA damaging stimuli and failure to activate cell cycle checkpoints in response to IR^[28,85]. Finally, over-expressing active ATR could restore S phase checkpoint defect in A-T cells, suggesting that ATM and ATR may complement each other in the cellular genotoxic stress response^[85].

Down-regulation of ATM and ATR

Once the sensors detect DNA damage and initiate the signaling pathway, and the biological consequences (including DNA repair, cell cycle arrest, and apoptosis) take effect, the signals need to be inactivated or attenuated. The regulation of some downstream components in the cellular genotoxic stress response has been rather clearly defined, and usually involves a negative feedback mechanism. One such example is the p53-Mdm2 regulation loop. In this loop p53 could activate the expression of Mdm2, and Mdm2 could mediate the rapid degradation of p53 through the ubiquitin pathway^[62]. MAPKs have a similar feedback regulation mechanism with MKPs. MAPKs could induce the expression of MKPs, and MKPs then could interact with specific MAPKs to deactivate them through dephosphorylation^[1]. On the other hand, the mechanisms for the regulation of ATM and ATR, remain obscure, although some recent studies have significantly advanced our understanding.

In contrast to the vast volume of reports about the activation of ATM under genotoxic stress, very few studies have been conducted to evaluate how ATM was inactivated. The results from these studies so far all pointed toward inactivation of ATM through Caspase-mediated cleavage during apoptosis^[86–88]. This same mechanism has also been shown to regulate many other proteins involved in apoptosis, including serine/threonine protein kinase C δ (PKC δ), Mdm2, PARP, replication factor C, 70 kDa U1snRNP, fodrin and lamins^[87]. It was reported that during apoptosis induced by c-Myc or DNA-damaging agents (such as etoposide or IR), ATM but not ATR, was specifically cleaved by members of the Caspase family. Detailed studies revealed that the Caspase responsible for this

cleavage was either Caspase-3 or -7, but not Caspase-6. This cleavage abrogated the kinase activity of ATM to phosphorylate p53, although the resulting two fragments retained their DNA binding ability and interacted with each other. This finding led to the hypothesis that cleaved ATM protein, without its kinase activity, might act in a trans-dominant-negative fashion to compete with the intact ATM, thus preventing DNA repair and DNA damage signaling through its binding to DNA^[86-88].

Even less information is available regarding the inactivation of ATR. However, the recent identification of an ATR-interacting protein (ATRIP) might provide a lead for future studies^[89]. ATRIP is an 86-kDa protein with a coiled-coil domain near its N-terminal and its expression is regulated by ATR. The deletion of ATR mediated by Cre recombinase could cause the loss of both ATR and ATRIP expression, along with the loss of DNA damage checkpoint responses and cell death. ATRIP could be phosphorylated by ATR and co-localized at intranuclear foci with ATR after DNA damage caused by hydroxyurea (HU), IR, or UV, or inhibition of DNA replication. Conversely, ATRIP could also regulate the expression of ATR, as inhibition of ATRIP expression with small interference RNA (siRNA) would result in decreased ATR protein expression, while ATR mRNA levels would not be affected. Interference with ATRIP function could cause the same loss of G2-M response to DNA damage as that seen in the case of ATR deletion, suggesting that these two proteins work as mutually dependent partners in cell cycle checkpoint pathways^[89].

CONCLUSION

Human cancer is a major health issue for society, causing millions of deaths each year and huge economical losses. Since most of human carcinogens are genotoxins^[90,91], considerable resources have been and are being expended in efforts to understand the mechanism of genotoxin-induced carcinogenesis, thus leading to a better prevention or even the treatment of cancer. Since the sensing of DNA damage is one of the earliest steps in the cellular response to genotoxic stress, identification of these "sensors" is the most prominent challenge. As discussed in this review, ATM and ATR are showing their promise as potential candidates. However, what we should keep in mind is that detection of DNA damage may not be such a simple process, and may require more than just one or two proteins to fulfill this role. Supporting this idea is the finding of "foci" at damaged DNA sites, where many proteins involved in DNA repair and maintenance aggregate. It is more likely that interactions of these proteins, combined with some unidentified factors might function as DNA damage sensors^[92]. Further elucidation of these "foci" will be an exciting area for future research.

REFERENCES

- 1 **Yang J**, Yu Y, Duerksen-Hughes PJ. Protein kinases and their involvement in the cellular responses to genotoxic stress. *Mutat Res* 2003; **543**: 31-58
- 2 **Liu Y**, Guyton KZ, Gorospe M, Xu Q, Lee JC, Holbrook NJ. Differential activation of ERK, JNK/SAPK, and p38/CSBP/RK map kinase family members during the cellular response to arsenite. *Free Radic Biol Med* 1996; **21**: 771-781
- 3 **Liu ZG**, Baskaran R, Lea-Chou ET, Wood LD, Chen Y, Karin M, Wang JY. Three distinct signalling responses by murine fibroblasts to genotoxic stress. *Nature* 1996; **384**: 273-276
- 4 **Sanchez-Prieto R**, Rojas JM, Taya Y, Gutkind JS. A role for the p38 mitogen-activated protein kinase pathway in the transcriptional activation of p53 on genotoxic stress by chemotherapeutic agents. *Cancer Res* 2000; **60**: 2464-2472
- 5 **Kharbanda S**, Saxena S, Yoshida K, Pandey P, Kaneki M, Wang Q, Cheng K, Chen YN, Campbell A, Sudha T, Yuan ZM, Narula J, Weichselbaum R, Nalin C, Kufe D. Translocation of SAPK/JNK to mitochondria and interaction with Bcl-x(L) in response to DNA damage. *J Biol Chem* 2000; **275**: 322-327
- 6 **Zhang Y**, Zhong S, Dong Z, Chen N, Bode AM, Ma W, Dong Z. UVA induces Ser381 phosphorylation of p90RSK/MAPKAP-K1 via ERK and JNK pathways. *J Biol Chem* 2001; **276**: 14572-14580
- 7 **She QB**, Chen N, Dong Z. ERKs and p38 kinase phosphorylate p53 protein at serine 15 in response to UV radiation. *J Biol Chem* 2000; **275**: 20444-20449
- 8 **Akechi M**, Ito M, Uemura K, Takamatsu N, Yamashita S, Uchiyama K, Yoshioka K, Shiba T. Expression of JNK cascade scaffold protein JSAP1 in the mouse nervous system. *Neurosci Res* 2001; **39**: 391-400
- 9 **Tawadros T**, Formenton A, Dudler J, Thompson N, Nicod P, Leisinger HJ, Waeber G, Haefliger JA. The scaffold protein IB1/JIP-1 controls the activation of JNK in rat stressed urothelium. *J Cell Sci* 2002; **115**(pt2): 385-393
- 10 **Ito M**, Akechi M, Hirose R, Ichimura M, Takamatsu N, Xu P, Nakabeppu Y, Tadayoshi S, Yamamoto K, Yoshioka K. Isoforms of JSAP1 scaffold protein generated through alternative splicing. *Gene* 2000; **255**: 229-234
- 11 **Yang J**, Duerksen-Hughes P. A new approach to identifying genotoxic carcinogens: p53 induction as an indicator of genotoxic damage. *Carcinogenesis* 1998; **19**: 1117-1125
- 12 **Wahl GM**, Linke SP, Paulson TG, Huang LC. Maintaining genetic stability through TP53 mediated checkpoint control. *Cancer Surv* 1997; **29**: 183-219
- 13 **Lowndes NF**, Murguia JR. Sensing and responding to DNA damage. *Curr Opin Genet Dev* 2000; **10**: 17-25
- 14 **Abraham RT**. Cell cycle checkpoint signaling through the ATM and ATR kinases. *Genes Dev* 2001; **15**: 2177-2196
- 15 **Rouse J**, Jackson SP. Interfaces between the detection, signaling, and repair of DNA damage. *Science* 2002; **297**: 547-551
- 16 **O'Connell MJ**, Walworth NC, Carr AM. The G2-phase DNA-damage checkpoint. *Trends Cell Biol* 2000; **10**: 296-303
- 17 **Green CM**, Erdjument-Bromage H, Tempst P, Lowndes NF. A novel Rad24 checkpoint protein complex closely related to replication factor C. *Curr Biol* 2000; **10**: 39-42
- 18 **Roos-Mattjus P**, Vroman BT, Burtelow MA, Rauen M, Eapen AK, Karnitz LM. Genotoxin-induced Rad9-Hus1-Rad1 (9-1-1) chromatin association is an early checkpoint signaling event. *J Biol Chem* 2002; **277**: 43809-43812
- 19 **Durocher D**, Jackson SP. DNA-PK, ATM and ATR as sensors of DNA damage: variations on a theme? *Curr Opin Cell Biol* 2001; **13**: 225-231
- 20 **Rotman G**, Shiloh Y. ATM: a mediator of multiple responses to genotoxic stress. *Oncogene* 1999; **18**: 6135-6144
- 21 **Chan ED**, Winston BW, Jarpe MB, Wynes MW, Riches DW. Preferential activation of the p46 isoform of JNK/SAPK in mouse macrophages by TNF alpha. *Proc Natl Acad Sci U S A* 1997; **94**: 13169-13174
- 22 **Bao S**, Tibbetts RS, Brumbaugh KM, Fang Y, Richardson DA, Ali A, Chen SM, Abraham RT, Wang XF. ATR/ATM-mediated phosphorylation of human Rad17 is required for genotoxic stress responses. *Nature* 2001; **411**: 969-974
- 23 **Plumb MA**, Smith GC, Cunniffe SM, Jackson SP, O'Neil P. DNA-PK activation by ionizing radiation-induced DNA single-strand breaks. *Int J Radiat Biol* 1999; **75**: 553-561
- 24 **Jackson SP**. DNA-dependent protein kinase. *Int J Biochem Cell Biol* 1997; **29**: 935-938
- 25 **Gately DP**, Hittle JC, Chan GK, Yen TJ. Characterization of ATM expression, localization, and associated DNA-dependent protein kinase activity. *Mol Biol Cell* 1998; **9**: 2361-2374
- 26 **Pandita TK**, Lieberman HB, Lim DS, Dhar S, Zheng W, Taya Y, Kastan MB. Ionizing radiation activates the ATM kinase throughout the cell cycle. *Oncogene* 2000; **19**: 1386-1391
- 27 **Andegeko Y**, Moyal L, Mittelman L, Tsarfaty I, Shiloh Y, Rotman G. Nuclear retention of ATM at sites of DNA double strand breaks. *J Biol Chem* 2001; **276**: 38224-38230
- 28 **Wright JA**, Keegan KS, Herendeen DR, Bentley NJ, Carr AM, Hoekstra MF, Concannon P. Protein kinase mutants of human ATR increase sensitivity to UV and ionizing radiation and abrogate cell cycle checkpoint control. *Proc Natl Acad Sci U S A* 1998; **95**: 7445-7450

- 29 **Hekmat-Nejad M**, You Z, Yee MC, Newport JW, Cimprich KA. Xenopus ATR is a replication-dependent chromatin-binding protein required for the DNA replication checkpoint. *Curr Biol* 2000; **10**: 1565-1573
- 30 **Wahl GM**, Carr AM. The evolution of diverse biological responses to DNA damage: insights from yeast and p53. *Nature Cell Biol* 2001; **3**: E227-E286
- 31 **Suzuki K**, Kodama S, Watanabe M. Recruitment of ATM protein to double strand DNA irradiated with ionizing radiation. *J Biol Chem* 1999; **274**: 25571-25575
- 32 **Smith GC**, Cary RB, Lakin ND, Hann BC, Teo SH, Chen DJ, Jackson SP. Purification and DNA binding properties of the ataxia-telangiectasia gene product ATM. *Proc Natl Acad Sci U S A* 1999; **96**: 11134-11139
- 33 **Guo Z**, Kumagai A, Wang SX, Dunphy WG. Requirement for Atr in phosphorylation of Chk1 and cell cycle regulation in response to DNA replication blocks and UV-damaged DNA in *Xenopus* egg extracts. *Genes Dev* 2000; **14**: 2745-2756
- 34 **Unsal-Kacmaz K**, Makhov AM, Griffith JD, Sancar A. Preferential binding of ATR protein to UV-damaged DNA. *Proc Natl Acad Sci U S A* 2002; **99**: 6673-6678
- 35 **Wang Y**, Cortez D, Yazdi P, Neff N, Elledge SJ, Qin J. BASC, a super complex of BRCA1-associated proteins involved in the recognition and repair of aberrant DNA structures. *Genes Dev* 2000; **14**: 927-939
- 36 **Kim GD**, Choi YH, Dimtchev A, Jeong SJ, Dritschilo A, Jung M. Sensing of ionizing radiation-induced DNA damage by ATM through interaction with histone deacetylase. *J Biol Chem* 1999; **274**: 31127-31130
- 37 **Zou L**, Cortez D, Elledge SJ. Regulation of ATR substrate selection by Rad17-dependent loading of Rad9 complexes onto chromatin. *Genes Dev* 2002; **16**: 198-208
- 38 **Tibbetts RS**, Cortez D, Brumbaugh KM, Scully R, Livingston D, Elledge SJ, Abraham RT. Functional interactions between BRCA1 and the checkpoint kinase ATR during genotoxic stress. *Genes Dev* 2000; **14**: 2989-3002
- 39 **Schmidt DR**, Schreiber SL. Molecular association between ATR and two components of the nucleosome remodeling and deacetylating complex, HDAC2 and CHD4. *Biochemistry* 1999; **38**: 14711-14717
- 40 **Wang JY**. Cellular responses to DNA damage. *Curr Opin Cell Biol* 1998; **10**: 240-247
- 41 **Wen ST**, Van Etten RA. The PAG gene product, a stress-induced protein with antioxidant properties, is an Abl SH3-binding protein and a physiological inhibitor of c-Abl tyrosine kinase activity. *Genes Dev* 1997; **11**: 2456-2467
- 42 **Kharbanda S**, Ren R, Pandey P, Shafman TD, Feller SM, Weichselbaum RR, Kufe DW. Activation of the c-Abl tyrosine kinase in the stress response to DNA-damaging agents. *Nature* 1995; **376**: 785-788
- 43 **Shafman T**, Khanna KK, Kedar P, Spring K, Kozlov S, Yen T, Hobson K, Gatei M, Zhang N, Watters D, Egerton M, Shiloh Y, Kharbanda S, Kufe D, Lavin MF. Interaction between ATM protein and c-Abl in response to DNA damage. *Nature* 1997; **387**: 520-523
- 44 **Baskaran R**, Wood LD, Whitaker LL, Canman CE, Morgan SE, Xu Y, Barlow C, Baltimore D, Wynshaw-Boris A, Kastan MB, Wang JY. Ataxia telangiectasia mutant protein activates c-Abl tyrosine kinase in response to ionizing radiation. *Nature* 1997; **387**: 516-519
- 45 **Shangary S**, Brown KD, Adamson AW, Edmonson S, Ng B, Pandita TK, Yalowich J, Taccioli GE, Baskaran R. Regulation of DNA-dependent protein kinase activity by ionizing radiation-activated Abl kinase is an ATM-dependent process. *J Biol Chem* 2000; **275**: 30163-30168
- 46 **Takao N**, Mori R, Kato H, Shinohara A, Yamamoto K. c-Abl tyrosine kinase is not essential for ataxia telangiectasia mutated functions in chromosomal maintenance. *J Biol Chem* 2000; **275**: 725-728
- 47 **Yuan ZM**, Huang Y, Whang Y, Sawyers C, Weichselbaum R, Kharbanda S, Kufe D. Role for c-Abl tyrosine kinase in growth arrest response to DNA damage. *Nature* 1996; **382**: 272-274
- 48 **Wen ST**, Jackson PK, van Etten RA. The cytosolic function of c-Abl is controlled by multiple nuclear localization signals and requires the p53 and Rb tumor suppressor gene products. *EMBO J* 1996; **15**: 1583-1595
- 49 **Sionov RV**, Moallem E, Berger M, Kazaz A, Gerlitz O, Ben-Neriah Y, Oren M, Haupt Y. C-Abl neutralizes the inhibitory effect of Mdm2 on p53. *J Biol Chem* 1999; **274**: 8371-8374
- 50 **Sionov RV**, Coen S, Goldberg Z, Berger M, Bercovich B, Ben-Neriah Y, Ciechanover A, Haupt Y. C-Abl regulates p53 levels under normal and stress conditions by preventing its nuclear export and ubiquitination. *Mol Cell Biol* 2001; **21**: 5869-5878
- 51 **Huang Y**, Yuan ZM, Ishiko T, Nakada S, Utsugisawa T, Kato T, Kharbanda S, Kufe DW. Pro-apoptotic effect of the c-Abl tyrosine kinase in the cellular response to 1-beta-D-arabinofuranosylcytosine. *Oncogene* 1997; **15**: 1947-1952
- 52 **Yuan ZM**, Huang Y, Ishiko T, Kharbanda S, Weichselbaum R, Kufe D. Regulation of DNA damage-induced apoptosis by the c-Abl tyrosine kinase. *Proc Natl Acad Sci U S A* 1997; **94**: 1437-1440
- 53 **Shaul Y**. C-Abl: activation and nuclear targets. *Cell Death Differ* 2000; **7**: 10-16
- 54 **Gong JG**, Costanzo A, Yang HQ, Melino G, Kaelin WG Jr, Levrero M, Wang JY. The tyrosine kinase c-Abl regulates p73 in apoptotic response to cisplatin-induced DNA damage. *Nature* 1999; **399**: 806-809
- 55 **Agami R**, Blandino G, Oren M, Shaul Y. Interaction of c-Abl and p73alpha and their collaboration to induce apoptosis. *Nature* 1999; **399**: 809-813
- 56 **Canman CE**, Lim DS, Cimprich KA, Taya Y, Tamai K, Sakaguchi K, Appella E, Kastan MB, Siliciano JD. Activation of the ATM kinase by ionizing radiation and phosphorylation of p53. *Science* 1998; **281**: 1677-1679
- 57 **Banin S**, Moyal L, Shieh S, Taya Y, Anderson CW, Chessa L, Smorodinsky NI, Prives C, Reiss Y, Shiloh Y, Ziv Y. Enhanced phosphorylation of p53 by ATM in response to DNA damage. *Science* 1998; **281**: 1674-1677
- 58 **Nakagawa K**, Taya Y, Tamai K, Yamaizumi M. Requirement of ATM in phosphorylation of the human p53 protein at serine 15 following DNA double-strand breaks. *Mol Cell Biol* 1999; **19**: 2828-2834
- 59 **Tibbetts RS**, Brumbaugh KM, Williams JM, Sarkaria JN, Cliby WA, Shieh SY, Taya Y, Prives C, Abraham RT. A role for ATR in the DNA damage-induced phosphorylation of p53. *Genes Dev* 1999; **13**: 152-157
- 60 **Waterman MJ**, Stavridi ES, Waterman JL, Halazonetis TD. ATM-dependent activation of p53 involves dephosphorylation and association with 14-3-3 proteins. *Nat Genet* 1998; **19**: 175-178
- 61 **Saito S**, Goodarzi AA, Higashimoto Y, Noda Y, Lees-Miller SP, Appella E, Anderson CW. ATM mediates phosphorylation at multiple p53 sites, including Ser(46), in response to ionizing radiation. *J Biol Chem* 2002; **277**: 12491-12494
- 62 **Alarcon-Vargas D**, Ronai Z. p53-Mdm2—the affair that never ends. *Carcinogenesis* 2002; **23**: 541-547
- 63 **Hirao A**, Kong YY, Matsuoka S, Wakeham A, Ruland J, Yoshida H, Liu D, Elledge SJ, Mak TW. DNA damage-induced activation of p53 by the checkpoint kinase Chk2. *Science* 2000; **287**: 1824-1827
- 64 **Chehab NH**, Malikzay A, Appel M, Halazonetis TD. Chk2/hCds1 functions as a DNA damage checkpoint in G₁ by stabilizing p53. *Genes Dev* 2000; **14**: 278-288
- 65 **Chehab NH**, Malikzay A, Stavridi ES, Halazonetis TD. Phosphorylation of Ser-20 mediates stabilization of human p53 in response to DNA damage. *Proc Natl Acad Sci U S A* 1999; **96**: 13777-13782
- 66 **Khosravi R**, Maya R, Gottlieb T, Oren M, Shiloh Y, Shkedy D. Rapid ATM-dependent phosphorylation of MDM2 precedes p53 accumulation in response to DNA damage. *Proc Natl Acad Sci U S A* 1999; **96**: 14973-14977
- 67 **de Toledo SM**, Azzam EI, Dahlberg WK, Gooding TB, Little JB. ATM complexes with HDM2 and promotes its rapid phosphorylation in a p53-independent manner in normal and tumor human cells exposed to ionizing radiation. *Oncogene* 2000; **19**: 6185-6193
- 68 **Maya R**, Balass M, Kim ST, Shkedy D, Leal JF, Shifman O, Moas M, Buschmann T, Ronai Z, Shiloh Y, Kastan MB, Katzir E, Oren M. ATM-dependent phosphorylation of Mdm2 on serine 395: role in p53 activation by DNA damage. *Genes Dev* 2001; **15**: 1067-1077
- 69 **Tang D**, Wu D, Hirao A, Lahti JM, Liu L, Mazza B, Kidd VJ, Mak TW, Ingram AJ. ERK activation mediates cell cycle arrest and apoptosis after DNA damage independently of p53. *J Biol Chem*

- 2002; **277**: 12710-12717
- 70 **Zhang Y**, Ma WY, Kaji A, Bode AM, Dong Z. Requirement of ATM in UVA-induced signaling and apoptosis. *J Biol Chem* 2002; **277**: 3124-3131
- 71 **Wang X**, McGowan CH, Zhao M, He L, Downey JS, Fearn C, Wang Y, Huang S, Han J. Involvement of the MKK6-p38 γ cascade in γ -radiation-induced cell cycle arrest. *Mol Cell Biol* 2000; **20**: 4543-4552
- 72 **Sanchez-Prieto R**, Sanchez-Arevalo VJ, Servitja JM, Gutkind JS. Regulation of p73 by c-Abl through the p38 MAP kinase pathway. *Oncogene* 2002; **21**: 974-979
- 73 **Pandey P**, Raingeaud J, Kaneki M, Weichselbaum R, Davis RJ, Kufe D, Kharbanda S. Activation of p38 mitogen-activated protein kinase by c-Abl-dependent and -independent mechanisms. *J Biol Chem* 1996; **271**: 23775-23779
- 74 **Cong F**, Goff SP. C-Abl-induced apoptosis, but not cell cycle arrest, requires mitogen-activated protein kinase kinase 6 activation. *Proc Natl Acad Sci U S A* 1999; **96**: 13819-13824
- 75 **Ito Y**, Pandey P, Sathyanarayana P, Ling P, Rana A, Weichselbaum R, Tan TH, Kufe D, Kharbanda S. Interaction of hematopoietic progenitor kinase 1 and c-Abl tyrosine kinase in response to genotoxic stress. *J Biol Chem* 2001; **276**: 18130-18138
- 76 **Liu RY**, Fan C, Liu G, Olashaw NE, Zuckerman KS. Activation of p38 mitogen-activated protein kinase is required for tumor necrosis factor- α -supported proliferation of leukemia and lymphoma cell lines. *J Biol Chem* 2000; **275**: 21086-21093
- 77 **Bar-Shira A**, Rashi-Elkeles S, Zlochover L, Moyal L, Smorodinsky NI, Seger R, Shiloh Y. ATM-dependent activation of the gene encoding MAP kinase phosphatase 5 by radiomimetic DNA damage. *Oncogene* 2002; **21**: 849-855
- 78 **Ejima Y**, Yang L, Sasaki MS. Aberrant splicing of the ATM gene associated with shortening of the intronic mononucleotide tract in human colon tumor cell lines: a novel mutation target of microsatellite instability. *Int J Cancer* 2000; **86**: 262-268
- 79 **Shen CY**, Yu JC, Lo YL, Kuo CH, Yue CT, Jou YS, Huang CS, Lung JC, Wu CW. Genome-wide search for loss of heterozygosity using laser capture microdissected tissue of breast carcinoma: an implication for mutator phenotype and breast cancer pathogenesis. *Cancer Res* 2000; **60**: 3884-3892
- 80 **Worgul BV**, Smilenov L, Brenner DJ, Junk A, Zhou W, Hall EJ. Atm heterozygous mice are more sensitive to radiation-induced cataracts than are their wild-type counterparts. *Proc Natl Acad Sci U S A* 2002; **99**: 9836-9839
- 81 **Spring K**, Ahangari F, Scott SP, Waring P, Purdie DM, Chen PC, Hourigan K, Ramsay J, McKinnon PJ, Swift M, Lavin MF. Mice heterozygous for mutation in Atm, the gene involved in ataxia-telangiectasia, have heightened susceptibility to cancer. *Nat Genet* 2002; **32**: 185-190
- 82 **Concannon P**. ATM heterozygosity and cancer risk. *Nat Genet* 2002; **32**: 89-90
- 83 **Brown EJ**, Baltimore D. ATR disruption leads to chromosomal fragmentation and early embryonic lethality. *Genes Dev* 2000; **14**: 397-402
- 84 **de Klein A**, Muijtjens M, van Os R, Verhoeven Y, Smit B, Carr AM, Lehmann AR, Hoeijmakers JH. Targeted disruption of the cell-cycle checkpoint gene ATR leads to early embryonic lethality in mice. *Curr Biol* 2000; **10**: 479-482
- 85 **Cliby WA**, Roberts CJ, Cimprich KA, Stringer CM, Lamb JR, Schreiber SL, Friend SH. Overexpression of a kinase-inactive ATR protein causes sensitivity to DNA-damaging agents and defects in cell cycle checkpoints. *EMBO J* 1998; **17**: 159-169
- 86 **Smith GC**, d'Adda di Fagagna F, Lakin ND, Jackson SP. Cleavage and inactivation of ATM during apoptosis. *Mol Cell Biol* 1999; **19**: 6076-6084
- 87 **Hotti A**, Jarvinen K, Siivola P, Holtta E. Caspases and mitochondria in c-Myc-induced apoptosis: identification of ATM as a new target of caspases. *Oncogene* 2000; **19**: 2354-2362
- 88 **Tong X**, Liu B, Dong Y, Sun Z. Cleavage of ATM during radiation-induced apoptosis: caspase-3-like apoptotic protease as a candidate. *Int J Radiat Biol* 2000; **76**: 1387-1395
- 89 **Cortez D**, Guntuku S, Qin J, Elledge SJ. ATR and ATRIP: partners in checkpoint signaling. *Science* 2001; **294**: 1713-1716
- 90 **Williams GM**, Weisburger JH. Chemical Carcinogenesis. New York, NY, Pergamon Press 1991
- 91 **Smart RC**. Carcinogenesis. Norwalk, CT, Appleton Lange 1994
- 92 **Yang J**, Yu Y, Hamrick HE, Duerksen-Hughes PJ. ATM, ATR, and DNA-PK: initiators of the cellular genotoxic stress responses. *Carcinogenesis* 2003; **24**: 1571-1580

Edited by Zhu LH and Wang XL

Effect of staurosporine on cycle human gastric cancer cell

Min-Wen Ha, Ke-Zuo Hou, Yun-Peng Liu, Yuan Yuan

Min-Wen Ha, Yuan Yuan, Cancer Institute of the First Affiliated Hospital of China Medical University, Shenyang 110001, Liaoning Province, China

Ke-Zuo Hou, Yun-Peng Liu, Department of Oncology of the First Affiliated Hospital of China Medical University, Shenyang 110001, Liaoning Province, China

Supported by The China State Key Basic Research Program, No. G1998051203

Correspondence to: Professor Yuan Yuan, Cancer Institute of the First Affiliated Hospital of China Medical University, 155 Northern Nanjing Street, Heping District, Shenyang 110001, Liaoning Province, China. yyuan@mail.cmu.edu.cn

Telephone: +86-24-23256666 **Fax:** +86-24-22703576

Received: 2003-06-05 **Accepted:** 2003-07-24

Abstract

AIM: To study the effect of staurosporine (ST) on the cell cycle of human gastric cancer cell lines MGC803 and SGC7901.

METHODS: Cell proliferation was evaluated by trypan blue dye exclusion method. Apoptotic morphology was observed under a transmission electron microscope. Changes of cell cycle and apoptotic peaks of cells were determined by flow cytometry. Expression of *p21^{WAF1}* gene was examined using immunohistochemistry and RT-PCR.

RESULTS: The growth of MGC803 and SGC7901 cells was inhibited by ST. The inhibitory concentrations against 50% cells (IC_{50}) at 24 h and 48 h were 54 ng/ml and 23 ng/ml for MGC803, and 61 ng/ml and 37 ng/ml for SGC7901. Typical apoptotic bodies and apoptotic peaks were observed 24 h after cells were treated with ST at a concentration of 200 ng/ml. The percentage of cells at G_0/G_1 phase was decreased and that of cells at G_2/M was increased significantly in the group treated with ST at the concentrations of 40 ng/ml, 60 ng/ml, 100 ng/ml for 24 h, compared with the control group ($P < 0.01$). The expression levels of *p21^{WAF1}* gene in both MGC803 and SGC7901 cells were markedly up-regulated after treatment with ST.

CONCLUSION: ST can cause arrest of gastric cancer cells at G_2/M phase, which may be one of the mechanisms that inhibit cell proliferation and cause apoptosis in these cells. Effect of ST on cells at G_2/M phase may be attributed to the up-regulation of *p21^{WAF1}* gene.

Ha MW, Hou KZ, Liu YP, Yuan Y. Effect of staurosporine on cycle human gastric cancer cell. *World J Gastroenterol* 2004; 10(2): 161-166

<http://www.wjgnet.com/1007-9327/10/161.asp>

INTRODUCTION

Protein kinase C (PKC) isoforms are serine/threonine kinases involved in signal transduction pathways that govern a wide range of physiological processes including differentiation, proliferation, gene expression, membrane transport and

organization of cytoskeletal and extracellular matrix proteins^[1]. PKC isoforms are often overexpressed in disease states such as cancer. The important role they play in the processes relevant to neoplastic transformation, carcinogenesis and tumor cell invasion renders PKC a potentially suitable target for anticancer therapy^[2].

Staurosporine (ST), a microbial alkaloid (indolocarbazole produced by *Streptomyces sp.*), has been shown to be a potent inhibitor of a wide range of protein kinases, including different serine/threonine and tyrosine protein kinases, which acts by competing with the ATP-binding region of the kinase catalytic domain^[3]. Staurosporine has been reported to exert various pharmacological actions involving protein kinase C both *in vivo* and *in vitro*, such as diminishing thrombin enhanced procoagulant activity, reducing carbachol-induced insulin secretion^[4-7]. PKC function is altered in some neoplasias, and this dysfunction has been related to uncontrolled proliferation^[8,9].

Completion of the cell cycle requires the coordination of a variety of macromolecular syntheses, assemblies, and movements^[10]. Coordination of the timing and order of these processes are achieved by a regulatory system that responds to checkpoints at major transitions in the cycle. Two key checkpoints are at the G_1/S and G_2/M phase transitions. G_1 and G_2 cyclins, the cyclin-dependent kinases and cycle kinase inhibitors (CKI) are responsible for controlling the transitions. Here, we investigated the effect of the potent phospholipid/ Ca^{2+} -dependent kinase (PKC) inhibitor, ST, on cell cycle of human gastric cancer cell lines, MGC803 and SGC7901.

MATERIALS AND METHODS

Cell lines and cell culture

Human gastric mucinous adenocarcinoma cell line, MGC803, was obtained from Department of Immunity, China Medical University and human gastric carcinoma metastatic lymph node cell line, SGC7901, was obtained from Laboratory of Oncology, the First Affiliated Hospital of China Medical University. The derived cell lines were grown in RPMI 1640 medium supplemented with 10% heat-inactivated fetal calf serum, 50 U/ml penicillin and 50 μ g/ml streptomycin. The cells were maintained at 37 °C in a humidified atmosphere containing 5% CO_2 . Viability of the cells used in these experiments was consistently more than 95% when evaluated by the trypan blue exclusion method. Staurosporine was purchased from Sigma Company (St. Louis, USA).

Analysis of cell viability

Effect of ST on cell growth and viability was measured by directly counting the number of cells by means of trypan blue dye exclusion. Cells at a density of 2.5×10^5 /ml were seeded onto 24-well plates, and then treated with ST at different concentrations for 24 and 48 h. Control cells were also cultured at the same time. Cell proliferation and inhibition curves were drawn, and the inhibitory concentration against 50% cells (IC_{50}) was determined.

Cell morphological analysis with transmission electron microscope

Transmission electronic microscope was employed to observe

the effect of ST on cell apoptosis. Cells (1×10^6) were collected after being treated with ST at 200 ng/ml for 24 h, washed twice with PBS solution, centrifuged for 5 min at 1 500 rpm, then fixed in 2% glutaraldehyde at 4 °C for 72 h, then placed in 1% phosphotungstic acid. The cells were desiccated with gradients, and embedded with EPON-812. Ultrathin sections were prepared and observed after double staining with uranium and plumbum under a transmission electron microscope. Each experiment was repeated four times. At the same time, the cells without treatment with ST were used as a control group.

Cell cycle analysis

Flow cytometry was employed to determine the DNA content and the apoptotic peaks of the cells. The cells were seeded on 100 mm-dishes and grown in RPMI-1640 supplemented with 10% FCS. After treated with ST at the concentrations of 40 ng/ml, 60 ng/ml, 100 ng/ml, 200 ng/ml, 500 ng/ml for 24 h respectively, the cells were harvested, trypsinized, washed with D-PBS, fixed by adding slowly 2 ml of cold 70% ethanol into the tube and then stored at 4 °C. After fixation, the cells were washed, centrifuged, and resuspended in 0.05 mg/ml propidium iodide (Fluka Co, MILWAUKEE, USA), 100 units/ml RNase (Fluka Co, MILWAUKEE, USA) in PBS. The sample was incubated at room temperature for 30 min, and analyzed on a FACSCalibur (BD PharMingen, FRANKLIN Lakes, USA). Cell cycle data originally obtained with Cell Quest software (BD PharMingen, FRANKLIN Lakes, USA) were re-analyzed using MODFIT software (Verity Software House, Topsham, USA). At the same time negative controls were constructed.

Immunohistochemistry

p21 protein was detected by immunohistochemistry using specific monoclonal antibody (Maxin Co, Fuzhou, China). After treated with ST at the concentrations 40 ng/ml, 60 ng/ml, 100 ng/ml for 24 h, respectively, the cells were harvested. At the same time the negative controls were constructed. The cells were smeared on a slide with cell smear centrifugal apparatus, and stained using conventional S-P immunohistochemical method. Color was developed with DAB reagent and counterstained with hematoxylin. The cells were observed under a light microscope. The cells clearly showing brown color in their nuclei and plasma were considered to be positive for p21 protein.

Semiquantitative reverse transcription-PCR

The expression of p21 mRNA was determined by RT-PCR. After treated with ST at the concentration of 60 ng/ml, the cells were harvested. At the same time the negative controls were constructed. The cells were washed, and total RNA was extracted with the Qiagen RNA isolation kit (GIBCO Co., New York, USA). Aliquots containing 5 µg/ml of RNA from each treatment were used for the first-strand cDNA synthesis (TaKaRa Co., Dalian, China). In each reaction, 100 µl solution containing 3 µM of random hexamers, 25 mM Tris-HCl, 37 mM KCl, 1.5 mM MgCl₂, 10 mM DTT, 0.25 mM dNTP, 40 units of RNasin, an RNase inhibitor, 50 U/ml Super Taq DNA polymerase, and 200 units of reverse transcriptase was used. The annealing mixture was incubated at room temperature for 15 min, and then incubated in a water bath at 41 °C for 60 min. The reverse transcriptase enzyme was inactivated by heating the solution to 95 °C for 5 min. PCR was then carried out using the Perkin-Elmer PCR reaction kit and primers. The PCR was performed using a thermocycler for 30 cycles consisting of denaturation at 94 °C for 1 min, annealing at 57 °C for 1 min, and extension at 72 °C for 2 min. The PCR products were separated on 2% agarose gel. The primers used for PCR

were as follow: p21 sense (5' -GGG GAC AGC AGA GGA AGA C-3'), p21 antisense (5' -CGG CGT TTG GAG TGG TAG A-3'); β-actin sense (5' -GAT TGC CTC AGG ACA TTT CTG- 3'), β-actin antisense (5' -GAT TGC TCA GGA CAT TTC TG-3'). Gene primers were synthesized by Beijing Oake Company (Beijing, China).

Statistical analysis

Student's *t*-test was used to compare the difference between control and ST treated groups. Data of cell growth were presented as $\bar{x} \pm s$. A *P* value less than 0.05 was considered statistically significant.

RESULTS

ST inhibited proliferation of MGC803 and SGC7901 cells in a time-dependent and concentration-dependent manner

In this study, the exponentially grown MGC803 and SGC7901 cells were treated with 40 ng/ml, 60 ng/ml, 100 ng/ml ST, respectively, and the cell proliferation was measured 24 and 48 h after ST addition. Figures 1 and 2 show the cell proliferation curves at various ST concentrations. The inhibition of proliferation of MGC803 and SGC7901 cells by ST was clearly observed in a time-dependent and concentration-dependent manner. The IC₅₀ was 54 ng/ml and 23 ng/ml for MGC803 and 61 ng/ml and 37 ng/ml for SGC7901 at 24 and 48 h.

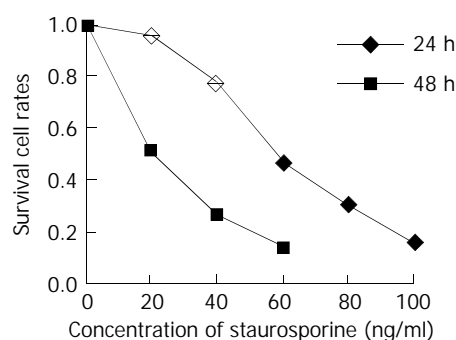


Figure 1 Inhibition of staurosporine on MGC-803 cell proliferation.

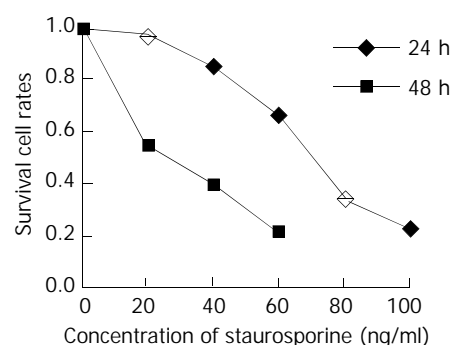


Figure 2 Inhibition of staurosporine on SGC-7901 cell proliferation.

Morphological observation of ST treatment effects

Cell morphological changes were observed under a transmission electron microscope after treatment with ST at the concentration of 200 ng/ml for 24 h. The ultrastructural appearances showed the typical changes in the cell morphology, including blebbing of the plasma membrane, chromatin condensation and formation of apoptotic bodies. Figure 3 shows the morphological changes of MGC803 and SGC7901 cells under a electron microscope after treatment with ST.

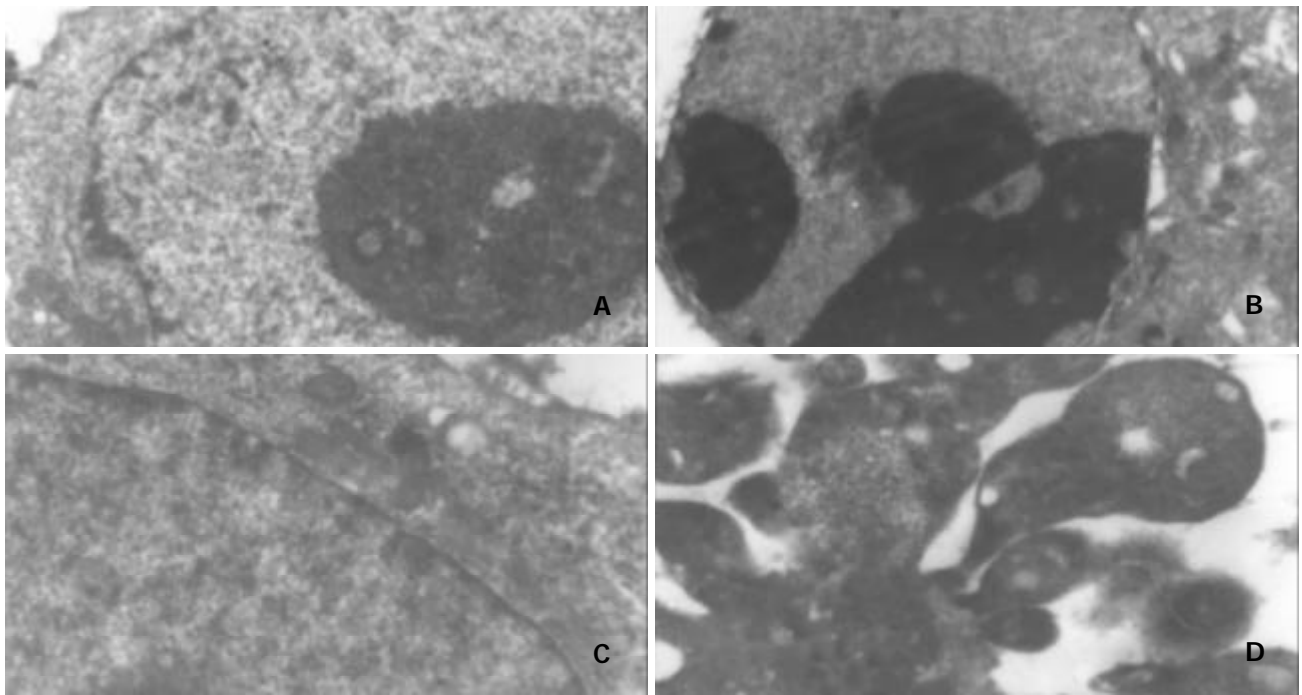


Figure 3 Morphological changes in MGC803 and SGC7901 cells under electron microscope after treatment with ST (200 ng/ml), $\times 5000$. A: MGC803 control cells, B: 200 ng/ml ST-induced MGC803 cells, C: SGC7901 control cells, D: 200 ng/ml ST-induced SGC7901 cells. Note: chromatin condensation and formation of apoptotic bodies.

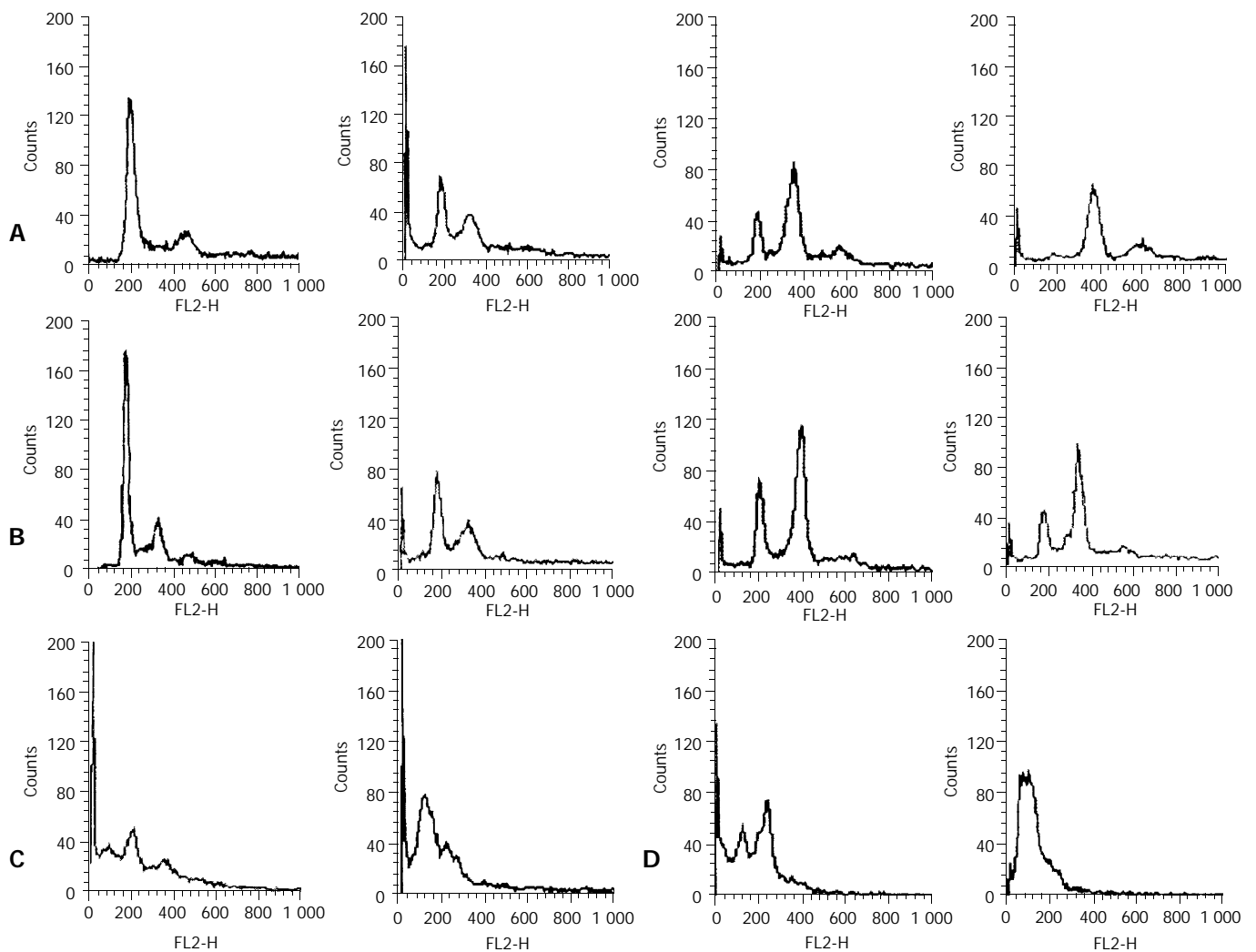


Figure 4 Effect of ST on cell cycle of human gastric cancer cells. A: Changes of cell cycle in MGC803 cells after ST-treatment for 24h, B: Changes of cell cycle in SGC7901 cells after ST-treatment for 24 h, C: ST-induced apoptosis in MGC-803 cells, D: ST-induced apoptosis in SGC-7901 cells.

Table 1 Effect of ST on cell cycle of MGC803 and SGC7901 cells ($\bar{x}\pm s$)

	MGC803				SGC7901			
	G ₀ /G ₁ (%)	S(%)	G ₂ /M(%)	AI	G ₀ /G ₁ (%)	S(%)	G ₂ /M(%)	AI
Control	54.3±3.1	15.2±0.6	13.5±0.2	3.1±0.2	52.5±4.4	10.1±0.6	13.5±2.2	2.8±0.2
40 ng/ml	23.6±1.8 ^a	13.9±1.1	22.6±4.0 ^a	3.8±0.9	27.1±1.4 ^a	12.4±0.1	21.9±2.6 ^a	3.3±0.3
60 ng/ml	11.6±0.7 ^a	12.6±2.8	35.5±0.4 ^a	4.0±0.3	17.0±3.4 ^a	13.4±2.0	39.5±4.9 ^a	3.7±0.6
100 ng/ml	3.3±0.2 ^a	10.9±1.7	36.8±5.5 ^a	5.2±0.4	13.7±0.7 ^a	12.7±0.9	38.4±3.1 ^a	4.4±1.1

AI, apoptotic incidence; ^a $P<0.01$ vs Control.

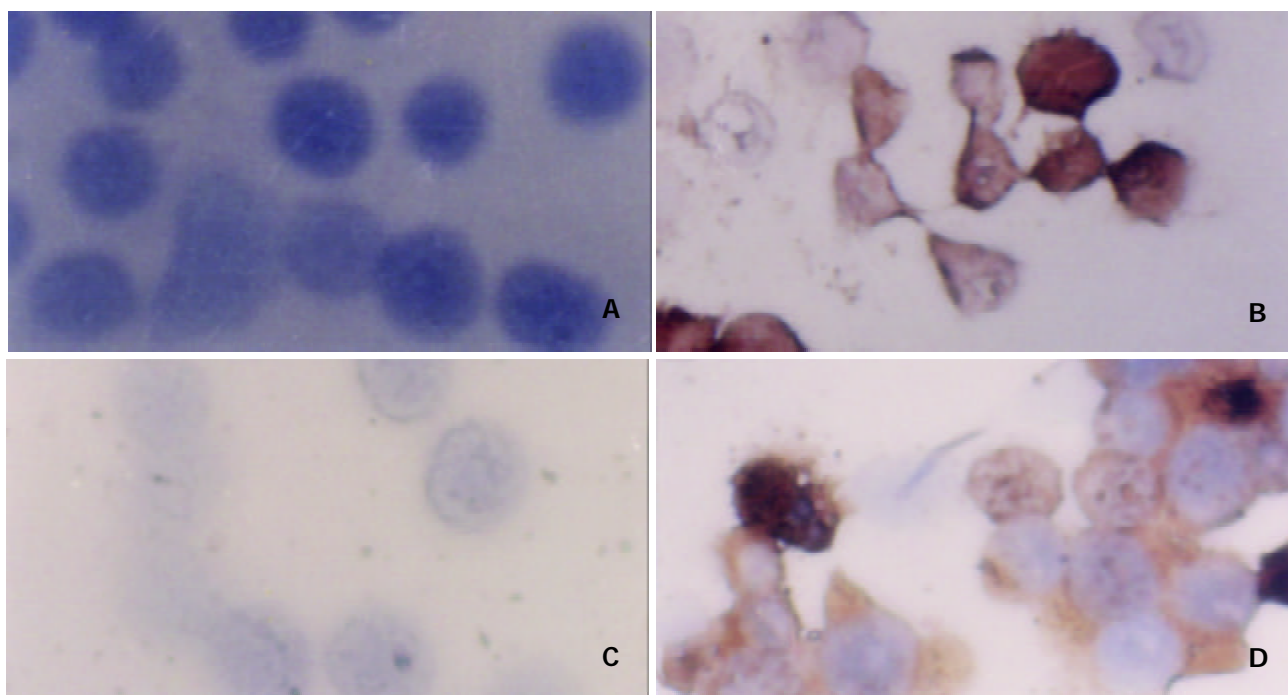


Figure 5 Expression of p21 protein in MGC803 and SGC7901 cells after ST-treatment as determined by immunohistochemistry (SP×400). A: MGC803 control cells, B: MGC803 cells treated with 60 ng/ml ST, C: SGC7901 control cells, D: SGC7901 cells treated with 60 ng/ml ST.

ST induced MGC803 and SGC7901 cells G₂/M phase arrest

The effects of ST on cell cycle progression, population distribution and apoptotic incidence in MGC803 and SGC7901 cells were determined using flow cytometry. ST-induced effects were detected by comparing the cell cycle profiles between ST treated and untreated cells. Notably, the cells demonstrated significant G₂/M arrest 24 h after ST treatment ($P<0.01$), in comparison to untreated cells. Interestingly, the S phase population was also increased, but to a lesser extent as compared with untreated cells. The percentage of cells in the S, G₁, and G₂/M phases are shown in Table 1. Apoptotic peaks were observed and cell apoptotic incidence was determined 24 h after treatment with ST at the concentrations of 200 ng/ml and 500 ng/ml. The apoptotic incidence increased to 50.2% and 89.6% in MGC803 cells, and 34.6% and 80.7% in SGC7901 cells after ST treatment. Figure 4 shows ST-induced apoptosis in MGC803 and SGC7901 cells.

ST resulted in an increase of p21 expression

The effect of ST on p21 protein levels was determined by immunohistochemistry analysis. Normally, p21 was not expressed in MGC803 and SGC7901 cells. However, p21 was significantly expressed, the positive rates were 19.3%, 26.6%, 31.8% in MGC803 cells, and 20.5%, 24.2%, 30.3% in SGC7901 cells after treatment with ST at the concentration 40 ng/ml, 60 ng/ml, 100 ng/ml for 24 h. Figure 5 shows the

levels of p21 expression in MGC803 and SGC7901 cells by immunohistochemistry.

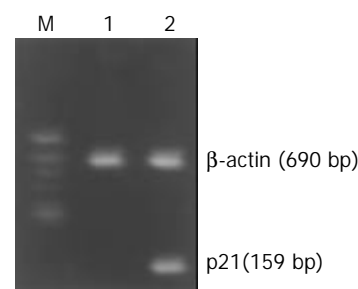


Figure 6 Effect of ST treatment on p21^{WAF1} mRNA expression in MGC803 cells. M: DNA Marks, 1: control cells, 2: cells treated with 60 ng/ml ST.

ST upregulated p21^{WAF1} expression

Normally, p21^{WAF1} mRNA was almost not expressed in MGC803 and SGC7901 cells when detected by RT-PCR. However, treatment with ST at the concentration of 60 ng/ml induced the upregulation of p21^{WAF1} mRNA in MGC803 and SGC7901 cells. Figures 6 and 7 show that p21^{WAF1} mRNA expression was upregulated in MGC803 and SGC7901 cells after treatment with ST.

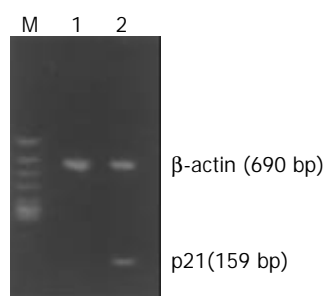


Figure 7 Effect of ST treatment on p21^{WAF1} mRNA expression in SGC7901 cells. M: DNA Marks, 1: control cells, 2: cells treated with 60 ng/ml ST.

DISCUSSION

Cancer cells have been found to be different from normal cells in many important characteristics, including loss of differentiation and decrease of apoptosis^[11,12]. These differences did not arise simply from uncontrolled cellular growth but rather from a process of cellular evolution^[13-15]. Cell cycle plays an important role in the modulation of tumor cell growth, and attention has been paid to preventing unlimited proliferation of tumor cells by cell cycle control^[16].

Twenty years ago, staurosporine (ST) was isolated from bacteria and identified as a potent inhibitor of PKC activity^[17-19]. In this study, the proliferation of human gastric cell lines, MGC803 and SGC7901, was significantly inhibited in a time- and concentration-dependent manner and classical apoptosis (sub-diploid peak on flow cytometry, and typical morphological changes) was observed after treated with ST. ST also blocked the G₂/M phase of the cell cycle. In order to examine the distribution of DNA content, the cells treated with ST were detected using flow cytometry. The first peak (2C C=haploid DNA content) was produced by the cell population in G₁ phase, the second (4C) was produced by the cells in G₂/M phase with or without cells in G₁ phase at a higher DNA ploidy (tetraploidy, G_{1t}), and the third (8C) was produced by cells in G₂ phase at a higher DNA ploidy (tetraploidy, G_{2t}). The results presented in this study indicated that the cells were blocked in G₂/M phase. These results lead to the suggestion that, ST can make damaged cells stagnate at G₂/M phase of cell cycle, and inhibit proliferation of cells, allowing them to repair the damage. If this happens, cells will reenter the cycle, otherwise, they will undergo apoptosis or death. More importantly, ST affects the selectively on G₂/M phase of these cells and participates in the regulation of the cell cycle, and thus the blocking effect of ST on cells in G₂/M phase might be the mechanism of its antitumor effect. These observations may provide some useful information that ST can be used as an antitumor agent.

The present study was undertaken to delineate the mechanism of ST effect on the G₂/M phase arrest of cells, and techniques including immunohistochemistry and RT-PCR were used to detect the expression of p21^{WAF1} protein and gene. Our results revealed that p21^{WAF1} expression was low in MGC803 and SGC7901 cells. However, ST significantly increased the expression of p21 in MGC803 and SGC7901 cells. Cell cycle events, including microtubule dynamics, membrane organization and DNA synthesis, were tightly controlled, and specific changes were induced at particular points in the eukaryotic cell cycle during cell proliferation^[20,21]. Negative controls on cell cycle progression were exerted during development, differentiation, senescence, and cell death. These negative controls might play an important role in preventing tumorigenesis. p21^{WAF1}, the pioneer member of p21 family of cyclin-CDK inhibitor class of proteins, has been implicated as a growth arrest mediator in cell terminal differentiation and

apoptosis^[22]. Regulation of cell cycle progression is orchestrated by a family of CDKs, which can be negatively regulated by CDK inhibitors, such as p21^{WAF1}. p21^{WAF1} is a downstream effector of p53 that mediates both G₁ and G₂/M phase arrest. Mechanistically, the p21^{WAF1}-mediated arrest of the G₂/M cell cycle transition has been suggested to include a p21^{WAF1}-CDK2 and p21^{WAF1}-PCNA protein interaction^[23,24]. p21 is the strongest kinase inhibitor, and has been found to inhibit the CDK4/6-cyclinD complex when overexpressed, leading to growth arrest and, under some conditions, to apoptosis^[25-27]. Although our knowledge on cell cycle checkpoints is still limited, it is clear that many such control points existed within the cell cycle and that they played a major role in maintaining the integrity of the genome^[28,29]. At least two checkpoints could detect DNA damage, one at the G₁-S transition and another at the G₂-M transition^[30-32]. ST up-regulates p21^{WAF1}, which then affects cell growth by repressing G₂/M phase, probably through interaction with cyclin-CDK complex. However, this hypothesis needs to be further investigated.

In conclusion, the present study demonstrates that ST can effectively inhibit the proliferation of human gastric cancer MGC803 and SGC7901 cells, induces apoptosis, blocks these cells in G₂/M phase, and up-regulates the p21^{WAF1} expression. This study provides some experimental data for the use of ST in the treatment of gastric carcinoma.

REFERENCES

- 1 **Caponigro F**, French RC, Kaye SB. Protein Kinase C: a worthwhile target for anticancer drugs? *Anticancer Drugs* 1997; **8**: 26-33
- 2 **Aiello LP**, Bursell SE, Clermont A, Duh E, Ishii H, Takagi C, Mori F, Ciulla TA, Ways K, Jirousek M, Smith LE, King GL. Vascular endothelial growth factor-induced retinal permeability is mediated by protein kinase C *in vivo* and suppressed by an orally effective beta-isoform-selective inhibitor. *Diabetes* 1997; **46**: 1473-1480
- 3 **Toledo LM**, Lydon NB, Elbaum D. The structure-based design of ATP-site directed protein kinase inhibitors. *Curr Med Chem* 1999; **6**: 775-805
- 4 **Zaugg K**, Rocha S, Resch H, Hegyi I, Oehler C, Glanzmann C, Fabbro D, Bodis S, Pruschy M. Differential p53-dependent mechanism of radiosensitization *in vitro* and *in vivo* by the protein kinase C-specific inhibitor PKC412. *Cancer Res* 2001; **61**: 732-738
- 5 **Gescher A**. Analogs of staurosporine: potential anticancer drugs? *Gen Pharmacol* 1998; **31**: 721-728
- 6 **Xia M**, Xue SB, Xu CS. Shedding of TNFR1 in regenerative liver can be induced with TNF alpha and PMA. *World J Gastroenterol* 2002; **8**: 1129-1133
- 7 **Li MS**, Li PF, He SP, Du GG, Li G. The promoting molecular mechanism of alpha-fetoprotein on the growth of human hepatoma Bel7402 cell line. *World J Gastroenterol* 2002; **8**: 469-475
- 8 **Ouyang GL**, Li QF, Peng XX, Liu QR, Hong SG. Effects of tachyplesin on proliferation and differentiation of human hepatocellular carcinoma SMMC-7721 cells. *World J Gastroenterol* 2002; **8**: 1053-1058
- 9 **Han Y**, Han ZY, Zhou XM, Shi R, Zheng Y, Shi YQ, Miao JY, Pan BR, Fan DM. Expression and function of classical protein kinase C isoenzymes in gastric cancer cell line and its drug-resistant sublines. *World J Gastroenterol* 2002; **8**: 441-445
- 10 **Gescher A**. Staurosporine analogues - pharmacological toys or useful antitumor agents? *Crit Rev Oncol Hematol* 2000; **34**: 127-135
- 11 **Chen B**, He L, Savell VH, Jenkins JJ, Parham DM. Inhibition of the interferon- γ /signal transducers and activators of transcription (STAT) pathway by hypermethylation at a STAT-binding site in the p21^{WAF1} promoter region. *Cancer Res* 2000; **60**: 3290-3298
- 12 **Zeng YX**, el-Deiry WS. Regulation of p21^{WAF1}/CIP1 expression by p53-independent pathways. *Oncogene* 1996; **12**: 1557-1564
- 13 **Wu Q**, Kirschmeier P, Hockenberry T, Yang TY, Brassard DL, Wang L, McClanahan T, Black S, Rizzi G, Musco ML, Mirza A, Liu S. Transcriptional regulation during p21^{WAF1}/CIP1 induced apoptosis in human ovarian cancer cells. *J Biol Chem* 2002; **277**: 36329-36337

- 14 **Kovalsky O**, Lung FD, Roller PP, Fornace AJ Jr. Oligomerization of human Gadd45a Protein. *J Biol Chem* 2001; **276**: 39330-39339
- 15 **Mihalik R**, Uher F, Pocsik EE, Berczi L, Benczur M, Kopper L. Detection of drug-induced apoptosis by flow cytometry after alkaline extraction of ethanol fixed cells. *Pathol Oncol Res* 1996; **2**: 78-83
- 16 **Heerdts BG**, Houston MA, Mariadason JM, Augenlicht LH. Dissociation of staurosporine-induced apoptosis from G2-M arrest in SW620 human colonic carcinoma cells: initiation of the apoptotic cascade is associated with elevation of the mitochondrial membrane potential (deltapsim). *Cancer Res* 2000; **60**: 6704-6713
- 17 **Salvioli S**, Dobrucki J, Moretti L, Troiano L, Fernandez MG, Pinti M, Pedrazzi J, Franceschi C, Cossarizza A. Mitochondrial heterogeneity during staurosporine-induced apoptosis in HL60 cells: analysis at the single cell and single organelle level. *Cytometry* 2000; **40**: 189-197
- 18 **He SW**, Shen KQ, He YJ, Xie B, Zhao YM. Regulatory effect and mechanism of gastrin and its antagonists on colorectal carcinoma. *World J Gastroenterol* 1999; **5**: 408-416
- 19 **Bernard B**, Fest T, Pretet JL, Mougin C. Staurosporine-induced apoptosis of HPV positive and negative human cervical cancer cells from different points in the cell cycle. *Cell Death Differ* 2001; **8**: 234-244
- 20 **Stokke T**, Smedshammer L, Jonassen TS, Blomhoff HK, Skarstad K, Steen HB. Uncoupling of the order of the S and M phases: effects of staurosporine on human cell cycle kinases. *Cell Prolif* 1997; **30**: 197-218
- 21 **Zeng ZC**, Jiang GL, Wang GM, Tang ZY, Curran WJ, Iliakis G. DNA-PKcs subunits in radiosensitization by hyperthermia on hepatocellular carcinoma hepG2 cell line. *World J Gastroenterol* 2002; **8**: 797-803
- 22 **Bertrand R**, Solary E, O' Connor P, Kohn KW, Pommier Y. Induction of a common pathway of apoptosis by staurosporine. *Exp Cell Res* 1994; **211**: 314-321
- 23 **Fang JY**, Lu YY. Effects of histone acetylation and DNA methylation on p21(WAF1) regulation. *World J Gastroenterol* 2002; **8**: 400-405
- 24 **Wartenberg M**, Fischer K, Hescheler J, Sauer H. Modulation of intrinsic P-glycoprotein expression in multicellular prostate tumor spheroids by cell cycle inhibitors. *Biochim Biophys Acta* 2002; **1589**: 49-62
- 25 **Yuste VJ**, Sanchez-Lopez I, Sole C, Encinas M, Bayascas JR, Boix J, Comella JX. The prevention of the staurosporine-induced apoptosis by Bcl-X(L), but not by Bcl-2 or caspase inhibitors, allows the extensive differentiation of human neuroblastoma cells. *J Neurochem* 2002; **80**: 126-139
- 26 **Shimizu T**, Takahashi N, Tachibana K, Takeda K. Complex regulation of CDK2 and G1 arrest during neuronal differentiation of human prostatic cancer TSU-Prl cells by staurosporine. *Anticancer Res* 2001; **21**: 893-898
- 27 **Narita Y**, Asai A, Kuchino Y, Kirino T. Actinomycin D and staurosporine, potent apoptosis inducers *in vitro*, are potentially effective chemotherapeutic agents against glioblastoma multiforme. *Cancer Chemother Pharmacol* 2000; **45**: 149-156
- 28 **Chen X**, Lowe M, Herliczek T, Hall MJ, Danes C, Lawrence DA, Keyomarsi K. Protection of normal proliferating cells against chemotherapy by staurosporine-mediated, selective, and reversible G(1) arrest. *J Natl Cancer Inst* 2000; **92**: 1999-2008
- 29 **Sausville EA**, Johnson J, Alley M, Zaharevitz D, Senderowicz AM. Inhibition of CDKs as a therapeutic modality. *Ann N Y Acad Sci* 2000; **910**: 207-221
- 30 **Shchepina LA**, Popova EN, Pletjushkina OY, Chernyak BV. Respiration and mitochondrial membrane potential are not required for apoptosis and anti-apoptotic action of Bcl-2 in HeLa cells. *Biochemistry* 2002; **67**: 222-226
- 31 **Swe M**, Sit KH. Staurosporine induces telophase arrest and apoptosis blocking mitosis exit in human Chang liver cells. *Biochem Biophys Res Commun* 1997; **236**: 594-598
- 32 **Stepczynska A**, Lauber K, Engels IH, Janssen O, Kabelitz D, Wesselborg S, Schulze-Osthoff K. Staurosporine and conventional anticancer drugs induce overlapping, yet distinct pathways of apoptosis and caspase activation. *Oncogene* 2001; **20**: 1193-1202

Edited by Xia HHX and Wang XL

Inhibition of β -ionone on SGC-7901 cell proliferation and upregulation of metalloproteinases-1 and -2 expression

Jia-Ren Liu, Bao-Feng Yang, Bing-Qing Chen, Yan-Mei Yang, Hong-Wei Dong, You-Qiang Song

Jia-Ren Liu, Bing-Qing Chen, Yan-Mei Yang, Hong-Wei Dong, Public Health College, Harbin Medical University, Harbin 150001, Heilongjiang Province, China

Bao-Feng Yang, Department of Pharmacology, Harbin Medical University, Harbin 150086, Heilongjiang Province, China

You-Qiang Song, Department of Biochemistry and the Genome Research Centre, The University of Hong Kong, Hong Kong, China

Supported by the National Natural Science Foundation of China, No. 30200229 and the Youth Foundation of Harbin Medical University, China

Correspondence to: Dr. Jia-Ren Liu, Public Health College, Harbin Medical University, 199 Dongdazhi Street, Nangang District, Harbin 150001, Heilongjiang Province, China. jiarl@ems.hrbmu.edu.cn

Telephone: +86-451-3641309 **Fax:** +86-451-3648617

Received: 2003-03-04 **Accepted:** 2003-04-01

Abstract

AIM: To observe the effect of β -ionone on the proliferation of human gastric adenocarcinoma cell line SGC-7901 and the inhibition of metalloproteinase.

METHODS: Using growth inhibition, Zymograms assays and reverse transcription-polymerase-chain reaction (RT-PCR), we examined cell growth rates, activities of matrix metalloproteinases-2 (MMP-2) and -9 (MMP-9), and expression of metalloproteinases-1 (TIMP-1) and -2 (TIMP-2) in SGC-7901 cells after the treatment with β -ionone for 24 h and 48 h, respectively.

RESULTS: β -ionone had an inhibitory effect on the growth of SGC-7901 cells. Eight days after the treatment with β -ionone at concentrations of 25, 50, 100 and 200 $\mu\text{mol/L}$, the inhibition rates were 25.9%, 28.2%, 74.4% and 90.1%, respectively. The IC_{50} value of β -ionone for SGC-7901 cells was estimated to be 89 $\mu\text{mol/L}$. The effects of β -ionone on MMP-2 and MMP-9 activities in SGC-7901 cells were not observed. However, the levels of TIMP-1 and TIMP-2 transcripts were elevated in cells treated with β -ionone in a dose-dependent manner.

CONCLUSION: β -ionone can inhibit the proliferation of SGC-7901 cells, upregulate the expression of TIMP-1 and TIMP-2 expression, and may influence metastasis of cancer.

Liu JR, Yang BF, Chen BQ, Yang YM, Dong HW, Song YQ. Inhibition of β -ionone on SGC-7901 cell proliferation and upregulation of metalloproteinases-1 and -2 expression. *World J Gastroenterol* 2004; 10(2): 167-171

<http://www.wjgnet.com/1007-9327/10/167.asp>

INTRODUCTION

Epidemiological data showed that regular consumption of fruits and vegetables was associated with a reduced risk of chronic diseases such as cancer and cardiovascular diseases^[1-4]. Isoprenoid is an important group of nutritious elements found in fruits,

vegetables and cereal grains, giving rise to about 22 000 secondary products during its metabolism in these plants. It has been found that these compounds shared a common precursor, mevalonic acid^[14]. Isoprenoids have been shown to suppress chemically-induced carcinogenesis^[5-10] and the growth of cancer cells^[11-13]. β -ionone, an end-ring analog of β -carotenoid, represents a subclass of cyclic isoprenoids and has been demonstrated to have an anticancer effect^[15]. β -ionone was effective in chemoprevention of 7,12-dimethylben[a]anthracene-induced mammary carcinogenesis in SD rats, with its tumor multiplicity reduced by 45%^[16]. It has also been found to be associated with growth inhibition of melanoma and breast cancer cells as well as metastasis of tumor cells^[17-20]. However, the exact mechanisms remain to be clarified, and the effect of β -ionone on gastric cancer cells is unknown.

Chemoprevention has been an approach to treat advanced cancers^[21-25]. Gastric cancer is one of the most common malignancies in China and in other parts of the world^[26-34]. Understanding the mechanisms of the possible inhibitory effect of β -ionone on proliferation of gastric adenocarcinoma cells could provide a way to prevent this disease. Therefore, in this study, we studied the effect of β -ionone on the proliferation of human gastric adenocarcinoma cell line SGC-7901 and on the regulative factors of tissue metalloproteinases and investigated the underlying mechanism.

MATERIALS AND METHODS

Cell culture

Human gastric adenocarcinoma cell line SGC-7901, provided by Beijing Cancer Research Institute, was grown in RPMI 1640 medium (Gibco BRL, Life Technologies Inc, Gaithersburg, MD, USA), supplemented with 100 ml/L calf serum, 100×10^3 U/L penicillin and 100 mg/L streptomycin at 37 °C in a humidified atmosphere containing 5% CO_2 .

IC50 and cell growth assessment

β -ionone (purity >95%) (Sigma, USA) was dissolved in absolute ethanol and further diluted to the concentrations of 25, 50, 100 and 200 $\mu\text{mol/L}$, respectively.

The SGC-7901 cells were seeded into six 24-well plates (Nuc, Denmark) with 2×10^4 cells/well after 24 h culture. Twenty-four hour later, the medium was replaced with the media supplemented with at different concentrations of β -ionone. In the next 8 days, the cells were treated with a trypsin-EDTA solution at 37 °C for 2 minutes and harvested from 3 wells per day for each plate. The cells were pelleted by a short spin at 1 000 g and resuspended in phosphate-buffered saline (PBS). Typan blue exclusion test was used to count viable cells by a hemocytometer. The number of cells at 24 h was deducted from the final cell counts to provide an estimate of the net increase. The β -ionone concentration required to inhibit the net increase in the 48 h cell count by 50% (IC_{50}) was measured by plotting data obtained from three or more times. The means were obtained on each of the eight days and used to draw a cell growth curve. The inhibitory rate (IR) was calculated according to the formula: $\text{IR} (\%) = (\text{total number of cells in}$

negative control - number of cells in test group)/total number of cells in negative control $\times 100\%$.

Zymograms assay for activities of gelatinase

Although many kinds of proteinase are involved in tumor metastasis, members of the matrix metalloproteinase (MMPs, gelatinase) and TIMP families, play a pivotal role in these events. MMPs are a group of zinc-dependent endopeptidase molecules that have the potential to degrade proteins of the extracellular matrix. MMP activity was under regulation at several levels, including activation of the MMP zymogens and specific inhibition by the tissue inhibitors of metalloproteinase (TIMPs)^[54]. We determined the activities of gelatinase in SGC-7901 cells treated with β -ionone.

The SGC-7901 cells were seeded in 100 ml bottles, each containing 5×10^6 cells. After incubation for 24 h, the medium was replaced with 400 μ L of serum-free medium supplemented with β -ionone at different concentrations for 24 h and 48 h. The serum-free media were loaded onto a 100 g/L SDS-polyacrylamide gel co-polymerized with 1 g/L gelatin (Amresco Corp, USA) and separated under a non-denaturing condition for 3-4 h. Then, the gels were incubated in 25 g/L Triton X-100 (Sigma, USA) for 1 h and subsequently in a substrate buffer (50 μ mol/L Tris, pH 7.5, containing 10 mmol/L CaCl_2 , 200 mmol/L NaCl and 1 μ mol/L ZnCl_2) for 12 to 16 h at 37 $^\circ\text{C}$. Finally, the gels were stained in a solution containing 1 g/L Coomassie blue R250, 450 g/L methanol and 100 g/L acetic acid, and the gelatinolytic activity was indicated by bands in a blue background.

RT-PCR

Tissue inhibitor of TIMP-1 and TIMP-2 were related to several tumorigenic processes in lung, stomach, and mammary gland^[56]. We examined the expression of TIMP-1 and TIMP-2 in SGC-7901 cells exposed to different concentrations of β -ionone.

SGC-7901 cells (5×10^6) were incubated at different concentrations of β -ionone for 24 h and 48 h, the total cellular RNA was isolated. Concentrations and purity of total RNA were determined. RT-PCR was performed following the manufacturer's instructions (Takara Biotech, Dalian, China). Total RNA (5 μ g) and AMV reverse transcriptase XL were used to synthesize cDNA. Twenty-five μ L PCR mixture containing 4 μ L of RT reaction product, 2.5 U *Taq* DNA polymerase and 20 pmol primers, was heated for 5 min at 94 $^\circ\text{C}$ for pre-denaturation, and then subjected to 35 PCR cycles, denaturation at 94 $^\circ\text{C}$ for 30 s, annealing at 60 $^\circ\text{C}$ for 30 s for and extension at 72 $^\circ\text{C}$ for 45 s, in a PTC-100 thermocycler (MJ Research, USA). TIMP-1 and TIMP-2 genes were amplified with specific primers, with the gene for β -actin as an internal control (Table 1). The amplified products were resolved in a 20 g/L agarose gel containing ethidium bromide, and visualized under ultraviolet light. The density and area of each band were analyzed using the ChemiImagerTM 4 000 digital system (Alpha Innotech Corp, USA).

Table 1 Primer sequences and size of TIMP-1 and TIMP-2 in expected PCR products for RT-PCR

Genes	Primer sequences	Product size (bp)
TIMP-1	Sense: 5'-CTGTTGGCTGTGAGGAATGCACAG-3'	106
	Antisense: 5'-TTCAGAGCCTTGGAGGAGCTGGTC-3'	
TIMP-2	Sense: 5'-AGACGTAGTGATCGGGCCA-3'	490
	Antisense: 5'-GTACCACGCGCAAGAACCCT-3'	
β -actin	Sense: 5'-AAGGATTCCTATGTGGGC-3'	532
	Antisense: 5'-CATCTCTTGCTCGAAGTC-3'	

Statistical analysis

Student's *t* test was used for analysis of data. $P < 0.05$ was considered statistically significant.

RESULTS

Cell growth inhibition of β -ionone

The inhibitory effect of β -ionone on the growth of SGC-7901 cells was shown in Figure 1. Growth of the cells in the media containing 200 μ mol/L and 100 μ mol/L β -ionone was markedly slower than that of the negative control within 8 d ($P < 0.01$). The change was less obvious the cells treated with 50 μ mol/L and 25 μ mol/L of β -ionone. The inhibitory rates were 25.9%, 28.2%, 74.4% and 90.1%, respectively. The IC_{50} of β -ionone was 89 μ mol/L.

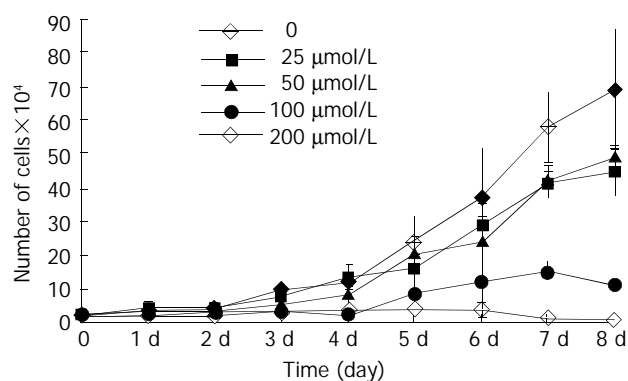


Figure 1 Proliferation kinetics of SGC-7901 cells treated at various concentrations of β -ionone.

Expression of type IV collagenases

The effects of β -ionone on type IV collagenase activities (97kD for MMP-9 and 72kD for MMP-2) in SGC-7901 cells were presented in Figure 2. In the serum-free supernatants of SGC-7901 cells preincubated in the media supplemented with various concentrations of β -ionone, the activities of type IV collagenases (both MMP-9 and MMP-2) were not different in comparison with the negative control. No effect of β -ionone on the activities of type IV collagenases in SGC-7901 cells was shown.

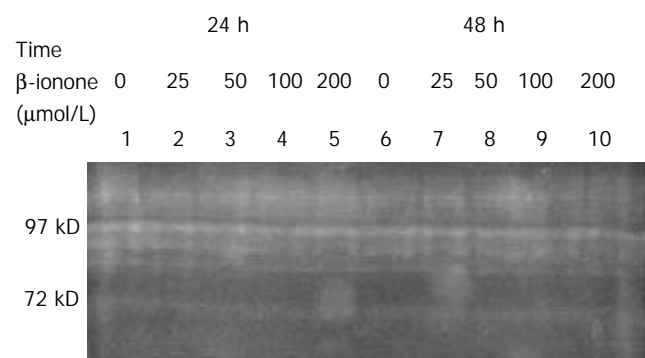


Figure 2 Effect of β -ionone on gelatinase/type IV collagenase secretion (97kD for MMP-9 and 72kD for MMP-2) in SGC-7901 cells.

Levels of TIMP-1 and TIMP-2 mRNA in SGC-7901 cells

As shown in Figures 3 and 4, the levels of TIMP-1 and TIMP-2 transcripts in SGC-7901 cells were gradually elevated with increase of the β -ionone concentration, indicating an upregulation effect of β -ionone on the expression of TIMP-1 and TIMP-2 in SGC-7901 cells.

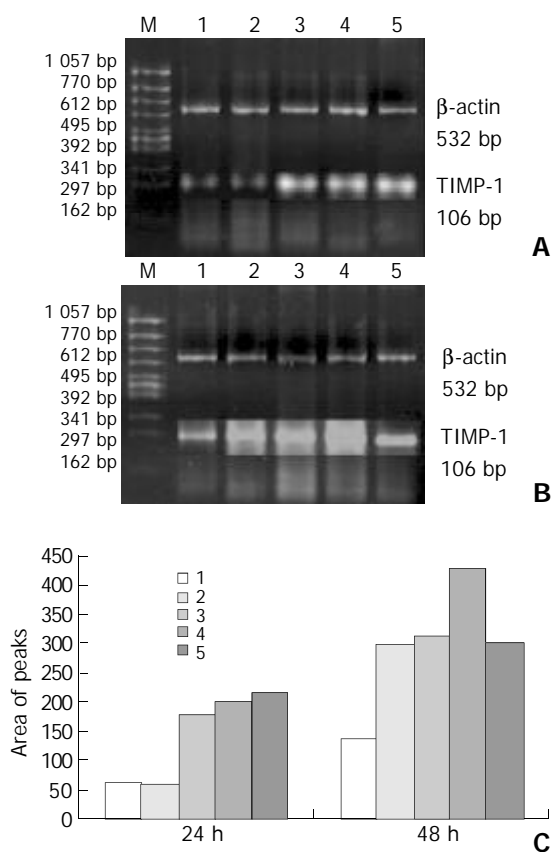


Figure 3 RT-PCR result: expression of TIMP-1 mRNA in SGC-7901 cells treated by β -ionone for 24 h (A) and 48 h (B). C: area of peaks; Lanes 1-5: 0, 25, 50, 100 and 200 μ mol/L of β -ionone; M: molecular weight markers.

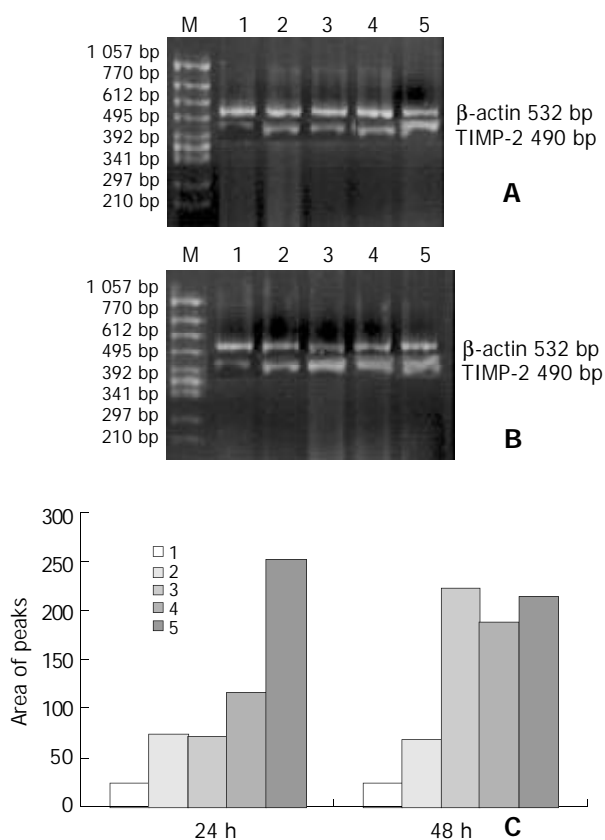


Figure 4 RT-PCR results showing expression of TIMP-2 mRNA in SGC-7901 cells treated by β -ionone for 24 h (A) and 48 h (B). C: chart of area of peaks; Lanes 1-5: 0, 25, 50, 100 and 200 μ mol/L of β -ionone; M: molecular weight markers.

DISCUSSION

Interactions between cells and extracellular matrix (ECM) were critical for many cellular functions including division, migration, differentiation, and apoptosis^[35]. In different mature normal tissues, ECM is specified by its structures and compositions to maintain tissue homeostasis and cellular quiescence. It has been found that remodeling of the ECM occurred during embryonic development and certain normal pathological processes such as wound-healing^[36,37]. However, restructuring of the ECM has also been implicated in the pathogenesis of various human diseases including impaired wound-healing and fibrosis^[38], rheumatoid arthritis^[39], restenosis following balloon angioplasty^[40], atherosclerosis^[41], tumor development, invasion and metastasis^[35,42].

Tumor invasion is a complex biological process, during which tumor cells detach from the primary tumor and infiltrate the surrounding tissues. This process has been found to require loss of cell contacts between tumor cells, active cell migration, adhesion to ECM and proteolytic degradation of the ECM^[43,44]. Different molecules including cadherins, integrins, proteases, and growth factors were implicated in the regulation of invasion of tumor cells^[44].

A major group of enzymes responsible for ECM degradation in cancer tissue has been found to be the MMP family, including collagenases, gelatinase, and stromelysins^[45-49]. Collagenases can cleave fibrillar collagens at neutral conditions and play an important role in matrix remodeling. The largest sub-family of the MMPs is membrane-type (MT). MT-MMPs play a dual role in cell surface proteolysis. They can cleave a variety of extracellular components, and activate some secreted MMPs. Evidence has suggested that proteolytic activities at cell surface could promote cell invasion^[50]. MMP-2, a 72-kDa type IV collagenase, is a cell surface-associated type I collagen-degrading MMP, which was found to designate gelatinase A^[51]. Its overexpression has been observed in different types of tumors, and it was believed to be involved in tumor metastasis, primary tumor growth and angiogenesis^[52]. MMP-2 is also regarded as a type IV collagenase involved in cell invasion across basement membrane. Thus, serum and tissue MMP profiles have been used as prognostic factors in certain types of malignant tumors including gastric and breast cancers^[53]. MMP-9, a 97-kDa type IV collagenase also designating gelatinase B, was found to be associated with tumor invasion as well, its expression has been proven to be correlated with the differentiation grade of some malignancies^[54]. In the present study, we did not find any effect of β -ionone on MMP-9 and MMP-2 activities in SGC-7901 cells. The growth inhibition on SGC-7901 cells appeared to be independence of the type IV collagenase activity.

TIMPs (TIMP-1, -2, -3 and -4) have been found to be the key regulators of MMP activity and ECM degradation^[60]. The MMP inhibitors, TIMP-1 and TIMP-2 have been associated to several tumorigenic processes including development, invasion and metastasis of bronchial cancer^[55-59]. Recent transgenic animal studies have demonstrated that alteration of the MMP/TIMP balance *in vivo* in favor of TIMP-1 activity could block neoplastic proliferation in the SV40 T antigen-induced murine hepatocellular carcinoma^[61]. Active MT1-MMP was found to bind to amino-terminal domain of TIMP-2^[62], whereas an interaction between the carboxyl-terminal domains of TIMP-2 and pro-MMP-2 was also described^[63]. TIMP-2 might prevent SH2-protein-tyrosine phosphatase-1 (SHP-1) dissociation from immunoprecipitable epidermal growth factor receptor complex and a selective increase in total SHP-1 activity^[64]. Our results showed that β -ionone might increase the expression of TIMP-1 and TIMP-2 in SGC-7901 cells. Clearly, further studies are needed to elucidate whether β -ionone inhibits metastasis of the cancer cells.

In summary, β -ionone can inhibit SGC-7901 cell growth

and proliferation and has an effect on upregulating TIMP-1 and TIMP-2 expression in SGC-7901 cells. It seems to be related to potential tumor metastasis in SGC-7901 cells induced by β -ionone. However, the mechanism of the inhibitory effect of β -ionone inhibits cell proliferation remains to be clarified.

ACKNOWLEDGEMENT

We thank Dr. Dong-Yan Jin for his critically reading and revising of the manuscript.

REFERENCES

- 1 **Michaud DS**, Pietinen P, Taylor PR, Virtanen M, Virtamo J, Albanes D. Intakes of fruits and vegetables, carotenoids and vitamins A, E, C in relation to the risk of bladder cancer in the ATBC cohort study. *Br J Cancer* 2002; **87**: 960-965
- 2 **Ito LS**, Inoue M, Tajima K, Yamamura Y, Kadera Y, Hirose K, Takezaki T, Hamajima N, Kuroishi T, Tominaga S. Dietary factors and the risk of gastric cancer among Japanese women. A comparison between the differentiated and non-differentiated subtypes. *Ann Epidemiol* 2003; **13**: 24-31
- 3 **Willett WC**. Balancing life-style and genomics research for disease prevention. *Science* 2002; **296**: 695-698
- 4 **Block G**, Patterson B, Subar A. Fruit, vegetables, and cancer prevention: a review of the epidemiological evidence. *Nutr Cancer* 1992; **18**: 1-29
- 5 **Elson CE**. Suppression of mevalonate pathway activities by dietary isoprenoids: protective roles in cancer and cardiovascular disease. *J Nutr* 1995; **125**: 1666-1672
- 6 **Elson CE**, Yu SG. The chemoprevention of cancer by mevalonate-derived constituents of fruits and vegetables. *J Nutr* 1994; **124**: 607-614
- 7 **Huang C**, Huang Y, Li J, Hu W, Aziz R, Tang MS, Sun N, Cassady J, Stoner GD. Inhibition of benzo(a)pyrene diol-epoxide-induced transactivation of activated protein 1 and nuclear factor kappaB by black raspberry extracts. *Cancer Res* 2002; **62**: 6857-6863
- 8 **Serafini M**, Bellocco R, Wolk A, Ekstrom AM. Total antioxidant potential of fruit and vegetables and risk of gastric cancer. *Gastroenterology* 2002; **123**: 985-991
- 9 **Pandey M**, Shukla VK. Diet and gallbladder cancer: a case-control study. *Eur J Cancer Prev* 2002; **11**: 365-368
- 10 **Devasena T**, Menon VP. Enhancement of circulatory antioxidants by fenugreek during 1,2-dimethylhydrazine-induced rat colon carcinogenesis. *J Biochem Mol Biol Biophys* 2002; **6**: 289-292
- 11 **Agarwal C**, Singh RP, Agarwal R. Grape seed extract induces apoptotic death of human prostate carcinoma DU145 cells via caspases activation accompanied by dissipation of mitochondrial membrane potential and cytochrome c release. *Carcinogenesis* 2002; **23**: 1869-1876
- 12 **Ohyama K**, Akaike T, Hirobe C, Yamakawa T. Cytotoxicity and apoptotic Inducibility of vitex agnus-castus fruit extract in cultured human normal and cancer cells and effect on growth. *Biol Pharm Bull* 2003; **26**: 10-18
- 13 **Dietrich M**, Block G, Norkus EP, Hudes M, Traber MG, Cross CE, Packer L. Smoking and exposure to environmental tobacco smoke decrease some plasma antioxidants and increase gamma-tocopherol *in vivo* after adjustment for dietary antioxidant intakes. *Am J Clin Nutr* 2003; **77**: 160-166
- 14 **Bach TJ**. Some new aspects of isoprenoid biosynthesis in plants—a review. *Lipids* 1995; **30**: 191-202
- 15 **Mo H**, Elson CE. Apoptosis and cell-cycle arrest in human and murine tumor cells are initiated by isoprenoids. *J Nutr* 1999; **129**: 804-813
- 16 **Yu SG**, Anderson PJ, Elson CE. Efficacy of β -ionone in the chemoprevention of rat mammary carcinogenesis. *J Agric Food Chem* 1995; **43**: 2144-2147
- 17 **He L**, Mo H, Hadisusilo S, Qureshi AA, Elson CE. Isoprenoids suppress the growth of murine B16 melanomas *in vitro* and *in vivo*. *J Nutr* 1997; **127**: 668-674
- 18 **Nangia MP**, Hogan V, Honjo Y, Baccarini S, Tait L, Bresalier R, Raz A. Inhibition of human cancer cell growth and metastasis in nude mice by oral intake of modified citrus pectin. *J Natl Cancer Inst* 2002; **94**: 1854-1862
- 19 **Kimura Y**, Taniguchi M, Baba K. Antitumor and antimetastatic effects on liver of triterpenoid fractions of *Ganoderma lucidum*: mechanism of action and isolation of an active substance. *Anti-cancer Res* 2002; **22**: 3309-3318
- 20 **Dabrosin C**, Chen J, Wang L, Thompson LU. Flaxseed inhibits metastasis and decreases extracellular vascular endothelial growth factor in human breast cancer xenografts. *Cancer Lett* 2002; **185**: 31-37
- 21 **Tovey FI**, Hobsley M. Post-gastrectomy patients need to be followed up for 20-30 years. *World J Gastroenterol* 2000; **6**: 45-48
- 22 **Morgner A**, Miehlke S, Stolte M, Neubauer A, Alpen B, Thiede C, Klann H, Hierlmeier FX, Ell C, Ehninger G, Bayerdörffer E. Development of early gastric cancer 4 and 5 years after complete remission of *Helicobacter pylori*-associated gastric low-grade marginal zone B-cell lymphoma of MALT type. *World J Gastroenterol* 2001; **7**: 248-253
- 23 **Niu WX**, Qin XY, Liu H, Wang CP. Clinicopathological analysis of patients with gastric cancer in 1200 cases. *World J Gastroenterol* 2001; **7**: 281-284
- 24 **Deng DJ**. Progress of gastric cancer etiology: N-nitrosamides in the 1990s. *World J Gastroenterol* 2000; **6**: 613-618
- 25 **Wang X**, Liu FK, Li X, Li JS, Xu GX. Inhibitory effect of endostatin expressed by human liver carcinoma SMMC7721 on endothelial cell proliferation *in vitro*. *World J Gastroenterol* 2002; **8**: 253-257
- 26 **Cao WX**, Ou JM, Fei XF, Zhu ZG, Yin HR, Yan M, Lin YZ. Methionine-dependence and combination chemotherapy on human gastric cancer cells *in vitro*. *World J Gastroenterol* 2002; **8**: 230-232
- 27 **Liu JR**, Chen BQ, Yang YM, Wang XL, Xue YB, Zheng YM, Liu RH. Effect of apoptosis on gastric adenocarcinoma cell line SGC-7901 induced by *cis*-9, *trans*-11-conjugated linoleic acid. *World J Gastroenterol* 2002; **8**: 999-1004
- 28 **Li Y**, Lu YY. Applying a highly specific and reproducible cDNA RDA method to clone garlic up-regulated genes in human gastric cancer cells. *World J Gastroenterol* 2002; **8**: 213-216
- 29 **Sun ZJ**, Pan CE, Liu HS, Wang GJ. Anti-hepatoma activity of resveratrol *in vitro*. *World J Gastroenterol* 2002; **8**: 79-81
- 30 **Liu JR**, Li BX, Chen BQ, Han XH, Xue YB, Yang YM, Zheng YM, Liu RH. Effect of *cis*-9, *trans*-11-conjugated linoleic acid on cell cycle of gastric adenocarcinoma cell line (SGC-7901). *World J Gastroenterol* 2002; **8**: 224-229
- 31 **Wang X**, Lan M, Shi YQ, Lu J, ZhongYX, Wu HP, Zai HH, Ding J, Wu KC, Pan BR, Jin JP, Fan DM. Differential display of vincristine-resistance-related genes in gastric cancer SGC-7901 cells. *World J Gastroenterol* 2002; **8**: 54-59
- 32 **Gao F**, Yi J, Shi GY, Li H, Shi XG, Tang XM. The sensitivity of digestive tract tumor cells to As_2O_3 is associated with the inherent cellular level of reactive oxygen species. *World J Gastroenterol* 2002; **8**: 36-39
- 33 **Chen BQ**, Xue YB, Liu JR, Yang YM, Zheng YM, Wang XL, Liu RH. Inhibition of conjugated linoleic acid on mouse forestomach neoplasia induced by benzo(a)pyrene and chemopreventive mechanisms. *World J Gastroenterol* 2003; **9**: 44-49
- 34 **Wu K**, Li Y, Zhao Y, Shan YJ, Xia W, Yu WP, Zhao L. Roles of Fas signaling pathway in vitamin E succinate-induced apoptosis in human gastric cancer SGC-7901 cells. *World J Gastroenterol* 2002; **8**: 982-986
- 35 **Lukashev ME**, Werb Z. ECM signalling: orchestrating cell behaviour and misbehaviour. *Trends Cell Biol* 1998; **8**: 437-441
- 36 **Werb Z**, Chin JR. Extracellular matrix remodeling during morphogenesis. *Ann NY Acad Sci* 1998; **857**: 110-118
- 37 **Raghow R**. The role of extracellular matrix in postinflammatory wound healing and fibrosis. *FASEB J* 1994; **8**: 823-831
- 38 **Friedman S**. Seminars in medicine of the Beth Israel Hospital, Boston. The cellular basis of hepatic fibrosis. Mechanisms and treatment strategies. *N Engl J Med* 1993; **328**: 1828-1835
- 39 **Cawston T**. Matrix metalloproteinases and TIMPs: properties and implications for the rheumatic diseases. *Mol Med Today* 1998; **4**: 130-137
- 40 **Batchelor WB**, Robinson R, Strauss BH. The extracellular matrix in balloon arterial injury: a novel target for restenosis prevention. *Prog Cardiovasc Dis* 1998; **41**: 35-49
- 41 **Newby AC**, Zaltsman AB. Fibrous cap formation or destruction—the critical importance of vascular smooth muscle cell proliferation, migration and matrix formation. *Cardiovasc Res* 1999; **41**: 345-360
- 42 **Stenlicht MD**, Lochter A, Sympon CJ, Huey B, Rougie JP, Gray JW, Pindel D, Bissell MJ, Werb Z. The stromal proteinase MMP3/

- stromelysin-1 promotes mammary carcinogenesis. *Cell* 1999; **98**: 137-146
- 43 **Mareel MM**, Van Roy FM, Bracke ME. How and when do tumor cells metastasize? *Crit Rev Oncog* 1993; **4**: 559-594
- 44 **Engers R**, Gabbert HE. Mechanisms of tumor metastasis: cell biological aspects and clinical implications. *J Cancer Res Clin Oncol* 2000; **126**: 682-692
- 45 **Nagase H**, Woessner JF Jr. Matrix metalloproteinases. *J Biol Chem* 1999; **274**: 21491-21494
- 46 **Birkedal-Hansen H**, Moore WG, Bodden MK, Windsor LJ, Birkedal-Hansen B, DeCarlo A, Engler JA. Matrix metalloproteinases: a review. *Crit Rev Oral Biol Med* 1993; **4**: 197-250
- 47 **Stetler-Stevenson WG**. Matrix metalloproteinases in angiogenesis: a moving target for therapeutic intervention. *J Clin Invest* 1999; **103**: 1237-1241
- 48 **Nelson AR**, Fingleton B, Rothenberg ML, Matrisian LM. Matrix metalloproteinases: biologic activity and clinical implications. *J Clin Oncol* 2000; **18**: 1135-1149
- 49 **Onodera S**, Nishihira J, Koyama KI, Yoshida K, Tanaka S, Minami A. Macrophage Migration Inhibitory Factor Up-regulates Matrix Metalloproteinase-9 and -13 in Rat Osteoblasts. *J Biol Chem* 2002; **277**: 7865-7874
- 50 **Murphy G**, Gavrilovic J. Proteolysis and cell migration: creating a path? *Curr Opin Cell Biol* 1999; **11**: 614-621
- 51 **Zhuge Y**, Xu J. Rac1 Mediates Type I Collagen-dependent MMP-2 Activation. *J Biol Chem* 2001; **276**: 16248-16256
- 52 **Sato H**, Seiki M. Membrane-type matrix metalloproteinases (MT-MMPs) in tumor metastasis. *J Biochem* 1996; **119**: 209-215
- 53 **McCawley LJ**, Matrisian LM. Matrix metalloproteinases: multifunctional contributors to tumor progression. *Mol Med Today* 2000; **6**: 149-156
- 54 **Rao JS**, Yamamoto M, Mohaman S, Gokaslan ZL, Fuller GN, Stetler-Stevenson WG, Rao VH, Liotta LA, Nicolson GL, Sawaya RE. Expression and localization of 92 kDa type IV collagenase/gelatinase B (MMP-9) in human gliomas. *Clin Exp Metastasis* 1996; **14**: 12-18
- 55 **Brand K**. Cancer gene therapy with tissue inhibitors of metalloproteinases (TIMPs). *Curr Gene Ther* 2002; **2**: 255-271
- 56 **Jiang Y**, Goldberg ID, Shi YE. Complex roles of tissue inhibitors of metalloproteinases in cancer. *Oncogene* 2002; **21**: 2245-2252
- 57 **Chang C**, Werb Z. The many faces of metalloproteases: cell growth, invasion, angiogenesis and metastasis. *Trends Cell Biol* 2001; **11**: 37-43
- 58 **Giannelli G**, Antonaci S. Gelatinases and their inhibitors in tumor metastasis: from biological research to medical applications. *Histol Histopathol* 2002; **17**: 339-345
- 59 **Chung AS**, Yoon SO, Park SJ, Yun CH. Roles of matrix metalloproteinases in tumor metastasis and angiogenesis. *J Biochem Mol Biol* 2003; **36**: 128-137
- 60 **Gomez DE**, Alonso DF, Yoshiji H, Thorgeirsson UP. Tissue inhibitors of metalloproteinases: structure, regulation and biological functions. *Eur J Cell Biol* 1997; **74**: 111-122
- 61 **Martin DC**, Sanchez-Sweatman OH, Ho AT, Inderdeo DS, Tsao MS, Khokha R. Transgenic TIMP-1 inhibits simian virus 40 T antigen-induced hepatocarcinogenesis by impairment of hepatocellular proliferation and tumor angiogenesis. *Lab Invest* 1999; **79**: 225-234
- 62 **Zucker S**, Drews M, Conner C, Foda HD, DeClerck YA, Langley KE, Bahou WF, Docherty AJ, Cao J. Tissue inhibitor of metalloproteinase-2 (TIMP-2) binds to the catalytic domain of the cell surface receptor, membrane type 1-matrix metalloproteinase 1 (MT1-MMP). *J Biol Chem* 1998; **273**: 1216-1222
- 63 **Overall CM**, Tam E, McQuibban GA, Morrison C, Wallon UM, Bigg HF, King AE, Roberts CR. Domain interactions in the gelatinase A.TIMP-2.MT1-MMP activation complex. The ectodomain of the 44-kDa form of membrane type-1 matrix metalloproteinase does not modulate gelatinase A activation. *J Biol Chem* 2000; **275**: 39497-39506
- 64 **Hoegy SE**, Oh HR, Corcoran ML, Stetler-Stevenson WG. Tissue Inhibitor of Metalloproteinases-2 (TIMP-2) Suppresses TKR-Growth Factor Signaling Independent of Metalloproteinase Inhibition. *J Biol Chem* 2001; **276**: 3203-3214

Edited by Ren SY and Wang XL

Correlation of thymidylate synthase, thymidine phosphorylase and dihydropyrimidine dehydrogenase with sensitivity of gastrointestinal cancer cells to 5-fluorouracil and 5-fluoro-2'-deoxyuridine

Tao Ma, Zheng-Gang Zhu, Yu-Bao Ji, Yi Zhang, Ying-Yan Yu, Bing-Ya Liu, Hao-Ran Yin, Yan-Zhen Lin

Tao Ma, Zheng-Gang Zhu, Yu-Bao Ji, Yi Zhang, Ying-Yan Yu, Bing-Ya Liu, Hao-Ran Yin, Yan-Zhen Lin, Shanghai Institute of Digestive Surgery, Ruijin Hospital, Shanghai Second Medical University, Shanghai 200025, China

Correspondence to: Dr. Zheng-Gang Zhu, Shanghai Institute of Digestive Surgery, Ruijin Hospital, Shanghai Second Medical University, Shanghai 200025, China. digsurg@online.sh.cn

Telephone: +86-21-64373909 **Fax:** +86-21-64373909

Received: 2003-08-06 **Accepted:** 2003-08-28

Abstract

AIM: To determine the expression levels of three metabolic enzymes of fluoropyrimidines: thymidylate synthase (TS), thymidine phosphorylase (TP) and dihydropyrimidine dehydrogenase (DPD) in seven human gastrointestinal cancer cell lines, and to compare the enzyme levels with the sensitivity to 5-fluorouracil (5-FU) and 5-fluoro-2'-deoxyuridine (FdUrd).

METHODS: TS, TP and DPD mRNA levels were assessed by semi-quantitative RT-PCR, TP and DPD protein contents were measured by ELISA. Fifty percent inhibitory concentrations of growth (IC50), representing the sensitivity to drugs, were determined by MTT assay.

RESULTS: IC50 values ranged from 1.28 to 12.26 μ M for 5-FU, and from 5.02 to 24.21 μ M for FdUrd, respectively. Cell lines with lower DPD mRNA and protein levels tended to be more sensitive to 5-FU ($P < 0.05$), but neither TS nor TP correlated with 5-FU IC50 ($P > 0.05$). Only TS mRNA level was sharply related with FdUrd sensitivity ($P < 0.05$), but TP and DPD were not ($P > 0.05$). A correlation was found between mRNA and protein levels of DPD ($P < 0.05$), but not TP ($P < 0.05$).

CONCLUSION: DPD and TS enzyme levels may be useful indicators in predicting the antitumor activity of 5-FU or FdUrd, respectively.

Ma T, Zhu ZG, Ji YB, Zhang Y, Yu YY, Liu BY, Yin HR, Lin YZ. Correlation of thymidylate synthase, thymidine phosphorylase and dihydropyrimidine dehydrogenase with sensitivity of gastrointestinal cancer cells to 5-fluorouracil and 5-fluoro-2'-deoxyuridine. *World J Gastroenterol* 2004; 10(2): 172-176 <http://www.wjgnet.com/1007-9327/10/172.asp>

INTRODUCTION

The antimetabolite, 5-fluorouracil (5-FU), remains to be widely prescribed in the treatment of gastrointestinal carcinoma. Although it was originally synthesized 46 years ago, and the deoxyribonucleoside derivative of 5-FU, 5-fluoro-2'-deoxyuridine (FdUrd) is also applied in clinics through regional administration^[1-3].

The response rate of gastrointestinal carcinoma to 5-FU as a single agent, however, is only 10%-30%, and differs greatly among patients^[1,4]. So it is imperative to identify some indexes which could be applied to predict the efficacy of 5-FU in clinical settings. As a pyrimidine analog, 5-FU is metabolized *in vivo* similarly to uracil, and exerts its antitumor effects through anabolism, which is determined by the rate of catabolism. Thus, the expression level of genes coding for key enzymes in the metabolism within tumor cells may play a pivotal role in the sensitivity and efficacy of 5-FU^[1,4,5].

The primary biochemical mechanism responsible for cytotoxicity of 5-FU and FdUrd is the formation of 5-fluorouridine monophosphate (FdUMP), which can bind tightly to and inhibit thymidylate synthase (TS) in the presence of 5, 10-methylene tetrahydrofolate (CH_2FH_4). TS catalyzes the reductive methylation of deoxyuridine-5'-monophosphate (dUMP) to deoxythymidine-5'-monophosphate (dTMP), which is the only pathway for *de novo* synthesis of dTMP, so the inhibition of TS by FdUMP disrupts intracellular nucleotide pools necessary for DNA synthesis^[1,3]. As the main target of fluoropyrimidines, the expression level of TS is assumed to influence the response of chemotherapy, although the amount of TS is not unanimously recognized as a determinant factor of 5-FU sensitivity^[6-8].

Thymidine phosphorylase (TP) is known to be elevated in tumors compared with surrounding normal tissue. When 5-FU is administered, it is anabolized to FdUMP by TP present in the tumor, and FdUrd can be converted to 5-FU by TP^[9-11]. TP levels might affect the sensitivity of 5-FU, the transfection of TP cDNA into cancer cells increased their sensitivity to 5-FU^[12]. The expression of TP was reported to be useful for predicting the efficacy and survival of fluoropyrimidine chemotherapy^[13,14], but this tendency was not confirmed in a recent clinical trial of colorectal carcinoma^[15]. The relationship between TP and the sensitivity of fluoropyrimidines needs to be further explored.

In contrast to anabolism of 5-FU, much less attention has been focused on its catabolism. In human, dihydropyrimidine dehydrogenase (DPD) is the initial and rate-limiting enzyme of 5-FU catabolism, 85% of an administered dose of 5-FU is degraded to inactive metabolites by DPD, with only 1-3% of the drug anabolized. While anabolism is essential for the antitumor activity of 5-FU, catabolism by indirectly controlling the availability of 5-FU for anabolism is a critical determinant of 5-FU cytotoxicity^[4,5,16,17]. Several studies have shown a great interindividual difference in DPD activity, and suggested that DPD activity could be used as a predictive marker of 5-FU response^[18-20].

We measured the expression levels of TS, DPD and TP on a panel of seven gastrointestinal cancer cell lines to probe the correlation between TS/DPD/TP and 5-FU or FdUrd sensitivity.

MATERIALS AND METHODS

Chemicals

5-FU was kindly provided by Faulding Pharmaceuticals Co,

FdUrd and MTT were obtained from Sigma-Aldrich Chemicals Co.

Cell culture

Seven cancer cell lines of human origin were adopted, including four gastric carcinoma cells (MKN45, SGC7901, MKN28 and AGS) and three colorectal carcinoma cells (SW1116, Lovo and HCT-8). Cells were routinely cultured in RPMI-1640 media (Gibco BRL), supplemented with 10% heat-inactivated fetal bovine serum (Gibco BRL), 100 u/ml penicillin and 100 ug/ml streptomycin in a humidified incubator at 37 °C with an atmosphere containing 5% CO₂.

Evaluation of 5-FU and FdUrd-induced cytotoxicity by MTT assay

Cells were dispersed into 96-well microtitration plates, and the initial cell density was 5 000-10 000 cells per well, so that the cells were in a Log growth phase. Twenty-four hours after plating, the cells were exposed to a series of 10-fold dilutions of 5-FU or FdUrd (10⁻²-10⁻⁹M) for 72 hours. Each concentration was performed in quadruplicate, the percentage of growth inhibition was assessed by MTT assay, and determined according to the following equation: $[1-(T-T_0)/(C-T_0)] \times 100\%$, where T is the absorbance of the experimental wells after 72 h of 5-FU or FdUrd exposure, and T₀ is that of background control with the same drug concentrations, C is that of cell control wells (without drug) after 72 h incubation. The 5-FU or FdUrd concentrations causing a 50% growth inhibition as compared to cell controls (IC₅₀) were calculated by modified Kärbers method^[21]: $IC_{50} = 10^{i-1} [X_k - i(\sum P - 0.5)]$, in which X_k represents logarithm of the highest drug concentration, i is that of ratio of adjacent concentration, $\sum P$ equals the sum of the percentage of growth inhibition at various concentrations, and 0.5 is a constant of experience. All experiments were repeated 4 times, from which we reported the mean and standard deviation of IC₅₀.

Semi-quantification of TS/DPD/TP mRNA by RT-PCR

Total RNA from seven gastrointestinal cancer cell lines was extracted using TRIzol (Gibco BRL) and quantified by UV spectrophotometry. First-strand cDNA was synthesized from 1 µg of total RNA with oligo (dT)₁₅ primer and avian myeloblastosis virus reverse transcriptase using an RT-PCR kit (Promega) following the conditions of the manufacturer. PCR primers were designed based on the sequences of human TS/DPD/TP and GAPDH mRNA (internal standard), and the specificity of all primers was confirmed by DNA sequencing of the PCR products amplified with them (Table 1).

Table 1 Primers for TS, DPD, TP and GAPDH amplification

mRNA	Bases	Sequences (5' → 3')	Product size (bp)
TS	613-632	accaaccctgacgacagaag	405
	998-1017	atcgaggattgtacccttcaa	
DPD	1325-1344	tgcttcggacagagaagaatg	400
	1705-1724	cttcaatccggcatttcta	
TP	390-408	aggagacctggtgctgac	402
	772-791	tgagaatggaggctgtgatg	
GAPDH	109-127	gaaggtgaaggtcggagtc	226
	315-334	gaagatggtgatgggatttc	

TS/DPD/TP was co-amplified with GAPDH in 50 µl of PCR mixture containing 4 µg of cDNA template, 2.5 mM MgCl₂, 5 µl 10×buffer, 0.4 mM dNTP, 2.5 u Taq polymerase (Promega), 12.5pmol of each sense and anti-sense primer. The PCR profile of TS consisted of an initial 4 min denaturation at

95 °C, followed by 25 PCR cycles (at 94 °C for 1 min, at 60 °C for 30 s, and at 72 °C for 1 min) and a final 7 min extension (33 cycles of amplification for DPD and 35 cycles for TP). The PCR products were separated by ethidium bromide-stained 2% agarose gel electrophoresis, the images were scanned and analyzed by densitometry using Fluro-s™ image software (Bio-Rad). The relative amount of mRNA was calculated by determining the product intensity ratio of TS/DPD/TP to GAPDH within the linear amplification range of PCR, and four separate experiments were repeated.

Protein contents of TP and DPD

Cell lines in a Log growth phase were harvested and washed twice by phosphate buffered saline (PBS, pH 7.4). After the last wash, cell pellets were resuspended in 500 µl PBS and lysed by a sonifier (pulses, 10 min), then the lysates were centrifuged at 13 000×g for 15 min, and the supernatants were carefully collected, the protein concentration of which were determined using a BCA protein assay reagent kit (Pierce).

The protein contents of DPD and TP in cell lines were determined by sandwich ELISA (Roche), according to the manufacturer's instructions. Enzyme levels were expressed as U/mg protein, where one U of TP is an amount equivalent to 1 µg 5-FU generated in an hour, and one U of DPD is an amount equivalent to catabolizing 1pmol of 5-FU per minute.

Determination of population doubling time

As described before^[22], 1-2×10⁵ cells were cultured in a 25 ml flask containing 2.5 ml of RPMI-1640, and the number of cells per flask was counted every 24 hours for 7 days. When the cells were in a Log growth phase, the population doubling time (dt) was determined by the following formula: $dt = 1 \text{ g} / 2 \text{ g} (C_t / C_0) \times t$, where t means the time between cell counts C_t and C₀, C₀ is the initial count, and C_t is the count after time t.

Statistics

Linear regression analysis and paired t-test were performed by SPSS software, P<0.05 was regarded as statistically significant.

RESULTS

Sensitivity of cell lines to 5-FU and FdUrd

Table 2 shows the parameters of interest for the whole cell line panel. After 72-hour drug exposure, the chemosensitivity of cell lines presented a marked difference, with IC₅₀ values ranged from 1.28 to 12.26µM for 5-FU (9.57-fold), and from 5.02 to 24.21µM (4.83-fold) for FdUrd, respectively. The IC₅₀ value of 5-FU was 2.8-fold lower than that of FdUrd (P<0.01), and there was no significant correlation between IC₅₀ values of these two drugs among seven gastrointestinal cancer cell lines (P>0.05).

TS mRNA levels

TS mRNA was highly expressed in the seven cell lines, and the TS:GAPDH product intensity ratio varied from 0.84 to 2.69 (Figure 1A, Table 2). TS mRNA expression was significantly correlated with the sensitivity of cell lines to FdUrd (r=0.81, P=0.028), where low TS mRNA levels were associated with the high sensitivity to FdUrd (Figure 2), but the sensitivity to 5-FU was not influenced by TS mRNA levels.

DPD mRNA and protein levels

DPD mRNA expression was measurable in all cell lines but HCT-8 (Figure 1B). Although cDNA of DPD was amplified by PCR with 8 more cycles, DPD mRNA expression was much lower than TS expression, as shown in Table 2. DPD protein content, representing enzyme activity, ranged from 1.16 to

Table 2 Sensitivity to 5-FU or FdUrd and enzyme levels for cell lines

Cell line	IC50 ^a		TS mRNA ^b	DPD		TP		Doubling time (hours)
	5-FU	FdUrd		mRNA ^b	protein ^c	mRNA ^b	protein ^c	
MKN45	12.26±2.13	16.85±2.28	1.13±0.22	0.57±0.17	10.13	0.72±0.13	5.11	22.9
SGC7901	8.97±1.55	12.45±1.46	1.04±0.17	0.50±0.09	9.13	0.59±0.06	1.78	25.8
MKN28	3.44±0.36	5.02±1.32	0.84±0.21	0.36±0.12	4.57	0.70±0.12	0.55	20.5
AGS	2.77±0.58	19.31±1.85	1.27±0.23	0.35±0.08	4.95	0.67±0.20	3.835	29.5
SW1116	5.45±0.47	24.21±3.26	2.69±0.36	0.47±0.11	5.99	0.57±0.11	2.60	22.2
Lovo	4.86±0.92	14.41±0.96	1.19±0.12	0.31±0.05	1.83	0.70±0.08	0.04	33.9
HCT-8	1.28±0.43	17.62±1.84	1.54±0.31	ND ^d	1.16	0.10±0.06	0.67	28.1

a: values of IC50 ($\bar{x}\pm s$), b: TS/DPD/TP mRNA levels, expressed as TS/DPD/TP:GAPDH product intensity ratio ($\bar{x}\pm s$), c: DPD/TP protein levels, in U/mg protein, d: not detectable.

10.13 U/mg protein (8.73-fold), and there was a statistically significant correlation between mRNA and protein level of DPD ($r=0.88$, $P=0.009$, Figure 3A).

Linear regression analysis showed that both mRNA ($r=0.82$, $P=0.025$) and protein level of DPD ($r=0.88$, $P=0.009$) were significantly correlated to the sensitivity to 5-FU (Figure 4). The greater the enzyme level was, the higher the IC50 of 5-FU. The most sensitive cell line (HCT-8) exhibited the lowest DPD mRNA and protein level, and the most resistant cell line (MKN45) had the greatest DPD mRNA and protein level. But the correlation between mRNA or protein level of DPD and the IC50 of FdUrd was not found ($P>0.05$).

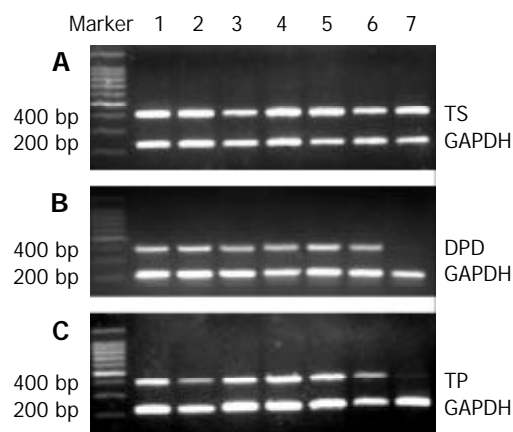


Figure 1 mRNA expression of seven gastrointestinal cancer cell lines by RT-PCR. (A) the bands of TS and GAPDH; (B) the bands of DPD and GAPDH; (C) the bands of TP and GAPDH (1-MKN45; 2-SGC7901; 3-MKN28; 4-AGS; 5-SW1116; 6-Lovo; 7-HCT-8). The relative amount of mRNA was expressed as the intensity ratio of TS/DPD/TP to GAPDH RT-PCR products, as showed in Table 2.

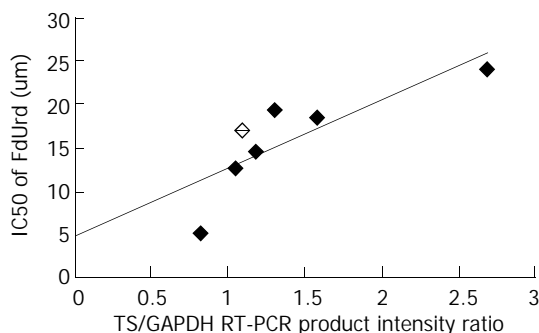


Figure 2 Linear regression for the sensitivity to FdUrd as a function of TS mRNA level (FdUrd-IC50=7.89TS mRNA+4.77, $r=0.81$, $P=0.028$). Scatter plot shows the correlation between TS mRNA levels and IC50 of FdUrd.

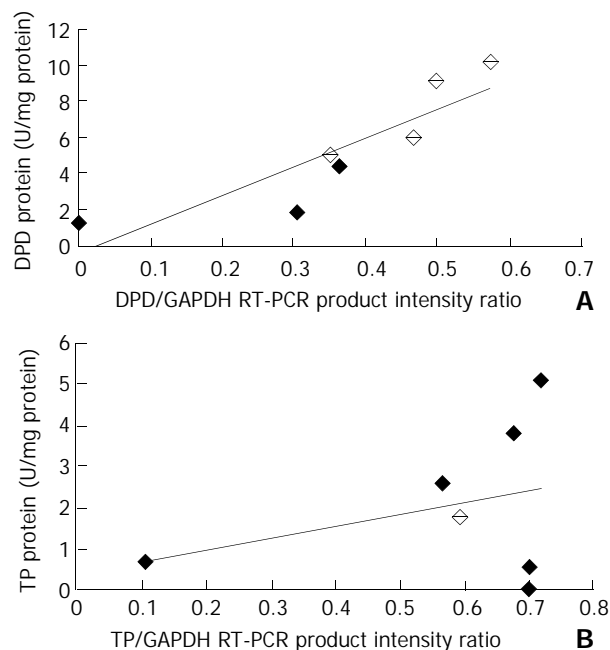


Figure 3 (A) Correlation between mRNA and protein level of DPD ($r=0.88$, $P=0.009$); (B) Correlation between mRNA and protein level of TP ($r=0.33$, $P=0.466$).

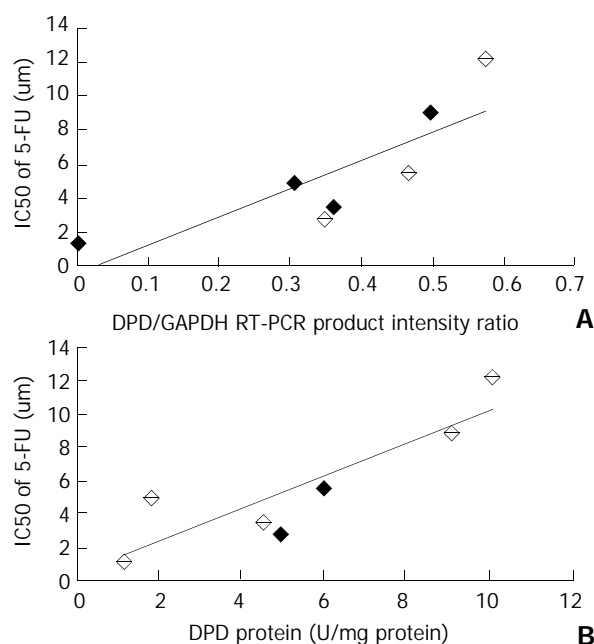


Figure 4 (A) Linear regression for the sensitivity to 5-FU as a function of DPD mRNA level (5-FU-IC50=16.77DPD mRNA-0.54, $r=0.82$, $P=0.025$). (B) Linear regression for the sensitivity to

5-FU as a function of of DPD protein level (5-FU-IC₅₀=1.00DPD protein+0.20, $r=0.88$, $P=0.009$). Scatter plot shows the correlation between DPD mRNA or protein levels and IC₅₀ of 5-FU.

TP mRNA and protein levels

Both mRNA and protein of TP had lower expression levels compared to TS or DPD (Figure 1C, Table 2). Figure 3B shows no correlation between TP/GAPDH RT-PCR product intensity ratio and TP protein level ($r=0.33$, $P=0.466$). Although it was expected that mRNA and protein level of TP would predict the sensitivity to 5-FU or FdUrd, no significant correlation was shown ($P>0.05$).

Doubling time of cell lines

The cell doubling time ranged from 20.5 (MKN28) to 33.9 hours (Lovo), and no correlation was demonstrated between the doubling time and IC₅₀ of 5-FU or FdUrd. Cell doubling time did not correlate with either TS/DPD/TP mRNA or protein levels ($P>0.05$).

DISCUSSION

There is a high prevalence of gastrointestinal cancer, including gastric and colorectal cancer in China, but most of the diagnoses are established at advanced stages, when chemotherapy is regarded as one of the main treatments. At present, 5-FU has been considered as the principal component of chemotherapy regimen for gastrointestinal cancer in both advanced disease and the adjuvant setting^[2,23], and FdUrd is also available commercially for chemotherapy, especially for intraarterial and intracavitary infusion. But the response of gastrointestinal cancer to fluoropyrimidines was still unsatisfactory and their efficacy varied greatly among individuals, so how to enhance the chemotherapeutic response of 5-FU has become a very interesting subject^[24,25]. The identification of predictive markers of chemosensitivity through pharmacogenomics means could clarify which subset of patients might benefit, and enable clinicians to design individualized chemotherapy regimens^[26].

It has been demonstrated in our study that the sensitivity of seven gastrointestinal cancer cell lines to 5-FU corresponded to DPD mRNA or DPD protein levels linearly. The cancer cells with lower DPD levels were more sensitive to 5-FU, and DPD mRNA was even undetectable in the most sensitive cell line HCT-8. But no correlation between TS or TP levels and sensitivity to 5-FU was found in the present study, in view of the known relevance of TS or TP as a determinant of response of 5-FU in some preclinical and clinical studies^[6,7,27], therefore the results obtained from the study of seven cancer cell lines must be interpreted scrupulously.

The low expression levels of TP could partly explain our finding, besides inhibition of TS activity through anabolism to FdUMP by TP catalyzation. 5-FU exerted its antitumor activity by converting to FdUTP and FUTP for incorporating into DNA and RNA, respectively^[1], thereby interfering with their normal structure and function, so there was no correlation between TS or TP levels and 5-FU sensitivity. On the other hand, Nita *et al.*^[28] also observed DPD expression and predicted 5-FU sensitivity in colorectal cancer cell lines. Etienne *et al.*^[29] confirmed this association in tumor biopsy tissues from the patients of head and neck cancers, but no relationship was demonstrated between TS activity and 5-FU response, either. Our findings, similar to these results, suggested that most of 5-FU within insensitive tumor cells was quickly catabolized by a higher DPD level, which regulated the amount of 5-FU available for anabolism, thereby affecting its cytotoxicity. In addition, these results suggested that DPD inhibitors, such as eniluracil^[30], uracil^[31], 5-chloro-2,4-dihydroxypyrimidine (CDHP)^[32], and BOF-A2^[33], might be used as a novel type of biochemical

modulators for elevating the antitumor activity of 5-FU.

It has been indicated in our work that TS may contribute greatly to the sensitivity of FdUrd, and the higher the TS mRNA levels, the higher the IC₅₀ of FdUrd. Because both TP mRNA and protein levels of this panel of cell lines were rather low, and only little amount of FdUrd could be converted to 5-FU, the suppression of TS through conversion to FdUMP was the principal mechanism of action of FdUrd^[1,10,11]. Therefore TS may serve as a predictive marker of FdUrd. Given the metabolic characteristics of FdUrd, it is comprehensible that there was no correlation between TP or DPD levels and FdUrd sensitivity.

Grem *et al.*^[8] found cell doubling time was a potentially important variable in drug sensitivity, and cell lines with faster doubling times tended to have higher TS activities, but we did not observe the similar trend. In their study, the cytotoxicity was determined by MTT assay after 48 hours of drug exposure, whilst we did it after 72 hours by the same protocol. Since the cell doubling time, ranging from 20.5 to 33.9 hours, was relatively shorter in our study than Grem's, the influence of doubling time on fluoropyrimidines seemed to be much weaker.

We used semi-quantitative RT-PCR and ELISA to determine DPD/TP mRNA and protein level, respectively, and found a statistically significant correlation between mRNA level and protein content of DPD. Compared to traditional radioisotopic enzyme activity assay^[34], RT-PCR and ELISA were less laborious, less expensive, and more feasible in most laboratories. In general, even small amounts (≤ 100 mg) of tissues were enough for them, and the correlation between DPD activity and mRNA or protein levels has been already confirmed in several preclinical and clinical trials^[18,35-38]. But there was no such a correlation in TP, a close look showed three cell lines had extremely low TP protein contents, and even TP enzyme level of MKN45, the highest one, was only 5.11 U/mg protein. A recent clinical trial disclosed that the range of TP level in primary colorectal cancer was 13.8-196.0 U/mg protein^[36], which might explain this apparent discrepancy between mRNA and protein level. Griffiths also pointed out by immunohistochemistry that the predominant cells positive for TP were macrophages and other stroma cells within tumor tissues, and the activation of fluoropyrimidines in human might rely on the paracrine of TP by these stroma cells, but not tumor cells^[10]. As the low expression of TP could directly influence the sensitivity of these seven cell lines to fluoropyrimidines, the role of TP in gastrointestinal cancer cells sensitive to 5-FU and FdUrd needs to be more deeply explored.

In summary, we found that DPD and TS were potential indicators in predicting tumor sensitivity to 5-FU and FdUrd. However, the conclusions were drawn from the limited *in vitro* experiment. This study was merely a first step toward the goal of individualized fluoropyrimidine chemotherapy for gastrointestinal cancers. Controlled, prospective clinical trials are required to confirm our results and to establish the advantage of pre-treatment tumor biopsy for TS/DPD screening, which permits a more rational decision on whether to proceed a fluoropyrimidine-based therapy as first-line treatment. So patients who are unlikely to respond may spare unnecessary toxicity and can be treated with alternative drugs such as CPT-11, oxaliplatin, or with potent biochemical modulators of fluoropyrimidine.

REFERENCES

- 1 **Grem JL.** 5-Fluoropyrimidines. in: Chabner BA, Longo DL eds. *Cancer Chemotherapy and Biotherapy* 3rd ed. Philadelphia: Lippincott Raven 2001: 186-264
- 2 **Ren G,** Cai R, Chen Q. The update advance in chemotherapy of gastric cancer. *Shijie Huaren Xiaohua Zazhi* 2002; **10**: 83-85
- 3 **Nakagawa H,** Maeda N, Tsuzuki T, Suzuki T, Hirayama A, Miyahara E, Wada K. Intracavitary chemotherapy with 5-fluoro-

- 2'-deoxyuridine (FdUrd) in malignant brain tumors. *Jpn J Clin Oncol* 2001; **31**: 251-258
- 4 **Diasio RB**, Johnson MR. The role of pharmacogenetics and pharmacogenomics in cancer chemotherapy with 5-fluorouracil. *Pharmacology* 2000; **61**: 199-203
 - 5 **Diasio RB**. Improving fluorouracil chemotherapy with novel orally administered fluoropyrimidines. *Drugs* 1999; **58**(Suppl 3): 119-126
 - 6 **Van Triest B**, Peters GJ. Thymidylate synthase: a target for combination therapy and determinant of chemotherapeutic response in colorectal cancer. *Oncology* 1999; **57**: 179-194
 - 7 **Leichman CG**, Lenz HJ, Leichman L, Danenberg K, Baranda J, Groshen S, Boswell W, Metzger R, Tan M, Danenberg PV. Quantitation of intratumoral thymidylate synthase expression predicts for disseminated colorectal cancer response and resistance to protracted-infusion fluorouracil and weekly leucovorin. *J Clin Oncol* 1997; **15**: 3223-3229
 - 8 **Grem JL**, Danenberg KD, Behan K, Parr A, Young L, Danenberg PV, Nguyen D, Drake J, Monks A, Allegra CJ. Thymidine kinase, thymidylate synthase, and dihydropyrimidine dehydrogenase profiles of cell lines of the National Cancer Institute's Anticancer Drug Screen. *Clin Cancer Res* 2001; **7**: 999-1009
 - 9 **Ikeguchi M**, Makino M, Kaibara N. Thymidine phosphorylase and dihydropyrimidine dehydrogenase activity in colorectal carcinoma and patients prognosis. *Langenbecks Arch Surg* 2002; **387**:240-245
 - 10 **Griffiths L**, Stratford IJ. Platelet-derived endothelial cell growth factor thymidine phosphorylase in tumour growth and response to therapy. *Br J Cancer* 1997; **76**: 689-693
 - 11 **Creaven PJ**, Rustum YM, Petrelli NJ, Meropol NJ, Raghavan D, Rodriguez-Bigas M, Levine EG, Frank C, Udvary-Nagy S, Proefrock A. Phase I and pharmacokinetic evaluation of floxuridine /leucovorin given on the Roswell Park weekly regimen. *Cancer Chemother Pharmacol* 1994; **34**: 261-265
 - 12 **Marchetti S**, Chazal M, Dubreuil A, Fischel JL, Etienne MC, Milano G. Impact of thymidine phosphorylase surexpression on fluoropyrimidine activity and on tumour angiogenesis. *Br J Cancer* 2001; **85**: 439-445
 - 13 **Mader RM**, Sieder AE, Braun J, Rizovski B, Kalipciyan M, Mueller MW, Jakesz R, Rainer H, Steger GG. Transcription and activity of 5-fluorouracil converting enzymes in fluoropyrimidine resistance in colon cancer *in vitro*. *Biochem Pharmacol* 1997; **54**: 1233-1242
 - 14 **Saito H**, Tsujitani S, Oka S, Kondo A, Ikeguchi M, Maeta M, Kaibara N. The expression of thymidine phosphorylase correlates with angiogenesis and the efficacy of chemotherapy using fluorouracil derivatives in advanced gastric carcinoma. *Br J Cancer* 1999; **81**: 484-489
 - 15 **Metzger R**, Danenberg K, Leichman CG, Salonga D, Schwartz EL, Wadler S, Lenz HJ, Groshen S, Leichman L, Danenberg PV. High basal level gene expression of thymidine phosphorylase (platelet-derived endothelial cell growth factor) in colorectal tumors is associated with nonresponse to 5-fluorouracil. *Clin Cancer Res* 1998; **4**: 2371-2376
 - 16 **Fischel JL**, Etienne MC, Spector T, Formento P, Renee N, Milano G. Dihydropyrimidine dehydrogenase: a tumoral target for fluorouracil modulation. *Clin Cancer Res* 1995; **1**: 991-996
 - 17 **Mattison LK**, Soong R, Diasio RB. Implications of dihydropyrimidine dehydrogenase on 5-fluorouracil pharmacogenetics and pharmacogenomics. *Pharmacogenomics* 2002; **3**: 485-492
 - 18 **Tanaka-Nozaki M**, Onda M, Tanaka N, Kato S. Variations in 5-fluorouracil concentrations of colorectal tissues as compared with dihydropyrimidine dehydrogenase(DPD) enzyme activities and DPD messenger RNA levels. *Clin Cancer Res* 2001; **7**: 2783-2787
 - 19 **Ishikawa Y**, Kubota T, Otani Y, Watanabe M, Teramoto T, Kumai K, Takechi T, Okabe H, Fukushima M, Kitajima M. Dihydropyrimidine dehydrogenase and messenger RNA levels in gastric cancer: possible predictor for sensitivity to 5-fluorouracil. *Jpn J Cancer Res* 2000; **91**: 105-112
 - 20 **Milano G**, McLeod HL. Can dihydropyrimidine dehydrogenase impact 5-fluorouracil-based treatment? *Eur J Cancer* 2000; **36**: 37-42
 - 21 **Liu GF**. Median effective dose. in: Jiang ZJ eds. Medical statistics. 1sted. Beijing: People's Medical Publishing House 1997: 136-153
 - 22 **Feng RH**, Zhu ZG, Li JF, Liu BY, Yan M, Yin HR, Lin YZ. Inhibition of human telomerase in MKN-45 cell line by antisense hTR expression vector induces cell apoptosis and growth arrest. *World J Gastroenterol* 2002; **8**: 436-440
 - 23 **Hu JK**, Chen ZX, Zhou ZG, Zhang B, Tian J, Chen JP, Wang L, Wang CH, Chen HY, Li YP. Intravenous chemotherapy for resected gastric cancer: meta-analysis of randomized controlled trials. *World J Gastroenterol* 2002; **8**: 1023-1028
 - 24 **Shi YQ**, Xiao B, Miao JY, Zhao YQ, You H, Fan DM. Construction of eukaryotic expression vector pBK-fas and MDR reversal test of drug-resistant gastric cancer cells. *Shijie Huaren Xiaohua Zazhi* 1999; **7**: 309-312
 - 25 **Xiao B**, Shi YQ, Zhao YQ, You H, Wang ZY, Liu XL, Yin F, Qiao TD, Fan DM. Transduction of fas gene or bcl-2 antisense RNA sensitizes cultured drug resistant gastric cancer cells to chemotherapeutic drugs. *Huaren Xiaohua Zazhi* 1998; **6**: 675-679
 - 26 **McLeod HL**, Evans WE. Pharmacogenomics: unlocking the human genome for better drug therapy. *Annu Rev Pharmacol Toxicol* 2001; **41**: 101-121
 - 27 **Wong NA**, Brett L, Stewart M, Leitch A, Longley DB, Dunlop MG, Johnston PG, Lessells AM, Jodrell DI. Nuclear thymidylate synthase expression, p53 expression and 5FU response in colorectal carcinoma. *Br J Cancer* 2001; **85**: 1937-1943
 - 28 **Nita ME**, Tominaga O, Nagawa H, Tsuruo T, Muto T. Dihydropyrimidine dehydrogenase but not thymidylate synthase expression is associated with resistance to 5-fluorouracil in colorectal cancer. *Hepatogastroenterology* 1998; **45**: 2117-2122
 - 29 **Etienne MC**, Cheradame S, Fischel JL, Formento P, Dassonville O, Renee N, Schneider M, Thyss A, Demard F, Milano G. Response to fluorouracil therapy in cancer patients: the role of tumoral dihydropyrimidine dehydrogenase activity. *J Clin Oncol* 1995; **13**: 1663-1670
 - 30 **Mani S**, Hochster H, Beck T, Chevlen EM, O'Rourke MA, Weaver CH, Bell WN, White R, McGuirt C, Levin J, Hohneker J, Schilsky RL, Lokich J. Multicenter phase I study to evaluate a 28-day regimen of oral fluorouracil plus eniluracil in the treatment of patients with previously untreated metastatic colorectal cancer. *J Clin Oncol* 2000; **18**: 2894-2901
 - 31 **Colevas AD**, Amrein PC, Gomolin H, Barton JJ, Read RR, Adak S, Benner S, Costello R, Posner MR. A phase II study of combined oral uracil and ftorafur with leucovorin for patients with squamous cell carcinoma of the head and neck. *Cancer* 2001; **92**: 326-331
 - 32 **Takechi T**, Fujioka A, Matsushima E, Fukushima M. Enhancement of the antitumour activity of 5-fluorouracil(5-FU) by inhibiting dihydropyrimidine dehydrogenase activity(DPD) using 5-chloro-2,4-dihydroxypyridine(CDHP) in human tumour cells. *Eur J Cancer* 2002; **38**: 1271-1277
 - 33 **Sugimachi K**, Maehara Y. A phase II trial of a new 5-fluorouracil derivative, BOF-A2 (Emitofur), for patients with advanced gastric cancer. *Surg Today* 2000; **30**: 1067-1072
 - 34 **Johnson MR**, Yan J, Shao L, Albin N, Diasio RB. Semi-automated radioassay for determination of dihydropyrimidine dehydrogenase (DPD) activity. Screening cancer patients for DPD deficiency, a condition associated with 5-fluorouracil toxicity. *J Chromatogr B Biomed Sci Appl* 1997; **696**: 183-191
 - 35 **Hiroyasu S**, Shiraishi M, Samura H, Tokashiki H, Shimoji H, Isa T, Muto Y. Clinical relevance of the concentrations of both pyrimidine nucleoside phosphorylase(PyNPase) and dihydropyrimidine dehydrogenase (DPD) in colorectal cancer. *Jpn J Clin Oncol* 2001; **31**: 65-68
 - 36 **Nishimura G**, Terada I, Kobayashi T, Ninomiya I, Kitagawa H, Fushida S, Fujimura T, Kayahara M, Shimizu K, Ohta T, Miwa K. Thymidine phosphorylase and dihydropyrimidine dehydrogenase levels in primary colorectal cancer show a relationship to clinical effects of 5'-deoxy-5-fluorouridine as adjuvant chemotherapy. *Oncol Rep* 2002; **9**: 479-482
 - 37 **Hoque MO**, Kawamata H, Nakashiro KI, Omotehara F, Shinagawa Y, Hino S, Begum NM, Uchida D, Yoshida H, Sato M, Fujimori T. Dihydropyrimidine dehydrogenase mRNA level correlates with the response to 5-fluorouracil-based chemio-immuno-radiation therapy in human oral squamous cell cancer. *Int J Oncol* 2001; **19**: 953-958
 - 38 **Johnson SJ**, Ridge SA, Cassidy J, McLeod HL. Regulation of dihydropyrimidine dehydrogenase in colorectal cancer. *Clin Cancer Res* 1999; **5**: 2566-2570

Expression of NF- κ B and human telomerase reverse transcriptase in gastric cancer and precancerous lesions

Wei Wang, He-Sheng Luo, Bao-Ping Yu

Wei Wang, He-Sheng Luo, Bao-Ping Yu, Department of Gastroenterology, Renmin Hospital of Wuhan University, Wuhan 430060, Hubei Province, China

Correspondence to: Professor He-Sheng Luo, Department of Gastroenterology, Renmin Hospital of Wuhan University, Wuhan 430060, Hubei Province, China. luotang@public.wh.hb.cn

Telephone: +86-27-88041911-2134

Received: 2003-06-16 **Accepted:** 2003-07-24

Abstract

AIM: To investigate the expression of NF- κ Bp65 protein and human telomerase reverse transcriptase (hTERT) and their correlation in gastric cancer and precancerous lesions.

METHODS: Forty-one patients with primary gastric cancer, 15 with dysplasia, 23 intestinal metaplasia and 10 with normal gastric mucosa were included in this study. Expression of NF- κ Bp65 protein, hTERT mRNA and protein were determined by immunohistochemistry and *in situ* hybridization.

RESULTS: The rate of p65 expression in normal gastric mucosa, intestinal metaplasia, dysplasia and carcinoma was 0%, 34.78%, 53.33% and 60.98%, respectively, while the rate of hTERT mRNA expression was 10.00%, 39.13%, 66.67% and 85.37% and the rate of hTERT protein expression was 0%, 30.43%, 60.00% and 78.05%, respectively. All the three parameters were significantly increased in dysplasia and carcinoma compared to normal mucosa, while the expression levels were also significantly higher in carcinoma than in intestinal metaplasia ($P < 0.05$). In gastric cancer tissues, nuclear staining rates of p65 and hTERT protein were both significantly associated with the degree of differentiation, lymph node metastasis, clinical stage and invasion depth ($P < 0.05$). However, hTERT mRNA expression was only significantly associated with clinical stage. There was a positive correlation between p65 and hTERT mRNA ($r_s = 0.661-0.752$, $P < 0.01$), and between hTERT protein and hTERT mRNA ($r_s = 0.609-0.750$, $P < 0.01$).

CONCLUSION: NF- κ Bp65 and hTERT expressions are upregulated at the early stage of gastric carcinogenesis. NF- κ B activation may contribute to hTERT expression and thereby enhance telomerase activity, which represents an important step in carcinogenesis progress.

Wang W, Luo HS, Yu BP. Expression of NF- κ B and human telomerase reverse transcriptase in gastric cancer and precancerous lesions. *World J Gastroenterol* 2004; 10(2): 177-181
<http://www.wjgnet.com/1007-9327/10/177.asp>

INTRODUCTION

NF- κ B is a family of dimeric transcription factors that play a critical role in host defense by regulating the expression of immune and inflammatory genes^[1-3]. The most common dimer is RelA (p65)/NF- κ B1 (p50) heterodimer. In resting cells, NF-

κ B is localized in the cytoplasm, which is noncovalently associated with the cytoplasmic inhibitory protein I κ B. Upon stimulation with a variety of pathogenic inducers such as viruses, mitogens, bacteria, agents providing oxygen radicals, and inflammatory cytokines, I κ B is phosphorylated, ubiquitinated, and degraded in the cytoplasm, and the NF- κ B complex migrates into the nucleus and binds to DNA recognition sites in the regulatory regions of target genes^[4]. Recently, there were several reports on the role of NF- κ B gene products in cell proliferation, transformation, and tumor development^[5-9]. Recent studies have also indicated that NF- κ B is constitutively activated in several tumors^[10-13]. However, the biological significance of NF- κ B activation remains unclear in gastric carcinogenesis although gastric cancer is one of the most aggressive forms of cancer.

Telomerase is a key enzyme that catalyzes the synthesis of telomere DNA participating in cell immortalization through stabilization of chromosomal structure^[14]. Telomerase is expressed in germ tissues as well as in majority of human tumors, including gastrointestinal carcinomas, but is low and difficult to detect in somatic cells generally^[15-19]. So it may be a useful molecular marker for cancer diagnosis and therapeutic strategies. Human telomerase reverse transcriptase (hTERT) has been identified as a putative catalytic subunit of human telomerase^[20]. Recent reconstitution experiments, both *in vitro* and *in vivo*, also strongly suggest that hTERT is the major determinant of human telomerase activity^[21,22]. Overexpression of hTERT in cancer cells is thought to contribute to tumor development and angiogenesis^[23-25]. However, the mechanism by which hTERT is overexpressed in cancer cells remains unclear. There are evidences that hTERT expression may be regulated by the highly inducible NF- κ B transcription factor^[26]. So it is interesting to investigate the relation between NF- κ B and hTERT at cellular level.

We undertook the present study to determine whether NF- κ B was constitutively activated in precancerous and cancerous tissues of the stomach, to examine whether expression of hTERT gene correlated with NF- κ B activation, and to evaluate the relationship between clinicopathological features and NF- κ B activation as well as hTERT gene expression.

MATERIALS AND METHODS

Tissue samples

Gastric tissues were obtained by surgical resection from 89 patients: 10 with normal gastric mucosa, 23 with intestinal metaplasia, 15 with dysplasia and 41 with gastric cancer. Patients with gastric cancer were admitted to Renmin Hospital of Wuhan University from February to December in 2000, and had not been treated with chemotherapy or radiation therapy before operation. Histological examinations were performed, according to the criteria of the Japanese Gastric Cancer Association^[27]. All specimens were fixed in 10 % buffered neutral formalin and embedded in paraffin. Serial tissue sections (4.5 μ m thick) were placed on glass slides coated with 3-aminopropyltriethoxysilane (Sigma, USA), and then used in the following experiments.

Immunohistochemistry for NF- κ B p65 and hTERT proteins

Immunostaining was performed as described previously with slight modification^[28]. Briefly, slides were treated overnight at 4 °C with either anti-p65 mAb (4 μ g/ml) or anti-hTERT polyclonal antibody (3 μ g/ml). Both antibodies were from Santa Cruz Biotechnology (USA). Then, slides were incubated with secondary antibody by using a streptavidin-peroxidase kit (Maixin-Bio, Fujian). Finally, the antigen sites were visualized by incubating with diaminobendizine (DAB) solution (Zhongshan Biotechnical Co, Beijing), and the nuclei were weakly counterstained with Mayer's hematoxylin (Maixin-Bio, Fujian). The specificity of immunostaining was determined by replacement of the primary antibody with PBS. Positive reaction was detected as nuclear stain presenting in brown-yellow color. Slides positively stained were further stratified from 1+ to 3+ based on the overall intensity and percentage of the stained tumor cells, with an estimated scale of <25% cell positive =1+, 25% to 50% =2+, and >50% =3+. Staining was defined as negative if positive cells were <5%.

In situ hybridization for hTERT mRNA

hTERT mRNA ISH detection kit and antisense polyoligonucleotide probe (digoxin-labeled) were purchased from Boster Biological Technology Ltd. (Wuhan). In brief, deparaffinized sections were incubated with 3% hydrogen peroxide for 30 min and then with 1 μ g/ml pepsin for 15 min. The prehybridization was performed at 37 °C for 2 h, and the hybridization was conducted in a 42 °C water bath for 18 h with each section covered with a soil coverslip. After thorough washing, tissue sections were preblocked for 20 min with blocking solution. Then, rabbit anti-digoxin antibody was added for 60 min at 37 °C. After washed in PBS, the sections were visualized according to the manufacturer's instructions. A negative control was prepared by using a hybridization solution without the probe. A positive reaction was detected as plasmatic stain presenting in brown-yellow color. Slides positively stained were further stratified from 1+ to 3+ as described above.

Statistics

Statistical analysis was performed using chi-squared test, Fisher's exact test, and spearman rank test. A *P* value <0.05 (one-sided) was accepted as statistically significant.

RESULTS

Staining of NF- κ Bp65 protein, hTERT mRNA and protein

P65 immunostaining was significantly enhanced both in cytoplasm and in nuclei of the tumor cells in comparison to that in normal epithelial cells (Figure 1). Since nuclear staining, which indicated nuclear transportation of p65, was considered as a marker of NF- κ B activation, we only counted the number of nuclear stained cells and took them into calculation of the percentage of positively stained cells. Similarly, hTERT protein was mainly localized in the nuclei of tumor cells, and only a small number of cells showed a positive reaction in the cytoplasm (Figure 2). Stromal cells such as endothelial cells and smooth muscle cells (except lymphocytes) showed no reaction for hTERT. Weak staining of p65 and hTERT proteins was observed in some epithelial cells in the lower two-thirds of the glands of nonneoplastic mucosa.

In situ hybridization

Revealed that hTERT mRNA was significantly enhanced in the cytoplasm of tumor cells (Figure 3). Only a few signals were seen in nonneoplastic cells, which were slightly increased in the replicating basal layer, and in intestinal metaplastic cells as well as in activated lymphocytes, while the surface epithelia were negative (Figure 4).

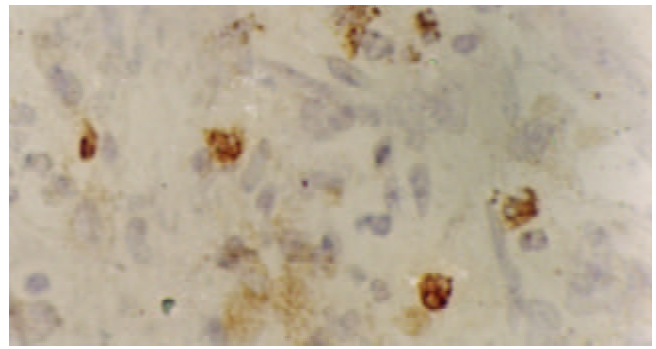


Figure 1 Immunohistochemical detection of NF- κ Bp65 protein in gastric carcinoma showing cytoplasmic and nuclear staining SP \times 400.

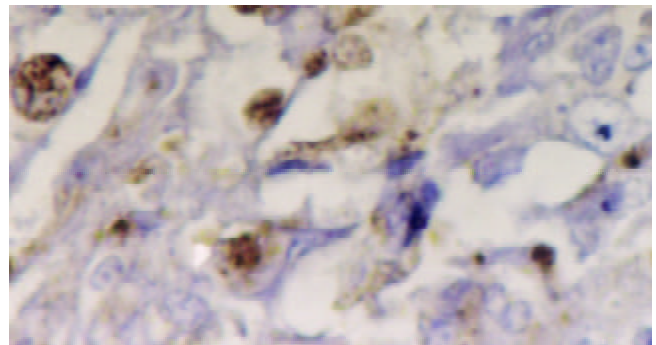


Figure 2 Immunohistochemical detection of hTERT protein in poorly differentiated gastric carcinoma. A positive reaction was shown in the nuclei of cancer cells. SP \times 400.

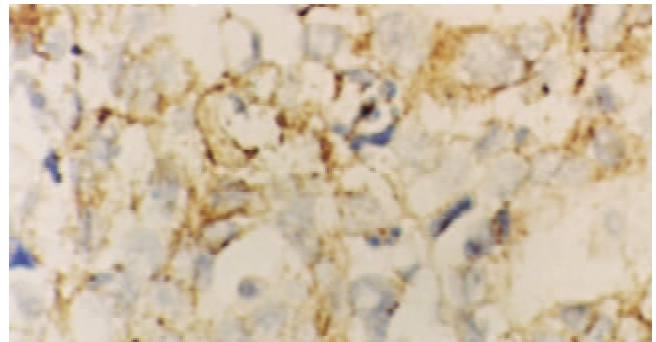


Figure 3 Detection of hTERT mRNA in a mucinous adenocarcinoma. Most tumor cells displayed strong signals that were localized in the cytoplasm. ISH \times 400.

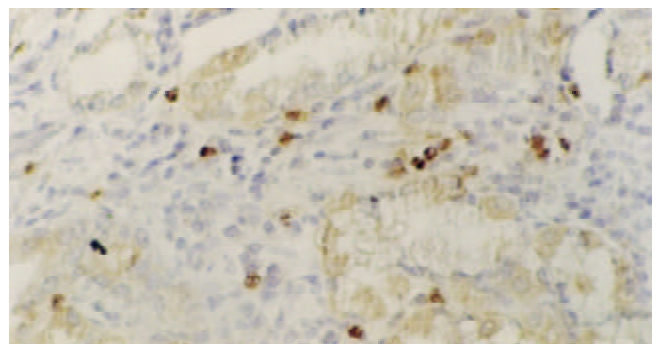


Figure 4 Detection of hTERT mRNA in intestinal metaplasia. The reaction was localized in the cytoplasm of intestinal metaplastic cells, activated lymphocytes, as well as replicating cells in basal layer, while the surface epithelia were negative. ISH \times 100.

Table 1 Expression of NF- κ Bp65 protein, hTERT mRNA and protein in precancerous lesions and gastric cancer

Lesion	Cases	NF- κ Bp65				hTERT mRNA				hTERT protein			
		+	++	+++	Total (%)	+	++	+++	Total (%)	+	++	+++	Total (%)
Normal	10	0	0	0	0 (0)	1	0	0	1 (10.00)	0	0	0	0 (0)
Intestinal metaplasia	23	7	1	0	8 (34.78) ^b	6	3	0	9 (39.13) ^b	5	2	0	7 (30.43) ^b
Dysplasia	15	7	1	0	8 (53.33) ^a	7	3	0	10 (66.67) ^a	7	2	0	9 (60.00) ^a
Cancer	41	7	14	4	25 (60.98) ^a	6	20	9	35 (85.37) ^a	6	20	6	32 (78.05) ^a

^a $P < 0.05$, vs normal mucosa group; ^b $P < 0.01$, vs cancer group.

Expression of NF- κ Bp65 protein, hTERT mRNA and protein

Expression of p65 protein, hTERT mRNA and protein in gastric precancerous and cancerous tissues was increased compared with normal mucosa (Table 1). The nuclear staining rates of p65 (active form) were higher in gastric cancer than in intestinal metaplasia ($P < 0.05$), or normal mucosa ($P < 0.05$). The rates were also significantly higher in dysplasia than in normal mucosa. Similarly, expression of hTERT mRNA and protein was increased in precancerous and cancerous tissues (Table 1).

The relations between clinicopathological features and expression of p65 and hTERT in the 41 patients with gastric carcinoma were further analyzed (Table 2). Nuclear staining rates of p65 and hTERT proteins were both significantly associated with the degree of differentiation, lymph node metastasis, clinical stage and the depth of invasion ($P < 0.01-0.05$). Furthermore, the nuclear staining of p65 was significantly higher in tumors ≥ 5 cm than in those < 5 cm. With respect to expression of hTERT mRNA, we found that carcinomas at advanced stage showed a significantly higher level than those at early stage. However, there was no significant association between expression of hTERT mRNA and other clinicopathological features.

Table 2 Correlation between expression of NF- κ Bp65 protein, hTERT mRNA and protein and clinicopathological features

Factor	Cases	NF- κ B p65 (%)	hTERT mRNA (%)	hTERT protein (%)
Gender				
Male	30	16 (53.33)	24 (80.00)	24 (80.00)
Female	11	9 (81.82)	11 (100.00)	8 (72.73)
Age (years)				
< 60	24	14 (58.33)	21 (87.50)	20 (83.33)
≥ 60	17	11 (64.71)	14 (82.35)	12 (70.59)
Histology (type)				
Intestinal	16	7 (43.75)	12 (75.00)	10 (62.50)
Diffuse	25	18 (72.00)	23 (92.00)	22 (88.00)
Differentiation				
Well	13	3 (23.08) ^b	9 (69.23)	7 (53.85) ^a
Poor	28	22 (78.57)	26 (92.86)	25 (89.29)
Lymph node metastasis				
Negative	16	4 (25.00) ^b	12 (75.00)	9 (56.25) ^a
Positive	25	21 (84.00)	23 (92.00)	23 (92.00)
Stage				
Early	12	2 (16.67) ^b	7 (58.33) ^b	5 (41.67) ^b
Advanced	29	23 (79.31)	28 (96.55)	27 (93.10)
Tumor size (cm)				
< 5	19	6 (31.58) ^b	14 (73.68)	13 (68.42)
≥ 5	22	19 (86.36)	21 (95.45)	19 (86.36)
Depth of invasion				
m, sm	10	2 (20.00) ^a	6 (60.00)	4 (40.00) ^a
ms, ss	17	11 (64.71)	16 (94.12)	15 (88.24)
se, si	14	12 (85.71)	13 (92.86)	13 (92.86)

^a $P < 0.05$, ^b $P < 0.01$, From comparison in each group of clinicopathologic feature by chi-square test or Fisher's exact test. m: mucosa,

sm: submucosa, mp: muscularis propria, ss: subserosa, se: invasion to serosa, si: invasion to other organ. Tumor size was defined as the largest size in extension on the gastric mucosa.

Correlation between NF- κ B activation and expression of hTERT

There was a positive correlation between NF- κ B activation and hTERT mRNA expression in patients with intestinal metaplasia ($r_s = 0.665$), dysplasia ($r_s = 0.661$) and gastric cancer ($r_s = 0.752$). Similarly, hTERT mRNA expression was also positively correlated with hTERT protein in these three groups ($P < 0.05$), with the r_s values of 0.609, 0.750 and 0.730, respectively.

DISCUSSION

The present study reported the detection of NF- κ B activation and hTERT gene expression, as well as their correlation, in cancerous and precancerous tissues of stomach.

NF- κ B, an important transcription factor, consists of dimeric complexes. We used immunohistochemistry to detect NF- κ B activation. The polyclonal antibody we used, could bind to the active and inactive forms of p65, one of NF- κ B subunits, as shown in a previous study^[29]. We only quantified the nuclear staining (active form) to evaluate NF- κ B activation. With such an analysis, nuclear translocation of p65 could be estimated at single-cell level. We found that active NF- κ B was not only in the nuclei of tumor cells but also in the nuclei of infiltrating inflammatory cells, especially lymphocytes, which was accordant with the role of NF- κ B involved in immune and inflammatory responses^[30,31]. Isomoto *et al*^[32] also reported that in *Helicobacter pylori*-associated gastritis, activated NF- κ B was expressed in macrophages, vascular endothelial cells and B lymphocytes in addition to epithelial cells, which might be involved in the inflammation process.

Using *in situ* hybridization and immunohistochemistry methods, we detected the expression of hTERT at both RNA and protein levels. Importantly, the *in situ* detection enabled us to differentiate whether telomerase activity was due to proliferative normal cells or lymphocytes. Therefore immunohistochemical detection of hTERT might be a novel tool for the diagnosis of gastric cancer^[33]. In this study, we demonstrated that, besides tumor cells, hTERT mRNA and protein were also expressed, albeit weakly in normal gastric fundic mucosa. These epithelial cells were terminally differentiated. It is possible that low levels of hTERT expression might be the characteristics of physically regenerating tissues containing stem cells, and hTERT-positive cells might be competent for regeneration if severe mucosal damage occurred^[28]. Although the level of hTERT mRNA correlated significantly with that of hTERT protein in our study, their expression levels were not always coincident in precancerous and cancerous lesions. It is likely that post-translational modifications, such as phosphorylation by akt kinase, might be involved in hTERT expression^[28,34].

The present study revealed that NF- κ Bp65 nuclear staining rates were higher in cancer tissues, followed by dysplasia,

intestinal metaplasia and normal mucosa. This is the first report on NF- κ Bp65 detection in gastric precancerous tissues. As to the expression of hTERT gene, previous studies revealed that carcinomas could express hTERT more frequently than noncancerous tissues^[25,35-38]. Our findings support these results. The present study indicated that NF- κ B and telomerase were both activated in precancerous lesions, suggesting that NF- κ B activation and increased hTERT gene expression emerge at the early stage of gastric carcinogenesis, and that they may be the prerequisites for malignant transformation. Therefore, NF- κ B and telomerase might be potentially important targets for the development of anti-tumor therapies for gastric carcinoma^[15,39,40].

Sasaki *et al*^[29] reported that NF- κ B activation was positively correlated with tumor size, lymphatic invasion, depth of invasion and peritoneal metastasis. Besides that, our study also revealed significantly positive correlations between nuclear staining of NF- κ B p65 and differentiation degree and clinical stage. Therefore, NF- κ B activation might be associated with tumor growth, invasion and metastasis.

It has been reported that hTERT expression might be downstream of NF- κ B activation^[26,41]. Yin *et al*^[26] found a potential NF- κ B binding site at 350 base pairs upstream from the translational start site of mouse TERT promoters and NF- κ B was found to contribute to the activation of TERT expression. In addition, Akiyama *et al*^[41] showed that NF- κ B interacted directly with hTERT protein in multiple myeloma cells. In the present study we examined the relationship between nuclear staining of NF- κ Bp65 and hTERT mRNA at the cellular level by immunohistochemistry and *in situ* hybridization. We observed that both p65 and hTERT mRNA were overexpressed in gastric cancer with the positive staining rates of 60.98% and 85.37%, respectively. In fact, most specimens showing a high p65 level also showed high hTERT mRNA expression and *vice versa*. Furthermore, the expression of p65 and hTERT mRNA showed a significant correlation in cancerous and precancerous tissues (intestinal metaplasia and dysplasia). And in nonneoplastic mucosa, the positive staining of p65 and hTERT mRNA were detected simultaneously in proliferative glands and activated lymphocytes. All of these suggested that NF- κ Bp65 cooperated with hTERT in gastric carcinogenesis. We speculate that NF- κ Bp65 may induce hTERT promoter activity and upregulate telomerase activity and contribute to the aggressiveness of gastric carcinoma.

However, our study was limited by the high specificity of p65 mAb for the p65 subunit, and thus we could not evaluate other NF- κ B dimers. The relationship between other NF- κ B subunits and gastric cancer needs further studies.

In conclusion, we demonstrated the presence of activated NF- κ Bp65 and increased hTERT expression in gastric cancerous and precancerous tissues. The levels of p65 and hTERT expression were higher in gastric cancer than in normal mucosa, and NF- κ B activation was associated with tumor growth, invasion and metastasis. Our findings suggest that NF- κ Bp65 cooperates with hTERT in gastric carcinogenesis.

REFERENCES

- Baeuerle PA**, Baltimore D. NF-kappa B: ten years after. *Cell* 1996; **87**: 13-20
- Jia CK**, Zheng SS, Li QY, Zhang AB. Immunotolerance of liver allotransplantation induced by intrathymic inoculation of donor soluble liver specific antigen. *World J Gastroenterol* 2003; **9**: 759-764
- Gong JP**, Liu CA, Wu CX, Li SW, Shi YJ, Li XH. Nuclear factor κ B activity in patients with acute severe cholangitis. *World J Gastroenterol* 2002; **8**: 346-349
- Thanos D**, Maniatis T. NF-kappa B: a lesson in family values. *Cell* 1995; **80**: 529-532
- Pahl HL**. Activators and target genes of Rel/NF-kappaB transcription factors. *Oncogene* 1999; **18**: 6853-6866
- de Martin R**, Schmid JA, Hofer-Warbinek R. The NF-KappaB/Rel family of transcription factors in oncogenic transformation and apoptosis. *Mutat Res* 1999; **437**: 231-243
- Li HL**, Chen DD, Li XH, Zhang HW, Lu YQ, Ye CL, Ren XD. Changes of NF- κ B, p53, Bcl-2 and caspase in apoptosis induced by JTE-522 in human gastric adenocarcinoma cell line AGS cells: role of reactive oxygen species. *World J Gastroenterol* 2002; **8**: 431-435
- La Rosa FA**, Pierce JW, Sonenshein GE. Differential regulation of the c-myc oncogene promoter by the NF-kappa B rel family of transcription factors. *Mol Cell Biol* 1994; **14**: 1039-1044
- Sonenshein GE**. Rel/NF- κ B transcription factors and the control of apoptosis. *Semin Cancer Biol* 1997; **8**: 113-119
- Zhu JW**, Yu BM, Ji YB, Zheng MH, Li DH. Upregulation of vascular endothelial growth factor by hydrogen peroxide in human colon cancer. *World J Gastroenterol* 2002; **8**: 153-157
- Wang W**, Abbruzzese JL, Evans DB, Larry L, Cleary KR, Chiao PJ. The nuclear factor-kappa B RelA transcription factor is constitutively activated in human pancreatic adenocarcinoma cells. *Clin Cancer Res* 1999; **5**: 119-127
- Sovak MA**, Bellas RE, Kim DW, Zanieski GJ, Rogers AE, Traish AM, Sonenshein GE. Aberrant nuclear factor-kappaB/Rel expression and the pathogenesis of breast cancer. *J Clin Invest* 1997; **100**: 2952-2960
- Guo SP**, Wang WL, Zhai YQ, Zhao YL. Expression of nuclear factor-kappa B in hepatocellular carcinoma and its relation with the X protein of hepatitis B virus. *World J Gastroenterol* 2001; **7**: 340-344
- Blackburn EH**. Telomerases. *Annu Rev Biochem* 1992; **61**: 113-129
- Burger AM**, Bibby MC, Double JA. Telomerase activity in normal and malignant mammalian tissues: feasibility of telomerase as a target for cancer chemotherapy. *Br J Cancer* 1997; **75**: 516-522
- Lu JP**, Mao JQ, Li MS, Lu SL, Hu XQ, Zhu SN, Nomura S. *In situ* detection of TGF betas, TGF beta receptor II mRNA and telomerase activity in rat cholangiocarcinogenesis. *World J Gastroenterol* 2003; **9**: 590-594
- Liao C**, Zhao MJ, Zhao J, Song H, Pineau P, Marchio A, Dejean A, Tiollais P, Wang HY, Li TP. Mutation analysis of novel human liver-related putative tumor suppressor gene in hepatocellular carcinoma. *World J Gastroenterol* 2003; **9**: 89-93
- Shen ZY**, Xu LY, Chen MH, Shen J, Cai WJ, Zeng Y. Progressive transformation of immortalized esophageal epithelial cells. *World J Gastroenterol* 2002; **8**: 976-981
- Feng RH**, Zhu ZG, Li JF, Liu BY, Yan M, Yin HR, Lin YZ. Inhibition of human telomerase in MKN-45 cell line by antisense hTR expression vector induces cell apoptosis and growth arrest. *World J Gastroenterol* 2002; **8**: 436-440
- Meyerson M**, Counter CM, Eaton EN, Ellisen LW, Steiner P, Caddle SD, Ziaugra L, Beijersbergen RL, Davidoff MJ, Liu Q, Bacchetti S, Haber DA, Weinberg RA. hEST2, the putative human telomerase catalytic subunit gene, is up-regulated in tumor cells and during immortalization. *Cell* 1997; **90**: 785-795
- Weinrich SL**, Pruzan R, Ma L, Ouellette M, Tesmer VM, Holt SE, Bodnar AG, Lichtsteiner S, Kim NW, Trager JB, Taylor RD, Carlos R, Andrews WH, Wright WE, Shay JW, Harley CB, Morin GB. Reconstitution of human telomerase with the template RNA component hTR and the catalytic protein subunit hTERT. *Nat Genet* 1997; **17**: 498-502
- Nakayama J**, Tahara H, Tahara E, Saito M, Ito K, Nakamura H, Nakanishi T, Tahara E, Ide T, Ishikawa F. Telomerase activation by hTERT in human normal fibroblasts and hepatocellular carcinomas. *Nat Genet* 1998; **18**: 65-68
- Shao JC**, Wu JF, Wang DB, Qin R, Zhang H. Relationship between the expression of human telomerase reverse transcriptase gene and cell cycle regulators in gastric cancer and its significance. *World J Gastroenterol* 2003; **9**: 427-431
- Pallini R**, Pierconti F, Falchetti ML, D' Arcangelo D, Fernandez E, Maira G, D' Ambrosio E, Larocca LM. Evidence for telomerase involvement in the angiogenesis of astrocytic tumors: expression of human telomerase reverse transcriptase messenger RNA by vascular endothelial cells. *J Neurosurg* 2001; **94**: 961-971
- Kumaki F**, Kawai T, Hiroi S, Shinomiya N, Ozeki Y, Ferrans VJ, Torikata C. Telomerase activity and expression of human

- telomerase RNA component and human telomerase reverse transcriptase in lung carcinomas. *Hum Pathol* 2001; **32**: 188-195
- 26 **Yin L**, Hubbard AK, Giardina C. NF-kappa B regulates transcription of the mouse telomerase catalytic subunit. *J Biol Chem* 2000; **275**: 36671-36675
- 27 **Japanese Gastric Cancer Association**. Japanese Classification of Gastric Carcinoma - 2nd English Edition -. *Gastric Cancer* 1998; **1**: 10-24
- 28 **Yasui W**, Tahara E, Tahara H, Fujimoto J, Naka K, Nakayama J, Ishikawa F, Ide T, Tahara E. Immunohistochemical detection of human telomerase reverse transcriptase in normal mucosa and precancerous lesions of the stomach. *Jpn J Cancer Res* 1999; **90**:589-595
- 29 **Sasaki N**, Morisaki T, Hashizume K, Yao T, Tsuneyoshi M, Noshiro H, Nakamura K, Yamanaka T, Uchiyama A, Tanaka M, Katano M. Nuclear factor-kappaB p65 (RelA) transcription factor is constitutively activated in human gastric carcinoma tissue. *Clin Cancer Res* 2001; **7**: 4136-4142
- 30 **Cong B**, Li SJ, Yao YX, Zhu GJ, Ling YL. Effect of cholecystokinin octapeptide on tumor necrosis factor α transcription and nuclear factor-kappaB activity induced by lipopolysaccharide in rat pulmonary interstitial macrophages. *World J Gastroenterol* 2002; **8**: 718-723
- 31 **Meng AH**, Ling YL, Zhang XP, Zhang JL. Anti-inflammatory effect of cholecystokinin and its signal transduction mechanism in endotoxic shock rat. *World J Gastroenterol* 2002; **8**: 712-717
- 32 **Isomoto H**, Mizuta Y, Miyazaki M, Takeshima F, Omagari K, Murase K, Nishiyama T, Inoue K, Murata I, Kohno S. Implication of NF-kappaB in *Helicobacter pylori*-associated gastritis. *Am J Gastroenterol* 2000; **95**: 2768-2776
- 33 **Yasui W**, Tahara H, Tahara E, Fujimoto J, Nakayama J, Ishikawa F, Ide T, Tahara E. Expression of telomerase catalytic component, telomerase reverse transcriptase, in human gastric carcinomas. *Jpn J Cancer Res* 1998; **89**: 1099-1103
- 34 **Kang SS**, Kwon T, Kwon DY, Do SI. Akt protein kinase enhances human telomerase activity through phosphorylation of telomerase reverse transcriptase subunit. *J Biol Chem* 1999; **274**: 13085-13090
- 35 **Lan J**, Xiong YY, Lin YX, Wang BC, Gong LL, Xu HS, Guo GS. *Helicobacter pylori* infection generated gastric cancer through p53-Rb tumor-suppressor system mutation and telomerase reactivation. *World J Gastroenterol* 2003; **9**: 54-58
- 36 **Yao XX**, Yin L, Sun ZC. The expression of hTERT mRNA and cellular immunity in gastric cancer and precancerosis. *World J Gastroenterol* 2002; **8**: 586-590
- 37 **Kammori M**, Kanauchi H, Nakamura K, Kawahara M, Weber TK, Mafune K, Kaminishi M, Takubo K. Demonstration of human telomerase reverse transcriptase in human colorectal carcinomas by *in situ* hybridization. *Int J Oncol* 2002; **20**: 15-21
- 38 **Jong HS**, Park YI, Kim S, Sohn JH, Kang SH, Song SH, Bang YJ, Kim NK. Up-regulation of human telomerase catalytic subunit during gastric carcinogenesis. *Cancer* 1999; **86**: 559-565
- 39 **Ueda M**, Kokura S, Imamoto E, Naito Y, Handa O, Takagi T, Yoshida N, Yoshikawa T. Blocking of NF-kappaB activation enhances the tumor necrosis factor alpha-induced apoptosis of a human gastric cancer cell line. *Cancer Lett* 2003; **193**: 177-182
- 40 **Akari H**, Bour S, Kao S, Adachi A, Strebel K. The human immunodeficiency virus type 1 accessory protein Vpu induces apoptosis by suppressing the nuclear factor kappaB-dependent expression of antiapoptotic factors. *J Exp Med* 2001; **194**: 1299-1311
- 41 **Akiyama M**, Hideshima T, Hayashi T, Tai YT, Mitsiades CS, Mitsiades N, Chauhan D, Richardson P, Munshi NC, Anderson KC. Nuclear factor-kappaB p65 mediates tumor necrosis factor alpha-induced nuclear translocation of telomerase reverse transcriptase protein. *Cancer Res* 2003; **63**: 18-21

Edited by Xia HXH and Wang XL

Correlation of tumor-positive ratio and number of perigastric lymph nodes with prognosis of gastric carcinoma in surgically-treated patients

Yong-Bin Ding, Guo-Yu Chen, Jian-Guo Xia, Xi-Wei Zang, Hong-Yu Yang, Li Yang, Yue-Xian Liu

Yong-Bin Ding, Guo-Yu Chen, Jian-Guo Xia, Xi-Wei Zang, Hong-Yu Yang, Li Yang, Department of General Surgery, First Affiliated Hospital of Nanjing Medical University, Nanjing 210029, Jiangsu Province, China

Yue-Xian Liu, Nanjing University of Traditional Chinese Medicine, Nanjing 210029, Jiangsu Province, China

Correspondence to: Yong-Bin Ding, Department of General Surgery, First Affiliated Hospital of Nanjing Medical University, Nanjing 210029, Jiangsu Province, China. njdyb@sina.com

Telephone: +86-25-86563750

Received: 2003-03-04 **Accepted:** 2003-04-19

Abstract

AIM: To evaluate the tumor-positive ratio and number of perigastric lymph nodes as prognostic factors of gastric carcinoma in surgically-treated patients.

METHODS: The postoperative survival of 169 patients with gastric cancer who were performed D₂ curative gastrectomy was analyzed with regard to its lymph node metastasis ratio and number. Meanwhile correlation of tumor-positive ratio and number of perigastric lymph nodes with pathological parameters of these patients was studied.

RESULTS: The overall 5-year survival rate of all the patients studied was 29.6%. The 5-year cumulative survival rate in patients with 1%-20% and more than 20% of tumor-positive lymph nodes was 70.6% and 12.0% respectively, and 46.6% and 17.4% in those with 1-5 and more than 5 of tumor-positive lymph nodes respectively, which were significantly decreased with the increment of involved lymph nodes assessed by either numbers or ratio ($P < 0.05$). Multiple stepwise regression analysis showed that both the positive ratio and number of tumor-involved lymph nodes were sensitive prognostic factors in these surgically-treated patients, which were also significantly correlated with tumor size and depth of submucosal invasion ($P < 0.05$).

CONCLUSION: Tumor-positive ratio and number of perigastric lymph nodes are associated with cancer progression and five-year survival rate, and may serve as valuable prognostic factors of gastric cancer in surgically-treated patients.

Ding YB, Chen GY, Xia JG, Zang XW, Yang HY, Yang L, Liu YX. Correlation of tumor-positive ratio and number of perigastric lymph nodes with prognosis of gastric carcinoma in surgically-treated patients. *World J Gastroenterol* 2004; 10(2): 182-185 <http://www.wjgnet.com/1007-9327/10/182.asp>

INTRODUCTION

It has been well recognized that lymph node metastasis in patients with gastric cancer is one of the important prognostic factors^[1-4]. In 1997, the International Union Contrele Cancer

(UICC) and American Joint Commission for Cancer (AJCC) redefined metastatic status of lymph node on the basis of the involved node number rather than its location, in which pN1 was defined as 1-6 local lymph nodes being involved, pN2 as 7-15 local lymph nodes being involved and pN3 as more than 15 local lymph nodes being involved^[5-7]. Some reports strongly suggested that this classification was more sensitive with a higher reproducibility in the prognostic evaluation of gastric cancer patients than that assessed by the metastatic locations of lymph node^[8,9]. However, In China there are few reports concerning the correlation of local lymph node metastatic ratio and number with the prognosis of gastric cancer patients, which was the motivation for us to initiate the present study of such cases in the Chinese population.

MATERIALS AND METHODS

Patients and materials

Between January 1995 and November 1997, 304 patients with primary gastric cancer were performed D₂ radical gastrectomy in the Department of General Surgery, First Affiliated Hospital of Nanjing Medical University. Of them, 121 male and 48 female cases aging from 32 to 78 years (mean, 58.4 years) were found to have lymph node metastasis, and analyzed in the present study, with a following-up time from 0 to 61 months postoperation.

Methods

The status of lymph nodes was assessed according to the staging system formulated by UICC/AJCC in 1997. Of the 169 patients with positive lymph nodes, 32 were found to have remote lymphatic metastasis such as that in the retropancreatic, mesenteric and paraortic regions. The total number of resected lymph nodes was 10 223 (mean: 34.1, range: 11-122), the median number of examined lymph nodes was 26 (mean: 31.1, range: 12 to 91) for all 304 patients, the median number of involved regional lymph nodes was 5.0 (mean: 7.1, range: 1 to 42). Lymph node metastasis ratio was defined as the number of metastatic lymph nodes to the total number of resected ones.

To elucidate the prognostic significance of metastatic lymph nodes, the clinical and histopathological records of these 169 patients were analyzed. The relationships of 5-year survival rate with sex, age, tumor location, histopathological grading, macroscopic type, lymph node resection and depth of tumor invasion were determined. Tumor location, macroscopic type, and lymph node resection were graded according to the Japanese classification of gastric carcinoma proposed by Japanese Gastric Carcinoma Association (JGCA). Histopathological grading was defined according to the fifth edition of TNM classification. Following-up information was obtained from routine clinical examinations.

Statistical analysis

Statistical analysis was carried out using SPSS 10.0 for Windows. The 5-year survival rate of those performed using D₂ radical gastrectomy was analyzed by cox's proportional

hazard models. The log rank test was used to compare the survival data between groups. Comparison between qualitative results for the PN categories and clinical or histopathological parameters was performed using the χ^2 test. Independent predictors of postoperation survival were identified by logistic regression analysis. Kaplan-Meier curves were used to demonstrate survival distribution.

RESULTS

Among the 304 patients, 169(55.6%) had lymph node metastasis. The 5-year survival rate was 29.6% for the node-positive patients, and was 91.2% for the node-negative patients. The cancer -specific 5-year survival rate of patients with lymph node metastasis was significantly lower than that of those without lymph node metastasis ($P<0.05$).

Correlation between lymph node metastatic ratio and 5-year survival rate

The patients were divided into two groups by the ratio of metastatic lymph node number to the total number of resected lymph nodes. The 5-year survival rate of 51 patients with metastatic lymph nodes less than 20% was 70.6%(36 cases), while that of 118 patients with 21% or more was 12% (14 cases). A significant difference was noted between the two groups ($P<0.05$, Table 1). As the ratio of lymph node metastasis increased, the 5-year survival rate decreased (Figure 1).

Table 1 Correlation between lymph node metastatic ratio and survival years

Ratio of positive lymph nodes	n	Survival years					P
		1	2	3	4	5	
<20%	51	51	49	45	39	36	<0.05
>21%	118	104	87	66	43	14 ^a	

^a $P<0.05$ vs the group with lymph node metastatic ratio less than 20%.

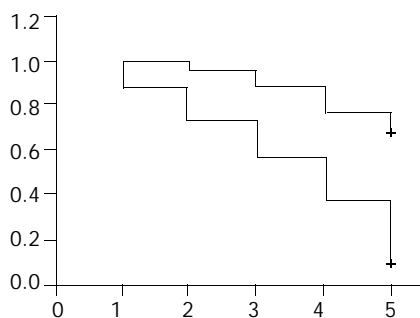


Figure 1 Negative correlation between survival years and ratio of metastatic lymph nodes in patients with gastric cancer. +: patients with metastatic ratio of lymph node less than 20%; -: patients with metastatic ratio of lymph node more than 21%.

Relation between lymph node metastasis number and 5-year survival rate

There was no significant difference in the outcome of patients with 1, 2, 3, 4 or 5 positive nodes, but there was a sharp decrease in survival rate when the sixth node was involved (Table 1), So the patients were divided into two groups according to the lymph node metastatic number. Group A having less than 5 and group B having more than 6. The 5-year survival rate of 71 patients with less than 5 metastatic lymph nodes was 46.6%(33 cases), and the 5-year survival rate of 98 patients with more than 6 metastatic lymph nodes was 17.4% (17 cases).

A sharp decrease in survival was seen between two groups ($P<0.05$, Table 2). The 5-year survival rate decreased as the number of lymph node metastases increased (Figure 2).

Table 2 Correlation between lymph node metastatic number and survival years

Number of positive lymph node	n	Survival years					P
		1	2	3	4	5	
1	9	9	9	8	6	5	
2	20	20	19	18	15	10	0.908
3	12	12	12	10	9	5	1.0
4	11	11	9	8	6	5	0.79
5	19	17	16	14	11	8	0.704
6	41	36	30	22	11	10	0.009
7	20	18	16	13	9	5	0.555
8	16	14	11	9	7	3	0.698
≥9	21	18	13	9	8	3	0.688
1-5	71	69	66	58	47	33	
>5	98	86	70	53	35	17	0.00072 ^a

^a $P<0.05$, vs the group with lymph node metastatic number more than 5.

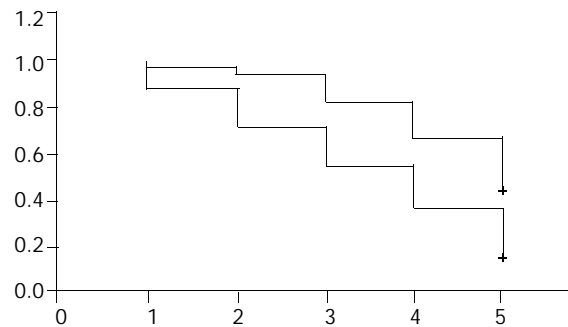


Figure 2 Negative correlations between survival years and number of metastatic lymph nodes in patients with gastric cancer. +: patients with metastatic number of lymph nodes less than 5; -: patients with metastatic number of lymph nodes more than 6.

Correlation between positive ratio of lymph node metastasis and tumor characteristics

As shown in Table 3, lymph node metastatic ratio was positively correlated to tumor size, depth of invasion. No significant difference was found between lymph node metastatic ratio and tumor location.

Table 3 Correlation between lymph node metastatic ratio and tumor characteristics

Pathological characteristics	Lymph node <20% metastatic ratio	>21%	P
Size of tumor			
<4 cm	42	43	
≥4 cm	9	74 ^a	0.48
location			
Lower third	5	8	
Middle third	22	47	
Upper third	24	63	<0.001
Depth of invasion			
Mucosa and submucosa	12	9	
Muscle and subserosa	16	6	
Serosa	23	103 ^b	<0.001

^a $P<0.05$, ^b $P<0.05$ vs the group with lymph node metastatic ratio less than 20%.

Correlation between number of positive lymph nodes and tumor characteristics

As shown in Table 4, tumors with one to five involved lymph nodes compared with those with six or more involved lymph nodes were significantly characterized by size, depth of invasion, there was no significant difference between the number of involved lymph nodes and tumor location.

Table 4 Correlation between number of involved lymph nodes and tumor characteristics

Pathological characteristics	Number of positive lymph nodes 1-5	>5	P
Size of tumor			
<4 cm	51	34	
≥4 cm	20	64 ^a	0.48
location			
Lower third	7	6	
Middle third	31	38	
Upper third	33	54	<0.05
Depth of invasion			
Mucosa and submucosa	20	1	
Muscle and subserosa	18	4	
Serosa	33	93 ^b	<0.05

^aP<0.05, ^bP<0.05 vs the group with lymph node metastatic number more than 5.

DISCUSSION

Gastric carcinoma, one of the most common human malignant tumors, is as the first leading cause of gastrointestinal cancer-related mortality. Over 50% of patients with gastric cancer operated in China had lymph node metastasis, which resulted in poor prognosis of these patients^[10-13]. As yet, lymph node status has been considered as the major determinant of gastric cancer recurrence for patients undergoing a curative gastrectomy^[14-16]. However, some authors suggested that the prognostic assessment of these patients by counting the number of positive lymph nodes related to tumor locations was too complicated to be used in routine practice. A simple and easy system for lymph node staging has been considered to be urgently needed^[14-16].

In the present study, we observed the effect of metastatic lymph node number on the survival years of gastric cancer patients. The result showed that the five-year survival rate in patients with 0, 1-5 and more than 5 tumor-positive lymph nodes was 91.2%, 46.6% and 17.4% respectively, indicating that considerable differences in the five-year survival rate existed between the patients. However, There was no significant difference observed between the outcomes of patients with 1, 2, 3, 4 and 5 tumor-positive lymph nodes. Thus it is more reasonable to classify gastric cancer patients with criteria of tumor-positive node numbers rather than tumor-positive nodes. Similar results have been revealed in a previous report by Wu *et al.* They divided the gastric cancer patients into two groups according to the number of involved lymph nodes, and found that the number of positive nodes rather than lymph node involvement was suitable for the classification of nodal stages in gastric cancer^[8,17,18].

Lymph node metastatic ratio, namely the number of metastatic lymph nodes to the total number of resected lymph nodes, has also been found to be an important prognostic factor^[19-22]. We observed that the 5-year survival rate in patients with the metastatic lymph node ratio of 0, 1-20% and more than 21%, was 91.2%, 70.6% and 12% respectively. Similar results have been shown by Kwon and his colleagues that the

metastatic ratio of lymph nodes was one of the main factors in determining the five-year survival rate of gastric cancer patients. Furthermore, the lymph node metastatic ratio has also been found to be more objective and reliable than the metastatic number in the prognosticating outcomes of these patients, because the former could effectively eliminate the influence of variance in resected lymph number on the prognosis of gastric cancer patients^[23-27].

It is generally accepted the depth of cancer invasion is an other important prognostic indicator in gastric cancer. Yasuda *et al* showed that the metastatic rate of lymph nodes was correlated with the depth of submucosal invasion in early stage of gastric carcinoma^[28,29], which was in accordance with our present results. We found that the number and ratio of metastatic lymph nodes were positively related with the depth of cancer invasion and tumor size in gastric cancer cases.

In conclusion, gastric cancer patients with 5 or more positive lymph nodes and 20% or more of positive lymph node metastasis associated with a poor prognosis. The positive number and ratio of lymph node metastasis are simple and useful indicators in evaluating the surgical results of patients with gastric cancer^[19,30,31].

REFERENCES

- 1 **Manfe AZ**, Segalina P, Maffei Faccioli A. Prognostic factors in gastric cancer. Our experience and review of the literature. *Minerva Chir* 2000; **55**: 299-305
- 2 **Takagane A**, Terashima M, Abe K, Araya M, Irinoda T, Yonezawa H, Nakaya T, Inaba T, Oyama K, Fujiwara H, Saito K. Evaluation of the ratio of lymph node metastasis as a prognostic factor in patients with gastric cancer. *Gastric Cancer* 1999; **2**: 122-128
- 3 **Yokota T**, Kunii Y, Teshima S, Yamada Y, Saito T, Takahashi M, Kikuchi S, Yamauchi H. Significant prognostic factors in patients with early gastric cancer. *Int Surg* 2000; **85**: 286-290
- 4 **Ding YB**, Chen GY, Xia JG, Zang XW, Yang HY, Yang L. Association of VCAM-1 Overexpression with oncogenesis, tumor angiogenesis and metastasis of gastric carcinoma. *World J Gastroenterol* 2003; **9**: 1409-1414
- 5 **Jahne J**. Lymphadenectomy in gastric carcinoma? *Zentralbl Chir* 2002; **127**: 550-553
- 6 **Hayashi H**, Ochiai T, Suzuki T, Shimada H, Hori S, Takeda A, Miyazawa Y. Superiority of a new UICC-TNM staging system for gastric carcinoma. *Surgery* 2000; **127**: 129-135
- 7 **Omejc M**, Juvan R, Jelenc F, Repse S. Lymph node metastases in gastric cancer: correlation between new and old UICC TNM classification. *Int Surg* 2001; **86**: 14-19
- 8 **Wu CW**, Hsieh MC, Lo SS, Shen KH, Lui WY, P'eng FK. Comparison of the UICC/AJCC 1992 and 1997 pN categories for gastric cancer patients after surgery. *Hepatogastroenterology* 2001; **48**: 279-284
- 9 **Katai H**, Yoshimura K, Maruyama K, Sasako M, Sano T. Evaluation of the New International Union Against Cancer TNM staging for gastric carcinoma. *Cancer* 2000; **88**: 1796-1800
- 10 **Abe N**, Watanabe T, Suzuki K, Machida H, Toda H, Nakaya Y, Masaki T, Mori T, Sugiyama M, Atomi Y. Risk factors predictive of lymph node metastasis in depressed early gastric cancer. *Am J Surg* 2002; **183**: 168-172
- 11 **Yamaguchi T**, Sano T, Katai H, Sasako M, Maruyama K. Node-positive mucosal gastric cancer: a follow-up study. *Jpn J Clin Oncol* 2001; **31**: 153-156
- 12 **de Manzoni G**, Verlato G, di Leo A, Guglielmi A, Laterza E, Ricci F, Cordiano C. Perigastric lymph node metastases in gastric cancer: comparison of different staging systems. *Gastric Cancer* 1999; **2**: 201-205
- 13 **Chen CY**, Wu CW, Lo SS, Hsieh MC, Lui WY, Shen KH. Peritoneal carcinomatosis and lymph node metastasis are prognostic indicators in patients with Borrmann type IV gastric carcinoma. *Hepatogastroenterology* 2002; **49**: 874-877
- 14 **Pan W**, Ishii H, Ebihara Y, Gobe G. Prognostic use of growth characteristics of early gastric cancer and expression patterns of apoptotic, cell proliferation, and cell adhesion proteins. *J Surg*

- Oncol* 2003; **82**: 104-110
- 15 **Nakamura K**, Morisaki T, Sugitani A, Ogawa T, Uchiyama A, Kinukawa N, Tanaka M. An early gastric carcinoma treatment strategy based on analysis of lymph node metastasis. *Cancer* 1999; **85**: 1500-1505
 - 16 **Kodera Y**, Yamamura Y, Shimizu Y, Torii A, Hirai T, Yasui K, Morimoto T, Kato T, Kito T. Lymph node status assessment for gastric carcinoma: is the number of metastatic lymph nodes really practical as a parameter for N categories in the TNM Classification? *Tumor Node Metastasis. J Surg Oncol* 1998; **69**: 15-20
 - 17 **Shimada S**, Yagi Y, Honmyo U, Shiomori K, Yoshida N, Ogawa M. Involvement of three or more lymph nodes predicts poor prognosis in submucosal gastric carcinoma. *Gastric Cancer* 2001; **4**: 54-59
 - 18 **Bouvier AM**, Haas O, Piard F, Roignot P, Bonithon-Kopp C, Faivre J. How many nodes must be examined to accurately stage gastric carcinomas? Results from a population based study. *Cancer* 2002; **94**: 2862-2866
 - 19 **Inoue K**, Nakane Y, Iiyama H, Sato M, Kanbara T, Nakai K, Okumura S, Yamamichi K, Hioki K. The superiority of ratio-based lymph node staging in gastric carcinoma. *Ann Surg Oncol* 2002; **9**: 27-34
 - 20 **Yasuda K**, Shiraishi N, Suematsu T, Yamaguchi K, Adachi Y, Kitano S. Rate of detection of lymph node metastasis is correlated with the depth of submucosal invasion in early stage gastric carcinoma. *Cancer* 1999; **85**: 2119-2123
 - 21 **Bando E**, Yonemura Y, Taniguchi K, Fushida S, Fujimura T, Miwa K. Outcome of ratio of lymph node metastasis in gastric carcinoma. *Ann Surg Oncol* 2002; **9**: 775-784
 - 22 **Hyung WJ**, Noh SH, Yoo CH, Huh JH, Shin DW, Lah KH, Lee JH, Choi SH, Min JS. Prognostic significance of metastatic lymph node ratio in T3 gastric cancer. *World J Surg* 2002; **26**: 323-329
 - 23 **Yin T**, Ji XL, Shen MS. Relationship between lymph node sinuses with blood and lymphatic metastasis of gastric cancer. *World J Gastroenterol* 2003; **9**: 40-43
 - 24 **Lee E**, Chae Y, Kim I, Choi J, Yeom B, Leong AS. Prognostic relevance of immunohistochemically detected lymph node micrometastasis in patients with gastric carcinoma. *Cancer* 2002; **94**: 2867-2873
 - 25 **Choi HJ**, Kim YK, Kim YH, Kim SS, Hong SH. Occurrence and prognostic implications of micrometastases in lymph nodes from patients with submucosal gastric carcinoma. *Ann Surg Oncol* 2002; **9**: 13-19
 - 26 **Tsujitani S**, Kaibara N. Clinical significance of molecular biological detection of micrometastases in gastric carcinoma. *Nippon Geka Gakkai Zasshi* 2001; **102**: 741-744
 - 27 **Fukagawa T**, Sasako M, Mann GB, Sano T, Katai H, Maruyama K, Nakanishi Y, Shimoda T. Immunohistochemically detected micrometastases of the lymph nodes in patients with gastric carcinoma. *Cancer* 2001; **92**: 753-760
 - 28 **Monig SP**, Zirbes TK, Schroder W, Baldus SE, Lindemann DG, Dienes HP, Holscher AH. Staging of gastric cancer: correlation of lymph node size and metastatic infiltration. *Am J Roentgenol* 1999; **173**: 365-367
 - 29 **Saiura A**, Umekita N, Inoue S, Maeshiro T, Miyamoto S, Matsui Y, Asakage M, Kitamura M. Clinicopathological features and outcome of hepatic resection for liver metastasis from gastric cancer. *Hepatogastroenterology* 2002; **49**: 1062-1065
 - 30 **Yoshizumi Y**, Matuyama T, Koike H, Aiko S, Sugiura Y, Maehara T. Long-term survival after gastric cancer and liver and paraaortic lymph node metastases: report of a case. *Surg Today* 2001; **31**: 159-162
 - 31 **Kologlu M**, Kama NA, Reis E, Doganay M, Atli M, Dolapci M. A prognostic score for gastric cancer. *Am J Surg* 2000; **179**: 521-526

Edited by Zhu L and Wang XL

Construction of a targeting Adenoviral vector carrying AFP promoter for expressing EGFP gene in AFP producing hepatocarcinoma cell

Yu-Jun Shi, Jian-Ping Gong, Chang-An Liu, Xu-Hong Li, Ying Mei, Can Mi, Yan-Ying Huo

Yu-Jun Shi, Jian-Ping Gong, Chang-An Liu, Xu-Hong Li, Ying Mei, Department of General Surgery, the Second College of Clinical Medicine and the Second Affiliated Hospital of Chongqing University of Medical Sciences, Chongqing 400010, China

Can Mi, Department of Pathology, Basic Medical College, Chongqing University of Medical Sciences, Chongqing 400016, China

Yan-Ying Huo, Institute for Radiology, Military Academy of Medical Sciences, Beijing 100850, China

Supported by the Key Program of Medical Science Foundation of Chongqing Public Health Bureau, [2001] 01-1-018

Correspondence to: Professor Chang-An Liu, Department of General Surgery, the Second College of Clinical Medicine and the Second Affiliated Hospital of Chongqing University of Medical Science, Chongqing 400010, China. shiyujun1128@hotmail.com

Telephone: +86-23-63848842

Received: 2003-08-11 **Accepted:** 2003-10-23

Abstract

AIM: To construct a recombinant adenoviral vector carrying AFP promoter and EGFP gene for specific expression of EGFP gene in AFP producing hepatocellular carcinoma (HCC) HepG2 cells.

METHODS: Based on the Adeno-X™ expression system, the human immediate early cytomegalovirus promoter (P_{CMV IE}) was removed from the plasmid, *pshuttle*, and replaced by a 0.3 kb α -fetoprotein (AFP) promoter that was synthesized by polymerase chain reaction (PCR). The enhanced green fluorescent protein (EGFP) gene was inserted into the multi-clone site (MCS), and then the recombinant adenovirus vector carrying the 0.3 kb AFP promoter and EGFP gene was constructed. Cells of a normal liver cell line (LO2), a hepatocarcinoma cell line (HepG2) and a cervical cancer cell line (HeLa) were transfected with the adenovirus. Northern blot and fluorescence microscopy were used to detect the expression of the EGFP gene at mRNA or protein level in three different cell lines.

RESULTS: The 0.3 kb AFP promoter was synthesized through PCR from the human genome. The AFP promoter and EGFP gene were directly inserted into the plasmid *pshuttle* as confirmed by restriction digestion and DNA sequencing. Northern blot showed that EGFP gene was markedly transcribed in HepG2 cells, but only slightly in LO2 and HeLa cells. In addition, strong green fluorescence was observed in HepG2 cells under a fluorescence microscopy, but fluorescence was very weak LO2 and HeLa cells.

CONCLUSION: Under control of the 0.3 kb human AFP promoter, the recombinant adenovirus vector carrying EGFP gene can be specially expressed in AFP-producing HepG2 cells. Therefore, this adenovirus system can be used as a novel, potent and specific tool for gene-targeting therapy for the AFP positive primary hepatocellular carcinoma.

Shi YJ, Gong JP, Liu CA, Li XH, Mei Y, Mi C, Huo YY. Construction of a targeting Adenoviral vector carrying AFP promoter for

expressing EGFP gene in AFP producing hepatocarcinoma cell. *World J Gastroenterol* 2004; 10(2): 186-189

<http://www.wjgnet.com/1007-9327/10/186.asp>

INTRODUCTION

In recent years, research in tumor gene therapy has made great progress in laboratory. However, there is an urgent need for gene therapy in clinical practice. Recombinant adenovirus is one of the most popular and promising tools for gene therapy^[1,2]. But how to construct a proper recombinant adenovirus vector carrying the interested gene that is specifically expressed only in target tumor cells has become the bottle neck which restricts the application of the vector in clinical gene therapy for tumors^[3,4]. The aim of this study was to construct a recombinant adenovirus vector carrying a 0.3 kb AFP promoter, and to investigate the expression of enhanced green fluorescent protein (EGFP) gene that was inserted into the vector in AFP positive hepatocarcinoma cells.

MATERIALS AND METHODS

Reagents

EX Taq DNA polymerase, T4 ligase, DNA isolation and purification kit were purchased from Promega (USA), restriction endonucleases and the DNA marker from Takara Biotechnology, Dalian (China), Lipofectamin™ 2000 from Invitrogen (USA), and RPMI 1640 medium and fetal calf serum from Hyclone (USA).

Cell lines

Hepatocarcinoma cell line, HepG2, was a gift from Professor Wei-Xue Tang, Department of Pathophysiology, Chongqing University of Medical Sciences. A normal hepatocyte cell line, LO2, and human cervical cancer cell line, HeLa, were preserved in our laboratory. Low-passage HEK 293 cells were obtained from the Institute for Cytobiology, Chinese Academy of Sciences, Shanghai. All cells were cultured in RPMI-1640 medium containing 10% fetal calf serum at 37 °C in saturated humidified air with 5% CO₂. The cells were subcultured once every three days.

Vectors

Adenovirus vector Adeno-X™ expression system and *pEGFP-C1* were purchased from Clontech Corporation (USA).

Polymerase chain reaction (PCR)

PCR was employed to amplify human AFP promoter and EGFP gene from HepG2 cell genomic DNA and *pEGFP-C1*, respectively. Specific primers for AFP promoter were as follows: 5' -GCG CTA GCA TTC TGT AGT TTG AGG AG-3' (sense), 5' -ATG GGC CCA TTG GCA GTG GTG GAA-3' (antisense). *NheI* and *PstI* sites were introduced into the sense and antisense primer, respectively, as underlined. Specific primers for EGFP gene were as follows: 5' -AAG GGC CCT TTA GTG AAC CGT CAG AT-3' (sense), 5' -GCCTTA AGT

TAT CTA GAT CCG GTG GAT-3' (antisense). *ApaI* and *AflIII* sites were introduced into the sense and antisense primer, respectively.

To remove the p_{CMVIE} from the *pshuttle*, PCR was used to amplify the 99-744 region of *pshuttle*, and specific primers were as follows: 5' -AGC CAG TAT CTG CTC CCT GCT TGT G-3' (sense), 5' -ATG CTA GCG GTG CCA AAA CAA ACT CCC A-3' (antisense). *NheI* site was introduced into the antisense primer.

PCR was performed in a total volume of 50 μ l consisting of 1 μ M each primer, 200 μ M each dNTP, 5 μ l 10 \times polymerase reaction buffer, 1.25U EX taq DNA polymerase and 1 μ l DNA template. The samples were heated to 94 $^{\circ}$ C for 5 min followed by amplification for 30 cycles at 94 $^{\circ}$ C for 30 s, 55 $^{\circ}$ C for 30 s, and 72 $^{\circ}$ C for 50 s. After the last cycle, a final extension step was at 72 $^{\circ}$ C for 7 min. Then 5 μ l of each product was analyzed by 1% agarose gel (containing 0.5 μ g/ml EB) electrophoresis. PCR products were purified from the agarose gel using DNA purification kit.

Construction of the adenoviral vector

pshuttle and the PCR products of 99-744 region were both doubly digested with *MluI* and *NheI*, and the digested products were ligated with T4 ligase. *MluI* site was 256, and the *NheI* was 921 in *pshuttle*. The 256-921 region of the *pshuttle* was removed from the plasmid, and replaced by the region of 256-744, then the 744-921 region containing the p_{CMVIE} was removed from *pshuttle*. Thus, a new plasmid p_{CMV}^{-} was constructed.

Subsequently, the p_{CMV}^{-} and *AFP* PCR products were doubly digested with *NheI* and *ApaI*. The 0.3 kb *AFP* promoter was inserted into the p_{CMV}^{-} , which was called *pAFP*. Then the p_{CMVIE} was replaced by the *AFP* promoter.

To insert the *EGFP* gene into the *pAFP*, both the *pAFP* and *EGFP* PCR products were doubly digested with *ApaI* and *AflIII*. The digested products were ligated to construct *pAFP-EGFP*.

The newly constructed plasmid *pAFP-EGFP* was then doubly digested with *PI-SceI/Ceu I* (New England Biolabs, UK), and the purified product was ligated with Adeno-X genome DNA. It was amplified in *E. coli DH5a*. The HEK293 cells were transfected with recombinant adenovirus which was linearized with *PacI*, as described in the manual. In brief, the HEK293 cells were cultured in a 60 mm plate, and 10 μ l *Pac I*-digested Adeno-X DNA was added in the culture medium when the cells were 50-70% confluent, then the cells were transfected with Lipofectamin and incubated for another week. For virus collection, the cells were lysed with three consecutive freeze-thaw cycles, and the virus was collected from supernatant. The titer of the virus was about 1×10^7 pfu/ml, which was determined with end-point dilution assay.

Northern blot analysis

HepG2, LO2 and HeLa cells were cultured in 6-well plates, and the medium was removed after 24 h, followed by addition of adenovirus at multiplicity of infection (M.O.I) of 100 plaque-forming units (pfu)/cell, and fresh culture medium was added 4 h later. After 48 h of normal culture, total RNA was extracted from the cells for Northern blot. In brief, 10 μ g total RNA of each sample was added to 10 g \cdot L $^{-1}$ formaldehyde denatured agarose gel, and electrophoresis was performed. mRNA was transferred onto the nitrocellular (NC) membranes by capillary blot, and exposed to 254 nm ultraviolet for 1 min ($600 \times 100 \mu$ J \cdot cm $^{-1}$) to fix mRNA. The NC membranes were pre-hybridized for 3 h at 42 $^{\circ}$ C. The cDNA probes were labeled by a random primer method. The probes were added and hybridized at 42 $^{\circ}$ C for 20 h. Then the membranes were washed,

dried and used for X-ray film autoradiography at -70 $^{\circ}$ C in a black box for 48 h. The relative amount of *EGFP* cDNA was semi-quantified from relative optical density of the band, using a Bio-image analysis system (Bio-Rad Doc Gel 2000, USA).

Fluorescence microscopy

The cells were cultured and transfected with the recombinant adenovirus as described above. Fluorescent images were captured at 490 nm using a Nikon Eclipse E1000 microscope.

RESULTS

PCR amplification and DNA sequencing of *AFP* promoter

Electrophoretic results of PCR product of the human 0.3 kb *AFP* promoter are shown in Figure 1. The sequence of the promoter was described as below:

```
gcgctagcat tctgtagttt gaggagaata ttgttatat ttgcaaaata aaataagttt
NheI -229
gcaagttttt ttttctgcc ccaaagagct ctgtgctct gaacataaaa tacaataaac
GRE
cgctctgctg taattattg gcaaatgtcc cattttcaac ctaaggaaat accataaagt
HNF-1
aacagatata ccaacaaaag gttactagtt aacaggcatt gctgaaaag agtataaaaag
HNF-1
aattcageca tgattttcca tattgtgcttc caccactgcc aatgggccc a
+25 Apa I
```

The *AFP* promoter region of -229 to 25 was indicated with italics; GRE: glucocorticoid response element; HNF-1: hepatocyte nuclear factor; *tata*: TATA Box.

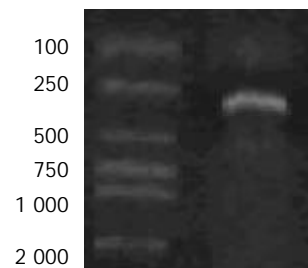


Figure 1 Human 0.3 kb *AFP* promoter.

Enzyme digestion analysis of the recombinant *pshuttle*

The plasmid *pshuttle* and the 99-744 region of the PCR product were both doubly digested with *MluI* and *NheI* (Figure 2). A 670 bp fragment was released from *pshuttle*, and replaced by a 490 bp fragment that was digested from the PCR product. The p_{CMVIE} was removed from the *pshuttle*.

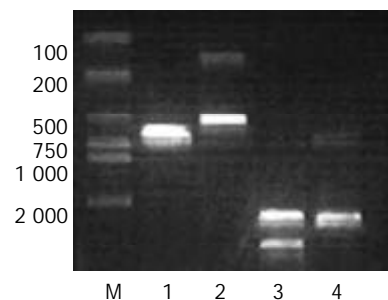


Figure 2 Plasmid *pshuttle* and PCR product doubly-digested with *MluI/NheI*. M: marker, 1: the PCR product of 99-744 region of *pshuttle*, 2: the product of PCR doubly digested with *MluI/NheI*, 3: *pshuttle*, 4: doubly-digested *pshuttle* with *MluI/NheI*, a 670 bp fragment was released from *pshuttle*.

Specific expression of EGFP gene in HepG2 cells

As shown in Figure 3, strong expression of *EGFP* mRNA was observed in HepG2 cells but was weak in AFP negative LO2 and HeLa cells, only 38% and 17% of that in HepG2 cells, respectively.

Under fluorescence microscopy, green fluorescence indicating expression of EGFP was strong in HepG2 cells (Figure 4A) but very weak in LO2 (Figure 4B) and invisible in HeLa cells.

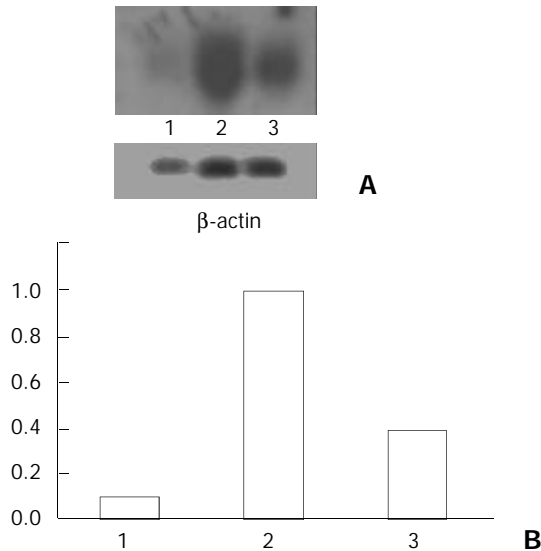


Figure 3 A: Transcription levels of *EGFP* shown by Northern blot in three different cell lines, B: Transcription levels of *EGFP* gene detected by semi-quantity analysis in three cell lines. Lane 1, HeLa cell; lane 2, HepG2 cell; lane 3, LO2 cell.

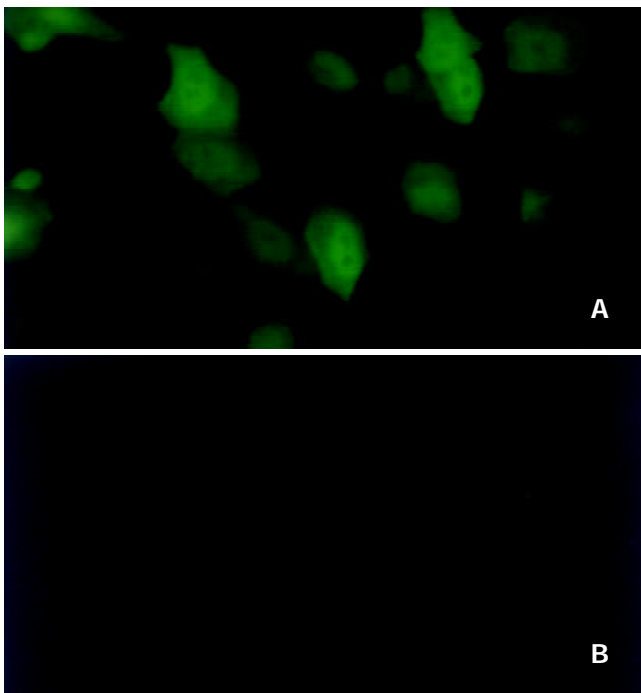


Figure 4 Expression of *EGFP* mRNA in HepG2 cells (A) and LO2 cells (B) $\times 200$.

DISCUSSION

Hepatocellular carcinoma (HCC) is one of the most common malignancies worldwide. All the treatment strategies used today had a poor outcome^[5-7]. Gene therapy might be a promising

way^[8,9]. Gene transfer into specific tissues or cell types is a key technique in the development of gene therapy. A tissue-specific promoter has been found to be potentially valuable for the study of specific gene function and for gene therapy^[10-14], as it permitted a linked cytotoxic or any other gene to be expressed specifically in target cells^[15-17]. The AFP could be re-expressed in the majority of hepatocellular carcinomas^[18,19], and thus utility of the *AFP* promoter for gene therapy against HCC might be a rational approach^[20-22].

Adenoviral gene transfer is one of the most reliable methods for introducing genes into almost all types of mammalian cells and for expressing the genes at high levels since many cells receive multiple copies of the recombinant genome. Gene therapy using replication-competent adenovirus that selectively propagates in tumor cells might be an effective treatment for cancer^[23,24]. We developed an adenovirus carrying an *AFP* promoter, thus the replication of the target gene was restricted specifically in AFP-producing HCC^[25]. The full length *AFP* promoter was 5.1 kb^[26,27], previous studies have shown that the 0.3 kb of the *AFP* promoter had an enough activity to stimulate *AFP* transcription containing a glucocorticoid response element and two binding sites of hepatocyte nuclear factor (HNF)-1, a hepatocyte-specific transcriptional factor, and a TATA box, but no typical CCAAT sequence^[28,29].

In this study, primers containing specific enzyme-cutting sites were designed to amplify the 0.3 kb *AFP* promoter from human genome, and the 0.3 kb sequence was cloned into the plasmid *pshuttle* to replace the primary *CMV* promoter. *EGFP* gene as a target gene was inserted into the downstream of *AFP* promoter. Then AFP expressing hepatocarcinoma cells (HepG2), AFP negative normal hepatocytes (LO2) and HeLa cells were transfected with the recombinant adenovirus. Northern blot showed that *EGFP* gene was dramatically transcribed in HepG2 cells, however, in LO2 and HeLa cells, the transcription was very weak. Under fluorescent microscopy, green fluorescence was strong in HepG2 cells, but very weak in the other two cell lines. Therefore, this recombinant adenovirus carrying the 0.3 kb *AFP* promoter can be used as a proper vector to express the interested gene in AFP expressing hepatocarcinoma cells or tissues.

It has been reported that the promoter activity of 0.3 kb *AFP* promoter was limited for transcription of downstream genes^[30,31]. For this reason, several enhancers have been inserted into the upstream of the promoter in order to upgrade its activity^[32-35]. In our study, the original enhancer in *pshuttle* was reserved, which might contribute to the satisfactory transcription of the downstream gene using the 0.3 kb promoter.

REFERENCES

- 1 **Alemay R**, Lai S, Lou YC, Jan HY, Fang X, Zhang WW. Complementary adenoviral vectors for oncolysis. *Cancer Gene Ther* 1999; **6**: 21-25
- 2 **Kanai F**. Transcriptional targeted gene therapy for hepatocellular carcinoma by adenovirus vector. *Mol Biotechnol* 2001; **18**: 243-250
- 3 **Murayama Y**, Tadakuma T, Kunitomi M, Kumai K, Tsutsui K, Yasuda T, Kitajima M. Cell-specific expression of the diphtheria toxin A-chain coding sequence under the control of the upstream region of the human alpha-fetoprotein gene. *J Surg Oncol* 1999; **70**: 145-149
- 4 **Bui LA**, Butterfield LH, Kim JY, Ribas A, Seu P, Lau R, Glaspy JA, McBride WH, Economou JS. *In vivo* therapy of hepatocellular carcinoma with a tumor-specific adenoviral vector expressing interleukin-2. *Hum Gene Ther* 1997; **8**: 2173-2182
- 5 **Tang ZY**. Hepatocellular carcinoma—cause, treatment and metastasis. *World J Gastroenterol* 2001; **7**: 445-454
- 6 **Di Maio M**, De Maio E, Perrone F, Pignata S, Daniele B. Hepatocellular carcinoma: systemic treatments. *J Clin Gastroenterol* 2002; **35**(5 Suppl 2): S109-114

- 7 **Lin DY**, Lin SM, Liaw YF. Non-surgical treatment of hepatocellular carcinoma. *J Gastroenterol Hepatol* 1997; **12**: S319-328
- 8 **Raper SE**, Wilson JM. Gene therapy for human liver disease. *Prog Liver Dis* 1995; **13**: 201-230
- 9 **Huang TG**, Savontaus MJ, Shinozaki K, Sauter BV, Woo SL. Telomerase-dependent oncolytic adenovirus for cancer treatment. *Gene Ther* 2003; **10**: 1241-1247
- 10 **Sato Y**, Tanaka K, Lee G, Kanegae Y, Sakai Y, Kaneko S, Nakabayashi H, Tamaoki T, Saito I. Enhanced and specific gene expression via tissue-specific production of Cre recombinase using adenovirus vector. *Biochem Biophys Res Commun* 1998; **244**: 455-462
- 11 **Igarashi T**, Suzuki S, Takahashi M, Tamaoki T, Shimada T. A novel strategy of cell targeting based on tissue-specific expression of the ecotropic retrovirus receptor gene. *Hum Gene Ther* 1998; **9**: 2691-2698
- 12 **Dachs GU**, Dougherty GJ, Stratford IJ, Chaplin DJ. Targeting gene therapy to cancer: a review. *Oncol Res* 1997; **9**: 313-325
- 13 **Kanai F**, Lan KH, Shiratori Y, Tanaka T, Ohashi M, Okudaira T, Yoshida Y, Wakimoto H, Hamada H, Nakabayashi H, Tamaoki T, Omata M. *In vivo* gene therapy for alpha-fetoprotein-producing hepatocellular carcinoma by adenovirus-mediated transfer of cytosine deaminase gene. *Cancer Res* 1997; **57**: 461-465
- 14 **Xu GW**, Sun ZT, Forrester K, Wang XW, Coursen J, Harris CC. Tissue-specific growth suppression and chemosensitivity promotion in human hepatocellular carcinoma cells by retroviral-mediated transfer of the wild-type p53 gene. *Hepatology* 1996; **24**: 1264-1268
- 15 **Hanke P**, Serwe M, Dombrowski F, Sauerbruch T, Caselmann WH. DNA vaccination with AFP-encoding plasmid DNA prevents growth of subcutaneous AFP-expressing tumors and does not interfere with liver regeneration in mice. *Cancer Gene Ther* 2002; **9**: 346-355
- 16 **Vollmer CM Jr**, Eilber FC, Butterfield LH, Ribas A, Dissette VB, Koh A, Montejo LD, Lee MC, Andrews KJ, McBride WH, Glaspy JA, Economou JS. Alpha-fetoprotein-specific genetic immunotherapy for hepatocellular carcinoma. *Cancer Res* 1999; **59**: 3064-3067
- 17 **Wang XW**, Xu B. Several new targets of antitumor agents. *Zhongguo Yaoli Xuebao* 1997; **18**: 289-292
- 18 **Johnson PJ**. Role of alpha-fetoprotein in the diagnosis and management of hepatocellular carcinoma. *J Gastroenterol Hepatol* 1999; **14**(Suppl): S32-36
- 19 **Chen XP**, Zhao H, Zhao XP. Alternation of AFP-mRNA level detected in blood circulation during liver resection for HCC and its significance. *World J Gastroenterol* 2002; **8**: 818-821
- 20 **Lu SY**, Sui YF, Li ZS, Pan CE, Ye J, Wang WY. Construction of a regulable gene therapy vector targeting for hepatocellular carcinoma. *World J Gastroenterol* 2003; **9**: 688-691
- 21 **Wills KN**, Huang WM, Harris MP, Macherer T, Maneval DC, Gregory RJ. Gene therapy for hepatocellular carcinoma: chemosensitivity conferred by adenovirus-mediated transfer of the HSV-1 thymidine kinase gene. *Cancer Gene Ther* 1995; **2**: 191-197
- 22 **Barajas M**, Mazzolini G, Genove G, Bilbao R, Narvaiza I, Schmitz V, Sangro B, Melero I, Qian C, Prieto J. Gene therapy of orthotopic hepatocellular carcinoma in rats using adenovirus coding for interleukin12. *Hepatology* 2001; **33**: 52-61
- 23 **Ferry N**. Gene therapy of primary cancers of the liver: hopes and realities. *Bull Cancer* 1997; **84**: 431-434
- 24 **Kaneko S**, Hallenbeck P, Kotani T, Nakabayashi H, McGarrity G, Tamaoki T, Anderson WF, Chiang YL. Adenovirus-mediated gene therapy of hepatocellular carcinoma using cancer-specific gene expression. *Cancer Res* 1995; **55**: 5283-5287
- 25 **Ohashi M**, Kanai F, Tateishi K, Taniguchi H, Marignani PA, Yoshida Y, Shiratori Y, Hamada H, Omata M. Target gene therapy for alpha-fetoprotein-producing hepatocellular carcinoma by E1B55k-attenuated adenovirus. *Biochem Biophys Res Commun* 2001; **282**: 529-535
- 26 **Nakabayashi H**, Hashimoto T, Miyao Y, Tjong KK, Chan J, Tamaoki T. A position-dependent silencer plays a major role in repressing alpha-fetoprotein expression in human hepatoma. *Mol Cell Biol* 1991; **11**: 5885-5893
- 27 **Kaneko S**, Tamaoki T. Gene therapy vectors harboring AFP regulatory sequences. Preparation of an adenoviral vector. *Mol Biotechnol* 2001; **19**: 323-330
- 28 **Tamaoki T**. Human alpha-fetoprotein transcriptional regulatory sequences. Application to gene therapy. *Adv Exp Med Biol* 2000; **465**: 47-56
- 29 **Ido A**, Nakata K, Kato Y, Nakao K, Murata K, Fujita M, Ishii N, Tamaoki T, Shiku H, Nagataki S. Gene therapy for hepatoma cells using a retrovirus vector carrying herpes simplex virus thymidine kinase gene under the control of human alpha-fetoprotein gene promoter. *Cancer Res* 1995; **55**: 3105-3109
- 30 **Bilbao R**, Gerolami R, Bralet MP, Qian C, Tran PL, Tennant B, Prieto J, Brechot C. Transduction efficacy, antitumoral effect, and toxicity of adenovirus-mediated herpes simplex virus thymidine kinase/ganciclovir therapy of hepatocellular carcinoma: the woodchuck animal model. *Cancer Gene Ther* 2000; **7**: 657-662
- 31 **Ohguchi S**, Nakatsukasa H, Higashi T, Ashida K, Nouse K, Ishizaki M, Hino N, Kobayashi Y, Uematsu S, Tsuji T. Expression of alpha-fetoprotein and albumin genes in human hepatocellular carcinomas: limitations in the application of the genes for targeting human hepatocellular carcinoma in gene therapy. *Hepatology* 1998; **27**: 599-607
- 32 **Cao G**, Kuriyama S, Tsujinoue H, Chen Q, Mitoro A, Qi Z. A novel approach for inducing enhanced and selective transgene expression in hepatocellular carcinoma cells. *Int J Cancer* 2000; **87**: 247-252
- 33 **Ido A**, Uto H, Moriuchi A, Nagata K, Onaga Y, Onaga M, Hori T, Hirono S, Hayashi K, Tamaoki T, Tsubouchi H. Gene therapy targeting for hepatocellular carcinoma: selective and enhanced suicide gene expression regulated by a hypoxia-inducible enhancer linked to a human alpha-fetoprotein promoter. *Cancer Res* 2001; **61**: 3016-3021
- 34 **Ishikawa H**, Nakata K, Mawatari F, Ueki T, Tsuruta S, Ido A, Nakao K, Kato Y, Ishii N, Eguchi K. Utilization of variant-type of human alpha-fetoprotein promoter in gene therapy targeting for hepatocellular carcinoma. *Gene Ther* 1999; **6**: 465-470
- 35 **Cao G**, Kuriyama S, Gao J, Nakatani T, Chen Q, Yoshiji H, Zhao L, Kojima H, Dong Y, Fukui H, Hou J. Gene therapy for hepatocellular carcinoma based on tumour-selective suicide gene expression using the alpha-fetoprotein (AFP) enhancer and a housekeeping gene promoter. *Eur J Cancer* 2001; **37**: 140-147

Edited by Xia HHX and Wang XL

Effects of p53 on apoptosis and proliferation of hepatocellular carcinoma cells treated with transcatheter arterial chemoembolization

En-Hua Xiao, Jing-Qing Li, Jie-Fu Huang

En-Hua Xiao, Department of Radiology, the Second Xiangya Hospital, Central South University, Changsha 410011, Hunan Province, China

Jin-Qing Li, Jie-Fu Huang, Liver Cancer Research Center, Sun Yat-Sen University of Medical Sciences, Guangzhou 510060, Guangdong Province, China

Supported by the National Natural Science Foundation of China, No. 30070235

Correspondence to: Dr. En-Hua Xiao, Department of Radiology, the Second Xiangya Hospital, Central South University, Changsha 410011, Hunan Province, China. xiaogdk@sohu.com

Telephone: +86-731-5550355

Received: 2003-06-05 **Accepted:** 2003-07-30

Abstract

AIM: To evaluate the effects of p53 on apoptosis and proliferation of hepatocellular carcinoma (HCC) cells treated with transcatheter arterial chemoembolization (TACE).

METHODS: A total of 136 patients with HCC received TACE and other management before surgery were divided into TACE group and non-TACE group. TACE group included 79 patients who had 1-5 courses of TACE before surgery, of them, 11 patients had 1-4 courses of chemotherapy (group A), 33 patients had 1-5 courses of chemotherapy combined with iodized oil (group B), 23 patients had 1-3 courses of chemotherapy, iodized oil and gelatin sponge (group C), 12 patients had 1-3 courses of chemotherapy combined with iodized oil, ethanol and gelatin sponge (group D). Non-TACE group included the remaining 57 patients who had surgery only. The extent of apoptosis was analyzed by transferase mediated dUTP nick end labeling (TUNEL) staining. The expressions of p53, Bcl-2, Bax, Ki-67 and PCNA protein were detected by immunohistochemical method.

RESULTS: P53 protein expressions in trabecular and clear cells in HCC specimens were significantly lower than that in pseudoglandular, solid, poorly differentiated or undifferentiated and sclerosis HCC ($P < 0.05$). Expression of p53 protein in HCC cells increased with the increase of pathological grades ($P < 0.05$), and correlated positively with expressions of Ki-67 and PCNA protein, and negatively with Bcl-2 to Bax protein expression rate and AI ($P < 0.05$). Expression of p53 protein was significantly higher in group A than in groups B, C, D and the non-TACE group, and was higher in group B than in groups C and D, and lower in group D than in the non-TACE group ($P < 0.05$).

CONCLUSION: Expression of p53 protein can enhance proliferation of HCC cells and suppress apoptosis of HCC cells after TACE.

Xiao EH, Li JQ, Huang JF. Effects of p53 on apoptosis and proliferation of hepatocellular carcinoma cells treated with transcatheter arterial chemoembolization. *World J Gastroenterol* 2004; 10(2): 190-194

<http://www.wjgnet.com/1007-9327/10/190.asp>

INTRODUCTION

Hepatocellular carcinoma (HCC) is one of the most common malignancies. Surgical resection has been recognized as the most effective method for the treatment of HCC^[1,2], but it is only indicated for small number of HCC patients. Transcatheter arterial chemoembolization (TACE) has become one of the most popular and effective palliative methods for HCC. Various mixtures of anticancer drugs, Lipiodol and gelatin sponge have been used as TACE agents. There have been a few reports on comparison of the efficacy of different TACE regimens on HCC patients^[3].

Cellular homeostasis in tissue depends on the balance between apoptosis and cell proliferation. Wild-type p53 protein inhibits the growth of tumor by arrest of cell proliferation and induction of apoptosis^[4]. Bcl-2 and Bax protein are important regulators of apoptosis^[5]. Bcl-2 proteins can prolong cell survival by suppressing apoptosis, and Bax proteins can enhance apoptosis^[6]. PCNA and Ki-67 protein are useful markers for proliferative activity^[7]. PCNA functions as a cofactor of DNA-polymerase and an important mark for evaluating the proliferation of colon cancer^[8], gastric adenocarcinoma^[9], *H. pylori* associated gastric epithelial lesions^[10], lung cancer^[11], ovarian cancer^[12], large intestine polyps^[13] and HCC^[14,15].

As far as we know, the effect of p53 on apoptosis and proliferation of HCC cells treated with different TACE regimens has not been investigated yet. In particular, it is unclear whether p53 can affect apoptosis and proliferation of HCC cells treated with TACE by modulating the expressions of Bcl-2, Bax, PCNA and Ki-67 proteins. In the present study, we examined the effects of p53 on apoptosis and proliferation of HCC cells treated with TACE alone or in combination with others.

MATERIALS AND METHODS

Patients

From February 1992 to February 2001, 136 patients with HCC were referred to our hospital for surgery, including 122 men and 14 women with a mean age of 45 years (range 20 to 70 years). Preoperative ultrasound (US), computed tomography (CT), magnetic resonance (MRI), digital subtraction angiography (DSA) and plasma AFP levels were used to diagnose the conditions and the diagnosis was finally confirmed with pathological biopsy.

Surgical procedure

The patients were divided into TACE or non-TACE group. In TACE group, 79 patients underwent 1-5 courses chemoembolization prior to liver resection. Of them, 11 patients had 1-4 courses of chemotherapy only (group A), 33 patients had 1-5 courses of chemotherapy combined with iodized oil (group B), 23 patients had 1-3 courses of chemotherapy, iodized oil and gelatin sponge (group C), 12 patients had 1-3 courses of chemotherapy combined with iodized oil, ethanol and gelatin - sponge (group D). Considering the course of TACE, 50 patients underwent one course, 19 patients underwent two courses, 10 patients underwent three or more courses. The interval from the last TACE to the surgery was 52.8 ± 12.2 days ($\bar{x} \pm s$), 25 patients had

1 month or less, 29 patients had 2 months or less, 16 patients had 3 months or less, 9 patients had over 3 months. In non-TACE group, 57 patients had surgery without preoperative TACE. The types of hepatectomy were dependent on the location of tumor, the severity of concomitant hepatic cirrhosis and preoperative hepatic function.

TUNNEL staining

Transferase-mediated dUTP nick end labeling (TUNEL) staining was used to examine apoptosis. Positive control slides were treated with DNase-1 and negative controls were stained in the absence of terminal deoxynucleotidyl transferase enzyme. Dark brown nuclei with nuclear condensation in stained cells were considered as TUNEL positive. Apoptotic index was the ratio of the number of positively stained tumor cells to the total number of tumor cells.

Immunohistochemical method

The formalin-fixed, paraffin-embedded specimens were examined immunohistochemically using respective antibodies to p53 M7001 (dilution: 1:100), Bcl-2 MO887(dilution: 1:60), Bax A3533 (dilution: 1:200), Ki-67 M7187(dilution: 1:50) and PCNA M0879 (dilution: 1:200) (LSAB kit Dako). Positive controls were selected cases known to be positive for the primary antibody, such as laryngeal carcinoma or normal lymph nodes. Negative controls were stained with a nonspecific Ig G (normal rabbit Ig G) and Tris-buffered saline. Brown-yellow staining in nuclei of cancer was found in p53, Ki-67 and PCNA positive cells, while brown-yellow staining in cytoplasm and/or cell membrane was observed in Bcl-2 and Bax positive cells. All slides were reviewed and scored by two independent observers in blind. A few cases with discrepant scoring were reevaluated to reach a final agreement.

Statistical analysis

Data were expressed as $\bar{x} \pm s$ and analyzed by means of SPSS 10.0 software package (SPSS, Chicago, IL, USA, 1999). The Student *t* test, the Crosstabs (chi-square and Fisher's exact probability test), K independent samples and Pearson rank correlation coefficient test were used to test the correlation between parameters. A *P* value <0.05 was considered statistically significant.

RESULTS

P53 expression in different histopathologic types

P53 protein expression in trabecular and clear cells of HCC was significantly lower than that in pseudoglandar, solid, poorly differentiated or undifferentiated and sclerosis HCC (*P*<0.05, Table 1).

Table 1 P53 protein expression of different types of HCC

Groups	Histological types					
	Trabecular	Pseudoglandar	Solid	Clear cell	Poorly differentiated	Sclerosis
Non-TACE	63.66±19.96	72.29±12.47	70.83±24.45	68.27±19.22	74.79±16.18	72.11±0.00
TACE	56.90±17.12	72.35±13.70	74.93±8.76	62.15±11.78	73.66±8.54	
<i>P</i>	>0.05	>0.05	>0.05	>0.05	>0.05	

Table 3 Correlation p53 expression with Ki-67, PCNA, Bax, Bcl-2 and AI

		Ki-67	PCNA	bcl-2	bax	bcl-2/bax	AI	
Non-TCAE group	P53	PC	0.454 ^a	0.331 ^a	-0.141	0.054	-0.375 ^a	-0.198
TACE group	p53	PC	0.553 ^a	0.577 ^a	0.007	-0.142	0.001	-0.459 ^a

^aCorrelation is significant at the 0.05 level (2-tailed), PC: Pearson correlation.

P53 expression in different pathological grades

Pathological grades were divided into four groups. Expression of p53 protein in HCC cells increased as the increase of pathological grade in non-TACE or TACE group (*P*<0.05). P53 protein expression in grade II specimens in TACE group was significantly lower than that in non-TACE group (*P*<0.05, Table 2).

Table 2 Expressions of proteins in different grades of HCC

Treat groups	I	II	III	IV
Non-TACE	60.99±30.58	67.22±15.53	72.98±20.60	93.47±0.00
TACE	32.59±11.68	60.02±14.67	74.69±8.65	82.64±1.11
<i>P</i>	>0.05	<0.05	>0.05	>0.05

P53 expression in HCC cells

Expression of p53 protein in HCC cells was 69.37±18.81% in the non-TACE group, 65.09±15.71% in TACE group, 75.34±5.36% in group A, 69.34±12.59% in group B, 60.94±17.24% in group C, and was 53.41±18.13% in group D. Expression of p53 protein was significantly higher in group A than in groups B, C, D and non-TACE group, and was higher in group B than in groups C and D, and lower in group D than in non-TACE group (*P*<0.05, Figures 1-4).

Correlation between courses of TACE and p53 protein expression

Expression of p53 protein in HCC cells was 69.37±18.81% in non-TACE group, 65.76±13.96% in one-course of TACE group, 64.09±19.81% in two-courses of TACE group, and 65.19±17.80% in three or more courses of TACE group. No statistical difference was found among groups (*P*>0.05).

Correlation between interval of TACE and p53 protein expression

Considering the interval from the last TACE to the operation, expression of p53 protein was 69.37±18.81% in non-TACE group, 63.54±13.72% in TACE group with an interval ≤1 month, 61.17±18.32% in TACE group with a 1-2 months interval, 70.87±15.06% in TACE group with a 2-3 months interval, and 73.67±5.87% in TACE group with an interval >3 months. P53 protein expression was significantly lower in patients with an interval ≤2 months than that in patients with an interval >3 months (*P*<0.05).

Correlation of p53 expression with Ki-67, PCNA, Bax, Bcl-2 protein expressions and AI

In non-TCAE group, p53 expression (69.37±18.81%) had a positive correlation with expressions of Ki-67 protein

($44.43 \pm 20.70\%$, $P < 0.05$), PCNA ($62.92 \pm 17.21\%$, $P < 0.05$), and Bax ($44.29 \pm 23.73\%$, $P > 0.05$), and a negative correlation with the ratio of Bcl-2 to Bax (0.48 ± 0.64 , $P < 0.05$), AI (5.71 ± 1.38 , $P > 0.05$) and Bcl-2 ($12.72 \pm 4.92\%$, $P > 0.05$) (Table 3).

In TACE group, expression of p53 protein ($65.09 \pm 15.71\%$) had a positive correlation with expression of Ki-67 ($40.24 \pm 16.59\%$, $P < 0.05$), PCNA ($59.95 \pm 17.75\%$, $P < 0.05$), and Bcl-2 ($7.47 \pm 6.41\%$, $P > 0.05$), Bcl-2 to Bax ratio (0.21 ± 0.29 , $P > 0.05$), and a negative correlation with AI ($14.69 \pm 6.29\%$, $P < 0.05$) and Bax ($54.59 \pm 23.63\%$, $P > 0.05$) (Table 3).

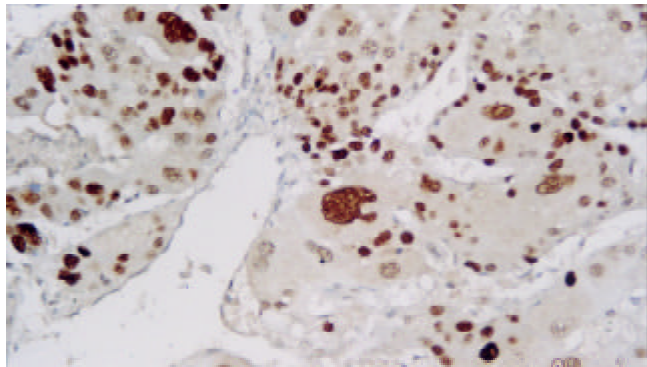


Figure 1 P53 immunostaining cells in one representative HCC specimen in non-TACE group (Dako Envision, peroxidase method $\times 200$).

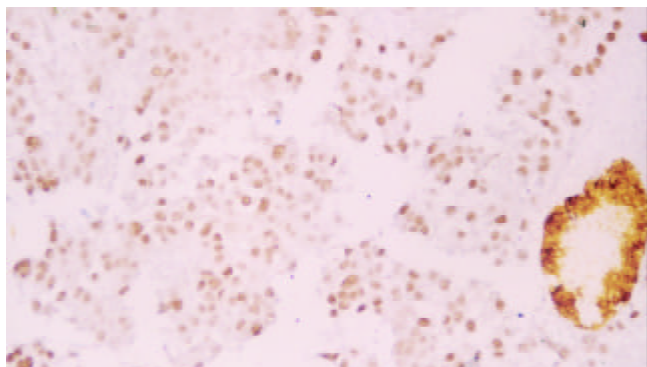


Figure 2 P53 staining cells in HCC in group B (Dako Envision, peroxidase method $\times 200$).

DISCUSSION

HCC is one of the most common malignant neoplasms. Most HCC patients are treated palliatively to improve the resectable rate and prolong survival. The best therapeutic method for HCC with tumor thrombi in portal vein (PVTT) has been regional hepatic TACE treatment after hepatic resection with removal of tumor thrombi^[16]. TACE has become one of the most common and effective palliative approaches. The prognosis of patients treated with TACE was dependent on both the effect of TACE and tumor factors^[17].

To our knowledge, few data regarding the molecular mechanism of TACE treatment for HCC are available, the current study is the first report to describe the correlations between p53 expression and different TACE regimens.

Our study showed that the frequency of p53 expression was higher in group A than in group B, non-TACE group and TACE group, the lowest in group C and D ($P < 0.05$). Our previous study showed that multidrug resistant gene product-Pgp protein was significantly increased in chemotherapy group alone^[18], suggesting that p53 expression increased after chemotherapy with the development of chemoresistance. p53 status might be an important determinant of tumor response to

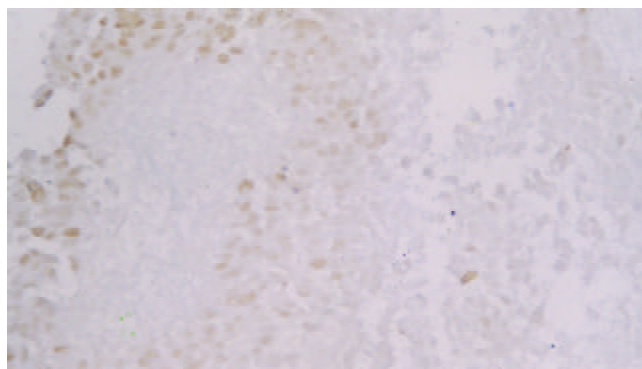


Figure 3 P53 staining cells in HCC in group D (Dako Envision, peroxidase method $\times 200$).

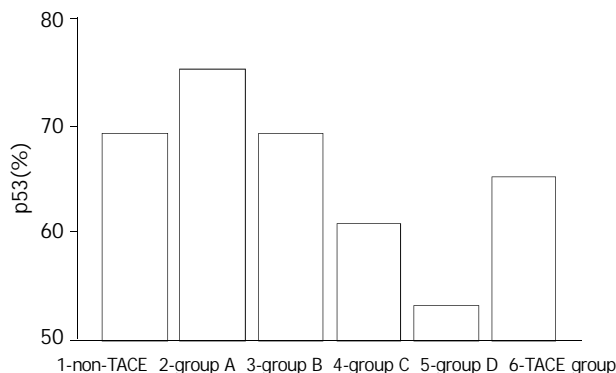


Figure 4 P53 expressions in different groups.

chemotherapy. Tumors with P53 (-) expression might respond to chemotherapy. Inversely, chemotherapy was not effective in patients with P53 (+) expression^[19]. This study demonstrated that p53 protein expression had no significant difference between the TACE and non-TACE groups^[20].

The reverse correlation between AI and p53 protein expression of HCC cells was found in both TACE and non-TACE groups in this study. Most p53 protein measured was the mutant-type. AI was significantly positively correlated with wild-type p53 which enhanced apoptosis by activating proapoptotic Bax and by down-regulating antiapoptotic Bcl-2^[21].

The current study demonstrated that p53 expression was positively related to Ki-67 and PCNA protein expression in the non-TACE and TACE groups, suggesting that the mutated p53 protein could enhance the growth of HCC. Our previous study showed both PCNA and p53 expressions had a significantly parallel correlation, the overexpression of mutated p53 resulted in cancer immortalization, high tumor recurrence risk, more aggressive growth and poor survival^[22] and Kieser *et al* found that a mutated p53 gene could provide an advantage for tumor proliferation^[23]. Igarashi *et al* reported that expression of p53 protein like Ki-67 labeling index was a useful indicator for high proliferative activity^[24]. A mutated p53 gene provided an advantage for tumor proliferation not only by allowing escape from apoptosis, but also by leading to formation of a vascular-rich microenvironment^[25]. However, it has been known that wild-type p53 could inhibit the expression of PCNA^[26].

Wild-type p53 is a positive transcriptional activator for human Bax gene and a negative transcriptional activator for human Bcl-2 gene. The activation of p53 pathway could lead to the down-regulation of Bcl-2 and up-regulation of Bax^[27]. The current study demonstrated that p53 protein expression was positively related to Bax expression, and negatively to Bcl-2 expression in the non-TACE group. Bcl-2 expression had an inverse correlation with mutant p53, and wild-type p53

and majority of mutant p53 proteins could down-regulate Bcl-2 expression and up-regulate Bax expression *in vitro* and *in vivo*^[28]. Moreover, Bcl-2 and p53 could cooperate in regulating pathogenetic pathways in the processes of tumor invasion and metastasis^[29].

The current study demonstrated that p53 protein expression was negatively related to Bax expression, and positively to Bcl-2 expression in the TACE group, which was in accordance with the previous report that Bax expression was significantly increased in tumors with wild-type p53 gene after chemotherapy but did not increase in tumors with mutant p53 gene^[21].

This study demonstrated that discrepancy of P53 existed in different types of HCC. P53 protein expression was significantly lower in trabecular and clear cells of HCC than that in solid and poorly differentiated or undifferentiated HCC, in both non-TACE and TACE groups, Zhao *et al* reported that p53 gene mutation varied in histological types and the mutated rate was 10.5% in trabecular cells, 37.5% in pseudoglandular cells, 60.0% in solid cells and 33.3% in sclerosis ($P < 0.05$)^[30]. Our previous study showed that trabecular and clear cells were more sensitive to TACE than solid, poorly or undifferentiated, and small cells of HCC^[31]. Wang *et al* also found that the clear cells of HCC were more sensitive to TAE than small cells of HCC and poorly differentiated or undifferentiated HCCs^[32]. Yamashita *et al* found that most HCCs responded to TACE well^[33]. These suggest that p53 protein expression would influence the effects of TACE on HCC. Further study is needed to clarify the correlation between p53 protein expression and tumor necrosis and patient survival.

This study also demonstrated that P53 protein expression increased as grades increased in both non-TACE and TACE groups ($P < 0.05$), which was inconsistent with the study of Zhao *et al*^[30].

P53 protein expression of grade II HCC was significantly lower in TACE group than in non-TACE group, suggesting that influences of the molecular markers were very complicated and discrepancy in therapeutic effect of TACE on different histopathological types of HCC was existed. It would be the best choice to use TACE in an individualized mode.

The best interval of treatment for repeated TACE or second stage resection is controversial. In this study, we found that p53 protein expression of HCC cells was significantly lower in the group with a 2 months or less interval than in the group with an over 3 month treatment interval ($P < 0.05$). We found that the best interval between treatment with TACE or second stage resection was 2-3 months.

In conclusion, discrepancy of histological types and pathological grades in p53 protein expression is existed in HCC. P53 protein expression can enhance proliferation of HCC cells and suppress apoptosis of HCC cells after TACE. P53 protein expression would influence effects of TACE on HCC. We need further study to clarify the correlation between p53 protein expression, tumor necrosis and patient survival.

REFERENCES

- Parks RW**, Garden OJ. Liver resection for cancer. *World J Gastroenterol* 2001; **7**: 766-771
- Tang ZY**. Hepatocellular Carcinoma-Cause, Treatment and Metastasis. *World J Gastroenterol* 2001; **7**: 445-454
- Ueno K**, Miyazono N, Inoue H, Nishida H, Kanetsuki I, Nakajo M. Transcatheter arterial chemoembolization therapy using iodized oil for patients with unresectable hepatocellular carcinoma: evaluation of three kinds of regimens and analysis of prognostic factors. *Cancer* 2000; **88**: 1574-1581
- Xie X**, Clausen OP, De Angelis P, Boysen M. The prognostic value of spontaneous apoptosis, Bax, Bcl-2, and p53 in oral squamous cell carcinoma of the tongue. *Cancer* 1999; **86**: 913-920
- Oltvai ZN**, Milliman CL, Korsmeyer SJ. Bcl-2 heterodimerizes *in vivo* with a conserved homolog, Bax, that accelerates programmed cell death. *Cell* 1993; **74**: 609-619
- Xu HY**, Yang YL, Guan XL, Song G, Jiang AM, Shi LJ. Expression of regulating gene and apoptosis index in primary liver cancer. *World J Gastroenterol* 2000; **6**: 721-724
- Perry A**, Jenkins RB, O' Fallon JR, Schaefer PL, Kimmel DM, Mahoney MR, Scheithauer BW, Smith SM, Hill EM, Sebo TJ, Levitt R, Krook J, Tschetter LK, Morton RF, Buckner JC. Clinicopathologic study of 85 similarly treated patients with anaplastic astrocytic tumors: An analysis of DNA content (ploidy), cellular proliferation, and p53 expression. *Cancer* 1999; **86**: 672-683
- Kanazawa Y**, Onda M, Tanaka N, Seya. Proliferation cell nuclear antigen and p53 protein expression in submucosal invasive colorectal carcinoma. *J Nippon Medical School* 2000; **67**: 242-249
- Elpek GO**, Gelen T, Aksoy NH, Karpuzoglu T, Keles N. Microvessel count, proliferating cell nuclear antigen and Ki-67 indices in gastric adenocarcinoma. *Pathol Oncol Res* 2000; **6**: 59-64
- Zhang Z**, Yuan Y, Gao H, Dong M, Wang L, Gong YH. Apoptosis, proliferation and p53 gene expression of *H pylori* associated gastric epithelial lesions. *World J Gastroenterol* 2001; **7**: 779-782
- Fukuse T**, Hirata T, Naiki H, Hitomi S, Wada H. Expression of proliferating cell nuclear antigen and CD44 variant isoforms in the primary and metastatic sites of nonsmall cell lung carcinoma with intrapulmonary metastases. *Cancer* 1999; **86**: 1174-1181
- Wu X**, Zhang Z, Cai S. Proliferating cell nuclear antigen(PCNA) in ovarian carcinoma and its relation to lymph node metastasis and prognosis. *Zhonghua Zhongliu Zazhi* 1998; **20**: 68-70
- Luo YQ**, Ma LS, Zhao YL, Wu KC, Pan BR, Zhang XY. Expression of proliferating cell nuclear antigen in polyps from large intestine. *World J Gastroenterol* 1999; **5**: 160-164
- Wu WY**, Xu Q, Shi LC, Zhang WB. Inhibitory effects of *Curcuma aromatica* oil on proliferation of hepatoma in mice. *World J Gastroenterol* 2000; **6**: 216-219
- Lin GY**, Chen ZL, Lu CM, Li Y, Ping XJ, Huang R. Immunohistochemical study on p53, H-rasp21, c-erbB-2 protein and PCNA expression in HCC tissues of Han and minority ethnic patients. *World J Gastroenterol* 2000; **6**: 234-238
- Fan J**, Wu ZQ, Tang ZY, Zhou J, Qiu SJ, Ma ZC, Zhou XD, Ye SL. Multimodality treatment in hepatocellular carcinoma patients with tumor thrombi in portal vein. *World J Gastroenterol* 2001; **7**: 28-32
- Rose DM**, Chapman WC, Brockenbrough AT, Wright JK, Rose AT, Meranze S, Mazer M, Blair T, Blanke CD, Debelak JP, Pinson CW. Transcatheter arterial chemoembolization as primary treatment for hepatocellular carcinoma. *Am J Surg* 1999; **177**: 405-410
- Xiao EH**, Hu GD, Liu PC, Hu DY, Liu SC, Hao CY. The effect of different interventional treatment on P-glycoprotein in different histopathological types of primary hepatocellular carcinoma. *Zhonghua Fangshexue Zazhi* 1999; **33**: 150-152
- Okumura H**, Natsugoe S, Nakashima S, Matsumoto M, Sakita H, Nakano S, Kusano C, Baba M, Takao S, Furukawa T, Akiyama SI, Aikou T. Apoptosis and cell proliferation in esophageal squamous cell carcinoma treated by chemotherapy. *Cancer Lett* 2000; **158**: 211-216
- Huang JF**, He XS, Lin XJ. Effect of preoperative transcatheter arterial chemoembolization on tumor cell activity in hepatocellular carcinoma. *Chin Med J* 2000; **113**: 446-448
- Sato S**, Kigawa J, Minagawa Y, Okada M, Shimada M, Takahashi M, Kamazawa S, Terakawa N. Chemosensitivity and p53-dependent apoptosis in epithelial ovarian carcinoma. *Cancer* 1999; **86**: 1307-1313
- Li JQ**, Zhang CQ, Feng KT. PCNA, p53 protein and prognosis in primary liver cancer. *China Natl J New Gastroenterol* 1996; **2**: 220-222
- Kieser A**, Weich HA, Brander G, Marme D, Kolch W. Mutant p53 potentiates protein kinase C induction of vascular endothelial growth factor expression. *Oncogene* 1994; **9**: 963-969
- Igarashi N**, Takahashi M, Ohkubo H, Omata K, Iida R, Fujimoto S. Predictive value of Ki-67, p53 protein, and DNA content in the diagnosis of gastric carcinoma. *Cancer* 1999; **86**: 1449-1454
- Matsuura T**, Fukuda Y, Fujitaka T, Nishisaka T, Sakatani T, Ito

- H. Preoperative treatment with Tegafur Suppositories enhances apoptosis and reduces the intratumoral microvessel density of human colorectal carcinoma. *Cancer* 2000; **88**: 1007-1015
- 26 **Deb S**, Jackson CT, Subler MA, Martin DW. Modulation of cellular and viral promoters by mutant human p53 proteins found in tumor cells. *J Virol* 1992; **66**: 6164-6170
- 27 **Miyashita T**, Krajewski S, Krajewska M, Wang HG, Lin HK, Liebermann DA, Hoffman B, Reed JC. Tumor suppressor p53 is a regulator of bcl-2 and bax gene expression *in vitro* and *in vivo*. *Oncogene* 1994; **9**: 1799-1805
- 28 **Ioachim E**, Malamou-Mitsi V, Kamina SA, Goussia AC, Agnantis NJ. Immunohistochemical expression of Bcl-2 protein in breast lesions: Correlation with Bax, p53, Rb, C-erbB-2, EGFR and proliferation indices. *Anticancer Res* 2000; **20**: 4221-4226
- 29 **Giatromanolaki A**, Stathopoulos GP, Tsiobanou E, Papadimitriou C, Georgoulas V, Gatter KC, Harris AL, Koukourakis MI. Combined role of tumor angiogenesis, bcl-2, and p53 expression in the prognosis of patients with colorectal carcinoma. *Cancer* 1999; **86**: 1421-1430
- 30 **Zhao P**, Yang GH, Mao X. A molecular pathological study of p53 gene in hepatocellular carcinoma. *Zhonghua Binglixue Zazhi* 1993; **22**: 16-18
- 31 **Xiao EH**, Hu GD, Li JQ, Zhang YQ, Chen MS, Guo YP, Lin XG, Li SP, Shi M. The effect of transcatheter arterial chemoembolization on the different histopathological types of hepatocellular carcinoma. *Zhonghua Gandanwaikexue Zazhi* 2001; **7**: 411-414
- 32 **Wang YP**, Zhang JS, Gao YA. Therapeutic efficacy of transcatheter arterial embolization of primary hepatocellular carcinoma: discrepancy in different histopathological types of HCC. *Zhonghua Fangshexue Zazhi* 1997; **31**: 586-591
- 33 **Yamashita Y**, Matsukawa T, Arakawa A, Hatanaka Y, Urata J, Takahashi M. Us-guided liver biopsy: Predicting the effect of interventional treatment of hepatocellular carcinoma. *Radiology* 1995; **196**: 799-804

Edited by Ren SY and Wang XL

Expression of co-stimulator 4-1BB molecule in hepatocellular carcinoma and adjacent non-tumor liver tissue, and its possible role in tumor immunity

Yun-Le Wan, Shu-Sen Zheng, Zhi-Cheng Zhao, Min-Wei Li, Chang-Ku Jia, Hao Zhang

Yun-Le Wan, Shu-Sen Zheng, Zhi-Cheng Zhao, Min-Wei Li, Chang-Ku Jia, Hao Zhang, Key Laboratory of Combined Multi-organ Transplantation, Ministry of Public Health, Department of Hepatobiliary and Pancreatic Surgery, First Affiliated Hospital, School of Medicine, Zhejiang University, Hangzhou 310000, Zhejiang Province, China

Correspondence to: Dr. Yun-Le Wan, Department of Hepatobiliary and Pancreatic Surgery, First Affiliated Hospital, School of Medicine, Zhejiang University, Hangzhou 310000, Zhejiang Province, China. wanyl036@sina.com

Telephone: +86-571-87236570 **Fax:** +86-571-87236570

Received: 2003-06-05 **Accepted:** 2003-08-16

Abstract

AIM: To investigate the expression of 4-1BB molecule in hepatocellular carcinoma (HCC) and its adjacent tissues.

METHODS: Reverse transcription-polymerase chain reaction (RT-PCR) was used to determine the gene expression of 4-1BB in hepatocarcinoma and its adjacent tissues, and peripheral blood mononuclear cells (PBMCs) from both HCC and health control groups. Flow cytometry was used to analyse the phenotypes of T cell subsets from the blood of HCC patients and healthy volunteers, and further to determine whether 4-1BB molecules were also expressed on the surface of CD4⁺ and CD8⁺ T cells. The localization of 4-1BB proteins on tumor infiltrating T cells was determined by direct immunofluorescence cytochemical staining and detected by confocal microscopy.

RESULTS: 4-1BB mRNA, which was not detectable in normal liver, was found in 19 liver tissues adjacent to tumor edge (<1.0 cm). Low expression of 4-1BB mRNA was shown in 8 tumor tissues and 6 liver tissues located within 1 to 5 cm away from tumor edge. In PBMCs, 4-1BB mRNA was almost not detected. Percentage of CD4⁺, CD8⁺ and CD3⁺/CD25⁺ T cells, as well as ratio of CD4 to CD8 revealed no difference between groups ($P>0.05$, respectively), while a significant lower percentage of CD3⁺ T cell was found in HCC group as compared to healthy control group ($P<0.05$). However, 4-1BB molecules were almost not found on the surface of CD4⁺ and CD8⁺ T cells in HCC and healthy control group. Double-staining of 4-1BB⁺/CD4⁺ and 4-1BB⁺/CD8⁺ immunofluorescence on tumor infiltrating T cells was detected in 13 liver tissues adjacent to tumor edge (<1.0 cm) by confocal microscopy.

CONCLUSION: Although HCC may escape from immune attack by weak immunogenicity or downregulated expression of MHC-1 molecules on the tumor cell surface, tumor infiltrating T cells can be activated via other costimulatory signal pathways to exert a limited antitumor effect on local microenvironment. The present study also implicates that modulating 4-1BB/4-1BBL costimulatory pathway may be an effective immunotherapy strateg to augment the host response.

Wan YL, Zheng SS, Zhao ZC, Li MW, Jia CK, Zhang H. Expression of co-stimulator 4-1BB molecule in hepatocellular carcinoma and adjacent non-tumor liver tissue, and its possible role in tumor immunity. *World J Gastroenterol* 2004; 10(2): 195-199

<http://www.wjgnet.com/1007-9327/10/195.asp>

INTRODUCTION

Hepatocellular carcinoma (HCC) has a very poor prognosis owing to its high malignancy, and it ranks second cause of cancer death in China^[1]. Curative tumour resection or orthotopic liver transplantation (LTx) seems to be an optimal treatment. Nevertheless, the recurrence rate remains high both after tumour resection and LTx^[2-10]. Chemotherapy and embolisation are at best palliative with few impacts on survival^[3]. Recently, immunotherapy has been used with some success for such tumours as melanoma^[11-14] and renal-cell carcinoma^[15,16] that are associated with an inflammatory or immune response. However, like most solid tumours, HCC has long been considered poorly immunogenic and substantially refractory to immunotherapy. Since a better prognosis of HCC attributes to the anti-tumor effect induced by cellular immunity of infiltrating CD8⁺ and CD4⁺ T lymphocytes^[17], these tumor infiltrating lymphocytes (TILs) might be in an activated status and play a limited immune protection in microenvironment.

The 4-1BB receptor, a recently identified molecule of tumor necrosis factor- receptor (TNFR) superfamily, is a type I membrane protein expressed on activated cytolytic and helper T cells^[18,19], as well as NK cells^[20]. The ligand for 4-1BB receptor is a 4-1BB ligand (4-1BBL), which is expressed on APCs including B cells, macrophages, and dendritic cells^[21,22]. Ligation of 4-1BB with 4-1BB ligand plays an important role in sustaining T cells activation, amplifying cytotoxic T lymphocyte (CTL) response, as well as inducing IL-2 production in the complete absence of a signal through CD28 molecule^[22,23]. A recent research demonstrated that immunomodulatory gene therapy with 4-1BB ligand could induce long-term remission of liver metastases in a mouse model and augment CTL response against tumor^[24]. The present study was to detect whether 4-1BB molecules were expressed on infiltrating CD4⁺ and CD8⁺ T cells in HCC and its adjacent tissues, and to illustrate the role of 4-1BB/4-1BBL pathway in tumor immunity.

MATERIALS AND METHODS

Patients

Nineteen patients with HCC confirmed by histopathologic examination were selected. Among them, 14 were male and 5 female aged from 28 to 68 years (average, 49.67±13.04 years). Three liver specimens from mismatched cadaver donor and 22 healthy peripheral blood specimens from Blood Center of Zhejiang Province were served as controls.

Reagents

Fluorescein isothiocyanate (FITC) -conjugated mouse

monoclonal antibodies (mAbs) specific for human surface antigens including anti-CD4 (IgG1k clone RPA-T4), anti-CD8 (IgG1k clone RPA-T8), anti-CD3 (IgG1k clone UCHT1), phycoerythrin (PE)-conjugated anti-CD25 (IgG1k clone M-A251), anti-4-1BB (IgG1k clone 4B4-1), and FITL or PE-conjugated mouse IgG1k (clone MOPC-21) as isotype controls were purchased from Becton Dickinson, San Jose, CA. RevertAid™ M-MuLV reverse transcriptase and Taq DNA polymerase were obtained from Promega, USA.

Peripheral blood mononuclear cell preparation

In order to isolate PBMCs, 5 ml heparinized blood was diluted 1:1 with PBS containing 0.6% Na₃-citrate and layered over a 5 ml Ficoll cushion. After centrifugation (20 min, 700×g), the interface containing PBMCs was collected and washed twice with PBS. This precipitate contained approximately 25% monocytes and 75% lymphocytes.

Reverse transcriptase-polymerase chain reaction (RT-PCR)

Semi-quantitative assessment of 4-1BB mRNA expression was performed using RT-PCR on a PTC-200 DNA engine (MJ Research, USA). Briefly, total RNA was prepared from PBMCs and liver tissues using TRIZOL (Gibco BRL Life Technologies, Breda, the Netherlands). cDNA was synthesized with 2 µg of total RNA template using the superscript pre-amplification system (Promega, USA) and random primers in a final volume of 20 µl. The cDNA used as template was checked in respect to human β₂-MG amplification. The following primers (Shanghai Sangon, China) were used: β₂-MG sense primer: 5' -CCAGCAGAGAATGGAAAGTC-3', β₂-MG antisense primer: 5' -GATGCTGCTTACATGTCTCG-3', 4-1BB sense primer: 5' -TCAGGACCAGGAAGGAGTGT-3', 4-1BB antisense primer: 5' -AACGGAGCGTGAGGAAGAAC-3'. Using these primers, fragments of 240 bp, and 414 bp were expected to result from amplification of β₂-MG and 4-1BB cDNAs, respectively. PCR reactions contained 20 pmol of each primer for 4-1BB, 2.5 u of Taq polymerase, 1 µl of 25 mM dNTPs, 1.2 µl of 25 mM MgCl₂ and 10×PCR buffer in a final volume of 25 µl. For β₂-MG amplification, 1 µl of each primer at a 1:8 diluted concentration to 4-1BB primers was used for the reaction. PCR products (8 µl) were analyzed on 1.5% agarose gel containing ethidium bromide using Kodak DNA analyser (Gibco BRL) with Kodak digital science 1S 2.0 software. The expression level of 4-1BB mRNA was described as the ratio of 4-1BB/β₂-MG×100.

Flow cytometric analysis

One hundred microliters of heparinized peripheral blood were incubated with monoclonal antibody at room temperature in dark for 15 min to 30 min according to the manufacturer's instructions. Another 100 µl of heparinized peripheral blood incubated with FITL or PE-conjugated mouse IgG1k (clone MOPC-21) was used as negative isotype control. Erythrocytes were lysed in turn with ImmunoPrep A, B, and C haemolytic solution on Coulter Q-Prep (Beckman-coulter). Alignment was checked using immunocheck beads (Beckman-coulter). All results were obtained using EPICS® XL FACScan (Beckman-coulter) with system™ software.

Direct immunofluorescence histochemical staining protocol

Tissues were stored at -70 °C until use. Four µm-thick frozen sections (on poly-L-lysine coated slides) were fixed in acetone for 10 min at 4 °C. The sections were blocked in phosphate buffered saline (PBS) and 1% bovine serum albumin (BSA) for 1 h, followed by incubation with FITC and PE labeled antibodies or conjugated isotype matched control antibodies for 16 h at 4 °C. After extensively washed (overnight), stained sections were covered in PBS and kept in dark at 4 °C.

Confocal microscopy

LEICA TCS-SP confocal microscope (Germany) was equipped with argon lasers and Leica inverted research biological microscope with an oil immersion objective lens of ×40 (NA1.30). The sections processed for immunocytochemistry were viewed under LEICA TCS-SP confocal microscope. After standard fluorescence observations, 4-1BB and CD4 or CD8 localization on TIL was automatically scanned by laser emitted at 488 nm and imaged by using PowerScanner physiology software. FITC and PE fluorescence emissions were captured through grating at 530/30-nm and 605/30-nm respectively.

Statistical analysis

Data were expressed as mean±SD. Statistical analysis was performed using one-way ANOVA with SPSS 10.0 software. Kruskal-Wallis H test and Student's *t* test were also used for the nonparametric and parametric data analysis between two groups, respectively. A *P* value ≤ 0.05 was considered significant.

RESULTS

Expression of 4-1BB mRNA in tumor tissues but almost not in PBMCs

4-1BB mRNA was not detectable in normal liver, but was detected in all 19 liver tissues adjacent to tumor edge (<1.0 cm). Low expression of 4-1BB mRNA was shown in 8 tumor tissues and 6 liver tissues located within 1 to 5 cm away from tumor edge. However, in PBMCs, 4-1BB mRNA expression was not detected in samples from 18 healthy controls (81.82%, 18/22) and 13 patients with HCC (68.42%, 13/19). Very low expression of 4-1BB mRNA was detected in another 4 healthy volunteers and 6 patients with HCC. However, the median level of 4-1BB mRNA expression from PBMCs in each group was 0 (*P*>0.05) (Figures 1, 2).

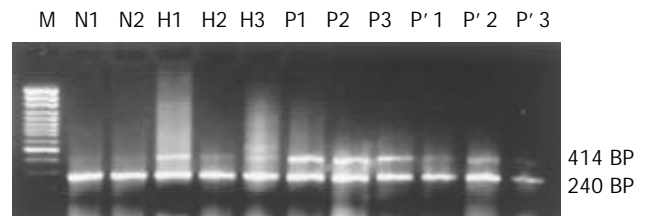


Figure 1 Representative RT-PCR results of 4-1BB mRNA expression in normal liver, and HCC tissues as well as its adjacent tissues. (M, GeneRuler™ 100 bp DNA Ladder Plus; N, normal liver; H, HCC tissues; P, adjacent tissues to HCC (<1 cm), P': liver tissues located within 1 to 5 cm away from tumor edge)

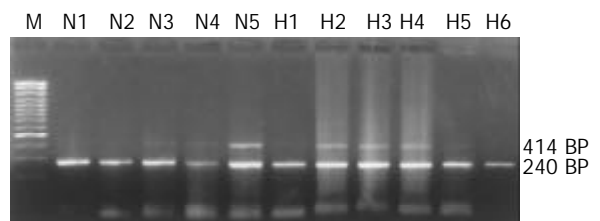


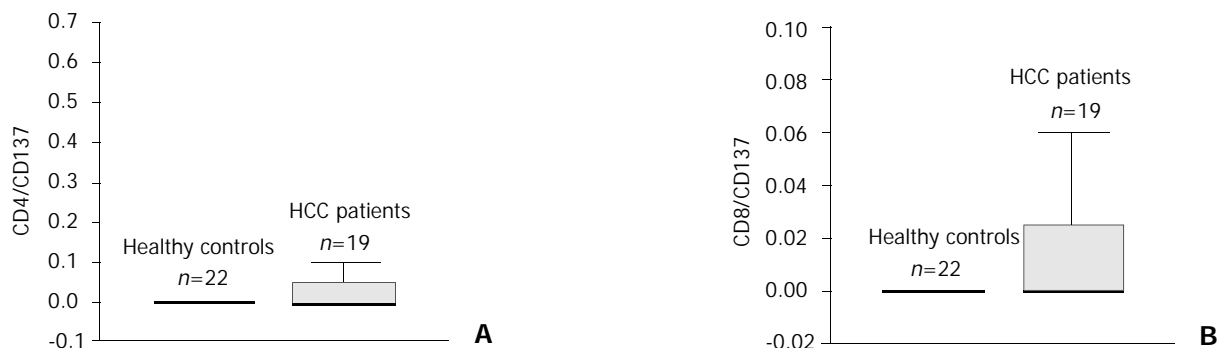
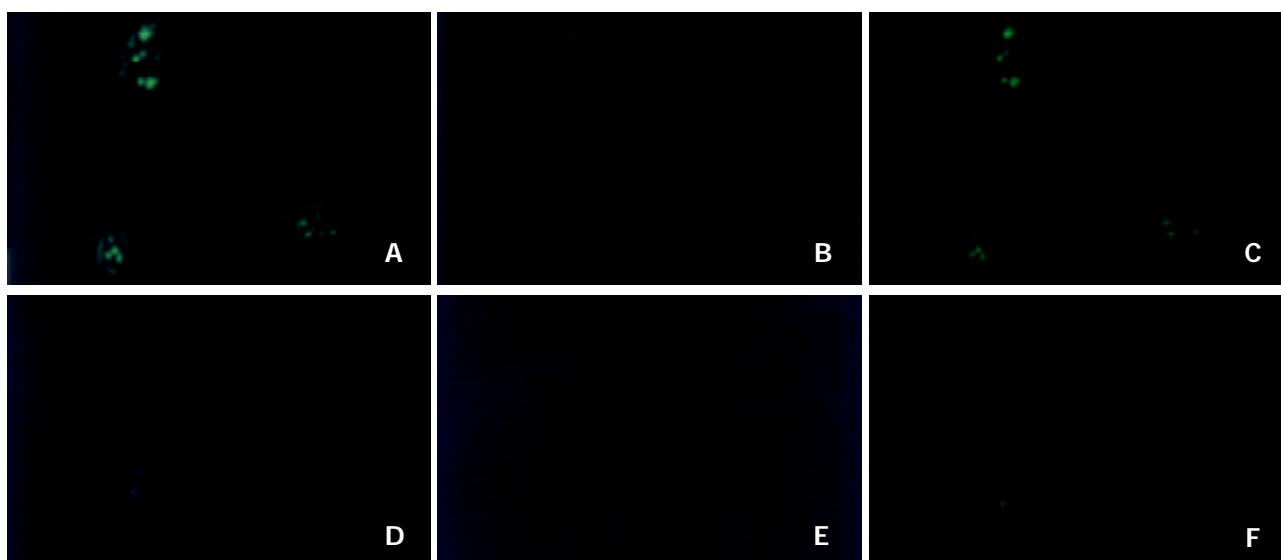
Figure 2 Representative RT-PCR results of 4-1BB mRNA expression in PBMCs (M, GeneRuler™ 100 bp DNA Ladder Plus; N, healthy control; H, HCC group).

Almost no detection of 4-1BB molecules on CD4⁺ or CD8⁺ T cells in PBMCs

In order to analyze T cell phenotypes, and determine whether 4-1BB molecules expressed on T cells from PBMCs, flow

Table 1 Analysis of T cells phenotypes of PBMCs from healthy controls and HCC patients (Mean±SD)

Groups	<i>n</i>	CD4	CD8	CD3	CD3/CD25	CD4/CD8
Normal control	22	34.74±6.19	28.70±5.11	66.56±10.24	1.22±0.13	1.20±0.18
HCC	19	31.40±4.70	25.83±3.98	61.30±4.61	1.22±0.12	1.26±0.17
<i>P</i> value		0.058	0.051	0.038	0.918	0.279

**Figure 3** Comparison of 4-1BB molecules on CD4⁺ or CD8⁺ PBMCs between healthy controls and HCC patients.**Figure 4** Confocal laser micrographs of TILs in HCC adjacent tissues processed for the immunocytochemical detection of 4-1BB and CD4 or CD8 molecules. (A and D, FITC immunofluorescence for CD4 and CD8 molecules respectively; B and E, PE immunofluorescence for 4-1BB molecules; C and F, automatically synthetic micrographs by computer soft for A and B, and D and E, respectively).

cytometric analysis was used. The results are shown in Table 1. Percentages of CD4⁺, CD8⁺ T cells and CD3⁺CD25⁺ T cells, as well as the ratio of CD4 to CD8 had no significant differences between the groups ($P>0.05$). However, a significantly higher percentage of CD3⁺ T cells was found in healthy control group as compared to HCC group ($P<0.05$). 4-1BB molecules were almost not found on the surface of CD4⁺ and CD8⁺ T cells in HCC and healthy control group. The percentage of 4-1BB⁺/CD4⁺ or CD8⁺ T cells in two groups was not more than 0.1%, and the median value in each group was 0 ($P=0.406$ for 4-1BB⁺/CD4⁺, $P=0.209$ for 4-1BB⁺/CD8⁺, respectively). (Table 1, Figure 3).

Co-localization of 4-1BB and CD4 or CD8 on TILs

To determine whether TILs were the same clones as T lymphocytes from peripheral blood, confocal laser microscopy was used to detect 4-1BB expressions on TILs. As expected, we did not find any PE conjugated 4-1BB and FITC conjugated CD4 or CD8 fluorescence located within 3 normal liver tissues. However, co-localization of 4-1BB⁺/CD4⁺ or CD8⁺ on TIL was visualized by confocal laser microscopy in 3 tumor tissues and

1 liver tissue located within 1 to 5 cm away from tumor edge, as well as 13 tumor adjacent tissues within 1 cm. (Figure 4).

DISCUSSION

It seems that a better prognosis of HCC could attribute to the anti-tumor effect induced by cellular immunity of infiltrating CD8⁺ and CD4⁺ T lymphocytes^[17]. However, like most solid tumours, HCC has long been considered poorly immunogenic. Tumor cells were capable of delivering antigen-specific signals to T cells clone, but could not deliver costimulatory signals, e.g., a B7/CD28 interaction^[25-27], necessary for full T cell activation, could lead to the evasion of immune surveillance by malignant cells^[28]. Moreover, evidences have demonstrated that TILs can down-regulate the expression of CD28 molecules, but still could retain a limited immune protection in local tumor microenvironment^[27]. Therefore, other molecules may involve in sustaining T cells activation and amplifying cytotoxic T lymphocytes response.

In this study, we found that 4-1BB mRNA transcripts were

not detectable in normal liver, but were detected in all 19 liver tissues adjacent to tumor edge (<1.0 cm). In some tumor and liver tissues located within 1 to 5 cm away from tumor edge, low expression of 4-1BB mRNA was also detected. Since 4-1BB molecules were mainly expressed on activated T lymphocytes^[18,19], 4-1BB transcripts might derive from TILs. To identify this hypothesis, direct immunofluorescence staining of 4-1BB and CD4 or CD8 on TILs was examined by confocal microscope. Co-localization of 4-1BB⁺/CD4⁺ or CD8⁺ fluorescence located on TILs was visualized by confocal microscopy in tumor and liver tissue within 1 to 5 cm away from tumor edge, as well as tumor adjacent tissues within 1 cm. Previous researches reported that interaction of 4-1BB with 4-1BB ligand played an important role in sustaining T cells activation, amplifying cytotoxic T lymphocyte (CTL) response, as well as inducing IL-2 production in the complete absence of a signal through CD28 molecule^[22,23]. A recent report indicated that under the condition of repeated Ag-stimulation, down-regulated expression of CD28 molecule on activated T cells could lead to activation-induced cell death (AICD)^[29], while very few 4-1BB molecules might supply sufficient costimulatory signals to sustain T cells activation, and inhibit AICD^[30,31]. In fact, accumulative evidence has confirmed that 4-1BB/4-1BB ligand pathway plays a role in transplant immunity^[32-34] and autoimmune disease^[35-37]. Therefore, the present study may provide an important clue that 4-1BB molecules are also involved in the process of infiltrating CD4⁺ and CD8⁺ T cells activation, at least partly, and that modulating 4-1BB/4-1BB ligand pathway might augment CTL response against tumor^[24,38-40].

However, even if these infiltrating lymphocytes are functionally activated via 4-1BB signals or the others, and are truly specific for tumor cells, why they could not inhibit the tumour growth? This phenomenon was inexplicable. Cytotoxic T cells propagated from biopsies showed a specific killing of the tumor cells *in vitro*, confirming that the complex microenvironment inside the tumor tissue was not able to provide the optimal condition for TILs to fully exert their functions in inhibiting tumor growth, or even to induce apoptosis of TILs through Fas/Fas ligand system^[41,42].

To explore if the TILs were the same clones as T lymphocytes from peripheral blood, we analyzed the phenotypes of peripheral blood lymphocytes, and examined 4-1BB molecules and its mRNA transcripts by flow cytometry and RT-PCR respectively. To our surprise, we failed to detect 4-1BB mRNA in peripheral blood lymphocytes and 4-1BB molecules on peripheral CD4⁺ or CD8⁺ T cells from HCC patients. But our results confirmed that a significantly lower percentage of CD3⁺ T cells was found in HCC group as compared to healthy control group, which was coincided with other research data^[43]. Since the phenotype and function of lymphocytes collected from the peripheral blood were not the same as those of lymphocytes from tumor draining regional lymph nodes and tumor tissues, we found that 4-1BB molecules were existed in infiltrating CD4⁺ and CD8⁺ T cells but not in peripheral blood lymphocytes. Therefore, we may conclude that TILs and peripheral blood lymphocytes are not the same clones^[43-45].

In summary, we examined 4-1BB molecules expression in infiltrating T cells in HCC specimens, indicating that tumor infiltrating T cells can be activated via other costimulatory signals, e.g., 4-1BB, and exert a limited antitumor protection in local microenvironment. The present study also implicates that modulating 4-1BB/4-1BBL costimulatory pathway may be an effective immunotherapy strategy to augment the host response.

REFERENCES

- 1 **Tang ZY**, Yu YQ, Zhou XD, Ma ZC, Wu ZQ. Progress and prospects in hepatocellular carcinoma surgery. *Ann Chir* 1998; **52**: 558-563
- 2 **Zhao WH**, Ma ZM, Zhou XR, Feng YZ, Fang BS. Prediction of recurrence and prognosis in patients with hepatocellular carcinoma after resection by use of CLIP score. *World J Gastroenterol* 2002; **8**: 237-242
- 3 **Qin LX**, Tang ZY. The prognostic significance of clinical and pathological features in hepatocellular carcinoma. *World J Gastroenterol* 2002; **8**: 193-199
- 4 **Kanematsu T**, Furui J, Yanaga K, Okudaira S, Shimada M, Shirabe K. A 16-year experience in performing hepatic resection in 303 patients with hepatocellular carcinoma: 1985-2000. *Surgery* 2002; **131**(Suppl 1): S153-158
- 5 **Chiappa A**, Zbar AP, Audisio RA, Leone BE, Biella F, Staudacher C. Factors affecting survival and long-term outcome in the cirrhotic patient undergoing hepatic resection for hepatocellular carcinoma. *Eur J Surg Oncol* 2000; **26**: 387-392
- 6 **Ouchi K**, Sugawara T, Fujiya T, Kamiyama Y, Kakugawa Y, Mikuni J, Yamanami H, Nakagawa K. Prediction of recurrence and extratumor spread of hepatocellular carcinoma following resection. *J Surg Oncol* 2000; **75**: 241-245
- 7 **Otto G**, Heuschen U, Hofmann WJ, Krumm G, Hinz U, Herfarth C. Survival and recurrence after liver transplantation versus liver resection for hepatocellular carcinoma: a retrospective analysis. *Ann Surg* 1998; **227**: 424-432
- 8 **Philosophie B**, Greig PD, Hemming AW, Cattral MS, Wanless I, Rasul I, Baxter N, Taylor BR, Langer B. Surgical management of hepatocellular carcinoma: resection or transplantation? *J Gastrointest Surg* 1998; **2**: 21-27
- 9 **Margarit C**, Charco R, Hidalgo E, Allende H, Castells L, Bilbao I. Liver transplantation for malignant diseases: selection and pattern of recurrence. *World J Surg* 2002; **26**: 257-263
- 10 **Hemming AW**, Cattral MS, Reed AI, Van Der Werf WJ, Greig PD, Howard RJ. Liver transplantation for hepatocellular carcinoma. *Ann Surg* 2001; **233**: 652-659
- 11 **Lucas ML**, Heller L, Coppola D, Heller R. IL-12 plasmid delivery by *in vivo* electroporation for the successful treatment of established subcutaneous B16.F10 melanoma. *Mol Ther* 2002; **5**: 668-675
- 12 **Hsueh EC**, Essner R, Foshag LJ, Ollila DW, Gammon G, O' Day SJ, Boasberg PD, Stern SL, Ye X, Morton DL. Prolonged survival after complete resection of disseminated melanoma and active immunotherapy with a therapeutic cancer vaccine. *J Clin Oncol* 2002; **20**: 4549-4554
- 13 **Dreno B**, Nguyen JM, Khammari A, Pandolfino MC, Tessier MH, Bercegeay S, Cassidanius A, Lemarre P, Billaudel S, Labarriere N, Jotereau F. Randomized trial of adoptive transfer of melanoma tumor-infiltrating lymphocytes as adjuvant therapy for stage III melanoma. *Cancer Immunol Immunother* 2002; **51**: 539-546
- 14 **Labarriere N**, Pandolfino MC, Gervois N, Khammari A, Tessier MH, Dreno B, Jotereau F. Therapeutic efficacy of melanoma-reactive TIL injected in stage III melanoma patients. *Cancer Immunol Immunother* 2002; **51**: 532-538
- 15 **Mickisch GH**, Garin A, van Poppel H, de Prijck L, Sylvester R. Radical nephrectomy plus interferon-alfa-based immunotherapy compared with interferon alfa alone in metastatic renal-cell carcinoma: a randomised trial. *Lancet* 2001; **358**: 966-970
- 16 **Stadler WM**, Kuzel T, Dumas M, Vogelzang NJ. Multicenter phase II trial of interleukin-2, interferon-alpha, and 13-cis-retinoic acid in patients with metastatic renal-cell carcinoma. *J Clin Oncol* 1998; **16**: 1820-1825
- 17 **Wada Y**, Nakashima O, Kutami R, Yamamoto O, Kojiro M. Clinicopathological study on hepatocellular carcinoma with lymphocytic infiltration. *Hepatology* 1998; **27**: 407-414
- 18 **Kwon BS**, Weissman SM. cDNA sequences of two inducible T-cell genes. *Proc Natl Acad Sci U S A* 1989; **86**: 1963-1967
- 19 **Pollok KE**, Kim YJ, Zhou Z, Hurtado J, Kim KK, Pickard RT, Kwon BS. Inducible T cell antigen 4-1BB. Analysis of expression and function. *J Immunol* 1993; **150**: 771-781
- 20 **Melero I**, Johnston JV, Shufford WW, Mittler RS, Chen L. NK1.1 cells express 4-1BB (CDw137) costimulatory molecule and are required for tumor immunity elicited by anti-4-1BB monoclonal antibodies. *Cell Immunol* 1998; **190**: 167-172
- 21 **Pollok KE**, Kim YJ, Hurtado J, Zhou Z, Kim KK, Kwon BS. 4-1BB T-cell antigen binds to mature B cells and macrophages, and

- costimulates anti- μ -primed splenic B cells. *Eur J Immunol* 1994; **24**: 367-374
- 22 **DeBenedette MA**, Shahinian A, Mak TW, Watts TH. Costimulation of CD28- T lymphocytes by 4-1BB ligand. *J Immunol* 1997; **158**: 551-559
- 23 **Chu NR**, DeBenedette MA, Stiernholm BJ, Barber BH, Watts TH. Role of IL-12 and 4-1BB ligand in cytokine production by CD28⁺ and CD28⁻ T cells. *J Immunol* 1997; **158**: 3081-3089
- 24 **Martinet O**, Ermekova V, Qiao JQ, Sauter B, Mandeli J, Chen L, Chen SH. Immunomodulatory gene therapy with interleukin 12 and 4-1BB ligand: long- term remission of liver metastases in a mouse model. *J Natl Cancer Inst* 2000; **92**: 931-936
- 25 **Tatsumi T**, Takehara T, Katayama K, Mochizuki K, Yamamoto M, Kanto T, Sasaki Y, Kasahara A, Hayashi N. Expression of costimulatory molecules B7-1 (CD80) and B7-2 (CD86) on human hepatocellular carcinoma. *Hepatology* 1997; **25**: 1108-1114
- 26 **Qiu YR**, Yang CL, Chen LB, Wang Q. Analysis of CD8⁺ and CD8⁻CD28⁻ cell subsets in patients with hepatocellular carcinoma. *Diyi Junyi Daxue Xuebao* 2002; **22**: 72-73
- 27 **Tang KF**, Chan SH, Loh KS, Chong SM, Wang D, Yeoh KH, Hu H. Increased production of interferon-gamma by tumour infiltrating T lymphocytes in nasopharyngeal carcinoma: indicative of an activated status. *Cancer Lett* 1999; **140**: 93-98
- 28 **Chavan SS**, Chiplunkar SV. Immunophenotypes and cytotoxic functions of lymphocytes in patients with hepatocellular carcinoma. *Tumori* 1997; **83**: 762-767
- 29 **Kim YJ**, Kim SH, Mantel P, Kwon BS. Human 4-1BB regulates CD28 co-stimulation to promote Th1 cell responses. *Eur J Immunol* 1998; **28**: 881-890
- 30 **DeBenedette MA**, Chu NR, Pollok KE, Hurtado J, Wade WF, Kwon BS, Watts TH. Role of 4-1BB ligand in costimulation of T lymphocyte growth and its upregulation on M12 B lymphomas by cAMP. *J Exp Med* 1995; **181**: 985-992
- 31 **Hurtado JC**, Kim YJ, Kwon BS. Signals through 4-1BB are costimulatory to previously activated splenic T cells and inhibit activation-induced cell death. *J Immunol* 1997; **158**: 2600-2609
- 32 **Blazar BR**, Kwon BS, Panoskaltis-Mortari A, Kwak KB, Peschon JJ, Taylor PA. Ligation of 4-1BB (CDw137) regulates graft-versus-host disease, graft-versus-leukemia, and graft rejection in allogeneic bone marrow transplant recipients. *J Immunol* 2001; **166**: 3174-3183
- 33 **DeBenedette MA**, Wen T, Bachmann MF, Ohashi PS, Barber BH, Stocking KL, Peschon JJ, Watts TH. Analysis of 4-1BB ligand (4-1BBL)-deficient mice and of mice lacking both 4-1BBL and CD28 reveals a role for 4-1BBL in skin allograft rejection and in the cytotoxic T cell response to influenza virus. *J Immunol* 1999; **163**: 4833-4841
- 34 **Tan JT**, Ha J, Cho HR, Tucker-Burden C, Hendrix RC, Mittler RS, Pearson TC, Larsen CP. Analysis of expression and function of the costimulatory molecule 4-1BB in alloimmune responses. *Transplantation* 2000; **70**: 175-183
- 35 **Sun Y**, Lin X, Chen HM, Wu Q, Subudhi SK, Chen L, Fu YX. Administration of agonistic anti-4-1BB monoclonal antibody leads to the amelioration of experimental autoimmune encephalomyelitis. *J Immunol* 2002; **168**: 1457-1465
- 36 **Michel J**, Langstein J, Hofstadter F, Schwarz H. A soluble form of CD137 (ILA/4-1BB), a member of the TNF receptor family, is released by activated lymphocytes and is detectable in sera of patients with rheumatoid arthritis. *Eur J Immunol* 1998; **28**: 290-295
- 37 **Sharief MK**. Heightened intrathecal release of soluble CD137 in patients with multiple sclerosis. *Eur J Neurol* 2002; **9**: 49-54
- 38 **Giuntoli RL 2nd**, Lu J, Kobayashi H, Kennedy R, Celis E. Direct costimulation of tumor-reactive CTL by helper T cells potentiate their proliferation, survival, and effector function. *Clin Cancer Res* 2002; **8**: 922-931
- 39 **Ye Z**, Hellstrom I, Hayden-Ledbetter M, Dahlin A, Ledbetter JA, Hellstrom KE. Gene therapy for cancer using single-chain Fv fragments specific for 4-1BB. *Nat Med* 2002; **8**: 343-348
- 40 **Martinet O**, Divino CM, Zang Y, Gan Y, Mandeli J, Thung S, Pan PY, Chen SH. T cell activation with systemic agonistic antibody versus local 4-1BB ligand gene delivery combined with interleukin-12 eradicate liver metastases of breast cancer. *Gene Ther* 2002; **9**: 786-792
- 41 **Bennett MW**, O'Connell J, O' Sullivan GC, Brady C, Roche D, Collins JK, Shanahan F. The Fas counterattack in vivo: apoptotic depletion of tumor-infiltrating lymphocytes associated with Fas ligand expression by human esophageal carcinoma. *J Immunol* 1998; **160**: 5669-5675
- 42 **Bodey B**, Bodey B Jr, Siegel SE, Kaiser HE. Immunocytochemical detection of leukocyte-associated and apoptosis-related antigen expression in childhood brain tumors. *Crit Rev Oncol Hematol* 2001; **39**: 3-16
- 43 **Santin AD**, Ravaggi A, Bellone S, Pecorelli S, Cannon M, Parham GP, Hermonat PL. Tumor-infiltrating lymphocytes contain higher numbers of type 1 cytokine expressors and DR⁺ T cells compared with lymphocytes from tumor draining lymph nodes and peripheral blood in patients with cancer of the uterine cervix. *Gynecol Oncol* 2001; **81**: 424-432
- 44 **Echchakir H**, Dorothee G, Vergnon I, Menez J, Chouaib S, Mami-Chouaib F. Cytotoxic T lymphocytes directed against a tumor-specific mutated antigen display similar HLA tetramer binding but distinct functional avidity and tissue distribution. *Proc Natl Acad Sci U S A* 2002; **99**: 9358-9363
- 45 **Santin AD**, Hermonat PL, Ravaggi A, Bellone S, Roman JJ, Smith CV, Pecorelli S, Radominska-Pandya A, Cannon MJ, Parham GP. Phenotypic and functional analysis of tumor-infiltrating lymphocytes compared with tumor-associated lymphocytes from ascitic fluid and peripheral blood lymphocytes in patients with advanced ovarian cancer. *Gynecol Obstet Invest* 2001; **51**: 254-261

Edited by Zhang JZ and Wang XL

Antitumor immunopreventive effect in mice induced by DNA vaccine encoding a fusion protein of α -fetoprotein and CTLA4

Geng Tian, Ji-Lin Yi, Ping Xiong

Geng Tian, Ji-Lin Yi, Department of General Surgery, Tongji Hospital, Tongji Medical College, Huazhong University of Science and Technology, Wuhan 430030, Hubei Province, China

Ping Xiong, Department of Immunology, Tongji Medical College, Huazhong University of Science and Technology, Wuhan 430030, Hubei Province, China

Correspondence to: Geng Tian, Department of General Surgery, Tongji Hospital, Tongji Medical College, Huazhong University of Science and Technology, Wuhan 430030, Hubei Province, China. geng_tian707@hotmail.com

Telephone: +86-27-83663402

Received: 2003-07-12 **Accepted:** 2003-07-30

Abstract

AIM: To develop a tumor DNA vaccine encoding a fusion protein of murine AFP and CTLA4, and to study its ability to induce specific CTL response and its protective effect against AFP-producing tumor.

METHODS: Murine α -fetoprotein (mAFP) gene was cloned from total RNA of Hepa1-6 cells by RT-PCR. A DNA vaccine was constructed by fusion murine α -fetoprotein gene and extramembrane domain of murine CTLA4 gene. The DNA vaccine was identified by restriction enzyme analysis, sequencing and expression. EL-4 (mAFP) was developed by stable transfection of EL-4 cells with pmAFP. The frequency of cells producing IFN- γ in splenocytes harvested from the immunized mice was measured by ELISPOT. Mice immunized with DNA vaccine were inoculated with EL-4 (mAFP) cells in back to observe the protective effect of immunization on tumor. On the other hand, blood samples were collected from the immunized mice to check the functions of liver and kidney.

RESULTS: 1.8 kb mAFP cDNA was cloned from total RNA of Hepa1-6 cells by RT-PCR. The DNA vaccine encoding a fusion protein of mAFP-CTLA4 was constructed and confirmed by restriction enzyme analysis, sequencing and expression. The expression of mAFP mRNA in EL-4 (mAFP) was confirmed by RT-PCR. The ELISPOT results showed that the number of IFN- γ -producing cells in pmAFP-CTLA4 group was significantly higher than that in pmAFP, pcDNA3.1 and PBS group. The tumor volume in pmAFP-CTLA4 group was significantly smaller than that in pmAFP, pcDNA3.1 and PBS group, respectively. The hepatic and kidney functions in each group were not altered.

CONCLUSION: AFP-CTLA4 DNA vaccine can stimulate potent specific CTL responses and has distinctive antitumor effect on AFP-producing tumor. The vaccine has no impact on the function of mouse liver and kidney.

Tian G, Yi JL, Xiong P. Antitumor immunopreventive effect in mice induced by DNA vaccine encoding a fusion protein of α -fetoprotein and CTLA4. *World J Gastroenterol* 2004; 10 (2): 200-204

<http://www.wjgnet.com/1007-9327/10/200.asp>

INTRODUCTION

Hepatocellular carcinoma (HCC) is a major cause of cancer death with more than 1.2 million global annual incidences. The incidence of HCC has been increasing rapidly in both Asian and Western countries because of the global pandemic of hepatitis B and C infections^[1]. Surgery and liver transplantation are the only effective treatments, but most HCC patients are not eligible due to the advanced stage of disease or poor hepatic function concomitant with cirrhosis^[2-8]. It is important to develop novel therapies for HCC, and some genes and immunotherapeutic strategies for HCC are under investigation.

Understanding of antigen processing and presentation by antigen-presenting cells, as well as the conditions of induction of T-cell immunity, has spawned the discipline of genetic immunotherapy. DNA-based immunization can induce strong cellular immune responses to a variety of antigens, including tumor antigens, such as antigens associated with malignant melanoma^[9-11], ovarian carcinoma^[12], breast cancer^[13,14], small-cell lung cancer^[15], neuroblastoma^[16] and prostate carcinoma^[17].

Two major obstacles in developing rational strategies in tumor immunotherapy are identification of suitable target tumor antigens and effective process and presentation by professional antigen-presenting cells to induce T cell immunity.

Recent studies on the immunodominant epitopes of AFP have provided a solution to the obstacle of HCC immunotherapy. The majority of human HCCs overexpress the oncofetal antigen AFP, M_r 70 000 glycoprotein. AFP is produced at fetal liver at high levels, and transcriptionally repressed at birth and is present thereafter at low serum levels throughout life^[18]. Butterfield *et al*^[19-21] found recently that 4 peptides of human AFP processed and presented in the context of HLA-A0201, could be recognized by the human T cell repertoire, and could be used to generate AFP-specific CTL in human T cell cultures and HLA-A0201/ K^b -transgenic mice. It was also found that the murine immune system could generate T-cell responses to this oncofetal antigen^[22-24]. AFP can serve as an effective tumor-specific antigen but its immunogenicity is weak^[19-25].

Cytotoxic T-lymphocyte antigen 4 (CTLA4) is a glycoprotein expressed on activated T cells. It has a strong binding affinity to both B7-1 (CD80) and B7-2 (CD86) molecules^[26], which are primarily expressed on APCs. CTLA4 is a homodimer, but dimerization of CTLA4 is not required for B7 binding^[27]. CTLA4-Ig has been used as an immunosuppressive drug in animal models of transplantation and autoimmune diseases^[28,29].

In the present study, we investigated whether the immunogenicity of mouse AFP could be improved by targeting to APCs through B7-1 and B7-2 molecules. We constructed a plasmid DNA encoding mAFP and the extramembrane domain of mouse CTLA4 and found this DNA vaccine could stimulate potent specific CTL responses and had distinctive antitumor effect on AFP-producing tumor.

MATERIALS AND METHODS

Cell lines and plasmids

Hepa 1-6 (murine HCC) and EL-4 (murine lymphoma) cell lines were gifts from Dr Wang Hao (The Second Military

Medical University, Shanghai, China). CHO cells were provided by China Center for Type Culture Collection (Wuhan, China). The plasmid pmCTLA4-Ig encoding murine CTLA4-Ig was kindly provided by Professor Wang DW (Tongji Medical College, Huazhong University of Science and Technology, Hubei, China). Eukaryotic expression vector pcDNA3.1/myc-His was from Invitrogen Company.

Main reagents

TRIzol was a product of Gibco Company. RT-PCR kit was purchased from TaKaRa Biotechnology Company. Lipofectamine 2000 was a product of Invitrogen Company. Goat anti-AFP polyclonal antibody was purchased from Sant Cruz Company. Biotinylated rabbit anti-CTLA4 polyclonal antibody was purchased from PepraTech Company. Primers were synthesized by the Shanghai Bioasia Biocompany. ECL Western blotting detection reagents were products of Pharmacia Company. Murine IFN- γ ELISPOT kit was a product of Diaclone Company.

Construction of Plasmids

The 1.8 kb mAFP cDNA was cloned from total RNA of Hepa1-6 cells by RT-PCR. Total RNA was isolated from Hepa1-6 cells by the TRIzol method. RT-PCR primers were designed to include the entire mAFP coding region, including the signal sequence. The primers used were 5' -CTCAGGAATTCGCC ATGAAGTGGATCACAC-3' and 5' -CTCTGCTCTAGATT ACTCGAGAACGCCCAAAGCATCACG-3'. The 1.8 kb mAFP cDNA PCR product was cloned into pcDNA3.1/myc-His to construct the plasmid pmAFP. The plasmid pmCTLA4-Ig was used as a temple to get the extramembrane domain of CTLA4 through PCR. To construct the mAFP-mCTLA4 fusion protein expression vector, we used overlap PCR to add a GGGGSGGGGS peptide linker upstream of the extramembrane domain of mouse CTLA4 gene. The forward primer 5' -TATGGCGGGGCTCGATGGAAGCCATAC AGGTG-3' and the reverse primer 5' -CTCTCTCTAGATC AAGAATCCGGGCATGGT-3' were used in the first round PCR on the mouse CTLA4-Ig gene. The PCR product was used as a template to perform a second round PCR using the same reverse primer and a second forward primer 5' -TTATATTCTC GAGGGAGGCGGGGCTCGGGAGGCGGGGCTCGATGG-3'. The 5' side of the first forward primer and the 3' side of the second forward primer were overlapped for 17 nucleotides. The N terminal of extramembrane domain of CTLA4 with linker was fused in frame with the C terminal of mAFP in pmAFP to construct the mAFP-mCTLA4 fusion protein expression plasmid pmAFP-CTLA4. The recombinant vector was identified by restriction enzyme analysis and sequencing.

Western blot

Lipofectamine 2000 was used for transient transfection of CHO cells according to the manufacturer's instructions. Proteins were separated on SDS-PAGE, and transferred onto a nitrocellulose membrane by semidry electroblotting. Proteins were stained with goat anti-AFP polyclonal antibody or biotinylated rabbit anti-CTLA4 polyclonal antibody, followed by anti-goat IgG-HRP or HRP-avidin. The blot was developed with ECL Western blotting detection reagents.

Stable transfection of EL-4 cells with plasmids pmAFP

EL-4 (mAFP) was developed by stable transfection of EL-4 cells with pmAFP by Lipofectamine 2000 according to the manufacturer's instructions. Transfectants were selected and maintained with G418 (0.3 mg/ml) in RPMI1640 complete media. The expression of mAFP mRNA in EL-4(mAFP) was assessed by RT-PCR.

Immunization and ELISPOT assay

Twenty-four female C57BL/6 mice were divided into pmAFP-CTLA4 group, pmAFP group, pcDNA3.1 group and PBS group, each group had 6 mice. For each mouse, 100 μ g plasmid was administered in the left anterior tibialis muscle on day 0 and day 14, respectively. On day 28 of study, all mice were killed. The splenic lymphocytes were separated for ELISPOT and the blood was drawn for examination of the functions of liver and kidney. The splenocytes were restimulated *in vitro* by EL-4(mAFP) as reported^[22]. In brief, splenocytes were cultured with irradiated EL-4 (mAFP) cells containing 10 unit/ml human IL-2 for 48 h at 37 °C. The anti-IFN- γ antibody coated ELISPOT plate was incubated with restimulated cells at 37 °C for 24 h.

Protective effect of DNA vaccine against tumor

Another 24 C57BL female mice were grouped and immunized as above. Two weeks after the last immunization, all mice were injected by 2×10^5 EL-4 (mAFP) on the back subcutaneously. Tumor mass was assessed two times weekly as the follow formula: $4/3\pi r^3$ (r = radius).

Examination of functions of liver and kidney

The serum ALT and creatinine were measured with ALT assay kit and creatinine assay kit, respectively.

Statistical analysis

Software SPSS 10.0 was employed to process the data. The *t* test was used for statistical analysis. $P < 0.05$ was considered significant.

RESULTS

Plasmids construction

The 1.8 kb mAFP cDNA was isolated from murine HCC cell line Hepa1-6 by RT-PCR and subcloned into pcDNA3.1 to construct plasmid pmAFP. We cloned the extracellular domain of mouse CTLA4 from plasmid pmCTLA4-Ig, and added a flexible linker (GGGGSGGGGS) before CTLA4 by overlap PCR. The N terminal of extramembrane domain of CTLA4 with linker was fused in frame with the C terminal of mAFP in pmAFP to construct the mAFP-mCTLA4 fusion protein expression plasmid pmAFP-CTLA4. Correct orientation of the ligations was determined by restriction enzyme analysis (Figure 1). Sequencing analysis showed that the reading frame was correct.

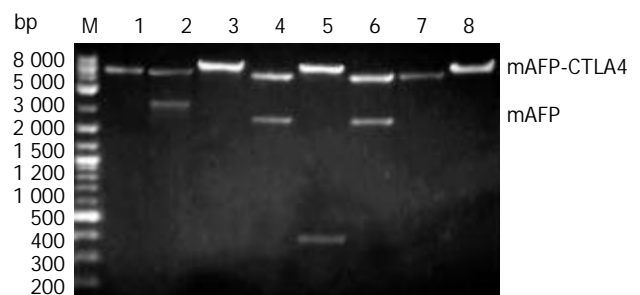


Figure 1 Identification of pmAFP and pmAFP-CTLA4 with restriction enzyme analysis. M: DNA marker, Lane 1: pcDNA3.1/EcoRI, Lane 2: pmAFP-CTLA4/EcoRI+XbaI, Lane 3: pmAFP-CTLA4/EcoRI, Lane 4: pmAFP-CTLA4/EcoRI+XhoI, Lane 5: pmAFP-CTLA4/XhoI+XbaI, Lane 6: pmAFP/EcoRI+XbaI, Lane 7: pcDNA3.1/EcoRI, Lane 8: pmAFP/EcoRI.

Western blot

Expression of plasmids pmAFP and pmAFP-CTLA4 in transient transfection of CHO cells was analyzed with Western blotting, the expected two protein bands (-70 and -84 kDa)

were shown (Figure 2). The expression of mAFP mRNA in EL-4(mAFP) was confirmed by RT-PCR(data not shown).

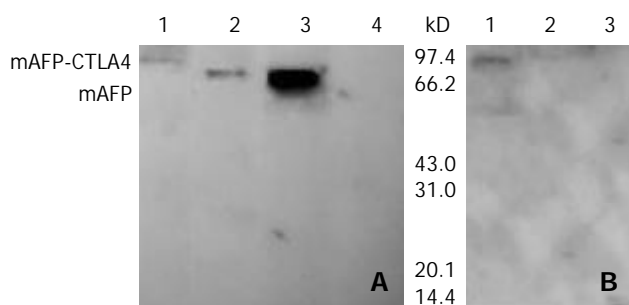


Figure 2 Detection of protein expression of plasmids by Western blotting. A: the blot was probed with anti-AFP. Lane 1: CHO/pmAFP-CTLA, Lane 2: CHO/pmAFP, Lane 3: Hepa 1-6, Lane 4: CHO/pcDNA3.1, B: the blot was probed with anti-CTLA4. Lane 1: CHO/pmAFP-CTLA, Lane 2: CHO/pmAFP, Lane 3: CHO/pcDNA3.1.

ELISPOT assay

ELISPOT results showed the number of IFN- γ -producing cells in pmAFP-CTLA4 group was significantly higher than that in pmAFP group ($P < 0.01$), pcDNA3.1 group ($P < 0.01$) and PBS group ($P < 0.01$) (Figure 3).

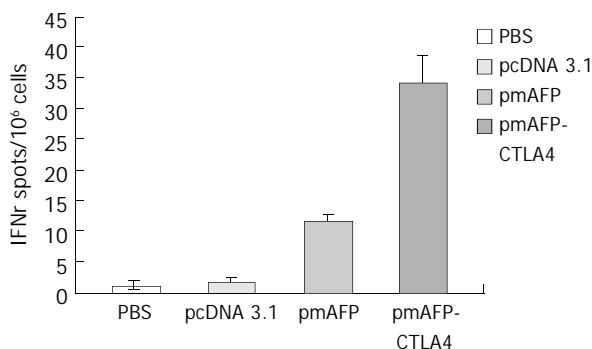


Figure 3 Number of IFN- γ -producing cells in 4 different groups.

Protective effect of DNA vaccine against tumor

The tumor growth in pmAFP-CTLA4 group was slower than that in other groups. Twenty two days after tumor challenge, the tumor volume of pmAFP-CTLA4 group was significantly smaller than that in pmAFP group ($P < 0.01$), pcDNA3.1 group ($P < 0.01$) and PBS group ($P < 0.01$) (Figure 4).

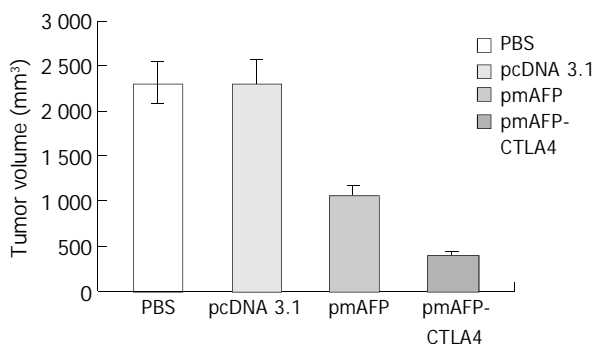


Figure 4 Comparison of tumor masses in 4 groups on 22 days following tumor challenge.

Functions of liver and kidney

The serum level of ALT and creatinine in each group was

unchanged (Table 1), suggesting that the immunization had no impact on the function of liver and kidney.

Table 1 Serum level of ALT and creatinine after immunization with DNA vaccine

Groups	<i>n</i>	ALT/U·mL ⁻¹ ($\bar{x} \pm s$)	Creatinine/ μ mol·L ⁻¹ ($\bar{x} \pm s$)
PBS	6	51.1 \pm 1.7	119.4 \pm 6.9
pcDNA3.1	6	50.9 \pm 1.5	116.6 \pm 9.7
pmAFP	6	51.6 \pm 2.5	116.4 \pm 6.0
pmAFP-CTLA4	6	52.5 \pm 3.2	118.6 \pm 11.5

DISCUSSION

Many tumors express tumor-associated or tumor-specific antigens but do not elicit an efficient immune response. Various experimental strategies have been explored to enhance the immunogenicity of tumor vaccines. Targeting immunogens to APCs with Abs against class MHC^[30,31], Fc γ R^[30], 33D1^[31], or surface Ig^[32] could substantially increase Ab responses. Antigens could be presented to APCs more efficiently by conjugating with Fc γ R^[33], IP10^[34], MCP-3^[34], L-selectin^[35] and CTLA4^[35,36], and lead to significant antitumor immunity^[34,36]. A DNA vaccine that can express carcinoembryonic Ag (CEA), AFP, and CD40 ligand trimer fusion protein, could break peripheral T cell tolerance against CEA and achieve effective tumor-protective immunity against murine colon carcinoma in CEA-transgenic mice^[37].

HCC is a highly malignant tumor with a poor prognosis and few therapeutic options. AFP is a HCC-associated Ag but can not elicit efficient immune response. Some experimental strategies have been explored to enhance the immunogenicity of HCC vaccines based on AFP. Previous experiments of AFP-specific genetic immunotherapy for HCC included AFP plasmid immunization, AFP-transduced DCs immunization and AFP plasmid prime-AFP adenovirus boost immunization. Plasmid AFP immunization resulted in detectable but low levels of AFP-specific T-cell responses and poorly reproducible protective immunity^[22-25]. DCs engineered to express murine AFP demonstrated a powerful ability to generate AFP-specific T-cell responses and protective immunity in mice^[22,23]. However, the need for costly cell culture procedures precluded their wide availability for clinical use, and minor variation in the culture technique or antigen loading might yield sub optimal, even tolerating vaccines^[38,39]. AFP plasmid prime-AFP adenovirus boost immunization could generate significant AFP-specific T-cell responses and protective immunity in mice^[23]. But this method at least has two steps. In the present study, we tested a novel strategy for inducing anti-HCC immunity by specifically targeting APCs with a DNA vaccine encoding both AFP and CTLA4 in mice. We found that the vaccine elicited strong AFP-specific T-cell responses and had distinctive preventive effect on AFP-producing tumor.

We attributed the successful α -fetoprotein specific T cell responses in mice to the CTLA4 moiety targets APCs for efficient receptor-mediated uptake and processing of mAFP. CTLA4 could likely provide such a strong adjuvant activity due to its strong binding affinity to B7 molecules on APCs. CTLA4 could bind to both B7-1 and B7-2 with a 20- to 50-fold higher affinity than CD28^[40]. A CTLA4-Ig fusion protein composed of CTLA4 and IgG Fc was 4-fold high of that in draining lymph nodes, levels of nontargeted protein within 2-24 hours administration^[41]. Monomeric CTLA4 also has binding activity for B7-1 and B7-2, though its binding activity is low when compared with dimeric CTLA4.

CTLA4-Ig has been used as an immunosuppressive drug in animal models of transplantation and autoimmune

diseases^[28,29]. Our current study showed the enhanced immunogenicity of mAFP-CTLA4. CTLA4 had 20 to 50-fold higher affinity to both B7-1 and B7-2 than CD28. The immune suppression mediated by CTLA4-Ig was likely through its inhibition of CD28-B7 interactions, which provide an important positive signal for T-cell proliferation and cytokine release^[42]. The different immunomodulating effects of CTLA4 might be caused by varied doses of CTLA4 administered. In previous studies, to achieve maximal immune suppression, 50-500 µg CTLA4-Ig was applied before and after transplantation for several consecutive days. But when fusion protein Id-CTLA4 was used as vaccine in another experiment, only twice administration of 0.1-50 µg Id-CTLA4 was sufficient enough to elicit strong immune response to Id^[36]. Vaccination with DNA encoding CTLA4-Ig provided an additional evidence that CTLA4-Ig at low levels could increase both Ab and T-cell proliferation responses^[35,43].

In summary, the result suggests that a DNA vaccine encoding AFP and CTLA4 can elicit strong AFP-specific T-cell responses and has distinctive antitumor effect on AFP-producing tumor.

REFERENCES

- Schafer DF**, Sorrell MF. Hepatocellular carcinoma. *Lancet* 1999; **353**: 1253-1257
- Tang ZY**. Hepatocellular carcinoma—cause, treatment and metastasis. *World J Gastroenterol* 2001; **7**: 445-454
- Qin LX**, Tang ZY. The prognostic significance of clinical and pathological I features in hepatocellular carcinoma. *World Gastroenterol* 2002; **8**: 193-199
- Zhang G**, Long M, Wu ZZ, Yu WQ. Mechanical properties of hepatocellular carcinoma cells. *World J Gastroenterol* 2002; **8**: 243-246
- Tang ZY**, Sun FX, Tian J, Ye SL, Liu YK, Liu KD, Xue Q, Chen J, Xia JL, Qin LX, Sun HC, Wang L, Zhou J, Li Y, Ma ZC, Zhou XD, Wu ZQ, Lin ZY, Yang BH. Metastatic human hepatocellular carcinoma models in nude mice and cell line with metastatic potential. *World J Gastroenterol* 2001; **7**: 597-601
- Zheng WW**, Zhou KR, Chen ZW, Shen JZ, Chen CZ, Zhang SJ. Characterization of focal hepatic lesions with SPIO-enhanced MRI. *World J Gastroenterol* 2002; **8**: 82-86
- Fu JM**, Yu XF, Shao YF. Telomerase and primary liver cancer. *Shijie Huaren Xiaohua Zazhi* 2000; **8**: 461-463
- Su YH**, Zhu SN, Lu SL, Gu YH. HCV genotypes expression in hepatocellular carcinoma by reverse transcription *in situ* polymerase chain reaction. *Shijie Huaren Xiaohua Zazhi* 2000; **8**: 874-878
- Mendiratta SK**, Thai G, Eslahi NK, Thull NM, Matar M, Bronte V, Pericle F. Therapeutic tumor immunity induced by polyimmunization with melanoma antigens gp100 and TRP-2. *Cancer Res* 2001; **61**: 859-862
- Wagner SN**, Wagner C, Luhrs P, Weimann TK, Kutil R, Goos M, Stinge G, Schneeberger A. Intracutaneous genetic immunization with autologous melanoma-associated antigen Pmel17/gp100 induces T cell-mediated tumor protection *in vivo*. *J Invest Dermatol* 2000; **115**: 1082-1087
- Park JH**, Kim CJ, Lee JH, Shin SH, Chung GH, Jang YS. Effective immunotherapy of cancer by DNA vaccination. *Mol Cells* 1999; **9**: 384-391
- Neglia F**, Orengo AM, Cilli M, Meazza R, Tomassetti A, Canevari S, Melani C, Colombo MP, Ferrini S. DNA vaccination against the ovarian carcinoma-associated antigen folate receptor- α (Fr α) induces cytotoxic T lymphocyte and antibody responses in mice. *Cancer Gene Ther* 1999; **6**: 349-357
- Pupa SM**, Invernizzi AM, Forti S, Di Carlo E, Musiani P, Nanni P, Lollini PL, Meazza R, Ferrini S, Menard S. Prevention of spontaneous neu-expressing mammary tumor development in mice transgenic for rat proto-neu by DNA vaccination. *Gene Ther* 2001; **8**: 75-79
- Lachman LB**, Rao XM, Kremer RH, Ozpolat B, Kiriakova G, Price JE. DNA vaccination against neu reduces breast cancer incidence and metastasis in mice. *Cancer Gene Ther* 2001; **8**: 259-268
- Ohwada A**, Nagaoka I, Takahashi F, Tominaga S, Fukuchi Y. DNA vaccination against HuD antigen elicits antitumor activity in a small-cell lung cancer murine model. *Am J Respir Cell Mol Biol* 1999; **21**: 37-43
- Lode HN**, Pertl U, Xiang R, Gaedicke G, Reissfeld RA. Tyrosine hydroxylase-based DNA vaccination is effective against murine neuroblastoma. *Med Pediatr Oncol* 2000; **35**: 641-646
- Kim JJ**, Yang JS, Dang K, Manson KH, Weiner DB. Engineering enhancement of immune responses to DNA-based vaccines in a prostate cancer model in rhesus macaques through the use of cytokine gene adjuvants. *Clin Cancer Res* 2001; **7**: 882s-889s
- Deutsch HF**. Chemistry and biology of α -fetoprotein. *Adv Cancer Res* 1991; **56**: 253-311
- Butterfield LH**, Koh A, Meng W, Vollmer CM, Ribas A, Dissette VB, Lee E, Glaspy JA, McBride WH, Economou JS. Generation of human T cell responses to an HLA-A2.1-restricted peptide epitope from α Fetoprotein. *Cancer Res* 1999; **59**: 3134-3142
- Butterfield LH**, Meng WS, Koh A, Vollmer CM, Ribas A, Dissette VB, Faull K, Glaspy JA, McBride WH, Economou JS. T cell responses to HLA-A*0201-restricted peptides derived from α -fetoprotein. *J Immunol* 2001; **166**: 5300-5308
- Meng WS**, Butterfield LH, Ribas A, Heller JB, Dissette VB, Glaspy JA, McBride WH, Economou JS. Fine specificity analysis of an HLA-A2.1-restricted immunodominant T cell epitope derived from human alpha-fetoprotein. *Mol Immunol* 2000; **37**: 943-950
- Vollmer CM Jr**, Eilber FC, Butterfield LH, Ribas A, Dissette VB, Koh A, Montejó L, Andrews K, McBride WH, Glaspy JA, Economou JS. α fetoprotein-specific immunotherapy for hepatocellular carcinoma. *Cancer Res* 1999; **59**: 3064-3067
- Meng WS**, Butterfield LH, Ribas A, Dissette VB, Heller JB, Miranda GA, Glaspy JA, McBride WH, Economou JS. α -fetoprotein-specific tumor immunity induced by plasmid prime-adenovirus boost genetic vaccination. *Cancer Res* 2001; **61**: 8782-8786
- Grimm CF**, Ortman D, Mohr L, Michalak S, Krohne TU, Meckel S, Eisele S, Encke J, Blum HE, Geissler M. Mouse α -fetoprotein-specific DNA-based immunotherapy of hepatocellular carcinoma leads to tumor regression in mice. *Gastroenterology* 2000; **119**: 1104-1112
- Bei R**, Budillon A, Reale MG, Capuano G, Pomponi D, Budillon G, Frati L, Muraro R. Cryptic epitopes on α -fetoprotein induce spontaneous immune responses in hepatocellular carcinoma, liver cirrhosis, and chronic hepatitis patients. *Cancer Res* 1999; **59**: 5471-5474
- Linsley PS**, Ledbetter JA. The role of the CD28 receptor during T cell responses to antigen. *Annu Rev Immunol* 1993; **11**: 191-212
- Linsley PS**, Nadler SG, Bajorath J, Peach R, Leung HT, Rogers J, Bradshaw J, Stebbins M, Leytze G, Brady W, Malacko AR, Marquardt H, Shaw SY. Binding stoichiometry of the cytotoxic T lymphocyte-associated molecule-4. *J Biol Chem* 1995; **270**: 15417-15424
- Lin H**, Bolling SF, Linsley PS. Long-term acceptance of major histocompatibility complex mismatched cardiac allografts induced by CTLA4Ig plus donor-specific transfusion. *J Exp Med* 1993; **178**: 1801-1806
- Frinck BK**, Linsley PS, Wofsy D. Treatment of murine lupus with CTLA4Ig. *Science* 1994; **265**: 1225-1227
- Snider DP**, Kaubisch A, Segal DM. Enhanced antigen immunogenicity induced by bispecific antibodies. *J Exp Med* 1990; **171**: 1957-1963
- Carayanniotis G**, Skea DL, Luscher MA, Barber BH. Adjuvant-independent immunization by immunotargeting antigens to MHC and non-MHC determinants *in vivo*. *Mol Immunol* 1991; **28**: 261-267
- Kawamura H**, Berzofsky JA. Enhancement of antigenic potency *in vitro* and immunogenicity *in vivo* by coupling the antigen to anti-immunoglobulin. *J Immunol* 1986; **136**: 58-65
- Gosselin EJ**, Wardwell K, Gosselin DR, Alter N, Fisher JL, Guyre PM. Enhanced antigen presentation using human Fc gamma receptor (monocyte/macrophage)-specific immunogens. *J Immunol* 1992; **149**: 3477-3481
- Biragyn A**, Tani K, Grimm MC, Weeks S, Kwak LW. Genetic fusion of chemokines to a self tumor antigen induces protective, T-cell dependent antitumor immunity. *Nat Biotechnol* 1999; **17**: 253-258

- 35 **Boyle JS**, Brady JL, Lew AM. Enhanced responses to a DNA vaccine encoding a fusion antigen that is directed to sites of immune induction. *Nature* 1998; **392**: 408-411
- 36 **Huang TH**, Wu PY, Lee CN, Huang HI, Hsieh SL, Kung J, Tao MH. Enhanced antitumor immunity by fusion of CTLA4 to a self tumor antigen. *Blood* 2000; **96**: 3663-3670
- 37 **Xiang R**, Primus FJ, Ruehlmann JM, Niethammer AG, Silletti S, Lode HN, Dolman CS, Gillies SD, Reisfeld RA. A dual-function DNA vaccine encoding carcinoembryonic antigen and CD40 ligand trimer induces T cell-mediated protective immunity against colon cancer in carcinoembryonic antigen-transgenic mice. *J Immunol* 2001; **167**: 4560-4565
- 38 **Steinman RM**, Turley S, Mellman I, Inaba K. The induction of tolerance by dendritic cells that have captured apoptotic cells. *J Exp Med* 2000; **191**: 411-416
- 39 **Chakraborty A**, Li L, Chakraborty NG, Mukherji B. Stimulatory and inhibitory differentiation of human myeloid dendritic cells. *Clin Immunol* 2000; **94**: 88-98
- 40 **Linsley PS**, Greene JL, Brady W, Bajorath J, Ledbetter JA, Peach R. Human B7-1 (CD80) and B7-2 (CD86) bind with similar avidities but distinct kinetics to CD28 and CTLA4 receptors. *Immunity* 1994; **1**: 793-801
- 41 **Deliyannis G**, Boyle JS, Brady JL, Brown LE, Lew AM. A fusion DNA vaccine that targets antigen-presenting cells increases protection from viral challenge. *Proc Natl Acad Sci U S A* 2000; **97**: 6676-6680
- 42 **Lenschow DJ**, Walunas TL, Bluestone JA. CD28/B7 system of T cell costimulation. *Annu Rev Immunol* 1996; **14**: 233-258
- 43 **Chaplin PJ**, De Rose R, Boyle JS, McWaters P, Kelly J, Tennent JM, Lew AM, Scheerlinck JP. Targeting improves the efficacy of a DNA vaccine against *Corynebacterium pseudotuberculosis* in sheep. *Infect Immun* 1999; **67**: 6434-6438

Edited by Ren SY and Wang XL

Enhancement of osteopontin expression in HepG2 cells by epidermal growth factor via phosphatidylinositol 3-kinase signaling pathway

Guo-Xin Zhang, Zhi-Quan Zhao, Hong-Di Wang, Bo Hao

Guo-Xin Zhang, Zhi-Quan Zhao, Hong-Di Wang, Bo Hao, Department of Gastroenterology, the First Affiliated Hospital, Nanjing Medical University, Nanjing 210029, Jiangsu Province, China

Correspondence to: Dr. Guo-Xin Zhang, 300 Guangzhou Road, Department of Gastroenterology, the First Affiliated Hospital, Nanjing Medical University, Nanjing 210029, Jiangsu Province, China. guoxinz2002@yahoo.com

Telephone: +86-25-3718836 **Fax:** +86-25-3724440

Received: 2003-06-21 **Accepted:** 2003-08-16

Abstract

AIM: Osteopontin (OPN) is a phosphorylated glycoprotein with diverse functions including cancer development, progression and metastasis. It is unclear how osteopontin is regulated in HepG2 cells. The aim of this study was to investigate the effect of epidermal growth factor on the expression of osteopontin in HepG2 cells, and to explore the signal transduction pathway mediated this expression.

METHODS: Osteopontin expression was detected by RNAase protection assay and Western blot. Wortmannin, a specific inhibitor of PI3K, was used to see if PI3K signal transduction was involved in the induction of osteopontin gene expression.

RESULTS: HepG2 cells constitutively expressed low levels of osteopontin. Treatment with epidermal growth factor increased osteopontin mRNA and protein level in a dose- and time-dependent manner. Application of wortmannin caused a dramatic reduction of epidermal growth factor-induced osteopontin expression.

CONCLUSION: Osteopontin gene expression can be induced by treatment of HepG2 cells with epidermal growth factor. Epidermal growth factor may regulate osteopontin gene expression through PI3K signaling pathway. Several potential targets in the pathway can be manipulated to block the synthesis of osteopontin and inhibit liver cancer metastasis.

Zhang GX, Zhao ZQ, Wang HD, Hao B. Enhancement of osteopontin expression in HepG2 cells by epidermal growth factor via phosphatidylinositol 3-kinase signaling pathway. *World J Gastroenterol* 2004; 10(2): 205-208

<http://www.wjgnet.com/1007-9327/10/205.asp>

INTRODUCTION

Osteopontin (OPN) is a secreted arginine-glycine-aspartate (RGD)-containing phosphoprotein with cell adhesive and chemotactic properties *in vitro* and *in vivo*^[1-3]. It is closely associated with infiltrating macrophages in tumors and can directly stimulate macrophage migration, which has made it a key target as a molecule likely to be important in mediating tumor metastasis^[4]. It has been shown that osteopontin is up-regulated in many kinds of cancer, including hepatocellular

carcinoma^[5,6], breast cancer^[7-9], prostate cancer^[10,11], ovarian cancer^[12,13], brain cancer^[14,15] and lung cancer^[16]. Elevated osteopontin transcription often correlates with increased metastatic potential of cancers.

Epidermal growth factor (EGF) receptor (EGFR) is a member of the ErbB family of ligand-activated tyrosine kinase receptors, which play a central role in the proliferation, differentiation, and/or oncogenesis of epithelial cells, neural cells, and fibroblasts^[17,18]. It has been reported that EGF can induce osteopontin expression of breast cancer cells^[19], rat kidney epithelial cells^[20] and HL60 cells^[21], and the induction of osteopontin may involve in signaling pathway related to PKC and tyrosine kinase^[22]. The mechanism responsible for osteopontin up-regulation in HCC is unknown, but may involve induction by specific cytokines. We have investigated this hypothesis by testing the effects of epidermal growth factor on osteopontin regulation in hepatocellular carcinoma cell line, HepG2. Using RNase protection assay, Western blot, we found that HepG2 cells constitutively expressed low levels of osteopontin mRNA and protein. EGF is a potent inducer of osteopontin mRNA and protein in HepG2 cells. Wortmannin, a specific PI3-K inhibitor, blocks the EGF-induced OPN expression. Our study suggests that OPN expression induced by EGF is dependent on PI3-K signaling pathway in HepG2 cells.

MATERIALS AND METHODS

Cell line and culture

HepG2 cell line was obtained from Cell Biology Institute (Shanghai, China). Cells were cultured in DMEM (Gibco BRL) containing 10% fetal calf serum (Hyclone).

Induction of growth factor signaling

Cells were plated at 1×10^5 per well in 6-well plates, and were grown overnight. Next morning, the cultures were washed twice with PBS and maintained in serum-free medium (containing 0.05% BSA) for 24 hours. The cells were then stimulated with the indicated amounts of EGF (Sigma) for the indicated time frames before harvesting and analysis.

To assess signal transduction molecules involved in the induction of osteopontin gene expression, the PI3-Kinase inhibitor wortmannin (Calbiochem) was added to the cells. The cells were pretreated with respective inhibitors or vehicle (DMSO) alone for half an hour and then treated in combination with EGF for 8 hours. Preliminary dose-response experiments had defined the concentrations of 100nM wortmannin to be effective and non-toxic.

DNA constructs and *in vitro* transcription

Plasmid pGEM-OPN containing osteopontin fragments was constructed in our laboratory. A 486bp of OPN fragment was obtained by reverse transcription-PCR from plasmid pBlueScript-OPN containing full length human osteopontin (a kind gift from Dr. Chambers, Canada) using the sense primer 5' -ATGGATCCGATGACACTGATGATTCTCAC-3' and

antisense primer 5'-GCGAATTCGAATTCACGGCTGACAAA-3'. The resultant BamHI-EcoRI cDNA fragment was ligated into the vector pGEM, and confirmed by direct sequencing.

To make RNA probes for OPN and β -actin (a linearized plasmid containing β -actin fragment included in the kit), *in vitro* transcription was performed with a commercial kit (Ambion), according to the user's instructions.

RNA isolation and RNase protection assay

Total RNA was isolated using the RNeasy Mini kit (QIAGEN GmbH, Germany). RNase protection assay was performed with a commercial kit (Ambion). α^{32} P-UTP labeled probes were mixed with sample RNA and co-precipitated. Hybridization was proceeded for 10 minutes at 68 °C, followed by digestion with RNase A-T1 for 30 minutes at 37 °C, and separation of hybridized RNA on 5% acrylamide and 8M urea gels. The gels were dried on filter paper for 40 minutes at 80 °C, and exposed to X-ray film. The autoradiographs were scanned using an AlphaImager 2200 spot densitometer (Alpha Innotech Corporation), and the integrated densities of areas were recorded.

Western blot

Cultured cells were lysed in RIPA buffer (50 mM Tris-HCL pH 7.5, 150 mM NaCl, 1% NP-40, 0.5% Na-deoxycholate,

0.1% sodium dodecyl sulfate). Cell lysates were denatured at 100 °C for 5 minutes, and equal amounts of protein were loaded onto 10% SDS-polyacrylamide gels. The separated proteins were transferred to PVDF membranes (ROCHE) and probed with antibodies to osteopontin (Calbiochem). Membranes were stripped and re-probed with antibodies to tubulin as an internal control.

RESULTS

OPN expression in HepG2 cells induced by EGF-treatment

In order to examine the regulators of osteopontin expression in hepatocellular carcinoma cells, HepG2 cells were incubated in serum-free medium and then treated with epidermal growth factor that had been implicated in HCC. As shown in Figures 1 and 2, HepG2 cells constitutively expressed low levels of osteopontin, stimulation of the cells with EGF increased osteopontin mRNA expression as well as protein level in a dose-dependent and time-dependent manner. To quantitate this finding, densitometry of osteopontin mRNA levels was recorded (Figure 1B and Figure 2B). Osteopontin expression was elevated after treatment with EGF within a 8-hour period, expression levels were further increased at 16 hours and 24 hours following treatment.

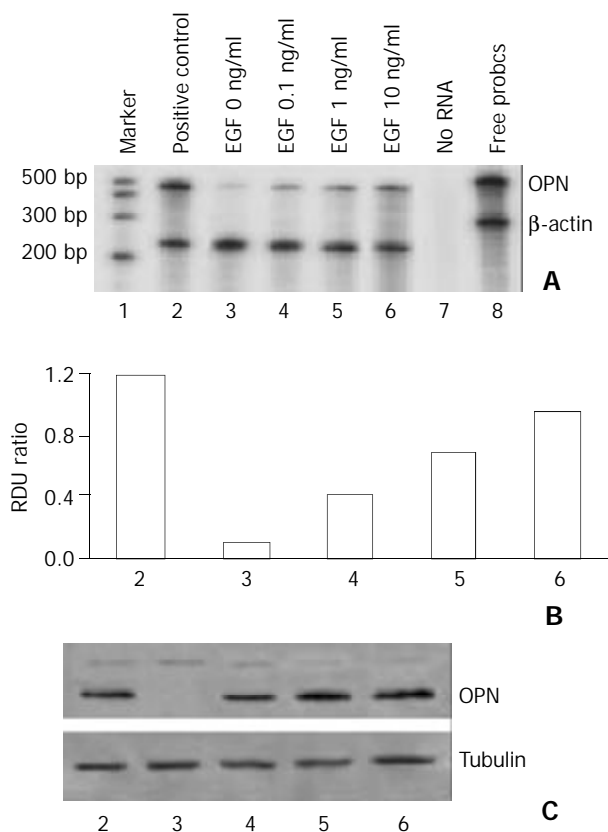


Figure 1 Dose-dependent effect of EGF on osteopontin expression in HepG2 cells. 1×10^5 cells were plated in 6-well plates. Next morning, cell cultures (near 80% confluent) were incubated in serum-free medium for 24 hours. The cells were stimulated dose-dependently by epidermal growth factor. Positive control denotes cells in normal growth medium containing 10% fetal calf serum. A. Osteopontin mRNA level was analyzed by RNase protection assay on total RNA using a 486 base-pair probe and controlling the loading with a probe for β -actin. B. Quantitation of osteopontin mRNA levels is shown in (A). RDU ratio reflects relative density units of osteopontin mRNA divided by β -actin mRNA. C. The results from RNase protection assay were confirmed by Western blot of osteopontin protein. Tubulin was served as loading control.

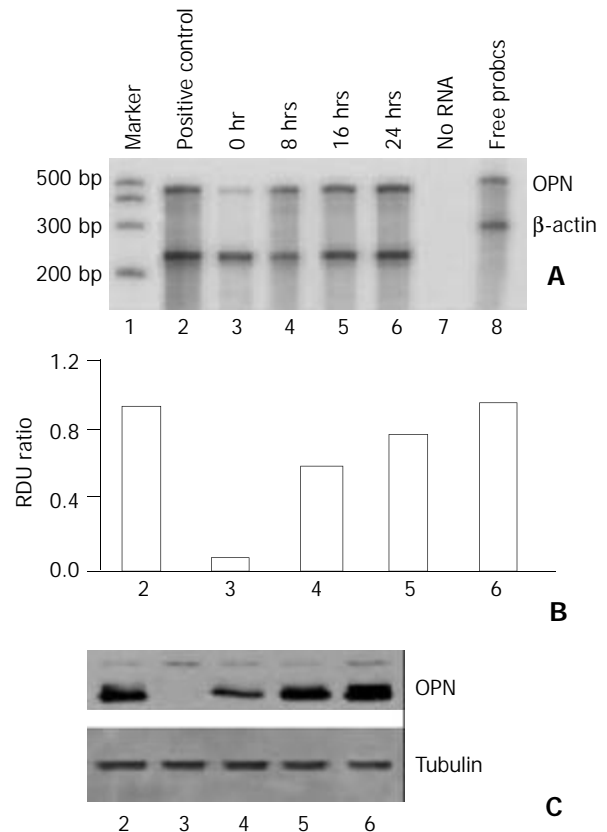


Figure 2 Time course showing effect of EGF on osteopontin expression in HepG2 cells. 1×10^5 cells were plated in 6-well plates. Next morning, cell cultures (near 80% confluent) were incubated in serum-free medium for 24 hours. The cells were stimulated time-dependently by 10 ng/ml EGF. Positive control denotes cells in normal growth medium containing 10% fetal calf serum. A. Osteopontin gene expression was analyzed by RNase protection assay on total RNA using a 486 base pair probe and standardized by comparison to β -actin. B. Quantitation of osteopontin mRNA levels is shown in (A). RDU ratio reflects relative density units of osteopontin mRNA divided by β -actin mRNA. C. Western blot of osteopontin protein by cell lysates confirmed the results from RNase protection assay. Tubulin was served as loading control.

- cancer metastasis. *Clin Cancer Res* 2002; **8**: 61-74
- 8 **Reinholz MM**, Iturria SJ, Ingle JN, Roche PC. Differential gene expression of TGF-beta family members and osteopontin in breast tumor tissue: analysis by real-time quantitative PCR. *Breast Cancer Res Treat* 2002; **74**: 255-269
- 9 **Tuck AB**, Chambers AF. The role of osteopontin in breast cancer: clinical and experimental studies. *J Mammary Gland Biol Neoplasia* 2001; **6**: 419-429
- 10 **Tozawa K**, Yamada Y, Kawai N, Okamura T, Ueda K, Kohri K. Osteopontin expression in prostate cancer and benign prostatic hyperplasia. *Urol Int* 1999; **62**: 155-158
- 11 **Angelucci A**, Festuccia C, D'Andrea G, Teti A, Bologna M. Osteopontin modulates prostate carcinoma invasive capacity through RGD-dependent upregulation of plasminogen activators. *Biol Chem* 2002; **383**: 229-234
- 12 **Kim JH**, Skates SJ, Uede T, Wong Kk KK, Schorge JO, Feltmate CM, Berkowitz RS, Cramer DW, Mok SC. Osteopontin as a potential diagnostic biomarker for ovarian cancer. *JAMA* 2002; **287**: 1671-1679
- 13 **Tiniakos DG**, Yu H, Liapis H. Osteopontin expression in ovarian carcinomas and tumors of low malignant potential (LMP). *Hum Pathol* 1998; **29**: 1250-1254
- 14 **Weber GF**, Ashkar S. Molecular mechanisms of tumor dissemination in primary and metastatic brain cancers. *Brain Res Bull* 2000; **53**: 421-424
- 15 **Ding Q**, Stewart J Jr, Prince CW, Chang PL, Trikha M, Han X, Grammer JR, Gladson CL. Promotion of malignant astrocytoma cell migration by osteopontin expressed in the normal brain: differences in integrin signaling during cell adhesion to osteopontin versus vitronectin. *Cancer Res* 2002; **62**: 5336-5343
- 16 **Zhang J**, Takahashi K, Takahashi F, Shimizu K, Ohshita F, Kameda Y, Maeda K, Nishio K, Fukuchi Y. Differential osteopontin expression in lung cancer. *Cancer Lett* 2001; **171**: 215-222
- 17 **Walker F**, Kato A, Gonez LJ, Hibbs ML, Pouliot N, Levitzki A, Burgess AW. Activation of the ras/mitogen-activated protein kinase pathway by kinase-defective epidermal growth factor receptors results in cell survival but not proliferation. *Mol Cell Biol* 1998; **18**: 7192-7204
- 18 **Zhang K**, Sun J, Liu N, Wen D, Chang D, Thomason A, Yoshinaga SK. Transformation of NIH 3T3 cells by HER3 or HER4 receptors requires the presence of HER1 or HER2. *J Biol Chem* 1996; **271**: 3884-3890
- 19 **Zhang G**, He B, Weber GF. Growth factor signaling induces metastasis genes in transformed cells: molecular connection between akt kinase and osteopontin in breast cancer. *Mol Cell Biol* 2003; **23**: 6507-6519
- 20 **Malyankar UM**, Almeida M, Johnson RJ, Pichler RH, Giachelli CM. Osteopontin regulation in cultured rat renal epithelial cells. *Kidney Int* 1997; **51**: 1766-1773
- 21 **Atkins KB**, Simpson RU, Somerman MJ. Stimulation of osteopontin mRNA expression in HL-60 cells is independent of differentiation. *Arch Biochem Biophys* 1997; **343**: 157-163
- 22 **Chackalaparampil I**, Peri A, Nemir M, Mckee MD, Lin PH, Mukherjee BB, Mukherjee AB. Cells *in vivo* and *in vitro* from osteopetrotic mice homozygous for c-src disruption show suppression of synthesis of osteopontin, a multifunctional extracellular matrix protein. *Oncogene* 1996; **12**: 1457-1467
- 23 **Bosch FX**, Ribes J, Borrás J. Epidemiology of primary liver cancer. *Semin Liver Dis* 1999; **19**: 271-285
- 24 **El-Serag HB**, Mason AC. Rising incidence of hepatocellular carcinoma in the United States. *N Engl J Med* 1999; **340**: 745-750
- 25 **Taylor-Robinson SD**, Foster GR, Arora S, Hargreaves S, Thomas HC. Increase in primary liver cancer in the UK, 1979-94. *Lancet* 1997; **350**: 1142-1143
- 26 **Yuki K**, Hirohashi S, Sakamoto M, Kanai T, Shimosato Y. Growth and spread of hepatocellular carcinoma: A review of 240 consecutive autopsy cases. *Cancer* 1990; **66**: 2174-2179
- 27 **Genda T**, Sakamoto M, Ichida T, Asakura H, Kojiro M, Narumiya S, Hirohashi S. Cell motility mediated by rho and Rho-associated protein kinase plays a critical role in intrahepatic metastasis of human hepatocellular carcinoma. *Hepatology* 1999; **30**: 1027-1036
- 28 **Weber GF**. The metastasis gene osteopontin: a candidate target for cancer therapy. *Biochim Biophys Acta* 2001; **1552**: 61-85
- 29 **Oates AJ**, Barraclough R, Rudland PS. The identification of osteopontin as a metastasis-related gene product in a rodent mammary tumor model. *Oncogene* 1996; **13**: 97-104
- 30 **Denhardt DT**, Mistretta D, Chambers AF, Krishna S, Porter JF, Raghuram S, Rittling SR. Transcriptional regulation of osteopontin and the metastatic phenotype: evidence for a Ras-activated enhancer in the human OPN promoter. *Clin Exp Metastasis* 2003; **20**: 77-84
- 31 **Denhardt DT**, Guo X. Osteopontin: a protein with diverse functions. *FASEB J* 1993; **7**: 1475-1482
- 32 **Laverdure GR**, Banerjee D, Chackalaparampil I, Mukherjee BB. Epidermal and transforming growth factors modulate secretion of a 69 kDa phosphoprotein in normal rat kidney fibroblasts. *FEBS Lett* 1987; **222**: 261-265
- 33 **Pianetti S**, Arsura M, Romieu-Mourez R, Coffey RJ, Sonenshein GE. Her-2/neu overexpression induces NF-kappaB via a PI3-kinase/Akt pathway involving calpain-mediated degradation of I-kappaB-alpha that can be inhibited by the tumor suppressor PTEN. *Oncogene* 2001; **20**: 1287-1299

Edited by Zhang JZ and Wang XL

Genetic detection of Chinese hereditary nonpolyposis colorectal cancer

Long Cui, Hei-Ying Jin, Hui-Yu Cheng, Yu-Di Yan, Rong-Gui Meng, De-Hong Yu

Long Cui, Hei-Ying Jin, Hui-Yu Cheng, Rong-Gui Meng, De-Hong Yu, Department of Colorectal Surgery, Changhai Hospital, The Second Military Medical University, Shanghai 200433, China
Yu-Di Yan, Department of Colorectal Surgery, Gansu People's Hospital, Lanzhou 730000, Gansu Province, China

Supported by the National Natural Science Foundation of China, No. 30170927

Correspondence to: Dr. Long Cui, Department of Colorectal Surgery, Changhai Hospital, The Second Military Medical University, 174 Changhai Road, Shanghai 200433, China. cuilongdr@yahoo.com

Telephone: +86-21-25072073 **Fax:** +86-21-65492727

Received: 2003-06-04 **Accepted:** 2003-07-30

Abstract

AIM: To explore the germline mutations of the two main DNA mismatch repair genes (*hMSH2* and *hMLH1*) between patients with hereditary non-polyposis colorectal cancer (HNPCC) and suspected (atypical) HNPCC.

METHODS: Genomic DNA was extracted from the peripheral blood of the index patient of each family, and germline mutations of *hMSH2* and *hMLH1* genes were detected by PCR-single strand conformation polymorphism (PCR-SSCP) and DNA sequencing techniques.

RESULTS: For PCR-SSCP analysis, 67% (4/6) abnormal exons mobility in typical group and 33% (2/6) abnormal exons mobility in atypical group were recognized. In direct DNA sequencing, 50% (3/6) mutation of MMR genes in typical group and 33% (2/6) mutation of MMR genes in atypical group were found, and 4/6 (66.67%) and 1/6 (16.67%) mutations of *hMSH2* and *hMLH1* were identified in typical HNPCC and atypical HNPCC, respectively.

CONCLUSION: Mutation detection of the patients is of benefit to the analysis of HNPCC and, PCR-SSCP is an effective strategy to detect the mutations of HNPCC equivalent to direct DNA sequence. It seems that there exist more complicated genetic alterations in Chinese HNPCC patients than in Western countries.

Cui L, Jin HL, Cheng HY, Yan YD, Meng RG, Yu DH. Genetic detection of Chinese hereditary nonpolyposis colorectal cancer. *World J Gastroenterol* 2004; 10(2): 209-213

<http://www.wjgnet.com/1007-9327/10/209.asp>

INTRODUCTION

Hereditary nonpolyposis colorectal cancer (HNPCC) is characterized by early onset of colorectal cancer, location of tumors in the proximal colon, and an increased risk of neoplasms of extracolonic organs, including endometrium, stomach, urothelium, small intestine, and ovary^[1-6]. The International Collaborative Group on HNPCC (ICG-HNPCC) proposed a set of clinical diagnostic criteria (Amsterdam Criteria I) for HNPCC in 1990 and has revised them recently

(Amsterdam Criteria II) to provide a uniformity in collaborative studies^[7,8]. According to these criteria, there should have at least three patients in two consecutive generations who had colorectal cancer or the other extracolonic malignancies including endometrial cancer, small bowel cancer, cancer of the ureter and cancer of the renal pelvis. One of them should be a first-degree relative of the other two, one cancer should be diagnosed before age 50, and familial adenomatous polyposis (FAP) should be excluded. In Asia, on the other hand, the Japan Research Society for Cancer of the Colon and Rectum developed the clinical criteria (Japanese criteria) for HNPCC in 1991^[9]. According to these criteria, at least two relatives in at least two successive generations should have colorectal cancer, and one of them should be a first-degree relative of the other, also, we called them atypical HNPCC.

Nevertheless, according to those criteria above, all families that are diagnosed as having HNPCC are identified on the basis of a family history of colorectal or other certain malignancies. Sometimes the accuracy and reliability of the family history provided by patients themselves and their relatives or recorded by physicians are questionable, as there is much variability for the family history. Therefore, the requirements for establishing objective strategies to identify this disease are imperative. In the last decade, the progress in genetic study that DNA mismatch repair genes have been identified as being mutated in HNPCC including *hMSH2*, *hMLH1*, *hPMS1*, *hPMS2*, and *hMSH6* makes it possible to identify the cohort of patients through genetic test. Totally, these genes are now believed to account for about 50%-70% of all families with HNPCC and over 90% of the identified mutations focused on the two genes, *hMSH2* and *hMLH1*^[10-18]. There are many studies about the procedures of genetic testing of HNPCC, such as microsatellite instability (MSI), PCR-SSCP, immunohistochemistry (IHC) and direct DNA sequencing^[19-24]. However, much knowledge and a higher grade of technical development are required, before this strategy becomes applicable to the general population.

It has no doubt that there is a large population of HNPCC in China^[25,26]. Unfortunately, there have been few reports about clinical and genetic characteristics of HNPCC^[27]. In this study, six HNPCC families and six atypical HNPCC families were enrolled and, the germline mutations of *hMSH2* and *hMLH1* in the index patients from each family were investigated.

MATERIALS AND METHODS

Subjects

The project was approved by the Institutional Review Board and informed consent was obtained from each participant before the procedures were carried out. Personal and family cancer history was obtained from the proband and participating relatives, and cancer diagnosis and deaths were confirmed by review of medical records, pathological reports or death certificates. Families were identified by the Amsterdam or Japanese criteria for HNPCC. Patients and families were classified as the HNPCC group according to the Amsterdam criteria, suspected HNPCC group according to the Japanese criteria and control group without any family history.

Genetic testing

Preparation of peripheral blood samples and DNA amplification Genetic analysis was performed on a blood specimen from the proband in each family. Specimens were collected and immediately frozen in liquid nitrogen. DNA was extracted from blood specimens using the Wizard genomic purification kit (Qiagen, Shanghai) according to the manufacturer's instructions. Each of the exons from hMSH2 and hMLH1 genes was amplified by polymerase chain reaction (PCR). Next, the samples were heat-treated at 95 °C for 5 minutes to inactivate the enzyme, and used as the template DNA. All DNA amplification was performed in a 50 µl volume containing 100 ng template DNA, 10⁻³ M Tris-HCl (pH 8.9), 50⁻³M KCl, 2.5 mM MgCl₂, 0.2⁻³M of each dNTP, 10 pmol each primer, and 1U Taq polymerase was subjected to 35 PCR cycles (5 mins at 94 °C, 40 s at 94 °C, 60 s at 55 °C, and 40 s at 72 °C). Oligonucleotide sequences were designed from the sequences published in Genbank.

PCR-SSCP analysis and direct sequencing

Single-strand conformation polymorphism (SSCP) The technique of single-strand conformational polymorphism (SSCP) was used to identify mutations in the mismatch repair genes^[28,29]. Each exon of *hMSH2* and *hMLH1* was amplified specifically using PCR (details of oligonucleotide sequences and conditions are available from the authors). PCR products were electrophoresed on 10% non-denaturing polyacrylamide gels with an acrylamide: bisacrylamide ratio of 30:0.8 at 70volt for 12 h at room temperature. DNA was detected by silver staining according to the methods described by others. Those single stranded DNAs that took up an altered conformation appeared as aberrantly migrating bands on the electrophoresis gel.

Direct sequencing

The nucleotide sequence of PCR products showing an abnormal mobility on SSCP was determined by direct sequencing. The PCR products were purified with 1.5% low melted point agarose, and then performed using automated DNA

sequencer. Sequence alterations with an allele frequency of at least 5% were considered as normal variants (polymorphisms) and not reported.

Statistical analysis

The genetic differences of the typical HNPCC groups and the suspected HNPCC groups were analyzed for statistical significance using the chi square test. $P < 0.05$ was considered statistically significant.

RESULTS

Results of genetic testing

Characterization of the variants of PCR-SSCP and DNA sequencing analysis found in the 12 families/individuals in the study is presented in Table 1. A total of seven abnormal motilities were identified in PCR-SSCP including five in typical group and two in atypical group (part of PCR-SSCP analysis is shown in Figure 1). DNA sequencing found 6/7 (85.7%) abnormal motilities of PCR-SSCP, which were proven to be pathogenic germline mutations of *hMSH2* and *hMLH1*. The other abnormal mobility, an "A" insertion in *hMLH1* intron 10 occurred in the C10-1 patient, was proven to be polymorphism.

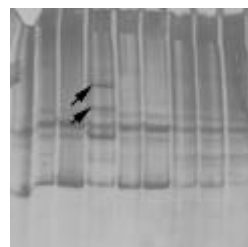


Figure 1 Results of PCR-SSCP in C13 family (*hMSH2*-exon11). Arrow shows the abnormal mobility.

Totally, five patients were found to harbor MMR gene mutations in the direct DNA sequencing. Three of six (50%)

Table 1 Characterization of variants in PCR-SSCP and sequence detection

Family	Abnormal mobility	DNA change	Mutation	Group
C4-1	<i>hMLH1</i> exon18 <i>hMSH2</i> exon15	T insert in 2 081 C insert in 2 469 G insert in 2 471	Frameshift Frameshift Frameshift	Typical HNPCC
C13-1	<i>hMSH2</i> exon11	T insert in 1 760 A→C missense in 1 688	Frameshift Tyr563Ser	Typical HNPCC
C11-1	<i>hMSH2</i> exon13	T to A missense in 2 091	Cys697	Typical HNPCC
C1-1	<i>hMLH1</i> exon11	A insert in 934	Terminator Condon Frameshift	Atypical HNPCC
C8-2	<i>hMLH1</i> exon12	C to G missense in 1 198 C to G missense in 1 261 C insert in 1 364 and 1 372	Leu400Val Val421Leu Frameshift	Atypical HNPCC
C10-1	<i>hMLH1</i> intron10	-	Polymorphism	Typical HNPCC

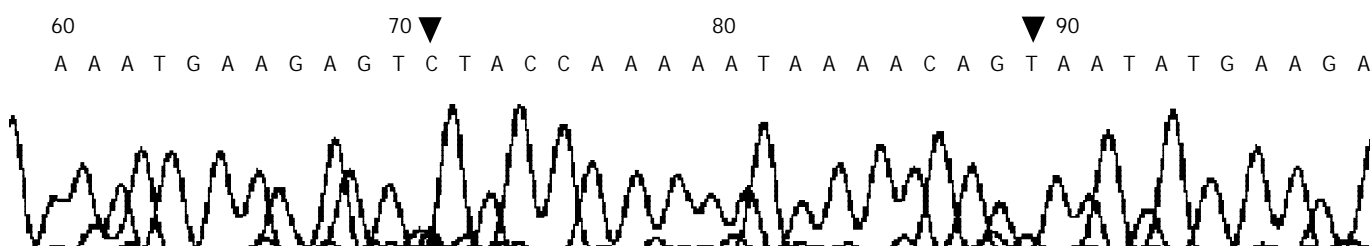


Figure 2 Results of direct sequencing of exon 11 of *hMSH2* in C13 family (A to C substitution in 1 688 and T insertion in 1 706).

patients with HNPCC and 2/6 (33%) patients with suspected HNPCC were found to harbor mutations. However, we found the mutations were complicated as the total number of mutations was more than five and all the mutations we found were novel and of unknown pathogenicity (part of sequence analysis is shown in Figure 2).

In typical HNPCC, the germline mutation of *hMLH1* and *hMSH2* was detected in 3 of 6 HNPCC families. Seven novel mutations were found in 3 exons of *hMSH2* and 1 exon of *hMLH1*, two mutations were detected at 11 exons of *hMSH2* in C13 family, one was the frame shift mutation resulted from an insertion of "T" at 1 760 so that a terminate cordon appeared ahead, the other was "A to C" missense mutation at 1 688 leading to Tyr-Ser substitution. A "T to A" substitution at 2 091 of exon 13 of *hMSH2* in C11 family resulted in a terminate cordon at 697. The mutations in C4 family were worthy of specific comment, as the mutation occurred in *hMLH1* as well as *hMSH2*, there was a frame shift mutation resulted from an insertion of T at 2 081 of exon 18 of *hMLH1*, there were "C, G" inserts at 2 469, 2 471 respectively. However, all families without germline *hMSH2* and *hMLH1* mutations were combined with extracolonic tumors.

In atypical HNPCC, only the germline mutation of *hMLH1* was detected in 2 of 6 HNPCC families, one was the frame shift mutation in exon 11 resulted from an insertion of "A" at 934 in C13 family. In C8 family, the mutation occurred at four locations, one was "C to G" missense mutation at 1 198 leading to Leu400Val substitution, one was "C to G" missense mutation at 1 261 leading to Val421Leu substitution and the other two shift mutations occurred at 1 364 and 1 372 resulted from the A insertion at the two locations respectively. The detailed results of sequencing are shown in Table 2.

Table 2 Comparison of two kinds of HNPCC with PCR-SSCP and sequencing

	Typical HNPCC (n=6)	Atypical HNPCC (n=6)	P
PCR-SSCP	4 (67%)	2 (33%)	0.269
Sequencing	3 (50%)	2 (33%)	0.575

DISCUSSION

To date, HNPCC is defined either by the so-called Amsterdam I+II criteria or by detection of a mutation in one of the mismatch repair genes. Once the positive mutation is identified, predictive testing of family members at risk is available. Screening recommendations for clinically identified families, mutation carriers, and their unaffected relatives at risk must be defined for clinical management^[30].

Recently, Watson *et al.*^[31] published their results about that carrier risk status changes resulted from mutation testing in hereditary non-polyposis colorectal cancer and hereditary breast-ovarian cancer. They concluded that mutation testing could raise the accuracy of carrier risk assessments, and lower the number of persons at high carrier risk. The most common risk assessment change resulted from DNA testing was a change from those at risk to non-carriers. To the extent that these persons were aware of their carrier risk and were obtaining heightened cancer surveillance test, this could be expected to lead to a reduced emotional toll and a reduced pressure on limited medical resources.

A better understanding of the molecular basis of hereditary colorectal cancer syndromes such as hereditary nonpolyposis colorectal cancer syndrome (HNPCC) and familial adenomatous polyposis (FAP) would have profound consequences for both the diagnosis and (prophylactic) treatment of (pre)malignant neoplastic lesions^[32] Clinically, when we see a patient with

colorectal cancer with a family history of suspected HNPCC, we need to work out our surgical strategies for this patient, the same as we do for the patients with HNPCC, in whom colonoscopy surveillance or prophylaxis surgeries such as subtotal colectomy are needed. One of the evidences of special surgical treatment has been found to be genetic detection^[33,34]. Since HNPCC is resulted from the dysfunction of mismatch repair genes and some reports indicated that mutation of *hMSH2* and *hMLH1* accounted for 40%-70% HNPCC^[35-39], we decided to detect the germline mutation of *hMSH2* and *hMLH1* in this study. In PCR-SSCP analysis of genomic DNA of 12 probands, we identified seven abnormal mobilities, five in typical HNPCC and two in suspected HNPCC and six of them were testified to be mutations by DNA sequencing. When we compared the genetic investigation of two groups we studied, we also concluded that there were no statistical differences in the results of both PCR-SSCP and direct sequence.

We also found that the mutations occurred both in typical HNPCC group and in atypical HNPCC group. Beck *et al.* found germline HNPCC mutations in six families in which none fulfilled the Amsterdam criteria. They highlighted that if germline mutations of the mismatch repair genes were common in families with features of HNPCC, but not fulfilling the Amsterdam criteria, then it was very important that all such families were also referred to cancer clinics for assessment and possible genetic testing^[40]. It was suggested that many suspected HNPCC patients might not be recognized and might be excluded from genetic counseling^[41,42].

Upon reviewing the literature and checking the variants registried in the ICG-HNPCC mutation database (<http://www.nfdht.nl>), we found that all the mutations were novel. It is rarely reported that there exist multiple mutations in the same exons. However, it seemed to be common in our analysis, two mutations were found at 11 exons of *hMSH2* in C13 family and C8 family. The mutation occurred at four locations, one was "C to G" missense mutation at 1 198 leading to Leu400Val substitution, one was "C to G" missense mutation at 1 261 leading to Val421Leu substitution and the other two shift mutations occurred at 1 364 and 1 372 resulted from the A insertion at the two locations, respectively. Furthermore, it is the first report that the mutation occurred in both *hMLH1* and *hMSH2* in C4 family.

Several techniques for genetic detection of HNPCC have been developed including MSI, immunohistochemistry, SSCP, denaturing gradient gel electrophoresis (DGGE) and sequencing. SSCP was considered inefficient in detecting mutations^[43,44] and was expected to miss approximately 20% of point and frameshift mutations. Furthermore, it was unable to detect the whole exon deletions, which occurred in some HNPCC families^[45]. We chose SSCP first because it was relatively simple, quick and cheap, and did not require special apparatus. In our study, 12 abnormal bands found in SSCP were proven to represent 11 mutations (91.7%). We found it was a practical procedure for the genetic screening of HNPCC.

Given the limitations of current techniques, direct PCR product sequencing analysis is more efficient for detecting mutations, but it is laborious, more expensive in term of reagents and data analysis time and not 100% efficient. It is much more acceptable clinically to take the screening techniques, such as SSCP, first and use sequencing to analyze the details of the mutation. Recently, some studies demonstrated that large genomic rearrangements accounted for 10%-20% of all *hMSH2* mutations, and a lower proportion of all *hMLH1* mutations. Nakagawa^[46] used the multiplex ligation-dependent probe amplification (MLPA) method to screen *hMSH2* and *hMLH1* deletions in 70 patients whose colorectal or endometrial tumors were MSI positive, yet no mutation was found by genomic exon-by-exon sequencing of *hMSH2*, *hMLH1*, and *hMSH6*. They

identified five candidates with four different hMSH2 deletions and one candidate with an hMLH1 deletion.

In summary, our study demonstrates that the Amsterdam criteria are important but inappropriate for the establishment of diagnosis, some atypical families not fulfilling all the Amsterdam criteria probably possess the similar genetic alterations. We conclude that the mutation detection of patients is of benefit to the analysis of HNPCC and, PCR-SSCP is as effective as direct DNA sequence in detecting the mutations of HNPCC. Furthermore, it seems that there exist more complicated genetic alterations in Chinese HNPCC patients than in Western countries.

However, there are also some cases without any mutation, further investigations should be carried out such as detection of other mismatch repair genes as well as detection of gene methylation of hMLH1.

REFERENCES

- Lynch HT, Lynch JF. Hereditary nonpolyposis colorectal cancer. *Semin Surg Oncol* 2000; **18**: 305-313
- Vasen HF, Watson P, Mecklin JP, Jass JR, Green JS, Nomizu T, Muller H, Lynch HT. The epidemiology of endometrial cancer in hereditary nonpolyposis colorectal cancer. *Anticancer Res* 1994; **14**(4B): 1675-1678
- Jass JR. Pathology of hereditary nonpolyposis colorectal cancer. *Ann N Y Acad Sci* 2000; **910**: 62-73; 73-74
- Vasen HF, Sanders EA, Taal BG, Nagengast FM, Griffioen G, Menko FH, Kleibeuker JH, Houwing-Duistermaat JJ, Meera Khan P. The risk of brain tumours in hereditary non-polyposis colorectal cancer (HNPCC). *Int J Cancer* 1996; **65**: 422-425
- Song YM, Zheng S. Analysis for phenotype of HNPCC in China. *World J Gastroenterol* 2002; **8**: 837-840
- Dunlop MG, Farrington SM, Carothers AD, Wyllie AH, Sharp L, Burn J, Liu B, Kinzler KW, Vogelstein B. Cancer risk associated with germline DNA mismatch repair gene mutations. *Hum Mol Genet* 1997; **6**: 105-110
- Vasen HF, Mecklin JP, Khan PM, Lynch HT. The International Collaborative Group on HNPCC. *Anticancer Res* 1994; **14**(4B): 1661-1664
- Vasen HF, Watson P, Mecklin JP, Lynch HT. New clinical criteria for hereditary nonpolyposis colorectal cancer (HNPCC, Lynch syndrome) proposed by the International Collaborative group on HNPCC. *Gastroenterology* 1999; **116**: 1453-1456
- Fujita S, Moriya Y, Sugihara K, Akasu T, Ushio K. Prognosis of hereditary nonpolyposis colorectal cancer (HNPCC) and the role of Japanese Criteria for HNPCC. *Jpn J Oncol* 1996; **26**: 351-355
- Lynch HT, Lynch JF. The Lynch Syndrome: Melding natural history and molecular genetics to genetic counseling and cancer control. *Cancer Control* 1996; **3**: 13-19
- Peltomaki P, Aaltonen L, Sistonen P, Pylkkanen L, Mecklin J-P, Jarvinen H, Green JS, Jass JR, Weber JL, Leach FS, Petersen GM, Hamilton SR, de la Chapelle A, Vogelstein B. Genetic mapping of a locus predisposing to human colorectal cancer. *Science* 1993; **260**: 810-812
- Leach FS, Nicolaides NC, Papadopoulos N, Liu B, Jen J, Parsons R, Peltomaki P, Sistonen P, Aaltonen LA, Nystrom-Lahti M, Guan XY, Zhang J, Metzler PS, Yu JW, Kao FT, Chen DJ, Cerosaletti KM, Fournier REK, Todd S, Lewis T, Leach RJ, Naylor SL, Weissbach J, Mecklin JP, Jarvinen H, Petersen GM, Hamilton SR, Green J, Jass J, Watson P, Lynch HT, Trent JM, de la Chapelle A, Kinzler KW, Vogelstein B. Mutations of a mutS homolog in hereditary nonpolyposis colorectal cancer. *Cell* 1993; **75**: 1215-1225
- Fishel R, Lescoe MK, Rao MR, Copeland NG, Jenkins NA, Garber J, Kane M, Kolodner R. The human mutator gene homolog MSH2 and its association with hereditary nonpolyposis colon cancer. *Cell* 1993; **75**: 1027-1038
- Nicolaides NC, Papadopoulos N, Liu B, Wei YF, Carter KC, Ruben SM, Rosen CA, Haseltine WA, Fleischmann RD, Fraser CM, Adams MD, Venter JC, Dunlop MG, Hamilton SR, Petersen GM, de la Chapelle A, Vogelstein B, Kinzler KW. Mutations of two PMS homologs in hereditary nonpolyposis colon cancer. *Nature* 1994; **371**: 75-80
- Nystrom-Lahti M, Parsons R, Sistonen P, Pylkkanen L, Aaltonen LA, Leach FS, Hamilton SR, Watson P, Bronson E, Fusaro R. Mismatch repair genes on chromosomes 2p and 3p account for a major share of hereditary nonpolyposis colorectal cancer families evaluable by linkage. *Am J Hum Genet* 1994; **55**: 659-665
- Papadopoulos N, Nicolaides NC, Wei YF, Ruben SM, Carter KC, Rosen CA, Haseltine WA, Fleischmann RD, Fraser CM, Adams MD. Mutation of a mutL homolog in hereditary colon cancer. *Science* 1994; **263**: 1625-1629
- Bronner CE, Baker SM, Morrison PT, Warren G, Smith LG, Lescoe MK, Kane M, Earabino C, Lipford J, Lindblom A. Mutation in the DNA mismatch repair gene homologue hMLH1 is associated with hereditary non-polyposis colon cancer. *Nature* 1994; **368**: 258-261
- Peltomaki P, de la Chapelle A. Mutations predisposing to hereditary nonpolyposis colorectal cancer. *Adv Cancer Res* 1997; **71**: 93-119
- Wijnen J, Vasen H, Khan PM, Menko FH, van der Klift H, van Leeuwen C, van den Broek M, van Leeuwen-Cornelisse I, Nagengast F, Meijers-Heijboer A. Seven new mutations in hMSH2, an HNPCC gene, identified by denaturing gradient-gel electrophoresis. *Am J Hum Genet* 1995; **56**: 1060-1066
- Ikenaga M, Tomita N, Sekimoto M, Ohue M, Yamamoto H, Miyake Y, Mishima H, Nishisho I, Kikkawa N, Monden M. Use of microsatellite analysis in young patients with colorectal cancer to identify those with hereditary nonpolyposis colorectal cancer. *J Surg Oncol* 2002; **79**: 157-165
- Merkelbach-Bruse S, Kose S, Losen I, Bosserhoff AK, Buettner R. High throughput genetic screening for the detection of hereditary non-polyposis colon cancer (HNPCC) using capillary electrophoresis. *Comb Chem High Throughput Screen* 2000; **3**: 519-524
- Holinski-Feder E, Muller-Koch Y, Friedl W, Moeslein G, Keller G, Plaschke J, Ballhausen W, Gross M, Baldwin-Jedele K, Jungck M, Mangold E, Vogelsang H, Schackert HK, Lohse P, Murken J, Meitinger T. DHPCL mutation analysis of the hereditary nonpolyposis colon cancer (HNPCC) genes hMLH1 and hMSH2. *J Biochem Biophys Methods* 2001; **47**: 21-32
- Kurzawski G, Safranow K, Suchy J, Chlubek D, Scott RJ, Lubinski J. Mutation analysis of MLH1 and MSH2 genes performed by denaturing high-performance liquid chromatography. *J Biochem Biophys Methods* 2002; **51**: 89-100
- Wahlberg SS, Schmeits J, Thomas G, Loda M, Garber J, Syngal S, Kolodner RD, Fox E. Evaluation of microsatellite instability and immunohistochemistry for the prediction of germ-line MSH2 and MLH1 mutations in hereditary nonpolyposis colon cancer families. *Cancer Res* 2002; **62**: 3485-3492
- Cai SJ, Xu Y, Cai GX, Lian P, Guan ZQ, Mo SJ, Sun MH, Cai Q, Shi DR. Clinical characteristics and diagnosis of patients with hereditary nonpolyposis colorectal cancer. *World J Gastroenterol* 2003; **9**: 284-287
- Cai Q, Sun MH, Lu HF, Zhang TM, Mo SJ, Xu Y, Cai SJ, Zhu XZ, Shi DR. Clinicopathological and molecular genetic analysis of 4 typical Chinese HNPCC families. *World J Gastroenterol* 2001; **7**: 805-810
- Beck NE, Tomlinson IP, Homfray T, Frayling I, Hodgson SV, Harocopos C, Bodmer WF. Use of SSCP analysis to identify germline mutations in HNPCC families fulfilling the Amsterdam criteria. *Hum Genet* 1997; **99**: 219-224
- Viel A, Genuardi M, Capozzi E, Leonardi F, Bellacosa A, Paravatou-Petsotas M, Pomponi MG, Fornasari M, Percesepe A, Roncucci L, Tamassia MG, Benatti P, Ponz de Leon M, Valenti A, Covino M, Anti M, Foletto M, Boiocchi M, Neri G. Characterization of MSH2 and MLH1 mutations in Italian families with hereditary nonpolyposis colorectal cancer. *Genes Chromosomes Cancer* 1997; **18**: 8-18
- Moslein G. Clinical implications of molecular diagnosis in hereditary nonpolyposis colorectal cancer. *Recent Results Cancer Res* 2003; **162**: 73-78
- Watson P, Narod SA, Fodde R, Wagner A, Lynch JF, Tinley ST, Snyder CL, Coronel SA, Riley B, Kinarsky Y, Lynch HT. Carrier risk status changes resulting from mutation testing in hereditary non-polyposis colorectal cancer and hereditary breast-ovarian cancer. *J Med Genet* 2003; **40**: 591-596

- 31 **Church JM.** Prophylactic colectomy in patients with hereditary nonpolyposis colorectal cancer. *Ann Med* 1996; **28**: 479-482
- 32 **Hanna NN, Mentzer RM Jr.** Molecular genetics and management strategies in hereditary cancer syndromes. *J Ky Med Assoc* 2003; **101**: 100-107
- 33 **Lynch HT, Watson P, Shaw TG, Lynch JF, Harty AE, Franklin BA, Kapler CR, Tinley ST, Liu B, Lerman C.** Clinical impact of molecular genetic diagnosis, genetic counseling, and management of hereditary cancer. Part II: Hereditary nonpolyposis colorectal carcinoma as a model. *Cancer* 1999; **86**(11 Suppl): 2457-2463
- 34 **Boland CR.** Molecular genetics of hereditary nonpolyposis colorectal cancer. *Ann N Y Acad Sci* 2000; **910**: 50-61
- 35 **Jacob S, Praz F.** DNA mismatch repair defects: role in colorectal carcinogenesis. *Biochimie* 2002; **84**: 27-47
- 36 **Bocker T, Ruschoff J, Fishel R.** Molecular diagnostics of cancer predisposition: hereditary non-polyposis colorectal carcinoma and mismatch repair defects. *Biochim Biophys Acta* 1999; **1423**: 1-10
- 37 **Planck M, Koul A, Fernebro E, Borg A, Kristoffersson U, Olsson H, Wenngren E, Mangell P, Nilbert M.** hMLH1, hMSH2 and hMSH6 mutations in hereditary non-polyposis colorectal cancer families from southern Sweden. *Int J Cancer* 1999; **83**: 197-202
- 38 **Kruger S, Plaschke J, Jeske B, Gorgens H, Pistorius SR, Bier A, Kreuz FR, Theissig F, Aust DE, Saeger HD, Schackert HK.** Identification of six novel MSH2 and MLH1 germline mutations in HNPCC. *Hum Mutat* 2003; **21**: 445-446
- 39 **Beck NE, Tomlinson IP, Homfray T, Hodgson SV, Harocopus CJ, Bodmer WF.** Genetic testing is important in families with a history suggestive of hereditary non-polyposis colorectal cancer even if the Amsterdam criteria are not fulfilled. *Br J Surg* 1997; **84**: 233-237
- 40 **Wang Q, Desseigne F, Lasset C, Saurin JC, Navarro C, Yagci T, Keser I, Bagci H, Luleci G, Gelen T, Chayvialle JA, Puisieux A, Ozturk M.** Prevalence of germline mutations of hMLH1, hMSH2, hPMS1, hPMS2, and hMSH6 genes in 75 French kindreds with nonpolyposis colorectal cancer. *Hum Genet* 1999; **105**: 79-85
- 41 **Wagner A, Hendriks Y, Meijers-Heijboer EJ, de Leeuw WJ, Morreau H, Hofstra R, Tops C, Bik E, Brocker-Vriends AH, van Der Meer C, Lindhout D, Vasen HF, Breuning MH, Cornelisse CJ, van Krimpen C, Niermeijer MF, Zwinderman AH, Wijnen J, Fodde R.** Atypical HNPCC owing to MSH6 germline mutations: analysis of a large Dutch pedigree. *J Med Genet* 2001; **38**: 318-322
- 42 **Moslein G, Pistorius S, Saeger HD, Schackert HK.** Preventive surgery for colon cancer in familial adenomatous polyposis and hereditary nonpolyposis colorectal cancer syndrome. *Langenbecks Arch Surg* 2003; **388**: 9-16
- 43 **Syngal S, Fox EA, Eng C, Kolodner RD, Garber JE.** Sensitivity and specificity of clinical criteria for hereditary non-polyposis colorectal cancer associated mutations in MSH2 and MLH1. *J Med Genet* 2000; **37**: 641-645
- 44 **Liu B, Parsons R, Papadopoulos N, Nicolaidis NC, Lynch HT, Watson P, Jass JR, Dunlop M, Wyllie A, Peltomaki P, de la Chapelle A, Hamilton SR, Vogelstein B, Kinzler KW.** Analysis of mismatch repair genes in hereditary non-polyposis colorectal cancer patients. *Nat Med* 1996; **2**: 169-174
- 45 **Nakagawa H, Hampel H, Chapelle Ad Ade L.** Identification and characterization of genomic rearrangements of MSH2 and MLH1 in Lynch syndrome (HNPCC) by novel techniques. *Hum Mutat* 2003; **22**: 258

Edited by Ma JY and Wang XL

Expression of estrogen receptor β in human colorectal cancer

Li-Qun Xie, Jie-Ping Yu, He-Sheng Luo

Li-Qun Xie, Jie-Ping Yu, He-Sheng Luo, Department of Gastroenterology Renmin Hospital, Wuhan University, Wuhan 430060, Hubei Province, China

Correspondence to: Jie-Ping Yu, Department of Gastroenterology, Renmin Hospital, Wuhan University, 283 Jie-Fang Road, Wuhan 430060, Hubei Province, China. xieliquan1966@sohu.com

Received: 2003-05-13 **Accepted:** 2003-06-07

Abstract

AIM: To determine the expression of estrogen receptor (ER) β in Chinese colorectal carcinoma (CRC) patients.

METHODS: ER β expression in CRC was investigated by immunohistochemical staining of formalin-fixed, paraffin-embedded tissue sections from 40 CRCs, 10 colonic adenomas, and 10 normal colon mucosa biopsies. The percentage of positive cells was recorded, mRNA expression of ER α and ER β in 12 CRC tissues and paired normal colon tissues were detected by RT-PCR.

RESULTS: Positive ER immunoreactivity was present in part of normal epithelium of biopsy (2/10), adenomas (3/10), and the sections of CRC tissue, most of them were nuclear positive. In CRCs, nuclear ER β immunoreactivity was detected in over 10% of the cancer cells in 57.5% of the cases and was always associated with cytoplasmic immunoreactivity. There was no statistical significance between ER β positive and negative groups in regard to depth of invasion and nodal metastases. Of the 12 CRC tissues and paired normal colon tissues, the expression rate of ER α mRNA in CRC tissue and corresponding normal colon tissue was 25% and 16.6%, respectively. ER β mRNA was expressed in 83.3% CRC tissue and 91.7% paired normal colon tissue, respectively. There was no significant difference in ER β mRNA level between CRC tissues and paired normal colon tissues.

CONCLUSION: A large number of CRCs are positive for ER β , which can also be detected in normal colonic epithelia. There is a different localization of ER β immunoreactivity among normal colon mucosae, adenomas and CRCs. ER α and ER β mRNA can be detected both in CRC tissue and in corresponding normal colon tissue. A post-transcriptional mechanism may account for the decrease of ER β protein expression in CRC tissues.

Xie LQ, Yu JP, Luo HS. Expression of estrogen receptor β in human colorectal cancer. *World J Gastroenterol* 2004; 10(2): 214-217
<http://www.wjgnet.com/1007-9327/10/214.asp>

INTRODUCTION

Epidemiological data have shown that the risk of colorectal cancer is reduced among postmenopausal hormone users, compared with those who have never used these hormones. Animal models showed that male rats had a higher risk developing colon cancer compared with their female counterparts when exposed to dimethylhydrazine, an experimental carcinogen. The results indicated that 17 β -

oestradiol (E₂) treatment could significantly reduce the frequency of dimethylhydrazine-induced large intestinal tumors in rats^[1-3]. These evidences suggest that estrogen maybe involved in the growth of colonic tumors. Estrogen receptor locates at the cellular nuclei of target tissues, estrogen molecules diffuse into cytoplasm, and bind to estrogen receptors, then modulate gene expression by interaction with promoter response elements or other transcription factors. The estrogen receptor discovered in 1986 is named ER α , and another ER subtype identified in 1997 is called ER β . ER β protein contains 485 amino acids, with a molecular weight of 54.2 Kda. The DNA binding domain (DBD) contains a two-zinc finger structure which plays an important role in receptor dimerization and in binding of receptors to specific DNA sequence. The DBDs of ER α and ER β are highly homologous^[4]. Up to now, several ER β isoforms have been identified such as ER β 1, ER β 2, ER β 3, ER β 4, ER β 5, etc^[5]. However, the physiological significance of these ER β isoforms is still unknown. Meanwhile, published data about the expression of ER α and ER β in colon cancer tissues were often controversial^[6-20]. Therefore it is reasonable to reevaluate ER status and hormonal modulation of cell growth in colon cancer. In this study, immunohistochemistry and reverse transcription-polymerase chain reaction (RT-PCR) techniques were used to explore the precise mechanism of hormonal modulation of colon cancer.

MATERIALS AND METHODS

Patients and tissues

The study was performed in tissue sections of CRC from 40 patients who underwent surgical resection of colorectal cancer in the Department of Surgery of Renmin Hospital, Wuhan University from June 1998 to December 2000. The age of the patients ranged from 38 to 78 years (average age 65 years). Ten sections of colonic adenoma were studied, and 10 sections of normal colonic mucosa biopsy were used as control. Information about depth of invasion and nodal metastases was obtained from a review of the pathology reports. Fresh tumor tissues and corresponding normal colon tissue were obtained from 12 patients who underwent surgical resection of colon cancer in the Department of Surgery of Affiliated Hospital of Wujing Medical College and Tianjin First Central Hospital from June 2001 to December 2002. The patients were comprised of 8 men and 4 women aged 49-79 years (mean 63.3 years). The tumorous and paired normal tissues were divided into two parts. One part was fixed in 10% formalin, embedded in paraffin and stained with hematoxylin-eosin for pathological diagnosis. The other part was frozen in liquid nitrogen and stored at -80 °C until RNA was extracted. ER α and ER β mRNA were detected by RT-PCR.

Immunohistochemistry

Rabbit anti-rat or human ER β polyclonal antibody was purchased from Santa Cruz, USA. S-P kit and DAB kit were purchased from Fuzhou Maixin Biotechnology Company.

Formalin-fixed and paraffin-embedded tissue sections from 40 CRCs, 10 colonic adenomas, and 10 normal colonic mucosa biopsies were immunostained by SP technique with the following procedures. The slides were washed in 0.01 M phosphate-buffered saline (PBS). Endogenous peroxidase was

blocked by 0.3% H_2O_2 for 25 minutes, followed by incubation in normal goat serum for 15 minutes at room temperature. Then the slides were incubated with a 1:75 dilution of the primary ER β polyclonal antibody for 2 hours at room temperature. After that the slides were washed with a reagent (biotinylated anti-immunoglobulin) for 20 minutes at room temperature. After rinsed in PBS, the slides were incubated with the peroxidase-conjugated streptavidin label for 20 minutes at room temperature, and incubated with diaminobenzidine and H_2O_2 for 5 minutes. Finally the sections were counterstained with hematoxylin.

RT-PCR amplification

Total RNA was isolated with TRIZOL reagent (Life Technologies, USA), and quantified by spectrometry ($\lambda 260$ nm). Only those RNA preparations with $260/280 > 1.7$ were used in this study.

Reverse transcription was performed using a reverse transcription system (revertaidTM first strand cDNA synthesis kit, MBI). RT of RNA was performed in a final volume of 20 μ l containing 5 \times first strand buffer (containing 1 mM Tris-HCl, pH 8.3, 1.5 mM KCl and 60 μ M MgCl₂), 25 μ M dNTP mixture, 200 pM random primer, 100 units of Moloney murine leukemia virus reverse transcriptase, 2 μ g total RNA. Then DEPC treated water was added to 20 μ l. RT reaction procedure was as follows: at 70 $^{\circ}$ C for 1 min \rightarrow at 37 $^{\circ}$ C for 5 min \rightarrow at 42 $^{\circ}$ C for 60 min \rightarrow at 98 $^{\circ}$ C for 5 min. ER α , ER β and β -actin were amplified using several pairs of appropriate oligonucleotide primers as follows: ER α (530 bp): (sense) 5' -ATGTGGGAGAGGAT GAGG AG-3', (antisense) 5' -AACCGAGATGATGTAGCCAGCAGC-3'. ER β (259 bp): (sense) 5' -TAGG GTCCATGGCCAGTTAT-3', (antisense) 5' -GGGAGCCACACT TC ACCAT-3'. β -actin (control) (540 bp): (sense) 5' -GTGGG GCGCC CCAGG CAC CA-3', (antisense) 5' -CTTCC TTAAT GTCAC GCACG ATTTC-3' (Figure 1).

PCR was performed in a final volume of 50 μ l containing 4 μ l 10 \times pc buffer, 2.5 U recombinant Taq DNA polymerase (Taraka, Japan), 0.1 mM MgCl₂, 100 μ M dNTP mixture, and 50 pM of each primer. PCR was performed for 40 cycles (denaturation at 94 $^{\circ}$ C for 1 min, annealing at 55 $^{\circ}$ C for 1 min, and extension at 72 $^{\circ}$ C for 1.5 min). The PCR condition for inter control β -actin was 35 cycles (denaturation at 94 $^{\circ}$ C for 45 seconds, annealing at 60 $^{\circ}$ C for 45 seconds, and extension at 72 $^{\circ}$ C for 45 seconds). The PCR products were separated by electrophoresis on a 2% agarose gel and visualized by ethidium bromide staining and UV illumination.

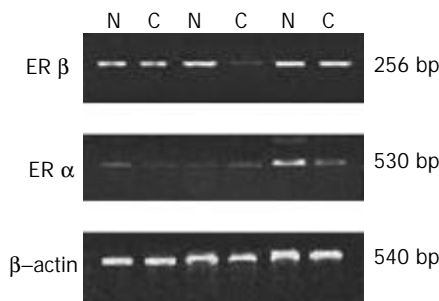


Figure 1 mRNA expression of ER α and ER β in paired representative tissues from cancer and adjacent normal mucosa. C: cancer, N: normal mucosa. RT-PCR result of β -actin was used to show equal loading.

Statistical analysis

The association between expression of ER α and ER β , the significance of ER α and ER β in groups dichotomized according to clinical and histopathologic characteristics of the patients were compared and assessed by Chi-square test and Student's *t*-test. A *P* value < 0.05 was considered significant.

RESULTS

Expression of ER α and ER β protein

Using immunoperoxidase technique, ER β immunoreactivity was detected in or near the nuclei of normal colonic mucosa in the same sections of carcinoma. ER immunoreactivity was present in some of normal epithelia (2/10), and adenomas (3/10). Nuclear immunoreactivity was consistently found in part of normal colonic mucosa, and in all areas of the crypt epithelium, and most abundant at the bottom (Figures 2A,2B). One section of rectal tubular adenocarcinoma showed strong positive nuclear and cytoplasmic staining of ER β (Figure 2C). A few stromal cells, smooth muscle cells and vascular endothelial cells were also positive (Figure 2D). In CRCs, nuclear ER β immunoreactivity was associated with cytoplasmic immunoreactivity. Some sections showed only cytoplasmic staining of ER β (Figure 2E). Positive ER β was detected in more than 10% of the cancer cells in 57.5% of the CRC cases (Figure 3).

Three of the 12 randomly selected cases stained with anti-ER α antibody showed positive. None of the 10 normal colonic mucosa biopsies was stained positive with anti-ER α antibody. There were no statistically significant differences between positive and negative ER β groups in regard to the depth of invasion, and nodal metastases (Tables 1-2).

Table 1 Expression of ER β and ER α in CRCs, colonic adenomas and normal colonic mucosa

Group	<i>n</i>	ER α positive (%)	<i>n</i>	ER β positive (%)
Normal colon mucosa	10	0 (0%)	10	2 (20%)
CRCs	12	3 (25%)	40	23 (57.5%)
Colonic adenoma			10	3 (30%)

Table 2 Clinicopathological characteristics of patients with CRCs and their association with ER β expression

Category	<i>n</i>	ER β negativity	ER β positivity (%)	<i>P</i> value
Age (years)				> 0.05
<50	4	2	2 (50.0)	
≥ 50	36	15	21 (58.3)	
Sex				> 0.05
Male	23	9	14 (60.9)	
Female	17	8	9 (52.9)	
Lymph node metastasis				> 0.05
0	18	7	11 (61.1)	
≥ 1	22	10	12 (54.5)	
Duke's type				> 0.05
A	15	5	10 (66.7)	
B	10	3	7 (70.0)	
C	7	3	4 (57.1)	
D	3	1	2 (66.7)	
Histological grading				> 0.05
Well-differentiated	15	5	10 (66.7)	
Moderately-differentiated	15	7	8 (53.3)	
Poorly-differentiated	10	5	5 (50.5)	

Table 3 Expression of ER α mRNA in CRC tissue and adjacent normal mucosa tissue

Tissue type	<i>n</i>	+	Positive rate (%)
CRCs	12	3	25%
Normal tissue	12	2	16.6%

Table 4 Expression of ER β mRNA in CRC tissue and adjacent normal mucosa tissue

Tissue type	<i>n</i>	+	Expression rate (%)	Level of ER β mRNA	<i>P</i>
CRCs	12	10	83.3%	91.15 \pm 3.56	> 0.05
Normal tissue	12	11	91.7%	95.38 \pm 2.79	

ER α and ER β mRNA expression

Table 3 and Table 4 show that the expression of ER α mRNA in CRC tissue and corresponding normal colon tissue was 25% and 16.6%, respectively. ER β mRNA was predominantly expressed in CRC tissue and paired normal colon tissue, the positive rate was 83.3% and 91.7%, respectively. There was no statistically significant difference.

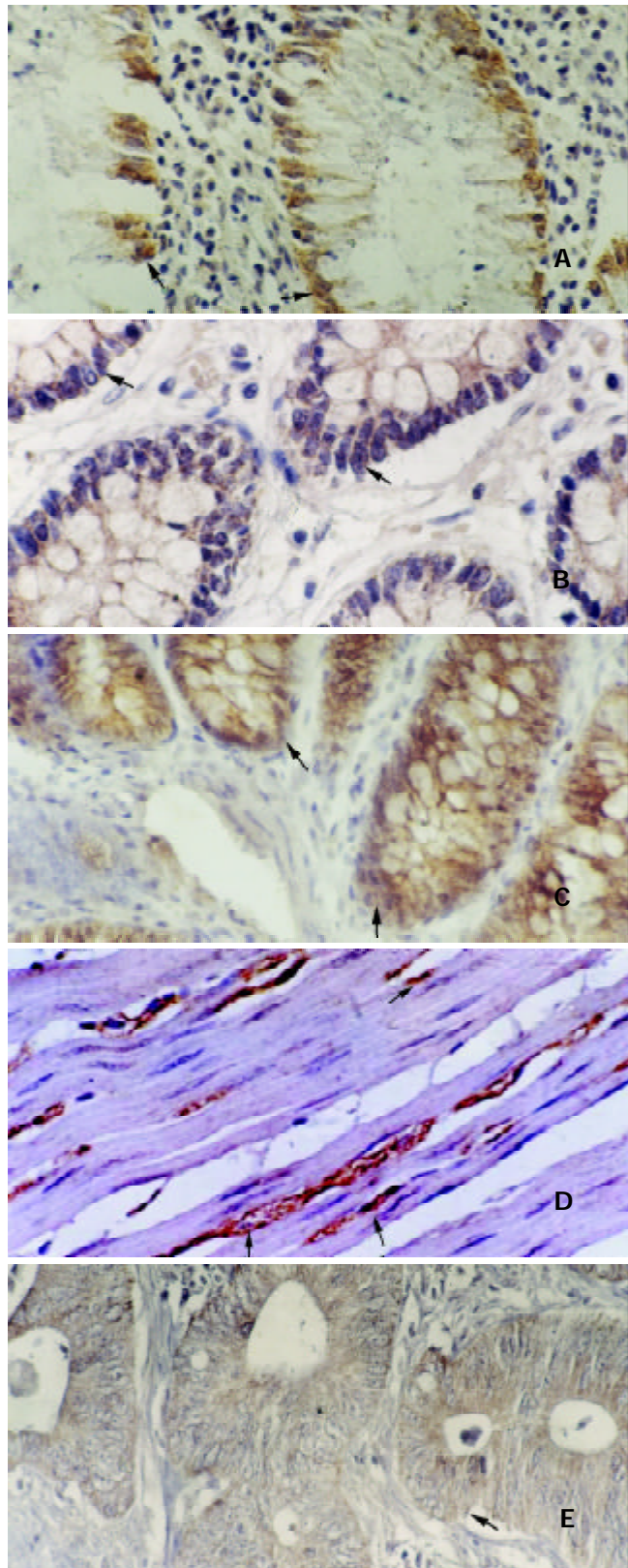


Figure 2 Immunohistochemical staining of ER β in CRC and normal colonic mucosa. A: shows the ER β positive epithelium. $\times 200$. B: shows the ER β positive crypt cell. $\times 200$. C: shows the nuclear

and cytoplasmic staining in rectal tubular adenocarcinoma. $\times 200$. D: shows the ER β positive smooth muscle cell and stromal cell. $\times 400$. E shows diffuse cytoplasmic staining in CRC. $\times 400$.

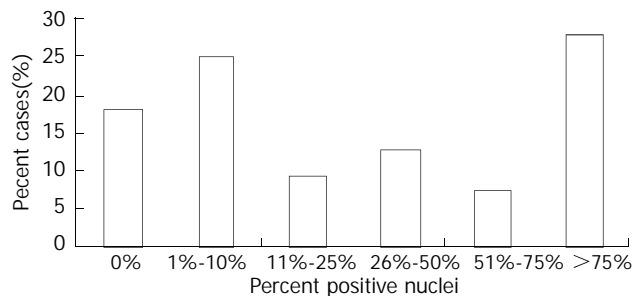


Figure 3 Extent of nuclear ER- β immunoreactivity in 40 cases of CRC.

DISCUSSION

Several epidemiologic studies have shown that colon cancer might be influenced by steroid hormones^[1-3], and estrogen use might be associated with a low risk of colon cancer^[21-27]. Some experimental results indicated that estrogen had a trophic effect on colon cancer^[11,11-12]. However, the effect of estrogen on colon cancer is controversial according to some reports. For example, Qiu *et al*^[28] reported that estradiol could induce apoptosis in colo205, a colon cancer cell line expressing only ER β . The question is whether ER expresses in normal colon mucosa or CRC. Earlier studies using biochemical ER-binding assay concluded that there was no ER in human colon. A more recent study concluded that ER was present in normal human colon and CRC tissues. Several immunohistochemical studies from China or Japan have shown that ER was present in normal human colon and CRC tissues^[12-18]. Similarly, our immunohistochemical study using ER antibodies (clone number 1D5), which are specific for ER α , showed that ER α was present in normal colon mucosa and CRC. However, the expression rate of ER α was about 20-40%, which was lower than that of ER β .

In 1997, the second type of ER (ER β) was cloned, and recent studies indicated ER β was distributed in human tissues^[5]. Several basic studies have shown that different distribution and regulatory mechanism of these two types of ER played different roles^[29,30]. ER β expression in normal colonic epithelium, especially at the bottom portion of colonic crypts, suggests that estrogens may play an important role in the growth and regeneration of normal colonic mucosa. ER β expression in a large number of CRCs indicates that estrogens may exert effects on these cancers, which may have significant implications for the treatment and prevention of CRC.

According to some published reports, ER α was also present in gastric or colon cancer^[11-18]. Our results support this conclusion. However, the positive rate of ER α in CRC was less than that of ER β in CRC. Some research results indicated that ER α and ER β could interact with the fos/jun transcription factor complex on AP1 sites to stimulate gene expression. However, they had opposite effects in the presence of estradiol. In the presence of ER α , estradiol functioned as an agonist in the AP1 pathway. In contrast, in the presence of ER β , tamoxifen and raloxifene behaved as fully competent agonists in the AP1 pathway, while estradiol acted as an antagonist, inhibiting the activity of both tamoxifen and raloxifene^[29,30]. It is the presence of two ERs that explains the conflicting experimental results. We deduced that estradiol might have trophic effects via combining with ER α . However, estradiol could inhibit tumour growth by combining with ER β .

In this study, we found no significant correlation between ER β expression and clinicopathologic features, including

Duke's types, lymph node metastasis and differentiation. Because of the relatively small sample size in this study, a study using a larger sampled study is necessary to further investigate the relationship between ER β expression and clinicopathologic characteristics and survival of colorectal cancer patients.

Our RT-PCR results showed that ER α and ER β mRNA were both expressed in CRC, semiquantitative RT-PCR revealed there was no statistical significance in ER β mRNA level between CRC tissue and paired normal colon tissue. Our immunohistochemical results showed that some sections were only cytoplasmically stained. Foley *et al*^[33] reported that Western blot analysis revealed very low levels of ER α protein in tumor and normal colon tissue. However, malignant colon tissue showed a selective loss of ER β protein expression when compared to normal colon tissue in the same patient. A post-transcriptional mechanism may account for the decrease of ER β protein expression in CRC tissue. Another reason is the different expressions of ER β isoforms in CRC. There are at least 5 different ER β isoforms, which show different amino acid sequences at the COOH terminus and are differently expressed in tumor cell lines^[31-35]. Campbell-Thompson *et al*^[35] and Witte *et al*^[36] showed that ER β was the predominant ER subtype between human colon and that the decreased levels of ER β 1 and ER β 2 mRNA were associated with colonic tumorigenesis in females. Their data suggest that there is a change in the relative expression of ER β isoforms. Therefore, It is possible that the cytoplasmic immunoreactivity in CRC tissue is caused by one of the overexpressed ER β subtypes. Further study should determine not only whether there are different ER β isoform expressions between normal colon and CRC, but also whether different isoforms are associated with different responses to estrogens and antiestrogens.

REFERENCES

- Singh S**, Langman MJ. Oestrogen and colonic epithelial cell growth. *Gut* 1995; **37**: 737-739
- Di Leo A**, Messa C, Cavallini A, Linsalata M. Estrogens and colorectal cancer. *Curr Drug Targets Immune Endocr Metabol Disord* 2001; **1**: 1-12
- Al-Azzawi F**, Wahab M. Estrogen and colon cancer: current issues. *Climacteric* 2002; **5**: 3-14
- Dardes RC**, Jordan VC. Novel Agents to modulate oestrogen action. *Br Med Bull* 2000; **56**: 773-786
- Enmark E**, Peltö-Huikko M, Grandien K, Lagercrantz S, Lagercrantz J, Fried G, Nordenskjöld M, Gustafsson JA. Human estrogen receptor β -gene structure, chromosomal localization, and expression pattern. *J Clin Endocrinol Metab* 1997; **82**: 4258-4265
- Leygue E**, Dotzlaw H, Watson PH, Murphy LC. Expression of estrogen receptor beta 1, beta2, and beta5 messenger RNAs in human breast tissue. *Cancer Res* 1999; **59**: 1175-1179
- Tong D**, Schuster E, Seifert M, Czerwenka K, Leodolte S, Zeillinger R. Expression of estrogen receptor beta isoforms in human breast cancer tissues and cell lines. *Breast Cancer Res Treat* 2002; **71**: 249-255
- Poola I**, Abraham J, Baldwin K. Identification of ten exon deleted ERbeta mRNAs in human ovary, breast, uterus and bone tissues: alternate splicing pattern of estrogen receptor beta mRNA is distinct from that of estrogen receptor alpha. *FEBS Lett* 2002; **516**: 133-138
- Shiau AK**, Barstad D, Radek JT, Meyers MJ, Nettles KW, Katzenellenbogen BS, Katzenellenbogen JA, Agard DA, Greene GL. Structural characterization of a subtype-selective ligand reveals a novel mode of estrogen receptor antagonism. *Nat Struct Biol* 2002; **9**: 359-364
- Yi P**, Driscoll MD, Huang J, Bhagat S, Hilf R, Bambara RA, Muyan M. The effects of estrogen-responsive element- and ligand-induced structural changes on the recruitment of cofactors and transcriptional responses by ER alpha and ER beta. *Mol Endocrinol* 2002; **16**: 674-693
- Sciascia C**, Olivero G, Comandone A, Festa T, Fiori MG, Enrichens F. Estrogen receptors in colorectal adenocarcinomas and in other large bowel diseases. *Int J Biol Markers* 1990; **5**: 38-42
- Slattery ML**, Samowitz WS, Holden JA. Estrogen and progesterone receptors in colon tumors. *Am J Clin Pathol* 2000; **113**: 364-368
- Oshima CT**, Wonraht DR, Catarino RM, Mattos D, Forones NM. Estrogen and progesterone receptors in gastric and colorectal cancer. *Hepatogastroenterology* 1999; **46**: 3155-3158
- Zhang ZS**, Zhang YL. Progress in research of colorectal cancer in China. *Shijie Huaren Xiaohua Zazhi* 2001; **9**: 489-494
- Qin ZK**, Lian JY, Wan DS, Hou JH, Lin HL. Expression and Prognostic Values of p21 Protein and Estrogen Receptor in Colorectal Cancers. *Ai zheng* 2001; **20**: 77-78
- Jiang YA**, Zhang YY, Luo HS, Xing SF. Mast cell density and the context of clinicopathological parameters and expression of p185, estrogen receptor, and proliferating cell nuclear antigen in gastric carcinoma. *World J Gastroenterol* 2002; **8**: 1005-1008
- Zhao XH**, Gu SZ, Liu SX, Pan BR. Expression of estrogen receptor and estrogen receptor messenger RNA in gastric carcinoma tissues. *World J Gastroenterol* 2003; **9**: 665-669
- Gao MX**, Zhang NZ, Ji CX. Estrogen receptor and PCNA in gastric carcinomas. *Shijie Huaren Xiaohua Zazhi* 2000; **8**: 1117-1120
- Xie LQ**, Yu JP, Luo HS. Estrogen receptor beta expression in Chinese colorectal adenocarcinoma. *Shijie Huaren Xiaohua Zazhi* 2002; **10**: 774-778
- Konstantinopoulos PA**, Kominea A, Vandoros G, Sykiotis GP, Andricopoulos P, Varakis I, Sotiropoulou-Bonikou G, Papavassiliou AG. Oestrogen receptor beta (ERbeta) is abundantly expressed in normal colonic mucosa, but declines in colon adenocarcinoma paralleling the tumour's dedifferentiation. *Eur J Cancer* 2003; **39**: 1251-1258
- Grodstein F**, Newcomb PA, Stampfer MJ. Postmenopausal Hormone therapy and the risk of colorectal cancer: A review and meta-analysis. *Am J Med* 1999; **106**: 574-582
- Moghissi KS**. Hormone replacement therapy for menopausal women. *Compr Ther* 2000; **26**: 197-202
- Gambacciani M**, Monteleone P, Sacco A, Genazzani AR. Hormone replacement therapy and endometrial, ovarian and colorectal cancer. *Best Pract Res Clin Endocrinol Metab* 2003; **17**: 139-147
- Burkman RT**. Reproductive hormones and cancer: ovarian and colon cancer. *Obstet Gynecol Clin North Am* 2002; **29**: 527-540
- Giovannucci E**. Obesity, gender, and colon cancer. *Gut* 2002; **51**: 147
- Adlercreutz H**. Phyto-oestrogens and cancer. *Lancet Oncol* 2002; **3**: 364-373
- Barrett-Connor E**, Stuenkel CA. Hormone replacement therapy (HRT)—risks and benefits. *Int J Epidemiol* 2001; **30**: 423-426
- Qiu Y**, Waters CE, Lewis AE, Langman MJ, Eggo MC. Oestrogen-induced apoptosis in colonocytes expressing oestrogen receptor beta. *J Endocrinol* 2002; **174**: 369-377
- Ing NH**, Spencer TE, Bazer FW. Estrogen enhances endometrial estrogen receptor gene expression by a posttranscriptional mechanism in the ovariectomized ewe. *Biol Reprod* 1996; **54**: 591-599
- Yeap BB**, Krueger RG, Leedman PJ. Differential posttranscriptional regulation of androgen receptor gene expression by androgen in prostate and breast cancer cells. *Endocrinology* 1999; **140**: 3282-3291
- Fiorelli G**, Picariello L, Martinetti V, Tonelli F, Brandi ML. Functional estrogen receptor beta in colon cancer cells. *Biochem Biophys Res Commun* 1999; **261**: 521-527
- Arai N**, Strom A, Rafter JJ, Gustafsson JA. Estrogen receptor beta mRNA in colon cancer cells: growth effects of estrogen and genistein. *Biochem Biophys Res Commun* 2000; **270**: 425-431
- Foley EF**, Jazaeri AA, Shupnik MA, Jazaeri O, Rice LW. Selective loss of estrogen receptor beta in malignant human colon. *Cancer Res* 2000; **60**: 245-248
- Vladusic EA**, Hornby AE, Guerra-Vladusic FK, Lakins J, Lupu R. Expression and regulation of estrogen receptor beta in human breast tumors and cell lines. *Oncol Rep* 2000; **7**: 157-167
- Campbell-Thompson M**, Lynch II, Bhardwaj B. Expression of estrogen receptor (ER) subtypes and ER beta isoforms in colon cancer. *Cancer Res* 2001; **61**: 632-640
- Witte D**, Chirala M, Younes M, Li Y, Younes M. Estrogen receptor beta is expressed in human colorectal adenocarcinoma. *Hum Pathol* 2001; **32**: 940-944

Ethylene diamine tetraacetic acid induced colonic crypt cell hyperproliferation in rats

Qing-Yong Ma, Kate E Williamson, Brian J Rowlands

Qing-Yong Ma, Department of Surgery, First Hospital of Xi'an Jiaotong University, Xi'an 710061, Shaanxi Province, China

Kate E Williamson, Department of Pathology, Institute of Clinical Science, The Queen's University of Belfast, Belfast, UK

Brian J Rowlands, Department of Surgery, School of medical and Surgical Sciences, University of Nottingham, Nottingham, NG7 2UH, UK

Supported by DHSS of Northern Ireland

Correspondence to: Professor Qing-Yong Ma, Department of Surgery, First Hospital of Xi'an Jiaotong University, Xi'an 710061, Shaanxi Province, China. qyma0@163.com

Telephone: +86-29-85324009

Received: 2003-06-05 **Accepted:** 2003-08-16

Abstract

AIM: To investigate the effect of ethylene diamine tetraacetic acid (EDTA) on proliferation of rat colonic cells.

METHODS: EDTA was administered into Wistar rats, carcinogenesis induced by 1,2-dimethylhydrazine (DMH) in rats was studied with immunohistochemistry.

RESULTS: Marked regional differences in cell proliferation were found in all groups. In EDTA-treated animals, total labelling indexes in both proximal (10.00 ± 0.44 vs 7.20 ± 0.45) and distal (11.05 ± 0.45 vs 8.65 ± 0.34) colon and proliferative zone size (21.67 ± 1.13 vs 16.75 ± 1.45 , 27.73 ± 1.46 vs 21.74 ± 1.07) were significantly higher than that in normal controls ($P < 0.05$) and lower than that in DMH group (10.00 ± 0.44 vs 11.54 ± 0.45 , 11.05 ± 0.45 vs 13.13 ± 0.46 , 21.67 ± 1.13 vs 35.52 ± 1.58 , 27.73 ± 1.46 vs 39.61 ± 1.32 , $P < 0.05$). Cumulative frequency distributions showed a shift of the EDTA distal curve to the right ($P < 0.05$) while the EDTA proximal curve did not change compared to normal controls. Despite the changes of proliferative parameters, tumours did not develop in EDTA treated animals.

CONCLUSION: Hyperproliferation appears to be more easily induced by EDTA in distal colon than in proximal colon. Hyperproliferation may need to exceed a threshold to develop colonic tumours. EDTA may work as a co-factor in colonic tumorigenesis.

Ma QY, Williamson KE, Rowlands BJ. Ethylene diamine tetraacetic acid induced colonic crypt cell hyperproliferation in rats. *World J Gastroenterol* 2004; 10(2): 218-222

<http://www.wjgnet.com/1007-9327/10/218.asp>

INTRODUCTION

Colonic epithelial hyperproliferation has been considered as a high risk factor in both human and animal colonic cancer models^[1-19]. Evidence from animal studies has shown that experimental colonic tumours induced by procarcinogen 1, 2-dimethylhydrazine (DMH) are of epithelial origin with a similar histology, morphology and anatomy to human colonic

neoplasms^[2,3,20,21]. Furthermore, prior to the development of colonic cancer, injections of DMH could result in increased colonic crypt cellularity, colonic crypt cell proliferation and colonic crypt proliferative zone^[22,23]. This procarcinogen thus provides an adequate model for kinetic and therapeutic studies of the colorectal cancer.

It is important to compare cell proliferation in the distal and proximal colon. As in normal rats, the location of stem cells and the direction of colonocyte migration differ in these two regions^[24]. In addition, differences in the incidence, morphology and clinical behaviour of colonic carcinoma in the proximal and distal colon have been reported^[25,26].

EDTA is widely used as a vehicle solution in chemical-induced colorectal carcinogenesis. However, little is known about the nature of its effect on cell proliferation. *In vitro*, EDTA could inhibit cell proliferation^[27,29] and DNA synthesis^[30]. Inhibition on cell growth is not associated with EDTA's chelational stability^[28]. *In vivo*, EDTA has been shown to stimulate cell proliferation in a neural crest tumour model^[31]. In the present study BrdUrd *in vivo* cell labelling was employed to determine crypt cell proliferation patterns in proximal and distal rat colons from normal, EDTA and DMH-induced colon cancer animals.

MATERIALS AND METHODS

Animals and treatment

Forty eight male Wistar rats (weighing 180-220 g) were divided equally into DMH group and EDTA group. Three animals were housed in each cage in a containment isolator with negative pressure to protect experimenters against the effects of the carcinogen. A specific colonic procarcinogen 1, 2-dimethylhydrazine (DMH, Aldric, Poole, Dorset) at a dosage of 20 mg/kg body weight was administered subcutaneously to the animals weekly for 20 weeks. DMH was dissolved in 1 mM EDTA (BDH Ltd, Poole, Dorset), and adjusted to pH 6.5 with 10% sodium hydroxide (BDH Ltd, Poole, Dorset) immediately before injection. Animals in EDTA group were given weekly subcutaneous injection of EDTA for 20 weeks, and sacrificed 2 weeks after the last injection. In addition, six normal rats were used as controls for BrdUrd immunohistochemistry.

In vivo BrdUrd labelling and tissue sampling

Eighteen rats (6 per group) from normal controls, EDTA-treated group and DMH-treated group were used for a crypt cell proliferation study. Fifteen minutes before removal of the colon, the anaesthetised animals had a peritoneal injection with 50 mg/kg body weight of 2% BrdUrd (Sigma B-5002) between 9 and 11 a.m. to avoid diurnal variation. The colon was removed and rinsed with tap water. Following excision of the caecum and rectum, the remaining colon was divided into proximal and distal halves. A 1-2 cm segment of each end of the proximal and distal colon was discarded. After fixation in 70% ethanol for 4 hours the segments were rolled prior to processing and embedding in paraffin wax.

BrdUrd immunohistochemistry

Several 3 μ m thick sections were cut and placed on poly-L-

lysine coated slides. The slides were dewaxed before DNA was denatured in 1M HCl at 37 °C for 12 minutes. After rinsed in phosphate buffered saline (PBS, pH 7.1) the sections were incubated with 30 µl of mouse anti-BrdUrd monoclonal antibody (M 744 Dako, Bucks, England) diluted 1:50 in PBS with 0.05% Tween 20 (PBST) with added normal rat serum diluted 1:25 for 60 minutes at room temperature. After a further rinsing in PBS the sections were incubated with biotinylated rabbit anti-mouse F(ab')₂ antibody (E 413 Dako, Bucks, England) at a dilution of 1:200 in PBST with added rat serum for 30 minutes at room temperature. The slides were again rinsed in PBS and then incubated with streptavidin-biotin peroxidase complex (K 377 Dako, Bucks, England) for 30 minutes at room temperature. Finally the reaction product was visualised using diaminobenzidine hydrochloride (DAB) (Sigma, Dorset, England) primed with 100 µl of 30% H₂O₂ (diluted 1:20 with distilled water) for approximately 5 minutes. After DAB was washed off with distilled water the sections were lightly counterstained in Harris haematoxylin before dehydration and mounting in DPX.

Counting and scoring criteria

Only complete well-orientated longitudinally sectioned crypts which extended from the luminal surface into the muscularis mucosae and contained at least 30 cells per hemicrypt were used for analysis. To facilitate scoring each crypt was divided at the base into 2 crypt columns (hemicrypts). Starting at the base of the hemicrypt, cells were numbered up to the luminal surface of the colon to determine the number of cells per hemicrypt. Crypts were then divided into 5 compartments each containing the same number of cells. The number and the position of BrdUrd-labelled cells in the hemicrypt were recorded. The proliferative zone, which was expressed as a percentage, was obtained by calculating the difference between the highest and lowest labelled cells in each hemicrypt and dividing this figure by the total number of cells in the hemicrypt. Labelling index (LI) was determined for the whole hemicrypt, for each compartment and for the proliferative zone as follows, $\text{equation} = (\frac{\text{number of labelled cells}}{\text{number of total cells}}) \times 100$. Each hemicrypt was then normalised to a notional 100 cell positions. The frequency of BrdUrd positive cells in each of the 100 normalised positions was recorded.

Statistical analysis

Mean and standard error of the mean were calculated where appropriate. Since the sample size for crypt cell proliferation was more than 100 except in one group (normal proximal colon group in which the sample size was 78) and all groups appeared to have normal distribution, a two sided Student's *t* test was used to identify the differences between individual variables. Kolmogorov-Smirnov 2 sample test^[16] was used to compare the BrdUrd cumulative labelling frequency curves with reference to the presence of EDTA or DMH treatment and the site of origin of the sample from the colon. Results were considered as significant when $P < 0.05$. Statistics were analysed running the SPSS package for Windows.

RESULTS

Characterisation of tumours

All animals survived to the time when they were sacrificed. In the EDTA control animals no macroscopical changes were observed in the mucosa of large intestine after 20 weeks of treatment. However, in the DMH group a total of 66 tumours were found in 23 animals (96%) and 1 rat was tumour free. Most of the tumours (73%) were located in the distal colon. Microscopically, the tumours were either adenoma or

adenocarcinoma. Most rats had one or more types of lesions, indicating that the response to DMH was heterogeneous. The number and distribution of both adenoma and adenocarcinoma are summarised in Table 1.

Table 1 Characterisation of colorectal tumours

Location	Adenoma	Carcinoma	Total (%)
Caecum	0	1	1 (1.5)
Proximal	2	6	8 (12.1)
Flexure	4	4	8 (12.1)
Distal	12	36	48 (72.7)
Rectum	0	1	1 (1.5)
Total	18	48	66

Differences between proximal and distal colon

The number of cells per hemicrypt in the proximal colon was significantly higher than that in the distal colon in all respective groups ($P < 0.05$, Table 2). Although the number of labelled cells per hemicrypt was similar in the proximal and distal colon in all groups, the total LI was significantly higher in distal colon compared to proximal colon both in normal control group ($P < 0.05$) and in DMH treated animals ($P < 0.05$). In EDTA treated group, the total LI in the distal colon was higher than that in the proximal colon with no statistical significance ($P = 0.11$). The size of the proliferative zone was higher in distal colon than that in proximal colon in all groups ($P < 0.05$) while the LI in proliferative zone did not significantly change. In the normal controls, BrdUrd labelled cells in the proximal colon were located predominantly in compartments 2 and 3 (88.4%), whereas the labelled cells in the distal colon were mostly in compartments 1 and 2 (85.3%). In compartment 1, the LI was significantly higher in the distal colon than in the proximal colon ($P < 0.05$), while in compartment 3 the LI was significantly lower in the distal colon than in the proximal colon ($P < 0.05$). None of the labelled cells appeared in compartment 5. When the cumulative labelling distribution curves of the proximal and distal colon of normal rats were compared, the distal colon showed a significant shift to the left ($P < 0.05$, Figure 1).

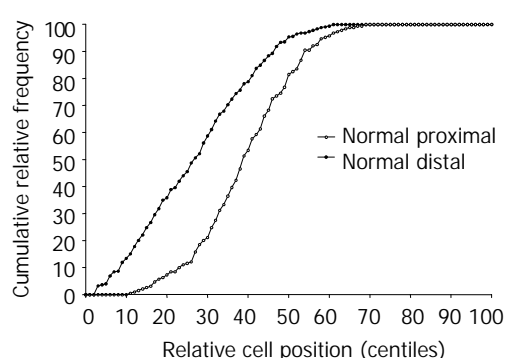


Figure 1 Different patterns of cumulative labelling distributions in proximal and distal rat colons of normal controls. The curve was significantly shifted to the right when the proximal colon was compared to the distal colon.

Effect of EDTA

In EDTA-treated animals, the number of cells per hemicrypt, labelled cells per hemicrypt and total LI were all significantly increased in both the proximal and distal colons when compared to normal controls. In addition, the size of proliferative zone in EDTA treated animals was significantly higher in both proximal and distal colons than in normal controls. However, the LI in proliferative zone was not changed. In the proximal colon, the increase in LI was limited

to compartment 3 while in the distal colon the increase in LI was extended from compartment 2 to compartment 4. When compared to the normal controls cumulative frequency distributions of the EDTA distal curve shifted to the right ($P < 0.05$, Figure 2) but the EDTA proximal curve did not change ($P > 0.05$, Figure 3).

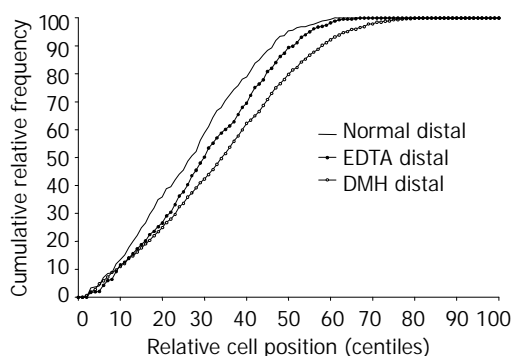


Figure 2 Cumulative labelling distribution in normal, EDTA and DMH treated distal rat colons, respectively. The curve was significantly shifted to the right in EDTA distal colon compared to normal distal colons. The curve was further shifted to the right in DMH distal colon compared to either normal or EDTA distal colon.

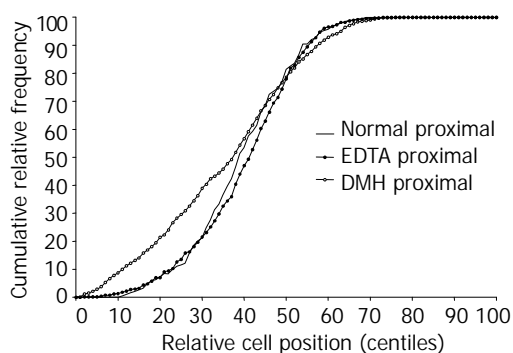


Figure 3 Cumulative labelling distribution in normal, EDTA and DMH treated proximal rat colons. The curve of EDTA

treated proximal rat colon did not change compared to the normal proximal curve. Whereas the curve of DMH treated proximal rat colon was initially significantly shifted to the left and then at higher centiles shifted to the right.

Effect of DMH treatment

DMH treatment significantly increased the number of cells per hemi-crypt in both proximal and distal colons in comparison with either normal controls or EDTA treated animals. The number of labelled cells per hemi-crypt and total LI were also significantly increased following DMH injections in both proximal and distal colons. Additionally, DMH increased the size of the proliferative zone in both proximal and distal colonic crypts. However, the LI of proliferative zone was reduced because of the increased denominator (Table 2). In the proximal colon the increase in LI was in compartments 1, 3 and 4, whereas in the distal colon the increase in LI in DMH rats was most marked in compartments 2, 3 and 4. The extent of LI in compartment 3 in the distal colon was significantly greater than that in the proximal colon ($P < 0.05$). Further analysis of the cumulative labelling distributions showed a shift of the DMH distal curve to the 81st centile which was to the right of the plateau of the normal distal colon located at the 61st centile ($P < 0.05$) and EDTA distal colon located at the 67th centile ($P < 0.05$, Figure 2). In contrast, the cumulative labelling distribution curve in DMH proximal colon demonstrated a shift to the left in the lower crypt cell positions and then shifted to the right high up the crypt compared with normal ($P < 0.05$) and EDTA ($P < 0.05$) proximal cumulative frequency curves (Figure 3).

DISCUSSION

This study supported the findings that adenoma and adenocarcinoma of intestine could be obtained, using DMH or its metabolites in Wistar rats^[20,32,33]. Another advantage of DMH and its metabolites is the specificity for the large bowel. The incidences of cancer at small intestine and extra-intestine were very low^[34]. In our study the vast majority of colon tumours occurred distally and were mainly polypoid neoplasms or adenocarcinomas. The types of the proximal colon tumours were reported to be variable histopathologically, dominated

Table 2 Features of proliferative colonic crypt cells in 6 groups

Group	LC	CPC	TLI	LI 1	LI 2	LI 3	LI 4	PZone	LIPZ
NP(76)	2.49±0.16	34.45±0.39	7.20±0.45	3.11±0.11	18.78±1.64	13.21±1.50	0.90±0.39	16.75±1.45	59.43±3.39
ND(198)	2.74±0.11	31.45±0.2	8.65±0.34	17.33±1.06	19.54±1.21	6.38±0.76	0.00	21.74±1.07	55.13±2.17
EP(134)	3.71±0.16	37.68±0.27	10.00±0.44	3.36±0.62	19.46±1.41	24.45±1.55	1.67±0.43	21.67±1.13	55.87±2.22
ED(130)	3.58±0.15	32.55±0.21	11.05±0.47	14.76±1.33	23.74±1.66	15.49±1.29	0.9±0.31	27.73±1.46	51.68±2.43
DP(138)	5.7±0.24	49.09±0.65	11.54±0.45	12.87±1.11	21.72±1.41	19.72±1.21	3.47±0.62	35.52±1.58	39.84±1.77
DD(182)	5.67±0.23	42.68±0.53	13.13±0.46	18.23±1.08	24.86±1.31	18.83±1.19	3.43±0.6	39.61±1.32	38.89±1.50
<i>P</i> Values									
ND:NP	0.21	0.000	0.019	0.000	0.731	0.000	0.000	0.011	0.3
ED:EP	0.571	0.000	0.107	0.000	0.05	0.000	0.151	0.001	0.203
DD:DP	0.94	0.000	0.017	0.003	0.107	0.604	0.966	0.047	0.682
ND:ED	0.000	0.000	0.000	0.131	0.037	0.000	0.000	0.001	0.3
ND:DD	0.000	0.000	0.000	0.556	0.003	0.000	0.000	0.000	0.000
ED:DD	0.000	0.000	0.002	0.043	0.593	0.062	0.001	0.000	0.000
NP:EP	0.000	0.000	0.000	0.798	0.765	0.000	0.237	0.009	0.365
NP:DP	0.000	0.000	0.000	0.000	0.195	0.001	0.004	0.000	0.000
EP:DP	0.000	0.000	0.016	0.000	0.259	0.017	0.019	0.000	0.000

Values represented as $\bar{x} \pm S_x$, NP(76): Normal proximal, 76 hemi-crypts were counted, ND: Normal distal, EP: EDTA proximal, ED: EDTA distal, DP: DMH proximal, DD: DMH distal, LC: Labelled cells per hemi-crypt, CPC: Cells per hemi-crypt, TLI: Total labelling index, LI1: Labelling index of compartment 1, Pzone: Proliferative zone size, LIPZ: Labelling index of proliferative zone Size.

with the mucinous type of adenocarcinoma^[35]. The different responses of bowel segments to DMH, and the reasons for the predilection of colonic neoplasia to distal colon as well as the differences in morphological type of tumours between the proximal and distal colon are not fully understood. However it is known that the structure and function of intestinal mucosa differed significantly between humans^[36] and experimental animals^[37-39]. An understanding of these inherent regional differences may be pivotal in study of the mechanisms of colonic tumorigenesis.

Significant regional differences in the distribution of BrdUrd-labelled cells in proximal and distal rat colon were demonstrated in this study. The differences in distribution of proliferative cells between proximal and distal colons were previously shown with ³H-thymidine autoradiography and immunohistochemistry. ³H-thymidine LI and proliferative zone size were reported to be significantly greater distally than proximally^[40]. In the distal colon PCNA expression was strictly confined to the lower third of the crypt, whereas in the proximal colon it was located in the mid-crypt^[23].

Sunter noted that the peak LI in the proximal colon was located in the middle third of the crypt while the peak of LI in the distal colon was located in the lower third near the base of the crypt^[41]. These findings, together with ours, tended to support the theory of crypt cell origin and colonocyte migration given by Sato and Ahnen^[24]. After a double labelling with ³H-thymidine and BrdUrd, Sato and Ahnen investigated the location of stem cells and the direction of colonocyte migration in normal rat colonic crypt, and reported that distal stem cells were located in the crypt base while proximal stem cells in the mid-crypt, thus postulating that colonocytes migrated up toward the luminal surface in the distal colon in contrast to the bidirectional migration, i.e. up toward the luminal surface and down toward the crypt base in the proximal colon.

Our results showed that after EDTA treatment, the number of proliferative colonic crypt cells was significantly increased in the distal and proximal colon. The LI in the proliferative zone in the EDTA animals did not increase which could be attributable to the concomitant increase of the zone size. In the EDTA treated animals, LIs in all compartments in the distal colon increased except the LI in compartment 1, a significant increase of LI in the proximal colon was found in compartment 3 only. This was corroborated by the cumulative labelling distribution curves. In comparison with normal control, the distal curve shifted toward to the right, but the proximal curve did not change. The fact that the proximal curve did not shift might be important. If hyperproliferation preceded tumour formation and was a cause of tumor formation, then these findings indicated that the distal colon was more susceptible. EDTA did not induce colorectal tumours after administration for 20 weeks, but prolonged EDTA treatment might induce tumours. Another hypothesis is that hyperproliferation in EDTA animals is a co-factor in DMH-induced colonic tumour formation.

DMH treatment further increased colonic crypt cell proliferation. Although DMH treatment increased the LI in both the proximal and distal colon, the cumulative labelling distribution was markedly shifted to the right in the distal colon whereas the proximal curve shifted to the left (*i.e.* downwards in the crypt). The distribution of DMH-induced colorectal cancer resembled human colorectal carcinoma^[42-44]. We found that when the total colon was exposed to the procarcinogen DMH, 73% of tumours occurred distally and only 12% proximally.

Further investigation is required to understand the differences of tumour distribution, and their relationship to the proliferation of different crypt cells and differentiation patterns in the proximal and distal colon. It has been shown that in the proximal colon, mucous cells were predominant in the lower third of the crypt, whereas columnar cells in the

upper third^[45]. In contrast, crypts of the distal colon contained only a small number of mucous cells in basal positions. The undifferentiated cells or the cells with the lowest level of differentiation (presumptive stem cells) were the vacuolated cells located near or at the base of crypt^[46]. The progeny of the vacuolated cells migrated upward to differentiate into columnar cells and downward to differentiate into mucous cells^[47].

In this study we observed a great number of cells in the crypt in the proximal colon than in the distal colon, which was in contrary to published data^[39,40]. This disparity might be due to different criteria for recoding the overlapping nuclei, selecting crypts or ascertaining the top of the crypt. In this study longitudinally well-oriented crypts were selected and all visible nuclei were counted.

EDTA increased crypt cell proliferation but all of the increased parameters were significantly lower than those in the DMH group. The number of crypt cells in hyperproliferation induced by a carcinogen might reach or exceed a limited value (threshold) before colonic tumours developed. While proliferative crypt cells that did not exceed this threshold as in the EDTA animals, might act as a promoting agent to stimulate tumour growth. In conclusion, EDTA's effect of increasing crypt cell proliferation may be a co-factor in this model.

ACKNOWLEDGEMENT

We thank Dr. Hin LY for his statistical advice and Dr. Hamilton PW for his critical suggestions.

REFERENCES

- Huang ZH**, Fan YF, Xia H, Feng HM, Tang FX. Effects of TNP-470 on proliferation and apoptosis in human colon cancer xenografts in nude mice. *World J Gastroenterol* 2003; **9**: 281-283
- Ma QY**, Williamson KE, Rowlands BJ. Variability of cell proliferation in the proximal and distal colon of normal rats and rats with dimethylhydrazine induced carcinogenesis. *World J Gastroenterol* 2002; **8**: 847-852
- Ma QY**, Williamson KE, O'rouke D, Rowlands BJ. The effects of l-arginine on crypt cell hyperproliferation in colorectal cancer. *J Surg Res* 1999; **81**: 181-188
- Chen XX**, Lai MD, Zhang YL, Huang Q. Less cytotoxicity to combination therapy of 5-fluorouracil and cisplatin than 5-fluorouracil alone in human colon cancer cell lines. *World J Gastroenterol* 2002; **8**: 841-846
- Li J**, Guo WJ, Yang QY. Effects of ursolic acid and oleanolic acid on human colon carcinoma cell line HCT15. *World J Gastroenterol* 2002; **8**: 493-495
- Jia XD**, Han C. Chemoprevention of tea on colorectal cancer induced by dimethylhydrazine in Wistar rats. *World J Gastroenterol* 2000; **6**: 699-703
- Chapkin RS**, Lupton JR. Colonic cell proliferation and apoptosis in rodent species. Modulation by diet. *Adv Exp Med Biol* 1999; **470**: 105-118
- Mills SJ**, Mathers JC, Chapman PD, Burn J, Gunn A. Colonic crypt cell proliferation state assessed by whole crypt microdissection in sporadic neoplasia and familial adenomatous polyposis. *Gut* 2001; **48**: 41-46
- Ochsenkuhn T**, Bayerdorffer E, Meining A, Schinkel M, Thiede C, Nussler V, Sackmann M, Hatz R, Neubauer A, Paumgartner G. Colonic mucosal proliferation is related to serum deoxycholic acid levels. *Cancer* 1999; **85**: 1664-1669
- Akedo I**, Ishikawa H, Ioka T, Kaji I, Narahara H, Ishiguro S, Suzuki T, Otani T. Evaluation of epithelial cell proliferation rate in normal-appearing colonic mucosa as a high-risk marker for colorectal cancer. *Cancer Epidemiol Biomarkers Prev* 2001; **10**: 925-930
- Barnes CJ**, Hardman WE, Cameron IL. Presence of well-differentiated distal, but not poorly differentiated proximal, rat colon carcinomas is correlated with increased cell proliferation in and lengthening of colon crypts. *Int J Cancer* 1999; **80**: 68-71
- Wong WM**, Wright NA. Cell proliferation in gastrointestinal mucosa. *J Clin Pathol* 1999; **52**: 321-333

- 13 **Kozoni V**, Tsioulis G, Shiff S, Rigas B. The effect of lithocholic acid on proliferation and apoptosis during the early stages of colon carcinogenesis: differential effect on apoptosis in the presence of a colon carcinogen. *Carcinogenesis* 2000; **21**: 999-1005
- 14 **Lipkin M**, Blattner WE, Fraumeni JF Jr, Lynch HT, Deschner E, Winawer S. Tritiated thymidine (fp, fh) labelling distribution as a marker for hereditary predisposition to colon cancer. *Cancer Res* 1983; **43**: 1899-1904
- 15 **Lipkin M**, Blattner WE, Gardner EJ, Burt RW, Lynch H, Deschner E, Winawer S, Fraumeni JF Jr. Classification and risk assessment of individuals with familial polyposis, Gardner's syndrome, and familial non-polyposis colon cancer from [³H]-thymidine labelling patterns in colonic epithelial cells. *Cancer Res* 1984; **44**: 4201-4207
- 16 **Wilson RG**, Smith AN, Bird CC. Immunohistochemical detection of abnormal cell proliferation in colonic mucosa of subjects with polyps. *J Clin Pathol* 1990; **43**: 744-747
- 17 **Roncucci L**, Pedroni M, Vaccina F, Benatti P, Marzona L, De Pol A. Aberrant crypt foci in colorectal carcinogenesis. Cell and crypt dynamics. *Cell Prolif* 2000; **33**: 1-18
- 18 **Terpstra OT**, van Blankenstein M, Dees J, Eilers GAM. Abnormal pattern of cell proliferation in the entire colonic mucosa of patients with colon adenoma or cancer. *Gastroenterology* 1987; **92**: 704-708
- 19 **Yamada K**, Yoshitke K, Sato M, Ahnen DJ. Proliferating cell nuclear antigen expression in normal, preneoplastic colonic epithelium of the rat. *Gastroenterology* 1992; **103**: 160-167
- 20 **Ma QY**, Hoper M, Anderson N, Rowlands BJ. Effect of supplemental L-arginine in a chemical-induced model of colorectal cancer. *World J Surg* 1996; 1087-1091
- 21 **Maskens AP**. Histogenesis and growth pattern of 1,2-dimethylhydrazine induced rat colon adenocarcinoma. *Cancer Res* 1976; **36**: 1585-1592
- 22 **Richards TC**. Early changes in the dynamics of crypt cell populations in mouse colon following administration of 1,2-dimethylhydrazine. *Cancer Res* 1977; **37**: 1680-1685
- 23 **Heitman DW**, Grubbs BG, Heitman TO, Cameron IL. Effects of 1,2-dimethylhydrazine treatment and feeding regimen on rat colonic epithelial cell proliferation. *Cancer Res* 1983; **43**: 1153-1162
- 24 **Sato M**, Ahnen D. Regional variability of colonocyte growth and differentiation in the rat. *Anat Record* 1992; **233**: 409-414
- 25 **Freeman HJ**, Kim YS, Kim YS. Glycoprotein metabolism in normal proximal and distal rat colon and changes associated with 1, 2-dimethylhydrazine induced colonic neoplasia. *Cancer Res* 1978; **38**: 3385-3390
- 26 **Greene FL**. Distribution of colorectal neoplasm. A left to right shift of polyps and cancer. *Am Surg* 1983; **49**: 62-65
- 27 **Krishnamurti C**, Saryan LA, Petering DH. Effects of ethylenediaminetetraacetic acid and 1, 10-phenanthroline on cell proliferation and DNA synthesis of Ehrlich ascites cells. *Cancer Res* 1980; **40**: 4092-4099
- 28 **Skehan P**. Nonchelational cell growth inhibition by EDTA. *Life Science* 1986; **39**: 1787-1793
- 29 **Grummt F**, Weinmann-Dorsch C, Schneider-Schaulies J, Lux A. Zinc as a second messenger of mitogenic induction: effects of diadenosine tetraphosphate (Ap₄A) and DNA synthesis. *Exp Cell Res* 1986; **163**: 191-200
- 30 **Rubin H**. Inhibition of DNA synthesis in animal cells by ethylene diamine tetraacetate, and its reversal by zinc. *Proc Natl Acad Sci* 1972; **69**: 713-716
- 31 **Nozue AT**. Effect of EDTA in newborn mice with special reference to neural crest cells. *Anatomischer Anzeiger* 1988; **166**: 209-217
- 32 **Pozharisski K**. Morphology and morphogenesis of experimental epithelial tumors of the intestine. *JNCI* 1975; **54**: 1115-1135
- 33 **Sunter JP**, Appleton DR, Wright NA, Watson AJ. Kinetics of changes in the crypts of the jejunal mucosa of dimethylhydrazine-treated rats. *Br J Cancer* 1978; **37**: 662-672
- 34 **Martin MS**, Martin F, Michiels R, Bastien H, Justrabo E, Bordes M, Viry B. An experimental model for cancer of the colon and rectum. Intestinal carcinoma induced in the rat by 1,2-dimethylhydrazine. *Digestion* 1973; **8**: 22-34
- 35 **Ward JM**, Yamamoto RS, Brown CA. Pathology of intestinal neoplasm and other lesions in rats exposed to azoxymethane. *JNCI* 1973; **51**: 1029-1039
- 36 **Filipe MI**, Branfoot AC. Abnormal pattern of mucus secretion in apparently normal mucosa of large intestine with carcinoma. *Cancer* 1974; **34**: 282-290
- 37 **Reid PE**, Culling CFA, Dunn WL, Ramey CW, Clay MG. Differences in chemical composition between the epithelial glycoproteins of the upper and lower halves of rat colon. *Can J Biochem* 1975; **53**: 1328-1332
- 38 **Freeman HJ**, Kim Y, Kim YS. Glycoprotein metabolism in normal proximal and distal rat colon and changes associated with 1, 2-dimethylhydrazine-induced colonic neoplasia. *Cancer Res* 1978; **38**: 3385-3390
- 39 **Mian N**, Cowen DM, Nutman CA. Glycosidases heterogeneity among dimethylhydrazine induced rat colonic tumours. *Br J Cancer* 1974; **30**: 231-237
- 40 **McGarrity TJ**, Perffer LP, Colony PC. Cellular proliferation in proximal and distal rat colon during 1,2-dimethylhydrazine-induced carcinogenesis. *Gastroenterology* 1988; **95**: 343-348
- 41 **Sunter JP**, Watson AJ, Wright NA, Appleton DR. Cell proliferation at different sites along the length of the rat colon. *Virchows Arch B Cell Path* 1979; **32**: 75-87
- 42 **Rodgers AE**, Nauss KM. Rodent model for carcinoma of the colon. *Dig Dis Sci* 1985; **30**: 87S-102S
- 43 **Shamsuddin AK**, Trump BF. Colon Epithelium: II. *In vivo* studies of colon carcinogenesis. Light microscopic, histochemical, and ultrastructural studies of histogenesis of azoxymethane-induced colon carcinogenesis in Fischer 344 rats. *JNCI* 1981; **66**: 389-401
- 44 **Sunter JP**, Hull DL, Appleton DR, Watson AJ. Cell proliferation of colonic neoplasms in dimethylhydrazine-treated rats. *Br J Cancer* 1980; **42**: 95-102
- 45 **Shamsuddin AK**, Trump BF. Colon Epithelium: I. Light microscopic, histochemical, and ultrastructural features of normal colon epithelium of male Fischer 344 rats. *JNCI* 1981; **66**: 375-388
- 46 **Nabeyama A**. Presence of cells combining features of two different cell types in the colonic crypt and pyloric glands of the mouse. *Am J Anat* 1975; **142**: 471-484
- 47 **Chang WWL**, Leblond CP. Renewal of the epithelium in the descending colon of the mouse. I. Presence of three cell populations: vacuolated-columnar, mucous and argentaffin. *Am J Anat* 1971; **131**: 73-99

Low grade gastric MALTOMA: Treatment strategies based on 10 year follow-up

Sang Kil Lee, Yong Chan Lee, Jae Bock Chung, Chae Yoon Chon, Young Myoung Moon, Jin Kyung Kang, In-Suh Park, Chang Ok Suh, Woo Ik Yang

Sang Kil Lee, Yong Chan Lee, Jae Bock Chung, Chae Yoon Chon, Young Myoung Moon, Jin Kyung Kang, Division of Gastroenterology, Department of Internal Medicine, Yonsei University College of Medicine, Seoul, South Korea

In-Suh Park, Department of Internal Medicine, NHIC Ilsan Hospital, Ilsan, South Korea

Chang Ok Suh, Department of Radiation Oncology, Yonsei University College of Medicine, Seoul, South Korea

Woo Ik Yang, Department of Pathology, Yonsei University College of Medicine, Seoul, South Korea

Correspondence to: Dr. Jae Bock Chung, Division of Gastroenterology, Department of Internal Medicine, Yonsei University College of Medicine, 134 Shinchon-dong, Seodaemun-gu, Seoul, South Korea. jbchung@yumc.yonsei.ac.kr

Telephone: +82-2-361-5410 **Fax:** +82-2-393-6884

Received: 2003-07-17 **Accepted:** 2003-09-24

Abstract

AIM: To deduce strategic guideline of gastric mucosa associated lymphoid tissue lymphoma (MALTOMA) by evaluating the long-term outcome of patients in respect to various treatment modalities.

METHODS: A total of 55 patients with MALTOMA from May 1992 to August 2002 were retrospectively reviewed.

RESULTS: Complete remission was obtained in 24 (82.8%) of 29 patients treated with anti *Helicobacter pylori* (*H pylori*) regimen only. The duration to reach complete remission was 12 months (85 percentile, 2-33 months). Five patients showed complete remission with radiation therapy (26-86 months). Two of them were *H pylori* treatment failure cases.

CONCLUSION: *H pylori* eradication is an effective primary treatment option for low grade MALTOMA and radiation therapy could be considered in patients with no evidence of *H pylori* infection or who do not respond to *H pylori* eradication therapy 12 months after successful eradication.

Lee SK, Lee YC, Chung JB, Chon CY, Moon YM, Kang JK, Park IS, Suh CO, Yang WI. Low grade gastric MALTOMA: Treatment strategies based on 10 year follow-up. *World J Gastroenterol* 2004; 10(2): 223-226

<http://www.wjgnet.com/1007-9327/10/223.asp>

INTRODUCTION

In 1983, Isaacson and Wright introduced the term MALTOMA to characterize primary low grade gastric B-cell lymphoma and immunoproliferative small-intestinal disease^[1]. Subsequently, the definition of MALTOMA was extended to include several other extranodal low grade B-cell lymphomas, with a similar histology to Peyer's patches, including those of the salivary gland, lung, and thyroid, but gastric form is the most common and best characterized MALTOMA^[2].

Low grade MALTOMA is composed of small cells with dense nuclear chromatin and a low proliferation fraction; the converse is true for diffuse large B cell lymphoma. Low grade gastric MALTOMA is a neoplasia with a very indolent course and an excellent prognosis. It has a tendency to remain localized to the gastric wall and seldom involve lymph nodes and bone marrow.

In the past, primary low grade gastric MALTOMA was treated with surgery in the same way as adenocarcinoma. This often necessitated a total gastrectomy due to the multi-focal or diffuse nature of gastric lymphomas. Since the introduction of *H pylori* concept, the association of this bacterium with chronic active gastritis, peptic ulcer and gastric cancer has been demonstrated^[3-5]. Furthermore, *H pylori* is suggested to be associated with low-grade gastric MALTOMA. It was proposed that low grade gastric MALTOMA was formed by the immune response to *H pylori* infection in the gastric mucosa^[6,7]. The discovery of a causal role for *H pylori* in the development of gastric marginal zone lymphoma of the MALT type has dramatically altered the therapeutic approach to patients with early stage disease^[8,9]. According to recent data, durable complete remissions might be achieved in up to 80% of patients with early stage MALTOMA following eradication of the bacteria^[9]. In the patients who failed to respond to *H pylori* eradication or had low grade gastric MALTOMA without *H pylori* infection, radiotherapy, chemotherapy or surgery has been tried.

However, the long-term follow-up result of *H pylori* eradication on low grade MALT lymphoma has been seldom reported. Furthermore, a clear-cut time is difficult to define the failure to *H pylori* eradication therapy and currently there has been no standard guideline to assess the result of eradication therapy. Also the time interval to perform endoscopic examination to evaluate histologic and morphologic remission is unclear. Consequently, a suitable strategic guideline to decide subsequent treatment option when one fails has not been well proposed. We aimed to evaluate the long-term outcome of patients with low grade gastric MALTOMA in respect to various treatment modalities. We also tried to deduce suitable strategic guideline to treat low grade gastric MALTOMA.

MATERIALS AND METHODS

Patients

We retrospectively studied 55 patients of primary low grade gastric MALTOMA aged 23 to 74 years from May 1992 to August 2002. All the patients were pathologically confirmed as low grade gastric MALTOMA. The diagnosis of low grade gastric MALTOMA was made according to the criteria of Isaacson^[10] and scoring system of Wotherspoon *et al*^[11]. The initial staging procedures included a complete physical examination, chest roentgenogram, bone marrow examination, abdominal CT scan and endoscopic ultrasonography (EUS).

Methods

We evaluated the patients' initial presenting symptoms and the status of *H pylori* infection. *H pylori* infection was diagnosed by rapid urease test (CLOTM, Delta West, Bentley,

Western Austria), and/or histologic examination. *H pylori* status was considered positive if any of the two tests was positive. Endoscopic findings included the shape, size, location and number of lesions. Gross phenotype was classified according to the endoscopic features into seven types: 1) gastritis: only mucosal color change, 2) granular: small nodules on the lesion, 3) ulcerative: one or more ulceration, 4) ulceroinfiltrative: one or more ulceration with surrounding mucosal infiltration, 5) depressed: depressed or EGC IIc like lesion, 6) protruding: elevated or polypoid, and 7) mixed, and then was categorized into diffuse and localized type according to the pattern of distribution.

RESULTS

Clinical and endoscopic features of patients

The male to female ratio was 1:1.3. The mean age of the patients was 47.8 years (23-74). All but three of the patients were symptomatic at presentation: The main symptoms were abdominal pain (56.4%), indigestion (23.6%), epigastric discomfort (12.7%) and vomiting (1%). A total of 48 (48/53, 90.5%) met the case definition for *H pylori* positivity (Table 1). When each test was considered individually, *H pylori* infection was detected by histology and rapid urease test in 42 (87.5%) and 39 (81.3%) patients, respectively. Initial endoscopic findings are summarized in Table 2.

Table 1 Clinical features of patients and *H pylori* state (n=55)

Age (years)	47.8±11.3 (23-74)	
Sex	Male:Female=24:31	
<i>H pylori</i> status ^a	Positive	48 (90.5%)
	Negative	5 (9.5%)

^aExcluding two cases of unknown *H pylori* status.

Table 2 Endoscopic findings and location of low grade MALTOMA (n=55)

Location	No. of cases (%)	Findings	No. of cases (%)
Body only	21 (38.2)	Ulcerative	15 (27.3)
Antrum only	11 (20.0)	Mixed	15 (27.3)
Antrum & body	20 (36.4)	Ulceroinfiltrative	10 (18.2)
Fundus/Cardia	3 (5.4)	Depressed	6 (10.9)
		Gastritis	5 (9.1)
		Protruding	3 (5.5)
		Granular	1 (1.8)

Treatment modalities and outcomes

Treatment modalities included *H pylori* eradication, surgery, radiotherapy and combination therapy (Table 3). A total of twenty nine patients were treated with *H pylori* eradication therapy (omeprazole + amoxicillin + metronidazole or clarithromycin for 2 weeks). All but one was positive in urease test or histologic examination for *H pylori*. Endoscopic ultrasonography was done before *H pylori* eradication and cases with lymph node metastasis or involvement beyond the submucosal layer were excluded. For determination of the response, two months after the end of eradication therapy, biopsy specimens were collected from the multiple sites including the lesion for histologic examination. One additional specimen was obtained for rapid urease test. For the remission failure case, a repeat endoscopy was performed every two to three months until complete remission was achieved. In cases with complete remission, endoscopic examination and biopsy were performed every 6-12 months. Overall *H pylori* eradication rate was 96.4% (27/28). Complete remission of

low grade MALTOMA was achieved in 24 out of 29 cases (82.8%). The median time to get complete remission was 4 months (2-33) (Table 3). In terms of histologic remission of the low grade gastric MALTOMA, the mucosal lesions changed to atrophic or endoscopically normal appearance (Figure 1). There were five treatment failures to *H pylori* eradication therapy. Radiation treatment was given in two patients who failed to respond to anti *H pylori* treatment after 6 months and 9 months of follow-up, respectively. One underwent operation. They all had complete remission in the subsequent follow-up. The remaining two patients were recommended to receive other treatment with persistence of localized MALTOMA.

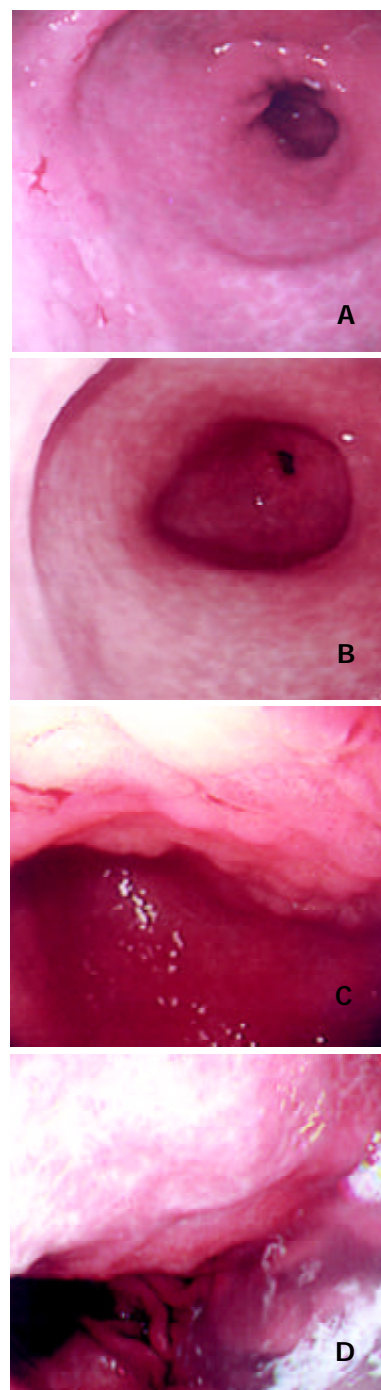


Figure 1 A: A case with irregular ulceration on the anterior wall of antrum before eradication. B: 3 months after *H pylori* eradication therapy, ulceration was disappeared. C: A case with mucosal nodularities on the posterior wall of the upper body before eradication. D: 2 months after *H pylori* eradication therapy, the lesion was replaced by atrophic mucosa.

Sixteen patients underwent surgery, including 11 total gastrectomies and 5 subtotal gastrectomies (Table 3). Most of them were treated by surgery because they were suspected to have lymph node metastasis or infiltration beyond the submucosal layer in endoscopic ultrasonographic examination. Among the sixteen patients, 4 patients showed lymph node metastasis. Three patients received additional radiation therapy or chemotherapy after surgery because of lymph node metastasis or perigastric fat infiltration of low grade gastric MALTOMA.

Five patients received radiation therapy. These cases included two patients with *H pylori* negativity, two patients with failure to *H pylori* eradication, and one case with recurrence in remnant stomach after surgery (Table 3). The median radiation dose was 30.6 Gy (range 30-39) with a daily fraction of 1.5-1.8 Gy.

The comparative study among different endoscopic types of low grade MALT lymphoma patients who showed failure to eradication treatment disclosed no significant correlation. However, the lesion of localized mass type showed the tendency to higher treatment failure (Table 4).

Table 3 Initial treatments and outcomes of low grade MALTOMA

	<i>H pylori</i> eradication (n=29)	Surgery (n=16)	Radiotherapy (n=5)
Complete remission (%)	24 (82.8%)	16 (100%)	5 (100%)
Failure (%)	5 (17.2%)	0	0
Recurrence (%)	1 (4.2%)	1	0
Median follow-up (months)	24 (2-74)	46.5 (12-120)	35.5 (26-86)
Time to get CR in 85 percentile of patients (interval) (months)	12 (2-33)		

CR: Complete remission.

Table 4 Failures of *H pylori* eradication treatment according to endoscopic findings

Endoscopic types	Treatment cases	Failure cases (%) ^a
Diffuse	13	1 (17.7) ^b
Gastritis	2	0 (0)
Granular	1	0 (0)
Mixed	10	1 (10.0)
Localized	16	4 (25.0) ^a
Ulcerative	8	2 (25.0)
Ulceroinfiltrative	3	1 (33.3)
Depressed	4	0 (0)
Protruding	1	1 (100.0)
Total	29	5 (17.2)

^aFailure rate of each endoscopic type, ^b $P > 0.05$ by χ^2 test.

DISCUSSION

The relationship between *H pylori* and low grade gastric MALTOMA is strong, and therefore treatment strategies are aimed at *H pylori* eradication in early stages. Recently, durable complete remissions have been supposed to achieve in up to 80% of patients with early stage MALTOMA following eradication of the bacteria^[9]. In the largest MALTOMA study to date, 120 patients with early stage low grade gastric MALTOMA were treated with *H pylori* eradication therapy and followed^[12]. After mean follow-up period of 48 months, 81% of patients were in complete remission. Relapse after complete remission occurred in less than 10% of cases, and whether this was always caused by *H pylori* reinfection has been unknown^[13-24]. Follow-up is essential in patients with

MALTOMA treated with *H pylori* eradication therapy. Endoscopic follow-up with biopsy for histology and *H pylori*, and EUS at least yearly after remission was recommended^[12,25]. Because some residual cells lay dormant after clinical and histological remission was achieved, some investigators insisted that molecular studies should be included in addition to histologic study^[20]. At present, histologic study is considered as the gold standard.

Because eradication therapy is never 100% successful, it is also important to choose the most suitable additional treatment for treatment failure. MALTOMA that were not *H pylori* positive or did not respond to eradication therapy could be treated with surgery, radiation, or chemotherapy. Radical gastrectomy has 5- and 10-yr survival rates of 90% and 70%, but lead to significant morbidity^[26]. Monotherapy with alkylating agents was tried in MALTOMA patients who did not respond to *H pylori* eradication therapy. In this study, remission could be achieved with chlorambucil in only 58% of the nonresponding patients to *H pylori* eradication therapy^[25].

Our results showed 82.8% of remission induction in low grade gastric MALTOMA by *H pylori* eradication alone with a single relapse. About 50% of patients with low grade gastric MALTOMA showed complete remission by 4 months after *H pylori* eradication. However, delayed response by up to 33 months occurred in one case. Overall, complete remission was achieved within 12 months in 85 percentile. We propose that it is necessary to wait for 12 months after initial eradication therapy of *H pylori* to define the time for *H pylori* eradication failure, because relapse is relatively rare after 12 months and nearby all the cases would have complete remission by 12 months. In addition, other treatment modalities could be used 12 months after initial *H pylori* eradication therapy, such as radiation therapy, surgery or chemotherapy.

A recent series from the memorial Sloan-Kettering Cancer Center and Yonsei Cancer Center reported a 100% complete remission rate with radiation alone. Especially, radiation therapy was chosen in the management of low grade gastric MALTOMA in patients with no evidence of *H pylori* infection or who showed no response to *H pylori* eradication therapy^[27,28]. In our study, complete remission was obtained in all the patients after various treatment modalities. All the patients who received radiotherapy tolerated the treatment well and completed the treatment course without significant acute or delayed toxicities. Radiation therapy was superior to surgery or chemotherapy because it had significant advantages of gastric preservation and lower morbidity.

Our results provide further supports to the recommendation by Issacson and Spencer that eradication of *H pylori* is harmless and inexpensive and should be the first-line treatment for localized low grade gastric MALTOMA. If no response is observed by 12 months after eradication therapy, radiotherapy should be considered.

Several investigators evaluated endoscopic appearance of primary gastric lymphoma^[29,30]. In low grade lymphoma, endoscopic findings were often interpreted as a benign condition, in contrast to high grade lymphoma, for which carcinoma was the most frequently suspected diagnosis. Our results were consistent with previous reports that low grade gastric MALTOMA was found at a relatively high frequency (94.6%) in the middle third of the stomach^[31]. The most frequent endoscopic appearance of gastric lymphoma was ulceration, while the finding of polypoid lesions or other forms (as gastritis or erosions) had a lower frequency^[32]. Also in this study, the majority of the endoscopic features of low grade gastric MALTOMA was superficial, such as shallow ulceration or mixed type, and was multiple rather than single. But these cases also exhibited variegated pictures. In terms of the result of *H pylori* eradication therapy, we did not see any correlation

with the endoscopic findings. It might be due to the small number of cases of *H pylori* eradication failure and complexity of endoscopic findings of low grade MALTOMA. However, the lesion of localized mass type showed the tendency to higher treatment failure (Table 4). Nevertheless, if we consider the fact that high grade lymphoma is often accompanied with deep ulceration or protruding mass in the stomach, our results might be valuable on the presumption that mixed type MALTOMA might exist which was responsible for the treatment failure.

REFERENCES

- 1 **Isaacson P**, Wright DH. Malignant lymphoma of mucosa-associated lymphoid tissue. A distinctive type of B-cell lymphoma. *Cancer* 1983; **52**: 1410-1416
- 2 **Zhou Q**, Xu TR, Fan QH, Zhen ZX. Clinicopathologic study of primary intestinal B cell malignant lymphoma. *World J Gastroenterol* 1999; **5**: 538-540
- 3 **Marshall BJ**, Warren JR. Unidentified curved bacilli in the stomach of patients with gastritis and peptic ulceration. *Lancet* 1984; **16**: 1311-1315
- 4 **NIH Consensus conference**. *Helicobacter pylori* in peptic ulcer disease. NIH Consensus Development Panel on *Helicobacter pylori* in Peptic Ulcer Disease. *JAMA* 1994; **272**: 65-69
- 5 **Parsonnet J**, Friedman GD, Vandersteen DP, Chang Y, Vogelstein JH, Orentreich N, Sibley RK. *Helicobacter pylori* infection and the risk of gastric carcinoma. *N Engl J Med* 1991; **325**: 1127-1131
- 6 **Wyatt JL**, Rathbone BJ. Immune response of the gastric mucosa to *Campylobacter pylori*. *Scand J Gastroenterol Suppl* 1988; **142**: 44-49
- 7 **Stolte M**, Eidt S. Lymphoid follicles in antral mucosa: immune response to *Campylobacter pylori*? *J Clin Pathol* 1989; **42**: 1269-1271
- 8 **Isaacson PG**. Gastric MALT lymphoma: from concept to cure. *Ann Oncol* 1999; **10**: 637-645
- 9 **Neubauer A**, Thiede C, Morgner A, Alpen B, Ritter M, Neubauer B, Wundisch T, Ehninger G, Stolte M, Bayerdorffer E. Cure of *Helicobacter pylori* infection and duration of remission of low-grade gastric mucosa-associated lymphoid tissue lymphoma. *J Natl Cancer Inst* 1997; **89**: 1350-1355
- 10 **Isaacson PG**. Gastrointestinal lymphoma. *Hum pathol* 1994; **25**: 1020-1029
- 11 **Wotherspoon AC**, Doglioni C, Diss TC, Pan L, Moschini A, de Boni M, Isaacson PG. Regression of primary low-grade B-cell gastric lymphoma of mucosa-associated lymphoid tissue type after eradication of *Helicobacter pylori*. *Lancet* 1993; **342**: 575-577
- 12 **Stolte M**, Bayerdorffer E, Morgner A, Alpen B, Wundisch T, Thiede C, Neubauer A. *Helicobacter* and gastric MALT lymphoma. *Gut* 2002; **50**: 19-24
- 13 **Isaacson PG**, Diss TC, Wotherspoon AC, Barbazza R, De Boni M, Doglioni C. Long-term follow-up of gastric MALT lymphoma treated by eradication of *H pylori* with antibodies. *Gastroenterology* 1999; **117**: 750-751
- 14 **Du MQ**, Isaacson PG. Gastric MALT lymphoma: from aetiology to treatment. *Lancet Oncol* 2002; **3**: 97-104
- 15 **Roggero E**, Zucca E, Pinotti G, Pascarella A, Capella C, Savio A, Pedrinis E, Paterlini A, Venco A, Cavalli F. Eradication of *Helicobacter pylori* infection in primary low-grade gastric lymphoma of mucosa-associated lymphoid tissue. *Ann Intern Med* 1995; **122**: 767-769
- 16 **Savio A**, Franzin G, Wotherspoon AC, Zamboni G, Negrini R, Buffoli F, Diss TC, Pan L, Isaacson PG. Diagnosis and posttreatment follow-up of *Helicobacter pylori*-positive gastric lymphoma of mucosa-associated lymphoid tissue: histology, polymerase chain reaction, or both? *Blood* 1996; **87**: 1255-1260
- 17 **Sackmann M**, Morgner A, Rudolph B, Neubauer A, Thiede C, Schulz H, Kraemer W, Boersch G, Rohde P, Seifert E, Stolte M, Bayerdorffer E. Regression of gastric MALT lymphoma after eradication of *Helicobacter pylori* is predicted by endosonographic staging. MALT Lymphoma Study Group. *Gastroenterology* 1997; **113**: 1087-1090
- 18 **Montalban C**, Manzanal A, Boixeda D, Redondo C, Alvarez I, Calleja JL, Bellas C. *Helicobacter pylori* eradication for the treatment of low-grade gastric MALT lymphoma: follow-up together with sequential molecular studies. *Ann Oncol* 1997; **8**(Suppl 2): 37-39
- 19 **Papa A**, Cammarota G, Tursi A, Gasbarrini A, Gasbarrini G. *Helicobacter pylori* eradication and remission of low-grade gastric mucosa-associated lymphoid tissue lymphoma: a long-term follow-up study. *J Clin Gastroenterol* 2000; **31**: 169-171
- 20 **Montalban C**, Santon A, Boixeda D, Redondo C, Alvarez I, Calleja JL, de Argila CM, Bellas C. Treatment of low grade gastric mucosa-associated lymphoid tissue lymphoma in stage I with *Helicobacter pylori* eradication. Long-term results after sequential histologic and molecular follow-up. *Haematologica* 2001; **86**: 609-617
- 21 **Ruskone-Fourmestraux A**, Lavergne A, Aegerter PH, Megraud F, Palazzo L, de Mascarel A, Molina T, Rambaud JL. Predictive factors for regression of gastric MALT lymphoma after anti-*Helicobacter pylori* treatment. *Gut* 2001; **48**: 297-303
- 22 **Steinbach G**, Ford R, Globber G, Sample D, Hagemester FB, Lynch PM, McLaughlin PW, Rodriguez MA, Romaguera JE, Sarris AH, Younes A, Luthra R, Manning JT, Johnson CM, Lahoti S, Shen Y, Lee JE, Winn RJ, Genta RM, Graham DY, Cabanillas FF. Antibiotic treatment of gastric lymphoma of mucosa-associated lymphoid tissue: An uncontrolled trial. *Ann Intern Med* 1999; **131**: 88-95
- 23 **Nakamura S**, Matsumoto T, Suekane H, Takeshita M, Hizawa K, Kawasaki M, Yao T, Tsuneyoshi M, Iida M, Fujishima M. Predictive value of endoscopic ultrasonography for regression of gastric low grade and high grade MALT lymphomas after eradication of *Helicobacter pylori*. *Gut* 2001; **48**: 454-460
- 24 **Cheng H**, Wang J, Zhang CS, Yan PS, Zhang XH, Hu PZ, Ma FC. Clinicopathologic study of mucosa-associated lymphoid tissue lymphoma in gastroscopic biopsy. *World J Gastroenterol* 2003; **9**: 1270-1272
- 25 **Levy M**, Copie-Bergman C, Traulle C, Lavergne-Slove A, Brousse N, Flejou JF, de Mascarel A, Hemery F, Gaulard P, Delchier JC. Conservative treatment of primary gastric low-grade B-cell lymphoma of mucosa-associated lymphoid tissue: predictive factors of response and outcome. *Am J Gastroenterol* 2002; **97**: 292-297
- 26 **Radaszkiewicz T**, Dragosics B, Bauer P. Gastrointestinal malignant lymphomas of the mucosa-associated lymphoid tissue: factors relevant to prognosis. *Gastroenterology* 1992; **102**: 1628-1638
- 27 **Park HC**, Park W, Hahn JS, Kim CB, Lee YC, Noh JK, Suh CO. Low grade MALT lymphoma of the stomach: treatment outcome with radiotherapy alone. *Yonsei Med J* 2002; **43**: 601-606
- 28 **Schechter NR**, Portlock CS, Yahalom J. Treatment of mucosa-associated lymphoid tissue lymphoma of the stomach with radiation alone. *J Clin Oncol* 1998; **16**: 1916-1921
- 29 **Taal BG**, den Hartog Jager FC, Burgers JM, van Heerde P, Tio TL. Primary non-Hodgkin's lymphoma of the stomach: Changing aspects and therapeutic choices. *Eur J Cancer Clin Oncol* 1989; **25**: 439-450
- 30 **Seifert E**, Schulte F, Weismuller J, de Mas CR, Stolte M. Endoscopic and biopptic diagnosis of malignant non-Hodgkin's lymphoma of the stomach. *Endoscopy* 1993; **25**: 497-501
- 31 **Hiyama T**, Haruma K, Kitadai Y, Masuda H, Miyamoto M, Ito M, Kamada T, Tanaka S, Uemura N, Yoshihara M, Sumii K, Shimamoto F, Chayama K. Clinicopathological features of gastric mucosa-associated lymphoid tissue lymphoma: a comparison with diffuse large B-cell lymphoma without a mucosa-associated lymphoid tissue lymphoma component. *J Gastroenterol Hepatol* 2001; **16**: 734-739
- 32 **Isaacson PG**. Recent developments in our understanding of gastric lymphomas. *Am J Surg Pathol* 1996; **20**(Suppl): S1-7

Effect of *Helicobacter pylori* infection on expressions of Bcl-2 family members in gastric adenocarcinoma

Hao Zhang, Dian-Chun Fang, Rong-Quan Wang, Shi-Ming Yang, Hai-Feng Liu, Yuan-Hui Luo

Hao Zhang, Dian-Chun Fang, Rong-Quan Wang, Shi-Ming Yang, Hai-Feng Liu, Yuan-Hui Luo, Department of Gastroenterology of Southwest Hospital, Third Military Medical University, Chongqing 400038, China

Supported by the National Natural Science Foundation of China, No.30070043, and the Key Programs of the Military Medical and Health Foundation during the 10th Five-Year Plan Period, No.01Z075

Correspondence to: Professor Dian-Chun Fang, Department of Gastroenterology of Southwest Hospital, Chongqing 400038, China. fangdianchun@hotmail.com

Telephone: +86-23-68754124

Received: 2003-07-12 **Accepted:** 2003-08-16

Abstract

AIM: To investigate the effect of *Helicobacter pylori* (*H pylori*) infection on the expressions of Bcl-2 family members in gastric adenocarcinoma.

METHODS: Gastric adenocarcinoma and resection margin tissues of 95 patients were studied. Semi-quantitative RT-PCR was used to measure Bid, Bax and Bcl-2 mRNA expressions.

RESULTS: Expressions of Bid and Bax in gastric adenocarcinoma tissues without *H pylori* infection, with *cagA*⁻ *H pylori* infection and *cagA*⁺ *H pylori* infection increased significantly in turn (Bid, 0.304, 0.422 and 0.855 respectively, $P < 0.05$; Bax, 0.309, 0.650 and 0.979 respectively, $P < 0.05$). Bcl-2 mRNA levels increased significantly in gastric adenocarcinoma tissues with *cagA*⁻ *H pylori* infection and *cagA*⁺ *H pylori* infection, compared with those without *H pylori* infection (0.696 and 0.849 vs 0.411, $P < 0.05$). Expressions of Bid, Bax and Bcl-2 in resection margin tissues without *H pylori* infection, with *cagA*⁻ *H pylori* infection and *cagA*⁺ *H pylori* infection increased significantly in turn (Bid, 0.377, 0.686 and 0.939 respectively, $P < 0.05$; Bax, 0.353, 0.645 and 1.001 respectively, $P < 0.05$; Bcl-2, 0.371, 0.487 and 0.619 respectively, $P < 0.05$). In *H pylori* negative specimens, expressions of Bid and Bax correlated negatively with that of Bcl-2 respectively in adenocarcinoma tissues (Bid vs Bcl-2, $r = -0.409$, $P < 0.05$; Bax vs Bcl-2, $r = -0.451$, $P < 0.05$). In *H pylori* positive specimens, expressions of Bid and Bax did not correlate with that of Bcl-2 in adenocarcinoma tissues (Bid vs Bcl-2, $r = 0.187$, $P > 0.05$; Bax vs Bcl-2, $r = 0.201$, $P > 0.05$), but correlated positively with that of Bcl-2 respectively in resection margin tissues (Bid vs Bcl-2, $r = 0.331$, $P < 0.05$; Bax vs Bcl-2, $r = 0.295$, $P < 0.05$).

CONCLUSION: *H pylori* may enhance Bid, Bax and Bcl-2 mRNA levels and cause deregulation of these apoptosis-associated genes expressions, which may play a role during development of gastric adenocarcinoma induced by *H pylori*.

Zhang H, Fang DC, Wang RQ, Yang SM, Liu HF, Luo YH. Effect of *Helicobacter pylori* infection on expressions of Bcl-2 family members in gastric adenocarcinoma. *World J Gastroenterol* 2004; 10(2): 227-230

<http://www.wjgnet.com/1007-9327/10/227.asp>

INTRODUCTION

Helicobacter pylori (*H pylori*) infection is the most common chronic infection in humans and is the major cause of gastritis worldwide. This infection is also accepted as the etiological factor of the majority of peptic ulcers. It has been implicated as a significant contributing factor in the development of gastric malignancy, both gastric MALT lymphoma and gastric adenocarcinoma^[1-14], and *H pylori* was classified as a group 1 carcinogen for gastric cancer in 1994 by the WHO and International Agency for Research on Cancer (IARC)^[15]. The role of *H pylori* infection in the gastric carcinogenesis is not clear. It might be involved in imbalance between apoptosis and proliferation^[16-33]. Bcl-2 family members have been closely related to apoptosis, which could either promote cell survival (Bcl-2, Bcl-x_L, A1, Mcl-1, and Bcl-w) or promote cell death (Bax, Bak, Bcl-x_S, Bad, Bid, Bik, Bim, Hrk, Bok)^[34-36]. In the present study, we investigated the effect of *H pylori* infection on the expressions of Bcl-2 family members in gastric adenocarcinoma and resection margin tissues.

MATERIALS AND METHODS

Tissue specimens

Specimens of gastric adenocarcinoma of 95 patients (72 males and 23 females, age range 31 to 84 years, mean 56 years), who had undergone resection surgical at the Southwest Hospital in Chongqing and had not taken anti-*H pylori* drugs before operation, were collected from 2001 to 2002. Gastric adenocarcinoma tissues were examined microscopically. Resection margin tissues were also examined to verify that they did not contain malignant cells. The histological diagnosis was confirmed by a professional pathologist. The remaining specimens were snap-frozen and stored at -80 °C until assayed. Warthin-Starry silver staining and polymerase chain reaction (PCR) analysis for *H pylori* urease gene A (*ureA*) were performed to detect *H pylori* infection. PCR analysis for *H pylori cagA* gene was performed to verify *cagA*⁺ *H pylori* infection. Fifty-eight patients whose both Warthin-Starry staining and PCR for *ureA* showed positive results were diagnosed as suffering from *H pylori* infection and 37 were *cagA*⁺ *H pylori*.

RT-PCR analysis of Bid, Bax and Bcl-2 mRNA

According to references^[37,38], primers were designed for β -actin (GenBank accession No.BC013380), 5' -GTG GGG CGC CCC AGG CAC CA-3' (sense) and 5' -CTC CTT AAT GTC ACG CAC GAT TTC-3' (antisense), 540 bp product; for Bid (GenBank accession No.AF087891), 5' -ATG GAC TGT TGA GGT CAA CAA C-3' (sense) and 5' -TCA GTC CAT CCC ATT TCT GGC T-3' (antisense), 588 bp product; for Bax (GenBank accession No.AY217036), 5' -ACC AAG AAG CTG AGC GAG TGT C-3' (sense) and 5' -ACA AAG ATG GTC ACG GTC TGC C-3' (antisense), 332 bp product; and for Bcl-2 (GenBank accession No.M13994), 5' -TGC ACC TGA CGC CCT TCA C-3' (sense), 5' -AGA CAG CCA GGA GAA ATC AAA CAG-3' (antisense), 293 bp product.

Total RNA was prepared from gastric adenocarcinoma

tissues and resection margin tissues by using TriPure isolation reagent (Roche) according to the manufacturer's protocol. Reverse transcription (RT) was performed for first-strand cDNA by using 2 µg of total RNA and 1 µl of oligo(dT)18 primer in the presence of 5 unit AMV reverse transcriptase (Promega), 20 unit RNase inhibitor, 0.5 mmol/L of each dNTP and 1×buffer in 20 µl for 60 min at 42 °C. Then 2 µl reverse transcription products were used for PCR. In a total of 20 µl reactive mixture, 5 pmol/L sense primer and 5 pmol/L antisense primer, 0.25 mmol/L of each dNTP, 1×reaction buffer and 1.5 unit Taq polymerase were mixed. The reaction was run for 33 cycles, and each consisted of denaturation at 94 °C for 60 s, annealing at 58 °C for 60 s, extension at 72 °C for 60 s and final extension prolonged for 7 min at 72 °C. PCR-amplified products (8 µl each) were analyzed on 1.5% agarose gels after ethidium bromide staining. Expression levels of Bid, Bax and Bcl-2 were quantitated using Quantity One quantitation software (Bio-Rad Laboratories) and were reported to be normalized to β-actin levels.

Statistical analysis

All data were presented as means ± standard error. Differences in means were examined by ANOVA, and correlations were analyzed by using Spearman's rank correlation coefficient (SPSS 10.0 for Windows). A *P* value < 0.05 was considered significant.

RESULTS

Effect of *H pylori* on expressions of Bid, Bax and Bcl-2 mRNA

In gastric adenocarcinoma tissues, expressions of Bid and Bax mRNA in *H pylori* negative group, *cagA*⁻ *H pylori* infection group and *cagA*⁺ *H pylori* infection group increased in an ascending pattern, respectively (*P* < 0.05). Expression of Bcl-2 in *H pylori* negative group was significantly lower than that in *H pylori* infection group (*P* < 0.05). Levels of Bcl-2 mRNA between *cagA*⁻ *H pylori* infection group and *cagA*⁺ *H pylori* infection group did not show any significant difference.

In resection margin tissues, expressions of Bid, Bax and Bcl-2 mRNA in *H pylori* negative group, *cagA*⁻ *H pylori* infection group and *cagA*⁺ *H pylori* infection group increased in turn (*P* < 0.05) (Figure 1, Tables 1-3).

Table 1 Effect of *H pylori* infection on expression of Bid

	Adenocarcinoma	Resection margin
<i>H pylori</i> (-)	0.304±0.113	0.377±0.119
<i>H pylori</i> (+) <i>cagA</i> (-)	0.422±0.149 ^a	0.686±0.285 ^a
<i>H pylori</i> (+) <i>cagA</i> (+)	0.855±0.305 ^{ac}	0.939±0.383 ^{ac}

^a*P* < 0.05, vs *H pylori* negative group, ^c*P* < 0.05, vs *cagA*⁻ *H pylori* infection group.

Table 2 Effect of *H pylori* infection on expression of Bax

	Adenocarcinoma	Resection margin
<i>H pylori</i> (-)	0.309±0.123	0.353±0.139
<i>H pylori</i> (+) <i>cagA</i> (-)	0.650±0.393 ^a	0.645±0.327 ^a
<i>H pylori</i> (+) <i>cagA</i> (+)	0.979±0.375 ^{ac}	1.001±0.361 ^{ac}

^a*P* < 0.05, vs *H pylori* negative group, ^c*P* < 0.05, vs *cagA*⁻ *H pylori* infection group.

Table 3 Effect of *H pylori* infection on expression of Bcl-2

	Adenocarcinoma	Resection margin
<i>H pylori</i> (-)	0.411±0.132	0.371±0.153
<i>H pylori</i> (+) <i>cagA</i> (-)	0.696±0.318 ^a	0.487±0.241 ^a
<i>H pylori</i> (+) <i>cagA</i> (+)	0.849±0.352 ^a	0.619±0.243 ^{ac}

^a*P* < 0.05, vs *H pylori* negative group, ^c*P* < 0.05, vs *cagA*⁻ *H pylori* infection group.

Correlation among levels of Bid, Bax and Bcl-2 mRNA

In *H pylori* negative group, levels of Bid and Bax mRNA correlated negatively with that of Bcl-2 in gastric adenocarcinoma tissues (Bid vs Bcl-2, *r* = -0.409, *P* < 0.05; Bax vs Bcl-2, *r* = -0.451, *P* < 0.05). In *H pylori* positive group, expressions of Bid and Bax did not correlate with that of Bcl-2 in adenocarcinoma tissues (Bid vs Bcl-2, *r* = 0.187, *P* > 0.05; Bax vs Bcl-2, *r* = 0.201, *P* > 0.05), but correlated positively with that of Bcl-2 respectively in resection margin tissues (Bid vs Bcl-2, *r* = 0.331, *P* < 0.05; Bax vs Bcl-2, *r* = 0.295, *P* < 0.05).

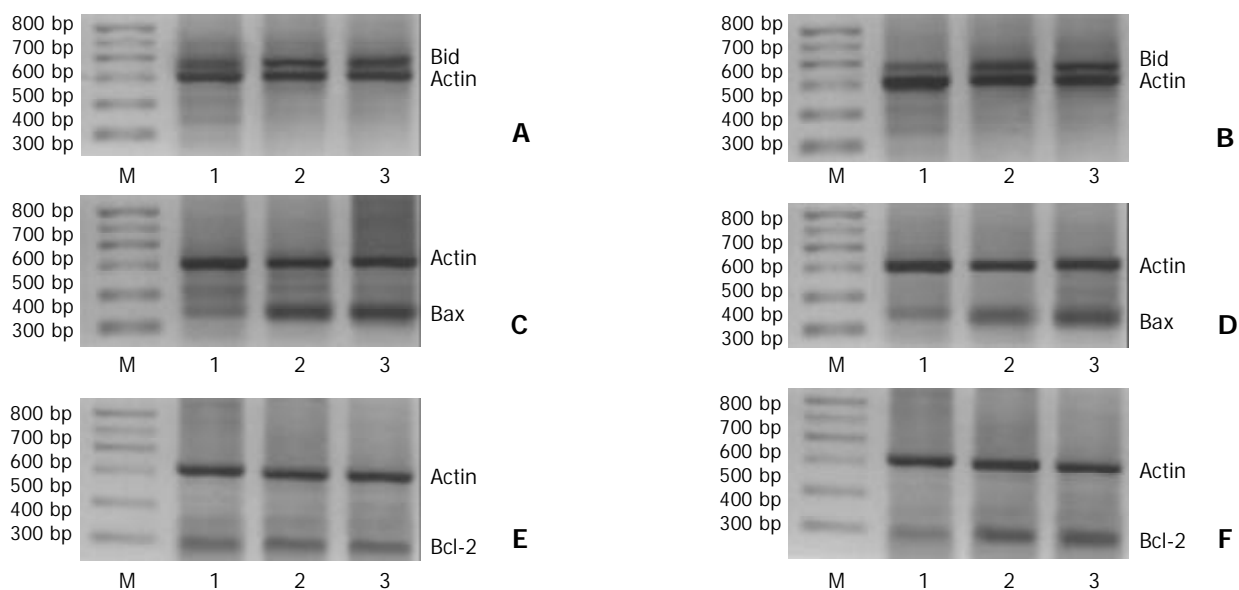


Figure 1 Effect of *H pylori* infection on mRNA expressions of Bcl-2 family members in gastric adenocarcinoma and resection margin tissues. A: Expression of Bid in gastric adenocarcinoma, B: Expression of Bid in resection margin, C: Expression of Bax in gastric adenocarcinoma, D: Expression of Bax in resection margin, E: Expression of Bcl-2 in gastric adenocarcinoma, F: Expression of Bcl-2 in resection margin, 1: *H pylori* negative group, 2: *cagA*⁻ *H pylori* group, 3: *cagA*⁺ *H pylori* group.

DISCUSSION

Bid, Bax and Bcl-2 are representative members of Bcl-2 family. Bid and Bax are pro-apoptosis members. Bcl-2 is an anti-apoptosis member. In the mechanism of regulating apoptosis, Bid as a BH3 domain protein, is one of the initiators to apoptosis and Bax is the key member. Either Bid or Bcl-2 must rely on Bax to induce or inhibit apoptosis^[39-43].

Studies have shown that *H pylori* infection could induce Fas antigen (Fas Ag) expression in gastric epithelial cells^[44]. In addition, *H pylori* infection was also associated with increased mucosal inflammatory cytokines, including TNF- α ^[45] and IFN- γ ^[46]. The cytokines generated during the immune response to *H pylori* also increased expression of Fas Ag in gastric cell lines^[47]. Fas Ag, after binding specifically to its ligand (Fas L), trimerizes and activates Caspase-8. Activation of Caspase-8 could result in the cleavage of cytosolic Bid to truncate tBID, which could translocate to mitochondria and initiate apoptosis^[48]. Shibayama et al^[31] found that *H pylori* infection induced the activation of Caspase-8 and the expression of Bid in human gastric epithelial cells, and inhibition of Caspase-8 suppressed the expression of Bid. In the present study, we found that *H pylori* infection upregulated expression of Bid mRNA in both gastric adenocarcinoma and resection margin tissues. That might be due to the upregulation of Fas and the activation of Caspase-8.

Bax is a cytosolic protein and translocates from the cytosol to the mitochondria for integration into the membrane following a proapoptotic stimulus. This action then results in cytochrome C release and initiates apoptosis. We have previously demonstrated that *H pylori* infection could promote Bax protein expression in chronic gastritis and premalignant lesions. Expression of Bax correlated positively with apoptotic index. The apoptotic index in Bax expression positive group in intestinal metaplasia, gastric dysplasia and gastric carcinoma was significantly higher than that in Bax negative group. In the present study, we found *H pylori* infection also increased levels of Bax mRNA in both gastric adenocarcinoma and resection margin tissues, and the effect was stronger in CagA⁺ *H pylori* group than cagA⁻ *H pylori* group. These results showed *H pylori* infection might promote apoptosis in gastric adenocarcinoma and its resection margin tissues.

Bcl-2 is an important anti-apoptosis protein. We found that Bcl-2 mRNA levels in *H pylori* negative group in gastric adenocarcinoma tissues were lower than in *H pylori* positive group. In resection margin tissues, Bcl-2 mRNA levels in *H pylori* negative group, cagA⁻ *H pylori* infection group and cagA⁺ *H pylori* infection group respectively increased in turn, suggesting that *H pylori* might promote expression of Bcl-2 in both gastric adenocarcinoma and resection margin tissues.

Although *H pylori* could promote expressions of Bid, Bax and Bcl-2, the correlations among them are still unclear. In the present study, it showed that levels of Bid and Bax mRNA were correlated negatively with that of Bcl-2 in gastric adenocarcinoma tissues without *H pylori* infection. This result is correspondent with the findings that apoptosis decreases in tumor tissues. In *H pylori* positive group, levels of Bid, Bax and Bcl-2 mRNA in gastric adenocarcinoma all increased. Besides, levels of Bid, Bax, and Bcl-2 did not correlate with each other. In the resection margin tissues, levels of Bid and Bax mRNA were correlated positively with that of Bcl-2. These results indicated that although *H pylori* could promote expressions of Bid, Bax and Bcl-2, it might play a different role in the development of gastric adenocarcinoma. In benign gastric lesions, *H pylori* infection might mainly upregulate expressions of pro-apoptotic genes such as Bid and Bax, and this effect might be stronger than its upregulatory effect on Bcl-2, which is consistent with the phenomena that *H pylori* infection increases apoptosis in atrophic gastritis and gastric

ulcer. During development of gastric adenocarcinoma, upregulatory effect of *H pylori* on anti-apoptotic genes, for example Bcl-2, might increase gradually and counteract pro-apoptosis effect of Bid and Bax, which may induce or worsen deregulation of apoptosis-associated genes expressions during the course of the formation of gastric adenocarcinoma.

Recently, it was found that not only excessive proliferation played an important role in gastric adenocarcinoma, but also reduction of apoptosis contributed to the carcinogenesis of gastric mucosa. The abnormal expressions of Bid, Bax and Bcl-2 induced by *H pylori* might result in inhibition of apoptosis, which may play an important role during development of gastric adenocarcinoma induced by *H pylori*^[49]. The detailed mechanism still remains to be studied.

REFERENCES

- 1 Jones RG, Trowbridge DB, Go MF. *Helicobacter pylori* infection in peptic ulcer disease and gastric malignancy. *Front Biosci* 2001; **6**: E213-226
- 2 Parsonnet J, Hansen S, Rodriguez L, Gelb AB, Warnke RA, Jellum E, Orentreich N, Vogelstein JH, Friedman GD. *Helicobacter pylori* infection and gastric lymphoma. *N Engl J Med* 1994; **330**: 1267-1271
- 3 Huang JQ, Sridhar S, Chen Y, Hunt RH. Meta-analysis of the relationship between *Helicobacter pylori* seropositivity and gastric cancer. *Gastroenterology* 1998; **114**: 1169-1179
- 4 Matsukura N. Relation between *Helicobacter pylori* and diseases: knowledge for clinician. *J Nippon Med Sch* 2002; **69**: 200-204
- 5 Miwa H, Go MF, Sato N. *H pylori* and gastric cancer: the Asian enigma. *Am J Gastroenterol* 2002; **97**: 1106-1112
- 6 Lan J, Xiong YY, Lin YX, Wang BC, Gong LL, Xu HS, Guo GS. *Helicobacter pylori* infection generated gastric cancer through p53-Rb tumor-suppressor system mutation and telomerase reactivation. *World J Gastroenterol* 2003; **9**: 54-58
- 7 Gao HJ, Yu LZ, Bai JF, Peng YS, Sun G, Zhao HL, Miu K, Lü XZ, Zhang XY, Zhao ZQ. Multiple genetic alterations and behavior of cellular biology in gastric cancer and other gastric mucosal lesions: *H pylori* infection, histological types and staging. *World J Gastroenterol* 2000; **6**: 848-854
- 8 Wang RT, Wang T, Chen K, Wang JY, Zhang JP, Lin SR, Zhu YM, Zhang WM, Cao YX, Zhu CW, Yu H, Cong YJ, Zheng S, Wu BQ. *Helicobacter pylori* infection and gastric cancer: evidence from a retrospective cohort study and nested case-control study in China. *World J Gastroenterol* 2002; **8**: 1103-1107
- 9 Xue FB, Xu YY, Wan Y, Pan BR, Ren J, Fan DM. Association of *H pylori* infection with gastric carcinoma: a Meta analysis. *World J Gastroenterol* 2001; **7**: 801-804
- 10 Cai L, Yu SZ, Zhang ZF. *Helicobacter pylori* infection and risk of gastric cancer in Changle County, Fujian Province, China. *World J Gastroenterol* 2000; **6**: 374-376
- 11 Zhang ZW, Farthing MJ. Molecular mechanisms of *H pylori* associated gastric carcinogenesis. *World J Gastroenterol* 1999; **5**: 369-374
- 12 Hu GY, Yu BP, Dong WG, Li MQ, Yu JP, Luo HS, Rang ZX. Expression of TFF2 and *Helicobacter pylori* infection in carcinogenesis of gastric mucosa. *World J Gastroenterol* 2003; **9**: 910-914
- 13 Yang YL, Xu B, Song YG, Zhang WD. Overexpression of c-fos in *Helicobacter pylori*-induced gastric precancerosis of Mongolian gerbil. *World J Gastroenterol* 2003; **9**: 521-524
- 14 Guo XL, Wang LE, Du SY, Fan CL, Li L, Wang P, Yuan Y. Association of cyclooxygenase-2 expression with Hp-cagA infection in gastric cancer. *World J Gastroenterol* 2003; **9**: 246-249
- 15 Schistosomes, liver flukes and *Helicobacter pylori*. IARC working Group on the Evaluation of Carcinogenic Risks to Humans. Lyon, 7-14 June 1994. *IARC Monogr Eval Carcinog Risks Hum* 1994; **61**: 1-241
- 16 Jang TJ, Kim JR. Proliferation and apoptosis in gastric epithelial cells of patients infected with *Helicobacter pylori*. *J Gastroenterol* 2000; **35**: 265-271
- 17 Chan AO, Wong BC, Lam SK. Gastric cancer: past, present and future. *Can J Gastroenterol* 2001; **15**: 469-474
- 18 Liu HF, Liu WW, Fang DC, Men RP. Expression and significance of proapoptotic gene Bax in gastric carcinoma. *World J Gastroenterol* 1999; **5**: 15-17

- 19 **Liu HF**, Liu WW, Fang DC, Liu FX, He GY. Clinical significance of Fas antigen expression in gastric carcinoma. *World J Gastroenterol* 1999; **5**: 90-91
- 20 **Maeda S**, Yoshida H, Mitsuno Hirata Y, Ogura K, Shiratori Y, Omata M. Analysis of apoptotic and antiapoptotic signalling pathways induced by *Helicobacter pylori*. *Gut* 2002; **50**: 771-778
- 21 **Wu YL**, Sun B, Zhang XJ, Wang SN, He HY, Qiao MM, Zhong J, Xu JY. Growth inhibition and apoptosis induction of Sulindac on Human gastric cancer cells. *World J Gastroenterol* 2001; **7**: 796-800
- 22 **Hamajima N**, Matuo K, Watanabe Y, Suzuki T, Nakamura T, Matsuura A, Yamao K, Ohashi K, Tominaga S. A pilot study to evaluate stomach cancer risk reduction by *Helicobacter pylori* eradication. *Am J Gastroenterol* 2002; **97**: 764-765
- 23 **Kodama M**, Fujioka T, Kodama R, Takahashi K, Kubota T, Murakami K, Nasu M. p53 expression in gastric mucosa with *Helicobacter pylori* infection. *J Gastroenterol Hepatol* 1998; **13**: 215-219
- 24 **Zhu GH**, Yang XL, Lai KC, Ching CK, Wong BC, Yuen ST, Ho J, Lam SK. Nonsteroidal antiinflammatory drugs could reverse *Helicobacter pylori*-induced apoptosis and proliferation in gastric epithelial cells. *Dig Dis Sci* 1998; **43**: 1957-1963
- 25 **Kohda K**, Tanaka K, Aiba Y, Yasuda M, Miwa T, Koga Y. Role of apoptosis induced by *Helicobacter pylori* infection in the development of duodenal ulcer. *Gut* 1999; **44**: 456-462
- 26 **Konturek PC**, Pierzchalski P, Konturek SJ, Meixner H, Faller G, Kirchner T, Hahn EG. *Helicobacter pylori* induces apoptosis in gastric mucosa through an upregulation of Bax expression in humans. *Scand J Gastroenterol* 1999; **34**: 375-383
- 27 **Fan X**, Crowe SE, Behar S, Gunasena H, Ye G, Haeberle H, Van Houten N, Gourley WK, Ernst PB, Reyes VE. The effect of class II major histocompatibility complex expression on adherence of *Helicobacter pylori* and induction of apoptosis in gastric epithelial cells: a mechanism for T helper cell type 1-mediated damage. *J Exp Med* 1998; **187**: 1659-1669
- 28 **Anti M**, Armuzzi A, Iascone E, Valenti A, Lippi ME, Covino M, Vecchio FM, Pierconti F, Buzzi A, Pignataro G, Bonvicini F, Gasbarrini G. Epithelial-cell apoptosis and proliferation in *Helicobacter pylori*-related chronic gastritis. *Ital J Gastroenterol Hepatol* 1998; **30**: 153-159
- 29 **Watanabe S**, Takagi A, Koga Y, Kamiya S, Miwa T. *Helicobacter pylori* induces apoptosis in gastric epithelial cells through inducible nitric oxide. *J Gastroenterol Hepatol* 2000; **15**: 168-174
- 30 **Takagi A**, Watanabe S, Igarashi M, Koike J, Hasumi K, Deguchi R, Koga Y, Miwa T. The effect of *Helicobacter pylori* on cell proliferation and apoptosis in gastric epithelial cell lines. *Aliment Pharmacol Ther* 2000; **14**(Suppl 1): 188-192
- 31 **Shibayama K**, Doi Y, Shibata N, Yagi T, Nada T, Inuma Y, Arakawa Y. Apoptotic signaling pathway activated by *Helicobacter pylori* infection and increase of apoptosis-inducing activity under serum-starved conditions. *Infect Immun* 2001; **69**: 3181-3189
- 32 **Igarashi M**, Kitada Y, Yoshiyama H, Takagi A, Miwa T, Koga Y. Ammonia as an accelerator of tumor necrosis factor alpha-induced apoptosis of gastric epithelial cells in *Helicobacter pylori* infection. *Infect Immun* 2001; **69**: 816-821
- 33 **Xia HH**, Talley NJ. Apoptosis in gastric epithelium induced by *Helicobacter pylori* infection: implications in gastric carcinogenesis. *Am J Gastroenterol* 2001; **96**: 16-26
- 34 **Puthalakath H**, Strasser A. Keeping killers on a tight leash: transcriptional and post-translational control of the pro-apoptotic activity of BH3-only proteins. *Cell Death Differ* 2002; **9**: 505-512
- 35 **Adams JM**, Cory S. The Bcl-2 protein family: arbiters of cell survival. *Science* 1998; **281**: 1322-1326
- 36 **Gross A**, McDonnell JM, Korsmeyer SJ. BCL-2 family members and the mitochondria in apoptosis. *Genes Dev* 1999; **13**: 1899-1911
- 37 **Lee EH**, Wan XH, Song J, Kang JJ, Cho JW, Seo KY, Lee JH. Lens epithelial cell death and reduction of anti-apoptotic protein Bcl-2 in human anterior polar cataracts. *Mol Vis* 2002; **8**: 235-240
- 38 **Tafani M**, Karpinich NO, Hurster KA, Pastorino JG, Schneider T, Russo MA, Farber JL. Cytochrome c release upon Fas receptor activation depends on translocation of full-length bid and the induction of the mitochondrial permeability transition. *J Biol Chem* 2002; **277**: 10073-10082
- 39 **Zong WX**, Lindsten T, Ross AJ, MacGregor GR, Thompson CB. BH3-only proteins that bind pro-survival Bcl-2 family members fail to induce apoptosis in the absence of Bax and Bak. *Genes Dev* 2001; **15**: 1481-1486
- 40 **Letai A**, Bassik MC, Walensky LD, Sorcinelli MD, Weiler S, Korsmeyer SJ. Distinct BH3 domains either sensitize or activate mitochondrial apoptosis, serving as prototype cancer therapeutics. *Cancer Cell* 2002; **2**: 183-192
- 41 **Theodorakis P**, Lomonosova E, Chinnadurai G. Critical requirement of BAX for manifestation of apoptosis induced by multiple stimuli in human epithelial cancer cells. *Cancer Res* 2002; **62**: 3373-3376
- 42 **Cheng EH**, Wei MC, Weiler S, Flavell RA, Mak TW, Lindsten T, Korsmeyer SJ. BCL-2, BCL-X(L) sequester BH3 domain-only molecules preventing BAX- and BAK-mediated mitochondrial apoptosis. *Mol Cell* 2001; **8**: 705-711
- 43 **Shangary S**, Johnson DE. Peptides derived from BH3 domains of Bcl-2 family members: a comparative analysis of inhibition of Bcl-2, Bcl-x(L) and Bax oligomerization, induction of cytochrome c release, and activation of cell death. *Biochemistry* 2002; **41**: 9485-9495
- 44 **Houghton J**, Macera-Bloch LS, Harrison L, Kim KH, Korah RM. Tumor necrosis factor alpha and interleukin 1beta up-regulate gastric mucosal Fas antigen expression in *Helicobacter pylori* infection. *Infect Immun* 2000; **68**: 1189-1195
- 45 **D'Elia MM**, Manghetti M, De Carli M, Costa F, Baldari CT, Burrioni D, Telford JL, Romagnani S, Del Prete G. T helper 1 effector cells specific for *Helicobacter pylori* in the gastric antrum of patients with peptic ulcer disease. *J Immunol* 1997; **158**: 962-967
- 46 **Harris PR**, Mobley HL, Perez-Perez GI, Blaser MJ, Smith PD. *Helicobacter pylori* urease is a potent stimulus of mononuclear phagocyte activation and inflammatory cytokine production. *Gastroenterology* 1996; **111**: 419-425
- 47 **Houghton J**, Korah RM, Condon MR, Kim KH. Apoptosis in *Helicobacter pylori*-associated gastric and duodenal ulcer disease is mediated via the Fas antigen pathway. *Dig Dis Sci* 1999; **44**: 465-478
- 48 **Wei MC**, Lindsten T, Mootha VK, Weiler S, Gross A, Ashiya M, Thompson CB, Korsmeyer SJ. tBID, a membrane-targeted death ligand, oligomerizes BAK to release cytochrome c. *Genes Dev* 2000; **14**: 2060-2071
- 49 **Konturek PC**, Konturek SJ, Pierzchalski P, Bielanski W, Duda A, Marlicz K, Starzynska T, Hahn EG. Cancerogenesis in *Helicobacter pylori* infected stomach—role of growth factors, apoptosis and cyclooxygenases. *Med Sci Monit* 2001; **7**: 1092-1107

Edited by Wang XL Proofread by Zhu LH

Chinese literature associated with diagnosis of *Helicobacter pylori*

Yi Wan, Yong-Yong Xu, Jian-Hui Jiang, Fan-Shu Kong, Fu-Bo Xue, Yu-Xiang Bai, Bo-Rong Pan, Jun Ren, Dai-Ming Fan

Yi Wan, Yong-Yong Xu, Jian-Hui Jiang, Fu-Bo Xue, Yu-Xiang Bai, Department of Health Statistics, Fourth Military Medical University, Xi'an 710032, Shaanxi Province, China

Fan-Shu Kong, Department of Postgraduate, Fourth Military Medical University, Xi'an 710032, Shaanxi Province, China

Bo-Rong Pan, Jun Ren, Department of Oncology of Xijing Hospital, Fourth Military Medical University, Xi'an 710032, Shaanxi Province, China

Dai-Ming Fan, Department of Gastroenterology of Xijing Hospital, Fourth Military Medical University, Xi'an 710032, Shaanxi Province, China

Supported by the National Natural Science Foundation of China, No. 30024002 and the University Key Teachers Fund of Ministry of Education of China, No. 2000-65

Correspondence to: Dai-Ming Fan, Department of Gastroenterology of Xijing Hospital, Fourth Military Medical University, Xi'an 710032, Shaanxi Province, China. fandaim@fmmu.edu.cn

Telephone: +86-29-3375221 **Fax:** +86-29-2539041

Received: 2003-06-16 **Accepted:** 2003-08-28

Abstract

AIM: To synthetically analyze and probe into the diagnosis of *H pylori* infection, we followed the principles of evidence-based medicine.

METHODS: A total of 22 papers of prevalence survey and case-control studies were selected for studying about diadynamic methods. Using meta-analysis, we analyzed the different diadynamic methods of *H pylori* in China.

RESULTS: Through meta-analysis, among the five diadynamic methods, the accuracy of polymerase chain reaction (PCR) was the highest (98.47%) and PCR was the most sensitive method (*Sp*: 99.03%).

CONCLUSION: Among the five diadynamic methods, the accuracy of PCR is the highest and PCR is the most sensitive method to diagnose the infection of *H pylori*.

Wan Y, Xu YY, Jiang JH, Kong FS, Xue FB, Bai YX, Pan BR, Ren J, Fan DM. Chinese literature associated with diagnosis of *Helicobacter pylori*. *World J Gastroenterol* 2004; 10(2): 231-233 <http://www.wjgnet.com/1007-9327/10/231.asp>

INTRODUCTION

Since *Helicobacter pylori* (*H pylori*) was first isolated in 1982,

the association of *H pylori* and related diseases has become the hot spot of gastroenterological studies. The distribution of *H pylori* infection is worldwide, and the prevalence rate of *H pylori* among populations is very high. With the deepening of *H pylori* researches, studies about *H pylori*, which aimed at effectively controlling the infection, were of great significance in preventing and curing the chronic stomach troubles. Because of the independence of each study and limit to the region and sample source, a great majority of studies did not have enough evidence and totally unanimous conclusion, which influenced the reliability of the conclusion. However, meta-analysis method could appraise and analyze synthetically the results of study with the same research purpose^[1], thus improving the efficiency of statistics, solving the problem with inconsistent results of studies, and making the conclusion of study more reliable. Therefore, we used meta-analysis to analyze synthetically the results of studies associated with *H pylori* diagnosis so as to express them more accurately.

MATERIALS AND METHODS

Literature selection and data

A Chinese biology and medicine database (CBM) search of non-review articles since 1995 was performed with the MeSH headings "*Helicobacter pylori*", "diagnosis", "polymerase chain reaction", "enzyme-linked immunosorbent assay" and "urea enzymes test".

Standard of selection The research objects were the population who could possibly suffer from *H pylori*, and the results of study had intact statistics.

***H pylori*-positive result judgment** *H pylori* cultivation was positive or one or two of the followings were positive: *H pylori* morphology (smear, histology or immunohistochemistry), urea enzyme test (RUT, ¹³C or ¹⁴C-urea breath test), PCR detection, serologic test (ELISA or immunoblotting test, etc.).

Standard of rejection The sample size was too small for statistical study, children less than one year old who possibly carried mother's antibody, studies without definite detection of *H pylori* or strict quality control.

Study on diadynamic methods of *H pylori* The literature search result were classified as follows. Twenty-two reports^[2-23] appraised synthetically according to 5 commonly used clinical diagnostic methods, the evaluation targets included sensitivity (*Se*), specificity (*Sp*) and accuracy (π). Bibliographic retrieval results of ¹³C-urea breath test, ¹⁴C-urea breath test, ELISA, RUT and PCR are shown in Tables 1-5.

Table 1 Related literature of ¹³C-urea breath test

Study No. (i)	<i>H pylori</i> positive		<i>H pylori</i> negative		<i>Se</i> (%)	<i>Sp</i> (%)	π (%)	<i>PV</i> (%)	<i>PV</i> ₊ (%)
	a	c	b	d					
1	36	0	0	24	100	98.50	99.40	100	100
2	148	5	0	165	96.70	100	98.41	97.06	100
3	13	0	1	23	100	95.83	97.41	100	92.86
4	39	3	0	10	92.86	100	94.23	76.92	100
5	42	0	0	10	100	96.97	99.42	100	100
6	52	2	3	13	96.30	81.25	92.86	94.55	86.67
7	47	1	0	32	97.92	100	98.75	97.14	100
8	147	3	0	3	98	90.70	97.86	96.10	95.30
9	74	3	0	49	96	100	97.56	94.23	100

Table 2 Related literature of ¹⁴C-urea breath test

Study No. (i)	<i>H pylori</i> positive		<i>H pylori</i> negative		Se (%)	Sp (%)	π (%)	PV. (%)	PV ₊ (%)
	a	c	b	d					
1	81	2	2	52	97.06	96.12	96.69	95.12	97.06
2	52	5	0	23	91.23	100	93.73	82.14	100
3	51	1	2	16	97.36	88.89	95.47	97.36	96.23
4	56	3	1	59	94.92	98.33	96.61	95.16	98.25
5	83	0	3	75	100	96.15	98.35	100	96.51
6	78	5	2	76	93.98	97.44	95.65	93.83	97.50
7	79	4	2	76	95.18	97.44	96.27	95	97.53

Table 3 Related literature of ELISA

Study No. (i)	<i>H pylori</i> positive		<i>H pylori</i> negative		Se (%)	Sp (%)	π (%)	PV. (%)	PV ₊ (%)
	a	c	b	d					
1	85	11	2	38	88.54	95	90.41	77.55	97.70
2	55	2	2	26	96.49	92.86	95.25	92.86	96.49
3	38	6	2	13	86.36	86.67	86.44	68.42	95
4	43	1	1	14	97.37	93.33	96.34	93.33	97.73
5	37	7	4	11	84.09	73.33	81.35	61.11	90.24
6	64	2	2	15	96.97	88.23	95.18	88.24	96.97
7	44	0	3	12	100	80	94.92	100	93.62

Table 4 Related literature of RUT

Study No. (i)	<i>H pylori</i> positive		<i>H pylori</i> negative		Se (%)	Sp (%)	π (%)	PV. (%)	PV ₊ (%)
	a	c	b	d					
1	34	2	0	24	94.44	100	96.64	92.31	100
2	32	10	0	10	76.19	100	80.77	50	100
3	38	4	1	9	89.74	90.91	89.97	69.23	97.44
4	30	2	2	17	93.75	89.47	92.16	89.74	93.75
5	55	4	7	53	93.22	88.33	90.73	92.98	88.71
6	62	4	4	13	93.94	76.47	90.36	76.47	93.94
7	46	8	4	12	85.52	75	83.12	60	92
8	151	50	11	47	75.12	81.03	76.35	48.45	93.21
9	171	30	7	51	85.07	87.93	85.84	62.96	96.07
10	72	15	0	63	82.76	100	90.02	80.77	100
11	227	22	6	29	91.16	82.86	90.05	56.86	97.42
12	73	14	0	63	83.91	100	90.66	81.82	100
13	58	7	1	30	89.23	96.77	91.65	81.08	98.31
14	34	0	7	28	100	80	89.86	100	82.93
15	64	15	3	13	81.01	81.25	81.05	46.43	95.52

Table 5 Related literature of PCR

Study No. (i)	<i>H pylori</i> positive		<i>H pylori</i> negative		Se (%)	Sp (%)	π (%)	PV. (%)	PV ₊ (%)
	a	c	b	d					
1	178	0	0	98	100	100	100	100	100
2	32	0	5	14	100	73.68	90.19	100	86.49
3	34	0	1	34	100	97.14	98.53	100	97.14
4	34	2	1	34	94.44	97.14	95.73	94.44	97.14
5	149	0	0	10	100	100	100	100	100
6	77	2	2	14	97.47	87.50	95.82	87.50	97.47

Methods

In the statistical analysis of data, Meta-analysis method with a fixed effect model and a random effect model was used to reach an integrated conclusion^[24-26].

RESULTS

Among the five diadynamic methods, the accuracy of PCR was the highest and PCR was the most sensitive method, specificity of ¹³C-urea breath test was the highest, the sensitivity and accuracy of RUT were the lowest, specificity of ELISA

was the lowest (Table 6).

Table 6 Synthetic evaluation of five diadynamic methods

Diadynamic methods	Se (%)	Sp (%)	π (%)
¹³ C-urea breath test	99.34	95.09	97.78
¹⁴ C-urea breath test	97.56	94.96	96.40
ELISA	93.96	81.78	90.09
PCR	98.25	99.03	98.47
RUT	95.58	71.19	87.02

DISCUSSION

This study used bibliographic retrieval to collect the relevant materials of *H pylori* infection, and meta-analysis, including combination of statistics in many studies by weight and equalized test, to analyze the diagnosis of *H pylori* infection.

The five diadynamic methods of *H pylori* infection all had a high sensitivity, specificity and accuracy, among which PCR was most sensitive and accurate. ¹³C-urea breath test was the most specific. As an ideal diadynamic method, it should have the following advantages: a high sensitivity and specificity, minimal incursions into or no damage to patients, simple and convenient in manipulation, less sophisticated technique or equipment, low cost and easy acceptance by patients. However, in fact, it is difficult for one diadynamic method to possess all these qualities. Above all, among the five diadynamic methods of *H pylori* infection, ELISA is the most convenient, which has the lowest cost and damage, therefore, serological positivity can merely explain the situation of whether patients have been infected or being infected. ¹³C-urea breath test has no harm, and can provide the whole infection information of stomach, which is relatively ideal, but it is difficult to popularize for the need of equipments and high expense. Although ¹⁴C-urea breath test can be done by well-equipped hospital and has lower cost than ¹³C-urea breath test, it has some radioactivity risk. RUT belongs to indirect test, whose intensity is determined by bacterial density of biopsy specimen. PCR is more sensitive than other methods. PCR can also detect *H pylori*, which cannot be detected by other methods, and at present it has been widely used in detection of various kinds of clinical specimens^[27]. So which diadynamic methods would be adopted in clinical detection must be determined according to the specific situation and different requirements^[28-32].

H pylori infection is common and study of *H pylori* infection involves a wide extent. A large number of researches and works on this aspect have been done in China, and have achieved a great progress, although some problems were found in these studies such as flaw in experimental design, scattered data, deficiency of objective and reliable conclusion. Therefore, many aspects of *H pylori* infection are still to be studied to obtain accurate and consummate results.

REFERENCES

- Schweitzer IL**, Dun AEG, Peters RL, Spears RL. Viral hepatitis B in neonates and infants. *Am J Med* 1973; **55**: 762-771
- Zhu RM**, Lu YK, Wang L. Analysis on antibodies of *Helicobacter pylori* in serum and saliva. *Zhonghua Xiaohua Zazhi* 1997; **17**: 342-344
- Xie Y**, Wang CW, Zhu JQ, Zhang KH. IgA to *Helicobacter pylori* in gastric juice and its clinical significance. *Zhonghua Weishengwuxue He Mianyixue Zazhi* 1997; **17**: 430-432
- Lu YK**, Xu GM, Zhou ZQ, Zhang HF. Purification of the specific antigens of *Helicobacter pylori* for semiquantitative serodiagnosis. *Dier Junyi Daxue Xuebao* 1997; **18**: 449-451
- Chen JP**, Xu CP, Cheng SJ, Xu QW, Liu FX, Wang ZH, Fuang DC, Guao PH. Microdose capsule-based ¹⁴C-urea breath test for the diagnosis of *Helicobacter pylori* infection. *Disan Junyi Daxue Xuebao* 1997; **19**: 317-320
- Qu HT**, Fang ZH, Liu Y, Yang XL. A modified PCR assay for detection of *Helicobacter pylori* in gastric biopsy specimens. *Zhonghua Xiaohua Neijing Zazhi* 1997; **14**: 207-210
- Xu CP**, Xu H, Cheng SJ, Xu QW, Liu FX, Wang ZH. ¹⁴C-urea breath test in the diagnosis of *Helicobacter pylori* infection in the stomach. *Zhonghua Neike Zazhi* 1995; **34**: 239-242
- Zhang WQ**, You JF, Hu B, Xiang ZQ, Xu CD. Reliability of ¹³C-urea breath test in detection of *Helicobacter pylori* infections in children. *Zhonghua Erke Zazhi* 1999; **37**: 484-485
- Kang HZ**, Ma JZ, Shu MJ, Cha JZ, Li BB, Wu YL, Xiang ZQ. ¹³C-urea breath test for the diagnosis of *Helicobacter pylori* infection in pediatric patients. *Linchuang Erke Zazhi* 1999; **17**: 137-140
- Li ZJ**, Zou WM, Jiang T. Evaluation of Salivary anti-*Hp* IgG detection in the diagnosis of *Helicobacter pylori* infection. *Linchuang Neike Zazhi* 1999; **16**: 88-89
- Peng H**, Pan GZ, Cao SZ, Zhao RG. The significance of detection of *Helicobacter pylori* in saliva. *Zhonghua Neike Zazhi* 1999; **38**: 171-173
- Wu LJ**, Zhang WJ, Zhang H, Deng GG. Comparison of three rapid diagnosis of *Helicobacter pylori* infection. *Disan Junyi Daxue Xuebao* 1999; **21**: 301-302
- Shu HJ**, Ge ZZ, Xiang ZQ, Liu Y, Ren WP, Xiao SD. Evaluation of detecting methods of *Helicobacter pylori* infection-histology, serology, ¹³Curea breath test, and Rapid urease tests. *Zhonghua Xiaohua Zazhi* 1998; **18**: 260-262
- Wu SM**, Shi Y, Liu WZ, Zhang DZ, Xiao SD, Xiang ZQ. Reliability of ¹³C-urea breath test (UBT) in detection of *Helicobacter pylori* infection. *Zhonghua Xiaohua Zazhi* 1998; **18**: 263-264
- Wang WH**, Hu FL, Jia BQ, Wang HH. Detection of *Helicobacter pylori* from gastric mucosa by using polymerase chain reaction. *Xin Xiaohuabingxue Zazhi* 1997; **5**: 11-12
- Zhang DR**, Hu GH, Wu F, Xiao SD, Yuan JM, Xiang ZQ. ¹⁴C-urea breath test in diagnosing *Helicobacter pylori* infection. *Shanghai Yixue* 1996; **19**: 373-375
- Huang QD**, Zheng PF, Cheng L, Cheng JX, Zhao L. Evaluation of trace of ¹⁴C-urea breath test in diagnosing *Helicobacter pylori* infection. *Linchuang Neike Zazhi* 1999; **16**: 80-81
- Zhang XY**, Xu SF, Yuan JP, Zhang HJ, Zhao ZQ. Parallel detection of *Helicobacter pylori* infection. *Zhonghua Xiaohua Neijing Zazhi* 1998; **15**: 166-167
- Jiang K**, Pan GZ, Wen SH, Yang XO, Bei L, Jiang J, Zhang CX. Evaluation of diagnostic methods of *Helicobacter pylori* infection. *Zhongguo Shiyong Neike Zazhi* 1998; **18**: 33-34
- Zhang WQ**, You JK, Lu YM, Yao PY, Cao LF, Ying CM, Xiang ZQ, Xiu CD. Comparison of rapid diagnosis of *Helicobacter pylori* infection in pediatric patients. *Linchuang Erke Zazhi* 1999; **17**: 140-141
- Su YQ**, Li CQ. Low dosage ¹³C-urea breath test in detection of *Helicobacter pylori* infection. *Zhongguo Neijing Zazhi* 1996; **2**: 39-41
- Zhu RM**, Lu YK, Wang L. Detection of antibodies of *Helicobacter pylori* in saliva. *Zhonghua Neike Zazhi* 1997; **36**: 469-470
- Zhao R**, Lin SR. Detection of *Helicobacter pylori* from gastric juices by using polymerase chain reaction. *Zhonghua Neike Zazhi* 1998; **37**:701-702
- Li LS**. Principle and Method for Study in Clinical medicine, Practical Clinical Epidemiology. 1sted. Xi'an. *Shaanxi Kexue Jishu Chubanshe* 2000: 357-372
- Guo ZC**. Yixue Tongjixue. 1sted. Beijing. *Renmin Junyi Chubanshe* 1999: 152-154
- Zhao N**, Yu SZ. The relationship of smoking and lung cancer in china: a Meta analysis. *Zhonghua Liuxingbingxue Zazhi* 1993; **14**: 350-353
- Guo MX**, Xu HJ, Zhao SL, Xiao HM, Hong FZ. Clinical significance of PCR in *Helicobacter pylori* DNA detection in human gastric disorders. *China Natl J New Gastroenterol* 1997; **2**: 98-100
- Liu YB**, Su LY. ¹⁴C-urea breath test to diagnosis *Helicobacter pylori*. *Xuzou Yixueyuan Xuebao* 1998; **18**: 118-119
- Yuan MB**, Liu XF. Laboratory diagnosis of *Helicobacter pylori*. *Yishi Jinxu Zazhi* 2002; **25**: 3-5
- Yan Y**, Qian LS, Wang WF. Research on of rapid diagnosis of *Helicobacter pylori*. *Fudan Xuebao* 2002; **29**: 410-413
- Lin H**, Zheng DZ, Ye HQ, Wei L, Wang QG, Tang FK. Comparison of five detection methods for *Helicobacter pylori*. *Haixia Yufang Yixue Zazhi* 2001; **7**: 38-39
- Li XB**, Liu WZ, Ge ZZ, Ran ZH, Chen XY, Xiu WW, Xiao SD. Evaluate of normal diagnosis of *Helicobacter pylori*. *Zhonghua Xiaohua Zazhi* 2002; **22**: 691-693

Stable expression of human cytochrome P450 2D6*10 in HepG2 cells

Jian Zhuge, Ying-Nian Yu, Xiao-Dan Wu

Jian Zhuge, Ying-Nian Yu, Department of Pathology and Pathophysiology, School of Medicine, Zhejiang University, Hangzhou 310031, Zhejiang Province, China

Xiao-Dan Wu, Center of Analysis, Zhejiang University, Hangzhou 310031, Zhejiang Province, China

Supported by National Natural Science Foundation of China, No. 39770868 and Natural Science Foundation of Zhejiang Province, No. 397490

Correspondence to: Professor Ying-Nian Yu, Department of Pathology and Pathophysiology, School of Medicine, Zhejiang University, Hangzhou 310031, Zhejiang Province, China. ynyu@mail.hz.zj.cn
Telephone: +86-571-87217149 **Fax:** +86-571-87217149

Received: 2003-06-26 **Accepted:** 2003-08-16

Abstract

AIM: Over 90% of drugs are metabolized by the cytochrome P-450 (CYP) family of liver isoenzymes. The most important enzymes are CYP1A2, 3A4, 2C9/19, 2D6 and 2E1. Although CYP2D6 accounts for <2% of the total CYP liver enzyme content, it mediates metabolism in almost 25% of drugs. In order to study its enzymatic activity for drug metabolism, its cDNA was cloned and a HepG2 cell line stably expressing CYP2D6 was established.

METHODS: Human *CYP2D6* cDNA was amplified with reverse transcription-polymerase chain reaction (RT-PCR) from total RNA extracted from human liver tissue and cloned into pGEM-T vector. cDNA segment was identified by DNA sequencing and subcloned into a mammalian expression vector pREP9. A cell line was established by transfecting the recombinant plasmid of pREP9-CYP2D6 to hepatoma HepG2 cells. Expression of mRNA was validated by RT-PCR. Enzyme activity of catalyzing dextromethorphan *O*-demethylation in postmitochondrial supernatant (S9) fraction of the cells was determined by high performance liquid chromatography (HPLC).

RESULTS: The cloned cDNA had 4 base differences, e.g. 100 C→T, 336 T→C, 408 C→G and 1 457 G→C, which resulted in P34S, and S486T amino acid substitutions, and two samesense mutations were 112 F and 136 V compared with that reported by Kimura *et al* (GenBank accession number: M33388). P34S and S486T amino acid substitutions were the characteristics of *CYP2D6*10* allele. The relative activity of S9 fraction of HepG2-CYP2D6*10 metabolized dextromethorphan *O*-demethylation was found to be 2.31 ± 0.19 nmol·min⁻¹·mg⁻¹ S9 protein ($n=3$), but was undetectable in parental HepG2 cells.

CONCLUSION: cDNA of human *CYP2D6*10* can be successfully cloned. A cell line, HepG2-CYP2D6*10, expressing CYP2D6*10 mRNA and having metabolic activity, has been established.

Zhuge J, Yu YN, Wu XD. Stable expression of human cytochrome P450 2D6*10 in HepG2 cells. *World J Gastroenterol* 2004; 10 (2): 234-237

<http://www.wjgnet.com/1007-9327/10/234.asp>

INTRODUCTION

Over 90% of drugs are metabolized by the cytochrome P-450 (CYP) family of liver isoenzymes^[1]. The most important enzymes are CYP1A2, 3A4, 2C9/19, 2D6 and 2E1. Although CYP2D6 accounts for <2% of the total CYP liver enzyme content, it mediates metabolism in almost 25% of drugs. Among these are many antipsychotics and antidepressants, beta-blockers, antiarrhythmic agents and opiates^[2,3]. *CYP2D6* exhibits extensive polymorphism. Over 40 *CYP2D6* allelic variants have been discovered^[4] (<http://www.imm.ki.se/CYPalleles/cyp2d6.htm>).

Human CYP1A1^[5], CYP2B6^[5], CYP2A6^[6], CYP3A4^[7], CYP2C9^[8], CYP2C18^[9] and a phase II metabolism enzyme UDP-glucuronosyltransferase, UGT1A9^[10] have been stably expressed in Chinese hamster lung CHL cells in our laboratory. Among the human hepatic cell lines, HepG2 is derived from a human liver tumor and characterized by many xenobiotic-metabolizing activities as compared to fibroblasts. Therefore, HepG2 cell is useful in the prediction of the metabolism and cytotoxicity of chemicals in human liver^[11]. But it does not produce a significant amount of CYP^[12,13]. Yoshitomi *et al*^[14] have established stable expression of a series of human CYP subtypes, e.g. CYP1A1, CYP1A2, CYP2A6, CYP2B6, CYP2C8, CYP2C9, CYP2C19, CYP2D6, CYP2E1 and CYP3A4, respectively in the HepG2 cells.

In this study human *CYP2D6*10* cDNA was amplified with reverse transcription-polymerase chain reaction (RT-PCR), and a cell line stably expressing CYP2D6.10 was established.

MATERIALS AND METHODS

Materials

Restriction endonucleases and Moloney murine leukemia virus (M-MuLV) reverse transcriptase were supplied by MBI Fermentas AB, Lithuania. PCR primers, DNA sequence primers, random hexamer primers and dNTPs were synthesized or supplied by Shanghai Sangon Biotechnology Co. Expand fidelity PCR system and NADPH were from Roche Molecular Biochemicals. DNA sequencing kit was purchased from Perkin-Elmer Co. TRIzol reagent, G418, Dulbecco's modified Eagle's medium (DMEM) and newborn bovine calf sera were from Gibco. Diethyl pyrocarbonate (DEPC), dextromethorphan HBr and dextrophan D-tartrate were purchased from Sigma/RBI. T4 DNA ligase and pGEM-T vector system were from Promega. HPLC solvents and other chemicals were all of the highest grade from commercial sources.

Methods

Cloning of human *CYP2D6* cDNA from human liver Total RNA was extracted from a surgical specimen of human liver with TRIzol reagent according to the manufacture's instructions. RT-PCR amplifications using expand fidelity PCR system were described before. Two specific 28-mer oligonucleotide PCR primers were designed according to the cDNA sequence of *CYP2D6* reported by Kimura *et al*^[15] (GenBank accession no.M33388). The sense primer corresponding to base position -12 to 13 was CYP2D6 F1: 5' -

CTCGAGGCAGGTATGGGGCTAGAAG-3', with a restriction site of *Xho* I, and the anti-sense one, corresponding to the base position from 1 503 to 1 530, was CYP2D6 R1: 5' - GGATCCTGAGCAGGCTGGGGACTAGGTA-3', with a restriction site of *Bam*HI. The anticipated PCR products were 1.543 kb in length. PCR was performed at 94 °C for 5 min, then 35 cycles at 94 °C for 60 s, at 62 °C for 60 s, at 72 °C for 2 min, and a final extension at 72 °C for 10 min. An aliquot (10 µL) from PCR was subjected to electrophoresis in a 1% agarose gel stained with ethidium bromide.

Construction of recombinant pGEM-CYP2D6 and sequencing of CYP2D6 cDNA^[8] The PCR products were ligated with pGEM-T vector, and transformed to *E. coli* DH5α. cDNA of *CYP2D6* cloned in pGEM-T was sequenced by dideoxy chain-termination method marked with BigDye with primers of T7, SP6 promoters and two specific primers of 5' - ACCTCATGAATCACGGCAGT-3' (1 088-1 069), and 5' - CCGTGTCCAACAGGAGA-3' (987-1 003). The termination products were dissolved and detected using an automated DNA sequencer (Perkin-Elmer-ABI Prism 310).

Construction of pREP9 based expression plasmid for CYP2D6^[8] *Xho* I/*Bam*HI fragment having the total span of human *CYP2D6* cDNA in pGEM-CYP2D6 was subcloned to a mammalian expression vector pREP9 (Invitrogen). The recombinant was transformed to *E. coli* Top 10, screened by ampicillin resistant and identified by restriction mapping.

Transfection and selection^[8, 16] HepG2 cells were maintained as monolayer cell cultures at 37 °C in DMEM supplemented with 10% new born calf sera. HepG2 cells were transfected with the resultant recombinant plasmid, pREP9-CYP2D6, using a modified calcium phosphate method. A cell line named HepG2-CYP2D6 was established by selecting in the culture medium containing G418.

RT-PCR assay of CYP2D6 mRNA expression in HepG2-CYP2D6 and HepG2 cells Total RNA was prepared from G-418-resistant clones by TRIzol reagent. RT-PCR was performed as described before^[8], using 200 mmol·L⁻¹ of CYP2D6F1 and CYP2D6R1 primers and 200 mmol·L⁻¹ primers of beta-actin as internal control. The sense and anti-sense primers used for PCR amplification of beta-actin (GenBank accession no. NM_001101) are 5' -TCCCTGGAGAAGAGCTACGA-3' (776-795) and 5' -CAAGAAAGGGTGTACGCAAC-3' (1 217-1 237), respectively. PCR was performed at 94 °C for 2 min, then 35 cycles at 94 °C for 30 s, at 62 °C for 30 s, at 72 °C for 90 s, and a final extension at 72 °C for 7 min. The anticipated beta-actin PCR products were 462 bp in length and that of *CYP2D6* were 1 543 bp in length. An aliquot (10 µL) from PCR was subjected to electrophoresis in a 1.2% agarose gel stained with ethidium bromide.

Preparation of postmitochondrial supernant (S9) of HepG2-CYP2D6 The procedure for the preparation of S9 fraction was described before^[8]. The protein in S9 was determined by Lowry's method, with bovine serum albumin as standard.

Dextromethorphan O-demethylation assays^[17-20] *CYP2D6* dextromethorphan *O*-demethylation activity of S9 was determined by reversed phase high performance liquid chromatography (HPLC). Briefly, incubation reactions were performed in 50 mmol·L⁻¹ potassium phosphate buffer (pH7.4), containing 3 mmol·L⁻¹ MgCl₂, 1 mmol·L⁻¹ EDTA, 40 mmol·L⁻¹ dextromethorphan and 200 µg S9 protein in a final volume of 200 µL. Reactions were initiated by addition of 1 mmol·L⁻¹ NADPH and terminated with 30% acetic acid after incubation for 10 min at 37 °C. Protein was precipitated by centrifugation at 10 000 g for 4 min, and the supernatant was stored at -20 °C for analysis. On HPLC analysis, 10 µL of supernatant was injected into a Water HPLC equipped with a Shimadzu RF-535 fluorescence detector. A CLC phenyl column (15 cm×4.5-mm

i.d.) was used to separate the metabolites. The mobile phase consisted of a mixture of 30% acetonitrile, 1% acetic acid, and 0.05% triethylamine in water. The flow rate through the column at 25 °C was 0.75 ml·min⁻¹. The excitation and emission wavelengths of the fluorescence detector were 285 nm and 310 nm, respectively. The rates of product formation were determined from standard curves prepared by adding varying amounts of dextrophan D-tartrate to incubations conducted without NADPH.

RESULTS

Construction of human CYP2D6*10 cDNA recombinants

The pGEM-CYP2D6 recombinant was constructed by inserting human *CYP2D6* cDNA into the pGEM-T vector. Selection and identification of the recombinant were carried out by *Xho* I/*Bam*HI endonuclease digestion, agarose gel electrophoresis (Figure 1) and DNA sequencing. Compared with the cDNA sequence reported by Kimura *et al.*^[15] (GenBank accession no. M33388), differences were found in 100 C→T, 336 T→C, 408 C→G and 1457 G→C, that result in P34S and S486T amino acid substitutions, and two samesense mutations of 112 F and 136 V.

The *Xho* I/*Bam*HI fragment (1.543 kb) containing the complete *CYP2D6* cDNA was subcloned into the *Xho* I/*Bam*HI site of mammalian expression vector pREP9. Selection and identification of the recombinant were carried out by *Xho* I/*Bam*HI endonuclease digestion and agarose gel electrophoresis (Figure 1). The resulting plasmid was designated as pREP9-CYP2D6 and contained the entire coding region, along with 11 bp of the 5' and 35 bp of the 3' untranslated region of *CYP2D6* cDNA, respectively.

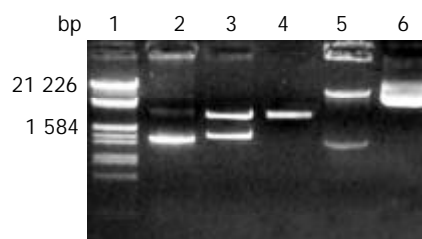


Figure 1 Electrophoresis identification of pGEM-CYP2D6 and pREP9-CYP2D6 recombinants. Lane 1: Marker (λ /*Eco*R I and *Hind* III), 2: PCR products of *CYP2D6* (1.543 kb), 3: Recombinant of pGEM-CYP2D6 digested by *Xho* I and *Bam*HI, 4: pGEM-T vector (3 kb), 5: Recombinant of pREP9-CYP2D6 digested by *Xho* I and *Bam*HI, 6: pREP9 vector (10.5 kb).

Establishment of cell line HepG2-CYP2D6

HepG2 cells were transfected with pREP9-CYP2D6, and selected with G418. The surviving clones were subcultured and the cell line termed HepG2-CYP2D6 was established.

RT-PCR assay of CYP2D6 mRNA expression in HepG2-CYP2D6 cells

CYP2D6 mRNA expression in HepG2-CYP2D6 cells was detected by RT-PCR with CYP2D6F1 and CYP2D6R1 primers. It was easily to identify a 1.5 kb band from HepG2-CYP2D6 cells, but not from HepG2 cells (Figure 2).

Dextromethorphan O-demethylation activity in HepG2-CYP2D6 cells

The dextromethorphan *O*-demethylation activity in S9 of HepG2-CYP2D6 cells was assayed by reverse HPLC. A typical elution profile of metabolites in supernatant was shown (Figure 3). The retention times for dextrophan and dextromethorphan

were 6.5 min and 16.8 min, respectively. The CYP2D6 enzyme activity towards dextromethorphan *O*-demethylation was found to be $2.31 \pm 0.19 \text{ nmol} \cdot \text{min}^{-1} \cdot \text{mg}^{-1}$ S9 protein ($n=3$), but was undetectable in parent HepG2 cells.

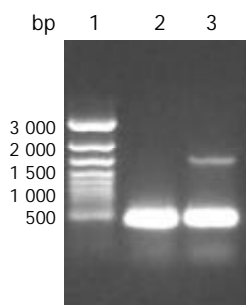


Figure 2 Identification of CYP2D6 mRNA expression in HepG2-CYP2D6 and HepG2 cells by RT-PCR with beta-actin as internal control. Lane 1: 1 kb ladder marker, 2: RT-PCR products of HepG2 cells showing a 462 bp of beta-actin, 3: RT-PCR products of HepG2-CYP2D6 cells showing a 462 bp of beta-actin and 1.5 kb of CYP2D6.

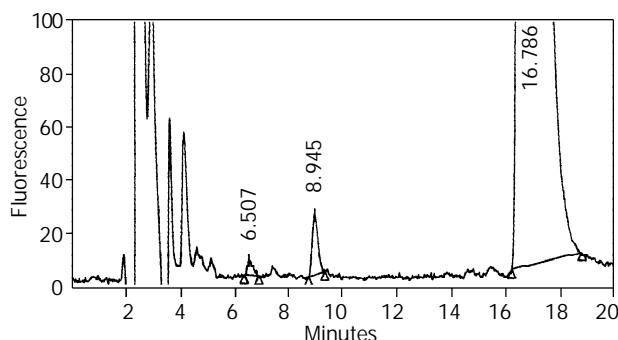


Figure 3 Representative chromatograms of metabolites in supernatant. 10 μL of supernatant was injected into a Water HPLC equipped with a Shimadzu RF-535 fluorescence detector. A CLC phenyl column (15 $\text{cm} \times 4.5\text{-mm}$ i.d.) was used to separate the metabolites. The mobile phase consisted of a mixture of 30% acetonitrile, 1% acetic acid, and 0.05% triethylamine in water. The flow rate through the column at 25 $^{\circ}\text{C}$ was $0.75 \text{ mL} \cdot \text{min}^{-1}$. The excitation and emission wavelengths of the fluorescence detector were 285 nm and 310 nm, respectively. The retention times for dextrophan and dextromethorphan were 6.5 min and 16.8 min, respectively. The retention time of an unidentified metabolite was 8.9 min.

DISCUSSION

The gene encoding CYP2D6 enzyme is localized on chromosome 22. Three major mutant alleles, termed *CYP2D6**3, *4, and *5, associated with the poor metabolizer (PM) phenotype, were found early on in Caucasians^[3]. *CYP2D6* gene has turned out to be extremely polymorphic with 44 alleles described to 10-Nov-2003 (<http://www.imm.ki.se/CYPalleles/cyp2d6.htm>). Three fairly population specific alleles have been found with *CYP2D6**4 in Caucasians, *10 in Asians and *17 in Africans^[3]. The *CYP2D6**10 allele with 100 C→T and 1457 G→C, can result in P34S and S486T amino acids substitute and an unstable enzyme with decreased catalytic activity. This allele occurred from 38% to 70% in Asian population^[4]. The most frequent allele in Chinese was *CYP2D6**10 allele with a frequency of about 51.3%^[21], it was 57.2% in Guangdong Chinese population^[22], 41.17% in Hong Kong Chinese population^[23]. The *CYP2D6* cDNA we cloned has the characteristics of *CYP2D6**10 allele with 2 amino acid substitutions of P34S and S486T.

Ramamoorthy *et al*^[24] have compared CYP2D6.10 with CYP2D6.1 *in vitro* in a baculovirus expression system using various substrates, such as dextromethorphan, *P*-methoxyamphetamine, 1-methyl-4-phenyl-1, 2, 3, 6-tetrahydropyridine and (+/-)-3, 4-methylenedioxymethamphetamine, the ratio of intrinsic clearance ($V_{\text{max}}/K_{\text{m}}$) of CYP2D6.1 to CYP2D6.10 was 50, 34, 22 and 123, respectively.

Yu *et al*^[25] reported that the purified CYP2D6.10 enzyme prepared from *in vitro* and to a high homogeneity was reconstituted with lipid and cytochrome P450 reductase, and exhibited an estimated enzyme efficiency (as $V_{\text{max}}/K_{\text{m}}$) 50-fold lower for dextromethorphan *O*-demethylation and 100-fold lower for fluoxetine *N*-demethylation when compared with CYP2D6.1, whereas no measurable catalytic activity was observed for this variant toward codeine.

The intrinsic clearances ($V_{\text{max}}/K_{\text{m}}$) in reconstituted microsomes expressing CYP2D6.10 were reduced by 135-fold with (+/-)-3, 4-methylenedioxymethamphetamine and by 164-fold with dextromethorphan compared with that of wild-type CYP2D6.1^[26].

Bufuralol 1'-hydroxylase activity in microsomes of yeast expressing CYP2D6.10 was rapidly decreased by heat treatment, supporting the idea that the thermal stability of the enzyme was reduced by amino acid replacement. Thermal instability together with the reduced intrinsic clearance of CYP2D6.10 is one of the causes responsible for the known fact that Orientals show lower metabolic activities than Caucasians for drugs metabolized mainly by CYP2D6^[27].

Subjects homozygous for *CYP2D6**10 had higher total areas under the plasma concentration-time curve, lower apparent oral clearances, and longer mean plasma half-life of nortriptyline than subjects in the *CYP2D6**1/*1 and the heterozygous groups^[28].

The plasma haloperidol concentration/dose ratio was significantly higher in older subjects (at least 50 years old) than in younger subjects with non-*2D6**10 homozygous genotypes, but not for those with *2D6**10 homozygous genotype^[29]. No significant differences in plasma concentration of fluvoxamine divided by daily dose of fluvoxamine per body weight ratio were found between subjects with no, one or two *CYP2D6**10 alleles in Japanese subjects^[30].

Cai *et al*^[31] found that patients with homozygous mutant of *CYP2D6**10 not only had a plasma concentration at peak (C_{max}) of propafenone two times as high as those of wild-type genotype, but also showed a two-fold higher inhibitory rate of ventricular premature contractions compared with those with homozygous *CYP2D6**1.

Venlafaxine, a new antidepressant, is metabolized mainly by CYP2D6 to an active metabolite, *O*-desmethylvenlafaxine. C_{max} and areas under the plasma concentration-time curve of venlafaxine were 184% and 484% higher in the *CYP2D6**10/*10 subjects than in the *CYP2D6**1/*1 subjects^[32].

Bufuralol 1'-hydroxylation has been commonly used by pharmaceutical industry to study *in vitro* drug interactions for CYP2D6^[33]. Dextromethorphan has been a widely used probe drug for human CYP2D6 activity both *in vitro* and *in vivo*^[34]. In humans, dextromethorphan is metabolized to dextrophan, 3-methoxymorphinan and 3-hydroxymorphinan. CYP2D6 contributes at least 80% to the formation of dextrophan, and CYP3A4 contributes more than 90% to the formation of 3-hydroxymorphinan. Dextromethorphan as a marker for monitoring both CYP2D6 and CYP3A activities has been found to be practical in human liver microsomal preparation^[35].

The expression of CYP2D6*10 mRNA was validated by RT-PCR. The dextromethorphan *O*-demethylation of HepG2-CYP2D6*10 was $2.31 \pm 0.19 \text{ nmol} \cdot \text{min}^{-1} \cdot \text{mg}^{-1}$ S9 protein, which was higher than baculovirus expressed CYP2D6 ($1.3420 \pm 0.1466 \text{ nmol} \cdot \text{min}^{-1} \cdot \text{mg}^{-1}$ protein) and human liver

microsome 0.17 to 0.30 nmol·min⁻¹·mg⁻¹ protein^[36]. This cell line is a useful tool for further studies of the function and biochemical mechanism of CYP2D6.10 enzyme.

REFERENCES

- Danielson PB.** The cytochrome P450 superfamily: biochemistry, evolution and drug metabolism in humans. *Curr Drug Metab* 2002; **3**: 561-597
- Anzenbacher P,** Anzenbacherova E. Cytochromes P450 and metabolism of xenobiotics. *Cell Mol Life Sci* 2001; **58**: 737-747
- Bertilsson L,** Dahl ML, Dalen P, Al-Shurbaji A. Molecular genetics of CYP2D6: clinical relevance with focus on psychotropic drugs. *Br J Clin Pharmacol* 2002; **53**: 111-122
- Bradford LD.** CYP2D6 allele frequency in European Caucasians, Asians, Africans and their descendants. *Pharmacogenomics* 2002; **3**: 229-243
- Wu J,** Dong H, Cai Z, Yu Y. Stable expression of human cytochrome CYP2B6 and CYP1A1 in Chinese hamster CHL cells: their use in micronucleus assays. *Chin Med Sci J* 1997; **12**: 148-155
- Yan L,** Yu Y, Zhuge J, Xie HY. Cloning of human cytochrome P450 2A6 cDNA and its expression in mammalian cells. *Zhongguo Yaolixue Yu Dulixue Zazhi* 2000; **14**: 31-35
- Chen Q,** Wu J, Yu Y. Establishment of transgenic cell line CHL-3A4 and its metabolic activation. *Zhonghua Yufang Yixue Zazhi* 1998; **32**: 281-284
- Zhuce J,** Yu YN, Li X, Qian YL. Cloning of cytochrome P-450 2C9 cDNA from human liver and its expression in CHL cells. *World J Gastroenterol* 2002; **8**: 318-322
- Zhuce J,** Yu YN, Qian YL, Li X. Establishment of a transgenic cell line stably expressing human cytochrome P450 2C18 and identification of a CYP2C18 clone with exon 5 missing. *World J Gastroenterol* 2002; **8**: 888-892
- Li X,** Yu YN, Zhu GJ, Qian YL. Cloning of UGT1A9 cDNA from liver tissues and its expression in CHL cells. *World J Gastroenterol* 2001; **7**: 841-845
- Rueff J,** Chiapella C, Chipman JK, Darroudi F, Silva ID, Duvergeran Bogaert M, Fonti E, Glatt HR, Isern P, Laires A, Leonard A, Llagostera M, Mossesso P, Natarajan AT, Palitti F, Rodrigues AS, Schinoppi A, Turchi G, Werle-Schneider G. Development and validation of alternative metabolic systems for mutagenicity testing in short-term assays. *Mutat Res* 1996; **353**: 151-176
- Rodriguez-Antona C,** Donato MT, Boobis A, Edwards RJ, Watts PS, Castell JV, Gomez-Lechon MJ. Cytochrome P450 expression in human hepatocytes and hepatoma cell lines: molecular mechanisms that determine lower expression in cultured cells. *Xenobiotica* 2002; **32**: 505-520
- Jover R,** Bort R, Gomez-Lechon MJ, Castell JV. Cytochrome P450 regulation by hepatocyte nuclear factor 4 in human hepatocytes: a study using adenovirus-mediated antisense targeting. *Hepatology* 2001; **33**: 668-675
- Yoshitomi S,** Ikemoto K, Takahashi J, Miki H, Namba M, Asahi S. Establishment of the transformants expressing human cytochrome P450 subtypes in HepG2, and their applications on drug metabolism and toxicology. *Toxicol In Vitro* 2001; **15**: 245-256
- Kimura S,** Umeno M, Skoda RC, Meyer UA, Gonzalez FJ. The human debrisoquine 4-hydroxylase (CYP2D) locus: sequence and identification of the polymorphic CYP2D6 gene, a related gene, and a pseudogene. *Am J Hum Genet* 1989; **45**: 889-904
- Sambrook J,** Fritsch EF, Maniatis T. Molecular Cloning, A Laboratory Manual, 2nd ed. New York: Cold Spring Harbor Laboratory Press 1989: 6.28-6.29
- Kronbach T,** Mathys D, Umeno M, Gonzalez FJ, Meyer UA. Oxidation of midazolam and triazolam by human liver cytochrome P450III A4. *Mol Pharmacol* 1989; **36**: 89-96
- Palamanda JR,** Casciano CN, Norton LA, Clement RP, Favreau LV, Lin C, Nomeir AA. Mechanism-based inactivation of CYP2D6 by 5-fluoro-2-[4-[(2-phenyl-1H-imidazol-5-yl)methyl]-1-piperazinyl]pyrimidine. *Drug Metab Dispos* 2001; **29**: 863-867
- Yu A,** Dong H, Lang D, Haining RL. Characterization of dextromethorphan O- and N-demethylation catalyzed by highly purified recombinant human CYP2D6. *Drug Metab Dispos* 2001; **29**: 1362-1365
- Barecki ME,** Casciano CN, Johnson WW, Clement RP. *In vitro* characterization of the inhibition profile of loratadine, desloratadine, and 3-OH-desloratadine for five human cytochrome P-450 enzymes. *Drug Metab Dispos* 2001; **29**: 1173-1175
- Ji L,** Pan S, Marti-Jaun J, Hanseler E, Rentsch K, Hersberger M. Single-step assays to analyze CYP2D6 gene polymorphisms in Asians: allele frequencies and a novel *14B allele in mainland Chinese. *Clin Chem* 2002; **48**: 983-988
- Gao Y,** Zhang Q. Polymorphisms of the GSTM1 and CYP2D6 genes associated with susceptibility to lung cancer in Chinese. *Mutat Res* 1999; **444**: 441-449
- Garcia-Barcelo M,** Chow LY, Chiu HF, Wing YK, Lee DT, Lam KL, Waye MM. Genetic analysis of the CYP2D6 locus in a Hong Kong Chinese population. *Clin Chem* 2000; **46**: 18-23
- Ramamoorthy Y,** Tyndale RF, Sellers EM. Cytochrome P450 2D6.1 and cytochrome P450 2D6.10 differ in catalytic activity for multiple substrates. *Pharmacogenetics* 2001; **11**: 477-487
- Yu A,** Kneller BM, Rettie AE, Haining RL. Expression, purification, biochemical characterization, and comparative function of human cytochrome P450 2D6.1, 2D6.2, 2D6.10, and 2D6.17 allelic isoforms. *J Pharmacol Exp Ther* 2002; **303**: 1291-1300
- Ramamoorthy Y,** Yu AM, Suh N, Haining RL, Tyndale RF, Sellers EM. Reduced (+/-)-3,4-methylenedioxymethamphetamine ("Ecstasy") metabolism with cytochrome P450 2D6 inhibitors and pharmacogenetic variants *in vitro*. *Biochem Pharmacol* 2002; **63**: 2111-2119
- Nakamura K,** Ariyoshi N, Yokoi T, Ohgiya S, Chida M, Nagashima K, Inoue K, Kodama T, Shimada N, Kamataki T. CYP2D6.10 present in human liver microsomes shows low catalytic activity and thermal stability. *Biochem Biophys Res Commun* 2002; **293**: 969-973
- Yue QY,** Zhong ZH, Tybring G, Dalen P, Dahl ML, Bertilsson L, Sjoqvist F. Pharmacokinetics of nortriptyline and its 10-hydroxy metabolite in Chinese subjects of different CYP2D6 genotypes. *Clin Pharmacol Ther* 1998; **64**: 384-390
- Ohara K,** Tanabu S, Ishibashi K, Ikemoto K, Yoshida K, Shibuya H. Effects of age and the CYP2D6*10 allele on the plasma haloperidol concentration/dose ratio. *Prog Neuropsychopharmacol Biol Psychiatry* 2003; **27**: 347-350
- Ohara K,** Tanabu S, Ishibashi K, Ikemoto K, Yoshida K, Shibuya H. CYP2D6*10 alleles do not determine plasma fluvoxamine concentration/dose ratio in Japanese subjects. *Eur J Clin Pharmacol* 2003; **58**: 659-661
- Cai WM,** Xu J, Chen B, Zhang FM, Huang YZ, Zhang YD. Effect of CYP2D6*10 genotype on propafenone pharmacodynamics in Chinese patients with ventricular arrhythmia. *Acta Pharmacol Sin* 2002; **23**: 1040-1044
- Fukuda T,** Yamamoto I, Nishida Y, Zhou Q, Ohno M, Takada K, Azuma J. Effect of the CYP2D6*10 genotype on venlafaxine pharmacokinetics in healthy adult volunteers. *Br J Clin Pharmacol* 1999; **47**: 450-453
- Yuan R,** Madani S, Wei XX, Reynolds K, Huang SM. Evaluation of cytochrome p450 probe substrates commonly used by the pharmaceutical industry to study *in vitro* drug interactions. *Drug Metab Dispos* 2002; **30**: 1311-1319
- Streetman DS,** Bertino JS Jr, Nafziger AN. Phenotyping of drug-metabolizing enzymes in adults: a review of *in vivo* cytochrome P450 phenotyping probes. *Pharmacogenetics* 2000; **10**: 187-216
- Yu A,** Haining RL. Comparative contribution to dextromethorphan metabolism by cytochrome P450 isoforms *in vitro*: can dextromethorphan be used as a dual probe for both CYP2D6 and CYP3A activities? *Drug Metab Dispos* 2001; **29**: 1514-1520
- Abdel-Rahman SM,** Marcucci K, Boge T, Gotschall RR, Kearns GL, Leeder JS. Potent inhibition of cytochrome P-450 2D6-mediated dextromethorphan O-demethylation by terbinafine. *Drug Metab Dispos* 1999; **27**: 770-775

Dynamic changes of capillarization and peri-sinusoid fibrosis in alcoholic liver diseases

Guang-Fu Xu, Xin-Yue Wang, Gui-Ling Ge, Peng-Tao Li, Xu Jia, De-Lu Tian, Liang-Duo Jiang, Jin-Xiang Yang

Guang-Fu Xu, Xin-Yue Wang, De-Lu Tian, Liang-Duo Jiang, Jin-Xiang Yang, Digestive Department of the Affiliated Dongzhimen Hospital, Beijing University of Traditional Chinese Medicine, Beijing 100700, China

Gui-Ling Ge, Central Electronic Microscope Examination Studio of Beijing University of TCM, Beijing 100029, China

Peng-Tao Li, Xu Jia, Basic Medical College of Beijing University of TCM, Beijing 100029, China

Correspondence to: Dr. Guang-Fu Xu, Digestive Department of the Affiliated Dongzhimen Hospital, Beijing University of TCM, Beijing 100700, China. guangfuxu@hotmail.com

Telephone: +86-10-84290755

Received: 2003-05-12 **Accepted:** 2003-06-07

Abstract

AIM: To investigate the dynamic changes of capillarization and peri-sinusoid fibrosis in an alcoholic liver disease model induced by a new method.

METHODS: Male SD rats were randomly divided into 6 groups, namely normal, 4 d, 2 w, 4 w, 9 w and 11 w groups. The animals were fed with a mixture of alcohol for designated days and then decollated, and their livers were harvested to examine the pathological changes of hepatocytes, hepatic stellate cells, sinusoidal endothelial cells, sinusoid, peri-sinusoid. The generation of three kinds of extra cellular matrix was also observed.

RESULTS: The injury of hepatocytes became severer as modeling going on. Under electronic microscope, fatty vesicles and swollen mitochondria in hepatocytes, activated hepatic stellate cells with fibrils could be seen near or around it. Fenestrae of sinusoidal endothelial cells were decreased or disappeared, sinusoidal basement was formed. Under light microscopy typical peri-sinusoid fibrosis, gridding-like fibrosis, broaden portal areas, hepatocyte's fatty and balloon denaturation, iron sediment, dot necrosis, congregated lymphatic cells and leukocytes were observed. Type I collagen showed an increasing trend as modeling going on, slightly recovered when modeling stopped for 2 weeks. Meanwhile, type IV collagen decreased rapidly when modeling began and recovered after modeling stopped for 2 weeks. Laminin increased as soon as modeling began and did not recover when modeling stopped for 2 weeks.

CONCLUSION: The pathological changes of the model were similar to that of human ALD, but mild in degree. It had typical peri-sinusoid fibrosis, however, capillarization seemed to be instable. It may be related with the reduction of type IV collagen in the basement of sinusoid during modeling.

Xu GF, Wang XY, Ge GL, Li PT, Jia X, Tian DL, Jiang LD, Yang JX. Dynamic changes of capillarization and peri-sinusoid fibrosis in alcoholic liver diseases. *World J Gastroenterol* 2004; 10 (2): 238-243

<http://www.wjgnet.com/1007-9327/10/238.asp>

INTRODUCTION

In China alcoholic liver disease patients have been on the rise. Acetaldehyde and hydroxy free radicals oxidized from alcohol can injure hepatocytes and activate lipid peroxidation. Hydroxy free radicals are able to activate phagocytes to secrete cytokines and activate hepatic stellate cells (HSC). The activation of HSC leads to the production of various components of extracellular matrix (ECM). Researchers have reported that peri-sinusoid fibrosis, capillarization, gridding-like fibrosis, bridging fibrosis and even cirrhosis are most typical morphological changes in alcoholic consumers for more than 10 or even 20 years. But mild and/or moderate drinkers may not experience such severe damages of the liver. Among the ECM produced during fibrosis, types I and IV collagen and laminin are closely related to the formation of capillarization and peri-sinusoid fibrosis. The Tsukamoto-French model has been used to investigate ALD, but it is expensive and complicated. Many researchers like to make use of the gavage model because of its simplicity and convenience, but there are many inconsistent reports about the content of alcohol ingested, the time of modeling, *etc.* In order to probe into the mechanism of ALD and find a more suitable model, we investigated the dynamic changes of capillarization and peri-sinusoid fibrosis, the contents of types I and IV collagen and laminin, *etc.* in male SD rats during modeling so as to explore whether it was acceptable.

MATERIALS AND METHODS

Materials

Male SD rats, weighing 150±5g, were purchased from Beijing Vital River Company. Corn oil was from Carrefour Supermarket. Xanthan gum and maltose were from Beijing Chemical Agent Company. Edible alcohol was from Beijing General Alcohol Brewing Company. Carbonyl iron and pirazole were from Sigma, USA. First antibody to type I collagen, type IV collagen and laminin were from Antibody Diagnostic Inc, ADI, USA. PV-6001 Kits were from Power Vision, USA. ZLI-9030 and ZLI9001 were from Beijing Zhongshan Company.

Methods

Fifty-six rats were divided into normal(6), 4 d(8), 2 w(8), 4 w(10), 9 w(12), 11 w(12) groups.

ALD model was induced by intragastric infusion of a mixture made of alcohol (5 g/d·kg), pirazole (30 mg/d·kg), corn oil (3 ml/d·kg), carbonyl iron (35 mg/d·kg, which was decreased to 15 mg after 4 w), a little xanthan gum and maltose once a day for 5 days consecutively, with 2 days off per week, until 9 w. The rats were fed with normal diet and water *ad libitum*.

The rats were executed at the end of 4 d, 2 w, 4 w, 9 w and 11 w, respectively. Harvested livers were split and fixed for electron microscopy, hematoxylin and eosin, and Masson complex staining. A portion was snap frozen for biochemical and molecular analysis. Histological analysis of each liver was undertaken. Further sections were cut from each liver, deparaffinized and subjected to amylopin antigen retrieval before being immunostained with primary antigen and second envision agents for types I and IV collagen and laminin. Semi-quantitative computation of types I and IV collagen and laminin

was done by the image analyzing system MIS-2000, which was from 3Y Company, USA. The slides for electron microscopic examination were made according to routine protocol, sub-cellular morphology was investigated and photographed under JEM-1200EX (80KV).

Statistics

SPSS Version 10.0 was used. All values were expressed as mean \pm SD. One-way ANOVA was used to determine the

significance of differences among the six groups. $P < 0.05$ was considered statistically significant.

RESULTS

HE staining

Normal hepatocytes in neat plates, had big and round nuclei, with a clear profile. Hepatocytes in Four d group became swollen and turbid, or balloon denatured. Sinus stricture was

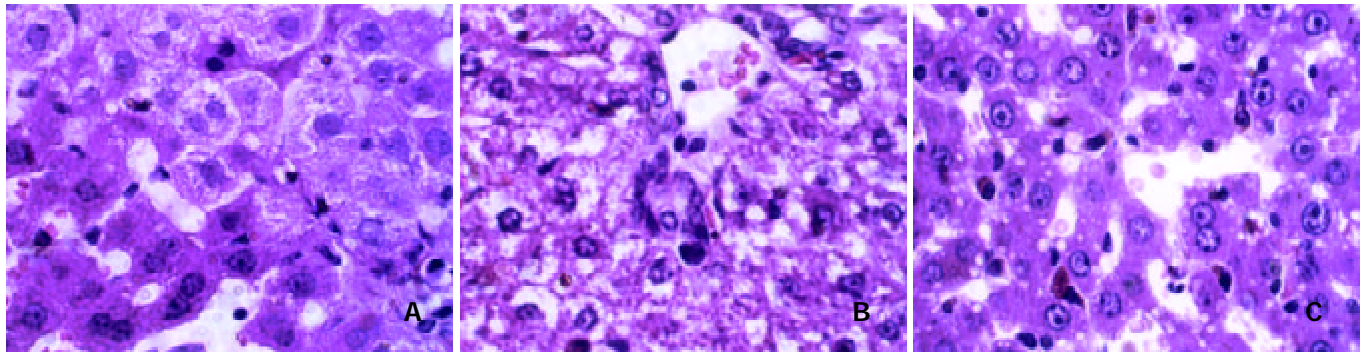


Figure 1 Changes of hepatocytes after HE staining. A: normal HE, B: 4 d HE, C: 4 w HE.

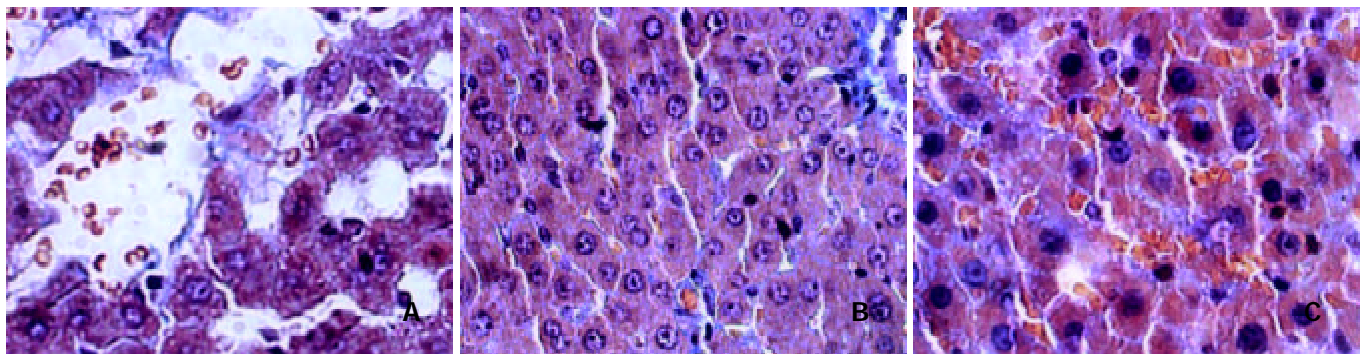


Figure 2 Changes of hepatocytes after Masson staining. A: normal Masson, B: 4 w Masson, C: 11 w Masson

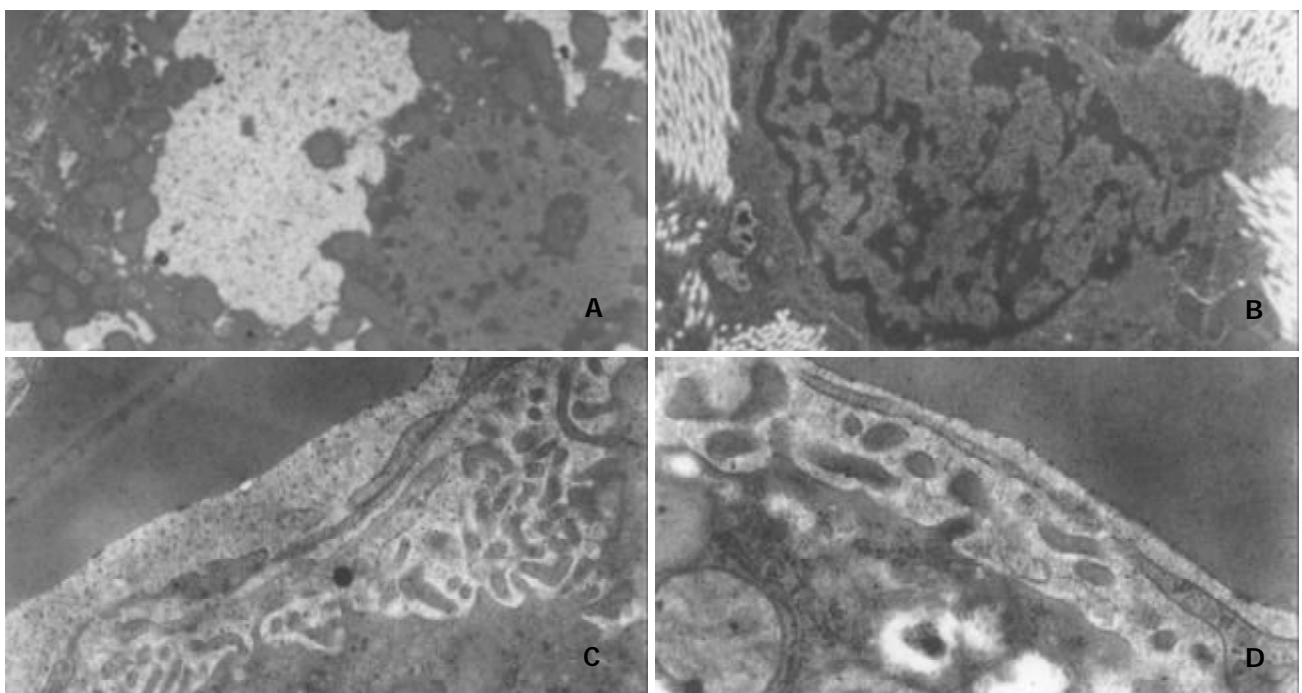


Figure 3 Changes of hepatocytes observed by electron microscopy. A: fatty vesicle in hepatocytes, B: activated HSC and fibril, C: sinusoidal endothelium and basement, D: endothelium, less fenestrae.

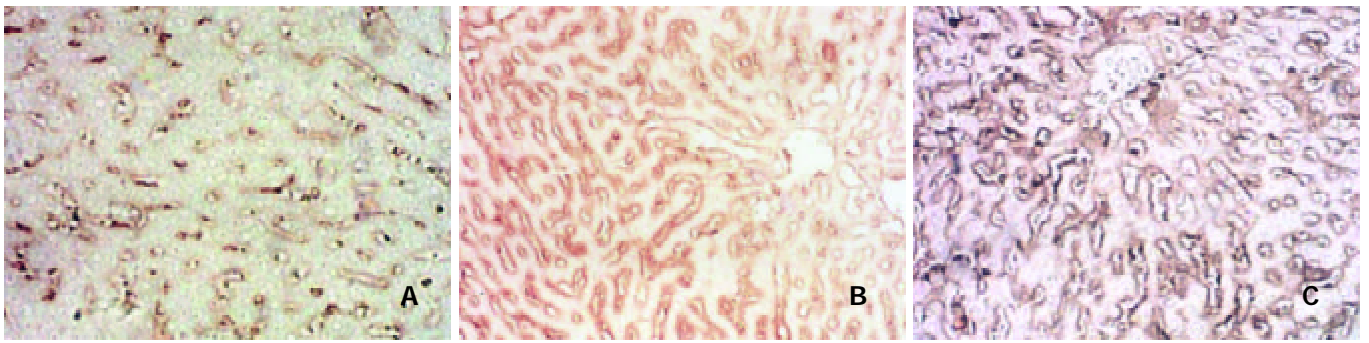


Figure 4 Changes of type I collagen after immunohistochemical staining. A: col-I Normal group, B: Col-I in 4 w group, C: Col-I in 9 w group.

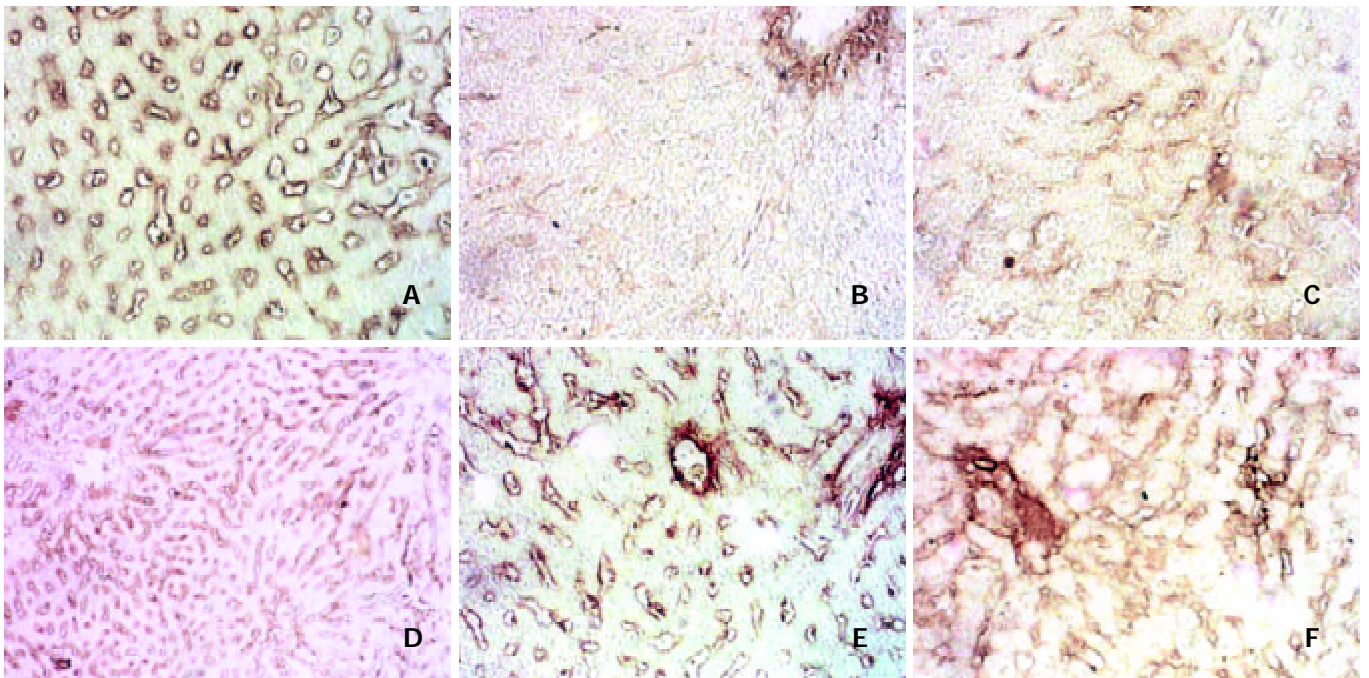


Figure 5 Changes of type IV collagen after immunohistochemical staining. A: col-IV Normal group, B: Col-IV in 4 d group, C: Col-IV in 2 w group, D: Col-IV in 4 w group, E: Col-IV in 9 w group, F: Col-IV in 11 w group.

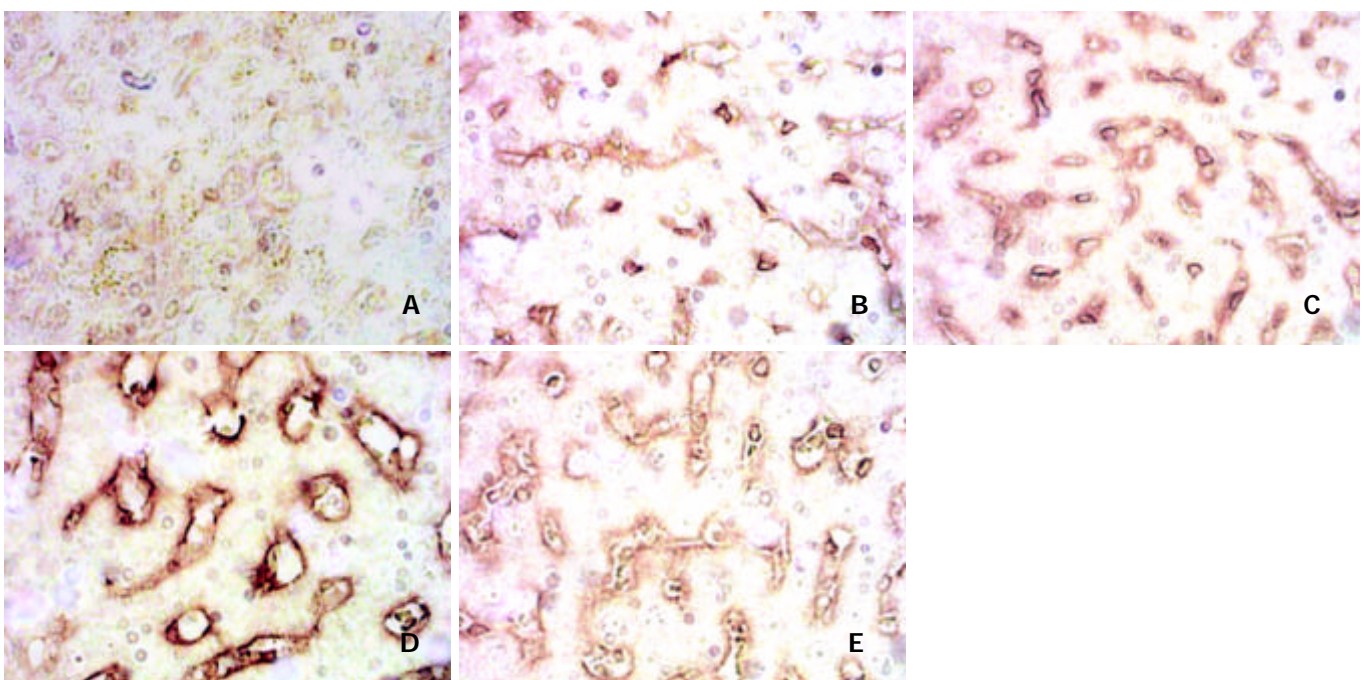


Figure 6 Changes of laminin after immunohistochemical staining. A: laminin Normal group, B: Laminin in 4 d group, C: Laminin in 4 w group, D: Laminin in 9 w group, E: Laminin in 11 w group.

evident. Hepatocytes in 2 w group showed bridging balloon denaturation at around-lobules and portal area, dot necrosis and congregating inflammatory cells could be seen. Four w group exhibited evident hepatocytes coagulation necrosis, mesenchymal cells hyperplasia, broadened portal area with fibrosis. In the Nine w group Mallory body and widespread fatty vesicle denaturation in hepatocytes, piecemeal necrosis, congregating inflammatory cells and fibrosis could be seen. Eleven w group had denatured hepatocytes and a little necrosis, hepatic stellate cells showed dark nuclei (Figure 1. A, B, C)

HE-masson staining

Normal group showed very light stain of the basement of central veins of lobules, Which was mildly evident in blood vessels at the portal area. Four d group showed more evident stain of central vein basement, parts of the hepatocytes were surrounded by gridding-like stains. Two w group showed more gridding-like stains. In 4 w group almost all hepatocytes were surrounded by gridding-like fibrosis and thicker basements of central veins were seen. Thick fibers in portal area bridged with those in hepatic lobules. The fibrotic changes in 9 w group deteriorated. In 11 w group the gridding-like fibrosis slightly ameliorated, but no evident changes were seen in central veins and portal areas (Figure 2. A, B, C).

Electron microscopic examination

Normal hepatocytes had round and clear nuclei, many microvilli extended to touch sinusoidal endothelial cells, or encircle hepatic stellate cells. Its mitochondria presented oval profiles and clear crests. Sinusoidal endothelial cells had many fenestrae and flat nuclei, without obvious basement and fibril underneath. HSC showed tight nuclear chromatin, few in number, and without fibril surrounded by. As modeling going on, the microvilli of hepatocytes became swollen and broken, rough endoplasmic reticulum showed turbulence, mitochondria became swollen and crest broken. The nuclei of sinusoidal endothelial cells became darker and thicker, nuclei chromatin grew crassitude. Fewer fenestrae and basement could be seen under which a large amount of fibrils was found. HSC proliferated actively, with nuclear chromatin turned into crassitude, and lots of fibril surrounded lay (Figure 3. A, B, C, D).

Table 1 Dynamic changes of types I and IV collagen and laminin ($\bar{x}\pm s$)

Group	Type I Collagen	Type IV Collagen	Laminin
Normal	0.2874±0.0224	0.3421±0.0217	0.2263±0.0010
4 d	0.2811±0.0151	0.2907±0.0109 ^a	0.2975±0.0034 ^a
2 w	0.2912±0.0122	0.2463±0.0062 ^a	0.2962±0.0048 ^a
4 w	0.3853±0.0401 ^a	0.3165±0.0049 ^a	0.3336±0.0091 ^a
9 w	0.4262±0.0992 ^a	0.3202±0.0039 ^a	0.3523±0.0108 ^a
11 w	0.3734±0.1239 ^a	0.3249±0.0119	0.3549±0.0120 ^a

^aP<0.05 vs normal.

Immunohistochemical staining

The content of type I collagen grew gradually from Two w and reached the peak in Nine w. After 2 week recovery, it dropped a little in 11 week but was still higher than that of normal rats (Figure 4. A, B, C).

The content of type IV collagen in normal rats was moderate, but it rapidly decreased after the infusion of alcohol mixture, and was sustained at a low level during the course of modeling. However, it recovered in Eleven w (Figure 5. A, B, C, D, E, F).

There were few positive stains of laminin in normal rats, but as soon as the modeling began, its content increased rapidly,

maintaining at high levels during the course, and did not return to normal in 11 w group, but much higher than that of normal rats (Figure 6. A, B, C, D, E, Table 1).

DISCUSSION

The viewpoints^[1-3] that moderate drinking might be beneficial to heart and vascular system or might improve the ability of senior citizens to cognize imply that the disadvantages of alcohol have not been sufficiently recognized. Investigations on pathological changes of mild and moderate drinkers in the liver, especially capillarization and peri-sinusoid fibrosis are not so profound.

Alcohol abuse has become a severe problem in China. The modeling method for the purpose of ALD research is one of the key factors. ALD may be formed in more than 10 or even 20 years, meanwhile have been found many differences due to their various genotypes^[4,5]. As to modeling, pure alcohol intake was difficult in inducing a successful model in a relative short period of time^[6]. Tsukamoto-French model can do so by means of consecutive infusion of alcohol into stomach through a gastric fistula and does not need quite a long time, but it is complicated and expensive. At present the most widely used method of modeling is “gavage” of alcohol^[7,8]. In order to make a model in a relative short period of time, other assisting materials besides alcohol must be added to promote the pathological progress. But the materials added should be of or about the same mechanism as that of alcohol, and the contents of them have to be restrained in order not to overcome alcohol. The core is whether the model has similar pathological changes to ALD and suitable for drug researches, whether it can illustrate the mechanism of treatment so to serve clinic investigation reliably.

The mechanism of ALD has been thought to have a close relation to many factors such as lipid peroxidation^[9], endotoxin^[10-13], acetaldehyde and immunological injuries it induced^[14-16], gender^[17], sediment of iron^[18-25], free radicals^[26], *etc.* Analysis^[27] of alcohol-responsive genes showed that alcohol might injure the liver omnidirectionally, causing not only fatty liver, necrosis and inflammation, hepatocyte apoptosis and hyperhomocysteinemia, but also turbulence in glucose metabolism and DNA damages, *etc.* It has been recognized that the occurrence of fibrosis induced by alcohol or other factors is due to the activation of hepatic stellate cells^[28-41]. All materials added besides alcohol such as iron, polyunsaturated fatty acid and endotoxin during modeling should be designed to strengthen the common mechanism. Our model accepted iron as an additive to promote the course of lipid peroxidation. Corn oil had similar functions. Pirazole could delay the course of alcohol to be cleared from plasmid. Meanwhile we used pirazole to cause or promote blood stasis and flatulence of the intestinal tract, this might be due to its stimulating effect on local mucosa. It needs more evidences to say that pirazole can promote endotoxin absorption. But whether the fibrosis model induced by alcohol and CCl₄ is suitable for ALD research should be under further observation^[42].

Some researchers reported^[43] that capillarization, peri-sinusoid fibrosis and gridding-like fibrosis were typical morphological changes in alcoholic cirrhosis of human beings which are rather different from that of fibrosis or cirrhosis induced by virus infection, yet we do not know whether it would happen in average moderate drinkers, and how the extracellular matrix was involved in changes of types I and IV collagen and laminin. Since there was no unification about the species of rats, the dosage of alcohol and additives used during modeling, we introduced a model established by intragastric infusion of a new mixture of alcohol for 9 weeks consecutively and studied the dynamic changes of types I and IV collagen as

well as laminin, in order to find out whether this model was suitable or not for ALD research^[44,45].

The end products of alcohol in the liver include acetaldehyde and hydroxy free radicals which can injure hepatocytes and activate lipid peroxidation. Phagocytes are susceptible to the course, and would excrete many cytokines such as TNF- α , TGF- β 1, which in turn activate hepatic stellate cells. Activation of HSC is the key event of various kinds of fibrosis. We found in this model, however, as modeling going on, the pathological changes of hepatocytes and fibrosis were gradually deteriorated. The rats in 2 w group were low in spirit with hair standing and diarrhea, the rats in 4 w group became worse and even died. However, because of sustained alcohol intake, after 4 w the rats seemed to get better in spirits and activities, implying that they might develop some mechanisms to adapt to alcohol intake.

In this model we found that the pathological changes of hepatocytes, HSC, endothelia under electronic microscopy, HE stain, HE-masson complex stain were consistent with that of ALD in human beings. Histological analysis showed that the degree of fibrosis was stages I-II^[46,47]. This model may be a good representative of average moderate drinkers who have extensive mild pathological injuries of the liver. Our study may provide some clues for investigation about mild and moderate drinkers in clinic.

Capillarization was a process in which the liver sinusoid became consecutive capillaries with evident basement around. The morphological changes mainly included decreased fenestrae in number or even disappearance in endothelia, and the formation of evident basement^[48-51]. The progression of fibrosis was directly linked to the activation of HSC, and always accompanied by the activation of matrix metalloproteinase2 (MMP-2), without strong expression of the family of tissue inhibitor of matrix metalloproteinases (TIMPS) which was usually observed at the primary stages of fibrosis. Capillarization might not be always stably formed. Our observation demonstrated this might be true, because the content of type IV collagen was low and changed during the modeling, the basement might be mainly composed of laminin. Some of the basements of the liver sinusoid in the rats of 4 w and 9 w groups were not so typical but indeed existed.

The laminin content showed a consecutive high level during the modeling, and did not return to normal even after 2 week recovery. It implied that decomposition of laminin in this model was slightly tough. It deserves further investigation in human ALD. Thus MMP-2's activity alone may not be able to promote the reverse of capillarization.

The content of type I collagen is less than that of type III collagen in normal rats' liver, but it is not so when fibrosis occurs. In normal rats we saw few fibrils near the sinusoid, as modeling going on, many fibrils appeared around sinusoidal endothelial cells. We postulate that type I collagen may take part in this course. Because most researchers believed that type I collagen was not involved in the formation of basement during capillarization. We conclude that the peri-sinusoid fibrosis may be mainly composed of fibrils consisting of type I collagen. Electron microscopic observation showed that peri-sinusoid fibrils were not prone to decomposition after modeling stopped. Immunohistochemical staining observation was consistent with this.

This model had stable alcohol intake during modeling, this ensured less deaths but resulted in moderate pathological changes. If we increase the content of alcohol intake after 4 w and last it for a longer time, or do not reduce the content of iron intake, there may be more severe injuries of the liver such as cirrhosis, but also more dead animals would come forth which may lead to modeling ending in failure. However, the model still needs further improvements.

REFERENCES

- 1 **Laatikainen T**, Manninen L, Poikolainen K, Vartiainen E. Increased mortality related to heavy alcohol intake pattern. *J Epidemiol Community Health* 2003; **57**: 379-384
- 2 **Ambler G**, Royston P, Head J. Non-linear models for the relation between cardiovascular risk factors and intake of wine, beer and spirits. *Stat Med* 2003; **22**: 363-383
- 3 **Zuccala G**, Onder G, Pedone C, Cesari M, Landi F, Bernabei R, Cocchi A. Dose-related impact of alcohol consumption on cognitive function in advanced age: results of a multicenter survey. *Alcohol Clin Exp Res* 2001; **25**: 1743-1748
- 4 **Tadic SD**, Elm MS, Li HS, Van Londen GJ, Subbotin VM, Whitcomb DC, Eagon PK. Sex differences in hepatic gene expression in a rat model of ethanol-induced liver injury. *J Appl Physiol* 2002; **93**: 1057-1068
- 5 **Wang G**, Wang B, Liu C. Relation between activities of hepatic and gastric alcohol dehydrogenases and formation of chronic alcoholic liver diseases. *Zhonghua Ganzangbing Zazhi* 2001; **9**: 265-267
- 6 **Ren C**, Paronetto F, Mak KM, Leo MA, Lieber CS. Cytokeratin 7 staining of hepatocytes predicts progression to more severe fibrosis in alcohol-fed baboons. *J Hepatol* 2003; **38**: 770-775
- 7 **Li J**, French BA, Fu P, Bardag-Gorce F, French SW. Mechanism of the alcohol cyclic pattern: role of catecholamines. *Am J Physiol Gastrointest Liver Physiol* 2003; **285**: G442-448
- 8 **French SW**. Intra-gastric ethanol infusion model for cellular and molecular studies of alcoholic liver disease. *J Biomed Sci* 2001; **8**: 20-27
- 9 **Chen WH**, Liu P, Xu GF, Lu X, Xiong WG, Li FH, Liu CH. Role of lipid peroxidation in liver fibrogenesis induced by dimethylnitrosamine in rats. *Shijie Huaren Xiaohua Zazhi* 2001; **9**: 645-648
- 10 **Murohisa G**, Kobayashi Y, Kawasaki T, Nakamura S, Nakamura H. Involvement of platelet-activating factor in hepatic apoptosis and necrosis in chronic ethanol-fed rats given endotoxin. *Liver* 2002; **22**: 394-403
- 11 **Tamai H**, Horie Y, Kato S, Yokoyama H, Ishii H. Long-term ethanol feeding enhances susceptibility of the liver to orally administered lipopolysaccharides in rats. *Alcohol Clin Exp Res* 2002; **26** (8 Suppl): 75S-80S
- 12 **Keshavarzian A**, Choudhary S, Holmes EW, Yong S, Banan A, Jakate S, Fields JZ. Preventing gut leakiness by oats supplementation ameliorates alcohol-induced liver damage in rats. *J Pharmacol Exp Ther* 2001; **299**: 442-448
- 13 **Mathurin P**, Deng QG, Keshavarzian A, Choudhary S, Holmes EW, Tsukamoto H. Exacerbation of alcoholic liver injury by enteric endotoxin in rats. *Hepatology* 2000; **32**: 1008-1017
- 14 **Jarvelainen HA**, Vakeva A, Lindros KO, Meri S. Activation of complement components and reduced regulator expression in alcohol-induced liver injury in the rat. *Clin Immunol* 2002; **105**: 57-63
- 15 **Shimada S**, Yamauchi M, Takamatsu M, Uetake S, Ohata M, Saito S. Experimental studies on the relationship between immune responses and liver damage induced by ethanol after immunization with homologous acetaldehyde adducts. *Alcohol Clin Exp Res* 2002; **26** (8 Suppl): 86S-90S
- 16 **Searashi Y**, Yamauchi M, Sakamoto K, Ohata M, Asakura T, Ohkawa K. Acetaldehyde-induced growth retardation and micro-heterogeneity of the sugar chain in transferrin synthesized by HepG2 cells. *Alcohol Clin Exp Res* 2002; **26** (8 Suppl): 32S-37S
- 17 **Colantoni A**, Emanuele MA, Kovacs EJ, Villa E, Van Thiel DH. Hepatic estrogen receptors and alcohol intake. *Mol Cell Endocrinol* 2002; **193**: 101-104
- 18 **Boireau A**, Marechal PM, Meunier M, Dubedat P, Moussaoui S. The anti-oxidant ebselen antagonizes the release of the apoptogenic factor cytochrome c induced by Fe²⁺/citrate in rat liver mitochondria. *Neurosci Lett* 2000; **289**: 95-98
- 19 **Karbownik M**, Reiter RJ, Garcia JJ, Cabrera J, Burkhardt S, Osuna C, Lewinski A. Indole-3-propionic acid, a melatonin-related molecule, protects hepatic microsomal membranes from iron-induced oxidative damage: relevance to cancer reduction. *J Cell Biochem* 2001; **81**: 507-513
- 20 **Schumann K**. Safety aspects of iron in food. *Ann Nutr Metab* 2001; **45**: 91-101
- 21 **Valerio LG Jr**, Petersen DR. Characterization of hepatic iron over-

- load following dietary administration of dicyclopentadienyl iron (Ferrocene) to mice: cellular, biochemical, and molecular aspects. *Exp Mol Pathol* 2000; **68**: 1-12
- 22 **MacDonald GA**, Bridle KR, Ward PJ, Walker NI, Houghlum K, George DK, Smith JL, Powell LW, Crawford DH, Ramm GA. Lipid peroxidation in hepatic steatosis in humans is associated with hepatic fibrosis and occurs predominately in acinar zone 3. *J Gastroenterol Hepatol* 2001; **16**: 599-606
- 23 **Raynard B**, Balian A, Fallik D, Capron F, Bedossa P, Chaput JC, Naveau S. Risk factors of fibrosis in alcohol-induced liver disease. *Hepatology* 2002; **35**: 635-638
- 24 **De Feo TM**, Fargion S, Duca L, Cesana BM, Boncinelli L, Lozza P, Cappellini MD, Fiorelli G. Non-transferrin-bound iron in alcohol abusers. *Alcohol Clin Exp Res* 2001; **25**: 1494-1499
- 25 **Tsukamoto H**. Iron regulation of hepatic macrophage TNF α expression. *Free Radic Biol Med* 2002; **32**: 309-313
- 26 **Kono H**, Bradford BU, Rusyn I, Fujii H, Matsumoto Y, Yin M, Thurman RG. Development of an intragastric enteral model in the mouse: studies of alcohol-induced liver disease using knock-out technology. *J Hepatobiliary Pancreat Surg* 2000; **7**: 395-400
- 27 **Ji C**, Kaplowitz N. Betaine decreases hyperhomocysteinemia, endoplasmic reticulum stress, and liver injury in alcohol-fed mice. *Gastroenterology* 2003; **124**: 1488-1499
- 28 **Friedman SL**. Stellate cell activation in alcoholic fibrosis—an overview. *Alcohol Clin Exp Res* 1999; **23**: 904-910
- 29 **Okuno M**, Sato T, Kitamoto T, Imai S, Kawada N, Suzuki Y, Yoshimura H, Moriwaki H, Onuki K, Masushige S, Muto Y, Friedman SL, Kato S, Kojima S. Increased 9,13-di-cis-retinoic acid in rat hepatic fibrosis: implication for a potential link between retinoid loss and TGF-beta mediated fibrogenesis *in vivo*. *J Hepatol* 1999; **30**: 1073-1080
- 30 **Friedman SL**. Cytokines and fibrogenesis. *Semin Liver Dis* 1999; **19**: 129-140
- 31 **Li D**, Friedman SL. Liver fibrogenesis and the role of hepatic stellate cells: new insights and prospects for therapy. *J Gastroenterol Hepatol* 1999; **14**: 618-633
- 32 **Whalen R**, Rockey DC, Friedman SL, Boyer TD. Activation of rat hepatic stellate cells leads to loss of glutathione S-transferases and their enzymatic activity against products of oxidative stress. *Hepatology* 1999; **30**: 927-933
- 33 **Eng FJ**, Friedman SL. Fibrogenesis I. New insights into hepatic stellate cell activation: the simple becomes complex. *Am J Physiol Gastrointest Liver Physiol* 2000; **279**: G7-G11
- 34 **Boireau A**, Marechal PM, Meunier M, Dubedat P, Moussaoui S. The anti-oxidant ebselen antagonizes the release of the apoptogenic factor cytochrome c induced by Fe $^{2+}$ /citrate in rat liver mitochondria. *Neurosci Lett* 2000; **289**: 95-98
- 35 **Albanis E**, Friedman SL. Hepatic fibrosis. Pathogenesis and principles of therapy. *Clin Liver Dis* 2001; **5**: 315-334
- 36 **Eng FJ**, Friedman SL. Transcriptional regulation in hepatic stellate cells. *Semin Liver Dis* 2001; **21**: 385-395
- 37 **Nieto N**, Friedman SL, Cederbaum AI. Stimulation and proliferation of primary rat hepatic stellate cells by cytochrome P450 2E1-derived reactive oxygen species. *Hepatology* 2002; **35**: 62-73
- 38 **Reeves HL**, Friedman SL. Activation of hepatic stellate cells—a key issue in liver fibrosis. *Front Biosci* 2002; **7**: d808-826
- 39 **Saxena NK**, Ikeda K, Rockey DC, Friedman SL, Anania FA. Leptin in hepatic fibrosis: evidence for increased collagen production in stellate cells and lean littermates of ob/ob mice. *Hepatology* 2002; **35**: 762-771
- 40 **Safadi R**, Friedman SL. Hepatic fibrosis—role of hepatic stellate cell activation. *Med Gen Med* 2002; **4**: 27
- 41 **Albanis E**, Safadi R, Friedman SL. Treatment of hepatic fibrosis: almost there. *Curr Gastroenterol Rep* 2003; **5**: 48-56
- 42 **Chae HB**, Jang LC, Park SM, Son BR, Sung R, Choi JW. An experimental model of hepatic fibrosis induced by alcohol and CCl $_4$: can the lipopolysaccharide prevent liver injury induced by alcohol and CCl $_4$? *Taehan Kan Hakhoe Chi* 2002; **8**: 173-178
- 43 **Zhao JB**, Wang TL, Zhang DM. Morphological study on 40 cases of alcoholic liver disease. *Zhonghua Binglixue Zazhi* 1994; **23**: 14-16
- 44 **Bo AH**, Tian CS, Xue GP, Du JH, Xu YL. Morphology of immune and alcoholic liver diseases in rats. *Shijie Huaren Xiaohua Zazhi* 2001; **9**: 157-160
- 45 **Lin H**, Lü M, Zhang YX, Wang BY, Fu BY. Induction of a rat model of alcoholic liver diseases. *Shijie Huaren Xiaohua Zazhi* 2001; **9**: 24-28
- 46 **Hepatic Fibrosis Research Branch of Chinese Hepatic Diseases Associate**. Some agreements evaluating the diagnosis and curative effects of hepatic fibrosis. *Zhonghua Ganzangbing Zazhi* 2002; **10**: 327-328
- 47 **Infectious, parasitic and hepatic diseases branch of Chinese Medical Association**. Prevention and treatment program for Virus Hepatitis. *Zhonghua Ganzangbing Zazhi* 2000; **8**: 324-329
- 48 **Xu GF**, Tian DL. Progress in capillarization research of hepatic sinusoid. *Zhongguo Zhongxiyi Jiehe Xiaohua Zazhi* 2002; **10**: 314-316
- 49 **Lu X**, Xu GF, Chen WH, Liu CH, Liu P. The dynamic changes of capillarization during hepatic fibrosis induced by DMN in rats. *Shijie Huaren Xiaohua Zazhi* 2000; **8**: 1415-1416
- 50 **Lu X**, Liu CH, Xu GF, Chen WH, Liu P. Successive observation of laminin and collagen IV on hepatic sinusoid during the formation of the liver fibrosis in rats. *Shijie Huaren Xiaohua Zazhi* 2001; **9**: 260-262
- 51 **Cheng J**. The biology of molecules of extracellular matrix and the relation with clinical diseases. 1st ed, Beijing: *The Publishing Company of Beijing University of Medical Sciences* 1999

Edited by Wang XL and Zhu LH

Preparation and property analysis of a hepatocyte targeting pH-sensitive liposome

Si-Yuan Wen, Xiao-Hong Wang, Li Lin, Wei Guan, Sheng-Qi Wang

Si-Yuan Wen, Xiao-Hong Wang, Li Lin, Wei Guan, Sheng-Qi Wang, Beijing Institute of Radiation Medicine, Beijing 100850, China
Supported by the grants of the State 863 High Technology Project of China, No. 102-08-04-01

Correspondence to: Professor Sheng-Qi Wang, Beijing Institute of Radiation Medicine, No. 27 Taiping Road, Beijing 100850, China. sqwang@nic.bmi.ac.cn

Telephone: +86-10-66932211 **Fax:** +86-10-66932211

Received: 2003-04-02 **Accepted:** 2003-06-04

Abstract

AIM: To develop a hepatocyte targeting pH-sensitive liposome for drug delivery based on active targeting technology mediated by asialoglycoprotein receptors.

METHODS: Four types of targeting molecules with galactose residue were synthesized and mixed with pH-sensitive lipids DC-chol/DOPE to prepare liposome with integrated property of hepatocyte specificity and pH sensitivity. Liposome 18-gal was selected with the best transfection activity through cellular uptake experiment. Property analysis was made through experiments of competitive inhibition of receptors, red blood cell hemolysis, *in vitro* cytotoxicity test by MTS assay and mediation of inhibitory effects of antisense phosphorothioate ODN on gene expression, *etc.*

RESULTS: Liposome 18-gal had the desired properties of hepatocyte specificity, pH sensitivity, low cytotoxicity, and high transfection efficiency.

CONCLUSION: Liposome 18-gal can be further developed as a potential hepatocyte-targeting delivery system.

Wen SY, Wang XH, Lin L, Guan W, Wang SQ. Preparation and property analysis of a hepatocyte targeting pH-sensitive liposome. *World J Gastroenterol* 2004; 10(2): 244-249
<http://www.wjgnet.com/1007-9327/10/244.asp>

INTRODUCTION

Previous studies have suggested a promising future of antisense oligodeoxynucleotide (ODN) in the treatment of viral hepatitis^[1-6]. However, as a polyanionic macromolecule, antisense ODN has two major limitations: poor efficiency of cellular uptake and rapid degradation. The realization of its *in vivo* biological effect is accomplished under the mediation of liposome. In recent years, with the advent of cationic liposome and active targeting technology^[7-10], liposome technology has been widely applied in the transfer of antisense ODNs for its virtues of high transfection efficiency, protection for the entrapped and ease of chemical modification.

The effectiveness of cationic liposome in the mediation of antisense ODN transfer in clinical trials was reported^[11-15], while its deficiency lay in the lack of tissue specificity. To improve the targeting property, active targeting technology based on specific receptor-ligand recognition reaction has been applied.

Hepatocytes exclusively expressed large numbers of high affinity asialoglycoprotein receptors which can recognize the ligand molecules with galactose residues and mediate their endocytosis^[16-20]. In this study, four types of targeting molecules bearing galactose residue were synthesized and mixed with the pH-sensitive lipids DC-chol/DOPE to prepare liposome with integrated property of hepatocyte specificity and pH sensitivity.

MATERIALS AND METHODS

Chemicals and reagents

Chloroformylcholesterol, N,N-dimethylethylenediamine, dioleoylphosphatidylethanol-amine, hydrolytic lactose were purchased from Sigma Chemicals (St. Louis, MO), DC-chol was synthesized according to the published methods^[21]. Enzymes, vectors, luciferase assay system and Celltiter 96@AQ_{ueous} non-radioactive cell proliferation assay test kit were obtained from Promega Corp (Madison, WI). All other reagents were analytically pure.

Plasmid and transgenic cell line HepG2.9706^[22]

pHCV-neo4 was constructed by cloning the complete 5' NCR (non-coding region) and part C region of fusion protein of Chinese HCV genome into pGL3 luciferase reporter vector in which the start codon was deleted without frameshift. In pHCV-neo4, the expression of luciferase gene could be suppressed by blocking the HCV 5' NCR. Transgenic cell strain HepG2.9706 with permanent expression of luciferase gene was constructed by selection of the transfected HepG2 cell with pHCV-neo4 using G418.

Phosphorothioate oligodeoxynucleotide

Phosphorothioate ODN HCV363a (5' GAG-GTT-TAG-GAT-TCG-TGC-TCA-TG 3') is a 23-mer sequence complimentary to part of HCV 5' NCR (noncoding region). HCV363s (5' CAT-GAG-CAC-GAA-TCC-TAA-ACC-TC 3') is the reverse complimentary sequence to HCV363a. NSC (non-specific control: 5' GCA-GAG-GTG-AAA-AAG-TTG-CAT 3') is a random sequence with low homology to HCV5' NCR. The oligonucleotides were synthesized with the automatic DNA synthesizer (390Z, Applied Biosystems, Inc) and purified by HPLC (Micro Pure II reverse phase column).

Synthesis of targeting molecule

Four types of amphiphilic glycolipid molecules (octodecyl galactoside, octodecyl lactoside, cholesteryl galactoside, cholesteryl lactoside) bearing galactose residues were synthesized according to the published method^[23,24] with some modifications. Hydrophilic groups were galactose and lactose, and hydrophobic groups were octadecanol and cholesterol. Structure confirmation was made through element analysis, nuclear magnetic resonance and mass spectrum (data not shown).

Preparation of liposome

Targeting molecule: DC-chol:DOPE (optimum:6:4 molar ratio) was dissolved in the solvent mixture of ethanol/chloroform

(1:1 v/v), evaporated to a thin film in a rotating evaporator, resuspended in the sterile PBS buffer (pH 7.4) and incubated overnight at 4 °C with gentle stirring. The suspension was sonicated in a bath sonicator for 30 minutes and passed through a polycarbonate membrane (pore diameter 0.4 µm) filter for sterility and granular uniformity. The particle size of the liposomes was measured in a dynamic light scattering spectrophotometer (LS-900, Otsuka Electronics, Osaka, Japan). Lipid concentration in stock solution was determined by phosphorus assay.

Plasmid transfection experiment

Cells (HepG2, GLC) were maintained in DMEM supplement with 10% FBS at 37 °C under an atmosphere of 5% CO₂ in air. The cells were seeded onto a 96-well plate at a density of 10⁴/well and cultivated in 0.2 mL DMEM supplemented with 10% FBS. After 24 h, the culture medium was replaced with DMEM containing plasmid DNA/liposome complexes. Five hours later, the incubation medium was replaced again with DMEM supplemented with 10% FBS and incubated for an additional period of 36 h. The cells were then collected and washed with PBS buffer twice, mixed with 30 µL/well cell lysis solution. Ten minutes later, 100 µL/well luciferase substrate buffer was added and the light produced was immediately measured using a luminometer. The activity was indicated as the relative light units per mg protein. The protein content of the cell suspension was determined by a modified Lowry method using BSA as a standard. In the experiment of competitive inhibition of receptors, the galactose/glucose solution was added 5 minutes before plasmid DNA/liposome complexes, and all other procedures were the same. All assays were performed in triplicate.

Red blood cell hemolysis experiment

A series of 0.1 mol/L PBS buffer with gradient pH value (4.0, 5.0, 6.0, 7.0, 8.0) were prepared. Eighty µL 1% (v/v) newly prepared chicken red blood cell suspension and 20 µL plasmid DNA/liposome complexes (1:5 wt/wt, lipid concentration: 0.5 µg/µL) were mixed in 100 µL 0.1M PBS buffer of different pH value. The mixture was shaken at 37 °C, and an aliquot of suspension was taken at the given time periods (10 min, 30 min and 90 min), centrifuged at 1 000×g. Absorbance value of the supernatant was measured at wavelength 540nm in a photometer (Multiscan MS). Controls were set as follows:
Parallel control: 100 µL PBS buffer + 80 µL 1% (v/v) RBC + 20 µL saline;
Negative control: 120 µL saline + 80 µL 1% (v/v) RBC.

In vitro cytotoxicity assay

DNA/liposome (1:5 wt/wt) complexes were diluted with DMEM supplemented with 2% FBS in an index gradient way (index number: 2, initial lipid concentration: 0.5 µg/µL). HepG2 cells were seeded onto a 96-well plate at a density of 10⁴/well and cultivated in 0.2 mL DMEM supplemented with 10% FBS. After 24 h, the culture medium was replaced with DMEM containing DNA/liposome complexes prepared, and cells were incubated for an additional period of 24 h. Cytotoxicity was evaluated by MTS assay according to the instructions of Celltiter 96@AQ_{ueous} non-radioactive cell proliferation assay test kit, and commercially available cationic liposome Lipofectin served as the control.

Delivery of phosphorothioate ODN to HepG2.9706 cells

Phosphorothioate ODNs were dissolved in DMEM at various concentrations (0.2 µmol/L, 0.4 µmol/L and 0.8 µmol/L), alone or in combination with liposome 18-gal (octadecanol-galactoside:DC-chol:DOPE 1:6:4) at a ratio of 1:5 (wt/wt).

The HepG2.9706 cells seeded onto a 24-well plate at a density of 2×10⁴/well were incubated in DMEM supplement with 10% FBS. After 24 h, the culture medium was replaced with DMEM containing phosphorothioate ODNs. Five hours later, the incubation medium was replaced again with DMEM supplemented with 10% FBS and incubated for an additional period of 24 h. Then the activity of luciferase enzyme was determined as in the plasmid transfection experiment.

RESULTS

Analysis of liposomal transfection efficiency and targeting property

Four types of targeting liposomes (denoted as 18-gal, 18-lac, chol-gal and chol-lac respectively) were prepared by mixing glycolipids with DC-chol/DOPE in a molar ratio of 1:6:4, respectively. A fixed amount of (0.4 µg/well) plasmid DNA encoding a luciferase gene was complexed with these liposomes at a ratio of 1:5 (wt/wt). Figure 1 shows the expression of luciferase gene in HepG2 cells (liver cells) and GLC cells (lung cells lacking asialoglycoprotein receptor) treated with the DNA/liposome complexes. The transfection activity of DC-chol/DOPE was similar in the two cell lines, whereas the transfection activity of the targeting liposomes was significantly higher in HepG2 cells than in GLC cells. When compared with the transfection activity of DC-chol/DOPE in HepG2 cells, there was a significant increase in that of 18-gal ($P<0.01$) while a relatively significant decrease in those of 18-lac and chol-lac ($P<0.05$), and no significant difference was observed between those of chol-gal and DC-chol/DOPE ($P>0.05$). In GLC cells, the transfection activity of the targeting liposomes was significantly lower than that of DC-chol/DOPE ($P<0.05$). These results suggested that the addition of poorly soluble and electrically neutral glycoside molecules could impair the transfection activity of DC-chol/DOPE to some extent. However, asialoglycoprotein receptor-mediated internalization induced by targeting molecules with galactose residues could specifically enhance the transfection activity of targeting liposomes in HepG2 cells, especially that of 18-gal.

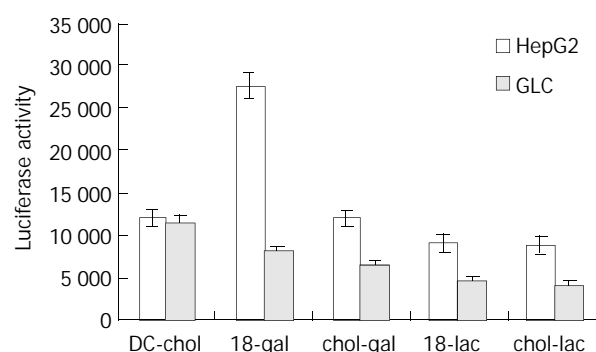


Figure 1 Transfection activity of plasmid DNA/liposome complexes in HepG2 cells and GLC cells. Four types of targeting liposomes (18-gal, 18-lac, chol-gal and chol-lac) were prepared by mixing the targeting molecules with DC-chol/DOPE at a molar ratio of 1:6:4, respectively. A fixed amount (0.4 µg/well) of plasmid DNA was complexed with liposomes at a ratio of 1:5 (wt/wt). Each value represents $\bar{x} \pm s$ ($n=3$).

The following experiments were performed with liposome 18-gal. To optimize the lipid composition, the molar ratio of octadecanol-galactoside to lipid DC-chol/DOPE varied from 0:6:4 to 5:6:4. The liposomal transfection activity showed a bell-shape dependence on the molar percentage of octadecanol-galactoside in liposomal composition. The maximum gene

expression (about 3 times that of DC-chol/DOPE) was observed at the ratio of octadecanol-galactoside:DC-chol:DOPE 1:6:4 (Figure 2). When the molar percentage of octadecanol-galactoside exceeded 20%, the colloidal solution was easy to agglomerate into turbidity, and the liposomal transfection efficiency dropped significantly. Therefore, the maximum molar proportion of octadecanol-galactoside in the liposomal formula should not exceed 20 mol%.

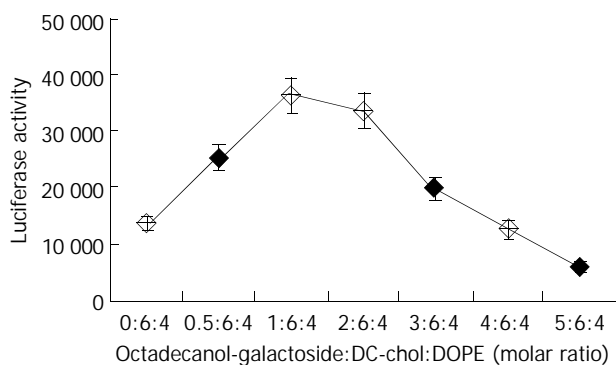


Figure 2 Effect on liposomal transfection activity in HepG2 cells of molar ratio of octadecanol-galactoside (targeting molecules) in liposome composition. The molar ratio of octadecanol-galactoside to lipid DC-chol/DOPE varied from 0:6:4 to 5:6:4. A fixed amount (0.4 $\mu\text{g}/\text{well}$) of plasmid DNA was complexed with liposomes at a ratio of 1:5 (wt/wt). Each value represents $\bar{x} \pm s$ ($n=3$).

A fixed amount of plasmid DNA (0.4 $\mu\text{g}/\text{well}$) was complexed with liposome 18-gal (octadecanol-galactoside:DC-chol:DOPE 1:6:4) in different ratios (1:2.5, 1:5, 1:10, 1:20 wt/wt) to treat HepG2 cells. The greatest gene expression was achieved at the ratio of 1:5-1:10 (Figure 3).

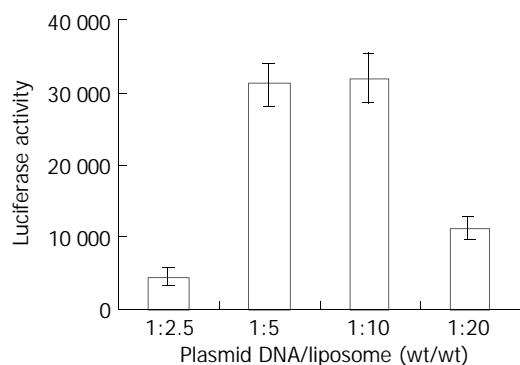


Figure 3 Transfection activity of plasmid DNA/liposome complexes at various ratios (wt/wt) in HepG2 cells. Liposomal composition was octadecanol-galactoside:DC-chol:DOPE 1:6:4 (molar ratio). Plasmid DNA amount was fixed at 0.4 $\mu\text{g}/\text{well}$ in all experiments. Each value represents $\bar{x} \pm s$ ($n=3$).

To investigate whether the cellular uptake of liposome 18-gal in HepG2 cells was partly mediated by asialoglycoprotein receptors, the inhibitory effect of 20 mmol/L galactose solution on the transfection activity of liposome 18-gal of different compositions (the ratio of octadecanol-galactoside to DC-chol/DOPE ranging from 0:6:4 to 2:6:4) was measured. As shown in Figure 4A, the transfection efficiency of liposome 18-gal was significantly inhibited ($P < 0.01$, the mean inhibition rates were 35%, 40% and 46% respectively) in the presence of galactose, but not that of DC-chol/DOPE(6:4). On the other hand, no significant difference was found in the gene expression of DNA/liposome 18-gal complexes in the presence or absence of glucose (Figure 4B).

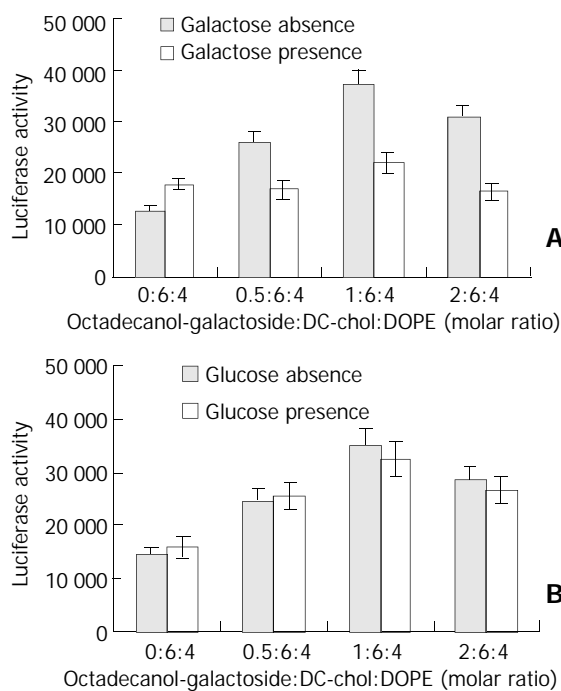


Figure 4 Effect of copresence of 20 mmol/L galactose (A) and glucose (B) on transfection activity of liposomes of different composition in HepG2 cells. Cells were transfected with DNA/liposome complexes in the presence (\square) and absence (\blacksquare) of galactose or glucose. A fixed amount (0.4 $\mu\text{g}/\text{well}$) of plasmid DNA was complexed with liposomes at a ratio of 1:5 (wt/wt). Each value represents $\bar{x} \pm s$ ($n=3$).

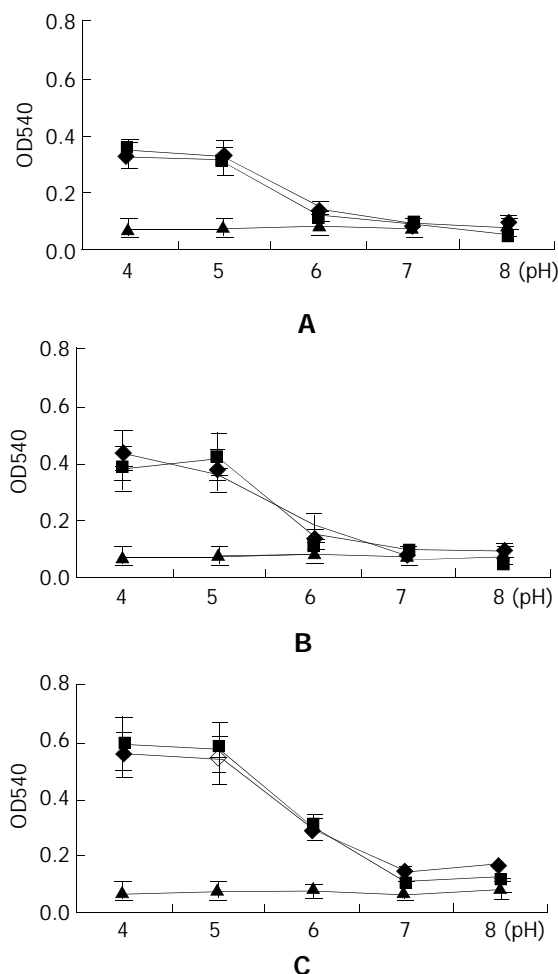


Figure 5 Fusion of plasmid DNA/liposome complexes with chicken hematocyte at various pH values. \blacksquare DC-chol/DOPE

6:4, ◆ octadecanol-galactoside:DC-chol:DOPE 1:6:4, ▲ PBS buffer. Plasmid DNA was complexed with liposomes (lipid concentration: $0.5 \mu\text{g}/\mu\text{L}$) at a ratio of 1:5 (wt/wt). The release of hemachrome was determined at 10 min (A), 30 min (B) and 90 min (C). Each value represents $\bar{x} \pm s$ ($n=3$).

Characterization of liposomal pH sensitivity

To characterize the liposomal pH sensitivity, plasmid DNA/liposome complexes were mixed with chicken hematocyte in different pH conditions, and release of hemachrome which indicates cell membrane fusion was determined at 10 min, 30 min and 90 min. As shown in Figure 5, there was no difference ($P>0.05$) at the release of hemachrome in the PBS buffer of various pH values. They were close to the negative control (the mean value of negative control: 10 min, 0.076; 30 min, 0.077; 90 min, 0.082). The membrane fusion of red blood cells with DNA/liposome complexes was significantly dependent on the pH value. There was a significant difference between the release amounts of hemachrome in the intervals before and after pH=6 ($P<0.01$).

In vitro cytotoxicity of liposome

The cytotoxicity of liposome 18-gal was tested and compared with that of lipofectin. As shown in Figure 6, within lipid concentrations of 0.5, 0.25, 0.125 and $0.0625 \mu\text{g}/\mu\text{L}$, the cytotoxicity of lipofectin was significantly higher than that of liposome 18-gal and DC-Chol/DOPE at corresponding concentrations, the latter two only demonstrated certain cytotoxicity at the concentration of $0.5 \mu\text{g}/\mu\text{L}$ (about 25%). When the concentration that generated 25% cytotoxicity (IC_{25}) was compared, the cytotoxicity of lipofectin was 16 (2^4) times higher than that of the other two liposomes. This results confirmed that DC-Chol/DOPE was a type of cationic liposome with low cytotoxicity, and the addition of octadecanol-galactoside in the liposomal formula did not increase the cytotoxicity.

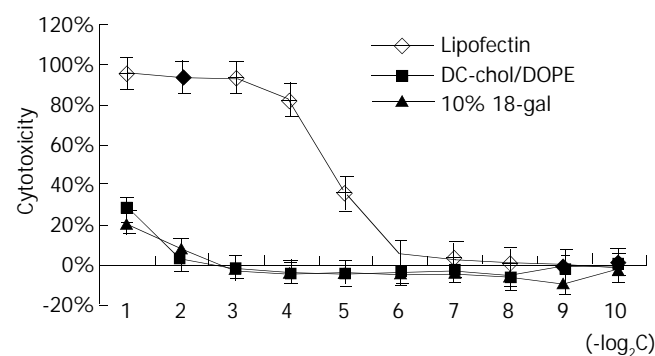


Figure 6 *In vitro* cytotoxicity of cationic liposomes (◆ lipofectin, ■ DC-chol/DOPE 6:4, ▲ octadecanol-galactoside:DC-chol:DOPE 1:6:4). The DNA/liposome (1:5 wt/wt) complexes were diluted with DMEM supplemented with 2% FBS in an index gradient way (initial lipid concentration: $0.5 \mu\text{g}/\mu\text{L}$). Each value represents $\bar{x} \pm s$ ($n=3$).

Assessment of liposomal activity in mediating phosphorothioate ODNs delivery

HepG2.9706 cells were treated with phosphorothioate ODNs at different concentrations (0.2, 0.4 and $0.8 \mu\text{mol}/\text{L}$), alone or in combination with liposome 18-gal. As shown in Figure 7, within the range of 0.2- $0.8 \mu\text{mol}/\text{L}$, HCV363a/18-gal complexes had a significantly dose-dependent inhibitory activity on the expression of luciferase gene, and the inhibition rate was 31%, 43% and 54% respectively. HCV363s/18-gal complexes showed stimulating effects on gene expression to some extent. The stimulating effects of sense oligonucleotides on gene expression were also reported by other researchers^[25,26], but

the cause has been unclear. NSC/18-gal complexes had nonspecific inhibitory effects on gene expression of no more than 15%. Treatment with phosphorothioate ODNs alone showed no inhibitory effects on the expression of luciferase gene in HepG2.9706 within the concentration of $0.8 \mu\text{mol}/\text{L}$.

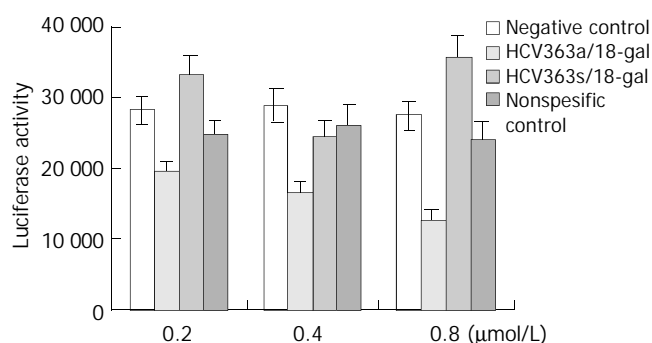


Figure 7 Effects of phosphorothioate ODNs transfected by liposome 18-gal on luciferase gene expression in HepG2.9706 cells. Phosphorothioate ODNs were dissolved in DMEM at various concentrations ($0.2 \mu\text{mol}/\text{L}$, $0.4 \mu\text{mol}/\text{L}$, $0.8 \mu\text{mol}/\text{L}$) and complexed with liposome 18-gal (octadecanol-galactoside:DC-chol:DOPE 1:6:4) at a ratio of 1:5 (wt/wt). Each value represents $\bar{x} \pm s$ ($n=3$).

In addition, the effect of administration time on the inhibitory activity of HCV363a/18-gal complexes was also investigated. HepG2.9706 cells were consecutively treated 3 times with HCV363a/18-gal complexes and the activity of luciferase enzyme was determined each time 24h after HCV363a/18-gal complexes were administered. As shown in Figure 8, the inhibitory effects of HCV363a/18-gal complexes increased with the administration time.

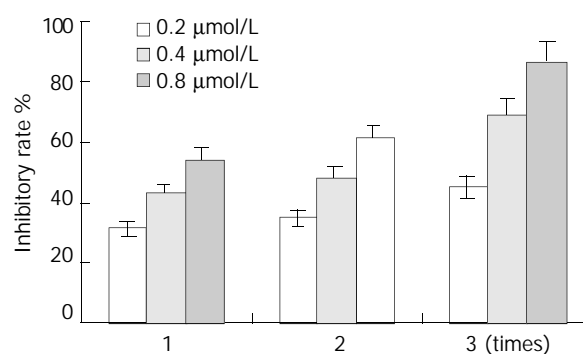


Figure 8 Effect of administration time on inhibitory efficiency of HCV363a in HepG2.9706. Phosphorothioate ODN (HCV363a) was dissolved in DMEM at various concentrations ($0.2 \mu\text{mol}/\text{L}$, $0.4 \mu\text{mol}/\text{L}$, $0.8 \mu\text{mol}/\text{L}$) and complexed with liposome 18-gal (octadecanol-galactoside:DC-chol:DOPE 1:6:4) at a ratio of 1:5 (wt/wt). HepG2.9706 cells were consecutively treated 3 times with HCV363a/18-gal complexes and the activity of luciferase enzyme was determined each time 24 h after HCV363a/18-gal complexes was administered. Each value represents $\bar{x} \pm s$ ($n=3$).

DISCUSSION

In the present study, we synthesized targeting molecules with galactose residue and developed a novel formula for a hepatocyte-targeting pH sensitive liposome. Liposome 18-gal was selected with the best transfection activity that was greatly mediated by asialoglycoprotein receptor in HepG2 cells. The hepatocyte specificity of liposome 18-gal was confirmed by the following facts: (1) There was a significant difference

($P < 0.01$) in the transfection efficiencies of DNA/18-gal complexes between HepG2 cells (liver cells) and GLC cells (lung cells lacking asialoglycoprotein receptors). (2) Within a certain proportion (<20 mol%), the addition of octadecanogalactoside greatly increased the transfection efficiency of DC-chol/DOPE in HepG2 cells (maximum: about 3 folds). This effect was significantly inhibited by galactose but not by glucose. In comparison, the transfection activity of DC-chol/DOPE was similar in the presence or absence of galactose or glucose in HepG2 cells.

In the presence of excessive proportion of targeting molecules (>20 mol%, molar percentage in liposome composition), the colloidal solution was easy to form turbidity, and the transfection efficiency of prepared liposomes dropped significantly. It was because that a large amount of electrically neutral targeting molecules reduced the positive charge density of cationic liposome. Studies with phospholipid containing liposomes have shown that an increase in a glycolipid or gangliosides greater than 10 mol% resulted in the solubility of liposome into micelles. Due to the potential shielding of the cationic lipid interaction with plasmid DNA by the carbohydrate head group, a heterogeneous population of mixed micelles could be generated at a high molar percent, thus explaining the bell shaped curve for expression. The poor solubility of glycoside molecules in organic solvent also affected the preparation and property of liposome to some extent.

pH-sensitivity is another important property of liposome, which was considered as a mechanism to amass the enclosed antisense ODN at the action site of cytoplasm^[27-29]. In brief, liposome is selectively uptaken by specific cells based on active targeting mechanism. The pH sensitivity inducing the liposomal escape from endosome/lysosome at low pH value makes the entrapped antisense ODN release at cytoplasm to take action. In the present study, the significant dependence on the pH value of membrane fusion of chicken hematocytes with DNA/liposome complexes confirmed the pH sensitivity of the two liposomes, and the similarity of the two liposomes in the membrane fusion experiment strongly indicated the pH-sensitivity of liposome 18-gal as that of DC-chol/DOPE which has been proved to be a pH sensitive liposome^[30].

Transgenic cell strain HepG2.9706 with permanent expression of luciferase gene is a convenient cell model purposely constructed to evaluate the inhibitory effect of antisense ODNs on the HCV 5' NCR. The comparison between the effects on gene expression of phosphorothioate ODNs with or without liposome 18-gal mediation showed that liposome 18-gal was highly efficient in mediating the delivery of phosphorothioate ODNs into HepG2.9706 cells.

In conclusion, the liposome 18-gal prepared in this study has the desired properties of hepatocyte specificity, pH sensitivity, low cytotoxicity, and high transfection efficiency. It can be further developed as a potential hepatocyte-targeting ODN delivery system.

REFERENCES

- 1 Heintges T, Encke J, zu Putlitz J, Wands JR. Inhibition of hepatitis C virus NS3 function by antisense oligodeoxynucleotides and protease inhibitor. *J Med Virol* 2001; **65**: 671-680
- 2 Robaczewska M, Guerret S, Remy JS, Chemin I, Offensperger WB, Chevallier M, Behr JP, Podhajka AJ, Blum HE, Trepo C, Cova L. Inhibition of hepatitis C viral replication by polyethylenimine-based intravenous delivery of antisense phosphodiester oligodeoxynucleotides to the liver. *Gene Ther* 2001; **8**: 874-881
- 3 Alt M, Eisenhardt S, Serwe M, Renz R, Engels JW, Caselmann WH. Comparative inhibitory potential of differently modified antisense oligodeoxynucleotides on hepatitis C virus translation. *Eur J Clin Invest* 1999; **29**: 868-876
- 4 Alt M, Renz R, Hofschneider PH, Caselmann WH. Core specific antisense phosphorothioate oligodeoxynucleotides as potent and specific inhibitors of hepatitis C viral translation. *Arch Virol* 1997; **142**: 589-599
- 5 Alt M, Renz R, Hofschneider PH, Paumgartner G, Caselmann WH. Specific inhibition of hepatitis C viral gene expression by antisense phosphorothioate oligodeoxynucleotides. *Hepatology* 1995; **22**: 707-717
- 6 Liu Y, Chen Z, He N. Inhibition of hepatitis C virus by antisense oligodeoxynucleotide *in vitro*. *Zhonghua Yixue Zazhi* 1997; **77**: 567-570
- 7 Zabner J. Cationic lipids used in gene transfer. *Adv Drug Deliv Rev* 1997; **27**: 17-28
- 8 Kim JK, Choi SH, Kim CO, Park JS, Ahn WS, Kim CK. Enhancement of polyethylene glycol (PEG)-modified cationic liposome-mediated gene deliveries: effects on serum stability and transfection efficiency. *J Pharm Pharmacol* 2003; **55**: 453-460
- 9 Abra RM, Bankert RB, Chen F, Egilmez NK, Huang K, Saville R, Slater JL, Sugano M, Yokota SJ. The next generation of liposome delivery systems: recent experience with tumor-targeted, sterically-stabilized immunoliposomes and active-loading gradients. *J Liposome Res* 2002; **12**: 1-3
- 10 Mastrobattista E, Koning GA, Storm G. Immunoliposomes for the targeted delivery of antitumor drugs. *Adv Drug Deliv Rev* 1999; **40**: 103-127
- 11 Hyde SC, Southern KW, Gileadi U, Fitzjohn EM, Mofford KA, Waddell BE, Gooi HC, Goddard CA, Hannavy K, Smyth SE, Egan JJ, Sorgi FL, Huang L, Cuthbert AW, Evans MJ, Colledge WH, Higgins CF, Webb AK, Gill DR. Repeat administration of DNA/liposomes to the nasal epithelium of patients with cystic fibrosis. *Gene Ther* 2000; **7**: 1156-1165
- 12 Stopeck AT, Jones A, Hersh EM, Thompson JA, Finucane DM, Gutheil JC, Gonzalez R. Phase II study of direct intralesional gene transfer of allovectin-7, an HLA-B7/beta2-microglobulin DNA-liposome complex, in patients with metastatic melanoma. *Clin Cancer Res* 2001; **7**: 2285-2291
- 13 Hortobagyi GN, Ueno NT, Xia W, Zhang S, Wolf JK, Putnam JB, Weiden PL, Willey JS, Carey M, Branham DL, Payne JY, Tucker SD, Bartholomeusz C, Kilbourn RG, De Jager RL, Sneige N, Katz RL, Anklesaria P, Ibrahim NK, Murray JL, Theriault RL, Valero V, Gershenson DM, Bevers MW, Huang L, Lopez-Berestein G, Hung MC. Cationic liposome-mediated E1A gene transfer to human breast and ovarian cancer cells and its biologic effects: a phase I clinical trial. *J Clin Oncol* 2001; **19**: 3422-3433
- 14 Hui KM, Ang PT, Huang L, Tay SK. Phase I study of immunotherapy of cutaneous metastases of human carcinoma using allogeneic and xenogeneic MHC DNA-liposome complexes. *Gene Ther* 1997; **4**: 783-790
- 15 Gill DR, Southern KW, Mofford KA, Seddon T, Huang L, Sorgi F, Thomson A, MacVinish LJ, Ratcliff R, Bilton D, Lane DJ, Littlewood JM, Webb AK, Middleton PG, Colledge WH, Cuthbert AW, Evans MJ, Higgins CF, Hyde SC. A placebo-controlled study of liposome-mediated gene transfer to the nasal epithelium of patients with cystic fibrosis. *Gene Ther* 1997; **4**: 199-209
- 16 Gao S, Chen J, Xu X, Ding Z, Yang YH, Hua Z, Zhang J. Galactosylated low molecular weight chitosan as DNA carrier for hepatocyte-targeting. *Int J Pharm* 2003; **255**: 57-68
- 17 Kunath K, von Harpe A, Fischer D, Kissel T. Galactose-PEI-DNA complexes for targeted gene delivery: degree of substitution affects complex size and transfection efficiency. *J Control Release* 2003; **88**: 159-172
- 18 Yuan L, He S, Guan C, Pang Q. The preparation and study on hepatic targeting tendency of galactosyl-anti-CD3-McAb in mice. *Huaxi Yike Daxue Xuebao* 2001; **32**: 424-426
- 19 Kawakami S, Yamashita F, Nishikawa M, Takakura Y, Hashida M. Asialoglycoprotein receptor-mediated gene transfer using novel galactosylated cationic liposomes. *Biochem Biophys Res Commun* 1998; **252**: 78-83
- 20 Hara T, Kuwasawa H, Aramaki Y, Takada S, Koike K, Ishidate K, Kato H, Tsuchiya S. Effects of fusogenic and DNA-binding amphiphilic compounds on the receptor-mediated gene transfer into hepatic cells by asialofetuin-labeled liposomes. *Biochim Biophys Acta* 1996; **1278**: 51-58

- 21 **Gao X**, Huang L. A novel cationic liposome reagent for efficient transfection of mammalian cells. *Biochem Biophys Res Commun* 1991; **179**: 280-285
- 22 **Wang XH**, Wang SQ, Li MD, Zhu BZ. Establishment of a HCV 5' NCR transgenic cell model. *Bingdu Xuebao* 1998; **14**: 296-301
- 23 **Smits E**, Ernberts FN, Kellogg RM. Reliable method for the synthesis of aryl b-D-glucopyranosides, using boron trifluoride-diethyl ether as catalysts. *J Chem Soc Perkin Trans* 1996; **2873-2877**
- 24 **Lubineu A**, Queneau Y. Aqueous cycloadditions using gluco-organic substrates 1. stereo- chemical course of the reaction. *J Org Chem* 1987; **52**: 1001-1009
- 25 **Wakita T**, Wands JR. Specific inhibition of hepatitis C virus expression by antisense oligodeoxynucleotides. *In vitro* model for selection of target sequence. *J Biol Chem* 1994; **269**: 14205-14210
- 26 **Chen J**, Simon RP, Nagayama T, Zhu R, Loeffert JE, Watkins SC, Graham SH. Suppression of endogenous bcl-2 expression by antisense treatment exacerbates ischemic neuronal death. *J Cereb Blood Flow Metab* 2000; **20**: 1033-1039
- 27 **Venugopalan P**, Jain S, Sankar S, Singh P, Rawat A, Vyas SP. pH-sensitive liposomes: mechanism of triggered release to drug and gene delivery prospects. *Pharmazie* 2002; **57**: 659-671
- 28 **Simoes S**, Slepushkin V, Duzgunes N, Pedroso de Lima MC. On the mechanisms of internalization and intracellular delivery mediated by pH-sensitive liposomes. *Biochim Biophys Acta* 2001; **1515**: 23-37
- 29 **Simoes S**, Slepushkin V, Pires P, Gaspar R, de Lima MP, Duzgunes N. Mechanisms of gene transfer mediated by lipoplexes associated with targeting ligands or pH-sensitive peptides. *Gene Ther* 1999; **6**: 1798-1807
- 30 **Wrobel I**, Collins D. Fusion of cationic liposomes with mammalian cells occurs after endocytosis. *Biochim Biophys Acta* 1995; **1235**: 296-304

Edited by Ma JY and Wang XL

Effects of estradiol on liver estrogen receptor- α and its mRNA expression in hepatic fibrosis in rats

Jun-Wang Xu, Jun Gong, Xin-Ming Chang, Jin-Yan Luo, Lei Dong, Ai Jia, Gui-Ping Xu

Jun-Wang Xu, Xin-Ming Chang, Ai Jia, Gui-Ping Xu, Department of Gastroenterology, First Hospital of Xi'an Jiaotong University, Xi'an 710061, Shaanxi Province, China

Jun Gong, Jin-Yan Luo, Lei Dong, Department of Gastroenterology, Second Hospital of Xi'an Jiaotong University, Xi'an 710031, Shaanxi Province, China

Supported by the Doctorate Foundation of Xi'an Jiaotong University, No.2001-13

Correspondence to: Dr. Jun-Wang Xu, Department of Gastroenterology, First Hospital of Xi'an Jiaotong University, Xi'an 710061, Shaanxi Province, China. xujw@pub.xaonline.com

Telephone: +86-29-85323507 **Fax:** +86-29-85263190

Received: 2003-05-11 **Accepted:** 2003-06-07

(18.7 \pm 3.8, 23.1 \pm 3.7) fibrotic groups (P <0.05).

CONCLUSION: The increase in hepatic ER and mRNA expression may be part of the molecular mechanisms underlying the suppressive effect of estradiol on liver fibrosis induced by CCl₄ administration.

Xu JW, Gong J, Chang XM, Luo JY, Dong L, Jia A, Xu GP. Effects of estradiol on liver estrogen receptor- α and its mRNA expression in hepatic fibrosis in rats. *World J Gastroenterol* 2004; 10(2): 250-254

<http://www.wjgnet.com/1007-9327/10/250.asp>

Abstract

AIM: Estradiol treatment regulates estrogen receptor (ER) level in normal rat liver. However, little information is available concerning the role of estrogen in regulating liver ER in hepatic fibrosis in rats. The present study was conducted to determine whether estradiol treatment in CCl₄-induced liver fibrosis of female and ovariectomized rats altered liver ER α and its mRNA expression, and to investigate the possible mechanisms.

METHODS: Seventy female rats were divided into seven groups with ten rats in each. The ovariectomy groups were initiated with ovariectomies and the sham operation groups were initiated with just sham operations. The CCl₄ toxic fibrosis groups received 400 mL/L CCl₄ subcutaneously at a dose of 2 mL/kg twice weekly. Estrogen groups were treated subcutaneously with estradiol 1 mg/kg, the normal control group and an ovariectomy group received injection of peanut oil vehicle twice weekly. At the end of 8 weeks, all the rats were killed to detect their serum and hepatic indicators, their hepatic collagen content, and liver ER and ER mRNA expression.

RESULTS: Estradiol treatment in both ovariectomy and sham ovariectomy groups reduced liver levels of ALT (from 658 \pm 220 nkat/L to 311 \pm 146 nkat/L and 540 \pm 252 nkat/L to 314 \pm 163 nkat/L, P <0.05) and AST (from 697 \pm 240 nkat/L to 321 \pm 121 nkat/L and 631 \pm 268 nkat/L to 302 \pm 153 nkat/L, P <0.05), increased serum nitric oxide (NO) level (from 53.7 \pm 17.1 μ mol/L to 93.3 \pm 24.2 μ mol/L and 55.3 \pm 23.1 μ mol/L to 87.5 \pm 23.6 μ mol/L, P <0.05) and hepatic nitric oxide synthase (NOS) activity (from 1.73 \pm 0.71 KU/g to 2.49 \pm 1.20 KU/g and 1.65 \pm 0.46 KU/g to 2.68 \pm 1.17 KU/g, P <0.05), diminished the accumulation of hepatic collagen, decreased centrolobular necrotic areas as well as the inflammatory reaction in rats subjected to CCl₄. The positive signal of ER and ER mRNA distributed in parenchymal and non-parenchymal hepatic cells, especially near the hepatic centrolobular and periportal areas. Ovariectomy decreased ER level (from 10.2 \pm 3.2 to 4.3 \pm 1.3) and ER mRNA expression (from 12.8 \pm 2.1 to 10.9 \pm 1.3) significantly (P <0.05). Hepatic ER and ER mRNA concentrations were elevated after treatment with estradiol in both ovariectomy (15.8 \pm 2.4, 20.8 \pm 3.1) and sham ovariectomy

INTRODUCTION

The progression of various forms of chronic liver diseases is more rapid in men than in women. This has been specifically noted in hepatic cirrhosis and hepatocellular carcinoma^[1-3]. The specific mechanisms underlying these clinical findings are unclear. Hepatic fibrosis is a consequence of severe liver damage, which occurs in many chronic liver diseases as a forerunner to cirrhosis. We recently found^[4] that estradiol treatment inhibited the proliferation of hepatic stellate cells, suppressed hepatic collagen content and reduced hepatic type I collagen in fibrotic rats induced by CCl₄ administration, and thus improved liver fibrosis. The mechanisms of the antifibrogenic effect of estradiol have been hypothesized by an indirect way—a hepatocellular membrane protection and a radical scavenging action.

Chronic fibrotic diseases can differ from each other in etiology. But, in terms of pathogenesis, they share some basic common features^[5]. For instance, three serious chronic diseases—atherosclerosis, glomerulosclerosis, and liver fibrosis—have many properties in common. Therefore, factors that affect the development of atherosclerosis or glomerulosclerosis may affect liver fibrosis by similar mechanisms. Studies showed^[6] that estradiol could suppress atherosclerosis and glomerulosclerosis in rats by directly affecting the estrogen receptor (ER) on smooth muscle cells and mesangial cells. The liver is not considered as a kind of classic estrogen-dependent tissue, as are the breast and uterus, but livers in both male and female rats have shown to contain high affinity, low capacity of ER and respond to estrogen by regulating liver function^[7]. Previous data have shown^[4] that tamoxifen, an antiestrogen agent, acts by occupying the estrogen-binding site of the receptor protein, increases fibrogenesis in CCl₄-induced fibrosis of the liver. It was proposed that estrogen might suppress hepatic fibrosis also by a receptor mechanism. In the liver, ER α is the dominant form of ER, while the other subtype, ER β , has not yet been demonstrated^[8]. Hence, only ER α would be further considered in this paper.

Previously published data indicated that 17 β -estradiol treatment could regulate the levels of ER in normal rat liver^[9]. However, little information is available concerning the role of estrogen in the regulation of liver ER in fibrotic rats. The present study was conducted to determine whether estradiol treatment in CCl₄-induced liver fibrosis of female and

ovariectomy rats altered the liver ER and its mRNA expression, and to investigate the possible mechanisms.

MATERIALS AND METHODS

Animals

Seventy female Sprague-Dawley rats (obtained from the Experimental Animal Holding Unit of Shaanxi Province, China), weighing 209 ± 19 g, with an average age of approximately 10 weeks, were housed in a temperature-humidity-controlled environment with 12 h light-dark cycles (lights on from 07:00 AM to 19:00 PM) and had free access to food and water. They were randomly divided into seven groups with ten rats in each. Ovariectomy groups were initiated with a bilateral ovariectomy and sham operation groups were initiated with just a sham operation. For two CCl₄ toxic fibrosis groups, with bilateral ovariectomy (CCl₄+Ovx) and sham operation (CCl₄), 400 mL/L CCl₄ in peanut oil was injected subcutaneously at a dose of 2 mL/kg twice weekly, and the first dosage was doubled. The two estrogen groups, with bilateral ovariectomy (CCl₄+Ovx+E) and sham operation (CCl₄+E), were treated subcutaneously with estradiol (benzoic estradiol) 1 mg/kg twice weekly (The Ninth Pharmaceutical Factory of Shanghai, China). All of the above four groups were fed with a modified high fat diet containing 5 g/kg cholesterol and 200 g/kg pig oil. CCl₄ and estradiol were used 2 weeks after operation. A control ovariectomy treated group (Ovx+E) was just given estradiol 1 mg/kg twice weekly. The normal control group (Control) and an ovariectomy group (Ovx) were given normal food and water, and received injection of peanut oil vehicle twice weekly. At the end of a 8-week experimental period, all the rats were fasted overnight and sacrificed by cervical dislocation after anaesthetised by intramuscular injection of sodium pentobarbital (40 mg/kg). Blood was collected from the animals and serum was analysed. The livers were removed immediately.

Estimation of serum indicators and hepatic nitric oxide synthase

Activities of serum aspartate aminotransferase (AST) and alanine aminotransferase (ALT) were assayed by a 917-Hitachi automatic analyzer. Serum nitric oxide (NO) and hepatic nitric oxide synthase (NOS) were measured following the instructions of the reagent kit (purchased from Jiancheng Medical Institute, Nanjing, China).

Histopathological study

Liver tissues excised from each rat were fixed in 100 mL/L neutral formalin, embedded in paraffin, and stained with hematoxylin-eosin (HE) and Masson's trichrome. Evaluation of hepatic fibrosis was determined by a semi-quantitative method to assess the degree of histologic injury, applying the following scores^[10,11]: 0, absence of fibrosis; 1, perivenular and/or pericellular fibrosis; 2, septal fibrosis; 3, bridging fibrosis (incomplete cirrhosis); 4, complete cirrhosis.

Immunohistochemical examination for estrogen receptor- α

Liver tissue sections were mounted on slides, deparaffinized in xylene, and rehydrated in alcohol. Estrogen receptor- α (ER α) was assessed and semi-quantitated by immunohistochemistry using a commercial antibody against ER α (Boster, Wuhan, China) followed by DAB detection. For each sample, ten random fields were evaluated for positively stained cells. The results were expressed as the percentage of positive cells to the total number of cells counted.

In situ hybridization for estrogen receptor mRNA of liver tissue

In situ hybridization kit was purchased from Boster Biological

Technology Limited Company (Wuhan, China, No. MK1069 α). In situ hybridization was performed according to the manufacturer's instructions. Briefly, the paraffin embedded serial sections (thickness of 4 μ m) were dried at 80 °C, and their paraffin was removed by xylene and rehydrated with graded ethanol. The sections were acidified in HCl for 30 min, and blocked in 3 mL of 300 mL/L H₂O₂ for 10 min before digestion in proteinase K for 30 min, and then dehydrated with graded ethanol. After prehybridization at 37–40 °C for 2 h, the labeled cDNA probes of ER α were denatured in hybridization buffer at 95 °C for 10 min, then at -20 °C for 10 min, then added into tissues prehybridized at 37 °C overnight. Sections were washed in turn with 2 \times SSC, 1 \times SSC, 0.2 \times SSC, and Buffer I, blocking water was added at room temperature for 20 min, and then mouse anti-digoxin serum at 37 °C for 60 min, biotinylated goat anti-mouse serum at 37 °C for 30 min, SABC at 37 °C for 30 min, finally DAB was added to be stained. After several times of washing, the sections were counterstained with hematoxylin, dehydrated with ethanol, rinsed in xylene and mounted with gum for microscopic examination and photography. For each sample, ten random fields were evaluated for positively stained cells. The results were expressed as the percentage of positive cells to the total number of cells counted.

Statistical analysis

Data were presented as $\bar{x} \pm s$ unless otherwise indicated. Mann-Whitney *u* test for nonparametric and unpaired values, Student's *t*-test or Fisher's exact test was used as appropriate. Results were considered significant when $P < 0.05$.

RESULTS

Estimation of serum indicators and hepatic nitric oxide synthase

At the end of a 8-week experimental period, 5 rats died because of infection at the site of injection and hepatic crack due to improper handling. It was evident that CCl₄ produced a marked increase in the activities of serum ALT and AST in both ovariectomy and sham ovariectomy rats. The extent of increase was lower in sham ovariectomy group than in ovariectomy group, but without statistical significance ($P > 0.05$). CCl₄ plus estradiol in both ovariectomy and sham ovariectomy groups showed a significant decrease in enzyme levels. However, they were still higher than those of control groups. The enzyme levels in the ovariectomy and estradiol treatment groups were similar to those in control group. The levels of serum NO₂⁻/NO₃⁻ and hepatic NOS activity increased significantly in both ovariectomy and sham ovariectomy rats when CCl₄ was injected, especially in estradiol treatment groups (Table 1). Ovariectomy itself had no influence on the above parameters.

Table 1 Serum ALT, AST, NO₂⁻/NO₃⁻ and hepatic NOS activity ($\bar{x} \pm s$)

Group	<i>n</i>	ALT (nkat/L)	AST (nkat/L)	NO ₂ ⁻ /NO ₃ ⁻ (μ mol/L)	NOS (KU/g)
Control	10	35.8 \pm 7.9	64.5 \pm 20.8	21.8 \pm 13.7	0.65 \pm 0.08
Ovx	10	31.6 \pm 6.5	66.4 \pm 18.3	19.3 \pm 11.2	0.54 \pm 0.33
Ovx+E	9	38.5 \pm 11.2	68.4 \pm 21.2	84.8 \pm 24.9 ^c	2.57 \pm 1.06 ^{ac}
CCl ₄	9	540 \pm 252 ^a	631 \pm 268 ^a	55.3 \pm 23.1 ^a	1.65 \pm 0.46 ^a
CCl ₄ +Ovx	10	658 \pm 220 ^a	697 \pm 240 ^a	53.7 \pm 17.1 ^a	1.73 \pm 0.71 ^a
CCl ₄ +E	8	314 \pm 163 ^c	302 \pm 153 ^c	87.5 \pm 23.6 ^c	2.68 \pm 1.17 ^c
CCl ₄ +Ovx+E	9	311 \pm 146 ^c	321 \pm 121 ^c	93.3 \pm 24.2 ^c	2.49 \pm 1.20 ^c

^a $P < 0.05$, vs control; ^c $P < 0.05$, vs CCl₄.

Histopathological changes

The control livers showed a normal lobular architecture with central veins and radiating hepatic cords. Prolonged administration of CCl₄ caused severe pathological damages such as fat accumulation, inflammation, necrosis, and collagen deposition, especially in ovariectomy group. Administration of estradiol reduced the accumulation of hepatic collagen, decreased centrolobular necrotic areas as well as inflammatory reaction in rats subjected to CCl₄. Semi-quantitative hepatic collagen staging scores are shown in Table 2.

Table 2 Effects of ovariectomy and estradiol on histological scores of CCl₄-induced hepatic fibrosis

Group	n	Hepatic fibrosis scores				
		-	+	++	+++	++++
Control	10	10	0	0	0	0
Ovx	10	10	0	0	0	0
Ovx+E	9	9	0	0	0	0
CCl ₄	9	0	2	2	3	1
CCl ₄ +Ovx ^a	10	0	0	2	5	3
CCl ₄ +E ^a	8	0	4	2	1	0
CCl ₄ +Ovx+E ^a	9	0	5	2	2	0

^aP<0.05, vs control.

Immunohistochemical staining and *in situ* hybridization for estrogen receptor- α

By immunohistochemical detection, the positive signal of ER α as brown particles was scattered or diffused only in cytoplasm other than in nuclei of parenchymal (hepatocytes) and non-parenchymal hepatic cells, especially near the hepatic centrolobular and periportal areas. The positive signal of *in situ* hybridization for ER α mRNA also showed brown particles, and distributed in cytoplasm and partly in nuclei (Figure 1).

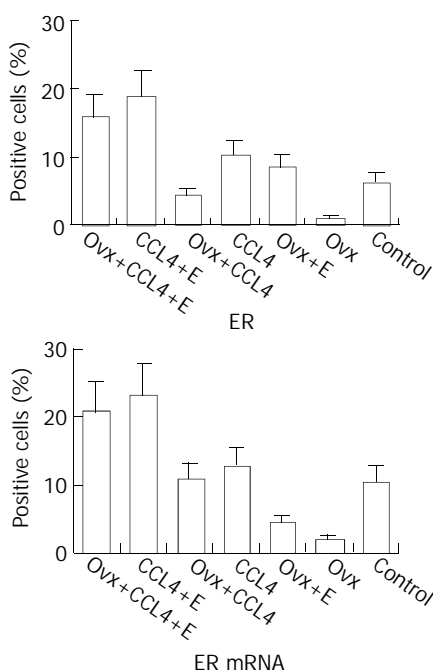


Figure 1 ER α and ER α mRNA in female rat liver.

It showed that livers of female rats contained ER, and ovariectomy decreased ER level and ER mRNA expression significantly ($P<0.05$). Treatment with estradiol at a high dose restored the liver ER and ER mRNA levels. CCl₄ administration

in control and ovariectomized groups was associated with an increase in ER level and ER mRNA expression, but the difference was not significant in control group ($P>0.05$). Hepatic ER and ER mRNA concentrations were elevated significantly after treatment with estradiol in CCl₄ induced fibrotic rats ($P<0.05$, Figures 2 and 3).

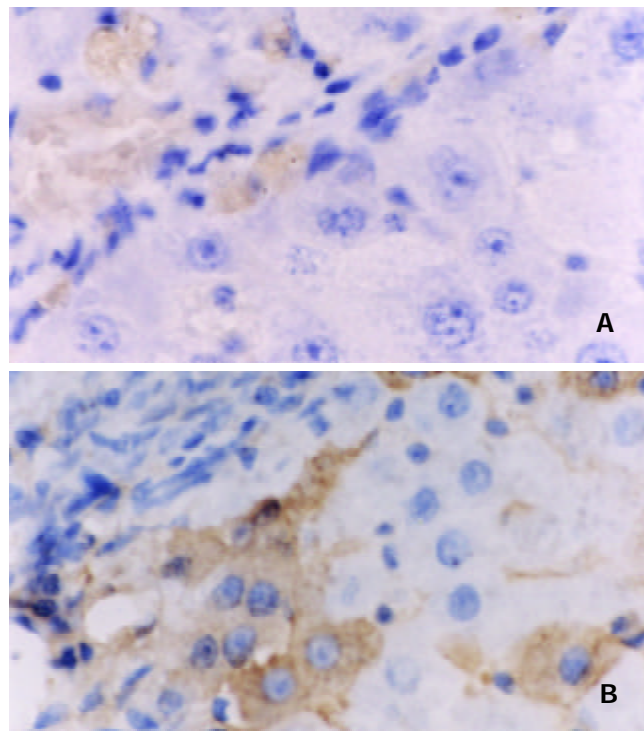


Figure 2 Positive signal of ER in female rat liver (Immunohistochemistry staining PAP method, magnification $\times 400$). 2A: CCl₄ group, 2B: Estradiol treatment group shows increased ER expression compared with 2A.

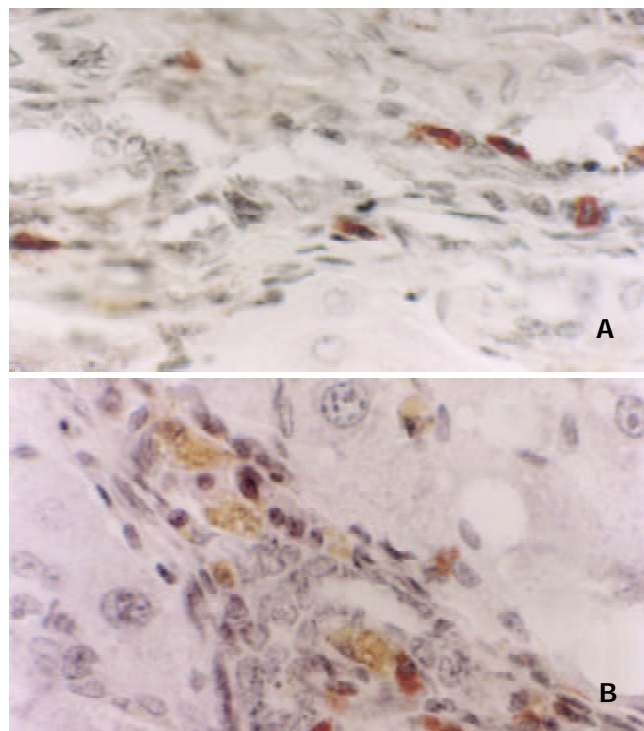


Figure 3 Positive signal of ER mRNA in female rat liver (*in situ* hybridization staining, SP method, magnification $\times 400$). 3A: CCl₄ group, 3B: Estradiol treatment group shows increased ER mRNA expression compared with 3A.

DISCUSSION

Hormone receptors are generally down regulated by high concentrations of their own ligands. This also seems to be the case with ER in reproductive tissues such as the uterus, ovaries, and mammary glands where estrogens are involved in cell growth and differentiation^[12]. In the liver, however, ER has an entirely different function and the hepatic responses to estrogens appear to require high concentrations of estrogens. Some data indicated^[9] that treatment with a low (physiological) dose of estradiol could increase ER and ER mRNA in livers of male rats. But the regulation of hepatic ER and ER mRNA in female rats by estrogen has been reported differently^[13,14]. The majority of studies concerning estrogenic effects have been performed in ovariectomized female rats. Some data showed^[15] that hepatic sinusoidal endothelial cell and Kupffer cell in the livers of female rats contained ER, and they were decreased by ovariectomy. Long-term treatment of 17 β -estradiol elevated the level of ER in hepatic sinusoidal endothelial cell and Kupffer cell in ovariectomized rats. On the other hand, ovariectomy has also been reported to increase ER level and decrease ER mRNA level in hepatocytes from female rats^[12]. This is somewhat divergent to what was seen in this study, where as ovariectomy decreased ER level and ER mRNA expression in parenchymal and non-parenchymal hepatic cells of female rats, and treatment with estradiol at a high dose restored their levels. These observations confirmed a reported increase in hepatic ER mRNA after estrogen treatment in ovariectomized female rats^[16]. An explanation for the mechanism whereby hepatic ER was increased is difficult based on our limited observations. It is possible that the effect of estrogen-treatment on ER levels in ovariectomized female rats was affected indirectly through the pituitary, or by increased hepatic growth hormone receptors. Treatment with 17 β -estradiol in combination with growth hormone and dexamethasone was reported to increase ER levels to eightfold, while estradiol treatment alone had a minimal influence on them in cultured hepatocytes from female rats^[12]. This may suggest that the regulation of hepatic ER is under a more complex control involving other factors.

It has been shown^[17] that prolonged alcohol abuse induced a marked increase in ER levels in livers of both male and female patients, especially in patients who had histological evidence of acute liver damage (alcoholic hepatitis). As we know, CCl₄-induced hepatitis and fibrosis shared several characteristics with human hepatitis and fibrosis of different etiologies^[18-24]. In this study, prolonged administration of CCl₄ induced increases in hepatic ER and ER mRNA expression in female rats, especially in ovariectomized group. The increase extent of ER and ER mRNA was correlated histologically with inflammation, fat accumulation, necrosis, activities of serum ALT and AST, and hepatic collagen disposition. As it is impossible to provide a detailed explanation of the regulation of hepatic ER in normal female rats, we can not establish whether the increase in ER is due CCl₄ administration in our study. Further investigations are thus required to clarify this point. Within these limitations, our data indicate that prolonged CCl₄ administration can affect ER levels and ER mRNA expression in female rat livers.

In our study, hepatic ER and ER mRNA concentrations were significantly elevated after treatment with estradiol in CCl₄-induced fibrotic rats, and the elevation of ER was correlated with a marked decrease in hepatic damage and fibrosis. It suggested that estradiol might suppress hepatic fibrosis by a receptor mechanism. This finding has not been reported previously^[25,26] but is in line with the experimental data obtained from cultured hepatic sinusoidal endothelial cells in rats. In the experiment^[27], ER was demonstrated in hepatic sinusoidal endothelial cells, and estrogen increased NOS activity and upregulated NO production in the cells through

an ER-mediated system, and then regulated the hepatic sinusoidal microcirculation. It has been found that in the liver, NO is produced by hepatic sinusoidal endothelial cells, Kupffer cells, hepatic stellate cells and hepatocytes^[28-32], and NO is synthesized by NOS from L-arginine as a substrate^[33,34]. It was observed that endogenous NO could protect the liver from lipid peroxidation, damage, and fibrosis^[35]. In the present study, estradiol treatment led to a paralleled increase in ER with serum NO and hepatic NOS activity in fibrotic rats. These findings suggest that in liver fibrosis, estrogen may promote NO synthesis through hepatic ER, resulting in improvements of liver damage and fibrosis in rats.

The liver has been found to be extremely sensitive to the action of sex hormones^[4,26], estrogen-dependent regulation of hepatic function could occur through ER present in the liver^[7]. We demonstrated that administration of estradiol elevated ER levels in hepatic fibrotic rats, and ER was distributed in parenchymal (hepatocytes) and non-parenchymal hepatic cells, especially near the hepatic centrolobular and periportal areas where non-parenchymal cells were mainly located. Although we could not identify the exact location of ER in hepatic cells in the present study, we know that the high affinity ER in Kupffer cells of rat liver could exhibit the same characteristics as that presented in hepatocytes^[15]. Therefore, estrogen may modulate Kupffer cell function. Kupffer cells upon stimulation, could produce mediators such as TNF, IL-6 and IL-10, and therefore playing a central role in the regulation of CCl₄-induced liver injury and fibrotic progression^[17,36-42].

As is generally believed that the expression of specific genes and cell responses to steroid hormones are related to the amount of receptors, the increase in hepatic ER and its mRNA as described in this paper may be part of the molecular mechanisms underlying the suppressive effect of estradiol on liver fibrosis induced by CCl₄ administration.

REFERENCES

- 1 **Becker U**, Deis A, Sorensen TI, Gronbaek M, Borch-Johnsen K, Muller CF, Schnohr P, Jensen G. Prediction of risk of liver disease by alcohol intake, sex, and age: a prospective population study. *Hepatology* 1996; **23**: 1025-1029
- 2 **Pinzani M**, Romanelli RG, Magli S. Progression of fibrosis in chronic liver diseases: time to tally the score. *J Hepatol* 2001; **34**: 764-767
- 3 **Yan JC**, Ma JY, Pan BR, Ma LS. Study of hepatitis B in China. *Shijie Huaren Xiaohua Zazhi* 2001; **9**: 611-616
- 4 **Xu JW**, Gong J, Chang XM, Luo JY, Dong L, Hao ZM, Jia A, Xu GP. Estrogen reduces CCl₄-induced liver fibrosis in rats. *World J Gastroenterol* 2002; **8**: 883-887
- 5 **Tan E**, Gurjar MV, Sharma RV, Bhalla RC. Estrogen receptor- α gene transfer into bovine aortic endothelial cells induces eNOS gene expression and inhibits cell migration. *Cardiovasc Res* 1999; **43**: 788-797
- 6 **Kwan G**, Neugarten J, Sherman M, Ding Q, Fotadar U, Lei J, Silbiger S. Effect of sex hormones on mesangial cell proliferation and collagen synthesis. *Kidney Int* 1996; **50**: 1173-1179
- 7 **Porter LE**, Elm MS, Van Thiel DH, Dugas MC, Eagon PK. Characterization and quantitation of human hepatic estrogen receptor. *Gastroenterology* 1983; **84**: 704-712
- 8 **Kuiper GG**, Carlsson B, Grandien K, Enmark E, Haggblad J, Nilsson S, Gustafsson JA. Comparison of the ligand binding specificity and transcript tissue distribution of estrogen receptor α and β . *Endocrinology* 1997; **138**: 863-870
- 9 **Koritnik DR**, Koshy A, Hoversland RC. 17 β -estradiol treatment increases the levels of estrogen receptor and its mRNA in male rat liver. *Steroids* 1995; **60**: 519-529
- 10 **George J**, Rao KR, Stern R, Chandrakasan G. Dimethylnitrosamine-induced liver injury in rats: the early deposition of collagen. *Toxicology* 2001; **156**: 129-138
- 11 **Pilette C**, Rousselet MC, Bedossa P, Chappard D, Oberti F, Rifflet H, Maiga MY, Gallois Y, Cales P. Histopathological evaluation

- of liver fibrosis: quantitative image analysis vs Semi-quantitative scores. Comparison with serum markers. *J Hepatol* 1998; **28**: 439-446
- 12 **Stavreus-Evers AC**, Feyschuss B, Eriksson HA. Hormonal regulation of the estrogen receptor in primary cultures of hepatocytes from female rats. *Steroids* 1997; **62**: 647-654
- 13 **Stavreus-Evers A**, Parini P, Freyschuss B, Elger W, Reddersen G, Sahlin L, Eriksson H. Estrogenic influence on the regulation of hepatic estrogen receptor- α and serum level of angiotensinogen in female rats. *J Steroid Biochem Mol Biol* 2001; **78**: 83-88
- 14 **Ignatenko LL**, Mataradze GD, Rozen VB. Endocrine mechanisms for the formation of sex-related differences in hepatic estrogen receptor content and their significance for the realization of an estrogen effect on angiotensinogen blood level in rats. *Hepatology* 1992; **15**: 1092-1098
- 15 **Vickers AE**, Lucier GW. Estrogen receptor levels and occupancy in hepatic sinusoidal endothelial and Kupffer cells are enhanced by initiation with diethylnitrosamine and promotion with 17 α -ethynylestradiol in rats. *Carcinogenesis* 1996; **17**: 1235-1242
- 16 **Shupnik MA**, Gordon MS, Chin WW. Tissue-specific regulation of rat estrogen receptor mRNAs. *Mol Endocrinol* 1989; **3**: 660-665
- 17 **Colantoni A**, Emanuele MA, Kovacs EJ, Villa E, Van Thiel DH. Hepatic estrogen receptors and alcohol intake. *Mol Cell Endocrinol* 2002; **193**: 101-104
- 18 **Du WD**, Zhang YE, Zhai WR, Zhou XM. Dynamic changes of type I, III and IV collagen synthesis and distribution of collagen-producing cells in carbon tetrachloride induced rat liver fibrosis. *World J Gastroenterol* 1999; **5**: 397-403
- 19 **Wu CH**. Fibrodynamics-elucidation of the mechanisms and sites of liver fibrogenesis. *World J Gastroenterol* 1999; **5**: 388-390
- 20 **Liu HL**, Li XH, Wang DY, Yang SP. Matrix metalloproteinase-2 and tissue inhibitor of metalloproteinase -1 expression in fibrotic rat liver. *World J Gastroenterol* 2000; **6**: 881-884
- 21 **Wei HS**, Li DG, Lu HM, Zhan YT, Wang ZR, Huang X, Zhang J, Cheng JL, Xu QF. Effects of AT1 receptor antagonist, losartan, on rat hepatic fibrosis induced by CCl₄. *World J Gastroenterol* 2000; **6**: 540-545
- 22 **Wang JY**, Zhang QS, Guo JS, Hu MY. Effects of glycyrrhetic acid on collagen metabolism of hepatic stellate cells at different stages of liver fibrosis in rats. *World J Gastroenterol* 2001; **7**: 115-119
- 23 **Zhang YT**, Chang XM, Li X, Li HL. Effects of spironolactone on expression of type I/III collagen proteins in rat hepatic fibrosis. *Shijie Huaren Xiaohua Zazhi* 2001; **9**: 1120-1124
- 24 **Wang LT**, Zhang B, Chen JJ. Effect of anti-fibrosis compound on collagen expression of hepatic cells in experimental liver fibrosis of rats. *World J Gastroenterol* 2000; **6**: 877-880
- 25 **Shimizu I**, Mizobuchi Y, Yasuda M, Shiba M, Ma YR, Horie T, Liu F, Ito S. Inhibitory effect of oestradiol on activation of rat hepatic stellate cells *in vivo* and *in vitro*. *Gut* 1999; **44**: 127-136
- 26 **Liu Y**, Shimizu I, Omoya T, Ito S, Gu XS, Zuo J. Protective effect of estradiol on hepatocytic oxidation damage. *World J Gastroenterol* 2002; **8**: 363-366
- 27 **Sakamoto M**, Uen T, Nakamura T, Hashimoto O, Sakata R, Kin M, Ogata R, Kawaguch T, Torimura T, Sata M. Estrogen upregulates nitric oxide synthase expression in cultured rat hepatic sinusoidal endothelial cells. *J Hepatol* 2001; **34**: 858-864
- 28 **Huang YQ**, Zhang DZ, Mo JZ, Li RR, Xiao SD. Nitric oxide concentration of esophageal tissues and hemodynamics in cirrhotic rats. *Xin Xiaohuabingxue Zazhi* 1997; **5**: 558-559
- 29 **Yang CJ**, Zhen CE, Yao XX. Study on relationship between plasma NO and sex hormones in patients with hepatic cirrhosis. *Huaren Xiaohua Zazhi* 1998; **6**: 976-978
- 30 **Huang YQ**, Xiao SD, Zhang DZ, Mo J. Nitric oxide synthase distribution in esophageal mucosa and hemodynamic changes in rats with cirrhosis. *World J Gastroenterol* 1999; **5**: 213-216
- 31 **Qin JM**, Zhang YD. Intestinal expressions of eNOSmRNA and iNOSmRNA in rats with acute liver failure. *World J Gastroenterol* 2001; **7**: 652-656
- 32 **Wang X**, Zhong YX, Zhang ZY, Lu J, Lan M, Miao JY, Guo XG, Shi YQ, Ding J, Wu KC, Pan BR, Fan DM. Effect of L-NAME on nitric oxide and gastrointestinal motility alterations in cirrhotic rats. *World J Gastroenterol* 2002; **8**: 328-332
- 33 **Zhou JF**, Cai D, Zhu YG, Yang JL, Peng CH, Yu YH. A study on relationship of nitric oxide, oxidation, peroxidation, lipoperoxidation with chronic chole-cystitis. *World J Gastroenterol* 2000; **6**: 501-507
- 34 **Pei WF**, Xu GS, Sun Y, Zhu SL, Zhang DQ. Protective effect of electroacupuncture and moxibustion on gastric mucosal damage and its relation with nitric oxide in rats. *World J Gastroenterol* 2000; **6**: 424-427
- 35 **Muriel P**. Nitric oxide protection of rat liver from lipid peroxidation, collagen accumulation, and liver damage induced by carbon tetrachloride. *Biochem Pharmacol* 1998; **56**: 773-779
- 36 **Li D**, Zhang LJ, Chen ZX, Huang YH, Whang XZ. Effects of TNF α , IL-6 and IL-10 on the development of experimental rat liver fibrosis. *Shijie Huaren Xiaohua Zazhi* 2001; **9**: 1242-1245
- 37 **Jian HQ**, Zhang XL. The mechanisms of hepatic fibrosis. *Shijie Huaren Xiaohua Zazhi* 2000; **8**: 687-689
- 38 **Weng HL**, Cai WM, Liu RH. Animal experiment and clinical study of effect of gamma-interferon on hepatic fibrosis. *World J Gastroenterol* 2001; **7**: 42-48
- 39 **Dai WJ**, Jiang HC. Advances in gene therapy of liver cirrhosis: a review. *World J Gastroenterol* 2001; **7**: 1-8
- 40 **Tang NH**, Chen YL, Wang XQ, Li XJ, Yin FZ, Wang XZ. Construction of IL-2 gene-modified human hepatocyte and its cultivation with microcarrier. *World J Gastroenterol* 2003; **9**: 79-83
- 41 **Li D**, Wang XZ. Relationship of liver fibrosis and TNF α , IL-6 and IL-10. *Shijie Huaren Xiaohua Zazhi* 2001; **9**: 808-810
- 42 **Parola M**, Robino G. Oxidative stress-related molecules and liver fibrosis. *J Hepatol* 2001; **35**: 297-306

Edited by Zhu LH and Wang XL

Expression of liver insulin-like growth factor 1 gene and its serum level in rats with diabetes

Jian-Bo Li, Cheng-Ya Wang, Jia-Wei Chen, Zhen-Qing Feng, Hong-Tai Ma

Jian-Bo Li, Jia-Wei Chen, Department of Endocrinology, First Affiliated Hospital of Nanjing Medical University, Nanjing 210029, Jiangsu Province, China

Cheng-Ya Wang, Molecular Laboratory, First Affiliated Hospital of Nanjing Medical University, Nanjing 210029, Jiangsu Province, China

Zhen-Qing Feng, Hong-Tai Ma, Department of Pathology, Nanjing Medical University, Nanjing 210029, Jiangsu Province, China

Supported by the National Natural Science Foundation of China, No. 39770355

Correspondence to: Dr. Jian-Bo Li, Department of Endocrinology, First Affiliated Hospital of Nanjing Medical University, Nanjing 210029, Jiangsu Province, China. ljbjlx18@yahoo.com.cn

Telephone: +86-25-3718836-6983 **Fax:** +86-25-3724440

Received: 2003-06-04 **Accepted:** 2003-08-16

Abstract

AIM: To explore the effect of diabetic duration and blood glucose level on insulin like growth factor 1 (IGF-1) gene expression and serum IGF-1 level.

METHODS: Diabetes was induced into Sprague Dawley rats by alloxan and then the rats were subdivided into different groups with varying blood glucose level and diabetic duration. The parameters were measured as follows: IGF-1 mRNA by reverse transcriptase-polymerase chain reaction (RT-PCR), IGF-1 peptide and serum IGF-1 concentration by enzyme-linked immunosorbent assay (ELISA).

RESULTS: During early diabetic stage (week 2), in comparison with normal control group (NC), IGF-1 mRNA (1.17 ± 0.069 vs 0.79 ± 0.048 , $P < 0.001$; 1.17 ± 0.069 vs 0.53 ± 0.023 , $P < 0.0005$, respectively), IGF-1 peptide contents [(196.66 ± 14.9) ng·mg⁻¹ vs (128.2 ± 11.25) ng·mg⁻¹, $P < 0.0005$; (196.66 ± 14.9) ng·mg⁻¹ vs (74.43 ± 5.33) ng·mg⁻¹, $P < 0.0001$, respectively] were reduced in liver tissues of diabetic rats. The IGF-1 gene downregulation varied with glucose control level of the diabetic state, and deteriorated gradually further with duration of diabetes. By month 6, hepatic tissue IGF-1 mRNA was 0.71 ± 0.024 vs 1.12 ± 0.056 , $P < 0.001$; 0.47 ± 0.021 vs 1.12 ± 0.056 , $P < 0.0005$, respectively. IGF-1 peptide was (114.35 ± 8.09) ng·mg⁻¹ vs (202.05 ± 15.73) ng·mg⁻¹, $P < 0.0005$; (64.58 ± 3.89) ng·mg⁻¹ vs (202.05 ± 15.73) ng·mg⁻¹, $P < 0.0001$ respectively. Serum IGF-1 was also lowered in diabetic group with poor control of blood glucose. On week 2, serum IGF-1 concentrations were (371.0 ± 12.5) ng·mg⁻¹ vs (511.2 ± 24.7) ng·mg⁻¹, $P < 0.0005$, (223.2 ± 9.39) ng·mg⁻¹ vs (511.2 ± 24.7) ng·mg⁻¹, $P < 0.0001$ respectively. By month 6, (349.6 ± 18.62) ng·mg⁻¹ vs (520.7 ± 26.32) ng·mg⁻¹, $P < 0.0005$, (188.5 ± 17.35) vs (520.7 ± 26.32) ng·mg⁻¹, $P < 0.0001$, respectively. Serum IGF-1 peptide change was significantly correlated with that in liver tissue ($r = 0.99$, $P < 0.001$). Furthermore, No difference was found in the above parameters between diabetic rats with euglycemia and non-diabetic control group.

CONCLUSION: The influence of diabetic status on IGF-1

gene expression in liver tissues is started from early diabetic stage, causing down regulation of IGF-1 expression, and progresses with the severity and duration of diabetic state. Accordingly serum IGF-1 level decreases. This might indicate that liver tissue IGF-1 gene expression is greatly affected in diabetes, thus contributing to reduction of serum IGF-1 level.

Li JB, Wang CY, Chen JW, Feng ZQ, Ma HT. Expression of liver insulin-like growth factor 1 gene and its serum level in rats with diabetes. *World J Gastroenterol* 2004; 10(2): 255-259

<http://www.wjgnet.com/1007-9327/10/255.asp>

INTRODUCTION

Insulin like growth factor-1 (IGF-1) is widely present in tissues of mammalian animals and has a number of bioactivities including regulation of metabolism and enhancement of growth and development of tissues^[1-4]. Recently its research has attracted much attention. IGF-1 may probably be involved in metabolic abnormality and complications associated with diabetes. Liver might be the main source of circulating IGF-1^[1,5]. Recent studies have shown that there was early reduction in hepatic tissue IGF-1 gene expression in experimental diabetes^[6]. However, further investigation on it is lacking. Upon this basis, we further explored the effect of chronic diabetic status on liver tissue IGF-1 gene expression and IGF-1 concentration in the circulation and hoped to help elucidating the pathogenesis of diabetes related disorder of metabolism and complications and lay a basis for premise of intervention.

MATERIALS AND METHODS

Diabetic animal model

Randomly selected Sprague Dawley rats, weighing 180-200 g, were injected *ip*, with alloxan saline solutions at a dose of 240 mg·g⁻¹ body weight. Rats in non-diabetic normal control group (NC group, $n = 28$) were injected *ip*, with an equivalent volume of saline solution^[7]. After 48 hours, blood samples were collected. Diabetic model was established in the rats injected with alloxan, whose blood glucose concentration was > 20 mmol·L⁻¹ (diabetic group, $n = 90$). The mean glucose concentration of the NC group was 5.14 ± 0.91 mmol·L⁻¹. The diabetic group was reassigned into 3 subgroups ($n = 30$ for each group): ID-1 group [(4.93 ± 0.72) - (4.88 ± 0.67) mmol·L⁻¹], ID-2 group [(11.4 ± 0.56) - (10.86 ± 0.94) mmol·L⁻¹] and ID-3 group [(18.34 ± 1.03) - (17.50 ± 1.05) mmol·L⁻¹] with sixteen rats in each group based on glucose level regulated by pork regular insulin combined with protamine zinc insulin (2:1) injected subcutaneously. Both blood glucose level and aminofructose level were regularly measured.

Measurement of liver tissue IGF-1 mRNA contents

After rats were anaesthetized, 1 g liver tissue of the rats was taken. The total RNAs from the tissues were extracted by one-step method^[8,9]. Both quantity and purity of the RNA were determined with the 752 spectrophotometer. Through reverse

transcription polymerase chain reaction (RT-PCR), tissue IGF-1 mRNA was semi-quantitated. The RT-PCR kit was provided by Promega Company (USA) and rat β -actin was used as an internal standard^[8]. According to IGF-1 gene sequence, we designed RT-PCR IGF-1 upstream/downstream primer sequences 5' CTTTGC GGGGCTGAGCTGGT 3', 5' CTT CAGCGAGCAGTACA 3', respectively. All the primers were synthesized by Shanghai BioEngineer Company. The following was optimal reaction condition: reverse transcription at 48 °C for 45 min, denaturation of RNA/DNA hybrid and inactivation of reverse transcriptase at 94 °C for 2 min. PCR for 40 cycles, denaturation at 94 °C for 30 s, annealing at 60 °C for 1 min, extension at 68 °C for 2 min, final extension at 68 °C for 7 min. RT-PCR was performed on the Perkin Elmer (USA). The RT-PCR bands were 184 bp IGF-1 cDNA and 357 bp β -actin cDNA, respectively. Electrophoresis was carried out on 2% agarose gel containing ethidium bromide and semi-quantitated on the Gel DOC 1000 densitometry (Bio-RAD, USA). IGF-1 mRNA contents were calculated and expressed as cDNA relative densitometric units (ratio of IGF-1 cDNA/ β -actin).

Measurement of liver tissue IGF-1 peptide contents

One gram liver tissue was excised from each rat, then frozen in liquid nitrogen and homogenized in a mortar. The homogenates were extracted with 1 mmol·L⁻¹ acetic acid (precooled) and centrifuged. The supernatants were collected, then mixed with 0.05 mmol·L⁻¹ Tris·HCl (PH 7.8) to neutralization and finally stored under -70 °C for future use^[10]. An aliquot of the samples treated as above was taken to measure both total protein content by Brodford method and IGF-1 peptide concentration by enzyme linked immunosorbent assay (ELISA, Diagnostic Systems Laboratory, Inc.). DG-3022 type A was used to measure IGF-1 concentration with a maximum absorbance of 450 nm. IGF-1 tissue content was calculated and expressed as IGF-1 ng·mg⁻¹ total protein.

Measurement of serum IGF-1 peptide concentration

Serum samples from rat heart blood were frozen immediately for future analysis. The samples were pre-treated before assessment of IGF-1 peptide serum concentration (ng·ml⁻¹) with the methods used in ELISA^[11].

Statistical analysis

Data values were presented as $\bar{x}\pm s$. Significance of difference between groups was analyzed by one-way analysis of variance, nonparametric *t'* pair test, Wilcoxon test and χ^2 test. $P<0.05$ was considered statistically significant.

RESULTS

Blood glucose metabolic parameters

At the end of experiment, ID-1 group and NC group had no difference in glucose level, amino fructose level, and body weight. Both blood glucose level and fructose level were significantly higher in ID-2 group and especially in ID-3 group when compared with NC group ($P<0.0001$). Significant differences were also found in the above parameters between ID-2 and ID-3 groups ($P<0.0001$). Within each group, there was no significant difference in aminofructose level (Table 1).

Effects of diabetes on tissue IGF-1 gene expression

Two weeks after diabetic model was established, the liver tissue IGF-1 mRNA contents (IGF-1 cDNA/ β -actin cDNA) were decreased in both ID-2 group ($P<0.001$) and ID-3 group ($P<0.0005$) with a drop of 31% and 53% respectively. They were further decreased with progression of diabetes. On month 6, in comparison with NC group, obvious differences were shown in ID-2 group ($P<0.0005$) and ID-3 group ($P<0.0001$) with a drop of 36% and 59%. Between the two diabetic groups with poor diabetic control, ID-3 group had a significantly lower IGF-1 level than ID-2 group. The drop was 5% and 6% at week 2. Between group ID-1 and NC group, there was no significant difference (Table 2, Figure 1).

The change in tissue IGF-1 peptide content (IGF-1 peptide ng·mg⁻¹ total protein) nearly paralleled that in mRNA content. At the 2nd week, compared with NC group, ID-2 group ($P<0.0005$) and ID-3 group ($P<0.005$) showed a decrease of 32%, 62%, respectively. Both were further decreased over the time course, with a drop of 34% and 65% by the end of the 6th month ($P<0.0001$). A drop of 2% and 3% was found at week 2. ID-3 group had a significantly lower IGF-1 level than ID-2 group ($P<0.001$). There was no significant difference between ID-1 and NC groups (Table 2).

Table 1 Glucose metabolic parameters during the experiment

Group	Duration (month)	n	Initial weight (g)	Weight (g)	Blood (mmol·L ⁻¹)	Aminofructose (mmol·L ⁻¹)
NC	0.5	5	198.41±9.76	249.33±16.02	5.14±0.91	0.82±0.07
	2	5	202.53±17.67	351.20±18.23	5.3±0.44	0.85±0.08
	3	6	200.06±13.03	402.05±37.10	4.91±0.26	0.81±0.09
	6	5	199.65±15.22	544.54±30.41	5.21±0.47	0.85±0.05
ID-1	0.5	5	196.25±14.22	254.31±20.97	4.93±0.72	0.79±0.05
	2	4	202.34±19.12	345.75±23.48	5.10±0.62	0.84±0.08
	3	5	196.42±11.41	411.31±47.37	4.88±0.67	0.78±0.06
	6	6	198.68±12.64	538.52±31.62	4.94±0.58	0.84±0.07
ID-2	0.5	5	192.00±5.70	217.00±9.64 ^a	11.4±0.56 ^c	1.02±0.14 ^c
	2	5	199.00±16.73	241.00±16.44 ^c	10.94±1.08 ^c	1.00±0.29 ^c
	3	6	198.66±14.36	256.83±14.98 ^c	10.86±0.94 ^c	0.98±0.08 ^c
	6	5	201.37±14.11	266.24±13.53 ^c	12.13±0.63 ^c	1.10±0.14 ^c
ID-3	0.5	5	208.60±13.08	205.75±15.34 ^b	18.34±1.03 ^{ce}	1.20±0.12 ^{ce}
	2	5	198.60±16.66	192.80±13.35 ^{cd}	17.48±0.62 ^{ce}	1.18±0.21 ^{ce}
	3	5	211.50±11.37	204.8±11.03 ^{ce}	17.50±1.05 ^{ce}	1.21±0.19 ^{ce}
	6	6	204.35±12.34	185.22±14.36 ^{ee}	16.89±0.95 ^{ce}	1.2±0.34 ^{ee}

Data expressed as mean \pm SD. NC, normal control group; ID-1,-2,-3, insulin treatment group. vs NC, ^a $P<0.0025$, ^b $P<0.001$, ^c $P<0.0001$; vs ID-2 (for the same period), ^d $P<0.001$, ^e $P<0.0001$.

Table 2 Liver tissue IGF-1mRNA ,peptide contents and IGF-1serum concentration

Group	Duration (month)	n	Liver tissue mRNA contents*	Liver tissue IGF-1 peptide (ng·mg ⁻¹)**	Serum IGF-1 (ng·ml ⁻¹)
NC	0.5	5	1.15±0.09	196.66±14.9	511.2±24.7
	2	5	1.17±0.069	198.13±15.25	544.6±22.4
	3	6	1.12±0.056	202.05±15.73	525±30.2
	6	5	1.14±0.066	197.11±12.55	520.7±26.32
ID-1	0.5	5	1.20±0.064	196.7±17.4	536±18.1
	2	4	1.21±0.054	204.1±16.5	540.5±32.5
	3	5	1.18±0.047	200.42±14.9	520.2±14.4
	6	6	1.22±0.044	199.38±16.56	536.54±25.14
ID-2	0.5	5	0.79±0.048 ^b	128.2±11.25 ^c	371.0±12.5 ^c
	2	5	0.74±0.028 ^b	121.3±7.27 ^c	366.4±16.0 ^c
	3	6	0.71±0.024 ^{bh}	114.35±8.09 ^{ci}	353.5±22.4 ^{ce}
	6	5	0.68±0.035 ^{bh}	110.38±10.57 ^{ci}	349.6±18.62 ^{ci}
ID-3	0.5	5	0.53±0.023 ^{cf}	74.43±5.33 ^{df}	223.2±9.39 ^{dc}
	2	5	0.49±0.016 ^{cf}	67.4±6.07 ^{df}	205.6±12.7 ^{dc}
	3	5	0.47±0.02 ^{dgi}	64.58±3.89 ^{dgi}	196.4±15.67 ^{dgi}
	6	6	0.44±0.08 ^{dgi}	62.91±4.32 ^{dgi}	188.5±17.35 ^{dgi}

Data expressed as mean ±SD. *IGF-1relative mRNA contents: IGF-1 cDNA/β-actin cDNA, **tissue IGF-1peptide content: IGF-1 ng·mg⁻¹ total protein. ID-1,-2 ,-3 vs NC (for the same period): ^bP<0.001, ^cP<0.0005, ^dP<0.0001; vs ID-2 group (for the same period): ^eP<0.025, ^fP<0.0025, ^gP<0.001; vs ID-2 (week 2): ^hP<0.05, ⁱP<0.01; vs ID-3 (week 2): ^jP<0.01.

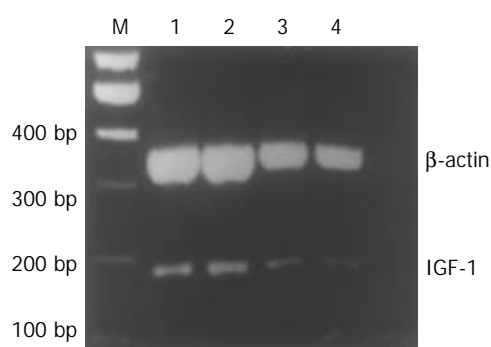


Figure 1 At month 6 of the experiment, liver tissue IGF-1 cDNA/β-actin mRNA RT-PCR product electrophoresis. (1: Control group, 2: ID-1 group, 3: ID-2 group, 4: ID-3 group).

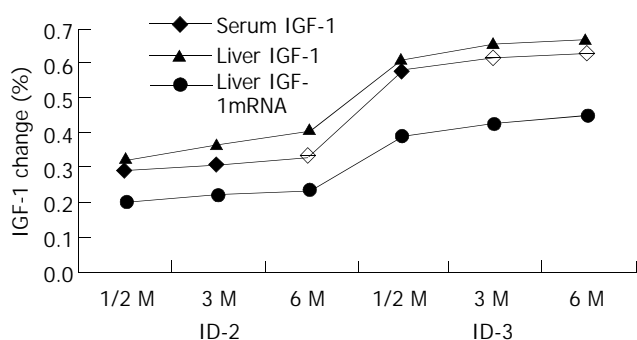


Figure 2 The trend of change in serum IGF-1, liver IGF-1 and mRNA over time course of DM ($r_1=0.99$, $P_1<0.001$; $r_2=0.966$, $P_2<0.001$).

Serum IGF-1 concentration

At week 2, in comparison with NC group, ID-2 and ID-3 groups showed a significant decrease in serum IGF-1 level: 371.0 ± 12.5 ng·mg⁻¹, $P<0.0005$ and 223.2 ± 9.39 ng·mg⁻¹, $P<0.0001$, a drop of 29% and 57%. By the sixth month, serum IGF-1 level was further lowered in both ID-2 and ID-3 groups [349.6 ± 18.62 ng·mg⁻¹, $P<0.0005$; 188.5 ± 17.35 ng·mg⁻¹, $P<0.0001$, respectively], with a fall of 33% and 63%. A drop of 4% and 6% was found at week 2. ID-3 group had a significantly

lower IGF-1 level than ID-2 group ($P<0.001$). There was no significant difference between ID-1 and NC groups.

Relationship between changes in liver IGF-1 mRNA, peptide and serum IGF-1 level

Correlation analysis showed that the trend of serum IGF-1 change was consistent with that occurred in liver IGF-1 peptide ($r_1=0.99$, $P_1<0.001$), and IGF-1mRNA ($r_2=0.99$, $P_2<0.001$) over the time course of diabetes (Figure 2).

DISCUSSION

The study made a preliminary exploration of the effect of chronic diabetic status (e.g. long duration and different glucose levels) on the hepatic IGF-1 gene expression and IGF-1 concentration of circulation.

Insulin like growth factors (IGFs) have similar structures and functions like those of insulin, and can be divided into IGF-1 and IGF-2, the latter of which exerts its biological action on embryonic development and growth. The action of IGF-1 peaks around puberty period and decreases gradually with aging. IGF-1, a single polypeptide with 70 amino acids, was widely expressed in mammal tissues^[1,2]. *In situ* hybridization and immunohistochemical techniques have proven the presence of IGF-1 gene expression (IGF-1 mRNA and peptide) in hepatic cells^[5]. The liver was found to have the highest concentration among all tissues and was probably the main source of circulating IGF-1^[1,5,12], which exert its effect by binding to specific receptors on target cells in endocrine pattern. Human IGF-1 gene is on the long arm of chromosome 12, spanning a minimum of 90 kb which contains 6 exons. Exons 1 and 2 encode 5' untranslated region and amino residue terminal end of IGF-1 peptide, 5' end of Exon 3 encodes carboxyl terminal end of IGF-1 signal peptide. The remaining exon 3 and the main part of exon 4 encode mature IGF-1 peptide including B, C, A, D domains. The 5' end of the remaining exons 4, 5 and 6 encodes signal peptide and 3' untranslated region. Human exon 5 contains stop codon. Gene transcription initiates at exon 1 or 2, varying with tissue specificity. Growth hormone (GH) might affect initiation activity of exon 1 and/or exon 2 to regulate liver IGF-1 gene expression. Insulin may directly regulate liver IGF-1 expression or indirectly by increasing the

number of GH receptors on hepatic cells. Nutritional state and corticosteroid hormones have been found in factors influencing IGF-1 gene expression^[1,5].

In our study, liver tissue IGF-1 gene expression was significantly downregulated in rats with poorly controlled blood glucose (ID-3 and ID-2 groups), as compared to that in rats with normally controlled blood glucose (ID-1 group). Among them, the rats with a higher blood glucose (ID-3) showed more abnormal IGF-1 than those with a relatively low blood glucose (ID-2), the severity of which varied with levels of blood glucose. We continued the observation of the rats with the same level of blood glucose for 6 months after 2 weeks and found that the liver tissue IGF-1 gene expression was gradually decreased with the time course in the rats with hyperglycemia, especially severe hyperglycemia. This showed its association with the progression of diabetes, but to a lower degree. It may indicate the effect of chronic diabetic state on IGF-1 gene expression is less significant than that of the severity of blood glucose. However, the discrepancy in IGF-1 drop rate between the two conditions may reflect a fraction of other tissue's contribution to the circulating IGF-1.

Our study, using RT-PCR technique, demonstrated the early reduction in IGF-1 mRNA contents in liver tissues of alloxan-induced diabetic rats, which was consistent with the previous studies using Northern blot and RT-PCR^[5,6]. However, Veronica MC and Goya *et al* did not study the changes in liver tissue IGF-1 protein and effect of different blood glucose level and duration. We furthermore observed the effect of chronic duration and different severity of hyperglycemia on hepatic IGF-1 gene expressions. In our study, liver tissue IGF-1 gene expression was significantly downregulated in the rats with poorly controlled blood glucose (ID-3 and ID-2 groups), as compared with the rats with normally controlled blood glucose (ID-1 group). Among them, the rats with a higher blood glucose (ID-3) showed more abnormal IGF-1 than those with a relatively low blood glucose (ID-2), the severity of the abnormality varied with the level of blood glucose. We continued the observation of rats with the same level of blood glucose for 6 months after 2 weeks and found that liver tissue IGF-1 gene expression continued to go down gradually with the time course in rats with hyperglycemia, especially severe hyperglycemia. This showed its association with the progression of diabetes, but to a lesser degree. It may indicate the effect of chronic state on IGF-1 gene expression is less significant than severity of hyperglycemia. We are the first to find this. We also found that at translation level, hepatic IGF-1 peptide changed in similar extent as that of mRNA content, indicating the same effect of diabetic status on different translational level. We also demonstrated that serum IGF-1 concentration had a parallel change of hepatic tissue IGF-1. Thus further evidence was provided that the liver might remain to be the main endocrine source of IGF-1 in experimental diabetes. However, the discrepancy in IGF-1 drop rate between the two conditions might reflect a fraction of other tissue's contribution to the circulating IGF-1. The IGF-1 down-regulation was prevented when hyperglycemia was corrected by subcutaneous injection of exogenous insulin, suggesting insulin might be a major regulator of IGF-1 gene expression during diabetes and exclude the possible direct influence of alloxan on IGF-1 gene expression.

Diabetes could result in down-regulation of gene expression, the major factors of which might be insulin secretion deficiency and/or its resistance. Some studies showed that tissue IGF-1 gene expression might be affected by systemic or local factors or both in diabetes, i.e. decrease of GH receptors in target cells and its binding affinity^[13], and by reduced or absent pulsatile pattern secretion of GH, metabolic abnormality of insulin like growth factor binding proteins (IGFBPs)^[6,14], negative nitrogen balance^[15,16] *etc.* All these may probably lead to a decline of

IGF-1. However, the deficiency of insulin or insulin resistance might be the main cause of IGF-1 gene downregulation^[1,17]. In diabetes, IGF-1 in most tissues were down regulated at different degrees, varying with specific tissues^[1,5,18,19]. In the liver it was down regulated^[1,6]. Insulin that corrects hyperglycemia can correct the abnormal IGF-1 gene expression. Our study further supported it. It is known that IGF-1 transcription started at exons 1 and 2 regulated by different initiators and mRNA products that varied in length and affluence with tissue specificity^[1,5,18]. The exact mechanism of insulin controlling IGF-1 gene expression remains to be elucidated.

We successfully established the animal model and found that the hepatic tissue IGF-1 gene expression was down regulated in the diabetic rats, the severity of which depended on glucose level and duration of diabetes. Accordingly, circulating IGF-1 was also decreased. The model established in our experiment is expected to mimic human diabetic status which will help us to interpret the role of IGF-1 in diabetic state. Diabetes can lead to a fall in IGF-1 of endocrine origin. IGF-1 it been found that has a number of bioactivities including mediating action of growth hormone, increasing glucose taken by tissues, inhibiting hepatic glycogenesis, improving insulin sensitivity, decreasing oxidation of lipid, lowering free fatty acids, increasing nucleotide synthesis, proliferation and differentiation of cells^[20-25]. These researches would inevitably help understand the molecular pathogenesis of disturbances of glucose, lipid, protein metabolism associated with diabetes, diabetic peripheral neuropathy and diabetic foot^[4,26-28] and probably might provide the premise of future molecular therapeutic intervention^[29,30].

REFERENCES

- 1 **Pankov YA.** Growth hormone and a partial mediator of its biological action, insulin-like growth factor I. *Biochemistry* 1999; **64**: 1-7
- 2 **Thraikill KM.** Insulin-like growth factor-I in diabetes mellitus: its physiology, metabolic effects, and potential clinical utility. *Diabetes Technol Ther* 2000; **2**: 69-80
- 3 **Cusi K, DeFronzo R.** Recombinant human insulin-like growth factor I treatment for 1 week improves metabolic control in type 2 diabetes by ameliorating hepatic and muscle insulin resistance. *J Clin Endocrinol Metab* 2000; **85**: 3077-3084
- 4 **Zhuang HX, Wuarin L, Fei ZJ, Ishii DN.** Insulin-like growth factor (IGF) gene expression is reduced in neural tissues and liver from rats with non-insulin-dependent diabetes mellitus, and IGF treatment ameliorates diabetic neuropathy. *J Pharmacol Exp Ther* 1997; **283**: 366-374
- 5 **Catanese VM, Scivolino PJ, Lango MN.** Discordant, organ-specific regulation of insulin-like growth factor-1 messenger ribonucleic acid in insulin-deficient diabetes in rats. *Endocrinology* 1993; **132**: 496-503
- 6 **Goya L, Rivero F, Martin MA, Alvarez C, Ramos S, de la Puente A, Pascual-Leone AM.** Liver mRNA expression of IGF-I and IGFBPs in adult undernourished diabetic rats. *Life Sci* 1999; **64**: 2255-2271
- 7 **Okada M, Shibuya M, Yamamoto E, Murakami Y.** Effect of diabetes on vitamin B6 requirement in experimental animals. *Diabetes Obes Metab* 1999; **1**: 221-225
- 8 **Onoue H, Maeyama K, Nomura S, Kasugai T, Tei H, Kim HM, Watanabe T, Kitamura Y.** Absence of immature mast cells in the skin of Ws/Ws rats with a small deletion at tyrosine kinase domain of the c-kit gene. *Am J Pathol* 1993; **142**: 1001-1007
- 9 **Wang P, Li N, Li JS, Li WQ.** The role of endotoxin, TNF-alpha, and IL-6 in inducing the state of growth hormone insensitivity. *World J Gastroenterol* 2002; **8**: 531-536
- 10 **Stiles AD, Sosenko IR, D' Ercole AJ, Smith BT.** Relation of kidney tissue somatomedin-C/insulin-like growth factor I to postnephrectomy renal growth in the rat. *Endocrinology* 1985; **117**: 2397-2401
- 11 **Assy N, Paizi M, Gaitini D, Baruch Y, Spira G.** Clinical implication of VEGF serum levels in cirrhotic patients with or without

- portal hypertension. *World J Gastroenterol* 1999; **5**: 296-300
- 12 **Sjogren K**, Jansson JO, Isaksson OG, Ohlsson C. A transgenic model to determine the physiological role of liver-derived insulin-like growth factor I. *Minerva Endocrinol* 2002; **27**: 299-311
- 13 **Landau D**, Segev Y, Eshet R, Flyvbjerg A, Phillip M. Changes in the growth hormone-IGF-I axis in non-obese diabetic mice. *Int J Exp Diabetes Res* 2000; **1**: 9-18
- 14 **Kobayashi K**, Amemiya S, Kobayashi K, Sawanobori E, Mochizuki M, Ishihara T, Higashida K, Miura M, Nakazawa S. The involvement of growth hormone-binding protein in altered GH-IGF axis in IDDM. *Endocr J* 1999; **46**(Suppl): S67-69
- 15 **Heo YR**, Kang CW, Cha YS. L-Carnitine changes the levels of insulin-like growth factors (IGFs) and IGF binding proteins in streptozotocin-induced diabetic rat. *J Nutr Sci Vitaminol* 2001; **47**: 329-334
- 16 **McCarty MF**. Hepatic monitoring of essential amino acid availability may regulate IGF-I activity, thermogenesis, and fatty acid oxidation/synthesis. *Med Hypotheses* 2001; **56**: 220-224
- 17 **Kaytor EN**, Zhu JL, Pao CI, Phillips LS. Physiological concentrations of insulin promote binding of nuclear proteins to the insulin-like growth factor I gene. *Endocrinology* 2001; **142**: 1041-1049
- 18 **Butler AA**, LeRoith D. Minireview: tissue-specific versus generalized gene targeting of the *igf1* and *igf1r* genes and their roles in insulin-like growth factor physiology. *Endocrinology* 2001; **142**: 1685-1688
- 19 **Duan J**, Zhang HY, Adkins SD, Ren BH, Norby FL, Zhang X, Benoit JN, Epstein PN, Ren J. Impaired cardiac function and IGF-I response in myocytes from calmodulin-diabetic mice: role of Akt and RhoA. *Am J Physiol Endocrinol Metab* 2003; **284**: E366-376
- 20 **Scharf JG**, Ramadori G, Dombrowski F. Analysis of the IGF axis in preneoplastic hepatic foci and hepatocellular neoplasms developing after low-number pancreatic islet transplantation into the livers of streptozotocin diabetic rats. *Lab Invest* 2000; **80**: 1399-1411
- 21 **Cusi K**, DeFronzo R. Recombinant human insulin-like growth factor I treatment for 1 week improves metabolic control in type 2 diabetes by ameliorating hepatic and muscle insulin resistance. *J Clin Endocrinol Metab* 2000; **85**: 3077-3084
- 22 **Butler ST**, Marr AL, Pelton SH, Radcliff RP, Lucy MC, Butler WR. Insulin restores GH responsiveness during lactation-induced negative energy balance in dairy cattle: effects on expression of IGF-I and GH receptor 1A. *J Endocrinol* 2003; **176**: 205-217
- 23 **Sjogren K**, Sheng M, Moverare S, Liu JL, Wallenius K, Tornell J, Isaksson O, Jansson JO, Mohan S, Ohlsson C. Effects of liver-derived insulin-like growth factor I on bone metabolism in mice. *J Bone Miner Res* 2002; **17**: 1977-1987
- 24 **Price JA**, Kovach SJ, Johnson T, Koniaris LG, Cahill PA, Sitzmann JV, McKillop IH. Insulin-like growth factor I is a comitogen for hepatocyte growth factor in a rat model of hepatocellular carcinoma. *Hepatology* 2002; **36**: 1089-1097
- 25 **Reinmuth N**, Fan F, Liu W, Parikh AA, Stoeltzing O, Jung YD, Bucana CD, Radinsky R, Gallick GE, Ellis LM. Impact of insulin-like growth factor receptor-I function on angiogenesis, growth, and metastasis of colon cancer. *Lab Invest* 2002; **82**: 1377-1389
- 26 **Busiguina S**, Fernandez AM, Barrios V. Neurodegeneration is associated to changes in serum insulin-like growth factors. *Neurobiol Dis* 2000; **7**(6 Pt B): 657-665
- 27 **Pierson CR**, Zhang W, Murakawa Y, Sima AA. Early gene responses of trophic factors in nerve regeneration differ in experimental type 1 and type 2 diabetic polyneuropathies. *J Neuropathol Exp Neurol* 2002; **61**: 857-871
- 28 **Li J**, Wang C, Chen J, Li X, Feng Z, Ma H. The role of insulin-like growth factor-I gene expression abnormality in pathogenesis of diabetic peripheral neuropathy. *Zhonghua Neike Zazhi* 2001; **40**: 93-97
- 29 **Savage MO**, Camacho-Hubner C, Dunger DB, Ranke MB, Ross RJ, Rosenfeld RG. Is there a medical need to explore the clinical use of insulin-like growth factor I? *Growth Horm IGF Res* 2001; **11** (Suppl A): S65-69
- 30 **Torrado J**, Carrascosa C. Pharmacological characteristics of parenteral IGF-I administration. *Curr Pharm Biotechnol* 2003; **4**: 123-140

Edited by Wang XL

Long term persistence of T cell memory to HBsAg after hepatitis B vaccination

Ru-Xiang Wang, Greet J. Boland, Jan van Hattum, Gijsbert C. de Gast

Ru-Xiang Wang, Shenyang Center for Disease Control and Prevention, Shenyang 110031, Liaoning Province, China

Greet J. Boland, Jan van Hattum, Department of Gastroenterology, University Hospital Utrecht, the Netherlands

Gijsbert C. de Gast, Netherlands Cancer Institute, Amsterdam, the Netherlands

Correspondence to: Dr. Ru-Xiang Wang, Shenyang Center for Disease Control and Prevention, 37 Qishan Zhong Lu, Huanggu District, Shenyang 110031, Liaoning Province China. rxwtzh@pub.sy.ln.cn

Telephone: +86-24-86853243 **Fax:** +86-24-86863778

Received: 2003-04-12 **Accepted:** 2003-10-11

Abstract

AIM: To determine if the T cell memory to HBsAg can persist for a long time after hepatitis B (HB) vaccination.

METHODS: Thirty one vaccine recipients who were healthcare workers (18 females and 13 males aged 34-58 years) from Utrecht University Hospital, Netherlands, and had previously received a standard course of vaccination for hepatitis B were investigated and another 9 unvaccinated healthy volunteers from the same hospital were used as the control. Blood samples were taken just before the experiment to test serum anti-HBs levels and the subjects were classified into different groups according to their serum titers of anti-HBs and vaccination history. Their peripheral blood mononuclear cells (PBMC) were isolated from freshly heparinized venous blood and the proliferative response of T lymphocytes to the recombinant hepatitis B surface antigen (HBsAg) was investigated.

RESULTS: Positive serum anti-HBs was found in 61.3% (19/31) vaccine recipients and a significant *in vitro* lymphocyte proliferative response to recombinant HBsAg was observed in all the vaccinees with positive anti-HBs. Serum anti-HBs level ≤ 10 IU/L was found in 38.7% (12/31) subjects. In this study, we specially focused on lymphocyte proliferative response to recombinant HBsAg in those vaccine recipients with serum anti-HBsAg less than 10 IU/L. Most of them had received a standard course of vaccination about 10 years before. T lymphocyte proliferative response was found positive in 7 of the 12 vaccine recipients. These results confirmed that HBsAg-specific memory T cells remained detectable in the circulation for a long time after vaccination, even when serum anti-HBs level had been undetectable.

CONCLUSION: The T cell memory to HBsAg can persist for at least 10 years after HB vaccination. Further booster injection is not necessary in healthy responders to HB vaccine.

Wang RX, Boland GJ, van Hattum J, de Gast GC. Long term persistence of T cell memory to HBsAg after hepatitis B vaccination. *World J Gastroenterol* 2004; 10(2): 260-263
<http://www.wjgnet.com/1007-9327/10/260.asp>

INTRODUCTION

Since the introduction of hepatitis B vaccination in the early 1980s, many epidemiological studies have been done to determine the efficacy of the vaccine in eliciting protective immunity against HBV infection. The antibody response to HB vaccine has been found occurring in more than 90% of the healthy vaccinees^[1-15]. Kinetic studies showed serum anti-HBs levels decreased with time following vaccination^[5,9,14,16]. Several demographic and behavioral factors have been found to be associated with a lower rate of antibody response to hepatitis B vaccine^[17,18]. In a considerable percentage of vaccinated persons the anti-HBs level was expected to drop to below 10 IU/L after 5-10 years^[5,19,20]. The decline seemed to be proportional to the antibody titer originally obtained^[15,21]. The necessity of implementing booster injections for those with their anti-HBs levels less than 10 IU/L has remained to be determined^[13,16,20,22,23].

A correlation between *in vivo* antibody production and *in vitro* T cell proliferative response following immunization with HBsAg vaccine has been reported^[24,25]. In previous studies we demonstrated that the B cell memory to HBsAg persisted for a long time after HB vaccination^[26]. The purpose of this study was to determine whether the HBsAg-specific T lymphocyte memory could persist for a long time after HB vaccination especially in vaccine recipients whose serum anti-HBs level was less than 10 IU/L in an attempt to determine the optimal policy of booster vaccination.

MATERIALS AND METHODS

Lymphocytes donor

Forty healthy healthcare personnel from Utrecht University Hospital, the Netherlands participated in the study. Of them, 31 subjects (18 females and 13 males aged 34-58 years) had previously received a standard course of hepatitis B vaccination of 10 or 20 μ g HB vaccine from Merck Sharp & Dohme, West Point, PA, USA (MSD) or Smith Kline and Beecham (SKB, Rixensart, Belgium) at 0, 1, and 6 months about 10 years before. Another 9 unvaccinated healthy volunteers (5 females and 4 males aged 29-57 years) from the same hospital functioned as the control.

Reagents

Recombinant HBsAg free of preservatives was a gift from Merck Sharp & Dohme, West Point, PA, USA. Hepatitis B vaccine used *in vivo* in the study was HB-Vax (MSD). Anti-HBs levels were measured in the study by means of Ausab EIA test (Abbott, Chicago, IL, USA).

Study protocol

The serum from all the volunteers was tested for HBV markers and the subjects were classified into four groups according to their serum titers of anti-HBs and vaccination history. Group I, unvaccinated ($n=9$); group II, vaccinated and with anti-HBs ≤ 10 IU/L ($n=12$); group III, vaccinated and with anti-HBs 10-100 IU/L ($n=6$); group IV vaccinated and with anti-HBs greater than 100 IU/L ($n=13$). The unvaccinated healthy

Table 1 Lymphocyte proliferation to HBsAg in controls and vaccine recipients

Group	<i>n</i>	anti-HBs Titer (IU/L)	Net count (mean)	T cell proliferation positive	ConA stimulation (mean ± SD)	Tetanus + diphtheria (mean ± SD)
1	9	unvaccinated	252 ^a	0/9 (0%)	61 000±29 058	19 075±13 688
2	12	≤10	2 810 ^{a, b}	7/12 (58%)	55 203±25 071	10 651±7 533
3	6	11-100	4 718 ^b	6/6 (100%)	35 273±33 140	19 448±16 171
4	13	>100	12 167	13/13	40 668±20 695	21 266±17 025

net count = mean cpm of medium, ^a*P*-value of statistical comparison of net counts of group II (anti-HBs ≤10 IU/L) with group I (unvaccinated control): *P*=0.0093, ^b*P*-value of statistical comparison of group II with group III + group IV (anti-HBs >10 IU/L): *P*=0.0022 (Mann-Whitney).

volunteers had no evidence of natural HBV infection (negative in the detection of serum HBsAg, anti-HBc or anti-HBs). Blood from all the subjects was collected, serum was tested for anti-HBs levels and peripheral mononuclear cells (PBMCs) were used for lymphocyte proliferation. All the subjects from whom blood was drawn gave their written informed consent for the study. This study was approved by the Medical Ethical Committee of Utrecht Hospital, the Netherlands, under No 92/82.

Cell culture and proliferation assays

PBMCs were isolated from freshly heparinized venous blood by Ficoll-Hypaque density gradient centrifugation. Blood samples were taken just before the experiment.

PBMCs were suspended in RPMI 1640 culture medium supplemented with 10% heat-inactivated pooled human AB serum (Red Cross Blood Bank, Utrecht, the Netherlands), 25 mM HEPES, 2 mmol/L L-glutamine, 50 U/ml penicillin and 50 µg/ml streptomycin. PBMCs (4×10⁵ cells/well) from each sample were prepared in 96-well U-bottom plates and stimulated with different doses of HBsAg (10 ng/mL, 30 ng/mL, 100 ng/mL, 300 ng/mL and 1.0 µg/ml) for 7 days at 37 °C in 95% humidified air with 5% CO₂. Concanavalin A (Con A) at 240 µg/ml, tetanus toxoid and diphtheria toxoid at 3.3 µg/ml served as each sample's positive control for lymphocyte proliferation. Negative control cultures were made by incubating cells in medium alone. During the final 18 h incubation, the cells were pulsed with 1.0 µCi of (³H)-thymidine per well. Sixteen to twenty hours after the cultures were harvested onto glass filters using a multichannel cell harvester the incorporated (³H)-thymidine was measured by liquid scintillation counting. Since there were individual variations in the concentration of maximal stimulation and 300 ng/mL and 1.0 µg/ml of HBsAg gave the maximal stimulation and the least variability in the triplicates, we chose the maximal stimulation at the concentration of 300 ng/mL and 1.0 µg/ml of HBsAg as the optimal result for each subject. Results were expressed as net counts (the value of (³H)-thymidine incorporation of HBsAg stimulation culture minus the value of (³H)-thymidine incorporation of medium). A net count was considered positive if the value of (³H)-thymidine incorporation was higher than the average in the unvaccinated control group + 2 SD.

Statistical method

ANOVA and Mann-Whitney *U*-test were used to compare the results between the different groups and the different concentrations.

RESULTS

HBsAg-induced *in vitro* proliferative response in vaccinated groups

The lymphocyte proliferation correlated with serum antibody levels. The highest proliferative response was observed in those vaccinated with serum anti-HBs greater than 100 IU/L (Table 1).

The difference of proliferative responses between those with serum anti-HBs levels ≤10 IU/L and those with serum anti-HBs level >10 IU/L was statistically significant (*P*=0.0022). The PBMCs from the unvaccinated control group did not respond to HBsAg (in comparison with those with serum anti-HBs levels ≤10 IU/L, *P*=0.0093). As shown in Figure 1, neither the proliferative response to diphtheria and tetanus toxoid, nor the response to mitogen ConA did differ significantly between groups I-IV.

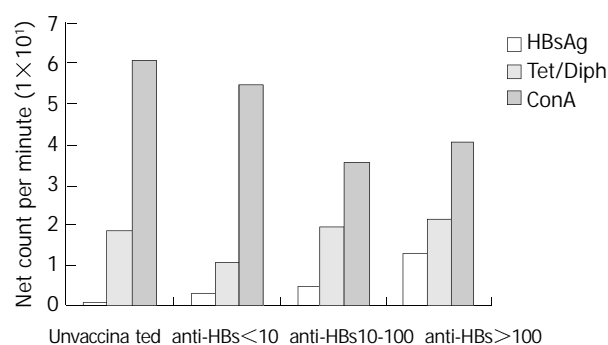


Figure 1 T cell proliferation to HBsAg, ConA and Tet/diph toxoid. The lymphocyte proliferation correlates with serum anti-HBs levels. Neither the proliferative response to diphtheria and tetanus toxoid nor to the mitogen ConA did differ significantly between groups I-IV.

Table 2 Lymphocyte proliferation to HBsAg in vaccine recipients with anti-HBs serum levels ≤10 IU/L

Donor	Sex	Time from vacc. to testing (years)	Time of vaccination	Serum anti-HBs (IU/L)	Net count
1	F	12	1983	4	304
2	F	11	1984	9	2 387 ^a
3	M	12	1983	0	2 853 ^a
4	F	8	1987	0	6 147 ^a
5	F	3	1992	9	11 729 ^a
6	F	9	1986	9	1 769 ^a
7	F	11	1984	0	1 346 ^a
8	M	11	1984	0	2 587 ^a
9	M	7	1988	10	254
10	M	12	1983	2	620
11	F	8	1987	6	475
12	M	11	1984	10	73

^aIf the net count of a subject was more than the net count of unvaccinated control group + 2 SD, it was considered positive. Abbreviation: F = female, M = male.

Lymphocyte proliferative response in vaccine recipients with serum anti-HBs less than 10 IU/L

A positive lymphocyte proliferative response was observed in 7 of the 12 subjects with serum anti-HBs less than 10 IU/L.

Compared with other groups (with anti-HBs >10 IU/L), the mean proliferative response was lower. There was no correlation between the presence of low anti-HBs titer (4-10 IU/L) or the absence of anti-HBs (≤ 2 IU/L) with the proliferative response, nor with the time from vaccination to testing (Table 2).

DISCUSSION

The humoral immune response to hepatitis B after vaccination has been studied systematically. However, duration and the quality of long term protection from HB infection in healthy vaccinees remain a matter of discussion^[1-8]. Especially the T cell response to hepatitis B vaccine has not been fully characterized. Several studies were performed to detect the lymphocyte proliferative response *in vitro* with purified HBsAg, recombinant HBsAg, preS1, preS2 and peptides of HBsAg, but results were not consistent^[26-29]. The immune response to HBsAg *in vitro* was difficult to detect and might not be detected in all vaccinated individuals^[27]. T cell responses *in vitro* after vaccination in individuals responding to vaccination were significantly diminished after 12 weeks, a time when the antibody response was still vigorous^[30]. It has been suggested that there were many variables such as geometry of the wells, the quality of culture media and in particular that of the added serum that influenced the assay results. In addition, the number of cultured PMBCs and duration of the culture might be important^[24]. In our previous experiments, we tested the influence of variables such as cell density, culture time and dose of antigen for lymphocyte proliferation. We observed that 1.0 $\mu\text{g/ml}$ HBsAg, 4×10^5 cells/well, use of human AB⁺ serum and 6 days of culture achieved optimal results. These results confirmed the assay conditions described by G. Leroux-Roels^[8].

To our knowledge, few reports have elucidated the long term efficacy of hepatitis B vaccination on T- cell immunity. In the past, a few groups have induced HBsAg-specific lymphocyte proliferative response in culture of fresh PBMCs from the individuals who were just vaccinated with hepatitis B vaccine or received a booster dose during the experiment^[24,30,31]. In our study 31 healthy persons (healthcare personnel) volunteered to give blood to test the specific response to hepatitis B. All of them were vaccinated several years ago. Our data showed that a lymphocyte proliferative response to HBsAg should be detected *in vitro* in all the vaccine recipients with positive anti-HBs. This result further confirms that *in vivo* humoral and *in vitro* cellular immune responses to HBsAg are closely correlated. In addition, we found that the HB vaccine has the capacity to stimulate the cellular immune response *in vitro*.

However, the most interesting group in our study was the vaccine recipients with serum anti-HBs levels less than 10 IU/L. We observed positive lymphocyte proliferative responses in 7 of the 12 subjects, although the maximal proliferation was lower than that in vaccine recipients with positive serum anti-HBs. We previously reported that an immunological B cell memory to hepatitis B after a vaccination existed in healthcare personnel though serum anti-HBs titers were decreased with time or not measurable in some cases^[32]. The long term efficacy of hepatitis B vaccination was also investigated in China and it was found that the protective efficacy of hepatitis B vaccination was still existed with a low risk of becoming a carrier and a low serum level of neutralizing antibody even at the time of 12 years after vaccination^[9]. These findings suggest that immunity can persist for a long time after vaccination even when the serum antibody levels are below 10 IU/L. It is therefore possible that the T cell immune response plays an important role in protecting against hepatitis B virus infection and becoming a carrier in the absence of antibodies, either directly

or indirectly by providing help to produce antibodies.

Our group previously showed a sensitive *in vitro* method for the study of B cell memory to HBsAg^[33]. A good correlation between *in vitro* mitogen induced IgG anti-HBs spots and immune memory after a booster dose of HB vaccination was observed in naturally infected subjects and vaccine recipients. Our results that 58% of the HB vaccine recipients with anti-HBs ≤ 10 IU/L have kept lymphocyte proliferative responses many years after vaccination could confirm that HB vaccine not only induces humoral immunity but also cell-mediated immunity and that T cell memory often persists longer than serum anti-HBs titers.

We conclude that T cell memory to HBsAg can be demonstrated by lymphocyte proliferation many years after HB vaccination, even in the majority of persons with serum anti-HBs ≤ 10 IU/L. Booster vaccination in those persons is probably not necessary as T cell memory is still existed, which means that the protective antibodies will reappear rapidly or that effector cytotoxic T cells can rapidly eliminate virus infected hepatocytes after exposure to HBV. Our results are of practical value because of high prevalence of hepatitis B in Asia, especially in China.

REFERENCES

- 1 **Liao SS**, Li RC, Li H, Yang JY, Zeng XJ, Gong J, Wang SS, Li YP, Zhang KL. Long-term efficacy of plasma-derived hepatitis B vaccine among Chinese children: a 12-year follow-up study. *World J Gastroenterol* 1999; **5**: 165-166
- 2 **Li H**, Li RC, Liao SS, Yang JY, Zeng XJ, Wang SS. Persistence of hepatitis B vaccine immune protection and response to hepatitis B booster immunization. *World J Gastroenterol* 1998; **4**: 493-496
- 3 **Kojouharova M**, Teoharov P, Bahtchevanova T, Maeva I, Eginlian A, Deneva M. Safety and immunogenicity of a yeast-derived recombinant hepatitis B vaccine in Bulgarian newborns. *Infection* 2001; **29**: 342-344
- 4 **Rendi-Wagner P**, Kundi M, Stemberger H, Wiedermann G, Holzmann H, Hofer M, Wiesinger K, Kollaritsch H. Antibody-response to three recombinant hepatitis B vaccines: comparative evaluation of multicenter travel-clinic based experience. *Vaccine* 2001; **19**: 2055-2060
- 5 **Ozaki T**, Mochizuki H, Ichikawa Y, Fukuzawa Y, Yoshida S, Morimoto M. Persistence of hepatitis B surface antibody levels after vaccination with a recombinant hepatitis B vaccine: a 3-year follow-up study. *J Oral Sci* 2000; **42**: 147-150
- 6 **Jain A**, Mathur US, Jandwani P, Gupta RK, Kumar V, Kar P. A multicentric evaluation of recombinant DNA hepatitis B vaccine of Cuban origin. *Trop Gastroenterol* 2000; **21**: 14-17
- 7 **Al-Faleh FZ**, Al-Jeffri M, Ramia S, Al-Rashed R, Arif M, Rezeig M, Al-Toraif I, Bakhsh M, Mishkhas A, Makki O, Al-Freih H, Mirdad S, AlJuma A, Yasin T, Al-Swailem A, Ayoola A. Seroepidemiology of hepatitis B virus infection in Saudi children 8 years after a mass hepatitis B vaccination programme. *J Infect* 1999; **38**: 167-170
- 8 **Li H**, Li RC, Liao SS, Gong J, Zeng XJ, Li YP. Long-term effectiveness of infancy low-dose hepatitis B vaccine immunization in Zhuang minority Area in China. *World J Gastroenterol* 1999; **5**: 122-124
- 9 **Liu HB**, Meng ZD, Ma JC, Han CQ, Zhang YL, Xing ZC, Zhang YW, Liu YZ, Cao HL. A 12-year cohort study on the efficacy of plasma-derived hepatitis B vaccine in rural newborns. *World J Gastroenterol* 2000; **6**: 381-383
- 10 **Li H**, Wang L, Wang SS, Gong J, Zeng XJ, Li RC, Nong Y, Huang YK, Chen XR, Huang ZN. Research on optimal immunization strategies for hepatitis B in different endemic areas in China. *World J Gastroenterol* 2000; **6**: 392-394
- 11 **Zeng XJ**, Yang GH, Liao SS, Chen AP, Tan J, Huang ZJ, Li H. Survey of coverage, strategy and cost of hepatitis B vaccination in rural and urban areas of China. *World J Gastroenterol* 1999; **5**: 320-323
- 12 **Shokri F**, Jafarzadeh A. High seroprotection rate induced by low doses of a recombinant hepatitis B vaccine in healthy Iranian neonates. *Vaccine* 2001; **19**: 4544-4548
- 13 **Trivello R**, Chiaramonte M, Ngatchu T, Baldo V, Majori S,

- Moschen ME, Simoncello I, Renzulli G, Naccarato R. Persistence of anti-HBs antibodies in health care personnel vaccinated with plasma-derived hepatitis B vaccine and response to recombinant DNA HB booster vaccine. *Vaccine* 1995; **13**: 139-141
- 14 **Whittle HC**, Maine N, Pikington J, Mendy M, Fortuin M, Bunn J, Allison L, Howard C, Hall A. Long-term efficacy of continuing hepatitis B vaccination in infancy in two Gambian villages. *Lancet* 1995; **345**: 1089-1092
- 15 **Jilg W**, Schmidt M, Deinhardt F. Decline of anti-HBs after hepatitis B vaccination and timing of revaccination. *Lancet* 1990; **335**: 173-174
- 16 **Wismans PJ**, Van Hattum J, Mudde GC, Endeman HJ, Poel J, de Gast GC. Is booster injection with hepatitis B vaccination necessary in healthy responders? A study of the immune response. *J Hepatol* 1988; **1**: 1-5
- 17 **Wood RC**, MacDonald KL, White KE, Hedberg CW, Hanson M, Osterholm MT. Risk factors for lack of detectable antibody following hepatitis B vaccination of Minnesota health care workers. *JAMA* 1993; **270**: 2935-2939
- 18 **Roome AJ**, Walsh SJ, Cartter ML, Hadler JL. Hepatitis B vaccine responsiveness in the Connecticut public safety personnel. *JAMA* 1993; **270**: 2931-2934
- 19 **Watson B**, West DJ, Chilkatowsky A, Piercy S, Ioli VA. Persistence of immunologic memory for 13 years in recipients of a recombinant hepatitis B vaccine. *Vaccine* 2001; **19**: 3164-3168
- 20 **Wistrom J**, Ahlm C, Lundberg S, Settergren B, Tarnvik A. Booster vaccination with recombinant hepatitis B vaccine four years after priming with one single dose. *Vaccine* 1999; **17**: 2162-2165
- 21 **Banatvala J**, Van Damme P, Oehen S. Lifelong protection against hepatitis B: the role of vaccine immunogenicity in immune memory. *Vaccine* 2000; **19**: 877-885
- 22 **Garcia Llop L**, Asensi Alcoverro A, Coll Mas P, Ramada Benedito MA, Grafia Juan C. Anti-HBs titers after a vaccination program in children and adolescents. Should a booster dose be given? *An Esp Pediatr* 2001; **54**: 32-37
- 23 **Huang LM**, Chiang BL, Lee CY, Lee PI, Chi WK, Chang MH. Long-term response to hepatitis B vaccination and response to booster in children born to mothers with hepatitis B e antigen. *Hepatology* 1999; **29**: 954-959
- 24 **Leroux-Roels G**, Van Hecke E, Michiels W, Voet P, Hauser P, Petre J. Correlation between *in vivo* humoral and *in vitro* cellular immune responses following immunization with hepatitis B surface antigen (HBsAg) vaccines. *Vaccine* 1994; **12**: 812-815
- 25 **Are booster immunisations needed for lifelong hepatitis B immunity?** European Consensus Group on Hepatitis B Immunity. *Lancet* 2000; **355**: 561-565
- 26 **De Gast GC**, Houwen B, Nieweg HO. Specific lymphocyte stimulation by purified heat-inactivated hepatitis B antigen. *Br Med J* 1973; **4**: 707-709
- 27 **Fernan A**, Cayzer CJ, Cooksley WG. HBsAg-induced antigen-specific T and B lymphocyte response in chronic hepatitis B virus carriers and immune individuals. *Clin Exp Immunol* 1989; **76**: 222-226
- 28 **Ferrari G**, Penna A, Bertolotti A, Cavalli A, Valli A, Schianchi C, Fiaccadori F. The preS1 antigen of hepatitis B virus is highly immunogenic at T cell level in man. *J Clin Invest* 1989; **84**: 1314-1319
- 29 **Cupps TR**, Tibbles J, Hurmi WM, Miller WJ, Ellis RW, Milich D, Wettter N. *In vitro* T cell immune responses to the PreS2 antigen of the hepatitis B virus envelope protein in PreS2+S vaccine recipients. *J Immunol* 1993; **151**: 3353-3360
- 30 **Deulofeut H**, Iglesias A, Mikeal N, Bing DH, Awdeh Z, Yunis J, Marcus-Bagley D, Kruskal MS, Alper CA, Yunis EJ. Cellular recognition and HLA restriction of a midsequence HBsAg peptide in hepatitis B vaccinated individuals. *Mol Immunol* 1993; **30**: 941-948
- 31 **Degrassi A**, Mariani E, Honorati MC, Roda P, Miniero R, Capelli M, Faccini A. Cellular response and anti-HBs synthesis *in vitro* after vaccination with yeast-derived recombinant hepatitis B vaccine. *Vaccine* 1992; **10**: 617-621
- 32 **Wismans PJ**, van Hattum J, de Gast GC, Bouter KP, Diepersloot RJ, Maikoe T, Mudde GC. A prospective study of *in vitro* anti-HBs producing B cells (spot-ELISA) following primary and supplementary vaccination with a recombinant hepatitis B vaccine in insulin dependent diabetic patients and matched controls. *J Med Virol* 1991; **35**: 216-222
- 33 **Wismans PJ**, van Hattum J, de Gast GC, Endeman HJ, Poel J, Stolk B, Maikoe T, Mudde GC. The spot-ELISA: a sensitive *in vitro* method to study the immune response to hepatitis B surface antigen. *Clin Exp Immunol* 1989; **78**: 75-79

Establishment of transgenic mice carrying gene encoding human zinc finger protein 191

Jian-Zhong Li, Xia Chen, Hua Yang, Shui-Liang Wang, Xue-Lian Gong, Hao Feng, Bao-Yu Guo, Long Yu, Zhu-Gang Wang, Ji-Liang Fu

Jian-Zhong Li, Hua Yang, Shui-Liang Wang, Ji-Liang Fu, Department of Medical Genetics, Second Military Medical University, Shanghai 200433, China

Zhu-Gang Wang, Ji-Liang Fu, Shanghai Nanfang Research Center for Biomodel Organism, Shanghai 201203, China

Long Yu, Genetics Institute, Fudan University, Shanghai 200433, China

Jian-Zhong Li, Xue-Lian Gong, Hao Feng, Bao-Yu Guo, Department of Biochemical Pharmacy, Second Military Medical University, Shanghai 200433, China

Xia Chen, Shanghai Research Center of Biotechnology, Chinese Academy of Sciences, Shanghai 200233, China

Supported by the National Natural Science Foundation of China, No.39830360

Correspondence to: Professor Ji-Liang Fu, Department of Medical Genetics, Second Military Medical University, 800 Xiangyin Road, Shanghai 200433, China. jlfu@guomai.sh.cn

Telephone: +86-21-25070027 **Fax:** +86-21-25070027

Received: 2003-06-16 **Accepted:** 2003-07-24

Wang ZG, Fu JL. Establishment of transgenic mice carrying gene encoding human zinc finger protein 191. *World J Gastroenterol* 2004; 10(2): 264-267

<http://www.wjgnet.com/1007-9327/10/264.asp>

INTRODUCTION

Transcriptional regulation is controlled through interactions between DNA and protein complex, the latter contains transcription factors with highly conserved protein motifs. The most well known motifs are helix-turn-helix, helix-loop-helix, and zinc finger. During cell differentiation and development, each of these domains is involved in the binding of transcription factors to their cognate DNA recognition sites, resulting in specific activation or repression of gene expression^[1].

Zinc finger gene family belongs to one of the largest human gene families and plays an important role in the regulation of transcription. This large family may be divided into many subfamilies such as Cys₂/His₂ type, glucocorticoid receptor, ring finger, GATA-1 type, GAL4 type, and LIM family^[2-4]. In the Cys₂/His₂ type of zinc finger genes, there is a highly conserved consensus sequence TGEKPYX (X representing any amino acid) between adjacent zinc finger motifs. The zinc finger proteins containing this specific structure are named Krüppel-like zinc finger proteins because the structure was first found in *Drosophila* Krüppel protein^[1].

ZNF191 is a putative transcription factor belonging to Krüppel-like zinc finger gene family. It contains four Cys₂/His₂ zinc fingers in its C-terminus, and one SCAN box element (also known as LeR domain for leucine-rich) in its N-terminus^[5-7]. Biochemical binding studies showed SCAN as a selective heterologous and homologous oligomerization domain^[7,8]. Tissue mRNA analysis showed that ZNF191 gene was ubiquitously expressed^[5,9]. ZNF191 can specifically bind to the TCAT repeats (*HUMTH01*) in the first intron of the human tyrosine hydroxylase (*TH*) gene. *HUMTH01* may regulate transcription of *TH* gene, which encodes the rate-limiting enzyme in the synthesis of catecholamines^[9-11]. The disturbances of catecholaminergic neurotransmission have been implicated in neuropsychiatric and cardiovascular diseases^[12-17]. These studies suggested that ZNF191 might be relevant to these diseases. Analysis of amino acid sequence of ZNF191 showed 94% identity with the murine sequence of ZF-12^[18]. Mouse ZF-12 gene likely represents the murine counterpart of human ZNF191. ZF-12 also contains four zinc finger motifs of the Cys₂/His₂ type and one SCAN box. ZF-12 mRNA is expressed during embryonic development and in different organs in adult^[19]. ZF-12 may play an important role in cartilage differentiation and basic cellular processes^[19].

To facilitate the functional studies of ZNF191, we established transgenic mice carrying ZNF191 gene. Four transgenic mice were identified by PCR and Southern blot, and used as founders to establish transgenic mouse lineages. The results of F1 identification with PCR showed that ZNF191 gene could be transmitted stably. RT-PCR analysis demonstrated that ZNF191 gene was expressed in multiple tissues of transgenic mice.

Abstract

AIM: Human zinc finger protein 191 (ZNF191) was cloned and characterized as a Krüppel-like transcription factor, which might be relevant to many diseases such as liver cancer, neuropsychiatric and cardiovascular diseases. Although progress has been made recently, the biological function of ZNF191 remains largely unidentified. The aim of this study was to establish a ZNF 191 transgenic mouse model, which would promote the functional study of ZNF191.

METHODS: Transgene fragments were microinjected into fertilized eggs of mice. The manipulated embryos were transferred into the oviducts of pseudo-pregnant female mice. The offsprings were identified by PCR and Southern blot analysis. ZNF 191 gene expression was analyzed by RT-PCR. Transgenic founder mice were used to establish transgenic mouse lineages. The first generation (F1) and the second generation (F2) mice were identified by PCR analysis. Ten-week transgenic mice were used for pathological examination.

RESULTS: Four mice were identified as carrying copies of ZNF191 gene. The results of RT-PCR showed that ZNF 191 gene was expressed in the liver, testis and brain in one of the transgenic mouse lineages. Genetic analysis of transgenic mice demonstrated that ZNF 191 gene was integrated into the chromosome at a single site and could be transmitted stably. Pathological analysis showed that the expression of ZNF 191 did not cause obvious pathological changes in multiple tissues of transgenic mice.

CONCLUSION: ZNF 191 transgenic mouse model would facilitate the investigation of biological functions of ZNF191 *in vivo*.

Li JZ, Chen X, Yang H, Wang SL, Gong XL, Feng H, Guo BY, Yu L,

Pathological analysis results demonstrated that over-expression of ZNF191 did not cause obvious pathological changes in multiple tissues of the transgenic mice.

MATERIALS AND METHODS

Plasmid

pcDNA3-ZNF191 containing full length ZNF191 cDNA under control of CMV promoter.

Animals

C57, CBA mice were maintained by Shanghai Nanfang Research Center for Biomodel Organism. Transgenic mice were raised and bred in the Laboratory Animal Centre of Second Military Medical University, Shanghai.

Generation of transgenic mice

The 6.5 kb linearized pcDNA3-ZNF191 was purified from agarose gel with QIAGEN gel extraction kit (Qiagen), adjusted to a final concentration of 2 µg/ml in TE buffer and used as DNA solution in microinjection. The first generation (F1) female hybrids of C57 and CBA mice were hormonally superovulated and mated with F1 male hybrids. The next morning fertilized one-cell eggs were collected from the oviduct. The eggs were microinjected with the DNA solution under a microscope. The injected fertilized eggs were transplanted into the oviduct of pseudo-pregnant F1 hybrids of C57 and CBA mice.

Identification of transgenic mice

Founder (G0) mice were identified by PCR and Southern blotting analysis. For PCR analysis, genomic DNA was extracted from tails, and amplified using pcDNA3-ZNF191 primers (P1: 5' -ATGCGGTGGGCTCTATG-3' ; P2: 5' -CGGCTTCCATCCGAGTA-3') which produced a 1 353 bp fragment from mice carrying the transgene. For Southern blotting analysis, genomic DNA was digested overnight with *HindIII* and subjected to electrophoresis in a 0.7% agarose gel and transferred to nylon membrane (Millipore Co., Ltd). Hybridization was performed under stringent conditions with a random-primed (α -³²P)-labeled ZNF191 cDNA probe.

Expression of transgene

One of the transgenic mouse lineages was used to study the expression of transgene. Total RNA was isolated from tissues with TRIzol reagent (Invitrogen), according to the manufacturer's instructions. After digestion of the RNA with DNase I (RNase free), first strand cDNA was synthesized by reverse transcription (Promega). RT-PCR reactions were performed using primers (P3:5' -GTACTAGTAGAAGACATGGT-3' , P4:5' -CGCACACAAAAGAACAATCT-3') for ZNF191 cDNA, which produced a 394 bp fragment. PCR reactions were performed 35 cycles at 95 °C for 45 s, at 55 °C for 1 min, and at 72 °C for 1 min. The PCR products were electrophoresed on 1.2% agarose gel.

Transmission of transgene

To study transmission of the transgene in mice, transgenic founder mice were mated with normal C57 mice to produce the first generation (F1) which was identified by PCR analysis using primers P1/P2. F1 mice of the same founder carrying the transgene were mated between brother and sister mice to produce the second generation (F2). F2 mice were also identified by PCR analysis.

Histological examination

Various organs were dissected from the 10 weeks old mice and fixed in 10% formalin. Sections were obtained from

paraffin-embedded tissue samples, stained with H&E, and examined under a microscope and photographed. Pathological analysis was carried out in the Department of Pathology, Changhai Hospital of Second Military Medical University, Shanghai.

RESULTS

Establishment of ZNF191 transgenic mice

The transgene fragment containing full length ZNF191 cDNA was microinjected into the male pronuclei of 582 fertilized oocytes of F1 hybrids between C57 and CBA mice. The injected eggs were implanted into the oviducts of 27 pseudo-pregnant foster mothers, of which 15 mice became pregnant and gave birth to 81 offsprings. Four offsprings were identified to carry ZNF191 cDNA by PCR and Southern blotting analysis (Figures 1 and 2). The ratio of transgene integration was 4.9% by PCR and Southern blotting analysis.

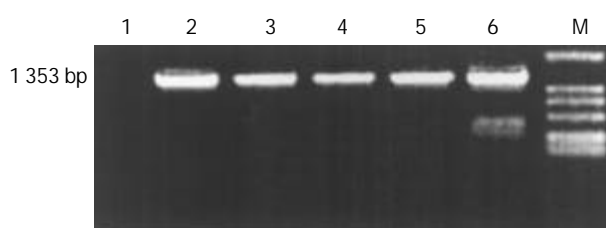


Figure 1 PCR results in transgenic mice. M: DL-2000 Marker, 1: Negative control (wild type mouse), 2-5: Transgenic founder mice, 6: Positive control (pcDNA3-ZNF191).

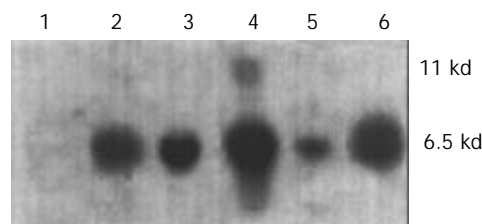


Figure 2 Results of genomic DNA Southern blotting analysis in transgenic mice. 1: Negative control (wild type mouse), 2-5: Transgenic founder mice, 6: Positive control (pcDNA3-ZNF191).

ZNF191 transgene expression in multiple tissues of transgenic mice

The transgene was driven by CMV promoter. To study whether it could be expressed in multiple tissues of transgenic mice, we analysed the tissue expression profile of ZNF191 transgene by RT-PCR. The results (Figure 3) showed that ZNF191 transgene was expressed in the liver, testis and brain.



Figure 3 RT-PCR results in transgene expression. M: DL-2000 Marker, 1-3: Transgenic mice tissues, 4-5: Negative control (non-reverse transcribed RNA), 6:C57 mouse liver, 7: Positive control (pcDNA3-ZNF191).

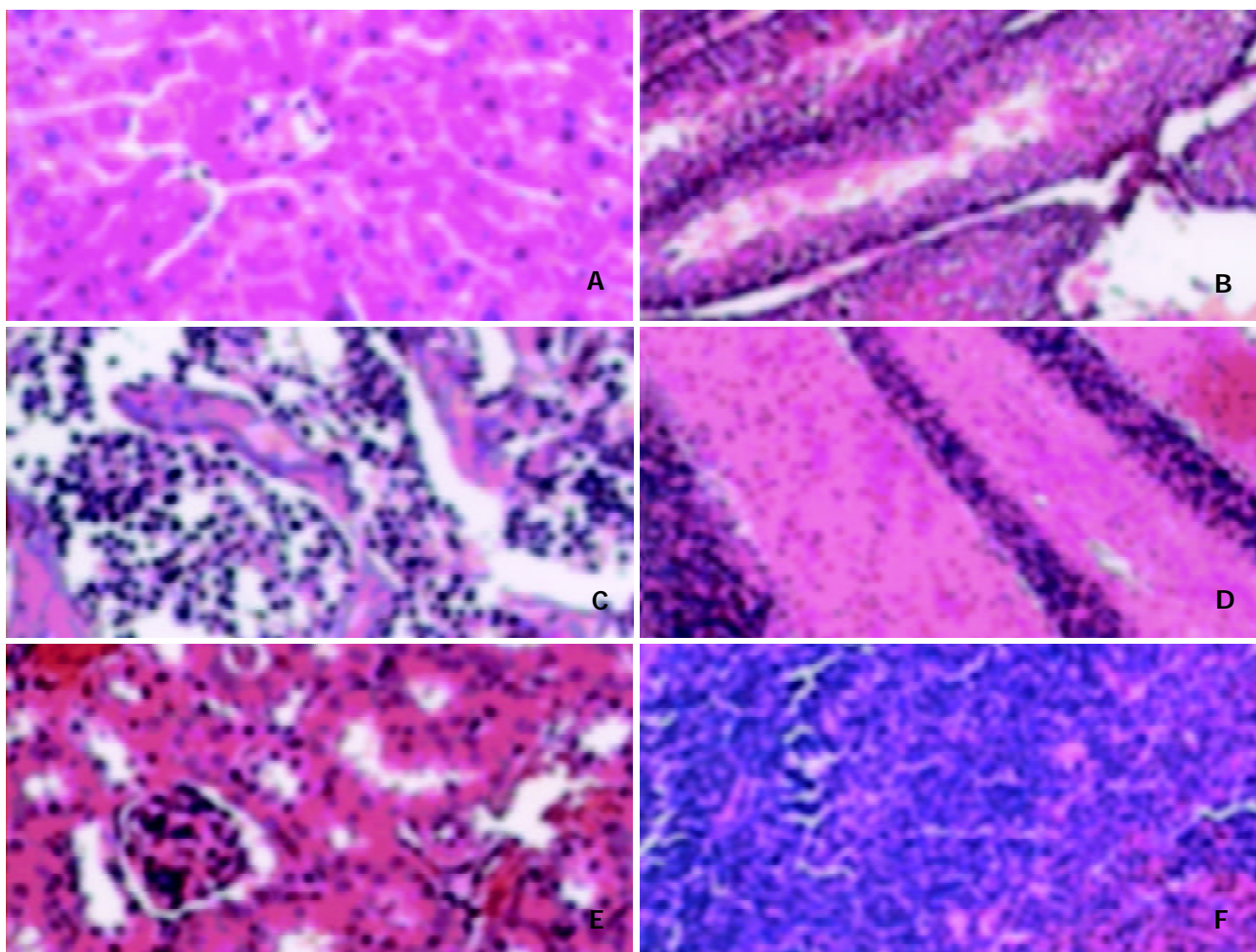


Figure 4 Morphology of tissues of transgenic mouse. A: Liver, B: Testis, C: Marrow, D: Brain, E: Kidney, F: Spleen.

Genetics of transgenic mice

To establish transgenic mouse lineages, the founder mice were mated to C57 mice to produce F1 mice. Among the 43 mice of first generation, 19 were identified as carrying *ZNF191* cDNA transgene by PCR analysis. The ratio of transgene transmission was 44.2%. F1 mice from the same founder were mated with each other to produce F2 mice. Sixty-one out of 86 F2 mice were *ZNF191* transgenic mice, with a transgene transmission ratio of 71%. These results showed that the inheritance of *ZNF191* transgene was in accordance with Mendel's laws, and the transgene was integrated into the chromosome at a single site and could be transmitted stably.

Pathological analysis of tissues

Pathological analysis was carried out to see whether the expression of *ZNF191* transgene would cause any pathological changes in tissues of the transgenic mice. The results (Figure 4) showed there were no obvious pathological changes in the tissues examined. Therefore, so far as the tissues examined, the expression of exogenous *ZNF191* did not cause any pathological consequences in the transgenic mice.

DISCUSSION

Cys₂/His₂ type zinc finger gene family is one of the largest gene families, and each member has repeated zinc finger motifs containing a finger-like structure, in which two cysteines and two histidines could covalently bind to one zinc ion^[20]. It is estimated that in this huge family, about one third of the members are *Krüppel*-like genes as characterized by the presence of highly conserved connecting sequences "TGEKPYX" between

adjacent zinc finger motifs. Substantial evidences indicate that *Krüppel* proteins are important players in many physiological processes as transcriptional regulators. *Krüppel*-like zinc finger genes are key transcriptional repressors in the development of *Drosophila*. In mammalian animals and human, these genes have been found involved in embryo development and carcinogenesis. For example, *KLF6* was reported as a tumor suppressor gene in prostate cancer^[21-23]. Gut-enriched *Krüppel*-like factor (GKLF) was expressed abundantly in epithelial cells of gastrointestinal tract, and deregulation of GKLF was linked to several types of cancer^[24-27].

ZNF191 gene is a novel member of the *Krüppel*-like zinc finger gene family. It was previously cloned from bone marrow and promyelocytic leukemia cell line NB4 using homologous PCR amplification with primers based on conserved sequences of the *Krüppel*-like family of transcription factors^[5]. This first identification suggested that *ZNF191* played a role in hematopoiesis. *ZNF191* has been found to contain a SCAN domain mediating selective protein oligomerization^[6-8]. *ZNF191* specifically binds to *HUMTH01* *in vitro*. The microsatellite *HUMTH01*, located at the first intron of tyrosine hydroxylase (*TH*) gene, is characterized by a TCAT repeated motif and has been used in genetic studies of neuropsychiatric and cardiovascular diseases, in which disturbances of catecholaminergic neurotransmission were implicated^[10-17]. Allelic variations of *HUMTH01* had a quantitative silencing effect on *TH* gene expression *in vitro*, and correlated with quantitative and qualitative changes in the binding by *ZNF191*^[9]. Since TCAT repeated sequence is widespread throughout the genome, this phenomenon might be relevant to the quantitative expression of several genes implicated in complex genetic traits, both

normal and pathological^[28-31]. These studies suggested that ZNF191 might be relevant to neuropsychiatric and cardiovascular diseases. It is vital to have a transgenic or knock-out animal model for the study of the biological role of ZNF191. So far, the attempt to produce ZNF191 transgenic and knock-out mice has not been reported. To our knowledge, we have generated the first transgenic mice carrying ZNF191 transgene and ZF-12^{+/-} mice (to be reported in another paper).

In *in vivo* situation, ZNF191 transcript was found in various organs^[5,9]. Moreover, ZNF191 expression was significantly up-regulated in liver cancer (personal communication), suggesting that ZNF191 might be relevant to hepatocellular carcinogenesis. In this study, ZNF191 transgene was expressed in multiple tissues, which are capable of expressing endogenous ZF-12 *in vivo*. Therefore, the ZNF191 transgenic mouse we generated would be an invaluable animal model not only for the investigation of ZNF191 functions in hepatic tissues, but also in other tissues, which may ultimately reveal the undefined biological functions of ZNF191.

Given that ZNF191 has important biological functions and is relevant to many diseases, it is somewhat unexpected that no pathological changes occurred in the ten-week transgenic mice with ZNF191 over-expression. It is possible that overexpression of exogenous ZNF191 may trigger a negative feedback response to the expression of endogenous ZF-12. It remains to be determined whether the expression of endogenous ZF-12 would change in cells overexpressing exogenous ZNF191. On the other hand, liver cancer, neuropsychiatric and cardiovascular diseases involve many factors and usually have a long incubation time before any pathological phenotypes can be observed. So, it is necessary to continue the investigation into possible pathological changes in a long term follow-up.

In conclusion, we reported here the successful generation of a transgenic mouse model expressing ZNF191 gene. Future studies should focus on the physiological and pathological changes in this mouse model using powerful analytic methods such as microarray comparisons of gene expression profiles among normal, transgenic, ZF-12^{+/-} and ZF-12^{-/-} mice.

REFERENCES

- Klug A, Schwabe JW. Protein motifs 5. Zinc fingers. *FASEB J* 1995; **9**: 597-604
- Borden KL, Freemont PS. The RING finger domain: a recent example of a sequence-structure family. *Curr Opin Struct Biol* 1996; **6**: 395-401
- Hammarstrom A, Berndt KD, Sillard R, Adermann K, Otting G. Solution structure of a naturally-occurring zinc-peptide complex demonstrates that the N-terminal zinc-binding module of the Lasp-1 LIM domain is an independent folding unit. *Biochemistry* 1996; **35**: 12723-12732
- Barlow PN, Luisi B, Milner A, Elliott M, Everett R. Structure of the C3HC4 domain by 1H-nuclear magnetic resonance spectroscopy. A new structural class of zinc-finger. *J Mol Biol* 1994; **237**: 201-211
- Han ZG, Zhang QH, Ye M, Kan LX, Gu BW, He KL, Shi SL, Zhou J, Fu G, Mao M, Chen SJ, Yu L, Chen Z. Molecular cloning of six novel Kruppel-like zinc finger genes from hematopoietic cells and identification of a novel transregulatory domain KRNB. *J Biol Chem* 1999; **274**: 35741-35748
- Collins T, Stone JR, Williams AJ. All in the family: the BTB/POZ, KRAB, and SCAN domains. *Mol Cell Biol* 2001; **21**: 3609-3615
- Stone JR, Maki JL, Blacklow SC, Collins T. The SCAN domain of ZNF174 is a dimer. *J Biol Chem* 2002; **277**: 5448-5452
- Schumacher C, Wang H, Honer C, Ding W, Koehn J, Lawrence Q, Coulis CM, Wang LL, Ballinger D, Bowen BR, Wanger S. The SCAN domain mediates selective oligomerization. *J Biol Chem* 2000; **275**: 17173-17179
- Albanese V, Biguet NF, Kiefer H, Bayard E, Mallet J, Meloni R. Quantitative effects on gene silencing by allelic variation at a tetranucleotide microsatellite. *Hum Mol Genet* 2001; **10**: 1785-1792
- Meloni R, Albanese V, Ravssard P, Treihou F, Mallet J. A tetranucleotide polymorphic microsatellite, located in the first intron of the tyrosine hydroxylase gene, acts as a transcription regulatory element *in vitro*. *Hum Mol Genet* 1998; **7**: 423-428
- Mallet J. The TiPS/TINS lecture. Catecholamines: from gene regulation to neuropsychiatric disorders. *Trends Pharmacol Sci* 1996; **17**: 129-135
- Sharma P, Hingorani A, Jia H, Ashby M, Hopper R, Clayton D, Brown MJ. Positive association of tyrosine hydroxylase microsatellite marker to essential hypertension. *Hypertension* 1998; **32**: 676-682
- Meloni R, Leboyer M, Bellivier F, Barbe B, Samolyk D, Allilaire JF, Mallet J. Association of manic-depressive illness with tyrosine hydroxylase microsatellite marker. *Lancet* 1995; **345**: 932
- Perez de Castro I, Santos J, Torres P, Visedo G, Saiz-Ruiz J, Llinares C, Fernandez-Piqueras J. A weak association between TH and DRD2 genes and bipolar affective disorder in a Spanish sample. *J Med Genet* 1995; **32**: 131-134
- Serretti A, Macchiardi F, Verga M, Cusin C, Pedrini S, Smeraldi E. Tyrosine hydroxylase gene associated with depressive symptomatology in mood disorder. *Am J Med Genet* 1998; **81**: 127-130
- Meloni R, Laurent C, Campion D, Ben Hadjali B, Thibaut F, Dollfus S, Petit M, Samolyk D, Martinez M, Poirier MF, Mallet J. A rare allele of a microsatellite located in the tyrosine hydroxylase gene found in schizophrenic patients. *C R Acad Sci III* 1995; **318**: 803-809
- Wei J, Ramchand CN, Hemmings GP. Possible association of catecholamine turnover with the polymorphic (TCAT)_n repeat in the first intron of the human tyrosine hydroxylase gene. *Life Sci* 1997; **61**: 1341-1347
- Li JZ, Chen X, Wang SL, Sun X, Zhang YZ, Yu L, Fu JL. Cloning, genomic organization and promoter activity of the mouse zinc finger protein gene ZF-12. *Yichuan Xuebao* 2003; **30**: 311-316
- Prost JF, Negre D, Cornet-Javaux F, Cortay JC, Cozzone AJ, Herbage D, Mallein-Gerin F. Isolation, cloning, and expression of a new murine zinc finger encoding gene. *Biochim Biophys Acta* 1999; **1447**: 278-283
- Jacobs GH. Determination of the base recognition positions of zinc fingers from sequence analysis. *EMBO J* 1992; **11**: 4507-4517
- Chen C, Hyytinen ER, Sun X, Helin HJ, Koivisto PA, Frierson HF Jr, Vessella RL, Dong JT. Deletion, mutation, and loss of expression of KLF6 in human prostate cancer. *Am J Pathol* 2003; **162**: 1349-1354
- Narla G, Heath KE, Reeves HL, Li D, Giono LE, Kimmelman AC, Glucksman MJ, Narla J, Eng FJ, Chan AM, Ferrari AC, Martignetti JA, Friedman SL. KLF6, a candidate tumor suppressor gene mutated in prostate cancer. *Science* 2001; **294**: 2563-2566
- Narla G, Friedman SL, Martignetti JA. Kruppel cripples prostate cancer: KLF6 progress and prospects. *Am J Pathol* 2003; **162**: 1047-1052
- Stone CD, Chen ZY, Tseng CC. Gut-enriched Kruppel-like factor regulates colonic cell growth through APC/beta-catenin pathway. *FEBS Lett* 2002; **530**: 147-152
- Wang N, Liu ZH, Ding F, Wang XQ, Zhou CN, Wu M. Down-regulation of gut-enriched Kruppel-like factor expression in esophageal cancer. *World J Gastroenterol* 2002; **8**: 966-970
- Chen ZY, Shie JL, Tseng CC. Gut-enriched Kruppel-like factor represses ornithine decarboxylase gene expression and functions as checkpoint regulator in colonic cancer cells. *J Biol Chem* 2002; **277**: 46831-46839
- Katz JP, Perreault N, Goldstein BG, Lee CS, Labosky PA, Yang VW, Kaestner KH. The zinc-finger transcription factor Klf4 is required for terminal differentiation of goblet cells in the colon. *Development* 2002; **129**: 2619-2628
- Meloni R, Biguet NF, Mallet J. Post-genomic era and gene discovery for psychiatric diseases: there is a new art of the trade? The example of the HUMTH01 microsatellite in the Tyrosine Hydroxylase gene. *Mol Neurobiol* 2002; **26**: 389-403
- Schadt EE, Monks SA, Drake TA, Luskis AJ, Che N, Colinao V, Ruff TG, Milligan SB, Lamb JR, Cavet G, Linsley PS, Mao M, Stoughton RB, Friend SH. Genetics of gene expression surveyed in maize, mouse and man. *Nature* 2003; **422**: 297-302
- Mackay TF. The genetic architecture of quantitative traits. *Annu Rev Genet* 2001; **35**: 303-339
- Reif A, Lesch KP. Toward a molecular architecture of personality. *Behav Brain Res* 2003; **139**: 1-20

Effects of depression on parameters of cell-mediated immunity in patients with digestive tract cancers

Ke-Jun Nan, Yong-Chang Wei, Fu-Ling Zhou, Chun-Li Li, Chen-Guang Sui, Ling-Yun Hui, Cheng-Ge Gao

Ke-Jun Nan, Yong-Chang Wei, Fu-Ling Zhou, Chun-Li Li, Chen-Guang Sui, Department of Medical Oncology, First Hospital of Xi'an Jiaotong University, Xi'an 710061, Shaanxi Province, China
Ling-Yun Hui, Research Center of Medical Laboratory, First Hospital of Xi'an Jiaotong University, Xi'an 710061, Shaanxi Province, China
Cheng-Ge Gao, Department of Psychology, First Hospital of Xi'an Jiaotong University, Xi'an 710061, Shaanxi Province, China
Supported by the Natural Science Foundation of Shaanxi Province, No. 99SM50

Correspondence to: Dr. Ke-Jun Nan, Department of Medical Oncology, First Hospital of Xi'an Jiaotong University, Xi'an 710061, Shaanxi Province, China. alisantra0351@sina.com

Telephone: +86-29-3705937 **Fax:** +86-29-5324086

Received: 2003-03-12 **Accepted:** 2003-04-14

CONCLUSION: Depression occurs with a high incidence in patients with cancers of the digestive tract, which probably is not the sole factor leading to the impairment of immunological functions in these cases. However, comprehensive measures including psychological support should be taken in order to improve the immunological function, quality of life and clinical prognosis of these patients.

Nan KJ, Wei YC, Zhou FL, Li CL, Sui CG, Hui LY, Gao CG. Effects of depression on parameters of cell-mediated immunity in patients with digestive tract cancers. *World J Gastroenterol* 2004; 10(2): 268-272

<http://www.wjgnet.com/1007-9327/10/268.asp>

Abstract

AIM: To evaluate the effects of depression on parameters of cell-mediated immunity in patients with cancers of the digestive tract.

METHODS: One hundred and eight adult patients of both sexes with cancers of the digestive tract admitted between March 2001 and February 2002 in the Department of Medical Oncology, First Affiliated Hospital of Xi'an Jiaotong University were randomly enrolled in the study. The Zung self-rating depression scale (SDS), Zung self-rating anxiety scale (SAS), numeric rating scale (NRS) and social support rating scale (SSRS) were employed to evaluate the degree of depression and their contributing factors. In terms of their SDS index scores, the patients were categorized into depression group (SDS \geq 50) and non-depression group (SDS < 50). Immunological parameters such as T-lymphocyte subsets and natural killer (NK) cell activities in peripheral blood were determined and compared between the two groups of patients.

RESULTS: The SDS index was from 33.8 to 66.2 in the 108 cases, 50% of these patients had a SDS index more than 50. Similarly, the SAS index of all the patients ranged from 35.0 to 62.0 and 46.3% of the cases had a SAS index above 50. Cubic curve estimation showed that the depression was positively correlated with anxiety and negatively with social support. Furthermore, the depression correlated with the tumor type, which manifested in a descending order as stomach, gallbladder, pancreas, intestine, esophagus, duodenum and rectum, according to their correlativity. Step-wise regression analysis suggested that hyposexuality, dispiritment, agitation, palpitation, low CD₅₆ and anxiety were the significant factors contributing to depression. More severe anxiety (49.7 \pm 7.5 vs 45.3 \pm 6.9, P <0.05), pain (6.5 \pm 2.8 vs 4.6 \pm 3.2, P <0.05), poor social support (6.8 \pm 2.0 vs 7.6 \pm 2.1, P <0.05), as well as decline of lymphocyte count (0.33 \pm 0.09 vs 0.39 \pm 0.07, P <0.05) and CD₅₆ (0.26 \pm 0.11 vs 0.29 \pm 0.11, P <0.05) were noted in the depression group compared with those of the non-depression patients. However, fewer obvious changes in CD₄/CD₈ ratio and other immunological parameters were found between the two groups.

INTRODUCTION

Cancers of the digestive tract continue to be one of the most common malignancies in human worldwide^[1-14], in which gastric, esophageal, colorectal and liver cancers are among the top ten malignant tumors in China and account for 63% of total cancer mortality^[11]. Depressive symptoms such as pervasive senses of hopeless, helpless, valueless, despair, guilty, punishment and self-deprecatory thinking are often found in cancer patients. When severely enough, it may cause negative effects on the antitumor therapy, immunological function, prognosis, as well as the quality of life^[15,16]. However, up to the present, much attention has been paid to the effects of depression on patients with several kinds of malignancies^[17-20] except that of the digestive tract. Besides, despite mounting evidence that psychiatric depression heightens risk for cancerous morbidity and mortality, little is known about the detailed mechanisms responsible for this association, which is no doubt of importance in the improvement of therapy for cancer patients.

In the present study, we therefore investigated the effects of depression on cell-mediated immunity and its contributing factors in 108 patients with cancers of the digestive tract by SDS^[21] and other questionnaires, as well as immunological parameters including T-lymphocyte subsets and natural killer (NK) cell activities in peripheral blood, in an attempt to provide evidence for the necessities of psychological therapy of these cancer patients.

MATERIALS AND METHODS

Patients

One hundred and eight adult patients of both sexes with cancers of the digestive tract including 24 esophageal, 36 gastric, 4 duodenal, 4 gallbladder, 4 pancreatic, 28 colonic and 8 rectal cancer cases admitted between March 2001 and February 2002 in the Department of Medical Oncology, First Affiliated Hospital of Xi'an Jiaotong University were randomly enrolled in the study. The medical records of these patients were reviewed by investigators and their characteristics such as the family history of cancer and main symptoms were abstracted. Subjects with a history of abnormal mentality or cognitive disorders were excluded from the investigation. All the cancer cases were finally verified by histopathological examinations

and clinically diagnosed as stage I in 14, stage II in 34, stage III in 28 and stage IV in 32 according to TNM classification and the Union International Center of Cancer (UICC) system. The average disease course of the patients was 14 ± 11 months and the average age was 58 ± 9 years with the education background of 7 being graduated from primary school, 25 from junior high school and 76 from senior high school or above. Their performance status (PS) was defined by Eastern Cooperative Oncology Group (ECOG) and social information such as marital and employment status was obtained through an interview. The patients were categorized into depression group and non-depression group in terms of their SDS index scores. The study protocol was in accordance with the guideline for clinical research and approved by the Ethical and Research Committee of the hospital.

Psychological measurements

Zung self-rating depression scale (SDS) The Zung SDS system harbors 20 items of self-evaluation measurements for depressive symptoms^[21]. In the study, the patients were asked to rate each of the items regarding how they felt during the preceding week by a 4-point Likert scale with the 4 representing the most unfavorable response. After the scores of 10 reversely-graded items were adjusted in line with that of the sequentially-scored items, a raw score that was turned out from the total value of 20 items was further converted into a depression-judging variable termed as SDS index, based on which the cases were categorized into 2 levels of psychological conditions. Level 1, SDS index below 50, was considered not significant psychopathologically. Level 2, SDS index equal to or above 50, was suggested the presence of depression. It was not meant for SDS index to offer a strict diagnostic guideline but rather denote levels of depression in symptomatology that might be of clinical significance. Overall, the SDS index was shown to be relatively valid with a high internal consistency that was exhibited by an alpha coefficient of 0.84^[22].

Zung Self-rating anxiety scale (SAS) Just like Zung SDS system, Zung SAS also has 20 items to be scored with the 4-point Likert scale except that there are 5 reversely-scored items, in which the 4 represents the most unfavorable response^[23]. After the scores of 5 reversely-graded items were adjusted in line with that of the sequentially-scored items, a raw score that was turned out from the total value of 20 items was further converted into an anxiety-judging variable termed as SAS index, based on which the cases were categorized into 2 levels of psychological conditions. Level 1, SAS index below 50, was considered not significant psychopathologically. Level 2, SAS index equal to or above 50, was suggested the presence of anxiety.

Numeric rating scale (NRS) NRS consisting of four questions covering pain, nausea, insomnia and appetite was evaluated by using a 0-10 scale, with 0 meaning without symptoms and 10 indicating the situation being as bad as imagined, which was found to be a simple and valid pain measurement in some disease states^[24]. In this study, the patients were asked to circle the number that best described the symptom at its worst during a one-week period.

Social support rating scale (SSRS) SSRS was employed to evaluate the levels of objective, subjective and total social support, as well as the utility of this support^[25].

Study protocols

Two days before the investigation, each item for the psychological measurements was explained by specialized doctors in order to make the patients understand and complete the questionnaires correctly by themselves in a quiet condition to exclude any possible influence. If it could not be completed by the patients for some reasons as sickness or poor education, family members or

physicians in charge were prescribed to do it instead.

On the experimental day, 3.5 ml of peripheral blood was drawn from each patient and anticoagulated by ethylenediaminetetraacetic acid (EDTA), in which 50 μ l of blood was quantified with the Sysmes KX-21 blood counter (Japan) for the measurement of white blood cells, erythrocytes, thrombocytes, and fractions of lymphocytes, granulocytes and monocytes. The other 3.0 ml of blood sample was used to determine natural killer cells (CD₅₆) and T lymphocyte subsets with the EPICS ELITE flow cytometer (American) by individuals blinded to the clinical data of the patients in our immunology laboratory.

Statistical analysis

Experimental data were expressed as $\bar{x} \pm s$. Comparisons between experimental groups were performed by *t*-test to examine the variables with normal distribution and by Mann-Whitney *U* test to assess the other kinds of numerical values. Demographic variables were analyzed by descriptive statistics to evaluate the clinical and sociodemographic characteristics of the studied samples. Curve estimation, stepwise multiple or univariate linear regression and Pearson correlations were adopted to assess the correlation of depression with its possible contributing factors. A *P* value less than 0.05 was considered statistically significant. All statistical procedures were performed with statistical package of SPSS for social science (2000).

RESULTS

Incidence of depression in cancer patients

Questionnaires answered by the enrolled patients were correctly filled in according to the experimental protocol. The scores of SDS 4 grade evaluation are listed in Table 1. In the present study, SDS index was approximately a normal distribution in the 108 cases, ranging from 33.8 to 66.2 and averaging at 50.4 ± 8.8 . Fifty percent of the patients had a SDS index score more than 50. Similarly, SAS index of all the patients ranged from 35.0 to 62.0 and averaged at 46.9 ± 7.7 , 46.3% of the cases had a SAS index score above 50, 29.6% of the enrolled patients had scores above 50 simultaneously for both SDS and SAS indexes. The social support score was between 28 and 56 and averaged at 43.8 ± 7.2 . Curve estimation showed that the depression was positively correlated with anxiety and negatively with social support. Furthermore, the depression correlated with the tumor type, which manifested in a descending order as stomach, gallbladder, pancreas, intestine, esophagus, duodenum and rectum, according to their correlativity.

Factors contributing to depression

Many factors were associated with depression such as cancer pain, anxiety, poor economic status, tumor type, anorexia (X5: I eat as much as I used to), hyposexuality (X6: I enjoy looking at, talking to and being with attractive men/women), dispiritment (X1: I feel downhearted, blue and sad), agitation (X13: I am restless and can not keep still), palpitation (X9: My heart beats faster than usual), fatigue without apparent reasons (X10: I get tired for no reason), CD₅₆₊, *etc.* However, step-wise regression analysis suggested that hyposexuality, dispiritment, agitation, palpitation, CD₅₆ and anxiety were the significant factors contributing to depression (Table 2).

Effects of depression on cell-mediated immunity

More severe anxiety and poor social support were noted in the depression group compared with those of the non-depression patients. As for the parameter changes of cell-mediated immunity in peripheral blood, an increase of granulocyte count and a decline in T-lymphocyte subsets (CD₃, CD₄ and CD₈), erythrocyte and monocyte counts were observed in depression cases, but did not reach a significant level. Lymphocyte count

Table 1 SDS 4 grading of depressive manifestations in patients with gut cancers

Item	Factors	$\bar{x}\pm s$	Grade			
			1	2	3	4
X1	I feel downhearted, blue and sad	1.9±0.8	34	50	18	6
X2	Morning is when I feel best	2.6±1.1	18	42	18	30
X3	I have crying spells or feel like it	1.5±0.9	75	14	14	5
X4	I have trouble sleeping through the night	2.1±1.0	42	22	34	10
X5	I eat as much as I used to	2.6±1.0	22	22	46	18
X6	I enjoy looking at, talking to, and being with attractive men/women	2.6±1.1	25	26	26	31
X7	I notice that I am losing weight	2.4±1.0	18	46	22	22
X8	I have trouble with constipation	2.2±1.1	38	30	22	18
X9	My heart beats faster than usual	1.3±0.6	76	16	8	8
X10	I get tired for no reason	2.3±1.1	34	30	22	22
X11	My mind is as clear as it used to be	1.8±0.9	50	30	22	6
X12	I find it easy to do the things I used to do	2.3±0.9	22	42	30	14
X13	I am restless and can't keep still	1.6±0.9	62	22	18	6
X14	I feel hopeful about the future	2.2±0.9	30	30	42	6
X15	I am more irritable than usual	1.7±1.0	58	26	14	10
X16	I find it easy to make decisions	2.3±1.1	34	26	26	22
X17	I feel that I am useful and needed	1.9±1.0	42	42	10	14
X18	My life is pretty full	1.8±0.8	38	50	14	6
X19	I feel that others would be better off if I were dead	1.4±0.7	70	30	2	6
X20	I still enjoy the things I used to do	2.2±1.0	30	42	18	18

Table 2 Multivariate analysis of contributing factors of depression with step-wise regression

Variable	Unstandardized coefficients (B)	Standardized coefficients (β)	t	P value	Pearson correlation
X1 ^a	4.47	0.36	19 193 329	0.00	0.64
X6 ^a	4.13	0.51	19 076 980	0.00	-0.80
X9 ^a	0.97	0.07	3 266 595.5	0.00	0.65
X13 ^a	1.78	0.15	4 232 747.7	0.00	0.08
Anxiety ^a	6.04E-02	0.06	3 691 620.2	0.00	0.32
CD ₅₆ ^a	-2.33	-0.10	-28 074 903	0.00	-0.18

^aP<0.05 vs nondepression group.

and CD₅₆ were significantly decreased in the depression group compared with those of the non-depression patients ($P<0.05$) as shown in Table 3. However, fewer changes in CD₄/CD₈ ratio and other immunological parameters were found between the two groups.

Table 3 Multiple factors between depression and nondepression groups ($\bar{x}\pm s$)

Parameters	Depressive state	Non-depressive state	P
Anxiety	49.7±7.5 ^b	45.3±6.9	0.003
Pain	6.5±2.8 ^a	4.6±3.2	0.025
Social support	44.0±6.8	44.6±7.7	0.670
Objective support	11.9±3.0	12.5±3.0	0.360
Subjective support	24.8±3.8	24.5±4.4	0.630
Utilization of support	6.8±2.0 ^a	7.6±2.1	0.043
Cells in peripheral blood			
Erythrocyte (10 ¹² /L)	3.4±1.2	3.8±1.8	0.460
Lymphocyte (0.00)	0.33±0.09 ^a	0.39±0.87	0.032
Granulocyte (0.00)	0.61±0.12	0.56±0.88	0.240
Monocyte (0.00)	0.04±0.01	0.06±0.05	0.900
Thrombocyte (10 ⁹ /L)	137.5±12.5 ^a	167.7±43.2	0.020
T lymphocyte subsets			
CD ₃ (0.00)	0.53±0.11	0.59±0.11	0.070
CD ₄ (0.00)	0.27±0.07	0.30±0.11	0.440
CD ₈ (0.00)	0.32±0.10	0.35±0.10	0.240
Natural killer			
CD ₅₆ (0.00)	0.26±0.11 ^a	0.29±0.11	0.041

^aP<0.05, ^bP<0.01, vs nondepression group.

DISCUSSION

Depression is a psychotic or neurotic condition characterized by inability to concentrate, insomnia, and feelings of extreme sadness, dejection and hopelessness, which commonly occur in cancer patients. It has been estimated that the incidence of severe depression in these patients is about 3%-50% depending on tumor site, stage, assessment methods, and a lot of other contributing factors, with an average overall incidence of approximately 20%^[18,26,27]. However, depression remains an often unrecognized source of suffering among cancer patients, which is partially because of the lack of recognition by clinical physicians. Under such circumstances, particularly when the depression was confused with symptoms resulted from the underlying disease, clinicians were usually inclined to dismiss even severe depression on the assumption that these "symptoms" are understandable^[27]. In fact, untreated depression in these patients might cause more frequent clinic visits, higher medical costs, longer hospital stay, as well as noncompliance with therapeutic measures, poor quality of life, bad prognosis, and even accidental death^[20,28-32].

In the present study, we investigated the effects of depression on the parameters of cell-mediated immunity and its contributing factors in patients with cancers of the digestive tract. To our knowledge, it is one of the few clinical reports in recent years concerning depression in patients with digestive tract cancers. It was revealed that depression occurred in 50% of the cases, which was higher than the average total incidence among all tumor patients. Besides, there was also a higher percentage of cases with both SDS and SAS scores equal to or more than 50 in our study, accounting for 29.6% of the investigated patients. The exact reason for these has not yet been fully elucidated, it

is probably because the gut function relates so closely to people's daily life that a malignant disorder in the digestive tract might affect the psychological status of patients more easily compared with tumors of the other sites.

Lots of factors are closely related to the depression of cancer patients including physiological, immunological and psychosocial impacts. Although this correlation has been established as a whole in tumor cases^[33,34], however, little is known about the contributing factors to the depression in patients with cancer of the digestive tract according to the new bio-psycho-social model. Our study revealed that despite many factors such as cancer pain, poor economic status, tumor type, anorexia (X5), fatigue without apparent reasons (X10) might play a role, hyposexuality (X6), dispiritment (X1), agitation (X13), palpitation (X9), CD₅₆ and anxiety were the significant factors contributing to the depression of these patients by step-wise regression analysis.

Impairment of immunologic functions has been noted to be one of the major negative effects exerted by depression in cancer patients^[35]. Some immunological parameters such as T lymphocyte subsets and natural killer (NK) cells have been believed to be the major effectual mechanism against tumors^[36-43]. For instance, the growth of malignancies was inhibited by activated tumor-specific T cells^[44,45] and the depressed activity of NK cells was probably related to tumor enlargement and dissemination^[46]. Papadopoulos and his associates^[42] reported that the depletion of cytotoxic T cell (CD₈₊) and NK cell (CD₅₆₊) in advanced papillary ovarian cancer might in part explain the poor clinical outcomes of those patients. However, in our study, although significantly reduced NK cells (CD₅₆) and thrombocyte count were found in the depressive patients, T lymphocyte subset, CD₄/CD₈ ratio and other immunological parameters did not exhibit significant alterations between the two groups, suggesting that depression was probably not a necessarily factor leading to impairment of immune functions in patients with cancers of the digestive tract.

In summary, our study reveals that the incidence of depression is as high as 50% in patients with cancers of the digestive tract. Hyposexuality, dispiritment, agitation, palpitation, low CD₅₆ and anxiety are the significant factors contributing to the depression. Although significantly reduced NK cells (CD₅₆) and thrombocyte count are found in the depressive patients, T lymphocyte subset, CD₄/CD₈ ratio and other immunological parameters do not exhibit significant alterations between the depressive and non-depressive patients. Comprehensive measures including psycho-logical support therefore should be taken in order to improve their immunological functions, quality of life and clinical prognosis of cancer patients.

REFERENCES

- Newnham A**, Quinn MJ, Babb P, Kang JY, Majeed A. Trends in oesophageal and gastric cancer incidence, mortality and survival in England and Wales 1971-1998/1999. *Aliment Pharmacol Ther* 2003; **17**: 655-664
- Shibuya K**, Mathers CD, Boschi-Pinto C, Lopez AD, Murray CJ. Global and regional estimates of cancer mortality and incidence by site: II. Results for the global burden of disease 2000. *BMC Cancer* 2002; **2**: 37
- Ke L**. Mortality and incidence trends from esophagus cancer in selected geographic areas of China circa 1970-1990. *Int J Cancer* 2002; **102**: 271-274
- Le Vu B**, de Vathaire F, de Vathaire CC, Paofaite J, Roda L, Soubiran G, Lhoumeau F, Laudon F. Cancer incidence in French Polynesia 1985-1995. *Trop Med Int Health* 2000; **5**: 722-731
- Mohandas KM**, Jagannath P. Epidemiology of digestive tract cancers in India. VI. Projected burden in the new millennium and the need for primary prevention. *Indian J Gastroenterol* 2000; **19**: 74-78
- Zhang YL**, Zhang ZS, Wu BP, Zhou DY. Early diagnosis for colorectal cancer in China. *World J Gastroenterol* 2002; **8**: 21-25
- Shen ZY**, Shen WY, Chen MH, Shen J, Cai WJ, Yi Z. Nitric oxide and calcium ions in apoptotic esophageal carcinoma cells induced by arsenite. *World J Gastroenterol* 2002; **8**: 40-43
- Gu ZP**, Wang YI, Li JG, Zhou YA. VEGF165 antisense RNA suppresses oncogenic properties of human esophageal squamous cell carcinoma. *World J Gastroenterol* 2002; **8**: 44-48
- Chen K**, Cai J, Liu XY, Ma XY, Yao KY, Zheng S. Nested case-control study on the risk factors of colorectal cancer. *World J Gastroenterol* 2003; **9**: 99-103
- Tsukuma H**, Ajiki W, Oshima A. Time-trends in cancer incidence and mortality in Japan. *Gan To Kagaku Ryoho* 2001; **28**: 137-141
- Sun X**, Mu R, Zhou Y, Dai X, Qiao Y, Zhang S, Huangfu X, Sun J, Li L, Lu F. 1990-1992 mortality of stomach cancer in China. *Zhonghua Zhongliu Zazhi* 2002; **24**: 4-8
- Zhang S**, Li L, Lu F. Mortality of primary liver cancer in China from 1990 through 1992. *Zhonghua Zhongliu Zazhi* 1999; **21**: 245-249
- Zheng S**, Liu XY, Ding KF, Wang LB, Qiu PL, Ding XF, Shen YZ, Shen GF, Sun QR, Li WD, Dong Q, Zhang SZ. Reduction of the incidence and mortality of rectal cancer by polypectomy: a prospective cohort study in Haining County. *World J Gastroenterol* 2002; **8**: 488-492
- Wan J**, Zhang ZQ, Zhu C, Wang MW, Zhao DH, Fu YH, Zhang JP, Wang YH, Wu BY. Colonoscopic screening and follow-up for colorectal cancer in the elderly. *World J Gastroenterol* 2002; **8**: 267-269
- Murr C**, Widner B, Sperner-Unterweger B, Ledochowski M, Schubert C, Fuchs D. Immune reaction links disease progression in cancer patients with depression. *Med Hypotheses* 2000; **55**: 137-140
- Skarstein J**, Aass N, Fossa SD, Skovlund E, Dahl AA. Anxiety and depression in cancer patients: relation between the Hospital Anxiety and Depression Scale and the European Organization for Research and Treatment of Cancer Core Quality of Life Questionnaire. *J Psychosom Res* 2000; **49**: 27-34
- Sarna L**, Padilla G, Holmes C, Tashkin D, Brecht ML, Evangelista L. Quality of life of long-term survivors of non-small-cell lung cancer. *J Clin Oncol* 2002; **20**: 2920-2929
- Hopwood P**, Stephens RJ. Depression in patients with lung cancer: prevalence and risk factors derived from quality-of-life data. *J Clin Oncol* 2000; **18**: 893-903
- Gallagher J**, Parle M, Cairns D. Appraisal and psychological distress six months after diagnosis of breast cancer. *Br J Health Psychol* 2002; **7**(Part 3): 365-376
- Hjerl K**, Andersen EW, Keiding N, Mouridsen HT, Mortensen PB, Jorgensen T. Depression as a prognostic factor for breast cancer mortality. *Psychosomatics* 2003; **44**: 24-30
- Passik SD**, Lundberg JC, Rosenfeld B, Kirsh KL, Donaghy K, Theobald D, Lundberg E, Dugan W. Factor analysis of the Zung Self-Rating Depression Scale in a large ambulatory oncology sample. *Psychosomatics* 2000; **41**: 121-127
- Dugan W**, McDonald MV, Passik SD, Rosenfeld BD, Theobald D, Edgerton S. Use of the Zung Self-Rating Depression Scale in cancer patients: feasibility as a screening tool. *Psychooncology* 1998; **7**: 483-493
- Zung WW**. A rating instrument for anxiety disorders. *Psychosomatics* 1971; **12**: 371-379
- Paice JA**, Cohen FL. Validity of a verbally administered numeric rating scale to measure cancer pain intensity. *Cancer Nurs* 1997; **20**: 88-93
- Hu MY**, Zhou CJ, Xiao SY. Psychological health level and related psychosocial factors of nurses in Changsha. *Zhonghua Huli Zazhi* 1997; **32**: 192-195
- Chochinov HM**. Depression in cancer patients. *Lancet Oncol* 2001; **2**: 499-505
- Goldman LS**, Nielsen NH, Champion HC. Awareness, diagnosis, and treatment of depression. *J Gen Intern Med* 1999; **14**: 569-580
- DiMatteo MR**, Lepper HS, Croghan TW. Depression is a risk factor for noncompliance with medical treatment: meta-analysis of the effects of anxiety and depression on patient adherence. *Arch Intern Med* 2000; **160**: 2101-2107
- Watson M**, Haviland JS, Greer S, Davidson J, Bliss JM. Influence of psychological response on survival in breast cancer: a population-based cohort study. *Lancet* 1999; **354**: 1331-1336

- 30 **Breitbart W**, Rosenfeld B, Pessin H, Kaim M, Funesti-Esch J, Galietta M, Nelson CJ, Brescia R. Depression, hopelessness, and desire for hastened death in terminally ill patients with cancer. *JAMA* 2000; **284**: 2907-2911
- 31 **Akechi T**, Okamura H, Nishiwaki Y, Uchitomi Y. Predictive factors for suicidal ideation in patients with unresectable lung carcinoma. *Cancer* 2002; **95**: 1085-1093
- 32 **Nie J**, Liu S, Di L. Cancer pain and its influence on cancer patients' quality of life. *Zhonghua Zhongliu Zazhi* 2000; **22**: 432-434
- 33 **Lissoni P**, Cangemi P, Pirato D, Roselli MG, Rovelli F, Brivio F, Malugani F, Maestroni GJ, Conti A, Laudon M, Malysheva O, Gianni L. A review on cancer-psycho-spiritual status interactions. *Neuroendocrinol Lett* 2001; **22**: 175-180
- 34 **Schussler G**, Schubert C. The influence of psychosocial factors on the immune system (psychoneuroimmunology) and their role for the incidence and progression of cancer. *Z Psychosom Med Psychother* 2001; **47**: 6-41
- 35 **Mafune K**, Tanaka Y. Influence of multimodality therapy on the cellular immunity of patients with esophageal cancer. *Ann Surg Oncol* 2000; **7**: 609-616
- 36 **Dhodapkar MV**, Young JW, Chapman PB, Cox WI, Fonteneau JF, Amigorena S, Houghton AN, Steinman RM, Bhardwaj N. Paucity of functional T-cell memory to melanoma antigens in healthy donors and melanoma patients. *Clin Cancer Res* 2000; **6**: 4831-4838
- 37 **Ochsenbein AF**, Sierro S, Odermatt B, Pericin M, Karrer U, Hermans J, Hemmi S, Hengartner H, Zinkernagel RM. Roles of tumour localization, second signals and cross priming in cytotoxic T-cell induction. *Nature* 2001; **411**: 1058-1064
- 38 **Marzo AL**, Kinnear BF, Lake RA, Frelinger JJ, Collins EJ, Robinson BW, Scott B. Tumor-specific CD₄⁺ T cells have a major "post-licensing" role in CTL mediated anti-tumor immunity. *J Immunol* 2000; **165**: 6047-6055
- 39 **Ferreira C**, Barthlott T, Garcia S, Zamoyska R, Stockinger B. Differential survival of naive CD₄ and CD₈ T cells. *J Immunol* 2000; **165**: 3689-3694
- 40 **Echchakir H**, Bagot M, Dorothee G, Martinvalet D, LeGouvello S, Bousmell L, Chouaib S, Bensussan A, Mami-Chouaib F. Cutaneous T cell lymphoma reactive CD₄⁺ cytotoxic T lymphocyte clones display a Th1 cytokine profile and use a fas-independent pathway for specific tumor cell lysis. *J Invest Dermatol* 2000; **115**: 74-80
- 41 **Wolf AM**, Wolf D, Steurer M, Gastl G, Gunsilius E, Grubeck-Loebenstien B. Increase of Regulatory T Cells in the Peripheral Blood of Cancer Patients. *Clin Cancer Res* 2003; **9**: 606-612
- 42 **Papadopoulos N**, Kotini A, Cheva A, Jivannakis T, Manavis J, Alexiadis G, Lambropoulou M, Vavetsis S, Tamiolakis D. Gains and losses of CD₈, CD₂₀ and CD₅₆ expression in tumor stroma-infiltrating lymphocytes compared with tumor-associated lymphocytes from ascitic fluid and lymphocytes from tumor draining lymph nodes in serous papillary ovarian carcinoma patients. *Eur J Gynaecol Oncol* 2002; **23**: 533-536
- 43 **Zhai SH**, Liu JB, Zhu P, Wang YH. CD₅₄, CD₈₀, CD₈₆ and HLA-ABC expressions in liver cirrhosis and hepatocarcinoma. *Shijie Huaren Xiaohua Zazhi* 2000; **8**: 292-295
- 44 **Pardoll D**. T cells take aim at cancer. *Proc Natl Acad Sci U S A* 2002; **99**: 15840-15842
- 45 **Dudley ME**, Wunderlich JR, Robbins PF, Yang JC, Hwu P, Schwartzentruber DJ, Topalian SL, Sherry R, Restifo NP, Hubicki AM, Robinson MR, Raffeld M, Duray P, Seipp CA, Rogers-Freezer L, Morton KE, Mavroukakis SA, White DE, Rosenberg SA. Cancer regression and autoimmunity in patients after clonal repopulation with antitumor lymphocytes. *Science* 2002; **298**: 850-854
- 46 **Takeuchi H**, Maehara Y, Tokunaga E, Koga T, Kakeji Y, Sugimachi K. Prognostic significance of natural killer cell activity in patients with gastric carcinoma: a multivariate analysis. *Am J Gastroenterol* 2001; **96**: 574-578

Edited by Zhu LH and Wang XL

Estimating medical costs of gastroenterological diseases

Li-Fang Chou

Li-Fang Chou, Department of Public Finance, National Chengchi University, Taipei, Taiwan, China

Correspondence to: Professor Li-Fang Chou, Department of Public Finance, National Chengchi University, 64, Sec. 2, Chih-Nan Road, Taipei 11623, Taiwan, China. lifang@nccu.edu.tw

Telephone: +886-2-29387310 **Fax:** +886-2-29390074

Received: 2003-06-05 **Accepted:** 2003-08-02

Abstract

AIM: To estimate the direct medical costs of gastroenterological diseases within the universal health insurance program among the population of local residents in Taiwan.

METHODS: The data sources were the first 4 cohort datasets of 200 000 people from the National Health Insurance Research Database in Taipei. The ambulatory, inpatient and pharmacy claims of the cohort in 2001 were analyzed. Besides prevalence and medical costs of diseases, both amount and costs of utilization in procedures and drugs were calculated.

RESULTS: Of the cohort with 183 976 eligible people, 44.2% had ever a gastroenterological diagnosis during the year. The age group 20-39 years had the lowest prevalence rate (39.2%) while the elderly had the highest (58.4%). The prevalence rate was higher in women than in men (48.5% vs. 40.0%). Totally, 30.4% of 14 888 inpatients had ever a gastroenterological diagnosis at discharge and 18.8% of 51 359 patients at clinics of traditional Chinese medicine had such a diagnosis there. If only the principal diagnosis on each claim was considered, 16.2% of admissions, 8.0% of outpatient visits, and 10.1% of the total medical costs (8 469 909 US dollars/83 830 239 US dollars) were attributed to gastroenterological diseases. On average, 46.0 US dollars per insured person in a year were spent in treating gastroenterological diseases. Diagnostic procedures related to gastroenterological diseases accounted for 24.2% of the costs for all diagnostic procedures and 2.3% of the total medical costs. Therapeutic procedures related to gastroenterological diseases accounted for 4.5% of the costs for all therapeutic procedures and 1.3% of the total medical costs. Drugs related to gastroenterological diseases accounted for 7.3% of the costs for all drugs and 1.9% of the total medical costs.

CONCLUSION: Gastroenterological diseases are prevalent among the population of local residents in Taiwan, accounting for a tenth of the total medical costs. Further investigations are needed to differentiate costs in screening, ruling out, confirming, and treating.

Chou LF. Estimating medical costs of gastroenterological diseases. *World J Gastroenterol* 2004; 10(2): 273-278
<http://www.wjgnet.com/1007-9327/10/273.asp>

INTRODUCTION

The cost analysis of disease management is essential for health policymaking in resource allocation and medical manpower

planning^[1-8]. Among all medical specialties, gastroenterology has played a major role because of disease prevalence and advanced technology^[9-12]. While the literature about economic assessments in gastroenterology dealt mainly with cost-effectiveness of single pharmaceuticals, diagnostic measures or therapeutic interventions^[13-23], analyses of the entire specialty are relatively scarce. One of the reasons might be that the complete utilization data of the total population or a representative sample are not easily available. The more decisive reason is the lack of a standardized analysis framework and operational measures.

The aim of this study was to estimate the direct medical costs of gastroenterological diseases among the population of local residents in Taiwan. Besides the diagnosis-based approach, the costs would also be sorted by diagnostic procedure, therapeutic procedure, and drug. The strength of this study was to use the complete claim data of a representative cohort of 200 000 people within the universal health insurance program in Taiwan. Not only the nominal costs of gastroenterological diseases but also their relative ratio in total medical costs could be measured.

MATERIALS AND METHODS

Data sources

The data of the first 4 cohort datasets (R01-R04) in 2001 from the National Health Insurance Research Database (NHIRD; <http://www.nhri.org.tw/nhird/>) in Taipei were used for the analysis. The NHIRD owned all claims in electronic form from the national health insurance (NHI) program that has started in 1995 and covered nearly all inhabitants in Taiwan (21 653 555 beneficiaries at the end of 2001)^[24]. The NHIRD has retrieved dozens of datasets publicly available for researchers. For each cohort dataset, the NHIRD at first randomly sampled 50 000 people from 23 753 407 people who had ever been insured from March 1, 1995 to December 31, 2000. Then, all insurance claims belonging to these people were drawn to make up one specific cohort dataset.

A cohort dataset included one registration file of the insured people and 6 files of original claim data: inpatient expenditures by admissions, details of inpatient orders, ambulatory care expenditures by visits, details of ambulatory care orders, expenditures for prescriptions dispensed at contracted pharmacies, and details of prescriptions dispensed at contracted pharmacies. The structure of the insurance claim files had been described in details on the NHIRD web site and in other published literature^[25-28].

Among the 4 cohort datasets in 2001, there were totally 183 976 eligible people, 22 746 admissions, 1 241 760 inpatient prescription items, 2 607 646 visits (including 234 598 visits for traditional Chinese medicine), 11 765 537 outpatient prescription items, 127 008 dispensed prescriptions at pharmacies, and 513 231 dispensed prescription items at pharmacies. The ambulatory sector included medical care services at clinics of Western medicine, traditional Chinese medicine, and dentistry, and pharmaceutical services at pharmacies. Because the separation of prescribing and dispensing was not yet thoroughly executed in Taiwan, relatively few outpatient prescriptions had been dispensed at independent pharmacies.

Besides, the fee schedule of 4 837 medical service items and the list of 21 146 approved drug items of Western medicine in Taiwan were downloaded from the web site of the Bureau of National Health Insurance (<http://www.nhi.gov.tw/>, accessed January 12, 2002). Each drug of different brand, strength and form had an official unique identifier for claims. The BNHI also offered a list of ATC codes (the Anatomical Therapeutic Chemical classification system, version 2000)^[29] for each drug item.

Study design

The costs of gastroenterological diseases were estimated in 4 dimensions: diagnosis, diagnostic procedure, therapeutic procedure, and drug. The reason for separate approaches was that on the one hand an admission or a visit with a gastroenterological diagnosis might contain service items not related to the gastroenterological diagnosis, and on the other hand a procedure or drug for gastroenterological diseases might not be associated with any gastroenterological diagnosis on the claim because of the coding error or limitation (5 diagnosis fields on an admission claim and 3 on a visit claim).

The age-sex prevalence of patients having any gastroenterological diagnosis during the year was at first calculated. All 5 diagnoses on an admission record and all 3 diagnoses on a visit record were taken into account. Then, medical costs of visits and admissions because of gastroenterological diseases as the principal diagnosis were calculated and stratified by major disease category.

The definition and categorization of gastroenterological diseases were based on the scheme of the Clinical Classifications Software (CCS for ICD-9-CM) developed by the Agency for Healthcare Research and Quality (AHRQ) of the U.S. Department of Health and Human Services^[30]. The single-level diagnosis CCS aggregated illnesses and conditions of over 12 000 diagnosis codes within the International Classification of Diseases, 9th Revision, Clinical Modification (ICD-9-CM) into 259 mutually exclusive categories. The single-level CSS categories 6, 12-18, 120, 135, 138-155, 214, 250, and 251 were deemed as gastroenterological diseases. Some codes such as benign neoplasm, injury, and screening that were dispersedly included in other CSS categories were also identified as gastroenterological diseases.

The fee schedule of the NHI included mainly consultation and rehabilitation fees, charges for diagnostic procedures (*e.g.* laboratory tests and radiological examinations), therapeutic procedures (*e.g.* general treatments, radiological interventions and surgeries) and materials, and case payments based on diagnosis-related groups. Among 1 470 items of diagnostic procedures and 2 435 items of therapeutic procedures, 132 and 338 items were related to gastroenterological diseases respectively.

Drugs for treating gastroenterological diseases in the current study included all drug items of the groups A02 (antacids, drugs for treatment of peptic ulcer and flatulence), A03 (antispasmodic and anticholinergic agents and propulsives), A04 (antiemetics and antinauseants), A05 (bile and liver therapy), A06 (laxatives), A07 (antidiarrheals, intestinal antiinflammatory/antiinfective agents), A09 (digestives, including enzymes), C05A (antihemorrhoidals for topical use), P01A (agents against amoebiasis and other protozoal diseases), and P02 (anthelmintics) in the ATC classification system. The items in the group J07BC (hepatitis vaccines) were not included because they were not reimbursable within the NHI. A total of 2 269 drug items for treating gastroenterological diseases had been registered in Taiwan since 1995. Some drugs might be no more available on the market or not reimbursable by the insurance during the study period.

In describing utilization and costs of diagnostic procedures, therapeutic procedures, and drugs related to gastroenterological diseases, the number of recipients, the number of orders, and the total costs were calculated and stratified either by individual item of procedures or by group of drugs at the ATC 3rd and 4th levels. The original monetary values in unit of New Taiwan dollars were converted into U.S. currency based on the average exchange rate in 2001 (1 U.S. dollar [USD]=33.8003 New Taiwan dollars) according to the Central Bank of China in Taiwan (<http://www.cbc.gov.tw/>, accessed 6 February 2003).

Statistical analysis

The database software of Microsoft SQL Server 2000 was used for data linkage and processing. The regular statistics were displayed.

RESULTS

General information of the cohort

Among the 200 000-person cohort, only 183 976 people were still insured in 2001. There were more men than women (92 566 vs 91 394), and the status of sex was unknown in 16 persons (Table 1). The mean age of the eligible people was 33.9 (SD 20.3) years.

Table 1 Age-sex specific prevalence of gastroenterological diseases among cohorts (*n*=183 976) in 2001

Age group in year	No. of patients			Prevalence in percent		
	All	Female	Male	All	Female	Male
Sampling cohort^a						
<20	51 029	24 644	26 384			
20-39	63 800	32 115	31 670			
40-59	45 432	23 061	22 371			
>=60	23 715	11 574	12 141			
Total	183 976	91 394	92 566			
Patients with any gastroenterological diagnosis at both inpatient and ambulatory sectors^{b,c}						
<20	22 006	10 728	11 277	43.1	43.5	42.7
20-39	25 035	14 988	10 044	39.2	46.7	31.7
40-59	20 412	11 497	8 915	44.9	49.9	39.9
>=60	13 845	7 090	6 755	58.4	61.3	55.6
Total	81 298	44 303	36 991	44.2	48.5	40.0
Patients with any gastroenterological diagnosis at inpatient sector						
<20	947	388	559	1.9	1.6	2.1
20-39	792	301	491	1.2	0.9	1.6
40-59	1 056	431	625	2.3	1.9	2.8
>=60	1 738	737	1 001	7.3	6.4	8.2
Total	4 533	1 857	2 676	2.5	2.0	2.9
Patients with any gastroenterological diagnosis at ambulatory sector^d						
<20	21 931	10 698	11 232	43.0	43.4	42.6
20-39	24 932	14 955	9 974	39.1	46.6	31.5
40-59	20 310	11 459	8 851	44.7	49.7	39.6
>=60	13 643	6 996	6 647	57.5	60.4	54.7
Total	80 816	44 108	3 6704	43.9	48.3	39.7
Patients with any gastroenterological diagnosis at clinics of traditional Chinese medicine						
<20	1 833	1 005	828	3.6	4.1	3.1
20-39	3 608	2 259	1 349	5.7	7.0	4.3
40-59	2 892	1 687	1 205	6.4	7.3	5.4
>=60	1 310	731	579	5.5	6.3	4.8
Total	9 643	5 682	3 961	5.2	6.2	4.3

^aThose born after January 1, 2001 were not included in the cohort. The status of sex was unknown in 16 persons. ^b Patients with gastroenterological diseases included 4 persons of

unknown sex. All diagnoses of a patient during the year were taken into account, not confined to principal diagnosis at each admission or visit. The ambulatory sector included physician offices, hospital outpatient departments, and emergency departments of Western medicine, dentistry, and traditional Chinese medicine.

The medical care benefits of these people in 2001 totaled 83 830 239 USD, of which 26 443 645 USD (31.5%) was claimed at the inpatient sector and 57 386 595 USD (68.5%) at the ambulatory sector. The clinics of traditional Chinese medicine and independent pharmacies only accounted for 4.2% (3 499 397 USD) and 0.8% (677 908 USD) of the total costs respectively.

The utilization and costs of all kinds of procedures and drugs among the cohort were as following: 1 119 629 orders of diagnostic procedures summing to 7 858 087 USD (9.4% of the total costs), 774 340 orders of therapeutic procedures with 23 582 229 USD (28.1% of the total costs), and 8 683 664 prescribed or dispensed items of drugs with 21 193 285 USD (25.3% of the total costs).

Age-sex specific prevalence of gastroenterological diseases

Table 1 also displays the number of patients with any gastroenterological diagnosis in 2001 and their prevalence among the eligible cohort, stratified by age group, sex, and setting. Totally, 44.2% of the insured people had at least one gastroenterological diagnosis. The age group 20-39 years had the lowest prevalence rate while the elderly had the highest. The prevalence rate was higher in women than in men (48.5% vs 40.0%). But, men had a slightly higher prevalence rate (2.9%) at the inpatient sector than women (2.0%). During the year, 14 888 patients were admitted to hospitals. In other words, 30.4% of inpatients had ever a gastroenterological diagnosis at discharge. Physicians of traditional Chinese medicine made gastroenterological diagnoses in 9 643 patients, i.e. in 5.2% of the entire cohort and in 18.8% of the 51 359 patients having visited the clinics of traditional Chinese medicine during 2001.

Prevalence and costs of gastroenterological diseases by major disease category

Table 2 shows the aggregate costs of visits and admissions due to gastroenterological diseases. The analysis took account of the principal diagnosis into consideration on each claim only, the results were stratified by major disease category, and the numbers of affected patients were also calculated. Totally, 67 073 patients (36.5% of the cohort) were involved and medical care costs in value of 8 469 909 USD (10.1% of the total medical costs) were consumed. On average, 46.0 USD per insured person in a year was spent in treating gastroenterological diseases.

Besides, 16.2% ($n=3\ 676$) of all admissions, 8.0% ($n=209\ 254$) of all visits, and 10.4% ($n=24\ 429$) of all visits to traditional Chinese medicine during 2001 were primarily attributed to gastroenterological causes. While the largest patient group was noninfectious gastroenteritis (9.6% of the cohort), followed by other gastrointestinal disorders (8.7%), abdominal pain (7.7%), gastritis and duodenitis (7.7%), and other disorders of stomach and duodenum (4.2%), the top 5 diagnosis groups with higher total charges were gastroduodenal ulcer (10.6% of the costs related to gastroenterological diseases/1.1% of the total medical costs), other liver diseases (6.7%/0.7%), other gastrointestinal disorders (6.7%/0.7%), hepatitis (6.5%/0.7%), and biliary tract disease (6.0%/0.6%).

Utilization and costs of diagnostic procedures related to gastroenterological diseases

Among the cohort during 2001, 36 004 (19.6%) patients utilized 210 156 (18.8%) diagnostic procedures related to gastroenterological diseases with costs of 1 900 752 USD (24.2%

of the costs for all diagnostic procedures and 2.3% of the total medical costs). The computer tomography with 3 fee items took almost a two-fifth share of the costs for GI-related diagnostic procedures. The other two items with higher costs were abdominal sonography (18.4% of the costs for GI-related diagnostic procedures) and upper GI panendoscopy (13.0%). But, the most common procedures belonged to biochemical tests of blood: glutamic-pyruvic transaminase (GPT) with 47 523 orders and glutamic-oxalacetic transaminase (GOT) with 45 653 orders. Nearly a seventh of the cohort received these two tests (Table 3).

Table 2 Prevalence and costs of gastroenterological diseases among cohorts ($n=183\ 976$) in 2001 by major disease category, according to principal diagnosis only

CSS ^a code	Single-level CCS diagnosis categories	Patients		Total cost	
		No.	Mean age (SD)	US \$	%
6	Hepatitis	6 356	44.3 (16.1)	547 599	6.5%
12	Cancer of esophagus	67	47.4 (22.3)	193 853	2.3%
13	Cancer of stomach	110	64.0 (15.0)	207 765	2.5%
14	Cancer of colon	230	63.2 (14.3)	308 903	3.6%
15	Cancer of rectum and anus	180	65.9 (12.8)	328 540	3.9%
16	Cancer of liver and intrahepatic bile duct	242	60.5 (14.4)	448 114	5.3%
17	Cancer of pancreas	30	67.9 (13.4)	148 490	1.8%
18	Cancer of other GI organs, peritoneum	40	67.5 (11.5)	70 893	0.8%
120	Hemorrhoids	2 110	45.6 (17.1)	236 477	2.8%
135	Intestinal infection	7 727	25.3 (22.2)	175 479	2.1%
138	Esophageal disorders	967	46.9 (20.9)	145 264	1.7%
139	Gastroduodenal ulcer (except hemorrhage)	6 214	48.1 (18.5)	898 028	10.6%
140	Gastritis and duodenitis	14 112	36.7 (21.9)	348 621	4.1%
141	Other disorders of stomach and duodenum	7 736	38.7 (23.1)	285 697	3.4%
142	Appendicitis and other appendiceal conditions	362	33.1 (18.8)	217 212	2.6%
143	Abdominal hernia	515	35.6 (27.9)	228 586	2.7%
144	Regional enteritis and ulcerative colitis	1 406	31.4 (22.5)	29 259	0.3%
145	Intestinal obstruction without hernia	543	39.4 (29.3)	112 282	1.3%
146	Diverticulosis and diverticulitis	45	58.2 (20.9)	29 713	0.4%
147	Anal and rectal conditions	366	41.8 (21.4)	87 506	1.0%
148	Peritonitis and intestinal abscess	72	49.5 (21.5)	54 941	0.6%
149	Biliary tract disease	1 000	54.2 (17.5)	509 960	6.0%
150	Liver disease, alcohol-related	156	48.5 (12.3)	39 179	0.5%
151	Other liver diseases	2 102	47.7 (16.9)	569 503	6.7%
152	Pancreatic disorders (not diabetes)	157	50.0 (17.0)	116 327	1.4%
153	Gastrointestinal hemorrhage	1 385	52.4 (20.2)	442 493	5.2%
154	Noninfectious gastroenteritis	17 717	28.9 (21.9)	401 586	4.7%
155	Other gastrointestinal disorders	16 080	36.7 (22.6)	563 336	6.7%
214	Digestive congenital anomalies	84	31.2 (22.2)	15 785	0.2%
250	Nausea and vomiting	926	25.5 (24.3)	19 924	0.2%
251	Abdominal pain	14 113	34.4 (20.1)	404 085	4.8%
-	Others	997	37.6 (23.1)	284 509	3.4%
	Total	67 073	34.8 (21.8)	8 469 909	100.0%

^aCCS: Clinical Classifications Software by the Agency for Healthcare Research and Quality (AHRQ), Rockville, MD, USA.

Table 3 Utilization and costs of diagnostic procedures related to gastroenterological diseases among cohorts ($n=183\ 976$) in 2001: top 20 by total cost

Item of diagnostic procedures ^a	No. of patients	No. of orders	Total cost		
			US \$	%	Cum.%
Whole body computer tomography (without contrast)	2 541	3 092	374 106	19.7%	19.7%
Abdominal sonography	11 132	15 730	349 690	18.4%	38.1%
Whole body computer tomography (with/without contrast)	1 644	2 106	320 943	16.9%	55.0%
Upper GI panendoscopy	4 693	5 606	247 458	13.0%	68.0%
Serum GPT	25 427	47 523	69 765	3.7%	71.7%
Serum GOT	24 265	45 653	67 676	3.6%	75.2%
Whole body computer tomography (with contrast)	337	437	59 522	3.1%	78.3%
Colon fiberoscopy	730	780	50 698	2.7%	81.0%
Double-contrast study of lower GI series	421	432	29 421	1.5%	82.6%
AFP (RIA)	1 461	2 408	28 361	1.5%	84.1%
AFP (EIA)	2 363	3 570	20 865	1.1%	85.2%
Plain abdomen X-ray	2 338	2 856	18 498	1.0%	86.1%
Serum bilirubin, total	6 345	12 553	18 307	1.0%	87.1%
HbsAg (EIA)	3 678	3 999	17 237	0.9%	88.0%
Serum albumin	6 989	14 638	15 522	0.8%	88.8%
CEA (EIA)	856	1 308	15 293	0.8%	89.6%
Alkaline phosphatase	5 686	10 091	14 159	0.7%	90.4%
Upper GI series	296	315	13 347	0.7%	91.1%
CEA (RIA)	647	1 127	13 344	0.7%	91.8%
Sigmoid fiberoscopy	311	327	11 620	0.6%	92.4%
Others			144 922	7.6%	100.0%
Total ^b	36 004	210 156	1 900 752	100.0%	

^aMagnet resonance imaging (MRI) was excluded from analysis because the fee schedule of the National Health Insurance did not differentiate MRI for abdomen from MRI for other body parts. ^bNumbers might not add to totals because of rounding.

Table 4 Utilization and costs of therapeutic procedures (treatment and surgery) related to gastroenterological diseases among cohorts ($n=183\ 976$) in 2001

Item of therapeutic procedure	No. of patients	No. of orders	Total cost		
			US \$	%	Cum.%
Nasal feeding	917	28 352	167 762	15.7%	15.7%
Repair of inguinal hernia (without bowel resection)	322	359	94 046	8.8%	24.5%
Appendectomy	226	226	74 145	7.0%	31.5%
Laparoscopic cholecystectomy	83	84	68 081	6.4%	37.9%
Hemorrhoidectomy, internal & external	198	199	59 994	5.6%	43.5%
Trans-arterial embolization (T.A.E.)	65	96	57 634	5.4%	48.9%
Insertion of nasogastric tube	1 745	5 370	25 609	2.4%	51.3%
Heat probe during endoscopy	162	185	21 893	2.1%	53.4%
Cholecystectomy	58	58	18 485	1.7%	55.1%
Endoscopic papillectomy	31	32	17 893	1.7%	56.8%
Colonoscopic polypectomy	153	157	17 140	1.6%	58.4%
Internal hemorrhoid ligation	216	356	16 795	1.6%	60.0%
Gastric decompression	900	3 712	16 473	1.5%	61.5%
Percutaneous transhepatic cholangiography drainage (PTCD)	38	54	15 735	1.5%	63.0%
Choledocholithotomy with T-tube drainage	28	28	15 282	1.4%	64.4%
Radical gastrectomy	14	14	15 061	1.4%	65.8%
Radical proctectomy	11	11	14 723	1.4%	67.2%
Radical hemicolectomy with ascending colon anastomosis	23	23	13 973	1.3%	68.5%
Restorative proctectomy with colo-anal anastomosis	11	11	13 948	1.3%	69.8%
Vagotomy and pyloroplasty	20	20	13 911	1.3%	71.1%
Others			307 915	28.9%	100.0%
Total ^a	8 349	60 245	1 066 497	100.0%	

^aNumbers might not add to totals because of rounding.

Table 5 Utilization and costs of drugs related to gastroenterological diseases among cohorts ($n=183\ 976$) in 2001, by the fourth level of ATC classification system

ATC code	Drug group name	No. of patients	No. of orders	Total cost		
				US \$	%	Cum. %
A02BA	H ₂ -receptor antagonists	26 690	85 228	269 851	17.4%	17.4%
A02BC	Proton pump inhibitors	2 223	7 100	219 823	14.2%	31.6%
A02AF	Antacids with antifatulents	98 197	385 623	156 244	10.1%	41.6%
A05BA	Liver therapy	3 234	12 990	113 482	7.3%	49.0%
A02AD	Combinations and complexes of aluminium, calcium and magnesium compounds	83 569	305 357	108 399	7.0%	55.9%
A03FA	Propulsives	46 418	140 278	108 006	7.0%	62.9%
A02AB	Aluminium compounds	20 845	50 850	71 820	4.6%	67.5%
A06AB	Contact laxatives	8 775	37 266	59 022	3.8%	71.3%
A02AG	Antacids with antispasmodics	53 966	160 086	52 394	3.4%	74.7%
A06AC	Bulk producers	2 327	5 851	47 848	3.1%	77.8%
A09AA	Enzyme preparations	15 041	37 149	35 754	2.3%	80.1%
A03AA	Synthetic anticholinergics, esters with tertiary amino group	19 071	43 779	28 953	1.9%	82.0%
A07EC	Aminosalicic acid and similar agents	248	1 504	24 494	1.6%	83.6%
A03AX	Other synthetic anticholinergic agents	2 264	4 110	22 682	1.5%	85.0%
A04AA	Serotonin (5HT ₃) antagonists	108	375	22 612	1.5%	86.5%
A02DA	Antifatulents	38 126	97 683	16 448	1.1%	87.5%
A03AB	Synthetic anticholinergics, quaternary ammonium compounds	8 413	15 312	16 205	1.0%	88.6%
A03BB	Belladonna alkaloids, semisynthetic, quaternary ammonium compounds	20 940	39 494	15 415	1.0%	89.6%
A06AD	Osmotically acting laxatives	513	1 485	15 401	1.0%	90.6%
A05AA	Bile acid preparations	409	1 580	15 064	1.0%	91.5%
-	Others			131 330	8.5%	100.0%
	Total ^a	149 062	1719 500	1 551 250	100.0%	

^aNumbers might not add to totals because of rounding.

Utilization and costs of therapeutic procedures related to gastroenterological diseases

Among the cohort during 2001, 8 349 (4.5%) patients utilized 60 245 (7.8%) therapeutic procedures related to gastroenterological diseases with costs of 1 066 497 USD (4.5% of the costs for all therapeutic procedures and 1.3% of the total medical costs). The most common general treatments were nasal feeding, insertion of nasogastric tube, and gastric decompression. The most common surgeries were hernioplasty, appendectomy, cholecystectomy, hemorrhoidectomy, and trans-arterial embolization. The utilization of surgeries was far less frequent than that of general treatments (Table 4).

Utilization and costs of drugs related to gastroenterological diseases

Over four-fifths of the cohort received drugs for treating gastroenterological diseases in value of 1 551 250 USD (7.3% of the costs for all drugs and 1.9% of the total medical costs). The most popular drugs were antacids (ATC group A02A) prescribed to 141 185 (76.7%) patients, drugs for treatment of peptic ulcer (A02B) with 29 181 (15.9%) recipients had the largest (33.1%) share of drug costs related to gastroenterological diseases. Table 5 gives a breakdown of the utilization into the fourth level of ATC classification. Despite fewer recipients, proton pump inhibitors (A02BC) were the second in aggregate cost only to H₂-receptor antagonists (A02BA). Another noteworthy fact was that drugs for liver therapy were prescribed to 7.1% of the cohort.

DISCUSSION

The current study offered concrete and considerable details about prevalence and costs of gastroenterological diseases among the population of local residents in Taiwan. The major findings were as the following: 44.2% of the insured people had ever a gastroenterological diagnosis during the study year. 16.2% of admissions, 8.0% of outpatient visits, and 10.1% of the total medical costs were attributed to gastroenterological diseases as principal diagnoses. GI-related diagnostic procedures accounted for 24.2% of costs for all diagnostic procedures and 2.3% of the total medical costs. GI-related therapeutic procedures accounted for 4.5% of costs for all therapeutic procedures and 1.3% of the total medical costs. GI-related drugs accounted for 7.3% of costs for all drugs and 1.9% of the total medical costs.

The current study focused only on the direct medical costs within the health insurance system. Those services beyond the insurance coverage were not taken into analysis. Although the NHI in Taiwan reimbursed visits and drugs at clinics of traditional Chinese medicine, the popular utilization of various kinds of folklore medicine by the Chinese people remained yet unknown.

The feature of the current study was to estimate costs of gastroenterological diseases from 4 dimensions. The reason of adopting such an approach was mentioned in the subsection of study design. It was initially difficult to define diagnoses related to gastroenterological diseases. If directly the ninth chapter (diseases of the digestive system) of ICD-9-CM was chosen, not only the scope of dentistry would be included, but also it would miss some GI-related infections, neoplasms, injuries, symptoms and signs coded in other chapters. The analysis did not proceed from the specialties of gastroenterologists and general surgeons either, because it might include breast, thyroid diseases and others then. Besides, other specialists and general practitioners might take care of gastroenterological diseases, too. Consequently, the current study followed a popular and public grouping system (CSS for ICD-9-CM) from the U.S.A.

to facilitate international comparisons in the future.

The other dimensions of the current study had limitations, too. With respect to diagnostic procedures, some tests, *e.g.* serum albumin, were not specific to diagnosing gastroenterological diseases. Besides, some tests, *e.g.* serum GOT, GPT, and bilirubin, almost belonged to screening routines on admission, so their utilization could not reflect the prevalence of diseases. Magnetic resonance imaging (MRI) as a popular and expensive procedure was absent in the analysis because the fee schedule of the NHI did not differentiate MRI for abdomen from MRI for other body parts.

With respect to therapeutic procedures, general treatments such as nasal feeding and insertion of nasogastric tube might not be directly related to gastroenterological diseases. In case payments based on diagnosis-related groups, the reimbursement per admission was fixed no matter whether the actual service items aggregately cost more. Because of the discrepancy between nominal and real values, costs of procedures within case payments, *i.e.* hernioplasty, appendectomy, cholecystectomy, and hemorrhoidectomy, might not be estimated accurately.

Drugs for treating gastroenterological diseases in the current study did not include antineoplastic and immunomodulating agents because these drugs were not specific in indications. Antivirals such as lamivudine or ribavirin were not included in the analysis either because they had been not yet reimbursed by the NHI in Taiwan. Although physicians of traditional Chinese medicine also used ICD-9-CM on claims, the lack of a corresponding classification for traditional Chinese drugs limited the analysis. Furthermore, the widespread use of antacids might be a unique phenomenon that reflected the habit of Chinese physicians in co-prescribing antacids^[25].

Finally, it cannot be denied that the diagnoses on insurance claims serve primarily for administrative purposes. They are rather tentative diagnoses than definite ones. Only in combination with conventional epidemiological surveys or data verification, the costs of screening, ruling out, confirming, and treating can be further differentiated.

ACKNOWLEDGMENTS

This study was based in part on data from the National Health Insurance Research Database provided by the Bureau of National Health Insurance, Department of Public Health and managed by National Health Research Institutes in Taiwan. The interpretation and conclusions contained herein do not represent those of Bureau of National Health Insurance, Department of Public Health or National Health Research Institutes. Besides, the author thanks Dr. med. Tzeng-Ji Chen for the professional advice.

REFERENCES

- 1 A primer on outcomes research for the gastroenterologist: report of the American Gastroenterology Association task force on outcomes research. *Gastroenterology* 1995; **109**: 302-306
- 2 **Bodger K**, Daly MJ, Heatley RV, Williams DR. Clinical economics review: gastroenterology. *Aliment Pharmacol Ther* 1996; **10**: 55-60
- 3 **Provenzale D**, Lipscomb J. A reader's guide to economic analysis in the GI literature. *Am J Gastroenterol* 1996; **91**: 2461-2470
- 4 **Hoffman C**, Rice D, Sung HY. Persons with chronic conditions. Their prevalence and costs. *JAMA* 1996; **276**: 1473-1479
- 5 **Provenzale D**. Economic considerations for the hepatologist. *Hepatology* 1999; **29**(Suppl 1): 13S-17S
- 6 **Glick HA**, Polsky D. Analytic approaches for the evaluation of costs. *Hepatology* 1999; **29**(Suppl 1): 18S-22S
- 7 **Sandler RS**, Everhart JE, Donowitz M, Adams E, Cronin K, Goodman C, Gemmen E, Shah S, Avdic A, Rubin R. The burden of selected digestive diseases in the United States. *Gastroenterology* 2002; **122**: 1500-1511

- 8 **Marshall JK**, Cawdron R, Yamamura DL, Ganguli S, Lad R, O'Brien BJ. Use and misuse of cost-effectiveness terminology in the gastroenterology literature: a systematic review. *Am J Gastroenterol* 2002; **97**: 172-179
- 9 OECD Health Data 2001. Paris: *OECD (Organisation for Economic Co-operation and Development)* 2001
- 10 **Drossman DA**, Li Z, Andruzzi E, Temple RD, Talley NJ, Thompson WG, Whitehead WE, Janssens J, Funch-Jensen P, Corazziari E, Richter JE, Koch GG. U.S. householder survey of functional gastrointestinal disorders. Prevalence, sociodemography, and health impact. *Dig Dis Sci* 1993; **38**: 1569-1580
- 11 **Sonnenberg A**, Everhart JE. Health impact of peptic ulcer in the United States. *Am J Gastroenterol* 1997; **92**: 614-620
- 12 **Westbrook JI**. Trends in the utilization of diagnostic upper GI endoscopy in New South Wales, Australia, 1988 to 1998. *Gastrointest Endosc* 2002; **55**: 847-853
- 13 **Bloom BS**, Fox NA, Jacobs J. Patterns of care and expenditures by California Medicaid for peptic ulcer and other acid-related diseases. *J Clin Gastroenterol* 1989; **11**: 615-620
- 14 **Talley NJ**, Gabriel SE, Harmsen WS, Zinsmeister AR, Evans RW. Medical costs in community subjects with irritable bowel syndrome. *Gastroenterology* 1995; **109**: 1736-1741
- 15 **Segal R**, Russell WL, Ben-Joseph R, Mansheim B. Cost of acid peptic disorders in a managed-care organization. *Clin Ther* 1996; **18**: 319-333
- 16 **Greenberg PD**, Koch J, Cello JP. Clinical utility and cost effectiveness of *Helicobacter pylori* testing for patients with duodenal and gastric ulcers. *Am J Gastroenterol* 1996; **91**: 228-232
- 17 **Jönsson B**, Karlsson G. Economic evaluation in gastrointestinal disease. *Scand J Gastroenterol Suppl* 1996; **220**: 44-51
- 18 **Taylor JL**, Zagari M, Murphy K, Freston JW. Pharmacoeconomic comparison of treatments for the eradication of *Helicobacter pylori*. *Arch Intern Med* 1997; **157**: 87-97
- 19 **Levin TR**, Schmittiel JA, Kunz K, Henning JM, Henke CJ, Colby CJ, Selby JV. Costs of acid-related disorders to a health maintenance organization. *Am J Med* 1997; **103**: 520-528
- 20 **Levin TR**, Schmittiel JA, Henning JM, Kunz K, Henke CJ, Colby CJ, Selby JV. A cost analysis of a *Helicobacter pylori* eradication strategy in a large health maintenance organization. *Am J Gastroenterol* 1998; **93**: 743-747
- 21 **Moayyedi P**, Soo S, Deeks J, Forman D, Mason J, Innes M, Delaney B. Systematic review and economic evaluation of *Helicobacter pylori* eradication treatment for non-ulcer dyspepsia. Dyspepsia Review Group. *BMJ* 2000; **321**: 659-664
- 22 **Westbrook JI**, Duggan AE, McIntosh JH. Prescriptions for anti-ulcer drugs in Australia: volume, trends, and costs. *BMJ* 2001; **323**: 1338-1339
- 23 **van Hout BA**, Klok RM, Brouwers JR, Postma MJ. A pharmacoeconomic comparison of the efficacy and costs of pantoprazole and omeprazole for the treatment of peptic ulcer or gastroesophageal reflux disease in the Netherlands. *Clin Ther* 2003; **25**: 635-646
- 24 **Bureau of National Health Insurance**. 2001 National Health Insurance Annual Statistical Report. Taipei: *Bureau of National Health Insurance* 2002
- 25 **Liu JY**, Chen TJ, Hwang SJ. Concomitant prescription of non-steroidal anti-inflammatory drugs and antacids in the outpatient setting of a medical center in Taiwan: a prescription database study. *Eur J Clin Pharmacol* 2001; **57**: 505-508
- 26 **Chen TJ**, Chou LF, Hwang SJ. Trends in prescribing proton pump inhibitors in Taiwan: 1997-2000. *Int J Clin Pharmacol Ther* 2003; **41**: 207-212
- 27 **Chen TJ**, Chou LF, Hwang SJ. Prevalence of anti-ulcer drug use in a Chinese cohort. *World J Gastroenterol* 2003; **9**: 1365-1369
- 28 **Chen TJ**, Chou LF, Hwang SJ. Utilization of hepatoprotectants within the National Health Insurance in Taiwan. *J Gastroenterol Hepatol* 2003; **18**: 868-872
- 29 Guidelines for ATC Classification and DDD Assignment, 3rd ed. Oslo: *WHO Collaborating Centre for Drug Statistics Methodology* 2000
- 30 Clinical Classifications Software (ICD-9-CM) Summary and Download. Summary and Downloading Information. January 2003. Agency for Health Care Policy and Research, Rockville, MD. Available from: URL: <http://www.ahrq.gov/data/hcup/ccs.htm>

Edited by Wang XL

Expression of *bcl-2* family of genes during resection induced liver regeneration: Comparison between hepatectomized and sham groups

Kamil Can Akcali, Aydin Dalgic, Ahmet Ucar, Khemaais Ben Haj, Dilek Guvenc

Kamil Can Akcali, Ahmet Ucar, Khemaais Ben Haj, Department of Molecular Biology and Genetics, Bilkent University, Ankara, Turkey, 06800

Dilek Guvenc, Department of Mathematics, Bilkent University, Ankara, Turkey, 06800

Aydin Dalgic, Department of Surgery, Gazi University Medical School, Ankara, Turkey, 06510

Supported by Bilkent University Faculty Development Grant and Bilkent University Research Grant

Correspondence to: Dr. Kamil Can Akcali, Department of Molecular Biology and Genetics, Bilkent University, Bilkent, Ankara, Turkey, 06800. akcali@fen.bilkent.edu.tr

Telephone: +90-312-2902418 **Fax:** +90-312-2665097

Received: 2003-09-06 **Accepted:** 2003-10-12

Abstract

AIM: During liver regeneration cellular proliferation and apoptosis result in tissue remodeling to restore normal hepatic mass and structure. Main regulators of the apoptotic machinery are the Bcl-2 family proteins but their roles are not well defined throughout the liver regeneration. We aimed to analyze the expression levels of *bcl-2* gene family members during resection induced liver regeneration.

METHODS: We performed semi-quantitative RT-PCR to examine the expression level of *bak*, *bax*, *bcl-2* and *bcl-x_L* in the 70% hepatectomized rat livers during the whole regeneration process and compared to that of the sham and normal groups.

RESULTS: The expression of *bak* and *bax* were decreased whereas *bcl-2* and *bcl-x_L* were increased in hepatectomized animals compared to normal liver at most time points. We also reported for the first time that sham group of animals had statistically significant higher expression of *bak* and *bax* compared to hepatectomized animals. In addition, the area under the curve (AUC) values of these genes were more in sham groups than the hepatectomized groups.

CONCLUSION: We conclude that the expressional changes of *bak*, *bax*, *bcl-2* and *bcl-x_L* genes were altered not only due to regeneration, but also due to the effects of surgical operations.

Akcali KC, Dalgic A, Ucar A, Ben Haj K, Guvenc D. Expression of *bcl-2* family of genes during resection induced liver regeneration: Comparison between hepatectomized and sham groups. *World J Gastroenterol* 2004; 10(2): 279-283

<http://www.wjgnet.com/1007-9327/10/279.asp>

INTRODUCTION

Liver regeneration is a complex physiological response that takes place after the loss of hepatocytes caused by toxic or

viral injury or secondary to liver resection^[1,2]. During regeneration, series of reactions take place to maintain the homeostasis and virtually all of the surviving hepatocytes undergo mitosis^[3]. Experimentally partial hepatectomy (PH) has been a useful model to study the cellular mechanisms of hepatic regeneration.

Post-hepatectomy-induced proliferative response led to full restoration of the hepatic mass in rats in 14 days^[4,5]. Several converging lines of evidence from recent works have established that growth factors and cytokines including hepatocyte growth factor (HGF), tumor necrosis factor- α (TNF- α), interleukin-6 (IL-6), epidermal growth factor (EGF), transforming growth factor- α (TGF- α), fibroblast growth factor (FGF), vascular endothelial growth factor (VEGF), transforming growth factor- β 1 (TGF- β 1) and hormones such as insulin, glucagon, sex hormones, thyroid hormone, norepinephrine, nitric oxide and vasopressin are important components of liver regeneration^[5-9]. Multiple signaling pathways are then activated by these components^[10,11].

During liver regeneration, apoptosis occurs as a response to eliminate the defective cells that appear due to rapid cellular divisions after PH, resulting in fine-tuning of the liver size and tissue remodeling^[5,12-14]. Therefore, control of apoptosis plays a crucial role in liver regeneration. Among the regulators of apoptosis, the Bcl-2 family of proteins determines the life-or-death of a cell by controlling the releases of mitochondrial apoptogenic factors, cytochrome C and apoptosis inducing factors (AIF), which activate the downstream executional phases, including the activation of the caspases^[15,16]. Bcl-2 family of genes consists of both pro- and anti-apoptotic genes and by forming dimers, they exert their function^[17]. Since Bcl-2 family of proteins is the most important and critical regulators of apoptosis^[18], they should be tightly regulated during regeneration in a time-dependent manner. Existing data suggests the involvement of these proteins in regeneration process during the initial stages of this process^[19-23]. These studies investigated the expression of these genes during the first four days after hepatectomy, however the expression pattern of the Bcl-2 family members were not examined throughout the regeneration process. Therefore, the purpose of the present study was to quantitate the expression levels of some members of *bcl-2* family of genes (*bcl-2*, *bcl-x_L*, *bax*, *bak*) by using semi-quantitative RT-PCR within a time spectrum that extended to 14 days after hepatectomy, which was needed for the completion of the regeneration process. We also compared the expression levels of these genes with the levels of the corresponding sham group of animals. For this purpose, we used the "area under the curve" method as used in pharmacodynamic studies and other liver injury and stress models.

MATERIALS AND METHODS

Animals

Nine weeks old and 200-250 grams male Sprague-Dawley rats were used. They were housed under controlled environmental

conditions (22 °C) with a 12-hour light and 12 hour dark cycle in the animal holding facility of Bilkent University, Turkey. All the animals received care according to the criteria outlined in the "Guide for Care and Use of Laboratory Animals" prepared by the National Academy of Science and this study protocol complied with Bilkent University's guidelines on humane care and use of laboratory animals.

Experimental groups, partial hepatectomy and sham groups

Three randomly selected three animals were used for each time point. After injecting Ketamine (Ketalar, Park Davis) subcutaneously at a dose of 30 mg/kg, liver resections consisting of 70% of the liver mass were performed in PH group^[24]. Sham group of animals underwent the same per operative anesthesia with the PH group. All the surgical operations were done the same as PH, but the liver lobes were not resected. All the operations were performed between 8:00 AM and 12:00 PM to minimize diurnal effects. After the completion of the procedure, the animals were placed under a lamp to prevent the hypothermy and then put into cages (one animal per cage) with continuous supply of food and water. The animals in the PH and corresponding sham groups were sacrificed at 0.5, 2, 8, 18, 36 hours, 3 days, 7 days and 14 days after the operation. The group of animals in which no surgery was performed, as used as normal liver group and mentioned time "0" in quantitated graphs. After sacrificing the animal by cervical dislocation, the remnant liver lobes were excised and washed in DMEM medium, then immediately frozen in liquid nitrogen.

Total RNA isolation and reverse transcription

The RNAs were isolated from all the liver samples using Tripure solution (Roche- Boehringer, Mannheim) according to the manufacturer's protocol. The integrity of the isolated RNA samples was determined by denaturing- (formaldehyde-) agarose gel electrophoresis. The cDNA samples were synthesized from the total RNA samples with the RevertAid First Strand cDNA Synthesis Kit (MBI Fermentas) by using the manufacturer's protocol.

Primer design and semi-quantitative PCR

We designed primers for *bcl-2*, *bcl-x_L* and *bax* by using the cDNA sequences of rat homologues of these genes (GenBank accession numbers of rat homologues of *bcl-2* is NM_016993, *bcl-x_L* is U34963, and *bax* is S76511). In the case of *bak*, the cDNA sequences of mouse (Y13231) and human (U23765) were aligned by Blast (NCBI), and primers were chosen from the longest conserved regions by selecting the mouse sequences in the regions of mismatches. As a housekeeping gene, we used *cyclophilin*, and primers were designed by using the rat cDNA sequence (GenBank accession number: M19533). The primer pairs used for each gene were as follows: *cyclophilin*: GGAAGGTGAAAGAAGGCAT and GAGAGCAGAG ATTACAGGGT; *bcl-2*: CCTGGCATCTTCTCCTTC and TGCTGACCTCACTTGTGG; *bcl-x_L*: TCAATGGCAACC CTTCTG and ATCCGACTACCAATACCTG; *bax*: ACGCATCCACCAAGAAGC and GAAGTCCAGAGTC CAGCC; *bak*: CCGGAATTCCAGGACACAGAGGA and CCAAGCTTGCCCAACAGAACCAC.

In all the reactions, the negative control group was done by using ddH₂O instead of cDNA. For each gene, we determined the cycle number of PCR reactions in which the PCR reaction was not saturated. Based on this, we used the following PCR conditions: The initial denaturation step was at 95 °C, followed by 18 (*cyclophilin*), 33 (*bcl-2*), 37 (*bcl-x_L*), 28 (*bax*), 29 (*bak*) cycles of denaturation for 30 seconds at 95 °C, annealing for 30 seconds at either 55 °C (*cyclophilin*, *bcl-2*, *bak*) or 52 °C

(*bcl-x_L*), or 60 °C (*bax*), and extension for 30 seconds at 72 °C. A final extension at 72 °C for 10 minutes was applied to all the reactions and the PCR products were electrophoresed on a 1.2% agarose gel. Each PCR reaction was replicated three times. The quantitated values for the expression of *bcl-2* family members were normalized with the quantitated values for the *cyclophilin* for each sample respectively by comparing with the expression level of *cyclophilin* in normal liver. The normalized values were then analyzed using Multi-Analyst software and the graphs were drawn.

Calculation of AUC

Area under the curve (AUC) calculations was performed as shown by Tygstrup *et al*^[25]. Results of the expression levels of the *bcl-2* family genes by RT-PCR are given as mean ± SEM. As a measure of the change in expression level during the experimental period, the area of the expression level/time curve (AUC: cDNA level x time) was calculated as the sum of the area of the intervals between the samplings for PH and sham groups. Since the time intervals were different, in order to standardize the calculations, we used hour as the unit of X-axis i.e. between 7 days and 14 days, we multiplied with 168 (24x7) to calculate the area under the curve. To determine the hourly changes at the AUC, we divided the AUC values by the hour difference between each two-time points; i.e. between 2 and 8 hour groups, AUC value was calculated and divided by 6.

Statistical tests

For each group of three animals the mean expression level was calculated at the given time points. The means of PH and sham groups were compared using Mann-Whitney test. Since sham group animals seemed to have higher levels of expression of these genes than the hepatectomized animals, one-sided significance level (*P* value) of 0.05 was used. The null hypothesis of no difference between the expression of *bax*, *bak*, *bcl-2*, and *bcl-x_L* in PH and sham groups was tested versus the research hypothesis that PH group had lower level of expression than the sham group.

RESULTS

Since the transcriptional control of *bcl-2* gene family has been known to be important, we performed semi-quantitative RT-PCR to examine the changes in the expression levels of the transcripts of *bcl-2*, *bcl-x_L*, *bax* and *bak* in the livers of rats that were subjected to either 70% PH, or sham operation at different time points (Figures 1-4). In all the experiments, the expression at "time 0" was the quantitated expression of each gene in normal livers and accepted as "1" in order to make a comparison with the subsequent time groups.

Expression pattern of pro-apoptotic genes

Two hours after hepatectomy, in 70% PH groups, we observed that the transcript level of *bak* was decreased by twofold compared with that in normal liver (Figure 1, "time 0"). Although *bak* expression levels reached the levels observed in normal liver at 8 hours and 7 days, *bak* was expressed less in comparison with that in the normal liver at other time points (Figure 1, solid circles). On the other hand, in sham group of animals, the expression of *bak* mRNA was higher than that in the normal liver and hepatectomized group at every time point (Figure 1, open circles). The expression of *bak* was significantly higher in sham group than in PH group (*P*<0.001).

Another pro-apoptotic gene, *bax* mRNA expression, like *bak*, was increased at 0.5 hour after hepatectomy and then decreased to below the level in normal liver by 2 hours (Figure 2, solid circles). During the 14-day period except the increase

at 8 hours after hepatectomy, *bax* expression showed a steady pattern and by 14 days after hepatectomy, it reached almost the expression level of the normal liver (Figure 2, solid circles). The expression of *bax* in sham group did not show any sharp changes and unlike *bak*, it remained close to the levels of normal liver by 14 days (Figure 2, open circles). The test results revealed that the expression of *bax* was significantly higher in sham group than in PH group ($P < 0.05$).

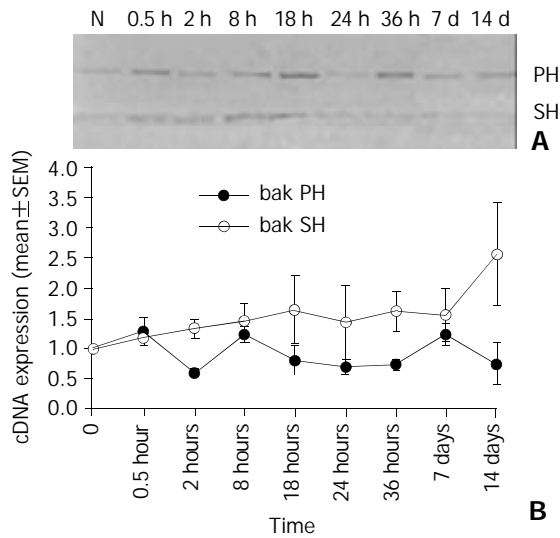


Figure 1 A: The expression of *bak* in 70% hepatectomized (PH) and sham (SH) groups shown in 1.2% agarose gel. B: The quantitated expression of *bak* in 70% PH (—●—) or sham (—○—) groups. Results were expressed as mean \pm SEM of triplicate animals with $n=3$ rats per time point. The expressions were quantitated with the expression of *cyclophilin* for each sample and analyzed using the Multi-Analyst software. The expression at “time 0” denoted the quantitated expression of *bak* in normal liver and was accepted as “1”. In comparison among the mean values at each time point, it was revealed that the means for *bak* in PH group were significantly less than those in SH group ($P < 0.001$ Mann Whitney U test).

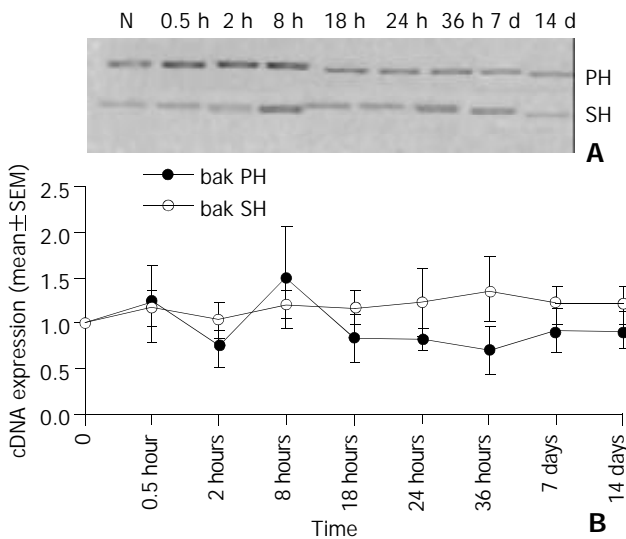


Figure 2 A: The expression of *bax* in 70% hepatectomized (PH) and sham (SH) groups shown in 1.2% agarose gel. B: The quantitated expression of *bax* in 70% PH (—●—) or sham (—○—) groups. Results were expressed as mean \pm SEM of triplicate animals with $n=3$ rats per time point. The expressions were quantitated with the expression of *cyclophilin* for each sample and analyzed using the Multi-Analyst software. The expression at “time 0” denoted the quantitated expression of *bax* in normal liver and was accepted as “1”. In comparison among the mean values at

each time point, it was revealed that the *bax* values in PH group were less than those in SH group (one-tailed $P < 0.05$, Mann Whitney U test).

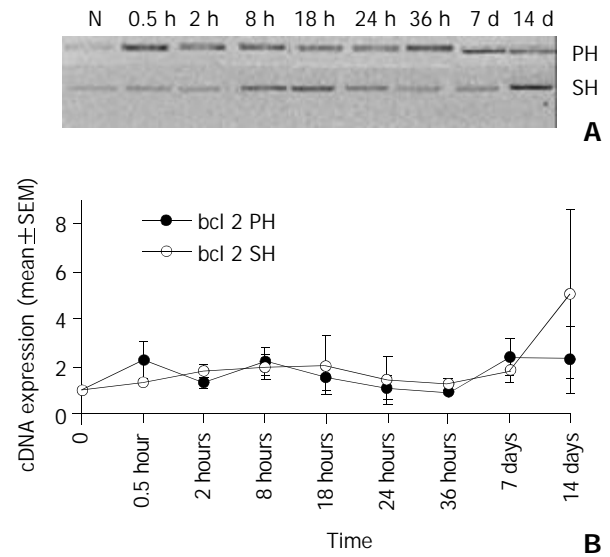


Figure 3 A: The expression of *bcl-2* in 70% hepatectomized (PH) and sham (SH) groups shown in 1.2% agarose gel. B: The quantitated expression of *bcl-2* in 70% PH (—●—) or sham (—○—) groups. Results were expressed as mean \pm SEM of triplicate animals with $n=3$ rats per time point. The expressions were quantitated with the expression of *cyclophilin* for each sample and analyzed using the Multi-Analyst software. The expression at “time 0” denoted the quantitated expression of *bcl-2* in normal liver and was accepted as “1”. Comparing the mean values at each time point, we found no difference in *bcl-2* values between PH and SH group.

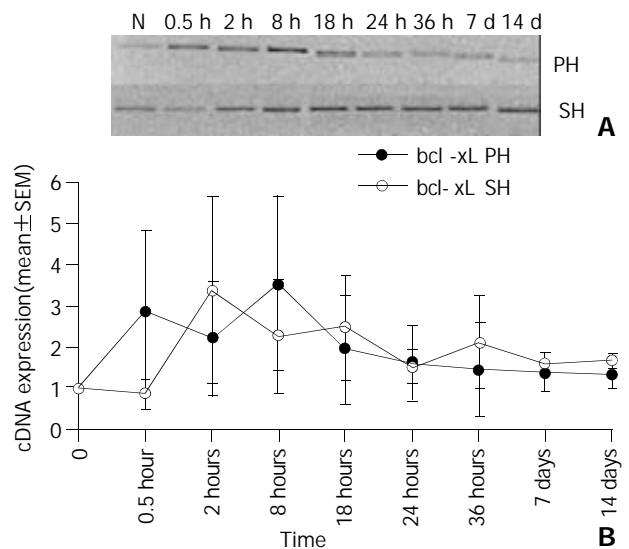


Figure 4 A: The expression of *bcl-x_L* in 70% hepatectomized (PH) and sham (SH) groups shown in 1.2% agarose gel. B: The quantitated expression of *bcl-x_L* in 70% PH (—●—) or sham (—○—) groups. Results were expressed as mean \pm SEM of triplicate animals with $n=3$ rats per time point. The expressions were quantitated with the expression of *cyclophilin* for each sample and analyzed using the Multi-Analyst software. The expression at “time 0” denoted the quantitated expression of *bcl-x_L* in normal liver and was accepted as “1”. Comparing the mean values at each time points, no difference in *bcl-x_L* values between PH and SH groups was found.

Expression pattern of anti-apoptotic genes

Amongst the anti-apoptotic members of *bcl-2* gene family, *bcl-*

2 mRNA expression did not decrease to below the level in normal liver both in PH and sham groups. Its level was increased 0.5 hour after hepatectomy and peaked at 8 hours and 7 days after hepatectomy, more than 2-fold that of the normal liver (Figure 3, solid circles). In the sham group of animals, the expression of this gene also increased by 0.5 hour after surgery and then followed a steady level until day 14. The expression of *bcl-2* in PH and sham group showed a similar pattern except at 14 day. At this time point, *bcl-2* expression was more than two-fold in sham group compared to PH group (Figure 3, open circles).

The expression of another anti-apoptotic gene *bcl-x_L* showed more than 3-fold increase by 8 hours after hepatectomy whereas at the same time interval, the sham group had almost two-fold increase compared to normal liver. The amount of *bcl-x_L* expression decreased afterwards both in PH and sham group (Figure 4). However, in both groups, the expression level was always above the levels in normal liver at all time points.

AUC calculation

In order to better compare the expression levels of *bak*, *bax*, *bcl-2* and *bcl-x_L* during the whole regeneration process, we calculated the AUC values for partially hepatectomized and sham groups, i.e.; the area between the lines connecting cDNA levels of different time and zero. It is important to emphasize that AUC is an arbitrary value but provides a comparison between the total expression of these genes in PH and sham groups. The AUC values for PH and sham groups for each gene analyzed are shown in Table 1. AUC values of all the genes were higher in sham group compared with those in the PH group. Interestingly however, the difference was more obvious for pro-apoptotic genes (*bak* and *bax*) than for anti-apoptotic genes (*bcl-2* and *bcl-x_L*). We detected an 87% and 64% increase in expression levels of pro-apoptotic genes (*bak* and *bax* respectively) in sham group compared to PH group, whereas, this difference was 25% in *bcl-2* and 21% in *bcl-x_L*.

Since the time intervals ranged from 0.5 hour to 7 days, we calculated hourly changes of AUC values in our experiments for each of *bcl-2* family of genes in hepatectomized and sham group of animals. We measured AUC value for each time group and divided this value by the hours of that particular group (Table 2). The values for *bak* and *bax* were found to be significantly higher in sham group than in hepatectomized group ($P < 0.05$). No significant difference was found for *bcl-2* and *bcl-x_L* values.

Table 1 AUC of cDNA expression for members of the *bcl-2* family of genes

	AUC (70% PH)	AUC (SH)	Change
<i>bak</i>	324	609	87%
<i>bax</i>	245	402	64%
<i>bcl-2</i>	666	837	25%
<i>bcl-x_L</i>	494	601	21%

Table 2 Hourly changes of AUC values for the members of the *bcl-2* family of genes

	<i>bak</i> PH ^a	<i>bak</i> SH ^a	<i>bax</i> PH ^a	<i>bax</i> SH ^a	<i>bcl-2</i> PH	<i>bcl-2</i> SH	<i>bcl-x_L</i> PH	<i>bcl-x_L</i> SH
0.5-2 h	0.94	1.25	1.12	2.36	1.81	1.56	2.53	2.13
2-8 h	0.91	1.37	0.8	1.12	1.76	1.88	2.86	2.82
8-18 h	1.01	1.5	1.15	1.19	1.86	2	2.73	2.36
18-24 h	0.75	1.53	0.8	1.19	1.33	1.73	1.78	1.99
24-36 h	0.7	1.52	0.75	1.03	1	1.28	1.53	1.82
36-168 h	0.97	1.58	0.45	1.29	1.65	1.53	1.41	1.87
168-33 6h	0.98	2.1	0.9	1.2	2.35	3.42	1.37	1.64

^a $P < 0.05$ vs the expression of *bak* and *bax* was significantly higher in sham group than that in the hepatectomized group.

DISCUSSION

During liver regeneration, apoptosis allows hepatocytes to die without provoking a potentially harmful inflammatory response. The harmony amongst these complex biological responses is crucial since abnormal regeneration may result in fulminant liver failure, cirrhosis and primary liver cancers^[26]. Since programmed cell death is a major component of hepatic regeneration mechanism, and the *bcl-2* family members are the main regulators of this cellular death pathway, we concentrated on the expression level of these genes throughout the regeneration of liver induced by partial hepatectomy. For all of the members of this family, it has been shown that the transcriptional activation or suppression is critical^[27,28]. Existing data in literature suggests the involvement of these genes in regeneration process however, the expression of these genes has been shown for only 4 days after hepatectomy^[19-23]. Liver regeneration is a long lasting event but there have been no studies regarding the expression of these genes during the later stages of liver regeneration. Since apoptosis is a homeostatic mechanism, the expression of the genes that regulate apoptosis should be important during the whole regeneration process. Therefore, in this study, we quantitated the expression levels of *bak*, *bax*, *bcl-2* and *bcl-x_L* up to 14 days post-hepatectomy, which is the time needed for the completion of regeneration process. In addition, we also examined the expression of these genes in corresponding sham group of animals.

Our data regarding the expression of *bak*, *bax* and *bcl-x_L* during early stages of regeneration (within the first four days) were consistent with previous studies^[19-23]. However contradictory data have been published about the expression of *bcl-2* in normal liver prior to hepatectomy. It has been reported that by using Northern blot Tzung *et al*^[29] did not find any *bcl-2* expression, whereas Kren *et al*^[21] did. Similar to our results Masson *et al*^[22] also found a basal expression of *bcl-2* by using RT-PCR. Since the source of *bcl-2* is non-parenchymal cells, a more sensitive method such as RT-PCR is a better choice of analyzing its expression.

According to our results, the expression levels of *bax* and *bak* in PH group were lower than those in the normal liver except 0.5 and 8 hours after 70% hepatectomy. On the other hand, the anti-apoptotic genes, *bcl-2* and *bcl-x_L* had higher expression levels than those in the normal liver at most of the time points. Amongst them, the expression of *bcl-x_L* in hepatectomized animals was higher than that of normal liver at all the time points. We observed an overall decrease in the pro-apoptotic genes (*bax* and *bak*) and an increase in the anti-apoptotic genes (*bcl-2* and *bcl-x_L*) expression compared to that in normal liver. Recently, Locker *et al* has also shown increased antiapoptotic regulators and down-regulated proapoptotic regulators by using microarray technology during liver regeneration in mouse^[30]. Thus, the increase in the ratio of anti- vs. pro-apoptotic gene expression was in favor of survival of the liver tissue throughout the regeneration process.

In our study, we also compared the total expression of these

genes between sham and partially hepatectomized groups by calculating AUC as used by Tygstrup *et al*^[25]. In their study AUC calculation was used to show and compare the mRNA profiles of a set of liver function related and repair related genes in different liver injury and stress models. By comparing AUC values, they have shown that the expressions of several genes related to liver function were reduced^[25]. By calculating AUC values, we found an interesting phenomenon that had not been reported in previous studies. The AUC values of all the *bcl-2* family of genes were higher in sham group than that of PH group, suggesting the overall expression levels of apoptotic regulator genes in sham group were increased more than those in the hepatectomized group. Since the sham group of animals had undergone the same period of anesthesia and were sacrificed at the same time, the effect of circadian rhythms on the expression of these genes could be ruled out. In addition, when we measured the hourly changes of the expression of these genes, we found an increase in all the genes that we studied in the sham group compared to PH group except for the first 18 hours in *bcl-x_L*. The increase in the case of *bak* and *bax* were statistically significant. This indicated that the expressions of *bak* and *bax* were up regulated in sham group compared to those in hepatectomized group. Therefore, many of the previous findings of expressional changes in transcript levels of *bcl-2*, *bcl-x_L*, *bax* and *bak* might be due to not only regeneration, but also the effects of surgical operations.

The reduction in the expression of proapoptotic *bak* and *bax* in PH group compared to sham group may be related to the enhanced effects of some growth factors on liver proliferation to prevent apoptosis and to ensure the survival of the tissue. It has also been reported that the majority of the rats that had undergone PH, later developed tumors in their remnant liver^[31]. Therefore it is tempting to speculate that decreased expression of proapoptotic genes might be responsible for this outcome. However, the cause for the reduction in the expression of anti-apoptotic *bcl-2* family of genes in PH group compared to sham group has been unclear. In the case of *bcl-2*, since it is expressed exclusively by non-parenchymal cells and especially cholangiocytes, removal of a large portion of the liver might be the explanation for this reduction. Thus, it could be speculated that upon removal of a large portion of the tissue, the liver conferred priority to the expression of vitally most important genes.

REFERENCES

- 1 **Sell S.** Is there a liver stem cell? *Cancer Res* 1990; **50**: 3811-3815
- 2 **Fausto N.** Hepatology- A Textbook of Liver Disease, 2nd ed., Philadelphia: Saunders 1990: 49-64
- 3 **Fausto N,** Webber EM. Liver Regeneration In: Arias IM, Boyer JL, Fausto N, Jakoby WB, Schachter DA, Shafritz DA, eds. The Liver: Biology and Pathobiology. New York: Raven 1994: 1059-1084
- 4 **Fausto N,** Thomson NL, Braun L. Cell separation: Methods and selected applications. Orlando: Academic Press 1986: 45-75
- 5 **Fausto N.** Liver regeneration. *J Hepatol* 2000; **32**(1 Suppl): 19-31
- 6 **Bucher NLR.** Liver regeneration then and now In: Jirtle RL, ed. Liver regeneration and carcinogenesis, Molecular and Cellular Mechanisms. San Diego: Academic Press 1995: 1-25
- 7 **Michalopoulos G,** Defrances M. Liver regeneration. *Science* 1997; **276**: 60-66
- 8 **Xia M,** Xue SB, Xu CS. Shedding of TNFR1 in regenerative liver can be induced with TNF alpha and PMA. *World J Gastroenterol* 2002; **8**: 1129-1133
- 9 **Li YC,** Xu CS, Zhu WL, Li WQ. Isolation and analysis of a novel gene over-expressed during liver regeneration. *World J Gastroenterol* 2003; **9**: 1282-1286
- 10 **Brenner DA.** Signal transduction during liver regeneration. *J Gastroenterol Hepatol* 1998; **13**: S93-95
- 11 **Stolz DB,** Mars WM, Petersen BE, Kim TH, Michalopoulos GK. Growth factor signal transduction immediately after two-thirds partial hepatectomy in the rat. *Cancer Res* 1999; **59**: 3954-3960
- 12 **Fan G,** Kren BT, Steer CJ. Regulation of apoptosis associated genes in the regenerating liver. *Semin Liver Dis* 1998; **18**: 123-140
- 13 **Kren BT,** Trembley JH, Fan G, Steer CJ. Molecular regulation of liver regeneration. *Ann N Y Acad Sci* 1997; **831**: 361-381
- 14 **Sakamoto T,** Liu Z, Murase N, Ezure T, Yokomuro S, Poli V, Demetris AJ. Mitosis and apoptosis in the liver of interleukin-6-deficient mice after partial hepatectomy. *Hepatology* 1999; **29**: 403-411
- 15 **Martinou JC,** Green DR. Breaking the mitochondrial barrier. *Nat Rev Mol Cell Biol* 2001; **2**: 63-67
- 16 **Zamzami N,** Kroemer G. The mitochondrion in apoptosis: how Pandora's box opens. *Nat Rev Mol Cell Biol* 2001; **2**: 67-71
- 17 **Adams JM,** Cory S. The Bcl-2 protein family: Arbiters of cell survival. *Science* 1998; **281**: 1322-1326
- 18 **Cory S,** Adams JM. The Bcl-2 family: regulators of the cellular life-or-death switch. *Nat Rev Cancer* 2002; **2**: 647-656
- 19 **Kamimukai N,** Togo S, Hasegawa S, Kubota T, Kurosawa H, Li XK, Suzuki S, Shimada H. Expression of Bcl-2 family reduces apoptotic hepatocytes after excessive hepatectomy. *Eur Surg Res* 2001; **33**: 8-15
- 20 **Taira K,** Hiroyasu S, Shiraishi M, Muto Y, Koji T. Role of the Fas system in liver regeneration after a partial hepatectomy in rats. *Eur Surg Res* 2001; **33**: 334-341
- 21 **Kren BT,** Trembley JH, Krajewski J, Behren TW, Reed JC, Steer CJ. Modulation of apoptosis-associated genes *bcl-2*, *bcl-x*, and *bax* during rat liver regeneration. *Cell Growth Differ* 1996; **7**: 1633-1642
- 22 **Masson S,** Scotte M, Garnier S, Francois A, Hiron M, Teniere P, Fallu J, Salier JP, Daveau M. Differential expression of apoptosis-associated genes post-hepatectomy in cirrhotic vs normal rats. *Apoptosis* 2000; **5**: 173-179
- 23 **Karavias DD,** Tsamandas AC, Tepetes K, Kritikos N, Kourelis T, Ravazoula P, Vagenas K, Siasos N, Mirra N, Bonikos DS. BCL-2 and BAX expression and cell proliferation, after partial hepatectomy with and without ischemia, on cholestatic liver in rats: an experimental study. *J Surg Res* 2003; **110**: 399-408
- 24 **Wang X,** Parsson H, Anderson R, Soltesz V, Johansson K, Bengmark S. Bacterial translocation, intestinal ultrastructure and cell membrane permeability early after major liver resection in the rat. *Br J Surg* 1994; **81**: 579-584
- 25 **Tygstrup N,** Bangert K, Ott P, Bisgaard HC. Messenger RNA profiles in liver injury and stress: A comparison of lethal and nonlethal rat models. *Biochem Biophys Res Comm* 2002; **290**: 518-525
- 26 **Diehl AM.** Liver generation. *Front Biosci* 2002; **7**: e301-314
- 27 **Gross A,** McDonnell JM, Korsmeyer SJ. Bcl-2 family members and the mitochondria in apoptosis. *Genes Dev* 1999; **13**: 1899-1911
- 28 **Tsujimoto Y,** Shimizu S. Bcl-2 family: Life-or-death switch. *FEBS Lett* 2000; **466**: 6-10
- 29 **Tzung SP,** Fausto N, Hockenberry DM. Expression of Bcl-2 family during liver regeneration and identification of *bcl-x* as a delayed early response gene. *Am J Pathol* 1997; **150**: 1985-1995
- 30 **Locker J,** Tian J, Carver R, Concas D, Cossu C, Ledda-Columbano GM, Columbano A. A common set of immediate-early response genes in liver regeneration and hyperplasia. *Hepatology* 2003; **38**: 314-325
- 31 **Picardo A,** Karpoff HM, Ng B, Lee J, Brennan MF, Fong Y. Partial hepatectomy accelerates local tumor growth: potential roles of local cytokine activation. *Surgery* 1998; **124**: 57-64

Complications of stent placement for benign stricture of gastrointestinal tract

Ying-Sheng Cheng, Ming-Hua Li, Wei-Xiong Chen, Ni-Wei Chen, Qi-Xin Zhuang, Ke-Zhong Shang

Ying-Sheng Cheng, Ming-Hua Li, Qi-Xin Zhuang, Ke-Zhong Shang, Department of Radiology, Sixth People's Hospital, Shanghai Jiaotong University, Shanghai 200233, China

Wei-Xiong Chen, Ni-Wei Chen, Department of Gastroenterology, Sixth People's Hospital, Shanghai Jiaotong University, Shanghai 200233, China

Supported by the National Key Medical Research and Development Program of China during the 9th Five-year Plan Period, No.96-907-03-04; Shanghai Nature Science Funds, No.02Z1314073; Shanghai Medical Development Funds, No.00419

Correspondence to: Dr. Ying-Sheng Cheng, Department of Radiology, Sixth People's Hospital, Shanghai Jiaotong University, Shanghai 200233, China. chengys@sh163.net

Telephone: +86-21-64368920 **Fax:** +86-21-64701361

Received: 2003-05-13 **Accepted:** 2003-06-02

Abstract

AIM: To observe the frequent complications of stent placement for stricture of the gastrointestinal tract and to find proper treatment.

METHODS: A total number of 140 stents were inserted in 138 patients with benign stricture of the gastrointestinal tract. The procedure was completed under fluoroscopy in all of the patients.

RESULTS: Stents were successfully placed in all the 138 patients. Pains occurred in 23 patients (16.7%), slight or dull pains were found in 21 patients and severe chest pain in 2 respectively. For the former type of pain, the patients received only analgesia or even no treatment, while peridural anesthetics was conducted for the latter condition. Reflux occurred in 16 of these patients (11.6%) after stent placement. It was managed by common antireflux procedures. Gastrointestinal bleeding occurred in 13 patients (9.4%), and was treated by hemostat. Restenosis of the gastrointestinal tract occurred in 8 patients (5.8%), and was apparently associated with hyperplasia of granulation tissue. In 2 patients, the second stent was placed under X-ray guidance. The granulation tissue was removed by cauterization through hot-node therapy under gastroscopie guidance in 3 patients, and surgical reconstruction was performed in another 3 patients. Stent migration occurred in 5 patients (3.6%), and were extracted with the aid of a gastroscopie. Food-bolus obstruction was encountered in 2 patients (1.4%) and was treated by endoscope removal. No perforation occurred in all patients.

CONCLUSION: Frequent complications after stent placement for benign stricture of the gastrointestinal tract include pain, reflux, bleeding, restenosis, stent migration and food-bolus obstruction. They can be treated by drugs, the second stent placement or gastroscopic procedures depend on the specific condition.

Cheng YS, Li MH, Chen WX, Chen NW, Zhuang QX, Shang KZ. Complications of stent placement for benign stricture of gastrointestinal tract. *World J Gastroenterol* 2004; 10(2): 284-286 <http://www.wjgnet.com/1007-9327/10/284.asp>

INTRODUCTION

Stricture of the gastrointestinal tract is a common complication associated with various diseases of the gastrointestinal tract. Previously, such conditions were treated surgically in most patients. Operational difficulties and increased expense have limited its application. The recently established non-vascular stent technology could provide a new approach for such patients^[1]. The procedure has been proved to be effective, but it has various complications^[2-5]. Since 1994, we have placed gastrointestinal stents for benign stricture in 138 patients. Various complications were encountered and treated effectively.

MATERIALS AND METHODS

Materials

Our cohort comprised 138 patients (81 males, 57 females; ages, 18 to 82 years, mean 53.6 years) with benign stricture of gastrointestinal tract. All patients were examined by endoscopy or gastrointestinal barium radiography. Among the 138 patients, 8 had simple sclerosis stricture after radiation therapy for esophageal carcinoma, 86 had achalasia, 36 had esophageal and esophago-gastric anastomosis stricture (complicated with anastomosis fistula in 2), 4 had gastro-duodenal anastomosis stricture, and 4 had esophageal chemical corrosive stricture. All the patients had dysphagia, frequent vomiting, and/or dysphoria before stent placement. The follow-up lasted for 1 week to 8 years.

Methods

Stents were placed in all of the 138 patients under X-ray guidance. For the patients with serious stricture, a probe or saccule was used repeatedly to expand the lesion before stent placement. A total of 140 stents were placed, with two stents at the same site in 2 patients.

RESULTS

Various complications encountered are listed in Table 1.

Table 1 Complications of stent placement for benign stricture of gastrointestinal tract

Type of complication	Patients (n)	Incidence (%)
Pain	23	16.7
Slight or mild	21	15.2
Severe	2	1.5
Reflux	16	11.6
Bleeding	13	9.4
Restonsis	8	5.8
Stent migration	5	3.6
Food-bolus obstruction	2	1.4

Complications were treated according to the specific conditions in each patient. Slight or mild pains (n=21) that did not affect work and rest were not treated (n=12) and that affecting work and rest were treated with analgesics (n=9). For the 2 patients who had severe pain, an analgesic was first

used. This was not effective, peridural anesthesia was conducted and the pain disappeared within 2 days. Sixteen patients had gastro-esophageal or duodenum-gastro biliary regurgitation. Thirteen patients who had gastro-esophageal reflux after stent placement in cardiac achalasia were treated with antacid agent (omeprazole), gastric mucosa protectant (sucralfate) and dynamic medicine (domperidone) for 2 weeks or longer. Administration of medicines was reduced or suspended when symptoms palliated. Thirteen patients exhibited bleeding after stent placement. The bleeding disappeared 2 weeks after venous injection of adrenobazonum. Recurrence of the stricture was observed after stent placement in 8 patients. The second stent was placed in 2 patients under X-ray guidance. Hyperplasia of granulation tissue was cauterized by hot-node therapy in 3 patients under gastroscopie and surgically reconstructed in 3 patients. Stent migration was encountered in 5 patients, and the stent was extracted with the aid of a gastroscopie. Two patients had food-bolus obstruction. It was removed under gastroscopie guidance. No perforation occurred in this series.

DISCUSSION

Complications were frequently encountered after stent placement in benign stricture of gastrointestinal tract^[1-3]. The application of this approach would be hampered if these complications were not well treated. The occurrence of complications was related to the material and structure of stents and skill of the operator. It was also associated with the region and nature of pathological changes and physiques of the patients^[4-6]. However, treatment of the complications remains difficult.

Pain is one of the common complications after stent placement in benign stricture of gastrointestinal tract, and it usually disappears within 2-4 weeks. The causes of pain are diverse. In terms of stent-related reasons, one is the resulted physical expansion, the other is that pain occurs more frequently in patients with severe lesions. Pain is also closely associated with sites of the lesions. The upper part of the esophagus is sensitive to pain, and mucosa erosion occurs more frequently in lower part due to reflux, resulting in a burning sensation. A stent with a diameter of 16 mm was used for patients with serious stricture, stricture at the upper or lower part of the esophagus. This reduced the pain markedly. Severe pain occurred in 2 patients after stent placement. When omeprazole was suspended, a severe chest pain was complained by the patients 3 days later. Treatment with dolantin was not satisfactory, and venous injection of omeprazole and peridural anesthesia were used for 2 days to relieve the pain. In terms of pain after stent placement, the incidence (16.7%) was slightly higher than those reported previously^[7-26]. This may be attributable to the types of lesions and size of the stents. In our series, all patients had benign stricture and large diameter stents were used.

Reflux was mostly associated with pathological changes at the lower part of the esophagus. Expansion by the stents often caused disruption of the lower sphincter of esophagus, resulting in reflux. This problem could cause reflux esophagitis. After stent placement in cardiac achalasia, both reflux and bleeding occurred in three patients and disappeared after treatment with antacid agent, hemostat, and antireflux agent. The incidence of reflux esophagitis (11.6%) in our patients was similar to those previously reported (10-50%). The incidence of bleeding (9.4%) was also similar to those described by other authors^[27-34].

Restenosis of the gastrointestinal tract is a thorny problem after stent placement. Benign restenosis is primarily caused by hyperplasia of granulation tissue, this was particularly true, while uncovered stents were used. We adopted one of the procedures for the restenosis including placement of the second stent, or cauterization through hot-node therapy or surgical reconstruction. However, in some patients covered stents could

not be used for anatomical and pathological reasons, such as the ampullary region (open end of the choledochus) or the descending part of the duodenum. Covered stents could easily cause obstructive jaundice, and uncovered stents were used in such patients. The incidence of restenosis in our series (5.8%) was among the range as reported by other authors (3-20%)^[35-38].

Stent migration was a complication that occurred within one to four weeks in most patients after stent placement in the gastrointestinal tract. In a few patients it occurred 3 months after stent placement. Typically, this occurred most frequently in patients with covered stents. The displaced stents were extracted under gastroscopie guidance. The incidence of stent displacement in our series (3.6%) was in the range as reported previously (0-12.5%)^[39-42].

The incidence of food-bolus obstruction reported in other countries ranged from 7% to 20%^[11], while it was 1.4% in our series. After stent placement, we provided the patients with a fluid or semi-fluid diet at the early stage, a small amount each time and several times a day. Patient compliance with this advice could explain, at least partially, the low incidence of food-bolus obstruction in our series. When this complication occurred, food-bolus could be removed under gastroscopie. Perforation in the gastrointestinal tract was rare^[43-46]. If happened, a second covered stent should be placed or surgery should be conducted immediately.

In patients with malignant pathological changes, stent placement in the gastrointestinal tract was very useful for improving their quality of life. For patients with benign strictures, however, caution was required when placing a stent, especially when it was intended to be permanent. Recoverable stents and biologically degradable stents can be expected to overcome the difficulties and prevent restenosis. This would also reduce the incidence of stent-related complications.

REFERENCES

- 1 **Wong VS**, Garvey CJ, Morris AI. Splitting of the polyethylene coverings as a previously unrecognized complication of oesophageal metallic covered stent (Gianturco-Rosch) inserted for malignant stricture. *Endoscopy* 1998; **30**: 557
- 2 **Boullis NM**, Armstrong WS, Chandler WF, Orringer MB. Epidural abscess: a delayed complication of esophageal stenting for benign stricture. *Ann Thorac Surg* 1999; **68**: 568-570
- 3 **Mayoral W**, Fleischer D, Salcedo J, Roy P, Al-Kawas F, Benjamin S. Nonmalignant obstruction is a common problem with metal stents in the treatment of esophageal cancer. *Gastrointest Endosc* 2000; **51**: 556-559
- 4 **Mauro MA**, Koehler RE, Baron TH. Advances in gastrointestinal intervention: the treatment of gastroduodenal and colorectal obstructions with metallic stents. *Radiology* 2000; **215**: 659-669
- 5 **Wang MQ**, Sze DY, Wang ZP, Wang ZQ, Gao YA, Dake MD. Delayed complications after esophageal stent placement for treatment of malignant esophageal obstructions and esophagorespiratory fistulas. *J Vasc Interv Radiol* 2001; **12**: 465-474
- 6 **Power C**, Rynne M, O'Gorman T, Maguire D, McAnena OJ. An unusual complication following intubation of a benign oesophageal stricture. *Endoscopy* 2001; **33**: 642
- 7 **Rajjman I**, Siddique I, Ajani J, Lynch P. Palliation of malignant dysphagia and fistulae with coated expandable metal stents: experience with 101 patients. *Gastrointest Endosc* 1998; **48**: 172-179
- 8 **Laasch HU**, Nicholson DA, Kay CL, Attwood S, Bancewicz J. The clinical effectiveness of the Gianturco oesophageal stent in malignant oesophageal obstruction. *Clin Radiol* 1998; **53**: 666-672
- 9 **Karras PJ**, Barawi M, Webb B, Michalos A. Squamous cell papillomatosis of esophagus following placement of a self-expanding metal stent. *Dig Dis Sci* 1999; **44**: 457-461
- 10 **Park HS**, Do YS, Suh SW, Choo SW, Lim HK, Kim SH, Shim YM, Park KC, Choo IW. Upper gastrointestinal tract malignant obstruction: initial results of palliation with a flexible covered stent. *Radiology* 1999; **210**: 865-870
- 11 **Pron G**, Common A, Simons M, Ho CS. Interventional radiology

- and the use of metal stents in nonvascular clinical practice: a systematic overview. *J Vasc Interv Radiol* 1999; **10**: 613-628
- 12 **Morgan R**, Adam A. The radiologist's view of expandable metallic stents for malignant esophageal obstruction. *Gastrointest Endosc Clin N Am* 1999; **9**: 431-435
- 13 **Camunez F**, Echenagusia A, Simo G, Turegano F, Vazquez J, Barreiro-Meiro I. Malignant colorectal obstruction treated by means of self-expanding metallic stents: effectiveness before surgery and in palliation. *Radiology* 2000; **216**: 492-497
- 14 **Law WL**, Chu KW, Ho JW, Tung HM, Law SY, Chu KM. Self-expanding metallic stent in the treatment of colonic obstruction caused by advanced malignancies. *Dis Colon Rectum* 2000; **43**: 1522-1527
- 15 **Gomez Herrero H**, Paul Diaz L, Pinto Pabon I, Lobato Fernandez R. Placement of a colonic stent by percutaneous colostomy in a case of malignant stenosis. *Cardiovasc Intervent Radiol* 2001; **24**: 67-69
- 16 **Tominaga K**, Yoshida M, Maetani I, Sakai Y. Expandable metal stent placement in the treatment of a malignant anastomotic stricture of the transverse colon. *Gastrointest Endosc* 2001; **53**: 524-527
- 17 **Maetani I**, Ukita T, Inone H, Yoshida M, Igarashi Y, Sakai Y. Knitted nitinol stent insertion for various intestinal stenoses with a modified delivery system. *Gastrointest Endosc* 2001; **54**: 364-367
- 18 **Mao AW**, Gao ZD, Xu JY, Yang RJ, Xiao XS, Jiang TH, Jiang WJ. Treatment of malignant digestive tract obstruction by combined intraluminal stent installation and intra-arterial drug infusion. *World J Gastroenterol* 2001; **7**: 587-592
- 19 **Adler DG**, Baron TH, Geels W, Morgan DE, Monkemuller KE. Placement of PEG tubes through previously placed self-expanding esophageal metal stents. *Gastrointest Endosc* 2001; **54**: 237-241
- 20 **Razzaq R**, Laasch HU, England R, Marriott A, Martin D. Expandable metal stents for the palliation of malignant gastroduodenal obstruction. *Cardiovasc Intervent Radiol* 2001; **24**: 313-318
- 21 **McGrath JP**, Browne M, Riordan C, Ravi N, Reynolds JV. Expandable metal stents in the palliation of malignant dysphagia and oesophageal-respiratory fistulae. *Ir Med J* 2001; **94**: 270-272
- 22 **Decker P**, Lippler J, Decker D, Hirner A. Use of the Polyflex stent in the palliative therapy of esophageal carcinoma: results in 14 cases and review of the literature. *Surg Endosc* 2001; **15**: 1444-1447
- 23 **Aviv RI**, Shyamalan G, Watkinson A, Tibballs J, Ogunbaye G. Radiological palliation of malignant colonic obstruction. *Clin Radiol* 2002; **57**: 347-351
- 24 **Martinez-Santos C**, Lobato RF, Fradejas JM, Pinto I, Ortega-Deballon P, Moreno-Azcoita M. Self-expandable stent before elective surgery vs emergency surgery for the treatment of malignant colorectal obstructions: comparison of primary anastomosis and morbidity rates. *Dis Colon Rectum* 2002; **45**: 401-406
- 25 **Sanchez W**, Baron TH. Palliative colonic stent placement. *Gastrointest Endosc* 2002; **56**: 735
- 26 **Zhong J**, Wu Y, Xu Z, Liu X, Xu B, Zhai Z. Treatment of medium and late stage esophageal carcinoma with combined endoscopic metal stenting and radiotherapy. *Chin Med J* 2003; **116**: 24-28
- 27 **Keymling M**. Colorectal stenting. *Endoscopy* 2003; **35**: 234-238
- 28 **May A**, Ell C. Palliative treatment of malignant esophagorespiratory fistulas with Gianturco-Z stents. A prospective clinical trial and review of the literature on covered metal stents. *Am J Gastroenterol* 1998; **93**: 532-535
- 29 **Bastos I**, Gomes D, Gregorio C, Baranda J, Gouveia H, Donato A, de Freitas D. An unusual foreign body in the rectum. *Hepatogastroenterology* 1998; **45**: 1587-1588
- 30 **Davies N**, Thomas HG, Eyre-Brook IA. Palliation of dysphagia from inoperable oesophageal carcinoma using Atkinson tubes or self-expanding metal stents. *Ann R Coll Surg Engl* 1998; **80**: 394-397
- 31 **Conio M**, Caroli-Bosc F, Demarquay JF, Sorbi D, Maes B, Delmont J, Dumas R. Self-expanding metal stents in the palliation of neoplasms of the cervical esophagus. *Hepatogastroenterology* 1999; **46**: 272-277
- 32 **Sandha GS**, Marcon NE. Expandable metal stents for benign esophageal obstruction. *Gastrointest Endosc Clin N Am* 1999; **9**: 437-446
- 33 **Paul L**, Pinto I, Gomez H, Fernandez-Lobato R, Moyano E. Metallic stents in the treatment of benign diseases of the colon: preliminary experience in 10 cases. *Radiology* 2002; **223**: 715-722
- 34 **Lee A**, Forbes K. Esophageal stents may interfere with the swallowing reflex: an illustrative case history. *J Pain Symptom Manage* 1998; **16**: 254-258
- 35 **McManus K**, Khan I, McGuigan J. Self-expanding oesophageal stents: strategies for re-intervention. *Endoscopy* 2001; **33**: 601-604
- 36 **Kaneko K**, Ito H, Konishi K, Kurahashi T, Katagiri A, Katayose K, Kitahara T, Ohtsu A, Mitamura K. Implantation of self-expanding metallic stent for patients with malignant stricture after failure of definitive chemoradiotherapy for T3 or T4 esophageal squamous cell carcinomas. *Hepatogastroenterology* 2002; **49**: 699-705
- 37 **Nemoto K**, Takai Y, Ogawa Y, Kakuto Y, Ariga H, Matsushita H, Wada H, Yamada S. Fatal hemorrhage in irradiated esophageal cancer patients. *Acta Oncol* 1998; **37**: 259-262
- 38 **Kennedy C**, Steger A. Fatal hemorrhage in stented esophageal carcinoma: tumor necrosis of the aorta. *Cardiovasc Intervent Radiol* 2001; **24**: 443-444
- 39 **Sen S**, Balaratnam N, Wood LA, Allison MC. Buckling of redundant expansile stent distal to an oesophageal cancer: endoscopic management. *Endoscopy* 1998; **30**: 422-424
- 40 **Von Schonfeld J**. Endoscopic retrieval of a broken and migrated esophageal metal stent. *Z Gastroenterol* 2000; **38**: 795-798
- 41 **De Palma GD**, Iovino P, Catanzano C. Distally migrated esophageal self-expanding metal stents: wait and see or remove? *Gastrointest Endosc* 2001; **53**: 96-98
- 42 **Di Fiore F**, Lecleire S, Antonietti M, Savoye G, Savoye-Collet C, Herve S, Roque I, Hochain P, Ben Soussan E. Spontaneous passage of a dislocated esophageal metal stent: report of two cases. *Endoscopy* 2003; **35**: 223-225
- 43 **Banerjee A**, Rao KS, Nachiappan M. Intrathoracic oesophageal perforations following bougienage: a protocol for management. *Aust N Z J Surg* 1989; **59**: 563-566
- 44 **Pajarinen J**, Ristkari SK, Mokka RE. A report of three cases with an oesophageal perforation treated with a coated self-expanding stent. *Ann Chir Gynaecol* 1999; **88**: 332-334
- 45 **Kim HC**, Han JK, Kim TK, Do KH, Kim HB, Park JH, Choi BI. Duodenal perforation as a delayed complication of placement of an esophageal stent. *J Vasc Interv Radiol* 2000; **11**: 902-904
- 46 **Sarmiento RI**, Lee DW, Wong SK, Chan AC, Chung SC. Mesenteric perforation of an obstructing sigmoid colon tumor after endoluminal stent insertion. *Endoscopy* 2003; **35**: 94

Edited by Wang XL

Long-term outcome of esophageal myotomy for achalasia

Jun-Feng Liu, Jun Zhang, Zi-Qiang Tian, Qi-Zhang Wang, Bao-Qing Li, Fu-Shun Wang, Fu-Min Cao, Yue-Feng Zhang, Yong Li, Zhao Fan, Jian-Jing Han, Hui Liu

Jun-Feng Liu, Zi-Qiang Tian, Qi-Zhang Wang, Bao-Qing Li, Fu-Shun Wang, Fu-Min Cao, Yue-Feng Zhang, Yong Li, Zhao Fan, Jian-Jing Han, Hui Liu, Department of Thoracic Surgery, Fourth Hospital, Hebei Medical University, Shijiazhuang 050011, Hebei Province, China

Jun Zhang, Department of Surgery, Shenzhou City Hospital, Shenzhou 052860, Hebei Province, China

Correspondence to: Jun-Feng Liu, Department of Thoracic Surgery, Fourth Hospital, Hebei Medical University, 12 Jiankang Road, Shijiazhuang 050011, Hebei Province, China. liujf@heinfo.net

Telephone: +86-311-6033941 **Fax:** +86-311-6077634

Received: 2003-06-21 **Accepted:** 2003-07-24

Abstract

AIM: Modified Heller's myotomy is still the first choice for achalasia and the assessment of surgical outcomes is usually made based on the subjective sensation of patients. This study was to objectively assess the long-term outcomes of esophageal myotomy for achalasia using esophageal manometry, 24-hour pH monitoring, esophageal scintigraphy and fiberoptic esophagoscopy.

METHODS: From February 1979 to October 2000, 176 patients with achalasia underwent modified Heller's myotomy, including esophageal myotomy alone in 146 patients, myotomy in combination with Gallone or Dor antireflux procedure in 22 and 8 patients, respectively. Clinical score, pressure of the lower esophageal sphincter (LES), esophageal clearance rate and gastroesophageal reflux were determined before and 1 to 22 years after surgery.

RESULTS: After a median follow-up of 14 years, 84.5% of patients had a good or excellent relief of symptoms, and clinical scores as well as resting pressures of the esophageal body and LES were reduced compared with preoperative values ($P < 0.001$). However, there was no significant difference in DeMeester score between pre- and postoperative patients ($P = 0.51$). Esophageal transit was improved in postoperative patients, but still slower than that in normal controls. The incidence of gastroesophageal reflux in patients who underwent esophageal myotomy alone was 63.6% compared to 27.3% in those who underwent myotomy and antireflux procedure ($P = 0.087$). Three (1.7%) patients were complicated with esophageal cancer after surgery.

CONCLUSION: Esophageal myotomy for achalasia can reduce the resting pressures of the esophageal body and LES and improve esophageal transit and dysphagia. Myotomy in combination with antireflux procedure can prevent gastroesophageal reflux to a certain extent, but further randomized studies should be carried out to demonstrate its efficacy.

Liu JF, Zhang J, Tian ZQ, Wang QZ, Li BQ, Wang FS, Cao FM, Zhang YF, Li Y, Fan Z, Han JJ, Liu H. Long-term outcome of esophageal myotomy for achalasia. *World J Gastroenterol* 2004; 10(1): 287-291

<http://www.wjgnet.com/1007-9327/10/287.asp>

INTRODUCTION

Achalasia is an esophageal motility disorder characterized by failure of lower esophageal sphincter (LES) to relax with swallowing and by the absence of esophageal peristalsis. Up to now, surgical treatment is still the first choice for the disease although dilatation and medication have been reported extensively^[1-5]. Because pathophysiological changes of achalasia could not be rectified by any measures, the treatment usually aims at the reduction of LES pressure in order to increase esophageal transit and relieve dysphagia^[6].

The outcomes of myotomy for achalasia have been assessed usually according to the subjective sensation of patients in other studies^[7], which lack objective criteria. Until now, there have been no reports about the objective evaluation on long-term outcomes of Heller's myotomy for achalasia in a large group of patients in China. The aim of this study was to objectively evaluate the long-term outcomes of Heller's myotomy for achalasia by 24-hour pH monitoring, esophageal manometry, esophageal scintigraphy and esophagoscopy.

MATERIALS AND METHODS

General materials

From February 1979 to October 2000, 176 patients underwent modified Heller's myotomy for achalasia at the Department of Thoracic Surgery, Fourth Hospital, Hebei Medical University. There were 78 men and 98 women, ranging from 8 to 62 years (mean 32.9 years). All patients (100%) had varying extent of dysphagia for a mean of 4.8 years (range 2 months to 37 years) before operation. One hundred and thirteen (64.2%) patients had vomiting, 54 (30.7%) regurgitation at night, 8 (4.5%) chest pain or substernal discomfort and 2 (1.1%) heartburn. Symptoms were evaluated by a clinical scoring system proposed by Eckardt *et al*^[8], in which a sum of the individual scores of three major symptoms including dysphagia, heartburn and chest pain was calculated. Each of these symptoms was graded as followings: 0, absent; 1, occasional; 2 daily; 3, with each meal. Therefore, the highest score was 9.

Pre-operative examination

Before surgery, esophagography was performed for all patients, esophagoscopy (Olympus GIF 100) for 114, esophageal manometry (Synectics Medical, Stockholm, Sweden) for 50, 24-hour esophageal pH monitoring (Synectics Medical, Stockholm, Sweden) for 12, esophageal scintigraphy as previously described^[9] for 12 patients and 12 normal subjects as controls. Existence of gastroesophageal reflux was defined if a DeMeester score was more than 14.72 by 24-hour esophageal pH monitoring.

Surgery

Myotomy was performed from 5 cm above the esophagogastric junction to 1.5 cm distal to the esophagogastric junction for all of the 176 patients. As an antireflux procedure, Gallone operation^[10] was added for 22 patients and Dor operation^[11] for 8 patients. Thus, 146 patients underwent esophageal myotomy only, and 30 patients underwent combined esophageal myotomy and antireflux procedure in the present study.

Follow-up study

Fifty-eight patients were followed up from 1 year to 22 years after surgery, with a median follow-up of 14 years. The patients were inquired for dysphagia, heartburn and chest pain. Clinical scores were calculated according to Eckardt *et al*^[8] and compared with preoperative values. According to the method described by Devaney *et al*^[12], the efficacy of operation was graded as excellent (completely asymptomatic), good (mild symptoms requiring no treatment), fair (symptoms requiring occasional treatment such as dilatation or anti-diarrhea medication), and poor (symptoms requiring regular treatment). Postoperatively, esophageal manometry was performed for 30 patients, 24-hour pH monitoring for 22, esophageal scintigraphy for 42, and esophagoscopy for 15.

Statistical analysis

Data on clinical scores, resting pressures of the esophageal body and LES, and DeMeester scores were expressed as mean±SD, and analysed with Student's *t* test. The incidence of gastroesophageal reflux and esophagitis was assessed with Chi-square test. Statistical analyses were performed using a SPSS 10.0 software package, and the differences were considered as significant if $P < 0.05$.

RESULTS

In the present study, 84.5% (49/58) of patients had a good or excellent relief of dysphagia after a median follow-up of 14 years. Table 1 shows pre- and post-operative clinical scores, resting pressures of the esophageal body and LES, and DeMeester scores. Clinical scores and resting pressures of the esophageal body and LES were significantly reduced after Heller's myotomy ($P < 0.001$). After a long-term follow-up study, both clinical scores and LES pressures still remained lower than preoperative values, but had a trend of elevation

with the lapse of postoperative time (Figures 1 and 2). There were no significant differences in DeMeester score between pre- and post-operative patients ($P = 0.512$). DeMeester scores were above normal value in 33.3% (4/12) of preoperative patients, and in 45.5% (10/22) of postoperative patients ($P = 0.717$). In contrast, esophagitis was detected with esophagoscopy in 21.9% (25/114) of the patients before surgery and in 46.7% (7/15) after surgery ($P = 0.054$). Compared with preoperative patients, the esophageal clearance rate was improved in postoperative patients, but did not reach normal until the fifth minute after swallowing of isotope-labeled semi-liquid food (Table 2).

In group of esophageal myotomy with anti-reflux procedure, clinical scores were similar to those in group of esophageal myotomy alone ($P = 0.27$). Also, there was no significant difference in objective parameters including LES resting pressure and DeMeester score between the 2 groups ($P > 0.05$) (Table 3). Twenty-four-hour esophageal pH monitoring showed that the incidence of gastroesophageal reflux in patients undergoing esophageal myotomy with anti-reflux procedure was 27.3% (3/11) compared to 63.6% (7/11) in those undergoing esophageal myotomy only ($P = 0.087$).

Four patients were found to have varying extents of resumption of esophageal peristalsis by esophageal manometry at 20 months, 7, 15 and 20 years after esophageal myotomy, respectively (Figure 3). Three (1.7%) patients underwent re-operation, of whom 2 underwent myotomy again at 1 year and 4 years after surgery respectively for severe dysphagia due to scar formation around abdominal segment of the esophagus, and the remaining 1 underwent resection of the lower third of the esophagus at the third postoperative year due to repeated bleeding resulted from gastroesophageal reflux. Squamous cell carcinoma occurred in 3 (1.7%) patients at 6, 17 and 18 years after Heller's myotomy, respectively, and esophagectomy was performed for these patients.

Table 1 Objective and subjective parameters from patients with achalasia before and after Heller's myotomy

	Before surgery		After surgery		<i>t</i>	<i>P</i>
	<i>n</i>	mean±SD	<i>n</i>	mean±SD		
Clinical score	176	4.11±0.93	58	1.84±1.26	14.66	0.000
RP of the LES (cm H ₂ O)	50	31.14±10.54	30	18.05±8.90	5.76	0.000
RP of the EB (cm H ₂ O)	50	13.66±5.49	30	4.96±4.86	7.15	0.000
DeMeester score	12	33.87±54.2	22	49.75±73.4	0.663	0.512

RP=resting pressure, EB=esophageal body.

Table 2 Esophageal clearance rates for pre- and post-myotomy patients and normal controls (mean±SD%)

<i>n</i>	Times after isotope labeled semi-liquid meal intaken				
	5 th second	1 st minute	2 nd minute	5 th minute	
Normal controls	12	91.7±1.4	92.5±1.9	92.8±2.1	93.0±2.5
Pre-myotomy pts	12	7.5±2.1 ^a	40.4±28.2 ^a	45.5±30.1 ^a	50.5±35.5 ^a
Post-myotomy pts	42	33.7±8.8 ^b	80.2±19.1 ^c	85.4±12.2 ^c	94.4±5.1

^a $P < 0.01$ vs normal controls and post-myotomy patients, ^b $P < 0.01$ vs normal controls, ^c $P < 0.05$ vs normal controls.

Table 3 Subjective and objective parameters from patients who underwent Heller's myotomy alone and in combination with antireflux procedure

	Heller alone		Heller+antireflux		<i>t</i>	<i>P</i>
	<i>n</i>	mean±SD	<i>n</i>	mean±SD		
Clinical score	47	1.79±1.19	11	2.27±1.62	1.11	0.27
LES RP(cm H ₂ O)	25	18.4±9.80	5	16.6±3.23	0.44	0.66
DeMeester score	11	44.4±38.5	11	55.1±29.3	0.34	0.74

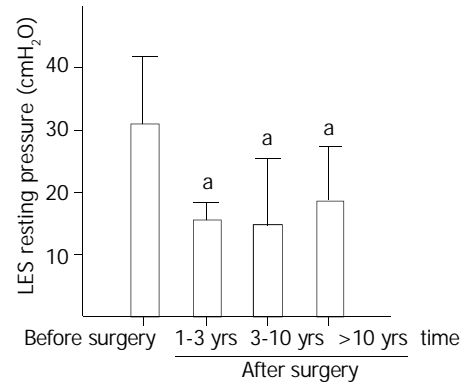
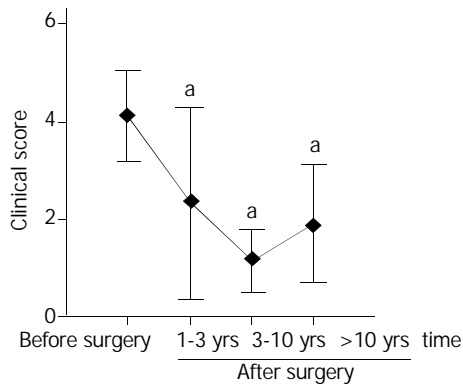


Figure 1 Clinical scores before and at various intervals after Heller's myotomy. Data were expressed as mean±SD. ^a*P*<0.001 vs before surgery.

Figure 2 Lower esophageal sphincter (LES) pressure before and at various times after Heller's myotomy. Data were expressed as mean±SD. ^a*P*<0.001 vs before surgery.

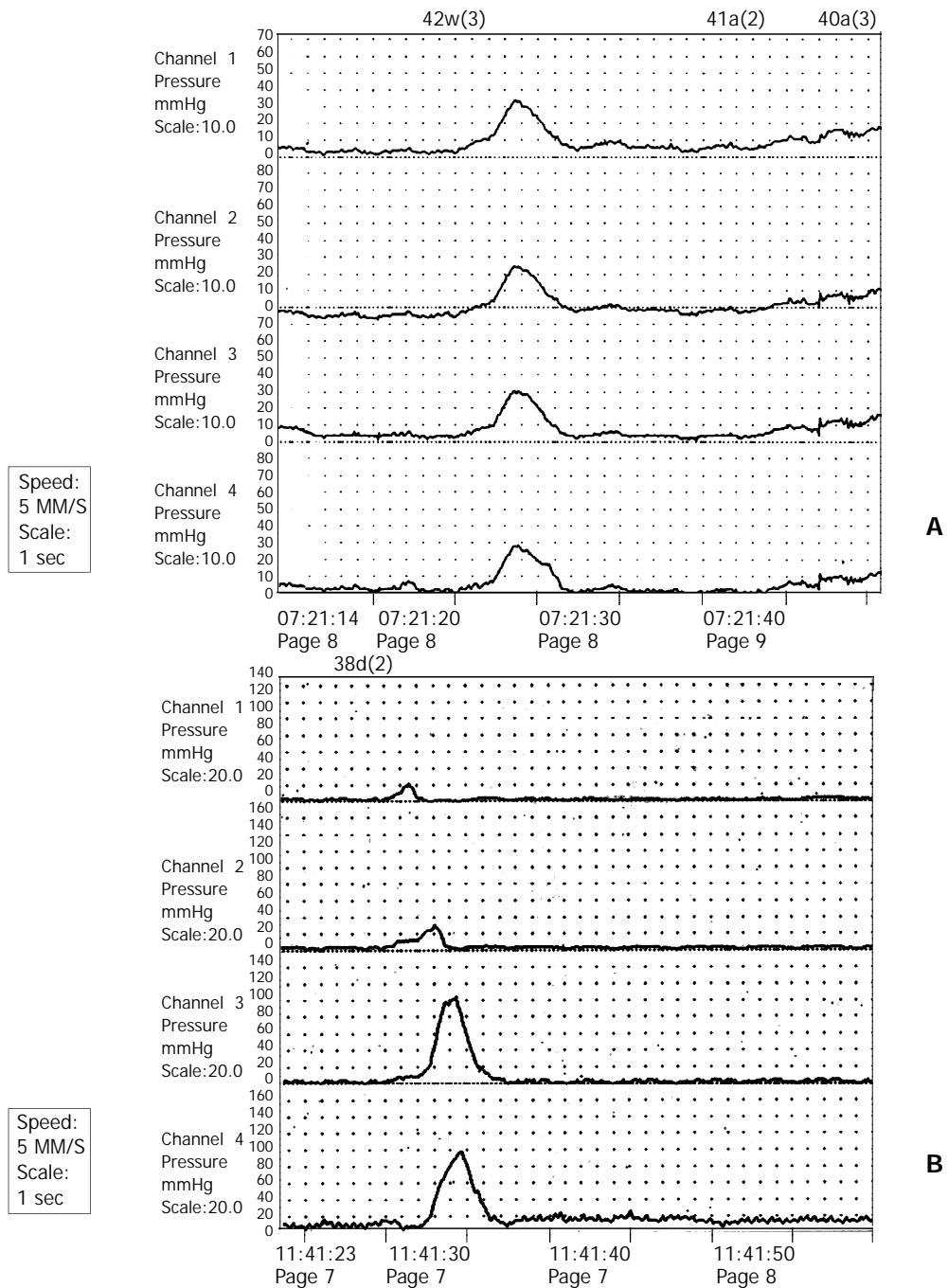


Figure 3 Esophageal manometric tracings obtained from a 29-y female patient with achalasia before and after Heller's myotomy. A, Preoperative manometry showed simultaneous contractions of the esophagus, suggestive of no pulsive peristalsis. B, Esophageal manometry revealed peristaltic contractions seven years after Heller's myotomy.

DISCUSSION

Achalasia is an uncommon disease. Although there are no epidemiological data in China, its incidence is one per 100 000 population in Western countries^[13-16]. The major pathophysiological changes of achalasia are aperistalsis of the smooth muscle portion of the esophagus and absent or incomplete relaxation of LES with swallowing. Neuroanatomic data suggest ganglion cell is degenerated in the esophageal myenteric plexus. Although the cause of achalasia is unknown, it has been hypothesized to be related to class II HLA antigen DQw1^[16], and herpes zoster^[17] or measles virus infections^[18]. The finding of antimyenteric neuron antibodies in achalasia patients has shown it is an autoimmune pathogenesis^[19].

In general, aperistalsis of the esophagus in achalasia patients is not reversible after esophageal myotomy. For this reason, its treatment usually aims at the reduction of LES resting pressure. In the currently used methods, medication and dilation have been found to have a certain efficacy, but the duration of dysphagia relief was short^[20,21]. Thus, up to now, myotomy has been the first choice for achalasia. In the present study, both LES resting pressure and clinical score were significantly decreased after Heller's myotomy, and 84.5% of patients had a good or excellent relief of dysphagia. This figure was consistent with other reports^[22,23]. Furthermore, the relief of clinical symptoms was permanent after Heller's myotomy in the present study. In contrast, the effective relief of symptoms has been reported to present in only 15%-30% of patients one year after intra-sphincter injection of botulinum toxin^[3,24], and in 50% of patients one year after pneumatic dilatation^[3].

Our results of esophageal manometry showed that resting pressure of the esophageal body was also decreased along with the drop of LES pressure after esophageal myotomy. This may be resulted from the reduction or disappearance of intra-esophageal content after Heller's myotomy. Generally, aperistaltic esophagus could not become peristaltic after Heller's myotomy. However, we found that aperistaltic esophagus resumed peristalsis in 4 patients at 20 months, 7, 15 and 20 years after surgery, respectively. In these patients, the mean time of dysphagia was 1.1 years (range 2 months to 8 years) before surgery, which was shorter than that in the entire group (4.8 years), and there were 2 patients with moderate dilation of the esophagus and 2 with mild dilation. Although the reason is unknown, this finding indicates that it is potential for a few achalasia patients to resume their esophageal peristalsis after Heller's myotomy. Chen and colleagues^[25] found that the return of peristalsis was seen mainly in patients with a short clinical evolution, and a little esophageal dilation with preserved contractile capacity. Therefore, we suggest that Heller's myotomy should be performed as early as possible once achalasia is diagnosed.

In the present study, DeMeester scores had no significant changes after Heller's myotomy compared with preoperative values. It was reported that gastroesophageal reflux seldom occurred in patients with achalasia before Heller's myotomy, and the reasons for higher DeMeester scores in aperistaltic esophagus were due to the increase of lactic acid resulted from fermentation of retained food in the esophagus^[26,27]. In the present study, 24-hour esophageal pH monitoring showed that DeMeester scores were above the normal level in 33.3% of patients before surgery, which is higher than the incidence in normal populations. After Heller's myotomy, gastroesophageal reflux may occur because of the destruction of anti-reflux barrier. Our results also showed that the overall incidence of gastroesophageal reflux was 45.5% in patients undergoing Heller's myotomy. In the literature, the corresponding figure was 25% in those who had undergone esophageal myotomy in combination with anti-reflux procedure^[28].

In the present study, 3 (1.7%) patients developed squamous cell carcinoma, while the reported incidence varied between

1.7% and 20%^[22,29]. Ribeiro *et al*^[30] indicated that chronic irritation of the esophagus appeared to participate in the process of carcinogenesis in patients with achalasia. Although esophageal emptying has been significantly improved after Heller's myotomy, it could not reach normal level because of the aperistaltic esophagus. For this reason, epithelial hyperplasia of the esophagus caused by chronic irritation before surgery may develop into cancer after surgery. Thus, the incidence of squamous cell carcinoma in achalasia patients who have undergone Heller's myotomy is still higher than that in normal population. For this reason, esophagoscopy should be performed for achalasia patients before surgery and at postoperative follow-up to rule out cancer.

It has been a controversy whether an anti-reflux procedure should be performed with Heller's myotomy^[31]. In the present study, the postoperative incidence of gastroesophageal reflux in patients who underwent Heller's myotomy in combination with antireflux procedure was 27.3% compared to 63.6% in those undergoing Heller's myotomy only. In addition, esophagitis was found in 46.7% of patients at postoperative follow-up, and most of them might be resulted from gastroesophageal reflux. However, there were no significant differences in DeMeester and clinical scores between Heller's myotomy only and myotomy in combination with antireflux procedure. Esophageal bleeding resulted from gastroesophageal reflux occurred in one patient who underwent myotomy alone and severe dysphagia occurred in 2 patients who underwent myotomy in combination with anti-reflux procedure due to scar formation around the abdominal segment of the esophagus. Therefore, there is no overwhelming evidence to indicate myotomy in combination with anti-reflux procedure is better than myotomy only for achalasia, and a large number of patients should be studied randomly before the dispute is settled. In our experience, partial rather than total fundoplication should be performed with myotomy because aperistaltic esophagus has a poor emptying ability, and total fundoplication hinders esophageal transit more severely than partial fundoplication does.

Up to now, modified Heller's myotomy is still the best choice for achalasia because of its high rate of symptom relief and permanent efficacy. Heller's myotomy in combination with antireflux procedure could stop gastroesophageal reflux to a certain extent, but a large number of patients should be studied randomly to further demonstrate its efficacy.

REFERENCES

- 1 **Anselmino M**, Perdakis G, Hinder RA, Polishuk PV, Wilson P, Terry JD, Lanspa SJ. Heller myotomy is superior to dilatation for the treatment of early achalasia. *Arch Surg* 1997; **132**: 233-240
- 2 **Katz PO**, Gilbert J, Castell DO. Pneumatic dilatation is effective long-term treatment for achalasia. *Dig Dis Sci* 1998; **43**: 1973-1977
- 3 **Mikaeli J**, Fazel A, Montazeri G, Yaghoobi M, Malekzadeh R. Randomized controlled trial comparing botulinum toxin injection to pneumatic dilatation for the treatment of achalasia. *Aliment Pharmacol Ther* 2001; **15**: 1389-1396
- 4 **Cuilliere C**, Ducrotte P, Zerbib F, Metman EH, de Looze D, Guillemot F, Hudziak H, Lamouliatte H, Grimaud JC, Ropert A, Dapigny M, Bost R, Lemann M, Bigard Denis P, Auget JL, Galmiche JP, Bruley des Varannes S. Achalasia: outcome of patients treated with intrasphincteric injection of botulinum toxin. *Gut* 1997; **41**: 87-92
- 5 **Pasricha PJ**, Ravich WJ, Hendrix TR, Sostre S, Jones B, Kalloo AN. Treatment of achalasia with intrasphincteric injection of botulinum toxin: A pilot trial. *Ann Intern Med* 1994; **121**: 590-591
- 6 **Spieess AE**, Kahrilas PJ. Treating achalasia: from whalebone to laparoscope. *JAMA* 1998; **280**: 638-642
- 7 **Torbey CF**, Achkar E, Rice TW, Baker M, Richter JE. Long-term outcome of achalasia treatment: the need for closer follow-up. *J Clin Gastroenterol* 1999; **28**: 125-130
- 8 **Eckardt VF**, Aignherr C, Bernhardt G. Predictors of outcome in patients with achalasia treated by pneumatic dilation. *Gastroen-*

- terology* 1992; **103**: 1732-1738
- 9 **Liu JF**, Wang QZ, Li WQ, Li BQ, Wang FS, Cao FM, Tian ZQ, Zhang YF. Esophageal scintigraphy to quantitate esophageal transit of the achalasia patients after Heller's myotomy. *Zhonghua Heyixue Zazhi* 1995; **15**: 228-229
 - 10 **Gallone L**, Peri G, Galliera M. Proximal gastric vagotomy and anterior fundoplication as complementary procedures to Heller's operation for achalasia. *Surg Gynecol Obstet* 1982; **155**: 337-341
 - 11 **Bonavina L**, Nosadini A, Bardini R, Baessato M, Peracchia A. Primary treatment of esophageal achalasia. Long-term results of myotomy and Dor fundoplication. *Arch Surg* 1992; **127**: 222-226
 - 12 **Devaney EJ**, Lannettoni MD, Orringer MB, Marshall B. Esophagectomy for achalasia: patient selection and clinical experience. *An Thorac Surg* 2001; **72**: 854-858
 - 13 **Mayberry JF**, Atkinson M. Studies of incidence and prevalence of achalasia in the Nottingham area. *Q J Med* 1985; **56**: 451-456
 - 14 **Earlham RJ**, Ellis FH Jr, Nobrega FT. Achalasia of the esophagus in a small urban community. *May Clin Proc* 1969; **44**: 478-483
 - 15 **Howard PJ**, Maher L, Pryde A, Cameron EW, Heading RC. Five year prospective study of the incidence, clinical features, and diagnosis of achalasia in Edinburgh. *Gut* 1992; **33**: 1011-1015
 - 16 **Wong RK**, Maydonovitch CL, Metz SJ, Baker JR Jr. Significant DQw1 association in achalasia. *Dig Dis Sci* 1989; **34**: 349-352
 - 17 **Robertson CS**, Martin BA, Atkinson M. Varicella-zoster virus DNA in the oesophageal myenteric plexus in achalasia. *Gut* 1993; **34**: 299-302
 - 18 **Jones DB**, Mayberry JF, Rhodes J, Munro J. Preliminary report of an association between measles virus and achalasia. *J Clin Pathol* 1983; **36**: 655-657
 - 19 **Verne GN**, Sallustio JE, Eaker EY. Anti-myenteric neuronal antibodies in patients with achalasia: A prospective study. *Dig Dis Sci* 1997; **42**: 307-313
 - 20 **Gelfond M**, Rozen P, Gilat T. Isosorbide dinitrate and nifedipine treatment of achalasia: a clinical, manometric and radionuclide evaluation. *Gastroenterology* 1982; **83**: 963-969
 - 21 **Traube M**, Hongo M, Magyar L, McCallum RW. Effects of nifedipine in achalasia and in patients with high-amplitude peristaltic esophageal contractions. *JAMA* 1984; **252**: 1733-1736
 - 22 **Shai SE**, Chen CY, Hsu CP, Hsia JY, Yang SS. Transthoracic oesophagomyotomy in the treatment of achalasia-a 15-year experience. *Scand Cardiovasc J* 1999; **33**: 333-336
 - 23 **Ionescu NG**, Pereni O, Maghiar A, Ionescu C, Ionescu S, Maghiar T. Oesophageal: Surgical consideration in the management of achalasia. *Br J Surg* 1995; **82**: 105
 - 24 **Bassotti G**, Annese V. Review article: Pharmacological options in achalasia. *Aliment Pharmacol Ther* 1999; **13**: 1391-1396
 - 25 **Chen LQ**, Chughtai T, Sideris L, Nastos D, Taillefer R, Ferraro P, Duranceau A. Long-term effects of myotomy and partial fundoplication for esophageal achalasia. *Dis Esophagus* 2002; **15**: 171-179
 - 26 **Spechler SJ**, Souza RF, Rosenberg SJ, Ruben RA, Goyal RK. Heartburn in patients with achalasia. *Gut* 1995; **37**: 305-308
 - 27 **Smart HL**, Mayberry JF, Atkinson M. Achalasia following gastro-oesophageal reflux. *J R Soc Med* 1986; **79**: 71-73
 - 28 **Ponce J**, Juan M, Garrigues V, Pascual S, Berenguer J. Efficacy and safety of cardiomyotomy in patients with achalasia after failure of pneumatic dilatation. *Dig Dis Sci* 1999; **44**: 2277-2282
 - 29 **Sandler RS**, Nyren O, Ekblom A, Eisen GM, Yuen J, Josefsson S. The risk of esophageal cancer in patients with achalasia: A population-based study. *JAMA* 1995; **274**: 1359-1362
 - 30 **Ribeiro U Jr**, Posner MC, Safatle-Ribeiro AV, Reynolds JC. Risk factors for squamous cell carcinoma of the oesophagus. *Br J Surg* 1996; **83**: 1174-1185
 - 31 **Cosentini E**, Berlakovich G, Zacherl J, Stacher-Janotta G, Merio R, Wenzl E, Bergmann H, Stacher G. Achalasia. Results of myotomy and antireflux operation after failed dilatations. *Arch Surg* 1997; **132**: 143-147

Edited by Wang XL and Proofread by Zhu LH

Expression of COX-2 proteins in gastric mucosal lesions

Lian-Zhen Yu, Heng-Jun Gao, Jian-Feng Bai, Gu Sun, Han-Lin Zhao, Liang Sun, Kun Miu, Zhi-Quan Zhao

Lian-Zhen Yu, Heng-Jun Gao, Liang Sun, Kun Miu, Zhi-Quan Zhao, Department of Gastroenterology, the First Affiliated Hospital of Nanjing Medical University, Nanjing 210029, Jiangsu Province, China

Jian-Feng Bai, Gu Sun, Han-Lin Zhao, Department of General Surgery, the First Affiliated Hospital of Nanjing Medical University, Nanjing 210029, Jiangsu Province, China

Supported by the Natural Science Fund of the Educational Committee of Jiangsu Province, No.125FA9608 and Fund of Nanjing Medical University for Outstanding Young Faculty

Correspondence to: Heng-Jun Gao, Department of Gastroenterology, the First Affiliated Hospital of Nanjing Medical University, Nanjing 210029, Jiangsu Province, China

Received: 2003-04-02 **Accepted:** 2003-05-17

Abstract

AIM: To investigate the expression of COX-2 proteins in gastric mucosal lesions and to assess the relationship between COX-2 expression and type, pathologic stage, differentiation, or lymph node metastasis in gastric cancer and the relationship between COX-2 expression and *H pylori* infection in gastric mucosal lesions.

METHODS: Thirty patients with gastric carcinoma underwent surgical resection. Samples were taken from tumor site and paracancerous tissues, and ABC immunohistochemical staining was used to detect the expression of COX-2 proteins. *H pylori* was determined by rapid urea test combined with pathological staining/¹⁴C urea breath test.

RESULTS: The positive rate and staining intensity of mutant COX-2 gene expression in gastric cancer were significantly higher than those in paracancerous tissues (66.7% vs 26.7%) ($P < 0.01$, $P < 0.001$). There was a significant correlation between COX-2 and pathologic stage or lymph node metastasis type of gastric carcinoma (76.0% vs 20.0%, 79.2% vs 16.7%) ($P < 0.05$). No correlation was found between COX-2 expression and type or grade of differentiation ($P > 0.05$). COX-2 expression of intestinal metaplasia (IM) or dysplasia (DYS) with positive *H pylori* was significantly higher than that with negative *H pylori* (50.6% vs 18.1%, 60.0% vs 33.3%) ($P < 0.05$).

CONCLUSION: COX-2 overexpression was found in a large proportion of gastric cancer tissues compared with matched non-cancerous tissues and was significantly associated with advanced tumor stage and lymph node metastasis. Overexpression of COX-2 plays an important role in tumor progression of gastric cancer. COX-2 may also play a role in the early development/promotion of gastric carcinoma and is associated with *H pylori* infection.

Yu LZ, Gao HJ, Bai JF, Sun G, Zhao HL, Sun L, Miu K, Zhao ZQ. Expression of COX-2 proteins in gastric mucosal lesions. *World J Gastroenterol* 2004; 10(2): 292-294
<http://www.wjgnet.com/1007-9327/10/292.asp>

INTRODUCTION

Recently, a number of researches show that COX-2 was expressed at a very high level in gastrointestinal tumors. However, we know less about COX-2 expression in gastric cancer, especially the relationship between COX-2 overexpression and typing, degree, differentiation, lymphonic metastasis of gastric cancer. In this paper, we investigated the expression of COX-2 proteins in gastric mucosal lesions and assessed the relationship between COX-2 expression and the type, pathologic stage, differentiation, or lymph node metastasis in gastric cancer and the relationship between expression of COX-2 and *H pylori* infection in gastric mucosal lesions.

MATERIALS AND METHODS

Materials

Tissue samples were acquired from 30 patients with gastric cancer diagnosed between April 1996 and March 1998 in our hospital, including a piece of tumor tissue and a piece of paracancerous tissue obtained from the surgery. Samples were then fixed quickly into formalin solution at pH 7.0, embedded in paraffin and cut into slices (4 μ m thick). Slides were used for HE staining and ABC immunohistochemical staining, the latter was used to detect the expression of COX-2 proteins. *H pylori* was determined by rapid urea test combined with pathological staining/¹⁴C urea breath test.

Methods

ABC immunohistochemical staining Polyclone antibody against COX-2 was obtained from Gene Company Limited, ABC immunohistochemical kits and DAB substrate solution were from Vector Laboratories Inc, USA. Slides were treated with 0.01 mol/L citric acid buffer to recover the antigen activity, and developed with routine ABC immunohistochemical staining at an antibody concentration of 1:50, and the second antibody with labeled biotin at 1:200. The negative control was used with PBS buffer replacing the polyclone antibody, and positive control was also set up with a tissue sample with a known positive reaction. The criteria for positive reactions were as follows: positive staining of COX-2 protein located within cytosol, but without stain in the nucleus, being pale yellow to deep pale yellow, even pale red. In evaluation of the positive activity, the positive cell number and reaction level were two useful parameters. When over 10% cells were dyed, it could be considered as a positive expression, and the positive reaction levels were shown as weakly positive (+), moderately positive (++) and strongly positive (+++).

Statistics

Statistical analysis system (SAS) software package was used for χ^2 test, and rank sum test for the degree of group data.

RESULTS

COX-2 expression in gastric cancer tissue and paracancerous tissue

The positive rate and intensity of COX-2 expression in gastric cancer tissue were all significantly higher than those in paracancerous tissues ($P < 0.01$, $P < 0.001$, Table 1).

Table 2 COX-2 expression in gastric mucosa with *H pylori* infection, n (%)

	CG (n=30)		IM (n=19)		DYS (n=11)		GC (n=30)	
	Hp+	Hp -	Hp+	Hp -	Hp +	Hp -	Hp +	Hp -
n	25	5	9	11	5	6	11	19
COX-2	2(8.0%)	1(0%)	5(50.6%) ^a	2(18.1%)	3(60.0%) ^a	2(33.3%)	8(72.7%)	12(63.5%)

^aP<0.05, IM or DYS (*H pylori* positive) vs IM or DYS (*H pylori* negative).

Table 1 COX-2 expression in gastric cancer and paracancerous tissues

	Number	COX-2 expression intensity ^b				Positive rate ^d n (%)
		-	+	++	+++	
Gastric cancer	30	10	4	8	8	20 (66.7)
Paracancerous tissue	30	22	6	2	0	8 (26.7)

^bP<0.001 gastric cancer vs paracancerous tissue; ^dP<0.01 gastric cancer vs paracancerous tissue.

COX-2 expression in gastric mucosa with *H pylori* infection

COX-2 expression of IM or DYS with positive *H pylori* was significantly higher than that with negative *H pylori* ($P<0.05$), (Table 2).

Relationship between COX-2 expression and type, pathologic stage, differentiation, or lymph node metastasis of gastric cancer

The relationship between COX-2 expression and type, pathologic stage, differentiation, or lymph node metastasis of gastric cancer is shown in Table 3. COX-2 positive expression in gastric cancer tissue at the developing stage (76.0%) was significantly higher than that at the early stage (20.0%) ($P<0.05$). The positive rate in gastric cancer with lymph node metastasis (79.2%) was significantly higher than that without lymph node metastasis (16.7%) ($P<0.05$). But the COX-2 positive expression in intestinal gastric cancer (66.7%) was the same as that in gastric type of gastric cancer (66.7%). The positive rate in gastric cancer with low or no differentiation (80%) was not higher than that with high or moderate differentiation (57.1%) ($P>0.05$), (Table 3).

Table 3 COX-2 expression in gastric cancer tissues

Groups	Number	COX-2 n (%)
Type		
Intestinal type	24	16 (66.7)
Gastric type	6	4 (66.7)
Stage		
Early stage	5	1 (20.0)
Developing	25	19 (76.0) ^a
Differentiation (Intestinal type)		
High and moderate	14	8 (57.1)
Low and no differentiation	10	8 (80.0)
Lymph node metastasis		
Without metastasis	6	1 (16.7)
With metastasis	24	19 (79.2) ^a

^aP<0.05, developing stage vs early stage; metastasis vs no metastasis.

DISCUSSION

New COX isozyme-COX-2, is not expressed in normal tissues, but expressed at a high level in inflammatory tissues. It has

been shown in animal studies that COX-2 expression can enhance PGE2 production, which induces cell proliferation and bcl-2 expression. These can destroy the balance between proliferation and apoptosis and induce tumors. More and more studies have shown that COX-2 could express at a high level in human colorectal tumor^[1-5] and other gastrointestinal tumors^[6-8]. COX-2 overexpression was found in well-differentiated epidermoid carcinoma of the esophagus. Ratnasinghe^[9] studied the COX-2 expression in epidermoid carcinoma of the esophagus and found that COX-2 expressed at a high level in well-differentiated tissues, at a low positive level in the normal esophagus, and negative in poorly-differentiated tissues. Hao^[10] found COX-2 protein expressed at a high level in adenocarcinoma and adenoma of colon, compared with normal mucosal tissues. COX-2 mRNA expressed in tumor tissues at a significantly higher level than that in normal tissues. There was neither a relationship between COX-2 protein expression and proliferation degree or volume of adenoma, nor a relationship between COX-2 expression and tumor differentiation, Duke's stage as well as lymph node metastasis ($P>0.05$). Interestingly, COX-2 expressed in the tissues near adenocarcinoma or adenoma at a higher level than in normal mucosal tissues ($P<0.0001$), but lower than that in adenocarcinoma or adenoma itself ($P<0.001$, $P<10^5$).

It has been found that the positive rate of COX-2 expression in gastric cancer tissue was 60%-70%^[6-8]. Ratnasinghe^[6] found that COX-2 expressed positively in 36% cardia adenocarcinoma and 60% gastric body adenocarcinoma in his research on 19 patients with cardia adenocarcinoma and 15 patients with gastric body adenocarcinoma. COX-2 overexpression was found in most of gastric body adenocarcinoma and some cardia adenocarcinoma tissues. It is necessary to further confirm the status of COX-2 expression in gastric cancer tissues, especially the characteristics of COX-2 overexpression related to typing, degree, differentiation and lymph node metastasis^[11-15]. We studied the COX-2 expression at gene and protein levels in tissues with gastric mucosal lesion, and explored the relationship between COX-2 expression and gastric carcinoma and *H pylori* infection at pathological and pathophysiological levels.

Our study based on 30 tissue samples with gastric cancer as well as paracancerous tissues showed that COX-2 protein expressed at a high level in tumor tissues, which was significantly higher than that in paracarcinoma tissues ($P<0.01$), and also significantly higher in tumor tissues ($P<0.01$). COX-2 positive expression in gastric cancer tissues at the developing stage was significantly higher than that at early stage, the positive rate in gastric cancer with lymph node metastasis was significantly higher than that without lymph node metastasis ($P<0.05$), but the COX-2 positive expression in intestine type of gastric cancer was the same as that in gastric type of gastric cancer. The positive rate in gastric cancer with low or no differentiation was not higher than that with high or moderate differentiation ($P>0.05$). Our results were similar to those of foreign investigators^[7,8]. In conclusion, abnormal expression of COX-2 protein was related to the progress of gastric carcinoma as well as lymph node metastasis, while it was not significantly related to the type of gastric cancer and degree of pathological differentiation^[13,15].

We also found that COX-2 expression in tissues with *H pylori* positive intestinal metastasis or dysplasia was significantly higher than that in tissues with *H pylori* negative infection. *H pylori* could induce acute and chronic inflammation of gastric mucosa, and the production of cell factors such as IL-8 and IL-1 β , and the secondary high COX-2 expression which caused gastric mucosal lesions. *H pylori* infection could also induce gastric mucosal cell proliferation by COX-2 expression. COX-2 gene expression was one of the related factors mediating the progress from gastritis with *H pylori* infection to pre-carcinoma lesions even gastric carcinoma^[16,17]. Based on this study, treatment of *H pylori* infection and special COX-2 inhibitor could be useful for the prevention of gastric carcinoma^[18].

REFERENCES

- Eberhart CE**, Coffey RJ, Radhika A, Giardiello FM, Ferrenbach S, DuBois RN. Up-regulation of cyclooxygenase-2 gene expression in human colorectal adenomas and adenocarcinomas. *Gastroenterology* 1994; **107**: 1183-1188
- Sano H**, Kawahito Y, Wilder RL, Hashiramoto A, Mukai S, Asai K, Kimura S, Kato H, Kondo M, Hla T. Expression of cyclooxygenase-1 and -2 in human colorectal cancer. *Cancer Res* 1995; **55**: 3785-3789
- Reddy BS**, Rao CV, Seibert K. Evaluation of cyclooxygenase-2 inhibitor for potential chemopreventive properties in colon carcinogenesis. *Cancer Res* 1996; **56**: 4566-4569
- Tsuji M**, Kawano S, DuBios RN. Cyclooxygenase-2 expression in human colon cancer cells increases metastatic potential. *Proc Natl Acad Sci U S A* 1997; **94**: 3336-3340
- Watson AJ**. Chemopreventive effects of NSAIDs against colorectal cancer: regulation of apoptosis and mitosis by COX-1 and COX-2. *Histol Histopathol* 1998; **13**: 591-597
- Ratnasinghe D**, Tangrea JA, Roth MJ, Dawsey SM, Anver M, Kasprzak BA, Hu N, Wang QH, Taylor PR. Expression of cyclooxygenase-2 in human adenocarcinomas of the gastric cardia and corpus. *Oncol Rep* 1999; **6**: 965-968
- Murata H**, Kawano S, Tsuji S, Tsuji M, Sawaoka H, Kimura Y, Shiozaki H, Hori M. Cyclooxygenase-2 overexpression enhances lymphatic invasion and metastasis in human gastric carcinoma. *Am J Gastroenterol* 1999; **94**: 451-455
- Yamamoto H**, Itoh F, Fukushima H, Hinoda Y, Imai K. Overexpression of cyclooxygenase-2 protein is less frequent in gastric cancers with microsatellite instability. *Int J Cancer* 1999; **84**: 400-403
- Ratnasinghe D**, Tangrea J, Roth MJ, Dawsey S, Hu N, Anver M, Wang QH, Taylor PR. Expression of cyclooxygenase-2 in human squamous cell carcinoma of the esophagus; an immunohistochemical survey. *Anticancer Res* 1999; **19**(1A): 171-174
- Hao X**, Bishop AE, Wallace M, Wang H, Willcocks TC, Maclouf J, Polak JM, Knight S, Talbot IC. Early expression of cyclooxygenase-2 during sporadic colorectal carcinogenesis. *J Pathol* 1999; **187**: 295-301
- Ristimaki A**, Honkanen N, Jankala H, Sipponen P, Harkonen M. Expression of cyclooxygenase-2 in human gastric carcinoma. *Cancer Res* 1997; **57**: 1276-1280
- Sawaoka H**, Kawano S, Tsuji S, Tsujii M, Murata H, Hori M. Effects of NSAIDs on proliferation of gastric cancer cells *in vitro*: possible implication of cyclooxygenase-2 in cancer development. *J Clin Gastroenterol* 1998; **27**(Suppl 1): S47-52
- Saukkonen K**, Nieminen O, van Rees B, Vilkkii S, Harkonen M, Juhola M, Mecklin JP, Sipponen P, Ristimaki A. Expression of cyclooxygenase-2 in dysplasia of the stomach and in intestinal-type gastric adenocarcinoma. *Clin Cancer Res* 2001; **7**: 1923-1931
- Van Rees BP**, Saukkonen K, Ristimaki A, Polkowski W, Tytgat GN, Drilenburg P, Offerhaus GJ. Cyclooxygenase-2 expression during carcinogenesis in the human stomach. *J Pathol* 2002; **196**: 171-179
- Yamagata R**, Shimoyama T, Fukuda S, Yoshimura T, Tanaka M, Munakata A. Cyclooxygenase-2 expression is increased in early intestinal-type gastric cancer and gastric mucosa with intestinal metaplasia. *Eur J Gastroenterol Hepatol* 2002; **14**: 359-363
- Walker MM**. Cyclooxygenase-2 expression in early gastric cancer, intestinal metaplasia and *Helicobacter pylori* infection. *Eur J Gastroenterol Hepatol* 2002; **14**: 347-349
- Wambura C**, Aoyama N, Shirasaka D, Sakai T, Ikemura T, Sakashita M, Maekawa S, Kuroda K, Inoue T, Ebara S, Miyamoto M, Kasuga M. Effect of *Helicobacter pylori*-induced cyclooxygenase-2 on gastric epithelial cell kinetics: implication for gastric carcinogenesis. *Helicobacter* 2002; **7**: 129-138
- Sung JJ**, Leung WK, Go MY, To KF, Cheng AS, Ng EK, Chan FK. Cyclooxygenase-2 expression in *Helicobacter pylori*-associated premalignant and malignant gastric lesions. *Am J Pathol* 2000; **157**: 729-735

Edited by Ma JY and Wang XL

Effects of *zhaoyangwan* on chronic hepatitis B and posthepatic cirrhosis

Cui-Ping Zhang, Zi-Bin Tian, Xi-Shuang Liu, Qing-Xi Zhao, Jun Wu, Yong-Xin Liang

Cui-Ping Zhang, Zi-Bin Tian, Xi-Shuang Liu, Qing-Xi Zhao, Jun Wu, Yong-Xin Liang, Department of Gastroenterology, the Affiliated Hospital of Qingdao Medical College, Qingdao University, Qingdao, 266003, Shandong Province, China

Supported by the Natural Science Foundation of Shandong Province, No.1999CA1CKB3

Correspondence to: Dr. Cui-Ping Zhang, Department of Gastroenterology, the Affiliated Hospital of Qingdao Medical College, Qingdao University, Qingdao 266003, Shandong Province, China. tianzbsun@public.qd.sd.cn
Telephone: +86-532-2911304

Received: 2003-05-13 **Accepted:** 2003-06-02

Abstract

AIM: To study the therapeutic effects of *zhaoyangwan* (ZYW) on chronic hepatitis B and hepatic cirrhosis and the anti-virus, anti-fibrosis and immunoregulatory mechanisms of ZYW.

METHODS: Fifty cases of chronic hepatitis B and posthepatic cirrhosis with positive serum HBsAg, HBeAg, anti-Hbc and HBV-DNA were divided randomly and single-blindly into the treatment group (treated with ZYW) and the control group (treated with interferon). After 3 month treatment, the effects of the treatment group and the control group were evaluated.

RESULTS: The serum ALT normalization was 83.3%(30/36) in the treatment group and 85.7%(12/14) in the control group, with no significant difference ($\chi^2=0.043$, $P>0.05$). After the course, the negative expression rates of the serum HBV-DNA and HBeAg were 44.4%(16/36) and 50%(18/36) in the treatment group, and 50%(7/14) and 50%(7/14) in the control group, respectively, with no significant difference ($\chi^2=0.125$, $\chi^2=0.00$, both $P>0.05$). Negative HBsAg and positive HBsAb appeared in 4 cases of the treatment group and 1 case of the control group. Serum anti-HBc turned negative in 6 cases of the treatment group and 1 case of the control group, respectively. After the ZYW treatment, serum CD₃⁺, CD₄⁺, CD₈⁺, CD₄⁺/CD₈⁺ and NK cell activation were significantly increased. Only serum CD₃⁺ and NK cell activation were significantly increased in the control group with a significant difference between the two groups. The serum C₄, C_{1q}, C₃, B and C₉ were significantly increased in the treatment group. In the control group only the serum C₄ was increased. The concentration of serum interferon had no change after treatment with ZYW, while it was significantly increased in the control group after treatment with interferon. The ultrastructure of the liver restored, which helped effectively to reduce the degeneration and necrosis of hepatic cells, infiltration of inflammatory cells and hepatic cirrhosis.

CONCLUSION: ZYW is a pure Chinese herbal medicine. It can exert potent therapeutic effects on chronic hepatitis B and posthepatic cirrhosis. ZYW has similar therapeutic effects to those of interferon. It is cheap and easily administered with no obvious side-effects. It can be widely used in clinical practice.

Zhang CP, Tian ZB, Liu XS, Zhao QX, Wu J, Liang YX. Effects of *zhaoyangwan* on chronic hepatitis B and posthepatic cirrhosis. *World J Gastroenterol* 2004; 10(2): 295-298

<http://www.wjgnet.com/1007-9327/10/295.asp>

INTRODUCTION

HBV is highly prevalent in China. HBsAg-positive rate is 8-10% among young adults, some of them may develop chronic hepatitis B (CHB), with poor liver function and positive HBeAg and HBV-DNA. Therefore, it is urgent to improve the immunity of CHB patients to make the virus unable to replicate so as to reduce the damage to the liver and to slow down the progress of CHB to fibrosis and cancer. Anti-virus treatment is the key point^[1-7], and great attention has been paid to it. However, no specific therapy has been found. The use of interferon and lamivudine is clinically limited because they are expensive and the patients are easy to relapse^[8-14]. An urgent issue of top priority is how to treat CHB and other virus infection with traditional Chinese medicine according to syndrome differentiation. Insufficiency of experience and the complexity of the drug ingredients result in the lack of objective parameters. This study used the proprietary Chinese medicine of *zhaoyangwan* (Morning Sun Pill) invented by Professor Jiang Tingdong. Interferon was used as controls. Fifty patients with hepatitis B were observed for the changes in liver function, cellular immunity function, NK cell activity, serum complement, serum marker of HBV, HBV-DNA, ultrastructure of the liver and serum interferon before and after treatment with ZYW to investigate the mechanisms of the anti-virus, anti-fibrosis activity in the liver and immuno-regulatory of traditional Chinese medicine and to provide theoretic basis for the treatment of chronic hepatic diseases with Chinese herbs.

MATERIALS AND METHODS

Materials

The 50 patients were all HBsAg, HBeAg, Anti-HBc and HBV-DNA positive. Thirty-four were males and 16 females, aged 15 to 57 years, with an average of 38.5 years. They were classified according to the diagnostic criteria devised on the Beijing Conference of Infectious and Parasitic Diseases in 1995. Thirty-eight cases were CHB, 22 cases were post-hepatitis active hepatocirrhosis(in compensation). They had no such chronic diseases as other types of hepatitis, diabetes or tuberculosis.

Methods

The 50 patients were divided into *zhaoyangwan* (ZYW) group and interferon group (control group). The 36 patients in ZYW group took orally 2 packs of ZYW a day, one in the morning and one in the evening, for 3 months. The 14 patients in the control group were administered intramuscularly with α -interferon made by Changchun Bio-product Institute, 3 mU once every other day for 3 months. Vitamins might be added to the patients in both groups, but no other anti-virus, immuno-

regulatory or liver enzyme reduction drugs were used during the treatment. One therapeutic course lasted for 3 months. Serum marker of HBV, T-cell subgroup, NK cell activity, contents of serum complement, and level of serum interferon were examined before and after the treatment, respectively. The liver function was examined once a week. Liver puncture and electrodiaphanoscopy were performed for some patients to observe the ultrastructure of the liver before and after the treatment.

Assay methods

HBVDNA was assayed with PCR, T-cell sub-group with direct method of bacterial ring, NK cell activity with MTT colorimetry, serum complement with one-direction immunity diffusion, and serum interferon with ELISA, with reagent produced by Endogen of USA. The ultrastructure of the liver was observed under electrodiaphanoscope.

RESULTS

Changes of symptoms and signs before and after treatment

Changes of symptoms and signs in both groups before treatment (BT) and after treatment (AT) are compared in Table 1, which showed that the symptom disappearance rate (DR) of the treated group was similar to or higher than that of the control group, but the sign disappearance rate was lower, with no statistical significance.

Changes of liver function and serum markers before and after treatment

Serum glutamic-pyruvic transaminase (ALT) was evidently improved in both groups. The serum ALT returned to normal in 83.3% (30/36) of the treated group and 85.7% (12/14) of the control group. No significant difference was found between

both groups. ($\chi^2=0.043, P>0.05$). The negative conversion rate of HBVDNA and HBeAg in the treated group was 44.4% (16/36) and 50% (18/36), respectively, while in the control group, it was 50% (7/14) and 50% (7/14), respectively, with no significant difference ($\chi^2=0.123, \chi^2=0.00$, both $P>0.05$). HBsAg turned negative in 4 cases of the treated group and 1 case of the control group, and their HBsAb turned positive. Anti-HBc turned negative in 6 cases of the treated group and 2 cases of the control group.

Changes of T-cell sub-group and NK cell activity before and after the treatment

Serum CD3⁺, CD4⁺, CD8⁺, CD4⁺/CD8⁺ and NK cell activity were significantly increased in the ZYW treated group ($t=8.921-13.380$, all $P<0.001$), while in the control group, only CD3⁺ and NK cell activity were significantly increased ($t=7.473, 10.101, P<0.001$). The results of the two groups were significantly different after the treatment ($t=6.812-14.108$, all $P<0.001$), as shown in Table 2.

Changes of serum complement elements before and after treatment

The five serum complement elements, ie. C₄, C_{1q}, C₃, BF, and C₉, increased significantly compared with those before the treatment in the ZYW group ($t=4.437-24.330, P<0.001$), while in the control group, only C₄ increased ($t=5.044, P<0.001$). The results of the two groups were significantly different after the treatment ($t=3.972-12.910, P<0.001$), as shown in Table 3.

Changes of serum interferon concentration

The serum interferon concentration changed little in the ZYW group, while in the interferon group, it rose significantly. The results of the two groups were significantly different after treatment ($t=2.723, P<0.001$), as seen in Table 4.

Table 1 Improvement of symptoms and signs in both groups before and after treatment

Symptoms and signs	Treated group			Control group			χ^2	P
	BT	AT	DR(%)	BT	AT	DR(%)		
Fatigue	29	14	51.7	12	6	50	0.10	>0.05
Abdominal distension	31	9	71	13	5	61.5	0.375	>0.05
Nausea	12	7	41.7	8	6	25	0.586	>0.05
Anorexia	23	6	73.9	11	4	63.6	0.379	>0.05
Hepatic pain	17	10	41.2	7	5	28.6	0.336	>0.05
Sallow complexion	14	4	71.4	5	3	40	1.564	>0.05
Hepatomegaly	20	12	40	6	3	50	0.189	>0.05
Splenomegaly	9	7	22.2	4	3	25	0.012	>0.05
Percussion pain of liver	21	12	42.9	9	5	44.4	0.006	>0.05

Table 2 Changes of T-cell sub-group and NK cell activity before and after treatment (%)

	n	CD3 ⁺	CD4 ⁺	CD8 ⁺	CD4 ⁺ /CD8 ⁺	NK
Treated group BT	36	47.14±4.76	41.56±5.06	30.10±3.03	1.41±0.24	43.62±5.92
AT	36	57.81±5.83	54.81±5.64 ^{ab}	23.07±4.47 ^{ab}	2.49±0.72 ^{ab}	56.69±5.29 ^{ab}
Control group BT	14	39.93±5.00	28.38±3.40	23.38±3.40	1.40±0.18	40.36±5.90
AT	14	52.28±7.18 ^b	29.17±1.86	29.17±1.86	1.34±0.88	59.40±4.97 ^b

^aThe treated group vs control group after treatment, $P<0.001$, ^bResults after treatment vs those before treatment for both groups, $P<0.001$.

Table 3 Changes of 5 serum complement elements before and after treatment (mg/L)

	n	C ₄	C _{1q}	C ₃	BF	C ₉
Treated group BT	36	339.68±35.40	245.09±47.11	842.13±62.51	220.91±32.84	746.28±62.79
AT	36	529.48±42.49 ^b	349.32±35.01 ^b	1 114.05±218.22 ^b	279.71±52.86 ^b	819.31±103.17 ^b
Control group BT	14	331.84±42.63	240.08±25.32	838.54±44.32	219.56±25.08	715.06±77.58
AT	14	427.57±112.18 ^{ab}	238.35±23.59 ^a	843.89±50.32 ^a	225.08±26.85 ^a	732.08±51.12 ^a

^aThe treated group vs control group after treatment, $P<0.001$, ^bResults after treatment vs those before treatment for both groups, $P<0.001$.

Table 4 Changes of serum interferon concentration before and after treatment

	Case number	BT	AT	t	P
Treated group	13	156.25±17.62	155.93±19.76	0.046	>0.05
Control group	8	143.27±21.44	218.72±63.34	3.193	<0.05

After treatment, the serum interferon concentration of the two groups was significantly different ($t=2.723$, $P<0.05$).

Changes of hepatic ultrastructure

Degeneration, necrosis, cholestasis, fibrosis, and lysis of the organelles existed in different degrees in the liver cells before treatment, while after treatment, the necrotic cells of the liver resiled to a certain extent.

Side effects of ZYW

No evident side effects appeared in the ZYW group. Xerostomia and constipation appeared in one case and slight dizziness in another case, but they disappeared automatically with the continuous use of the pills. More side effects appeared in the interferon group, including influenza-like symptoms, symptoms of the digestive tract, sore and painful muscles. However, the patients continued taking their drugs after patient persuasion of the doctors.

DISCUSSION

Some studies indicated that ZYW had two-way immune modulation functions^[15]. It could improve the function of Kupffer cells of the liver and the activity of natural killer (NK) cells. It also could induce interferon to produce antiviral activity and turn HBeAg negative. We investigated the effects of ZYW on chronic hepatitis by random single-blind ways. The effects of three-month short-term therapy were good and the overall effectiveness was 83.3% (30/36). Some main symptoms such as fatigue, abdominal distension, nausea, anorexia were improved or disappeared after the treatment. The effects of the treatment group were better than those of the control group and were statistically significantly different. In most patients, the color of facial skin turned from dark and gloomy to bright red, with their vigor improved, hepatosplenomegaly improved, percussive pain of the liver region disappeared and state of general health apparently improved. Liver function tests turned normal in half of the patients including 6 patients with slight jaundice which completely disappeared, and serum bilirubin turned normal after the three-month therapy. In the control group, the rate of ALT normalization was 85.7% (12/14) with no statistical significance compared with the treatment group ($P>0.05$). ZYW has some antiviral activity. After the treatment, the rates of negative conversion of HBVDNA and HBeAg were 44.4% (16/36) and 50% (18/36) in the treatment group. There was no statistical significance compared with the control group, in which the rates were 50% (7/14) and 50% (7/14). The HBsAg of four patients in the treatment group and one patient in the control group turned from positive to negative and their HBsAb turned positive. The HBeAb of six patients in the treatment group and two patients in the control group turned negative. Therefore, ZYW has high antiviral activity and the effectiveness is similar to that of interferon. Because the treatment was short-termed, we did not investigate the incidence of recurrence. If the course of treatment is lasted for six months, it would have better efficiency.

Hepatitis B virus infection is the primary cause of viral hepatitis. Persistent existence of hepatitis B virus in the body is the primary cause of chronic hepatitis B^[16-19]. Hepatitis B virus infection leads to chronic hepatitis and persistent damage

to the liver function. Low antiviral immunity of the body and abnormal immunity modulation are also the primary cause of chronicity^[20-25]. Some studies have found that there are different degrees of low cellular immunity^[26,27], which represent deficient T cell immunity and decreased activity of NK cells in patients with chronic hepatitis B and liver cirrhosis. NK cells of the liver are important to antiviral immunity and against tumor metastasis^[28-31]. Kakimi *et al*^[32] injected lactate(activator of NK-T cell) into HBV-transgenic mouse and found that interferon- γ in the liver of the mouse increased, reproduction of HBV stopped and OK-T cells decreased. They believed that activated OK-T cells could activate NK cells, release lots of cytokines and prevent virus from reproducing. It indicates that NK cell is important in the process of erasing HBV. The results of our study showed that there were different levels of modulation disturbance of cellular immunity, such as elevation of CD3⁺, CD4⁺, CD8⁺ and decrease of CD4⁺/CD8⁺ and activity of NK cells in the patients of hepatitis B before ZYW treatment. After ZYW treatment, values of CD3⁺, CD4⁺, CD8⁺ and CD4⁺/CD8⁺ and activity of NK cells improved differently, indicating that ZYW can improve cellular immunity, especially the total amount of T lymphocyte and function of NK cells. It remains to be further studied whether it can be used as an activator of NK cells.

Besides, low cellular immunity, the level of blood complement decreased differently in patients with chronic hepatitis B. HBV antigen is highly compatible with liver cells. The complex of HBV-antibody-complement can damage the liver cells by activating the typical route as common complexes, or by adhering to the liver cells as half-antigen through the typical route of antibody-complement^[33]. Our study indicated that low serum complement was improved differently in patients with chronic hepatitis B after treatment with ZYW and interferon, especially in the ZYW treated group.

Interferon is a broad-spectrum antiviral protein and has some antiviral activity. It does not kill viruses directly but prevents viruses from replication by mediating RNA-dependent PKR or RHA-activated enzyme. Interferon can also improve phagocytosis of phagocytes and activity of T killer cells and NK cells^[29,34-36]. Our study indicated that the activity of NK cells was only slightly elevated in some patients and had no change in patients treated with interferon, indicating that the immuno-modulating function of interferon is not evident. Besides, it is difficult for interferon to be widely used due to its high price and poor tolerance in practice. So other medications which can modulate and improve immunity are suggested to be used in conjunction with interferon, which is mainly used for antiviral treatment.

Liver fibrosis is a pathologic process in which abnormal hyperplasia of fibro-connective tissue develops after inflammatory necrosis has occurred in the liver. The liver can worsen the inflammatory necrosis by cytokines or microcirculation in the liver. The activity of lesions in the liver means the activity of liver fibrosis. Some authors^[37] have suggested that drugs that can prevent or slow down liver fibrosis would cure most of chronic hepatitis. Thus, preventing or delaying liver fibrosis and treating viruses are two aspects of chronic hepatitis B therapy. Today drugs for anti-liver fibrosis are rare and the curative effect is not certain. Our study found that ultramicrocirculation in the liver and liver fibrosis were improved differently after ZYW treatment in patients with chronic hepatitis B and early-stage liver fibrosis. Since the case number was small, and it needs to be further studied.

Patina in ZYW is one of its characteristic ingredients that is different from other drugs in treating chronic hepatitis in practice. Modern medicine believes that copper is an important ingredient for blood-production in the body. Taking appropriate copper orally can improve retina cells and hemoglobin in the bone marrow and blood, and stimulate and repair the liver.

Copper combined with protein in the body produces copper-protein compounds which can restrain hepatitis viruses and induce the body to produce interferon. Our results indicated that the liver function and immunity index of the patients with chronic hepatitis B were differently improved after ZYW treatment and the rate of negative conversion of chronic hepatitis B markers was similar to that of interferon group. The level of serum interferon was elevated after ZYW treatment, but the difference was not statistically significant. Because our case number was small, this needs to be further investigated. We believe that ZYW has a good curative effect and fewer side-effects in treating chronic viral hepatitis. It is also cheap and can be easily taken. So it can be widely used in practice.

REFERENCES

- Guidotti LG**, Rochford R, Chung J, Shapiro M, Purcell R, Chisari FV. Viral clearance without destruction of infected cells during acute HBV infection. *Science* 1999; **284**: 825-829
- Suri D**, Schilling R, Lopes AR, Mullerova I, Colucci G, Williams R, Naoumov NV. Non-cytolytic inhibition of Hepatitis B virus replication in human hepatocytes. *J Hepatol* 2001; **35**: 790-797
- Lau GK**, Tsiang M, Hou J, Yuen S, Carman WF, Zhang L, Gibbs CS, Lam S. Combination therapy with Lamivudine and Famciclovir for chronic hepatitis B infected Chinese patients: a viral dynamic study. *Hepatology* 2000; **32**: 394-399
- Shiratori Y**, Yoshida H, Omata M. Management of hepatocellular carcinoma: advances in diagnosis, treatment and prevention. *Expert Rev Anticancer Ther* 2001; **1**: 277-290
- Okuno M**, Kojima S, Moriwaki H. Chemoprevention of hepatocellular carcinoma: concept, progress and perspectives. *J Gastroenterol Hepatol* 2001; **16**: 1329-1335
- Merle P**, Zoulim F, Vitvitski L, Trepo C. The prophylaxis of hepatocellular carcinoma by interferon-alpha in virus-induced cirrhosis. *Gastroenterol Clin Biol* 2000; **24**: 1166-1176
- Hajnicka V**, Proost P, Kazar J, Fuchsberger N. Comparison of manganese superoxide dismutase precursor induction ability in human hepatoma cells with or without hepatitis B virus DNA insertion. *Acta Virol* 2000; **44**: 343-347
- Korba BE**, Cote P, Hornbuckle W, Schinazi R, Gangemi JD, Tennant BC, Gerin JL. Enhanced antiviral benefit of combination therapy with Lamivudine and alpha interferon against WHV replication in chronic carrier woodchucks. *Antivir Ther* 2000; **5**: 95-104
- Mutimer D**, Dowling D, Cane P, Ratcliffe D, Tang H, O' Donnell K, Shaw J, Elias E, Pillay D. Additive antiviral effects of Lamivudine and alpha interferon in chronic hepatitis B infection. *Antivir Ther* 2000; **5**: 273-277
- Han HL**, Lang ZW. Changes in serum and histology of patients with chronic hepatitis B after interferon alpha-2b treatment. *World J Gastroenterol* 2003; **9**: 117-121
- Yang SS**, Hsu CT, Hu JT, Lai YC, Wu CH. Lamivudine does not increase the efficacy of interferon in the treatment of mutant type chronic viral hepatitis B. *World J Gastroenterol* 2002; **8**: 868-871
- Terrault NA**. Combined interferon and lamivudine therapy: is this the treatment of choice for patients with chronic hepatitis B virus infection? *Hepatology* 2000; **32**: 675-677
- Tamam L**, Yerdelen D, Ozpoyraz N. Psychosis associated with interferon alfa therapy for chronic hepatitis B. *Ann Pharmacother* 2003; **37**: 384-387
- Jung MC**, Gruner N, Zachoval R, Schraut W, Gerlach T, Diepolder H, Schirren CA, Page M, Bailey J, Birtles E, Whitehead E, Trojan J, Zeuzem S, Pape GR. Immunological monitoring during therapeutic vaccination as a prerequisite for the design of new effective therapies: induction of a vaccine-specific CD4+ T-cell proliferative response in chronic hepatitis B carriers. *Vaccine* 2002; **4**: 3598-3612
- Zhaoyangwan study group**. The development of research on zaoyangwan. Beijing: *Military Medical Sciences Press* 1997: 1-201
- Rabe C**, Pilz T, Klostermann C, Berna M, Schild HH, Sauerbruch T, Caselmann WH. Clinical characteristics and outcome of a cohort of 101 patients with hepatocellular carcinoma. *World J Gastroenterol* 2001; **7**: 208-215
- Lan GK**. Hepatitis B infection in China. *Clin Liver Dis* 2001; **5**: 361-379
- Zhang DF**. To pursuit novel therapeutic approaches based on the mechanism of clearance of HBV infection. *Zhonghua Ganzangbing Zazhi* 2001; **9**: 196-202
- Protzer U**, Schaller H. Immune escape by hepatitis B viruses. *Virus Genes* 2000; **21**: 27-37
- Schalm SW**. Lamivudine-interferon combination therapy for chronic hepatitis B: further support but no conclusive evidence. *J Hepatol* 2001; **35**: 419-420
- Liu S**, Tan D, Li C. Specific cellular and humoral immune responses induced by intramuscular injection of DNA vaccine containing HBV HBsAg gene in mice. *Hunan Yike Daxue Xuebao* 1999; **24**: 313-315
- Koziel MJ**. What once was lost, now is found: restoration of hepatitis B-specific immunity after treatment of chronic hepatitis B. *Hepatology* 1999; **29**: 1331-1333
- Luers C**, Sudhop T, Speugler U, Berthold HK. Improvement of sarcoidosis under therapy with interferon-alpha 2b for chronic hepatitis B virus infection. *J Hepatol* 1999; **30**: 347
- Liaw YF**. Treatment of chronic hepatitis B: a need for consensus. *J Gastroenterol Hepatol* 1999; **14**: 1-2
- Zhang HY**, Lu H, Li XM, Duan HY. Therapeutic effect of alpha 1b interferon on patients with chronic hepatitis B: changes in serological fibrosis markers and histology. *Zhonghua Ganzangbing Zazhi* 2003; **11**: 117-118
- Sing GK**, Ladham A, Arnold S, Parmar H, Chen X, Cooper J, Butterworth L, Stuart K, D' Arcy D, Cooksley WG. A longitudinal analysis of cytotoxic T lymphocyte precursor frequencies to the hepatitis B virus in chronically infected patients. *J Viral Hepat* 2001; **8**: 19-29
- Liu CJ**, Chen PJ, Lai MY, Kao JH, Jeng YM, Chen DS. Ribavirin and interferon is effective for hepatitis C virus clearance in hepatitis B and C dually infected patients. *Hepatology* 2003; **37**: 568-576
- Valiante NM**, D' Andrea A, Crotta S, Lechner F, Klennerman P, Nuti S, Wack A, Abrignani S. Life, activation and death of intrahepatic lymphocytes in chronic hepatitis C. *Immunol Rev* 2000; **174**: 77-89
- Schirren CA**, Jung MC, Gerlach JT, Worzfeld T, Baretton G, Mamin M, Hubert Gruener N, Houghton M, Pape GR. Liver-derived hepatitis C virus (HCV)-specific CD4(+)T cells recognize multiple HCV epitopes and produce interferon gamma. *Hepatology* 2000; **32**: 597-603
- Webster GJ**, Reignat S, Maini MK, Whalley SA, Ogg GS, King A, Brown D, Amlot PL, Williams R, Vergani D, Dusheiko GM, Bertolotti A. Incubation phase of acute hepatitis B in man: dynamic of cellular immune mechanisms. *Hepatology* 2000; **32**: 1117-1124
- Kakimi K**, Lane TE, Chisari FV, Guidotti LG. Cutting edge: Inhibition of hepatitis B virus replication by activated NK T cells does not require inflammatory cell recruitment to the liver. *J Immunol* 2001; **167**: 6701-6705
- Kakimi K**, Guidotti LG, Koezuka Y, Chisari FV. Natural killer T cell activation inhibits hepatitis B virus replication *in vivo*. *J Exp Med* 2000; **192**: 921-930
- Zhang CP**, Zhang DX, Shen LQ, Zhang ZG. The measurement and clinical significance of complement system in serum of patients with liver cirrhosis and cancer. *Linchuang Gandanbing Zazhi* 1993; **9**: 19-21
- Weng HL**, Cai WM, Liu RH. Animal experiment and clinical study of effect of gamma-interferon on hepatic fibrosis. *World J Gastroenterol* 2001; **7**: 42-48
- Xu KC**, Wei BH, Yao XX, Zhang WD. Recent therapy for chronic hepatitis B by combined transitional Chinese and Western medicine. *Shijie Huaren Xiaohua Zazhi* 1999; **7**: 970-974
- Yang LM**, Xu KC, Zhao YL, Wu ZR, Chen DF, Qin ZY, Zuo JS, Wei BH, Zhang WD. Clinic-pathological study on therapeutic efficacy of Qianggan capsule for hepatic fibrosis of chronic hepatitis B. *Weichang Bingxue Yu Ganbingxue Zazhi* 2001; **10**: 247-249
- Bongiovanni M**, Viberti L, Pecchioni C, Papotti M, Thonhofer R, Hans Popper H, Sapino A. Steroid hormone receptor in pleural solitary fibrous tumours and CD34+ progenitor stromal cells. *J Pathol* 2002; **198**: 252-257

Enhancement of migration and invasion of hepatoma cells via a Rho GTPase signaling pathway

De-Sheng Wang, Ke-Feng Dou, Kai-Zong Li, Zhen-Shun Song

De-Sheng Wang, Ke-Feng Dou, Kai-Zong Li, Zhen-Shun Song,
Department of Hepatobiliary Surgery, Xijing Hospital, Fourth Military
Medical University, Xi'an 710032, Shannxi Province, China

Correspondence to: De-Sheng Wang, MD., Department of Hepatobiliary
Surgery, Xijing Hospital, Fourth Military Medical University, Xi'an,
710032, Shannxi Province, China. wangdesh@163.com

Telephone: +86-29-3375259 **Fax:** +86-29-3375255

Received: 2003-08-05 **Accepted:** 2003-09-18

Abstract

AIM: Intrahepatic extension is the main cause of liver failure and death in hepatocellular carcinoma patients. The small GTPase Rho and one of its effector molecules ROCK regulate cytoskeleton and actomyosin contractility, and play a crucial role in cell adhesion and motility. We investigated the role of small GTPase Rho in biological behaviors of hepatocellular carcinoma to demonstrate the importance of Rho in cancer invasion and metastasis.

METHODS: Using Western blotting, we quantitated Rho protein expression in SMMC-7721 cells induced by Lysophosphatidic acid (LPA). Furthermore, we examined the role of Rho signaling in regulating the motile and invasive properties of tumor cells.

RESULTS: Rho protein expression was stimulated by LPA. Using the Rhotekin binding assay to assess Rho activation, we observed that the level of GTP-bound Rho was elevated transiently after the addition of LPA, and Y-27632 decreased the level of active Rho. LPA enhanced the motility of tumor cells and facilitated their invasion. Rho played an essential role in the migratory process, as evidenced by the inhibition of migration and motility of cancer cells by a specific inhibitor of ROCK, Y-27632.

CONCLUSION: The finding that invasiveness of hepatocellular carcinoma is facilitated by the Rho/Rho-kinase pathway is likely to be relevant to tumor progression and Y-27632 may be a new potential effective agent for the prevention of intrahepatic extension of human liver cancer.

Wang DS, Dou KF, Li KZ, Song ZS. Enhancement of migration and invasion of hepatoma cells via a Rho GTPase signaling pathway. *World J Gastroenterol* 2004; 10(2): 299-302
<http://www.wjgnet.com/1007-9327/10/299.asp>

INTRODUCTION

Hepatocellular carcinoma is one of the most common cancers worldwide, especially in Asia^[1]. It frequently shows early invasion into blood vessels together with intrahepatic extensions and later extrahepatic metastasis^[2]. A better understanding of the processes involved in the development of the metastasis might improve future prognosis by facilitating treatment strategies.

Tumor invasion is a complex biological process, during

which tumor cells detach from the primary tumor and infiltrate the surrounding tissue. This process requires loss of cell contacts between tumor cells, active cell migration, adhesion to the extracellular matrix and proteolytic degradation of the extracellular matrix^[3-5]. Rho, a member of the Ras family of small GTP-binding proteins, has a molecular weight of approximately 27 kDa and is located under the cell membrane, potentially functioning in signal transduction pathways^[6]. Small GTPase Rho protein is known to work as a molecular switch for the regulation of signal transduction of intracellular events related to cell motility, cytoskeletal dynamics, and tumor progression^[7,8]. In the present study, we hypothesized that Rho protein might be associated with the development of hepatocellular carcinoma.

Lysophosphatidic acid (LPA) is a product of phospholipid metabolism. Exogenous LPA binds to surface G protein-coupled receptors and its biological activities are mediated in part by the cytosolic small GTPase Rho^[9-11]. The motility of tumor cells could be regulated by the target of Rho, Rho-associated coiled-coil forming protein kinase (p160ROCK), through reorganization of the actin cytoskeleton^[12]. A recently described specific inhibitor of p160ROCK, the (+)-(R)-*trans*-4-(1-Aminoethyl)-N-(4-pyridyl) cyclohexanecarboxamide dihydrochloride (Y-27632), was reported to inhibit Rho-mediated cell migration as well as smooth muscle contraction both *in vivo* and *in vitro*^[13-15].

Given the recent interest in the participation of Rho in cell migration, we analyzed the role of Rho associated signal transduction pathways during the LPA-induced transmigration of human hepatocellular cells, and more importantly the activity of Rho regulated by LPA and inhibitor of p160ROCK.

MATERIALS AND METHODS

Cell lines and treatment

SMMC-7721 cell, originally isolated from a poorly differentiated hepatocellular carcinoma, was used in all experiments. SMMC-7721 cell was cultured in modified minimum essential medium (MEM) containing 2-fold concentrated amino acids and vitamins supplemented with 10% fetal calf serum (FCS) at 37 °C in a humidified atmosphere of 5% CO₂ in air. The cells were used within 15-20 passages after the initiation of cultures. Before each experiment, cells were cultured under serum-free conditions (in medium containing 0.1% bovine serum albumin) for 24 h.

Western blot analysis

Cells were starved in serum-free culture medium for 24 h and subsequently treated with LPA at 37 °C for various times. The cells were washed twice with PBS and lysed in ice-cold lysis buffer (20 mM Tris, pH 7.4, 150 mM NaCl, 1% Triton X-100, 1 mM EDTA, 1 mM EGTA, 2.5 mM sodium pyrophosphate, 1 mM glycerolphosphate, 1 mM sodium orthovanadate, 1 µg/ml leupeptin, and 1 mM phenylmethylsulfonyl fluoride). The extracts were centrifuged to remove cellular debris, and protein content of the supernatants was determined using the Bio-Rad protein assay reagent. Samples were resolved by SDS-polyacrylamide gel electrophoresis and transferred to

Hybond-P. The transferred samples were incubated with the anti-rho antibody indicated, and then incubated with HRP-conjugated IgG, and the immunoblotted proteins were visualized with ECL reagents.

Rho activation assay

A commercial pull-down assay (Rho activation assay kit, Upstate) was used to measure the effect of LPA and Y-27632 on Rho activity in SMMC-7721 cells. The cells were washed twice with modified MEM and incubated in fresh modified MEM without serum for 24 h, 25 μ M LPA with or without Y-27632 (25 μ mol/L) was added and the cell suspension was centrifuged at the indicated time after LPA addition, and then the cell pellet was lysed (lysis buffer, Upstate) and the activated Rho pull-down assay was performed according to the manufacturer's protocol. A protein assay was performed prior to beginning pull-down assay to equalize the total protein concentration of each treatment group. Positive and negative controls were also performed according to the manufacturer's protocol. Briefly, lysates of cells were preincubated with 100 μ M nonhydrolyzable GTP γ S (positive Rho activation) or 100 μ M GDP (negative Rho activation) prior to undergoing precipitation by the Rhotekin GTP-Rho binding domain.

Morphological changes by Rho-kinase pathway

The cells were cultured in serum-free culture medium, and the dishes were incubated for an additional period of 24 hours. LPA (5 μ mol/L) was then added to the dishes with or without different concentrations of Y-27632 (5, 25, 125 μ mol/L) and cultured for 1 hour. The cells were examined using a phase-contrast microscope.

Cell motility assay

Random motility was determined by using the gold-colloid assay^[16]. Gold colloid was layered onto glass coverslips and placed into 6-well plates. Cells were seeded onto the coverslips and allowed to adhere for 1 h at 37 °C in a CO₂ incubator (12 500 cells/3 ml in serum-free medium). To stimulate the cells, the serum-free medium was replaced with 5% FBS containing LPA (5 μ mol/L) with or without Y-27632 (25 μ mol/L) and allowed to incubate for 24 h at 37 °C. The medium was aspirated and the cells were fixed with 2% glutaraldehyde. The coverslips were then mounted onto glass microscope slides and areas of clearing in the gold colloid corresponding to phagokinetic cell tracks were counted.

Cell invasion assay

Chemotactic directional migration was evaluated using a modified Boyden chamber^[17,18]. In this invasion assay, tumor cells had to overcome a reconstituted basement membrane by a sequential process of proteolytic degradation of the substrate and active migration. Costar transwells (pore size 8 μ m) were coated with matrigel, dried at 37 °C in an atmosphere of 5% CO₂, and reconstituted with serum-free medium. Cells (3×10^4) were plated in the upper chamber in medium containing LPA with or without Y-27632 and allowed to migrate for 4.5 h. Nonmigrating cells were removed from the upper chamber with a cotton swab and migrating cells adherent to the underside of the filter were fixed and stained with Mayer's hematoxylin solution and counted with an ocular micrometer. All experiments were performed in triplicate, and at least 10 fields/filter were counted. Data were expressed as relative migration (number of cells/field) and represented as $\bar{x} \pm s$ of at least three independent experiments.

Statistical analysis

All data were expressed as $\bar{x} \pm s$. Statistical analysis was done

by statistical package of SPSS for window release 9.0. Differences between the mean were tested with the Mann-Whitney test. $P < 0.05$ was considered statistically significant.

RESULTS

Increase of Rho protein levels as a result of LPA treatment

Using Western blot analysis with Rho polyclonal antibody, we detected the changes of the level of Rho family protein in SMMC-7721 cell extracts. The protein level of Rho rapidly increased within 5 h and reached the nearly maximal level at 25 h after the treatment with LPA, with more than 2-fold increase over the untreated control value (Figure 1).

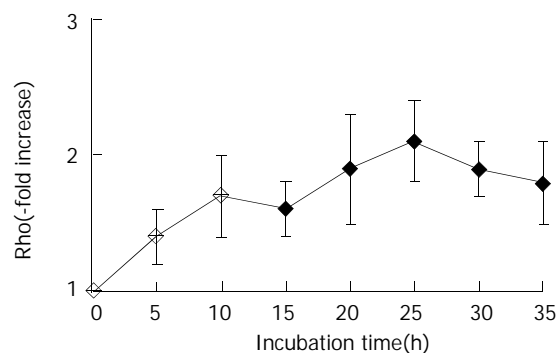


Figure 1 Changes in levels of Rho family protein in SMMC-7721 cells induced by LPA. The levels of Rho protein were analyzed by Western blot analysis. The data shown are expressed as $\bar{x} \pm s$ from three different experiments.

Inhibition of LPA-induced Rho activation by Y-27632

We measured the intracellular levels of the GTP-bound active form of Rho by the pull-down assay system^[19]. Activated GTP-Rho was precipitated by the Rho-binding domain of Rhotekin, a downstream Rho effector that specifically binds to only activated GTP-Rho^[20]. The level of GTP-bound Rho was elevated transiently after the addition of LPA and reached the peak level at 30 min after LPA addition, whereas Y-27632 decreased the level of active Rho. Since the total amount of Rho in each lysate was almost constant, Y-27632 inhibited Rho activation. This result was controlled by equalizing the harvested protein levels from each treatment with an appropriate dilution of buffer determined by a protein concentration assay prior to beginning the pull-down assay. A positive and negative control for active or inactive Rho was also performed in parallel. Lysates of cells were preincubated with nonhydrolyzable GTP γ S (positive Rho activation) or GDP (negative Rho activation) prior to undergoing precipitation by Rhotekin. Similar levels of active Rho were detected in cells grown on LPA and in cells incubated with GTP γ S. Thus, the result indicated that LPA might stimulate an increase in activated Rho and Y-27632 might inhibit the activation of Rho.

Morphological changes induced by Rho-kinase inhibitor and LPA

The effect of Y-27632 on morphologic changes induced by LPA in serum-starved SMMC-7721 cells was observed under a phase-contrast microscope. In serum starvation, cells formed relatively cohesive colonies, and after addition of LPA, they formed dissociated and scattered lamellipodial extensions at the cells' edges. Addition of Y-27632 at a concentration of 25 μ mol/L or more inhibited these LPA-induced morphologic changes, and SMMC-7721 cells remained cohesive with each other.

Inhibition of LPA-induced motility and invasion by Y-27632

To evaluate the effect of Rho-mediated cellular motility, we

assessed the treated cell line in colloidal-gold random motility assay. Cells were seeded onto glass coverslips overlaid with a gold colloid and stimulated with LPA to induce motility. Discernable and quantifiable tracks were left as the cells moved and phagocytized the gold colloid. As determined by the trypan blue dye exclusion assay, the reduction in cell motility was not caused by a decrease in the number of viable cells. At 24 h after stimulation, the cells treated with LPA were 2.2 fold more motile than their untreated counterparts ($P < 0.01$) and Y-27632 significantly suppressed the LPA-induced motility (Figure 2).

As shown in Figure 3, when the cells were tested for their ability to invade through a matrigel-coated filter in response to a chemoattractant, the LPA-treated cells were 2.3 fold more invasive than the untreated cells. Addition of Y-27632 at a concentration of 25 $\mu\text{mol/L}$ significantly inhibited the LPA-induced invasion ($P < 0.01$). Taken together, these data suggested that treatment of SMMC-7721 cells with Y-27632 could lead to the inhibition of LPA-mediated motility and invasion.

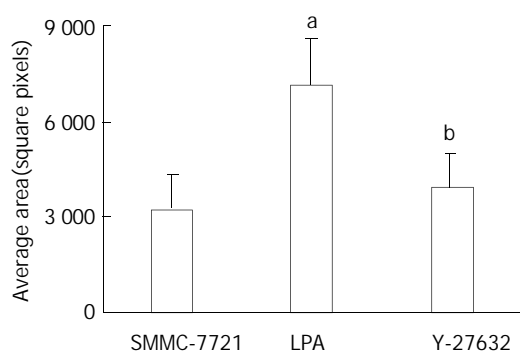


Figure 2 Tumor cell random motility determined by gold-colloid assay. Cells were seeded onto the coverslips and allowed to adhere for 1 h and then incubated in FBS containing LPA with or without Y-27632 for 24 h. The areas of clearing in the gold colloid corresponding to phagokinetic cell tracks were counted and represented as $\bar{x} \pm s$ from triplicate experiments. ^a $P < 0.01$ LPA treated cells vs SMMC-7721 control cells, ^b $P < 0.01$ Y-27632 treated cells vs LPA treated cells.

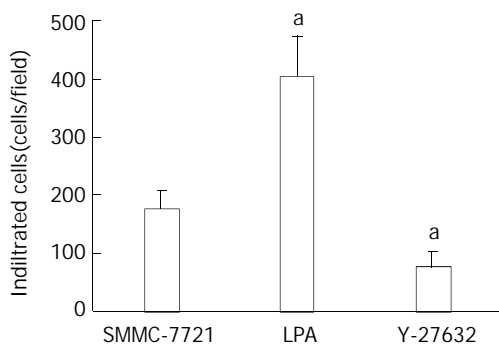


Figure 3 Inhibition of LPA-induced tumor cell invasion by Y-27632. Serum-starved cells were seeded onto porous filters. After incubation of the filters with Y-27632 in the presence of LPA 25 μM for 4.5 h to permit penetration of the cells, nonmigrating cells were removed from the upper chamber and migrating cells adherent to the underside of the filters were counted in a minimum of 10-high power fields. Data were expressed as relative migration (number of cells/field) and represented as $\bar{x} \pm s$ from triplicate experiments. ^a $P < 0.01$ relative to SMMC-7721 control cells.

DISCUSSION

Generally, metastasis has been found to be a multistep process, which includes detachment of cancer cells from primary tumor, migration, adhesion and invasion of cancer cells into the blood

or lymphatic vessels, extravasation out of the vessel, and finally, interactions with the target tissue and the formation of metastatic foci in distant organs^[21,22]. In spite of recent advances in diagnostic and therapeutic methods, the prognosis of HCC patients with intrahepatic metastasis was poor^[1]. Accordingly, analysis of the mechanism of the migration of cancer cells might lead to new strategies for preventing the progression of hepatocellular carcinoma. The molecular and cellular mechanisms of intrahepatic metastasis have not been fully understood, although cell motility mediated by Rho signaling pathway was recently shown to play a critical role in metastasis of various tumor cells.

Rho is a small GTPase that was found to play an essential role in a variety of cellular processes^[6,23]. The active GTP-bound form was involved in cytoskeletal responses to extracellular signaling pathways, resulting in the formation of stress fibres and focal adhesions^[24]. Other Rho effects included important roles in signaling pathways that control gene transcription, cell cycle regulation, apoptosis, and tumor progression^[25]. Rho proteins could oscillate between an active GTP-bound state and inactive GDP-bound state. The ratio between these two forms is regulated by two classes of proteins: GTPase-activating proteins (GAPs), which promote hydrolysis of GTP bound to the active form and accumulation of the inactive GDP-bound form, and guanine nucleotide exchange factors (GEFs), which promote the exchange of GDP for GTP and therefore induce accumulation of the activated GTP-bound form. In resting cells, inactive GDP-bound Rho proteins were found in the cytosol in complex with another class of regulatory proteins, nucleotide dissociation inhibitors (RhoGDIs). Upon activation, dissociation of RhoGDIs from the complex was required to enable interaction with GEFs and exchange of GDP for GTP^[26,27]. To exert their function, activated Rho proteins need to associate with the cell membrane and this in turn depends on their posttranslational modification.

It has been demonstrated that the role of Rho in inducing the invasion could be substituted for by one of its downstream effectors, the Rho-associated kinase (ROCK)^[28]. Invasion by tumor cells is a process composed of proteolytic degradation of extracellular matrix barriers and the migration of the cells through the modified region. Contraction of the actomyosin system is important for cell migration, and ROCK regulates the myosin light chain (MLC) phosphorylation by direct phosphorylation of MLC and by inactivation of myosine phosphatase, which was found to result in an increase in actomyosin-based contractility^[29,30]. Lysophosphatidic acid is a simple phospholipid that nonetheless has the properties of an extracellular growth factor, mediating diverse cellular responses through the activation of multiple signal transduction pathways. LPA could trigger actin-cytoskeletal events through Rho GTPases, thereby influencing transcellular migration^[31]. LPA could induce MLC phosphorylation through Rho activation, leading to the stimulation of cell contractility and motility of fibroblasts and cancer cells^[32].

Overexpression of Rho family members increases migration and invasion in various cell lines and culture models, this suggests that such an overexpression in carcinomas might profoundly affect metastatic potential *in vivo*^[33]. The result of Western blot showed that the level of activation of Rho was augmented by LPA. In our study, we extended this observation by providing the evidence that a specific inhibitor of Rho kinase, Y-27632, could inhibit LPA induced Rho activation by GTP-bound Rho pull-down assay. The Rho pathway through a G protein-coupled receptor appeared to be an important process of LPA-mediated signaling.

Y-27632 had an excellent selectivity to inhibit Rho-kinase as compared to other kinases, such as protein kinase C and myosin light-chain kinase in a cell-free system^[34]. Thus, Y-

27632 is a powerful tool to investigate the role of the Rho/Rho-kinase system, especially *in vivo*, although more potent Rho-kinase inhibitors have been synthesized^[35]. Y-27632 was reported to inhibit transcellular invasion and reduce the extent of local peritoneal metastases by MM1 rat hepatoma and also *in vivo* dissemination of prostate cancer cells^[36]. In the present study, Y-27632 blocked LPA-mediated SMMC-7721 cell transmonolayer invasion, suggesting the essential role of Rho-Rho kinase pathway in LPA-mediated cell migration. We also observed that Y-27632 induced morphological changes in SMMC-7721 cells, characterized by remaining relatively cohesive colonies, suggesting that Rho-kinase was necessary as a downstream effector of Rho for cell morphologies. Previous reports also demonstrated that Y-27632 inhibited LPA-induced morphologic changes in various cell lines *in vitro*.

As cell migration, invasion, cellular proliferation, and survival are advantageous to tumor cells for the formation of metastases, the finding that invasiveness of hepatocellular carcinoma is facilitated by the Rho/Rho-kinase pathway is likely to be relevant to tumor progression and the Rho/Rho-kinase may be useful as a prognostic indicator and also in the development of novel therapeutic strategies. Y-27632 may be a new potentially effective agent for the prevention of intrahepatic extension of human HCC.

REFERENCES

- Tang ZY**. Hepatocellular carcinoma—cause, treatment and metastasis. *World J Gastroenterol* 2001; **7**: 445-454
- Poon RT**, Fan ST, Ng IO, Wong J. Prognosis after hepatic resection for stage IVA hepatocellular carcinoma: a need for reclassification. *Ann Surg* 2003; **237**: 376-383
- Bartsch JE**, Staren ED, Appert HE. Adhesion and migration of extracellular matrix-stimulated breast cancer. *J Surg Res* 2003; **110**: 287-294
- Mareel M**, Leroy A. Clinical, cellular, and molecular aspects of cancer invasion. *Physiol Rev* 2003; **83**: 337-376
- Gupta MK**, Qin RY. Mechanism and its regulation of tumor-induced angiogenesis. *World J Gastroenterol* 2003; **9**: 1144-1155
- Wang P**, Bitar KN. Rho A regulates sustained smooth muscle contraction through cytoskeletal reorganization of HSP27. *Am J Physiol* 1998; **275**: G1454-G1462
- Nishimura Y**, Itoh K, Yoshioka K, Ikeda K, Himeno M. A role for small GTPase RhoA in regulating intracellular membrane traffic of lysosomes in invasive rat hepatoma cells. *Histochem J* 2002; **34**: 189-213
- Stice LL**, Forman LW, Hahn CS, Faller DV. Desensitization of the PDGFbeta receptor by modulation of the cytoskeleton: the role of p21(Ras) and Rho family GTPases. *Exp Cell Res* 2002; **275**: 17-30
- Wojciak-Stothard B**, Ridley AJ. Rho GTPases and the regulation of endothelial permeability. *Vascul Pharmacol* 2002; **39**: 187-199
- Hashimoto T**, Yamashita M, Ohata H, Momose K. Lysophosphatidic acid enhances *in vivo* infiltration and activation of guinea pig eosinophils and neutrophils via a Rho/Rho-associated protein kinase-mediated pathway. *J Pharmacol Sci* 2003; **91**: 8-14
- Sawada K**, Morishige K, Tahara M, Kawagishi R, Ikebuchi Y, Tasaka K, Murata Y. Alendronate inhibits lysophosphatidic acid-induced migration of human ovarian cancer cells by attenuating the activation of rho. *Cancer Res* 2002; **62**: 6015-6020
- Kawaguchi A**, Ohmori M, Harada K, Tsuruoka S, Sugimoto K, Fujimura A. The effect of a Rho kinase inhibitor Y-27632 on superoxide production, aggregation and adhesion in human polymorphonuclear leukocytes. *Eur J Pharmacol* 2000; **403**: 203-208
- Ai S**, Kuzuya M, Koike T, Asai T, Kanda S, Maeda K, Shibata T, Iguchi A. Rho-Rho kinase is involved in smooth muscle cell migration through myosin light chain phosphorylation-dependent and independent pathways. *Atherosclerosis* 2001; **155**: 321-327
- Itoh K**, Yoshioka K, Akedo H, Uehata M, Ishizaki T, Narumiya S. An essential part for Rho-associated kinase in the transcellular invasion of tumor cells. *Nat Med* 1999; **5**: 221-225
- Somlyo AV**, Bradshaw D, Ramos S, Murphy C, Myers CE, Somlyo AP. Rho-kinase inhibitor retards migration and *in vivo* dissemination of human prostate cancer cells. *Biochem Biophys Res Commun* 2000; **269**: 652-659
- Albrecht-Buehler G**. The phagokinetic tracks of 3T3 cells. *Cell* 1977; **11**: 395-404
- van Golen KL**, Risin S, Staroselsky A, Berger D, Tainsky MA, Pathak S, Price JE. Predominance of the metastatic phenotype in hybrids formed by fusion of mouse and human melanoma clones. *Clin Exp Metastasis* 1996; **14**: 95-106
- van Golen KL**, Bao L, DiVito MM, Wu Z, Prendergast GC, Merajver SD. Reversion of RhoC GTPase-induced inflammatory breast cancer phenotype by treatment with a farnesyl transferase inhibitor. *Mol Cancer Ther* 2002; **1**: 575-583
- Ren XD**, Kiosses WB, Schwartz MA. Regulation of the small GTP-binding protein Rho by cell adhesion and the cytoskeleton. *EMBO J* 1999; **18**: 578-585
- Wahl S**, Barth H, Ciossek T, Aktories K, Mueller BK. Ephrin-A5 induces collapse of growth cones by activating Rho and Rho kinase. *J Cell Biol* 2000; **149**: 263-270
- Qin LX**, Tang ZY. The prognostic molecular markers in hepatocellular carcinoma. *World J Gastroenterol* 2002; **8**: 385-392
- Bartsch JE**, Staren ED, Appert HE. Adhesion and migration of extracellular matrix-stimulated breast cancer. *J Surg Res* 2003; **110**: 287-294
- Matozaki T**, Nakanishi H, Takai Y. Small G-protein networks: their crosstalk and signal cascades. *Cell Signal* 2000; **12**: 515-524
- Greenberg DL**, Mize GJ, Takayama TK. Protease-activated receptor mediated RhoA signaling and cytoskeletal reorganization in LNCaP cells. *Biochemistry* 2003; **42**: 702-709
- Van Aelst L**, D' Souza-Schorey C. Rho GTPases and signaling networks. *Genes Dev* 1997; **11**: 2295-2322
- Zwartkruis FJ**, Bos JL. Ras and Rap1: two highly related small GTPases with distinct function. *Exp Cell Res* 1999; **253**: 157-165
- Geyer M**, Wittinghofer A. GEFs, GAPs, GDIs and effectors: taking a closer (3D) look at the regulation of Ras-related GTP-binding proteins. *Curr Opin Struct Biol* 1997; **7**: 786-792
- Riento K**, Ridley AJ. Rocks: multifunctional kinases in cell behaviour. *Nat Rev Mol Cell Biol* 2003; **4**: 446-456
- Chen BH**, Tzen JT, Bresnick AR, Chen HC. Roles of Rho-associated kinase and myosin light chain kinase in morphological and migratory defects of focal adhesion kinase-null cells. *J Biol Chem* 2002; **277**: 33857-33863
- Katoh K**, Kano Y, Amano M, Onishi H, Kaibuchi K, Fujiwara K. Rho-kinase-mediated contraction of isolated stress fibers. *J Cell Biol* 2001; **153**: 569-584
- Panetti TS**, Nowlen J, Mosher DF. Sphingosine-1-phosphate and lysophosphatidic acid stimulate endothelial cell migration. *Arterioscler Thromb Vasc Biol* 2000; **20**: 1013-1019
- Amano M**, Chihara K, Nakamura N, Fukata Y, Yano T, Shibata M, Ikebe M, Kaibuchi K. Myosin II activation promotes neurite retraction during the action of Rho and Rho-kinase. *Genes Cells* 1998; **3**: 177-188
- Steeg PS**. Metastasis suppressors alter the signal transduction of cancer cells. *Nat Rev Cancer* 2003; **3**: 55-63
- Feng J**, Ito M, Kureishi Y, Ichikawa K, Amano M, Isaka N, Okawa K, Iwamatsu A, Kaibuchi K, Hartshorne DJ, Nakano T. Rho-associated kinase of chicken gizzard smooth muscle. *J Biol Chem* 1999; **274**: 3744-3752
- Uehata M**, Ishizaki T, Satoh H, Ono T, Kawahara T, Morishita T, Tamakawa H, Yamagami K, Inui J, Maekawa M, Narumiya S. Calcium sensitization of smooth muscle mediated by a Rho-associated protein kinase in hypertension. *Nature* 1997; **389**: 990-994
- Somlyo AV**, Bradshaw D, Ramos S, Murphy C, Myers CE, Somlyo AP. Rho-kinase inhibitor retards migration and *in vivo* dissemination of human prostate cancer cells. *Biochem Biophys Res Commun* 2000; **269**: 652-659

Determination of chemical composition of gall bladder stones: Basis for treatment strategies in patients from Yaounde, Cameroon

Fru F. Angwafo III, Samuel Takongmo, Donald Griffith

Fru F. Angwafo III, Samuel Takongmo, Department of Surgery, Faculty of Medicine and Biomedical Sciences, The University of Yaounde I, Cameroon

Donald Griffith, Department of Urology, Baylor University, Houston, Texas, USA

Correspondence to: Fru F. Angwafo III, MD, Department of Surgery, Faculty of Medicine, The University of Yaounde I, PO Box 1364, Yaounde, Cameroon. asanji25@hotmail.com, fobuzshi@yahoo.com

Telephone: +237-7705749 **Fax:** +237-2315733

Received: 2003-06-04 **Accepted:** 2003-09-13

Abstract

AIM: Gallstone disease is increasing in sub-saharan Africa (SSA). In the west, the majority of stones can be dissolved with bile salts, since the major component is cholesterol. This medical therapy is expensive and not readily accessible to poor populations of SSA. It was therefore necessary to analyze the chemical composition of biliary stones in a group of patients, so as to make the case for introducing bile salt therapy in SSA.

METHODS: All patients with symptomatic gallstones were recruited in the study. All stones removed during cholecystectomy were sent to Houston for x-ray diffraction analysis. Data on age, sex, serum cholesterol, and the percentage by weight of cholesterol, calcium carbonate, and amorphous material in each stone was entered into a pre-established proforma. Frequencies of the major components of the stones were determined.

RESULTS: Sixteen women and ten men aged between 27 and 73 (mean 44.9) years provided stones for the study. The majority of patients (65.38%) had stones with less than 25% of cholesterol. Amorphous material made up more than 50% and 100% of stones from 16 (61.53%) and 9 (34.61%) patients respectively.

CONCLUSION: Cholesterol is present in small amounts in a minority of gallstones in Yaounde. Dissolution of gallstones with bile salts is unlikely to be successful.

Angwafo III FF, Takongmo S, Griffith D. Determination of chemical composition of gall bladder stones: Basis for treatment strategies in patients from Yaounde, Cameroon. *World J Gastroenterol* 2004; 10(2): 303-305

<http://www.wjgnet.com/1007-9327/10/303.asp>

INTRODUCTION

Biliary lithiasis has been a common disease in Europe and the USA for decades. Over half of the cases are asymptomatic, usually detected by an abdominal ultrasound^[1]. For a very long time, biliary stone disease was said to be rare in Sub-Saharan Africa (SSA). Archampong reported a 0.4% prevalence of all admissions in the Korle Bu Teaching Hospital in 1969 in Ghana^[2]. Today the prevalence of gallstone disease has increased considerably with the widespread use of ultrasonography^[3].

This increase has also been observed in African populations of Jamaica^[4] and SSA^[2,5].

Many studies to identify risk factors for biliary lithiasis in the West have focused on supersaturation of cholesterol in bile in the nucleation process, a critical step in the genesis of bile stones^[1,6]. The high concentration of cholesterol in gallstones has been the basis for the widespread use of bile acids, a nonsurgical treatment for the dissolution of gall bladder stones. These stones account for as much as 80% of Western stones^[6]. Unfortunately, gall bladder stone composition is heterogeneous, and differs within and without populations around the world^[3-8].

The increasing frequency of biliary stones in SSA, with its different epidemiological factors and diseases, prompted us to carry out a chemical analysis of gallstones. This study would demonstrate the role of cholesterol in our stones and therefore the necessity of using bile salts for gall stone dissolution in SSA.

MATERIALS AND METHODS

This was a cross-sectional study of a series of stones removed from patients at the University Hospital Center (UHC) of the University of Yaounde I from January 1, 1989 to December 31, 1998. All stones removed during surgery were placed on sterile gauze to air dry, transferred into a paper envelope bearing the name, age, and sex of the patient as well as the date. The first batch of stones from 19 patients was sent to the Urolithiasis laboratory in Houston, Texas in January 1996. A second collection of stones from 7 patients was sent to the same laboratory in May 1999.

All stone specimens were first examined for shape, size, and color. They were classified as cholesterol, black or brown pigmented stones, examined under a polarized microscope. The composition of the nidus, the internal and external shells was determined by X-ray diffraction as described previously^[9]. The percentage of cholesterol, calcium carbonate, and amorphous material such as black bilirubinate, black phosphate, glycoproteins and salts was determined. A descriptive analysis was done for stones from each patient. Patients who were able to pay for a serum cholesterol assay did so. Hemoglobin electrophoresis was not asked in this mainly adult population who did not give histories of sickle cell disease or crisis.

RESULTS

Patient population

There were 26 Cameroonian patients, all black Africans, aged between 27 and 73 years (mean 44.9 years). There were 16 women and 10 men, a 1.6 female to male sex ratio. The men were aged between 36 and 62 years whereas 6 women were less than 35 years (23.07%). All our patients resided in the city. They consumed mainly an African traditional diet made of local vegetarian menus mixed with imported processed Western items such as rice and wheat. The serum cholesterol level was normal in all 10 patients who did it.

Stone analyses

The percentage of cholesterol in the stones by weight is

depicted in Table 1. Seventeen patients (65.38%) had stones with less than 25% cholesterol. Of these, 11 (42.30%) had cholesterol free stones. Seven patients (26.92%) and 9 others (34.61%) had stones with 50% and 80% cholesterol content, respectively.

Calcium carbonate was detected in stones from 4 (15.38%) patients, three of whom were female. Two of these females had mixed stones containing cholesterol, calcium carbonate and amorphous material.

Table 2 shows the distribution of amorphous material by weight in these stones. Stones from 16 (61.53%) patients contained more than 50% amorphous material. The entire stone was made of amorphous material in 9 (34.61%) cases.

Table 1 Percent by weight of cholesterol in the gallstones from 26 patients

% by weight	Males	Females	Patient (%)
0	6	5	11 (42.30)
<25	1	5	6 (23.07)
> or =25 and <50	0	0	0
> or = 50 and <80	1	1	2 (7.69)
> or = 80 <100	0	4	4 (15.38)
100	2	1	3 (11.53)
	10	16	26 (100)

Table 2 Percent by weight of amorphous material in the gallstones from 26 patients

% by weight	Males	Females	Patient (%)
0	2	1	3 (11.53)
<25	0	5	5 (19.23)
> or = 25 and <50	1	1	2 (7.69)
> or = 50 and <80	1	0	1 (3.84)
> or = 80 and <100	0	6	6 (23.07)
100	6	3	9 (34.61)
	10	16	26 (100)

DISCUSSION

The results from this hospital-based nonrandomized study cannot be extrapolated to the community due to several limitations. In this group there were no children. Yet, it is known that children with hemolytic diseases develop cholesterol-poor, bilirubin-rich gallstones^[2]. Even in children without hemolytic disease, the composition of gallstones was different from those of adults in Leeds, England^[7]. Limitations to recruiting a potentially representative population of patients include poverty, in the absence of a financial scheme for health care coverage, ignorance and cultural factors that dissuade people from attending hospital services. Nonetheless, this pilot study permits us to raise the hypothesis that dissolution of gall bladder stones with bile salts is not a cost-effective alternative to surgical treatment.

A recent series of biliary lithiasis revealed a 4-fold increase of symptomatic gall bladder stone disease in Ghana from 1966-1999. This series also reported that the majority of Ghanaian stones were not cholesterol rich. Furthermore, cholesterol stones were more common in females and only 34% of their stones contained 75% or more of cholesterol by weight. They also showed that the external appearance of the stone was a poor predictor of its composition^[2]. This means that even in the poorer regions of the world, such as Sub-Saharan Africa, all attempts should be made to chemically analyze stones.

The treatment of gallstone diseases runs the gamut from bile salts dissolution, to fragmentation with laser^[10], pulverization with extracorporeal shock wave lithotripsy^[11], endoscopic

extraction, and classical surgery, whereas noninvasive medical therapy is appealing, bile acid therapy is only effective in some cholesterol gallstones. Bile acids are not effective in treating calcium bilirubinate or calcium carbonate/phosphate stones. It is therefore imperative that the composition of the stone be determined to tailor treatment for the individual patient^[12].

To determine stone composition, there are many possibilities offered by different technologies. On simple X-ray, radiologically undetectable stone calcification reduces the probability of dissolution and calcified structures appearing in stones during treatment are composed of calcium carbonate. A radio-opaque stone would suggest that medical therapy is unlikely to succeed. Stone composition is also determined on computed tomography. Results from polarizing microscopy of gall bladder bile suggest that the presence of cholesterol crystals is a sensitive measure of cholesterol and vaterite microspheruliths confirm presence of calcium carbonate in the gallstone^[13].

In the less technically developed areas the chemical composition of stones was determined from its external appearance. This has been shown to be inaccurate. Frequently the stones are homogenized and chemically analyzed. Our stones were analyzed with X-ray diffraction where cholesterol, calcium carbonate, and amorphous material were detected. The components of the amorphous material (bilirubine, glycerophosphates and bile salts) were not identifiable on X-ray diffraction. Infra-red spectroscopy and scanning electron microscopy were used to show that black and brown pigment gallstones differ in microstructure and micro-composition, suggesting that they form by different mechanisms. Black carbonate and brown stones layered structure suggests that stone growth is dependent on cyclical changes in biliary substances^[14]. This may explain the permissive or causal role endogenous hormones have in gallstone formation^[15]. Stone formation begins with nucleation where the interaction of pronucleators and antinucleators leads to formation of cholesterol crystals and these develop into gallstones^[6,16]. Hepatic cholesterol hypersecretion is associated with the increased unsaturated fatty acid proportion in biliary phospholipids and gallbladder mucin secretion, thereby causing rapid crystal nucleation^[17]. It is evident that gallstone disease has a multifactorial causation, including gall bladder infection,^[18] decreased gall bladder motility after surgery for obesity and/or weight loss^[19], ileal disease (Crohn's)^[20], hemolytic diseases^[2], familial hypercholesterolemia^[21], and metabolic defects in hepatic bilirubin glucuronidation^[22].

A shortcoming in our study is the absence of hemoglobin electrophoresis in a population where the prevalence of the sickle trait varies between 10% and 20% and that of the disease is about 1%^[2]. We did not explore many of the risk factors mentioned above largely due to technical and financial limitations. The absence of calcium in the stones of 22 (84.61%) patients correlates with a small number of gallstones detected on plain X-ray of the abdomen in our region. The extremely infrequent occurrence of pure cholesterol gallstones is a strong argument against the introduction of oral dissolution agents in SSA.

CONCLUSION

There is a corresponding variation in prevalence of cholesterol rich stones as a variation in composition of gallstones. This variation seems to be related to genes and the environment. Stone composition determines the therapeutic approaches in each locality. This pilot study suggests that oral bile salt dissolution therapy would not be effective in 70% of our patients. As populations in SSA undergo epidemiologic transition from infectious diseases to noncommunicable diseases, there will be increasing prevalence of biliary lithiasis.

REFERENCES

- 1 **Bartoli E**, Capron JP. Epidemiology and natural history of cholelithiasis. *Rev Prat* 2000; **50**: 2112-2116
- 2 **Darko R**, Archampong EQ, Qureshi Y, Muphy GM, Dowling RH. How often are Ghanaian gallbladder stones cholesterol-rich. *West Afr J Med* 2000; **19**: 64-70
- 3 **Kratzer W**, Mason RA, Kachele V. Prevalence of gallstones in sonographic surveys worldwide. *J Clin Ultrasound* 1999; **27**: 1-7
- 4 **Walker TM**, Hambleton IR, Serjeant GR. Gallstones in sickle cell disease: observations from the Jamaican cohort study. *J Pediatr* 2000; **136**: 80-85
- 5 **Akute OO**, Marinho AO, Kalejaiye AO, Sogo K. Prevalence of gallstones in a group of antenatal women in Ibadan. *Nigeria Afr J Med Sci* 1999; **3-4**: 159-161
- 6 **Kaloo AN**, Kanstevoev SV. Gallstones and biliary disease. *Prim Care* 2001; **28**: 591-606
- 7 **Stringer MD**, Taylor DR, Soloway RD. Gallstone composition: are children different? *J Pediatr* 2003; **142**: 435-440
- 8 **Kim MH**, Lim BC, Myung SJ, Lee SK, Ohor HC, Kim YT, Roe IH, Kim JH, Chung JB, Kim CD, Shim SC, Yun YB, Min YI, Yang US, Kang JK. Epidemiological study of Korean gallstone disease: a nationwide cooperative study. *Dig Dis Sci* 1999; **44**: 1674-1683
- 9 **Bassi N**, Aggio L, Ghio S, Meggiato T, Di Mario F, Del Favero G, Scalon P, Molin M, D' Amico D, Naccarato R. X-ray diffraction study of biliary calculi. Morphological and composition correlations of calculi. *G Clin Med* 1990; **71**: 331-335
- 10 **Shi W**, Vari S, Papaioannou T, Daykovsky L, Grundfest W. Biliary calculi fragmentation by a 308 mm excimer laser. *J Clin Laser Med Surg* 1991; **9**: 139-141
- 11 **Ertran A**. Treatment of gall stones by extracorporeal shock wave lithotripsy. *Am J Gastroenterol* 2002; **97**: 831-832
- 12 **Ros E**, Navarro S, Fernandez I, Reixach M, Ribo JM, Rodes J. Utility of biliary microscopy for the prediction of the chemical composition of gall stones and outcome of dissolution therapy with ursodexycolic acid. *Gastroenterology* 1986; **91**: 703-712
- 13 **Nakai K**, Tazuma S, Ochi H, Chayama K. Does bilirubin play a role in the pathogenesis of both cholesterol and pigment gallstone formation? Direct and indirect influences of bilirubin on bile lithogenicity. *Biochim Biophys Acta* 2001; **1534**: 78-84
- 14 **Kleiner O**, Ramesh J, Huleihel M, Cohen B, Kantarovich K, Levi C, Polyak B, Marks RS, Mordechai J, Cohen Z, Mordechai S. A comparative study of gallstones from children and adults using FTIR spectroscopy and fluorescence microscopy. *BMC Gastroenterol* 2002; **2**: 3-15
- 15 **Russo F**, Cavallini A, Messa C, Mangini V, Guerra V, D' Amato G, Misciagna G, Di Leo A. Endogenous sex hormones and cholesterol gallstones: a case-control study in an echographic survey of gallstones. *Am J Gastroenterol* 1993; **88**: 712-717
- 16 **Portincasa P**, Moschetta A, Calamita G, Margari A, Palasciano G. Pathobiology of cholesterol gallstone disease: from equilibrium ternary phase to agents preventing cholesterol crystallization and stone formation. *Curr Drug Targets Immune Endocr Metabol Disord* 2003; **3**: 67-81
- 17 **Hatsushika S**, Tasuma S, Kajiyama G. Nucleation time and fatty acid composition of lecithin in human gallbladder bile. *Scand J Gastroenterol* 1993; **28**: 131-136
- 18 **Stewart L**, Ponce R, Oesterk AL, Griffiss JM, Way LW. Pigment gallstones pathogenesis: slime production by biliary bacteria is more important than beta-glucuronidase production. *J Gastrointest Surg* 2000; **4**: 547-553
- 19 **Al-Jiffry BO**, Shaffer EA, Saccone GT, Downey P, Kow L, Toouli J. Changes in gall bladder motility and gall stone formation following laparoscopic banding for morbid obesity. *Can J Gastroenterol* 2003; **17**: 169-174
- 20 **Lapidus A**, Bangstad M, Astrom M, Muhrheck O. The prevalence of gallstones disease in a defined cohort of patient with Crohn's disease. *Am J Gastroenterol* 1999; **94**: 1130-1132
- 21 **Hoogerbrugge-vd LN**, de Rooy FW, Jansen H, van Blankenstein M. Effect of pravastatin on biliary lipid composition and bile acid synthesis on familial hypercholesterolemia. *Gut* 1990; **31**: 348-350
- 22 **Duvaldestin P**, Manu JL, Metreau JM, Arondel J, Preaux AM, Berthelot P. Possible role of defect in hepatic bilirubin glucuronidation in the initiation of cholesterol gallstones. *Gut* 1980; **21**: 650-655

Edited by Ma JY

Can HB vaccine yield a booster effect on individuals with positive serum anti-HBs and anti-HBc markers?

Ru-Xiang Wang, Ying Guo, Chang-Hong Yang, Yu Song, Juan Chen, Fu-Sheng Pang, Shao-Ping Lei, Xiao-Ming Jia, Jin-Ying Wen, Christina Y. Shi

Ru-Xiang Wang, Ying Guo, Yu Song, Juan Chen, Shenyang Center for Disease Control and Prevention, Shenyang 110031, Liaoning Province, China

Chang-Hong Yang, Dongling District Anti-epidemic Station, Dongling District, Shenyang 110015, Liaoning Province, China

Fu-Sheng Pang, Shao-Ping Lei, Liaoning Center for Disease Control and Prevention, Shenyang, 110003, Liaoning Province, China

Xiao-Ming Jia, No.2 Hospital of China Medical University, Shenyang 110004, Liaoning Province, China

Jin-Ying Wen, Shenyang 606 Hospital, Shenyang 110015, Liaoning Province, China

Christina Y. Shi, Vita-Tech Canada, 1345 Denison Street, Markham, Ontario, Canada L3R 5V2

Correspondence to: Dr. Ru-Xiang Wang, Shenyang Center for Disease Control and Prevention, 37 Qishanzhong Road, Huanggu District, Shenyang 110031, China. rxwtxh@pub.sy.ln.cn

Telephone: +86-24-86853243 **Fax:** +86-24-86863778

Received: 2003-04-12 **Accepted:** 2003-10-11

Abstract

AIM: To evaluate if HB vaccination can yield a booster effect on the anti-HBs level of those naturally acquired HBV positive markers.

METHODS: Sera were collected from 1399 newly enrolled university students aged between 18-20 years at the entrance medical examination in 2001. Forty-four students (28 males and 16 females) with positive serum anti-HBs and anti-HBc markers served as an observation group and another 44 students (24 males and 20 females) without any HBV markers as the control. HB vaccination was given to all the students without positive serum HBsAg according to 0, 1, 6 month regimen and the peripheral venous blood was sampled from those of both observation and control groups for anti-HBs detection one month after the second and third doses. Anti-HBs levels were measured by ELISA.

RESULTS: The seroconversion rate of anti-HBs in the control group was 100% after the second dose, but the geometric mean titers (GMTs) were low. The tendency of serum anti-HBs changes after the 3rd dose was completely different between the two groups. Although more than half of those with positive anti-HBs and anti-HBc showed a mild increase of anti-HBs levels after the 2nd boosting dose (mean anti-HBs level was 320:198 mIU), but the increase of serum anti-HBs titer was much smaller than that in the control group. The averages of their initial serum anti-HBs levels and the levels after the 2nd and 3rd doses were 198, 320 and 275 mIU respectively. All the subjects from the control group had an obvious increase in their serum anti-HBs levels which was nearly 4 times the baseline level (302:78 mIU).

CONCLUSION: HB vaccination can not enhance anti-HBs levels in those with positive serum anti-HBs and anti-HBc markers.

Wang RX, Guo Y, Yang CH, Song Y, Chen J, Pang FS, Lei SP, Jia

XM, Wen JY, Shi CY. Can HB vaccine yield a booster effect on individuals with positive serum anti-HBs and anti-HBc markers? *World J Gastroenterol* 2004; 10(2): 306-308

<http://www.wjgnet.com/1007-9327/10/306.asp>

INTRODUCTION

HB vaccination program has been well developed for neonates and younger adults in China. Nowadays, according to Chinese regulation all the newly enrolled university students are required to have their blood detected for HBsAg and those with negative HBsAg are eligible to receive HB vaccination. Since it has been well demonstrated that an additional dose can induce a booster effect on vaccinees' serum anti-HBs titers, it is natural for most people to get the idea that the more doses they get, the more benefits they will gain. Our previous survey in a group of university students showed that HBsAg carrier rate in those of the 18-20 age group was about 4-6% and when gained entrance to the university more than 50% students with positive serum anti-HBs or anti-HBc or both were vaccinated each year. Is it necessary to vaccinate the people with positive anti-HBc and anti-HBs markers? To answer this question, we followed up the newly enrolled students from a university to observe the changes of their serum anti-HBs titers after HB vaccination, especially those with positive serum anti-HBs and anti-HBc markers before. The changes of serum anti-HBs titers in students without any HBV markers before the vaccination were observed after HB vaccination as the experimental control. The results might be helpful for the establishment of a scientific, reasonable and economic vaccination program against HBV infection in the adult population.

MATERIALS AND METHODS

Reagents

Ten μ g of yeast recombinant HB vaccine (Lot No: 2990104-1) was produced in Kangtai Biological Pharmaceutical Company, China. ELISA kits of HBV markers were from Sino-American Biotechnology Company, Luoyang, China. ELISA kit of Measles antibody was provided by Institute of Virus, Chinese Center of Disease Control and Prevention, Beijing, China.

Subjects and vaccination methods

Forty-four students with positive serum anti-HBs and anti-HBc and 44 without any HB markers who experienced a regular medical examination in one college were selected to be investigated after vaccinated with HB vaccine according to 0, 1, 6 month scheme, in which the vaccine was intramuscularly injected into the deltoid muscle. All the subjects were also injected measles vaccine one week before the first dose of HB vaccination. An informed consent was given by each participant before the beginning of observation.

Determination of serum anti-HBs antibody

Serum anti-HBs antibody was measured respectively at one

month after the 2nd and 3rd doses of HB vaccine. The sera were randomly chosen from 35 subjects with positive anti-HBs and anti-HBc to measure the antibodies (IgG) to both measles and HBsAg according to the manufacturer's instructions. The resulting value was determined according to Holliger formula: $mIU=418 \times [EXP \times 0.9(S-N)/(P-N)-1]$ in the light of OD values. mIU of anti-HBs titers greater than 10 was considered as positive anti-HBs. *t* test was used to compare GMTs between groups and the difference was considered significant when $P < 0.05$.

Table 1 Comparison of booster effect on anti-HBs levels between two groups

No.	Anti-HBs (anti-HBc pos.)			Anti-HBs (anti-HBc neg.)		
	Before	After 2 nd dose	After 3 rd dose	No.	After 2 nd dose	After 3 rd dose
23338	161	578	362	22404	48	471
23306	266	293	163	13236	25	268
23310	406	295	293	13240	45	598
23304	168	417	337	24332	48	324
23116	44	86	76	24327	63	144
23140	30	37	43	24311	186	314
23139	372	456	344	24105	344	656
23129	309	459	225	17239	135	83
23105	145	451	461	17238	58	253
23119	162	269	252	17226	83	598
27138	592	387	533	17214	53	384
27128	406	494	449	23240	63	268
27130	341	272	199	23201	40	370
27103	182	148	145	23141	201	340
27137	53	328	211	23108	26	512
27001	326	424	269	17129	22	970
27109	99	122	116	17125	178	318
27133	573	373	316	17122	45	22
27120	151	420	207	17118	78	466
22222	115	438	588	17108	236	414
22225	442	417	338	17106	88	350
22214	283	293	466	17102	197	264
22206	176	282	208	13139	186	291
22205	547	275	377	13129	17	158
22201	183	193	158	13126	73	264
24120	128	558	393	13125	93	191
24107	239	356	257	13118	17	176
24140	35	426	409	13114	53	263
24141	212	275	231	13108	216	280
22138	392	534	659	13107	35	338
22130	660	643	504	13102	130	252
13214	247	331	244	13101	113	216
13223	491	315	176	14130	320	520
23235	106	232	199	14131	65	407
24137	108	472	280	14129	320	365
22202	61	205	253	18302	30	63
18238	244	302	303	18310	73	336
23322	422	463	503	16119	53	395
18223	333	314	389	16112	30	370
25122	355	315	286	16122	200	375
25139	206	361	337	16104	45	420
25129	116	391	303	16108	30	365
25121	38	119	204	16107	441	476
18220	65	507	506	16110	107	499
Total GMT	198	320	275	GMT	78	302

RESULTS

Anti-HBs titers before and after HB vaccination in those with positive anti-HBs and anti-HBc

The tendency of serum anti-HBs changes after the 3rd dose was completely different between the two groups. Although more than half of those with positive anti-HBs and anti-HBc markers showed a mild increase of serum anti-HBs titer after the 2nd booster dose, the increase of serum anti-HBs titer (mean anti-HBs level was 198:320 mIU) was much smaller than that in the control group, in which 100% subjects had an obvious increase in their serum anti-HBs levels which was nearly 4 times their baseline (302:78 mIU).

It was interesting to note that the serum anti-HBs levels did not change in most of the subjects with positive anti-HBs and anti-HBc markers after the 3rd dose. The mean serum anti-HBs level of the baseline, after the 2nd and 3rd doses was 198, 320 and 275 mIU (Table 1) respectively.

Effect of a boost dose on antibody titers of HBsAb and measles Ab

In order to confirm that all the subjects in this study had a normal immune competence, the serum antibodies to measles were detected in 35 subjects and an increased antibody level was observed in 91.4% (32/35) subjects after a booster dose. A comparison of antibody levels before and after a booster dose was made and the difference was statistically significant ($P < 0.05$, Table 2).

Table 2 Effect of a boost on antibody titers of HBsAb and measles Ab

Boost	A-HBsAb		B-HBsAb		C-HBsAb		MeaslesAb	
	No.	GMT	No.	GMT	No.	GMT	No.	GMT
Before	44	198	44	198	44	78	35	322
After	44	320	44	275	44	302	35	1 207

Comparison of anti-HBs induced by HB vaccination before and after a boost in HBV negative group, $P < 0.05$.

DISCUSSION

Hepatitis B vaccination has been implemented for 20 years, however, the disease remains a global problem^[1-4]. Although the safety and efficacy of HB vaccine have been well demonstrated^[5-16], few papers regarding the immune response of those with positive anti-HBs and anti-HBc to HB vaccination are available. In this study, we observed if a booster effect and a better protection against HBV infection could be obtained after HB vaccination in those with positive serum anti-HBs and anti-HBc markers.

It has been well demonstrated that the HB vaccine-induced antibody might gradually decline or was even undetectable some years after primary immunization^[17-20]. It is not clear if such persons could be protected against HB infection following exposure to HBV^[21]. Although some studies have proved that memory cells to HBsAg might exist in vaccinees for a long time even the serum anti-HBs was undetectable^[19,22,23]. Whether additional booster doses should be used has been under discussion^[17-20,23-25]. Considering the available data on measles vaccine, which showed that loss of detectable antibody following vaccination was correlated with the waning of immunity^[26], a booster HB vaccination might be necessary.

Our data revealed that the serum anti-HBs levels in the subjects with positive serum anti-HBs and anti-HBc markers did not significantly increase one month after the 2nd dose of HB vaccination. Although a mild increase was seen in some cases, the elevation of serum anti-HBs levels in the observatory

group was much less than that in the control in which 100% subjects had an obvious increase of serum anti-HBs levels that was nearly 4 times their baseline. After the 3rd dose, anti-HBs levels remained unchanged in most of the subjects with positive serum anti-HBs and anti-HBc markers compared with that in the control, in which a sharp increase of serum anti-HBs levels was observed after the 3rd dose. The phenomenon might be related to the following possibilities. First, the subjects with positive serum anti-HBs and anti-HBc markers before the vaccination might not be in a normal condition of immune competence during the observation period. In the present study, their increased response to measles after the booster dose was observed in 91.4% (32/35) subjects. Because measles vaccination has been well practiced in China and normally all the subjects have to be vaccinated in their early age, the increased immunological response could prove that the subjects had the normal immune competence. Second, the immune response to viruses can damage the host via the formation of immune complexes, or directly damage the infected cells. Thus, the poor response to the HB vaccine might probably relate to the damage caused by HBV before the vaccination.

HB vaccination program is implemented in children and adults in China. But the problem is that our current vaccination regimen is not completely suitable for adult vaccination. An appropriate vaccination program for the adult population has to be established to prevent the prevalence of HBV. Our results indicate that it is not necessary to vaccinate those with positive serum anti-HBs and anti-HBc because no significant increase of anti-HBs titers was observed after a standard HB vaccination. It suggests that the vaccine-induced anti-HBs can not be elevated in those infected with HBV naturally before the HB vaccination.

REFERENCES

- Cassidy WM.** Adolescent hepatitis B vaccination. *Minerva Pediatr* 2001; **53**: 559-566
- Kralj N, Hofmann F, Michaelis M, Berthold H.** Current hepatitis B epidemiology in Germany. *Gesundheitswesen* 1998; **60**: 450-455
- Bayas JM, Bruguera M, Vilella A, Carbo JM, Vidal J, Navarro G, Nebot X, Prat A, Salleras L.** Prevalence of hepatitis B and hepatitis A virus infection among health sciences students in Catalonia, Spain. *Med Clin* 1996; **107**: 281-284
- Bonanni P.** Universal hepatitis B immunization: infant, and infant plus adolescent immunization. *Vaccine* 1998; **16**(Suppl): S17-22
- Kojouharova M, Teoharov P, Bahtchevanova T, Maeva I, Eginlian A, Deneva M.** Safety and immunogenicity of a yeast-derived recombinant hepatitis B vaccine in Bulgarian newborns. *Infection* 2001; **29**: 342-344
- Liao SS, Li RC, Li H, Yang JY, Zeng XJ, Gong J, Wang SS, Li YP, Zhang KL.** Long-term efficacy of plasma-derived hepatitis B vaccine among Chinese children: a 12-year follow-up study. *World J Gastroenterol* 1999; **5**: 165-166
- Li H, Li RC, Liao SS, Yang JY, Zeng XJ, Wang SS.** Persistence of hepatitis B vaccine immune protection and response to hepatitis B booster immunization. *World J Gastroenterol* 1998; **4**: 493-496
- Rendi-Wagner P, Kundi M, Stemberger H, Wiedermann G, Holzmann H, Hofer M, Wiesinger K, Kollaritsch H.** Antibody-response to three recombinant hepatitis B vaccines: comparative evaluation of multicenter travel-clinic based experience. *Vaccine* 2001; **19**: 2055-2060
- Ozaki T, Mochizuki H, Ichikawa Y, Fukuzawa Y, Yoshida S, Morimoto M.** Persistence of hepatitis B surface antibody levels after vaccination with a recombinant hepatitis B vaccine: a 3-year follow-up study. *J Oral Sci* 2000; **42**: 147-150
- Jain A, Mathur US, Jandwani P, Gupta RK, Kumar V, Kar P.** A multicentric evaluation of recombinant DNA hepatitis B vaccine of Cuban origin. *Trop Gastroenterol* 2000; **21**: 14-17
- Al-Faleh FZ, Al-Jeffri M, Ramia S, Al-Rashed R, Arif M, Rezeig M, Al-Toraifi I, Bakhsh M, Mishkhas A, Makki O, Al-Freih H, Mirdad S, AlJuma A, Yasin T, Al-Swailem A, Ayoola A.** Seroprevalence of hepatitis B virus infection in Saudi children 8 years after a mass hepatitis B vaccination programme. *J Infect* 1999; **38**: 167-170
- Li H, Li RC, Liao SS, Gong J, Zeng XJ, Li YP.** Long-term effectiveness of infancy low-dose hepatitis B vaccine immunization in Zhuang minority area in China. *World J Gastroenterol* 1999; **5**: 122-124
- Liu HB, Meng ZD, Ma JC, Han CQ, Zhang YL, Xing ZC, Zhang YW, Liu YZ, Cao HL.** A 12-year cohort study on the efficacy of plasma-derived hepatitis B vaccine in rural newborns. *World J Gastroenterol* 2000; **6**: 381-383
- Li H, Wang L, Wang SS, Gong J, Zeng XJ, Li RC, Nong Y, Huang YK, Chen XR, Huang ZN.** Research on optimal immunization strategies for hepatitis B in different endemic areas in China. *World J Gastroenterol* 2000; **6**: 392-394
- Zeng XJ, Yang GH, Liao SS, Chen AP, Tan J, Huang ZJ, Li H.** Survey of coverage, strategy and cost of hepatitis B vaccination in rural and urban areas of China. *World J Gastroenterol* 1999; **5**: 320-323
- Shokri F, Jafarzadeh A.** High seroprotection rate induced by low doses of a recombinant hepatitis B vaccine in healthy Iranian neonates. *Vaccine* 2001; **19**: 4544-4548
- Peces R, Lares AS.** Persistence of immunologic memory in long-term hemodialysis patients and healthcare workers given hepatitis B vaccine: role of a booster dose on antibody response. *Nephron* 2001; **89**: 172-176
- Li H, Li R, Liao S, Yang J, Zeng X.** Persistence of HB vaccine immune protection and response to hepatitis B booster immunization. *Zhongguo Yixue Kexueyuan Xuebao* 1998; **20**: 54-59
- Watson B, West DJ, Chilkatowsky A, Piercy S, Ioli VA.** Persistence of immunologic memory for 13 years in recipients of a recombinant hepatitis B vaccine. *Vaccine* 2001; **19**: 3164-3168
- Garcia Llop L, Asensi Alcoverro A, Coll Mas P, Ramada Benedito MA, Grafia Juan C.** Anti-HBs titers after a vaccination program in children and adolescents. Should a booster dose be given? *An Esp Pediatr* 2000; **54**: 32-37
- Wood RC, MacDonald KL, White KE, Hedberg CW, Hanson M, Osterholm MT.** Risk factors for lack of detectable antibody following B vaccination of Minnesota health care workers. *JAMA* 1993; **270**: 2935-2939
- Wismans PJ, Van Hattum J, De Gast GC, Endeman HJ, Poel J, Stolk B, Maikoe T, Mudde GC.** The spot-ELISA: a sensitive *in vitro* method to study the immune response to hepatitis B surface antigen. *Clin Exp Immunol* 1989; **78**: 75-78
- Trivello P, Chiamonte M, Ngatchu T, Baldo V, Majori S, Moschen ME, Simoncello I, Renzulli G, Naccarato R.** Persistence of anti-HBs antibodies in health care personnel vaccinated with plasma-derived hepatitis B vaccine and response to recombinant DNA HB booster vaccine. *Vaccine* 1995; **13**: 139-141
- Coursaget P, Yvonnet B, Chotard J, Sarr M, Vincelot P, N' doye R, Diop-Mar I, Chiron JP.** Seven-year study of hepatitis B vaccine efficacy in infants from an endemic area (Senegal). *Lancet* 1986; **15**: 1143-1144
- Hadler SC, Francis DP, Maynard JE, Thompson SE, Judson EN, Echenberg DF, Ostrow DG, O' Malley PM, Penley KA, Altman NL.** Long-term immunogenicity and efficacy of hepatitis B vaccine in homosexual men. *N Engl J Med* 1986; **315**: 209-215
- Center for Disease Control.** Measles prevention: recommendation of the Immunization Practices Advisory Committee. *MMWR Morb Mortal Wkly Rep* 1989; **38**: S-9

Key role of mast cells and their major secretory products in inflammatory bowel disease

Shao-Heng He

Shao-Heng He, Allergy and Inflammation Research Institute, Medical College, Shantou University, Shantou 515031, Guangdong Province, China
Supported by the Li Ka Shing Foundation, Hong Kong, China, No. C0200001 and the Planned Science and Technology Project of Guangdong Province, China, No. 2003B31502

Correspondence to: Professor Shao-Heng He, Allergy and Inflammation Research Institute, Medical College, Shantou University 22 Xin-Ling Road, Shantou 515031, Guangdong Province, China. shoahenghe@hotmail.com

Telephone: +86-754-8900405 **Fax:** +86-754-8900192

Received: 2003-12-23 **Accepted:** 2004-01-11

Abstract

Historically, mast cells were known as a key cell type involved in type I hypersensitivity. Until last two decades, this cell type was recognized to be widely involved in a number of non-allergic diseases including inflammatory bowel disease (IBD). Markedly increased numbers of mast cells were observed in the mucosa of the ileum and colon of patients with IBD, which was accompanied by great changes of the content in mast cells such as dramatically increased expression of TNF α , IL-16 and substance P. The evidence of mast cell degranulation was found in the wall of intestine from patients with IBD with immunohistochemistry technique. The highly elevated histamine and tryptase levels were detected in mucosa of patients with IBD, strongly suggesting that mast cell degranulation is involved in the pathogenesis of IBD. However, little is known of the actions of histamine, tryptase, chymase and carboxypeptidase in IBD. Over the last decade, heparin has been used to treat IBD in clinical practice. The low molecular weight heparin (LMWH) was effective as adjuvant therapy, and the patients showed good clinical and laboratory response with no serious adverse effects. The roles of PGD₂, LTC₄, PAF and mast cell cytokines in IBD were also discussed. Recently, a series of experiments with dispersed colon mast cells suggested there should be at least two pathways in man for mast cells to amplify their own activation-degranulation signals in an autocrine or paracrine manner. The hypothesis is that mast cell secretagogues induce mast cell degranulation, release histamine, then stimulate the adjacent mast cells or positively feedback to further stimulate its host mast cells through H₁ receptor. Whereas released tryptase acts similarly to histamine, but activates mast cells through its receptor PAR-2. The connections between current anti-IBD therapies or potential therapies for IBD with mast cells were discussed, implicating further that mast cell is a key cell type that is involved in the pathogenesis of IBD. In conclusion, while pathogenesis of IBD remains unclear, the key role of mast cells in this group of diseases demonstrated in the current review implicates strongly that IBD is a mast cell associated disease. Therefore, close attentions should be paid to the role of mast cells in IBD.

He SH. Key role of mast cells and their major secretory products in inflammatory bowel disease. *World J Gastroenterol* 2004; 10(3):309-318

<http://www.wjgnet.com/1007-9327/10/309.asp>

INTRODUCTION

Historically, mast cells were known as a key cell type involved in type I hypersensitivity^[1]. Until last two decades, this cell type was recognized to be widely involved in a number of non-allergic diseases in internal medicine including chronic obstructive pulmonary disease (COPD), Crohn's disease, ulcerative colitis, liver cirrhosis, cardiomyopathy, multiple sclerosis and rheumatoid arthritis, *etc.* (Table 1). This article will focus solely on the relationships between mast cells and inflammatory bowel disease, give evidence for a hypothesis of self-amplification mechanism of mast cell degranulation in gut and discuss the potential therapies for the treatment of inflammatory bowel disease (IBD).

Table 1 Mast cells involved in non-allergic diseases in internal medicine

Disease	Evidence
Chronic obstructive pulmonary disease (COPD)	Mast cell hyperplasia in epithelia and bronchial glands ^[2,3] , tryptase and histamine release in BALF ^[4]
Cor pulmonale	Mast cell hyperplasia in bronchial and vascular tissues ^[5]
Bronchiectasis	Increased numbers of degranulated mast cells in lung tissue, and higher tryptase concentrations in BALF ^[6]
Acute respiratory distress syndrome (ARDS)	Mast cell hyperplasia ^[7] and degranulation ^[8]
Bronchiolitis obliterans-organizing pneumonia	Mast cell hyperplasia ^[9] and degranulation ^[10]
Cystic fibrosis	Mast cell hyperplasia ^[11] and degranulation ^[12] in lung
Interstitial lung diseases	Mast cell hyperplasia ^[13] and degranulation ^[14]
Silicosis	Mast cell hyperplasia ^[15]
Sarcoidosis	Mast cell hyperplasia ^[16] , and degranulation ^[17] in lung
Lung cancer	Mast cell hyperplasia ^[18]
Tuberculosis	Mast cell degranulation ^[19]
Gastritis	Mast cell hyperplasia ^[20] and degranulation ^[21]
Peptic ulcer	Mast cell hyperplasia ^[22] and degranulation ^[23]
Hepatocellular carcinoma	Mast cell hyperplasia ^[24]
Ulcerative colitis	Mast cell hyperplasia ^[25,26] and degranulation ^[27]
Crohn's disease	Mast cell hyperplasia ^[28] and degranulation ^[29]
Liver cirrhosis	Mast cell hyperplasia ^[30]
Hepatitis	Mast cell hyperplasia ^[31,32]
Pancreatitis	Mast cell hyperplasia and degranulation ^[33]
Atherosclerosis	Mast cell hyperplasia ^[34]
Myocardial infarction	Mast cell hyperplasia and degranulation ^[35,36]
Congenital heart disease	Mast cell hyperplasia and subtype change ^[37]
Myocarditis	Mast cell hyperplasia ^[38]
Cardiomyopathy	Mast cell hyperplasia ^[39] and degranulation ^[40]
Diabetes	Mast cell hyperplasia ^[41]
Thyroiditis	Mast cell hyperplasia ^[42]
Osteoporosis	Mast cell hyperplasia ^[43]
Glomerulonephritis	Mast cell hyperplasia ^[44]
Nephropathy	Mast cell hyperplasia ^[45]
Multiple sclerosis	Mast cell hyperplasia ^[46]
Rheumatoid arthritis	Mast cell degranulation ^[47]
Osteoarthritis	Mast cell hyperplasia ^[48]
Rheumatic arthritis	Mast cell hyperplasia ^[49]

MAST CELLS

Morphology

Mast cell is the cell that contains numerous metachromatically stained basophilic granules in its cytoplasm. It has various sizes between species with diameters of up to 30 μm reported in humans, and from 3.5 μm to 22 μm in rodents^[28,50]. In human lung, for example, the range of mast cell diameters has been reported to be between 9.9 μm and 18.4 μm ^[51] and in human skin between 4 μm and 18 μm ^[52]. The shape of mast cell varies as well, it has been described as polyhedral, fusiform, ovoid, and rectangular, and appears dependent on tissue locations. Mast cell nuclei are usually round or oval and have peripherally dispersed heterochromatin^[53].

Up to 40% of the volume of mast cell is occupied by membrane-enclosed secretory granules^[54]. There are 50 to 500 secretory granules in one mature human mast cell, each with a diameter ranging from 0.2 to 0.5 μm . Within a given mast cell, these granules are usually of a uniform size, but there is variability from cell to cell^[55]. Mast cell granules originate from the Golgi apparatus, which is responsible for the synthesis and organization of the preformed mediators contained therein^[56].

Mediators

Upon activation mast cell can release its mediators to fulfill its biological functions. Among preformed mediators, histamine is a primary amine synthesized from histidine in the Golgi apparatus, from where it is transported to the granule for storage in ionic association with the acidic residues of glycosaminoglycans side chains of heparin and proteinases^[57,58]. The histamine content of mast cells dispersed from human lung and skin is similar at 2 to 5 pg/cell, and the stored histamine ranges from 10 to 12 $\mu\text{g/g}$ in both tissues^[53]. As only mast cell and basophil contain histamine in man, and few basophils in human tissue histamine can be used as a marker of mast cell degranulation.

Proteoglycans in human mast cells include heparin and chondroitin sulphate, which contains several highly sulphated glycosaminoglycan side chains attached to a single chain protein core. They comprise the major supporting matrix of the mast cell granule with the sulphate groups binding to histamine, proteinases and acid hydrolases.

Neutral proteases of mast cells are also preformed mediators. Three mast cell unique neutral proteinases (tryptase, chymase and carboxypeptidase) have been isolated in man and there is evidence also for a proteinase with antigenic and enzymatic properties similar to those of neutrophil cathepsin G in mast cells^[59,60]. Mast cell tryptase, chymase and carboxypeptidase are reliable markers of mast cell degranulation. Based on their content of proteinases, mast cells can be classified into two types in man, with MC_T cells defined as those containing tryptase but not chymase, and MC_{TC} cells as those containing both tryptase and chymase^[61]. Subsequently both carboxypeptidase^[62] and cathepsin G like proteases^[63,64] have been found to be localised exclusively in the MC_{TC} population.

Newly generated mediators include eicosanoids and platelet activating factor (PAF). Eicosanoids are a group of newly generated mediators of mast cells. Immunological activation of mast cells results in the liberation of arachidonic acid from phospholipids in the cell membrane. This 20-carbon fatty acid is then rapidly oxidized along either of two independent pathways, namely the cyclooxygenase pathway to form PGD₂ and the lipoxygenase pathway to form LTC₄. These are the only two eicosanoids produced by human mast cells^[65]. PAF is also a product of phospholipid metabolism in mast cells.

Mast cell cytokines may constitute a third category in that they may be both preformed and newly synthesized. For instance, it has been reported that approximately 75%, 10%, 35%, and 35% of mast cells contain IL-4, IL-5, IL-6 and TNF α ,

respectively in the nasal mucosa and bronchus^[66]. Mast cell contains also IL-1 β , IL-3, IL-8, IL-9, IL-10, IL-13, IL-16, IL-18, IL-25, granulocyte-macrophage colony-stimulating factor (GM-CSF), stem cell factor macrophage chemotactic peptide (MCP)-1, 3, 4, regulated on activation of normal T cell-expressed and secreted protein (RANTES) and eotaxin^[67].

Mast cell activation

Mast cell activation is a crucial step in mast cell involved events because it seems that only activated mast cells are able to cause pathophysiological changes. There are a number of compounds that can activate mast cells. They are antigens, anti-IgE and ionophores. Skin mast cells but not those of lung, tonsil or gut can be activated by other diverse compounds including substance P, VIP, C5a and C3a, somatostatin, compound 48/80, morphine, pepstatin, MBP, PAF, platelet factor 4 and very-low-density lipoproteins^[68,53]. Stem cell factor^[69], eosinophil cationic protein^[70] and tryptase^[71] have also been found to be able to activate human mast cells.

The mechanisms of mast cell activation differ with different classes of triggers. Human skin mast cells are able to respond to non-crosslinking stimuli, such as neuropeptides, morphine, and complement fragments^[68]. IgE-dependent mast cell activation is a complicated process. It involves a specific IgE bound to its high affinity receptor (Fc ϵ R1) on the surface of mast cells, a multivalent antigen (Ag) crosslinking specific IgEs bound to Fc ϵ R1 and a signal transduction and translation process in mast cells.

Models for mast cell degranulation

While normal human mast cell line is not available, dispersed and purified mast cells are essential for investigating mast cell functions. Human mast cells have been dispersed from skin, lung, tonsil, synovium heart and intestine tissues by incubation with collagenase and hyaluronidase. These dispersed cells have appreciable morphological and functional properties of mast cells. Since dispersed cells can be evenly distributed in experiment, it is the most popular method at present. However, the purity of mast cells with this system is only 0.5-10% depending on tissues.

Chopped tissue fragments were also used for mast cell degranulation study. We found that it was difficult to evenly distribute cells in tissue fragments, therefore causing large experimental errors.

Laboratory animal tissues or mast cells are widely used in mast cell degranulation study. Thus, rat and mouse peritoneum, guinea pig lung and cultured mouse bone marrow derived mast cells are the most popular models. However, it is always adequate to use human mast cells to investigate the pathophysiological process of human disease.

INCREASED NUMBERS OF MAST CELLS IN IBD

As early as in 1980, Dvorak and colleagues^[28] reported that the number of mast cells was markedly increased in the involved area of the ileum of patients with Crohn's disease. In 1990, Nolte *et al.*^[72] found that the mast cell count in patients with ulcerative colitis was increased compared with that in control subjects and patients with Crohn's disease. In an individual patient, the mast cell count obtained from inflamed tissue was greater than that of normal tissue. This finding was taken further by King *et al.*^[26] in 1992 that the number of mast cells in active ulcerative colitis was 6.3 in active inflammation, 19.5 at the line of demarcation and 15.8 in normal mucosa. The accumulation of mast cells at the visible line of demarcation between normal and abnormal mucosa suggested that mast cells played a crucial role in the pathogenesis of the disease, either causing further damage or limiting the expansion of damage. Recently, a report^[73] provided us an even more convincing evidence and clear picture on the elevated number

of mast cells in inflammatory bowel disease. Nishida and colleagues found that there were greater numbers of mast cells than macrophages in the lamina propria of patients with inflammatory bowel disease though this was not found in patients with collagenous colitis. Interestingly, increased numbers of mast cells were observed throughout the lamina propria, particularly in the upper part of lamina propria, whereas increased numbers of macrophages were only seen in the lower part of lamina propria in patients with inflammatory bowel disease. This could result from that accumulated mast cells released their proinflammatory mediators, and these mediators, at least tryptase^[74] and chymase^[75], induced macrophage accumulation in the lower part of lamina propria. Dramatically increased numbers of mast cells were also observed in the hypertrophied and fibrotic muscularis propria of strictures in Crohn's disease compared with normal bowel ($81.3/\text{mm}^2$ vs $1.5/\text{mm}^2$)^[76].

Not only the number of mast cells was elevated^[77], but also the contents of mast cells were greatly changed in inflammatory bowel disease in comparison with normal subjects. Laminin, a multi-functional non-collagenous glycoprotein, which is normally found in extracellular matrix was detected in mast cells in muscularis propria (but not those in submucosa), indicating that mast cells may be actively involved in the tissue remodeling in Crohn's disease^[76]. Similarly, the number of TNF- α positive mast cells was greater in the muscularis propria of patients with Crohn's disease than that in normal controls^[78]. In the submucosa of involved ileal wall of Crohn's disease, more TNF- α positive mast cells were found in inflamed area than uninfamed area. Since those TNF- α positive mast cells were mast cell type that expressed TNF- α in ileal wall, the successful treatment of Crohn's disease with anti-TNF- α antibody could well be the consequence that the antibody neutralized the excessively secreted TNF- α from mast cells. This indirectly proved the important contribution of mast cells to the development of Crohn's disease. Increased number of IL-16 positive mast cells, which was correlated well with increased number of CD4⁺ lymphocytes, was also observed in active Crohn's disease^[79], indicating that this chemokine may selectively attract CD4⁺ lymphocytes to the involved inflammatory area^[80,81]. In chronic ulcerative colitis, increased number of substance P positive mast cells was observed in gut wall, particularly in mucosa^[82], indicating the possibility of neuronal elements being involved in the pathogenesis of the disease.

Increased number of mast cells was also seen in a number of diseases closely related to inflammatory bowel disease. Primary sclerosing cholangitis and chronic sclerosing sialadenitis showed similar marked mast cell infiltration pattern with inflammatory bowel disease^[83]. Focal active gastritis is a typical pathological change in Crohn's disease^[84], in which large number of mast cells accumulate at the border of the lesions^[20]. In the animal models, increased number of mast cells in gastrointestinal tract was observed in dogs with inflammatory bowel disease in comparison with healthy dogs^[85]. When given 3% dextran sulphate sodium for 10 days^[86] or water avoidance stress for 5 days^[87], pathological changes such as mucosal damage and edema were developed in rats, and these were accompanied by mast cell hyperplasia and activation. However, the same treatment had little effect on mast cell deficient Ws/Ws rats, implying the importance of mast cells in the development of inflammatory bowel disease.

EVIDENCE OF MAST CELL DEGRANULATION IN IBD

As early as in 1975, Lloyd and colleagues observed that there were marked degranulation of mast cells and IgE-containing cells in the bowel wall of patients with Crohn's disease^[29], and this observation later became an important investigation area

for understanding the pathogenesis of Crohn's disease. In 1980, Dvorak *et al.* described in more detail the degranulation of mast cells in the ileum of patients with Crohn's disease^[28] with transmission electron microscopy technique. Similarly, with electron microscopy technique, degranulation of mast cells was seen in the intestinal biopsies of patients with ulcerative colitis^[88]. Using immunohistochemistry technique with antibodies specific to human tryptase or chymase, both of which are exclusive antigens of human mast cells, mast cell degranulation was found in the mucosa of bowel walls of patients with Crohn's disease, ulcerative colitis^[89] and chronic inflammatory duodenal bowel disorders^[90].

INVOLVEMENT OF HISTAMINE IN PATHOGENESIS OF IBD

Using segmental jejunal perfusion system with a two-balloon, six channel small tube, Knutson and colleagues found that the histamine secretion rate was increased in patients with Crohn's disease compared with normal controls, and the secretion of histamine was related to the disease activity, indicating strongly that degranulation of mast cells was involved in active Crohn's disease^[91]. The highly elevated mucosal histamine levels were also observed in patients with allergic enteropathy and ulcerative colitis^[27]. Moreover, enhanced histamine metabolism was found in patients with collagenous colitis and food allergy^[92], and increased level of N-methylhistamine, a stable metabolite of the mast cell mediator histamine, was detected in the urine of patients with active Crohn's disease or ulcerative colitis^[93,94]. Since increased level of N-methylhistamine was significantly correlated to clinical disease activity, the above finding further strongly suggested the active involvement of histamine in the pathogenesis of these diseases.

Interestingly, mast cells originated from the resected colon of patients with active Crohn's disease or ulcerative colitis were able to release more histamine than those from normal colon when being stimulated with an antigen, colon derived murine epithelial cell associated compounds^[95]. Similarly, cultured colonrectal endoscopic samples from patients with IBD secreted more histamine towards substance P alone or substance P with anti-IgE than the samples from normal control subjects under the same stimulation^[96]. In a guinea pig model of intestinal inflammation induced by cow's milk proteins and trinitrobenzenesulfonic acid, both IgE titers and histamine levels were higher than normal control animals^[97].

As a proinflammatory mediator, histamine is selectively located in the granules of human mast cells and basophils and released from these cells upon degranulation. To date, a total of four histamine receptors H₁, H₂, H₃ and H₄ have been discovered^[98] and the first three of them have been located in human gut^[99,100], proving that there are some specific targets on which histamine can work in intestinal tract. Histamine was found to cause a transient concentration-dependent increase in short-circuit current, a measure of total ion transport across the epithelial tissue in gut^[101]. This could be due to the interaction of histamine with H₁-receptors that increased Na and Cl ions secretion from epithelium^[102]. The finding that H₁-receptor antagonist pyrilamine was able to inhibit anti-IgE induced histamine release and ion transport^[103] suggests further that histamine is a crucial mediator responsible for diarrhea in IBD and food allergy. The ability of SR140333, a potent NK1 antagonist in reducing mucosal ion transport was most likely due to its inhibitory actions on histamine release from colon mast cells^[104].

INVOLVEMENT OF MAST CELL PROTEASES IN PATHOGENESIS OF IBD

Tryptase is a tetrameric serine proteinase that constitutes some

20% of the total protein within human mast cells and is stored almost exclusively in the secretory granules of mast cells^[105] in a catalytically active form^[106]. The ability of tryptase to induce microvascular leakage in the skin of guinea pig^[107], to accumulate inflammatory cells in the peritoneum of mouse^[74] and to stimulate release of IL-8 from epithelial cells^[108], and the evidence that relatively higher secretion of tryptase has been detected in ulcerative colitis^[109] implicated that this mediator is involved in the pathogenesis of intestinal diseases. However, little is known about its actions in IBD. Recently, proteinase activated receptor (PAR)-2, a highly expressed receptor in human intestine^[110] was recognized as a receptor of human mast cell tryptase^[111]. Colonic administration of PAR-2 agonists up-regulated PAR-2 expression, induced granulocyte infiltration, colon wall edema and damage and stimulated an increased paracellular permeability of colon mucosa^[112]. PAR-2 agonists were also able to stimulate intestinal electrolyte secretion^[113]. Interestingly, some 60% and 46% of mast cells in ulcerative colitis tissues expressed PAR-2 or TNF- α , respectively. PAR-2 agonists were able to stimulate TNF- α secretion from mast cells^[114] and secreted TNF- α could then enhance PAR-2 expression in a positive feedback manner^[113]. These findings indicated further the importance of TNF- α and mast cells in the pathogenesis of IBD.

Chymase is a serine proteinase exclusively located in the same granules as tryptase and could be released from granules together with other preformed mediators. Large quantity of active form chymase (10 pg per mast cell) in mast cells^[115] implicates that this mast cell unique mediator may play a role in mast cell related diseases. Indeed, chymase has been found to be able to induce microvascular leakage in the skin of guinea pig^[116], stimulate inflammatory cell accumulation in peritoneum of mouse^[75], and alter epithelial cell monolayer permeability *in vitro*^[117]. However, little is known about its actions in IBD. Mast cell carboxypeptidase is a unique product of MC_{TC} subtype mast cells. There is some 10 pg in each mast cells. No information about the relationship between mast cell carboxypeptidase and IBD is available, but the successful cloning of mast cell carboxypeptidase from human gut tissue and obtaining of recombinant human mast cell carboxypeptidase [chen 2004] will certainly help to initiate the investigation of the role of mast cell carboxypeptidase in IBD. It is astonishing to learn the fact that the potential roles of mast cell neutral proteinases in IBD have been almost completely ignored till today. Since they are the most abundant granule products of mast cells and have been demonstrated to possess important actions in inflammation, they should certainly contribute to the occurrence and development of IBD.

INVOLVEMENT OF HEPARIN IN PATHOGENESIS OF IBD

Over the last decade, heparin, a unique product of human mast cells and basophils, has been used to treat IBD in clinical practice. Using combined heparin and sulfasalazine therapy, Gaffney and colleagues successfully treated 10 patients with ulcerative colitis poorly controlled on sulfasalazine and prednisolone^[119]. Similarly, Evans *et al.* found that heparin was effective in treating corticosteroid-resistant ulcerative colitis^[120], and Yoshikane *et al.* reported that heparin was very effective in the treatment of disseminated intravascular coagulation (DIC) caused by ulcerative colitis^[121]. Recently, heparin was even suggested as a first line therapy in the treatment of severe colonic inflammatory bowel disease^[122], but should be administered in hospitalized patients only because of the risk of possible serious bleeding^[123]. To overcome bleeding side effect, low molecular weight heparin (LMWH) was employed as adjuvant therapy^[124], and the patients showed good clinical and laboratory response with

no severe adverse effects^[125,126].

Apart from anticoagulation activity, the mechanisms by which heparin was able to treat IBD were considered to include its ability to inhibit the recruitment of neutrophils, reduce production of pro-inflammatory cytokines^[127] and restore the high-affinity receptor binding of antiulcerogenic growth factor^[128,129]. The ability of heparin to inhibit neutrophil activation, adhesion, and chemotaxis was also found in a mouse model of inflammatory bowel disorder^[130,131], suggesting that balanced interactions between mast cells and neutrophils might be important for the development of IBD. In rat models of IBD, heparin revealed its ability to attenuate TNF α induced leucocyte rolling and CD11b dependent adhesion^[132], reduce serum IL-6 level and improve microcirculatory disturbance in rectal walls^[133,134]. Thus, preformed mast cell mediators seemed to have dual actions on the pathogenesis of IBD. On the one hand, tryptase, histamine, and TNF- α can cause damage in the intestinal wall, and on the other hand, heparin can protect the intestinal wall from damage.

INVOLVEMENT OF PGD₂, LTC₄ AND PAF IN PATHOGENESIS OF IBD

It was reported that mast cells in the actively involved areas of ulcerative colitis released greater amount of PGD₂, in parallel to histamine and LTC₄^[135]. In a rat experimental colitis model, the time for stimulating PGD₂ release was initiated within 1 h and increased 4 fold within 3 h^[136]. This was accompanied by a significant granulocyte infiltration, indicating the likelihood of involvement of PGD₂ in IBD. The basal release of LTC₄ was enhanced in the gut of Crohn's disease patients^[137], but the meaning of this enhancement still remains uninvestigated.

It was found that mast cell activators, calcium ionophore A23187 and anti-IgE, were able to stimulate more PAF release from colon with ulcerative colitis than from normal colon, and this increased PAF release could be inhibited by steroids and 5-aminosalicylic acid^[138,139]. The increased secretion of PAF was detected in the stool of patients with active Crohn's disease, but not in that of patients with irritable bowel syndrome^[140]. The level of PAF was also higher in colonic mucosa of patients with Crohn's disease than in colonic mucosa of healthy controls^[141]. These indicated that PAF might be involved in the pathogenesis of Crohn's disease^[142]. The elevated level of PAF in colon was likely to be the result of increased production by colonic epithelial cells^[143], lamina propria mononuclear cells^[144] and mast cells, and decreased PAF acetylhydrolase (the major PAF degradation enzyme activity)^[145]. In patients with ulcerative colitis, colonic production of PAF was increased in comparison with control patients^[146], and the level of PAF in the stool of patients with ulcerative colitis was much higher than that in the stool of healthy volunteers^[147]. Since increased colonic production of PAF was correlated to local injury and inflammation^[146], it implicates strongly that PAF is involved in the pathogenesis of ulcerative colitis. However, a randomized controlled trial with a specific PAF antagonist SR27417A showed that this compound had no significant effect on patients with active ulcerative colitis though it was safe in humans^[148].

INVOLVEMENT OF CYTOKINES IN PATHOGENESIS OF IBD

Dozens of proinflammatory cytokines were reported to be involved in the pathogenesis of IBD, but only several of them have been considered to be therapeutic targets. TNF α was considered being secreted mainly from intestinal mast cells in IBD^[78], and bacteria and anti-IgE were able to substantially enhance their release from mast cells^[149]. The released mast cell products TNF α and histamine could then synergistically stimulate ion secretion from intestinal epithelium^[150]. The anti-

TNF α therapy will be described below. In IBD, most intestinal mast cells produce IL-3, and this increased expression of IL-3 could be inhibited by administration of steroid^[151]. IL-10, a cytokine which can be produced by human mast cells^[152], was reported to have some anti-inflammatory role in IBD^[153]. However, the results from clinical trials were heterogeneous^[154]. IL-1 was found to be excessively released from patients with ulcerative colitis and could stimulate the short-circuit current response to IL-1^[155]. As for IL-3, steroid could significantly inhibit IL-1 release in IBD^[156]. Mast cells from healthy controls did not produce IL-5, but mast cells from patients with intestinal inflammatory disease could release a relatively large amount of IL-5^[157]. However, the effect of IL-5 on IBD needs to be investigated. It is still in early days to understand the role of cytokines in IBD, therefore it is difficult to draw a conclusive line on the issue whether cytokine related therapy is beneficial for IBD.

HYPOTHESIS OF SELF-AMPLIFICATION MECHANISM OF MAST CELL DEGRANULATION IN GUT

Tryptase has been proved to be a unique marker of mast cell degranulation *in vitro* as it is more selective than histamine to mast cells. Inhibitors of tryptase^[71,158] and chymase^[159] have been discovered to possess the ability to inhibit histamine or tryptase release from human skin, tonsil, synovial^[160] and colon mast cells^[161,162], suggesting that they are likely to be developed as a novel class of mast cell stabilizers. Recently, a series of experiments with dispersed colon mast cells suggested there should be at least two pathways in man for mast cells to amplify their own activation-degranulation signals in an autocrine or paracrine manner, which may partially explain the phenomena that when a sensitized individual contacts allergen only once the local allergic response in the involved tissue or organ may last for days or weeks. These findings included both anti-IgE and calcium ionophore were able to induce significant release of tryptase and histamine from colon mast cells^[163], histamine was a potent activator of human colon mast cells^[164] and the agonists of PAR-2 and trypsin were potent secretagogues of human colon mast cells^[165]. Since tryptase was reported to be able to activate human mast cells^[71] and H₁ receptor antagonists terfenadine and cetirizine^[166] were capable of inhibiting mast cell activation, the hypothesis of mast cell degranulation self-amplification mechanisms is that mast cell secretagogues induce mast cell degranulation, release histamine, then stimulate the adjacent mast cells or positively feedback to further stimulate its host mast cells through H₁ receptor, whereas released tryptase acts similarly to histamine through its receptor PAR-2 on mast cells (Figure 1).

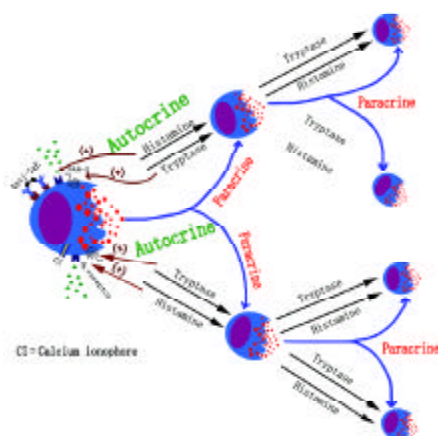


Figure 1 Hypothesis of self-amplification mechanism of mast cell degranulation in gut.

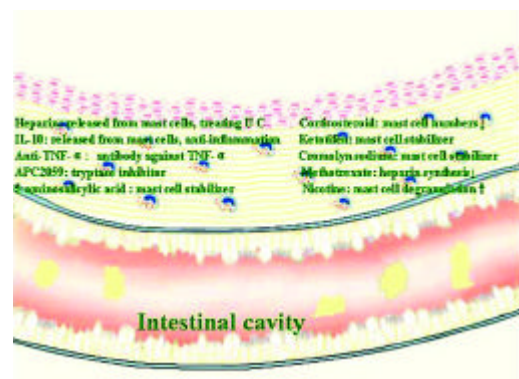


Figure 2 Association of mast cells with IBD therapies.

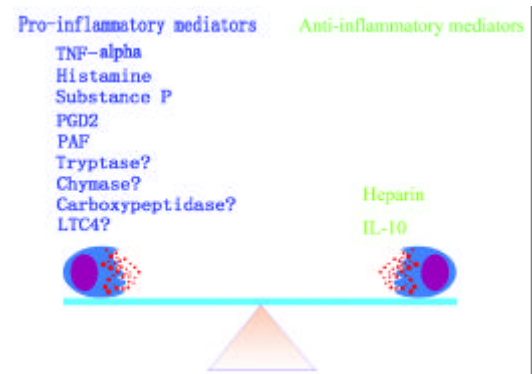


Figure 3 Balance between “pro-inflammatory” and “anti-inflammatory” mast cell mediators in IBD.

RELATIONSHIP BETWEEN THERAPIES FOR IBD AND MAST CELLS

Although aminosalicylates and corticosteroids remain the mainstream therapeutic drugs for the treatment of IBD^[167], the mast cell related therapy should be given some close attentions. Besides heparin therapy mentioned above, anti-TNF α monoclonal antibody^[168,169], infliximab in particular^[170] showed promising results in treating Crohn’s disease. Thalidomide, an agent with antiangiogenic and immunomodulatory properties^[171], possessed inhibitory activity towards TNF α ^[172] and was therapeutically effective in IBD^[173]. Mast cell tryptase inhibitor APC2059 was also effective and safe in treating ulcerative colitis^[174]. Even 5-aminosalicylic acid, an aminosalicylate drug was an effective inhibitor of anti-IgE induced histamine and PGD2 release from human intestinal mast cells^[175]. Thus the beneficial effects of 5-aminosalicylic acid on IBD were at least partially due to its mast cell stabilizing activity. Similarly, the effective treatment of IBD by corticosteroids might also be partially associated with its action on mast cells as significantly reduced numbers of mast cells were observed in the colon throughout steroid therapy^[176].

The ineffective treatment of ulcerative colitis by mast cell stabilizer, cromolyn sodium^[177] was most likely due to the drug that did not affect release of histamine from colon mast cells^[178]. However, it was recently found to be effective in treating chronic or recurrent enterocolitis in patients with Hirschsprung’s disease^[179]. In 1992, Eliakim and colleagues found that ketotifen, a mast cell stabilizer, was able to significantly decrease mucosal damage of ulcerative colitis in an experimental colitis model^[180] and inhibit accumulation of PGE2, ITB4 and LTC4 in ulcerative colitis colon mucosa organ-culture^[181], suggesting that this anti-asthma drug may be useful for the treatment of IBD. Indeed, ketotifen was revealed to be effective in treating IBD with 5-aminosalicylate intolerance^[182], and acute ulcerative colitis in

children^[183], most likely through inhibition of mast cell and neutrophil degranulation^[184].

It was surprising to learn that even immunomodulatory drug methotrexate, which showed promise in Crohn's disease therapy^[185] was able to inhibit heparin synthesis in mast cells^[186], suggesting that the beneficial action of methotrexate on Crohn's disease might be due to the reduction of heparin secretion from mast cells. Nicotine, an addictive component of tobacco, had a dual effect on IBD. It could ameliorate disease activity of ulcerative colitis but deteriorate disease process of Crohn's disease^[187]. Since nicotine was reported to be able to induce degranulation of mast cells^[188], its dual action on IBD could be related to the locally imbalanced quantities of mast cell products, such as histamine and heparin. The association of these therapies with mast cells strongly indicates that mast cells are key cells in the development of IBD (Figure 2).

CONCLUSION

Mast cells are a key cell type, which is actively involved in the pathogenesis of IBD. The different actions of mast cell mediators in IBD suggest that there must be a balance between 'pro-IBD' and 'anti-IBD' mast cell mediators (Figure 3). Breaking this balance may cause diseases. There are at least two pathways, histamine pathway and tryptase pathway, for mast cells to amplify their degranulation signals. Each of them is likely to act in either autocrine or paracrine manner. These mast cell degranulation signal amplification mechanisms may be the key event in the pathophysiological process of long-lasting local response of mast cell associated diseases such as IBD, asthma and rhinitis.

REFERENCES

- 1 **Walls AF**, He SH, Buckley MG, McEuen AR. Roles of the mast cell and basophil in asthma. *Clin Exp Allergy Review* 2001; **1**: 68-72
- 2 **Sun G**, Stacey MA, Vittori E, Marini M, Bellini A, Kleimberg J, Mattoli S. Cellular and molecular characteristics of inflammation in chronic bronchitis. *Eur J Clin Invest* 1998; **28**: 364-372
- 3 **Pesci A**, Rossi GA, Bertorelli G, Aufiero A, Zanon P, Olivieri D. Mast cells in the airway lumen and bronchial mucosa of patients with chronic bronchitis. *Am J Respir Crit Care Med* 1994; **149**: 1311-1316
- 4 **Kalenderian R**, Raju L, Roth W, Schwartz LB, Gruber B, Janoff A. Elevated histamine and tryptase levels in smokers' bronchoalveolar lavage fluid. Do lung mast cells contribute to smokers' emphysema? *Chest* 1988; **94**: 119-123
- 5 **Daum S**. Pathophysiology of pulmonary hypertension and chronic cor pulmonale. *Z Gesamte Inn Med* 1993; **48**: 525-531
- 6 **Sepper R**, Konttinen YT, Kempainen P, Sorsa T, Eklund KK. Mast cells in bronchiectasis. *Ann Med* 1998; **30**: 307-315
- 7 **Liebler JM**, Qu Z, Buckner B, Powers MR, Rosenbaum JT. Fibroproliferation and mast cells in the acute respiratory distress syndrome. *Thorax* 1998; **53**: 823-829
- 8 **Vucicevic Z**, Suskovic T. Acute respiratory distress syndrome after aprotinin infusion. *Ann Pharmacother* 1997; **31**: 429-432
- 9 **Barbato A**, Panizzolo C, D' Amore ES, La Rosa M, Saetta M. Bronchiolitis obliterans organizing pneumonia (BOOP) in a child with mild-to-moderate asthma: evidence of mast cell and eosinophil recruitment in lung specimens. *Pediatr Pulmonol* 2001; **31**: 394-397
- 10 **Pesci A**, Majori M, Piccoli ML, Casalini A, Curti A, Franchini D, Gabrielli M. Mast cells in bronchiolitis obliterans organizing pneumonia. Mast cell hyperplasia and evidence for extracellular release of tryptase. *Chest* 1996; **110**: 383-391
- 11 **Hubeau C**, Puchelle E, Gaillard D. Distinct pattern of immune cell population in the lung of human fetuses with cystic fibrosis. *J Allergy Clin Immunol* 2001; **108**: 524-529
- 12 **Henderson WR Jr**, Chi EY. Degranulation of cystic fibrosis nasal polyp mast cells. *J Pathol* 1992; **166**: 395-404
- 13 **Pesci A**, Bertorelli G, Gabrielli M, Olivieri D. Mast cells in fibrotic lung disorders. *Chest* 1993; **103**: 989-996
- 14 **Hunt LW**, Colby TV, Weiler DA, Sur S, Butterfield JH. Immunofluorescent staining for mast cells in idiopathic pulmonary fibrosis: quantification and evidence for extracellular release of mast cell tryptase. *Mayo Clin Proc* 1992; **67**: 941-948
- 15 **Hamada H**, Vallyathan V, Cool CD, Barker E, Inoue Y, Newman LS. Mast cell basic fibroblast growth factor in silicosis. *Am J Respir Crit Care Med* 2000; **161**: 2026-2034
- 16 **Amano H**, Kurosawa M, Ishikawa O, Chihara J, Miyachi Y. Mast cells in the cutaneous lesions of sarcoidosis: their subtypes and the relationship to systemic manifestations. *J Dermatol Sci* 2000; **24**: 60-66
- 17 **Flint KC**, Leung KB, Hudspeth BN, Brostoff J, Pearce FL, Geraint-James D, Johnson NM. Bronchoalveolar mast cells in sarcoidosis: increased numbers and accentuation of mediator release. *Thorax* 1986; **41**: 94-99
- 18 **Nagata M**, Shijubo N, Walls AF, Ichimiya S, Abe S, Sato N. Chymase-positive mast cells in small sized adenocarcinoma of the lung. *Virchows Arch* 2003; **443**: 565-573
- 19 **Munoz S**, Hernandez-Pando R, Abraham SN, Enciso JA. Mast cell activation by Mycobacterium tuberculosis: mediator release and role of CD48. *J Immunol* 2003; **170**: 5590-5596
- 20 **Furusu H**, Murase K, Nishida Y, Isomoto H, Takeshima F, Mizuta Y, Hewlett BR, Riddell RH, Kohno S. Accumulation of mast cells and macrophages in focal active gastritis of patients with Crohn's disease. *Hepatogastroenterology* 2002; **49**: 639-643
- 21 **Sulik A**, Kemon A, Sulik M, Oldak E. Mast cells in chronic gastritis of children. *Pol Merkuriusz Lek* 2001; **10**: 156-160
- 22 **Nakajima S**, Krishnan B, Ota H, Segura AM, Hattori T, Graham DY, Genta RM. Mast cell involvement in gastritis with or without *Helicobacter pylori* infection. *Gastroenterology* 1997; **113**: 746-754
- 23 **Plebani M**, Basso D, Rugge M, Vianello F, Di Mario F. Influence of *Helicobacter pylori* on tryptase and cathepsin D in peptic ulcer. *Dig Dis Sci* 1995; **40**: 2473-2476
- 24 **Terada T**, Matsunaga Y. Increased mast cells in hepatocellular carcinoma and intrahepatic cholangiocarcinoma. *J Hepatol* 2000; **33**: 961-966
- 25 **Balazs M**, Illyes G, Vadasz G. Mast cells in ulcerative colitis. Quantitative and ultrastructural studies. *Virchows Arch B Cell Pathol Incl Mol Pathol* 1989; **57**: 353-360
- 26 **King T**, Biddle W, Bhatia P, Moore J, Miner PB Jr. Colonic mucosal mast cell distribution at line of demarcation of active ulcerative colitis. *Dig Dis Sci* 1992; **37**: 490-495
- 27 **Raitel M**, Matek M, Baenkler HW, Jorde W, Hahn EG. Mucosal histamine content and histamine secretion in Crohn's disease, ulcerative colitis and allergic enteropathy. *Int Arch Allergy Immunol* 1995; **108**: 127-133
- 28 **Dvorak AM**, Monahan RA, Osage JE, Dickersin GR. Crohn's disease: transmission electron microscopic studies. II. Immunologic inflammatory response. Alterations of mast cells, basophils, eosinophils, and the microvasculature. *Hum Pathol* 1980; **11**: 606-619
- 29 **Lloyd G**, Green FH, Fox H, Mani V, Turnberg LA. Mast cells and immunoglobulin E in inflammatory bowel disease. *Gut* 1975; **16**: 861-866
- 30 **Nakamura A**, Yamazaki K, Suzuki K, Sato S. Increased portal tract infiltration of mast cells and eosinophils in primary biliary cirrhosis. *Am J Gastroenterol* 1997; **92**: 2245-2249
- 31 **Matsunaga Y**, Kawasaki H, Terada T. Stromal mast cells and nerve fibers in various chronic liver diseases: relevance to hepatic fibrosis. *Am J Gastroenterol* 1999; **94**: 1923-1932
- 32 **Bardadin KA**, Scheuer PJ. Mast cells in acute hepatitis. *J Pathol* 1986; **149**: 315-325
- 33 **Zimnoch L**, Szynaka B, Puchalski Z. Mast cells and pancreatic stellate cells in chronic pancreatitis with differently intensified fibrosis. *Hepatogastroenterology* 2002; **49**: 1135-1138
- 34 **Atkinson JB**, Harlan CW, Harlan GC, Virmani R. The association of mast cells and atherosclerosis: a morphologic study of early atherosclerotic lesions in young people. *Hum Pathol* 1994; **25**: 154-159
- 35 **Laine P**, Kaartinen M, Penttila A, Panula P, Paavonen T, Kovanen PT. Association between myocardial infarction and the mast cells in the adventitia of the infarct-related coronary artery. *Circulation* 1999; **99**: 361-369

- 36 **Kovanen PT**, Kaartinen M, Paavonen T. Infiltrates of activated mast cells at the site of coronary atheromatous erosion or rupture in myocardial infarction. *Circulation* 1995; **92**: 1084-1088
- 37 **Hamada H**, Terai M, Kimura H, Hirano K, Oana S, Niimi H. Increased expression of mast cell chymase in the lungs of patients with congenital heart disease associated with early pulmonary vascular disease. *Am J Respir Crit Care Med* 1999; **160**: 1303-1308
- 38 **Turlington BS**, Edwards WD. Quantitation of mast cells in 100 normal and 92 diseased human hearts. Implications for interpretation of endomyocardial biopsy specimens. *Am J Cardiovasc Pathol* 1988; **2**: 151-157
- 39 **Patella V**, de Crescenzo G, Lamparter-Schummert B, De Rosa G, Adt M, Marone G. Increased cardiac mast cell density and mediator release in patients with dilated cardiomyopathy. *Inflamm Res* 1997; **46**(Suppl 1): S31-32
- 40 **Patella V**, Marino I, Arbustini E, Lamparter-Schummert B, Verga L, Adt M, Marone G. Stem cell factor in mast cells and increased mast cell density in idiopathic and ischemic cardiomyopathy. *Circulation* 1998; **97**: 971-978
- 41 **Ruger BM**, Hasan Q, Greenhill NS, Davis PF, Dunbar PR, Neale TJ. Mast cells and type VIII collagen in human diabetic nephropathy. *Diabetologia* 1996; **39**: 1215-1222
- 42 **Toda S**, Tokuda Y, Koike N, Yonemitsu N, Watanabe K, Koike K, Fujitani N, Hiromatsu Y, Sugihara H. Growth factor-expressing mast cells accumulate at the thyroid tissue-regenerative site of subacute thyroiditis. *Thyroid* 2000; **10**: 381-386
- 43 **McKenna MJ**. Histomorphometric study of mast cells in normal bone, osteoporosis and mastocytosis using a new stain. *Calcif Tissue Int* 1994; **55**: 257-259
- 44 **Toth T**, Toth-Jakatics R, Jimi S, Ihara M, Urata H, Takebayashi S. Mast cells in rapidly progressive glomerulonephritis. *J Am Soc Nephrol* 1999; **10**: 1498-1505
- 45 **Kurusu A**, Suzuki Y, Horikoshi S, Shirato I, Tomino Y. Relationship between mast cells in the tubulointerstitium and prognosis of patients with IgA nephropathy. *Nephron* 2001; **89**: 391-397
- 46 **Toms R**, Weiner HL, Johnson D. Identification of IgE-positive cells and mast cells in frozen sections of multiple sclerosis brains. *J Neuroimmunol* 1990; **30**: 169-177
- 47 **Woolley DE**, Tetlow LC. Mast cell activation and its relation to proinflammatory cytokine production in the rheumatoid lesion. *Arthritis Res* 2000; **2**: 65-74
- 48 **Dean G**, Hoyland JA, Denton J, Donn RP, Freemont AJ. Mast cells in the synovium and synovial fluid in osteoarthritis. *Br J Rheumatol* 1993; **32**: 671-675
- 49 **Godfrey HP**, Ilardi C, Engber W, Graziano FM. Quantitation of human synovial mast cells in rheumatoid arthritis and other rheumatic diseases. *Arthritis Rheum* 1984; **27**: 852-856
- 50 **Galli SJ**, Dvorak AM, Dvorak HF. Basophils and mast cells: morphologic insights into their biology, secretory patterns, and function. *Prog Allergy* 1984; **34**: 1-141
- 51 **Schulman ES**, Kagey-Sobotka A, MacGlashan DW Jr, Adkinson NF Jr, Peters SP, Schleimer RP, Lichtenstein LM. Heterogeneity of human mast cells. *J Immunol* 1983; **131**: 1936-1941
- 52 **Benyon RC**, Lowman MA, Church MK. Human skin mast cells: their dispersion, purification and secretory characterization. *J Immunol* 1987; **138**: 861-867
- 53 **Church MK**, Caulfield JP. Mast cell and basophil functions. In: Holgate ST, Church MK, ed. *Allergy*. London: Gower Medical Publishing 1993: 5.1-5.12
- 54 **Schwartz LB**. Tryptase from human mast cells: Biochemistry, biology and clinical utility: In: Schwartz LB, ed. *Neutral Proteases of Mast Cells*. Basel Karger: Monogr Allergy 1990: 90-113
- 55 **Church MK**, Benyon RC, Clegg LS, Holgate ST. Immunopharmacology of mast cells. In: Greaves MW, Schuster S, eds. *Handbook of experimental pharmacology*. Berlin Heidelberg: Springer-Verlag 1989: 129-166
- 56 **Caulfield JP**, Lewis RA, Hein A, Austen KF. Secretion in dissociated human pulmonary mast cells. Evidence of solubilization of granule contents before discharge. *J Cell Biol* 1980; **85**: 299-312
- 57 **Johnson RG**, Carty SE, Fingerhoff BJ, Scarpa A. The internal pH of mast cell granules. *FEBS Lett* 1980; **120**: 75-79
- 58 **Lagunoff D**, Rickard A. Evidence for control of mast cell granule protease *in situ* by low pH. *Exp Cell Res* 1983; **144**: 353-360
- 59 **Irani AA**, Schwartz LB. Neutral protease as indicators of human mast cell heterogeneity. In: Schwartz LB, ed. *Neutral proteases of mast cells*. Basel Karger: Monogr Allergy 1990: 146-162
- 60 **Goldstein SM**, Kaempfer CE, Kealey JT, Wintroub BU. Human mast cell carboxypeptidase. Purification and characterization. *J Clin Invest* 1989; **83**: 1630-1636
- 61 **Irani AA**, Schechter NM, Craig SS, DeBlois G, Schwartz LB. Two types of human mast cells that have distinct neutral protease compositions. *Proc Natl Acad Sci U S A* 1986; **83**: 4464-4468
- 62 **Irani AA**, Goldstein SM, Wintroub BU, Bradford T, Schwartz LB. Human mast cell carboxypeptidase. Selective localization to MCTC cells. *J Immunol* 1991; **147**: 247-253
- 63 **Meier HL**, Heck LW, Schulman ES, MacGlashan DW Jr. Purified human mast cells and basophils release human elastase and cathepsin G by an IgE-mediated mechanism. *Int Arch Allergy Appl Immunol* 1985; **77**: 179-183
- 64 **Schechter NM**, Irani AM, Sprows JL, Abernethy J, Wintroub B, Schwartz LB. Identification of a cathepsin G-like proteinase in the MCTC type of human mast cell. *J Immunol* 1990; **145**: 2652-2661
- 65 **Robinson C**, Benyon C, Holgate ST, Church MK. The IgE- and calcium-dependent release of eicosanoids and histamine from human purified cutaneous mast cells. *J Invest Dermatol* 1989; **93**: 397-404
- 66 **Bradding P**, Walls AF, Church MK. Role of mast cells and basophils in inflammatory responses. In: Holgate ST, ed. *Immunopharmacology of the respiratory system*. Harcourt Brace Company, Publishers: Academic press 1995: 53-84
- 67 **Holgate ST**. The role of mast cells and basophils in inflammation. *Clin Exp Allergy* 2000; **30**(Suppl 1): 28-32
- 68 **Peters SP**. Mechanism of mast cell activation. In: Busse WW, Holgate ST, eds. *Asthma and Rhinitis*. Oxford: Blackwell 1995: 221-230
- 69 **Nagai S**, Kitani S, Hirai K, Takaishi T, Nakajima K, Kihara H, Nonomura Y, Ito K, Morita Y. Pharmacological study of stem-cell-factor-induced mast cell histamine release with kinase inhibitors. *Biochem Biophys Res Commun* 1995; **208**: 576-581
- 70 **Patella V**, de Crescenzo G, Marinò I, Genovese A, Adt M, Gleich GJ, Marone G. Eosinophil granule proteins activate human heart mast cells. *J Immunol* 1996; **157**: 1219-1225
- 71 **He SH**, Gaça MD, Walls AF. A role for tryptase in the activation of human mast cells: modulation of histamine release by tryptase and inhibitors of tryptase. *J Pharmacol Exp Ther* 1998; **286**: 289-297
- 72 **Nolte H**, Spjeldnaes N, Kruse A, Windelborg B. Histamine release from gut mast cells from patients with inflammatory bowel diseases. *Gut* 1990; **31**: 791-794
- 73 **Nishida Y**, Murase K, Isomoto H, Furusu H, Mizuta Y, Riddell RH, Kohno S. Different distribution of mast cells and macrophages in colonic mucosa of patients with collagenous colitis and inflammatory bowel disease. *Hepatology* 2002; **49**: 678-682
- 74 **He SH**, Peng Q, Walls AF. Potent induction of a neutrophil and eosinophil-rich infiltrate *in vivo* by human mast cell tryptase: selective enhancement of eosinophil recruitment by histamine. *J Immunol* 1997; **159**: 6216-6225
- 75 **He SH**, Walls AF. Human mast cell chymase induces the accumulation of neutrophils, eosinophils and other inflammatory cells *in vivo*. *Br J Pharmacol* 1998; **125**: 1491-1500
- 76 **Gelbmann CM**, Mestermann S, Gross V, Kollinger M, Scholmerich J, Falk W. Strictures in Crohn's disease are characterised by an accumulation of mast cells colocalised with laminin but not with fibronectin or vitronectin. *Gut* 1999; **45**: 210-217
- 77 **Sasaki Y**, Tanaka M, Kudo H. Differentiation between ulcerative colitis and Crohn's disease by a quantitative immunohistochemical evaluation of T lymphocytes, neutrophils, histiocytes and mast cells. *Pathol Int* 2002; **52**: 277-285
- 78 **Lilja I**, Gustafson-Svard C, Franzen L, Sjobahl R. Tumor necrosis factor-alpha in ileal mast cells in patients with Crohn's disease. *Digestion* 2000; **61**: 68-76
- 79 **Middel P**, Reich K, Polzien F, Blaschke V, Hemmerlein B, Herms J, Korabiowska M, Radzun HJ. Interleukin 16 expression and phenotype of interleukin 16 producing cells in Crohn's disease. *Gut* 2001; **49**: 795-803
- 80 **Lynch EA**, Heijens CA, Horst NF, Center DM, Cruikshank WW. Cutting Edge: IL-16/CD4 Preferentially induces Th1 cell migration: requirement of CCR5. *J Immunol* 2003; **171**: 4965-4968

- 81 **Schreiber S.** Monocytes or T cells in Crohn's disease: does IL-16 allow both to play at that game? *Gut* 2001; **49**: 747-748
- 82 **Stoyanova II.** Gulubova MV. Mast cells and inflammatory mediators in chronic ulcerative colitis. *Acta Histochem* 2002; **104**: 185-192
- 83 **Tsuneyama K.** Saito K, Ruebner BH, Konishi I, Nakanuma Y, Gershwin ME. Immunological similarities between primary sclerosing cholangitis and chronic sclerosing sialadenitis: report of the overlapping of these two autoimmune diseases. *Dig Dis Sci* 2000; **45**: 366-372
- 84 **Halme L.** Karkkainen P, Rautelin H, Kosunen TU, Sipponen P. High frequency of helicobacter negative gastritis in patients with Crohn's disease. *Gut* 1996; **38**: 379-383
- 85 **Locher C.** Tipold A, Welle M, Busato A, Zurbriggen A, Griot-Wenk ME. Quantitative assessment of mast cells and expression of IgE protein and mRNA for IgE and interleukin 4 in the gastrointestinal tract of healthy dogs and dogs with inflammatory bowel disease. *Am J Vet Res* 2001; **62**: 211-216
- 86 **Araki Y.** Andoh A, Fujiyama Y, Bamba T. Development of dextran sulphate sodium-induced experimental colitis is suppressed in genetically mast cell-deficient Ws/Ws rats. *Clin Exp Immunol* 2000; **119**: 264-269
- 87 **Santos J.** Yang PC, Soderholm JD, Benjamin M, Perdue MH. Role of mast cells in chronic stress induced colonic epithelial barrier dysfunction in the rat. *Gut* 2001; **48**: 630-636
- 88 **Dvorak AM.** McLeod RS, Onderdonk A, Monahan-Earley RA, Cullen JB, Antonioli DA, Morgan E, Blair JE, Estrella P, Cisneros RL. Ultrastructural evidence for piecemeal and anaphylactic degeneration of human gut mucosal mast cells *in vivo*. *Int Arch Allergy Immunol* 1992; **99**: 74-83
- 89 **Bischoff SC.** Wedemeyer J, Herrmann A, Meier PN, Trautwein C, Cetin Y, Maschek H, Stolte M, Gebel M, Manns MP. Quantitative assessment of intestinal eosinophils and mast cells in inflammatory bowel disease. *Histopathology* 1996; **28**: 1-13
- 90 **Crivellato E.** Finato N, Isola M, Ribatti D, Beltrami CA. Low mast cell density in the human duodenal mucosa from chronic inflammatory duodenal bowel disorders is associated with defective villous architecture. *Eur J Clin Invest* 2003; **33**: 601-610
- 91 **Knutson L.** Ahrenstedt O, Odland B, Hallgren R. The jejunal secretion of histamine is increased in active Crohn's disease. *Gastroenterology* 1990; **98**: 849-854
- 92 **Schwab D.** Hahn EG, Raithel M. Enhanced histamine metabolism: a comparative analysis of collagenous colitis and food allergy with respect to the role of diet and NSAID use. *Inflamm Res* 2003; **52**: 142-147
- 93 **Winterkamp S.** Weidenhiller M, Otte P, Stolper J, Schwab D, Hahn EG, Raithel M. Urinary excretion of N-methylhistamine as a marker of disease activity in inflammatory bowel disease. *Am J Gastroenterol* 2002; **97**: 3071-3077
- 94 **Weidenhiller M.** Raithel M, Winterkamp S, Otte P, Stolper J, Hahn EG. Methylhistamine in Crohn's disease (CD): increased production and elevated urine excretion correlates with disease activity. *Inflamm Res* 2000; **49**(Suppl 1): S35-36
- 95 **Fox CC.** Lichtenstein LM, Roche JK. Intestinal mast cell responses in idiopathic inflammatory bowel disease. Histamine release from human intestinal mast cells in response to gut epithelial proteins. *Dig Dis Sci* 1993; **38**: 1105-1112
- 96 **Raithel M.** Schneider HT, Hahn EG. Effect of substance P on histamine secretion from gut mucosa in inflammatory bowel disease. *Scand J Gastroenterol* 1999; **34**: 496-503
- 97 **Fargeas MJ.** Theodorou V, More J, Wal JM, Fioramonti J, Bueno L. Boosted systemic immune and local responsiveness after intestinal inflammation in orally sensitized guinea pigs. *Gastroenterology* 1995; **109**: 53-62
- 98 **Repka-Ramirez MS.** New concepts of histamine receptors and actions. *Curr Allergy Asthma Rep* 2003; **3**: 227-231
- 99 **Bertaccini G.** Coruzzi G. An update on histamine H3 receptors and gastrointestinal functions. *Dig Dis Sci* 1995; **40**: 2052-2063
- 100 **Rangachari PK.** Histamine: mercurial messenger in the gut. *Am J Physiol* 1992; **262**(1 Pt 1): G1-G13
- 101 **Homaidan FR.** Tripodi J, Zhao L, Burakoff R. Regulation of ion transport by histamine in mouse cecum. *Eur J Pharmacol* 1997; **331**: 199-204
- 102 **Traynor TR.** Brown DR, O'Grady SM. Effects of inflammatory mediators on electrolyte transport across the porcine distal colon epithelium. *J Pharmacol Exp Ther* 1993; **264**: 61-66
- 103 **Crowe SE.** Luthra GK, Perdue MH. Mast cell mediated ion transport in intestine from patients with and without inflammatory bowel disease. *Gut* 1997; **41**: 785-792
- 104 **Moriarty D.** Goldhill J, Selve N, O'Donoghue DP, Baird AW. Human colonic anti-secretory activity of the potent NK(1) antagonist, SR140333: assessment of potential anti-diarrhoeal activity in food allergy and inflammatory bowel disease. *Br J Pharmacol* 2001; **133**: 1346-1354
- 105 **Abraham WM.** Tryptase: potential role in airway inflammation and remodelling. *Am J Physiol Lung Cell Mol Physiol* 2002; **282**: L193-L196
- 106 **McEuen AR.** He SH, Brander ML, Walls AF. Guinea pig lung tryptase: Localisation to mast cells and characterisation of the partially purified enzyme. *Biochem Pharmacol* 1996; **52**: 331-340
- 107 **He SH.** Walls AF. Human mast cell tryptase: a stimulus of microvascular leakage and mast cell activation. *Eur J Pharmacol* 1997; **328**: 89-97
- 108 **Cairns JA.** Walls AF. Mast cell tryptase is a mitogen for epithelial cells. Stimulation of IL-8 production and intercellular adhesion molecule-1 expression. *J Immunol* 1996; **156**: 275-283
- 109 **Raithel M.** Winterkamp S, Pacurar A, Ulrich P, Hochberger J, Hahn EG. Release of mast cell tryptase from human colorectal mucosa in inflammatory bowel disease. *Scand J Gastroenterol* 2001; **36**: 174-179
- 110 **Kunzelmann K.** Schreiber R, Konig J, Mall M. Ion transport induced by proteinase-activated receptors (PAR2) in colon and airways. *Cell Biochem Biophys* 2002; **36**: 209-214
- 111 **Molino M.** Barnathan ES, Numerof R, Clark J, Dreyer M, Cumashi A, Hoxie JA, Schechter N, Woolkalis M, Brass LF. Interactions of mast cell tryptase with thrombin receptors and PAR-2. *J Biol Chem* 1997; **272**: 4043-4049
- 112 **Cenac N.** Coelho AM, Nguyen C, Compton S, Andrade-Gordon P, MacNaughton WK, Wallace JL, Hollenberg MD, Bunnett NW, Garcia-Villar R, Bueno L, Vergnolle N. Induction of intestinal inflammation in mouse by activation of proteinase-activated receptor-2. *Am J Pathol* 2002; **161**: 1903-1915
- 113 **Mall M.** Gonska T, Thomas J, Hirtz S, Schreiber R, Kunzelmann K. Activation of ion secretion via proteinase-activated receptor-2 in human colon. *Am J Physiol Gastrointest Liver Physiol* 2002; **282**: G200-G210
- 114 **Kim JA.** Choi SC, Yun KJ, Kim DK, Han MK, Seo GS, Yeom JJ, Kim TH, Nah YH, Lee YM. Expression of protease-activated receptor 2 in ulcerative colitis. *Inflamm Bowel Dis* 2003; **9**: 224-229
- 115 **Krishnaswamy G.** Kelley J, Johnson D, Youngberg G, Stone W, Huang SK, Bieber J, Chi DS. The human mast cell: functions in physiology and disease. *Front Biosci* 2001; **6**: D1109-1127
- 116 **He SH.** Walls AF. The induction of a prolonged increase in microvascular permeability by human mast cell chymase. *Eur J Pharmacol* 1998; **352**: 91-98
- 117 **Scudamore CL.** Jepson MA, Hirst BH, Miller HR. The rat mucosal mast cell chymase, RMCP-II, alters epithelial cell monolayer permeability in association with altered distribution of the tight junction proteins ZO-1 and occludin. *Eur J Cell Biol* 1998; **75**: 321-330
- 118 **Chen ZQ.** He SH. Cloning and expression of human colon mast cell carboxypeptidase. *World J Gastroenterol* 2004; **10**: 342-347
- 119 **Gaffney PR.** Doyle CT, Gaffney A, Hogan J, Hayes DP, Annis P. Paradoxical response to heparin in 10 patients with ulcerative colitis. *Am J Gastroenterol* 1995; **90**: 220-223
- 120 **Evans RC.** Wong VS, Morris AI, Rhodes JM. Treatment of corticosteroid-resistant ulcerative colitis with heparin—a report of 16 cases. *Aliment Pharmacol Ther* 1997; **11**: 1037-1040
- 121 **Yoshikane H.** Sakakibara A, Ayakawa T, Taki N, Kawashima H, Arakawa D, Hidano H. Disseminated intravascular coagulation in an ulcerative colitis case not associated with surgery. *Hepatogastroenterology* 2000; **47**: 1608-1610
- 122 **Ang YS.** Mahmud N, White B, Byrne M, Kelly A, Lawler M, McDonald GS, Smith OP, Keeling PW. Randomized comparison of unfractionated heparin with corticosteroids in severe active inflammatory bowel disease. *Aliment Pharmacol Ther* 2000; **14**: 1015-1022
- 123 **Folwaczny C.** Wiebecke B, Loeschke K. Unfractionated heparin in

- the therapy of patients with highly active inflammatory bowel disease. *Am J Gastroenterol* 1999; **94**: 1551-1555
- 124 **Dotan I**, Hallak A, Arber N, Santo M, Alexandrowitz A, Knaani Y, Hershkovitz R, Brazowski E, Halpern Z. Low-dose low-molecular weight heparin (enoxaparin) is effective as adjuvant treatment in active ulcerative colitis: an open trial. *Dig Dis Sci* 2001; **46**: 2239-2244
- 125 **Vrij AA**, Jansen JM, Schoon EJ, de Bruine A, Hemker HC, Stockbrugger RW. Low molecular weight heparin treatment in steroid refractory ulcerative colitis: clinical outcome and influence on mucosal capillary thrombi. *Scand J Gastroenterol Suppl* 2001; **234**: 41-47
- 126 **Torkvist L**, Thorlacius H, Sjoqvist U, Bohman L, Lapidus A, Flood L, Agren B, Raud J, Lofberg R. Low molecular weight heparin as adjuvant therapy in active ulcerative colitis. *Aliment Pharmacol Ther* 1999; **13**: 1323-1328
- 127 **Papa A**, Danese S, Gasbarrini A, Gasbarrini G. Review article: potential therapeutic applications and mechanisms of action of heparin in inflammatory bowel disease. *Aliment Pharmacol Ther* 2000; **14**: 1403-1409
- 128 **Michell NP**, Lalor P, Langman MJ. Heparin therapy for ulcerative colitis? Effects and mechanisms. *Eur J Gastroenterol Hepatol* 2001; **13**: 449-456
- 129 **Day R**, Forbes A. Heparin, cell adhesion, and pathogenesis of inflammatory bowel disease. *Lancet* 1999; **354**: 62-65
- 130 **McCarty MF**. Vascular heparan sulfates may limit the ability of leukocytes to penetrate the endothelial barrier—implications for use of glucosamine in inflammatory disorders. *Med Hypotheses* 1998; **51**: 11-15
- 131 **Wan MX**, Liu Q, Wang Y, Thorlacius H. Protective effect of low molecular weight heparin on experimental colitis: role of neutrophil recruitment and TNF-alpha production. *Inflamm Res* 2002; **51**: 182-187
- 132 **Salas A**, Sans M, Soriano A, Reverter JC, Anderson DC, Pique JM, Panes J. Heparin attenuates TNF-alpha induced inflammatory response through a CD11b dependent mechanism. *Gut* 2000; **47**: 88-96
- 133 **Dobosz M**, Mionskowska L, Dobrowolski S, Dymecki D, Makarewicz W, Hrabowska M, Wajda Z. Is nitric oxide and heparin treatment justified in inflammatory bowel disease? An experimental study. *Scand J Clin Lab Invest* 1996; **56**: 657-663
- 134 **Fries W**, Pagiaro E, Canova E, Carraro P, Gasparini G, Pomerri F, Martin A, Carlotto C, Mazzon E, Sturniolo GC, Longo G. The effect of heparin on trinitrobenzene sulphonic acid-induced colitis in the rat. *Aliment Pharmacol Ther* 1998; **12**: 229-236
- 135 **Fox CC**, Lazenby AJ, Moore WC, Yardley JH, Bayless TM, Lichtenstein LM. Enhancement of human intestinal mast cell mediator release in active ulcerative colitis. *Gastroenterology* 1990; **99**: 119-124
- 136 **Ajuebor MN**, Singh A, Wallace JL. Cyclooxygenase-2-derived prostaglandin D(2) is an early anti-inflammatory signal in experimental colitis. *Am J Physiol Gastrointest Liver Physiol* 2000; **279**: G238-G244
- 137 **Casellas F**, Guarner F, Antolin M, Rodriguez R, Salas A, Malagelada JR. Abnormal leukotriene C4 released by unaffected jejunal mucosa in patients with inactive Crohn's disease. *Gut* 1994; **35**: 517-522
- 138 **Eliakim R**, Karmeli F, Razin E, Rachmilewitz D. Role of platelet-activating factor in ulcerative colitis. Enhanced production during active disease and inhibition by sulfasalazine and prednisolone. *Gastroenterology* 1988; **95**: 1167-1172
- 139 **Rachmilewitz D**, Karmeli F, Eliakim R. Platelet-activating factor—a possible mediator in the pathogenesis of ulcerative colitis. *Scand J Gastroenterol Suppl* 1990; **172**: 19-21
- 140 **Denizot Y**, Chaussade S, Nathan N, Colombel JF, Bossant MJ, Cherouki N, Benveniste J, Couturier D. PAF-acether and acetylhydrolase in stool of patients with Crohn's disease. *Dig Dis Sci* 1992; **37**: 432-437
- 141 **Sobhani I**, Hochlaf S, Denizot Y, Vissuzaine C, Rene E, Benveniste J, Lewin MM, Mignon M. Raised concentrations of platelet activating factor in colonic mucosa of Crohn's disease patients. *Gut* 1992; **33**: 1220-1225
- 142 **Thornton M**, Solomon MJ. Crohn's disease: in defense of a microvascular aetiology. *Int J Colorectal Dis* 2002; **17**: 287-297
- 143 **Riehl TE**, Stenson WF. Platelet-activating factor acetylhydrolases in Caco-2 cells and epithelium of normal and ulcerative colitis patients. *Gastroenterology* 1995; **109**: 1826-1834
- 144 **Ferraris L**, Karmeli F, Eliakim R, Klein J, Fiocchi C, Rachmilewitz D. Intestinal epithelial cells contribute to the enhanced generation of platelet activating factor in ulcerative colitis. *Gut* 1993; **34**: 665-668
- 145 **Kald B**, Smedh K, Olaison G, Sjodahl R, Tagesson C. Platelet-activating factor acetylhydrolase activity in intestinal mucosa and plasma of patients with Crohn's disease. *Digestion* 1996; **57**: 472-477
- 146 **Guimbaud R**, Izzo A, Martinolle JP, Vidon N, Couturier D, Benveniste J, Chaussade S. Intraluminal excretion of PAF, lysoPAF, and acetylhydrolase in patients with ulcerative colitis. *Dig Dis Sci* 1995; **40**: 2635-2640
- 147 **Hocke M**, Richter L, Bosseckert H, Eitner K. Platelet activating factor in stool from patients with ulcerative colitis and Crohn's disease. *Hepatogastroenterology* 1999; **46**: 2333-2337
- 148 **Stack WA**, Jenkins D, Vivet P, Hawkey CJ. Lack of effectiveness of the platelet-activating factor antagonist SR27417A in patients with active ulcerative colitis: a randomized controlled trial. The Platelet Activating Factor Antagonist Study Group in Ulcerative Colitis. *Gastroenterology* 1998; **115**: 1340-1345
- 149 **Bischoff SC**, Lorentz A, Schwengberg S, Weier G, Raab R, Manns MP. Mast cells are an important cellular source of tumour necrosis factor alpha in human intestinal tissue. *Gut* 1999; **44**: 643-652
- 150 **Oprins JC**, van der Burg C, Meijer HP, Munnik T, Groot JA. Tumour necrosis factor alpha potentiates ion secretion induced by histamine in a human intestinal epithelial cell line and in mouse colon: involvement of the phospholipase D pathway. *Gut* 2002; **50**: 314-321
- 151 **Ligumsky M**, Kuperstein V, Nechushtan H, Zhang Z, Razin E. Analysis of cytokine profile in human colonic mucosal Fc epsilonRI-positive cells by single cell PCR: inhibition of IL-3 expression in steroid-treated IBD patients. *FEBS Lett* 1997; **413**: 436-440
- 152 **Royer B**, Varadarajalou S, Saas P, Gabiot AC, Kantelip B, Feger F, Guillosson JJ, Kantelip JP, Arock M. Autocrine regulation of cord blood-derived human mast cell activation by IL-10. *J Allergy Clin Immunol* 2001; **108**: 80-86
- 153 **Scheinin T**, Butler DM, Salway F, Scallon B, Feldmann M. Validation of the interleukin-10 knockout mouse model of colitis: antitumour necrosis factor-antibodies suppress the progression of colitis. *Clin Exp Immunol* 2003; **133**: 38-43
- 154 **Asadullah K**, Sterry W, Volk HD. Interleukin-10 therapy—review of a new approach. *Pharmacol Rev* 2003; **55**: 241-269
- 155 **Wardle TD**, Turnberg LA. Potential role for interleukin-1 in the pathophysiology of ulcerative colitis. *Clin Sci* 1994; **86**: 619-626
- 156 **Rachmilewitz D**, Eliakim R, Simon P, Ligumsky M, Karmeli F. Cytokines and platelet-activating factor in human inflamed colonic mucosa. *Agents Actions* 1992; Spec No: C32-C36
- 157 **Lorentz A**, Schwengberg S, Mierke C, Manns MP, Bischoff SC. Human intestinal mast cells produce IL-5 *in vitro* upon IgE receptor cross-linking and *in vivo* in the course of intestinal inflammatory disease. *Eur J Immunol* 1999; **29**: 1496-1503
- 158 **He SH**, McEuen AR, Blewett SA, Li P, Buckley MG, Leufkens P, Walls AF. The inhibition of mast cell activation by neutrophil lactoferrin: uptake by mast cells and interaction with tryptase, chymase and cathepsin G. *Biochem Pharmacol* 2003; **65**: 1007-1015
- 159 **He SH**, Gaça MD, McEuen AR, Walls AF. Inhibitors of chymase as mast cell-stabilizing agents: the contribution of chymase in the activation of human mast cells. *J Pharmacol Exp Ther* 1999; **291**: 517-523
- 160 **He SH**, Gaca MD, Walls AF. The activation of synovial mast cells: modulation of histamine release by tryptase and chymase and their inhibitors. *Eur J Pharmacol* 2001; **412**: 223-229
- 161 **He SH**, Xie H. Modulation of histamine release from human colon mast cells by protease inhibitors. *World J Gastroenterol* 2004; **10**: 337-341
- 162 **He SH**, Xie H. Inhibition of tryptase release from human colon mast cells by protease inhibitors. *World J Gastroenterol* 2004; **10**: 332-336
- 163 **He SH**, Xie H, He YS. Induction of tryptase and histamine release from human colon mast cells by IgE-dependent or -inde-

- pendent mechanisms. *World J Gastroenterol* 2004; **10**: 319-322
- 164 **He SH**, Xie H. Modulation of tryptase secretion from human colon mast cells by histamine. *World J Gastroenterol* 2004; **10**: 323-326
- 165 **He SH**, He YS, Xie H. Activation of human colon mast cells through proteinase activated receptor-2. *World J Gastroenterol* 2004; **10**: 327-331
- 166 **Okayama Y**, Benyon RC, Lowman MA, Church MK. *In vitro* effects of H1-antihistamine on histamine and PGD₂ release from mast cells of human lung, tonsil, and skin. *Allergy* 1994; **49**: 246-253
- 167 **Jani N**, Regueiro MD. Medical therapy for ulcerative colitis. *Gastroenterol Clin North Am* 2002; **31**: 147-166
- 168 **Baert FJ**, Rutgeerts PJ. Medical therapies for ulcerative colitis and Crohn's disease. *Curr Gastroenterol Rep* 2000; **2**: 446-450
- 169 **Wolf JM**, Lashner BA. Inflammatory bowel disease: sorting out the treatment options. *Cleve Clin J Med* 2002; **69**: 621-626
- 170 **Cheifetz A**, Smedley M, Martin S, Reiter M, Leone G, Mayer L, Plevy S. The incidence and management of infusion reactions to infliximab: a large center experience. *Am J Gastroenterol* 2003; **98**: 1315-1324
- 171 **Witzens M**, Moehler T, Neben K, Fruehauf S, Hartschuh W, Ho AD, Goldschmidt H. Development of leukocytoclastic vasculitis in a patient with multiple myeloma during treatment with thalidomide. *Ann Hematol* 2003; **19**: [Epub ahead of print]
- 172 **Zhu X**, Giordano T, Yu QS, Holloway HW, Perry TA, Lahiri DK, Brossi A, Greig NH. Thiothalidomides: novel isosteric analogues of thalidomide with enhanced TNF-alpha inhibitory activity. *J Med Chem* 2003; **46**: 5222-5229
- 173 **Ogata H**, Hibi T. Cytokine and anti-cytokine therapies for inflammatory bowel disease. *Curr Pharm Des* 2003; **9**: 1107-1113
- 174 **Tremaine WJ**, Brzezinski A, Katz JA, Wolf DC, Fleming TJ, Mordenti J, Strenkoski-Nix LC, Kurth MC. Treatment of mildly to moderately active ulcerative colitis with a tryptase inhibitor (APC 2059): an open-label pilot study. *Aliment Pharmacol Ther* 2002; **16**: 407-413
- 175 **Fox CC**, Moore WC, Lichtenstein LM. Modulation of mediator release from human intestinal mast cells by sulfasalazine and 5-aminosalicylic acid. *Dig Dis Sci* 1991; **36**: 179-184
- 176 **Goldsmith P**, McGarity B, Walls AF, Church MK, Millward-Sadler GH, Robertson DA. Corticosteroid treatment reduces mast cell numbers in inflammatory bowel disease. *Dig Dis Sci* 1990; **35**: 1409-1413
- 177 **Babb RR**. Cromolyn sodium in the treatment of ulcerative colitis. *J Clin Gastroenterol* 1980; **2**: 229-231
- 178 **Rampton DS**, Brown MJ, Causon R, Sahib M. The effect of disodium cromoglycate on rectal mucosal histamine release, eosinophil exudation and disease activity in active ulcerative colitis. *Clin Allergy* 1982; **12**: 243-248
- 179 **Rintala RJ**, Lindahl H. Sodium cromoglycate in the management of chronic or recurrent enterocolitis in patients with Hirschsprung's disease. *J Pediatr Surg* 2001; **36**: 1032-1035
- 180 **Eliakim R**, Karmeli F, Okon E, Rachmilewitz D. Ketotifen effectively prevents mucosal damage in experimental colitis. *Gut* 1992; **33**: 1498-1503
- 181 **Eliakim R**, Karmeli F, Chorev M, Okon E, Rachmilewitz D. Effect of drugs on colonic eicosanoid accumulation in active ulcerative colitis. *Scand J Gastroenterol* 1992; **27**: 968-972
- 182 **Marshall JK**, Irvine EJ. Ketotifen treatment of active colitis in patients with 5-aminosalicylate intolerance. *Can J Gastroenterol* 1998; **12**: 273-275
- 183 **Jones NL**, Roifman CM, Griffiths AM, Sherman P. Ketotifen therapy for acute ulcerative colitis in children: a pilot study. *Dig Dis Sci* 1998; **43**: 609-615
- 184 **Luk HH**, Ko JK, Fung HS, Cho CH. Delineation of the protective action of zinc sulfate on ulcerative colitis in rats. *Eur J Pharmacol* 2002; **443**: 197-204
- 185 **Robinson M**. Medical therapy of inflammatory bowel disease for the 21st century. *Eur J Surg Suppl* 1998; **582**: 90-98
- 186 **Marcondes S**, Bau EC, Antunes E, Dietrich CP, Nader HB, De Nucci G. Inhibition of heparin synthesis by methotrexate in rats *in vivo*. *Biochem Pharmacol* 2002; **64**: 169-175
- 187 **Eliakim R**, Karmeli F, Cohen P, Heyman SN, Rachmilewitz D. Dual effect of chronic nicotine administration: augmentation of jejunitis and amelioration of colitis induced by iodoacetamide in rats. *Int J Colorectal Dis* 2001; **16**: 14-21
- 188 **Felsenfeld H**, Corrado LA. Nicotine and pyrrolidine-induced release of 5-hydroxytryptamine and histamine from neoplastic mast cells. *Biochem Pharmacol* 1973; **22**: 2381-2390

Edited by Wang XL

Induction of tryptase and histamine release from human colon mast cells by IgE dependent or independent mechanisms

Shao-Heng He, Hua Xie, Yong-Song He

Shao-Heng He, Hua Xie, Allergy and Inflammation Research Institute, Shantou University Medical College, Shantou 515031, Guangdong Province, China

Shao-Heng He, Yong-Song He, Immunopharmacology Group, University of Southampton, Southampton, UK

Supported by the National Natural Science Foundation of China, No. 30140023, and the Li Ka Shing Foundation, Hong Kong, China, No. C0200001

Correspondence to: Professor Shao-Heng He, Allergy and Inflammation Research Institute, Shantou University Medical College, 22 Xin-Ling Road, Shantou 515031, Guangdong Province, China. shoahenghe@hotmail.com

Telephone: +86-754-8900405 **Fax:** +86-754-8900192

Received: 2003-10-08 **Accepted:** 2003-11-19

Abstract

AIM: To investigate the tryptase and histamine release ability of human colon mast cells upon IgE dependent or independent activation and the potential mechanisms.

METHODS: Enzymatically dispersed cells from human colons were challenged with anti-IgE or calcium ionophore A23187, and the cell supernatants after challenge were collected. Both concentration dependent and time course studies with anti-IgE or calcium ionophore A23187 were performed. Tryptase release was determined with a sandwich ELISA procedure and histamine release was measured using a glass fibre-based fluorometric assay.

RESULTS: Both anti-IgE and calcium ionophore were able to induce dose dependent release of histamine from colon mast cells with up to approximately 60% and 25% net histamine release being achieved with 1 µg/mL calcium ionophore and 10 µg/mL anti-IgE, respectively. Dose dependent release of tryptase was also observed with up to approximately 19 ng/mL and 21 ng/mL release of tryptase being achieved with 10 µg/mL anti-IgE and 1 µg/mL calcium ionophore, respectively. Time course study revealed that both tryptase and histamine release from colon mast cells stimulated by anti-IgE initiated within 10 sec and reached their maximum release at 6 min following challenge. Pretreatment of cells with metabolic inhibitors abolished the actions of anti-IgE as well as calcium ionophore. Tryptase and histamine release, particularly that induced by calcium ionophore was inhibited by pretreatment of cells with pertussis toxin.

CONCLUSION: Both anti-IgE and calcium ionophore are able to induce significant release of tryptase and histamine from colon mast cells, indicating that this cell type is likely to contribute to the pathogenesis of colitis and other mast cell associated intestinal diseases.

He SH, Xie H, He YS. Induction of tryptase and histamine release from human colon mast cells by IgE dependent or independent mechanisms. *World J Gastroenterol* 2004; 10(3):319-322
<http://www.wjgnet.com/1007-9327/10/319.asp>

INTRODUCTION

Increased numbers of mast cells have been found in the epithelium of intestine of the patients with ulcerative colitis and Crohn's disease^[1,2]. Through releasing its proinflammatory mediators including tryptase, histamine, heparin, and other preformed or newly synthesized mast cell products^[3], mast cells actively participate in the pathogenesis of inflammatory bowel diseases^[4].

Tryptase is a tetrameric serine proteinase that constitutes some 20% of the total protein within human mast cells and is stored almost exclusively in the secretory granules of mast cells^[5] in a catalytically active form^[6]. Upon degranulation, tryptase is released from mast cells along with chymase, histamine, and other mast cell products. In recent years, evidence has been emerging that this major secretory product of human mast cells may be a key mediator of allergic inflammation and a promising target for therapeutic intervention^[3] as it has been found to be able to induce microvascular leakage in the skin of guinea pig^[7], bronchoconstriction^[8] in allergic sheep airways, inflammatory cell accumulation in peritoneum of mouse^[9] and release of IL-8 from epithelial cells^[10].

For more than four decades, histamine has been widely used as a marker of mast cell degranulation *in vitro*, and numerous anti-allergic drugs such as sodium cromoglycate, lodoxamide, salbutamol, ketotifen, terfenadine and cetirizine^[11,12] and salmeterol^[13] were reported to be able to inhibit anti-IgE induced histamine release from human tonsil, skin or lung mast cells. However, little is known of the properties of tryptase release from human mast cells, and even histamine release properties of human colon mast cells were relatively less studied. We therefore parallelly investigated the tryptase and histamine release properties of human colon mast cells by using the same preparations of challenged mast cells in the current study.

MATERIALS AND METHODS

Reagents

The following compounds were purchased from Sigma (St. Louis, USA): collagenase (type I), hyaluronidase (type I), bovine serum albumin (BSA, fraction V), penicillin and streptomycin, calcium ionophore A23187, antimycin A, 2-deoxy-D-glucose, pertussis toxin. Goat anti-human IgE (inactivated) was from Serotec (Kidlington, Oxford, UK). FCS and minimum essential medium (MEM) containing 25 mM *N*-2-hydroxyethylpiperazine-*N'*-2-ethane sulphonic acid (HEPES) were from Gibco (Paisley, Renfrewshire, UK). A polyclonal antibody and a monoclonal antibody against tryptase were donated by Dr Andrew F. Walls (University of Southampton, UK). Histamine plate was from RefLab (Copenhagen, Denmark). HEPES and all other chemicals were of analytical grade.

Dispersion of mast cells

Human colon tissue was obtained from patients with carcinoma of colon at colectomy. Only macroscopically normal tissue was used for the study. After removing fat, tissue was washed and chopped finely with scissors into fragments of 0.5-2.0 mm³, and then incubated with 1.5 mg/ml collagenase and 0.75 mg/ml

hyaluronidase in MEM containing 2% fetal calf serum (1 g colon/10 ml buffer) for 70 min at 37 °C. Dispersed cells were separated from undigested tissue by filtration through nylon gauze (pore size 100 µm diameter), washed and maintained in MEM (containing 10% FCS, 200 U/ml penicillin, 200 µg/ml streptomycin) on a roller overnight at room temperature. Mast cell purity, as determined by light microscopy after stained by alcine blue, ranged from 3.5% to 5.4%.

Mast cell challenge

Dispersed cells were resuspended in HEPES buffered salt solution (HBSS, pH 7.4) with CaCl₂ and MgCl₂ (complete HBSS), and 100 µl aliquots containing 4-6×10⁵ mast cells were added to a 50 µl anti-IgE, calcium ionophore or control buffer alone and incubated for 15 min at 37 °C. The reaction was terminated by the addition of 150 µl ice cold incomplete HBSS and the tubes were centrifuged immediately (500 g, 10 min, 4 °C). All experiments were performed in duplicate. For the experiments with pertussis toxin, cells were incubated with 0.1 or 1.0 µg/ml pertussis toxin for four hours at 37 °C, and then washed with HBSS before adding stimulus. Similarly, for the experiments with metabolic inhibitors, cells were incubated with 2-deoxy-D-glucose (10 mM) and antimycin A (1 µM) for 40 min at 37 °C before challenged with stimulus. For the measurement of total histamine concentration, in certain tubes the suspension was boiled for 6 min. Supernatants were stored at -20 °C until use.

Tryptase and histamine measurement

Tryptase concentrations were measured with a sandwich ELISA procedure with a specific polyclonal antibody against human tryptase as the capture antibody and AA5 a monoclonal antibody specific for human tryptase as the detecting antibody^[14]. Histamine concentrations were determined using a glass fibre-based fluorometric assay^[15].

Statistical analysis

Data are shown as mean±SEM for the number of experiments (*n*) indicated, and the paired Student's *t* test was applied to evaluate two independent samples. In all analyses *P*<0.05 was taken as statistically significant.

RESULTS

Effect of anti-IgE and calcium ionophore on tryptase and histamine release from colon mast cells

Both anti-IgE and calcium ionophore were able to induce a dose dependent release of histamine from colon mast cells with up to approximately 60% and 25% net histamine release being achieved with 1 µg/mL calcium ionophore and 10 µg/mL anti-IgE, respectively. Increasing the concentrations of calcium ionophore up to 10 µg/mL and anti-IgE up to 100 µg/mL failed to provoke any further release of histamine from colon mast cells (Figure 1). Dose dependent release of tryptase was also observed when dispersed colon mast cells were incubated with calcium ionophore or anti-IgE. Up to approximately 19 ng/mL and 21 ng/mL release of tryptase were achieved with 10 µg/mL anti-IgE and 1 µg/mL calcium ionophore, respectively. Only as little as 0.1 µg/mL calcium ionophore and 1 µg/mL anti-IgE were required to elicit a significant release of tryptase. Similar to histamine release, increasing the concentrations of calcium ionophore to more than 1 µg/mL and anti-IgE more than 10 µg/mL did not stimulate more tryptase release from colon mast cells (Figure 2). There was a significant correlation between the quantities of histamine and tryptase released in response to anti-IgE (Pearson correlation: *r*=0.939, *P*=0.005) and calcium ionophore (Pearson correlation: *r*=0.973, *P*=0.001).

Time course study revealed that both tryptase and histamine release from colon mast cells stimulated by anti-IgE initiated within 10 sec when cells were incubated with the stimulus, the release was then steadily increased while incubation periods were prolonged. Tryptase and histamine reached their maximum release at 6 min following incubation. Prolonging the incubation period from 6 min to 15 min had little effect on the release of tryptase and histamine (Figure 3). The time course pattern of tryptase release provoked by calcium ionophore was similar to that induced by anti-IgE with approximately 45% tryptase released within 10 sec. This was different from the time course for calcium ionophore induced histamine release, which showed as much as approximately 70% of histamine released within 10 sec of challenge (Figure 4).

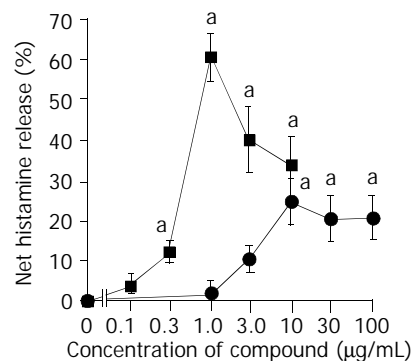


Figure 1 Anti-IgE and calcium ionophore induced histamine release from colon mast cells. The values shown are mean±SEM for four separate experiments. Stimulus or HBSS alone was incubated with cells for 15 min before termination of the reactions. ^a*P*<0.05 compared with spontaneous release group (paired Student's *t* test).

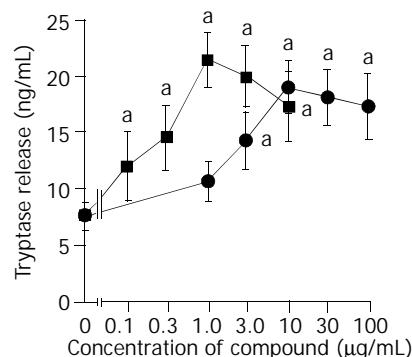


Figure 2 Anti-IgE and calcium ionophore induced tryptase release from colon mast cells. The values shown are mean±SEM for four separate experiments. Stimulus or HBSS alone was incubated with cells for 15 min before termination of the reactions. ^a*P*<0.05 compared with spontaneous release group (paired Student's *t* test).

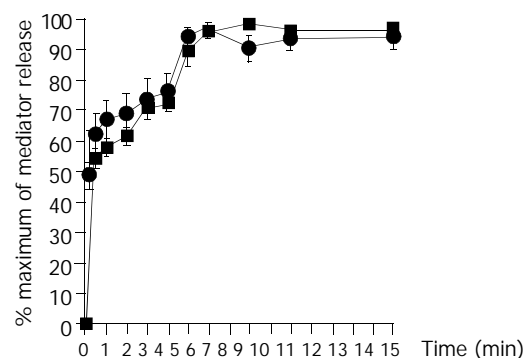


Figure 3 Time course for anti-IgE (10 µg/ml) induced release of tryptase (—■—) and histamine (—●—) from colon mast cells. Data shown are mean±SEM of four separate experiments.

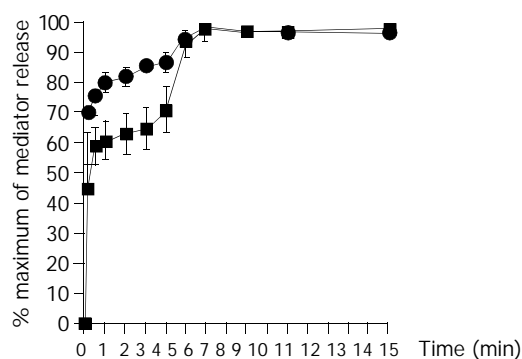


Figure 4 Time course for calcium ionophore (1 µg/ml) induced release of tryptase (■) and histamine (●) from colon mast cells. Data shown are mean±SEM of four separate experiments.

Inhibition of anti-IgE and calcium ionophore induced tryptase and histamine release by pertussis toxin and metabolic inhibitors

Pretreatment of cells with metabolic inhibitors abolished the actions of anti-IgE as well as calcium ionophore. Tryptase and histamine release, particularly that induced by calcium ionophore was inhibited by pretreatment of cells with pertussis toxin (Table 1, Table 2).

Table 1 Effects of pertussis toxin and metabolic inhibitors on anti-IgE induced histamine and tryptase release from colonic mast cells

Treatment	Net mediator release (ng/mL)	
	Tryptase	Histamine
Untreated	11.4±2.7	14.0±3.2
Pertussis toxin 0.1 µg/mL	3.2±1.3 ^a	5.4±1.7 ^a
1.0 µg/mL	4.0±1.6 ^a	4.0±1.9 ^a
Metabolic inhibitors	-2.1±1.7 ^a	-2.6±1.7 ^a

The values shown are mean±SEM of four separate experiments performed in duplicate. ^a*P*<0.05 compared with the untreated group (paired Student's *t* test). Metabolic inhibitors=1 µM antimycin A+10 mM 2-deoxy-D-glucose.

Table 2 Effects of pertussis toxin and metabolic inhibitors on calcium ionophore induced tryptase and histamine release from colonic mast cells

Treatment	Mediator release (ng/mL)	
	Tryptase	Histamine
Untreated	13.8±2.4	34.3±3.4
Pertussis toxin 0.1 µg/mL	4.0±1.6 ^a	2.7±2.8 ^a
1.0 µg/mL	1.4±1.8 ^a	-0.1±1.3 ^a
Metabolic inhibitors	2.0±1.4 ^a	1.8±2.6 ^a

The values shown are mean±SEM of four separate experiments performed in duplicate. ^a*P*<0.05 compared with the untreated group (paired Student's *t* test). Metabolic inhibitors=1 µM antimycin A+10 mM 2-deoxy-D-glucose.

DISCUSSION

We have reported for the first time the *in vitro* tryptase release ability of human colon mast cells. This is particularly important when tryptase and histamine, the two major mast cell mediators were investigated in the same experiments, which would not only prove that the two mediators were released from mast cells unnecessarily at a constantly parallel ratio, but also revealed that histamine was released slightly faster than tryptase upon

degranulation.

Approximately 25% histamine and 10% tryptase (presumably 10 pg tryptase per mast cell^[16], and 5000 cells in each test tube) were released from colon mast cells in response to IgE dependent provocation, indicating that only a proportion of mast cells was activated or the granule contents in activated mast cells were partially released. The maximum release of histamine and tryptase was induced by 10 µg/mL rather than higher concentrations of anti-IgE, suggesting that colon mast cells would give their maximum response to a sufficient stimulation, but not an excess stimulation, which showed a self-protection mechanism of colon mast cells.

Approximately 45% degranulation occurred within 10 sec of IgE dependent stimulation, suggesting that colon mast cells were able to quickly respond to allergen challenge, but they required about 6 min to reach their full capacity (maximum histamine or tryptase release). The time course also revealed that histamine was released slightly faster than tryptase upon degranulation, and this was particularly evident with calcium ionophore. The peak histamine release induced by anti-IgE and calcium ionophore occurred at 6 min following stimulation of colon mast cells, and appeared much faster than the occurrence of peak histamine release with lung mast cells, which required at least 15 min to reach its peak following anti-IgE and calcium ionophore stimulation^[17].

Pretreatment of cells with metabolic inhibitors antimycin A, which blocks the oxidative phosphorylation process of cells, and 2-deoxy-D-glucose which blocks anaerobic metabolism pathway in cells, abolished the actions of anti-IgE as well as calcium ionophore, indicating that the induced release of these two mediators was a non-cytotoxic process, and was dependent on cell energy supply. Tryptase and histamine release, particularly that induced by calcium ionophore was inhibited by pretreatment of cells with pertussis toxin, suggesting that the degranulation process elicited by anti-IgE and calcium ionophore was associated with activation of G-protein coupled receptors.

Over the last decade, a number of functions of mast cell tryptase have been discovered. However, the mechanism by which tryptase acts on cells is still unclear. The finding that proteinase-activated receptor-2 (PAR-2) on cos cells could be a receptor for tryptase^[18] suggested that the effects of tryptase on various types of cells were associated with this type of receptor. Since both tryptase^[7,15] and PAR-2 agonists^[19] were able to activate human mast cells, it is likely that there is a self-amplification mechanism of mast cell degranulation, which would contribute largely to the pathogenesis of mast cell related diseases including inflammatory bowel diseases. The report that induction of intestinal inflammation in mouse by activation of PAR-2^[20] and PAR-2 as an anti-inflammatory signal for colonic lamina propria lymphocytes in a mouse model of colitis^[21] suggested the potential roles of PAR-2 in inflammatory bowel diseases.

Histamine has long been accepted as a specific marker of mast cell degranulation. Tryptase however, is seldom used in the same way though it has been employed as a specific marker of mast cells since 1980's. Based on the results in the current study and the evidence that these two mediators are located in the same secretory granules of mast cells, we believe that human tryptase can serve as an indicator of mast cell degranulation *in vitro*. In conclusion, both anti-IgE and calcium ionophore are able to induce a significant release of tryptase and histamine from colon mast cells, indicating that this cell type is likely to contribute to the pathogenesis of colitis and other mast cell associated intestinal diseases.

REFERENCES

- 1 **Sasaki Y**, Tanaka M, Kudo H. Differentiation between ulcerative

- colitis and Crohn's disease by a quantitative immunohistochemical evaluation of T lymphocytes, neutrophils, histiocytes and mast cells. *Pathol Int* 2002; **52**: 277-285
- 2 **Furusu H**, Murase K, Nishida Y, Isomoto H, Takeshima F, Mizuta Y, Hewlett BR, Riddell RH, Kohno S. Accumulation of mast cells and macrophages in focal active gastritis of patients with Crohn's disease. *Hepatogastroenterology* 2002; **49**: 639-643
- 3 **Walls AF**, He SH, Buckley MG, McEuen AR. Roles of the mast cell and basophil in asthma. *Clin Exp Allergy Review* 2001; **1**: 68-72
- 4 **Stoyanova II**, Gulubova MV. Mast cells and inflammatory mediators in chronic ulcerative colitis. *Acta Histochem* 2002; **104**: 185-192
- 5 **Abraham WM**. Tryptase: potential role in airway inflammation and remodelling. *Am J Physiol Lung Cell Mol Physiol* 2002; **282**: L193-L196
- 6 **McEuen AR**, He SH, Brander ML, Walls AF. Guinea pig lung tryptase: Localisation to mast cells and characterisation of the partially purified enzyme. *Biochem Pharmacol* 1996; **52**: 331-340
- 7 **He SH**, Walls AF. Human mast cell tryptase: A potent stimulus of microvascular leakage and mast cell activation. *Eur J Pharmacol* 1997; **328**: 89-97
- 8 **Molinari JF**, Scuri M, Moore WR, Clark J, Tanaka R, Abraham WM. Inhaled tryptase causes bronchoconstriction in sheep via histamine release. *Am J Respir Crit Care Med* 1996; **154**: 649-653
- 9 **He SH**, Peng Q, Walls AF. Potent induction of neutrophil- and eosinophil-rich infiltrate *in vivo* by human mast cell tryptase: selective enhancement of eosinophil recruitment by histamine. *J Immunol* 1997; **159**: 6216-6225
- 10 **Cairns JA**, Walls AF. Mast cell tryptase is a mitogen for epithelial cells: Stimulation of IL-8 production and intercellular adhesion molecule-1 expression. *J Immunol* 1996; **156**: 275-283
- 11 **Okayama Y**, Church MK. Comparison of the modulatory effect of ketotifen, sodium cromoglycate, procaterol and salbutamol in human skin, lung and tonsil mast cells. *Int Arch Allergy Appl Immunol* 1992; **97**: 216-225
- 12 **Okayama Y**, Benyon RC, Lowman MA, Church MK. *In vitro* effects of H₁-antihistamine and PGD₂ release from mast cells of human lung, tonsil, and skin. *Allergy* 1994; **49**: 246-253
- 13 **Butchers PR**, Vardey CJ, Johnson M. Salmeterol: a potent and long-acting inhibitor of inflammatory mediator release from human lung. *Br J Pharmacol* 1991; **104**: 672-676
- 14 **Buckley MG**, Walters C, Brander M, Wong WM, Cawley MI, Ren S, Schwartz LB, Walls AF. Mast cell activation in arthritis: detection of α - and β -tryptase, histamine and eosinophil cationic protein in synovial fluid. *Clin Sci* 1997; **93**: 363-370
- 15 **He SH**, Gaça MDA, Walls AF. A role for tryptase in the activation of human mast cells: Modulation of histamine release by tryptase and inhibitors of tryptase. *J Pharmacol Exp Ther* 1998; **286**: 289-297
- 16 **Schwartz LB**, Irani AM, Roller K, Castells MC, Schechter NM. Quantitation of histamine, tryptase, and chymase in dispersed human T and TC mast cells. *J Immunol* 1987; **138**: 2611-2615
- 17 **Holgate ST**, Burns GB, Robinson C, Church MK. Anaphylactic- and calcium-dependent generation of prostaglandin D₂ (PGD₂), thromboxane B₂, and other cyclooxygenase products of arachidonic acid by dispersed human lung cells and relationship to histamine release. *J Immunol* 1984; **133**: 2138-2144
- 18 **Molino M**, Barnathan ES, Numerof R, Clark J, Dreyer M, Cumashi A, Hoxie JA, Schechter NM, Woolkalis M, Brass LF. Interactions of mast cell tryptase with thrombin receptors and PAR-2. *J Biol Chem* 1997; **272**: 4043-4049
- 19 **He SH**, Xie H, He YS. Effect of a proteinase-activated receptor-2 (PAR2) agonist on tryptase release from human mast cells. *Acta Physiol Sin* 2002; **54**: 531-534
- 20 **Cenac N**, Coelho AM, Nguyen C, Compton S, Andrade-Gordon P, MacNaughton WK, Wallace JL, Hollenberg MD, Bunnett NW, Garcia-Villar R, Bueno L, Vergnolle N. Induction of intestinal inflammation in mouse by activation of proteinase-activated receptor-2. *Am J Pathol* 2002; **161**: 1903-1915
- 21 **Fiorucci S**, Mencarelli A, Palazzetti B, Distrutti E, Vergnolle N, Hollenberg MD, Wallace JL, Morelli A, Cirino G. Proteinase-activated receptor 2 is an anti-inflammatory signal for colonic lamina propria lymphocytes in a mouse model of colitis. *Proc Natl Acad Sci U S A* 2001; **98**: 13936-13941

Edited by Wang XL Proofread by Zhu LH

Modulation of tryptase secretion from human colon mast cells by histamine

Shao-Heng He, Hua Xie

Shao-Heng He, Hua Xie, Allergy and Inflammation Research Institute, Medical College, Shantou University, Shantou 515031, Guangdong Province, China

Shao-Heng He, Immunopharmacology Group, University of Southampton, Southampton, UK

Supported by the National Natural Science Foundation of China, No. 30140023, and the Li Ka Shing Foundation, Hong Kong, China, No. C0200001

Correspondence to: Professor Shao-Heng He, Allergy and Inflammation Research Institute, Medical College, Shantou University, 22 Xin-Ling Road, Shantou 515031, Guangdong Province, China. shoahenghe@hotmail.com

Telephone: +86-754-8900405 **Fax:** +86-754-8900192

Received: 2003-12-23 **Accepted:** 2004-01-11

Abstract

AIM: To investigate the ability of histamine to modulate tryptase release from human colon mast cells and the potential mechanisms.

METHODS: Enzymatically dispersed cells from human colons were challenged with histamine, anti-IgE or calcium ionophore A23187 (CI), and the cell supernatants after challenge were collected. Tryptase release was determined with a sandwich ELISA procedure.

RESULTS: Histamine at concentrations from 1 ng/mL was able to induce a "bell" shape dose related release of tryptase from colon mast cells. The maximum release of tryptase was approximately 3.5 fold more than spontaneous release. As little as 10 ng/mL histamine showed a similar potency to 10 µg/mL anti-IgE in induction of tryptase release. Histamine induced release of tryptase initiated at 10 s when histamine (100 ng/mL) was added to cells, gradually increased thereafter, and completed at 5 min. Both pertussis toxin or metabolic inhibitors were able to inhibit histamine induced tryptase release. When histamine and anti-IgE were added to colon mast cells at the same time, the quantity of tryptase released was similar to that induced by anti-IgE alone. The similar results were observed with CI. However, when various concentrations of histamine were incubated with cells for 20 min before adding anti-IgE or CI, the quantity of tryptase released was similar to that was induced by histamine alone.

CONCLUSION: Histamine is a potent activator of human colon mast cells, which represents a novel and pivotal self-amplification mechanism of mast cell degranulation.

He SH, Xie H. Modulation of tryptase secretion from human colon mast cells by histamine. *World J Gastroenterol* 2004; 10(3):323-326

<http://www.wjgnet.com/1007-9327/10/323.asp>

INTRODUCTION

It has been reported that mast cells and their inflammatory mediators are closely associated to a number of intestinal

diseases including idiopathic inflammatory bowel disease^[1], chronic ulcerative colitis^[2], Crohn's disease^[3] and collagenous colitis^[4]. Through release their proinflammatory mediators including histamine, tryptase, chymase, heparin and some cytokines^[5], mast cells actively participate in the pathogenesis of these intestinal diseases.

Tryptase is a tetrameric serine proteinase that constitutes some 20% of the total protein within human mast cells and is stored almost exclusively in the secretory granules of mast cells^[6] in a catalytically active form^[7]. Relatively higher secretion of tryptase has been detected in ulcerative colitis^[8], implicating that this mediator is involved in the pathogenesis of intestinal diseases. Evidence is emerging that tryptase may be a key mediator of allergic inflammation and a promising target for therapeutic intervention^[9] as it has been found to be able to induce microvascular leakage in the skin of guinea pig^[10], bronchoconstriction^[11] in allergic sheep airways, inflammatory cell accumulation in peritoneum of mouse^[12] and release of IL-8 from epithelial cells^[13]. Moreover, tryptase has long been recognised as a marker of mast cells^[14,15], and an indicator of mast cell degranulation *in vivo*^[16,17]. However, the application of tryptase as a unique marker of mast cell degranulation in mast cell challenge study *in vitro* was only started recently^[18]. This was largely due to the lack of adequate assay to detect this mast cell product.

Histamine, on the other hand, has been widely employed as a marker of mast cell degranulation in mast cell challenge studies over the last four decades. But as a activator of mast cells it has hardly been examined. Since increased levels of histamine or enhanced histamine metabolism have been observed in collagenous colitis, food allergy^[19], Crohn's disease^[20], ulcerative colitis^[20,21] and allergic enteropathy^[21], this proinflammatory mediator is likely to participate in the pathogenesis of these diseases. In the current study, we investigated the potential of histamine to activate human colon mast cells *in vitro* in order to understand further the role of histamine in inflammatory bowel diseases.

MATERIALS AND METHODS

Reagents

The following compounds were purchased from Sigma (St. Louis, Mo., USA): CI, histamine dihydrochloride, collagenase (type I), hyaluronidase (type I), antimycin A, 2-deoxy-D-glucose, pertussis toxin, bovine serum albumin (BSA, fraction V), penicillin and streptomycin, extravidin peroxidase, *o*-phenylene diamine, biotin conjugate sheep anti-mouse immunoglobulins, extr-avidin peroxidase. Minimum essential medium (MEM) containing 25 mM *N*-2-hydroxyethylpiperazine-*N'*-2-ethane sulphonic acid (HEPES) and FCS was from Gibco (Paisley, Renfrewshire, UK). Goat anti-human IgE (inactivated) was from Serotec (Kidlington, Oxford, UK). A polyclonal antibody and a monoclonal antibody against tryptase were donated by Dr. Andrew F. Walls (University of Southampton, UK). HEPES and all other chemicals were of analytical grade.

Dispersion of mast cells

The mast cell dispersion procedure was similar to that described

previously^[21,22]. Human colon tissue was obtained from patients with carcinoma of colon at colectomy. Only macroscopically normal tissue was used for the study. After removal of fat, the tissue was washed and chopped finely with scissors into fragments of 0.5-2.0 mm³, and then incubated with 1.5 mg/mL collagenase and 0.75 mg/mL hyaluronidase in MEM containing 2% fetal calf serum (1 g colon/10 mL buffer) for 70 min at 37 °C. Dispersed cells were separated from the undigested tissue by filtration through a nylon gauze (pore size 100 µm diameter), washed and maintained in MEM (containing 10% FCS, 200 U/mL penicillin, 200 µg/mL streptomycin) on a roller overnight at room temperature. Mast cell purity, as determined by light microscopy after staining by Alcine blue, ranged from 3.6% to 5.8%.

Mast cell challenge

Dispersed cells were resuspended in HEPES buffered salt solution (HBSS, pH 7.4) with 1.8 mM CaCl₂ and 0.5 mM MgCl₂ (complete HBSS), and 100 µL aliquots containing 4-6×10³ mast cells was added to 50 µL histamine, anti-IgE, CI or buffer alone and incubated for 15 min at 37 °C. The reaction was terminated by the addition of 150 µL ice cold incomplete HBSS and the tubes were centrifuged immediately (500 g, 10 min, 4 °C). All experiments were performed in duplicate. For the experiments with pertussis toxin, cells were incubated with 0.1 or 1.0 µg/mL pertussis toxin for four hours at 37 °C, and then washed with HBSS before adding stimulus. Similarly, for the experiments with metabolic inhibitors, cells were incubated with 2-deoxy-D-glucose (10 mmol/L) and antimycin A (1 µmol/L) for 40 min at 37 °C before challenged with stimulus. Supernatants were stored at -20 °C until use. As reported previously that 10 µg/mL anti-IgE and 1 µg/mL CI were the optimal concentrations for the induction of tryptase released from human colon mast cells^[18], therefore they were selected as the standard concentrations throughout the study.

Tryptase measurement

Tryptase concentrations were measured using a sandwich ELISA procedure with a specific polyclonal antibody against human tryptase as the capture antibody and AA5 a monoclonal antibody specific for human tryptase as the detecting antibody^[23].

Statistical analysis

Data were shown as mean±SEM for the number of experiments (*n*) indicated, and the paired Student's *t* test was applied to evaluate two independent samples. In all analyses, *P*<0.05 was taken as statistically significant.

RESULTS

Induction of tryptase release by histamine

Histamine at the concentration of 1 ng/mL was able to induce a 'bell' shape dose related release of tryptase from colon mast cells. The maximal release of tryptase was approximately 3.5 fold more than spontaneous release provoked by 100 ng/mL histamine. Relatively less tryptase was released when 1 000 ng/mL and 10 000 ng/mL histamine were incubated with mast cells. As little as 10 ng/mL histamine showed a similar potency to 10 µg/mL anti-IgE in induction of tryptase release from colon mast cells (Figure 1).

Time course for histamine induced tryptase release

Histamine induced release of tryptase initiated at 10 s when histamine (100 ng/mL) was added to cells, gradually increased thereafter, and completed at 5 min (Figure 2).

Effects of pertussis toxin and metabolic inhibitors on histamine induced tryptase release

Tryptase release induced by histamine was reduced to the

baseline level by pretreatment of colon mast cells with pertussis toxin or metabolic inhibitors. The same treatment was also able to slightly decrease the spontaneous tryptase release from mast cells (Table 1).

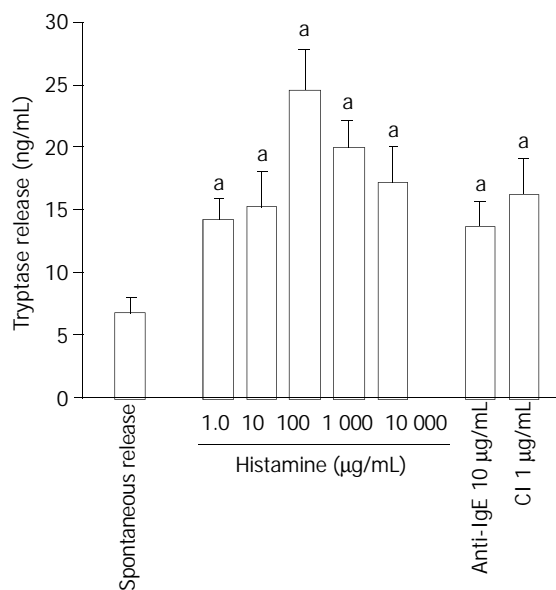


Figure 1 Histamine, anti-IgE and calcium ionophore (CI) induced tryptase release from colon mast cells. The values shown are mean±SEM for six separate experiments. Stimulus or HBSS alone was incubated with cells for 15 min before termination of the reactions. ^a*P*<0.05 compared with spontaneous release group (paired Student's *t* test).

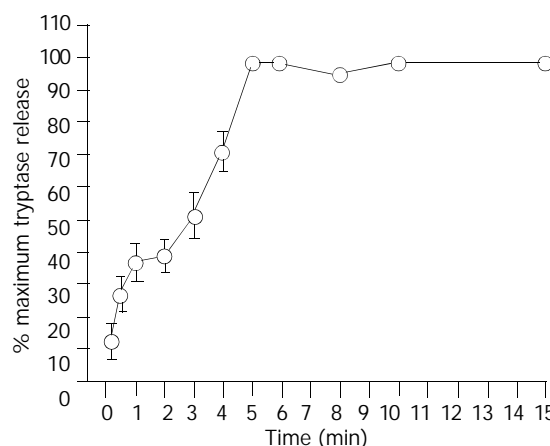


Figure 2 Time course for histamine (100 ng/mL) induced release of tryptase from colon mast cells. Data shown are mean±SEM of five separate experiments.

Table 1 Effects of pertussis toxin (1.0 µg/mL) and metabolic inhibitors on histamine induced tryptase release from colon mast cells

Treatment	Tryptase release (ng/mL)		
	Hist 100 µg/mL	Hist 1 000 µg/mL	Buffer alone
Untreated	32±5.5	30.5±3.9	20.5±2.8
Pertussis toxin	17.1±1.8 ^a	16.7±1.7 ^a	17.6±2.7
Metabolic inhibitors	18.8±3.5 ^a	17.5±1.9 ^a	16.3±1.9

The values shown are mean±SEM of five separate experiments performed in duplicate. ^a*P*<0.05 compared with the untreated group (paired Student's *t* test). Metabolic inhibitors=1 µM antimycin A+10 mM 2-deoxy-D-glucose. Hist=histamine.

Effect of histamine on anti-IgE and CI induced tryptase release

When 100 ng/mL or 1 000 ng/mL histamine and anti-IgE were added to colon mast cells at the same time, tryptase release was significantly less than that induced by addition of the corresponding concentration of histamine alone. The similar results were observed when the same concentrations of histamine were added to cells at the same time with CI, though there was no significant difference between histamine alone and histamine plus CI (Figure 3). However, addition of various concentrations of histamine to colon mast cells 20 min before placing anti-IgE or CI, tryptase release was similar to that induced by the corresponding histamine alone, except for 10 ng/mL histamine with CI, indicating a synergistic action between them (Figure 4).

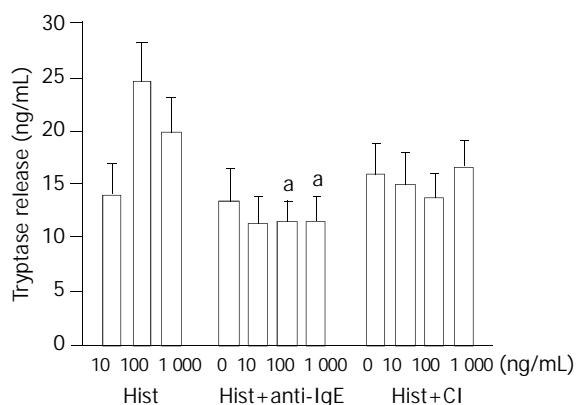


Figure 3 Effect of co-addition of histamine (hist) and anti-IgE or calcium ionophore (CI) on tryptase release from colon mast cells. The values shown are mean \pm SEM for six separate experiments. Various concentrations of histamine and anti-IgE or CI were added to cells at the same time, and then incubated with cells for 15 min before termination of the reactions. ^a $P < 0.05$ compared with the corresponding histamine alone group (paired Student's *t* test).

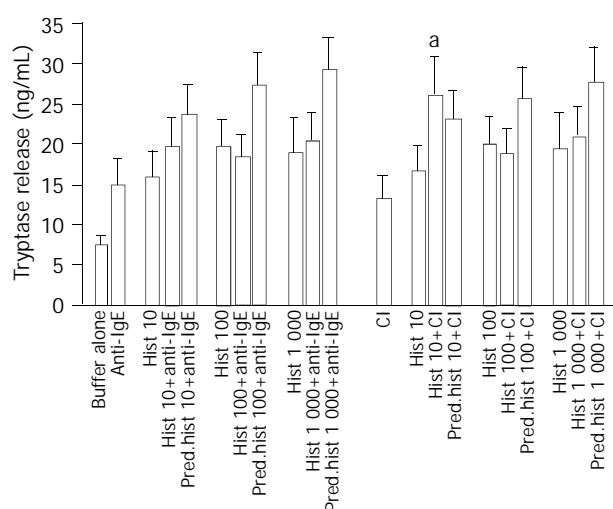


Figure 4 Effect of histamine (hist) on anti-IgE or calcium ionophore (CI) induced tryptase release from colon mast cells. The values shown are mean \pm SEM for six separate experiments. Various concentrations of histamine were incubated with cells for 20 min before addition of anti-IgE or CI. ^a $P < 0.05$ compared with the corresponding histamine alone group (paired Student's *t* test). Pred.hist + anti-IgE or CI = the sum of tryptase release induced by histamine alone and anti-IgE or CI alone.

DISCUSSION

The finding that histamine is a potent activator of human colon

mast cells demonstrated a novel and pivotal self-amplification mechanism of human mast cell degranulation, that is mast cells release histamine upon degranulation, and then the released histamine activates the adjacent mast cells. Thus, there are at least two self-amplification mechanisms in human mast cells upon degranulation, including tryptase and PAR-2 feedback process previously reported^[22,23] and histamine inducing tryptase release.

Histamine appeared a potent secretagogue of tryptase, as little as 10 ng/mL histamine could share a similar potency of 10 μ g/mL anti-IgE. This was a surprising result, but it clearly demonstrate a novel self-amplification mechanism of mast cell degranulation as the concentration of histamine inside the mast cell granules was estimated over 100 m mol/mL^[24]. Interestingly, histamine concentration at 1 000 ng/mL or above was able to induce less tryptase release from mast cells than 100 ng/mL, which may represent a novel self-protection mechanism of mast cells. Histamine induced tryptase release started slower than that elicited by anti-IgE, CI^[18] or tc-LIGRLO^[23], but completed 1 min earlier than that induced by anti-IgE and CI, indicating that it has its own activation-degranulation pathway in mast cells. Pretreatment of cells with metabolic inhibitors antimycin A which blocks the oxidative phosphorylation process of cells, and 2-deoxy-D-glucose which blocks anaerobic metabolism pathway in cells, abolished the action of histamine, indicating that histamine induced release of tryptase is a non-cytotoxic process depending on cell energy supply. Tryptase release provoked by histamine was also inhibited by pretreatment of cells with pertussis toxin, suggesting that the degranulation process is associated with the activation of G-protein coupled receptors^[25].

When histamine and anti-IgE were placed to mast cells at the same time, the quantity of released tryptase was similar to that elicited by anti-IgE alone, much less than that provoked by histamine alone, implicating that tryptase released from colon mast cells was mainly induced by anti-IgE, rather than by histamine. The reason for this was that the initiation of anti-IgE induced tryptase release was quicker than that induced by histamine, and mast cells only accepted one type of stimulation at a time^[26,27]. Similar phenomena were observed with CI, and CI provoked mast cell degranulation apparently faster than that induced by histamine. In contrast, addition of various concentrations of histamine to colon mast cells 20 min before placing anti-IgE or CI, tryptase release was similar to that induced by the corresponding histamine alone, which proved further that colon mast cells were only able to respond to one optimal activation at a time, and the desensitized mast cells did not respond to any further stimulation. This behavior is an effective self-protection mechanism of mast cells. However, a synergistic action between 10 ng/mL histamine and CI, but not anti-IgE was observed, suggesting that mast cells experiencing a non-optimal stimulation may still have ability to respond to a further stimulation. In conclusion, histamine is a potent activator of human colon mast cells, and represents a novel and pivotal self-amplification mechanism of mast cell degranulation.

REFERENCES

- 1 **Fox CC**, Lichtenstein LM, Roche JK. Intestinal mast cell responses in idiopathic inflammatory bowel disease. Histamine release from human intestinal mast cells in response to gut epithelial proteins. *Dig Dis Sci* 1993; **38**: 1105-1112
- 2 **Stoyanova II**, Gulubova MV. Mast cells and inflammatory mediators in chronic ulcerative colitis. *Acta Histochem* 2002; **104**: 185-192
- 3 **Nishida Y**, Murase K, Isomoto H, Furusu H, Mizuta Y, Riddell RH, Kohno S. Different distribution of mast cells and macrophages in colonic mucosa of patients with collagenous colitis and inflammatory bowel disease. *Hepatogastroenterology* 2002; **49**: 678-682

- 4 **Schwab D**, Raithel M, Hahn EG. Evidence for mast cell activation in collagenous colitis. *Inflamm Res* 1998; **47**(Suppl 1): S64-S65
- 5 **Walls AF**, He SH, Buckley MG, McEuen AR. Roles of the mast cell and basophil in asthma. *Clin Exp Allergy Rev* 2001; **1**: 68-72
- 6 **Abraham WM**. Tryptase: potential role in airway inflammation and remodelling. *Am J Physiol Lung Cell Mol Physiol* 2002; **282**: L193-L196
- 7 **McEuen AR**, He SH, Brander ML, Walls AF. Guinea pig lung tryptase. Localisation to mast cells and characterisation of the partially purified enzyme. *Biochem Pharmacol* 1996; **52**: 331-340
- 8 **Raithel M**, Winterkamp S, Pacurar A, Ulrich P, Hochberger J, Hahn EG. Release of mast cell tryptase from human colorectal mucosa in inflammatory bowel disease. *Scand J Gastroenterol* 2001; **36**: 174-179
- 9 **Walls AF**. Structure and function of human mast cell tryptase. In: Marone G, editor. Mast cells and basophils. New York: Academic Press 2000: p. 291-309
- 10 **He SH**, Walls AF. Human mast cell tryptase: a stimulus of microvascular leakage and mast cell activation. *Eur J Pharmacol* 1997; **328**: 89-97
- 11 **Molinari JF**, Scuri M, Moore WR, Clark J, Tanaka R, Abraham WM. Inhaled tryptase causes bronchoconstriction in sheep via histamine release. *Am J Respir Crit Care Med* 1996; **154**(3 Pt 1): 649-653
- 12 **He SH**, Peng Q, Walls AF. Potent induction of a neutrophil and eosinophil-rich infiltrate *in vivo* by human mast cell tryptase: selective enhancement of eosinophil recruitment by histamine. *J Immunol* 1997; **159**: 6216-6225
- 13 **Cairns JA**, Walls AF. Mast cell tryptase is a mitogen for epithelial cells. Stimulation of IL-8 production and intercellular adhesion molecule-1 expression. *J Immunol* 1996; **156**: 275-283
- 14 **Proud D**, Bailey GS, Naclerio RM, Reynolds CJ, Cruz AA, Eggleston PA, Lichtenstein LM, Togias AG. Tryptase and histamine as markers to evaluate mast cell activation during the responses to nasal challenge with allergen, cold, dry air, and hyperosmolar solutions. *J Allergy Clin Immunol* 1992; **89**: 1098-1110
- 15 **He SH**, Li P, Buckley MG, Walls AF. Identification of mast cell subtypes by double labeling immunohistochemistry technique. *Chin J Pathol* 2000; **29**: 383-384
- 16 **Schwartz LB**, Metcalfe DD, Miller JS, Earl H, Sullivan T. Tryptase levels as an indicator of mast-cell activation in systemic anaphylaxis and mastocytosis. *N Engl J Med* 1987; **316**: 1622-1626
- 17 **Laroche D**, Vergnaud MC, Sillard B, Soufarapis H, Bricard H. Biochemical markers of anaphylactoid reactions to drugs. Comparison of plasma histamine and tryptase. *Anesthesiology* 1991; **75**: 945-949
- 18 **He SH**, Xie H, He YS. Induction of tryptase and histamine release from human colon mast cells by IgE-dependent or independent mechanisms. *World J Gastroenterol* 2004; **10**: 319-322
- 19 **Schwab D**, Hahn EG, Raithel M. Enhanced histamine metabolism: a comparative analysis of collagenous colitis and food allergy with respect to the role of diet and NSAID use. *Inflamm Res* 2003; **52**: 142-147
- 20 **Winterkamp S**, Weidenhiller M, Otte P, Stolper J, Schwab D, Hahn EG, Raithel M. Urinary excretion of N-methylhistamine as a marker of disease activity in inflammatory bowel disease. *Am J Gastroenterol* 2002; **97**: 3071-3077
- 21 **Raithel M**, Matek M, Baenkler HW, Jorde W, Hahn EG. Mucosal histamine content and histamine secretion in Crohn's disease, ulcerative colitis and allergic enteropathy. *Int Arch Allergy Immunol* 1995; **108**: 127-133
- 22 **He SH**, Gaça MD, Walls AF. A role for tryptase in the activation of human mast cells: modulation of histamine release by tryptase and inhibitors of tryptase. *J Pharmacol Exp Ther* 1998; **286**: 289-297
- 23 **He SH**, He YS, Xie H. Activation of human colon mast cells through proteinase activated receptor-2. *World J Gastroenterol* 2004; **10**: 327-331
- 24 **Schwartz LB**, Irani AM, Roller K, Castells MC, Schechter NM. Quantitation of histamine, tryptase, and chymase in dispersed human T and TC mast cells. *J Immunol* 1987; **138**: 2611-2615
- 25 **Piliponsky AM**, Gleich GJ, Nagler A, Bar I, Levi-Schaffer F. Non-IgE-dependent activation of human lung- and cord blood-derived mast cells is induced by eosinophil major basic protein and modulated by the membrane form of stem cell factor. *Blood* 2003; **101**: 1898-1904
- 26 **Shalit M**, Levi-Schaffer F. Challenge of mast cells with increasing amounts of antigen induces desensitization. *Clin Exp Allergy* 1995; **25**: 896-902
- 27 **Rubinchik E**, Shalit M, Levi-Schaffer F. Responsiveness of human skin mast cells to repeated activation: an *in vitro* study. *Allergy* 1998; **53**: 14-19

Edited by Wang XL

Activation of human colon mast cells through proteinase activated receptor-2

Shao-Heng He, Yong-Song He, Hua Xie

Shao-Heng He, Hua Xie, Allergy and Inflammation Research Institute, Shantou University Medical College, Shantou 515031, Guangdong Province, China

Shao-Heng He, Yong-Song He, Immunopharmacology Group, University of Southampton, Southampton, UK

Supported by the National Natural Science Foundation of China, No. 30140023, and the Li Ka Shing Foundation, Hong Kong, China, No. C0200001

Correspondence to: Professor Shao-Heng He, Allergy and Inflammation Research Institute, Shantou University Medical College, 22 Xin-Ling Road, Shantou 515031, Guangdong Province, China. shoahenghe@hotmail.com

Telephone: +86-754-8900405 **Fax:** +86-754-8900192

Received: 2003-10-10 **Accepted:** 2003-11-19

Abstract

AIM: To investigate the ability of agonists of PAR-2 to stimulate release of tryptase and histamine from human colon mast cells and the potential mechanisms.

METHODS: Enzymatically dispersed cells from human colons were challenged with tc-LIGRLO, tc-OLRGIL, SLIGKV, VKGILS, trypsin, anti-IgE or calcium ionophore A23187, and the cell supernatants after challenge were collected. Tryptase release was determined with a sandwich ELISA procedure and histamine release was measured using a glass fibre-based fluorometric assay.

RESULTS: Both PAR-2 agonists tc-LIGRLO-NH₂ and SLIGKV-NH₂ were able to induce dose dependent release of tryptase and histamine from colon mast cells. More than 2.5 fold increase in both tryptase and histamine release was provoked by 100 μmol/mL tc-LIGRLO-NH₂, in comparison with only 2.0 fold increase being stimulated by SLIGKV-NH₂. The reverse peptides tc-OLRGIL-NH₂ and VKGILS-NH₂ at the concentrations tested had no effect on the release of these two mediators. The maximum tryptase release elicited by tc-LIGRLO-NH₂ was similar to that induced by anti-IgE (10 μg/mL) or calcium ionophore (1 μg/mL), though the latter was a more potent stimulus for histamine release. Both histamine and tryptase release in response to tc-LIGRLO-NH₂ were completed within 3 min. Trypsin at concentrations from 1.0 to 100 μg/mL was capable of provoking a dose dependent release of tryptase as well as histamine with a maximum of 16 ng/mL tryptase and 14 ng/mL histamine release being achieved. An approximately 80% and 70% inhibition of trypsin induced release of tryptase and histamine were observed with SBTI, respectively. Pretreatment of cells with metabolic inhibitors or pertussis toxin abolished the actions of tc-LIGRLO-NH₂, SLIGKV-NH₂ and trypsin.

CONCLUSION: The agonists of PAR-2 and trypsin are potent secretagogues of human colon mast cells, which are likely to contribute to the development of inflammatory disorders in human gut.

He SH, He YS, Xie H. Activation of human colon mast cells

through proteinase activated receptor-2. *World J Gastroenterol* 2004; 10(3):327-331

<http://www.wjgnet.com/1007-9327/10/327.asp>

INTRODUCTION

PAR-2 is a 7-transmembrane G protein-coupled receptor, which can be activated by serine proteinase trypsin and mast cell tryptase^[1], and some synthetic peptides corresponding to the N-terminal tethered ligand sequences that are unmasked by proteolytic cleavage including SLIGKV in man^[2] and SLIGRL in rodent^[3].

In gastrointestinal tract, PAR-2 activation has been found to be actively involved in a number of inflammatory processes including induction of granulocyte infiltration, colon edema, tissue damage in mouse^[4,5], induction of gastric mucus secretion and mucosal cytoprotection^[6] in rat, excitation of submucosal neurons of guinea pig small intestine^[7,8] and activation of ion secretion from human colon^[9]. Moreover, upregulation of expression of PAR-2 in ulcerative colitis^[10] suggested a strong possibility of involvement of mast cell tryptase and trypsin in inflammatory bowel disease.

Indeed, increased numbers of mast cells were observed in chronic ulcerative colitis^[11] and Crohn's disease^[12], elevated histamine levels or enhanced histamine metabolism were found in collagenous colitis, food allergy^[13], Crohn's disease^[14], ulcerative colitis^[14,15] and allergic enteropathy^[15] and increased levels of tryptase were detected in ulcerative colitis^[16], indicating that these two proinflammatory mediators are involved in the pathogenesis of certain gastrointestinal diseases.

We have reported previously that mast cell tryptase was able to activate mast cells^[17,18], which presents a self-amplification mechanism of mast cell degranulation. Since the receptor of tryptase, PAR-2 was localized on human mast cells^[19] and PAR-2 agonists were reported to be capable of activating rat peritoneal mast cells^[20], it is likely that PAR-2 agonists and trypsin may have ability to activate human mast cells. We therefore examined the effect of trypsin and PAR-2 agonists on tryptase and histamine release from human colon mast cells in the current study.

MATERIALS AND METHODS

Reagents

The following compounds were purchased from Sigma (St. Louis, USA): collagenase (type I), hyaluronidase (type I), soy bean trypsin inhibitor (SBTI), bovine serum albumin (BSA, fraction V), penicillin and streptomycin, calcium ionophore A23187, antimycin A, human trypsin, 2-deoxy-D-glucose, pertussis toxin. Goat anti-human IgE (inactivated) was from Serotec (Kidlington, Oxford, UK). FCS and minimum essential medium (MEM) containing 25 mM N-2-hydroxyethylpiperazine-N'-2-ethane sulphonic acid (HEPES) were from Gibco (Paisley, Renfrewshire, UK). Peptides SLIGKV-NH₂, VKGILS-NH₂, trans-cinnamoyl-Leu-Ile-Gly-Arg-Leu-Orn-amide (tc-LIGRLO) and trans-cinnamoyl-Orn-Leu-Arg-Gly-Ile-Leu-amide

(tc-OLRGIL) were >98% purity and from Meilian Corporation (Xian, China). A polyclonal antibody and a monoclonal antibody against tryptase were donated by Dr Andrew F. Walls (University of Southampton, UK). Histamine plate was from RefLab (Copenhagen, Denmark). HEPES and all other chemicals were of analytical grade.

Dispersion of mast cells

The mast cell dispersion procedure was similar to the one described previously^[21,22]. Human colon tissue was obtained from patients with carcinoma of colon at colectomy. Only macroscopically normal tissue was used for the study. After removal of fat, tissue was washed and chopped finely with scissors into fragments of 0.5-2.0 mm³, and then incubated with 1.5 mg/mL collagenase and 0.75 mg/mL hyaluronidase in MEM containing 2% fetal calf serum (1 g colon/10 mL buffer) for 70 min at 37 °C. Dispersed cells were separated from undigested tissue by filtration through nylon gauze (pore size 100 µm diameter), washed and maintained in MEM (containing 10% FCS, 200 U/mL penicillin, 200 µg/mL streptomycin) on a roller overnight at room temperature. Mast cell purity, as determined by light microscopy after stained by alcian blue, ranged from 3.5% to 5.5%.

Mast cell challenge

Dispersed cells were resuspended in HEPES buffered salt solution (HBSS, pH 7.4) with 1.8 mM CaCl₂ and 0.5 mM MgCl₂ (complete HBSS), and 100 µL aliquots containing 4-6×10³ mast cells were added to a 50 µL tc-LIGRLO, tc-OLRGIL, SLIGKV, VKGILS, trypsin, control secretagogue or buffer alone and incubated for 15 min at 37 °C. The reaction was terminated by the addition of 150 µL ice cold incomplete HBSS and the tubes were centrifuged immediately (500 g, 10 min, 4 °C). All experiments were performed in duplicate. For the experiments with pertussis toxin, cells were incubated with 0.1 or 1.0 µg/mL pertussis toxin for four hours at 37 °C, and then washed with HBSS before adding stimulus. Similarly, for the experiments with metabolic inhibitors, cells were incubated with 2-deoxy-D-glucose (10 mmol/L) and antimycin A (1 µmol/L) for 40 min at 37 °C before challenged with stimulus. For the measurement of total histamine concentration

in certain tubes, the suspension was boiled for 6 min. Supernatants were stored at -20 °C until use.

Tryptase and histamine measurement

Tryptase concentrations were measured with a sandwich ELISA procedure with a specific polyclonal antibody against human tryptase as the capture antibody and AA5 a monoclonal antibody specific for human tryptase as the detecting antibody^[23]. Histamine concentrations were determined using a glass fibre-based fluorometric assay^[17].

Statistical analysis

Data are shown as mean±SEM for the number of experiments (*n*) indicated, and the paired Student's *t* test was applied to evaluate two independent samples. In all analyses *P*<0.05 was taken as statistically significant.

RESULTS

Induction of tryptase release by agonists of PAR-2

Both PAR-2 agonists tc-LIGRLO-NH₂ and SLIGKV-NH₂ were able to induce dose dependent release of tryptase from colon mast cells (Figure 1). More than 2.5 fold increase in tryptase release was provoked by 100 µmol/mL tc-LIGRLO-NH₂, even at a concentration as low as 1.0 µmol/mL tc-LIGRLO-NH₂ was able to elicit a 2.2 fold increase in the release of tryptase. Although the potency of SLIGKV-NH₂ appeared slightly weaker than that of tc-LIGRLO-NH₂, it could still stimulate as much as two fold increase in the release of tryptase from colon mast cells. The reverse peptides tc-OLRGIL-NH₂ and VKGILS-NH₂ had no effect on the release of tryptase when being added at the concentrations from 0.1 to 300 µmol/mL (Figure 1). The quantity of tryptase released elicited by tc-LIGRLO-NH₂ (100 µmol/mL) was similar to that induced by 10 µg/mL anti-IgE or 1 µg/mL calcium ionophore. Trypsin at the concentrations of 1.0-100 µg/mL was capable of provoking a dose dependent release of tryptase with a maximum of 16 ng/mL tryptase being released by 100 µg/mL trypsin (Figure 1). Approximately 80% trypsin induced release of tryptase was diminished by SBTI when trypsin and SBTI were added to cells at the same time (Figure 1).

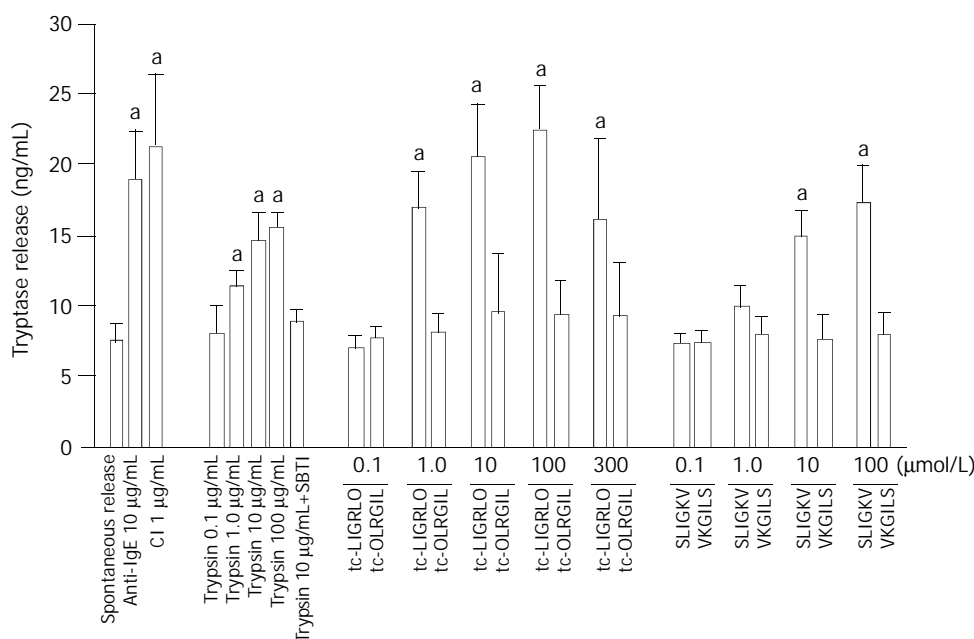


Figure 1 Effects of tc-LIGRLO, tc-OLRGIL, SLIGKV, VKGILS, trypsin, anti-IgE and calcium ionophore A23187 (CI) on tryptase release from colon mast cells. The values shown are mean±SEM for four separate experiments. Stimulus or control was incubated with cells for 15 min before termination of the reactions. ^a*P*<0.05 compared with buffer alone group (paired Student's *t* test).

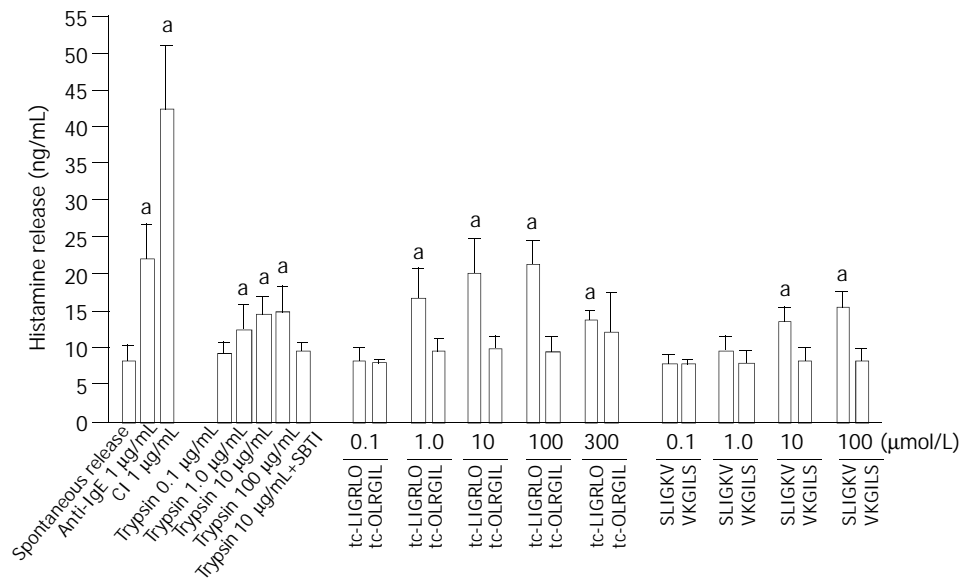


Figure 2 Effects of tc-LIGRLO, tc-OLRGIL, SLIGKV, VKGILS, trypsin, anti-IgE and calcium ionophore A23187 (CI) on histamine release from colon mast cells. The values shown are mean±SEM for four separate experiments. Stimulus or control was incubated with cells for 15 min before termination of the reactions. ^a*P*<0.05 compared with buffer alone group (paired Student's *t* test).

Induction of histamine release by agonists of PAR-2

Both PAR-2 agonists tc-LIGRLO-NH₂ and SLIGKV-NH₂ were also able to induce a dose dependent release of histamine from colon mast cells. More than 2.5 and 2.0 fold increases in histamine release were provoked by 100 µmol/mL tc-LIGRLO-NH₂ and SLIGKV-NH₂, respectively. However, histamine release elicited by tc-LIGRLO-NH₂ (100 µmol/mL) was less than that induced by anti-IgE (10 µg/mL) and only half of that provoked by calcium ionophore (1 µg/mL). The reverse peptides tc-OLRGIL-NH₂ and VKGILS-NH₂ had no effect on the release of histamine when being added at concentrations up to 300 µmol/mL (Figure 2). Trypsin at the concentrations from 1.0 to 100 µg/mL was capable of provoking a dose dependent release of histamine with a maximum of 14 ng/mL histamine being released by 100 µg/mL trypsin. Approximately 70% trypsin induced release of histamine was reduced by SBTI when trypsin and SBTI were added at the same time to cells (Figure 2).

Time course for tc-LIGRLO-NH₂

The release of trypsin and histamine in response to tc-LIGRLO-NH₂ was maximized within 3 min following addition of 100 µmol/mL tc-LIGRLO-NH₂ to colon mast cells. The maximum release of trypsin and histamine was then maintained for at least 15 min (Figure 3). When tc-LIGRLO-NH₂, anti-IgE and calcium ionophore were incubated with cells for a prolonged period of 30 min, the amount of trypsin and histamine released appeared not being increased (Table 1).

Table 1 Effects of tc-LIGRLO, tc-OLRGIL, anti-IgE and calcium ionophore A23187 (CI) on trypsin and histamine release from colon mast cells following 30 min incubation period

Concentration of stimulus	Trypsin (ng/mL)	Histamine (ng/mL)
Buffer alone	8.2±0.6	9.5±1.7
tc-LIGRLO 100 µmol/mL	22±3.0 ^a	17±1.3 ^a
tc-OLRGIL 100 µmol/mL	8.4±2.8	10±1.9
Anti-IgE 10 µg/mL	19±4.1 ^a	19±4.8 ^a
CI 1.0 µg/mL	13±0.6 ^a	34±4.3 ^a

The values shown are mean±SEM for four separate experiments performed in duplicate. ^a*P*<0.05 compared with buffer alone group (paired Student's *t* test).

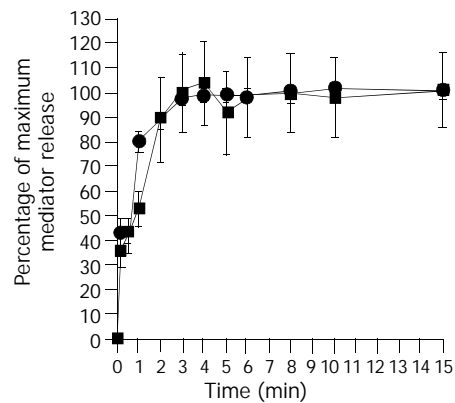


Figure 3 Time course for tc-LIGRLO (100 µM) induced release of trypsin (■) and histamine (●) from colon mast cells. Data shown are mean±SEM of four separate experiments.

Effects of pertussis toxin and metabolic inhibitors on trypsin and histamine release

Trypsin release induced by tc-LIGRLO-NH₂, SLIGKV-NH₂ and trypsin was abolished by pretreatment of colon mast cells with metabolic inhibitors or pertussis toxin (Table 2). The same treatment was also able to almost completely inhibit histamine release from mast cells (Table 3).

Table 2 Inhibition of tc-LIGRLO, SLIGKV, trypsin, anti-IgE or calcium ionophore A23187 (CI) induced trypsin release from colon mast cells by pertussis toxin (1 µg/mL) and metabolic inhibitors

Concentration of stimulus	% inhibition of trypsin release	
	Pertussis toxin	Metabolic inhibitors
tc-LIGRLO 100 µmol/mL	85±9.6 ^a	91±3.9 ^a
SLIGKV 100 µmol/mL	91±4.8 ^a	94±3.6 ^a
Trypsin 10 µg/mL	100±0 ^a	95±4.0 ^a
Anti-IgE 10 µg/mL	87±10 ^a	99±0.5 ^a
CI 1.0 µg/mL	84±8.8 ^a	89±4.7 ^a

The values shown are mean±SEM for four separate experiments performed in duplicate. ^a*P*<0.05 compared with the uninhibited control group (paired Student's *t* test).

Table 3 Inhibition of tc-LIGRLO, SLIGKV, trypsin, anti-IgE or calcium ionophore A23187 (CI) induced histamine release from colon mast cells by pertussis toxin (1 µg/mL) and metabolic inhibitors

Concentration of stimulus		% inhibition of histamine release	
		Pertussis toxin	Metabolic inhibitors
tc-LIGRLO	100 µmol/mL	92±5.4 ^a	98±2.0 ^a
SLIGKV	100 µmol/mL	95±5.9 ^a	92±3.8 ^a
Trypsin	10 µg/mL	84±6.8 ^a	88±8.7 ^a
Anti-IgE	10 µg/mL	84±5.2 ^a	99±1.1 ^a
CI	1.0 µg/mL	97±2.4 ^a	99±0.1 ^a

The values shown are mean±SEM for four separate experiments performed in duplicate. ^a*P*<0.05 compared with the uninhibited control group (paired Student's *t* test).

DISCUSSION

The finding in the current study that PAR-2 agonists were able to activate human mast cells fulfilled our hypothesis that human mast cells possess a self-amplification mechanism to IgE dependent activation through their mediator tryptase. That is to say that upon activation, mast cells release tryptase, and the released tryptase then activates their neighbouring mast cells or acts on its host mast cells through PAR-2.

The maximum 22.5 ng/mL tryptase and 21 ng/mL histamine release induced by tc-LIGRLO-NH₂ were comparable to those induced by 10 µg/mL anti-IgE, indicating that the PAR-2 agonist is a potent stimulus of mast cells. SLIGKV was also able to provoke a significant tryptase and histamine release from colon mast cells, but its action appeared slightly weaker than tc-LIGRLO-NH₂. This could be due to the structural difference between the two molecules. As little as 1.0 µmol/mL tc-LIGRLO-NH₂ was able to stimulate a significant release of tryptase and histamine, suggesting further that this compound is a potent mast cell secretagogue, and the concentration of the stimulus is easy to be achieved under physiological conditions. It was little surprised to observe that trypsin was able to activate colon mast cells as there should be a relatively high concentration of trypsin in human intestinal tract, and some of them should be able to penetrate through the epithelial lining of intestine, particularly when paracellular permeability of colon was increased upon PAR-2 activation^[4]. Nevertheless, it should be interesting to learn the physiological or pathophysiological role of mast cell activation by trypsin in gastrointestinal tract in future. The fact that reversed peptides of PAR-2 agonists had little effect on tryptase and histamine release from colon mast cells proved further the specificity of the PAR-2 agonists on mast cells. The maximum release of tryptase and histamine from colon mast cells was achieved at 3 min after adding tc-LIGRLO-NH₂ to cells, suggesting that its action on mast cells was slower than that of neuropeptide substance P, which reached peak histamine release within 20 sec of incubation^[24], but faster than that induced by anti-IgE and calcium ionophore, which required at least 6 min to complete^[21].

The inhibition of trypsin induced tryptase and histamine release by SBTI, a mixed type of inhibitor of tryptic enzymes^[25], indicating that the process was not cytotoxic and required an intact catalytic site of trypsin. Pretreatment of cells with metabolic inhibitors antimycin A which blocks the oxidative phosphorylation process of cells, and 2-deoxy-D-glucose which blocks anaerobic metabolism pathway in cells, abolished the actions of tc-LIGRLO-NH₂, SLIGKV, trypsin, anti-IgE as well as calcium ionophore, indicating that the release of tryptase and histamine induced by them was a non-cytotoxic process,

and was dependent on cell energy supply. Tryptase and histamine release provoked by tc-LIGRLO-NH₂, SLIGKV, trypsin, anti-IgE and calcium ionophore were also inhibited by pretreatment of cells with pertussis toxin, suggesting that the degranulation process elicited by them was associated with the activation of G-protein coupled receptors^[26].

Over the last decade, a number of functions of mast cell tryptase have been discovered. These include induction of microvascular leakage^[27], accumulation and activation of eosinophils and neutrophils^[28,29], provocation of release of IL-8 from epithelial cells^[30]. Similarly, PAR-2 agonists were found to be able to provoke the inflammatory response in the rat paw^[31,32] and mediate eosinophil infiltration and hyperreactivity in allergic inflammation of the airway^[33]. Of particular importance is the finding that the delayed onset of inflammation was observed in protease-activated receptor-2-deficient mice^[34]. These highlighted the crucial role of tryptase and its receptor PAR-2 in inflammation. The finding that PAR-2 agonists were able to activate human colon mast cells in the current study added a new concept to the tryptase and PAR-2 theory, indicating further the importance of them in the pathogenesis of inflammation. In conclusion, the agonists of PAR-2 and trypsin are potent secretagogues of human colon mast cells, which are likely to contribute to the development of inflammatory disorders in human gut.

REFERENCES

- Molino M**, Barnathan ES, Numerof R, Clark J, Dreyer M, Cumashi A, Hoxie JA, Schechter NM, Woolkalis M, Brass LF. Interactions of mast cell tryptase with thrombin receptors and PAR-2. *J Biol Chem* 1997; **272**: 4043-4049
- Hollenberg MD**, Saifeddine M, al-Ani B, Kawabata A. Proteinase-activated receptors: structural requirements for activity, receptor cross-reactivity, and receptor selectivity of receptor-activating peptides. *Can J Physiol Pharmacol* 1997; **75**: 832-841
- Al-Ani B**, Saifeddine M, Hollenberg MD. Detection of functional receptors for the proteinase-activated-receptor-2-activating polypeptide, SLIGRL-NH₂, in rat vascular and gastric smooth muscle. *Can J Physiol Pharmacol* 1995; **73**: 1203-1207
- Cenac N**, Coelho AM, Nguyen C, Compton S, Andrade-Gordon P, MacNaughton WK, Wallace JL, Hollenberg MD, Bunnett NW, Garcia-Villar R, Bueno L, Vergnolle N. Induction of intestinal inflammation in mouse by activation of proteinase-activated receptor-2. *Am J Pathol* 2002; **161**: 1903-1915
- Cenac N**, Garcia-Villar R, Ferrier L, Larauche M, Vergnolle N, Bunnett NW, Coelho AM, Fioramonti J, Bueno L. Proteinase-activated receptor-2-induced colonic inflammation in mice: possible involvement of afferent neurons, nitric oxide, and paracellular permeability. *J Immunol* 2003; **170**: 4296-4300
- Kawabata A**, Kinoshita M, Nishikawa H, Kuroda R, Nishida M, Araki H, Arizono N, Oda Y, Kakehi K. The protease-activated receptor-2 agonist induces gastric mucus secretion and mucosal cytoprotection. *J Clin Invest* 2001; **107**: 1443-1450
- Gao C**, Liu S, Hu HZ, Gao N, Kim GY, Xia Y, Wood JD. Serine proteases excite myenteric neurons through protease-activated receptors in guinea pig small intestine. *Gastroenterology* 2002; **123**: 1554-1564
- Reed DE**, Barajas-Lopez C, Cottrell G, Velazquez-Rocha S, Dery O, Grady EF, Bunnett NW, Vanner SJ. Mast cell tryptase and proteinase-activated receptor 2 induce hyperexcitability of guinea-pig submucosal neurons. *J Physiol* 2003; **547**: 531-542
- Mall M**, Gonska T, Thomas J, Hirtz S, Schreiber R, Kunzelmann K. Activation of ion secretion via proteinase-activated receptor-2 in human colon. *Am J Physiol Gastrointest Liver Physiol* 2002; **282**: G200-G210
- Kim JA**, Choi SC, Yun KJ, Kim DK, Han MK, Seo GS, Yeom JJ, Kim TH, Nah YH, Lee YM. Expression of protease-activated receptor 2 in ulcerative colitis. *Inflamm Bowel Dis* 2003; **9**: 224-229
- Stoyanova II**, Gulubova MV. Mast cells and inflammatory mediators in chronic ulcerative colitis. *Acta Histochem* 2002; **104**: 185-192

- 12 **Furusu H**, Murase K, Nishida Y, Isomoto H, Takeshima F, Mizuta Y, Hewlett BR, Riddell RH, Kohno S. Accumulation of mast cells and macrophages in focal active gastritis of patients with Crohn's disease. *Hepatogastroenterology* 2002; **49**: 639-643
- 13 **Schwab D**, Hahn EG, Raithel M. Enhanced histamine metabolism: a comparative analysis of collagenous colitis and food allergy with respect to the role of diet and NSAID use. *Inflamm Res* 2003; **52**: 142-147
- 14 **Winterkamp S**, Weidenhiller M, Otte P, Stolper J, Schwab D, Hahn EG, Raithel M. Urinary excretion of N-methylhistamine as a marker of disease activity in inflammatory bowel disease. *Am J Gastroenterol* 2002; **97**: 3071-3077
- 15 **Raithel M**, Matek M, Baenkler HW, Jorde W, Hahn EG. Mucosal histamine content and histamine secretion in Crohn's disease, ulcerative colitis and allergic enteropathy. *Int Arch Allergy Immunol* 1995; **108**: 127-133
- 16 **Raithel M**, Winterkamp S, Pacurar A, Ulrich P, Hochberger J, Hahn EG. Release of mast cell tryptase from human colorectal mucosa in inflammatory bowel disease. *Scand J Gastroenterol* 2001; **36**: 174-179
- 17 **He SH**, Gaça MDA, Walls AF. A role for tryptase in the activation of human mast cells: modulation of histamine release by tryptase and inhibitors of tryptase. *J Pharmacol Exp Ther* 1998; **286**: 289-297
- 18 **He SH**, Gaça MDA, Walls AF. The activation of synovial mast cells: modulation of histamine release by tryptase and chymase and their inhibitors. *Eur J Pharmacol* 2001; **412**: 223-229
- 19 **D' Andrea MR**, Rogahn CJ, Andrade-Gordon P. Localization of protease-activated receptors-1 and -2 in human mast cells: indications for an amplified mast cell degranulation cascade. *Biotech Histochem* 2000; **75**: 85-90
- 20 **Stenton GR**, Nohara O, Dery RE, Vliagoftis H, Gilchrist M, Johri A, Wallace JL, Hollenberg MD, Moqbel R, Befus AD. Proteinase-activated receptor (PAR)-1 and -2 agonists induce mediator release from mast cells by pathways distinct from PAR-1 and PAR-2. *J Pharmacol Exp Ther* 2002; **302**: 466-474
- 21 **He SH**, Xie H, He YS. Induction of tryptase and histamine release from human colon mast cells by IgE-dependent or -independent mechanisms. *World J Gastroenterol* 2004; **10**: 319-322
- 22 **He SH**, Xie H. Modulation of histamine release from human colon mast cells by protease inhibitors. *World J Gastroenterol* 2004; **10**: 337-341
- 23 **Buckley MG**, Walters C, Wong WM, Cawley MID, Ren S, Schwartz LB, Walls AF. Mast cell activation in arthritis: detection of α - and β -tryptase, histamine and eosinophil cationic protein in synovial fluid. *Clin Sci* 1997; **93**: 363-370
- 24 **Lowman MA**, Benyon RC, Church MK. Characterisation of neuropeptide-induced histamine release from human dispersed skin mast cells. *Br J Pharmacol* 1988; **95**: 121-130
- 25 **He SH**, Gaça MDA, McEuen AR, Walls AF. Inhibitors of chymase as mast cell stabilising agents: the contribution of chymase in the activation of human mast cells. *J Pharmacol Exp Ther* 1999; **291**: 517-523
- 26 **Piliponsky AM**, Gleich GJ, Nagler A, Bar I, Levi-Schaffer F. Non-IgE-dependent activation of human lung- and cord blood-derived mast cells is induced by eosinophil major basic protein and modulated by the membrane form of stem cell factor. *Blood* 2003; **101**: 1898-1904
- 27 **He SH**, Walls AF. Human mast cell tryptase: A potent stimulus of microvascular leakage and mast cell activation. *Eur J Pharmacol* 1997; **328**: 89-97
- 28 **He SH**, Peng Q, Walls AF. Potent induction of neutrophil- and eosinophil-rich infiltrate *in vivo* by human mast cell tryptase: selective enhancement of eosinophil recruitment by histamine. *J Immunol* 1997; **159**: 6216-6225
- 29 **Temkin V**, Kantor B, Weg V, Hartman ML, Levi-Schaffer F. Tryptase activates the mitogen-activated protein kinase/activator protein-1 pathway in human peripheral blood eosinophils, causing cytokine production and release. *J Immunol* 2002; **169**: 2662-2669
- 30 **Cairns JA**, Walls AF. Mast cell tryptase is a mitogen for epithelial cells: Stimulation of IL-8 production and intercellular adhesion molecule-1 expression. *J Immunol* 1996; **156**: 275-283
- 31 **Vergnolle N**, Hollenberg MD, Sharkey KA, Wallace JL. Characterization of the inflammatory response to proteinase-activated receptor-2 (PAR2)-activating peptides in the rat paw. *Br J Pharmacol* 1999; **127**: 1083-1090
- 32 **Vergnolle N**. Proteinase-activated receptor-2-activating peptides induce leukocyte rolling, adhesion, and extravasation *in vivo*. *J Immunol* 1999; **163**: 5064-5069
- 33 **Schmidlin F**, Amadesi S, Dabbagh K, Lewis DE, Knott P, Bunnett NW, Gater PR, Geppetti P, Bertrand C, Stevens ME. Protease-activated receptor 2 mediates eosinophil infiltration and hyper-reactivity in allergic inflammation of the airway. *J Immunol* 2002; **169**: 5315-5321
- 34 **Lindner JR**, Kahn ML, Coughlin SR, Sambrano GR, Schauble E, Bernstein D, Foy D, Hafezi-Moghadam A, Ley K. Delayed onset of inflammation in protease-activated receptor-2-deficient mice. *J Immunol* 2000; **165**: 6504-6510

Inhibition of tryptase release from human colon mast cells by protease inhibitors

Shao-Heng He, Hua Xie

Shao-Heng He, Hua Xie, Allergy and Inflammation Research Institute, Shantou University Medical College, Shantou 515031, Guangdong Province, China

Shao-Heng He, Immunopharmacology Group, University of Southampton, Southampton, UK

Supported by the National Natural Science Foundation of China, No. 30140023, and the Li Ka Shing Foundation, Hong Kong, China, No. C0200001

Correspondence to: Professor Shao-Heng He, Allergy and Inflammation Research Institute, Shantou University Medical College, 22 Xin-Ling Road, Shantou 515031, Guangdong Province, China. shoahenghe@hotmail.com

Telephone: +86-754-8900405 **Fax:** +86-754-8900192

Received: 2003-10-10 **Accepted:** 2003-11-19

Abstract

AIM: To investigate the ability of protease inhibitors to modulate tryptase release from human colon mast cells.

METHODS: Enzymatically dispersed cells from human colon were challenged with anti-IgE or calcium ionophore A23187 in the absence or presence of tryptase and chymase inhibitors, and tryptase release was determined.

RESULTS: IgE dependent tryptase release from colon mast cells was inhibited by up to approximately 37%, 40% and 36.6% by chymase inhibitors Z-Ile-Glu-Pro-Phe-CO₂Me (ZIGPFM), *N*-tosyl-L-phenylalanyl-chloromethyl ketone (TPCK), and α_1 -antitrypsin, respectively. Similarly, the inhibitors of tryptase leupeptin, *N*-tosyl-L-lysine chloromethyl ketone (TLCK) and lactoferrin were also able to inhibit anti-IgE induced tryptase release by a maximum of 39.4%, 47.6% and 36.6%, respectively. The inhibitory actions of chymase inhibitors, but not tryptase inhibitors on colon mast cells were enhanced by preincubation of them with cells for 20 min before challenged with anti-IgE. At a concentration of 10 μ g/mL, protamine was able to inhibit anti-IgE and calcium ionophore induced tryptase release. However, at 100 μ g/mL, protamine elevated tryptase levels in supernatants. A specific inhibitor of aminopeptidase amastatin had no effect on anti-IgE induced tryptase release. The significant inhibition of calcium ionophore induced tryptase release was also observed with the inhibitors of tryptase and chymase examined. The inhibitors tested by themselves did not stimulate tryptase release from colon mast cells.

CONCLUSION: It was demonstrated for the first time that both tryptase and chymase inhibitors could inhibit IgE dependent and calcium ionophore induced tryptase release from dispersed colon mast cells in a concentration dependent manner, which suggest that they are likely to be developed as a novel class of anti-inflammatory drugs to treat chronic of colitis in man.

He SH, Xie H. Inhibition of tryptase release from human colon mast cells by protease inhibitors. *World J Gastroenterol* 2004; 10(3):332-336

<http://www.wjgnet.com/1007-9327/10/332.asp>

INTRODUCTION

It has been reported that increased number of mast cells and mast cell degranulation are closely associated with a number of gastrointestinal diseases including idiopathic inflammatory bowel disease^[1], chronic ulcerative colitis^[2], Crohn's disease^[3-5], gastritis^[5] and collagenous colitis^[6,7], irritable bowel syndrome^[8,9] and chronic inflammatory duodenal bowel disorders^[10]. Through releasing their proinflammatory mediators including histamine, tryptase, chymase, heparin and some cytokines^[11], mast cells actively participate in the pathogenesis of these intestinal diseases.

Tryptase is a tetrameric serine proteinase that constitutes about 20% of the total protein within human mast cells and is stored almost exclusively in the secretory granules of mast cells^[12] in a catalytically active form^[13]. Relatively higher secretion of tryptase has been detected in ulcerative colitis^[14], implicating that this mediator is involved in the pathogenesis of intestinal diseases. Evidence is emerging that tryptase may be a key mediator of allergic inflammation and a promising target for therapeutic intervention^[15] as it has been found to be able to induce microvascular leakage in the skin of guinea pig^[16], bronchoconstriction^[17] in allergic sheep airways, inflammatory cell accumulation in peritoneum of mouse^[18] and release of IL-8 from epithelial cells^[19]. Moreover, tryptase has been proved to be a unique marker of mast cell degranulation *in vitro* as it is more selective than histamine to mast cells^[20].

In recent years, inhibitors of tryptase^[21,22] and chymase^[23] were discovered to possess the ability to inhibit histamine release from human skin, tonsil, synovial^[24] and colon mast cells^[25], suggesting these inhibitors are likely to be developed as a novel class of mast cell stabilizers. However, little is known of the actions of tryptase and chymase inhibitors on tryptase release from human colon mast cells. We therefore investigated the effects of these two groups of inhibitors on IgE dependent or independent tryptase release from human colon mast cells in the current study.

MATERIALS AND METHODS

Dispersion of mast cells

Human colon tissue was obtained from patients with carcinoma of colon at colectomy. Only macroscopically normal tissue was used for the study. After removal of fat, tissue was washed and chopped finely with scissors into fragments of 0.5-2.0 mm³, and then incubated with 1.5 mg/mL collagenase (Sigma) and 0.75 mg/mL hyaluronidase (Sigma) in minimum essential medium (MEM) containing 2% fetal calf serum (1 g colon/10 mL buffer) for 70 min at 37 °C. Dispersed cells were separated from undigested tissue by filtration through nylon gauze (pore size 100 μ m in diameter), washed and maintained in MEM (Gibco) (containing 10% FCS, 200 U/mL penicillin, 200 μ g/mL streptomycin) on a roller overnight at room temperature. Mast cell purity, as determined by light microscopy after stained by alcian blue, ranged from 3.5% to 5.4%.

Mast cell challenge

Dispersed cells were resuspended in HEPES buffered salt solution (HBSS, pH 7.4) with CaCl₂ and MgCl₂ (complete HBSS), and 100 μ L aliquots containing 4-6 \times 10³ mast cells

were added to a 50 μ L anti-IgE (Serotec, UK), calcium ionophore (Sigma), or inhibitor in complete HBSS and incubated for 15 min at 37 °C. The reaction was terminated by addition of 150 μ L ice cold incomplete HBSS and the tubes were centrifuged immediately (500 g, 10 min, 4 °C). All experiments were performed in duplicate. Supernatants were stored at -20 °C until tryptase concentrations were determined.

Inhibition of release of tryptase

For some experiments, protease inhibitor was preincubated with cells for 20 min before anti-IgE or calcium ionophore was added. Protease inhibitor and anti-IgE or calcium ionophore were also added to cells at the same time (no preincubation period). Data were expressed as the percentage inhibition of tryptase release, taking into account tryptase release in the presence and absence of the inhibitor. As for our previous experiments, the optimal tryptase release from colon mast cells was induced by 10 μ g/mL anti-IgE or 1 μ g/mL calcium ionophore^[20], and therefore they were chosen as standard concentrations throughout the study.

Tryptase measurement

Tryptase concentrations were measured with a sandwich ELISA procedure with a specific polyclonal antibody against human tryptase as the capture antibody and AA5 a monoclonal antibody specific for human tryptase as the detecting antibody^[26].

Statistical analyses

Statistical analyses were performed with SPSS software. Data were expressed as mean \pm SEM. Analysis of variance indicated significant differences between groups with ANOVA. For the preplanned comparison of interest, Student's *t* test was applied. For all analyses, $P < 0.05$ was taken as statistically significant.

RESULTS

Effects of secretagogues and inhibitors on tryptase release from mast cells

At 15 min following incubation, anti-IgE at 10 μ g/mL and calcium ionophore at 1 μ g/mL were able to induce 41.6 \pm 4.3 ng/mL and 38.8 \pm 3.0 ng/mL tryptase release from colon mast cells, respectively, whereas at the same time point spontaneous tryptase release (buffer alone) was 22.4 \pm 3.2 ng/mL. The same concentrations of anti-IgE and calcium ionophore were also able to provoke a significant tryptase release from colon mast cells following a 35 min incubation period (Table 1). All protease inhibitors tested had no stimulatory effect on colon mast cells following a 15 min or a 35 min incubation period (data not shown).

Table 1 Spontaneous and anti-IgE or calcium ionophore induced tryptase release from human colon mast cells

Compound	Tryptase released (ng/mL)	
	15 min	35 min
Buffer alone	22.4 \pm 3.2	20.5 \pm 2.8
Anti-IgE 10 μ g/mL	41.6 \pm 4.3 ^a	37.6 \pm 2.6 ^a
CI 1.0 μ g/mL	38.8 \pm 3.0 ^a	38.4 \pm 3.6 ^a

The values shown are mean \pm SEM for six separate experiments. ^a $P < 0.05$ compared with buffer alone control (Student's *t* test).

Inhibition of anti-IgE induced tryptase release from mast cells

The concentration dependent inhibition of anti-IgE induced release of tryptase from colon mast cells was observed when anti-IgE and various concentrations of chymase inhibitors ZIGPFM, TPCK, and α_1 -antitrypsin were added to cells at the same time. Up to approximately 37%, 40% and 36.6%

inhibition of IgE dependent tryptase release were achieved with ZIGPFM, TPCK, and α_1 -antitrypsin, respectively (Figure 1). As little as 10 ng/mL ZIGPFM was able to significantly inhibit IgE dependent tryptase release. Preincubation of ZIGPFM and TPCK with cells for 20 min before challenged with anti-IgE was able to moderately enhance their inhibitory actions on cells (Figure 2).

The inhibitors of tryptase leupeptin, TLCK and lactoferrin were also able to inhibit anti-IgE induced tryptase release in a concentration dependent manner, and a maximum of some 39.4%, 47.6%, and 36.6% of inhibition was achieved with 200 μ mol/mL leupeptin, 100 μ mol/mL TLCK, and 30 μ mol/mL lactoferrin, respectively (Figure 1). Preincubation of inhibitors of tryptase with cells for 20 min before anti-IgE was added had little effect on their abilities to inhibit anti-IgE induced tryptase release (Figure 2). A specific inhibitor of aminopeptidase, amastatin had no effect on anti-IgE induced tryptase release. When 10 μ g/mL protamine was added to cells at the same time with anti-IgE, or when 1.0 μ g/mL protamine was preincubated with cells before addition of the stimulus, anti-IgE induced tryptase release was significantly inhibited. However, when 100 μ g/mL protamine and anti-IgE was added to cells at the same time, tryptase concentrations measured in cell supernatants were much higher than those induced by anti-IgE alone (Table 2).

Table 2 Effect of protamine on anti-IgE or calcium ionophore (CI) induced tryptase release from human colon mast cells

Protamine concentration (μ g/mL)	% inhibition of tryptase release			
	No preincubation		20 min preincubation	
	Anti-IgE	CI	Anti-IgE	CI
0.1	4.0 \pm 2.3	5.1 \pm 4.5	nd	nd
1.0	17.3 \pm 5.2	16.7 \pm 4.6	21.4 \pm 3.8 ^a	19.5 \pm 2.9 ^a
10	20.9 \pm 4.3 ^a	17.1 \pm 3.8	-0.7 \pm 1.8	-9.7 \pm 11
100	-54.7 \pm 13 ^b	-24.9 \pm 8.9 ^b	nd	nd

The values shown are mean \pm SEM for six separate experiments. Protamine was either added to cells at the same time with anti-IgE or CI, or preincubated with cells for 20 min before challenged with anti-IgE or CI. ^alevels of tryptase reduced in comparison with the uninhibited control ($P < 0.05$, Student's *t* test). ^blevels of tryptase elevated in comparison with the uninhibited control ($P < 0.05$, Student's *t* test). nd=not done.

Inhibition of calcium ionophore induced tryptase release from mast cells

The concentration dependent inhibition of calcium ionophore induced tryptase release from colon mast cells was observed when calcium ionophore and various concentrations of chymase inhibitors ZIGPFM, TPCK, and α_1 -antitrypsin were added to cells at the same time. Up to approximately 27.6%, 35.3% and 23% inhibition of IgE dependent tryptase release were achieved with ZIGPFM, TPCK, and α_1 -antitrypsin, respectively (Figure 3). Preincubation of the inhibitors with cells for 20 min before challenged with calcium ionophore enhanced the inhibitory ability of ZIGPFM, but not TPCK (Figure 4).

Calcium ionophore stimulated tryptase release was also reduced by addition of the various concentrations of inhibitors of tryptase to cells. Leupeptin, TLCK and lactoferrin were able to inhibit calcium ionophore stimulated tryptase release by up to approximately 27.1%, 44.1% and 38.2% respectively, when they were added to cells together with calcium ionophore (Figure 3). The extent of inhibition by leupeptin and TLCK was not affected by preincubation of them with cells for 20 min before calcium ionophore was added (Figure 4). Protamine at a concentration of 1 μ g/mL was also able to inhibit calcium ionophore induced tryptase release (Table 2).

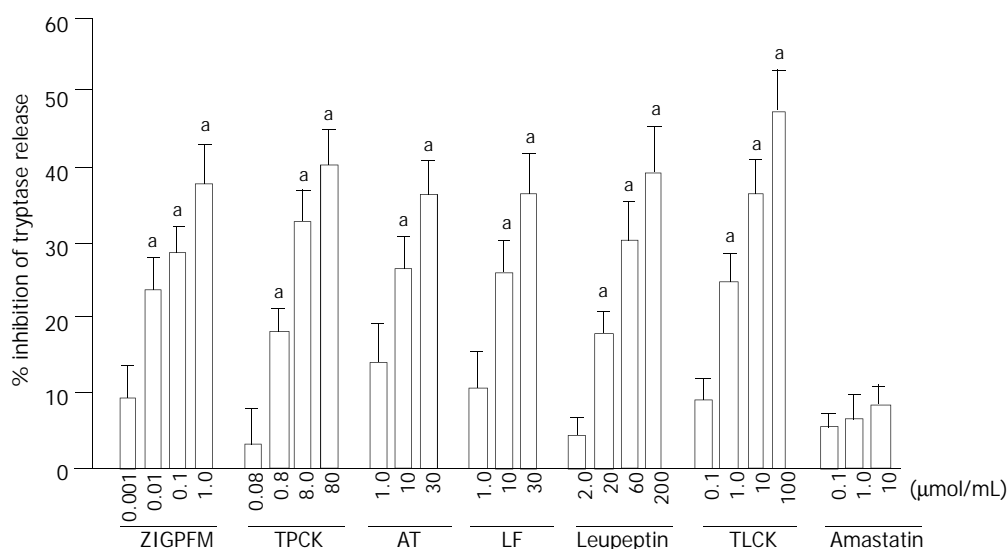


Figure 1 Inhibition of anti-IgE (10 µg/mL) induced tryptase release from dispersed colon mast cells by protease inhibitors. The inhibitors and anti-IgE were added to cells at the same time (no preincubation). Data are presented as mean±SEM for four to six separate experiments performed in duplicate. ^a*P*<0.05 compared with the responses with uninhibited controls. AT=α₁-antitrypsin; LF=lactoferrin.

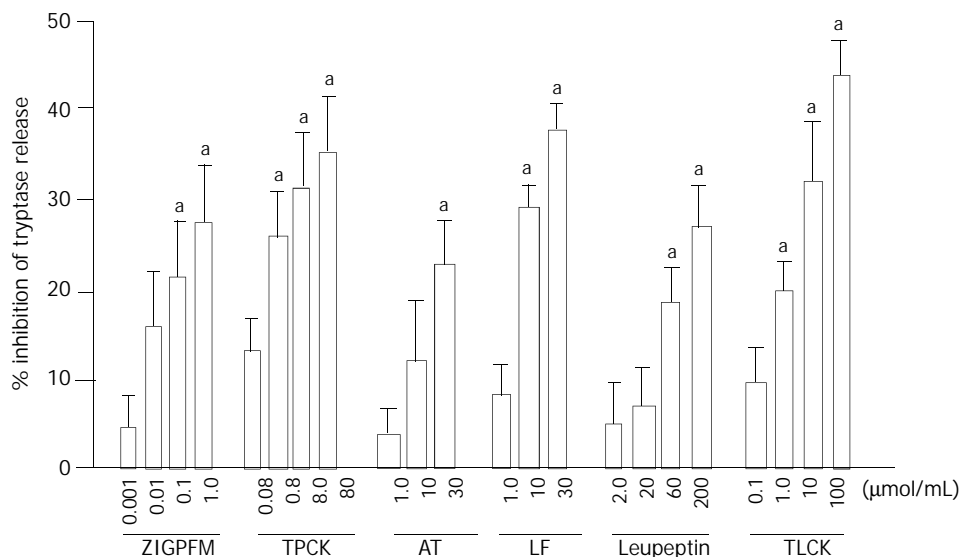


Figure 2 Inhibition of anti-IgE (10 µg/mL) induced tryptase release from dispersed colon mast cells by protease inhibitors. The inhibitors were preincubated with cells for 20 min before anti-IgE was added. Data are presented as mean±SEM for four to six separate experiments performed in duplicate. ^a*P*<0.05 compared with the responses of uninhibited controls.

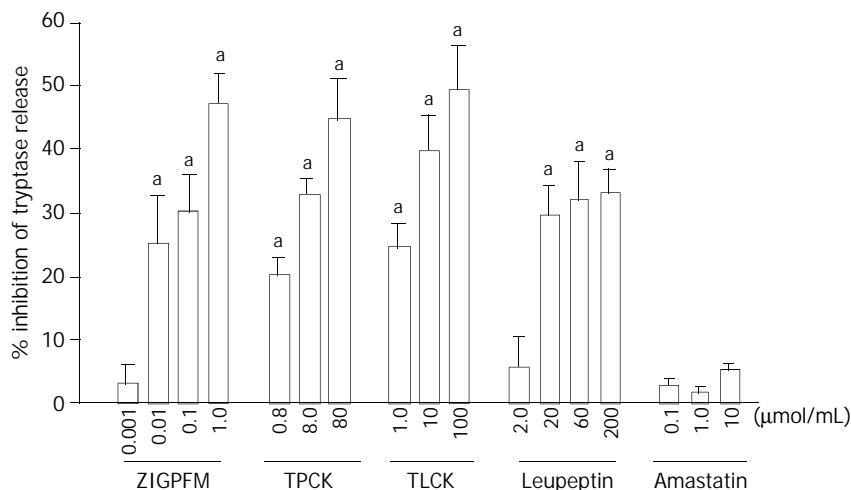


Figure 3 Inhibition of calcium ionophore (1 µg/mL) induced tryptase release from dispersed colon mast cells by protease inhibitors. The inhibitors and anti-IgE were added to cells at the same time (no preincubation). Data are presented as mean±SEM for four to six separate experiments performed in duplicate. ^a*P*<0.05 compared with the responses with uninhibited controls. AT=α₁-antitrypsin; LF=lactoferrin.

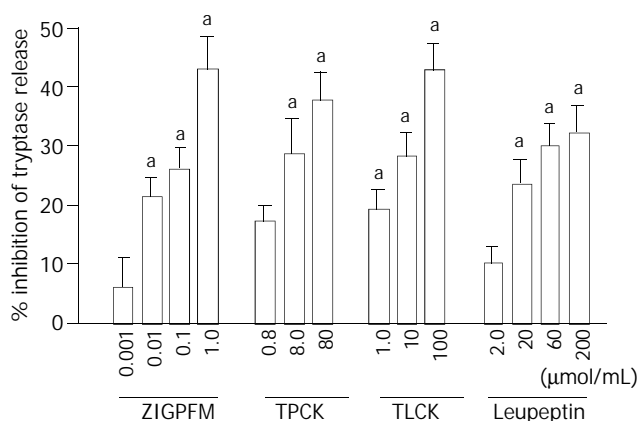


Figure 4 Inhibition of calcium ionophore (1 $\mu\text{g}/\text{mL}$) induced tryptase release from dispersed colon mast cells by protease inhibitors. The inhibitors were preincubated with cells for 20 min before calcium ionophore was added. Data are presented as mean \pm SEM for four to six separate experiments performed in duplicate. ^a $P < 0.05$ compared with the responses of uninhibited controls.

DISCUSSION

We have found for the first time that inhibitors of tryptase and chymase were able to inhibit anti-IgE and calcium ionophore induced tryptase release from dispersed human colon mast cells, which may indicate a potential of a novel therapy for inflammatory bowel disease or other mast cell related intestinal diseases.

Up to approximately 40% inhibition of IgE dependent tryptase release from colon mast cells was observed with inhibitors of chymase, indicating that a chymase activity was involved in the process of IgE dependent gut mast cell degranulation. This was consistent with our previous finding that chymase inhibitors inhibited IgE dependent histamine release, which has indirectly proved that tryptase and histamine are likely to share a similar degranulation process. Unlike inhibition of histamine release, preincubation of ZIGPFM and TPCK with cells for 20 min before challenged with anti-IgE appeared to further reduce the quantity of tryptase released from mast cells, implicating that there may be some difference between tryptase and histamine release processes. Similar to chymase inhibitors, tryptase inhibitors inhibited up to some 47.6% anti-IgE induced tryptase release from colon mast cells, which implicated that a tryptase activity was likely to be involved in the process of colon mast cell degranulation. Once again, this was consistent with our previous finding that tryptase inhibitors were able to inhibit IgE dependent histamine release.

Since the majority of these inhibitors at the concentrations used in the current study were able to inhibit more than 95% tryptase or chymase activity in enzyme assays^[27], the incomplete inhibition of tryptase release from mast cells may suggest that some pathways other than tryptase and chymase pathways are involved in the anti-IgE induced degranulation of gut mast cells. A specific inhibitor of aminopeptidase amastatin, which did not inhibit chymotrypsin and trypsin activities^[28], was used as an irrelevant protease inhibitor control. It had no significant effects on anti-IgE induced tryptase release from colon mast cells, which proved the specificity of actions of tryptase and chymase inhibitors on tryptase release from mast cells.

Calcium ionophore is a calcium carrier that could help to elevate the calcium concentration in cytoplasm of mast cells^[29], and therefore acts on the downstream site of the process of mast cell degranulation. The inhibition of calcium ionophore induced tryptase release by the inhibitors of tryptase and chymase in the current study might also suggest the

involvement of tryptase and chymase activities in mast cell degranulation process was at the downstream site and most likely after influx of calcium ions into mast cells. The evidence that tryptase and chymase are sited in the granules of mast cells in their fully active form supports further the likelihood that these two mast cell serine proteases are involved in IgE dependent activation of colon mast cells. The results that tryptase levels were elevated when 100 $\mu\text{g}/\text{mL}$ protamine was added to cells at the same time with unexpected anti-IgE. This was most likely due to the tetrameric structure of tryptase being dissociated by protamine^[30], thus more tryptase monomers existed in supernatants, and were recognized by AA5 as an intact tryptase molecule.

Some of the latest reports on tryptase inhibitors demonstrated the importance of these potential anti-inflammatory drugs. Inhaled APC366 was able to attenuate allergen-induced late-phase airway obstruction in asthma^[31], and APC2059 could improve the symptomatic scores of patients with mildly to moderately active ulcerative colitis in an open-label pilot study^[32]. Our findings in the current study may at least partially explain why tryptase inhibitors could treat these diseases. Moreover, the successful treatment of acute ulcerative colitis^[33] and Crohn's disease^[34] with mast cell stabilizer ketotifen further strongly suggests that inhibitors of tryptase and chymase are likely to become a novel class of anti-inflammatory drugs with their anti-inflammatory actions and mast cell stabilizing properties.

In conclusion, the inhibitors of both tryptase and chymase are able to inhibit anti-IgE dependent and calcium ionophore induced tryptase release from colon mast cells, indicating that they are likely to be developed as a novel class of anti-inflammatory drugs to treat chronic colitis in man.

REFERENCES

- 1 **Fox CC**, Lichtenstein LM, Roche JK. Intestinal mast cell responses in idiopathic inflammatory bowel disease. Histamine release from human intestinal mast cells in response to gut epithelial proteins. *Dig Dis Sci* 1993; **38**: 1105-1112
- 2 **Stoyanova II**, Gulubova MV. Mast cells and inflammatory mediators in chronic ulcerative colitis. *Acta Histochem* 2002; **104**: 185-192
- 3 **Gelbmann CM**, Mestermann S, Gross V, Kollinger M, Scholmerich J, Falk W. Structures in Crohn's disease are characterised by an accumulation of mast cells colocalised with laminin but not with fibronectin or vitronectin. *Gut* 1999; **45**: 210-217
- 4 **Bischoff SC**, Wedemeyer J, Herrmann A, Meier PN, Trautwein C, Cetin Y, Maschek H, Stolte M, Gebel M, Manns MP. Quantitative assessment of intestinal eosinophils and mast cells in inflammatory bowel disease. *Histopathology* 1996; **28**: 1-13
- 5 **Beil WJ**, Schulz M, McEuen AR, Buckley MG, Walls AF. Number, fixation properties, dye-binding and protease expression of duodenal mast cells: comparisons between healthy subjects and patients with gastritis or Crohn's disease. *Histochem J* 1997; **29**: 759-773
- 6 **Nishida Y**, Murase K, Isomoto H, Furusu H, Mizuta Y, Riddell RH, Kohno S. Different distribution of mast cells and macrophages in colonic mucosa of patients with collagenous colitis and inflammatory bowel disease. *Hepatogastroenterology* 2002; **49**: 678-682
- 7 **Schwab D**, Raithe M, Hahn EG. Evidence for mast cell activation in collagenous colitis. *Inflamm Res* 1998; **47**(Suppl 1): S64-S65
- 8 **O'Sullivan M**, Clayton N, Breslin NP, Harman I, Bountra C, McLaren A, O'Morain CA. Increased mast cells in the irritable bowel syndrome. *Neurogastroenterol Motil* 2000; **12**: 449-457
- 9 **Pang X**, Boucher W, Triadafilopoulos G, Sant GR, Theoharides TC. Mast cell and substance P-positive nerve involvement in a patient with both irritable bowel syndrome and interstitial cystitis. *Urology* 1996; **47**: 436-438
- 10 **Crivellato E**, Finato N, Isola M, Ribatti D, Beltrami CA. Low mast cell density in the human duodenal mucosa from chronic inflammatory duodenal bowel disorders is associated with defective

- villous architecture. *Eur J Clin Invest* 2003; **33**: 601-610
- 11 **Walls AF**, He SH, Buckley MG, McEuen AR. Roles of the mast cell and basophil in asthma. *Clin Exp Allergy Rev* 2001; **1**: 68-72
- 12 **Abraham WM**. Tryptase: potential role in airway inflammation and remodelling. *Am J Physiol Lung Cell Mol Physiol* 2002; **282**: L193-L196
- 13 **McEuen AR**, He SH, Brander ML, Walls AF. Guinea pig lung tryptase: Localisation to mast cells and characterisation of the partially purified enzyme. *Biochem Pharmacol* 1996; **52**: 331-340
- 14 **Raithel M**, Winterkamp S, Pacurar A, Ulrich P, Hochberger J, Hahn EG. Release of mast cell tryptase from human colorectal mucosa in inflammatory bowel disease. *Scand J Gastroenterol* 2001; **36**: 174-179
- 15 **Walls AF**. Structure and function of human mast cell tryptase. In: Marone G, editor. Mast cells and basophils. New York: Academic Press 2000: p 291-309
- 16 **He SH**, Walls AF. Human mast cell tryptase: A potent stimulus of microvascular leakage and mast cell activation. *Eur J Pharmacol* 1997; **328**: 89-97
- 17 **Molinari JF**, Scuri M, Moore WR, Clark J, Tanaka R, Abraham WM. Inhaled tryptase causes bronchoconstriction in sheep via histamine release. *Am J Respir Crit Care Med* 1996; **154**: 649-653
- 18 **He SH**, Peng Q, Walls AF. Potent induction of neutrophil- and eosinophil-rich infiltrate *in vivo* by human mast cell tryptase: selective enhancement of eosinophil recruitment by histamine. *J Immunol* 1997; **159**: 6216-6225
- 19 **Cairns JA**, Walls AF. Mast cell tryptase is a mitogen for epithelial cells: Stimulation of IL-8 production and intercellular adhesion molecule-1 expression. *J Immunol* 1996; **156**: 275-283
- 20 **He SH**, Xie H, He YS. Induction of tryptase and histamine release from human colon mast cells by IgE-dependent or -independent mechanisms. *World J Gastroenterol* 2004; **10**: 319-322
- 21 **He SH**, Gaça MDA, Walls AF. A role for tryptase in the activation of human mast cells: Modulation of histamine release by tryptase and inhibitors of tryptase. *J Pharmacol Exp Ther* 1998; **286**: 289-297
- 22 **He SH**, McEuen AR, Blewett SA, Li P, Buckley MG, Leufkens P, Walls AF. The inhibition of mast cell activation by neutrophil lactoferrin: uptake by mast cells and interaction with tryptase, chymase and cathepsin G. *Biochem Pharmacol* 2003; **65**: 1007-1015
- 23 **He SH**, Gaça MDA, McEuen AR, Walls AF. Inhibitors of chymase as mast cell stabilising agents: the contribution of chymase in the activation of human mast cells. *J Pharmacol Exp Ther* 1999; **291**: 517-523
- 24 **He SH**, Gaca MD, Walls AF. The activation of synovial mast cells: modulation of histamine release by tryptase and chymase and their inhibitors. *Eur J Pharmacol* 2001; **412**: 223-229
- 25 **He SH**, Xie H. Modulation of histamine release from human colon mast cells by protease inhibitors. *World J Gastroenterol* 2004; **10**: 337-341
- 26 **Buckley MG**, Walters C, Wong WM, Cawley MID, Ren S, Schwartz LB, Walls AF. Mast cell activation in arthritis: detection of α - and β -tryptase, histamine and eosinophil cationic protein in synovial fluid. *Clin Sci* 1997; **93**: 363-370
- 27 **He SH**, Chen P, Chen HQ. Modulation of enzymatic activity of human mast cell tryptase and chymase by proteinase inhibitors. *Acta Pharmacol Sin* 2003; **24**: 923-929
- 28 **Rich DH**, Moon BJ, Harbeson S. Inhibition of aminopeptidases by amastatin and bestatin derivatives. Effect of inhibitor structure on slow-binding processes. *J Med Chem* 1984; **27**: 417-422
- 29 **Foreman JC**, Mongar JL, Gomperts BD. Calcium ionophores and movement of calcium ions following the physiological stimulus to a secretory process. *Nature* 1973; **245**: 249-251
- 30 **Hallgren J**, Estrada S, Karlson U, Alving K, Pejler G. Heparin antagonists are potent inhibitors of mast cell tryptase. *Biochemistry* 2001; **40**: 7342-7349
- 31 **Krishna MT**, Chauhan A, Little L, Sampson K, Hawksworth R, Mant T, Djukanovic R, Lee T, Holgate ST. Inhibition of mast cell tryptase by inhaled APC366 attenuates allergen-induced late-phase airway obstruction in asthma. *J Allergy Clin Immunol* 2001; **107**: 1039-1045
- 32 **Tremaine WJ**, Brzezinski A, Katz JA, Wolf DC, Fleming TJ, Mordenti J, Strenkoski-Nix LC, Kurth MC. Treatment of mildly to moderately active ulcerative colitis with a tryptase inhibitor (APC 2059): an open-label pilot study. *Aliment Pharmacol Ther* 2002; **16**: 407-413
- 33 **Jones NL**, Roifman CM, Griffiths AM, Sherman P. Ketotifen therapy for acute ulcerative colitis in children: a pilot study. *Dig Dis Sci* 1998; **43**: 609-615
- 34 **Marshall JK**, Irvine EJ. Ketotifen treatment of active colitis in patients with 5-aminosalicylate intolerance. *Can J Gastroenterol* 1998; **12**: 273-275

Edited by Wang XL Proofread by Zhu LH

Modulation of histamine release from human colon mast cells by protease inhibitors

Shao-Heng He, Hua Xie

Shao-Heng He, Hua Xie, Allergy and Inflammation Research Institute, Shantou University Medical College, Shantou 515031, Guangdong Province, China

Shao-Heng He, Immunopharmacology Group, University of Southampton, Southampton, UK

Supported by the National Natural Science Foundation of China, No. 30140023, and the Li Ka Shing Foundation, Hong Kong, China, No. C0200001

Correspondence to: Professor Shao-Heng He, Allergy and Inflammation Research Institute, Shantou University Medical College, 22 Xin-Ling Road, Shantou 515031, Guangdong Province, China. shoahenghe@hotmail.com

Telephone: +86-754-8900405 **Fax:** +86-754-8900192

Received: 2003-10-10 **Accepted:** 2003-11-19

Abstract

AIM: To investigate the ability of protease inhibitors to modulate histamine release from human colon mast cells.

METHODS: Enzymatically dispersed cells from human colon were challenged with anti-IgE or calcium ionophore A23187 in the absence or presence of tryptase and chymase inhibitors, and histamine release was determined.

RESULTS: IgE dependent histamine release from colon mast cells was inhibited by up to approximately 37%, 26% and 36.8% by chymase inhibitors Z-Ile-Glu-Pro-Phe-CO₂Me (ZIGPFM), N-Tosyl-L-phenylalanyl-chloromethyl ketone (TPCK), and α_1 -antitrypsin, respectively. Similarly, inhibitors of tryptase leupeptin, N-tosyl-L-lysine chloromethyl ketone (TLCK), lactoferrin and protamine were also able to inhibit anti-IgE induced histamine release by a maximum of some 48%, 37%, 40% and 34%, respectively. Preincubation of these inhibitors with cells for 20 min before challenged with anti-IgE had small effect on the inhibitory actions of these inhibitors on colon mast cells. A specific inhibitor of aminopeptidase amastatin had no effect on anti-IgE induced histamine release. The significant inhibition of calcium ionophore induced histamine release was also observed with the inhibitors of tryptase and chymase examined. Apart from leupeptin and protamine, the inhibitors tested by themselves did not stimulate colon mast cells.

CONCLUSION: It was demonstrated that both tryptase and chymase inhibitors could inhibit IgE dependent and calcium ionophore induced histamine release from dispersed colon mast cells in a concentration dependent of manner, which suggest that they are likely to be developed as a novel class of anti-inflammatory drugs to treat chronic of colitis in man.

He SH, Xie H. Modulation of histamine release from human colon mast cells by protease inhibitors. *World J Gastroenterol* 2004; 10(3):337-341

<http://www.wjgnet.com/1007-9327/10/337.asp>

INTRODUCTION

It has been reported that mast cells and their inflammatory

mediators are closely associated with a number of intestinal diseases including idiopathic inflammatory bowel disease^[1], chronic ulcerative colitis^[2], Crohn's disease^[3] and collagenous colitis^[4]. Through release their proinflammatory mediators including histamine, tryptase, chymase, heparin and some cytokines^[5], mast cells actively participate in the pathogenesis of these intestinal diseases.

As a proinflammatory mediator, histamine is selectively located in the granules of human mast cells and basophils and released from these cells upon degranulation. To date, a total of four histamine receptors H₁, H₂, H₃ and H₄ have been discovered^[6] and the first three of them are located in human gut^[7,8], which prove that there are some specific targets that histamine can work on in intestinal tract. Indeed, increased levels of histamine or enhanced histamine metabolism have been observed in collagenous colitis, food allergy^[9], Crohn's disease^[10], ulcerative colitis^[10,11] and allergic enteropathy^[11], indicating that this mediator is involved in the pathogenesis of these diseases.

For more than four decades, histamine has been widely used as a marker of mast cell degranulation *in vitro*, and numerous anti-allergic drugs such as sodium cromoglycate, lodoxamide, salbutamol, ketotifen, terfenadine and cetirizine^[12,13] and salmeterol^[14] were reported to be able to inhibit anti-IgE induced histamine release from human mast cells. In recent years, inhibitors of tryptase^[15,16] and chymase^[17] have been discovered to possess the ability to inhibit histamine release from human skin, tonsil and synovial mast cells^[18], suggesting these inhibitors are likely to be developed as a novel class of mast cell stabilizers. However, little is known of the actions of tryptase and chymase inhibitors on histamine release from human colon mast cells. We therefore investigated the effects of these two groups of inhibitors on IgE dependent or independent histamine release from human colon mast cells in the current study.

MATERIALS AND METHODS

Dispersion of mast cells

Human colon tissue was obtained from patients with carcinoma of colon at colectomy. Only macroscopically normal tissue was used for the study. After removal of fat, tissue was washed and chopped finely with scissors into fragments of 0.5-2.0 mm³, and then incubated with 1.5 mg/mL collagenase (Sigma) and 0.75 mg/mL hyaluronidase (Sigma) in minimum essential medium (MEM) containing 2% fetal calf serum (1 g colon/10 mL buffer) for 70 min at 37 °C. Dispersed cells were separated from undigested tissue by filtration through nylon gauze (pore size 100 μ m diameter), washed and maintained in MEM (Gibco) (containing 10% FCS, 200 U/mL penicillin, 200 μ g/mL streptomycin) on a roller overnight at room temperature. Mast cell purity, as determined by light microscopy after stained by alcian blue, ranged from 3.5% to 5.4%.

Mast cell challenge

The challenge procedure was performed as described previously^[19]. Dispersed cells were resuspended in HEPES

buffered salt solution (HBSS, pH 7.4) with CaCl₂ and MgCl₂ (complete HBSS), and 100 µL aliquots containing 4-6×10³ mast cells were added to a 50 µL anti-IgE (Serotec, UK), calcium ionophore (Sigma), or inhibitor in complete HBSS and incubated for 15 min at 37 °C. The reaction was terminated by addition of 150 µL ice cold incomplete HBSS and the tubes were centrifuged immediately (500 g, 10 min, 4 °C). All experiments were performed in duplicate. For the measurement of total histamine concentration, in certain tubes the suspension was boiled for 6 min. Supernatants were stored at -20 °C until histamine concentrations were determined.

Inhibition of release of histamine

For some experiments, protease inhibitor was preincubated with cells for 20 min before anti-IgE or calcium ionophore being added. Protease inhibitor and anti-IgE or calcium ionophore were also added to cells at the same time (no preincubation period). Data were expressed as the percentage of inhibition of histamine release, taking into account of histamine release in the presence and absence of the inhibitor. As for our previous experiments, the optimal histamine release from colon mast cells was induced by 10 µg/mL anti-IgE or 1 µg/mL calcium ionophore^[20], and therefore they were chosen as standard concentrations throughout the study.

Histamine measurement

Histamine concentrations were determined using a glass fibre-based fluorometric assay^[15]. The procedure involved the binding of histamine to a glass-fiber matrix (RafLab, Copenhagen, Denmark) and its detection spectrophotometrically with Perkin-Elmer LS 2 detector (Denmark) following addition of o-phthalaldehyde (OPT). Histamine release was expressed as a percentage of total cellular histamine levels, and corrected for the spontaneous release measured in tubes in which cells had been incubated with the HBSS diluent alone.

Statistical analyses

Statistical analyses were performed with SPSS software. Data were expressed as mean±SEM. Where analysis of variance indicated significant differences between groups with ANOVA, for the preplanned comparisons of interest, Student's *t* test was applied. For all analyses, *P*<0.05 was taken as statistically significant.

RESULTS

Effects of protease inhibitors on histamine release from mast cells

At 15 min following incubation, leupeptin at concentration 200 µmol/mL and protamine at 100 µg/mL were able to provoke small but nevertheless significant histamine release from colon mast cells (Table 1). The same concentration of leupeptin was also capable of eliciting histamine release following a 35 min incubation period (Table 2). All the other protease inhibitors tested had no stimulatory action on colon mast cells. Leupeptin and protamine at all other concentrations did not induce a significant histamine release from colon mast cells. In the same experiments, anti-IgE and calcium ionophore were able to induce up to 11% and 21.8% net histamine release, respectively.

Inhibition of anti-IgE induced histamine release from mast cells

The concentration dependent inhibition of anti-IgE induced release of histamine from colon mast cells was observed when anti-IgE and various concentrations of chymase inhibitors ZIGPFM, TPCK, and α₁-antitrypsin were added to cells at

the same time. Up to approximately 37%, 26% and 36.8% inhibition of IgE dependent histamine release were achieved with ZIGPFM, TPCK, and α₁-antitrypsin, respectively (Figure 1). Preincubation of ZIGPFM and TPCK with cells for 20 min before challenged with anti-IgE was able to slightly enhance their inhibitory actions (Figure 2).

The inhibitors of trypsin leupeptin, TLCK, lactoferrin and protamine were also able to inhibit anti-IgE induced histamine release in a concentration dependent manner, and a maximum of 48%, 37%, 40% and 34% inhibition was achieved with 200 µmol/mL leupeptin, 100 µmol/mL TLCK, 30 µmol/mL lactoferrin and 100 µg/mL protamine, respectively (Figure 1). In contrast to inhibitors of chymase, preincubation of inhibitors of trypsin with cells for 20 min before the addition of anti-IgE had little effect on their abilities to inhibit anti-IgE induced histamine release (Figure 2). A specific inhibitor of aminopeptidase, amastatin had no effect on anti-IgE induced histamine release (data not shown).

Table 1 The effects of protease inhibitors on histamine release from human colon mast cells at 15 min incubation period

Compound	Concentration	Net histamine release (%)
ZIGPFM	0.001 µmol/mL	-0.9±0.8
	0.01 µmol/mL	0±1.1
	0.1 µmol/mL	0.8±0.6
	1.0 µmol/mL	0.2±1.2
TPCK	0.08 µmol/mL	3.1±2.0
	0.8 µmol/mL	2.1±1.0
	8.0 µmol/mL	2.0±1.2
	80 µmol/mL	0.7±1.1
α ₁ -antitrypsin	1.0 µmol/mL	0.9±0.5
	10 µmol/mL	1.1±0.6
	30 µmol/mL	1.5±0.6
Lactoferrin	1.0 µmol/mL	-1.0±0.8
	10 µmol/mL	0.8±0.6
	30 µmol/mL	0.5±1.0
TLCK	0.1 µmol/mL	1.7±2.1
	1.0 µmol/mL	1.1±0.6
	10 µmol/mL	2.7±1.7
	100 µmol/mL	3.5±1.2
Amastatin	0.1 µmol/mL	1.5±0.4
	1.0 µmol/mL	2.3±0.6
	10 µmol/mL	3.9±0.6
Leupeptin	2.0 µmol/mL	1.2±0.7
	20 µmol/mL	2.0±1.4
	60 µmol/mL	0.6±0.5
	200 µmol/mL	4.7±0.8 ^a
Protamine	0.1 µg/mL	1.7±1.3
	1.0 µg/mL	1.9±1.4
	10 µg/mL	0.2±2.1
	100 µg/mL	4.5±0.5 ^a
Anti-IgE	10 µg/mL	11±2.7 ^a
Calcium ionophore	1.0 µg/mL	18±3.6 ^a

The values shown are mean±SEM for four to six separate experiments. Cells were incubated with each concentration of the compound for 15 min at 37 °C. Spontaneous histamine release from these cells was 9.2±1.3%. ^a*P*<0.05 compared with buffer alone control (Student's *t* test).

Table 2 The effects of protease inhibitors on histamine release from human colon mast cells at 35 min incubation period

Compound	Concentration	Net histamine release (%)
ZIGPFM	0.001 $\mu\text{mol/mL}$	0.3 \pm 0.3
	0.01 $\mu\text{mol/mL}$	1.0 \pm 0.8
	0.1 $\mu\text{mol/mL}$	1.8 \pm 1.3
	1.0 $\mu\text{mol/mL}$	1.9 \pm 0.6
TPCK	0.8 $\mu\text{mol/mL}$	0.9 \pm 2.1
	8.0 $\mu\text{mol/mL}$	1.8 \pm 1.3
	80 $\mu\text{mol/mL}$	1.7 \pm 3.6
TLCK	1.0 $\mu\text{mol/mL}$	0 \pm 2.4
	10 $\mu\text{mol/mL}$	0.7 \pm 1.9
	100 $\mu\text{mol/mL}$	0.7 \pm 2.2
Amastatin	0.1 $\mu\text{mol/mL}$	1.0 \pm 1.7
	1.0 $\mu\text{mol/mL}$	-1.9 \pm 3.3
	10 $\mu\text{mol/mL}$	0 \pm 3.6
Leupeptin	2.0 $\mu\text{mol/mL}$	1.0 \pm 0.7
	20 $\mu\text{mol/mL}$	1.2 \pm 0.7
	60 $\mu\text{mol/mL}$	0 \pm 0.7
	200 $\mu\text{mol/mL}$	5.1 \pm 0.5 ^a
Protamine	1.0 $\mu\text{g/mL}$	1.2 \pm 2.9
	10 $\mu\text{g/mL}$	1.0 \pm 2.5
Anti-IgE	10 $\mu\text{g/mL}$	10.1 \pm 2.5 ^a
Calcium ionophore	1.0 $\mu\text{g/mL}$	21.8 \pm 3.8 ^a

The values shown are mean \pm SEM for four to six separate experiments. Spontaneous histamine release from these cells was 9.8 \pm 1.7%. ^a P <0.05 compared with buffer alone control (Student's *t* test).

Inhibition of calcium ionophore induced histamine release from mast cells

The concentration dependent inhibition of calcium ionophore induced histamine release from colon mast cells was observed when calcium ionophore and various concentrations of chymase inhibitors ZIGPFM, TPCK, and α_1 -antitrypsin were added to cells at the same time. Up to approximately 35%, 24% and 23.6% inhibition of IgE dependent histamine release

were achieved with ZIGPFM, TPCK, and α_1 -antitrypsin, respectively (Figure 3). Preincubation of TPCK with cells for 20 min before challenged with calcium ionophore slightly enhanced its inhibitory ability, whereas the same treatment did not improve the inhibitory ability of ZIGPFM (Figure 4).

Calcium ionophore stimulated histamine release was also reduced by addition of the various concentrations of inhibitors of tryptase to cells. Leupeptin, TLCK, lactoferrin and protamine were able to inhibit calcium ionophore stimulated histamine release by up to approximately 25%, 26%, 25% and 32%, respectively when they were added to cells together with calcium ionophore (Figure 3). The extent of inhibition by leupeptin and TLCK was increased when colon mast cells were preincubated with them for 20 min before calcium ionophore was added. However, the same treatment failed to improve the inhibitory action of protamine (Figure 4).

DISCUSSION

We have found that inhibitors of tryptase and chymase were able to inhibit anti-IgE and calcium ionophore induced histamine release from dispersed human colon mast cells, which may indicate a potential of a novel therapy for inflammatory bowel disease or other mast cell related intestinal diseases.

Up to approximately 37% inhibition of IgE dependent histamine release from colon mast cells was observed with inhibitors of chymase, indicating that a chymase activity was involved in the process of IgE dependent gut mast cell degranulation. This was consistent with our previous findings with human skin, lung^[17] and synovium tissues^[18], which demonstrated that chymase was involved in the mast cell activation-degranulation process. Comparing mast cells from different human tissues, the order of extent of maximum inhibition by chymase inhibitors was skin (82%) > lung (80%) > synovium (69%) > colon (37%). This might represent a novel type of mast cell heterogeneity, and could also be resulted from an inhibitor of chymase, chymostatin was not used for colon cells, but for the cells from other tissues.

Similar to chymase inhibitors, tryptase inhibitors inhibited

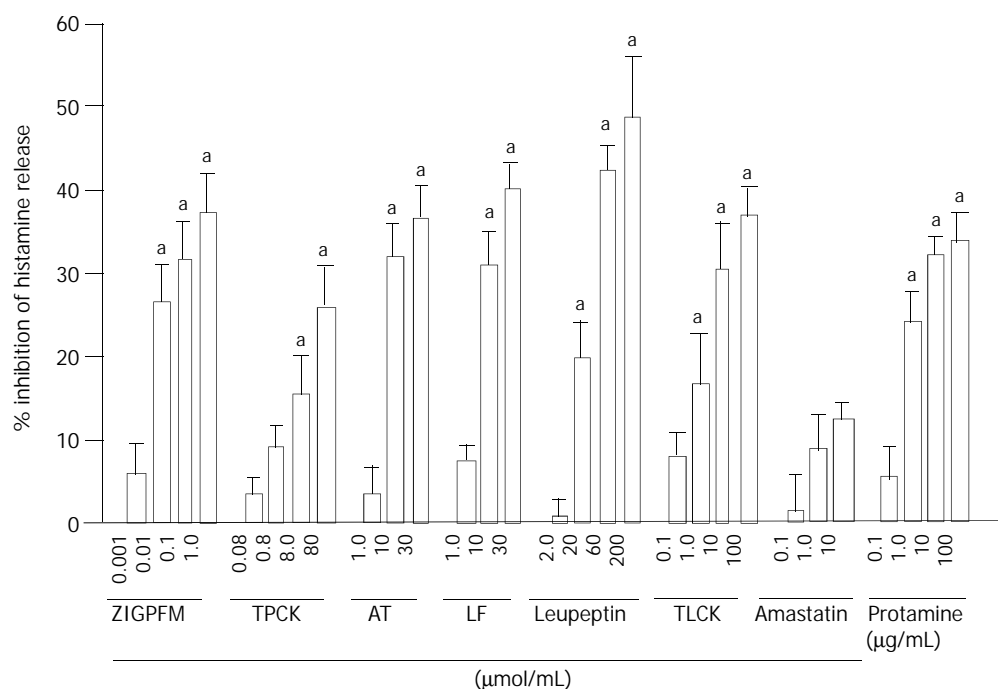


Figure 1 Inhibition of anti-IgE (10 $\mu\text{g/mL}$) induced histamine release from dispersed colon mast cells by the protease inhibitors. The inhibitors and anti-IgE were added to cells at the same time (no preincubation). Data are presented as mean \pm SEM for four to six separate experiments performed in duplicate. ^a P <0.05 compared with the responses with uninhibited controls. AT= α_1 -antitrypsin; LF=lactoferrin.

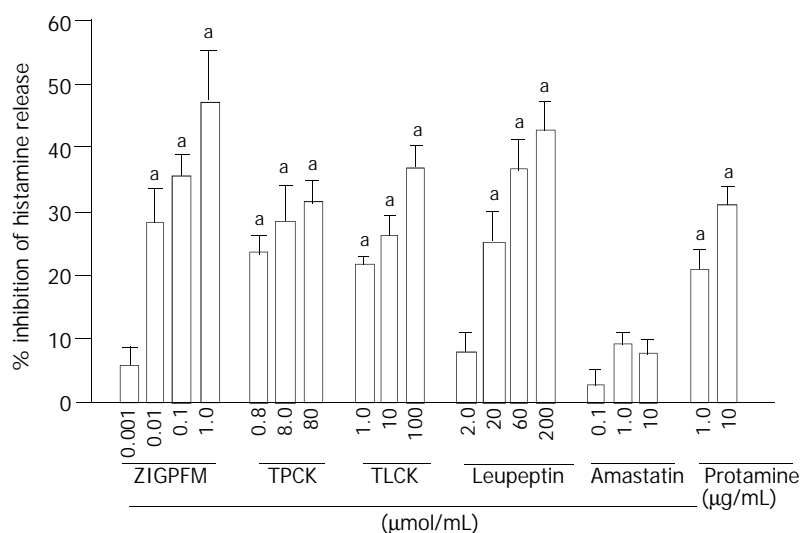


Figure 2 Inhibition of anti-IgE (10 µg/mL) induced histamine release from dispersed colon mast cells by the protease inhibitors. The inhibitors were preincubated with cells for 20 min before anti-IgE was added. Data are presented as mean±SEM for four to six separate experiments performed in duplicate. * $P < 0.05$ compared with the responses with uninhibited controls.

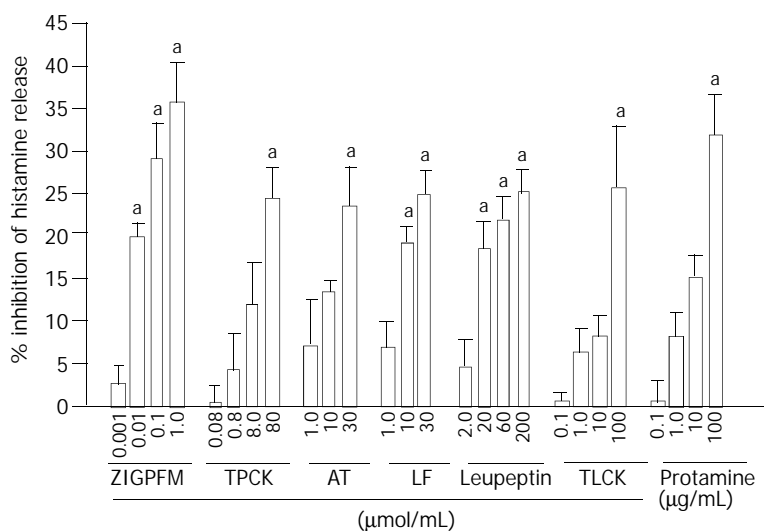


Figure 3 Inhibition of calcium ionophore (1 µg/mL) induced histamine release from dispersed colon mast cells by the protease inhibitors. The inhibitors and anti-IgE were added to cells at the same time (no preincubation). Data are presented as mean±SEM for four to six separate experiments performed in duplicate. * $P < 0.05$ compared with the responses with uninhibited controls. AT=α₁-antitrypsin; LF=lactoferrin.

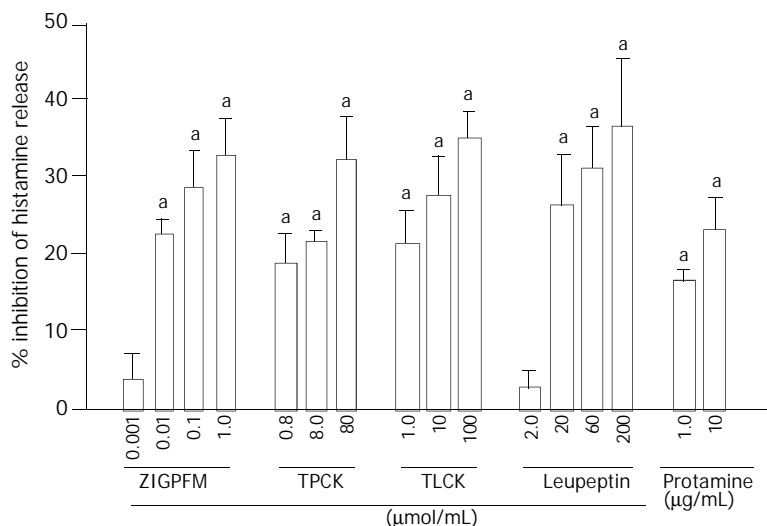


Figure 4 Inhibition of calcium ionophore (1 µg/mL) induced histamine release from dispersed colon mast cells by the protease inhibitors. The inhibitors were preincubated with cells for 20 min before calcium ionophore being added. Data are presented as mean±SEM for four to six separate experiments performed in duplicate. * $P < 0.05$ compared with the responses with uninhibited controls.

up to some 48% anti-IgE induced histamine release from colon mast cells, which implicated that a tryptase activity was likely to be involved in the process of colon mast cell degranulation. Once again, this was consistent with our previous findings with cells from other human tissues including skin, tonsil^[15] and synovium^[18]. Comparing mast cells from different human tissues, the order of extent of maximum inhibition by tryptase inhibitors was skin (90%) > synovium (70%) > colon (48%) > tonsil (35%).

Since the majority of these inhibitors at the concentrations used in the current study were able to inhibit more than 95% tryptase or chymase activity in enzyme assays^[20], the incomplete inhibition of histamine release from mast cells may suggest that some pathways other than tryptase and chymase pathways are involved in the anti-IgE induced degranulation of gut mast cells. A specific inhibitor of aminopeptidase amastatin, which did not inhibit chymotrypsin and trypsin activities^[21], was used as an irrelevant protease inhibitor control. It had no significant effects on anti-IgE induced histamine release from colon mast cells, which proved the specificity of actions of tryptase and chymase inhibitors on mast cells. The observation that preincubation of the inhibitors with cells for 20 min before challenged with anti-IgE had little impact on inhibition of IgE dependent histamine release was unexpected, nevertheless it may suggest that the actions of these inhibitors are rather rapid and the involvement of tryptase and chymase activities in anti-IgE induced histamine release is likely at the downstream site of the degranulation process. Since calcium ionophore is a calcium carrier that can help to elevate the calcium concentration in cytoplasm of mast cells, and therefore acts on the downstream site of the process of mast cell degranulation, the inhibition of calcium ionophore induced histamine release by the inhibitors of tryptase and chymase in the current study might also suggest that the involvement of tryptase and chymase activities in mast cell degranulation process was at the downstream site and most likely after influx of calcium ions into mast cells. The evidence that tryptase and chymase are sited in the granules of mast cells in their fully active form supports further the likelihood that these two mast cell serine proteases are involved in IgE dependent activation of colon mast cells.

Over the years, many compounds including sodium cromoglycate, lodoxamide, salbutamol, ketotifen, terfenadine and cetirizine have been recognized as mast cell stabilizers or histamine receptor antagonists, and used as anti-allergic drugs in clinical practice. However, only less than 40% inhibition of IgE dependent mast cell degranulation could be achieved with these compounds, much less than that with inhibitors of tryptase and chymase in the similar experimental system^[15,17]. Moreover, mast cell stabilizer drug ketotifen was successfully used to treat acute ulcerative colitis^[22] and Crohn's disease^[23]. These strongly suggest that inhibitors of tryptase and chymase are likely to become a novel class of anti-inflammatory drugs with their anti-inflammatory actions and mast cell stabilizing properties.

In conclusion, inhibitors of both tryptase and chymase are able to inhibit anti-IgE dependent and calcium ionophore induced histamine release from colon mast cells, indicating that they are likely to be developed as a novel class of anti-inflammatory drugs to treat chronic colitis in man.

REFERENCES

- 1 **Fox CC**, Lichtenstein LM, Roche JK. Intestinal mast cell responses in idiopathic inflammatory bowel disease. Histamine release from human intestinal mast cells in response to gut epithelial proteins. *Dig Dis Sci* 1993; **38**: 1105-1112
- 2 **Stoyanova II**, Gulubova MV. Mast cells and inflammatory mediators in chronic ulcerative colitis. *Acta Histochem* 2002; **104**: 185-192
- 3 **Nishida Y**, Murase K, Isomoto H, Furusu H, Mizuta Y, Riddell RH, Kohno S. Different distribution of mast cells and macrophages in colonic mucosa of patients with collagenous colitis and inflammatory bowel disease. *Hepatogastroenterology* 2002; **49**: 678-682
- 4 **Schwab D**, Raithel M, Hahn EG. Evidence for mast cell activation in collagenous colitis. *Inflamm Res* 1998; **47**(Suppl 1): S64-S65
- 5 **Walls AF**, He SH, Buckley MG, McEuen AR. Roles of the mast cell and basophil in asthma. *Clin Exp Allergy Rev* 2001; **1**: 68-72
- 6 **Repka-Ramirez MS**. New concepts of histamine receptors and actions. *Curr Allergy Asthma Rep* 2003; **3**: 227-231
- 7 **Bertaccini G**, Coruzzi G. An update on histamine H3 receptors and gastrointestinal functions. *Dig Dis Sci* 1995; **40**: 2052-2063
- 8 **Rangachari PK**. Histamine: mercurial messenger in the gut. *Am J Physiol* 1992; **262**: G1-G13
- 9 **Schwab D**, Hahn EG, Raithel M. Enhanced histamine metabolism: a comparative analysis of collagenous colitis and food allergy with respect to the role of diet and NSAID use. *Inflamm Res* 2003; **52**: 142-147
- 10 **Winterkamp S**, Weidenhiller M, Otte P, Stolper J, Schwab D, Hahn EG, Raithel M. Urinary excretion of N-methylhistamine as a marker of disease activity in inflammatory bowel disease. *Am J Gastroenterol* 2002; **97**: 3071-3077
- 11 **Raithel M**, Matek M, Baenkler HW, Jorde W, Hahn EG. Mucosal histamine content and histamine secretion in Crohn's disease, ulcerative colitis and allergic enteropathy. *Int Arch Allergy Immunol* 1995; **108**: 127-133
- 12 **Okayama Y**, Church MK. Comparison of the modulatory effect of ketotifen, sodium cromoglycate, procaterol and salbutamol in human skin, lung and tonsil mast cells. *Int Arch Allergy Appl Immunol* 1992; **97**: 216-225
- 13 **Okayama Y**, Benyon RC, Lowman MA, Church MK. *In vitro* effects of H₁-antihistamine on PGD₂ release from mast cells of human lung, tonsil, and skin. *Allergy* 1994; **49**: 246-253
- 14 **Butchers PR**, Vardey CJ, Johnson M. Salmeterol: a potent and long-acting inhibitor of inflammatory mediator release from human lung. *Br J Pharmacol* 1991; **104**: 672-676
- 15 **He SH**, Gaça MDA, Walls AF. A role for tryptase in the activation of human mast cells: Modulation of histamine release by tryptase and inhibitors of tryptase. *J Pharmacol Exp Ther* 1998; **286**: 289-297
- 16 **He SH**, McEuen AR, Blewett SA, Li P, Buckley MG, Leufkens P, Walls AF. The inhibition of mast cell activation by neutrophil lactoferrin: uptake by mast cells and interaction with tryptase, chymase and cathepsin G. *Biochem Pharmacol* 2003; **65**: 1007-1015
- 17 **He SH**, Gaça MDA, McEuen AR, Walls AF. Inhibitors of chymase as mast cell stabilising agents: the contribution of chymase in the activation of human mast cells. *J Pharmacol Exp Ther* 1999; **291**: 517-523
- 18 **He SH**, Gaca MD, Walls AF. The activation of synovial mast cells: modulation of histamine release by tryptase and chymase and their inhibitors. *Eur J Pharmacol* 2001; **412**: 223-229
- 19 **He SH**, Li P. Mast cell activation and histamine measurement. *Xuaxi Yikedaxue Xuebao* 2002; **33**: 586-588
- 20 **He SH**, Xie H, He YS. Induction of tryptase and histamine release from human colon mast cells by IgE dependent or independent mechanisms. *World J Gastroenterol* 2004; **10**: 319-322
- 21 **He SH**, Chen P, Chen HQ. Modulation of enzymatic activity of human mast cell tryptase and chymase by proteinase inhibitors. *Acta Pharmacol Sin* 2003; **24**: 923-929
- 22 **Rich DH**, Moon BJ, Harbeson S. Inhibition of aminopeptidases by amastatin and bestatin derivatives. Effect of inhibitor structure on slow-binding processes. *J Med Chem* 1984; **27**: 417-422
- 23 **Jones NL**, Roifman CM, Griffiths AM, Sherman P. Ketotifen therapy for acute ulcerative colitis in children: a pilot study. *Dig Dis Sci* 1998; **43**: 609-615
- 24 **Marshall JK**, Irvine EJ. Ketotifen treatment of active colitis in patients with 5-aminosalicylate intolerance. *Can J Gastroenterol* 1998; **12**: 273-275

• MAST CELL AND INFLAMMATORY BOWEL DISEASE •

Cloning and expression of human colon mast cell carboxypeptidase

Zhang-Quan Chen, Shao-Heng He

Zhang-Quan Chen, Shao-Heng He, Allergy and Inflammation Research Institute, Medical College, Shantou University, Shantou 515031, Guangdong Province, China

Supported by the Li Ka Shing Foundation, Hong Kong, China. No. C0200001

Correspondence to: Professor Shao-Heng He, Allergy and Inflammation Research Institute, Medical College, Shantou University, 22 Xin-Ling Road, Shantou 515031, Guangdong Province, China. shoahenghe@hotmail.com

Telephone: +86-754-8900405 **Fax:** +86-754-8900192

Received: 2003-12-23 **Accepted:** 2004-01-11

Abstract

AIM: To clone and express the human colon mast cell carboxypeptidase (MC-CP) gene.

METHODS: Total RNA was extracted from colon tissue, and the cDNA encoding human colon mast cell carboxypeptidase was amplified by reverse-transcription PCR (RT-PCR). The product cDNA was subcloned into the prokaryotic expression vector pMAL-c2x and eukaryotic expression vector pPIC9K to construct prokaryotic expression vector pMAL/human MC-CP (hMC-CP) and eukaryotic pPIC9K/hMC-CP. The recombinant fusion protein expressed in *E. coli* was induced with IPTG and purified by amylose affinity chromatography. After digestion with factor Xa, recombinant hMC-CP was purified by heparin agarose chromatography. The recombinant hMC-CP expressed in *Pichia pastoris* (*P. pastoris*) was induced with methanol and analyzed by SDS-PAGE, Western blot, N-terminal amino acid sequencing and enzyme assay.

RESULTS: The cDNA encoding the human colon mast cell carboxypeptidase was cloned, which had five nucleotide variations compared with skin MC-CP cDNA. The recombinant hMC-CP protein expressed in *E. coli* was purified with amylose affinity chromatography and heparin agarose chromatography. SDS-PAGE and Western blot analysis showed that the recombinant protein expressed by *E. coli* had a molecular weight of 36 kDa and reacted to the anti-native hMC-CP monoclonal antibody (CA5). The N-terminal amino acid sequence confirmed further the product was hMC-CP. *E. coli* generated hMC-CP showed a very low level of enzymatic activity, but *P. pastoris* produced hMC-CP had a relatively high enzymatic activity towards a synthetic substrate hippuryl-L-phenylalanine.

CONCLUSION: The cDNA encoding human colon mast cell carboxypeptidase can be successfully cloned and expressed in *E. coli* and *P. pastoris*, which will contribute greatly to the functional study on hMC-CP.

Chen ZQ, He SH. Cloning and expression of human colon mast cell carboxypeptidase. *World J Gastroenterol* 2004; 10(3):342-347
<http://www.wjgnet.com/1007-9327/10/342.asp>

INTRODUCTION

Mast cells and their inflammatory mediators have been

implicated to play a pivotal role in intestinal diseases such as inflammatory bowel disease^[1-7], collagenous colitis^[8,9], intestinal anaphylaxis^[10,11] and irritable bowel syndrome^[11,12]. Mast cell neutral proteases constitute more than 50% granule proteins in mast cells. They are tryptase, MC-CP, chymase, and a cathepsin G-like protease^[13-16]. Upon degranulation, these neutral proteases are released and carry out numerous functions in tissues nearby or distant as pro-inflammatory mediators. Recently it was found that mast cell products tryptase and histamine might play an important role in the amplification of degranulation signals in human^[17-21].

hMC-CP is a distinctive carboxypeptidase, which is exclusively located in MC_{TC} mast cells, possesses pancreatic carboxypeptidase A (CPA)-like activity, but has a closer amino acid sequence identical to carboxypeptidase B (CPB)^[13,22]. The evolution analysis demonstrated that MC-CP originated from a gene duplication along the pancreatic CPB lineage rather than along the pancreatic CPA lineage^[22,23]. Although hMC-CP has been detected in skin, lung, and intestinal tissues with immunohistochemistry^[13,22,24], and hMC-CP genes from skin and lung were cloned^[22,23,25], hMC-CP gene from intestinal tissue is still unknown.

Investigations on the structures and functions of human tryptase and chymase have made impressive progress and a number of potent functions of these two mast cell proteases were found in last decade. These include induction of microvascular leakage in skin of guinea pig^[26], stimulation of inflammatory cell accumulation in peritoneum of mouse^[27,28] and modulation of mast cell degranulation^[29,30], indicating that they may be key mediators of allergic inflammation and promising targets for diagnosis and therapeutic intervention^[31-35]. However, little is known about the function of hMC-CP except for its ability to cleave angiotension I^[13]. This could be resulted from lack of sufficient amount of hMC-CP. In the current study, a procedure for cloning and expression of hMC-CP was developed and enzymatically active human intestinal recombinant MC-CP was produced.

MATERIALS AND METHODS

Materials

RNA extract kit, total RNA purification system, multi-copy *Pichia* expression kit were purchased from Invitrogen (Carlsbad, CA, USA). First strand cDNA synthesis kit, restriction endonucleases, T₄ DNA ligase, the expression vector pMAL-c2x, *E. coli* hosts TB1 and amylose resin were obtained from Biolabs (Beverly, MA, USA). Antibiotics, isopropyl thio-β-D-galactopyranoside (IPTG), heparin agarose, extr-Avidin peroxidase, biotinylated sheep anti-mouse IgG, for *E. coli* growth medium and *P. Pichia* growth medium were from Sigma (Saint Louis, MO, USA). Qiaquick gel extraction kit and *Taq* polymerase were from Qiagen (Hilden, Germany). Protein molecular weight markers were from Bio-Rad (Hercules, CA, USA). A monoclonal antibody against human mast cell carboxypeptidase (CA5) was donated by University of Southampton, UK. All other chemicals were of analytical grade.

Tissue preparation

Human colon tissue was obtained from patients with carcinoma

of colon at colectomy. Only macroscopically normal tissue was used for the study. The specimens were kept in liquid nitrogen until use.

Extraction of RNA

Total cellular RNA was extracted from normal colon tissues according to the manufacturer's protocol. The purity of RNA was confirmed by formaldehyde denaturing agarose gel electrophoresis, and the concentration of RNA was determined with a spectrophotometer (DU640, Beckman).

Synthesis of cDNA

cDNAs were generated from total RNA by using the ProtoScript™ first strand cDNA synthesis kit. A total of 10 µL of RNA (1 µg), 2 µL of oligo (dT) primer and 4 µL of 2.5 mM dNTP were heated at 70 °C for 5 min. Reverse transcription was performed for 1 h at 42 °C in a solution (20 µL of total volume) containing 1 µL of 25U/µL M-MuLV reverse transcriptase. The reaction was terminated by incubating the mixture at 95 °C for 5 min, and placed on ice immediately.

PCR amplification and cloning of cDNAs

Based on the published DNA sequence of human skin mast cell carboxypeptidase^[22], a pair of primers (P1: 5' -GCTATGAGGCTCATCCTGCCTGT-3'; P2: 5' -GCTTTAGGAAGTATGCTTGAGGATATAC-3') were used to amplify hMC-CP cDNA. A hot-star PCR protocol was followed under the condition: at 95 °C for 15 min prior to amplification, then at 94 °C for 30 s, at 57 °C for 30 s, and at 72 °C for 1 min. The amplification was carried out for 30 cycles, followed by incubation at 72 °C for 10 min. The PCR products were analyzed with 1% agarose gel electrophoresis, and recovered with a Qiaquick gel extraction kit. The purified PCR product was cloned to pGEM-T Easy vector, forming a new plasmid pGEM/hMC-CP. The ligation mixtures were transformed into *E. coli* Dh5α. The positive recombinant clones were seeded on LB/agar plates with 100 µg/mL ampicillin, and the clones were further determined by PCR and DNA sequencing using a DNA sequencer (ABI 377 PRISM).

Construction of expression vector

To express hMC-CP in *E. coli*, an expression plasmid comprising the expression vector pMAL-C2x and hMC-CP cDNA was constructed. For this construction, a pair of specific primers (P3: 5' -GCTGAATTCATCGAGGGAAGGATCCCAGGCAGGCACAGCTAC-3'; P4: -GCTCTGCAGTTAGGAAGTATGCTTGAGGATATAC-3') were designed and used to amplify the coding region of the mature hMC-CP. The forward primer contained the recognition sequences for *EcoR* I, coding sequences for Factor Xa rEcognition sequence and the N-terminal region of the mature hMC-CP, and the reverse primer contained the rEcognition sequences for *Pst* I, and the coding sequence of the C-terminal region of the mature hMC-CP. pGEM/hMC-CP was used as the template for PCR. The resulting PCR fragments and pMAL-c2x plasmid were digested with *EcoR* I and *Pst* I. The fragments of interests were recovered from agarose gel, purified and ligated by T4 DNA ligase, which resulted in the expression plasmid pMAL/hMC-CP. The ligation mixtures were used to transform *E. coli* TB1 cells. The positive recombinant products were selected on LB agar plates with 100 µg/mL ampicillin, and confirmed by PCR and DNA sequencing.

To express hMC-CP in *pichia pastoris*, another expression plasmid comprising the expression vector pPIC9K and hMC-CP cDNA was constructed. For this construction, a pair of specific primers (P5: 5' -GCTGAATTCATCCCAGGCAGGCACAGCTAC-3'; P6: -TACGCGGCCGCTTAGGAAG

TATGCTTGAGGATATAC-3') were designed and used to amplify the coding region of the mature hMC-CP. The forward primer contained the recognition sequences for *EcoR* I, and the reverse primer contained the recognition sequences for *Pst* I. pGEM/hMC-CP was used as the template for PCR. The resulting PCR fragments and pPIC9K plasmid were digested with *EcoR* I and *Not* I. The fragments of interests were recovered from agarose gel, purified and ligated by T4 DNA ligase, which resulted in the expression plasmid pPIC9K/hMC-CP. The ligation mixtures were used to transform *E. coli* DH5α cells. The positive recombinant products were selected on LB agar plates with 100 µg/mL ampicillin. The nucleotide sequences of cDNA insert and flanking sequence were verified. The expression plasmid pPIC9K/hMC-CP was linearized by digestion with *Bgl* II. Competent cells of *P. pastoris* GS115 were prepared for electroporation with the linearized plasmid pPIC9K/hMC-CP. The electroporation was performed in a 2 mm gap cuvette at 2.0 kV, 25 µF, and 200Ω using a gene-pulsar (Bio-Rad). Transformants were screened for a His^r pheNotype on minimal dextrose (MD) agar plates. MD and minimal methanol (MM) plates were used to identify Mut^s clones. YPD plates containing Geneticin at a final concentration of 0.25, 0.5, 0.75, 2.0, 3.0, 4.0 mg/mL were used to screen multiple inserts for further expression.

Expression of recombinant hMC-CP

E. coli TB1 cells harboring the expression plasmid pMAL/hMC-CP were inoculated into LB medium containing 100 µg/mL ampicillin overnight at 37 °C in an orbital shaker (220 rpm). IPTG was added to a final concentration of 0.3 mM before the culture mixture was transferred to a 23 °C air shaker.

For the expression of hMC-CP in *P. pastoris*, a single colony of GS115 harboring the expression plasmid pPIC9K/hMC-CP was inoculated into 200 mL of buffered minimal glycerol complex medium (BMGY), and grew at 30 °C until the culture reached an A₆₀₀=2.0. Cultured cells were harvested by centrifugation and transferred to 1/10 of the original culture volume of buffered minimal methanol complex medium (BMMY), then grew at 30 °C. Methanol was added to a final concentration of 0.5% (v/v) every 24 h to maintain induction.

Purification of recombinant hMC-CP

At 24 h after induction, the bacterial cells were harvested by centrifugation at 5 000 g for 10 min at 4 °C. The pellet was resuspended in 50 mL ice-cold cells lysis buffer (20 mM Tris, 200 mM NaCl, 0.01% Triton X-100) at pH 8.0, then sonicated 6 times for 10 s (300 w) at 30 s intervals. The clarified cell extract was obtained by centrifugation at 20 000 g for 20 min, at 4 °C.

Amylose resin was used for purification of the fusion protein, and equilibrated with the running buffer (20 mM Tris, 200 mM NaCl, pH8.0), then the cell extract was loaded onto the column at a flow rate. The fusion protein was eluted from column with a buffer containing 10 mM maltose. In order to obtain the recombinant hMC-CP, the fusion protein was cleaved with factor Xa in 20 mM Tris, pH 8.0, containing 100 mM NaCl, 2 mM CaCl₂. The digestion was performed at 23 °C for 3 h. The above cleavage mixture was applied to heparin agarose in an equilibration buffer (20 mM Tris, 200 mM NaCl, pH8.0), and eluted from heparin agarose by the elution buffer containing 20 mM Tris, 2 M NaCl, pH 8. The fractions containing hMC-CP were collected and stored at -80 °C. The procedures above were mainly performed at 4 °C.

SDS-PAGE and Western blotting analysis

SDS-PAGE was performed on a 15% polyacrylamide gel. The gel was then stained with 0.25% Coomassie brilliant blue R-250

or transferred to polyvinylidene fluoride (PVDF) membranes for Western blotting. The membranes were incubated for 1 h at room temperature in PBS containing 4% BSA and 0.02% Tween-20 in order to prevent nonspecific binding. After incubated with CA5, biotinylated sheep anti-mouse antibody followed by extr-avidin peroxidase was added to the strips. The immunoreactive protein was visualized by DAB.

N-terminal amino acid sequence analysis

Protein was sequenced by automated Edman degradation on a model 491A protein sequencer (Applied Biosystem). Purified protein was applied to a SDS-PAGE. After blotting, the polyvinylidene difluoride membranes were stained with Coomassie brilliant blue R-250, the protein bands of interest were cut out for N-terminal amino acids sequence determination.

Protein assay

Protein concentration was determined using the method of Bradford with the protein assay dye reagent concentrator (Bio-Rad) and bovine serum albumin (BSA) was used as a standard protein.

Enzyme activity assay

In this study, the hMC-CP activity was measured spectrophotometrically by hydrolyzing a substrate of synthesis peptide of hippuryl-L-phenylalanine^[13]. The rate of hydrolysis of hippuryl-L-phenylalanine was determined by measuring the increase in absorbance at 254 nm. The assay mixtures contained 1 mM substrate in 0.05 M Tris-HCl, pH 7.5, 0.5 M NaCl. $\Delta A_{254}/\text{minute}$ from the initial linear portion of the curve was determined. Unit definition: One unit hydrolyzes one micromole of hippuryl-L-phenylalanine per minute at pH 7.5 and 25 °C. Bovine pancreatic CPA (51 U/mg, Sigma) was used as positive control.

RESULTS

RT-PCR amplification of hMC-CP cDNA

RT-PCR was performed with total RNA template extracted from human colon tissues. The PCR product showed a single band about 1 250 bp on 1% agarose gel (Figure 1A).

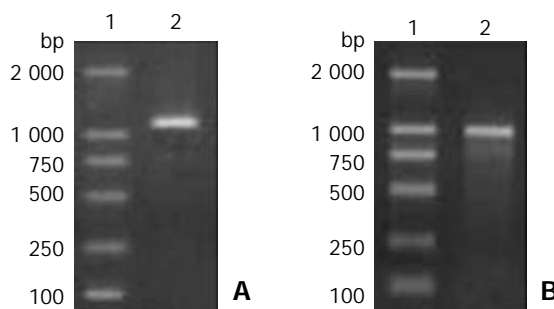


Figure 1 Agarose gel electrophoresis of PCR product. A: hMC-CP cDNA (lane 1: DNA molecular marker; lane 2: hMC-CP cDNA). B: coding region of mature human colon MC-CP cDNA (lane 1: DNA molecular marker; lane 2: PCR product of colon MC-CP cDNA).

DNA sequencing revealed that the human colon MC-CP cDNA had 1 254 bp. The DNA sequence and deduced amino acid sequence of human colon MC-CP are shown in Figure 2. The DNA sequence of human colon MC-CP cDNA was identical to the skin MC-CP except for five nucleotides at the positions 109, 575, 576, 708, 737: C→G, C→T, T→C, A→C, A→T (nucleotide numbering starts from the first codon of mature enzyme). Only the fourth (A1035→C) of the nucleotide differences described above did not represent an altered amino acid residue in the putative protein products. The other 4

```

1  ATC CCA GGC AGG CAC AGC TAC GCA AAA TAC AAT AAT TGG GAA AAG ATT GTG GCT TGG ACT
   I  P  G  R  H  S  Y  A  K  Y  N  N  W  E  K  I  V  A  W  T
61  GAA AAG ATG ATG GAT AAG TAT CCT GAA ATG GTC TCT CGT ATT AAA ATT GGA TCT ACT GTT
   E  K  M  M  D  K  Y  P  E  M  V  S  R  I  K  I  G  S  T  V
121 GAA GAT AAT CCA CTA TAT GTT CTG AAG ATT GGG GAA AAG AAT GAA AGA AGA AAG GCT ATT
   E  D  N  P  L  Y  V  L  K  I  G  E  K  N  E  R  R  K  A  I
181 TTT ATG GAT TGT GGC ATT CAC GCA CGA GAA TGG GTC TCC CCA GCA TTC TGC CAG TGG TTT
   F  M  D  C  G  I  H  A  R  E  W  V  S  P  A  F  C  Q  W  F
241 GTC TAT CAG GCA ACC AAA ACT TAT GGG AGA AAC AAA ATT ATG ACC AAA CTC TTG GAC CGA
   V  Y  Q  A  T  K  T  Y  G  R  N  K  I  M  T  K  L  L  D  R
301 ATG AAT TTT TAC ATT CTT CCT GTG TTC AAT GTT GAT GGA TAT ATT TGG TCA TGG ACA AAG
   M  N  F  Y  I  L  P  V  F  N  V  D  G  Y  I  W  S  W  T  K
361 AAC CGC ATG TGG AGA AAA AAT CGT TCC AAG AAC CAA AAC TCC AAA TGC ATC GGC ACT GAC
   N  R  M  W  R  K  N  R  S  K  N  Q  N  S  K  C  I  G  T  D
421 CTC AAC AGG AAT TTT AAT GCT TCA TGG AAC TCC ATT CCT AAC ACC AAT GAC CCA TGT GCA
   L  N  R  N  F  N  A  S  W  N  S  I  P  N  T  N  D  P  C  A
481 GAT AAC TAT CGG GGC TCT GCA CCA GAG TCC GAG AAA GAG ACG AAA GCT GTC ACT AAT TTC
   D  N  Y  R  G  S  A  P  E  S  E  K  E  T  K  A  V  T  N  F
541 ATT AGA AGC CAC CTG AAT GAA ATC AAG GTT TAC ATC ACC TTC CAT TCC TAC TCC CAG ATG
   I  R  S  H  L  N  E  I  K  V  Y  T  F  H  S  Y  S  Q  M
601 CTA TTG TTT CCC TAT GGA TAT ACA TCA AAA CTG CCA CCT AAC CAT GAG GAC TTG GCC AAA
   L  L  F  P  Y  G  Y  T  S  K  L  P  P  N  H  E  D  L  A  K
661 GTT GCA AAG ATT GGC ACT GAT GTT CTA TCA ACT CGA TAT GAA ACC CGC TAC ATC TAT GGC
   V  A  K  I  G  T  D  L  S  T  R  Y  E  T  R  Y  I  Y  G
721 CCA ATA GAA TCA ACA ATT TAC CCG ATA TCA GGT TCT TCT TTA GAC TGG GCT TAT GAC CTG
   P  I  E  S  T  Y  P  I  S  G  S  S  L  D  W  A  Y  D  L
781 GGC ATC AAA CAC ACA TTT GCC TTT GAG CTC CGA GAT AAA GGC AAA TTT GGT TTT CTC CTT
   G  I  K  H  T  F  A  F  E  L  R  D  K  G  K  F  G  F  L  L
841 CCA GAA TCC CGG ATA AAG CCA ACG TGC AGA GAG ACC ATG CTA GCT GTC AAA TTT ATT GCC
   P  E  S  R  I  K  P  T  C  R  E  T  M  L  A  V  K  F  I  A
901 AAG TAT ATC CTC AAG CAT ACT TCC TAA
   K  Y  I  L  K  H  T  S  stop

```

Figure 2 Nucleotide sequence and deduced amino acid sequences of mature human colon MC-CP. The nucleotide variations and amino acid substitutions different from the skin MC-CP are underlined and boxed, respectively.

nucleotide variations caused 3 amino acid substitutions at the positions 146, 301, 355. The human colon MC-CP had Gly¹⁴⁶, Ile³⁰¹ and Ile³⁵⁵ residues, whereas the skin MC-CP had Arg¹⁴⁶, Thr¹⁴⁶ and Asn³⁵⁵ residues. In contrast, the colon MC-CP cDNA was 100% identical to the lung MC-CP cDNA.

Construction of expression vector

A 924 bp of PCR product was obtained following amplification of the coding region of the mature hMC-CP (Figure 1B). DNA sequencing showed that the recombinant pMAL/hMC-CP and pPIC9K/hMC-CP plasmids had the correct open reading frame coding for 308 amino acids mature polypeptide and no substitutions were introduced by PCR.

Expression of recombinant hMC-CP in *E. coli*

As shown in Figure 3A, a high level of expression of an induced protein of about 80 kDa was achieved after the *E. coli* harbouring expression plasmid pMAL/hMC-CP, which was in agreement with the expected molecular mass of the fusion protein MBP (45 kDa) and hMC-CP (36 kDa). Figure 3B showed a band at about 80 kDa (expected in *E. coli* cells with IPTG induction) reacted to CA5, suggesting that the recombinant protein had a good immunological activity. The best expression of the recombinant protein after IPTG induction was at 23 °C for 16 h (Figure 4). The recombinant products generated by the above procedures were mainly insoluble inclusion body with a small proportion of the soluble recombinant proteins (Figure 5).

In *P. pastoris* expression, 2 colonies resistant to 4.0 mg/ml Geneticin were screened and used for the expression of recombinant protein. There was a substantial quantity of recombinant proteins in cell-free supernatant, and SDS-PAGE showed a major band of approximately 37 kDa (Figure 6A), which reacted to CA5 on Western blot (Figure 6B).

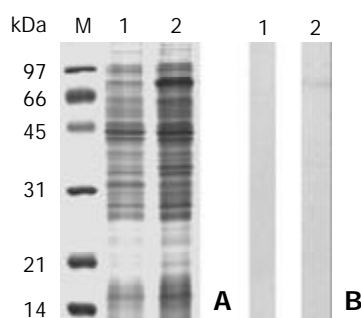


Figure 3 Analysis of recombinant proteins expressed in *E. coli*. A: SDS-PAGE. B: Western blots. M: molecular mass markers; lane 1: without IPTG induction; lane 2: with IPTG induction.

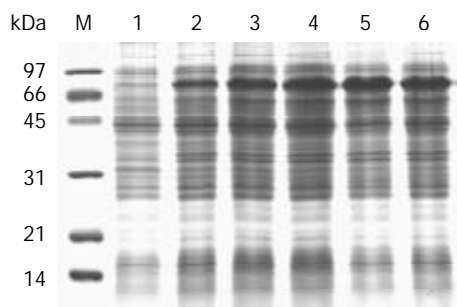


Figure 4 SDS-PAGE analysis of time course of recombinant proteins expressed in *E. coli*. lane 1: before induction; lane 2: 8 h after induction; lane 3: 16 h after induction; lane 4: 24 h after induction; lane 5: 32 h after induction.

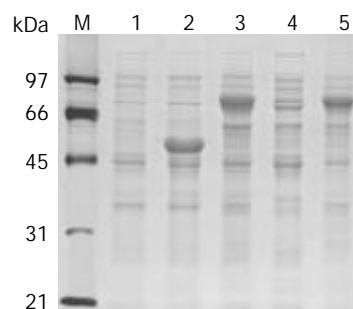


Figure 5 SDS-PAGE analysis of rhMC-CP expressed in *E. coli* TB1 cells. M: molecular weight markers; lane 1: total cellular protein of *E. coli* TB1 cells without IPTG induction; lane 2: total cellular protein of *E. coli* TB1 cells with IPTG induction (control vector); lane 3: total cellular protein of *E. coli* TB1 cells with IPTG induction; lane 4: soluble fraction of cell lysate from *E. coli* TB1 with IPTG induction; lane 5: precipitated fraction of cell lysate from *E. coli* TB1 with IPTG induction.

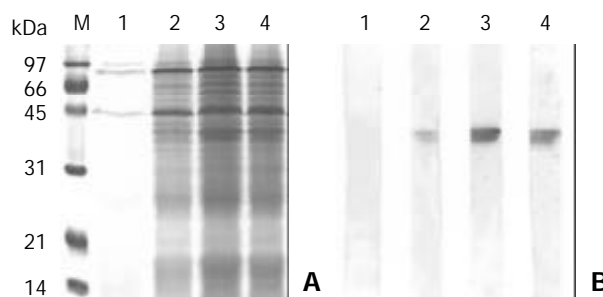


Figure 6 Induction of recombinant HMC-CP expressed in *P. pastoris*. A: secreted proteins analyzed by SDS-PAGE. B: Western blot analysis of secreted proteins with HMC-specific monoclonal antibody, clone CA5. M: molecular weight markers; lane 1: 0 h; lane 2: 24 h; lane 3: 48 h; lane 4: 72 h.

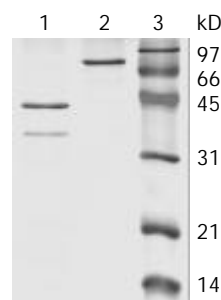


Figure 7 SDS-PAGE analysis of fusion protein cleavage (lane 1: cleaved by factor Xa; lane 2: uncleaved by factor Xa; lane 3: molecular weight marker).

Purification of rhMC-CP

Maltose-binding protein (MBP) was used as a fusion partner to provide a “tag” which could be used for the subsequent purification. The yield of the recombinant fusion protein was 12 mg/L of bacterial culture. The purified fusion protein showed a single protein band of approximately 80 kDa on SDS-PAGE.

After the fusion protein cleavage, SDS-PAGE analysis showed that the fusion protein was completely cleaved by factor Xa (Figure 7). The cleavage mixtures were loaded to heparin agarose, and the target protein showed one band about 36 kDa on SDS-PAGE, which was corresponding to the molecular weight of the native hMC-CP published previously (Figure 8A). About 1.2 mg pure recombinant protein was obtained from 5 mg fusion protein following the above procedures. The Western blot showed that this 36 kDa protein band strongly

reacted to CA5 (Figure 8B), suggesting that the recombinant protein had a good immunology activity. The N-terminal sequence of the purified recombinant protein expressed in *E. coli* was IPGRHSYAKY, and no additional amino acids were found at the N-terminus.

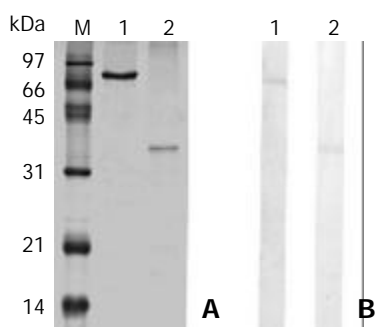


Figure 8 Analysis of purified recombinant protein. A: SDS-PAGE analysis of purified recombinant protein. B: Western blot analysis of purified fusion protein with CA5. Lane 1: purified fusion protein after MBP affinity chromatography; lane 2: purified recombinant hMC-CP after heparin agarose affinity chromatography.

Analysis of enzymatic activity

The purified recombinant hMC-CP expressed in *E. coli* had a very low level of enzymatic activity. In contrast, enzymatic activity in cell-free supernatant of *P. pastoris* culture was 11.7 U/mg secreted protein.

DISCUSSION

A cDNA of human colon hMC-CP was cloned and active enzyme was expressed in the current study, which will offer an essential tool for investigating the functions of hMC-CP, a zinc containing metalloexopeptidase.

Our result revealed that the human colon MC-CP cDNA comprised 1 251 bp, which agreed with the skin and lung mast cell carboxypeptidase^[22,23,26]. The hMC-CP was predicted to be translated as a 417 amino acid preproenzyme which includes a 15 amino acid signal peptide, a 94 amino acid activation peptide and 308 amino acid mature mast cell carboxypeptidase. When comparison of the DNA sequence of human colon MC-CP cDNA with skin MC-CP cDNA, five variations were found which caused 3 amino acid substitutions, but there was not any difference between the human colon and skin MC-CP. The meaning of these variations between tissues in man requires more investigations.

Since the role of hMC-CP in man remains unclear and human mast cells contain large amount of MC-CP, there is a pressing need to investigate the functions of this enzyme. One of the difficulties in investigating the potential functions of MC-CP over the years was that it was uneasy to obtain a substantial quantity of the active enzyme. Purification of MC-CP from human tissues was not only hard to perform, but also difficult to collect enough tissues for purification. Therefore, development of an efficient heterologous expression system for the production of recombinant hMC-CP is an alternative for obtaining a sufficient quantity of hMC-CP. There are a number of options for heterologous recombinant expressions, among them *E. coli* expression system is the most convenient and frequently used, therefore, *E. coli* expression system was used to express hMC-CP. The pMAL-C2x plasmid^[36,37], a vector that allows the fusion of the target protein N-terminus to the MBP tag, made the purification of recombinant proteins much easier.

The extra residue(s) is often added to the C-terminus or N-terminus of recombinant protein. In this study, a pair of

specific primers were designed. The upstream primer contained the sequences for a factor Xa recognition site just before the sequence for N-terminus of hMC-CP, and the downstream primer contained a terminator. The PCR product was inserted into the expression vector pMAL-c2x, which yielded the recombinant protein without extra residues after the fusion protein was cut with factor Xa. The result of N-terminal amino acid sequencing also showed that the N-terminus of recombinant hMC-CP had no extra residue.

After induction with IPTG, the recombinant protein was expressed in *E. coli*, with a molecular weight of about 80 kDa. This was in agreement with the expected molecular mass of the fusion proteins MBP (45 kD) and hMC-CP (36 kD). It was reported that the target gene fused to bacterial gene could improve the expression level and increase the solubility of recombinant proteins^[37]. The expression vector pMAL-2x containing *malE* gene of *E. coli* encoding MBP was used for fusion expression. The target gene was inserted downstream from the *malE* gene, which resulted in the expression of hMC-CP fused to MBP. The solubility of recombinant proteins generally could be increased when the cell culture temperature decreased^[38]. In our case, although the culture temperature was reduced to 23 °C, insoluble recombinant proteins were still the major products. Since purification of recombinant proteins from inclusion body was a complicated process, we only used soluble products to isolate active recombinant hMC-CP.

Fusion protein was purified with one-step affinity chromatography with maltose. Once the fusion protein was isolated, it was necessary to remove the tag. In this study, the linker sequence recognized by factor Xa was designed between the MBP and target protein, because there were no such sequences in MBP and hMC-CP. After the fusion protein cleavage, usually ion exchange chromatography and hydroxyapatite chromatography were used in separating the protein of interest from MBP^[36,39]. But in this study, the recombinant protein was purified by heparin agarose chromatography as MC-MBP could tightly bind to heparin^[40]. In comparison with ion exchange chromatography and hydroxyapatite chromatography, heparin agarose chromatography was simpler and more convenient. Approximately 1.2 mg target protein was obtained from 5 mg fusion protein following the established procedures. N-terminal amino acid sequencing showed that the first 10 amino acids of the recombinant hMC-CP were in good agreement with the human skin and lung MC-CP. Western blotting analysis showed that the recombinant protein had the similar immuno-reactivity with its natural counterpart, indicating that the recombinant hMC-CP could be used as an antigen to produce a specific antibody.

Our studies revealed that the purified recombinant hMC-CP expressed in *E. coli* had a very low level of enzymatic activity to substrate hippuryl-L-phenylalanine. It might be possible that the *E. coli* expression system is a prokaryotic expression system, which can not carry out post-translation modifications. In order to obtain higher levels of enzymatic activity of recombinant hMC-CP, we used *P. pastoris* to express hMC-CP. The enzymatic assay showed that the hMC-CP expressed in *P. asporis* had a relatively high activity (11.7 U/mg secreted protein) towards hippuryl-L-phenylalanine. It is possible that *P. asporis* is an eukaryotic expression system, which has the ability to perform eukaryotic post-translational modifications, such as glycosylation, disulfide bond formation and proteolytic processing^[41]. Our result showed that the supernatant of *P. pastoris* culture had the highest enzymatic activity on the second day after induction by methanol, the enzymatic activity would decrease when induction time increased. It is possible that the secreted recombinant protein was degraded with the increase of induction time.

In conclusion, cDNA encoding human colon MC-CP can

be cloned and expressed in *E.coli* and *P.asptoris*. The expression of recombinant hMC-CP can facilitate its functional study including its role in intestinal diseases.

REFERENCES

- 1 **He SH.** Key role of mast cells and their major secretory products in inflammatory bowel disease. *World J Gastroenterol* 2004; **10**: 309-318
- 2 **Crowe SE,** Luthra GK, Perdue MH. Mast cell mediated ion transport in intestine from patients with and without inflammatory bowel disease. *Gut* 1997; **41**: 785-792
- 3 **Raithel M,** Winterkamp S, Pacurar A, Ulrich P, Hochberger J, Hahn EG. Release of mast cell tryptase from human colorectal mucosa in inflammatory bowel disease. *Scand J Gastroenterol* 2001; **36**: 174-179
- 4 **Stoyanova II,** Gulubova MV. Mast cells and inflammatory mediators in chronic ulcerative colitis. *Acta Histochem* 2002; **104**: 185-192
- 5 **Sasaki Y,** Tanaka M, Kudo H. Differentiation between ulcerative colitis and Crohn's disease by a quantitative immunohistochemical evaluation of T lymphocytes, neutrophils, histiocytes and mast cells. *Pathol Int* 2002; **52**: 277-285
- 6 **Furusu H,** Murase K, Nishida Y, Isomoto H, Takeshima F, Mizuta Y, Hewlett BR, Riddell RH, Kohno S. Accumulation of mast cells and macrophages in focal active gastritis of patients with Crohn's disease. *Hepatogastroenterology* 2002; **49**: 639-643
- 7 **Gelbmann CM,** Mestermann S, Gross V, Kollinger M, Scholmerich J, Falk W. Strictures in Crohn's disease are characterized by an accumulation of mast cells colocalised with laminin but not with fibronectin or vitronectin. *Gut* 1999; **45**: 210-217
- 8 **Nishida Y,** Murase K, Isomoto H, Furusu H, Mizuta Y, Riddell RH, Kohno S. Different distribution of mast cells and macrophages in colonic mucosa of patients with collagenous colitis and inflammatory bowel disease. *Hepatogastroenterology* 2002; **49**: 678-682
- 9 **Schwab D,** Raithel M, Hahn EG. Evidence for mast cell activation in collagenous colitis. *Inflamm Res* 1998; **47**(Suppl 1): S64-65
- 10 **Stenton GR,** Vliangoftis H, Befus AD. Role of intestinal mast cells in modulating gastrointestinal pathophysiology. *Ann Allergy Asthma Immunol* 1998; **81**: 1-11
- 11 **Gui XY.** Mast cells: a possible link between psychological stress, enteric infection, food allergy and gut hypersensitivity in the irritable bowel syndrome. *J Gastroenterol Hepatol* 1998; **13**: 980-989
- 12 **O' Sullivan M,** Clayton N, Breslin NP, Harman I, Bountra C, McLaren A, O' Morain CA. Increased mast cells in the irritable bowel syndrome. *Neurogastroenterol Motil* 2000; **12**: 449-457
- 13 **Goldstein SM,** Kaempfer CE, Kealy JP, Wintroub BU. Human mast cell carboxypeptidase. Purification and characterization. *J Clin Invest* 1989; **83**: 1630-1636
- 14 **Welle M.** Development, significance, and heterogeneity of mast cells with particular regard to the mast cell-specific proteases chymase and tryptase. *J Leukoc Biol* 1997; **61**: 233-245
- 15 **Schechter NM,** Choi JK, Slavin DA, Deresienski DT, Sayama S, Dong G, Lavker RM, Proud D, Lazarus GS. Identification of a chymotrypsin-like proteinase in human mast cells. *J Immunol* 1986; **137**: 962-970
- 16 **Schechter NM,** Irani AM, Sprows JL, Abernethy J, Wintroub B, Schwartz LB. Identification of a cathepsin G-like proteinase in the MCTC type of human mast cell. *J Immunol* 1990; **145**: 2652-2661
- 17 **He SH,** Xie H, He YS. Induction of tryptase and histamine release from human colon mast cells by IgE dependent or independent mechanisms. *World J Gastroenterol* 2004; **10**: 319-322
- 18 **He SH,** Xie H. Modulation of tryptase secretion from human colon mast cells by histamine. *World J Gastroenterol* 2004; **10**: 323-326
- 19 **He SH,** Xie H. Inhibition of tryptase release from human colon mast cells by protease inhibitors. *World J Gastroenterol* 2004; **10**: 332-336
- 20 **He SH,** He YS, Xie H. Activation of human colon mast cells through proteinase activated receptor-2. *World J Gastroenterol* 2004; **10**: 327-331
- 21 **He SH,** Xie H. Modulation of histamine release from human colon mast cells by protease inhibitors. *World J Gastroenterol* 2004; **10**: 337-341
- 22 **Natsuaki M,** Stewart CB, Vanderslice P, Schwartz LB, Natsuaki M, Wintroub BU, Rutter WJ, Golstein SM. Human skin mast cell carboxypeptidase: functional characterization, cDNA cloning, and genealogy. *J Invest Dermatol* 1992; **99**: 138-145
- 23 **Reynolds DS,** Gurley DS, Austen KF. Cloning and characterization of the novel gene for mast cell carboxypeptidase A. *J Clin Invest* 1992; **89**: 273-282
- 24 **Irani AM,** Goldstein SM, Wintroub BU, Bradford T, Schwartz LB. Human mast cell carboxypeptidase. Selective localization to MCTC cells. *J Immunol* 1991; **147**: 247-253
- 25 **Reynolds D,** Gurley DS, Stevens RL, Sugarbaker DJ, Austen KF, Serafin WE. Cloning of cDNAs that encode human mast cell carboxypeptidase A, and comparison of the protein with mouse mast cell carboxypeptidase A and rat pancreatic carboxypeptidases. *Proc Natl Acad Sci U S A* 1989; **86**: 9480-9484
- 26 **He SH,** Walls AF. The induction of a prolonged increase in microvascular permeability by human mast cell chymase. *Eur J Pharmacol* 1998; **352**: 91-98
- 27 **He SH,** Peng Q, Walls AF. Potent induction of a neutrophil and eosinophil-rich infiltrate *in vivo* by human mast cell tryptase: selective enhancement of eosinophil recruitment by histamine. *J Immunol* 1997; **159**: 6216-6225
- 28 **He SH,** Walls AF. Human mast cell chymase induces the accumulation of neutrophils, eosinophils and other inflammatory cells *in vivo*. *Br J Pharmacol* 1998; **125**: 1491-1500
- 29 **He SH,** Gaca MD, Walls AF. A role for tryptase in the activation of human mast cells: modulation of histamine release by tryptase and inhibitors of tryptase. *J Pharmacol Exp Ther* 1998; **286**: 289-297
- 30 **He SH,** Gaca MD, Walls AF. The activation of synovial mast cells: modulation of histamine release by tryptase and chymase and their inhibitors. *Eur J Pharmacol* 2001; **412**: 223-229
- 31 **Tomimori Y,** Tsuruoka N, Fukami H, Saito K, Horikawa C, Saito M, Muto T, Sugiura N, Yamashiro K, Sumida M, Kakutani S, Fukuda Y. Role of mast cell chymase in allergen-induced biphasic skin reaction. *Biochem Pharmacol* 2002; **64**: 1187
- 32 **Dell' Italia LJ,** Husain A. Dissecting the role of chymase in angiotensin II formation and heart and blood vessel diseases. *Curr Opin Cardiol* 2002; **17**: 374-379
- 33 **Tomimori Y,** Muto T, Fukami H, Saito K, Horikawa C, Tsuruoka N, Saito M, Sugiura N, Yamashiro K, Sumida M, Kakutani S, Fukuda Y. Chymase participates in chronic dermatitis by inducing eosinophil infiltration. *Lab Invest* 2002; **82**: 789-794
- 34 **Leskinen MJ,** Lindstedt KA, Wang Y, Kovanen PT. Mast cell chymase induces smooth muscle cell apoptosis by a mechanism involving fibronectin degradation and disruption of focal adhesions. *Arterioscler Thromb Vasc Biol* 2003; **23**: 238-243
- 35 **Buckley MG,** Variend S, Walls AF. Elevated serum concentrations of beta-tryptase, but not alpha-tryptase, in Sudden Infant Death Syndrome (SIDS). An investigation of anaphylactic mechanisms. *Clin Exp Allergy* 2001; **31**: 1696-1704
- 36 **Riggs P.** Expression and purification of recombinant proteins by fusion to maltose-binding protein. *Mol Biotechnol* 2000; **15**: 51-63
- 37 **Lazos SA,** Tsiftoglou AS. Production and purification of recombinant human cytokines (rhIL-4, rhGM-CSF and rhIL-1beta) from generically engineered *E.coli* cells bearing pMAL expression vector constructs. *J Protein Chem* 1998; **17**: 517-519
- 38 **Schein CH.** Optimizing protein folding to the native state in bacteria. *Curr Opin Biotechnol* 1991; **2**: 746-750
- 39 **Ding Y,** Qin L, Kottenko SV, Pestka S, Bromberg JS. A single amino acid determines the immunostimulatory activity of interleukin 10. *J Exp Med* 2000; **191**: 213-224
- 40 **Goldstein SM,** Leong J, Schwartz LB, Cooke D. Protease composition of exocytosed human skin mast cell protease-proteoglycan complexes. Tryptase resides in a complex distinct from chymase and carboxypeptidase. *J Immunol* 1992; **148**: 2475-2482
- 41 **Cereghino JL,** Cregg JM. Heterologous protein expression in the methylotrophic yeast *Pichia pastoris*. *FEMS Microbiol Rev* 2000; **24**: 45-66

Apoptosis of human gastric adenocarcinoma cells induced by β -ionone

Jia-Ren Liu, Bing-Qing Chen, Bao-Feng Yang, Hong-Wei Dong, Chang-Hao Sun, Qi Wang, Guo Song, You-Qiang Song

Jia-Ren Liu, Bing-Qing Chen, Hong-Wei Dong, Chang-Hao Sun, Qi Wang, Public Health College, Harbin Medical University, Harbin 150001, Heilongjiang Province, China

Bao-Feng Yang, Guo Song, Department of Pharmacology, Harbin Medical University, Harbin 150086, Heilongjiang Province, China

You-Qiang Song, Department of Biochemistry and The Genome Research Center, The University of Hong Kong, Hong Kong, China

Supported by The National Natural Science Foundation of China, No. 30200229 and The Postdoctoral Foundations of China and Heilongjiang Province, China

Correspondence to: Dr. Bao-Feng Yang, Department of Pharmacology, Harbin Medical University, Harbin 150086, Heilongjiang Province, China. jiarl@ems.hrbmu.edu.cn

Telephone: +86-451-53641309 **Fax:** +86-451-53648617

Received: 2003-08-26 **Accepted:** 2003-10-12

Abstract

AIM: To investigate the effect of β -ionone on the growth and apoptosis of gastric adenocarcinoma cell line SGC-7901.

METHODS: Using MTT, fluorescence dye (Hoechst-33258), transmission electron microscopy and the TUNEL assay, we examined growth and apoptosis of SGC-7901 cells treated with β -ionone at various concentrations (*i.e.* 25, 50, 100 and 200 $\mu\text{mol/L}$) for 24 h, 48 h.

RESULTS: The growth of SGC-7901 cells was inhibited by β -ionone. Seven days after treatment with β -ionone at four concentrations, the inhibition rates were 12.04%, 30.59%, 78.25% and 94.15%, respectively. The IC_{50} value of β -ionone for SGC-7901 cells was estimated to be 89 $\mu\text{mol/L}$. The apoptotic morphology was demonstrated in SGC-7901 cells treated with β -ionone by Hoechst-33258 staining and electron microscopy. Apoptosis was also shown in β -ionone-treated SGC-7901 cells by the TUNEL assay.

CONCLUSION: β -ionone can inhibit cell proliferation and induce apoptosis of SGC-7901 cells. However, the mechanism needs to be further investigated.

Liu JR, Chen BQ, Yang BF, Dong HW, Sun CH, Wang Q, Song G, Song YQ. Apoptosis of human gastric adenocarcinoma cells induced by β -ionone. *World J Gastroenterol* 2004; 10(3):348-351
<http://www.wjgnet.com/1007-9327/10/348.asp>

INTRODUCTION

Following the dietary guidelines^[1,2] that emphasize the importance of fruits, vegetables and grains could lead to an estimated 35% reduction in cancer deaths^[3], fruits, vegetables and grains are potential sources of anticarcinogenic agents^[4-11], such as nondigestible carbohydrates and micronutrients including β -ionone, ascorbic acid, γ -tocopherol, isoprenoids and folic acid. Epidemiological evidence suggested that intake of these constituents could lead to a reduced risk of chronic diseases such as cancer and cardiovascular disorders^[3,12-14]. β -ionone, enriched in many fruits, vegetables and grains, is a

common intermediate product of up to 22 000 isoprenoids^[15] and could exert potent anticarcinogenic and antitumor activities at the pharmacological level^[16,17]. It has been documented that β -ionone could suppress the proliferation of melanoma, breast cancer and meningioma cells^[18-21]. β -ionone has also been shown to have an effect on apoptosis of vascular endothelial cells^[22] and tumor cells^[23,24]. Although its exact mechanisms are not clear, the inhibitory effect of β -ionone on the proliferation of rapidly dividing cells has been demonstrated. In many instances, growth inhibition following terminal differentiation or anticancer drug treatment results in apoptosis.

Gastric cancer is one of the most frequent neoplasms in China and some other parts of the world^[25-33]. Chemoprevention is always used as the main treatment for advanced cancer, and has been under intense investigation^[34-49]. Understanding the mechanisms through which β -ionone suppresses the proliferation of gastric adenocarcinoma cells could provide a way to prevent this disease in general population. Therefore, in this study, we explored whether and how β -ionone induced apoptosis of human gastric adenocarcinoma cells.

MATERIALS AND METHODS

β -ionone

β -ionone, 4-(2, 6, 6-trimethyl-1-cyclohexenyl)-3-buten-2-one with >95 % purity, was purchased from Sigma (USA). It was dissolved in absolute ethanol and diluted to the following concentrations: 25, 50, 100 and 200 $\mu\text{mol/L}$.

Cell culture

Human gastric adenocarcinoma cell line, SGC-7901 (Cancer Research Institute of Beijing, China), was cultured in RPMI 1640 medium (pH 7.2-7.4), supplemented with fetal calf serum 10%, penicillin (100 U/ml) and streptomycin (100 $\mu\text{g/ml}$) at 37 °C with a humidified atmosphere of 5% CO_2 . The cells were sub-cultured with a mixture of ethylenedinitrile tetracetic acid (EDTA) and trypsin (Sigma).

MTT assay for determination of cell growth

SGC-7901 cells were seeded in eight 96-well plates, each well containing 3.0×10^3 cells. After 24 h, different concentrations of β -ionone were added with. On the next day, 0.05 mL of 1.0 mg/ml 3-(4,5-dimethylthiazole-2-yl)-2,5-diphenyltetrazolium bromide (MTT, Sigma) was added to one of the eight plates. After 4 h, culture media were discarded followed by addition of 0.2 ml dimethyl sulfoxide (DMSO) and vibration for 2 min. The absorbance was measured at 570 nm using a model 550 microplate Reader. β -ionone concentration required to inhibit the net increase in the 48 h cell count by 50 % (IC_{50}) was calculated based on the plots of data from three or more evaluations. The means were obtained on each of seven days and used to draw a curve of cell proliferation. The inhibitory rates (IR) on the 7th day were calculated as follows:

$$\text{IR}(\%) = \frac{\text{Total absorbance in negative control (7 d)} - \text{Total absorbance in the tested group (7 d)}}{\text{Total absorbance in negative control (7 d)}} \times 100\%$$

Hoechst-33258 staining for determination of morphological changes of apoptotic cells

Morphological changes of apoptotic cells were determined by fluorescence microscopy. Briefly, the cells were collected and fixed in 100% ethanol, stained with 0.5 mmol/L Hoechst-33258 (Sigma) for 3 min at 37 °C, then visualized under a fluorescence microscope with ultraviolet (UV) excitation at 300-500 nm. The cells with nuclei containing condensed chromatin or cells with fragmented nuclei were defined as apoptotic cells.

Observation of apoptotic cells with transmission electron microscopy

The cultured SGC-7901 cells treated with β -ionone at different concentrations were scraped off and harvested. Subsequently, the cells were immersed with Epon 821, embedded in capsules and converged at 60 °C for 72 h, and then ultrathin sections (60 nm) were prepared and stained with uranyl acetate and lead citrate. The ultrastructure of cells was examined by transmission electron microscopy.

TUNEL assay for determination of apoptosis cells

The TUNEL reaction could preferentially label DNA strand

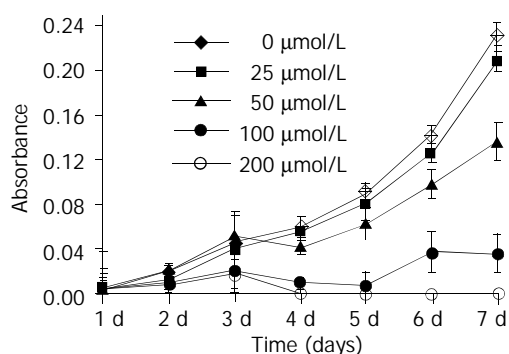


Figure 1 Proliferation kinetics of SGC-7901 cells treated with β -ionone at various concentrations.

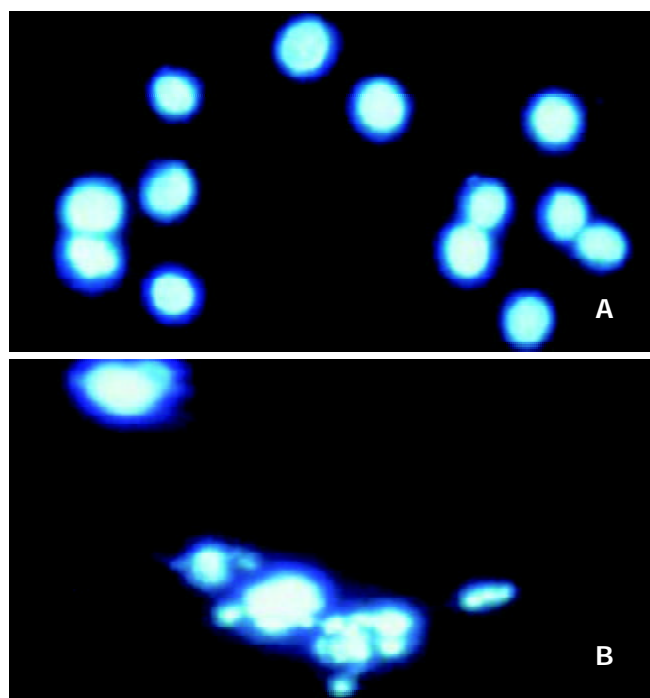


Figure 2 β -ionone-induced apoptosis in SGC-7901 cells stained with Hoechst-33258 ($\times 400$). A: control SGC-7901 cells, B: experimental cells treated with β -ionone showing nuclear shrinkage or fragmentation.

breaks generated during apoptosis, and allow discrimination of apoptosis from necrosis and primary DNA strand breaks induced by cancer chemoprevention agents. SGC-7901 cells were treated for 24 h and 48 h with β -ionone at various concentrations and collected by centrifugation. Specimens were fixed immediately in 4% formaldehydum polymerisatum and embedded in paraffin. Apoptosis of SGC-7901 cells was evaluated by using an *in situ* cell death detection kit (Roche Co. Ltd, Germany). The sections were deparaffinized in xylene and rehydrated through graded alcohol, treated with proteinase K and then 0.3% H_2O_2 , labeled with fluorescein dUTP in a humidified box for 1 h at 37 °C. The cells were then combined with POD-horseradish peroxidase, colorized with diaminobenzidine tetrahydrochloride (DAB). Controls consisted of omission of fluorescein dUTP. Cells were visualized under a light microscope. The apoptotic index (AI) was calculated as follows: $\text{AI} = (\text{number of apoptotic cells} / \text{total number counted}) \times 100\%$.

Statistical analysis

Data were expressed as mean \pm SD. Analysis of data was performed using the Student's *t* test or one-way ANOVA. $P < 0.05$ was considered as statistically significant.

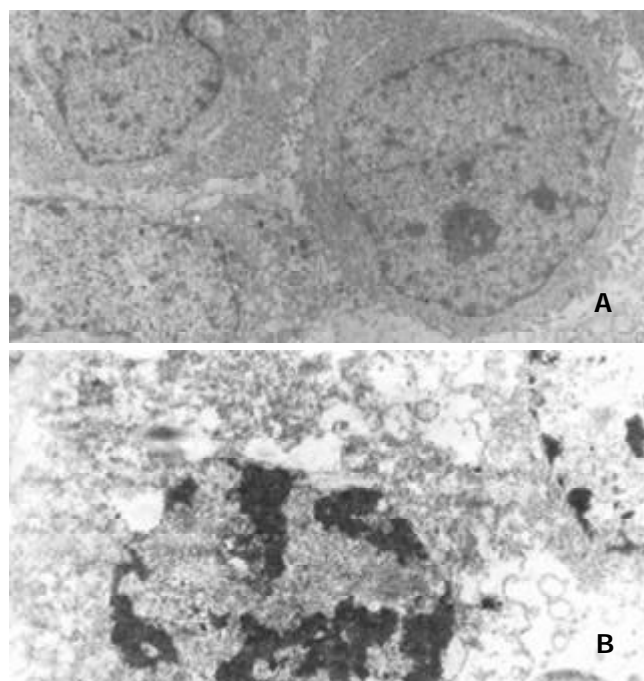


Figure 3 Ultrastructural changes of SGC-7901 cells treated with 100 $\mu\text{mol/L}$ β -ionone for 24 h ($\times 15000$). A: SGC-7901 cells in the control group, B: experimental SGC-7901 cells treated with β -ionone showing early changes of apoptosis in which nuclear chromatin condensation and cell shrinkage were observed.

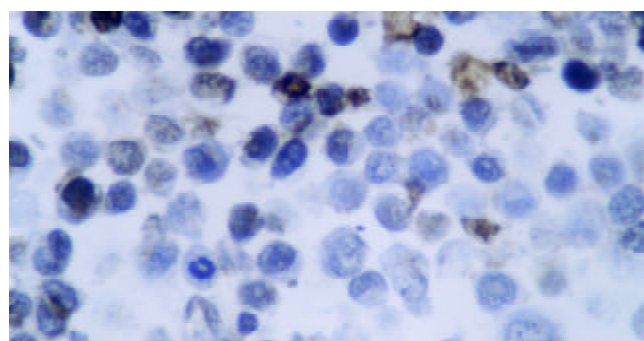


Figure 4 Apoptotic cells induced by β -ionone (200 $\mu\text{mol/L}$ 48 h) in SGC-7901 cells detected TUNEL assay ($\times 400$).

RESULTS

Inhibition of SGC-7901 cell proliferation by β -ionone

SGC-7901 cells were treated with β -ionone at various concentrations for 1-7 days, and the cell viability was determined as described above by MTT assay. As shown in Figure 1, β -ionone inhibited the growth of gastric adenocarcinoma cells in a dose- and time-dependent manner. The growth of the cells treated with β -ionone at concentrations of 100 and 200 $\mu\text{mol/L}$ was significantly slower than that of the negative control within 7 days ($P < 0.05$). SGC-7901 cells incubated with 25 and 50 $\mu\text{mol/L}$ of β -ionone grew slower, albeit not significantly than the negative control. β -ionone at 100 $\mu\text{mol/L}$ and 200 $\mu\text{mol/L}$ had an inhibitory effect of more than 90% on tumor cell growth 3 days after treatment. The inhibitory rate at the four progressively increasing concentrations of β -ionone was 12.04%, 30.59%, 78.25% and 94.15% 7 days after treatment. The IC_{50} value for β -ionone was estimated to be 89 $\mu\text{mol/L}$.

Morphological changes of apoptotic SGC-7901 cells treated with β -ionone

SGC-7901 cells in the negative control group exhibited a round shape, clear edge and homogeneous staining (Figure 2A). However, after 24 h and 48 h exposure to β -ionone, SGC-7901 cells began to show morphologic features of apoptosis, such as cell shrinkage, chromatin condensation and nuclear pyknosis (Figure 2B). The ultrastructural changes were observed by electron microscopy showing early changes of apoptosis including nuclear chromatin condensation and cell shrinkage (Figures 3A & 3B).

Apoptosis detected by TUNEL assay in SGC-7901 cells treated with β -ionone

The cells with positive staining in the nuclei were defined as apoptotic cells (Figure 4). The results showed that after treatment of SGC-7901 cells with β -ionone at different concentrations for 24 h and 48 h, the AIs were significantly increased in a dose- and time-dependent manner (Table 1).

Table 1 Apoptotic index (AI) of SGC-7901 cells treated by β -ionone

β -ionone ($\mu\text{mol/L}$)	AI (%) ^a	
	24 h	48 h
0	0.15 \pm 0.087	-
25	0.12 \pm 0.03	0.87 \pm 0.23 ^b
50	0.47 \pm 0.15	3.43 \pm 1.00 ^b
100	1.67 \pm 0.53 ^{b,c}	8.50 \pm 19.2 ^{b,c}
200	4.78 \pm 1.32 ^{b,c,d}	11.85 \pm 3.83 ^{b,c,d}

a: X experiments were performed and Y cells were counted in each experiment, b: $P < 0.05$, comparison between 24 h and 48 h, c: $P < 0.05$ compared with negative control, d: $P < 0.05$ as determined by one-way ANOVA.

DISCUSSION

Epidemiologic studies have revealed a strong inverse association between frequency of intake of plant-derived foods and cancer incidence^[3]. β -ionone, widely distributed in fruits and vegetables, has been found to be a common intermediate product of up to 22 000 isoprenoids^[15] and many other phytochemicals. It could exert broad and potent anticarcinogenic and antitumor activities when fed at pharmacological levels. β -ionone could also suppress the proliferation of melanoma and breast cancer cells^[16-18]. However, the effects of β -ionone on gastric adenocarcinoma cells have not been reported.

Isoprenoid-mediated suppression of cell growth is clearly independent of a mutated *ras* function. β -ionone could suppress

the proliferation of B16 and HL-60 cells that express *ki-ras* and *n-ras*, respectively. The study from Mo *et al*^[16] showed that β -ionone also suppressed the proliferation of Caco-2 and MCF-7 cells which express wild-type *ras*. The action, like that of lovastatin, is independent of *ras* function. Both β -ionone and lovastatin can arrest HL-60 promyelocytic leukemia cells in the G_1 phase of the cell cycle in a concentration-dependent manner. The present study demonstrated that β -ionone inhibited the growth of human gastric adenocarcinoma SGC-7901 cells in a dose- and time-dependent manner. The inhibition rates were 12.04%, 30.59%, 78.25% and 94.15% 7 days after treatment with β -ionone at 25, 50, 100 and 200 $\mu\text{mol/L}$, respectively. The IC_{50} value for β -ionone was estimated to be 89 $\mu\text{mol/L}$.

Apoptosis, also known as programmed cell death, is a natural process of cell suicide which plays a critical role in the development and homeostasis of metazoans^[50,51]. It is a complex process regulated by a variety of factors such as Bcl-2^[52], Fas^[53] and p53^[54]. The isoprenoid-mediated initiation of apoptosis might be independent of a mutated p53 function. β -ionone could initiate apoptosis in B16 and MCF-7 cells which express wild type p53 and in Caco-2 cells which express mutated p53 as well as in p53-null HL-60 cells^[55]. However, whether β -ionone has any effect on the other apoptotic pathways in cancer cells is not understood.

In conclusion, β -ionone can inhibit cell growth and proliferation and induce apoptosis of SGC-7901 cells. However, the mechanism by which β -ionone blocks cell proliferation and induces apoptosis of SGC-7901 cells needs to be further investigated.

ACKNOWLEDGEMENT

We thank Dr. Dong-Yan Jin for critically reading and revising the manuscript.

REFERENCES

- 1 Shikany JM, White GL Jr. Dietary guidelines for chronic disease prevention. *South Med J* 2000; **93**: 1138-1151
- 2 Kant AK, Schatzkin A, Graubard BI, Schairer C. A prospective study of diet quality and mortality in women. *JAMA* 2000; **283**: 2109-2115
- 3 Block G, Patterson B, Subar A. Fruit, vegetables, and cancer prevention: a review of the epidemiological evidence. *Nutr Cancer* 1992; **18**: 1-29
- 4 Jaga K, Duvvi H. Risk reduction for DDT toxicity and carcinogenesis through dietary modification. *J R Soc Health* 2001; **121**: 107-113
- 5 Witte JS, Longnecker MP, Bird CL, Lee ER, Frankl HD, Haile RW. Relation of vegetable, fruit, and grain consumption to colorectal adenomatous polyps. *Am J Epidemiol* 1996; **144**: 1015-1025
- 6 Elson CE. Suppression of mevalonate pathway activities by dietary isoprenoids: protective roles in cancer and cardiovascular disease. *J Nutr* 1995; **125**(6 Suppl): 1666S-1672S
- 7 Elson CE, Yu SG. The chemoprevention of cancer by mevalonate-derived constituents of fruits and vegetables. *J Nutr* 1994; **124**: 607-614
- 8 Huang C, Huang Y, Li J, Hu W, Aziz R, Tang MS, Sun N, Cassidy J, Stoner GD. Inhibition of benzo(a)pyrene diol-epoxide-induced transactivation of activated protein 1 and nuclear factor kappaB by black raspberry extracts. *Cancer Res* 2002; **62**: 6857-6863
- 9 Serafini M, Bellocco R, Wolk A, Ekstrom AM. Total antioxidant potential of fruit and vegetables risk of gastric cancer. *Gastroenterology* 2002; **123**: 985-991
- 10 Pandey M, Shukla VK. Diet and gallbladder cancer: a case-control study. *Eur J Cancer Prev* 2002; **11**: 365-368
- 11 Devasena T, Menon VP. Enhancement of circulatory antioxidants by fenugreek during 1,2-dimethylhydrazine-induced rat colon carcinogenesis. *J Biochem Mol Biol Biophys* 2002; **6**: 289-292
- 12 Michaud DS, Pietinen P, Taylor PR, Virtanen M, Virtamo J, Albanes D. Intakes of fruits and vegetables, carotenoids and vitamins A, E, C in relation to the risk of bladder cancer in the

- ATBC cohort study. *Br J Cancer* 2002; **87**: 960-965
- 13 **Ito LS**, Inoue M, Tajima K, Yamamura Y, Kodera Y, Hirose K, Takezaki T, Hamajima N, Kuroishi T, Tominaga S. Dietary factors and the risk of gastric cancer among Japanese women. a comparison between the differentiated and non-differentiated subtypes. *Ann Epidemiol* 2003; **13**: 24-31
- 14 **Willett WC**. Balancing life-style and genomics research for disease prevention. *Science* 2002; **296**: 695-698
- 15 **Bach TJ**. Some new aspects of isoprenoid biosynthesis in plants-a review. *Lipids* 1995; **30**: 191-202
- 16 **Mo H**, Elson CE. Apoptosis and cell-cycle arrest in human and murine tumor cells are initiated by isoprenoids. *J Nutr* 1999; **129**: 804-813
- 17 **Yu SG**, Anderson PJ, Elson CE. Efficacy of β -ionone in the chemoprevention of rat mammary carcinogenesis. *J Agric Food Chem* 1995; **43**: 2144-2147
- 18 **He L**, Mo H, Hadisusilo S, Qureshi AA, Elson CE. Isoprenoids suppress the growth of murine B16 melanomas *in vitro* and *in vivo*. *J Nutr* 1997; **127**: 668-674
- 19 **Riebeling C**, Forsea AM, Raisova M, Orfanos CE, Geilen CC. The bisphosphonate pamidronate induces apoptosis in human melanoma cells *in vitro*. *Br J Cancer* 2002; **87**: 366-371
- 20 **Tatman D**, Mo H. Volatile isoprenoid constituents of fruits, vegetables and herbs cumulatively suppress the proliferation of murine B16 melanoma and human HL-60 leukemia cells. *Cancer Lett* 2002; **175**: 129-139
- 21 **Johnson MD**, Woodard A, Okediji EJ, Toms SA, Allen GS. Lovastatin is a potent inhibitor of meningioma cell proliferation: evidence for inhibition of a mitogen associated protein kinase. *J Neurooncol* 2002; **56**: 133-142
- 22 **Newton CJ**, Xie YX, Burgoyne CH, Adams I, Atkin SL, Abidia A, McCollum PT. Fluvastatin induces apoptosis of vascular endothelial cells: blockade by glucocorticoids. *Cardiovasc Surg* 2003; **11**: 52-60
- 23 **Elson CE**, Peffley DM, Hentosh P, Mo H. Isoprenoid-mediated inhibition of mevalonate synthesis: potential application to cancer. *Proc Soc Exp Biol Med* 1999; **221**: 294-311
- 24 **Burke YD**, Ayoubi AS, Werner SR, McFarland BC, Heilman DK, Ruggeri BA, Crowell PL. Effects of the isoprenoids perillyl alcohol and farnesol on apoptosis biomarkers in pancreatic cancer chemoprevention. *Anticancer Res* 2002; **22**: 3127-3134
- 25 **Ding Y**, Le XP, Zhang QX, Du P. Methylation and mutation analysis of p16 gene in gastric cancer. *World J Gastroenterol* 2003; **9**: 423-426
- 26 **Guo HQ**, Guan P, Shi HL, Zhang X, Zhou BS, Yuan Y. Prospective cohort study of comprehensive prevention to gastric cancer. *World J Gastroenterol* 2003; **9**: 432-436
- 27 **Tovey FI**, Hobsley M. Post-gastrectomy patients need to be followed up for 20-30 years. *World J Gastroenterol* 2000; **6**: 45-48
- 28 **Morgner A**, Miehke S, Stolte M, Neubauer A, Alpen B, Thiede C, Klann H, Hierlmeier FX, Ell C, Ehninger G, Bayerdorffer E. Development of early gastric cancer 4 and 5 years after complete remission of *Helicobacter pylori* associated gastric low grade marginal zone B cell lymphoma of MALT type. *World J Gastroenterol* 2001; **7**: 248-253
- 29 **Niu WX**, Qin XY, Liu H, Wang CP. Clinicopathological analysis of patients with gastric cancer in 1200 cases. *World J Gastroenterol* 2001; **7**: 281-284
- 30 **Xin Y**, Li XL, Wang YP, Zhang SM, Zheng HC, Wu DY, Zhang YC. Relationship between phenotypes of cella-function differentiation and pathobiological behavior of gastric carcinomas. *World J Gastroenterol* 2001; **7**: 53-59
- 31 **Yao YL**, Xu B, Song YG, Zhang WD. Overexpression of cyclin E in Mongolian gerbil with *Helicobacter pylori*-induced gastric precancerosis. *World J Gastroenterol* 2002; **8**: 60-63
- 32 **Deng DJ**. progress of gastric cancer etiology: N-nitrosamides 1999s. *World J Gastroenterol* 2000; **6**: 613-618
- 33 **Cao WX**, Ou JM, Fei XF, Zhu ZG, Yin HR, Yan M, Lin YZ. Methionine-dependence and combination chemotherapy on human gastric cancer cells *in vitro*. *World J Gastroenterol* 2002; **8**: 230-232
- 34 **Oliveira CPMS**, Kassab P, Lopasso FP, Souza HP, Janiszewski M, Laurindo FRM, Iriya K, Laudanna AA. Protective effect of ascorbic acid in experimental gastric cancer: reduction of oxidative stress. *World J Gastroenterol* 2003; **9**: 446-448
- 35 **Chen C**, Liu FK, Qi XP, Li JS. The study of chemiluminescence in gastric and colonic carcinoma cell lines treated by anti-tumor drugs. *World J Gastroenterol* 2003; **9**: 242-245
- 36 **Zhou HB**, Zhu JR. Paclitaxel induces apoptosis in human gastric carcinoma cells. *World J Gastroenterol* 2003; **9**: 442-445
- 37 **Wu YL**, Sun B, Zhang XJ, Wang SN, He HY, Qiao MM, Zhong J, Xu JY. Growth inhibition and apoptosis induction of Sulindac on Human gastric cancer cells. *World J Gastroenterol* 2001; **7**: 796-800
- 38 **Liu S**, Wu Q, Chen ZM, Su WJ. The effect pathway of retinoic acid through regulation of retinoic acid receptor α in gastric cancer cells. *World J Gastroenterol* 2001; **7**: 662-666
- 39 **Wang X**, Lan M, Shi YQ, Lu J, ZhongYX, Wu HP, Zai HH, Ding J, Wu KC, Pan BR, Jin JP, Fan DM. Differential display of vincristine-resistance-related genes in gastric cancer SGC7901 cell. *World J Gastroenterol* 2002; **8**: 54-59
- 40 **Wang X**, Liu FK, Li X, Li JS, Xu GX. Inhibitory effect of endostatin expressed by human liver carcinoma SMMC7721 on endothelial cell proliferation *in vitro*. *World J Gastroenterol* 2002; **8**: 253-257
- 41 **Xu CT**, Huang LT, Pan BR. Current gene therapy for stomach carcinoma. *World J Gastroenterol* 2001; **7**: 752-759
- 42 **Chen BQ**, Xue YB, Liu JR, Yang YM, Zheng YM, Wang XL, Liu RH. Inhibition of conjugated linoleic acid on mouse forestomach neoplasia induced by benzo(a)pyrene and chemopreventive mechanisms. *World J Gastroenterol* 2003; **9**: 44-49
- 43 **Liu JR**, Chen BQ, Yang YM, Wang XL, Xue YB, Zheng YM, Liu RH. Effect of apoptosis on gastric adenocarcinoma cell line SGC-7901 induced by *cis*-9,*trans*-11- conjugated linoleic acid. *World J Gastroenterol* 2002; **8**: 999-1004
- 44 **Li Y**, Lu YY. Applying a highly specific and reproducible cDNA RDA method to clone garlic up-regulated genes in human gastric cancer cells. *World J Gastroenterol* 2002; **8**: 213-216
- 45 **Wu K**, Li Y, Zhao Y, Shan YJ, Xia W, Yu WP, Zhao L. Roles of Fas signaling pathway in vitamin E succinate-induced apoptosis in human gastric cancer SGC-7901 cells. *World J Gastroenterol* 2002; **8**: 982-986
- 46 **Liu JR**, Li BX, Chen BQ, Han XH, Xue YB, Yang YM, Zheng YM, Liu RH. Effect of *cis*-9, *trans*-11-conjugated linoleic acid on cell cycle of gastric adenocarcinoma cell line (SGC-7901). *World J Gastroenterol* 2002; **8**: 224-229
- 47 **Xu AG**, Li SG, Liu JH, Gan AH. Function of apoptosis and expression of the proteins Bcl-2, p53 and C-myc in the development of gastric cancer. *World J Gastroenterol* 2001; **7**: 403-406
- 48 **Gao F**, Yi J, Shi GY, Li H, Shi XG, Tang XM. The sensitivity of digestive tract tumor cells to As_2O_3 is associated with the inherent cellular level of reactive oxygen species. *World J Gastroenterol* 2002; **8**: 36-39
- 49 **Morse MA**, Stoner GD. Cancer chemoprevention: principles and prospects. *Carcinogenesis* 1993; **14**: 1737-1746
- 50 **Green DR**, Reed JC. Mitochondria and apoptosis. *Science* 1998; **281**: 1309-1312
- 51 **Ashkenazi A**, Dixit VM. Apoptosis control by death and decoy receptors. *Curr Opin Cell Biol* 1999; **11**: 255-260
- 52 **Wang NS**, Vnkila MT, Reineks EZ, Distelhorst CW. Transient expression of wild-type or mitochondrially targeted Bcl-2 induces apoptosis, whereas transient expression of endoplasmic reticulum-targeted Bcl-2 is protective against Bax-induced cell death. *J Biol Chem* 2001; **276**: 44117-44128
- 53 **Luschen S**, Ussat S, Scherer G, Kabelitz D, Adam-Klages S. Sensitization to death receptor cytotoxicity by inhibition of fas-associated death domain protein (FADD)/caspase signaling. Requirement of cell cycle progression. *J Biol Chem* 2000; **275**: 24670-24678
- 54 **Marchenko ND**, Zaika A, Moll UM. Death signal-induced localization of p53 protein to mitochondria. A potential role in apoptotic signaling. *J Biol Chem* 2000; **275**: 16202-16212
- 55 **David-Pfeuty T**, Chakrani F, Ory K, Nouvian-Dooghe Y. Cell cycle-dependent regulation of nuclear p53 traffic occurs in one subclass of human tumor cells and in untransformed cells. *Cell Growth Differ* 1996; **7**: 1211-1225

Expression and significance of VEGF-C and FLT-4 in gastric cancer

Xing-E Liu, Xiao-Dong Sun, Jin-Min Wu

Xing-E Liu, Jin-Min Wu, Center of Oncology, the Affiliated Sir Run Run Shaw Hospital, Medical College, Zhejiang University, Hangzhou 310016, Zhejiang Province, China

Xiao-Dong Sun, Department of General Surgery, the Affiliated Sir Run Run Shaw Hospital, Medical College, Zhejiang University, Hangzhou 310016, Zhejiang Province, China

Correspondence to: Dr. Xing-E Liu, Center of Oncology, the Affiliated Sir Run Run Shaw Hospital, Medical College, Zhejiang University, Hangzhou 310016, Zhejiang Province, China. xingel001@yahoo.com

Telephone: +86-571-86090073 **Fax:** +86-571-86044817

Received: 2003-08-05 **Accepted:** 2003-09-01

Abstract

AIM: To investigate the expression of pathological factors of VEGF-C and its receptor FLT-4 in primary gastric cancer and adjacent normal tissues.

METHODS: The expression of VEGF-C and FLT-4 was studied in 80 primary gastric cancers and adjacent normal tissues from the same patients by semi-quantitative reverse transcriptase-polymerase chain reaction (RT-PCR) and immunohistochemistry.

RESULTS: Both primary gastric cancer and adjacent normal tissue could express VEGF-C and FLT-4, and FLT-4 expression was also detected in endothelial cells of stromal blood vessels and lymphatic vessels. There was a significant difference in expression of VEGF-C between primary tumor and adjacent normal tissue samples ($P=0.01$), and a statistical correlation between VEGF-C and FLT-4 expression in tumors ($P=0.00886$). With regard to VEGF-C expression, there was a significant difference between moderate-poor differential type and high differential type ($P=0.032$), and a significant difference between positive and negative lymph node metastases ($P=0.024$). However, there was no significant difference between positive and negative serosal invasions ($P=0.219$).

CONCLUSION: VEGF-C and its receptor FLT-4 play a role in the development of gastric cancer, and the tumors with expression of VEGF-C and FLT-4 are more likely to have lymph node metastasis.

Liu XE, Sun XD, Wu JM. Expression and significance of VEGF-C and FLT-4 in gastric cancer. *World J Gastroenterol* 2004; 10 (3):352-355

<http://www.wjgnet.com/1007-9327/10/352.asp>

INTRODUCTION

Invasion and metastasis are the characteristics of malignant tumor. Epithelial malignancy spreads predominantly through lymphatic system, and its metastatic degree is closely related to patient's prognosis^[1]. However, very little is known about the mechanism of lymphangiogenesis and lymph node metastasis. Recent studies have shown that VEGF-C can bind to specific receptor VEGFR3/FLT-4 that express in lymphatic endothelium, stimulate lymphangiogenesis, and promote

lymphatic metastasis^[2-4]. We investigated the expression and significance of VEGF-C and its receptor FLT-4 in gastric cancer.

MATERIALS AND METHODS

Materials

Reagents Trizol liquid, AMV reverse transcriptase, Oligd(T)₁₄, RNAsin, dNTP, Taq DNA polymerase were purchased from Shanghai Sangon Biological Engineering Technology and Service Co.Ltd, PCR primers were synthesized by Shanghai Sangon Biological Engineering Technology and Service Co. Ltd. The antibodies of VEGF-C and FLT-4 were purchased from Santa Cruz Company.

Clinical data A total of 80 patients with primary gastric cancer were analyzed, with a mean age of 53.5 years, arranging from 38 to 72 years. Routine pathological diagnosis showed that 59 cases were adenocarcinoma and 21 cases were signet carcinoma. Among them, 54 cases presented lymph node metastasis, and 26 cases had no lymph node metastasis.

Methods

Detection of expression of VEGF-C AND FLT-4 Expression of VEGF-C and FLT-4 was assessed in each gastric cancer sample and its adjacent normal tissues by semi-quantitative RT-PCR.

RNA extraction Total RNA was extracted by Trizol one-step procedure, and suspended in DEPC-treated reverse osmosis-H₂O, and conserved at -70 °C for reverse transcription. RNA yield and purity were determined by standard UV spectrophotometric assay. The ratio of A260/A280 was 1.80.

First strand cDNA synthesis Five µg of the total RNA was dissolved in 20 µl of mixture containing 2 µl 10× first-strand buffer, 20 U AMV reverse transcriptase, 2 µl dNTP, 20 U RNAsin, 500 ng Oligd(T)₁₄, and DEPC-treated reverse osmosis-H₂O. The reaction conditions were as follows: at 42 °C for 60 min, and at 95 °C for 5 min. The first strand cDNA was stored at -20 °C until use.

PCR amplification The primers of VEGF-C, FLT-4 and β-actin were synthesized according to the primer design principles, all primers span an intron to control against amplification of genomic DNA sequences. Four µl first strand cDNA was amplified in 20 µl volume. The primers of VEGF-C yielded 206 bp product as follows: 5'-end primer: 5'-AAGGAGGCTGGCAACATAAC-3', 3'-end primer: 5'-CCACATCTGTAGACGGACAC-3'. Following an initial denaturation at 94 °C for 5 min, the samples were amplified by 30 cycles of denaturation at 94 °C for 30 s, annealing at 58 °C for 30 s, extension at 72 °C for 30 s, and ended by extension at 72 °C for 10 min. The primers of FLT-4 yielded a 298 bp product as follows: 5'-end primer: 5'-AGCCATTCATCAACAAGCCT-3', 3'-end primer: 5'-GGCAACAGCTGGATGTCATA-3'. Following an initial denaturation at 94 °C for 5 min, the samples were amplified by 28 cycles of denaturation at 94 °C for 30 s, annealing at 58 °C for 1 min, extension at 72 °C for 1 min, and ended by extension at 72 °C for 10 min. The primers of β-actin, which was amplified with VEGF-C and FLT-4 as an internal control, yielded a 644 bp product as follows: 5'-end primer: 5'-ACGTTATGGATGATGATATCGC-3', 3'-end primer: 5'-CTTAATGTACGCACGATTTCC-3'. The PCR products

were separated on 1.7% agarose gel, stained with ethidium bromide, and analyzed with Quantity one 4.1.0 software. The ratios of VEGF-C/ β -actin, and FLT-4/ β -actin were used to semiquantify the levels of VEGF-C and FLT-4.

Immunohistochemistry Immunohistochemical studies of VEGF-C and FLT-4 expression in gastric cancer and adjacent normal tissues were performed by the avidin-biotin-peroxidase technique, as previously described^[5].

Statistical analysis Statistical analyses were made with SPSS software, version 10.0.

RESULTS

Results of RT-PCR

Eighty primary gastric cancers and adjacent normal tissues from the same patients were examined for the expression of VEGF-C and FLT-4 by RT-PCR. In 80 cases of primary tumors, VEGF-C and FLT-4 were expressed in 58 (72.5%) and 51 (63.75%) cases, respectively. However, in 80 adjacent normal samples, VEGF-C and FLT-4 were expressed in 13 (16.25%) and 16 (20%), respectively. The expression of VEGF-C and FLT-4 in primary gastric cancer was significantly different from that in adjacent normal tissues ($P=0.01$ and $P=0.038$ respectively, Figure 1, Table 1).

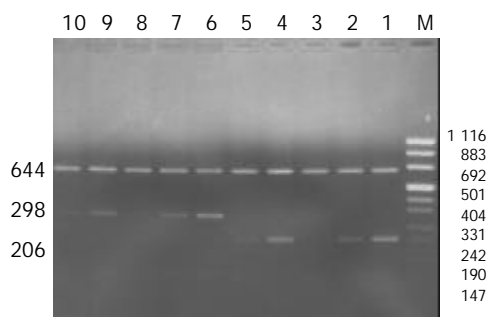


Figure 1 Semi-quantitative RT-PCR amplified products of VEGF-C and FLT-4 in primary gastric cancer and adjacent normal tissues. Lane-M: puc mix marker 8 (116, 883, 692, 501, 404, 331, 242, 190, 147, 110, 67, 34, 26, 19) bp, 644 bp: internal standards, 298 bp: FLT-4 expression, 206 bp: VEGF-C expression, Lane 1: Control of VEGF-C positive expression in placenta, Lane 6: Control of FLT-4 positive expression in placenta, Lanes 2,4: VEGF-C expression in primary gastric cancer, Lanes 3,5: VEGF-C expression in adjacent normal tissues, Lanes 7,9: FLT-4 expression in primary gastric cancer, Lanes 8, 10: FLT-4 expression in adjacent normal tissues.

Table 1 Expression of VEGF-C and FLT-4 in primary gastric cancers and adjacent normal tissues detected by semi-quantitative RT-PCR (mean \pm SD)

	Cases	VEGF-C	FLT-4
Primary gastric cancers	80	0.555 \pm 0.399 ^a	0.335 \pm 0.261 ^b
Adjacent normal tissues	80	0.146 \pm 0.311 ^c	0.153 \pm 0.275 ^d

^a $P=0.01$ vs group c, ^b $P=0.038$ vs group d.

Meanwhile, in 58 cases of gastric cancer with VEGF-C positive expression, FLT-4 was coexpressed in 42 cases (82.35%), but 22 cases of gastric cancer with VEGF-C negative expression showed FLT-4 expression in 9 cases (40.91%). The VEGF-C expression in primary tumors was significantly correlated with FLT-4 ($P=0.00886$).

Result of immunohistochemistry

Human placenta served as a positive control. Positive expression

of VEGF-C and FLT-4 showed brown staining in the cytoplasm of tumor or normal cells, more than 500 cells were calculated in different microscopic fields of slides, and percentage of positive cells was evaluated. Staining intensities were scored according to the following scale: -, no cells stained; +, less than 25% of cells stained; ++, 26% to 50% of cells stained; +++, 51% to 75% of cells stained; +++++, more than 75% of cells stained.

Immunohistochemical staining revealed that VEGF-C was expressed in 55 of 80 primary tumors (68.75%) and 11 of 80 adjacent normal tissues (13.75%), FLT-4 was expressed in 49 of 80 primary tumors (61.25%) and 14 of 80 adjacent normal tissues (17.5%), FLT-4 also expressed in endothelium of small blood and lymphatic vessels. There was a significant difference in the expression of VEGF-C and FLT-4 between gastric cancer and adjacent normal tissues (Table 2, Figure 2).

Table 2 Expression of VEGF-C and FLT-4 in primary gastric cancers and adjacent normal tissues detected by immunohistochemistry

Positive expression	Primary gastric cancer (cases)		Adjacent normal tissue (cases)	
	VEGF-C	FLT-4	VEGF-C	FLT-4
+	3	2	2	3
++	7	8	4	5
+++	20	18	3	3
++++	25	21	2	3

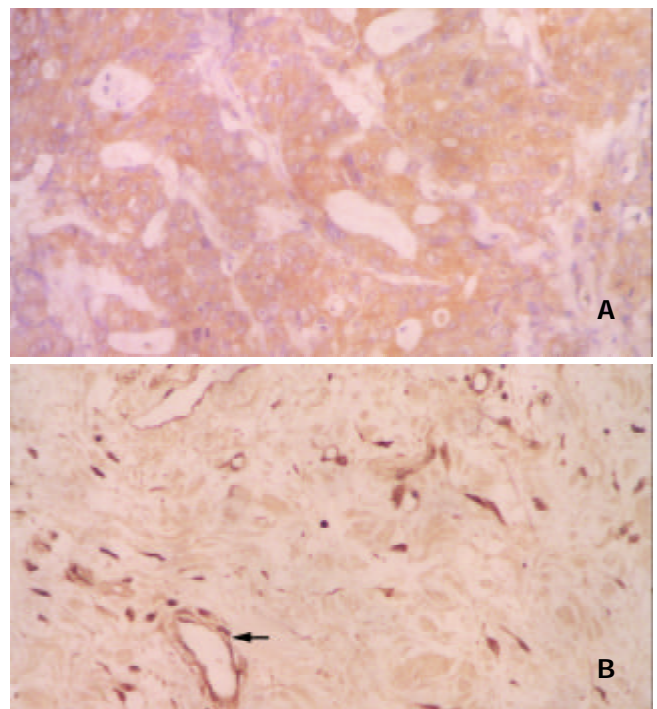


Figure 2 Expression of VEGF-C and FLT-4 in gastric cancer. A: VEGF-C positive expression in gastric cancer, $\times 400$. B: FLT-4 positive expression in gastric cancer, $\times 200$. (\leftarrow endothelial cells of vessels).

Pathologic factors affecting expression of VEGF-C

Several pathological factors, including histological type, lymph node metastasis, serosal invasion, were investigated to predict the expression of VEGF-C in gastric cancer. The results showed that there was a significant difference in expression of VEGF-C between moderately-poorly differentiated type and highly differentiated type ($P=0.032$), and a significant difference between positive lymph node metastasis and negative lymph

node metastasis ($P=0.024$). However, there was no significant difference between positive and negative serosal invasions ($P=0.219$, Table 3).

Table 3 Correlation between pathological factors and VEGF-C expression in 80 primary gastric cancers

Pathological factors	No. of cases	VEGF-C mRNA (mean±SD)	P
Histological type			
Moderately-Poorly differential	51	0.485±0.345	$P=0.032$
Highly differential	29	0.200±0.290	
Lymph node metastasis			
Positive	54	0.579±0.290	$P=0.024$
Negative	26	0.282±0.314	
Serosal invasion			
Positive	59	0.567±0.268	$P=0.219$
Negative	21	0.390±0.330	

DISCUSSION

In the 1970's, Folkman first found that tumor growth and metastasis were dependent on intratumoral angiogenesis. Since then, a large number of studies have emphasized the angiogenesis of tumors, but the roles of lymphatic vessels in tumor growth and metastasis were neglected. However, it is well known that lymphatic metastasis is mainly responsible for the spread of epithelial malignant tumors, and its metastasis degree is closely related to the prognosis of patients. Consisting of simple endothelium, without tight junction, and incomplete, even defect of basic membrane, accordingly, the permeability of small lymphatic vessels is larger than that of small blood vessels, and it is beneficial to tumor metastasis. However, up to now, it is still controversial about intratumoral lymphangiogenesis, mechanism of lymphangiogenesis and relationship between lymphangiogenesis and tumor metastasis.

VEGF-C family is a group of highly conservative secreted glycoproteins, which regulate vasculogenesis, lymphangiogenesis, and vascular permeability, and have been implicated in many physiological and pathological processes^[6-8]. VEGF-C is a member of the VEGF family, its encoding gene is located in 4q34, VEGF-C has 7 exons and shares 30% autologousity with VEGF. The studies showed that VEGF-C expressed in normal placenta, ovary, small intestine, skeleton muscle, spleen, colon, etc.^[9-12].

VEGFR-3/FLT-4, which belongs to the platelet-derived growth factor for receptor subfamily of receptor tyrosine kinase, was extensively expressed in embryonic tissues^[13-16]. In adult however, VEGFR-3/FLT-4 was mainly expressed in lymphatic endothelia, so it was regarded as a special marker of lymphatic endothelia. The density and distribution of lymphatic vessels could be detected by VEGFR-3/FLT-4 antibody^[17-21].

Recent studies showed that, the binding of VEGF-C to its special receptor FLT-4, could induce tyrosine phosphorylation of receptors, activate MAPK via intracellular kinase reaction, and finally promote proliferation of lymphatic endothelia, and lymphangiogenesis^[22-25].

Karpanen's results showed that VEGF-C could promote growth of tumor cells, which was correlated with the growth of lymphatic vessels around tumors and the intralymphatic spread of cancer^[26]. Several clinical studies have proved that overexpression of VEGF-C in solide tumors, such as squamous cell carcinomas of head and neck, thyroid carcinoma, prostate cancer, gastric cancer, colorectal carcinoma, breast cancer, esophageal squamous carcinoma, cervical cancer, lung cancer, was relevant to lymphatic spread^[27-31].

Akagi^[32] examined the relationship between expression of VEGF-C in 99 primary tumors and 18 metastatic lymph nodes from colorectal cancer and clinicopathological features by semi-quantitative reverse transcriptase-polymerase chain reaction (RT-PCR) and immunohistochemistry. The results showed that the expression of VEGF-C was correlated with lymphatic involvement, lymph node metastasis, and depth of invasion. To study the correlation between lymphogenous metastasis in early gastric carcinoma (EGC) and the expression of VEGF-C, Kabashima^[33] selected 35 cases of lymph node metastasis-positive [n(+)] EGC and 70 cases of lymph node metastasis-negative [n(-)] EGC. Clinicopathologically, there were significant differences in median size, lymphatic invasion, and venous invasion between the two groups, the incidence of positive-expression of VEGF-C in n(+) EGC was significantly higher than that in n(-) EGC. In breast cancer, the expression of VEGF-C was correlated with lymphatic vessel invasion, the 5-year disease free survival rate of the VEGF-C positive group was significantly poorer than that of the VEGF-C negative group^[34]. The expression of VEGF-C in breast cancer cells could increase intratumoral lymphangiogenesis, resulting in significantly enhanced metastasis to regional lymph nodes and lungs, and the degree of tumor lymphangiogenesis was highly correlated with the extent of lymph node and lung metastases^[35].

Most of the studies demonstrated that VEGF-C was mainly produced by cancer cells, and VEGFR-3/FLT-4 by endothelial cells of the stromal lymphatic vessels, the incidence of VEGF-C was closely correlated with VEGFR-3/FLT-4 expression in the primary tumors. VEGF-C produced by cancer cells might induce the expression of VEGFR-3/FLT-4 on lymphatic endothelial cells, consequently, the activation of VEGF-C/FLT-4 paracrine loop induced the lymphangiogenesis^[36].

However, the study by Gumingham^[37] obtained opposite results, in which a significant correlation was found between expression of VEGF-C and VEGFR-3/FLT-4 in breast cancer, but no significant difference in VEGF-C expression between normal and neoplastic breast tissues and no association between VEGF-C and either lymph node status or number of involved nodes, patient age, tumor size, estrogen receptor status, or tumor grade were found.

We studied the correlation between VEGF-C and VEGFR-3/FLT-4 expression in 80 primary gastric cancers and adjacent normal tissues by semi-quantitative reverse transcriptase-polymerase chain reaction (RT-PCR) and immunohistochemistry. The results showed that there was a significant difference in VEGF-C expression between primary tumor and adjacent normal tissue samples, and a significant correlation between expression of VEGF-C and VEGFR-3/FLT-4 in tumor tissues. The present study also clearly demonstrated that expression of VEGF-C and VEGFR-3/FLT-4 was closely related to the histological type of tumors and lymph node metastasis. Expressions of VEGF-C and VEGFR-3/FLT-4 were detected both in primary gastric cancer and in adjacent normal tissues. However, the former was significantly higher than the latter. Meanwhile, VEGFR-3/FLT-4 expression was detected in endothelial cells of stromal blood vessels and lymphatic vessels.

Tumor cell metastasis to regional lymph nodes is an early event in tumor spread, and this index is frequently used to predict disease prognosis^[38]. VEGF-C is the first growth factor related to lymphangiogenesis, and the study of lymphangiogenesis of tumors is only at its beginning. Its mechanisms and mediators await further studies.

REFERENCES

- Gershenwald JE, Fidler IJ. Cancer. Targeting lymphatic metastasis. *Science* 2002; **296**: 1811-1812
- Karkkainen MJ, Petrova TV. Vascular endothelial growth factor

- receptors in the regulation of angiogenesis and lymphangiogenesis. *Oncogene* 2000; **19**: 5598-5605
- 3 **Parr C**, Jiang WG. Quantitative analysis of lymphangiogenic markers in human colorectal cancer. *Int J Oncol* 2003; **23**: 533-539
 - 4 **Arinaga M**, Noguchi T, Takeno S, Chujo M, Miura T, Uchida Y. Clinical significance of vascular endothelial growth factor C and vascular endothelial growth factor receptor 3 in patients with nonsmall cell lung carcinoma. *Cancer* 2003; **97**: 457-464
 - 5 **Kishimoto K**, Sasaki A, Yoshihama Y, Mese H, Tsukamoto G, Matsumura T. Expression of vascular endothelial growth factor-C predicts regional lymph node metastasis in early oral squamous cell carcinoma. *Oral Oncol* 2003; **39**: 391-396
 - 6 **Pepper MS**. Lymphangiogenesis and tumor metastasis: myth or reality? *Clin Cancer Res* 2001; **7**: 462-468
 - 7 **Cao Y**, Linden P, Farnebo J, Cao R, Eriksson A, Kumar V, Qi JH, Claesson-Welsh L, Alitalo K. Vascular endothelial growth factor C induces angiogenesis *in vivo*. *Proc Natl Acad Sci U S A* 1998; **95**: 14389-14394
 - 8 **Enholm B**, Paavonen K, Ristimaki A, Kumar V, Gunji Y, Klefstrom J, Kivinen L, Laiho M, Olofsson B, Joukov V, Eriksson U, Alitalo K. Comparison of VEGF, VEGF-B, VEGF-C and Ang-1 mRNA regulation by serum, growth factors, oncoproteins and hypoxia. *Oncogene* 1997; **14**: 2475-2483
 - 9 **Lee J**, Gray A, Yuan J, Luoh SM, Avraham H, Wood WI. Vascular endothelial growth factor-related protein: A ligand and specific activator of the tyrosine kinase receptor Flt4. *Proc Natl Acad Sci U S A* 1996; **93**: 1988-1992
 - 10 **Laitinen M**, Ristimaki A, Honkasalo M, Narko K, Paavonen K, Ritvos O. Differential hormonal regulation of vascular endothelial growth factors VEGF, VEGF-B, and VEGF-C messenger ribonucleic acid levels in cultured human granulosa-luteal cells. *Endocrinology* 1997; **138**: 4748-4756
 - 11 **Ohta Y**, Shridhar V, Bright RK, Kalemkerian GP, Du W, Carbone M, Watanabe Y, Pass HI. VEGF and VEGF type C play an important role in angiogenesis and lymphangiogenesis in human malignant mesothelioma tumours. *Br J Cancer* 1999; **81**: 54-61
 - 12 **Boardman KC**, Swartz MA. Interstitial flow as a guide for lymphangiogenesis. *Circ Res* 2003; **92**: 801-808
 - 13 **Pajusola K**, Aprelikova O, Korhonen J, Kaipainen A, Pertovaara L, Alitalo R, Alitalo K. Flt4 receptor tyrosine kinase contains seven immunoglobulin-like loops and is expressed in multiple human tissues and cell lines. *Cancer Res* 1992; **52**: 5738-5743
 - 14 **Lymboussaki A**, Partanen TA, Olofsson B, Thomas-Crusells J, Fletcher CD, de Waal RM, Kaipainen A, Alitalo K. Expression of the vascular endothelial growth factor C receptor VEGFR-3 in lymphatic endothelium of the skin and in vascular tumors. *Am J Pathol* 1998; **153**: 395-403
 - 15 **Salven P**, Mustjoki S, Alitalo R, Alitalo K, Rafii S. VEGFR-3 and CD133 identify a population of CD34+ lymphatic/vascular endothelial precursor cells. *Blood* 2003; **101**: 168-172
 - 16 **Hamrah P**, Chen L, Zhang Q, Dana MR. Novel expression of vascular endothelial growth factor receptor (VEGFR)-3 and VEGF-C on corneal dendritic cells. *Am J Pathol* 2003; **163**: 57-68
 - 17 **Clarijs R**, Schalkwijk L, Hofmann UB, Ruitter DJ, de Waal RM. Induction of vascular endothelial growth factor receptor-3 expression on tumor microvasculature as a new progression marker in human cutaneous melanoma. *Cancer Res* 2002; **62**: 7059-7065
 - 18 **Jussila L**, Valtola R, Partanen TA, Salven P, Heikkila P, Matikainen MT, Renkonen R, Kaipainen A, Detmar M, Tschachler E, Alitalo R, Alitalo K. Lymphatic endothelium and Kaposi's sarcoma spindle cells detected by antibodies against the vascular endothelial growth factor receptor-3. *Cancer Res* 1998; **58**: 1599-1604
 - 19 **Valtola R**, Salven P, Heikkila P, Taipale J, Joensuu H, Rehn M, Pihlajaniemi T, Weich H, deWaal R, Alitalo K. VEGFR-3 and its ligand VEGF-C are associated with angiogenesis in breast cancer. *Am J Pathol* 1999; **154**: 1381-1390
 - 20 **Kaipainen A**, Korhonen J, Mustonen T, van Hinsbergh VW, Fang GH, Dumont D, Breitman M, Alitalo K. Expression of the fms-like tyrosine kinase 4 gene becomes restricted to lymphatic endothelium during development. *Proc Natl Acad Sci U S A* 1995; **92**: 3566-3570
 - 21 **Lymboussaki A**, Olofsson B, Eriksson U, Alitalo K. Vascular endothelial growth factor (VEGF) and VEGF-C show overlapping binding sites in embryonic endothelia and distinct sites in differentiated adult endothelia. *Circ Res* 1999; **85**: 992-999
 - 22 **Kawakami M**, Furuhashi T, Kimura Y, Yamaguchi K, Hata F, Sasaki K, Hirata K. Quantification of vascular endothelial growth factor-C and its receptor-3 messenger RNA with real-time quantitative polymerase chain reaction as a predictor of lymph node metastasis in human colorectal cancer. *Surgery* 2003; **133**: 300-308
 - 23 **Kubo H**, Cao R, Brakenhielm E, Makinen T, Cao Y, Alitalo K. Blockade of vascular endothelial growth factor receptor-3 signaling inhibits fibroblast growth factor-2-induced lymphangiogenesis in mouse cornea. *Proc Natl Acad Sci U S A* 2002; **99**: 8868-8873
 - 24 **Dias S**, Choy M, Alitalo K, Rafii S. Vascular endothelial growth factor (VEGF)-C signaling through FLT-4 (VEGFR-3) mediates leukemic cell proliferation, survival, and resistance to chemotherapy. *Blood* 2002; **99**: 2179-2184
 - 25 **Karkkainen MJ**, Saaristo A, Jussila L, Karila KA, Lawrence EC, Pajusola K, Bueler H, Eichmann A, Kauppinen R, Kettunen MI, Yla-Herttuala S, Finegold DN, Ferrell RE, Alitalo K. A model for gene therapy of human hereditary lymphedema. *Proc Natl Acad Sci U S A* 2001; **98**: 12677-12682
 - 26 **Karpanen T**, Egeblad M, Karkkainen MJ, Kubo H, Yla-Herttuala S, Jaattela M, Alitalo K. Vascular endothelial growth factor C promotes tumor lymphangiogenesis and intralymphatic tumor growth. *Cancer Res* 2001; **61**: 1786-1790
 - 27 **Neuchrist C**, Erovc BM, Handisurya A, Fischer MB, Steiner GE, Hollemann D, Gedlicka C, Saaristo A, Burian M. Vascular endothelial growth factor C and vascular endothelial growth factor receptor 3 expression in squamous cell carcinomas of the head and neck. *Head Neck* 2003; **25**: 464-474
 - 28 **Ishikawa M**, Kitayama J, Kazama S, Nagawa H. Expression of vascular endothelial growth factor C and D (VEGF-C and -D) is an important risk factor for lymphatic metastasis in undifferentiated early gastric carcinoma. *Jpn J Clin Oncol* 2003; **33**: 21-27
 - 29 **Tsurusaki T**, Kanda S, Sakai H, Kanetake H, Saito Y, Alitalo K, Koji T. Vascular endothelial growth factor-C expression in human prostatic carcinoma and its relationship to lymph node metastasis. *Br J Cancer* 1999; **80**: 309-313
 - 30 **Kitadai Y**, Amioka T, Haruma K, Tanaka S, Yoshihara M, Sumii K, Matsutani N, Yasui W, Chayama K. Clinicopathological significance of vascular endothelial growth factor (VEGF)-C in human esophageal squamous cell carcinomas. *Int J Cancer* 2001; **93**: 662-666
 - 31 **Hashimoto I**, Kodama J, Seki N, Hongo A, Yoshinouchi M, Okuda H, Kudo T. Vascular endothelial growth factor-C expression and its relationship to pelvic lymph node status in invasive cervical cancer. *Br J Cancer* 2001; **85**: 93-97
 - 32 **Akagi K**, Ikeda Y, Miyazaki M, Abe T, Kinoshita J, Maehara Y, Sugimachi K. Vascular endothelial growth factor-C (VEGF-C) expression in colorectal cancer tissues. *Br J Cancer* 2000; **83**: 887-891
 - 33 **Kabashima A**, Maehara Y, Kakeji Y, Sugimachi K. Overexpression of vascular endothelial growth factor C is related to lymphogenous metastasis in early gastric carcinoma. *Oncology* 2001; **60**: 146-150
 - 34 **Kinoshita J**, Kitamura K, Kabashima A, Saeki H, Tanaka S, Sugimachi K. Clinical significance of vascular endothelial growth factor-C (VEGF-C) in breast cancer. *Breast Cancer Res Treat* 2001; **66**: 159-164
 - 35 **Skobe M**, Hawighorst T, Jackson DG, Prevo R, Janes L, Velasco P, Riccardi L, Alitalo K, Claffey K, Detmar M. Induction of tumor lymphangiogenesis by VEGF-C promotes breast cancer metastasis. *Nat Med* 2001; **7**: 192-198
 - 36 **Yonemura Y**, Fushida S, Bando E, Kinoshita K, Miwa K, Endo Y, Sugiyama K, Partanen T, Yamamoto H, Sasaki T. Lymphangiogenesis and the vascular endothelial growth factor receptor (VEGFR)-3 in gastric cancer. *Eur J Cancer* 2001; **37**: 918-923
 - 37 **Gunningham SP**, Currie MJ, Han C, Robinson BA, Scott PA, Harris AL, Fox SB. The short form of the alternatively spliced flt-4 but not its ligand vascular endothelial growth factor C is related to lymph node metastasis in human breast cancers. *Clin Cancer Res* 2000; **6**: 4278-4286
 - 38 **Yin T**, Ji XL, Shen MS. Relationship between lymph node sinuses with blood and lymphatic metastasis of gastric cancer. *World J Gastroenterol* 2003; **9**: 40-43

Activating mechanism of transcription factor NF- κ B regulated by hepatitis B virus X protein in hepatocellular carcinoma

Tao Wang, Yi Wang, Meng-Chao Wu, Xin-Yuan Guan, Zheng-Feng Yin

Tao Wang, Yi Wang, Meng-Chao Wu, Zheng-Feng Yin, Department of Molecular Oncology, Eastern Hepatobiliary Surgery Hospital, Shanghai 200438, China

Xin-Yuan Guan, Department of Clinical Oncology, The University of Hong Kong, Hong Kong, China

Supported by the National Natural Science Foundation of China, No. 30171046

Correspondence to: Dr. Yi Wang, Department of Molecular Oncology, Eastern Hepatobiliary Surgery Hospital, 225 Changhai Road, Shanghai 200438, China. yiwang6151@yahoo.com

Telephone: +86-21-25070754 **Fax:** +86-21-25070859

Received: 2003-06-06 **Accepted:** 2003-08-16

Abstract

AIM: To investigate the mechanism and significance of NF- κ B activation regulated by hepatitis B virus X protein (HBx) in hepatitis B virus (HBV)-associated hepatocellular carcinoma (HCC).

METHODS: The expression levels of HBx, p65, I κ B- α and ubiquitin were detected by immunohistochemistry in HCC tissue microarrays (TMA) respectively, and I κ B- α was detected by Western blot in HCC and corresponding liver tissues.

RESULTS: The percentage of informative TMA samples was 98.8% in 186 cases with a total of 367 samples. Compared with corresponding liver tissues (60.0%), the HBx expression was obviously decreased in HBV-associated HCC (47.9%, $u=2.24$, $P<0.05$). On the contrary, the expressions of p65 (20.6% vs 45.3%, $u=4.85$, $P<0.01$) and ubiquitin (8.9% vs 59.0%, $u=9.68$, $P<0.01$) were notably elevated in HCC. In addition, I κ B- α had a tendency to go up. Importantly, positive relativity was observed between HBx and p65 ($\chi^2=10.26$, $P<0.01$), p65 and I κ B- α ($\chi^2=16.86$, $P<0.01$), I κ B- α and ubiquitin ($\chi^2=8.90$, $P<0.01$) in HCC, respectively.

CONCLUSION: Both active and non-active forms of NF- κ B are increased in HBV-associated HCC. Variant HBx is the major cause of the enhancement of NF- κ B activity. The activation always proceeds in nucleus and the proteasome complexes play an important role in the activation.

Wang T, Wang Y, Wu MC, Guan XY, Yin ZF. Activating mechanism of transcription factor NF- κ B regulated by hepatitis B virus X protein in hepatocellular carcinoma. *World J Gastroenterol* 2004; 10 (3):356-360

<http://www.wjgnet.com/1007-9327/10/356.asp>

INTRODUCTION

Hepatocellular carcinoma (HCC) is a malignant tumor with a poor prognosis. Hepatitis B virus (HBV) has been shown to be linked epidemiologically to the HCC development and about eighty percent of the tumors in China are induced by HBV. As a unique non-structure protein, hepatitis B virus X protein (HBx) performs a variety of biological functions, such as gene

transactivation^[1], interaction with p53^[2], interference with host DNA repair^[3], repression of physiological proteolysis^[4], modulation of cell proliferation and apoptosis^[5,6], induction of malignant cell migration^[7,8]. These functions may play an important role in the initiation and development of HCC associated with HBV infection. NF- κ B, a crucial transcription factor, takes part in almost all aspects of cell regulation, including immune cell activation, stress response, proliferation, apoptosis, differentiation and oncogenic transformation. Currently, more attentions have been paid to the carcinogenesis of HBx transactivating NF- κ B^[9]. However, the active state of NF- κ B in HCC has been seldom studied. As a new high-throughput technology introduced in 1999, tissue microarray (TMA) is worthy of popularization. In our study, the expression levels of HBx, p65, I κ B- α and ubiquitin were detected by immunohistochemistry on TMA respectively, as well as I κ B- α was detected by Western blot, in order to investigate the mechanism and significance of HBx activating NF- κ B.

MATERIALS AND METHODS

Tissue samples

Paraffin specimens were prepared from operatively-resected HCC and non-HCC counterparts between 1997 and 2000, including 171 cases of serum HBV-positive HCC, 10 cases of serum HBV-negative HCC and their corresponding liver tissues, 5 cases of normal control liver tissues (Table 1). In addition, 24 couples of fresh HCC and its corresponding liver tissues were collected between March and October in 2001, stored at -80 °C until experiment.

Tissue microarray construction

All formalin-fixed and paraffin-embedded HCC tissues used in this study were sectioned and stained with hematoxylin-eosin (H&E). The H&E-stained sections were carefully diagnosed, and the representative regions of the tumor and its corresponding liver tissue for microarray were defined as well. HCC TMA was constructed according to the procedure described by Kononen *et al*^[10]. Briefly, core tissue specimens, 0.6 mm in diameter, were taken from selected regions of individual donor blocks and precisely arrayed into recipient paraffin blocks (45 mm×22 mm) using a tissue-arraying instrument (Beecher Instruments, Silver Spring, MD, USA). After construction, the recipient paraffin block was incubated at 37 °C for one hour and the surface of the block was smoothed. Five-micrometer consecutive sections of this TMA block were cut with a microtome. The presence and morphology of tumor and liver tissues on arrayed samples were identified by H&E stained sections.

Immunohistochemistry

TMA section was deparaffinized through xylene and dehydrated with graded alcohol. Endogenous peroxidase was then blocked with 0.3% H₂O₂ diluted in methanol for 30 min at room temperature. Antigen retrieval was performed by treating the slide in citrate buffer in a microwave for 10 min. The slide was incubated in a moist chamber with HBx mouse monoclonal

antibody (1:100; Chemicon, USA), p65 mouse monoclonal antibody (Santa Cruz, USA), I κ B- α rabbit polyclonal antibody (Santa Cruz, USA) and ubiquitin rabbit polyclonal antibody (Neomarkers, USA) at 4 °C overnight respectively. After a brief wash in PBS, the slide was treated with goat anti-mouse antibody and goat anti-rabbit antibody (EnVision™ +Kits, DAKO, Denmark), respectively, for 45 min at 37 °C. After a brief wash in PBS, the slide was developed in 0.05% freshly prepared diaminobenzidine solution (DAB, Sigma, St. Louis, MO) for 8 min, and then counterstained with hematoxylin. More than 5% cells stained were identified as a positive result.

Western blot

Western blot was carried out based on the protocol of *molecular clone*^[11]. Briefly, frozen tissues were lysed in a single eradicator buffer (150 mmol/L NaCl, 50 mmol/L pH 8.0 Tris-HCl, 0.02% natriumazid, 1 ug/ml aprotinin, 100 ug/ml PMSF, 1% Triton X-100) and quantified by BCA method. The samples were boiled, loaded, separated on 12% SDS gel electrophoresis, transferred to nitrocellulose membrane, and reacted with I κ B- α rabbit polyclonal antibody (1:1 000, Santa Cruz, USA). At last, the membrane was exposed several minutes after ECL substrate incubation.

Statistical analysis

HBx, p65, I κ B- α , ubiquitin expression differences between HBV-associated HCC and corresponding liver tissues were analyzed statistically using *u* test. The relativity between HBx, I κ B- α , p65, ubiquitin was analyzed statistically using χ^2 test or adjusted χ^2 test.

RESULTS

Tissue microarray

In this study, two HCC TMA blocks were constructed which

contained a total of 181 cases with 367 samples. One thousand four hundred fifty-one informative samples were totally detected by immunohistochemistry on arrays and the observed ratio was up to 98.8% (1 451/1 468 samples). HE-stained sections showed that the morphology of tissues and cells could be seen clearly. The HCC array HE-stained sections and several types of the tumor are shown in Figure 1.

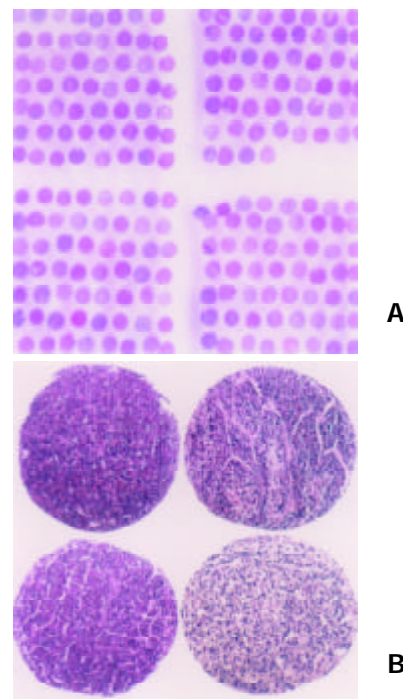


Figure 1 Overview of HCC TMA. A: TMA overview of H&E-staining section, B: HCC morphology on TMA stained by H&E.

Table 1 Clinicopathologic information of patients used in TMA

Group	HBV			Sex		Age	Diameter	Grade			Cirrhosis	
	Total	Positive	Negative	Man	Female	mean±SD (year)	mean±SD (cm)	II	III	IV	Yes	No
HCC	181	171	10	158	23	49.3±10.6	7.2±3.5	28	141	12	166	15
Normal	5	0	5	2	3	42.4±9.6	9.3±5.8				0	5

Table 2 Expressions of HBx, p65, I κ B- α and ubiquitin in HCC and corresponding liver tissues

Group	HBx			p65			I κ B- α			Ubiquitin		
	Total	Positive	%	Total	Positive	%	Total	Positive	%	Total	Positive	%
HCC	169	81	47.9	170	77	45.3	170	124	72.9	166	98	59.0
Control	170	102	60.0	170	35	20.6	171	116	67.0	168	15	8.9
Statistics	<i>u</i> =2.24 ^a			<i>u</i> =4.85 ^b			<i>u</i> =1.19			<i>u</i> =9.68 ^b		

^a*P*<0.05, ^b*P*<0.01.

Table 3 Relativity analysis between HBx, I κ B- α , p65 and ubiquitin in HCC and corresponding liver tissues

	HBx		P65		Ubiquitin	
	Negative	Positive	Negative	Positive	Negative	Positive
HBx	Negative		58(52)	30(16)	39(57)	46(8)
	Positive		33(83)	47(19)	28(95)	52(7)
Statistics			$\chi^2=10.26^b(0.60)$		$\chi^2=2.02(1.44)$	
I κ B- α	Negative	29(21)	17(34)	36(46)	9(9)	26(50)
	Positive	59(47)	63(68)	56(89)	68(26)	42(103)
Statistics	$\chi^2=2.28(0.11)$		$\chi^2=16.86^b(1.02)$		$\chi^2=8.90^b(0.04)$	

^b*P*<0.01, vs Corresponding liver tissue.

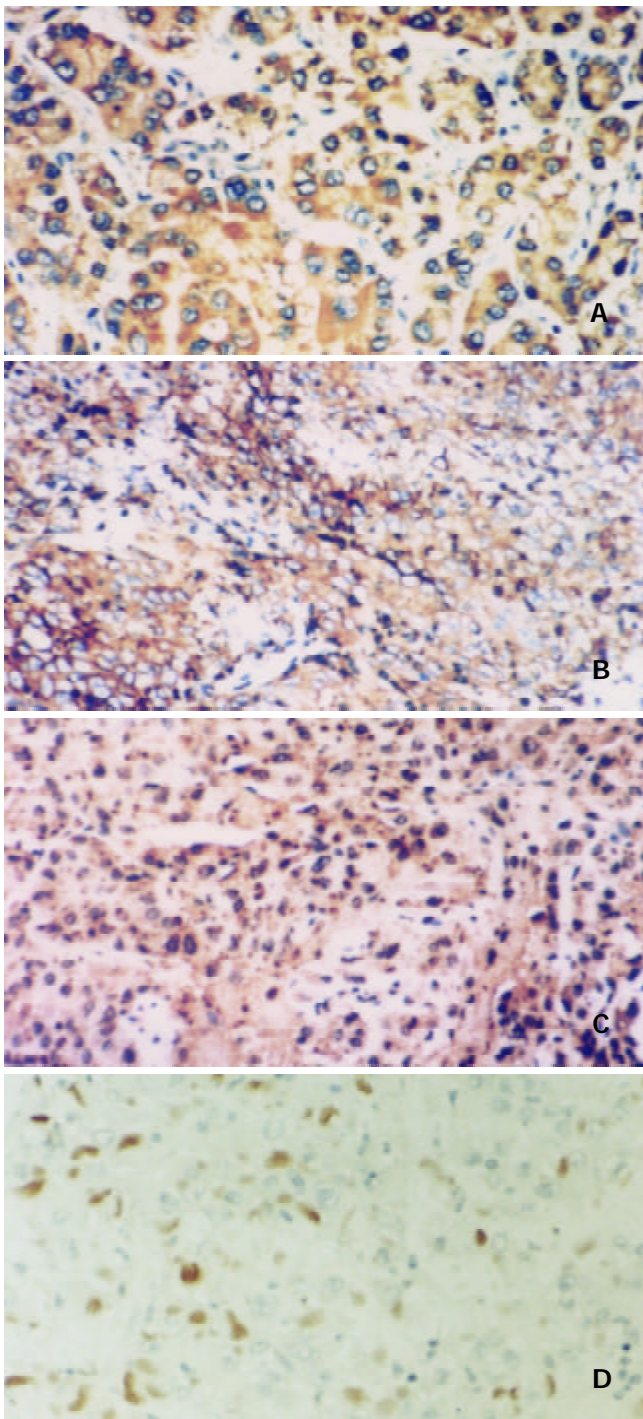


Figure 2 Expressions and locations of HBx, p65, IκB-α and ubiquitin in HCC detected by immunohistochemistry, EnVision $\times 200$. A: HBx expression in cytoplasm, B: p65 immunostaining in cytoplasm and nuclei, C: IκB-α distribution in cytoplasm and nuclei, D: ubiquitin location in nuclei.

Expression differences of four proteins in HCC and corresponding liver tissues

The expression of HBx was restricted exclusively to cytoplasmic location in both HCC and liver tissues. The positive immunostainings of p65 and IκB-α were seen only in cytoplasm of liver tissues, but in both cytoplasm and nuclei of HCC. The positive signal of ubiquitin was distributed predominantly in cytoplasm of liver tissues and in nuclei of HCC (Figure 2).

In serum HBV-positive cases, the HBx expressions in HCC (81/169, 47.9%) were significantly decreased as compared with the corresponding liver tissues (102/170, 60.0%, $P < 0.05$). On the contrary, the expressions of p65 and ubiquitin were notably

elevated in HCC (45.3%, 59.0% respectively) as compared with corresponding liver tissues (20.6%, 8.9% respectively, $P < 0.01$). The positive rate of immunostaining reaction of IκB-α in HCC and corresponding liver tissues was 72.9% and 67% respectively. The difference was not significant, though the staining in HCC was more intense (Table 2).

In serum HBV-negative cases, the expressions of HBx, p65, IκB-α, ubiquitin in HCC were detected in 2/10 cases, 5/9 cases, 7/9 cases and 5/10 cases respectively. In corresponding liver tissues, their expressions were detected in 2/10 cases, 2/9 cases, 7/9 cases and 2/10 cases respectively.

In five normal liver tissues, all expressions of HBx, p65 and ubiquitin were negative, whereas, IκB-α was demonstrated to be weakly positive.

Western blot of IκB-α

Compared with corresponding liver tissues, elevated levels of IκB-α were detected in 10 HCC cases, decreased in 1 case. In the other 13 couples of HCC and corresponding liver tissues, no obvious difference of expression was detected (Figure 3).

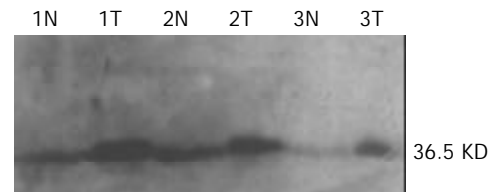


Figure 3 IκB-α expression levels detected by Western blot. IκB-α levels were elevated in 3 cases of HCC compared with their corresponding liver tissues.

Relativity analysis between HBx, IκB-α, p65 and ubiquitin

χ^2 test showed that no relativity existed between HBx, IκB-α, p65 and ubiquitin in corresponding liver tissues, but a positive relativity was observed between HBx and p65, p65 and IκB-α, IκB-α and ubiquitin in HCC (Table 3).

DISCUSSION

TMA is a new technology first introduced in 1999. It contains hundreds or even thousands of small tissue samples arranged into a grid for rapid, cost efficient and high-throughput analysis. TMA has been used widely in gene or protein expression analysis, antibody screening, tissue specificity detection of proteins, phenotype versus genotype analysis, RNA or DNA *in situ*-hybridization^[10,12,13]. Based on TMA, we studied the expressions of HBx, NF-κB, IκB-α, ubiquitin and their interrelationship in HCC.

The result of HBx expression detection in HBV-associated HCC showed that HBx expression was reduced in cancer tissue as compared with the corresponding liver tissue. The result might be ascribed to the existing form of HBV in tumor tissue. Many researches indicated that integration was the major form of HBV in HCC, so the viral copies were far less than that in non-tumor tissues where free virus prevails^[14]. The expression of HBx in samples with serum HBV-negative implicated quite a few patients were once infected with HBV. Moreover, the cytoplasmic location of HBx was consistent with the previous reports^[15].

NF-κB plays a vital role in almost all aspects of cell regulation such as immune cell activation, proliferation, apoptosis, stress response, differentiation and oncogenic transformation. Activated NF-κB can mediate the expression of a large (more than 150) and diverse set of inflammatory and immune response mediators. It has been considered as a central regulator of cellular responses and played a pivotal

role both at the stage of initiation and perpetuation of chronic inflammation^[16-19]. NF- κ B is sequestered in the cytosol of unstimulated cells via non-covalent interactions with a class of inhibitor proteins, called I κ Bs. Signals that induce NF- κ B activity cause the phosphorylation of I κ Bs, their dissociation and subsequent ubiquitination and degradation in 26S proteasome complex, allowing NF- κ B proteins to enter the nucleus and induce gene expression by binding κ B site in DNA. As one of the NF- κ B activation products, I κ B- α could induce NF- κ B export from the nucleus by reuniting NF- κ B and terminating associated gene activation. The negative feedback loop could keep NF- κ B sensitivity to signals by returning rapidly to baseline activity^[20-22].

Because p65 is one of the most common members in NF- κ B family, and I κ B- α is the most important inhibitor, detection of p65 and I κ B- α expression can reflect the state of NF- κ B metabolism. In our test, low expression rate of p65 and weakly positive expression of I κ B- α represented the nonactive state of NF- κ B in non-cancerous tissues, but the activation enhancement of NF- κ B in HCC was in accord with the previous reports^[23,24]. The expression of I κ B- α in HCC and its corresponding liver tissue has not been reported yet. In our study, no statistical difference was found in positive rates between HCC and its corresponding liver tissue, the discrimination of immunostaining intensity was scented. Furthermore, Western blot validated the concentration augmentation of I κ B- α in HCC, while in the meantime, molecular weight alteration was not observed. The results illustrated that I κ B- α regulation gave priority to quantity change in HCC. The location of p65 and I κ B- α represented the activation or non-activation form of NF- κ B. Quite a few cytoplasm locations of p65 and I κ B- α observed in our test accounted for the non-activated NF- κ B increase in HCC, which contradicted with cytoplasm decrease of p65 and I κ B- α observed *in vivo* system^[25]. We ascribed the contradiction of NF- κ B metabolism to the persistence in HCC and the transience *in vivo* system. The lasting activation of NF- κ B can automatically regulate the production of I κ B- α and possibly even p65 or p50. A great deal of non-activated NF- κ B repertory is in favor of lasting activation of NF- κ B.

I κ B- α proteolysis is by the ubiquitin-proteasome pathway, but the exact locality is still not clear. Birbach *et al* expatiated I κ B- α shuttle mechanism between cytoplasm and nucleus^[26]. It is recognized now that besides I κ B- α , up-stream kinases such as NIK and MAPKK can shuttle between cytoplasm and nucleus. The present study is the first to show the distribution and expression of ubiquitin in HCC. The results of nuclear location of ubiquitin and its relativity with I κ B- α indicated the proteolysis of I κ B- α was processed in tumor cell nuclei. Of course, another likelihood was that transcription of ubiquitin would be promoted after NF- κ B activation^[27]. There is no relativity between ubiquitin and HBx, so whether the proteolysis of HBx passes through non-ubiquitin pathway or not remains to be determined.

Positive relativity between HBx and p65 in HCC indicated that HBx existed in tumor tissues was one cause of inducing NF- κ B activation. It has been found in some studies that HBx mutation was common in HCC compared with corresponding liver tissues^[28]. Frequent types of HBx mutation were COOH-terminal truncation and hotspot mutations in certain amino acids^[29-31]. COOH-terminally truncated HBx is encoded by truncated X gene, which usually derives from HBV integrated into host genome. Base mutation and frame-shift are the other causes. Usually, it was considered that HBx activated NF- κ B relied on its transactivation domains, and COOH-terminal transactivation domain was important to its transactivation function^[32,33]. In our study, NF- κ B activation was elevated in HCC with a low HBx expression compared with corresponding liver tissues. Therefore, the results implied that HBx might

activate NF- κ B by other unknown mechanisms but not its transactivation ability. One likeness was that C-terminally truncated HBx lost its ability to suppress proteasome complex and facilitated I κ B- α degradation and NF- κ B activation^[4]. The high percentage of ubiquitin expressions in HCC (59.0%) from our results in part supports the opinion. The detailed mechanism of NF- κ B activation in HBV-associated hepatocellular carcinoma remains to be further studied.

In conclusion, NF- κ B activation induced by HBx could not only facilitate infected cell survival and HBV escape from immune clearance, but also promote liver cell malignant transformation and tumor cell advantageous growth^[34]. Variant HBx plays an important role in potentiating NF- κ B activation.

REFERENCES

- 1 **Caselmann WH.** Trans-activation of cellular genes by hepatitis B virus proteins: a possible mechanism of hepatocarcinogenesis. *Adv Virus Res* 1996; **47**: 253-302
- 2 **Lee SG, Rho HM.** Transcriptional repression of the human p53 gene by hepatitis B viral X protein. *Oncogene* 2000; **19**: 468-471
- 3 **Jia L, Wang XW, Harris CC.** Hepatitis B virus X protein inhibits nucleotide excision repair. *Int J Cancer* 1999; **80**: 875-879
- 4 **Fischer M, Runkel L, Schaller H.** HBx protein of hepatitis B virus interacts with the C-terminal portion of a novel human proteasome alpha-subunit. *Virus Genes* 1995; **10**: 99-102
- 5 **Huo TI, Wang XW, Forgues M, Wu CG, Spillare EA, Giannini C, Brechot C, Harris CC.** Hepatitis B virus X mutants derived from human hepatocellular carcinoma retain the ability to abrogate p53-induced apoptosis. *Oncogene* 2001; **20**: 3620-3628
- 6 **Schuster R, Hildt E, Chang SF, Terradillos O, Pollicino T, Lanford R, Gerlich WH, Will H, Schaefer S.** Conserved transactivating and pro-apoptotic functions of hepadnaviral X protein in ortho- and avihepadnaviruses. *Oncogene* 2002; **21**: 6606-6613
- 7 **Lara-Pezzi E, Gomez-Gaviro MV, Galvez BG, Mira E, Iniguez MA, Fresno M, Martinez AC, Arroyo AG, Lopez-Cabrera M.** The hepatitis B virus X protein promotes tumor cell invasion by inducing membrane-type matrix metalloproteinase-1 and cyclooxygenase-2 expression. *J Clin Invest* 2002; **110**: 1831-1838
- 8 **Lara-Pezzi E, Serrador JM, Montoya MC, Zamora D, Yanez-Mo M, Carretero M, Furthmayr H, Sanchez-Madrid F, Lopez-Cabrera M.** The hepatitis B virus X protein (HBx) induces a migratory phenotype in a CD44-dependent manner: possible role of HBx in invasion and metastasis. *Hepatology* 2001; **33**: 1270-1281
- 9 **Chirillo P, Falco M, Puri PL, Artini M, Balsano C, Levrero M, Natoli G.** Hepatitis B virus pX activates NF-kappa B-dependent transcription through a Raf-independent pathway. *J Virol* 1996; **70**: 641-646
- 10 **Kononen J, Bubendorf L, Kallioniemi A, Barlund M, Schraml P, Leighton S, Torhorst J, Mihatsch MJ, Sauter G, Kallioniemi OP.** Tissue microarrays for high-throughput molecular profiling of tumor specimens. *Nat Med* 1998; **4**: 844-847
- 11 **Sambrook J, Fritsch EF, Maniatis T.** Molecular Cloning: A laboratory manual. 2nd ed. New York: Cold Spring Harbor Laboratory Press 1989
- 12 **Zhang DH, Salto-Tellez M, Chiu LL, Shen L, Koay ES.** Tissue microarray study for classification of breast tumors. *Life Sci* 2003; **73**: 3189-3199
- 13 **Bubendorf L, Kononen J, Koivisto P, Schraml P, Moch H, Gasser TC, Willi N, Mihatsch MJ, Sauter G, Kallioniemi OP.** Survey of gene amplifications during prostate cancer progression by high-throughput fluorescence *in situ* hybridization on tissue microarrays. *Cancer Res* 1999; **59**: 803-806
- 14 **Wang Y, Wu MC, Sham JS, Tai LS, Fang Y, Wu WQ, Xie D, Guan XY.** Different expression of hepatitis B surface antigen between hepatocellular carcinoma and its surrounding liver tissue, studied using a tissue microarray. *J Pathol* 2002; **197**: 610-616
- 15 **Majano P, Lara-Pezzi E, Lopez-Cabrera M, Apolinario A, Moreno-Otero R, Garcia-Monzon C.** Hepatitis B virus X protein transactivates inducible nitric oxide synthase gene promoter through the proximal nuclear factor kappaB-binding site: evidence that cytoplasmic location of X protein is essential for gene transactivation. *Hepatology* 2001; **34**: 1218-1224

- 16 **Pahl HL**. Activators and target genes of Rel/NF-KappaB transcription factors. *Oncogene* 1999; **18**: 6853-6866
- 17 **Li X**, Stark GR. NFkappaB-dependent signaling pathways. *Exp Hematol* 2002; **30**: 285-296
- 18 **Karin M**, Delhase M. The I kappa B kinase (IKK) and NF-kappa B: key elements of proinflammatory signalling. *Semin Immunol* 2000; **12**: 85-98
- 19 **Jobin C**, Sartor RB. The I kappa B/NF-kappa B system: a key determinant of mucosal inflammation and protection. *Am J Physiol Cell Physiol* 2000; **278**: C451-462
- 20 **Baldwin AS Jr**. The NF-kappa B and I kappa B proteins: new discoveries and insights. *Annu Rev Immunol* 1996; **14**: 649-683
- 21 **Baeuerle PA**, Baltimore D. NF-kappa B: ten years after. *Cell* 1996; **87**: 13-20
- 22 **Brown K**, Gerstberger S, Carlson L, Franzoso G, Siebenlist U. Control of I kappa B-alpha proteolysis by site-specific, signal-induced phosphorylation. *Science* 1995; **267**: 1485-1488
- 23 **Tai DI**, Tsai SL, Chang YH, Huang SN, Chen TC, Chang KS, Liaw YF. Constitutive activation of nuclear factor kappaB in hepatocellular carcinoma. *Cancer* 2000; **89**: 2274-2281
- 24 **Guo SP**, Wang WL, Zhai YQ, Zhao YL. Expression of nuclear factor-kappa B in hepatocellular carcinoma and its relation with the X protein of hepatitis B virus. *World J Gastroenterol* 2001; **7**: 340-344
- 25 **Rice NR**, Ernst MK. *In vivo* control of NF-KappaB activation by I Kappa B alpha. *EMBO J* 1993; **12**: 4685-4695
- 26 **Birbach A**, Gold P, Binder BR, Hofer E, de Martin R, Schmid JA. Signaling molecules of the NF-kappaB pathway shuttle constitutively between cytoplasm and nucleus. *J Biol Chem* 2002; **277**: 10842-10851
- 27 **Wu CG**, Forgues M, Siddique S, Farnsworth J, Valerie K, Wang XW. SAGE transcript profiles of normal primary human hepatocytes expressing oncogenic hepatitis B virus X protein. *FASEB J* 2002; **16**: 1665-1667
- 28 **Poussin K**, Dienes H, Sirma H, Urban S, Beaugrand M, Franco D, Schirmacher P, Brechot C, Paterlini-Brechot P. Expression of mutated hepatitis B virus X genes in human hepatocellular carcinomas. *Int J Cancer* 1999; **80**: 497-505
- 29 **Lin X**, Ma ZM, Yao X, Zhang YP, Wen YM. Replication efficiency and sequence analysis of full-length hepatitis B virus isolates from hepatocellular carcinoma tissues. *Int J Cancer* 2002; **102**: 487-491
- 30 **Hsia CC**, Nakashima Y, Tabor E. Deletion mutants of the hepatitis B virus X gene in human hepatocellular carcinoma. *Biochem Biophys Res Commun* 1997; **241**: 726-729
- 31 **Hsia CC**, Yuwen H, Tabor E. Hot-spot mutations in hepatitis B virus X gene in hepatocellular carcinoma. *Lancet* 1996; **348**: 625-626
- 32 **Kim H**, Lee YH, Won J, Yun Y. Through induction of juxtaposition and tyrosine kinase activity of Jak1, X-gene product of hepatitis B virus stimulates Ras and the transcriptional activation through AP-1, NF-kappaB, and SRE enhancers. *Biochem Biophys Res Commun* 2001; **286**: 886-894
- 33 **Tu H**, Bonura C, Giannini C, Mouly H, Soussan P, Kew M, Paterlini-Brechot P, Brechot C, Kremsdorf D. Biological impact of natural COOH-terminal deletions of hepatitis B virus X protein in hepatocellular carcinoma tissues. *Cancer Res* 2001; **61**: 7803-7810
- 34 **Barkett M**, Gilmore TD. Control of apoptosis by Rel/NF-kappaB transcription factors. *Oncogene* 1999; **18**: 6910-6924

Edited by Xu JY and Wang XL

Purification of heat shock protein 70-associated tumor peptides and its antitumor immunity on hepatoma in mice

Dai-Xiong Chen, Yan-Rong Su, Gen-Ze Shao, Zhen-Chao Qian

Dai-Xiong Chen, Key Laboratory of Cell Engineering of Guizhou Province, Affiliated Hospital of Zunyi Medical College, Zunyi 563003, Guizhou Province, China

Yan-Rong Su, Gen-Ze Shao, Department of Pathophysiology and Department of Biochemistry, Shantou University Medical College, Shantou 515031, Guangdong Province, China

Zhen-Chao Qian, Research Center of Cancer Biotherapy, Institute of Cancer Research, Dalian Medical University, Dalian 116027, Lianing Province, China

Supported by the National Natural Science Foundation of China, No.3973440-II

Correspondence to: Professor Dai-Xiong Chen, Key Laboratory of Cell Engineering of Guizhou Province, Affiliated Hospital of Zunyi Medical College, Dalian Road, Zunyi 563003, Guizhou Province, China. cellgene@163.com

Telephone: +86-852-8608812 **Fax:** +86-852-8638630

Received: 2003-03-12 **Accepted:** 2003-06-02

Abstract

AIM: To purify the heat shock protein (HSP) 70-associated tumor peptides and to observe its non-MHC-I molecule restrictive antitumor effect.

METHODS: By ConA-sepharose affinity chromatography, ADP-agarose affinity chromatography, and DEAE anion exchange chromatography, we were able to purify HSP70-associated peptides from mouse hepatoma (HCaF) cells treated in heat shock at 42 °C. Specific active immunization and adoptive cellular immunization assay were adopted to observe the immunoprotective effect elicited by HSP70-associated peptide complexes isolated from HcaF.

RESULTS: The finally purified HSP-associated peptides had a very high purity and specificity found by SDS-PAGE and Western blot. Mice immunized with HSP70-associated peptide complexes purified from HCaF cells were protected from HCaF living cell challenge. This effect was dose dependent. Adoptive immunization of immune spleen cells of mice immunized with HSP70-associated peptide complexes could elicit immunity against HCaF challenge, and the tumor-free mice could resist repeated challenges. This effect could be continuously enhanced by repeated challenge with HCaF living cells. The tumor-free mice could tolerate the challenge for as high as 1×10^7 HCaF cells. The mice immunized once with spleen cells pulsed with HSP70-associated peptide complexes *in vitro* could also result in a certain adoptive immunity against HCaF.

CONCLUSION: High purity and specificity of HSP70-associated peptides could be achieved from tumor cells by the low-pressure affinity chromatography method used in this study. HSP70-associated peptide complexes derived from the HCaF can elicit non-MHC-I molecule restrictive immunoprotective effect against HCaF. This effect can be transferred by adoptive immunization to mice and enhanced by repeated challenge with HCaF live cells.

Chen DX, Su YR, Shao GZ, Qian ZC. Purification of heat shock protein 70-associated tumor peptides and its antitumor immunity on hepatoma in mice. *World J Gastroenterol* 2004; 10(3):361-365

<http://www.wjgnet.com/1007-9327/10/361.asp>

INTRODUCTION

Heat shock proteins (HSPs) are molecular chaperones which are emerging as biochemical regulators of cell growth, apoptosis, protein homeostasis and cellular targets of peptides. Numerous studies have demonstrated that HSP70 preparations derived from a tumor can elicit cancer-specific immunity against the same tumor by virtue of their ability to bind tumor-specific peptides^[1-7]. Further studies indicated that tumor immunity elicited by immunization with HSP peptide complexes, including HSP70 and gp96 family, is mediated by CD8⁺ T lymphocytes, and its mechanism involves MHC-I class molecule restricted response which is required to channel the peptides into class I presentation pathway^[8-10]. In this study, we isolated successfully HSP70-associated peptides from mouse hepatoma HCaF by low-pressure chromatography system and investigated the non-MHC-I class molecule restrictive anti-tumor immunity elicited by purified HSP70 associated peptide complexes.

MATERIALS AND METHODS

Materials

Animals and tumor strain BALB/c mice (H-2^d), weighing 18-20 g, were purchased from Xipuerbikai Experimental Animal Ltd, Shanghai, China. Mouse hepatoma HCaF(non-MHC-I class molecule expression) was obtained from Cancer Institute, Dalian Medical University, China.

Reagents ConA-sepharose was purchased from Pharmacia Inc. ADP, ADP-agarose from Sigma Corp. Macro-Pre DEAE support, Macro-Prep High Q from Bio-Rad Corp. Low-molecule weight standard protein and IgG of goat anti-mouse labeled with horseradish peroxidase from B.M Corp, RPMI1640 and new born bovine serum from GIBCO Corp, and anti-HSP70 McAb(mouse anti-mouse) from Wuhan Boster Corp. All other reagents used were of analytic grade.

Methods

Purification of HSP70-associated peptides The ascites of mice which had been inoculated intraperitoneally with HCaF cells for 6-7 days were used. HCaF cells were washed three times in PBS, and then suspended in RPMI1640 complete medium with water immersion at 42 °C for 12 hours. The HCaF cell pellets harvested were homogenized in hypotonic buffer (10 mM NaHCO₃, 0.5 mM PMSF, pH7.1) and centrifuged at 100 000×g for 90 min at 4 °C, and the supernatant was collected. The supernatant concentrated by PEG(MW600) was applied to a ConA-sepharose column in the presence of ConA-sepharose bound buffer C (20 mM Tris-acetate, pH 7.5, 0.5 mM NaCl, 2 mM CaCl₂, 2 mM MgCl₂, 15 mM 2 ME, 0.5 mM PMSF), and fluid was collected at a flow rate of 12 ml/h, that was the

ConA-sepharose unbound protein. The fraction was dialyzed against buffer D (20 mM Tris-acetate, pH7.5, 20 mM NaCl, 3 mM MgCl₂, 15 mM 2ME, 0.5 mM PMSF) overnight at 4 °C. The sample was applied to an ADP-agarose column equilibrated previously with buffer D at a flow rate of 12 ml/h. The proteins were eluted by buffer D containing 0.5M NaCl and buffer D until the protein was not detected by Bradford method. The column was eluted by 25 ml buffer D containing 3 mM ADP. The harvested elute was concentrated and dialyzed against DEAE ion-exchange buffer A (20 mM Na₃PO₄, 20 mM NaCl, pH7.2). The sample was applied on a DEAE column equilibrated with buffer A at a flow rate of 10 ml/h. After buffer A equilibrium for 30 min, the target protein was eluted at a linear gradient of 20 mM-1 000 mM NaCl in buffer A (20 mM Na₃PO₄, 1M NaCl, pH7.0, ranging from 0%-100%). Various fractions harvested were detected with SDS-PAGE and silver staining. The fractions of HSP70 protein were collected, pooled and dried with freeze-drying, and stored at -20 °C until further use.

Identification of HSP70-associated tumor peptides HSP70 proteins were resolved on 10% SDS-PAGE, subjected to electrophoresis, detected by silver staining, and blotted using mAb specific for HSP70. Manipulation of SDS-PAGE and Western blot were performed according to the method described by Sambrook *et al*^[11]. The protein content was determined by Bradford standard curve method^[12].

Active immunization assays BALB/c mice were immunized subcutaneously with HSP70-associated peptide complexes, supernatant from homogenate of HCaF cells treated with heat shock (S-HCaF), supernatant from homogenate of liver cells treated with heat shock (S-HC), and PBS twice at weekly intervals separately and challenged by subcutaneous injection of the indicated number of HCaF living cells (5×10⁴ cells in 100 μl PBS) one week after the last immunization.

Adoptive immunoprotection experiment BALB/c mice were immunized with tail vein injection of immune spleen cells (ISC, 1×10⁷ cells in 200 μl PBS) of mice immunized with HSP70-associated peptides and free of tumor, twice at 5 days intervals, and challenged subcutaneously by 5×10⁴ HCaF living cells in 100 μl PBS 3 days after the last immunization. The mice with complete protection were challenged by 1×10⁵ HCaF living cells again 50 days after the first challenge. The mice which tolerated the second HCaF challenge, were challenged by 1×10⁷ HCaF living cells again. In another experiment, the mice were immunized by tail vein injection of spleen cells (1×10⁷ cells in 200 μl PBS) pulsed with HSP70-associated peptides *in vitro* and challenged subcutaneously by 5×10⁴ HCaF living cells in 100 μl PBS 3 days after immunization. Corresponding control groups were set in above experiment.

Statistical analysis

Values were expressed as mean±SD or percent (%). The data were analyzed with SPSS 8.0 software package. The results were considered statistically significant when $P < 0.05$.

RESULTS

Purity and specificity of HSP70-associated peptides

Purified HSP70-associated peptides showed one was bond on SDS-PAGE (Figure 1). Western blotting showed that molecular weight of HSP70-associated peptides purified from HCaF was about 70KD, which was consistent with the expected maker (Figure 2). The results indicated that HSP70-associated peptide complexes isolated from HCaF had a very high purity and specificity.

Active immunoprotective effect of HSP70-associated peptides derived from HCaF

As shown in Figure 3 and Table 1, different degrees of

immunoprotection against HCaF challenge could be elicited by immunization with HCaF-70 associated peptide complexes derived from HCaF. The effect on female groups was much better than that on male groups. This effect was dose-dependent. In the female groups, mice immunized with 600 μg/kg HSP70-associated peptides showed better protection than those immunized with 300 μg/kg HSP70-associated peptides. The survival rate of the two groups was 83.3% and 60%, respectively. The female mice immunized with S-HCaF also could result in a certain extent of protective effect against HCaF challenge, and the survival rate and mean survival time of tumor-bearing mice had significant differences from S-HC and PBS control groups ($P < 0.01$).

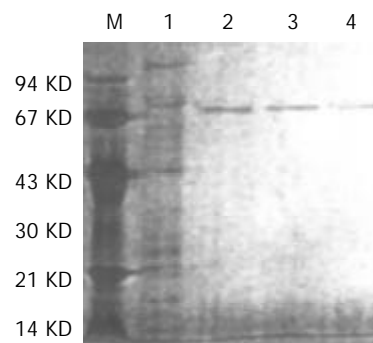


Figure 1 SDS-PAGE analysis of HSP70-tumor peptide complexes (silver staining). M: protein molecular weight marker, 1: protein eluted with 250-350 mmol/L NaCl buffer, after ADP-agarose chromatography (eluted with 0.5 mol/L NaCl buffer, PH7.5, containing 20 mmol/L Tris-acetate) and DEAE-ion exchange, 2-4: protein eluted with 250-350 mmol/L NaCl buffer, after ADP-agarose chromatography (eluted with 3 mmol ADP/L buffer, pH7.5, containing 20 mmol/L Tris-acetate) and DEAE-ion exchange.

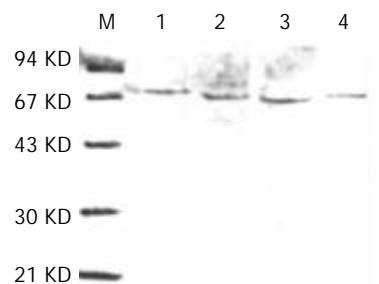


Figure 2 Western blot identification of HSP70-tumor peptide complexes purified from HCaF cells. The notes are the same with Figure 1.

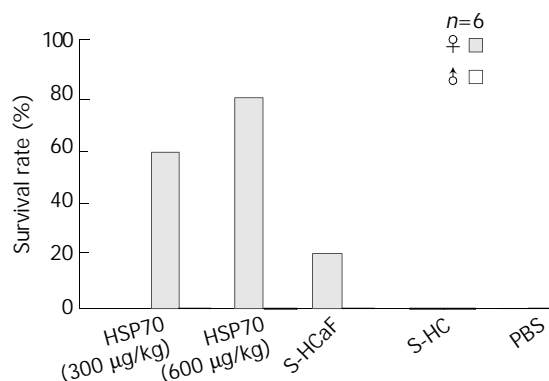


Figure 3 Immunoprotective effect of HSP70-associated peptides against tumor.

Table 1 Comparison of survival time of tumor-bearing mice after immunized by HSP70-peptide complexes

Groups	Sex	No. of tumor-bearing/ No. of mice challenged	Survival days of tumor-bearing (mean±SD)	Extended survival rate (%)
HSP70 300 µg/kg	Female	2/6	48.0±8.5 ^{ad}	67.4 ^{bd}
	Male	6/6	31.0±13.2	49.7 ^c
600 µg/kg	Female	1/6	33	
	Male	6/6	30.7±12.7	48.4 ^c
S-HCaF	Female	5/6	59.2±10.0 ^{bd}	106.5 ^{bd}
	Male	6/6	20.3±0.9	-2.0
S-HC	Female	6/6	24.0±5.8	-16.3
	Male	6/6	18.5±0.6	-10.5
PBS	Female	6/6	28.7±11.6	
	Male	6/6	20.7±6.1	

^a*P*<0.05, vs PBS; ^b*P*<0.01, vs PBS; ^c*P*<0.01, vs S-HC; ^d*P*<0.05, vs S-HC.

$$\text{Extended survival rate} = \frac{\text{MST of experimental group} - \text{MST of control group}}{\text{MST of control group}} \times 100\%$$

Table 2 Comparison of tumor growth in mice immunized with HSP70-peptide complexes

Groups	Sex	No. of tumor-bearing mice	10 days after HCaF challenge		15 days after HCaF challenge	
			Size of tumor (mm ³)	Inhibition rate (%)	Size of tumor (mm ³)	Inhibition rate (%)
HSP70 300 µg/kg	Female	2	0.88 ^{bc}	97.0 ^{ac}	6.66 ^{bd}	98.5 ^{ad}
	Male	6	61.98 ^{bd}	80.2 ^{bd}	384.77 ^{bc}	83.2 ^{bc}
600 µg/kg	Female	1	0.45	98.4	5.74	
	Male	6	64.49 ^b	79.4 ^{bd}	515.10 ^{bc}	77.6 ^{bc}
S-HCaF	Female	5	3.09 ^{bc}	89.2 ^{bc}	10.21 ^{bc}	97.7 ^{bc}
	Male	6	24.27 ^{bd}	92.2 ^{bd}	501.55 ^b	78.2 ^{bd}
S-HC	Female	6	30.00	-4.5	402.17	8.2
	Male	6	204.89	34.5	1 554.30	32.3
PBS	Female	6	28.70		438.17	
	Male	6	312.83		2 295.52	

^a*P*<0.05, vs PBS; ^b*P*<0.01, vs PBS; ^c*P*<0.01, vs S-HC; ^d*P*<0.05, vs S-HC.

$$\text{Inhibition rate (\%)} = 1 - \frac{\text{Tumor size of experimental group}}{\text{Tumor size of control group (PBS)}} \times 100\%$$

Table 3 Comparison of tumor weight and spleen weight after tumor-bearing mice death (mean±SD)

Groups	No. of tumor-bearing mice	Female		No. of tumor-bearing mice	Male	
		Tumor wt. (g)	Spleen wt. (g)		Tumor wt. (g)	Spleen wt. (g)
HSP70 300 µg/kg	2	14.40±6.22 ^{bce}	0.93±0.18 ^{bde}	6	7.06±2.59	0.19±0.04
	600 µg/kg	1	6.5	0.4	6	7.51±2.33
S-HCaF	6	8.68±1.65 ^a	0.53±0.22 ^{be}	6	5.06±0.71	0.24±0.10
S-HC	5	4.72±1.65	0.17±0.08	6	4.98±1.04	0.14±0.02
PBS	6	6.78±1.34	0.25±0.06	6	6.30±2.18	0.12±0.07

^a*P*<0.05, vs S-HC; ^b*P*<0.01, vs S-HC; ^c*P*<0.05, vs S-HCaF; ^d*P*<0.01, vs S-HCaF; ^e*P*<0.01, vs PBS.

Table 4 Adoptive immunoprotective effect against HCaF challenge elicited by ISC transfer

Group	Survival rate (%) (No. of death/No. of mice challenged)	Survival days of tumor-bearing mice (mean±SD)	Extended survival rate (%)	Tumor wt. (g) (mean±SD)	Spleen wt. (g) (mean±SD)
ISC	75 (2/8) ^a	50.5±9.2 ^b	71.0 ^b	14.92±0.42 ^{bc}	0.39±0.01 ^{bc}
SC	0 (8/8)	36.8±12.9	24.6	7.73±2.14	0.18±0.05
Chal. control	0 (8/8)	29.5±3.9	0	7.35±1.16	0.21±0.05

^a*P*<0.05, vs chal. Control; ^b*P*<0.01, vs chal. Control; ^c*P*<0.01, vs SC.

On the 10th day and 15th day after HCaF challenge, the tumor volume of tumor-bearing mice in both HSP70-associated peptides and S-HCaF groups was apparently smaller than that in S-HC and PBS groups (Table 2). In females, tumor weight and spleen weight of dead mice in both HSP70-associated peptides and S-HCaF groups were significantly larger than those in S-HC and PBS groups (Table 3).

Adoptive immunoprotective effect

Adoptively transferred immune spleen cells of mice, which had been immunized with HSP70-associated peptides and were free of tumor, could provoke immunoprotection against HCaF challenge. The survival rate of ISC-immunized mice was 75%, and the mean survival time of tumor-bearing mice was significantly prolonged compared with both non-immune spleen cells (SC) group and challenge control (Table 4).

The mice which tolerated HCaF challenge were challenged by 1×10^5 HCaF living cells, and the survival rate was 83.3%, while all of the challenge controls died within 27.5 days. The mice which tolerated the second challenge could tolerate repeated challenges for as high as 1×10^7 HCaF living cells, while all the challenge controls died within 22 days (Figure 4).

The mice immunized once with spleen cells pulsed with HSP70-associated peptides *in vitro* could lead to a certain extent of protection against HCaF challenge. Although the survival rate of mice was only 20%, the mean survival time of tumor-bearing mice was 42 days, all the mice treated with S-HCaF, S-HC, SC or PBS died within 33 days.

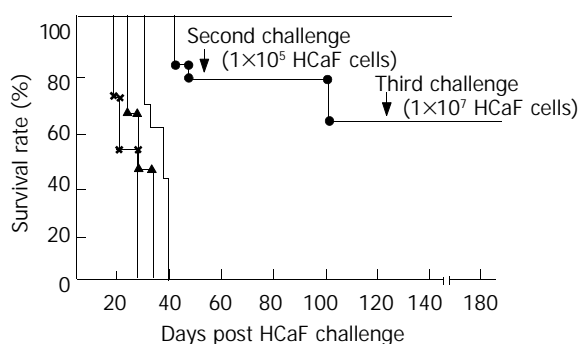


Figure 4 Protective effect of transferred immune spleen cells against repeated challenges with HCaF. -▲-▲ ×-× First, second, and third challenge controls. ●-● Transferred immune spleen cell group.

DISCUSSION

Intracellular HSP70 is very low in content of cells and makes up approximately 0.01% of the cell wet weight. At present, ConA-sepharose affinity chromatography or ADP-agarose affinity chromatography in combination with fast protein liquid chromatography^[13,14] has been the typical method for purifying HSP70. The recovery of HSP70 isolated by the above methods was lower than 50 mg/L cell pellet^[4]. The purification protocol used in our experiment resulted in a relatively high recovery compared with the traditional method of HSP70 purification, being for 50-100 mg/L wet weight of cell pellet. This purification method might be used as a universal technique due to its easy and reproducible isolation of antigenic HSP from other tissues of different sources.

Numerous investigations have shown that HSP itself had no antigenicity and its immunogenicity has been attributed to the peptide chaperoned carried by itself^[1-4]. In this experiment, tumor rejection assay demonstrated that HSP70 purified from HCaF could elicit tumor immunity. We therefore conclude that purified HSP70 identified by both SDS-PAGE and Western

blot should be regarded as HSP70-associated tumor peptides.

Our experiment indicated that HSP70-associated peptides derived from HCaF could elicit anti-tumor immunity. Mice immunized with 600 µg/kg HSP70-associated peptides showed better protection than those immunized with 300 µg/kg. This effect was dose-dependent, and was consistent with other reports^[4]. In this study, we found the transferred immune spleen cells of mice immunized with HSP70-associated peptide complexes could elicit immunity against HCaF challenge, and the tumor-free mice could resist repeated HCaF challenges. This effect could be continuously enhanced by repeated challenges with HCaF living cells. The mice so treated could tolerate a challenge for as high as 1×10^7 HCaF cells. Our results demonstrated that adoptively transferred immune spleen cells immunized with HSP70-associated tumor peptides could result in immunoprotection against the same tumor. This evidence indicates that anti-tumor immunity elicited by HSP70-associated peptides has a considerable stability of immunoprotection and specific immunologic memory.

It has been generally believed that tumor immunity elicited by immunization with exogenous HSP70-peptide complexes is mediated by antigen-presenting cells and presented by MHC class I molecules^[15-24]. It is worth pointing out that the tumor model of HCaF used in our experiment did not express MHC class I molecule protein. Therefore, the tumor immunity elicited by HSP70-associated peptides derived from HCaF might not be mediated by CD8⁺ CTL. Several studies have shown that HSP70-associated peptides could directly activate $\gamma \delta$ T lymphocytes or nature killer cells as superantigen without being dependent on the stimulation of MHC-Ia and I b class molecules^[25-30]. It is possible that HSP70-associated peptides derived from HCaF can elicit antitumor immunity in a similar manner.

In addition, we found that the supernatants of HCaF cell homogenate could also result in a certain tumor immunity. This effect might be related to the expression of HSP in HCaF cells induced by heat shock.

Compared spleen weight of tumor-bearing mice in various groups, the mean spleen weight of tumor-bearing mice in HSP70-associated peptide complexes group was significantly higher than that in the controls. Our results further showed that adoptively transferred spleen cells pulsed with purified HSP70-associated peptides could also provoke a certain protection against HCaF challenge. These results indicated that spleen cells might play an important role in tumor immunity mediated by HSP70-associated peptides.

It is of great interest to note that the protective effect in the female mice immunized with HSP70-associated peptide complexes was significantly better than that in the male group. The difference may be associated with estrogens, its mechanisms remain to be explored further.

REFERENCES

- 1 **Srivastava PK**, DeLeo AB, Old LJ. Tumor rejection antigens of chemically induced sarcomas of inbred mice. *Proc Natl Acad Sci U S A* 1986; **83**: 3407-3411
- 2 **Palladino MA Jr**, Srivastava PK, Oettgen HF, DeLeo AB. Expression of a shared tumor-specific antigen by two chemically induced BALB/c sarcomas. *Cancer Res* 1987; **47**: 5074-5079
- 3 **Srivastava PK**, Udono H. Heat shock protein-peptide complexes in cancer immunotherapy. *Curr Opin Immunol* 1994; **6**: 728-732
- 4 **Udono H**, Srivastava PK. Heat shock protein70-associated peptides elicit specific cancer immunity. *J Exp Med* 1993; **178**: 1391-1396
- 5 **Ciupitu AM**, Petersson M, Kono K, Charo J, Kiessling R. Immunization with heat shock protein 70 from methylcholanthrene-induced sarcomas induces tumor protection correlating with *in vitro* T cell responses. *Cancer Immunol Immunother* 2002; **51**: 163-170
- 6 **Basu S**, Srivastava PK. Heat shock proteins: the fountainhead

- of innate and adoptive immune responses. *Cell Stress Chaperones* 2000; **5**: 443-451
- 7 **Przeziorka D**, Srivastava PK. Heat shock protein-peptide complexes as immunotherapy for human cancer. *Mol Med Today* 1998; **4**: 478-484
 - 8 **Meng SD**, Gao F, Tien P. Role of heat shock protein-peptide complexes on tumor and infectious diseases immunity. *Shenwu Gongcheng Xuebao* 2000; **16**: 425-428
 - 9 **Singh-Jasuja H**, Toes RE, Spee P, Munz C, Hilf N, Schoenberger SP, Ricciardi-Castagnoli P, Neefjes J, Rammensee HG, Arnold-Schild D, Schild H. Cross-presentation of glycoprotein 96-associated antigen on major histocompatibility complex class I molecules requires receptor-mediated endocytosis. *J Exp Med* 2000; **191**: 1965-1974
 - 10 **Srivastava PK**. Purification of heat shock protein-peptide complexes for use in vaccination against cancers and intracellular pathogens. *Methods* 1997; **12**: 165-171
 - 11 **Sambrook J**, Fritsch EF, Maniatis T. Molecular cloning: A laboratory manual. Second Edition. USA: Cold Spring Harbor Laboratory Press 1989: 18.47-18.75
 - 12 **Marshak DR**, Kadoyama JT, Burgess RR, Knuth MW, Brennan JR, Lin SH. Strategies for protein purification and characterization: A laboratory course manual. Beijing: China Science Press 1999: 158-159
 - 13 **Peng P**, Menoret A, Srivastava PK. Purification of immunogenic heat shock protein 70-peptide complexes by ADP-affinity chromatography. *J Immunol Methods* 1997; **204**: 13-21
 - 14 **Suto R**, Srivastava PK. A mechanism for the specific immunogenicity of heat shock protein-chaperoned peptides. *Science* 1995; **269**: 1585-1588
 - 15 **Srivastava PK**, Udono H, Blachere NE, Li Z. Heat shock proteins transfer peptides during antigen processing and CTL priming. *Immunogenetics* 1994; **39**: 93-98
 - 16 **Udono H**, Srivastava PK. Comparison of tumor-specific immunogenicities of stress-induced protein gp96, hsp90, and hsp70. *J Immunol* 1994; **152**: 5398-5403
 - 17 **Basu S**, Binder RJ, Ramalingam T, Srivastava PK. CD91 is a common receptor for heat shock proteins gp96, hsp90, hsp70, and calreticulin. *Immunity* 2001; **14**: 303-313
 - 18 **Dressel R**, Lubbers M, Walter L, Herr W, Gunther E. Enhanced susceptibility to cytotoxic T lymphocytes without increase of MHC class II antigen expression after conditional overexpression of heat shock protein 70 in target cells. *Eur J Immunol* 1999; **29**: 3925-3935
 - 19 **Basu S**, Srivastava PK. Calreticulin, a peptide-binding chaperone of the endoplasmic reticulum, elicits tumor- and peptide-specific immunity. *J Exp Med* 1999; **189**: 797-802
 - 20 **Ishii T**, Udono H, Yamano T, Ohta H, Uenaka A, Ono T, Hizuta A, Tanaka N, Srivastava PK, Nakayama E. Isolation of MHC class I-restricted tumor antigen peptide and its precursors associated with heat shock protein hsp70, hsp90, and gp96. *J Immunol* 1999; **162**: 1303-1309
 - 21 **Suzue K**, Zhou X, Eisen HN, Young RA. Heat shock fusion proteins as vehicles for antigen delivery into the major histocompatibility complex class I presentation pathway. *Proc Natl Acad Sci U S A* 1997; **94**: 13146-13151
 - 22 **Blachere NE**, Li Z, Chandawarkar RY, Suto R, Jaikaria NS, Basu S, Udono H, Srivastava PK. Heat shock protein-peptide complexes, reconstituted *in vitro*, elicit peptide-specific cytotoxic T lymphocyte response and tumor immunity. *J Exp Med* 1997; **186**: 1315-1322
 - 23 **Heike M**, Noll B, Meyer zum Buschenfelde KH. Heat shock protein-peptide complexes for use in vaccines. *J Leukoc Biol* 1996; **60**: 153-158
 - 24 **Ojcius DM**, Delarbre C, Kourilsky P, Gachelin G. Major histocompatibility complex class II molecules and resistance against intracellular pathogens. *Crit Rev Immunol* 1994; **14**: 193-220
 - 25 **Kaur I**, Voss SD, Gupta RS, Schell K, Fisch P, Sondel PM. Human peripheral $\gamma\delta$ T cells recognize hsp60 molecules on Daudi Burkitt's lymphoma cells. *J Immunol* 1993; **150**: 2046-2055
 - 26 **Thomas ML**, Samant UC, Deshpande RK, Chiplunkar SV. Gamma delta T cells lyse autologous and allogenic oesophageal tumors: involvement of heat-shock proteins in the tumour cell lysis. *Cancer Immunol Immunother* 2000; **48**: 653-659
 - 27 **Multhoff G**, Botzler C, Issels R. The role of heat shock proteins in the stimulation of an immune response. *Biol Chem* 1998; **379**: 295-300
 - 28 **Botzler C**, Li G, Issels RD, Multhoff G. Definition of extracellular localized epitopes of Hsp70 involved in an NK immune response. *Cell Stress Chaperones* 1998; **3**: 6-11
 - 29 **Multhoff G**, Mizzen L, Winchester CC, Milner CM, Wenk S, Eissner G, Kampinga HH, Laumbacher B, Johnson J. Heat shock protein 70 (Hsp70) stimulates proliferation and cytolytic activity of natural killer cells. *Exp Hematol* 1999; **27**: 1627-1636
 - 30 **Multhoff G**. Activation of natural killer cells by heat shock protein70. *Int J Hyperthermia* 2002; **18**: 576-585

Edited by Ma JY and Wang XL

Antisense oligonucleotide targeting at the initiator of hTERT arrests growth of hepatoma cells

Su-Xia Liu, Wen-Sheng Sun, Ying-Lin Cao, Chun-Hong Ma, Li-Hui Han, Li-Ning Zhang, Zhen-Guang Wang, Fa-Liang Zhu

Su-Xia Liu, Wen-Sheng Sun, Ying-Lin Cao, Chun-Hong Ma, Li-Hui Han, Li-Ning Zhang, Zhen-Guang Wang, Fa-Liang Zhu, Institute of Immunology, Medical School of Shandong University, Wenhua West Road 44, Jinan 250012, Shandong Province, China
Supported by the National Natural Science Foundation of China, No.30070341

Correspondence to: Dr. Wen-Sheng Sun, Institute of Immunology, Medical School of Shandong University, Wenhua West Road 44, Jinan 250012, Shandong Province, China. wangjd@jn-public.sd.cninfo.net
Telephone: +86-531-8382038 **Fax:** +86-531-8382084
Received: 2002-09-14 **Accepted:** 2002-10-28

Abstract

AIM: To evaluate the inhibitory effect of antisense phosphorothioate oligonucleotide (asON) complementary to the initiator of human telomerase catalytic subunit (hTERT) on the growth of hepatoma cells.

METHODS: The as-hTERT was synthesized by using a DNA synthesizer. HepG2.2.15 cells were treated with as-hTERT at the concentration of 10 μ mol/L. After 72 h, these cells were obtained for detecting growth inhibition, telomerase activity using the methods of MTT, TRAP-PCR-ELISA, respectively. BALB/c(nu/nu) mice were injected HepG2.2.15 cells and a human-nude mice model was obtained. There were three groups for anti-tumor activity study. Once tumors were established, these animals in the first group were administered as-hTERT and saline. Apoptosis of tumor cells was detected by FCM. In the 2nd group, the animals were injected HepG2.2.15 cells together with as-hTERT. In the third group, the animals were given as-hTERT 24 hours postinjection of HepG2.2.15 cells. The anti-HBV effects were assayed with ELISA *in vitro* and *in vivo*.

RESULTS: Growth inhibition was observed in cells treated with as-hTERT *in vitro*. A significant different in the value of $A_{570}-A_{630}$ was found between cells treated with as-hTERT and control ($P < 0.01$) by MTT method. The telomerase activity of tumor cells treated with as-hTERT was reduced, the value of A_{450} nm was 0.42 compared to control (1.49) with TRAP-PCR-ELISA. The peak of apoptosis in tumor cells given as-hTERT was 21.12%, but not seen in saline-treated control. A prolonged period of carcinogenesis was observed in the second and third group animals. There was inhibitory effect on the expression of HBsAg and HBeAg *in vivo* and *in vitro*.

CONCLUSION: As-hTERT has an anti-tumor activity, which may be useful for gene therapy of tumors.

Liu SX, Sun WS, Cao YL, Ma CH, Han LH, Zhang LN, Wang ZG, Zhu FL. Antisense oligonucleotide targeting at the initiator of hTERT arrests growth of hepatoma cells. *World J Gastroenterol* 2004; 10(3):366-370

<http://www.wjgnet.com/1007-9327/10/366.asp>

INTRODUCTION

Human hepatocellular carcinoma (HCC) is a critical disease threatening human health. It is one of the most common malignant tumors worldwide, however there is no effective treatment at present. It is very necessary to explore new methods for the therapy of HCC. The developments in molecular biochemistry have afforded the possibility for this purpose.

Telomerase, a ribonucleoprotein enzyme that synthesizes telomeric DNA, is thought to be necessary for cellular immortality and carcinogenesis^[1,2], and consists of human telomerase RNA component (hTERC), human telomerase protein 1(hTEP1), and human telomerase reverse transcriptase (hTERT). Among them, only the expression of hTERT mRNA is correlated with telomerase^[3], and mainly regulates the expression of human telomerase enzymatic activity^[4-6]. hTERT is a useful marker for telomerase activation^[7,8]. It is associated with the majority of malignant human cancers. Therefore, telomerase is the target of anti-tumor drugs research. For example, many scientists declared that ribozyme which cleaved telomerase mRNA and PS-ODNs complementary to the repeat sequence of the mammalian telomere (5' TTAGGG3') could arrest tumor cells^[9-13] in cell lines. In this study, we observed the inhibitory effect of as-hTERT both *in vivo* and *in vitro*.

In HCC, the activity of telomerase played a very important role during the occurrence of HCC and cirrhotic livers^[14]. The positive hTERT mRNA was 89.47% in HCC tissues^[15]. Though many factors were related to hepatocarcinogenesis^[16], infection of HBV and HCV^[17] was the most important. Tahara *et al*^[18] discovered that telomerase activity was 100% in HCC tissues with HBV positivity. These studies indicated that there might be a close relationship between HBV infection and telomerase activity during hepatocarcinogenesis. Therefore, in this study, HepG2.2.15 cells, a cell line in which HBV genome was integrated into the chromosome, were the target cells and as-hTERT complementary to hTERT promoter was added to these cells, and the anti-tumor effects and inhibitory action on HBV gene expression of as-hTERT were studied *in vitro* and *in vivo*.

MATERIALS AND METHODS

Materials

The oligomers used in this study were prepared by Shengong Co. The solutions were suspended in sterile phosphate-buffered saline (PBS) and filtered into 1.5 ml sterile Eppendorf tube, and stored at 4 °C until use. AsON used in this study targeted at the promoter area of human hTERT with the sequence 5' GCC ACG TGG GAA GCG 3' (-192--176 site). In this area, there is a potential binding site of upstream stimulating factors, such as pro-oncogene c-myc. The random sequence (5' TTG CCG AGC GGG GTA 3') was used as control. HepG2.2.15 was used as targeted cells. This cell line was purchased from Beijing Institute of Medical Biology. Fetal calf serum (FCS) and G418 were purchased from GIBCO and Sigma respectively. The quantitative detection kit of telomerase (PCR-ELISA) was purchased from Roche Molecular Biochemicals, Germany.

Cell culture

The experimental protocols were similar to those as previously described^[19,20]. HepG2.2.15 was a hepatoma cell line which was integrated with HBV genome, and could replicate intact HBV DNA and extract HBsAg and HBeAg. The cells were grown *in vitro* in a 25 ml flask at a concentration of 5×10^4 cells per milliliter in MEM media supplemented with 10% fetal bovine serum containing 380 $\mu\text{g/ml}$ G418^[21,22]. The cells were tested for HBsAg and HBeAg and found to replicate HBV DNA. When the cells grew to 75% confluence, they were digested and used for the *in vitro* and *in vivo* studies.

MTT assay

The cells were cultured in 60 mm² dishes with 2×10^5 cells per dish. The next day as-hTERT and control sequence were added at a concentration of 10 μM . After 72 h incubation, these cells were added 20 μL of MTT per dish. Four hours later, the cells were given 100 μL of DMSO per dish and the absorbance of the sample was measured at 570 nm and 630 nm using an ELISA microtiter plate reader. The value of absorbance at 570 nm and 630 nm was named A_{570} and A_{630} .

Determination of telomerase activity

Telomerase activity assay was performed according to a polymerase chain reaction-based telomeric repeat amplification protocol as described previously^[23-26] using a kit from Roche (Germany). The cells (10^5 - 10^6 per dish) were harvested after 72 h incubation with as-hTERT and control sequence.

Preparation of extracts from cells The cells were put in a 1.5 ml Eppendorf tube and pelleted at 3 000 \times g for 10 min in a refrigerated centrifuge at 4 °C. Then these cells were washed once in cold PBS. For one tube, 200 μl pre-cooled lysis reagent was added and incubated on ice for 30 min and centrifuged at 10 000 \times g for 20 min at 4 °C. A total of 175 μl supernatant was carefully transferred to a fresh Eppendorf tube. These cell extracts were used for the telomerase assay using the telomerase PCR-ELISA procedure.

Telomeric repeat amplification protocol (TRAP reaction)

For each sample, 25 μl reaction mixture was transferred into a PCR tube. Three μl cell extract and sterile water were transferred to a final volume of 50 μl . Then a combined primer elongation reaction was performed according to the following protocol (Table 1).

Table 1 Protocol of TRAP reaction

Step	Time	Temperature	Cycle number
Primer elongation	30 min	25 °C	1
Telomerase inactivation	5 min	94 °C	2
Amplification			3-32
Denaturation	30 s	94 °C	
Annealing	30 s	50 °C	
Polymerization	90 s	72 °C	
	10 min	72 °C	33

Hybridization and ELISA procedure The product of PCR was aliquoted, denatured, bound to a streptavidin-coated 96 well plate, and hybridized to a DIG-labelled telomeric-repeat specific probe. An antibody to DIG conjugated to peroxidase was subsequently bound to DIG. Then tetramethyl benzidine (TMB) was metabolized, the substrates of the enzyme was added to produce a colored reaction product. The absorbance of the sample was measured at 450 nm using an ELISA microtiter plate reader within 30 min after adding the stop reagent. The value of absorbance at 450 nm was named A_{450} .

Animal studies

BALB/c (*nu/nu*) mice (weighing approximately 18-20 g) were purchased from the Experimental Animals Center of Chinese Academy of Sciences. The mice were divided into eight teams randomly. These animals were placed into fresh cages with free access to sterile water. All the solutions were filtered into sterile bottles. In order to compare the different curative effects of as-hTERT by different administration routes, the study was divided into three study groups.

Group I: Each mouse was injected subcutaneously 5×10^6 cells at the left axilla and tumor progression was measured daily. Two weeks postinjection, the mice with tumors about 0.5 cm in diameter were selected, and as-hTERT and control sequence were injected into the tumors subcutaneously. These animals were divided into two teams, one team ($n=12$) was injected as-hTERT 100 $\mu\text{g}/\text{mouse}/\text{day}$, the other ($n=6$) was treated with saline 100 $\mu\text{l}/\text{mouse}/\text{day}$. Five days postinjection, the mice were killed by removing the eyeballs and the tumor tissues were removed, and stored in 10% formalin for FCM. These tumor samples were also embedded in paraffin, and sectioned into slices about 5 μm in thickness. The sections were stained with hematoxylin and eosin for histological examination. In this group, the serum were harvested and stored at -20 °C for detecting HBsAg and HBeAg.

Group II: Each mouse was injected subcutaneously 5×10^6 cells at the left axilla and as-hTERT 100 $\mu\text{g}/\text{mouse}$ ($n=7$) simultaneously, the controls with saline 100 $\mu\text{l}/\text{mouse}$ ($n=6$) and random controls with as-hTERT 100 $\mu\text{g}/\text{mouse}$ ($n=6$), and tumor progression was measured daily.

Group III: Each mouse was injected subcutaneously 5×10^6 cells at the left axilla. One day postinjection, each mouse was injected as-hTERT 100 $\mu\text{g}/\text{mouse}$ ($n=12$), saline 100 $\mu\text{l}/\text{mouse}$ ($n=8$) and random controls with as-hTERT 100 $\mu\text{g}/\text{mouse}$ ($n=8$) at the same axilla. Three weeks postinjection, no tumors were detected in 10 animals treated with as-hTERT. These mice were divided further into another two teams: one team ($n=6$) was injected subcutaneously as-hTERT at the dosage of 30 $\mu\text{g}/\text{mouse}$ at the same place as the first time, the other ($n=4$) was given saline.

In each group, tumor progression was measured, and observations on animal behavior were recorded daily during the study period.

HBV antigen detection

According to the protocol of antigen detection kit (Lizhu Co. Shenzhen, China), the concentrations of HBsAg and HBeAg in the supernatant were detected using an ELISA microtiter plate reader. The results were illustrated with P/N value ($P/N = \text{sample A}/\text{negative control A}$. A stands for the amount of light absorbance).

Statistical analysis

All the data were expressed as the mean \pm standard error of the mean (SE). The *P* values were calculated by ANOVA or exact probability method. A *P* value less than 0.05 was considered statistically significant.

RESULTS

as-hTERT on activity of telomerase

The results were shown with the value of $A_{450\text{nm}}$. $A_{450\text{nm}}$ of as-hTERT treated cells, random sequence control, positive control were 0.42, 1.49 and 1.51 respectively (Figure 1). That of the negative control was 0.08. Telomerase activity was inhibited with the addition of 17-base as-hTERT at a concentration of 10 μM .

Antiproliferation effect of as-hTERT on HepG2.2.15 cells

Seventy-two hours after incubation with the drugs, as-hTERT caused significant ($F=251.13$, $P=0.0001$) inhibition of cell growth as shown in Figure 1, but not in random sequence controls and saline controls.

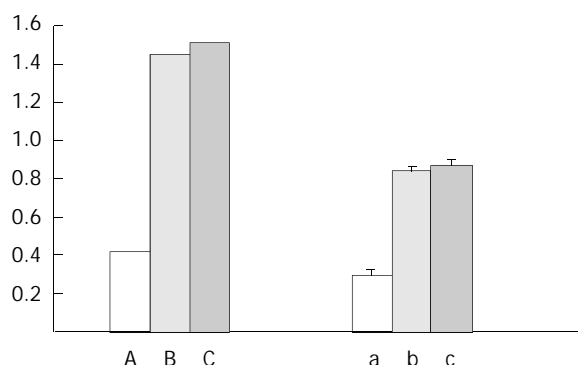


Figure 1 Inhibition effects on HepG2.2.15 cells of as-hTERT *in vitro*. A, B and C: Growth inhibition by MTT method. a, b, and c: Inhibitory effects on telomerase activity by PCR-ELISA. A and a: as-hTERT treated cells, B and b: Random sequence treated cells, C and c: Saline treated cells.

Growth arrest of human hepatocarcinoma *in vivo*

The drugs were injected into the tumors. After seven days, the peaks of apoptosis of tumor cells treated with as-hTERT, saline control were 21.12% and 7.92% respectively (Figure 2). Inflammation was observed in tissues treated with as-hTERT, but not in controls. The conformation of the animals' liver was normal.

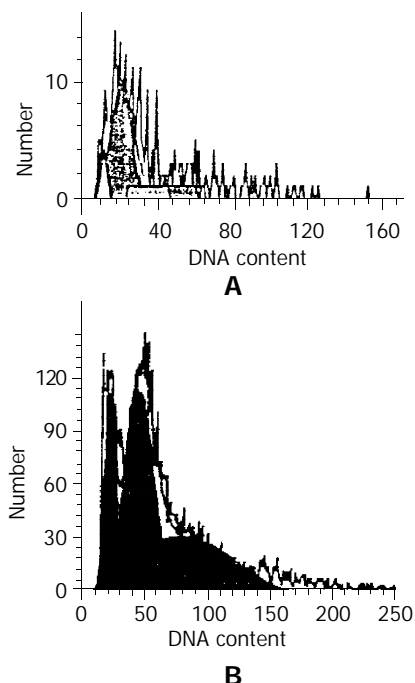


Figure 2 Cell cycle of tumor cells treated with as-hTERT/saline *in vivo*. A: Cell cycle of tumor cells treated with saline. The apoptosis peak was 7.92% (#). B: Cell cycle of tumor cells treated with as-hTERT. The apoptosis peak was 21.12%(*).

As-hTERT could retard tumor cell growth. In the group in which the drugs were injected in combination with HepG2.2.15 cells, tumors were undetectable subcutaneously during the whole study period (10 weeks, 0%, 0/7), while the saline and random sequence controls failed to inhibit tumor growth. In

two weeks, tumors were developed in all of the animals in control teams (100%, 8/8). There was a significant difference between as-hTERT treated and control animals ($P<0.01$).

If the drugs were injected 24 h after the animals were injected with the cells, in three weeks, tumors were detectable in all of the animals in control teams (100%, 8/8), while in team of animals treated with as-hTERT tumors began to appear in two (16.7%, 2/12), and grew very slowly. Furthermore, if the animals without tumor were injected supplementary drugs, subcutaneous tumor was undetectable during the later 6w (0%, 0/6), while in the team of animals without extra addition of the drugs, tumors developed (Figure 3).

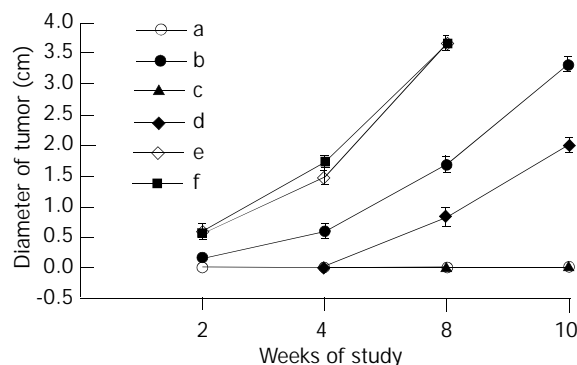


Figure 3 Inhibition effects of tumor cells *in vitro*. a: as-hTERT and HepG2.2.15 cells were injected into animals together. There was no tumor growth in ten weeks. So the diameter of tumor was 0 during the whole study period. b: as-hTERT was injected 24 hours postinjection of the cells. Tumor was not grown in animals which were treated with as-hTERT supplementary (c), otherwise (d), tumors grew again, but very slowly. In random (e) and saline control (f), there was no retarding effect on tumorcell growth. Tumors grew very fast, and after eight weeks, the animals died naturally.

Alteration of HBV antigen expression

as-hTERT could inhibit HBV expression *in vitro* and *in vivo*. *In vitro*, the inhibition peaks on HBsAg and HBeAg were 76% and 56% respectively, while *in vivo*, the inhibition peaks were 38% and 73%.

DISCUSSION

Hepatocarcinogenesis is a very complicated event, and many factors were involved in this process, such as activation of oncogenes, inactivation of tumor suppressor genes and hepatitis virus infection^[27]. But the most important is the activation of telomerase. Therefore, to inhibit telomerase activity so as to arrest tumor cell growth by antisense technique is of great significance. In most researches, the target gene was hTR, which is the replication template for telomere, but not the regulatory region of hTERT, the most important region which regulates the activity of telomerase.

Recent studies suggested that hTERT gene expression was controlled mainly at the transcriptional level^[28]. Many cis-elements and trans-acting factors that regulate the hTERT gene transcription have been identified^[29-31]. Among the potential transcription factor binding sites within hTERT promoter region, a typical E-box (CACGTG, -178--182) which belongs to the bHLHZ family of transcription factors (such as oncogene c-myc), was likely to play an important role in hTERT gene transcription^[32-38]. Our results showed that as-hTERT targeting at the binding site of E-box in hTERT promoter region could inhibit the growth of HepG2.2.15 cells *in vitro*. The probable reason was that the regulating effect of E-box on hTERT transcription was eliminated due to as-hTERT complementary

to E-box binding site. Therefore, telomerase activity was decreased, telomere was shortened to the crisis point, and cell growth was arrested, and apoptosis was increased. However, asON could not completely inhibit telomerase activity. This result indicated that E-box is one of the cis-elements which regulate telomerase transcription. Furthermore, it is very important to study on cis-element and transcriptional factors regulating telomerase activity.

AsON targeting at the promoter region of telomerase could inhibit hepatoma cell growth of mice model *in vivo*. Different ways of drugs administration demonstrated different growth inhibitory effects. Apoptosis was detected in tumors injected as-hTERT, but not in cells treated with saline controls. The best growth inhibitory effect on tumor cells was observed in animals injected as-hTERT in combination with the cells. In another team, tumor growth was observed in the mice which were given as-hTERT 24 hours postinjection of HepG2.2.15 cells at the same site, but the tumors grew very slowly. It could not inhibit tumor cell growth completely through this way. However, if the mice were given a smaller dosage of the drug continually, tumor cell growth would be inhibited completely. These results demonstrated that as-hTERT could inhibit tumor cell growth, the earlier the drug were given, the better the effect was. It suggests that as-hTERT can be an effective drug for eliminating the remaining tumor cells after operation.

HBV genome could integrate into the telomerase gene^[32,39]. HBV was a potential cis-activation factor which regulated telomerase activity^[40]. The expression of HBV gene could increase telomerase activity^[41]. This study demonstrated that as-hTERT could affect the expression of HBV antigen both *in vitro* and *in vivo*. The reason may be that as-hTERT inhibited telomerase activity, and cell growth was retarded. Therefore, HBsAg and HBeAg expressions were inhibited. Maybe, there is some relationship between telomerase activity and HBV, which needs to be further clarified.

Furthermore, there was no toxicity on the mice. In summary, we have demonstrated that a short asON which targets at the initiator of hTERT is capable of inhibiting telomerase activity and retarding tumor cell growth both *in vitro* and *in vivo* in a sequence-dependent manner. These results provide further evidence that drugs targeting at telomerase have a therapeutic potential.

REFERENCES

- Avilion AA**, Piatyszek MA, Gupta J, Shay JW, Bacchetti S, Greider CW. Human telomerase RNA and telomerase activity in immortal cell lines and tumor tissues. *Cancer Res* 1996; **56**: 645-650
- Kim NW**, Piatyszek MA, Prowse KR, Harley CB, West MD, Ho PL, Coviello GM, Wright WE, Weinrich SL, Shay JW. Specific association of human telomerase activity with immortal cells and cancer. *Science* 1994; **266**: 2011-2015
- Yeh TS**, Chen TC, Chen MF. Dedifferentiation of human hepatocellular carcinoma up-regulates telomerase and Ki-67 expression. *Arch Surg* 2000; **135**: 1334-1339
- Tominaga T**, Kashimura H, Suzuki K, Nakahara A, Tanaka N, Noguchi M, Itabashi M, Ohkawa J. Telomerase activity and expression of human telomerase catalytic subunit gene in esophageal tissues. *J Gastroenterol* 2002; **37**: 418-427
- Yang Y**, Chen Y, Zhang C, Huang H, Weissman SM. Nucleolar localization of hTERT protein is associated with telomerase function. *Exp Cell Res* 2002; **277**: 201-209
- Cao Y**, Li H, Deb S, Liu JP. TERT regulates cell survival independent of telomerase enzymatic activity. *Oncogene* 2002; **21**: 3130-3138
- Toshikuni N**, Nouse K, Higashi T, Nakatsukasa H, Onishi T, Kaneyoshi T, Kobayashi Y, Kariyama K, Yamamoto K, Tsuji T. Expression of telomerase-associated protein 1 and telomerase reverse transcriptase in hepatocellular carcinoma. *Br J Cancer* 2000; **82**: 833-837
- Kotoula V**, Hytiroglou P, Pырpasopoulou A, Saxena R, Thung SN, Papadimitriou CS. Expression of human telomerase reverse transcriptase in regenerative and precancerous lesions of cirrhotic livers. *Liver* 2002; **22**: 57-69
- Ludwig A**, Saretzki G, Holm PS, Tiemann F, Lorenz M, Emrich T, Harley CB, Von Zglinicki T. Ribozyme cleavage of telomerase mRNA sensitizes breast epithelial cells to inhibitors of topoisomerase. *Cancer Res* 2001; **61**: 3053-3061
- Qu Y**, Liu SQ, Peng WZ, Liu BL. Inhibition of telomerase activity by ribozyme targeted to human telomerase transcriptase. *Shengwu Huaxue Yu Shengwu Wuli Xuebao* 2002; **34**: 323-328
- Yokoyama Y**, Takahashi Y, Shinohara A, Wan X, Takahashi S, Niwa K, Tamaya T. The 5' -end of hTERT mRNA is a good target for hammerhead ribozyme to suppress telomerase activity. *Biochem Biophys Res Commun* 2000; **273**: 316-321
- Mei M**, Yu H, Zhang W, Shi J, Yang J. Inhibition of hTR activity for suppression of lung cancer cell proliferation using antisense phosphorothioate oligonucleotides. *Zhonghua Binglixue Zazhi* 2000; **29**: 204-207
- Kushner DM**, Paranjape JM, Bandyopadhyay B, Cramer H, Leaman DW, Kennedy AW, Silverman RH, Cowell JK. 2-5A antisense directed against telomerase RNA produces apoptosis in ovarian cancer cells. *Gynecol Oncol* 2000; **76**: 183-192
- Zhang R**, Wang X, Guo L, Xie H. Growth inhibition of BEL-7404 human hepatoma cells by expression of mutant telomerase reverse transcriptase. *Int J Cancer* 2002; **97**: 173-179
- Nagao K**, Tomimatsu M, Endo H, Hisatomi H, Hikiji K. Telomerase reverse transcriptase mRNA expression and telomerase activity in hepatocellular carcinoma. *J Gastroenterol* 1999; **34**: 83-87
- Qin LX**, Tang ZY. The prognostic molecular markers in hepatocellular carcinoma. *World J Gastroenterol* 2002; **8**: 385-392
- Nita ME**, Alves VA, Carrilho FJ, Ono-Nita SK, Mello ES, Gama-Rodrigues JJ. Molecular aspects of hepatic carcinogenesis. *Rev Inst Med Trop Sao Paulo* 2002; **44**: 39-48
- Tahara H**, Nakanishi T, Kitamoto M, Nakashio R, Shay JW, Tahara E, Kajiyama G, Ide T. Telomerase activity in human liver tissues: comparison between chronic liver disease and hepatocellular carcinomas. *Cancer Res* 1995; **55**: 2734-2736
- Ma CH**, Sun WS, Tian PK, Gao LF, Liu SX, Wang XY, Zhang LN, Cao YL, Han LH, Liang XH. A novel HBV antisense RNA gene delivery system targeting hepatocellular carcinoma. *World J Gastroenterol* 2003; **9**: 463-467
- Ma CH**, Sun WS, Liu SX, Wang XY, Zhang LN, Cao YL, Han LH. Inhibition of HBV DNA replication and expression in 2.2.15 hepatoma cells infected with AFP-mediated HBX antisense RNA. *Zhonghua Ganzhangbing Zazhi* 2003; **11**: 291-294
- Hirschman SZ**, Price P, Garfinkel E, Christman J, Acs G. Expression of cloned hepatitis B virus DNA in human cell cultures. *Proc Natl Acad Sci U S A* 1980; **77**: 5507-5511
- Christman JK**, Gerber M, Price PM, Flordellis C, Edelman J, Acs G. Amplification of expression of hepatitis B surface antigen in 3T3 cells cotransfected with a dominant-acting gene and cloned viral DNA. *Proc Natl Acad Sci U S A* 1982; **79**: 1815-1819
- Wu WJ**, Liu LT, Huang CH, Chang SF, Chang LL. Telomerase activity in human bladder tumors and bladder washing specimens. *Kaohsiung J Med Sci* 2001; **17**: 602-609
- Bhaduri S**. Comparison of multiplex PCR, PCR-ELISA and fluorogenic 5' nuclease PCR assays for detection of plasmid-bearing virulent *Yersinia enterocolitica* in swine feces. *Mol Cell Probes* 2002; **16**: 191-196
- Yang HZ**, Hu CP, Su XL. Detection of telomerase activity level in human non-small-cell lung cancer. *Hunan Yike Daxue Xuebao* 2001; **26**: 549-550
- Yan SN**, Deng B, Gong ZJ. Effect of cell cycle on telomerase activity of hepatoma cells and its relationship with replication of hepatitis B virus. *Ai Zheng* 2003; **22**: 504-507
- Niu ZS**, Li BK, Wang M. Expression of p53 and C-myc genes and its clinical relevance in the hepatocellular carcinomatous and pericarcinomatous tissues. *World J Gastroenterol* 2002; **8**: 822-826
- Gunes C**, Lichtsteiner S, Vasserot AP, Englert C. Expression of the hTERT gene is regulated at the level of transcriptional initiation and repressed by Mad1. *Cancer Res* 2000; **60**: 2116-2121
- Nozawa K**, Maehara K, Isobe KI. Mechanism for the reduction

- of telomerase expression during muscle cell differentiation. *J Biol Chem* 2001; **276**: 22016-22023
- 30 **Fujimoto K**, Kyo S, Takakura M, Kanaya T, Kitagawa Y, Itoh H, Takahashi M, Inoue M. Identification and characterization of negative regulatory elements of the human telomerase catalytic subunit (hTERT) gene promoter: possible role of MZF-2 in transcriptional repression of hTERT. *Nucleic Acids Res* 2000; **28**: 2557-2562
- 31 **Liu JP**. Studies of the molecular mechanisms in the regulation of telomerase activity. *FASEB J* 1999; **13**: 2091-2104
- 32 **Biroccio A**, Amodei S, Benassi B, Scarsella M, Cianciulli A, Mottolise M, Del Bufalo D, Leonetti C, Zupi G. Reconstitution of hTERT restores tumorigenicity in melanoma-derived c-Myc low-expressing clones. *Oncogene* 2002; **21**: 3011-3019
- 33 **Yago M**, Ohki R, Hatakeyama S, Fujita T, Ishikawa F. Variant forms of upstream stimulatory factors (USFs) control the promoter activity of hTERT, the human gene encoding the catalytic subunit of telomerase. *FEBS Lett* 2002; **520**: 40-46
- 34 **Szutorisz H**, Palmqvist R, Roos G, Stenling R, Schorderet DF, Reddel R, Lingner J, Nabholz M. Rearrangements of minisatellites in the human telomerase reverse transcriptase gene are not correlated with its expression in colon carcinomas. *Oncogene* 2001; **20**: 2600-2605
- 35 **Pallini R**, Pierconti F, Falchetti ML, D' Arcangelo D, Fernandez E, Maira G, D' Ambrosio E, Larocca LM. Evidence for telomerase involvement in the angiogenesis of astrocytic tumors: expression of human telomerase reverse transcriptase messenger RNA by vascular endothelial cells. *J Neurosurg* 2001; **94**: 961-971
- 36 **Drissi R**, Zindy F, Roussel MF, Cleveland JL. c-Myc-mediated regulation of telomerase activity is disabled in immortalized cells. *J Biol Chem* 2001; **276**: 29994-30001
- 37 **Sagawa Y**, Nishi H, Isaka K, Fujito A, Takayama M. The correlation of TERT expression with c-myc expression in cervical cancer. *Cancer Lett* 2001; **168**: 45-50
- 38 **Horikawa I**, Cable PL, Afshari C, Barrett JC. Cloning and characterization of the promoter region of human telomerase reverse transcriptase gene. *Cancer Res* 1999; **59**: 826-830
- 39 **Gozuacik D**, Murakami Y, Saigo K, Chami M, Mugnier C, Lagorce D, Okanoue T, Urashima T, Brechot C, Paterlini-Brechot P. Identification of human cancer-related genes by naturally occurring Hepatitis B Virus DNA tagging. *Oncogene* 2001; **20**: 6233-6240
- 40 **Horikawa I**, Barrett JC. cis-Activation of the human telomerase gene (hTERT) by the hepatitis B virus genome. *J Natl Cancer Inst* 2001; **93**: 1171-1173
- 41 **Zhou W**, Shen Q, Gu B, Ren H, Zhang D. Effects of hepatitis B virus X gene on apoptosis and the activity of telomerase in HepG (2) cells. *Zhonghua Ganzangbing Zazhi* 2000; **8**: 212-214

Edited by Wang XL and Zhu LH

Nuclear and mitochondrial DNA microsatellite instability in Chinese hepatocellular carcinoma

Dian-Chun Fang, Li Fang, Rong-Quan Wang, Shi-Ming Yang

Dian-Chun Fang, Li Fang, Rong-Quan Wang, Shi-Ming Yang,
Department of Gastroenterology, Southwest Hospital, Third Military
Medical University, Chongqing 400038, China

Supported by the National Natural Science Foundation of China,
No. 30070043

Correspondence to: Dian-Chun Fang, M.D., Ph.D. Southwest
Hospital, Third Military Medical University, Chongqing 400038,
China. fangdianchun@hotmail.com

Telephone: +86-23-68754624 **Fax:** +86-23-68754124

Received: 2003-06-05 **Accepted:** 2003-08-16

Abstract

AIM: To study the nuclear microsatellite instability (nMSI) at BAT26 and mitochondrial microsatellite instability (mtMSI) in the occurrence and development of hepatocellular carcinoma and the relationship between nMSI and mtMSI.

METHODS: nMSI was observed with PCR and mtMSI with PCR-SSCP in 52 cases of hepatocellular carcinoma.

RESULTS: mtMSI was detected in 11 out of the 52 cases of hepatocellular carcinoma (21.2%). Among the 11 cases of hepatocellular carcinoma with mtMSI, 7 occurred in one locus and 4 in 2 loci. The frequency of mtMSI in the 52 cases of hepatocellular carcinoma showed no correlation to sex, age, infection of hepatitis B, liver cirrhosis as well as positive AFP of the patients ($P>0.05$). In addition, nMSI was detected in 3 out of 52 cases of hepatocellular carcinoma (5.8%) and there was no correlation of the incidence of mtMSI to that of nMSI ($P>0.05$).

CONCLUSION: mtMSI may be involved in the occurrence and development of hepatocellular carcinoma and it is independent of nMSI.

Fang DC, Fang L, Wang RQ, Yang SM. Nuclear and mitochondrial DNA microsatellite instability in Chinese hepatocellular carcinoma. *World J Gastroenterol* 2004; 10(3):371-375

<http://www.wjgnet.com/1007-9327/10/371.asp>

INTRODUCTION

Mitochondria are the energy-transducing organelles of eukaryotic cells in which fuels to drive cellular metabolism are converted into cellular adenosine triphosphate (ATP) through the process of oxidative phosphorylation. Mitochondria are responsible for generating approximately 90% of ATP. The mitochondrion is the only organelle in the cell, aside from the nucleus, which contains its own genome and genetic machinery^[1]. Mitochondrial DNA (mtDNA) is a 16 569 base-pair, double-stranded and closed circular molecule, and encodes 13 polypeptides. All of the polypeptides are components of the respiratory chain/OXPHOS system, plus 24 genes, specifying two ribosomal RNAs (rRNAs) and 22 transfer RNAs (tRNAs), which are required to synthesize the 13 polypeptides. Mitochondrial genome is far more vulnerable to oxidative

damage and undergoes a higher rate of mutation than nuclear genome due to its lack of histone protection, limited repair capacity, and close proximity to the electron transport chain, which constantly generates superoxide radicals^[2-5]. Accumulation of mutations in mtDNA is approximately tenfold greater than that in nuclear DNA^[6].

A high frequency of mtDNA mutations has been identified in cancer of the colon^[7], stomach^[8], liver^[9], pancreas^[10], lung^[11], breast^[12], kidney^[13], prostate^[14], ovary^[15], Barrett's esophagus^[16] and leukemia^[17]. The majority of these somatic mutations were homoplasmic, suggesting that mutant mtDNA becomes dominant in tumor cells. In addition, microsatellite instability has also been shown in mtDNA of colorectal and gastric carcinomas^[18,19]. Further studies demonstrated that mononucleotide could repeat alteration, missense mutation, and small deletion in NADH dehydrogenase genes and alteration in a polycytidine (C)_n tract in the D-loop region of mtDNA could occur in colorectal carcinomas^[20]. These results imply that microsatellite instability in mtDNA (mtMSI) of colorectal carcinoma may be resulted from certain deficiencies in DNA repair. Therefore, it has been proposed that somatic mutations and mtMSI play a role in tumorigenesis and development of cancer^[21].

Hepatocellular carcinoma (HCC) is one of the most common causes of cancer related mortality worldwide. The incidence of HCC shows a considerable geographical variation with a very high incidence in China. Epidemiological studies in high-risk populations have identified chronic hepatitis B virus (HBV) and chronic hepatitis C virus (HCV) infection as well as dietary exposure to aflatoxin B1 (AFB1) as major factors in the etiology of this disease^[22]. It has been reported that the amount of AFB1 combined to hepatocellular mtDNA is 3-4 fold larger than that combined to nuclear DNA (nDNA). This combined product of aflatoxin cannot easily be expelled and stays in mtDNA for a long period^[22]. Since there is a prolonged period between initial HBV and HCV infection and emergence of HCC, multiple genetic events may occur to promote the malignant transformation of hepatocytes. Many chromosomal aberrations have been frequently reported in HCCs including loss of heterozygosity (LOH) at numerous loci^[23,24]. The repeated destruction and regeneration of liver tissue associated with chronic viral hepatitis would lead to accumulation of mtDNA mutations^[25]. Although MSI in nuclear DNA (nDNA) of HCCs has been detected^[26-32], little attention has been paid to MSI in mtDNA (mtMSI) in this tumor. In order to elucidate the role of mtMSI in the hepatocarcinogenesis, we examined mtMSI and nMSI in a set of 52 Chinese HCCs.

MATERIALS AND METHODS

Fresh tissues were collected from 52 HCC patients undergoing hepatic resection in the Southwest Hospital, Third Military Medical University, Chongqing, China from 1996 to 2002. Neoplastic and nonneoplastic liver tissues were frozen in liquid nitrogen immediately and kept at -70 °C until processing. The 52 patients consisted of 42 males and 10 females, their age ranged from 22 to 71 years with an average of 48.8 years at

Table 1 Sequences of primer for PCR analysis

Repeat sequence	mtDNA region	Position	Annealing (°C)	Primer (5' -3')
(C) _n	270-425	D-loop	58	TCCACACAGACATCAATAACA AAAGTGCATACCGCCAAAAG
(CA) _n	467-556	D-loop	55	CCCATACTACTAATCTCATCAA TTTGGTTGGTTCGGGGTATG
(C) ₆	3529-3617	ND1	55	CCGACCTTAGCTCTCACCAT AATAGGAGGCCTAGGTTGAG
(A) ₇	4555-4644	ND2	55	CCTGAGTAGGCCTAGAAAATAAA ACTTGATGGCAGCTTCTGTG
(T) ₇	9431-9526	COIII	55	CCAAAAAGGCCTTCGATACG GCTAGGCTGGAGTGGTAAAA
(C) ₆ and (A) ₈	12360-12465	ND5	55	CACCCTAACCTGACTTCC GGTGGATGCGACAATGGATT
(CCT) ₃ and (AGC) ₃	12940-13032	ND5	55	GCCCTTCTAAACGCTAATCC TCAGGGGTGGAGACCTAATT

diagnosis. Thirty-two patients were positive and 20 were negative for hepatitis B surface antigen (HBsAg). Hepatitis C virus antibody (Anti-HCV) was negative for all cases. Hematoxylin and eosin-stained sections were prepared from the same samples used for mtMSI and nMSI studies and the diagnosis of HCC was confirmed by histology. None of the patients included in the present series had a family history suggestive of HNPCC and none had received previous chemotherapy or radiation therapy. Necrotic tumors were excluded from the study. The tumor samples contained more than 70% malignant cells. Genomic DNA was isolated from tumor and non-tumor liver tissues and blood, using standard proteinase-K digestion and phenol-chloroform extraction protocols.

PCR-single strand conformation polymorphism (PCR-SSCP) was performed to amplify the microsatellite sequence of mtDNA using published primers^[18]. The primer consisted of 2 D-loop regions and 5 coding regions (Table 1). The reaction conditions and procedures were similar to those reported by Hebano *et al*^[18].

Each PCR was digested by appropriate restriction enzymes and electrophoresed at 300V at 22°C for 2 hr on a 7.5% polyacrylamide gel containing 50 mmol/L boric acid, 1 mmol/L EDTA and 2.5% glycerol. After silver staining, PCR products showing mobility shifts were directly sequenced using appropriate internal primer and analyzed using 373A automated DNA sequencer (Perkin Elmer Cetus). All analyses were performed twice to rule out PCR artifact.

MSI at BAT26 microsatellite locus was analyzed using PCR method. The sequence of upper stream primer was 5' -TGACTACTTTGACTTCAGCC-3' and that of down stream primer was 5' -AACCATTCA ACA TTT TTA ACC C-3'. PCR was performed in 20 µl of reaction mixture containing 10 mmol/L Tris-HCl (pH8.3), 50 mmol/L KCl, 1.5 mmol/L MgCl₂, 200 µmol/L each deoxynucleotide triphosphate, 0.5 µmol/L of each primer, 0.5 unit Ampli Taq polymerase (Perkin-Elmer Cetus, Nowak), 100 ng genomic DNA and 0.5 µCi [³³P] dATP. The reaction was carried out in a thermal cycler at 94 °C for 1 min, at 55 °C-62 °C for 1 min, and at 72 °C for 1min, for 35 cycles with an initial denaturation step at 94 °C for 5 min and final extension step at 72 °C for 10 min. The PCR products were then separated on 5% polyacrylamide 7M urea denaturing gel, and visualized by autoradiography. MSI was defined as the presence of a band shift in the tumor DNA not present in the corresponding normal DNA.

χ^2 test was used for statistical analysis and $P < 0.05$ was considered as statistically significant.

RESULTS

Fifty-two HCC samples were screened for mtMSI at seven repeat sites using the PCR-RFLP method. Figure 1 exhibits a representative mobility-shift band compared with normal counterpart. mtMSI affecting at least one locus was observed in 11 out of 52 cases (21.2%), in which 7 cases affected 1 locus and 4 cases affected 2 loci. mtMSI occurred in D-loop in 10 cases (19.2%), in which 8 cases occurred in (C)_n region and 2 cases in (CA)_n region. mtMSI occurred in the coding region in 5 cases (9.6%), and concomitant mtMSI locus was found in the D-loop in 4 out of the 5 cases. The frequency of mtMSI in 52 cases of HCC showed no correlation to sex, age, HBV infection, liver cirrhosis and positive AFP of the patients ($P > 0.05$, Table 2).

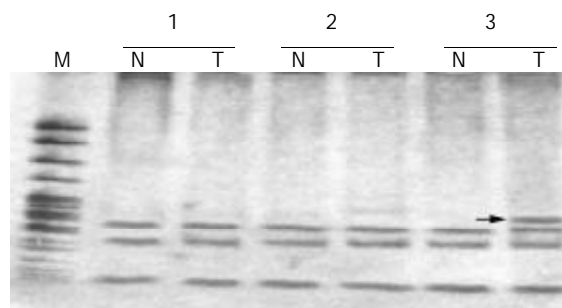


Figure 1 mtMSI in hepatocellular cancer. Arrows indicate conformational variants associated with mtMSI, N: normal DNA, T: tumor DNA.

Table 2 Relationship between MSI and clinical parameters

		n	mtMSI positive	mtMSI negative
Sex	Male	42	10	32
	Female	10	1	9
Age	<30	1	1	0
	30-60	41	8	33
	≥60	10	2	8
HBsAg	Positive	38	8	30
	Negative	14	3	11
Cirrhosis	Positive	37	9	28
	Negative	15	2	13
AFP	Positive	26	6	20
	Negative	26	5	21

The mobility shift in tumor DNA compared to corresponding normal DNA samples representing nMSI is shown in Figure 2. nMSI was found in 3 of 52 cases of HCC (5.8%). In the 3 cases of nMSI, only 1 case showed mtMSI simultaneously. No correlation was found between nMSI and mtMSI in the 52 cases of HCC.



Figure 2 MSI at BAT-26 in hepatocellular cancer. Arrows indicate conformational variants associated with MSI. N: normal DNA, T: tumor DNA.

DISCUSSION

It has been discovered so far that mitochondria are the only organelle to have their own genome and to undergo replication, transcription and translation without dependence on nuclear DNA. They are called as the “25th chromosome of human body”. Many diseases have been found to be related to the structural and functional defects of mitochondria and consequently they are known as mitochondrial diseases^[33]. mtMSI has been found to be a very common phenomenon accompanying gastric carcinoma, colorectal carcinoma and breast carcinoma and may play an important role in the carcinogenesis of these malignant diseases^[12,18-21]. To study the role of mtMSI in liver carcinogenesis, we analyzed 52 cases of HCC using seven microsatellite markers known to be altered in gastrointestinal carcinomas. mtMSI in at least one locus was found in 11 of the 52 cases (21.2%) of HCC, implying that mtMSI might occur not only in gastrointestinal cancers but also in hepatic cancers, and it may play an important role in the occurrence of a certain number of HCC.

Unlike other types of cancer, HCC has been found usually preceded by chronic inflammation due to viral infection^[34-37]. Matsuyama *et al*^[11] reported that the frequency of mtDNA mutations was markedly increased in both noncancerous and cancerous liver specimens compared with control liver tissue. Accumulation of mtDNA mutations in HCC tissue could reflect its malignant potency. The frequency of mtDNA mutations was significant higher in HBV infection-related HCC than in other tumors, which implies that repeated destruction and regeneration of the liver tissue associated with chronic viral hepatitis would lead to accumulation of mtDNA mutations. In the current study, we did not find any obvious relationship between mtMSI and HBsAg, suggesting that HBV infection might play a limited role in the mtMSI pathway of HCC. In addition, we did not find an obvious relationship between mtMSI and sex, age, cirrhosis as well as positive AFP.

MtDNA contains several mono- and dinucleotide repeats. The most frequently used mtDNA in the test of mtMSI is a (CA)_n microsatellite starting at 514 bp position of the D-loop^[38] and a homopolymeric C tract extending from 16 184 to 16 193 bp of the D-loop, which could be interrupted by a T at 16 189 bp position^[39]. Alonso *et al*^[40] studied mutations in the mtDNA D-loop region and found three mutations in eight gastric tumors. Richard *et al*^[41] studied 40 pairs of normal/cancer breast specimens for the presence of mtMSI and found a 216-fold increase in the D-loop point mutations of cancer cells with regard to the spontaneous rate detected in female

gametes. Maximo *et al*^[19] utilized PCR-SSCP to examine mtDNA large deletions and mutations in 32 gastric carcinomas and found that most of the mutations corresponded to insertions/deletions in the D-loop region or transitions in ND1, ND5, and COXI. Earlier studies revealed the presence of mutations in the D-loop of both non-malignant and malignant gastric tumors^[42,43]. Analysis of HCCs indicated that mutations in the D-loop were a frequent event and could be used as a molecular tool for the determination of clonality^[9,44]. Two recent studies reported the frequency of D-loop mutations in esophageal cancer. One group focused on adenocarcinomas of Barrett’s esophagus. In that study, D-loop alterations were identified in 40% of the patients examined^[16]. The other study showed that D-loop mutations were much less frequent in esophageal cancer, occurring in only 5% of the specimens analyzed^[45]. Clearly, analysis of mtDNA from more esophageal tumor samples is needed in order to determine the frequency of D-loop mutations and their relevance in this type of cancer. In our series of 52 cases of HCC, mtMSI was found in 11 (21.2%). MtMSI occurred in the D-loop region of 10 cases and in the coding region of 5 cases. Among the 10 cases, mtMSI occurred in (C)_n region of 8 cases and in (CA)_n region of 2 cases, So (C)_n region of D-loop is the site at which mtMSI occurs more frequently than in other regions. Our findings are consistent to those reported by Habano *et al.* and Maximo *et al*^[18-20].

Microsatellite markers might provide evidences of faulty DNA mismatch repair (MMR) via the detection of MSI^[46-49]. The choice of microsatellite markers may impact on the MSI detection rate. BAT-26, a repeat of 26 deoxyadenosine localized in intron 5 of hMSH2 gene, has been reported as a reliable indicator of replication error phenotype in colorectal cancers, enabling analysis of tumour DNA in the absence of paired normal DNA^[50]. The frequency of nMSI in hepatic cancer varied in different reports^[51,52]. Karachristos *et al*^[52] studied 27 cases of HCC and found none of the tumors examined showed alterations in BAT-26. In our series of 52 cases, 3 cases were found to have nMSI at BAT26 (5.8%). Our finding indicates that nMSI at BAT26 is not common in cases of HCC and support the hypothesis that HCC is a “low” MSI tumor in China. Carcinogenesis of HCC may undergo a different molecular route other than that of nMSI.

Mutation of mtDNA may result in the occurrence of tumor but its mechanism remains unknown. Further studies are required to determine if mtDNA mutations are correlated with malignant transformation. Recently, scholars have shifted their attention to the interactions between mtDNA and nDNA. Fragments of mtDNA are sometimes found in nuclear genes, and the insertion of mtDNA has been suggested as a mechanism by which oncogenes are activated^[53]. For example, sequences representing subunits ND4 (Complex I) and subunits cytochrome C oxidases I, II and III (complex IV) have been found in the nuclear DNA of various tissues^[53]. In yeast cells, migration of DNA from the mitochondria to the nucleus occurred 100 000 times more frequently than in the opposite direction^[54]. In our series of 52 cases of HCC, nMSI was detected in 5.8% and coexistence of nMSI and mtMSI in only 1 out of 3 cases. We failed to confirm there was a correlation of mtMSI to nMSI in our cases of HCC. This finding is in agreement with the recently published data on gastrointestinal cancer^[55].

In conclusion, mtMSI could play an important role at multiple stages in the process of carcinogenesis. The mitochondrial production of ROS might be involved in the initiation and promotion of carcinogenesis, in part due to ROS-triggered mutagenesis of both mtDNA and nDNA^[56]. Also, other evidences exists for a mechanism of nDNA mutagenesis involving the integration of mtDNA fragments. Many primary tumors revealed a high frequency of mtDNA mutations and

the majority of these somatic mutations were homoplasmic in nature, indicating that the mutant mtDNA has become dominant in tumor cells. The mutated mtDNA was readily detectable in paired bodily fluids from each type of cancer and was 19 to 220 times as abundant as mutated nuclear p53 DNA. By virtue of their clonal nature and high copy number, mitochondrial mutations might provide a powerful molecular marker for noninvasive detection of cancer^[57]. Important areas for future research should include intergenomic signaling pathways in carcinogenesis and the potential role of mitochondria and mtDNA mutations in immunological surveillance of tumor cells. Finally, the role of mitochondria in stimulating apoptosis could be exploited in cancer therapeutics^[58].

REFERENCES

- 1 **Anderson S**, Bankier AT, Barrell BG, de Bruijn MH, Coulson AR, Drouin J, Eperon IC, Nierlich DP, Roe BA, Sanger F, Schreier PH, Smith AJ, Staden R, Young IG. Sequence and organization of the human mitochondrial genome. *Nature* 1981; **290**: 457-465
- 2 **Yakes FM**, Van Houten B. Mitochondrial DNA damage is more extensive and persists longer than nuclear DNA damage in human cells following oxidative stress. *Proc Natl Acad Sci U S A* 1997; **94**: 514-519
- 3 **Marcelino LA**, Thilly WG. Mitochondrial mutagenesis in human cells and tissues. *Mutat Res* 1999; **434**: 177-203
- 4 **Kunkel TA**, Loeb LA. Fidelity of mammalian DNA polymerases. *Science* 1981; **213**: 765-767
- 5 **Shay JW**, Werbin H. Are mitochondrial DNA mutations involved in the carcinogenic process? *Mutat Res* 1987; **186**: 149-160
- 6 **Johns DR**. Seminars in medicine of the Beth Israel Hospital, Boston. Mitochondrial DNA and disease. *N Engl J Med* 1995; **333**: 638-644
- 7 **Polyak K**, Li Y, Zhu H, Lengauer C, Willson JK, Markowitz SD, Trush MA, Kinzler KW, Vogelstein B. Somatic mutations of the mitochondrial genome in human colorectal tumours. *Nat Genet* 1998; **20**: 291-293
- 8 **Habano W**, Sugai T, Nakamura SI, Uesugi N, Yoshida T, Sasou S. Microsatellite instability and mutation of mitochondrial and nuclear DNA in gastric carcinoma. *Gastroenterology* 2000; **118**: 835-841
- 9 **Nomoto S**, Yamashita K, Koshikawa K, Nakao A, Sidransky D. Mitochondrial D-loop mutations as clonal markers in multicentric hepatocellular carcinoma and plasma. *Clin Cancer Res* 2002; **8**: 481-487
- 10 **Jones JB**, Song JJ, Hempen PM, Parmigiani G, Hruban RH, Kern SE. Detection of mitochondrial DNA mutations in pancreatic cancer offers a "mass"-ive advantage over detection of nuclear DNA mutations. *Cancer Res* 2001; **61**: 1299-1304
- 11 **Matsuyama W**, Nakagawa M, Wakimoto J, Hirotsu Y, Kawabata M, Osame M. Mitochondrial DNA mutation correlates with stage progression and prognosis in non-small cell lung cancer. *Hum Mutat* 2003; **21**: 441-443
- 12 **Tan DJ**, Bai RK, Wong LJ. Comprehensive scanning of somatic mitochondrial DNA mutations in breast cancer. *Cancer Res* 2002; **62**: 972-976
- 13 **Nagy A**, Wilhelm M, Kovacs G. Mutations of mtDNA in renal cell tumours arising in end-stage renal disease. *J Pathol* 2003; **199**: 237-242
- 14 **Jeronimo C**, Nomoto S, Caballero OL, Usadel H, Henrique R, Varzim G, Oliveira J, Lopes C, Fliss MS, Sidransky D. Mitochondrial mutations in early stage prostate cancer and bodily fluids. *Oncogene* 2001; **20**: 5195-5198
- 15 **Liu VW**, Shi HH, Cheung AN, Chiu PM, Leung TW, Nagley P, Wong LC, Ngan HY. High incidence of somatic mitochondrial DNA mutations in human ovarian carcinomas. *Cancer Res* 2001; **61**: 5998-6001
- 16 **Miyazono F**, Schneider PM, Metzger R, Warnecke-Eberz U, Baldus SE, Dienes HP, Aikou T, Hoelscher AH. Mutations in the mitochondrial DNA D-Loop region occur frequently in adenocarcinoma in Barrett's esophagus. *Oncogene* 2002; **21**: 3780-3783
- 17 **Ivanova R**, Lepage V, Loste MN, Schachter F, Wijnen E, Busson M, Cayuela JM, Sigaux F, Charron D. Mitochondrial DNA sequence variation in human leukemic cells. *Int J Cancer* 1998; **76**: 495-498
- 18 **Habano W**, Nakamura S, Sugai T. Microsatellite instability in the mitochondrial DNA of colorectal carcinomas: evidence for mismatch repair systems in mitochondrial genome. *Oncogene* 1998; **17**: 1931-1937
- 19 **Maximo V**, Soares P, Seruca R, Rocha AS, Castro P, Sobrinho-Simoes M. Microsatellite instability, mitochondrial DNA large deletions, and mitochondrial DNA mutations in gastric carcinoma. *Genes Chromosomes Cancer* 2001; **32**: 136-143
- 20 **Habano W**, Sugai T, Yoshida T, Nakamura S. Mitochondrial gene mutation, but not large-scale deletion, is a feature of colorectal carcinomas with mitochondrial microsatellite instability. *Int J Cancer* 1999; **83**: 625-629
- 21 **Hochhauser D**. Relevance of mitochondrial DNA in cancer. *Lancet* 2000; **356**: 181-182
- 22 **Niranjan BG**, Bhat NK, Avadhani NG. Preferential attack of mitochondrial DNA by aflatoxin B1 during hepatocarcinogenesis. *Science* 1982; **215**: 73-75
- 23 **Rashid A**, Wang JS, Qian GS, Lu BX, Hamilton SR, Groopman JD. Genetic alterations in hepatocellular carcinomas: association between loss of chromosome 4q and p53 gene mutations. *Br J Cancer* 1999; **80**: 59-66
- 24 **Okabe H**, Ikai I, Matsuo K, Satoh S, Momoi H, Kamikawa T, Katsura N, Nishitai R, Takeyama O, Fukumoto M, Yamaoka Y. Comprehensive allelotyping study of hepatocellular carcinoma: potential differences in pathways to hepatocellular carcinoma between hepatitis B virus-positive and -negative tumors. *Hepatology* 2000; **31**: 1073-1079
- 25 **Nishikawa M**, Nishiguchi S, Shiomi S, Tamori A, Koh N, Takeda T, Kubo S, Hirohashi K, Kinoshita H, Sato E, Inoue M. Somatic mutation of mitochondrial DNA in cancerous and noncancerous liver tissue in individuals with hepatocellular carcinoma. *Cancer Res* 2001; **61**: 1843-1845
- 26 **Kondo Y**, Kanai Y, Sakamoto M, Mizokami M, Ueda R, Hirohashi S. Genetic instability and aberrant DNA methylation in chronic hepatitis and cirrhosis—A comprehensive study of loss of heterozygosity and microsatellite instability at 39 loci and DNA hypermethylation on 8 CpG islands in microdissected specimens from patients with hepatocellular carcinoma. *Hepatology* 2000; **32**: 970-979
- 27 **Wang G**, Zhao Y, Liu X, Wang L, Wu C, Zhang W, Liu W, Zhang P, Cong W, Zhu Y, Zhang L, Chen S, Wan D, Zhao X, Huang W, Gu J. Allelic loss and gain, but not genomic instability, as the major somatic mutation in primary hepatocellular carcinoma. *Genes Chromosomes Cancer* 2001; **31**: 221-227
- 28 **Salvucci M**, Lemoine A, Saffroy R, Azoulay D, Lepere B, Gaillard S, Bismuth H, Reynes M, Debuire B. Microsatellite instability in European hepatocellular carcinoma. *Oncogene* 1999; **18**: 181-187
- 29 **Kondo Y**, Kanai Y, Sakamoto M, Mizokami M, Ueda R, Hirohashi S. Microsatellite instability associated with hepatocarcinogenesis. *J Hepatol* 1999; **31**: 529-536
- 30 **Takagi K**, Esumi M, Takano S, Iwai S. Replication error frequencies in primary hepatocellular carcinoma: a comparison of solitary primary versus multiple primary cancers. *Liver* 1998; **18**: 272-276
- 31 **Kazachkov Y**, Yoffe B, Khaoustov VI, Solomon H, Klintmalm GB, Tabor E. Microsatellite instability in human hepatocellular carcinoma: relationship to p53 abnormalities. *Liver* 1998; **18**: 156-161
- 32 **Macdonald GA**, Greenon JK, Saito K, Cherian SP, Appelman HD, Boland CR. Microsatellite instability and loss of heterozygosity at DNA mismatch repair gene loci occurs during hepatic carcinogenesis. *Hepatology* 1998; **28**: 90-97
- 33 **Pulkes T**, Hanna MG. Human mitochondrial DNA diseases. *Adv Drug Deliv Rev* 2001; **49**: 27-43
- 34 **Shen LJ**, Zhang HX, Zhang ZJ, Li JY, Chen MQ, Yang WB, Huang R. Detection of HBV, PCNA and GST- π in hepatocellular carcinoma and chronic liver diseases. *World J Gastroenterol* 2003; **9**: 459-462
- 35 **Tang ZY**. Hepatocellular carcinoma—cause, treatment and metastasis. *World J Gastroenterol* 2001; **7**: 445-454
- 36 **Guo SP**, Wang WL, Zhai YQ, Zhao YL. Expression of nuclear factor-kappa B in hepatocellular carcinoma and its relation with the X protein of hepatitis B virus. *World J Gastroenterol* 2001; **7**:

- 340-344
- 37 **Gao FG**, Sun WS, Cao YL, Zhang LN, Song J, Li HF, Yan SK. HBx-DNA probe preparation and its application in study of hepatocarcinogenesis. *World J Gastroenterol* 1998; **4**: 320-322
- 38 **Szibor R**, Michael M, Spitsyn VA, Plate I, Ginter EK, Krause D. Mitochondrial D-loop 3' (CA)_n repeat polymorphism: optimization of analysis and population data. *Electrophoresis* 1997; **18**: 2857-2860
- 39 **Bendall KE**, Sykes BC. Length heteroplasmy in the first hypervariable segment of the human mtDNA control region. *Am J Hum Genet* 1995; **57**: 248-256
- 40 **Alonso A**, Martin P, Albarran C, Aquilera B, Garcia O, Guzman A, Oliva H, Sancho M. Detection of somatic mutations in the mitochondrial DNA control region of colorectal and gastric tumors by heteroduplex and single-strand conformation analysis. *Electrophoresis* 1997; **18**: 682-685
- 41 **Richard SM**, Bailliet G, Paez GL, Bianchi MS, Peltomaki P, Bianchi NO. Nuclear and mitochondrial genome instability in human breast cancer. *Cancer Res* 2000; **60**: 4231-4237
- 42 **Tamura G**, Nishizuka S, Maesawa C, Suzuki Y, Iwaya T, Sakata K, Endoh Y, Motoyama T. Mutations in mitochondrial control region DNA in gastric tumours of Japanese patients. *Eur J Cancer* 1999; **35**: 316-319
- 43 **Burgart LJ**, Zheng J, Shu Q, Strickler JG, Shibata D. Somatic mitochondrial mutation in gastric cancer. *Am J Pathol* 1995; **147**: 1105-1111
- 44 **Liu MR**, Pan KF, Li ZF, Wang Y, Deng DJ, Zhang L, Lu YY. Rapid screening of mitochondrial DNA mutation by using denaturing high-performance liquid chromatography. *World J Gastroenterol* 2002; **8**: 426-430
- 45 **Hibi K**, Nakayama H, Yamazaki T, Takase T, Taguchi M, Kasai Y, Ito K, Akiyama S, Nakao A. Detection of mitochondrial DNA alterations in primary tumors and corresponding serum of colorectal cancer patients. *Int J Cancer* 2001; **94**: 429-431
- 46 **Fang DC**, Wang RQ, Yang SM, Yang JM, Liu HF, Peng GY, Xiao TL, Luo YH. Mutation and methylation of hMLH1 in gastric carcinomas with microsatellite instability. *World J Gastroenterol* 2003; **9**: 655-659
- 47 **Fang DC**, Luo YH, Yang SM, Li XA, Ling XL, Fang L. Mutation analysis of APC gene in gastric cancer with microsatellite instability. *World J Gastroenterol* 2002; **8**: 787-791
- 48 **Cai Q**, Sun MH, Lu HF, Zhang TM, Mo SJ, Xu Y, Cai SJ, Zhu XZ, Shi DR. Clinicopathological and molecular genetic analysis of 4 typical Chinese HNPCC families. *World J Gastroenterol* 2001; **7**: 805-810
- 49 **Fang DC**, Yang SM, Zhou XD, Wang DX, Luo YH. Telomere erosion is independent of microsatellite instability but related to loss of heterozygosity in gastric cancer. *World J Gastroenterol* 2001; **7**: 522-526
- 50 **Cravo M**, Lage P, Albuquerque C, Chaves P, Claro I, Gomes T, Gaspar C, Fidalgo P, Soares J, Nobre-Leitao C. BAT-26 identifies sporadic colorectal cancers with mutator phenotype: a correlative study with clinico-pathological features and mutations in mismatch repair genes. *J Pathol* 1999; **188**: 252-257
- 51 **Martins C**, Kedda MA, Kew MC. Characterization of six tumor suppressor genes and microsatellite instability in hepatocellular carcinoma in southern African blacks. *World J Gastroenterol* 1999; **5**: 470-476
- 52 **Karachristos A**, Liloglou T, Field JK, Deligiorgi E, Kouskouni E, Spandidos DA. Microsatellite instability and p53 mutations in hepatocellular carcinoma. *Mol Cell Biol Res Commun* 1999; **2**: 155-161
- 53 **Corral M**, Baffet G, Kitzis A, Paris B, Tichonicky L, Kruh J, Guguen-Guillouzo C, Defer N. DNA sequences homologous to mitochondrial genes in nuclei from normal rat tissues and from rat hepatoma cells. *Biochem Biophys Res Commun* 1989; **162**: 258-264
- 54 **Thorsness PE**, Fox TD. Escape of DNA from mitochondria to the nucleus in *Saccharomyces cerevisiae*. *Nature* 1990; **346**: 376-379
- 55 **Schwartz S Jr**, Perucho M. Somatic mutations in mitochondrial DNA do not associate with nuclear microsatellite instability in gastrointestinal cancer. *Gastroenterology* 2000; **119**: 1806-1808
- 56 **Li JM**, Cai Q, Zhou H, Xiao GX. Effects of hydrogen peroxide on mitochondrial gene expression of intestinal epithelial cells. *World J Gastroenterol* 2002; **8**: 1117-1122
- 57 **Fliss MS**, Usadel H, Caballero OL, Wu L, Buta MR, Eleff SM, Jen J, Sidransky D. Facile detection of mitochondrial DNA mutations in tumors and bodily fluids. *Science* 2000; **287**: 2017-2019
- 58 **Shen ZY**, Shen J, Li QS, Chen CY, Chen JY, Zeng Y. Morphological and functional changes of mitochondria in apoptotic esophageal carcinoma cells induced by arsenic trioxide. *World J Gastroenterol* 2002; **8**: 31-35

Edited by Zhang JZ and Wang XL

Hemizygous deletion and hypermethylation of RUNX3 gene in hepatocellular carcinoma

Wen-Hua Xiao, Wei-Wen Liu

Wen-Hua Xiao, Department of Oncology, 304th Hospital of PLA, Beijing 100037, China

Wei-Wen Liu, Department of Gastroenterology, Southwest Hospital, Third Military Medical University, Chongqing 400038, China

Correspondence to: Wen-Hua Xiao, PhD, Associate Professor, Department of Oncology, 304th Hospital of PLA, Beijing 100037, China. w_hxiao@hotmail.com

Telephone: +86-10-66867324 **Fax:** +86-10-66867672

Received: 2003-05-11 **Accepted:** 2003-06-02

Abstract

AIM: To analyze the genetic and epigenetic alterations of RUNX3 gene, a potential putative tumor suppressor gene, in hepatocellular carcinoma (HCC).

METHODS: PCR-based loss of heterozygosity (LOH) detection, analysis of mutation with PCR-single strand conformational polymorphism (SSCP) and sequencing, and methylation study with methylation specific PCR (MSP) were performed on RUNX3 gene in a series of 62 HCCs along with their matched normal tissues.

RESULTS: Mutation of RUNX3 gene was not found, but one single nucleotide polymorphism with T to A transversion at the second nucleotide of the 18th codon was found. Nine of 26 informative cases (34.6%) showed allelic loss on the polymorphic site and 30 cases (48.4%) revealed hypermethylation of RUNX3 gene in promoter CpG islands. Furthermore, of the 9 cases with LOH, 8 (88.9%) also had hypermethylation.

CONCLUSION: Our findings indicate that inactivation of RUNX3 gene through allelic loss and promoter hypermethylation might be one of the major mechanisms in hepatocellular carcinogenesis.

Xiao WH, Liu WW. Hemizygous deletion and hypermethylation of RUNX3 gene in hepatocellular carcinoma. *World J Gastroenterol* 2004; 10(3):376-380

<http://www.wjgnet.com/1007-9327/10/376.asp>

INTRODUCTION

Transforming growth factor- β (TGF- β) is a multifunctional cytokine known to be a potent growth inhibitor for most epithelial cells^[1,2]. TGF- β signaling pathway is composed of TGF- β type I, type II receptors and Smad proteins, and is transduced by forming heteromeric complex with its type I and type II transmembrane Ser/Thr kinase receptors. Activated type I receptors then activate the cytoplasmic Smad 2 and Smad 3 by phosphorylation, allowing them to form a heteromeric complex with Smad 4. This Smad complex can activate TGF- β responsive gene transcription only after it is translocated to nucleus and bound to the specific target nuclear matrix site^[2]. However, the key process of nuclear translocation and subnuclear distribution for regulating transcription of TGF- β -

responsive gene needs a broad range of nuclear proteins^[3]. Recently, RUNX proteins, including RUNX3 gene were proved to interact through their C-terminal segment with Smads and recruit Smads to subnuclear sites of active transcription, thus exerting their biological control^[4]. The function of RUNX proteins has been considered as the subnuclear acceptor proteins for signal transduction. On the contrary, Smads cannot be directed to the nuclear matrix in the absence of RUNX proteins^[4]. Therefore, TGF- β -Smad signal pathway would be disrupted. RUNX3, one member of the RUNT domain family, was recently found with a loss of 40-60% of expression due to a highly frequency of hemizygous deletion and hypermethylation in gastric cancer^[5]. Also, the gastric mucosa of RUNX3 knocked out mouse exhibited hyperplasia and suppressed apoptosis and growth-inhibition induced by TGF- β in epithelial cells^[5]. Taken together, it is strongly suggested that RUNX3 gene be a novel tumor-suppressor gene.

Hepatocellular carcinoma (HCC) is one of the most common causes of cancer death in the world, especially in Asia and Africa^[6,7]. HCC, like many other kinds of human malignancy, has been reported to overexpress TGF- β ^[8]. The serum concentration of TGF- β is also elevated with tumor progression^[9]. Therefore, HCC cells resistant to the anti-proliferative function of TGF- β may be a critical step in the development of HCC^[10]. However, until the present no molecular event has been found to contribute to the impairment of TGF- β signal pathway in HCC^[11]. It is well documented that aberrance of molecules of the pathway including TGF- β receptor, Smads 2, 3, 4, 6 and 7 was very rare in HCC^[12-14]. The exact mechanism of HCC with loss of TGF- β responsiveness still remains unknown. A growing body of evidence showed that chromosome 1p36 was a common deletion region where just loci of RUNX3 gene exist^[15,16]. Several putative tumor suppressor genes are believed to be in this region. But, different types of tumor have different regions of consensus deletion. For example, the consensus deletion of neuroblastoma has been mapped to 1p36.2-36.3, a region distal to the deleted region in HCC. While in HCC, a minimally deleted region of about 4 Mb on chromosome 1p36 was well defined^[17]. Within the common deletion region, another candidate tumor suppressor gene, retinoblastoma protein (Rb)-interacting zinc finger gene (RIZ) was also identified^[18]. Unfortunately, mutation of RIZ gene was not found in HCC^[15]. Its role in hepatocarcinogenesis has not been clarified yet. Most notably, LOH encompassing RUNX3 gene occurs in early stage of HCC, even in precancerous condition^[19,20]. In the current paper, we studied the genetic and epigenetic alterations of RUNX3 gene in HCC in order to find out new clues to the development of HCC.

MATERIALS AND METHODS

Tissue samples

Sixty-two frozen HCC specimens and their adjacent normal liver tissue specimens were obtained from Southwest Hospital, Third Military Medical University, Chongqing, China. Informed consents were obtained from every patient. The patients' age ranged 29-72 years with an average of 48.6 years. The male to female ratio was 52:10. The background liver showed cirrhosis in 53 (85.4%) cases, chronic persistent hepatitis in 6 cases

(9.7%), and non-specific change in 3 (3.2%) cases. HBV was detected in 49 cases (79.0%), HCV was detected in 5 (8.1%) and non-virus hepatitis in 8 (12.8%). The number of cases with histological grades I, II and III was 8, 26, 28, respectively. Three pathologists reviewed independently one 5 μ m thick section stained with hematoxylin and eosin.

DNA extraction

Frozen tissue samples were ground into very fine powder in liquid nitrogen, suspended in lysis buffer and treated with proteinase K. DNA was extracted by phenol-chloroform-isoamyl alcohol and ethanol precipitation^[21]. Adjacent normal liver tissues were used as corresponding normal controls.

Single strand conformational polymorphism (SSCP) and DNA sequencing

A total of 6 exons of RUNX3 gene were screened for inactivation mutations with PCR-SSCP, cyclic sequencing on genomic DNA templates. The primers were designed with OLIGO software program (version 5.0; National Bioscience Inc., Plymouth, MN) using the genomic sequences obtained from GenBank (accession No. NT_004391). PCR primer pairs for amplification of RUNX3 gene are described in Table 1. Each PCR reaction except for exon 2 was performed under standard conditions in a 10 μ l reaction mixture containing 1 μ l of template DNA, 0.5 μ M of each primer, 0.2 mM of each dNTP, 1.5 mM MgCl₂, 0.5 unit of Taq polymerase (Ampli Taq Gold™ containing antibody to Taq, Roche), 0.5 μ Ci of ³²P-dCTP (Amersham, Buckinghamshire, UK), and 1 μ l of 10X buffer. Advantage^R-GC genomic PCR kit (Clontech Laboratories, Inc., CA, USA) was used to amplify exon 2 containing CpG-rich sequence according to the user manual. The reaction mixture was denatured for 5 min at 95 °C and incubated for 35 cycles (denaturing for 30 s at 95 °C, annealing for 30 s at 51-67 °C, and extending for 30 s at 72 °C). A final extension was continued for 5 min at 72 °C in a thermal cycler (PE 480, USA). After amplification, the PCR products were denatured for 5 min at 95 °C at 1:1 dilution of sample buffer containing 98% formamide/5 mmol/L NaOH and loaded onto a SSCP gel (FMC mutation detection enhancement system, Intermountain Scientific, Kaysville, UT) with 10% glycerol. After electrophoresis, the gels were transferred to 3-mm Whatman paper and dried, and autoradiography was performed with Kodak X-OMAT film (Eastman Kodak, Rochester, NY). For the detection of mutations, DNAs showing mobility shifts were cut out from the dried gel, and reamplified for 30 cycles using the same primer set. Sequencing kit (Perkin-Elmer, Foster City, CA) was used according to the manufacturer's recommendations. Cycling sequencing products were resolved on a 6% denatured sequencing gel (USB™, Cleveland, USA).

Loss of heterozygosity (LOH) analysis

We found 1 polymorphic site during SSCP and sequencing analysis using the primer sets covering 6 exons. The polymorphic site had highly frequent information of heterozygote in HCC patients. This made it feasible as an intragenic polymorphic marker for LOH analysis of RUNX3 gene. PCR and SSCP conditions for LOH analysis were exactly the same as described above. PCR products from the corresponding normal and tumor DNAs were run on SSCP gel. Allelic loss was scored when the band intensity of one allelic marker was significantly decreased (more than 70% reduction) in tumor DNA as compared with that in normal DNA.

DNA methylation analysis of RUNX3 gene by methylation specific PCR (MSP)

The methylation status of RUNX3 gene was determined by

sodium bisulfate treatment of DNA followed by methylation-specific polymerase chain reaction (MSP), as described with modification^[22,23]. In brief, about 100 ng DNA was incubated in 0.2 M NaOH at 42 °C for 30 minutes in a total volume of 50 μ l. After the addition of 350 μ l of 3.6 M sodium bisulfate (Sigma) containing 1 mM hydroquinone at pH 5, the samples were incubated for 4-5 hours at 55 °C in the dark. The modified DNA was recovered with 5 μ l of glassmilk (BIO 101, Inc., CA, USA) and 800 μ l of 6 M NaI. The glassmilk catching the modified DNA was washed three times with 70% ethanol at room temperature, and then treated with 0.3 M NaOH/90% ethanol once, washed twice again with 90% ethanol. The DNA was finally eluted from the dried pellet with 30 μ l of 1 mM Tris-HCl (pH 8.0) for 15 minutes at 55 °C. Five μ l of bisulfate-modified DNA was subjected to MSP using two sets of primer specific for methylation detection and unmethylation detection as reported previously^[5]. PCR was performed in a total volume of 30 μ l containing 5 μ l template DNA, 0.5 μ M of each primer, 0.2 mM of each dNTP, 1.5 mM MgCl₂, 0.5 unit of Taq polymerase (Ampli Taq Gold™ containing antibody to Taq, Roche) and 3 μ l of 10X buffer. The reaction solution was initially denatured at 95 °C for 1 minute. Amplification was carried out for 40 cycles at 95 °C for 30 s, at 63 °C for 30 s and at 72 °C for 30 s, followed by a final extension at 72 °C for 5 min. Controls without DNA were performed for each set for PCRs. Ten μ l of PCR products was directly loaded onto 2% agarose gel containing ethidium bromide, and directly visualized under UV illumination, and photographed. The size of PCR products was 234 bp.

RESULTS

Frequency of LOH in RUNX3 gene and its clinical significance

We failed to detect a mutation in all six exons and partial intron adjacent to exon in 62 HCCs by PCR-SSCP and sequencing. But the polymorphic site with T to A transition at the second nucleotide of codon 18 was found at exon 1, a relatively high frequency of heterozygotes (26/62) was used as an intragenic marker to examine LOH of RUNX3 gene, and 34.6% (9/26) of informative cases showed allelic loss (Figure 1).

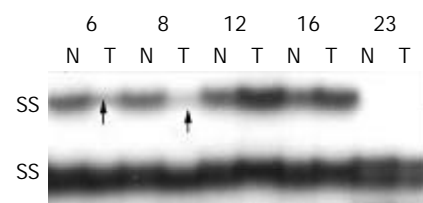


Figure 1 Allelic loss of RUNX3 gene in HCC. N: normal, T: tumor, Arrow indicate allelic loss.

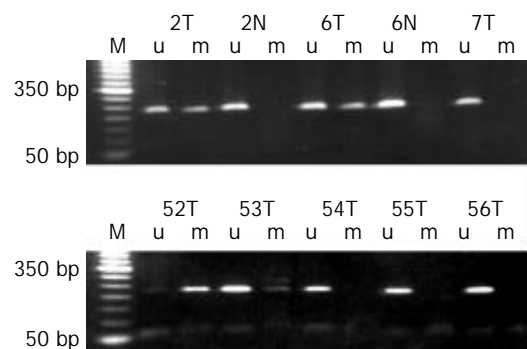


Figure 2 Methylation state of RUNX3 gene in HCC. M: Molecular weight of 50 bp DNA ladder, u: unmethylation, m: methylation, N: normal, T: tumor.

Table 1 Primers used for PCR amplification of RUNX3 gene

Name	Exon	Primer sequence	Annealing Tm(°C)	Size (bp)
RUNX3_E1	1	F:5' -CTGGCCACAGTCCCCACC-3' R:5' -ATCCCAACCCAACCCCTGAAG-3'	64	158
RUNX3_E2-1	2	F:5' -CTGCTTTCCCGCTTCTCGCGGCAGC-3' R:5' -CGCCGCTGTCTCGCCCATCTTGCC-3'	62	212
RUNX3_E2-2	2	F:5' -CCAAGCACCAGCCGCGCTTCACAC-3' R:5' -GAGGAAGTTGGGGCTGTCGGTGCGC-3'	65	207
RUNX3_E2-3	2	F:5' -CTCGATGGTGGACGTGCTGGCGGAC-3' R:5' -GTCTCGGGCACCTCCCATCCCCACT-3'	62	230
RUNX3_E3	3	F:5' -TGCCATTGCCAATGCTGAA-3' R:5' -TAAGCTGTCCCCCTGCATCC-3'	58	240
RUNX3_E4	4	F:5' -GCACTGGACCTCCTCCC-3' R:5' -CACCTGCCTCTATTCCCCACT-3'	60	187
RUNX3_E5	5	F:5' -CGCTGCAGCCCCTCCCTC-3' R:5' -GGGAAGCAACGGCTGATGG-3'	65	225
RUNX3_E6-1	6	F:5' -GTTGTTAGGGTCCCCGCCTCC-3' R:5' -CTACCCGCATGCTGGCCTCTT-3'	63	224
RUNX3_E6-2	6	F:5' -CGCTGCTGGTGCAAGAGG-3' R:5' -ACCAGCCGCTTCCACCATAC-3'	63	205
RUNX3_E6-3	6	F:5' -TGGCGGGAGGTAGGTATGGTG-3' R:5' -GCCAACCTCACGGAGAGC-3'	63	166
RUNX3_E6-4	6	F:5' -AATGCATCTGGGGTCTGG-3' R:5' -GGGTTGTCTCGAGCTGGAAC-3'	61	150

Frequent hypermethylation of RUNX3 gene in HCC

On the basis of the presence of a CpG island in the 5' region of RUNX3 gene, we examined the promoter 2 hypermethylation using two sets of primers specific for MSP reported by Li^[5], and 48.4% (30/62) HCCs were found to have hypermethylation (Figure 2). Notably, we found the degree of hypermethylation was quite different among individual tumors by comparing with the intensity between unmethylation and methylation bands under the same PCR conditions. Although our methods could not be used to quantitate methylation, hypermethylation was not found in the matching normal liver tissues.

Biallelic aberrant of RUNX3 gene in HCC

LOH and hypermethylation are two distinct ways to inactivate tumor suppressor gene. It is widely known that both of them were often involved in complete loss of gene function through cooperation. We, here, found 8 cases had hypermethylation in the 9 cases with LOH of RUNX3 gene.

DISCUSSION

RUNX3 gene has been found belonging to the runt domain family of transcription factors acting as master regulators of gene expression in major developmental pathway^[3]. At present, three RUNX genes, RUNX1, RUNX2 and RUNX3, have been identified. All the three genes have been found to share a highly conserved region, called runt domain^[24]. They have been shown to interact with Smads 1, 2, 3 and 5, and are indispensable in mediating Smads compound nuclear distribution and Smads specific binding to target DNA^[25,4]. Therefore, RUNX proteins are important targets of TGF-beta-Smads signaling pathway. It is well documented that mutation of RUNX1 gene was associated with the development of acute myelogenous leukemia, while mutation of RUNX2 contributed to celeidocranial dysplasia (CCD)^[25]. Recently, RUNX3 gene was found to play

an important role during the development of gastric cancer. Its absence would lead to abnormal proliferation of gastric epithelial cells, lack of responsiveness to apoptosis and growth-inhibitory effect induced by TGF-beta in knock out mouse. Moreover, wild type RUNX3 gene significantly reduced the tumorigenesis ability of tumor cells, whereas mutant type RUNX3 gene would abolish the tumor suppressor action of RUNX3 in nude mice and drive tumor cells to grow much faster. In human primary gastric tumor, 60% cases do not significantly express RUNX3 gene because of hemizygous deletion and hypermethylation. Correlation between hypermethylation and under-expression or no expression was further confirmed in *in vitro* experiment^[5]. These evidences strongly suggest that RUNX3 gene be a tumor suppressor gene.

It is commonly known that TGF-beta-Smad signal pathway is disrupted in HCC, but the exact mechanism of disruption of the signal pathway has still remained to be worked out^[8]. Furthermore, LOH of 1p36 encompassing RUNX3 gene was a common event in pathogenesis of HCC^[19]. So, it is reasonable to consider RUNX3 gene as a most possible target gene in the development of HCC. In this study, we found 34.6% of HCC showed LOH of RUNX3. This result is in concordance with the previously reported 30% more or less frequency of LOH at 1p36, an early event in the development of HCC^[17,20]. Unfortunately, no mutation was discovered in 62 HCCs.

Hypermethylation is a regional event that occurs frequently in GC-rich sequences, called CpG islands, often located within the 5' regulatory regions of non-transcribed genes. In contrast, actively transcribed genes are always in unmethylation status. Inactivation of genes by hypermethylation of their CpG islands has been well clarified^[21,26,27]. Now, it has been recognized that hypermethylation of CpG islands in the promoter region is an alternative way to silence some cancer-associated gene as effectively as inactivation by mutation or deletion^[28,29]. To date, genes involved in regulation of cell cycle^[21,30], DNA repair^[31],

angiogenesis^[32], and apoptosis^[33,34] have been shown to be inactivated by hypermethylation which is also a frequent event in many human cancers including hepatocellular carcinoma^[35-37]. For RUNX3 gene, transcription is regulated by two distinct promoters, P1 and P2. The major RUNX3 mRNA is transcribed from P2. The genomic region surrounding the P2 promoter constituted a large (4.2 kb) CpG island with a GC content of 64%^[24]. These features showed P2 possessed the hallmark characteristics of GC-rich promoters. So, it is rational that transcription from P2 should be regulated by DNA methylation in theory. In practice, Li *et al*^[5] confirmed the presumption in *in vitro* experiment. Our analysis of RUNX3 gene in HCCs provided evidence of promoter hypermethylation, a common alteration as well as an early event. Thus, methylation of the promoter region appears to be the dominant mode of inactivation of RUNX3 gene in human HCC, just the same as in human gastric cancer. Unfortunately, we did not detect the expression of RUNX3 gene due to unavailability of the sample and antibody. However, methylation changes are considered as a surrogate for altered expression of the gene product, thus, the detection of any abnormally methylated site is a strong indication that this mechanism could alter the expression levels of target genes. It was reported that hypermethylation correlated with LOH and often occurred before the allelic loss^[38]. We found in our study 48.3%(30/62) of HCCs showed hypermethylation, which was higher than LOH (34.6%), and 88.9%(8/9) of HCCs with LOH had hypermethylation in the promoter of RUNX3 gene, hence being in line with Knudson's two hit hypothesis and consistent with previous reports.

In summary, we have demonstrated a high frequency of RUNX3 gene aberration-allelic loss together with hypermethylation of the remaining alleles in HCC. These observations can provide the evidence that promoter hypermethylation and allelic loss are the major mechanisms for inactivation of RUNX3 gene in HCC. RUNX3 gene may be one of the key tumor suppressor genes at 1p36 which is the common deletion site of RUNX3 gene in HCC. Inactivation of RUNX3 gene functions, resulting in impairment of TGF-beta-Smads signal pathway and other tumor suppressor function, may be closely associated with the development of HCC.

REFERENCES

- Kloos DU**, Choi C, Wingender E. The TGF-beta-Smad network: introducing bioinformatic tools. *Trends Genet* 2002; **18**: 96-103
- Moustakas A**, Pardali K, Gaal A, Heldin C. Mechanisms of TGF-beta signaling in regulation of cell growth and differentiation. *Immunol Lett* 2002; **82**: 85-91
- Leboy P**, Grasso-Knight G, D' Angelo M, Volk SW, Lian JV, Drissi H, Stein GS, Adams SL. Smad-Runx interactions during chondrocyte maturation. *J Bone Joint Surg Am* 2001; **83A** (Pt 1): S15-22
- Zaidi SK**, Sullivan AJ, van Wijnen AJ, Stein JL, Stein GS, Lian JB. Integration of Runx and Smad regulatory signals at transcriptionally active subnuclear sites. *Proc Natl Acad Sci U S A* 2002; **99**: 8048-8053
- Li QL**, Ito K, Sakaura C, Fukamachi H, Inoue K, Chi XZ, Lee KY, Nomura S, Lee CW, Han SB, Kim HM, Kim WJ, Yamamoto H, Yamashita N, Yano T, Ikeda T, Itohara S, Inazawa J, Abe T, Hagiwara A, Yamagishi H, Ooe A, Kaneda A, Sugimura T, Ushijima T, Bae SC, Ito Y. Causal relationship between the loss of RUNX3 expression and gastric cancer. *Cell* 2002; **109**: 113-124
- Korn WM**. Moving toward an understanding of the metastatic process in hepatocellular carcinoma. *World J Gastroenterol* 2001; **7**: 777-778
- Qin LX**, Tang ZY. The prognostic significance of clinical and pathological features in hepatocellular carcinoma. *World J Gastroenterol* 2002; **8**: 193-199
- Bedossa P**, Peltier E, Terris B, Franco D, Poynard T. Transforming growth factor-beta1 (TGF-beta1) and TGF-beta1 receptors in normal, cirrhotic, and neoplastic human livers. *Hepatology* 1995; **21**: 760-766
- Shirai Y**, Kawata S, Tamura S, Ito N, Tsushima H, Takaishi K, Kiso S, Matsuzawa Y. Plasma transforming growth factor-beta 1 in patients with hepatocellular carcinoma. Comparison with other liver diseases. *Cancer* 1994; **73**: 2275-2279
- Song BC**, Chung YH, Kim JA, Choi WB, Suh DD, Pyo SI, Shin JW, Lee HC, Lee YS, Suh DJ. Transforming growth factor-beta1 as a useful serologic marker of small hepatocellular carcinoma. *Cancer* 2002; **94**: 175-180
- Matsuzaki K**, Date M, Furukawa F, Tahashi Y, Matsushita M, Sugano Y, Yamashiki N, Nakagawa T, Seki T, Nishizawa M, Fujisawa J, Inoue K. Regulatory mechanisms for transforming growth factor beta as an autocrine inhibitor in human hepatocellular carcinoma: implications for roles of smads in its growth. *Hepatology* 2000; **32**: 218-227
- Kawate S**, Takenoshita S, Ohwada S, Mogi A, Fukusato T, Makita F, Kuwano H, Morishita Y. Mutation analysis of transforming growth factor beta type II receptor, Smad2, and Smad4 in hepatocellular carcinoma. *Int J Oncol* 1999; **14**: 127-131
- Kawate S**, Ohwada S, Hamada K, Koyama T, Takenoshita S, Morishita Y, Hagiwara K. Mutational analysis of the Smad 6 and Smad 7 genes in hepatocellular carcinoma. *Int J Mol Med* 2001; **8**: 49-52
- Schutte M**, Hruban RH, Hedrick L, Cho KR, Nadasdy GM, Weinstein CL, Bova GS, Isaacs WB, Cairns P, Nawroz H, Sidransky D, Casero RA Jr, Meltzer PS, Hahn SA, Kern SE. DPC4 gene in various tumor types. *Cancer Res* 1996; **56**: 2527-2530
- Simon D**, Knowles BB, Weith A. Abnormalities of chromosome 1 and loss of heterozygosity on 1p in primary hepatomas. *Oncogene* 1991; **6**: 765-770
- Yeh SH**, Chen PJ, Chen HL, Lai MY, Wang CC, Chen DS. Frequent genetic alterations at the distal region of chromosome 1p in human hepatocellular carcinomas. *Cancer Res* 1994; **54**: 4188-4192
- Fang W**, Piao Z, Simon D, Sheu JC, Huang S. Mapping of a minimal deleted region in human hepatocellular carcinoma to 1p36.13-p36.23 and mutational analysis of the RIZ (PRDM2) gene localized to the region. *Genes Chromosomes Cancer* 2000; **28**: 269-275
- Huang S**. The retinoblastoma protein-interacting zinc finger gene RIZ in 1p36-linked cancers. *Front Biosci* 1999; **4**: D528-D532
- Kuroki T**, Fujiwara Y, Tsuchiya E, Nakamori S, Imaoka S, Kanematsu T, Nakamura Y. Accumulation of genetic changes during development and progression of hepatocellular carcinoma: loss of heterozygosity of chromosome arm 1p occurs at an early stage of hepatocarcinogenesis. *Genes Chromosomes Cancer* 1995; **13**: 163-167
- Sun M**, Eshleman JR, Ferrell LD, Jacobs G, Sudilovsky EC, Tuthill R, Hussein MR, Sudilovsky O. An early lesion in hepatic carcinogenesis: loss of heterozygosity in human cirrhotic livers and dysplastic nodules at the 1p36-p34 region. *Hepatology* 2001; **33**: 1415-1424
- Liu LH**, Xiao WH, Liu WW. Effect of 5-Aza-2'-deoxycytidine on the p16 tumor suppressor gene in hepatocellular carcinoma cell line HepG2. *World J Gastroenterol* 2001; **7**: 131-135
- Lehmann U**, Hasemeier B, Lilischkis R, Kreipe H. Quantitative analysis of promoter hypermethylation in laser-microdissected archival specimens. *Lab Invest* 2001; **81**: 635-638
- Grunau C**, Clark SJ, Rosenthal A. Bisulfite genomic sequencing: systematic investigation of critical experimental parameters. *Nucleic Acids Res* 2001; **29**: E65
- Bangsow C**, Rubins N, Glusman G, Bernstein Y, Negreanu V, Goldenberg D, Lotem J, Ben-Asher E, Lancet D, Levanon D, Groner Y. The RUNX3 gene-sequence, structure and regulated expression. *Gene* 2001; **279**: 221-232
- Cohen MM Jr**. RUNX genes, neoplasia, and cleidocranial dysplasia. *Am J Med Genet* 2001; **104**: 185-188
- Baylin SB**, Herman JG, Graff JR, Vertino PM, Issa JP. Alterations in DNA methylation: a fundamental aspect of neoplasia. *Adv Cancer Res* 1998; **72**: 141-196
- Esteller M**, Corn PG, Baylin SB, Herman JG. A gene hypermethylation profile of human cancer. *Cancer Res* 2001; **61**: 3225-3229

- 28 **Jones PA**, Laird PW. Cancer epigenetics comes of age. *Nat Genet* 1999; **21**: 163-167
- 29 **Wajed SA**, Laird PW, DeMeester TR. DNA methylation: an alternative pathway to cancer. *Ann Surg* 2001; **234**: 10-20
- 30 **Roncalli M**, Bianchi P, Bruni B, Laghi L, Destro A, Di Gioia S, Gennari L, Tommasini M, Malesci A, Coggi G. Methylation framework of cell cycle gene inhibitors in cirrhosis and associated hepatocellular carcinoma. *Hepatology* 2002; **36**: 427-432
- 31 **Esteller M**, Hamilton SR, Burger PC, Baylin SB, Herman JG. Inactivation of the DNA repair gene O6-methylguanine-DNA methyltransferase by promoter hypermethylation is a common event in primary human neoplasia. *Cancer Res* 1999; **59**: 793-797
- 32 **Li Q**, Ahuja N, Burger PC, Issa JP. Methylation and silencing of the Thrombospondin-1 promoter in human cancer. *Oncogene* 1999; **18**: 3284-3289
- 33 **Teitz T**, Lahti JM, Kidd VJ. Aggressive childhood neuroblastomas do not express caspase-8: an important component of programmed cell death. *J Mol Med* 2001; **79**: 428-436
- 34 **Jones PA**. Cancer. Death and methylation. *Nature* 2001; **409**: 141-144
- 35 **Shen L**, Ahuja N, Shen Y, Habib NA, Toyota M, Rashid A, Issa JP. DNA methylation and environmental exposures in human hepatocellular carcinoma. *J Natl Cancer Inst* 2002; **94**: 755-761
- 36 **Zhong S**, Tang MW, Yeo W, Liu C, Lo YM, Johnson PJ. Silencing of GSTP1 gene by CpG island DNA hypermethylation in HBV-associated hepatocellular carcinomas. *Clin Cancer Res* 2002; **8**: 1087-1092
- 37 **Yoshikawa H**, Matsubara K, Qian GS, Jackson P, Groopman JD, Manning JE, Harris CC, Herman JG. SOCS-1, a negative regulator of the JAK/STAT pathway, is silenced by methylation in human hepatocellular carcinoma and shows growth-suppression activity. *Nat Genet* 2001; **28**: 29-35
- 38 **Makos M**, Nelkin BD, Reiter RE, Gnarr JR, Brooks J, Isaacs W, Linehan M, Baylin SB. Regional DNA hypermethylation at D17S5 precedes structural changes in the progression of renal tumour. *Cancer Res* 1993; **53**: 2719-2722

Edited by Zhu LH and Wang XL

Evaluation of high-resolution computed tomography and pulmonary function tests in patients with chronic hepatitis C virus infection

Oguzhan Okutan, Zafer Kartaloglu, Ahmet Ilvan, Ali Kutlu, Erkan Bozkanat, Emir Silit

Oguzhan Okutan, Zafer Kartaloglu, Ahmet Ilvan, Erkan Bozkanat, GATA Haydarpaşa Training Hospital, Department of Pulmonary Diseases, Istanbul, Turkey

Ali Kutlu, Gumussuyu Military Hospital, Department of Pulmonary Diseases, Istanbul, Turkey

Emir Silit, GATA Haydarpaşa Training Hospital, Department of Radiology, Istanbul, Turkey

Correspondence to: Dr. Oguzhan Okutan, GATA Camlica Gogus Hastaliklari Hastanesi 81020 Acibadem, Istanbul, Turkey. oguzhanokutan@hotmail.com

Telephone: +90-216-3257250 **Fax:** +90-216-3257257

Received: 2003-08-23 **Accepted:** 2003-11-20

Abstract

AIM: To investigate pulmonary involvement via pulmonary function tests (PFT) and high-resolution computed tomography (HRCT) in patients with chronic hepatitis C virus (HCV) infection.

METHODS: Thirty-four patients with chronic HCV infection without diagnosis of any pulmonary diseases and 10 healthy cases were enrolled in the study. PFT and HRCT were performed in all cases.

RESULTS: A decrease lower than 80% of the predicted value was detected in vital capacity in 9/34 patients, in forced expiratory volume in one second in 8/34 patients, and in forced expiratory flow 25-75 in 15/34 patients, respectively. Carbon monoxide diffusing capacity (DLCO) was decreased in 26/34 patients. Findings of interstitial pulmonary involvement were detected in the HRCT of 16/34 patients. Significant difference was found between controls and patients with HCV infection in findings of HRCT ($\chi^2=4.7$, $P=0.003$). Knodell histological activity index (KHA1) of 28/34 patients in whom liver biopsy was applied was 9.0 ± 4.7 . HRCT findings, PFT values and DLCO were not affected by KHA1 in patients with HCV infection. In these patients, all the parameters were related with age.

CONCLUSION: We suggest that chronic hepatitis C virus infection may cause pulmonary interstitial involvement without evident respiratory symptoms.

Okutan O, Kartaloglu Z, Ilvan A, Kutlu A, Bozkanat E, Silit E. Evaluation of high-resolution computed tomography and pulmonary function tests in patients with chronic hepatitis C virus infection. *World J Gastroenterol* 2004; 10(3):381-384
<http://www.wjgnet.com/1007-9327/10/381.asp>

INTRODUCTION

Hepatitis C virus (HCV) is a common infectious agent, and it is estimated that 3% of the world population are infected with HCV. It was reported that HCV caused 20% of acute hepatitis and 70% of chronic hepatitis^[1,2]. HCV could be stimulated chronically by immune system^[3,4]. There are few studies about

pulmonary involvement of chronic HCV infection. These have been done with small patient groups and results on the association between chronic HCV infection and pulmonary involvement could not be found from these studies^[5,6].

Although idiopathic pulmonary fibrosis is considered to be idiopathic, inhaled substances are suggested to be responsible for the manifestation of this clinical presentation^[7,8]. Onset of symptoms following a viral infection or common cold in some patients suggests that development of the disease may be due to the injury related to the infection. There is evidence that hepatitis C virus, Epstein-Barr virus (EBV), and adenoviruses may be responsible for the fibrosis^[9-11].

This study was to investigate the relationship between HCV infection and interstitial pulmonary involvement, and to reveal the relationship among involvement and age, sex, cigarette smoking, severity of hepatitis, and respiratory functions.

MATERIALS AND METHODS

Patients and study design

Thirty-four patients with chronic HCV infection at outpatient clinics of our hospital, were included in the study. Written informed consent was obtained from each patient prior to participation. Ten healthy subjects (6 males, 4 females) were enrolled in the study as control group. Their age, sex characteristics, and smoking habit were similar to the patient group.

Diagnosis of chronic HCV infection was established by the 3rd generation ELISA test (AxSYM HCV version 3.0, Abbott, Wiesbaden-Delkenheim, Germany) and liver biopsy. When liver biopsy was impossible (6 cases), HCV RNA positivity was accepted for the diagnosis.

Patients with previous diagnosis of another pulmonary disease, decompensated cirrhosis, congestive heart failure, suspected malignancy, collagen tissue disease, leukopenia ($<3\ 000/\text{mm}^3$), thrombocytopenia ($<80\ 000/\text{mm}^3$), hepatitis B carriers and drug addicts (current and past users) were excluded. Cases having a history of chronic alcoholism were also not included in the study. All the patients did not receive any treatment for HCV infection.

Medical history was recorded and physical examination was performed in cases who fulfilled the above criteria for study entry. Their age, sex and quantity of cigarette smoking (pack-year) were recorded. Chest X-ray was obtained.

Pulmonary function test (PFT), diffusion test and high-resolution computerized tomography (HRCT) were performed in all cases.

Pulmonary function test

Measurements of vital capacity (VC), forced vital capacity (FVC), forced expiratory volume in first second (FEV1), forced mid-expiratory flow rate (FEF25-75), carbon monoxide diffusion capacity (DLCO) and ratio of DLCO to alveolar ventilation (DLCO/VA) were done in accordance with American Thoracic Society criteria^[13] by using the Vmax 22 device (Sensor Medics, Yorba Linda, CA, USA) with single breath diffusion method. None of the patients had received bronchodilator drugs prior to the tests. Measurements were

recorded as the percentage of the predicted value, 80% and above were considered as normal.

High resolution computerized tomography

HRCT images were obtained by the Somatom DRH device (Siemens, Erlangen, Germany), without contrast administration, and with 10 mm interval, 2 mm thick section, 310 mAs, 125 kVp, 4 seconds of imaging time, in bone algorithm, 512x512 reconstruction matrix, and 1 600/-400 parenchymal and 350/50 mediastinal window range.

For evaluation of interstitial involvement with HRCT, the method described by Remy-Jardin *et al*^[13] was used. HRCT scans were evaluated for the presence, distribution, and extent of the following signs: [a] ground-glass attenuation, [b] nodular areas of high attenuation, [c] consolidation, [d] linear areas of high attenuation, classified as nonseptal lines, [e] septal lines, [f] honeycombing, and [g] architectural distortion.

Extension of the involvement was assessed independently for each of the three zones of the thorax defined as follows. The upper zones were above the level of the main carina, the middle zones were between the level of the main carina and the inferior pulmonary veins, and the lower zones were under the level of the inferior pulmonary veins. HRCT scores in the upper, middle, and lower pulmonary zones were determined by visually estimating the extent of the disease in each zone. The HRCT score was based on the percentage of pulmonary parenchyma that showed evidence of each recorded abnormality, and was estimated to be 5% of parenchymal involvement: 25% and below as 1 point, 26%-50% as 2 points, 51%-75% as 3 points, 76% and above as 4 points. The scores for each zone were then added to obtain a global extent score, ranging from 0 to 12, and referred to as the HRCT extent score of each HRCT abnormality. A total score of pulmonary involvement was obtained by summation of the global extent score of all HRCT abnormalities, ranging from 0 to 84, which was the feature referred to as the overall HRCT of disease severity.

Pulmonary interstitial involvement was confirmed with prone position scanning in patients who had HRCT findings. HRCT scans were interpreted in random order by two radiologists without any clinical data, the two observers assessed the scans together to reach a decision by consensus.

Evaluation of liver biopsy

Liver biopsy was performed in 28/34 patients. Histological evaluation of liver biopsy reflecting the activity level of the disease was done according to the Knodell histological activity index (KHAI) described by Knodell *et al*^[14]. Inflammation in portal areas, piecemeal appearance and bridging necrosis at periportal areas and necro-inflammatory activity observed in parenchyma were considered in the evaluation of the severity of hepatitis.

Statistical analysis

Quantitative data were presented as mean±SD. Statistical

analysis was performed by Mann-Whitney *U* test for comparison of PFTs of patients with HCV infection and control group, and Fisher's exact (chi-square) test for comparison of HRCT findings. Relation among KHAI and age, sex was evaluated by multiple linear regression analysis. HRCT and PFT were considered as dependent variables, KHAI and factors possibly affecting pulmonary pathologies including age, sex and amount of cigarette smoking were considered as independent variables, then separate multiple linear regression analyses for HRCT score, VC, FVC, FEV1, FEF25-75, DLCO, DLCO/VA were performed. *P*<0.05 was considered statistically significant.

RESULTS

Thirty-four patients (15 women and 19 men) with a mean age of 47.6±17.5 years (20-72) were enrolled in the study. Eighteen patients had a history of cigarette smoking and the mean amount of cigarette smoking was 16.5±9.7 pack-year. Ten healthy control cases (6 men and 4 women) with a mean age of 46.2±2.6 years (21-65) were enrolled into the study. Four of them had a history of cigarette smoking.

PFT measurements revealed that VC, FVC, FEV1, and FEF25-75 were below 80% of the predicted value in 9/34, 8/34, 5/34 and 15/34 patients with HCV infection, respectively. DLCO was decreased in 26/34 patients and DLCO/VA ratio was decreased in 18/34 patients. But, there was no significant difference between controls and patients with HCV infection in mean PFT parameters (Table 1). KHAI values were between 2-16 in 28 patients in whom liver biopsy was performed and the mean KHAI was 9.0±4.7 points.

Table 1 Knodell histological activity index (KHAI) and pulmonary function tests (mean±SD) in patients with chronic hepatitis C virus infection and controls

Features	Patients with HCV (n=34)	Controls (n=10)	P
KHAI	9.0±4.7	-	-
VC ^a	86.3±10.9	83.6±7.9	NS
FVC ^a	85.8±12.0	80.6±8.3	NS
FEV1 ^a	86.5±11.0	82.3±6.7	NS
FEF25-75 ^a	78.2±18.8	81.7±13.5	NS
DLCO ^a	66.3±21.3	80.7±15.3	NS
DLCO/VA ^a	77.7±18.0	85.2±14.5	NS

^a: % predicted; NS: Not significant.

Interstitial pulmonary involvement was found in 16/34 patients with HRCT. Only one case (1/10) had distortion in the controls in HRCT. HRCT findings excluded other causes such as pneumonia, cancer or tuberculosis in patients and control cases. There was a significant difference between controls and patients with HCV infection in HRCT for interstitial involvement ($\chi^2=4.7$, *P*=0.03) (Table 2). All of our

Table 2 High-resolution computed tomography (HRCT) findings in patients with chronic hepatitis C virus infection and controls

HRCT Findings	Patients with HCV infection			Controls		
	n	%	HRCT scores	n	%	HRCT scores
Ground-glass attenuation	1	2.9	2	0	0	-
Nodular areas of high attenuation	6	17.6	3.6±1.5	0	0	-
Consolidation	0	0	-	0	0	-
Non-septal lines	5	14.7	2.7±1.7	0	0	-
Septal lines	4	11.7	3.9±1.6	0	0	-
Honeycombing	0	0	-	0	0	-
Distortion	0	0	-	1	10	2

P=0.03, $\chi^2=4.7$.

Table 3 Multiple linear regression analysis of Knodell histological activity index (KHAI) and age and sex in patients with chronic hepatitis C virus infection

Dependent variable	Independent variables								
	Whole regression equation			Age			Sex		
	R ²	F	p	β	t	p	β	t	p
KHAI	0.61	38.8	<0.001	0.78	6.2	<0.001	a	a	a

a: Not significant, R²: squared multiple correlation coefficient, F: F value, β: Partial correlation coefficients, t: t value of regression coefficients.

Table 4 Multiple linear regression analysis of high-resolution computed tomography (HRCT) score, pulmonary function test, Knodell histological activity index (KHAI), age, sex and smoking in patients with chronic hepatitis C virus infection

Dependent variables	Independent variables														
	Whole regression equation			KHAI			Age			Sex			Smoking		
	R ²	F	p	β	t	p	β	t	p	β	t	p	β	t	p
HRCT score	0.17	5.4	0.028	a	a	a	0.42	2.3	0.028	a	a	a	a	a	a
VC	0.19	6.1	0.020	a	a	a	-0.44	-2.5	0.020	a	a	a	a	a	a
FVC	0.24	8.0	0.009	a	a	a	-0.49	-2.8	0.009	a	a	a	a	a	a
FEV1	0.25	8.6	0.007	a	a	a	-0.50	-2.9	0.007	a	a	a	a	a	a
FEF25-75	0.30	11.1	0.003	a	a	a	-0.55	-3.3	0.003	a	a	a	a	a	a
DLCO	0.16	4.9	0.036	a	a	a	-0.40	-2.1	0.036	a	a	a	a	a	a
DLCO/VA	0.22	3.5	0.047	0.55	2.2	0.04	-0.66	-2.6	0.015	a	a	a	a	a	a

a: Not significant, R²: squared multiple correlation coefficient, F: F value, β: Partial correlation coefficients, t: t value of regression coefficients.

16 patients in whom interstitial pulmonary involvement was found in HRCT had HRCT scores consistent with mild parenchymal abnormalities, there was a negative correlation between HRCT score and DLCO, FVC ($r=-0.364$, $P=0.035$; $r=-0.400$, $P=0.019$, respectively).

Multiple linear regression analysis in which age and sex were considered as independent variables and KHAI was considered as dependent variable, revealed that KHAI was not affected by sex and was related with age, while KHAI was increased with age (Table 3). In order to investigate the possible association between liver pathology (KHAI) and pulmonary data (HRCT, PFT), pulmonary data were considered as dependent variables, KHAI and possible factors affecting pulmonary pathologies including age, sex and amount of cigarette smoking were considered as independent variables, then separate multiple linear regression analyses for HRCT score, VC, FVC, FEV1, FEF25-75, DLCO, DLCO/VA were performed. HRCT score, VC, FVC, FEV1, FEF25-75, DLCO, and DLCO/VA were related with age. HRCT score was positively correlated with age, whereas others decreased with increasing age (negative correlation). When multiple linear regression analysis was used, no significant relation was found between liver pathology and any of the PFT (except DLCO/VA) or HRCT score (Table 4). Although 16 patients had signs consistent with interstitial involvement in HRCT, our findings showed that this was not directly related with liver pathology.

DISCUSSION

In our study, some patients with HCV infection had a mild decrease in PFTs. However, there was no significant difference between patients and controls in PFTs. We determined that there was a significant difference between patients and controls according to the findings in thorax HRCT. The age was related with both pulmonary involvement and liver pathology.

Although the relationship between pulmonary fibrosis and HCV infection was first suggested by Ueda *et al*^[9], Irving *et al*^[15] held on opposite point. In a study, which investigated 300 patients with clinically evident HCV infection for the presence

of pulmonary fibrosis, HRCT assessments revealed a moderate degree of pulmonary fibrosis in 4 cases and severe pulmonary fibrosis in another 4 cases. In all of these 8 cases, there were various degrees of decreases in diffusion capacity that correlated with HRCT findings and less frequently restriction in PFT parameters^[5].

In our study, FEF25-75 was below 80% of the predicted value in a small group of patients (5 patients) with normal FEV1 and VC. Decrease in FEF25-75 and normal VC and FEV1 might be an indicator of an early stage small airway disease. Similar to our findings, Mimori *et al*^[16] stated that in sarcoidosis patients with normal FEV1 and VC, the increase in the ratio of maximum expiratory flow rate at 50% of vital capacity (V50) to maximum expiratory flow rate at 25% of vital capacity (V25) was a finding of the early stage manifestation of small airway disease.

There are contradictory results in the literature about correlations between PFT and HRCT score in patients with pulmonary fibrosis. Also, studies generally revealed a negative correlation between PFT and HRCT score^[5,13,17]. We detected a negative correlation among HRCT, FVC and DLCO in patients with HCV infection.

As HCV infections generally follow a silent course and as they are rarely diagnosed at the acute phase, onset of the disease usually could not be determined^[2]. So, duration of the disease was not investigated among factors that would possibly affect the development of pulmonary involvement. HRCT score and PFT parameters were related with age. In our opinion, because duration of HCV infection may not be accurately determined, age may indirectly be a sign of the duration of the disease.

KHAI was related with DLCO/VA and age in our study. Chronic HCV infection is known to result in moderate to severe disorders in liver, particularly in elderly and alcoholics^[18]. In our patients, neither any of the PFT parameters except DLCO/VA nor HRCT score was affected by KHAI (Table 3). Change in DLCO was probably related with age. Because KHAI is for the evaluation of liver parenchyma, we believe that it does not reflect the intensity of extrahepatic manifestations.

It is clearly revealed that HCV infection does not only affect

the liver, it also has many systemic manifestations. However few studies about its effect on the lung showed that there was an uncertain relationship between HCV infection and pulmonary involvement^[4,18]. We found a negative correlation between HRCT score and DLCO in chronic HCV patients. In some patients (six cases), there was a decrease in DLCO despite normal HRCT findings. Many studies have shown that DLCO could decrease without presence of any radiological finding in the early stage of fibrosis and this decrease might become more significant later^[19-21].

Chronic hepatitis C virus infections may cause mild pulmonary involvement without any pulmonary symptoms resulting in a minimal decrease in PFT. In our study, we found that pulmonary involvement was not related with the degree of liver pathology. The relationship between liver pathology and pulmonary involvement must be investigated in large patient population, and also, it should be detected whether alveolitis can demonstrate the early stage pulmonary involvement. However, we suggest that chronic HCV infection patients, particularly elder ones, might be carefully evaluated by HRCT and DLCO even though they have normal chest X-ray or other PFT parameters.

REFERENCES

- 1 **Alter MJ**. Epidemiology of hepatitis C in the west. *Semin Liver Dis* 1995; **15**: 5-14
- 2 **Hoofnagle JH**. Hepatitis C: The clinical spectrum of disease. *Hepatology* 1997; **26**(Suppl 1): 15S-20S
- 3 **Ferri C**, Monti M, La Civita L, Longombardo G, Greco F, Pasero G, Gentilini P, Bombardieri S, Zignego AL. Infection of peripheral blood mononuclear cells by hepatitis C virus in mixed cryoglobulinemia. *Blood* 1993; **82**: 3701-3704
- 4 **Pawlotsky JM**, Roudot-Thoraval F, Simmonds P, Mellor J, Ben Yahia MB, Andre C, Voisin MC, Intrator L, Zafrani ES, Duval J, Dhumeaux D. Extrahepatic immunologic manifestations in chronic hepatitis C and hepatitis C virus serotypes. *Ann Intern Med* 1995; **122**: 169-173
- 5 **Ferri C**, La Civita L, Fazzi P, Solfanelli S, Lombardini F, Begliomini E, Monti M, Longombardo G, Pasero G, Zignego AL. Interstitial lung fibrosis and rheumatic disorders in patients with hepatitis C virus infection. *Br J Rheumatol* 1997; **36**: 360-365
- 6 **Weidensaul D**, Imam T, Holyst MM, King PD, McMurray RW. Polymyositis, pulmonary fibrosis and hepatitis C virus. *Arthritis Rheum* 1995; **38**: 437-439
- 7 **Hubbard R**, Lewis S, Richards K, Johnston I, Britton J. Occupational exposure to metal or wood dust and aetiology of cryptogenic fibrosing alveolitis. *Lancet* 1996; **347**: 284-289
- 8 **Scott J**, Johnston I, Britton J. What causes cryptogenic fibrosing alveolitis? A case-control study of environmental exposure to dust. *BMJ* 1990; **301**: 1015-1017
- 9 **Ueda T**, Ohta K, Suzuki N, Yamaguchi M, Hirai K, Horiuchi T, Watanabe J, Miyamoto T, Ito K. Idiopathic pulmonary fibrosis and high prevalence of serum antibodies to hepatitis C virus. *Am Rev Respir Dis* 1992; **146**: 266-268
- 10 **Vergnon JM**, Vincent M, De The G, Mornex JF, Weynants P, Brune J. Cryptogenic fibrosing alveolitis and Epstein-Barr Virus: An association? *Lancet* 1984; **2**: 768-771
- 11 **Kuwano K**, Nomoto Y, Kunitake R, Hagimoto N, Matsuba T, Nakanishi Y, Hara N. Detection of adenovirus E1A DNA in pulmonary fibrosis using nested polymerase chain reaction. *Eur Respir J* 1997; **10**: 1145-1149
- 12 **O'Donnell DE**, McGuire M, Samis L, Webb KA. The impact of exercise reconditioning on breathlessness in severe chronic airflow limitation. *Am J Respir Crit Care Med* 1995; **152**(6 Pt 1): 2005-2013
- 13 **Remy-Jardin M**, Giraud F, Remy J, Wattinne L, Wallaert B, Duhamel A. Pulmonary sarcoidosis: Role of CT in the evaluation of disease activity and functional impairment and in prognosis assessment. *Radiology* 1994; **191**: 675-680
- 14 **Knodell RG**, Ishak KG, Black WC, Chen TS, Craig R, Kaplowitz N, Kiernan TW, Wollman J. Formulation and application of numerical scoring system for assessing histological activity in asymptomatic chronic active hepatitis. *Hepatology* 1981; **1**: 431-435
- 15 **Irving WL**, Day S, Johnston ID. Idiopathic pulmonary fibrosis and hepatitis C virus infection. *Am Rev Respir Dis* 1993; **148**: 1683-1684
- 16 **Mimori Y**. Sarcoidosis: Correlation of HRCT findings with results of pulmonary function tests and serum angiotensin-converting enzyme assay [abstract]. *Kurume Med J* 1998; **45**: 247-256
- 17 **Fenlon HM**, Doran M, Sant SM, Breatnach E. High-resolution chest CT in systemic lupus erythematosus. *Am J Roentgenol* 1996; **166**: 301-307
- 18 **Terrault NA**, Wright TL. Viral hepatitis A through G. In: Feldman M, Scharschmidt BF, Sleisenger MH, eds. *Gastrointestinal and Liver Disease*. 6th ed. Los Angeles: WB Saunders 1998: 1123-1170
- 19 **Kanengiser LC**, Rapoport DM, Epstein H, Goldring RM. Volume adjustment of mechanics and diffusion in interstitial lung disease. Lack of clinical relevance. *Chest* 1989; **96**: 1036-1042
- 20 **Javaheri S**, Sicilian L. Lung function, breathing pattern and gas exchange in interstitial lung disease. *Thorax* 1992; **47**: 93-97
- 21 **Crapo RO**, Forster RE 2nd. Carbon monoxide diffusing capacity. *Clin Chest Med* 1989; **10**: 187-198

Edited by Wang XL Proofread by Zhu LH

Expression of platelet-derived growth factor-BB in liver tissues of patients with chronic hepatitis B

Song-Mei Lou, You-Ming Li, Kai-Ming Wang, Wei-Min Cai, Hong-Lei Weng

Song-Mei Lou, Department of Gastroenterology, Hangzhou First People's Hospital, Hangzhou 310006, Zhejiang Province, China

You-Ming Li, Kai-Ming Wang, Wei-Min Cai, Hong-Lei Weng, First Affiliated Hospital, College of Medicine, Zhejiang University, Hangzhou 310003, Zhejiang Province, China

Correspondence to: Song-Mei Lou, Department of Gastroenterology, Hangzhou First People's Hospital, Hangzhou 310006, Zhejiang Province, China. lousm_72@hotmail.com

Telephone: +86-571-87065701-2184

Received: 2003-05-11 **Accepted:** 2003-07-05

Abstract

AIM: To study the relationship between expression of platelet-derived growth factor-BB (PDGF-BB) and fibrogenesis in chronic hepatitis B.

METHODS: Hepatic tissues from 43 patients with chronic hepatitis B were embedded in paraffin. The sections were stained with HE and picric acid-sirius red to determine inflammatory activity and fibrosis stages. PDGF-BB expression was detected by immunohistochemistry and assessed semiquantitatively. Levels of serum hyaluronic acid (HA), pro-collagen III (PCIII), collagen IV (IV-C) and laminin (LN) were examined by radioimmunoassay (RIA).

RESULTS: The expression level of PDGF-BB was found to be positively correlated with inflammatory activity, fibrosis stage and grade of histological findings ($\tau=0.58, 0.55, 0.55, P<0.01$). The positive correlation was also observed between tissue level of PDGF-BB expression and contents of HA, PCIII, IV-C and LN in the circulation ($r=0.52, 0.32, 0.40, 0.33, P<0.05$).

CONCLUSION: PDGF-BB may play some role in the development and progression of liver fibrosis.

Lou SM, Li YM, Wang KM, Cai WM, Weng HL. Expression of platelet-derived growth factor-BB in liver tissues of patients with chronic hepatitis B. *World J Gastroenterol* 2004; 10(3):385-388 <http://www.wjgnet.com/1007-9327/10/385.asp>

INTRODUCTION

In chronic liver diseases, fibrosis is one of the parameters indicating a progressive process leading to cirrhosis. Hepatic stellate cells (HSCs) are considered to play a central role in the pathogenesis of liver fibrosis^[1,2]. During the process, HSCs proliferate and differentiate into myofibroblast-like cells, synthesizing various extracellular matrix (ECM) components including collagen^[2,3].

Platelet-derived growth factor (PDGF) is the most potent mitogen for HSCs^[4-6], which were currently indicated as the principle cells producing connective tissue in fibrotic liver^[7-9]. PDGF was currently indicated as a major inflammatory growth factor playing a central role in the repair process after acute and chronic tissue injuries. Several recent studies have

demonstrated a pathogenic role of PDGF in several chronic inflammatory disorders including glomerulonephritis^[10,11], scleroderma^[12], rheumatoid arthritis^[13], idiopathic pulmonary fibrosis^[14] and atherosclerosis^[15,16]. The presence of inflammatory infiltrates and the excessive deposition of collagenous matrix are the prominent features of chronic hepatitis. Along these lines, PDGF may also be involved in hepatic fibrogenesis.

PDGF consists of two polypeptide chains (A and B). Three isoforms have been described, namely PDGF-AA, -AB, -BB^[17-19]. Recent studies have shown that PDGF-AB and -BB isoforms are more mitogenic for HSCs than PDGF-AA^[6]. Thus, the expression of the B chain is thought to be more important in hepatic fibrogenesis than that of the A chain.

In this study we used immunohistological methods to detect PDGF-BB in human liver biopsy specimens from 43 patients with chronic hepatitis B. In addition, the levels of serum hyaluronic acid (HA), pro-collagen type III (PCIII), collagen type IV (IV-C) and laminin (LN) were examined by radioimmunoassay. The relationship between expression of PDGF-BB, histologic and serum parameters were evaluated.

MATERIALS AND METHODS

Liver and serum samples

Liver tissue samples with various necroinflammatory activities and at different fibrosis stages were obtained by percutaneous liver biopsies from 43 patients with HBV-related chronic hepatitis during routine diagnostic procedures. All of the patients did not receive any anti-inflammatory or anti-fibrotic treatments, such as steroids or interferon. Informed consent was obtained from the patients for the use of their specimens in the investigation. The biopsy specimens were fixed in 10% neutral formalin and embedded in paraffin. Sections of 6 μ m in thickness were used for morphological and immunohistochemical examinations. Serum samples were collected and stored at -20 °C.

Histology

Paraffin sections were stained with hematoxylin and eosin (H&E). Alternatively, the Sirius red stain method was used to demonstrate fibrous tissue components. A polarization microscope (DMLB, Leica, Wetzlar, Germany) was used to distinguish type I from type III collagen fibers^[20]. Grades of necroinflammation (0-4) and stages of fibrosis (0-4) were assessed according to the well-established criteria^[21,22]. The grades and stages were scored as follows: 0=2⁰, 1=2¹, 2=2², 3=2³, and 4=2⁴.

Immunohistochemistry

The deparaffinized sections were washed with phosphate-buffered saline (PBS; pH 7.4) and incubated in 3% H₂O₂/methanol for 20 minutes to block endogenous peroxidase. After washed three times in PBS, 5 min each, the sections were heated for 10 min in 0.01 M citrate buffer (pH 6.0) using a microwave oven, and then washed three times in PBS, 5 min each, and incubated with a rabbit antibody against human PDGF-BB (Santa Cruz Biotechnology, Inc., Santa Cruz, California, USA)

at a dilution of 1:50 in PBS at room temperature for 5 hours. After washed, the immunologic reaction was demonstrated using a kit (Beijing Zhongshan Biotechnology Co., Ltd. Beijing, China) and visualized in a solution containing 3, 3'-diaminobenzidine tetrahydrochloride (DAB). The slides were rinsed in distilled water, counterstained with hematoxylin, dehydrated, air dried, and mounted. PBS was used to substitute for the primary antibody as a negative control.

Sera-assays for hepatic fibrosis

Serum hepatic fibrosis parameters including HA, C-IV, PCIII and LN, were assessed by radioimmunoassays using the kits from Shanghai Navy Medical Institute according to the manufacturer's instructions.

Statistical analysis

Results were expressed as mean±SD. Statistical analyses were performed with the one-way ANOVA, Kendall and Spearman rank correlation. Two-tailed tests were done. $P < 0.05$ was considered statistically significant.

RESULTS

Histological evaluation

The liver tissues of all patients showed various degrees of chronic inflammation and fibrosis. The fibrosis stage was 0 in 7 patients, 1 in 17, 2 in 8, 3 in 6, and 4 in 4. The stage of inflammatory activity was 1 in 13 patients, 2 in 14, 3 in 12, and 4 in 3.

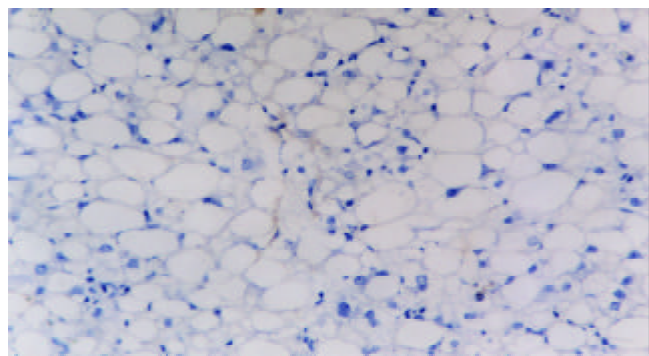


Figure 1 Immunohistochemical detection of PDGF-BB in liver biopsy of a patient with chronic hepatitis B. This case was diagnosed as stage 0. DAB, ×200.

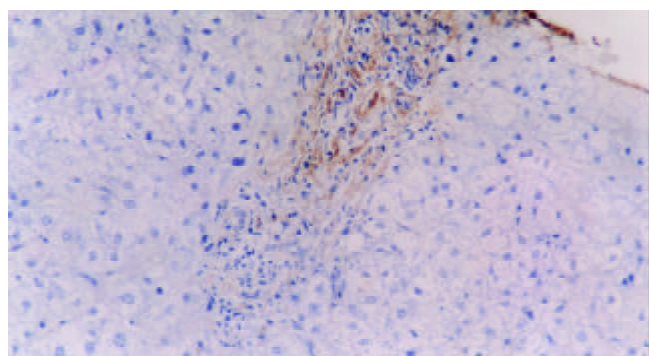


Figure 2 Immunohistochemical detection of PDGF-BB in liver biopsy of a patient with chronic hepatitis B. This case was diagnosed as stage 1. DAB, ×200.

Expression of PDGF-BB in liver biopsy samples

PDGF-BB immunoreactivity was found in a few mesenchymal cells of portal areas and fibrous septa with its products localized

diffusely in the cytoplasm compartment. In intralobular areas, some perisinusoidal cells were also immunoreactive in the areas with necroinflammation. The number of positive cells increased with progression of fibrosis (Figures 1-5) and inflammation. Tables 1- 3 describe PDGF-BB expression levels of different groups respectively. Expression level of PDGF-BB was found to be positively correlated with inflammatory activity, fibrosis stages and grades of histological findings ($\tau = 0.58, 0.55, 0.55, P < 0.01$) in Table 4.

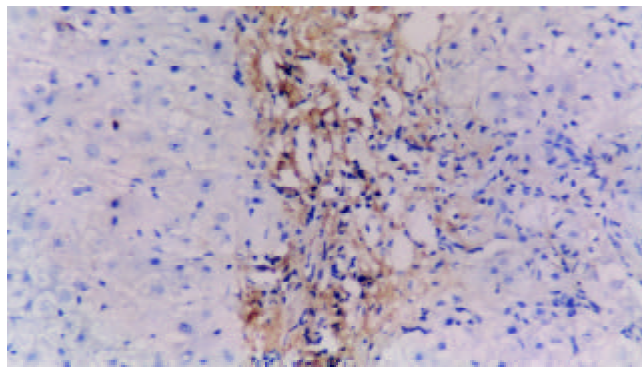


Figure 3 Immunohistochemical detection of PDGF-BB in liver biopsy of a patient with chronic hepatitis B. This case was diagnosed as stage 2. DAB, ×200.

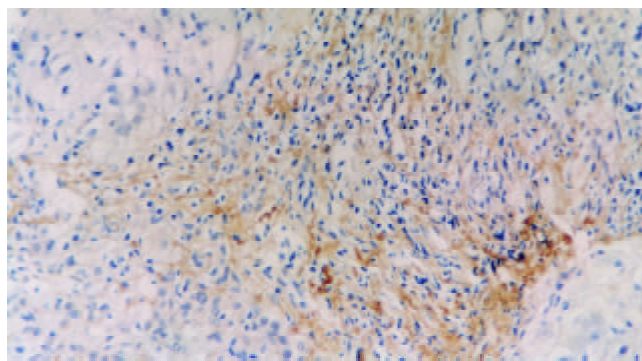


Figure 4 Immunohistochemical detection of PDGF-BB in liver biopsy of a patient with chronic hepatitis B. This case was diagnosed as stage 3. DAB, ×200.

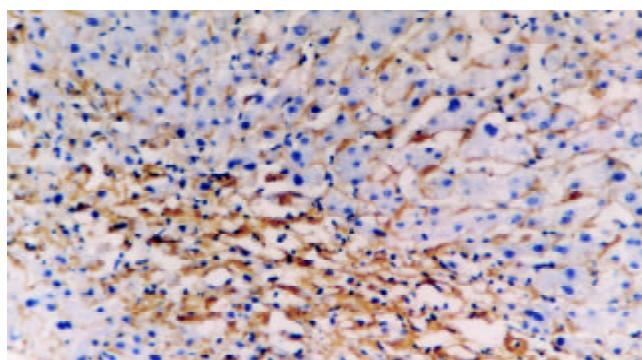


Figure 5 Immunohistochemical detection of PDGF-BB in liver biopsy of a patient with chronic hepatitis B. This case was diagnosed as stage 4. DAB, ×200.

Levels of serum hepatic fibrosis

Positive correlations were found between PDGF-BB expression levels and four serum parameters for hepatic fibrosis, including HA, LN, PC III and C-IV, and their coefficient was 0.38, 0.33, 0.32, and 0.40 ($P < 0.05$), respectively (Table 5).

Table 1 PDGF-BB expression levels in liver samples with different stages of fibrosis

Stages of fibrosis	Case numbers	Expression levels (mean±SD)
S ₀	7	4.71±1.50
S ₁	17	6.47±2.50
S ₂	8	11.63±5.66 ^a
S ₃	6	9.33±2.73 ^a
S ₄	5	16.50±5.74 ^a

^aP<0.05 vs S₀.

Table 2 PDGF-BB expression levels in liver tissues with different grades of necroinflammatory activity

Grades of inflammatory activity	Case numbers	Expression levels (mean±SD)
G ₁	13	4.85±1.57
G ₂	14	8.21±4.17 ^a
G ₃	12	10.67±4.12 ^b
G ₄	4	17.33±6.11 ^b

^aP<0.05 vs G₁; ^bP<0.01 vs G₁.

Table 3 PDGF-BB expression scores in liver tissues of different histological grading groups

Grades of histological finding	Cases numbers	Expression levels (mean±SD)
Mild	27	6.59±3.58
Moderate	10	10.20±4.16 ^a
Sever	6	15.60±5.37 ^b

^aP<0.05 vs mild group; ^bP<0.01 vs mild group.

Table 4 Relationship between PDGF-BB expression levels in liver tissues of different fibrosis stages, necroinflammatory activity and histological grades

	Coefficients as compared with PDGF-BB expression levels (τ)
Stages of fibrosis	0.55 ^b
Grades of inflammatory activity	0.58 ^b
And histological findings	0.55 ^b

^aP<0.05; ^bP<0.01.

DISCUSSION

Liver fibrosis has been to be resulted from architectural remodeling and progressive deposition of ECM components such as proteoglycans, fibronectin, and collagen molecules^[23]. It is one of the major factors affecting the clinical course of

chronic liver diseases. Active fibrogenesis is frequently preceded by, and associated with inflammation. Fibrogenic growth factors and cytokines released by inflammatory cells can promote the proliferation of fat-storing cells, and designate HSCs, which were considered to be the main cellular source of matrix proteins in the liver^[24,25]. In HSCs isolated from rat, mouse or human liver and activated in culture, the dimeric forms of PDGF, either PDGF-AB or -BB, appeared significantly more potent than that of -AA^[26-28]. The results of these *in vitro* studies implicated that an increased expression of PDGF might occur also *in vivo* after liver tissue injury. The current study showed that most of the cells immunoreactive for PDGF-BB were located in portal areas. In intralobular areas, the positive cells were seen mainly in the areas with necroinflammation. In addition, the number of cells expressing PDGF-BB was correlated both to the inflammatory activity and to the fibrosis progression. We consider that PDGF may enhance the tissue repair after acute liver injury. In chronic liver diseases, however, the presence of reiterative tissue damage associated with a persistent inflammatory state may cause a sustained release of PDGF involved in the deposition of extracellular matrix. In this context, the prolonged effects of this growth factor on fat-storing cells may contribute to the development of tissue fibrosis rather than to effective tissue repair. Therefore, PDGF-BB may play an essential role in the development and progression of liver fibrosis. The management of PDGF activity by antagonists may prevent aggressive liver fibrosis and improve prognosis of hepatitis B.

It has been well known that collagen type I was the predominant ECM component in fibrosis and cirrhosis, but it required specific procedures to discriminate different collagen fibers on tissue sections^[29,30]. We used sirius red stain to subtype the fibers as described by Zhang *et al*^[20]. Under the polarization microscope, collagen types I and III were stained red and green, respectively.

Our data showed that the expression levels of PDGF-BB in the liver were correlative with the proposed serum parameters for hepatic fibrosis, including HA, LN, PC III and C-IV. ECM is a complex of macromolecules that includes collagens, proteoglycans and glycoproteins. In fibrotic liver tissue there is an increase in all of these matrix components, and they increase in serum in patients with chronic hepatitis B or liver cirrhosis. These ECM components have been used as a serum marker of hepatic fibrosis. Therefore, serum levels of connective tissue metabolites are related, to some extent, with the amount of ECM in the liver. Wang *et al*^[31] reported that serum fibrosis markers were fairly well correlated with the staging of fibrosis. Regarding the correlation observed in this study between the serum parameters and the expression of PDGF-BB in liver specimens, tissue PDGF-BB levels may be correlative with the stages of hepatic fibrosis. These findings suggest that measurement of serum PDGF-BB may be useful in estimating the active hepatic fibrogenesis of chronic hepatitis B.

Table 5 Relationship between serum fibrosis parameters and PDGF-BB expression levels in liver tissues of different fibrosis stages

Staging of fibrosis(S)	Cases	PDGF-BB	HA (μg/L)	LN(μg/L)	PCIII(μg/L)	IV-C(μg/L)
S ₀	7	4.71±1.50	102.67±60.38	138.23±17.69	137.80±35.57	58.71±17.40
S ₁	17	6.47±2.50	168.74±159.76	129.97±30.15	143.91±51.13	64.12±20.26
S ₂	8	11.63±5.66	434.86±360.58	156.39±39.06	163.74±70.56	86.04±41.94
S ₃	6	9.33±2.73	430.60±325.37	172.65±39.77	192.65±40.05	115.60±30.62
S ₄	5	16.50±5.74	392.30±245.53	163.25±26.26	154.68±22.24	122.10±21.34
Coefficients (r)	...		0.38 ^a	0.33 ^a	0.32 ^a	0.40 ^b

^aP<0.05; ^bP<0.01.

REFERENCES

- 1 **Blomhoff R**, Wake K. Perisinusoidal stellate cells of the liver: important roles in retinal metabolism and fibrosis. *FASEB J* 1991; **5**: 271-277
- 2 **Burt AD**. Cellular and molecular aspects of hepatic fibrosis. *J Pathol* 1993; **170**: 105-144
- 3 **Schuppan D**. Structure of the extracellular matrix in normal and fibrotic liver: collagens and glycoproteins. *Semin Liver Dis* 1990; **10**: 1-10
- 4 **Pinzani M**, Gesualdo L, Sabbah GM, Abboud HE. Effects of platelet-derived growth factor and other polypeptide mitogens on DNA synthesis and growth of cultured rat liver fat-storing cells. *J Clin Invest* 1989; **84**: 1786-1793
- 5 **Friedman SL**, Arthur MJ. Activation of cultured rat hepatic lipocytes by Kupffer cell conditioned medium: Direct enhancement of matrix synthesis and stimulation of cell proliferation via induction of platelet-derived growth factor receptors. *J Clin Invest* 1989; **84**: 1780-1785
- 6 **Pinzani M**, Knauss TC, Pierce GF, Hsieh P, Kenney W, DUBYAK GR, Abboud HE. Mitogenic signals for platelet-derived growth factor isoforms in liver fat-storing cells. *Am J Physiol* 1991; **260**(3 Pt 1): C485-491
- 7 **Mak KM**, Lieber CS. Lipocytes and transitional cells in alcoholic liver disease: a morphometric study. *Hepatology* 1988; **8**: 1027-1033
- 8 **Milani S**, Grappone C, Pellegrini G, Schuppan D, Herbst H, Calabro A, Casini A, Pinzani M, Surrenti C. Undulin RNA and protein expression in normal and fibrotic human liver. *Hepatology* 1994; **20**(4 Pt 1): 908-916
- 9 **Maher JJ**, McGuire RF. Extracellular matrix gene expression increases preferentially in rat lipocytes and sinusoidal endothelial cells during hepatic fibrosis *in vivo*. *J Clin Invest* 1990; **86**: 1641-1648
- 10 **Yoshimura A**, Gordon K, Alpers CE, Floege J, Pritzl P, Ross R, Couser WG, Bowen-Pope DF, Johnson RJ. Demonstration of PDGF B-chain mRNA in glomeruli in mesangial proliferative nephritis by *in situ* hybridization. *Kidney Int* 1991; **40**: 470-476
- 11 **Gesualdo L**, Pinzani M, Floriano JJ, Hassan MO, Nagy NU, Schena FP, Emancipator SN, Abboud HE. Platelet-derived growth factor expression in mesangial proliferative glomerulonephritis. *Lab Invest* 1991; **65**: 160-167
- 12 **Gay S**, Jones RE Jr, Huang GQ, Gay RE. Immunohistologic demonstration of platelet-derived growth factor(PDGF) and sis-oncogene expression in scleroderma. *J Invest Dermatol* 1989; **92**: 301-303
- 13 **Reuter Dahl C**, Tingstrom A, Terracio L, Funa K, Heldin CH, Rubin K. Characterization of platelet-derived growth factor beta-receptor expressing cells on the vasculature of human rheumatoid synovium. *Lab Invest* 1991; **64**: 321-329
- 14 **Nagaoka I**, Trapnell BC, Crystal RG. Upregulation of platelet-derived growth factor-A and -B gene expression in alveolar macrophages of individuals with idiopathic pulmonary fibrosis. *J Clin Invest* 1990; **85**: 2023-2027
- 15 **Wilcox JN**, Smith KM, Williams LT, Schwartz SM, Gordon D. Platelet-derived growth factor mRNA detection in human atherosclerotic plaques by *in situ* hybridization. *J Clin Invest* 1988; **82**: 1134-1143
- 16 **Ross R**, Masuda J, Raines EW, Gown AM, Katsuda S, Sasahara M, Malden LT, Masuko H, Sato H. Localization of PDGF-B protein in macrophages in all phases of atherosclerosis. *Science* 1990; **248**: 1009-1012
- 17 **Ross R**, Raines EW, Bowen-Pope DF. The biology of platelet-derived growth factor. *Cell* 1986; **46**: 155-169
- 18 **Seifert RA**, Hart CE, Phillips PE, Forstrom JW, Ross R, Murray MJ, Bowen-Pope DF. Two different subunits associate to create isoform-specific platelet-derived growth factor receptors. *J Biol Chem* 1989; **264**: 8771-8778
- 19 **Kelly JD**, Haldeman BA, Grant FJ, Murray MJ, Seifert RA, Bowen-Pope DF, Cooper JA, Kazlauskas A. Platelet-derived growth factor(PDGF) stimulates PDGF receptor subunit dimerization and intersubunit trans-phosphorylation. *J Biol Chem* 1991; **266**: 8987-8992
- 20 **Zhang J**, He JW, Wang TL, Zhao JB. Discriminate collagen type I and collagen typeIII by Sirius red stain and polarization microscopy. *Zhonghua Binglixue Zazhi* 1996; **25**: 180-181
- 21 **Desmet VJ**, Gerber M, Hoofnagle JH, Manns M, Scheuer PJ. Classification of chronic hepatitis: diagnosis, grading and staging. *Hepatology* 1994; **19**: 1513-1520
- 22 **Batts KP**, Ludwig J. Chronic hepatitis: An update on terminology and reporting. *Am J Surg Pathol* 1995; **19**: 1409-1417
- 23 **Bissell DM**, Friedman SL, Maher JJ, Roll FJ. Connective tissue biology and hepatic fibrosis: report of a conference. *Hepatology* 1990; **11**: 488-498
- 24 **Gressner AM**, Bachem MG. Cellular sources of noncollagenous matrix proteins: role of fat-storing cells in fibrogenesis. *Semin Liver Dis* 1990; **10**: 30-46
- 25 **Friedman SL**. Cellular sources of collagen and regulation of collagen production in liver. *Semin Liver Dis* 1990; **10**: 20-29
- 26 **Pinzani M**, Knauss TC, Pierce GF, Hsieh P, Kenney W, DUBYAK GR, Abboud HE. Mitogenic signals for platelet-derived growth factor isoforms in liver fat-storing cells. *Am J Physiol* 1991; **260**(3 Pt 1): C485-C491
- 27 **Pinzani M**, Abboud HE, Gesualdo L, Abboud SL. Regulation of macrophage colony-stimulating factor in liver fat-storing cells by peptide growth factors. *Am J Physiol* 1992; **262**(4 Pt 1): C876-C881
- 28 **Pinzani M**, Gentilini A, Caligiuri A, De Franco R, Pellegrini G, Milani S, Marra F, Gentilini P. Transforming growth factor- β 1 regulates platelet-derived growth factor receptor β subunit in human liver fat-storing cells. *Hepatology* 1995; **21**: 232-239
- 29 **Alpini G**, Elias I, Glaser SS, Rodgers RE, Phinizy JL, Robertson WE, Francis H, Lasater J, Richards M, LeSage GD. Gamma-Interferon inhibits secretin-induced cholestasis and cholangiocyte proliferation in a murine model of cirrhosis. *J Hepatol* 1997; **27**: 371-380
- 30 **Brenner DA**, Westwick J, Breindl M. Type I collagen gene regulation and the molecular pathogenesis of cirrhosis. *Am J Physiol* 1993; **264**(4 Pt 1): G589-G595
- 31 **Wang TL**, Wang BE, Liu X, Jia JD, Zhao JB, Li XM, Zhang J, Li NZ. Correlation of serum markers with fibrosis staging in chronic viral hepatitis. *Zhonghua Binglixue Zazhi* 1998; **27**: 185-190

Edited by Su Q and Wang XL

Viral replication modulated by synthetic peptide derived from hepatitis B virus X protein

Chang-Zheng Song, Qing-Wei Wang, Chang-Cheng Song, Zeng-Liang Bai

Chang-Zheng Song, Zeng-Liang Bai, Laboratory of Immunobiology, College of Life Sciences, Shandong University, Jinan 250100, Shandong Province, China

Chang-Zheng Song, Shandong Research Center for Medical Biotechnology, Shandong Academy of Medical Sciences, Jinan 250062, Shandong Province, China

Qing-Wei Wang, Cancer Research Center, Qilu Hospital of Shandong University, Jinan 250012, Shandong Province, China

Chang-Cheng Song, Basic Research Laboratory, National Cancer Institute at Frederick, MD 21702, USA

Correspondence to: Dr. Chang-Zheng Song, Project of Viral Vaccine, Shandong Research Center for Medical Biotechnology, Shandong Academy of Medical Sciences, Jinan 250062, Shandong Province, China. songcz@life.sdu.edu.cn

Telephone: +86-531-2919607

Received: 2003-08-06 **Accepted:** 2003-09-24

Abstract

AIM: A strategy for viral vaccine design is the use of conserved peptides to overcome the problem of sequence diversity. At present it is still unclear whether conserved peptide is safe as a candidate vaccine. We reported it here for the first time not only to highlight the biohazard issue and safety importance for viral peptide vaccine, but also to explore the effect of a fully conserved peptide on HBV replication within the carboxyl terminus of HBx.

METHODS: We synthesized the fully conserved peptide (CP) with nine residues, FVLGGCRHK. HBV-producing 2.2.15 cells were treated with or without 3.5 μ M CP for 36 hours. Quantitative detection of viral DNA was performed by real-time PCR. HBV antigens were determined by enzyme-linked immunosorbent assay (ELISA). Quantitative analyses of p53 and Bax proteins were based on immunofluorescence. Flow cytometry was performed to detect cell cycle and apoptosis.

RESULTS: Both extracellular and intracellular copies of HBV DNA per ml were significantly increased after incubation with 3.5 μ M of CP. HBsAg and HBeAg in the cultured medium of CP-treatment cells were as abundant as untreated control cells. CP influenced negatively the extracellular viral gene products, and 3.5 μ M CP could significantly inhibit intracellular HBsAg expression. In response to CP, intracellular HBeAg displayed an opposite pattern to that of HBsAg, and 3.5 μ M CP could efficiently increase the level of intracellular HBeAg. Flow cytometric analyses exhibited no significant changes on cell cycle, apoptosis, p53 and Bax proteins in 2.2.15 cells with or without CP.

CONCLUSION: Together with the results generated from the synthetic peptide, we address that the conserved region, a domain of HBx, may be responsible for modulating HBV replication. As conserved peptides from infectious microbes are used as immunogens to elicit immune responses, their latent biological hazard for human beings should be evaluated.

Song CZ, Wang QW, Song CC, Bai ZL. Viral replication modulated by synthetic peptide derived from hepatitis B virus X protein. *World J Gastroenterol* 2004; 10(3):389-392

<http://www.wjgnet.com/1007-9327/10/389.asp>

INTRODUCTION

Human hepatitis B virus (HBV) is known as an important cause of acute and chronic hepatitis, cirrhosis, and hepatocellular carcinoma^[1]. Although the incidence of new infections has decreased after the introduction of vaccination programmes, HBV infection remains an important global health problem, with the number of chronic HBV carriers exceeding 350 million worldwide^[2]. HBV is a small DNA virus belonging to the hepadnavirus family that includes hepatitis viruses of woodchuck, ground squirrel, Peking duck, *etc.* These viral species all contain a highly conserved small open reading frame (ORF) encoding HBV x protein (HBx). HBx is a multifunctional viral regulator that modulates transcription, signaling pathways, protein degradation, and cell responses to genotoxic stress. These modulations affect viral replication and viral proliferation, directly or indirectly. HBx also affects cell cycle checkpoints, cell death, and carcinogenesis^[3].

HBx is well conserved among the mammalian hepadnaviruses^[4,5]. Regarding the viral life cycle, in related woodchuck hepatitis viruses, ablation of their X protein start codon or creation of C-terminal truncations has been found to decrease viral replication *in vitro* and to inhibit the establishment of productive infection *in vivo*^[6,7]. It is not known which pathways influenced by HBx are needed or sufficient to establish an environment required for viral replication. HBx could not only form intracellular aggregates by itself^[8-11], but also involve clumping and organelle aggregation leading to an abnormal mitochondrial distribution^[12,13]. The precise role of HBx in the HBV life cycle remains uncertain.

Several novel HBV therapeutic peptides containing immunodominant T helper (Th) and cytotoxic T lymphocyte responses (CTL) epitopes of HBV have been screened out. Epitope-based HBV vaccines were designed and synthesized^[14]. Epitope peptides derived from HBx have been used in peptide vaccines to induce specific cellular immunity^[15]. In order to overcome the problem of sequence diversity, a strategy for vaccine design was the use of conserved peptides^[16]. The biological importance of HBx in HBV replication remains largely undefined. In transient transfection assays the full-length X-gene encoding a product in cells appeared to form intracellular aggregates and to accumulate in large granules, with a tendency of apoptosis^[9]. There was a fully conserved nine amino acid sequence within the carboxyl terminus of all HBx. Deletion of this segment resulted in a drastic loss of transactivation activity of HBx^[17]. To obtain a different approach to investigate the possible functions of the X gene in HBV replication, we recently performed experiments with synthetic peptide derived from HBx. The peptide could avoid forming aggregates and be employed to investigate the effect of HBx on HBV replication. We report it here for the first

time to highlight the biohazard issue and safety importance regarding the synthetic peptide used as a candidate vaccine.

MATERIALS AND METHODS

In vitro synthesis of conserved peptide

HBx sequences of hepadnaviruses used for analysis were taken from GenBank. Accession numbers were as follows: arctic ground squirrel hepatitis B virus, U29144; woodchuck hepatitis virus, M19183; woolly monkey hepatitis B Virus, NC_001896; orangutan hepadnavirus, NC_002168; hepatitis B virus subtype adr, D12980; and hepatitis B virus subtype adw, M54923. Sequence alignment was performed with the software provided by Vector NTI (USA). The fully conserved peptide of nine residues from HBx, FVLGGCRHK (Figure 1), was synthesized by the solid-phase method (GL Biochem Ltd.). Purity (>97%) was assessed by high-pressure liquid chromatography, amino acid analysis, and molecular weight determination by mass spectrometry.

Arctic ground squirrel hepatitis B virus	123	SRLPL <u>FVLGGCRHK</u> YKM
Woodchuck hepatitis virus	123	PRLSIF <u>FVLGGCRHK</u> CM
Woollymonkey hepatitis B virus	125	PRLKV <u>FVLGGCRHK</u> LV
Orangutan hepadnavirus	127	IRLKV <u>FVLGGCRHK</u> LV
Hepatitis B virus subtype adr	127	IRLKV <u>FVLGGCRHK</u> LV
Hepatitis B virus subtype adw	127	IRLKV <u>FVLGGCRHK</u> LV

Figure 1 Alignment of amino acid sequences of HBx from six mammalian hepadnaviruses.

The numbers refer to the first amino acid of each peptide. Underlined region is a fully conserved sequence.

Cell culture treated with peptide

2.2.15 cell line containing HBV ayw strain genome derived from a human hepatoblastoma HepG2 cells^[18], was grown and cultured in Dulbecco's modified Eagle's medium (Gibco Life Technologies) supplemented with 10% heat-inactivated fetal calf serum. 2.2.15 cells were seeded into 24-well tissue culture plates. Once cell culture dishes were subconfluent ($\sim 5 \times 10^6$ cells), the culture medium was replaced by the same amount of fresh media harboring CP. Cells were incubated with 3.5 μ M CP for 36 hours, the culture medium was collected for the analysis of extracellular HBV DNA and HBV antigens. The cells were washed and detached from the dishes. The collected cells were lysed. After centrifugation, the supernatant was stored for the analysis of intracellular HBV genomic forms and HBV antigens. The protein concentration was estimated by Bradford method.

Real-time PCR assay

Fluorescence quantitation of HBV DNA was performed with real-time PCR reagent kit (Shenzhen PG Biotech, China). The primers and probe were selected in the S gene of HBV genome and generated a product of 70 bp. HBV DNA was extracted from 100 μ l of the sample. Real time PCR was done using 2 μ l of HBV DNA, 0.06 μ l of UNG (1 u/ μ l), 0.4 μ l Taq (5 u/ μ l) and 37.6 μ l PCR mix. After incubation for 5 min at 37 °C, the DNA polymerase was activated at 94 °C for 1 min. The PCR cycling program consisted of 42 two-step cycles of 5 s at 95 °C and 30 s at 60 °C. Viral DNA was extracted and purified from 100 μ l of the sample. Amplification and detection were performed with a Line-gene real-time PCR analysis system (Japan). Three independent experiments were performed.

HBsAg and HBeAg assay

Hepatitis B surface antigen (HBsAg) and hepatitis B e antigen (HBeAg) were determined using licensed ELISA kits (Wantai

Biotech Inc., Beijing) following the manufacturer's package insert procedure.

Flow cytometric analysis

2.2.15 cells treated with or without 3.5 μ M CP for 36 hours were released by trypsinization and resuspended in phosphate-buffered saline at a density of 2×10^6 cells/ml. Quantitative analyses of p53 and Bax proteins were based on immunofluorescence of cells stained with fluorescein isothiocyanate-conjugated monoclonal antibodies (PharMingen, USA) respectively. Cell cycle and apoptosis were monitored using propidium iodide staining of nuclei. Flow cytometry was performed and analyzed on a Becton Dickinson flow cytometer using CellQuest software.

Statistical analysis

Statistical analysis was performed by Student's *t* test. The data were analyzed with SigmaPlot 2000 software (SPSS Inc., USA). Differences were considered statistically significant when *P* value was less than 0.05.

RESULTS

Enhancement of HBV DNA replication after CP treatment of 2.2.15 cells

Parallel cultures, with or without CP, were maintained at 37 °C for 36 hours, and then investigated for the presence of viral DNA in cell lysates. HBV DNA was analyzed in a quantitative manner for the overall levels of HBV DNA (both extracellular and intracellular DNA) and the relative rate of HBV replication (intracellular DNA). HBV DNA was analyzed by real-time PCR. As shown in Figure 2, both extracellular and intracellular copies of HBV DNA per ml were significantly increased after incubation with 3.5 μ M of CP. We observed that HBV DNA replication of treated 2.2.15 cells was substantially enhanced by the conserved peptide.

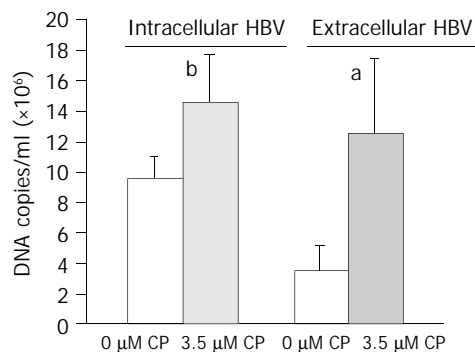


Figure 2 Quantitative detection of HBV DNA by real-time PCR. HBV DNA levels were significantly increased by 3.5 μ M of CP (^a*P*=0.005, ^b*P*=0.038).

Effects of CP on expression of HBV antigens

Cell lysates and culture medium were analyzed for intracellular and extracellular viral gene products. ELISA results revealed that CP affected the expression of HBV antigens differently. As shown in Figure 3, there were no significant differences in extracellular HBsAg from 2.2.15 cells treated with or without CP, and 3.5 μ M CP could significantly inhibit intracellular HBsAg expression. Changes in HBeAg were evaluated as well. It was found that there was no statistically significant difference of extracellular HBeAg when the cells were treated with CP or without CP (Figure 4). In response to CP, the intracellular HBeAg displayed an opposite pattern to that of HBsAg. We observed that CP could efficiently increase the level of intracellular HBeAg (Figure 4).

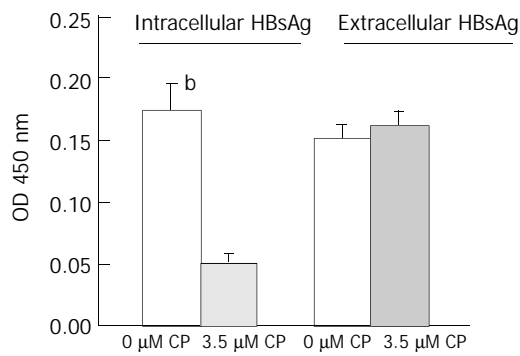


Figure 3 ELISA detection of HBsAg. Three and a half μM CP could significantly inhibit intracellular HBsAg expression (^b $P < 0.001$).

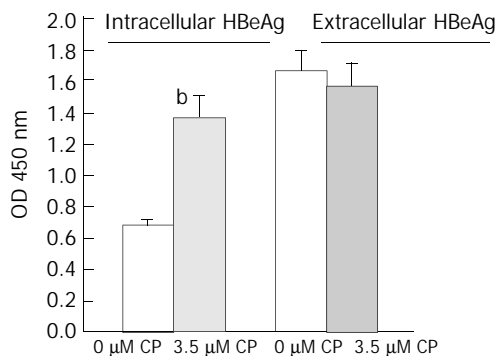


Figure 4 ELISA detection of HBeAg. The level of intracellular HBeAg was significantly increased by 3.5 μM CP (^b $P < 0.001$).

Flow cytometric analysis of virus-host cells treated with CP

When fluorescein isothiocyanate-conjugated monoclonal antibodies were used to assess p53 and Bax proteins, 2.2.15 cells treated with CP or without CP displayed no significant changes (Figure 5). As shown in Table 1, the results exhibited no significant changes of cell cycle and apoptosis in 3.5 μM CP treated cells compared with the cells not treated by CP.

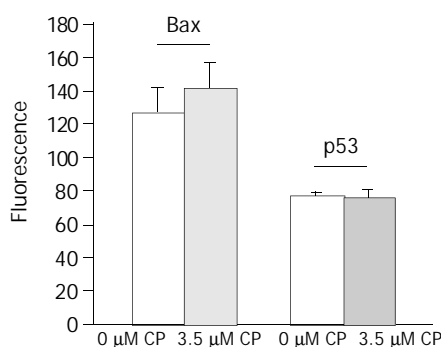


Figure 5 Flow cytometric analysis of Bax and p53 proteins.

Table 1 Percentage of apoptosis and cell cycle phase

HepG2 cells	Apoptosis	G0/G1	G2-M	S
0 μM CP	0.39±0.01	81.21±0.51	11.09±2.11	7.71±2.62
3.5 μM CP	0.62±0.27	79.87±1.22	10.24±0.99	9.89±0.30

DISCUSSION

HBV is a 3.2 Kb DNA virus with only four genes having been identified namely C, S, P, and X^[19]. The C gene codes for the core protein and the e antigen, the S gene codes for three related viral envelope proteins known as surface antigens, the P gene

codes for the viral DNA polymerase, and the X gene codes for a 16.5-kDa protein. HBV molecule is well organized. The X gene could overlap the viral polymerase gene and the precore gene^[20,21], thus increasing the utilization of the small genome. Uchida and colleagues analyzed nucleotide (nt) sequences of HBx from more than 130 clinical HBV isolates. They attempted to establish the correlation of nt substitutions with clinical pathological characteristics. They found the X gene (465nt) was crucial for the replication and expression of HBV because HBx could transactivate HBV DNA, and contained the core promoter, enhancer II, and two direct repeats. There were several mutational hotspots, some of which seemed to relate to the immunological epitopes of the X protein. One was an 8-nt deletion between nt 1 770 and 1 777, which could truncate 20 amino acids from the carboxyl terminus of HBx. This deletion could lead to the suppression of replication of HBV DNA^[22]. There was a fully conserved nine amino acid sequence within the carboxyl terminus of all HBx. We synthesized the fully conserved peptide with nine residues, FVLGGCRHK, and queried for its physiological role in regulation of HBV replication.

HBx is regarded as an important multifunctional protein for the viral life cycle and viral-host interactions. HBx has been shown to be essential for viral proliferation in the woodchuck^[6,7], but was not central to HBV replication and virion export^[23]. In the absence of a convenient animal model system for studying HBV replication, the transgenic mouse could provide an alternative choice. The transgenic mice HBx was not absolutely essential for HBV replication and virion secretion, but replication was significantly decreased in the absence of X protein^[24]. Utilizing real time quantitative PCR, we found that CP could increase both the level of intracellular HBV DNA and the production of HBV DNA secretion.

HBsAg and HBeAg were translated from preS/S mRNA and precore mRNA individually. In this report, we demonstrated that CP could induce intracellular HBeAg expression and downregulate intracellular HBsAg expression. The results agreed closely with a recent observation of Xu *et al.*, who found that the presence of HBx increased the level of C gene transcripts approximately three folds in mtTg04 mice. HBx had no apparent effect on the RNA level of the S gene in this mouse line^[25]. Our result was also supported by the findings of Reifenberg's research group^[26]. They found that the X gene provided in trans could stimulate the expression of C gene when they studied transgenic mice carrying subgenomic HBV DNA. Our data suggest that HBsAg and HBeAg in cultured medium of CP-treated cells were as abundant as untreated control cells. This might be due to the basal level released from 2.2.15 cells before incubated with CP. CP had a negative influence on extracellular viral gene products. Considering the possible influence of CP on the status of host cells might alter the biologic properties of HBV, we performed analysis of cell cycle and apoptosis. Our results showed no significant cellular changes by CP. Despite the association of multiple activities with HBx, none of them appeared to provide a uniform hypothesis regarding the true biological functions of HBx^[27]. Taking advantage of the synthetic peptide, we are in an attempt to identify different roles of a domain in HBx in HBV replication.

Synthetic peptide derived HBx may be responsible for modulating HBV replication. HBx has been found to be a short-lived protein and proteolysed by a ubiquitin proteasome pathway^[28,29]. We think that some short peptides converted from HBx through intracellular degradation process may still remain their basic functions for HBV replication.

REFERENCES

- 1 Lee YH, Yun Y. HBx protein of hepatitis B virus activates Jak1-STAT signaling. *J Biol Chem* 1998; **273**: 25510-25515

- 2 **Lee WM.** Hepatitis B virus infection. *N Engl J Med* 1997; **337**: 1733-1745
- 3 **Murakami S.** Hepatitis B virus X protein: a multifunctional viral regulator. *J Gastroenterol* 2001; **36**: 651-660
- 4 **Seeger C, Mason WS.** Hepatitis B virus biology. *Microbiol Mol Biol Rev* 2000; **64**: 51-68
- 5 **Murakami S.** Hepatitis B virus X protein: structure, function and biology. *Intervirology* 1999; **42**: 81-99
- 6 **Zoulim F, Saputelli J, Seeger C.** Woodchuck hepatitis virus X protein is required for viral infection *in vivo*. *J Virol* 1994; **68**: 2026-2030
- 7 **Chen HS, Kaneko S, Girones R, Anderson RW, Hornbuckle WE, Tennant BC, Cote PJ, Gerin JL, Purcell RH, Miller RH.** The woodchuck hepatitis X gene is important for establishment of virus infection in woodchucks. *J Virol* 1993; **67**: 1218-1226
- 8 **Henkler F, Hoare J, Waseem N, Goldin RD, McGarvey MJ, Koshy R, King IA.** Intracellular localization of the hepatitis B virus HBx protein. *J Gen Virol* 2001; **82**(Pt 4): 871-882
- 9 **Song CZ, Bai ZL, Song CC, Wang QW.** Aggregate formation of hepatitis B virus X protein affects cell cycle and apoptosis. *World J Gastroenterol* 2003; **9**: 1521-1524
- 10 **Pal J, Somogyi C, Szmolenszky AA, Szekeres G, Sipos J, Hegedus G, Martzinovits I, Molnar J, Nemeth P.** Immunohistochemical assessment and prognostic value of hepatitis B virus X protein in chronic hepatitis and primary hepatocellular carcinomas using anti-HBxAg monoclonal antibody. *Pathol Oncol Res* 2001; **7**: 178-184
- 11 **Urban S, Hildt E, Eckerskorn C, Sirma H, Kekule A, Hofschneider PH.** Isolation and molecular characterization of hepatitis B virus X-protein from a baculovirus expression system. *Hepatology* 1997; **26**: 1045-1053
- 12 **Rahmani Z, Huh KW, Lasher R, Siddiqui A.** Hepatitis B virus X protein colocalizes to mitochondria with a human voltage-dependent anion channel, HVDAC3, and alters its transmembrane potential. *J Virol* 2000; **74**: 2840-2846
- 13 **Takada S, Shirakata Y, Kaneniwa N, Koike K.** Association of hepatitis B virus X protein with mitochondria causes mitochondrial aggregation at the nuclear periphery, leading to cell death. *Oncogene* 1999; **18**: 6965-6973
- 14 **Guan XJ, Wu YZ, Jia ZC, Shi TD, Tang Y.** Construction and characterization of an experimental ISCOMS-based hepatitis B polypeptide vaccine. *World J Gastroenterol* 2002; **8**: 294-297
- 15 **Hwang YK, Kim NK, Park JM, Lee K, Han WK, Kim HI, Cheong HS.** HLA-A2 1 restricted peptides from the HBx antigen induce specific CTL responses *in vitro* and *in vivo*. *Vaccine* 2002; **20**: 3770-3777
- 16 **Nakamura Y, Kameoka M, Tobiume M, Kaya M, Ohki K, Yamada T, Ikuta K.** A chain section containing epitopes for cytotoxic T, B and helper T cells within a highly conserved region found in the human immunodeficiency virus type 1 Gag protein. *Vaccine* 1997; **15**: 489-496
- 17 **Kumar V, Jayasuryan N, Kumar R.** A truncated mutant (residues 58-140) of the hepatitis B virus X protein retains transactivation function. *Proc Natl Acad Sci U S A* 1996; **93**: 5647-5652
- 18 **Sells MA, Chen ML, Acs G.** Production of hepatitis B virus particles in Hep G2 cells transfected with cloned hepatitis B virus DNA. *Proc Natl Acad Sci U S A* 1987; **84**: 1005-1009
- 19 **Lee JH, Ku JL, Park YJ, Lee KU, Kim WH, Park JG.** Establishment and characterization of four human hepatocellular carcinoma cell lines containing hepatitis B virus DNA. *World J Gastroenterol* 1999; **5**: 289-295
- 20 **Okamoto H, Tsuda F, Akahane Y, Sugai Y, Yoshida M, Moriyama K, Tanaka T, Miyakawa Y, Mayumi M.** Hepatitis B virus with mutations in the core promoter for an e antigen-negative phenotype in carriers with antibody to e antigen. *J Virol* 1994; **68**: 8102-8110
- 21 **Yuh CH, Chang YL, Ting LP.** Transcriptional regulation of precore and pregenomic RNAs of hepatitis B virus. *J Virol* 1992; **66**: 4073-4084
- 22 **Uchida T, Saitoh T, Shinzawa H.** Mutations of the X region of hepatitis B virus and their clinical implications. *Pathol Int* 1997; **47**: 183-193
- 23 **Blum HE, Zhang ZS, Galun E, von Weizsacker F, Garner B, Liang TJ, Wands JR.** Hepatitis B virus X protein is not central to the viral life cycle *in vitro*. *J Virol* 1992; **66**: 1223-1227
- 24 **Reifenberg K, Nusser P, Lohler J, Spindler G, Kuhn C, von Weizsacker F, Kock J.** Virus replication and virion export in X-deficient hepatitis B virus transgenic mice. *J Gen Virol* 2002; **83**(Pt 5): 991-996
- 25 **Xu Z, Yen TS, Wu L, Madden CR, Tan W, Slagle BL, Ou JH.** Enhancement of hepatitis B virus replication by its X protein in transgenic mice. *J Virol* 2002; **76**: 2579-2584
- 26 **Reifenberg K, Wilts H, Lohler J, Nusser P, Hanano R, Guidotti LG, Chisari FV, Schlicht HJ.** The hepatitis B virus X protein transactivates viral core gene expression *in vivo*. *J Virol* 1999; **73**: 10399-10405
- 27 **Seeger C.** The hepatitis B virus X protein: the quest for a role in viral replication and pathogenesis. *Hepatology* 1997; **25**: 496-498
- 28 **Hu Z, Zhang Z, Doo E, Coux O, Goldberg AL, Liang TJ.** Hepatitis B virus X protein is both a substrate and a potential inhibitor of the proteasome complex. *J Virol* 1999; **73**: 7231-7240
- 29 **Kim JH, Kang S, Kim J, Ahn BY.** Hepatitis B virus core protein stimulates the proteasome-mediated degradation of viral X protein. *J Virol* 2003; **77**: 7166-7173

Edited by Wu XN and Wang XL

Antiangiogenic effect of somatostatin receptor subtype 2 on pancreatic cancer cell line: Inhibition of vascular endothelial growth factor and matrix metalloproteinase-2 expression *in vitro*

Manoj Kumar, Zheng-Ren Liu, Laxmi Thapa, Qing Chang, Da-Yu Wang, Ren-Yi Qin

Manoj Kumar, Zheng-Ren Liu, Qing Chang, Da-Yu Wang, Ren-Yi Qin, Department of Surgery, Tongji Hospital, Tongji Medical College, Huazhong University of Science and Technology, Wuhan, 430030, Hubei Province, China

Laxmi Thapa, Department of Obstetrics and Gynecology, Tongji Hospital, Tongji Medical College, Huazhong University of Science and Technology, Wuhan, 430030, Hubei Province, China

Supported by National Natural Science Foundation of China, No. 30271473

Correspondence to: Manoj Kumar/Ren-Yi Qin, Department of Surgery, Tongji Hospital, Tongji Medical College, Huazhong University of Science and Technology, Wuhan, 430030, Hubei Province, China. ryqin@tjh.tjmu.edu.cn

Telephone: +86-27-83662389

Received: 2003-08-06 **Accepted:** 2003-10-07

Abstract

AIM: To investigate the anti-angiogenic effect of somatostatin receptor subtype 2 (SSTR2) gene transfer into pancreatic cancer cell line PC-3, and the mechanisms involved in this effect.

METHODS: The full length human SSTR2 cDNA was introduced into pancreatic cancer cell line PC-3 by lipofectamine-mediated transfection. Positive clones were screened by G418 and stable expression of SSTR2 was detected by immunohistochemistry SABC methods and RT-PCR. Enzyme-linked immunosorbent assay (ELISA) was used to detect vascular endothelial growth factor (VEGF) levels in the cell culture supernatants of SSTR2-expressing cells, vector control and mock control cells. Furthermore, the expressions of VEGF and matrix metalloproteinase-2 (MMP-2) were detected by immunohistochemistry SABC methods and RT-PCR in these cells.

RESULTS: VEGF levels in the cell culture supernatants were significantly reduced in the SSTR2-expressing cells (first week, 172.63±21.2 ng/L and after two months, 198.85±26.44 ng/L) compared with the vector control (first week, 790.39±86.52 ng/L and after two months, 795.69±72.35 ng/L) and mock control (first week, 786.42±90.62 ng/L and after two months, 805.32±84.36 ng/L) ($P<0.05$). The immunohistochemical assay showed a significant reduction of the integral optical density of VEGF and MMP-2 in the SSTR2-expressing cells (42.25±8.6 and 70.5±6.25, respectively) compared with the vector control (85.75±12.9 and 110.52±13.5, respectively) and mock control (82.6±9.28 and 113.56±9.62, respectively) ($P<0.05$). Conversely, the average gray value of VEGF and MMP-2 was significantly increased in the SSTR2-expressing cells (121.56±8.43 and 134.46±19.95, respectively) compared with the vector control (55.72±5.6 and 62.26±12.68, respectively) and mock control cells (58.48±6.2 and 65.49±9.16, respectively) ($P<0.05$). Moreover, the expressions of VEGF mRNA and MMP-2 mRNA were significantly reduced in the SSTR2-expressing cells (0.1384±0.017 and 0.2343±0.070, respectively) compared

with the vector control (1.024±0.117 and 0.806±0.119, respectively) and mock control (1.085±0.105 and 0.714±0.079, respectively) ($P<0.05$).

CONCLUSION: The expression of reintroduced human SSTR2 gene exerts its antiangiogenic effects by down-regulating the expressions of the factors involved in tumor angiogenesis and metastasis, suggesting SSTR2 gene transfer as a new strategy of gene therapy for pancreatic cancer.

Kumar M, Liu ZR, Thapa L, Chang Q, Wang DY, Qin RY. Antiangiogenic effect of somatostatin receptor subtype 2 on pancreatic cancer cell line: Inhibition of vascular endothelial growth factor and matrix metalloproteinase-2 expression *in vitro*. *World J Gastroenterol* 2004; 10(3):393-399

<http://www.wjgnet.com/1007-9327/10/393.asp>

INTRODUCTION

The antiproliferative action of somatostatin (SS)/analogues is signaled by specific G-protein coupled receptors, and up to date, six different subtypes (SSTR-1, -2A, -2B, -3, -4, and -5) have been cloned and functionally characterized in various cell systems, including pancreas, adrenal cortex, and brain tissue^[1]. However, several studies demonstrated that somatostatin receptor subtypes (SSTRs) were strongly expressed in the normal pancreas, whereas not only a desensitization or mutation of these receptors occurred in pancreatic tumors^[2], but also expression of these receptors, especially SSTR2, was frequently lost in human pancreatic adenocarcinomas^[3-5]. Despite remarkable biochemical properties of SS analogues *in vitro*, poor therapeutic results with them in Phase I/II clinical trials against the majority of cases of pancreatic cancers^[5-7], were due to the loss of gene expression for SSTR2 in pancreatic cancers and relatively low expressions of SSTR3 and SSTR5^[8].

VEGF, also known as a vascular permeability factor, is highly expressed in various types of tumors, and is an endothelial cell (EC) specific mitogen. VEGF via binding to its high affinity receptors (Flt-1/VEGFR-1, Flk-1/KDR/VEGFR-2), exerts its mitogenic effect by promoting EC proliferation and migration, thereby playing a crucial role in tumor neovascularization^[9,10]. Gupta *et al* reported VEGF as a survival factor for EC, rendering these cells more radioresistant^[11]. Several studies showed positive correlations between tumor cell VEGF expression, blood vessel density, tumor growth and metastasis, disease progression and poor prognosis in pancreatic carcinomas^[12-14], and suppression of VEGF expression attenuated pancreatic cancer cell tumorigenicity^[10], suggesting that over-expression of VEGF might be associated with the aggressive phenotype of this disease and that VEGF should be an important target for anticancer therapy.

On the other hand, matrix metalloproteinases (MMPs) were reported to enhance the degradation of extracellular matrix

(ECM), and thereby hydrolyze the important components of ECM and basement membrane such as types IV, V, VII, X collagens and fibronectin, elastin, *etc* and were closely associated with the invasiveness and metastasis of tumors^[15-20]. MMP-2 was the most commonly expressed MMPs in pancreatic tumor specimens but not in normal pancreas and was correlated with the aggressive phenotype (invasive and metastatic potential) of pancreatic carcinomas^[21-24]. Ellenrieder *et al* demonstrated that increased expression and activation levels of MMP-2 were strongly associated with elevated expression levels of its activators MT1-MMP (Membrane type 1-MMP) and MT2-MMP (Membrane type 2-MMP) and that it played a significant role in pancreatic tumor cell invasion^[25]. The selective MMP-2 and MMP-9 inhibitor MMI-166 exerted its antitumor effects on pancreatic cancer by inhibiting its invasion and angiogenesis^[26].

In the present study, we evaluated the potency of introduction of exogenous SSTR2 gene as negative regulators of VEGF and MMP-2 production in pancreatic cancer cell line PC-3 for the following reasons: (1) SSTR2 was strongly expressed in normal pancreas whereas it was frequently lost in human pancreatic adenocarcinoma^[2-4]. (2) Antitumor effects of SSTR2 occurred as a consequence of an SSTR2-dependent negative feedback autocrine loop, whereby SSTR2 induced the expression of its own ligand, SS, which also constitutively activated SSTR2^[4,27]. (3) SS/analogues exhibited antiseecretory effects by the inhibition of release of growth factors and trophic hormones, *e.g.*, growth hormone, insulin-like growth factor-1, insulin, gastrin^[2]. In addition, since pancreatic cancer is characterized by the over-expression of several angiogenic factors such as VEGF, bFGF, MMP-2, *etc*, it is necessary to elucidate the effects of the genes or molecules with antiangiogenic properties on pancreatic cancer. Previous studies have reported the antiangiogenic properties of SS/analogues and SSTRs in various tumors^[28,29], however the mechanisms involved in the antiangiogenic effects of SSTR2 have been poorly elucidated in this pancreatic cancer cell line PC-3 as yet. Hence, our present study demonstrated that the reexpression of SSTR2 gene in the pancreatic cancer cell line PC-3 devoid of SSTR2, exhibited its antiangiogenic effects by down-regulating the expression of angiogenic factors *in vitro* both at protein and mRNA levels.

MATERIALS AND METHODS

Materials

PC-3, a human pancreatic cancer cell line, was obtained from Shanghai Institute of Cell Biology, Chinese Academy of Sciences. Dulbecco's modified eagles medium (DMEM), fetal bovine serum (FBS), lipofectamine and geneticin (G418) were purchased from Gibco BRL. The full-length cDNA of human SSTR2 was kindly provided by G. I. Bell (Howard Hughes Medical Institute, Chicago, IL). Monoclonal antibody of SSTR2, mouse anti-VEGF polyclonal antibody, mouse anti-MMP-2 monoclonal antibody, SABC kit were purchased from Santa Cruz Biotechnology, Inc. (Santa Cruz, CA, USA). TRIZOL® reagent, RNasin, oligo(dt) 15, dNTPs, M-MLV reverse transcriptase, Taq DNA polymerase and VEGF ELISA kit were from Promega. Eukaryotic expression vector pcDNA3.1 was purchased from Invitrogen (Invitrogen, San Diego, CA).

Plasmid construction and gene transfer

Human SSTR2 cDNA was digested with *EcoRI/XbaI* and cloned in the *EcoRI/XbaI* site of pcDNA3.1. The sequence encoding the signal peptide from alkaline phosphatase was inserted into the *HindIII/EcoRI* site upstream of SSTR2 and an epitope tag derived from influenza virus hemagglutinin A (HA) was fused in the *EcoRI* site between the signal peptide and SSTR2. Recombinant plasmid was purified by QIA prep

spin miniprep kit (QIAGEN Co).

PC-3 cells were routinely cultured in DMEM media supplemented with 10% heat-inactivated FBS, 100 u/ml penicillin and 100 u/ml streptomycin, and incubated at 37 °C in a humidified atmosphere containing 5% CO₂ in air. Gene transfer was performed according to the manufacturer's protocol of lipofectamine (Gibco BRL). Briefly, about 3×10⁵ cells per well containing 2 ml appropriate complete growth medium were seeded in a six-well culture plate, and incubated at 37 °C in a CO₂ incubator until the cells were 70% to 80% confluent. A cover slip was plated in each well before seeding. After the cells were ringed with serum free and antibiotics-free medium, the cells were transfected separately with pcDNA3.1-SSTR2 1 µg/lipofectamine 3 µL (experimental group), pcDNA3.1 1 µg/lipofectamine 3 µL (vector control), and only lipofectamine 3 µL (mock control), followed by incubation at 37 °C in a CO₂ incubator for 6 hours. Then the medium was replaced by DMEM culture medium containing 20% FBS. After 48 hours, two wells in each group were taken out to detect the transient expression of SSTR2 by immunohistochemical SABC methods, whereas others were continuously cultured for stable expression of SSTR2. G418 (500 mg/L) was added to select the resistant clones after 48 hours. Six days later, when most of the cells died, the concentration of G418 was decreased to 300 mg/L and cells were cultured with G418 for another 6 days. Then the medium was changed every 3 or 4 days and colonies were collected approximately 2 weeks later for the examination of stable expression of SSTR2 by immunohistochemical SABC methods and RT-PCR assay.

Confirmation of SSTR2 protein expression by immunohistochemical staining

The stable expression of SSTR2 in the experimental group cells was detected by using immunohistochemical SABC methods. All the cover slips were dried at room temperature and washed twice with PBS solution (pH 7.2), followed by the treatment with 3% H₂O₂ for 10 min at room temperature. Then the cover slips were incubated in 5% bovine serum albumin in PBS solution for 20 min to block the nonspecific antibody-binding. The cover slips were then incubated with mouse anti-human SSTR2 antibody, diluted in 1:50 in 0.5% bovine serum albumin in PBS for 12 hours at 4 °C. The bridging antibody (biotinylated goat anti-mouse IgG) and SABC complex were diluted to 1:100 and incubated with the specimens for 20 min at 30 °C. Finally diaminobenzidine tetrachloride (DAB) was used for color development and the cover slips were counterstained with hematoxylin. Positive rate (brown color cells) was automatically measured with the biological image analysis system 2000 (Opton Germany).

Confirmation of SSTR2 mRNA expression by RT-PCR

Total RNA was extracted separately from PC-3 cells of each group with TRIZOL® reagent following the manufacturer's instructions. A 2 µg (treated in 5 µL DEPC water in an Ep tube) sample of total RNA was denaturalized by incubating at 70 °C for 5 min, and the tube was placed to ice for 3 min, and then reverse-transcribed into complementary DNA (cDNA) by using Moloney murine leukemia virus reverse transcriptase (M-MLV). Briefly, the denaturalized RNA (5 µL) was incubated for 60 min at 37 °C and for 5 min at 95 °C with 4 µL 5×reverse transcriptase buffer, 1 µL oligo (dt) 15, 1 µL RNasin (50 u/µL), 1 µL dNTPs (10 mmol/L), 1 µL reverse transcriptase (200 u/µL), and 7 µL DEPC water in a total volume of 20 µL. For polymerase chain reaction (PCR), 5 µL of the resulting cDNA, 31 µL of triple-distilled H₂O, 5 µL of 10×PCR buffers, 3 µL of MgCl₂ (25 mmol/L), 1 µL of dNTPs, 1 µL of each of sense and antisense primers (10 pmol/L), 1 µL of each of sense

and antisense β -actin, and 1 μ L Taq DNA polymerase (3 u/ μ L) in a total volume of 50 μ L were added. The samples were amplified through 35 cycles, each amplification consisting of denaturation at 94 °C for 40 s, primer annealing at 55 °C for 40 s and extension at 72 °C for 1 min. Cycles were preceded by incubation at 94 °C for 5 min to ensure full denaturation of the target gene, followed by an extra incubation at 72 °C for 10 min to ensure full extension of the products. PCR products were analyzed on 1.5% agarose gel containing ethidium bromide. The sequences of the primers for SSTR2 were sense 5' -CCCCAGCCCTTAAAGGCATGT-3' and antisense 5' -GGTCTCCATTGAGGAGGGTCC-3' (234 bp) and for β -actin, sense 5' -GTGCGTGACATTAAGGAG-3' and antisense 5' -CTAAGTCATAGTCCGCCT-3' (520 bp).

Detection of VEGF mRNA and MMP-2 mRNA expression by RT-PCR

Total RNA was extracted separately from PC-3 cells of each group with TRIZOL® reagent following the manufacturer's instructions. RT-PCR was carried out as described above except some changes in conditions of amplification cycles. For mRNA expression of VEGF, samples of each group were subjected to PCR at an annealing temperature from 60 °C to 50 °C decreased by 0.5 °C per cycle for 20 cycles, followed by an additional 15 cycles at an annealing temperature of 50 °C for 35 s. PCR products were analyzed on 1.5% agarose gel containing ethidium bromide and quantified by a complete gel documentation and analysis system. VEGF mRNA expression level was determined by the ratio of VEGF/ β -actin protein. The sequences of primers for VEGF were sense 5' -TTGCTGCTCTACCTCCAC-3' and antisense 5' -CTCCAGGCCCTCGTCATT-3' (240 bp) and for β -actin, sense 5' -GTGCGTGACATTAAGGAG-3' and antisense 5' -CTAAGTCATAGTCCGCCT-3' (520 bp).

For mRNA expression of MMP-2, samples of each group were subjected to PCR for 33 cycles, each cycle consisting of denaturation at 94 °C for 1 min, primer annealing at 55 °C for 35 s and extension at 72 °C for 1 min. PCR products were analyzed on 1.5% agarose gel containing ethidium bromide and quantified by a complete gel documentation and analysis system. MMP-2 mRNA expression level was determined by the ratio of MMP-2/ β -actin protein. The sequences of primers for MMP-2 were sense 5' -GCGGATCCAGCGCCCAGAGAGACAC-3' and antisense 5' -TTAAGCTTCCACTCCGGGCAGGATT-3' (473 bp) and for β -actin were sense 5' -CCTTCCTGGGCATGGAGTCCTG-3' and antisense 5' -GGAGCAATGATCTTGATCTTC-3' (205 bp).

Determination of VEGF concentration in cultured supernatants by ELISA

After successful stable transfection, VEGF protein levels in the supernatants secreted by the cultured human pancreatic cancer cells of experimental group, vector control and mock control were quantitated by ELISA. To generate the conditioned medium, the cells of each group (4×10^5 /well) were incubated in 1.5 ml DMEM for 48 hours. The conditioned medium was then collected and centrifuged at 12 000 rpm at 4 °C for 15 min, and then ELISA analysis was performed according to the manufacturer's instructions. Furthermore, to observe the long-term antisecretory effect of SSTR2, ELISA analysis was performed two months after stable transfection. The value of OD (A_{450} values) of each well was measured at 450 nm. The supernatants were harvested in triplicate and the experiment was performed twice.

Detection of VEGF and MMP-2 expressions in vitro by immunohistochemistry

Two cover slips were plated in each well of six-well culture

plates, and then the cells of each group (10^5 cells) containing 2 ml appropriate complete growth medium were seeded in each well, and incubated at 37 °C in a CO₂ incubator for 48 hours. All the cover slips were dried and washed three times with PBS (pH 7.2) at room temperature, followed by the treatment with the 1:1 mixture of 100% acetone and formaldehyde for 10 min at room temperature. The expressions of VEGF and MMP-2 were detected by using immunohistochemical SABC methods as described above by using mouse anti-human VEGF polyclonal antibody and MMP-2 monoclonal antibody. Under the light microscope, positive staining (brown yellow) was located in cytoplasm and membrane for VEGF and MMP-2. For the image analysis, 150 cells of clear outline from 10 microscopic fields (15 cells in each field) were selected randomly from each group under 10 \times 40 magnification, and the average gray value and integral optical density of each group were automatically measured by using HPIAS-1000, high resolution pathological image analysis.

Statistical analysis

Results were expressed as mean \pm SD and the mean values were compared by using the ANOVA (SNK, Student-Newman-Keuls test) in the SAS 8.1 software and $P < 0.05$ was considered statistically significant.

RESULTS

Reexpression of SSTR2 after transfection

After 48 h *in vitro* transfection, most of the cells in experimental group demonstrated positive staining for SSTR2 as detected by immunohistochemical SABC methods, whereas almost no positive SSTR2 stainings were detected in vector control and mock control. The cells in experimental group were continuously cultured by adding G418 (500 mg/L) with 20% FBS, and then we were able to select a population of PC-3 cells resistant to the toxic effects of G418. After 2 weeks, all of these cells demonstrated positive staining for SSTR2 detected by immunohistochemical SABC methods (Figure 1). Furthermore, RT-PCR analysis of total RNA extracted from the cells of each group showed SSTR2 mRNA expression in experimental group, but not in vector control and mock control (Figure 2). The results suggested that the exogenous SSTR2 gene was successfully reexpressed in PC-3 cell line devoid of SSTR2.

Effect of SSTR2 on VEGF production in cultured supernatants

In the first week after stable transfection, VEGF levels in the cultured supernatants were significantly decreased in the cells of experimental group (172.63 \pm 21.2 ng/L) compared with those of vector control (790.39 \pm 86.52 ng/L) and mock control (786.42 \pm 90.62 ng/L) ($P < 0.05$, Figure 3). Similarly, two months after stable transfection, there was still a significant inhibition of VEGF production in the cells of experimental group (198.85 \pm 26.44 ng/L) compared with those of vector control (795.69 \pm 72.35 ng/L) and mock control (805.32 \pm 84.36 ng/L) ($P < 0.05$, Figure 3), however the inhibition of VEGF production in the cells of experimental group was slightly less than that in the first week (Figure 3). There were no statistical difference in VEGF levels between the vector control and mock control (Figure 3). Thus, SSTR2 could suppress the production of VEGF secreted by the cells of experimental group.

Effect of SSTR2 on VEGF mRNA and MMP-2 mRNA expression in vitro

RT-PCR analysis showed that the expression of VEGF mRNA was significantly decreased in the experimental group (0.1384 \pm 0.017) compared with the vector control (1.024 \pm 0.11)

and mock control (1.085 ± 0.105) ($P < 0.05$, Figures 4 and 6). Similarly, the expression of MMP-2 mRNA was also significantly reduced in the experimental group (0.2343 ± 0.07) compared with the vector control (0.806 ± 0.119) and mock control (0.714 ± 0.079) ($P < 0.05$, Figures 5 and 6). But there was no statistical difference either in VEGF mRNA or in MMP-2 mRNA expression between the vector control and mock control. These results suggested that the reexpression of SSTR2 gene could suppress the expression of VEGF and MMP-2 at mRNA level *in vitro*.

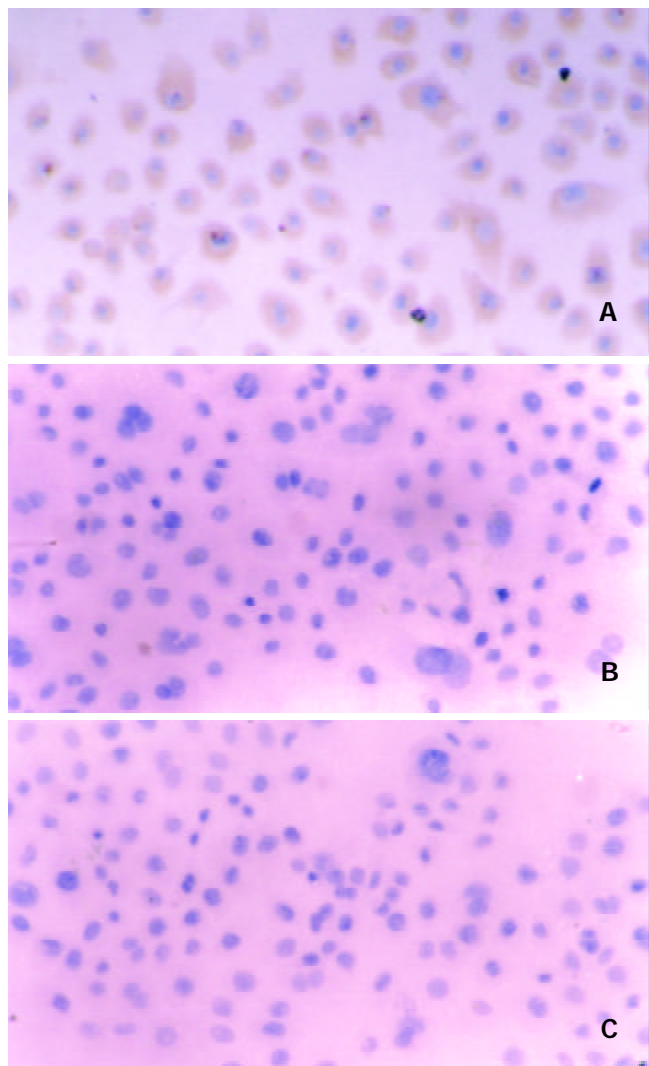


Figure 1 Immunohistochemical staining of SSTR2 expression after stable transfection. The cytoplasmic brown yellow staining represents SSTR2 expression. (A) experimental group, (B) vector control, and (C) mock control (SABC×150).

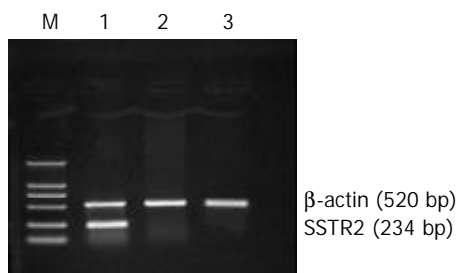


Figure 2 Expression of SSTR2 mRNA by RT-PCR analysis in experimental group, but not in vector control and mock control. Lane M: DNA marker DL 2000, Lane 1: experimental group, Lane 2: vector control, Lane 3: mock control.

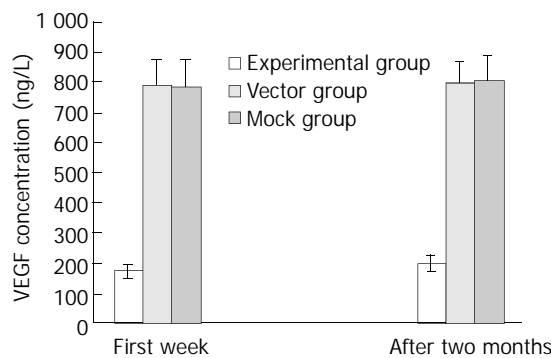


Figure 3 Inhibition of VEGF production in cultured supernatants by SSTR2. VEGF was determined in cultured supernatants by ELISA in the first week and two months after stable transfection. VEGF secretion was significantly reduced in the experimental group compared with the vector and mock controls ($P < 0.05$). Values were expressed as mean±SD.

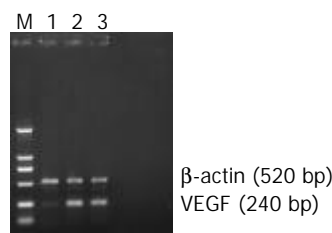


Figure 4 Weak expression of VEGF mRNA in experimental group but strong expression in vector and mock control shown by RT-PCR analysis. The expected length of PCR products was 240 bp (VEGF) and 520 bp (β-actin). Lane M: DNA marker DL 2000, Lane 1: experimental group, Lane 2: vector control, Lane 3: mock control.

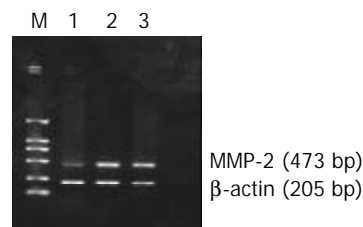


Figure 5 Weak expression of MMP-2 mRNA in experimental group but strong expression in vector and mock control shown by RT-PCR. The expected length of PCR products was 473 bp (MMP-2) and 205 bp (β-actin). Lane M: DNA marker DL 2000, Lane 1: experimental group, Lane 2: vector control, Lane 3: mock control.

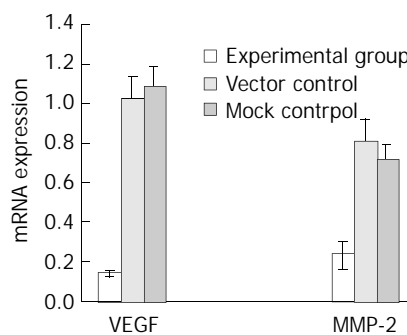


Figure 6 Significant inhibition of VEGF mRNA and MMP-2 mRNA in experimental group compared with vector control and mock control shown by quantification analysis of PCR products of VEGF and MMP-2 mRNA on 1.5% agarose gel containing ethidium bromide ($P < 0.05$). Values were expressed as mean±SD.

Down-regulation of VEGF and MMP-2 protein expression by SSTR2

Positive staining of VEGF (Figure 7) and MMP-2 (Figure 9) was located in the cytoplasm and membrane of the cells. The immunohistochemical staining showed a significant decrease in the expression of both VEGF and MMP-2 protein in the experimental group compared with the vector control and mock control ($P < 0.05$). According to HPIAS-1000 and statistical analysis, the integral optical density of VEGF staining was significantly reduced in the experimental group (42.25 ± 8.6) compared with the vector control (85.75 ± 12.9) and mock control (82.6 ± 9.28) and the average gray value of VEGF staining was significantly increased in the experimental group (121.56 ± 8.43) compared with the vector control (55.72 ± 5.6) and mock control (58.48 ± 6.2) ($P < 0.05$, Figure 8). However, no significant difference was observed between the vector control and mock control.

Similarly, according to HPIAS-1000 and statistical analysis, the integral optical density of MMP-2 staining was significantly reduced in the experimental group (70.5 ± 6.25) compared with the vector control (110.52 ± 13.5) and mock control (113.56 ± 9.62) and the average gray value of MMP-2 staining was significantly increased in the experimental group (134.46 ± 19.95) compared with the vector control (62.26 ± 12.68) and mock control (65.49 ± 9.16) ($P < 0.05$, Figure 10). However, no significant difference was observed between the vector control and mock control.

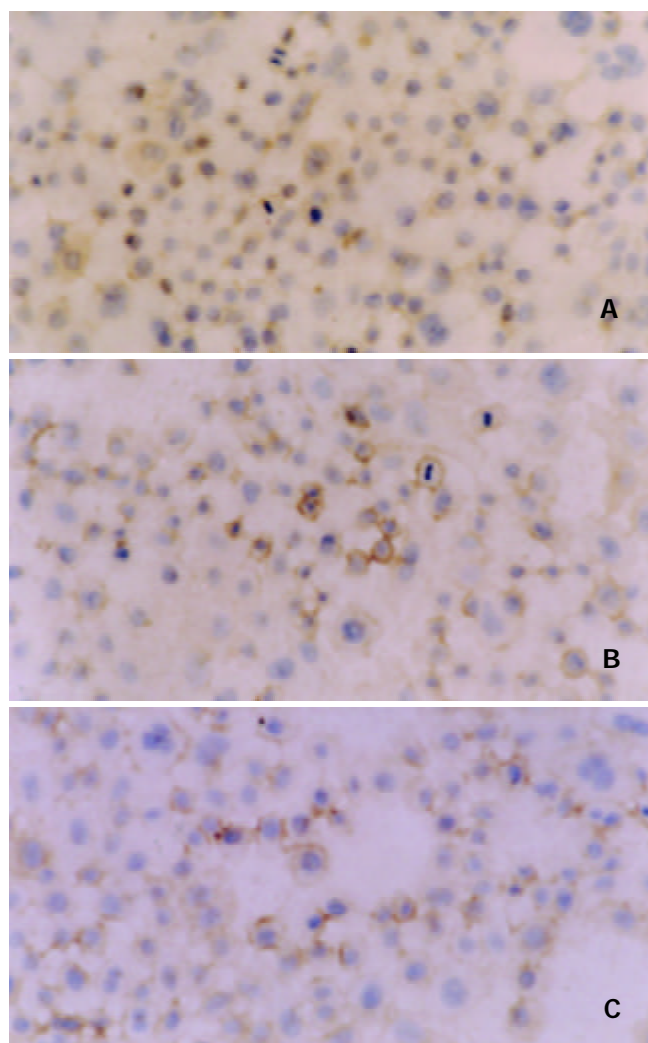


Figure 7 Location of immunohistochemical staining of expression of VEGF in cytoplasm and membrane. A: experimental group, B: vector control, C: mock control.

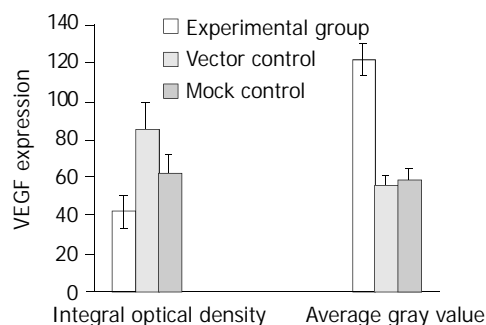


Figure 8 Down-regulation of VEGF protein expression by SSTR2. The expression of VEGF was significantly decreased in experimental group compared with vector control and mock control ($P < 0.05$). Values were expressed as mean ± SD.

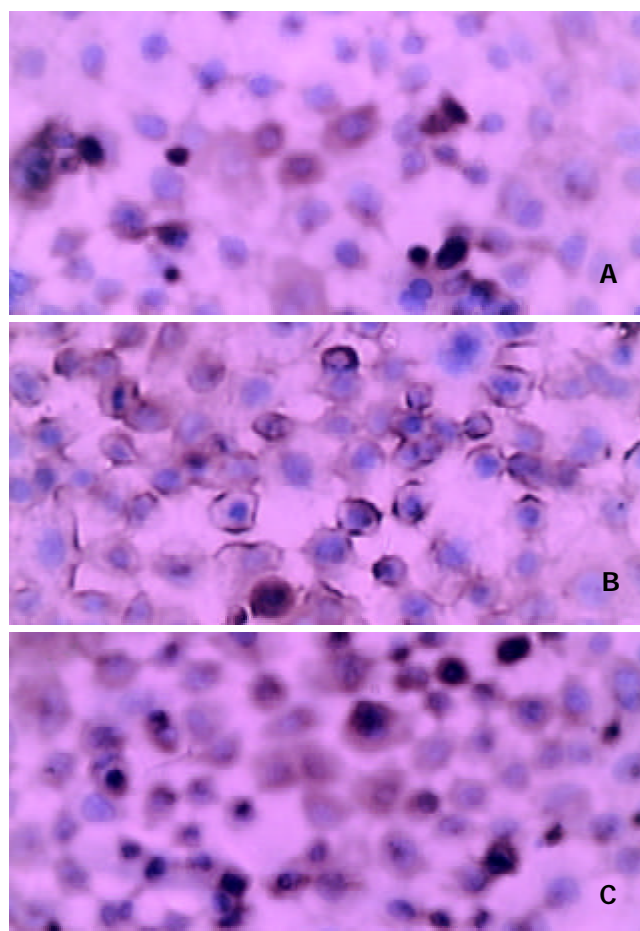


Figure 9 Location of immunohistochemical staining of expression of MMP-2 in cytoplasm and membrane. A: experimental group, B: vector control, C: mock control (SABC×400).

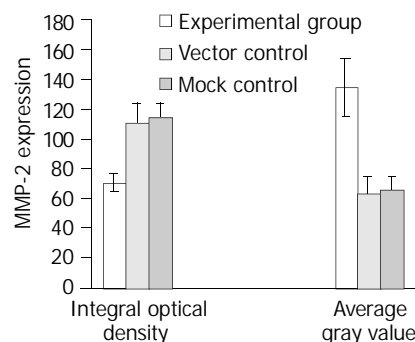


Figure 10 Down-regulation of MMP-2 protein expression by SSTR2. The expression of MMP-2 was significantly decreased

in experimental group compared with vector control and mock control ($P < 0.05$). Values were expressed as mean \pm SD.

DISCUSSION

The properties of tumor cells to release and induce several angiogenic and antiangiogenic factors which play a crucial role in regulating EC proliferation, migration, apoptosis or survival, cell-cell and cell-matrix adhesion through different intracellular signalings, have been thought to be the essential mechanisms during tumor-induced angiogenesis^[9]. The important steps during tumor angiogenesis, such as degradation of basement membrane by proteases and proliferation and migration of EC, were associated with the over-expression of angiogenic factors^[9]. Since fundamental requirements of tumor growth are dependent on the blood supply, the antiangiogenic therapy of cancer represents a highly effective strategy for destroying tumors. In addition, antiangiogenic agents, if administered before a tumor develops or becomes vascular supply-dependent, would therefore theoretically act similarly to a vaccine in preventing tumor development, not just tumor growth. Similarly, transfer of antiangiogenic or molecules with antiangiogenic properties constitutes one of the new therapeutic approaches to cancer. SSTR2 could act as an antiangiogenic in human pancreatic cancer cells and its antiproliferative and antimetastatic effects could occur as a consequence of an SSTR2-dependent negative feedback autocrine loop^[4,27]. Furthermore, the loss of SSTR2 during pancreatic tumorigenesis^[3-5] was found to be responsible for the poor therapeutic efficacy^[5-7] and the aggressive behaviours of pancreatic carcinoma. However, to our knowledge, whether the aberrant expression of SSTR2 is associated with pancreatic tumor angiogenesis, has not been reported as yet. But several previous investigations have shown that SS/analogues as well as SSTRs exhibited their antitumor effects through different pathways such as inhibition of release of growth factors and trophic hormones, *e.g.*, growth hormone, insulin-like growth factor-1, insulin, gastrin, *etc*^[2]. In CAM model, the study showed that unlabeled SS analogues inhibited angiogenesis which was proportional to the ability of the analogues to inhibit growth hormone production^[8]. Moreover, Mentlein *et al* reported that VEGF produced by cultured glioma cell lines constantly over-expressing SSTRs, especially SSTR2, was reduced to 25% to 80% by co-cubation with SS or SSTR2-selective agonists (octreotide and L-054 522) in a dose-dependent manner^[30]. Interestingly, transfer of SSTR2 gene was found to restore the responsiveness of SSTR2-negative cells to SS analogues, and inhibited the tumorigenicity of pancreatic tumor cells *in vitro* without administration of exogenous SSTR2 ligands^[4]. Similar to these, in our study, we successfully reexpressed exogenous human SSTR2 gene in pancreatic cancer cell line PC-3 by lipofectamine-mediated stable transfection and investigated its antiangiogenic mechanisms in the absence of SSTR2 ligand, SS.

The most commonly found angiogenic growth factors such as VEGF could contribute to the progression of many solid tumors by promoting the "angiogenic switch"^[31]. In patients with pancreatic cancer, hypervascularity which was correlated with the over-expression of several angiogenic factors such as VEGF, PD-ECGF, MMP-2, *etc*, was significantly associated with tumor extension, lymph node status and shorter median survival time^[9,14,32]. And also since VEGF via binding to its high affinity receptors (VEGFR) on EC, exerted its mitogenic effect by promoting EC proliferation and migration, resulting in tumor neovascularization^[9,10], the VEGF-VEGFR system has been considered as a promising target for the development of antiangiogenic tumor therapy^[33-37]. In our study, we observed a significant decrease in VEGF production levels in the cultured supernatants of the experimental group (cells reexpressed

SSTR2) when compared with the vector control and mock control ($P < 0.05$). We further observed that the antisecretory effect of SSTR2 was similar to or even more durable than that of SS/analogues which was time- and dose-dependent^[29], because in our experiment, we observed a significant inhibition of VEGF production in the cultured supernatants of the experimental group, which persisted for at least two months after stable transfection and the inhibitory rate of SSTR2 was slightly less after two months than in the first week after stable transfection, suggesting that there was a long-term induction of SS (ligand of SSTR2) by the SSTR2-dependent negative feedback autocrine loop. By contrast, Hipkin *et al* reported that the inhibitory effects of SSTR2 gene were not permanent and stable because of its down-regulation or desensitization by long-term exposure to SS^[38]. In addition, we observed a significant inhibitory effect of SSTR2 on VEGF expression both at protein and mRNA levels *in vitro* detected by immunohistochemical and RT-PCR assay, respectively. All of these antisecretory events evoked by SSTR2 expression in PC-3 cell may explain the antiangiogenic effect observed *in vitro*.

On the other hand, up-regulation of MMPs activity favoured proteolytic degradation of the basement membrane and ECM, thereby releasing angiogenic mitogens stored within the matrix, and has been linked to tumor growth and metastasis, as well as tumor-associated angiogenesis^[9]. Furthermore, the aggressive phenotype of pancreatic carcinoma has been reported to be associated with over-expression of MMP-2^[21-24]. Due to the high level expression of MMP-2 in clinical and experimental models of pancreatic cancer, inhibition of MMP-2 has shown a great promise with synthetic inhibitors as antitumor agents (antiangiogenesis, antiproliferative and antimetastasis) in preclinical models^[39]. Here, we observed that MMP-2 was significantly down-regulated both at protein and mRNA levels *in vitro* in the experimental group when compared with the vector control and mock control, suggesting that the reexpression of SSTR2 in pancreatic cancer cell line PC-3 could decrease the aggressive phenotype of pancreatic carcinoma. Similarly, Wang *et al* reported that administration of SS analogue, octreotide, was found to inhibit the migration and invasion of gastric cancer cells *in vitro* and the metastasis of cancer *in vivo* via down-regulation of MMP-2 and VEGF expressions, thereby decreasing tumor angiogenesis^[29].

In conclusion, our present study shows that the reexpression of SSTR2 gene can inhibit angiogenesis in pancreatic carcinoma by decreasing endogenous levels of VEGF and MMP-2, suggesting that restoration of SSTR2 in pancreatic cancer cells may offer an avenue for antiangiogenic therapy.

REFERENCES

- 1 **Reisine T.** Somatostatin receptors. *Am J Physiol* 1995; **269**(6 Pt 1): G813-G820
- 2 **Buscail L,** Vernejoul F, Faure P, Torrisani J, Susini C. Regulation of cell proliferation by somatostatin. *Ann Endocrinol* 2002; **63**(2 Pt 3): 2S13-2S18
- 3 **Buscail L,** Saint-Laurent N, Chastre E, Vaillant JC, Gespach C, Capella G, Kalthoff H, Lluís F, Vaysse N, Susini C. Loss of sst2 somatostatin receptor gene expression in human pancreatic and colorectal cancer. *Cancer Res* 1996; **56**: 1823-1827
- 4 **Delesque N,** Buscail L, Esteve JP, Saint-Laurent N, Muller C, Weckbecker G, Bruns C, Vaysse N, Susini C. sst2 somatostatin receptor expression reverses tumorigenicity of human pancreatic cancer cells. *Cancer Res* 1997; **57**: 956-962
- 5 **Reubi JC,** Horisberger U, Essed CE, Jeckel J, Klijn JG, Lamberts SW. Absence of somatostatin receptors in human exocrine pancreatic adenocarcinomas. *Gastroenterology* 1988; **95**: 760-763
- 6 **Sulkowski U,** Buchler M, Pederzoli P, Arnold R, Dinse P, Kay A, Haus U, Beger HG. A phase II study of high-dose octreotide in patients with unresectable pancreatic carcinoma. *Eur J Cancer* 1999; **35**: 1805-1808

- 7 **Burch PA**, Block M, Schroeder G, Kugler JW, Sargent DJ, Braich TA, Mailliard JA, Michalak JC, Hatfield AK, Wright K, Kurross SA. Phase III evaluation of octreotide versus chemotherapy with 5-fluorouracil or 5-fluorouracil plus leucovorin in advanced exocrine pancreatic cancer: a North Central Cancer Treatment Group study. *Clin Cancer Res* 2000; **6**: 3486-3492
- 8 **Fisher WE**, Doran TA, Muscarella P 2nd, Boros LG, Ellison EC, Schirmer WJ. Expression of somatostatin receptor subtype 1-5 genes in human pancreatic cancer. *J Natl Cancer Inst* 1998; **90**: 322-324
- 9 **Gupta MK**, Qin RY. Mechanism and its regulation of tumor-induced angiogenesis. *World J Gastroenterol* 2003; **9**: 1144-1155
- 10 **Korc M**. Pathways for aberrant angiogenesis in pancreatic cancer. *Mol Cancer* 2003; **2**: 8
- 11 **Gupta VK**, Jaskowiak NT, Beckett MA, Mauceri HJ, Grunstein J, Johnson RS, Calvin DA, Nodzinski E, Pejovic M, Kufe DW, Posner MC, Weichselbaum RR. Vascular endothelial growth factor enhances endothelial cell survival and tumor radioresistance. *Cancer J* 2002; **8**: 47-54
- 12 **Itakura J**, Ishiwata T, Friess H, Fujii H, Matsumoto Y, Buchler MW, Korc M. Enhanced expression of vascular endothelial growth factor in human pancreatic cancer correlates with local disease progression. *Clin Cancer Res* 1997; **3**: 1309-1316
- 13 **Seo Y**, Baba H, Fukuda T, Takashima M, Sugimachi K. High expression of vascular endothelial growth factor is associated with liver metastasis and a poor prognosis for patients with ductal pancreatic adenocarcinoma. *Cancer* 2000; **88**: 2239-2245
- 14 **Ikeda N**, Adachi M, Taki T, Huang C, Hashida H, Takabayashi A, Sho M, Nakajima Y, Kanehiro H, Hisanaga M, Nakano H, Miyake M. Prognostic significance of angiogenesis in human pancreatic cancer. *Br J Cancer* 1999; **79**: 1553-1563
- 15 **Stock UA**, Wiederschain D, Kilroy SM, Shum-Tim D, Khalil PN, Vacanti JP, Mayer JE Jr, Moses MA. Dynamics of extracellular matrix production and turnover in tissue engineered cardiovascular structures. *J Cell Biochem* 2001; **81**: 220-228
- 16 **Uria JA**, Lopez-Otin C. Matrilysin-2, a new matrix metalloproteinase expressed in human tumors and showing the minimal domain organization required for secretion, latency, and activity. *Cancer Res* 2000; **60**: 4745-4751
- 17 **Deng SJ**, Bickett DM, Mitchell JL, Lambert MH, Blackburn RK, Carter HL 3rd, Neugebauer J, Pahel G, Weiner MP, Moss ML. Substrate specificity of human collagenase 3 assessed using a phage-displayed peptide library. *J Biol Chem* 2000; **275**: 31422-31427
- 18 **Stracke JO**, Hutton M, Stewart M, Pendas AM, Smith B, Lopez-Otin C, Murphy G, Knauper V. Biochemical characterization of the catalytic domain of human matrix metalloproteinase 19. Evidence for a role as a potent basement membrane degrading enzyme. *J Biol Chem* 2000; **275**: 14809-14816
- 19 **Marchenko GN**, Ratnikov BI, Rozanov DV, Godzik A, Deryugina EI, Strongin AY. Characterization of matrix-metalloproteinase-26, a novel metalloproteinase widely expressed in cancer cells of epithelial origin. *Biochem J* 2000; **356**(Pt 3): 705-718
- 20 **Nar H**, Werle K, Bauer MM, Dollinger H, Jung B. Crystal structure of human macrophage elastase (MMP-12) in complex with a hydroxamic acid inhibitor. *J Mol Biol* 2001; **312**: 743-751
- 21 **Bramhall SR**, Neoptolemos JP, Stamp GW, Lemoine NR. Imbalance of expression of matrix metalloproteinases (MMPs) and tissue inhibitors of the matrix metalloproteinases (TIMPs) in human pancreatic carcinoma. *J Pathol* 1997; **182**: 347-355
- 22 **Koshiha T**, Hosotani R, Wada M, Miyamoto Y, Fujimoto K, Lee JU, Doi R, Arai S, Imamura M. Involvement of matrix metalloproteinase-2 activity in invasion and metastasis of pancreatic carcinoma. *Cancer* 1998; **82**: 642-650
- 23 **Matsuyama Y**, Takao S, Aikou T. Comparison of matrix metalloproteinase expression between primary tumors with or without liver metastasis in pancreatic and colorectal carcinomas. *J Surg Oncol* 2002; **80**: 105-110
- 24 **Koshiha T**, Hosotani R, Wada M, Fujimoto K, Lee JU, Doi R, Arai S, Imamura M. Detection of matrix metalloproteinase activity in human pancreatic cancer. *Surg Today* 1997; **27**: 302-304
- 25 **Ellenrieder V**, Alber B, Lacher U, Hendler SF, Menke A, Boeck W, Wagner M, Wilda M, Friess H, Buchler M, Adler G, Gress TM. Role of MT-MMPs and MMP-2 in pancreatic cancer progression. *Int J Cancer* 2000; **85**: 14-20
- 26 **Matsushita A**, Onda M, Uchida E, Maekawa R, Yoshioka T. Antitumor effect of a new selective matrix metalloproteinase inhibitor, MMI-166, on experimental pancreatic cancer. *Int J Cancer* 2001; **92**: 434-440
- 27 **Raully I**, Saint-Laurent N, Delesque N, Buscail L, Esteve JP, Vaysse N, Susini C. Induction of a negative autocrine loop by expression of sst2 somatostatin receptor in NIH3T3 cells. *J Clin Invest* 1996; **97**: 1874-1883
- 28 **Koizumi M**, Onda M, Tanaka N, Seya T, Yamada T, Takahashi Y. Antiangiogenic effect of octreotide inhibits the growth of human rectal neuroendocrine carcinoma. *Digestion* 2002; **65**: 200-206
- 29 **Wang C**, Tang C. Inhibition of human gastric cancer metastasis by octreotide *in vitro* and *in vivo*. *Zhonghua Yixue Zazhi* 2002; **82**: 19-22
- 30 **Mentlein R**, Eichler O, Forstreuter F, Held-Feindt J. Somatostatin inhibits the production of vascular endothelial growth factor in human glioma cells. *Int J Cancer* 2001; **92**: 545-550
- 31 **Hanahan D**, Folkman J. Patterns and emerging mechanisms of the angiogenic switch during tumorigenesis. *Cell* 1996; **86**: 353-364
- 32 **Stipa F**, Lucandri G, Limiti MR, Bartolucci P, Cavallini M, Di Carlo V, D'Amato A, Ribotta G, Stipa S. Angiogenesis as a prognostic indicator in pancreatic ductal adenocarcinoma. *Anticancer Res* 2002; **22**: 445-449
- 33 **Ferrara N**. Role of vascular endothelial growth factor in the regulation of angiogenesis. *Kidney Int* 1999; **56**: 794-814
- 34 **Ferrara N**, Alitalo K. Clinical applications of angiogenic growth factors and their inhibitors. *Nat Med* 1999; **5**: 1359-1364
- 35 **Kim KJ**, Li B, Winer J, Armanini M, Gillett N, Phillips HS, Ferrara N. Inhibition of vascular endothelial growth factor-induced angiogenesis suppresses tumor growth *in vivo*. *Nature* 1993; **362**: 841-844
- 36 **Millauer B**, Shawver LK, Plate KH, Risau W, Ullrich A. Glioblastoma growth inhibited *in vivo* by a dominant-negative Flk-1 mutant. *Nature* 1994; **367**: 576-579
- 37 **Zhang W**, Ran S, Sambade M, Huang X, Thorpe PE. Monoclonal antibody that blocks VEGF binding to VEGFR2 (KDR/Flk-1) inhibits vascular expression of Flk-1 and tumor growth in an orthotopic human breast cancer model. *Angiogenesis* 2002; **5**: 35-44
- 38 **Hipkin RW**, Friedman J, Clark RB, Eppler CM, Schonbrunn A. Agonist-induced desensitization, internalization, and phosphorylation of the sst2A somatostatin receptor. *J Biol Chem* 1997; **272**: 13869-13876
- 39 **Bloomston M**, Zervos EE, Rosemurgy AS 2nd. Matrix metalloproteinases and their role in pancreatic cancer: a review of preclinical studies and clinical trials. *Ann Surg Oncol* 2002; **9**: 668-674

Herpes simplex virus thymidine kinase and ganciclovir suicide gene therapy for human pancreatic cancer

Jing Wang, Xiao-Xuan Lu, Dao-Zhen Chen, Shu-Feng Li, Li-Shan Zhang

Jing Wang, Xiao-Xuan Lu, Dao-Zhen Chen, Shu-Feng Li, Li-Shan Zhang, Genetics Research Center, School of Basic-Medicine, Southeast University, Nanjing 210009, Jiangsu Province, China
Supported by the Science and Technology Foundation of Southeast University

Correspondence to: Professor Li-Shan Zhang, Genetics Research Center, School of Basic-Medicine, Southeast University, Nanjing 210009, Jiangsu Province, China. wjing18@sohu.com
Telephone: +860-25-3220761 **Fax:** +860-25-3220761
Received: 2003-01-11 **Accepted:** 2003-03-05

Abstract

AIM: To investigate the *in vitro* effects of suicide gene therapy system of herpes simplex virus thymidine kinase gene (HSV-TK) in combination with the treatment of nucleotide analog-ganciclovir (GCV) on human pancreatic cancer, and to provide a novel clinical therapeutic method for human pancreatic cancer.

METHODS: We used a replication defective recombinant retrovirus vector GINaTK (bearing HSV-TK gene) to make packaging cell PA317 produce progeny virions. We then transferred the HSV-TK gene to target cells SW1990 using these progeny virions, and treated these gene-modified tumor cells with GCV to study the sensitivity of the cells to GCV and their bystander effects by routine MTT-method.

RESULTS: Packaging cell PA317/TK was successfully constructed, and we acquired SW1990/TK through virus progeny infection. These gene-modified pancreatic cancer cells were sensitive to the treatment of GCV compared with unmodified tumor cells ($t=4.15$, $n=10$, $P<0.0025$). We also observed a remarkable bystander effect by mixing two kinds of cells at different ratio.

CONCLUSION: Our data demonstrate that HSV-TK/GCV suicide gene therapy system is effective for treating experimental human pancreatic cancer, which is largely resistant to the common therapies, so the suicide gene therapy system may be a potential treatment approach for pancreatic cancer.

Wang J, Lu XX, Chen DZ, Li SF, Zhang LS. Herpes simplex virus thymidine kinase and ganciclovir suicide gene therapy for human pancreatic cancer. *World J Gastroenterol* 2004; 10(3):400-403
<http://www.wjgnet.com/1007-9327/10/400.asp>

INTRODUCTION

Pancreatic cancer is an aggressive malignancy with less than 5% of the patients alive at 5 years and 92% of the patients dead at 2 years^[1,2]. Despite of the development in the three routine therapeutic methods of surgery^[3], chemotherapy, and radiotherapy, the cure rate for pancreatic cancer has improved only minimally, and the overall survival of patients remains

dismal. Its prognosis is extremely poor with current modes of treatment^[4,5]. Therefore, it is urgent to develop effective approaches to this lethal disease. With great progresses of gene therapy in recent years^[6], much of interest and effort have been focused on the treatment of pancreatic cancer. The use of pro-drug-activating genes is a promising approach for cancer gene therapy, especially herpes simplex virus thymidine kinase gene (HSV-TK) in combination with ganciclovir (GCV), which is currently used in gene therapy-based experimental trials for cancer treatment, and in clinical treatment of brain tumors^[7,8].

Virus-originated HSV-TK gene is different from that of mammals, its product thymidine kinase is able to metabolize the nontoxic prodrug, GCV, into a monophosphate derivative, then phosphorylate it further into GCV triphosphate. This metabolite is incorporated into replicating DNA strands and acts as both a DNA synthesis inhibitor and a cell cycle blocker, finally leading to cell apoptosis and death^[9,10], which is also called "suicide gene". The therapeutic effect of this system is also based on a "bystander effect" whereby HSV-TK gene modified tumor cells are toxic to nearby unmodified tumor cells when exposed to the antiviral drug GCV. In this study, we wanted to see whether suicide gene therapy system was effective for the treatment of human pancreatic cancer.

MATERIALS AND METHODS

Cell culture

Murine fibroblasts NIH3T3 cells and packaging cell PA317 were propagated in DMEM (Gibico) with low and high concentrations of glucose separately supplemented with 10% heat-inactivated fetal bovine serum (FBS). Human pancreatic cancer cell line SW1990 was maintained in RPMI1640 (Gibico) supplemented with 20% FBS. Transgenic cell PA317/TK and SW1990/TK were maintained in DMEM (10%FBS) and RPMI1640 (20% FBS) respectively, both with 300 µg/ml of G418 (Promega).

Construction of package cell PA317/TK

HSV-TK gene was inserted downstream of the cytomegalovirus (CMV) promoter in a GINa plasmid containing neo open reading frame (NeoORF), the neomycin resistance gene, which is resistant to neomycin analogue G418. Packaging cells PA317 were transfected with a GINaTK plasmid vector (a gift from the Genetic Research Center of Fudan University, Shanghai, China) using Lipofectin as recommended by the manufacturer (Gibico). Transfected cells were selected with 300 µg/ml of G418 in DMEM supplemented with 10% FBS for weeks. Single-clones were selected, expanded, and maintained in G418-containing medium until further experiments. Total cell DNA were extracted for PCR using specific primer sets for HSV-TK gene (Prime 1: 609 bp-630 bp: 5' -CTACACCACACAAC ACCGCTC-3' ; Prime 2: 1 012 bp-991 bp: 5' -TCGCAGCCAGCATAGC CAGGTC-3'). We also used scanning-electron microscope (SEM) to confirm the success of gene transfer and the production of viral progeny. Virus titers were determined on NIH3T3 cells by plaque assay.

Transfer of HSV-TK gene to pancreatic cancer cells

One day before transfection, we seeded cells to be infected with a density that would allow them to grow logarithmically for at least 2-3 days. The transfection protocol was that the culture supernatant of PA317/TK containing progeny virion was collected and then replaced by fresh DMEM (10% FBS, without G418) within 24 hours before transfection, and passed through a 0.22 μm filter. Then the cell growth medium of SW1990 was replaced with 5 ml of viral supernatant containing 8 $\mu\text{g}/\text{ml}$ polybrene to help the adhesion of viruses. Cells were returned to the incubator and incubated for 2 hours, and then 5 ml of growth medium was added and incubated overnight. The next day the supernatant was removed and the cells were fed with. Two days post-infection the selection was started with 300 $\mu\text{g}/\text{ml}$ of G418 in RPMI1640. In order to confirm the successful infection we performed PCR as described before. We also extracted total RNA and did RT-PCR to assess the expression of TK gene.

Test of cell sensitivity to GCV

We planted gene-modified pancreatic cell SW1990/TK in 96-well (Nunc) plates with 5 000 cells/well. The next day, GCV was added at a concentration ranging from 0 to 500 $\mu\text{g}/\text{ml}$. five days later, cell survival rate (SR) was determined using routine MTT-method, absorbance (A) values were read on a Bio-Rad micro-plate auto-reader at 490 nm wavelength. Survival percentage was determined by ratios of absorbance values from test conditions over absorbance values from non-infected cells. $\text{SR} = (\text{A value of the test well} \div \text{A value of the control}) \times 100\%$.

Study of bystander effect

SW1990 and SW1990/TK cells were seeded at a total density of 10 000 cells/well in 96-well plates with various proportions. GCV was added at a concentration of 50 $\mu\text{g}/\text{ml}$. Then MTT assay was performed as routine protocols, each ratio was tested at least three times.

Statistical analysis

Uni-variate two-sided analysis of matched *t*-test for dependent samples was used, the dose-response curve was obtained using Microsoft Excel.

RESULTS

Through PCR, we obtained a 404 bp long fragment, which was the expected product of HSV-TK gene (Figure 1). From SEM, we can see easily that the cell surface of transfected PA317 had a lot of progeny viruses compared with their parent cells (Figure 2). These confirmed that TK gene was successfully integrated into the genome of packaging cell PA317, which was secreting virion progeny steadily, so we named it as PA317/TK. The virus titer was 40 000 CFU/ml.

Both PCR and RT-PCR confirmed the successful infection and expression of TK gene in gene-modified SW1990 (RT-PCR product electrophoretogram see Figure 3), and we named this cell as SW1990/TK.

Our experiment demonstrated that transgenic SW1990/TK cells were sensitive to prodrug GCV compared to SW1990 ($t=4.15$, $n=10$, $P<0.0025$). With increase of GCV concentration, SW1990/TK presented typical morphological changes of apoptosis and cell death such as nuclear condensation and oligonucleosomal DNA fragmentation, and finally lyses (Figure 4). The survival rate decreased sharply, especially at 0.5 to 50 $\mu\text{g}/\text{ml}$ GCV, while the growth of SW1990 cells was not affected. At the same time, we found that the growth of unmodified cancer cells was inhibited when the concentration

was more than 100 $\mu\text{g}/\text{ml}$, as seen in Figure 5.

SW1990/TK exhibited a "bystander effect" when mixed with TK-negative cells at different ratios. From Figure 6 we can see that the cell survival rate was 40%, 20% and 0% when there was 15%, 30% and 80% of SW1990/TK cells in all, the inhibitory rate ($\text{IR} = 1 - \text{SR}$) was 60%, 80%, 100% respectively. Apparently the IR was much higher than the percentage of SW1990/TK, which reflected the bystander effect.

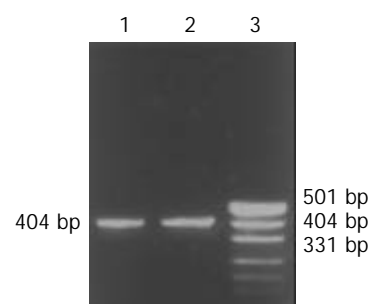


Figure 1 Electrophoretic results of PCR products. 1. GINaTK, 2. PA317/TK, 3. Marker (puc19DNA/MSP I).

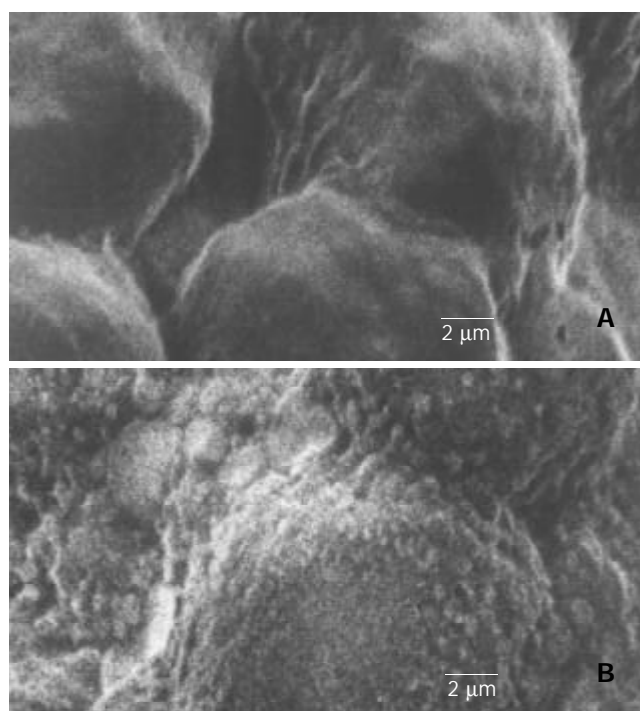


Figure 2 Results of scanning electron microscope. A: The surface of PA317 cell are very smooth, B: There are a lot of bumps on the surface of PA317/TK cells because these gene-modified cells are secreting virus particles.

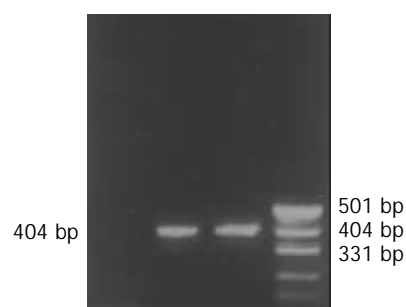


Figure 3 Results of RT-PCR. 1. SW1990, 2. SW1990/TK, 3. GINaTK, 4. Marker.

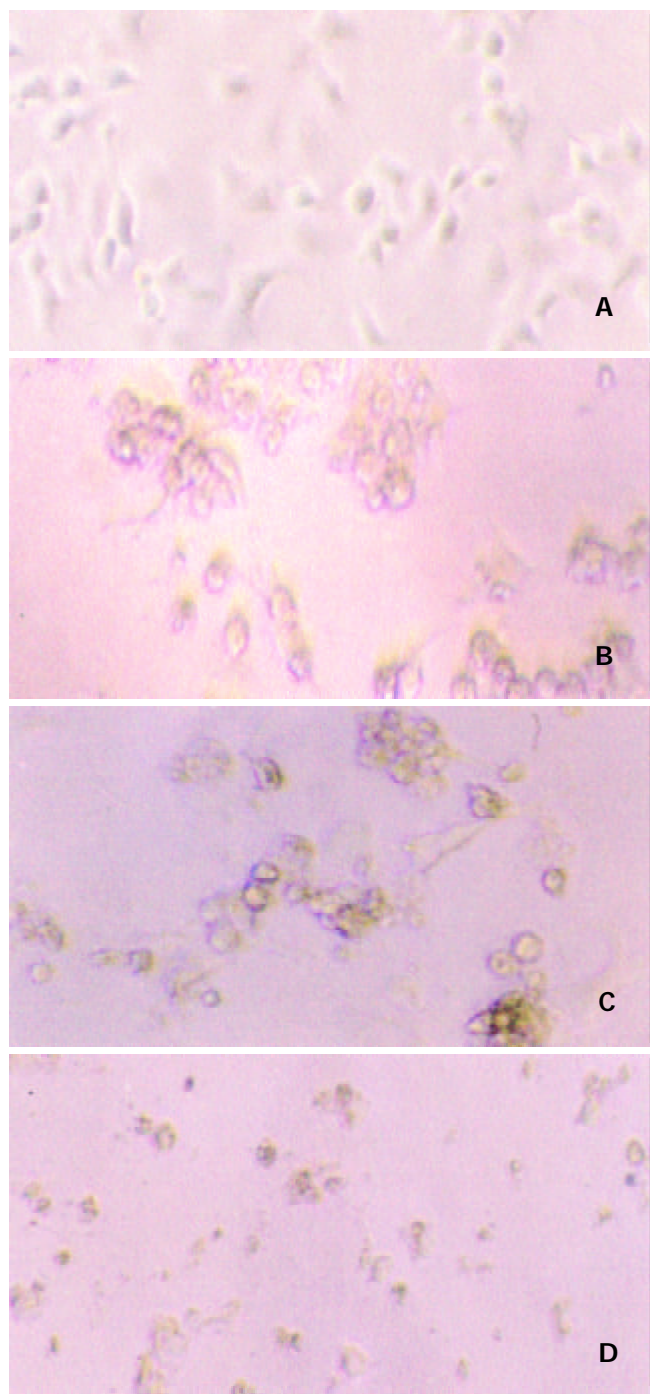


Figure 4 Typical morphological changes in SW1990/TK cells when exposed to GCV (50 µg/ml). A: SW1990/TK cells without GCV. B: Two days after adding 50 µg/ml of GCV, cells became round and smaller, losing their normal morphology. C: Four days after adding GCV, cells gathered to balls. D: Five days later, cells clasped into small fragments.

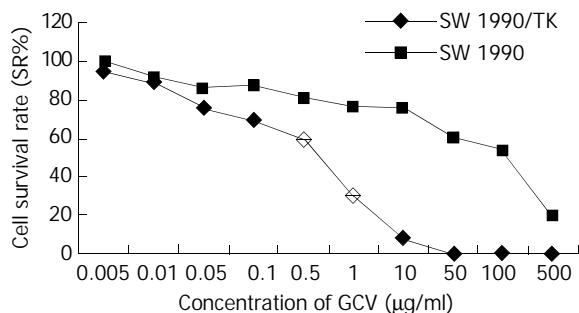


Figure 5 Sensitivity of SW1990/TK to GCV.

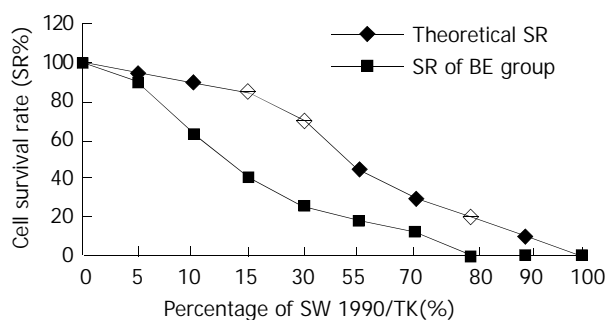


Figure 6 Bystander effects of SW1990/TK cell line.

DISCUSSION

Pancreatic cancer has an extremely poor prognosis due to lack of early diagnostic and therapeutic approaches, few are suitable for surgery and respond to chemo-radiation therapy, mainly because of its silent course and explosive fatal outcome. Most patients had locally advanced or metastatic diseases at the time of diagnosis and were therefore not amenable to resection, whilst chemotherapy and radiotherapy were by and large ineffective^[11]. HSV-TK/GCV suicide gene therapy system has been widely studied these years, and is a promising approach to tumor therapy, but its use in human pancreatic cancer has been limited.

In our study, the retrovirus was used as a target gene vector. Among various vectors, retrovirus-mediated gene transfer is restricted to cells that are proliferating and synthesizing DNA at the time of infection but not nondividing cells. It is suitable to gene transfer of malignant cells with rapid proliferation and can improve the targeting of gene transfer. With 40 000 CFU/ml virus titer, it transfers target gene effectively.

Besides the advantage of retrovirus, HSV-TK/GCV suicide gene therapy system shows another superiority: bystander effect. Both the transduction efficiency and bystander effect are essential factors for the success of the anti-tumor effect of HSV-TK and prodrug GCV suicide gene therapy system. Bystander effect is described when nontransduced or genetically unmodified cells are killed as the result of enzyme-prodrug activation during the death of genetically modified tumor cells transduced with a suicide gene. The “bystander effect” greatly amplifies the efficacy of HSV-TK/GCV gene therapy for cancer in which only a fraction of the cells are targeted. The *in vitro* bystander effect in C6/C6-TK5 co-culture was highly significant, the presence of only 5% of C6-TK5 cells led to an overall 78% decrease in cell survival after 5 days of GCV treatment^[12]. In our experiment, 15% of SW1990/TK cells could lead 60% cells to death. However, the mechanism of bystander effect is still controversial. Some investigators suggested that intercellular communication was essential for the bystander effect. The correlation between gap junction communication (GJIC) and the extent of bystander effect suggested a role of GJIC in mediating the bystander effect, which could provide a useful system for selective killing of gene-modified tumor cells^[13]. Some provided evidences for a role of cell membrane in signal pathways leading to bystander effect.

As we all know, everything has two sides. Inevitably, this system had its own side effect. The most common side effects of GCV in immunocompromised patients were leukemia (7-42%), thrombocytopenia (8-57%), and abnormal liver-function tests (2%). However, side effects in patients with intact immune system have not been reported^[14]. As we can see in Figure 5, once the dose of GCV exceeded 500 µg/ml, it did harm to unmodified cells, so control of the dosage of drug administration is important in clinical practice.

The current trend of gene therapy for tumor is to combine

two or even more approaches in order to improve its anti-tumor effect and reduce its side effects. The combination of both suicide systems of cytochrome p450 2b1 (CYP2B1)/CPA and HSV-TK/GCV *in vitro* resulted in a potentiation of the killing effect. This suggested that in order to achieve a potentiation in cell killing when two suicide systems were combined, co-expression of both genes in the same tumor cell would be necessary^[15]. Gene therapy with p53 and K-ras modulated herpes viruses might become a palliative treatment option and could be used easily by regional chemotherapy techniques^[11]. Pancreatic ductal adenocarcinomas (PDACs) could overexpress various cell-surface tyrosine kinase receptors, including type I high-affinity fibroblast growth factor receptor (FGFR-1). In view of the overexpression of high-affinity FGFRs in cancer cells in PDAC, Kleeff's findings suggested that combined use of AdTK, ganciclovir, and FGF2-Fab' might ultimately be a promising therapeutic approach in a subgroup of patients with PDAC^[16].

Besides suicide gene therapy system, there are many other approaches for pancreatic cancer therapy. Based on the relative uniformity in its molecular abnormalities, about 80-90% of tumors have dominant oncogene K-ras mutations and disruption of p16/RB tumor suppressor pathway, about 60-75% have p53 mutations, and more than 50% have SMAD4/DPC4 disruptions, transfer of wild-type p53 and p16 could produce significant growth suppression of pancreatic cancer *in vitro* and *in vivo*^[17-19]. The results of Kawakami *et al.* showed that IL-4 receptor-targeted cytotoxin represented a potent agent that might provide an effective therapy for pancreatic cancer^[20]. Yan and his group found that adenovirus-mediated E2F-1 gene transfer could sensitize melanoma cells to some chemotherapeutic agents, particularly topoisomerase II poisons *in vitro* and *in vivo*. These results suggested a new chemosensitization strategy for melanoma gene therapy^[21]. With the discovery of RNA-interference, some researchers suggested it might be used in tumor therapy^[22-24].

Our results indicated that gene modified tumor cells SW1990/TK were sensitive to antiviral prodrug GCV, and showed a remarkable bystander effect on killing tumor cells. In conclusion, HSV-TK/GCV suicide gene therapy system is a promising approach for the treatment of pancreatic cancer. As increasingly more researchers focus on the diagnosis and therapy of this lethal malignancy, we believe that some effective ways would be discovered for clinical treatment of pancreatic cancer.

ACKNOWLEDGMENTS

First of all, I thank my family and my boyfriend for offering their all-out support to my work. Secondly, I appreciate the academic advice and technical support by Professor Zhang LS and Mrs. Lu.

REFERENCES

- Lorenz M**, Heinrich S. Regional chemotherapy. *Hematol Oncol Clin North Am* 2002; **16**: 199-215
- Gustin A**, Pederson L, Miller R, Chan C, Vickers SM. Application of molecular biology studies to gene therapy treatment strategies. *World J Surg* 2002; **26**: 854-860
- Shankar A**, Russell RC. Recent advances in the surgical treatment of pancreatic cancer. *World J Gastroenterol* 2001; **7**: 622-626
- McAuliffe PF**, Jarnagin WR, Johnson P, Delman KA, Federoff H, Fong Y. Effective treatment of pancreatic tumors with two multimitated herpes simplex oncolytic viruses. *J Gastrointest Surg* 2000; **4**: 580-588
- Makinen K**, Loimas S, Wahlfors J, Alhava E, Janne J. Evaluation of herpes simplex thymidine kinase mediated gene therapy in experiment pancreatic cancer. *J Gene Med* 2000; **2**: 361-367
- Xu CT**, Huang LT, Pan BR. Current gene therapy for stomach carcinoma. *World J Gastroenterol* 2001; **7**: 752-759
- Fukui T**, Hayashi Y, Kagami H, Yamamoto N, Fukuhara H, Tohnai I, Ueda M, Mizuno M, Yoshida J. Suicide gene therapy for human oral squamous cell carcinoma cell lines with adeno-associated virus vector. *Oral Oncol* 2001; **37**: 211-215
- Jiang BJ**, Sun RX, Lin H, Gao YF. Study on the risk factors of lymphatic metastasis and the indications of less in vasive operations in early gastric cancer. *World J Gastroenterol* 2000; **6**: 553-556
- Robe PA**, Princen F, Martin D, Malgrange B, Stevenaert A, Moonen G, Gielen J, Merville M, Bours V. Pharmacological modulation of the bystander effect in the herpes simplex virus thymidine kinase/ganciclovir gene therapy system: effects of dibutyryl adenosine 3', 5'-cyclic monophosphate, alpha-glycyrrhetic acid, and cytosine arabinoside. *Biochem Pharmacol* 2000; **60**: 241-249
- Craferi D**, Vicat JM, Nissou MF, Mathieu J, Baudier J, Benabid AL, Verna JM. Increased bax expression is associated with cell death induced by ganciclovir in a herpes thymidine kinase gene-expressing glioma cell line. *Hum Gene Ther* 1999; **10**: 679-688
- Halloran CM**, Ghaneh P, Neoptolemos JP, Costello E. Gene therapy for pancreatic cancer—current and prospective strategies. *Surg Oncol* 2000; **9**: 181-191
- Gilliam AD**, Watson SA. Emerging biological therapies for pancreatic carcinoma. *Eur J Surg Oncol* 2002; **28**: 370-378
- Nagasawa H**, Cremesti A, Kolesnick R, Fuks Z, Little JB. Involvement of membrane signaling in the bystander effect in irradiated cells. *Cancer Res* 2002; **62**: 2531-2534
- Shalev M**, Miles BJ, Thompson TC, Ayala G, Butler EB, Aguilar-Cordova E, Kadmon D. Suicide gene therapy for prostate cancer using a replication-deficient adenovirus containing the herpes virus thymidine kinase gene. *World J Urol* 2000; **18**: 125-129
- Carrio M**, Visa J, Cascante A, Estivill X, Fillat C. Intratumoral activation of cyclophosphamide by retroviral transfer of the cytochrome P450 2B1 in a pancreatic tumor model. Combination with the HSVtk/GCV system. *J Gene Med* 2002; **4**: 141-149
- Kleeff J**, Fukahi K, Lopez ME, Friess H, Buchler MW, Sosnowski BA, Korc M. Targeting of suicide gene delivery in pancreatic cancer cells via FGF receptors. *Cancer Gene Ther* 2002; **9**: 522-532
- Gazdar AF**, Minna JD. Targeted therapies for killing tumor cells. *Proc Natl Acad Sci U S A* 2001; **98**: 10028-10030
- Ghaneh P**, Greenhalf W, Humphreys M, Wilson D, Zumstein L, Lemoine NR, Neoptolemos JP. Adenovirus-mediated transfer of p53 and p16(INK4a) results in pancreatic cancer regression *in vitro* and *in vivo*. *Gene Ther* 2001; **8**: 199-208
- Zheng M**, Liu LX, Zhu AL, Qi SY, Jiang HC, Xiao ZY. K-ras gene mutation in the diagnosis of ultrasound guided fine-needle biopsy of pancreatic masses. *World J Gastroenterol* 2003; **9**: 188-191
- Kawakami K**, Kawakami M, Husain SR, Puri RK. Targeting interleukin-4 receptors for effective pancreatic cancer therapy. *Cancer Res* 2002; **62**: 3575-3580
- Dong YB**, Yang HL, Elliott MJ, McMasters KM. Adenovirus-mediated E2F-1 gene transfer sensitizes melanoma cells to apoptosis induced by topoisomerase II inhibitors. *Cancer Res* 2002; **62**: 1776-1783
- Brummelkamp TR**, Bernards R, Agami R. A system for stable expression of short interfering RNAs in mammalian cells. *Science* 2002; **296**: 550-553
- Paddison PJ**, Caudy AA, Hannon GJ. Stable suppression of gene expression by RNAi in mammalian cells. *Proc Natl Acad Sci U S A* 2002; **99**: 1443-1448
- Borkhardt A**. Blocking oncogenes in malignant cells by RNA interference—new hope for a highly specific cancer treatment? *Cancer Cell* 2002; **2**: 167-168

Striking elevation in incidence and prevalence of inflammatory bowel disease in a province of western Hungary between 1977-2001

Laszlo Lakatos, Gabor Mester, Zsuzsanna Erdelyi, Mihaly Balogh, Istvan Szipocs, Gyorgy Kamaras, Peter Laszlo Lakatos

Laszlo Lakatos, Gabor Mester, Zsuzsanna Erdelyi, 1st Department of Medicine, Csolnok F. Province Hospital, Veszprem, Hungary
Mihaly Balogh, Department of Medicine, Grof Eszterhazy Hospital, Papa, Hungary

Istvan Szipocs, Department of Medicine, Municipal Hospital, Tapolca, Hungary

Gyorgy Kamaras, Department of Infectious Diseases, Magyar Imre Hospital, Ajka, Hungary

Peter Laszlo Lakatos, 1st Department of Medicine, Semmelweis University, Budapest, Hungary

Correspondence to: Laszlo Lakatos, MD, 1st Department of Medicine, Csolnok F. Province Hospital, Korhaz u.1, Veszprem, H-8200 Hungary. laklaci@hotmail.com

Telephone: +36-20-911-9339 **Fax:** +36-1-313-0250

Received: 2003-08-11 **Accepted:** 2003-09-24

Abstract

AIM: An investigation into inflammatory bowel disease and colorectal cancer in Veszprem Province was conducted from 1977 to 2001.

METHODS: Both hospital and outpatient records were collected and reviewed comprehensively. The majority of patients were followed up regularly.

RESULTS: The population of the province was decreased from 386 000 to 376 000 during the period. Five hundred sixty new cases of ulcerative colitis (UC), 212 of Crohn's disease (CD), and 40 of indeterminate colitis (IC) were diagnosed. The incidence rates increased from 1.66 to 11.01 cases per 100 000 persons for UC, from 0.41 to 4.68 for CD and from 0.26 to 0.74 for IC. The prevalence rate at the end of 2001 was 142.6 for UC and 52.9 cases per 100 000 persons for CD. The peak onset age in UC patients was between 30 and 40 years, in CD between 20 and 30 years. A family history of IBD was present in 3.4 % in UC and 9.9 % in CD patients. Smoking increased the risk for CD (OR=1.94) while it decreased the risk for UC (OR=0.25). Twelve colorectal carcinomas were observed in this cohort, the cumulative colorectal cancer risk after 10 years in UC was 2%, after 20 years 8.8%, after 30 years 13.3%.

CONCLUSION: The incidence and prevalence rates of IBD have increased steadily in Veszprem Province, now equivalent to that in Western European countries. Rapid increase in incidence rates supports a probable role for environmental factors. The rate of colorectal cancers in IBD is similar to that observed in Western countries.

Lakatos L, Mester G, Erdelyi Z, Balogh M, Szipocs I, Kamaras G, Lakatos PL. Striking elevation in incidence and prevalence of inflammatory bowel disease in a province of western Hungary between 1977-2001. *World J Gastroenterol* 2004; 10(3):404-409 <http://www.wjgnet.com/1007-9327/10/404.asp>

INTRODUCTION

The pathogenesis of ulcerative colitis (UC) and Crohn's disease

(CD) has only been partly understood. Inflammatory bowel disease (IBD) is a multifactorial polygenic disease with probable genetic heterogeneity. Based on this hypothesis, the disease may develop in a genetically predisposed host as a consequence of dysregulated immune response to environmental factors, in particular enteric antigens, resulting in continuous immune-mediated inflammation^[1,2]. However, the disease phenotype may be affected by various other factors.

IBD represents an important public health problem, as it tends to afflict young people and has a protracted and relapsing clinical course, affecting education, working abilities, social life and quality of life.

Several studies have been done on the epidemiology of IBD^[3,4]. The geographical incidence of IBD varies considerably, the highest incidence rates were reported in Northern and Western Europe as well as North America, whereas they were lower in Africa, South America and Asia, including China^[5]. It is more common in developed, more industrialized countries, urban residency seems to be a risk factor. The incidence rate of UC varies greatly between 0.5-24.5/100 000 inhabitants, that of Crohn's disease between 0.1-11/100 000 inhabitants worldwide.

Previous studies in Europe suggested that the incidence was decreased from North to South^[6,7], but in the early nineties the European IBD Study Group found comparable rates in Southern and Northern Europe^[8]. This tendency may be explained by the relative stable incidence in previous high incidence areas, whereas in previous low incidence areas the incidence rose continuously. A further difference is that the previously reported predominance of UC is diminishing, as CD is becoming more prevalent. The reported average incidence of UC in Europe was 10.4, that of CD was 5.6.

Few data have been available about the frequency of IBD in the Eastern European countries. In the early eighties, Vucelic *et al.*^[9,10] conducted a prospective survey on the incidence of IBD in Zagreb, Croatia. They reported an incidence rate of 1.5/100 000 inhabitants in UC and 0.7 in CD. Similarly low incidence of UC (1.7) and CD (1.4) was reported in another prospective study in Estonia^[11]. Nagy *et al.*^[12] reported epidemiological data in IBD from the early 60's to the late 80's among Hungarians. The reported incidence rate was 3.6 in UC and 1.0 in CD. These data were based mainly on hospital reports. No population based survey has been reported.

The elevated colorectal cancer (CRC) risk in patients with long standing IBD has been widely accepted since Crohn's original report. Recent observations suggested that the prevalence of CRC was also higher in CD^[13]. The magnitude of the risk complicating IBD varied greatly in different geographic areas and in different studies. From Eastern Europe we found only one publication about CRC in IBD^[14].

Recently we reported on the prevalence of extraintestinal manifestations in a large IBD cohort in a long-term follow-up study^[15]. The aim of the present study was to determine the incidence and prevalence of IBD and the main epidemiological features of the disease in a province of Hungary in a population based survey.

MATERIALS AND METHODS

Demographical data

Veszprem Province is located in the Western part of Hungary. The province consists of both industrial and agricultural regions.

The number of permanent population was relatively stable, with a slight decrease from 386 462 to 376 211 from 1980 to 1998 (Table 1). The rate of Gypsies is below the Hungarian average (2.5%), few Jewish people live in the province. The ratio of urban/rural residence was also relative stable (the data in 1991 were used for comparison, Table 2).

There are 7 general hospitals in the province, each is staffed by at least one gastroenterologist or internist with special interest in gastroenterology. The majority of the patients (74% of UC patients and 94% of CD patients) were followed-up in the Csolnok F. Province Hospital in Veszprem. The main data sources were the hospital records, outpatient clinical reports, endoscopic, radiological and pathological reports collected from the Internal Medicine Department, Surgery Department, Outpatient Units and family doctors. Both inpatients and outpatients permanently residing in the investigated area were included in the study. Most of the patients were followed up regularly. Diagnoses (based on hospitalization records, outpatient visits, endoscopic, radiological and histological evidence) generated in each hospital and outpatient unit were reviewed thoroughly, using the Lennard-Jones criteria^[16].

Cases having another readily identifiable cause of colitis, such as infectious colitis (including pseudomembranous) were excluded. Anticoncipient or NSAID associated colitis and ischemic colitis cases were also excluded. UC cases with involvement outside the colon, with the exception of "backwash ileitis", were excluded. In some cases the final diagnosis was made years after the beginning of symptoms.

The term indeterminate colitis (IC) was first described by Price in 1978^[17] for cases operated on because of non-differentiable fulminating colitis. Today it has been used for IBD colitis cases, when the data were insufficient to differentiate between UC and CD^[8].

Before the early eighties the diagnosis was based mainly on rectoscopy, histology, barium enema and upper GI series. Later colonoscopy, double-contrast barium enema and selective enterography were the basic diagnostic methods, CT and in some cases leukocyte scintigraphy were also more frequently performed to help make a more accurate diagnosis (*e.g.* location, activity and complications).

The location in UC was determined by colonoscopy and/or double-contrast colonography based on the macroscopic picture. Patients were classified according to the greatest known extent. In mild to moderately severe active UC cases the location was determined during the active phase, in more severe disease shortly after the active period.

The study was retrospective. Data of IBD patients were summarized yearly, in some cases the diagnosis was changed after re-evaluation. IBD patient data were collected every year from the 7 general hospitals and gastroenterology outpatient units. The provincial IBD register data were centralized in Veszprem, which is the secondary referral center for IBD patients in the province. Patients diagnosed in the same calendar year were included in the incidence calculations. All the residents and IBD patients permanently residing in the province on the 31st of December 1991 and 2001 were included in the prevalence calculations (including patients who had moved to Veszprem Province after diagnosis).

Regular colonoscopic dysplasia-cancer surveillance program with multiple biopsies was carried out in patients with extensive colitis after 8 years, with left-sided colitis after 12 years.

The source of demographic data was the Hungarian Central Statistical Office (KSH).

Table 1 Population of Veszprem Province between 1980-1998

Years	Total	Women	Men
1980	386.462	194.855	191.607
1990	379.246	192.867	186.462
1998	376.211	192.296	183.915

Male/female ratio in 1990: 0.966.

Table 2 Proportion of patients according to places of residence (in 1991) (OR: Odds ratio)

	Urban (n)	Rural (n)	Total (n)
Veszprem Province	208.284	173.089	381.373
Ulcerative colitis	339	221	560
	OR: 1.27 (95% CI: 1.07-1.52)		
Crohn's disease	122	90	212
	OR: 1.13 (95% CI: 0.85-1.49)		

Statistical methods

For statistical comparison of the data, Statistica 6.0 (Statsoft Inc., USA) was used. Odds ratio (OR) was calculated for potential factors that influenced the prevalence of IBD, including residence (urban versus rural) and smoking habits. For comparisons within group ANOVA analysis with Scheffe post hoc test was used. Yates-corrected Chi-square analysis was performed to compare differences in incidence according to the location of UC or CD during the observed period. Results were expressed as mean±SD if otherwise not stated (NS=not statistically significant).

RESULTS

Incidence

During the observation period 560 new patients with UC (M/F: 288/272, ratio: 1.058) and 212 new patients with CD (M/F: 108/104, ratio: 1.038) were diagnosed in Veszprem Province.

The mean incidence rate for UC was 5.89 (95% CI: 2.15-9.63) cases per 100 000 persons per year. The sex-standardized incidence appeared slightly higher in men (6.19, 95% CI: 2.30-10.08) than in women (5.64, 95% CI: 2.39-8.89), however, the difference was not statistically significant. For the calculation of the sex standardized incidence rates, gender specific population data of Veszprem Province were used (Hungarian Central Statistical Office, KSH). In CD the average 25-year incidence was 2.23 (95% CI: 0.5-3.96), in men: 2.31 (95% CI: 0.64-3.98 and in women: 2.17 (95% CI: 0.34-4). Indeterminate colitis was diagnosed in forty cases (M/F: 22/18), the mean incidence rate was 0.42 cases per 100 000 persons per year.

The incidence of IBD in 5-year intervals is shown in Figure 1. A sharp increase in incidence of UC was observed from 1.66 during 1977-1981 to 11.01 during 1997-2001 (in men from 1.77 to 11.96 and in women from 1.54 to 10.09). For CD, a similar tendency was observed. The incidence rose from 0.41 to 4.68, in men from 0.21 to 5.76, in women from 0.41 to 3.64. An almost continuous rise in incidence was observed for both UC and CD. The incidence of IC also rose during the observed period (from 0 to 0.74).

In contrast to UC, for which the highest incidence rate recorded was in 2001 in both sexes (in men 16.85, in women 11.96), for CD the peak incidence recorded in men was 9.24 in 1998, whereas in women it was 5.72 in 2001.

The ratio of UC/CD incidence rates decreased from 4.05 to 2.35 during the observed periods.

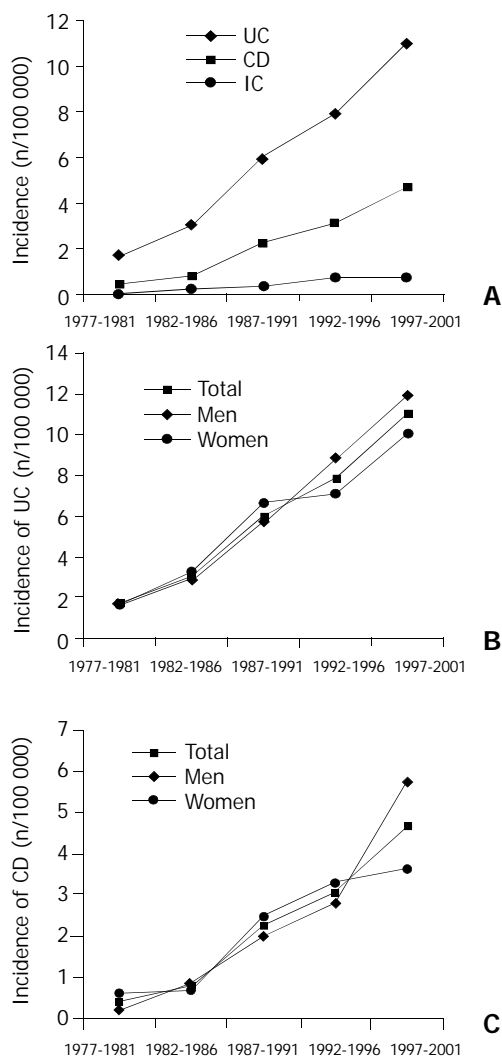


Figure 1 Average and sex-specific incidence of UC, CD and IC in Veszprem Province between 1977-2001.

Age standardized incidence rates

The mean age at diagnosis was 31.7 ± 12.8 years for CD, 38.9 ± 15.5 years for UC and 36.8 ± 13.9 years for IC. For the calculation of age standardized incidence rates, age specific population data of Veszprem Province were used (Hungarian Central Statistical Office, KSH). We observed only one peak incidence. For UC the highest incidence rate was in 31-40-year olds, but the 21-30-year olds incidence rate was in the same range (10.96 vs 9.26). For CD the peak incidence was in the 21-30-year olds (Figures 2A and B). The youngest UC patient was diagnosed at the age of 9 years, while the oldest patient just passed 80 years at the time of diagnosis. The youngest CD-diagnosed-patient was 12, the oldest 80 years old.

Prevalences

All the patients permanently living in Veszprem Province were included in the prevalence calculation (even patients diagnosed before 1977, 33 UC cases and 3 CD cases were not included as incidence cases).

On the 31st of December 1991, the prevalence of UC was 59.2 cases per 100 000 persons, that of CD was 17.1 cases per 100 000 persons. On this day the prevalence of IC was 2.9/100 000. The prevalences were significantly increased by the 31st of December 2001. For UC the prevalence was 142.6, while for CD 52.9 cases per 100 000 persons.

The urban/rural ratio was 1.205 in general population in 1991, which was relatively stable during the observed period. Urban residency seemed to increase the risk of UC (OR: 1.27), but it did not affect significantly the risk for CD (Table 2).

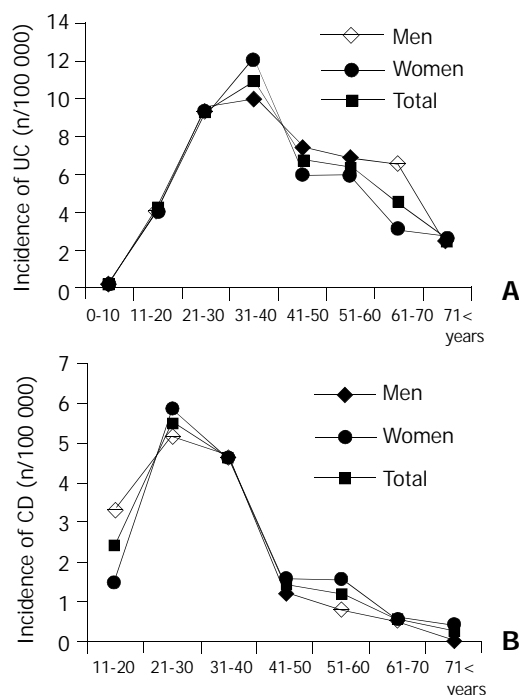


Figure 2 Age and sex-specific incidence of UC and CD in Veszprem Province between 1977-2001.

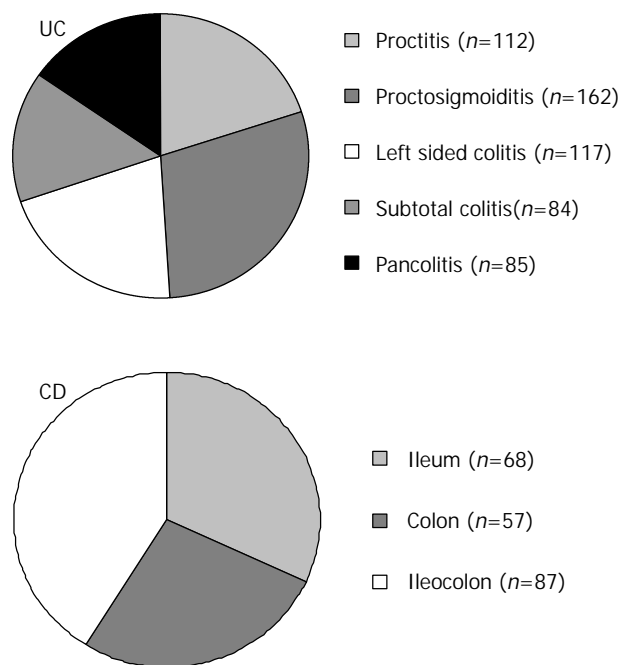


Figure 3 Location of UC or CD (n=number of patients).

Location and disease behavior

According to our information 112 of the UC patients had proctitis, 162 proctosigmoiditis, 117 left sided colitis, 84 subtotal and 85 pancolitis (Figure 3A). The age at diagnosis did not affect the location of the disease.

Location of UC did change in the past 25 years, proctitis became more prevalent in the last decade compared to the first 10 years (8.6% vs 24.0%, $P=0.002$), while pancolitis cases

were relatively less frequent (39.8% vs 27.8%, $P=0.034$). The percentage of left sided colitis did not change (51.6% vs 48.2%).

The Vienna classification^[18] defines CD patients according to the age at onset, location and disease behavior. In CD ileal disease (L1) was found in 32.1%, colonic (L2) in 26.9% and ileocolonic (L3) in 41.0% of the patients (Figure 3B). Location of CD did also change in the observed period. There was a tendency of colonic location becoming more frequent in the last decade compared to the first one, while the percentage of ileocolonic cases was decreased (L1: 19.2% vs 24.1%, $P=NS$, L2: 19.2% vs 36.5%, $P=NS$, L3: 61.5% vs 39.4%, $P=0.05$). The most commonly associated location was perianal (48 cases). All the patients with upper gastrointestinal location (L4) had lower gastrointestinal involvement, and were classified according to this location (L1-3). In 5 cases the jejunum, in 2 the duodenum, in 5 the stomach and in 2 the esophagus were also affected. Only histologically proven cases were included in the calculation of associated locations. There was no correlation between the location and age at diagnosis.

According to the disease behavior 63 of our CD patients were defined as non-stricturing, non-penetrating (B1), 54 as stricturing (B2) and 95 as penetrating (B3). Fifty-three patients of the 95 penetrating cases had parallel strictures.

In UC group 6.4% of the patients had at least one bowel operation, a much higher frequency was observed in CD (60%, Table 5). There was an association between disease location and the frequency of operations (L1=0.98, L2=0.21, L3=1.93 operations on average, $P<0.01$ among all the groups, ANOVA-Scheffe post hoc test).

Familial incidence

Of the UC patients 19 had one or more close relatives with confirmed UC or CD (Table 3). In CD patients IBD was apparent in 9.9% of the families. The occurrence of IBD was more pronounced in families of CD patients with stricturing disease than in those of CD cases with non-stricturing, non-penetrating disease (B1: 6.6% (4/60), B2: 24.5% (13/53) and B3: 11.7% (11/94), $P=0.04$).

Table 3 Familial occurrence of IBD

Relationship	UC (n=560)	CD (n=212)
First-degree relative with IBD	17	15
Second-degree relative with IBD	2	6
Familial IBD	3.4 %	9.9%

Smoking

Sixty-seven UC patients (14.3%) were smokers at the time of diagnosis, while the rate of ex-smokers and nonsmokers was 18.4% and 67.3%, respectively (Table 4). In CD patients 102 were smokers at the time of diagnosis (50.5%, which was higher than the Hungarian average of 40.5%, 1991 data, KSH). Among the patients with CD, 13 ex-smokers and 87 nonsmokers were identified. Smoking decreased the risk for UC by 75%, while it almost doubled the risk for CD (OR: 1.94, 95% CI: 1.46-2.59).

Colorectal carcinoma

Colon tumor was observed in 10 patients with UC (Table 6). The average duration of IBD at the diagnosis of colorectal cancer was 18.4 years. The average age at the diagnosis of CRC was 53.4 (27-65) years, 15 years younger than the age of patients with non-IBD CRC at diagnosis (68.2 years, 2000 data, KSH). The male/female ratio was one (5/5). Seven out of the ten patients had pancolitis. Two colorectal cancers occurred in CD patients with a short follow-up (3 and 6 years) period. The location of CD was colonic without ileal involvement. No

family history of IBD was apparent in IBD cases with CRC. Only one out of the twelve patients with IBD and CRC had a family history of CRC.

The cumulative risk for colorectal cancer in patients with UC for 10 years was 2%, for 20 years 8.8%, and for 30 years 13.3%, respectively.

Table 4 Smoking habits in IBD patients at presentation

	UC n (%)	CD n (%)
Non-smoker	315 (67.3%)	87 (43.1%)
Ex-smoker	86 (18.4%)	13 (6.4%)
Smoker	67 (14.3%)	102 (50.5%)
No data	92	10
Odds ratio for smoking	0.25 (95% CI: 0.19-0.32)	1.94 (95% CI: 1.46-2.59)

(Prevalence of smoking in Hungary in 1991: 40.5%).

Table 5 Surgery in IBD

Surgery in UC	Surgery in CD
<ul style="list-style-type: none"> • Resection: 8 • Proctocolectomy: 28 - J Pouch: 25 	Not operated: 86 (40.6 %) <ul style="list-style-type: none"> • Operated: 126 (59.4 %) <ul style="list-style-type: none"> • 1 operation: 63 (29.7 %) • 2-3 operations: 50 (23.6 %) • 4-8 operations: 13 (6.1 %)

Table 6 Colorectal carcinoma in IBD

Carcinomas	Age at diagnosis	Duration of IBD	Location of IBD	Location of tumor
UC (n=10)	35 yrs (20-56 yrs)	18.4 yrs (9-33 yrs)	Pancolitis: 7 Left sided colitis: 3	Ascending: 2 Transverse: 4 Descending: 2 Rectum: 2
CD (n=2)	24 and 45 yrs	3 and 6 yrs	Right colon: 2	Transverse: 2

DISCUSSION

The incidence of IBD varied greatly worldwide. Genetic and environmental factors were assumed to play a significant role in the etiology of the disease^[1,2]. The role of genetic factors was supported by ethnical and familial differences and also by twin studies^[19-22], while the differences in incidence rates among various geographical areas suggest a role for certain environmental factors. There has been an important change in incidence of IBD in the last few decades. In high incidence countries in Western Europe the incidence rate remained relatively stable, while in previous low incidence areas^[9,12] as supported by our data as well, the disease has become more common.

The continuous increase in incidence rates of both UC and CD observed in this study raises further questions. What could be the cause of this change? In the first years the lower incidence rates could be explained partly by the use of less up-to-date diagnostic procedures (*e.g.* the relative low availability of selective enterography or colonoscopy). It is possible that better awareness, either by physicians or by patients, may result in the diagnosis of mild cases that previously might have gone unnoticed. There has also been an important change in patients' behavior in Hungary, as patients tend to seek medical advice more often and with milder symptoms than they did two decades ago. We believe that the increase in the incidence of IBD in the second part of the observed period is real and not

solely due to an improved diagnosis or more extensive search. This idea is also supported by the increase in severe cases that could only be interpreted as real. Our incidence rates in UC (11.01) and CD (4.68) in the last five-year period (1997-2001) were in the range as previously observed in high incidence Nordic countries^[7,8,23,24] and they were much higher than the rates reported in Hungary two decades ago^[12].

Most studies reported the peak onset of both UC and CD at late puberty - early adulthood period. In some studies a second peak of onset was observed in 50-70 year-olds^[25]. The EC-IBD study^[8] reported one peak onset in CD in both sexes around the age of 20 (incidence rate in men was around 6.0 and in women 7.7) followed by a continuous decrease. In UC the peak incidence was observed in both sexes in 25-30-year olds (incidence rate was 11.2 in men and 10.7 in women), followed by a continuous decrease in women, while the incidence remained relatively stable in men. In the present study we observed one peak incidence in UC in 30-40 year olds (in men 10.0 and in women 12.1) and also in CD in 20-30 year olds (in men 5.2 and in women 5.9).

IBD could affect both sexes almost equally, with a slight predominance of women in CD, and a male/female ratio ranging from 1.1 to 2.0 in UC^[5,8,23]. In our present study the male to female ratio was almost similar with a slight male predominance.

In UC the proportion of extensive colitis was higher, while the percentage of proctitis cases was lower than those in the recent EC-IBD study^[8]. Location of UC cases only mildly changed in the observed period. The percentage of pancolitis cases was decreased, in contrast, proctitis became more prevalent. However it was still less frequent than observed in the Western-European epidemiological studies^[8].

In CD ileal disease was found in one third of the patients, and ileocolonic in 41.0% of the patients. A recent study reported a higher frequency of ileocolonic disease while the percentage of ileal disease was lower^[8]. In the current study colonic involvement was observed in almost two-thirds of the patients, and there seemed to be a shift from ileal to colonic location during the observed period.

The rapid increase in incidence rates might support a role for possible environmental factors^[26]. Diet, as a luminal antigen was thought to be an important factor in the pathogenesis of IBD^[1,27]. In the last two decades there has been a change in the lifestyle in Hungary, as the standard way of living including the diet became more "Western". Other possible environmental factors, such as perinatal events, infections in childhood or measles have not been investigated in this study^[26,28,29]. Measles vaccination is universal in Hungary, and the disease is very rare. The birth rate is one of the lowest ones in Europe. Early childhood hygiene is developed, supporting the "oversheltered child" theory^[30].

One of the most important environmental factors considered in the etiology of IBD was smoking^[1,31]. In concordance with previous data we could identify smoking as a protective factor in patients with UC (OR: 0.25). In contrast, smoking increased the risk for CD almost 2-fold.

The percentage of operations in UC in our study was below the 10-20% rate reported in most series. The reason for this could be the more conservative practice in Hungary and also the greater resistance of patients to surgery. The majority of the operations were proctocolectomies with ileal pouch anal anastomosis (IPAA). The proportion of surgically treated patients in CD was similar to that previously published (60-80%). Almost one third of the CD patients had multiple operations.

There is an increased risk of CRC in IBD, but the reported incidence rates varied greatly. Earlier studies from tertiary referral centers reported rather high cumulative incidence rates of CRC (>10% at 20 years, >30% at 30 years). However, it might

reflect referral biases, because of overrepresentation of more serious diseases in these centers that did not represent the usual spectrum of IBD^[32]. In population-based studies, that followed a larger number of patients for a long time, in a certain area, lower CRC rates were reported (5.5% at 20 years, 13.5% at 30 years). The rate of colorectal cancers in our study was similar to that reported in previous population-based studies.

The two most important risk factors were the disease duration and extent (in CD the colonic involvement)^[32,33]. Other factors involved are early age at onset, pharmacotherapy, disease activity (relapsing-chronically active, number and severity of relapses), smoking habits, family history of CRC, the presence of primary sclerosing cholangitis, backwash ileitis. In our study the UC patients with CRC were non-smokers while the two CD patients were smokers during the follow-up, however our numbers were relatively small to make a reasonable conclusion.

Prophylactic colectomy, regular mesalamine and folic acid treatment, and colonoscopic surveillance might reduce the elevated CRC risk^[34,35]. In our study all the patients with IBD and CRC received 5-ASA. In concordance with previous results CRC was diagnosed in only one out of 32 patients with UC and in none of 66 patients with CD taking azathioprine, such azathioprine did not seem to increase cancer risk. Colonoscopic surveillance was the most widely used method to reduce CRC risk, but evidences of its benefits were controversial^[36,37]. We also performed colonoscopic surveillance, which might have reduced cancer risk.

There is an additional increased risk of both colorectal and hepatobiliary malignancies in the subset of patients with primary sclerosing cholangitis (PSC) and IBD^[38]. In our cohort three colorectal carcinomas developed in the 13 PSC patients, showing an increased risk in this subgroup. The reason for the short interval (3 and 6 years) between the diagnosis of CD and colorectal cancer is not clear. One may hypothesize that the asymptomatic course of IBD may be responsible for the early occurrence of colorectal cancers.

In conclusion, the incidence and prevalence have been steadily rising in the last 25 years and Now it reaches the levels reported in Western European countries. We observed no gender differences. There was a relative high incidence of colorectal cancers in IBD, similar to Western countries. The cause of the continuous rapid increase in the incidence of IBD is unknown, but the incidence supports a possible role for environmental (*e.g.* diet, lifestyle) factors.

ACKNOWLEDGEMENT

The authors thank the following doctors for their help in data collection: Gyula David, M.D., Agnes Horvath, M.D. and Tunde Pandur, M.D. (Veszprem), Sandor Meszaros MD, Pal Küronya, M.D. and Csaba Molnar, M.D. (Ajka), Zsuzsa Balogh, M.D. (Papa) and Arpad Tollas, M.D. (Varpalota), and Mrs. Gabriella Deményi for her technical assistance.

REFERENCES

- 1 **Podolsky DK**. Inflammatory bowel disease. *N Engl J Med* 2002; **347**: 417-429
- 2 **Tibble JA**, Bjarnason I. Non-invasive investigation of inflammatory bowel disease. *World J Gastroenterol* 2001; **7**: 460-465
- 3 **Delco F**, Sonnenberg A. Commonalities in the time trends of Crohn's disease and ulcerative colitis. *Am J Gastroenterol* 1999; **94**: 2171-2176
- 4 **Niv Y**, Abuksis G, Fraser GM. Epidemiology of Crohn's disease in Israel: a survey of Israeli Kibbutz Settlements. *Am J Gastroenterol* 1999; **94**: 2961-2965
- 5 **Xia B**, Shivananda S, Zhang GS, Yi JY, Crusius JBA, Peka AS. Inflammatory bowel disease in Hubei province of China. *China Natl J New Gastroenterol* 1997; **3**: 119-120

- 6 **Tsianos EV**, Masalas CN, Merkouropoulos M, Dalekos GN, Logan RF. Incidence of inflammatory bowel disease in north west Greece: rarity of Crohn's disease in an area where ulcerative colitis is common. *Gut* 1994; **35**: 369-372
- 7 **Stewenius J**, Adnerhill I, Ekelund G, Floren CH, Fork FT, Janzon L, Lindstrom C, Mars I, Nyman M, Rosengren JE. Ulcerative colitis and indeterminate colitis in the city of Malmo, Sweden. A 25-year incidence study. *Scand J Gastroenterol* 1995; **30**: 38-43
- 8 **Shivananda S**, Lennard-Jones J, Logan R, Fear N, Price A, Carpenter L, van Blankenstein M. Incidence of inflammatory bowel disease across Europe: is there a difference between north and south? Results of the European Collaborative Study on Inflammatory Bowel Disease (EC-IBD). *Gut* 1996; **39**: 690-697
- 9 **Vucelic B**, Korac B, Sentic M, Milicic D, Hadzic N, Juresa V, Bozikov J, Rotkvic I, Buljevac M, Kovacevic I. Ulcerative colitis in Zagreb, Yugoslavia: incidence and prevalence 1980-1989. *Int J Epidemiol* 1991; **20**: 1043-1047
- 10 **Vucelic B**, Korac B, Sentic M, Milicic D, Hadzic N, Juresa V, Bozikov J, Rotkvic I, Buljevac M, Kovacevic I. Epidemiology of Crohn's disease in Zagreb, Yugoslavia: a ten-year prospective study. *Int J Epidemiol* 1991; **20**: 216-220
- 11 **Salupere R**. Inflammatory bowel disease in Estonia: a prospective epidemiologic study 1993-1998. *World J Gastroenterol* 2001; **7**: 387-388
- 12 **Nagy G**, Minik K, Ujszaszy L, Juhasz L. Epidemiology of inflammatory bowel diseases in Borsod-Abauj-Zemplen county 1963-1992. *LAM* 1994; **4**: 424-430
- 13 **Friedman S**, Rubin PH, Bodian C, Goldstein E, Harpaz N, Present DH. Screening and surveillance colonoscopy in chronic Crohn's colitis. *Gastroenterology* 2001; **120**: 820-826
- 14 **Maratka Z**, Nedbal J, Kocianova J, Havelka J, Kudrman J, Hendl J. Incidence of colorectal cancer in proctocolitis: a retrospective study of 959 cases over 40 years. *Gut* 1985; **26**: 43-49
- 15 **Lakatos L**, Pandur T, David G, Balogh Z, Kuronya P, Tollas A, Lakatos PL. Association of extraintestinal manifestations of inflammatory bowel disease in a province of western Hungary with disease phenotype: results of a 25-year follow-up study. *World J Gastroenterol* 2003; **9**: 2300-2307
- 16 **Lennard-Jones JE**. Classification of inflammatory bowel disease. *Scand J Gastroenterol Suppl* 1989; **170**: 2-6
- 17 **Price AB**. Overlap in the spectrum of non-specific inflammatory bowel disease-„colitis indeterminate”. *J Clin Pathol* 1978; **31**: 567-577
- 18 **Louis E**, Collard A, Oger AF, Degroote E, Aboul Nasr El Yafi FA, Belaiche J. Behaviour of Crohn's disease according to the Vienna classification: changing pattern over the course of the disease. *Gut* 2001; **49**: 777-782
- 19 **Loftus EV Jr**, Silverstein MD, Sandborn WJ, Tremaine WJ, Harmsen WS, Zinsmeister AR. Ulcerative colitis in Olmsted County, Minnesota, 1940-1993: incidence, prevalence, and survival. *Gut* 2000; **46**: 336-343
- 20 **Zheng CQ**, Hu GZ, Zeng ZS, Lin LJ, Gu GG. Progress in searching for susceptibility gene for inflammatory bowel disease by positional cloning. *World J Gastroenterol* 2003; **9**: 1646-1656
- 21 **Kinouchi Y**, Matsumoto K, Negoro K, Takagi S, Takahashi S, Hiwatashi N, Shimosegawa T. Hla-B genotype in Japanese patients with Crohn's disease. *Dis Colon Rectum* 2003; **46**(10 Suppl): S10-14
- 22 **Pena AS**. Genetics of inflammatory bowel diseases-pats present, and future. *Dig Dis* 2003; **21**: 85-90
- 23 **Björnsön S**, Johannsson JH. Inflammatory bowel disease in Iceland, 1990-1994: a prospective, nationwide, epidemiological study. *Eur J Gastroenterol Hepatol* 2000; **12**: 31-38
- 24 **Lindberg E**, Jornerot G. The incidence of Crohn's disease is not decreasing in Sweden. *Scand J Gastroenterol* 1991; **26**: 495-500
- 25 **Stowe SP**, Redmond SR, Stormont JM, Shah AN, Chessin LN, Segal HL, Chey WY. An epidemiological study of inflammatory bowel disease in Rochester, New York. Hospital incidence. *Gastroenterology* 1990; **98**: 104-110
- 26 **Kugathasan S**, Judd RH, Hoffmann RG, Heikenen J, Telega G, Khan F, Weisdorf-Schindele S, San Pablo W Jr, Perrault J, Park R, Yaffe M, Brown C, Rivera-Bennett MT, Halabi I, Martinez A, Blank E, Werlin SL, Rudolph CD, Binion DG. Epidemiologic and clinical characteristics of children with newly diagnosed inflammatory bowel disease in Wisconsin: a statewide population-based study. *J Pediatr* 2003; **143**: 525-531
- 27 **Cashman KD**, Shanahan F. Is nutrition an aetiological factor for inflammatory bowel disease? *Eur J Gastroenterol Hepatol* 2003; **15**: 607-613
- 28 **Delco F**, Sonnenberg A. Exposure to risk factors for ulcerative colitis occurs during an early period of life. *Am J Gastroenterol* 1999; **94**: 679-684
- 29 **Elliman DA**, Bedford HE. Measles, mumps and rubella vaccine, autism and inflammatory bowel disease: advising concerned parents. *Paediatr Drugs* 2002; **4**: 631-635
- 30 **Gilat T**, Hachoen D, Lilos P, Langman MJ. Childhood factors in ulcerative colitis and Crohn's disease. An international cooperative study. *Scand J Gastroenterol* 1987; **22**: 1009-1024
- 31 **Picco MF**, Bayless TM. Tobacco consumption and disease duration are associated with fistulizing and stricturing behaviors in the first 8 years of Crohn's disease. *Am J Gastroenterol* 2003; **98**: 363-368
- 32 **Munkholm P**. Review article: the incidence and prevalence of colorectal cancer in inflammatory bowel disease. *Aliment Pharmacol Ther* 2003; **18** (Suppl 2): 1-5
- 33 **Eaden JA**, Mayberry JF. Colorectal cancer complicating ulcerative colitis: a review. *Am J Gastroenterol* 2000; **95**: 2710-2719
- 34 **Shanahan F**. Review article: colitis-associated cancer – time for new strategies. *Aliment Pharmacol Ther* 2003; **18**(Suppl 2): 6-9
- 35 **Eaden J**. Review article: the data supporting a role for aminosalicylates in the chemoprevention of colorectal cancer in patients with inflammatory bowel disease. *Aliment Pharmacol Ther* 2003; **18** (Suppl 2): 15-21
- 36 **Hata K**, Watanabe T, Kazama S, Suzuki K, Shinozaki M, Yokoyama T, Matsuda K, Muto T, Nagawa H. Earlier surveillance colonoscopy programme improves survival in patients with ulcerative colitis associated colorectal cancer: results of a 23-year surveillance programme in the Japanese population. *Br J Cancer* 2003; **89**: 1232-1236
- 37 **Karlen P**, Kornfeld D, Brostrom O, Lofberg R, Persson PG, Ekblom A. Is colonoscopic surveillance reducing colorectal cancer mortality in ulcerative colitis? A population based case control study. *Gut* 1998; **42**: 711-714
- 38 **Shetty K**, Rybicki L, Brzezinski A, Carey WD, Lashner BA. The risk for cancer or dysplasia in ulcerative colitis patients with primary sclerosing cholangitis. *Am J Gastroenterol* 1999; **94**: 1643-1649

Comparative observation on different intervention procedures in benign stricture of gastrointestinal tract

Ying-Sheng Cheng, Ming-Hua Li, Wei-Xiong Chen, Ni-Wei Chen, Qi-Xin Zhuang, Ke-Zhong Shang

Ying-Sheng Cheng, Ming-Hua Li, Qi-Xin Zhuang, Ke-Zhong Shang, Department of Radiology, Sixth People's Hospital, Shanghai Jiaotong University, Shanghai 200233, China
Wei-Xiong Chen, Ni-Wei Chen, Department of Gastroenterology, Sixth People's Hospital, Shanghai Jiaotong University, Shanghai 200233, China

Supported by the National Key Medical Research and Development Program of China during the 9th Five-year Plan Period, No.96-907-03-04; Shanghai Nature Science Funds, No.02Z1314073; Shanghai Medical Development Funds, No.00419

Correspondence to: Dr. Ying-Sheng Cheng, Department of Radiology, Sixth People's Hospital, Shanghai Jiaotong University, Shanghai 200233, China. chengys@sh163.net

Telephone: +86-21-64368920 **Fax:** +86-21-64701361

Received: 2003-05-13 **Accepted:** 2003-06-02

Abstract

AIM: To determine the most effective intervention procedure by evaluation of mid and long-term therapeutic efficacy in patients of stricture of the gastrointestinal tract (GIT).

METHODS: Different intervention procedures were used to treat benign stricture of GIT in 180 patients including pneumatic dilation (group A, $n=80$), permanent (group B, $n=25$) and temporary (group C, $n=75$) placement of expandable metallic stents.

RESULTS: The diameters of the strictured GIT were significantly greater after the treatment of all procedures employed ($P<0.01$). For the 80 patients in group A, 160 dilations were performed (mean, 2.0 times per patient). Complications in group A included chest pain ($n=20$), reflux ($n=16$), and bleeding ($n=6$). Dysphagia relapse occurred in 24 (30%) and 48 (60%) patients respectively during 6-and-12 month follow-up periods in group A. In group B, 25 uncovered or partially covered or antireflux covered expandable metallic stents were placed permanently, complications included chest pain ($n=10$), reflux ($n=15$), bleeding ($n=3$), and stent migration ($n=4$), and dysphagia relapse occurred in 5 (20%) and 3 patients (25%) during the 6-and-12 month follow-up periods, respectively. In group C, the partially covered expandable metallic stents were temporarily placed in 75 patients and removed after 3 to 7 days via gastroscope, complications including chest pain ($n=30$), reflux ($n=9$), and bleeding ($n=12$), and dysphagia relapse occurred in 9 (12%) and 8 patients (16%) during the 6-and-12 month follow-up periods, respectively. The placement and withdrawal of stents were all successfully performed. The follow-up of all patients lasted for 6 to 96 months (mean 45.3 ± 18.6 months).

CONCLUSION: The effective procedures for benign GIT stricture are pneumatic dilation and temporary placement of partially-covered expandable metallic stents. Temporary placement of partially-covered expandable metallic stents is one of the best methods for benign GIT strictures in mid and long-term therapeutic efficacy.

Cheng YS, Li MH, Chen WX, Chen NW, Zhuang QX, Shang KZ. Comparative observation on different intervention procedures in benign stricture of gastrointestinal tract. *World J Gastroenterol* 2004; 10(3):410-414

<http://www.wjgnet.com/1007-9327/10/410.asp>

INTRODUCTION

Benign stricture of gastrointestinal tract (GIT) is caused by postsurgical anastomoses, ingestion of corrosive agents, simple sclerosis after radiation therapy for tumors, digestive ulcer and functional disturbances, which involve different sites including esophagus, stomach, duodenum, colon and rectum. From July 1994, 180 patients with benign GIT stricture were treated with intervention procedures. Our experiences and follow-up data are reported herein.

MATERIALS AND METHODS

Materials

Our cohort comprised 180 patients with benign GIT stricture (101 males, 79 females; age, 12 to 78 years, mean 48.7 years). The subjects were divided into three groups according to the intervention procedures used: 80 patients with pneumatic dilation (group A), 25 with permanent uncovered or partially covered or antireflux covered metallic stent dilation (group B), and 75 with temporary partially covered metallic stent dilation (group C). Among the 180 patients, 8 had simple sclerosis stricture after radiation therapy for esophageal carcinoma, 132 had achalasia, 32 had esophageal and esophagogastric anastomosis stricture (complicated with anastomosis fistula in two patients), 4 had gastroduodenal anastomosis stricture, and 4 had esophageal chemical corrosive stricture. All patients were examined by barium radiography of GIT and gastroscopy before the intervention procedures.

Methods

The GIT was emptied for at least 4 h before intervention procedures. Bleeding and clotting times were examined. The devices used were as follows. The catheter was an SY dumbbell-like catheter (Sanyuan Medical Instrument Research Institute, Jinan, Shandong, China) with a length of 75 cm. The diameters upon saccule dilation were 28 mm, 30 mm, and 32 mm, and length of the saccule was 8 cm. There were two types of metallic stents, one was an imported covered Z-stent made from stainless steel wire (Wilson-Cook Medical Inc, NC, USA), the other made domestically from nitinol and uncovered or partially covered or antireflux covered (Zhiye Medical Instrument Research Institute, Changzhou, Jiangsu, China; Youyi Yijin Advanced Materials Co. Ltd, Beijing, China). The body of the partially covered metallic stents was coated with intracavity silica gel. The areas within 2 cm of both ends of the stent were not membrane covered. The stents were 4 to 14 cm in length and 16 to 30 mm in diameter, with one or two horns (diameter, 20 to 35 mm).

Patients for pneumatic dilation were placed in a supine or

Table 1 Incidence of complications following treatment with different intervention procedures (%)

Groups	Patient numbers (<i>n</i>)	Number (%) with pain (<i>n</i>)	Number (%) with reflux (<i>n</i>)	Number (%) with bleeding (<i>n</i>)	Number (%) with stent migration (<i>n</i>)
A	80	20 (25.0%)	16 (20.0%)	6 (7.5%)	-
B	25	10 (40.0%)	15 (60.0%)	3 (12.0%)	4 (16.0%)
C	75	30 (40.0%)	9 (12.0%)	12 (16.0%)	-

Table 2 Dysphagia relapse rate during follow-up

Group	6 months follow-up		12 months follow-up	
	Number tested (<i>n</i>)	Number (%) with DR (<i>n</i>)	Number tested (<i>n</i>)	Number (%) with DR(<i>n</i>)
A	80	24(30%)	80	48(60%)
B	25	5(20%)	12	3(25%)
C	75	9(12%)	50	8(16%)

DR: dysphagia relapse.

sitting position. Surface anesthesia was first applied to the pharynx. The guidewire was inserted through the mouth and passed through the stricture section as demonstrated by X-ray examination. The catheter with a diameter of 28 mm was introduced through the region of benign esophageal stricture via the guidewire, with the center of sacculi at the most-strictered section. The sacculi was injected using an injector with the diluted contrast medium or gas. Under fluoroscopy and according to the pain reaction of the patient, pressurization was applied to gradually dilate the sacculi. The central portion of the sacculi was dumbbell-shaped. When further pressurization flattened the surface of the sacculi or when the pressure did not further change, the piston was turned off. The pressure of the sacculi was maintained for 5 to 30 min. After the sacculi pressure had reduced for 5 min, pressurization was again applied. Typically each treatment involved 3 to 5 dilations, and then the catheter was withdrawn. The second and third treatments with graded pneumatic dilation were carried out using dilators with diameters of 30 mm and 32 mm, respectively. In some patients, the treatment was conducted every 2 weeks until clinical symptoms disappeared.

The placement of metallic stents was performed as follows. In upper GIT, lidocaine (1%) was first sprayed (as a mist) for anaesthesia on the pharynx. Patients were placed in a sitting position or lying on the side. Applicable false tooth were removed and a tooth bracket was mounted. A 260 cm long exchange guidewire was inserted into the stomach. The stent was mounted on the propeller whose front end was coated with sterilized liquid paraffin. Guided by the wire, the propeller on which the stent was mounted was moved through the section of pathological change. Under fluoroscopic control, the outer sheath was slowly withdrawn and the stent was expanded under its own tension. After placing a stent, GIT radiography was performed to observe the patency of the GIT. In group C, 500 to 1 000 ml ice-cold water was injected via a bioptic hole under gastroscopy for 3 to 7 days after stent placement, which resulted in retraction of the stent and reduced its diameter. Bioptic pliers were then used to withdraw the stent using a gastroscopy. Gastroscopy was performed again to detect complications, such as bleeding, mucosa tearing, or perforation. Patients returned to the ward and consumed cold drinks and liquid food for 2 days before resuming a normal diet. It was preferable for patients to eat solid food since the natural expansion of the food reduced the retraction of the GIT. The criterion for therapeutic efficacy was the diameter of the most-strictered gastrointestinal segment before and after dilation.

For postoperative treatment of pneumatic dilation, barium radiography of the GIT was performed immediately after

intervention procedure to observe the patency of the GIT and check the presence of perforations and submucous hematoma. Patients drank fluids 2 h after intervention procedure and were treated with antibiotics, antacids, antireflux drugs, and analgesics. For postoperative treatment of stent placement, barium radiography was used to observe the patency of the GIT. Patients ate semisolid food on the day following intervention procedure. Within one week after stent removal, barium radiography of the GIT was again used to observe the patency of the GIT. Patients were followed-up by telephone and out-patients after 1 month, 6 months, 1 year.

RESULTS

The diameters of the strictured GIT were significantly greater after the treatment of all procedures employed ($P < 0.01$). The 80 patients in group A involved 160 dilations (mean 2.0 times per patient). Among them, five graded dilations of increasing diameters were performed in 1 patient, three in 29 patients, two in 18 patients and a single dilation in 32 patients. In the 25 patients of group B, uncovered or partially covered or antireflux covered stents were placed. Stent placement was successful in 100% of the patients. In the 75 patients of group C, 75 partially covered stents were placed and removed under gastroscopy guidance 3 to 7 days after intervention procedure. The success rate of stent placement and extraction was 100%. The complications of the treatment are listed in Table 1, and the relapse rates of dysphagia are listed in Table 2.

DISCUSSION

Benign stricture of the GIT is a common complication of gastrointestinal diseases. Its causes are diverse, its treatment is usually difficult. The procedures used included surgery, bougienage, pneumatic dilation, permanent metallic and temporary metallic stent dilation, each having their own advantages and drawbacks^[1-7]. Bougienage is now uncommon since it has a poor therapeutic efficacy and many complications. The use of surgery is declining due to the associated large lesion, high risk, and high relapse rate, but it is still one of the most common methods of treatment. Pneumatic dilation was primarily used in the plasty of angiodysplasia, and then applied gradually to other organs for its reliable therapeutic efficacy. It exhibits a remarkable therapeutic efficacy when used in benign esophageal stricture. Currently, it has been widely used in the nonsurgical treatment of benign GIT stricture. According to most authors^[8-31], the graded dilation is more effective than single dilation.

Permanent metallic stent dilation was primarily used in the treatment of malignant obstruction of the GIT, and exhibited a remarkable palliative therapeutic efficacy^[32-40]. Cwikiel *et al*^[2] reported an experimental and clinical study of the treatment of benign esophageal stricture with expandable metallic stents. We used uncovered or partially covered or antireflux covered stents in 25 patients of benign GIT stricture in order to reduce the possibility of stent migration. After placement of the uncovered stent, dilation of the stricture was excellent and dysphagia disappeared. Thus we achieved the treatment goal. However, the patients were accompanied by new problems including gastroesophageal reflux or biliary regurgitation, followed by occurrence of restenosis (hyperplasia of granulation tissue). Reflux could be treated with drugs, but this took a long time. Restenosis was reduced after cauterization using hot-point therapy under gastroscope guidance, but it was easy to relapse. Even though an antireflux stent was used, many unexpected results appeared. These difficulties led to dilation using temporary partially covered metallic stents. After their clinical trials, they not only produced fewer complications, but also exhibited excellent therapeutic efficacy. Now their use has been gradually accepted by clinicians.

For the temporary metallic stents, optimal placement time remains to be determined. If the therapeutic efficacy is poor, stents cannot be easily removed after a long-time placement. Usually, the stents are placed within 1 week. Cwikiel *et al*^[2] placed a covered metallic stent in the esophagus of the pigs in an experimental study. One week later, granulation tissue grew and merged with the noncovered area of the stent, resulting in difficulties for removing the stent. The stent could not be removed following the placement for 10 to 14 days or longer. By our experience, stent migration occurred mostly within 1 week. Therefore, after the placement of a partially covered metallic stent, it should be extracted within 1 week. In our series, the stent was easily removed on the third to fourth day, but this became quite difficult on the fifth day, and extremely difficult after 6 to 7 days. Song *et al*^[3] reported the removal of a stent 2 months after its placement. In such patients the stent should be completely coated (including its outer layer) so that granulation tissue cannot grow into the lumen. However, the use of this type of stent should be limited to patients with tumor, since in patients of benign GIT stricture, it migrates easily. In terms of the degree of acceptance of patients, therapeutic efficacy, extent of tissue lesion, and incidence of complications, the best method for malignant stricture or obstruction of the GIT is the partially covered metallic stent, and for benign stricture of the GIT, graded pneumatic dilation or temporary partially covered metallic stent dilation should be recommended^[41-45].

Sixty percent of patients with the follow-up of 1 year or longer had dysphagia relapse, demonstrating that pneumatic dilation of benign stricture of the GIT had an excellently immediate therapeutic efficacy but a poor mid and long-term therapeutic efficacy. First, this was associated with the diameter of sacculae. Kadakia *et al*^[4] suggested that the diameter of the sacculae in pneumatic dilation should be 35 to 45 mm, but the incidence of complications was very high (*e.g.*, 15% presented esophageal perforation). We used sacculae with a diameter of 28 to 32 mm in order to reduce the incidence of serious complications, but the mid and long-term therapeutic efficacy was not satisfactory. Second, the therapeutic efficacy was associated with the frequency of dilation. One dilation did not produce excellent therapeutic efficacy, since it was affected by various factors such as the correct location of the sacculae pressure applied to the sacculae, and variations in the anatomy of GIT. The graded dilation was suggested by most authors. Third, the therapeutic efficacy was associated to the course of the disease. When the course was long, the GIT muscularis would

become fleshy and lose elasticity.

Permanent uncovered or partially covered metallic stents were used in the treatment of malignant stricture or obstruction of the GIT with excellently immediate therapeutic efficacy and poor mid and long-term therapeutic efficacy. This was mainly due to tumor growth. Since uncovered or partially covered metallic stents could only provide palliative treatment for the obstruction, only by adopting a combined therapy for the tumor, can mid and long-term therapeutic efficacy be achieved. In our series, permanent uncovered or partially covered or antireflux covered metallic stent dilations were used in 25 patients of benign GIT stricture, their immediate therapeutic efficacy was excellent and the mid and long-term efficacies were unsatisfactory. The poor mid and long-term outcome for permanent uncovered metallic stent dilation was mainly due to frequent gastroesophageal reflux or biliary regurgitation and restenosis. Three uncovered stents could not be extracted after a 12-month follow-up period, and hence the cardia had to be excised with the stent and surgically reconstructed. Therefore, permanent uncovered metallic stent dilation was not suitable for patients with functional GIT stricture^[46-49]. Permanent partially covered metallic stent dilation had poor mid and long-term therapeutic effects. This was mainly due to reflux and stent migration. Temporary partially covered metallic stent dilation used for benign GIT stricture resulted in excellent immediate effect, thus becoming the best method for mid and long-term therapeutic efficiencies. First, design of the stent coincided with the physiological structure of the gastrointestinal tract and the specific pathological manifestations of the benign stricture. The upper outlet of the stent was a large horn without cover, increasing stability of the stent. However, this made removal of the stent more difficult. Second, the diameter of the stents used in this group was 16 to 30 mm. Upon stent dilation, the stricture returned almost to the maximum normal diameter of gastrointestinal dilation. Third, the duration of dilation was very long, with a typical period of stent placement for 3 to 7 days. Why was the therapeutic efficacy of temporary partially covered metallic stent dilation better than that of pneumatic dilation? We thought that this was mainly due to the stent expanding the strictured gastrointestinal region, causing chronic tearing of the strictured wall muscularis. As a stent gradually expanded with the body temperature of the patient, it took 12 to 24 h for a stent to reach 36 °C. The stent thus expanded completely to reach the expected diameter. In our consideration, the wall muscularis was torn regularly by the metallic stent, and scars were relatively few when repaired. This resulted in a markedly lower incidence of restenosis compared to that for pneumatic dilation.

Table 3 Strategies of intervention procedure for different benign strictures in upper gastrointestinal tract

Types of GIT stricture	Strategies
AS	TCSD > PD > PCSD > PUCSD
AS with fistula	PCSD > TCSD
New scar stricture	TCSD > PD > PCSD
Scar stricture	PCSD > TCSD > PD
Functional stricture (achalasia)	TCSD > PD > PCSD with antireflux

AS: anastomosis stricture, TCSD: temporary covered stent dilation, PD: pneumatic dilation, PCSD: permanent covered stent dilation, PUCSD: permanent uncovered stent dilation.

With different intervention procedures compared in consideration of the extents of lesion, incidences of complication, therapeutic efficacies, and degrees of acceptance of patients,

we found that partially covered metallic stents could provide excellent therapeutic effect. However, different strategies should be adopted to different types of lesion (Table 3). Development of biologically removable stents, which can be catabolized in 2 months after their placement, may provide a much longer retention time with no necessity for extraction^[50-56].

REFERENCES

- 1 **Cheng YS**, Shang KZ, Zhuang QX, Li MH, Xu JR, Yang SX. Interventional therapy and cause of restenosis of esophageal benign stricture. *Huaren Xiaohua Zazhi* 1998; **6**: 791-794
- 2 **Cwikiel W**, Willen R, Stridbeck H, Liol G, Von Holstein CS. Self-expanding stent in the treatment of benign esophageal strictures: experimental study in pigs and presentation of clinical cases. *Radiology* 1993; **187**: 667-671
- 3 **Song HY**, Park SI, Do YS, Yoon HK, Sung KB, Sohn KH, Min YI. Expandable metallic stent placement in patients with benign esophageal strictures: results of long-term follow-up. *Radiology* 1997; **203**: 131-136
- 4 **Kadakia SC**, Wong RK. Graded pneumatic dilation using Rigidflex achalasia dilators in patients with primary esophageal achalasia. *Am J Gastroenterol* 1993; **88**: 34-38
- 5 **Cheng YS**, Yang RJ, Mao AW, Zhuang QX, Shang KZ. Common complications of stent insertion in patients with GI tract stricture or obstruction. *Huaren Xiaohua Zazhi* 1998; **6**: 856-858
- 6 **Huang QH**, Jin ZD, Xu GM. Ultrasonographic endoscopy and microultrasound probe in the diagnosis and treatment of cardiac achalasia. *Shijie Huaren Xiaohua Zazhi* 1999; **7**: 787-788
- 7 **Shang KZ**, Cheng YS, Wu CG, Zhuang QX. Pharyngoesophageal dynamic imaging in diagnosis of patients with deglutition disorders. *Shijie Huaren Xiaohua Zazhi* 1999; **7**: 52-54
- 8 **Lisy J**, Hetkova M, Snajdauf J, Vyhnanek M, Tuma S. Long-term outcomes of balloon dilation of esophageal strictures in children. *Acad Radiol* 1998; **5**: 832-835
- 9 **Chawda SJ**, Watura R, Adams H, Smith PM. A comparison of barium swallow and erect esophageal transit scintigraphy following balloon dilation for achalasia. *Dis Esophagus* 1998; **11**: 181-188
- 10 **Yoneyama F**, Miyachi M, Nimura Y. Manometric findings of the upper esophageal sphincter in esophageal achalasia. *World J Surg* 1998; **22**: 1043-1047
- 11 **Katz PO**, Gilbert J, Castell DO. Pneumatic dilatation is effective long-term treatment for achalasia. *Dig Dis Sci* 1998; **43**: 1973-1977
- 12 **Vaezi MF**, Richter JE. Current therapies for achalasia: comparison and efficacy. *J Clin Gastroenterol* 1998; **27**: 21-35
- 13 **Khan AA**, Shah SW, Alam A, Butt AK, Shafqat F, Castell DO. Pneumatic balloon dilation in achalasia: a prospective comparison of balloon distention time. *Am J Gastroenterol* 1998; **93**: 1064-1067
- 14 **Muehldorfer SM**, Schneider TH, Hochberger J, Martus P, Hahn EG, Ell C. Esophageal achalasia: intrasphincteric injection of botulinum toxin A versus balloon dilation. *Endoscopy* 1999; **31**: 517-521
- 15 **Beckingham IJ**, Callanan M, Lonw JA, Bornman PC. Laparoscopic cardiomyotomy for achalasia after failed balloon dilation. *Surg Endosc* 1999; **13**: 493-496
- 16 **Seelig MH**, DeVault KR, Seelig SK, Klingler PJ, Branton SA, Floch NR, Bammer T, Hinder RA. Treatment of achalasia: recent advances in surgery. *J Clin Gastroenterol* 1999; **28**: 202-207
- 17 **Khan AA**, Shah SW, Alam A, Butt AK, Shafqat F, Castell DO. Massively dilated esophagus in achalasia: response to pneumatic balloon dilation. *Am J Gastroenterol* 1999; **94**: 2363-2366
- 18 **Panaccione R**, Gregor JC, Reynolds RP, Preiksaitis HG. Intrasphincteric botulinum toxin versus pneumatic dilatation for achalasia: a cost minimization analysis. *Gastrointest Endosc* 1999; **50**: 492-498
- 19 **Gideon RM**, Castell DO, Yarze J. Prospective randomized comparison of pneumatic dilatation technique in patients with idiopathic achalasia. *Dig Dis Sci* 1999; **44**: 1853-1857
- 20 **Singh V**, Duseja A, Kumar A, Kumar P, Rai HS, Singh K. Balloon dilatation in achalasia cardia. *Trop Gastroenterol* 1999; **20**: 68-69
- 21 **Vaezi MF**. Achalasia: diagnosis and management. *Semin Gastrointest Dis* 1999; **10**: 103-112
- 22 **Gaudric M**, Sabate JM, Artru P, Chaussade S, Couturier D. Results of pneumatic dilatation in patients with dysphagia after antireflux surgery. *Br J Surg* 1999; **86**: 1088-1091
- 23 **Vaezi MF**, Baker ME, Richter JE. Assessment of esophageal emptying post-pneumatic diation: use of the timed barium esophagram. *Am J Gastroenterol* 1999; **94**: 1802-1807
- 24 **Torbey CF**, Achkar E, Rice TW, Baker M, Richter JE. Long-term outcome of achalasia treatment: the need for closer follow-up. *J Clin Gastroenterol* 1999; **28**: 125-130
- 25 **Metman EH**, Lagasse JP, d'Alteroche L, Picon L, Scotto B, Barbieux JP. Risk factors for immediate complications after progressive pneumatic dilation for achalasia. *Am J Gastroenterol* 1999; **94**: 1179-1185
- 26 **Vaezi MF**, Richter JE, Wilcox CM, Schroeder PL, Birgisson S, Slaughter RL, Koehler RE, Baker ME. Botulinum toxin versus pneumatic dilation in the treatment of achalasia: a randomised trial. *Gut* 1999; **44**: 231-239
- 27 **Smout AJ**. Back to the whale bone. *Gut* 1999; **44**: 149-150
- 28 **Alonso P**, Gonzalez-Conde B, Macenlle R, Pita S, Vazquez-Iglesias JL. Achalasia: the usefulness of manometry for evaluation of treatment. *Dig Dis Sci* 1999; **44**: 536-541
- 29 **Prakash C**, Freedland KE, Chan MF, Clouse RE. Botulinum toxin injections for achalasia symptoms can approximate the short term efficacy of a single pneumatic dilation: a survival analysis approach. *Am J Gastroenterol* 1999; **94**: 328-333
- 30 **Horgan S**, Pellegrini CA. Botulinum toxin injections for achalasia symptoms. *Am J Gastroenterol* 1999; **94**: 300-301
- 31 **Hamza AF**, Awad HA, Hussein O. Cardiac achalasia in children. Dilatation or surgery? *Eur J Pediatr Surg* 1999; **9**: 299-302
- 32 **De Palma GD**, Catanzano C. Removable self-expanding metal stents: a pilot study for treatment of achalasia of the esophagus. *Endoscopy* 1998; **30**: S95-96
- 33 **Kozarek RA**. Esophageal stenting-when should metal replace plastic? *Endoscopy* 1998; **30**: 575-577
- 34 **Ell C**, May A. Self-expanding metal stents for palliation of stenosing tumors of the esophagus and cardia: a critical review. *Endoscopy* 1997; **29**: 392-398
- 35 **Ell C**, May A, Hahn EG. Self-expanding metal endoprosthesis in palliation of stenosing tumors of the upper gastrointestinal tract. Comparison of experience with three stent types in 82 implantations. *Dtsch Med Wochensch* 1995; **120**: 1343-1348
- 36 **Yates MR 3rd**, Morgan DE, Baron TH. Palliation of malignant gastric and small intestinal strictures with self-expandable metal stents. *Endoscopy* 1998; **30**: 266-272
- 37 **De Gregorio BT**, Kinsman K, Katon RM, Morrison K, Saxon RR, Barton RE, Keller FS, Rosch J. Treatment of esophageal obstruction from mediastinal compressive tumor with covered, self-expanding metallic Z-stents. *Gastrointest Endosc* 1996; **43**: 483-489
- 38 **Spinelli P**, Cerrai FG, Dal Fante M, Mancini A, Meroni E, Pizzetti P. Endoscopic treatment of upper gastrointestinal tract malignancies. *Endoscopy* 1993; **25**: 675-678
- 39 **Pinto IT**. Malignant gastric and duodenal stenosis: palliation by peroral implantation of a self-expanding metallic stent. *Cardiovasc Intervent Radiol* 1997; **20**: 431-434
- 40 **Strecker EP**, Boos I, Husfieldt KJ. Malignant duodenal stenosis: palliation with peroral implantation of a self-expanding nitinol stent. *Radiology* 1995; **196**: 349-351
- 41 **Acunas B**, Poyanli A, Rozanes I. Intervention in gastrointestinal tract: the treatment of esophageal, gastroduodenal and colorectal obstructions with metallic stents. *Eur J Radiol* 2002; **42**: 240-248
- 42 **Wan XJ**, Li ZS, Xu GM, Wang W, Zhang W, Wu RP. Pathologic study on esophagus after "Z" and "reticular" stenting. *Shijie Huaren Xiaohua Zazhi* 2000; **8**: 5-9
- 43 **Wan XJ**, Li ZS, Xu GM, Wang W, Zhan XB, Liu J. Study on changes of mucosal blood flow and permeability after esophageal "Z" stenting. *Shijie Huaren Xiaohua Zazhi* 2000; **8**: 10-14
- 44 **Mao AW**, Gao ZD, Yang RJ, Jiang WJ, Cheng YS, Fan H, Jiang TH. Malignant obstruction of digestology tract of 198 cases with stent. *Shijie Huaren Xiaohua Zazhi* 2000; **8**: 369-370
- 45 **Mauro MA**, Koehler RE, Baron TH. Advances in gastrointestinal intervention: the treatment of gastroduodenal and

- colorectal obstructions with metallic stents. *Radiology* 2000; **215**: 659-669
- 46 **Chen WX**, Cheng YS, Yang RJ, Li MH, Zhuang QX, Chen NW, Xu JR, Shang KZ. Interventional therapy of achalasia with temporary metal internal stent dilatation and its intermediate and long term follow-up. *Shijie Huaren Xiaohua Zazhi* 2000; **8**: 896-899
- 47 **Cheng YS**, Shang KZ. Gastrointestinal imageology in China: a 50 year evolution. *Shijie Huaren Xiaohua Zazhi* 2000; **8**: 1225-1232
- 48 **Cheng YS**, Yang RJ, Li MH, Shang KZ, Chen WX, Chen NW, Chu YD, Zhuang QX. Interventional procedure for benign or malignant stricture or obstruction of upper gastrointestinal tract. *Shijie Huaren Xiaohua Zazhi* 2000; **8**: 1354-1360
- 49 **Chen WX**, Cheng YS, Yang RJ, Li MH, Shang KZ, Zhuang QX, Chen NW. Metal stent dilation in the treatment of benign esophageal stricture by interventional procedure: a follow-up study. *Shijie Huaren Xiaohua Zazhi* 2002; **10**: 333-336
- 50 **Shang KZ**, Cheng YS. Making more attention to issue of swallowing disorders. *Shijie Huaren Xiaohua Zazhi* 2002; **10**: 1241-1242
- 51 **Cheng YS**, Shang KZ. Interventional therapy in dysphagia. *Shijie Huaren Xiaohua Zazhi* 2002; **10**: 1312-1314
- 52 **Therasse E**, Oliva VL, Lafontaine E, Perreault P, Giroux MF, Soulez G. Balloon dilation and stent placement for esophageal lesions: indications, methods, and results. *Radiographics* 2003; **23**: 89-105
- 53 **Zhong J**, Wu Y, Xu Z, Liu X, Xu B, Zhai Z. Treatment of medium and late stage esophageal carcinoma with combined endoscopic metal stenting and radiotherapy. *Chin Med J* 2003; **116**: 24-28
- 54 **Sakakura C**, Hagiwara A, Kato D, Deguchi K, Hamada T, Itoi Y, Mitsufuji S, Kashima K, Yamagishi H. Successful treatment of intractable esophagothoracic fistula using covered self-expandable stent. *Hepatogastroenterology* 2003; **50**: 77-79
- 55 **Dormann AJ**, Eisendrath P, Wigglinghaus B, Huchzermeyer H, Deviere J. Palliation of esophageal carcinoma with a new self-expanding plastic stent. *Endoscopy* 2003; **35**: 207-211
- 56 **Keymling M**. Colorectal stenting. *Endoscopy* 2003; **35**: 234-238

Edited by Su Q and Wang XL

Survivin expression induced by doxorubicin in cholangiocarcinoma

Qing Chang, Zheng-Ren Liu, Da-Yu Wang, Manoj Kumar, Yi-Bei Chen, Ren-Yi Qin

Qing Chang, Zheng-Ren Liu, Da-Yu Wang, Manoj Kumar, Yi-Bei Chen, Ren-Yi Qin, Department of Surgery, Tongji Hospital, Tongji Medical College, Huazhong University of Science and Technology, Wuhan 430030, Hubei Province, China

Supported by National Natural Science Foundation of China, No. 30271473

Correspondence to: Professor Ren-Yi Qin, Department of Surgery, Tongji Hospital, Tongji Medical College, Huazhong University of Science and Technology, Wuhan 430030, Hubei Province, China. ryqin@tjh.tjmu.edu.cn

Telephone: +86-27-83662389

Received: 2003-08-06 **Accepted:** 2003-10-07

Abstract

AIM: To study the role of survivin expression induced by chemotherapy agent (doxorubicin) in the development and anti-chemotherapy of cholangiocarcinoma.

METHODS: Expression of survivin was detected by SP immunohistochemical technique in 33 cases of cholangiocarcinoma, 28 cases of adjacent noncancerous bile duct, and 5 cases of benign bile duct lesions. Low concentration of doxorubicin (0.05 mg/l) was added in cultured cholangiocarcinoma cell line (QBC939). The expression of survivin was detected by RT-PCR and Western blot at 24 h and 48 h after adding doxorubicin.

RESULTS: Survivin was expressed in 24 of 33 cholangiocarcinoma cases (72.7%). In contrast, no expression of survivin in adjacent noncancerous and benign bile duct lesions was observed ($P < 0.01$). No correlation was found between survivin expression and clinical features. Doxorubicin could markedly ($P < 0.001$) up-regulate survivin mRNA and protein expression of QBC939 cells.

CONCLUSION: Overexpression of survivin in cholangiocarcinomas may play an important role in the development of cholangiocarcinoma, its relationship with prognosis of cholangiocarcinoma deserves further investigation. Higher expression of survivin is induced by doxorubicin in QBC939. Survivin expression may resist apoptosis induced by chemotherapy agents.

Chang Q, Liu ZR, Wang DY, Kumar M, Chen YB, Qin RY. Survivin expression induced by doxorubicin in cholangiocarcinoma. *World J Gastroenterol* 2004; 10(3):415-418

<http://www.wjgnet.com/1007-9327/10/415.asp>

INTRODUCTION

Survivin, a member of the inhibitors of apoptosis protein (IAP) family, is characterized by a unique structure that discriminates it from other members of the IAP family. It contains only a single BIR repeat and lacks a carboxy terminal RING finger domain. Survivin is expressed in the G₂/M phase of cell cycle in a cycle-regulated manner^[1]. It directly binds to and inhibits both Caspase-3 and Caspase-7 activity, leading to arrest of apoptosis^[2].

Survivin expression is not detectable in differentiated normal adult cells of any organ^[3], but it is abundantly expressed in embryonic tissues and in a wide range of cancer tissues^[4] including neuroblastoma^[5], colorectal^[6], stomach^[7] and breast^[8] carcinomas. It has been demonstrated recently that survivin is also frequently expressed in malignant pancreatic ductal tumors^[9] and pancreatic adenocarcinoma^[10]. Furthermore, the prognostic value of survivin expression has been reported in several human cancers^[11].

Inducing apoptosis is the mechanism of chemotherapy agents killing tumor cells. But tumor cells resist chemotherapy agents because not only they overexpress MDR1/P-glycoprotein (P-gp) but also resist apoptosis induced by chemotherapy agents. Studies demonstrating resistance of survivin-transfected cells to anticancer drug-induced apoptosis^[2] and sensitization to chemotherapy by survivin antisense treatment^[12] have shown that survivin is implicated in sensitization to chemotherapy.

But in cholangiocarcinoma, survivin distribution and its implication for apoptosis inhibition are not clear at present. This study aimed to study the role of survivin expression induced by chemotherapy agent (doxorubicin) in the development and anti-chemotherapy of cholangiocarcinoma.

MATERIALS AND METHODS

Materials

Thirty-three specimens were obtained from patients with cholangiocarcinoma at the Department of General Surgery, Tongji Hospital of Tongji Medical College during the period from 1993 to 2001. There were 21 males and 12 females, and the mean age of the patients was 55.1 years (range from 34 to 79 years). The patients did not receive chemotherapy, radiation therapy or immunotherapy before surgery. Five specimens of benign bile duct lesions were also obtained. Formalin-fixed, paraffin-embedded blocks of tissue samples were taken from pathological archives. Serial sections of 4 μm were prepared from the cut surface of the blocks at the maximum cross-section of the tissue sample. Representative sections were stained with H&E in order to confirm the histopathological diagnosis. Human extrahepatic cholangiocarcinoma cell line QBC939 was established by Professor Wang SG (Third Military Medical University, China) and offered to us as a gift^[13]. The cells were maintained as monolayers in RPMI 1640 medium supplemented with 10% fetal bovine serum (FBS, Gibco, USA), 100 units/ml penicillin and 100 mg/ml streptomycin in a humidified atmosphere of 50 mL/L CO₂ at 37 °C.

Methods

Immunohistochemical staining Immunohistochemical staining was carried out with the SP technique using the SP kit (Zhongshan Biotech Co., Beijing, China) after antigen retrieval by microwave pretreatment. Briefly, deparaffinized sections were immersed in a 0.1 M sodium citrate buffer (pH 6.0) and heated three times for 5 min each at a 15 min interval in a microwave oven at 600 W. After quenched in 3 % hydrogen peroxide and blocked, the sections were incubated with rabbit survivin polyclonal antibody (Neomarkers, USA; dilution 1:200) overnight at 4 °C. Biotinylated antirabbit immunoglobulin and streptavidin conjugated to horseradish peroxidase were

subsequently applied. Finally, 3', 3'-diaminobenzidine was used for color development, and hematoxylin was used for counterstaining. As a negative control, the sections were processed in the absence of primary antibody. Tissue sections from a hepatocellular carcinoma with a known strong expression of survivin were used as a positive control. A scoring method was used to quantitate the survivin expression in various samples examined. A mean percentage of positive tumor cells was determined in at least five areas at $\times 400$ magnification. Patients with scores of less than 5% were defined as negative, otherwise they were defined as positive.

RT-PCR Low concentration of doxorubicin (0.05 mg/l, Pharmacia & Upjohn Co. Ltd.) was added in cultured cholangiocarcinoma cell line (QBC939). Expression of survivin was detected by RT-PCR before adding doxorubicin and at 24 h and 48 h after adding doxorubicin. Total RNA was prepared from subconfluent cultures with TRIzol reagent (Gibco, USA) according to the manufacture's instructions. The primers were designed to amplify a fragment of survivin cDNA based on the reported sequence for human survivin. To normalize the amount of input RNA, RT-PCR was performed with primers for constitutively expressed β -actin gene. The survivin primers were 5' -CCCCATAGAGAACATAAAA-3' (sense) and 5' -GGAATAAACCTGGAAGTG-3' (antisense), giving rise to a 273 base pair polymerase chain reaction product. The β -actin primers were 5' -GTGCGTGACATTAAGGAG-3' (sense) and 5' -CTAAGTCATAGTCCGCCT-3' (antisense), giving rise to a 520 base pair polymerase chain reaction product. The first strand cDNA synthesis and the subsequent PCR were performed with RNA PCR kit (AMV) using a programmed temperature control system set for 35 cycles, each consisting of denaturation at 94 °C for 45 s, annealing at 50 °C for 45 s, and extension at 72 °C for 45 s. Ten μ L reaction mixture was electrophoresed on a 1.5% agarose gel, and the PCR products were visualized by ethidium bromide staining and quantified by an ImageQuant software. Survivin mRNA expression level was determined by survivin/ β -actin protein.

Western blot Low concentration of doxorubicin (0.05 mg/l) was added in cultured cholangiocarcinoma cell line (QBC939). Expression of survivin was detected by Western blot before adding doxorubicin and at 24 h and 48 h after adding doxorubicin. Total cells were lysed with cell-lysis buffer [50 mM Tris-Cl, pH 8.0, 150 mM NaCl, 0.02% NaN_3 , 0.1% SDS, 100 μ g/ml PMSF, 1 μ g/ml Aprotinin, 1% NP-40]. Twenty μ g of protein was separated on 10% of SDS-PAGE gels and transferred to NC membranes. After blocked with 5% non-fat milk, the membranes were incubated with rabbit survivin polyclonal antibody (1:1 000 dilution) at 4 °C overnight. After washed three times the membranes were incubated with goat anti-rabbit IgG at room temperature for 1 hour. The signals were developed with the ECL kit (Amersham Pharmacia Biotechnology Inc.).

Statistical analysis

Association between survivin expression and various clinical and pathological variables was examined using χ^2 test or Fisher's exact test. The data of PCR and Western blot were expressed as mean \pm SD. Student's *t*-test was used for statistical analysis. $P < 0.05$ was considered statistically significant.

RESULTS

Expression of survivin and associated clinicopathological variables

Survivin was prominently found in 24 of 33 cholangiocarcinoma cases (72.7%) by immunohistochemistry. Positive staining for survivin was located in the cytoplasm of tumor cells (Figure

1). In contrast, expression of survivin was observed neither in adjacent noncancerous bile ducts nor in benign bile duct lesions ($P < 0.01$). No correlation was found between survivin expression and clinical features (Table 1).

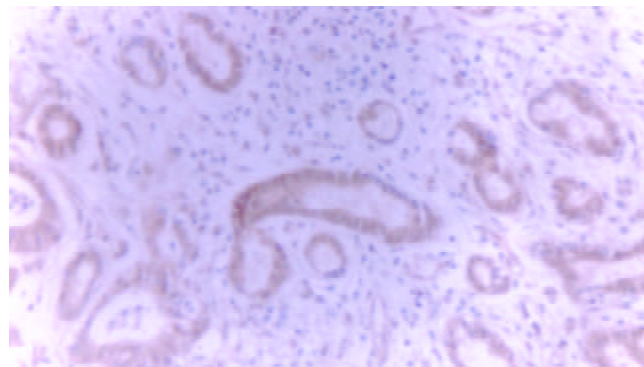


Figure 1 Expression of survivin in cholangiocarcinoma ($\times 200$, SP).

Table 1 Correlation between clinicopathological factors and survivin expression in cholangiocarcinoma

Clinical features	n	Survivin expression		χ^2	P
		n	%		
All patients	33	24	72.7		
Age (years)					
≤ 60	18	13	72.2	0.0051	0.9431
> 60	15	11	73.5		
Sex					
Male	21	15	71.4	0.0491	0.8246
Female	12	9	75.0		
Tumor size (cm)					
≤ 2	13	10	76.9	0.1904	0.6626
> 2	20	14	70.6		
Differentiation level					
High & Middle	29	21	72.4	0.0119	0.9133
Low	4	3	75.0		
Metastasis					
Positive	7	5	71.4	0.0076	0.9307
Negative	26	19	73.1		

Expression level of survivin mRNA

Doxorubicin could markedly ($P < 0.001$) up-regulate survivin mRNA expression of QBC939 cells (Figure 2, Table 2).

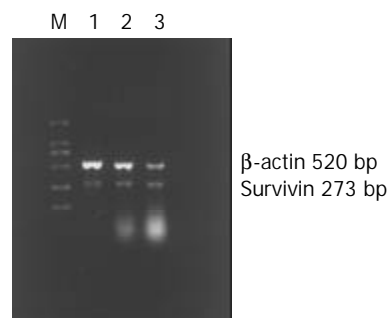


Figure 2 Expression of survivin in a human cholangiocarcinoma cell line. β -actin served as control. M: DL2 000 marker, 1: Normal Qbc939, 2: 24 h after adding doxorubicin, 3: 48 h after adding doxorubicin.

Table 2 Expression level of survivin mRNA

Group	n	Survivin/ β -actin	t	P
A	7	0.4210 \pm 0.0551	^b t=45.89, ^d t=12.54	^b P, ^d P<0.001
B	7	0.8481 \pm 0.0713	^b t=26.11	^b P<0.001
C	7	1.7034 \pm 0.0493		

Survivin mRNA expression level was determined by survivin/ β -actin protein. Data were expressed as mean \pm SD, b vs C (48 h after adding doxorubicin), d vs B (24 h after adding doxorubicin), A: Normal Qbc939.

Expression level of survivin protein

Doxorubicin could markedly ($P<0.001$) up-regulate survivin protein expression of QBC939 cells (Figure 3, Table 3).

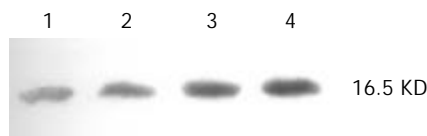


Figure 3 Expression of survivin in a human cholangiocarcinoma cell line. 1 and 2: Normal Qbc939, 3: 24 h after adding doxorubicin, 4: 48 h after adding doxorubicin.

Table 3 Expression level of survivin protein

Group	n	OD value	t	P
A	6	204.568 \pm 1.387	^b t=17.99, ^d t=11.23	^b P, ^d P<0.001
B	6	311.105 \pm 1.539	^b t=11.02	^b P<0.001
C	6	339.989 \pm 1.872		

Data were expressed as mean \pm SD, b vs C (48 h after adding doxorubicin), d vs B (24 h after adding doxorubicin), A: Normal Qbc939.

DISCUSSION

Expression of survivin was detected in 72.7% of cholangiocarcinomas. In contrast, no expression of survivin in adjacent noncancerous and benign bile duct lesions was observed ($P<0.01$). Using a similar polyclonal antibody, survivin expression was detected in 93% of malignant melanomas^[14], 81% of basal cell carcinomas, 92% of cutaneous squamous cell carcinomas^[15], 70% of hepatocellular carcinomas^[16], 88% of gastric carcinomas^[17], 100% of oesophageal cancers^[18], 88% of pancreatic adenocarcinomas^[10] and 74% of ovarian carcinomas^[19]. Our study demonstrated a high expression of survivin in cholangiocarcinoma as in other human malignancies.

There was no correlation between survivin expression and any clinical or pathological characteristics of cholangiocarcinoma. A similar absence of correlation was also noted in previous observations including gastric^[7,20], colorectal^[6,21] and breast cancers^[8]. Though many reports have shown that survivin was an independent prognostic factor for various cancers^[19,22-27], such a distribution of clinicopathological features and the high prevalence of survivin expression in cholangiocarcinoma might have rendered the power of this study insufficient to demonstrate any correlation between survivin expression and any clinical or pathological characteristics. Thus, the relationship with prognosis deserves further investigation.

Substantial evidences have also shown that during chemotherapy, changes in expression levels of survivin might provide information about chemo-sensitivity or chemo-resistance of tumors^[28,29]. In the present study, low concentration of chemotherapy agent doxorubicin (0.05 mg/l) could markedly ($P<0.001$) up-regulate survivin mRNA and protein expression

of QBC939 cells. These results suggested a direct link between survivin expression and bile duct carcinoma cell susceptibility to doxorubicin. That is, higher survivin expression may directly down-regulate chemo-sensitivity. It may be one of the mechanisms of anti-chemotherapy in cholangiocarcinoma.

In summary, a high expression of survivin in cholangiocarcinoma may play an important role in the development of cholangiocarcinoma, the relationship with prognosis deserves further investigation. Higher expression of survivin could be induced by doxorubicin in QBC939 and might resist apoptosis induced by chemotherapy agents. These results provide several exciting therapeutic possibilities. Initial evidence *in vitro* and *in vivo* has shown that targeting survivin may provide a viable approach to kill cancer cells selectively^[30,31]. Inhibition of survivin expression by molecular manipulation has been reported to improve the effectiveness of chemotherapy^[12,31-33] and produce impact on radiation therapy^[34-37].

REFERENCES

- 1 **Li F**, Ambrosini G, Chu EY, Plescia J, Tognin S, Marchisio PC, Altieri DC. Control of apoptosis and mitotic spindle checkpoint by survivin. *Nature* 1998; **396**: 580-584
- 2 **Tamm I**, Wang Y, Sausville E, Scudiero DA, Vigna N, Oltersdorf T, Reed JC. IAP-family protein survivin inhibits caspase activity and apoptosis induced by Fas (CD95), Bax, caspases, and anti-cancer drugs. *Cancer Res* 1998; **58**: 5315-5320
- 3 **Ambrosini G**, Adida C, Altieri DC. A novel anti-apoptosis gene, survivin, expressed in cancer and lymphoma. *Nat Med* 1997; **3**: 917-921
- 4 **Yamamoto T**, Tanigawa N. The role of survivin as a new target of diagnosis and treatment in human cancer. *Med Electron Microsc* 2001; **34**: 207-212
- 5 **Adida C**, Berrebi D, Peuchmaur M, Reyes-Mugica M, Altieri DC. Anti-apoptosis gene, survivin, and prognosis of neuroblastoma. *Lancet* 1998; **351**: 882-883
- 6 **Kawasaki H**, Altieri DC, Lu CD, Toyoda M, Tenjo T, Tanigawa N. Inhibition of apoptosis by survivin predicts shorter survival rates in colorectal cancer. *Cancer Res* 1998; **58**: 5071-5074
- 7 **Lu CD**, Altieri DC, Tanigawa N. Expression of novel anti-apoptosis gene, survivin, correlated with tumor cell apoptosis and p53 accumulation in gastric carcinomas. *Cancer Res* 1998; **58**: 1808-1812
- 8 **Tanaka K**, Iwamoto S, Gon G, Nohara T, Iwamoto M, Tanigawa N. Expression of survivin and its relationship to loss of apoptosis in breast carcinomas. *Clin Cancer Res* 2000; **6**: 127-134
- 9 **Satoh K**, Kaneko K, Hirota M, Masamune A, Satoh A, Shimosegawa T. Expression of survivin is correlated with cancer cell apoptosis and is involved in the development of human pancreatic duct cell tumors. *Cancer* 2001; **92**: 271-278
- 10 **Sarella AI**, Verbeke CS, Ramsdale J, Davies CL, Markham AF, Guillou PJ. Expression of survivin, a novel inhibitor of apoptosis and cell cycle regulatory protein, in pancreatic adenocarcinoma. *Br J Cancer* 2002; **86**: 886-892
- 11 **Altieri DC**, Marchisio PC, Marchisio C. Survivin apoptosis: an interloper between cell death and cell proliferation in cancer. *Lab Invest* 1999; **79**: 1327-1333
- 12 **Olie RA**, Simoes-Wust AP, Baumann B, Leech SH, Fabbro D, Stahel RA, Zangemeister-Wittke U. A novel antisense oligonucleotide targeting survivin expression induces apoptosis and sensitizes lung cancer cells to chemotherapy. *Cancer Res* 2000; **60**: 2805-2809
- 13 **Wang SG**, Han BL, Duan HC, Chen YS, Peng ZM. Establishment of the extrahepatic cholangiocarcinoma cell line. *Chin J Exp Sur* 1997; **14**: 67-68
- 14 **Grossman D**, McNiff JM, Li F, Altieri DC. Expression and targeting of the apoptosis inhibitor, survivin, in human melanoma. *J Invest Dermatol* 1999; **113**: 1076-1081
- 15 **Grossman D**, McNiff JM, Li F, Altieri DC. Expression of the apoptosis inhibitor, survivin, in nonmelanoma skin cancer and gene targeting in a keratinocyte cell line. *Lab Invest* 1999; **79**: 1121-1126
- 16 **Ito T**, Shiraki K, Sugimoto K, Yamanaka T, Fujikawa K, Ito M, Takase K, Moriyama M, Kawano H, Hayashida M, Nakano T,

- Suzuki A. Survivin promotes cell proliferation in human hepatocellular carcinoma. *Hepatology* 2000; **31**: 1080-1085
- 17 **Okada E**, Murai Y, Matsui K, Isizawa S, Cheng C, Masuda M, Takano Y. Survivin expression in tumor cell nuclei is predictive of a favorable prognosis in gastric cancer patients. *Cancer Lett* 2001; **163**: 109-116
- 18 **Beardsmore DM**, Verbeke CS, Sarela AI, Li AGK, Davis CL, Guillou PJ. The expression of survivin, an inhibitor of apoptosis, in esophageal cancer. *Gastroenterology* 2001; **120**: 660-668
- 19 **Cohen C**, Lohmann CM, Cotsonis G, Lawson D, Santoianni R. Survivin expression in ovarian carcinoma: correlation with apoptotic markers and prognosis. *Mod Pathol* 2003; **16**: 574-583
- 20 **Zhu XD**, Lin GJ, Qian LP, Chen ZQ. Expression of survivin in human gastric carcinoma and gastric carcinoma model of rats. *World J Gastroenterol* 2003; **9**: 1435-1438
- 21 **Sarela AI**, Scott N, Ramsdale J, Markham AF, Guillou PJ. Immunohistochemical detection of the anti-apoptosis protein, survivin, predicts survival after curative resection of stage II colorectal carcinomas. *Ann Surg Oncol* 2001; **8**: 305-310
- 22 **Ikeguchi M**, Ueda T, Sakatani T, Hirooka Y, Kaibara N. Expression of survivin messenger RNA correlates with poor prognosis in patients with hepatocellular carcinoma. *Diagn Mol Pathol* 2002; **11**: 33-40
- 23 **Ikehara M**, Oshita F, Kameda Y, Ito H, Ohgane N, Suzuki R, Saito H, Yamada K, Noda K, Mitsuda A. Expression of survivin correlated with vessel invasion is a marker of poor prognosis in small adenocarcinoma of the lung. *Oncol Rep* 2002; **9**: 835-838
- 24 **Ikeguchi M**, Kaibara N. Survivin messenger RNA expression is a good prognostic biomarker for oesophageal carcinoma. *Br J Cancer* 2002; **87**: 883-887
- 25 **Takai N**, Miyazaki T, Nishida M, Nasu K, Miyakawa I. Survivin expression correlates with clinical stage, histological grade, invasive behavior and survival rate in endometrial carcinoma. *Cancer Lett* 2002; **184**: 105-116
- 26 **Kappler M**, Kotzsch M, Bartel F, Fussel S, Lautenschlager C, Schmidt U, Wurl P, Bache M, Schmidt H, Taubert H, Meye A. Elevated expression level of survivin protein in soft-tissue sarcomas is a strong independent predictor of survival. *Clin Cancer Res* 2003; **9**: 1098-1104
- 27 **Kennedy SM**, O' Driscoll L, Purcell R, Fitz-Simons N, McDermott EW, Hill AD, O' Higgins NJ, Parkinson M, Linehan R, Clynes M. Prognostic importance of survivin in breast cancer. *Br J Cancer* 2003; **88**: 1077-1083
- 28 **Ikeguchi M**, Nakamura S, Kaibara N. Quantitative analysis of expression levels of bax, bcl-2, and survivin in cancer cells during cisplatin treatment. *Oncol Rep* 2002; **9**: 1121-1126
- 29 **Zaffaroni N**, Pennati M, Colella G, Perego P, Supino R, Gatti L, Pilotti S, Zunino F, Daidone MG. Expression of the anti-apoptotic gene survivin correlates with taxol resistance in human ovarian cancer. *Cell Mol Life Sci* 2002; **59**: 1406-1412
- 30 **Zaffaroni N**, Daidone MG. Survivin expression and resistance to anticancer treatments: perspectives for new therapeutic interventions. *Drug Resist Updat* 2002; **5**: 65-72
- 31 **Altieri D**. Blocking survivin to kill cancer cells. *Methods Mol Biol* 2003; **223**: 533-542
- 32 **Yamamoto T**, Manome Y, Nakamura M, Tanigawa N. Downregulation of survivin expression by induction of the effector cell protease receptor-1 reduces tumor growth potential and results in an increased sensitivity to anticancer agents in human colon cancer. *Eur J Cancer* 2002; **38**: 2316-2324
- 33 **Chen T**, Tian FZ, Cai ZH, Yin ZL, Zhao TJ. The signal transduction pathway related to hepatocellular carcinoma apoptosis induced by survivin antisense oligonucleotide. *Zhonghua Yixue Zazhi* 2003; **83**: 425-429
- 34 **Asanuma K**, Moriai R, Yajima T, Yagihashi A, Yamada M, Kobayashi D, Watanabe N. Survivin as a radioresistance factor in pancreatic cancer. *Jpn J Cancer Res* 2000; **91**: 1204-1209
- 35 **Asanuma K**, Kobayashi D, Furuya D, Tsuji N, Yagihashi A, Watanabe N. A role for survivin in radioresistance of pancreatic cancer cells. *Jpn J Cancer Res* 2002; **93**: 1057-1062
- 36 **Rodel C**, Haas J, Groth A, Grabenbauer GG, Sauer R, Rodel F. Spontaneous and radiation-induced apoptosis in colorectal carcinoma cells with different intrinsic radiosensitivities: survivin as a radioreistance factor. *Int J Radiat Oncol Biol Phys* 2003; **55**: 1341-1347
- 37 **Pennati M**, Binda M, Colella G, Folini M, Citti L, Villa R, Daidone MG, Zaffaroni N. Radiosensitization of human melanoma cells by ribozyme-mediated inhibition of survivin expression. *J Invest Dermatol* 2003; **120**: 648-654

Edited by Zhang JZ and Wang XL

Effects of gastric pacing on gastric emptying and plasma motilin

Min Yang, Dian-Chun Fang, Qian-Wei Li, Nian-Xu Sun, Qing-Lin Long, Jian-Feng Sui, Lu Gan

Min Yang, Dian-Chun Fang, Qing-Lin Long, PLA, Research and Clinical Center of Gastroenterology, Southwest Hospital, Chongqing 400038, China

Jian-Feng Sui, Department of Physiology, Third Military Medical University, Chongqing 400038, China

Qian-Wei Li, Department of Nuclear Medicine, Southwest Hospital, Chongqing 400038, China

Nian-Xu Sun, Lu Gan, Department of Surgery, Southwest Hospital, Chongqing 400038, China

Correspondence to: Dian-Chun Fang, M.D., Ph.D, Southwest Hospital, Third Military Medical University, Chongqing 400038, China. fangdianchun@hotmail.com

Telephone: +86-23-68754624 **Fax:** +86-23-68754124

Received: 2003-06-10 **Accepted:** 2003-08-16

Abstract

AIM: To investigate the effects of gastric pacing on gastric emptying and plasma motilin level in a canine model of gastric motility disorders and the correlation between gastric emptying and plasma motilin level.

METHODS: Ten healthy Mongrel dogs were divided into: experimental group of six dogs and control group of four dogs. A model of gastric motility disorders was established in the experimental group undergone truncal vagotomy combined with injection of glucagon. Gastric half-emptying time ($GET_{1/2}$) was monitored with single photon emission computerized tomography (SPECT), and the half-solid test meal was labeled with an isotope- ^{99m}Tc sulfur colloid. Plasma motilin concentration was measured with radioimmunoassay (RIA) kit. Surface gastric pacing at 1.1-1.2 times the intrinsic slow-wave frequency and a superimposed series of high frequency pulses (10-30 Hz) was performed for 45 min daily for a month in conscious dogs.

RESULTS: After surgery, $GET_{1/2}$ in dogs undergone truncal vagotomy was increased significantly from 56.35 ± 2.99 min to 79.42 ± 1.91 min ($P < 0.001$), but surface gastric pacing markedly accelerated gastric emptying and significantly decreased $GET_{1/2}$ to 64.94 ± 1.75 min ($P < 0.001$) in animals undergone vagotomy. There was a significant increase of plasma level of motilin at the phase of IMCIII (interdigestive myoelectrical complex, IMCIII) in the dogs undergone bilateral truncal vagotomy (baseline vs vagotomy, 184.29 ± 9.81 pg/ml vs 242.09 ± 17.22 pg/ml; $P < 0.01$). But plasma motilin concentration (212.55 ± 11.20 pg/ml; $P < 0.02$) was decreased significantly after a long-term treatment with gastric pacing. Before gastric pacing, $GET_{1/2}$ and plasma motilin concentration of the dogs undergone vagotomy showed a positive correlation ($r = 0.867$, $P < 0.01$), but after a long-term gastric pacing, $GET_{1/2}$ and motilin level showed a negative correlation ($r = -0.733$, $P < 0.04$).

CONCLUSION: Surface gastric pacing with optimal pacing parameters can improve gastric emptying parameters and significantly accelerate gastric emptying and can resume or alter motor function in a canine model of motility disorders. Gastric emptying is correlated well with plasma motilin level before and after pacing, which suggests that

motilin can modulate the mechanism of gastric pacing by altering gastric motility.

Yang M, Fang DC, Li QW, Sun NX, Long QL, Sui JF, Gan L. Effects of gastric pacing on gastric emptying and plasma motilin. *World J Gastroenterol* 2004; 10(3):419-423

<http://www.wjgnet.com/1007-9327/10/419.asp>

INTRODUCTION

The incidence of gastric motility disorder has been increasing, but the mechanisms of the development of this disease remain obscure, and specific and effective therapy are lacking. The current treatment mainly relies on conventional prokinetic agents. However, some patients with motility disorder can not undergo a chronic treatment with prokinetic drugs because of their side effects^[1-3]. In addition, tachyphylaxis may occur sooner or later and refractoriness to prokinetic agents is observed in a large number of patients. The limited efficacy of drugs in gastric motility disorder has led investigators to examine the effect of gastric pacing on gastric emptying. In the wake of cardiac pacing, some investigators hope that gastric pacing would be a new way to treat refractory gastric motility disorder. The role of gastric pacing with application of implanted gastric serosa electrodes, suction intraluminal electrodes or gastric mucosal electrodes in gastrointestinal (GI) tract has been greatly discussed in western countries^[4-23]. Most studies were restricted to animal experiments because of the invasiveness, substantial risk, and complications associated with the surgical procedure. However, the study of surface gastric pacing was rarely reported in medical literature. To determine the therapeutic efficacy of surface gastric pacing, we combined bilateral truncal vagotomy with administration of glucagon to establish a canine model of gastric motility disorder. Then, we observed the effects of surface gastric pacing on gastric emptying and plasma motilin level before and after pacing, and also explored the possible mechanism of gastric pacing.

MATERIALS AND METHODS

Animals and surgical preparation

Ten healthy Mongrel dogs were divided into: experimental group of six dogs (four males and two females) 12.5-17.5 (average 14.5) kg and control group of four dogs (two males and two females) 13.0-17.0 (average 15.5) kg. Bilateral truncal vagotomy was performed in the experimental group under aseptic conditions with intravenous anaesthesia of pentobarbital sodium after an overnight fasting. The initial dosage of the anaesthetics was 30 mg/kg, which was supplemented with 3 mg/kg if necessary on the basis of corneal reflex. Artificial ventilation was given during surgery. After surgery, the animal was first transferred to an intensive care cage for a few hours and then to the regular cage after a complete recovery from anaesthesia. The protocol was approved by the Institution of Animal Care of the Third Military Medical University.

Experimental procedure

The dogs were allowed to recover completely from surgery for 2 to 3 wk before any study. The study was conducted in

three sessions for each dog and experiments were performed on all the dogs in awake state. The dogs stood quietly on a table in a canvas support sling when gastric pacing was administered and gastric emptying was assessed. In the first session, we established the basic characteristics for gastric emptying in both control dogs and experimental dogs. In the second session, an intravenous injection of glucagon (500 $\mu\text{g}/\text{kg}$)^[4,24] was administered. Gastric emptying of semi-solid food was monitored in all 10 dogs in the first 5 min after glucagon injection. Three days later, a second experiment with glucagon was performed, and we utilized gastric pacing to observe if the effects on drug could be altered, and gastric emptying was monitored for 2 h with gastric pacing. In the third session, gastric pacing was performed for 45 min after meal daily for a month in dogs of the experimental group to observe the chronic efficacy of a long-term treatment with gastric pacing, and gastric emptying was assessed for 2 h after cessation of gastric pacing.

Gastric pacing

In order to simulate the basic electrical rhythm (BER) and induce release of acetylcholine from intramural cholinergic fibers, gastric pacing stimulus consisted of two signals: a continuous similar-sine basic wave with a low-frequency (1.1-1.2 times the intrinsic slow-wave frequency) and a superimposed series of high frequency pulses (10-30 Hz), the number of a series of pulse was 15-40/cycle. The pacing signals from a pacemaker were delivered with a pair of bipolar skin electrodes. Stimulating electrodes were placed on commonly used positions of the abdominal region (localization through X ray). A long-term surface gastric pacing was performed for 45 min after meal daily for a month.

Measurement of gastric emptying

Gastric emptying was monitored with single photon emission computerized tomography (SPECT) (GE Inc., USA). The semi-solid test meal consisted of 90 mg of commercial black sesame powder labeled with 74 MBq of ^{99m}Tc-sulfur colloid and 120 ml water. The study of gastric emptying consisted of two procedures, with or without gastric pacing, in a randomized order. On the day of gastric emptying test, the animal was fasted over 16 h. Immediately after the intake of isotope-labeled semi-solid meal, the maximum count rates were determined. After a first image was taken, the other sets were taken at an interval of 15 min for 2 h. The gastric region of interest was outlined by hand on the initial image by a nuclear medicine technologist who had no interest in the outcome of the study. To reduce the error resulted from the physical radioactive decay of isotope ^{99m}Tc, we corrected and normalized the percentage of semi-solid food retained in the stomach over time and chose the linear-fitting decay program to extrapolate $\text{GET}_{1/2}$.

Measurement of plasma concentration of motilin

Plasma level of motilin was determined with commercially available RIA (radioimmunoassay) kits. Blood was collected before and after vagotomy and after a long-term treatment of gastric pacing at the start of phase III of interdigestive myoelectric complex (IMCIII) respectively. Samples of peripheral venous blood were collected in lyophilized tubes containing 40 μl of 0.3 mol/L Na_2EDTA and 2 000 u trasytol. Immediately, plasma was separated with centrifugation at 4 000 r/min at 4 $^{\circ}\text{C}$. The plasma should be frozen within 2 hours and then stored at -70 $^{\circ}\text{C}$ for batch assay with a well-established motilin immunoassay^[20] (The motilin kit was supplied by the Radioimmunologic Center of PLA General Hospital, China).

Statistical analysis

Analysis of variance and paired Student's *t* test and linear

correlation analysis (SPSS 10.0 software) were performed to investigate the effects of gastric pacing on gastric emptying and plasma motilin level in dogs of the two groups. Statistical significance was assigned for $P < 0.05$. All data were presented as means \pm SD.

RESULTS

Basic condition

All dogs generally tolerated well the surgical procedure and surface gastric pacing. Large doses of glucagon injected intravenously triggered hyperglycemia in the diabetic setting and plasma glucose levels were increased sharply from 81-114 mg/dl to 200-233 mg/dl. Only two of the ten dogs were sensitively induced by glucagon to show nausea and vomiting, but the adverse symptoms rapidly disappeared and did not lead to any complication. Long-term gastric pacing resulted in a significant weight gain. The average weight (11.3 \pm 2.4 kg) after surgery was significantly lower than that before surgery (15.5 \pm 3.2 kg, $P < 0.01$), but after a long-term treatment with gastric pacing weight gain was found to be 14.7 \pm 2.7 kg ($P < 0.05$) in dogs of the experimental group.

Effects of vagotomy and glucagon on gastric emptying

Gastric emptying data were collected from each dog in all conditions. Results are summarized in Table 1 and Figure 1. The data before and after vagotomy were compared, and $\text{GET}_{1/2}$ of the dogs undergone truncal vagotomy was significantly increased from 56.35 \pm 2.99 min to 79.42 \pm 1.91 min ($P < 0.001$). To observe the effects of glucagon alone on gastric emptying, we compared the $\text{GET}_{1/2}$ of control dogs and the dogs undergone vagotomy before and after glucagon was administered (no gastric pacing was applied). In comparison with that before injection of glucagon, the $\text{GET}_{1/2}$ of the dogs undergone vagotomy was significantly longer after glucagon was administered (108.24 \pm 10.75 min, $P < 0.01$). However, the delay of gastric emptying in control dogs after injection of glucagon was not statistically significant (57.73 \pm 1.65 min vs 56.15 \pm 2.34 min, $P > 0.05$).

Table 1 Effects of gastric pacing on gastric emptying parameters

Groups	n	$\text{GET}_{1/2}$ (min)		
		No pacing	Acute pacing	Long-term pacing
Control	4	56.15 \pm 2.34	58.52 \pm 4.77	
Control + glucagon	4	57.73 \pm 1.65	56.90 \pm 2.53	
Vagotomy	6	79.42 \pm 1.91 ^a	74.41 \pm 6.10	64.94 \pm 1.75 ^d
Vagotomy+ glucagon	6	108.24 \pm 10.75 ^b	76.93 \pm 8.55 ^c	

All the data were expressed as means \pm SD. ^a $P < 0.001$ vs control, ^b $P < 0.01$ vs before injection of glucagon, ^c $P < 0.05$ vs before acute pacing, ^d $P < 0.001$ vs before a long-term pacing.

Effects of acute gastric pacing on gastric emptying

To investigate the acute effects of gastric pacing on gastric emptying in dogs undergone truncal vagotomy in combination with injection of glucagon and in control dogs with injection of glucagon, we observed gastric emptying for 2 h during gastric pacing. The $\text{GET}_{1/2}$ of the dogs undergone vagotomy and injection of glucagon was significantly shorter with pacing than that without pacing (108.24 \pm 10.75 min vs 76.93 \pm 8.55 min, $P < 0.01$). However, such an acute pacing had no significant effect on the $\text{GET}_{1/2}$ of control dogs with injection of glucagon (57.73 \pm 1.65 min vs 56.90 \pm 2.53 min, $P = 0.4$) or when only

vagotomy was performed (79.42 ± 1.91 min vs 74.41 ± 6.10 min, $P=0.3$).

Effects of chronic gastric pacing on gastric emptying

To investigate the effects of chronic gastric pacing on gastric emptying, we compared the $GE_{t_{1/2}}$ before pacing with that after a long-term gastric pacing of 30 d in the dogs undergone vagotomy. Gastric pacing significantly accelerated gastric emptying in animals undergone vagotomy (79.42 ± 1.91 min vs 64.94 ± 1.75 min, $P < 0.001$) and significantly decreased retention of gastric isotope (Figure 1).

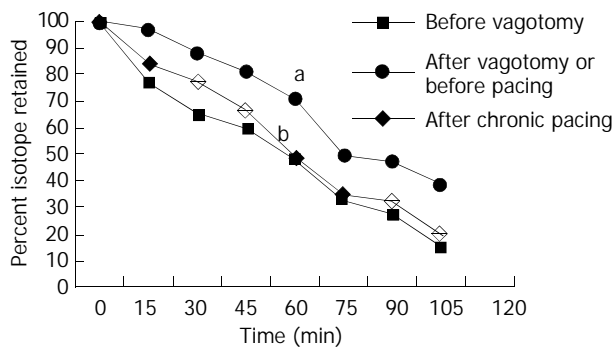


Figure 1 Effects of vagotomy and gastric pacing on gastric isotope retention during monitoring for 120 min. Data were expressed as means \pm SD, $n=6$. ^a $P < 0.005$ vs before vagotomy, ^b $P < 0.005$ vs before pacing (by analysis of variance at 120 min).

Effects of gastric pacing on plasma gastric motilin

There was a significant increase of plasma motilin concentration in the phase of IMCIII after bilateral truncal vagotomy (baseline vs vagotomy, 242.09 ± 17.22 pg/ml vs 184.29 ± 9.81 pg/ml; $P < 0.01$). But plasma motilin concentration was significantly lower after a long-term surface gastric pacing than that before gastric pacing (212.55 ± 11.20 pg/ml; $P < 0.02$).

Correlation of plasma gastric motilin and gastric emptying

Statistic analysis indicated that $GE_{t_{1/2}}$ (79.42 ± 1.91 min) and plasma motilin concentration (242.09 ± 17.22 pg/ml) in the phase of IMCIII of the dogs undergone vagotomy had a positive correlation ($r = 0.867$, $P < 0.01$) before surface gastric pacing, that is, vagotomy evoked the increase of plasma motilin level which clearly disrupted gastric emptying. But after a long-term gastric pacing, $GE_{t_{1/2}}$ (64.94 ± 1.75 min) and plasma motilin level (212.55 ± 11.20 pg/ml) had a negative correlation ($r = -0.733$, $P < 0.04$), that is, plasma motilin release was inclined to restore its normal level, which might be helpful to improve gastric emptying.

DISCUSSION

We used bilateral truncal vagotomy in combination administration of glucagon to establish a canine model of gastric motility disorders, which can simulate some aspects of diabetic gastroparesis. Our study demonstrated that surface gastric pacing at 1.1-1.2 times the intrinsic slow-wave frequency superimposed series of high frequency pulses (10-30 Hz) was able to entrain propagated slow waves to replace the spontaneous ones and to improve gastric emptying in dogs after vagotomy and injection of glucagon. It is considered that gastric pacing could be proven to be an effective therapeutic approach for the treatment of gastric motility disorders^[13,20-22,25-27].

Complete abdominal vagotomy has been shown to induce gastric stasis and delay emptying of solid food in both humans and animals^[4,11]. It could change the contractile pattern during interdigestive migrating motor complex III (IMCIII)^[28].

Extrinsic denervation of the antrum could diminish the frequency of antral action potentials and retard gastric emptying of solids. Our study indicated that gastric emptying of semi-solid food was obviously impaired after vagotomy in six dogs and confirmed the finding of previous researchers^[4,11] despite difference in their techniques of measuring gastric emptying. Previous studies have demonstrated that glucagon could delay gastric emptying of intact dogs^[29], but our study did not find that glucagon was able to delay gastric emptying in the healthy dogs, suggesting that the dogs undergone vagotomy were more susceptible to gastric motility disorder. The mechanisms by which glucagon delayed gastric emptying in both humans and dogs have not been fully understood. This delay might associate with acute hyperglycemia-evoked gastric slow wave dysrhythmias by endogenous prostaglandins^[24,30], such as tachygastria, tachyarrhythmia, bradyarrhythmia, asystolia (electrical silence), and gastric fibrillation which is a complete disorganization of gastric electrical activity due to impairment of coupling and propagation of gastric slow waves causing unpropagated antral contractions and exacerbating the hyperglycemia-evoked antral hypomotility^[31-33]. In addition, hyperglycemia might have inhibitory effects on the spike potentials that could induce antral contractions or possible indirect effects of glucagon on gastric emptying through the release of hormones or neurotransmitters^[4].

At present, controversial findings were reported about the effects of gastric pacing on gastric emptying. McCallum *et al.*^[13,20,22] showed that there was an increase in gastric emptying. On the other hand, Eagon *et al.*^[6] observed that neither the motility index nor gastric emptying rate was consistently changed by stimulation at any frequency. In our study, we employed a 1.1-1.2 times the intrinsic physiologic slow-wave frequency superimposed series of high frequency pulses (10-30 Hz) in surface gastric pacing which resulted in a significant acceleration of gastric emptying of semi-solid food in dogs undergone vagotomy but not in intact dogs. Our findings were consistent with those of Bellahsene *et al.*^[4] who employed a frequency similar to or slightly higher than the intrinsic slow-wave frequency.

Our study also evaluated the effects of total abdominal vagotomy and surface gastric pacing on plasma concentration of motilin in the phase of IMCIII. Motilin is a straight chain peptide containing 22 amino acids and has a molecular weight of approximately 2700. It has been found that plasma motilin levels varied in a cyclic fashion during the fasting state in accordance with the interdigestive migrating motor complex (IMMC), and IMMC III was concurrent with the peak of plasma motilin level^[34]. Motilin has been known to induce IMMC III contractions through cholinergic neural pathways, 5-hydroxytryptamine (HT) receptors, and alpha receptors^[35,36]. IMMC can clean large indigestible food residues, enhance antroduodenal and gallbladder coordination, stimulate pancreatic and bile secretion, and keep the small intestine free from stasis^[37]. Our results showed that there was a significant difference in plasma motilin concentration in the phase of IMCIII before and after the operation and after gastric pacing. The significant increase of plasma motilin level in the dogs after truncal vagotomy might be explained that total abdominal vagotomy or a complete extrinsic vagal gastric denervation could markedly delay gastric empty and induce gastric stasis, and reduce the sensitivity of motilin receptors, which might feedbackly lead to the release of plasma motilin. After a long-term surface gastric pacing, the delay of gastric emptying was improved and plasma motilin level gradually restored normal. At present, its mechanism is not clearly determined. In addition, our study showed gastric emptying was correlated well with plasma motilin level in the phase of IMCIII before and after gastric pacing, which implies that there is a possibility for

motilin to mediate the process of gastric pacing by altering gastric motility.

It has been found that gastrointestinal motility is regulated by a spatio-temporally-coordinated electrical pattern called gastrointestinal myoelectrical activity (GMA) that is paced by the GI pacemaker^[38]. Recently, it has been recognized that interstitial cells of Cajal known as pacemaker cells could generate rhythmically electrical pacemaker activities (or electrical slow waves) which regulate the frequency of contractions of the tunica muscularis for GI motility^[39-44]. The normal patterns of GMA present temporal evolution from endogenous rhythmic oscillation to bursting of spikes associated with contractions, and also order spatial propagation of the oscillating waves. Spatio-temporal modeling of the GMA has been established, thanks to the advances in electronic technology. Therefore, we employed a continuous similar-sine basic wave with a low-frequency (10%-20% high than intrinsic gastric frequency) superimposed a series of high frequency pulses (10-30 Hz) as signals of surface gastric electrical pacing. In contrast to gastric pacing through implanted serosal electrodes and the suction intraluminal electrodes in gastrointestinal tract, surface gastric pacing is more simple and noninvasive. In addition, surface gastric pacing does not require any surgical procedures such as laparotomy or laparoscopy. So this technique is a very attractive, reliable and acceptable candidate method to treat gastric motility disorders.

Although gastric pacing could restore a normal pattern of slow wave and an efficient gastric motor function and improve gastric emptying, its mechanism remains unclear^[45]. Recently, Qian *et al.*^[15] reported gastric pacing at a frequency similar to or just above that of the native slow wave to induce gastric slow wave was not via the cholinergic nerves, because although atropine was used to block the vagal activity, gastric pacing could still entrain and normalize the irregular rhythm of gastric slow wave. Moreover, spectral analysis of heart rate indicated that gastric pacing had no effect on the extrinsic autonomic functions. Accordingly, we presume that the mechanism of gastric pacing at a frequency slightly higher than the intrinsic frequency to induce gastric slow wave may be via some other neurohumoral pathways or directly leads to local activation of interstitial cells of Cajal and/or smooth muscle cells. Gastric electrical stimulation with a frequency much higher (about 10-1 200 cycles/min) than that of the intrinsic slow wave probably could act on sensory fibers directed to the central nervous system^[46]. Gastric electrical stimulation with a frequency 10-100 Hz might be possibly associated with autonomic and enteric nervous system changes, likely induce the release of acetylcholine from the intramural cholinergic fibers, which in turn stimulated the muscular cell contraction, because its effect was prevented by a previous administration of atropine^[47-49]. In addition, gastrointestinal hormones such as motilin or NANC neurotransmitter VIP might also mediate the process of gastric pacing^[47,50].

REFERENCES

- 1 **Wang SH**, Lin CY, Huang TY, Wu WS, Chen CC, Tsai SH. QT interval effects of cisapride in the clinical setting. *Int J Cardiol* 2001; **80**: 179-183
- 2 **Kyrmizakis DE**, Chimona TS, Kanoupakis EM, Papadakis CE, Velegarakis GA, Helidonis ES. QT prolongation and torsades de pointes associated with concurrent use of cisapride and erythromycin. *Am J Otolaryngol* 2002; **23**: 303-307
- 3 **Smalley W**, Shatin D, Wysowski DK, Gurwitz J, Andrade SE, Goodman M, Chan KA, Platt R, Schech SD, Ray WA. Contraindicated use of cisapride: Impact of food and drug administration regulatory action. *JAMA* 2000; **284**: 3036-3039
- 4 **Bellahsene BE**, Lind CD, Schirmer BD, Updike OL, McCallum RW. Acceleration of gastric emptying with electrical stimulation in a canine model of gastroparesis. *Am J Physiol* 1992; **262**(5 Pt 1): G826-834
- 5 **Eagon JC**, Kelly KA. Effects of gastric pacing on canine gastric motility and emptying. *Am J Physiol* 1993; **265**(4 Pt 1): G767-774
- 6 **Eagon JC**, Kelly KA. Effect of electrical stimulation on gastric electrical activity, motility and emptying. *Neurogastroenterol Motil* 1995; **7**: 39-45
- 7 **Familoni BO**, Abell TL, Voeller G, Salem A, Gaber O. Electrical stimulation at a frequency higher than basal rate in human stomach. *Dig Dis Sci* 1997; **42**: 885-891
- 8 **Familoni BO**, Abell TL, Nemoto D, Voeller G, Johnson B. Efficacy of electrical stimulation at frequencies higher than basal rate in canine stomach. *Dig Dis Sci* 1997; **42**: 892-897
- 9 **Soboocki J**, Thor PJ, Popiela T, Wasowicz P, Herman RM. Stomach electrostimulation—new possibility for treating gastroparesis. *Folia Med Cracov* 1999; **40**: 63-75
- 10 **Mintchev M**, Bowes K. Computer model of gastric electrical stimulation. *Ann Biomed Eng* 1997; **25**: 726-730
- 11 **Yokota M**, Ando N, Ozawa S, Imazu Y, Kitajima M. Enhanced motility of the vagotomized canine stomach by electrical stimulation. *J Gastroenterol Hepatol* 1997; **12**: 338-346
- 12 **Lin ZY**, McCallum RW, Schirmer BD, Chen JD. Effects of pacing parameters on entrainment of gastric slow waves in patients with gastroparesis. *Am J Physiol* 1998; **274**(1 Pt 1): G186-191
- 13 **McCallum RW**, Chen JD, Lin Z, Schirmer BD, Williams RD, Ross RA. Gastric pacing improves emptying and symptoms in patients with gastroparesis. *Gastroenterology* 1998; **114**: 456-461
- 14 **Mintchev MP**, Sanmiguel CP, Otto SG, Bowes KL. Microprocessor-controlled movement of liquid gastric content using sequential neural electrical stimulation. *Gut* 1998; **43**: 607-611
- 15 **Qian L**, Lin X, Chen JD. Normalization of atropine-induced postprandial dysrhythmias with gastric pacing. *Am J Physiol* 1999; **276**(2 Pt 1): G387-392
- 16 **Xing J**, Brody F, Rosen M, Chen JD, Soffer E. The effect of gastric electrical stimulation on canine gastric slow waves. *Am J Physiol* 2003; **284**: G956-962
- 17 **Mintchev MP**, Sanmiguel CP, Amaris M, Bowes KL. Microprocessor-controlled movement of solid gastric content using sequential neural electrical stimulation. *Gastroenterology* 2000; **118**: 258-263
- 18 **Lin Z**, Forster J, Sarosiek I, McCallum RW. Treatment of gastroparesis with electrical stimulation. *Dig Dis Sci* 2003; **48**: 837-848
- 19 **Lin X**, Peters LJ, Hayes J, Chen JD. Entrainment of segmental small intestinal slow waves with electrical stimulation in dogs. *Dig Dis Sci* 2000; **45**: 652-656
- 20 **Forster J**, Sarosiek I, Delcore R, Lin Z, Raju GS, McCallum RW. Gastric pacing is a new surgical treatment for gastroparesis. *Am J Surg* 2001; **182**: 676-681
- 21 **Chang CS**, Chou JW, Ko CW, Wu CY, Chen GH. Cutaneous electrical stimulation of acupuncture points may enhance gastric myoelectrical regularity. *Digestion* 2002; **66**: 106-111
- 22 **Abell TL**, Van Cutsem E, Abrahamsson H, Huizinga JD, Konturek JW, Galmiche JP, Voeller G, Filez L, Everts B, Waterfall WE, Domschke W, Bruley des Varannes S, Familoni BO, Bourgeois IM, Janssens J, Tougas G. Gastric electrical stimulation in intractable symptomatic gastroparesis. *Digestion* 2002; **66**: 204-212
- 23 **Chen JD**, Qian L, Ouyang H, Yin J. Gastric electrical stimulation with short pulses reduces vomiting but not dysrhythmias in dogs. *Gastroenterology* 2003; **124**: 401-409
- 24 **Hasler WL**, Soudah HC, Dulai G, Owyang C. Mediation of hyperglycemia-evoked gastric slow-wave dysrhythmias by endogenous prostaglandins. *Gastroenterology* 1995; **108**: 727-736
- 25 **Abell TL**, Minocha A. Gastroparesis and the gastric pacemaker: a revolutionary treatment for an old disease. *J Miss State Med Assoc* 2002; **43**: 369-375
- 26 **Shafik A**, El-Sibai O, Shafik AA, Ahmed I. The motor efficacy of the artificial colonic pacemaker in colonic inertia patients. *Front Biosci* 2002; **7**: b6-13
- 27 **Chen JD**, Lin HC. Electrical pacing accelerates intestinal transit slowed by fat-induced ileal brake. *Dig Dis Sci* 2003; **48**: 251-256
- 28 **Tanaka T**, Kendrick ML, Zyromski NJ, Meile T, Sarr MG. Vagal innervation modulates motor pattern but not initiation of canine gastric migrating motor complex. *Am J Physiol Gastrointest Liver Physiol* 2001; **281**: G283-292

- 29 **Chernish SM**, Brunelle RR, Rosenak BD, Ahmadzai S. Comparison of the effects of glucagon and atropine sulfate on gastric emptying. *Am J Gastroenterol* 1978; **70**: 581-586
- 30 **Kim TW**, Beckett EA, Hanna R, Koh SD, Ordog T, Ward SM, Sanders KM. Regulation of pacemaker frequency in the murine gastric antrum. *Am J Physiol* 2002; **538**(Pt 1): 145-157
- 31 **Petrakis IE**, Kogerakis N, Vrachassotakis N, Stiakakis I, Zacharioudakis G, Chalkiadakis G. Hyperglycemia attenuates erythromycin-induced acceleration of solid-phase gastric emptying in healthy subjects. *Abdom Imaging* 2002; **27**: 309-314
- 32 **Schvarcz E**, Palmer M, Aman J, Horowitz M, Stridsberg M, Berne C. Physiological hyperglycemia slows gastric emptying in normal subjects and patients with insulin-dependent diabetes mellitus. *Gastroenterology* 1997; **113**: 60-66
- 33 **Petrakis IE**, Kogerakis N, Prokopakis G, Zacharioudakis G, Antonakakis S, Vrachassotakis N, Chalkiadakis G. Hyperglycemia attenuates erythromycin-induced acceleration of liquid-phase gastric emptying of hypertonic liquids in healthy subjects. *Dig Dis Sci* 2002; **47**: 67-72
- 34 **Tanaka T**, VanKlombenberg LH, Sarr MG. Selective role of vagal and nonvagal innervation in initiation and coordination of gastric and small bowel patterns of interdigestive and postprandial motility. *J Gastrointest Surg* 2001; **5**: 418-433
- 35 **Itoh Z**, Mizumoto A, Iwanaga Y, Yoshida N, Torii K, Wakabayashi K. Involvement of 5-hydroxytryptamine 3 receptor in regulation of interdigestive gastric contraction by motilin in the dog. *Gastroenterology* 1991; **100**: 901-908
- 36 **Haga N**, Mizumoto A, Satoh M, Mochiki E, Mizusawa F, Ohshima K, Itoh Z. Role of endogenous 5-hydroxytryptamine in the regulation of gastric contractions by motilin in dogs. *Am J Physiol* 1996; **270**(1 Pt 1): G20-28
- 37 **Testoni PA**, Bagnolo F, Masci E, Colombo E, Tittobello A. Different interdigestive antroduodenal motility patterns in chronic antral gastritis with and without *Helicobacter pylori* infection. *Dig Dis Sci* 1993; **38**: 2255-2261
- 38 **Wang ZS**, Cheung JY, Gao SK, Chen JD. Spatio-temporal non-linear modeling of gastric myoelectrical activity. *Methods Inf Med* 2000; **39**: 186-190
- 39 **Sanders KM**. A case for interstitial cells of Cajal as pacemakers and mediators of neurotransmission in the gastrointestinal tract. *Gastroenterology* 1996; **111**: 492-515
- 40 **Der-Silaphet T**, Malysz J, Hagel S, Larry Arsenault A, Huizinga JD. Interstitial cells of cajal direct normal propulsive contractile activity in the mouse small intestine. *Gastroenterology* 1998; **114**: 724-736
- 41 **Hanani M**, Freund HR. Interstitial cells of Cajal—their role in pacing and signal transmission in the digestive system. *Acta Physiol Scand* 2000; **170**: 177-190
- 42 **Horiguchi K**, Semple GS, Sanders KM, Ward SM. Distribution of pacemaker function through the tunica muscularis of the canine gastric antrum. *Am J Physiol* 2001; **537**(Pt 1): 237-250
- 43 **Ward SM**, Sanders KM. Physiology and pathophysiology of the interstitial cell of Cajal: from bench to bedside. I. Functional development and plasticity of interstitial cells of Cajal networks. *Am J Physiol* 2001; **281**: G602-611
- 44 **Takayama I**, Horiguchi K, Daigo Y, Mine T, Fujino MA, Ohno S. The interstitial cells of Cajal and a gastroenteric pacemaker system. *Arch Histol Cytol* 2002; **65**: 1-26
- 45 **Bortolotti M**. The “electrical way” to cure gastroparesis. *Am J Gastroenterol* 2002; **97**: 1874-1883
- 46 **Chou JW**, Chang YH, Chang CS, Chen GH. The effect of different frequency electrical ac-stimulation on gastric myoelectrical activity in healthy subjects. *Hepatogastroenterology* 2003; **50**: 582-586
- 47 **Furgala A**, Thor PJ, Kolasinska-Kloch W, Krygowska-Wajs A, Kopp B, Laskiewicz J. The effect of transcutaneous nerve stimulation (TENS) on gastric electrical activity. *J Physiol Pharmacol* 2001; **52**(4 Pt 1): 603-610
- 48 **Amaris MA**, Rashev PZ, Mintchev MP, Bowes KL. Microprocessor controlled movement of solid colonic content using sequential neural electrical stimulation. *Gut* 2002; **50**: 475-479
- 49 **Lin J**, Cai G, Xu JY. A comparison between Zhishi Xiaopiwan and cisapride in treatment of functional dyspepsia. *World J Gastroenterol* 1998; **4**: 544-547
- 50 **Li W**, Zheng TZ, Qu SY. Effect of cholecystokinin and secretin on contractile activity of isolated gastric muscle strips in guinea pigs. *World J Gastroenterol* 2000; **6**: 93-95

Surgical salvage therapy of anal canal cancer

Yue-Kui Bai, Wen-Lan Cao, Ji-Dong Gao, Jun Liang, Yong-Fu Shao

Yue-Kui Bai, Ji-Dong Gao, Yong-Fu Shao, Department of General Surgical Oncology, Cancer Hospital of Chinese Academy of Medical Sciences, Peking Union Medical College, Beijing 100021, China

Jun Liang, Department of Radiotherapy, Cancer Hospital of Chinese Academy of Medical Sciences, Peking Union Medical College, Beijing 100021, China

Wen-Lan Cao, Department of Radiotherapy, Central Hospital, Yuncheng 044000, Shanxi Province, China

Correspondence to: Yong-Fu Shao, Department of General Surgical Oncology, Cancer Hospital of Chinese Academy of Medical Sciences, Peking Union Medical College, Beijing 100021, China. 5151bai@yahoo.com.cn

Telephone: +86-10-87708385

Received: 2003-05-12 **Accepted:** 2003-06-19

Abstract

AIM: To evaluate the results of salvage resection in the management of persistent or locally recurrent anal canal cancer.

METHODS: Details of all patients with anal canal cancer treated from 1978 to 1994 at Cancer Hospital of Chinese Academy of Medical Sciences (CAMS) were reviewed retrospectively. Sixteen patients who presented with persistent or locally recurrent anal canal cancer received salvage surgery. Before surgery all of the patients had received radiotherapy alone as their primary treatments.

RESULTS: Of the 16 patients, 14 received salvage abdominoperineal resection (APR) and two had transanal local excision. There were no deaths attributable to operation. Delayed healing of the perineal wound occurred in eight patients. Complications unrelated to the perineal wound were found in five patients. The median follow-up time was 120 (range 5-245) months after salvage surgery. Nine patients died of disease progression, with a median survival time of 16 (range 5-27) months. Six patients had a long-term survival.

CONCLUSION: Salvage resection after radiotherapy can yield a long-time survival in selected patients with anal canal cancer. However it offers little hope to patients with T₄ and/or N_{2,3} tumors.

Bai YK, Cao WL, Gao JD, Liang J, Shao YF. Surgical salvage therapy of anal canal cancer. *World J Gastroenterol* 2004; 10 (3):424-426

<http://www.wjgnet.com/1007-9327/10/424.asp>

INTRODUCTION

Anal canal cancer is rare and only accounts for 2% to 4% of all anorectal neoplasms^[1,2]. Radiotherapy alone or concomitant chemoradiotherapy currently is considered as a standard treatment for most of the patients^[3,4]. Although disease control was reported to be excellent, as many as 33% of patients would develop locoregional disease progression^[3-5]. Because this disease is uncommon, there has been no randomized study that compares different salvage approaches^[6]. The aim of this

study was to review our experience in salvage surgery for patients who developed local disease recurrence after radiotherapy.

MATERIALS AND METHODS

Materials

From 1978 to 1994, 83 patients with biopsy-proven anal canal cancer were treated with curative intent at Cancer Hospital of Chinese Academy of Medical Sciences (CAMS). Primary radiotherapy failed to produce any regression of the primary tumor in 16 patients. These 16 patients, including eleven who presented with a persistent disease and five patients who had a recurrent disease, were treated with salvage surgery. Primary tumors were staged in accordance with the criteria of the American Joint Committee on Cancer (AJCC)^[7]. Diagnosis of lymph node metastasis was made clinically, with radiological investigations such as computerized tomography scanning, and confirmed histologically. Pretreatment characteristics of these patients are listed in Table 1.

Table 1 Pretreatment characteristics (n=16)

Characteristics	No. of patients (n)
Demographics	
Median age(y)(range)	56(45-70)
Males/females	9/7
Histology	
Squamous	15
Basaloid	1
Clinical stage (UICC TNM)	
T ₁	1
T ₂	15
T ₃	2
T ₄	1
N ₀	7
N ₂	6
N ₃	3
Stage II	7
Stage IIIB	9

Treatment

Of the 16 patients, 15 received external beam radiation therapy (EBRT) alone. The mean dose of EBRT was 40 Gy(range 30-75 Gy). One patient was implanted with ¹⁹²Ir sources after EBRT. The brachytherapy dose was 14 Gy. No patients received adjuvant or concomitant chemotherapy. After completion of primary treatment, the patients were followed up according to a standard protocol^[8].

RESULTS

Surgical results

Among the 16 patients who failed initial therapy, 14 underwent salvage abdominoperineal resection (APR) and two had transanal local excision. Partial prostatic resection was performed on two males. There were no deaths attributable to operation. Fourteen patients had their perineal wounds packed open for hip bath. Healing time of the perineal wound

exceeding 3 months was considered to be delayed, which occurred in eight patients. In four patients the healing time of perineal wound exceeded six months and in one patient the healing was not achieved within two years. Other complications unrelated to perineal wound were recorded in five patients. These included one small bowel obstruction treated conservatively, one perineourethra fistula after prostatic resection, one abdominal wound infection and two neurocystitis.

Oncological results

All the patients were followed up. The median follow-up time was 120 (range 5-245) months after salvage surgery. At the time of the last follow-up nine patients died of disease progression, with a mean survival time of 16(range 5-27) months. In these patients, eight presented with a persistent disease and one had a recurrent disease. The median follow-up time among survivors was 173 (range 98-245) months. Six patients survived for more than 10 years. According to the initial tumor stage, one of seven patients with T₂N₀M₀ died 18 months after resection whereas eight of nine patients with T₁₋₄N₂₋₃M₀ disease were not controlled. Of the 16 patients, only one patient presented with a second locoregional disease recurrence and was salvaged with radiotherapy.

DISCUSSION

Despite progresses in chemoradiotherapy of anal epidermoid cancer^[3,4,9,10], a substantial percentage of patients, particularly those with more advanced disease, still developed a local failure and demand salvage therapy^[11,12]. Surgical resection was often recommended as the most appropriate salvage method^[13-15]. The overall survival rate for surgical salvage at 5 years was about 30-60%^[16,17]. Some investigators reported disappointingly low success rates^[18] and alternative approaches have been suggested, such as low dose radiotherapy or combined chemoradiotherapy^[19]. In the present study, six of the 16 patients who underwent appropriate surgical treatment survived for more than 10 years. These results are similar to those of Longo *et al*^[20], who reported a survival rate of 53% among 17 patients and Ellenhorn *et al*^[21], who noted that 44% of 38 patients survived for 5 years after salvage resection.

It is well known that delayed healing of perineal wounds is a common complication for patients after radiotherapy. Earlier investigators reported the perineal wound complication rate was up to 30%^[16,17,21]. In the study by Nilsson *et al*^[22], the rate of delayed healing was 66 % (22 of 35). No difference was detected in the radiation dose delivered between patients with delayed healing and those in whom healing was achieved within 3 months. Also in rectal cancer, preoperative radiotherapy whether given in 5.0-Gy fractions or using conventional 1.8-2.0-Gy fractions, always made the healing of perineal wounds delay^[23]. In 14 patients who received salvage APR, eight presented with a delayed perineal wound healing and one did not have a wound healing within two years. It might help the healing of large defects created in an irradiated field by using an omentoplasty or musculo-cutaneous flap^[24,25].

Of the five patients who presented with local recurrence after having achieved complete disease remission, three survived for more than 10 years. In contrast, among the 11 patients who presented with persistent diseases, eight died of the diseases within 3 years. There was a better 10-year survival among patients with recurrences compared with that in patients with a persistent disease. These findings are consistent with those of Nilssio *et al*^[22], who reported a significantly better 5-year survival among patients with recurrences (82% versus 33%) and Allal *et al*^[17](56% versus 23%), but contradicted with those of Pocard *et al*^[16], who reported that patients with a persistent disease had a longer survival time (74 versus 25

months). The difference may be related to the tumors' stage and nodal status at initial presentation, or, alternatively, may reflect more aggressive biologic phenotypes of tumors that are different in response to radiotherapy.

The effect of salvage surgery appeared to correlate with the initial disease stage^[26-28]. In the study by Allal *et al*^[17], 41% of patients who failed local treatment of T₂₋₃N₀M₀ anal canal cancer were successfully salvaged, compared with 17% of patients with T₁₋₄N₂₋₃M₀ anal canal cancer. The effects of initial lymph node involvement and tumor extent on patients' outcome after surgical salvage therapy also were stressed by Ellenhorn *et al*^[21]. In the present study, eight of 9 patients who died of the disease presented with T₁₋₄N₂₋₃M₀ anal canal cancer, whereas most of the survivors had a T₂N₀M₀ anal canal cancer.

In summary, salvage APR after radiotherapy has a high complication rate, but can bring a long-time survival in selected patients with anal canal cancer. Since patients with T₄ and/or N₂₋₃ tumors could not obtain much benefit from salvage surgery, salvage chemoradiotherapy needs to be further investigated.

REFERENCES

- 1 **Whiteford MH**, Stevens KR Jr, Oh S, Deveney KE. The evolving treatment of anal cancer: How are we doing? *Arch Surg* 2001; **136**: 886-891
- 2 **Lai MD**, Luo MJ, Yao JE, Chen PH. Anal cancer in Chinese: human papillomavirus infection and altered expression of p53. *World J Gastroenterol* 1998; **4**: 298-302
- 3 **Anonymous**. Epidermoid anal cancer: results from the UKCCCR randomised trial of radiotherapy alone versus radiotherapy, 5-fluorouracil, and mitomycin. UKCCCR Anal Cancer Trial Working Party. UK Co-ordinating Committee on Cancer Research. *Lancet* 1996; **348**: 1049-1054
- 4 **Bartelink H**, Roelofs F, Eschwege F, Rougier P, Bosset JF, Gonzalez DG, Peiffert D, van Glabbeke M, Pierart M. Concomitant radiotherapy and chemotherapy is superior to radiotherapy alone in the treatment of locally advanced anal cancer: results of a phase III randomized trial of the European Organization for Research and Treatment of Cancer Radiotherapy and Gastrointestinal Cooperative Groups. *J Clin Oncol* 1997; **15**: 2040-2049
- 5 **Cummings BJ**. Concomitant radiotherapy and chemotherapy for anal cancer. *Semin Oncol* 1992; **19**(4 Suppl 11): 102-108
- 6 **Esiashvili N**, Landry J, Matthews RH. Carcinoma of the anus: strategies in management. *Oncologist* 2002; **7**: 188-199
- 7 **Minsky BD**, Hoffman JP, Kelsen DP. Cancer: principles and Practice of Oncology. 6thd. Philadelphia: *Lippincott Williams Wilkins* 2001: 1319-1342
- 8 **Cummings BJ**, Keane TJ, O' Sullivan B, Wong CS, Catton CN. Epidermoid anal cancer: treatment by radiation alone or by radiation and 5-fluorouracil with and without mitomycin C. *Int J Radiat Oncol Biol Phys* 1991; **21**: 1115-1125
- 9 **Weber DC**, Kurtz JM, Allal AS. The impact of gap duration on local control in anal canal carcinoma treated by split-course radiotherapy and concomitant chemotherapy. *Int J Radiat Oncol Biol Phys* 2001; **50**: 675-680
- 10 **Beck DE**, Karulf RE. Combination therapy for epidermoid carcinoma of the anal canal. *Dis Colon Rectum* 1994; **37**: 1118-1125
- 11 **Spratt JS**. Cancer of the anus. *J Surg Oncol* 2000; **74**: 173-174
- 12 **Faynsod M**, Vargas HI, Tolmos J, Udani VM, Dave S, Arnell T, Stabile BE, Stamos MJ. Patterns of recurrence in anal canal carcinoma. *Arch Surg* 2000; **135**: 1090-1093
- 13 **Ryan DP**, Compton CC, Mayer RJ. Carcinoma of the anal canal. *N Engl J Med* 2000; **342**: 792-800
- 14 **Gao JD**, Shao YF, Bi JJ, Shi SS, Liang J, Hu YH. Local excision carcinoma in early stage. *World J Gastroenterol* 2003; **9**: 871-873
- 15 **Grabenbauer GG**, Matzel KE, Schneider IH, Meyer M, Wittekind C, Matsche B, Hohenberger W, Sauer R. Sphincter preservation with chemoradiation in anal canal carcinoma: abdominoperineal resection in selected cases? *Dis Colon Rectum* 1998; **41**: 441-450
- 16 **Pocard M**, Turet E, Nugent K, Dehni N, Parc R. Results of salvage abdominoperineal resection for anal cancer after radiotherapy. *Dis Colon Rectum* 1998; **41**: 1488-1493

- 17 **Allal AS**, Laurencet FM, Reymond MA, Kurtz JM, Marti MC. Effectiveness of surgical salvage therapy for patients with locally uncontrolled anal carcinoma after sphincter-conserving treatment. *Cancer* 1999; **86**: 405-409
- 18 **Zelnick RS**, Haas PA, Ajlouni M, Szilagyi E, Fox TA Jr. Results of abdominoperineal resections for failures after combination chemotherapy and radiation therapy for anal canal cancers. *Dis Colon Rectum* 1992; **35**: 574-577
- 19 **Flam M**, John M, Pajak TF, Petrelli N, Myerson R, Doggett S, Quivey J, Rotman M, Kerman H, Coia L, Murray K. Role of mitomycin in combination with fluorouracil and radiotherapy, and of salvage chemoradiation in the definitive nonsurgical treatment of epidermoid carcinoma of the anal canal: results of a phase III randomized intergroup study. *J Clin Oncol* 1996; **14**: 2527-2539
- 20 **Longo WE**, Vernava AM 3rd, Wade TP, Coplin MA, Virgo KS, Johnson FE. Recurrent squamous cell carcinoma of the anal canal. Predictors of initial treatment failure and results of salvage therapy. *Ann Surg* 1994; **220**: 40-49
- 21 **Ellenhorn JD**, Enker WE, Quan SH. Salvage abdominoperineal resection following combined chemotherapy and radiotherapy for epidermoid carcinoma of the anus. *Ann Surg Oncol* 1994; **1**: 105-110
- 22 **Nilsson PJ**, Svensson C, Goldman S, Glimelius B. Salvage abdominoperineal resection in anal epidermoid cancer. *Br J Surg* 2002; **89**: 1425-1429
- 23 **Glimelius B**, Isacsson U. Preoperative radiotherapy for rectal cancer—is 5 x 5 Gy a good or a bad schedule? *Acta Oncol* 2001; **40**: 958-967
- 24 **de Haas WG**, Miller MJ, Temple WJ, Kroll SS, Schusterman MA, Reece GP, Skibber JM. Perineal wound closure with the rectus abdominis musculocutaneous flap after tumor ablation. *Ann Surg Oncol* 1995; **2**: 400-406
- 25 **Giampapa V**, Keller A, Shaw WW, Colen SR. Pelvic floor reconstruction using the rectus abdominis muscle flap. *Ann Plast Surg* 1984; **13**: 56-59
- 26 **Myerson RJ**, Kong F, Birnbaum EH, Fleshman JW, Kodner IJ, Picus J, Ratkin GA, Read TE, Walz BJ. Radiation therapy for epidermoid carcinoma of the anal canal, clinical and treatment factors associated with outcome. *Radiother Oncol* 2001; **61**: 15-22
- 27 **Gerard JP**, Chapet O, Samiei F, Morignat E, Isaac S, Paulin C, Romestaing P, Favrel V, Mornex F, Bobin JY. Management of inguinal lymph node metastases in patients with carcinoma of the anal canal: experience in a series of 270 patients treated in Lyon and review of the literature. *Cancer* 2001; **92**: 77-84
- 28 **Smith AJ**, Whelan P, Cummings BJ, Stern HS. Management of persistent or locally recurrent epidermoid cancer of the anal canal with abdominoperineal resection. *Acta Oncol* 2001; **40**: 34-36

Edited by Zhu LH and Wang XL

Utility of serum CA19-9 in diagnosis of cholangiocarcinoma: In comparison with CEA

Xing-Lei Qin, Zuo-Ren Wang, Jing-Sen Shi, Min Lu, Lin Wang, Quan-Ru He

Xing-Lei Qin, Zuo-Ren Wang, Jing-Sen Shi, Lin Wang, Department of Hepatobiliary Surgery, First Hospital of Xi'an Jiaotong University, Xi'an 710061, Shaanxi Province, China
Min Lu, Quan-Ru He, Luoyang Central Hospital, Luoyang 471009, Henan Province, China

Correspondence to: Dr. Xing-Lei Qin, M.D., Department of Hepatobiliary Surgery, First Hospital of Xi'an Jiaotong University, Xi'an 710061, Shaanxi Province, China. qinxinglei@yahoo.com.cn
Telephone: +86-29-5274739 **Fax:** +86-29-5269313
Received: 2003-06-05 **Accepted:** 2003-07-24

Abstract

AIM: The diagnosis of cholangiocarcinoma is often difficult, making management approaches problematic. A reliable serum marker for cholangiocarcinoma would be a useful diagnostic test. The aims of our study were to evaluate the usefulness of a serum CA19-9 determination in the diagnosis of cholangiocarcinoma.

METHODS: We prospectively measured serum CA19-9 and CEA concentrations in patients with cholangiocarcinoma ($n=35$), benign biliary diseases ($n=92$), and healthy individuals ($n=15$). Serum CA19-9 and CEA concentrations were measured by an immunoradiometric assay without knowledge of the clinical diagnosis.

RESULTS: The sensitivity of a CA19-9 value >37 KU·L⁻¹ and a CEA value >22 μg·L⁻¹ in diagnosing cholangiocarcinoma were 77.14% and 68.57%, respectively. When compared with the benign biliary diseases group, the true negative rates of serum CA19-9 and CEA were 84.78% and 81.52%, respectively. The false positive rates of serum CA19-9 and CEA were 15.22% and 18.48%, whereas the accuracy of serum CA19-9 and CEA were 82.68% and 77.95%, respectively. Serum CA19-9 and CEA concentrations were significantly elevated ($P<0.001$ and $P<0.05$) in patients with cholangiocarcinoma (290.31 ± 5.34 KU·L⁻¹ and 36.46 ± 18.03 μg·L⁻¹) compared with patients with benign biliary diseases (13.38 ± 2.59 KU·L⁻¹ and 13.84 ± 3.85 μg·L⁻¹) and healthy individuals (12.78 ± 3.69 KU·L⁻¹ and 11.48 ± 3.37 μg·L⁻¹). In 15 patients undergoing curative resection of cholangiocarcinoma, the mean serum CA19-9 concentration was decreased from a preoperative level of 286.41 ± 4.36 KU·L⁻¹ to a postoperative level of 62.01 ± 17.43 KU·L⁻¹ ($P<0.001$), and the mean serum CEA concentration from 39.41 ± 24.35 μg·L⁻¹ to 28.69 ± 11.03 μg·L⁻¹ ($P<0.05$). In patients with cholangiocarcinoma, however, no correlation was found between serum CEA and CA19-9 concentrations ($r=0.036$).

CONCLUSION: These data suggest that the serum CA19-9 determination is a useful addition to the available tests for the differential diagnosis of cholangiocarcinoma. Serum CA19-9 is an effective tumor marker in diagnosing cholangiocarcinoma, deciding whether the tumor has been radically resected and monitoring effect of treatment.

Qin XL, Wang ZR, Shi JS, Lu M, Wang L, He QR. Utility of

serum CA19-9 in diagnosis of cholangiocarcinoma: In comparison with CEA. *World J Gastroenterol* 2004; 10(3): 427-432

<http://www.wjgnet.com/1007-9327/10/427.asp>

INTRODUCTION

Cholangiocarcinoma is a malignant tumor arising from bile duct epithelium. Unlike most human cancers, a pathological diagnosis of cholangiocarcinoma is often extremely difficult because of its location, size, and desmoplastic characteristics^[1-3]. Percutaneous fine needle aspiration is frequently not possible because many of these tumors are located in the liver hilum amid large vascular structures^[4,5]. Furthermore, tumor masses are often not even identifiable by CT, ultrasound, or magnetic resonance imaging^[6-8]. Endoscopic approaches are also of limited usefulness in tissue diagnosis because of the desmoplastic nature of these cancers. Indeed, bile cytology obtained at endoscopic retrograde cholangiography has a sensitivity of only 33-56%^[1,9-11], endobiliary brush cytology of 50-68%^[12-14], and endoscopic transpapillary biopsy of 53-86% for detecting cholangiocarcinoma^[15-18]. Because of the problems in obtaining diagnostic tissues, treatment and management decisions for patients with biliary disease that may be malignant are problematic.

Of the two possible tumor markers available for detecting cholangiocarcinomas, carcinoembryonic antigen (CEA) is a glycoprotein tumor marker with the immunodeterminant present on the protein moiety of the molecule. The other, carbohydrate antigen 19-9 (CA19-9), is a mucin-type glycoprotein in serum with the immunodeterminant present on the carbohydrate moiety of the molecule. Both tumor markers have been investigated for the diagnosis of malignancies in the stomach, colon and pancreas^[19-23] but have not been gained widespread use in bile duct. It has been reported that the sensitivity and specificity for CA19-9 value >37 KU·L⁻¹ for cholangiocarcinoma with primary sclerosing cholangitis (PSC) were 60% to 93% and 78% to 98%, respectively^[9,16,21,24-27]. The corresponding indexes of CEA value >22 μg·L⁻¹ were 53% to 84% and 50% to 79%^[25-30]. Although widely used as a tumor marker, the clinical value of serum CA19-9 determination in the diagnosis of cholangiocarcinoma in the absence of PSC is unknown. Thus, the objective of this study was to determine the clinical usefulness of CA19-9 value for cholangiocarcinoma.

MATERIALS AND METHODS

Patients

From January 1995 to February 2003, we prospectively obtained serum samples from patients undergoing evaluation for benign and malignant biliary disease at the First Hospital of Xi'an Jiaotong University and Luoyang Central Hospital. Serum samples were also prospectively obtained from healthy individuals who served as the disease control group. Patients with the diagnosis of PSC were excluded from this study. Clinical information was obtained by a thorough review of

the medical histories. This study included 35 patients with cholangiocarcinoma, 92 patients with benign biliary diseases, and 15 healthy individuals. Of the 35 patients with cholangiocarcinoma, the diagnosis was established by surgical biopsy in 25 patients, endoscopic biopsy and brushing in six patients, and fine needle aspiration in four patients. In patients with cholangiocarcinoma, the stage and resectability of the tumors were ascertained using information obtained by imaging studies or at the time of surgery. Unresectability was defined by Bismuth stage 4 cancer arising from the right and left hepatic ducts and extending intrahepatically. Patients with intra- and extrahepatic metastasis were also deemed unresectable.

The benign biliary diseases group consisted of 92 patients and included 26 patients with benign bile duct stricture, 36 patients with cholecystolithiasis, 20 patients with cholecystic polyp, and 10 patients with chronic cholecystitis. The other control group consisted of 15 healthy individuals without any disease.

Methods

Blood samples obtained from patients were stored at -20°C until used. CA19-9 and CEA were assayed by means of an immunoradiometric method with a commercially available CA19-9 RIA diagnostic kit (ELISA-CA19-9, CIS Bio International, France) and CEA RIA diagnostic kit (CIS Bio Industries, Gif-Sur-Yvette, France). Cutoff values recommended for diagnostic purpose were $37\text{ KU}\cdot\text{L}^{-1}$ for CA19-9 and $22\text{ }\mu\text{g}\cdot\text{L}^{-1}$ for CEA. Values above the cutoff concentrations were considered positive in this study. Sensitivity in detecting each group was compared between CA19-9 and CEA.

Statistics

The results were expressed as mean values \pm standard deviation of the mean (mean \pm SD). Statistical analysis was performed using a statistical program (SPSS, 11.0 Inc, Chicago, IL). Statistical significance in mean values was evaluated by the Student's *t* test. The one-way analysis of variance (ANOVA) was used to compare the different groups, and the Mann-Whitney rank sum

test was used for intergroup comparisons. The relationships between CA19-9 and CEA, total bilirubin, alkaline phosphatase, or AST were determined by linear regression analysis.

RESULTS

Patients' characteristics

The Table 1 shows some of the characteristics of the different groups. Patients with cholangiocarcinoma were significantly older than either patients with benign biliary diseases or healthy individuals. However, the mean total serum bilirubin and serum alkaline phosphatase values were significantly higher in patients with cholangiocarcinoma, compared to the other two groups ($P<0.05$). Thus, the patients with cholangiocarcinoma had a more marked cholestatic profile than the other two groups of patients.

Serum CA19-9 and CEA values in cholangiocarcinoma, benign biliary diseases and healthy individuals

The mean CA19-9 and CEA concentrations were significantly greater in the cholangiocarcinoma group than those in the benign biliary diseases group or healthy individuals group (Figure 1). Table 1 shows the mean serum CA19-9 concentration in patients with cholangiocarcinoma was $290.31\pm 5.34\text{ KU}\cdot\text{L}^{-1}$ in comparison with $13.38\pm 2.59\text{ KU}\cdot\text{L}^{-1}$ in the benign biliary diseases group and $12.78\pm 3.69\text{ KU}\cdot\text{L}^{-1}$ in the healthy individuals group ($P<0.001$). Their corresponding mean serum CEA concentrations were $36.46\pm 18.03\text{ }\mu\text{g}\cdot\text{L}^{-1}$, $13.84\pm 3.85\text{ }\mu\text{g}\cdot\text{L}^{-1}$ and $11.48\pm 3.37\text{ }\mu\text{g}\cdot\text{L}^{-1}$, respectively ($P<0.05$).

Comparison of CA19-9 and CEA levels in serum in patients with cholangiocarcinoma and benign diseases

Table 2 shows the distribution of serum CA19-9 and CEA values in patients with cholangiocarcinoma and benign biliary diseases. Of the 35 patients with cholangiocarcinoma, 27 (77.14%) had a concentration exceeding $37\text{ KU}\cdot\text{L}^{-1}$ in serum CA19-9. Using a CA19-9 concentration of $37\text{ KU}\cdot\text{L}^{-1}$, the true negative rate of a CA19-9 for cholangiocarcinoma was 84.78% when

Table 1 Patients' characteristics in three groups (mean \pm SD)

Characteristics	Cholangiocarcinoma	Benign biliary diseases	Healthy individuals
N	35	92	15
Age (yr)	60.37 \pm 11.2	49.78 \pm 10.6	27.6 \pm 4.7
Sex (M/F)	19/16	39/53	15/0
Total bilirubin ($\mu\text{mol/L}$)	47.4 \pm 2.1 ^a	8.3 \pm 0.7	8.6 \pm 0.9
AST (U/L)	79 \pm 21.2 ^a	26 \pm 3.5	21 \pm 4.6
ALP (U/L)	193 \pm 41.8 ^a	114 \pm 50.6	90 \pm 18.3
CA19-9 (KU/L)	290.31 \pm 5.34 ^{bc}	13.38 \pm 2.59	12.78 \pm 3.69
CEA ($\mu\text{g/L}$)	36.46 \pm 18.03 ^a	13.84 \pm 3.85	11.48 \pm 3.37

^a $P<0.05$, ^b $P<0.001$ vs benign biliary diseases or healthy individuals. ^c $P<0.05$ vs serum CEA. AST=aspartate aminotransferase, ALP=alkaline phosphatase, CA19-9=carbohydrate antigen 19-9, CEA=carcinoembryonic antigen.

Table 2 Comparison of serum CA19-9 and CEA levels in patients with cholangiocarcinoma and benign biliary diseases

	CA19-9 ^Δ	CA19-9	CEA	CA19-9 or CEA	CA19-9 and CEA
Sensitivity (true positive) [*]	65.71%(23/35)	77.14%(27/35) ^a	68.57%(24/35)	91.43%(32/35)	62.86%(22/35)
Specificity (true negative) ^{**}	88.04%(81/92)	84.78%(78/92)	81.52%(75/92)	76.09%(70/92)	86.96%(80/92)
Positive predictive value	67.65%(23/34)	65.85%(27/41)	58.54%(24/41)	59.26%(32/54)	64.71%(22/34)
Negative predictive value	87.10%(81/93)	90.70%(78/86)	87.21%(75/86)	95.89%(70/73)	88.89%(80/90)
Accuracy	81.89%(104/127)	82.68%(105/127)	77.95%(99/127)	80.31%(102/127)	80.31%(102/127)
False positive rate	11.98%(11/92)	15.22%(14/92)	18.48%(17/92)	23.91%(22/92)	13.04%(12/92)

^{*}Number of positive tests/number of patients with cholangiocarcinoma. ^{**}Number of negative tests/number of patients with benign biliary diseases. ^a $P<0.05$ vs CEA. ^ΔWhen the cutoff value of serum CA19-9 was $100\text{ KU}\cdot\text{L}^{-1}$.

assessed as the benign biliary diseases. The sensitivity (true positive) and specificity (true negative) of CEA were 68.57% and 81.52%, respectively (Table 2). Among the 92 patients with benign biliary diseases, the false positive rates of serum CA19-9 > 37 KU·L⁻¹ and CEA > 22 µg·L⁻¹ were 15.22% (14/92) and 18.48% (17/92), respectively. The combination of CA19-9 and CEA showed the highest sensitivity and specificity, they were 91.43% and 76.09% when CA19-9 or CEA was positive, and they were 62.86% and 86.96% when both CA19-9 and CEA were positive, respectively. If the cutoff value was increased from 37 KU·L⁻¹ to 100 KU·L⁻¹, the sensitivity and specificity of CA19-9 were 65.71% (23/35) and 88.04% (81/92), respectively.

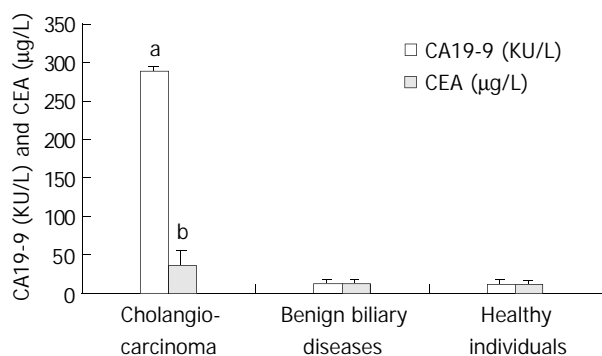


Figure 1 Mean serum CA19-9 and CEA concentrations. ^a*P*<0.001, ^b*P*<0.05 vs benign biliary diseases or healthy individuals. ^c*P*<0.05 vs serum CEA.

Correlation between serum CA19-9 and total bilirubin, ALP, AST or CEA in patients with cholangiocarcinoma

In patients with cholangiocarcinoma, no correlation was found between CEA and CA19-9 concentration (*r*=0.036). Likewise, no correlation was found among serum CA19-9, or ALP, AST, and total bilirubin (*r*=0.015, *r*=0.037 and *r*=0.145, respectively). Thus, elevated serum CA19-9 value could not be attributed to either cholestasis or hepatocellular injury.

Decrease of serum CA19-9 values in patients with cholangiocarcinoma after undergoing curative resection

Of the 35 patients with cholangiocarcinoma, 15 patients underwent curative resection and 20 had unresectable cancer. The mean preoperative and postoperative serum CA19-9 levels in the resectable group were 286.41±4.36 KU·L⁻¹ and 62.01±17.43 KU·L⁻¹, respectively. The corresponding indexes of serum CEA were 39.41±24.35 µg·L⁻¹ and 28.69±11.03 µg·L⁻¹, respectively (Figure 2 and Table 3). Thus, patients after curative resection had significantly lower mean serum CA19-9 and CEA concentrations than those before operation (*P*<0.001 and *P*<0.05). The mean serum CA19-9 concentration in the resectable group was 286.41±4.36 KU·L⁻¹ as compared to 391.37±5.76 KU·L⁻¹ in the unresectable group (Figure 2 and Table 3). Thus, patients with unresectable disease had a significantly higher mean serum CA19-9 concentration than those with resectable disease (*P*<0.05).

Table 3 Preoperative and postoperative change of serum CA19-9 and CEA concentrations in patients with cholangiocarcinoma undergoing curative resection (mean±SD)

Groups	CA19-9 (KU/L)	CEA(µg/L)
After the resectable (<i>n</i> =15)	62.01±17.43 ^a	28.69±11.03 ^c
Before the resectable (<i>n</i> =15)	286.41±4.36	39.41±24.35
The unresectable (<i>n</i> =20)	391.37±5.76 ^b	43.28±20.68

^a*P*<0.001, ^b*P*<0.01, ^c*P*<0.05 vs before the resectable group.

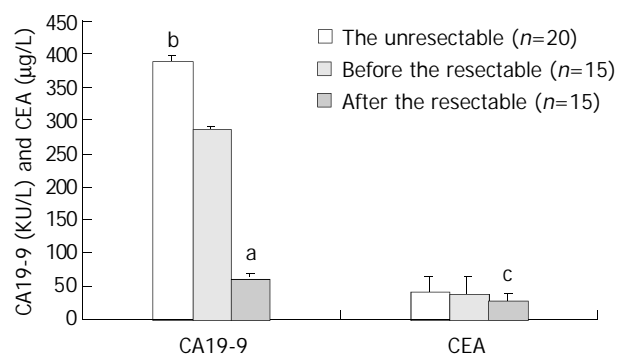


Figure 2 Mean postoperative serum CA19-9 and CEA levels of resectable group and mean serum CA19-9 and CEA levels of the unresectable group.

Relation between serum CA19-9 and CEA values and clinicopathologic features in 35 patients with cholangiocarcinoma

Perineural invasion by malignant cells was found in 23 of the 33 patients and more frequently encountered in cancer of the upper portion of extrahepatic bile ducts. Of the 35 tumors, lymph node metastasis was seen in 18 and venous invasion in 17. Histologically, 35 examples of cholangiocarcinoma were composed of 16 well-differentiated adenocarcinomas, 12 moderately-differentiated adenocarcinomas, 5 poorly-differentiated adenocarcinomas, 1 anaplastic carcinoma, and 1 adenosquamous carcinoma (Table 4). Table 4 shows statistically significant differences in serum CA19-9 and CEA between positive and negative lymph node metastases (*P*<0.01, *P*<0.05), perineural invasion (*P*<0.01, *P*<0.05), and venous invasion (*P*<0.05). However, there appears to be no relationship between the degrees of differentiation of carcinomas and the values of serum CEA and CA19-9.

Table 4 Relation between serum CA19-9 and CEA levels and clinicopathologic features of tumors in 35 patients with cholangiocarcinoma (mean±SD)

	No. of patients	CA19-9 (KU/L)	CEA (µg/L)
Well-differentiated adenocarcinoma	16	261.67±6.31	34.37±11.29
Moderately-differentiated adenocarcinoma	12	270.56±4.57	38.42±19.23
Poorly-differentiated adenocarcinoma	5	302.71±5.81	48.23±23.64
Anaplastic carcinoma	1	468	64
Adenosquamous carcinoma	1	293	27
Perineural infiltration			
Positive	23	310.12±7.11 ^a	37.64±10.35 ^b
Negative	10	195.16±6.48	21.28±13.15
Venous invasion			
Positive	17	318.49±3.27 ^b	39.78±18.41 ^b
Negative	18	253.08±5.37	29.67±20.13
Lymph node metastasis			
Positive	18	345.66±4.23 ^a	46.37±9.46 ^b
Negative	17	265.30±4.58	31.89±16.46

^a*P*<0.01, ^b*P*<0.05 vs negative groups.

DISCUSSION

Since koprowski *et al.*^[19] discovered CA19-9 from the human colon cancer cell line, which has been commonly used in the

diagnosis of pancreatic and biliary malignant diseases. Recently, its usefulness has been demonstrated in the staging, evaluation of resectability, and assessment of prognosis and recurrence, as well as in the initial diagnosis of malignant disorders, especially pancreatic cancer^[31-37].

Elevated concentration of serum CA19-9 (>37 KU·L⁻¹) in bile duct cancers has been frequently reported. Torzilli *et al.*^[38] described a positive rate of 97% in patients with cholangiocarcinoma, whereas Hulcrantz *et al.*^[39] described a rate of 76%, and Caturelli *et al.*^[40] described a 68% rate. We have also found an elevation of CA19-9 in 77.14% of cholangiocarcinomas, which was comparable to the rates reported in other studies. Furthermore, as shown in Table 2, the application of CA19-9 for differentiating cancer from benign biliary diseases was inspiring in our study because of its high sensitivity and specificity. The sensitivity and specificity in our study were 77.14% and 84.78%, respectively, which were similar to 78.2% and 81.4% reported by Kau *et al.*^[41]. However, the concentration of CA19-9 could raise in patients with benign inflammatory conditions as well as in malignant disease^[42-45]. Indeed, Ahrendt *et al.*^[46] reported a moderate increase in CA19-9 concentration in 13.8% of patients with benign biliary tract diseases. The positive serum rate was 28% in patients with acute cholangitis, as reported by Ker *et al.*^[47], and 35.6% in patients with bile duct stones, as reported by Shiozawa *et al.*^[48]. In our present study, an increased concentration of CA19-9 was found in 15.22% of patients with benign biliary diseases. According to Ker *et al.*^[47], CA19-9 was synthesized by normal biliary ductal cells and malignant cells. If bile flow is blocked by biliary obstruction in benign conditions, such as choledocholithiasis, epithelial cells will be markedly impaired by inflammation and will proliferate concurrently. As a result, more CA19-9 may be secreted and leaked out into the bloodstream. An elevated CA19-9 level often returns to normal with appropriate decompression of the common duct or relief of acute cholangitis. However, the increment of CA19-9 in benign diseases is usually not significant, and a concentration of CA19-9 exceeding 480 KU·L⁻¹ is rare. In our study, only 2(2.17%) patients with benign biliary diseases exhibited CA19-9 levels >480 KU·L⁻¹.

CEA is mainly secreted by digestive glandular cancers and their metastases. It has also been found in other types of cancer such as breast, lung, ovary, thyroid cancers. The sensitivity and specificity of serum CEA in our study were 68.57% and 81.52%, respectively, which were similar to 63.3% and 78.4% reported by Ramage *et al.*^[49]. The false positive rate of serum CEA was 18.48% (14/92). Serum CA19-9 was obviously superior to serum CEA in the diagnosis of cholangiocarcinoma and often considered the standard marker for pancreatic cancer and cholangiocarcinoma, with which other markers were compared^[50-53]. Our data also showed a much higher sensitivity with serum CA19-9 than with serum CEA in detecting cholangiocarcinomas, but the sensitivity and specificity could be raised by combining these two tumor markers. Furthermore, no correlation between the levels of serum CEA and CA19-9 was found ($r=0.036$).

Serum CA19-9 has been reported to be able to predict resectability of cholangiocarcinoma^[54-57]. In our study, marked elevation of serum CA19-9 tended to associate with advanced and unresectable biliary cancers. Both serum CA19-9 and CEA levels had a positive correlation with tumor stage. This positive correlation is theoretically helpful in assessing the therapeutic effect and monitoring tumor recurrence after treatment. CA19-9 and CEA have been claimed to have a prognostic value in cholangiocarcinomas^[7,21,24,30,58]. When applied to cholangiocarcinomas, both tumor markers could provide valuable prognostic information. In our study, serum CA19-9 and CEA concentrations were measured in 15 of 35 patients

with cholangiocarcinoma after undergoing curative resection. Within two weeks after operation, the average concentration of serum CA19-9 and CEA was $62.01 \pm 17.43 \text{ KU} \cdot \text{L}^{-1}$ and $28.69 \pm 11.03 \text{ } \mu\text{g} \cdot \text{L}^{-1}$, respectively, with an obvious decrease compared with those before operation ($P < 0.001$ and $P < 0.05$). Hence, serum CA19-9 could provide more important diagnostic and prognostic values than CEA in cholangiocarcinoma.

In summary, serum CA19-9 is an effective tumor marker in diagnosing cholangiocarcinoma, deciding whether the tumor has been radically resected and monitoring the effect of treatment. Serum CA19-9 determination is a useful adjunct in our diagnostic armamentarium for cholangiocarcinoma. However, serum CA19-9 has limitations in diagnosing cholangiocarcinoma. Indeed, our data clearly demonstrated that a negative test could not exclude cholangiocarcinoma. Moreover, for a patient suspected of having biliary cancer, consideration of the presence of acute cholangitis or cholestasis is suggested. If the patient has no evidence of acute cholangitis or cholestasis, a cutoff value of $37 \text{ KU} \cdot \text{L}^{-1}$ may be appropriate. However, if a patient shows symptoms and signs of acute cholangitis or cholestasis, application of CA19-9 should be delayed until after recovery from acute conditions or a cutoff value of $100 \text{ KU} \cdot \text{L}^{-1}$ should be used. Additional bile- or serum-based tests are needed in the diagnosis of cholangiocarcinoma. Ultimately, a profile of tests analogous to liver biochemistry measurement of serum or bile tumor markers and genetic analysis for cholangiocarcinoma-associated mutations will need to be developed to assist in the diagnosis of this disease.

ACKNOWLEDGMENT

This work was supported by the Department of Hepatobiliary Surgery, First Hospital of Xi'an Jiaotong University and Luoyang Central Hospital.

REFERENCES

- 1 Ohtsuka M, Ito H, Kimura F, Shimizu H, Togawa A, Yoshidome H, Miyazaki M. Results of surgical treatment for intrahepatic cholangiocarcinoma and clinicopathological factors influencing survival. *Br J Surg* 2002; **89**: 1525-1531
- 2 Ueno N, Sano T, Kanamaru T, Tanaka K, Nishihara T, Idei Y, Yamamoto M, Okuno T, Kawaguchi K. Adenosquamous cell carcinoma arising from the papilla major. *Oncol Rep* 2002; **9**: 317-320
- 3 Saito M, Hige S, Takeda H, Tomaru U, Shibata M, Asaka M. Combined hepatocellular carcinoma and cholangiocarcinoma growing into the common bile duct. *J Gastroenterol* 2001; **36**: 842-847
- 4 Matsumoto A, Imamura M, Akagi Y, Kaibara A, Ohkita A, Mizobe T, Isomoto H, Aoyagi S. A case report of disseminated recurrence of inferior bile duct carcinoma in PTCF fistula. *Kurume Med J* 2002; **49**: 71-75
- 5 Siqueira E, Schoen RE, Silverman W, Martin J, Rabinovitz M, Weissfeld JL, Abu-Elmagd K, Madariaga JR, Slivka A, Martini J. Detecting cholangiocarcinoma in patients with primary sclerosing cholangitis. *Gastrointest Endosc* 2002; **56**: 40-47
- 6 Qin LX, Tang ZY. Hepatocellular carcinoma with obstructive jaundice: diagnosis, treatment and prognosis. *World J Gastroenterol* 2003; **9**: 385-391
- 7 Kinoshita H, Tanimura H, Uchiyama K, Tani M, Onishi H, Yamaue H. Prognostic factors of intrahepatic cholangiocarcinoma after surgical treatment. *Oncol Rep* 2002; **9**: 97-101
- 8 Kijima H, Takeshita T, Suzuki H, Tanahashi T, Suto A, Izumika H, Miki H, Terasaki Y, Nakamura M, Watanabe H, Tamaoki N, Omiya H. Carcinosarcoma of the ampulla of Vater: a case report with immunohistochemical and ultrastructural studies. *Am J Gastroenterol* 1999; **94**: 3055-3059
- 9 Desa LA, Akosa AB, Lazzara S, Domizio P, Krausz T, Benjamin IS. Cytodiagnosis in the management of extrahepatic biliary stricture. *Gut* 1991; **32**: 1188-1191

- 10 **Davidson B**, Varsamidakis N, Dooley J, Deery A, Dick R, Kurzawinski T, Hobbs K. Value of exfoliative cytology for investigating bile duct strictures. *Gut* 1992; **33**: 1408-1411
- 11 **Shiota K**, Taguchi J, Nakashima O, Nakashima M, Kojiro M. Clinicopathologic study on cholangiolocellular carcinoma. *Oncol Rep* 2001; **8**: 263-268
- 12 **Jiao W**, Yakushiji H, Kitajima Y, Ogawa A, Miyazaki K. Establishment and characterization of human hilar bile duct carcinoma cell line and cell strain. *J Hepatobiliary Pancreat Surg* 2000; **7**: 417-425
- 13 **Chalasanani N**, Baluyut A, Ismail A, Zaman A, Sood G, Ghalib R, McCashland TM, Reddy KR, Zervos X, Anbari MA, Hoen H. Cholangiocarcinoma in patients with primary sclerosing cholangitis: a multicenter case-control study. *Hepatology* 2000; **31**: 7-11
- 14 **Kurzawinski T**, Deery A, Dooley J, Dick R, Hobbs K, Davidson B. A prospective controlled study comparing brush and bile exfoliative cytology for diagnosing bile duct strictures. *Gut* 1992; **33**: 1675-1677
- 15 **Ferrari Junior AP**, Lichtenstein DR, Slivka A, Chang C, Carr-Locke DL. Brush cytology during ERCP for the diagnosis of biliary and pancreatic malignancies. *Gastrointest Endosc* 1994; **40**(2 Pt 1): 140-145
- 16 **Sugiyama M**, Atomi Y, Wada N, Kuroda A, Muto T. Endoscopic transpapillary bile duct biopsy without sphincterotomy for diagnosing biliary strictures: a prospective comparative study with bile and brush cytology. *Am J Gastroenterol* 1996; **91**: 465-467
- 17 **Pugliese V**, Conio M, Nicolo G, Saccomanno S, Gatteschi B. Endoscopic retrograde forceps biopsy and brush cytology of biliary strictures: a prospective study. *Gastrointest Endosc* 1995; **42**: 520-526
- 18 **Lindberg B**, Arnelo U, Bergquist A, Thorne A, Hjerpe A, Granqvist S, Hansson LO, Tribukait B, Persson B, Broome U. Diagnosis of biliary strictures in conjunction with endoscopic retrograde cholangiopancreatography, with special reference to patients with primary sclerosing cholangitis. *Endoscopy* 2002; **34**: 909-916
- 19 **Koprowski H**, Stepiewski Z, Mitchell K, Herlyn M, Herlyn D, Fubrer P. Colorectal carcinoma antigens detected by hybridoma antibodies. *Somatic Cell Genet* 1979; **5**: 957-971
- 20 **Louhimo J**, Finne P, Alfthan H, Stenman UH, Haglund C. Combination of HCGbeta, CA19-9 and CEA with logistic regression improves accuracy in gastrointestinal malignancies. *Anticancer Res* 2002; **22**: 1759-1764
- 21 **Nanashima A**, Yamaguchi H, Nakagoe T, Matsuo S, Sumida Y, Tsuji T, Sawai T, Yamaguchi E, Yasutake T, Ayabe H. High serum concentrations of sialyl Tn antigen in carcinomas of the biliary tract and pancreas. *J Hepatobiliary Pancreat Surg* 1999; **6**: 391-395
- 22 **Safi F**, Schlosser W, Falkenreck S, Beger HG. Prognostic value of CA 19-9 serum course in pancreatic cancer. *Hepatogastroenterology* 1998; **45**: 253-259
- 23 **Zheng CX**, Zhan WH, Zhao JZ, Zheng D, Wang DP, He YL, Zheng ZQ. The prognostic value of preoperative serum levels of CEA, CA19-9 and CA72-4 in patients with colorectal cancer. *World J Gastroenterol* 2001; **7**: 431-434
- 24 **Hyman J**, Wilczynski SP, Schwarz RE. Extrahepatic bile duct stricture and elevated CA 19-9: malignant or benign? *South Med J* 2003; **96**: 89-92
- 25 **Chen CY**, Shiesh SC, Tsao HC, Lin XZ. The assessment of biliary CA 125, CA 19-9 and CEA in diagnosing cholangiocarcinoma—the influence of sampling time and hepatolithiasis. *Hepatogastroenterology* 2002; **49**: 616-620
- 26 **Kitagawa Y**, Iwai M, Muramatsu A, Tanaka S, Mori T, Harada Y, Okanoue T, Kashima K. Immunohistochemical localization of CEA, CA19-9 and DU-PAN-2 in hepatitis C virus-infected liver tissues. *Histopathology* 2002; **40**: 472-479
- 27 **Qin XL**, Shi JS, Shi L, Wang ZR, Wang L. Clinical value of CA19-9 determination in patients with bile duct carcinoma. *Shijie Huaren Xiaohua Zazhi* 1999; **7**: 814-815
- 28 **Giannini E**, Borro P, Botta F, Chiarbonello B, Fasoli A, Malfatti F, Romagnoli P, Testa E, Risso D, Lantieri PB, Antonucci A, Boccato M, Milone S, Testa R. Cholestasis is the main determinant of abnormal CA 19-9 levels in patients with liver cirrhosis. *Int J Biol Markers* 2000; **15**: 226-230
- 29 **Watanabe M**, Chigusa M, Takahashi H, Nakamura J, Tanaka H, Ohno T. High level of CA19-9, CA50, and CEA-producible human cholangiocarcinoma cell line changes in the secretion ratios *in vitro* or *in vivo*. *In Vitro Cell Dev Biol Anim* 2000; **36**: 104-109
- 30 **Qin XL**, Li ZQ, Shi JS, Zhang L, Wang ZR, Wang L. Value of bile and serum CA19-9 and CEA in diagnosing biliary tract Carcinoma. *Chin J Bases Clin Genet Surg* 2000; **7**: 161-163
- 31 **Haglund C**, Ylatupa S, Mertaniemi P, Partanen P. Cellular fibronectin concentration in the plasma of patients with malignant and benign diseases: a comparison with CA 19-9 and CEA. *Br J Cancer* 1997; **76**: 777-783
- 32 **Botzger TC**, Junginger T. Treatment of tumors of the pancreatic head with suspected but unproved malignancy: is a nihilistic approach justified? *World J Surg* 1999; **23**: 158-162
- 33 **Ogawa T**, Yokoi H, Kawarada Y. A case of inflammatory pseudotumor of the liver causing elevated serum CA19-9 levels. *Am J Gastroenterol* 1998; **93**: 2551-2555
- 34 **Montgomery RC**, Hoffma JP, Ross EA, Riley LB, Ridge JA, Eisenberg BL. Biliary CA 19-9 values correlate with the risk of hepatic metastases in patients with adenocarcinoma of the pancreas. *J Gastrointest Surg* 1998; **2**: 28-35
- 35 **Goetz M**, Steen PD. False elevation of CA 19-9 levels in a patient with a history of pancreatic cancer. *Am J Gastroenterol* 1997; **92**: 1390-1391
- 36 **Brown RW**, Campagna LB, Dunn JK, Cagle PT. Immunohistochemical identification of tumor markers in metastatic adenocarcinoma. A diagnostic adjunct in the determination of primary site. *Am J Clin Pathol* 1997; **107**: 12-19
- 37 **Zhao XY**, Yu SY, Da SP, Bai L, Guo XZ, Dai XJ, Wang YM. A clinical evaluation of serological diagnosis for pancreatic cancer. *World J Gastroenterol* 1998; **4**: 147-149
- 38 **Torzilli G**, Makuuchi M, Ferrero A, Takayama T, Hui AM, Abe H, Inoue K, Nakahara K. Accuracy of the preoperative determination of tumor markers in the differentiation of liver mass lesions in surgical patients. *Hepatogastroenterology* 2002; **49**: 740-745
- 39 **Hultcrantz R**, Olsson R, Danielsson A, Jarnerot G, Loof L, Ryden BO, Wahren B, Broome U. A 3-year prospective study on serum tumor markers used for detecting cholangiocarcinoma in patients with primary sclerosing cholangitis. *J Hepatol* 1999; **30**: 669-673
- 40 **Caturelli E**, Bisceglia M, Villani MR, de Maio G, Siena DA. CA19-9 production by a cystadenoma with mesenchymal stroma of the common hepatic duct: a case report. *Liver* 1998; **18**: 221-224
- 41 **Kau SY**, Shyr YM, Su CH, Wu CW, Lui WY. Diagnostic and prognostic values of CA19-9 and CEA in periampullary cancers. *J Am Coll Surg* 1999; **188**: 415-420
- 42 **Minato H**, Nakanuma Y, Terada T. Expression of blood group-related antigens in cholangiocarcinoma in relation to non-neoplastic bile ducts. *Histopathology* 1996; **28**: 411-419
- 43 **Bjornsson E**, Kilander A, Olsson R. CA19-9 and CEA are unreliable markers for cholangiocarcinoma in patients with primary sclerosing cholangitis. *Liver* 1999; **19**: 501-508
- 44 **Lin CL**, Changchien CS, Chen YS. Mirizzi's syndrome with a high CA19-9 level mimicking cholangiocarcinoma. *Am J Gastroenterol* 1997; **92**: 2309-2310
- 45 **Horsmans Y**, Laka A, van Beers BE, Descamps C, Gigot JF, Geubel AP. Hepatobiliary cystadenocarcinoma without ovarian stroma and normal CA19-9 levels. Unusually prolonged evolution. *Dig Dis Sci* 1997; **42**: 1406-1408
- 46 **Ahrendt SA**, Pitt HA, Nakeeb A, Klein AS, Lillemoe KD, Kalloo AN, Cameron JL. Diagnosis and management of cholangiocarcinoma in primary sclerosing cholangitis. *J Gastrointest Surg* 1999; **3**: 357-367
- 47 **Ker CG**, Chen JS, Lee KT, Sheen PC, Wu CC. Assessment of serum and bile levels of CA19-9 and CA125 in cholangitis and bile duct carcinoma. *J Gastroenterol Hepatol* 1991; **6**: 505-508
- 48 **Shiozawa K**, Ishii K, Mori T, Takamura N, Ikehara T, Shinohara M, Kawafune T, Sumino Y, Nonaka H. Heterochronous development of intrahepatic cholangiocellular carcinoma following hepatocellular carcinoma in a hepatitis B virus carrier. *Intern Med*

- 2001; **40**: 624-630
- 49 **Ramage JK**, Donaghy A, Farrant JM, Iorns R, Williams R. Serum tumor markers for the diagnosis of cholangiocarcinoma in primary sclerosing cholangitis. *Gastroenterology* 1995; **108**: 865-869
- 50 **Haglund C**, Lundin J, Kuusela P, Roberts PJ. CA 242, a new tumor marker for pancreatic cancer: a comparison with CA 19-9, CA 50 and CEA. *Br J Cancer* 1994; **70**: 487-492
- 51 **Shimada M**, Yamashita Y, Aishima S, Shirabe K, Takenaka K, Sugimachi K. Value of lymph node dissection during resection of intrahepatic cholangiocarcinoma. *Br J Surg* 2001; **88**: 1463-1466
- 52 **Tsuji M**, Kashihara T, Terada N, Mori H. An immunohistochemical study of hepatic atypical adenomatous hyperplasia, hepatocellular carcinoma, and cholangiocarcinoma with alpha-fetoprotein, carcinoembryonic antigen, CA19-9, epithelial membrane antigen, and cytokeratins 18 and 19. *Pathol Int* 1999; **49**: 310-317
- 53 **Ramage JK**, Donaghy A, Farrant JM, Iorns R, Williams R. Serum tumor markers for the diagnosis of cholangiocarcinoma in primary sclerosing cholangitis. *Gastroenterology* 1995; **108**: 865-869
- 54 **Dorandeu A**, Raoul JL, Siriser F, Leclercq-Rioux N, Gosselin M, Martin ED, Ramee MP, Launois B. Carcinoma of the ampulla of Vater: prognostic factors after curative surgery: a series of 45 cases. *Gut* 1997; **40**: 350-355
- 55 **Forsmark CE**, Lambiase L, Vogel SB. Diagnosis of pancreatic cancer and prediction of unresectability using the tumor-associated antigen CA19-9. *Pancreas* 1994; **9**: 731-734
- 56 **Yasue M**, Sakamoto J, Teramukai S, Morimoto T, Yasui K, Kuno N, Kurimoto K, Ohashi Y. Prognostic values of preoperative and postoperative CEA and CA19-9 levels in pancreatic cancer. *Pancreas* 1994; **9**: 735-740
- 57 **Nakamura S**, Suzuki S, Sakaguchi T, Konno H, Baba S, Kosugi I, Muro H. Second cancer during long-term survival after resection of biliary tract carcinoma. *J Gastroenterol* 1996; **31**: 289-293
- 58 **Su WC**, Chan KK, Lin XZ, Lin PW, Chow NH, Shin JS, Chen CY, Tsao CJ. A clinical study of 130 patients with biliary tract cancers and periampullary tumors. *Oncology* 1996; **53**: 488-493

Edited by Zhang JZ and Wang XL

Extraction of protoporphyrin disodium and its inhibitory effects on HBV-DNA

Chao-Pin Li, Li-Fa Xu, Qun-Hong Liu, Chao Zhang, Jian Wang, Yu-Xia Zhu

Chao-Pin Li, Li-Fa Xu, Qun-Hong Liu, Chao Zhang, Jian Wang, Yu-Xia Zhu, Medical College, Anhui University of Science and Technology, Huainan 232001, Anhui Province, China

Supported by the Natural Science Foundation of Anhui Province, No. 2000j1222

Correspondence to: Dr. Chao-Pin Li, Department of Etiology and Immunology, Huainan 232001, Anhui Province, China. cpli@aust.edu.cn

Telephone: +86-554-6658770 **Fax:** +86-554-6662469

Received: 2003-04-10 **Accepted:** 2003-10-07

Abstract

AIM: To explore an ideal method for extracting protoporphyrin disodium (PPN) from unanticoagulated animal blood, and to study the inhibitory effects of PPN on HBV-DNA duplication and its cytotoxicity to 2.2.15 cell strain.

METHODS: Protoporphyrin methyl ester and other intermediate products were prepared with protoheme separated from protein hydrolysates of coagulated animal blood, which were finally made into PPN and detected quantitatively with an ultraviolet fluorescent analyzer. Ten $\mu\text{g/ml}$, 20 $\mu\text{g/ml}$, 40 $\mu\text{g/ml}$, 80 $\mu\text{g/ml}$ and 160 $\mu\text{g/ml}$ of PPN-aqueous solution were added into culture medium for 2.2.15 cells respectively. Eight days later, the drug concentration in supernatant from the culture medium was detected when inhibition rate of HBeAg, cell survival rate when inhibition rate of HBeAg was 50% (ID50), and when survival cells in experimental group were 50% of those in control group (CD50), and the therapeutic index (TI) was also detected. PPN with different concentration of 10 $\mu\text{g/ml}$, 20 $\mu\text{g/ml}$, 40 $\mu\text{g/ml}$, 80 $\mu\text{g/ml}$ and 160 $\mu\text{g/ml}$ was respectively mixed and cultivated with HepG2 2.2.15 cell suspension, and then the inhibition of PPN against HBV-DNA was judged by PCR.

RESULTS: The extract of henna crystal was identified to be PPN. When the concentrations of PPN were 160 $\mu\text{g/ml}$ and 80 $\mu\text{g/ml}$, the inhibition rates of HBeAg were 89.8% and 82.4%, and the cell survival rates were 98.7% and 99.2%.

CONCLUSION: It is suggested that PPN can be extracted from unanticoagulated animal blood. PPN can inhibit HBV-DNA expression and duplication *in vitro*, and has no cytotoxicity to liver cells. Further study and application of PPN are warranted.

Li CP, Xu LF, Liu QH, Zhang C, Wang J, Zhu YX. Extraction of protoporphyrin disodium and its inhibitory effects on HBV-DNA. *World J Gastroenterol* 2004; 10(3):433-436

<http://www.wjgnet.com/1007-9327/10/433.asp>

INTRODUCTION

Protoporphyrin disodium (PPN) is a macrocyclic compound with a conjugated double bond, which is consisted of four

pyrrole rings connected by four methylene bonds, and is a derivative of porphine. PPN can be prepared with extracted haemachrome originated from ferrohemoglobin in serum and other chemicals. PPN is a pharmaceuticals to improve liver functions and can be used in clinical therapy for recovery of injured liver cells.

PPN could be obtained from fresh anticoagulant animal blood according to reports^[1-3]. But the PPN in this study was obtained from fresh unanticoagulated animal blood, and the method has not been reported in the literature.

Hepatitis B is widely occurred in China, and severely affects people's health and the quality of life. In order to find out the relationship between PPN and the expression and duplication of HBV-DNA, hoping to seek for an effective therapy of Hepatitis B, we designed an experimental *in vitro* study.

MATERIALS AND METHODS

Reagents

Unanticoagulated pig blood (from Huainan area), NaOH, zinc powder, chloroform, skellysolve G, 2.2.15 cell strain (from the Institute of Infectious Disease, Peking Medical University), kit for ELISA (from Huamei Biological Engineering Co.,Ltd), kit for PCR (from Huamei Biological Engineering Co.,Ltd).

Instruments

Tissue homogenate instrument (from Shanghai Biaomo), magnetic stirring apparatus, glassy device of reflux, glassy filter, chromatography column with neutral aluminium oxide (from Shanghai-Jinhua Chromatography Equipment Factory), drying oven by electrothermal blow (from Shanghai-Yuejin Equipment Factory), gamma radio immunoassay counters (from State-Operated Factory 262), CO₂ incubator (from Japan), SLT-Spectra-I enzyme analyzer (from America), DNA amplifier (from Zhuhai Hema Bio-Tech Institute), ultraviolet fluorescent analyzer (from Shanghai-Kanghua Biochemical Instrument Manufactory).

Methods

Extraction of protoheme 1L homogenate of unanticoagulated pig bloods was added to a container, and 100 g NaOH was added simultaneously during stirring until they were well mixed. When the mixture changed into dilute solution after placement for 24 h, it was heated and stirred by magnetic stirring apparatus at the 80 °C to 90 °C for 12 hours. When the mixture was naturally cooled to 60 °C, 1M HCL aqueous solution was added into the mixture till precipitation of protoheme occurred. The precipitation was taken out, washed 3 times with water and dried. Finally about 1.7g of protoheme was obtained.

Preparation of crude protoporphyrin 1.5 g zinc powder divided into six portions was added into the mixture of 250 ml formic acid aqueous solution (85%) and 5 g protoheme under the condition of heating, stirring and regurgitating respectively. Each addition had an interval of 5 minutes. Then they were heated and regurgitated once more for 20 min and then cooled and filtered. Ammonium acetate aqueous solution (20%) was

added into the filtrate, then the solution was filtered when crystals occurred after placement for 12 h. After the crystals were dissolved with 600 ml ammonia water (2%), ammonium acetate aqueous solution (30%) was added into the solute and placed for 12 h till crystallization occurred. The crystals were filtered out and washed 3 times with 600 ml ammonium acetate aqueous solution (2%) and 90 ml distilled water, respectively. Then it was dried into crude protoporphyrin, which was a kind of brown crystalline materials of about 2 g.

Preparation of protoporphyrin methyl ester 5 g crude protoporphyrin was dissolved in 200 ml hydrochloric methanol aqueous solution (1%), and the reactants were heated, regurgitated for 20 min. Then 1 000 ml ammonium carbonate aqueous solution (1%) was added into the above cooled reactants and placed till crystallization occurred. The crystalline materials were taken, and washed 3 times with distilled water, then dissolved in 200 ml chloroform and the solute was taken to pass through chromatography column with 1 000 g neutral aluminium oxide. After the elution with prepared eluting agent of chloroform and petroleum ether with volumetric proportion at the ratio of 1 to 3 was completed, the eluent of protoporphyrin methyl ester was collected and evaporated, and a kind of brown crystalline materials was obtained. Then the brown crystalline materials were crystallized 2 times with chloroform and methanol, and 2 g protoporphyrin methyl ester was acquired.

Preparation of pure protoporphyrin 5 g protoporphyrin methyl ester was dissolved in 150 ml HCL aqueous solution (25%). After placed for 8 h, the reactants were neutralized with NaOH aqueous solution (30%), then crystallization occurred. The crystalline materials were isolated and washed 3 times with distilled water. After being dried, the crystalline materials were re-crystallized 2 times with pyridine, and 2.5 g brown pure protoporphyrin was obtained.

Preparation of PPN The mixture of 10 g pure protoporphyrin, 5 g NaOH and 500 ml anhydrous alcohol was heated and regurgitated for 2 h. Crystalline materials occurred after the mixture was cooled. Then the crystalline materials were isolated, washed 3 times with anhydrous alcohol and dried. Finally, 9 g brown crystalline materials of PPN was obtained.

Inhibitory effects of PPN on HBV-DNA expression *in vitro* 2.2.15 cell strain was prepared based on human cancer cell strain of the liver, HepG₂, which had been infected with HBV-DNA, could express all marks of duplications of HBV-DNA effectively^[4-17]. Regarding 2.2.15 cell strain as the target cell, the effect of PPN on HBV-DNA was confirmed by detecting the levels of HBeAg in culture supernatants with quantitative methods.

Procedure was as follows: 1×10^5 /ml cell suspension was prepared with 2.2.15 cell strain which grew well. One ml cell suspension was added into each of the 24-hole plastic plate respectively and cultivated. After incubation at 37 °C for 48 h, fresh culture media with different concentrations of PPN (10 µg/ml, 20 µg/ml, 40 µg/ml, 80 µg/ml, 160 µg/ml) were then replaced every 3 days. Eight days later, supernatants were collected and stored at 20 °C for detection of HBeAg levels and cytotoxicity of PPN to liver cells. ELISA was used for detection of HBeAg. The detailed procedure followed the operating instructions. Inhibition rate (%)=(P/N values of the control holes- P/N values of the study holes)/(P/N values of the control holes -2.1)×100%, and ID₅₀ represented the concentration of PPN when the inhibition rate of HBeAg was 50%. The cytotoxicity of PPN to liver cells was detected by MTT to determine the survival rate of liver cells. The survival rate of liver cells (%)=values of the study holes (A₅₉₅-A₆₅₀)/ values of the control holes (A₅₉₅-A₆₅₀)×100%. CD₅₀ represented the concentration of PPN when the number of the survival cells in the detected holes to the survival cells in the study holes was 50%.

Inhibitory effects of PPN on HBV were evaluated with TI (TI=CD₅₀/ID₅₀). When TI<1, PPN was cytotoxic and poorly effective on liver cells. When 1<TI<2, PPN was cytotoxic and effective. When TI≥2, PPN was mildly cytotoxic and effective. The higher the values of TI, the greater the inhibitory effects of PPN on HBV and the less the cytotoxicity of PPN to liver cells^[18,19] (Table 1).

Inhibitory effects of PPN on HBV-DNA duplication *in vitro* PPN was diluted to a series of solutions with different concentrations (including 10 µg/ml, 20 µg/ml, 40 µg/ml, 80 µg/ml and 160 µg/ml) by aseptic techniques for further use. HepG₂ 2.2.15 cells in good cultivation were dispensed to the suspension with a concentration of 1×10^5 /ml, 6 identical shares of it were subsequently taken out, PPN with the concentration of 10 µg/ml, 20 µg/ml, 40 µg/ml, 80 µg/ml and 160 µg/ml respectively was added to 5 of 6, the remaining one had no PPN. After a period of cultivation, the cells were collected, then whole genome DNA of them was extracted by using CASSupper blood genomic DNA isolation kit and further amplified by PCR. The amplification system included 10×buffer 25 ul, dNTP 3 ul, sense 0.5 ul, anti-sense 0.5 ul, TaqE 1.5 ul and template 2 ul. The parameters included at 95 °C for 5 min, at 94 °C for 30 s, at 55 °C for 30 s, at 72 °C for 30 s, 35 cycles and extension at 72 °C for 5 min. The final products with DGL-2000 were further performed with routine electrophoresis. During the process of analysing by using agarose gel electrophoresis containing EB, each hole was added 10 ul of products and placed at 80-100V for 20 min. Lastly, the agar plates were observed by ultraviolet fluorescence analysis.

RESULTS

General characteristics of PPN

The prepared PPN was brown crystalline materials, soluble in water, slightly soluble in methyl alcohol, but not soluble in chloroform, diethyl ether or dimethyl ketone. PPN displayed absorption peaks at wavelengths of 600 nm, 556 nm and 408 nm, and the maximal absorption wavelength was 408 nm. When exposed to ultraviolet, strong fluorescence could be observed in red^[3].

Quantitative detection of PPN

According to the fact that when PPN was dissolved in 1.37M HCL and placed at wavelength of 408 nm, the $E_{1\text{cm}}^{1\%}$ was 4.81×10^3 , the purity of PPN extract was detected to be 97.3%.

Inhibitory effects of PPN on HBV-DNA *in vitro*

Table 1 Inhibition of PPN on HBV-DNA expression *in vitro*

PPN (µg/ml)	OD	Inhibition rate of HBeAg (%)	Survival rate of liver cell (%)
160	1.20	89.8	98.7
80	1.30	82.4	99.2
40	1.50	56.7	100
20	1.85	32.3	100
10	2.30	5.5	100

CD₅₀=279.4 µg/ml, ID₅₀=37.4 µg/ml, TI=7.47.

Table 1 shows that when the concentrations of PPN were 160 µg/ml and 80 µg/ml, the inhibition rates of HBeAg were 89.8% and 82.4% respectively and cellular survival rates were 98.7% and 99.2%, TI=7.47.

It was obvious that the luminance of amplified bands of samples without addition of PPN was the brightest, while that of samples with addition of PPN decreased gradually accompanying increased concentration of PPN.

DISCUSSION

While fresh anticoagulated animal blood was used as raw materials to prepare PPN, the harvest, transportation, and preservation of the raw materials needed a strict condition, which made the source of raw materials limited, working cost increased and the scale of production limited. In this study, unanticoagulated animal blood was used as raw materials to prepare PPN, that is, the form of the raw materials was improved. Using unanticoagulated animal blood as raw materials to prepare PPN, fine PPN could be obtained. The method is an ideal way of preparing PPN at present. Meanwhile, it can solve the problems mentioned. In addition, during the whole process of preparation, the special, expensive reagents are not necessary and also some reagents can be retrieved for reuse. The method is simple and convenient in its process of preparation and its production cost is lower. If some of amino acids produced during the preparation were studied, analyzed and purified, the additional value of the raw materials would be increased, so that large amount of animal blood resource can be fully utilized.

Protoporphyrin is the necessary component of ferroheme, myoheme, cytochrome, catalase and tryptophan pyrrolase in human body. Protoporphyrin showed a circular structure in somatic cells, and could easily combine with metallic ion to form metallic porphyrin^[21]. In the case of liver disease, liver functions might be in disorder, porphyrin and metallic porphyrin in bile decrease as well as the activity of catalase in liver would decrease. Therefore, PPN could activate the biosynthesis of porphyrin and metallic porphyrin in cells as demonstrated by *in vitro* test, increase the quantity of metallic porphyrin in cells, inhibit the decrease of activity of catalase, improve cellular respiration and regeneration, and decrease the necrosis of liver cells with recovery of its function. Based upon the above metabolic properties, PPN could improve blood flow and utilization rate of oxygen by liver and other related organs, accelerate the respiration of histocytes, improve metabolism of proteins and carbohydrates, enhance effects of complement fixation, and enhance immunity, anti-inflammation and anti-anaphylaxis potentials of the organism. Thus, PPN has been constantly studied and applied as an improving agent of liver functions^[22-32]. At present, PPN is being studied for its antineoplastic effects in foreign countries. Inhibitory effects of PPN on expression and duplication of HBV-DNA *in vitro* was studied by us from another point of view. As table 1 shows, PPN could inhibit expression of HBV-DNA *in vitro* and had no cytotoxic action, and it is not difficult to see that the luminance of amplified bands decreased gradually with increased concentration of PPN. The mechanism of action in the above results might be that some intermediary metabolites of PPN in liver cells could affect antisense oligonucleotides (ASONs) located at pre-C and C gene regions of HBV and also adjust genes ENH I of HBV through ASONs. Then it could finally inhibit the duplication of HBV-DNA and the expression of HBeAg in host cells^[33-35]. Therefore, further study and application of PPN in clinical therapy of hepatitis B should be carried out.

ACKNOWLEDGEMENTS

The authors thank the staff of Department of Biochemistry for their help and the instruction of Professor YE Ke-qiang for the instruction.

REFERENCES

- 1 **Chamberlain MP**, Lock EA, Gaskell BA, Reed CJ. The role of glutathione S-transferase- and cytochrome P450-dependent metabolism in the olfactory toxicity of methyl iodide in the rat. *Arch Toxicol* 1998; **72**: 420-428
- 2 **Ratra GS**, Cottrell S, Powell CJ. Effects of induction and inhibition of cytochromes P450 on the hepatotoxicity of methapyrilene. *Toxicol Sci* 1998; **46**: 185-196
- 3 **Ackley KL**, Day JA, Caruso JA. Separation of metalloporphyrins by capillary electrophoresis with UV detection and inductively coupled plasma mass spectrometric detection. *J Chromatogr A* 2000; **888**: 293-298
- 4 **Zhang S**, Wang S, Wang Y. Inhibition of hepatitis B virus replication *in vitro* by phosphorothioate and tetradecyl phosphorothioate analogs of antisense oligonucleotide directed against precore and core regions. *Zhonghua Neike Zazhi* 1996; **35**: 95-98
- 5 **Ji W**, St CW. Inhibition of hepatitis B virus by retroviral vectors expressing antisense RNA. *J Viral Hepat* 1997; **4**: 167-173
- 6 **Lara-Pezzi E**, Majano PL, Gomez-Gonzalo M, Garcia-Monzon C, Moreno-Otero R, Levrero M, Lopez-Cabrera M. The hepatitis B virus X protein up-regulates tumor necrosis factor alpha gene expression in hepatocytes. *Hepatology* 1998; **28**: 1013-1021
- 7 **Ji W**, Wang Q, Yu M. Transfer and expression of antisense genes of hepatitis B virus (HBV) and their anti-HBV effects. *Zhonghua Yixue Zazhi* 1997; **77**: 425-429
- 8 **Zhang J**, Chen F, Zhong S, Tang K, Shi X, Wang M, Peng J. Anti-HBV effect of targeted antisense RNA against HBV C gene. *Zhonghua Ganzangbing Zazhi* 2000; **8**: 169-170
- 9 **Yang Z**, Deng X, Zhang F, Wu W, Lei C, Zhu Y. The effect of attenuated varicella-zoster virus on replication of HBV. *Zhonghua Ganzangbing Zazhi* 2001; **9**: 28-30
- 10 **Lu X**, Lu Y, Geschwindt R, Dwek RA, Block TM. Hepatitis B virus MHBs antigen is selectively sensitive to glucosidase-mediated processing in the endoplasmic reticulum. *DNA Cell Biol* 2001; **20**: 647-656
- 11 **Wu C**, Zeng Z, Wang Q. Experimental study of inhibition of hepatitis B by dual-target antisense RNA. *Zhonghua Yixue Zazhi* 2001; **81**: 605-608
- 12 **Cao H**, Tao P. Anti-hepatitis B virus effects of lamivudine and other five drugs *in vitro*. *Zhonghua Yixue Zazhi* 2001; **81**: 1004-1007
- 13 **Chih HW**, Chiu HF, Tang KS, Chang FR, Wu YC. Bullatacin, a potent antitumor annonaceous acetogenin, inhibits proliferation of human hepatocarcinoma cell line 2.2.15 by apoptosis induction. *Life Sci* 2001; **69**: 1321-1331
- 14 **Zhong S**, Wen S, Zhang D. Inhibition of HBV gene expression by antisense oligonucleotides using galactosylated poly (L-lysine) as a hepatotropic carrier. *Zhonghua Shiyuan He Linchuang Bingduxue Zazhi* 2001; **15**: 150-153
- 15 **Sun D**, Hu D, Wu G, Hu X, Li J, Fan G. Construction and expression of recombinant retrovirus vector carrying HBV vector. *Zhonghua Shiyuan He Linchuang Bingduxue Zazhi* 2002; **16**: 162-165
- 16 **Dandri M**, Burda MR, Burkle A, Zuckerman DM, Will H, Rogler CE, Greten H, Petersen J. Increase in de novo HBV DNA integrations in response to oxidative DNA damage or inhibition of poly (ADP-ribosyl) ation. *Hepatology* 2002; **35**: 217-223
- 17 **Tan TM**, Zhou L, Houssais S, Seet BL, Jaenicke S, Peter F, Lim SG. Intracellular inhibition of hepatitis B virus S gene expression by chimeric DNA-RNA phosphorothioate minimized ribozyme. *Antisense Nucleic Acid Drug Dev* 2002; **12**: 257-264
- 18 **Oh SH**, Yeh BI, Kim SH. Inhibition of HBV replication by antisense oligodeoxyribonucleotides in HepG2 cells transfected with a cloned HBV DNA. *Yonsei Med J* 1995; **36**: 527-533
- 19 **Zhong S**, Zheng SJ, Chen F, Wen SM, Wang SQ, Zhang JJ, Deng CL. *In vivo* inhibition of hepatitis B virus replication and gene expression by targeted phosphorothioate modified antisense oligodeoxynucleotides. *Zhonghua Ganzangbing Zazhi* 2002; **10**: 283-286
- 20 **Zekri AR**, Awlia AA, El Mahalawi H, Ismail EF, Mabrouk GM. Evaluation of blood units with isolated anti HBC for the presence of HBVDNA. *Dis Markers* 2002; **18**: 107-110
- 21 **Jacob Blackmon B**, Dailey TA, Lianchun X, Dailey HA. Characterization of a human and mouse tetrapyrrole-binding protein. *Arch Biochem Biophys* 2002; **407**: 196-201
- 22 **Fiala ES**, Sohn OS, Li H, El-Bayoumy K, Sodum RS. Inhibition of 2-nitropropane-induced rat liver DNA and RNA damage by benzyl selenocyanate. *Carcinogenesis* 1997; **18**: 1809-1815
- 23 **Cable EE**, Gildemeister OS, Pepe JA, Lambrecht RW, Bonkovsky HL. Mechanism of induction of heme oxygenase by

- metalloporphyrins in primary chick embryo liver cells: evidence against a stress-mediated response. *Mol Cell Biochem* 1997; **169**: 13-20
- 24 **Iyer S**, Woo J, Cornejo MC, Gao L, McCoubrey W, Maines M, Buelow R. Characterization and biological significance of immunosuppressive peptide D2702.75-84(E→V) binding protein. Isolation of heme oxygenase-1. *J Biol Chem* 1998; **273**: 2692-2697
- 25 **Woo J**, Iyer S, Cornejo MC, Mori N, Gao L, Sipos I, Maines M, Buelow R. Stress protein-induced immunosuppression: inhibition of cellular immune effector functions following overexpression of haem oxygenase (HSP 32). *Transpl Immunol* 1998; **6**: 84-93
- 26 **Chamberlain MP**, Lock EA, Gaskell BA, Reed CJ. The role of glutathione S-transferase- and cytochrome P450-dependent metabolism in the olfactory toxicity of methyl iodide in the rat. *Arch Toxicol* 1998; **72**: 420-428
- 27 **Ratra GS**, Cottrell S, Powell CJ. Effects of induction and inhibition of cytochromes P450 on the hepatotoxicity of methapyrilene. *Toxicol Sci* 1998; **46**: 185-196
- 28 **Amersi F**, Buelow R, Kato H, Ke B, Coito AJ, Shen XD, Zhao D, Zaky J, Melinek J, Lassman CR, Kolls JK, Alam J, Ritter T, Volk HD, Farmer DG, Ghobrial RM, Busuttil RW, Kupiec-Weglinski JW. Upregulation of heme oxygenase-1 protects genetically fat Zucker rat livers from ischemia/reperfusion injury. *J Clin Invest* 1999; **104**: 1631-1639
- 29 **Shan Y**, Pepe J, Lu TH, Elbirt KK, Lambrecht RW, Bonkovsky HL. Induction of the heme oxygenase-1 gene by metalloporphyrins. *Arch Biochem Biophys* 2000; **330**: 219-227
- 30 **Kato H**, Amersi F, Buelow R, Melinek J, Coito AJ, Ke B, Busuttil RW, Kupiec-Weglinski JW. Heme oxygenase-1 overexpression protects rat livers from ischemia/reperfusion injury with extended cold preservation. *Am J Transplant* 2001; **1**: 121-128
- 31 **Redaelli CA**, Tian YH, Schaffner T, Ledermann M, Baer HU, Dufour JF. Extended preservation of rat liver graft by induction of heme oxygenase-1. *Hepatology* 2002; **35**: 1082-1092
- 32 **Shan Y**, Pepe J, Lambrecht RW, Bonkovsky HL. Mapping of the chick heme oxygenase-1 proximal promoter for responsiveness to metalloporphyrins. *Arch Biochem Biophys* 2002; **399**: 159-166
- 33 **Zhou S**, Wen SM, Zhang DF, Wang QL, Wang SQ, Ren H. Sequencing of PCR amplified HBV DNA pre-c and c regions in the 2.2.15 cells and antiviral action by targeted antisense oligonucleotide directed against sequence. *World J Gastroenterol* 1998; **4**: 434-436
- 34 **Zhou S**, Wen S, Zhang D. Inhibition of HBV gene expression by antisense oligonucleotides using galactosylated poly (L-lysine) as a hepatotropic carrier. *Zhonghua Shiyan He Linchuang Bingduxue Zazhi* 2001; **15**: 150-153
- 35 **Schulte-Frohlinde E**, Seidler B, Burkard I, Freilinger T, Lersch C, Erfle V, Foster GR, Classen M. Different activities of type I interferons on hepatitis B virus core promoter regulated transcription. *Cytokine* 2002; **17**: 214-220

Edited by Xu JY and Wang XL

Mechanism of intrauterine infection of hepatitis B virus

Shu-Lin Zhang, Ya-Fei Yue, Gui-Qin Bai, Lei Shi, Hui Jiang

Shu-Lin Zhang, Department of Infectious Disease, First Hospital of Xi'an Jiaotong University, Xi'an 710061, Shaanxi Province, China
Ya-Fei Yue, Gui-Qin Bai, Lei Shi, Department of Gynecology and Obstetrics, First Hospital of Xi'an Jiaotong University, Xi'an 710061, Shaanxi Province, China

Hui Jiang, Hospital of Women's and Children's Health Care, Zhaoqing 526060, Guangdong Province, China

Supported by the Science and Technology Bureau of Shaanxi Province, 90KY-G10

Correspondence to: Dr. Shu-Lin Zhang, Department of Infectious Disease, First Hospital of Xi'an Jiaotong University, Jiankang Road 1#, Xi'an 710061, Shaanxi Province, China. zhangsl451206@vip.163.com

Telephone: +86-029-5252812 **Fax:** +86-029-5252812

Received: 2003-06-16 **Accepted:** 2003-08-18

Abstract

AIM: To explore the possible mechanism of intrauterine infection of hepatitis B virus (HBV).

METHODS: HBV DNA was detected in vaginal secretion and amniotic fluid from 59 HBsAg-positive mothers and in venous blood of their newborns by PCR. HBsAg and HbCag in placenta were determined by ABC immunohistochemistry.

RESULTS: The rate of HBV intrauterine infection was 40.1% (24/59). HBV DNA was detected in 47.5% of amniotic fluid samples and 52.5% of vaginal secretion samples respectively. HBsAg and HbCag were detected in placentas from HBsAg-positive mothers. The concentration of the two antigens decreased from the mother's side to the fetus's side, in the following order: maternal decidual cells > trophoblastic cells > villous mesenchymal cells > villous capillary endothelial cells. However, in 4 placentas the distribution was in the reverse order. HBsAg and HbCag were detected in amniotic epithelial cells from 32 mothers.

CONCLUSION: The main route of HBV transmission from mother to fetus is transplacental, from the mother side of placenta to the fetus side. However, HBV intrauterine infection may take place through other routes.

Zhang SL, Yue YF, Bai GQ, Shi L, Jiang H. Mechanism of intrauterine infection of hepatitis B virus. *World J Gastroenterol* 2004; 10(3):437-438

<http://www.wjgnet.com/1007-9327/10/437.asp>

INTRODUCTION

Hepatitis B virus infection is a worldwide health problem. China is one of the high prevalent areas, with a positive rate of HBsAg in population more than 10%^[1]. Recent data indicate that the rate of intrauterine infection of HBV is 10%-44.4%^[2,3]. Intrauterine infection is one of important routes of HBV transmission, and the main cause of HBV chronic infection. To explore the possible mechanism of intrauterine infection, we detected HBV DNA in the vaginal secretion and amniotic fluid from HBsAg-positive mothers and venous blood from the neonates by PCR, and also detected the

distribution of HBsAg and HbCag in the placenta by ABC immunohistochemical method.

MATERIALS AND METHODS

Patients

Pregnant women who gave birth in the Hospital of Women's and Children's Health Care in Zhaoqing, Guangdong Province, China and their full-term newborns were recruited into this study. All the mothers received a regular prenatal examination in the clinic during pregnancy, and were detected for HBV serum markers (HBVM) by ELISA. Fifty-nine HBsAg-positive mothers and their newborns were studied, 10 HBsAg-negative mothers and their newborns served as control. All the mothers had no threatened abortion or related history, no pregnancy related complications. There was no difference in age, pregnant frequency of mother and gestational age of fetus between the two groups. Sixty-nine mothers gave birth to sixty-nine newborns.

HBV DNA detection

Vaginal secretion of mothers was taken before amnion rupture. After entering labor of the mother, at a proper time or just after amnion rupture, amniotic fluid was taken, and strictly prevented from blood contamination. After birth, 3 ml of neonatal venous blood was taken and separated for serum. All specimens were stored at -20 °C and HBV DNAs were detected simultaneously. PCR test kits were purchased from Hua Mei Biological Engineering Company. The tests were performed strictly according to the manufacturer's instructions.

Determination of HBsAg and HbCag in placenta

Placental tissues of 1 cm×1 cm×2 cm, were taken from the fetal side and the maternal side respectively, fixed in 10% formalin, embedded with paraffin according to routine procedure and sliced in 5 μm thickness. Rabbit McAb against HbCag and mouse McAb against HBsAg were used for immunohistochemical test and DAB staining kits were purchased from Wuhan BoShide Biological Engineering Ltd Company. HBsAg and HbCag positive livers from autopsy were used as positive control, and placentas from HBVM negative mothers served as negative control. At the same time, we used PBS instead of the first antibody as blank control. Dark brown yellow in cytoplasm or nucleus was regarded as strongly positive, brown yellow as positive, and light brown yellow as weakly positive.

Diagnosis of intrauterine infection

The presence of HBV DNA in neonatal venous blood was regarded as intrauterine infection.

RESULTS

HBV DNA status in amniotic fluid, vaginal secretion and neonatal venous blood

The positive rates of HBV DNA in amniotic fluid and vaginal secretions were 47.5% (28/59) and 55.9% (31/59) respectively. No HBV DNA was detected in amniotic fluid and vaginal secretion in control group. Of the 59 newborns born to mothers with HBsAg-positive, 24 were HBV DNA positive in neonatal venous blood, the rate of intrauterine infection was 40.1%

(24/59). No HBV DNA was detected in neonatal venous blood from newborns whose mothers were HBsAg-negative.

HBsAg and HBcAg in placenta

The positive rates of HBsAg and HBcAg in placentas from 59 mothers with HBsAg- positive were 81.4% (48/59) and 61.1% (36/59) respectively. HBsAg in placenta appeared as inhomogeneous dark brown yellow granules in plasma of all kinds of cells. It was 76.27% (45/59) in maternal decidual cells, 72.88% (43/59) in trophoblastic cells, 62.71% (37/59) in villous mesenchymal cells, 52.54% (31/59) in villous capillary endothelial cells, 54.24% (32/59) in amniotic epidermic cells. The positive coloration of HBsAg was seen in part of the villous interstices. The distribution of positive cells was patchy or conglomerate. The stained HBcAg in placentas was homogeneous granule, existing in nuclei of the positive cells which were distributed in focus or dispersion, mainly including 59.32% (35/59) of maternal decidual cells, 55.93% (33/59) of trophoblastic cells, 50.85% (30/59) of villous mesenchymal cells, 44.07% (26/59) of villous capillary endothelial cells, 49.15% (29/59) of amniotic epidermic cells. No HBsAg or HBcAg was detected in placentas of the control. The number of positive cells of HBsAg or HBcAg and the degree of staining were gradually decreased from maternal decidual cells to villous capillary endothelial cells.

On the contrary, the distribution of HBsAg- and HBcAg-stained cells in 4 placentas was gradually decreased from villous capillary endothelial cells to maternal decidual cells. The staining degree of HBsAg and HBcAg was also decreased in the same order.

DISCUSSION

Most researchers hold that the mechanism of HBV intrauterine infection is transplacental infection. In 1987, Lin detected 32 placentas of HBsAg and HBcAg positive mothers using PAP immunohistochemistry, and did not find HBsAg^[4]. Tang detected HBV DNA in placentas of induced labor from HBsAg-positive mothers using dot blot hybridization, and found HBV DNA in 2 cases^[5]. Lucifora detected 12 placentas of HBsAg carriers with no symptoms by immunohistochemistry and found HBsAg and HBcAg in villous capillary endothelial cells^[6,7]. Xu^[8] and Yan^[9] detected placentas from HBsAg-positive mothers by ABC immunohistochemistry and *in situ* hybridization and found HBsAg, HBcAg and HBV DNA in all kinds of placental cells. Wang *et al* detected 24 placentas of HBsAg and HBcAg positive mothers using *in situ* hybridization and found HBV DNA was mainly distributed in maternal decidual cells, while no HBV DNA- positive cells were in the villi^[10]. The results above were different obviously. In the present study, by using PCR for the determination of intrauterine HBV infection and ABC immunohistochemistry for the detection of the presence of HBsAg and HBcAg in placenta, we detected 59 placentas of HBsAg-positive mothers and found the positive rates of HBsAg and HBcAg were 81.4% (48/59) and 61.1% (36/59) respectively. The detection rate of HBsAg and HBcAg, the proportion of positive cells and the degree of staining were gradually decreased from the maternal side to the fetus side of placenta (decidual cells > trophoblastic cells > villous mesenchymal cells > villous capillary endothelial cells). The villous capillary endothelial cells were infected by HBV in 31 mothers, from whom 22 newborns had HBV intrauterine infection. These results indicated that HBV could infect all kinds of cells in placenta, which was the possible mechanism of intrauterine infection that HBV infected cells from maternal decidua to villous capillary endothelia or that HBV infected trophoblastic cells directly, then to villous mesenchymal cells

and villous capillary endothelial cells resulting in fetus infection.

In our study, the number of HBsAg- and HBcAg- positive cells was gradually decreased from villous capillary endothelial cells to maternal decidual cells in 4 placentas. The degree of staining was decreased in the same order from the fetus side to the mother side of placenta. HBV DNA was positive in 2 of the venous blood samples. This indicated that HBV infected the fetus first, and then infected cells in different layers of placenta. In these 4 cases HBsAg and HBcAg were detected in amniotic epidermic cells, HBV DNA in amniotic fluid and vaginal secretion was also detected, suggesting that the ascending infection from vagina might exist, that is to say, HBV in vaginal secretion infected fetal membrane, amniotic fluid, fetus and cells of different layers in placenta or HBV infected fetal membrane first then infected cells in different layers of placenta from the fetus side to the mother's side.

From the 1980's, researchers all over the world have proved that HBV DNA was existent in all generations of spermatogenic cells and sperms in HBV-infected males. Researchers studied male HBV carriers whose wives were not infected with HBV, and their fetuses. The results of HBV DNA sequencing showed that the homology between the father and his son or daughter was 98%-100%. Some researchers found HBsAg in follicular fluid of HBsAg-positive women by immunohistochemistry. Still others found HBV DNA in ovary from a woman who died of severe hepatitis using *in situ* hybridization. HBV DNA was mainly in plasma of ovum and interstitial cells. Now that human oocytes can be infected by HBV, the possibility of HBV transmission through oocytes may exist. In our study, although the fetus HBV infection through oocyte has not been proved in the 2 cases, we could not exclude the possibility.

In conclusion, intrauterine HBV infection is mainly transmitted through the placenta from the maternal blood to the fetus. HBV infection through vagina or oocytes may exist.

REFERENCES

- Xu DZ.** The epidemic state of hepatitis B virus in present. *Zhonghua Linchuang Yisheng* 2002; **30**: 2-3
- Ruff TA,** Gertig DM, Otto BF, Gust ID, Sutanto A, Soewarso TI, Kandun N, Marschner IC, Maynard JE. Lombok Hepatitis B Model Immunization Project:toward universal infant hepatitis B immunization in Indonesia. *J Infect Dis* 1995; **171**: 290-296
- Zhang SL,** Han XB, Yue YF. Relationship Between HBV viremia level of pregnant women and intrauterine infection:neated PCR for detection of HBV DNA. *World J Gastroenterol* 1998; **4**: 61-63
- Lin HH,** Lee TY, Chen DS, Sung JL, Ohto H, Etoh T, Kawana T, Mizuno M. Transplacental leakage of HBeAg-positive maternal blood as the most likely route in causing intrauterine infection with hepatitis B virus. *J Pediatr* 1987; **111**(6 Pt 1): 877-881
- Tang SX,** Yu GL, Cheng SY. Study on the mechanism and effected factors of HBV intrauterine infection. *Zhonghua Liuxingbingxue Zazhi* 1991; **12**: 325-327
- Lucifora G,** Martines F, Calabro S, Carroccio G, Brigandi A, de Pasquale R. HBcAg identification in the placental cytotypes of symptom-free HBsAg-carrier mother: a study with the immunoperoxidase method. *Am J Obstet Gynecol* 1990; **163**(1 Pt 1): 235-239
- Lucifora G,** Calabro S, Carroccio G, Brigandi A. Immunocytochemical HBsAg evidence in placentas of asymptomatic carrier mothers. *Am J Obstet Gynecol* 1988; **159**: 839-842
- Xu DZ,** Yan YP, Zou S, Choi BC, Wang S, Liu P, Bai G, Wang X. Role of placental tissues in the intrauterine transmission of hepatitis B virus. *Am J Obstet Gynecol* 2001; **185**: 981-987
- Yan YP,** Xu DZ, Wang WL, Liu B, Liu ZH, Men K, Zhang JX, Xu JQ. The HBV infection of HBsAg positive women with different pregnant periods placentas. *Zhonghua Yixue Zazhi* 1998; **78**: 76-77
- Wang FS,** Li ZL, Zhang Y, Xu DZ, Wang CJ. The detection and significance of HBV DNA in PBMC and placental tissue of HBVM-positive mothers. *Zhongguo Yishi Zazhi* 1999; **1**: 31-32

Quantitative study of multiple biomarkers of colorectal tumor with diagnostic discrimination model

Wen Jin, Mei-Qin Gao, Zhi-Wu Lin, Dai-Xing Yang

Wen Jin, Mei-Qin Gao, Dai-Xing Yang, Department of Pathology, Fujian Medical University, Fuzhou 350004, Fujian Province, China
Zhi-Wu Lin, Department of Oncology, Fujian Provincial Hospital, Fuzhou 350004, Fujian Province, China

Supported by the Education Fund for Scientific Research in Fujian Province, No. 97A068

Correspondence to: Wen Jin, Department of Pathology, Fujian Medical University, Fuzhou 350004, Fujian Province, China. jinwen9484@sina.com

Received: 2003-06-04 **Accepted:** 2003-07-30

Abstract

AIM: To evaluate the multiple biomarkers of colorectal tumor and their potential usage in early diagnosis of colorectal cancers.

METHODS: Multiple biomarkers (DNA contents, AgNOR, PCNA, p53, c-erbB-2) in 10 normal colorectal mucosae, 37 colorectal adenomas and 55 colorectal cancers were analyzed quantitatively in the computed processing imaging system. Discrimination patterns were employed to evaluate the significance of single and multiple indices in diagnosis of colorectal cancers.

RESULTS: The mean values of the analyzed parameters increased in order of the normal mucosa, adenoma and adenocarcinoma, and this tendency reflected the progression of colorectal malignancy. The parameters including DNA index, positive rates, densities of AgNOR, c-erbB-2, and p53, shape and density of nucleus were relatively valuable for diagnoses. Then a diagnostic discrimination model was established. The samples were confirmed with the model, the sensitivity rates in cancer group and adenoma group were 96.36% and 89.19%, respectively. The value of proliferating cell nuclear antigen (PCNA) in early diagnosis of colorectal cancers was uncertain.

CONCLUSION: The quantitative evaluation of some parameters for colorectal tumor can provide reproducible data for differential diagnosis. The established diagnostic discrimination model may be of clinicopathological value, and can make the early diagnosis of colorectal cancer possible.

Jin W, Gao MQ, Lin ZW, Yang DX. Quantitative study of multiple biomarkers of colorectal tumor with diagnostic discrimination model. *World J Gastroenterol* 2004; 10(3):439-442
<http://www.wjgnet.com/1007-9327/10/439.asp>

INTRODUCTION

Colorectal carcinoma is one of the most common malignant tumors worldwide. Quantitative changes in nucleus, DNA content, PCNA, AgNOR were observed in the progression of tumor^[1-6]. Genes such as p53, *cerbB-2* might play a significant role in carcinogenesis^[7-13]. Although the biologic parameters of tumors have been assessed extensively, measurement of

these parameters has little impact on histological diagnosis. Furthermore, analysis of a single parameter is insufficient to evaluate tumor malignancy. Meanwhile, distinguishing benign from malignant lesions has traditionally been subjective; a quantifiable test is useful for the diagnosis of colorectal cancer. In this study, we used quantitative analysis to examine the potential usage of multiple biomarkers (DNA contents, AgNOR, PCNA, p53, c-erbB-2) in early diagnosis of colorectal cancer.

MATERIALS AND METHODS

Materials

Pathological specimens were obtained from Department of Pathology at Fujian Medical University from 1991 to 1996, including 55 cases of colorectal carcinoma, 37 cases of colorectal adenoma and 10 cases of normal colonic mucosae. The diagnosis was confirmed pathologically. The patients included 35 males, and 20 females with a mean age of 57 ± 12.83 years (range 31 to 84 years). Histologically, there were 15 highly differentiated types, 19 moderately differentiated types, 21 poorly differentiated types, and 13 cases had a local lymph node metastasis and 1 case had the liver metastasis.

Reagents and methods

Schiff reagent, AgNOR staining fluid, antibodies against PCNA, c-erbB-2 and p53 and SP immunohistochemical reagent were purchased from Fujian Maxin Co.Ltd.

Formalin-fixed, paraffin-embedded specimens were cut in to 5 μ m in thickness. The slices were stained with Feulgen, AgNOR and the detected antigen, and those in the control group were stained without primary antibody.

Semi-quantitative evaluation

Some silver stained black particles were observed in nuclei and classified. The positive staining rate was calculated^[14]. A semi-quantitative evaluation system was used to determine the antigen expression in specimens^[15]. Expression of p53 and c-erbB-2 was graded as the following scale: <10% “-”, 10-25% “+”, 26-50% “++”, 51-75% “+++”, >75% “++++”. Expression of PCNA was graded as the following scale: <25% “+”, 26-50% “++”, 51-75% “+++”, >75% “++++”.

Quantitative evaluation

The specimens were examined for multiple biomarkers with quantitative analysis using the computer processing image system (American Image Co. 8000 Type). Under the same power field of microscope, 150-200 cells were examined. Multiple biomarkers stained with silver or PCNA included DNA content, DNA index, nucleus area, Abs, granular shape factor, width and length of nuclei, the widest and longest diameter, and density of nucleus.

Statistical analysis

Student's *t* test was used for analysis of variance. Discriminant analysis was done for multiple parameters and indices. The selected significant parameters were used to set up a diagnostic discrimination model. The SAS system for windows (version 6.12) was used for completing all the statistical analyses.

RESULTS

Multiple biomarkers (DNA contents, AgNOR, PCNA, p53, c-erbB-2) were quantitatively processed using the computer processing image system in 10 normal colonic mucosae, 37 colorectal adenomas and 55 colorectal carcinomas. The values of most parameters were increased in the order of normal mucosa, adenoma and adenocarcinoma. The tendency reflected the progression of colorectal malignancy. But the PCNA content was peaked in adenoma and decreased in carcinoma. The values were subjected to discrimination pattern method to evaluate the significance of parameters in multiple indices in order to set up the discrimination model. Then the model was used to recheck the samples. DNA index, shape factor, the widest diameter and density of nuclei were demonstrated to be the valuable parameters in feulgen-stained sections. The concordance rate was 86.02% for cancer group and 80.06% for adenoma group. The relatively valuable parameters in silver stained slides were average number, positive rate, density and aspect factor of particles. The concordance rate of the established model was 79.57% for cancer group and 78.65% for adenoma group. The valuable parameters in PCNA stained specimens were positive rate and density, and the concordance rate was 76.34% for cancer group and 73.55% for adenoma group. The valuable parameters in c-erbB-2 stained samples were Abs, positive rate and density, the concordance rate was 90.32% for cancer group and 90.14% for adenoma group. The valuable parameters in p53 stained positive samples were total positive area and density, and the concordance rate was 86.02% for cancer group and 83.55% for adenoma group. Discriminant analysis was performed for the above parameters. DNA index (X_1), positive rate (X_2), density (X_3) and aspect factor of AgNOR (X_4), density of c-erbB-2 (X_5), density of p53 (X_6), shape factor (X_7) and density of nucleus (X_8) were demonstrated to be the relatively valuable indices. Then a diagnostic discrimination model was established, and the model rechecked the samples, the concordance rates in cancer group and adenoma group were 96.36% and 89.19%, respectively. The models were as follows.

$$Y(1) = -412.86 - 7.30X_1 + 34.83X_2 + 1.15X_3 + 2.54X_4 + 500.07X_5 + 17.34X_6 + 2.54X_7 + 409.68X_8$$

$$Y(2) = -480.40 - 7.04X_1 + 34.33X_2 + 0.98X_3 + 2.81X_4 + 560.55X_5 + 26.85X_6 + 2.47X_7 + 375.14X_8$$

$$Y(3) = -432.76 - 4.58X_1 + 41.97X_2 + 0.75X_3 + 2.63X_4 + 529.44X_5 + 52.13X_6 + 2.26X_7 + 321.11X_8$$

DISCUSSION

Relationship among DNA content, shape parameters of nucleus and colorectal carcinoma

Most tumor cells had a certain amount of abnormal DNA; DNA content of tumor was closely related to biological behaviors^[1,2]. Our study showed that the level of DNA content was increased in the order of normal mucosa, adenoma and adenocarcinoma with different significances. It has been confirmed that DNA content is a reliable and objective marker in early diagnosis of colorectal carcinoma and in distinguishing benign from malignant tumors.

In diagnosis of colorectal carcinoma with quantitative analysis as reported^[1,2], the results varied with selected parameters. We believed that abnormalities of nuclei were the most important phenomena in hypertrophy of neoplastic cells in addition to abnormal structure of cells or tissues. It is well known that increased mitotic nuclei, multi-hierarchical structure, enlargement and pleomorphism of nuclei are expressed in most rapidly growing neoplasms. We suspected that increased nucleus area and much more irregular shape of nucleus were in accordance with the normal mucosa-adenoma-adenocarcinoma

sequence. Parameters of nuclear shape and density of DNA reflected the malignancy of tumor significantly.

Although we considered that area of nucleus would play an important role in diagnosis of tumor with three-dimensional (3D) image processing, this study failed to show that areas of nuclei could reflect hyperplastic degree of tumor quantitatively. This might be due to the limitation of bi-dimension that could not reveal the whole nucleus.

Previous studies reported that Abs was an objective parameter to reflect the nucleus. But discriminant analysis showed that Abs was not relatively valuable. While Abs and density of nucleus had significant differences among the groups. We reason that sectional shape of nucleus is different from its real shape, so average area of Abs (density of nucleus) reflects of DNA content more objectively.

Relationship between AgNOR and colorectal carcinoma

Variation of the number of nucleolar organizer regions (NORs) could reveal the conditions of cellular activity^[16-20]. It was suggested that AgNOR dot count of cells had a potential role in distinguishing benign from malignant tumors and in their early diagnosis^[21]. Our results revealed that the count of AgNOR was increased in accordance with the normal mucosa-adenoma-adenocarcinoma sequence. Due to the strong correlation among type of particles, irregular factor and shape factor, irregular factor was rejected from the equations by discriminant analysis first. Type of particles used to be regarded as an important parameter^[21], and turned out to have a limited value. The parameters, such as average number, positive rate, density and surface factor of particles were demonstrated to be valuable, and could reflect the characteristics of particles. The concordance rate was 79.57% for cancer group and 78.65% for adenoma group indicating this improved system is sensitive and very precise for quantifying the AgNOR dot count in cells and can provide a valuable objective measurement in differentiating benign from malignant tumors.

Relationship between PCNA and colorectal carcinoma

PCNA is a cell cycle related protein that is maximally elevated in late G1 and S-phase of proliferating cells and a key cycle regulator. It can be used as a marker of proliferation, and directly assessed using a thymidine analogue in suitably labeled pathological materials. Cellular proliferative activity has been accepted as a useful indicator of biologic aggressiveness in colorectal carcinoma^[5-17]. PCNA immunohistochemistry could be used as a reliable marker of the proliferative compartment in both normal and neoplastic colonic mucosae^[22]. The results revealed that all the parameters were significantly higher in adenoma and adenocarcinoma than in normal tissue, and the parameters in adenoma were higher than those in adenocarcinoma, indicating that multiplicative growth presented in G1 and S-phase when adenoma progressed to adenocarcinoma, and in other phase or in shock period while in adenocarcinoma. So the parameters of PCNA were descent in adenocarcinoma. Therefore we considered that the value of PCNA could distinguish benign from malignant lesions in the earlier stage of tumor.

Relationship among c-erbB-2, p53 and colorectal carcinoma

The c-erbB2 gene could be amplified in human adenocarcinomas, leading to elevated levels of expression of its encoded product, p185^[11-23]. It has been shown that the accumulation of several alterations in p53 genes is most important for the conversion of adenoma to carcinoma. Critical genetic changes, including activation of oncogenes, mutation and deletion of tumor suppressor genes and disturbances in transcriptional regulatory sequences, might bring about aberrant expression of growth factors and their receptors in gastrointestinal carcinomas^[10].

Mutations in the tumor suppressor gene p53 occur prevalently in a wide range of human tumors. Detection of a mutated p53 could provide useful information for the clinical management of colorectal neoplasms^[24-29]. The p53 gene mutation and its subsequent over-expression in colorectal adenomas might therefore be a fundamental genetic event underlying the dysplasia and loss of proliferative control that are the characteristics of adenomas with a malignant potential^[30]. Mutant p53 tumor suppressor gene and c-erbB-2 proto-oncogene were involved in human carcinogenesis, and detection of their protein product in human malignancies might influence the evolution of many neoplasms^[31,32]. Therefore the aim of this study was to investigate the correlation of c-erbB-2, p53 with occurrence, progression of colorectal carcinoma and to determine the prognostic significance of oncogenes. The results showed that the values of c-erbB-2, p53 were increased in accordance with normal mucosa-adenoma-adenocarcinoma sequence ($P < 0.01$), and the levels of c-erbB-2 were obviously increased in normal tissue and adenoma, suggesting that the occurrence of colorectal carcinoma was associated with activation of c-erbB-2, and c-erbB-2 could be considered as a more significant predictor of the occurrence of colorectal carcinoma. Meanwhile the value of total positive area and density of p53 were obviously increased in adenoma and carcinoma, indicating that p53 was a key oncogene in the progression of colorectal carcinoma. These results confirmed that p185 overexpression was associated with the early stages of colorectal cancer, whereas p53 was associated with more advanced stages^[31].

Precancerous lesion of colorectal adenoma

The rate of carcinogenesis is associated with proliferation. To evaluate the proliferative degree of colorectal tumor with imaging analysis is helpful for the diagnosis of tumors. Our study of DNA contents, AgNOR, PCNA, p53, c-erbB-2 provided some useful prognostic information, their determination was useful for accurate evaluation of the prognosis.

The entity of carcinomatous change is a complicated process from quantitative to qualitative change. We studied the proliferative lesion with a mathematics model in order to provide the objective markers for accurate diagnosis. The result showed that DNA index, positive rates, density and aspect factor of AgNOR, densities of c-erbB-2, p53, shape factor and density of nucleus were relatively valuable. The result also showed that normal group was correctly diagnosed with the model ($F > 0.8$). The 4 fault samples of papillary adenoma with grade 2-3 atypical hyperplasia by pathologic diagnosis were fault diagnosis of adenocarcinoma by the model ($F < 0.8$). The 2 highly differentiated colorectal tumors were fault diagnosis of adenoma ($F < 0.8$). Comprehensive evaluation showed the strong discriminating power of the model.

This study examined the value of PCNA. No parameter of PCNA was selected for the final model. As strong correlations were observed between PCNA and p53^[33,34] we believed that the discriminating power of PCNA was hid by p53 due to the complex interface among the parameters. On the other hand, we doubted the value of PCNA in early cancer. However, some parameters of DNA, AgNOR, p53, c-erbB-2 were selected for the model, and the diversity of tumor and occurrence and progression of colorectal tumor were related with multiple factors. Meanwhile, all the 4 indexes played a major role in the diagnosis of colorectal tumor, and inactivation of anti-oncogene and activation of oncogene were existed in the progression of colorectal malignancy.

Quantitative evaluation of some indices of colorectal tumor could provide reproducible data for its differential diagnosis. The discrimination model established can offer subjective parameters for distinguishing benign from malignant tumors.

REFERENCES

- 1 **Meng QK**, Yang HM, Wang H. Clinical significance of DNA in colorectal carcinoma. *Shiyong Zhongliuxue Zazhi* 1999; **13**: 93-94
- 2 **Xu SY**, Zhang YL, Zhou DY, Wen B. Computerized analysis of nuclear morphology in the differential diagnosis of protuberant colorectal lesions. *Zhongguo Zhongliu Linchuang* 1998; **25**: 85-87
- 3 **Derezini M**, Trere D, Pession A, Govoni M, Sirri V, Chieco P. Nucleolar size indicates the rapidity of cell proliferation in cancer tissues. *J Pathol* 2000; **191**: 181-186
- 4 **Eminovic-Behrem S**, Trobonjaca Z, Petrovecki M, Dobi-Babic R, Dujmovic M, Jonjic N. Prognostic significance of DNA ploidy pattern and nucleolar organizer regions (AgNOR) in colorectal carcinoma. *Croat Med J* 2000; **41**: 154-158
- 5 **Feng S**, Song JD, Tian XR. Significance of proliferating cell nuclear antigen expression in colorectal carcinoma. *Hauren Xiaohua Zazhi* 1998; **6**: 146-147
- 6 **Lavezzi AM**, Ottaviani G, De Ruberto F, Fichera G, Maturri L. Prognostic significance of different biomarkers (DNA content, PCNA, karyotype) in colorectal adenomas. *Anticancer Res* 2002; **22**: 2077-2081
- 7 **Sugai T**, Nakamura SI, Habano W, Uesugi N, Sato H, Yoshida T, Orii S. Usefulness of proliferative activity, DNA ploidy pattern and p53 products as diagnostic adjuncts in colorectal adenomas and intramucosal carcinomas. *Pathol Int* 1999; **49**: 617-625
- 8 **Freitas D**, Goulao MH, Camacho E, Figueiredo P, Ministro P, Ferreira M, Portela F, Andrade P, Donato A, Martins MI. Clinical relevance of proliferation biomarkers and p53 expression in rectal mucosa and sporadic colonic adenomas: a prospective study. *Hepatogastroenterology* 2002; **49**: 1269-1274
- 9 **Zhuang XQ**, Lai RQ, Sun GH, Wang XH, Luo ZQ, Yuan SZ. Expression and prognostic significance of p53 protein during colorectal tumorigenesis. *Shijie Huaren Xiaohua Zazhi* 1998; **6**: 280-281
- 10 **Di Stefano A**, Fisichella P, Catanuto G, Di Blasi M, La Greca G, Grasso G, Russello D. Characterization and prognostic value of colorectal adenomas with molecular genetic markers. *Minerva Chir* 2000; **55**: 99-104
- 11 **Zhu WL**, Li QX. An oncogene c-erbB-2 and cancer. *Linchuang Yu Shiyang Binglixue Zazhi* 1998; **14**: 79-81
- 12 **Wu W**, Zhang X, Yan X, Wang J, Zhang J, Li Y. Expressions of beta-catenin, p53 and proliferating cell nuclear antigen in the carcinogenesis of colorectal adenoma. *Zhonghua Zhongliu Zazhi* 2002; **24**: 264-267
- 13 **He Q**, Ohaki Y, Tanaka N, Asano G. The relationship between p53 protein and c-erb B-2 expression and apoptosis in colorectal cancer. *Nippon Ika Daigaku Zasshi* 1999; **66**: 181-187
- 14 **Xu LZ**. AgNOR Standard Regimen. *Aizheng* 1996; **15**: 75
- 15 **Su JM**, Zhou YP, Xu WL, Cao LH, Zha XL. E-Cadherin expression in four kinds of carcinoma and their relations to differentiation and metastasis. *Chin J Cancer Res* 2001; **13**: 13-17
- 16 **Pich A**, Margaria E, Chiusa L. Significance of the AgNOR in tumor pathology. *Pathologica* 2002; **94**: 2-9
- 17 **Nakae S**, Nakamura T, Ikegawa R, Yoshioka H, Shirono J, Tabuchi Y. Evaluation of argyrophilic nucleolar organizer region and proliferating cell nuclear antigen in colorectal cancer. *J Surg Oncol* 1998; **69**: 28-35
- 18 **Trere D**. AgNOR staining and quantification. *Micron* 2000; **31**: 127-131
- 19 **Derezini M**, Trere D. Silver-stained Nucleolar Organizer Regions (AgNOR). *Pathologica* 2001; **93**: 99-105
- 20 **Derezini M**. The AgNORs. *Micron* 2000; **31**: 117-120
- 21 **Liu J**, Zhao FD, Shi Y. Value of AgNORs determination in diagnosis of benign and malignant lesions of gastric mucosa. *Practical J Cancer* 1998; **13**: 276-277
- 22 **Tanaka K**, Murata N, Yanai H, Okita K. Immunohistological study on the expression of proliferating cell nuclear antigen (PCNA/cyclin) in human colorectal lesions. *Nippon Shokakibyo Gakkai Zasshi* 1992; **89**: 493-497
- 23 **Terzuoli L**, Carlucci F, Martino AD, Froisi B, Porcelli B, Minacci C, Vernillo R, Baldi L, Marinello E, Pagani R, Tabucchi A. Determination of p185 and adenylsuccinate lyase (ASL) activity in preneoplastic colon lesions and intestinal mucosa of human subjects. *Clin Biochem* 1998; **31**: 523-528

- 24 **Chang FH**, Tzeng DS, Lee TM, Chen TC, Hsu LS, Lung FW. Mutations in the p53 tumor suppressor gene in colorectal cancer in Taiwan. *Kaohsiung J Med Sci* 2003; **19**: 151-158
- 25 **Sugai T**, Takahashi H, Habano W, Nakamura S, Sato K, Orii S, Suzuki K. Analysis of genetic alterations, classified according to their DNA ploidy pattern, in the progression of colorectal adenomas and early colorectal carcinomas. *J Pathol* 2003; **200**: 168-176
- 26 **Guzinska-Ustymowicz K**, Sulkowska M, Famulski W, Sulkowski S. Tumour 'budding' and its relationship to p53 and Bcl-2 expression in colorectal cancer. *Anticancer Res* 2003; **23**: 649-653
- 27 **Kanavaros P**, Stefanaki K, Valassiadou K, Vlachonikolis J, Mavromanolakis M, Vlychou M, Kakolyris S, Gorgoulis V, Tzardi M, Georgoulis V. Expression of p53, p21/waf, bcl-2, bax, Rb and Ki67 proteins in colorectal adenocarcinomas. *Med Oncol* 1999; **16**: 23-30
- 28 **Sulkowska M**, Famulski W, Guzinska-Ustymowicz K, Sulkowski S. Study of P53 protein expression in colorectal cancer. *Folia Histochem Cytobiol* 2001; **39**: 157-158
- 29 **Saleh HA**, Jackson H, Banerjee M. Immunohistochemical expression of bcl-2 and p53 oncoproteins: correlation with Ki67 proliferation index and prognostic histopathologic parameters in colorectal neoplasia. *Appl Immunohistochem Mol Morphol* 2000; **8**: 175-182
- 30 **Pignatelli M**, Stamp GW, Kafiri G, Lane D, Bodmer WF. Overexpression of p53 nuclear oncoprotein in colorectal adenomas. *Int J Cancer* 1992; **50**: 683-688
- 31 **Porcelli B**, Frosi B, Terzuoli L, Arezzini L, Marinello E, Vernillo R, De Martino A, Vatti R, Minacci C. Expression of p185 and p53 in benign and malignant colorectal lesions. *Histochem J* 2001; **33**: 51-57
- 32 **Wu JT**. C-erbB2 oncoprotein and its soluble ectodomain: a new potential tumor marker for prognosis early detection and monitoring patients undergoing Herceptin treatment. *Clin Chim Acta* 2002; **322**: 11-19
- 33 **Zhuang XQ**, Lai RQ, Shun GH, Wang XH, Yuan SZ. p53 expression and PCNA expression as prognostic significance in colorectal neoplasmas. *Shijie Huaren Xiaohua Zazhi* 1999; **7**: 616
- 34 **McKay JA**, Douglas JJ, Ross VG, Curran S, Loane JF, Ahmed FY, Cassidy J, McLeod HL, Murray GI. Analysis of key cell-cycle checkpoint proteins in colorectal tumours. *J Pathol* 2002; **196**: 386-393

Edited by Wang XL Proofread by Zhu LH

Effect of antisense oligodeoxynucleotide of telomerase RNA on telomerase activity and cell apoptosis in human colon cancer

Ying-An Jiang, He-Sheng Luo, Li-Fang Fan, Chong-Qing Jiang, Wei-Jin Chen

Ying-An Jiang, He-Sheng Luo, Department of Gastroenterology, Renming Hospital of Wuhan University, Wuhan 430060, Hubei Province, China

Li-Fang Fan, Department of Pathology, Medical College of Wuhan University, Wuhan 430071, Hubei Province, China

Chong-Qing Jiang, Department of General Surgery, Zhongnan Hospital of Wuhan University, Wuhan 430071, Hubei Province, China

Wei-Jin Chen, Department of Medical Information, Central Hospital of Huangshi City, Huangshi 435000, Hubei Province, China

Supported by the Science and Technology Research Project of Hubei Province, No. 2002AA301C72

Correspondence to: Ying-An Jiang, Central Hospital of Huangshi City, 43 Wuhan Road, Huangshi 435000, Hubei Province, China. weijin@hs.hb.cninfo.net

Telephone: +86-714-6283783 **Fax:** +86-714-6233931

Received: 2003-10-12 **Accepted:** 2003-11-15

Abstract

AIM: To explore the effect of antisense oligodeoxynucleotide (As-ODN) of telomerase RNA on telomerase activity and cell apoptosis in human colon cancer.

METHODS: As-ODN was transfected into SW480 cells by liposomal transfection reagent. Telomerase activity of SW480 cells was examined by telomeric repeat amplification protocol (TRAP) and enzyme-linked immunosorbent assay (ELISA). Apoptosis was analyzed by morphology and flow cytometry.

RESULTS: The telomerase activity in SW480 cells transfected with 1.0 $\mu\text{mol/L}$ of As-ODN for 2-5 days, was significantly decreased in a time-dependent manner, and the cells underwent apoptosis. The missense ODN (Ms-ODN) and the control group transfected with SW480 cells did not show these changes.

CONCLUSION: As-ODN can specifically inhibit the telomerase activity of SW480 cells and induce apoptosis.

Jiang YA, Luo HS, Fan LF, Jiang CQ, Chen WJ. Effect of antisense oligodeoxynucleotide of telomerase RNA on telomerase activity and cell apoptosis in human colon cancer. *World J Gastroenterol* 2004; 10(3):443-445

<http://www.wjgnet.com/1007-9327/10/443.asp>

INTRODUCTION

Colon cancer is one of the most common malignancies both in the world and in China^[1]. More and more patients with early colon cancer can now be found due to the improvement in the diagnostic techniques. Although surgery and chemotherapy are effective on patients with localized tumors, the prognosis of patients with advanced or metastatic tumors is not ideal. As a result, it is absolutely necessary to explore a novel treatment modality, namely the gene therapy. Just like other kinds of cancer, colon cancer is now recognized as a genetic disease. Colon cancer cells contain many genetic alterations which accumulate as tumor develops. This makes it possible to treat

cancer with gene therapy^[2-3].

Telomerase is a ribonucleoprotein consisting of two components, RNA and protein. The RNA gene of telomerase is termed as human telomerase RNA (hTR). Two protein subunits have been found, which were named as human telomerase-associated protein (TEP1) and human telomerase catalytic subunit or human telomerase reverse transcriptase (hTERT)^[4,5]. Telomerase activity in humans has been detected in germline and tumor tissues as well as in established cultured cell lines^[6]. In normal somatic cells, the absence or low expression of telomerase is thought to result in progressive telomeric shortening with each cell division^[7,8]. Therefore, it has been suggested that reactivation of telomerase is a critical step in tumorigenesis and that interference with the regulation of telomerase activity may serve as a basis for cancer therapy^[9,10]. However, to our knowledge, whether antisense gene therapy directing against hTR is effective on colon cancer is unknown. We reported here the effect of antisense oligodeoxynucleotide of telomerase RNA on human colon cancer cell line, and investigated the potential value of telomerase as a target for antisense gene therapy of colon cancer.

MATERIALS AND METHODS

Cell culture

SW480 cells, a human colon cancer cell line, were provided by Department of Biology, Wuhan University, China, and maintained in RPMI 1640-10% fetal bovine serum supplemented with 1 mmol/L L-glutamine, 100 U/ml of penicillin plus 100 $\mu\text{g/ml}$ of streptomycin at 37 °C under 5% CO₂.

Cell counting

SW480 cells were counted with 5 g/L of trypan blue staining.

Oligodeoxynucleotide synthesis

Two oligodeoxynucleotides were synthesized as described by Feng *et al* and Norton *et al*^[11,12]. Antisense oligodeoxynucleotides (As-ODN) with the sequence 5' TAGGGTTAGACAA-3', which can recognize the RNA template region of telomerase, and missense oligodeoxynucleotide (Ms-ODN) with the sequence 5' TGTAAGGAACTAG 3' were synthesized by Beijing SBS Biotechnology Engineering Company using the 391 DNA synthesizer. The synthesized oligodeoxynucleotides were subjected to electrophoresis (PAGE) and purified (300V, 1.5 h).

Transfection of oligodeoxynucleotides

Transfection of phosphorothiate oligodeoxynucleotides (ODNs) was carried out with liposomal transfection reagent DOSPER (Roche Diagnostic GmbH) according to the manufacturer's protocol. Briefly, cells were plated onto 6-well plates and incubated until the cells reached 70-80% confluence. The DOSPER was diluted with serum-free medium the day before transfection. Then, the desired amount of ODNs was incubated for 15 minutes with diluted DOSPER. The ODNs/DOSPER mixture (100 μl) was added dropwise into 900 μl of serum-free RPMI 1640. After incubated for 6 hours at 37 °C, 1 ml of RPMI 1640 containing 20% FBS was added into each

Table 1 Inhibitory effect of telomerase activity by ODNs (mean±SD)

Groups	Active duration				
	24 h	48 h	72 h	96 h	120 h
As-ODN 10 μmol/L	0.872±0.194	0.406±0.232	0.386±0.146	0.307±0.203	0.289±0.213
Ms-ODN 10 μmol/L	1.063±0.249	1.285±0.179	0.959±0.273	0.109±0.243	1.247±0.178
Positive control	1.725±0.267	1.571±0.418	1.243±0.186	1.236±0.235	1.098±0.347
Negative control	0.349±0.092	0.312±0.076	0.283±0.089	0.063±0.072	0.057±0.023

well. Cells were harvested and analysed after 48, 72, 96 and 120 hours, respectively.

Telomerase activity assay

Telomerase activity was measured by polymerase chain reaction and enzyme linked immunosorbent assay (PCR-ELISA). Briefly, 2×10^6 cells were isolated, mixed with 200 μl of protein extraction buffer by vortex, and left on ice for 30 minutes. One hundred and seventy-five μl of supernatant was collected after centrifugation (16 000×g, 20 minutes, 4 °C). PCR was performed in a system of 50 μl containing 25 μl of transfer reaction mixture, 2 μl protein extract and 2 μl primers, and 23 μl of nuclease-free water was added. The PCR condition was as the follows: at 25 °C for 30 minutes for primer elongation, at 94 °C for 5 minutes for telomerase inactivation. Thirty cycles of amplification were performed, each cycle was performed at 94 °C for 30 s for denaturation, at 50 °C for 30 s for annealing, and at 72 °C for 90 s for polymerization. Five μl of the amplified product and 20 μl of the denatured reagent were incubated at room temperature, 225 μl of hybridization buffer was then added and mixed, and 100 μl of them was distributed in the wells of a microtitering plate. After 2 hours of incubation (37 °C, 300 rpm), 100 μl of anti-DIG-POD working solution was added and incubated for another 30 minutes, followed by the addition of 100 μl of TMB substrate solution, and 100 μl of stop reagent was added at last. The OD value in each well was read at the wave lengths 450 nm and 655 nm on a microtiter plate reader (Bio-RAD Model 550 microplate reader). The result of OD₄₅₀ minus OD₆₅₅ greater than 1.5 unit was judged as a positive control using a protein extract from immortalized telomerase-positive human embryonic kidney cells (293 cells). The negative control was considered as OD₄₅₀ minus OD₆₅₅ less than 0.2 unit by reading the protein extract pretreated with RNase A at 65 °C for 10 minutes. Telomerase activity was considered positive when the value of OD₄₅₀ minus OD₆₅₅ of a sample was at least 0.2 unit higher than that of the negative control, otherwise it was considered negative. Each sample was examined more than twice. The final value was presented as mean±SD after a statistical treatment by using *t* test.

Apoptotic features

To determine whether SW480 transfected with AS-ODN displayed an apoptotic morphology, the transfected cells were observed under Olympus optical microscope and Hitach transmission electron microscope.

To determine the apoptotic rate and cell cycle distribution, the cells were fixed and stained by propidium iodide (PI, Sigma product), and analyzed by a FACSORT flow cytometer (Becton Dickinson). Briefly, cells were trypsinized, washed once in ice-cold PBS, and incubated with annexin-V-fluorescein/PI, and then analyzed immediately by FACSORT flow cytometry. All data were analyzed using the Cell Quest software.

Statistical analysis

Results were expressed as mean±SD. Statistical analyses were carried out with the software package SPSS10.0. A *P* value less than 0.05 was considered statistically significant.

RESULTS

Inhibitory effect of antisense hTR ODNs on telomerase activity

SW480 cells were transfected with As-ODN (1.0 μmol/L) and Ms-ODN (1.0 μmol/L), and collected at 24, 48, 72, 96 and 120 hours after transfection respectively. Telomerase activities were measured by TRAP-ELISA. Following results were found. The telomerase activity of SW480 cells transfected with As-ODN was greatly inhibited compared with that in the Ms-ODN. The telomerase activity of SW480 cells transfected with As-ODN at 72 and 96 hours after transfection was significantly lower than that both at 24 hours and in positive control as shown in Table 1. These findings suggested that this inhibitory action was sequence specific and in a time-dependent manner.

Effect of antisense hTR ODNs on induction of SW480 cell apoptosis

Cytologic morphological changes SW480, transferred with 1 μmol/L As-ODN for 3 days, cytologic morphology was observed under Olympus optical microscope and Hitach transmission electron microscope. It was found that cells rounded up off the plastids, exhibiting cytoplasmic blebbing, fragmentation and chromatin condensation, features of apoptosis. No apoptotic features (normal morphology) were observed in SW480 transfected with 10 μmol/L Ms-ODN (Figure 1).

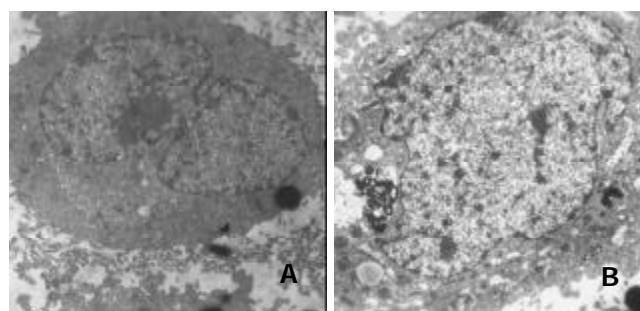


Figure 1 Morphologic observation under transmission electron microscope. A: cells had no apoptotic features. B: cell rounded up off the plastic, exhibiting cytoplasmic blebbing, fragmentation and chromatin condensation, features of apoptosis.

Table 2 Effect of ODNs on induction of SW480 cell apoptosis (mean±SD)

Groups	Active duration		
	48 h	72 h	96 h
As-ODN 1 μmol/L	4.99±0.54	8.63±0.59	9.96±0.41
Ms-ODN 1 μmol/L	3.86±0.39	4.88±0.57	4.92±0.67
HRT blank	1.57±0.18	1.79±0.21	1.71±0.32

Detection of apoptotic cells

To determine the apoptotic rate, SW480 cells were transfected with 1 μmol/L As-ODN and Ms-ODN for 2 days. After permeabilization, the cells were stained with propidium iodide and analysed by flow cytometry. The apoptotic rate of SW480 cells transfected with As-ODN increased (4.99±0.54, 8.63±0.59,

and 9.96 ± 0.41 at 48 h, 72 h and 96 h, respectively, $P < 0.001$), but no significant changes of apoptosis were observed in SW480 cells transfected with 1 $\mu\text{mol/L}$ Ms-ODN as shown in Table 2, indicating that this apoptotic induction was sequence specific and in a time-dependent manner.

DISCUSSION

Compared with normal somatic cells, cancer cells have an unlimited replicating capacity. This important characteristic of cancer, named immortality, has been gaining more and more attention, seeing that cancer cells might achieve cellular immortality through only a major pathway, the activation of telomerase^[13]. Telomerase has been found to play an important role in carcinogenesis, thus becoming the basis of the widely held view of telomerase as a highly selective target for antisense gene therapy of cancer^[14].

The RNA component of telomerase (hTR) was crucial to the telomerase activity^[15-17]. Human cell lines expressing hTR mutated in the template region could generate the predictive mutant telomerase activity. Recent experiments have shown that antisense gene therapy directing against telomerase RNA component could effectively inhibit telomerase activity and induce apoptotic cell death in ovarian cancer, prostate cancer, bladder cancer, malignant gliomas and human breast epithelial cells^[18-22]. However, whether such an anti-cancer effect can be obtained in human colon cancer is still unknown. Therefore, we examined the effect of antisense hTR oligodeoxynucleotide on human colon cancer cell line. As the results showed, our experiment clearly demonstrated that antisense-hTR oligodeoxynucleotide could significantly inhibit telomerase activity and induce apoptosis of human colon cancer cells, which was supported by the results obtained in our previous experiment^[23]. All these findings provide the strong evidence that telomerase may be an ideal target for antisense gene therapy of human colon cancer.

Recently, it has been showed that telomerase activity was the dominant mechanism providing telomere maintenance to human immortalized cells. However, the exact mechanisms of how telomerase activity is regulated in tumour cells remain poorly understood. Some researchers have shown that telomerase activity correlated with the growth rate of immortal cells^[24-26], whereas others found no significant association between telomerase activity and proliferation index in tissue specimens from breast carcinoma^[27], gastric carcinoma^[28], and Wilm's tumour^[29].

Inhibition of telomerase activity has been proposed as a potential method for the treatment of human malignancies. It is suggested that telomerase inhibition may serve as an effective tool for eliminating tumour cells that have short telomeres. Such tumours may provide reasonable targets for agents that inhibit telomerase. These experiments await the development of specific inhibitors for the components of telomerase complex.

REFERENCES

- 1 **Parkin DM.** Global cancer statistics in the year 2000. *Lancet Oncol* 2001; **2**: 533-543
- 2 **Tominaga K,** Suto R, Sasaki E, Watanabe T, Fujiwara Y, Higuchi K, Arakawa T, Shokei K, Iwao H. Gene therapy for colon cancer. *Nippon Rinsho* 2003; **61**(Suppl 7): 490-494
- 3 **Wang YQ,** Ugai S, Shimozato O, Yu L, Kawamura K, Yamamoto H, Yamaguchi T, Saisho H, Tagawa M. Induction of systemic immunity by expression of interleukin-23 in murine colon carcinoma cells. *Int J Cancer* 2003; **105**: 820-824
- 4 **Blackburn EH.** Structure and function of telomeres. *Nature* 1991; **350**: 569-573
- 5 **Nakamura TM,** Morin GB, Chapman KB, Weinrich SL, Andrews WH, Lingner J, Harley CB, Cech TR. Telomerase catalytic subunit homologs from fission yeast and human. *Science* 1997; **277**:955-959
- 6 **Holt SE,** Shay JW, Wright WE. Refining the telomere-telomerase hypothesis of aging and cancer. *Nat Biotechnol* 1996; **14**: 836-839
- 7 **Hoos A,** Hepp HH, Kaul S, Ahlert T, Bastert G, Wallwiener D. Telomerase activity correlates with tumor aggressiveness and reflects therapy effect in breast cancer. *Int J Cancer* 1998; **79**: 8-12
- 8 **Kyo S,** Takakura M, Tanaka M, Kanaya T, Inoue M. Telomerase activity in cervical cancer is quantitatively distinct from that in its precursor lesions. *Int J Cancer* 1998; **79**: 66-70
- 9 **Dahsc R,** Fiedler W, Ernst G. Telomeres and telomerase: biological and clinical importance. *Clin Chem* 1997; **43**: 708-714
- 10 **Yan P,** Conidre JM, Benhattar J, Bosman FT, Guillou L. Telomerase activity and human telomerase reverse transcriptase mRNA expression in soft tissue tumors: correlation with grade, histology, and proliferative activity. *Cancer Res* 1999; **59**: 3166-3170
- 11 **Feng J,** Funk WD, Wang SS, Weinrich SL, Avilion AA, Chiu CP, Adams RR, Chang E, Allsopp RC, Yu J. The RNA component of human telomerase. *Science* 1995; **269**: 1236-1241
- 12 **Norton JC,** Piatyszek MA, Wright WE, Shay JW, Corey DR. Inhibition of human telomerase activity by peptide nucleic acids. *Nat Biotechnol* 1996; **14**: 615-619
- 13 **Shammas MA,** Simmons CG, Corey DR, Shmookler Reis RJ. Telomerase inhibition by peptide nucleic acids reverses "immortality" of transformed human cells. *Oncogene* 1999; **18**: 6191-6200
- 14 **Neidle S,** Kelland LR. Telomerase as an anti-cancer target: current status and future prospects. *Anticancer Drug Des* 1999; **14**:341-347
- 15 **Weilbaecher RG,** Lundblad V. Assembly and regulation of telomerase. *Curr Opin Chem Biol* 1999; **3**: 573-577
- 16 **Gilley D,** Blackburn EH. The telomerase RNA pseudoknot is critical for the stable assembly of a catalytically active ribonucleoprotein. *Proc Natl Acad Sci U S A* 1999; **96**: 6621-6625
- 17 **Liu JP.** Studies of the molecular mechanisms in the regulation of telomerase activity. *FASEB J* 1999; **13**: 2091-2104
- 18 **Kushner DM,** Paranjape JM, Bandyopadhyay B, Cramer H, Leaman DW, Kennedy AW, Silverman RH, Cowell JK. 2-5A antisense directed against telomerase RNA produces apoptosis in ovarian cancer cells. *Gynecol Oncol* 2000; **76**: 183-192
- 19 **Kondo Y,** Koga S, Komata T, Kondo S. Treatment of prostate cancer *in vitro* and *in vivo* with 2-5A-anti-telomerase RNA component. *Oncogene* 2000; **19**: 2205-2211
- 20 **Koga S,** Kondo Y, Komata T, Kondo S. Treatment of bladder cancer cells *in vitro* and *in vivo* with 2-5A antisense telomerase RNA. *Gene Ther* 2001; **8**: 654-658
- 21 **Mukai S,** Kondo Y, Koga S, Komata T, Barna BP, Kondo S. 2-5A antisense telomerase RNA therapy for intracranial malignant gliomas. *Cancer Res* 2000; **60**: 4461-4467
- 22 **Herbert BS,** Pitts AE, Baker SI, Hamilton SE, Wright WE, Shay JW, Corey DR. Inhibition of human telomerase in immortal human cells leads to progressive telomere shorting and cell death. *Proc Natl Acad Sci U S A* 1999; **96**: 14276-14281
- 23 **Jiang YA,** Luo HS, Zhang YY, Fan LF, Jiang CQ, Chen WJ. Telomerase activity and cell apoptosis in colon cancer cell by human telomerase reverse transcriptase gene antisense oligodeoxynucleotide. *World J Gastroenterol* 2003; **9**: 1981-1984
- 24 **Belair CD,** Yeager TR, Lopez PM, Reznikoff CA. Telomerase activity: a biomarker of cell proliferation, not malignant transformation. *Proc Natl Acad Sci U S A* 1997; **94**: 13677-13682
- 25 **Holt SE,** Glinsky VV, Ivanova AB, Glinsky GV. Resistance to apoptosis in human cells conferred by telomerase function and telomere stability. *Mol Carcinog* 1999; **25**: 241-248
- 26 **Greider W.** Telomerase activity, cell proliferation, and cancer. *Proc Natl Acad Sci U S A* 1998; **95**: 90-92
- 27 **Bednarek AK,** Sahin A, Brenner AJ, Johnston DA, Aldaz CM. Analysis of telomerase activity levels in breast cancer: positive detection at the *in situ* breast carcinoma stage. *Clin Cancer Res* 1997; **3**: 11-16
- 28 **Okusa Y,** Shinomiya N, Ichikura T, Mochizuki H. Correlation between telomerase activity and DNA ploidy in gastric cancer. *Oncology* 1998; **55**: 258-264
- 29 **Dome JS,** Chung S, Bergemann T, Umbricht CB, Saji M, Carey LA, Grundy PE, Perlman EJ, Breslow NE, Sukumar S. High telomerase reverse transcriptase (hTERT) messenger RNA level correlates with tumor recurrence in patients with favourable histology Wilms' tumor. *Cancer Res* 1999; **59**: 4301-4307

Clinical and epidemiological data of patients with clonorchiasis

Ke-Xia Wang, Rong-Bo Zhang, Yu-Bao Cui, Ye Tian, Ru Cai, Chao-Pin Li

Ke-Xia Wang, Rong-Bo Zhang, Yu-Bao Cui, Ye Tian, Ru Cai, Chao-Pin Li, Department of Etiology and Immunology, School of Medicine, Anhui University of Science and Technology, Huainan 232001, Anhui Province, China

Correspondence to: Dr. Chao-Pin Li, Department of Etiology and Immunology, School of Medicine, Anhui University of Science and Technology, Huainan 232001, Anhui Province, China. cpli@aust.edu.cn

Telephone: +86-554-6658770 **Fax:** +86-554-6662469

Received: 2003-06-05 **Accepted:** 2003-10-07

Abstract

AIM: To study the clinical and epidemiological features of patients with clonorchiasis so as to provide scientific evidences for the diagnosis and prevention of clonorchiasis.

METHODS: Stools from 282 subjects suspected of having clonorchiasis were examined for helminth eggs with modified Kato's thick smear and sedimentation methods, and their sera were tested for HAV-DNA, HBV-DNA, HCV-RNA, HDV-RNA and HEV-RNA with polymerase chain reaction (PCR). Clinical symptoms of patients with clonorchiasis only were analyzed, and their blood samples were tested for circulating antigen (CAg) with Dot-ELISA, eosinophilic granulocyte count, and alanine aminotransferase (ALT). Meanwhile, they were asked to provide data of occupation, eating habit, hygienic habit and knowledge of clonorchiasis. In addition, the ecosystem of the environment in epidemic areas was surveyed.

RESULTS: Among the 282 patients, 61 (21.43%) were infected with *clonorchis sinensis* only, 97 (34.64%) were co-infected with *clonorchis sinensis* and other pathogens, 92 (32.86%) were infected with hepatitis virus only and 31 (11.07%) neither with *clonorchis sinensis* nor hepatitis virus. Among the 61 patients with clonorchiasis only, there were 14 (22.95%) subjects with discomfort over hepatic region or epigastrium, 12 (19.67%) with general malaise or discomfort and inertia in total body, 6 (9.84%) with anorexia, indigestion and nausea, 4 (6.56%) with fever, dizziness and headache (6.56%), and 25 (40.98%) without any symptoms; sixty one (100%) with CAg (+), 98.33% (59/60) with eosinophilic granulocytes increased and 65.00% (39/60) with ALT increased. B-mode ultrasonography revealed 61 cases with dilated and thickened walls of intrahepatic bile duct, and blurred patchy echo acoustic image in liver. Twenty-six cases had stones in the bile duct, 39 cases had slightly enlarged liver with diffuse coarse spots in liver parenchyma. Twenty cases had enlarged gallbladder with thickened coarse wall and image of floating plaques, 9 cases had slightly enlarged spleen. By analysis of epidemiological data, we found that the ecologic environment was favorable for the epidemiology of clonorchiasis. Most patients with clonorchiasis were lack of knowledge about the disease. Their living environment, hygienic habits, eating habits and their occupations were the related factors that caused the prevalence of the disease.

CONCLUSION: The clinical symptoms of clonorchiasis are non-specific, and the main evidences for diagnosis of clonorchiasis should be provided by etiologic examination,

B-mode ultrasonography and clinical history. The infection of *clonorchis sinensis* is related to occupations, bad eating habits and lack of knowledge about prevention of the disease.

Wang KX, Zhang RB, Cui YB, Tian Y, Cai R, Li CP. Clinical and epidemiological data of patients with clonorchiasis. *World J Gastroenterol* 2004; 10(3):446-448

<http://www.wjgnet.com/1007-9327/10/446.asp>

INTRODUCTION

Clonorchiasis, a food-borne infection by eating raw fish contaminated with *Clonorchis sinensis* metacercariae, is more frequently found in individuals along the great rivers and streams in areas of China, northern Vietnam, Korea and other Eastern Asia countries^[1-8]. After oral infection, *C. sinensis* often engulfs the biliary epithelial tissues and blood cells in the intestine, and causes cholangitis with marked eosinophilic infiltration, biliary adenomatous hyperplasia, bile duct obstruction, and subsequently cholangiofibrosis^[9-21]. In an effort to provide scientific evidences for diagnosis of this disease, clinical and epidemiological data of patients with clonorchiasis were analyzed in this study.

MATERIALS AND METHODS

Subjects

Two hundred and eighty-two individuals suspected of being infected with clonorchiasis were involved in this study, including 187 males and 95 females. Their age distribution was as follows: 29 aged 10-16 years, 182 aged 17-55 years and 71 aged 55-67 years.

Methods

Etiological examination Stools from 282 subjects were examined for helminth eggs with modified Kato's thick smear and sedimentation methods, and sera of them were tested for HAV-DNA, HBV-DNA, HCV-RNA, HDV-RNA and HEV-RNA with polymerase chain reaction (PCR).

Analysis of clinical symptoms Clinical symptoms of the patients only with clonorchiasis diagnosed by microscopic fecal examinations were expressed as percentages according to the formula (the number of patients with some symptoms/the total number of the patients with clonorchiasis)×100% and subsequently statistical analysis was conducted.

Laboratory examination Blood samples of patients only with clonorchiasis were detected for circulating antigen (CAg) with Dot-ELISA, counted for eosinophilic granulocytes, and tested for alanine aminotransferase (ALT). The number of eosinophilic granulocytes above $0.5 \times 10^9/L$ was regarded as increased, and the value of alanine aminotransferase (ALT) above 30 u/L was judged as abnormal.

Examination by B-mode ultrasonography Abdominal part of the patients only with *C. sinensis* eggs in their stools was examined by B-mode ultrasonography.

Analysis of epidemiological data A questionnaire was given to the patients only with clonorchiasis, including occupation, eating habits, hygienic habits and knowledge about prevention

of clonorchiasis. In addition, we surveyed the ecosystem environments in the epidemic areas.

RESULTS

Etiological examination

Of the 282 individuals investigated, 21.43% (61/282) were confirmed to be infected with *C. sinensis* only by etiological examination, 34.64% (97/282) were infected with *C. sinensis* and other pathogens, 32.86% (92/282) were infected with hepatitis virus only, and 11.07% (31/282) with neither *C. sinensis* nor hepatitis virus (Table 1).

Table 1 Results of etiological examination

Types of pathogens	Case numbers	Percentages (%)
Infection of <i>C. sinensis</i> only	61	21.63
Infection of <i>C. sinensis</i> and other pathogens	97	34.40
Infection of <i>C. sinensis</i> and other helminth	32	11.35
Infection of <i>C. sinensis</i> and hepatitis virus	24	8.51
Infection of <i>C. sinensis</i> , other helminth and hepatitis virus	41	14.54
Infection of hepatitis virus only	92	32.62
Neither with <i>C. sinensis</i> nor hepatitis virus	32	11.35
Totally	282	100

Analysis of clinical manifestations

Among the 61 patients with clonorchiasis only, 14 (22.95%) subjects had discomfort over hepatic region or epigastrium, 12 (19.67%) had general malaise or discomfort, 6 (9.84%) had anorexia, indigestion and nausea, 4 (6.56%) had fever, dizziness and headache, and 25 (40.98%) had not any symptoms.

Laboratory examination

The results of laboratory examination of the 61 patients with clonorchiasis only showed that the positive rates of CAg were 100%, eosinophilic granulocytes increased in 98.33% (59/60) patients and the values of ALT increased in 65.00% (39/60).

Examination by B-mode ultrasonography

In B-mode ultrasonography, 61 cases had dilated and thickened walls of intrahepatic bile ducts. Blurred patchy acoustic image was seen in liver. Twenty-six cases had calculi of intrahepatic ducts, 39 cases had slightly enlarged liver with diffuse coarse spots in liver parenchyma. Twenty cases had enlargement of gallbladder with thickened rough wall, floating plaques with postural variation were seen in the gallbladder. Nine cases had slightly enlarged spleen.

Analysis of epidemiological data

Occupational structure The constituent ratios of the occupation of 61 patients with clonorchiasis only were: fishermen 37.7%, fishmongers 9.84%, workers in processing fish products 16.39%, officials 19.67%, students 9.84% and others 6.56%.

Eating habits According to the results of questionnaires sent to 61 patients with clonorchiasis only, there were 26 subjects with habits of eating raw fishes and shrimps, 41 eating undercooked fish and shrimps, 48 with kitchen knives used in both raw and cooked food, 30 grasping food directly after contacting live fish and shrimps with unwashed hands, and 11 drinking unclean or unboiled crude water.

Knowledge about prevention of clonorchiasis All patients, did not have any knowledge about metacercaria of *C. sinensis* that might be in fish and shrimps of Huaihe River System. They had no idea about the possible infection with *C. sinensis* after ingestion of raw and undercook fish and shrimps. Even

if infected with *C. sinensis*, symptoms such as epigastric pain, diarrhea, decreased appetite, dizziness, *etc.*, would occur.

Ecologic survey Among the sixty-one patients confirmed to be infected with *C. sinensis* only, 18 lived in villages along the Huaihe River, 19 lived near fishponds. We found a crowd of domestic animals coming and going on both banks of the river, such as chickens, ducks, dogs, pigs, *etc.*, and murine animals, hares and wild cats running in brushes and weeds near the river. In addition, wild ducks and birds, frolic king were looking for food on the river. Some mollusca, like *viviparidae*, *unionidar*, *bithyniidae*, *lymnaeidae*, and some fish and shrimps, such as *Pseudorasbora parva*, *Ctenopharyngodon idellus*, *Mylopharyngodon aethops*, *Cyprinus carpio*, *Lobstergrow* were found in waterweeds in the river.

About two thousand kinds of mollusca were collected and examined for cercaria of *C. sinensis*, and the positive rate was 0.25% (5/2000). When *Ctenopharyngodon idellus* was infected with cercaria, we could separate encysted metacercaria from its body. Similarly, the adult worms could be found from cats that were infected by encysted metacercaria. In addition, the positive rate of encysted metacercaria in fish and shrimps was 9.50% (19/200).

DISCUSSION

Clonorchiasis is endemic in East Asian countries and about seven million subjects were estimated to be infected with the fluke^[22,23]. After oral infection with *C. sinensis* metacercariae, the organism excysts in the digestive tract and migrates up to the bile duct where it grows into adult worms. Infected humans excrete faeces containing *C. sinensis* eggs, and human infections could be diagnosed by microscopic fecal examination with demonstration of the characteristic eggs^[24-26]. In the present study, we examined 282 subjects suspected of being infected with *C. sinensis* with methods of modified Kato's thick smear and sedimentation, and 61 individuals were found to be infected with *C. sinensis* only, while 97 were co-infected with *C. sinensis* and other pathogens, 92 were infected with hepatitis virus only, 31 had neither *C. sinensis* nor hepatitis virus. Etiological examination is a major method in the differential diagnosis of clonorchiasis and other diseases of the liver and biliary tract.

The prevalence of clinical symptoms was determined by the fluke quantity, frequency of infection and the hosts immunities. Subjects with mild infection of *C. sinensis*, often had symptoms or only some epigastric discomfort, anorexia, dyspepsia, *etc.* Subjects with moderate infection often had inertia, lassitude, dyspepsia, abdominal pain and other mild complaints, all of which could also be obviously observed in the subjects with severe infection and cirrhosis of liver. Portal hypertension and ascitis might finally occur^[27-32]. The outcome of this study showed there were 40.98% of patients without any symptoms and others with symptoms of epigastric discomfort, general malaise, inertia, anorexia, dyspepsia, nausea, fever, dizziness, headache, *etc.* had no specificity. Differential diagnosis should include schistosomiasis Japonica, fascioliasis and fasciolopsiasis.

During the development of *C. sinensis* in human body, CAg was produced and released into circulation. Generally, CAg might be detected in sera of the subjects three days after infection^[33,34]. For this reason, detection of CAg may be used to examine whether live worms exist in human body or not, and for check up of treatment effects. By Dot-ELISA, all of the 61 *C. sinensis* egg-positive individuals were positive, although 40.98% of them had no symptoms. So detection of CAg may provide an evidence for diagnosis of clonorchiasis. In addition, results from this study showed that eosinophilic granulocytes were increased in 98.33% patients, ALT was increased in 65% patients and image changes were found in

liver with B-mode ultrasonography in all patients. These are all helpful in the diagnosis of clonorchiasis.

Both natural and social factors affect transmission of *C. sinensis*. We investigated the ecologic system in the Huaihe River on the spot and saw various kinds of mollusca crawling on water plants and some fish and shrimps swimming in the river, all of which are intermediate hosts of *C. sinensis*. Near the river, a large number of domestic animals, livestock, murine animals, hares and wild cats are reservoir hosts. Moreover, the villagers have got accustomed to feeding fish with their own stools and domestic animals with raw fish and shrimps, which help *C. sinensis* to be transmitted from one host to another. On both banks of the river, simple toilets and pigsties are arranged everywhere, and the villagers brush chamber pots in the river without scruple. Terribly, they live on water untreated from the river. All of these natural environments and human activities contribute to overflowing of *C. sinensis* in this area.

The incidence of clonorchiasis was shown in this study to vary greatly and was related to occupations, and was higher in fishermen, fishmongers, workers in processing fish products, officials than in those with other occupations. Because of bad working and eating habits, they have chances to be infected with encysted metacercaria. Therefore, knowledge about prevention of clonorchiasis should be strengthened in these populations to correct their bad eating and health habits and to reinforce their protection consciousness.

REFERENCES

- Yong TS**, Park SJ, Lee DH, Yang HJ, Lee JW. Identification of IgE-reacting *Clonorchis sinensis* antigens. *Yonsei Med J* 1999; **40**: 178-183
- Park SY**, Lee KH, Hwang YB, Kim KY, Park SK, Hwang HA, Sakanari JA. Characterization and Large-scale expression of the recombinant cysteine proteinase from adult clonorchis sinensis. *J Parasitol* 2001; **87**: 1454-1458
- Kim BJ**, Ock MS, Kim IS, Yeo UB. Infection status of *Clonorchis sinensis* in residents of Hamyang-gun, Gyeongsangnam-do, Korea. *Korean J Parasitol* 2002; **40**: 191-193
- Park GM**, Yong TS. Geographical variation of the liver fluke, *Clonorchis sinensis*, from Korea and China based on the karyotypes, zymodeme and DNA sequences. *Southeast Asian J Trop Med Public Health* 2001; **32**(Suppl 2): 12-16
- Wang JJ**, Chung LY, Lee JD, Chang EE, Chen ER, Chao D, Yen CM. Haplorchis infections in intermediate hosts from a clonorchiasis endemic area in Meinung, Taiwan, Republic of China. *J Helminthol* 2002; **76**: 185-188
- Kino H**, Inaba H, Van De N, Van Chau L, Son DT, Hao HT, Toan ND, Cong LD, Sano M. Epidemiology of clonorchiasis in Ninh Binh Province, Vietnam. *Southeast Asian J Trop Med Public Health* 1998; **29**: 250-254
- Guoqing L**, Xiaozhu H, Kanu S. Epidemiology and control of *Clonorchis sinensis* in China. *Southeast Asian J Trop Med Public Health* 2001; **32**(Suppl 2): 8-11
- Lee GS**, Cho IS, Lee YH, Noh HJ, Shin DW, Lee SG, Lee TY. Epidemiological study of clonorchiasis and metagonimiasis along the Geum-gang (River) in Okcheon-gun (county), Korea. *Korean J Parasitol* 2002; **40**: 9-16
- Carpenter HA**. Bacterial and parasitic cholangitis. *Mayo Clin Proc* 1998; **73**: 473-478
- Kim YH**. Eosinophilic cholecystitis in association with clonorchis sinensis infestation in the common bile duct. *Clin Radiol* 1999; **54**: 552-554
- Leung JW**, Yu AS. Hepatolithiasis and biliary parasites. *Baillieres Clin Gastroenterol* 1997; **11**: 681-706
- Na BK**, Lee HJ, Cho SH, Lee HW, Cho JH, Kho WG, Lee JS, Lee JS, Song KJ, Park PH, Song CY, Kim TS. Expression of cysteine proteinase of *Clonorchis sinensis* and its use in serodiagnosis of clonorchiasis. *J Parasitol* 2002; **88**: 1000-1006
- Kim KH**, Kim CD, Lee HS, Lee SJ, Jeon YT, Chun HJ, Song CW, Lee SW, Um SH, Choi JH, Ryu HS, Hyun JH. Biliary papillary hyperplasia with clonorchiasis resembling cholangiocarcinoma. *Am J Gastroenterol* 1999; **94**: 514-517
- Kim YH**. Eosinophilic cholecystitis in association with clonorchis sinensis infestation in the common bile duct. *Clin Radiol* 1999; **54**: 552-554
- Kim YH**. Extrahepatic cholangiocarcinoma associated with clonorchiasis: CT evaluation. *Abdom Imaging* 2003; **28**: 68-71
- Saito S**, Endo I, Yamagishi S, Tanaka K, Ichikawa Y, Togo S, Shimada H, Amano T, Ueda M, Kawano N. Multiple cancer of the common bile duct associated with clonorchiasis. *Nippon Shokakibyo Gakkai Zasshi* 2002; **99**: 518-522
- Fry LC**, Monkemuller KE, Baron TH. Sclerosing cholangitis caused by *Clonorchis sinensis*. *Gastrointest Endosc* 2002; **56**: 114
- Chan HH**, Lai KH, Lo GH, Cheng JS, Huang JS, Hsu PI, Lin CK, Wang EM. The clinical and cholangiographic picture of hepatic clonorchiasis. *J Clin Gastroenterol* 2002; **34**: 183-186
- Watanapa P**, Watanapa WB. Liver fluke-associated cholangiocarcinoma. *Br J Surg* 2002; **89**: 962-970
- Abdel-Rahim AY**. Parasitic infections and hepatic neoplasia. *Dig Dis* 2001; **19**: 288-291
- Kim SH**, Park YN, Yoon DS, Lee SJ, Yu JS, Noh TW. Composite neuroendocrine and adenocarcinoma of the common bile duct associated with *Clonorchis sinensis*: a case report. *Hepatogastroenterology* 2000; **47**: 942-944
- Tinga N**, Van De N, Vien HV, Van Chau L, Toan ND, Kager PA, de Vries PJ. Little effect of praziquantel or artemisinin on clonorchiasis in northern Vietnam. A pilot study. *Trop Med Int Health* 1999; **4**: 814-818
- Kim TY**, Kang SY, Park SH, Sukontason K, Sukontason K, Hong SJ. Cystatin capture enzyme-linked immunosorbent assay for serodiagnosis of human clonorchiasis and profile of captured antigenic protein of *Clonorchis sinensis*. *Clinical Diagnostic Laborat Immunol* 2001; **8**: 1076-1080
- Yoon BI**, Jung SY, Hur K, Lee JH, Joo KH, Lee YS, Kim DY. Differentiation of hamster liver oval cell following *Clonorchis sinensis* infection. *J Vet Med Sci* 2000; **62**: 1303-1310
- Hong SJ**, Kim TY, Song KY, Sohn WM, Kang SY. Antigenic profile and localization of *Clonorchis sinensis* proteins in the course of infection. *Korean J Parasitol* 2001; **39**: 307-312
- Yoon BI**, Lee JH, Joo KW, Lee YS, Kim DY. Isolation of liver oval cells from hamsters treated with diethylnitrosamine and 2-acetylaminofluorene. *J Vet Med Sci* 2000; **62**: 255-261
- Joo CY**, Chung MS, Kim SJ, Kang CM. Changing patterns of *Clonorchis sinensis* infections in Kyongbuk, Korea. *Korean J Parasitol* 1997; **35**: 155-164
- Yoon BI**, Choi YK, Kim DY, Hyun BH, Joo KH, Rim HJ, Lee JH. Infectivity and pathological changes in murine clonorchiasis: comparison in immunocompetent and immunodeficient mice. *J Vet Med Sci* 2001; **63**: 421-425
- Lee HJ**, Lee CS, Kim BS, Joo KH, Lee JS, Kim TS, Kim HR. Purification and characterization of a 7-kDa protein from clonorchis sinensis adult worms. *J Parasitol* 2002; **88**: 499-504
- Lee WJ**, Lim HK, Jang KM, Kim SH, Lee SJ, Lim JH, Choo IW. Radiologic spectrum of cholangiocarcinoma: emphasis on unusual manifestations and differential diagnoses. *Radiographics* 2001; **21**: S97-S116
- Suh KS**, Roh HR, Koh YT, Lee KU, Park YH, Kim SW. Clinicopathologic features of the intraductal growth type of peripheral cholangiocarcinoma. *Hepatology* 2000; **31**: 12-17
- Su KE**, Wang FY, Chi PY. Worm recovery and precipitin antibody response in guinea pigs and rats infected with *Clonorchis sinensis*. *J Microbiol Immunol Infect* 1998; **31**: 211-216
- Wang X**, Li S, Zhou Z. A rapid one-step method of EIA for detection of circulating antigen of *Schistosoma japonicum*. *Chin Med J* 1999; **112**: 124-128
- Liu XM**. Comparative studies on detecting CAg in urine of acute schistosomiasis patients by mAb-RIHA and mAb-DotELISA. *Southeast Asian J Trop Med Public Health* 1999; **30**: 29-31

Effects of Cd^{+2} , Cu^{+2} , Ba^{+2} and Co^{+2} ions on *Entamoeba histolytica* cysts

Umit Aksoy, Sebnem Ustun, Hande Dagci, Süleyman Yazar

Umit Aksoy, Department of Parasitology, Medical Faculty, Dokuz Eylül University, ȳnciraltı, ȳzmir-Turkey

Sebnem Ustun, Department of Gastroenterology, Medical Faculty, Ege University, Bornova, ȳzmir-Turkey

Hande Dagci, Department of Parasitology, Medical Faculty, Ege University, Bornova, ȳzmir-Turkey

Süleyman Yazar, Department of Parasitology, Medical Faculty, Erciyes University, Kayseri-Turkey

Correspondence to: Süleyman Yazar, Department of Parasitology, Medical Faculty, Erciyes University, 38039, Kayseri, Turkey. syazar@erciyes.edu.tr

Telephone: +90-352-4374937 Ext 23401

Received: 2003-09-06 **Accepted:** 2003-09-20

Abstract

AIM: The effects of cobalt, copper, cadmium and barium ions on the cysts of *Entamoeba histolytica* (*E. histolytica*), an amebic dysentery agent, cultured in Robinson medium were investigated.

METHODS: *E. histolytica* cysts and trophozoites isolated from a patient with amebiasis were cultivated in the medium, incubated at 37 °C for a period of 4 days and 40×10^4 /ml amebic cysts were then transferred to a fresh medium. At the second stage, 0.05, 0.1 and 0.2 mM of selected metal ions were added to the medium, and the effects of these ions on parasitic reproduction compared with the control group were observed.

RESULTS: It was determined that the number of living parasites in all the groups containing metal ions decreased significantly starting from 30 minutes ($P < 0.01$). CuCl_2 showed the highest lethal effect on *E. histolytica* cysts, whereas the lowest lethal effect was observed with CoCl_2 . It was also seen that the number of living cells was decreased as the ion concentration and exposure time were increased, and that there were no living parasites in the medium at the end of 24 h ($P < 0.01$).

CONCLUSION: It may be stated that the effect of ever-increasing contamination of the environment with metal waste materials on parasites should be investigated further.

Aksoy U, Ustun S, Dagci H, Yazar S. Effects of Cd^{+2} , Cu^{+2} , Ba^{+2} and Co^{+2} ions on *Entamoeba histolytica* cysts. *World J Gastroenterol* 2004; 10(3):449-451

<http://www.wjgnet.com/1007-9327/10/449.asp>

INTRODUCTION

Amebiasis, which infects nearly 10% of the world population and is responsible for mortality and morbidity in developing countries in particular is caused by a protozoan, *Entamoeba histolytica* (*E. histolytica*)^[1]. The form of the agent infecting humans is the 4 nuclei cysts, shed into the environment with feces. The cysts, which can survive in the environment for a long time, can carry on their life cycle with fecal-oral contamination^[2,3].

Like many other protozoa, this particular parasite develops complex metabolic structures under different environmental conditions^[4]. Reproduction of *E. histolytica* in *in vitro* culture provides a better understanding of its biological characteristics, its pathogenesis and adaptation to environmental conditions^[2]. The metabolism of the parasite in a medium environment varies according to the age of the culture, its oxidation-reduction potential, as well as the composition, the temperature of the medium and the accompanying bacteria^[5,6]. It was reported that *E. histolytica* cysts reproduced under axenic conditions had cyst walls, which were different from, and weaker than those found under natural conditions^[7]. For this reason, it is believed that it would be more appropriate to use xenic media as they reflect the morphological structure and living conditions of the parasite^[8]. One of the most commonly and successfully used xenic media is the one defined by Robinson^[9].

In these complex biochemical reactions of microorganisms, certain metal cations play an important role as trace elements^[10]. However, some of them are not favored by the ecosystems of living cells, and doses which accumulate in the cell in time (metal ions) do not agree with life^[11,12]. Heavy metal ions in particular bind to sulphhydryl (-SH) groups and form complexes, leading to toxic effects on living cells. This situation can be determined by the blurring of the reproduction media of microorganisms especially in the experimental studies carried out with *in vitro* cultures^[13]. Setting out from this point, knowing the reaction of *E. histolytica* cysts shed into the environment with feces to the metal ions found in the area for various reasons will especially help understand the impact of the contamination by these ions on the parasite population^[14,15].

In this study, we investigated the effects of cadmium (Cd^{+2}), copper (Cu^{+2}), barium (Ba^{+2}) and cobalt (Co^{+2}) ions on *E. histolytica* clinical isolate xenically produced in Robinson medium. In the light of the data we obtained, we also investigated what kinds of effects these metal ions produced with different intracellular concentrations in the parasite depended on time, and whether there were any differences among these ions with respect to their tendency to produce such effects.

MATERIALS AND METHODS

Clinical isolate and culture

E. histolytica fresh clinical isolate was obtained from a patient with amebiasis who came to the laboratory of Dokuz Eylül University Medical Faculty Department of Parasitology. As a result of an examination of the stool samples of the patient by wet mount and Lugol's iodine and trichrome staining methods, *E. histolytica* cysts and trophozoites were determined and the specimen was cultivated in Robinson medium^[9]. The tubes were incubated at 37 °C for 4 days without subculturing. The cysts were then washed with sterile distilled water at pH 7 and counted with a haemocytometer. The 40×10^4 /ml amebae cysts were transferred to a fresh medium under the same conditions and ions prepared at different molarities were immediately added to the tubes.

Cd^{+2} , Cu^{+2} , Ba^{+2} and Co^{+2} ion concentrations

Cd^{+2} [Cadmium chloride ($\text{CdCl}_2 \cdot 5/2\text{H}_2\text{O}$) (Merck; NJ, USA)],

Cu^{+2} [Cupric chloride ($\text{CuCl}_2 \cdot 2\text{H}_2\text{O}$) (Merck; NJ, USA)], Ba^{+2} [Bariumchloride ($\text{BaCl}_2 \cdot 2\text{H}_2\text{O}$) (Riedel-de Haën; Seelze, Germany)] and Co^{+2} [Cobalt chloride ($\text{CoCl}_2 \cdot 6\text{H}_2\text{O}$) (Carlo Erba Reagenti; Rodano (Mi), Italy)] ions prepared at 3 different molarities, namely 0.05, 0.1 and 0.2 mM, were added to the study group^[15]. The remaining tubes, on the other hand, were kept as control group without addition of metal ions, and also serum was added to the control tubes. Three tubes were prepared for each ion molarity and also for control group. Each determination was performed in triplicate.

Parasite counting

All the medium tubes were incubated at 37 °C. After 0.5, 1, 2, 3, 5, 7 and 24 h, the tubes were stirred for 5-10 seconds to achieve a homogeneous distribution and a drop of medium specimen was taken with the help of a Pasteur pipet. A drop of 1% eosin saline solution was added to the specimen. Unstained cystic structures were considered to be alive, whereas those which let pink-red stains in were regarded to be dead. Living cysts were counted with a haemocytometer and the measurements were recorded.

Statistical analysis

All the groups in this study were evaluated by means of GLM-repeated measures, post hoc Tukey in the SPSS for windows 8.0 statistical program and Mann-Whitney *U* test within themselves. $P < 0.05$ was considered significant.

RESULTS

The number of living amebae per ml determined in each tube at 0.5, 1, 2, 3, 5, 7 and 24 h after metal ions and serum were added to the medium environment, is shown in Figure 1. The numbers of living cells were significantly decreased in all the groups compared to control group ($P < 0.01$). It was determined that the most effective metal ion was Cu^{+2} ($P < 0.01$), in contrast the least effective metal ion was Co^{+2} . In all the groups, the number of living cells was decreased as the concentration of the metal ions was increased ($P < 0.01$).

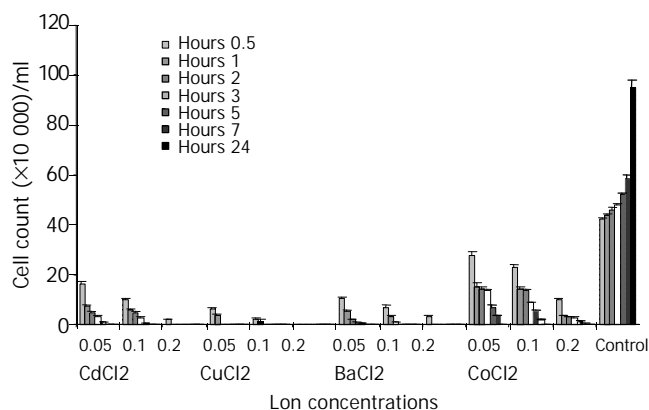


Figure 1 Effect of different concentrations of metal ions on *E. histolytica* cysts. X-axis: the molarities of ion concentration. Y-axis: The alteration of living parasite counts dependent on time and ion molarities.

Judging from the facts that they let 1% eosin-saline solution in themselves and that their cell walls degenerated and degranulated, it was found that the amebae cysts were dead after 24 h at each of the 3 concentrations of all the metal ions. It was also observed that heavy metals with larger atomic numbers affected the functions of intracellular physiologic cations, forming metal complexes. Such a complex formed with Cu^{+2} was seen at any concentration for Cd^{+2} , however, the

formation of complexes was started from 0.1 mM. The formation of this complex was indicated by the blurring of the medium.

As for the effect of Co^{+2} , it was found that *E. histolytica* cysts survived until the end of the 7th h at 0.05 and 0.1 mM concentrations, whereas this was not the case for the other metal ions. Similarly, it was observed that at 0.2 mM of Co^{+2} living amebae cysts were found at the end of the first hour only ($P < 0.01$).

It was also observed that most of the cysts in the control group tubes, cultivated in a fresh medium, transformed into trophozoites and started to reproduce.

DISCUSSION

To be aware of the effects of toxic metals on living things is of great importance, especially in view of the ever-increasing environmental pollution. A number of researches about the effects of metal ions on the physiologic functions of various microorganisms are available^[16-18].

It is believed that the toxic effect of Cd^{+2} , an important heavy metal, might be associated with the denaturation of proteins as a result of its binding to the thiol groups in living cells or with membrane damage stemming from its interaction with Ca^{+2} ^[17]. It was reported that the toxic effect of Cd^{+2} on the culture medium of *Trypanosoma brucei brucei* was at 0.045 mM level^[19]. We determined in this study that when we used 0.05 mM Cd^{+2} as the lowest concentration, the lethal effect leading to the death of living *E. histolytica* cysts started at 0.5 h and was increased time-dependently. We also observed that, Cd^{+2} made the most complexes in the medium starting from 0.1 mM. In this context, the result we obtained was comparable with relevant literature data^[19].

Cu^{+2} , however, can interact with radicals, oxygen in particular. These radicals also cause Cu^{+2} to become toxic. A study carried out on pseudomonas by means of spectroscopy, reported that Cu^{+2} caused greater damage than Co^{+2} did^[20]. In the present study, we discovered that the lethal effect of metal ions at different concentrations was dependent on time rather than the extent of damage and found that Cu^{+2} ions were more effective than Co^{+2} . Another study in which the toxic effect of cadmium acetate and copper sulphate salts on the mouse trachea culture was investigated, reported that the effect of cadmium acetate was shown after 35 minutes, while that of copper sulphate came about after 85 minutes although equal amounts were added to the medium, accordingly the effect of cadmium acetate on the cell was greater^[21]. As a different view, in a study where the cytotoxic effect of cadmium and copper was investigated in the culture of *Merceneria mercenaria*, the cytotoxicity concentration of Cd^{+2} was started at 0.1-1.5 mM and that of Cu^{+2} at 0.01-0.1 mM^[22]. In our study, however, we investigated the effect of 0.05, 0.1 and 0.2 mM metal ions on *E. histolytica* cysts in a culture environment. When the effect of both metal ions was investigated starting as early as 0.5 h, we found the toxic effect of Cu^{+2} on amebae cysts to be greater. Cu^{+2} ions also bound to various compounds and formed complexes. These complexes were determined by the blurring of the medium environment and led to toxic effects on *E. histolytica* cysts at each molarity.

On the other hand, Co^{+2} enters the composition of B_{12} , the main cofactor. This element accumulates in the core structure of microorganism cells. Ermolli *et al.* reported that 0.475 mM Co^{+2} produced a toxic effect on HaCaT human keratinocytes and that this effect could only be observed after 4 h^[23]. It was found in our study however, the lethal effect of Co^{+2} on *E. histolytica* was presented at lower concentrations such as 0.05 mM and was increased dose-dependently. It was also observed that amebae cysts maintained their vitality, though at a minimal level, at all the three concentrations at the end of

the 7th h and that no living parasite remained in the culture medium at the end of the 24th h. In the light of these data, we believe that Co⁺² at low concentrations has a slowly developing lethal effect on *E. histolytica* cysts.

Certain studies aiming at determining the effects of Ba⁺² have been carried out in cell cultures^[24,25]. Borella *et al.* reported that addition of 10⁽⁻⁴⁾ -10⁽⁻⁶⁾ mol/L Ba⁺² to the culture medium did not have any effect on reproduction^[24]. When we investigated the effect of 0.05, 0.1 and 0.2 mM Ba⁺² on *E. histolytica* cysts in Robinson medium, we found that the lethal effect was dependent on both the dose and time.

CdCl₂, CuCl₂, BaCl₂ and CoCl₂ were used for evaluating the effects of these metal ions on the growth of *E. histolytica* cysts. As it was shown the only anion was chlor, all differed in the metal cations.

It would not be surprising to predict that investigating the effects of various factors causing environmental pollution on the life cycle of parasites, which have an important place among microorganisms, would be one of the objectives of future scientific studies. Accordingly, when the effect of Cd⁺², Cu⁺², Ba⁺² and Co⁺² ions on *E. histolytica* was investigated, we determined that these metal ions, led by Cu⁺², prepared at concentrations of 0.05, 0.1 and 0.2 mM had a lethal effect on the parasite. Considering the fact that the life cycle of *E. histolytica* depends on mature cysts with 4 nuclei shed into the environment with feces, this particular result may have a considerable significance in terms of the ecological balance of the environment, which is being contaminated by various metal waste materials.

REFERENCES

- 1 **Walsh JA.** Problems in recognition and diagnosis of amebiasis. Estimation of the global magnitude of morbidity and mortality. *Rev Infect Dis* 1986; **8**: 228-238
- 2 **Belding DL.** The parasitic amoebae of man. Textbook of Parasitology,.3th Edition. Appleton-Century-Crafts, New York 1965: 31-51
- 3 **Markell EK,** John DT, Krotoski WA. Lumen-dwelling protozoa. In: Ozmat S editor. Markell and Voge' s Medical Parasitology, 8 th ed. Saunders Company Mexica 1999: 24-89
- 4 **Bruhn H,** Leippe M. Novel putative saposin-like proteins of Entamoeba histolytica different from amoebapores. *Biochim Biophys Acta* 2001; **1514**: 14-20
- 5 **Clarck CG,** Diamond LS. Methods for cultivation of luminal parasitic protists of clinical importance. *Clin Microbiol Rev* 2002; **15**: 329-341
- 6 **Diamond LS.** A new liqued medium for xenic cultivation of Entamoeba histolytica and other lumen-dwelling protozoa. *J Parasitol* 1982; **68**: 958-959
- 7 **Said-Fernandez S,** Mata-Cardenas BD, Gonzales-Garza MT, Navarro-Marmolejo L, Rodriguez- Perez E. Entamoeba histolytica cysts with a defective wall formed under axenic conditions. *Parasitol Res* 1993; **79**: 200-203
- 8 **Diamond LS.** Axenic cultivation of Entamoeba histolytica: progress and problems. *Arch Invest Med* 1980; **11**: 47-54
- 9 **Robinson GL.** The laboratory diagnosis of human parasitic amoebae. *Trans Roy Soc Trop Med Hyg* 1968; **62**: 285-294
- 10 **Unz RF,** Shuttleworth KL. Microbial mobilization and immobilization of heavy metals. *Curr Opin Biotechnol* 1996; **7**: 307-310
- 11 **Agranoff DD,** Krishna S. Metal ion homeostasis and intracellular parasitism. *Mol Microbiol* 1998; **28**: 403-412
- 12 **Vargas E,** Alvarez AH, Cervantes C. Bacterial systems for expelling toxic metals. *Rev Latinoam Microbiol* 1998; **40**: 53-71
- 13 **Nelson N.** Metal ion transporters and homeostasis. *EMBO J* 1999; **18**: 4361-4371
- 14 **Campos-Gongora E,** Viader-Salvado JM, Martinez-Rodriguez HG, Zunica-Charles MA, Galindo JM, Sait-Fernandez S. Mg, Mn and Co ions enhance the formation of Entamoeba histolytica cyst-like structures resistant to sodium dodecyl sulfate. *Arch Med Res* 2000; **31**: 162-168
- 15 **Nies DH.** Microbial heavy-metal resistance. *Appl Microbiol Biotechnol* 1999; **51**: 730-770
- 16 **Kachur AV,** Koch CJ, Biaglow JE. Mechanims of copper-catalyzed oxidation of glutatione. *Free Radical Res* 1998; **28**: 259-269
- 17 **Nies DH,** Silver S. Ion efflux systems involved in bacterial metal resistances. *J Ind Microbiol* 1995; **14**: 186-199
- 18 **Weast RC.** CRC handbook of chemistry and physics. 64 ed. CRC, Boca Raton, Fla 1984
- 19 **Nyarko E,** Hara T, Grab DJ, Tabata M, Fukama T. Toxic effects of mercury (II), cadmium (II) and lead (II) porphyrins on Trypanosoma brucei brucei growth. *Chem Biol Interact* 2002; **139**: 177-185
- 20 **Ivanov A,** Gavriushkin AV, Siunova TV, Khasanova LA, Khasanova ZM. Resistance of certain strains of Pseudomonas bacteria to toxic effect of heavy metal ions. *Mikrobiologiya* 1999; **68**: 366-374
- 21 **Olsen I,** Jonsen J. Effects of cadmium acetate, copper sulphate and nickel chloride on organ cultures of mouse trachea. *Acta Pharmacol Toxicol* 1979; **44**: 120-127
- 22 **Zaroogian G,** Anderson S, Voyer RA. Individual and combined cytotoxic effects of cadmium, copper, and nickel on brown cells of Mercenaria mercenaria. *Ecotoxicol Environ Saf* 1992; **24**: 328-337
- 23 **Ermolli M,** Menne C, Pozzi G, Serra MA, Clerici LA. Nickel, cobalt and chromium-induced cytotoxicity and intracellular accumulation in human hacat keratinocytes. *Toxicology* 2001; **159**: 23-31
- 24 **Borella P,** Manni S, Giardino A. Cadmium, nickel, chromium and lead accumulate in human lymphocytes and interfere with PHA-induced proliferation. *J Trace Elem Electrolytes Health Dis* 1990; **4**: 87-95
- 25 **Deineka SE,** Prodanchuk NG, Petrunik IO, Davydenko IS, Sinchenko VG, Shelifost AV. The cytotoxic action of metal stearates and its correlation with the toxicity for animals. *Gig Tr Prof Zabol* 1992; **4**: 17-20

Edited by Zhu LH and Wang XL

Frequency of toxoplasmosis in patients with cirrhosis

Sebnem Ustun, Umit Aksoy, Hande Dagci, Galip Ersoz

Sebnem Ustun, Department of Gastroenterology, School of Medicine, University of Ege, 35100 Bornova, Izmir, Turkey

Umit Aksoy, Department of Parasitology, School of Medicine, University of Dokuz Eylul, Izmir, Turkey

Hande Dagci, Department of Parasitology, School of Medicine, University of Ege, Izmir, Turkey

Galip Ersoz, Department of Gastroenterology, School of Medicine, University of Ege, Izmir, Turkey

Correspondence to: Sebnem Ustun, MD, Department of Gastroenterology, School of Medicine, University of Ege, 35100 Bornova, Izmir, Turkey. sustun@med.ege.edu.tr

Telephone: +90-232-3881969-181

Received: 2003-08-26 **Accepted:** 2003-10-23

Abstract

AIM: It is known that toxoplasmosis rarely leads to various liver pathologies, most common of which is granulomatose hepatitis in patients having normal immune systems. Patients who have cirrhosis of the liver are subject to a variety of cellular as well as humoral immunity disorders. Therefore, it may be considered that toxoplasmosis can cause more frequent and more severe diseases in patients with cirrhosis and is capable of changing the course of the disease. The aim of this study was to investigate the frequency of toxoplasmosis in patients with cirrhosis.

METHODS: Serum samples were taken from 108 patients with cirrhosis under observation in the Hepatology Polyclinic of the Gastroenterology Clinic, and a control group made up of 50 healthy blood donors. IFAT and ELISA methods were used to investigate the IgG and IgM antibodies, which had developed from these sera.

RESULTS: Toxoplasma IgG and IgM antibody positivity was found in 74 (68.5%) of the 108 cirrhotic patients and 24 (48%) of the 50 people in the control group. The difference between them was significant ($P < 0.05$).

CONCLUSION: In conclusion, it was found that the toxoplasma sero-prevalence in the cirrhotic patients in this study was higher. Cirrhotic patients are likely to form a toxoplasma risk group. More detailed studies are needed on this subject.

Ustun S, Aksoy U, Dagci H, Ersoz G. Frequency of toxoplasmosis in patients with cirrhosis. *World J Gastroenterol* 2004; 10(3): 452-454

<http://www.wjgnet.com/1007-9327/10/452.asp>

INTRODUCTION

Toxoplasmosis is a protozoan disease that infects 35-40% of the adult population of the world and demonstrates varying clinical manifestations. Its active agent is *Toxoplasmosis gondii* (*T. gondii*). In man tissue parasitism during the proliferative phase may occur without signs of symptoms. It may lead to a transient illness characterized by lymphadenopathy, fever and fatigue, or a severe disease. Severe manifestations of the disease

most commonly occur in patients with impaired immunity^[1].

In most countries, seroprevalence of toxoplasma ranges between 20% and 60%. The prevalence is quite low in extremely dry and cold regions. It has been reported that the prevalence is rather high in warm and humid areas^[2].

Cats, small mammals and birds take place in the usual life cycle of *T. gondii* in nature. Humans join this chain as a result of their close relationship with cats. Toxoplasmosis is never encountered in the small Pacific islands where there are no cats. In the group investigated for toxoplasmosis, the prevalence in Turkey ranged between 44% and 55%^[3,4].

Toxoplasmosis may rarely cause various liver pathologies due to granulomatose hepatitis in patients with normal immune systems^[1,5-8].

Patients with cirrhosis of the liver demonstrate various cellular and humoral immunity disorders^[9-12]. For this reason, it may be thought that toxoplasmosis may lead to more frequent and more severe diseases in patients with cirrhosis and change the course of the disease.

What was investigated in this study was the frequency of *T. gondii* antibodies in the cases of cirrhosis associated with various reasons.

MATERIALS AND METHODS

One hundred and eight patients with cirrhosis from the Hepatology Polyclinic of the Gastroenterology Clinic, and a control group comprising 50 healthy blood donors of similar age and sex were taken in the study. Serum samples were taken from the patients and control group and kept at -20 °C until toxoplasma serological tests were performed.

IgM and IgG antibodies from the sera were investigated by IFAT and ELISA methods.

ELISA method

Dissolved antigen was prepared based upon literature data provided by Herlow *et al*, Naot *et al*^[13,14]. Serum samples were diluted up to 1/64, 1/256, 1/1 024, 1/4 096 to determine IgM antibodies and up to 1/256, 1/1 024, 1/4 096, 1/8 000, 1/32 000 to determine IgG antibodies. The sera were read at a 405λ wavelength ELISA reader (Titertek II). The mean absorbance values of negative controls were added to the 2 standard deviation values of these absorbance values. Those above the cut-off value obtained were accepted as positive and compared with the values expressed by the control sera to assess the suspected sera. For IgG 1/1 024 and above and for IgM 1/256 and above were accepted as significant titers with regard to active disease^[15].

IFAT method

Particle antigen was prepared according to data from Garin *et al*, Remington *et al*^[16,17]. Serum samples were diluted and assessed semiquantatively. The dilution of the sera within the scope of the study was 1/16, 1/64, 1/128, 1/256, 1/512, 1/1 024, 1/4 096 for both IgG and IgM. The results obtained were assessed by a fluorescence microscope (Nikon) at 490 nm stimulation, 510 nm barrier filter wavelength and 20×10 magnification. For IgG 1/256 and above and for IgM 1/16 and above were accepted as significant titers with regard to

Table 1 Cirrhosis etiology of 108 patients

	Number of patients	%
Hepatitis B	37	34.3
Hepatitis C	27	25
Autoimmune hepatitis	5	4.6
Alcoholic cirrhosis	18	16.7
Primary biliary cirrhosis	12	11.1
With unknown etiology	9	8.3
Total	108	

Table 2 Toxoplasma IgG and IgM positivity of patients and control groups

	Number of patients	Sex W/M	Age	IFAT and ELISA IgG(+)	IFAT and ELISA IgM(+)	Active disease significant with respect to	
						Ig G(+)	IgM(+)
Cirrhosis	108	38/70	51.5±10.2	74 (68.5) ^a	2	31(28.7) ^a	2
Control	50	19/31	40±6.7	24 (48)	-	4 (8)	-

^a $P < 0.05$.

active disease^[15].

Comparisons between the cirrhotic patients and the control group pertaining to antibody positivity and sex were performed according to Fisher exact age distribution *t* test.

RESULTS

Cirrhosis etiology in patients is shown in Table 1. The cirrhotic patients and the control group demonstrated similar sex and age distributions (Table 2). Toxoplasma IgG and IgM antibody positivity was determined in 74 (68.5%) of the 108 cirrhotic patients and 24 (48%) of the 50 individuals in the control group. The difference was significant ($P < 0.05$). Significant titers were found with respect to active disease (IgG 1/1 024 and above, IgM 1/256 and above for ELISA, and IgG1/256 and above, IgM 1/16 and above for IFAT) were found in 31 (28.7%) of the cirrhotic patients and 4 (8%) of the control group. The difference was significant (Table 2).

DISCUSSION

Toxoplasmosis is a protozoan disease that is widespread all over the world and demonstrates varying clinical manifestations. Determination of its incidence in various risk groups in the society and establishment of these risk groups play a significant role in taking the necessary precautions against this disease.

In this study toxoplasma IFAT and ELISA antibody positivity was significantly higher in cirrhotic patients. Besides, the significant titers were found to be higher with regard to active disease.

Toxoplasmosis can be frequently found in the general population all over the world. It has been reported that it was encountered at a higher rate in warm and humid regions compared to cold and dry places^[2]. No sero-epidemiologic studies that would properly demonstrate the toxoplasmosis prevalence in the whole population in Turkey have been reported so far. The studies carried out merely reflect the results of those that have been brought to and evaluated in various laboratories with suspicion of toxoplasmosis. In a study carried out in Elazığ, a region of Turkey that is comparatively underdeveloped from the socio-economic point of view, Asci *et al.* found toxoplasma antibodies in 55% of 1 641 serum samples^[3]. In a study covering the Aegean region between 1991-1995, Altintas *et al.* determined toxoplasma seropositivity in 4 651 (49.4%) of 9 410 individuals in their study^[18]. Sutcu *et al.*

found the toxoplasma IgM positivity was 10% and IgG positivity was 44% in Konya province between 1993 and 1997^[4]. The seropositivity rate in Turkey generally varies between 44% and 55%. These values are quite close to the rates we have determined in our control group (48%), but lower than those in cirrhotic patients (68.5%). No other study has investigated the toxoplasma antibody frequency in cirrhotic patients. This study is probably the first one investigating the toxoplasma seroprevalence in cirrhotic patients.

The reasons why both the antibody positivity and titers were significant with regard to active disease are not known. Could toxoplasma, known to cause partial damage to the liver, have a role in the onset and clinical course of cirrhosis?

This study did not contain any research into the activity of toxoplasma. Nevertheless, the fact that antibody titers are higher in cirrhotic patients leads one to think that these people might have an active disease. We are also planning another study to determine whether active disease develops in cirrhotic patients by monitoring the changes in the long-term toxoplasma titers.

To sum up, the toxoplasma sero-prevalence in cirrhotic patients in our study was found to be higher. Cirrhotic patients may well form a risk group for toxoplasma. More detailed studies need to be carried out on this particular subject.

REFERENCES

- 1 Jones TC. Toxoplasmosis. In *Cecil Textbook of medicine* Neeson PB, McDermott W, Wyngaarden JB, (Eds), part X, 15th ed. London: W.B. Saunders Co 1979: 594-598
- 2 Beaman MH, McCabe RE, Wong S, Remington JS. *Toxoplasma gondii*. In *Principles and Practice of Infections Diseases*. Mandell GL, Benett JE, Dolin R (eds). Fourth edition, New York: Churchill Livingstone 1995: 2393-2525
- 3 Asci Z, Seyrek A, Kizirgil A, Doymaz MZ, Yilmaz M. Toxoplazma supheli hasta serumlarında anti-*Toxoplasma gondii* IgG ve IgM antikorlarının araştırılması. *Türkiye Parazitoloji Dergisi* 1997; **21**: 245-247
- 4 Sutcu A, Tuncer I, Kuru C, Baykan M. Konya ve çevresinde *Toxoplasma gondii* IgM ve IgG prevalansı. *Türkiye Parazitoloji Dergisi* 1998; **22**:5-7
- 5 Duvic C, Herody M, Didelot F, Nedelec G. Acute toxoplasmic hepatitis in an immunocompetent adult. *Ann Med Interne*1997; **148**: 323-324
- 6 Frenkel JK, Remington JS. Hepatitis in toxoplasmosis. *N Engl J Med* 1980; **302**: 178-179
- 7 Masur H, Jones TC. Hepatitis in acquired toxoplasmosis. *N Engl*

- J Med* 1979; **301**: 613
- 8 **Schoukry NA**, Farrag SA, Makarem SS, el Nassr MS, Baddar MR, el Lamei OI, Labib MH. *Toxoplasma gondii* in acute and chronic hepatitis. *J Egypt Soc Parasitol* 1986; **16**: 531-539
- 9 **Fiere J**, Finley F. Deficient serum bactericidal activity against *Echerichia coli* in patients with cirrhosis of the liver. *J Clin Invest* 1979; **63**: 912-921
- 10 **Nouri-Aria KT**, Alexander GJ, Portmann BC, Hegarty JE, Eddleston AL, Williams R. T and B cell function in alcoholic liver disease. *J Hepatol* 1986; **2**: 195-207
- 11 **Rajkovic IA**, Williams R. Abnormalities of neutrophil phagocytosis, intracellular killing and metabolic activity in alcoholic cirrhosis and hepatitis. *Hepatology* 1986; **6**: 252-262
- 12 **Trevisani F**, Castelli E, Foschi FG, Parazza M, Loggi E, Bertelli M, Meloti C, Domenicali M, Zoli G, Bernardi M. Impaired tuftsin activity in cirrhosis: relationship with splenic function and clinical outcome. *Gut* 2002; **50**: 707-712
- 13 **Herlow ED**, Lane D. Antibodies. *A laboratory manual*. Cold Spring Harbour Laboratory 1998: 561-591
- 14 **Naot Y**, Remington JS. An enzyme-linked immunosorbent assay for detection of IgM antibodies of *Toxoplasma gondii*: use for diagnosis of acute acquired toxoplasmosis. *J Infect Dis* 1980; **142**:757-766
- 15 **Garcia LS**, Bruckner DA. Serodiagnosis of Parasitic Diseases. *Diagnostic Medical Parasitology*. Washington DC: American Soc. for Microbiology 1993: 392-406
- 16 **Garin JP**, Ambroise-Thomas P. The serological diagnosis of toxoplasmosis by fluorescent antibody method (indirect technic). *La Presse Medicale* 1963; **71**: 2485
- 17 **Remington JS**, Mcleod R, Desmont G. Toxoplasmosis. In *Infectious diseases of the fetus newborn infant*. Remington JS, Klein JO (eds), 4th edition. Philadelphia: WB Saunders Company 1995: 140-268
- 18 **Altintas N**, Kuman HA, Akisu C, Aksoy U, Atambay M. Toxoplasmosis in last four year in Aegean region, Turkey. *J Egypt Soc Parasitol* 1997; **27**: 439-443

Edited by Wang XL Proofread by Zhu LH

Probiotics inhibit TNF- α -induced interleukin-8 secretion of HT29 cells

Ai-Ping Bai, Qin Ouyang, Wen Zhang, Chun-Hui Wang, Sheng-Fu Li

Ai-Ping Bai, Qin Ouyang, Chun-Hui Wang, Department of Gastroenterology, Huaxi Hospital, Sichuan University, Chengdu 610041, Sichuan Province, China

Wen Zhang, Department of Hepatology, First Hospital of Xiangfan City, Xiangfan 441000, Hubei Province, China

Sheng-Fu Li, Institute of Transplantation and Immunology, Huaxi Hospital, Sichuan University, Chengdu 610041, Sichuan Province, China

Correspondence to: Ai-Ping Bai, Department of Gastroenterology, Huaxi Hospital, Sichuan University, Chengdu 610041, Sichuan Province, China. baiap@163.com

Telephone: +86-28-85422386

Received: 2003-06-05 **Accepted:** 2003-07-30

Abstract

AIM: To study the effect of probiotics on interleukin-8 secretion in intestinal epithelia when stimulated by proinflammatory cytokines.

METHODS: Colonic adenocarcinoma HT29 cells were cultured and divided into four groups: control, TNF- α (group T in short), bifidobacterium (group B), lactobacillus (group L). *B. Longum* and *L. bulgaricus* were suspended in culture medium with a concentration of 1×10^8 cfu/ml and added into 24 wells respectively. One hour later TNF- α (10 ng/ml) was added into each well of groups T, B, L. The supernatants were collected and measured for IL-8 after 3 hours, nuclear factor- κ B (NF- κ B) p65 was also examined by Western blotting.

RESULTS: There was less interleukin-8 secretion in HT29 cells when preincubated with *B. Longum* or *L. bulgaricus* compared with group T. Less p65 appeared in nuclei in groups B and L compared with group T, as detected by Western blot.

CONCLUSION: Probiotics can suppress interleukin-8 secretion in intestinal epithelia when stimulated by proinflammatory cytokines, which is most likely mediated by NF- κ B.

Bai AP, Ouyang Q, Zhang W, Wang CH, Li SF. Probiotics inhibit TNF- α -induced interleukin-8 secretion of HT29 cells. *World J Gastroenterol* 2004; 10(3):455-457

<http://www.wjgnet.com/1007-9327/10/455.asp>

INTRODUCTION

Intestinal epithelium is an important factor of gut mucosal barrier, and participates in innate immunity. Intestinal epithelia are capable of releasing some proinflammatory cytokines such as IL-8 when stimulated by cytokines like TNF- α , and can response to enteric pathogens and release some proinflammatory cytokines which in turn direct the movement of inflammatory cells of the lamina propria^[1]. Probiotics, including bifidobacterium, lactobacillus play an essential role in the completeness of intestinal mucosa barrier. For example, some probiotic strains could modulate intestinal mucosal immune response, some could play protective roles by inhibiting the adhesion of pathogenic bacteria to intestinal epithelia. The

present study was to investigate the effect of probiotics on IL-8 secretion of intestinal epithelium induced by TNF- α , and its possible mechanism.

MATERIALS AND METHODS

Reagents

rh TNF- α was obtained from Pepro Tech Ec Ltd, UK. Rabbit anti-human NF- κ B p65 polyclonal antibody, peroxidase-conjugated goat anti-rabbit IgG were purchased from Santa Cruz Biotechnology Inc., USA. Human IL-8 ELISA kit was supplied by Jingmei Biotech Co. Ltd., China. BHI-agar was provided by Oxoid Co., UK. TMB membrane peroxidase substrate system was provided by KPL Inc., USA.

Methods

Bacteria *Bifidobacterium longum* and *Lactobacillus bulgaricus* LB10 were provided by the Department of Microbiology, Huaxi School of Stomatology, Si chuan University. The strains were grown at 37 °C in static, nonaerated BHI-agar to reach the mid-log phase. Bacteria were harvested by centrifugation at 2 500 g for 15 min at 20 °C. After two washes in sterile PBS pH 7.4, at 25 °C, the bacteria were resuspended in PBS. Cell counts in the bacteria suspension were estimated by optical density at 600 nm absorbance (BioMerieux, Germany). Then the bacteria were added to the cell culture wells at appropriate dilution to reach a final concentration of 10^8 cfu/ml of medium.

Cells and bacteria coculture HT29 cells were grown in RPMI1640 with 10% fetal calf serum, and divided into four groups: control, TNF- α (group T in short), bifidobacterium (group B), lactobacillus (group L). When grown to confluence in single layer, cells were washed three times with PBS pH 7.4, to remove culture medium and nonadherent cells. The bacteria in culture medium were transferred into individual wells respectively. TNF- α (10 ng/ml) was added into each well of groups T, B, L 1 hour later. The supernatants were collected and centrifuged for measurement of IL-8 after 3 hours.

IL-8 enzyme-linked immunosorbent assays IL-8 enzyme-linked immunosorbent assays (ELISA) were performed according to the manufacturer's instructions. In short, polyclonal goat anti-human IL-8 antibodies were used as capturing antibodies, biotinylated polyclonal rabbit anti-human IL-8 antibodies as detecting antibodies. Streptavidin-HRP and TMBS were added as color indicator. Plates were read at 450 nm of wavelength right after color reaction was stopped with acid. All procedures were performed at room temperature.

Assessment of NF- κ B activation by Western blotting Nuclear extracts were prepared according to the protocol described by Schreiber, *et al*^[2]. Nuclear proteins were separated by SDS-polyacrylamide mini-gel electrophoresis at a constant current of 30 mA for 150 min, then transferred to nitrocellulose membranes and stained with ponceau S to verify equal protein loading. Membranes were blocked in 5% milk in Tris-buffered saline for 4 h at 4 °C, incubated overnight at 4 °C with anti-human p65 polyclonal antibody (at a dilution of 1:1 000) followed by 1 h incubation at room temperature with peroxidase-conjugated goat anti-rabbit IgG (1:2 000). Finally,

the membranes were incubated in TMB membrane peroxidase substrate solution.

RESULTS

IL-8 secretion

Concentrations of IL-8 in supernatants of each group are shown in Figure 1. The concentration of IL-8 in control was only 172.2±42.1 ng/L. When stimulated by TNF- α , HT29 cells secreted a large number of IL-8, and the concentration of IL-8 in group T was 639.5±62.3 ng/L. However, when preincubated with *B. Longum* or *L. bulgaricus*, HT29 cells produced less IL-8, compared with group T, and the concentrations of IL-8 were 461.8±76.7 ng/L, 515.4±55.4 ng/L in groups B and L, respectively.

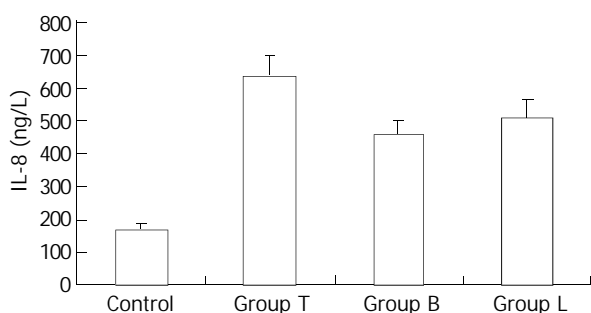


Figure 1 Concentrations of IL-8 in each group (mean±SD). Natural interleukin-8 expression was seldom found in HT29 cells of control group. When stimulated by TNF- α (10 ng/ml), HT29 cells secreted a large number of IL-8, and the concentrations IL-8 in groups T, B and L were significantly increased than that in control ($P < 0.001$). However, there was some difference in the concentration of IL-8 among groups T, B and L. There was less interleukin-8 secretion in HT29 cells when preincubated with *B. Longum* or *L. bulgaricus* in groups B and L compared with group T ($P = 0.002, 0.01$, respectively), but there was no difference in concentration of IL-8 between groups B and L ($P = 0.068$).

Detection of nuclear p65

There was little NF- κ B p65 in nuclei of normal epithelia without any stimuli, and it was very difficult to detect p65 in those cells by Western blotting. The epithelia expressed high levels of nuclear NF- κ B p65 when stimulated by TNF- α . Decreased expression of nuclear NF- κ B p65 appeared in cells of groups B and L, in contrast to group T, as Western blotting showed (Figure 2).



Figure 2 Expression of nuclear NF- κ B p65 in each group. Line 1: group T, Line 2: control, Line 3: group L, Line 4: group B.

DISCUSSION

Intestinal epithelia constitute mucosal barrier of the bowel, and participate in inflammatory or immune responses in gut^[3,4]. In some gastrointestinal infectious and inflammatory conditions, such as inflammatory bowel disease (IBD), acute gastroenteritis, inflammatory cells including monocytes, lymphocytes, were activated and accumulated in lamina propria. The cells secrete excessive inflammatory products,

such as TH1 type cytokines, chemokines and a lot of active oxides. Overproduction of cytokines could affect the biological action of epithelial cells. For instance, TNF- α could induce epithelial cells to secrete IL-8, and express membrane Toll-like receptor 4 (TLR4) excessively^[5,6]. TLR4 could enable intestinal epithelia hyperreactive in response to lipopolysaccharides (LPS), the component of bacteria walls, and IL-8 had leukocytes chemotactic and stimulatory properties^[7]. As more inflammatory cells infiltrate, the inflammatory reaction is therefore amplified.

The normal flora of human gastrointestinal tract contains diverse populations of bacteria which play an essential role in the development of gut mucosal barrier and innate immunity. Some intestinal microflora could exert a protective role against pathogens^[8]. Aberrance of gut microflora has been reported in IBD and acute gastroenteritis^[9,10]. The aberrant microflora dysregulates mucosal immune reaction. Invasion of some virulent strains into epithelia could break down the integrity of intestinal mucosa, and induce inflammatory cell infiltration^[11]. Some researchers found that manipulating the normal intestinal flora using probiotics had a beneficial effect on health by altering the microbial environment, and some components of the flora could down-regulate inflammation when supplemented to patients with gastrointestinal diseases^[12,13]. Some studies have been undergoing to explore the possible mechanisms of probiotic action on gut epithelium and mucosal immune system.

In order to imitate the inflammatory condition of gut *in vitro*, we used TNF- α to stimulate human colonic adenocarcinoma HT29 cells, which has basically the same biological properties as normal colonic epithelia. As some probiotic strains could adhere to human intestinal cell surface^[14,15], two probiotic strains, *B. longum* and *L. bulgaricus*, inhibited the secretion of IL-8 in HT29 cells when stimulated with TNF- α one hour after coculture with the two probiotic strains. It indicated that the strains could trigger anti-inflammatory pathways within the gut epithelium. The epithelia attached to the strains showed immune hyporeaction to TNF- α , and produced less IL-8. Because transcriptional control of IL-8 was mediated by transcription factor NF- κ B^[15], we investigated the expression of nuclear NF- κ B p65 in HT29 cells. There was little NF- κ B p65 in nuclei of normal epithelia without any stimuli. TNF- α highly up-regulated the expression levels of nuclear NF- κ B p65. However, the epithelia pre-cocultured with two probiotic strains before TNF- α treatment showed a decreased expression of nuclear NF- κ B p65. We postulated that such normal florae down-regulated inflammation by inhibiting NF- κ B activation in gut epithelium.

Neish reported some nonvirulent *Salmonella* strains attenuated the synthesis of inflammatory effector molecules in model human epithelia elicited by proinflammatory stimuli by blockade of I κ B degradation^[16]. In order to investigate such an effect of the bacteria in gut, we selected and cultured two strains of bifidobacterium and lactobacillus under anaerobic conditions. The two strains successfully inhibited IL-8 secretion and NF- κ B activation in intestinal epithelia in the experiment. At present, some probiotic compounds have been used in management of some diseases, such as maintenance therapy in IBD^[17,18]. Although the mechanism of probiotic action has not been fully understood, the beneficial effects were consistent with an anti-inflammatory state conferred by probiotics^[19,20]. More researches need to be done in order to understand the beneficial effect of probiotics on human beings.

REFERENCES

- Gewirtz AT, McCormick B, Neish AS, Petasis NA, Gronert K, Serhan CN, Madara JL. Pathogen-induced chemokine secretion from model intestinal epithelium is inhibited by lipoxin A4 analogs. *J Clin Invest* 1998; **101**: 1860-1869

- 2 **Schreiber E**, Matthias P, Muller MM, Schaffner W. Rapid detection of octamer binding proteins with 'mini-extracts', prepared from a small number of cells. *Nucleic Acids Res* 1989; **17**: 6419
- 3 **Gordon JI**, Hooper LV, McNevin MS, Wong M, Bry L. Epithelial cell growth and differentiation. III. Promoting diversity in the intestine: conversations between the microflora, epithelium, and diffuse GALT. *Am J Physiol* 1997; **273**(3 Pt 1): G565-G570
- 4 **Campbell N**, Yio XY, So LP, Li Y, Mayer L. The intestinal epithelial cell: processing and presentation of antigen to the mucosal immune system. *Immunol Rev* 1999; **172**: 315-324
- 5 **Hausmann M**, Kiessling S, Mestermann S, Webb G, Spottl T, Andus T, Scholmerich J, Herfarth H, Ray K, Falk W, Rogler G. Toll-like receptors 2 and 4 are up-regulated during intestinal inflammation. *Gastroenterology* 2002; **122**: 1987-2000
- 6 **Wolfs TG**, Buurman WA, van Schadewijk A, de Vries B, Daemen MA, Hiemstra PS, van't Veer C. *In vivo* expression of Toll-like receptor 2 and 4 by renal epithelial cells: IFN- γ and TNF- α mediated up-regulation during inflammation. *J Immunol* 2002; **168**: 1286-1293
- 7 **Aderem A**, Ulevitch RJ. Toll-like receptors in the induction of the innate immune response. *Nature* 2000; **406**: 782-787
- 8 **Isolauri E**, Kirjavainen PV, Salminen S. Probiotics: a role in the treatment of intestinal infection and inflammation? *Gut* 2002; **50** (Suppl 3): III54-59
- 9 **Duchmann R**, Kaiser I, Hermann E, Mayet W, Ewe K, Meyer zum Buschenfelde KH. Tolerance exists towards resident intestinal flora but is broken in active inflammatory bowel disease (IBD). *Clin Exp Immunol* 1995; **102**: 448-455
- 10 **Masseret E**, Boudeau J, Colombel JF, Neut C, Desreumaux P, Joly B, Cortot A, Darfeuille-Michaud A. Genetically related *Escherichia coli* strains associated with Crohn's disease. *Gut* 2001; **48**: 320-325
- 11 **Resta-Lenert S**, Barrett KE. Enteroinvasive bacteria alter barrier and transport properties of human intestinal epithelium: role of iNOS and COX-2. *Gastroenterology* 2002; **122**: 1070-1087
- 12 **Guandalini S**. Use of Lactobacillus-GG in paediatric Crohn's disease. *Dig Liver Dis* 2002; **34**(Suppl 2): S63-65
- 13 **Rembacken BJ**, Snelling AM, Hawkey PM, Chalmers DM, Axon AT. Non-pathogenic *Escherichia coli* versus mesalazine for the treatment of ulcerative colitis: a randomised trial. *Lancet* 1999; **354**: 635-639
- 14 **Bernet MF**, Brassart D, Neeser JR, Servin AL. Lactobacillus acidophilus LA 1 binds to cultured human intestinal cell lines and inhibits cell attachment and cell invasion by enterovirulent bacteria. *Gut* 1994; **35**: 483-489
- 15 **Adlerberth I**, Ahrne S, Johansson ML, Molin G, Hanson LA, Wold AE. A mannose-specific adherence mechanism in Lactobacillus plantarum conferring binding to the human colonic cell line HT-29. *Appl Environ Microbiol* 1996; **62**: 2244-2251
- 16 **Neish AS**, Gewirtz AT, Zeng H, Young AN, Hobert ME, Karmali V, Rao AS, Madara JL. Prokaryotic regulation of epithelial responses by inhibition of I κ B- α ubiquitination. *Science* 2000; **289**: 1560-1563
- 17 **Malin M**, Suomalainen H, Saxelin M, Isolauri E. Promotion of IgA immune response in patients with Crohn's disease by oral bacteriotherapy with Lactobacillus GG. *Ann Nutr Metab* 1996; **40**: 137-145
- 18 **Gionchetti P**, Rizzello F, Venturi A, Brigidi P, Matteuzzi D, Bazzocchi G, Poggioli G, Miglioli M, Campieri M. Oral bacteriotherapy as maintenance treatment in patients with chronic pouchitis: a double-blind, placebo-controlled trial. *Gastroenterology* 2000; **119**: 305-309
- 19 **Madsen KL**, Doyle JS, Jewell LD, Tavernini MM, Fedorak RN. Lactobacillus species prevents colitis in interleukin 10 gene-deficient mice. *Gastroenterology* 1999; **116**: 1107-1114
- 20 **Shibolet O**, Karmeli F, Eliakim R, Swennen E, Brigidi P, Gionchetti P, Campieri M, Morgenstern S, Rachmilewitz D. Variable response to probiotics in two models of experimental colitis in rats. *Inflamm Bowel Dis* 2002; **8**: 399-406

Edited by Zhu LH and Wang XL

Dysentery caused by *Balantidium coli* in a patient with non-Hodgkin's lymphoma from Turkey

Süleyman Yazar, Fevzi Altuntas, Izzet Sahin, Metin Atambay

Süleyman Yazar, Izzet Sahin, Department of Parasitology, Medical Faculty, Erciyes University, Kayseri-Turkey

Fevzi Altuntas, Department of Haematology, Medical Faculty, Erciyes University, Kayseri-Turkey

Metin Atambay, Department of Parasitology, Medical Faculty, Inonu University, Malatya-Turkey

Correspondence to: Süleyman Yazar, Department of Parasitology, Medical Faculty, Erciyes University, 38039, Kayseri, Turkey. syazar@erciyes.edu.tr

Telephone: +90-352-4374937 Ext 23401

Received: 2003-09-06 **Accepted:** 2003-09-20

Abstract

Balantidium coli is the only parasitic ciliate of man. It is a flattened oval organism covered with cilia, and a gullet at the anterior end. It is infrequently pathogenic for man, although epidemic buds in tropical zones have been described. The infection fundamentally affects the colon and causes variable clinic pictures, from asymptomatic to serious dysenteric forms. We present a case of parasitologically diagnosed as causes of diarrhea in a patient with non-Hodgkin's lymphoma from Turkey. In order to find out the causative etiologic agent of diarrhea, stool samples were examined by native, lugol and flotation methods and we detected moving trophozoites, which were approximately 60 µm long and 35 µm wide. These bodies were diagnosed as *Balantidium coli*. This case underlines that *Balantidium coli* should also be considered as a possible pathogen in immunocompromised patients with diarrhea.

Yazar S, Altuntas F, Sahin I, Atambay M. Dysentery caused by *Balantidium coli* in a patient with non-Hodgkin's lymphoma from Turkey. *World J Gastroenterol* 2004; 10(3):458-459

<http://www.wjgnet.com/1007-9327/10/458.asp>

INTRODUCTION

Balantidium coli (*B. coli*), the largest protozoan affecting humans, is a ciliate organism often associated with pigs. The greenish-yellow trophozoites may measure up to 120×150 µm and are capable of attacking the intestinal epithelium, creating ulcers and causing bloody diarrhea similar to that of amebic dysentery. It commonly infects primates, rats and pigs, and has a world-wide distribution. It is the only parasite of the family of *Balantidiidae* that, in rare instances, is pathogenic for humans. Balantidiasis is an infection of the large intestine by the ciliate protozoan, *B. coli*. In many infections (perhaps 80 percent) *B. coli* lives as a commensal in the lumen of the colon and causes no symptoms. A variety of gastrointestinal symptoms, including cramping, abdominal pain, nausea and foul breath, also occur. Encystment usually occurs in the intestinal lumen or stool (human or swine), and the large round cysts transmit the infection through contaminated food or water. Pigs act as carriers and are not often adversely affected by this organism^[1,2].

Fortunately, balantidiasis is uncommon in temperate

climates. It is found in association with pigs throughout the tropics, especially the Philippines^[1]. Evidence indicates that some infected humans may become asymptomatic cyst carriers, whereas others clear the infection spontaneously. As with amebiasis, this condition probably runs the gamut between mild colitis and severe, potentially fatal dysentery. Treatment of adults and older children is usually accomplished with tetracycline, 500 mg four times daily for 20 days and metronidazole, 750 mg three times daily for five days^[3].

Our study in this paper is the first reported case of balantidiasis in a patient with non-Hodgkin's lymphoma from Turkey.

CASE REPORT

A 47 year-old female patient with non-Hodgkin's lymphoma and complaining of diarrhea and abdominal pain was admitted to our hospital. In the patient's history, there were watery, bad smelling, bloody diarrhea (ten times per day) and abdominal pain.

Physical examination revealed mild abdominal tenderness and increased sounds of intestine. In laboratory examination, blood routine tests were found as follows: Hb: 9.6 g/dl, Htc: 31.4%, white blood cells: $0.4 \times 10^9/L$ (with 20% granulocytes and 80% lymphocytes), platelets: $56 \times 10^9/L$ and sedimentation rate: 40 mm/h. Biochemical tests results were as follows: Fbg: 82 mg/dl, BUN: 40 mg/dl, creatinin: 0.7 mg/dl, total protein: 7.6 gr/dl, AST: 30 U/L, ALT: 32 U/L, ALP: 231 U/L, GGT: 43 U/L, LDH: 342 U/L, albumin: 4.1 gr/dl.

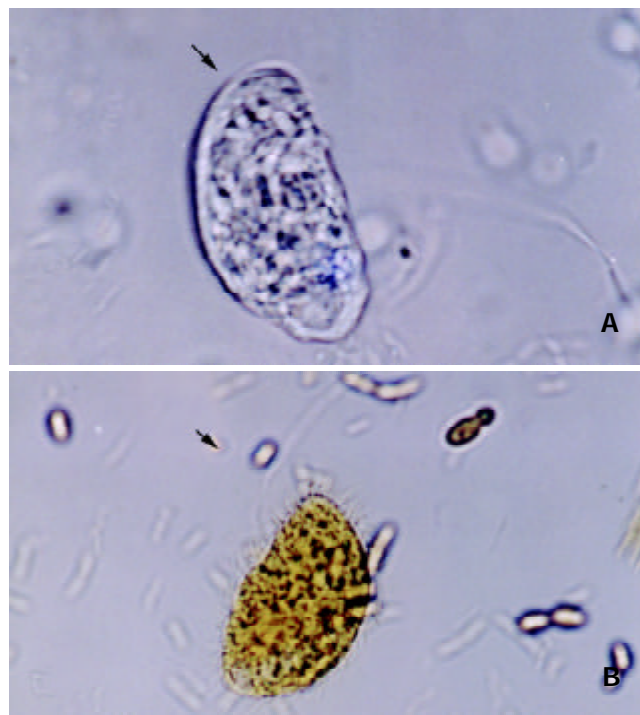


Figure 1 *Balantidium coli* trophozoites in native (A) and lugol (B) preparations (original magnification ×400).

We did not obtain any abnormalities in abdominal ultrasonography and direct X-ray. There was no growth of any pathogens in stool and blood culture.

In order to find the causative etiologic agent of diarrhea, stool samples were obtained from the patient and sent to the laboratory. The stool samples were examined parasitologically by native, lugol and flotation methods. Approximately 60 µm long and 35 µm broad moving trophozoites with cilia were seen. These bodies were diagnosed as *Balantidium coli* (Figure 1).

Consequently, we diagnosed this organism as *Balantidium coli*. The patient was treated with metronidazole 750 mg three times daily for five days. Following the treatment, the symptoms rapidly and completely resolved. Re-examination of a stool sample, however, did not reveal the presence of any organism.

DISCUSSION

Balantidium coli is a protozoon and the only one ciliate that is able to cause disease in man. The trophozoite or vegetative state has oval form covered by a great amount of cilia grouped in row. In its forcebody they are peristoma and citostoma that continue with citofaringe. The later end finishes in the anal pore or citopigio. The cysts are oval or spherical, they measure from 45 to 65 µm in length^[2].

Although the distribution of *B.coli* is cosmopolitan, infection in humans takes place by the ingestion of cysts coming from leas of the parasite guests. Of this form, different epidemic buds like the one arising in the Truk Islands after a typhoon, have taken place. That typhoon caused an extensive contamination of superficial and underground water with leas of pigs, which provided the source of water for the population^[4] and led to a severe prevalence in psychiatric hospitals^[5,6].

Sporadic transmission was also produced by the water, contaminated vegetables crude and fecal-oral mechanism. People in contact with pigs were more likely to be infected, thus, it is said that the Aymara children of the Plateau of Bolivia had a greater prevalence of this infection, although usually they remained asymptomatic^[7]. Our patient was personally questioned, she had not contacted with a pig. Probably, she might have got this parasite either via contaminated food or water. This case underlines that *B. coli* should also be considered as a possible pathogen in immunocompromised patients with diarrhea even if they have no contact with pigs.

REFERENCES

- 1 **Schmidt GD**, Roberts LS. Phylum coli. In: Schmidt GD, Roberts LS. Foundation of parasitology. 4th ed. St. Louis: *Times Mirror/Mosby College Publication* 1989: 175-180
- 2 **Gonzalez de Canales Simon P**, del Olmo Martinez L, Cortejoso Hernandez A, Arranz Santos T. Colonic balantidiasis. *Gastroenterol Hepatol* 2000; **23**: 129-131
- 3 **Juckett G**. Intestinal protozoa. *Am Fam Physician* 1996; **53**: 2507-2516
- 4 **Walzer PD**, Judson FN, Murphy KB, Healy GR, English DK, Schultz MG. Balantidiasis outbreak in Truk. *Am J Trop Med Hyg* 1973; **22**: 33-41
- 5 **Giacometti A**, Cirioni O, Balducci M, Drenaggi D, Quarta M, De Federicis M, Ruggeri P, Colapinto D, Ripani G, Scalise G. Epidemiologic features of intestinal parasitic infections in Italian mental institutions. *Eur J Epidemiol* 1997; **13**: 825-830
- 6 **Areán VM**, Koppisch E. Balantidiasis. A review and report of cases. *Am J Pathol* 1956; **32**: 1089-1115
- 7 **Esteban JG**, Aguirre C, Angles R, Ash R, Mas-Coma S. Balantidiasis in Aymara children from the northern Bolivian Altiplano. *Am J Trop Med Hyg* 1998; **59**: 922-927

Edited by Zhu LH Proofread by Wang XL

Unusual manifestations of gastric inflammatory fibroid polyp in a child

Voranush Chongsrisawat, Phisek Yimyeam, Naruemon Wisedopas, Dusit Viravaidya, Yong Poovorawan

Voranush Chongsrisawat, Phisek Yimyeam, Yong Poovorawan,
Department of Pediatrics, Faculty of Medicine, Chulalongkorn
University, Bangkok 10330, Thailand

Naruemon Wisedopas, Department of Pathology, Faculty of Medicine,
Chulalongkorn University, Bangkok 10330, Thailand

Dusit Viravaidya, Department of Surgery, Faculty of Medicine,
Chulalongkorn University, Bangkok 10330, Thailand

Supported by the Thailand Research Fund and Center of Excellence,
Viral Hepatitis Research Unit, Chulalongkorn University

Correspondence to: Professor Dr. Yong Poovorawan, Department
of Pediatrics, Faculty of Medicine, Chulalongkorn University,
Bangkok, 10330 Thailand. yong.p@chula.ac.th

Telephone: +662-256-4909 **Fax:** +662-256-4929

Received: 2003-10-08 **Accepted:** 2003-11-20

Abstract

AIM: Inflammatory fibroid polyp (IFP) is a rare benign lesion that may occur throughout the digestive tract. IFP is more commonly found in the antrum of the stomach in particular. It mostly affects adults at the average age of 60 years. These polyps are able to cause abdominal pain, gastrointestinal bleeding, intestinal obstruction or intussusception. In this paper we report a case of gastric IFP with unusual presenting features.

METHODS: A child with gastric IFP was described and the literature was reviewed.

RESULTS: A 4-year-old girl presented with fever for 2 months, arthralgia of knees and ankles, iron deficiency anemia, and hypoalbuminemia. Her stool examination was positive for occult blood. The upper gastrointestinal study demonstrated a large lobulated mass at the upper part of gastric body. Partial gastrectomy *en bloc* with this 5cm×8 cm mass was subsequently performed. Pathological examination was consistent with IFP. Following the mass excision, her fever abruptly declined and disappeared together with anemia and arthralgia. She remained asymptomatic and the abdominal ultrasonography performed at the 24-month follow-up demonstrated no recurrence of the tumor.

CONCLUSION: The etiopathogenesis of IFP still remains unclear. The presence of IFP throughout the gastrointestinal tract and its variable clinical appearances make it difficult to diagnose. The inflammatory symptoms found in this patient support the hypothesis of inflammatory benign lesions of IFP.

Chongsrisawat V, Yimyeam P, Wisedopas N, Viravaidya D, Poovorawan Y. Unusual manifestations of gastric inflammatory fibroid polyp in a child. *World J Gastroenterol* 2004; 10(3): 460-462

<http://www.wjgnet.com/1007-9327/10/460.asp>

INTRODUCTION

Gastric neoplasms are exceedingly rare in children. Murphy *et al.* reviewed 1 403 pediatric gastric pathology reports and found only 3 benign gastric tumors^[1]. Attard *et al.* reported

hyperplastic-inflammatory polyp was the most common gastric polyps (42%) found in pediatric population^[2].

Inflammatory fibroid polyp (IFP) is a solitary polypoid or sessile lesion with an inflammatory basis. It is a rare benign lesion that may occur throughout the digestive tract, but is most often seen in the stomach (approximately 80%)^[3]. IFP in the stomach is usually located in the antrum or prepyloric region^[4,5]. In large retrospective studies of gastric polyps, 3.1-4.5% were found to be IFP^[6,7]. It is slightly more common in women (female:male ratio 1.6:1)^[5]. It is found in all age groups, although not often in children, and its maximal incidence is in the sixth decade^[7]. The symptomatology is determined by its site. In the stomach, it causes pyloric obstruction, and often in the small bowel, intussusception which is the most common presentation in children.

We report a case of gastric IFP who presented with prolonged fever, arthralgia, hypoalbuminemia, and iron deficiency anemia. Surgical excision led to a complete resolution of those symptoms.

CASE REPORT

A 4-year-old girl presented with high fever for 2 months, arthralgia of knees and ankles, and anemia that required multiple packed red cell transfusions. The lowest hemoglobin was 3.9 g/dL. A provisional diagnosis of juvenile rheumatoid arthritis was made. She was treated with aspirin and prednisolone, but had no improvement. Later she was referred to our hospital in June 2001.

On her admission, the patient's weight was 15 kg (25th percentile for gender and age). Physical examination revealed pale conjunctivae, pitting edema of both legs, the rest was unremarkable. Laboratory tests after multiple blood transfusions showed a white blood cell count of 41 400/mm³, 76% PMNs, 16% lymphocytes, 6% monocytes, and 2% atypical lymphocytes; hemoglobin was 11.4 g/dL (MCV 76 fL, MCH 21.1 pg, MCHC 27.9 g/dL, RDW 21.2%), and platelet count was 684 000/mm³. Stool occult blood was positive. Serum albumin and globulin were 2.1 g/dL and 3.2 g/dL, respectively. Anti DNA, ANA, ANCA, anti Smith, rheumatoid factor, VDRL and LE cell were negative. β_2 C was 176.9 mg/dL. ESR was 82 mm/h. Culture of blood, urine, stool, and bone marrow aspirate were negative. Upper GI series demonstrated a large lobulated mass at the upper part of gastric body (Figure 1).



Figure 1 A large lobulated mass at the upper part of gastric body (arrow head) shown by radiography.

Table 1 Literature review of inflammatory fibroid polyp in children (since 1960 in English language)

Year	Reference	Age (y.)	Sex	Location	Clinical manifestations
1966	Samter ^[8]	4	Male	Colon	Abdominal pain, vomiting, concomitant ruptured colonic diverticulum
1966	Samter ^[8]	8	Female	Jejunum	Vomiting, intermittent diarrhea, anemia
1972	Persoff ^[9]	3	Male	Ileum	Abdominal pain, vomiting, diarrhea
1984	Pollice ^[10]	8	Male	Rectum	Lower GI bleeding, anemia
1987	Schroeder ^[11]	5	Female	Stomach	Abdominal pain, weakness, vomiting, anemia
Our study	Chongsrisawat	4	Female	Stomach	Prolonged fever, arthralgia, anemia, hypoalbuminemia

At laparotomy, a 5 cm×8 cm mass was found at the body of the stomach. Partial gastrectomy *en bloc* with the mass was performed. Light microscopic examination of the gastric mass showed foci of ulcerated mucosa, focal elongated distorted branching and dilated hyperplastic foveolar and glands, covering a mass consisting of proliferative fibroblasts and blood vessels admixed with mixed inflammatory cell infiltrates in the stroma (Figure 2). The histological finding was consistent with IFP.

The patient developed postoperative convulsion due to steroid-induced hypertension and encephalopathy. She was treated with phenytoin and nifedipine which were later discontinued after 2 and 4 months, respectively. Fever, arthralgia, hypoalbuminemia, and anemia resolved after removal of the polyp. She was discharged 12 days after the surgery. The abdominal ultrasonography performed at the 24-month follow-up demonstrated no recurrence of the tumor and she remained asymptomatic.

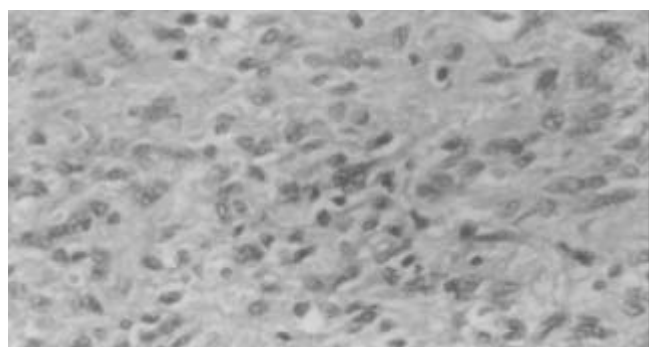


Figure 2 Packed spindle-shaped cells, proliferated vessels and inflammatory cells, mostly eosinophils observed in tumor (H&E, 10×40).

DISCUSSION

Current pediatric literature regarding IFP is limited to case reports and small case series as shown in Table 1. Clinical manifestations of IFP are variable, depending on the location and size of the lesion. Most are small and asymptomatic. Nevertheless, it is able to cause anemia due to gastrointestinal bleeding, abdominal pain, vomiting, weight loss, intestinal obstruction or intussusception. Physical examination is usually not conclusive. Imagings such as upper GI series, ultrasonography or computed tomography can help diagnose the mass, but the final diagnosis is generally based on endoscopy and histological examination.

Histologically IFP has been found to be characterized by a submucosal lesion with a mixture of proliferation of fibroblasts and small blood vessels, accompanying a marked eosinophilic infiltration^[12]. Since the distinctive structures for diagnosis are located within the submucosa and at the base of the mucosa, the diagnosis may not be possible in most of these polyps by

endoscopic biopsy specimen. In the past, IFP was reported under several terms, such as eosinophilic granuloma, submucosal granuloma with eosinophilic infiltration, hemangioendothelioma, hemangiopericytoma, and polypoid fibroma^[11,13]. The etiology and the pathogenesis of IFP remain unclear. It has been hypothesized that several factors could damage the gastrointestinal mucosa and expose the stroma to several irritants (chemical, mechanical and biological), and stimulate the formation of polyps among certain people^[14]. A polyp of this category is a specific response of gastrointestinal stromal tissue of unknown etiology. Electron microscopic study revealed that IFP represented a reactive lesion of myofibroblastic nature^[15]. Thus, it has been now generally accepted that IFP is not a neoplasia, but a reactive process, either to an allergy or a foreign body and has no malignant potential^[4-6].

An infective etiology has never been reported in IFP, although several reported cases showed its association with *Helicobacter pylori* infection^[3,14]. In one of these reports, the patient also had autoimmune diseases (sarcoidosis, rheumatoid arthritis, and ankylosing spondylitis)^[3]. This finding supports the possibility of an immunological reaction as a contributing factor. It is not exactly known that *H pylori* started an immunological reaction which caused the polyp, or it only complicated this finding. Surgery is the main therapy of IFP and the recurrence has not been observed after polyp removal. Small polyps up to 2 cm in diameter can be excised endoscopically.

Our case is unusual in several aspects, such as the patient's young age at the presentation, the location of the mass at the corpus of the stomach, and the autoimmune-like manifestations. We hypothesized that IFP might release cytokines that cause fever and other autoimmune-like symptoms in this patient.

CONCLUSION

Not only is IFP rare in children, but its presence throughout the gastrointestinal tract and its variable clinical appearance make it difficult to diagnose. Patients with IFP may present with inflammatory symptoms and disappearance of the symptoms after polyp removal found in this patient supports the hypothesis of inflammatory benign lesions of IFP.

ACKNOWLEDGEMENTS

We express our gratitude to Dr. Kridakorn Kesorncam for her effort in the present study. Lastly, we would like to thank Venerable Dr. Mettanando Bhikkhu of Wat Nakprok, Bangkok and Ms. Pisaneek Saiklin for reviewing the manuscript.

REFERENCES

- 1 **Murphy S**, Shaw K, Blanchard H. Report of three gastric tumors in children. *J Pediatr Surg* 1994; **29**: 1202-1204
- 2 **Attard TM**, Yardley JH, Cuffari C. Gastric polyps in pediatrics: an 18-year hospital-based analysis. *Am J Gastroenterol* 2002; **97**: 298-301

- 3 **Buciuto R**, Kullman E, Boeryd B, Borch K. *Helicobacter pylori* gastritis associated with a gastric inflammatory fibroid tumour and sarcoidosis. *Eur J Surg* 1996; **162**: 421-424
- 4 **Matsushita M**, Hajiro K, Okazaki K, Takakuwa H. Endoscopic features of gastric inflammatory fibroid polyps. *Am J Gastroenterol* 1996; **91**: 1595-1598
- 5 **Hizawa K**, Iida M, Tada S, Fuchigami T, Kuwano Y, Yao T, Fujishima M. Endoscopic evaluation of gastric inflammatory fibroid polyp. *Surg Endosc* 1995; **9**: 397-400
- 6 **Stolte M**, Sticht T, Eidt S, Ebert D, Finkenzeller G. Frequency, location, and age and sex distribution of various types of gastric polyp. *Endoscopy* 1994; **26**: 659-665
- 7 **Stolte M**, Finkenzeller G. Inflammatory fibroid polyp of the stomach. *Endoscopy* 1990; **22**: 203-207
- 8 **Samter TG**, Alstott DF, Kurlander GJ. Inflammatory fibroid polyps of the gastrointestinal tract: A report of 3 cases, 2 occurring in children. *Am J Clin Pathol* 1966; **45**: 420-436
- 9 **Persoff MM**, Arterburn JG. Eosinophilic granuloma causing intussusception in a three year old child. *Am J Surg* 1972; **124**: 676-678
- 10 **Pollice L**, Bufo P. Inflammatory fibroid polyp of the rectum. *Path Res Pract* 1984; **178**: 508-512
- 11 **Schroeder BA**, Wells RG, Sty JR. Inflammatory fibroid polyp of the stomach in a child. *Pediatr Radiol* 1987; **17**: 71-72
- 12 **Kim YI**, Kim WH. Inflammatory fibroid polyps of gastrointestinal tract. Evolution of histologic patterns. *Am J Clin Pathol* 1988; **89**: 721-727
- 13 **Blackshaw AJ**, Levison DA. Eosinophilic infiltrates of the gastrointestinal tract. *J Clin Pathol* 1986; **39**: 1-7
- 14 **Shalom A**, Wasserman I, Segal M, Orda R. Inflammatory fibroid polyp and *Helicobacter pylori*. Aetiology or coincidence? *Eur J Surg* 2000; **166**: 54-57
- 15 **Navas-Palacios JJ**, Colina-Ruizdelgado F, Sanchez-Larrea MD, Cortes-Cansino J. Inflammatory fibroid polyps of the gastrointestinal tract. An immunohistochemical and electron microscopic study. *Cancer* 1983; **51**: 1682-1690

Edited by Wang XL Proofread by Zhu LH

Roles of main pro- and anti-angiogenic factors in tumor angiogenesis

Zhi Huang, Shi-Deng Bao

Zhi Huang, School of Life Sciences, Xiamen University, Xiamen 361005, Fujian Province, China

Shi-Deng Bao, the Key Laboratory of the Ministry of Education for Cell Biology and Tumor Cell Engineering, School of Life Sciences, Xiamen University, Xiamen 361005, Fujian Province, China

Supported by the National Natural Science Foundation of China, No.30170463

Correspondence to: Zhi Huang, Cell Biology Research Lab, School of Life Sciences, Xiamen University, Xiamen 361005, Fujian Province, China. subhiv@hotmail.com

Telephone: +86-592-2186091 **Fax:** +86-592-2186091

Received: 2003-06-21 **Accepted:** 2003-07-24

Abstract

Tumor growth without size restriction depends on vascular supply. The ability of tumor to induce new blood-vessel formation has been a major focus of cancer research over the past decade. It is now known that members of the vascular endothelial growth factor and angiopoietin families, mainly secreted by tumor cells, induce tumor angiogenesis, whereas other endogenous angiogenic inhibitors, including thrombospondin-1 and angiostatin, keep tumor in dormancy. Experimental and clinical evidence has suggested that the process of tumor metastasis depends on angiogenesis or lymphangiogenesis. This article summarizes the recent research progress for some basic pro- or anti-angiogenic factors in tumor angiogenesis.

Huang Z, Bao SD. Roles of main pro- and anti-angiogenic factors in tumor angiogenesis. *World J Gastroenterol* 2004; 10(4): 463-470

<http://www.wjgnet.com/1007-9327/10/463.asp>

INTRODUCTION

In the early time of the 20th century, Lewis observed that the vascular architecture depended on the tumor type, and proposed that the tumor environment determined the growth and morphological characteristics of tumor vessels. Hitherto it is the cognition that tumor vascularization is a vital process for the progression of all solid tumors from a small, localized focus to a large tumor with the capability to metastasize^[1,2]. This progression begins with the sprouting or intussusception from pre-existing host vessels. Circulating endothelial precursors, shed from the vessel wall or mobilized from the bone marrow, also contribute to tumor angiogenesis^[3,4].

Contrarily, adult normal tissue vasculature is quiescent because of the balance between angiogenic promoters and inhibitors. The early development of tumor is dormant because of the same reason. Break of the balance results in physiological angiogenesis such as wound healing and pathological angiogenesis such as tumor angiogenesis.

Tumor-induced angiogenesis is thought to depend on the production of pro-angiogenic growth factors by the tumor cells, which affect the existing vessels^[5]. This turns on the tumor "angiogenic switch", and then promotes tumor growth and metastases.

ANGIOGENIC FACTORS

Vascular endothelial growth factors and vascular endothelial growth factor receptors

In 1983, Senger and his colleagues discovered a protein that induced vascular leakage and named it as tumor vascular permeability factor (VPF)^[6]. Subsequently Ferrara and Connolly showed that VPF and vascular endothelial growth factor (VEGF) were the same molecule^[7,8]. In 1992, Breier and Risau found that the expression of *VEGF* mRNA temporally and spatially correlated with blood-vessel growth in the developing mouse embryo. This supported the idea that VEGF was an angiogenic factor *in vivo*^[9]. Later Veikkola and Alitalo also demonstrated that inactivation of one of the two VEGF alleles in the mouse embryos led to severe defects in vascular formation, ultimately resulted in embryonic lethality, whereas increased expression of VEGF seemed to be essential for tumor growth beyond size restriction^[10]. *In-situ* hybridization studies have identified that the expression of *VEGF* mRNA is increased in renal^[11], ovarian^[12], gastric carcinomas^[13], and particularly the highly vascular and aggressive glioblastoma^[14]. VEGF is considered as a prognostic molecular marker in hepatocellular carcinoma^[15]. *VEGF* gene is localized on the short arm of chromosome 6^[16], with eight exons and seven introns^[17]. Predominant isoforms of *VEGF* are *VEGF*₁₈₉, *VEGF*₁₆₅, *VEGF*₁₂₁, and *VEGF*₂₀₅. They are generated by alternative mRNA splicing and proteolytic processing. *VEGF*₁₂₁ differs from all the other higher molecular weight species by the absence of the heparin-binding domain encoded by exon 7 that can bind to neuropilin-1 (NP-1)^[18,19]. Therefore, VEGF₁₂₁-diphtheria toxin (DT385) conjugation treatment completely prevents tumor angiogenesis *in vivo* without toxicity to NP-1^[20]. VEGF is a major inducer of angiogenesis and structurally resembles (placenta growth factor), VEGF-B, VEGF-C, VEGF-D and the Orf virus derived VEGF (also called VEGF-E)^[21-26].

Interestingly, VEGF is highly expressed in most ischemic areas of the tumor, indicating that VEGF expression might be induced by hypoxia. In hypoxic tissue the hypoxia inducible factor-1 (HIF-1) has been proven to play a central role in inducing the transcription of genes that are involved in glycolysis and angiogenesis, including VEGF^[27]. Subsequent studies have shown that the mechanisms of hypoxic regulation of VEGF and erythropoietin are similar^[28]. *VEGF* gene contains two hypoxia-regulated element (HRE) in the 5' and 3' regions (Figure 1). HIF-1 recognizes and binds HRE^[29,30]. Hypoxia also induces an RNA-binding protein, HuR, which can bind to the 3' untranslated region (UTR) of *VEGF* mRNA and increase the mRNA stability^[31]. Oncogenes including members of the *ras* and *erbB* families also up-regulate the expression of VEGF^[32,33]. The products of *ras* gene activate the HIF-1 α and promote the stability of the HIF-1 α via Raf/MEK/MAPK and PI3K/PDK-1/AKT pathways^[34]. The activated AKT increases the phosphorylation of GSK3 β on Ser9, and then enhances HIF-1 α stabilization, since unphosphorylated GSK3 β inhibits HIF-1 α accumulation^[35] (Figure 1). Recent studies have indicated that the chronic myelogenous leukemia (CML)-associated oncogene *BCR/ABL* induces VEGF expression in growth factor-dependent Ba/F3 cells by promoting the expression of HIF-1^[36]. However, the product of the von

Hippel-Lindau tumor suppressor gene (vHL) inhibits the expression of VEGF^[37,38]. The ubiquitin ligase E3 complex containing the vHL tumor suppressor protein increases the HIF-1 α degradation^[39]. In addition to vHL, other tumor suppressor proteins such as p53 also inhibit the transcriptional activity of HIF-1 by binding to the HIF-1/P300 complex and then promoting Mdm2-mediated ubiquitination and proteasomal degradation of the HIF-1 α , which ultimately results in the decrease of VEGF expression^[40,41]. These findings indicate that HIF-1 is critical for the regulation of VEGF expression. VEGF expression is also regulated by estradiol in human breast cancer cells^[42]. Similarly, 17 beta-estradiol also enhances VEGF expression via the regulation of adenylate cyclase in differentiated THP-1 cells^[43].

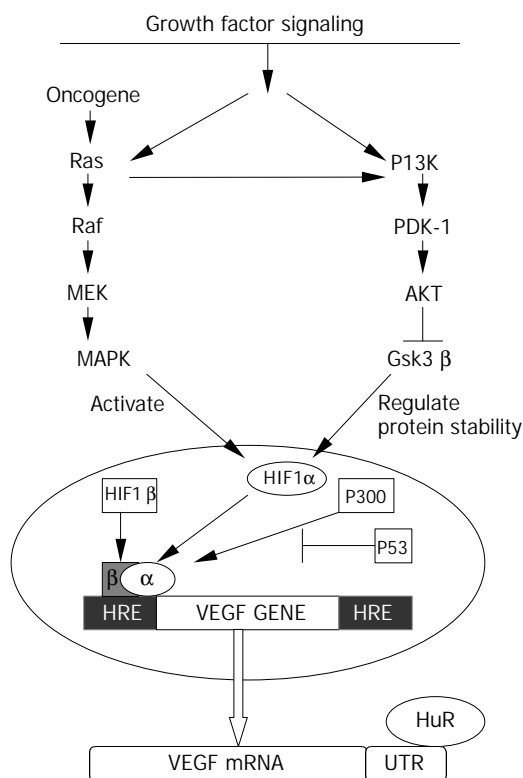


Figure 1 The regulation of the VEGF expression. HIF1 plays central roles in this regulation.

VEGFs induce angiogenesis through the binding to their relevant receptors that are mainly expressed in endothelial cells. The first VEGF receptor was identified to be Flt1 (FMS-like-tyrosine kinase), also known as VEGFR1^[44]. Subsequently, the other highly specific VEGF-binding receptors (KDR, Flk1, or VEGFR2) were discovered^[45,46]. Scientists investigated the function of VEGFR1 and VEGFR2 in endothelial cells via Flt1 or Flk1 mutant endothelial cells or an embryonic model. They counted the number of mitotic endothelial cells in embryo to confirm the effect of proliferation of endothelial cells. In VEGFR1 knockout mice, the reason causing early embryonic lethality was not the absence of vascularisation but the disorganized embryonic and extra-embryonic vasculature^[47]. This suggests that Flt1 signal pathways mainly regulate normal endothelial cell-cell or cell-matrix interactions during the process of vascular development. The ability of VEGFR1 to bind to VEGF is 10 times stronger than VEGFR2, but the activity of tyrosine kinase of VEGFR1 is weaker than that of VEGFR2. A study demonstrated that Flt1 null mutation resulted in early embryonic death, but Flt1 lacking tyrosine kinase domain homozygous mice developed normal vessels and survive^[48]. These observations indicate that Flt1 without

tyrosine kinase domain is sufficient to promote embryonic normal angiogenesis. The effects of VEGFR2 in endothelial cells, such as cell survival and proliferation, are not induced by treatment with VEGFR1 specific ligands or in the VEGFR1 overexpressing cells lacking VEGFR2^[49,50]. These data suggest that VEGFR2 plays the central role in VEGF signal transduction in endothelial cells. VEGFR1 is likely to be the antagonist of VEGFR2, acting as a negative regulator of angiogenesis via sequestering VEGF and thus blocking the VEGF signal transduction mediated by VEGFR2. Recent studies have confirmed this conclusion. The *Flt1* gene encodes not only the full-length Flt-1, but also a soluble short form of Flt-1, designated sFlt1. In placenta, sFlt-1 is abundant in the trophoblast layer during pregnancy, suggesting that it is a negative regulator to excess angiogenesis at the feto-maternal border in mammals^[51]. Subsequently Kearney confirmed that Flt-1 normally modulated vascular growth by controlling the rate of endothelial cell division *in vitro* and *in vivo*^[52]. The downstream signaling events of VEGF signal transduction pathway via VEGFR2 includes receptor dimerization, transphosphorylation of intracellular VEGFR2 tyrosine residues (Tyr951/996 and Tyr1054/1059)^[53], the activation of protein kinase C, and then the activation of the MEK/MAPK pathway to promote endothelial cell proliferation (Figure 2). However, Meyer's data showed that phosphorylation of tyrosine 1212 of VEGFR2 was also necessary for VEGFR2-mediated angiogenesis^[54]. In addition to VEGF, scientists have found that there are other molecules that activate VEGFR2 or enhance the expression of VEGFR2. Recent studies have indicated that tumor necrosis factor (TNF) has anti-tumor activity by down-regulating Flk-1 expression in tumor endothelial cells^[55]. Moreover, in cardiac capillary endothelial cells, Bradykinin (BK) also stimulates angiogenesis via the activation of the B2- type receptor, which leads to the tyrosine phosphorylation and dimerization of Flk-1 as does VEGF itself^[56]. This implies a novel mechanism by which a G protein-coupled receptor activates a receptor tyrosine kinase to generate biological response. In addition to the stimulation of endothelial cell migration and proliferation, VEGF also elevates the survival capacity of endothelial cells *in vitro*. The underlying mechanism is that VEGF activates VEGFR2, which further activates phosphatidylinositol 3-kinase (PI3-K) and Akt^[57]. VEGF also prolongs the survival of human dermal microvascular endothelial cells (HDMECs) *in vitro* by inducing expression of the anti-apoptotic protein Bcl-2^[58].

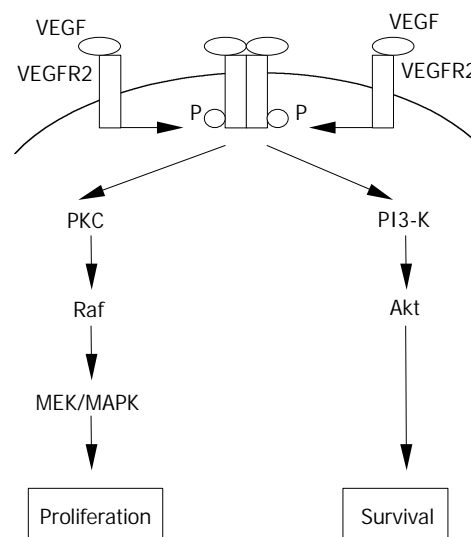


Figure 2 The intracellular downstream signaling of VEGF signal transduction via VEGFR2.

Interestingly, new data have revealed that NP-1, originally found to control the neuronal axon guidance, also enhances the mitogenic effects of VEGFR2 signaling in endothelial cells^[59]. So far, the potential role of NP-1 in pathologic angiogenesis remains unknown. Some experiments have indicated that VEGF up-regulates NP-1 via VEGFR2-dependent pathway. Endothelial proliferation stimulated by VEGF₁₆₅ is inhibited significantly by antibody neutralization of NP-1. In a murine model of VEGF-dependent angioproliferative retinopathy, intense NP1 mRNA expression was observed in the newly formed vessels^[60]. In breast carcinoma cells neuropilin expression also enhances VEGF-inducing cells survival signal^[61]. Furthermore, in rat uterus the neuropilins (NP-1 and NP-2) might participate in hormonally regulated changes occurring throughout the female reproductive cycle^[62].

The other factor VEGF-C and its receptor (VEGFR3) are essential to the lymphangiogenesis and play a direct role in the metastatic dissemination of tumor cells. It is known that VEGFR3 is mainly expressed in lymphatic endothelium during development^[63,64]. Later in embryonic development, VEGFR3 is expressed in lymphatic cells, and further induces lymphangiogenesis^[63,64]. However, in early embryonic development without lymphatic vessels, the embryos lacking VEGFR3 gene usually die due to cardiovascular failure^[65]. These data indicate that VEGFR3 is necessary in the formation of the primary cardiovascular network. In addition, VEGFR3 is also expressed in the tumor endothelial cells, which helps tumor neovascularization^[66].

Angiopoietins and Tie receptors

The second family of growth factors that specifically act on the vascular endothelium has been identified, namely the angiopoietins^[67,68]. To date, there are four members of this family, mainly including Ang-1 and Ang-2, which both only bind to the Tie-2 receptor and control the blood vessel stabilization signals^[67,68]. The results of early experiments showed that the mouse embryonic development lacking Ang-1 or Tie-2 died in the later stage of angiogenesis because the remodeling and stabilization of the primitive vasculature induced by VEGF was severely perturbed^[69-71]. Similarly, the increased Ang-1 expression in human cervical cancer HeLa cells by transgene promotes the growth of human cervical cancers in mice via promoting tumor angiogenesis^[72]. In addition to in the active angiogenesis tissue, Ang-1 seems to be widely expressed in the normal adult tissues^[73], indicating

that Ang-1 may act on the stabilization of existing vessels. The underlying mechanism is thought to modulate the interaction between endothelial cells and surrounding support cells, such as smooth muscle cells^[71,74]. Ang-2 was cloned in 1997. It is thought to be a natural antagonist for the Ang-1/Tie-2 interaction now. The transgenic overexpression of Ang-2 in embryo results in early embryonic lethality, similar to the phenomenon in embryonic development without Ang-1 or Tie-2^[68].

The relation of VEGF and angiopoietins in angiogenesis has become a research hotspot (Figure 3). In the onset of cerebral ischemia, the increase of VEGF mRNA goes with the decrease of Ang-1 mRNA. Later increased expression of VEGF/VEGFRs and Ang-1/Tie2 is detected^[75]. This data show that Ang-1 works at the later stage of angiogenesis. Other experiments directly demonstrate the above mentioned role of VEGF and Ang-1. The transgenic overexpression of VEGF in the skin of mice induces the formation of numerous leaky blood vessels. In contrast, overexpression of Ang-1 leads to an enlargement of dermal vessels with less leaking, instead of an increase in the number of vessels. If both VEGF and Ang-1 are overexpressed, the size and number of skin vessels are both increased. Furthermore, these vessels are not leaky. Remarkably, it is found that Ang-1 also reduces VEGF-stimulated inflammation by suppressing expression of adhesion molecules, including intercellular adhesion molecule-1 (ICAM-1), vascular cell adhesion molecule-1 (VCAM-1)^[76] and E-selectin^[77]. The expression of Ang-2 is not broader than that of Ang-1. Holash *et al* demonstrated that endothelial cells apoptosis occurred prior to the wide spread loss of tumor cells in the necrotic tumor core^[78]. This implies that there is a mechanism to induce this process. Ang-2 promotes endothelial cell death and vessel regression if the activity of VEGF is inhibited. By contrast, Ang-2 promotes a rapid increase in capillary diameter and stimulates sprouting of new blood vessels in the presence of endogenous VEGF *in vivo*^[79]. These results indicate that the pre-effect of existing blood vessels by Ang-2 is in favor of the step of VEGF-inducing angiogenesis. Thereby, in the regulation of angiogenesis, VEGF can convert the role of Ang-2 from an anti-angiogenic factor to a pro-angiogenic factor. Other data further confirm that Ang-2 expression precedes that of VEGF in the early stage of tumor angiogenesis^[80].

Altogether, VEGF/VEGFRs and angiopoietins/Ties co-regulate the tumor vessels regression, growth and maturation.

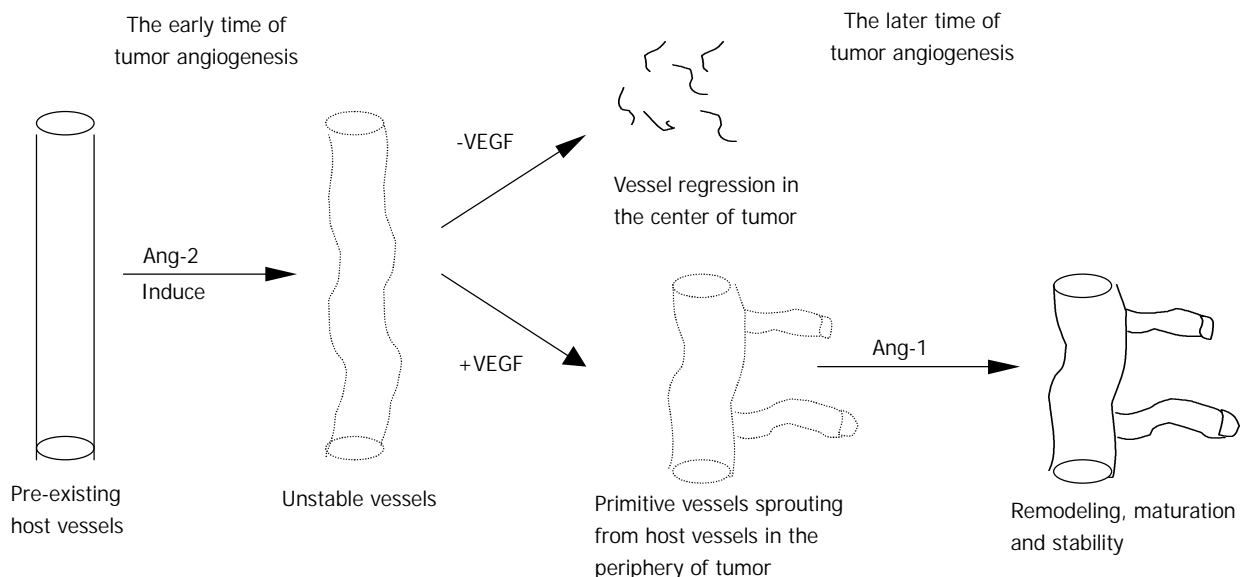


Figure 3 The interaction relation between VEGF and angiopoietins in the development of tumor angiogenesis.

Expression of Ang-2 without VEGF induces vessels regression in core of a necrotic tumor. Then, hypoxia induces tumor cells to express VEGF. The angiogenic properties of VEGF may be easier to act on the vessels, which are destabilized by Ang-2. Newly formed tumor vessels are abnormal, including highly disorganization, poor differentiation, tortuousness and excessive branch, because continuous expression of Ang-2 in newly tumor vessels inhibits the maturation and stabilization signals via Ang-1. In the later development of tumor angiogenesis, the increasing expression of Ang-1 promotes the maturation of neovascularization. In fact, hyper-vascular hepatomas with aberrant vasculature show high levels of Ang-2 expression in the endothelium.

Other angiogenic factors

The mechanism of tumor angiogenesis is complicated. It involves many factors and some different signal pathways. Therefore, if only one signal molecule (for example VEGF) is blocked, tumor may switch to another molecule (for example bFGF) for the induction of angiogenesis. The basic fibroblast growth factor (bFGF, also known as FGF-2) isolated from a chondrosarcoma was identified to be the first pro-angiogenic factor^[81]. bFGF is the main member of FGF family which is a structurally homologous protein family, including at least 20 members. FGF has a high affinity to heparin sulfate proteoglycans (HSPGs), which locates on the surface of most cells and within the extracellular matrix^[82].

Four receptor tyrosine kinases (known as FGFR-1,-2,-3,-4) can interact with FGF. The FGF/FGFRs signal pathway may play a crucial role in angiogenesis. The FGFR-1 mutant mouse embryos exhibited abnormal embryonic and extra-embryonic vascularization, suggesting that FGF/FGFR-1 plays a role in the development and maintenance of a matured vascular network in the embryo^[83]. The mechanisms for VEGF- and FGF-mediated angiogenesis are not the same. In astrocytoma, bFGF and VEGF expression levels positively correlated with tumor growth and angiogenesis. However, bFGF and VEGF expression levels were significantly different in various grades of astrocytoma^[84]. In the culture of embryonic stem cell-derived vascular precursors *in vitro*, bFGF and VEGF both exhibited effects on the survival of angioblasts. However, VEGF induced the formation of primitive endothelial tubes, whereas bFGF did not^[85]. This finding suggests that VEGF but not bFGF plays a major role in angiogenesis. The mitogen-activated protein kinase kinase (MEK) inhibitor PD98059 suppresses FGF-induced angiogenesis, indicating that the Ras-MEK-MAPK pathway is important for the biological effect of FGF^[86]. Subsequently, Cross *et al* found that the Shb adaptor protein binding to Tyr766 in the FGFR-1 promoted FRS2 phosphorylation, and further regulated the Ras-MEK-MAPK pathway^[87]. FGFR-1-mediated intracellular signal cascades include the Ras pathway, Src family tyrosine kinases, phosphoinositide 3-kinase (PI3K) and the PLC pathway^[88]. Some members of the FGF family (such as FGF-3) promote oncogenesis, and are identified as proto-oncogenes^[89].

ANTI-ANGIOGENIC FACTORS

In humans or vertebrates, normal vascularization is quiescent, suggesting that *in vivo* humans or vertebrates should have anti-angiogenic factors against angiogenic factors. Recently, experiments *in vitro* or *in vivo* confirm the presence of endogenous anti-angiogenic factors.

The primary anti-angiogenic factors include thrombospondins (TSP), angiostatin and endostatin. Now the TSP family includes five members, known as TSP-1, -2, -3, -4 and TSP-5/COMP. They play multiple functions via binding to matrix proteins, plasma proteins and cytokines^[90-93]. Some

reports have shown that TSP-1 and TSP-2 have anti-angiogenic properties. TSP-1 inhibits angiogenesis via a direct way that suppresses migration and induces apoptosis of endothelial cells or via an indirect way that inhibits the mobilization of pro-angiogenic factors and blocks their access to co-receptors on the endothelial cell surface^[94]. TSP-2 has the similar functions^[95]. The signal pathway of TSP includes TSP/CD36 receptor, cytoplasmic tyrosine kinase p59^{lyn}, caspase-3-like proteases and p38 mitogen-activated protein kinase (MAPK), and results in apoptosis of endothelial cells^[94,96,97]. It has been proven that TSP is an anti-angiogenic factor or acts as prognostic predictor in pancreatic ductal carcinoma^[98], bladder cancer^[99], non-small cell lung cancer^[100,101], breast cancer^[102], cervical cancer^[103] and colon cancer^[104]. TSP expression is regulated by several factors. Hypoxia increases TSP-1 expression in endothelial cells by promoting the post-transcriptional stabilization of the *TSP-1* mRNA^[105]. This property does not match with its anti-angiogenic property. Contrarily, *in vitro* hypoxia suppresses TSP-1 expression and induces VEGF expression in rodent cells, regardless of the p53 genotype^[106]. In cultured fibroblasts, loss of the wild-type allele of the p53 results in reduced expression of TSP-1. Transfection assays have revealed that p53 stimulates the expression of the endogenous *TSP-1* gene and positively regulate *TSP-1* gene promoter sequences^[107,108]. A novel p53-inducible gene, named *BAl1*, was found in 1997^[109]. *BAl1* contains five TSP-type 1 repeats, and significantly suppresses angiogenesis. Some oncogenes have been also found to regulate TSP1 expression, including *c-jun*^[110] and *H-ras*^[106]. These data indicate that oncogenes or loss of tumor suppressor genes also regulate TSP expression to turn on the angiogenic switch and promote tumor growth.

A number of experimental studies have demonstrated that a primary tumor inhibits a secondary distant tumor^[111,112], indicating that there are some inhibitors from the primary tumor to inhibit the growth of metastases. Endostatin is a circulatory inhibitor, and identified to be an anti-angiogenic factor^[113]. It is a 20 kD C-terminal fragment of collagen XVIII. Treatment with endostatin by transgene inhibits angiogenesis and liver tumor growth^[114]. In other similar diseases such as rheumatoid arthritis, treatment with endostatin showed beneficial effects^[115]. Interestingly, endostatin immunostaining was stronger in area accompanied with blood vessel maturation. Endostatin expression was significantly prominent in vessels of tumor marginal zone where angiogenesis was highly active. These observations suggest that endostatin inhibits angiogenesis by stabilization of newly formed endothelial tubes in angiogenic active region in tumors^[116]. Intracellular signaling mechanisms by endostatin remain poorly understood. Jiang *et al* found that endostatin increases intracellular Ca²⁺ concentration approximately three-fold, indicating that endostatin induces intracellular Ca²⁺ signal^[117]. Endostatin also modulates the Wnt signaling by regulating β -catenin stability via a novel glycogen synthase kinase 3(GSK3)-independent mechanism^[118].

Angiostatin is another circulatory anti-angiogenic factor. It was isolated from a lung carcinoma cell line and is particularly effective in suppressing metastatic growth when the primary tumor is removed^[119]. Angiostatin is a 38 kD fragment of plasminogen. Treatment with angiostatin inhibits angiogenesis in a murine breast cancer model^[120]. Now it is found that angiostatin plays a crucial role in inflammation via directly inhibiting neutrophil migration and neutrophil-mediated angiogenesis^[121]. Recent studies have shown that angiostatin has structural similarities to hepatocyte growth factor (HGF), which induces proliferation and migration of both endothelial cells and smooth muscle cells via its cell surface receptor, c-met. Therefore, the disruption of HGF/c-met

signaling is a novel mechanism for the anti-angiogenic effect of angiostatin^[122]. Experiments by Mauceri *et al* indicated that TNF- α enhances the production of angiostatin in tumor cells by inducing the activity of the plasminogen activator and the release of MMP-9 by tumor cells^[123].

CONCLUSIONS

Tumor angiogenesis plays crucial roles in tumor growth and metastases. Tumor angiogenesis is a complex process involving interactions of many molecules and several different or similar signal pathways. Despite the rapid research progress in the field, there are many mysteries regarding the molecular mechanism of tumor angiogenesis. Once we fully understand the precise functions of these pro- and anti-angiogenic factors in tumor angiogenesis, clinical application of those novel research results for tumor therapy would become practical.

REFERENCES

- Gupta MK**, Qin RY. Mechanism and its regulation of tumor-induced angiogenesis. *World J Gastroenterol* 2003; **9**: 1144-1155
- Folkman J**. Anti-angiogenesis: new concept for therapy of solid tumors. *Ann Surg* 1972; **175**: 409-416
- Asahara T**, Kalka C, Isner JM. Stem cell therapy and gene transfer for regeneration. *Gene Ther* 2000; **7**: 451-457
- Raffi S**. Circulating endothelial precursors: mystery, reality, and promise. *J Clin Invest* 2000; **105**: 17-19
- Hanahan D**, Folkman J. Patterns and emerging mechanisms of the angiogenic switch during tumorigenesis. *Cell* 1996; **86**: 353-364
- Senger DR**, Galli SJ, Dvorak AM, Perruzzi CA, Harvey VS, Dvorak HF. Tumor cells secrete a vascular permeability factor that promotes accumulation of ascites fluid. *Science* 1983; **219**: 983-985
- Leung DW**, Cachianes G, Kuang WJ, Goeddel DV, Ferrara N. Vascular endothelial growth factor is a secreted angiogenic mitogen. *Science* 1989; **246**: 1306-1309
- Keck PJ**, Hauser SD, Krivi G, Sanzo K, Warren T, Feder J, Connolly DT. Vascular permeability factor, an endothelial cell mitogen related to PDGF. *Science* 1989; **246**: 1309-1312
- Breier G**, Albrecht U, Sterrer S, Risau W. Expression of vascular endothelial growth factor during embryonic angiogenesis and endothelial cell differentiation. *Development* 1992; **114**: 521-532
- Veikkola T**, Alitalo K. VEGFs, receptors and angiogenesis. *Semin Cancer Biol* 1999; **9**: 211-220
- Takahashi A**, Sasaki H, Kim SJ, Tobisu K, Kakizoe T, Tsukamoto T, Kumamoto Y, Sugimura T, Terada M. Markedly increased amounts of messenger RNAs for vascular endothelial growth factor and placenta growth factor in renal cell carcinoma associated with angiogenesis. *Cancer Res* 1994; **54**: 4233-4237
- Olson TA**, Mohanraj D, Carson LF, Ramakrishnan S. Vascular permeability factor gene expression in normal and neoplastic human ovaries. *Cancer Res* 1994; **54**: 276-280
- Du JR**, Jiang Y, Zhang YM, Fu H. Vascular endothelial growth factor and microvascular density in esophageal and gastric carcinomas. *World J Gastroenterol* 2003; **9**: 1604-1606
- Plate KH**, Breier G, Weich HA, Risau W. Vascular endothelial growth factor is a potential tumour angiogenesis factor in human gliomas *in vivo*. *Nature* 1992; **359**: 845-848
- Qin LX**, Tang ZY. The prognostic molecular markers in hepatocellular carcinoma. *World J Gastroenterol* 2002; **8**: 385-392
- Vincenti V**, Cassano C, Rocchi M, Persico G. Assignment of the vascular endothelial growth factor gene to human chromosome 6p21.3. *Circulation* 1996; **93**: 1493-1495
- Tischer E**, Mitchell R, Hartman T, Silva M, Gospodarowicz D, Fiddes JC, Abraham JA. The human gene for vascular endothelial growth factor. Multiple protein forms are encoded through alternative exon splicing. *J Biol Chem* 1991; **266**: 11947-11954
- Soker S**, Fidler IJ, Neufeld G, Klagsbrun M. Characterization of novel vascular endothelial growth factor (VEGF) receptors on tumor cells that bind VEGF165 via its exon 7-encoded domain. *J Biol Chem* 1996; **271**: 5761-5767
- Soker S**, Gollamudi-Payne S, Fidler IJ, Charnahelli H, Klagsbrun M. Inhibition of vascular endothelial growth factor (VEGF)-induced endothelial cell proliferation by a peptide corresponding to the exon 7-encoded domain of VEGF165. *J Biol Chem* 1997; **272**: 31582-31588
- Wild R**, Dhanabal M, Olson TA, Ramakrishnan S. Inhibition of angiogenesis and tumour growth by VEGF121-toxin conjugate: differential effect on proliferating endothelial cells. *Br J Cancer* 2000; **83**: 1077-1083
- Ferrara N**, Davis-Smyth T. The biology of vascular endothelial growth factor. *Endocr Rev* 1997; **18**: 4-25
- Olofsson B**, Pajusola K, Kaipainen A, von Euler G, Joukov V, Saksela O, Orpana A, Pettersson RF, Alitalo K, Eriksson U. Vascular endothelial growth factor B, a novel growth factor for endothelial cells. *Proc Natl Acad Sci U S A* 1996; **93**: 2576-2581
- Hanrahan V**, Currie MJ, Gunningham SP, Morrin HR, Scott PA, Robinson BA, Fox SB. The angiogenic switch for vascular endothelial growth factor (VEGF)-A, VEGF-B, VEGF-C, and VEGF-D in the adenoma-carcinoma sequence during colorectal cancer progression. *J Pathol* 2003; **200**: 183-194
- Achen MG**, Jeltsch M, Kukk E, Makinen T, Vitali A, Wilks AF, Alitalo K, Stacker SA. Vascular endothelial growth factor D (VEGF-D) is a ligand for the tyrosine kinases VEGF receptor 2 (Flk1) and VEGF receptor 3 (Flt4). *Proc Natl Acad Sci U S A* 1998; **95**: 548-553
- Ogawa S**, Oku A, Sawano A, Yamaguchi S, Yazaki Y, Shibuya M. A novel type of vascular endothelial growth factor, VEGF-E (NZ-7 VEGF), preferentially utilizes KDR/Flk-1 receptor and carries a potent mitotic activity without heparin-binding domain. *J Biol Chem* 1998; **273**: 31273-31282
- Meyer M**, Clauss M, Lepple-Wienhues A, Waltenberger J, Augustin HG, Ziche M, Lanz C, Buttner M, Rziha HJ, Dehio C. A novel vascular endothelial growth factor encoded by Orf virus, VEGF-E, mediates angiogenesis via signalling through VEGFR-2 (KDR) but not VEGFR-1 (Flt-1) receptor tyrosine kinases. *EMBO J* 1999; **18**: 363-374
- Gleadle JM**, Ratcliffe PJ. Hypoxia and the regulation of gene expression. *Mol Med Today* 1998; **4**: 122-129
- Goldberg MA**, Schneider TJ. Similarities between the oxygen-sensing mechanisms regulating the expression of vascular endothelial growth factor and erythropoietin. *J Biol Chem* 1994; **269**: 4355-4359
- Minchenko A**, Salceda S, Bauer T, Caro J. Hypoxia regulatory elements of the human vascular endothelial growth factor gene. *Cell Mol Biol Res* 1994; **40**: 35-39
- Ladoux A**, Frelin C. Hypoxia is a strong inducer of vascular endothelial growth factor mRNA expression in the heart. *Biochem Biophys Res Commun* 1993; **195**: 1005-1010
- Levy NS**, Chung S, Furneaux H, Levy AP. Hypoxic stabilization of vascular endothelial growth factor mRNA by the RNA-binding protein HuR. *J Biol Chem* 1998; **273**: 6417-6423
- Okada F**, Rak JW, Croix BS, Lieubeau B, Kaya M, Roncari L, Shirasawa S, Sasazuki T, Kerbel RS. Impact of oncogenes in tumor angiogenesis: mutant K-ras up-regulation of vascular endothelial growth factor/vascular permeability factor is necessary, but not sufficient for tumorigenicity of human colorectal carcinoma cells. *Proc Natl Acad Sci U S A* 1998; **95**: 3609-3614
- Petit AM**, Rak J, Hung MC, Rockwell P, Goldstein N, Fendly B, Kerbel RS. Neutralizing antibodies against epidermal growth factor and ErbB-2/neu receptor tyrosine kinases down-regulate vascular endothelial growth factor production by tumor cells *in vitro* and *in vivo*: angiogenic implications for signal transduction therapy of solid tumors. *Am J Pathol* 1997; **151**: 1523-1530
- Sodhi A**, Montaner S, Miyazaki H, Gutkind JS. MAPK and Akt act cooperatively but independently on hypoxia inducible factor-1 α in rasV12 upregulation of VEGF. *Biochem Biophys Res Commun* 2001; **287**: 292-300
- Mottet D**, Dumont V, Deccache Y, Demazy C, Ninane N, Raes M, Michiels C. Regulation of Hypoxia-inducible Factor-1 α Protein Level during Hypoxic Conditions by the Phosphatidy-

- linositol 3-Kinase/Akt/Glycogen Synthase Kinase 3{beta} Pathway in HepG2 Cells. *J Biol Chem* 2003; **278**: 31277-31285
- 36 **Mayerhofer M**, Valent P, Sperr WR, Griffin JD, Sillaber C. BCR/ABL induces expression of vascular endothelial growth factor and its transcriptional activator, hypoxia inducible factor-1alpha, through a pathway involving phosphoinositide 3-kinase and the mammalian target of rapamycin. *Blood* 2002; **100**: 3767-3775
- 37 **Siemeister G**, Weindel K, Mohrs K, Barleon B, Martiny-Baron G, Marme D. Reversion of deregulated expression of vascular endothelial growth factor in human renal carcinoma cells by von Hippel-Lindau tumor suppressor protein. *Cancer Res* 1996; **56**: 2299-2301
- 38 **Gnarra JR**, Zhou S, Merrill MJ, Wagner JR, Krumm A, Papavassiliou E, Oldfield EH, Klausner RD, Linehan WM. Post-transcriptional regulation of vascular endothelial growth factor mRNA by the product of the VHL tumor suppressor gene. *Proc Natl Acad Sci U S A* 1996; **93**: 10589-10594
- 39 **Maxwell PH**, Ratcliffe PJ. Oxygen sensors and angiogenesis. *Semin Cell Dev Biol* 2002; **13**: 29-37
- 40 **Blagosklonny MV**, An WG, Romanova LY, Trepel J, Fojo T, Neckers L. p53 inhibits hypoxia-inducible factor-stimulated transcription. *J Biol Chem* 1998; **273**: 11995-11998
- 41 **Ravi R**, Mookerjee B, Bhujwalla ZM, Sutter CH, Artemov D, Zeng Q, Dillehay LE, Madan A, Semenza GL, Bedi A. Regulation of tumor angiogenesis by p53-induced degradation of hypoxia-inducible factor 1alpha. *Genes Dev* 2000; **14**: 34-44
- 42 **Hyder SM**, Nawaz Z, Chiappetta C, Stancel GM. Identification of functional estrogen response elements in the gene coding for the potent angiogenic factor vascular endothelial growth factor. *Cancer Res* 2000; **60**: 3183-3190
- 43 **Kanda N**, Watanabe S. 17beta-estradiol enhances vascular endothelial growth factor production and dihydrotestosterone antagonizes the enhancement via the regulation of adenylate cyclase in differentiated THP-1 cells. *J Invest Dermatol* 2002; **118**: 519-529
- 44 **de Vries C**, Escobedo JA, Ueno H, Houck K, Ferrara N, Williams LT. The fms-like tyrosine kinase, a receptor for vascular endothelial growth factor. *Science* 1992; **255**: 989-991
- 45 **Terman BI**, Dougher-Vermazen M, Carrion ME, Dimitrov D, Armellino DC, Gospodarowicz D, Bohlen P. Identification of the KDR tyrosine kinase as a receptor for vascular endothelial cell growth factor. *Biochem Biophys Res Commun* 1992; **187**: 1579-1586
- 46 **Millauer B**, Wizigmann-Voos S, Schnurch H, Martinez R, Moller NP, Risau W, Ullrich A. High affinity VEGF binding and developmental expression suggest Flk-1 as a major regulator of vasculogenesis and angiogenesis. *Cell* 1993; **72**: 835-846
- 47 **Fong GH**, Rossant J, Gertsenstein M, Breitman ML. Role of the Flt-1 receptor tyrosine kinase in regulating the assembly of vascular endothelium. *Nature* 1995; **376**: 66-70
- 48 **Hiratsuka S**, Minowa O, Kuno J, Noda T, Shibuya M. Flt-1 lacking the tyrosine kinase domain is sufficient for normal development and angiogenesis in mice. *Proc Natl Acad Sci U S A* 1998; **95**: 9349-9354
- 49 **Seetharam L**, Gotoh N, Maru Y, Neufeld G, Yamaguchi S, Shibuya M. A unique signal transduction from FLT tyrosine kinase, a receptor for vascular endothelial growth factor VEGF. *Oncogene* 1995; **10**: 135-147
- 50 **Kroll J**, Waltenberger J. The vascular endothelial growth factor receptor KDR activates multiple signal transduction pathways in porcine aortic endothelial cells. *J Biol Chem* 1997; **272**: 32521-32527
- 51 **Yamaguchi S**, Iwata K, Shibuya M. Soluble Flt-1 (soluble VEGFR-1), a potent natural antiangiogenic molecule in mammals, is phylogenetically conserved in avians. *Biochem Biophys Res Commun* 2002; **291**: 554-559
- 52 **Kearney JB**, Ambler CA, Monaco KA, Johnson N, Rapoport RG, Bautch VL. Vascular endothelial growth factor receptor Flt-1 negatively regulates developmental blood vessel formation by modulating endothelial cell division. *Blood* 2002; **99**: 2397-2407
- 53 **Dougher-Vermazen M**, Hulmes JD, Bohlen P, Terman BI. Biological activity and phosphorylation sites of the bacterially expressed cytosolic domain of the KDR VEGF-receptor. *Biochem Biophys Res Commun* 1994; **205**: 728-738
- 54 **Meyer RD**, Dayanir V, Majnoun F, Rahimi N. The presence of a single tyrosine residue at the carboxyl domain of vascular endothelial growth factor receptor-2/FLK-1 regulates its autophosphorylation and activation of signaling molecules. *J Biol Chem* 2002; **277**: 27081-27087
- 55 **Menon C**, Iyer M, Prabakaran I, Canter RJ, Lehr SC, Fraker DL. TNF-alpha downregulates vascular endothelial Flk-1 expression in human melanoma xenograft model. *Am J Physiol Heart Circ Physiol* 2003; **284**: H317-329
- 56 **Thuringer D**, Maulon L, Frelin C. Rapid transactivation of the vascular endothelial growth factor receptor KDR/Flk-1 by the bradykinin B2 receptor contributes to endothelial nitric-oxide synthase activation in cardiac capillary endothelial cells. *J Biol Chem* 2002; **277**: 2028-2032
- 57 **Gerber HP**, McMurtry A, Kowalski J, Yan M, Keyt BA, Dixit V, Ferrara N. Vascular endothelial growth factor regulates endothelial cell survival through the phosphatidylinositol 3'-kinase/Akt signal transduction pathway. Requirement for Flk-1/KDR activation. *J Biol Chem* 1998; **273**: 30336-30343
- 58 **Nor JE**, Christensen J, Mooney DJ, Polverini PJ. Vascular endothelial growth factor (VEGF)-mediated angiogenesis is associated with enhanced endothelial cell survival and induction of Bcl-2 expression. *Am J Pathol* 1999; **154**: 375-384
- 59 **Soker S**, Takashima S, Miao HQ, Neufeld G, Klagsbrun M. Neuropilin-1 is expressed by endothelial and tumor cells as an isoform-specific receptor for vascular endothelial growth factor. *Cell* 1998; **92**: 735-745
- 60 **Oh H**, Takagi H, Otani A, Koyama S, Kemmochi S, Uemura A, Honda Y. Selective induction of neuropilin-1 by vascular endothelial growth factor (VEGF): a mechanism contributing to VEGF-induced angiogenesis. *Proc Natl Acad Sci U S A* 2002; **99**: 383-388
- 61 **Bachelder RE**, Crago A, Chung J, Wendt MA, Shaw LM, Robinson G, Mercurio AM. Vascular endothelial growth factor is an autocrine survival factor for neuropilin-expressing breast carcinoma cells. *Cancer Res* 2001; **61**: 5736-5740
- 62 **Pavelock K**, Braas K, Ouafik L, Osol G, May V. Differential expression and regulation of the vascular endothelial growth factor receptors neuropilin-1 and neuropilin-2 in rat uterus. *Endocrinology* 2001; **142**: 613-622
- 63 **Kaipainen A**, Korhonen J, Mustonen T, van Hinsbergh VM, Fang GH, Dumont D, Breitman M, Alitalo K. Expression of the fms-like tyrosine kinase 4 gene becomes restricted to lymphatic endothelium during development. *Proc Natl Acad Sci U S A* 1995; **92**: 3566-3570
- 64 **Kukk E**, Lymboussaki A, Taira S, Kaipainen A, Jeltsch M, Joukov V, Alitalo K. VEGF-C receptor binding and pattern of expression with VEGFR-3 suggests a role in lymphatic vascular development. *Development* 1996; **122**: 3829-3837
- 65 **Dumont DJ**, Jussila L, Taipale J, Lymboussaki A, Mustonen T, Pajusola K, Breitman M, Alitalo K. Cardiovascular failure in mouse embryos deficient in VEGF receptor-3. *Science* 1998; **282**: 946-949
- 66 **Valtola R**, Salven P, Heikkila P, Taipale J, Joensuu H, Rehn M, Pihlajaniemi T, Weich H, deWaal R, Alitalo K. VEGFR-3 and its ligand VEGF-C are associated with angiogenesis in breast cancer. *Am J Pathol* 1999; **154**: 1381-1390
- 67 **Davis S**, Aldrich TH, Jones PF, Acheson A, Compton DL, Jain V, Ryan TE, Bruno J, Radziejewski C, Maisonpierre PC, Yancopoulos GD. Isolation of angiopoietin-1, a ligand for the TIE2 receptor, by secretion-trap expression cloning. *Cell* 1996; **87**: 1161-1169
- 68 **Maisonpierre PC**, Suri C, Jones PF, Bartunkova S, Wiegand SJ, Radziejewski C, Compton D, McClain J, Aldrich TH, Papadopoulos N, Daly TJ, Davis S, Sato TN, Yancopoulos GD. Angiopoietin-2, a natural antagonist for Tie2 that disrupts *in vivo* angiogenesis. *Science* 1997; **277**: 55-60
- 69 **Dumont DJ**, Gradwohl G, Fong GH, Puri MC, Gerstenstein M, Auerbach A, Breitman ML. Dominant-negative and targeted null mutations in the endothelial receptor tyrosine kinase, tek, reveal a critical role in vasculogenesis of the embryo. *Genes Dev* 1994; **8**: 1897-1909
- 70 **Sato TN**, Tozawa Y, Deutsch U, Wolburg-Buchholz K, Fujiwara

- Y, Gendron-Maguire M, Gridley T, Wolburg H, Risau W, Qin Y. Distinct roles of the receptor tyrosine kinases Tie-1 and Tie-2 in blood vessel formation. *Nature* 1995; **376**: 70-74
- 71 **Suri C**, Jones PF, Patan S, Bartunkova S, Maisonpierre PC, Davis S, Sato TN, Yancopoulos GD. Requisite role of angiopoietin-1, a ligand for the TIE2 receptor, during embryonic angiogenesis. *Cell* 1996; **87**: 1171-1180
- 72 **Shim WS**, Teh M, Bapna A, Kim I, Koh GY, Mack PO, Ge R. Angiopoietin 1 promotes tumor angiogenesis and tumor vessel plasticity of human cervical cancer in mice. *Exp Cell Res* 2002; **279**: 299-309
- 73 **Wong AL**, Haroon ZA, Werner S, Dewhirst MW, Greenberg CS, Peters KG. Tie2 expression and phosphorylation in angiogenic and quiescent adult tissues. *Circ Res* 1997; **81**: 567-574
- 74 **Folkman J**, D'Amore PA. Blood vessel formation: what is its molecular basis? *Cell* 1996; **87**: 1153-1155
- 75 **Zhang ZG**, Zhang L, Tsang W, Soltanian-Zadeh H, Morris D, Zhang R, Goussev A, Powers C, Yeich T, Chopp M. Correlation of VEGF and angiopoietin expression with disruption of blood-brain barrier and angiogenesis after focal cerebral ischemia. *J Cereb Blood Flow Metab* 2002; **22**: 379-392
- 76 **Ding YB**, Chen GY, Xia JG, Zang XW, Yang HY, Yang L. Association of VCAM-1 overexpression with oncogenesis, tumor angiogenesis and metastasis of gastric carcinoma. *World J Gastroenterol* 2003; **9**: 1409-1414
- 77 **Kim I**, Moon SO, Park SK, Chae SW, Koh GY. Angiopoietin-1 reduces VEGF-stimulated leukocyte adhesion to endothelial cells by reducing ICAM-1, VCAM-1, and E-selectin expression. *Circ Res* 2001; **89**: 477-479
- 78 **Holash J**, Maisonpierre PC, Compton D, Boland P, Alexander CR, Zagzag D, Yancopoulos GD, Wiegand SJ. Vessel cooption, regression, and growth in tumors mediated by angiopoietins and VEGF. *Science* 1999; **284**: 1994-1998
- 79 **Lobov IB**, Brooks PC, Lang RA. Angiopoietin-2 displays VEGF-dependent modulation of capillary structure and endothelial cell survival *in vivo*. *Proc Natl Acad Sci U S A* 2002; **99**: 11205-11210
- 80 **Peoch M**, Farion R, Hiou A, Le Bas JF, Pasquier B, Remy C. Immunohistochemical study of VEGF, angiopoietin 2 and their receptors in the neovascularization following microinjection of C6 glioma cells into rat brain. *Anticancer Res* 2002; **22**: 2147-2151
- 81 **Shing Y**, Folkman J, Sullivan R, Butterfield C, Murray J, Klagsbrun M. Heparin affinity: purification of a tumor-derived capillary endothelial cell growth factor. *Science* 1984; **223**: 1296-1299
- 82 **Vlodavsky I**, Bar-Shavit R, Ishai-Michaeli R, Bashkin P, Fuks Z. Extracellular sequestration and release of fibroblast growth factor: a regulatory mechanism? *Trends Biochem Sci* 1991; **16**: 268-271
- 83 **Lee SH**, Schloss DJ, Swain JL. Maintenance of vascular integrity in the embryo requires signaling through the fibroblast growth factor receptor. *J Biol Chem* 2000; **275**: 33679-33687
- 84 **Bian XW**, Du LL, Shi JQ, Cheng YS, Liu FX. Correlation of bFGF, FGFR-1 and VEGF expression with vascularity and malignancy of human astrocytomas. *Anal Quant Cytol Histol* 2000; **22**: 267-274
- 85 **Kazemi S**, Wenzel D, Kolossov E, Lenka N, Raible A, Sasse P, Hescheler J, Addicks K, Fleischmann BK, Bloch W. Differential role of bFGF and VEGF for vasculogenesis. *Cell Physiol Biochem* 2002; **12**: 55-62
- 86 **Fu XB**, Yang YH, Sun TZ, Chen W, Li JY, Sheng ZY. Rapid mitogen-activated protein kinase by basic fibroblast growth factor in rat intestine after ischemia/reperfusion injury. *World J Gastroenterol* 2003; **9**: 1312-1317
- 87 **Cross MJ**, Lu L, Magnusson P, Nyqvist D, Holmqvist K, Welsh M, Claesson-Welsh L. The Shb adaptor protein binds to tyrosine 766 in the FGFR-1 and regulates the Ras/MEK/MAPK pathway via FRS2 phosphorylation in endothelial cells. *Mol Biol Cell* 2002; **13**: 2881-2893
- 88 **Boilly B**, Vercoutter-Edouart AS, Hondermarck H, Nurcombe V, Le Bourhis X. FGF signals for cell proliferation and migration through different pathways. *Cytokine Growth Factor Rev* 2000; **11**: 295-302
- 89 **Kim HS**, Crow TJ. Human proto-oncogene Int-2/FGF-3. Map position 11q13.3-q13.4. *Chromosome Res* 1998; **6**: 579
- 90 **Mosher DF**. Physiology of thrombospondin. *Annu Rev Med* 1990; **41**: 85-97
- 91 **Frazier WA**. Thrombospondins. *Curr Opin Cell Biol* 1991; **3**: 792-799
- 92 **Bornstein P**. Diversity of function is inherent in matricellular proteins: an appraisal of thrombospondin 1. *J Cell Biol* 1995; **130**: 503-506
- 93 **Hogg PJ**, Hotchkiss KA, Jimenez BM, Stathkis P, Chesterman CN. Interaction of platelet-derived growth factor with thrombospondin 1. *Biochem J* 1997; **326**(Pt 3): 709-716
- 94 **Lawler J**. Thrombospondin-1 as an endogenous inhibitor of angiogenesis and tumor growth. *J Cell Mol Med* 2002; **6**: 1-12
- 95 **DiPietro LA**. Thrombospondin as a regulator of angiogenesis. *EXS* 1997; **79**: 295-314
- 96 **de Fraipont F**, Nicholson AC, Feige JJ, Van Meir EG. Thrombospondins and tumor angiogenesis. *Trends Mol Med* 2001; **7**: 401-407
- 97 **Bornstein P**, Armstrong LC, Hankenson KD, Kyriakides TR, Yang Z. Thrombospondin 2, a matricellular protein with diverse functions. *Matrix Biol* 2000; **19**: 557-568
- 98 **Tobita K**, Kijima H, Dowaki S, Oida Y, Kashiwagi H, Ishii M, Sugio Y, Sekka T, Ohtani Y, Tanaka M, Inokuchi S, Makuuchi H. Thrombospondin-1 expression as a prognostic predictor of pancreatic ductal carcinoma. *Int J Oncol* 2002; **21**: 1189-1195
- 99 **Goddard JC**, Sutton CD, Jones JL, O'Byrne KJ, Kockelbergh RC. Reduced thrombospondin-1 at presentation predicts disease progression in superficial bladder cancer. *Eur Urol* 2002; **42**: 464-468
- 100 **Mascaux C**, Martin B, Paesmans M, Verdebout JM, Verhest A, Vermeylen P, Bosschaerts T, Ninane V, Sculier JP. Expression of thrombospondin in non-small cell lung cancer. *Anticancer Res* 2002; **22**: 1273-1277
- 101 **Yamaguchi M**, Sugio K, Ondo K, Yano T, Sugimachi K. Reduced expression of thrombospondin-1 correlates with a poor prognosis in patients with non-small cell lung cancer. *Lung Cancer* 2002; **36**: 143-150
- 102 **Urquidí V**, Sloan D, Kawai K, Agarwal D, Woodman AC, Tarin D, Goodison S. Contrasting expression of thrombospondin-1 and osteopontin correlates with absence or presence of metastatic phenotype in an isogenic model of spontaneous human breast cancer metastasis. *Clin Cancer Res* 2002; **8**: 61-74
- 103 **Kodama J**, Hashimoto I, Seki N, Hongo A, Yoshinouchi M, Okuda H, Kudo T. Thrombospondin-1 and -2 messenger RNA expression in invasive cervical cancer: correlation with angiogenesis and prognosis. *Clin Cancer Res* 2001; **7**: 2826-2831
- 104 **Maeda K**, Nishiguchi Y, Kang SM, Yashiro M, Onoda N, Sawada T, Ishikawa T, Hirakawa K. Expression of thrombospondin-1 inversely correlated with tumor vascularity and hematogenous metastasis in colon cancer. *Oncol Rep* 2001; **8**: 763-766
- 105 **Phelan MW**, Forman LW, Perrine SP, Faller DV. Hypoxia increases thrombospondin-1 transcript and protein in cultured endothelial cells. *J Lab Clin Med* 1998; **132**: 519-529
- 106 **Laderoute KR**, Alarcon RM, Brody MD, Calaoagan JM, Chen EY, Knapp AM, Yun Z, Denko NC, Giaccia AJ. Opposing effects of hypoxia on expression of the angiogenic inhibitor thrombospondin 1 and the angiogenic inducer vascular endothelial growth factor. *Clin Cancer Res* 2000; **6**: 2941-2950
- 107 **Dameron KM**, Volpert OV, Tainsky MA, Bouck N. Control of angiogenesis in fibroblasts by p53 regulation of thrombospondin-1. *Science* 1994; **265**: 1582-1584
- 108 **Dameron KM**, Volpert OV, Tainsky MA, Bouck N. The p53 tumor suppressor gene inhibits angiogenesis by stimulating the production of thrombospondin. *Cold Spring Harb Symp Quant Biol* 1994; **59**: 483-489
- 109 **Nishimori H**, Shiratsuchi T, Urano T, Kimura Y, Kiyono K, Tatsumi K, Yoshida S, Ono M, Kuwano M, Nakamura Y, Tokino T. A novel brain-specific p53-target gene, BAI1, containing thrombospondin type 1 repeats inhibits experimental angiogenesis. *Oncogene* 1997; **15**: 2145-2150
- 110 **Mettouchi A**, Cabon F, Montreau N, Vernier P, Mercier G, Blangy D, Tricoire H, Vigier P, Binetruy B. SPARC and thrombospondin genes are repressed by the c-jun oncogene in rat embryo fibroblasts. *EMBO J* 1994; **13**: 5668-5678
- 111 **Prehn RT**. The inhibition of tumor growth by tumor mass. *Can-*

- cer Res* 1991; **51**: 2-4
- 112 **Prehn RT**. Two competing influences that may explain concomitant tumor resistance. *Cancer Res* 1993; **53**: 3266-3269
- 113 **O'Reilly MS**, Boehm T, Shing Y, Fukai N, Vasios G, Lane WS, Flynn E, Birkhead JR, Olsen BR, Folkman J. Endostatin: an endogenous inhibitor of angiogenesis and tumor growth. *Cell* 1997; **88**: 277-285
- 114 **Li X**, Fu GF, Fan YR, Shi CF, Liu XJ, Xu GX, Wang JJ. Potent inhibition of angiogenesis and liver tumor growth by administration of an aerosol containing a transferrin-liposome-endostatin complex. *World J Gastroenterol* 2003; **9**: 262-266
- 115 **Matsuno H**, Yudoh K, Uzuki M, Nakazawa F, Sawai T, Yamaguchi N, Olsen BR, Kimura T. Treatment with the angiogenesis inhibitor endostatin: a novel therapy in rheumatoid arthritis. *J Rheumatol* 2002; **29**: 890-895
- 116 **Ergun S**, Kilic N, Wurmbach JH, Ebrahimnejad A, Fernando M, Sevinc S, Kilic E, Chalajour F, Fiedler W, Lauke H, Lamszus K, Hammerer P, Weil J, Herbst H, Folkman J. Endostatin inhibits angiogenesis by stabilization of newly formed endothelial tubes. *Angiogenesis* 2001; **4**: 193-206
- 117 **Jiang L**, Jha V, Dhanabal M, Sukhatme VP, Alper SL. Intracellular Ca(2+) signaling in endothelial cells by the angiogenesis inhibitors endostatin and angiostatin. *Am J Physiol Cell Physiol* 2001; **280**: C1140-1150
- 118 **Hanai J**, Gloy J, Karumanchi SA, Kale S, Tang J, Hu G, Chan B, Ramchandran R, Jha V, Sukhatme VP, Sokol S. Endostatin is a potential inhibitor of Wnt signaling. *J Cell Biol* 2002; **158**: 529-539
- 119 **O'Reilly MS**, Holmgren L, Shing Y, Chen C, Rosenthal RA, Moses M, Lane WS, Cao Y, Sage EH, Folkman J. Angiostatin: a novel angiogenesis inhibitor that mediates the suppression of metastases by a Lewis lung carcinoma. *Cell* 1994; **79**: 315-328
- 120 **Gyorffy S**, Palmer K, Podor TJ, Hitt M, Gauldie J. Combined treatment of a murine breast cancer model with type 5 adenovirus vectors expressing murine angiostatin and IL-12: a role for combined anti-angiogenesis and immunotherapy. *J Immunol* 2001; **166**: 6212-6217
- 121 **Benelli R**, Morini M, Carrozzino F, Ferrari N, Minghelli S, Santi L, Cassatella M, Noonan DM, Albin A. Neutrophils as a key cellular target for angiostatin: implications for regulation of angiogenesis and inflammation. *FASEB J* 2002; **16**: 267-269
- 122 **Wajih N**, Sane DC. Angiostatin selectively inhibits signaling by hepatocyte growth factor in endothelial and smooth muscle cells. *Blood* 2003; **101**: 1857-1863
- 123 **Mauceri HJ**, Seetharam S, Beckett MA, Lee JY, Gupta VK, Gately S, Stack MS, Brown CK, Swedberg K, Kufe DW, Weichselbaum RR. Tumor production of angiostatin is enhanced after exposure to TNF-alpha. *Int J Cancer* 2002; **97**: 410-415

Edited by Xia HHX Proofread by Zhu LH

Values of mutations of K-ras oncogene at codon 12 in detection of pancreatic cancer: 15- year experience

De-Qing Mu, You-Shu Peng, Qiao-Jian Xu

De-Qing Mu, You-Shu Peng, Department of Surgery of the Second Affiliated Hospital, Medical College of Zhejiang University, Hangzhou 310009, Zhejiang Province, China

Qiao-Jian Xu, Undergraduate Medical College of Zhejiang University, Hangzhou 310009, Zhejiang Province, China

Correspondence to: Dr. De-Qing Mu, Department of surgery of the Second Affiliated Hospital, Medical College of Zhejiang University, Hangzhou 310009, Zhejiang Province, China. samier-1969@163.com

Telephone: +86-571-87783762

Received: 2003-05-11 **Accepted:** 2003-06-27

Abstract

AIM: To summarize progress in the study of K-ras gene studies in pancreatic cancer and its potential clinical significance in screening test for early detection of pancreatic cancer, and to differentiate pancreatic cancer from chronic pancreatitis in recent decade.

METHODS: Literature search (MEDLINE 1986-2003) was performed using the key words K-ras gene, pancreatic cancer, chronic pancreatitis, and diagnosis. Two kind of opposite points of view on the significance of K-ras gene in detection early pancreatic cancer and differentiation pancreatic cancer from chronic pancreatitis were investigated. The presence of a K-ras gene mutation at codon 12 has been seen in 75-100% of pancreatic cancers, and is not rare in patients with chronic pancreatitis, and represents an increased risk of developing pancreatic cancer. However, the significance of the detection of this mutation in specimens obtained by needle aspiration from pure pancreatic juice and from stools for its utilization for the detection of early pancreatic cancer, and differentiation pancreatic cancer from chronic pancreatitis remains controversial.

CONCLUSION: The value of K-ras gene mutation for the detection of early pancreatic cancer and differentiation pancreatic cancer from chronic pancreatitis remains uncertain in clinical practice. Nevertheless, K-ras mutation screening may increase the sensitivity of FNA and ERP cytology and may be useful in identifying pancreatitis patients at high risk for developing cancer, and as an adjunct with cytology to differentiate pancreatic cancer from chronic pancreatitis.

Mu DQ, Peng YS, Xu QJ. Values of mutations of K-ras oncogene at codon 12 in detection of pancreatic cancer: 15- year experience. *World J Gastroenterol* 2004; 10(4): 471-475
<http://www.wjgnet.com/1007-9327/10/471.asp>

INTRODUCTION

Cytology, for detection of pancreatic cancer is limited for the definitive diagnosis by a low sensitivity and accuracy^[1-4]. K-ras oncogene as a cytological adjunct can be date back to ten years ago^[5]. K-ras oncogene has been found to be activated by specific point mutations restricted to condon 12 in 75 to 100%

of pancreatic cancers, but rare in chronic pancreatitis^[6-8]. Attempt at detection of such genetic change have been made in plasm^[9-12], pancreatic juice samples^[13-16], fine needle tumour aspirates^[17-19], and stool samples^[20-22]. However, at present there exists completely different viewpoints about these preliminary results. In this article we review previous studies of prospective follow-up of patients with chronic pancreatitis positive for K-ras gene at codon 12 and evaluated its significance mutation in detecting early pancreatic cancer and in differentiating pancreatic cancer from chronic pancreatitis.

K-RAS GENE MUTATIONS

K-ras gene is the locus for the c-k-ras protooncogene, lying on chromosome 12p12, and is about 45 000 bp in lenth. It encodes for a 2.0 kb transcript which is highly conserved across species, and is translated into the p21-ras protein. These proteins are located in the plasma membrane and could transduce growth and differentiation signals from activated receptors to protein kinases within the cell^[23]. p21-ras protein are in a weak GTP-bound, active state, thereby altering transduction into the cell^[23]. The majority of mutations have been found at K-ras codons 12 and 13, and to a lesser extent, at codon 61^[24,25]. These mutations are somatic rather than in the germ-line, and consist of single base-pair substitutions which lead to the change of one amino acid in the protein. The wild-type K-ras gene encodes for glycine (GGT) at codon 12, and the most common amino acid substitution is aspartic acid for glycine (46%), followed by valine (32%), arginine (13%), cystein (5%), serine (1-2%), and alanine (<1%). These mutations presumably result in the K-ras protein product (p21-ras) remaining in the GTP-bound, activated state, which may promote cell proliferation. The reason for the specificity of these mutations to condon 12 is not entirely clear. This location appears to confer higher change in the p21 ras protein's 3 dimensional structure and ras-GAP binding characteristics.

K-ras mutations were thought to be an early event in pancreatic tumorigenesis^[24]. Is it true? In animal models, weekly exposed to doses of nitrosamines and serially sacrificed at 8,12, 14, 16, or 24 weeks, K-ras mutations were found in 26% of hyperplastic lesions,46% of papillary hyperplastic lesions,76% of carcinomas *in situ*, and 80% of invasive pancreatic carcinomas^[25]. In human pancreas, K-ras point mutation at codon 12 is found hyperplasia without dysplasia^[26,27], severe dysplasia^[26] or carcinoma *in situ*^[26] even within multifocal hyperplastic foci of ductal epithelium in histologically normal pancreas^[26]. K-ras point mutations rate seems to increase regularly from normal duct cells to flat or papillary hyperplasia observed in chronic pancreatitis tissue^[26]. Such epithelial lesions mainly associated with chronic pancreatitis are thought to be potentially premalignant ductal lesions. However, there existed completely different objections about the significance of presence of the presence of K-ras mutations^[28,29].

CLINICAL SIGNIFICANCES OF K-RAS MUTATIONS

K-ras mutation and pancreatic cancer screening test

Chronic pancreatitis (CP) was considered to be a risk factor

for the development of pancreatic carcinoma (PC)^[30,31]. The detection of K-ras mutations in the duodenal or pancreatic juice has been held to be a tool for pancreatic cancer early diagnosis. One application of K-ras mutation testing for pancreatic cancer is the screening of pancreatic juice samples. In order to evaluate the significance of K-ras mutation, a prospective follow-up of study of patients with CP in the detection of early pancreatic cancer and K-ras mutations at codon 12 has been carried out. In Berthelemy's series^[32], two patients free of pancreatic mass had no evidence of pancreatic cancer, when K-ras was first studied, but developed tumors 18 and 40 months, respectively, after identification of K-ras mutations. Boadas *et al*^[33] collected 50 patients' pancreatic juice samples, including 49 patients with CP and one patient proceeding from a PC family screening. K-ras mutation was detected by PCR-RFLP (restriction fragment length polymorphism). As a result, K-ras mutation was detected in 8/49 patients (16%) with CP, one of whom developed PC during the follow-up, allowing surgical resection of early cancer.

Another interesting clinical application of K-ras mutation testing for pancreatic cancer is the screening of stool samples. Caldas and colleagues^[20] tested stool samples from patients with pancreatic adenocarcinoma, cholangiocarcinoma, and chronic pancreatitis for K-ras mutations. Stool samples were frozen, then approximately 1 g was resuspended in buffer, extracted in phenol-chloroform, and precipitated. PCR products resulting from this template were subcloned and plaque hybridizations using specific oligonucleotide probes for different K-ras mutations. Positive stool samples were found in 6 of 11 patients with carcinoma of pancreas (all of which had mutations in paraffin-embedded tumor sections), in none of 3 chronic pancreatitis specimens (all negative on paraffin sections) and in 2 of 3 cholangiocarcinomas (one positive and one negative on paraffin sections, the one negative stool sample was positive for K-ras mutation on paraffin section). When mutations were detected in stool specimens, 5 of 6 cases had the same amino acid substitution as seen in the paraffin-embedded sections. Negative controls using *E. coli* DNA were performed, and no mutation was detected. The frequency of K-ras mutations approximates only 40-50% in pancreatic cancer, it was presumed that these mutations were derived from exfoliated cells from pancreatic cancer. The sensitivity and specificity of K-ras mutation as a screening tool were not high, and therefore its clinical application is limited at present.

The significance of codon 12 K-ras mutation in CP is still debated. Queneau *et al*^[34] examined the pure pancreatic juice from the diagnosed 36 patients with chronic pancreatitis based on the criteria of Cambridge and Marseilles classifications. Ten patients were positive for K-ras point mutation at codon 12, pancreatic cancer was discovered at an invasive stage in two patients, respectively in 7 and 17 months after disclosure of a K-ras mutation. Unfortunately the disclosure of pancreatic cancer after follow-up of patients with chronic pancreatitis positive for a K-ras mutation was not associated with an early stage at diagnosis and an improved prognosis. Lohr *et al*^[35] reported that K-ras gene mutation was found in 6 of 66 patients with chronic pancreatitis, pancreatic neoplasm occurred in none of the mutation in patients over a mean follow-up period of 26 (4-54) months, no pancreatic cancer developed during follow-up. Analysis of K-ras gene mutation seemed to have little use for detection pancreatic neoplasm in patients with chronic pancreatitis^[36,37].

Conflicting reports have raised the question whether K-ras gene mutations in chronic pancreatitis are related to the development of pancreatic neoplasm. According to epidemiological data: about 4%^[30] patients with chronic pancreatitis will develop pancreatic cancer during the course

of the disease. Interestingly, the risk of cancer seemed predominant in the first few years of chronic pancreatitis^[31]. No clinical, morphological, or histocytological information could help differentiate patients with cancer from the others during the follow-up of chronic pancreatitis. Moreover, K-ras mutations were found in 63-71% of the microdissected specimens of benign mucous cell hyperplasia of the pancreatic ductal epithelium with chronic inflammation^[26], only about 1% of patients harboring such precursor lesions were believed to develop pancreatic adenocarcinoma. Disclosure of a K-ras point mutation in chronic pancreatitis seemed not sufficiently predictive of malignant transformation, and even in some cases of chronic pancreatitis early occurrence of p53 gene but not K-ras mutations has been reported^[38]. Therefore, detection of K-ras mutation cannot be recommended at this time for screening pancreatic cancer.

Utility of K-ras mutation in differentiating pancreatic cancer from chronic pancreatitis

Fine needle aspiration (FNA) of pancreatic cancer and K-ras gene The knowledge that pancreatic cancer frequently harbor K-ras mutations has been applied to the histopathologic diagnosis of pancreatic mass. Because cytologic diagnosis from FNA depends upon accurate sampling, a negative test does not rule out carcinomas. However, in equivocal cases, detection of K-ras mutation might help to conform the diagnosis of pancreatic cancer. Urgell^[19] prospectively examined a total of 84 consecutive having a pancreatic mass who were clinically suspected of pancreatic cancer for the confirmation and follow-up of their chronic pancreatitis. Fine needle aspiration specimens were taken for both cytology and the presence of K-ras mutations. By cytology and/ or the patient's clinical course (death within a year), the authors concluded that the final diagnoses were 60 pancreatic cancers, 2 mucinous cystic tumours, 4 endocrine tumours and 6 other malignancies, 10 chronic pancreatitis, 1 acute pancreatitis and 1 tuberculosis. Cytology offered a conclusive diagnosis in 63 of 84 (75%) cases, inconclusive report in 21 cases (25%) (9 cases with suspicious cells and 12 cases with insufficient material). The presence of malignant cells in the FNA samples from patients with pancreatic cancer was 65%. No false-positives were detected in the remaining 24 conclusive FNAs. K-ras mutations were detected in 46 of 60 FNA samples (77%) from cancers and no mutations were detected in the remaining 24 FNA samples. The combined molecular and cytological approach offered an 88% sensitivity with a 100% specificity. A similar study was performed by Urban and colleagues^[17], who examined 20 consecutive patients undergoing FNA for pancreatic lesions. Sixteen samples were successfully amplified by PCR, 10 (of 11) pancreatic cancers and 1 (of 1) cystadenocarcinoma had K-ras mutations, while no mutations were found in 3 patients with chronic pancreatitis and 1 patient with an islet cell tumor. Two patients having a benign cytologic diagnosis had K-ras mutations and were ultimately proven to have pancreatic cancers. Pathologic diagnosis alone was established in 13 of 16 cases, but when pathology and K-ras mutations were combined, all the 16 patients were correctly diagnosed. When adequate samples were obtained, the sensitivity rate was 92% and specificity was 100% in this study. K-ras mutation in combination with cytologic analysis might be a helpful tool for the diagnosis of pancreatic carcinomas.

K-ras point mutation at codon 12 in pancreatic juice Differentiating pancreatic adenocarcinoma from chronic pancreatitis can be quite difficult particularly when both diseases coexist. Cytological distinction between chronic pancreatitis and pancreatic cancer is occasionally difficult because chronic pancreatitis can induce morphological changes

similar to those seen in well differentiated adenocarcinomas. In addition, pancreatic juice can induce the cell injury and degradation due to disadvantages of digestive utility induced by various proteases. The main advantages of the gene technique are its objectivity and the lack of dependence on cell integrity and number. Van Laethem *et al*^[39] analysed prospectively the presence of these mutations in brushing samples collected during ERCP in 45 patients (26 males, 19 females) showing a dominant stricture of the main pancreatic duct at pancreatography. Twenty-four were pancreatic adenocarcinoma, sixteen were chronic pancreatitis, and five intraductal mucin hypersecreting neoplasms. Twenty of 45 patients presented equivocal ERCP findings that did not permit a definite diagnosis. K-ras mutations at codon 12 were detected. Results were compared with those provided by routine brush cytology. A definitive diagnosis was established for each patient. Mutations were detected in 20 of 24 patients with pancreatic adenocarcinoma, but in none of the chronic pancreatitis patients and intraductal mucin hypersecreting neoplasms, irrespective of their locations. By contrast, only 13 (Carcinoma of the pancreas head) of 24 pancreatic adenocarcinoma were detected by cytological examination, which yielded four false negative and seven (Carcinoma of the body or tail of pancreas) non-contributive results. Sensitivity (due to the neoplastic site lying in the body or tail of pancreas), specificity, and accuracy of molecular biological and cytological methods were 83-76%, 100-83%, and 90-58%, respectively. Notably the mutations could be detected in six patients with small tumours. Watanabe^[40] found K-ras mutations from the pancreatic juice in 11 of 20 (55%) pancreatic cancer patients, and in none of 18 patients with chronic pancreatitis. Fifty percent of tumours of the pancreatic head (4 of 8), 67% of the body (6 of 9), and 33% of the tail (1 of 3) had K-ras mutation. When tumours were examined by size, 50% of T1 (1 of 2), 43% of T2 (3 of 7), 50% of T3 (3 of 6), and 80% of T4 (4 of 5) had K-ras mutations. Tada^[41] found K-ras mutations in the pancreatic juice from 6 of 6 patients with pancreatic cancer, and 1 with intraductal papillary neoplasm. In contrast, 3 patients with chronic pancreatitis were negative for mutations, and this method was sensitive enough to detect 3-30 mutant copies of K-ras in the presence of 3000 000 normal copies of the gene (which would be the equivalent to 0.01 ng of mutant DNA in 1 mg of total DNA).

On the contrary, Pugliese *et al*^[42] believed that cytology rather than mutation was useful in the diagnosis of pancreatic cancer. In their one report cytological examination, and detection of K-ras point mutation were performed, sensitivity of cytology was 74%, that of mutations in 87% in cancer and 40% in chronic pancreatitis. The specificity for cytology and mutation was 100% and 60% respectively. Combining cytology with mutation analysis increased the sensitivity to 93% but reduced the positive predictive value. Matsubayashi *et al*^[43] reported the occurrence of K-ras point mutations at codon 12 and compared it with cytology in pancreatic juice. K-ras point mutations at codon 12 were detected in seven of 14 (50%) pancreatic cancers, in four of 10 (40%) mucin-producing tumours, in four of 13 (31%) chronic pancreatitis, and in two of (10%) pancreas without definite disorders. K-ras point mutations were detected in nine of 18 (50%) pancreatic juice samples containing cancer cells, in eight of 18 (44%) pancreatic juice samples containing atypical cells, but in none of such samples containing only normal cells. It was concluded that K-ras mutations were not detected in pancreatic cancer exclusively, they could be detected in pancreatic cancer, and also other diseases.

Combining K-ras point mutation at codon 12 with cytology could increase its sensitivity and specificity. In Tada's series^[44], cytology and semiquantitatively mutant analysis were

performed using EUS-FNA specimens as well as in pancreatic juice in 34 patients with pancreatic masses (26 cancers and 8 chronic pancreatitis). Quantitative analysis of mutant ras gene supplemented with cytology was more effective in differential diagnosis of pancreatic cancer.

Evidence to date suggests that the progression to pancreatic adenocarcinoma is multifactorial, and perhaps undefined, genetic mutations play major roles. Molecular profiling indicated a large number of genes were differentially expressed in pancreatic cancer and normal pancreas, but the differences were not significant between pancreatic cancer and chronic pancreatitis^[45]. Combining other marker seemed to contribute to increase the sensitivity and specificity of detection of K-ras gene point mutation at codon 12 for differentiation of the pancreatic cancer from chronic pancreatitis. Myung *et al*^[46] examined the telomerase activity and K-ras gene mutations in pancreatic juice from 31 patients. Of them 12 had pancreatic cancer, 11 had chronic pancreatitis, and 8 were control patients. K-ras gene mutation was positive in 75% (9 of 12) of pancreatic cancers and in 27% (3 of 11) of cases of chronic pancreatitis but in none of the control patients. Telomerase activity was detected in 92% (11 of 12) of pancreatic cancers and in 18% (2 of 11) of cases of chronic pancreatitis. By combining these two methods, the specificity rose to 100%. Alterations of other genes such as p16, have been described in pancreatic cancer, but they have also been found in chronic pancreatitis^[47]. Positive for the two mutations could therefore be particularly predictive of malignant conditions and helpful to differentiating pancreatic cancer from chronic pancreatitis. An identical approach has been evaluated with K-ras gene and p53 or p16 alterations, and has given promising results^[47, 48].

CONCLUSIONS

Usefulness and status of K-ras gene point mutation at codon 12 are contradictory, the mutation indicates a preneoplastic condition, or cancer at an early stage, and therefore disclosure of K-ras gene point mutation in chronic pancreatitis seems not sufficiently predictive of malignant transformation, and its detection in combination with clinical and morphological follow-up should not be recommended at this time for screening pancreatic cancer, but can be used as an adjunct to cytology for the differentiation of pancreatic cancer from chronic pancreatitis. The finding of K-ras point mutations at codon 12 in cytology or biopsy samples from pancreatic mass can not specifically confirm the diagnosis of pancreatic cancer. Only raises the possibility for early surgical intervention if these patients are at high risk of developing pancreatic cancer in the future. Further studies are needed to define the value of K-ras mutation screening in patients with other evidences suggesting the presence of pancreatic cancer. Chronic pancreatitis may be positive for the mutation in the absence of cancer, and pancreatic cancer does not necessarily have the mutation. The ultimate goal is to detect pancreatic cancer at an early stage and avoid unnecessary pancreaticoduodenectomies for chronic pancreatitis.

REFERENCES

- 1 **Yeaton P**, Sears RJ, Ledent T, Salmon I, Kiss R, Decaestecker C. Discrimination between chronic pancreatitis and pancreatic adenocarcinoma using artificial intelligence-related algorithms based on image cytometry-generated variables. *Cytometry* 1998; **32**: 309-316
- 2 **Lee JG**, Leung J. Tissue sampling at ERCP in suspected pancreatic cancer. *Gastrointest Endosc Clin N Am* 1998; **8**: 221-235
- 3 **Gress F**, Gottlieb K, Sherman S, Lehman G. Endoscopic ultrasonography-guided fine-needle aspiration biopsy of suspected pancreatic cancer. *Ann Intern Med* 2001; **134**: 459-464

- 4 **Afify AM**, al-Khafaji BM, Kim B, Scheiman JM. Endoscopic ultrasound-guided fine needle aspiration of the pancreas. Diagnostic utility and accuracy. *Acta Cytol* 2003; **47**: 341-348
- 5 **Motojima K**, Kohara N, Furui J, Terada M, Tsunoda T, Nagata Y, Urano K. Detection of point mutation of Kirsten ras oncogene in pancreatic carcinoma by polymerase chain reaction. *Nippon Geka Gakkai Zasshi* 1991; **92**: 453-458
- 6 **Tada M**, Omata M, Ohto M. Clinical application of ras gene mutation for diagnosis of pancreatic adenocarcinoma. *Gastroenterology* 1991; **100**: 233-238
- 7 **Lemoine NR**, Jain S, Hughes CM, Staddon SL, Maillet B, Hall PA, Kloppel G. Ki-ras oncogene activation in preinvasive pancreatic cancer. *Gastroenterology* 1992; **102**: 230-236
- 8 **Orth M**, Gansauge F, Gansauge S, Beger HG, Adler G, Schmid RM. K-ras mutations at codon 12 are rare events in chronic pancreatitis. *Digestion* 1998; **59**: 120-124
- 9 **Yamada T**, Nakamori S, Ohzato H, Oshima S, Aoki T, Higaki N, Sugimoto K, Akagi K, Fujiwara Y, Nishisho I, Sakon M, Gotoh M, Monden M. Detection of K-ras gene mutations in plasma DNA of patients with pancreatic adenocarcinoma: correlation with clinicopathological features. *Clin Cancer Res* 1998; **4**: 1527-1532
- 10 **Castells A**, Puig P, Mora J, Boadas J, Boix L, Urgell E, Sole M, Capella G, Lluís F, Fernandez-Cruz L, Navarro S, Farre A. K-ras mutations in DNA extracted from the plasma of patients with pancreatic carcinoma: diagnostic utility and prognostic significance. *J Clin Oncol* 1999; **17**: 578-584
- 11 **Mulcahy H**, Farthing MJ. Diagnosis of pancreatico-biliary malignancy: detection of gene mutations in plasma and stool. *Ann Oncol* 1999; **10**(Suppl 4): 114-117
- 12 **Theodor L**, Melzer E, Sologov M, Idelman G, Friedman E, Bar-Meir S. Detection of pancreatic carcinoma: diagnostic value of K-ras mutations in circulating DNA from serum. *Dig Dis Sci* 1999; **44**: 2014-2019
- 13 **Sawabu N**, Watanabe H, Yamaguchi Y, Okai T. Mutations of the K-ras oncogene in pancreatic carcinoma, and application of its detection in pancreatic juice to diagnose pancreatic carcinoma. *Nippon Rinsho* 1995; **53**: 511-517
- 14 **Watanabe H**, Sawabu N, Songur Y, Yamaguchi Y, Yamakawa O, Satimura Y, Ohta H, Motoo Y, Okai T, Wakabayashi T. Detection of K-ras point mutations at codon 12 in pure pancreatic juice for the diagnosis of pancreatic cancer by PCR-RFLP analysis. *Pancreas* 1996; **12**: 18-24
- 15 **Watanabe H**, Yamaguchi Y, Ha A, Hu YX, Motoo Y, Okai T, Yoshimura T, Sawabu N. Quantitative determination of K-ras mutations in pancreatic juice for diagnosis of pancreatic cancer using hybridization protection assay. *Pancreas* 1998; **17**: 341-347
- 16 **Kimura W**, Zhao B, Futakawa N, Muto T, Makuuchi M. Significance of K-ras codon 12 point mutation in pancreatic juice in the diagnosis of carcinoma of the pancreas. *Hepatogastroenterology* 1999; **46**: 532-539
- 17 **Urban T**, Ricci S, Grange JD, Lacave R, Boudghene F, Breittmayer F, Languille O, Roland J, Bernaudin JF. Detection of c-Ki-ras mutation by PCR/RFLP analysis and diagnosis of pancreatic adenocarcinomas. *J Natl Cancer Inst* 1993; **85**: 2008-2012
- 18 **Pabst B**, Arps S, Binmoeller K, Thul R, Walsemann G, Fenner C, Klapdor R. Analysis of K-ras mutations in pancreatic tissue after fine needle aspirates. *Anticancer Res* 1999; **19**: 2481-2483
- 19 **Urgell E**, Puig P, Boadas J, Capella G, Queralto JM, Boluda R, Antonijuan A, Farre A, Lluís F, Gonzalez-Sastre F, Mora J. Prospective evaluation of the contribution of K-ras mutational analysis and CA19.9 measurement to cytological diagnosis in patients with clinical suspicion of pancreatic cancer. *Eur J Cancer* 2000; **36**: 2069-2075
- 20 **Caldas C**, Hahn SA, Hruban RH, Redston MS, Yeo CJ, Kern SE. Detection of K-ras mutations in the stool of patients with pancreatic adenocarcinoma and pancreatic ductal hyperplasia. *Cancer Res* 1994; **54**: 3568-3573
- 21 **Berndt C**, Haubold K, Wenger F, Brux B, Muller J, Bendzko P, Hillebrand T, Kottgen E, Zanow J. K-ras mutations in stools and tissue samples from patients with malignant and nonmalignant pancreatic disease. *Clin Chem* 1998; **44**: 2103-2107
- 22 **Wenger FA**, Zieren J, Peter FJ, Jacobi CA, Muller JM. K-ras mutations in tissue and stool samples from patients with pancreatic cancer and chronic pancreatitis. *Langenbecks Arch Surg* 1999; **384**: 181-186
- 23 **Barbacid M**. Ras genes. *Annu Rev Biochem* 1987; **56**: 779-827
- 24 **Bos JL**, Fearon ER, Hamilton SR, Verlaan-de Vries M, van Boom JH, van der Eb AJ, Vogelstein B. Prevalence of ras gene mutations in human colorectal cancers. *Nature* 1987; **327**: 293-297
- 25 **Cerny WL**, Mangold KA, Scarpelli DG. K-ras mutation is an early event in pancreatic duct carcinogenesis in the Syrian golden hamster. *Cancer Res* 1992; **52**: 4507-4513
- 26 **Luttges J**, Schlehe B, Menke MA, Vogel I, Henne-Bruns D, Kloppel G. The K-ras mutation pattern in pancreatic ductal adenocarcinoma is usually identical to that in associated normal, hyperplastic, and metaplastic ductal epithelium. *Cancer* 1999; **85**: 1703-1710
- 27 **Matsubayashi H**, Watanabe H, Yamaguchi T, Ajioka Y, Nishikura K, Iwafuchi M, Yamano M, Kijima H, Saito T. Multiple K-ras mutations in hyperplasia and carcinoma in cases of human pancreatic carcinoma. *Jpn J Cancer Res* 1999; **90**: 841-848
- 28 **Tabate T**, Fujimori T, Maeda S, Yamamoto M, Saitoh Y. The role of Ras mutation in pancreatic cancer, precancerous lesions, and chronic pancreatitis. *Int J Pancreatol* 1993; **14**: 237-244
- 29 **Tada M**, Ohashi M, Shiratori Y, Okudaira T, Komatsu Y, Kawabe T, Yoshida H, Machinami R, Kishi K, Omata M. Analysis of K-ras gene mutation in hyperplastic duct cells of the pancreas without pancreatic disease. *Gastroenterology* 1996; **110**: 227-231
- 30 **Lowenfels AB**, Maisonneuve P, Cavallini G, Ammann RW, Lankisch PG, Andersen JR, Dimagno EP, Andren-Sandberg A, Domellof L. Pancreatitis and the risk of pancreatic cancer. International Pancreatitis Study Group. *N Engl J Med* 1993; **328**: 1433-1437
- 31 **Karlson BM**, Ekblom A, Josefsson S, McLaughlin JK, Fraumeni JF Jr, Nyren O. The risk of pancreatic cancer following pancreatitis: an association duo to confounding? *Gastroenterology* 1997; **113**: 587-592
- 32 **Berthelemy P**, Bouisson M, Escourrou J, Vaysse N, Rumeau JL, Pradayrol L. Identification of K-ras mutations in pancreatic juice in the early diagnosis of pancreatic cancer. *Ann Intern Med* 1996; **124**: 1014-1015
- 33 **Boadas J**, Mora J, Urgell E, Puig P, Roca M, Cusso X, Capella G, Lluís F, Farre A. Clinical usefulness of K-ras gene mutation detection and cytology in pancreatic juice in the diagnosis and screening of pancreatic cancer. *Eur J Gastroenterol Hepatol* 2001; **13**: 1141-1142
- 34 **Queneau PE**, Adessi GL, Thibault P, Cleau D, Heyd B, Mantion G, Carayon P. Early detection of pancreatic cancer in patients with chronic pancreatitis: diagnostic utility of a K-ras point mutation in the pancreatic juice. *Am J Gastroenterol* 2001; **96**: 700-704
- 35 **Lohr M**, Muller P, Mora J, Brinkmann B, Ostwald C, Farre A, Lluís F, Adam U, Stubbe J, Plath F, Nizze H, Hopt UT, Barten M, Capella G, Liebe S. P53 and K-ras mutations in pancreatic juice samples from patients with chronic pancreatitis. *Gastrointest Endosc* 2001; **53**: 734-743
- 36 **Furuya N**, Kawa S, Akamatsu T, Furihata K. Long-term follow-up of patients with chronic pancreatitis and K-ras gene mutation detected in pancreatic juice. *Gastroenterology* 1997; **113**: 593-598
- 37 **Nakaizumi A**, Uehera H, Takenaka A, Uedo N, Sakai N, Yano H, Ohigashi H, Ishikawa O, Ishiguro S, Sugano K, Tatsuta M. Diagnosis of pancreatic cancer by cytology and measurement of oncogene and tumor markers in pure pancreatic juice aspirated by endoscopy. *Hepatogastroenterology* 1999; **46**: 31-37
- 38 **Gansauge S**, Schmid RM, Muller J, Alder G, Mattfeldt T, Berger HG. Genetic alterations in chronic pancreatitis: evidence for early occurrence of p53 but not K-ras mutations. *Br J Surg* 1998; **85**: 1015
- 39 **Van Laethem JL**, Vertongen P, Deviere J, Van Rampelbergh J, Rickaert F, Cremer M, Robberecht P. Detection of c-Ki-ras gene codon 12 mutations from pancreatic duct brushings in the diagnosis of pancreatic tumours. *Gut* 1995; **36**: 781-787
- 40 **Watanabe H**, Sawabu N, Ohta H, Satomura Y, Yamakawa O, Motoo Y, Okai T, Takahashi H, Wakabayashi T. Identification

- of K-ras oncogene mutations in the pure pancreatic juice of patients with ductal pancreatic cancers. *Jpn J Cancer Res* 1993; **84**: 961-965
- 41 **Tada M**, Omata M, Kawai S, Saisho H, Ohto M, Saiki RK, Sninsky JJ. Detection of ras gene mutations in pancreatic juice and peripheral blood of patients with pancreatic adenocarcinoma. *Cancer Res* 1993; **53**: 2472-2474
- 42 **Pugliese V**, Pujic N, Saccomanno S, Gatteschi B, Pera C, Aste H, Ferrara GB, Nicolo G. Pancreatic intraductal sampling during ERCP in patients with chronic pancreatitis and pancreatic cancer: cytologic studies and K-ras-2 codon 12 molecular analysis in 47 cases. *Gastrointest Endosc* 2001; **54**: 595-599
- 43 **Matsubayashi H**, Watanabe H, Ajioka Y, Nishikura K, Yamano M, Seki T, Saito T, Matsubayashi T. Different amounts of K-ras mutant epithelial cells in pancreatic carcinoma and mass-forming pancreatitis. *Pancreas* 2000; **21**: 77-85
- 44 **Tada M**, Komatsu Y, Kawabe T, Sasahira N, Isayama H, Toda N, Shiratori Y, Omata M. Quantitative analysis of K-ras gene mutation in pancreatic tissue obtained by endoscopic ultrasonography-guided fine needle aspiration: clinical utility for diagnosis of pancreatic tumor. *Am J Gastroenterol* 2002; **97**: 2263-2270
- 45 **Logsdon CD**, Simeone DM, Binkley C, Arumugam T, Greenson JK, Giordano TJ, Misek DE, Hanash S. Molecular profiling of pancreatic adenocarcinoma and chronic pancreatitis identifies multiple genes differentially regulated in pancreatic cancer. *Cancer Res* 2003; **63**: 2649-2657
- 46 **Myung SJ**, Kim MH, KimYS, Kim HJ, Park ET, Yoo KS, Lim BC, Wan SED, Lee SK, Min YT, Kim JY. Telomerase activity in pure pancreatic juice for the diagnosis of pancreatic cancer may be complementary to K-ras mutation. *Gastrointest Endosc* 2000; **51**: 708-713
- 47 **Gerdes B**, Ramaswamy A, Kersting M, Ernst M, Lang S, Schuermann M, Wild A, Bartsch DK. P16(INK4a) alterations in chronic pancreatic-indicator for high-risk lesions for pancreatic cancer. *Surgery* 2001; **129**: 490-497
- 48 **Lu X**, Xu T, Qian J. An application value of detecting K-ras and p53 gene mutation in the stool and pure pancreatic juice for diagnosis of early pancreatic cancer. *Zhonghua Yixue Zazhi* 2001; **81**: 1050-1053

Edited by Zhu LH and Wang XL

Expression of Egr-1, c-fos and cyclin D1 in esophageal cancer and its precursors: An immunohistochemical and *in situ* hybridization study

Ming-Yao Wu, Chu-Xiang Zhuang, Huan-Xing Yang, Ying-Rui Liang

Ming-Yao Wu, Huan-Xing Yang, Department of Pathology, Shantou University Medical College, Shantou 515031, Guangdong Province, China

Chu-Xiang Zhuang, Department of Physiology, Shantou University Medical College, Shantou 515031, Guangdong Province, China

Ying-Rui Liang, Department of Pathology, The First People's Hospital of Foshan, Foshan 528000, Guangdong Province, China

Supported by the National Natural Science Foundation of China, No. 39670298

Correspondence to: Ming-Yao Wu, Department of Pathology, Shantou University Medical College, 22 Xinling Road, Shantou 515031, Guangdong Province, China. mywu@stu.edu.cn

Telephone: +86-754-8900486 **Fax:** +86-754-8557562

Received: 2003-06-05 **Accepted:** 2003-09-24

Abstract

AIM: To examine the expression of Egr-1, c-fos and cyclin D1 at both transcript and protein levels in esophageal carcinoma and to correlate the level of their expressions with precancerous and paracancerous esophageal lesions and esophageal carcinoma.

METHODS: *In situ* hybridization and immunohistochemistry were used respectively to detect the expression of mRNA and proteins of Egr-1, c-fos and cyclin D1 in 70 cases of esophageal squamous cell carcinoma and their corresponding para-cancerous mucosa and upper cut edge mucosa.

RESULTS: *In situ* hybridization and immunohistochemistry showed positive staining of all three mRNAs in the cytoplasm and those of the proteins in nuclei. Overexpression of Egr-1, c-fos and cyclin D1 mRNAs and their proteins was found in dysplasia and squamous carcinomas. The expression level of Egr-1 and c-fos was high, and cyclin D1 was low in dysplasia mucosa, whereas the expression of Egr-1 was decreased, c-fos was maintained and cyclin D1 was increased in the cancers. The expression of both c-fos and cyclin D1 was consistent between the mRNA and protein in their corresponding high expression lesions.

CONCLUSION: The expression of Egr-1, c-fos and cyclin D1 varies in esophageal precancerous lesions and cancer tissues, suggesting an involvement of these genes in the development of esophageal carcinoma.

Wu MY, Zhuang CX, Yang HX, Liang YR. Expression of Egr-1, c-fos and cyclin D1 in esophageal cancer and its precursors: An immunohistochemical and *in situ* hybridization study. *World J Gastroenterol* 2004; 10(4): 476-480

<http://www.wjgnet.com/1007-9327/10/476.asp>

INTRODUCTION

Esophageal carcinoma is one of the most common malignant

tumors in China^[1,2]. Its pathogenesis and development are closely related to the expression of some proto-oncogenes and their products^[3,4]. Our previous studies have shown that Egr-1 inhibited the growth of esophageal carcinoma cell line Eca109 after exogenous introduction of Egr-1 gene^[5,6], but there has been no report on the expression of Egr-1, c-fos, and cyclin D1 mRNAs and their proteins so far. In this study, we examined the expression of Egr-1, c-fos and cyclin D1 mRNAs by *In situ* hybridization and their proteins by immunohistochemistry in 70 specimens from esophageal carcinoma, upper cut edge mucosa and para-cancerous tissues. The purpose was to understand the expression of Egr-1, c-fos and cyclin D1 in esophageal carcinoma and their association with the development of tumor.

MATERIALS AND METHODS

Sample collecting and processing

Fresh surgical resection specimens of esophagus including tumor mass, the upper cut edge mucosa and adjacent mucosa of the tumor mass were taken from 70 patients with esophageal carcinomas who had not received chemotherapy or radiotherapy before the operation. All specimens were collected from Department of Pathology, Shantou University Medical College, between January and December of 2001. The specimens were fixed in 10% neutrally buffered formalin containing 1/1000 of diethyl pyrocarbonate (DEPC, Sigma Chemical Co., USA), paraffin embedded, sectioned to 4 μ m thickness, and HE stained.

Histopathology analysis

The diagnosis of esophageal epithelial para-cancer was made by histopathology according to the criteria of Liu *et al.*, which identified 42 cases of normal epithelium, 54 cases of simple hyperplasia and 44 cases of dysplasia. Seventy cases of esophageal carcinoma were diagnosed using WHO histological tumor classification. These included 2 cases of carcinoma *in situ*, 23 cases of grade I, 33 cases of grade II and 12 cases of grade III squamous cell carcinoma. There were 23 cases with invasion of the tumor into the superficial muscular layer, and others into the serosa. In addition, 26 of 70 cases showed lymphatic metastasis.

In situ hybridization

Eukaryotic expression vector of PCMV-Egr-1 plasmid was donated by Dr. Huang RP (Molecular Medicine, Northwest Hospital, WA, USA). The final construct contains the neogene (5.5 kb fragment) driven by the respiratory syncytial virus (RSV) promoter and the Egr-1 gene (2.1kb fragment) driven by the human cytomegalovirus (CMV) promoter. The plasmid was confirmed by gene amplification, purification and double endonuclease cutting, then the products were determined by agarose gel electrophoresis, the 327 bp DNA fragments was recovered by promega DNA purification kit and was labeled with digoxigenin using random priming method (Boehringer Mannheim Biochemica, Germany). The expression of Egr-1

was detected by enhanced sensitive *in situ* hybridization detection kit I (POD) from a commercial Kit (Boster Company, China) according to the manufacturer's instructions. Sections were dewaxed in xylene, hydrated in graduated ethanol, and then incubated in 3% hydrogen peroxide in methanol for 30 min. The tissue was then digested in 20 µg/ml proteinase K at 37°C for 20 min, fixed in 40 g/L PFA for 10 min, and cooled in 90% ethanol at -20°C for 5 min. The digoxigenin-labeled cDNA probe was denatured in hybridization buffer (1:40) at 95-100°C for 10 min and cooled at -20°C for 3 min. The tissues were then overlaid with the probe, covered with a coverslip and incubated at 42°C overnight. The expressions of c-fos mRNA and cyclin D1 mRNA were also detected by *in situ* hybridization with digoxigenin-labeled gene probes, which were supplied in commercial kits (Boster Company, China), according to the manufacturer's instructions. Following hybridizations, the sections were washed with SSC and incubated with mouse anti-digoxigenin antibody, biotinylated goat anti-mouse and then streptavidin-biotin complex (SABC) for 30 min respectively. The staining was visualized with 3.3'-diaminobenzidine (DAB). The human breast tissue and the known positive esophageal carcinoma tissue were used as positive controls. The hybridization buffer without the probe and sections pre-digested by RNase (10 µg/ml) before Egr-1, c-fos and cyclin D1 detection were used as negative controls.

Immunohistochemistry

The expression of Egr-1, c-fos and cyclin D1 proteins was analyzed using Egr-1 (SC-110) and c-fos (SC-52) rabbit polyclonal antiserum (1:200) and cyclin D1 (A-12) monoclonal antibody (1:100) (Santa Cruz Biot Co, USA) and the SABC and DAB visualization methods according to the manufacturer's instructions (Boster Company, China). The human breast tissue and the known positive esophageal carcinoma tissue were used as positive controls. Negative controls were designed by using PBS instead of Egr-1, c-fos antiserum or cyclin D1 monoclonal antibody.

Assessment of the staining

In situ hybridization showed brown signals of Egr-1, c-fos and cyclin D1 mRNAs in the cytoplasm. The positive

immunostaining of Egr-1, c-fos and cyclin D1 proteins was shown as brown signals in the nuclei. The percentage of positively stained cells was evaluated for each tissue section by counting approximately 1000 cells at a high power field. The cases having positive cancer cells accounting for more than 75% of all cancer cells on the slide were defined as a score of 3+ (strong), about 25-75% of all cancer cells were defined as a score of 2+ (moderate), and less than 25% were defined as a score of 1+ (weak). The score of - (negative) was given to cases having no positive cancer cells seen.

Statistical analysis

Statistical analyses were performed using χ^2 test and χ^2 rectified test. A P value less than 0.05 were considered to be statistically significant.

RESULTS

Expression of Egr-1, c-fos and cyclin D1 in esophageal precancerous lesions and cancer tissues

In normal epithelia of esophageal mucosa, the expression of Egr-1 mRNA and protein was found in the basal layer of mucosa (Figure 1). The level of expression increased gradually from simple hyperplasia epithelia to dysplasia, but decreased significantly in cancer tissues in which only a few cases of well-differentiated squamous cell carcinoma had Egr-1 expression (Figure 2). A very few cases of normal epithelia and simple hyperplasia epithelia showed c-fos mRNA and protein expression, and the highest expression level was seen in dysplasia of para-cancerous area and squamous cell carcinomas (Figure 3). The cyclin D1 mRNA and protein were found in a few simple hyperplasia epithelia and dysplasia epithelia, but showed the highest expression level in cancer tissues (Figure 4). The expression levels between mRNA and protein in both c-fos and cyclinD1 genes were consistent in their correspondent highest expression lesions. However, the expression levels of both Egr-1 and cyclin D1 were significantly different between cancer group and dysplasia epithelia group ($P<0.01$, $P<0.01$). The expressions of Egr-1, c-fos and cyclinD1 mRNAs and their proteins in esophageal precancerous lesions and cancer tissues are shown in Table 1.

Table 1 Expression of Egr-1, c-fos and cyclin D1 mRNAs and their proteins in esophageal precancerous lesions and cancer tissues

Groups	n	Egr-1 positivity		c-fos positivity		cyclin D1 positivity	
		ISH(%)	IHC(%)	ISH(%)	IHC(%)	ISH(%)	IHC(%)
Normal epithelia	42	13 (31.0)	3 (7.1)	2 (4.8)	1 (2.4)	2 (4.8)	0(0.0)
Simple hyperplasia	54	18 (33.3)	8 (14.8)	3 (5.6)	3 (5.6)	5 (9.3)	3 (5.6)
Dysplasia	44	27 (61.4)	21 (47.7)	30 (68.2)	29 (65.9)	6 (13.6)	6 (13.6)
Carcinoma <i>in situ</i>	2	1 (50.0)	1 (50.0)	1 (50.0)	1 (50.0)	0 (0.0)	0 (0.0)
Invasive carcinoma	68	12 (17.6)	9 (13.2) ^b	35 (51.5)	36 (52.9)	35 (51.5)	33 (48.5) ^d

^b $P<0.01$, $\chi^2=16.206$, compared with dysplasia group, ^d $P<0.01$, $\chi^2=16.367$, compared with dysplasia group.

Table 2 Association of expression of c-fos and cyclin D1mRNAs and their proteins with differentiation degree of cancer tissues

Groups	n	c-fos expression								cyclin D1 expression							
		ISH				IHC				ISH				IHC			
		-	+	++	+++	-	+	++	+++	-	+	++	+++	-	+	++	+++
Squamous carcinoma																	
Grade I	23	10	4	5	4	6	4	4	9	13	6	4	0	13	4	5	1
Grade II	33	14	7	8	4	16	3	5	9	17	7	6	3	19	6	5	3
Grade III	12	9	0	2	1	10	1	0	1	3	0	3	6	3	1	2	6 ^b

^b $P<0.01$, $\chi^2=11.256$, compared with squamous cell carcinoma grades I and II.

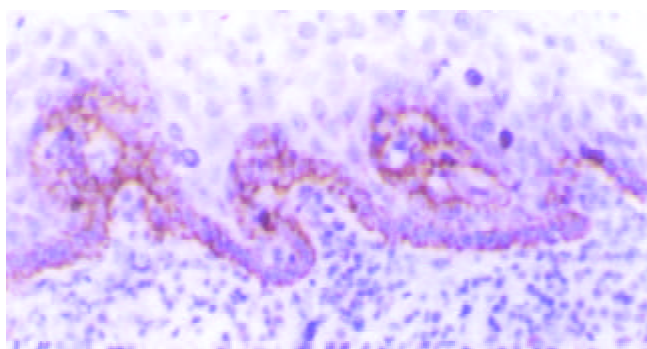


Figure 1 Egr-1 mRNA expression in basal mucosal layer in normal epithelia of esophagus. ISH $\times 200$.

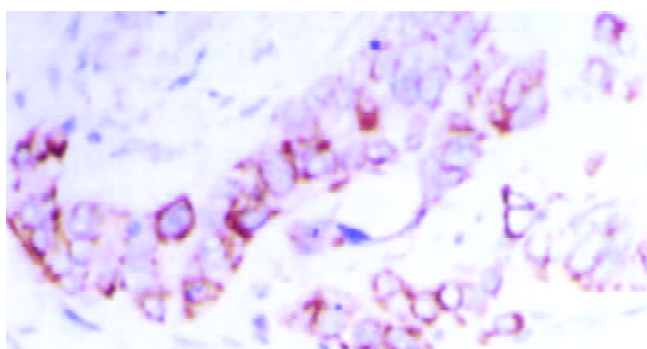


Figure 2 Positive expression of Egr-1 mRNA in cytoplasm of esophageal squamous cell carcinoma. ISH $\times 400$.

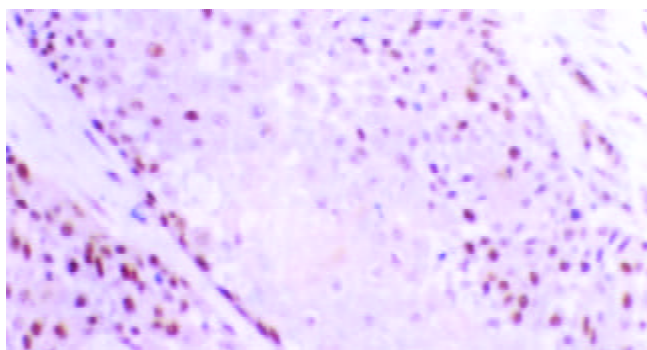


Figure 3 Positive expression c-fos proteins in nuclei of esophageal squamous cell carcinoma. IHC $\times 200$.

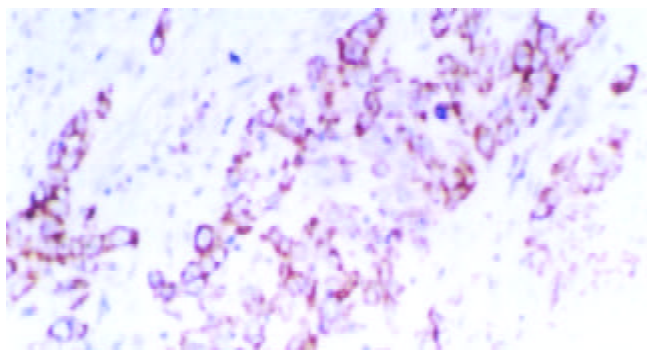


Figure 4 Positive expression of cyclin D1 mRNA in cytoplasm of esophageal squamous cell carcinoma. ISH $\times 200$.

Association of expression of c-fos and cyclin D1 with differentiation degree of cancer tissues

Of the three genes examined, the expression of Egr-1 mRNA and protein was low and the expression of c-fos and cyclin

D1 mRNAs and their proteins was high in esophageal cancer tissues. Furthermore, the expression of c-fos and cyclin D1 was different in different grades of esophageal carcinoma. The positive cases of c-fos appeared to be predominantly those with well or moderately differentiated squamous cell carcinoma, whereas the positive cases of cyclin D1 were mostly those with poorly differentiated squamous cell carcinoma. The cyclin D1 expression level in poorly differentiated squamous cell carcinoma group was significantly higher than that in well, or moderately differentiated squamous cell carcinoma group ($P < 0.01$). The expression status of c-fos and cyclin D1 mRNAs and their proteins in differently differentiated cancer tissues are shown in Table 2.

Association of expression of c-fos and cyclin D1 with lymphatic metastasis in esophageal carcinoma

Esophageal carcinomas were grouped according to different metastasis status and no association was found between the presence of lymphatic metastasis and the expression of c-fos and cyclin D1 mRNAs and their proteins in esophageal carcinomas ($P > 0.05$, $P > 0.05$, Table 3).

Table 3 Association of expression of c-fos and cyclin D1 with lymphic metastasis in esophageal carcinomas

Groups	n	c-fos positivity		cyclin D1 positivity	
		ISH	IHC	ISH	IHC
Lymphatic metastasis					
Negative	42	23	20	21	20
Positive	26	12	16 ^a	14	13 ^c

^a $P > 0.05$, $\chi^2 = 0.767$, compared with lymphatic metastasis negative group; ^c $P > 0.05$, $\chi^2 = 0.003$, compared with lymphatic metastasis negative group.

DISCUSSION

Regulations of cell growth are dependent on a number of gene families including proto-oncogene, growth factor, growth factor receptor and immediate early transcription factor gene. Egr-1, located on chromosome 5q31.1, is one of the immediate early gene families, and a nuclear protein that contains three zinc-finger domains and could regulate cell growth and differentiation by activating cyclin D1 to promote the progression of cells from G0/G1 phase into G2/M phase^[7-9]. It has been reported that Egr-1 was originally in dormancy but might be activated through membrane depolarization by induction of stress, ischemia, hypoxia, bacterial toxin, cell factors, ionizing radiation and some oncogenic factors^[10-12]. Using *in situ* hybridization and immunohistochemistry on a series of esophageal precancerous lesions and cancer tissues, Egr-1 mRNA and protein were detected in tissues of normal epithelia and simple hyperplastic epithelia of esophagus. However, the level of Egr-1 mRNA and protein expression was much higher (61.4% and 47.7%, respectively) in dysplasia but significantly decreased in cancerous tissues. It is possible that the precancerous mucosa might be subjected to a higher level of stimulation, which was consistent with the findings that Egr-1 expression could be activated by many factors^[13,14]. High expression of Egr-1 might preserve the stability of chromosome and suppress proliferation, and also improve differentiation and apoptosis of cells^[15,16].

C-fos proto-oncogene has been found belonging to a class of cellular genes known as one of the immediate early genes and its protein product is a transcription factor, which could be strongly induced by a number of mitogens^[17-19]. The present work found that the expression level of c-fos mRNA and

protein was very low in normal esophageal epithelia and simple hyperplasia epithelia, but was high in dysplasia mucous epithelia and cancer tissues of the esophagus. This finding was similar to those in some previous reports^[20-22]. The development of esophageal carcinoma has been identified as a successive course from simple hyperplasia of basal cells, dysplasia, and carcinoma *in situ* to invasive carcinomas. In the cases of c-fos expression, the abnormal expression might be an early molecular event of the pathogenesis and development of esophageal carcinoma. To a certain degree, the expression level could determine the progress or regression of the pathological changes.

Cyclins are a family of cell-cycle-associated nuclear proteins and cyclin D1 is a member of this family, which could contribute to cell cycle progression through G1 phase and has been found to be closely related to the regulation and control of cell cycle^[23]. The role of cyclin D1 in cell cycle control appeared to be mediated through the cyclin-dependent kinase (Cdk)/cyclin D1 complex. Some studies have indicated that cyclin D1 was involved in esophageal carcinoma and that its overexpression might be a useful prognostic factor^[24-28]. Others argued that the overexpression of cyclin D1 in esophageal cancer tissues might not predict the prognosis independently^[29-32]. In the current study, we found that cyclin D1 mRNA and protein expression was high in esophageal carcinoma compared with that in pre-cancerous tissue and the degree of positive expression was stronger in poorly differentiated squamous cell carcinomas. It seemed that the high level of expression of cyclin D1 indicated the poor prognosis. However, no correlation was found between cyclin D1 expression and lymphatic metastasis of squamous cell cancer. Our study suggested that overexpression of cyclin D1 could be used to help clinicians take more rational measures for post-operation patients who showed no metastasis to lymph nodes.

The pathogenesis of esophageal carcinoma is a course in which the oncogenes and tumor suppressor genes act or counter act to each other. This interaction could determine the development of esophageal carcinoma^[33-35]. The progress from normal esophageal mucous epithelia to simple hyperplasia, atypical hyperplasia and cancer is usually attributed to the decreased expression of tumor suppressor genes and increased expression of oncogenes. Our studies found that the expression of Egr-1 was decreased, c-fos was remained and cyclin D1 was increased during the progress of esophageal mucous epithelia from precancerous lesions to cancer. The activity of Egr-1 was reduced, but the activity of c-fos and cyclin D1 was enhanced. This resulted in abnormal regulation and control of cell cycle in the basal layer cells of esophageal mucous epithelia leading to the development of esophageal carcinoma. Nevertheless, the mechanism of the involvement of these genes in the development and progress of esophageal carcinoma remains to be further investigated.

REFERENCES

- 1 **Su M**, Lu SM, Tian DP, Zhao H, Li XY, Li DR, Zheng ZC. Relationship between ABO blood groups and carcinoma of esophagus and cardia in Chaoshan inhabitants of China. *World J Gastroenterol* 2001; **7**: 657-661
- 2 **He YT**, Hou J, Qiao CY, Chen ZF, Song GH, Li SS, Meng FS, Jin HX, Chen C. An analysis of esophageal cancer incidence in Cixian County from 1974 to 1996. *World J Gastroenterol* 2003; **9**: 209-213
- 3 **Su H, Hu N**, Shih J, Hu Y, Wang QH, Chuang EY, Roth MJ, Wang C, Goldstein AM, Ding T, Dawsey SM, Giffen C, Emmert-Buck MR, Taylor PR. Gene expression analysis of esophageal squamous cell carcinoma reveals consistent molecular profiles related to a family history of upper gastrointestinal cancer. *Cancer Res* 2003; **63**: 3872-3876
- 4 **Nie Y**, Liao J, Zhao X, Song Y, Yang GY, Wang LD, Yang CS. Detection of multiple gene hypermethylation in the development of esophageal squamous cell carcinoma. *Carcinogenesis* 2002; **23**: 1713-1720
- 5 **Wu MY**, Chen MH, Liang YR, Meng GZ, Yang HX, Zhuang CX. Experimental and clinicopathologic study on the relationship between transcription factor Egr-1 and esophageal carcinoma. *World J Gastroenterol* 2001; **7**: 490-495
- 6 **Hao MW**, Liang YR, Liu YF, Liu L, Wu MY, Yang HX. Transcription factor EGR-1 inhibits growth of hepatocellular carcinoma and esophageal carcinoma cell lines. *World J Gastroenterol* 2002; **8**: 203-207
- 7 **Nagamura-Inoue T**, Tamura T, Ozato K. Transcription factors that regulate growth and differentiation of myeloid cells. *Int Rev Immunol* 2001; **20**: 83-105
- 8 **Thiel G**, Cibelli G. Regulation of life and death by the zinc finger transcription factor Egr-1. *J Cell Physiol* 2002; **193**: 287-292
- 9 **Krishnaraju K**, Hoffman B, Liebermann DA. Early growth response gene 1 stimulates development of hematopoietic progenitor cells along the macrophage lineage at the expense of the granulocyte and erythroid lineages. *Blood* 2001; **97**: 1298-1305
- 10 **Kaufmann K**, Thiel G. Epidermal growth factor and platelet-derived growth factor induce expression of Egr-1, a zinc finger transcription factor, in human malignant glioma cells. *J Neuro Sci* 2001; **189**: 83-91
- 11 **Kaufmann K**, Bach K, Thiel G. The extracellular signal-regulated protein kinases Erk1/Erk2 stimulate expression and biological activity of the transcriptional regulator Egr-1. *Biol Chem* 2001; **382**: 1077-1081
- 12 **Nishi H**, Nishi KH, Johnson AC. Early Growth Response-1 gene mediates up-regulation of epidermal growth factor receptor expression during hypoxia. *Cancer Res* 2002; **62**: 827-834
- 13 **Meyer RG**, Kupper JH, Kandolf R, Rodemann HP. Early growth response-1 gene (Egr-1) promoter induction by ionizing radiation in U87 malignant glioma cells *in vitro*. *Eur J Biochem* 2002; **269**: 337-346
- 14 **Pawlinski R**, Pedersen B, Kehrl B, Aird WC, Frank RD, Guha M, Mackman N. Regulation of tissue factor and inflammatory mediators by Egr-1 in a mouse endotoxemia model. *Blood* 2003; **101**: 3940-3947
- 15 **Wu MY**, Liang YR, Wu XY, Zhuang CX. Relationship between Egr-1 gene expression and apoptosis in esophageal carcinoma and precancerous lesions. *World J Gastroenterol* 2002; **8**: 971-975
- 16 **Pignatelli M**, Luna-Medina R, Perez-Rendon A, Santos A, Perez-Castillo A. The transcription factor early growth response factor-1 (EGR-1) promotes apoptosis of neuroblastoma cells. *Biochem J* 2003; **373**(Pt 3): 739-746
- 17 **Berthoud HR**, Patterson LM, Zheng H. Vagal-enteric interface: vagal activation-induced expression of c-Fos and p-CREB in neurons of the upper gastrointestinal tract and pancreas. *Anat Rec* 2001; **262**: 29-40
- 18 **Nephew KP**, Choi CM, Polek TC, McBride R, Bigsby RM, Khan SA, Husseinzadeh N. Expression of fos and jun proto-oncogenes in benign versus malignant human uterine tissue. *Gynecol Oncol* 2000; **76**: 388-396
- 19 **Weisstein JS**, Majeska RJ, Klein MJ, Einhorn TA. Detection of c-fos expression in benign and malignant musculoskeletal lesions. *J Orthop Res* 2001; **19**: 339-345
- 20 **Pacheco MM**, Kowalski LP, Nishimoto IN, Brentani MM. Differential expression of c-jun and c-fos mRNAs in squamous cell carcinoma of the head and neck: associations with uPA, gelatinase B, and matrilysin mRNAs. *Head Neck* 2002; **24**: 24-32
- 21 **de Sousa SO**, Mesquita RA, Pinto DS Jr, Gutkind S. Immunolocalization of c-Fos and c-Jun in human oral mucosa and in oral squamous cell carcinoma. *J Oral Pathol Med* 2002; **31**: 78-81
- 22 **Feng DY**, Zheng H, Tan Y, Cheng RX. Effect of phosphorylation of MAPK and Stat3 and expression of c-fos and c-jun proteins on hepatocarcinogenesis and their clinical significance. *World J Gastroenterol* 2001; **7**: 33-36
- 23 **Shinohara M**, Aoki T, Sato S, Takagi Y, Osaka Y, Koyanagi Y, Hatooka S, Shinoda M. Cell cycle-regulated factors in esophageal cancer. *Dis Esophagus* 2002; **15**: 149-154
- 24 **Sarbia M**, Stahl M, Fink U, Heep H, Dutkowski P, Willers R,

- Seeber S, Gabbert HE. Prognostic significance of cyclin D1 in esophageal squamous cell carcinoma patients treated with surgery alone or combined therapy modalities. *Int J Cancer* 1999; **84**: 86-91
- 25 **Shamma A**, Doki Y, Shiozaki H, Tsujinaka T, Yamamoto M, Inoue M, Yano M, Monden M. Cyclin D1 overexpression in esophageal dysplasia: a possible biomarker for carcinogenesis of esophageal squamous cell carcinoma. *Int J Oncol* 2000; **16**: 261-266
- 26 **Toyoda H**, Nakamura T, Shinoda M, Suzuki T, Hatooka S, Kobayashi S, Ohashi K, Seto M, Shiku H, Nakamura S. Cyclin D1 expression is useful as a prognostic indicator for advanced esophageal carcinomas, but not for superficial tumors. *Dig Dis Sci* 2000; **45**: 864-869
- 27 **Natsugoe S**, Nakashima S, Matsumoto M, Sakita H, Sakamoto F, Okumura H, Baba M, Yoshinaka H, Takao S, Aikou T. Biologic and imaging diagnosis of lymph node metastasis in esophageal carcinoma. *J Surg Oncol* 2002; **81**: 25-32
- 28 **Shiozaki H**, Doki Y, Yamana H, Isono K. A multi-institutional study of immunohistochemical investigation for the roles of cyclin D1 and E-cadherin in superficial squamous cell carcinoma of the esophagus. *J Surg Oncol* 2002; **79**: 166-173
- 29 **Ikeda G**, Isaji S, Chandra B, Watanabe M, Kawarada Y. Prognostic significance of biologic factors in squamous cell carcinoma of the esophagus. *Cancer* 1999; **86**: 1396-1405
- 30 **Kuwahara M**, Hirai T, Yoshida K, Yamashita Y, Hihara J, Inoue H, Toge T. p53, p21(Waf1/Cip1) and cyclin D1 protein expression and prognosis in esophageal cancer. *Dis Esophagus* 1999; **12**: 116-119
- 31 **Shiozaki H**, Doki Y, Kawanishi K, Shamma A, Yano M, Inoue M, Monden M. Clinical application of malignancy potential grading as a prognostic factor of human esophageal cancers. *Surgery* 2000; **127**: 552-561
- 32 **Arber N**, Gammon MD, Hibshoosh H, Britton JA, Zhang Y, Schonberg JB, Rotterdam H, Fabian I, Holt PR, Weinstein IB. Overexpression of cyclin D1 occurs in both squamous carcinomas and adenocarcinomas of the esophagus and in adenocarcinomas of the stomach. *Hum Pathol* 1999; **30**: 1087-1092
- 33 **Mandard AM**, Hainaut P, Hollstein M. Genetic steps in the development of squamous cell carcinoma of the esophagus. *Mutat Res* 2000; **462**: 335-342
- 34 **Xu SH**, Qian LJ, Mou HZ, Zhu CH, Zhou XM, Liu XL, Chen Y, Bao WY. Difference of gene expression profiles between esophageal carcinoma and its pericancerous epithelium by gene chip. *World J Gastroenterol* 2003; **9**: 417-422
- 35 **Zhou J**, Zhao LQ, Xiong MM, Wang XQ, Yang GR, Qiu ZL, Wu M, Liu ZH. Gene expression profiles at different stages of human esophageal squamous cell carcinoma. *World J Gastroenterol* 2003; **9**: 9-15

Edited by Liu HX and Wang XL

Expression of pituitary tumor transforming gene in human gastric carcinoma

Chun-Yang Wen, Toshiyuki Nakayama, Ai-Ping Wang, Masahiro Nakashima, Yi-Tao Ding, Masahiro Ito, Hiromi Ishibashi, Mutsumi Matsuu, Kazuko Shichijo, Ichiro Sekine

Chun-Yang Wen, Toshiyuki Nakayama, Mutsumi Matsuu, Kazuko Shichijo, Ichiro Sekine, Department of Molecular Pathology, Atomic Bomb Disease Institute, Nagasaki University Graduate School of Biomedical Sciences, 1-12-4 Sakamoto, Nagasaki 852-8523, Japan

Chun-Yang Wen, Ai-Ping Wang, Department of Digestive Disease, Nanjing Drum Tower Hospital, Medical School of Nanjing University, Nanjing 210008, Jiangsu Province, China

Masahiro Nakashima, Tissue and Histopathology Section Division of Scientific Data Registry, Atomic Bomb Disease Institute, Nagasaki University Graduate School of Biomedical Sciences, 1-12-4 Sakamoto, Nagasaki 852-8523, Japan

Yi-Tao Ding, Department of Hepatobiliary Surgery, Nanjing Drum Tower Hospital, Medical School of Nanjing University, Nanjing 210008, Jiangsu Province, China

Masahiro Ito, Department of Pathology, National Nagasaki Medical Center, 2-1001-1 Kubara, Omura, Nagasaki 856-8562, Japan

Hiromi Ishibashi, Clinical Research Center, National Nagasaki Medical Center, 2-1001-1 Kubara, Omura, Nagasaki 856-8562, Japan

Correspondence to: Chun Yang Wen, M.D., Ph.D., Department of Molecular Pathology, Atomic Bomb Disease Institute, Nagasaki University Graduate School of Biomedical Sciences, 1-12-4 Sakamoto, Nagasaki 852-8523, Japan. cywen518@net.nagasaki-u.ac.jp or chunyangwen@yahoo.com.cn

Telephone: +81-95-849-7107 **Fax:** +81-95-849-7108

Received: 2003-12-23 **Accepted:** 2004-01-08

Abstract

AIM: Pituitary tumor transforming gene (PTTG1) is overexpressed in a variety of tumors, including carcinomas of the lung, breast, colon, as well as in leukemia, lymphoma and pituitary adenomas. However, there is little information on its expression in gastric carcinoma. We sought to investigate the expression of PTTG1 in gastric carcinoma and to explore the relationship between its expression and clinicopathological factors.

METHODS: We studied 75 primary human gastric adenocarcinomas, including 17 mucosal carcinomas, 21 submucosal infiltrative carcinomas, 12 carcinomas invading proprial muscle layers, 6 carcinomas reaching the subserosa, and 19 carcinomas penetrating the serosal surface. Immunohistochemical analysis was performed using paraffin-embedded sections of gastric adenocarcinomas.

RESULTS: PTTG1 was expressed heterogeneously in carcinomas. Positive PTTG1 staining was observed in 65.3% of the carcinomas (49 of 75). Its expression did not correlate significantly with either the histological type or the depth of infiltration of the gastric carcinomas. However, a statistical analysis showed significant differences between the primary adenocarcinomas and the associated metastatic lymph nodes.

CONCLUSION: The results of this study demonstrate that PTTG1 expression is enhanced in metastatic lymph nodes in comparison to that in primary carcinomas. We suggest

that PTTG1 may contribute to lymph node metastases in gastric carcinoma.

Wen CY, Nakayama T, Wang AP, Nakashima M, Ding YT, Ito M, Ishibashi H, Matsuu M, Shichijo K, Sekine I. Expression of pituitary tumor transforming gene in human gastric carcinoma. *World J Gastroenterol* 2004; 10(4): 481-483

<http://www.wjgnet.com/1007-9327/10/481.asp>

INTRODUCTION

Gastric carcinoma is one of the most common causes of malignancy-related death worldwide. Recent molecular biological studies suggest that genetic instability may play an important role in the pathogenesis of gastric carcinogenesis^[1]. There are at least two distinct genetic instabilities in gastric tumorigenesis. One is chromosomal instability and the other is instability of the microsatellites. In the former, diminished expression of tumor suppressor genes, such as p53, Rb, APC, MCC and DCC, plays an important role in carcinogenesis. Whereas in the latter, the defective repair of mismatched bases results in an increase in the rate of point mutations^[2-4].

Aneuploidy is a numerical imbalance in chromosomes caused by missegregation during cell division. A critical event that promotes equal partitioning of chromosomes during mitosis is the proper and timely separation of sister chromatids attached to each other and to the mitotic spindle. Interestingly, pituitary tumor transforming gene (PTTG1) is a securin that acts as an inhibitor of chromatid separation^[5].

PTTG1 is a novel oncogene that has been identified by Pei *et al*^[6]. PTTG1 overexpression in mouse fibroblasts and NIH 3T3 cells induced cellular proliferation and transformation, both *in vitro* and *in vivo*^[6,7]. PTTG1 is overexpressed in a variety of tumors, including carcinomas of the lung, breast, colon, as well as in leukemia, lymphoma and pituitary adenomas^[8-11]. The expression of PTTG1 in normal tissues is restricted with the highest expression occurring in the testis^[6,8,9]. PTTG1 is expressed in a stage-specific manner in germ cells during the spermatogenic cycle, suggesting that it may play a role in male germ cell differentiation^[12]. PTTG1 also regulates the secretion of basic fibroblast growth factor^[8].

In the present study, we investigated PTTG1 expression and explored the relationship between its expression and clinicopathological factors in 75 gastric carcinoma specimens.

MATERIALS AND METHODS

We studied 75 primary human gastric adenocarcinomas, including 17 mucosal carcinomas, 21 submucosal infiltrative carcinomas, 12 carcinomas invading proprial muscle layers, 6 carcinomas reaching the subserosa, and 19 carcinomas penetrating the serosal surface. All tumor specimens were obtained from patients at the Nagasaki University Hospital between 2001 and 2002. Each tumor was assigned a histological type and a depth grading of infiltration according to the

Japanese Classification of Gastric Carcinoma by the Japanese Gastric Cancer Association^[13]. The primary human gastric adenocarcinomas were classified histologically as follows: 4 papillary adenocarcinomas, 18 tubular adenocarcinomas of the well differentiated type, 22 tubular adenocarcinomas of the moderately differentiated type, 7 poorly differentiated adenocarcinomas of the solid type, 10 poorly differentiated adenocarcinomas of the nonsolid type, 12 signet-ring cell carcinomas, and 2 mucinous adenocarcinomas. Diagnosis was established by two independent pathologists (CY Wen and T Nakayama) and cases of questionable diagnosis were omitted from the study.

Immunohistochemistry

Formalin-fixed and paraffin-embedded tissues were cut into 4 μm sections, deparaffinized in xylene, and rehydrated in phosphate-buffered saline. Deparaffinized sections were subsequently preincubated in 3% H_2O_2 for 30 min, followed by incubation in normal bovine serum to prevent nonspecific binding and subsequently incubated overnight at 4°C in a primary polyclonal antibody directed against human PTTG1 (2 $\mu\text{g}/\text{ml}$) (Zymed Laboratories, Inc. South San Francisco, CA, USA). Next, the slides were incubated in biotinylated anti-rabbit immunoglobulin G followed by avidin-horseradish peroxidase and the reaction product was resolved using diaminobenzidine (DAB) (Vectastain ABC kit; Vector Laboratories, Burlingame, CA, USA). For the PTTG1 expression, pituitary adenoma served as a positive control, and the slide with the primary antibody omitted was used as a negative control. Analysis of the immunohistochemical staining was performed by two investigators (CY Wen and T Nakayama). PTTG1 expression was classified into three categories depending on the percentage of cells stained and/or the intensity of staining: -, 0% to 10% positive tumor cells; +, 10% to 50% positive tumor cells; and ++, >50% positive tumor cells.

Statistical analysis

Statistical analyses were performed using Spearman's correlation coefficient by rank test and the Mann-Whitney *U* test. A *P* value <0.05 was accepted as statistically significant.

RESULTS

PTTG1 protein was detected in the cytoplasm. Benign gastric epithelia showed focal and patchy immunoreactivity of PTTG1 with faint to mild staining intensity. The results of immunohistochemical analysis are summarized in Table 1. PTTG1 was expressed heterogeneously in carcinomas. Positive PTTG1 staining was observed in 65.3% of carcinomas (in 49 out of 75). The correlation between PTTG1 immunoreactivity and tumor histological type is shown in Table 1. Tubular adenocarcinomas of the well and moderately differentiated types

were stained strongly for PTTG1 (Figure 1). However, poorly differentiated adenocarcinomas of the solid and nonsolid types exhibited weak PTTG1 expression (Figure 2) and mucinous adenocarcinomas were negative for antibody reaction.

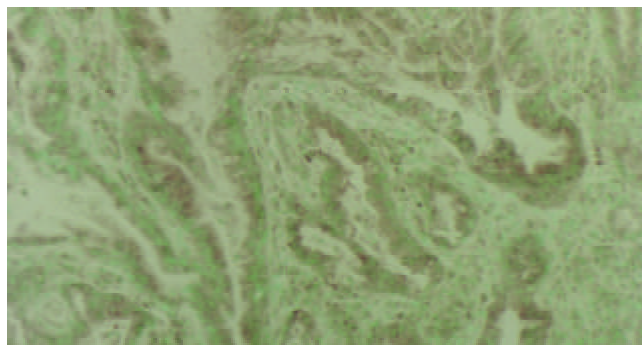


Figure 1 Immunohistochemical demonstration of PTTG1 staining in tumor cell cytoplasm. Tubular adenocarcinomas of the well differentiated type were stained strongly for PTTG1. ($\times 200$).

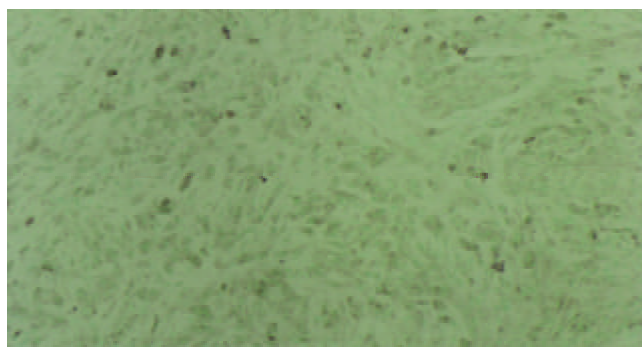


Figure 2 Relatively weak PTTG1 expression, poorly differentiated adenocarcinomas of the solid type. ($\times 200$).

The relationship between immunoreactivity and the depth of tumor infiltration is shown in Table 2. PTTG1 staining was positive for tumors with mucosal infiltration (74.7%) or submucosal infiltration (76.2%), whereas expression was markedly weaker in tumors infiltrating proprial muscle layers, subserosa, and serosal surface. PTTG1 expression did not correlate with either histological type or depth of infiltration of gastric carcinomas (Tables 1,2).

PTTG1 expression in primary adenocarcinomas and metastatic lymph nodes are compared in Table 3. PTTG1 staining was mostly negative for the primary sites, *i.e.*, 7 out of 19 tumors were positive (36.8%), whereas 79% of the metastatic sites were immunoreactive (15 out of 19). Statistical analysis showed a significant difference in staining intensity

Table 1 Histological types of gastric adenocarcinomas and immunohistochemical PTTG1 staining (75 cases) n(%)

	<i>n</i>	-	+	++	<i>P</i> value
Total carcinomas	75	26(34.7)	31(41.3)	18(24.0)	
Papillary adenocarcinomas	4	1(25.0)	2(50.0)	1(25.0)	
Tubular adenocarcinomas					
Well differentiated	18	6(33.3)	6(33.3)	6(33.3)	
Moderately differentiated	22	7(31.8)	7(31.8)	8(36.4)	
Poorly differentiated adenocarcinomas					
Solid types	7	4(40.0)	2(28.6)	1(14.3)	
Nonsolid type	10	4(40.0)	6(60.0)	0(0.0)	
Signet-ring cell carcinoma	12	4(33.3)	7(58.3)	1(8.3)	
Mucinous adenocarcinoma	2	2(100.0)	0(0.0)	0(0.0)	>0.05

See Materials and Methods for classification of staining intensity.

between primary adenocarcinomas and metastatic lymph nodes ($P < 0.005$, Table 3).

Table 2 Invasive grades of gastric adenocarcinomas and PTTG1 immunohistochemistry (75 cases) *n*(%)

	<i>n</i>	-	+	++	<i>P</i> value
m	17	6(35.3)	5(29.4)	6(35.3)	
sm	21	5(23.8)	11(52.4)	5(23.8)	
mp	12	5(41.7)	4(33.3)	3(25.0)	
ss	6	2(33.3)	4(66.7)	0(0.0)	
se	19	8(42.1)	7(36.8)	4(21.1)	>0.05
Total	75	26(34.7)	31(41.3)	18(24.0)	

m, mucosal carcinomas; sm, submucosal infiltrative carcinomas; mp, carcinomas invading the proprial muscle layers; ss, carcinomas reaching the subserosa; se, carcinomas penetrating the serosal surface.

Table 3 PTTG1 expression in primary adenocarcinomas and metastatic lymph nodes (19 cases) *n*(%)

	<i>n</i>	-	+	++	<i>P</i> value
Primary adenocarcinomas	19	12(63.2)	7(36.8)	0(0.0)	
Metastatic lymph nodes	19	4(21.0)	9(47.2)	6(31.6)	<0.005

DISCUSSION

It is now widely accepted that cancer results from the accumulation of mutations in genes that regulate cell birth or death. An underlying genetic instability might be a prerequisite for the generation of multiple mutations that lead to cancer^[14,15]. For example, losses or gains in the number of whole chromosomes (aneuploidy) have been found in nearly all major human tumor types, including gastric cancers^[16,17].

A large number of potential targets made putative cancer cells susceptible to several mechanisms that may lead to chromosome instability^[18]. The finding that PTTG1 codes for a securin involved in regulating chromatid separation during cell division suggested that securin overexpression might disrupt cell division, generate chromosomal instability and, thereby, increase cell susceptibility to mutations during subsequent divisions^[5].

In the present study, we investigated the correlation between PTTG1 expression and histological classification, invasive depth and lymph node metastasis in gastric carcinomas. PTTG1 expression was enhanced in metastatic lymph nodes in comparison to that found in primary carcinomas. Shibata *et al*^[19] recently showed a significant correlation between high PTTG1 expression, advanced pathological stage of cancer and lymph node metastasis in esophageal cancer. Heaney *et al* reported that high PTTG1 expression correlated with extension to the bowel wall, metastasis, vascularity and Dukes' staging^[10]. These findings suggest that enhanced PTTG1 expression may be a marker for invasive carcinoma.

Pei^[20] recently reported that PTTG1 could bind to the c-myc promoter near the transcription initiation site and activate c-myc transcription in transfected cells. These findings suggest that PTTG1 may act as a transcription activator and may be involved in cellular transformation and tumorigenesis via activation of the c-myc oncogene. Furthermore, PTTG1 induces angiogenesis, a key determinant and rate-limiting step in tumor progression and metastatic spread, through basic fibroblast growth factor. Poor prognosis in patients exhibiting high PTTG mRNA expression might reflect an angiogenic phenotype in addition to the acquisition of chromosome instability^[6,21].

In conclusion, the results of this study demonstrate that PTTG1 expression is enhanced in metastatic lymph nodes in comparison to that in primary carcinomas. We suggest that PTTG1 is a marker of lymph node metastasis in gastric carcinomas.

REFERENCES

- Fang DC**, Jass JR, Wang DX, Zhou XD, Luo YH, Young J. Infrequent loss of heterozygosity of APC/MCC and DCC genes in gastric cancer showing DNA microsatellite instability. *J Clin Pathol* 1999; **52**: 504-508
- Fang DC**, Yang SM, Zhou XD, Wang DX, Luo YH. Telomere erosion is independent of microsatellite instability but related to loss of heterozygosity in gastric cancer. *World J Gastroenterol* 2001; **7**: 522-526
- Martins C**, Kedda MA, Kew MC. Characterization of six tumor suppressor genes and microsatellite instability in hepatocellular carcinoma in southern African blacks. *World J Gastroenterol* 1999; **5**: 470-476
- Wu BP**, Zhang YL, Zhou DY, Gao CF, Lai ZS. Microsatellite instability, MMR gene expression and proliferation kinetics in colorectal cancer with familial predisposition. *World J Gastroenterol* 2000; **6**: 902-905
- Zou H**, McGarry TJ, Bernal T, Kirschner MW. Identification of a vertebrate sister-chromatid separation inhibitor involved in transformation and tumorigenesis. *Science* 1999; **285**: 418-422
- Pei L**, Melmed S. Isolation and characterization of a pituitary tumor-transforming gene. *Mol Endocrinol* 1997; **11**: 433-441
- Kakar SS**, Jennes L. Molecular cloning and characterization of the tumor transforming gene (TUTR 1): A novel gene in human tumorigenesis. *Cytogenet Cell Genet* 1999; **84**: 211-216
- Zhang X**, Horwitz GA, Prezant TR, Valentini A, Nakashima M, Bronstein MD, Melmed S. Structure, expression and function of human pituitary transforming gene (PTTG). *Mol Endocrinol* 1999; **13**: 156-166
- Dominguez A**, Ramos-Morales F, Romero F, Rios RM, Dreyfus F, Tortolero M, Pintor-Toro JA. Hpttg, a human homologue of rat pttg, is overexpressed in hematopoietic neoplasms. Evidence for a transcriptional activation function of hPTTG. *Oncogene* 1998; **17**: 2187-2193
- Heaney AP**, Singson R, McCabe CJ, Nelson V, Nakashima M, Melmed S. Expression of pituitary-transforming gene in colorectal tumors. *Lancet* 2000; **355**: 716-719
- Saez C**, Japon MA, Ramos-Morales F, Romero F, Segura DI, Tortolero M, Pintor-toro JA. Hpttg is over-expressed in pituitary adenomas and other primary epithelial neoplasias. *Oncogene* 1999; **18**: 5473-5476
- Pei L**. Genomic organization and identification of an enhancer element containing binding sites for multiple proteins in rat pituitary tumor-transforming gene. *J Biol Chem* 1998; **273**: 5219-5225
- Japanese Gastric Cancer Association**: Japanese Classification of Gastric Carcinoma (The 13th Edition). Edited by Japanese Gastric Cancer Association, Tokyo, Kenohara Press 1999
- Loeb LA**. Mutator phenotype may be required for multistage carcinogenesis. *Cancer Res* 1991; **51**: 3075-3079
- Hartwell L**. Defects in a cell cycle checkpoint may be responsible for the genomic instability of cancer cells. *Cell* 1992; **71**: 543-546
- Furuya T**, Uchiyama T, Murakami T, Adachi A, Kawauchi S, Oga A, Hirano T, Sasaki K. Relationship between chromosomal instability and intratumoral regional DNA ploidy heterogeneity in primary gastric cancers. *Clin Can Res* 2000; **6**: 2815-2820
- Choma D**, Daures JP, Quantin X, Pujol JL. Aneuploidy and prognosis of non-small-cell lung cancer: a meta-analysis of published data. *Br J Cancer* 2001; **85**: 14-22
- Lengauer C**, Kinzler KW, Vogelstein B. Genetic instabilities in human cancers. *Nature* 1998; **396**: 643-649
- Shibata Y**, Haruki N, Kuwabara Y, Nishiwaki T, Kato J, Shinoda N, Sato A, Kimura M, Koyama H, Toyama T, Ishiguro H, Kudo J, Tarashita Y, Konishi S, Fujii Y. Expression of PTTG (Pituitary Tumor Transforming Gene) in esophageal cancer. *Jpn J Clin Oncol* 2002; **32**: 233-237
- Pei L**. Identification of c-myc as a down-stream target for pituitary tumor-transforming gene. *J Biol Chem* 2001; **276**: 8484-8491
- Zetter BR**. Angiogenesis and tumor metastasis. *Annu Rev Med* 1998; **49**: 407-424

Anti-neoplastic efficacy of Haimiding on gastric carcinoma and its mechanisms

Yu-Bin Ji, Shi-Yong Gao, Hong-Rui Ji, Qi Kong, Xiu-Juan Zhang, Bao-Feng Yang

Yu-Bin Ji, Shi-Yong Gao, Hong-Rui Ji, Qi Kong, Postdoctoral Research Station, Institute of Materia Medica, Harbin Commercial University, Harbin 150076, Heilongjiang Province, China
Xiu-Juan Zhang, Department of Pharmaceutical Engineering, Harbin Commercial University, Harbin 150076, Heilongjiang Province, China

Bao-Feng Yang, Department of Pharmacology, Harbin Medical University, Harbin 150086, Heilongjiang Province, China
Supported by the National Natural Science Foundation of China, No. 30271598; Outstanding Post Doctoral Research Foundation of China, No. 17(1999); Heilongjiang Province Foundation for Talented Youth No. J 9906; Natural Science Foundation of Heilongjiang Province, China, No. D00-18; Innovative Fund for Distinguished University and College Teachers of Heilongjiang Province, No. 2001015

Correspondence to: Dr. Yu-Bin Ji, Postdoctoral Research Station, Institute of Materia Medica, Harbin Commercial University, 138 Tongda Street, Daoli District, Harbin 150076, Heilongjiang Province, China. sygao2002@sina.com

Telephone: +86-451-84866001 **Fax:** +86-451-84866001

Received: 2003-05-11 **Accepted:** 2003-06-07

Abstract

AIM: To study the anti-neoplastic effect of Haimiding and its mechanisms of action.

METHODS: Experiments using MTT and colony formation were carried out to study the *in vitro* anti-neoplastic action of Haimiding, its *in vivo* anti-neoplastic action was studied by observing its effect on the weight of tumors in FC mice and S₁₈₀, H₂₂ tumor bearing mice, as well as their life spans. The effect of Haimiding on cell apoptosis and different stages of cell cycles in human gastric carcinoma cells were studied by flow cytometry. Its effect on [Ca²⁺]_i of human gastric carcinoma cells and the source of Ca²⁺ during the change of [Ca²⁺]_i were observed by confocal laser scanning technique.

RESULTS: Haimiding showed a definite cytotoxicity to 8 human tumor cell lines, which was most prominent against BGC-823, E_{ca-109} and HCT-8 tumor cells. It also exhibited an obvious inhibition on colony formation of the above tumor cell lines, which was most prominent in E_{ca-109} tumor cells. It showed obvious inhibition on the growth of tumor in FC mice and S₁₈₀ bearing mice as well as prolonged the life span of H₂₂ bearing mice. It was able to induce apoptosis and elevate intracellular [Ca²⁺]_i concentration of tumor cells. The source of Ca²⁺ came from both extracellular Ca²⁺ influx and intracellular Ca²⁺ release.

CONCLUSION: Haimiding is composed of a TCM preparation and 5-fluorouracil. Its anti-neoplastic potency is highly enhanced by synergism as compared with either one of its components. Its mechanisms of anti-neoplastic action can be attributed to its action to initiate apoptosis of tumor cells by opening the membrane calcium channel and inducing intracellular Ca²⁺ release to elevate [Ca²⁺]_i of the tumor cells.

Ji YB, Gao SY, Ji HR, Kong Q, Zhang XJ, Yang BF. Anti-neoplastic efficacy of Haimiding on gastric carcinoma and its mechanisms. *World J Gastroenterol* 2004; 10(4): 484-490
<http://www.wjgnet.com/1007-9327/10/484.asp>

INTRODUCTION

Haimiding (HMD) is an anti-neoplastic preparation made of a traditional Chinese medicine (TCM) preparation and 5-fluorouracil (5-Fu). Its TCM preparation consists of active ingredients from the extracts of *Sargassum fusiforme* (Harv.) Setch, *Ecklonia kurome* Okam, *Astragalus chrysopterus* Buge, and *Sophora flavescens* Aits. The present study was to observe the *in vivo* and *in vitro* anti-neoplastic activities of HMD, and the effect of HMD on apoptosis of human gastric carcinoma SGC-7901 and intracellular [Ca²⁺]_i, so to better understand the mechanism of its anti-neoplastic action.

MATERIALS AND METHODS

Materials

Drug samples Sterile HMD powder with or without 5-Fu for parenteral use (Lot No.010606) was prepared by the Pharmaceutical Laboratory, Institute of Materia Medica, Harbin Commercial University. 5-Fu (Lot No. 990304) was provided by Haipo Pharmaceutical Factory, Shanghai, China.
Cancer cell lines Human oral epithelial KB, human esophageal carcinoma cell E_{ca-109}, human proventriculus BGC-823, human pulmonary adenocarcinoma A-549, human colon HCT-8, human breast MCF-7, human ovary A₂₇₈₀ and human liver Bel-7402 were provided by the Department of Pharmacology, Institute of Materia Medica, Chinese Academy of Medical Sciences. SGC-7901 was from College of Public Health, Harbin Medical University.

Test animals Kunming strain mice were provided by Veterinary Department of Harbin Medical University, pure 615 strain mice were provided by Institute of Materia Medica, Chinese Academy of Medical Sciences.

Tumor bearing mice strain FC mice, S₁₈₀ A and H₂₂ mice of same sex weighing 20±2 g were supplied by Institute of Materia Medica, Chinese Academy of Medical Sciences.

Reagents Bovine serum and RPMI-1640 culture medium were products of Gibco. MTT was provided by Sigma. Fluo-3/AM fluorescence probe was from Molecular Probe Co., USA. Verapamil was a product of Heng Rui Pharmaceutical Factory, Jiangsu Province, China.

Methods

Anti-neoplastic study *in vitro*

MTT test^[1,2] About 1200 cells were added to each well of a 96 multi-well culture plate. After 24 h each dose of the drug was added to 3 different wells in the test group. Vehicle was added as control in another group. The plate was placed into a humidified incubator (CAN-111, Japan) containing 5% CO₂ and incubated at 37°C for 4 d. Ten μl MTT stock solution (5 mg/ml) was added to each well and shaken well, the incubation was continued for a further 4 h. One hundred μl

acidified 10% sodium dodecanoate sulfonate (SDS) (pH=4.7) was added to each well, which was then left overnight. The absorbance was determined by an EI-311 enzyme labeling apparatus (EI-311, Bio-Tek, USA) at a wave length of 570 nm and a reference wave length of 630 nm. The drug concentration inhibiting 50% of cell growth (IC_{50}) was measured.

Experiments on formation of colonies^[3,4] About 100 test cells were inoculated onto a 35 mm plastic petridish for 24 h and the assigned dose of test drugs was added to each dish. The culture liquid was discarded on the 9th day and the residue was washed 3 times in PBS. The cells were fixed in 10% formaldehyde solution and stained with 0.25% gentian violet. The number of colonies containing more than 50 cells in each dish was counted under a microscope. Vehicles were used instead of test drugs as blank control.

Anti-neoplastic studies *in vivo*

Effect of HMD on tumor weight of FC mice^[5] Tumor cells were transplanted to 615 FC mice. Nine days after transplantation, FC mice bearing the well growing tumor were placed in an ice basin inside an enclosed aseptic working table. Tumor tissues, were separated and then cut into small pieces and homogenized with a glass homogenizer. The homogenate was made into a suspension containing about 5.6×10^6 /ml of tumor cells with sterile normal saline in the conventional way^[6], and 0.2 ml of the suspension was transplanted to the right axilla of each 615 strain mouse. After 24 h, the mice were weighed and randomized into 3 HMD groups (treated respectively *ip* with high, medium and low doses of HMD, equivalent to 27.05 g/kg, 13.53 g/kg and 6.76 g/kg of crude drugs in 0.4 ml injectable solution, once daily), a 5-Fu group treated *ip* with 25 mg/kg 5-Fu in 0.4 ml solution once daily, and a compound TCM group treated *ip* with HMD (without 5-Fu) equivalent to 13.50 g/kg of crude drug in 0.4 ml solution daily. A blank control group was treated *ip* with 0.4 ml normal saline once daily. All drugs were withdrawn on the 11th day. The animals were sacrificed on the next day and their tumors were resected and weighed. Results of 3 repeated experiments were collected and the data were statistically analyzed. The rate of tumor inhibition was calculated according to the following equation:

$$\text{Rate of inhibition (\%)} = \frac{\text{Mean tumor wt of blank} - \text{mean wt of test group}}{\text{Mean tumor wt of blank}} \times 100$$

Effect of HMD on tumor weight of S₁₈₀ bearing mice^[5] S₁₈₀ tumor cells were transplanted into Kunming strain mice. After 7 days, ascites was drawn from the mice bearing well growing tumor under aseptic condition. The tumor cells were diluted with sterile normal saline in ice-bath to 4:1 to produce a suspension containing about 5.8×10^6 /ml of tumor cells. This suspension should have a semi-transparent creamy appearance. Any ascitic fluid with blood streaks should not be used. The mice were transplanted by *sc* injection of 0.2 ml of the suspension to the right axilla of each Kunming mouse according to the procedure described in "National Requirements for *in vivo* Screening of Anti-neoplastic Drugs"^[7]. After 24 h, the transplanted mice were weighed and randomized into groups to be treated with different doses of test drugs. Their tumors were resected, weighed and the rate of tumor inhibition was calculated as above (results of 3 repeated trials).

Effect of HMD on life span of H₂₂ bearing mice^[8] Kunming mice were transplanted with H₂₂ tumor cells. The mice bearing well growing transplanted tumor were selected after 7 d, and their ascites were drawn under aseptic condition and diluted in ice-cold sterile normal saline to a concentration of 4:1. The tumor cells were mixed well to generate a suspension containing about 6×10^6 tumor cells/ml, and 0.2 ml of the

suspension was transplanted *ip* to each Kunming mouse. After 24 h, the mice were weighed and randomized to different dosage groups as described above. The number of dead mice was recorded every day until no survival left. The rate of life prolongation was calculated according to the following equation:

$$\text{Rate of life prolongation (\%)} = \frac{\text{Survial days in treated group} - \text{survial days in blank}}{\text{Survial days in blank control}} \times 100$$

Effect of HMD on apoptosis of gastric carcinoma cells^[9]

Culturing of tumor cells: Human gastric carcinoma SGC-7901 cells were resuscitated conventionally and cultured in RPMI 1640 culture medium (Gibo) containing 0.1 mass fraction of bovine serum and incubated at 37°C with 95% relative humidity in an incubator containing a volume fraction of 0.05 CO₂. The cells were generated every 2-3 days.

Experimental groups: Culture flasks containing human gastric carcinoma SGC-7901 cells were divided into 5 groups, 10 flasks each. HMD was added to each flask in the 3 dosage groups to a final concentration of 50 µl/ml, 100 µl/ml and 200 µl/ml, respectively. 5-Fu was added to another group of 10 flasks to a final concentration of 100 µl/ml. A similar amount of culture media was added to the remaining 10 flasks as blank control. They were incubated in an incubator containing 5% CO₂ for 24 h.

Determination of cell apoptosis by flow cytometry^[7]: Nine volumes of 70% ethanol were added to 1 volume (about 10⁶ cells) of cell suspension and fixed at -20°C for 12 h. The cells were kept in 70% ethanol at -20°C for 2-3 weeks, centrifuged and washed in PBS solution. The resulting cells were again suspended in 1 ml of PI staining solution, and stained at room temperature for 30 min. The red fluorescence FCM was detected with a laser (488 nm) or blue light (BG 12 light filter).

Effect of HMD on [Ca²⁺]_i of gastric cancer cells **Culturing of cells** Human gastric carcinoma SGC-7901 Cells, after resuscitated conventionally, were cultured in RPMI-1640 medium containing 0.1 mass fraction of bovine serum and incubated at 37°C with 95% relative humidity in an incubator containing 0.05 volume fraction of CO₂. Every 2-3 days were taken for a generation.

Experimental grouping and treatment with test drugs Trypan blue was used to show the number of cells, which was adjusted to about 2×10^5 /ml with culture medium, and stored in different culture bottles.

The experiments consisted of 6 groups (A, B, C₁, C₂, C₃ and D) and 4 different periods of time (12, 24, 36 and 48 h). Groups A and B were negative and positive controls respectively. Groups C₁, C₂ and C₃ were low, medium and high HMD dose groups, and group D was medium dose of HMD plus verapamil.

When the cells attached to the wall after culturing, the culture medium of each group was adjusted to different concentrations. Group B was adjusted to a final concentration of 50 µg/mL of 5-Fu, groups C₁, C₂ and C₃ to a final concentration of 200 µg/ml, 100 µg/ml and 50 µg/ml of HMD, respectively and group D to a final concentration of 100 µg/mL of HMD plus 20 µg/mL of verapamil. Group A, as a negative control was cultured in RPMI-1640 medium containing 10% bovine serum. These media were cultured for 12, 24, 36 and 48 h respectively, and the resulting cells were collected.

Determination of free Ca²⁺ concentration in cells^[9] SGC-7901 human gastric carcinoma cells, digested after addition of test drugs at different times, were collected and washed twice with 0.1 mass fraction RPMI-1640 and then stained with 0.25 mass fraction of trypan blue. The viable cell count was over 95%. The cell suspension was preheated at 37°C for 5 min and then washed 2-3 times in PBS and calcium free Dakins solution, stained with 100 µl Fluo-3/AM solution at 37°C for 45 min. A cell suspension was prepared with an appropriate amount of

calcium free Dakins solution. The change of intracellular Ca^{2+} concentration was examined under a confocal laser scanning microscope (Insight Plus-type IQ, meridian, USA), using the intensity of fluorescence light as the criteria of Ca^{2+} concentration, and was observed with a 40× objective lens at an exciting wavelength of 488 nm.

Statistical analysis

t test was used for statistical analysis and results were expressed as mean±SD.

RESULTS

Anti-neoplastic activity of HMD in vitro

Cytocidal activities of HMD against 8 human cancer cell lines are shown in Table 1. It demonstrated that the actions were more prominent in BGC-823, E_{ca-109} and HCT-8 cell lines in a dose dependent manner. Results from regression calculation showed that IC₅₀ of HMD against BGC-823, E_{ca-109} and HCT-8 was 25.28 mg/ml, 12.78 mg/ml and 28.29 mg/ml (equivalent to the crude drug) respectively.

Effect of HMD on formation of BGC-823, E_{ca-109} and HCT-8 cell colonies in cell culture

HMD had an obvious inhibitory effect on colony formation of BGC-823, E_{ca-109} and HCT-8 tumor cell lines, being most prominent in E_{ca-109} in a positive dose-effect manner. The data are shown in Table 2.

Anti-neoplastic action of HMD in vivo

Effect of HMD on tumor weight of FC mice HMD at doses of 27.05 g/kg·d, 13.53 g/kg·d and 6.76 g/kg·d demonstrated

an obvious inhibitory effect on the growth of tumor in FC mice in a positive dose-effect manner. The inhibitory effect of 13.53 g/kg HMD (containing 25 mg 5-Fu) was more potent than 25 mg/kg of 5-Fu alone with statistical significance ($P<0.05$). Results are shown in Table 3.

Effect of HMD on tumor weight of S₁₈₀ bearing mice HMD at doses of 27.05 g/kg·d, 13.53 g/kg·d and 6.76 g/kg·d significantly inhibited the growth of S₁₈₀ sarcoma in tumor-bearing mice in a positive dose-effect manner ($P<0.01$, $P<0.05$). Results are shown in Table 4.

Effect of HMD on life span of H₂₂ bearing mice HMD at doses of 27.05 g/kg·d, 13.53 g/kg·d, and 6.76 g/kg·d obviously prolonged the life span of H₂₂ bearing mice in a positive dose-effect manner. HMD at 13.53 g/kg (containing 25mg 5-Fu) showed a more potent effect than that of 5-Fu alone ($P<0.05$), and HMD without 5-Fu ($P<0.05$). Results are shown in Table 5.

Effect of HMD on tumor cell apoptosis and their cell cycles

Studies on the effects of HMD on cell apoptosis and cell cycles of tumor cell lines showed that HMD was able to induce cell apoptosis to a certain degree (Tables 6 and 7), which was statistically significant ($P<0.01$) as compared with the blank control. 5-Fu, however, was devoid of such an effect. HMD caused a decrease of cells at stage S, resulting in cells differentiation at G₀-G₁ and G₂-M stages. But most cells remained at stage G₂-M with an increase of HMD doses.

Effect of HMD on intracellular [Ca²⁺]_i of tumor cells Changes of intracellular [Ca²⁺]_i in human gastric carcinoma cells after treated with HMD for 12 h. It showed that HMD significantly increased the intracellular free calcium ion concentration ($P<0.001$) in a dose dependent manner (Tables 8-11). Calcium ion concentration of the verapamil group

Table 1 Cytotoxicity of HMD to human tumor cell lines (MTT assay)

Drug	IC ₅₀ (mg/ml)							
	KB	BGC-823	A549	MCF-7	A ₂₇₈₀	Bel-7420	HCT-8	E _{ca-109}
HMD	83.89	25.28	292.41	34.14	16.84	36.57	28.29	12.78
5-Fu	0.12	0.06	0.19	0.10	0.08	0.09	0.08	0.04
HMD without 5-Fu	428.58	274.90	685.70	365.00	124.65	295.60	187.58	100.42

Table 2 Effect of HMD on formation of colonies in culture of BGC-823, E_{ca-109} and HCT-8 cell lines (n=8)

Drug	Percentage of colony formation (mean±SD)			
	Dose (mg/ml)	BGC-823	HCT-8	E _{ca-109}
HMD	10.00	72.18±7.29 ^c	83.18±9.01	61.58±4.12 ^a
HMD	20.00	50.21±5.18 ^d	59.45±6.78 ^c	22.43±3.65 ^d
HMD	40.00	28.43±3.42 ^d	30.15±4.20 ^d	0
5-Fu	0.04	61.18±4.27 ^c	68.70±5.15 ^a	69.27±5.48 ^a
HMD without 5-Fu	19.63	90.51±7.42	82.15±7.92	78.29±6.25 ^a
Blank control		98.27±6.58	95.68±9.12	97.14±8.26 ^c

^a $P<0.05$, ^b $P<0.01$ vs blank control; ^c $P<0.05$, ^d $P<0.01$ vs HMD without 5-Fu.

Table 3 Effect of HMD on tumor weight of FC mice

Drug	Dose (g/kg)	Route of administration	No. of animals	Average weight of tumor (g)	Rate of inhibition (%)
HMD	27.05	<i>ip</i>	30	0.42±0.21 ^{bd}	76.92
HMD	13.53	<i>ip</i>	30	0.58±0.30 ^{bc}	68.13
HMD	47.63	<i>ip</i>	30	0.88±0.34 ^a	51.65
HMD					
Without 5-Fu	13.50	<i>ip</i>	30	1.21±0.45	33.52
5-Fu	0.03	<i>ip</i>	30	0.89±0.40	51.10
Normal saline		<i>ip</i>	30	1.82±0.43	

^a $P<0.05$, ^b $P<0.01$ vs HMD without 5-Fu; ^c $P<0.05$, ^d $P<0.01$ vs 5-Fu.

Table 4 Effect of HMD on tumor weight of S₁₈₀ bearing mice

Drug	Dose (g/kg)	Route	No. of animals	Average weight of tumor (g)	Rate of inhibition (%)
HMD	27.05	<i>ip</i>	30	0.28±0.10 ^{bc}	73.33
HMD	13.53	<i>ip</i>	30	0.40±0.15 ^a	61.91
HMD	6.76	<i>ip</i>	30	0.49±0.31 ^a	53.33
HMD					
Without 5-Fu	13.50	<i>ip</i>	28	0.79±0.33	24.76
5-Fu	0.03	<i>ip</i>	28	0.54±0.21	48.57
Normal saline		<i>ip</i>	29	1.05±0.32 ^d	

^a*P*<0.05, ^b*P*<0.01 vs HMD without 5-Fu; ^c*P*<0.05, ^d*P*<0.01 vs 5-Fu.

Table 5 HMD at doses of 27.05 g/kg·d, 13.53 g/kg·d and 6.76 g/kg·d prolonged life span of H₂₂- bearing mice

Drug	Dose (g/kg)	Route	No. of animals	Life-span(d)	Rate of life prolongation (%)
HMD	27.05	<i>iv</i>	27	21.1±1.6 ^{ac}	74.4
HMD	13.53	<i>iv</i>	28	18.6±2.9 ^{ac}	53.7
HMD	6.76	<i>iv</i>	30	17.1±3.2	41.3
HMD					
Without 5-Fu	13.50	<i>iv</i>	30	15.8±2.5	30.6
5-Fu	0.03	<i>iv</i>	29	14.6±2.7	20.7
Normal saline		<i>iv</i>	30	12.1±3.1	

^a*P*<0.05, ^b*P*<0.01 vs HMD without 5-Fu; ^c*P*<0.05, ^d*P*<0.01 vs 5-Fu.

Table 6 Effect of HMD on cell cycle of human gastric carcinoma

Group	Dose(μg/ml)	No. of cases	G ₀ /G ₁ (%)	G ₂ /M (%)	S (%)
Blank	Media only	10	22.20±5.06	4.09±1.27	73.56±12.10
5-Fu	50	10	44.81±10.25	0.03±0.01	55.13±7.28 ^b
HMD	50	10	22.63±3.34	11.01±3.56	63.38±7.31 ^a
HMD	100	10	26.70±7.99	19.33±4.67	52.83±10.03 ^b
HMD	200	10	12.65±2.43	31.36±7.06	54.27±8.33 ^b

^a*P*<0.05 vs blank control; ^b*P*<0.01 vs blank control.

(group D) was between that of the negative control and medium dose HMD group, both of which were statistically significant (*P*<0.01).

Table 7 Effect of HMD on cell apoptosis of human gastric carcinoma

Group	Dose (μg/ml)	No. of cases	APO (%)
Blank control	Media only	10	0.15±0.04
5-Fu	50	10	0.17±0.06
HMD	50	10	1.16±0.23 ^b
HMD	100	10	1.14±0.20 ^b
HMD	200	10	1.72±0.41 ^b

^b*P*<0.01 vs blank control.

Table 8 Changes of intracellular [Ca²⁺]_i in human gastric carcinoma cells after treated with HMD for 12 h

Group	Concentration of drug (μg/ml)	No. of cells	[Ca ²⁺] _i (FI)
A	Same vol. of medium	20	320.26±147.99
B	50	22	386.00±163.85 ^b
C ₁	200	25	1 367.56±133.98 ^d
C ₂	100	28	916.78±151.46 ^d
C ₃	50	26	724.26±151.33 ^d
D	100+20	24	776.36±144.10 ^f

^b*P*<0.01 vs negative control; ^d*P*<0.001 vs negative control; ^f*P*<0.01 vs medium dose group and negative control.

Table 9 Changes of intracellular [Ca²⁺]_i in human gastric carcinoma cells after treated with HMD for 24 h

Group	Concentration (μg/ml)	No. of cells	[Ca ²⁺] _i (FI)
A	Same vol. of medium	22	323.50±141.35
B	50	25	382.67±135.02 ^b
C ₁	200	23	824.63±155.65 ^d
C ₂	100	23	672.65±165.16 ^d
C ₃	50	27	532.46±146.76 ^d
D	100+20	26	579.16±147.20 ^f

^b*P*<0.01, ^d*P*<0.001 vs negative control; ^f*P*<0.01 vs medium dose group and negative control, respectively.

Table 10 Changes of intracellular [Ca²⁺]_i in human gastric carcinoma cells after treated with HMD for 36 h

Group	Concentration of drug (μg/ml)	No. of cells	[Ca ²⁺] _i (FI)
A	Same vol of medium	30	339.97±150.19
B	50	23	399.83±159.52 ^b
C ₁	200	25	833.84±133.10 ^d
C ₂	100	26	684.31±148.45 ^d
C ₃	50	23	519.00±170.92 ^d
D	100+20	32	583.67±144.80 ^f

^b*P*<0.01, ^d*P*<0.001 vs negative control; ^f*P*<0.01 vs medium dose group and negative control group separately.

Table 11 Changes of intracellular $[Ca^{2+}]_i$ in human gastric carcinoma cells after treated with HMD for 48 h

Group	Concentration of drug given ($\mu\text{g/ml}$)	No. of cells	$[Ca^{2+}]_i$ (FI)
A	Same vol. of medium	22	328.45 \pm 135.15
B	50	36	380.42 \pm 151.46 ^b
C ₁	200	33	1 119.55 \pm 193.94 ^d
C ₂	100	28	787.00 \pm 178.19 ^d
C ₃	50	21	547.29 \pm 142.25 ^d
D	100+20	26	693.38 \pm 168.15 ^f

^b $P < 0.01$, ^d $P < 0.001$ vs negative control; ^f $P < 0.01$ vs separately medium dose group and negative control group.

Table 12 Changes of $[Ca^{2+}]_i$ in human gastric carcinoma cells after treated with HMD for different times

Different durations of treatment (h)	No. of cells	$[Ca^{2+}]_i$ (FI)
12	28	916.78 \pm 151.46
24	23	672.65 \pm 165.16
36	26	684.31 \pm 148.41
48	28	787.00 \pm 178.19

The experimental results indicated that when HMD was used for treatment of tumor cells, an increase of intracellular free calcium ion concentration was observed regardless of the duration of treatment. But comparatively, at the early stage of treatment (12 h), the range of increase was most evident (Table 12).

DISCUSSION

Gastric carcinoma, as one of the most common human malignant tumors, ranks the first leading cause of gastrointestinal cancer-related mortality worldwide. In China, it now ranks the second. It has been shown that tumor apoptosis played an important role in its growth, invasion, metastasis and recurrence^[10-29].

HMD is a compound TCM preparation for injection in combination with modern synthetic drugs. It has an obvious anti-neoplastic activity shown by extensive pharmacological studies. In the present study *in vitro* experiments with MTT and cell colony formation were carried out to assess its inhibition on 8 human cancer cell lines. It showed that HMD could inhibit the growth of cancer cell lines. The anti-neoplastic activity of HMD was most prominent against human gastric carcinoma BGC-823, human esophagus carcinoma E_{ca-109}, and human colon carcinoma HCT-8 cell lines in a dose dependent manner. These results were consistent with the clinical effects of HMD on dysphagia and regurgitation, suggesting that HMD was extremely sensitive to carcinomas of the digestive tract. *In vivo* anti-neoplastic activity of HMD was studied by transplanting various cancer cell lines (proventricular FC, S₁₈₀ sarcoma and H₂₂ liver cancer) into experimental animals to observe its inhibition on tumor growth. It showed that HMD could inhibit the growth of FC and S₁₈₀ tumors in a positive dose-effect manner. It also significantly prolonged the life span of H₂₂ bearing mice, though its potency was not comparable to those obtained in FC and S₁₈₀-bearing mice. This indicates that HMD is more potent for solid tumors than ascitic carcinoma, which also conforms with the clinical observations.

HMD injection is composed of 2 parts, a compound TCM formula and a synthetic drug 5-fluorouracil (5-Fu). In the above *in vivo* and *in vitro* anti-neoplastic studies, controls with TCM formula or 5-Fu alone were included to compare their individual and combined efficacy. Results showed that the anti-

neoplastic action of HMD injection exceeded that of TCM formula or 5-Fu alone (at the same dosage level). Thus, it seemed that TCM formula and 5-Fu had an excellent synergism when used in combination.

To obtain a deeper understanding of the mechanism of the anti-neoplastic action of HMD on human gastric carcinoma, we carried out further studies on the induction of cell apoptosis of human gastric carcinoma SGC-7901 by HMD.

Cell apoptosis, as an autonomic process of organisms, is intrinsically different from necrosis in pathological conditions. Cell apoptosis is a "suicidal" process on its own accord under physiological condition, though it may also involve some pathological events. But, undoubtedly it plays an important role in the recovery and maintenance of normal physiological function. Carcinogenesis is not merely due to abnormal cell proliferation and differentiation, but the mechanisms of cell apoptosis, which leads to neoplastic occurrence, development, evolution, metastasis and eventually death of tumor-bearing hosts should also be duly considered. The mechanism of cell apoptosis in the etiology of carcinogenesis might be induced by many factors, such as inactivation and mutagenesis of apoptotic gene or inhibition of the process of apoptotic gene expression, apoptotic mechanism caused by chemical carcinogens or virus, apoptosis insufficiency of precancerous cell, apoptosis insufficiency of cancer cells due to immunological response of the organism, inhibition of tumor cell apoptosis by adhesion factor and growth factor of the host, attempts of tumor cells to avoid apoptosis by lowering their dependence on survival signal while enhancing their survival competence thereby aggravating the disease with metastasis^[30].

The relationship between cell apoptosis and carcinogenesis provides us a new pharmacological mechanism and target for the study of anti-neoplastic drugs. As an anti-neoplastic drug, if it is very potent to induce tumor cell apoptosis and to activate the programmed cell death process, then it can avoid a great number of untoward side effects due to the release of waste material resulted from cell necrosis, and alleviate the damage of normal cells caused by chemotherapy and prolong the life of patients.

Experimental studies of the effect of HMD on apoptosis of human gastric cancer cell line showed that there was a definite trend to promote cell apoptosis, but with the increase of dosage no further increase of cell apoptosis could be observed. This might be due to the fact that the increased dose caused a sufficient amount of tissue necrosis, which overshadowed cell apoptosis. The positive control 5-Fu was found unable to induce cell apoptosis which coincided with the finding that 5-Fu could enhance the tolerability of cells toward apoptosis as reported in the literature^[30]. Therefore it seems to be possible that the effective ingredient responsible for the induction of apoptosis is the polysaccharides present in HMD formula. Sea weed polysaccharides is known to possess cytotoxicity that can inhibit and kill cancer cells directly, and when excited by low doses of a cytotoxic agent it can induce cell apoptosis, while polysaccharides from *astragalus chrysopterur* can enhance the cytotoxicity of NK cells of mice. Such NK cell induced death of the target cell is known as apoptosis.

It has been found that the majority of active cells were proliferating at the S stage of DNA synthesis, while the differentiated cells were stagnant at the G₁/G₀ stage^[31], when DNA synthesis was not in progress. Anti-neoplastic agents can markedly change the kinetic features of cell cycle such as that occurred in tumor cells from S₁₈₀ mice by the action of HMD. Moreover, different doses of HMD had different effects on cell cycle kinetics. At small (50 $\mu\text{g/ml}$) and medium (100 $\mu\text{g/ml}$) doses, HMD could block cell growth at G₁/G₀ stage and S stage. Larger doses of HMD could cause the cells to remain at G₂ and M stage resulting in an obvious increase of G₂ and M cells,

indicating that different doses of HMD showed different anti-neoplastic mechanisms. Regarding its induction of cell apoptosis, HMD also showed several different mechanisms.

HMD exerts its anti-neoplastic action by inducing cell apoptosis of the tumor cells. Ca^{2+} has been found to play an important role in the transmission system of this pathway^[37]. To clarify the relationship between the mechanisms of the anti-neoplastic activity of HMD and the intracellular Ca^{2+} concentration, we tried to observe the effect of HMD on the Ca^{2+} concentration in cancer cells by confocal laser scanning microscopic technique.

Calcium presents in the body in two different forms: the combined form and the ionic form (Ca^{2+}). Only the ionic form shows physiological activity. Such calcium ions are divided into intracellular and extracellular types. It was shown that Ca^{2+} concentration in extracellular fluid was about 10^{-3} mol/L, while the intracellular concentration was only 10^{-7} mol/L. They were always maintained at this definite level with intracellular concentration being only 1/10 000 of that of the extracellular one. It has become increasingly evident nowadays that this seemingly negligible change of intracellular Ca^{2+} concentration interferes with many physiological and metabolic functions, especially transmission of cellular signals. At present, Ca^{2+} is regarded as a rather important second messenger and at the same time, participates in or coordinates with the metabolism of other second messengers and the regulation of cell functions.

In the transmission of cell signals, either intrinsic or extrinsic signals pass through the cell membrane to get into cytoplasm and enter into cell nuclei to induce changes of gene expression. Three pathways for a signal to cross over cell membrane have been found^[38]: through the mediation of tyrosine protein kinase, G-protein or the ionic channel^[32]. The signal transmission in cytoplasm was mainly accomplished by the messenger adenylate cyclase, lipositol and calcium calmodulin^[33]. Five corresponding transmission pathways which can induce apoptosis may be derived from the above 3 messengers. They are the Ca^{2+} signal system in cells, the cAMP/PKA signal system, the DG/PKC signal system, the tyrosine protein kinase system, and the acylsphingosine pathway. The main signal molecules in these messengers include cAMP, IP_3 , PKC and Ca^{2+} , in which Ca^{2+} could play a pivotal role in the transmission^[7,38]. Therefore, in our study on the mechanism of transmission of apoptosis signal to tumor cells, Ca^{2+} was first selected.

In the present study, Fluo-3/AM was used as the fluorescence indicator, and confocal laser scanning microscopy technique was used to determine the dynamic change of $[\text{Ca}^{2+}]_i$ in human gastric carcinoma SGC-7901 cell line after different durations of drug administration. Therefore, the study was performed at 4 different stages of 12, 24, 36 and 48 h. In each stage, the dose-dependent manner of the effect of HMD on intracellular $[\text{Ca}^{2+}]_i$ was observed. Experimental results showed that the Ca^{2+} concentration of all the HMD treated groups, regardless of the stage, was higher than that of the negative blank control ($P < 0.001$), and the extent of elevation by high, medium and low dosage of HMD was dose-dependent. As to groups dosed for different length of time, the group dosed for 12 h showed a most drastic elevation of Ca^{2+} concentration. All the other time groups showed a larger Ca^{2+} concentration change than the negative control though smaller than that of the 12 h group. This result conformed with literature reports that the elevation of Ca^{2+} was closely related to the early apoptosis.

Cohen and Duke^[34] found a continual increase of $[\text{Ca}^{2+}]_i$ when apoptosis of thymocytes was induced by glucocorticoid. Further studies found that the intrinsic endonuclease which caused DNA fragmentation was Ca^{2+} and Mg^{2+} dependent and the activity of this enzyme was obviously enhanced as the

concentration in cytoplasm was elevated. Similarly, when VP-16 or TNF was used to induce apoptosis of breast cancer cells, $[\text{Ca}^{2+}]_i$ was also elevated to activate the Ca^{2+} dependent endonuclease, causing DNA fragmentation and cell apoptosis^[35]. As shown in the present study HMD could induce apoptosis of cancer cells, and cause an increase of intracellular $[\text{Ca}^{2+}]_i$ similar to the changes of $[\text{Ca}^{2+}]_i$ when apoptosis of other cancer cell lines occurred^[38], which could explain why Ca^{2+} could activate Ca^{2+} dependent endonuclease leading to apoptosis.

While Ca^{2+} , with its pivotal role in those signal transmission systems may induce cell apoptosis through several different approaches: (1) to activate the Ca^{2+} dependent endonuclease causing apoptosis; (2) the elevation of Ca^{2+} activates PKC directly and at the same time helps DG to activate PKC, which is a bifunctional kinase that not only regulates cell differentiation but also induces cell apoptosis; (3) after the elevation of Ca^{2+} , it combines with CaM to form a complex Ca-CaM, which activates adenylate cyclase (AC) resulting in the activation of cAMP/PKA signal system, thereby activating PKA to induce tumor cell apoptosis; (4) Ca^{2+} could control the activity of glutamyl transferase resulting in cell apoptosis, though its exact mechanism is still unclear. In brief, Ca^{2+} plays a specific role in transmission of cell signals of apoptosis. HMD is capable of inducing tumor cell apoptosis by elevating intracellular $[\text{Ca}^{2+}]_i$.

Ca^{2+} comes from two sources when cellular $[\text{Ca}^{2+}]_i$ increases. One is the inflow of Ca^{2+} from extracellular sources, mainly by opening calcium channels, The other is the release of Ca^{2+} from intracellular calcium storage. Ca^{2+} in cells is mainly stored in endoplasmic reticulum/seroplasmic reticulum and is mainly regulated by IP_3 . To trace the source of Ca^{2+} when intracellular $[\text{Ca}^{2+}]_i$ in gastric carcinoma cells was elevated by HMD, we tried on an additional "verapamil group", with the use of a calcium channel blocker added to the medium dosage group of HMD. We deduced that one of the following results might occur. (1) If Ca^{2+} only came from extracellular calcium inflow, the $[\text{Ca}^{2+}]_i$ value should be similar to that of the negative control. (2) If Ca^{2+} came only from the release of intracellular storage, the $[\text{Ca}^{2+}]_i$ value should be similar to that of the medium dose of HMD group. (3) If the Ca^{2+} came from both extracellular Ca^{2+} inflow and intracellular Ca^{2+} release, the $[\text{Ca}^{2+}]_i$ value should be between those of negative control and medium dose HMD with statistical significance. Results of the experiment showed that the $[\text{Ca}^{2+}]_i$ value was higher than that of the negative control, but lower than that of the medium dose HMD group with statistical significance ($P < 0.001$). It indicated that HMD elevated intracellular $[\text{Ca}^{2+}]_i$ to induce tumor cell apoptosis and caused the opening of calcium channels, which facilitated Ca^{2+} inflow and interacted with receptors on the membrane to produce IP_3 for the release of Ca^{2+} from its storage.

From this study we conclude that HMD shows a remarkable cytotoxicity against tumor cells. Its mechanism of action is to increase intracellular $[\text{Ca}^{2+}]_i$ by opening the calcium channels of cell membrane, and initiate the release of Ca^{2+} from its storage to induce tumor cell apoptosis.

REFERENCES

- 1 **Chen W**, Zhou X, Xu Q, Guo W, Lin L. Chemosensitivity testing of oral and maxillofacial cancer with biopsy specimens. *Zhonghua Kouqiang Yixue Zazhi* 2002; **37**: 404-407
- 2 **Gui LR**, Zhou Y, Zhang BL, Li WB. Pituitary adenylate cyclase activating polypeptide protects neuro-2a cells from beta amyloid protein cytotoxicity by modulating intracellular calcium. *Shengli Xuebao* 2003; **55**: 42-46
- 3 **Han R**, Xu CX, Li ZR. The Research and Laboratory Technique of Anti-tumor Drug. Beijing: The United Press of Beijing Medical University and Peking Union Medical College 1997: 283

- 4 **Wang Q**, Wu LM, Li AY, Zhao Y, Wang NP. Experimental studies of antitumor effect of artesunate on liver cancer. *Zhongguo Zhongyao Zazhi* 2001; **26**: 707-708
- 5 **Wang LJ**, Wang Y, Chen SW, Ma JS, Fu Q, Wang BX. The antitumor activity of Diosgenin *in vivo* and *in vitro*. *Zhongguo Zhongyao Zazhi* 2002; **27**: 777-779
- 6 **Gao J**. Basic and Experiment of Oncolog. Beijing: The United Press of Beijing Medical University and Peking Union Medical College 1992: 61-67
- 7 **Han R**. The Research and Laboratory. Technique of Anti-tumor Drug. Beijing: The United Press of Beijing Medical University and Peking Union Medical College 1997: 400
- 8 **Wang Z**, Wang Y, Huang Z, Zhong S, Wu Y, Yu L. Study on antitumor effect and mechanism of aloe polysaccharides. *Zhongyao Cai* 2001; **24**: 350-353
- 9 **Huang YH**, Zhen YS. Rhein induces apoptosis in cancer cells and shows synergy with mitomycin. *Yaoxue Xuebao* 2001; **36**: 334-338
- 10 **Zhang T**, Cao EH, Li JF. A laser scanning confocal microscopy method. Simultaneous detection of intracellular Ca²⁺ and apoptosis using Fluo-3 and Hoechst 33342. *Anal Quant Cytol Histol* 2000; **22**: 93-97
- 11 **Miao ZH**, Tang T, Zhang YX, Zhang JS, Ding J. Cytotoxicity, apoptosis induction and downregulation of MDR-1 expression by the anti-topoisomerase II agent salivicine, in multidrug-resistant tumor cells. *Int J Cancer* 2003; **106**: 108-115
- 12 Gupta MK, Qin RY. Mechanism and its regulation of tumor-induced angiogenesis. *World J Gastroenterol* 2003; **9**: 1144-1155
- 13 **Kaledin VI**, Nikolin VP, Baimak TY, Galyamova MR, Popova Andreeva EM. Phenobarbital modifies antitumor effect of cyclophosphamide depending on the type of tumor cell death caused by it. *Bull Exp Biol Med* 2003; **135**: 289-292
- 14 **Kasibhatla S**, Tseng B. Why target apoptosis in cancer treatment? *Mol Cancer Ther* 2003; **2**: 573-580
- 15 **Guzman E**, Langowski JL, Owen-Schaub L. Mad dogs, Englishman and apoptosis: The role of cell death in UV-induced skin cancer. *Apoptosis* 2003; **8**: 315-325
- 16 **Steinbach JP**, Wolburg H, Klumpp A, Probst H, Weller M. Hypoxia-induced cell death in human malignant glioma cells: energy deprivation promotes decoupling of mitochondrial cytochrome c release from caspase processing and necrotic cell death. *Cell Death Differ* 2003; **10**: 823-832
- 17 **Kim WH**, Hong F, Radaeva S, Jaruga B, Fan S, Gao B. STAT1 plays an essential role in LPS/D-galactosamine induced liver apoptosis and injury. *Am J Physiol Gastrointest Liver Physiol* 2003; **285**: G761-768
- 18 **Westphal S**, Kalthoff H. Apoptosis: Targets in Pancreatic Cancer. *Mol Cancer* 2003; **2**: 6
- 19 **Kountouras J**, Zavos C, Chatzopoulos D. Apoptosis in hepatocellular carcinoma. *Hepatogastroenterology* 2003; **50**: 242-249
- 20 **Hood JD**, Cheresch DA. Role of integrins in cell invasion and migration. *Nat Rev Cancer* 2002; **2**: 91-100
- 21 **Folkman J**. Angiogenesis and apoptosis. *Semin Cancer Biol* 2003; **13**: 159-167
- 22 **Oleinick NL**, Morris RL, Belichenko I. The role of apoptosis in response to photodynamic therapy: what, where, why, and how. *Photochem Photobiol Sci* 2002; **1**: 1-21
- 23 **Altieri DC**. Survivin and apoptosis control. *Adv Cancer Res* 2003; **88**: 31-52
- 24 **Schmitt CA**. Senescence, apoptosis and therapy-cutting the lifelines of cancer. *Nat Rev Cancer* 2003; **3**: 286-295
- 25 **Nijhawan R**, Hemachandran M, Joshi K. Apoptosis in breast cancer. *Acta Cytol* 2003; **47**: 193-196
- 26 **Tsuruo T**. Molecular cancer therapeutics: recent progress and targets in drug resistance. *Intern Med* 2003; **42**: 237-243
- 27 **Tsuruo T**, Naito M, Tomida A, Fujita N, Mashima T, Sakamoto H, Haga N. Molecular targeting therapy of cancer: drug resistance apoptosis and survival signal. *Cancer Sci* 2003; **94**: 15-21
- 28 **Hernandez MO**, Neves I, Sales JS, Carvalho DS, Sarno EN, Sampaio EP. Induction of apoptosis in monocytes by mycobacterium leprae *in vitro*: a possible role for tumour necrosis factor-alpha. *Immunology* 2003; **109**: 156-164
- 29 **Liu JD**, Wang YI, Chen CH, Yu CF, Chen LC, Lin JK, Liang SY, Ho YS. Molecular mechanisms of G0/G1 cell-cycle arrest and apoptosis induced by terfenadine in human cancer cells. *Mol Carcinog* 2003; **37**: 39-50
- 30 **Wu H**, Goel V, Haluska FG. PTEN signaling pathways in melanoma. *Oncogene* 2003; **22**: 3113-3122
- 31 **Zhao WH**. Apoptosis. Zhengzhou: Henan Medical University Press 1997: 89
- 32 **Han R**. The Research and Laboratory Technique of Anti-tumor Drug Beijing: The Union Press of Beijing Medical University and Peking Union Medical College 1997: 346
- 33 **Lee YS**, Jin DQ, Kwon EJ, Park SH, Lee ES, Jeong TC, Nam DH, Huh K, Kim JA. Asiatic acid, a triterpene, induces apoptosis through intracellular Ca²⁺ release and enhanced expression of p53 in HepG2 human hepatoma cells. *Cancer Lett* 2002; **186**: 83-91
- 34 **Xing C**, Chen J, Xu H. Changes in [Ca²⁺]_i and IP₃ levels in the process of cisplatin-induced apoptosis of gastric carcinoma. *Zhonghua Zhongliu Zazhi* 1999; **21**: 256-258
- 35 **Sun DY**, Guo YL, Ma LG. Cell Signal Transduction (the second edition). Beijing: Science and Technology Press 1998: 28,42
- 36 **Cao ZY**. Hormone Acceptor and Clinical Application. Beijing: The Union Press of Beijing Medical University and Peking Union Medical College 1993: 48-70
- 37 **Cohen JJ**, Duke RC. Glucocorticoid activation of a calcium-dependent endonuclease in thymocyte nuclei leads to cell death. *J Immunol* 1984; **132**: 38-42
- 38 **Robinson JM**, Smith DF, Davis EM, Gilliam EB, Capetillo SC, Walborg EF Jr. Partial characterization of rat hepatoma cell-surface glycopeptides possessing concanavalin A receptor activity. *Biochem Biophys Res Commun* 1976; **72**: 81-88

Edited by Wang XL and Zhu LH

Expression of nuclear factor-kappa B and target genes in gastric precancerous lesions and adenocarcinoma: Association with *Helicobacter pylori* cagA (+) infection

Gui-Fang Yang, Chang-Sheng Deng, Yong-Yan Xiong, Ling-Ling Gong, Bi-Cheng Wang, Jun Luo

Gui-Fang Yang, Yong-Yan Xiong, Ling-Ling Gong, Bi-Cheng Wang, Jun Luo, Department of Pathology, Zhongnan Hospital, Wuhan University, Wuhan 430071, Hubei Province, China

Chang-Sheng Deng, Department of Gastroenterology, Zhongnan Hospital, Wuhan University, Wuhan 430071, Hubei Province, China
Supported by grants from the Bureau of Science and Technology of Hubei Province, No. 2003AA301C27

Correspondence to: Dr. Gui-Fang Yang, Department of Pathology, Zhongnan Hospital, Wuhan University, Wuhan 430071, Hubei Province, China. caiyang@public.wh.hb.cn

Telephone: +86-27-67813159

Received: 2003-06-05 **Accepted:** 2003-07-24

Abstract

AIM: To examine the expression of nuclear factor kappaB (NF- κ B) and its target genes in intestinal metaplasia (IM), dysplasia (DYS) and gastric carcinoma (GC) infected with *Helicobacter pylori* (*H. pylori*) and to investigate the mechanism underlying *H. pylori* cytotoxin associated gene A (cag A) infection leading to gastric adenocarcinoma.

METHODS: Expressions of NF- κ B/p65 and its target genes: c-myc, cyclinD1 and bcl-x1 were immunohistochemically examined in 289 cases of gastric biopsy and resection specimens from patients with IM, DYS and GC infected with *H. pylori*. *H. pylori* in the above mentioned tissues was detected by Warthin-Starry stain and rapid urease tests. IgG antibody to cagA in sera of the patients was measured by ELISA.

RESULTS: The positive rates of NF- κ B/p65 were significantly higher in groups with cagA of IM I-II(28/33), IM III(48/52), DYS I(27/31), DYS II-III(28/32), GC(35/40) than in groups without cagA of IM I-II(4/17), IM III(3/20), DYS I(3/20), DYS II-III(6/21), GC(10/23). The expressions of c-myc, cyclinD1, and bcl-x1 were significantly higher in groups with cagA of IM III(47/52, 49/52, 46/52), DYS II-III(29/32, 26/32, 25/32) than in groups without cagA of IM I-II(8/20, 7/20, 5/20), DYS II-III(10/21, 8/21, 3/21), which were in conformity with the expression of NF- κ B in IM III, and DYS II-III. A significantly higher expression level of NF- κ B/p65, c-myc, cyclinD1 and bcl-x1 was detected in intestinal type GC(27/28, 18/28, 22/28, 24/28) than in diffuse type GC(8/12, 3/12, 3/12, 6/12), respectively.

CONCLUSION: There may be two different molecular mechanisms in the occurrence of intestinal and diffuse type gastric carcinomas. Intestinal type gastric carcinoma is strongly associated with high expression of c-myc, cyclinD1 and bcl-x1 through NF- κ B/p65 activated by *H. pylori* cagA. Inhibiting the activity of NF- κ B is an effective and promising way to prevent intestinal type gastric carcinoma.

Yang GF, Deng CS, Xiong YY, Gong LL, Wang BC, Luo J. Expression of nuclear factor-kappa B and target genes in gastric

precancerous lesions and adenocarcinoma: Association with *Helicobacter pylori* cagA (+) infection. *World J Gastroenterol* 2004; 10(4): 491-496

<http://www.wjgnet.com/1007-9327/10/491.asp>

INTRODUCTION

A close link between gastric carcinoma and *H. pylori* infection has been found^[1-6]. Animal models of gastric carcinoma induced by *H. pylori* provide strong evidence^[7-10]. There is a close association between *H. pylori* cagA infection and non-cardio gastric carcinoma^[11-13]. However, the exact mechanism of *H. pylori* cagA leading to gastric carcinoma remains indistinct.

NF- κ B is a sequence-specific transcription factor known to be involved in inflammatory and immune responses. A wide variety of genes regulated by NF- κ B includes those encoding cytokines, antimicrobial peptides, adhesion molecules^[14]. Recently, it has been found that NF- κ B contributes to the activation of genes encoding regulators of anti-apoptosis and cell proliferation. Hence, the role of NF- κ B in tumorigenesis has attracted increasing attention. It is well documented that cagA of *H. pylori* can activate NF- κ B and *H. pylori* cagA infection often causes chronic atrophic gastritis accompanied by intestinal metaplasia and dysplasia. NF- κ B is not only involved in inflammatory responses but also related to carcinogenesis^[15-18]. We deduce that NF- κ B may be an important link between these two processes. This study was to investigate the possible association between *H. pylori* cagA infection and the expression of NF- κ B/p65 and its target genes in GC. Warthin-Starry staining and rapid urease tests were performed to detect *H. pylori*. ELISA was employed to measure IgG antibody to cagA. HID/AB/PAS staining method was used to distinguish sulphates, neutral and acid mucin. Immunohistochemical techniques were employed to determine the expression of NF- κ B/p65 and its target genes in specimens of IM, DYS, and GC.

MATERIALS AND METHODS

Patients and specimens

A total of 289 cases were recruited from patients suffering from gastritis who underwent endoscopic examination and biopsy and from gastric cancer patients received surgical resections from 2001 to 2002 at Zhongnan Hospital, Wuhan. Among the 289 cases, 179 were male and 110 were female. The average age was 48.5 years (range, 19-75 years). From each patient four samples were taken from gastric antrum and corpus, respectively. Rapid urease tests were done first. Patients who obtained positive results had their blood samples taken, which were stored at -20°C until ELISA assay. No patients had received chemotherapy or radiation therapy before surgery. Samples were fixed in 10% neutrally buffered formalin for histological, histochemical and immunohistochemical studies.

Pathological analysis

For histological evaluation, formalin-fixed tissues were embedded in paraffin, cut into 4 μm thick sections and stained with H&E. GC was histologically divided into early stage and advanced stage, with or without lymph node metastasis, intestinal type and diffuse type^[19].

Intestinal metaplasia was classified into three sub-types according to both morphological and histochemical criteria. Dysplasia was divided into three grades^[20-21].

ELISA

The presence of serum anti-cagA IgG antibody was tested with commercial enzyme-linked immunosorbent assay (ELISA) kits (Jing Ying Biotechnology Company, Shanghai). Briefly, a recombinant protein fragment of cagA, a purified form of *Escherichia coli* cell lysates, was used as an antigen and fixed to a 96-well plate in carbonate-bicarbonate buffer. After incubation of treated wells with serum diluted 1:100, alkaline phosphatase-conjugated goat anti-human IgG was added. After addition of phosphatase substrate, absorbance was read at 405 nm. Based on the results from *H pylori*-negative controls, a value of ≥ 0.18 was considered to be positive of IgG antibodies.

Histochemistry

Mucin histochemical studies were performed using HID/AB/PAS staining described by Walsh *et al* and Xin *et al*^[22,23]. IM I (complete type) showed a positive staining of AB (blue color). IM II (incomplete small intestinal type) had PAS (magenta color) and AB positive staining. IM III (incomplete colonic metaplasia) had both positive A B (blue color) and HID staining (sulphomucins brown in color) (as shown in Figure 1).

Warthin-Starry stain was carried out using standard histological laboratory methods. Positive *H pylori* showed dark-brown-stained bacillary structures in epithelium of mucosa or in glandular recess (as shown in Figure 2). Samples of positive ELISA and rapid urease test or Warthin-Starry stain were considered to be *H pylori* cagA positive. Samples of positive rapid urease test and Warthin-Starry stain were considered to be *H pylori* positive.

Immunohistochemistry

Serial 4 μm thick sections were made and mounted on poly L-lysine coated slides. Paraffin sections were immersed in xylene for 5 minutes and hydrated using a gradient series of alcohol. Antigen retrieval was routinely performed by immersing the sections in citric acid buffer (pH 6.0), in a microwave oven for 15 min. Endogenous peroxidase activity was blocked with 3% hydrogen peroxide for 10 min and then incubated with a primary antibody in a humidified chamber at 4°C overnight. Primary antibody was monoclonal mouse anti-NF- κB /p65 antibody (Santa Cruze) at 1:200 dilution. Monoclonal mouse anti-cyclinD1, *c-myc* antibody (Maixin Biotechnology Company), monoclonal mouse anti-bcl-xl antibody (Beijing Zhongsheng Biotechnology Company) and ultrasensitive SP kit were obtained from the above-mentioned two companies. Sections were counterstained for 5 min with Delafield's haematoxylin and then mounted. Human colon cancer having infiltration of lymphatic cells with intense staining for NF- κB , *c-myc*, cyclinD1, bcl-xl was used as a positive control. As a negative control, PBS was used instead of primary antibodies. Expressions of NF- κB , *c-myc*, cyclinD1, bcl-xl in carcinoma cells, metaplastic and dysplastic epithelia were evaluated according to the ratio of positive cells and defined as negative (0-9%) and positive (10-100%). Positive cells of NF- κB /p65 mainly showed a plasmatic staining (Figure 3). Positive cells of *c-myc*, cyclin D1 showed nuclear and plasmatic staining and bcl-xl showed a plasmatic staining (Figure 3).

Statistical analysis

Differences among groups were evaluated by using Chi-square test and Fisher's exact test. Differences were considered to be statistically significant at $P < 0.05$.

RESULTS

The highest positive rates of NF- κB /p65 and its target genes were in IM III among IM I-II, IM II, DYS I, DYS II-III and GC, but there were no significant differences among them (Table 1). The expression of NF- κB /p65 was significantly

Table 1 Expression of NF- κB /p65 and its target genes in IM, DYS, GC infected with *H pylori*

	<i>n</i>	NF- κB /p65 positive(<i>n</i>)	%	C-myc positive (<i>n</i>)	%	CyclinD ₁ positive (<i>n</i>)	%	Bcl-xl positive (<i>n</i>)	%
IM I-II	50	32	64.00	35	70.00	34	68.00	33	66.00
IM III	72	51	70.83	55	76.39	56	77.78	51	70.83
DYS I	51	33	64.71	36	70.59	35	68.63	34	66.67
DYS II-III	53	34	64.15	39	73.58	34	64.15	28	52.83
GC	63	45	71.43	33	52.38	37	58.73	44	69.84

Table 2 Expression of NF- κB /p65 and target genes in IM, DYS, GC infected with and without cagA *H pylori*

	CagA (<i>n</i>)	NF- κB /P65 positive(<i>n</i>)	χ^2	Exact	C-myc positive (<i>n</i>)	χ^2	Exact	CyclinD ₁ positive (<i>n</i>)	χ^2	Exact	Bcl-xl positive (<i>n</i>)	χ^2	Exact
IM I-II	+33	28	18.311	0.000	22	0.514	0.533	21	0.849	0.524	21	0.242	0.757
	-17	4			13			13			12		
IM III	+52	48	41.785	0.000	47	20.331	0.000	49	29.319	0.000	46	28.158	0.000
	-20	3			8			7			5		
Dys I	+31	27	26.089	0.000	22	0.005	1.000	22	0.201	0.760	21	0.041	1.000
	-20	3			14			13			13		
Dys II-III	+32	28	19.154	0.000	29	12.065	0.001	26	10.268	0.001	25	20.736	0.000
	-21	6			10			8			3		
GC	+40	35	13.867	0.000	21	0.128	0.721	25	0.642	0.432	30	1.384	0.239
	-23	10			11			12			14		

Table 3 Relationship between expression of NF- κ B/p65, its target genes and clinicopathology of GC infected with *cagA H pylori*

Clinicopathology	n	NF- κ B/p65 positive (n)	χ^2	P	C-myc positive (n)	χ^2	P	CyclinD ₁ positive (n)	χ^2	P	Bcl-xl positive (n)	χ^2	P
Early stage	13	9	5.877	0.031	3	6.687	0.017	7	0.615	0.498	5		
Advanced stage	27	26			18			18			10	0.008	1.000
Intestinal type	28	27	6.803	0.022	18	5.199	0.038	22	10.286	0.003	24		
Diffuse type	12	8			3			3			6	5.714	0.041
Metastasis of LN	30	26	0.076	1.000	19	5.647	0.028	16	4.302	0.060	22		
No metastasis of LN	10	9			2			9			8	0.178	1.000

higher in groups with *H pylori cagA* of IMI-II(28/33), IM III (48/52), DYSI(27/31), DYSII-III(28/32), GC(35/40) than in groups without *H pylori cagA* of IMI-II(4/17), IM III(3/20), DYSI(3/20), DYSII-III(6/21), GC(10/23) as shown in Table 2. The expression of *c-myc*, cyclinD1, *bcl-xl* was significantly higher in groups with *cagA* of IM III(47/52, 49/52, 46/52), DYSII-III(29/32, 26/32, 25/32) than in groups without *cagA* of IM III(8/20, 7/20, 5/20), DYSII-III(10/21, 8/21, 3/21) (Figure 4), which was conformable to the expression of NF- κ B in IM III, DYSII-III, as shown in Table 2.

The expression of NF- κ B/p65, *c-myc*, cyclinD1, and *bcl-xl* was significantly higher in intestinal type GC(27/28, 18/28, 22/28, 24/28) than in diffuse type GC(8/12, 3/12, 3/12 and 6/12), respectively (Figure 5), as shown in Table 3. It was also observed that the expression of NF- κ B/p65, *c-myc* was higher in advanced GC (26/27, 18/27) than in early stage GC(9/13, 3/13) ($P<0.05$). The expression of *c-myc* was higher in groups with lymph node metastasis(19/30) than in groups without lymph node metastasis (2/10) ($P<0.05$) (Table 3).

We also observed the expression of NF- κ B/p65, *c-myc*, cyclinD1 in inflammatory cells of gastric lamina propria and stroma, and 5.6% nuclear staining of NF- κ B/p65 was in the groups with *H pylori cagA* in the tissues of IM, DYS and GC.

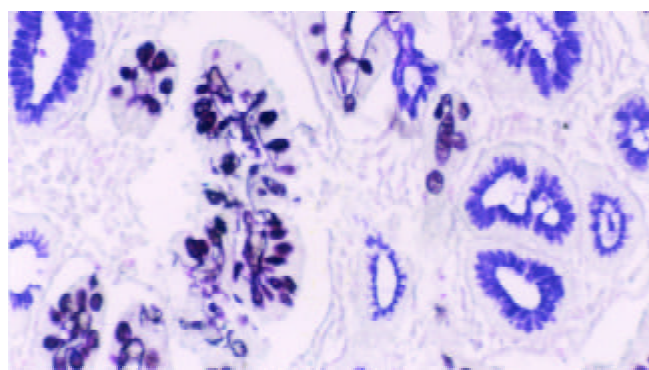


Figure 1 Type III intestinal metaplasia. Blue and brown stained mucin in cells. HID/AB/PAS stain $\times 200$.

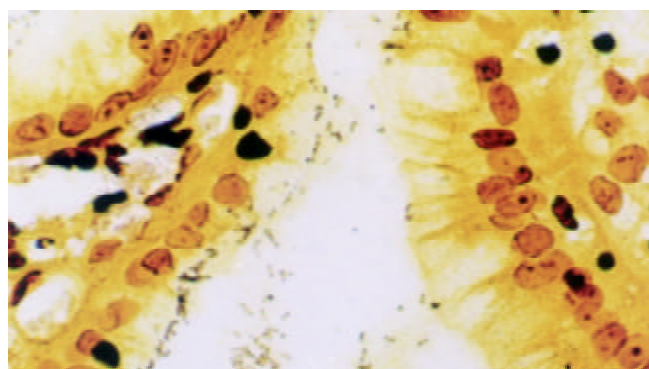


Figure 2 Dark-brown stained bacillary structures of positive *H pylori* in epithelium of mucosa. Warthin-Starry stain $\times 400$.

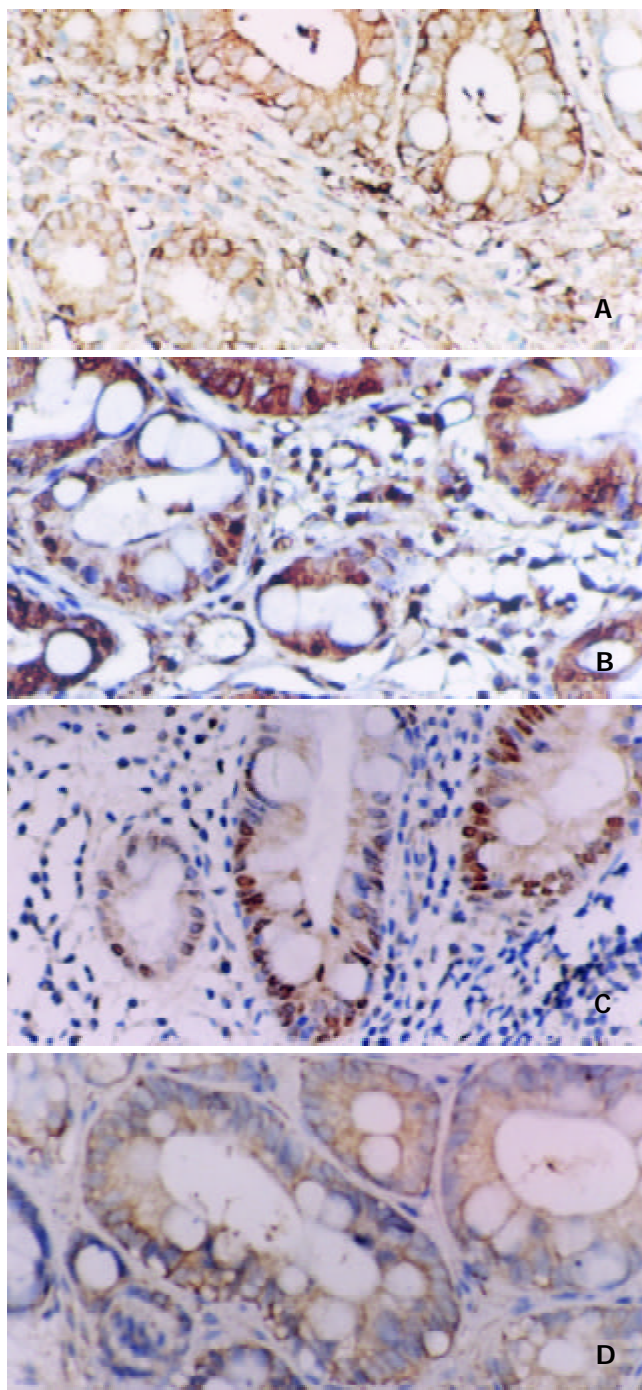


Figure 3 A: Positive expression of NF- κ B/p65 in IM. Some inflammatory cells showed plasmatic stain. Immunohistochemical stain $\times 200$. B: Positive expression of cyclinD1 in IM. Some inflammatory cells showed nuclear and plasmatic stains. Immunohistochemical stain $\times 200$. C: Positive expression of *c-myc* in IM. Some inflammatory cells showed nuclear and plasmatic stains. Immunohistochemical stain $\times 200$. D: Positive expression of *bcl-xl* in IM. Some inflammatory cells showed plasmatic stain. Immunohistochemical stain $\times 200$.

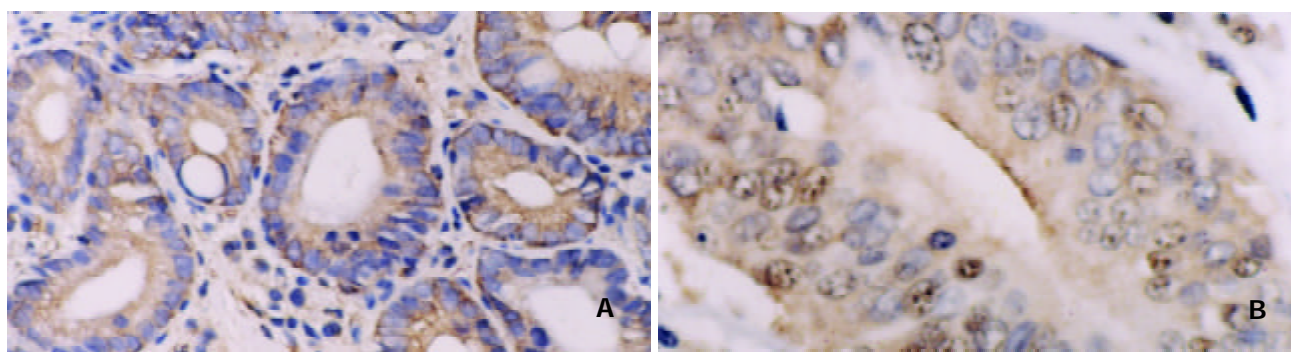


Figure 4 A: Positive expression of NF- κ B/p65 in DYS. Some inflammatory cells showed plasmatic stain. Immunohistochemical stain $\times 200$. B: Positive expression of c-myc in DYS III. Some inflammatory cells showed nuclear and plasmatic stains. Immunohistochemical stain $\times 400$.

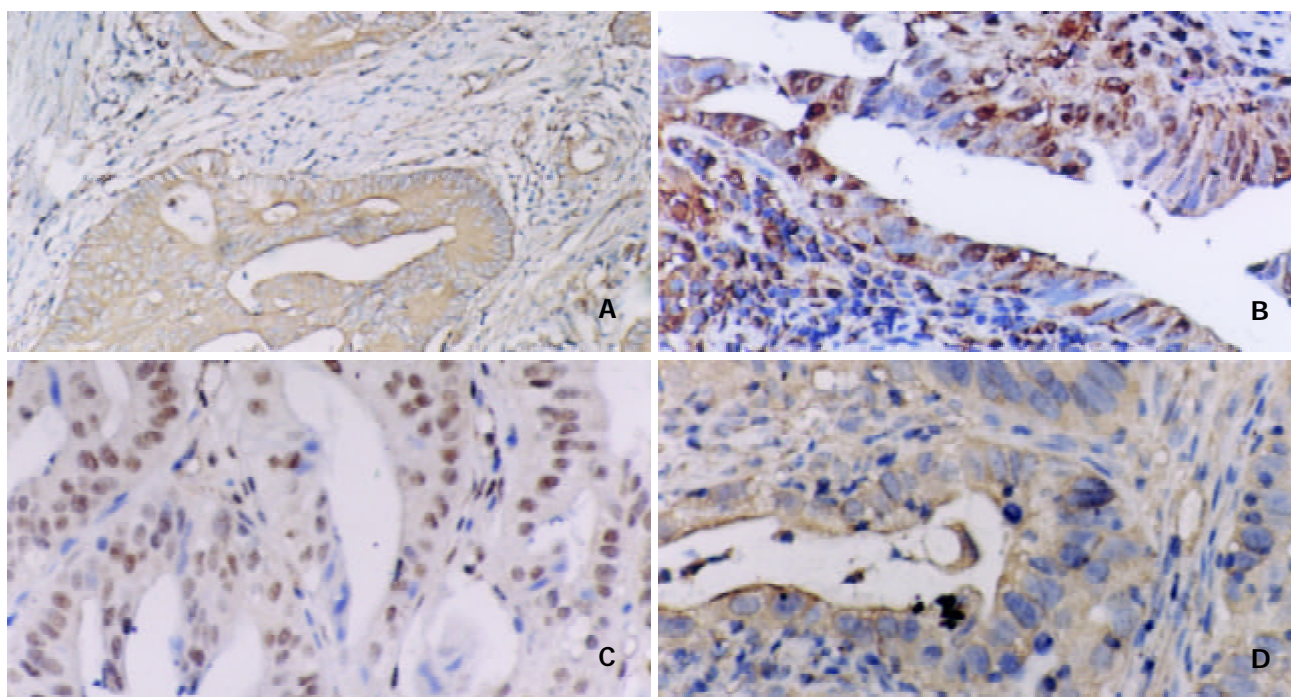


Figure 5 A: Positive expression of NF- κ B/p65 in intestinal type gastric carcinoma. Immunohistochemical stain $\times 200$. B: Positive expression of c-myc in intestinal type gastric carcinoma. Immunohistochemical stain $\times 200$. C: Positive expression of cyclinD1 in intestinal type gastric carcinoma. Immunohistochemical stain $\times 200$. D: Positive expression of bcl-xl in intestinal type gastric carcinoma. Immunohistochemical stain $\times 400$.

DISCUSSION

NF- κ B was first identified as a regulator of expression of the kappa light chain gene in murine B lymphocytes but has subsequently been found in many different cells^[14]. NF- κ B is made up of protein dimers that bind to a common sequence motif known as the κ B site. The activated form of NF- κ B is a heterodimer, which usually consists of two proteins: a p65 subunit and a p50 subunit. In unstimulated cells, NF- κ B is found in cytoplasm and is bound to I κ B, which prevents it from entering nuclei. When cells are stimulated, specific kinase phosphorylate I κ B results in I κ B's rapid degradation by proteasomes. The release of NF- κ B from I κ B would result in passage of NF- κ B into nuclei, where it binds to specific sequences in promoter regions of target genes and further activates target genes^[24-28].

H pylori cagA is one of the virulent strains of *H pylori*. Studies have demonstrated that activation of NF- κ B by *H pylori* requires genes in cag PAI (pathogenicity island). CagA protein of *H pylori* PAI can be translocated into gastric epithelial cells by a type IV secretion system encoded by cagPAI and is tyrosine-phosphorylated. Tyrosine phosphorylated cagA could

induce changes in the tyrosine phosphorylation status of distinct cellular proteins and further activate NF- κ B^[29-32]. In the present study, we found that high expression of NF- κ B/p65 was detected in the tissues of *H pylori* cagA group with metaplasia, dysplasia and gastric carcinoma. We also observed that expression of NF- κ B/p65 was mainly localized in cytoplasm. Although nuclear localization of NF- κ B was considered as equivalent to NF- κ B activation, it showed 5.6% positive rate in *H pylori* cagA group in our study, which was similar to that of Nakayama *et al*^[33]. Though it seems difficult to determine whether immunohistological detection of a certain protein reflects its dynamic localization, we believe that large amounts of NF- κ B/p65 in the cytoplasm of tissues infected with *H pylori* cagA may be easily activated by cagA of *H pylori*, even by a slight stimulation of cagA protein. NF- κ B/p65 activated by cagA up-regulated the expression of target genes in IM, DYS and GC, and might play an important role in the occurrence and development of gastric carcinoma caused by *H pylori* cagA infection. As one of the NF- κ B target genes^[34,35], bcl-xl belongs to the anti-apoptosis gene family and exerts its anti-apoptosis effect by inhibiting the release of apoptosis inducing factors.

Some investigations showed that tumor cells with activated NF- κ B were not sensitive to radio and chemotherapeutic agents, while inhibition of NF- κ B activity could enhance the radio- and chemosensitivity of cancer treatment^[36,37].

Activated NF- κ B has also been shown to directly stimulate the transcription of genes that encode *c-myc* and cyclinD1 because a κ B binding site is present within the *c-myc*, and cyclinD1 promoter^[16,38-40]. *c-myc* is known to be a strong inducer of proliferation and is believed to be critical for the oncogenic properties. Studies showed that aberrant *c-myc* expression was widespread in tumor cells and important for multistep carcinogenesis^[41,42]. However, proliferation induced by *c-myc* requires the concomitant mutant of p53. In gastric precancerous lesions infected with *H pylori*, mutants of p53 were often confirmed^[43,44]. cyclinD1 is a cell cycle regulatory gene. It is essential for G1 phase progression and has been implicated in the pathogenesis of several human malignancies, including gastric carcinoma^[45-47].

As evidenced here, high expressions of *c-myc*, cyclinD1, bcl-x1 concomitant with NF- κ B/p65 in the tissues of cagA+ of IM III and DYS II-III could drive cells inappropriately through the cell cycle to evade apoptosis, resulting in uncontrolled proliferation characteristic of neoplastic cells. In addition, weak to moderate staining of NF- κ B/p65, *c-myc*, cyclinD1 of inflammatory cells in the stroma of gastric lesions was observed. The above results, taken together, could be explained in two ways. First, *H pylori* cagA infection led to gastritis, and activated NF- κ B. Activated NF- κ B could promote inflammatory cells and epithelium of gastritis to produce large amounts of reaction oxygen species (ROS), cyclooxygenase-2 (COX-2), IL-6, and IL-8^[48-53]. ROS played an important role in damaging DNA of epithelium of gastric lesions^[54,55]. COX-2 could suppress epithelial cell apoptosis leading to cell proliferation. Some studies showed that overexpression of COX-2 had a strong association with gastric carcinoma^[56,57]. IL-6, and IL-8 could directly induce proliferation of epithelium^[58,59]. Second, cagA of *H pylori* activated NF- κ B in IM III and DYS II-III. Activated NF- κ B up-regulated the expression of *c-myc*, cyclinD1, bcl-x1, and prevented the death of epithelial cells that had undergone chromosomal rearrangements or other types of DNA damage. *c-myc*, cyclinD1 enhanced the proliferation of epithelial cells with mutant genes, leading to gastric carcinoma. Such cells are normally eliminated by means of checkpoint control, such as the p53 pathway. As previously mentioned, mutated p53 was often found in precancerous lesions of gastritis infected with *H pylori* cagA. The present study showed that the expression of NF- κ B/p65, *c-myc*, cyclinD1 and bcl-x1 was significantly higher in intestinal type carcinoma than in diffuse type carcinoma, suggesting that the occurrence of the two types of gastric adenocarcinomas may have different molecular mechanisms, which is similar to other author's viewpoint^[60,61]. *H pylori* cagA infection can lead to intestinal type gastric carcinoma which is strongly associated with the up-regulation of *c-myc*, cyclinD1 and bcl-x1 through NF- κ B. Moreover, the expression of NF- κ B and *c-myc* was higher in advanced stage than in early stage GC. There was no relationship between stages of gastric adenocarcinoma and expression of *c-myc*, cyclinD1, while higher expression of *c-myc* was detected in the group with lymph node metastasis as compared with the group without. It is concluded that high expression of NF- κ B/p65 and its target genes in *H pylori* cagA group of IM III, DYS II-III and intestinal type GC may play an important role in various stages of *H pylori* cagA induced intestinal type gastric carcinoma. In GC infected with *H pylori* cagA, the expression of NF- κ B/p65, *c-myc* is associated with infiltration of gastric carcinoma. Moreover, expression of *c-myc* is linked with lymph node metastasis of gastric carcinoma.

Our results suggest that there may be two different molecular

mechanisms in the development of intestinal and diffuse type gastric carcinomas. Intestinal type gastric carcinoma is associated with the high expression of *c-myc*, cyclinD1 and bcl-x1 through NF- κ B/p65 activated by *H pylori* cagA. A better understanding of the molecular mechanisms would contribute to the prevention and prognosis of gastric carcinoma.

REFERENCES

- Krejs GJ.** *Helicobacter pylori* and stomach cancer. *Acta Med Austriaca* 2000; **27**: 129-130
- Gschwantler M, Dragosics B.** Physiopathology of *Helicobacter pylori* infections. *Acta Med Austriaca* 2000; **27**: 117-121
- Koop H.** Prevention of gastric cancer: *Helicobacter*-eradication and immunization. *Schweiz Rudsch Med Rrax* 1998; **87**: 1233-1235
- Vandenplas Y.** *Helicobacter pylori* infection. *World J Gastroenterol* 2000; **6**: 20-31
- Zhuang XQ, Lin SR.** Research of *Helicobacter pylori* infection in precancerous gastric lesions. *World J Gastroenterol* 2000; **6**: 428-429
- Zhang ZW, Farthing MJG.** Molecular mechanisms of *H pylori* associated gastric carcinogenesis. *World J Gastroenterol* 1999; **5**: 369-374
- Yao YL, Xu B, Song YG, Zhang WD.** Overexpression of cyclin E in Mongolian gerbil with *Helicobacter pylori*-induced gastric precancerosis. *World J Gastroenterol* 2002; **8**: 60-63
- Fujioka T, Honda S, Tokieda M.** *Helicobacter pylori* infection and gastric carcinoma in animal models. *J Gastroenterol Hepatol* 2000; **15**(Suppl): D55-59
- Fujioka T, Murakami K, Kodama M, Kagawa J, Okimoto T, Sato R.** *Helicobacter pylori* and gastric carcinoma-from the view point of animal model. *Keio J Med* 2002; **51**(Suppl 2): 69-73
- Gao HJ, Yu LZ, Bai JF, Peng YS, Sun G, Zhao HL, Miu K, Lü XZ, Zhang XY, Zhao ZQ.** Multiple genetic alterations and behavior of cellular biology in gastric cancer and other gastric mucosal lesions: *H pylori* infection, histological types and staging. *World J Gastroenterol* 2000; **6**: 848-854
- Debets-Ossenkopp YJ, Reyes G, Mulder J, Aan De Stegge BM, Peters JT, Savelkoul PH, Tanca J, Pena AS, Vandenbroucke-Grauls CM.** Characteristics of clinical *Helicobacter pylori* strains from Ecuador. *J Antimicrob Chemother* 2003; **51**: 141-145
- Wu AH, Crabtree JE, Bernstein L, Hawtin P, Cockburn M, Tseng CC, Forman D.** Role of *Helicobacter pylori* CagA+strains and risk of adenocarcinoma of the stomach and esophagus. *Int J Cancer* 2003; **103**: 815-821
- Lawniczak M, Starzynska T.** *Helicobacter pylori* CagA (+) infection in gastric cancer patients. *PoI Merkurisz Lek* 2002; **13**: 216-220
- Barnes PJ, Karin M.** Nuclear factor-kappaB: a pivotal transcription factor in chronic inflammatory diseases. *N Engl J Med* 1997; **336**: 1066-1071
- Ghosh S, Karin M.** Missing pieces in the NF- κ B puzzle. *Cell* 2002; **109**(Suppl): S81-96
- Karin M, Gao Y, Creten FR, Li ZW.** NF-kappa B in cancer: from innocent bystander to major culprit. *Nat Rev Cancer* 2002; **2**: 301-310
- Lin A, Karin M.** NF-kappa B in cancer: a marked target. *Semin Cancer Biol* 2003; **13**: 107-114
- Sasaki N, Morisaki T, Hashizume K, Yao T, Tsuneyoshi M, Noshiro H, Nakamura K, Yamanaka T, Uchiyama A, Tanaka M, Katano M.** Nuclear factor-kappaB p65 (RelA) transcription factor is constitutively activated in human gastric carcinoma tissue. *Clin Cancer Res* 2001; **7**: 4136-4142
- Lauren P.** Histogenesis of intestinal and diffuse types of gastric carcinoma. *Scand J Gastroenterol Suppl* 1991; **180**: 160-164
- Rugge M, Correa P, Dixon MF, Hattori T, Leandro G, Lewin K, Riddell RH, Sipponen P, Watanabe H.** Gastric dysplasia: the padova international classification. *Am J Surg Pathol* 2000; **24**: 167-176
- Dixon MF, Genta RM, Yardley JH, Correa P.** Classification and grading of gastritis. The updated Sydney System. International Workshop on the Histopathology of Gastritis, Houston 1994. *Am J Surg Pathol* 1996; **20**: 1169-1181
- Walsh MD, Jass JR.** Histologically based methods for detection of mucin. *Methods Mol Biol* 2000; **125**: 29-44
- Xin Y, Li XL, Wang YP, Zhang SM, Zheng HC, Wu DY, Zhang YC.** Relationship between phenotypes of cell-function differentiation and pathobiological behavior of gastric carcinomas. *World J Gastroenterol* 2001; **7**: 53-59

- 24 **Siebenlist U.** Signal transduction. Barriers come down. *Nature* 2001; **412**: 601-602
- 25 **Isomoto H,** Mizuta Y, Miyazaki M, Takeshima F, Omagari K, Murase K, Nishiyama T, Inoue K, Murata I, Kohno S. Implication of NF-kappaB in *Helicobacter pylori*-associated gastritis. *Am J Gastroenterol* 2000; **95**: 2768-2776
- 26 **Foryst-Ludwig A,** Naumann M. p21-activated kinase 1 activates the nuclear factor kappa B (NF-kappa B)-inducing kinase-Ikappa B kinases NF-kappa B pathway and proinflammatory cytokines in *Helicobacter pylori* infection. *J Biol Chem* 2000; **275**: 39779-39785
- 27 **Naumann M.** Nuclear factor-kappa B activation and innate immune response in microbial pathogen infection. *Biochem Pharmacol* 2000; **60**: 1109-1114
- 28 **Maeda S,** Akanuma M, Mitsuno Y, Hirata Y, Ogura K, Yoshida H, Shiratori Y, Omata M. Distinct mechanism of *Helicobacter pylori*-mediated NF-kappa B activation between gastric cancer cells and monocytic cells. *J Biol Chem* 2001; **30**: 44856-44864
- 29 **Peek RM Jr,** Blaser MJ. *Helicobacter pylori* and gastrointestinal tract adenocarcinomas. *Nat Rev Cancer* 2002; **2**: 28-37
- 30 **Odenbreit S,** Puls J, Sedlmaier B, Gerland E, Fischer W, Haas R. Translocation of *Helicobacter pylori* CagA into gastric epithelial cells by type IV secretion. *Science* 2000; **287**: 1497-1500
- 31 **Keates S,** Hitti YS, Upton M, Kelly CP. *Helicobacter pylori* infection activates NF-kappa B in gastric epithelial cells. *Gastroenterology* 1997; **113**: 1099-1109
- 32 **Backert S,** Muller EC, Jungblut PR, Meyer TF. Tyrosine phosphorylation patterns and size modification of the *Helicobacter pylori* cagA protein after translocation into gastric epithelial cells. *Proteomics* 2001; **1**: 608-617
- 33 **Nakayama H,** Ikebe T, Beppu M, Shirasuna K. High expression levels of nuclear factor kappa B, Ikappa B Kinase and Akt kinase in squamous cell carcinoma of the oral cavity. *Cancer* 2001; **92**: 3037-3044
- 34 **Mori N,** Fujii M, Cheng G, Ikeda S, Yamasaki Y, Yamada Y, Tomonaga M, Yamamoto N. Human T-cell leukemia virus type I tax protein induces the expression of anti-apoptotic gene Bcl-xL in human T-cells through nuclear factor-kappaB and c-AMP responsive element binding protein pathways. *Virus Genes* 2001; **22**: 279-287
- 35 **Chiao PJ,** Na R, Niu J, Sclabas GM, Dong Q, Curley SA. Role of Rel/NF-kappaB transcription factors in apoptosis of human hepatocellular carcinoma cells. *Cancer* 2002; **95**: 1696-1705
- 36 **Cusack JC Jr,** Liu R, Houston M, Abendroth K, Elliott PJ. Enhanced chemosensitivity to CPT-11 with proteasome inhibitor PS-341: implications for systemic nuclear factor-kappaB inhibition. *Cancer Res* 2001; **61**: 3535-3540
- 37 **Russo SM,** Tepper JE, Baldwin AS Jr, Liu R, Adams J, Elliott P. Enhancement of radiosensitivity by proteasome inhibition: implications for a role of NF-kappaB. *Int J Radiat Oncol Biol Phys* 2001; **50**: 183-193
- 38 **Grumont RJ,** Strasser A, Gerondakis S. B cell growth is controlled by phosphatidylinositol 3-kinase-dependent induction of Rel/NF-kappaB regulated c-myc transcription. *Mol Cell* 2002; **10**: 1283-1294
- 39 **Kim JS,** Yoo YD. c-Myc exerts a protective function through ornithine decarboxylase against cellular insults. *Mol Pharmacol* 2002; **62**: 1400-1408
- 40 **Hinz M,** Krappmann D, Eichten A, Heder A, Scheiderei C, Strauss M. NF-kappaB function in growth control: regulation of cyclin D1 expression and G0/G1-to-S-phase transition. *Mol Cell Biol* 1999; **19**: 2690-2698
- 41 **Yokozaki H.** Molecular characteristics of eight gastric cancer cell lines established in Japan. *Pathol Int* 2000; **50**: 767-777
- 42 **Chen JP,** Lin C, Xu CP, Zhang XY, Fu M, Deng YP, Wei Y, Wu M. Molecular therapy with recombinant antisense c-myc adenovirus for human gastric carcinoma cells *in vitro* and *in vivo*. *J Gastroenterol Hepatol* 2001; **16**: 22-28
- 43 **Murakami K,** Fujioka T, Kodama M, Honda S, Okimoto T, Oda T, Nishizono A, Sato R, Kubota T, Kagawa J, Nasu M. Analysis of p53 mutations and *Helicobacter pylori* infection in human and animal models. *J Gastroenterol* 2002; **37**(Suppl 13): 1-5
- 44 **Teh M,** Tan KB, Seet BL, Yeoh KG. Study of p53 immunostaining in the gastric epithelium of cagA-positive and cagA-negative *Helicobacter pylori* gastritis. *Cancer* 2002; **95**: 499-505
- 45 **Umekita Y,** Ohi Y, Sagara Y, Yoshidar H. Overexpression of cyclin D1 predicts for poor prognosis in estrogen receptor-negative breast cancer patients. *Int J Cancer* 2002; **98**: 415-418
- 46 **Shao JC,** Wu JE, Wang DB, Qin R, Zhang H. Relationship between the expression of human telomerase reverse transcriptase gene and cell cycle regulators in gastric cancer and its significance. *World J Gastroenterol* 2003; **9**: 427-431
- 47 **Yu Z,** Wang W. The expressions of telomerase activity and cyclin D1 protein in laryngeal squamous cell carcinoma. *Linchuang Erbi Yanhouke Zazhi* 2002; **16**: 286-288
- 48 **Pastorelli A,** Di Caro S, Zannoni G, De Sole P, Gasbarrini G, Gasbarrini A. *Helicobacter pylori* cagA-positive strains affect oxygen free radicals generation by gastric mucosa. *Scand J Gastroenterol* 2001; **36**: 247-250
- 49 **Bhattacharyya A,** Pathak S, Datta S, Chattopadhyay S, Basu J, Kundu M. Mitogen-activated protein kinases and nuclear factor-kappaB regulate *Helicobacter pylori*-mediated interleukin-8 release from macrophages. *Biochem J* 2002; **368**(Pt 1): 121-129
- 50 **Kim JS,** Kim JM, Jung HC, Song IS. Expression of cyclooxygenase-2 in human neutrophils activated by *Helicobacter pylori* water-soluble proteins: possible involvement of NF-kappaB and MAP kinase signaling pathway. *Dig Dis Sci* 2001; **46**: 2277-2284
- 51 **Tu B,** Gong JP, Feng HY, Wu CX, Shi YJ, Li XH, Peng Y, Liu CA, Li SW. Role of NF-kappaB in multiple organ dysfunction during acute obstructive cholangitis. *World J Gastroenterol* 2003; **9**: 179-183
- 52 **Kim H,** Lim JW, Kim KH. *Helicobacter pylori*-induced expression of interleukin-8 and cyclooxygenase-2 in AGS gastric epithelial cells: mediation by nuclear factor-kappaB. *Scand J Gastroenterol* 2001; **36**: 706-716
- 53 **Kim H,** Lim JW, Seo JY, Kim KH. Oxidant-sensitive transcription factor and cyclooxygenase-2 by *Helicobacter pylori* stimulation in human gastric cancer cells. *J Environ Pathol Toxicol Oncol* 2002; **21**: 121-129
- 54 **Papa A,** Danese S, Sgambato A, Ardito R, Zannoni G, Rinelli A, Vecchio FM, Gentiloni-Silveri N, Cittadini A, Gasbarrini G, Gasbarrini A. Role of *Helicobacter pylori* cagA+ infection in determining oxidative DNA damage in gastric mucosa. *Scand J Gastroenterol* 2002; **37**: 409-413
- 55 **Smoot DT,** Elliott TB, Verspaget HW, Jones D, Allen CR, Vernon KG, Bremner T, Kidd LC, Kim KS, Groupman JD, Ashktorad H. Influence of *Helicobacter pylori* on reactive oxygen-induced gastric epithelial cell injury. *Carcinogenesis* 2000; **21**: 2091-2095
- 56 **Guo XL,** Wang LE, Du SY, Fan LC, Li L, Wang P, Yuan Y. Association of cyclooxygenase-2 expression with Hp-cagA infection in gastric cancer. *World J Gastroenterol* 2003; **9**: 246-249
- 57 **Li HX,** Chang XM, Song ZJ, He SX. Correlation between expression of cyclooxygenase-2 and angiogenesis in human gastric adenocarcinoma. *World J Gastroenterol* 2003; **9**: 674-677
- 58 **Galizia G,** Lieto E, De Vita F, Romano C, Orditura M, Castellano P, Imperatore V, Infusino S, Catalano G, Pignatelli C. Circulating levels of interleukin-10 and interleukin-6 in gastric and colon cancer patients before and after surgery: relationship with radicality and outcome. *J Interferon Cytokine Res* 2002; **22**: 473-482
- 59 **Zhang X,** Chen Y, Liu Y, Zhou X, Fan D. Local cytokines profile in gastric cancer lesions. *Zhonghua Zhongliu Zazhi* 2002; **24**: 14-16
- 60 **El-Zimaity HM,** Ota H, Graham DY, Akamatsu T, Katsuyama T. Patterns of gastric atrophy in intestinal type gastric carcinoma. *Cancer* 2002; **94**: 1428-1436
- 61 **Fukuda S,** Tanaka M, Soma Y, Shimoyama T, Mikami T, Crabtree JE, Saito H, Munakata A, Yoshida Y. Histological analysis of gastritis and *Helicobacter pylori* infection in patients with early gastric cancer: a case-control study. *J Gastroenterol Hepatol* 2000; **15**: 1370-1376

Differential expression of genes during aflatoxin B₁-induced hepatocarcinogenesis in tree shrews

Yuan Li, Da-Fang Wan, Jian-Jia Su, Ji Cao, Chao Ou, Xiao-Kun Qiu, Ke-Chen Ban, Chun Yang, Liu-Liang Qin, Dan Luo, Hui-Fen Yue, Li-Sheng Zhang, Jian-Ren Gu

Yuan Li, Jian-Jia Su, Ji Cao, Chao Ou, Ke-Chen Ban, Chun Yang, Liu-Liang Qin, Dan Luo, Hui-Fen Yue, Department of Experimental Pathology, Guangxi Cancer Institute, Nanning 530021, Guangxi Zhuang Autonomous Region, China

Da-Fang Wan, Xiao-Kun Qiu, Jian-Ren Gu, National Laboratory for Oncogene and Related Genes, Shanghai Cancer Institute, Shanghai 200032, China

Li-Sheng Zhang, Department of Molecular Biology, Guangxi Cancer Institute, Nanning 530021, Guangxi Zhuang Autonomous Region, China

Supported by National Natural Science Foundation of China, NO. 39860072 and NO. 39869001; and Natural Science Foundation of Guangxi Zhuang Autonomous Region, NO. 9817137

Co-first-authors: Yuan Li and Da-Fang Wan

Correspondence to: Dr. Yuan Li, Department of Experimental Pathology, Guangxi Cancer Institute, Nanning 530021, Guangxi Zhuang Autonomous Region, China. li-yuan@public.nn.gx.cn

Telephone: +86-771-5331100 **Fax:** +86-771-5312000

Received: 2003-06-16 **Accepted:** 2003-09-24

Abstract

AIM: Through exploring the regulation of gene expression during hepatocarcinogenesis induced by aflatoxin B₁ (AFB₁), to find out the responsible genes for hepatocellular carcinoma (HCC) and to further understand the underlying molecular mechanism.

METHODS: Tree shrews (*Tupaia belangeri chinensis*) were treated with or without AFB₁ for about 90 weeks. Liver biopsies were performed regularly during the animal experiment. Eight shares of total RNA were respectively isolated from 2 HCC tissues, 2 HCC-surrounding non-cancerous liver tissues, 2 biopsied tissues at the early stage (30th week) of the experiment from the same animals as above, 1 mixed sample of three liver tissues biopsied at the beginning (0th week) of the experiment, and another 1 mixed sample of two liver tissues from the untreated control animals biopsied at the 90th week of the experiment. The samples were then tested with the method of Atlas™ cDNA microarray assay. The levels of gene expression in these tissues taken at different time points during hepatocarcinogenesis were compared.

RESULTS: The profiles of differently expressed genes were quite different in different ways of comparison. At the same period of hepatocarcinogenesis, the genes in the same function group usually had the same tendency for up- or down-regulation. Among the checked 588 genes that were known to be related to human cancer, 89 genes (15.1%) were recognized as "important genes" because they showed frequent changes in different ways of comparison. The differentially expressed genes during hepatocarcinogenesis could be classified into four categories: genes up-regulated in HCC tissue, genes with similar expressing levels in both HCC and HCC-surrounding liver tissues which were higher than that in the tissues prior to the development of HCC,

genes down-regulated in HCC tissue, and genes up-regulated prior to the development of HCC but down-regulated after the development of HCC.

CONCLUSION: A considerable number of genes could change their expressing levels both in HCC and in HCC-surrounding non-cancerous liver tissues. A few modular genes were up-regulated only in HCC but not in surrounding liver tissues, while some apoptosis-related genes were down-regulated in HCC and up-regulated in surrounding liver tissues. To compare gene-expressing levels among the liver tissues taken at different time points during hepatocarcinogenesis may be helpful to locate the responsible gene (s) and understand the mechanism for AFB₁ induced liver cancer.

Li Y, Wan DF, Su JJ, Cao J, Ou C, Qiu XK, Ban KC, Yang C, Qin LL, Luo D, Yue HF, Zhang LS, Gu JR. Differential expression of genes during aflatoxin B₁-induced hepatocarcinogenesis in tree shrews. *World J Gastroenterol* 2004; 10(4): 497-504
<http://www.wjgnet.com/1007-9327/10/497.asp>

INTRODUCTION

Hepatocellular carcinoma (HCC) is one of the major malignant tumors with a high mortality worldwide, especially in some areas of Southeast Asia and sub-Saharan. The standardized incidence of HCC in these high-risk regions usually exceeds 100 cases per 100 000 population^[1]. HCC is also one of the few malignant tumors with a relatively defined etiology. It has been postulated that chronic hepatitis B virus (HBV) or hepatitis C virus (HCV) infection and exposure to dietary aflatoxins could contribute to an extraordinarily high risk of HCC in some regions^[2-7]. However, it is similar to most of other tumors that the molecular mechanism of tumorigenesis is still to be explored.

Tree shrews (*Tupaia belangeri chinensis*) are small, squirrel-like mammals. Formerly they were considered belonging to the primate order. Currently, they have been classified into a separate order Scandentia, and are considered to be independent of both primates and insectivores^[8]. Tree shrews have been used in biomedical researches since early in the 1960' s. Originally most of the researches were on tree shrew' s visual and nervous systems, until Reddy *et al.*^[9] successfully induced liver cancer in tree shrew by aflatoxin B₁ (AFB₁) in the 1970' s. Latterly, Yan *et al.*^[10,11] reported that tree shrews could be infected with human HBV and there was a synergistic effect between HBV infection and AFB₁ intake on inducing tree shrew' s HCC. Walter *et al.*^[12] reported their results from *in vivo* and *in vitro* studies on tree shrews infected with HBV. Tree shrews were then applied in studies on HCC chemoprevention, p53 gene mutation and oncogene expression in hepatocarcinogenesis^[13-16]. Since tree shrew is the only known animal that can be infected with human HBV, with the exception of chimpanzee, it has become an animal of interest in researches related to human hepatocarcinogenesis. The

experimental model of tree shrew's hepatocarcinogenesis was established by Yan *et al.* early in the 1980's^[10]. One of the characteristics of this model is that the animals can stand repeated liver biopsies during the experimental period. This makes it possible to observe dynamically the sequential changes in liver tissues from the same animal during the course of hepatocarcinogenesis.

cDNA array is a new technology developed in recent years, subsequent to the progress in the human genome project. This new technique can be used to analyze gene expression. It has been applied widely in many research areas including changes of gene expressing level in liver cancer^[17-23]. In this study, we used the technique of cDNA array to study gene-expressing patterns of tree shrews' liver at different time points during AFB₁-induced hepatocarcinogenesis. HCC and its surrounding non-cancerous liver tissues, liver tissues biopsied prior to the development of HCC from the same animals, and normal control animals at start of the experiment and at the time when HCC developed in AFB₁-treated animals, were compared. The dynamic changes of gene expression level by cDNA array during hepatocarcinogenesis are reported here.

MATERIALS AND METHODS

Animal experiment and collection of liver tissue samples

Adult tree shrews were purchased from Kunming Institute of Zoology, Chinese Academy of Sciences (Yunnan, China). Their body weights ranged from 100 to 160 g. After acclimatized to the facilities, all the animals were screened for sera alanine aminotransferase (ALT) and sera hepatitis B virus surface antigen (HBsAg), as well as histopathology of liver biopsies. The healthy animals were then divided into AFB₁ group and control group. Only tree shrews in AFB₁ group were fed with AFB₁ (150 µg/(kg·d), 5 d/w) in milk, from the 1st week to the 90th week of the experiment.

All the animals throughout the experiment were housed in suspended, stainless steel wire cages individually, under a controlled environmental condition with a 12 h light/dark photoperiod. They had free access to tap water and a diet containing rice, corn, wheat bran, soybean, egg, whole milk powder, sugar, salt, vitamins and minerals, *etc.* They were also fed with reconstituted powdered milk and fruit daily.

Liver biopsies were performed regularly during the experiment, under ketamine hydrochloride anesthesia. Tumors and their corresponding non-cancerous liver tissues were taken when animals were sacrificed. All tissue samples were immediately frozen by liquid nitrogen and stored at -80°C.

Eight shares of total RNA were prepared from the tissue samples, 2 from two cases of HCC and 2 from the non-cancerous counterparts respectively, 2 from the 30th-week (before HCC developed) biopsies of the same animals respectively, 1 mixed sample by three biopsies taken before the animals were grouped and treated with AFB₁ (0th week of the experiment), and another 1 mixed sample by two biopsies taken at the 90th-week (around the same time as HCC tissues were taken) from the control group. More detailed information of the samples is presented in Table 1. All liver tissues analyzed in this study were from female tree shrews.

Preparation of total RNA

Total RNAs were extracted from the specimens of liver tissue by a phenol/chloroform-based method. Briefly, 0.5 g of frozen tissue was pulverized in liquid nitrogen, lysed by adding 17.5 ml of denaturation solution (Trizol, GIBCO BRL), followed by phenol/chloroform extraction and isopropyl alcohol precipitation. The samples were then purified by DNase I and RNase inhibitor followed again by extraction and precipitation as above. Two µl and 5 µl RNA from each

sample were taken respectively for checking concentrations by measuring OD at 260 nm and 280 nm, and for checking quality by electrophoresis on a denaturing formaldehyde/agarose/EtBr gel. The purified total RNA samples were stored at -80°C prior to use.

Table 1 Sources of total RNA samples

Number and type of samples	Animal treatment
HCC tissue	
1	Tree shrew in AFB ₁ group died of HCC at the 88 th week of treatment with an amount of AFB ₁ up to 10.4 mg.
2	Tree shrew in AFB ₁ group died of HCC at the 89 th week of treatment with an amount of AFB ₁ up to 11.3 mg.
HCC-surrounding non-cancerous liver tissue	
3	Autopsy tissue from the same animal and at the same time as #1.
4	Autopsy tissue from the same animal and at the same time as #2.
Liver tissue taken before HCC developed	
5	Biopsy tissue from the same animal as #1, at the 30 th week of AFB ₁ -treatment with a total amount of 3.1 mg AFB ₁ .
6	Biopsy tissue from the same animal as #2, at the 30 th week of AFB ₁ -treatment with a total amount of 3.2 mg AFB ₁ .
Liver tissue taken before AFB₁-treatment	
7	Biopsy tissue mixture from 3 animals before they were grouped and treated (0 th week of the experiment).
Homochronous control	
8	Biopsy tissue mixture from 2 animals in control group at the 90 th week of the experiment.

Probe synthesis, labeling, purification and hybridization

Atlas™ human cDNA expression array (catalog No. 7740-1, lot No. 9090199) kits were purchased from Clontech Laboratories, Inc. (Palo Alto, CA, USA). There were 588 of human cDNAs for the known genes related to different kinds of human tumors, along with 9 housekeeping cDNAs as positive control for normalizing mRNA abundance. The 588 cDNAs were functionally divided into 16 classes. Each sequence of cDNA was 200-600 bp in length and spotted in duplicate with 10 ng of cDNA/dot on the array membrane. Some information of the genes and their functional categories are shown in Table 2.

Probe synthesis, labeling, purification and hybridization were performed according to the manufacturer's instructions. Briefly, cDNA probes were synthesized from 5 µg aliquots (2 µl) of the total RNA samples by the gene-specific CDS primer mix supplied with the Kits, labeled with α-³²P-dATP (10.0 mCi/ml, NEN Life Science Company, USA) by the method of reverse transcription and purified through column chromatography. Atlas array membrane was prehybridized for 2 hours and hybridized to the cDNA probes overnight (7 rpm, 68°C). After washed, the membranes were exposed to the phosphorimage system (BIO RAD, GS-525, USA) for 4 hours, the hybridized intensity of each dot was scanned and calculate. The membranes were finally exposed to Kodak X-ray film with intensifying screen for 24-72 hours at -80°C and then developed.

Data analysis

The intensity of each hybridized dot on each membrane was calibrated according to the formula: calibrated intensity of dot = (original intensity of dot - background intensity of membrane) / (intensity of housekeeping gene ubiquitin C - background intensity). The background intensity was taken from the middle of each membrane. The ratio of intensity between two compared dots ≥ 2.0 was considered as gene expression level up-regulated, ≤ 0.5 as down-regulated. If the same comparison of the two tissue specimens (*i.e.*, the two cases of HCC

compared to their corresponding non-cancerous liver tissues respectively) had the same pattern of change (*i.e.*, both up- or down-regulated), the average ratio was considered as “validated value”. Otherwise the ratio was considered as “invalidated value” perhaps due to individual variations or some other unknown factors.

The gene expressing levels in the 5 types of liver tissue were compared by 6 different ways, namely, liver tissues taken from AFB₁-treated animal before the development of HCC (30th week of the treatment, BC) and before AFB₁ treatment (0th week of the experiment, BA), HCC-surrounding non-cancerous liver tissue (NCL) and its corresponding BC, HCC and its corresponding NCL, HCC and its corresponding BC, HCC and BA, HCC and the liver tissue taken from control group around the same time as HCC (90th week of the treatment, C). Among these 6 ways of comparison, the first three were compared according to the possible sequence of hepatocarcinogenesis (normal liver → liver before HCC developed → HCC-surrounding non-cancerous liver → HCC), the last four were for comparing HCC tissues with the other 4 types of liver tissues. The genes showing changes at least twice among the first three ways of comparison or thrice among the last four ways of comparison, or in the 6th way plus any one of the other three among the last four ways of comparison were

considered as “important genes”.

All the data of hybridized dot' s intensity were analyzed with Excel software (Microsoft).

RESULTS

Up to the 90th week of the animal experiment, 2 cases showed HCC in AFB₁ group, and the first case of HCC appeared at the 88th week. The average amount of AFB₁ fed to animals in this group was 10.5 mg. All the HCCs were confirmed histopathologically. No HCC developed in control group until the 90th week of experiment.

The A₂₆₀/A₂₈₀ ratio for the 8 shares of total RNA was between 1.8-2.2. The electrophoresis showed intactness of all isolated RNA samples.

The intensity of ubiquitin C on each hybridized membrane was most distinct and steady among the 9 housekeeping genes. Generally, the profiles of differentially expressed genes were quite different in different ways of comparison, and the genes in the same function group usually had the same tendency for up- or down-regulation in a given type of comparison. Among the checked 588 genes, 89 (15.1%) were considered as “important genes” according to the criteria mentioned above. Table 2 shows the detailed information for these genes.

Table 2 Differential expressions of important genes

Coordinate	Genbank	Gene Name	1 BC/BA	2 NCL/BC	3 HCC/NCL	4 HCC/BC	5 HCC/BA	6 HCC/C
Oncogenes & tumor suppressors (1/57, 1.8%)								
A1i	X12795	v-erbA related protein 3 (EAR3)			↑ (3.56)	↑ (7.45)	↑ (4.80)	
Cell Cycle Regulators (1/41, 2.4%)								
A6i	L26584	cell division cycle 25 homolog (CDC25)				↑ (3.43)		↑ (5.92)
Ion channels & transport proteins (0/3)								
Modulators, effectors & intracellular transducers (5/88, 5.7%)								
B1f	M62424	thrombin receptor (TR)	↓ (0.15)	↑ (5.64)		↑ (10.75)		↑ (6.52)
B1l*	X74764	neurotrophic tyrosine kinase receptor-related 3		↑ (5.50)	↑ (2.63)	↑ (14.05)	↑ (25.36)	
B2j	D21878	bone marrow stromal antigen 1 (BST-1)	↓ (0.15)		↑ (11.14)			↑ (3.40)
B4l	U07707	epidermal growth factor receptor substrate 15 (EPS15)	↓ (0.40)			↑ (2.87)		↑ (2.18)
B5m*	M65066	cAMP-dependent protein kinase type I beta regulatory subunit (PRKAR1B)	↓ (0.02)	↑ (4.03)	↑ (11.35)	↑ (51.59)		
Stress response proteins (1/7, 14.3%)								
B7m	M11717	heat shock 70-kDa protein 1 (HSP70.1)	↑ (3.54)	↓ (0.26)		↓ (0.26)		↓ (0.17)
Apoptosis-associated proteins (15/64, 23.4%)								
C1g	M14694	p53 cellular tumor antigen			↓ (0.35)			↓ (0.10)
C1n	L07414	TNF-related activation protein (TRAP)			↓ (0.42)			↓ (0.24)
C3c	M25627	glutathione S-transferase A1 (GSTA1)				↓ (0.29)		↓ (0.23)
C3j	M13228	N-myc proto-oncogene	↑ (181.47)		↓ (0.30)		↑ (148.98)	↓ (0.18)
C3k	U25994	receptor (TNFRSF)-interacting serine-threonine kinase 1 (RIPK1)	↑ (4.61)		↓ (0.25)			↓ (0.06)
C3n	L11015	tumor necrosis factor C (TNFC)			↓ (0.24)			↓ (0.08)
C4c*	U15172	NIP1 (NIP1)			↓ (0.08)		↓ (0.16)	↓ (0.20)
C4d*	U15174	BCL2/adenovirus E1B 19-kDa-interacting protein 3 (BNIP3)			↓ (0.31)		↓ (0.34)	↓ (0.21)
C4f	U23765	BCL2 homologous antagonist/killer 1 (BAK1)			↓ (0.28)			↓ (0.12)
C4h	U29680	BCL2-related protein A1 (BCL2A1)		↑ (8.19)	↓ (0.16)			↓ (0.09)
C4k	U45880	inhibitor of apoptosis protein 3 (IAP3)	↑ (4.53)		↓ (0.42)			↓ (0.23)
C4m*	U57059	TNF-related apoptosis inducing ligand (TRAIL)	↓ (0.26)				↓ (0.20)	↓ (0.40)
C5c	Y09392	WSL protein+TRAMP+Apo-3+ death domain receptor 3 (DDR3)			↓ (0.39)			↓ (0.20)

C5f	U39613	cysteine protease ICE-LAP3			↓ (0.13)		↓ (0.03)
C5h	U71364	cytoplasmic antiproteinase 3 (CAP3)		↑ (44.85)	↓ (0.28)		↓ (0.13)
DNA synthesis, repair & recombinant proteins (15/34, 44.1%)							
C5k*	L07540	replication factor C 36-kDa subunit (RFC36)	↓ (0.24)	↑ (6.73)	↓ (0.26)		↓ (0.17)
C6a	M30938	nuclear factor IV			↓ (0.25)		↓ (0.07)
C6b	M31899	xeroderma pigmentosum group B complementing protein (XPB-ERCC3)			↓ (0.06)		↓ (0.04)
C6c	M32865	70-kDa thyroid autoantigen (TLAA)			↓ (0.44)		↓ (0.20)
C6e	M63488	replication protein A 70-kDa subunit (RPA70)			↓ (0.25)		↓ (0.07)
C6l	J04088	DNA topoisomerase II alpha (TOP2A)		↑ (4.00)	↓ (0.33)		↓ (0.30)
C7a	M13194	excision repair cross-complementing rodent repair deficiency complementation group 1 (ERCC1)			↓ (0.26)		↓ (0.09)
C7b	M13267	cytosolic superoxide dismutase 1 (SOD1)				↓ (0.39)	↓ (0.24)
C7c	U07418	colon cancer nonpolyposis type 2 protein (COCA2)			↓ (0.30)		↓ (0.10)
C7d*	D21090	UV excision repair protein RAD23 homolog B (hHR23B; XPC repair-complementing complex 58-kDa protein)			↓ (0.26)		↓ (0.08)
C7g	S40706	growth arrest & DNA damage-inducible protein 153 (GADD153)			↓ (0.29)		↓ (0.15)
C7i	U12134	DNA damage repair & recombination protein 52 homolog (RAD52)		↑ (6.02)	↓ (0.27)		↓ (0.12)
C7k	U63139	DNA damage repair & recombination protein 50 homolog (RAD50)			↓ (0.18)		↓ (0.08)
C7m	X84740	DNA ligase III (LIG3)		↑ (4.23)	↓ (0.21)		↓ (0.08)
C7n	X90392	muscle-specific DNase I-like (DNL1L)		↓ (5.36)	↓ (0.22)		↓ (0.12)
Transcription factors & DNA-binding proteins (8/98, 8.2%)							
D3a	D26155	SWI/SNF-related matrix-associated actin-dependent regulator of chromatin subfamily A member 2 (SMARCA2)	↓ (0.19)	↑ (3.85)		↑ (4.58)	↑ (2.55)
D4b*	M36542	octamer-binding transcription factor 2 (OCT2)		↑ (2.64)		↑ (8.32)	↑ (7.33) ↑ (3.30)
D4e	M62810	mitochondrial transcription factor 1 (MTTF1)				↑ (8.04)	↑ (25.07)
D4j	M76541	transcriptional repressor protein yin & yang 1 (YY1)	↓ (0.32)	↑ (2.73)		↑ (3.74)	↑ (3.10)
D5a*	M83234	nuclease-sensitive element DNA-binding protein (NSEP)			↑ (2.59)	↑ (3.24)	↑ (2.75) ↑ (5.21)
D5f	M96824	nucleobindin 1 (NUCB1)	↓ (0.24)	↑ (2.64)		↑ (3.00)	↑ (2.37)
D6h*	U10324	nuclear factor NF90				↑ (3.69)	↑ (2.34) ↑ (2.90)
D6l	U14575	activator of RNA decay (ARD-1)	↑ (72.46)	↑ (2.53)			↑ (93.75)
Growth factor & chemokine receptors (1/25, 4.0%)							
E1h	L06623	endothelin receptor type B (ETB)	↓ (0.37)	↑ (4.46)		↑ (2.07)	↑ (2.78)
Interleukin & interferon receptors (0/18)							
Hormone receptors (0/4)							
Neurotransmitter receptors (0/11)							
Cell surface antigens & adhesion proteins (3/40, 7.5%)							
E5l	M23197	myeloid cell surface CD33 antigen		↑ (6.68)		↑ (5.75)	↑ (3.26)
E6f*	M74777	dipeptidyl peptidase IV (DPP IV); T-cell activation CD26			↓ (0.32)		↓ (0.36) ↓ (0.28)
E7b	M35198	integrin beta 6 (ITGB6)		↑ (5.44)	↓ (0.44)		↓ (0.36)
Growth factors, cytokines & chemokines (20/64, 31.3%)							
F1f	X03438	granulocyte colony-stimulating factor (GCSF)	↑ (8.95)	↑ (3.32)	↓ (0.05)	↓ (0.18)	↓ (0.06)
F1j*	M16552	thrombomodulin (THBD)			↓ (0.10)		↓ (0.24) ↓ (0.23)
F2a	D16431	hepatoma-derived growth factor (HDGF)			↓ (0.39)		↓ (0.28)
F2c	J04130	T-cell activation protein 2 (AT2)			↓ (0.17)		↓ (0.20)
F2e	K03515	neuroleukin (NLK)	↑ (9.09)		↓ (0.40)		↓ (0.26)
F2f	L12260	neuregulin 1 (NRG1)	↑ (21.23)		↓ (0.10)		↑ (3.76) ↓ (0.13)

F2g	L12261	heregulin-beta3	↑ (6.10)	↓ (0.10)			↓ (0.14)	
F2h	L36052	thrombopoietin (THPO)	↑ (7.26)	↓ (0.04)	↓ (0.24)		↓ (0.06)	
F2m	M22491	bone morphogenetic protein 3 (BMP3)		↓ (0.05)			↓ (0.08)	
F3a	M24545	small inducible cytokine subfamily A member 2 (SCYA2)		↓ (0.36)			↓ (0.34)	
F3d	M30704	amphiregulin (AR)	↑ (3.69)	↓ (0.17)	↓ (0.41)		↓ (0.12)	
F3i	M57502	small inducible cytokine subfamily A member 1 (SCYA1)		↓ (0.22)			↓ (0.27)	
F3l	M60718	hepatocyte growth factor (HGF)		↓ (0.20)			↓ (0.30)	
F4c	M74178	hepatocyte growth factor-like protein	↓ (0.31)	↑ (5.11)		↑ (4.62)	↑ (2.28)	
F4e	M92934	connective tissue growth factor (CTGF)	↑ (3.86)	↑ (6.00)	↓ (0.30)		↑ (5.44) ↓ (0.24)	
F4h	U43142	vascular endothelial growth factor C (VEGFC)	↑ (8.75)	↑ (3.82)	↓ (0.14)		↑ (4.81) ↓ (0.15)	
F4i	X02530	small inducible cytokine subfamily B member 10 (SCYB10)	↑ (5.60)	↑ (4.14)	↓ (0.14)		↑ (3.17) ↓ (0.15)	
F4k	X06234	calgranulin A (CALA)			↓ (0.21)		↓ (0.21)	
F4n	X51943	AFGF + HBGF-1 + ECGF-beta			↓ (0.10)		↓ (0.19)	
F5e	X79929	OX40 ligand (OX40L)	↑ (5.42)		↓ (0.11)	↓ (0.31)	↓ (0.09)	
Interleukins & interferons (12/20, 60.0%)								
F5j	J04156	interleukin 7 (IL7)		↑ (3.62)	↓ (0.25)		↓ (0.27)	
F5k	A14844	interleukin 2 (IL2)	↑ (11.82)		↓ (0.14)	↓ (0.16)	↓ (0.13)	
F5l	X02851	interleukin 1 alpha (IL1-alpha)			↓ (0.19)		↓ (0.24)	
F5n	M14743	interleukin 3 (IL3)		↑ (11.18)	↓ (0.08)		↓ (0.06)	
F6a	M13982	interleukin 4 (IL4)	↑ (2.87)		↓ (0.26)		↓ (0.22)	
F6b*	X04602	interleukin 6 (IL6)		↑ (3.37)	↑ (2.73)	↑ (9.47)	↑ (12.41)	
F6d	M28622	interferon beta 1 (IFN-beta 1)			↓ (0.17)		↓ (0.16)	
F6g	L06801	interleukin 13 (IL13)	↓ (0.20)	↑ (5.04)		↑ (5.90)	↑ (2.36)	
F6i	M57765	interleukin 11 (IL11)		↑ (4.15)	↓ (0.11)	↓ (0.40)	↓ (0.10)	
F6j	M65290	interleukin 12 beta subunit (IL12-beta)	↑ (2.71)		↓ (0.19)		↓ (0.18)	
F6k	M65291	interleukin 12 alpha subunit (IL12-alpha)	↑ (3.78)		↓ (0.17)		↓ (0.14)	
F6l	U14407	interleukin 15 (IL15)		↑ (3.36)	↓ (0.24)		↓ (0.30)	
Hormones (7/14, 50.0%)								
F7d	A06925	prorelaxin H2 (RLN2)			↓ (0.23)		↓ (0.16)	
F7f	J04040	glucagon (GCG)		↑ (5.75)	↓ (0.17)		↓ (0.12)	
F7i	M31159	insulin-like growth factor-binding protein 3 (IGFBP3)			↓ (0.35)		↓ (0.35)	
F7j	M68867	cellular retinoic acid-binding protein II (CRABP2)		↑ (2.84)	↓ (0.27)		↓ (0.23)	
F7l	X58022	corticotropin-releasing factor-binding protein	↑ (5.00)	↑ (2.97)	↓ (0.12)	↓ (0.36)	↓ (0.16)	
F7m	U08098	estrogen sulfotransferase (STE; EST)	↑ (5.62)	↑ (3.44)			↑ (12.98)	
F7n	X54469	preprotachykinin beta (beta-PPT)	↑ (15.57)		↓ (0.07)	↓ (0.21)	↓ (0.09)	
Total amount		89/588, 15.1%	32	36	70	29	20	83
Up-regulation			20(62.5)	35(97.2)	5(7.1)	18(62.1)	13(65.0)	15(18.1)
Down-regulation			12(37.5)	1(2.8)	65(92.9)	11(37.9)	7(35.0)	68(81.9)

1 BA: liver tissue from animals before AFB1 treatment (0th week of the experiment). BC: liver tissue from the same HCC animals after AFB1 treatment for 30 weeks. HCC: hepatocellular carcinoma tissue from the same animal after AFB1 treatment. NCL: HCC-surrounding non-cancerous liver tissues from the same HCC animal. C: liver tissue from untreated animals taken at the time when HCC developed in AFB1 treated animals. 2 The numbers followed the name of functional classes are the amount of the important genes identified in this class and their percentage. 3 ↑ : up-regulation; ↓ : down-regulation. The numbers followed are the averages of the two checked samples. 4 *: Genes might be of more importance.

DISCUSSION

Tree shrew is a kind of animals classified more closely to human being than the common laboratory animals. Park *et al.* reported that tree shrew' s wild-type p53 showed 91.7% and 93.4% homologies with human p53 nucleotide and amino acid sequences respectively, and 77.2% and 73.7% homologies respectively with mice^[14]. With limited information of tree shrew' s genome and no commercial gene chip for tree shrew was currently available, in this study we used human cDNA-

array kit to explore tree shrew' s gene expression patterns during AFB₁-induced hepatocarcinogenesis. The results of hybridization implied that the method used in this study was practicable. Besides, the incidence of HCC (10/15 and 0/12 respectively for AFB₁ group and control group at the 135th week of the experiment, data unpublished) and the liver histopathological changes in this study were similar to those of our former experiments^[11,24], which demonstrated the tree shrew model of AFB₁-induced HCC was reliable.

In the former reports on differentially expressed genes of liver cancer, the usual method was to compare the levels of gene expression between HCC tissues and its surrounding tissues^[17-23,25,26]. These so-called "normal" HCC-surrounding tissues, however, frequently involve the changes of hepatitis and/or liver cirrhosis. The present study, by using biopsy tissue from a given animal at different time points during AFB₁-induced hepatocarcinogenesis, showed a dynamic profile of gene expression not reported previously. It is notable that a set of genes were up- or down-regulated in HCC-surrounding liver tissue but without any differences with the HCC counterpart. This phenomenon further indicated that the HCC-surrounding liver tissue was no longer normal even in terms of molecular biology. In these HCC-surrounding liver tissues, some growth factors, effectors or their receptors such as thrombin receptor, and some transcriptional factors such as SWI/SNF-related matrix-associated actin-dependent regulator of chromatin subfamily A member 2 (SMARCA 2) were up-regulated, but the genes related to apoptosis were down-regulated. These changes inevitably resulted in abnormality of the tissue response to the environment, and kept in anti-apoptosis condition. Apparently, the HCC-surrounding liver tissue was at a precancerous status at molecular level. Actually, there were only a few genes that were continuously up- or down-regulated during hepatocarcinogenesis. This study also showed that some genes were up-regulated during the early stage but down-regulated during the late stage of hepatocarcinogenesis, the reason of this phenomenon awaits further elucidation.

By comparing the 5 types of tissues taken at different time points, the genes differentially expressed during the course of AFB₁-induced hepatocarcinogenesis could be categorized into the following 4 types.

Type I, genes that were continuously up-regulated in HCC vs HCC-surrounding non-cancerous liver tissue (NCL) and NCL vs liver tissue taken before HCC developed (BC). This type of genes was rare. Only two were found among the 588 checked genes, namely genes for neurotrophic tyrosine kinase receptor-related protein 3 and cAMP-dependent protein kinase type I beta regulatory subunit (PRKAR1B). Their ratio for HCC vs NCL was 2.6 and 11.4 respectively, and the ratio for NCL vs BC was 5.5 and 4.0 respectively. The gene for nuclease-sensitive element DNA-binding protein (NSEP) probably would also be included into this type.

Type II, genes that had similar expressing levels in HCC and NCL tissues which were higher than that in BC. This type of genes included the genes in the functional group of modulators, effectors and intracellular transducers, and transcription factors and DNA-binding proteins, *etc.* This pattern of change might imply that these genes were up-regulated after the initiation of hepatocarcinogenesis but kept at a persistent level in the late stage. Moreover, it strongly indicated that a tremendous change in HCC-surrounding liver tissues at molecular level, implying the HCC-surrounding non-cancerous liver tissue was precancerous rather than normal.

Type III, genes that were down-regulated in HCC tissue vs NCL tissue. They included several groups of genes. (1) Genes related to apoptosis. Most of apoptosis-inducing genes were down regulated but a few of anti-apoptosis genes such as IAP were exceptionally down-regulated (0.4) too. The overall trend caused by this pattern of gene expression change, however, favored cell survival. This phenomenon was also seen in some other studies^[27-29]. (2) Genes for DNA-repairing were generally down-regulated. The down-regulation of this group of genes might imply the alteration of response of HCC cells to the signals from the surrounding environment. (3) Genes for growth factor, cytokines and chemokines. (4) Genes for interleukins, interferons and hormones.

Type IV, genes that were up-regulated before the appearance

of HCC but down-regulated after the development of HCC, including genes related to DNA-repair, genes related to growth factor and cytokines, genes for interleukins, and genes related to hormones. Their up-regulation might putatively imply the acute phase response of related genes to genotoxicity. The down-regulation might imply the defective expression of related genes during carcinogenesis, or some other up-regulated genes might functionally compensate for these genes. Table 3 shows the detailed information about these four types of genes.

Table 3 Four types of differentially expressed genes

Type I, genes that up-regulated both in HCC vs NCL and NCL vs BC.
Modulators, effectors & intracellular transducers
neurotrophic tyrosine kinase receptor-related 3
cAMP-dependent protein kinase type I beta regulatory subunit (PRKAR1B)
Type II, genes that had similar expressing level in HCC and NCL but higher than that in BC.
II-1. Modulators, effectors & intracellular transducers
thrombin receptor (TR)
epidermal growth factor receptor substrate 15 (EPS15)
II-2. Transcription factors & DNA-binding proteins
SWI/SNF-related matrix-associated actin-dependent regulator of chromatin subfamily A member 2 (SMARCA2)
octamer-binding transcription factor 2 (OCT2)
mitochondrial transcription factor 1 (MTTF1)
transcriptional repressor protein yin & yang 1 (YY1)
nucleobindin 1 (NUCB1)
II-3. Growth factor & chemokine receptors
endothelin receptor type B (ETB)
II-4. Cell surface antigens & adhesion proteins
myeloid cell surface CD33 antigen
II-5. Growth factors, cytokines & chemokines
hepatocyte growth factor-like protein
Type III, genes down-regulated in HCC vs NCL.
III-1. Apoptosis-associated proteins
p53 cellular tumor antigen
TNF-related activation protein (TRAP)
N-myc proto-oncogene
receptor (TNFRSF)-interacting serine-threonine kinase 1 (RIPK1)
tumor necrosis factor C (TNFC)
NIP1 (NIP1)
BCL2/adenovirus E1B 19-kDa-interacting protein 3 (BNIP3)
BCL2 homologous antagonist/killer 1 (BAK1)
inhibitor of apoptosis protein 3 (IAP3)
WSL protein + TRAMP + Apo-3 + death domain receptor 3 (DDR3)
cysteine protease ICE-LAP3
III-2. DNA synthesis, repair & recombination proteins
nuclear factor IV
xeroderma pigmentosum group B complementing protein (XPB; ERCC3)
70-kDa thyroid autoantigen (TLAA)
replication protein A 70-kDa subunit (RPA70)
excision repair cross-complementing rodent repair deficiency complementation group 1 (ERCC1)
colon cancer nonpolyposis type 2 protein (COCA2)
UV excision repair protein RAD23 homolog B (hHR23B;
XPC repair-complementing complex 58-kDa protein)
growth arrest & DNA damage-inducible protein 153 (GADD153)
DNA damage repair & recombination protein 50 homolog (RAD50)
III-3. Growth factors, cytokines & chemokines

- thrombomodulin (THBD)
 hepatoma-derived growth factor (HDGF)
 T-cell activation protein 2 (AT2)
 neuroleukin (NLK)
 neuregulin 1 (NRG1)
 bone morphogenetic protein 3 (BMP3)
 small inducible cytokine subfamily A member 2 (SCYA2)
 hepatocyte growth factor (HGF)
 calgranulin A (CALA)
 AFGF + HBGf-1 + ECGF-beta
- III-4. Interleukins & interferons
 interleukin 2 (IL2)
 interleukin 1 alpha (IL1-alpha)
 interleukin 4 (IL4)
 interferon beta 1 (IFN-beta 1)
 interleukin 12 beta subunit (IL12-beta)
 interleukin 12 alpha subunit (IL12-alpha)
- III-5. Hormones
 insulin-like growth factor-binding protein 3 (IGFBP3)
- Type IV, genes up-regulated before HCC appearance but down-regulated after HCC developed.
- IV-1. DNA synthesis, repair & recombination proteins
 replication factor C 36-kDa subunit (RFC36)
 DNA topoisomerase II alpha (TOP2A)
 DNA damage repair & recombination protein 52 homolog (RAD52)
 DNA ligase III (LIG3)
 muscle-specific DNase I-like (DNL1L)
- IV-2. Growth factors, cytokines & chemokines
 granulocyte colony-stimulating factor (GCSF)
 heregulin-beta3
 thrombopoietin (THPO)
 connective tissue growth factor (CTGF)
- IV-3. Interleukins & interferons
 interleukin 7 (IL7)
 interleukin 3 (IL3)
 interleukin 6 (IL6)
 interleukin 11 (IL11)
- IV-4. Hormones
 cellular retinoic acid-binding protein II (CRABP2)
 corticotropin-releasing factor-binding protein

It has to be noticed that cDNA array, the method used in this study has some limitations. First, this method only shows mRNA but not the protein expression level of related genes. Second, even if the expression level of mRNA may equally reflect the expression level of protein, it can not represent the functions of these gene products such as phosphorylation/dephosphorylation, methylation, acetylation or glycosylation. The status of protein phosphorylation is very critical for cellular signal transduction, and there is accumulating evidence that suggests the relationship between the status of methylation and activation of gene in hepatocarcinogenesis^[30-33]. Therefore, the genes showing differential expressions at mRNA level must be further studied on their protein expression level and their modified status. The present study, however, provides a preliminary clue to the differential expressions of mRNA during AFB₁- induced hepatocarcinogenesis, particularly at different stages of carcinogenesis from the same animals. Since the development of most human HCCs in China are attributed to the synergistic effects of AFB₁ and HBV, the study on tree shrew' s hepatocarcinogenesis induced by both AFB₁ and HBV is now in progress, and the preliminary result was published recently^[34].

ACKNOWLEDGMENT

The authors express their appreciation to Drs. Geng-Sun Qian and Yi-Qian Wu at Shanghai Cancer Institute for providing meaningful advice and discussion regarding the microarray work.

REFERENCES

- Yeh FS**, Yu MC, Mo CC, Luo S, Tong MJ, Henderson BE. Hepatitis B virus, aflatoxins, and hepatocellular carcinoma in southern Guangxi, China. *Cancer Res* 1989; **49**: 2506-2509
- Wang JS**, Huang T, Su J, Liang F, Wei Z, Liang Y, Luo H, Kuang SY, Qian GS, Sun G, He X, Kensler TW, Groopman JD. Hepatocellular carcinoma and aflatoxin exposure in Zhuqing Village, Fusui County, People' s Republic of China. *Cancer Epidemiol Biomarkers Prev* 2001; **10**: 143-146
- Wang LY**, Hatch M, Chen CJ, Levin B, You SL, Lu SN, Wu MH, Wu WP, Wang LW, Wang Q, Huang GT, Yang PM, Lee HS, Santella RM. Aflatoxin exposure and risk of hepatocellular carcinoma in Taiwan. *Int J Cancer* 1996; **67**: 620-625
- Oon CJ**, Chen WN, Goh KT, Mesenas S, Ng HS, Chiang G, Tan C, Koh S, Teng SW, Toh I, Moh MC, Goo KS, Tan K, Leong AL, Tan GS. Molecular characterization of hepatitis B virus surface antigen mutants in Singapore patients with hepatocellular carcinoma and hepatitis B virus carriers negative for HBsAg but positive for anti-HBs and anti-HBc. *J Gastroenterol Hepatol* 2002; **17** (Suppl): S491-496
- Sun CA**, Wu DM, Lin CC, Lu SN, You SL, Wang LY, Wu MH, Chen CJ. Incidence and cofactors of hepatitis C virus-related hepatocellular carcinoma: a prospective study of 12,008 men in Taiwan. *Am J Epidemiol* 2003; **157**: 674-682
- Cai RL**, Meng W, Lu HY, Lin WY, Jiang F, Shen FM. Segregation analysis of hepatocellular carcinoma in a moderately high-incidence area of East China. *World J Gastroenterol* 2003; **9**: 2428-2432
- Lai CL**, Ratziu V, Yuen MF, Poynard T. Viral hepatitis B. *Lancet* 2003; **362**: 2089-2094
- Bearder S**, Pitts RS. Chapter 36, Prosimians and tree shrews. In: Trevor BP eds. The UFAW Handbook on the Care and Management of Laboratory Animals, Sixth edition. Avon, Great Britain: Bath Press 1987: 551-567
- Reddy JK**, Svododa DJ, Rao SM. Induction of liver tumors by aflatoxin B1 in the tree shrew (*Tupaia glis*), a nonhuman primate. *Cancer Res* 1976; **36**: 151-160
- Yan RQ**, Su JJ, Huang DR, Gan YC, Yang C, Huang GH. Human hepatitis B virus and hepatocellular carcinoma. I. Experimental infection of tree shrews with hepatitis B virus. *J Cancer Res Clin Oncol* 1996; **122**: 283-288
- Yan RQ**, Su JJ, Huang DR, Gan YC, Yang C, Huang GH. Human hepatitis B virus and hepatocellular carcinoma. II. Experimental induction of hepatocellular carcinoma in tree shrews exposed to hepatitis B virus and aflatoxin B₁. *J Cancer Res Clin Oncol* 1996; **122**: 289-295
- Walter E**, Keist R, Niederost B, Pult I, Blum HE. Hepatitis B virus infection of tupaia hepatocytes *in vitro* and *in vivo*. *Hepatology* 1996; **24**: 1-5
- Li Y**, Su J, Qin L, Egner PA, Wang J, Groopman JD, Kensler TW, Roebuck BD. Reduction of aflatoxin B(1) adduct biomarkers by oltipraz in the tree shrew (*Tupaia belangeri chinensis*). *Cancer Lett* 2000; **154**: 79-83
- Park US**, Su JJ, Ban KC, Qin L, Lee EH, Lee YI. Mutations in the p53 tumor suppressor gene in tree shrew hepatocellular carcinoma associated with hepatitis B virus infection and intake of aflatoxin B1. *Gene* 2000; **251**: 73-80
- Su JJ**, Qin GZ, Yan RQ, Huang DR, Yang C, Lotlikar PD. The expression of insulin-like growth factor II, hepatitis B virus X antigen and p21 in experimental hepatocarcinogenesis in tree shrews. *Ann Acad Med Singapore* 1999; **28**: 62-66
- Li Y**, Su JJ, Qin LL, Yang C, Luo D, Ban KC, Kensler T, Roebuck B. Chemopreventive effect of oltipraz on AFB₁-induced hepatocarcinogenesis in tree shrew model. *World J Gastroenterol* 2000; **6**: 647-650
- Shirota Y**, Kaneko S, Honda M, Kawai HF, Kobayashi K. Identification of differentially expressed genes in hepatocellular carcinoma with cDNA microarrays. *Hepatology* 2001; **33**: 832-840

- 18 **Okabe H**, Satoh S, Kato T, Kitahara O, Yanagawa R, Yamaoka Y, Tsunoda T, Furukawa Y, Nakamura Y. Genome-wide analysis of gene expression in human hepatocellular carcinomas using cDNA microarray: identification of genes involved in viral carcinogenesis and tumor progression. *Cancer Res* 2001; **61**: 2129-2137
- 19 **Li Y**, Qiu MY, Wu CQ, Cao YQ, Tang R, Chen Q, Shi XY, Hu ZQ, Xie Y, Mao YM. Detection of differentially expressed genes in hepatocellular carcinoma using DNA microarray. *Yichuan Xuebao* 2000; **27**: 1042-1048
- 20 **Wu CG**, Salvay DM, Forgues M, Valerie K, Farnsworth J, Markin RS, Wang XW. Distinctive gene expression profiles associated with Hepatitis B virus X protein. *Oncogene* 2001; **20**: 3674-3682
- 21 **Lau WY**, Lai PB, Leung MF, Leung BC, Wong N, Chen G, Leung TW, Liew CT. Differential gene expression of hepatocellular carcinoma using cDNA microarray analysis. *Oncol Res* 2000; **12**: 59-69
- 22 **Kawai HF**, Kaneko S, Honda M, Shiota Y, Kobayashi K. alpha-fetoprotein-producing hepatoma cell lines share common expression profiles of genes in various categories demonstrated by cDNA microarray analysis. *Hepatology* 2001; **33**: 676-691
- 23 **Liu LX**, Jiang HC, Liu ZH, Zhou J, Zhang WH, Zhu AL, Wang XQ, Wu M. Integrin gene expression profiles of human hepatocellular carcinoma. *World J Gastroenterol* 2002; **8**: 631-637
- 24 **Li Y**, Su JJ, Qin LL, Yang C, Ban KC, Yan RQ. Synergistic effect of hepatitis B virus and aflatoxin B1 in hepatocarcinogenesis in tree shrews. *Ann Acad Med Singapore* 1999; **28**: 67-71
- 25 **Kurokawa Y**, Matoba R, Takemasa I, Nakamori S, Tsujie M, Nagano H, Dono K, Umeshita K, Sakon M, Ueno N, Kita H, Oba S, Ishii S, Kato K, Monden M. Molecular features of non-B, non-C hepatocellular carcinoma: a PCR-array gene expression profiling study. *J Hepatol* 2003; **39**: 1004-1012
- 26 **Wang ZX**, Hu GF, Wang HY, Wu MC. Expression of liver cancer associated gene HCCA3. *World J Gastroenterol* 2001; **7**: 821-825
- 27 **Kountouras J**, Zavos C, Chatzopoulos D. Apoptosis in hepatocellular carcinoma. *Hepatogastroenterology* 2003; **50**: 242-249
- 28 **Okano H**, Shiraki K, Inoue H, Kawakita T, Saitou Y, Enokimura N, Yamamoto N, Sugimoto K, Fujikawa K, Murata K, Nakano T. Over-expression of Smac promotes TRAIL-induced cell death in human hepatocellular carcinoma. *Int J Mol Med* 2003; **12**: 25-28
- 29 **Sun BH**, Zhang J, Wang BJ, Zhao XP, Wang YK, Yu ZQ, Yang DL, Hao LJ. Analysis of *in vivo* patterns of caspase 3 gene expression in primary hepatocellular carcinoma and its relationship to p21^{WAF1} expression and hepatic apoptosis. *World J Gastroenterol* 2000; **6**: 356-360
- 30 **Yu J**, Zhang HY, Ma ZZ, Lu W, Wang YF, Zhu JD. Methylation profiling of twenty four genes and the concordant methylation behaviours of nineteen genes that may contribute to hepatocellular carcinogenesis. *Cell Res* 2003; **13**: 319-333
- 31 **Okochi O**, Hibi K, Sakai M, Inoue S, Takeda S, Kaneko T, Nakao A. Methylation-mediated silencing of SOCS-1 gene in hepatocellular carcinoma derived from cirrhosis. *Clin Cancer Res* 2003; **9**: 5295-5298
- 32 **Kondoh N**, Hada A, Ryo A, Shuda M, Arai M, Matsubara O, Kimura F, Wakatsuki T, Yamamoto M. Activation of Galectin-1 gene in human hepatocellular carcinoma involves methylation-sensitive complex formations at the transcriptional upstream and downstream elements. *Int J Oncol* 2003; **23**: 1575-1583
- 33 **Fukai K**, Yokosuka O, Chiba T, Hirasawa Y, Tada M, Imazeki F, Kataoka H, Saisho H. Hepatocyte growth factor activator inhibitor 2/Placental bikunin (HAI-2/PB) gene is frequently hypermethylated in human hepatocellular carcinoma. *Cancer Res* 2003; **63**: 8674-8679
- 34 **Li Y**, Su JJ, Cao J, Ou C, Qiu XK, Yang C, Ban KC, Yue HF, Wei W, Ou SJ, Zhang LS, Wan DF, Gu JR. Differentially expressed genes in hepatocellular carcinoma of tree shrew induced by different factors. *Ai Zheng* 2003; **22**: 1018-1022

Edited by Wang XL

Comparison of transcatheter arterial chemoembolization, laparoscopic radiofrequency ablation, and conservative treatment for decompensated cirrhotic patients with hepatocellular carcinoma

Chung-Bao Hsieh, Hao-Ming Chang, Teng-Wei Chen, Chung-Jueng Chen, De-Chuan Chan, Jyh-Cherng Yu, Yao-Chi Liu, Tzu-Ming Chang, Kuo-Liang Shen

Chung-Bao Hsieh, Hao-Ming Chang, Teng-Wei Chen, Chung-Jueng Chen, De-Chuan Chan, Jyh-Cherng Yu, Yao-Chi Liu, Kuo-Liang Shen, Division of General Surgery, Department of Surgery, Department of Medicine, National Defense Medical Center, Tri-Service General Hospital, Taipei, Taiwan, China
Tzu-Ming Chang, Department of Surgery, Tungs' Taichung Metroharbor Hospital, Taichung, Taiwan, China
Correspondence to: Dr. Chung-Bao Hsieh, 325, Sec 2, Cheng-Kung Road, Taipei, Taiwan, China. albert0920@yahoo.com.tw
Telephone: +886-2-87927191 **Fax:** +886-2-87927273
Received: 2003-11-22 **Accepted:** 2003-12-16

Abstract

AIM: To compare the therapeutic effect of transcatheter arterial chemoembolization (TACE), laparoscopic radiofrequency ablation (LRFA), and conservative treatment for the therapy of decompensated liver cirrhosis patients with hepatocellular carcinomas (HCC).

METHODS: Between October 2000 and July 2003, one hundred patients with histologically proven primary HCC and clinical decompensated liver cirrhosis (Child classification B or C) were included in this study. Forty patients received LRFA (LRFA group), twenty received TACE (TACE group), and forty received conservative treatment (control group). We compared the survival, recurrence, and complication rates in these three groups, making adjustment using the tumor metastatic node staging system.

RESULTS: The major complication rate in the TACE group (9/20) was significantly higher than that in the LRFA group (7/40). For patients with TMN stage II HCC, the survival rate of the LRFA group was better than that of the TACE and control groups ($P=0.003$) but the recurrence rates between the LRFA and TACE groups did not differ.

CONCLUSION: The LRFA group of patients had better clinical outcomes in terms of survival and complication rates in comparison with the TACE group or conservative treatment in patients with decompensated liver cirrhosis, especially in TMN patients with stage II HCC. LRFA is thus an appropriate alternative treatment for poor liver function among patients with HCC.

Hsieh CB, Chang HM, Chen TW, Chen CJ, Chan DC, Yu JC, Liu YC, Chang TM, Shen KL. Comparison of transcatheter arterial chemoembolization, laparoscopic radiofrequency ablation, and conservative treatment for decompensated cirrhotic patients with hepatocellular carcinoma. *World J Gastroenterol* 2004; 10 (4): 505-508

<http://www.wjgnet.com/1007-9327/10/505.asp>

INTRODUCTION

Surgical resection is the preferred treatment for patients with hepatocellular carcinomas (HCC), as it offers the potential for cure of primary hepatic malignancies^[1,2]. Unfortunately, only 10% to 20% of patients with HCC are suitable candidates for resection because of constraints of size, location, extent of the tumors^[3] or poor liver function. The impaired liver function of HCC patients is thus a major limitation for surgical resection.

Over the last decade, other treatment modalities have been used in the management of these patients with unresectable HCC, such as cryoablation^[4], microwave coagulation therapy^[5,6], alcohol ablation, laser photocoagulation, high-intensity ultrasound, regional chemotherapy infusion^[7], transcatheter arterial chemoembolization (TACE)^[8], and radiofrequency ablation (RFA)^[9].

Recently both TACE and RFA have received increasing attention as promising treatments for patients with unresectable HCC^[4,8]. TACE is a liver-directed therapy that takes advantage of the relatively selective vascularization of hepatic arterial tumors. HCC derives approximately 80% to 85% of their blood supply from the hepatic artery, whereas the portal vein as well as the hepatic artery supply the normal hepatic parenchyma. Chemotherapeutic agents can thus be delivered angiographically with concomitant embolization to increase local chemotherapeutic dwell time and induce tumor ischemia^[10].

Investigation and use of thermal ablation have increased with advances in radiofrequency ablation (RFA) technology. This approach has been used to treat small lesions measuring 5 cm or less in diameter, and complete necrosis was achieved in 76-100% of lesions^[4]. It has few complications while achieving safe^[11] and excellent local control^[12].

The aim of this study was to compare the therapeutic effect of TACE, laparoscopic RFA (LRFA), and conservative treatment for patients with decompensated liver cirrhosis (Child classification B or C) with HCC.

MATERIALS AND METHODS

Between October 2000 and July 2003, one hundred patients with histologically proven primary hepatocellular carcinoma were included in this study. All patients were Child classification B or C^[12] and not suitable to receive surgical resection. Patients with tumor size larger than 5 cm or with more than three tumors were considered suitable for repeated TACE or conservative treatment. Patients with serum total bilirubin concentrations of more than 2 mg/dL were considered for LRFA or conservative treatment. Patients with fewer than three tumors smaller than 5 cm were considered for TACE, LRFA or conservative treatment, according to their own preferences or those of their families (Figure 1). Forty patients received LRFA (LRFA group), twenty received TACE (TACE group), and forty received conservative treatment (control group). We compared the

survival, recurrence, and complication rates in these three groups. The comparison was based on the AJCC TMN staging system modified in 1998^[13].

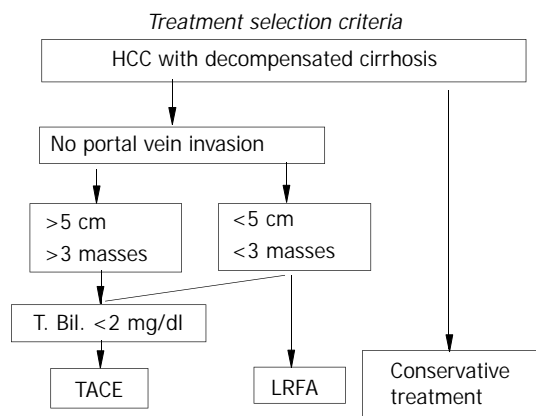


Figure 1 Criteria of treatment selection.

LRFA technique

Patients were considered for LRFA if they had less than three tumors smaller than 5 cm, regardless of the proximity of the lesions to major portal or hepatic vein branches. The LRFA needle was passed transcutaneously under laparoscopic ultrasound guidance in the operation room with the patient under general anesthesia. The Radio Therapeutics RF3000 system (Radio Therapeutics Corp, Mountain View, CA) was used in this study. It uses an insulated monopole LeVeen needle electrode consisting of ten hook-like projections that were deployed after the cannula was inserted into the target tissue. Once in place, power was applied by the RF3000 generator, which can deliver up to 100 W. Power was increased in a stepwise fashion beginning at 50 W until the maximum power was reached. Tumor ablation was continued at maximum power until tissue impedance increased to the point when power output fell rapidly (termed 'roll-off'). If roll-off was not achieved, ablation was continued at maximum power for 15 min. This procedure was repeated until roll-off, or for 10 min if roll-off could not be achieved.

Small tumors (less than 3 cm) were ablated after a single passage of the electrode array into the center of the lesions. For larger tumors (more than 3 cm), the electrode array was repositioned at 2 cm intervals and ablation was carried out as above to allow complete destruction of the tumor with a 1 cm margin. For tumors located in the posterior segment or lobes of the liver where trans-abdominal needle insertion was impossible, trans-thoracic needle insertion was performed using a chest tube.

TACE technique

Vascular access was obtained via the right common femoral artery and a guide wire was advanced under fluoroscopic guidance. A 5-French sheath was then inserted over the guide wire. The superior mesenteric artery was selected and an angiogram was completed to identify any aberrant arterial anatomy and verify portal vein patency. The celiac axis was then selected and an angiogram was completed. The catheter and guide wire were used to select the proper hepatic artery and a limited angiogram was completed to identify the branches of the hepatic artery. The right or left hepatic artery was selected for lesions in the right or left lobe, respectively, and an angiogram was completed. Any tumors were identified using a rapid contrast blush method.

Once the vascular supply of the tumor had been identified, chemoembolization of the supplying artery was started.

Doxorubicin (50 mg: NovaPlus, Novation, Irving, TX) with one-third of a vial of 250-355 μ m diameter polyvinyl alcohol particles (Boston Scientific, Natick, MA) was used as the chemoembolic agent. Successful embolization of the feeding vessel was confirmed by angiogram. The catheter and wire were then removed and direct pressure was applied for 20 minutes.

Follow-up

Computed tomographic (CT) scans were obtained from all patients one week postoperatively to document ablation. Follow-up CT scans were obtained every three months for one year and every six months thereafter. Serum Alpha-fetoprotein (AFP) concentrations were also monitored postoperatively. Elevated AFP concentrations, increases in size, or changes in the computer tomography (CT) contrast-enhanced appearance of the original tumors were used to diagnose any tumor recurrence.

Any mortality within one month after surgery (30 days) was recorded. Any complications were registered on a computer database for each patient. Major complications were regarded as any prolongation of stay in hospital caused by hepatic failure, pulmonary embolism, stroke, pneumonia, upper GI bleeding, or refractory ascites. Hepatic failure was defined based on symptoms such as hepatoencephalopathy, varices bleeding and the need for readmission and further treatment. Minor complications were regarded as those that did not cause any extension of hospital stay, such as pneumothorax, wound infections, burns and post embolization fever.

Statistical analysis

Analyses were performed using S-Plus[®]2000 for Windows statistical software (CANdiensten, Amsterdam, The Netherlands). The level of significance was set at $P < 0.05$ for all tests. Continuous variables were expressed as mean \pm SD, and tested using Student's *t* test and categorical variables were tested using Fisher's exact test. Survival rates were calculated using the Kaplan-Meier method and compared using the log-rank test.

RESULTS

The demographic data of these three groups of patients are summarized in Table 1. The mean ages and follow-up times of the three groups were not different. In this population, males predominated, the main etiology of HCC was hepatitis B virus (HBV) infection and the second was hepatitis C virus infection. This situation is common in Asia. All patients had decompensated liver cirrhosis and most were classified as Child class B, 33/100 were Child class C. Portal vein thromboses only appeared in the control group ($n=12$). The mean tumor diameter of the LRFA group was significantly smaller than that of the TACE and control groups (3.2 ± 1.0 cm vs 6.8 ± 3.7 cm and 6.5 ± 3.1 cm, respectively; $P < 0.05$). All three groups had patients with TNM stage II tumors (Table 2). We chose these patients to compare the survival and recurrence rate among the three different groups. The mean tumor diameter did not differ significantly. It was 3.4 ± 0.8 cm ($n=37$) for LRFA patients, 3.7 ± 1.0 cm ($n=9$) for TACE patients and 3.6 ± 0.9 cm ($n=10$) for the controls. There were 11/37, 1/9 and 4/10 TNM stage II patients with Child class C, respectively, among these groups (too few for statistical significance).

Two patients died of hepatic failure within one month, one in each experimental group. We excluded these from the survival analysis. The complication and recurrence rates are summarized in Table 2. The major complication rate of the LRFA group was significantly lower than that of the TACE group ($P < 0.05$). Three patients developed hepatic failure and two developed upper gastrointestinal tract (UGI) bleeding in both treatment groups. One patient in the LRFA group and

two in the TACE group developed refractory ascites after treatment. In the TACE group, one patient developed a pulmonary embolism and another had a stroke within three months. In the LRFA group, one patient developed pneumonia within three months. The minor complication and recurrence rates were not different after one and two years.

Patients classified as Child class B or C were also graded with TMN stage II tumors, the survival rate of the LRFA group was better than both the TACE and control groups (Figure 2) ($P=0.003$), whereas the recurrence rates for the LRFA and TACE groups were not significantly different (Figure 3).

Table 1 Demographic data

	LRFA	TACE	Conservative treatment
No. of patients	40	20	40
Age (years)	66.5±9.5	65.0±7.9	69.0±5.7
Sex (male/female)	35/5	17/3	32/8
Etiology (HBV/HCV)	29/11	11/9	26/14
Child-Pugh class B/C	28/12	17/3	22/18
AFP > 400 ng/ml	22	13	25
Portal vein thrombosis	0	0	12
Tumor diameter (cm):	3.2±1.0 ^a	6.8±3.7 ^a	6.5±3.1
–in TNM stage	3.4±0.8 (37)	3.7±1.0 (9)	3.6±0.9 (10)
II tumors ^b			
TNM stage I tumors	3	0	0
TNM stage II tumors	37	9	10
Child grade C in	11/37	1/9	4/10
TMN stage II tumors			
–in stage III tumors	0	11	14
–in stage IV tumors	0	0	16
Mean follow up (months and ranges)	12.5 (3–30)	11.3 (2.5–29)	10.5 (3.1–30)

^aMean tumor diameter in the LRFA group was significantly smaller than that in the TACE group ($P<0.05$). ^bTNM stage was allocated according to the 1998 modified edition^[13].

Table 2 Comparison between LRFA and TACE treatment groups in mortality, complication, and recurrence rates

	LRFA (n=40)	TACE (n=20)	P value
One-month mortality ^a	1 (2.5%)	1 (5%)	
Major complications: total	7 (17.5%)	9 (45%)	<0.05
Hepatic failure ^b	3	3	
Pulmonary embolism	0	1	
Stroke	0	1	
UGI ^c bleeding	2	2	
Pneumonia	1	0	
Refractory ascites	1	2	
Minor complications: total	7 (17.5%)	7 (35%)	
Pneumothorax	3	0	
Wound infection	2	0	
Burns	2	0	
Post embolization syndrome ^d	0	7	
Local recurrence rate			
One year	12	7	
Two years	19	11	

^aOne-month mortality, ^bHepatic failure: readmission due to chronic hepatic failure within three months after procedure, ^cUGI: upper gastrointestinal tract. ^dPost embolization syndromes included fever, pain, nausea, vomiting, leukocytosis and adynamic ileus.

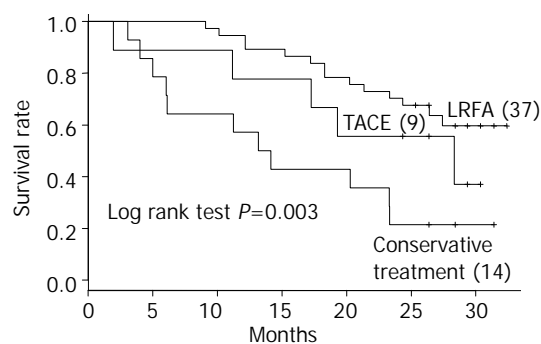


Figure 2 Kaplan-Meier curves of survival rates of TACE-, LRFA- and conservatively-treated groups of patients with TMN stage II hepatocarcinomas.

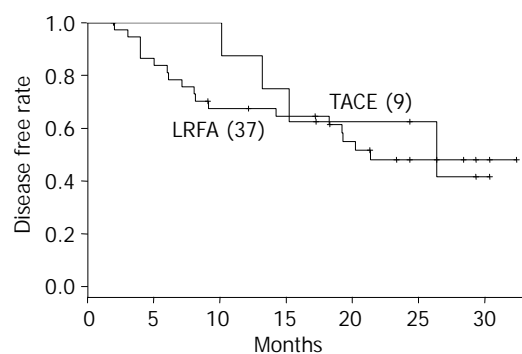


Figure 3 Kaplan-Meier curve of recurrence rate of TACE and LRFA in TMN stage II.

DISCUSSION

It is very difficult to perform randomized clinical trials among patients with HCC, as each treatment modality has its own specific indications and contraindications. In this study, there were some internal biases, such as tumor size and location, occurrence of portal vein thrombosis, treatment modalities, and liver functions. For example, if the tumor was larger than 5 cm or very near the artery, the patient could only choose TACE or conservative treatment. This made it difficult to compare these three different treatment modalities.

Systems for staging and classifying cancers are attracting interest worldwide. Such systems allow a selection between primary and adjuvant therapy, estimation of prognosis, assistance in evaluating the results of treatment, facilitation of the exchange of information among treatment centers, and contribution to the continuing investigation of human cancers^[13]. Among these scoring systems, Child classification^[14], Okuda, Cancer of the Liver Italian Program (CLIP), Barcelona Clinic Liver Cancer (BCLC), TMN^[15], and Child-Pugh staging are the most widely used for classifying patients with HCC. In this study, we needed a staging system that included both liver function parameters and tumor parameters and allowed the patient groups to be statistically comparable. We combined the Child classification (classes B and C patients) and the TMN staging system (less than three tumors with their diameter less than 5 cm) to select a comparable set of patients. Based on this analysis, the survival rate of the LRFA group was better than that of the TACE and control groups. Thus, LRFA is a good adjuvant therapy for decompensated cirrhotic patients with TMN stage II HCC tumors, especially if the tumors are smaller than 5 cm. The mechanism is unknown.

RFA had an advantage over surgical resection or other palliative treatments in that it could spare more normal liver tissue and pose less risk than surgery^[16]. It was more effective

and required less sessions than percutaneous ethanol injection (PEI), and had fewer complications than cryosurgery^[17]. As with resection of liver tumors, the goal of the RFA methods was to destroy the tumor and a small margin of the adjacent normal liver^[18]. RFA offered some significant advantages over other palliative techniques, such as brief treatment time, precise production of necrotic lesions, and minimal morbidity. RFA is thus a potentially valuable treatment for patients with unresectable liver tumors. It is safe, effective, and repeatable, and local control of hepatic tumors using RFA has been shown to be effective and to prolong the survival of patients with unresectable or advanced liver tumors^[11,19]. We found similar results here.

RFA can be performed by percutaneous, laparoscopic or exploratory surgical means. The laparoscopic approach could offer a minimally invasive procedure with the ability to perform intra-operative laparoscopic ultrasound guidance for better tumor detection and more accurate targeting^[20]. The decompensated liver was relatively small and lay low in the hepatic fossa, making the percutaneous RFA needle approach difficult. During laparoscopic RFA, achieving a pneumoperitoneum would cause elevation of the diaphragm, which increased the operative space to avoid adjacent organ injury and facilitated needle placement.

The goal of chemoembolization therapy is to prolong tumor exposure to the chemotherapeutic agent and to add an ischemic component (*i.e.*, particles) to enhance tumor necrosis. This treatment is based on the hypothesis that increased exposure time leads to improved response. The localized nature of this treatment could reduce many adverse side effects compared with systemic chemotherapy agents, which have been proven ineffective^[19]. By contrast, TACE has the disadvantage in that chemoembolization damages more normal liver tissue than RFA. This causes more postoperative complications, such as liver failure. We think that is why the survival rate of the TACE group of patients was lower than that of the LRFA group in this series.

The major complication rate among the LRFA-treated patients in this study (17.5%) was significantly higher than that reported by Iannitti *et al.* (7.1%)^[21] and Curley *et al.*^[22]. The complication rate was 8% in Child class A patients, 6.5% in Child class B patients and 27.6% in Child class C patients. All the patients in our study had significantly impaired liver function (Child class B or C) and a high major complication rate was expected. These major complications in the LRFA group arose from the decompensated cirrhotic liver except for the development of pneumonia.

The major complication rate seen in the TACE group in this study (45%) was significantly higher than that in other studies (20%)^[23]. As in the LRFA group, the major complications were caused by severely impaired liver function. TACE treatment could damage normal liver tissue and induce post-embolization hepatic failure. We believe that this caused the high complication rate in our study.

In conclusion, decompensated cirrhotic liver patients with TMN stage II HCC treated with LRFA had better clinical outcomes, such as survival and lower complication rates than those treated with TACE. We suggest that LRFA may be a better choice for treating Child class B or C patients with TMN stage I or II HCC.

REFERENCES

1 **Bloomston M**, Binitie O, Fraiji E, Murr M, Zervos E, Goldin S, Kudryk B, Zwiebel B, Black T, Fargher S, Rosemurgy AS.

- Transcatheter arterial chemoembolization with or without radiofrequency ablation in the management of patients with advanced hepatic malignancy. *Am Surgeon* 2002; **68**: 827-831
- 2 **Bowles BJ**, Machi J, Limm WML, Severino R, Oishi AJ, Furumoto NL, Wong LL, Oishi RH. Safety and efficacy of radiofrequency thermal ablation in advanced liver tumors. *Arch Surg* 2001; **136**: 864-869
- 3 **Holt DR**, Thiel DV, Edelstein JJ. Hepatic resections. *Arch Surg* 2000; **135**: 1353-1358
- 4 **Livraghi T**, Goldberg SN, Lazzaroni S, Meloni F, Solbiati L, Gazelle GS. Small hepatocellular carcinoma: treatment with radiofrequency ablation versus ethanol injection. *Radiology* 1999; **210**: 655-661
- 5 **Matsukawa T**, Yamashita Y, Arakawa A, Nishiharu T, Urata J, Murakami R, Takahashi M, Yoshimatsu S. Percutaneous microwave coagulation therapy in liver tumors: A 3-year experience. *Acta Radiol* 1997; **38**: 410-415
- 6 **Seki T**, Tamai T, Nakagawa T, Imamura M, Nishimura A, Yamashiki N, Ikeda K, Inoue K. Combination therapy with transcatheter arterial chemoembolization and percutaneous microwave coagulation therapy for hepatocellular carcinoma. *Cancer* 2000; **89**: 1245-1251
- 7 **Aguayo A**, Patt YZ. Nonsurgical treatment of hepatocellular carcinoma. *Semin Oncol* 2001; **28**: 503-513
- 8 **Rose DM**, Chapman WC, Brockenbrough AT, Wright JK, Rose AT, Meranze S, Mazer M, Blair T, Blanke CD, Debelak JP, Pinson CW. Transcatheter arterial chemoembolization as primary treatment for hepatocellular carcinoma. *Am J Surg* 1999; **177**: 405-410
- 9 **Kato T**, Reddy KR. Radiofrequency ablation for hepatocellular carcinoma: Help or hazard? *Hepatology* 2001; **33**: 1336-1337
- 10 **Liu CL**, Fan ST. Nonresectional therapies for hepatocellular carcinoma. *Am J Surg* 1997; **173**: 358-365
- 11 **Jiang HC**, Liu LX, Piao DX, Xu J, Zheng M, Zhu AL, Qi SY, Zhang WH, Wu LF. Clinical short-term results of radiofrequency ablation in liver cancers. *World J Gastroenterol* 2002; **8**: 624-630
- 12 **Cuschieri A**, Bracken J, Boni L. Initial experience with laparoscopic ultrasound-guided radiofrequency thermal ablation of hepatic tumours. *Endoscopy* 1999; **31**: 318-321
- 13 **Greene FL**, Page DL, Fleming ID, Fritz AG, Balch CM, Haller DG, Morrow M. AJCC cancer staging manual. 6th Ed. *Springer-Verlag* 2002: 3-8
- 14 **Pugh RN**, Murray-Lyon IM, Dawson JL, Pietroni MC, Williams R. Transection of the oesophagus for bleeding oesophagus varices. *Br J Surg* 1973; **60**: 646-649
- 15 **American Liver Tumor Study Group**. A randomized prospective multi-institutional trial of orthotopic liver transplantation or partial hepatic resection with or without adjuvant chemotherapy for hepatocellular carcinoma. *Investigator booklet and protocol* 1998
- 16 **Onik GM**, Atkinson D, Zemel R, Weaver M. Cryosurgery of liver cancer. *Semin Surg Oncol* 1993; **9**: 309-317
- 17 **Caridi J**. Radiofrequency ablation. Available from: http://www.miiit.com/2002/abst/caridi_rfa.pdf
- 18 **D'Agostino HB**, Solinas A. Percutaneous ablation therapy for hepatocellular carcinomas. *AJR* 1995; **164**: 1165-1167
- 19 **Scudamore CH**, Lee SI, Patterson EJ, Buczkowski AK, July LV, Chung SW, Buckley AR, Ho SGF, Owen DA. Radiofrequency ablation followed by resection of malignant liver tumors. *Am J Surg* 1999; **177**: 411-417
- 20 **Rospond RM**, Mills W. Hepatic artery chemoembolization therapy for hepatic tumors. *AORNJ* 1995; **61**: 573-576
- 21 **Iannitti DA**, Dupuy DE, Mayo-Smith WW, Murphy B. Hepatic radiofrequency ablation. *Arch Surg* 2002; **137**: 422-426
- 22 **Curley SA**, Izzo F, Ellis LM, Nicolas Vauthey J, Vallone P. Radiofrequency ablation of hepatocellular cancer in 110 patients with cirrhosis. *Ann Surg* 2000; **232**: 381-391
- 23 **Chan AO**, Yuen MF, Hui CK, Tso WK, Lai CL. A prospective study regarding the complications of transcatheter intraarterial lipiodol chemoembolization in patients with hepatocellular carcinoma. *Cancer* 2002; **94**: 1747-1752

Genes encoding Pir51, Beclin 1, RbAp48 and aldolase b are up or down-regulated in human primary hepatocellular carcinoma

Hai Song, Shuang-Luo Xia, Cheng Liao, Yi-Liang Li, Yi-Fei Wang, Tsai-Ping Li, Mu-Jun Zhao

Hai Song, Shuang-Luo Xia, Cheng Liao, Tsai-Ping Li, Mu-Jun Zhao, State Key Laboratory of Molecular Biology, Institute of Biochemistry and Cell Biology, Shanghai Institutes for Biological Sciences, Chinese Academy of Sciences, Shanghai 200031, China
Yi-Liang Li, East China Normal University, Shanghai 200062, China
Yi-Fei Wang, Department of Mathematics, Shanghai University, Shanghai 200436, China

Supported by the grants from National High Technology Research and Development Program of China (863 Program), No. 2001AA221021 and No. 2002BA711A02

Correspondence to: Professor Mu-Jun Zhao, P.O. Box 35, State Key Laboratory of Molecular Biology, Institute of Biochemistry and Cell Biology, Shanghai Institutes for Biological Sciences, Chinese Academy of Sciences, 320 Yue-Yang Road, Shanghai 200031, China. mjzhao@sibs.ac.cn

Telephone: +86-21-54921115 **Fax:** +86-21-54921011

Received: 2003-08-23 **Accepted:** 2003-10-07

Abstract

AIM: To reveal new tumor markers and target genes from differentially expressed genes of primary tumor samples using cDNA microarray.

METHODS: The ³³P labeled cDNAs were synthesized by reverse transcription of message RNA from the liver cancerous tissue and adjacent non-cancerous liver tissue from the same patient and used to hybridize to LifeGrid 1.0 cDNA microarray blot containing 8400 known and unique human cDNA gene targets, and an expression profile of genes was produced in one paired human liver tumor tissue. After a global analysis of gene expression of 8400 genes, we selected some genes to confirm the differential expression using Northern blot and RT-PCR.

RESULTS: Parallel analysis of the hybridized signals enabled us to get an expression profile of genes in which about 500 genes were differentially expressed in the paired liver tumor tissues. We identified 4 genes, the expression of three (Beclin 1, RbAp48 and Pir51) were increased and one (aldolase b) was decreased in liver tumor tissues. In addition, the expression of these genes in 6 hepatoma cell lines was also showed by RT-PCR analysis.

CONCLUSION: cDNA microarray permits a high throughput identification of changes in gene expression. The genes encoding Beclin 1, RbAp48, Pir51 and aldolase b are first reported that may be related with hepatocarcinoma.

Song H, Xia SL, Liao C, Li YL, Wang YF, Li TP, Zhao MJ. Genes encoding Pir51, Beclin 1, RbAp48 and aldolase b are up or down-regulated in human primary hepatocellular carcinoma. *World J Gastroenterol* 2004; 10(4): 509-513

<http://www.wjgnet.com/1007-9327/10/509.asp>

INTRODUCTION

Hepatocellular carcinoma (HCC), an aggressive malignancy

with poor prognosis and one of the most common tumors in human beings, has become a leading cause of cancer-related death in adults from Asia and sub-Saharan-Africa^[1]. The multiple pathogenic factors, including food contamination with aflatoxin B1 and infection with hepatitis B virus and hepatitis C virus and the subsequent multistage pathogenesis of HCC have been extensively studied. In addition, tumor suppressor genes, such as Rb and p53^[2], may play a significant role in hepatocarcinogenesis. However it is not clear how these disorders result in HCC. Recent advances in molecular genetics have identified various genetic abnormalities in tumors. However, little is known about the genetic alterations responsible for specific phenotypes of HCC.

With the advent of cDNA microarray technology, genome-wide expression of hundreds of genes can be simultaneously analyzed, facilitating differential expression monitoring of a large number of activated or suppressed genes under various biological conditions, including carcinogenesis^[3-5], drug discovery and development^[6]. With cDNA microarrays, it is now possible to perform a large-scale expression survey to identify candidate target genes^[7]. Efforts to classify human HCC based on gene expression profile using cDNA microarray have been successfully processed in recent year^[8-12]. Shirota *et al.* found that 10 genes were up-regulated and 9 genes were down-regulated in >50% HCC and identified the changes of 22 genes associated with the degree of differentiation of HCC^[8]. Kawai *et al.* showed that AFP-producing hepatoma cell lines shared a distinct expression profile of genes in various categories compared with those of AFP-negative hepatoma cell lines and non-hepatocellular cancer cell lines^[10]. Xu *et al.* identified that 156 genes were down-regulated and up-regulated in >50% of cancer samples of HCC^[12]. So much work has focused on HCC expression profile, however the data are still far less.

In this study, we used cDNA microarray representing 8400 cDNA clusters to analyze HCC specific expression profile. The aims were to identify complex alterations of genes expression responsible for the development of HCC and to identify differentially expressed genes and differentially expressed novel genes of potentially biological or medical importance for HCC. In this report, we showed that 523 genes were differentially expressed over 4 folds in the microarray analysis. We confirmed 4 genes which were consistently up or down-regulated in >50% of HCC samples.

MATERIALS AND METHODS

Tumor materials and cell lines

All samples were obtained from Eastern Hepatobiliary Surgery Hospital and Zhongshan Hospital (Shanghai, China). All patients were diagnosed as HCC. Tissue specimens were quickly frozen shortly after surgical resection and stored in liquid nitrogen. Tissue for cDNA microarray hybridization was obtained from a 47-year-old male patient with primary hepatocellular carcinoma stage III, HBV positive.

The HCC cell lines HepG2, SMMC-7721, Bel-7404, Bel-7402, HuH7 and the line of normal liver cells L02 were obtained from the Cell Bank of the Chinese Academy of Sciences

Table 1 Primer sequences and PCR conditions used for synthesis of amplicons applied as probes in Northern blot and RT-PCR

Genes name	Primer (5' -3')	PCR fragment size (bp)	Annealing temperature°C	Number of cycles
Pir51	F gtggaagatgatgttggtgggtg	527	58	32
	R aaggcggagactctgattgg			
RbAp48	F gaactgcctttcttcaatc	826	58	30
	R atggctcagacacctacctc			
Beclin 1	F cttaccacagcccaggegaaac	814	58	30
	R gccagagcatggagcagcaa			
Aldolase b	F gccacttcaacctcaatgc	423	55	32
	R tctccttccaacctaccac			
β -actin	F tgacgggggtcaccacactgtgcc	666	60	25
	R cttagaagcattgcggtggacgatg			

(Shanghai, P.R. China). HepG2, HuH7, Bel-7404 and Bel-7402 cells were cultured in Dulbecco's Modified Eagle Medium (DMEM; Life Technologies Inc., Grand Island NY, U.S.A.) supplemented with 10% fetal calf serum (FCS; Life Technologies Inc.) and L02 and SMMC-7721 cells were cultured in RPMI medium 1640 (Life Technologies Inc.) plus 10% FCS.

RNA preparation and poly A⁺ mRNA preparation

Total RNA was extracted with TRIZOL reagent (Life Technologies, Inc., N.Y., USA). Tissue samples were homogenized in 1ml of TRIZOL reagent per 50-100 mg of tissue and incubated for 5 min at room temperature, then 200 μ l chloroform was added and mixed vigorously and incubated at room temperature for 2-3 min. After centrifugation at 12000 rpm for 15 min at 4°C, the aqueous phase was transferred to a fresh tube, mixed with an equal volume of isopropanol, and incubated at room temperature for 10 min. Total RNA was collected and washed in 75% ethanol. Total RNA was run on a denaturing formaldehyde agarose gel to check quality. Poly A⁺ RNA was isolated using the oligotex mRNA mini kit (Qiagen, Hilden, Germany) according to the manufacture's instructions. Two hundred micrograms of total RNA was routinely used for mRNA isolation.

cDNA microarray hybridization

Gene expression was analyzed using the Human Life Grid 1.0 array (Incyte Genomics Inc. California, USA). Approximately 8400 human PCR products chosen from Incyte Genomics's library of proprietary clones were girded onto a 12x22 cm nylon membrane in a double-spotted pattern at a density of approximately 16800 spots and 27 controls. ³³P-labeled cDNA probe was generated by reverse transcription of 1 μ g of each analyzed polyA⁺ RNA sample in the presence of α -³³P dCTP and the percent label incorporation was not less than 40%. Each cDNA probe was then hybridized to a microarray. Overnight incubation was followed by stringent washing as recommended by the manual. Membranes were exposed to phosphor screen overnight. The data were analyzed by Incyte Genomics.

Northern blot and semi-quantitative RT-PCR

All probes were obtained by amplification of gene fragments by PCR under conditions listed in Table 1. For conventional Northern blot analysis, 15 μ g total RNA was fractionated by electrophoresis through 1% agarose gel containing formaldehyde and blotted in 20xSSC onto Hybond-N⁺ nylon membrane (Amersham Pharmacia Biotech, Ltd. Buckinghamshire, UK) by capillary force overnight. The blotted RNA was immobilized by incubating at 80°C for 1 h. Hybridization was performed at 68°C in ExpressHyb hybridization buffer (CLONTECH Inc.,

California, USA) for 3 h. Membranes were washed once in 2xSSC, 0.1% SDS at room temperature, twice in 0.1xSSC, 0.1% SDS at 68°C for 20 min and exposed to X-ray film (Eastman Kodak Co., Rochester MA) at -80°C for 1-6 d. Three μ g total RNA was reverse transcribed in 20 μ l reaction mixture with SuperscriptTM II (Life Technologies Inc., NY., USA). The PCR cycle number at the linear phase of amplification was chosen to compare differential gene expression among different genes.

RESULTS

Global gene expression analysis of HCC by high density cDNA microarray

The ³³P labeled cDNAs were synthesized by RT of message RNA from one liver cancerous tissue and adjacent normal liver tissue from the same patient and used to hybridize to Life Grid 1.0 cDNA microarray blot. General expression profile of 8400 genes was obtained (Figure 1A). We first performed a global analysis of gene expression of 8400 genes and compared the gene expression profiles for normal liver and liver tumor tissues. To eliminate data with low reliability, genes whose expression was regarded as absent in both normal liver and liver tumor by software analysis were excluded, and genes for which two spots were greater than 2.5 fold different and one of the spots was not 2 fold above background were also excluded. There were 6542 remaining genes in normal liver and liver tumor tissues. Fold changes in gene expression between normal liver and liver tumor are shown in Figure 1B. About 92% genes had no significant expression change. The result reflected the reliability of the gene expression profile. The scatter plot of intensity of all genes on arrays of liver tumor and adjacent normal liver was statistically examined to evaluate the accuracy of experiment (Figure 1C). A high correlation was observed. This result suggested a high reliability of the experiment for analysis of differentially displayed genes by cDNA microarray analysis of this sample.

Characterization of expression profile of HCC

Among the 6542 genes expressed in paired liver tumor tissue, 256 genes were up-regulated and 267 genes were down-regulated, which were greater or less than 4 fold in liver tumor tissue. Known functioning genes differentially expressed (>4 fold) in HCC were classified into six functional categories with respect to selected functional properties of their products. The six categories were included in cell division; cell, organism defense; metabolic enzymes, transporters ion channels; nuclear proteins; cell structure, extracellular matrix; cell signaling, communication. The numbers of classified genes are shown in Table 2. The group of 'other genes' summarized individual genes that could not be included in any of the above categories.

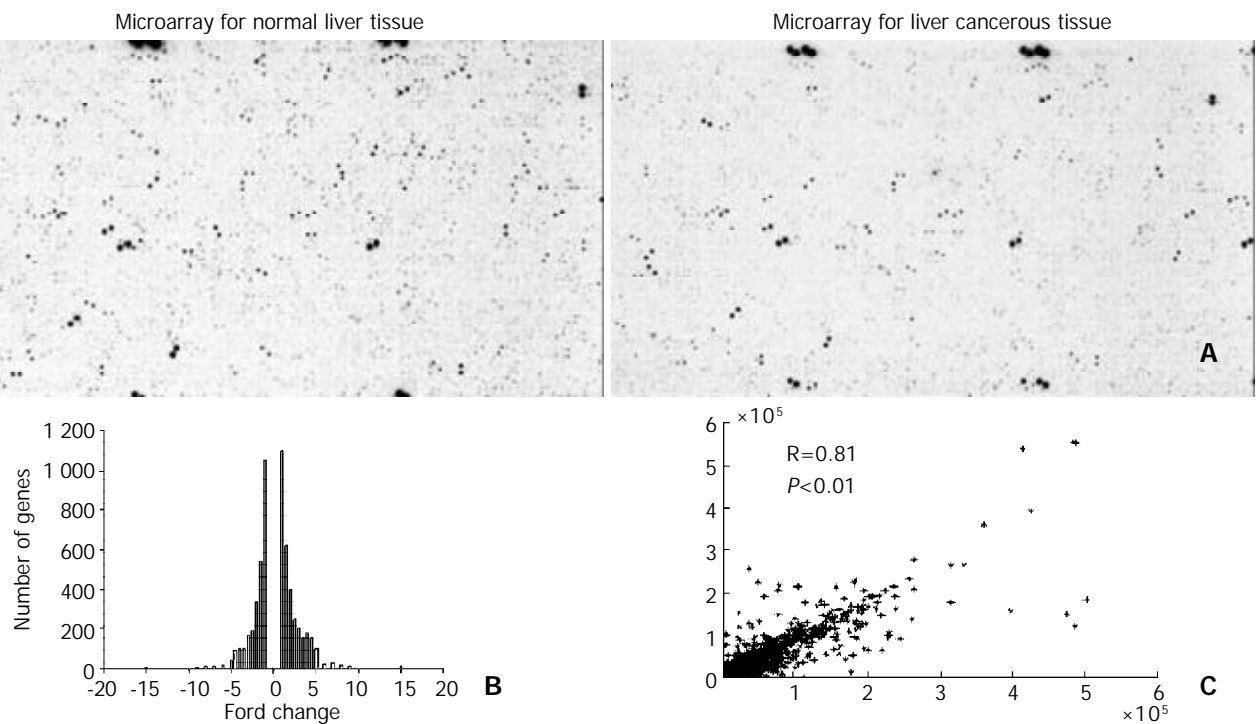


Figure 1 Parallel analysis of gene expression in paired human liver tumor sample (A). Histogram analysis of fold change in differentially expressed genes in cDNA microarray (B). Scatterplot of two cDNA microarray analyses of normal liver and liver tumor samples. Each point stands for a gene with the X coordinate value as the gene expression level in the normal liver microarray and the Y coordinate value as the gene expression level in the liver tumor microarray. A R of 0.81 was produced and suggested high reliability of the experiments (C).

Table 2 Classification of number of known functioning genes differentially expressed (>4 folds) in HCC

Gene functions	Number of down-regulated genes in HCC	Number of up-regulated genes in HCC
Cell division	17	14
Cell, organism defense	39	24
Metabolic enzymes, transporters ion channels	17	9
Nuclear proteins (transcription factors, DNA processing enzymes)	21	20
Cell structure, extracellular matrix	10	6
Cell signalling, communication	37	26
EST	41	53
Other genes	84	102

Verification of differentially expressed genes in cDNA microarray

To verify the data, we then performed Northern blot analysis and RT-PCR analysis. Only genes with expression levels that were altered by >4 fold between normal and tumor tissues were selected. These analyses were carried out with a total 10 paired HCC samples. We identified 4 genes that were differential expression in >50% paired samples. Three genes were up-regulated and one was down-regulated. Northern blot analysis of Beclin 1 and RbAp48 mRNA showed a significantly increased expression level in 50% paired tumor samples (Figure 2), which could not be detected in normal liver tissues. Northern blot analysis of aldolase b mRNA showed a significantly decreased expression level in 70% paired tumor samples. Northern blotting signal of Pir51 was difficult to obtain, the semi-quantitative RT-PCR carried out in the linear detection range was used to estimate the relative amount of mRNA. Pir51 mRNA was up-regulated by RT-PCR analysis in 60% paired tumor samples (Figure 2).

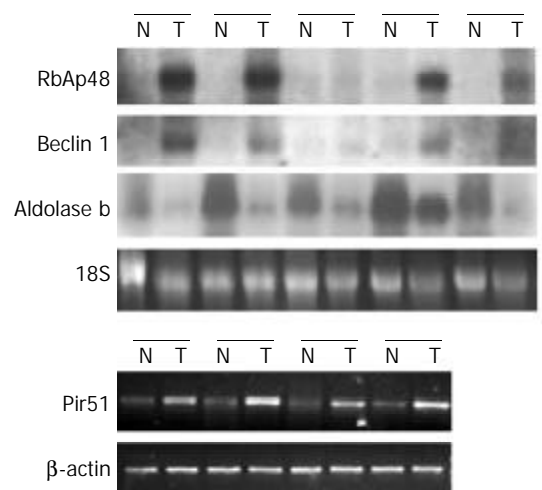


Figure 2 Northern blots of RbAp48, Beclin 1 and aldolase b genes in paired liver tumor (T) and normal liver tissues (N). RT-PCR analysis of Pir51 in the same paired HCC samples. 18S rRNA shown as a loading control.

In contrast we investigated the expression of Beclin 1, RbAp48, Pir51 and aldolase b in one hepato (L02) and 5 hepatoma cells lines by RT-PCR analysis. RbAp48 was detected in L02, Bel-7404, HepG2, Bel-7402 and HuH7, was undetectable in SMMC-7721. Beclin 1 was detected in L02, SMMC-7721, Bel-7404, and HepG2, was weak or undetectable in Bel-7402 and HuH7. Pir51 was expressed in all of hepatoma cell lines detected excluding HuH7. The data also showed that only HepG2 cells, most of cells had not, had a weak expression of aldolase b, (Figure 3). These results from cells coincided with that from tissues (Figure 2). The data of 4 genes obtained from microarray and Northern blot or RT-PCR are summarized in Table 3. The fold changes of the 4 genes by Northern blot analysis were significantly consistent with cDNA microarray.

Table 3 Genes showing differential expression levels in liver cancerous tissue and adjacent normal liver tissue

Gene Name	GenBank access number	Density in filter for tumor liver	Density in filter for normal liver	Fold change by microarray	Fold change by Northern blot
Beclin 1	AF077301	6 971	0	99	99
RbAp48	X74262	14 029.9	0	99	99
aldolase b	XM_005563	2 765	26 589	-9.65	-4.7
Pir51	NM_006479	8 654.61	323.2	26.8	5.7

GenBank access number, density, fold change verified by cDNA microarray and Northern blot were described.

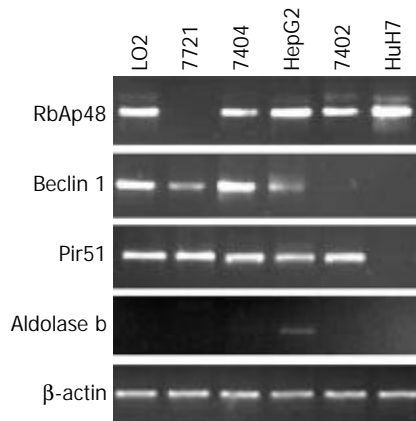


Figure 3 RT-PCR analysis of RbAp48, Beclin 1, Pir51 and aldolase b expression in one hepato (L02) and 5 hepatoma cell lines (SMMC-7721, Bel-7404, HepG2, Bel-7402, HuH7). β -actin was shown as an internal control.

DISCUSSION

In this study, we used cDNA microarray to identify the genes that may play roles in hepatocarcinogenesis. We demonstrated up- or down-regulated genes in liver cancerous tissues commonly found in patients, and compared them with those in adjacent normal tissues. Then we selected several differentially displayed genes for further verification by Northern blots or RT-PCR. Four genes (Beclin 1, RbAp48, Pir51 and aldolase b) were confirmed to have a differential expression pattern in normal and cancerous liver tissues. The low percentage appeared to be the heterogeneity of tumors^[12]. The genes identified through this approach are potential candidates for factors implicated in carcinogenesis, and are useful in both cancer diagnosis and HCC therapy.

Beclin 1 has been found to be a novel Bcl-2-interacting cellular protein which was mono-allelically deleted in 40-75% of sporadic human breast cancers and ovarian cancers^[13], and also a mammalian autophagy gene that could inhibit tumorigenesis and could be expressed at decreased levels in human breast carcinoma^[14]. It has been considered as a tumor suppressor gene in breast cancer^[14,15]. However, our results showed that the expression of Beclin 1 mRNA was increased in liver tumor tissues and HCC cell lines and could not be detected in normal liver tissues. Beclin 1 has an unknown function in HCC. Overexpression of Beclin 1 in neurons *in vivo* could inhibit Sindbis virus replication, reduce central nervous system (CNS) apoptosis, and provide protection against fatal Sindbis virus infection^[16]. 80% of HCC patients were infected with HBV or HCV, increased expression of Beclin 1 might be induced by the infection of virus. The enhanced expression of Beclin 1 in HCC provided us important information to further determine its new biological role.

RbAp48 was isolated as an Rb binding protein^[17]. RbAp48 was found to be one of the three subunits of chromatin

assembly factor 1^[18,19] and components of histone deacetylase complexes^[20,21]. RbAp48 could also interact with a complex of CREB binding protein and phosphorylated CREB^[22]. RbAp48 was physically associated in the presence of Rb and HDAC1, suggesting that RbAp48 could be involved in transcription repression of E2F responsive genes^[23]. Binding of RbAp48 correlated with the ability of Rb to block cell proliferation^[17,24]. Furthermore, the *C. elegans* homologues of both Rb and RbAp48 were recently cloned as two proteins that belong to the same Ras-inhibitory way^[25]. However, the mechanisms by which RbAp48 gene product regulated tumor growth are largely unknown. RbAp48 mRNA was also shown to increase in HCC tissues. Although the biological significance of this finding needs further study, our results showed that altered expression of RbAp48 gene might be related to HCC development.

Aldolase B, fructose-biphosphate Aldolase, an important enzyme for glucose and fructose metabolism, is a liver-specific gene. Some hepatic genes, for instance, albumin, ornitin transcarbamylase and transthyretin, were down-regulated in carcinogenesis of hepatocytes^[26,27]. This down-regulation was mainly attributed to the diminishing of some of liver-enriched transcription factors (LETf). Kovalenko *et al.*^[28] reported AIF-C1 enriched in fetal and regenerating livers, and down-regulated the aldolase B gene promoter in rat hepatoma cells. In our results, aldolase B was down-regulated in HCC samples and HCC cell lines, which may reflect the function change of liver cancer from metabolism to proliferation.

Pir51 protein could strongly interact with human Rad51 recombinase^[29]. Eukaryotic Rad51 protein has been reported to play a central role in homologous recombination by carrying out the pairing of homologous DNA molecules and initiating the strand exchange reaction^[30,31] and mammalian Rad51 was essential for cell proliferation. Rad51 activity is regulated by its associated proteins. Pir51 protein could bind to both single and double stranded DNA and was capable of aggregating DNA^[29]. However, functional significance of biochemical properties of pir51 is unclear.

In conclusion, our data demonstrate that profiling of HCC samples can help reveal genes that are commonly expressed in HCC. Information from these studies may be useful in the development of therapeutic drugs for liver cancer.

ACKNOWLEDGEMENTS

The authors thank Eastern Hepatobiliary Surgery Hospital for tumor materials and thank Mr. Sui-Quan Wang for reviewing the manuscript and helpful discussions.

REFERENCES

- 1 **Chen CJ**, Yu MW, Liaw YF. Epidemiological characteristics and risk factors of hepatocellular carcinoma. *J Gastroenterol Hepatol* 1997; **12**: S294-308
- 2 **Naka T**, Toyota N, Kaneko T, Kaibara N. Protein expression of p53, p21WAF1, and Rb as prognostic indicators in patients with surgically treated hepatocellular carcinoma. *Anticancer Res* 1998;

- 18:** 555-564
- 3 **Wang HT**, Kong JP, Ding F, Wang XQ, Wang MR, Liu LX, Wu M, Liu ZH. Analysis of gene expression profile induced by EMP-1 in esophageal cancer cells using cDNA Microarray. *World J Gastroenterol* 2003; **9**: 392-398
 - 3 **Liu LX**, Liu ZH, Jiang HC, Qu X, Zhang WH, Wu LF, Zhu AL, Wang XQ, Wu M. Profiling of differentially expressed genes in human Gastric carcinoma by cDNA expression array. *World J Gastroenterol* 2002; **8**: 580-585
 - 4 **Tan ZJ**, Hu XG, Cao GS, Tang Y. Analysis of gene expression profile of pancreatic carcinoma using cDNA microarray. *World J Gastroenterol* 2003; **9**: 818-823
 - 5 **Debouck C**, Goodfellow PN. DNA microarrays in drug discovery and development. *Nat Gene* 1999; **21**: 48-50
 - 6 **Khan J**, Saal LH, Bittner ML, Chen Y, Trent JM, Meltzer PS. Expression profiling in cancer using cDNA microarrays. *Electrophoresis* 1999; **20**: 223-229
 - 7 **Shirota Y**, Kaneko S, Honda M, Kawai HF, Kobayashi K. Identification of differentially expressed genes in hepatocellular carcinoma with cDNA microarrays. *Hepatology* 2001; **33**: 832-840
 - 8 **Liu LX**, Jiang HC, Liu ZH, Zhou J, Zhang WH, Zhu AL, Wang XQ, Wu M. Integrin gene expression profiles of human hepatocellular carcinoma. *World J Gastroenterol* 2002; **8**: 631-637
 - 9 **Kawai HF**, Kaneko S, Honda M, Shirota Y, Kobayashi K. alpha-fetoprotein-producing hepatoma cell lines share common expression profiles of genes in various categories demonstrated by cDNA microarray analysis. *Hepatology* 2001; **33**: 676-691
 - 10 **Liu LX**, Liu ZH, Jiang HC, Zhang WH, Qi SY, Hu J, Wang XQ, Wu M. Gene expression profiles of hepatoma cell line HLE. *World J Gastroenterol* 2003; **9**: 683-687
 - 11 **Xu L**, Hui L, Wang S, Gong J, Jin Y, Wang Y, Ji Y, Wu X, Han Z, Hu G. Expression profiling suggested a regulatory role of liver-enriched transcription factors in human hepatocellular carcinoma. *Cancer Res* 2001; **61**: 3176-3181
 - 12 **Aita VM**, Liang XH, Murty VV, Pincus DL, Yu W, Cayanis E, Kalachikov S, Gilliam TC, Levine B. Cloning and genomic organization of Beclin 1, a candidate tumor suppressor gene on chromosome 17q21. *Genomics* 1999; **59**: 59-65
 - 13 **Liang XH**, Jackson S, Seaman M, Brown K, Kempkes B, Hibshoosh H, Levine B. Induction of autophagy and inhibition of tumorigenesis by Beclin 1. *Nature* 1999; **402**: 672-676
 - 14 **Liang XH**, Yu J, Brown K, Levine B. Beclin 1 contains a leucine-rich nuclear export signal that is required for its autophagy and tumor suppressor function. *Cancer Res* 2001; **61**: 3443-3449
 - 15 **Liang XH**, Kleeman LK, Jiang HH, Gordon G, Goldman JE, Berry G, Herman B, Levine B. Protection against fatal Sindbis virus encephalitis by Beclin, a novel Bcl-2-interacting protein. *J Virol* 1998; **72**: 8586-8596
 - 16 **Qian YW**, Wang YC, Hollingsworth RE Jr, Jones D, Ling N, Lee EY. A retinoblastoma-binding protein related to a negative regulator of Ras in yeast. *Nature* 1993; **364**: 648-652
 - 17 **Verreault A**, Kaufman PD, Kobayashi R, Stillman B. Nucleosome assembly by a complex of CAF-1 and acetylated histones H3/H4. *Cell* 1996; **87**: 95-104
 - 18 **Tyler JK**, Bulger M, Kamakaka RT, Kobayashi R, Kadonaga JT. The p55 subunit of Drosophila chromatin assembly factor 1 is homologous to a histone deacetylase-associated protein. *Mol Cell Biol* 1996; **16**: 6149-6159
 - 19 **Zhang Y**, Iratni R, Erdjument-Bromage H, Tempst P, Reinberg D. Histone deacetylases and SAP18, a novel polypeptide, are components of a human Sin3 complex. *Cell* 1997; **89**: 357-364
 - 20 **Taunton J**, Hassig CA, Schreiber SL. A mammalian histone deacetylase related to the yeast transcriptional regulator Rpd3p. *Science* 1996; **272**: 408-411
 - 21 **Zhang Q**, Vo N, Goodman RH. Histone binding protein RbAp48 interacts with a complex of CREB binding protein and phosphorylated CREB. *Mol Cell Biol* 2000; **20**: 4970-4978
 - 22 **Nicolas E**, Morales V, Magnaghi-Jaulin L, Harel-Bellan A, Richard-Foy H, Trouche D. RbAp48 belongs to the histone deacetylase complex that associates with the retinoblastoma protein. *J Biol Chem* 2000; **275**: 9797-9804
 - 23 **Huang S**, Lee WH, Lee EY. A cellular protein that competes with SV40 T antigen for binding to the retinoblastoma gene product. *Nature* 1991; **350**: 160-162
 - 24 **Lu X**, Horvitz HR. lin-35 and lin-53, two genes that antagonize a *C. elegans* Ras pathway, encode proteins similar to Rb and its binding protein RbAp48. *Cell* 1998; **95**: 981-991
 - 25 **Clayton DF**, Weiss M, Darnell JE Jr. Liver-specific RNA metabolism in hepatoma cells: variations in transcription rates and mRNA levels. *Mol Cell Biol* 1985; **5**: 2633-2641
 - 26 **Herbst RS**, Nielsch U, Sladek F, Lai E, Babiss LE, Darnell JE Jr. Differential regulation of hepatocyte-enriched transcription factors explains changes in albumin and transthyretin gene expression among hepatoma cells. *New Biol* 1991; **3**: 289-296
 - 27 **Yabuki T**, Miyagi S, Ueda H, Saitoh Y, Tsutsumi K. A novel growth-related nuclear protein binds and inhibits rat aldolase B gene promoter. *Gene* 2001; **264**: 123-129
 - 28 **Kovalenko OV**, Golub EI, Bray-Ward P, Ward DC, Radding CM. A novel nucleic acid-binding protein that interacts with human rad51 recombinase. *Nucleic Acids Res* 1997; **25**: 4946-4953
 - 29 **Kowalczykowski SC**. Biochemistry of genetic recombination: energetics and mechanism of DNA strand exchange. *Annu Rev Biophys Chem* 1991; **20**: 539-575
 - 30 **Radding CM**. Helical interactions in homologous pairing and strand exchange driven by RecA protein. *J Biol Chem* 1991; **266**: 5355-5358
 - 31 **Tsuzuki T**, Fujii Y, Sakumi K, Tominaga Y, Nakao K, Sekiguchi M, Matsushiro A, Yoshimura Y, Morita T. Targeted disruption of the Rad51 gene leads to lethality in embryonic mice. *Proc Natl Acad Sci USA* 1996; **93**: 6236-6240

Edited by Zhang JZ and Wang XL

Inhibition of DNA primase and induction of apoptosis by 3,3'-diethyl-9-methylthia-carbocyanine iodide in hepatocellular carcinoma BEL-7402 cells

Zhi-Ming Li, Zong-Chao Liu, Zhong-Zhen Guan, Xiao-Feng Zhu, Jun-Min Zhou, Bing-Fen Xie, Gong-Kan Feng, Zhen-Yu Zhu, Wen-Qi Jiang

Zhi-Ming Li, Zong-Chao Liu, Zhong-Zhen Guan, Xiao-Feng Zhu, Jun-Min Zhou, Bing-Fen Xie, Gong-Kan Feng, Zhen-Yu Zhu, Wen-Qi Jiang, Cancer Hospital, Cancer Center, Sun Yat-sen University, Guangzhou 510060, Guangdong Province, China
Supported by the National High Technology Research and Development Program of China (863 Program), No. 2002AA2Z341C and the National Natural Science Foundation of China, No. 39870886
Correspondence to: Professor Wen-Qi Jiang, Cancer Hospital, Cancer Center, Sun Yat-sen University, Guangzhou 510060, Guangdong Province, China. wqjiang@yahoo.com
Telephone: +86-20-8734-3168 **Fax:** +86-20-8734-3392
Received: 2003-06-21 **Accepted:** 2003-08-25

Abstract

AIM: To evaluate the effects of 3,3'-diethyl-9-methylthia-carbocyanine iodide (DMTCCI) on DNA primase activity and on apoptosis of human hepatocellular carcinoma BEL-7402 cells.

METHODS: DNA primase assay was used to investigate DNA primase activity. MTT assay was applied to determine cell proliferation. Flow cytometric analysis, transmission electron microscopy, DNA fragmentation assay were performed to detect DMTCCI-induced apoptosis. Expression levels of p53, Bcl-2, Bcl-xL, Bad, Bax, survivin, Caspase-3 and poly (ADP-ribose) polymerase (PARP) were evaluated by immunoblot analysis. Caspase-3 activity was assessed with ApoAlert Caspase-3 colorimetric assay kit.

RESULTS: DMTCCI had inhibitory effects on eukaryotic DNA primase activity with IC₅₀ value of 162.2 nmol/L. It also inhibited proliferation of human hepatocellular carcinoma BEL-7402 cells with IC₅₀ value of 2.09 μmol/L. Furthermore, DMTCCI-induced BEL-7402 cell apoptosis was confirmed by DNA fragmentation (DNA ladders and sub-G1 formation) and transmission electron microscopy (apoptotic bodies formation). During the induction of apoptosis, expression of Bcl-2, Bcl-xL and survivin was decreased, and that of p53, Bad and Bax was increased. Caspase-3 was activated and poly (ADP-ribose) polymerase (PARP) was cleaved in BEL-7402 cells treated with DMTCCI.

CONCLUSION: The present data suggest that DMTCCI has inhibitory effects on eukaryotic DNA primase and can induce apoptosis of BEL-7402 cells. The modulation of expression of p53 and Bcl-2 family proteins, and activation of Caspase-3 might be involved in the induction of apoptosis.

Li ZM, Liu ZC, Guan ZZ, Zhu XF, Zhou JM, Xie BF, Feng GK, Zhu ZY, Jiang WQ. Inhibition of DNA primase and induction of apoptosis by 3,3'-diethyl-9-methylthia-carbocyanine iodide in hepatocellular carcinoma BEL-7402 cells. *World J Gastroenterol* 2004; 10(4): 514-520

<http://www.wjgnet.com/1007-9327/10/514.asp>

INTRODUCTION

In eukaryotes, DNA primase is the only enzyme catalyzing RNA primer synthesis and initiating DNA replication as well. DNA primase combines tightly with DNA polymerase α . The complex, consisting of four subunits with a molecular weight of 180 kD, 68 kD, 58 kD and 49 kD respectively, is formed. DNA primase consists of p58 and p49 subunit, and the latter is the catalytic core^[1]. PRIM1, the gene encoding DNA primase, is located on 12q13. It was found that 12q13-15 was amplified in many kinds of tumors, such as bladder cancer, glioblastoma, neuroblastoma, chronic lymphocytic leukemia, follicular central lymphoma, malignant fibrous histiocytoma, testicular germ cell tumor, breast cancer, sarcoma, primary alveolar rhabdomyosarcoma, Ewing's sarcoma and osteosarcoma. It was found that DNA primase activity in replicating cells was 5 to 6 times that in static cells. DNA primase could be regarded as a candidate target for cancer chemotherapy. In recent years, a few DNA primase inhibitors have been discovered, including fludarabine and its analogues, sphingosine, suramin, actinomycin, L-ATP, nucleotide analogues, Evans blue and aurintricarboxylic acid^[2-4]. However, there have been no anticancer drugs targeting DNA primase mainly in clinical use.

Hepatocellular carcinoma (HCC) is one of the most lethal malignancies in the world and there has been no effective preventive measure for this highly malignant disease up to date. In China, HCC has ranked the second of cancer mortality since 1990's^[5,6]. In this study, we found 3,3'-diethyl-9-methylthiacarbocyanine iodide (DMTCCI) could inhibit DNA primase activity. To explore the therapeutic potential of DMTCCI, we treated hepatocellular carcinoma BEL-7402 cells with DMTCCI and observed the proliferation inhibition and apoptosis induction effects. It was suggested that the modulation of expression of p53 and Bcl-2 family proteins, and activation of Caspase-3 might be involved in the induction of apoptosis.

MATERIALS AND METHODS

Drugs and reagents

DMTCCI (Figure 1), poly(dT) and MTT were purchased from Sigma-Aldrich (USA). RPMI-1640 medium was purchased from GIBCO. DE-52 was purchased from Serva. Phosphocellulose-11 was obtained from Whatman. [α -³²P]ATP was purchased from Amersham Biosciences. Anti-Caspase-3 antibody was obtained from Cell Signal Technology. Other antibodies were purchased from Santa Cruz Biotechnology. ApoAlert Caspase-3 colorimetric assay kit was purchased from Clontech. Ehrlich's ascites carcinoma (EAC) cells and hepatocellular carcinoma cell line BEL-7402 were obtained from the Cancer Center, Sun Yat-sen University, Guangzhou, China.

DNA primase assay

DNA primase-polymerase α complex was purified from mice EAC cells by chromatography (with DE-52 and

phosphocellulose-11 column) as described previously^[7]. The standard reaction mixture (30 μ L) contained 50 mmol/L Tris-HCl (pH 7.2), 0.1% PEG6000, 0.1 mg/mL bovine serum albumin (BSA), 3 mmol/L dithiothreitol (DTT), 6 mmol/L $MgCl_2$, 33 μ g/mL poly(dT), 2 mmol/L ATP, 400 μ mol/L [α -³²P] ATP (74 KBq), 10% glycerol and 5 units of mice DNA primase-polymerase α complex. Appropriate amounts of DMTCCI stock suspended in 0.1% DMSO were incubated with the standard reaction mixture for 30 min at 37°C. Then, the reaction products were spotted onto GF/C filters (Whatman), which were then washed three times in 5% trichoroacetic acid and twice in 95% ethanol. Filters were dried and the acid-precipitable radioactivity was determined with a liquid scintillation counter (Beckman). DNA primase reaction was measured by the formation of RNA oligomers. In order to explore the mode of inhibition of DMTCCI on DNA primase activity with respect to templet poly[dT], the concentrations of poly[dT] were established at 67, 100, 133, 167 and 200 mg/L with 0, 25 and 50 nmol/L of DMTCCI, respectively. The CPM counts were determined. In terms of Dixon plots, the mode of inhibition of DMTCCI on DNA primase activity was shown. K_i values of DMTCCI on DNA primase activity were calculated in accordance with Michaelis-Menton equation.

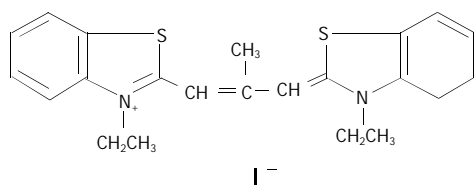


Figure 1 Chemical structure of 3, 3'-diethyl-9-methylthia-carbocyanine iodide (DMTCCI).

Cell culture

Human hepatocellular carcinoma cell line BEL-7402 was cultured in RPMI1640 medium supplemented with 10% fetal bovine serum, penicillin (100 IU/mL) and streptomycin (100 μ g/mL) at 37°C in a 5% CO₂ humidified atmosphere.

MTT assay

The logarithmically growing BEL-7402 cells were plated at a density of 1×10^4 cells/well into a 96-well plate. The stock of DMTCCI was diluted with medium, then added to the wells for the desired final concentrations. After 3 days' exposure to DMTCCI, 10 μ L MTT (5 mg/mL) was added to each well and incubated for an additional 4 h, and then the liquid in the wells was evaporated. To dissolve the formazan, 200 μ L of DMSO was added. Control wells were treated with 0.1% DMSO alone. The absorbance was detected in the microplate reader 550 model at 570 nm wavelength. Growth inhibition was equal to (1-absorbance of the treated wells)/(absorbance of the control wells) $\times 100\%$. IC₅₀ value was determined using a POMS software.

Flow cytometric analysis

Cells were harvested by trypsinization, washed twice with ice-cold PBS, resuspended in ice-cold PBS, and fixed with 70% ethanol. When ready to stain with propidium iodide (PI), the cells were centrifuged. After the ethanol was removed, the cells were washed once in PBS. The cell pellets were then resuspended in 1 mL of PI/Triton X-100 staining solution (0.1% Triton X-100 in PBS, 0.2 mg/mL RNase A, and 10 μ g/mL propidium iodide) and incubated for at least 30 min at room temperature. The stained cells were analyzed using a FACScan flow cytometer in combination with BD Lysis II Software (Becton Dickinson).

Transmission electron microscopy

BEL-7402 cells treated with DMTCCI (8 μ mol/L) for 48 h were collected and washed once in PBS. Cells were fixed in half-strength Karnofsky's fixative, postfixed in 1% collidine-buffered osmium tetroxide, dehydrated in a graded series of ethanol and propylene oxide, and embedded in LR white resin. Sections were cut and stained with both uranyl acetate and Reynold's lead stain. Electron micrographs were photographed with a JEM-1200 electron microscope.

DNA fragmentation assay

The integrity of DNA was assessed by agarose gel electrophoresis. Cells (1×10^6) were centrifuged for 5 min at 3000 g, washed once in PBS, and cell pellets were solubilized in 100 μ L of lysis buffer (50 mmol/L Tris-HCl, pH 8.0, 10 mmol/L tetraacetic acid, 0.4% SDS, 0.5 g/L proteinase K) and incubated for 8 h at 50°C, then 10 μ L of 0.5 g/L RNase A was added. The samples were incubated for 1 h at 50°C and heated to 70°C for 5 min, then 100 μ L of phenol:chloroform:isopropanol (25:24:1) was added. After centrifugation, the supernatants were transferred to new tubes, and twice volume ethanol (ice cold) was added. After centrifugation, the pellets were suspended in TE buffer (10 mmol/L Tris-HCl, 1 mmol/L tetraacetic acid) and loaded on 1.8% agarose gel for electrophoresis. The gel was stained with ethidium bromide, and photographed with UV illumination.

Immunoblot analysis

After treatment, the cells were washed in phosphate-buffered saline (PBS), and lysed in 100 μ L of lysis buffer (10 mmol/L Tris-HCl, pH 7.4, 5 mmol/L $MgCl_2$, 1 mmol/L EDTA, 25 mmol/L NaF, 100 μ mol/L fresh Na_3VO_4 and 1 mmol/L dithiothreitol). Cell lysates were centrifuged for 10 min at 14 000 g. Protein concentration in the supernatant was determined by Bradford protein assay. Equal amounts of protein (40 μ g) were resolved on 10% SDS-polyacrylamide gel, and transferred electrophoretically to PVDF membrane. The membranes were blocked with fat free dry milk (5%) in TBST (10 mmol/L Tris-HCl, pH 7.4, 150 mmol/L NaCl, 0.1% Tween-20), and then incubated with primary antibodies for 1 h at 4°C, washed three times in TBST for 30 min, and then incubated with secondary antibody (horseradish peroxidase-conjugated) for 2 h at room temperature. After the secondary antibody was washed, the bound antibody complex was detected using an ECL chemiluminescence reagent. All Western blots were performed three times in independent experiments.

Caspase-3 activity assay

To analyze Caspase-3 activity, DMTCCI-treated cells (1×10^6 cells) were washed twice in PBS and resuspended in cell lysis buffer (10 mmol/L HEPES, pH 7.4, 2 mmol/L EDTA, 0.1% CHAPS, 5 mmol/L DTT, 1 mmol/L PMSF, 10 μ g/mL pepstatin A, 10 μ g/mL aprotinin, and 20 μ g/mL leupeptin). The rest of the protocol followed the manufacturer's instructions (Bio-Rad). A specific inhibitor of Caspase-3, DEVD-fmk, was used to confirm the specificity, as suggested by the manufacturer. Absorbance was read with the microplate reader 550 model at 410 nm and the activity units were determined according to the instructions provided with the kit.

RESULTS

Inhibition of DNA primase activity by DMTCCI

DNA primase is responsible for the synthesis of RNA primers on both leading and lagging strand DNA during semi-conservative DNA replication. When DNA primase activity was assayed in the presence of various concentrations of DMTCCI, our data showed that at the concentrations of 18.5, 37.0, 111.0, 333.3 and 1 000 nmol/L of DMTCCI, the

inhibitory rates were (24.9±2.0)%, (31.4±5.0)%, (38.5±3.8)%, (52.5±6.4)% and (80.4±2.9)%, respectively, with IC₅₀ value of (162.2±7.8) nmol/L (Figure 2). The Dixon plot analysis demonstrated that DMTCCI inhibited mammalian DNA primase by a non-competitive mechanism (K_i=60.5 nmol/L) (Figure 3). The kinetics of the blockade indicated an allosteric modulation by DMTCCI of DNA primase activity.

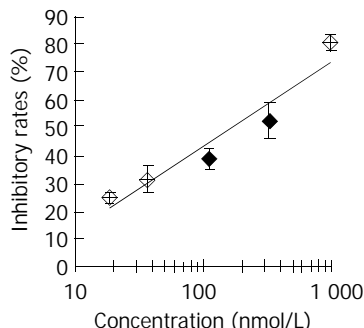


Figure 2 Inhibitory effect of DMTCCI on DNA primase activity. Appropriate amounts of DMTCCI were incubated with the standard reaction mixture containing DNA primase-polymerase α complex purified from mice Ehrlich's ascites carcinoma cells for 30 min at 37°C. DNA primase reaction was measured by the formation of RNA oligomers. Results were expressed as mean±SD for three independent experiments.

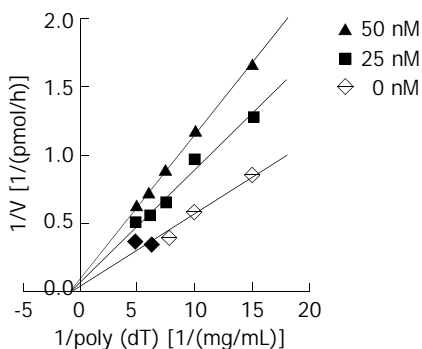


Figure 3 Kinetic analysis. Primase activity was measured in the absence or presence of DMTCCI using the indicated concentrations of DNA template poly[dT]. A Dixon plot was made on the basis of the data. Basically similar results were obtained in three separate repetitions of the experiment.

Growth inhibition of BEL-7402 cells by DMTCCI

After 3 days' exposure to DMTCCI, cell survival was analyzed by MTT assay. The results of MTT assay showed that DMTCCI inhibited cell proliferation of BEL-7402. At the concentrations of 0.3125, 0.625, 1.25, 2.5, 5, 10 and 20 μ mol/L, the inhibitory rates were 16.9%, 27.7%, 38.5%, 49.2%, 67.7%, 81.5% and 87.7% respectively. IC₅₀ value was 2.09 μ mol/L (Figure 4).

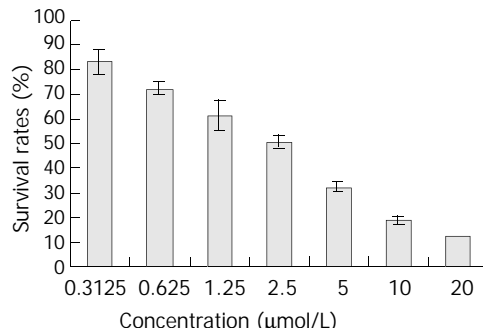


Figure 4 Effect of DNA primase inhibitor DMTCCI on proliferation of BEL-7402 cells. BEL-7402 cells were treated with various concentrations of DMTCCI as indicated for 72 h. Cell viability was determined with MTT assay and shown as survival rate.

Detection of apoptosis by flow cytometry

To examine whether BEL-7402 cells underwent apoptosis when they were treated with DMTCCI, the cells were stained with propidium iodide, followed by examination of the appearance of sub-G₁ population using flow cytometry. After treatment with 2 μ mol/L, 4 μ mol/L, 8 μ mol/L of DMTCCI for 24 h, cell death became apparent. As evidenced by the appearance of sub-G₁ population, the apoptotic indexes in BEL-7402 cells were 10.8%, 16.5% and 24.3%, respectively. At 36 h, the apoptotic indexes were 14.0%, 26.2% and 33.1%, respectively. At 48 h, the apoptotic indexes were 21.8%, 28.6% and 41.0%, respectively (Figure 5).

Transmission electron microscopy

Transmission electron microscopy showed that morphological changes typical of apoptosis were observed in BEL-7402 cells treated with DMTCCI. The cytoplasm shrank and the chromatin of cells became condensed and marginated. Chromatin was fragmented into apoptotic bodies in which

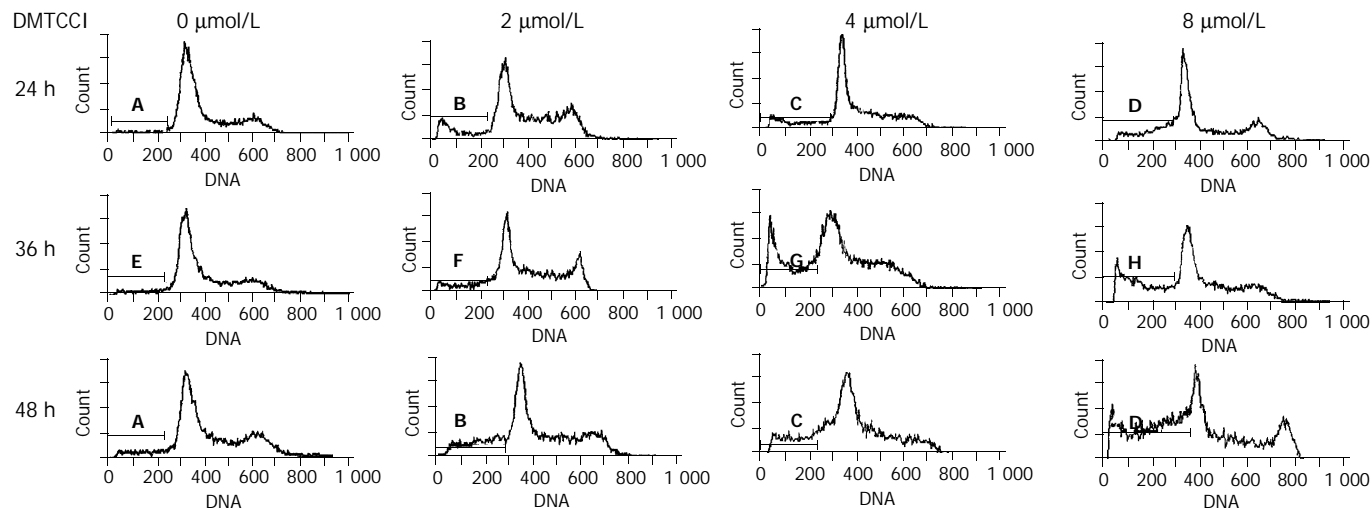


Figure 5 Flow cytometric analysis of BEL-7402 cells treated with DMTCCI. Untreated cells (control) or cells treated with DMTCCI were stained with propidium iodide, their DNA content was measured by flow cytometry. The data shown are representative of three experiments performed.

internal organelles were preserved, while most of control cells had centrally located round nuclei with prominent nucleoli and uniform morphology (Figure 6).

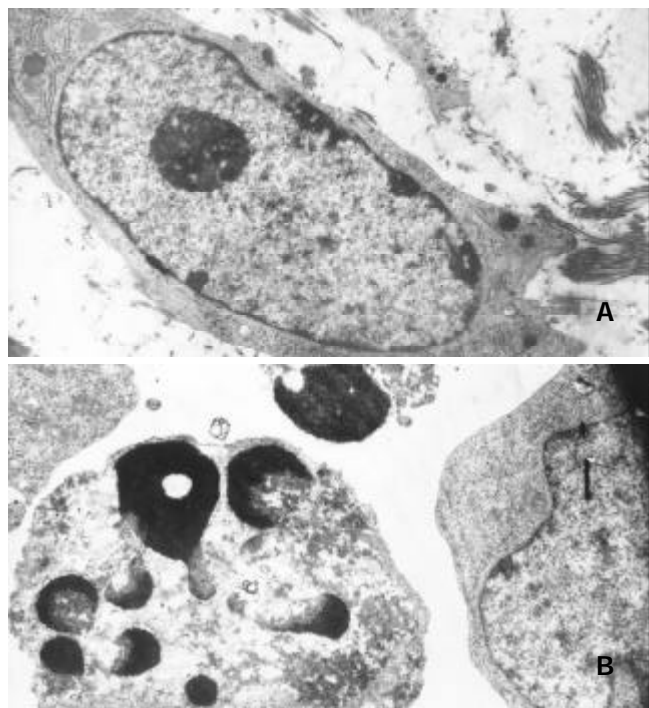


Figure 6 Morphological changes typical of apoptosis in BEL-7402 cells treated with 8 $\mu\text{mol/L}$ of DMTCCI for 24 h. BEL-7402 cells showed apoptotic morphological changes of the chromatin being condensed and margined. A: Control. $\times 5\ 000$; B: Treated with DMTCCI 8 $\mu\text{mol/L}$. $\times 7\ 000$.

Internucleosomal DNA damage in DMTCCI-treated BEL-7402 cells

Genomic DNA fragmentation was assayed as a hallmark of apoptotic cell death. As shown in Figure 7, agarose gel electrophoresis of DNA extracted from cells treated with DMTCCI revealed ladders of DNA fragmentation, indicative of induced apoptosis in BEL-7402 cells.

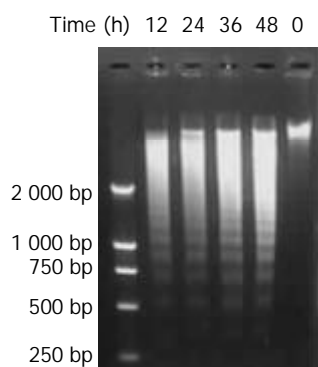


Figure 7 DNA fragmentation of BEL-7402 cells induced by DMTCCI. BEL-7402 cells were incubated in the absence or presence of DMTCCI 8 μM for 12 h, 24 h, 36 h, 48 h. Cells were harvested. DNA was isolated and DNA fragmentation was visualized as oligonucleosome-sized fragmentation in ethidium bromide after DNA agarose gel electrophoresis. This figure is a representative of three experiments.

Effect of DMTCCI on p53 in BEL-7402 cells

DNA damage could activate tumor suppressor gene p53, thereby inducing cell growth arrest, which could allow time

for DNA repair. To investigate whether p53 protein was associated with DMTCCI-induced apoptosis, we examined the change in p53 levels during the apoptotic process in BEL-7402 cells. Western blot analysis showed that the level of p53 protein increased following DMTCCI treatment in a time-dependent manner (Figure 8).

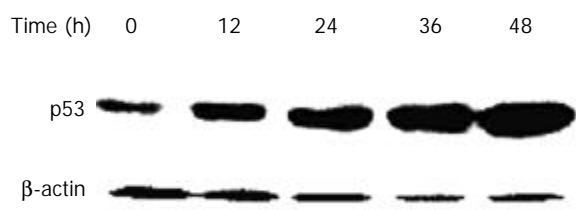


Figure 8 Down-regulation of p53 in BEL-7402 cells by DMTCCI. BEL-7402 cells were incubated with 8 μM DMTCCI for indicated time. Cells were harvested, lysed and resolved in 10% SDS-polyacrylamide gel. p53 protein levels were determined by immunoblot analysis. β -actin was used as a control.

Effect of DMTCCI on the expression of Bcl-2 family proteins

The Bcl-2 family proteins play a prominent role in the regulation of apoptosis. In this study, DMTCCI induced the expression of pro-apoptotic proteins, Bad and Bax, and downregulated the anti-apoptotic proteins, Bcl-2 and Bcl-xL in BEL-7402 cells. We deduced Bcl-2 family members might play a role in apoptosis induced by DMTCCI in BEL-7402 cells (Figure 9).

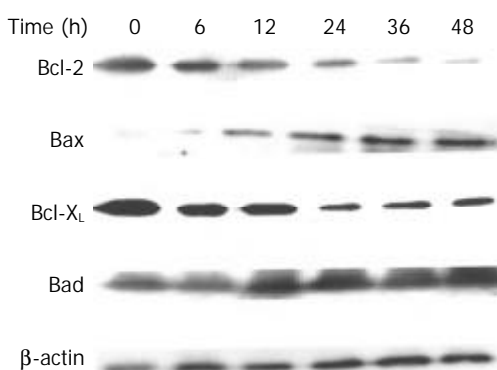


Figure 9 Effects of DMTCCI on levels of Bcl-2, Bax, Bcl-xL and Bad in BEL-7402 cells. BEL-7402 cells were treated with DMTCCI (8 μM) for indicated time, total protein was isolated by immunoblotting analysis. After electrophoresis on a 10% SDS-polyacrylamide gel, the protein was transferred to a PVDF membrane. The membrane was analyzed by immunoblotting with anti-Bcl-2, Bax, Bcl-xL and Bad antibodies, respectively. β -actin protein was used as a control.

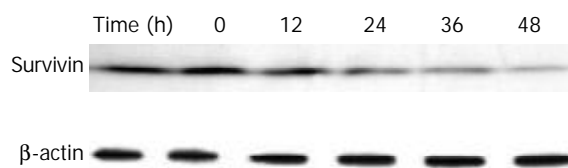


Figure 10 Down-regulation of survivin in BEL-7402 cells by DMTCCI. BEL-7402 cells were incubated with 8 μM DMTCCI for indicated time. Cells were harvested, lysed and resolved in 10% SDS-polyacrylamide gel. Survivin protein levels were determined by immunoblot analysis. β -actin was used as a control.

Effect of DMTCCI on survivin in BEL-7402 cells

Survivin is a member of the inhibitors of apoptosis protein family that is believed to play a role in oncogenesis. BEL-7402 cells treated with 8 μ M of DMTCCI for 6, 12, 24, 36 and 48 h were collected. Western blot analysis showed that the level of survivin protein decreased following DMTCCI treatment in a time-dependent manner (Figure 10).

Caspase-3 activity in DMTCCI-treated BEL-7402 cells

The results shown above indicated that DMTCCI induced apoptosis in BEL-7402 cells. To probe into the mechanism of apoptosis, we detected Caspase-3 activity following treatment of BEL-7402 with DMTCCI. As shown in Figure 11, Caspase-3 activity was apparently increased at 6 h and reached a peak at 24 h in response to DMTCCI treatment in BEL-7402 cells.

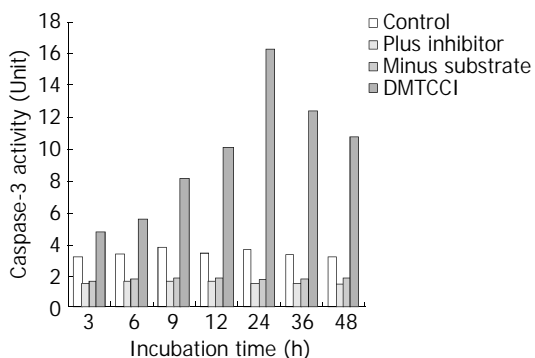


Figure 11 Inhibition of DMTCCI on activity of Caspase-3 in BEL-7402 cells. BEL-7402 cells were harvested after exposure to 8 μ mol/L of DMTCCI for indicated time. Activity of Caspase-3 was measured by ApoAlert caspase-3 assay kits. Cell lysates were prepared for each sample and used in the Caspase-3 activity assay using the colorimetric substrate DEVD-pNA. Absorbance was read at 410 nm and This figure is a representative of three experiments.

Cleavage of Caspase-3 induced by DMTCCI in BEL-7402 cells

Caspase-3, a member of the Caspase family, was shown to play an essential role in apoptosis induced by a variety of stimuli^[8-10]. We examined whether Caspase-3 was activated during DMTCCI-induced apoptosis in BEL-7402 cells. Activation of Caspase-3 was determined by monitoring proteolysis of the 35-kDa procaspase-3 to 17-kDa fragments. Figure 12 shows the appearance of the 17-kDa fragments of the active enzyme following exposure to 8 μ mol/L DMTCCI for 24 h, indicating that DMTCCI efficiently activated Caspase-3 in BEL-7402 cells.

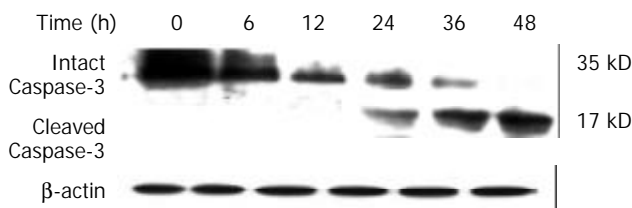


Figure 12 Effect of DMTCCI on levels of proteins of Caspase-3 in BEL-7402 cells. BEL-7402 cells were treated with 8 μ M DMTCCI for the indicated time. Western blot analysis was performed with anti-Caspase-3 antibody. β -actin was used as a control.

Cleavage of PARP induced by DMTCCI

Caspases are synthesized as inactive proenzymes. When activated, they could specifically cleave both relevant cellular

substrates and zymogens to promote apoptosis^[11,12]. One of the substrates for Caspase protease during apoptosis was PARP, an enzyme that appears to be involved in response to environment stress. Proteolytic cleavage of PARP could result in a characteristic shift of the protein upon electrophoresis from 116 to 89 kDa. PARP cleavage was used as an indicator of caspase activation in response to DMTCCI treatment. PARP could be cleaved 24 h after DMTCCI treatment (Figure 13).

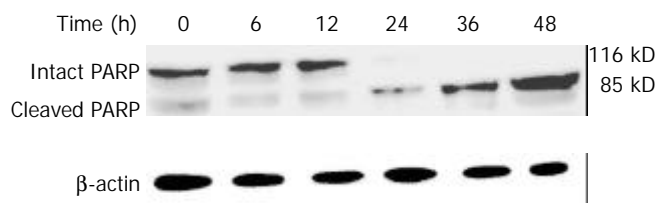


Figure 13 PARP cleavage in BEL-7402 cells induced by DMTCCI. After BEL-7402 cells were treated with 8 μ M DMTCCI for the indicated time, total protein was isolated by immunoblotting analysis. After electrophoresis on a 10% SDS-polyacrylamide gel, the protein was transferred to a PVDF membrane. The membrane was analyzed by immunoblotting with antibody against PARP. β -actin protein was used as a control.

DISCUSSION

In this study, we found DMTCCI could inhibit proliferation of hepatocellular carcinoma BEL-7402 cells. DNA replication is a prime target of cancer chemotherapeutics. For example, DNA polymerase α inhibitors have been widely used in chemotherapy. DNA primase could combine tightly with DNA polymerase α as a complex. It could play a critical role in coupling replication to repair and in checkpoint control during S phase, as well as in telomere maintenance^[1]. However, DNA primase has not been well studied as an anticancer target since its structure and function were not clarified until recently. DNA primase is considered as a key enzyme in DNA replication because it is the only enzyme that can initiate the synthesis of new DNA strands *de novo*. We believe new target helps improve existing treatment and overcome drug resistance. Nevertheless, our study showed DMTCCI could suppress cell proliferation at concentrations that were comparable to Ki values for its inhibition on DNA primase. The growth suppression of human hepatocellular carcinoma BEL-7402 cells by DMTCCI was well correlated with DNA primase inhibition.

Apoptosis plays important roles in the control of various biological systems, such as immune responses, hematopoiesis, embryonic development, and carcinogenesis. Apoptosis is an active cell death and could be triggered by a variety of pharmacological and physiological agents^[13-15]. In this study, we reported firstly that DMTCCI induced apoptosis in BEL-7402 cells demonstrated by DNA fragmentation, flow cytometry analysis and transmission electron microscopy.

P53 protein has been implicated in DNA damage recognition, DNA repair, cell cycle regulation and particularly in triggering apoptosis after genetic injury^[16-18]. To examine whether DMTCCI-induced apoptosis was associated with p53, we measured the level of p53 in BEL-7402 cells. Western blot analysis revealed that p53 protein level increased following DMTCCI treatment in a time-dependent manner, indicating that p53 might be involved in DMTCCI-mediated apoptosis.

It has been found that apoptotic process is controlled by several genes, including inducers and repressors, some of them belong to the Bcl-2 family^[19]. Bcl-2 family could be divided into two classes: those such as Bcl-2 and Bcl-xL, are able to

block apoptosis, and others, such as Bad and Bax, have proapoptotic effects^[20-22]. The balance between the anti-apoptotic and pro-apoptotic Bcl-2 family members may be critical to determine if a cell undergoes apoptosis. The death promoting protein Bax counteracts the anti-apoptotic effects of Bcl-2 by forming a heterodimer with Bcl-2. The ratio of Bcl-2 to Bax, rather than the levels of individual proteins, was considered to be critical in determining the survival/death of cells^[23-25]. Bad could compete for the binding to Bcl-xL and Bcl-2, thereby affecting the level of heterodimerization of these proteins with Bax^[26]. Our data showed that the expression level of protein Bad and Bax was increased, and that of Bcl-2 and Bcl-xL was decreased in BEL-7402 cells treated with DMTCCI. Taken together, the significant increase of Bad and Bax, and decrease of Bcl-2 and Bcl-xL would favor Bad to compete for Bcl-xL, resulting in much more free Bax into homodimers, which might induce apoptotic response in BEL-7402 cells.

Survivin has recently been identified as a novel inhibitor of apoptosis (IAP). Acting as one of the substrate inhibitors of Caspases, survivin blocks the activation of different effector Caspases. Overexpression of survivin could lead to the suppression of apoptosis triggered by diverse proapoptotic signals^[27-29]. In this study, DMTCCI decreased the level of survivin in BEL-7402 cells, indicating that survivin might be involved in DMTCCI-mediated apoptosis.

It has been found that apoptosis is coordinated by a family of cysteine proteases, the Caspases, which are activated upon receipt of divergent pro-apoptotic stimuli^[30-32]. In this study, we found that Caspase-3 was activated during DMTCCI-induced apoptosis in BEL-7402 cells. Caspase-3 is believed to be the main executioner Caspase and its activation has been shown to be essential for DNA fragmentation as well as chromatin condensation and proteolysis of certain Caspase substrates. During the process of DMTCCI-induced apoptosis, Caspase-3 activity was apparently increased at 6 h and reached a peak at 24 h in response to DMTCCI in BEL-7402 cells. One of the substrates for Caspase-3 during apoptosis was PARP, an enzyme that appears to be involved in response to environment stress. PARP cleavage was used as an indicator of Caspase-3 activation in response to DMTCCI treatment. PARP was cleaved 24 h after DMTCCI treatment. These results suggest that caspase-3 activation is involved in DMTCCI-mediated apoptosis in BEL-7402 cells.

In conclusion, DMTCCI could inhibit proliferation and induce apoptosis of human hepatocellular carcinoma BEL-7402 cells. In this study, the expression of Bcl-2, survivin and Bcl-xL was decreased, and that of Bad and Bax was increased in BEL-7402 cells treated with DMTCCI. Furthermore, we found that Caspase-3 was activated during apoptosis and the processing of Caspase-3 was accompanied by proteolytic cleavage of PARP. These finally led to apoptotic events including apoptotic bodies and DNA fragmentation. These results indicate that the induction of apoptosis by DMTCCI involves the modulation of expression of p53 and Bcl-2 family proteins and activation of Caspase-3. It can be a candidate for the development of new anti-tumor agents targeting DNA primase associated with human cancer, including human hepatocellular carcinoma.

REFERENCES

- Arezi B**, Kuchta RD. Eukaryotic DNA primase. *Trends Biochem Sci* 2000; **25**: 572-576
- Cloutier S**, Hamel H, Champagne M, Yotov WV. Mapping of the human DNA primase 1 (PRIM1) to chromosome 12q13. *Genomics* 1997; **43**: 398-401
- Grosse F**, Krauss G. The primase activity of DNA polymerase alpha from calf thymus. *J Biol Chem* 1985; **260**: 1881-1888
- Simbulan CM**, Tamiya-Koizumi K, Suzuki M, Shoji M, Taki T, Yoshida S. Sphingosine inhibits the synthesis of RNA primer by primase *in vitro*. *Biochemistry* 1994; **33**: 9007-9012
- Zhao WH**, Ma ZM, Zhou XR, Feng YZ, Fang BS. Prediction of recurrence and prognosis in patients with hepatocellular carcinoma after resection by use of CLIP score. *World J Gastroenterol* 2002; **8**: 237-242
- Roberts LR**, LaRusso NF. Potential roles of tumor suppressor genes and microsatellite instability in hepatocellular carcinogenesis in southern African blacks. *World J Gastroenterol* 2000; **6**: 37-41
- Tamiya-Koizumi K**, Murate T, Suzuki M, Simbulan CM, Nakagawa M, Takemura M, Furuta K, Izuta S, Yoshida S. Inhibition of DNA primase by sphingosine and its analogues parallels with their growth suppression of cultured human leukemic cells. *Biochem Mol Biol Int* 1997; **41**: 1179-1189
- Devarajan E**, Sahin AA, Chen JS, Krishnamurthy RR, Aggarwal N, Brun AM, Sapino A, Zhang F, Sharma D, Yang XH, Tora AD, Mehta K. Down-regulation of caspase 3 in breast cancer: a possible mechanism for chemoresistance. *Oncogene* 2002; **21**: 8843-8851
- Chen T**, Yang I, Irby R, Shain KH, Wang HG, Quackenbush J, Coppola D, Cheng JQ, Yeatman TJ. Regulation of caspase expression and apoptosis by adenomatous polyposis coli. *Cancer Res* 2003; **63**: 4368-4374
- Ceruti S**, Beltrami E, Matarrese P, Mazzola A, Cattabeni F, Malorni W, Abbracchio MP. A key role for caspase-2 and caspase-3 in the apoptosis induced by 2-chloro-2'-deoxy-adenosine (cladribine) and 2-chloro-adenosine in human astrocytoma cells. *Mol Pharmacol* 2003; **63**: 1437-1447
- Sharma K**, Wang RX, Zhang LY, Yin DL, Luo XY, Solomon JC, Jiang RF, Markos K, Davidson W, Scott DW, Shi YF. Death the Fas way: regulation and pathophysiology of CD95 and its ligand. *Pharmacol Ther* 2000; **88**: 333-347
- Nicholson DW**. Caspase structure, proteolytic substrates, and function during apoptotic cell death. *Cell Death Differ* 1999; **6**: 1028-1042
- Zimmermann KC**, Bonzon C, Green DR. The machinery of programmed cell death. *Pharmacol Ther* 2001; **92**: 57-70
- Pallis M**, Bradshaw TD, Westwell AD, Grundy M, Stevens MF, Russell N. Induction of apoptosis without redox catastrophe by thioredoxin-inhibitory compounds. *Biochem Pharmacol* 2003; **66**: 1695-1705
- Gil D**, Garcia LF, Rojas M. Modulation of macrophage apoptosis by antimycobacterial therapy: physiological role of apoptosis in the control of Mycobacterium tuberculosis. *Toxicol Appl Pharmacol* 2003; **190**: 111-119
- Adimoolam S**, Ford JM. p53 and DNA damage-inducible expression of the xeroderma pigmentosum group C gene. *Proc Natl Acad Sci U S A* 2002; **99**: 12985-12990
- Smith ND**, Rubenstein JN, Eggener SE, Kozlowski JM. The p53 tumor suppressor gene and nuclear protein: basic science review and relevance in the management of bladder cancer. *J Urol* 2003; **169**: 1219-1228
- Taylor WR**, Stark GR. Regulation of the G2/M transition by p53. *Oncogene* 2001; **20**: 1803-1815
- Konopleva M**, Konoplev S, Hu W, Zaritskey AY, Afanasiev BV, Andreeff M. Stromal cells prevent apoptosis of AML cells by up-regulation of anti-apoptotic proteins. *Leukemia* 2002; **16**: 1713-1724
- Panaretakis T**, Pokrovskaja K, Shoshan MC, Grandier D. Activation of Bak, Bax, and BH3-only proteins in the apoptotic response to doxorubicin. *J Biol Chem* 2002; **277**: 44317-44326
- Bellosillo B**, Villamor N, Lopez-Guillermo A, Marce S, Bosch F, Campo E, Montserrat E, Colomer D. Spontaneous and drug-induced apoptosis is mediated by conformational changes of Bax and Bak in B-cell chronic lymphocytic leukemia. *Blood* 2002; **100**: 1810-1816
- Zhou HB**, Zhu JR. Paclitaxel induces apoptosis in human gastric carcinoma cells. *World J Gastroenterol* 2003; **9**: 442-445
- Pettersson F**, Dalgleish AG, Bissonnette RP, Colston KW. Retinoids cause apoptosis in pancreatic cancer cells via activation of RAR-gamma and altered expression of Bcl-2/Bax. *Br J*

- Cancer* 2002; **87**: 555-561
- 24 **Zhou HB**, Yan Y, Sun YN, Zhu JR. Resveratrol induces apoptosis in human esophageal carcinoma cells. *World J Gastroenterol* 2003; **9**: 408-411
- 25 **Li SM**, Yao SK, Yamamura N, Nakamura T. Expression of Bcl-2 and Bax in extrahepatic biliary tract carcinoma and dysplasia. *World J Gastroenterol* 2003; **9**: 2579-2582
- 26 **Siervo-Sassi RR**, Marrangoni AM, Feng X, Naoumova N, Winans M, Edwards RP, Lokshin A. Physiological and molecular effects of Apo2L/TRAIL and cisplatin in ovarian carcinoma cell lines. *Cancer Lett* 2003; **190**: 61-72
- 27 **Xu ZX**, Zhao RX, Ding T, Tran TT, Zhang W, Pandolfi PP, Chang KS. Promyelocytic Leukemia protein 4 induces apoptosis by inhibition of survivin expression. *J Biol Chem* 2004; **279**: 1838-1844
- 28 **Yang L**, Cao Z, Yan H, Wood WC. Coexistence of high levels of apoptotic signaling and inhibitor of apoptosis proteins in human tumor cells: implication for cancer specific therapy. *Cancer Res* 2003; **63**: 6815-6824
- 29 **Carter BZ**, Wang RY, Schober WD, Milella M, Chism D, Andreeff M. Targeting survivin expression induces cell proliferation defect and subsequent cell death involving mitochondrial pathway in myeloid leukemic cells. *Cell Cycle* 2003; **2**: 488-493
- 30 **Li HL**, Chen DD, Li XH, Zhang HW, Lü JH, Ren XD, Wang CC. JTE-522-induced apoptosis in human gastric adenocarcinoma cell line AGS cells by caspase activation accompanying cytochrome C release, membrane translocation of Bax and loss of mitochondrial membrane potential. *World J Gastroenterol* 2002; **8**: 217-223
- 31 **Wolf BB**, Green DR. Suicidal tendencies: apoptotic cell death by caspase family proteinases. *J Biol Chem* 1999; **274**: 20049-20052
- 32 **Salvesen GS**, Dixit VM. Caspases: intracellular signaling by proteolysis. *Cell* 1997; **91**: 443-446

Edited by Zhu LH and Wang XL

Genomic instability of murine hepatocellular carcinomas with low and high metastatic capacities

Shu-Hui Zhang, Wen-Ming Cong, Jing-Quan Shi, Hong Wei

Shu-Hui Zhang, Wen-Ming Cong, Department of Pathology, Eastern Hepatobiliary Surgery Hospital, Second Military Medical University, Shanghai 200438, China

Jing-Quan Shi, Department of Pathology, Southwestern Hospital, Third Military Medical University, Chongqing 400038, China

Hong Wei, Laboratory Animal Center, Third Military Medical University, Chongqing 400038, China

Supported by the National Natural Science Foundation of China, No. 39900173 and the Major State Key Basic Research Development Program of China, No. G20000161061

Correspondence to: Dr. Shu-Hui Zhang, Department of Pathology, Eastern Hepatobiliary Surgery Hospital, Second Military Medical University, Shanghai 200433, China. zhangshuhui100@sohu.com

Telephone: +86-21-25070860 **Fax:** +86-21-25070854

Received: 2003-08-23 **Accepted:** 2003-09-25

Abstract

AIM: To investigate the frequency of genomic instability in murine hepatocellular carcinoma (HCC) cell lines Hca/A2-P (P) and Hca/163-F(F) with low and high metastatic capacity, and to explore its association with the occurrence and metastasis of hepatocellular carcinomas.

METHODS: Forty microsatellite markers were randomly selected to examine P and F cells for genomic instability using PCR-simple sequence length polymorphism (PCR-SSLP) analysis.

RESULTS: Allelic genes on the chromosomes of P cell line with thirty informative microsatellite loci were paralleled to those of inbred strain C₃H mouse, while those of F cell line with 28 loci were paralleled to those of inbred strain C₃H mice. The frequency of microsatellite alterations was 37.5% and 42.5% in P cell line and F cell line, respectively. There were different alterations of allelic band 9 at loci between P and F cells, among which, the frequency of microsatellite alterations was most commonly seen on chromosomes 3, 7, 11 and 16.

CONCLUSION: Genomic instability in mouse chromosomes 3, 7, 11 and 16 may play a more important role in the development and progression of HCC in mice. It is suggested that these two sub-clones derived from a same hepatic tumor in homozygous mouse present different genetic features.

Zhang SH, Cong WM, Shi JQ, Wei H. Genomic instability of murine hepatocellular carcinomas with low and high metastatic capacities. *World J Gastroenterol* 2004; 10(4): 521-524
<http://www.wjgnet.com/1007-9327/10/521.asp>

INTRODUCTION

Hepatocellular carcinoma (HCC) is one of the most frequent human cancers worldwide and has ranked second in China since 1990s^[1-3]. The development and progression of HCC are considered as a complex process involving genetic alterations,

such as chromosomal deletions, chromosomal translocation, point mutations, and gene amplification. These changes can lead to activation of oncogenes or inactivation of tumor suppressor genes at various stages of HCC^[4,5]. Genetic instability or genomic instability in human cancers can be divided into two types: microsatellite instability (MSI) which is usually equated with DNA polymerase errors, and chromosomal instability or loss of heterozygosity (LOH) which can result from errors in chromosome partitioning. Both LOH and MSI are considered as phenotypes of genomic instability^[6,7]. LOH is frequently observed on chromosomes 1p, 4q, 5q, 8p, 8q, 9p, 10q, 11p, 13q, 14q, 16q, 17p and 22q in HCC, suggesting that tumor suppressor genes may take part in hepatocarcinogenesis^[8-10]. MSI and mutations of defective mismatch repair genes can occur in hepatocytes in some chronic hepatitis, cirrhosis and HCC^[11-15]. Inbred strain mice provide the guarantee to study on comparison, reliability and accuracy of molecular genetics in neoplasms, because of their characteristics such as high genetic stability, phenotypic uniformity and homozygous alleles. Moreover, it is very valuable to understand the various molecular changes of development and progression in carcinogenesis^[16,17]. We examined genomic instability with microsatellite markers at 40 loci on four chromosomes in HCC with low and high metastatic capacity in mice and analyzed the association of microsatellite alterations and metastatic abilities, in order to provide experimental data for finding new tumor suppressor genes and metastasis associated genes.

MATERIALS AND METHODS

Hepatocellular carcinoma cell lines Hca/A2-P(P) and Hca/16-F(F) with low and high metastatic capacity were used in this study. Two cell lines were routinely cultured in 1640 medium (Gibco) supplemented with 10% fetal bovine serum (Hyclone) at 37°C with 5% CO₂. Inbred strain C₃H mice were provided by Sino-British SIPPR/BK Laboratory Animal Center (Shanghai, China).

DNA extraction

Genomic DNA was extracted from cancer cells and normal liver tissues of inbred C₃H mice using the standard phenol/chloroform extraction and ethanol precipitation methods^[18]. Briefly, normal tissues and cancer cells were incubated with 2 ml lysis/digestion buffer (1% sodium dodecyl sulfate, 1 mM EDTA, 50 mM Tris at pH 8.5, and 100 µg proteinase K/ml) at 52°C for 16 h. The digested lysate was subjected to two further extractions with an equal volume of chloroform:phenol:isoamyl alcohol (24:25:1). After centrifugation, DNA was precipitated from the aqueous phase by two volumes of cold absolute ethanol and collected with a glass rod^[19]. The DNA was further purified with RNase digestion, two steps of phenol/chloroform extractions, and precipitated and collected as described above. The concentration of DNA was determined with both spectrophotometric and fluorometric methods.

Microsatellite markers and polymerase chain reaction

The characteristics of microsatellite loci used in this study are

shown in Table 1. The polymerase chain reaction mixture contained more than 20 ng of genomic DNA, 200 μ mol/L of each dNTP, 1.5 mM MgCl₂, 0.5 units of AmpliTaq Gold DNA polymerase (PE Applied Biosystems, Foster City, CA), 0.5 μ mol/L of each primer, and 10 \times AmpliTaq Gold PCR buffer in a final volume of 10 μ L. After denaturation at 94°C for 12 minutes, DNA amplification was performed for 15 cycles of 94°C for 30 seconds, 63°C for 60 seconds (decreased 0.5°C of each cycle), and 72°C for 90 seconds, and then for 25 cycles of 94°C for 30 seconds, 56°C for 60 seconds, and 72°C for 90 seconds, with a final extension at 72°C for 10 minutes. PCR products were electrophoresized on 8% denatured polyacrylamide gel under a constant voltage of 30 V/cm for simple sequence length polymorphism (PCR-SSLP) analysis. The gel was stained with silver staining after electrophoresis.

Identification of genomic instability

We scored only the bands in cancer cells by preceding or succeeding compared with those in normal samples. Loss or gain of band(s) and clearly detectable changes in intensity were scored^[20]. Scoring was done by two independent observers. A change of band intensities was defined as an increase or decrease of the signal intensity by $\geq 50\%$ in tumor DNA compared to normal DNA by gray scanning function in an image analysis software.

RESULTS

Microsatellite alterations in HCC cell lines with low and high metastatic capacity in mice

Genomic instability was examined using 40 microsatellite markers spanning 4 chromosomes in HCC with low and high metastatic capacity in mice. The results showed that thirty

Table 1 Characteristics of microsatellite loci and summary of microsatellite alterations in mouse HCC cell lines

Locus name	Position (cM) ^a	Allele size (bp) ^a	Annealing (°C)	Hum homology region ^a	Hca/A2-P	Hca/16A3-F
D3Mit21	14.2	218	58	3q24-q28	additional band	additional band
D3Nds2	23.1	115	60	4q26-q28	additional band	additional band
D3Mit22	25.1	240	55	4q25-q28	240	240
D3Mit13	42.6	220	58	1q21	230	230
D3Mit15	45.9	145	55	1p36-q12.1q23-31	145	145
D3Mit16	45.9	186	53	1p36-q12.1q23-31	186	186
D3Mit17	50.3	180	54	1p13-p22	loss	additional band
D3Mit18	54.6	214	57	4q28-q31	loss	loss
D3Mit19	66.7	176	60	4q25-q28	176	176
D3Mit147	79.4	134	60	1p31	134	134
D7Mit20	5.5	107	62	19q13.2	loss	loss
D7Mit18	25.1	120	62	11p15-p14	shifted	shifted
D7Mit16	29.5	248	64	15q11-q13	248	248
D7Mit17	37.2	162	56	15q24-q26	shifted	additional band
D7Mit19	31.7	135	60	15q14	135	135
D7Mit10	62.3	150	62	10q24-q26	150	150
D7Mit12	62.3	197	56	10q24-q26	197	197
D7Mit13	62.3	195	60	10q24-q26	195	195
D7Mit14	64.5	147	58	10q24.3-ter	147	147
D7Mit15	66.7	138	62	10q26	loss	loss
D11Mit1	2.2	153	58	7p13-p11	153	153
D11Mit2	4.4	140	58	7p	140	140
D11Mit4	36.1	242	58	17p13-p11	loss	loss
D11Mit5	36.1	188	55	17p13-p11	shifted	loss
D11Mit7	40.4	144	64	17p13	loss	loss
D11Mit8	42.6	155	59	17p13	loss	loss
D11Mit10	64.5	100	55	17q11-qter	100	100
D11Mit13	65.6	162	63	17q24-q25	162	162
D11Mit11	72.1	238	64	17q11-qter	additional band	238
D11Mit12	75.4	147	59	17q25	147	147
D16Mit9	4.0	132	58	16q13	132	132
D16Mit1	17.5	106	61	22q11	106	106
D16Mit2	17.5	189	57	22q11	189	loss
D16Mit3	23	100	59	3q11-q13	100	loss
D16Mit4	25.1	123	58	3q13	shifted/additional band	loss
D16Mit5	32.8	160	59	3q21-qter	160	loss
D16Mit6	45.9	190	59	3p11	190	190
D16Mit7	45.9	162	60	3p11	loss	loss
D16Mit225	58	198	58	21q22	198	198
D16Mit71	69.2	154	58	21q22	loss	loss

^aData from GenBank.

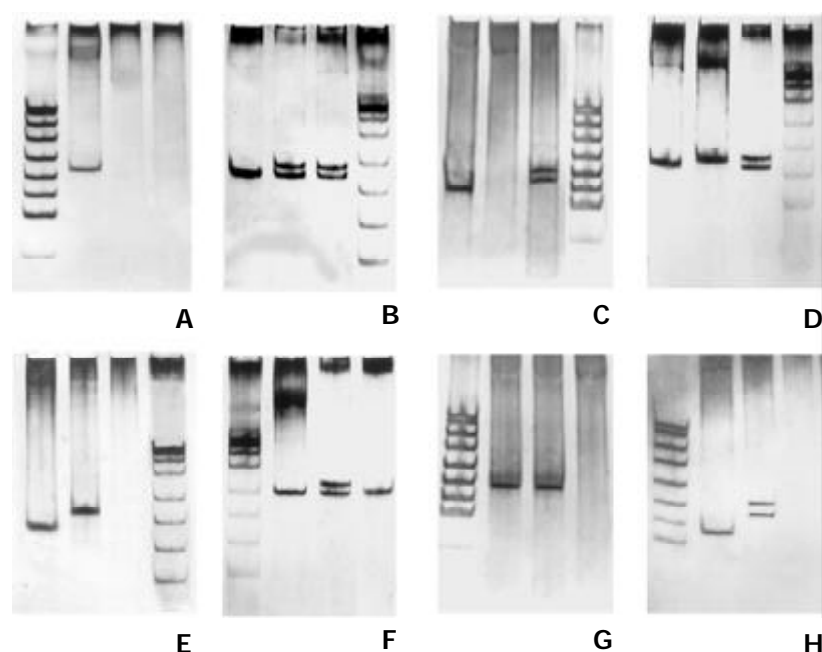


Figure 1 Genomic instability in murine hepatocellular carcinomas with low and high metastatic capacity, PCR-SSLP. A: D3Mit18, B: D3Nds2, C: D3Mit17, D: D7Mit17, E: D11Mit5, F: D11Mit11, G: D16Mit5, H: D16Mit4.

microsatellite loci were same as that of C₃H mice, they were D3Mit15, D3Mit16, D3Mit19, D3Mit22, D4Mit1, D4Mit2, D7Mit10, D7Mit12, D7Mit13, D7Mit14, D7Mit16, D7Mit19, D7Nds2, D11Mit1, D11Mit2, D11Mit10, D11Mit12, D11Mit13, D15Mit17, D15Nds1, D16Mit1 and D16Mit7. The results of microsatellite alterations in mouse HCC cell lines are shown in Table 1. Examples of genomic instability in hepatocellular carcinomas with low and high metastatic capacity in mice by PCR-SSLP method are shown in Figure 1. The frequency of microsatellite alterations was 37.5% in P cell line. The frequency of microsatellite alterations on chromosomes 3, 7, 11 and 16 was 40%, 40%, 50% and 20% in P cell line. The frequency of microsatellite alterations was 42.5% in F cell line. The frequency of microsatellite alterations on chromosomes 3, 7, 11 and 16 was 40%, 40%, 40% and 50% in F cell line. Microsatellite alterations at D3Mit18, D3Mit21, D3Nds2, D7Mit15, D7Mit18, D7Mit20, D11Mit4, D11Mit7, D11Mit8 and D16Mit7 in P cell line were same as those in F cell line. Microsatellite alterations at D3Mit17, D7Mit17, D11Mit5, D15Nds2, D16Mit2, D16Mit3, D16Mit4 and D16Mit5 in P cell line were different from those in F cell line. In contrast to inbred strain C₃H mice, the allelotypic sizes of 25 microsatellite loci were same as those of C₃H mice, 8 loci with loss of alleles, extra bands showing at 4 loci and band shifting at 3 loci in P cell line, while 23 loci were same as that of C₃H mice, allele loss at 11 loci, extra bands showing at 4 loci and band shifting at 1 locus in F cell line.

DISCUSSION

In the present study, we found that the frequent genomic instability on chromosomes 3, 7, 11 and 16 existed in hepatocellular carcinoma (HCC) cell lines Hca/A2-P(P) and Hca/163-F(F) with low and high metastatic capacity, both of which were derived from an inbred C₃H mouse. Microsatellite alterations at D3Mit18, D3Mit21, D3Nds2, D7Mit15, D7Mit18, D7Mit20, D11Mit4, D11Mit7, D11Mit8 and D16Mit7 in P cell line were same as those in F cell line. These results suggested that there were tumor suppressor genes in these points, inactivation of them might play an important role in the development of HCC in mice. Microsatellite alterations at D3Mit17, D7Mit17, D11Mit5, D15Nds2, D16Mit2,

D16Mit3, D16Mit4 and D16Mit5 in P cell line were different from those in F cell line. These results suggested that there were different genetic alterations in hepatocellular carcinoma (HCC) cell lines with high and low metastatic capacity derived from a homozygous mouse hepatic tumor.

Homologous regions between mouse and human chromosomes have been defined^[21]. Mouse chromosome 3 is syntenic to certain regions of human chromosomes 1p13-p22, 1p36-q12, 1q23-31, 3q24-q28, 4q25-q31 and 8. Previous studies suggested that 4q25 and 4q26-27 deletions occurred in human HCC^[22,23]. Epidermal growth factor locus is located at the former region. *Cyclin A* and *interleukin-2* loci are located at the latter region, which has a HBV integrated position. Mouse chromosome 7 is syntenic to certain regions of human chromosomes 10q26-ter, 11p15, 15q and 19q13. High frequencies of loss of heterozygosity (LOH) were observed on chromosome 10q26 in human hepatocellular carcinoma^[24]. *Ras* and *Bax* genes are located at 1.9cM distance from D7Mit18 locus. More than 50% of colon adenocarcinomas with human microsatellite mutator phenotype examined were found to have frameshift mutations in a tract of eight deoxyguanosines [(G)₈] within *BAX*, a gene that promotes apoptosis^[25]. Allelic loss and mutation of *Ha-ras* were seen in a variety of human and mice tumors^[26]. Mouse chromosome 11 is syntenic to certain regions of human chromosomes 17p13 and 17q21-qter. Previous studies have shown that high frequencies of LOH were found on chromosomes 17p13.1 and 17p13.3 in human HCC^[27,28]. Some studies have demonstrated LOH at the *p53* locus on chromosome 11 and mutational inactivation of the remaining *p53* allele in a significant percentage of carcinomas^[29], which also harbored for *BRCA1* tumor suppressor gene and candidate suppressor prohibitin^[30,31]. In the present study, we found that the allelic loss at D3Mit18, D7Mit15, D7Mit20, D11Mit4, D11Mit7 and D11Mit8 on 17p13 was present in P and F cells. We found an extra band at D3Mit21 (*IL-2* locus), D3Nds2 (*EGF* locus) and D7Mit18 in P and F cells. These results suggested that chromosomes 3, 7 and 11 might carry candidate tumor suppressor genes, and play important roles in the development of HCC in mice. Additionally, allelic loss occurred at D3Mit17 of P cells, while extra band appeared in F cells. Band shifting was present at D7Mit17 locus in P cells, while extra band appeared in F cells, suggesting that different

sub-clones of the same tumor have heterogeneity.

Mouse chromosome 16 is syntenic to certain regions of human chromosomes 3q21-ter, 12q, 16p, 21q and 22q. It was reported that human chromosome 3q carried a tumor suppressor gene for osteosarcoma, because this chromosomal region was frequently deleted in this type of tumors^[32]. LOH was frequently observed on 22q in HCC^[33]. Mafune *et al*^[34] found that mouse chromosome 16 was deleted in a clone of mouse fibrosarcoma 505 cells, suggesting that chromosome 16 may have a cognate of such candidate tumor suppressor genes and hence deletion of the region might confer malignancy related with metastasis. In the present study, genomic instability at D16Mit2, D16Mit3, D16Mit4 and D16Mit5 was found in mouse HCC with a high metastatic capacity. It was suggested that genes in chromosome 16 were closely related to tumor metastasis, their mutation could result in metastasis of HCC. Band shifting occurred at D16Mit4 locus in P cells, allelic loss was found in F cells due to continuous genomic instability during the development and progression of tumors. Genomic instability at some chromosomes of HCC in mice were studied and some loci related to hepatocarcinogenesis and progression were obtained which might be of great significance in searching new tumor associated genes.

In conclusion, genomic instability in mouse chromosomes 3, 7, 11 and 16 may play an important role in the development and progression of HCC in mice.

REFERENCES

- 1 **Wu MC**, Shen F. Progress in research of liver surgery in China. *World J Gastroenterol* 2000; **6**: 773-776
- 2 **Tang ZY**. Hepatocellular carcinoma—cause, treatment and metastasis. *World J Gastroenterol* 2001; **7**: 445-454
- 3 **Bosch FX**, Ribes J, Borrás J. Epidemiology of primary liver cancer. *Semin Liver Dis* 1999; **19**: 271-285
- 4 **Thorgeirsson SS**, Grisham JW. Molecular pathogenesis of human hepatocellular carcinoma. *Nat Genet* 2002; **31**: 339-346
- 5 **Feitelson MA**, Sun B, Satiroglu Tufan NL, Liu J, Pan J, Lian Z. Genetic mechanisms of hepatocarcinogenesis. *Oncogene* 2002; **21**: 2593-2604
- 6 **Loeb LA**, Loeb KR, Anderson JP. Multiple mutations and cancer. *Proc Natl Acad Sci U S A* 2003; **100**: 776-781
- 7 **Kawai H**, Suda T, Aoyagi Y, Isokawa O, Mita Y, Waguri N, Kuroiwa T, Igarashi M, Tsukada K, Mori S, Shimizu T, Suzuki Y, Abe Y, Takahashi T, Nomoto M, Asakura H. Quantitative evaluation of genomic instability as a possible predictor for development of hepatocellular carcinoma: comparison of loss of heterozygosity and replication error. *Hepatology* 2000; **31**: 1246-1250
- 8 **Buendia MA**. Genetics of hepatocellular carcinoma. *Semin Cancer Biol* 2000; **10**: 185-200
- 9 **Nagai H**, Pineau P, Tiollais P, Buendia MA, Dejean A. Comprehensive allelotyping of human hepatocellular carcinoma. *Oncogene* 1997; **14**: 2927-2933
- 10 **Li SP**, Wang HY, Li JQ, Zhang CQ, Feng QS, Huang P, Yu XJ, Huang LX, Liang QW, Zeng YX. Genome-wide analyses on loss of heterozygosity in hepatocellular carcinoma in Southern China. *J Hepatol* 2001; **34**: 840-849
- 11 **Dore MP**, Realdi G, Mura D, Onida A, Massarelli G, Dettori G, Graham DY, Sepulveda AR. Genomic instability in chronic viral hepatitis and hepatocellular carcinoma. *Hum Pathol* 2001; **32**: 698-703
- 12 **Karachristos A**, Liloglou T, Field JK, Deligiorgi E, Kouskouni E, Spandidos DA. Microsatellite instability and p53 mutations in hepatocellular carcinoma. *Mol Cell Biol Res Commun* 1999; **2**: 155-161
- 13 **Maggioni M**, Coggi G, Cassani B, Bianchi P, Romagnoli S, Mandelli A, Borzio M, Colombo P, Roncalli M. Molecular changes in hepatocellular dysplastic nodules on microdissected liver biopsies. *Hepatology* 2000; **32**: 942-946
- 14 **Roncalli M**, Bianchi P, Grimaldi GC, Ricci D, Laghi L, Maggioni M, Opocher E, Borzio M, Coggi G. Fractional allelic loss in non-end-stage cirrhosis: correlations with hepatocellular carcinoma development during follow-up. *Hepatology* 2000; **31**: 846-850
- 15 **Saeki A**, Tamura S, Ito N, Kiso S, Matsuda Y, Yabuuchi I, Kawata S, Matsuzawa Y. Lack of frameshift mutations in coding mononucleotide repeats in hepatocellular carcinoma in Japanese patients. *Cancer* 2000; **88**: 1025-1029
- 16 **Lee GH**. Genetic dissection of murine susceptibilities to liver and lung tumors based on the two-stage concept of carcinogenesis. *Pathol Int* 1998; **48**: 925-933
- 17 **Chabicovsky M**, Staniek K, Rossmanith W, Bursch W, Nohl H, Schulte-Hermann R. Hepatocarcinogenesis in the context of strain differences in energy metabolism between inbred strains of mice (C57BL/6J and C₃H/He). *Adv Exp Med Biol* 2001; **500**: 607-611
- 18 **Sood AK**, Buller RE. Genomic instability in ovarian cancer: a reassessment using an arbitrarily primed polymerase chain reaction. *Oncogene* 1996; **13**: 2499-2504
- 19 **Weber JL**, May PE. Abundant class of human DNA polymorphism which can be typed using the polymerase chain reaction. *Am J Hum Genet* 1989; **44**: 388-396
- 20 **Arzimanoglou II**, Gilbert F, Barber HR. Microsatellite instability in human solid tumors. *Cancer* 1998; **83**: 1808-1820
- 21 **Copeland NG**, Jenkins NA, Gilbert DJ, Eppig JT, Maltais LJ, Miller JC, Dietrich WF, Weaver A, Lincoln SE, Steen RG. A genetic linkage map of the mouse: current applications and future prospects. *Science* 1993; **262**: 57-66
- 22 **De-Mitri MS**, Pisi E, Brechot C, Paterlini P. Low frequency of allelic loss in the cyclin A gene in human hepatocellular carcinomas: a study based on PCR. *Liver* 1993; **13**: 259-261
- 23 **Chou YH**, Chung KC, Jeng LB, Chen TC, Liaw YF. Frequent allelic loss on chromosomes 4q and 16q associated with human hepatocellular carcinoma in Taiwan. *Cancer Lett* 1998; **123**: 1-6
- 24 **Nagai H**, Ponglikitmongkol M, Fujimoto J, Yamamoto H, Kim YS, Konishi N, Matsubara K. Genomic aberrations in early stage human hepatocellular carcinomas. *Cancer* 1998; **82**: 454-461
- 25 **Rampino N**, Yamamoto H, Ionov Y, Li Y, Sawai H, Reed JC, Perucho M. Somatic frameshift mutations in the BAX gene in colon cancers of the microsatellite mutator phenotype. *Science* 1997; **275**: 967-969
- 26 **Lumniczky K**, Antal S, Unger E, Wunderlich L, Hidvegi EJ, Safrany G. Carcinogenic alterations in murine liver, lung, and uterine tumors induced by in utero exposure to ionizing radiation. *Mol Carcinog* 1998; **21**: 100-110
- 27 **Rashid A**, Wang JS, Qian GS, Lu BX, Hamilton SR, Groopman JD. Genetic alterations in hepatocellular carcinomas: association between loss of chromosome 4q and p53 gene mutations. *Br J Cancer* 1999; **80**: 59-66
- 28 **Zhao X**, Li J, He Y, Lan F, Fu L, Guo J, Zhao R, Ye Y, He M, Chong W, Chen J, Zhang L, Yang N, Xu B, Wu M, Wan D, Gu J. A novel growth suppressor gene on chromosome 17p13.3 with a high frequency of mutation in human hepatocellular carcinoma. *Cancer Res* 2001; **61**: 7383-7387
- 29 **Fujii H**, Biel MA, Zhou W, Weitzman SA, Baylin SB, Gabrielson E. Methylation of the HIC-1 candidate tumor suppressor gene in human breast cancer. *Oncogene* 1998; **16**: 2159-2164
- 30 **Jupe ER**, Liu XT, Kiehlauch JL, McClung JK, Dell'Orco RT. Prohibitin in breast cancer cell lines: loss of antiproliferative activity is linked to 3' untranslated region mutations. *Cell Growth Differ* 1996; **7**: 871-878
- 31 **Sato T**, Sakamoto T, Takita K, Saito H, Okui K, Nakamura Y. The human prohibitin (PHB) gene family and its somatic mutations in human tumors. *Genomics* 1993; **17**: 762-764
- 32 **Kruzlock RP**, Murphy EC, Strong LC, Naylor SL, Hansen MF. Localization of a novel tumor suppressor locus on human chromosome 3q important in osteosarcoma tumorigenesis. *Cancer Res* 1997; **57**: 106-109
- 33 **Takahashi K**, Kudo J, Ishibashi H, Hirata Y, Niho Y. Frequent loss of heterozygosity on chromosome 22 in hepatocellular carcinoma. *Hepatology* 1993; **17**: 794-799
- 34 **Mafune Y**, Asakura H, Kominami R. Allelic losses and metastatic ability of mouse tumor cell clones derived from a heterozygous mouse. *Oncogene* 1994; **9**: 2191-2196

Expression of HIF-2 α /EPAS1 in hepatocellular carcinoma

Gassimou Bangoura, Lian-Yue Yang, Gen-Wen Huang, Wei Wang

Gassimou Bangoura, Lian-Yue Yang, Gen-We Huang, Wei-Wang, Department of General Surgery and Liver Cancer Laboratory, Xiangya Hospital, Central South University, Changsha 410008, Hunan Province, China

Supported by the National Key Technologies R and D Program, No. 2001BA703B04

Correspondence to: Professor Lian-Yue Yang, Department of General Surgery and Liver Cancer Laboratory, Xiangya Hospital, Central South University, Changsha 410008, Hunan Province, China. lianyueyang@hotmail.com

Telephone: +86-731-4327326 **Fax:** +86-731-4327232

Received: 2003-06-16 **Accepted:** 2003-10-07

Abstract

AIM: To investigate the expression of hypoxia-inducible factor (HIF)-2 α /endothelial PAS domain protein1 (EPAS1) in hepatocellular carcinoma (HCC).

METHODS: Expression of HIF-2 α /EPAS1 was investigated immunohistochemically on paraffin-embedded sections from 97 patients with HCC. To further confirm that HIF-2 α /EPAS1 in HCC tissues also correlated with angiogenesis, a parallel immunohistochemistry study of vascular endothelial growth factor (VEGF) was performed on these 97 cases.

RESULTS: HIF-2 α /EPAS1 could be detected in 50 of 97 cases (51.6%), including 19 weakly positive (19.8%), and 31 strongly positive (31.1%), the other 47 cases were negative (48.4%). The expression of HIF-2 α /EPAS1 was significantly correlated with tumor size, capsule infiltration, portal vein invasion, and necrosis. A parallel immunohistochemical analysis of VEGF demonstrated its positive correlation with capsule infiltration, portal vein invasion, and HIF-2 α /EPAS1 overexpression, which supported the correlation of HIF-2 α /EPAS1 up-regulation with tumor angiogenesis. No apparent correlation was observed between HIF-2 α /EPAS1 and capsular formation, presence of cirrhosis, and histological grade.

CONCLUSION: HIF-2 α /EPAS1 is expressed in most of HCC with capsular infiltration and portal vein invasion, which indicates a possible role of HIF-2 α /EPAS1 in HCC metastasis.

Bangoura G, Yang LY, Huang GW, Wang W. Expression of HIF-2 α /EPAS1 in hepatocellular carcinoma. *World J Gastroenterol* 2004; 10(4): 525-530

<http://www.wjgnet.com/1007-9327/10/525.asp>

INTRODUCTION

Hypoxia is an essential development and physiological stimulus and plays a key role in the physiology of cancer, heart attack, stroke, and other major causes of mortality^[1]. Recently, hypoxia-inducible factors HIF-1 α and HIF-2 α /endothelial PAS domain protein1 (EPAS1) have been identified. They are basic helix-loop-helix/Per-Arnt-Sim (PAS) transcription factors induced under hypoxia^[2,3]. When dimerized with aryl hydrocarbon nuclear translocator (also known as HIF-3 α , another basic helix-loop-helix family member), both HIF-1 α

and HIF-2 α can bind to the hypoxia response element in a battery of genes and transactivate their expression, including vascular endothelial growth factor (VEGF)^[3,4]. These genes are important for tumor adaptation to hypoxia, implicating the possible role of HIFs in tumor progression. Tumor can not grow larger than 1-2 mm³ in the absence of angiogenesis, because of the lack of oxygen in the center of tumors, which result in apoptosis and necrosis^[5]. Many tumors contain hypoxic microenvironments, a condition associated with poor prognosis and resistant to clinical treatment. Along with HIF-1 α , EPAS1 is also known as HIF-2 α ^[6,7], HIF-like factor^[8], and HIF-related factor^[9]. The expression of HIF-2 α /EPAS1 has been reported in many human malignancies^[10,11]. We chose to study HIF-2 α /EPAS1 expression in order to evaluate its clinical significance and identify the relation with some important markers of carcinoma progression, which are also predictors of metastasis.

MATERIALS AND METHODS

Clinical material

We examined 97 surgical resection specimens from patients (76 males, 21 females) with HCC, who underwent surgery at Xiangya hospital between January 1994 and December 2001. The age of patients ranged from 34 to 78 years (61.4 \pm 8.9 years). The clinical features of the patients were noted with reference to clinical reports and pathology reports, including Edmondson-Steiner classification. In principle, grades I, II and III-IV and the characteristics of these patients are summarized in Table 1.

Immunohistochemical determination

Tissues were fixed with 10% formaldehyde in phosphate-buffered saline, embedded in paraffin, and cut into 5 μ m-thick tissue sections. The sections were deparaffinized in xylene and rehydrated in grade ethanol. Endogenous peroxidase was blocked by immersing the sections in 3% H₂O₂ in 100% methanol for 20 minutes at room temperature. Antigen retrieval was achieved by micro-waving sections at 95 $^{\circ}$ C for 10 minutes in 0.001 M citrate buffer (pH 6.7). For immunohistochemical detection of diluted mouse monoclonal antibodies against HIF-2 α /EPAS1 (190b) (DAKO, Glostrup, Denmark) and 1:200 diluted mAb against VEGF (Ab3) (Fremont, CA). Substitution of the primary antibodies with normal mouse IgG was used as a negative control. After washing, specimens were incubated with peroxidase-conjugated goat anti-mouse IgG for 30 min at room temperature. The color reaction was developed by incubating the sections with 0.5 mg/ml 3,3'-diaminobenzidine and 3% (vol/vol) H₂O₂ in phosphate-buffer saline for 7 min. The sections were counterstained slightly with Meyer hematoxylin and mounted.

VEGF determination and assessment

Mouse monoclonal antibody Ab3, neomarker (Fremont, CA) for detecting a smaller isoform (VEGF₁₂₁) of VEGF were used for the identification and evaluation of VEGF expression in this study. Staining with VEGF monoclonal antibody required antigen retrieval, which was best done by microwave pretreatment. In brief, paraffin-fixed slides were autoclaved for 7 min in pretreatment before deparaffinization and

rehydration. Evaluation of staining was semiquantitatively graded based on score determination by intensity distribution as strong ++ (dark brown), weak + (brown), or negative - (no staining). The score was determined independently by at least three of four observers.

Statistical analysis

A computer software SPSS 10.0 program was used for statistical analysis. Spearman's correlation coefficient test was used to assess the relationship between HIF-2 α /EPAS1, VEGF expression versus histological grade and tumor size. χ^2 test was used to assess the correlation between HIF-2 α /EPAS1, VEGF, versus existence of necrosis, cirrhosis, capsular formation, capsular infiltration and portal vein invasion. $P < 0.05$ was considered to be statistically significant.

Table 1 Correlation between HIF-2 α /EPAS1 and clinicopathological features of HCC patients

Variant	HIF-2 α /EPAS1 expression (No of cases)			No of cases 97	Significance
	-	+	++		
Pathological grade					
Grade I	9	4	3	16	NS
Grade II	23	8	7	38	
Grade III-IV	15	7	221	43	
Tumor size					
≤ 2	22	3	8	33	
2-5	16	14	13	43	0.001 ^a
> 5	9	2	10	21	
Cirrhosis					
With	27	9	17	53	NS
Without	20	10	14	44	
Capsule formation					
With	8	1	9	18	NS
Without	39	18	22	79	
Capsule infiltration					
With	3	3	10	16	0.011 ^a
Without	44	16	21	81	
Portal vein invasion					
With	15	15	18	48	0.001 ^a
Without	32	4	13	49	
Necrosis					
With	19	12	23	54	0.010 ^a
Without	28	7	8	43	

^a $P < 0.05$ vs the expression of HIF-2 α /EPAS1 was significant in HCC tissues with capsule infiltration, portal vein invasion, necrosis, and tumor size. NS, not significant.

RESULTS

In the 97 cases studied, positive staining of HIF-2 α /EPAS1 protein was localized mainly in the cytoplasm, and occasionally and faintly in the membrane of HCC cells (Figures 1A and 1B). In general, most positive stains were observed in the perinecrotic regions near the tumor foci (Figure 1C). There was expression of HIF-2 α /EPAS1 in cancer cells, whereas no positive staining was seen in the stroma cells of HCC (Figure 1D). Immunoreactivity of HIF-2 α /EPAS1 was also observed in macrophages, as previously reported^[10]. In addition, we also found positive staining in the intraluminal surfaces of hepatic vessels. All the positive immunoreactivity in macrophages was in the cytoplasm. The immunoreactivity was even stronger in macrophages than that in tumor cells (Figure 1E). All the tumor cluster infiltrating to the tissue showed moderate to strong positive staining of HIF-2 α /EPAS1 (Figure 1F). Fifty of 97 cases (51.5%) were positive, including 31 strongly positive (31.9%), 19 weakly positive (19.8%). In the 50 HIF-2 α /EPAS1-positive cases, 35 cases (64.8%) had necrosis, and 15 cases

(16.27%) had no necrosis. Positive staining was seen in 33.3% of the small-sized HCC (≤ 2 cm), 62.7% of the medium-sized (2-5 cm), and 57.1% of the HCCs larger than 5 cm. HCC larger than 5 cm in diameter though not significantly different between the two groups, had a relatively lower HIF-2 α /EPAS1 expression compared to medium-sized tumors. HIF-2 α /EPAS1 staining was seen in 81.2% of HCC patients with capsule infiltration, and 45.6% in those without them. Positive staining was also seen in 68.7% in HCC patients with portal vein invasion, and 34.6% in those without them (Table 1). HIF-2 α /EPAS1 positivity was significantly correlated with tumor size, capsule infiltration, portal vein invasion, and existence of necrosis ($P < 0.05$ respectively). To further confirm whether HIF-2 α /EPAS1 expression in HCC tissues also correlated with angiogenesis, a parallel immunohistochemical study of VEGF was performed on these 97 cases, in which VEGF expression was assessed as a major marker for angiogenesis (Table 2). Positive staining was found mostly in the cytoplasm of tumor cells (Figures 2A and 2B), and only weaker staining in stroma areas was detectable. VEGF expression in tumors had strong correlation with capsule infiltration, portal vein invasion, and necrosis ($P < 0.05$ respectively). The overexpression of VEGF in capsule infiltration and portal vein invasion was found to correlate positively with HIF-2 α /EPAS1 expression ($P < 0.05$, Table 3), supporting the correlation of HIF-2 α /EPAS1 up-regulation with tumor metastasis and angiogenesis in HCC.

Table 2 Correlation between VEGF protein and clinicopathological features of HCC patients

Variants	NO of cases 97	VEGF expression			Significance
		-	+	++	
Pathological grade					
Grade I	6	6	0	0	NS
Grade II	76	28	22	26	
Grade III-IV	15	8	3	4	
Tumor size					
≤ 2	13	11	0	2	NS
2-5	49	16	14	19	
> 5	35	15	11	9	
Cirrhosis					
With	53	20	10	23	NS
Without	44	22	15	7	
Capsule formation					
With	18	7	5	6	NS
Without	79	35	20	24	
Capsule infiltration					
With	16	4	2	10	0.011 ^a
Without	81	38	23	20	
Portal vein infiltration					
With	48	14	16	18	0.020 ^a
Without	49	20	9	12	
Necrosis					
With	54	15	17	22	0.011 ^a
Without	43	27	8	8	

^a $P < 0.05$ vs the expression of VEGF was significant in HCC with capsule infiltration, portal vein invasion, and with necrosis. NS, not significant.

Table 3 Correlation between HIF-2 α /EPAS1 and VEGF protein expression in HCC tissues

Variants	NO of cases	Staining score			Significance
		-	+	++	
HIF-2 α /EPAS1	97	47	19	31	0.017
VEGF	97	42	25	30	

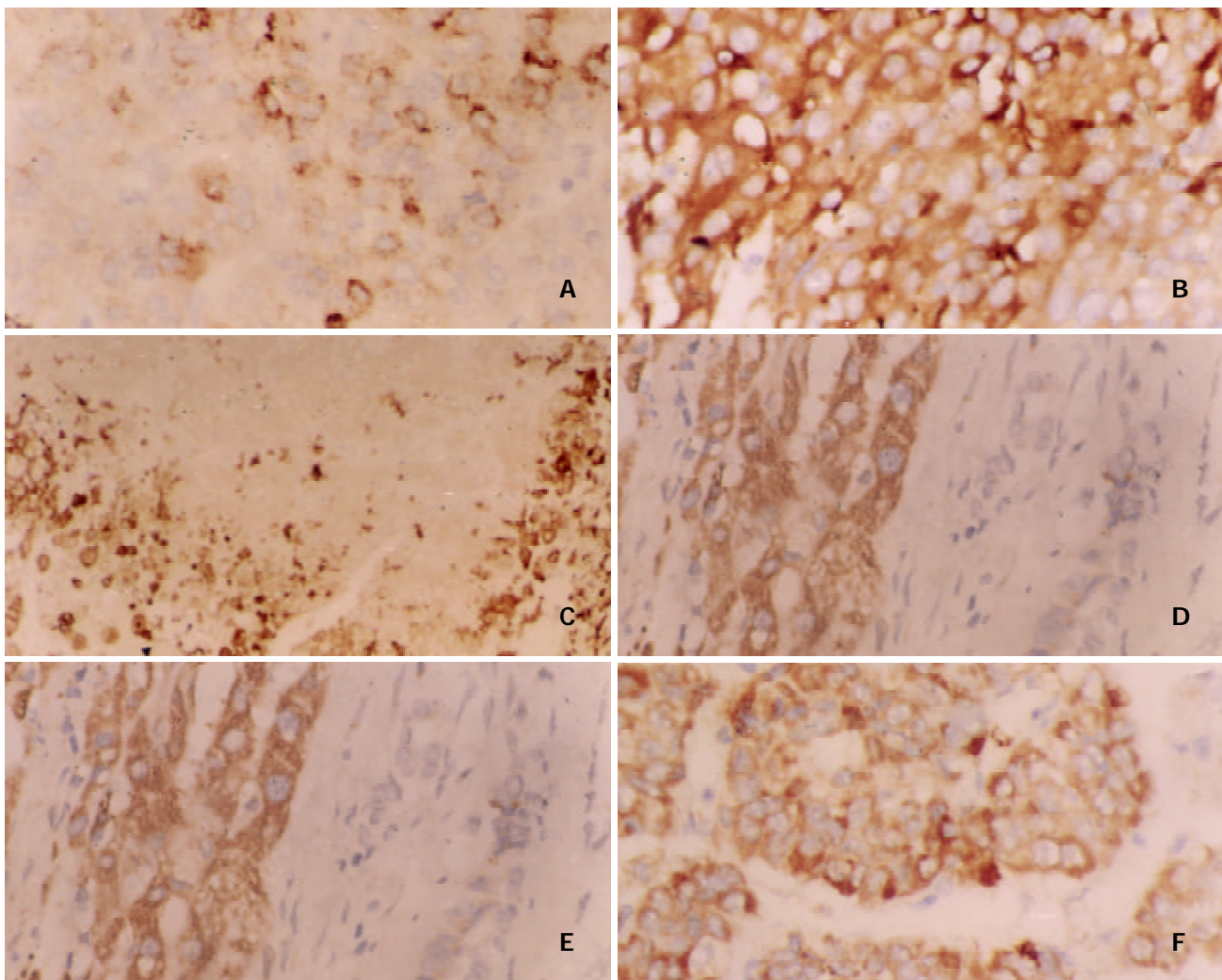


Figure 1 Characterization of HIF-2 α /EPAS1 expression in human hepatocellular carcinoma tissues by IHC technique. A: Weak expression of HIF-2 α /EPAS1 in membranes and cytoplasm of HCC cells ($\times 400$). B: Strong cytoplasmic immunoreactivity of HIF-2 α /EPAS1 in HCC cells ($\times 400$). C: HIF-2 α /EPAS1 positive staining (arrows) in perinecrotic region near tumor in a HCC sample (with capsular infiltration and portal vein invasion) ($\times 400$). D: Strong HIF-2 α /EPAS1 expression in HCC tissues whereas no staining in adjacent stroma cells ($\times 400$). E: Strong staining in the cytoplasm of macrophages compared with cancer cells, showing weak staining for HIF-2 α /EPAS1 ($\times 400$). F: Moderate to strong positive staining of HIF-2 α /EPAS1 in tumor clusters infiltrating to the tissue ($\times 400$).

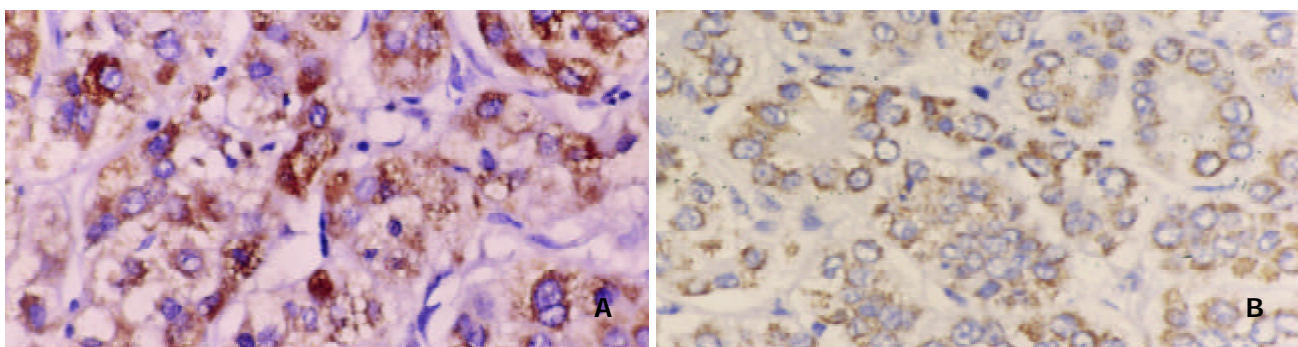


Figure 2 Parallel study of VEGF protein expression in HCC samples. A mAb against VEGF was used for immunostaining of slides from HCC patients. A: HCC with capsular infiltration and portal vein invasion showing strong staining (++) in the cytoplasm of tumor cells. B: HCC without capsular infiltration and portal vein invasion showing weak staining (+) ($\times 200$).

DISCUSSION

Angiogenesis appeared to be one of the crucial steps in tumor's transition from small, harmless cluster of mutated cells to a large, malignant growth, capable of spreading to other organs throughout the body^[12]. HCC is a typical hypervascular tumor of the digestive organs. It seems likely that the formation of

tumor vessels precedes tumor growth and is indispensable in maintaining tumor viability, because hepatic arterial embolization frequently causes necrosis and induces a marked reduction in tumor size. In the present study, we investigated the expression of HIF-2 α /EPAS1 in HCC tissues. To further confirm whether HIF-2 α /EPAS1 in HCC tissues also correlated

with angiogenesis, we performed an immunohistochemistry study of VEGF protein. We also examined the correlation between HIF-2 α /EPAS1, VEGF protein expression and clinicopathological features.

Our data showed that tumor size was correlated with HIF-2 α /EPAS1. Small HCC had significantly lower HIF-2 α /EPAS1 expression compared with medium-sized tumors. What was contrary to previous finding^[13,14] was that tumors with large sizes had higher expression than smaller and moderate sizes, even these tumors were relatively less vascular compared with the large-sized ones. However, it has been reported that the intercapillary distance increased as the tumor size or weight increased, possibly because of different rates of endothelial cells and neoplastic cell turnover^[15,16]. The turnover time of endothelial cells was 50 to 60 hours while that of the neoplastic cells was 22 hours, and significantly shorter^[17]. On the other hand, the characteristics of tumor microcirculation could offer another explanation for the reduction of HIF-2 α /EPAS1 expression as the tumor became smaller or larger. Generally, blood flow, oxygen pressure, and pH values were less in tumors than in the counterpart normal tissues^[18], and because of the absence of lymphatic vessels, the interstitial pressure was often high in tumors, leading further transport problems^[19]. As a result, hypoxia and necrosis were a general phenomenon of tumors, especially large ones^[20]. It was assumed that rapid cell proliferation at the center of tumor could lead to increased interstitial pressure, which may lead to compression closure of capillaries and consecutive tumor necrosis^[21]. The current results showed that HCCs of 2 to 5 cm in diameter had the highest HIF-2 α /EPAS1 expression compared with larger and smaller tumors. This observation could be considered important for regional chemotherapy, because intuitively, tumor, tumor metastasis, and tumor death should be closely correlated with tumor-induced hypoxia and necrosis. Cells in hypoxic regions have been thought to be more resistant to the effects of radiotherapy and many conventional chemotherapeutic agents than their normoxic counterparts^[22,23].

We also found strong immunoreactivity in macrophages. The significance of HIF-2 α /EPAS1 in these cells warrants further study. As they have been shown to be one of the terminally differentiated cells that can produce a number of potent angiogenic cytokines such as VEGF^[24,25], their chemotaxis, infiltration, degranulation may promote tumor angiogenesis and progression. A parallel IHC study of angiogenesis marker demonstrated that in HCC tissues, overexpression of both VEGF and HIF-2 α /EPAS1 was coincidentally found, supporting the notion that HIF-2 α /EPAS1 expression is correlated with angiogenesis in HCC.

In the current work, significantly more HIF-2 α /EPAS1 protein expression was present in perinecrotic regions. This, when taken with the fact that macrophages appeared to be more pro-angiogenic at these sites^[26] may help to explain our observation. As HIF-2 α /EPAS1 has been shown to be accumulated by hypoxic macrophages in human tumor^[11,27], our finding may indicate that HIF-2 α /EPAS1 protein may be released by macrophages and is part of the mechanism by which this protein is most expressed in perinecrotic regions. On the other hand, direct support for microenvironmental mechanisms of HIF- α activation in diverse types of human tumor could offer an alternative explanation.

Results from our analysis of HIF-2 α /EPAS1 expression in perinecrotic areas were consistent with a number of reports from clinical studies on breast^[28-30], ovarian^[31], and lung^[32,33] cancers and in hemangioblastomas^[10]. These reports all demonstrated that macrophage hotspots were remotely located from the vascular hotspots of tumors, suggesting that macrophages may preferentially migrate toward areas of relative hypoxia^[29]. This in turn might attract macrophages into

tumor, which then contribute to angiogenic process, giving rise to association between high levels of angiogenesis and extensive necrosis^[29]. Macrophages might be attracted to necrotic tumors by chemotactic factors, such as VEGF^[26,34,35].

As a potent pro-angiogenic cytokine, VEGF has been reported to be overexpressed in both malignant tumors^[30,36] and stroma cells^[30,34] and macrophages^[26,34,37]. Expression of VEGF was up-regulated in poorly vascularized areas of breast carcinomas^[28,29,38]. VEGF positive macrophages were restricted to areas of VEGF production^[26,28]. Evidence is accumulating that VEGF might be activated in stroma cells, especially in macrophages, with the process mediated by the VEGF receptor ftl-1^[35]. Thus, the subcellular mechanisms mediating hypoxia on VEGF gene by macrophages are not known at present. This most likely involved one or more of the pathways activated by hypoxia in transformed cells^[37,40], including the activation of such transcription factors as hypoxia-inducible factors (HIFs) 1, 2 (otherwise known as EPAS1). In this study, we observed the overexpression of VEGF protein in tumor and VEGF expression positively correlated with HIF-2 α /EPAS1 expression. We found that the highest VEGF expression was detectable mostly in tumor areas and only weaker staining in necrotic and stroma areas was detectable.

It is widely accepted that angiogenesis necessitates the degradation of extracellular matrix, this process requires protease activation and release. Plasmin was thought to be one of the key proteases involved in this process^[39]. Angiogenesis also appear to be involved in the invasion of tumors into surrounding tissues, because this invasion requires concomitant neovascularization through the sprouting of endothelial cells in the tumor stroma. It has been reported that VEGF induced both urokinase-type plasminogen activator (PA) and tissue type PA in endothelial cells^[40], and hypoxia might promote cellular invasion by stimulating the expression of urokinase type plasminogen activator (uPAR)^[41]. Therefore, enhanced expression of these angiogenic factors would likely indicate the ability of tumors to invade the tumor stroma as well as the ability to promote the development of new blood vessels. Based on these considerations, we examined both portal involvement and capsule infiltration. These two clinicopathological features have been thought to be the most important clinical factors in assessing liver tumor, and HCC in particular, as they were strongly correlated with the metastasis of HCC^[42-44]. Our results were in agreement with this concept. We found that the portal vein involvement and capsular infiltration were correlated with the expression of both HIF-2 α /EPAS1 and VEGF proteins. HCC patients with capsular infiltration and portal vein invasion had more HIF-2 α /EPAS1 and VEGF expression than those without them, indicating that HIF-2 α /EPAS1 and VEGF expression may be associated with a poor prognosis of patients with HCCs.

The clinical significance of HIF-2 α /EPAS1 expression in tumors remains largely unexplored as monoclonal antibodies available for immunohistochemistry have been recently developed. Talks *et al* recently reported the expression of HIF- α in a panel of normal human tissues and benign or malignant tumors and first showed the expression of the molecule in a good percentage of human carcinomas^[11]. However, studies on the HIF-2 α /EPAS1 expression with angiogenic factors and receptors, with microvessel density or with other molecular markers or with prognosis of human carcinomas are few. Investigations regarding these angiogenic factors which have been partially done for endothelial carcinoma^[3,33,45], and regarding the status of signal transduction via HIF-2 α /EPAS1 when the receptors do and do not bind to this protein and when dimerization with aryl hydrocarbon receptor nuclear translocator occurs between HIF-2 α /EPAS1 and other HIF- α protein family, should help clarify the significance

of HIF-2 α /EPAS1 in human cancers, including HCC.

In this study, we found cytoplasmic immunoreactivity of HIF-2 α /EPAS1, but equivocal staining was sometimes observed in the nuclear which we did not regard as positive. Although it was assumed that nuclear HIF was the active form, clearly it was synthesized and also degraded in the cytoplasm^[45,46]. These findings, at least in part, could explain the cytoplasmic location of HIF-2 α /EPAS1, which was a tumor specific finding and could better reflect the HIF up-regulation pathways in paraffin embedded material. This suggestion was in accordance with the scoring system proposed by Zhong *et al*^[46].

In conclusion, HIF-2 α /EPAS1 expression in HCC and its clinical association with necrosis seem to be a good predictive tool and possibly a target therapy for metastasis of liver cancer, especially HCC. The finding that medium-sized HCCs had the highest expression of HIF-2 α /EPAS1 compared with smaller and larger HCCs can be used, after further evaluation, as a therapeutic guide during the selection of cases for chemotherapy.

REFERENCES

- Iyer NV, Kotch LE, Agani F, Leung SW, Laughner E, Wenger RH, Gassmann M, Gearhart JD, Lawler AM, Yu AY, Semenza GL. Cellular and developmental control of O₂ homeostasis by hypoxia-inducible factor 1 alpha. *Genes Dev* 1998; **12**: 149-162
- Peng J, Zhang L, Drysdale L, Fong GH. The transcription factor EPAS1/hypoxia-inducible factor 2 alpha plays an important role in vascular remodeling. *Proc Natl Acad Sci U S A* 2000; **97**: 8386-8391
- Tian H, Mcknight SL, Russell DW. Endothelial PAS domain protein 1 (EPAS1), a transcription factor selectively expressed in endothelial cells. *Genes Dev* 1997; **11**: 72-82
- Semenza GL. HIF-1 and human disease: one highly involved factor. *Genes Dev* 2000; **14**: 1983-1991
- Morrow CS, Cowan KH. Antineoplastic drug resistance and breast cancer. *Ann NY Acad Sci* 1993; **698**: 289-312
- Wiesener MS, Turler H, Allen WE, William C, Eckardt KU, Talks KL, Wood SM, Gatter KC, Harris AL, Pugh CW, Ratcliffe PJ, Maxwell PH. Induction of endothelial PAS domain protein-1 by hypoxia: characterization and comparison with hypoxia-inducible factor-1 alpha. *Blood* 1998; **92**: 2260-2268
- Jain S, Maltepe E, Lu MM, Simon C, Bradfield CA. Expression of ARNT, ARNT2, HIF1 α , HIF2 α and Ah receptor mRNAs in the developing mouse. *Mech Dev* 1998; **73**: 117-123
- Ema M, Taya S, Yokotani N, Sogawa K, Matsuda Y, Fujii-Kuriyama Y. A novel bHLH-PAS factor with close sequence similarity to hypoxia-inducible factor 1 α regulates the VEGF expression and is potentially involved in lung and vascular development. *Proc Natl Acad Sci U S A* 1997; **94**: 4273-4278
- Flamme I, Frohlich T, von Reutern M, Kappel A, Damert A, Risau W. HRF, a putative basic helix-loop-helix-PAS-domain transcription factor is closely related to hypoxia-inducible factor-1 alpha and developmentally expressed in blood vessels. *Mech Dev* 1997; **63**: 51-60
- Flamme I, Krieg M, Plate KH. Up-regulation of vascular endothelial growth factor in stromal cells of hemangioblastomas is correlated with up-regulation of the transcription factor HRF/HIF-2 alpha. *Am J Pathol* 1998; **153**: 25-29
- Talks KL, Turley H, Gatter KC, Maxwell PH, Pugh CW, Ratcliffe PJ, Harris AL. The expression and distribution of the hypoxia-inducible factors HIF-1 alpha and HIF-2 alpha in normal human tissues, cancers, and tumor-associated macrophages. *Am J Pathol* 2000; **157**: 411-421
- Folkman J. Fighting cancer by attacking its blood supply. *Sci Am* 1996; **275**: 150-154
- Favier J, Plouin PF, Corvol P, Gasc JM. Angiogenesis and vascular architecture in pheochromocytomas: distinctive traits in malignant tumors. *Am J Pathol* 2002; **161**: 1235-1246
- Cayre A, Rossignal F, Clottes E, Penault LF. aHIF but not HIF-1alpha transcription a poor prognostic marker in human breast cancer. INSERMU484, Clermont-Ferrand, French. *Breast Cancer Res* 2003; **5**: 223-230
- Vaupel P. Hypoxia in neoplastic tissue. *Microvasc Res* 1977; **13**: 399-408
- Tannock IF, Steel GG. Quantitative techniques for study of the anatomy and function of small blood vessels in tumors. *J Natl Cancer Inst* 1969; **42**: 771-782
- Tannock IF, Hayashi S. The proliferation of capillary endothelial cells. *Cancer Res* 1972; **32**: 77-82
- Vaupel P, Kallinowski F, Okunieff P. Blood flow, oxygen and nutrient supply, and metabolic microenvironment of human tumors: a review. *Cancer Res* 1989; **49**: 6449-6465
- Jain RK. Transport of molecules, particles, and cells in solid tumors. *Annu Rev Biomed Eng* 1999; **1**: 241-263
- Lyng H, Skretting A, Rofstad EK. Blood flow in six human melanoma xenograft lines with different growth characteristics. *Cancer Res* 1992; **52**: 584-592
- Jain RK. Determinants of tumor blood flow: a review. *Cancer Res* 1988; **48**: 2641-2658
- Blancher C, Harris AL. The molecular basis of hypoxia response pathways: tumour hypoxia as a therapy target. *Cancer Metastasis Rev* 1998; **17**: 187-194
- Richard DE, Berra E, Pouyssegur J. Angiogenesis: how a tumor adapts to hypoxia. *Biochem Biophys Res Commun* 1999; **266**: 718-722
- Harmey JH, Dimitriadis E, Kay E, Redmond HP, Bouchier-Hayes D. Regulation of macrophage production of vascular endothelial growth factor (VEGF) by hypoxia and transforming growth factor beta-1. *Ann Surg Oncol* 1998; **5**: 271-278
- Gaudry M, Bregerie O, Andrieu V, El Benna J, Pocard MA, Hakim J. Intracellular pool of vascular endothelial growth factor in human neutrophils. *Blood* 1997; **90**: 4153-4161
- Lewis JS, Lee JA, Underwood JC, Harris AL, Lewis CE. Macrophage responses to hypoxia: relevance to disease mechanisms. *J Leukoc Biol* 1999; **66**: 889-900
- Griffiths L, Binley K, Iqbal S, Kan O, Maxwell P, Ratcliffe P, Lewis C, Harris AL, Kingsman S, Naylor S. The macrophage - a novel system to deliver gene therapy to pathological hypoxia. *Gene Ther* 2000; **7**: 255-262
- Leek RD, Hunt NC, Landers RJ, Lewis CE, Royds JA, Harris AL. Macrophage infiltration is associated with VEGF and EGFR expression in breast cancer. *J Pathol* 2000; **190**: 430-436
- Leek RD, Landers RJ, Harris AL, Lewis CE. Necrosis correlates with high vascular density and focal macrophage infiltration in invasive carcinoma of the breast. *Br J Cancer* 1999; **79**: 991-995
- Hlatky L, Tsionou C, Hahnfeldt P, Coleman CN. Mammary fibroblasts may influence breast tumor angiogenesis via hypoxia-induced vascular endothelial growth factor up-regulation and protein expression. *Cancer Res* 1994; **54**: 6083-6086
- Negus RP, Stamp GW, Hadley J, Balkwill FR. Quantitative assessment of the leukocyte infiltrate in ovarian cancer and its relationship to the expression of C-C chemokines. *Am J Pathol* 1997; **150**: 1723-1734
- Shoji M, Hancock WW, Abe K, Micko C, Casper KA, Baine RM, Wilcox JN, Danave I, Dillechay DL, Matthews E, Contrino J, Morrissey JH, Gordon S, Edgington TS, Kudryk B, Kreutzer DL, Rickles FR. Activation of coagulation and angiogenesis in cancer: immunohistochemical localization *in situ* of clotting proteins and vascular endothelial growth factor in human cancer. *Am J Pathol* 1998; **152**: 399-411
- Giatromanolaki A, Koukourakis MI, Siviridis E, Turley H, Talks K, Pezzella F, Gatter KC, Harris AL. Relation of hypoxia inducible factor 1 alpha and 2 alpha in operable non-small cell lung cancer to angiogenic/molecular profile of tumors and survival. *Br J Cancer* 2001; **85**: 881-890
- Polverini PJ, Leibovich SJ. Induction of neovascularization *in vivo* and endothelial proliferation *in vitro* by tumor-associated macrophages. *Lab Invest* 1984; **51**: 635-642
- Barleon B, Sozzani S, Zhou D, Weich HA, Mantovani A, Marme D. Migration of human monocytes in response to vascular endothelial growth factor (VEGF) is mediated via the VEGF receptor flt-1. *Blood* 1996; **87**: 3336-3343
- Huang GW, Yang LY, Sheng LX, Li HL, Qing JQ, Yang ZL. The relationship between VEGF and HIF-1 α protein in hepatocellular carcinoma. *Zhonghua Xiaohua Zazhi* 2000; **10**: 627-628

- 37 **Xiong M**, Elson G, Legarda D, Leibovich SJ. Production of vascular endothelial growth factor by murine macrophages: regulation by hypoxia, lactate, and the inducible nitric oxide synthase pathway. *Am J Pathol* 1998; **153**: 587-598
- 38 **Lewis JS**, Landers RJ, Underwood JC, Harris AL, Lewis CE. Expression of vascular endothelial growth factor by macrophages is up-regulated in poorly vascularized areas of breast carcinomas. *Pathol* 2000; **192**: 150-158
- 39 **Pepper MS**, Montesano R. Proteolytic balance and capillary morphogenesis. *Cell Differ Dev* 1990; **32**: 319-327
- 40 **Pepper MS**, Vassalli JD, Orci L, Montesano R. Proteolytic balance and capillary morphogenesis *in vitro*. *EXS* 1992; **61**: 137-145
- 41 **Graham CH**, Fitzpatrick TE, McCrae KR. Hypoxia stimulates urokinase receptor expression through a heme protein-dependent pathway. *Blood* 1998; **91**: 3300-3307
- 42 **Los M**, Zaemari S, Foekens JA, Gebbink MF, Voest EE. Regulation of the urokinase-type plasminogen activator system by the von Hippel-Lindau tumor suppressor gene. *Cancer Res* 1999; **59**: 4440-4445
- 43 **Arii S**, Tanaka J, Yamazoe Y, Minematsu S, Morino T, Fujita K, Maetani S, Tobe T. Predictive factors for intrahepatic recurrence of hepatocellular carcinoma after partial hepatectomy. *Cancer* 1992; **69**: 913-919
- 44 **Primary liver cancer in Japan**. Clinicopathologic features and results of surgical treatment. Liver Cancer Study Group of Japan. *Ann Surg* 1990; **211**: 277-287
- 45 **Hui EP**, Chan AT, Pezzella F, Turler H, To KF, Poon TC, Zee B, Mo F, Teo PM, Huang DP, Gatter KC, Johnson PJ, Harris AL. Coexpression of hypoxia-inducible factor 1 alpha and 2 alpha, carbonic anhydrase IX, and vascular endothelial growth factor in nasopharyngeal carcinoma and relationship to survival. *Clin Cancer Res* 2002; **8**: 2595-2604
- 46 **Zhong H**, De Marzo AM, Laughner E, Lim M, Hilton DA, Zagzag D, Buechler P, Issacs WB, Semenza GL, Simons JW. Overexpression of hypoxia-inducible factor 1 alpha in common human cancers and their metastases. *Cancer Res* 1999; **59**: 5830-5835

Edited by Gupta MK and Wang XL

Transfection efficiency of pORF lacZ plasmid lipopolyplex to hepatocytes and hepatoma cells

Xun Sun, Hong-Wei Zhang, Zhi-Rong Zhang

Xun Sun, Hong-Wei Zhang, Zhi-Rong Zhang, West China School of Pharmacy, Sichuan University, Chengdu 610041, Sichuan Province, China

Supported by the National High Technology Research and Development Program of China (863 program), No. 2001AA218021

Correspondence to: Zhi-Rong Zhang, West China School of Pharmacy, Sichuan University, Chengdu 610041, Sichuan Province, China. zrzrl@vip.sina.com

Telephone: +86-28-85501566 **Fax:** +86-28-85456898

Received: 2003-06-26 **Accepted:** 2003-07-24

Abstract

AIM: To develop a novel non-viral gene delivery system, which has a small particle size and a high transfection efficiency to hepatocyte and hepatoma cells.

METHODS: Lipid-polycation-DNA lipopolyplex (LPD) was prepared by mixing plasmid DNA and polylysine. The resulted polyplex was incubated for 10 min at room temperature, following the addition of preformed cationic liposomes. The morphology of LPD was observed by transmission electron microscopy. The diameter and surface charge of LPD were measured by photon correlation spectroscopy (PCS). The nuclease protection ability of LPD was evaluated by agarose gel electrophoresis. Estimation of the transfection efficiency was performed by galactosidase assay in Chang cells and SMMC-7721 cells.

RESULTS: LPD had a regular spherical surface. The average diameter and the zeta potential of LPD were 132.1 nm and 26.8 mV respectively. LPD could protect plasmid DNA from nuclease degradation after 2 hours incubation at 37°C while the naked DNA degraded rapidly. The average transfection efficiencies were 86.2±8.9% and 72.4±6.5% in Chang cells and SMMC-7721 cells respectively.

CONCLUSION: LPD has a rather small particle size and a high transfection activity. LPD may be a good non-viral vector for application in some gene delivery.

Sun X, Zhang HW, Zhang ZR. Transfection efficiency of pORF lacZ plasmid lipopolyplex to hepatocytes and hepatoma cells. *World J Gastroenterol* 2004; 10(4): 531-534
<http://www.wjgnet.com/1007-9327/10/531.asp>

INTRODUCTION

Gene therapy focuses on the therapeutic use of genes, and has achieved considerable advances in the treatment of both acquired and inherited diseases^[1,2]. The success of gene therapy rests on the development of a vector that can selectively and efficiently deliver a gene to the target cells with minimal toxicity^[3,4]. The vectors used to date can be classified into viral and non-viral groups.

Non-viral delivery systems for gene therapy have been increasingly proposed as safer alternatives to viral vectors.

They have the potential to be repeatedly used with minimal host immune response and are targetable, stable in storage, and easy to produce in large quantities. These advantages have provided the impetus to continue their development. So far, several non-viral delivery systems have been developed, such as liposomes^[5-7], nanoparticles^[8-10] hydrogel^[11] emulsion^[12] and peptide nucleic acid^[13]. Complexes formed between cationic liposomes and plasmid DNA are the predominant non-viral vectors employed for the transfection of eukaryotic cells in research laboratories^[14-16]. Currently, several cationic liposomal formulations have also undergone clinical evaluation as vectors for gene therapy in cancer and cystic fibrosis. However, the efficiency and specificity of non-viral delivery systems are not so high. To improve the transfection efficiency, some cationic lipids^[17] and polymers^[18-20] have been synthesized. Ligand or antibody mediated targeting of gene transfer has also been widely explored^[21-24]. Furthermore, nuclear localization sequences (NLS) are studied to help the entry of plasmid DNA from cytoplasm into nucleus^[25].

The liver possesses a variety of characteristics that make this organ very attractive for gene therapy^[26,27]. The proportion of administered macromolecules internalized by hepatocytes depends on their particle size and biochemical characteristics. Only relatively small molecules can pass the fenestrate of sinusoidal endothelial cells of the liver, since their diameter is about 100 nm^[28,29]. Polycations as a formulation component have been shown to enhance the efficiency of liposomes-mediated gene transfer both *in vitro* and *in vivo*. Specifically, lipid-polycation-DNA lipopolyplexes (LPD) have appeared promising as efficient gene-delivery vehicles for systemic administration^[30-33]. In this study, we developed a novel lipopolyplex formulation, which is small in particle size and high in transfection efficiency to hepatocytes and hepatoma cells.

MATERIALS AND METHODS

Materials

Plasmid pORF lacZ (3.54 kb) was purchased from Invivogen (USA). Poly-L-lysine (PLL, M_r 29 000), dimethyldioctadecyl ammonium bromide (DDAB) and β -galactosidase reporter gene staining kit were purchased from Sigma. Hepatoma cell line SMMC-7721 and hepatocyte cell line Chang were obtained from Shanghai Cell Institute, China Academy of Sciences. Cell culture media DMEM and RPMI 1640 were obtained from Gibco Co. (USA). Qiagen Giga Endo-free plasmid purification kit was purchased from Qiagen (CA, USA). All the other chemicals and reagents used were of the analytical grade obtained commercially.

Plasmid DNA preparation

Plasmid pORF lacZ (3.54 kb), is a eukaryotic expression vector containing the EF-1 α /HTLV hybrid promoter within an intron. The lacZ gene codes for the enzyme β -galactosidase, whose activity allows for quick determination of cells expressing the lacZ gene. pORF-lacZ plasmid DNA was isolated and purified from DH5- α E coli using the Qiagen Giga Endo-free plasmid purification kit. DNA concentration and purity were quantified

by UV absorbance at 260 nm and 280 nm on a GBC UV cintra 10e spectrophotometer. The structural integrity and topology of purified DNA were analyzed by agarose gel electrophoresis.

LPD preparation

Cationic liposomes composed of DDAB/cholesterol were prepared with the molar ratio of 1:1. The lipid mixture was dissolved in appropriate chloroform and a thin lipid film was formed in a round-bottomed flask by drying the solvent using a rotary evaporator. The film was hydrated at 60°C with the addition of 10 mM herpes buffer (pH7.4). The lipids were resuspended and then undergone ten passes through an extruder with 200, 100 nm polycarbonate membranes respectively. LPDs were formed by mixing equal volumes of DNA and PLL. DNA and PLL were both diluted from the stock with 10 mM herpes buffer. After mixed, the solution was briefly vortexed, and the resulting polyplexes were incubated for 10 min at room temperature. Concentrated cationic liposomes were subsequently added to the DNA/PLL mixture to achieve the desired final component concentrations and ratios.

Size and zeta potential

Diameter and surface charge of lipopolyplexes were measured by photon correlation spectroscopy (PCS) (Malvern zetasizer 3000 HS, Malvern Instruments Ltd., UK) with a 50 mV laser. Twenty μ l of LPD was diluted by 3 ml of 10 mM herpes buffer and added into the sample cell. The measurement time was set at 2 min (rapid measurement) and each run consisted of 10 subruns^[34]. The measurements were done at 25°C at an angle of 90°. The size distribution followed a lognormal distribution. The potential of the lipid carriers at the surface of spheres, called the zeta potential(ζ), was derived from the mobile particles in electric field by applying the smoluchowsky relationship, which was measured at least three times and at an average of appropriate concentrations of samples.

Negative stain electron microscopy

Just prior to use, the former-coated 100-mesh copper grids were prepared by glow discharging. The grids were then floated on 25 μ l of samples for 90 s, wicked off, and floated on drops of 1% aqueous uranyl acetate for 90 s. Finally, the samples were wicked off, dried in air and stored at room temperature. Negative stain electron micrographs of LPD were taken using a JEM-100SX electron microscope.

Stability in DNase I

Naked DNA or LPDs were incubated with DNase I solution (0.32 U/ μ g DNA) at 37°C for 5 min, 1 h and 2 h respectively. The enzyme reaction was stopped by addition of 0.5M EDTA^[35]. Triton X-100 (final concentration 1% v/v) was added to destroy the bilayer structure of liposomes and 0.9% w/v heparin was added to release DNA from PLL/DNA complexes^[36]. The samples were carefully added to the wells of a 0.8% agarose gel at a volume (representing 1 μ g of DNA per well). The gel was run in TBE buffer containing 0.5 μ g/ml EtBr at 100V for 1 h. Subsequently, the gel was removed from the tank and visualized under UV light by molecular analyst software.

Cell transfection

Chang cells and SMMC-7721 cells were cultured in DMEM and RPMI-1640 respectively with 10% fetal bovine serum and streptomycin (100 μ g/ml). The cells were seeded at 2×10^5 cells per well onto 6-well plates 24 h before transfection. The cells were about 70% confluence at the time of transfection. Then the cells were washed twice by PBS, and 1 ml of serum-free and antibiotics-free medium was added into each well^[37]. For

each well in a transfection, LPDs containing 5 μ g pORF-1acZ were overlaid and mixed gently. The cells were incubated with LPD for 5 hours at 37°C in a CO₂ incubator. Following incubation, LPD was removed and the cell surfaces were rinsed thoroughly and treated with 2 ml fresh complete medium. Then the cells were returned to the incubator for a further 45 h to allow intracellular gene expression to proceed.

X-gal staining

Estimation of the transfection efficiency was performed using galactosidase assay^[38,39]. After the desired time of incubation, the cells were washed with PBS twice and fixed with 2% formaldehyde and 0.2% glutaraldehyde for 10 minutes at room temperature. Then the cells were rinsed twice and stained by X-gal (20 mg/ml) according to the manufacture's instructions. The cells were incubated at 37°C overnight and observed under a microscope. The transfected cells were blue after X-gal staining. For each well, five visual fields were chosen randomly. Cells stained blue were counted and the transfection efficiency was calculated as the percentage of the blue cells in each field.

RESULTS

Morphology, particle size and zeta potential

Transmission electron microscopy (Figure 1) demonstrated the regular spherical surface of LPD. Figure 2 shows the average diameter of LPD being 132.1 nm with a very narrow distribution (polyindex 0.148). Figure 3 illustrates the zeta potential of LPD being 26.8 mV in 10 mM herpes buffer (pH 7.4).

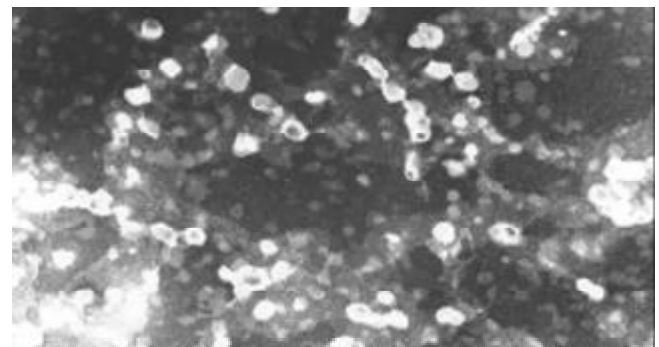


Figure 1 Electronic transmission microscopy of LPD ($\times 35\,000$).

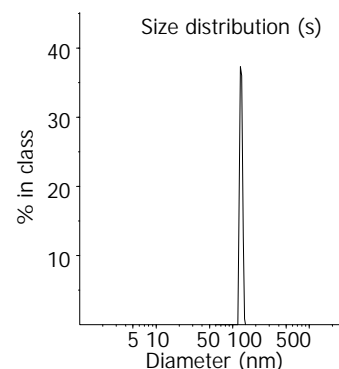


Figure 2 Size distribution of LPD. The particle size was measured by photon correlation spectroscopy (Malvern zetasizer 3000 HS). The average diameter of LPD is 132.1 nm.

Stability in DNase I

Figure 4 shows that LPD could protect plasmid DNA from nuclease degradation after 5 minutes, 1 hour and 2 hours of incubation at 37°C while the naked DNA degraded rapidly.

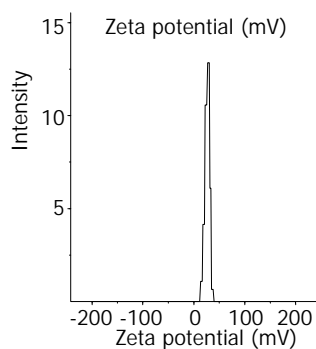


Figure 3 Zeta potential of LPD. The zeta potential of LPD was 26.8 mV in 10 mM herps buffer (pH 7.4).

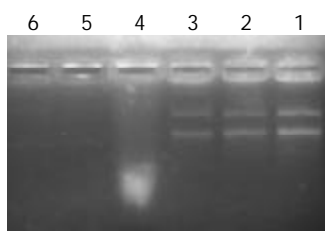


Figure 4 Agarose gel electrophoresis of naked DNA and LPD subjected to DNase degradation. Lane 1: LPD incubated with DNase for 5 minutes. Lane 2: LPD incubated with DNase for 1 hour. Lane 3: LPD incubated with DNase for 2 hours. Lane 4: Naked DNA incubated with DNase for 5 minutes. Lane 5: Naked DNA incubated with DNase for 1 hour. Lane 6: Naked DNA incubated with DNase for 2 hours.

Transfection efficiency

Figure 5 and 6 demonstrate that LPD had a rather high transfection efficiency both in Chang cells and in SMMC-7721 cells. The average transfection efficiencies were $86.2 \pm 8.9\%$ and $72.4 \pm 6.5\%$ in Chang cells and SMMC-7721 cells, respectively.



Figure 5 pORF LacZ lipopolyplex transfected Chang hepatocytes.

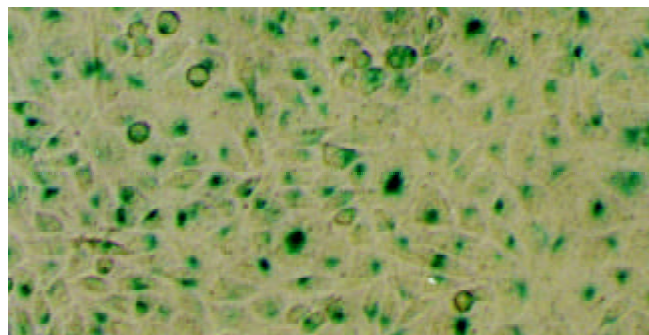


Figure 6 pORF LacZ lipopolyplex transfected SMMC-7721 hepatoma cells.

DISCUSSION

The amount of intact DNA present in LPD cannot be directly assayed by gel electrophoresis as the complexation hinders the binding between DNA and ethidium bromide. Therefore Triton X-100, a widely used detergent is employed to destroy the liposomal bilayer. Furthermore, dissociation of cationic polymer and DNA is also required. Traditionally, DNA is dissociated from PLL by digestion with trypsin and phenol extraction. This procedure is time-consuming and the lost DNA during extraction is immeasurable. Some new dissociation methods have been established based on the fact that the interaction between DNA and PLL was mainly due to electrostatic bonds^[40-43]. By raising the pH of electrophoretic buffer above the pKa of PLL, PLL could become less protonated, thus reducing the charge and thereby allowing the complexes to disassociation under electrophoretic conditions. However, when pH was higher than 11.6, ethidium bromide would lose its affinity for DNA and fluorescence was lost. In this study, heparin at final concentration of 0.9% (w/v) was added to release DNA from the complexes^[36]. Heparin, as an anionic polysaccharide can bind to PLL by electrostatic interaction. When enough amount of heparin was added, DNA could be completely released from PLL-DNA complexes. The presence of heparin did not interfere with the gel electrophoresis, so the sample could be loaded directly.

The size and surface charge of lipopolyplex could influence their physical stability, *in vivo* distribution, cellular interaction and extent of cell uptake. After intravenous administration, particles larger than 7 μm are normally filtered by the smallest capillaries of the lungs, and particles smaller than 7 μm in diameter may pass the smallest lung capillary beds and be entrapped in the capillary network of the liver and spleen. Particles between 100 nm and 2 μm in size are rapidly cleared from the bloodstream by the mononuclear phagocytic system (MPS). Typically in practice, 80-90% of hydrophobic particles were opsonized and taken up by fixed macrophages of the liver and spleen, often within a few minutes of intravenous administration^[1]. Zeta potential measurements can be a useful tool for characterizing colloidal drug delivery systems. They can give information about the surface properties of the carrier and therefore helping determine how the constituent molecules are organized. In this study, the LPDs had a positive zeta potential of 26.8mV. Therefore, they could interact with negatively charged cell surface, which resulted in cellular internalization. Furthermore, plasmid DNA in LPDs was shielded from nuclease digestion due to the formation of charge complexes.

It has become clear that cationic liposome plays several roles in the process of transfection, such as condensing and protecting DNA, binding to cell surface, triggering endocytosis and releasing DNA/lipid complexes from endosome. The size of condensed DNA is thought to be critical for *in vivo* delivery because the particle size influences not only the biodistribution but also the efficiency of cellular uptake through endocytosis. At an appropriate condition, cationic polymer PLL can precondense plasmid DNA more effectively than cationic liposomes. Therefore, LPD has a rather small particle size and a high transfection activity in hepatocytes and hepatoma cells. LPD may be a superior vector for some applications in gene delivery compared to regular DNA/liposome complexes. Structurally, this formulation has been found to be a virus-like particle, each containing a condensed genome as the core and a lipidic shell as the envelope. The liver possesses a variety of characteristics which make this organ very attractive for gene therapy. Although some of the virus-mediated gene transfer systems have been found to be quite effective, their usefulness is limited, given that they induce an immune response, leading to the rapid rejection of transduced cells. To overcome this

problem, our further work will focus on the use of LPD in the treatment of liver cancer.

REFERENCES

- Pouton CW**, Seymour LW. Key issues in non-viral gene delivery. *Adv Drug Deliv Rev* 2001; **46**: 187-203
- Liu F**, Huang L. Development of non-viral vectors for systemic gene delivery. *J Control Release* 2002; **78**: 259-266
- Nishikana M**, Huang L. Nonviral vectors in new millennium: delivery barriers in gene transfer. *Hum Gene Ther* 2001; **12**: 861-870
- Davis ME**. Non-viral gene delivery systems. *Curr Opin Biotechnol* 2002; **13**: 128-131
- Stuart DD**, Allen TM. A new liposomal formulation for antisense oligodeoxynucleotides with small size, high incorporation efficiency and good stability. *Biochim Biophys Acta* 2000; **1463**: 219-229
- Bailey AL**, Sullivan SM. Efficient encapsulation of DNA plasmids in small neutral liposomes induced by ethanol and calcium. *Biochim Biophys Acta* 2000; **1468**: 239-252
- Sudimack JJ**, Guo W, Tjarks W, Lee RJ. A novel pH-sensitive liposome formulation containing oleyl alcohol. *Biochim Biophys Acta* 2002; **1564**: 31-37
- Panyam J**, Labhassetwar V. Biodegradable nanoparticles for drug and gene delivery to cells and tissue. *Adv Drug Deliv Rev* 2003; **55**: 329-347
- Mao HQ**, Roy K, Troung-Le VL, Janes KA, Lin KY, Wang Y, August JT, Leong KW. Chitosan-DNA nanoparticles as gene carriers: synthesis, characterization and transfection efficiency. *J Control Release* 2001; **70**: 399-421
- Corsi K**, Chellat F, Yahia L, Fernandes JC. Mesenchymal stem cells, MG63 and HEK293 transfection using chitosan-DNA nanoparticles. *Biomaterials* 2003; **24**: 1255-1264
- Vinogradov SV**, Bronich TK, Kabanov AV. Nanosized cationic hydrogels for drug delivery: preparation, properties and interaction with cells. *Adv Drug Deliv Rev* 2002; **54**: 135-147
- Kim YJ**, Kim TW, Chung H, Kwon IC, Sung HC, Jeong SY. The effects of serum on the stability and the transfection activity of the cationic lipid emulsion with various oils. *Int J Pharm* 2003; **252**: 241-252
- Koppelhus U**, Nielsen PE. Cellular delivery of peptide nucleic acid (PNA). *Adv Drug Deliv Rev* 2003; **55**: 267-280
- Audouy SA**, de Leij LF, Hoekstra D, Molema G. *In vivo* characteristics of cationic liposomes as delivery vectors for gene therapy. *Pharm Res* 2002; **19**: 1599-1605
- Lesage D**, Cao A, Briane D, Lievre N, Coudert R, Raphael M, Salzman J, Taillandier E. Evaluation and optimization of DNA delivery into gliosarcoma 9L cells by a cholesterol-based cationic liposome. *Biochim Biophys Acta* 2002; **1564**: 393-402
- Templeton NS**. Cationic liposome-mediated gene delivery *in vivo*. *Biosci Rep* 2002; **22**: 283-295
- Ewert K**, Ahmad A, Evans HM, Schmidt HW, Safinya CR. Efficient synthesis and cell-transfection properties of a new multi-valent cationic lipid for nonviral gene delivery. *J Med Chem* 2002; **45**: 5023-5029
- Kabanov AV**, Lemieux P, Vinogradov S, Alakhov V. Pluronic block copolymers: novel functional molecules for gene therapy. *Adv Drug Deliv Rev* 2002; **54**: 223-233
- Maheshwari A**, Mahato RI, McGregor J, Han S, Samlowski WE, Park JS, Kim SW. Soluble biodegradable polymer-based cytokine gene delivery for cancer treatment. *Mol Ther* 2000; **2**: 121-130
- Lim YB**, Han SO, Kong HU, Lee Y, Park JS, Jeong B, Kim SW. Biodegradable polyester, poly [α -(4-aminobutyl)-l-glycolic acid], as a non-toxic gene carrier. *Pharm Res* 2000; **17**: 811-816
- Li WM**, Mayer LD, Bally MB. Prevention of antibody-mediated elimination of ligand-targeted liposomes by using poly(ethylene glycol)-modified lipids. *J Pharmacol Exp Ther* 2002; **300**: 976-983
- Mastrobattista E**, Kapel RH, Eggenhuisen MH, Roholl PJ, Crommelin DJ, Hennink WE, Storm G. Lipid-coated polyplexes for targeted gene delivery to ovarian carcinoma cells. *Cancer Gene Ther* 2001; **8**: 405-413
- Arango M**, Düzgünes N, Tros de Ilarduya C. Increased receptor-mediated gene delivery to the liver by protamine-enhanced-asialofetuin-lipoplexes. *Gene Ther* 2003; **10**: 5-14
- Fisher KD**, Ulbrich K, Subr V, Ward CM, Mautner V, Blakey D, Seymour LW. A versatile system for receptor-mediated gene delivery permits increased entry of DNA into target cells, enhanced delivery to the nucleus and elevated rates of transgene expression. *Gene Ther* 2000; **7**: 1337-1343
- Escriou V**, Carrière M, Scherman D, Wils P. NLS bioconjugates for targeting therapeutic genes to the nucleus. *Adv Drug Deliv Rev* 2003; **55**: 295-306
- Ghosh SS**, Takahashi M, Thummala NR, Parashar B, Chowdhury NR, Chowdhury JR. Liver-directed gene therapy: promises, problems and prospects at the turn of the century. *J Hepatol* 2000; **32**(1 Suppl): 238-252
- Hwang SH**, Hayashi K, Takayama K, Maitani Y. Liver-targeted gene transfer into a human hepatoblastoma cell line and *in vivo* by sterylucoside-containing cationic liposomes. *Gene Ther* 2001; **8**: 1276-1280
- Jain RK**. Delivery of molecular and cellular medicine to solid tumors. *Adv Drug Deliv Rev* 2001; **46**: 149-168
- Christie RJ**, Grainger DW. Design strategies to improve soluble macromolecular delivery constructs. *Adv Drug Deliv Rev* 2003; **55**: 421-437
- Guo W**, Gosselin MA, Lee RJ. Characterization of novel diolein-based LPDII vector for gene delivery. *J Control Release* 2002; **83**: 121-132
- Birchall JC**, Kellaway IW, Gumbleton M. Physical stability and *in vitro* gene expression efficiency of nebulised lipid-peptide-DNA complexes. *Int J Pharm* 2000; **197**: 221-231
- Li B**, Li S, Tan Y, Stolz DB, Watkins SC, Block LH, Huang L. Lyophilization of cationic lipid-protamine-DNA (LPD) Complexes. *J Pharm Sci* 2000; **89**: 355-364
- Tsai JT**, Furstoss KJ, Michnick T, Sloane DL, Paul RW. Quantitative physical characterization of lipid-polycation-DNA lipopolyplexes. *Biotechnol Appl Biochem* 2002; **36**(Pt 1): 13-20
- Dekie L**, Toncheva V, Dubrue P, Schacht EH, Barrett L, Seymour LW. Poly-L-glutamic acid derivatives as vectors for gene therapy. *J Control Release* 2000; **65**: 187-202
- Cui Z**, Mumper RJ. Plasmid DNA-entrapped nanoparticles engineered from microemulsion precursors: *in vitro* and *in vivo* evaluation. *Bioconjug Chem* 2002; **13**: 1319-1327
- Moret I**, Esteban Peris J, Guillem VM, Benet M, Revert F, Dasi F, Crespo A, Alino SF. Stability of PEI-DNA and DOTAP-DNA complexes: effect of alkaline PH, heparin and serum. *J Control Release* 2001; **76**: 169-181
- Dokka S**, Toledo D, Shi X, Ye J, Rojanasakul Y. High-efficiency gene transfection of macrophages by lipoplexes. *Int J Pharm* 2000; **206**: 97-104
- Sakurai F**, Nishioka T, Saito H, Baba T, Okuda A, Matsumoto O, Taga T, Yamashita F, Takakura Y, Hashida M. Interaction between DNA-cationic liposome complexes and erythrocytes is an important factor in systemic gene transfer via the intravenous route in mice: the role of the neutral helper lipid. *Gene Ther* 2001; **8**: 677-686
- Armeanu S**, Pelisek J, Krausz E, Fuchs A, Groth D, Curth R, Keil O, Quilici J, Rolland PH, Reszka R, Nikol S. Optimization of nonviral gene transfer of vascular smooth muscle cells *in vitro* and *in vivo*. *Mol Ther* 2000; **1**: 366-375
- Männistö M**, Vanderkerken S, Toncheva V, Elomaa M, Ruponen M, Schacht E, Urtti A. Structure-activity relationships of poly(L-lysines): effects of pegylation and molecular shape on physico-chemical and biological properties in gene delivery. *J Control Release* 2002; **83**: 169-182
- Parker AL**, Oupicky D, Dash PR, Seymour LW. Methodologies for monitoring nanoparticle formation by self-assembly of DNA with poly(L-lysine). *Anal Biochem* 2002; **302**: 75-80
- Hill IR**, Garnett MC, Bignotti F, Davis SS. Determination of protection from serum nuclease activity by DNA-polyelectrolyte complexes using an electrophoretic method. *Anal Biochem* 2001; **291**: 62-68
- Safinya CR**. Structures of lipid-DNA complexes: supramolecular assembly and gene delivery. *Curr Opin Struct Biol* 2001; **11**: 440-448

Inhibitory effect of antisense vascular endothelial growth factor 165 eukaryotic expression vector on proliferation of hepatocellular carcinoma cells

Song Gu, Chang-Jian Liu, Tong Qiao, Xue-Mei Sun, Lei-Lei Chen, Le Zhang

Song Gu, Chang-Jian Liu, Tong Qiao, Department of Vascular Surgery, Gulou Hospital, Affiliated Hospital of Medical College, Nanjing University, Nanjing 210008, Jiangsu Province, China
Xue-Mei Sun, Lei-Lei Chen, Le Zhang, Translational Science Laboratory, Gulou Hospital, Affiliated Hospital of Medical College, Nanjing University, Nanjing 210008, Jiangsu Province, China
Supported by the natural science foundation of Jiangsu Province, No. BK2003010, the special scientific research fund of Nanjing, Jiangsu Province, China, No. ZKS0012

Correspondence to: Dr. Song Gu, Department of Vascular Surgery, Gulou Hospital, Affiliated Hospital of Medical College, Nanjing University, Nanjing 210008, Jiangsu Province, China. gusong@263.net
Telephone: +86-25-3685061 **Fax:** +86-25-3317016
Received: 2003-09-06 **Accepted:** 2003-10-07

Abstract

AIM: To construct antisense VEGF₁₆₅ eukaryotic expression vector PCDNA₃-as-VEGF₁₆₅ and to study its expression and effect on the proliferation of hepatocarcinoma SMMC-7721 cells.

METHODS: VEGF₁₆₅ cDNA was inserted into polylinker sites of eukaryotic expression vector PCDNA₃ to construct PCDNA₃-as-VEGF₁₆₅. Then the vector was transferred into human hepatocarcinoma cell strain SMMC-7721 with cation lipofectamine 2000 mediated methods to evaluate the expression of VEGF protein and the inhibitory effect on the proliferation of hepatocarcinoma SMMC-7721 cells.

RESULTS: The detection indicated the presence of VEGF cDNA in normally cultured SMMC-7721 cells by PCR. VEGF mRNA expression was notably decreased in SMMC-7721 cells by RT-PCR after PCDNA₃-as-VEGF₁₆₅ transfection. The expression of VEGF protein was dramatically inhibited (142.01 ± 7.95 vs $1\ 625.52 \pm 64.46$ pg·ml⁻¹, $P < 0.01$) 2 days after transfection, which correlated with the dose of PCDNA₃-as-VEGF₁₆₅ gene. VEGF protein was most expressed in PCDNA₃ transferred SMMC-7721 cells but few in PCDNA₃-as-VEGF₁₆₅ transferred cells by immunohistochemical staining. The apoptotic rate of hepatocarcinoma SMMC-7721 cells was significantly promoted ($17.98 \pm 0.86\%$ vs $4.86 \pm 0.27\%$, $P < 0.01$) and the survival rate was notably decreased ($80.99 \pm 3.20\%$ vs $93.52 \pm 3.93\%$, $P < 0.05$) due to antisense VEGF₁₆₅ by flow cytometry (FCM). The transfection of antisense VEGF₁₆₅ gene resulted in the inhibitory effect on the proliferation of hepatocarcinoma cells by 3-(4, 5-dimethylthiazol-2-yl)-2, 5-diphenyltetrazolium bromide (MTT) and the death of all hepatocarcinoma cells on day 6 after transfection.

CONCLUSION: It is confirmed that antisense VEGF₁₆₅ can inhibit the expression of VEGF protein, interfere with the proliferation and induce the apoptosis of hepatocarcinoma cells in our study. Antisense VEGF₁₆₅ gene therapy may play an important role in the treatment of human hepatocarcinoma.

Gu S, Liu CJ, Qiao T, Sun XM, Chen LL, Zhang L. Inhibitory

effect of antisense vascular endothelial growth factor 165 eukaryotic expression vector on proliferation of hepatocellular carcinoma cells. *World J Gastroenterol* 2004; 10(4): 535-539
<http://www.wjgnet.com/1007-9327/10/535.asp>

INTRODUCTION

In recent years it has become clear that angiogenesis is not only important in physiological processes such as embryonic development, wound healing, and organ and tissue regeneration, but also plays a pivotal role in tumor progression and metastasis^[1]. Neovascularization is critical for the rapid growth of solid tumors^[2]. However, most if not all solid tumors appear to be dependent on angiogenesis for their further expansion and preventing tumor cell apoptosis when their size exceeds beyond 1-2 cubic millimeters^[3]. Tumor cells promote angiogenesis by secreting angiogenic factors, especially vascular endothelial growth factor (VEGF) or vascular permeability factor (VPF)^[4].

VEGF is a specific mitogen for endothelial cells that has been shown to be expressed in many tumor cell lines and vascular smooth muscle cells^[5,6] and is important not only for angiogenesis, but also for maintenance of existing blood vessels^[7]. VEGF characterized by rapidly growing solid tumors can also derive from immune cells that infiltrate tumors^[8]. Increased serum VEGF is found in cancer patients^[9] and elevated VEGF levels are reported to be a prognostic clinical factor correlated with decreased survival in patients with breast, ovarian, lung, gastric, liver and colon^[10,11] cancers.

Inhibition of VEGF action that controls tumor-induced angiogenesis on a molecular basis may therefore be a successful approach to the treatment of human hepatocarcinomas. Since VEGF is also known as the vascular permeability factor (VPF)^[12], inhibition of VEGF may induce a dual therapeutic effect (*e.g.*, antiangiogenic and anti-edematous) in patients with hepatocarcinoma^[13].

We constructed successfully antisense VEGF₁₆₅ eukaryotic expression vector PCDNA₃-as-VEGF₁₆₅ and transferred it into human hepatocarcinoma cells *in vitro* with cation lipofectamine 2000 mediated methods to evaluate the expression of VEGF protein and the inhibitory effect on the proliferation of hepatocarcinoma cells.

MATERIALS AND METHODS

Plasmid PCDNA₃-as-VEGF₁₆₅ constructions

The SMMC-7721 cell line had a high expression of endogenous VEGF protein, and used in antisense VEGF₁₆₅ transfection studies. The entire coding region of human VEGF₁₆₅ cDNA (0.6 kb) containing the 165 amino acid coding regions, was obtained from the PSV-VEGF₁₆₅ plasmid (Preserved by professor Bai-Gen Zhang, Renji Hospital, Shanghai, China), and subcloned into the Pbluescript M13- expression vector (preserved by Biochemistry Department of Nanjing University, Nanjing, China) generating the Pbluescript -VEGF₁₆₅ plasmid

with endonucleases EcoR I and Pst I (MBI) digested. Then the Pbluescript -VEGF₁₆₅ was digested by EcoR I and BamH I to obtain VEGF₁₆₅ cDNA that was reverse inserted into the PCDNA₃ eukaryon expression vector (preserved by Shanghai Institute for Biologic Science, Shanghai, China) generating the antisense VEGF₁₆₅ plasmid PCDNA₃-as-VEGF₁₆₅. It was confirmed by restriction endonuclease analysis, PCR (Roche) and nucleotide sequencing (Shanghai Sangon Biological Engineering Technology and Service Co. Ltd., China). Then the antisense VEGF₁₆₅ plasmid was amplified by transferring into activated Ecol. DH_{5α} was extracted with QIAGEN plasmid purification kit (QIAGEN) following the manufacturer's instructions.

ELISA for VEGF protein in cell culture supernatant

The day before transfection, the SMMC-7721 cells were trypsinized, counted, and plated in 24-well plates at 1×10^5 cells per well so that they were 90-95% confluent on the day of transfection. Cells were plated in 0.5 ml of DMEM containing 10% fetal bovine serum (FBS) and no antibiotics. For each well of cells to be transfected, 1.0 μg of DNA (PCDNA₃ or PCDNA₃-as-VEGF₁₆₅) and 3.0 μl of lipofectamine 2000 (LF2000) reagent were diluted respectively into 50 μl of DMEM without serum and antibiotics, and incubated for 5 min at room temperature. Once the LF2000 reagent was diluted, it was combined with DNA within 30 min, and then incubated at room temperature for 20 min to allow DNA-LF2000 reagent complexes to form. The DNA-LF2000 reagent complexes (100 μl) were added directly to each well and mixed gently by rocking the plate back and forth. The cells were incubated at 37°C in a CO₂ incubator for 48 h until they were ready to assay for transgene expression. The amount of human VEGF protein in cell culture supernatant was quantified by using an ELISA kit for human VEGF (Quantikine, R and D Systems)^[14].

Semiquantitative reverse transcription (RT)-PCR analysis^[15]

Tripure RNA isolation system (Roche) was used to isolate RNA from hepatocarcinoma SMMC-7721 cells after the transfection of DNA-LF2000 reagent complexes. According to the manufacturer's instructions, total RNA was resuspended in nuclease-free water (Promega), and the absorbance was read at A260 and A280. The quality of RNA was checked on a 1% denaturing agarose gel to ensure the presence of 28 S and 18 S ribosomal bands. VEGF mRNA expressions were measured using semiquantitative RT-PCR. One μg of total RNA was added to a 50 μl RT-PCR reaction (PCR-Access, Promega). The reaction master mix was prepared according to the manufacturer's instructions with β-actin (as an internal control for both qualitative and semiquantitative RT-PCR) and VEGF gene-specific primers. The primer sequences were 5'-GAGGGCAGAATCATCACGAAGT -3' (sense) and 5'-TCCTATGTGCTGGCCTTGGTGA -3' (antisense) for VEGF. The primer sequences for β-actin amplification were 5'-CCAAGGCCAACCGCGAGAAGATGAC -3' (sense) and 5'-AGGGTACATGGTGGTGCCGCCAGAC -3' (antisense). For quantitation of mRNA, primers were used in a reaction involving one cycle of reverse transcription at 48°C for 45 min and 30 cycles of denaturation at 94°C for 1 min, annealing at 55°C for 1 min, and extension at 72°C for 45 s. Then the resulting RT-PCR fragments were electrophoresed on 2% agarose gels at 110 V for 35 min.

VEGF165 cDNA PCR detection

Highpure DNA isolation system (Roche) was used to isolate DNA from normally cultured hepatocarcinoma SMMC-7721 cells. The primer sequences were 5'-GAGGGCAGAATCATCACGAAGT -3' (sense) and 5'-TCCTATGTGCTGG

CCTTGGTGA -3' (antisense) for VEGF. VEGF PCR was 30 cycles of denaturation at 94°C for 1 min, annealing at 55°C for 1 min, and extension at 72°C for 45 s. Then the fragments were identified by electrophoresis.

Flow cytometric analysis

The survival rate and apoptotic rate of hepatocarcinoma SMMC-7721 cells after antisense VEGF₁₆₅ transfections were determined by propidium iodide (PI) and annexin V staining. Hepatocarcinoma cells were digested by 0.25% trypsin at 37°C for 20 min and fixed with ice-cold 70% ethanol at a cell density of 1×10^6 ml⁻¹. PI and annexin V were then added and incubated with cells in the dark for 30 min until detected by flow cytometry^[16].

MTT assay

The day before PCDNA₃-as-VEGF₁₆₅ transfection, the hepatocarcinoma SMMC-7721 cells were trypsinized and counted, plated in 96-well plates at 1×10^4 cells per well. Cells were plated in 100 μl of DMEM containing serum and no antibiotics, and incubated at 37°C in a CO₂ incubator for 48 h until they were ready to transfer antisense VEGF₁₆₅. For each well of cells to be transfected, 0.2 μg of DNA (PCDNA₃ or PCDNA₃-as-VEGF₁₆₅) and 0.6 μl LF2000 were diluted respectively into 50 μl of DMEM without serum. The DNA-LF2000 reagent complexes (100 μl) were added directly to each well and mixed gently by rocking the plate back and forth. The cells were incubated at 37°C in a CO₂ incubator for 48 h until they were ready to assay for proliferation of hepatocarcinoma cells by MTT.

MTT assay was performed according to the methods of Mosmann^[17]. After the culture supernatant was sucked out, 100 μl 5 mg·ml⁻¹ MTT (Sigma) stock solution in PBS was respectively added to 4 wells each group each day for 5 days. After 4 h of incubation, 100 μl DMSO (Sigma) containing serum was added into each well. The plate was mixed gently by rocking back and forth until the blue sedimentation was completely dissolved. Then the absorbances were read by Tecan's sunrise absorbance microplate reader (A-5082)^[18].

Immunohistochemistry^[19]

The gene transferred hepatocarcinoma SMMC-7721 cells were trypsinized and sliced by cytofuge (Cytocentrifuge System M801-22, StatSpin). The slices containing SMMC-7721 cells were dried at 37°C overnight, rehydrated and exposed to 0.5 per cent hydrogen peroxide for 30 min to block the endogenous peroxidase activity. They were washed with distilled water and TRIS-HCL buffered saline (TBS) at PH 7.6, and then incubated with 1:5 normal rabbit serum for 10 min to reduce background staining. Next, the slices were incubated with diluted primary antibody at room temperature for 1 h. The antibody, a mouse monoclonal anti-human VEGF (DAKO, UK) was applied at a dilution of 1:200. The slices were then washed and a secondary antibody, horseradish peroxidase-conjugated rabbit anti-mouse immunoglobulin (DAKO, UK) at 1:50 dilution was applied for 30 min at room temperature. Thereafter, the slices were reacted in hydrogen peroxide-diaminobenzidine (DAB) solution to produce a brown color and counterstained with haematoxylin.

TBS was used as washing buffer between each stage of the staining and TBS containing 1 per cent bovine serum albumin was used to dilute the antibody.

Statistical calculations

The data were expressed as mean±SD. Besides a two-sided Student *t* test with a level of significance at 5%, a multiple-factor ANOVA (Tukey's test) was performed to analyze the

data of different groups. All the data were analyzed with the statistical software SPSS10.0.

RESULTS

Identification of eukaryotic expression vector PCDNA₃-as-VEGF₁₆₅

The eukaryotic expression vector PCDNA₃-as-VEGF₁₆₅ was identified by restriction endonucleases cut with EcoR I and BamH I and electrophoresis generating a 600 bp fragment according to the result from GeneBank. The fragment obtained from PCR was 258 bp in length. VEGF₁₆₅ cDNA was reverse subcloned into the site after T7 promoter appeared on the plasmid PCDNA₃ by nucleotide sequencing, coinciding completely with the sequence from GeneBank. There were no endonuclease cut sites of EcoR I, Pst I and BamH I by zymogram analysis.

Detection of SMMC 7721 cells after PCDNA₃-as-VEGF₁₆₅ transfection

VEGF cDNA was highly expressed in normally cultured hepatocarcinoma SMMC-7721 cells by PCR. But the VEGF mRNA expression was dramatically decreased after PCDNA₃-as-VEGF₁₆₅ transfection in hepatocarcinoma SMMC-7721 cells (Figure 1). The expression of VEGF protein in the culture supernatant of hepatocarcinoma SMMC-7721 cells was significantly inhibited (142.01 ± 7.95 vs 1625.52 ± 64.46 pg·ml⁻¹, $P < 0.01$) 2 days after antisense VEGF₁₆₅ transfection when compared to PCDNA₃ transfected controls, which correlated with the dose of antisense VEGF₁₆₅ gene. VEGF protein was highly expressed in most normally cultured hepatocarcinoma cells by immunohistochemical staining, but only in few hepatocarcinoma cells 2 days after antisense VEGF₁₆₅ transfection (Figure 2).

Evaluation of functions of eukaryotic expression vector PCDNA₃-as-VEGF₁₆₅

The apoptotic rate of hepatocarcinoma cells was significantly promoted ($17.98 \pm 0.86\%$ vs $4.86 \pm 0.27\%$, $P < 0.01$) and the survival

rate was notably decreased ($80.99 \pm 3.20\%$ vs $93.52 \pm 3.93\%$, $P < 0.05$) due to antisense VEGF₁₆₅ by flow cytometry (FCM). The transfection of antisense VEGF₁₆₅ gene resulted in the inhibition on the proliferation of hepatocarcinoma cells using MTT and the death of all hepatocarcinoma cells on day 6 after transfection (Figure 3).

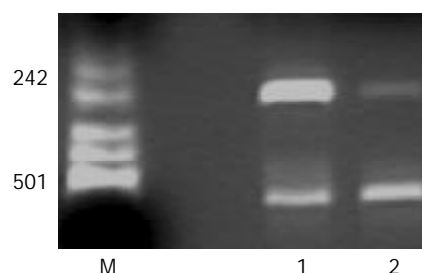


Figure 1 Effect of PCDNA₃-as-VEGF₁₆₅ on VEGF mRNA expression of hepatocarcinoma SMMC-7721 cells by RT-PCR. VEGF mRNA expression was negative after PCDNA₃-as-VEGF₁₆₅/LF2000 transfected. (Lane 1: PCDNA₃/LF2000 transfected, Lane 2: PCDNA₃-as-VEGF₁₆₅/LF2000 transfected; β-actin: 587 bp, VEGF 258 bp).

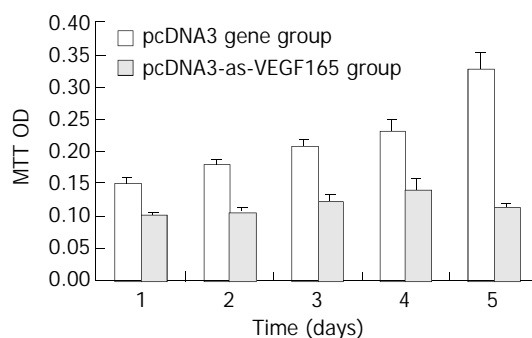


Figure 3 Effect of PCDNA₃-as-VEGF₁₆₅ on proliferation of hepatocarcinoma SMMC-7721 cells by MTT.

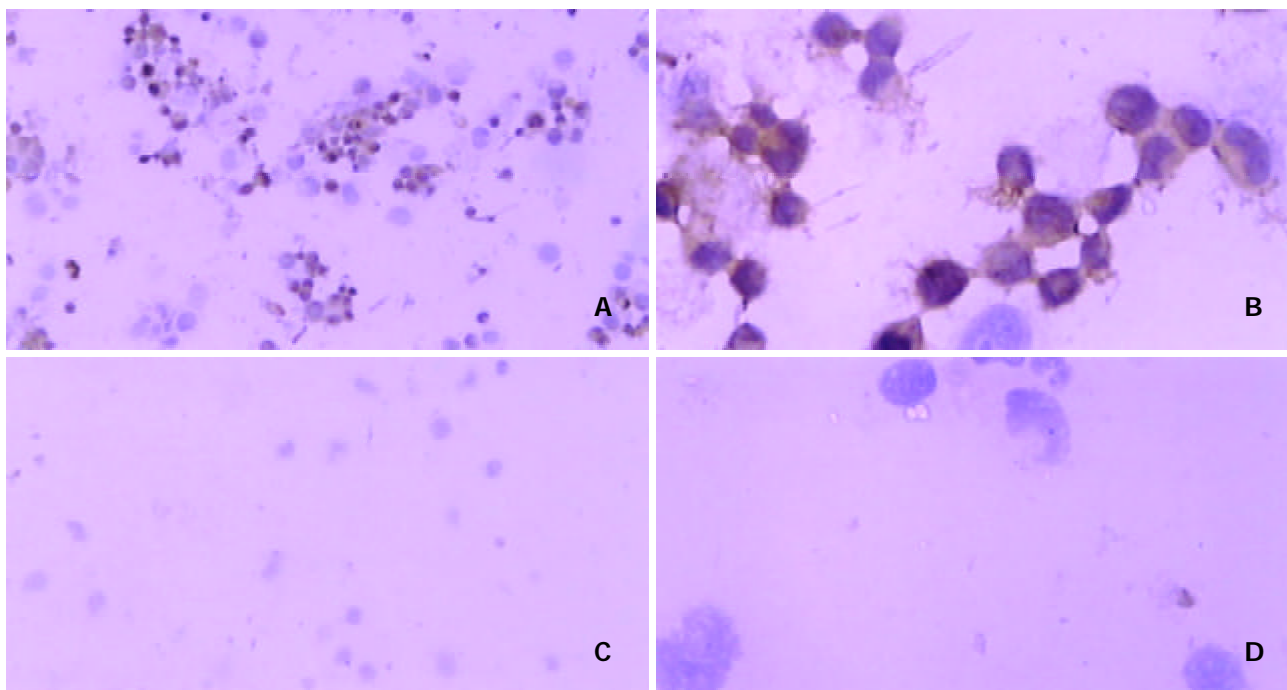


Figure 2 Immunohistochemical staining for expression of VEGF protein after DNA/LF2000 transfection in hepatocarcinoma SMMC-7721 cells. Positive signal for VEGF protein is brown and located in cytoplasm. A: ($\times 100$), B: ($\times 400$): PCDNA₃ transferred SMMC-7721 cells; C: ($\times 100$), D: ($\times 400$): PCDNA₃-as-VEGF₁₆₅ transferred.

DISCUSSION

The incidence of hepatic cancer has been gradually increasing in recent years in China. Currently surgical operation is considered exclusively as the sole option for the treatment of hepatocarcinoma, although less than 20% of patients were considered as candidates for resection^[20]. hepatocarcinoma is clearly a disease for which alternative therapies must be developed.

VEGF-mediated angiogenesis was considered to be a major contributor to tumor growth and metastasis^[21,22]. A number of VEGF antagonists have been developed for inhibiting VEGF-induced tumor angiogenesis and tumor growth. These antagonists include antisense VEGF oligonucleotides, VEGF antibodies, dominant-negative receptors, and soluble VEGF receptors^[23-26].

VEGF has been found to bind to two tyrosine kinase receptors, VEGFR-1 (Flt-1) and VEGFR-2 (KDR/Flk-1)^[27-29]. Both receptors were expressed on the surface of tumor endothelial cells, but not on tumor cells^[30]. Antisense VEGF cDNA^[31,32] significantly inhibited tumor angiogenesis and tumor growth *in vivo* with a paracrine signal transduction system. Angiogenesis played a key role in tumor growth and metastasis.

In previous studies, the putative anti-angiogenic effect of antisense VEGF₁₆₅ was investigated on stably transfected tumor cell lines. C6 and U87 glioma cells stably transfected with a vector encoding antisense VEGF₁₆₅ showed a significant growth inhibition when compared to sense VEGF transferred controls^[33,34]. These studies suggested that antisense VEGF₁₆₅ expression could be useful in controlling tumor angiogenesis and tumor growth *in vivo*.

In order to increase the effect of putative gene therapy, we implanted PCDNA₃-as-VEGF₁₆₅/LF2000 complexes into human hepatocarcinoma SMMC-7721 cells. We used hepatocarcinoma cells, because we previously observed that normally cultured hepatocarcinoma SMMC-7721 cells showed a high expression of VEGF protein^[35]. We achieved a significant promotion of SMMC-7721 cell apoptosis and complete hepatocarcinoma cell death on day 6 after antisense VEGF₁₆₅ transfection. VEGF mRNA expression was obviously blocked by antisense VEGF₁₆₅. Since the effect of antisense VEGF mRNA expression was temporary, it bound specifically to the sense counterpart and selectively neutralized the function of VEGF₁₆₅ gene^[36]. This approach may also require persistent expression of antisense VEGF or periodic administration of PCDNA₃-as-VEGF₁₆₅.

In summary, we succeeded in constructing the antisense VEGF₁₆₅ eukaryotic expression vector PCDNA₃-as-VEGF₁₆₅ acting as a VEGF₁₆₅ antagonist, and studied its anti-tumor activity. But the molecular mechanisms of PCDNA₃-as-VEGF₁₆₅ mediated apoptosis and inhibitory proliferation of hepatocarcinoma cells still need to be established. Finally, there may also exist other angiogenic pathways in hepatocarcinoma such as the angiopoietin/tie2 system that are not blocked by antisense VEGF₁₆₅^[37].

ACKNOWLEDGMENT

The authors thank Professor Bai-Gen Zhang for providing PSV-VEGF₁₆₅ and enthusiastic instructions to our study, and Lei Li and Jun-hao Chen in Translational Science Laboratory for their technical assistance.

REFERENCES

- 1 Hanahan D, Folkman J. Patterns and emerging mechanisms of the angiogenic switch during tumorigenesis. *Cell* 1996; **86**: 353-364

- 2 Folkman J. Role of angiogenesis in tumor growth and metastasis. *Semin Oncol* 2002; **29**(6 Suppl 16): 15-18
- 3 Bergers G, Hanahan D, Coussens LM. Angiogenesis and apoptosis are cellular parameters of neoplastic progression in transgenic mouse models of tumorigenesis. *Int J Dev Biol* 1998; **42**: 995-1002
- 4 Folkman J. New perspectives in clinical oncology from angiogenesis research. *Eur J Cancer* 1996; **32**: 2534-2539
- 5 Ferrara N, Houck K, Jakeman L, Leung DW. Molecular and biological properties of the vascular endothelial growth factor family of proteins. *Endocr Rev* 1992; **13**: 18-32
- 6 Dvorak HF, Brown LF, Detmar M, Dvorak AM. Vascular permeability factor/vascular endothelial growth factor, microvascular hyperpermeability, and angiogenesis. *Am J Pathol* 1995; **146**: 1029-1039
- 7 Berse B, Brown LF, Van de Water L, Dvorak HF, Senger DR. Vascular permeability factor (vascular endothelial growth factor) gene is expressed differentially in normal tissues, macrophages, and tumors. *Mol Biol Cell* 1992; **3**: 211-220
- 8 Freeman MR, Schneck FX, Gagnon ML, Corless C, Soker S, Niknejad K, Peoples GE, Klagsbrun M. Peripheral blood T lymphocytes and lymphocytes infiltrating human cancers express vascular endothelial growth factor: a potential role for T cells in angiogenesis. *Cancer Res* 1995; **55**: 4140-4145
- 9 Folkman J. What is the evidence that tumors are angiogenesis dependent? *J Natl Cancer Inst* 1990; **82**: 4-6
- 10 Paley PJ, Staskus KA, Gebhard K, Mohanraj D, Twigg LB, Carson LF, Ramakrishnan S. Vascular endothelial growth factor expression in early stage ovarian carcinoma. *Cancer* 1997; **80**: 98-106
- 11 Takahashi Y, Tucker SL, Kitadai Y, Koura AN, Bucana CD, Cleary KR, Ellis LM. Vessel counts and expression of vascular endothelial growth factor as prognostic factors in node-negative colon cancer. *Arch Surg* 1997; **132**: 541-546
- 12 Keck PJ, Hauser SD, Krivi G, Sanzo K, Warren T, Feder J, Connolly DT. Vascular permeability factor, an endothelial cell mitogen related to PDGF. *Science* 1989; **246**: 1309-1312
- 13 Plate KH. Gene therapy of malignant glioma via inhibition of tumor angiogenesis. *Cancer Metastasis Rev* 1996; **15**: 237-240
- 14 Ando S, Nojima K, Ishihara H, Suzuki M, Ando M, Majima H, Ando K, Kuriyama T. Induction by carbon-ion irradiation of the expression of vascular endothelial growth factor in lung carcinoma cells. *Int J Radiat Biol* 2000; **76**: 1121-1127
- 15 Kong HL, Crystal RG. Gene therapy strategies for tumor antiangiogenesis. *J Natl Cancer Inst* 1998; **90**: 273-286
- 16 Park JC, Sung HJ, Lee DH, Park YH, Cho BK, Suh H. Specific determination of endothelial cell viability in the whole cell fraction from cryopreserved canine femoral veins using flow cytometry. *Artif Organs* 2000; **24**: 829-833
- 17 Kendall RL, Thomas KA. Inhibition of vascular endothelial cell growth factor activity by an endogenously encoded soluble receptor. *Proc Natl Acad Sci U S A* 1993; **90**: 10705-10709
- 18 Mills J, Allison N. A rapid, quantitative microplate assay for NAD-linked D-mannitol dehydrogenase. *Lett Appl Microbiol* 1990; **11**: 211-213
- 19 Horiguchi N, Takayama H, Toyoda M, Otsuka T, Fukusato T, Merlino G, Takagi H, Mori M. Hepatocyte growth factor promotes hepatocarcinogenesis through c-Met autocrine activation and enhanced angiogenesis in transgenic mice treated with diethylnitrosamine. *Oncogene* 2002; **21**: 1791-1799
- 20 Wills KN, Huang WM, Harris MP, Machemer T, Maneval DC, Gregory RJ. Gene therapy for hepatocellular carcinoma: chemosensitivity conferred by adenovirus-mediated transfer of the HSV-1 thymidine kinase gene. *Cancer Gene Ther* 1995; **2**: 191-197
- 21 Dvorak HF, Sioussat TM, Brown LF, Berse B, Nagy JA, Sotrel A, Manseau EJ, Van de Water L, Senger DR. Distribution of vascular permeability factor (vascular endothelial growth factor) in tumors: concentration in tumor blood vessels. *J Exp Med* 1991; **174**: 1275-1278
- 22 Plate KH, Breier G, Weich HA, Risau W. Vascular endothelial growth factor is a potential tumour angiogenesis factor in human gliomas *in vivo*. *Nature* 1992; **359**: 845-848
- 23 Kendall RL, Thomas KA. Inhibition of vascular endothelial cell growth factor activity by an endogenously encoded soluble receptor. *Proc Natl Acad Sci U S A* 1993; **90**: 10705-10709

- 24 **Yang JC**, Haworth L, Sherry RM, Hwu P, Schwartzentruber DJ, Topalian SL, Steinberg SM, Chen HX, Rosenberg SA. A randomized trial of bevacizumab, an anti-vascular endothelial growth factor antibody, for metastatic renal cancer. *N Engl J Med* 2003; **349**: 427-434
- 25 **Millauer B**, Longhi MP, Plate KH, Shawver LK, Risau W, Ullrich A, Strawn LM. Dominant-negative inhibition of Flk-1 suppresses the growth of many tumor types *in vivo*. *Cancer Res* 1996; **56**: 1615-1620
- 26 **Lin P**, Sankar S, Shan S, Dewhirst MW, Polverini PJ, Quinn TQ, Peters KG. Inhibition of tumor growth by targeting tumor endothelium using a soluble vascular endothelial growth factor receptor. *Cell Growth Differ* 1998; **9**: 49-58
- 27 **Goldman CK**, Kendall RL, Cabrera G, Soroceanu L, Heike Y, Gillespie GY, Siegal GP, Mao X, Bett AJ, Huckle WR, Thomas KA, Curiel DT. Paracrine expression of a native soluble vascular endothelial growth factor receptor inhibits tumor growth, metastasis, and mortality rate. *Proc Natl Acad Sci U S A* 1998; **95**: 8795-8800
- 28 **Kendall RL**, Wang G, Thomas KA. Identification of a natural soluble form of the vascular endothelial growth factor receptor, FLT-1, and its heterodimerization with KDR. *Biochem Biophys Res Commun* 1996; **226**: 324-328
- 29 **De Vries C**, Escobedo JA, Ueno H, Houck K, Ferrara N, Williams LT. The fms-like tyrosine kinase, a receptor for vascular endothelial growth factor. *Science* 1992; **255**: 989-991
- 30 **Millauer B**, Witzmann-Voos S, Schnurch H, Martinez R, Moller NP, Risau W, Ullrich A. High affinity VEGF binding and developmental expression suggest Flk-1 as a major regulator of vasculogenesis and angiogenesis. *Cell* 1993; **72**: 835-846
- 31 **Terman BI**, Dougher-Vermazen M, Carrion ME, Dimitrov D, Armellino DC, Gospodarowicz D, Bohlen P. Identification of the KDR tyrosine kinase as a receptor for vascular endothelial cell growth factor. *Biochem Biophys Res Commun* 1992; **187**: 1579-1586
- 32 **Plate KH**, Breier G, Weich HA, Mennel HD, Risau W. Vascular endothelial growth factor and glioma angiogenesis: coordinate induction of VEGF receptors, distribution of VEGF protein and possible *in vivo* regulatory mechanisms. *Int J Cancer* 1994; **59**: 520-529
- 33 **Cheng SY**, Huang HJ, Nagane M, Ji XD, Wang D, Shih CC, Arap W, Huang CM, Cavenee WK. Suppression of glioblastoma angiogenicity and tumorigenicity by inhibition of endogenous expression of vascular endothelial growth factor. *Proc Natl Acad Sci U S A* 1996; **93**: 8502-8507
- 34 **Saleh M**, Stacker SA, Wilks AF. Inhibition of growth of C6 glioma cells *in vivo* by expression of antisense vascular endothelial growth factor sequence. *Cancer Res* 1996; **56**: 393-401
- 35 **Plate KH**, Breier G, Millauer B, Ullrich A, Risau W. Up-regulation of vascular endothelial growth factor and its cognate receptors in a rat glioma model of tumor angiogenesis. *Cancer Res* 1993; **53**: 5822-5827
- 36 **Sakakura C**, Hagiwara A, Tsujimoto H, Ozaki K, Sakakibara T, Oyama T, Ogaki M, Takahashi T. The anti-proliferative effect of proliferating cell nuclear antigen-specific antisense oligonucleotides on human gastric cancer cell lines. *Surg Today* 1995; **25**: 184-186
- 37 **Stratmann A**, Risau W, Plate KH. Cell type-specific expression of angiopoietin-1 and angiopoietin-2 suggests a role in glioblastoma angiogenesis. *Am J Pathol* 1998; **153**: 1459-1466

Edited by Wang XL

Effects of epidermal growth factor and its signal transduction inhibitors on apoptosis in human colorectal cancer cells

Jane CJ Chao, Wen Li Peng, Sheng-Hsuan Chen

Jane CJ Chao, Wen Li Peng, School of Nutrition and Health Sciences, Taipei Medical University, Taipei, 110 Taiwan, China
Sheng-Hsuan Chen, Department of Gastroenterology, Taipei Medical University Hospital, Taipei, 110 Taiwan, China

Correspondence to: Jane CJ Chao, School of Nutrition and Health Sciences, Taipei Medical University, 250 Wu Hsing Street, Taipei, 110 Taiwan, China. chenju@tmu.edu.tw

Telephone: +886-2-2736-1661 #6551~6556 Ext. 117

Fax: +886-2-2737-3112

Received: 2003-11-17 **Accepted:** 2003-12-16

Abstract

AIM: The study investigated if EGF signaling inhibitors, EGF antibody and tyrphostin 51 (a tyrosine kinase inhibitor), mediated the action of EGF on apoptosis and the expression of EGF receptors and p21 (a cyclin-dependent kinase inhibitor) of human colorectal cancer cells.

METHODS: Human colorectal adenocarcinoma cells (SW480) were incubated with 0.6 mL/L dimethyl sulfoxide (DMSO, the control group), 225 ng/mL (37.5 nmol/L) EGF in 0.6 mL/L DMSO, 225 ng/mL EGF+2.5 µg/mL (17 nmol/L) EGF antibody in 0.6 mL/L DMSO, or 225 ng/mL EGF+215 ng/mL (0.8 µmol/L) tyrphostin 51 in 0.6 mL/L DMSO.

RESULTS: After 48 h incubation, the levels of EGF in medium significantly increased ($P<0.05$) in the EGF-treated groups. The numbers of apoptotic cells were significantly fewer ($P<0.05$) in the EGF + EGF antibody and EGF + tyrphostin 51 groups than those in the control and EGF groups after 12 h treatments. The expression of phosphorylated EGF receptors in the EGF, EGF + EGF antibody, and EGF + tyrphostin 51 groups was 176.8%, 62.4%, and 138.1% of the control group, respectively. The expression of p21 protein in the EGF, EGF + EGF antibody, and EGF + tyrphostin 51 groups was 115.7%, 4.8%, and 61.5% of the control group, respectively.

CONCLUSION: The data suggest that EGF antibody and tyrphostin 51 can inhibit the action of EGF on apoptosis in human colorectal cancer cells through down-regulation of EGF receptor and p21 expression.

Chao JCJ, Peng WL, Chen SH. Effects of epidermal growth factor and its signal transduction inhibitors on apoptosis in human colorectal cancer cells. *World J Gastroenterol* 2004; 10(4): 540-544

<http://www.wjgnet.com/1007-9327/10/540.asp>

INTRODUCTION

Colorectal cancer is one of the most common human malignancies. The genetic alterations in colorectal cancer may drive the transition of normal colorectal epithelium to adenomas and adenocarcinomas through increased proliferation and decreased cell death or apoptosis. Several

peptide growth factors have been suggested as autocrine growth regulators in cancer cell lines^[1]. Anomalous expression of growth factors and/or growth factor receptors, as well as abnormal response to growth factors and/or their receptors may be involved in cellular transformation. Among these growth factors, epidermal growth factor (EGF) is known to play a major role in regulation of cell proliferation. Epidermal growth factor has been shown to be a potent mitogen both *in vitro* and *in vivo* studies to stimulate DNA, RNA, and protein synthesis in the digestive tract^[2,3].

Epidermal growth factor exerts its mitotic signal via a tyrosine kinase-type cell surface receptor, the EGF receptor (EGF-R). It has been reported that EGF-R is overexpressed in a number of human tumors^[4-6]. The EGF-R level in patients with primary colorectal carcinoma ranged between 4 and 79 fmol/mg membrane protein ($Kd=0.1-0.4\times 10^{-9} M$)^[7]. Messa *et al.*^[6] found that the expression of both EGF and EGF-R significantly increased in neoplastic tissues from patients with colorectal adenocarcinoma compared with that in their adjacent normal mucosa. The overexpression of EGF-R in human epidermoid carcinoma (A431) cells could allow selective growth advantage for tumor cells in the presence of normal or decreased ligand availability, and excessive ligand binding caused down-regulation of growth signaling and furthermore inhibition of growth and induction of apoptosis^[4].

Epidermal growth factor affects cell proliferation by modulating the activity of cyclin-dependent kinase complex, a cell cycle regulator^[8]. The cyclin-dependent kinase inhibitor p21 (also called WAF1, CAP20, Cip1, and Sdi1) may cause cell cycle arrest by both p53-dependent and -independent mechanisms^[9]. EGF has shown to induce p21 expression in different human cancer cell lines^[10-16].

Blockade of EGF signaling pathway by several methods affects the proliferation and/or apoptosis in a variety of tumor cell lines^[4,17-19]. The EGF/EGF-R inhibitors may have potential for the therapy of tumors that are dependent on EGF-R signaling pathway for proliferation or survival. The purposes of this study were to investigate if EGF signaling inhibitors, EGF antibody and tyrphostin 51 (a tyrosine kinase inhibitor), mediated the action of EGF on apoptosis of human epithelial-type colorectal adenocarcinoma cells with EGF-R expression, and if these inhibitors affected the expression of EGF-R and p21, which are involved in EGF signaling pathway and cell cycle regulation, respectively.

MATERIALS AND METHODS

Cell line and treatments

Human colorectal adenocarcinoma cell line (SW480; BCRC No. 60249) was purchased from Bioresources Collection and Research Center (BCRC) at Food Industry Research and Development Institute (Hsinchu, Taiwan). Cells were grown in 900 mL/L Leibovitz's L-15 medium with 100 mL/L fetal bovine serum at 37°C without CO₂. When cells reached 90% confluency, cells were switched to serum-free medium for 24 h to deplete growth factors in serum. Cells were then incubated with 0.6 mL/L dimethyl sulfoxide (DMSO, the

control group), 225 ng/mL (37.5 nmol/L, a physiological concentration) EGF in 0.6 mL/L DMSO, 225 ng/mL EGF + 2.5 µg/mL (17 nmol/L) EGF antibody (Research and Diagnostics Systems, Inc., Minneapolis, MN) in 0.6 mL/L DMSO, or 225 ng/mL EGF + 215 ng/mL (0.8 µmol/L) tyrphostin 51 (a tyrosine kinase blocker to inhibit the EGF receptor, Sigma-Aldrich Co., St. Louis, MO) in 0.6 mL/L DMSO serum-free medium for 12 or 48 h. Cells and conditioned medium were collected. Protein contents in cells and conditioned medium were measured by the modified method of Lowry *et al.*^[20] using a Bio-Rad DC protein kit (Bio-Rad Laboratories, Hercules, CA).

Measurement of EGF in medium

The secretion of EGF into conditioned medium was measured by a commercial EGF immunoassay kit (Quantikine™, Research and Diagnostics Systems, Inc.)^[21]. Serum-free conditioned medium (200 µL) was incubated with murine monoclonal EGF antibody coated in a 96-well plate for 2 h at room temperature, washed 3 times with wash buffer, and then incubated with 200 µL polyclonal EGF antibody conjugated to horseradish peroxidase for 1 h. After several washes, samples were incubated with 200 µL substrate (tetramethylbenzidine:H₂O₂=1:1) for 20 min. The reaction was terminated by 50 µL of 1 mol/L sulfuric acid. The levels of EGF were determined at 450 nm and corrected at 540 nm using an ELISA reader (Multiskan RC, Thermo Labsystems, Helsinki, Finland).

Detection of apoptosis

Apoptosis was analyzed by fluorescence microscopy using an annexin V-fluorescein isothiocyanate (FITC) apoptosis detection kit (Oncogene Research Products, Boston, MA). The externalization of phosphatidylserine was as a marker of early-stage apoptosis using annexin V-FITC binding^[22]. Cells (5×10⁵) were suspended in 0.5 mL binding buffer (10 mmol/L HEPES, pH 7.4/150 mmol/L NaCl/2.5 mmol/L CaCl₂/1 mmol/L MgCl₂/40 mg/L bovine serum albumin (BSA)), and incubated with 1.25 µL of 200 µg/mL annexin V-FITC in 50 mmol/L Tris (pH 7.4), 0.1 mol/L NaCl, 10 mg/L BSA, and 0.2 mg/L NaN₃ solution for 15 min in the dark. Cell suspension was centrifuged at 1 000 g for 5 min, resuspended in 0.5 mL binding buffer, and mixed with 10 µL of 30 µg/mL propidium iodide in PBS. Samples were placed on ice in the dark and analyzed by fluorescence microscopy immediately.

Measurement of EGF receptor and p21 proteins

Cell suspension (30 µg total protein) pooled from 7 independent experiments (*n*=7) was mixed with an equal volume of 2×SDS-PAGE sample buffer (0.125 mol/L Tris-HCl, pH 6.8/40 mg/L SDS/200 mL/L glycerol/100 mL/L 2-mercaptoethanol)^[23], denatured at 100 °C for 3 min, and applied to SDS-PAGE (Bio-Rad Mini-PROTEAN 3 Cell, Bio-Rad Laboratories). Proteins were separated by 7.5% or 10% resolving gel for EGF receptor or p21, respectively, with 4% stacking gel in the running buffer (25 mmol/L Tris, pH 8.3/192 mmol/L glycine/1 mg/L SDS) at 100 V for 1 h. After separation on the gel, proteins were then transferred onto the nitrocellulose membrane (0.45 µm) using a semi-dry transfer unit (Hofer TE 70, Amersham Biosciences Ltd. Taiwan Branch, Taipei, Taiwan) in Towbin buffer (25 mmol/L Tris/192 mmol/L glycine/1.3 mmol/L SDS/100 mL/L methanol)^[24] at 200 mA for 1 h. The membrane was washed briefly with PBS, and incubated with blocking buffer (50 mg/L skim milk/1 mL/L Tween-20 in PBS) for 1 h. After blocking, the membrane was incubated with 1 µg/mL mouse anti-human phosphorylated EGF receptor (eps15, BD Transduction Laboratories, San Diego, CA), p21 (p21^{Cip1/WAF1}, BD Transduction Laboratories), or α-tubulin (TU-02, Santa Cruz

Biotechnology, Inc., Santa Cruz, CA) antibody at room temperature for 1 h. The membrane was washed 3 times with wash buffer (1 mL/L Tween-20 in PBS), and incubated with 10 µg/mL goat anti-mouse IgG-horseradish peroxidase conjugate (Leinco Technologies, Inc., St. Louis, MO,) for 1 h. The blot was washed again 3 times with wash buffer, incubated with ECL™ Western blotting detection reagents (Amersham Biosciences Ltd. Taiwan Branch) for 1 min, and exposed to an X-ray film for 15 s. The bands were quantitated by an image analysis system (Gel analysis system, EverGene Biotechnology, Taipei, Taiwan) and Phoretix 1D Lite software (Phoretix International Ltd., Newcastle upon Tyne, UK).

Statistical analysis

Data are expressed as mean±SD. Data were analyzed by one-way ANOVA to determine the treatment effect using SAS (version 6.12, SAS Institute Inc., Cary, NC). Fisher's least significant difference test was used to make *post-hoc* comparisons if the main effect was demonstrated. Differences were considered significant at *P*<0.05.

RESULTS

The secretion of EGF into medium was significantly higher (*P*<0.05) in the EGF (8.35±0.82 ng/mg protein, *n*=7), EGF + EGF antibody (7.44±1.17 ng/mg protein, *n*=7), and EGF + tyrphostin 51 (8.28±0.84 ng/mg protein, *n*=7) groups than that in the control group (0.49±0.05 ng/mg protein, *n*=7) (Figure 1). However, the level of EGF did not significantly differ among the EGF-treated groups. Annexin V-FITC apoptosis detection assay showed that FITC-positive cells were significantly more often found (*P*<0.05) in the control (5.0±1.8/field) (Figure 2A) and EGF (6.0±1.3/field) (Figure 2B) groups, with a range of 2 to 8 positive cells per field (×100), compared with those in the EGF + EGF antibody (2.1±1.3/field) (Figure 2C) and EGF + tyrphostin 51 (1.9±1.3/field) (Figure 2D) groups, with a range of 0 to 4 cells per field (×100) after 12 h treatments. However, the numbers of apoptotic cells did not significantly differ between the control and EGF groups and between the EGF + EGF antibody and EGF + tyrphostin 51 groups. The expression of phosphorylated EGF-R in the EGF, EGF + EGF antibody, and EGF + tyrphostin 51 groups was 176.8%, 62.4%, and 138.1% of the control group, respectively (Figure 3). The expression of p21 protein in the EGF, EGF + EGF antibody, and EGF + tyrphostin 51 groups was 115.7%, 4.8%, and 61.5% of the control group, respectively (Figure 4).

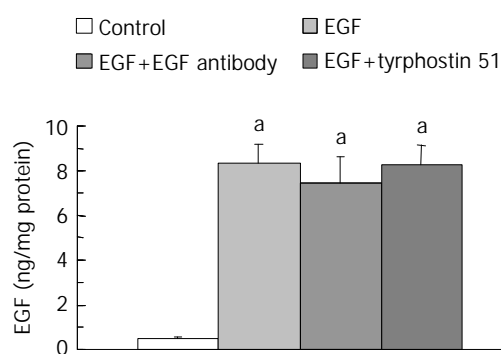


Figure 1 Levels of EGF in medium after incubation of SW480 cells with 0.06% dimethyl sulfoxide (DMSO, the control group), 225 ng/mL (37.5 nmol/L) EGF in 0.6 mL/L DMSO, 225 ng/mL EGF + 2.5 µg/mL (17 nmol/L) EGF antibody in 0.6 mL/L DMSO, or 225 ng/mL EGF + 215 ng/mL (0.8 µmol/L) tyrphostin 51 in 0.6 mL/L DMSO serum-free medium for 48 h. Data are expressed as mean±SD (*n*=7). **P*<0.05 significantly different between the control and EGF-treated groups.

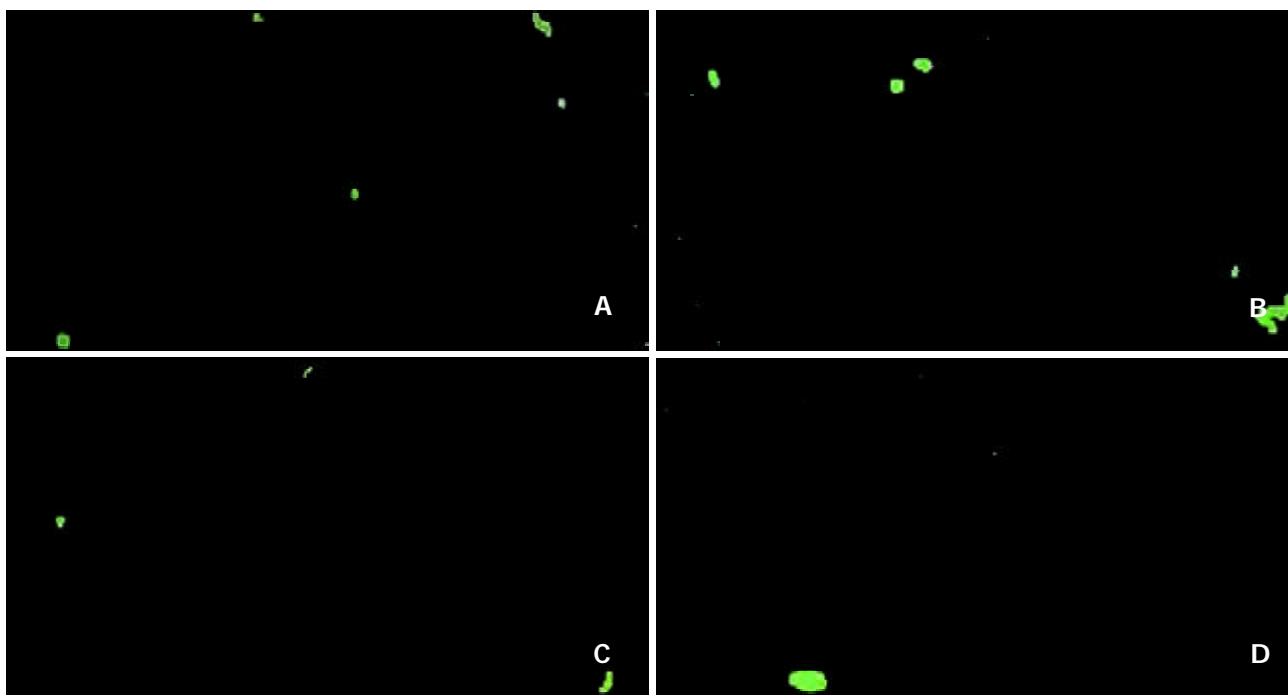


Figure 2 Apoptotic cells stained by annexin V-FITC binding (green) after incubation of SW480 cells with 0.6 mL/L dimethyl sulfoxide (DMSO, the control group) (A), 225 ng/mL (37.5 nmol/L) EGF in 0.6 mL/L DMSO (B), 225 ng/mL EGF + 2.5 μg/mL (17 nmol/L) EGF antibody in 0.6 mL/L DMSO (C), or 225 ng/mL EGF + 215 ng/mL (0.8 μmol/L) tyrphostin 51 in 0.6 mL/L DMSO serum-free medium (D) for 12 h. Micrograph magnified by ×100 is the representative of seven independent experiments (n=7).

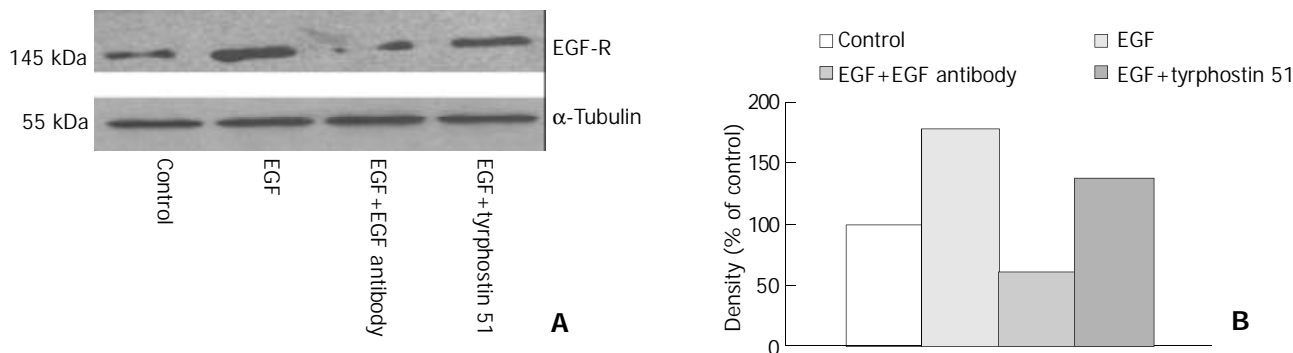


Figure 3 Expression of phosphorylated EGF receptor (EGF-R) with the molecular weight of 145 kDa visualized by Western blotting (A) and quantitated by an image analysis system (B) after incubation of SW480 cells with 0.6 mL/L dimethyl sulfoxide (DMSO, the control group), 225 ng/mL (37.5 nmol/L) EGF in 0.6 mL/L DMSO, 225 ng/mL EGF + 2.5 μg/mL (17 nmol/L) EGF antibody in 0.6 mL/L DMSO, or 225 ng/mL EGF + 215 ng/mL (0.8 μmol/L) tyrphostin 51 in 0.6 mL/L DMSO serum-free medium for 48 h. Samples were pooled from 7 independent experiments (n=7). Density was calibrated by an internal control, α-tubulin (55 kDa).

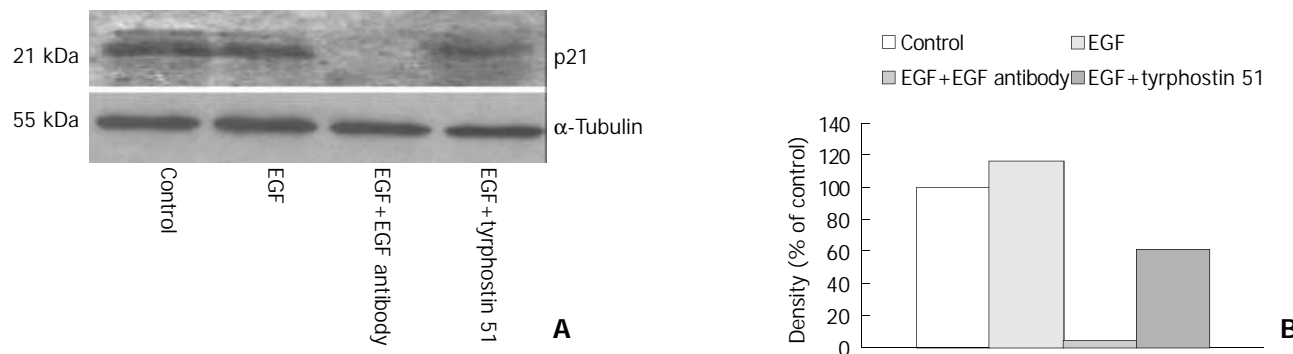


Figure 4 Expression of p21 protein with the molecular weight of 21 kDa visualized by Western blotting (A) and quantitated by an image analysis system (B) after incubation of SW480 cells with 0.6 mL/L dimethyl sulfoxide (DMSO, the control group), 225 ng/mL (37.5 nmol/L) EGF in 0.6 mL/L DMSO, 225 ng/mL EGF + 2.5 μg/mL (17 nmol/L) EGF antibody in 0.6 mL/L DMSO, or 225 ng/mL EGF + 215 ng/mL (0.8 μmol/L) tyrphostin 51 in 0.6 mL/L DMSO serum-free medium for 48 h. Samples were pooled from 7 independent experiments (n=7). Density was calibrated by an internal control, α-tubulin (55 kDa).

DISCUSSION

Our data showed that EGF treatment at a dose of 225 ng/mL (37.5 nmol/L) did not further stimulate apoptosis compared with the control group, but significantly increased to nearly 2-fold the expression of phosphorylated EGF-R. Gulli *et al.*^[4] demonstrated that exogenous EGF (60 ng/mL; 10 nmol/L) inhibited cell proliferation and induced morphological features of apoptosis in A431 cells with overexpressed EGF-R by induction of a 15-fold increase in EGF-R autophosphorylation, which down-regulated EGF signal transduction. At a lower concentration of EGF (0.06 ng/mL, 10 pmol/L), EGF-R autophosphorylation and cell proliferation increased to 2-fold compared with those in untreated cells^[4]. Previous studies showed the expression of EGF-R on the cell surface affected the action of EGF^[15,25]. A431 cells grown as three-dimensional spheroids showed growth stimulation in response to nanomolar concentrations of EGF, while monolayer cultures showed growth inhibition^[25]. The expression of EGF-R on monolayers of A431 cells was 20-fold greater than that on three-dimensional spheroids. Autophosphorylation of the EGF-R also increased in response to EGF in monolayer cultures of A431 cells. However, EGF prevented apoptosis of human bladder carcinoma 647V cells cultured as three-dimensional spheroids with lower expression of EGF-R^[15]. The data indicated that EGF could play a dual role in modulation of apoptosis depending on the level of EGF-R. The overexpression of EGF-R down-regulated growth-stimulating action of EGF when cells were grown in monolayer cultures.

Apoptosis occurred prior to and in response to EGF treatment in SW480 cells. Previous studies found that cell lines, such as A431^[4] and human mammary adenocarcinoma MDA-MB-468^[26] cells, which overexpress the EGF-R underwent apoptosis in response to EGF treatment. Additionally, apoptosis was greatly enhanced when cells were growth-arrested prior to EGF treatment^[26]. Our study showed that apoptosis was also induced in the control group, probably because cells were arrested after 24 h incubation in serum-free medium. However, apoptosis was induced to occur but not further enhanced by EGF compared with that without EGF (the control group) within 12 h. EGF-induced apoptosis may involve activation of activator protein-1^[26], inhibition of nuclear transcriptional factor-kappaB (NF- κ B)^[27] and protein kinase B (PKB/Akt) activation^[28], and cell detachment (a decline in cell adhesion)^[29,30].

Compared with the EGF group, apoptosis was inhibited after EGF signal transduction was blocked by EGF antibody or tyrosine kinase inhibitor. The expression of phosphorylated EGF-R and p21 decreased in the groups treated with EGF signaling inhibitors, especially in the EGF + EGF antibody group. Our data indicated that the inhibition of EGF signal transduction by EGF antibody or by EGF-R inhibitor decreased apoptosis of human colorectal adenocarcinoma cells, at least in part, through regulation of EGF-R and p21. SW480 cells produced the most transforming growth factor (TGF) β -like rather than TGF α -like activity and had no measurable TGF β membrane receptors, but EGF receptors were detectable^[31]. Additionally, the concentration of endogenous EGF detectable in conditioned medium of the control group was much lower than that of exogenous EGF in the EGF-treated groups. Therefore, apoptosis of SW480 cells was primarily mediated by exogenous EGF and EGF signaling inhibitors through EGF-R signaling pathway in a paracrine rather than an autocrine manner. Previous studies showed that inhibition of EGF signal transduction could reverse the action of EGF on cell proliferation^[4,17-19]. Anti-sense EGF-R RNA down-regulated the proliferation^[17] and invasive properties^[18] of human colon tumor cells. When A431 cells were simultaneously treated with EGF (60 ng/mL, 10 nmol/L) and EGF antibody (15 μ g/mL), a

significant reduction in EGF-R autophosphorylation reversed the action of EGF on cell proliferation^[4]. Tyrphostin, the most potent EGF-R kinase inhibitor, inhibited EGF-dependent proliferation of A431/clone 15 cells, but with little or no effect on EGF-independent cell growth^[32]. The phosphorylation of EGF-R was decreased by an inhibitor of EGF-R tyrosine kinase, RG-13022 (α -(3'-pyridyl)-3,4-dimethoxy)cinnamionitrile, in A431 cells^[4]. Additionally, another tyrosine kinase inhibitor, CP-358,774 ([6,7-bis(2-methoxy-ethoxy)-quinazolin-4-yl]-(3-ethynylphenyl)amine), inhibited proliferation and triggered apoptosis through arrest of cell cycle progression in the G1 phase by accumulation of p27^{KIP1}, a mitotic inhibitor, in human colorectal carcinoma (DiFi) cells^[19].

Similar to our findings, exposure to EGF at a nanomolar concentration reduced DNA synthesis, arrested cells in the G0/G1 phase, and elevated p21 protein in human squamous carcinoma cells, indicating that p21 plays a role in mediating EGF-induced growth inhibition^[10-12]. Additionally, EGF-mediated growth inhibition was associated with induction of p21 in human breast^[13,14], bladder^[15], and esophageal^[16] cancer cells. EGF-increasing p21 expression was by stabilization of p21 at the post-transcriptional and post-translational levels^[12], and activation of signal transducer and activator of transcription (STAT)1 and STAT3^[13,16,33]. Consistent with our study, EGF-induced p21 expression was inhibited by the EGF-R tyrosine kinase inhibitor, tyrphostin AG1478 in A431 cells^[10].

In conclusion, EGF antibody and tyrphostin 51 can inhibit the action of EGF on apoptosis in human colorectal cancer SW480 cells through down-regulation of EGF receptor and p21 expression. Furthermore, EGF at a higher concentration may have potential for the therapy of tumors with overexpressed EGF-R, which is dependent on EGF-R signaling pathway for proliferation.

REFERENCES

- 1 **Barnard JA**, Beauchamp RD, Russell WE, Dubois RN, Coffey RJ. Epidermal growth factor-related peptides and their relevance to gastrointestinal pathophysiology. *Gastroenterology* 1995; **108**: 564-580
- 2 **Gregory H**. *In vivo* aspects of urogastrone-epidermal growth factor. *J Cell Sci Suppl* 1985; **3**: 11-17
- 3 **Ménard D**, Arsénault P, Pothier P. Biological effects of epidermal growth factor in human fetal jejunum. *Gastroenterology* 1988; **94**: 656-663
- 4 **Gulli LE**, Palmer KC, Chen YQ, Reddy KB. Epidermal growth factor-induced apoptosis in A431 cells can be reversed by reducing the tyrosine kinase activity. *Cell Growth Differ* 1996; **7**: 173-178
- 5 **Messa C**, Russo F, Notarnicola M, Di Leo A. Demonstration of epidermal growth factor in colorectal adenocarcinoma by enzyme immunoassay. *Digestion* 1994; **55**: 103-107
- 6 **Messa C**, Russo F, Caruso MG, Di Leo A. EGF, TGF α and EGF-R in human colorectal adenocarcinoma. *Acta Oncol* 1998; **37**: 285-289
- 7 **Moorghen M**, Ince P, Finney KJ, Watson AJ, Harris AL. Epidermal growth factor receptors in colorectal carcinoma. *Anticancer Res* 1990; **10**: 605-611
- 8 **Alisi A**, Spagnuolo S, Leoni S. Treatment with EGF increases the length of S-Phase after partial hepatectomy in rat, changing the activities of cdk. *Cell Physiol Biochem* 2003; **13**: 239-248
- 9 **Gartel AL**, Tyner AL. The role of the cyclin-dependent kinase inhibitor p21 in apoptosis. *Mol Cancer Ther* 2002; **1**: 639-649
- 10 **Fan Z**, Lu Y, Wu X, DeBlasio A, Koff A, Mendelsohn J. Prolonged induction of p21Cip1/WAF1/CDK2/PCNA complex by epidermal growth factor receptor activation mediates ligand-induced A431 cell growth inhibition. *J Cell Biol* 1995; **131**: 235-242
- 11 **Jakus J**, Yeudall WA. Growth inhibitory concentrations of EGF induce p21 (WAF1/Cip1) and alter cell cycle control in squamous carcinoma cells. *Oncogene* 1996; **12**: 2369-2376
- 12 **Johannessen LE**, Knardal SL, Madshus IH. Epidermal growth factor increases the level of the cyclin-dependent kinase (CDK)

- inhibitor p21/CIP1 (CDK-interacting protein 1) in A431 cells by increasing the half-lives of the p21/CIP1 transcript and the p21/CIP1 protein. *Biochem J* 1999; **337**: 599-606
- 13 **Xie W**, Su K, Wang D, Paterson AJ, Kudlow JE. MDA468 growth inhibition by EGF is associated with the induction of the cyclin-dependent kinase inhibitor p21WAF1. *Anticancer Res* 1997; **17**: 2627-2633
- 14 **Thomas T**, Balabhadrapathruni S, Gardner CR, Hong J, Faaland CA, Thomas TJ. Effects of epidermal growth factor on MDA-MB-468 breast cancer cells: alterations in polyamine biosynthesis and the expression of p21/CIP1/WAF1. *J Cell Physiol* 1999; **179**: 257-266
- 15 **Dangles V**, Femenia F, Laine V, Berthelemy M, Le Rhun D, Poupon MF, Levy D, Schwartz-Cornil I. Two- and three-dimensional cell structures govern epidermal growth factor survival function in human bladder carcinoma cell lines. *Cancer Res* 1997; **57**: 3360-3364
- 16 **Ichiba M**, Miyazaki Y, Kitamura S, Kiyohara T, Shinomura Y, Matsuzawa Y. Epidermal growth factor inhibits the growth of TE8 esophageal cancer cells through the activation of STAT1. *J Gastroenterol* 2002; **37**: 497-503
- 17 **Rajagopal S**, Huang S, Moskal TL, Lee BN, el-Naggar AK, Chakrabarty S. Epidermal growth factor expression in human colon and colon carcinomas: anti-sense epidermal growth factor receptor RNA down-regulates the proliferation of human colon cancer cells. *Int J Cancer* 1995; **62**: 661-667
- 18 **Chakrabarty S**, Rajagopal S, Huang S. Expression of antisense epidermal growth factor receptor RNA down-modulates the malignant behavior of human colon cancer cells. *Clin Exp Metastasis* 1995; **13**: 191-195
- 19 **Moyer JD**, Barbacci EG, Iwata KK, Arnold L, Boman B, Cunningham A, DiOrio C, Doty J, Morin MJ, Moyer MP, Neveu M, Pollack VA, Pustilnik LR, Reynolds MM, Sloan D, Theleman A, Miller P. Induction of apoptosis and cell cycle arrest by CP-358,774, an inhibitor of epidermal growth factor receptor tyrosine kinase. *Cancer Res* 1997; **57**: 4838-4848
- 20 **Lowry OH**, Rosebrough NJ, Farr A, Randall RJ. Protein measurement with the Folin phenol reagent. *J Biol Chem* 1951; **193**: 265-275
- 21 **Abe Y**, Sagawa T, Sakai K, Kimura S. Enzyme-linked immunosorbent assay (ELISA) for human epidermal growth factor (hEGF). *Clin Chim Acta* 1987; **168**: 87-95
- 22 **Boersma AW**, Nooter K, Oostrum RG, Stoter G. Quantification of apoptotic cells with fluorescein isothiocyanate-labeled annexin V in Chinese hamster ovary cell cultures treated with cisplatin. *Cytometry* 1996; **24**: 123-130
- 23 **Laemmli UK**. Cleavage of Structural proteins during the assembly of the head of bacteriophage T4. *Nature* 1970; **227**: 680-685
- 24 **Towbin H**, Staehelin T, Gordon J. Electrophoretic transfer of proteins from polyacrylamide gels to nitrocellulose sheets: procedure and some applications. *Proc Natl Acad Sci U S A* 1979; **76**: 4350-4354
- 25 **Mansbridge JN**, Ausserer WA, Knapp MA, Sutherland RM. Adaptation of EGF receptor signal transduction to three-dimensional culture conditions: changes in surface receptor expression and protein tyrosine phosphorylation. *J Cell Physiol* 1994; **161**: 374-382
- 26 **Schaerli P**, Jaggi R. EGF-induced programmed cell death of human mammary carcinoma MDA-MB-468 cells is preceded by activation AP-1. *Cell Mol Life Sci* 1988; **54**: 129-138
- 27 **Anto RJ**, Venkatraman M, Karunakaran D. Inhibition of NF-kappaB sensitizes A431 cells to epidermal growth factor-induced apoptosis, whereas its activation by ectopic expression of RelA confers resistance. *J Biol Chem* 2003; **278**: 25490-25498
- 28 **Hognason T**, Chatterjee S, Vartanian T, Ratan RR, Ernewein KM, Habib AA. Epidermal growth factor receptor induced apoptosis: potentiation by inhibition of Ras signaling. *FEBS Lett* 2001; **491**: 9-15
- 29 **Kottke TJ**, Blajeski AL, Martins LM, Mesner PW Jr, Davidson NE, Earnshaw WC, Armstrong DK, Kaufmann SH. Comparison of paclitaxel-, 5-fluoro-2'-deoxyuridine-, and epidermal growth factor (EGF)-induced apoptosis. Evidence for EGF-induced anoikis. *J Biol Chem* 1999; **274**: 15927-15936
- 30 **Cao L**, Yao Y, Lee V, Kiani C, Spaner D, Lin Z, Zhang Y, Adams ME, Yang BB. Epidermal growth factor induces cell cycle arrest and apoptosis of squamous carcinoma cells through reduction of cell adhesion. *J Cell Biochem* 2000; **77**: 569-583
- 31 **Coffey RJ Jr**, Shipley GD, Moses HL. Production of transforming growth factors by human colon cancer lines. *Cancer Res* 1986; **46**: 1164-1169
- 32 **Gazit A**, Yaish P, Gilon C, Levitzki A. Tyrosinase I: synthesis and biological activity of protein tyrosine kinase inhibitors. *J Med Chem* 1989; **32**: 2344-2352
- 33 **Chin YE**, Kitagawa M, Su WC, You ZH, Iwamoto Y, Fu XY. Cell growth arrest and induction of cyclin-dependent kinase inhibitor p21WAF1/CIP1 mediated by STAT1. *Science* 1996; **272**: 719-722

Edited by Wang XL. Proofread by Zhu LH

Expression of thymidine phosphorylase by macrophages in colorectal cancer tissues

Ji-Min Zhang, Takayuki Mizoi, Ken-Ichi Shiiba, Iwao Sasaki, Seiki Matsuno

Ji-Min Zhang, Department of Gastrointestinal Surgery, The Second Hospital of Guangzhou Medical School, Guangzhou 510260, Guangdong Province, China

Takayuki Mizoi, Ken-ichi Shiiba, Iwao Sasaki, Seiki Matsuno, The First Department of Surgery, Tohoku University School of Medicine, Sendai 980-8574, Japan

Supported by Grants-in-Aid for Scientific Research from the Ministry of Education, Culture, Sports and Technology, Japan

Correspondence to: Ji-Min Zhang, MD, PhD, Department of Gastrointestinal Surgery, the Second Hospital of Guangzhou Medical School, Guangzhou 510260, Guangdong Province, China. arthur@basil.freemail.ne.jp

Telephone: +86-20-34152263 **Fax:** +86-20-82481695

Received: 2003-08-02 **Accepted:** 2003-09-24

Abstract

AIM: To detect the thymidine phosphorylase (dThdPase) expression in human colorectal cancer tissues and cells.

METHODS: Forty specimens resected from patients with colorectal cancer were immunohistochemically stained by 654-1, anti-dThdPase monoclonal antibody, PG-M1, anti-macrophage marker CD68 monoclonal antibody. Morphometrical analysis and positive cell counting were performed. In 27 of 40 specimens, dThdPase activity was also assayed by HPLC. Otherwise, the dThdPase level was measured by ELISA in 6 colorectal cancer cell lines, LS174T, Clone A, Colo320, CX-1, Lovo, and MIP101, as well as in 2 macrophage-like cell lines, THP-1 and U937.

RESULTS: dThdPase activity was significantly increased in cancer tissues compared with adjacent normal tissue ($P < 0.01$). In immunohistochemical analysis, it was confirmed that most cells expressed dThdPase were the stromal cells surrounding cancer nests or along the invasive margin of cancer. Based on their morphometrical characteristics, we found that most of them were tumor-associated macrophages (TAMs). The number of dThdPase-positive stromal cells was significantly correlated with the number of CD68-positive macrophages ($r = 0.76$, $P < 0.0001$). By ELISA, 18.2 unit/mg and 19.3 unit/mg of dThdPase protein were detected in THP-1 and U937, but only little was detected in 6 colorectal cancer cell lines.

CONCLUSION: The present data suggest that dThdPase expression is seldom detected in colorectal carcinoma cells. TAM is the most important source of dThdPase in colorectal cancer tissues.

Zhang JM, Mizoi T, Shiiba KI, Sasaki I, Matsuno S. Expression of thymidine phosphorylase by macrophages in colorectal cancer tissues. *World J Gastroenterol* 2004; 10(4): 545-549
<http://www.wjgnet.com/1007-9327/10/545.asp>

INTRODUCTION

Thymidine phosphorylase (dThdPase) is an enzyme involved

in pyrimidine nucleoside metabolism. It could catalyze the reversible phosphorolysis of thymidine, deoxyuridine and their analogues to their bases and 2-deoxyribose-1-phosphate^[1,2]. 5'-deoxy-5-fluorouridine (5'-DFUR), a prodrug of 5-fluorouracil (5-FU), must be activated by dThdPase in cancer tissues and converted into 5-FU, resulting in induction of the anticancer activity with few side effects in normal tissues^[3]. Previous studies have demonstrated that dThdPase is identical to platelet-derived endothelial cell growth factor (PD-ECGF), which is an endothelial cell mitogen^[4,5]. dThdPase/PD-ECGF could stimulate chemotaxis of endothelial cells *in vitro* and possess angiogenic activity *in vivo*^[5-8], however, the mechanisms by which dThdPase/PD-ECGF contributes to angiogenesis are still unclear.

Studies have reported that certain solid tumors including gastric and breast cancers could express elevated levels of dThdPase as compared with normal surrounding tissues^[9-12]. Thus it is reasonable that these tumors are susceptible to 5'-DFUR. In colorectal cancer, it is controversial whether cancer cells or stromal cells are responsible for the increased dThdPase levels. Some immunohistochemical studies reported that cancer cells had dThdPase expression^[12,13], while others believed that most cells expressing dThdPase were stromal cells, especially tumor-associated macrophages (TAMs), and lymphocytes^[14,15]. Therefore, it is uncertain how 5'-DFUR exerts its anticancer activity in colorectal cancer.

As we know, dThdPase plays an important role in cell proliferation, tumor angiogenesis, and in chemotherapy with 5'-DFUR. Here we focused on the expression of dThdPase in CD68-positive TAMs in colorectal cancer tissue with immunohistochemistry and an analysis of dThdPase level in 6 colorectal cancer cell lines by ELISA.

MATERIALS AND METHODS

Tissue preparation

Resected specimens from 40 patients with colorectal cancer in the First Department of Surgery, Tohoku University School of Medicine (Sendai, Japan) were used for immunohistochemical staining. In the 40 cases, 14 were well-differentiated adenocarcinomas, 25 were moderately differentiated carcinomas, and only 1 was poorly differentiated carcinoma.

Primary antibodies

654-1, a mouse monoclonal antibody that recognizes human dThdPase, was kindly provided by Nippon Roche Research Center (Kamakura, Japan). PG-M1, an anti-macrophage marker CD68 monoclonal antibody, was purchased from DAKO (Glostrup, Denmark). Non-specific mouse IgG1 (East Acres Biologicals, Southbridge, USA) was used as a control antibody.

Cell lines

Six human colorectal cancer cell lines, LS174T, Clone A, Colo320, CX-1, Lovo, and MIP101, and two human macrophage-like cell lines, THP-1 and U937, were used in this study. LS174T was obtained from the American Type Culture Collection (Rockville, MD). Clone A, CX-1, and MIP101 were provided by Dr. JM Jessup (University of Texas,

SA, USA). Colo320, Lovo, and THP-1, a human monocytic leukemia cell line, were purchased from Riken Cell Bank. U937, a human histiocytic lymphoma cell line, was obtained from Institute of Development, Aging and Cancer, Tohoku University (Sendai, Japan). THP-1 and U937 are suspension cell lines induced by phorbol-12-myristate-13-acetate (PMA). PMA-induced THP-1 and U937 were used in various experiments as macrophage-like cells because these cells could express many of normal macrophage characteristics including phagocytosis and adherence^[16-18]. All cell lines were cultured in RPMI1640 medium supplemented with 10% fetal calf serum (FCS) and 1% L-glutamine.

dThdPase activity assay

In 40 colorectal carcinoma specimens, 27 were frozen immediately at -80°C after removal by surgery. Then they were assayed with high performance liquid chromatography (HPLC) to detect dThdPase activity by Nippon Roche Research Center^[19].

Immunohistochemical staining

Streptavidin-biotin complex (SABC) method was adopted in formalin-fixed, paraffin-embedded sections. Sections were de-paraffinized and incubated with 1% hydrogen peroxide in methanol for 15 min to block the endogenous peroxidase activity. After washed with phosphate-buffered saline (PBS), the sections were incubated with 10% normal rabbit serum for 30 min at room temperature and then incubated with primary antibodies at 1.25 µg/ml for 654-1, 3.6 µg/ml for PG-M1 and 10 µg/ml for control mouse IgG overnight at 4°C. Followed by 3 washes with PBS, the sections were incubated with a second antibody (Histofine SAB-PO (M) kit, Nichirei, Tokyo, Japan) for 120 min at room temperature. After washed with PBS, the sections were then incubated with peroxidase-conjugated streptavidin (Histofine SAB-PO kit) for 30 min at room temperature, and then developed with 3, 3'-diaminobenzidine (Dojindo, Tokyo, Japan) in 0.05M Tris buffer (pH7.64), containing 0.07% sodium azide and 0.02% hydrogen peroxide for 5 min.

Morphometrical analysis

The dThdPase-positive cells were stained brown in cytoplasm and nuclei, occasionally, brown-stained nuclei alone could also be found. CD68-positive cells were also stained brown but a little darker than dThdPase. The number of dThdPase-positive cells and CD68-positive cells was quantified as follows. In each specimen, we selected five fields where the highest density of dThdPase-positive cells was observed after searching the whole field. In each field, immunoreactive cells were counted using an ocular grid (0.25mm×0.25mm) at magnification×400. Then CD68-positive cells were similarly counted in the corresponding five fields in the serial sections. The average number of positive cells in each section was expressed per 0.0625 mm².

Detection of dThdPase protein levels

dThdPase levels in 6 colorectal cancer cells and 2 macrophage-like cells, THP-1 and U937, were measured by ELISA in the study. At least 1×10⁷ cells of each cell line were prepared for this assay and ELISA was performed by Nippon Roche Research Center. It was reported that the dThdPase levels measured by this assay correlated well with a conventional enzyme assay^[19].

Statistical analysis

The significance of differences between means of dThdPase activities in tumor group and normal tissue group was tested by Student's *t* test, and the correlation between the number of dThdPase-positive cells and CD68-positive cells was evaluated

by Spearman's correlation coefficient test, the significance level was at 0.05.

RESULTS

dThdPase activity in tumor and normal mucosal tissues

The dThdPase activity in cancer tissues was 139.7±42.2 (µg 5-FU·hr⁻¹·ml⁻¹), significantly higher as compared with 61.5±21.4 (µg 5-FU·hr⁻¹·ml⁻¹) in the surrounding normal tissues (Figure 1, *P*<0.01).

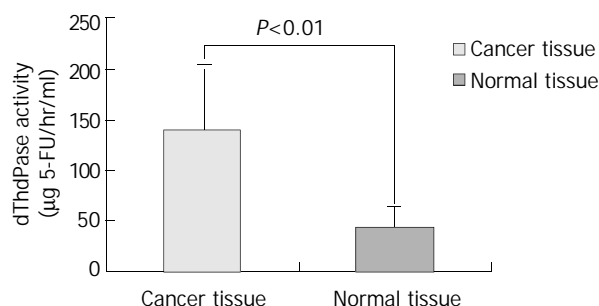


Figure 1 dThdPase activity analysis in 27 specimens of colorectal carcinoma. The dThdPase Activity was 139.7±42.2 (µg 5-FU/hr/ml) in cancer tissues, significantly higher than 61.5±21.4 (µg 5-FU/hr/ml) in adjacent normal tissue (*P*<0.01).

Immunohistochemical staining

In corresponding normal colorectal tissues, epithelial cells at the surface of mucosa were weakly immunoreactive for dThdPase and few stromal cells were positive (Figure 2A). Stromal cells were positive for dThdPase in all cancer tissues, while cancer cells were positive for dThdPase only in 3 out of the 40 cases (Figure 2B). The dThdPase-positive stromal cells were distributed mainly around the cancer nests (Figure 2C) or along the invasive margin of cancer (Figure 2D). In the corresponding areas, CD68-positive macrophages were also increased. The distribution patterns of CD68-positive cells (Figure 2E) were similar to those of the dThdPase-positive stromal cells (Figure 2F).

In the counting analysis of positive cells, the number of dThdPase-positive stromal cells was well correlated with the number of CD68-positive cells (*r*=0.76, *P*<0.0001), (Figure 3).

dThdPase levels in 6 colorectal cancer cell lines and 2 macrophage-like cell lines, were assessed by ELISA. The protein level of dThdPase was 0.5 unit/mg in LS174T, 8.9 unit/mg in Lovo, and not detected in the other 4 colorectal cancer cell lines. In macrophage-like cell lines, 18.2 unit/mg and 19.3 unit/mg of dThdPase were detected in THP-1 and U937, respectively (Table 1).

Table 1 dThdPase levels in 6 colorectal cancers cell lines and macrophage-like cell lines

	dThdPase level* (unit/mg)
Colorectal cancer cells	
LS174T	0.5
Clone A	<0.4 ^a
Colo 320	<1.1 ^a
CX-1	<0.3 ^a
Lovo	8.9
MIP101	<0.2 ^a
Macrophage-like cells	
THP-1	18.2
U937	19.3

*Figures indicate levels of detection limit.

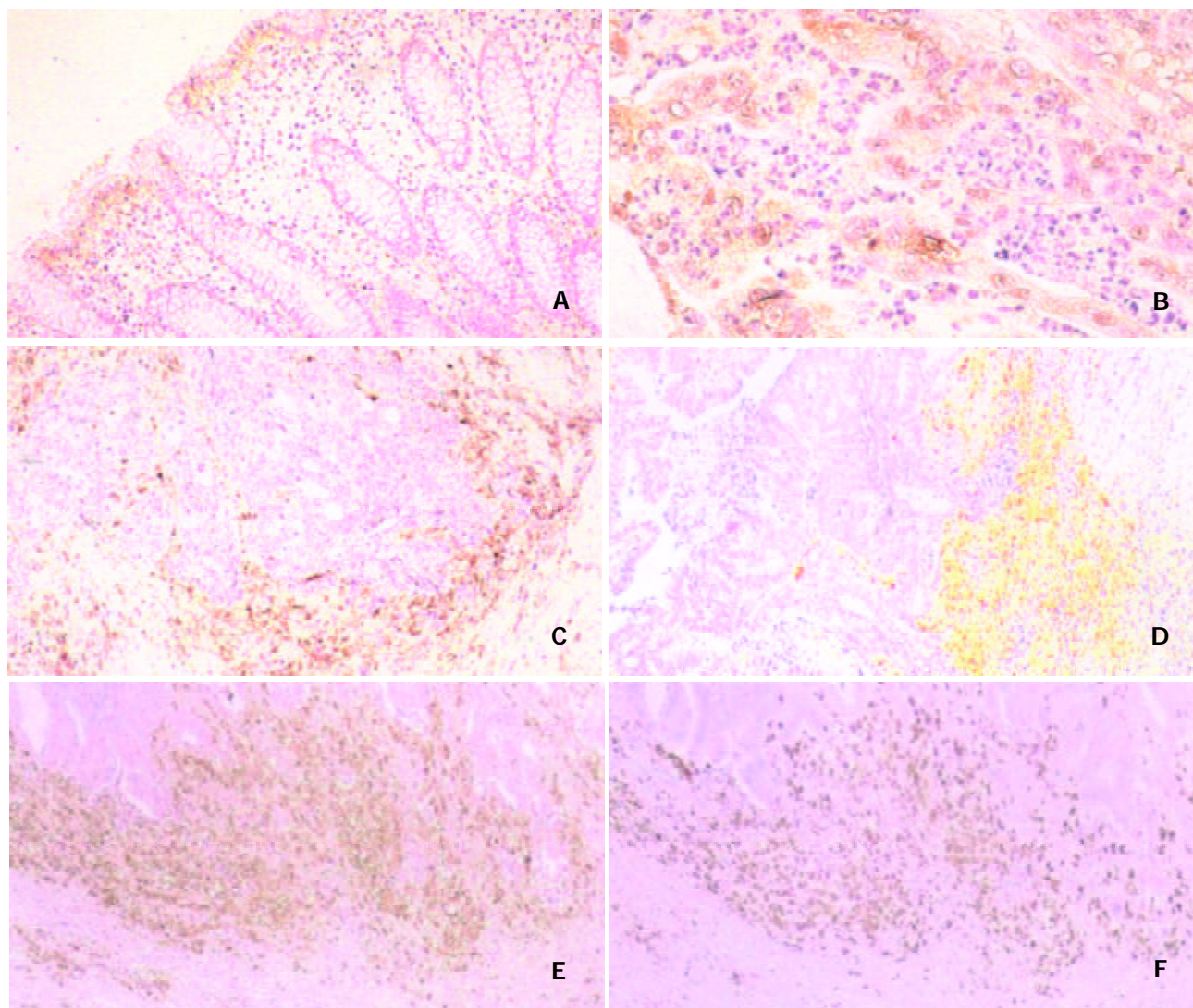


Figure 2 Immunohistochemical staining in colorectal cancer tissues. A: In normal colon mucosa, epithelial cells at the surface are weakly positive for dThdPase and few stromal cells are stained. B: In 3 of the 39 cases examined, cancer cells are positive for dThdPase. C: In most cases of colorectal cancers examined, stromal cells around the cancer nests are positive for dThdPase, while cancer cells are negative for dThdPase. D: In some cases, dThdPase-positive stromal cells are along the invasive margin of cancer, cancer cells are negative for dThdPase. E: Immunohistochemical staining for dThdPase and F: for CD68 in the corresponding area of colorectal cancer tissue. dThdPase-positive stromal cells are observed densely along the invasive margin of cancer. The distribution pattern of dThdPase-positive cells (E) is similar to that of CD68-positive cells (F).

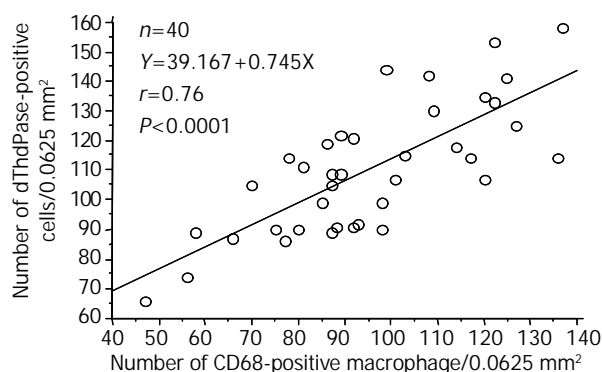


Figure 3 Correlation between number of CD68-positive macrophages and dThdPase-positive stromal cells in 40 cases of colorectal cancer. The significant correlation is judged by Spearman's coefficient rank test ($r=0.76$, $P<0.0001$).

DISCUSSION

It has been well known that dThdPase expression was selectively increased in various malignant tumor tissues

compared with adjacent normal tissues in the same organs^[9-12]. Our data of dThdPase activity analysis in cancer and normal tissues by *ELISA* are also supported the suggestion. However, the present immunohistochemical staining showed that stromal cells around the cancer nests or along the invasive margin of cancer strongly expressed dThdPase activity but few cancer cells did. A significant positive correlation was found between the number of dThdPase-positive stromal cells and CD68-positive macrophages ($r=0.76$, $P<0.0001$). We also detected certain dThdPase levels in macrophage-like cell lines, THP-1 and U937, but seldom detected it in colorectal cancer cell lines by *ELISA*. Takahashi^[20] reported that most cells stained with the same monoclonal antibody (654-1) were also positive for CD68 by double immunohistochemical staining in human colon cancer tissues, while Takebayashi^[9] reported that many colorectal cancer cells were also stained strongly as stromal cells did using the different antibody. These differences in dThdPase stained cancer cells were possibly caused by the different antibodies used, which may recognize the different epitopes. Taken together, TAMs should be a major source for dThdPase expression in colorectal carcinomas, although it's mechanism of expression in macrophage is still unclear.

Infiltration of mononuclear inflammatory cells including CD68-positive macrophages has been described as one of the important host reactions in colorectal cancer^[21]. These infiltrating cells are more abundantly distributed along the invasive margin of cancer tissues than in cancer tissues. These reports suggest that CD68-positive TAMs have various roles in interactions between host cells and cancer cells.

Macrophages belong to the mononuclear phagocyte system. They form a heterogeneous cell population and further differentiate into promonocytes and bone marrow monocytes, then enter into blood stream and migrate into tissues, where they undergo final differentiation to tissue macrophages, which are present ubiquitously in all tissues. Besides other functions, such as endocytosis, cytotoxicity, macrophages can secrete over 100 cell products. Many evidences showed that TAMs also appeared to be involved in tumor growth regulation, angiogenesis, host reaction, and antitumor immunity in various malignant tissues by some investigators^[22,23]. TAM has been found to play an important role in tumor angiogenesis by producing a number of angiogenic cytokines, including vascular endothelial growth factor (VEGF), basic fibroblast growth factor (bFGF), transforming growth factor alpha (TGF- α), tumor necrosis factor- α (TNF- α), and PD-ECGF/dThdPase^[24]. Because no macrophage cell line can pass and it is difficult to isolate macrophages, we detected the dThdPase level from macrophage-like cell lines, THP-1 and U937 instead of macrophages,

Using monoclonal antibody anti-CD68 (a macrophage marker), many investigators demonstrated that TAMs were associated with the tumor stage, invasive depth, survival, and angiogenesis in several malignancies^[12,13,15,22,25]. Therefore, CD68 is well known to be a best marker of tissue macrophages. Though it was reported that macrophages could express dThdPase in normal gastrointestinal tract tissues^[26], however, no report so far has dealt with whether colorectal carcinoma cells or macrophages express dThdPase *in vitro*, the mechanism of expression is still unknown.

It is necessary for 5'-DFUR to be converted into 5-FU by dThdPase expressed in cancer tissues during chemotherapy. De Cesare^[27] reported that the effect of 5'-DFUR on human colorectal carcinoma xenografts, it might be due to cytokines induced by TAMs, such as TNF- α , interleukin-1 α (IL-1 α), and interferon- γ (IFN- γ), resulting in an increase of dThdPase activity in cancer tissues. Some investigators have also reported that transfection of dThdPase cDNA could enhance the sensitivity of cancer cells to 5'-DFUR *in vitro*^[28-30], while our another analysis demonstrated that dThdPase was expressed in macrophage-like cells, THP-1, U937, and monocytes could modulate the conversion of 5'-DFUR into 5-FU and exert anticancer effect on 6 colorectal carcinoma cell lines^[31]. Further study is needed to investigate the mechanism, which may provide a future strategy for chemotherapy of colorectal cancer patients with 5'-DFUR.

ACKNOWLEDGEMENT

The authors would like to thank Dr. Yutaka Tanaka and Dr. Naohito Inagaki (Nippon Roche Research Center, Kamakura, Japan) for their valuable discussion and contributions to the measurement of dThdPase activity in colorectal cancer tissues with *HPLC*, and detection of dThdPase level in colorectal carcinoma cell lines and macrophage-like cell lines with *ELISA*. Also thank Ms. Emiko Shibuya and Ms. Keiko Inabe for their technical assistance.

REFERENCES

- 1 **Usuki K**, Saras J, Waltenberger J, Miyazono K, Pierce G, Thomason A, Heldin CH. Platelet-derived endothelial cell growth factor has thymidine phosphorylase activity. *Biochem Biophys Res Commun* 1992; **184**: 1311-1316
- 2 **Bodycote J**, Wolff S. Metabolic breakdown of [3H] thymidine and the inability to measure human lymphocyte proliferation by incorporation of radioactivity. *Proc Natl Acad Sci U S A* 1986; **83** (12 Pt 1): 4749-4753
- 3 **Armstrong RD**, Diasio RB. Selective activation of 5'-deoxy-5-fluorouridine by tumor cells as a basis for an improved therapeutic index. *Cancer Res* 1981; **41**: 4891-4894
- 4 **Miyazono K**, Okabe T, Urabe A, Takaku F, Heldin CH. Purification and properties of an endothelial cell growth factor from human platelets. *J Biol Chem* 1987; **262**: 4098-4103
- 5 **Ishikawa F**, Miyazono K, Hellman U, Drexler H, Wernstedt C, Hagiwara K, Usuki K, Takaku F, Risau W, Heldin CH. Identification of angiogenic activity and the cloning and expression of platelet-derived endothelial cell growth factor. *Nature* 1989; **338**: 557-562
- 6 **Furukawa T**, Yoshimura A, Sumizawa T, Haraguchi M, Akiyama S, Fukui K, Ishizawa M, Yamada Y. Angiogenic factor. *Nature* 1992; **356**: 668
- 7 **Haraguchi M**, Miyadera K, Uemura K, Sumizawa T, Furukawa T, Yamada K, Akiyama S, Yamada Y. Angiogenic activity of enzymes. *Nature* 1994; **368**: 198
- 8 **Miyadera K**, Sumizawa T, Haraguchi M, Yoshida H, Konstanty W, Yamada Y, Akiyama S. Role of thymidine phosphorylase activity in the angiogenic effect of platelet derived endothelial cell growth factor/thymidine phosphorylase. *Cancer Res* 1995; **55**: 1687-1690
- 9 **Takebayashi Y**, Yamada K, Miyadera K, Sumizawa T, Furukawa T, Kinoshita F, Aoki D, Okumura H, Yamada Y, Akiyama S, Aikou T. The activity and expression of thymidine phosphorylase in human solid tumours. *Eur J Cancer* 1996; **32A**: 1227-1232
- 10 **Maeda K**, Kang SM, Ogawa M, Onoda N, Sawada T, Nakata B, Kato Y, Chung YS, Sowa M. Combined analysis of vascular endothelial growth factor and platelet-derived endothelial cell growth factor expression in gastric carcinoma. *Int J Cancer* 1997; **74**: 545-550
- 11 **Toi M**, Ueno T, Matsumoto H, Saji H, Funata N, Koike M, Tominaga T. Significance of thymidine phosphorylase as a marker of protumor monocytes in breast cancer. *Clin Cancer Res* 1999; **5**: 1131-1137
- 12 **Takebayashi Y**, Akiyama S, Akiba S, Yamada K, Miyadera K, Sumizawa T, Yamada Y, Murata F, Aikou T. Clinicopathologic and prognostic significance of an angiogenic factor, thymidine phosphorylase, in human colorectal carcinoma. *J Natl Cancer Inst* 1996; **88**: 1110-1117
- 13 **Amaya H**, Tanigawa N, Lu C, Matsumura M, Shimomatsuya T, Horiuchi T, Muraoka R. Association of vascular endothelial growth factor expression with tumor angiogenesis, survival and thymidine phosphorylase/platelet-derived endothelial cell growth factor expression in human colorectal cancer. *Cancer Lett* 1997; **119**: 227-235
- 14 **Haba A**, Monden T, Sekimoto M, Ikeda K, Izawa H, Kanou T, Amano M, Kan'yama H, Monden M. PyNPase expression in human colon cancer. *Cancer Lett* 1998; **122**: 85-92
- 15 **Matsumura M**, Chiba Y, Lu C, Amaya H, Shimomatsuya T, Horiuchi T, Muraoka R, Tanigawa N. Platelet-derived endothelial cell growth factor/thymidine phosphorylase expression correlated with tumor angiogenesis and macrophage infiltration in colorectal cancer. *Cancer Lett* 1998; **128**: 55-63
- 16 **Kurosaka K**, Watanabe N, Kobayashi Y. Production of proinflammatory cytokines by phorbol myristate acetate-treated THP-1 cells and monocyte-derived macrophages after phagocytosis of apoptotic CTLL-2 cells. *J Immunol* 1998; **161**: 6245-6249
- 17 **Schwende H**, Fitzke E, Ambs P, Dieter P. Differences in the state of differentiation of THP-1 cells induced by phorbol ester and 1, 25-dihydroxyvitamin D3. *J Leukoc Biol* 1996; **59**: 555-561
- 18 **Hass R**, Bartels H, Topley N, Hadam M, Kohler L, Goppelt-Strube M, Resch K. TPA-induced differentiation and adhesion of U937 cells: changes in ultrastructure, cytoskeletal organization and expression of cell surface antigens. *Eur J Cell Biol* 1989; **48**: 282-293

- 19 **Nishida M**, Hino A, Mori K, Matsumoto T, Yoshikubo T, Ishitsuka H. Preparation of anti-human thymidine phosphorylase monoclonal antibodies useful for detecting the enzyme levels in tumor tissues. *Biol Pharm Bull* 1996; **19**: 1407-1411
- 20 **Takahashi Y**, Bucana CD, Liu W, Yoneda J, Kitadai Y, Cleary KR, Ellis LM. Platelet-derived endothelial cell growth factor in human colon cancer angiogenesis: role of infiltrating cells. *J Natl Cancer Inst* 1996; **88**: 1146-1151
- 21 **Hakansson L**, Adell G, Boeryd B, Sjogren F, Sjodahl R. Infiltration of mononuclear inflammatory cells into primary colorectal carcinomas: an immunohistological analysis. *Br J Cancer* 1997; **75**: 374-380
- 22 **Toritsu H**, Ono M, Kiryu H, Furue M, Ohmoto Y, Nakayama J, Nishioka Y, Sone S, Kuwano M. Macrophage infiltration correlates with tumor stage and angiogenesis in human malignant melanoma: possible involvement of TNF- α and IL-1 α . *Int J Cancer* 2000; **85**: 182-188
- 23 **Ueno T**, Toi M, Saji H, Muta M, Bando H, Kuroi K, Koike M, Inadera H, Matsushima K. Significance of macrophage chemoattractant protein-1 in macrophage recruitment, angiogenesis, and survival in human breast cancer. *Clin Cancer Res* 2000; **6**: 3282-3289
- 24 **Lewis CE**, Leek R, Harris A, McGee JO. Cytokine regulation of angiogenesis in breast cancer: the role of tumor-associated macrophages. *J Leukoc Biol* 1995; **57**: 747-751
- 25 **Leek RD**, Lewis CE, Whitehouse R, Greenall M, Clarke J, Harris AL. Association of macrophage infiltration with angiogenesis and prognosis in invasive breast carcinoma. *Cancer Res* 1996; **56**: 4625-4629
- 26 **Fox SB**, Moghaddam A, Westwood M, Turley H, Bicknell R, Gatter KC, Harris AL. Platelet-derived endothelial cell growth factor/thymidine phosphorylase expression in normal tissues: an immunohistochemical study. *J Pathol* 1995; **176**: 183-190
- 27 **De Cesare M**, Pratesi G, De Braud F, Zunino F, Stampino CG. Remarkable antitumor activity of 5'-deoxy-5-fluorouridine in human colorectal tumor xenografts. *Anticancer Res* 1994; **14**: 549-554
- 28 **Kato Y**, Matsukawa S, Muraoka R, Tanigawa N. Enhancement of drug sensitivity and a bystander effect in PC-9 cells transfected with a platelet-derived endothelial cell growth factor thymidine phosphorylase cDNA. *Br J Cancer* 1997; **75**: 506-511
- 29 **Kanyama H**, Tomita N, Yamano T, Miyoshi Y, Ohue M, Fujiwara Y, Sekimoto M, Sakita I, Tamaki Y, Monden M. Enhancement of the anti-tumor effect of 5'-deoxy-5-fluorouridine by transfection of thymidine phosphorylase gene into human colon cancer cells. *Jpn J Cancer Res* 1999; **90**: 454-459
- 30 **Evrard A**, Cuq P, Robert B, Vian L, Pelegrin A, Cano JP. Enhancement of 5-fluorouracil cytotoxicity by human thymidine-phosphorylase expression in cancer cells: *in vitro* and *in vivo* study. *Int J Cancer* 1999; **80**: 465-470
- 31 **Zhang J**, Mizoi T, Harada N, Shiiba K, Miyagawa K, Matsuno S, Sasaki I. Thymidine phosphorylase expressed in macrophages enhances antitumor effect of 5'-deoxy-5-fluorouridine on human colorectal carcinoma cells. *Anticancer Res* 2003; **23**: 323-329

Edited by Wu XW and Wang XL

Correlation of N-myc downstream-regulated gene 1 overexpression with progressive growth of colorectal neoplasm

Zhen Wang, Fang Wang, Wei-Qi Wang, Qian Gao, Wan-Li Wei, Yun Yang, Guo-Ying Wang

Zhen Wang, Fang Wang, Qian Gao, Yun Yang, Guo-Ying Wang,
Department of Pathology, Kunming Medical College, Kunming
650031, Yunnan Province, China

Wei-Qi Wang, Wan-Li Wei, Department of Pathology, the Third
Affiliated Hospital, Kunming Medical College, Kunming 650031,
Yunnan Province, China

Correspondence to: Dr. Fang Wang, Department of Pathology,
Kunming Medical College, 191 Renmin xilu, Kunming 650031,
Yunnan Province, China. wangfang_01@hotmail.com

Telephone: +86-871-5338845 **Fax:** +86-871-5709112-810

Received: 2003-06-21 **Accepted:** 2003-08-16

Abstract

AIM: To study the function of N-myc downstream-regulated gene 1 (NDRG1) in colorectal carcinogenesis and its correlation with tumor lymph node metastasis.

METHODS: NDRG1 was detected at its protein level by immunohistochemistry (IHC) and image analysis (IA), and NDRG1 mRNA was detected by *in situ* hybridization (ISH) in formalin-fixed and paraffin-embedded sections with a total of 190 specimens including 38 normal colorectal mucosae, 31 colorectal adenomas, 45 non-metastatic colorectal carcinomas (CRCs), 38 metastatic primary CRC and subsequently regional lymph nodes respectively. At the same time, the correlations of NDRG1 with sex, age of patients and histological types of colorectal carcinomas were observed.

RESULTS: NDRG1 proteins were gradually increased in colorectal carcinogenesis ($P < 0.05$ or $P < 0.01$). There was a significant difference in the expression of NDRG1 between non-metastatic and metastatic CRCs ($P < 0.05$), and the correlation was positive ($P < 0.01$, $r_s = 0.329$). However, there was no obvious difference in the expression of NDRG1 between the primary sites of CRCs and that in the metastatic sites of corresponding regional lymph nodes, nor was there an apparent difference in sex, age, and histological types. The expression of NDRG1 mRNA was generally in concordance with that of NDRG1 protein.

CONCLUSION: NDRG1 gene may play an important role in colorectal carcinogenesis. In addition, NDRG1 may be a putative tumor metastasis promoter gene and is regarded as one of the molecular biological markers that can forecast early metastasis of CRCs. NDRG1 gene in the metastatic sites of regional lymph nodes may preserve its expression characteristics in the primary sites of CRCs to some extent. The expression of NDRG1 is not affected by sex, age and histological types. The role of NDRG1 in tumor metastatic process can be demonstrated by *in vivo* and *in vitro*.

Wang Z, Wang F, Wang WQ, Gao Q, Wei WL, Yang Y, Wang GY. Correlation of N-myc downstream-regulated gene 1 overexpression with progressive growth of colorectal neoplasm. *World J Gastroenterol* 2004; 10(4): 550-554
<http://www.wjgnet.com/1007-9327/10/550.asp>

INTRODUCTION

N-myc downstream-regulated gene 1 (NDRG1) has been repeatedly isolated by different laboratories under different physiological conditions, and it was also called, human RTP (reducing agents and tunicamycin-responsive protein)^[1], Drg1 (differentiation related gene 1)^[2], cap43 (calcium activated protein)^[3], rit42 (reduced in tumor, 42kDa)^[4], PROXY-1 (protein regulated by OXYen-1)^[5], and the mouse homologue, designated Ndr1^[6], TDD5^[7], the rat homologue, designated Bdm1^[8]. In addition, mammalian NDRG1 has homologues in a wide variety of species, including zebra-fish, fruit fly, nematode, sunflower, *Arabidopsis thaliana*. The gene was later officially designated NDRG1 by the HUGO Gene Nomenclature Committee^[9]. Therefore, we used NDRG1 throughout this report. NDRG1 has been mapped to human chromosome 8q24.2^[10,11] and has a length of approximately 60 kb. NDRG1 cDNA contains an open-reading frame of 1 182 bp that encodes a cytoplasmic 43-kDa protein containing a tandem repeat of ten amino acids (GTRSRSTSE)^[12]. NDRG1 is one of the four members of a new gene family, which does not contain any protein motif with known functions^[13,14].

Guan *et al*^[15] investigated NDRG1 with 8 colon cancer cell lines and 10 colon cancer specimens. They reported that overexpression of NDRG1 induced morphological and molecular changes which were consistent with colon cancer cell differentiation and suppressed *in vitro* invasion and *in vivo* liver metastasis in nude mice. They proposed that NDRG1 suppress colon cancer metastasis by inducing colon cancer cell differentiation and partially reversing the metastatic phenotype, and suggested that NDRG1 might be a putative metastatic suppressor gene in human colon cancer. However, there are still no reports about the study of this gene in large samples of CRCs and progressive growth of colorectal cancer.

In the present report, we detected NDRG1 protein by immunohistochemistry (IHC), and NDRG1 mRNA by *in situ* hybridization (ISH) in patients with colorectal adenomas, non-metastatic and metastatic CRCs, as well as their corresponding regional lymph node metastatic sites and normal colorectal mucosa, to study its functions in colorectal carcinogenesis and its correlation with tumor lymph node metastasis.

MATERIALS AND METHODS

Materials

Specimens obtained from surgical resections, mucosa biopsies of colon and autopsies with a postmortem autolysis period of less than 24 h, were fixed in 10% formalin, embedded in paraffin, and stained by routine HE. They were divided into 5 groups: normal colorectal mucosa used as controls ($n=38$), colorectal adenomas ($n=31$), non-metastatic CRCs ($n=45$), metastatic CRCs ($n=38$) and their corresponding regional lymph node metastatic sites ($n=38$). Two pathologists examined all the specimens. The diagnosis of colorectal neoplasm was made according to the WHO's criteria in 2000^[16].

Methods

Immunohistochemistry Immunohistochemistry S-P method

was used to detect NDRG1 protein. Professor Bosman FT generously provided rabbit polyclonal antibody and immunostaining S-P kit was purchased from Fuzhou Maxim Biotechnical Company. Immunohistochemistry was performed as follows. (1) Four-micron sections of human tissues were deparaffinized by xylene, dehydrated in graded alcohol. Endogenous peroxidase activity was blocked with 3% H₂O₂ in methanol at room temperature for 15 min. (2) To retrieve the immunoreactivity, tissue sections were boiled twice in 10 mM sodium citrate, pH 6.0 for 5 min in an 800-W microwave oven. (3) Then, non-specific staining was blocked by incubating in normal non-immune serum at room temperature for 10 min. (4) The rabbit anti-NDRG1 was added to adjacent tissue sections and incubated overnight at 4°C. (5) Biotin-conjugated second antibody was added to the sections and incubated at room temperature for 10 min. (6) S-P complex was added at room temperature for 10 min and DAB was used for the color reaction, and then the slides were counterstained with hematoxylin. The tissue sections were washed with PBS (0.01M, pH 7.4) between each step. Positive and negative controls were simultaneously used to ensure the specificity and reliability of staining. The positive result showed yellow or brown coloration in cytoplasm and /or plasma membranes.

The degree of NDRG1 staining was estimated by semi-quantitative evaluation and categorized by the extent and intensity of staining as follows^[17]: (1) The extent of positive cells was estimated as 0=positive staining cells ≤5%, 1=positive staining cells in 6-25%, 2=positive staining cells in 26-50%, 3=positive staining cells in 51-75%, 4=positive staining cells >75%. (2) The intensity of staining was scored as 0=achromatic, 1=light yellow, 2=yellow, 3=brown. Combined staining score was used to evaluate the results of NDRG1 staining. The extent of positive cells was multiplied by the intensity of staining and scored as follows: (-)=0, (+)=1-4, (++)=5-8, (+++)=9-12. Two independent assessors unaware of the patient outcome carried out this semi-quantitative analysis.

Image analysis The immunostained sections were examined by using an Olympus microscope (×200) coupled to a video camera, connected to a computer-aided color video image analysis (VIA) system. After being captured and digitized onto the video screen, microscopic images were quantitatively analyzed by using an image analysis software program (HPIAS-1000, Microsoft Windows hosted image analysis system). We selected positive unit (PU)^[18] as the quantitatively analysis parameters. The higher the PU value was, the stronger the intensity of immunostaining.

Preparation of NDRG1 cDNA probe and *in situ* hybridization NDRG1 cDNA plasmid (1 ng/μl) was also a gift generously provided by Professor Bosman FT. We transformed bacteria JM109 and amplified NDRG1 cDNA plasmid, digested by KpnI and XbaI (Figure 1). The resulting NDRG1 cDNA fragment (nucleotide from 958 to 2 875, 1.9 kb) was labeled with biotin by using a random primer DNA biotinylation kit (TaKaRa Biotechnology Co., Ltd) according to the manufacturer's protocol. The concentration of NDRG1 cDNA probe was approximately 30 ng/μl.

In situ hybridization was used for the detection of NDRG1 mRNA. ISH-kit was purchased from Medical Faculty, Peking University. The main steps were as follows. (1) Four-micron sections of human tissues were deparaffinized by xylene, dehydrated in graded alcohol' treated with 0.1 N HCl at room temperature for 10 min and digested with proteinase K at 37°C for 15 min. (2) The biotin-labeled NDRG1 cDNA probe was added to adjacent tissue sections and incubated in a humidity chamber overnight at 4°C. (3) Then, non-specific staining was blocked by incubating in normal non-immune serum at room

temperature for 45 min. (4) SP-AP complex was added at 37°C for 1 h. (5) The substrate (BCIP/NBT) showed coloration at room temperature for 10-40 min, or till the coloration was developed and then the slides were counterstained with nuclear fast red. Positive and negative controls were simultaneously used to ensure the specificity and reliability of the staining. A known NDRG1 mRNA positive tissue section was taken as positive control while hybridization liquids without probe were used to replace the NDRG1 cDNA probe as negative control. The positive result showed blue coloration in the cytoplasm and was graded as follows^[19]. (-) negative, (+) a small quantity of scattering positive granules, (++) a large quantity of thick positive granules, (+++) positive granules distributed widely in a cluster. Expression of NDRG1 mRNA was compared with that of NDRG1 immunoreactivity to investigate the correlation between the two stainings.

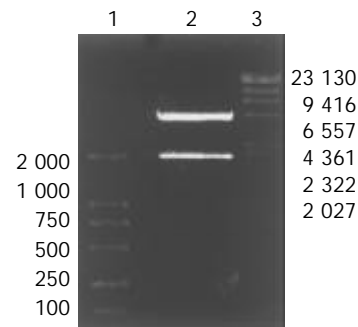


Figure 1 Electrophoretogram of NDRG1 cDNA plasmid cut by enzymes KpnI and XbaI. 1. DNA marker DL2000, 2. Products digested by KpnI and XbaI, 3. DNA marker λHindIII.

Statistical analysis

With statistical package for social science (SPSS) version 10.0, rank sum test was used to calculate the enumeration data, the measurement data were analyzed by one-way ANOVA. A Spearman's correlation coefficient was used for correlations between markers. $P < 0.05$ was considered statistically significant, all reported P values were two-sided.

RESULTS

Detection of NDRG1 protein

Immunoreactivity was not observed in negative control. In normal colorectal mucosa the surface epithelial cells were mainly stained and the majorities were yellow micro-granules located in the cytoplasm and/or plasma membranes while crypt cells were negative. In colorectal neoplasm, the positive staining showed yellow or brown coloration in the cytoplasm and /or plasma membranes distributed in scatter or in a cluster (Figures 2-3). The immunostaining results of all groups are summarized in Tables 1-3 and Figure 4. The correlation between the expression of NDRG1 and lymph node metastasis in CRCs is summarized in Table 4.

NDRG1 proteins were gradually increased in colorectal carcinogenesis ($P < 0.05$ or $P < 0.01$). There was a significant difference in expression of NDRG1 between non-metastatic and metastatic CRCs ($P < 0.05$) and the correlation was positive ($P < 0.01$, $r_s = 0.329$). That is, the higher the NDRG1 protein expression, the greater the possibility of lymph node metastasis. However, there was no obvious difference in expression of NDRG1 between the primary sites of CRCs and that in the metastatic sites corresponding regional lymph nodes. There was a good correlation between color VIA and semi quantitative evaluation of NDRG1 immune reactivity, confirming the validity of quantitative analysis.

Table 1 Comparison between positive rate and positive unit (PU) of NDRG1 protein in all groups

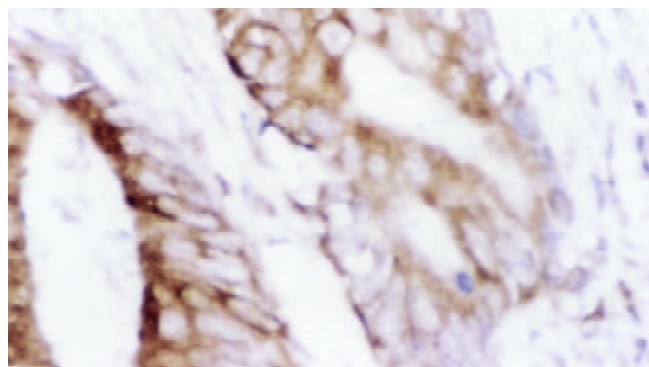
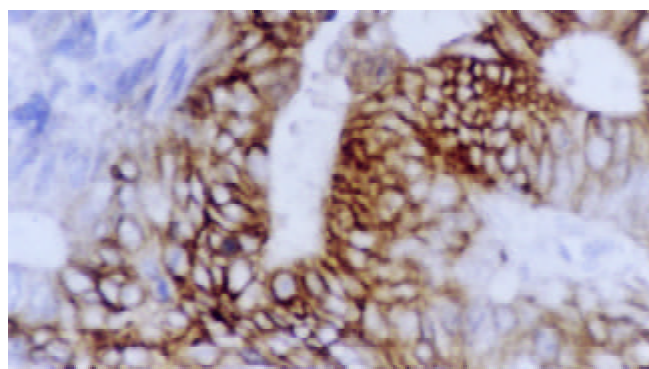
Group	Cases	Positive number and percentage					Positive unit mean±SD
		-	+	++	+++	%	
Normal colorectal mucosa	38	17	21	0	0	55.26	45.34±5.66
Colorectal adenomas	31	6	18	6	1	80.65	48.35±4.79
Non-metastatic CRCs	45	2	24	19	0	95.56	51.62±4.63
Metastatic CRCs	38	0	14	18	6	100.00	54.38±4.39
Regional lymph node metastatic sites	38	2	9	24	3	94.74	54.73±4.56

Table 2 Comparison of positive rates of NDRG1 protein in all groups (*P* value)

Group	Normal colorectal mucosa	Colorectal adenomas	Non-metastatic CRCs	Metastatic CRCs	Regional lymph node metastatic sites
Normal colorectal mucosa	--	^b <i>P</i> <0.01	^b <i>P</i> <0.01	^b <i>P</i> <0.01	^b <i>P</i> <0.01
Colorectal adenomas	^b <i>P</i> <0.01	--	^c <i>P</i> <0.05	^d <i>P</i> <0.01	^d <i>P</i> <0.01
Non-metastatic CRCs	^b <i>P</i> <0.01	^c <i>P</i> <0.05	--	^e <i>P</i> <0.05	^f <i>P</i> <0.01
Metastatic CRCs	^b <i>P</i> <0.01	^d <i>P</i> <0.01	^e <i>P</i> <0.05	--	
Regional lymph node metastatic sites	^b <i>P</i> <0.01	^d <i>P</i> <0.01	^f <i>P</i> <0.01		--

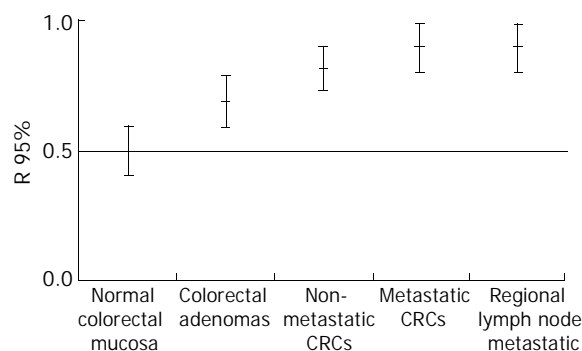
Table 3 Comparison of positive units (PU) of NDRG1 protein in all groups (*P* value)

Group	Normal colorectal mucosa	Colorectal adenomas	Non-metastatic CRCs	Metastatic CRCs	Regional lymph node metastatic sites
Normal colorectal mucosa	--	^a <i>P</i> <0.05	^b <i>P</i> <0.01	^b <i>P</i> <0.01	^b <i>P</i> <0.01
Colorectal adenomas	^a <i>P</i> <0.05	--	^d <i>P</i> <0.01	^d <i>P</i> <0.01	^d <i>P</i> <0.01
Non-metastatic CRCs	^b <i>P</i> <0.01	^d <i>P</i> <0.01	--	^e <i>P</i> <0.05	^f <i>P</i> <0.01
Metastatic CRCs	^b <i>P</i> <0.01	^d <i>P</i> <0.01	^e <i>P</i> <0.05	--	
Regional lymph node metastatic sites	^b <i>P</i> <0.01	^d <i>P</i> <0.01	^f <i>P</i> <0.01		--

**Figure 2** Expression of NDRG1 in cytoplasm of non-metastatic CRC. SP×200.**Figure 3** Overexpression of NDRG1 in cytoplasm of metastatic CRC. SP×200.**Detection of NDRG1 mRNA**

NDRG1 mRNA was not observed in negative control. The

positive results showed blue coloration in the cytoplasm distributed in scatter or in a cluster (Figures 5- 6). The expression of NDRG1 mRNA was generally in concordance with the expression of NDRG1 protein. However, the intensity of NDRG1 mRNA expression was weaker than that of NDRG1 protein. The positive cell percentage of NDRG1 mRNA expression was less than that of NDRG1 protein.

**Figure 4** Comparison of NDRG1 protein expressions in all groups.**Table 4** Correlation between expression of NDRG1 and lymph node metastasis in CRCs

Expression of NDRG1	LN (-)	LN (+)
-	2	0
+	24	14
++	19	18
+++	0	6
<i>P</i> value	<0.01	
Spearman correlation coefficient	0.329	

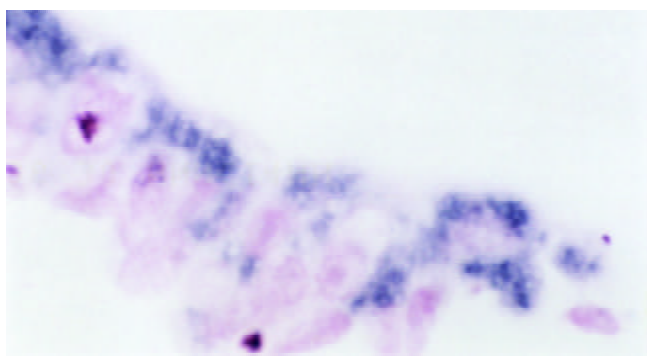


Figure 5 Expression of NDRG1 mRNA in cytoplasm of non-metastatic CRC. ISH×400.

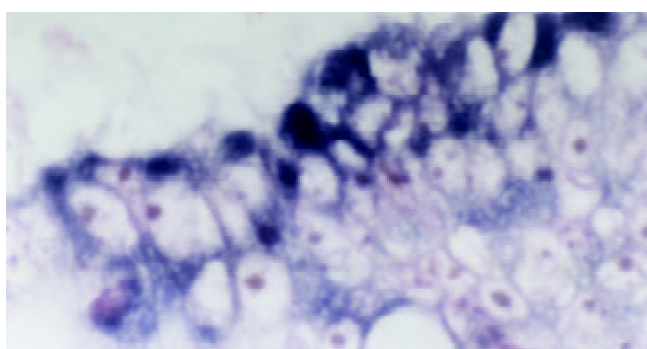


Figure 6 Overexpression of NDRG1 mRNA in cytoplasm of metastatic CRC. ISH×400.

Correlation of NDRG1 expression with clinicopathological parameters

The associations between NDRG1 expression in cancerous tissues and clinicopathologic variables are summarized in Table 5. There was no significant difference of NDRG1 expression in patients' age, sex, and tumor histological types.

Table 5 Association of clinicopathologic variables with NDRG1 expression in CRCs

	No. of cases	-	+	++	+++
Sex					
Male	51	1	26	20	4
Female	32	1	12	17	2
Age (years)					
<55	41	1	18	18	4
≥55	42	1	20	19	2
Histological differentiation					
High differentiation	23	2	10	11	0
Moderate differentiation	47	0	23	20	4
Poor differentiation	13	0	5	6	2

DISCUSSION

CRC is one of the most common malignant tumors in China. In the last decades, the incidence of CRC has been increasing^[19-22] and some reports indicate that the mortality of CRC has been increasing due to the early metastases. Because the dispensable nature of the colon allows removal of primary tumors, the prognosis of colon cancer was directly correlated with the extent of tumor invasion and metastases^[23]. How to diagnose and prevent early tumor metastasis was one of the most important topics in recent tumor studies. Molecules involved in cancer metastasis might serve as markers for early detection of metastasis, prognostic judgment and/or as targets for

therapeutic intervention^[24,25].

Most studies showed that NDRG1 was involved in cellular growth^[4,26-28], differentiation^[29-31], tumorigenesis^[32], metastasis^[14] and poor clinical outcome of some tumor^[33]. Our study showed that in normal colon NDRG1 protein was expressed mainly on the surface of epithelial cells that border the gut lumen, and the result was in accordance with recent reports^[12], indicating that NDRG1 protein was expressed late during differentiation, just before apoptosis and shedding of cells into the colon lumen.

There are many debates about the expression of NDRG1 in CRCs and other carcinomas. It was reported that NDRG1 gene was down regulated in several tumor cell lines and breast cancer, prostate cancer^[4,34,35] and renal cancer^[36]. In addition, Van Belzen *et al.*^[2] reported that compared to normal colon mucosa, NDRG1 mRNA expression was decreased in colon adenomas and adenocarcinoma. However, some studies^[37,38] indicated that in a variety of cancers, including lung, brain, melanoma, liver, prostate, breast, and renal cancers, NDRG1 protein was over-expressed in cancer cells. We observed that NDRG1 proteins were gradually increased during colorectal carcinogenesis (normal colorectal mucosa→colorectal adenomas→non-metastatic CRC→metastatic CRC) ($P<0.05$ or $P<0.01$), suggesting that NDRG1 gene might play an important role in colorectal carcinogenesis.

Okuda *et al.*^[14] reported that NDRG1 stable transfection of SW620 metastatic colon cancer cell line with Drg1 cDNA induced morphological changes and down-regulated metastatic colon cancer cells to nearly undetectable levels when compared with primary colon cancer. However, we observed different experimental results and found that there was a significant difference in expression of NDRG1 between non-metastatic and metastatic CRCs ($P<0.05$), and the correlation was positive ($P<0.01$, $r_s=0.329$), indicating that NDRG1 could not inhibit the metastatic ability. On the contrary, NDRG1 might play a role in promoting CRC regional lymph node metastasis. Our results combined with previous data on the NDRG1 gene products^[37-39] suggested that NDRG1 might be a putative tumor metastasis promoter gene and one of the molecular biological markers forecasting early metastasis of CRCs.

There was no obvious difference in expression of NDRG1 between the primary sites of CRCs and those in the metastatic sites of corresponding regional lymph nodes, nor was there an apparent difference in sex, age, and histological types, suggesting that NDRG1 gene in the metastatic sites of regional lymph nodes might still preserve its expressive characteristics in the primary sites of CRCs to some extent and the expression of NDRG1 might not be affected by these clinic pathologic variables.

The expression of NDRG1 mRNA was generally in concordance with the expression of NDRG1 protein. However, the intensity of NDRG1 mRNA expression was weaker than that of NDRG1 protein and the positive cell percentage of NDRG1 mRNA expression was less than that of NDRG1 protein. The discrepancies between mRNA expression and protein levels indicate that regulation at transcriptional, and the translational level might support the recent report^[35].

ACKNOWLEDGEMENTS

We would like to thank Professor Bosman FT and Dr. Pascale Lachat for their generously providing the NDRG1 antiserum and cDNA. We also want to thank Mrs. Wen Wang, Shuang Yang, and Xi-Nan Cao for their expert technical assistance. This publication represents the thesis work of Zhen Wang at Kunming Medical College.

REFERENCES

- 1 **Kokame K**, Kato H, Miyata T. Homocysteine-respondent genes

- in vascular endothelial cells identified by differential display analysis. GRP78/BiP and novel genes. *J Biol Chem* 1996; **271**: 29659-29665
- 2 **van Belzen N**, Dinjens WN, Diesveld MP, Groen NA, van der Made AC, Nozawa Y, Vlietstra R, Trapman J, Bosman FT. A novel gene which is up-regulated during colon epithelial cell differentiation and down-regulated in colorectal neoplasms. *Lab Invest* 1997; **77**: 85-92
- 3 **Zhou D**, Salnikow K, Costa M. Cap43, a novel gene specifically induced by Ni²⁺ compounds. *Cancer Res* 1998; **58**: 2182-2189
- 4 **Kurdistani SK**, Arizti P, Reimer CL, Sugrue MM, Aaronson SA, Lee SW. Inhibition of tumor cell growth by RTP/rit42 and its responsiveness to p53 and DNA damage. *Cancer Res* 1998; **58**: 4439-4444
- 5 **Park H**, Adams MA, Lachat P, Bosman F, Pang SC, Graham CH. Hypoxia induces the expression of a 43-kDa protein (PROXY-1) in normal and malignant cells. *Biochem Biophys Res Commun* 2000; **276**: 321-328
- 6 **Shimono A**, Okuda T, Kondoh H. N-myc-dependent repression of ndr1, a gene identified by direct subtraction of whole mouse embryo cDNAs between wild type and N-myc mutant. *Mech Dev* 1999; **83**: 39-52
- 7 **Lin TM**, Chang C. Cloning and characterization of TDD5, an androgen target gene that is differentially repressed by testosterone and dihydrotestosterone. *Proc Natl Acad Sci U S A* 1997; **94**: 4988-4993
- 8 **Yamauchi Y**, Hongo S, Ohashi T, Shioda S, Zhou C, Nakai Y, Nishinaka N, Takahashi R, Takesa F, Takeda M. Molecular cloning and characterization of a novel developmentally regulated gene, Bdm1, showing predominant expression in postnatal rat brain. *Brain Res Mol Brain Res* 1999; **68**: 149-158
- 9 **Wang Z**, Wang GY, Wang F. The relationship between N-myc downstream regulated gene 1 and neoplasms. *Zhonghua Binglixue Zazhi* 2003; **32**: 162-164
- 10 **van Belzen N**, Dinjens WN, Eussen BH, Bosman FT. Expression of differentiation-related genes in colorectal cancer: possible implications for prognosis. *Histol Histopathol* 1998; **13**: 1233-1242
- 11 **Kalaydjieva L**, Nikolova A, Turnev I, Petrova J, Hristova A, Ishpekova B, Petkova I, Shmarov A, Stancheva S, Middleton L, Merlini L, Trogu A, Muddle JR, King RH, Thomas PK. Hereditary motor and sensory neuropathy-Lom, a novel demyelinating neuropathy associated with deafness in gypsies: clinical, electrophysiological and nerve biopsy findings. *Brain* 1998; **121**: 399-408
- 12 **Lachat P**, Shaw P, Gebhard S, van Belzen N, Chaubert P, Bosman FT. Expression of NDRG1, a differentiation-related gene, in human tissues. *Histochem Cell Biol* 2002; **118**: 399-408
- 13 **Zhou RH**, Kokame K, Tsukamoto Y, Yutani C, Kato H, Miyata T. Characterization of the human NDRG gene family: a newly identified member, NDRG4, is specifically expressed in brain and heart. *Genomics* 2001; **73**: 86-97
- 14 **Okuda T**, Kondoh H. Identification of new genes ndr2 and ndr3 which are related to Ndr1/RTP/Drg1 but show distinct tissue specificity and response to N-myc. *Biochem Biophys Res Commun* 1999; **266**: 208-215
- 15 **Guan RJ**, Ford HL, Fu Y, Li Y, Shaw LM, Pardee AB. Drg-1 as a differentiation-related, putative metastatic suppressor gene in human colon cancer. *Cancer Res* 2000; **60**: 749-755
- 16 **Hamilton SR**, Aaltonen LA, eds. World Health Organization classification of tumors. Pathology and genetics of tumors of the digestive system. Lyon, France: IARC press, 2000: 103-143 [http://emice.nci.nih.gov/emice/mouse_models/organ_models/gastro_models/human_colorectal_cancer#1.2]
- 17 **Cao LY**, Zhang HF, Gong XY, Meng G. p53 and bcl-2 oncoprotein expression in colorectal tumor. *Linchuang Yu Shiyuan Binglixue Zazhi* 2000; **16**: 214-216
- 18 **Shen H**. Study on the quantitative method of immunohistochemistry (III). *Zhongguo Zuzhi Huaxue Yu Xibao Huaxue Zazhi* 1995; **4**: 89-91
- 19 **Fang SG**, Yang JZ, Yang F. Clinical characteristics of 610 cases with multiple primary malignant neoplasm's in digestive tract. *Shijie Huaren Xiaohua Zazhi* 1999; **7**: 812
- 20 **Wang MR**, Guo CH, Li MS, Yu GP, Yin XS, Cui GP, Geng CY, Yang JL. A case-control study on the dietary risk factors of upper digestive tract cancer. *Zhonghua Liuxingbingxue Zazhi* 1999; **20**: 95-97
- 21 **Yu BM**, Zhao R. Molecular biology of colorectal carcinoma. *Shijie Huaren Xiaohua Zazhi* 1999; **7**: 173-175
- 22 **Chen SY**, Wu TF, Liu HY, Wang JY, Zhang SS, Zhang XD. Hospital-based ten-year data of gastroendoscopy. *Shijie Huaren Xiaohua Zazhi* 1999; **7**: 15-17
- 23 **Liu LX**, Zhang WH, Jiang HC. Current treatment for liver metastases from colorectal cancer. *World J Gastroenterol* 2003; **9**: 193-200
- 24 **Zhao P**, Hu YC, Talbot IC. Expressing patterns of p16 and CDK4 correlated to prognosis in colorectal carcinoma. *World J Gastroenterol* 2003; **9**: 2202-2206
- 25 **Xiong B**, Yuan HY, Hu MB, Zhang F, Wei ZZ, Gong LL, Yang GL. Transforming growth factor- β 1 in invasion and metastasis in colorectal cancer. *World J Gastroenterol* 2002; **8**: 674-678
- 26 **Kokame K**, Kato H, Miyata T. Nonradioactive differential display cloning of genes induced by homocysteine in vascular endothelial cells. *Methods* 1998; **16**: 434-443
- 27 **Taketomi Y**, Sugiki T, Saito T, Ishii S, Hisada M, Suzuki-Nishimura T, Uchida MK, Moon TC, Chang HW, Natori Y, Miyazawa S, Kikuchi-Yanoshita R, Murakami M, Kudo I. Identification of NDRG1 as an early inducible gene during in vitro maturation of cultured mast cells. *Biochem Biophys Res Commun* 2003; **306**: 339-346
- 28 **Agarwala KL**, Kokame K, Kato H, Miyata T. Phosphorylation of RTP, an ER stress-responsive cytoplasmic protein. *Biochem Biophys Res Commun* 2000; **272**: 641-647
- 29 **Qu X**, Zhai Y, Wei H, Zhang C, Xing G, Yu Y, He F. Characterization and expression of three novel differentiation-related genes belong to the human NDRG gene family. *Mol Cell Biochem* 2002; **229**: 35-44
- 30 **Piquemal D**, Joulia D, Balaguer P, Basset A, Marti J, Commes T. Differential expression of the RTP/Drg1/Ndr1 gene product in proliferating and growth arrested cells. *Biochim Biophys Acta* 1999; **1450**: 364-373
- 31 **Kyuno J**, Fukui A, Michiue T, Asashima M. Identification and characterization of Xenopus NDRG1. *Biochem Biophys Res Commun* 2003; **309**: 52-57
- 32 **Gomez-Casero E**, Navarro M, Rodriguez-Puebla ML, Larcher F, Paramio JM, Conti CJ, Jorcano JL. Regulation of the differentiation-related gene Drg-1 during mouse skin carcinogenesis. *Mol Carcinog* 2001; **32**: 100-109
- 33 **Li J**, Kretzner L. The growth-inhibitory Ndr1 gene is a Myc negative target in human neuroblastomas and other cell types with overexpressed N- or C-myc. *Mol Cell Biochem* 2003; **250**: 91-105
- 34 **Bandyopadhyay S**, Pai SK, Gross SC, Hirota S, Hosobe S, Miura K, Saito K, Commes T, Hayashi S, Watabe M, Watabe K. The Drg-1 gene suppresses tumor metastasis in prostate cancer. *Cancer Res* 2003; **63**: 1731-1736
- 35 **Segawa T**, Nau ME, Xu LL, Chilukuri RN, Makarem M, Zhang W, Petrovics G, Sesterhenn IA, McLeod DG, Moul JW, Vahey M, Srivastava S. Androgen-induced expression of endoplasmic reticulum (ER) stress response genes in prostate cancer cells. *Oncogene* 2002; **21**: 8749-8758
- 36 **Masuda K**, Ono M, Okamoto M, Morikawa W, Otsubo M, Migita T, Tsuneyoshi M, Okuda H, Shuin T, Naito S, Kuwano M. Downregulation of Cap43 gene by von Hippel-Lindau tumor suppressor protein in human renal cancer cells. *Int J Cancer* 2003; **105**: 803-810
- 37 **Cangul H**, Salnikow K, Yee H, Zagzag D, Commes T, Costa M. Enhanced expression of a novel protein in human cancer cells: a potential aid to cancer diagnosis. *Cell Biol Toxicol* 2002; **18**: 87-96
- 38 **Cangul H**, Salnikow K, Yee H, Zagzag D, Commes T, Costa M. Enhanced overexpression of an HIF-1/hypoxia-related protein in cancer cells. *Environ Health Perspect* 2002; **110**(Suppl 5): 783-788
- 39 **Salnikow K**, Costa M, Figg WD, Blagosklonny MV. Hyperinducibility of hypoxia-responsive genes without p53/p21-dependent checkpoint in aggressive prostate cancer. *Cancer Res* 2000; **60**: 5630-5634

Abdominal aorta transplantation after programmed cryopreservation

Song Gu, Chang-Jian Liu, Tong Qiao, Xue-Mei Sun, Jun-Hao Chen

Song Gu, Chang-Jian Liu, Tong Qiao, Department of Vascular Surgery, Gulou Hospital, Affiliated Hospital of Medical College, Nanjing University, Nanjing 210008, Jiangsu Province, China

Xue-Mei Sun, Jun-Hao Chen, Scientific Research Department, Gulou Hospital, Affiliated Hospital of Medical College, Nanjing University, Nanjing 210008, Jiangsu Province, China

Supported by the Natural Science Foundation of Jiangsu Province, China, No. BK2003010; the Special Scientific Research Fund of Nanjing, Jiangsu Province, China, No. ZKS0012

Correspondence to: Dr. Song Gu, Department of Vascular Surgery, Gulou Hospital, Affiliated Hospital of Medical College, Nanjing University, Nanjing 210008, Jiangsu Province, China. njgusong@sohu.com

Telephone: +86-25-3685061 **Fax:** +86-25-3317016

Received: 2003-08-06 **Accepted:** 2003-10-07

Abstract

AIM: To study the morphologic and cellular immunologic changes after homologous transplantation of the abdominal aorta in rats after programmed cryopreservation (-196°C).

METHODS: Abdominal aorta was harvested from anesthetized Sprague Dawley (SD) rats for cryopreservation (group B) or immediate implantation (group A). The survival rates and apoptotic rates of aortic endothelial cells (ECs) were examined. The patency rates, histology and cellular immunologic changes of the abdominal aorta were examined on days 1, 3, 7, 14, 30, 60 after transplantation respectively.

RESULTS: The survival rate of ECs after programmed cryopreservation was $90.1 \pm 1.79\%$, about 3.4% lower than that of uncryopreservation ($93.5 \pm 1.96\%$). The apoptotic rates of ECs was increased after cryopreservation (7.15% vs 4.86%, $P < 0.05$). The patency rate of group B was significantly higher than that of group A ($91.6 \pm 12.9\%$ vs $62.5 \pm 26.2\%$, $P < 0.01$). CD4/CD8 ratio, TCR $\alpha\beta$ and CD11b/CD18 ratio of group B were significantly lower than those of group A ($P < 0.05$). Revivification of the cryopreserved abdominal aorta showed normal adventitia and intact smooth muscle cells.

CONCLUSION: Cryopreservation can reduce homologous abdominal aortic antigenicity. Even if without administration of immunosuppressive agents, it is still feasible to implement homologous artery grafting in rats.

Gu S, Liu CJ, Qiao T, Sun XM, Chen JH. Abdominal aorta transplantation after programmed cryopreservation. *World J Gastroenterol* 2004; 10(4): 555-559

<http://www.wjgnet.com/1007-9327/10/555.asp>

INTRODUCTION

Since the first implantation, human allograft vessels have been widely used for surgical treatment of vascular diseases^[1]. Approximately 1.5 million vascular reconstitutions are done each year in the United States^[2]. Great sphenoid veins are commonly used in coronary artery bypass and peripheral

vascular surgery^[3]. Arteries are candidates in the management of arterial infection^[4] and offer superior patency rates compared with veins^[5]. The availability of autologous fresh material is often limited and there is a definite need for cryopreserved substitutes. The long-term preservation of small-caliber arterial allografts has benefited from the improvement in organ harvesting and can be further improved by the advance of other cryobiology techniques^[6].

Preservation of vascular grafts at low temperatures using dimethyl sulfoxide (DMSO) as a cryoprotectant (CPA) has been repeatedly reported to be satisfactory after long-term storage. It has been reported that the mechanical properties of grafts and the functions of smooth muscle cells could be adequately preserved^[7] but the endothelium was often somehow compromised^[8]. Both the intact smooth muscle and endothelial cells are required to obtain full patency^[9] and impairment of either of these structures will alter the complete vessel functions. Relations between the viability of vascular endothelial cells at time of implantation and immunologic rejection are the subject of debate and remain poorly understood.

We therefore designed an abdominal aorta allograft model in rats, replicating and comparing in the same animal model most clinical and experimental situations, from fresh aortic autografts to cryopreserved allografts and studied the effects of cryopreservation on the survival rates and apoptotic rates of aortic endothelial cells (ECs), histology and the cellular immunologic changes.

MATERIALS AND METHODS

Experimental animals

Male or female Sprague Dawley rats (Laboratory Animal Center No. SCXK2002-0031 Jiangsu Province) weighing 250 g to 300 g were used as donors and recipients. They were housed in pathogen-free conditions with a 12 h light-dark cycle and were allowed to drink water. Animal care and the experimental protocol were in compliance with the guidelines of the European Community Standards on the Care and Use of Laboratory Animals (No.28871-22A9). The SD rats were fixed in the supine position^[10], and anesthetized with 100 mg/kg ketamine and the abdomen was opened with a median incision. The abdominal aorta with a diameter of 1.5 mm was dissociated. Then the blood stream was blocked, and the abdominal aorta was transected and washed with heparin saline. The aortic anastomosis was performed with 8/0 proline. The incision was sewed up and the rat was given 200 000 units of penicillin intramuscularly qd for 3 days.

Cryopreservation and thawing processes

The arteries were harvested according to sterile principle and "non-touch" technique^[11] and immersed in the culture medium RPMI1640 (Life Technologies, Gibco BRL.) with 20% fetal bovine serum (FBS) and 15% DMSO (Amresco Co.) contained in a beaker and kept at 4°C for 1 h. Programmed cryopreservation was performed in a biological freezer (Thermo Forma Co.) from 20°C to -100°C , following the cooling curve established by Gournier *et al*^[12,13]. The curve involved several stages of controlled time and temperature, and was designed to achieve a mean cooling rate of $1^{\circ}\text{C}/\text{min}$. Once frozen, aortic segments were stored in liquid nitrogen

(-196°C).

Before operation, frozen aortic segments were taken out of the liquid nitrogen and stored at RT for 5 min. Then they were incubated at 37°C in a water bath for 5 min and stored in RPMI1640 with 20% FBS.

Experimental design

The following groups were established. Control group (group A) included 24 fresh abdominal aortic segments and cryopreservation group (group B) included 24 abdominal aortic segments cryopreserved. Every four rats of two groups were sacrificed on days 1, 3, 7, 14, 30 and 60 after transplantation and the patency rate of the transplanted arteries was observed. The blood samples were collected from inferior vena cava and the donor arteries were harvested for examination.

Morphology

All transplanted aortae were observed for vascular patency^[14] and processed for pathologic study by light microscopy (LM). Specimens for LM were fixed by immersion in 10% formaldehyde and embedded in paraffin to obtain 5 µm-thick cuts. Sections were deparaffinated, hydrated, and stained with hematoxylin-eosin, Masson's trichrome stain and orcein.

Flow cytometric analysis

The survival and apoptotic rates of ECs were determined by propidium iodide (PI) and annexin V staining. Endothelial cells of abdominal aorta in rats were digested by 0.25% trypsin at 37°C for 20 min and fixed with ice-cold 70% ethanol at a cell density of $1 \times 10^6 \text{ ml}^{-1}$. PI and annexin V were then added and incubated with cells in the dark for 30 min until detection by flow cytometry^[15].

Monoclonal antibody (10 µl) (Simultest anti-CD4 and anti-CD8, anti-TCR α β^[16], Immunotech Co., anti-CD11b and anti-CD18^[17], Serotec Co., Simultest control (Becton-Dickinson)) was added to tubes with 25 µl whole blood (heparin anticoagulated). The tubes were incubated at 37°C in the dark for 30 min and 1 ml of lysing solution was added. After 15 min lysing time, the cells were washed twice with PBS and then 200 µl of fixation buffer (2% formaldehyde + 0.1% sodium azide in PBS (pH 7.4)) was added. The samples were thereafter kept at 4°C until they were analyzed by flow cytometer (FACSCalibur, BD Co.)^[18].

Statistical analysis

The data were expressed as mean±SD. Besides a two-sided Student test with a level of significance at 5%, a multiple-factor ANOVA (Tukey's test) was performed to analyze the difference between the two groups. All the data were analyzed with the statistical software SPSS10.0.

RESULTS

Survival rate and apoptotic rate of ECs in two groups

The survival rate of ECs without cryopreservation was $93.5 \pm 1.96\%$ and that of ECs with cryopreservation was $90.1 \pm 1.79\%$. But the apoptotic rate of uncryopreserved ECs was $4.86 \pm 0.252\%$ and that of cryopreserved ECs was $7.15 \pm 0.422\%$. There was a significant difference between the two groups ($n=4$, $P<0.05$).

Patency condition at each time point of two groups

Generally, all the external appearances of the arteries were normal, but the dissepiments were stiff and the intima was thickened, especially in group A. The inner-walls of vessels were smooth and had no mural thrombus. The patency rates of all six time points in group B were higher than those in group A (Table 1).

Table 1 Aortic patency of groups A and B after transplantation

Group	Patency/total number of aortae at each time point (days)						Patency rate (%)
	1	3	7	14	30	60	
A	4/4	3/4	3/4	2/4	2/4	1/4	62.5 ± 26.2
B	4/4	4/4	4/4	4/4	3/4	3/4	91.6 ± 12.9

Group A vs group B, $P<0.01$.

Subpopulation of T cells and TCRαβ

After transplantation, the number of CD4⁺ T cells was dramatically increased and reached the peak at 4 weeks post-transplantation. In the following days, the number of CD4⁺ T cells was maintained at a higher level. On the contrary, the number of CD8⁺ T cells was decreased. The ratio of CD4⁺/CD8⁺ was the highest at 4 weeks and there was a significant difference between groups A and B ($n=4$, $P<0.05$, Figure 1). The expression of TCRαβ was up-regulated soon after transplantation and the tendency of which was similar to that of the ratio CD4⁺/CD8⁺. There was also a significant difference between groups A and B. ($n=4$, $P<0.05$, Figure 2).

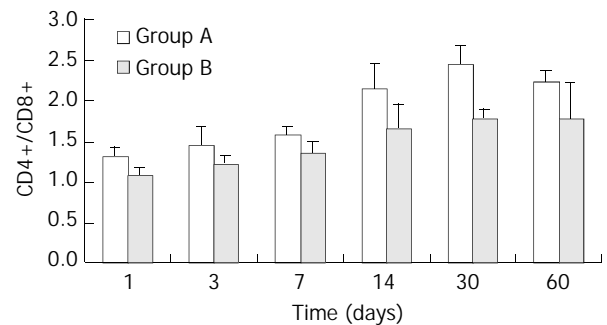


Figure 1 CD4⁺/CD8⁺ expression of groups A and B after transplantation ($n=4$).

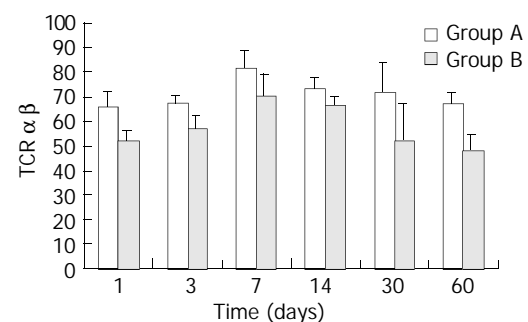


Figure 2 TCR α β expression in T cells of groups A and B after transplantation ($n=4$).

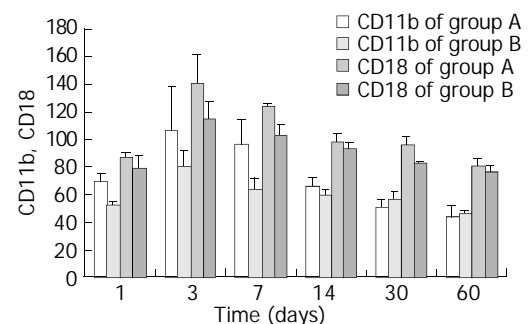


Figure 3 CD11b and CD18 expression on PMNs of groups A and B after transplantation ($n=4$).

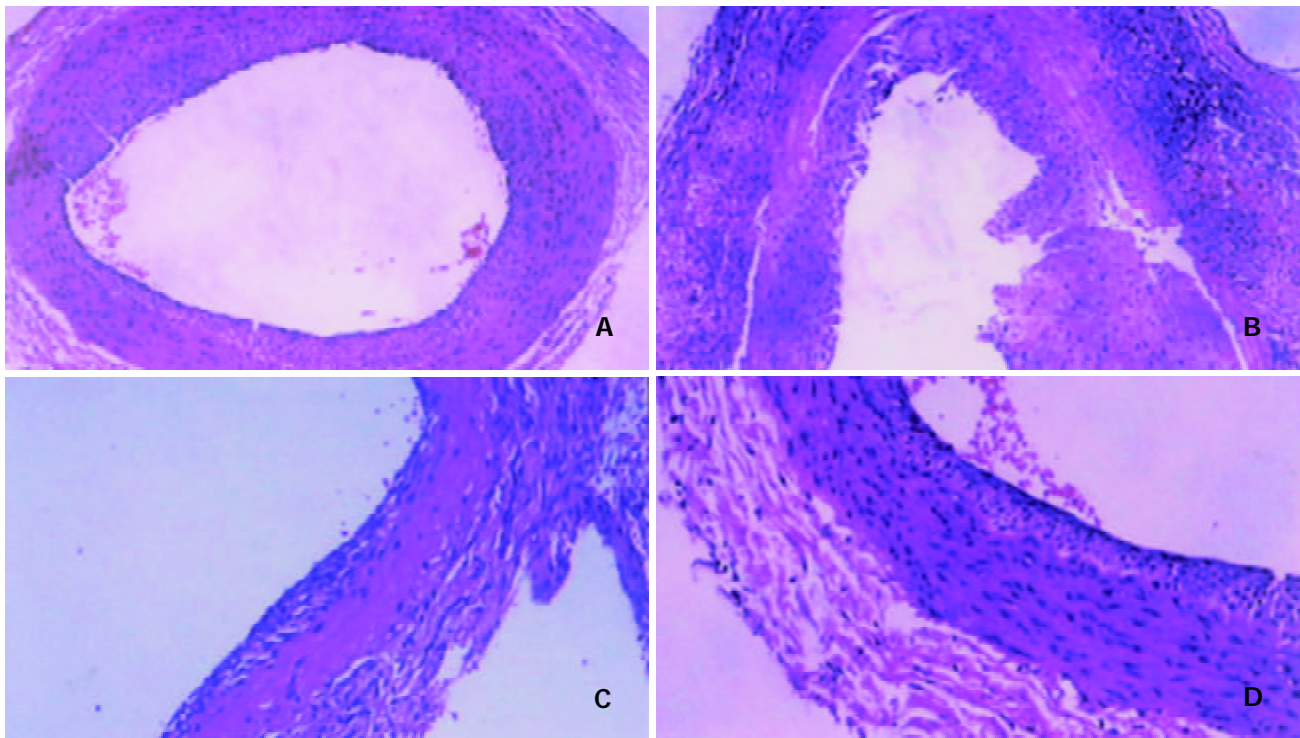


Figure 4 HE staining of abdominal aorta in rats after transplantation. A: Infiltration of T cells at 4 weeks in group A ($\times 100$), B: Excessively thickened intima at 8 weeks in group A ($\times 100$), C: Completely recovered ECs of cryopreserved aorta at 4 weeks in group B ($\times 100$), D: Intact and slightly thickened intima at 8 weeks in group B ($\times 100$).

Ratio of CD11b/CD18

The CD11b/CD18 ratio of the two groups after operation was increased. There was a significant difference at each time point between groups A and B ($n=4$, $P<0.05$, Figure 3).

Pathological and histological changes

Severe fragmental necrosis was observed in the intima of group A. The distribution of inflammatory cells in arteries was intensive, most of them intruded into tunica adventitia and media. Hyperplasia occurred in the intima 4 weeks after operation, smooth muscles in the media were thickened and the lumen of blood vessels became narrow. The intima was thickened excessively 8 weeks after operation and the lumen of blood vessels was markedly narrowed. Calcification and necrosis were observed in parts of the media. In group B few necrosis and fragments were observed and there was no obvious hyperplasia of smooth muscle in the media. ECs recovered completely and the intima remained intact and the intima of aorta was thickened slightly 4 and 8 weeks respectively after operation (Figure 4).

DISCUSSION

Methods of cryopreservation and thawing

Many methods could be used for the cryopreservation and thawing of blood vessel tissues^[19-21]. In our study, we cryopreserved the aorta using the biologic freezer with controlled rate and medium containing RPMI1640, 20% calf serum, and 15% DMSO was used as the protective agent. So the formation of ice crystals in tissues and cells was decreased, the thermal stress caused by the dilution shock and the temperature were also decreased, hence the damage to the vessels was minimally reduced. Some studies indicated that vascular endothelial cells cryopreserved by the biologic freezer with controlled rate could achieve a survival rate from 70% to 90%^[22-24]. Besides, these cryopreserved cells had similar proliferation and antithrombotic functions as normal cells after

revival^[25]. It was indicated that the competence of abdominal aorta in rats was almost entirely preserved in our stud, while the increase of apoptosis in group B was thought to be related with cryopreservation.

Cellular immunologic change after transplantation

Among all components of vascular dissepiment including ECs, smooth muscle cells (SMCs), elastic fibers and collagen fibers, ECs have the strongest antigenicity, which can offer all essential signals that result in the activation of T cells. Therefore, ABO blood type and histocompatibility should be determined and better in combination with the use of immuno-suppressive drugs. The correlation between immunosuppression and long-term patency rate has been confirmed in animal experiments. In our study we found that cell-mediated immunity caused by allografts was reduced dramatically in group B. T cell subpopulation changed after transplantation. Many sensitized CD4⁺ T cells entered into the peripheral blood and CD8⁺ T cells gathered at the part of grafts to perform the cytolytic function. The pathological study indicated that cellular immunologic reaction in group B was slight as compared with that in group A. The reduction of immunogenicity in group B might be related with the decrease of antigenicity and the adhesive ability of resuscitated ECs and the shedding of ECs caused by the brushing of blood stream.

The expression of CD11b/CD18 on the surface of polymorphonuclear leukocytes (PMNs) was gradually increased after transplantation, suggesting the activation of PMN. Recent studies have shown that white blood cells play an important role in the proliferation of SMCs and activated PMNs can promote activation of platelets, proliferation of SMCs, release of oxygen-derived free radicals and inhibition of nitrogen monoxide (NO) secreted by Ecs. Besides, the decrease of NO synthesis could reduce the inhibition of CD11b/CD18 expression, which reinforces the interaction between PMNs and Ecs through a feedback mechanism^[26]. Our study demonstrated that the lumens of aortas in group A were

markedly narrower than those in group B, but the expression of CD11b/CD18 on PMNs in group A was significantly higher than that in group B. It was confirmed that PMNs could take part in the process of vascular remodeling after transplantation, and the activation of PMNs was closely correlated with the restenosis and cellular immune rejection of allografts.

Effect evaluation

There were many reports about experiments of vascular allografting^[27,28]. Chaw *et al*^[29] reported that arteries had a patency rate of 84% 1 to 3 months after transplantation. Pratt *et al*^[30] found that arterial allografts had a patency rate of 93% 2 months after operation. Raman *et al*^[31] reported only 30% arterial patency rate in homologous transplantation 8 weeks after operation with the same method. We used DMSO as the cryoprotectant in programmed cryopreservation of abdominal aorta in rats and found the survival rate of ECs was 90.1% after cryopreservation. Some ECs were brushed out because of blood stream impact, but the remaining live ECs inhibited thrombosis formation after operation. Meanwhile cryopreservation decreased antigenicity of vascular allografts and cellular immune rejection and PMN infiltration, which would greatly promote the allograft restenosis after transplantation. The patency rate of group B was 91.6% 8 weeks after operation, which was significantly higher than that of group A.

The most obvious change of allografts after preservation and thawing was the rapid recovery of vascular endothelial cells and slight proliferation of SMCs intermedium. The recovery of ECs after cryopreservation was helpful to reduce thrombosis. The relative intact endothelium partly reduced excessive repair process after injury of blood vessels and excessive proliferation of SMCs intermedium. The recovered ECs were possibly from the hyperplasia of rest live ECs in donor arteries, the constitution of hyperplasia in recipients^[33-35] and the sedimentation of circulating Ecs on vascular walls. Our study showed that ECs of cryopreserved aorta recovered completely 4 weeks after transplantation and the endometrium hyperplasia was mild, while in group A the recovery of ECs was not complete 4 weeks after operation and the hyperplasia of vascular endometrium was severe and proliferation of SMCs intermedium was marked 8 weeks after operation.

Our study showed that ECs of the cryopreserved donor arteries still had strong activity at the time of homologous grafting. Due to the brushing of blood stream, a few ECs were shedded. But the rest live ECs still inhibited the formation of thrombus. Because of cryopreservation, the antigenicity of transplanted arteries, the cellular immune reaction and infiltration of PMNs were decreased. So the incidence of restenosis after homologous transplantation was greatly reduced.

In conclusion, the antigenicity of transplanted aorta can be decreased due to programmed cryopreservation and homologous transplantation of abdominal aorta can be performed in rats.

ACKNOWLEDGMENT

The authors thank Lei-Lei Chen, Li Lei and Le Zhang in Scientific Research Department for their technical assistance.

REFERENCES

- 1 **Concha M**, Casares J, Ross DN, Gonzalez-Lavin L, Franco M, Mesa D, Legarra JJ, Merino C, Garcia Jimenez MA, Roman M, Munoz I, Alados P, Chacon A. Aortic valve replacement with a pulmonary autograft (the Ross operation) in adult and pediatric patients. A preliminary study. *Rev Esp Cardiol* 1999; **52**: 113-120
- 2 **Langer R**, Vacanti JP. Tissue engineering. *Science* 1993; **260**: 920-926
- 3 **Cooper GJ**, Underwood MJ, Deverall PB. Arterial and venous conduits for coronary artery bypass. A current review. *Eur J Cardiothorac Surg* 1996; **10**: 129-140
- 4 **Vogt PR**, von Segesser LK, Goffin Y, Pasic M, Turina MI. Cryopreserved arterial homografts for *in situ* reconstruction of mycotic aneurysms and prosthetic graft infection. *Eur J Cardiothorac Surg* 1995; **9**: 502-506
- 5 **Gournier JP**, Adham M, Favre JP, Raba M, Bancel B, Lepetit JC, Barral X. Cryopreserved arterial homografts: preliminary study. *Ann Vasc Surg* 1993; **7**: 503-511
- 6 **Motomura N**, Eishi K, Kitoh H, Kawazoe K, Kitoh Y, Kawashima Y, Oka T. Cell viability of aortic allografts after long-term cryopreservation and clinical application to aortic root replacement in a patient with aortitis. *Cardiovasc Surg* 1995; **3**: 231-234
- 7 **Adham M**, Gournier JP, Favre JP, De La Roche E, Ducerf C, Baulieux J, Barral X, Pouyet M. Mechanical characteristics of fresh and frozen human descending thoracic aorta. *J Surg Res* 1996; **64**: 32-34
- 8 **Stanke F**, Riebel D, Carmine S, Cracowski JL, Caron F, Magne JL, Egelhoffer H, Bessard G, Devillier P. Functional assessment of human femoral arteries after cryopreservation. *J Vasc Surg* 1998; **28**: 273-283
- 9 **Furchgott RF**, Zawadzki JV. The obligatory role of endothelial cells in the relaxation of arterial smooth muscle by acetylcholine. *Nature* 1980; **288**: 373-376
- 10 **Schmitz-Rixen T**, Berwanger C, Lohe-Quast A, Addicks K, Hilgers RD, Pichlmaier H. Immunosuppression and cryopreservation of arterial allografts. *Vasa Suppl* 1992; **35**: 169-172
- 11 **Song YC**, Hunt CJ, Pegg DE. Cryopreservation the common carotid artery of the rabbit. *Cryobiology* 1994; **31**: 317-329
- 12 **Gournier JP**, Favre JP, Gay JL, Barral X. Cryopreserved arterial allografts for limb salvage in the absence of suitable saphenous vein: two-year results in 20 cases. *Ann Vasc Surg* 1995; **9**(Suppl): S7-14
- 13 **Mesa F**, Serra JM, Herreros J. Vascular cryopreservation in microsurgery. *J Reconstr Microsurg* 1997; **13**: 245-250
- 14 **Saito S**, Fukushima N, Kobayashi Y, Tori M, Tsukamoto Y, Shirakura R. Effects of cryopreservation of aortic xenografts on graft patency and immunogenicity. *Transplant Proc* 2000; **32**: 2398-2400
- 15 **Park JC**, Sung HJ, Lee DH, Park YH, Cho BK, Suh H. Specific determination of endothelial cell viability in the whole cell fraction from cryopreserved canine femoral veins using flow cytometry. *Artif Organs* 2000; **24**: 829-833
- 16 **Smith E**, De Young NJ, Drew PA. Immune cell subpopulations in regenerated splenic tissue in rats. *Aust N Z J Surg* 1999; **69**: 522-525
- 17 **Ng CJ**, Chen JC, Chiu DF, Chen MF, Chen HM. Role of prostacyclin on microcirculation in endotoxin-induced gastroprotection in rats: a microdialysis study. *Shock* 2002; **17**: 334-338
- 18 **Woo EY**, Chu CS, Goletz TJ, Schlienger K, Yeh H, Coukos G, Rubin SC, Kaiser LR, June CH. Regulatory CD4(+)CD25(+) T cells in tumors from patients with early-stage non-small cell lung cancer and late-stage ovarian cancer. *Cancer Res* 2001; **61**: 4766-4772
- 19 **Komorowska-Timek E**, Zhang F, Shi DY, Lineaweaver WC, Buncke HJ. Effect of cryopreservation on patency and histological changes of arterial isogeneic and allogeneic grafts in the rat model. *Ann Plast Surg* 2002; **49**: 404-409
- 20 **Showalter D**, Durham S, Sheppeck R, Berceci S, Greisler H, Brockbank K, Makaroun M, Webster M, Steed D, Siewers R. Cryopreserved venous homografts as vascular conduits in canine carotid arteries. *Surgery* 1989; **106**: 652-659
- 21 **Gottlob R**, Stockinger L, Gestring GF. Conservation of veins with preservation of viable endothelium. *J Cardiovasc Surg* 1982; **23**: 109-116
- 22 **Skop B**, Urbanek T, Bursig H, Ziája K, Wilczok T. The effect of prolonged ischaemia and cryopreservation on the cell viability of human aortic and femoral artery allografts. *Folia Histochem Cytobiol* 2002; **40**: 217-218

- 23 **Wusteman MC**, Pegg DE. Differences in the requirements for cryopreservation of porcine aortic smooth muscle and endothelial cells. *Tissue Eng* 2001; **7**: 507-518
- 24 **Rudderman RH**, Guyuron B, Mendelsohn G. The fate of fresh and preserved, noncrushed and crushed autogenous cartilage in the rabbit model. *Ann Plast Surg* 1994; **32**: 250-254
- 25 **Bambang LS**, Mazzucotelli JP, Moczar M, Beaujean F, Loisan D. Effects of cryopreservation on the proliferation and anticoagulant activity of human saphenous vein endothelial cells. *J Thorac Cardiovasc Surg* 1995; **110**(4 Pt 1): 998-1004
- 26 **Page CS**, Holloway N, Smith H, Yacoub M, Rose ML. Alloproliferative response of purified CD4+ and CD8+ T cells to endothelial cells in the absence of contaminating accessory cells. *Transplantation* 1994; **57**: 1628-1637
- 27 **Callow AD**. Arterial homografts. *Eur J Vasc Endovasc Surg* 1996; **12**: 272-281
- 28 **Orosz CG**, Pelletier RP. Chronic remodeling pathology in grafts. *Curr Opin Immunol* 1997; **9**: 676-680
- 29 **Chow SP**, So YC, Chan CW. Experimental microarterial grafts: freeze-dried allografts versus autografts. *Br J Plast Surg* 1983; **36**: 345-347
- 30 **Pratt MF**, Bank HL, Schmehl M, Horton WD. Freeze-dried microarterial replacement allografts in rabbits. *Laryngoscope* 1989; **99**(10 Pt 1): 1020-1026
- 31 **Raman J**, Hargrave JC. Freeze-dried microarterial allografts. *Plast Reconstr Surg* 1990; **85**: 248-251
- 32 **Jacobsen IA**, Pegg DE, Starklint H, Chemnitz J, Hunt C, Barfort P, Diaper MP. Effect of cooling and warming rate on glycerolized rabbit kidneys. *Cryobiology* 1984; **21**: 637-653
- 33 **Boren CH**, Roon AJ, Moore WS. Maintenance of viable arterial allografts by cryopreservation. *Surgery* 1978; **83**: 382-391
- 34 **Tice DA**, Zerbino VR, Isom OW, Cunningham JN, Engelman RM. Coronary artery bypass with freeze-preserved saphenous vein allografts. *J Thorac Cardiovasc Surg* 1976; **71**: 378-382

Edited by Xu JY and Wang XL

Effects of *Ginkgo biloba* extract on cytoprotective factors in rats with duodenal ulcer

Jane C.-J. Chao, Hwei-Chen Hung, Sheng-Hsuan Chen, Chia-Lang Fang

Jane C.-J. Chao, Hwei-Chen Hung, School of Nutrition and Health Sciences, Taipei Medical University, 250 Wu Hsing Street, Taipei, Taiwan 110, China

Sheng-Hsuan Chen, Department of Gastroenterology, Taipei Medical University Hospital, 252 Wu Hsing Street, Taipei, Taiwan 110, China

Chia-Lang Fang, Department of Pathology, Taipei Medical University, 250 Wu Hsing Street, Taipei, Taiwan 110, China

Correspondence to: Dr. Jane C.-J. Chao, School of Nutrition and Health Sciences, Taipei Medical University, 250 Wu Hsing Street, Taipei, Taiwan 110, China. chenju@tmu.edu.tw

Telephone: +886-2-2736-1661 #6551~6556 Ext. 117

Fax: +886-2-2737-3112

Received: 2003-10-30 **Accepted:** 2003-12-16

Abstract

AIM: To investigate the effects of *Ginkgo biloba* extract on cytoprotective factors in rats with duodenal ulcer.

METHODS: Sprague-Dawley rats were randomly divided into four groups: sham operation without ginkgo, sham operation with ginkgo, duodenal ulcer without ginkgo, and duodenal ulcer with ginkgo. Rats with duodenal ulcer were induced by 500 mL/L acetic acid. Rats with ginkgo were intravenously injected with *Ginkgo biloba* extract from the tail at a dose of 0.5 mg/(kg·d) for 7 and 14 days.

RESULTS: Pathological result showed that duodenal ulcer rats with ginkgo improved mucosal healing and inflammation compared with those without ginkgo after 7 d treatment. After 14 d treatment, duodenal ulcer rats with ginkgo significantly increased weight gain (34.0 ± 4.5 g versus 24.5 ± 9.5 g, $P < 0.05$) compared with those without ginkgo. Duodenal ulcer rats significantly increased cell proliferation (27.4 ± 4.0 and 27.8 ± 2.3 BrdU-labeled cells in duodenal ulcer rats with and without ginkgo versus 22.4 ± 3.5 and 20.8 ± 0.5 BrdU-labeled cells in sham operation rats with and without ginkgo, $P < 0.05$) compared with sham operation rats. Mucosal prostaglandin E₂ concentration significantly increased by 129% ($P < 0.05$) in duodenal ulcer rats with ginkgo compared with that in those without ginkgo. Duodenal ulcer rats without ginkgo significantly decreased superoxide dismutase activity in the duodenal mucosa and erythrocytes (19.4 ± 6.7 U/mg protein versus 38.1 ± 18.9 U/mg protein in the duodenal mucosa, and 4.87 ± 1.49 U/mg protein versus 7.78 ± 2.16 U/mg protein in erythrocytes, $P < 0.05$) compared with sham operation rats without ginkgo. However, duodenal ulcer rats with ginkgo significantly increased erythrocyte superoxide dismutase activity (8.22 ± 1.92 U/mg protein versus 4.87 ± 1.49 U/mg protein, $P < 0.05$) compared with those without ginkgo. Duodenal ulcer rats without ginkgo significantly increased plasma lipid peroxides (4.18 ± 1.12 $\mu\text{mol/mL}$ versus 1.60 ± 1.10 $\mu\text{mol/mL}$ and 1.80 ± 0.73 $\mu\text{mol/mL}$, $P < 0.05$) compared with sham operation rats without ginkgo and duodenal ulcer rats with ginkgo during the experimental period.

CONCLUSION: *Ginkgo biloba* extract can improve weight

gain and mucosal healing in duodenal ulcer rats by the actions of cytoprotection and antioxidation.

Chao CJ, Hung HC, Chen SH, Fang CL. Effects of *Ginkgo biloba* extract on cytoprotective factors in rats with duodenal ulcer. *World J Gastroenterol* 2004; 10(4): 560-566

<http://www.wjgnet.com/1007-9327/10/560.asp>

INTRODUCTION

Extract from the leaves of *Ginkgo biloba* (maidenhair tree) has been used therapeutically for centuries in the traditional Chinese pharmacopeia, and is used for the treatment of asthma and bronchitis^[1]. In Western countries, *Ginkgo biloba* extract is administered as film-coated tablets, a liquid, or by intravenous injection. In Germany and France, *Ginkgo biloba* extract is the most commonly prescribed medicine to improve circulation and cardiovascular health^[1]. Standard *Ginkgo biloba* extract, EGb 761, contains 240 mg/g flavonoids (ginkgo-flavone glycosides) and 60 mg/g terpenoids (ginkgolides and bilobalides) which are the most important active ingredients in the extract. *Ginkgo biloba* extract is well known for its antioxidant property to scavenge free radicals, especially oxygen-centered free radicals, such as OH·, O₂⁻, RO·, and ROO·, and to neutralize ferryl ion-induced peroxidation^[2]. It has been reported that the antioxidant activity of *Ginkgo biloba* extract can prove helpful in the prevention and treatment of diseases and degenerative processes associated with oxidative stress.

Oxygen-derived radicals are involved in the pathogenesis of duodenal ulceration^[3]. A previous study found that the pathogenesis of duodenal ulcer induced by diethyldithiocarbamate in rats could be significantly prevented by subcutaneous injection of antioxidative agents, such as superoxide dismutase (SOD, 50 000 units/kg), allopurinol (50 mg/kg), or glutathione (200 mg/kg), and antisecretory agent cimetidine (100 mg/kg)^[4]. Additionally, SOD injection significantly elevated the rate of alkaline secretion in the duodenum, suggesting that the mucosal antioxidative system including SOD may play a role in the regulation of alkaline secretion and contribute to duodenal mucosal defensive ability. In cysteamine-induced duodenal ulcer rats, Cu, Zn-SOD activity significantly decreased, but lipid peroxidation products determined by thiobarbituric acid reactants significantly increased^[5]. The results suggest that an increase of oxygen-derived free radicals and a decrease of Cu, Zn-SOD activity in the duodenal mucosa may be involved in the pathogenesis of cysteamine-induced duodenal ulcer. Non-smokers with peptic ulcer, clinically diagnosed as gastric or duodenal ulcer, had a higher level of malondialdehyde (MDA) in platelets, whereas platelet SOD activity significantly decreased compared with healthy subjects^[6].

Several mechanisms of gastroduodenal cytoprotection have been proposed, including increased formation of prostaglandins and scavenging of free radicals, to protect against gastroduodenal mucosal injury rather than inhibition or neutralization of gastric acid^[7]. There is no study yet to investigate the effect of *Ginkgo biloba* extract on peptic ulcer. Presumably, the property of a free radical scavenger for *Ginkgo biloba* extract can protect

duodenal ulcer from oxidative damage. Therefore, the purpose of this study was to investigate the effect of *Ginkgo biloba* extract on cytoprotective factors in rats with acetic acid-induced duodenal ulcer.

MATERIALS AND METHODS

Animals and duodenal ulcer operation

Male Sprague-Dawley rats (200–250 g) were purchased from the National Laboratory Animal Center (National Science Council, Taipei, Taiwan). The rats were housed in individual cages and had free access to food (powdered laboratory autoclavable rodent diet 5010, PMI Nutrition International Inc., Brentwood, MO), except for the fasting period. The light cycle was 12 hours and the room temperature was kept at 22–24°C. One hundred and forty-four rats were randomly divided into four groups: sham operation without ginkgo, sham operation with ginkgo, duodenal ulcer without ginkgo, and duodenal ulcer with ginkgo ($n=36$ per group). Rats with duodenal ulcer were induced by acetic acid^[8]. Prior to operation, the rats were fasted overnight, anesthetized by intraperitoneal injection with 50 mg/kg body weight thiopental sodium (Abbott Australasia Pty.Ltd., Kurnell, Australia), and the abdomen was then opened. A plastic tube (4.5 mm in inner diameter) filled with 70 µL of 500 mL/L acetic acid was applied tightly to the surface of the duodenum for 15 s. Due to different tolerance to acetic acid in various layers of the duodenum, it only caused immediate necrosis in the mucosa and submucosa, and a part of muscular layers exactly within the area of acetic acid application without penetration or perforation to the surrounding organs. Normal saline was used in sham operation rats instead of acetic acid. After operation, the rats were allowed to recover from anesthesia. Operated rats received only water on the day of operation (day 0), and were fed with a normal chow diet *ad libitum* next day (day 1) before treatment. Body weight of the rats was routinely recorded. All protocols were conducted under the guidelines of Animal Care and Use Committee, Taipei Medical University.

Treatment and pathological observation

The next day after operation, the rats were intravenously (iv) injected with *Ginkgo biloba* extract solution (Cerenin®, Dr. Willmar Schwabe GMBH & Co., Karlsruhe, Germany) from the tail at a single dose of 0.5 mg/(kg·d) for 7 and 14 days. The dose of *Ginkgo biloba* extract was calculated from the clinical recommendation of 35 mg intravenous injection (5 mL injection solution) for 70 kg adults (Cerenin®). Each mL of the injection solution contained 3.5 mg *Ginkgo biloba* extract (240 mg/g flavonoids and 60 mg/g terpenoids), 30 mg of 960 mL/L ethanol, 40 mg sorbitol, and 0.1 mol/L NaOH. The injection volume was adjusted daily by body weight. Rats without ginkgo were intravenously injected with the same volume of vehicle solution without ginkgo from the tail. Four rats in each group were killed on day 1 before ginkgo treatment to identify the formation of duodenal ulcer, and sixteen rats in each group were sacrificed for both biochemical analyses (8 rats) and pathological examination (8 rats) after 7 and 14 d treatment, respectively. The duodenum (5 mm×5 mm) was excised, preserved in 40 mg/L paraformaldehyde, and stained with haematoxylin and eosin. Under light microscope at a magnification of ×100 or ×200, coded specimens were evaluated by a pathologist in a blinded fashion.

Semiquantitation of cell proliferation

Rats were intraperitoneally (ip) injected with bromodeoxyuridine (BrdU; Sigma-Aldrich Co., St. Louis, MO) 5 mg/kg body weight one hour before sacrifice for immunohistochemical

analysis^[9]. The duodenum (4 µm thick) was fixed in formalin and embedded in paraffin. The duodenum sections were deparaffinized in xylene, dehydrated by graded ethanol series, and placed in 0.01 mol/L phosphate buffered saline (pH 7.4). Antigen retrieval was performed by boiling the duodenum sections in 0.1 mol/L citrate buffer (pH 6.0) for 10 min to deactivate endogenous alkaline phosphatase activity. The tissue sections were then exposed to 3% H₂O₂ to block endogenous peroxidases, and followed by partial denaturation of double-stranded DNA by treatment with 1 mol/L HCl. The sections were incubated with monoclonal mouse anti-BrdU antibody (1:50 dilution; DAKO, Denmark) for 1 h, and incubated with biotinylated anti-mouse IgG for 30 min. The sections were stained by a streptavidin-biotin complex method using a commercial kit (LSAB2 kit/HRP, DAKO), and detected by diaminobenzidine. The number of cells in the proliferation zone was calculated by counting the cells between the first stained cells of the serosal side and the last stained cells of the mucosal surface of a crypt under light microscope to evaluate the healing of the mucosa^[9]. The number of BrdU-labeled cells in the proliferation zone was counted by the number of positive cells from the serosal side to the mucosal surface of a crypt to evaluate DNA synthesis.

Prostaglandin E₂ concentration in duodenal mucosa

Prostaglandin E₂ (PGE₂) concentration in the duodenal mucosa was quantitated by ELISA using a commercial kit (DE2100, Research and Diagnostics Systems, Inc., Minneapolis, MN). The duodenal mucosa (100 mg wet weight) was homogenized with 1 mL of 150 mL/L methanol, and centrifuged at 8 000×g at 4°C for 10 min. The supernatant was applied to a C₁₈ Sep-Pak® minicolumn (Amersham Biosciences Ltd. Taiwan Branch, Taipei, Taiwan) at the flow rate of 0.5 mL/min. The column was washed with 2 mL petroleum ether followed by 2 mL of 150 mL/L methanol, and prostaglandin was eluted by 2 mL methyl formate. The elute was evaporated using nitrogen gas, and the residue was dissolved in 0.5 mL deionized water. The sample suspension or standards (100 µL) were added to a 96-well plate coated with goat anti-mouse polyclonal antibody, incubated with 50 µL prostaglandin E₂ conjugated to alkaline phosphatase and 50 µL mouse monoclonal anti-prostaglandin E₂ antibody at 2–8°C for 18–24 h. After several washes, the samples were incubated with 200 µL p-nitrophenyl phosphate substrate at 37°C for 1 h, and the reaction was terminated by 50 µL trisodium phosphate solution. The levels of prostaglandin E₂ were determined at 405 nm using an ELISA reader (Multiskan RC, Thermo Labsystems, Helsinki, Finland). Protein content in the duodenal mucosa was determined by the modified method of Lowry *et al.* using a Bio-Rad DC protein assay kit (Bio-Rad Laboratories, Hercules, CA)^[10].

Superoxide dismutase activity in duodenal mucosa and erythrocytes

The activity of SOD was determined spectrophotometrically at 525 nm using a commercial kit (Bioxytech®SOD-525™ assay, Oxis International, Inc., Portland, OR). Duodenal mucosa (15–20 mg) was homogenized in 0.25 mol/L sucrose solution, and centrifuged at 8 500×g at 4°C for 10 min. Blood samples (200 µL) were centrifuged at 2 500×g at 4°C for 5 min. The erythrocyte pellet was suspended in ice-cold water. The mucosa supernatant and erythrocyte suspension were extracted with ethanol/chloroform (62.6:37.5, v/v) for removal of hemoglobin interference. The samples were incubated with the chromogenic reagent (5,6,6a,11b-tetrahydro-3,9,10-trihydroxybenzo[c]fluorene) in alkaline condition (pH 8.8), and the absorbance was read at 525 nm within 1 min. The specific activity of SOD was expressed as unit/mg protein.

One SOD unit was defined as the activity that doubled the autooxidation rate in the absence of SOD.

Lipid peroxidation in plasma

Because of the limited amount of the duodenum specimen, lipid peroxidation was measured in the plasma. The concentration of lipid peroxides in the plasma was assessed colorimetrically at 586 nm using a commercial kit (Calbiochem 437634, Calbiochem-Novabiochem Cor., La Jolla, CA). The plasma (200 μ L) was mixed with 650 μ L of Reagent 1 (7.7 mM N-methyl-2-phenylindole in 750 mL/L acetonitrile and 250 mL/L methanol) and 150 μ L of Reagent 2 (15.4 M methanesulfonic acid) at 45 $^{\circ}$ C for 40 min. The levels of MDA and 4-hydroxy-2(E)-nonenal (4-HNE), the end products derived from peroxidation of polyunsaturated fatty acids and related esters, were measured at 586 nm.

Statistical analysis

The data are expressed as mean \pm SD. The data were analyzed by two-way ANOVA to determine the main effects of duodenal ulcer and ginkgo using SAS (version 6.12, SAS Institute, Cary, NC). *Post hoc* multiple comparisons between two groups were performed by Fisher's least significant difference test. Statistical significance was assigned at the 0.05 level.

RESULTS

The total dose of ginkgo was 108.7 \pm 4.1 mg/d, 105.3 \pm 8.0 mg/d for 7 d treatment, and 106.2 \pm 4.7 mg/d, 114.8 \pm 3.5 mg/d for 14 d treatment in sham operation and duodenal ulcer rats, respectively. Duodenal ulcer rats for 14 d treatment had higher ginkgo administration ($P<0.05$) compared with other rats. However, the total dose of ginkgo did not significantly differ among other rats. The initial weight on day 1 was 217.3 \pm 19.6 g, 206.6 \pm 9.1 g, 214.7 \pm 15.9 g, and 202.7 \pm 16.9 g for 7 d treatment, and 221.8 \pm 11.4 g, 199.8 \pm 10.5 g, 200.2 \pm 18.6 g, and 212.6 \pm 7.5 g for 14 d treatment in sham operation rats without ginkgo, sham operation rats with ginkgo, duodenal ulcer rats without ginkgo, and duodenal ulcer rats with ginkgo, respectively. The initial weight did not significantly differ among the groups. Weight gain did not significantly differ among four groups during the first week (Figure 1). Duodenal ulcer rats without ginkgo (24.5 \pm 9.5 g) had significantly lower weight gain ($P<0.05$) compared with sham operation rats without ginkgo (32.5 \pm 8.4 g) and duodenal ulcer rats with ginkgo (34.0 \pm 4.5 g) during the second week. However, weight gain did not significantly differ between sham operation rats with and without ginkgo (25.2 \pm 7.7 g versus 32.5 \pm 8.4 g), and between sham operation rats without ginkgo and duodenal ulcer rats with ginkgo (32.5 \pm 8.4 g versus 34.0 \pm 4.5 g).

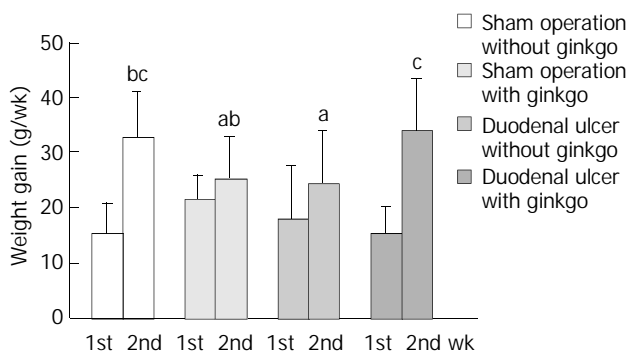


Figure 1 Weight gain of rats during the first and second weeks. Data are mean \pm SD ($n=8$). Values not sharing the same letter differ significantly ($P<0.05$) within the same week by Fisher's least significant difference test.

To identify the formation and healing of duodenal ulcer in rats after operation, gross morphological appearance magnified by $\times 100$ or $\times 200$ is shown in Figure 2. Compared with sham operation rats (Figure 2A), duodenal ulcer rats on day 1 before treatment had the discontinuous lining of the mucosal and submucosal layers, damage in the muscular layer, and serious inflammation with aggregation of the leukocytes (Figure 2B), which was similar to human duodenal ulcer in the pathology. The mean diameter of the ulcer damage was 2 mm under microscopic observation. After 7 d treatment, duodenal ulcer rats without ginkgo still had inflammation (Figure 2C). The mean diameter of the ulcer damage reduced to 1 mm. However, the inflammation almost recovered, and the microvilli proliferated in duodenal ulcer rats with ginkgo (Figure 2D). The mean diameter of the ulcer damage reduced to less than 1 mm. After 14 d treatment, the inflammation lessened and the microvilli increased proliferation in duodenal ulcer rats without ginkgo (Figure 2E). The mucosal healing and proliferation were more advanced in duodenal ulcer rats with ginkgo (Figure 2F). The diameter of the ulcer damage was undetectable in duodenal ulcer rats with and without ginkgo.

Cell proliferation of the duodenal mucosa was determined by anti-BrdU-immunohistochemical staining (Figure 3A). Duodenal ulcer rats had significantly higher number of total cells ($P<0.05$) in the proliferation zone than sham operation rats during the experimental period (Figure 3B). After 7 d treatment, duodenal ulcer rats with ginkgo (30.1 \pm 4.1) had significantly higher number of BrdU-labeled cells ($P<0.05$) in the proliferation zone compared with sham operation rats with (23.7 \pm 2.9) and without ginkgo (25.4 \pm 3.0) (Figure 3C). After 14 d treatment, duodenal ulcer rats (27.4 \pm 4.0 and 27.8 \pm 2.3 for those with and without ginkgo) had higher number of BrdU-labeled cells ($P<0.05$) in the proliferation zone than sham operation rats (22.4 \pm 3.5 and 20.8 \pm 0.5 for those with and without ginkgo). However, the number of both total and BrdU-labeled cells in the proliferation zone did not significantly differ between duodenal ulcer or sham operation rats with and without ginkgo during the experimental period.

The concentration of PGE₂ in the duodenal mucosa did not significantly differ among four groups after 7 d treatment (Figure 4). However, after 14 d treatment, duodenal ulcer rats with ginkgo (61.6 \pm 37.5 pg/mg protein) significantly increased PGE₂ concentration at least two-fold ($P<0.05$) compared with other rats (29.8 \pm 14.8 pg/mg, 28.0 \pm 25.2 pg/mg, and 26.9 \pm 11.9 pg/mg protein for sham operation rats without ginkgo, sham operation rats with ginkgo, and duodenal ulcer rats without ginkgo, respectively). Mucosal PGE₂ concentration did not significantly differ among other three groups.

The activity of SOD in the duodenal mucosa and erythrocytes did not significantly differ among four groups after 7 d treatment (Figure 5). After 14 d treatment, sham operation rats with ginkgo (21.0 \pm 6.9 U/mg protein) and duodenal ulcer rats without ginkgo (19.4 \pm 6.7 U/mg protein) significantly decreased the activity of SOD in the duodenal mucosa by 45% and 49% ($P<0.05$), respectively, compared with sham operation rats without ginkgo (38.1 \pm 18.9 U/mg protein) (Figure 5A). The activity of SOD in the duodenal mucosa did not significantly differ between duodenal ulcer rats with ginkgo (27.1 \pm 9.7 U/mg protein) and other rats. Duodenal ulcer rats without ginkgo (4.87 \pm 1.49 U/mg protein) significantly decreased the activity of SOD in the erythrocytes by 37% and 41% ($P<0.05$) compared with sham operation rats without ginkgo (7.78 \pm 2.16 U/mg protein) and duodenal ulcer rats with ginkgo (8.22 \pm 1.92 U/mg protein), respectively (Figure 5B). The activity of SOD in the erythrocytes did not significantly differ between sham operation rats with and without ginkgo (6.31 \pm 2.34 U/mg versus 7.78 \pm 2.16 U/mg protein), and between sham operation and duodenal ulcer rats with

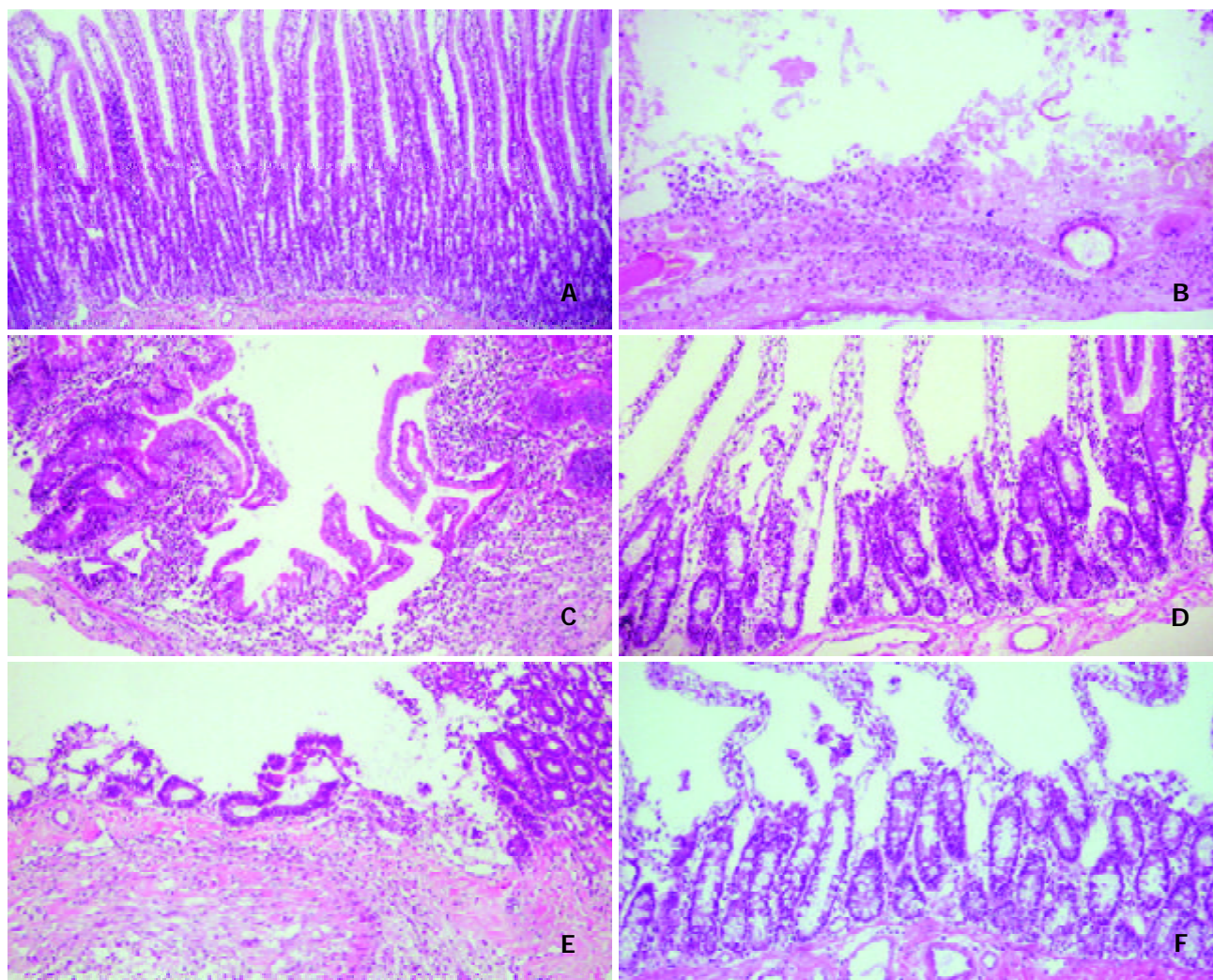


Figure 2 Representative micrographs of duodenal mucosa stained by haematoxylin and eosin. A: sham operation rats on day 1 before treatment ($\times 200$), B: duodenal ulcer rats on day 1 before treatment ($\times 100$), C: duodenal ulcer rats without ginkgo after 7 d treatment ($\times 100$), D: duodenal ulcer rats with ginkgo after 7 d treatment ($\times 200$), E: duodenal ulcer rats without ginkgo after 14 d treatment ($\times 100$), and F: duodenal ulcer rats with ginkgo after 14 d treatment ($\times 200$).

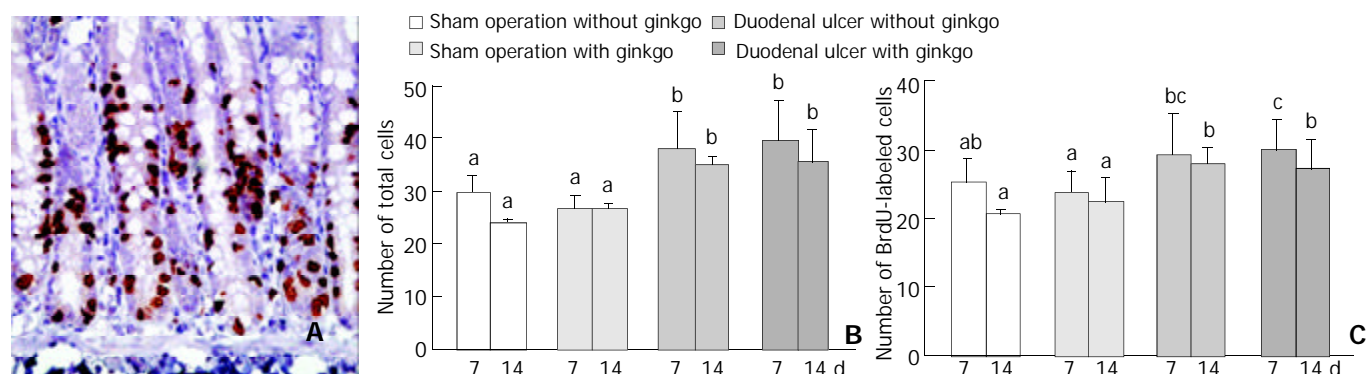


Figure 3 Representative micrographs ($\times 400$) stained by anti-bromodeoxyuridine (anti-BrdU) immunohistochemical method (A), and quantitation of the number of total (B) and BrdU-labeled (C) cells in the proliferation zone from the duodenal mucosa of the rats. Data are mean \pm SD ($n=8$). The nuclei of BrdU-labeled cells were stained in brown. The number of total and BrdU-labeled cells was obtained from three individual crypts for each rat. Values not sharing the same letter differ significantly ($P<0.05$) within the same day by Fisher's least significant difference test.

ginkgo (6.31 ± 2.34 U/mg versus 8.22 ± 1.92 U /mg protein). Sham operation rats with ginkgo (3.14 ± 1.21 $\mu\text{mol/mL}$) and duodenal ulcer rats without ginkgo (2.92 ± 0.90 $\mu\text{mol/mL}$) significantly increased lipid peroxides in the plasma by 85% and 72% ($P<0.05$), respectively, compared with sham operation rats without ginkgo (1.70 ± 0.76 $\mu\text{mol/mL}$) after 7 d treatment (Figure 6). After 14 d treatment, sham operation rats with

ginkgo (3.52 ± 0.99 $\mu\text{mol/mL}$) and duodenal ulcer rats without ginkgo (4.18 ± 1.12 $\mu\text{mol/mL}$) significantly increased lipid peroxides in the plasma by 120% and 161% ($P<0.05$), respectively, compared with sham operation rats without ginkgo (1.60 ± 1.10 $\mu\text{mol/mL}$). Duodenal ulcer rats with ginkgo after 7 (1.65 ± 0.69 $\mu\text{mol/mL}$) and 14 d treatment (1.80 ± 0.73 $\mu\text{mol/mL}$) significantly decreased lipid peroxides in the plasma by 43%

and 57% ($P<0.05$), respectively, compared with duodenal ulcer rats without ginkgo in the corresponding days. Lipid peroxidation in the plasma did not significantly differ between duodenal ulcer rats with ginkgo and sham operation rats without ginkgo during the experimental period.

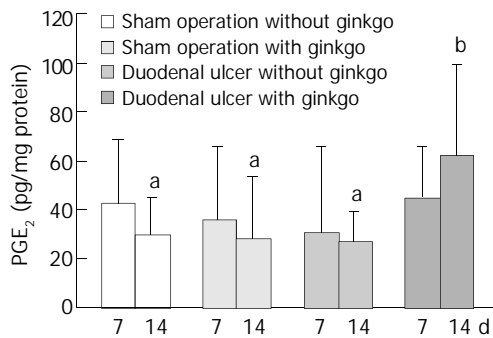


Figure 4 Concentration of prostaglandin E₂ (PGE₂) in duodenal mucosa of the rats during experimental period. Data are mean±SD ($n=8$). Values not sharing the same letter differ significantly ($P<0.05$) within the same day by Fisher's least significant difference test.

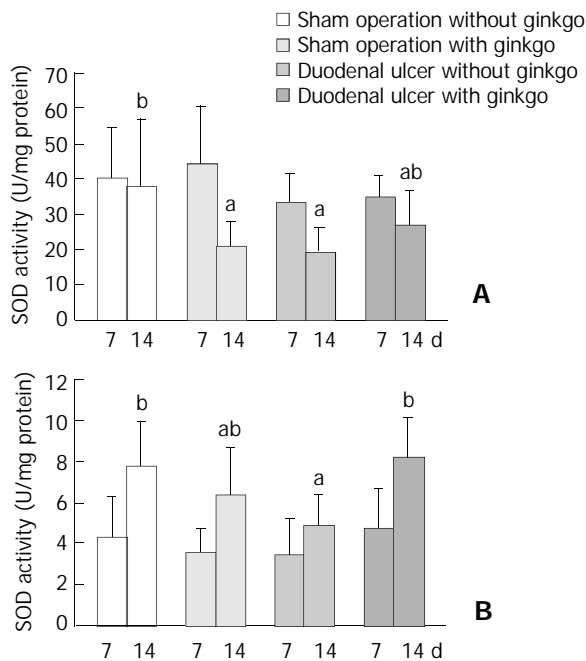


Figure 5 Activity of superoxide dismutase (SOD) in duodenal mucosa (A) and erythrocytes (B) of the rats during experimental period. Data are mean±SD ($n=8$). Values not sharing the same letter differ significantly ($P<0.05$) within the same day by Fisher's least significant difference test.

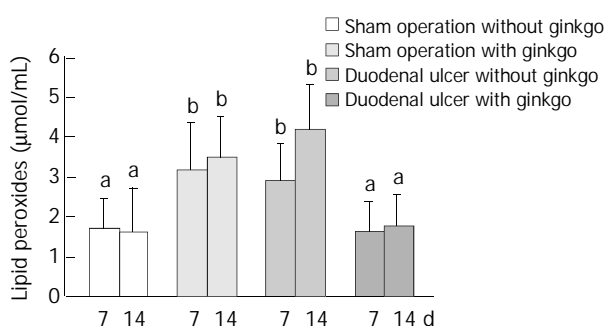


Figure 6 Concentration of lipid peroxides (malondialdehyde and 4-hydroxy-2(E)-nonenal) in plasma of the rats during ex-

perimental period. Data are mean±SD ($n=8$). Values not sharing the same letter differ significantly ($P<0.05$) within the same day by Fisher's least significant difference test.

DISCUSSION

Ginkgo biloba extract was administered by iv injection in this study. The precise dose of ginkgo was well controlled by iv injection into the rats, although oral administration was more convenient for humans. The dose of ginkgo administration was constant at 0.5 mg/(kg·d). However, the total dose was higher in duodenal ulcer rats for 14 d treatment, because weight gain was higher in duodenal ulcer rats with ginkgo after 14 d treatment.

Reactive oxygen species (ROS) could play an important role in the pathogenesis and aggravation of duodenal ulceration^[3,11]. Certain forms of ROS such as H₂O₂ might act as signal transduction messengers to activate transcription factors NF-κB and AP-1, which bind to the promoter region of a large variety of genes that are directly involved in the pathogenesis of diseases^[12]. Additionally, oxygen free radicals have been reported to trigger leukocyte adhesion and activation through modulating the expression of leukocyte adhesion molecules and CD markers^[13]. Pathological results in our study showed that *Ginkgo biloba* extract could eliminate inflammation caused by duodenal ulcer probably because of its antioxidant property. *Ginkgo biloba* extract or its component exerted an anti-inflammatory effect by suppressing the production of active oxygen and nitrogen species^[14,15]. Additionally, gross appearance found that more microvilli formation occurred in duodenal ulcer rats with ginkgo compared with those without ginkgo, indicating *Ginkgo biloba* extract could improve mucosal repair and proliferation. However, semiquantitation of cell proliferation demonstrated that only duodenal ulcer per se significantly increased numbers of total and BrdU-labeled cells in the proliferation zone of the duodenal mucosa. *Ginkgo biloba* extract did not influence these numbers in duodenal ulcer rats. It could be due to a small dose of BrdU (5 mg/kg, ip) and the short exposure time (1 h) to BrdU before sacrifice in our study compared with the administration of BrdU at 100 mg/kg (ip) 90 min prior to euthanasia in a previous study^[16]. It can not be ruled out the possibility that duodenal ulcer rats with ginkgo increase numbers of total and BrdU-labeled cells in the proliferation zone compared with those without ginkgo after administration of BrdU at a higher dose for a longer incorporation time. Dissimilar to this *in vivo* study, our *in vitro* study showed that EGb 761 at 1 000 mg/L significantly decreased cell proliferation to 45% and 39% of the control group in human hepatocellular carcinoma HepG2 and Hep3B cells^[17].

Prostaglandins E, F, and I have been found to exist in the mucosa and fluid of the gastrointestinal tract, and play important roles in modulating the mucosal integrity and various functions of the gastrointestinal tract^[18-20]. Besides the antisecretory property of prostaglandins^[21], several mechanisms of the gastroduodenal cytoprotective action for PGE₂ have been reported, including against disruption of gastric mucosal microvasculature^[22], stimulation of mucus and bicarbonate secretion^[23], elevation of blood flow^[18,24], stimulation of calcium efflux^[25], and stabilization of microtubules^[25]. Although PGE₂ concentration in the duodenal mucosa did not significantly differ among duodenal ulcer rats without ginkgo, sham operation rats with and without ginkgo during the experimental period, duodenal ulcer rats with ginkgo significantly increased PGE₂ concentration in the duodenal mucosa by 2.3-fold compared with those without ginkgo after 14 d treatment. Similarly, a previous study found that PGE₂ concentration in the duodenal mucosa significantly increased by 2- or 3.2-fold, respectively, after H₂-blocker drug treatment with famotidine

(40 mg daily) or ranitidine (150 mg twice daily) in duodenal ulcer patients for 4 weeks^[26]. The data suggest that *Ginkgo biloba* extract has similar effectiveness in increasing PGE₂ concentration in the duodenal mucosa to H₂-blocker drugs. Moreover, increased PGE₂ concentration in the duodenal mucosa may play an important role in duodenal cytoprotection to improve the repair of the duodenal mucosa.

Duodenal ulcer rats without ginkgo significantly decreased the activity of SOD in the duodenal mucosa and erythrocytes compared with sham operation rats without ginkgo after 14 days. Similarly, SOD activity markedly depleted in the ulcer edge of patients with duodenal ulcer compared with that in biopsies from the duodenal bulb of healthy control subjects, and increased after one month of anti-ulcer treatment^[27]. However, SOD activity in erythrocytes and serum did not differ between patients with duodenal ulcer and healthy control subjects. The decreased activity of SOD might attribute to the increased consumption of SOD for the defense of superoxide radicals generated in the duodenal ulcer rats. After 14 d treatment, *Ginkgo biloba* extract significantly restored SOD activity in erythrocytes of duodenal ulcer rats, but did not affect SOD activity in duodenal mucosa. The previous study demonstrated that coadministration of SOD and catalase protected against gastric mucosa lesions induced by water immersion restraint stress in rats, and suggested that the protective effect of SOD and catalase could be due to their antioxidant activity to scavenge ROS^[28]. *Ginkgo biloba* extract has been reported as a strong scavenger for superoxide anion^[2]. It is assumed that *Ginkgo biloba* extract given by intravenous injection may directly compensate the utilization of SOD in erythrocytes for the defense of superoxide anion. Whereas the trend for increased SOD activity in the duodenal mucosa of duodenal ulcer rats with ginkgo was not obvious as observed in erythrocytes, probably because the amount of ginkgo reached to the duodenal mucosa was less than that in the circulation, and the treatment duration was not long enough to significantly raise SOD activity in the duodenal mucosa.

Duodenal ulcer rats without ginkgo significantly increased plasma lipid peroxides compared with sham operation rats without ginkgo during the experimental period, suggesting that duodenal ulcer may be accompanied by oxidative damage to the body. The decreased SOD activity in erythrocytes of duodenal ulcer rats without ginkgo might be attributed to the increased utilization of SOD for the protection against the increased lipid peroxides in plasma. *Ginkgo biloba* extract significantly decreased the elevated lipid peroxides in plasma of duodenal ulcer rats after 7 and 14 d treatment. Similarly, *Ginkgo biloba* extract has been demonstrated to act as an antioxidant and a free radical scavenger to reduce the increased lipid peroxides induced by gentamicin in rat plasma and kidney^[29]. Unexpectedly, sham operation rats with ginkgo had lower SOD activity in the duodenal mucosa and higher lipid peroxides in plasma compared with those without ginkgo. In contrast with *Ginkgo biloba* extract as an antioxidant in previous studies^[2,14,29], it might play a prooxidant role in sham operation rats. Flavonoids with phenol rings in *Ginkgo biloba* extract could be metabolized by peroxidase to form prooxidant phenoxyl radicals which, in some cases, were sufficiently reactive to cooxidize glutathione or NADH accompanied by extensive oxygen uptake and reactive oxygen species formation^[30]. However, no report has directly pointed out the possibility of *Ginkgo biloba* extract as a prooxidant.

Overall, duodenal ulcer rats with ginkgo had less inflammation and more microvilli proliferation, and significantly reduced lipid peroxides in plasma compared with those without ginkgo after 7 d treatment. Additionally, duodenal ulcer rats with ginkgo tended to increase PGE₂ level in the duodenal mucosa and SOD activity in erythrocytes

compared with those without ginkgo, but not statistically significant. After 14 d treatment, besides further improvement in the healing of duodenal ulcer observed by gross appearance and a decrease in plasma lipid peroxides, duodenal ulcer rats with ginkgo significantly increased weight gain, PGE₂ concentration in the duodenal mucosa, and SOD activity in erythrocytes. Changes in the level of plasma lipid peroxides seemed to be more sensitive and were accompanied by the repair of the duodenal mucosa in duodenal ulcer rats after *Ginkgo biloba* extract treatment. In conclusion, *Ginkgo biloba* extract can increase PGE₂ level, SOD activity, and reduce oxidative damage by the actions of cytoprotection and antioxidation to improve the repair of the duodenal mucosa in duodenal ulcer rats.

REFERENCES

- 1 **Kleijnen J**, Knipschild P. *Ginkgo biloba*. *Lancet* 1992; **340**: 1136-1139
- 2 **Gardès-Albert M**, Ferradini C, Sekaki A, Droy-Lefaix MT. Oxygen-centered free radicals and their interactions with EGb 761 or CP 202. In: Ferradini C, Droy-Lefaix MT, Christen Y, eds. *Advances in Ginkgo biloba extract research: Ginkgo biloba extract (EGb 761) as a free-radical scavenger*. New York: Elsevier Science 1993: 1-11
- 3 **Zhang Q**, Dawodu JB, Etolhi G, Husain A, Gemmell CG, Russell RI. Relationship between the mucosal production of reactive oxygen radicals and density of *Helicobacter pylori* in patients with duodenal ulcer. *Eur J Gastroenterol Hepatol* 1997; **9**: 261-265
- 4 **Takeuchi K**, Nishiwaki H, Niida H, Ueshima K, Okabe S. Duodenal ulcers induced by diethyldithiocarbamate, a superoxide dismutase inhibitor, in the rat: role of antioxidative system in the pathogenesis. *Jpn J Pharmacol* 1991; **57**: 299-310
- 5 **Chen SH**, Pan S, Okita K, Takemoto T. Role of oxygen-derived free radicals in the mechanism of cysteamine-induced duodenal ulcer in rats. *J Formos Med Assoc* 1994; **93**: 11-14
- 6 **Kedziora-Kornatowska K**, Tkaczewski W, Blaszczyk J, Buczynski A, Chojnacki J, Kedziora J. Oxygen metabolism in blood of patients with gastric and duodenal ulcer disease. *Hepatogastroenterology* 1995; **42**: 246-249
- 7 **D'Souza RS**, Dhume VG. Gastric cytoprotection. *Indian J Physiol Pharmacol* 1991; **35**: 88-98
- 8 **Chao JCJ**, Liu KY, Chen SH, Fang CL, Tsao CW. Effect of oral epidermal growth factor on mucosal healing in rats with duodenal ulcer. *World J Gastroenterol* 2003; **9**: 2261-2265
- 9 **Yamaguchi T**, Nakajima N, Kuwayama H, Ito Y, Iwasaki A, Arakawa Y. Gastric epithelial cell proliferation and apoptosis in *Helicobacter pylori*-infected mice. *Aliment Pharmacol Ther* 2000; **14** (Suppl 1): 68-73
- 10 **Lowry OH**, Rosebrough NJ, Farr A, Randall RJ. Protein measurement with the Folin phenol reagent. *J Biol Chem* 1951; **93**: 265-275
- 11 **Sieron A**, Kawczyk-Krupka A, Gadowska-Cicha A. The role of free radicals in inflammatory states, ulceration, and ulcers of the stomach and duodenum. *Pol Merkuriusz Lek* 2001; **10**: 113-116
- 12 **Sen CK**, Packer L. Antioxidant and redox regulation of gene transcription. *FASEB J* 1996; **10**: 709-720
- 13 **Fratelli A**, Serrano CV Jr, Bochner BS, Capogrossi MC, Zweier JL. Hydrogen peroxide and superoxide modulate leukocyte adhesion molecule expression and leukocyte endothelial adhesion. *Biochim Biophys Acta* 1996; **1310**: 251-259
- 14 **Yoshikawa T**, Naito Y, Kondo M. *Ginkgo biloba* leaf extract: review of biological actions and clinical applications. *Antioxid Redox Signal* 1999; **1**: 469-480
- 15 **Kim HK**, Son KH, Chang HW, Kang SS, Kim HP. Inhibition of rat adjuvant-induced arthritis by ginkgetin, a biflavone from *Ginkgo biloba* leaves. *Planta Med* 1999; **65**: 465-467
- 16 **Lim CW**, Parker HM, Vesonder RF, Haschek WM. Intravenous fumonisins B1 induces cell proliferation and apoptosis in the rat. *Nat Toxins* 1996; **4**: 34-41
- 17 **Chao JCJ**, Chu CC. Effects of *Ginkgo biloba* extract on cell proliferation and cytotoxicity in human hepatocellular carcinoma cells. *World J Gastroenterol* 2004; **10**: 37-41
- 18 **Dajani EZ**, Agrawal NM. Protective effects of prostaglandins

- against nonsteroidal anti-inflammatory drug-induced gastrointestinal mucosal injury. *Int J Clin Pharmacol Res* 1989; **9**: 359-369
- 19 **Wallace JL**, Tigley AW. Review article: new insights into prostaglandins and mucosal defence. *Aliment Pharmacol Ther* 1995; **9**: 227-235
- 20 **Takeuchi K**, Kato S, Tanaka A. Gastrointestinal cytoprotection by prostaglandin E and EP receptor subtypes. *Nippon Yakurigaku Zasshi* 2001; **117**: 274-282
- 21 **Johansson C**, Bergstrom S. Prostaglandin and protection of the gastroduodenal mucosa. *Scand J Gastroenterol Suppl* 1982; **77**: 21-46
- 22 **Morris GP**. Prostaglandins and cellular restitution in the gastric mucosa. *Am J Med* 1986; **81**: 23-29
- 23 **Sugamoto S**, Kawauchi S, Furukawa O, Mimaki TH, Takeuchi K. Role of endogenous nitric oxide and prostaglandin in duodenal bicarbonate response induced by mucosal acidification in rats. *Dig Dis Sci* 2001; **46**: 1208-1216
- 24 **Yan CD**, Gu L, Tian SP, Chen QS, Dai YL, Li DS. Effects of gastric mucosal blood flow (GMBF) on the role of adaptive cytoprotection of rat gastric mucosa. *Shengli Xuebao* 1996; **48**: 469-476
- 25 **Banan A**, Smith GS, Deshpande Y, Rieckenberg CL, Kokoska ER, Miller TA. Prostaglandins protect human intestinal cells against ethanol injury by stabilizing microtubules: role of protein kinase C and enhanced calcium efflux. *Dig Dis Sci* 1999; **44**: 697-707
- 26 **Lezoche E**, Vagni V, D' Alessandro MD, Mariani P, Carlei F, Lomanto D, Nardovino M, Martelli A, Speranza V. Action of famotidine and ranitidine on prostaglandin E₂ (PGE₂) content of fundic and duodenal mucosa in duodenal ulcer patients. *Drugs Exp Clin Res* 1987; **13**: 655-658
- 27 **Klinowski E**, Broide E, Varsano R, Eshchar J, Scapa E. Superoxide dismutase activity in duodenal ulcer patients. *Eur J Gastroenterol Hepatol* 1996; **8**: 1151-1155
- 28 **Ohta Y**, Nishida K. Protective effect of coadministered superoxide dismutase and catalase against stress-induced gastric mucosal lesions. *Clin Exp Pharmacol Physiol* 2003; **30**: 545-550
- 29 **Naidu MU**, Shifow AA, Kumar KV, Ratnakar KS. *Ginkgo biloba* extract ameliorates gentamicin-induced nephrotoxicity in rats. *Phytomedicine* 2000; **7**: 191-197
- 30 **Galati G**, Sabzevari O, Wilson JX, O'Brien PJ. Prooxidant activity and cellular effects of the phenoxyl radicals of dietary flavonoids and other polyphenolics. *Toxicology* 2002; **177**: 91-104

Edited by Wang XL Proofread by Zhu LH

Insulin expression in livers of diabetic mice mediated by hydrodynamics-based administration

Chen-Xia He, Ding Shi, Wen-Jun Wu, You-Fa Ding, Deng-Min Feng, Bin Lu, Hao-Ming Chen, Ji-Hua Yao, Qi Shen, Da-Ru Lu, Jing-Lun Xue

Chen-Xia He, Ding Shi, Wen-Jun Wu, You-Fa Ding, Deng-Min Feng, Bin Lu, Hao-Ming Chen, Ji-Hua Yao, Qi Shen, Da-Ru Lu, Jing-Lun Xue, State Key Laboratory of Genetic Engineering, Institute of Genetics, School of Life Sciences, Fudan University, Shanghai 200433, China

Correspondence to: Jing-Lun Xue, State Key Laboratory of Genetic Engineering, Institute of Genetics, School of Life Sciences, Fudan University, Shanghai 200433, China. jlxue@fudan.ac.cn

Telephone: +86-21-65649899 **Fax:** +86-21-65649899

Received: 2003-05-10 **Accepted:** 2003-06-07

Abstract

AIM: Transfer and expression of insulin gene *in vivo* are an alternative strategy to improve glycemic control in type 1 diabetes. Hydrodynamics-based procedure has been proved to be very efficient to transfer naked DNA to mouse livers. The basal hepatic insulin production mediated by this rapid tail vein injection was studied to determine its effect on the resumption of glycemic control in type 1 diabetic mice.

METHODS: Engineered insulin cDNA was inserted into plasmid vectors under a CMV promoter, and transferred into STZ induced diabetic mice by hydrodynamic procedure. Glucose levels, body weight of treated mice, insulin levels, immunohistology of the liver, and quantity of insulin mRNA in the liver were assayed to identify the improvement of hyperglycemic complication after plasmid administration. *Sleeping Beauty*, a transposon system, was also used to prolong the insulin expression in the liver.

RESULTS: After plasmid administration, Plasma insulin was significantly increased in the diabetic mice and the livers were insulin-positive by immunostaining. At the same time the hyperglycemic complication was improved. The blood glucose levels of mice were reduced to normal. Glucose tolerance of the treated diabetic mice was improved. Body weight loss was also ameliorated. The rapid tail vein injection did not cause any fatal result.

CONCLUSION: Our results suggested that insulin gene could be efficiently transferred into the livers of diabetic mice via rapid tail vein injection and it resulted in high level of insulin expression. The basal hepatic insulin production mediated by hydrodynamics-based administration improved the glycemic control in type 1 diabetes dramatically and ameliorated diabetic syndromes. Hydrodynamics-based administration offers a simple and efficient way in the study of gene therapy for type 1 diabetes.

He CX, Shi D, Wu WJ, Ding YF, Feng DM, Lu B, Chen HM, Yao JH, Shen Q, Lu DR, Xue JL. Insulin expression in livers of diabetic mice mediated by hydrodynamics-based administration. *World J Gastroenterol* 2004; 10(4): 567-572

<http://www.wjgnet.com/1007-9327/10/567.asp>

INTRODUCTION

Type 1 or insulin-dependent diabetes mellitus is resulted from autoimmune destruction of the pancreatic β -cells^[1]. Due to severe deficiency of insulin, the key pancreatic hormone necessary for glucose homeostasis, patients with type 1 diabetes suffer from elevated blood glucose levels manifested as thirst, diuresis, overeating, ketoacidosis as well as weight loss. Development of long-term diabetic complications, such as nephropathy, retinopathy, neuropathy and macrovascular disease is also very dangerous and lethal. Currently, type 1 diabetic patients are treated with twice-daily insulin injection, which neither provides adequate glycemic control nor prevents the development of diabetic complications. Although oral and inhaled forms of insulin or insulin pump are used to achieve better glycemic control, these strategies need to be further improved^[2].

Insulin gene therapy, an alternative strategy to improve glycemic control in type 1 diabetes, can restore endogenous insulin production by insulin gene delivery. Although regulated insulin expression has been developed recently, the slow kinetics of insulin secretion limits its application in clinical research. On the other hand, basal insulin production has been proved to be an effective and adjuvant strategy in insulin therapy^[3]. The most intensely studied method for gene therapy utilizes viruses as a carrier to mediate long-term transgene expression, which is necessary for the chronic nature of diabetes, with improved safety profiles. Of the currently available gene delivery vehicles, only a few viral vectors, including lentiviral and adeno-associated viral (AAV) vectors meet these requirements. Except limited packaging size and the possibility of insertional mutagenesis following delivery of recombinant vectors, viral carriers usually require laborious procedures for preparation and purification^[4,5]. All these shortcomings make the viral carriers inconvenient in studying the function of gene products or the practicability of gene expression cassettes.

One of the alternatives currently under development is the direct use of naked DNA that is routine in preparation and safe after administration. But naked plasmid has obstacles in diabetic gene therapy because of its less efficiency to transfect animal cells. Low level expression of insulin fails to reduce blood glucose levels significantly^[6,7]. Liu and Zhang have developed a hydrodynamics-based procedure to mediate efficient expression of transgenes in the liver of mice by systemic administration of naked DNA^[8,9]. The liver, a surrogate organ for insulin gene transfer in most preclinical tests *in vivo*, showed the highest level of gene expression among the organs expressing transgenes. This strategy has been proved to be a convenient way in studying gene function and gene therapy. We used the hydrodynamics-based procedure, a convenient and safe strategy for naked DNA transfer, in the study of diabetes gene therapy.

In this report we injected naked plasmid with insulin precursor cDNA into diabetic mice via hydrodynamics-based procedure. The basal insulin production and its effect on the reversal of diabetic manifestations were evaluated. *Sleeping*

Beauty^[10], a TC-1 like transposon system, was also used to prolong the high level of insulin expression.

MATERIALS AND METHODS

Construction of plasmid vector

Engineered human proinsulin cDNA (mhINS) contained furin recognition sequences (Arg-X-Arg-Arg) at B/C and C/A junction regions. Such a genetical modification allowed proinsulin to be processed maturely by the ubiquitous protease furin in non-endocrine cells^[11]. An expression cassette containing mhINS cDNA driven by a CMV promoter in plasmid pcDNA3-mhINS^[12] (provided by Dr. Shen KT in Zhongshan Hospital) was recloned between two inverted reverse sequences in plasmid pT, a *Sleeping Beauty* transposon vector^[10] (provided by Dr. Zoltan Ivics). Plasmid used for transfection was purified with a purification kit (Qiagen) according to the instructions.

Animal studies

Male ICR mice (from BK Company, weighing 25-30 g) were used in this study. All the mice were fed at room temperature with sufficient water and food, and monitored for body weight every 3 days. To induce diabetes, the animals received intraperitoneal injection of streptozotocin (STZ dissolved in a 100 mmol/l sodium citrate solution pH 4.5, 150 mM NaCl, immediately before administration) at the dose of 150 mg/kg body weight. The mice with blood glucose levels in the range of 20-30 mmol/l were selected and used 7 days after STZ treatment. Blood glucose levels were determined with Precision Plus Electrodes (Medisense, MA). Plasma insulin levels were measured by human insulin radioimmunoassay (RIA, Linco Research, St. Louis, MO). Blood samples were collected by a retro-orbital technique into Eppendorf tubes. Subsequently, separated plasma from each of two to three mice in each group was mixed to obtain enough volume of samples for insulin evaluation assays.

Plasmid administration

Administration of mhINS vectors into STZ-induced diabetic mice was carried out by intravenous coinjection of 80 µg of pT-mhINS and 8 µg of pCMV-SB (plasmid expressing transposase), or intravenous injection of 80 µg of pcDNA3-mhINS in 2-3 ml (one tenth of the body weight in grams) of Ringer's solution (147 mM NaCl, 4 mM KCl, 1.13 mM CaCl₂) in 7 seconds^[9].

Glucose tolerance test

The mice were subjected to three hour fasting and injected intraperitoneally with 20% glucose at the dose of 2 g/kg body weight. Blood glucose was measured at 30-minute intervals before and after glucose infusion.

Identification of mhINS DNA and mRNA in livers

Genomic DNA prepared from livers of mice was used for PCR detection with primers specific for mhINS cDNA (forward, 5' -CGCAGCCTTTGTGAACCA-3'; and backward, 5' -TCCACAATGCCACGCCT-3'). Total RNA from livers was reversely transcribed and the resulting pool of cDNA was subjected to PCR detection with the same primers above. The reaction mixture for PCR amplification was subjected to 30 cycles of denaturation (95°C, 30 seconds), annealing (63°C, 30 seconds), and extension (72°C, 30 seconds). The amplified products were 204 bp in length and identified by agarose-gel electrophoresis. For β-actin RT-PCR, the sequences of primers were 5' -CCTTCCTGTGCATGGAGTCCT-3' and 5' -GGAGCAATGATCTTGATCTTC-3'. The PCR conditions involved denaturation at 95°C for 30 s, annealing at 55°C for

30 s, and extension at 72°C for 30 s for 30 cycles, and the PCR products were 202 bp in length. Here, β-actin RT-PCR was used as an internal control.

Quantitative RT-PCR analysis

On days 1, 7 and 14 after plasmid injection, we sacrificed the mice that had received pCMV-mhINS and pT-mhINS, and harvested the livers. The total RNA of the liver samples was isolated and the contaminated DNA was excluded with DNase I. Two micrograms of quantified RNA were first subjected to reverse transcription using an oligo(dT) primer and reverse transcriptase (RT, Gibco BRL, Rockville, MD, USA) to generate first-strand cDNA. To determine the levels of transgene-derived insulin mRNA in the liver, we performed quantitative real-time PCR analysis using an ABI PRISM 7000 system. Taqman Universal PCR MasterMix was used to provide critical components for PCR mixture. The primers and probe were as follows: forward primer, 5' -AACACCTGTGCGGCTCAGA-3'; backward, 5' -CGTTCCTCCGCACACTAGGTA-3'; FAM labeled MGB probe, FAM-5' -CTGGTGAAGCTCT-3' -MGB. The PCR process was at 50°C for 2 min, at 95°C for 10 min, then at 95°C for 15 s and at 60°C for 10 min for a total of 40 cycles. The length of expected products was 54 bp. The standard curve for mhINS plasmid was created. The quantity of insulin mRNA was expressed as pg/cDNA from 100 ng of total RNA.

Immunocytochemical analysis

For immunohistochemical (IHC) procedures, the tissues were fixed in 4% buffered paraformaldehyde. An antibody to human insulin (Linco Research) was used for immunostaining. The number of insulin-positive hepatocytes was counted on IHC sections from 3-4 animals.

RESULTS

Reduction of blood glucose in the diabetic mice treated with insulin precursor DNA

The expression constructs of human insulin precursor driven by CMV promoter are shown in Figure 1. Insulin precursor vectors were injected rapidly via tail vein into diabetic mice, and blood glucose of the mice was measured to determine the effect of insulin production after the naked vector delivery. As shown in Figure 2, the administration of insulin vectors resulted in a significant reduction in glucose concentration. In the eight animals co-transferred with pT-mhINS and pCMV-SB, their blood glucose levels were reduced to normal one day after plasmid injection, and three of them maintained the normal levels for two weeks. Glucose concentration was also reduced significantly one day after administration of the non-transposon vector pcDNA3-mhINS, but increased rapidly and reached pretreatment levels one week later. In contrast, Ringer's solution-treated animals remained the high glucose levels unchanged. The severe loss of body weight of the diabetic mice was ameliorated after delivery of pcDNA3-mhINS and pT-mhINS (Figure 3). Also, urination of the treated diabetic mice lessened dramatically. These results indicated that symptoms of diabetes were improved after hydrodynamics mediated insulin gene delivery. No diabetic mouse died from the rapid tail vein injection, which showed the safety of hydrodynamics-based DNA administration in the study of gene therapy for diabetes.

Insulin production in STZ-induced diabetic mice after insulin vector treatment

Insulin protein in mouse serum was measured by radioimmunity with human insulin polyclonal antibodies. Normal mice and STZ-induced diabetic mice treated with

Ringer's solution were used as controls. Insulin protein in pT-mhINS and pCMV-SB co-treated STZ mice was 97.2 μ U/ml, 33.3 μ U/ml, and 12.7 μ U/ml one day, seven days and fourteen days after treatment, respectively. In pcDNA3-mhINS treated mice it was 113 μ U/ml, 4.8 μ U/ml, and 3.4 μ U/ml one day, seven days and fourteen days after treatment, respectively (Table 1). Seven days after plasmid administration, insulin production was seven fold higher in serum of diabetic mice treated with transposon vector than that in serum of those treated with non-transposon vector, indicating transposon vector was more effective to mediate sustained basal insulin production.

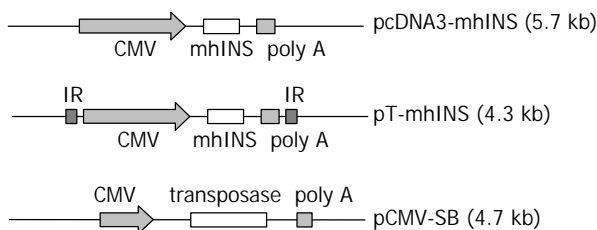


Figure 1 Structure of pcDNA3-mhINS, pT-mhINS, and pCMV-SB. CMV, CMV promoter; mhINS, engineered human insulin cDNA; IR, inverted repeat sequences of *Sleeping Beauty*.

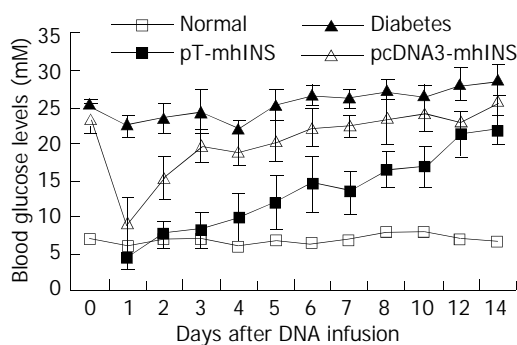


Figure 2 Reduction of blood glucose in diabetic mice treated with insulin precursor DNA. Data were plotted as the mean \pm SEM. $P < 0.01$ (1d). Vector administration was at day 0.

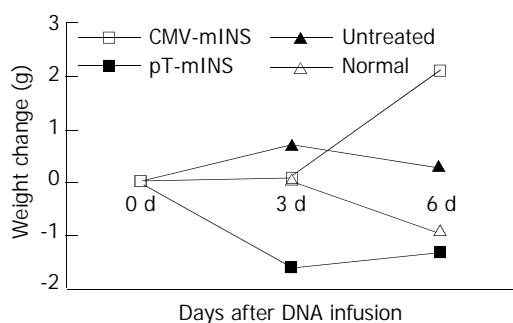


Figure 3 Weight increment of the mice after the mhINS vector treatment. Vectors were administrated at day 0.

Table 1 Insulin production in STZ-induced diabetic mice after insulin vector treatment (mean \pm SD)

Serum insulin Level (μ U/ml)	pCMV-mhINS	pT-mhINS+pCMV-SB	Diabetic control	Normal control
1 day after treatment	113.1 \pm 20.6	97.2 \pm 14.4	5.2 \pm 0.3	10-50
7 days after treatment	4.8 \pm 1.3	33.3 \pm 10.2	-	-
14 days after treatment	3.4 \pm 0.2	12.7 \pm 4.6	-	-

PCR and RT-PCR detection for mhINS cDNA and mRNA in livers

Total DNA and RNA were extracted for PCR and RT-PCR to detect if mhINS vectors were transfected into the mice livers and transcribed into mRNA. The PCR and RT-PCR products of 204 bp fragments were amplified from all livers of mice administrated pcDNA3-mhINS and pT-mhINS, but not from controls. In RT-PCR detection with β -actin primers, 202 bp fragments were found in all hepatic RNAs (Figure 4).

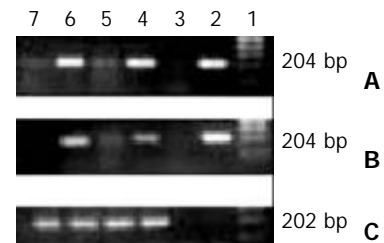


Figure 4 PCR and RT-PCR detection for mhINS cDNA and mRNA in livers. A, mhINS cDNA PCR; B, mhINS mRNA RT-PCR; C, β -actin RT-PCR. The number above the photo shows the number of positive control (2), negative control (3), livers of pT-mhINS treated mice 1 day (4) and 7 days (5) after administration, livers of pcDNA3-mhINS treated mice 1 day (6) and 7 days (7) after administration.

Quantitative real-time RT-PCR analysis for insulin mRNA in livers

To identify the difference of transcript levels of mhINS in the livers of diabetic mice treated with transposon and non-transposon vectors seven and fourteen days after injection, real-time RT-PCR was performed. The transcripts of mhINS in the livers of mice treated with transposon vector were more than those in the livers of mice treated with non-transposon vector seven days or fourteen days after delivery (Table 2). No mhINS transcripts were detected in the livers of negative control mice. To identify if the isolated RNA was contaminated by mhINS DNA, RNA isolated from the livers of plasmid-treated mice but not reversely transcribed was subjected to real-time PCR. Negative results suggested that the isolated RNA was not contaminated by mhINS DNA.

Table 2 Quantity of mhINS mRNA in mouse liver after plasmid infusion (mean \pm SD)

Quantity of mRNA (pg)	pCMV-mhINS	pT-mhINS+pCMV-SB	Diabetic control
7 days after treatment	0.21 \pm 0.14	3.41 \pm 1.48	0
14 days after treatment	0.13 \pm 0.04	1.24 \pm 1.06	0

Expression of insulin protein in livers of treated diabetic mice

To confirm that treatment of the diabetic mice with mhINS vectors resulted in insulin expression in the liver, immunohistological staining of liver sections with antibodies against insulin was performed. As shown in Figure 5, insulin-positive cells were observed in all livers of mhINS vector-treated mice. In contrast, it was negative in the livers of Ringer's solution-treated mice. To provide more quantitative information, liver sections from three cases in each group were randomly observed 7 days and 14 days after plasmid administration and the number of insulin-positive hepatocytes were counted. There were more positive cells in the livers of mice treated with transposon vector as compared with those treated with non-transposon vector (Table 3).

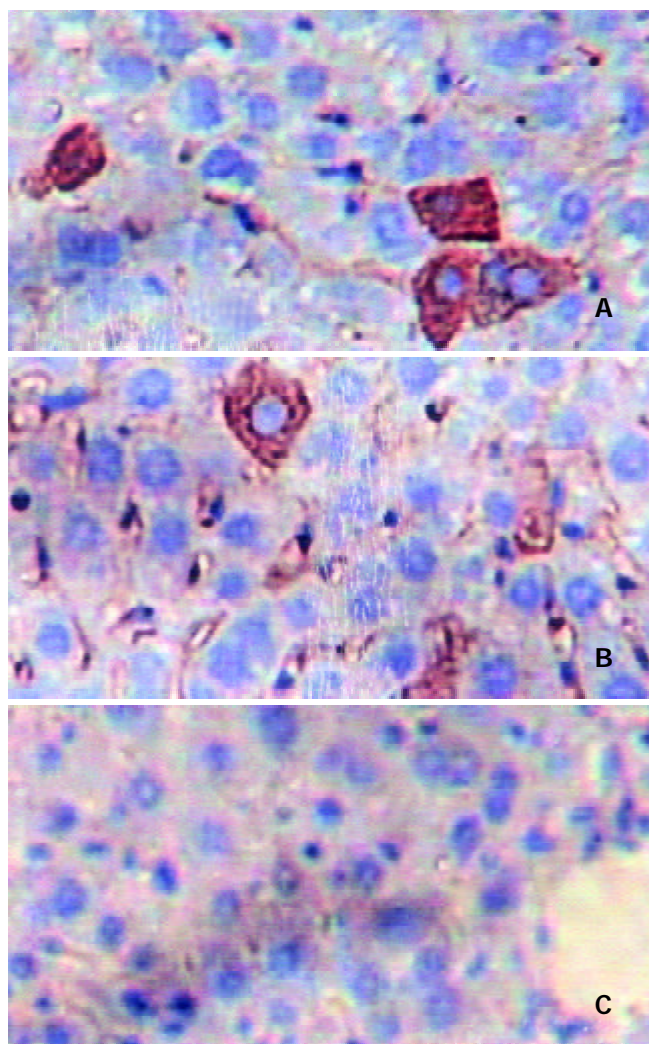


Figure 5 The expression of insulin protein in the livers of the treated diabetic mice. One day after pT-mhINS and pCMV-SB treatment (A), pcDNA3-mhINS treatment (B), and Ringer's solution-treatment (C), mice were sacrificed and liver sections were stained with antibodies to human insulin.

Table 3 Insulin-positive cells in mouse liver after plasmid infusion (mean±SD)

Positive cells	pCMV-mhINS	pT-mhINS+ pCMV-SB	Diabetic control
7 days after treatment	6.3±2.3	19.0±5.7	0
14 days after treatment	2.3±0.9	9.3±2.4	0

Effects of plasma insulin on glucose tolerance in diabetic mice treated with insulin vectors

To assess whether or not hepatic products of insulin at basal levels had any therapeutic effect on blood glucose disposal, glucose tolerance experiments were performed in the treated diabetic animals. As shown in Figure 6, blood glucose levels in normal control mice moderately rose to about 12 mM after glucose infusion, and rapidly restored to normal within 1.5 h. In contrast, glucose infusion further exacerbated the severity of hyperglycemia in diabetic animals, resulting in higher glucose concentration (over 22 mM), which persisted for more than 2 hours before slow decline. Blood glucose levels of the diabetic mice treated with insulin vectors were moderately elevated to the same degree as that of the normal mice after glucose challenge and returned to pre-challenge levels within

2 hours. These results suggested that sustained expression of hepatic insulin at basal levels could significantly enhance glucose tolerance in type 1 diabetic animals.

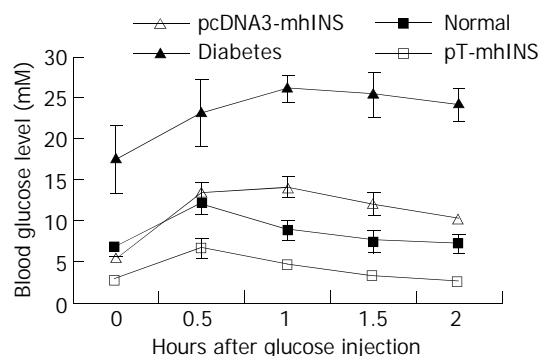


Figure 6 Effects of plasma insulin on glucose tolerance in the diabetic mice treated with the insulin vectors. Blood glucose levels at 30 min intervals prior to and after glucose challenge were determined and plotted as a function of time. Data were obtained 2 days after insulin vector treatment. Data are the mean±SEM, n=2 or 3.

DISCUSSION

One of the difficulties in gene therapy for diabetes is the requirement of high production of insulin to reduce blood glucose levels. Viral vectors, such as adenovirus^[13-15], AAV^[16-18], and retrovirus^[19] have been used. Productive transduction by retroviruses depends on cell division, which is a limiting factor for transducing postmitotic cells. In contrast, adenoviruses are effective for transducing non-dividing cells, but leaky expression of adenoviral proteins is immunogenic, consequently resulting in transient transgene expression. Recombinant AAV vectors have been widely used for gene transfer because of their inherently non-immunogenic nature and ability to stably transduce both dividing and non-dividing cells. Although rAAV is able to mediate stable transgene expression, efficient transduction of the liver by rAAV vector requires intraportal vein injection instead of peripheral intravenous infusion, and stable transgene expression is detected only in approximately 5% of liver cells. Naked plasmid vector, simpler, cheaper and more routine in preparation than viral vectors, is convenient in studying gene function and the practicability of gene expressing vectors. Hydrodynamics-based procedure can mediate naked DNA transfer to the liver most efficiently. It has been used in the study of transfer and expression of various genes, such as FIX^[20], IL-10^[21], LDL^[22], HDV^[23], hepatocyte growth factor^[24], etc. The method was proved to be very efficient for delivery of these genes into the mouse liver. The peak level of gene expression could be gained 24 hours after injection^[18,91]. Transaminase levels and liver histological results showed that rapid intravenous plasmid injection into mice could induce transient focal acute liver damage, which was rapidly repaired within 3 to 10 days. In the present study, we used hydrodynamics-based procedure to deliver insulin gene into STZ-induced type 1 diabetic mice. Insulin production was greatly improved after plasmid injection, and hyperglycemia was recovered to normal blood glucose levels. Most of all, no diabetic mice died from the procedure. These results indicated that hydrodynamics-based administration was a safe and very efficient way in the study of gene therapy for diabetes at the animal study stage.

Most preclinical tests of *in vivo* insulin gene transfer in the past chose the liver as a surrogate organ for insulin production^[2]. One attractive feature of hepatic insulin gene delivery is that hepatocytes are capable of responding to

changes in blood glucose concentrations. In addition, the liver is a major insulin target organ for glucose homeostasis and helps to maintain blood glucose concentrations in a narrow physiological range. Another advantageous feature of hepatic insulin production is related to the observation that portal insulin levels are relatively higher than peripheral insulin concentrations, as pancreatic insulin is released directly to portal circulation. Insulin gene expression in the liver is likely to restore to some extent portal/peripheral insulin concentration gradient in type 1 diabetes. Finally, the liver is a relatively large organ with a robust capacity for protein synthesis, and even a small fraction of hepatocytes transduced will be able to secrete sufficient amount of insulin for improving glycemic control in type 1 diabetes. Taken together, the liver is an excellent target site for insulin gene delivery. The limitation that the liver lacks pancreas-specific prohormone convertases PC2 and PC3 for insulin processing has largely been overcome by converting amino acid residues at B/C and C/A junction regions of the proinsulin polypeptide chain to a consensus furin recognition site^[25,26]. So proinsulin synthesized in hepatocytes will be processed by ubiquitously expressed enzyme furin. Hydrodynamics-based administration can efficiently deliver foreign gene into the liver. In this study, furin-cleaved proinsulin gene was injected into diabetic mice via rapid tail vein. There was a high expression of insulin mRNA and protein in the liver of mice treated with mhINS plasmid vectors. The glucose disposal of diabetic mice was also improved. These results indicated that hydrodynamics-mediated insulin expression in the liver was effective to improve the glucose control in type 1 diabetic mice.

One limitation of non- β cell expression of insulin gene is the lack of regulated protein secretory pathway. To overcome this limitation, different approaches have been taken to control hepatic insulin gene expression in the liver. While considerable progress has been made to achieve regulated insulin gene expression^[2,27], there are several issues concerning the safety and potential toxicity of such systems. A slow kinetics in insulin production and secretion from the liver in these reports was life-threatening^[28]. Sustained basal hepatic insulin production, another effective strategy in therapy of diabetes however, could be used as an adjuvant treatment to insulin therapy, and could confer profound therapeutic benefits to type 1 diabetes mellitus^[29]. Basal insulin represents an important physiological phase of insulin secretion in the post-absorption phase. In addition to providing the basal requirement for hormones in glucose metabolism, basal insulin played a key role in preventing the development of ketoacidosis^[3,18,26]. In the present study we transferred insulin expression plasmid controlled by a constitutive CMV promoter into STZ-induced diabetic mice. The results showed that non-regulated basal production of plasma insulin was significantly increased after plasmid administration. Blood glucose levels were reduced to normal and glucose tolerance was improved also. Weight loss was also ameliorated. Although the treated mice occurred hypoglycemia during fasting, controlling the dose of DNA injection could overcome it. Basal insulin production, when combined with twice-daily insulin injection, could achieve better glycemic control without the need of multiple daily insulin injections and excessive body weight gain, an inevitable consequence associated with intensive insulin therapy^[30].

Unlike mammalian promoter, CMV promoter delivered *in vivo* is known to induce cytokine production and cytokine-mediated effects could subsequently attenuate the promoter activity and limit transgene expression^[31,32]. We delivered mhINS under the promoter of rat liver pyruvate kinase gene (LPK) that has glucose response element. However, there was no difference in ameliorating hyperglycemia between two promoter-driven plasmids (data not shown). Elongation factor

promoter (EF) was also used to drive insulin expression. Though less DNA was required to normalize glucose concentration, there was no significant difference in prolonging the normalized state of glucose concentration between CMV and EF promoters (reported in another article). Some points would account for these results. A majority of DNA began to lose one day after injection and insulin expression declined below certain levels that can not significantly reduce blood glucose levels. So there was no significant difference in reduction of glucose level among CMV, EF and LPK promoters when the peak level expression of insulin was over. So how to stabilize DNA infused into hepatic cells and how to prevent gene silencing would be the most critical steps before hydrodynamics-based procedure can be used in gene therapy of diseases that need high levels of gene products.

Sleeping Beauty vector, one of mammalian transposon systems, was used in this study to prolong the high levels of insulin expression. *Sleeping Beauty* transposon could be efficiently inserted into mammalian chromosomes *in vivo* and might permit longer-term foreign gene expression with a single administration^[33]. The results indicated that the effect of transposon vector on hyperglycemia excelled that of non-transposon vector. Although the feature of unspecific insertion made transposon system unsafe in the practicality of gene therapy, it was still valuable in the study of gene function for diabetes therapy. Other safer systems to prolong naked DNA expression have been developed recently, such as phage ϕ 31 integration system^[34], combination of hepatic control region and hepatic promoter, *etc.*^[20,35-37]. These strategies, combined with hydrodynamics procedure, would be very valuable in the study of gene therapy for diabetes.

Although hydrodynamics-based procedure is unsuitable for clinical use, local gene transfer with such a high liquid pressure has been developed and is more practical^[38-42]. So hydrodynamics-based administration could be an efficient, safe and convenient way in the study of gene therapy for diabetes, especially in study of the function of gene products and the practicality of gene expressing vectors.

In conclusion, hydrodynamics-based approach can transfer insulin cDNA efficiently into diabetic mice livers. High level expression of insulin protein can result in significant reduction of blood glucose levels and improve diabetic syndromes. This intravenous procedure could be a convenient and efficient way in study of gene transfer and expression in diabetic mice.

ACKNOWLEDGEMENTS

We thank Professor Ding-Feng Su (Second Military Medical University, Shanghai, China) for his helpful discussion and suggestions.

REFERENCES

- 1 **Bach JF.** Insulin-dependent diabetes mellitus as an autoimmune disease. *Endocr Rev* 1994; **15**: 516-542
- 2 **Dong H, Anthony K, Morral N.** Challenges for gene therapy of type 1 diabetes. *Curr Gene Ther* 2002; **2**: 403-414
- 3 **Dong H, Altomonte J, Morral N, Meseck M, Thung SN, Woo SL.** Basal insulin gene expression significantly improves conventional insulin therapy in type 1 diabetic rats. *Diabetes* 2002; **51**: 130-138
- 4 **Chang LJ, Gay EE.** The molecular genetics of lentiviral vectors—current and future perspectives. *Curr Gene Ther* 2001; **1**: 237-251
- 5 **Kay MA, Glorioso JC, Naldini L.** Viral vectors for gene therapy: the art of turning infectious agents into vehicles of therapeutics. *Nat Med* 2001; **7**: 33-40
- 6 **Kon OL, Sivakumar S, Teoh KL, Lok SH, Long YC.** Naked plasmid-mediated gene transfer to skeletal muscle ameliorates diabetes mellitus. *J Gene Med* 1999; **1**: 186-194
- 7 **Yin D, Tang JG.** Gene therapy for streptozotocin-induced diabetic mice by electroporation transfer of naked human insulin

- precursor DNA into skeletal muscle *in vivo*. *FEBS Lett* 2001; **495**: 16-20
- 8 **Liu F**, Song Y, Liu D. Hydrodynamics-based transfection in animals by systemic administration of plasmid DNA. *Gene Ther* 1999; **6**: 1258-1266
- 9 **Zhang G**, Budker V, Wolff JA. High levels of foreign gene expression in hepatocytes after tail vein injections of naked plasmid DNA. *Hum Gene Ther* 1999; **10**: 1735-1737
- 10 **Ivics Z**, Hackett PB, Plasterk RH, Izsvak Z. Molecular reconstruction of Sleeping Beauty, a Tc1-like transposon from fish, and its transposition in human cells. *Cell* 1997; **91**: 501-510
- 11 **Hosaka M**, Nagahama M, Kim WS, Watanabe T, Hatsuzawa K, Ikemizu J, Murakami K, Nakayama K. Arg-X-Lys/Arg-Arg motif as a signal for precursor cleavage catalyzed by furin within the constitutive secretory pathway. *J Biol Chem* 1991; **266**: 12127-12130
- 12 **Qin XY**, Shen KT, Zhang X, Cheng ZH, Xu XR, Han ZG. Establishment of an artificial beta-cell line expressing insulin under the control of doxycycline. *World J Gastroenterol* 2002; **8**: 367-370
- 13 **Zhang W**, Lu D, Kawazu S, Komeda K, Takeuchi T. Adenoviral insulin gene therapy prolongs survival of IDDM model BB rats by improving hyperlipidemia. *Horm Metab Res* 2002; **34**: 577-582
- 14 **Auricchio A**, Gao GP, Yu QC, Raper S, Rivera VM, Clackson T, Wilson JM. Constitutive and regulated expression of processed insulin following *in vivo* hepatic gene transfer. *Gene Ther* 2002; **9**: 963-971
- 15 **Dong H**, Morral N, McEvoy R, Meseck M, Thung SN, Woo SL. Hepatic insulin expression improves glycemic control in type 1 diabetic rats. *Diabetes Res Clin Pract* 2001; **52**: 153-163
- 16 **Jindal RM**, Karanam M, Shah R. Prevention of diabetes in the NOD mouse by intra-muscular injection of recombinant adeno-associated virus containing the preproinsulin II gene. *Int J Exp Diabetes Res* 2001; **2**: 129-138
- 17 **Sugiyama A**, Hattori S, Tanaka S, Isoda F, Kleopoulos S, Rosenfeld M, Kaplitt M, Sekihara H, Mobbs C. Defective adenoassociated viral-mediated transfection of insulin gene by direct injection into liver parenchyma decreases blood glucose of diabetic mice. *Horm Metab Res* 1997; **29**: 599-603
- 18 **Lee HC**, Kim SJ, Kim KS, Shin HC, Yoon JW. Remission in models of type 1 diabetes by gene therapy using a single-chain insulin analogue. *Nature* 2000; **408**: 483-488
- 19 **Kolodka TM**, Finegold M, Moss L, Woo SL. Gene therapy for diabetes mellitus in rats by hepatic expression of insulin. *Proc Natl Acad Sci U S A* 1995; **92**: 3293-3297
- 20 **Miao CH**, Thompson AR, Loeb K, Ye X. Long-term and therapeutic-level hepatic gene expression of human factor IX after naked plasmid transfer *in vivo*. *Mol Ther* 2001; **3**: 947-957
- 21 **Jiang J**, Yamato E, Miyazaki J. Intravenous delivery of naked plasmid DNA for *in vivo* cytokine expression. *Biochem Biophys Res Commun* 2001; **289**: 1088-1092
- 22 **Holst HU**, Dagnaes-Hansen F, Corydon TJ, Andreasen PH, Jorgensen MM, Kolvraa S, Bolund L, Jensen TG. LDL receptor-GFP fusion proteins: new tools for the characterization of disease-causing mutations in the LDL receptor gene. *Eur J Hum Genet* 2001; **9**: 815-822
- 23 **Chang J**, Sigal L, Lerro A, Taylor J. Replication of the human hepatitis delta virus genome is initiated in mouse hepatocytes following intravenous injection of naked DNA or RNA sequences. *J Virol* 2001; **75**: 3469-3473
- 24 **Yang J**, Chen S, Huang L, Michalopoulos GK, Liu Y. Sustained expression of naked plasmid DNA encoding hepatocyte growth factor in mice promotes liver and overall body growth. *Hepatology* 2001; **33**: 848-859
- 25 **Dong H**, Woo SL. Hepatic insulin production for type 1 diabetes. *Trends Endocrinol Metab* 2001; **12**: 441-446
- 26 **Muzzin P**, Eisensmith RC, Copeland KC, Woo SL. Hepatic insulin gene expression as treatment for type 1 diabetes mellitus in rats. *Mol Endocrinol* 1997; **11**: 833-837
- 27 **Xu R**, Li H, Tse LY, Kung HF, Lu H, Lam KS. Diabetes gene therapy: potential and challenges. *Curr Gene Ther* 2003; **3**: 65-82
- 28 **Halban PA**, Kahn SE, Lernmark A, Rhodes CJ. Gene and cell-replacement therapy in the treatment of type 1 diabetes: how high must the standards be set? *Diabetes* 2001; **50**: 2181-2191
- 29 **Madsbad S**, Alberti KG, Binder C, Burrin JM, Faber OK, Krarup T, Regeur L. Role of residual insulin secretion in protecting against ketoacidosis in insulin-dependent diabetes. *Br Med J* 1979; **2**: 1257-1259
- 30 **DCCT**. The diabetes control and complications trial research group. Hypoglycemia in the diabetes control and complications trial. *Diabetes* 1997; **46**: 271-286
- 31 **Qin L**, Ding Y, Pahud DR, Chang E, Imperiale MJ, Bromberg JS. Promoter attenuation in gene therapy: interferon- γ and tumor necrosis factor- α inhibit transgene expression. *Hum Gene Ther* 1997; **8**: 2019-2029
- 32 **Harms JS**, Splitter GA. Interferon- γ inhibits transgene expression driven by SV40 or CMV promoters but augments expression driven by the mammalian MHC 1 promoter. *Hum Gene Ther* 1995; **6**: 1291-1297
- 33 **Yant SR**, Meuse L, Chiu W, Ivics Z, Izsvak Z, Kay MA. Somatic integration and long-term transgene expression in normal and haemophilic mice using a DNA transposon system. *Nat Genet* 2000; **25**: 35-41
- 34 **Olivares EC**, Hollis RP, Chalberg TW, Meuse L, Kay MA, Calos MP. Site-specific genomic integration produces therapeutic Factor IX levels in mice. *Nat Biotechnol* 2002; **20**: 1124-1128
- 35 **Chen ZY**, Yant SR, He CY, Meuse L, Shen S, Kay MA. Linear DNAs concatamerize *in vivo* and result in sustained transgene expression in mouse liver. *Mol Ther* 2001; **3**: 403-410
- 36 **Stoll SM**, Scimmenti CR, Baba EJ, Meuse L, Kay MA, Calos MP. Epstein-Barr virus/human vector provides high-level, long-term expression of alpha1-antitrypsin in mice. *Mol Ther* 2001; **4**: 122-129
- 37 **Cui FD**, Kishida T, Ohashi S, Asada H, Yasutomi K, Satoh E, Kubo T, Fushiki S, Imanishi J, Mazda O. Highly efficient gene transfer into murine liver achieved by intravenous administration of naked Epstein-Barr virus (EBV)-based plasmid vectors. *Gene Ther* 2001; **8**: 1508-1513
- 38 **Budker V**, Zhang G, Knechtle S, Wolff JA. Naked DNA delivered intraportally expresses efficiently in hepatocytes. *Gene Ther* 1996; **3**: 593-598
- 39 **Zhang G**, Vargo D, Budker V, Armstrong N, Knechtle S, Wolff JA. Expression of naked plasmid DNA injected into the afferent and efferent vessels of rodent and dog livers. *Hum Gene Ther* 1997; **8**: 1763-1772
- 40 **Zhang G**, Budker V, Williams P, Subbotin V, Wolff JA. Efficient expression of naked DNA delivered intraarterially to limb muscles of nonhuman primates. *Hum Gene Ther* 2001; **12**: 427-438
- 41 **Budker V**, Zhang G, Danko I, Williams P, Wolff J. The efficient expression of intravascularly delivered DNA in rat muscle. *Gene Ther* 1998; **5**: 272-276
- 42 **Eastman SJ**, Baskin KM, Hodges BL, Chu Q, Gates A, Dreusicke R, Anderson S, Scheule RK. Development of catheter-based procedures for transducing the isolated rabbit liver with plasmid DNA. *Hum Gene Ther* 2002; **13**: 2065-2077

Augmented regeneration of partial liver allograft induced by nuclear factor- κ B decoy oligodeoxynucleotides-modified dendritic cells

Ming-Qing Xu, Yu-Ping Suo, Jian-Ping Gong, Ming-Man Zhang, Lü-Nan Yan

Ming-Qing Xu, Jian-Ping Gong, Ming-Man Zhang, Lü-Nan Yan, Department of General Surgery, West China Hospital, Sichuan University, Chengdu 610041, Sichuan Province, China
Yu-Ping Suo, West China Second University Hospital, Sichuan University, Chengdu 610041, Sichuan Province, China
Supported by the Postdoctoral Science Foundation of China, No. 2003033531

Correspondence to: Professor Lü-Nan Yan, Department of General Surgery, West China Hospital, Sichuan University, Chengdu 610041, Sichuan Province, China. xumingqing0018@163.com

Telephone: +86-28-85582968

Received: 2003-08-26 **Accepted:** 2003-09-25

Abstract

AIM: To investigate the effect of NF- κ B decoy oligodeoxynucleotides (ODNs) - modified dendritic cells (DCs) on regeneration of partial liver allograft.

METHODS: Bone marrow (BM)- derived DCs from SD rats were propagated in the presence of GM-CSF or GM-CSF+IL-4 to obtain immature DCs or mature DCs, respectively. GM-CSF-propagated DCs were treated with double-strand NF- κ B decoy ODNs containing two NF- κ B binding sites or scrambled ODNs. Allogeneic (SD rat to LEW rat) 50% partial liver transplantation was performed. Normal saline (group A), GM-CSF -propagated DCs (group B), GM-CSF+IL-4 -propagated DCs (group C), and GM-CSF+NF- κ B decoy ODNs (group D) or scrambled ODNs -propagated DCs (group E) were injected intravenously into recipient LEW rats 7 days prior to liver transplantation and immediately after transplantation. DNA synthesis (BrdU labeling) and apoptosis of hepatocytes were detected with immunostaining and TUNEL staining postoperative 24 h, 48 h, 72 h and 84 h, respectively. Liver graft-resident NK cell activity, hepatic IFN- γ mRNA expression and recipient serum IFN- γ level at the time of the maximal liver allograft regeneration were measured with ^{51}Cr release assay, semiquantitative RT-PCR and ELISA, respectively.

RESULTS: Regeneration of liver allograft was markedly promoted by NF- κ B decoy ODNs-modified immature DCs but was significantly suppressed by mature DCs, the DNA synthesis of hepatocytes peaked at postoperative 72 h in group A, group B and group E rats, whereas the DNA synthesis of hepatocytes peaked at postoperative 84 h in group C rats and 48 h in group D rats, respectively. The maximal BrdU labeling index of hepatocytes in group D rats was significantly higher than that in the other groups rats. NF- κ B decoy ODNs-modified immature DCs markedly suppressed but mature DCs markedly promoted apoptosis of hepatocytes, liver-resident NK cell activity, hepatic IFN- γ mRNA expression and recipient serum IFN- γ production. At the time of the maximal regeneration of liver allograft, the minimal apoptosis of hepatocytes, the minimal activity of liver-resident NK cells, the minimal hepatic IFN- γ mRNA expression and serum IFN- γ production were detected in group D rats. The apoptotic index of hepatocytes, the activity

of liver- resident NK cells, the hepatic IFN- γ mRNA expression level and the serum IFN- γ level in group D rats were significantly lower than that in the other groups rats at the time of the maximal regeneration of liver allograft.

CONCLUSION: The data suggest that the augmented regeneration of partial liver allograft induced by NF- κ B decoy ODNs-modified DCs may be attributable to the reduced apoptotic hepatocytes, the suppressed activity of liver-resident NK cells and the reduced IFN- γ production.

Xu MQ, Suo YP, Gong JP, Zhang MM, Yan LN. Augmented regeneration of partial liver allograft induced by nuclear factor- κ B decoy oligodeoxynucleotides-modified dendritic cells. *World J Gastroenterol* 2004; 10(4): 573-578

<http://www.wjgnet.com/1007-9327/10/573.asp>

INTRODUCTION

Complete and prompt liver regeneration after living liver donation and transplantation could occur in both donor and recipient in most circumstances^[1-5]. Particularly in the transplant recipients, rejection^[6,7] and ischemic injury^[8] could result in inadequate regeneration, leading to hepatic insufficiency or overt liver failure. Early recognition and correction of these complications maximize the chance of liver graft salvage and good outcome for the patient.

Liver regeneration may be regulated cooperatively not only by humoral factors such as hormones, growth factors and growth inhibitory factors, but also by the immune system. It has been reported that regenerating hepatocytes became sensitive to the cytotoxic activity of normal liver-resident NK cells from partially hepatectomized mice^[9-15]. It has also been reported that during the acute phase of regeneration after partial hepatectomy in rats, NK cell functions were temporary suppressed, followed by their recovery at the termination of regeneration^[14], suggesting that such a selective suppression of NK cell functions during the acute phase represents an important regulatory mechanism for liver regeneration in the presence of hepatic NK cells. These observations indicate that liver-resident NK cells may be involved in regulating the extent of hepatocyte regeneration.

A recent study revealed that NKT cells proliferated in the liver after administration of IL-12^[16], were cytotoxic effector cells and the main antimetastatic lymphocyte population in the liver. NKT cells are thought to be responsible for the recognition and regulation of not only malignant cell proliferation but also benign cell proliferation, suggesting that NKT cells may be involved in the regulation of hepatocyte regeneration^[17].

It is accepted that both donor and recipient DCs mediate the rejection of graft in organ transplantation. Several studies have shown that immature donor DCs, deficient in surface costimulatory molecules, could induce T-cell hyporesponsiveness^[18-20] and prolong graft survival in unmodified hosts^[21-24]. Other studies showed that DCs treated with NF- κ B decoy oligodeoxynucleotides (ODNs)

containing specific NF- κ B binding sites, which are maintained in an immature state, could induce tolerance of cardiac allograft^[25,26]. Our recent study showed that NF- κ B decoy ODNs-modified DCs could induce tolerance of rat liver allograft by promoting apoptosis of liver graft-infiltrating cells (GIC) in the portal areas and suppressing IFN- γ mRNA expression in the liver graft^[27].

We hypothesize that the enhanced apoptosis of liver graft-infiltrating cells by NF- κ B decoy ODNs- modified DCs can reduce the total number of liver-resident NK cells and suppress the cytotoxicity of NK cells to the regenerating hepatocytes, and consequently promote liver graft regeneration. In the present study we reported for the first time that NF- κ B decoy ODNs-modified DCs could promote regeneration of partial liver allograft by suppressing hepatocyte apoptosis, liver-resident NK cell activity and IFN- γ production.

MATERIALS AND METHODS

NF- κ B decoy ODNs

Double-stranded NF- κ B decoy ODNs or scrambled ODNs (as a control for NF- κ B decoy ODNs) were generated using equimolar amounts of single-stranded sense and antisense phosphorothioate-modified oligonucleotide containing two NF- κ B binding sites (sense sequence 5' -AGGGACTTTCGCTG-GGGACTTTC-3', NF- κ B binding sites bold lines and underlined)^[25] and scrambled oligonucleotide (sense sequence 5' -TTGCCGTACCTGACTTAGCC-3')^[28]. Sense and antisense strands of each oligonucleotide were mixed in the presence of 150 mM PBS, heated to 100°C, and allowed to cool to room temperature to obtain double-stranded DNA.

Propagation of bone marrow-derived DC populations

Bone marrow cells harvested from femurs of normal SD rats were cultured in 24-well plates (2×10^6 per well) in 2 ml of RPMI 1640 complete medium supplemented with antibiotics, 10% fetal calf serum (FCS) and 4.0 ng/ml recombinant rat GM-CSF to obtain immature DCs. In addition to GM-CSF, 10 ng/ml recombinant rat IL-4 was added to cultures to obtain mature DCs. To select plates, 10 μ M NF- κ B decoy or scrambled ODNs was added at the initiation of culture of DCs^[25]. Cytokine-enriched medium was refreshed every 2 days, after gentle swirling of the plates, half of the old medium was aspirated and an equivalent volume of fresh, cytokine-supplemented medium was added. Thus, nonadherent granulocytes were depleted without dislodging clusters of developing DCs attached loosely to a monolayer of plastic-adherent macrophages. Nonadherent cells released spontaneously from the clusters were harvested after 7 days.

Liver transplantation

Eighty male LEW rats and eighty male SD rats weighing 250-300 g were used in all the experiments. Allogeneic liver transplantations were performed using a combination of SD rats with LEW rats. All operations were performed under ether anesthesia in sterile conditions. Orthotopic 50% partial liver transplantations were performed according to the method described in our previous study^[29]. Normal saline (group A), 1×10^7 GM-CSF-propagated DCs (group B), 1×10^7 GM-CSF+IL-4 - propagated DCs (group C), and 1×10^7 GM-CSF+NF- κ B decoy ODNs or scrambled ODNs - propagated DCs (group D or group E) were injected intravenously through the penile vein into recipient LEW rats 7 days prior to liver transplantation and immediately after liver transplantation, respectively. Liver graft samples and blood samples ($n=8$) were harvested at 24 h, 48 h, 72 h and 84 h postoperatively. Part of the liver grafts was immediately used for isolation of NK cells.

Part of the liver graft tissues was immediately frozen in liquid nitrogen and kept at -80°C for mRNA extraction and part of the liver graft tissues was preserved in 10% formalin for liver regeneration and apoptosis detection.

Liver allograft regeneration detection (BrdU labeling index)

Regeneration extent of liver allograft was indicated by BrdU labeling index of hepatocytes. The BrdU labeling index was determined as described previously. Briefly, BrdU administered intravenously at a dose of 50 mg/kg 30 min before death to measure DNA synthesis in the regenerative liver. Deparaffinized liver sections were incubated with anti-BrdU antibody for 60 min. Immunostaining for BrdU was performed by the avidin-biotin-immunoperoxidase method using ABC kit. A total of 1 000 hepatocytes were counted and the labeling index was calculated.

Apoptosis of hepatocytes

Apoptotic cells in tissue sections were detected with the *in situ* cell death detection kit. The liver graft tissue sections were dewaxed and rehydrated according to standard protocols. Tissue sections were incubated with proteinase K (20 μ g/ml in 10 mM Tris/HCl, pH 7.4-8.0) for 15 to 30 min at 21-37°C. Endogenous peroxidase activity was quenched with blocking solution (0.3% H₂O₂ in methanol) for 30 min at room temperature before exposure to TUNEL reaction mixture at 37°C for 60 min. After washed in stop wash buffer, POD (peroxidase) was added to react for 30 min at 37°C. DAB-substrate was used for color development, and the sections were counterstained with HARR' hematoxylin. TUNEL staining was mounted under glass coverslip and analysed under light microscope.

Activity of liver graft-resident NK cells

Hepatic mononuclear cells (MNCs) were isolated by the sinusoidal lavage method of Bouwens and Wisse^[30]. The cells were obtained by portal vein perfusion with 1% EDTA in PBS at 37°C and a pressure of 50 H₂O, and washed. Then, 30 mL of perfused fluid was collected from the inferior vena cava, and the erythrocytes and granulocytes were separated by the Ficoll (density 1.077) at 400 g for 25 min at 25°C. NK activity was measured by the ⁵¹Cr release method. After washed with PBS, RPMI 1640 medium containing 10% fetal bovine serum was added and the cell count was adjusted to 1×10^6 /ml. Next, the cultured K562 cells were harvested by centrifugation, 50 to 100 μ l of ⁵¹Cr was added, and the mixture was incubated at 37°C for 1 h. Also after the cells were washed with PBS, RPMI 1640 medium containing 10% fetal bovine serum was added and the cell count was adjusted to 1×10^6 /ml. Then the target cells were placed in each well of a microplate. 1 N HCl was added to obtain maximum release and RPMI 1640 medium containing 10% fetal bovine serum was added to obtain spontaneous release (controls). Liver MNCs were added to the other wells at an effector /target ratio of 20. Centrifugation was performed for 5 min at 800 rpm, using a plate centrifuge, followed by incubation for 3.5 h in 5% CO₂. The culture supernatant was collected from each well and radioactivity was measured with a g-scintillation counter. NK cells activity was calculated as follows:

$$\text{NK cell activity (\%)} = \frac{\text{Experimental release (cpm)} - \text{spontaneous release (cpm)}}{\text{Maximum release (cpm)} - \text{spontaneous release (cpm)}} \times 100$$

Semiquantitative RT-PCR assay for IFN-g mRNA expression in liver graft

IFN- γ mRNA expression was determined by semiquantitative

reverse transcription-PCR amplification in contrast with house-keeping gene β -actin. Total RNA from 10 mg liver allograft tissue was extracted using Tripure™ reagent. First-strand cDNA was transcribed from 1 μ g RNA using AMV and an Oligo (dT₁₅) primer. PCR was performed in a 25 μ l reaction system containing 10 μ l cDNA, 2 μ l 10 mM dNTP, 2.5 μ l 10 \times buffer, 2.5 μ l 25 mmol.L⁻¹ MgCl₂, 2 μ l specific primer, 5 μ l water and 1 μ l Taq (35 cycles: at 95 °C for 60 seconds, at 59 °C for 90 seconds, and at 72 °C for 10 seconds). The primers^[31,32] used in PCR reactions were as follows: IFN- γ , 5' primer 5' -AAGACAACCAGGCCATCAGCA-3', 3' primer 5' -AGCCACAGTGTGAGTTCAGTC -3', to give a 547 bp product. β -actin, 5' primer 5' -ATGCCATCCTGCGTCTGGACCTGGC-3', 3' primer 5' -AGCATTTGCGGTGCACGATGGAGGG-3', to give a 607 bp product. PCR products of each sample were subjected to electrophoresis in a 15 g.L⁻¹ agarose gel containing 0.5 mg.L⁻¹ ethidium bromide. Densitometrical analysis using NIH image software was performed for semiquantification of PCR products, and mRNA expression was evaluated by the band-intensity ratio of IFN- γ to β -actin, and presented as percent of β -actin (%).

Statistical analysis

Statistic analysis of data was performed using *t*-test, $P < 0.05$ was considered statistically significant.

RESULTS

Augmented regeneration of partial liver allograft by NF- κ B decoy ODNs-modified DCs

DNA synthesis by regenerating hepatocytes in the liver graft is shown in Figure 1. The BrdU labeling index of hepatocytes in liver graft peaked at postoperative 72 h in group A, group B and group E rats, whereas the BrdU labeling index of hepatocytes in liver graft peaked at postoperative 96 h in group C rats and 48 h in group D rats, respectively. The maximum BrdU labeling index of hepatocytes was 28.07 \pm 4.53% for group A rats, 34.46 \pm 6.72% for group B rats, 19.81 \pm 3.65% for group C rats, 48.62 \pm 9.07% for group D rats and 35.12 \pm 6.37% for group E rats, respectively. The maximum BrdU labeling index of hepatocytes was significantly higher in group D rats but significantly lower in group C rats than that in the other groups rats ($P < 0.01$ or $P < 0.001$). The data suggested that regeneration of partial liver allograft was promoted by NF- κ B decoy ODNs-modified DCs.

Suppression of apoptosis of hepatocytes by NF- κ B decoy ODNs-modified DCs

Some studies showed that liver regeneration was a process involving cell proliferation and inhibition of apoptosis^[33-35]. To determine the augmented regeneration of liver allografts induced by NF- κ B decoy ODNs-treated DCs was associated with the inhibited apoptotic death of hepatocytes, apoptotic activity in the liver graft at the time of maximal liver allograft regeneration was examined by TUNEL staining analysis. TUNEL staining of the liver graft sections revealed that the apoptosis index of hepatocytes was 13.07 \pm 3.27% for group A rats, 9.32 \pm 2.15% for group B rats, 17.76 \pm 3.89% for group C rats, 5.42 \pm 1.76% for group D rats and 9.75 \pm 2.53% for group E rats, respectively. The apoptosis index of hepatocytes was significantly lower in group D rats but significantly higher in group C rats than that in the other groups rats ($P < 0.05$ or $P < 0.01$ or $P < 0.001$). These data strongly suggested that the augmented regeneration of the partial liver allograft induced by NF- κ B decoy ODNs-modified DCs might be associated with the significantly suppressed apoptotic death of hepatocytes.

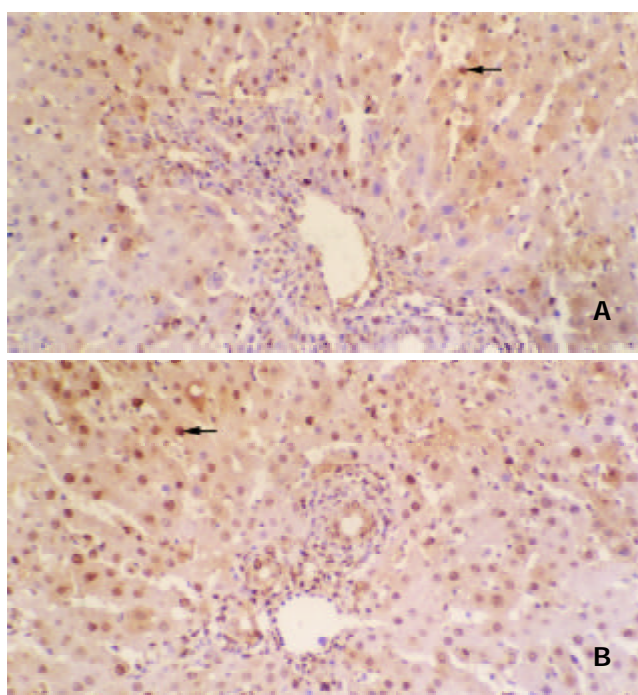


Figure 1 Augmented regeneration of partial liver allograft by NF- κ B decoy ODNs-modified DCs ($\times 200$). BrdU-positive hepatocytes in the liver allografts from group C rats (A) and group D rats (B).

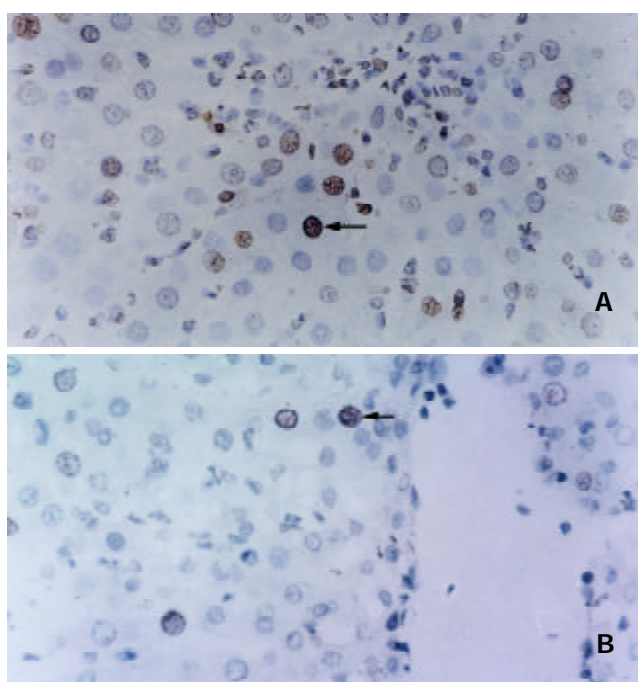


Figure 2 Suppression of apoptosis of hepatocytes in partial liver allografts by NF- κ B decoy ODNs-modified DCs ($\times 400$). Apoptosis of hepatocytes in the liver allografts from group C rats (A) and group D rats (B).

Suppression of activity of liver allograft-resident NK cells by NF- κ B decoy ODNs-modified DCs

Activity of the liver graft-resident NK cells at the time of the maximal liver allograft regeneration was measured with ⁵¹Cr release assay. A certain degree of activity of liver graft-resident NK cells was measured in group A rats. Activity of the liver graft-resident NK cells was partially suppressed by administration of immature DCs (group B and group E) but was significantly elevated by administration of IL-4 stimulated

mature DCs (Group C), whereas the activity of the liver graft-resident NK cells was significantly suppressed by administration of NF- κ B decoy ODNs-modified DCs (group D). The activity value of the liver graft-resident NK cells was $36.47 \pm 6.32\%$ for group A rats, $21.58 \pm 4.61\%$ for group B rats, $52.93 \pm 7.73\%$ for group C rats, $8.43 \pm 2.18\%$ for group D rats, and $23.06 \pm 5.27\%$ for group E rats, respectively. The activity of the liver graft-resident NK cells was significantly lower in group D rats but markedly higher in group C rats than that in the other groups rats ($P < 0.001$). The results suggested that the augmented regeneration of the partial liver allograft induced by NF- κ B decoy ODNs-modified DCs might be associated with the markedly suppressed activity of the liver allograft-resident NK cells.

Suppression of IFN- γ production by NF- κ B decoy ODNs-modified DCs

To determine the relationship of specific immunoregulator cytokine production to the regeneration of partial liver allograft, IFN- γ mRNA expression in the liver graft and serum level of IFN- γ at the time of the maximal liver allograft regeneration were examined by RT-PCR assay and ELISA (as shown in Figure 3 and Figure 4), respectively. A certain level of hepatic IFN- γ mRNA expression and a certain serum level of IFN- γ were detected in group A rats. Hepatic IFN- γ mRNA expression and serum IFN- γ production were partially down-regulated by administration of immature DCs (group B and group E) but were significantly up-regulated by administration of IL-4 stimulated mature DCs (Group C), whereas the hepatic IFN- γ mRNA expression and serum IFN- γ production were significantly suppressed by administration of NF- κ B decoy ODNs-modified DCs (group D). The hepatic IFN- γ mRNA expression level and the serum IFN- γ level were markedly lower in group D rats but markedly higher in group C rats than that in the other groups rats. The results suggested that the augmented regeneration of the partial liver allograft induced by NF- κ B decoy ODNs-modified DCs might be associated with the markedly suppressed hepatic IFN- γ mRNA expression and serum IFN- γ production.

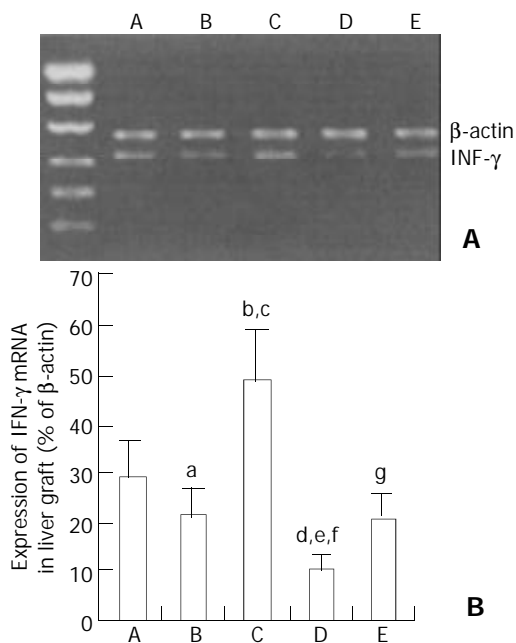


Figure 3 Suppression of IFN- γ mRNA expression in the liver allografts by NF- κ B decoy ODNs-modified DCs. ^a $P < 0.05$ vs group A, ^b $P < 0.001$ vs group A, ^c $P < 0.001$ vs group B, ^d $P < 0.001$ vs group A, ^e $P < 0.001$ vs group B, ^f $P < 0.001$ vs group C, ^g $P > 0.05$ vs group B.

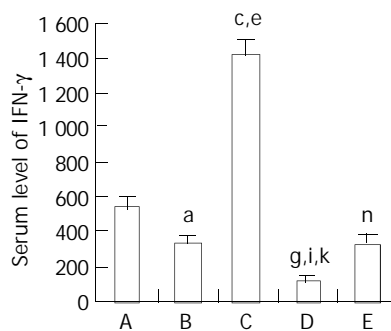


Figure 4 Down-regulation of serum IFN- γ level in recipient rats by NF- κ B decoy ODNs-modified DCs. ^a $P < 0.001$ vs group A, ^c $P < 0.001$ vs group A, ^e $P < 0.001$ vs group B, ^g $P < 0.001$ vs group A, ⁱ $P < 0.001$ vs group B, ^k $P < 0.001$ vs group C, ⁿ $P > 0.05$ vs group B.

DISCUSSION

Our and other studies have shown that NF- κ B decoy ODNs - modified immature DCs, which are stably deficient in surface costimulatory molecules and allosimulatory capacity, could inhibit alloantigen-specific T cell response and prolong cardiac and liver allograft survival in unmodified recipients^[25-27]. NF- κ B also has been found to be an important transcriptional regulator of liver regeneration^[36-39]. NF- κ B could prevent hepatocytes from undergoing apoptosis during development and liver regeneration, and inhibition of NF- κ B activation could induce apoptosis but not proliferation of hepatocytes. Whether the immature DCs modified with NF- κ B decoy ODNs, which inhibit NF- κ B activation, can interfere with the liver allograft regeneration is unknown. To study the effect of NF- κ B decoy ODNs-modified DCs on hepatic regeneration after liver transplantation, we measured the BrdU labeling index of hepatocytes in the partial liver allograft. Uchiyama *et al*^[6] demonstrated that DNA synthesis in liver was slower after an orthotopic transplantation than after a partial hepatectomy. In our partial liver transplantation model, the BrdU labeling index of hepatocytes peaked at 72 h after a allogeneic transplantation, in contrast to the maximum DNA synthesis at 24 h that has been documented after a partial hepatectomy^[40]. In the present study immature DCs or mature DCs were administered to recipient rats 7 days prior to liver transplantation and immediately after liver transplantation to detect whether NF- κ B decoy ODNs-modified DCs could improve the delayed liver graft regeneration. Our results showed that partial liver graft DNA synthesis peaked earlier in group D rats (pretreatment with NF- κ B decoy ODNs-modified immature DCs) but slower in group C rats (pretreatment with mature DCs) than that in the other groups rats. The maximum BrdU labeling index of hepatocytes in group D rats was significantly higher than that in the other groups rats, whereas the maximum BrdU labeling index of hepatocytes in group C rats was significantly lower than that in the other groups rats. In the present study, we also found that pretreatment with NF- κ B decoy ODNs-modified DCs could reduce apoptosis of hepatocytes in the liver graft, however, pretreatment with mature DCs could promote apoptosis of hepatocytes in the liver graft. *In situ* TUNEL staining of the liver graft sections revealed that the maximum apoptosis of hepatocytes was detected in group C rats and the minimum apoptosis of hepatocytes was detected in group D rats. Our results suggested that NF- κ B decoy ODNs-modified DCs could suppress apoptosis of hepatocytes and promote partial liver allograft regeneration.

The mechanisms by which NF- κ B decoy ODNs-modified DCs promote regeneration of partial liver allograft remain to be clarified. In the present study, we found that the augmented regeneration of liver graft induced by NF- κ B decoy ODNs-

modified DCs might be associated with the reduced activity of liver-resident NK cells and the decreased IFN- γ production. A negative correlation was observed between liver regeneration and immune reaction (NK cell activity) in other studies^[11,12], for the liver-resident and spleen-resident NK cells showed specific cytotoxicity against regenerating hepatocytes. Previous studies have shown that the liver grafts contained large numbers of NK cells and NK like cells with early lymphocyte activation before transplantation, and there was an influx of recipient NK and NK-like cells into the liver graft immediately after revascularization^[41] and their cytotoxic activity was significantly augmented in the rejected liver allograft^[42,43]. Other experimental studies have demonstrated that FasL expression on activated NK cells was augmented^[44,45], and FasL ligation to Fas expressed on hepatocytes could mediate hepatocytes apoptosis^[46,47]. Moreover, NK cells produce IFN- γ , which is involved in the aggravation of fulminant hepatitis. Thus, a decrease in NK cell activity may lead to reduction of IFN- γ . Although the definite role of NK cell activity and IFN- γ in liver regeneration is to be clarified, a rapid and profound suppression of a variety of spontaneous functions of NK cells in the liver or blood at the initiation phase of liver regeneration has been shown, including the rapidly decreased NK cell numbers and NK cell activity^[11,12]. Vujanovic *et al*^[14] found that depletion of NK cells by specific antibody accelerated rat liver regeneration after 70% partial hepatectomy. Tanigawa and Tamura^[11,12] also found that FK506 and augmenter of liver regeneration promoted liver regeneration by reducing NK cell activity. Liu *et al*^[9] recently suggested that the enhanced liver regeneration by oral ursodesoxycholic acid was mediated by suppression of NK cell activity in partially hepatectomized rats, and interleukin-2, a potent inducer of allograft rejection, could completely or partially block the decrease in NK activity and the increase in hepatocyte mitotic index. IFN- γ is secreted predominantly by activated T lymphocytes and activated NK cells interact *in vitro* in a complex network of mediators with other immune cytokines. IFN- γ is a potent stimulus for monocytes and macrophages that increases their expression of class II MHC antigens and Fc receptors. It also enhances TNF- α secretion. IFN- γ is also known to control the expression of mitochondrial transcription factor A, a nuclear gene responsible for mitochondrial metabolism. Moreover, IFN- γ could inhibit liver regeneration by stimulating MHC class II antigens expression by Kupffer cells in the regenerating liver^[48]. These MHC class II antigen-positive Kupffer cells act as antigen-presenting cells and present hepatocyte as antigen, the so-called abnormal "self", to helper and cytotoxic T cells. Both types of T cells, in turn, may suppress hepatocyte proliferation. In this respect, a synergistic effect was also observed with the combination of IL-2 and IFN- γ . A recent study demonstrated that administration of IFN- γ inhibited liver regeneration by decreasing the mitochondrial transcription factor A expression^[10]. These data suggested that augmentation of NK cell activity and IFN- γ production could inhibit liver regeneration. In the present study, we found that liver allograft-resident NK cell activity and hepatic IFN- γ mRNA expression and serum INF- γ production at the time of the maximal liver allograft regeneration were significantly suppressed by pretreatment with NF- κ B decoy ODNs-modified immature DCs, whereas liver allograft-resident NK cell activity and hepatic IFN- γ mRNA expression and serum INF- γ production at the time of the maximal liver allograft regeneration were significantly elevated by pretreatment with mature DCs. The results suggested that there was a negative relationship between liver allograft regeneration and NK cell activity and IFN- γ production in the present study.

The mechanisms by which NF- κ B decoy ODNs-modified immature DCs suppress the activity of liver allograft-resident NK cells and IFN- γ production after liver transplantation are

still to be clarified. In our previous study we found *in vitro* and *in vivo* evidences that the stably immature NF- κ B decoy ODNs-treated DCs could suppress T cell allostimulatory ability, promote apoptotic death of live graft-infiltrating lymphocytes, and consequently suppress Th1 immunostimulatory cytokines such as IL-2 and IFN- γ mRNA expression in the liver graft^[27]. We hypothesized that the enhanced apoptosis of liver graft-infiltrating lymphocytes by NF- κ B decoy ODNs-modified DCs could reduce the total number of the activated liver-resident NK cells and suppress the NK cell cytotoxicity to the regenerating hepatocytes. At the same time, the enhanced apoptosis of liver graft-infiltrating lymphocytes could decrease IFN- γ mRNA expression and IFN- γ production in the liver graft.

In summary, pretreatment with NF- κ B decoy ODNs-modified immature DCs can suppress liver allograft-resident NK cell activity and IFN- γ production. The suppressed liver allograft-resident NK cell activity and IFN- γ production, in turn, may suppress hepatocyte apoptosis and promote regeneration of partial liver allograft.

REFERENCES

- Kido M**, Ku Y, Fukumoto T, Tominaga M, Iwasaki T, Ogata S, Takenaga M, Takahashi M, Kuroda Y, Tahara S, Tanaka K, Hwang S, Lee S. Significant role of middle hepatic vein in remnant liver regeneration of right-lobe living donors. *Transplantation* 2003; **75**: 1598-1600
- Eguchi S**, Yanaga K, Sugiyama N, Okudaira S, Furui J, Kanematsu T. Relationship between portal venous flow and liver regeneration in patients after living donor right-lobe liver transplantation. *Liver Transpl* 2003; **9**: 547-551
- Maetani Y**, Itoh K, Egawa H, Shibata T, Ametani F, Kubo T, Kiuchi T, Tanaka K, Konishi J. Factors influencing liver regeneration following living-donor liver transplantation of the right hepatic lobe. *Transplantation* 2003; **75**: 97-102
- Kamel IR**, Erbay N, Warmbrand G, Kruskal JB, Pomfret EA, Raptopoulos V. Liver regeneration after living adult right lobe transplantation. *Abdom Imaging* 2003; **28**: 53-57
- Marcos A**, Fisher RA, Ham JM, Shiffman ML, Sanyal AJ, Luketic VA, Sterling RK, Fulcher AS, Posner MP. Liver regeneration and function in donor and recipient after right lobe adult to adult living donor liver transplantation. *Transplantation* 2000; **69**: 1375-1379
- Uchiyama H**, Yanaga K, Nishizaki T, Soejima Y, Yoshizumi T, Sugimachi K. Effects of deletion variant of hepatocyte growth factor on reduced-size liver transplantation in rats. *Transplantation* 1999; **68**: 39-44
- Selzner N**, Selzner M, Tian Y, Kadry Z, Clavien PA. Cold ischemia decreases liver regeneration after partial liver transplantation in the rat: A TNF- α /IL-6-dependent mechanism. *Hepatology* 2002; **36**(4 Pt 1): 812-818
- Cheung ST**, Tsui TY, Wang WL, Yang ZF, Wong SY, Ip YC, Luk J, Fan ST. Liver as an ideal target for gene therapy: expression of CTLA4Ig by retroviral gene transfer. *J Gastroenterol Hepatol* 2002; **17**: 1008-1014
- Liu L**, Sakaguchi T, Cui X, Shirai Y, Nishimaki T, Hatakeyama K. Liver regeneration enhanced by orally administered ursodesoxycholic acid is mediated by immunosuppression in partially hepatectomized rats. *Am J Chin Med* 2002; **30**: 119-126
- Polimeno L**, Margiotta M, Marangi L, Lisowsky T, Azzarone A, Ierardi E, Frassanito MA, Francavilla R, Francavilla A. Molecular mechanisms of augmenter of liver regeneration as immunoregulator: its effect on interferon-gamma expression in rat liver. *Dig Liver Dis* 2000; **32**: 217-225
- Tanigawa K**, Sakaida I, Masuhara M, Hagiya M, Okita K. Augmenter of liver regeneration (ALR) may promote liver regeneration by reducing natural killer (NK) cell activity in human liver diseases. *J Gastroenterol* 2000; **35**: 112-119
- Tamura F**, Masuhara A, Sakaida I, Fukumoto E, Nakamura T, Okita K. FK506 promotes liver regeneration by suppressing natural killer cell activity. *J Gastroenterol Hepatol* 1998; **13**: 703-708
- Francavilla A**, Vujanovic NL, Polimeno L, Azzarone A, Iacobellis

- A, Deleo A, Hagiya M, Whiteside TL, Starzl TE. The *in vivo* effect of hepatotrophic factors augments liver regeneration, hepatocyte growth factor, and insulin-like growth factor-II on liver natural killer cell functions. *Hepatology* 1997; **25**: 411-415
- 14 **Vujanovic NL**, Polimeno L, Azzarone A, Francavilla A, Chambers WH, Starzl TE, Herberman RB, Whiteside TL. Changes of liver-resident NK cells during liver regeneration in rats. *J Immunol* 1995; **154**: 6324-6338
- 15 **Ohnishi H**, Muto Y, Maeda T, Hayashi T, Nagaki M, Yamada T, Shimazaki M, Yamada Y, Sugihara J, Moriwaki H. Natural killer cell may impair liver regeneration in fulminant hepatic failure. *Gastroenterol Jpn* 1993; **28**(Suppl 4): 40-44
- 16 **Matsushita T**, Ando K, Kimura K, Ohnishi H, Imawari M, Muto Y, Moriwaki H. IL-12 induces specific cytotoxicity against regenerating hepatocytes *in vivo*. *Int Immunol* 1999; **11**: 657-665
- 17 **Sato Y**, Farges O, Buffello D, Bismuth H. Intra- and extrahepatic leukocytes and cytokine mRNA expression during liver regeneration after partial hepatectomy in rats. *Dig Dis Sci* 1999; **44**: 806-816
- 18 **Lee WC**, Zhong C, Qian S, Wan Y, Gauldie J, Mi Z, Robbins PD, Thomson AW, Lu L. Phenotype, function, and *in vivo* migration and survival of allogeneic dendritic cell progenitors genetically engineered to express TGF-beta. *Transplantation* 1998; **66**: 1810-1817
- 19 **Hayamizu K**, Huie P, Sibley RK, Strober S. Monocyte-derived dendritic cell precursors facilitate tolerance to heart allografts after total lymphoid irradiation. *Transplantation* 1998; **66**: 1285-1291
- 20 **Khanna A**, Steptoe RJ, Antonysamy MA, Li W, Thomson AW. Donor bone marrow potentiates the effect of tacrolimus on nonvascularized heart allograft survival: association with microchimerism and growth of donor dendritic cell progenitors from recipient bone marrow. *Transplantation* 1998; **65**: 479-485
- 21 **Lu L**, Li W, Zhong C, Qian S, Fung JJ, Thomson AW, Starzl TE. Increased apoptosis of immunoreactive host cells and augmented donor leukocyte chimerism, not sustained inhibition of B7 molecule expression are associated with prolonged cardiac allograft survival in mice preconditioned with immature donor dendritic cells plus anti-CD40L mAb. *Transplantation* 1999; **68**: 747-757
- 22 **Lutz MB**, Suri RM, Niimi M, Ogilvie AL, Kukutsch NA, Rossner S, Schuler G, Austyn JM. Immature dendritic cells generated with low doses of GM-CSF in the absence of IL-4 are maturation resistant and prolong allograft survival *in vivo*. *Eur J Immunol* 2000; **30**: 1813-1822
- 23 **Chiang YJ**, Lu L, Fung JJ, Qian S. Liver-derived dendritic cells induce donor-specific hyporesponsiveness: use of sponge implant as a cell transplant model. *Cell Transplant* 2001; **10**: 343-350
- 24 **Yoo-Ott KA**, Schiller H, Fandrich F, Oswald H, Richter K, Xhu XF, Kampen WU, Kronke M, Zavazava N. Co-transplantation of donor-derived hepatocytes induces long-term tolerance to cardiac allografts in a rat model. *Transplantation* 2000; **69**: 2538-2546
- 25 **Giannoukakis N**, Bonham CA, Qian S, Chen Z, Peng L, Harnaha J, Li W, Thomson AW, Fung JJ, Robbins PD, Lu L. Prolongation of cardiac allograft survival using dendritic cells treated with NF-kB decoy oligodeoxyribonucleotides. *Mol Ther* 2000; **1**(5 Pt 1): 430-437
- 26 **Bonham CA**, Peng L, Liang X, Chen Z, Wang L, Ma L, Hackstein H, Robbins PD, Thomson AW, Fung JJ, Qian S, Lu L. Marked prolongation of cardiac allograft survival by dendritic cells genetically engineered with NF-kappa B oligodeoxyribonucleotide decoys and adenoviral vectors encoding CTLA4-Ig. *J Immunol* 2002; **169**: 3382-3391
- 27 **Xu MQ**, Suo YP, Gong JP, Wang F, Yan LN. Tolerance of rat liver allograft induced by nuclear factor-kappa B decoy oligodeoxynucleotides - modified dendritic cells. *World J Gastroenterol* (In process)
- 28 **Abeyama K**, Eng W, Jester JV, Vink AA, Edelbaum D, Cockerell CJ, Bergstresser PR, Takashima A. A role for NF-kappaB-dependent gene transactivation in sunburn. *J Clin Invest* 2000; **105**: 1751-1759
- 29 **Xu MQ**, Yao ZX. Functional changes of dendritic cells derived from allogeneic partial liver graft undergoing acute rejection in rats. *World J Gastroenterol* 2003; **9**: 141-147
- 30 **Bouwens L**, Wisse E. Immuno-electron microscopic characterization of large granular lymphocytes (natural killer cells) from rat liver. *Eur J Immunol* 1987; **17**: 1423-1428
- 31 **Ikejima K**, Enomoto N, Iimuro Y, Ikejima A, Fang D, Xu J, Forman DT, Brenner DA, Thurman RG. Estrogen increases sensitivity of hepatic Kupffer cells to endotoxin. *Am J Physiol* 1998; **274**(4 Pt 1): G669-G676
- 32 **McKnight AJ**, Barclay AN, Mason DW. Molecular cloning of rat interleukin 4 cDNA and analysis of the cytokine repertoire of subsets of CD4+ T cells. *Eur J Immunol* 1991; **21**: 1187-1194
- 33 **Plumpe J**, Malek NP, Bock CT, Rakemann T, Manns MP, Trautwein C. NF-kappaB determines between apoptosis and proliferation in hepatocytes during liver regeneration. *Am J Physiol Gastrointest Liver Physiol* 2000; **278**: G173-G183
- 34 **Taira K**, Hiroyasu S, Shiraishi M, Muto Y, Koji T. Role of the Fas system in liver regeneration after a partial hepatectomy in rats. *Eur Surg Res* 2001; **33**: 334-341
- 35 **Masson S**, Scotte M, Garnier S, Francois A, Hiron M, Teniere P, Fallu J, Salier JP, Daveau M. Differential expression of apoptosis-associated genes post-hepatectomy in cirrhotic vs normal rats. *Apoptosis* 2000; **5**: 173-179
- 36 **Kirilova I**, Chaisson M, Fausto N. Tumor necrosis factor induces DNA replication in hepatic cells through nuclear factor kappaB activation. *Cell Growth Differ* 1999; **10**: 819-828
- 37 **Brenner DA**. Signal transduction during liver regeneration. *J Gastroenterol Hepatol* 1998; **13**(Suppl): S93-S95
- 38 **Iimuro Y**, Nishiura T, Hellerbrand C, Behrns KE, Schoonhoven R, Grisham JW, Brenner DA. NFkappaB prevents apoptosis and liver dysfunction during liver regeneration. *J Clin Invest* 1998; **101**: 802-811
- 39 **Chaisson ML**, Brooling JT, Ladiges W, Tsai S, Fausto N. Hepatocyte-specific inhibition of NF-kappaB leads to apoptosis after TNF treatment, but not after partial hepatectomy. *J Clin Invest* 2002; **110**: 193-202
- 40 **Xu MQ**, Han BL, Xue L, Gong JP. Ursodeoxycholic acid promotes liver regeneration after partial hepatectomy in bile duct obstructive rats. *Zhonghua Ganzangbing Zazhi* 2002; **10**: 103-105
- 41 **Navarro F**, Portales P, Candon S, Pruvot FR, Pageaux G, Fabre JM, Domergue J, Clot J. Natural killer cell and alphabeta and gammadelta lymphocyte traffic into the liver graft immediately after liver transplantation. *Transplantation* 2000; **69**: 633-639
- 42 **Li W**, Lu L, Wang Z, Wang L, Fung JJ, Thomson AW, Qian S. IL-12 antagonism enhances apoptotic death of T cells within hepatic allografts from Flt3 ligand-treated donors and promotes graft acceptance. *J Immunol* 2001; **166**: 5619-5628
- 43 **Navarro F**, Portales P, Pageaux JP, Perrigault PF, Fabre JM, Domergue J, Clot J. Activated sub-populations of lymphocytes and natural killer cells in normal liver and liver grafts before transplantation. *Liver* 1998; **18**: 259-263
- 44 **Hsieh CL**, Obara H, Ogura Y, Martinez OM, Krams SM. NK cells and transplantation. *Transpl Immunol* 2002; **9**: 111-114
- 45 **Kojima Y**, Kawasaki-Koyanagi A, Sueyoshi N, Kanai A, Yagita H, Okumura K. Localization of Fas ligand in cytoplasmic granules of CD8+ cytotoxic T lymphocytes and natural killer cells: participation of Fas ligand in granule exocytosis model of cytotoxicity. *Biochem Biophys Res Commun* 2002; **296**: 328-336
- 46 **Ariki N**, Morimoto Y, Yagi T, Oyama T, Cyouda Y, Sadamori H, Inagaki M, Urushihara N, Iwagaki H, Tanaka N. Activated T cells and soluble molecules in the portal venous blood of patients with cholestatic and hepatitis C virus-positive liver cirrhosis. Possible promotion of Fas/FasL-mediated apoptosis in the bile-duct cells and hepatocyte injury. *J Int Med Res* 2003; **31**: 170-180
- 47 **Wang J**, Li W, Min J, Qu Q, Chen J. Fas siRNA reduces apoptotic cell death of allogeneic-transplanted hepatocytes in mouse spleen. *Transplant Proc* 2003; **35**: 1594-1595
- 48 **Sato Y**, Tsukada K, Matsumoto Y, Abo T. Interferon-gamma inhibits liver regeneration by stimulating major histocompatibility complex class II antigen expression by regenerating liver. *Hepatology* 1993; **18**: 340-346

A novel method for preparation of tissue microarray

Han-Lei Dan, Ya-Li Zhang, Yan Zhang, Ya-Dong Wang, Zuo-Sheng Lai, Yu-Jie Yang, Hai-Hong Cui, Yan-Ting Jian, Jian Geng, Yan-Qing Ding, Chun-Hai Guo, Dian-Yuan Zhou

Han-Lei Dan, Ya-Li Zhang, Ya-Dong Wang, Zuo-Sheng Lai, Yu-Jie Yang, Hai-Hong Cui, Yan-Ting Jian, Dian-Yuan Zhou, Institute of Digestive Medicine, Nanfang Hospital, First Military Medical University, Guangzhou 510515, Guangdong Province, China
Yan Zhang, Jian Geng, Yan-Qing Ding, Department of Pathology, Nanfang Hospital, First Military Medical University, Guangzhou 510515, Guangdong Province, China

Chun-Hai Guo, Center Department of Chinese Academy of Engineering and Physics, Mianyang 621000, Sichuan Province, China

Co-correspondents: Han-Lei Dan and Ya-Li Zhang

Correspondence to: Dr. Han-Lei Dan, M.D., Institute of Digestive Medicine, Nanfang Hospital, First Military Medical University, Guangzhou 510515, Guangdong Province, China. henrydan@sina.com

Telephone: +86-20-61341531 **Fax:** +86-20-61341531

Received: 2003-05-11 **Accepted:** 2003-08-18

Abstract

AIM: To improve the technique of tissue microarray (tissue chip).

METHODS: A new tissue microarraying method was invented with a common microscope installed with a special holding needle, a sampling needle, and a special box fixing paraffin blocks on the microscope slide carrier. With the movement of microscope tube and objective stage on vertical and cross dimensions respectively, the holding procedure on the recipient paraffin blocks and sampling procedure of core tissue biopsies taken from the donor blocks were performed with the refitted microscope on the same platform. The precise observation and localization of representative regions in the donor blocks were also performed with the microscope equipped with a stereoscope.

RESULTS: Highly-qualified tissue chips of colorectal tumors were produced by a new method, which simplified the conventional microarraying procedure, and was more convenient and accurate than that employing the existing tissue microarraying instruments.

CONCLUSION: Using the refitted common microscope to produce tissue microarray is a simple, reliable, cost-effective and well-applicable technique.

Dan HL, Zhang YL, Zhang Y, Wang YD, Lai ZS, Yang YJ, Cui HH, Jian YT, Geng J, Ding YQ, Guo CH, Zhou DY. A novel method for preparation of tissue microarray. *World J Gastroenterol* 2004; 10(4): 579-582

<http://www.wjgnet.com/1007-9327/10/579.asp>

INTRODUCTION

Tissue microarray (TMA, tissue chip) is one of the most important biochip technologies, following the gene chip and protein chip. This technology was first illustrated by Kononen *et al*^[1] in the magazine of *Nature Medicine* in 1998, who then has been working with the National Human Genome Research Institute. Illuminated by the idea of DNA microarray (gene

chip), Kononen *et al* proposed a new method of tissue microarray to improve the conventional process of immunostaining and fluorescent *in situ* hybridization (FISH) of individual tissue sections, which was laborious, low-efficient, vulnerable to various factors affecting the experiments and poor comparability.

TMA technology is sharply distinguished from the methods illustrated by Battifora *et al*^[2] (1986) and Wan *et al*^[3] (1987), which involved manually randomized rearrangement of tissue specimens. The difference lies in that the spots on TMA chips are minute (0.6 mm-2.0 mm in diameter), the quantity is huge (up to 1000 arrays at present), the shape is regular and the arrays are ordinal. The results obtained from TMAs are more scientific and comparable while the research is more informative, efficient and requires less consumption of reagents. Besides, it paves the way to the standardization of inspection and automation of analysis, which eventually makes the molecular pathological research step forward on the way of standardization and advancement in technology^[4-7].

Nevertheless, the current facilities of tissue microarrays are not advanced as expected but are costly. Moreover, it is not convenient to observe and locate the exact sites in the donor tissue blocks, or to install, adjust and replace the holding and sampling needles. Thus, the whole procedure takes much time that restricts the wide application of this particular technology^[8,9]. To make up the inadequacy, we proposed a new methodology of TMA in the following section, which is convenient, up-to-date and well applicable.

MATERIALS AND METHODS

Technical design

The key techniques of TMA included high-adhesive glass slide preparation, reliable tissue specimen acquisition, tissue core arrangement, fine sectioning and section transferring techniques, as well as tissue staining and molecular pathological technology. The core technology was the acquisition of reliable tissue specimen and arrangement of tissue cores, which involved tissue fixation, collection, dehydration, embedding, tissue array design and sampling procedures, especially the exact location of needed tissue, instruments and methods of sampling and puncture, *etc.* To avoid the inadequacy of the current TMA method, we proposed a new method for fabrication of TMAs through re-equipping the common microscope. With the precise mechanical controls and sampling site observation of the microscope, the new procedure simplified the holding, sampling and inserting process, increased reliabilities, and reduced costs and was ready for wide application.

Equipments and articles

Following equipments and articles were required: a refitted common light microscope; a set of holding, sampling needles and related components (China patent No. 03113734.2), which were installed in the objective holder; a special paraffin-fixing box (China patent No. 03113733.4) placed on the slide carrier; turn buckles and screw nuts fitted by the microscope pillar for controlling the moving range of object stage or the lens; the buckles for fixing glass slide carrier; sufficient paraffin-

embedded donor and recipient blocks; a temperature controlling oven; adhesive-coated glass slides; a tissue sectioning and transferring system as well as instruments, equipments and reagents of routine staining and molecular pathology. A stereomicroscope, a scanning apparatus and a computer automation analysis system were needed if available.

Tissue sample acquisition

This method could be applied in fabrication of paraffin embedded tissue microarrays. We took surgically or endoscopically sectioned fresh tissue, and banked paraffin-embedded tissue blocks as the specimen. The acquisition procedure included tissue fixation, collection, dehydration, hyaline and paraffin embedding, which were basically not different from the routine ones. However, to ensure the quality of TMA, procedures such as the use of fixation solutions and fixing time should be standardized and mRNA in the specimen should be preserved as much as possible.

Paraffin TMA block construction

This was one of the key techniques in the new procedure. Illustrated in Figure 1(A, B, C, D), the basic process included holing in the recipient blocks, location on the donor blocks, tissue core sampling and inserting. A. Holing A recipient block is fixed in the paraffin-fixing box, and the holing needle is tuned to the working place, and punched into the exact site of the recipient block and then is drawn back with adjustment of the rotating screw. Then the core needle is pressed to squeeze out the paraffin in the needle. B. Location A donor block is fixed in the paraffin-fixing box, and the stereomicroscope lens is tuned to the working place, then the exact sampling site is observed and fixed in the center part of the microscopic vision field. C. Sampling The sampling needle is tuned to the working place, and inserted into the selected site of donor block, and retrieved with the adjustment of rotating screw. D. Inserting With the microscope stage moving, the recipient block moves under the sampling needle. When the sampling needle moves exactly above the recipient hole, the core needle is pressed to squeeze out the tissue core and then inserted it into the recipient hole.

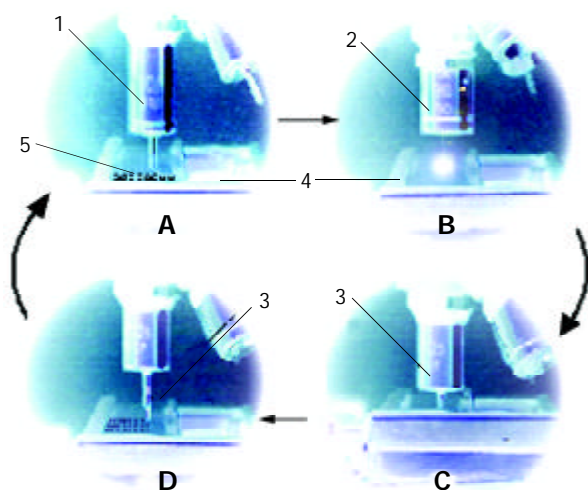


Figure 1 Procedures of paraffin-embed tissue micro-arraying. (1. holing needle, 2. stereomicroscope lens, 3. sampling needle, 4. paraffin block-fixing box, 5. recipient paraffin block).

Sectioning, transferring and staining or molecular pathological detecting

After insertion of all the samples, the recipient block was taken out from the fixing box and heated up to 58-65 °C and the tissue

core was flattened by a glass slide and then cooled down. The next procedures were sectioning, tissue slice transferring and routine staining (HE) or PCR, immunofluorescent *in situ* hybridization, *etc.* (Figures 3-4).

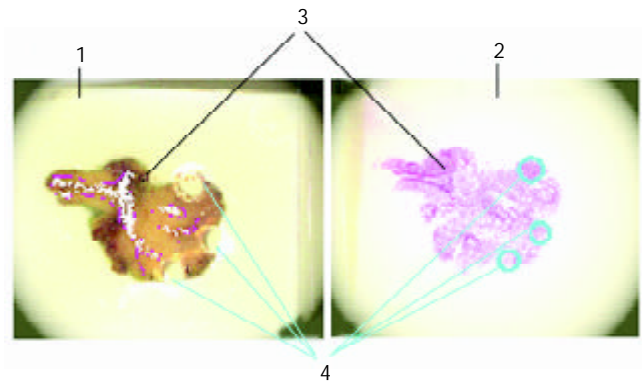


Figure 2 Defining accurate sampling sites in donor block under stereomicroscope. (1. Paraffin donor block and paraffin embedded tissue under stereomicroscope, 2. Routine section and HE staining of paraffin embedded donor tissue under stereomicroscope, 3. Regions of stroma, less cells or areas with no tissue, 4. Sampling locus.).

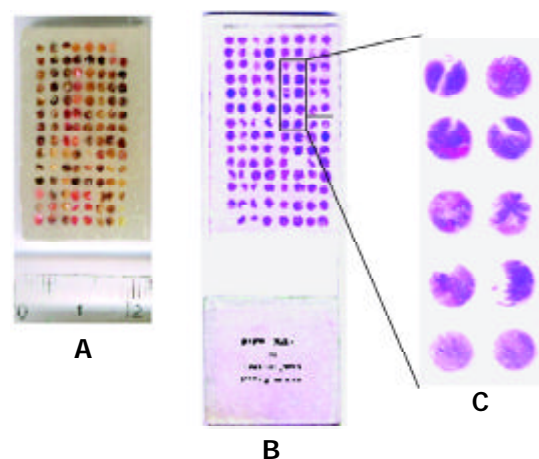


Figure 3 Pictures of paraffin-embedded tissue core arrangement (A), tissue spot arrays on slide (B) and magnified (X8) picture of selected array spots (C).

Computer imaging scan and data analysis

High-throughput digital imaging scanning and processing systems, as well as computer database programs such as Access, Excel were used to examine each core under microscope simultaneously. Data were analyzed with clinical information.

RESULTS

Employing the above method, high-quality tissue chips of colorectal tumors were successfully produced. Figure 3A is an image of the paraffin embedded tissue core arrays, which was 24 mm×35 mm in size. Every 3 core-specimens were obtained from each paraffin-embedded biopsy specimen, resulting in 111 cores from 35 colorectal tumor biopsy specimens (including colorectal adenocarcinoma, adenoma, non-adenoma polyps) and 2 normal colorectal tissue specimens. Each core was 1.3 mm in diameter and 0.7 mm in spacing.

The tissue micro-array of colorectal tumors on a glass slide (HE staining) is displayed in Figure 3B. The blank spot (dot array) on the left-hand corner was the location mark, and the blank spot in the center part was lost during sectioning and

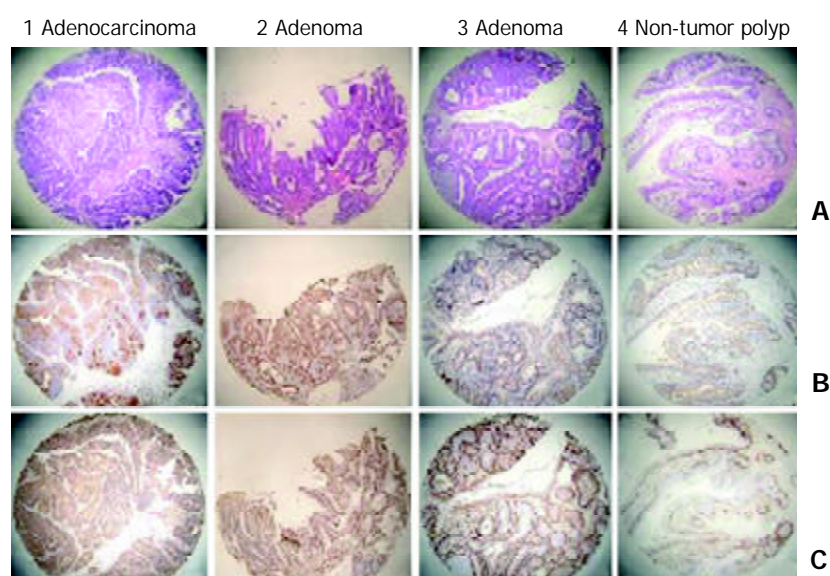


Figure 4 Photographs of different tissue array elements stained with HE(A) and immunohistochemistry (B: P53, C: PCNA).

Table 1 Comparison of gene, protein and tissue chips

	Gene chip	Protein chip	Tissue chip
Substrate	Definitive DNA or RNA (Oligo or cDNA)	Definitive proteins (antigens\ antibodies, <i>etc.</i>)	Many tissue samples
Probes	Labelled DNA or RNA (Cy3 and Cy5 -tyramide)	Labelled antigens or antibodies	Specific antigens or antibodies, as well as labelled DNA or RNA sequences
Target material	Various sequences of DNA or RNA	Multiple kinds of proteins	Morphology and DNA, RNA and proteins
Superiorities	Analyzing numerous genes simultaneously in the same sample	Analyzing numerous proteins simultaneously in the same sample	Profile of genes or proteins in numerous tissues or populations
Applications	Large-scale, parallel analysis of genetic alterations, functions and drug researches at DNA and RNA level	Large-scale, parallel analysis of concentrations, functional activities or interactions of proteins	Large-scale, parallel <i>in situ</i> analysis of DNA, RNA and proteins associated with clinical endpoints in hundreds of cell types or tissues at one time

staining, which made a rate of 0.8% non-evaluable core biopsy sections. The selected spots in Figure 3B were magnified (X8) in Figure 3C under a stereoscope and the dot arrays were in good order, sharp bordered, not crushed or deformed. All the arraying tissue specimens were representative of the interest regions, which coincidentally met the research demands.

Good staining quality was also attained on the same array sites in different slides stained with HE, immunohistochemistry and others respectively. The results were more comparable and sensitive on the chip slide as shown in Figure 4. Further detailed analyses would be reported soon.

DISCUSSION

As one of the three most important biochip technologies, tissue microarray has been accepted as a large-scale, parallel molecular analysis just like gene and protein chips^[3-6,10-15]. The results were more scientific, comparable, informative and efficient, and it needed less consumption of reagents^[16-23]. The difference lies in that the dot arrays of tissue chip were specimens from hundreds of different tissues and could show the features of morphology and expressions of DNA, RNA or proteins *in situ* associated with clinical endpoints at the same time. And the procedure was less complex and the results were more clinically applicable. Thus TMA is more feasible in the functional researches of gene and protein, especially in researches of gene or protein profiles in different tissues or populations. Therefore TMA has become one of the most

important methods in functional genomic and proteomic researches in the post-genomic era and, it has been expected to have wide applications in molecular pathology, drug discovery, monitoring of hygiene and environment, as well as national defense researches (Table 1)^[24,25].

However, the present technology of TMA is still not satisfactory. On the one hand, the instruments were not very advanced but costly. On the other hand, the present procedure took time and was not convenient to observe and locate the exact sites in donor tissue blocks^[8,9,26-32]. The new method to produce tissue microarray with refitted common microscope we presented here has the following advantages. (1) With the precise mechanical control of common microscope, the holing and sampling procedures in the paraffin recipient block and donor block are simpler and more accurate. (2) The punching procedure of holing and sampling needles is controlled by the adjustment of microscope stage or lens regulating screw, which frees us from direct finger operation and avoids needle gliding or trembling. This method is less laborious and easier and more accurate to control the holing and sampling depth. (3) The working place of holing and sampling needles and object lens changes with the rotation of objective holder and thus is easier to replace the needles and more convenient to apply the single-use holing and sampling needles in order to maintain a higher accuracy. (4) With this new method, the sampling sites can be easily and accurately observed and located under a microscope or a stereomicroscope and thus spares the efforts of marking the regions to punch on the face of the donor block and without

eyeballing, as is the case with the Beecher's instruments. (5) The whole process of holing, locating and sampling is performed with the same instrument on the same platform and thus spares uses of other platforms and instruments.

As TMA involves a number of related technologies and sciences, including engineering, surface physics and chemistry, pathology, molecular biology and information science, to produce high-quality tissue biochips, consideration should be also taken into the design of arrays, the qualities of holing and sampling needles, sectioning and transferring techniques, staining and other molecular pathological techniques. To improve the density and precision of arrays, the needles should be more minute in diameter and sharper in point. The arrangement of arrays should be in accordance with the research objectives and the computer imaging, and statistical tools should be provided for efficient management of a large amount of data generated from this high-throughput approach^[33-35].

REFERENCES

- Kononen J**, Bubendorf L, Kallioniemi A. Tissue microarrays for high-throughput molecular profiling of tumor specimens. *Nat Med* 1998; **4**: 844-847
- Battifora H**. The multitumor (sausage) tissue block: novel method for immunohistochemical antibody testing. *Lab Invest* 1986; **55**: 244-248
- Wan WH**, Fortuna MB, Furmanski P. A rapid and efficient method for testing immunohistochemical reactivity of monoclonal antibodies against multiple tissue samples simultaneously. *J Immunol Methods* 1987; **103**: 121-129
- Hsu FD**, Nielsen TO, Alkushi A. Tissue microarrays are an effective quality assurance tool for diagnostic immunohistochemistry. *Mod Pathol* 2002; **15**: 1374-1378
- Kallioniemi OP**. Biochip technologies in cancer research. *Ann Med* 2001; **33**: 142-147
- Stears RL**, Martinsky T, Schena M. Trends in microarray analysis. *Nat Med* 2003; **9**: 140-145
- Ball CA**, Sherlock G, Parkinson H, Rocca-Sera P, Brooksbank C, Causton HC, Cavalieri D, Gaasterland T, Hingamp P, Holstege F, Ringwald M, Spellman P, Stoeckert CJ Jr, Stewart JE, Taylor R, Brazma A, Quackenbush J. Microarray Gene Expression Data (MGED) Society. Standards for microarray data. *Science* 2002; **298**: 539
- Hoos A**, Cordon-Cardo C. Tissue microarray profiling of cancer specimens and cell lines: opportunities and limitations. *Lab Invest* 2001; **81**: 1331-1338
- Merseburger AS**, Kuczyk MA, Serth J, Bokemeyer C, Young DY, Sun L, Connelly RR, McLeod DG, Mostofi FK, Srivastava SK, Stenzl A, Moul JW, Sesterhenn IA. Limitations of tissue microarrays in the evaluation of focal alterations of bcl-2 and p53 in whole mount derived prostate tissues. *Oncol Rep* 2003; **10**: 223-228
- Torhorst J**, Bucher C, Kononen J, Haas P, Zuber M, Kochli OR, Mross F, Dieterich H, Moch H, Mihatsch M, Kallioniemi OP, Sauter G. Tissue microarrays for rapid linking of molecular changes to clinical endpoints. *Am J Pathol* 2001; **159**: 2249-2256
- Wang HT**, Kong JP, Ding F, Wang XQ, Wang MR, Liu LX, Wu M, Liu ZH. Analysis of gene expression profile induced by EMP-1 in esophageal cancer cells using cDNA Microarray. *World J Gastroenterol* 2003; **9**: 392-398
- Xu SH**, Qian LJ, Mou HZ, Zhu CH, Zhou XM, Liu XL, Chen Y, Bao WY. Difference of gene expression profiles between esophageal carcinoma and its pericancerous epithelium by gene chip. *World J Gastroenterol* 2003; **9**: 417-422
- Zhou J**, Zhao LQ, Xiong MM, Wang XQ, Yang GR, Qiu ZL, Wu M, Liu ZH. Gene expression profiles at different stages of human esophageal squamous cell carcinoma. *World J Gastroenterol* 2003; **9**: 9-15
- Zhu H**, Bilgin M, Bangham R, Hall D, Casamayor A, Bertone P, Lan N, Jansen R, Bidlingmaier S, Houfek T, Mitchell T, Miller P, Dean RA, Gerstein M, Snyder M. Global analysis of protein activities using proteome chips. *Science* 2001; **293**: 2101-2105
- Rao J**, Seligson D, Hemstreet GP. Protein expression analysis using quantitative fluorescence image analysis on tissue microarray slides. *Biotechniques* 2002; **32**: 924-926
- Van 't Veer LJ**, De Jong D. The microarray way to tailored cancer treatment. *Nat Med* 2002; **8**: 13-14
- Kim WH**, Rubin MA, Dunn RL. High-density tissue microarray. *Am J Surg Pathol* 2002; **26**: 1236-1238
- Bubendorf L**, Nocito A, Moch H, Sauter G. Tissue microarray (TMA) technology: miniaturized pathology archives for high-throughput in situ studies. *J Pathol* 2001; **195**: 72-79
- Rimm DL**, Camp RL, Charette LA, Costa J, Olsen DA, Reiss M. Tissue microarray: a new technology for amplification of tissue resources. *Cancer J* 2001; **7**: 24-31
- Moch H**, Kononen T, Kallioniemi OP, Sauter G. Tissue microarrays: what will they bring to molecular and anatomic pathology? *Adv Anat Pathol* 2001; **8**: 14-20
- Moch H**, Schraml P, Bubendorf L, Mirlacher M, Kononen J, Gasser T, Mihatsch MJ, Kallioniemi OP, Sauter G. High-throughput tissue microarray analysis to evaluate genes uncovered by cDNA microarray screening in renal cell carcinoma. *Am J Pathol* 1999; **154**: 981-986
- Nocito A**, Kononen J, Kallioniemi OP, Sauter G. Tissue microarrays (TMAs) for high-throughput molecular pathology research. *Int J Cancer* 2001; **94**: 1-5
- Andersen CL**, Hostetter G, Grigoryan A, Sauter G, Kallioniemi A. Improved procedure for fluorescence in situ hybridization on tissue microarrays. *Cytometry* 2001; **45**: 83-86
- Packeisen J**, Buerger H, Krech R, Boecker W. Tissue microarrays: a new approach for quality control in immunohistochemistry. *J Clin Pathol* 2002; **55**: 613-615
- Parker RL**, Huntsman DG, Lesack DW, Cupples JB, Grant DR, Akbari M, Gilks CB. Assessment of interlaboratory variation in the immunohistochemical determination of estrogen receptor status using a breast cancer tissue microarray. *Am J Clin Pathol* 2002; **117**: 723-728
- Chen W**, Foran DJ, Reiss M. Unsupervised imaging, registration and archiving of tissue microarrays. *Proc AMIA Symp* 2002: 136-139
- Chung GG**, Kielhorn EP, Rimm DL. Subjective differences in outcome are seen as a function of the immunohistochemical method used on a colorectal cancer tissue microarray. *Clin Colorectal Cancer* 2002; **1**: 237-242
- Rubin MA**, Dunn R, Strawderman M, Pienta KJ. Tissue microarray sampling strategy for prostate cancer biomarker analysis. *Am J Surg Pathol* 2002; **26**: 312-319
- Hendriks Y**, Franken P, Dierssen JW, De Leeuw W, Wijnen J, Dreef E, Tops C, Breuning M, Brocker-Vriends A, Vasen H, Fodde R, Morreau H. Conventional and tissue microarray immunohistochemical expression analysis of mismatch repair in hereditary colorectal tumors. *Am J Pathol* 2003; **162**: 469-477
- Wang Y**, Wu MC, Sham JS, Zhang W, Wu WQ, Guan XY. Prognostic significance of c-myc and AIB1 amplification in hepatocellular carcinoma. A broad survey using high-throughput tissue microarray. *Cancer* 2002; **95**: 2346-2352
- Gancberg D**, Di Leo A, Rouas G, Jarvinen T, Verhest A, Isola J, Piccart MJ, Larsimont D. Reliability of the tissue microarray based FISH for evaluation of the HER-2 oncogene in breast carcinoma. *J Clin Pathol* 2002; **55**: 315-317
- Sugita M**, Geraci M, Gao B, Powell RL, Hirsch FR, Johnson G, Lapadat R, Gabrielson E, Bremnes R, Bunn PA, Franklin WA. Combined use of oligonucleotide and tissue microarrays identifies cancer/testis antigens as biomarkers in lung carcinoma. *Cancer Res* 2002; **62**: 3971-3979
- Liu CL**, Prapong W, Natkunam Y, Alizadeh A, Montgomery K, Gilks CB, van de Rijn M. Software tools for high-throughput analysis and archiving of immunohistochemistry staining data obtained with tissue microarrays. *Am J Pathol* 2002; **161**: 1557-1565
- Rubin MA**, Dunn R, Strawderman M, Pienta KJ. Tissue microarray sampling strategy for prostate cancer biomarker analysis. *Am J Surg Pathol* 2002; **26**: 312-319
- Boguski MS**, McIntosh MW. Biomedical informatics for proteomics. *Nature* 2003; **422**: 233-237

Levels of v5 and v6 CD44 splice variants in serum of patients with colorectal cancer are not correlated with pT stage, histopathological grade of malignancy and clinical features

Bogdan Zalewski

Bogdan Zalewski, 2nd Department of General and Gastroenterological Surgery, Medical University of Bialystok, Poland

Correspondence to: Bogdan Zalewski M.D., 2nd Department of General and Gastroenterological Surgery, Medical University of Bialystok, M. Skłodowskiej-Curie st. 24a, 15-276 Bialystok, Poland. bogdan-zalewski@wp.pl

Telephone: +48-85-7468622 **Fax:** +48-85-7468622

Received: 2003-10-10 **Accepted:** 2003-11-20

Abstract

AIM: This study was designed to compare the levels of v5 and v6 splice variants of CD44 evaluated using ELISA test in the serum of patients with colorectal cancer in different stages of progression of the disease estimated in pT stage according to WHO score, histopathological grade of malignancy and some clinicopathological features.

METHODS: The serum obtained from 114 persons with colorectal adenocarcinomas was examined using ELISA method. pT stage and grade of malignancy of the tumour were examined in formalin fixed and paraffin embedded materials obtained during operation.

RESULTS: Only the level of CD44 v5 in the serum of patients before operation with G2 pT4 tumour was lower than that in other probes and the difference was statistically significant. We did not find any other correlations between the level of v5 and v6 CD44 variants and other evaluated parameters.

CONCLUSION: The level of CD44 v5 and v6 estimated by ELISA test in the serum can not be used as a prognostic factor in colorectal cancer.

Zalewski B. Levels of v5 and v6 CD44 splice variants in serum of patients with colorectal cancer are not correlated with pT stage, histopathological grade of malignancy and clinical features. *World J Gastroenterol* 2004; 10(4): 583-585
<http://www.wjgnet.com/1007-9327/10/583.asp>

INTRODUCTION

Neoplasms are the second, or according to some authors, the third cause of deaths all over the world just after the cardiovascular and infectious diseases, and just before communication accidents. Colorectal cancers are among other neoplasms on the third place in morbidity and mortality after the breast and lung and bronchus cancers in women and prostate and lung and bronchus cancers in men. According to American National Cancer Institute, 105 500 persons had a colon cancer and 42 000 rectum cancer in 2002 in the United States of America. Colorectal cancer is also the third cause of death among all neoplasms. It is estimated that over 57 000 persons died in 2003 in the United States due to colon cancer^[1]. According to World Health Organization data in 1990,

over 437 000 persons died and 783 000 became ill due to colorectal cancer. The incidence of this disease has been rising, and is more frequent in developed countries. The survival rate after radical operative treatment and chemo- or radiotherapy is still unsatisfactory. The 5-year survival after radical treatment was about 60% in the United States and Western Europe, whereas it was only about 40% in Eastern Europe^[2]. The recurrence of the disease is dependent on the progression of neoplasms metastases to lymph nodes and distal organs and is the most common cause of death^[3-6]. The routine examinations of specimens with the estimation of the pT according to WHO score as well as the histopathological grade of malignancy, clinical evaluation and even the changes in CEA levels in the serum evaluation are still insufficient to determine the precise prognosis about recurrence of the disease and survival rate. This is the reason, why a lot of medical investigations are concerned with understanding these problems and determining the prognostic factors in colorectal cancers, *i.e.* mutations of c-Ki-ras, C-Myc, APC, p53, DCC and other genes, CD44 protein in the tumour tissues and CEA and CA19.9 in the serum^[6-14]. The aim of this study was to determine if there were any differences between levels of variant 5 and 6 glycoprotein CD44 according to pT stage and histopathological grade of malignancy as well as some clinical features.

MATERIALS AND METHODS

Patients

One hundred and fourteen patients with colorectal adenocarcinoma were operated at the 2nd Department of General and Gastroenterological Surgery of Medical University of Bialystok, Poland in 1997-2001. There were 68 (59.65%) men and 46 (40.35%) women. The median age was 65 years (range: 32-87 years). The diagnosis was made based on clinical symptoms and endoscopic examination as well as histopathological study of tissue samples. Other types of cancer and polyps were excluded from the investigation. Fifty-nine cases (51.75%) of tumours were localized in the rectum and sigmoid colon and the rest, fifty-five cases (48.25%) were localized in other parts of the large bowel. Twelve tumours were inoperable. All the patients were divided into 6 groups according to the grade of malignancy and pT stage (Table 1, Table 2). The patients had not any preoperative chemo- or radiotherapy. All the patients were monitored after operation. Thirty-one (27.19%) of the controls died due to the recurrence of the disease (Table 3).

Tissue and serum samples

Tumour tissues were obtained during the operation. They were typically prepared and paraffin embedded sections were examined to estimate pT score and malignancy grade in G1-G3 score. The blood was collected from these patients before (sample A) and 10 days after the operation (sample B). The blood was centrifuged at 4 °C and the serum samples were

stored at -80°C until examination. The level of v5 and v6 variants of CD44 protein in the serum samples was estimated by ELISA test using kits for SCD44var(v5) and SCD44var(v6) ELISA (Bender MedSystem) according to the manufacturer's protocol. The values of levels obtained in our examination are presented in Table 4.

Statistical analysis

χ^2 Pearson, χ^2 NW, NIR and *U* Mann-Whitney tests were used to analyse the correlation between CD44v5 and CD44v6 expressions before (v5A, v6A) and after the operation (v5B, v6B), and such features as sex, age, location of the tumour in the large bowel (sigmo-rectal or the rest of the colon), the clinical stage according to pT stage and the grade of malignancy as well as the time of survival and the presence of recurrence. Student *t* test was used to analyse correlation between control and tested groups. *P* values less than 0.05 were considered to be statistically significant.

RESULTS

The level of CD44 v5 splice variant in the serum obtained from patients with colorectal adenocarcinoma evaluated by ELISA test before operation was lower in G2 pT4 stage of tumour than those in others probes and the difference was statistically significant. But there were not any other statistically significant correlations with clinicopathological features like sex, age, location of the tumour, pT stage and the grade of malignancy estimated in 3-stage score from G1 to G3. There were not any other differences between levels of that variant before and after operation as well.

The level of CD44 v6 evaluated in the serum obtained from patients did not correlate with any clinical and histopathological features. Also, there was not any statistically significant difference between its levels before and after operation.

The level of both v5 and v6 CD44 variants in the serum did not correlate with the recurrences of cancer and mortality (Table 4).

Table 1 Sex of patients, grade of malignancy (G) and pT stage

	Inoperable tumours	G2 pT2	G2 pT3	G2 pT4	G3 pT3	G3 pT4	All
Women	4 33.33%	4 44.44%	23 40.35%	5 41.67%	10 52.63%	0 0.00%	46 40.35%
Men	8 66.67%	5 55.56%	34 59.65%	7 58.33%	9 47.37%	5 100.00%	68 59.65%
All	12 10.53%	9 7.89%	57 50.00%	12 10.53%	19 16.67%	5 4.39%	114 100.00%

Table 2 Location of tumour, grade of malignancy (G) and pT stage

	Inoperable tumours	G2pT2	G2pT3	G2pT4	G3pT3	G3pT4	All
Sigmoid and rectum	6 59.00%	4 44.44%	34 59.65%	6 50.00%	7 36.84%	2 40.00%	59 51.75%
Colon	6 50.00%	5 55.56%	23 40.35%	6 50.00%	12 63.16%	3 60.00%	55 48.25%
All	12 10.53%	9 7.89%	57 50.00%	12 10.53%	19 16.67%	5 4.39%	114 100.00%

Table 3 Mortality, grade of malignancy (G) and pT stage

	Inoperable tumours	G2pT2	G2pT3	G2pT4	G3pT3	G3pT4	All
Alive	1 8.33%	8 88.89%	48 84.21%	11 91.67%	12 63.16%	3 60.00%	83 72.81%
Dead	11 91.67%	1 11.11%	9 15.79%	1 8.38%	7 36.84%	2 40.00%	31 27.19%
All	12 10.53%	9 7.89%	57 50.00%	12 10.53%	19 16.67%	5 4.39%	114 100.00%

Table 4 Mean values of CD44 v5 and CD44 v6 before and after operation (ng/ml)

	v5 A	v5 B	v6 A	v6 B
Age: <65	28.38	26.50	185.42	171.52
>65	25.18	27.61	178.78	183.18
Location: the sigmoid and the rectum	24.92	30.08	173.26	178.15
the colon	29.38	25.28	192.17	186.04
Inoperable tumours	29.88	25.92	178.42	189.17
G2 pT2	24.47	25.01	184.49	177.44
G2 pT3	26.98	27.87	181.96	181.78
G2 pT4	32.72	28.85	153.63	165.09
G3 pT3	23.21	23.76	181.74	183.00
G3 pT4	25.14	23.28	142.00	164.80

DISCUSSION

CD44 described at first by Dalchau in 1980 is a molecule which can take part in carcinogenesis and formation of metastases in lymph nodes and distal organs^[15]. It is a cell surface transmembrane glycoprotein which occurs in both healthy and neoplasm cells. The gene which codes for CD44 consists of 20 exons, and 10 of them can be combined, so there are a lot of its variants. It can also be modified just after the process of translation. The most common molecule with a molecular weight 85-90 kd is called standard molecule and is the main surface receptor of hyaluronic acid. It also takes an active part in intracellular communication and interactions between the cell and the extracellular matrix. It is responsible for T lymphocyte and natural killer cell activation, aggregation and B and T cell migration. It also induces the tumour necrosis factor and interleukin 1 release. So it is described as a main factor in the formation of metastases, however the precise mechanism of its function is still unknown^[16-19]. Examinations of standard CD44 molecule in tumour tissues and in neoplasm lymph nodes showed its higher expression^[6,20-23]. The examinations of some isoforms of CD44 in cancer and lymph nodes tissues showed the same results, but the number of examined patients was small^[24-26]. Especially v5 and v6 CD44 splice variant expression was higher in tumour tissues and depended on cancer progression^[6]. Elevated levels of sCD44v6 in malignant ascites was also described^[27]. Some publications about expression of v6 CD44 and v8-10CD44 isoform in the serum of patients with colorectal cancer did not show any correlation with pathological features and metastases^[28-30]. The same results of examination concerned with CD44 v5 and v6 were presented in this study. The lack of correlation between expression of v5 and v6 variants of CD44 and clinicopathological features could depend on the absence of these molecules in the soluble form in the serum.

In conclusion, there is no association between CD44v5 and v6 expression estimated in the serum and any clinicopathological features in patients with colorectal adenocarcinomas. Due to the short time of observation it is not implicated as a prognostic factor in colorectal cancer and it demands further investigations.

REFERENCES

- Jemal A**, Thomas A, Murray T, Thurn M. Cancer Statistics, 2003. *CA Cancer J Clin* 2003; **5**: 5-26
- Parkin M**, Pisani P, Ferlay J. Global Cancer Statistic. *Ca Cancer J Clin* 1999; **49**: 33-64
- Al-Mehdi AB**, Tozawa K, Fisher AB, Shientag L, Lee A, Muschel RJ. Intravascular origin of metastasis from the proliferation of endothelium - attached tumor cells: a new model for metastasis. *Nature Med* 2000; **6**: 100-102
- Fodde R**. The APC gene in colorectal cancer. *Eur J Cancer* 2002; **38**: 867-871
- Wielenga VJM**, van der Voort R, Taher TEI, Smit L, Beuling E, van Krimpen C, Spaargaren M, Pals ST. Expression of c-Met and Heparan-Sulfate proteoglycan forms of CD44 in colorectal cancer. *Am J Path* 2000; **157**: 1563-1573
- Zhang JC**, Wang ZR, Cheng YJ, Yang DZ, Shi JS, Liang AL, Liu NN, WangXM. Expression of proliferating cell nuclear antigen and CD44 variant exon 6 in primary tumors and corresponding lymph node metastases of colorectal carcinoma with Dukes' stage C or D. *World J Gastroenterol* 2003; **9**: 1482-1486
- Xu XM**, He C, Hu XT, Fang BL. Tumor necrosis factor-related apoptosis-inducing ligand gene on human colorectal cancer cell line HT29. *World J Gastroenterol* 2002; **9**: 965-969
- McArdle C**. Effectiveness of follow up. *BMJ serial online Nov* 2000; **321**: 1332-1335
- Kraemer M**, Wiratkapun S, Seow-Choen F, Nyam D. Stratifying Risk Factors for follow-up. A comparison of recurrent and non-recurrent colorectal cancer. *Dis Colon Rectum* 2001; **44**: 815-821
- Portera CA**, Berman RS, Ellis LM. Molecular determinants of colon cancer metastasis. *Surg Oncol* 1998; **7**: 183-195
- Meyer T**, Hart IR. Mechanisms of tumour metastasis. *Eur J Cancer* 1998; **34**: 214-221
- Zhang XM**, Sheng SR, Wang XY, Wang JR, Li J. Expression of tumor related genes NGX6, NAG-7, BRD7 in gastric and colorectal cancer. *World J Gastroenterol* 2003; **9**: 1729-1733
- Dunlop MG**. Science, medicine, and the future: Colorectal cancer. *BMJ serial online Jun* 1997; **314**: 1882-1988
- Sidransky D**. Emerging molecular markers of cancer. *Nat Rev Cancer* 2002; **2**: 210-219
- Dalchau R**, Kirkley J, Fahre JW. Monoclonal antibody to a human leukocyte-specific membrane glycoprotein probably homologous to the leukocyte-common (L-C) antigen of the rat. *Eur J Immunol* 1980; **10**: 737-744
- Ponta H**, Wainwright D, Herrlich P. The CD44 protein family. *Int J Biochem Cell Biol* 1998; **30**: 299-305
- Isacke C**, Yarwood H. The hyaluronan receptor, CD44. *Int J Biochem Cell Biol* 2002; **34**: 718-721
- Kincade PW**, Zhong Z, Shigeki K, Leif H. The importance of cellular environment to function of the CD 44 matrix receptor. *Curr Opin Cell Biol* 1997; **9**: 635-642
- Lindblom A**, Liljegen A. Tumour markers in malignancies. *BMJ serial online Feb* 2000; **320**: 424-427
- Liu PF**, Wu MC, Cheng H, Qian GX, Fu JL. Clinical significance of expression of metastasis-associated splice variants of CD44 mRNA in early primary liver cancer. *China Natl J New Gastroenterol* 1996; **2**: 112-114
- Fujisaki T**, Tanaka Y, Fujii K, Mine S, Saito K, Yamada S, Yamashita U, Irimura T, Eto S. CD44 stimulation induces integrin-mediated adhesion of colon cancer cell lines to endothelial cells by up-regulation of integrins and c-Met and activation of integrins. *Cancer Res* 1999; **59**: 4427-4434
- Llaneza A**, Gonzales A, Andicochea A, Fernandez JC, Allende MT, Garcia-Muniz JL, Vizoso F. CD44s, CD44v5 and CD44v6 protein contents in colorectal cancer and surrounding mucosa. *Int J Biol Marker* 2000; **15**: 192-194
- Zalewski B**, Famulski W, Sulkowska M, Sobaniec-Lotowska M, Piotrowski Z, Kisielewski W, Sulkowski S. CD44 expression in colorectal cancer. An immunohistochemical study including correlation with cathepsin D immunoreactivity and some tumour clinicopathological features. *Folia Histochem Cytobiol* 2001; **39**: 152-153
- Harada N**, Mizoi T, Kinouchi M, Hoshi K, Ishii S, Sasaki I, Matsuno S. Introduction of antisense CD44s cDNA down-regulates expression of overall CD44 isoforms and inhibits tumor growth and metastasis in highly metastatic colon carcinoma cells. *Int J Cancer* 2001; **91**: 67-75
- Wong LS**, Cantrill JE, Morris AG, Fraser IA. Expression of CD44 splice variants in colorectal cancer. *Br J Surg* 1997; **84**: 363-367
- Chun SJ**, Bae OS, Kim JB. The significance of CD44 variants expression in colorectal cancer and its regional lymph nodes. *J Korean Med Sci* 2000; **15**: 696-700
- Dong WG**, Sun XM, Yu BP, Luo HS, Yu JP. Role of VEGF and CD44v6 in differentiating benign from malignant ascites. *World J Gastroenterol* 2003; **11**: 2596-2600
- Weg-Remers S**, Hildebrandt U, Feifel G, Moser C, Zeitz M, Stallmach A. Soluble CD44 and CD44v6 Serum levels in patients with colorectal cancer are independent of tumor stage and tissue expression of CD44v6. *Am J Gastroenterol* 1998; **93**: 790-794
- Givvehchian M**, Worner S, Strater J, Zoller M, Heuschen U, Heuschen G, Lehnert T, Herfarth C, von Knebel Doeberitz M. No evidence for cancer-related splice variants in primary and metastatic colorectal cancer. *Eur J Cancer* 1998; **34**: 1099-1104
- Goi T**, Yamaguchi A, Seki K, Nakagawara G, Urano T, Shiku H, Furukawa K. Soluble protein encoded by CD44 variant exons 8-10 in the serum of patients with colorectal cancer. *Br J Surg* 1997; **84**: 1452-1453

Does recombinant human erythropoietin accelerate correction of post-ulcer-bleeding anaemia? A pilot study

Spiros D. Ladas, Dimitrios Polymeros, Thomas Pagonis, Konstantinos Triantafyllou, Gregorios Paspatis, Maria Hatzigiorgiou, Sotirios A. Raptis

Spiros D. Ladas, Dimitrios Polymeros, Thomas Pagonis, Konstantinos Triantafyllou, Maria Hatzigiorgiou, Sotirios A. Raptis, Gastroenterology Unit, 2nd Department of Internal Medicine, Athens University, Evangelismos Hospital, Athens, Greece
Gregorios Paspatis, Gastroenterology Department, Benizelion Hospital, Herakleion, Crete, Greece

Correspondence to: Associate Professor Spiros D. Ladas, MD, Gastroenterology Unit, 2nd Department of Internal Medicine, Athens University, Evangelismos Hospital, 23 Sisini street, 115 28 Athens, Greece. sdladas@hol.gr

Telephone: +3021 0 7210 213 **Fax:** +3021 0 7225 882

Received: 2003-08-11 **Accepted:** 2003-10-20

Abstract

AIM: Anaemia caused by acute upper gastrointestinal bleeding is treated with blood transfusion or iron, but patients usually face a two-month recovery period from post-haemorrhage anaemia. This prospective, randomised, open, pilot study was designed to investigate whether recombinant human erythropoietin (Epoetin) therapy accelerate haematocrit increase in the post-bleeding recovery period.

METHODS: We studied hospitalised patients admitted because of acute ulcer bleeding or haemorrhagic gastritis, who had a haematocrit of 27-33% and did not receive blood transfusions. One day after the endoscopic confirmation of cessation of bleeding, they were randomised either to erythropoietin (20 000 IU Epoetin alfa subcutaneously, on days 0, 4 and 6) plus iron (100 mg im, on days 1- 6, (G₁) or iron only (G₂). Haematocrit was measured on days 0, 6, 14, 30, 45, and 60, respectively.

RESULTS: One patient from G₁ and two from G₂ were lost to follow-up. Therefore, 14 and 13 patients from G₁ and G₂ respectively were analysed. Demographic characteristics, serum iron, ferritin, total iron binding capacity, reticulocytes, and haematocrit were not significantly different at entry to the study. Median reticulocyte counts were significantly different between groups on day six (G₁: 4.0, 3.0-6.4 vs G₂: 3.5, 2.1-4.4%, $P=0.03$) and median haematocrit on day fourteen [G₁: 35.9, 30.7-41.0 vs G₂: 32.5, 29.5-37.0% (median, range), $P=0.04$].

CONCLUSION: Erythropoietin administration significantly accelerates correction of anemia after acute ulcer bleeding. The haematocrit gain is equivalent to one unit of transfused blood two weeks after the bleeding episode.

Ladas SD, Polymeros D, Pagonis T, Triantafyllou K, Paspatis G, Hatzigiorgiou M, Raptis SA. Does recombinant human erythropoietin accelerate correction of post-ulcer-bleeding anaemia? A pilot study. *World J Gastroenterol* 2004; 10(4): 586-589
<http://www.wjgnet.com/1007-9327/10/586.asp>

INTRODUCTION

Following an episode of acute gastrointestinal bleeding from

peptic ulcer disease, patients face a two-month recovery period from post haemorrhage iron deficiency anaemia. If haematocrit is lower than 25%, corresponding to a haemoglobin value of 8 g/dl, patients are usually treated with blood transfusion supplemented with iron replenishment therapy. However, when haematocrit is higher than 30%, it slowly recovers with iron administration alone. During this recovery period patients are unable to work and face health-related reduced quality of life, because of iron deficiency anaemia, at least until haematocrit is increased to more than 35%. Therefore, shortening the recovery phase from post-haemorrhage anaemia is of clinical importance.

Erythropoietin is a glycoprotein hormone, synthesized predominantly in the kidney, that promotes the differentiation of erythroid progenitor cells and therefore it regulates the production of red blood cells. In addition, it stimulates the synthesis of haemoglobin^[1]. In the recent years, recombinant human erythropoietin (r-HuEPO, Epoetin Alfa) has become readily available and permitted the clinical investigation and application of this hormone to the treatment of anaemia. Epoetin Alfa has been shown to accelerate erythropoiesis and reduce the requirement for blood transfusion in patients undergoing gynaecologic surgery^[2] and those with anaemia because of chronic renal failure^[3], inflammatory bowel disease^[4], or human immunodeficiency virus infection^[5]. The success of Epoetin Alfa in treating anaemia in the post surgical recovery period^[6] suggests that it may be of benefit as an adjuvant therapy in treating the post haemorrhage anaemia due to peptic ulcer bleeding. The aim therefore of the present pilot study was to investigate whether adjuvant therapy with erythropoietin could be of benefit to this patient population, by accelerating an increase of the haematocrit during the recovery period from anaemia.

MATERIALS AND METHODS

Patients

Over a two-year period (1998-1999), 30 hospitalised adult patients admitted to our departments because of acute gastrointestinal bleeding from peptic ulcer or haemorrhagic gastritis were invited to participate in this prospective, randomised open pilot study. Patients included in the study fulfilled the following criteria. They did not require blood transfusion for resuscitation. They also had a stable haematocrit value at between 30-33% for men (normal range: 39-49%) and 25-30% for women (normal range: 33-43%) after confirming the cessation of the bleeding episode by endoscopy performed on the third day of hospitalisation. All patients should have a clean-based ulcer or red spot, indicating a low (<3%) rebleeding rate^[7]. Exclusion criteria were any known causes of anaemia including haematologic diseases, cancer, gastric surgery, or intention to use non-steroidal anti-inflammatory drugs following hospital discharge. Women of childbearing age, those with uncontrolled hypertension or seizure history and patients with severe chronic diseases were also excluded from the study.

Patients gave written informed consent to the study, after full explanation by the investigators. The study protocol was approved by our institution review board on human studies.

Methods

Study design Patients eligible to enter the study had haematocrit determinations on the second and third day of hospitalisation. If haematocrit had not changed by more than 1%, they were randomised according to a computer-generated randomisation list to Epoetin plus iron or iron therapy alone. Neither patients nor investigators were blinded to the therapy.

All patients were treated with intramuscular injections of 332 mg/2 ml ferric hydroxide polymaltose complex, corresponding to 100 mg of Fe³⁺, (Ferrum Hausmann®, Vifor, St. Gallen, Switzerland). Injections were given on days one to six. The total quantity of injected Fe³⁺ was 600 mg. Those randomised into the Epoetin group received adjuvant therapy with 20 000 IU of recombinant human erythropoietin (Epoetin Alfa, Eprex®, Cilag, Switzerland) given subcutaneously on days zero, four and six. The total quantity of Epoetin given was 60 000 IU. Patients were also treated with 20 mg of omeprazole twice daily, iv, for peptic ulcer bleeding over the initial 3-5 days of hospitalisation. They then resumed a normal diet and received 20 mg of omeprazole/day, orally, for one month. In those patients who were *H pylori* positive, eradication therapy was scheduled after completing follow-up, *i.e.*, two months after the bleeding episode.

Haematocrit and reticulocytes (normal value: 0.5-1.5%) were measured on days 0, 6, 14, 30, 45 and 60, respectively. Serum iron (normal values: 50-160 µg/dl), ferritin (normal values: 12-300 µg/dl) and total iron binding capacity (TIBC) (normal values: 250-400 µg/dl) were measured on days 0, 14, 30 and 45 from randomisation.

Statistical analysis

Data were analysed by the statistical packages SPSS 10.0.0 (SPSS Inc., Chicago, Illinois, USA) and Statgraphics Plus 4.0 (Manugistics Inc., Statistical Graphics Corp., Rockville, USA). Numerical data were assessed by the non-parametric Mann-Whitney two-sided *U*-test and the Kruskal-Wallis *t* test used for two- and multiple-sample comparison analysis, respectively.

Results in the text and table are presented as median with ranges. Data in figures are presented as box-and-whisker plots. The box includes 50% of the results falling between 25th and 75th percentile (interquartile distance). The median value is represented as a horizontal line inside the box. Outliers, *i.e.*, points more than 1.5 times the interquartile range from the end of the box are shown as open circles. A *P* value less than 0.05 was considered statistically significant.

RESULTS

Over the two-year study period, 30 adults fulfilling the inclusion criteria were randomised into the two treatment arms. Demographic and laboratory characteristics were not significantly different between the two groups at entry to the study (Table 1). Three patients were lost to follow up. Therefore, 14 patients in the Epoetin-iron treatment group and 13 patients in the iron treatment group were available for analysis.

Serum iron levels significantly increased over the study period within each group (Figure 1), but they were not significantly different between treatment groups anytime during the study period (Mann-Whitney *U* test>62, *P*>0.67). All the patients had normal serum ferritin levels during the study period. Ferritin did not significantly change over time either in the Epoetin-iron treatment group (Kruskal-Wallis *T*=0.07, *P*=0.1) or the iron treatment group (Kruskal-Wallis *T*=7.47, *P*=0.06). There was not any significant difference of

ferritin levels between treatment groups anytime during the study (Mann-Whitney *U* test>46.5, *P*>0.14). Similar results to ferritin were obtained for TIBC, which did not significantly change over time either within the Epoetin-iron (Kruskal-Wallis *T*=2.87, *P*=0.41) or the iron treatment group (Kruskal-Wallis *T*=3.50, *P*=0.32). In addition, there was not any significant difference of TIBC between treatment groups anytime during the study (Mann-Whitney *U* test>58.5, *P*>0.22).

Table 1 Demographic and laboratory data (median, range) of patients included in each treatment arm

	Epoetin+Iron (G ₁ , n=15)	Iron (G ₂ , n=15)	^a <i>P</i> -value
Male/female	10/ 5	10/ 5	
Age (years)	62, 36-70	58, 35-71	0.54
Ulcer/haemorrhagic gastritis	13/ 2	12/ 3	
Lost to follow up	1	2	
Haematocrit (%) ^b	29.0, 26.0-33.0	28.8, 26.0-32.5	0.9
Reticulocytes (%) ^b	3.3, 2.4-3.9	2.8, 2.3-4.2	0.63
Serum iron (µg/dl) ^b	37, 18-54	38, 24-63	0.37
Ferritin (µg/dl) ^b	78, 20-147	64, 41-173	0.96
TIBC (µg/dl) ^b	302, 224-392	302, 250-391	0.92

^aMann-Whitney two-sided *U*-test, ^bat entry to the study.

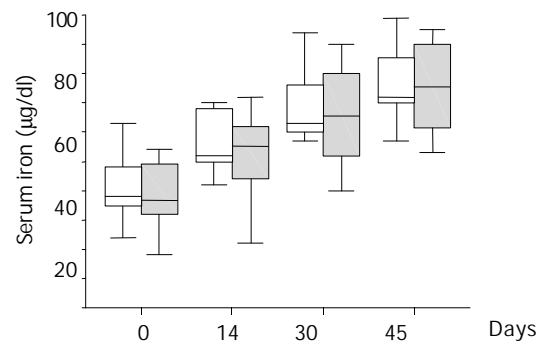


Figure 1 Box-and-whisker plots showing a progressive increase of serum iron levels over the recovery period from peptic ulcer bleeding of patients treated with either Epoetin alfa plus iron (G₁, dashed whiskers) or iron only (G₂, open whiskers). There were not any statistically significant differences between treatment groups anytime during the study (two-tailed Mann-Whitney *U* test>62, *P*>0.67).

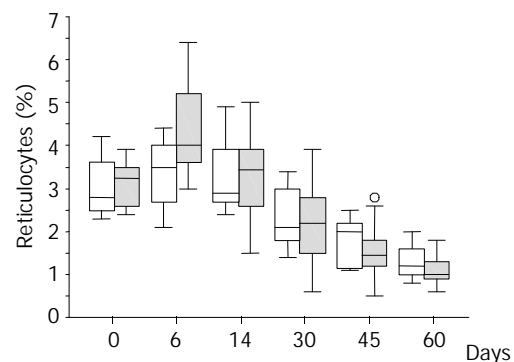


Figure 2 Box-and-whisker plots showing percent reticulocyte counts over the recovery period from peptic ulcer bleeding of patients treated with Epoetin alfa plus iron (G₁, dashed whiskers) and those treated with iron only (G₂, open whiskers). On day six patients in G₁ had significantly different (higher) median percent reticulocyte counts as compared with G₂ (two-tailed Mann-Whitney *U* test=46.5, *P*=0.03).

There was a brisk increase of reticulocyte counts in both groups on the sixth day of the study. This was the only date when there was a significant difference between the treatment groups in favour of the Epoetin-iron group (median: 4.0% versus 3.5%,) (Mann-Whitney U test=46.5, P <0.03) (Figure 2). Following the sixth day of the study, the reticulocyte counts were progressively decreased in both groups. Haematocrit increased over the study period within each group (Figure 3), but it was significantly different between treatment groups (higher in the Epoetin-iron group) only on the fourteenth day of the study (median: 35.85% versus 32.5%, range: 30, 7-41 versus 29, 5-37) (Mann-Whitney U test=49, P =0.041) (Figure 3). Epoetin therapy was not associated with any side effects in our study.

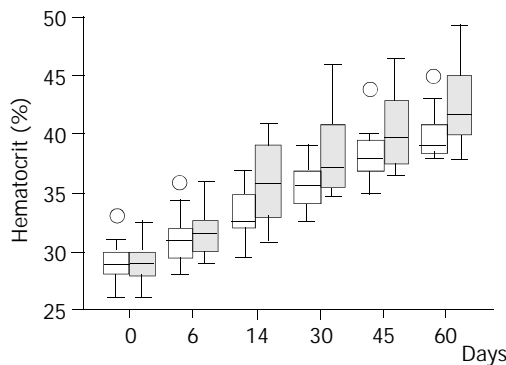


Figure 3 Box-and-whisker plots showing haematocrit values over the recovery period from peptic ulcer bleeding of patients treated with Epoetin alfa plus iron (G_1 , dashed whiskers) and those treated with iron only (G_2 , open whiskers). On day fourteen patients in G_1 had significantly different (higher) haematocrit values as compared with G_2 (two-tailed Mann-Whitney U test=49.0, P =0.041).

DISCUSSION

Acute upper gastrointestinal bleeding is a major cause of hospitalisation. Data from the USA and UK indicate that the overall incidence of acute upper gastrointestinal bleeding was about 100 hospital admissions per 100 000 adult population per year^[8,9]. In about 50% of these patients, the causes of bleeding were peptic ulcer or erosive-haemorrhagic gastritis. There are no guidelines dictating when patients with acute peptic ulcer bleeding should undergo transfusion. However, common sense dictates that stable patients, *i.e.*, those who did not continue to bleed and had a low risk of rebleeding^[10], as confirmed by emergency endoscopy, or a haematocrit higher than 25% should avoid blood transfusion^[11]. Hui and co-authors have recently shown that patients under the age of 60 admitted because of bleeding duodenal ulcer, having no stigmata of haemorrhage on emergency endoscopy and no concurrent serious medical illness might be discharged within 24 hours of endoscopy if haematocrit was above 30% and there were no clinical signs of circulatory instability^[12]. One might therefore, argue that our patients were candidates for early discharge. However, the prolongation of hospitalization in our study was only due to study practicalities, since the Epoetin-iron therapy could be safely administered on an outpatient basis.

Avoiding blood transfusion is wise in this group of patients. There is a worldwide concern of blood born transmission of infectious agents, and the risk of significant reduction in the blood donor pool with the planned introduction of testing for prior disease. The risk of infection per blood unit transfused was estimated by mathematical models to 1:676 000 for HIV, 1:103 000 for HCV and 1:63 000 for HBV infection^[13,14]. Transmission of hepatitis A or G virus was rare^[14] and occurred

primarily in the window period^[15]. The most common infectious agents transmitted were cytomegalovirus^[16] and *Yersinia enterocolitica*^[17]. The immunologic risks ranged from mild febrile nonhaemolytic reactions to fatal haemolytic ones^[18]. In addition, transfusion-associated graft-versus-host disease might be seen in immunocompetent patients^[18, 13].

Hospitalised patients for acute upper gastrointestinal bleeding may avoid blood transfusions, but following their discharge from the hospital they face a two-month recovery period from acute post haemorrhage anaemia. Symptoms experienced by anaemic patients included cold skin, dizziness, palpitations, or depression, which substantially affect patients' quality of life. Identifying patients most likely to benefit from blood conservation is not always easy. There was a recent debate about the threshold for transfusion at which the benefits outweigh the risks^[18]. No doubt even elderly patients might tolerate haematocrit of about 20-22%, especially those with megaloblastic anaemia. However, patients having haematocrit of about 30% at discharge might feel unable to work until haematocrit recovers to about 35%. It is therefore of clinical importance to improve the functional status of the anaemic patients by shortening the recovery period from iron deficiency anaemia.

Recombinant human erythropoietin (Epoetin Alfa) has been shown to accelerate erythropoiesis in certain anaemia states^[3-5,18]. It has also been used perioperatively in gynaecologic surgery^[2,6] and in a few cases of Jehovah's Witness hospitalised for acute gastrointestinal bleeding^[20-22,25]. Epoetin Alfa may therefore allow a lower value of haematocrit to be accepted, above which one would not transfuse. Our data agree with published studies showing an increase of haematocrit in the erythropoietin treated anaemic patients between one and two weeks post treatment^[2,6,23,24]. They also showed that patients with post haemorrhage anaemia treated with erythropoietin plus iron had a higher median haematocrit (35.9%) two weeks after the bleeding episode compared with controls treated with iron only (32.5%). This gain of 3.4% of haematocrit corresponds to one unit of transfused blood.

We used an adequate iron dose to replenish iron stores, as it was shown by normal ferritin and serum iron levels in all patients throughout the two-month study period. This is essential for patients treated with recombinant human erythropoietin, because it stimulates erythropoiesis and may quickly exhaust iron stores. We selected the intramuscular iron formulation to avoid dark-stained stools that might be mistaken for recurrence of bleeding. However, since oral iron is preferred to intramuscular injections, further studies are needed to investigate whether oral iron therapy may have the same beneficial result simplifying the therapeutic regime of iron-Epoetin, and avoiding possible side effects of iron injections.

Various doses of Epoetin have been used to stimulate erythropoiesis ranging from 50 to 600 IU/kg. In the study of Rutherford *et al*^[24] higher doses of Epoetin were associated with quicker stimulation of erythropoiesis, indicated by a significant increase of haematocrit by the sixth day. Our patients were treated with a lower dose of Epoetin (300 IU/kg), which may explain why they had a later response (day 14).

Our pilot study has demonstrated that patients who have been treated with Epoetin Alfa in addition to iron have accelerated response in terms of erythropoiesis. However, Epoetin is an expensive drug, the cost per treatment was 2.5 Euro for iron and 533.5 Euro for the Epoetin regime in our study. A larger study with a different design should address the secondary end-points of symptom scores and quality of life changes and also the socio-economic consequences like the time lost from work and the time of resumption of activities. The usefulness of Epoetin as a blood conserving adjuvant therapy should also be tested in the high-risk subgroup of

haemodynamically unstable patients who need transfusions. This has been suggested by case reports of severe GI bleeding in Jehovah's Witnesses who refused blood transfusions^[20,21,25].

REFERENCES

- 1 **Bieber E.** Erythropoietin, the biology of erythropoiesis and epoetin alfa. An overview. *J Reprod Med* 2001; **46**(5 Suppl): 521-530
- 2 **Larson B,** Bremme K, Clyne N, Nordstrom L. Preoperative treatment of anemic women with epoetin beta. *Acta Obstet Gynecol Scand* 2001; **80**: 559-562
- 3 **Silverberg DS,** Blum M, Agbaria Z, Deutsch V, Irony M, Schwatz D, Baruch R, Yachnin T, Steinbruch S, Iaina A. The effect of i.v. iron alone or in combination with low-dose erythropoietin in the rapid correction of anemia of chronic renal failure in the predialysis period. *Clin Nephrol* 2001; **55**: 212-219
- 4 **Gasche C,** Waldhoer T, Feichtenschlager T, Male C, Mayer A, Mittermayer C, Petritsch W. Prediction of response to iron sucrose in inflammatory bowel disease-associated anemia. *Am J Gastroenterol* 2001; **96**: 2382-2387
- 5 **Allen UD,** Kirby MA, Goeree R. Cost-effectiveness of recombinant human erythropoietin versus transfusions in the treatment of zidovudine-related anemia in HIV-infected children. *Pediatr AIDS HIV Infect* 1997; **8**: 4-11
- 6 **Atabek U,** Alvarez R, Pello MJ, Alexander JB, Camishion RC, Curry C, Spence RK. Erythropoietin accelerates hematocrit recovery in post-surgical anemia. *Am Surg* 1995; **61**: 74-77
- 7 **Laine L,** Peterson WL. Bleeding peptic ulcer. *N Eng J Med* 1994; **331**: 717-727
- 8 **Longstreth GF.** Epidemiology of hospitalization for acute upper gastrointestinal hemorrhage: a population-based study. *Am J Gastroenterol* 1995; **90**: 206-210
- 9 **Rockall TA,** Logan RF, Devlin HB, Northfield TC. Incidence of and mortality from acute upper gastrointestinal haemorrhage in the United Kingdom. Steering Committee members of the National Audit of Acute Upper Gastrointestinal Haemorrhage. *BMJ* 1995; **311**: 222-226
- 10 **Rockall TA,** Logan RF, Devlin HB, Northfield TC. Risk assessment after acute upper gastrointestinal haemorrhage. *Gut* 1996; **38**: 316-321
- 11 **Goodnough LT,** Bach RG. Anemia, transfusion, and mortality. *N Eng J Med* 2001; **345**: 1272-1274
- 12 **Hui WM,** Lai KC, Chin K, Lam SK. Can ulcer bleeding patients without stigmata of recent haemorrhage be discharged on the same day. A retrospective and prospective study. *Gastroenterol* 1992; **102**: A85
- 13 **AuBuchon JP,** Birkmeyer JD, Bush MP. Safety of the blood supply in the United States: opportunities and controversies. *Ann Intern Med* 1997; **127**: 904-909
- 14 **Goodnough LT,** Brecher ME, Kanter MH, AuBuchon JP. Transfusion medicine. First of two parts transfusion-blood. *N Engl J Med* 1999; **340**: 438-447
- 15 **Kleinman SH,** Busch MP, Korelitz JJ, Schreiber GB. The incidence/window period model and its use to assess the risk of transfusion-transmitted human immunodeficiency virus and hepatitis C virus infection. *Transfus Med Rev* 1997; **11**: 155-172
- 16 **Wilhelm JA,** Matter L, Schopfer K. The risk of transmitting cytomegalovirus to patients receiving blood transfusion. *J Infect Dis* 1986; **154**: 169-171
- 17 **No authors listed.** Red blood cell transfusions contaminated with *Yersinia enterocolitica* - United States, 1991-1996, and initiation of a national study to detect bacteria-associated transfusion reactions. *Morb Mortal Wkly Rep* 1997; **46**: 553-555
- 18 **Welch G,** Meehan KR, Goodnough LT. Prudent strategies for elective red blood cell transfusion. *Ann Intern Med* 1992; **116**: 393-401
- 19 **Seidenfeld J,** Piper M, Flamm C, Hasselblad V, Armitage JO, Bennett CL, Gordon MS, Lichtin AE, Wade JL 3rd, Woolf S, Aronson R. Epoetin treatment of anemia associated with cancer therapy: a systematic review and meta-analysis of controlled clinical trials. *J Natl Cancer Inst* 2001; **93**: 1204-1414
- 20 **Pousada L,** Fiorito J, Smyth C. Erythropoietin and anemia of gastrointestinal bleeding in a Jehovah's Witness. *Ann Intern Med* 1990; **112**: 552
- 21 **Smith SN,** Milov DE. Use of erythropoietin in Jehovah's Witness children following acute gastrointestinal blood loss. *J Fla Med Assoc* 1993; **80**: 103-105
- 22 **Koenig HM,** Levine EA, Resnick DJ, Meyer WJ. Use of recombinant human erythropoietin in a Jehovah's Witness. *J Clin Anesth* 1993; **5**: 244-247
- 23 **Yazicioglu L,** Eryilmaz S, Sirlak M, Inan MB, Aral A, Tasoz R, Eren NT, Kaya B, Akalin H. Recombinant human erythropoietin administration in cardiac surgery. *J Thorac Cardiovasc Surg* 2001; **122**: 741-745
- 24 **Rutherford CJ,** Schneider TJ, Dempsey H, Kirn DH, Brugnara C, Goldberg MA. Efficacy of different dosing regimens for recombinant human erythropoietin in a simulated perisurgical setting: the importance of iron availability in optimizing response. *Am J Med* 1994; **96**: 139-145
- 25 **Gannon CJ,** Napolitano LM. Severe anemia after gastrointestinal haemorrhage in a Jehovah's Witness: new treatment strategies. *Crit Care Med* 2002; **30**: 1933-1935

Edited by Wang XL Proofread by Zhu LH

Correlation of ATP7B genotype with phenotype in Chinese patients with Wilson disease

Xiao-Qing Liu, Ya-Fen Zhang, Tze-Tze Liu, Kwang-Jen Hsiao, Jian-Ming Zhang, Xue-Fan Gu, Ke-Rong Bao, Li-Hua Yu, Mei-Xian Wang

Xiao-Qing Liu, Jian-Ming Zhang, Ke-Rong Bao, Li-Hua Yu, Mei-Xian Wang, Department of Neurology, Xinhua Hospital, Shanghai Second Medical University, Shanghai 200092, China

Ya-Fen Zhang, Xue-Fan Gu, Shanghai Institute for Pediatric Research, Shanghai 200092, China

Tze-Tze Liu, Kwang-Jen Hsiao, Genome Research Center and Institute of Genetics, National Yang Ming University, and Department of Medical Research and Education, Taipei Veterans General Hospital, Taipei 11216, Taiwan, China

Supported by the National Ministry of Education Teacher Education Plan in China 2000 NO.1424

Correspondence to: Dr. Xiao-Qing Liu, Department of Neurology, Xinhua Hospital, Shanghai Second Medical University, 1665 Kongjiang Rd, Shanghai 200092, China. xqliu@public8.sta.net.cn

Telephone: +86-21-65790000 **Fax:** +86-21-65791316

Received: 2003-06-30 **Accepted:** 2003-07-30

Abstract

AIM: To determine the mutational characterization of P-type ATP7B gene and to explore the correlation of ATP7B genotype to phenotype in Chinese patients with Wilson disease (WD).

METHODS: Seventy-five patients with WD from 72 no-kinship families, 44 males and 31 females, were enrolled in this study. The age of onset ranged from 4 to 39 years, ≤ 18 years in 72 patients. Some exons of ATP7B gene mutations were analyzed in patients with WD by using biochemical methods, polymerase chain reaction-single strand configuration polymorphism (PCR-SSCP) and DNA sequence analysis. A total of 778 coding regions were identified with restriction enzyme Msp I. The activity of Cu-ATPase was assessed by measuring inorganic phosphorus.

RESULTS: Sixty-six of 75 patients (88%) had with hepatic manifestations, 39 of them had only hepatic manifestations, 27 patients had hepatic and neurological manifestations or other symptoms at the same time (16 patients had associated neurological manifestation, 3 patients had osteopathy, 8 patients had other symptoms). Eight of the 75 patients (10.7%) had only neurological symptoms, one patient (5 years old) had no symptom. Twelve changing patterns were detected in ATP7B gene by DNA sequencing, including seven mutations (R778L, C656X, G943D, V1140A, V1106I V1216M and 1384del17), six polymorphisms (IVS4-5t/c, A2495G, C2310G, IVS18+6c/t and IVS20+5a/g). R778L occurred in 49/66 patients (74%) with hepatic manifestations, homozygosity of R778L in 16 patients, heterozygosity of R778L in 33 patients. V1106I mutation of ATP7B gene occurred in 2 patients with delaying onset of clinical symptoms. Cu-ATPase activity of three patients with known mutations (R778L/V1106I/A2495G, R778L/V1216M and R778L/R778L) were determined, and the activity of Cu-ATPase was decreased by 44.55%, 88.23% and 69.49% respectively.

CONCLUSION: 1384del17bp is a novel mutation found in

WD patients. R778L is the most common mutation of ATP7B gene. There is a correlation between R778L and hepatic manifestations in WD patient.

Liu XQ, Zhang YF, Liu TT, Hsiao KJ, Zhang JM, Gu XF, Bao KR, Yu LH, Wang MX. Correlation of ATP7B genotype with phenotype in Chinese patients with Wilson disease. *World J Gastroenterol* 2004; 10(4): 590-593

<http://www.wjgnet.com/1007-9327/10/590.asp>

INTRODUCTION

Wilson disease (WD), or hepatolenticular degeneration, is an autosomal recessive disorder of copper metabolism caused by ATP7B gene mutation. The clinical manifestations of copper accumulation produced by enzyme deficiency usually presented after birth, but rarely occurred before 5 years old. Patients with WD most often present with either progressive liver degeneration or neurologic symptoms, or both. Three major clinical patterns of liver disease in WD are hepatic cirrhosis, chronic active hepatitis and fulminant hepatic failure. Neurological manifestations are bradykinesia, rigidity, tremor and dyskinesia, *etc.* Copper-transporting P-type ATP7B gene has been identified as a defective gene in WD. The WD locus (ATP7B, OMIM#277900), consisting of 21 exons, has been isolated by using YAC mapping on 13q14.3^[1]. Mutation screening in WD patients has led to the detection of at least 200 disease-specific mutations (HGMD). The published data suggest that some mutations appear to be population specific, while others are common to many populations. Arg778Leu has been identified as the most common mutation in the Asian population, accounting for 28-44% of WD chromosomes. The codon H1069Q mutation has been reported to have a high allele frequency in the eastern and northern European populations. This study was to investigate the mutational characterization of P-type ATP7B gene and to explore the correlation between genotype and phenotype in Chinese patients with WD.

MATERIALS AND METHODS

Subject

Seventy-five patients with WD from 72 no-kinship families, 44 males and 31 females, were enrolled in this study. All WD patients were from the Neurological Clinic in Xinhua Hospital and Shanghai Children's Medical Center, Shanghai Second Medical University. The age at onset of symptoms was 4 to 39 years, ≤ 18 years in 72 patients. The diagnosis of WD was confirmed by serum ceruloplasmin (or copper oxides activity), urinary copper of 24 h, liver and/or brain imaging features (CT or MRI).

Polymerase chain reaction (PCR)

DNA was isolated from peripheral blood. Some exons (3, 5, 7, 8, 10, 12, 15, 16, 17, 18 and 19) were amplified by PCR with the primers previously reported^[2]. Reactions were carried out in 50 μ l [H_2O 33 μ l, buffer (10 \times) 5 μ l, dNPT (10 mmol/L)

4 μ l, primer (12.5 μ mol/L) 4 μ l, Taq DNA polymerase 2 units]. Amplification was performed 35 cycles, 94°C for 40 s, each cycle was at 58–65°C for 1 min, at 72°C for 1 min, degeneration at 94°C for 5 min and a final extension at 72°C for 10 min.

Single strand configuration polymorphism (PCR-SSCP) and sequencing

Five μ l of PCR product and equivalence denaturing solution were degenerated at 95°C for 10 min, then they were placed directly on ice. Six μ l was added into a gel, using the auto-electrophoresis system (Pharmacia Biotech). Exons exhibiting an irregular shift by SSCP were subjected to direct sequencing for mutation identification. Before direct sequencing, PCR products were purified from agarose gel, using the Quik kit. Direct sequencing was performed using the ABI PRISM™ 377 DNA sequencer (PE Applied Biosystems).

Restriction-enzyme analysis

The CGG to CTG transition at exon 8 splice acceptor site was recognized by Msp I restriction-endonuclease. In normal exon 8, PCR product (296 bp) was amplified into two products of 256 bp and 40 bp. R778L would not be recognized, and PCR product (296 bp) was not digested.

Cu-ATPase activity

Ten ml peripheral venous blood was put in a heparinization bottle, lymphocytes were collected, and then split and membrane was collected^[3]. Cu-ATPase was assessed by a kit made in Nanjing Jiancheng Biotechnology Company, and protein was quantified by UV/spectrophotometer (PE).

RESULTS

Clinical features

Sixty-six of 75 patients (88%) had hepatic manifestations, 39 of them had only hepatic manifestations (Table 1), and 27 patients of them had hepatic manifestations and other symptoms at the same time. Among the 27 patients who had both hepatic and other symptoms, 16 patients were associated with neurological manifestations, 3 patients with musculoskeleton symptoms, 8 patients with other symptoms (hemolytic anemia

or renal lesions). Eight of the 75 patients had only neurological symptoms, one patient had no symptom identified by family screening and microsatellite DNA analysis^[4].

Table 1 Clinical manifestations of WD patients

Clinical manifestation	Patient No. (%)
Cirrhosis, chronic active hepatitis	66(88)
Enlargement	25(33)
Rigidity, tremor, ataxia, dyskinesia, dysarthria,	24(32)
Behavioral disturbances, psychosis	4(5)
K-F rings	49(65)
Hemolysis, petechia	6(8)
Hematuria, proteinuria	6(8)
Amenorrhea, menoxenia, hairiness	5(7)
Degenerative joint disease	3(4)

Analysis of mutated genes

Twelve changing patterns were detected in ATP7B gene by DNA sequencing, including five missense mutations (R778L, G943D, C656X, V1140A, V1106I and V1216M), one deletion (1384del17) (Figures 1 and 2) and six polymorphisms (IVS4-5t/c, 2495A>G, C2310G, IVS18+6c/t and IVS20+5a/g) (Table 2). With restriction-enzyme analysis and sequencing in exon 8, R778L and L/L770 were identified in 54/75 WD patients, 16 patients showed homozygous, and 38 patients heterozygous.

Correlation between genotype and phenotype

In 66 patients with hepatic manifestations, 49 patients (74%) carried R778L (arginine to leucine) mutation and L/L770 polymorphism (2310 site C to G). V1106I mutation occurred in two WD patients with later onset of illness and had presenting neurological manifestations when they were 39 and 48 years old respectively.

Cu-ATPase activity

Cu-ATPase activity was determined in 3 patients with known mutations (R778L/V1106I, R778L/V1216M and R778L/R778L), activity of cu-ATPase was decreased by 44.55%, 88.23% and 69.49% respectively, compared with normal value.

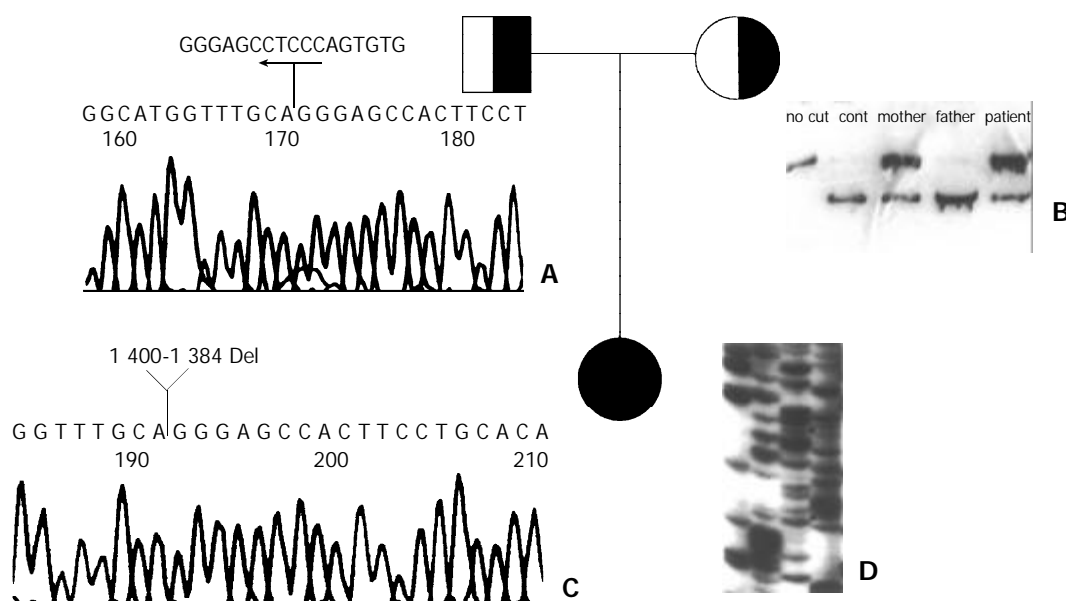


Figure 1 Family analysis of patient 038. A: Patients father carrying 1384Del17bp (ATP7B genes position 1 384-1 400 bp deletion). B: Msp I digested PCR product of ATP7B gene exon 8 of patients mother shows that she was R778L carrier. C and D: Patients genotypes are R778L/1384Del17 bp, 1384Del17 bp from his father and R778L from his mother.

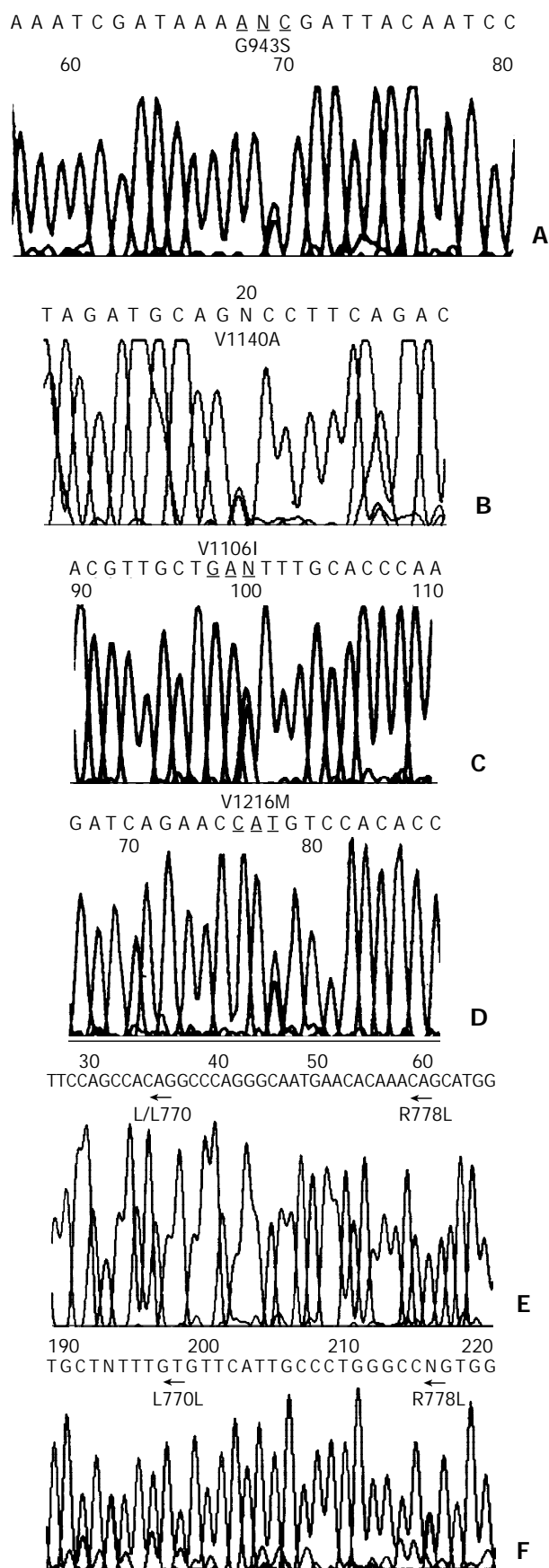


Figure 2 Nucleic acid sequence of PCR products of WD gene. A: Gly943Asp(G943D) heterozygous for a G-A mutation at position 2828, B: Val1140Ala (V1140A) heterozygous for a T-C mutation at position 3419, C: Val1106Ile (V1106I) heterozygous for a G-A mutation at position 3316, D: Val1216Met (V1216M) heterozygous for a G-A mutation at position 3646. E. and F: Arg778 Leu (R778L) homozygous and heterozygous for a G-T mutation at position 2333.

Table 2 Genotypes of ATP7B in WD patients

Exon	Mutation	Amino acid	Codon
3	1384del17	His stop	1384 delete 17 bp
7	C656X	Cys→X	1971 C splline
8	R778L	Arg→Leu (CGG→CTG)	2333 G→T
12	G943D	Gly→Asp (GGT→GAT)	2828 G→A
15	V1106I	Val→Ile (GTC→ATC)	3316 G→A
16	V1140A	Val→Ala (GTC→GCC)	3419 T→C
17	V1216M	Val→Met (GTG→ATG)	3646 G→A
<i>polymorphism</i>			
4	IVS4-5T/C		1708-5 t→c
8	L/L770		2310 C→G
10	2495A>G		2495 A→G
18	IVS18+6C/T		3903+6 c→t
20	IVS20+5A/G		4124+5 a→g
21	IVS21+3		4398+3 t→g

DISCUSSION

Wilson disease is an autosomal recessive disorder in copper transport. Disturbance of copper metabolism leads to accumulation of copper resulting in tissue damage, principally in the liver and brain. The disorder manifests as progressive liver degeneration, which is one of the important causes of chronic liver disease in childhood, although it is rare. Without early intervention, WD has a higher mortality and morbidity. ATP7B gene for WD is distributed worldwide, and has been demonstrated in almost all races. Epidemiological survey indicated that the prevalence of the disease was 1/30 000 live births, with a corresponding gene frequency of 0.3-0.7%, and a heterozygote carrier frequency of 1%^[5]. The prevalence of the disease is high in China.

There was a correlation between the age of onset and initial manifestations. Initial clinical feature was diverse. The age of onset ranged from 6 years to 15 years old in most patients with WD. In this group of patients, 72 patients were ≤ 18 years old, accounting for 96%, and 61 patients (81%) were ≤ 12 years old. In a large series of patients, the initial clinical manifestations were found to be 42% in liver, 34% in neurological system, 10% in psychiatric system, 12% in hematological system, 1% in kidney. Less commonly, patients had skeletal or other symptoms^[5]. In our patients, the initial clinical manifestations were found to 52% in liver (Cirrhosis, chronic active hepatitis), 21% in neurological system, 33% in saliva enlargement of spleen, 8% in kidney. Skeletal symptoms occurred in 3 patients (4%). The subjects in this study were most pediatric patients, it might be responsible for higher percentage of liver impairments in this study, compared with that in other reports.

To date, at least 200 different mutations have been identified in WD chromosomes. Some mutations appear to be population specific. H1069Q has been identified as the most common mutation in the eastern and northern European populations^[6-10]. Caca *et al* reported that an allele frequency of H1069Q was 63% in 82 WD patients, homozygous in 32 patients (39%), heterozygous in 39 patients (48%)^[11]. The H1069Q mutation was found in 27/42 WD patients (64.3%) from 39 Hungarian families, homozygous in 9, heterozygous in 18^[12]. The R778L has been reported to have a high allele frequency in the Oriental populations, such as Japanese, Korean, and Chinese. The allele frequency of R778L was 37.9% in Korean patients with WD^[13,14], 27% in Japanese WD^[15-19] and 28-44% in Chinese^[20-30]. In this study all the 75 WD patients were Han people. The R778L mutation was identified in 68/144 alleles with an allele frequency of 45.6%, in 54 WD patients (72%), homozygous in 16 patients, heterozygous in 38 patients. The average age of the patients was 9.5 years in homozygous, 10.7 years in heterozygous, there was no significant difference

between two groups. In our patients, we did not detect the H1069Q mutation, the most common WD mutation found in the European population. Our data showed that patients had clinical manifestations at preschool age or school age, liver impairment was the most common clinical manifestation, and allele frequency of the R778L was higher in patients with liver impairment. It is suggested that there might be a correlation between R778L mutation and liver impairment at initial evaluation.

The V1106I mutation was identified in two WD patients with late onset of phenotypes. One patient had neurological manifestations (tremor, and dysarthria) at the age of 39, progressing slowly. She was diagnosed as WD based on the decreased activity of Cu-ATPase and serum ceruloplasmin, Kayser-Fleischer rings, and increased urinary copper excretion. Treatment with oral D- penicillamine initiated at 9 months after diagnosis was made, showed clinical improvement. The genotype of the patient (014) was V1140A/V1106I. The other patient (026) having a past history of chronic hepatitis had psychiatric symptoms at the age of 48 years. Tremor gradually appeared and became progressively worse. After oral D- penicillamine clinical symptoms were remitted. Her genotype was R778L/V1106I. The other mutation did not detected by sequencing in exons 1 to 21 in these two patients. The results of family analysis of patient (038) with 1384De117bp/R778I genotype demonstrated that 1384De117bp was originated paternally and R778L maternally. R778L/V1216M (033) was found in one patient. G to A mutation at position 3646 occurred in exon 17 of ATP7B. The results demonstrated that the activity of Cu-ATPase was significantly decreased in lymphocytic membrane by 44.55% in patients with R778L/V1106I genotype, 88.23% in patients with R778L/V1216M genotype, 69.49% in patients with R778L/R778L (034) genotype. It can be presumed that the decreased degree of Cu-ATPase is correlated with the severity of clinical manifestations and genotypes.

REFERENCES

- Bull PC**, Barwell JA, Hannah HT, Pautler SE, Higgins MJ, Lal M, Cox DW. Isolation of new probes in the region of the Wilson disease locus, 13q14.2-q14.3. *Cytogenet Cell Genet* 1993; **64**: 12-17
- Thomas GR**, Forbes JR, Roberts EA, Walshe JM, Cox DW. The Wilson disease gene: spectrum of mutations and their consequences. *Nat Genet* 1995; **9**: 210-217
- Shah AB**, Chernov I, Zhang HT, Ross BM, Das K, Lutsenko S, Parano E, Pavone L, Evgrafov O, Ivanova-Smolenskaya IA, Annerén G, Westermarck K, Urrutia FH, Penchaszadeh GK, Sternlieb I, Scheinberg IH, Gilliam TC, Petrukhin K. Identification and Analysis of Mutations in the Wilson Disease Gene (ATP7B): Population Frequencies, Genotype-phenotype Correlation, and Functional Analyses. *Am J Hum Genet* 1997; **61**:317-328
- Liu XQ**, Zhang YF, Gu XF, Bao KR. Polymorphism analysis of ATP7B related microsatellite DNA haplotype in Wilson disease. *Lab Medicine* 2002; (Suppl): S50-51
- Gollan JL**, Gollan TJ. Wilson disease in 1998: genetic, diagnostic and therapeutic aspects. *J Hepatol* 1998; **28**: 28-36
- Czlonkowska A**, Rodo M, Gajda J, Ploos van Amstel HK, Juyn J, Houwen RHJ. Very high frequency of the His1069Gln mutation in Polish Wilson disease patients. *J Neurol* 1997; **244**: 591-599
- Ivanova-Smolenskaya IA**, Ovchinnikov IV, Karabanov AV, Deineko NL, Poleshchuk VV, Markova ED, Illarionov SN. The His1069Gln mutation in the ATP7B gene in Russian patients with Wilson disease. *J Med Genet* 1999; **36**: 174
- Tarnacka B**, Gromadzka G, Rodo M, Mierzejewski P, Czlonkowska A. Frequency of His1069Gln and Gly1267Lys mutations in Polish Wilson's Disease population. *Eur J Neurol* 2000; **7**: 495-498
- Loudianos G**, Dessi V, Lovicu M, Angius A, Altuntas B, Giacchino R, Marazzi M, Marcellini M, Sartorelli MR, Sturniolo GC, Kocak N, Yuce A, Akar N, Pirastu M, Cao A. Mutation analysis in patients of Mediterranean descent with Wilson disease: identification of 19 novel mutations. *J Med Genet* 1999; **36**: 833-836
- Palsson R**, Jonasson JG, Kristjansson M, Bodvarsson A, Goldin RD, Cox DW, Olafsson S. Genotype-phenotype interactions in Wilson's disease: insight from an Icelandic mutation. *Eur J Gastroenterol Hepatol* 2001; **13**: 433-436
- Caca K**, Ferenci P, Kühn HJ, Polli C, Willgerodt H, Kunath B, Hermann W, Mössner J, Berr F. High prevalence of the H1069Q mutation in East German patients with Wilson disease: rapid detection of mutations by limited sequencing and phenotype-genotype analysis. *J Hepatol* 2001; **35**: 575-581
- Firneisz G**, Lakatos PL, Szalay F, Polli C, Glant TT, Ferenci P. Common mutations of ATP7B in Wilson disease patients from Hungary. *Am J Med Genet* 2002; **108**: 23-28
- Yoo HW**. Identification of novel mutations and the three most common mutations in the human ATP7B gene of Korean patients with Wilson disease. *Genet Med* 2002; **4**: 43S-48S
- Kim EK**, Yoo OJ, Song KY, Yoo HW, Choi SY, Cho SW, Hahn SH. Identification of three novel mutations and a high frequency of the Arg778Leu mutation in Korean patients with Wilson disease. *Hum Mutat* 1998; **11**: 275-278
- Okada T**, Shiono Y, Hayashi H, Satoh H, Sawada T, Suzuki A, Takeda Y, Yano M, Michitaka K, Onji M, Mabuchi H. Mutational analysis of ATP7B and genotype-phenotype correlation in Japanese with Wilson's disease. *Hum Mutat* 2000; **15**: 454-462
- Shimizu N**, Nakazono H, Takeshita Y, Ikeda C, Fujii H, Watanabe A, Yamaguchi Y, Hemmi H, Shimatake H, Aoki T. Molecular analysis and diagnosis in Japanese patient with Wilson's disease. *Pediatr Int* 1999; **41**: 409-413
- Kusuda Y**, Hamaguchi K, Mori T, Shin R, Seike M, Sakata T. Novel mutations of the ATP7B gene in Japanese patients with Wilson disease. *J Hum Genet* 2000; **45**: 86-91
- Takeshita Y**, Shimizu N, Yamaguchi Y, Nakazono H, Saitou M, Fujikawa Y, Aoki T. Two families with Wilson disease in which siblings showed different phenotypes. *J Hum Genet* 2002; **47**: 543-547
- Nanji MS**, Nguyen VTT, Kawasoe JH, Inui K, Endo F, Nakajima T, Anezaki T, Cox DW. Haplotype and mutation analysis in Japanese patients with Wilson disease. *Am J Hum Genet* 1997; **60**: 1423-1429
- Lee CC**, Wu JY, Tsai FJ, Kodama H, Abe T, Yang CF, Tsai CH. Molecular analysis of Wilson disease in Taiwan: identification of one novel mutation and evidence of haplotype-mutation association. *J Hum Genet* 2000; **45**: 275-279
- Chuang LM**, Wu HP, Jang MH, Wang TR, Sue WC, Lin BJ, Cox DW, Tai TY. High frequency of two mutations in codon 778 in exon 8 of the ATP7B gene in Taiwanese families with Wilson disease. *J Med Gene* 1996; **33**: 521-523
- Fan Y**, Yu L, Jiang Y, Xu Y, Yang R, Han Y, Cui Y, Ren M, Zhao S. Identification of a mutation hotspot in exon 8 of Wilson disease gene by cycle sequencing. *Chin Med J* 2000; **113**: 172-174
- Yang RM**, Fan YX, Yu L, Cai YL, Shi SL, Wang XP, Han YZ, Ren MS, Zhao SY. Identification of a novel mutation in Wilson disease gene. *Zhonghua Yixue Zazhi* 1997; **77**: 344-347
- Wu ZY**, Wang N, Lin MT, Fang L, Murong SX, Yu L. Mutation analysis and the correlation between genotype and phenotype of Arg778Leu mutation in Chinese patients with Wilson disease. *Arch Neurol* 2001; **58**: 971-976
- Wang Y**, Wu ZY, Murong ZX, Lin MT, Fang L. Hot point mutations of Wilson disease gene in Chinese with DNA sequencing. *Zhonghua Shenjingke Zazhi* 1998; **31**: 20-24
- Xu P**, Liang X, Jankovic J, Le WD. Identification of a high frequency of mutation at exon 8 of the ATP7B gene in a Chinese population with Wilson disease by fluorescent PCR. *Arch Neurol* 2001; **58**:1879-1882
- Liu XQ**, Zhang JM, Gu XF, Wu J, Zhang YF, Xue HP, Xu XP, Bao KR, Chen RG. A study on the relationship between Arg778Leu mutation of ATP7B gene and clinical phenotype in Wilson disease. *Zhonghua Erke Zazhi* 1999; **37**: 359-361
- Liu XQ**, Zhang YF, Liu TT, Gu XF, Bao KR. Clinical application of D13S301 maker in the diagnosis of children with Wilson disease. *Linchuang Erke Zazhi* 2002; **20**: 614-616
- Wu Z**, Wang N, Murong S, Lin M. Identification and analysis of mutations of the Wilson disease gene in Chinese population. *Chin Med J* 2000; **113**: 40-43
- Tsai CH**, Tsai FJ, Wu JY, Chang JG, Lee CC, Lin SP, Yang CF, Jong YJ, Lo MC. Mutation analysis of Wilson disease in Taiwan and description of six new mutations. *Hum Mutat* 1998; **12**: 370-376

Effects of nitric oxide on gastric ulceration induced by nicotine and cold-restraint stress

Bo-Sheng Qui, Qi-Bing Mei, Li Liu, Kam-Meng Tchou-Wong

Bo-Sheng Qui, Kam-Meng Tchou-Wong, Departments of Medicine, Environmental Medicine and Microbiology, New York University School of Medicine, New York, USA

Qi-Bing Mei, Li Liu, Department of Pharmacology, The Fourth Military Medical University, Xian, China

Correspondence to: Dr. Kam-Meng Tchou-Wong, Departments of Medicine, Environmental Medicine, Microbiology, New York University School of Medicine, 550 First Avenue, MSB 141, New York, New York 10016, USA. tchouk02@med.nyu.edu

Telephone: +1-212-263-0243 **Fax:** +1-212-263-8902

Received: 2003-10-08 **Accepted:** 2003-12-24

Abstract

AIM: Stress induces gastric ulceration in human and experimental animals. People tend to smoke more cigarettes when under stress. Nitric oxide (NO) and nicotine have opposing effects on gastric integrity. The present study examined the possible therapeutic benefit of NO in nicotine-treated rats with stress-induced gastric ulceration.

METHODS: Rats drank a nicotine solution while control rats drank tap water for 20 days. The alkaloid was then replaced by water with or without supplementation of isosorbide dinitrate (NO donor) for an additional 10 days. Isosorbide dinitrate was given twice shortly before experiments (acute) or three times daily by oral gavages for 10 days after the rats stopped drinking nicotine solution. At the end of experiments, ulcer index, gastric adhesion mucus content and MPO activity were measured and analysed.

RESULTS: Nicotine treatment decreased gastric mucus content and intensified stress-induced gastric ulcer. A higher ulcer index persisted even after the rats stopped drinking nicotine solution for 10 days. Acute NO donor showed no benefit on both mucus and ulcer index in nicotine treatment or/and stress condition. Chronic NO donor treatment reversed the worsening action of nicotine in stomach. Stress increased gastric mucosal myeloperoxidase (MPO) activity, which was antagonized by chronic NO treatment. However, nicotine was unlikely to change mucosal MPO activity.

CONCLUSION: The intensifying action of nicotine on stress-induced gastric ulceration persists for 10 days after cessation. Nicotine treatment significantly decreases gastric mucus content that can be restored by chronic NO donor treatment. The present study suggests that NO antagonizes the ulcerogenic action of nicotine through a cytoprotective way.

Qui BS, Mei QB, Liu L, Tchou-Wong KM. Effects of nitric oxide on gastric ulceration induced by nicotine and cold-restraint stress. *World J Gastroenterol* 2004; 10(4): 594-597
<http://www.wjgnet.com/1007-9327/10/594.asp>

INTRODUCTION

Stress is well associated with cigarette smoking. It has been

reported that cigarettes help alleviate the feelings of stress which may underlie the tendency to smoke more cigarettes when under stress. However, smoking also further enhances stress levels because stress level has been shown to decline after smoking cessation^[1]. Hence, the vicious cycle of stress and smoking perpetuates. Clinical study and experiments have demonstrated that stress is a risk factor for gastrointestinal tract diseases^[2-5] and peptic ulcer disease is more common in smokers than in non-smokers. Although Western and traditional Chinese medicine^[6] have demonstrated efficacy in the treatment of peptic ulcer disease, peptic ulcers in smokers heal slowly and relapse frequently^[7].

Since nicotine accumulates in gastric juice, nicotine is thought to be the major culprit in cigarette smoking causing the detrimental effects of smoking in gastric ulceration^[7]. Nicotine also stimulates the central nervous system and chronic nicotine intake intensifies stress-induced gastric mucosal damages in rats^[8,9]. The interaction between stress and nicotine has been reported to work synergistically to intensify gastric ulceration^[10,11]. Smoking cessation could reduce the incidence and recurrence rate of peptic ulcer but only in people who were light smokers. However, in heavy smokers, smoking cessation did not reduce the incidence and recurrence rate of peptic ulcer. To treat peptic ulcer disease in these former smokers, more studies are needed to provide insights in to the restoration of the normal gastric integrity and the prevention of disease recurrence. Since gastric mucosal prostaglandin, nitric oxide (NO) and gastric adhesion mucus content^[12] could contribute significantly to maintaining normal gastric integrity, *i.e.*, cytoprotection, while neutrophil infiltration had an ulcerogenic effect^[13], these important parameters were, therefore, the focus of the present study.

In support of the role of prostaglandin, aspirin which inhibits prostaglandin synthesis has been shown to induce gastric mucosal damage. However, in the presence of an NO releasing compound, the ulcerogenic action of aspirin is abolished^[14]. In animal experiments, chronic nicotine treatment has been shown to markedly reduce gastric mucus content^[15], while other studies demonstrated that NO enhanced gastric mucus production^[16,17]. Inhibition of NO synthesis intensifies, while L-arginine (an NO substrate) reduces gastric ulceration in rats induced by cold-restraint stress^[18]. These studies suggest that NO may provide a therapeutic benefit to reverse the detrimental effects of nicotine, especially in heavy smokers. In this study, we used the cold-restraint stress-induced gastric ulceration model to evaluate the role of NO in restoring normal gastric integrity after chronic nicotine insult.

MATERIALS AND METHODS

General

In present study, we used male Sprague-Dawley rats (weighing 155-180 g). The animals were fed with a conventional pellet diet. Three rats were housed per cage and kept at room temperature (22±1 °C) with humidity of 65-70%. The rats were randomly assigned to tap water control group and nicotine group. In the nicotine group, the animals drank a nicotine solution [tap water containing nicotine bitartrate (50 µg/ml)

(Sigma)] for 20 days. NO donor was given to some nicotine-treated rats twice at 1 hour and at 10 min before experimentation. In the second experiment, rats drank the nicotine solution for 20 days and then the solution was replaced by tap water. NO donor was administered to some nicotine-treated rats for an additional 10 days. Solid food was withdrawn 48 hours before the start of experimentation. The animals were kept in fasting cages and allowed to drink a solution containing 8% sucrose in 0.2% NaCl (w/v). In the nicotine-treated group, rats were given the 8% sucrose/0.2% NaCl solution containing the same concentration of nicotine.

NO donor

Isosorbide dinitrite (Sigma) was used as an NO donor^[19] and administered at a dose of 10 mg/kg body weight. Isosorbide was freshly prepared. For acute treatment, the rats were given isosorbide by oral gavages twice at 1 hour and at 10 minutes before experimentation. In chronic experiments, NO donor was administered by oral gavages every 5 hours, three times daily for 10 days simultaneously after quitting nicotine.

Cold-restraint stress induced gastric ulcer

Rats were starved for 48 hours, and the drinking solution was removed 1 hour before starting experiments. For cold-restraint stress, the rats were restrained in individual close-fitting tubular wire-mesh cages at 4°C^[12] and the no stress control group was kept in starvation cages at 22°C. At the end of 2 hours, all the rats were sacrificed.

Gastric ulcer index

An observer who was unaware of the treatment regimen determined the severity of gastric mucosal lesions. The lesions were examined under an illuminated magnifier (3X). Lesion size (mm) was measured along its greatest length and in the case of patches, five such lesions were considered the equivalent of a 1 mm ulcer. The sum of the lesion lengths in each group of animals was divided by its number and expressed as the mean gastric hemorrhagic lesion index^[8].

Gastric adhesion mucus content

Gastric adhesion mucus content was determined by the Alcian blue method^[12,20]. The stomachs were removed, opened, and immediately soaked in Alcian blue solution for 2 hours. The Alcian blue dye complex attached to the gastric wall mucus and was separated from gastric wall by vortexing and subsequent extracting with magnesium chloride. The extracted solution was quantitated spectrophotometrically at 598 nm. The mucus content was correlated with the amount of Alcian blue per gram wet weight of glandular tissue.

Gastric mucosal myeloperoxidase activity (MPO)

MPO activity was measured as previously described^[21-24]. Firstly, the gastric mucosa was scraped after examination of ulcer index. The scrapings were then homogenized in ice-cold phosphate buffer. Hexadecyltrimethyl ammonium bromide (0.5% HTAB) (Sigma) was added to this phosphate buffer (50 mM, pH 6.0) to release MPO from the primary granules of neutrophils. Homogenates were then centrifuged and the supernatants were aspirated and mixed with *o*-dianisidine hydrogen peroxide reagent (Aldrich Chemical Co.) and absorbance at 460 nm was measured with a spectrophotometer. One unit of MPO activity was defined as that degrading 1 μmol of peroxide per minute at 25°C per g protein of gastric mucosa.

Statistics

All values in present study indicated mean±SD and were analyzed using the two-tailed Student's *t* test. Differences

between groups exposed to the same experimental conditions were analysed by the χ^2 test. The *P* value less than 5% was considered as statistically significant.

RESULTS

Effects of nicotine and acute NO treatment on stress-induced gastric ulceration

As summarized in Table 1A, only petechiae were found in the stomach of animals in the non-stressed control group and the mean ulcer index were unaffected by tap water, nicotine or acute NO donor treatments. Cold-restraint stress induced haemorrhagic ulcers in the glandular mucosa with a 100% incidence as indicated by the mean ulcer index in all stressed animals, whether given tap water, nicotine with or without NO donor (Table 1B). Treatment with nicotine for 20 days intensified stress-induced gastric ulceration significantly but had no effect on non-stressed group. Acute NO administration twice shortly before cold-restraint stress in nicotine-treated animals failed to reduce the ulcerogenic effect of nicotine (Table 1B).

Interestingly, nicotine treatment alone in the non-stressed group significantly reduced the gastric adhesion mucus content as compared to tap water control group, while acute NO treatment failed to reverse the effect of nicotine (Table 1A). When animals were subjected to stress, the adhesion mucus content was reduced to 50% of that of non-stressed group. Nicotine treatment further reduced the adhesion mucus content in stressed animals and acute NO treatment did not reverse the effects of nicotine (Table 1B).

Table 1 Effects of nicotine and acute nitric oxide treatment on gastric ulceration and adhesion mucus content in rats

Experimental group	No. of rats with lesions	Ulcer index (mm)	Adhesion mucus content (μg/g wet glandular tissue)
A. No stress (unrestrained at 22°C for 2 hours)			
Tap water	2 (7)	0.04±0.03	382±38
Nicotine alone	3 (8)	0.05±0.03	283±27 ^a
Nicotine + NO (acute)	2 (8)	0.06±0.04	276±28 ^a
B. Stress (restrained at 4°C for 2 hours)			
Tap water	8 (8) ^c	6.0±0.7	200±17 ^b
Nicotine alone	8 (8) ^c	19.0±1.7 ^{ad}	152±14 ^{ab}
Nicotine+ NO (acute)	7 (7) ^c	17.8±1.7 ^{ad}	143±15 ^{ab}

Values are mean±SD. Number of rats in each group is shown in parentheses. Lesions: Only petechiae in stomach were seen in non-stressed condition. Both petechiae and haemorrhagic ulcer in stomach were observed in stressed condition. Tap water: Rats drank water as control. Nicotine alone: Rats drank nicotine water (50 μg/ml) for 20 days. Nicotine + NO (acute): Rats drank nicotine water (50 μg/ml) for 20 days. Rats were given NO donor 60 min and 10 min twice by oral gavages before stress. ^a*P*<0.05 when compared to its own tap water control in A or B. ^b*P*<0.05, ^c*P*<0.01, ^d*P*<0.001 when compared to the corresponding control in A.

Effects of nicotine and chronic NO treatment on stress-induced gastric ulceration

To mimic the early effects of quitting smoking, animals were given nicotine solution for 20 days and nicotine was replaced by tap water for an additional 10 days and this treatment group was designated as quit nicotine. In the absence of cold-restraint stress, only petechiae but no ulcers were detected in the stomach in all groups: tap water control, quit nicotine cessation with or without chronic NO treatment (Table 2A). Interestingly, the adhesion mucus content was reduced even 10 days after nicotine cessation and chronic NO treatment for 10 days

restored the adherent mucus content to that of tap water control group (Table 2A). Hence, the damaging effect of nicotine on adhesion mucus content persisted even after nicotine cessation but could be reversed by chronic NO treatment.

As shown in Table 2B, cold-restraint stress induced haemorrhagic ulcers in the glandular mucosa in all treatment groups: tap water, quit nicotine with or without chronic NO treatment. The effects of nicotine persisted even after nicotine cessation as indicated by the increased gastric ulcer index in the quit nicotine group as compared to the tap water control group. Consistent with the protective effect of chronic NO treatment in restoring adhesion mucus content in non-stressed animals (Table 2A), the mean ulcer index induced by stress was reduced by NO treatment after nicotine cessation to the level of the tap water control group (Table 2B). In addition, chronic NO treatment after nicotine cessation in stressed animals also restored the mucus content to that of the tap water control group (Table 2B).

Table 2 Changes of ulcer index and adhesion mucus content after quit nicotine intake alone or with chronic nitric oxide donor (NO) treatment

Experimental group	No. of rats with lesions	Ulcer index (mm)	Adhesion mucus content ($\mu\text{g/g}$ wet glandular tissue)
A. No stress (unrestrained at 22°C for 2 hours)			
Tap water	2 (7)	0.03±0.02	391±39
Quit nicotine	3 (8)	0.04±0.02	278±29 ^a
Quit nicotine+NO (chronic)	2 (7)	0.04±0.03	386±37
B. Stress (restrained at 4°C for 2 hours)			
Tap water	8 (8) ^c	6.2±0.7 ^d	190±18 ^d
Quit nicotine	8 (8) ^c	9.0±0.9 ^{ad}	142±16 ^c
Quit nicotine+ NO (chronic)	7 (7) ^b	5.8±0.8 ^d	210±19 ^d

Values are mean±SD. Number of rats in each group is shown in parentheses. Lesions: Only petechiae in stomach were seen with non-stressed condition. Both petechiae and haemorrhagic ulcer in stomach were observed in stressed condition. Tap water: Rats drank water as control. Quit nicotine: Rats drank nicotine (50 $\mu\text{g/ml}$) for 20 days, then, nicotine was replaced by water for another 10 days. Quit nicotine + NO (chronic): Rats drank nicotine (50 $\mu\text{g/ml}$) for 20 days, then, nicotine was replaced by water, and rats were given NO donor three times daily by oral gavages for 10 days before experiment. ^a $P<0.05$ when compared to its own tap water control in A or B. ^b $P<0.05$, ^c $P<0.01$, ^d $P<0.001$ when compared to the corresponding control in A.

Effects of nicotine and NO on gastric mucosal MPO activity

Since gastric ulcer formation was associated with MPO activity, we next measured gastric MPO activity. As shown in Table 3, the gastric mucosal MPO activity in non-stressed tap water control group was used as a baseline for comparison with other

treatment groups. Cold-restraint stress alone induced MPO activity significantly. Although nicotine treatment intensified stress-induced gastric ulceration (Table 1B), the MPO activity was not further increased by nicotine treatment in stressed animals and was slightly but not significantly reduced by acute NO treatment (Table 3). After nicotine cessation, the higher MPO activity was maintained in stressed animals but was significantly suppressed by chronic NO treatment.

DISCUSSION

Gastric ulceration is resulted from an imbalance of gastric defensive and aggressive factors. The adherent mucus layer could provide a defensive barrier against self-digestion by gastric acid and pepsin^[25,26]. In a water immersion restraint stress model, gastric ulcer formation was associated with MPO activity^[13]. Because MPO is mainly produced by neutrophils, MPO activity is considered as an index for the evaluation of neutrophil infiltration^[13]. Since activated neutrophils produce many enzymes and free radicals that damage the gastric mucosa, neutrophil is considered as an aggressive factor in ulcer formation. Chow *et al.*^[27] reported that cigarette smoking significantly potentiated the formation of gastric mucosal lesions and enhanced gastric mucosal MPO activity. Reduction of NO production was well associated with enhancement in both neutrophil infiltration and gastric ulcer formation in water immersion restraint stress model^[28].

In the cold-restraint stress model, gastric ulcer formation was mainly due to gastric hypermotility, which could lead to mucosal over friction^[29]. Hence, the gastric mucus layer is extremely important and the mucus is generally believed to contribute to a cytoprotective action. Gastric mucus originates from the goblet cells and NO plays a critical role in the maintenance of goblet cell functions. NO donors could increase mucus release from gastric mucosal cells in rats^[30] and enhance mucus gel thickness in the rat stomach^[16]. Tobacco smoking has been reported to suppress NO release^[31-33] which might be explained in part by nicotine-induced damage of endothelial cells and lower NO synthesis^[34].

In the present study, we examined the effects of nicotine and NO in cold-restraint stress. To mimic the nicotine intake in heavy smokers, animals were given drinking water containing 50 $\mu\text{g/ml}$ of nicotine, a concentration reported to be comparable to the nicotine intake in heavy smokers^[8,35]. This concentration of nicotine in drinking water has been previously shown to intensify cold-restraint stress-induced gastric ulceration^[8,9,29]. Our data suggest that chronic nicotine treatment could significantly reduce the gastric mucus content and this latter effect persisted for even 10 days after nicotine cessation. Reduction of the gastric mucus content could lead to weakening of the gastric defensive capability which underlies the intensifying effect of nicotine on stress-induced gastric ulceration. Our results confirmed the previous observations that chronic nicotine administration could reduce the gastric mucus content^[36,37].

Table 3 Change in mucosal MPO activity after nicotine intake and nitric oxide donor (NO) treatment

	Tap water +no stress	Tap water +stress	Nicotine +stress	Nicotine +stress +NO (acute)	Quit nicotine +stress	Quit nicotine +stress +NO (chronic)
MPO (u/g protein):	6.3±0.7	9.3±1.1 ^a	9.1±1.0 ^a	7.9±0.9	9.4±1.2 ^a	5.7±0.9 ^b

Values are mean±SD. Each group had 8 rats. Stress: restrained at 4°C for 2 hours. Tap water: Rats drank water (control). Nicotine: Rats drank nicotine 50 $\mu\text{g/ml}$ for 20 days. Quit nicotine: Rats drank nicotine (50 $\mu\text{g/ml}$) for 20 days, then, nicotine was replaced by water for another 10 days. NO (acute): Rats drank nicotine (50 $\mu\text{g/ml}$) for 20 days, the rats were then given NO donor 60 and 10 min by oral gavages before stress. NO (chronic): Rats drank nicotine (50 $\mu\text{g/ml}$) for 20 days, then, nicotine was replaced by water, the rats were given NO donor three times daily by oral gavages for 10 days before experiment. ^a $P<0.05$ vs its own corresponding group in tap water + no stress control. ^b $P<0.05$ vs its own corresponding group in tap water +stress control.

Although nicotine intensified stress-induced gastric ulceration which was associated with enhanced MPO activity, nicotine had no additive effect on MPO activity, suggesting that the potentiating effect of nicotine is unrelated to gastric mucosal neutrophil infiltration. Acute NO donor treatment had no protective effect on animals subjected to chronic nicotine treatment and stress, while chronic NO donor treatment for 10 days after nicotine cessation could sufficiently restore the normal gastric mucosal integrity and increase the mucus content. Similarly, acute NO donor treatment did not significantly affect MPO activity in animals subjected to nicotine and stress. However, after nicotine cessation, the MPO activity was significantly reduced by chronic NO treatment in stressed animals. These results suggest that prolonged NO therapy may be necessary to restore the normal mucus layer and reduce MPO activity. Nevertheless, our data demonstrate that NO has a gastric mucosal cytoprotective activity and suggest that the protective role of NO in restoring the gastric mucosal integrity may be mediated via suppression of neutrophil infiltration and MPO activity. Our results are of clinical significance, and suggest that prolonged NO therapy may help to restore gastric mucosal integrity in heavy smokers, especially after they have stopped smoking.

REFERENCES

- Parrott AC.** Does cigarette smoking cause stress? *Am Psychol* 1999; **54**: 817-820
- Kim YH, Lee JH, Lee SS, Cho EY, Oh YL, Son HJ, Rhee PL, Kim JJ, Koh KC, Paik SW, Rhee JC, Choi KW.** Long-term stress and *Helicobacter pylori* infection independently induce gastric mucosal lesions in C57BL/6 mice. *Scand J Gastroenterol* 2002; **37**: 1259-1264
- Kwiecien S, Brzozowski T, Konturek PCH, Konturek SJ.** The role of reactive oxygen species in action of nitric oxide-donors on stress-induced gastric mucosal lesions. *J Physiol Pharmacol* 2002; **53**(4 Pt 2): 761-773
- Shen XZ, Chow JFL, Koo MWL, Cho CH.** Gene expression profiles in gastric mucosa of sleep deprivation rats. *World J Gastroenterol* 2000; **6**: 754-758
- Qiu BS, Vallance BA, Blennerhassett PA, Collins SM.** The role of CD4+ lymphocytes in the susceptibility of mice to stress-induced reactivation of experimental colitis. *Nat Med* 1999; **5**: 1178-1182
- Ma LS, Guo TM.** Combination of traditional Chinese medicine and Western medicine in the treatment of resistant peptic ulcer. *Chin Med J* 1994; **107**: 554-556
- Lindell G, Bukhave K, Lilja I, Madsen JR, Graffner H.** Acute effects of high-dose intragastric nicotine on mucosal defense mechanisms: an analysis of nicotine, prostaglandin E2, phospholipase A2, and phospholipids. *Dig Dis Sci* 1997; **42**: 640-644
- Qiu BS, Cho CH, Ogle CW.** Chronic nicotine treatment intensifies gastric ulceration by cold-restraint stress in rats. *Agents Actions* 1991; **33**: 367-370
- Qiu BS, Cho CH, Ogle CW.** Effects of nicotine on activity and stress-induced gastric ulcers in rats. *Pharmacol Biochem Behav* 1992; **43**: 1053-1058
- Chow JY, Ma L, Zhu M, Cho CH.** The potentiating actions of cigarette smoking on ethanol-induced gastric mucosal damage in rats. *Gastroenterology* 1997; **113**: 1188-1197
- Quan C, Talley NJ.** Management of peptic ulcer disease not related to *Helicobacter pylori* or NSAIDs. *Am J Gastroenterol* 2002; **97**: 2950-2961
- Qiu BS, Pfeiffer CJ, Cho CH.** Effects of chronic nitric oxide synthase inhibition in cold-restraint and ethanol-induced gastric mucosal damage in rats. *Digestion* 1996; **57**: 60-66
- Nishida K, Ohta Y, Kobayashi T, Ishiguro I.** Involvement of the xanthine-xanthine oxidase system and neutrophils in the development of acute gastric mucosal lesions in rats with water immersion restraint stress. *Digestion* 1997; **58**: 340-351
- Takeuchi K, Ukawa H, Konaka A, Kitamura M, Sugawa Y.** Effect of nitric oxide-releasing aspirin derivative on gastric functional and ulcerogenic responses in rats: comparison with plain aspirin. *J Pharmacol Exp Ther* 1998; **286**: 115-121
- Ogle CW, Qiu BS, Cho CH.** Nicotine and gastric ulcers in stress. *J Physiol Paris* 1993; **87**: 359-365
- Brown JF, Hanson PJ, Whittle BJ.** (1992) Nitric oxide donors increase mucus gel thickness in rat stomach. *Eur J Pharmacol* 1992; **223**: 103-104
- Nishida K, Ohta Y, Ishiguro I.** Relationship between constitutive nitric oxide synthase activity and mucus level in the gastric mucosa of rats with stress. *Pharmacol Res* 1998; **38**: 393-400
- Ogle CW, Qiu BS.** Nitric oxide inhibition intensifies cold-restraint induced gastric ulcers in rats. *Experientia* 1993; **49**: 304-307
- Stacher G, Schneider C, Steinringer H, Holzapfel A, Gaupmann G, Stacherjanotta G.** Effects of 3-days' intake of a sustained-release preparation of the nitric oxide donor, isosorbide, on oesophageal motility. *Aliment Pharmacol Ther* 1997; **11**: 967-971
- Corne SJ, Morrissey SM, Woods RJ.** Proceedings: A method for the quantitative estimation of gastric barrier mucus. *J Physiol* 1974; **242**: 116P-117P
- Qiu BS, Pfeiffer CJ, Keith JC Jr.** Protection by recombinant human interleukin-11 against experimental TNB-induced colitis in rats. *Dig Dis Sci* 1996; **41**: 1625-1630
- Krawisz JE, Sharon P, Stenson WF.** Quantitative assay for acute intestinal inflammation based on myeloperoxidase activity: assessment of inflammation in rat and hamster models. *Gastroenterology* 1984; **87**: 1344-1350
- Qiu BS, Pothoulakis C, Nikulasson Z, LaMont JT.** Nitric oxide inhibits rats intestinal secretion by *Clostridium difficile* toxin A but not *Vibrio cholerae* enterotoxin. *Gastroenterology* 1996; **111**: 409-418
- Qiu BS, Pothoulakis C, Nikulasson S, LaMont JT.** Participation of reactive oxygen metabolites in *Clostridium difficile* toxin A-induced enteritis in rats. *Am J Physiol* 1999; **276**(2 Pt 1): G485-490
- Ye YN, So HL, Liu ES, Shin VY, Cho CH.** Effect of polysaccharides from *Angelica sinensis* on gastric ulcer healing. *Life Sci* 2003; **72**: 925-932
- Pfeiffer CJ.** Experimental analysis of hydrogen ion diffusion in gastrointestinal mucus glycoprotein. *Am J Physiol* 1981; **240**: G176-182
- Chow JY, Ma L, Cho CH.** Involvement of free radicals and histamine in the potentiating action of cigarette smoke exposure on ethanol-induced gastric mucosal damage in rats. *Free Radic Biol Med* 1998; **24**: 1285-1293
- Nishida K, Ohta Y, Ishiguro I.** Contribution of NO synthases to neutrophil infiltration in the gastric mucosal lesions in rats with water immersion restraint stress. *FEBS Lett* 1998; **425**: 243-248
- Qiu BS, Cho CH, Ogle CW.** The influence of chronic nicotine treatment on stress-induced gastric ulceration and emptying rate in rats. *Experientia* 1992; **48**: 389-391
- Brown JF, Keates AC, Hanson PJ, Whittle BJ.** Nitric oxide generators and cGMP stimulate mucus secretion by rat gastric mucosal cells. *Am J Physiol* 1993; **265**: G418-422
- Robbins RA, Millatmal T, Lassi K, Rennard S, Daughton D.** Smoking cessation is associated with an increase in exhaled nitric oxide. *Chest* 1997; **112**: 313-318
- Ma L, Chow JY, Liu ES, Cho CH.** Cigarette smoke and its extract delays ulcer healing and reduces NO synthase activity and angiogenesis in rat stomach. *Clin Exp Pharmacol Physiol* 1999; **26**: 828-829
- Raza MW, Essery SD, Elton RA, Weir DM, Busuttill A, Blackwell C.** Exposure to cigarette smoke, a major risk factor for sudden infant death syndrome: effects of cigarette smoke on inflammatory responses to viral infection and bacterial toxins. *FEMS Immunol Med Microbiol* 1999; **25**: 145-154
- Krupski WC.** Peripheral vascular consequences of smoking. *Ann Vasc Surg* 1991; **5**: 291-304
- Moody PM.** The relationships of qualified human smoking behavior and demographic variables. *Soc Sci Med* 1980; **14A**: 49-54
- Wong D, Koo MWL, Shin VY, Liu ESL, Cho CH.** Pathogenesis of nicotine treatment and its withdrawal on stress-induced gastric ulceration in rats. *Eur J Pharmacol* 2002; **434**: 81-86
- Ma JJ, Hou DQ, Zhang QB, Korsten MA.** Reversal of the gastric effects of nicotine by nitric oxide donor treatment. *Digestion* 2001; **63**: 102-107

Helicobacter species sequences in liver samples from patients with and without hepatocellular carcinoma

Rinaldo Pellicano, Vincenzo Mazzaferro, Walter Franco Grigioni, Miguel Angel Cutufia, Sharmila Fagoonee, Lorenzo Silengo, Mario Rizzetto, Antonio Ponzetto

Rinaldo Pellicano, Mario Rizzetto, Antonio Ponzetto, Department of Gastro-Hepatology, Ospedale S. Giovanni Battista (Molinette), Torino, Italy

Vincenzo Mazzaferro, Surgery and Liver Transplantation Centre, Istituto Nazionale dei Tumori, Milano, Italy

Walter Franco Grigioni, Department of Pathology, Istituto Addarii, Bologna, Italy

Miguel Angel Cutufia, Sharmila Fagoonee, Lorenzo Silengo, Department of Biology, Biochemistry and Genetics, University of Torino, Italy

Supported by a grant from AIRC (Italian Association for Research on Cancer)

Correspondence to: Professor Antonio Ponzetto, Ambulatorio di Gastroenterologia, Ospedale S Giovanni Battista, Via Chiabrera 34, III piano, 10126 Torino, Italy. ponzetto@inwind.it

Telephone: +39-11-6336255 **Fax:** +39-11-6336250

Received: 2003-08-06 **Accepted:** 2003-10-23

Abstract

AIM: Only a minority of patients carrying a defined viral aetiological agent develop cirrhosis and ultimately hepatocellular carcinoma (HCC), the mechanism underlying the worsening is still undefined. Experimental infection by *Helicobacter hepaticus* in mice causes chronic hepatitis and HCC and recently, more *Helicobacter* species (*Helicobacter* spp.) have been detected in the liver of patients suffering from cholestatic diseases and HCC arising from non-cirrhotic liver. We investigated whether *Helicobacter* spp. sequences could be detected in the liver of patients with cirrhosis and HCC compared to subjects with metastasis to liver from colon cancer.

METHODS: Twenty-three liver samples from patients operated upon for HCC superimposed on hepatitis C virus (HCV)-related cirrhosis and 6 from patients with resected metastases from colorectal cancer, were tested by polymerase chain reaction for presence of genomic 16S rRNA of *Helicobacter* genus using specific primers. DNA sequencing and *cag A* gene analysis were also performed.

RESULTS: Genomic sequences of *Helicobacter* spp. were found in 17 of 20 (85%) liver samples from patients with HCC and in 2 of 6 samples from patients with liver metastasis. In three samples of the first group the result was uncertain. *H pylori* was revealed in 16 out of 17 positive samples and *Helicobacter pullorum* in the other.

CONCLUSION: *Helicobacter* spp., carcinogenic in mice, were found at a higher frequency in the liver of patients with HCV-related cirrhosis and HCC than those in patients without primary liver disease.

Pellicano R, Mazzaferro V, Grigioni WF, Cutufia MA, Fagoonee S, Silengo L, Rizzetto M, Ponzetto A. *Helicobacter* species sequences in liver samples from patients with and without hepatocellular carcinoma. *World J Gastroenterol* 2004; 10(4): 598-601
<http://www.wjgnet.com/1007-9327/10/598.asp>

INTRODUCTION

Hepatocellular carcinoma (HCC) is the fourth cause of cancer death worldwide^[1]. This tumor often follows chronic liver inflammation and longstanding cirrhosis. Cirrhosis of the liver is a diffuse process, characterised by fibrosis and nodule formation, which stems from hepatocellular injury. The cellular necrosis might originate from viral, toxic, metabolic and autoimmune sources^[2]. Moreover, hepatitis B and hepatitis C viruses (HBV and HCV) are well-known etiologic factors for liver cirrhosis, and have been classified by the International Agency for Research on Cancer (IARC) as type I liver carcinogens. Both viruses are highly prevalent in the adult population in Italy^[3,4]. Both viral and host characteristics have been reported to influence the outcome of HBV or HCV infection and the development of cirrhosis, but they do not explain all the epidemiological variations of the disease. For instance, in the case of HCV, the viral genotype 1b^[5] has been repeatedly connected with severity of liver outcome, although in other reports this issue has been debated^[6]. Host characteristics also play an important role in the pathogenesis of liver disease. For example, HLA class II haplotype DR5 has been shown to protect patients from the development of cirrhosis^[7].

Chronic inflammation *per se* is known to be a factor of progression towards cancer^[8], though HCV in itself does not appear to foster a strong inflammatory mechanism^[9]. It is thus not yet clear what factors most influence the outcome of the liver disease. Searching for other noxae has therefore become mandatory. A new infectious agent, *Helicobacter hepaticus* (*H. hepaticus*), that causes chronic active hepatitis and associated liver tumors in A/J Cr mice, has been described by Ward *et al*^[10]. Recently, other *Helicobacter* species (*Helicobacter* spp.), including *Helicobacter pylori* (*H. pylori*), bacteria associated with the pathogenesis of gastric^[11-14] and extradigestive manifestations^[15,16], have been detected in the liver of persons suffering from cholestatic diseases and HCC arising from non-cirrhotic liver^[17,18]. We have previously reported a high frequency of *H. pylori* and *Helicobacter pullorum* (*H. pullorum*) sequences detected by the polymerase chain reaction (PCR), in the liver of patients with cirrhosis and superimposed HCC^[19].

To demonstrate a role of the bacteria as a co-factor in the development of end-stage of liver disease in humans, it is fundamental to evidence whether *Helicobacter* occurs at the same frequency in the liver of patients without primary liver disease. The present study investigated whether *Helicobacter* spp. genomes could be detected in liver specimens from patients without any diagnosis of chronic active hepatitis, cirrhosis or HCC, compared with specimens from HCC patients. Therefore, we analysed liver samples from subjects operated upon for metastasis to the liver from colon cancer and, the presence of *Helicobacter* was assayed by molecular methods.

MATERIALS AND METHODS

Liver samples were obtained during the surgical excision for cure from 23 patients operated upon for HCC superimposed

on hepatitis C virus (HCV)-related cirrhosis and from 6 patients suffering from metastatic cancer to the liver, in whom surgery might obtain remission of the disease. All samples were immediately frozen in liquid nitrogen and stored at -80°C prior to testing. The architectural pattern and histologic grade of tumor differentiation of HCC were recorded in accordance with World Health Organisation (WHO) proposals^[20]. HCV infection was demonstrated by means of an ELISA (AxSYM System, Abbott Diagnostics) and an RIBA (RIBA II, LIA, HCV3, Sorin, Saluggia, Italy), and confirmed through detection of circulating HCV-RNA in a PCR.

DNA extraction from liver tissues

Approximately 3 mm³ of tissue was cut and incubated with 0.4 mg/ml proteinase K (Sigma, St Louis) in 0.5 ml extraction buffer (10 mM Tris-HCl, pH 7.5; 1 mM ethylene diamine tetra acetate or EDTA, pH 8; 0.25M sodium chloride; 0.2% sodium dodecyl sulphate or SDS) at 56°C on an agitator until total tissue digestion, the proteinase K was inactivated by boiling it for 10 min. The mixture was centrifuged at 14 000 rpm (Eppendorf centrifuge 5415 C) at room temperature, and to the supernatant, 1 volume of phenol/chloroform (1:1 ratio, equilibrated with 0.1 M phosphate buffered saline, pH 7.5) was added. After vortexed and centrifuged at 14 000 rpm, the aqueous phase was precipitated with 2 volumes of 100% ethanol containing 10% volume of 3M sodium acetate, pH 4.8 at -80°C for 20 min or at -20°C overnight. After two washes with 75% ethanol, the pellet was dried and resuspended in 300 μl TE buffer (10 mM Tris-HCl, pH 7.5, 5 mM EDTA, pH 8) for further use.

Nested-PCR

Amplification of 16S rRNA gene Samples were amplified by *Helicobacter* genus-specific 16S ribosomal RNA (16S rRNA) primers (designated Heli, Table 1) that could identify genomic sequences of 26 species of *Helicobacter*.

First amplification step Genomic DNA was amplified in a total volume of 50 μl containing PCR buffer (1X), 200 μM dNTP, 4 mM Mg²⁺, 0.2 μM primers (Heli-nest-S and Heli-nest-R, Table 1), 1 U *Taq* DNA polymerase (GibcoBRL, USA) and 1 μg of total DNA. The reaction mixture was initially denatured for 2 min at 94°C then amplified for 35 cycles as follows: denaturation for 30 s at 94°C , primer annealing for 30 s at 55°C and extension for 1.5 min at 72°C . A final extension step was done for 5 min at 72°C (Thermocycler HYBAID-OmniGene TR3 5M2-UK). An amplification product of 1 300 bp by the forward and reverse primers was expected. **Second amplification step** PCR was repeated as above with minor alterations: 1 μl of amplicon was used from the first amplification step, the annealing temperature was brought to 60°C , extension time lasted 30 s for 35 cycles and Heli-R/Heli-S primers (Table 1) were used. The expected size of the amplicon was 480 bp.

Amplification of *cag A* gene

Samples generating a positive result from the Nested-PCR were subsequently analysed with a different pair of primers (CagA, Table 1). The CagA-1 and CagA-2 primers used (Table 1) amplified a 290 bp product from the 128 KDa Cag A protein, typical of *H. pylori*^[21]. Fifty microliter of reaction mixture was prepared containing PCR buffer (1X), 2 mM of Mg²⁺, 200 μM dNTP, 0.2 μM primers, 1 U of *Taq* DNA polymerase and 1 μg of DNA. Amplification consisted of an initial denaturation for 2 min at 94°C then amplified for 50 cycles as follows: for 30 s at 94°C , for 30 s at 61°C and for 1 min at 72°C . Extension was continued for another cycle for 5 min at 72°C . The PCR products were analysed on a 2% agarose gel. Positive

and negative controls were included. VCS Hae III and VCS Hinf I were used as DNA size standard for amplification with Heli primers and Cag A primers, respectively.

Table 1 Primers used for amplification of 16S rRNA and *cag A* genes

Primers	Sequences 5' → 3'
Heli-nest-S	5' att agt ggc gca cgg gtg agt aa 3'
Heli-nest-R	5' ttt agc atc ccg act taa ggc 3'
Heli-S	5' gaa cct tac cta ggc ttg aca ttg 3'
Heli-R	5' ggt gag tac aag acc cgg gaa 3'
CagA-1	5' ata atg cta aat tag aca act tga gcg a 3'
CagA-2	5' tta gaa taa tca aca aac atc acg cca t 3'

Southern blot hybridisation

For this purpose, 10 μl of the amplified DNA samples was electrophoresed on a 1% agarose gel. The samples were then transferred to nylon hybond N+ membrane (Amersham Pharmacia Biotech Inc., UK) treated with denaturing agent (0.5 M sodium hydroxide, 1.5 M sodium chloride). The membrane was then neutralised with 5X SSC (0.75M sodium chloride and 0.075M sodium acetate) for 1 min. The membrane was prehybridised in buffer (5X SSPE (0.6 M NaCl, 40 mM NaH₂PO₄, 4 mM EDTA), 0.5% SDS, 5X Denhardt's solution, 0.02 mg/ml Salmon sperm) at 65°C for 4 h. A freshly denatured probe, amplified from *H. pullorum* DNA and labelled with P³²(Rediprime™ II, random labelling system, Amersham Pharmacia Biotech Inc., UK) according to the manufacturer's instructions, was purified using Microspin™ S-400 (HR Columns, Amersham Pharmacia Biotech Inc., New Jersey, USA). Hybridisation was performed overnight at 65°C in hybridisation solution containing blocking reagent (5X SSPE, 0.5% SDS, 5X Denhardt's solution) and the DNA probe. The nylon membrane was then washed in 2X SSC, 0.1% SDS for 15 min at RT, 2X SSC, 0.1% SDS for 15 min at 65°C , 1X SSC, 0.1% SDS for 15 min at 65°C and 0.5X SSC, 0.1% SDS for 10 min at 65°C . The bound probes were finally detected by autoradiography after 4 h at RT (Kodak scientific imaging film, X-OMAT/AR, Rochester, New York).

Sequencing of DNA

PCR-amplified *Helicobacter* genus-specific PCR products were run on a 2% agarose gel, purified using the QIAquick gel extraction kit (QIAGEN, Germany) and sequence analysis was performed with an Applied Biosystems DNA sequencer (Perkin-Elmer, Applied Biosystems, Warrington, Great Britain) following the procedure of the manufacturer, using the ABI PRISM 310 big dye terminator cycle sequencing kit. The sequences were entered, aligned and compared with known *Helicobacter* species using the BLAST programme (Genetics Computer Group, Madison, Wis.).

RESULTS

Screening for *Helicobacter* genus

We found DNA sequences typical of *Helicobacter* spp. in 17 of 20 (85%) livers from patients operated for HCC using *Helicobacter* genus-specific 16S rRNA primers. Three samples (15%) were negative, while in the remaining 3 out of 23, the results were uncertain. Two of 6 liver samples obtained from 6 patients whose livers were resected for metastasis due to colon cancer, contained sequences typical of *Helicobacter* spp.

The 480 bp product obtained in the second round of the nested-PCR with Heli primers is shown in Figure 1. The liver samples with a positive result by this method were all positive

by Southern blot hybridisation using P³²-labelled probe generated from *H. pullorum* DNA (data not shown). These results confirmed the presence of *Helicobacter* gene sequences in the liver samples analysed from patients with cirrhosis and HCC.

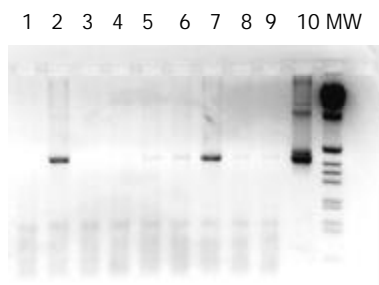


Figure 1 Agarose gel (2%) showing PCR products obtained with *Helicobacter* genus-specific 16S ribosomal RNA primers. Lane 1 negative control (DEPC-treated water). Lanes 3 and 4 liver samples from patients with metastatic liver cancer. Lanes 2, 5, 6, 7, 8 and 9 positive liver samples. Lane 10 positive control (*H. hepaticus* DNA). MW molecular-weight marker (VCS Hae III).

Type I *H. pylori* identification

The patients whose liver samples gave a signal typical for *Helicobacter* genus with Heli primers (Table 1), were analysed with primers specific for the amplification of a 290 bp stretch of the *cag A* gene^[21]. The bands amplified corresponded to the expected size (Figure 2).

Overall, 16 out of 17 (94%) liver tissues from patients who were positive when tested for *Helicobacter* genus, were also found to be positive when tested for the presence of a sequence that was typical only for type I *Helicobacter pylori*, i.e., the *cag A* gene.

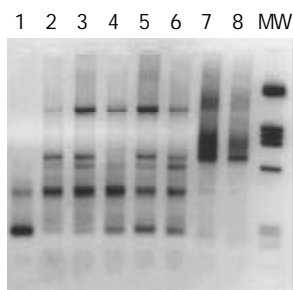


Figure 2 Analysis of *cagA*-specific PCR products from *Helicobacter* genus positive liver samples of patients with cirrhosis and HCC. The 290 bp fragments were examined on 2% agarose gel electrophoresis. Lane 1 negative control (DEPC-treated water). Lanes 2 to 6 *Helicobacter* genus positive liver samples. Lanes 7 and 8 positive controls (*cagA*-cDNA). MW molecular-weight marker (VCS Hinf I). Lanes 2, 3, 5, and 6 positive for amplified *cagA* fragment. Lane 4 negative for *cagA*.

Presence of *H. pylori* confirmed after DNA sequencing

The *Helicobacter* positive DNA fragments were sequenced. Comparison of DNA sequences of the genomic 16S rRNA amplicons with those of known *Helicobacter* spp. was performed using sequence alignment with the BLAST programme. The presence of *H. pylori* and *H. pullorum* sequences was thus confirmed in these liver samples.

DISCUSSION

Despite the profound impact of HCC on human health worldwide^[22], its pathogenesis remains uncertain. Thanks to the availability of very efficient vaccines that could prevent

HBV infection, WHO has sought to eradicate HBV infection and hence its long-term consequences such as HCC. However, in most industrialised countries, it has been shown that neither HBV nor *Schistosoma* infections play a major role in the development of HCC, instead, the majority of patients carry HCV. This virus does not integrate into host DNA, and it is likely that the mechanism of carcinogenesis differs from that of HBV. Therefore, the need to clarify the pathogenic mechanisms by which HCV may lead to liver cancer has become of prime importance.

Since the currently known risk factors cannot explain all aspects of its progression to HCC, other causal mechanisms should be explored^[23]. From an epidemiological aspect, several studies have evidenced a high seroprevalence of *H. pylori* among cirrhotic subjects^[24-26], but these data have not been ubiquitarily confirmed^[27]. Part of these differences might be explained by geographical and clinical differences in the population studied and the study-design^[23]. Experimentally, Ward *et al.* have fulfilled Koch's postulates as far as the association of *H. hepaticus* with chronic active hepatitis and HCC in mice was concerned^[10]. Whether *Helicobacter* spp. could act as a cofactor in the progression towards cirrhosis and carcinogenesis in humans with viral hepatitis, is still under review^[23].

Chronic hepatitis is an inflammatory disease and each inflammatory process is characterised by increased levels of pro-inflammatory cytokines such as interleukins 1, 6 (IL-1, IL-6), tumor necrosis factor (TNF) and by the presence of lympho-mono cellular infiltrate and lymphoid follicle formation^[28]. Viruses, such as HCV, are only capable of limited inflammation, due to shedding IL-1 receptor in circulation, thereby limiting the possibility of IL-1 binding to cellular receptors^[23]. *Helicobacters*, on the other hand, are strong inducers of the inflammatory cascade^[29], infection with them could lead to the accumulation of extraordinary number of lymphocytes and polymorphonuclear cells in the infected tissue. IL-1 gene cluster polymorphisms, thought to enhance IL-1 β production, confer an increased risk of cancer in patients infected with *H. pylori*^[30]. Furthermore, Meyer-ter-Vehn *et al.* have recently shown that strains of Cag-A-expressing *H. pylori* could activate the ERK/MAP kinase cascade, resulting in Elk-1 phosphorylation and increased *c-fos* transcription. Proto-oncogene activation might represent a crucial step in the pathomechanism of *H. pylori*-induced neoplasia. It has been shown that several *Helicobacter* spp. could also secrete a liver-specific toxin that causes hepatocyte necrosis in cell culture, and might therefore also be involved in damaging liver parenchyma *in vivo*.

The possibility that *Helicobacter* spp. could infect the biliary tract and the liver of humans has been reported by several studies in different settings. Fox *et al.* have shown the presence of *Helicobacter* spp. in the bile of Chileans with chronic cholecystitis. Avenaud and coworkers have demonstrated by PCR the presence of genomic sequences of *Helicobacter* spp. in the liver of 8 patients with HCC without primary diagnosis of cirrhosis, a further analysis by sequencing revealed that these species were *H. pylori* and *Helicobacter felis*^[18]. Similarly, we have reported the presence of the *cagA* gene sequences obtained from the liver tissue of cirrhotic patients with HCC^[19]. Furthermore, Nilsson *et al.* have identified *H. pylori* and *Helicobacter* spp. in human liver samples from patients suffering from primary sclerosing cholangitis and primary biliary cirrhosis^[17] and recently in liver samples of patients with cholangiocarcinomas or HCC.

Of great interest is the fact that the gene sequence obtained from positive *Helicobacter* spp. specific 16S rRNA PCR was usually most analogous to *H. pylori*. This encourages the speculation that the presence of *Helicobacter* DNA in human

liver tissue might reflect the transport of *H pylori* of gastric origin or its DNA to the liver. Studies have also indicated that intestinal *Helicobacter* might be implicated in hepatobiliary disease^[17]. Recently, for the first time, the culture of a *Helicobacter* strain from the human liver has been described. So far, few studies have been reported regarding the presence of *Helicobacter* spp. genomes in liver tissues from patients not suffering from primary chronic liver diseases.

We now report the infrequent presence of genomic sequences of *H pylori* in liver parenchyma of patients operated upon for metastasis to the liver arising from colon cancer. In contrast, the presence of genome of *Helicobacter* spp. was found with a higher frequency in the liver from patients with HCV-related cirrhosis and HCC. This finding lends support to the hypothesis that co-infection with *H pylori* or *Helicobacter* spp. might amplify the chronic inflammation of the parenchyma, thereby leading to cirrhosis and HCC^[23]. To date, we do not know whether bacterial infection of the liver could play a pathogenic role in the development of human HCC, analogous to what has been observed in the mouse model, and the question awaits clarification.

ACKNOWLEDGEMENT

We thank Dr. J. Stanley for providing *Helicobacter pullorum* DNA.

REFERENCES

- Parkin DM**, Pisani P, Ferlay J. Estimates of the worldwide incidence of 25 major cancers in 1990. *Int J Cancer* 1999; **80**: 827-841
- Sherlock S**, Dooley J. Diseases of the liver and biliary system. 10th Edition. Oxford: *Blackwell Scientific Publications* 1997
- Maio G**, D' Argenio P, Stroffolini T, Bozza A, Sacco L, Tosti ME, Intorcchia M, Fossi E, D' Alessio G, Anesti Kondili A, Rapicetta M, Mele A and the collaborating group. Hepatitis C virus infection and alanine transaminase levels in the general population: a survey in a southern Italian town. *J Hepatol* 2000; **33**: 116-120
- Guadagnino V**, Stroffolini T, Rapicetta M, Costantino A, Kondili LA, Menniti-Ippolito F, Caroleo B, Costa C, Griffo G, Loiacono L, Pisani V, Foca A, Piazza M. Prevalence, risk factors, and genotype distribution of hepatitis C virus infection in the general population: a community-based survey in southern Italy. *Hepatology* 1997; **26**: 1006-1011
- Silini E**, Bottelli R, Asti M, Bruno S, Candusso ME, Brambilla S, Bono F, Iamoni G, Tinelli C, Mondelli MU, Ideo G. Hepatitis C virus genotypes and risk of hepatocellular carcinoma in cirrhosis: a case-control study. *Gastroenterology* 1996; **111**: 199-205
- Wiese M**, Berr F, Lafrenz M, Porst H, Oesen U. Low frequency of cirrhosis in a hepatitis C (genotype 1b) single-source outbreak in Germany: a 20-year multicenter study. *Hepatology* 2000; **32**: 91-96
- Peano G**, Menardi G, Ponzetto A, Fenoglio L. HLA-DR5. A genetic factor influencing the outcome of hepatitis C virus infection? *Arch Intern Med* 1994; **154**: 2733-2736
- Cassell GH**. Infectious causes of chronic inflammatory diseases and cancer. *Emerging Infect Dis* 1998; **4**: 475-487
- Mosnier JF**, Scoazec JY, Marcellin P, Degott C, Behhamou JP, Feldmann G. Expression of cytokine-dependent immune adhesion molecules by hepatocytes and bile duct cells in chronic hepatitis C. *Gastroenterology* 1994; **107**: 1457-1468
- Ward JM**, Fox JG, Anver MR, Haines DC, George CV, Collins MJ, Gorelick PL, Nagashima K, Gonda MA, Gilden RV, Tully JG, Russell RJ, Benveniste RE, Paster BJ, Dewhirst FE, Donovan JC, Anderson LM, Rice JM. Chronic active hepatitis and associated liver tumors in mice caused by a persistent bacterial infection with a novel *Helicobacter* species. *J Natl Cancer Inst* 1994; **86**: 1222-1227
- Bulent K**, Murat A, Esin A, Fatih K, MMMurat H, Hakan H, Melih K, Mehmet A, Bulent Y, Fatih H. Association of *CagA* and *VacA* presence with ulcer and non-ulcer dyspepsia in a Turkish population. *World J Gastroenterol* 2003; **9**: 1580-1583
- Palmas F**, Pellicano R, Massimetti E, Berrutti M, Fagoonee S, Rizzetto M. Eradication of *Helicobacter pylori* infection with proton pump inhibitor-based triple therapy. A randomised study. *Panminerva Med* 2002; **44**: 145-147
- Testino G**, Cornaggia M, De Iaco F. *Helicobacter pylori* influence on gastric acid secretion in duodenal ulcer patients diagnosed for the first time. *Panminerva Med* 2002; **44**: 19-22
- Li S**, Lu AP, Zhang L, Li YD. Anti-*Helicobacter pylori* immunoglobulin G (IgG) and IgA antibody responses and the value of clinical presentations in diagnosis of *H pylori* infection in patients with precancerous lesions. *World J Gastroenterol* 2003; **9**: 755-758
- Roussos A**, Philippou N, Gourgoulialis KI. *Helicobacter pylori* infection and respiratory diseases: a review. *World J Gastroenterol* 2003; **9**: 5-8
- Yakoob J**, Jafri W, Abid S. *Helicobacter pylori* infection and micronutrient deficiencies. *World J Gastroenterol* 2003; **9**: 2137-2139
- Nilsson H**, Taneera J, Castedal M, Glatz E, Olsson R, Wadstrom T. Identification of *Helicobacter pylori* and *Helicobacter* species by PCR, hybridization and partial DNA sequencing in human liver samples from patients with primary sclerosing cholangitis or primary biliary cirrhosis. *J Clin Microbiol* 2000; **38**: 1072-1076
- Avenaud P**, Marais A, Monteiro L, Lebail B, Biouclac Sage P, Balabaud C, Mégraud F. Detection of *Helicobacter* species in the liver of patients with and without primary liver carcinoma. *Cancer* 2000; **89**: 1431-1439
- Ponzetto A**, Pellicano R, Leone N, Cutufia MA, Turrini F, Grigioni WF, D' Errico A, Mortimer P, Rizzetto M, Silengo L. *Helicobacter pylori* infection and cirrhosis in hepatitis C virus carriage: is it an innocent bystander or a troublemaker? *Med Hypotheses* 2000; **54**: 275-277
- Ishak KG**, Anthony PP, Sobin LH. Histological typing of tumors of the liver. World Health Organization. New York : *Springer Verlag* 1994
- Covacci A**, Censini S, Bugnoli M, Petracca R, Burrioni D, Macchia G, Massone A, Papini E, Xiang Z, Figura N, Rappuoli R. Molecular characterization of the 128 kDa immunodominant antigen of *Helicobacter pylori* associated with cytotoxicity and duodenal ulcer. *Proc Natl Acad Sci U S A* 1993; **90**: 5791-5795
- Sun HC**, Tang ZY. Preventive treatments for recurrence after curative resection of hepatocellular carcinoma-A literature review of randomized control trials. *World J Gastroenterol* 2003; **9**: 635-640
- Fagoonee S**, Pellicano R, Rizzetto M, Ponzetto A. The journey from hepatitis to hepatocellular carcinoma: bridging role of *Helicobacter* species. *Panminerva Med* 2001; **43**: 279-282
- Siringo S**, Vaira D, Menegatti M, Piscaglia F, Sofia S, Gaetani M, Miglioli M, Corinaldesi R, Bolondi L. High prevalence of *Helicobacter pylori* in liver cirrhosis: relationship with clinical and endoscopic features and the risk of peptic ulcer. *Dig Dis Sci* 1997; **42**: 2024-2030
- Spinzi G**, Pellicano R, Minoli G, Terreni N, Cutufia M, Fagoonee S, Rizzetto M, Ponzetto A. *Helicobacter pylori* seroprevalence in hepatitis C virus positive patients with cirrhosis: the Como cross-sectional study. *Panminerva Med* 2001; **43**: 85-87
- Pellicano R**, Leone N, Berrutti M, Cutufia MA, Fiorentino M, Rizzetto M, Ponzetto A. *Helicobacter pylori* seroprevalence in hepatitis C virus positive patients with cirrhosis. *J Hepatol* 2000; **33**: 648-650
- Chen JJ**, Chang-Chien CS, Tai DI, Chiou SS, Lee CM, Kuo CH. Role of *Helicobacter pylori* in cirrhotic patients with peptic ulcer. *Dig Dis Sci* 1994; **39**: 1565-1568
- Balkwill F**, Mantovani A. Inflammation and cancer: back to Virchow? *Lancet* 2001; **357**: 539-545
- Crabtree J**. Cytokine responses to *Helicobacter pylori* -induced infection. In: Riecken EO, Zeitz M, Stallmach A, Heise W editors. Malignancy and chronic inflammation in the gastro-intestinal tract: new concepts. Lancaster: *Kluwer Academic Publishers* 1995: 25-36
- El-Omar EM**, Carrington M, Chow WH, McColl KE, Bream JH, Young HA, Herrera J, Lissowska J, Yuan CC, Rothman N, Lanyon G, Martin M, Fraumeni JF Jr, Rabkin CS. Interleukin-1 polymorphisms associated with increased risk of gastric cancer. *Nature* 2000; **404**: 398-402

Genotypes of *Helicobacter pylori* in patients with peptic ulcer bleeding

Chin-Lin Perng, Hwai-Jeng Lin, Wen-Ching Lo, Guan-Ying Tseng, I-Chen Sun, Yueh-Hsing Ou

Chin-Lin Perng, I-Lan Hospital, Division of Gastroenterology, Department of Health, Taiwan, China

Hwai-Jeng Lin, I-Chen Sun, Division of Gastroenterology, Department of Medicine, VGH-TAIPEI, Taiwan, China

Wen-Ching Lo, Zhongxiao Municipal Hospital, Taipei, Taiwan, China

Guan-Ying Tseng, Ton-Yen General Hospital, Hsin-Chu, Taiwan, China

Yueh-Hsing Ou, Institute of Biotechnology in Medicine, School of Medical Technology and Engineering, and School of Medicine, National Yang-Ming University, Taiwan, China

Correspondence to: Professor Hwai-Jeng Lin, Division of Gastroenterology, Department of Medicine, VGH-TAIPEI, Shih-Pai Rd, Sec 2, Taipei, Taiwan, 11217, China. hjlin@vghtpe.gov.tw

Telephone: +886-2-28712121 Ext 2015 **Fax:** +886-2-28739318

Received: 2003-10-30 **Accepted:** 2003-12-15

Abstract

AIM: *Helicobacter pylori* causes chronic gastritis, peptic ulcer, gastric cancer and MALT-lymphoma. Different genotypes of *Helicobacter pylori* are confirmed from diverse geographic areas. Its association with bleeding peptic ulcer remains controversial. The aim of this study was to investigate the *Helicobacter pylori vacA* alleles, *cagA* and *iceA* in patients with bleeding peptic ulcer.

METHODS: We enrolled patients with bleeding, non-bleeding peptic ulcers and chronic gastritis. Biopsy specimens were obtained from the antrum of the stomach for rapid urease test, bacterial culture and PCR assay. DNA extraction and polymerase chain reaction were used to detect the presence or absence of *cagA* and to assess the polymorphism of *vacA* and *iceA*.

RESULTS: A total of 168 patients (60.4%) (25 patients with chronic gastritis, 26 patients with bleeding gastric ulcer, 51 patients with non-bleeding gastric ulcer, 26 patients with bleeding duodenal ulcer, and 40 patients with non-bleeding duodenal ulcer) were found to have positive PCR results between January 2001 and December 2002. Concerning genotypes, we found *cagA* (139/278, 50%), *vacA* s1a (127/278, 45.7%), and *iceA* A1 (125/278, 45%) predominated in all studied patients. In patients with bleeding peptic ulcers, *vacA* s1a and m1T were fewer than those in patients with non-bleeding peptic ulcers (37/106 vs 69/135, $P=0.017$, and 4/106 vs 21/135, $P=0.002$).

CONCLUSION: In patients with peptic ulcers, *H pylori vacA* s1a and m1T prevent bleeding complication.

Perng CL, Lin HJ, Lo WC, Tseng GY, Sun IC, Ou YH. Genotypes of *Helicobacter pylori* in patients with peptic ulcer bleeding. *World J Gastroenterol* 2004; 10(4): 602-605
<http://www.wjgnet.com/1007-9327/10/602.asp>

INTRODUCTION

Helicobacter pylori (*H pylori*) infection has been closely linked

to chronic gastritis, peptic ulcer, gastric cancer and MALT-lymphoma^[1]. It is one of the most common bacterial infections of humans^[2]. It remains to be answered why only a minority of *H pylori* carriers develop peptic ulcer disease. Host factors, *H pylori* strain variability, environmental factors, and NSAID play a role in the pathogenesis of peptic ulcer disease^[3-5]. The clinical outcome of *H pylori* infection is supposed to be linked to certain strains, e.g. vacuolating cytotoxin (*vacA*) and the cytotoxin-associated gene (*cagA*)^[6,7].

In patients with peptic ulcer disease, only a minority of them present with peptic ulcer hemorrhage. The incidence of peptic ulcer hemorrhage in patients with pre-existing peptic ulcer disease is less than 1% per year^[8]. Whether *H pylori* increases the risk of ulcer bleeding is controversial. Wu *et al* confirmed that *H pylori* increased the risk of peptic ulcer bleeding^[9]. Cullen *et al* had a similar finding (OR 2.8)^[10]. In addition, eradication of *H pylori* infection could decrease the chance of peptic ulcer bleeding^[11,12]. The above evidences strongly support the link of *H pylori* to peptic ulcer bleeding. However, the prevalence of *H pylori* has been found to be lower in bleeding ulcer patients than in non-bleeders^[13]. The most likely explanation is the use of NSAIDs in the absence of *H pylori* infection in these patients. Another reason may be false negative results in these patients^[14,15]. If we excluded the usage of NSAIDs in patients with duodenal ulcer bleeding, the prevalence of *H pylori* infection was 97%^[16].

Controversy exists concerning relationship of genotypes of *H pylori* with peptic ulcer bleeding. So far, there are only few reports concerning this topic^[17,18]. Although *H pylori* infection is very common, geographic distribution of different subtypes exists^[19,20]. Therefore, it is interesting to investigate the genotypes in patients with peptic ulcer bleeding. The aim of this study was to determine the genotypes of *H pylori* in bleeding ulcer patients in Taiwan.

MATERIALS AND METHODS

Between January 2001 and December 2002, patients with non-bleeding peptic ulcers (gastric ulcer or duodenal ulcer, at least 5 mm in diameter), bleeding peptic ulcers (spurting or oozing hemorrhage, non-bleeding visible vessel, blood clots or pigmented spots at the ulcer base) or chronic gastritis were invited to enter the study. There was no past history of upper gastrointestinal bleeding (hematemesis or melena) in patients with non-bleeding peptic ulcer in this study. Patients with pregnancy, bleeding tendency (platelet count less than 50 000/mm³, prothrombin time less than 30%, or taking anti-coagulants), gastric malignancy, age under 10, or over 90 years, anti-*H pylori* therapy 4 weeks prior to enrollment, and inability to cooperate were excluded from the study. The study was approved by the Clinical Research Committee of the Veterans General Hospital, Taipei.

Endoscopic examination and biopsy were performed after informed consent was obtained. We took three specimens from the antrum, one for rapid urease test, another for bacterial culture and the third for DNA extraction and PCR assay. Lysates of biopsied gastric mucosa were used for PCR assay. DNA of gastric biopsy specimens was extracted according to the method described by Boom^[21]. Briefly, biopsy specimens

were homogenized in guanidinium isothiocyanate, using a sterile micropestle. DNA was extracted, washed and eluted in 100 µl of 10 mM Tris-HCL (pH 8.3). Two µl of the eluted DNA was used for each PCR reaction.

The oligonucleotide primers for PCR amplification of specific segments are shown in Table 1^[5,22-25]. For *vacA* evaluation, the PCR program comprised 35 cycles of denaturation at 94°C for 1 min, annealing at 56°C for 2 min, extension at 72°C for 1 min, and one final extension at 72°C for 10 min. For *cagA*, amplification was performed with 35 cycles of denaturation at 94°C for 1 min, annealing at 56°C for 2 min, extension at 72°C for 1 min, and one final extension at 72°C for 5 min. For *iceA* amplification, amplifications were performed with 40 cycles of denaturation at 95°C for 30 s, annealing at 50°C for 45 s, extension at 72°C for 45 s and one final extension at 72°C for 10 min.

The association between *H pylori* genotypes and clinical diseases was determined using χ^2 test and Yates' correction or Fisher's exact test when appropriate. A *P* value less than 0.05 was considered statistically significant.

RESULTS

A total of 278 patients with bleeding or non-bleeding peptic ulcers and chronic gastritis (200 males and 78 females, mean age: 62.1 years, 95% CI: 60.1-64.1 years) fulfilling the admission criteria, were included in this study. A total of 168 patients (60.4%) were found to have a positive urease test. A total of 168 patients (60.4%) (25 patients with chronic gastritis, 26 patients with bleeding gastric ulcer, 51 patients with non-bleeding gastric ulcer, 26 patients with bleeding duodenal ulcer, and 40 patients with non-bleeding duodenal ulcer) were found

Table 1 Oligonucleotide primers used for *cagA*, *vacA* and *iceA* genotyping

Region detected	Primer designation	Primer sequence	Size of PCR product (bp)	References
s1 and s2	VA1-F	5' ATGGAAATACAACAAACACACC3'	259	21
	VA1-R	5' CTGCTTGAATGCGCCAAACTTTATC3'	286	
s1a	SS1-F	5' GTCAGCATCACACCGCAAC3'	190	9
s1b	SS3-F	5' AGCGCCATACCGCAAGAG3'	187	9
s1c	S1C-F	5' CTYGCTTTAGTRGGGYTA-3'	213	17
m1	VA3-F	5' GGTCAAAATGCGGTCATGG3'	290	9
	VA3-R	5' CCATTGGTACCTGTAGAAAC3'		
m1T	m1T-F	5' GGTCAAAATGCGGTCATGG3'	290	21
	m1T-R	5' CTCTTAGTGCCTAAAGAAACA3'		
m2	VA4-F	5' GGAGCCCCAGGAAACATTG3'	352	9
	VA4-R	5' CATAACTAGCGCCTTGAC3'		
iceA1	iceA1F	5' GTGTTTTTAACCAAAGTATC3'	247	16
	iceA1R	5' CTATAGCCASTYTCTTTGCA3'		
iceA2	iceA2F	5' GTTGGGTATATCACAATTTAT3'	229	16
	iceA2R	5' TTRCCCTATTTTCTAGTAGGT3'		
lcagA	lcagAD008	5' ATAATGCTAAATTAGACAACCTTGAGCGA3'	297	5
	lcagAR008	5' TTAGAATAATCAACAAACATCACGCCAT3'		

Table 2 Genotypes of *Helicobacter pylori* in patients with chronic gastritis, non-bleeding duodenal ulcers (DU), bleeding DU, non-bleeding gastric ulcers (GU) and bleeding GU

Diagnosis	No. of patients	No. of positive PCR	s1a	s1b	s1c	s2	m1	m1T	m2	<i>cagA</i>	<i>iceA1</i>	<i>iceA2</i>
Chronic gastritis	37	25	21(57)	0(0)	14(38)	0(0)	0(0)	8(22)	12(32)	22(59)	22(59)	2(5)
Non-bleeding DU	53	40	30(57)	4(8)	22(42)	0(0)	0(0)	11(21)	15(28)	29(55)	30(57)	3(6)
Bleeding DU	48	26	17(35)	4(8)	15(31)	2(4)	2(4)	3(6)	12(25)	25(52)	19(40)	7(15)
Non-bleeding GU	82	51	39(48)	0(0)	29(35)	0(0)	0(0)	10(12)	30(37)	41(50)	34(41)	13(16)
Bleeding GU	58	26	20(34)	1(2)	13(22)	0(0)	0(0)	1(2)	15(26)	22(38)	20(34)	4(7)

P>0.05 versus variables between non-bleeding DU and bleeding DU, between non-bleeding GU and bleeding GU.

Table 3 Genotypes of *Helicobacter pylori* in patients with non-bleeding peptic ulcers and bleeding peptic ulcers

Diagnosis	No. of patients	No. of positive PCR	s1a	s1b	s1c	s2	m1	m1T	m2	<i>cagA</i>	<i>iceA1</i>	<i>iceA2</i>
Non-bleeding PU	135	91	69 ^a (51)	4(3)	51(38)	0(0)	0(0)	21 ^b (16)	45(33)	70(52)	64(47)	16(12)
Bleeding PU	106	52	37(35)	5(5)	28(26)	2(2)	2(2)	4(4)	27(25)	47(44)	39(37)	11(10)

^a*P*=0.017 between non-bleeding peptic ulcers and bleeding peptic ulcers. ^b*P*=0.002 between non-bleeding peptic ulcers and bleeding peptic ulcers.

to have positive PCR results. The ages of patients with bleeding gastric ulcer (mean: 67.8 yr, 95% CI: 62.8-72.8), non-bleeding gastric ulcer (mean: 63.5 yrs, 95% CI: 59.8-67.2), bleeding duodenal ulcer (mean: 65.5 yrs, 95% CI: 59.2-71.8) were greater than those of patients with non-bleeding duodenal ulcer (mean: 54.6 yrs, 95% CI: 49.5-59.7, $P < 0.01$) and chronic gastritis (mean: 51.2 yrs, 95% CI: 42.8-59.6, $P < 0.01$).

In patients with bleeding gastric ulcer, there were blood clots inside the stomach in 8 patients, coffee grounds in 8 patients, and clear fluid in 10 patients. In patients with bleeding duodenal ulcers, there were blood clots inside the stomach in 8 patients, coffee grounds in two patients and clear fluid in 16 patients.

In patients with bleeding peptic ulcers, 52 (49.1%) were found to have positive PCR for *H pylori*. It was lower than that in those with non-bleeding peptic ulcers (91/135, 67.4%, $P = 0.006$) and chronic gastritis (25/37, 67.6%, $P = 0.008$).

The genotypes in patients with chronic gastritis, duodenal ulcers and gastric ulcers are described in Table 2. There was no statistical difference among variables in different groups.

Concerning genotypes, we found *cagA* (139/278, 50%), *vacA* s1a (127/278, 45.7%), and *iceA* A1 (125/278, 45%) predominated in all studied patients. In patients with bleeding peptic ulcers, *vacA* s1a and m1T were fewer than those in patients with non-bleeding peptic ulcers (37/106 vs 69/135, $P = 0.017$, and 4/106 vs 21/135, $P = 0.002$, Table 3).

DISCUSSION

H pylori is a world-wide infective agent ranging from 25% in developed countries to more than 80% in the developing world^[26,27]. However, not all individuals infected with *H pylori* develop gastric illness and this may be related to various factors such as environmental factors, host genetic factors, and bacterial virulent ability^[28,29].

This study determined using PCR the *cagA*, *vacA* and *iceA* status of 278 patients presenting for endoscopy by examining biopsy specimens from the antrum of each patient. Of them, 168 patients (60.4%) were found to have positive PCR. In this study, predominance of *vacA* s1a was found in patients with bleeding and non-bleeding peptic ulcer and chronic gastritis. Our finding was similar to those reported by other authors^[25,30,31]. In Hong Kong and Korea, a low incidence of *vacA* s1a subtype was found^[32,33].

The previous Taiwan reports gave no data concerning *vacA* s1c^[25,30]. *VacA* s1c was frequently found (93/278, 33.5%) in this study. In patients with bleeding peptic ulcers, *vacA* s1c was less than that in patients with non-bleeding peptic ulcers (26% vs 38%), but it did not reach statistical significance. The incidence of *vacA* s1c in this study was similar to the reports of Hong Kong^[32], Korea^[33], and Japan^[34], but different from those in Western world^[19,20]. In contrast, *vacA* s1b and s2 were rare. Our findings were compatible with that in mainland China^[31].

Concerning the m-region of *vacA*, m1 strains predominated in most Western reports^[19,20,27]. However, there were only 2% m1 subtypes in patients with bleeding peptic ulcers and none in patients with non-bleeding peptic ulcers in this study. We used a modified primer (m1T)^[25] and some peptic ulcer patients (bleeding: 3.8%, non-bleeding: 15.6%) with *H pylori* infection contained this genotype. m2 strains predominated (33% in patients with non-bleeding peptic ulcers, 25% in bleeding peptic ulcers) in this study. Our finding was consistent with reports from Taiwan^[25,30], Hong Kong^[32], and mainland China^[31]. In contrast, Japan and Korea had a much lower incidence of m2 strains^[24,33]. This indicates a great variation in the *vacA* region in Taiwan, particularly in the mid-region locus. *H pylori* may have a different geographic evolution in Taiwan

even compared with other East Asian countries.

IceA1 has been suggested to be related to peptic ulcer disease^[23,35]. But, this finding was doubted by other authors and us^[24,32,33]. In this study, we found *iceA1* was the predominant subtype and showed no difference between patients with bleeding and non-bleeding peptic ulcers. *IceA1* is the predominant subtype of *ice* in the East Asia, while *iceA2* is the predominant subtype in the USA and Columbia^[24].

Certain genotypes (e.g. *cagA*, *vacA* s1a) have been closely related to severe clinical outcomes and response to anti-*H pylori* therapy^[36-38]. However, these findings are not supported by other studies^[24,25,29-32,34]. The association between *H pylori* infection and peptic ulcer bleeding is less clear, but a strong argument for the etiological role is the fact that eradication of *H pylori* decreased recurrence of bleeding^[39]. Stack *et al* recently found that *cagA* positive *H pylori* was associated with an increased risk of ulcer bleeding^[17]. However, Illies *et al* found that presence of *cagA* antibody was similar both in patients with bleeding and in non-bleeding controls^[18]. In this study, there was no difference of *cagA* between patients with non-bleeding and those with bleeding peptic ulcers. However, there were fewer *vacA* s1a and m1T in patients with bleeding peptic ulcers than in patients with non-bleeding peptic ulcers.

In conclusion, in patients with bleeding peptic ulcers, *H pylori vacA* s1a and m1T are less than those in patients with non-bleeding peptic ulcers.

ACKNOWLEDGEMENT

This study was supported by VGH 92-230, NSC-91-2314-B-075-127. We are in debt to Miss Betty, Tzu-en Lin for their assistance in this study.

REFERENCES

- Dunn BE, Cohen H, Blaser MJ. *Helicobacter pylori*. *Clin Microbiol Rev* 1997; **10**: 720-741
- Blaser MJ. Ecology of *Helicobacter pylori* in the human stomach. *J Clin Invest* 1997; **100**: 759-762
- Olbe L, Fandriks L, Hamlet A, Svennerholm AM. Conceivable mechanisms by which *Helicobacter pylori* provokes duodenal ulcer disease. *Baillieres Best Pract Res Clin Gastroenterol* 2000; **14**: 1-12
- Dore MP, Graham DY. Pathogenesis of duodenal ulcer disease: the rest of the story. *Baillieres Best Pract Res Clin Gastroenterol* 2000; **14**: 97-107
- Henriksson AE, Edman AC, Nilsson I, Bergqvist D, Wadstrom T. *Helicobacter pylori* and the relation to other risk factors in patients with acute bleeding peptic ulcer. *Scand J Gastroenterol* 1998; **33**: 1030-1033
- Covacci A, Censini S, Bugnoli M, Petracca R, Burrone D, Macchia G, Massone A, Papini E, Xiang E, Figura N. Molecular characterization of the 128-kDa immunodominant antigen of *Helicobacter pylori* associated with cytotoxicity and duodenal ulcer. *Proc Natl Acad Sci* 1993; **90**: 5791-5795
- Cover TL. The vacuolating cytotoxin of *Helicobacter pylori*. *Mol Microbiol* 1996; **20**: 241-246
- Ohmann C, Thon K, Hengels KJ, Imhof M. Incidence and pattern of peptic ulcer bleeding in a defined geographical area. DUSUK Study Group. *Scand J Gastroenterol* 1992; **27**: 571-581
- Wu CY, Poon SK, Chen GH, Chang CS, Yeh HZ. Interaction between *Helicobacter pylori* and non-steroidal anti-inflammatory drugs in peptic ulcer bleeding. *Scand J Gastroenterol* 1999; **33**: 234-237
- Cullen DJE, Hawkey GM, Greenwood DC, Humphreys H, Shepherd U, Logan RF, Hawkey CJ. Peptic ulcer bleeding in the elderly: relative roles of *Helicobacter pylori* and non-steroidal anti-inflammatory drugs. *Gut* 1997; **41**: 459-462
- Rokkas T, Karameris A, Mavrogeorgis A, Rallis E, Gianni Kos N. Eradication of *Helicobacter pylori* reduces the possibility of rebleeding in peptic ulcer disease. *Gastrointest Endosc* 1995; **41**: 1-4
- Jaspersen D, Koerner T, Schorr W, Brennenstuehe M, Raschka C,

- Hammar CH. *Helicobacter pylori* eradication reduces the rate of rebleeding in ulcer hemorrhage. *Gastrointest Endosc* 1995; **41**: 5-7
- 13 **Vaira D**, Menegatti M, Giglioli M. What is the role of *Helicobacter pylori* in complicated ulcer disease? *Gastroenterology* 1997; **113**: S78-84
- 14 **Tu TC**, Lee CL, Wu CH, Chen TK, Chan CC, Huang SH, Lee MS SC. Comparison of invasive and noninvasive tests for detecting *Helicobacter pylori* infection in bleeding peptic ulcers. *Gastrointest Endosc* 1999; **49**(3 Pt 1): 302-306
- 15 **Colin R**, Czernichow P, Baty V, Touze I, Brazier F, Bretagne JF, Berkelmans I, Bartheemy P, Hemet J. Low sensitivity of invasive tests for the detection of *Helicobacter pylori* infection in patients with bleeding ulcer. *Gastroenterol Clin Biol* 2000; **24**: 31-35
- 16 **Gisbert JP**, Gonzalez L, de Pedro A, Valbuena M, Prieto B, Llorca I, BrizR, Khorrami S, Garcia-Gravalos R, Pajares JM. *Helicobacter pylori* and bleeding duodenal ulcer: prevalence of the infection and role of non-steroidal anti-inflammatory drugs. *Scand J Gastroenterol* 2001; **36**: 717-724
- 17 **Stack WA**, Atherton JC, Hawkey GM, Logan RF, Hawkey CJ. Interactions between *Helicobacter pylori* and other risk factors for peptic ulcer bleeding. *Aliment Pharmacol Ther* 2002; **16**: 497-506
- 18 **Illies G**, Reincke I, Nilius M, Dominguez-Munoz JE. *Helicobacter pylori* (HP) antibodies against cagA protein in bleeding and non-bleeding gastric and duodenal ulcers. *Gastroenterology* 1996; **110**: A 141
- 19 **van Doorn LJ**, Figueiredo C, Megráud F, Pena S, Midolo P, Queiroz DM, Carneiro F, Vanderborcht B, Pegado MD, Sanna R, De Boer W, Schneeberger PM, Correa P, Ng EK, Atherton J, Blaser MJ, Quint WG. Geographic distribution of *vacA* allelic types of *Helicobacter pylori*. *Gastroenterology* 1999; **116**: 823-830
- 20 **van Doorn LJ**, Figueiredo C, Sanna R, Pena S, Midolo P, Ng EK, Atherton JC, Blaser MJ, Quint WG. Expanding allelic diversity of *Helicobacter pylori vacA*. *J Clin Microbiol* 1998; **36**: 2597-2603
- 21 **Boom R**, Sol CJ, Salimans MM, Jansen CL, Wertheim-van Dillen PM, van der Nooraa J. Rapid and simple method for purification of nucleic acids. *J Clin Microbiol* 1990; **28**: 495-503
- 22 **Atherton JC**, Cao P, Peek RM, Tummuru MKR, Blaser M, Cover TL. Mosaicism in vacuolating cytotoxin alleles of *Helicobacter pylori*. *J Biol Chem* 1995; **270**: 17771-17777
- 23 **van Doorn LJ**, Figueiredo C, Sanna R, Plaisier A, Schneeberger P, de Boer W, Quint W. Clinical relevance of the *cagA*, *vacA* and *iceA* status of *Helicobacter pylori*. *Gastroenterology* 1998; **115**: 58-66
- 24 **Yamaoka Y**, Kodama T, Gutierrez O, Kim JG, Kashima K, Graham DY. Relationship between *Helicobacter pylori iceA*, *cagA*, and *vacA* status and clinical outcome: studies in four different countries. *J Clin Microbiol* 1999; **37**: 2274-2279
- 25 **Wang HJ**, Kuo CH, Yeh AAM, Chang PCL, Wang WC. Vacuolating toxin production in clinical isolates of *Helicobacter pylori* with different *vacA* genotypes. *J Inf Dis* 1998; **178**: 207-212
- 26 **Parsonnet JE**. The incidence of *Helicobacter pylori* infection. *Aliment Pharmacol Ther* 1995; **9**(Suppl 2): 45-52
- 27 **Pounder RE**. The prevalence of *Helicobacter pylori* in different countries. *Aliment Pharmacol Ther* 1995; **9**(Suppl 2): 33-40
- 28 **Campbell S**, Fraser A, Holliss B, Schmid J, O' Toole PW. Evidence for ethnic tropism of *Helicobacter pylori*. *Infect Immun* 1997; **65**: 3708-3712
- 29 **Malaty HM**, Graham DY. Importance of childhood socioeconomic status on the current prevalence of *Helicobacter pylori* infection. *Gut* 1994; **35**: 742-745
- 30 **Lin CW**, Wu SC, Lee SC, Cheng KS. Genetic analysis and clinical evaluation of vacuolating cytotoxin gene A and cytotoxin-associated gene A in Taiwanese *Helicobacter pylori* isolated from peptic ulcer patients. *Scand J Infect Dis* 2000; **32**: 51-57
- 31 **Pan ZJ**, Berg DE, van der Hulst RWM, Su WW, Raudonikiene A, Xiao SD, Dankert J, Tytgat GN, van der Ende A. Prevalence of vacuolating cytotoxin production and distribution of distinct *vacA* alleles in *Helicobacter pylori* from China. *J Infect Dis* 1998; **178**: 220-226
- 32 **Wong BC**, Yin Y, Berg DE, Xia HH, Zhang JZ, Wang WH, Wong WM, Hunag XR, Tang VS, Lam SK. Distribution of distinct *vacA*, *cagA* and *iceA* alleles in *Helicobacter pylori* in Hong Kong. *Helicobacter pylori* 2001; **6**: 317-324
- 33 **Kim SM**, Woo CW, Lee YM, Son BR, Kim JW, Chae HB, Youn SJ, Park SM. Genotyping *cagA*, *vacA* subtype, *iceA1*, and *BabA* of *Helicobacter pylori* isolates from Korean patients, and their association with gastroduodenal diseases. *J Korean Med Sci* 2001; **16**: 579-584
- 34 **Fukuta K**, Azuma T, Ito Y, Suto H, Keida Y, Wakabayashi H, Watanabe A, Kuriyama M. Clinical relevance of *cagE* gene from *Helicobacter pylori* strains in Japan. *Dig Dis Sci* 2002; **47**: 667-674
- 35 **Figura N**, Vindigni C, Covacci A, Presenti L, Burrioni D, Vernillo R, Banducci T, Roviello F, Marrelli D, Biscontri M, Kristodhullu S, Gennari C, Vaira D. *CagA* positive and negative *Helicobacter pylori* strains are simultaneously present in the stomach of most patients with non-ulcer dyspepsia: relevance to histological damage. *Gut* 1998; **42**: 772-778
- 36 **Figueiredo C**, Van Doorn LJ, Nogueira C, Soares JM, Pinho C, Figueira P. *Helicobacter pylori* genotypes are associated with clinical outcome in Portuguese patients and show a high prevalence of infections with multiple strains. *Scan J Gastroenterol* 2001; **36**: 128-135
- 37 **De Gusmão VR**, Mendes EN, de Magalhães Queiroz DM, Rocha GA, Rocha AMC, Ramadan Ashour AA, Teles Carvalho AS. *vacA* genotypes in *Helicobacter pylori* strains isolated from children with and without duodenal ulcer in Brazil. *J Clin Microbiol* 2000; **38**: 2853-2857
- 38 **Rudi J**, Kolb C, Maiwald M, Kuck D, Sieg A, Galle PR, Stremmel W. Diversity of *Helicobacter pylori vacA*, and *cagA* genes and relationship to *vacA* and *cagA* protein expression, cytotoxin production, and associated diseases. *J Clin Microbiol* 1998; **36**: 944-948
- 39 **van Leerdam ME**, Tytgat GNJ. Review article: *Helicobacter pylori* infection in peptic ulcer haemorrhage. *Aliment Pharmacol Ther* 2002; **16**: (S1) 66-78

Abnormal function of platelets and role of angelica sinensis in patients with ulcerative colitis

Wei-Guo Dong, Shao-Ping Liu, Hai-Hang Zhu, He-Sheng Luo, Jie-Ping Yu

Wei-Guo Dong, Shao-Ping Liu, He-Sheng Luo, Jie-Ping Yu,
Department of Gastroenterology, Renmin Hospital of Wuhan University, Wuhan 430060, Hubei Province, China

Hai-Hang Zhu, Department of Gastroenterology, the First Affiliated Hospital of Yangzhou University, Yangzhou 225001, Jiangsu Province, China

Supported by Key Project in Scientific and Technological Researches of Hubei Province, No. 2001AA308B

Correspondence to: Professor Wei-Guo Dong, Renmin Hospital of Wuhan University, 238 Jiefang Road, Wuhan 430060, Hubei Province, China. dongwg@public.wh.hb.cn

Telephone: +86-27-88054511

Received: 2003-08-06 **Accepted:** 2003-09-18

Abstract

AIM: To explore the abnormal function of platelets and the role of angelica sinensis injection (ASI) in patients with ulcerative colitis (UC).

METHODS: In 39 patients with active UC, 25 patients with remissive UC and 30 healthy people, α -granule membrane protein (GMP-140) and thromboxane B₂ (TXB₂) were detected by means of ELISA, 6-keto-PGF_{1a} was detected by radioimmunoassay, platelet count (PC) and 1 min platelet aggregation rate (1 min PAR) were detected by blood automatic tester and platelet aggregation tester respectively, and von Willebrand factor related antigen (vWF:Ag) was detected by the means of monoclonal -ELISA. The 64 patients with UC were divided into two therapy groups. After routine treatment and angelica sinensis injection (ASI) + routine treatment respectively for 3 weeks, all these parameters were also detected.

RESULTS: The PC, 1 min PAR and levels of GMP-140, TXB₂, and vWF:Ag in active UC were significantly higher than those in remissive UC and normal controls ($P < 0.05-0.01$). Meanwhile, 1 min PAR and levels of GMP-140, TXB₂, and vWF:Ag in remissive UC were still significantly higher than those in normal controls ($P < 0.05$). Furthermore, 6-keto-PGF_{1a} level in active and remissive UC was remarkably lower than that in normal control ($P < 0.05-0.01$). These parameters except 6-keto-PGF_{1a} were significantly improved after the treatment in ASI therapy group ($P < 0.05-0.01$), whereas they all were little changed in routine therapy group ($P > 0.05$).

CONCLUSION: Platelets can be significantly activated in UC, which might be related with vascular endothelium injury and imbalance between TXB₂ and 6-keto-PGF_{1a} in blood. ASI can significantly inhibit platelet activation, relieve vascular endothelial cell injury, and improve microcirculation in UC.

Dong WG, Liu SP, Zhu HH, Luo HS, Yu JP. Abnormal function of platelets and role of angelica sinensis in patients with ulcerative colitis. *World J Gastroenterol* 2004; 10(4): 606-609
<http://www.wjgnet.com/1007-9327/10/606.asp>

INTRODUCTION

Although the pathogenesis of ulcerative colitis (UC) still remains unknown, clinical observations have found that increased platelet number and platelet activation are notable characteristics of UC^[1-6]. Researches revealed that the extract of platelets from patients with UC could induce intense inflammatory reaction for a few hours after they were injected into the skin of healthy people while the extracts of neutrophils and basophils had no such effect, suggesting that platelet was an important inflammatory cell, and could directly cause inflammation response^[7,8]. Moreover, recent investigations indicated that the high blood coagulative state in patients with UC was closely related with the abnormal function of platelets, which resulted in high a probability of microvascular thrombosis and microcirculation dysfunction, main causative factors for UC^[9,10]. More and more studies suggested that the role of platelets might represent a previously unrecognized component of UC pathogenesis and that antiplatelet drugs may provide new therapeutic possibilities in the management of UC^[7,8,11-19].

The principal ingredient of ASI is sodium ferulate (SF), possesses various pharmacological effects on platelet function and blood circulation including regulating activity of platelets, inhibiting aggregation and liberation of platelets, improving microcirculation and decreasing consistency of blood^[20-25]. Moreover, ASI almost has no toxicity^[20]. So we presume that ASI might contribute to the treatment of UC. The aim of this study was to further explore the abnormal function of platelets and their mechanism in 64 patients with UC. At the same time, changes of the parameters related to platelet activation as well as clinical symptoms were observed before and after the treatment with ASI to investigate the effects of ASI on the abnormal function of platelets.

MATERIALS AND METHODS

Patients and grouping

A total of 64 patients with UC were recruited from Renmin Hospital of Wuhan University and Zhongnan Hospital of Wuhan University between January, 2000 and March, 2003. The diagnosis of UC was established according to the criteria reported in the literature^[15]. According to the evaluating criteria of Jones standards for UC phase^[26], 39 cases were evaluated as active UC (16 males, 23 females, aged 29 to 65, mean age 46.3 years, average disease course 10.6 months), 25 cases were evaluated as remissive UC (11 males, 14 females, mean age 43.6 years, average disease course 18.8 months). Thirty healthy volunteers without administration of antiplatelet medicine in recent 1 month (19 males, 11 females, mean age 42.8 years) were also enrolled in the study as normal control group. All the patients and healthy volunteers had no smoking history and administration of antiplatelet medicine. The 64 patients were randomly divided into routine therapy group and ASI therapy group according to the age. Among the 33 cases in routine therapy group and the 31 cases in ASI therapy group, 31 cases and 30 cases completed the experiment respectively. All groups showed comparable characteristics in sex and age.

Measurement of observed parameters

Venous blood samples 2 ml from the 64 patients without breakfast in the morning were obtained 24 hours after admission. At the same time, 2 ml blood sample was obtained from the 30 healthy volunteers under the same conditions. After mixed with 5% EDTA- Na_2 (v/v), an anticoagulant, the blood samples were quickly centrifuged at 3 000 \times g for 5 min. After separated from plasma, the blood samples were stored at -40°C until detection for α -granule membrane protein (GMP-140), thromboxane B₂ (TXB₂), 6-keto-prostaglandin F_{1a} (6-keto-PGF_{1a}) and von Willebrand factor related antigen (vWF:Ag). GMP-140 and TXB₂ were detected by using the ELISA kits, 6-keto-PGF_{1a} was detected by the radioimmunoassay kit, and vWF:Ag was detected by the monoclonal-ELISA kit following the manufacturer's instructions. All the above detection kits were purchased from Institute of Thrombosis and Coagulation, Medical College of Suzhou University in China. At the same time, platelet count (PC) and 1 min platelet aggregation rate (1 min PAR) were measured by a blood automatic tester (Beckman Co. USA) and a platelet aggregation rate tester (Wuxi Second Electronic Apparatus Factory) respectively using another venous blood sample obtained from all the subjects under the same condition. After the treatments for 3 weeks, venous blood samples from 64 patients were obtained again and all the observed parameters were detected for the second time.

Treatment

After admission, the 33 patients in routine therapy group received routine treatment for 3 weeks including having semifluid diet, correcting the disorder of liquid and electrolyte and 2 g/day Etiasa, modified-release microgranules in sachets produced by Laboratoires Ethypharm, 2-3 times a day. Based on the above routine treatment, 40 ml ASI produced by Pharmaceutical Factory of Zhongnan Hospital of Wuhan University was added to 250 ml 10% glucose iv. drop once a day for 3 weeks for the 31 patients in ASI therapy group.

Statistical analysis

Experimental results were expressed as mean \pm SD. Statistical differences between groups were determined by ANOVA followed by Student's *t* test. A *P* value less than 0.05 was considered statistically significant.

RESULTS

Change of all observed parameters in patients with UC

Compared with normal group, 1 min PAR and levels of GMP-140, TXB₂, and vWF:Ag in UC group and in remissive UC group and active UC group were all significantly increased while 6-keto-PGF_{1a} level was remarkably decreased ($P<0.05-0.01$). Meantime, PC in active UC group was obviously higher than that in normal group ($P<0.01$), whereas there was no significant difference in PC between remissive group and normal group ($P>0.05$). Furthermore, PC, 1 min PAR and levels of GMP-140, TXB₂, and vWF:Ag in active UC group were also significantly elevated compared with remissive group ($P<0.05$), while 6-keto-PGF_{1a} was little changed ($P>0.05$) (Table 1).

Effects of ASI on abnormal function of platelets in patients with UC

After the treatment for 3 weeks, all observed parameters had no obvious changes compared with those before the treatment in the routine therapy group ($P>0.05$), whereas the elevated PC, 1 min PAR and levels of PC, GMP-140, TXB₂, and vWF:Ag were significantly decreased in the ASI therapy group compared with those before the treatment ($P<0.05-0.01$), while 6-keto-PGF_{1a} level was still little changed ($P>0.05$) (Table 2).

DISCUSSION

Recent investigations indicate that platelets not only involve the increased incidence of systemic thromboembolism and a procoagulant blood state in UC but exhibit several proinflammatory properties including release of inflammatory and coagulant mediators such as platelet activated factor, thromboxane, thromboxin (5-HT), platelet factor 4, platelet beta-thromboglobulin, platelet-derived growth factors, and recruitment, chemotaxis and modulation of the activity of other inflammatory cells^[7-12, 27-31]. Moreover, platelet activation in UC might be responsible for the secondary activation of polymorphonuclear leukocytes (PMN) and increased the production of reactive oxygen species by PMN, which could account for the increase in PMN-mediated tissue injury associated with UC^[32]. In addition, Danese and his coworkers found that activated platelets in UC expressed enhanced levels of CD40 ligand and interacted with CD40-positive human intestinal microvascular endothelial cells, which could produce

Table 1 Changes of all observed parameters in patients with UC 24 h after admission (mean \pm SD)

Group	<i>n</i>	PC($\times 10^9$ /L)	GMP-140 (ug/L)	TXB ₂ (ng/L)	6-keto-PGF _{1a} (ng/L)	1 min PAR (%)	VWF:Ag (%)
Normal control	30	158.2 \pm 32.5	41.4 \pm 10.2	68.4 \pm 26.4	18.3 \pm 6.8	38.6 \pm 14.2	103.6 \pm 23.7
Patients with UC	64	189.8 \pm 68.3 ^a	52.1 \pm 17.8 ^b	98.8 \pm 55.4 ^b	12.9 \pm 8.2 ^b	58.2 \pm 21.5 ^b	143.6 \pm 52.7 ^b
Remissive UC	25	173.7 \pm 36.4 ^c	48.4 \pm 11.4 ^{ac}	87.4 \pm 32.7 ^{ac}	14.5 \pm 6.0 ^a	47.8 \pm 16.5 ^{ad}	127.9 \pm 46.1 ^{ac}
Active UC	39	201.8 \pm 48.6 ^b	54.9 \pm 13.2 ^b	115.5 \pm 46.8 ^b	11.3 \pm 6.4 ^b	65.5 \pm 19.2 ^b	154.5 \pm 48.9 ^b

^a $P<0.05$, ^b $P<0.01$ vs normal control, ^c $P<0.05$, ^d $P<0.01$, vs active UC group.

Table 2 Effects of ASI on abnormal function of platelet in patients with UC (mean \pm SD)

Group	<i>n</i>	PC($\times 10^9$ /L)	GMP-140 (ng/L)	TXB ₂ (ng/L)	6-keto-PGF _{1a} (ng/L)	1 min PAR (%)	VWF:Ag (%)
Routine therapy							
Before therapy	33	188.6 \pm 38.5	52.3 \pm 15.2	96.9 \pm 38.1	13.9 \pm 5.3	59.4 \pm 14.7	149.1 \pm 48.0
After therapy	31	179.3 \pm 36.2 ^c	48.8 \pm 13.7 ^c	87.7 \pm 28.6 ^c	16.2 \pm 5.7 ^c	53.1 \pm 15.6 ^c	137.3 \pm 48.2 ^c
ASI therapy							
Before therapy	31	193.9 \pm 41.4	51.1 \pm 13.8	99.3 \pm 33.1	12.7 \pm 5.3	56.8 \pm 17.2	139.5 \pm 50.2
After therapy	30	171.3 \pm 37.8 ^a	37.0 \pm 10.9 ^b	70.2 \pm 25.9 ^b	16.4 \pm 6.2 ^c	45.3 \pm 14.4 ^b	102.4 \pm 24.7 ^b

^a $P<0.05$, ^b $P<0.01$, ^c $P>0.05$ vs before therapy group.

proinflammatory mediators, up-regulate cell adhesion molecule expression and secrete chemokines such as IL-8, a very important proinflammatory interleukin in UC. Meantime, the expression of functional IL-1R and IL-8R on the surface membrane of platelets in UC was found to be significantly increased^[33,34].

GMP-140, a membrane glycoprotein, is mainly located in α -granule membrane of normal platelets. Only when platelets were activated and the granule were released, GMP-140 was expressed on the platelets surface and released into blood. Therefore, GMP-140 was commonly considered as the specific marker of platelet activation^[4,35]. Furthermore, investigations have proven that GMP-140 could aggravate inflammatory response in UC by adhesion of leukocytes, facilitate diapedesis and induce proinflammatory cytokine production from monocytes such as MCP-1, IL-8^[35]. At the same time, TXB₂ in blood and PRA have been found to be classic markers of platelet activation^[4,5,12]. In our study, 1 min PAR and levels of GMP-140 and TXB₂ in blood of patients with UC were significantly increased compared with those in normal controls. Meantime, these parameters in patients with active UC were much higher than those in patients with remissive UC. These results suggested that platelets in circulation were obviously activated in UC and degree of the platelet activation was parallel to the severity of UC. Our study also indicated that the number of activated platelets in active UC was remarkably increased compared with those in remissive UC and normal controls. So, numerous activated platelets took part in the inflammatory response.

Our study revealed the mechanisms underlying the activation of platelet in UC might be as follows: The intestine mucosal vascular endothelial cells might be damaged and the collagen was exposed, thus activating the platelets in circulation because vWF:Ag, a macromolecular glycoprotein mainly synthesized by vascular endothelial cell, was significantly increased in patients with UC in this study, which could sensitively reflect the injury of vascular endothelium. The parallel change between vWF:Ag and GMP-140 in this study also supported the hypothesis. Thromboxane A₂ (TXA₂), a strong vasoconstrictor, can intensely promote aggregation and activation of platelets while the effect of prostaglandin I₂ (PGI₂), a vasodilator, on platelet is just on the contrary. In normal situation, TXA₂ and PGI₂ are in dynamic balance and their stable metabolites are TXB₂ and 6-keto-PGF_{1 α} . In our study, significantly increased TXB₂ and remarkably decreased 6-keto-PGF_{1 α} in patients with UC showed the obvious imbalance between TXA₂ and PGI₂, thus promoting platelet activation as well as resulting in dysfunction of microcirculation. The above results demonstrated that inhibition of platelet activation and improvement of microcirculation should be involved in the treatment for UC.

Numerous investigations have demonstrated that SF, a ASI's principal ingredient, is not only a inhibitor of TXA₂ synthetase and cyclooxygenase-2, a crucial synthetase for arachidonic acid (AA) metabolism, but depresses the activity of phospholipase A₂, thus preventing the release of AA from phospholipid of cell membrane and effectly reducing the production of AA metabolites including TXA₂ and PGE₂^[36-40]. Meantime, SF could compensativly promote the synthesis of 6-keto-PGF_{1 α} during AA metabolism^[41]. As a result, ASI could partly correct the imbalance between TXA₂ and 6-keto-PGF_{1 α} in UC. Moreover, SF could directly inhibit 5-HT liberation and MDA synthesis from platelets^[7,41]. In addition, SF could reduce the content of fibrinogen in blood, increase the charges on cell membrane, thus inhibiting the cell aggregation, lowering the blood consistency. SF could prolong plasma prothrombin time (PPT) and reduce the weight and length of thrombus, thus ameliorating microcirculation^[20].

In our study, PC, 1 min PAR, and levels of GMP-140, TXB₂, and vWF:Ag were significantly decreased after 3 weeks treatment while 6-keto-PGF_{1 α} level was little changed compared with those before treatment in the ASI group. At the same time, there was no significant difference in all observed parameters before and after the treatment in the routine therapy group. Furthermore, clinical symptoms such as abdomen pain, diarrhea, occult blood, fever in the patients of ASI group were relieved and controlled more quickly than those in the patients of routine therapy group. The above results suggested that ASI remarkably inhibited the activation of platelets, attenuated the injury of vascular endothelial cells as well as improved the microcirculation in patients with UC, thus contributing to relieve the inflammatory response in UC. The protective effect of ASI on vascular endothelial cell might be related with SF's strong anti-oxidation property^[2,3,20,42-44].

In summary, the results of this study have shown that ASI can significantly inhibit platelet activation, relieve vascular endothelial cell injury in UC. ASI in combination with the well-established drugs may contribute to an optimal treatment for UC.

REFERENCES

- 1 **Jiang XL**, Quan QZ, Liu T, Dong XC. Recent advances in research of ulcerative colitis. *Shijie Huaren Xiaohua Zazhi* 2000; **8**: 216-218
- 2 **Xia B**. Etiology and pathogenesis of inflammatory bowel disease. *Shijie Huaren Xiaohua Zazhi* 2001; **6**: 245-250
- 3 **Kirsner JB**. Historical origins of current IBD concepts. *World J Gastroenterol* 2001; **7**: 175-184
- 4 **Collins CE**, Cahill MR, Newland AC, Rampton DS. Platelets circulate in an activated state in inflammatory bowel disease. *Gastroenterology* 1994; **106**: 840-845
- 5 **Collins CE**, Rampton DS, Rogers J, Williams NS. Platelet aggregation and neutrophil sequestration in the mesenteric circulation in inflammatory bowel disease. *Eur J Gastroenterol Hepatol* 1997; **9**: 1213-1217
- 6 **Kapsoritakis AN**, Koukourakis MI, Sfridakis A, Potamianos SP, Kosmadaki MG, Koutroubakis LE, Kouroumalis EA. Mean platelet volume: a useful marker of inflammatory bowel disease activity. *Am J Gastroenterol* 2001; **96**: 776-781
- 7 **Mannaioni PF**, Di Bello MG, Masini E. Platelets and inflammation: role of platelet-derived growth factor, adhesion molecules and histamine. *Inflamm Res* 1997; **46**: 4-18
- 8 **Webberley MJ**, Hart MT, Melikian V. Thromboembolism in inflammatory bowel disease: role of platelets. *Gut* 1993; **34**: 247-251
- 9 **Larsen TB**, Nielsen JN, Fredholm L, Lund ED, Brandslund I, Munkholm P, Hey H. Platelets and anticoagulant capacity in patients with inflammatory bowel disease. *Pathophysiol Haemost Thromb* 2002; **32**: 92-96
- 10 **Van Bodegraven AA**, Schoorl M, Baak JP, Linskens RK, Bartels PC, Tuynman HA. Hemostatic imbalance in active and quiescent ulcerative colitis. *Am J Gastroenterol* 2001; **96**: 487-493
- 11 **Collins CE**, Rampton DS. Platelet dysfunction: a new dimension in inflammatory bowel disease. *Gut* 1995; **36**: 5-8
- 12 **Collins CE**, Rampton DS. Review article: platelets in inflammatory bowel disease—pathogenetic role and therapeutic implications. *Aliment Pharmacol Ther* 1997; **11**: 237-247
- 13 **Cui HF**, Jiang XL. Treatment of corticosteroid-resistant ulcerative colitis with oral low molecular weight heparin. *World J Gastroenterol* 1999; **5**: 448-450
- 14 **Xu G**, Tian KL, Liu GP, Zhong XJ, Tang SL, Sun YP. Clinical significance of plasma D-dimer and von Willebrand factor levels in patients with ulcer colitis. *World J Gastroenterol* 2002; **8**: 575-576
- 15 **Jiang XL**, Quan QZ, Wan ZK. Diagnosis, typing and therapy of ulcerative colitis. *Shijie Huaren Xiaohua Zazhi* 2000; **8**: 332-334
- 16 **Das KM**, Farag SA. Current medical therapy of inflammatory bowel disease. *World J Gastroenterol* 2000; **6**: 483-489
- 17 **Rampton DS**. Management of difficult inflammatory bowel disease: where are we now? *World J Gastroenterol* 2000; **6**: 315-323
- 18 **Rigat B**, Reynaud D, Smiljanic-Georgijev N, Mahuran D. The GM2 activator protein, a novel inhibitor of platelet-activating factor. *Biochem Biophys Res Commun* 1999; **258**: 256-259

- 19 **Tyrell DJ**, Horne AP, Holme KR, Preuss JM, Page CP. Heparin in inflammation: potential therapeutic applications beyond anticoagulation. *Adv Pharmacol* 1999; **46**: 151-208
- 20 **Xie L**, Yang LH, Li XH. Resarch on the pharmacologic effects of *Angelica Sinensis*. *Zhong Yiyao Yanjiu* 2000; **16**: 56-58
- 21 **Zhang LF**, Bian RL, Wei EQ. Effects of platelets on histamine release of mast cell and influence of sodium ferulate. *Zhongguo Yaolixue Tongbao* 1995; **11**: 472-474
- 22 **Sun Y**, Lin AP, Zhang HQ, Bian RL. PAF-induced airway hyperresponsiveness and effects of sodium ferulate in guinea pigs. *Zhongguo Yaolixue Tongbao* 1996; **12**: 518-520
- 23 **Lin AP**, Sun Y, Zhang HQ, Bian RL. Effects of sodium ferulate on platelets immunol activation-induced airway hyperresponsiveness. *Liaoning Zhongyi Zazhi* 1995; **22**: 42-44
- 24 **Zhou JY**, Fan Y, Han ZF, Wu DZ, Hu ZB. Influence of ferulic acid sodium on the enhance of endothelial permeability induced by histamine. *Zhongguo Yaolixue Tongbao* 2000; **16**: 664-666
- 25 **Yi ZZ**, Zhang LY, Xu LN. [The effect of Dang-Gui (*Angelica sinensis*) and its ingredient ferulic acid on rat platelet aggregation and release of 5-HT (author' s transl)]. *Yaouxue Xuebao* 1980; **15**: 321-326
- 26 **Jones SC**, Crabtree JE, Rembacken BJ, Dixon MF, Trejdosiewicz LK, Whicher JT, Axon AT. Musosal interleukin-6 secretion in ulcerative colitis: effects of anti-inflammatory drugs and T-cell stimulation. *Scand J Gastroenterol* 1994; **29**: 722-728
- 27 **Yu FW**, Xiao GX, Fu WL, Yuan JC, Zhou LX, Qin XI. Pathogenetic effects of platelet activating factor on enterogenic endotoxemia after burn. *World J Gastroenterol* 2000; **6**: 451-453
- 28 **Wu JX**, Xu JY, Yuan YZ. Effect of emodin and sandostatin on metabolism of eicosanoids in acute necrotizing pancreatitis. *World J Gastroenterol* 2000; **6**: 293-294
- 29 **Nakamura T**, Sakaguchi T, Unno N, Sugatani J, Miwa M, Nakamura S. Relationship between the platelet activating factor acetylhydrolase gene and intractability of ulcerative colitis. *Dis Colon Rectum* 2002; **45**: 389-393
- 30 **Vrij AA**, Rijken J, Van Wersch JW, Stockbrugger RW. Platelet factor 4 and beta-thromboglobulin in inflammatory bowel disease and giant cell arteritis. *Eur J Clin Invest* 2000; **30**: 188-194
- 31 **Harhaj NS**, Barber AJ, Antonetti DA. Platelet-derived growth factor mediates tight junction redistribution and increases permeability in MDCK cells. *J Cell Physiol* 2002; **193**: 349-364
- 32 **Suzuki K**, Sugimura K, Hasegawa K, Yoshida K, Suzuki A, Ishizuka K, Ohtsuka K, Honma T, Narisawa R, Asakura H. Activated platelets in ulcerative colitis enhance the production of reactive oxygen species by polymorphonuclear leukocytes. *Scand J Gastroenterol* 2001; **36**: 1301-1306
- 33 **Schaufelberger HD**, Uhr MR, McGuckin C, Logan RP, Misiewicz JJ, Gordon-Smith EC, Beglinger C. Platelets in ulcerative colitis and Crohn' s disease express functional interleukin-1 and interleukin-8 receptors. *Eur J Clin Invest* 1994; **24**: 656-663
- 34 **Danese S**, de la Motte C, Sturm A, Vogel JD, West GA, Strong SA, Katz JA, Fiocchi C. Platelets trigger a CD40-dependent inflammatory response in the microvasculature of inflammatory bowel disease patients. *Gastroenterology* 2003; **124**: 1249-1264
- 35 **Fagerstam JP**, Whiss PA, Strom M, Andersson RG. Expression of platelet P-selectin and detection of soluble P-selectin, NPY and RANTES in patients with inflammatory bowel disease. *Inflamm Res* 2000; **49**: 466-472
- 36 **Wang Z**, Gao YH, Huang RS, Zhu GQ. Sodium ferulate is an inhibitor of thromboxane A2 synthetase. *Zhongguo Yaoli Xuebao* 1988; **9**: 430-433
- 37 **Gao SW**, Chen ZJ. Effects of sodium ferulate on platelet aggregation and TX thromboxane A2 of platelet in patients with coronary heart disease. *Zhongxiyi Jiehe Zazhi* 1988; **8**: 263-265
- 38 **Liu SP**, Dong WG, Wu DF, Luo HS, Yu JP, Mei Q. Effects of sodium ferulate on nitric oxide synthase and cyclooxygenase in colon of colitis rats. *Zhongguo Yaolixue Tongbao* 2003; **19**: 571-574
- 39 **Xu LN**, Yu WG, Tian JY, Liu QY. Effects of sodium ferulate on arachidonic acid metabolism. *Yaouxue Xuebao* 1990; **25**: 412-416
- 40 **Carty E**, Macey M, McCartney SA, Rampton DS. Ridogrel, a dual thromboxane synthase inhibitor and receptor antagonist: anti-inflammatory profile in inflammatory bowel disease. *Aliment Pharmacol Ther* 2000; **14**: 807-817
- 41 **Wang XJ**, Huang WZ, Zhang BY. Recent study on effect of *angelica sinensis* on the balance between TXA₂ and PGI₂ in human. *Hubei Zhongyi Zazhi* 2000; **22**: 53-54
- 42 **Cominacini L**, Pasini A, Garbin U, Evangelista S, Crea AE, Tagliacozzi D, Nava C, Davoli A, LoCascio V. Zofenopril inhibits the expression of adhesion molecules on endothelial cells by reducing reactive oxygen species. *Am J Hypertens* 2002; **15** (10 Pt 1): 891-895
- 43 **Zhang ZH**, Yu SZ, Li GS, Zhao BL. Influence of sodium ferulate on human neutrophil-derived oxygen metabolites. *Zhongguo Yaolixue Tongbao* 2001; **17**: 515-517
- 44 **Wang BH**, Ouyng JP, Tu SZ, Wei L, Liu YM, Zheng HQ, Yang JW. Protective effect of *Angelica Sinensis* on human endothelial cells injury induced by high level of oxidized low-density lipoprotein in serum. *Zhongguo Bingli Shengli Zazhi* 2000; **16**: 932

Edited by Zhang JZ and Wang XL

Effects of lipopolysaccharides stimulated Kupffer cells on activation of rat hepatic stellate cells

Xin Zhang, Wei-Ping Yu, Lei Gao, Kai-Bin Wei, Jiu-Long Ju, Jia-Zhang Xu

Xin Zhang, Wei-Ping Yu, Kai-Bin Wei, Basic Medical School, Southeast University, Nanjing 210009, Jiangsu Province, China

Xin Zhang, Lei Gao, Jiu-Long Ju, Jia-Zhang Xu, 81 Hospital of PLA, Nanjing 210002, Jiangsu Province, China

Correspondence to: Dr. Wei-Ping Yu, Department of Pathology and Pathophysiology, Basic Medical School, Southeast University, Nanjing 210009, Jiangsu Province, China

Telephone: +86-25-3272508

Received: 2003-07-04 **Accepted:** 2003-09-01

Abstract

AIM: To study the effects of Kupffer cell-conditioned medium (KCCM) derived from lipopolysaccharide (LPS) treatment on proliferation of rat hepatic stellate cells (HSC).

METHODS: HSC and Kupffer cells were isolated from the liver of Wistar rats by *in situ* perfusion with pronase and collagenase and density gradient centrifugation with Nycodenz and cultured. KCCM was prepared and 3-(4,5-dimethylthiazol-2-yl)-2,5-diphenyltetrazolium bromide (MTT) colorimetric assay was used to detect HSC proliferation. The content of type IV collagen and laminin secreted by HSC in the HSC-conditioned medium was determined by radioimmunoassay. TGF- β_1 production in the KCCM was detected by enzyme-linked immunosorbent assay (ELISA).

RESULTS: HSC and Kupffer cells isolated had high purity. One microgram per milliliter LPS-activated KCCM and unstimulated KCCM could significantly promote HSC proliferation [0.132 ± 0.005 and 0.123 ± 0.008 vs control group (0.100 ± 0.003), $P<0.01$], and there was a difference between them ($P<0.05$). Ten microgram per milliliter LPS-activated KCCM (0.106 ± 0.010) was unable to promote HSC proliferation ($P>0.05$). Adding anti-TGF- β_1 antibodies could suppress the proliferation promoted by unstimulated KCCM and LPS ($1\ \mu\text{g/ml}$)-activated KCCM (0.109 ± 0.009 vs 0.123 ± 0.008 , 0.115 ± 0.008 vs 0.132 ± 0.005 , $P<0.01$). LPS ($1\ \mu\text{g/ml}$ or $10\ \mu\text{g/ml}$) could not promote HSC proliferation immediately (0.096 ± 0.003 and 0.101 ± 0.004 vs 0.100 ± 0.003 , $P>0.05$). There was a parallel behavior between HSC proliferation and increased ECM level. One microgram per milliliter LPS-activated KCCM contained a larger amount of TGF- β_1 than unstimulated KCCM.

CONCLUSION: The technique for isolation of HSC and Kupffer cells described here is simple and reliable. KCCM stimulated by LPS may promote HSC proliferation and collagen accumulation, which are associated with hepatic fibrogenesis.

Zhang X, Yu WP, Gao L, Wei KB, Ju JL, Xu JZ. Effects of lipopolysaccharides stimulated Kupffer cells on activation of rat hepatic stellate cells. *World J Gastroenterol* 2004; 10 (4): 610-613

<http://www.wjgnet.com/1007-9327/10/610.asp>

INTRODUCTION

Hepatic fibrosis is now regarded as a common response to

chronic liver injury. Regardless of its nature (viral infections, alcohol abuse, and metal overload), it is also characterized by excessive deposition of extracellular matrix components^[1-3]. Hepatic stellate cells (HSC) are a major source of extracellular matrix in normal and pathological conditions^[4-6]. During fibrogenesis, HSC undergoes a process of activation, developing a myofibroblast-like phenotype associated with increased proliferation^[7-9] and collagen synthesis^[10,11]. As the data suggest, a paracrine mechanism may prevail over the stimulation of HSC proliferation and collagen synthesis *in vivo*^[12,13].

Lipopolysaccharide (LPS) is a critical component of the cell membrane of gram-negative bacteria and can mediate pathophysiological alterations during endotoxaemia. Systemic exposure to LPS could result in a cascade of events involving cellular and soluble mediators of inflammation, leading to injury to organs, including liver^[14,15]. Because LPS is known to activate Kupffer cells to release various kinds of cytokines^[16-18], there may be a chain of events to cause hepatic fibrosis.

The aim of this study was to evaluate whether paracrine stimuli derived from LPS-activated Kupffer cells could induce HSC proliferation and collagen synthesis or LPS could stimulate HSC proliferation immediately.

MATERIALS AND METHODS

Materials

Pronase E, collagenase type IV, deoxyribonuclease I, MTT, Nycodenz [(5-*N*-2, 3-dihydroxypropylaceta-mido)-2, 4, 6-tri-iodo-*N*, *N'* bis -(2, 3-dihydroxypropyl) isophthalamide] and lipopolysaccharide (LPS, *Escherichia coli*, serotype 0111: B4) were obtained from Sigma. All immunocytochemical reagents, including rabbit antihuman desmin and rabbit antihuman lysozyme, were purchased from Maixin Co. (Fuzhou, China). Culture media, Dulbecco's modified Eagle's medium (DMEM) and PRMI1640 were purchased from GIBCO (Grand Island, NY). Newborn bovine serum and fetal bovine serum were purchased from Sijiqing Co. (Hangzhou, China).

Methods

HSC and Kupffer cell isolation and culture^[19-25] HSC and Kupffer cells were isolated from rat livers by the pronase-collagenase method. Briefly, after the rat (male Wistar rats ranging from 350 g to 450 g of body weight) was anesthetized with sodium pentobarbital (40 mg/kg body weight, ip), the abdomen was opened and the portal vein was cannulated with 16-gauge cannula. The liver was perfused *in situ* for 15 min with Ca²⁺/Mg²⁺-free Hank's balanced salt solution (pH 7.4, 37°C) at a flow rate of 15 mL/min, and was then perfused with Hank's balanced salt solution (pH 7.4, 37°C) containing 0.1% pronase E and 0.05% collagenase type IV for an additional 30 min at a flow rate of 30 mL/min. After perfusion, the liver was removed, cut into small pieces, and incubated in a bath of Hank's balanced salt solution containing 0.02% pronase E and 0.05% collagenase type IV and 0.001% deoxyribonuclease at 37°C for 20 min. After passing through a filter (mesh size 74 μm), cells were washed twice with Hank's balanced salt

solution and HSC were obtained by centrifugation over 12% (wt/vol) Nycodenz gradient for 18 min at 1 450 g. After centrifugation, HSC were collected from the interface, washed with Hank's balanced salt solution, and resuspended at a concentration of 1×10^5 cells/ml, in DMEM supplemented with 20% newborn bovine serum, 2 mmol/L glutamine, and 1% antibiotic solution. Kupffer cells were synchronously collected under the interface, washed with Hank's balanced salt solution, and resuspended at a concentration of 1×10^6 cells/ml, in PRMI 1640 supplemented with 10% fetal bovine serum, 2 mmol/L glutamine, and 1% antibiotic solution. Cells were then cultured at 37°C in a humidified atmosphere containing 5% CO₂. The media of Kupffer cells were replaced 6 h after seeding and at every 48 h thereafter. Impurities caused by some endothelial cells were removed during the first medium change. The media of HSC were replaced 24 h after seeding and at every 48 h thereafter. Primary culture of HSC were allowed to grow to confluence 14 d after seeding, subcultured by trypsinization (0.125% trypsin) and then cultured in 96-well culture plates at a concentration of 1×10^5 cells/ml. HSC and Kupffer cells were identified by immunocytochemistry^[26]. HSC were also identified by vitamin A typical fluorescence at 328 nm excitation wavelength.

Preparation of Kupffer cell-conditioned medium (KCCM)

After a 72 h recovery period from isolation, the primary Kupffer cells were cultured in the presence or absence of 1 µg/ml or 10 µg/ml of LPS. Conditioned medium was collected after 48 h of culture and filtered with a 0.45 µm membrane filter, and stored at -70°C until use.

Modulation of HSC proliferation by KCCM or LPS

HSC were placed in 96-well plates and cultured for 48 h in the presence or absence of KCCM or LPS (1 µg/ml or 10 µg/ml). The HSC, with addition of KCCM, were cultured in the presence or absence of rabbit anti-human TGF-β₁ immunoglobulin. Conditioned media were collected and stored at -70°C until use. The remaining cells were added with 180 µl media and 20 µl MTT (5 g/L) at 37°C. The media were removed 4 h later and formazan product was dissolved with 100 µl/well of dimethyl sulphoxide (DMSO). After a few minutes at room temperature, to ensure that all crystals were dissolved, the optical density (OD) was read on an ELISA reader at test wavelength of 570 nm and referent wavelength of 630 nm.

Modulation of collagen type IV and laminin secretion by KCCM or LPS

The amount of type IV collagen and laminin, the most abundant type of ECM in early liver fibrosis, secreted by HSC in the HSC-conditioned medium was measured by radioimmunoassay.

Characterization of stimulatory factor in LPS-activated KCCM
TGF-β₁ production in the culture supernatant was measured by ELISA.

Statistical analysis

Data were expressed as mean±SD. Differences between any two groups were determined by new Duncan test and *t*-test. *P*<0.05 was considered statistically significant.

RESULTS

Isolation and culture of HSC and Kupffer cells

The HSC isolated with the aforementioned Nycodenz cushion ranged from 5×10^6 to 1×10^7 cells per liver, and Kupffer cell ranged from 3×10^6 to 5×10^6 cells per liver. The cell viability determined by trypan blue exclusion test varied considerably,

but was usually higher than 80%. HSC were identified by their typical dark-light microscopic appearance due to abundant vitamin A-containing vacuoles which showed intense fluorescence upon irradiation at 328 nm, and by positive immunocytochemical staining for desmin. Kupffer cells were identified by positive immunocytochemical staining for lysozyme. The initially isolated Kupffer cells were spherules with refraction which were much smaller than hepatocytes and HSC. Kupffer cells adhered to plates and some spread their pseudopods 4 h after seeding. During the first 24 h of HSC culture, the cells rounded up and flattened out. The major fraction contaminating nonadherent lymphocytes and endothelial cells, was removed with the first change of medium. After 2 to 3 d in culture, HSC developed a characteristic stellate shape. Lipid droplets had visible round nuclei and decreased with the time of culture. Confluence was reached on about the 14th day.

Effect of KCCM or LPS on HSC proliferation

When cells were cultured in the presence of 1 µg/ml or 10 µg/ml LPS, HSC proliferation was not observed (*P*>0.05). When cells were cultured in the presence of unstimulated KCCM and 1 µg/ml LPS-activated KCCM, HSC proliferated remarkably (*P*<0.01), and there was a difference between the two groups. Ten µg/ml LPS-activated KCCM could not promote HSC proliferation (*P*>0.05). In addition, HSC proliferation promoted by unstimulated KCCM and 1 µg/ml LPS-activated KCCM was suppressed partly in the presence of anti-TGF-β₁ antibodies (*P*<0.01), but there was a difference compared with control group (*P*<0.01) (Table 1).

Table 1 Effect of KCCM or LPS on HSC proliferation (mean±SD, *n*=12)

Treatment	A
LPS (1 µg/ml)	0.096±0.003
LPS (10 µg/ml)	0.101±0.004
KCCM1 (unstimulated)	0.123±0.008 ^a
KCCM2 (1 µg/ml LPS-activated)	0.132±0.005 ^a
KCCM3 (10 µg/ml LPS-activated)	0.106±0.010 ^d
KCCM1 + anti-TGF-β ₁ antibodies	0.109±0.009 ^b
KCCM2 + anti-TGF-β ₁ antibodies	0.115±0.008 ^d
KCCM3 + anti-TGF-β ₁ antibodies	0.106±0.010
Control group	0.100±0.003

^a*P*<0.01 vs control group; ^b*P*<0.01 vs unstimulated KCCM group; ^c*P*<0.05, ^d*P*<0.01 vs 1 µg/ml LPS-activated KCCM group.

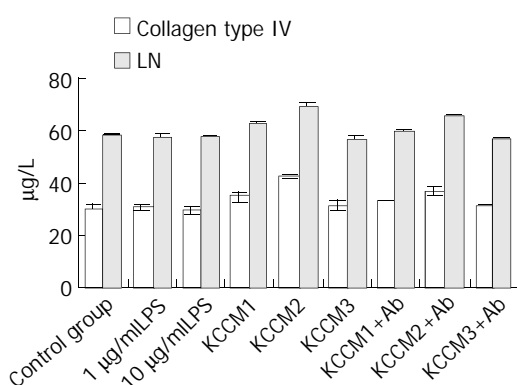
Effect of KCCM or LPS on collagen type IV and laminin secretion by HSC

When HSC were cultured in the presence of 1 µg/ml or 10 µg/ml LPS, the amount of collagen type IV secreted by HSC was 29.17±1.36 µg/L and 30.53±0.97 µg/L, respectively, and there was no difference between them (*P*>0.05). The amount of laminin was 56.61±2.39 ng/ml and 57.12±2.00 ng/ml respectively without statistical difference (*P*>0.05). When HSC were cultured in the presence of unstimulated KCCM and 1 µg/ml LPS-activated KCCM, collagen type IV and laminin secreted by HSC were markedly enhanced by LPS-stimulated KCCM (42.39±1.74 µg/L and 69.40±1.86 ng/ml), but were only slightly enhanced by unstimulated KCCM (37.99±1.41 µg/L and 63.54±2.25 ng/ml). Furthermore, this enhanced secretion was partly blocked in the presence of anti-TGF-β₁ antibodies. Ten microgram per milliliter LPS-activated KCCM could not promote collagen type IV and laminin secretion (31.12±0.84 µg/L and 56.34±2.17 ng/ml, *P*>0.05) (Table 2).

Table 2 Effect of KCCM or LPS on collagen type IV and laminin secretion by HSC (mean±SD, n=6)

Treatment	Collagen type IV (µg/L)	Laminin (ng/ml)
LPS (1 µg/ml)	30.53±0.9	57.12±2.00
LPS (10 µg/ml)	29.17±1.36	56.61±2.39
KCCM1 (unstimulated)	34.41±1.22 ^c	62.00±2.23 ^c
KCCM2 (1 µg/ml LPS-activated)	42.39±1.74 ^a	69.40±1.86 ^a
KCCM3 (10 µg/ml LPS-activated)	31.13±0.84 ^d	56.34±2.17 ^d
KCCM1+anti-TGF-β ₁ antibodies	32.18±1.71 ^b	58.87±2.31 ^b
KCCM2+anti-TGF-β ₁ antibodies	36.26±0.91 ^d	65.25±1.95 ^d
KCCM3+anti-TGF-β ₁ antibodies	30.76±1.88	56.16±2.62
Control group	30.34±1.02	57.56±1.56

^aP<0.01 vs control group; ^bP<0.01 vs unstimulated KCCM group; ^cP<0.05, ^dP<0.01 vs 1 µg/ml LPS-activated KCCM group.

**Figure 1** Effect of KCCM or LPS on ECM secretion by HSC.

Stimulatory factor assay

The concentration of TGF-β₁ in LPS-activated KCCM was markedly higher (0.941±0.114) than that in unstimulated KCCM (0.465±0.075).

Table 3 TGF-β₁ in LPS-activated and unstimulated KCCM (mean±SD, n=6)

Group	TGF-β ₁ (OD)
KCCM1(unstimulated)	0.465±0.075 ^a
KCCM2(1 µg/ml LPS-activated)	0.941±0.114 ^a
KCCM3(10 µg/ml LPS-activated)	0.669±0.093 ^a
Control group	0.089±0.010

^aP<0.01 vs control group.

DISCUSSION

It has been recognized that HSC are the major source of extracellular matrix in normal and pathological conditions^[1,5,9]. HSC activation during fibrogenesis, as a result of injury, is a dynamic process, which leads from a quiescent state to a myofibroblast-like phenotype with increased production of extracellular matrix and enhanced proliferation. Therefore, HSC play a central role in hepatic fibrogenesis. Previous studies have shown that the functions of adjacent cells were influenced by mediators released from Kupffer cells, such as protein synthesis in hepatocytes^[27] and sinusoidal endothelial cell functions^[28]. Several investigators have already evaluated the role of Kupffer cells in stimulating HSC, although the results were conflicting^[29]. Endotoxemia has been found in patients with chronic liver disease, such as hepatic cirrhosis and

hepatitis^[30,31]. Endotoxemia and hepatocytic damage could affect each other, but there is no evidence to show whether endotoxemia could promote HSC activation. So the relation between LPS and HSC was studied to demonstrate the possible mechanism in the fibrogenesis of endotoxemia.

We established an *in vitro* model of HSC and Kupffer cell-conditioned medium. The primary HSC grew very slowly and confluence was reached on about the 14th day in culture. The subcultured HSC grew much faster than the primary HSC, and lipid droplets decreased and even disappeared, which accorded with previous studies. In this study, Kupffer cells and HSC were cultured with LPS (1 µg/ml or 10 µg/ml), and Kupffer cell-conditioned medium was cultured with HSC. This mimicked the process that intestinal LPS affected liver cells *in vivo* when endotoxemia occurred. We measured HSC proliferation after HSC were cultured with LPS directly or indirectly to evaluate the degree of HSC activation. Our data showed that unstimulated KCCM could promote HSC proliferation. When HSC were cultured in the presence of 1 µg/ml LPS-activated KCCM, HSC proliferated more remarkably than the former. It was suggested that the primary Kupffer cells could secrete some factors and LPS could stimulate synthesis and secretion of these factors by Kupffer cells. When HSC were cultured in the presence of LPS directly, HSC proliferation could not be observed. Our results indicated that LPS affected HSC indirectly. Ten µg/ml LPS-activated KCCM could not promote HSC proliferation. It is difficult to assess and explain the reason why high concentration LPS could not activate HSC. One possibility was that high concentration LPS might decrease or suppress Kupffer cells to secrete cytokines, which could stimulate HSC proliferation. The other possibility was that cytokines secreted by Kupffer cells did not decrease, but Kupffer cells could secrete some other cytokines and counteract the promotion. So HSC did not undergo proliferation.

Overload ECM synthesis could lead to hepatic fibrosis. In our study, we measured the relative concentration of collagen type IV and laminin in HSC-conditioned media. Our results showed that there was a parallel behavior between increased HSC proliferation and increased ECM level. It was suggested that HSC proliferation was the direct reason of the overload ECM synthesis, which was probably related with the increased cell number and capability of single HSC to secrete ECM.

TGF-β₁ is the most powerful cytokine to promote fibrosis. During the period of HSC activation, TGF-β₁ was a very important initiation factor^[32]. In our study, HSC proliferation and ECM production by unstimulated KCCM and 1 µg/ml LPS-activated KCCM were suppressed partly in the presence of anti-TGF-β₁ antibodies, suggesting that HSC proliferation might be related with TGF-β₁ and some other cytokines, because anti-TGF-β₁ antibodies could completely not suppress the effect of proliferation. Our results suggested that Kupffer cells could be activated by a moderate concentration of LPS and probably release some soluble mediators, such as TGF-β₁, presented in the LPS-activated Kupffer cell-conditioned medium, which activated HSC from a quiescent state to a myofibroblast-like phenotype. It is clear that the stimulatory effect on both HSC proliferation and collagen synthesis is the main feature of liver fibrosis. It is easy to measure cytokines contained in LPS-activated KCCM by ELISA. Our results showed that moderate concentration of LPS-activated KCCM contained larger-activated KCCM and approve the above deducibility, *i.e.*, a high concentration of LPS might promote Kupffer cells to secrete a smaller amount of TGF-β₁ than 1 µg/ml LPS, and secrete other cytokines to counteract the effect of TGF-β₁.

In conclusion, LPS plays a role in the stimulation of HSC proliferation and collagen synthesis. Kupffer cells cultured in

the presence at a moderate concentration of LPS can release products, which stimulate HSC proliferation and collagen accumulation. These *in vitro* observations presumably mimic some profibrogenic situations *in vivo*, whereas HSC are activated in the presence of LPS.

REFERENCES

- 1 **Friedman SL.** Seminars in medicine of the Beth Israel Hospital. Boston cellular basis of hepatic fibrosis. Mechanisms and treatment strategies. *N Engl J Med* 1993; **328**: 1828-1835
- 2 **Fan JG, Zeng MD, Hong J, Li JQ, Qiu DK.** Effects of free unsaturated fatty acids on proliferation of L-02 and HLF cell lines and synthesis of extracellular matrix. *Shijie Huaren Xiaohua Zazhi* 1998; **6**: 502-504
- 3 **Lu LG, Zeng MD, Li JQ, Hua J, Fan JG, Qiu DK.** Study on the role of free fatty acids in proliferation of rat hepatic stellate cells (II). *World J Gastroenterol* 1998; **4**: 500-502
- 4 **Wu J, Zern MA.** Hepatic stellate cells: a target for the treatment of liver fibrosis. *J Gastroenterol* 2000; **35**: 665-672
- 5 **Friedman SL, Roll JF, Boyles J, Bissell DM.** Hepatic lipocytes: the principal collagen-producing cells of normal rat liver. *Proc Natl Acad Sci U S A* 1985; **82**: 8681-8685
- 6 **Crabb DW.** Pathogenesis of alcoholic liver disease: newer mechanisms of injury. *Keio J Med* 1999; **48**: 184-188
- 7 **Svegliati Baroni G, Ambrosio LD, Curto P, Casini A, Mancini R, Jezequel AM, Benedetti A.** Interferon gamma decreases hepatic stellate cell activation and extracellular matrix deposition in rat liver fibrosis. *Hepatology* 1996; **23**: 1189-1199
- 8 **Mancini R, Jezequel AM, Benedetti A, Paolucci F, Trozzi L, Orlandi F.** Quantitative analysis of proliferating sinusoidal cells in dimethylnitrosamine-induced cirrhosis. An immunohistochemical study. *J Hepatol* 1992; **15**: 361-366
- 9 **Geerts A, Lazou JM, De Bleser P, Wisse E.** Tissue distribution, quantitation and proliferation kinetics of fat-storing cells in carbon tetrachloride-injured rat liver. *Hepatology* 1991; **13**: 1193-1202
- 10 **Milani S, Herbst H, Schuppan D, Surrenti C, Riechen EO, Stein H.** Cellular localization of type I, III, and IV procollagen gene transcripts in normal and fibrotic human liver. *Am J Pathol* 1990; **137**: 59-70
- 11 **Svegliati-Baroni G, Ridolfi F, Di Sario A, Saccomanno S, Bendia E, Benedetti A, Greenwel P.** Intracellular signaling pathways involved in acetaldehyde-induced collagen and fibronectin gene expression in human hepatic stellate cells. *Hepatology* 2001; **33**: 1130-1140
- 12 **Friedman SL.** Parenchymal Fe and collagen gene expression: an iron-clad association? *Hepatology* 1995; **21**: 1197-1199
- 13 **Toda K, Kumagai N, Tsuchimoto K, Inagaki H, Suzuki T, Oishi T, Atsukawa K, Saito H, Morizane T, Hibi T, Ishii H.** Induction of hepatic stellate cell proliferation by LPS-stimulated peripheral blood mononuclear cells from patients with liver cirrhosis. *J Gastroenterol* 2000; **35**: 214-220
- 14 **Pearson JM, Schultze AE, Schwartz KA, Scott MA, Davis JM, Roth RA.** The thrombin inhibitor, hirudin, attenuates lipopolysaccharide-induced liver injury in the rat. *J Pharmacol Exp Ther* 1996; **278**: 378-383
- 15 **Han DW, Zhao LF.** The effect of intestinal endotoxemia in chronic hepatitis. *Jichu Yixue Yu Linchuang* 1999; **19**: 482-487
- 16 **Decker K.** Biologically active products of stimulated liver macrophages (Kupffer cells). *Eur J Biochem* 1990; **192**: 245-261
- 17 **Shimohashi N, Nakamuta M, Uchimura K, Sugimoto R, Iwamoto H, Enjoji M, Nawata H.** Selenoorganic compound, ebselen, inhibits nitric oxide and tumor necrosis factor-alpha production by the modulation of jun-N-terminal kinase and the NF-kappaB signaling pathway in rat Kupffer cells. *J Cell Biochem* 2000; **78**: 595-606
- 18 **Wang F, Wang LY, Wright D, Parmely MJ.** Redox imbalance differentially inhibits lipopolysaccharide-induced macrophage activation in mouse liver. *Infect Immun* 1999; **67**: 5409-5416
- 19 **Knook DL, Sleyster EC.** Separation of Kupffer and endothelial cells of the rat liver by centrifugal elutriation. *Exp Cell Res* 1976; **99**: 444-449
- 20 **Knook DL, Seffelaar AM, de Leeuw AM.** Fat-storing cells of the rat liver. Their isolation and purification. *Exp Cell Res* 1982; **139**: 468-471
- 21 **Friedman SL, Roll FJ.** Isolation and culture of hepatic lipocytes, Kupffer cells, and sinusoidal endothelial cells by density gradient centrifugation with stractan. *Anal Biochem* 1987; **161**: 207-218
- 22 **Blomhoff R, Smedsrod B, Eskild W, Granum PE, Berg T.** Preparation of isolated liver endothelial cells and Kupffer cells in high yield by means of an enterotoxin. *Exp Cell Res* 1984; **150**: 194-204
- 23 **Lu LG, Zeng MD, Fan JG, Li JQ, Hua J, Fan ZP.** Isolation, culture and characterization of Kupffer cells from rat liver. *Shanghai Yixue* 1998; **21**: 630-632
- 24 **Song SG, Yang Y, Cheng MZ.** Isolation and culture of Ito and Kupffer cell from rat liver. *Zhongguo Linchuang Yaolixue Yu Zhilixue* 2000; **5**: 351-353
- 25 **Alpini G, Phillips JO, Vroman B, LaRusso NF.** Recent advances in the isolation of liver cells. *Hepatology* 1994; **20**: 494-514
- 26 **Takase S, Leo MA, Nouchi T, Lieber CS.** Desmin distinguishes cultured fat-storing cells from myofibroblasts, smooth muscle cells and fibroblasts in the rat. *J Hepatol* 1988; **6**: 267-276
- 27 **West MA, Billiard TR, Curran RD, Hyland BJ, Simmons RL.** Evidence that rat Kupffer cells stimulate and inhibit hepatocyte protein synthesis *in vitro* by different mechanisms. *Gastroenterology* 1989; **96**: 1572-1582
- 28 **Deaciuc IV, Bagby GJ, Niesman MR, Skrepnik N, Spitzer JJ.** Modulation of hepatic sinusoidal endothelial cell function by Kupffer cells: an example of intercellular communication in the liver. *Hepatology* 1994; **19**: 464-470
- 29 **Shiratori Y, Geerts A, Ichida T, Kawase T, Wisse E.** Kupffer cells from CCl₄-induced fibrotic livers stimulate proliferation of fat-storing cells. *J Hepatol* 1986; **3**: 294-303
- 30 **Bode C, Kugler V, Bode JC.** Endotoxemia in patients with alcoholic and non-alcoholic cirrhosis and in subjects with no evidence of chronic liver disease following acute alcohol excess. *J Hepatol* 1987; **4**: 8-14
- 31 **Bjarnason I, Peters TJ, Wise RJ.** The leaky gut of alcoholism: possible route of entry for toxic compounds. *Lancet* 1984; **1**: 179-182
- 32 **Dooley S, Delvoux B, Streckert M, Bonzel L, Stopa M, ten Dijke P, Gressner AM.** Transforming growth factor beta signal transduction in hepatic stellate cells via Smad2/3 phosphorylation, a pathway that is abrogated during *in vitro* progression to myofibroblasts. TGFbeta signal transduction during transdifferentiation of hepatic stellate cells. *FEBS Lett* 2001; **502**: 1-3

Edited by Zhang JZ and Wang XL

Significance of perigastric lymph node involvement in periampullary malignant tumor

De-Qing Mu, You-Shu Peng, Feng-Guo Wang, Qiao-Jian Xu

De-Qing Mu, You-Shu Peng, Department of Surgery of the Second Affiliated Hospital, Medical College of Zhejiang University, Hangzhou 3100031, Zhejiang Province, China

Feng-Guo Wang, Department of Pathology of the Second Affiliated Hospital, Medical College of Zhejiang University, Hangzhou 310009, Zhejiang Province, China

Qiao-Jian Xu, Undergraduate Medical College of Zhejiang University, Hangzhou 310009, Zhejiang Province, China

Correspondence to: Dr. De-Qing Mu, Department of Surgery of the Second Affiliated Hospital, Medical College of Zhejiang University, Hangzhou 310009, Zhejiang Province, China. samier-1969@163.com
Telephone: +86-571-87783762

Received: 2003-05-11 **Accepted:** 2003-06-27

Abstract

AIM: To determine the perigastric lymph node involvement in periampullar tumors, in an attempt to optimize the surgical treatment of pylorus-preserving pancreatoduodenectomy.

METHODS: We retrospectively investigated the frequency of lymph nodes involvement in perigastric regions. Distribution and number of involved lymph nodes were examined from 112 patients with carcinoma of pancreas, 59 patients with distal bile duct carcinoma, and 41 patients with carcinoma of the papilla of Vater.

RESULTS: The frequency of lymphatic spread of carcinoma in pancreas; distal bile duct and papilla of Vater was 18.7%, 1.9%, 2.5% respectively. With regard to the mode of lymphatic spread in perigastric region, Infrapyloric nodes of carcinoma of the head of pancreas predominated over others, in carcinomas of the distal bile duct and the papilla of Vater, the left gastric artery, and the greater curvature lymph nodes was the only sole sites, respectively.

CONCLUSION: Understanding perigastric lymphatic involvement in periampullary tumors may be helpful for choosing the appropriate surgical approaches to pancreatoduodenectomy with preservation of pylorus.

Mu DQ, Peng YS, Wang FG, Xu QJ. Significance of perigastric lymph node involvement in periampullary malignant tumor. *World J Gastroenterol* 2004; 10(4): 614-616
<http://www.wjgnet.com/1007-9327/10/614.asp>

INTRODUCTION

Since the first pancreaticoduodenectomy was successfully performed, there have been many controversies^[1-3] among surgeons about the preservation of pylorus during pancreatoduodenectomy is the adequate strategy in periampullar malignant tumors. Usually the decision of pylorus-preserving is decided by the presence or absence of positive lymph node involvement in the perigastric lymph nodes. The goal of our study is to determine the perigastric lymph node involvement in periampullary tumors and to perform appropriate surgical

procedures for “periampullary tumors”.

MATERIALS AND METHODS

Materials

Specimens obtained from 112 patients with carcinoma of the pancreas of head including 23 cases of small carcinoma of pancreas, 51 patients of carcinoma of distal bile duct, 41 cases of carcinoma of the papilla of Vater. They all underwent consecutive resection at our Department of Surgery between January 1990 to December 2000. The 112 patients with carcinoma of pancreas were composed of 79 men and 33 women with a mean age of 67 years (range 41 to 73 years). The 51 patients with carcinoma of the distal bile duct were composed of 39 men and 12 women averaging at age of 61 years (range 39-81 years). The 41 patients with carcinoma of the papilla of Vater were composed of 27 men and 14 women averaging at age of 69.4 years (rang 47-79 years).

Methods

Patients with periampullar malignant tumors received radical operation. Primary group (N1) and secondary group (N2) lymph nodes were cleared together with neighboring connective tissue. The tertiary group(N3) lymph nodes with neighboring connective were appropriately cleared (Figures 1A and 1B).

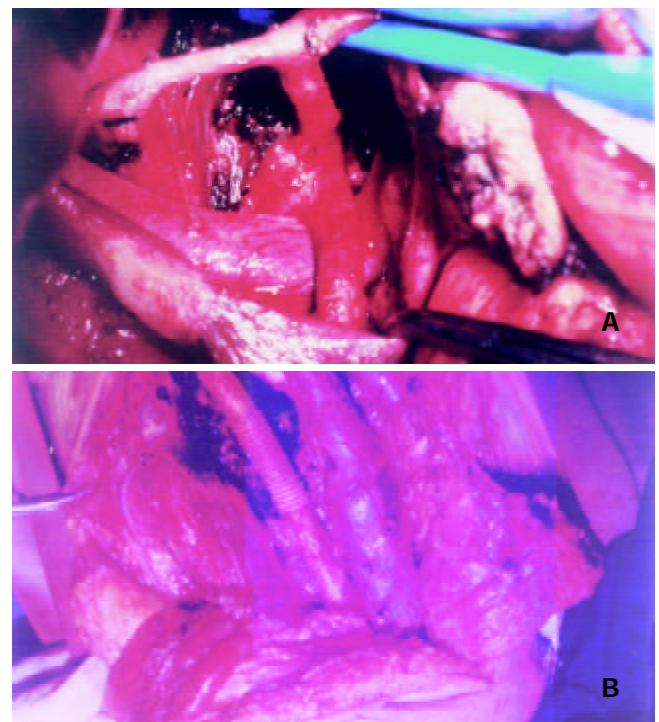


Figure 1 A and B Ranges of lymphatic and neighboring connective tissue dissection in periampullary malignant tumors. In Figure 1A n1, n2 and n3 (N07) nodes were cleared with neighboring connective tissue, In Figure 1B n2 nodes (N016) and connective tissue around the major vessels including aorta and inferior vein were cleared.

Immediately after operation The tumor locations were determined by close observation of the resected specimens. Lymph nodes macroscopically identified were separated from the fresh surgical specimen with the surrounding fatty tissues, in which small lymph nodes might be contained. Both the nodes and fatty tissues were embeded and cut into 5 μm sections and examined microscopically. Based on the guidelines of the General rules for Surgical and Pathological studies on Cancer of Pancreas by the Japanese society of Pancreatic Surgery^[3] (4rd edition, 1996), General Rules for Surgical and Pathological studies on cancer of Biliary Tract by the Japanese Society of Biliary Surgery (4rd edition 1997), perigastric lymph nodes were classified as right cardiac lymph nodes, left cardiac lymph nodes, lesser curvature lymph nodes, great curcature lymph nodes, suprapyloric lymph nodes, infrapyloric lymph nodes. Metastatic lymph nodes of carcinoma were confirmed by microscopic examination and the percentage of positive lymph nodes was calculated using the formula: [the number of sites positive for carcinoma metastasis]/[the number of sites dissected actually].

RESULTS

The number of dissected lymph nodes in each case range between seven and 19(mean 12) in patients with carcinoma of the pancreas of head,between 4 and 15(mean 9.7) in those with carcinoma of the distal bile duct,and between 3 and 16(mean 10.4) in those with carcinoma of the papilla of Vater.

The frequency of lymph node involvement was 18.7% of the patients with advanced carcinoma of the pancreas of head had perigastric lymph node involvement,5.6% patients with small carcinoma of pancreas had perigastric node involvement localized to the number 5 and 6, 1.9% patients with carcinoma of the distal bile duct had perigastric lymph node involvement in N₀7, 1.2% patients with carcinoma of the papilla of Vater had perigastric lymph node involvement only identified in N₀4. Pathological metastatic rates to perigastric regional lymph nodes in resected cases of carcinoma of periampulla are shown in Table1.

Table 1 Perigastric lymph node involvement in patients with carcinoma of periampulla

Carcinoma of pancreas			Carcinoma of distal bile duct			Carcinoma of papilla of Vater		
No	%	I/II	No	%	I/II	No	%	I/II
1	-	-	1	-	-	1	-	-
2	-	-	2	-	-	2	-	-
3	2.2	28/1261	3	0	0/145	3	0	0/498
4	1.2	17/1412	4	0	0/197	4	5.1	19/376
5	2.2	29/1319	5	0	0/216	5	0	0/512
6	7.2	116/1623	6	0	0/207	6	0	0/419
7	3.5	42/1174	7	3.1	17/557	7	0	0/517

I/II[the number of the sites positive for carcinoma metastasis]/[the number of sites dissected actually].

DISCUSSION

In this current study, periampulla cancer, includes three categories,namely carcinoma of ampulla, carcinoma of distal common bile duct, carcinonoma of pancreatic head.

Standard whipple operation for the treatment of resectable tumors of the periampullary region involves a radical pancreatoduodenectomy with an extensive gastric resection. The modified Whipple operation aims to preserve the stomache, pylorus and proximal duodenum so as to decreas

postgastrectomy complications and improve the patient’s quality of life. However, there were still many postoperative complications after pylous-preserving pancreatoduodenectomy (PPPD)^[4,5]. In addition, in malignant periampullary tumor the patient’s quality of life after resection depended more on recurrence of malignant diseases than on physiologic alterations related to the resection and reconstruction^[6,7]. There might exist two kinds of recurrence after PPPD, one was the possibility of cancerous infiltration of duodenal and gastric margins through lymph vessels^[8], the other was the perigastric region node involvement. Individual lymph nodes have been histologically proved metastasis to perigastric region. According to our investigation, the rate of metastasis to perigastric lymph nodes in patients with carcinoma of pancreas was 18.7%. In those with other types of periampullary carcinomas, such as carcinoma of the ampulla, distal bile duct, the rate was 1.9% and 1.2% respectively. The involved sites were extremely limited^[9-14]. So far as carcinoma of the pancreas of head concernd even small carcinoma of pancreas has a higher perigastric lymph node involvement^[15,16].

The presence of metastatic cancer in lymph nodes excised during pancreatoduodenectomy is generally accepted as an evidence of a surgically incurable disease, and lymph node dissection may therefore be considered as a prognostic factor. PPPD could not remove peripyloric or celiac lymph nodes. The expected 5-year survival rate after PPPD without perigastric lymph node clearance range from 30% to 50% in patients with carcinoma of the ampulla of Vater or the distal bile duct^[9,17,18]. However, impact on the negative survival of metastatic lymph nodes of carcinoma of pancreatic head has been observed in many studies and was associated with high rates of local and regional recurrence after PPPD^[19,20]. Taking all these into account, we hold that PPPD may be acceptable for carcinoma of the ampulla of Vater, distal bile duct. It may be indicated for carcinoma of pancreas of head if perigastric node involvement is not observed.

REFERENCES

- 1 **Miyazaki I**, Kayahara M, Nagakawa T. Changes in lymph node dissection for pancreatic cancer. *Nippon Geka Gakkai Zasshi* 1997; **98**: 610-614
- 2 **Ogata Y**, Hishinuma S. The impact of pylorus-preserving pancreatoduodenectomy on surgical treatment for cancer of the pancreatic head. *J Hepatobiliary Pancreat Surg* 2002; **9**: 223-232
- 3 **Roher HD**, Heise JW, Goretzki PE. Stomach saving duodenopan-createctomy. Indications and contraindications. The most important surgical steps. *Zentralbl Chir* 2000; **125**: 961-965
- 4 **Sakaguchi T**, Nakamura S, Suzuki S, Kojima Y, Tsuchiya Y, Konno H, Nakaoka J, Nishiyama R. Marginal ulceration after pylorus-preserving pancreaticoduodenectomy. *J Hepatobiliary Pancreat Surg* 2000; **7**: 193-197
- 5 **Park YC**, Kim SW, Jang JY, Ahn YJ, Park YH. Factors influencing delayed gastric emptying after pylorus-preserving pancreatod- uodenectomy. *J Am Coll Surg* 2003; **196**: 859-865
- 6 **Mcleod RS**. Quality of life, nutritional status and gastrointesti- nal hormone profile following the Whipple procedure. *Ann Oncol* 1999; **10**(Suppl 4): 281-284
- 7 **van Berge Henegouwen MI**, Moojen TM, van Gulik TM, Rauws EA, Obertop H, Gouma DJ. Postoperative weight gain after stan- dard Whipple’s procedure versus pylorous-preserving pancreatoduodenectomy: the influence of tumour status. *Br J Surg* 1998; **85**: 922-926
- 8 **Sharp KW**, Ross CB, Halter SA, Morrison JG, Richards WO, Wil- liams LF, Sawyers JL. Pancreatoduodenectomy with pyloric pres- ervation for carcinoma of the pancreas: a cautionary note. *Surg- ery* 1989; **105**: 645-653
- 9 **Sasaki R**, Takahashi M, Funato O, Nitta H, Murakami H, Kawamura H, Suto T, Kanno S, Saito K. Prognostic significance of lymph node involvement in middle and distal bile duct cancer. *Surgery* 2001; **129**: 677-683

- 10 **Kayahara M**, Nagakawa T, Ohta T, Kitagawa H, Tajima H, Miwa K. Role of nodal involvement and the periductal soft-tissue margin in middle and distal bile duct cancer. *Ann Surgery* 1999; **229**: 76-83
- 11 **Yoshida T**, Shibata K, Yokoyama H, Morii Y, Matsumoto T, Sasaki A, Kitano S. Patterns of lymph node metastasis in carcinoma of the distal bile duct. *Hepatogastroenterology* 1999; **46**: 1595-1598
- 12 **Yoshida T**, Matsumoto T, Sasaki A, Morii Y, Shibata K, Ishio T, Kitano S. Lymphatic spread differs according to tumor location in extrahepatic bile duct cancer. *Hepatogastroenterology* 2003; **50**: 17-20
- 13 **Shirai Y**, Ohtani T, Tsukada K, Hatakeyama K. Patterns of lymphatic spread of carcinoma of the ampulla of Vater. *Br J Surg* 1997; **84**: 1012-1016
- 14 **Yoshida T**, Matsumoto T, Shibata K, Yokoyama H, Morii Y, Sasaki A, Kitano S. Patterns of lymph node metastasis in carcinoma of the ampulla of Vater. *Hepatogastroenterology* 2000; **47**: 880-883
- 15 **Ishikawa O**, Ohigashi H, Sasaki Y, Kabuto T, Furukawa H, Nakamori S, Imaoka S, Iwanaga T, Kasugai T. Practical grouping of positive lymph nodes in pancreatic head cancer treated by an extended pancreatectomy. *Surgery* 1997; **121**: 244-249
- 16 **Kayahara M**, Nagakawa T, Kobayashi H, Mori K, Nakano T, Kadoya N, Ohta T, Ueno K, Miyazaki I. Lymphatic flow in carcinoma of the head of the pancreas. *Cancer* 1992; **70**: 2061-2066
- 17 **Roberts RH**, Krige JE, Bornman PC, Terblanche J. Pancreaticoduodenectomy of ampullary carcinoma. *Am Surg* 1999; **65**: 1043-1048
- 18 **Takao S**, Aikou T, Shinci H, Uchikura K, Kubo M, Imamura H, Maenohara S. Comparison of relapse and long-term survival between pylorus-preserving and Whipple pancreaticoduodenectomy in periampullary cancer. *Am J Surg* 1998; **176**: 467-470
- 19 **Benassai G**, Mastrorilla M, Quarto G, Cappiello A, Giani U, Forestieri P, Mazzeo F. Factors influencing survival after resection for ductal adenocarcinoma of the head of the pancreas. *J Surg Oncol* 2000; **73**: 212-218
- 20 **Millikan KW**, Deziel DJ, Silverstein JC, Kanjo TM, Christein JD, Doolas A, Prinz RA. Prognostic factors associated with respectable adenocarcinoma of the head of the pancreas. *Am Surg* 1999; **65**: 618-623

Edited by Zhu LH and Wang XL

Mechanisms for amplified mediator release from colonic mast cells: Implications for interstitial inflammatory diseases

Kim E. Barrett

Kim E. Barrett, Division of Gastroenterology, Department of Medicine, University of California, San Diego, School of Medicine, San Diego, CA 92103, USA

Supported by the grants from the National Institutes of Health, USA (DK33491 and AT01180) and the Crohn's and Colitis Foundation of America

Correspondence to: Kim E. Barrett, Ph.D., UCSD Medical Center, 8414, 200 west Arbor Drive (for courier delivery, use CTF-A108, 210 Dickinson Street), San Diego, CA 92103-8414, USA. kbarrett@ucsd.edu

Telephone: +1-619-543 3726 **Fax:** +1-619-543 6969

Received: 2004-02-11 **Accepted:** 2004-02-14

Barrett KE. Mechanisms for amplified mediator release from colonic mast cells: Implications for interstitial inflammatory diseases. *World J Gastroenterol* 2004; 10(5): 617-619
<http://www.wjgnet.com/1007-9327/10/617.asp>

The mast cell is an enigmatic cell type whose physiological function has preoccupied large numbers of investigators for decades^[1]. Some have concluded that the absence of mast cells is incompatible with life, at least in humans, because no human conditions have been documented where these cells are absent from the body. On the other hand, mice harboring specific mutations in certain growth factors, or their receptors, that lead to apparently an almost total ablation of the mast cell lineage, are viable, although they do have several documented abnormalities and may exhibit altered inflammatory responses in a variety of tissues^[2]. The viability of such animals may reflect redundancy in the murine system for specific mast cell functions, and/or that other cell types adapt to become repositories of characteristic mast cell mediators. But in any event, mast cells have long been considered to play specific roles in pathophysiology, particularly in disease states that are characterized by allergic inflammation^[1-5]. In the setting of the gastrointestinal tract, release of mast cell mediators has been thought to contribute to tissue injury and inflammation, as well as alterations in epithelial and smooth muscle function, in conditions such as food allergy, systemic anaphylaxis, ulcer disease and inflammatory bowel diseases, as well as, more controversially, irritable bowel syndrome^[3,5-13]. The spectrum of mast cell involvement has also been expanded by recognition that they can participate in biological events not classically related to allergic responses, such as innate immunity, the phagocytosis of bacteria and cross-talk with the peripheral and enteric nervous systems^[14-16].

Mast cells are activated classically by cross-linking of membrane IgE receptors^[17]. *In vivo*, this occurs when a genetically susceptible individual mounts an IgE antibody response to a foreign protein that would be seen as innocuous by the immune system of those who are not allergic. The IgE antibodies bind with great avidity to the mast cell IgE receptors. Thus, because mast cells in the tissues are also long-lived, the allergic individual becomes chronically sensitized, with mast cell IgE receptors occupied by allergen-specific IgE, priming the cell to be activated by a subsequent exposure to the allergen. Binding of allergen to adjacent IgE molecules on such primed

cells results, in turn, in apposition of the IgE receptors, thereby initiating a signal transduction cascade, involving, among other steps, mobilization of intracellular calcium and activation of protein kinases, that leads ultimately to release of mast cell mediators^[17,18]. The mediators that account for the biological effects of mast cell activation may be stored in cytoplasmic granules, such as histamine and a protease known as tryptase that were studied by He and co-workers in work reported in the *Journal*^[19-24]. Other potent mediators, including various cytokines and leukotrienes, are synthesized *de novo*, with delayed or rapid kinetics depending on whether gene transcription is or is not required, respectively^[19]. The process of mast cell activation can be mimicked *in vitro* by artificially stimulating aspects of the signaling cascade. He and co-workers accomplished this by using antibodies directed against the IgE molecule itself, which cause allergen-independent IgE receptor cross-linking, or a calcium ionophore, which causes an increase in the levels of cytoplasmic calcium.

In addition to the immunological activation of mast cells, it has been known for many years that various other substances can initiate or potentiate mast cell mediator release^[25]. These include neuropeptides, highly basic compounds, peptides from bee venom, and adenosine. The work from He *et al.*, conducted with mast cells isolated from human colonic specimens, extends this list to include histamine and proteases, including trypsin and mast cell tryptase itself^[20-24]. While these and other investigators had shown that proteases can activate some mast cell populations to release histamine, it was important to demonstrate directly that they were active against human intestinal mast cells due to the known existence of substantial functional and biochemical heterogeneity among mast cells isolated from different tissue sites and from different species^[26-29]. Moreover, the ability of histamine to activate tryptase release from intestinal mast cells had not previously been demonstrated; rather, in other mast cell populations, histamine has been shown to inhibit mediator release, although others have shown that histamine H₁ receptor antagonists can block mediator secretion from basophils, consistent with the findings of He *et al.*^[30,31]. The work from He and co-workers also implies important autoregulatory mechanisms that almost certainly contribute to the overall level of mediator release from mast cells *in vivo*. Thus, not only are histamine and tryptase released from mast cells, but they also likely stimulate further mediator release once present in the extracellular space. The concentrations of histamine capable of activating mediator release are well within the range that might be expected in the vicinity of activated mast cells^[20]. Likewise, the biological significance of the inferred effect of tryptase on mediator release is illustrated by the fact that inhibitors of the proteolytic activity of this enzyme significantly reduce mast cell mediator release evoked by IgE cross-linking^[23]. Overall, these findings suggest that mast cells participate in a self-perpetuating amplification mechanism that would be capable of sustaining mediator release, at least from the granule-associated pool, until released mediators had been cleared from the area by diffusion or metabolism. However, there also appear to be some "brakes" to the system that would preclude wholly uncontrolled release of the panoply of potent mast cell mediators. For histamine in

particular, the effect on mediator secretion was biphasic, with higher concentrations of the amine less effective than lower ones^[20]. Thus, released histamine would amplify ongoing mediator release from the cell of origin or others in the neighborhood, but only up to a certain point. The biphasic effect of histamine may also explain differences between the findings of He *et al.* and those reported previously by others^[20,30].

The authors also have begun to examine the specific receptors and other mechanisms that contribute to protease-activated mediator release from human colonic mast cells. The process is active rather than cytotoxic, and can be reproduced by peptide agonists specific for a member of a novel class of receptors, the proteinase-activated receptors, or PAR's^[32]. PAR's are G-protein coupled receptors that are activated by proteolytic cleavage, revealing a tethered ligand. The prototypic member of this class is the thrombin receptor, or PAR-1^[32]. In addition, PAR-2 has been shown to contribute to inflammatory reactions, including in the intestine, and is activated by both trypsin and tryptase, as well as by synthetic peptides that mimic the sequence of the tethered ligand^[32-36]. He *et al.* developed evidence that mast cells are likely activated by PAR-2 ligation, such as would be stimulated by release of tryptase itself^[21]. On the other hand, the receptor subtype mediating the effect of histamine on tryptase release from human colonic mast cells is not yet known.

Some minor caveats should be raised about the studies presented. First, the mast cells used for the experiments were studied as an unpurified preparation in which mast cells constituted only about 5% of the total cell number^[20-24]. Thus, the effects of either histamine and proteases on mediator release could in fact be indirect, and mediated secondarily by another substance released from a contaminating cell type responsive to either agent. However, this scenario does not necessarily detract from the clinical relevance of the responses studied by He and co-workers, because mast cells are not activated in isolation *in vivo*. Likewise, the presence of PAR-2, although not histamine receptors, has been demonstrated directly on human mast cells in a variety of tissues using immunohistochemistry. Second, the authors speculate that mast cells in the gut wall might constantly be exposed to pancreatic trypsin during the normal process of digestion, and that this might evoke mediator release. However, even if a small proportion of luminal trypsin does leak across the small intestinal epithelium in intact form to encounter subepithelial mast cells, and at concentrations comparable to those needed to activate mast cells *in vitro* (which is unproven at the present time), this is unlikely to occur in the colon, and so the studies would need to be repeated using mast cells isolated from the small intestine to understand fully whether the findings have physiological or pathophysiological relevance. Finally, we know little about the persistence of mast cell mediators in the interstitium following their release. While the concentrations of both histamine and proteases capable of activating colonic mast cells are at least theoretically within the biological range immediately following degranulation, it is unknown whether these concentrations remain elevated for long enough to contribute significantly to amplifying subsequent mediator release.

The caveats notwithstanding, the studies of He *et al.* enhance our understanding of the possible roles of mast cells in initiating and/or perpetuating intestinal disorders, including inflammatory bowel diseases and peptic ulcer disease. Knowledge of the mechanisms that regulate mediator release from intestinal mast cells specifically should aid in our ability to modulate the activity of this cell type, with potential therapeutic benefits given the wide range of adverse effects of released mediators. Indeed, He and co-workers themselves suggest that proteinase inhibitors might be attractive targets for drug development, although the biological actions of such

compounds would almost certainly extend beyond simply an effect on mast cell activation, given the wide distribution of PAR's^[23]. Further, the findings may shed light on pathogenic mechanisms in diseases not currently appreciated as being dependent on mast cells and their mediators. For example, colon cancer cells often release novel trypsins into their environment, and this in turn could conceivably account for the fact that mast cells are often observed at the margins of tumors examined histologically, based on the possibility that such cells are chronically activated by the tumor microenvironment^[37-39]. Overall, progress in this field should be expected to improve the understanding and treatment of a whole host of digestive disorders.

REFERENCES

- 1 **Galli SJ**. The Paul Kallos Memorial Lecture. The mast cell: a versatile effector cell for a challenging world. *Int Arch Allergy Immunol* 1997; **113**: 14-22
- 2 **Wershil BK**. Mast cell-deficient mice and intestinal biology. *Am J Physiol Gastrointest Liver Physiol* 2000; **278**: G343-G348
- 3 **Brandt EB**, Strait RT, Hershko D, Wang Q, Muntel EE, Scribner TA, Zimmermann N, Finkelman FD, Rothenberg ME. Mast cells are required for experimental oral allergen-induced diarrhea. *J Clin Invest* 2003; **112**: 1666-1677
- 4 **Barrett KE**. Immune regulation of intestinal ion transport: implications for inflammatory diarrhea. *Progr Inflamm Bowel Dis* 1991; **12**: 8-11
- 5 **Barrett KE**, Metcalfe DD. The mucosal mast cell and its role in gastrointestinal allergic disease. *Clin Rev Allergy* 1984; **2**: 39-53
- 6 **Chadwick VS**, Chen W, Shu D, Paulus B, Betwaite P, Tie A, Wilson I. Activation of the mucosal immune system in irritable bowel syndrome. *Gastroenterology* 2002; **122**: 1778-1783
- 7 **Myers CP**, Hogan DL, Yao B, Koss M, Isenberg JJ, Barrett KE. Inhibition of rabbit duodenal bicarbonate secretion by pro-ulcerogenic agents: histamine-dependent and -independent effects. *Gastroenterology* 1998; **114**: 527-535
- 8 **He SH**. Key role of mast cells and their major secretory products in inflammatory bowel disease. *World J Gastroenterol* 2004; **10**: 309-318
- 9 **Gelbmann CM**, Barrett KE. Role of inflammatory cell types In: Scholmerich J, Kruis W, Goebell H, Hohenberger W, Gross V, eds. *Inflammatory Bowel Diseases - Pathophysiology as Basis of Treatment*. Lancaster, UK: Kluwer Academic 1993: 62-79
- 10 **Gelbmann CM**, Barrett KE. Role of histamine in a rat model of colitis. *Inflamm Res* 1995; **44**: 386-392
- 11 **Perdue MH**, Masson S, Wershil BK, Galli SJ. Role of mast cells in ion transport abnormalities associated with intestinal anaphylaxis. Correction of the diminished secretory response in genetically mast cell-deficient *W/W^v* mice by bone marrow transplantation. *J Clin Invest* 1991; **87**: 687-693
- 12 **Perdue MH**, McKay DM. Integrative immunophysiology in the intestinal mucosa. *Am J Physiol* 1994; **267**: G151-G165
- 13 **Siddiqui AA**, Miner PB Jr. The role of mast cells in common gastrointestinal diseases. *Curr Allergy Asthma Rep* 2004; **4**: 47-54
- 14 **Mekori YA**, Metcalfe DD. Mast cells in innate immunity. *Immunol Rev* 2000; **173**: 131-140
- 15 **Malaviya R**, Abraham SN. Mast cell modulation of immune responses to bacteria. *Immunol Rev* 2001; **179**: 16-24
- 16 **Bauer O**, Razin E. Mast cell-nerve interactions. *News Physiol Sci* 2000; **15**: 213-218
- 17 **Sada K**, Yamamura H. Protein tyrosine kinases and adaptor proteins in FcεRI-mediated signaling in mast cells. *Curr Mol Med* 2003; **3**: 85-94
- 18 **Barker SA**, Lujan D, Wilson BS. Multiple roles for PI 3-kinase in the regulation of PLCγ activity and Ca²⁺ mobilization in antigen-stimulated mast cells. *J Leukocyte Biol* 1999; **65**: 321-329
- 19 **Schwartz LB**. Mast cells: function and contents. *Curr Opin Immunol* 1994; **6**: 91-97
- 20 **He SH**, Xie H. Modulation of tryptase secretion from human colon mast cells by histamine. *World J Gastroenterol* 2004; **10**: 323-326

- 21 **He SH**, He YS, Xie H. Activation of human colon mast cells through proteinase activated receptor-2. *World J Gastroenterol* 2004; **10**: 327-331
- 22 **He SH**, Xie H, He YS. Induction of tryptase and histamine release from human colon mast cells by IgE dependent or independent mechanisms. *World J Gastroenterol* 2004; **10**: 319-322
- 23 **He SH**, Xie H. Inhibition of tryptase release from human colon mast cells by protease inhibitors. *World J Gastroenterol* 2004; **10**: 332-336
- 24 **He SH**, Xie H. Modulation of histamine release from human colon mast cells by protease inhibitors. *World J Gastroenterol* 2004; **10**: 337-341
- 25 **Stassen M**, Hultner L, Schmitt E. Classical and alternative pathways of mast cell activation. *Crit Rev Immunol* 2002; **22**: 115-140
- 26 **He SH**, Walls AF. Human mast cell tryptase: a potent stimulus of microvascular leakage and mast cell activation. *Eur J Pharmacol* 1997; **328**: 89-97
- 27 **He SH**, Gaça MDA, Walls AF. A role for tryptase in the activation of human mast cells: modulation of histamine release by tryptase and inhibitors of tryptase. *J Pharmacol Exp Ther* 1998; **286**: 289-297
- 28 **He SH**, Xie H, He YS. Effect of a proteinase-activated receptor-2 (PAR2) agonist on tryptase release from human mast cells. *Acta Physiol Sin* 2002; **54**: 531-534
- 29 **Barrett KE**, Pearce FL. Heterogeneity of mast cells In: Uvnas B, ed. *Histamine and Histamine Antagonists*. Berlin:Springer Verlag 1991: 93-117
- 30 **Weltman JK**. Histamine as a regulator of allergic and asthmatic inflammation. *Allergy Asthma Proc* 2003; **24**: 227-229
- 31 **McGlashan D Jr**. Histamine: a mediator of inflammation. *J Allergy Clin Immunol* 2003; **112**(4 Suppl): S53-S59
- 32 **Schmidlin F**, Bunnett NW. Protease-activated receptors: how proteases signal to cells. *Curr Opin Pharmacol* 2001; **1**: 575-582
- 33 **Kawabata A**. Gastrointestinal functions of proteinase-activated receptors. *Life Sci* 2003; **74**: 247-254
- 34 **Cenac N**, Garcia-Villar R, Ferrier L, Larauche M, Vergnolle N, Bunnett NW, Coelho AM, Fioramonti J, Bueno L. Proteinase-activated receptor 2-induced colonic inflammation in mice: possible involvement of afferent neurons, nitric oxide, and paracellular permeability. *J Immunol* 2003; **170**: 4296-4300
- 35 **Cottrell GS**, Amadesi S, Schmidlin F, Bunnett N. Protease-activated receptor 2: activation, signalling and function. *Bioch Soc Trans* 2003; **31**: 1191-1197
- 36 **Cenac N**, Coelho AM, Nguyen C, Compton S, Andrade-Gordon P, MacNaughton WK, Wallace JL, Hollenberg MD, Bunnett NW, Garcia-Villar R, Bueno L, Vergnolle N. Induction of intestinal inflammation in mouse by activation of proteinase-activated receptor-2. *Am J Pathol* 2002; **161**: 1903-1915
- 37 **Yamamoto H**, Iku S, Adachi Y, Imsumran A, Taniguchi H, Noshu K, Min Y, Horiuchi S, Yoshida M, Itoh F, Imai K. Association of trypsin expression with tumor progression and matrilysin expression in human colorectal cancer. *J Pathol* 2003; **199**: 176-184
- 38 **Dimitriadou V**, Koutsilieris M. Mast cell-tumor cell interactions: for or against tumour growth and metastasis? *Anticancer Res* 1997; **17**: 1541-1549
- 39 **McKerrow JH**, Bhargava V, Hansell E, Huling S, Kuwahara T, Matley M, Coussens L, Warren R. A functional proteomics screen of proteases in colorectal cancer. *Mol Med* 2000; **6**: 450-460

Edited by Zhang JZ Proofread by Zhu LH

IL-10 and its related cytokines for treatment of inflammatory bowel disease

Ming-Cai Li, Shao-Heng He

Ming-Cai Li, Shao-Heng He, Allergy and Inflammation Research Institute, Shantou University Medical College, Shantou 515041, Guangdong Province, China

Supported by the Li Ka Shing Foundation, Hong Kong, China, No. C0200001

Correspondence to: Professor Shao-Heng He, Allergy and Inflammation Research Institute, Shantou University Medical College, 22 Xin Ling Road, Shantou 515041, Guangdong Province, China. shoahenghe@hotmail.com

Telephone: +86-754-8900405 **Fax:** +86-754-8900192

Received: 2003-10-24 **Accepted:** 2003-12-22

Abstract

Inflammatory bowel diseases (IBDs), including Crohn's disease and ulcerative colitis are chronic inflammatory disorders of gastrointestinal tract. Although the etiology is incompletely understood, initiation and aggravation of the inflammatory process seem to be due to a massive local mucosal immune response. Interleukin-10 (IL-10) is a regulatory cytokine which inhibits both antigen presentation and subsequent pro-inflammatory cytokine release, and it is proposed as a potent anti-inflammatory biological therapy in chronic IBD. Many methods of IL-10 as a treatment for IBD have been published. The new strategies of IL-10 treatment, including recombinant IL-10, the use of genetically modified bacteria, gelatine microsphere containing IL-10, adenoviral vectors encoding IL-10 and combining regulatory T cells are discussed in this review. The advantages and disadvantages of these IL-10 therapies are summarized. Although most results of recombinant IL-10 therapies are disappointing in clinical testing because of lacking efficacy or side effects, therapeutic strategies utilizing gene therapy may enhance mucosal delivery and increase therapeutic response. Novel IL-10-related cytokines, including IL-19, IL-20, IL-22, IL-24, IL-26, IL-28 and IL-29, are involved in regulation of inflammatory and immune responses. The use of IL-10 and IL-10-related cytokines will provide new insights into cell-based and gene-based treatment against IBD in near future.

Li MC, He SH. IL-10 and its related cytokines for treatment of inflammatory bowel disease. *World J Gastroenterol* 2004; 10 (5): 620-625

<http://www.wjgnet.com/1007-9327/10/620.asp>

INTRODUCTION

Inflammatory bowel diseases, including Crohn's disease and ulcerative colitis are chronic inflammatory and frequently relapsing diseases of the gut that ultimately lead to destruction of the intestinal tissue. Over recent decades the incidence of IBD has been rising in the world, and IBD will become increasingly common in Asia, as it has been in the last fifty years in Europe and North America^[1]. The pathogenesis of IBD likely involves multifactorial interactions among genetic factors, immunological factors and environmental triggers^[2].

Recent evidence suggests that a pathologic activation of the mucosal immune system in response to antigens is a key factor in the pathogenesis of IBD. In patients with IBD, a loss of immune tolerance occurs to some, but not all, commensal bacterial antigens coupled with alterations in T-cell regulation leads to relapsing chronic inflammation^[3,4]. There appear to be distinct pathways of inflammation in Crohn's disease and ulcerative colitis. In patients with Crohn's disease, the patterns of cytokines expressed by mucosal lymphocytes generally tend to be consistent with a T-helper-1(Th1) response, including an early increase in the expression of interferon (IFN), IL-2, and IL-12, followed by a subsequent increase in tumour necrosis factor- α (TNF- α) and IL-18^[5]. In addition, there also appears to be a compensatory increase in IL-10 and transforming growth factor- β (TGF- β) levels. In patients with ulcerative colitis, the pattern of cytokine expression differs from that seen in Crohn's disease, with an increased expression of IL-5, IL-6, IL-10, and IL-13^[5].

Current therapy of IBD is neither sufficient nor disease-modifying. Long-term treatment with non-specific anti-inflammatory drugs such as aminosaliculates, corticosteroids and immunosuppressants is often accompanied by undesirable and potentially serious side effects^[6]. Novel biologically-driven therapies are targeted to specific pathophysiological processes, offering the potential for better treatment outcomes. Several new therapeutic strategies are currently being tested in clinical practice, including recombinant anti-inflammatory cytokines (IFN- α , IL-10, IL-11) and inhibitors of cell adhesion molecules (ICAM), pro-inflammatory cytokines (TNF, IL-12) and their specific monoclonal antibodies or their receptors (TNFR, IL-6R)^[2].

The pathogenesis of IBD is characterized by an imbalanced activation of Th1- and Th2-lymphocytes. IL-10 represents an anti-inflammatory cytokine which downregulates the production of Th1-derived cytokines. The relative deficiency of IL-10 in patients with ulcerative colitis may contribute to persistent inflammatory changes^[7]. IL-10-deficient mice (IL-10(-/-)) spontaneously develop intestinal inflammation characterized by discontinuous transmural lesions affecting the small and large intestines and by dysregulated production of proinflammatory cytokines, indicating that endogenous IL-10 is a central regulator of the mucosal immune response^[8]. IL-10 is in clinical trial as an anti-inflammatory therapy for IBD and various autoimmune diseases such as psoriasis, rheumatoid arthritis, and multiple sclerosis. This review describes the current state of knowledge regarding IL-10-directed biological therapies in IBD.

BIOLOGICAL CHARACTERISTICS AND FUNCTIONS OF IL-10

IL-10 was first identified in 1989 as a cytokine synthesis inhibitor produced by a subset of murine T lymphocytes termed T-helper-2 (Th2) cells. It is an 18.5 ku cytokine with a broad immunoregulatory activity. It plays the role of a Th2 cell-derived cytokine, and is produced by several cell types, including monocytes, macrophages, T lymphocytes, B cells, dendritic cells, mast cells and various tumour cell lines. Its main biological functions seem to limit and terminate the

inflammatory responses, block the proinflammatory cytokine secretion and regulate the differentiation and proliferation of several immune cells such as T cells, B cells, natural killer cells, antigen-presenting cells, mast cells, and granulocytes^[9]. IL-10 acts on specific IL-10 receptors that have now been cloned, although the signal transduction pathways and kinases that lead to the widespread anti-inflammatory actions of this cytokine are not yet well understood.

Human IL-10 binds as a 2-fold symmetric homodimer to a functional tetrameric complex of two receptors^[10], consisting of two α - or R1 chains which bind to IL-10, and of two CRF2-4 chains (β - or R2) which initiate the IL-10-induced signal transduction events. CRF2-4 is a member of the class II cytokine receptor family (CRF2), which includes the IFN receptors and is encoded by the CRFB4 gene on chromosome 21^[11]. IL-10R generates its signals through the JAK1-STAT3 pathway and activates the SOCS-3 gene (suppressor of cytokine signalling-3) of which the expression results in inhibition of JAK/STAT-dependent signalling and the expression of many genes in the cells^[12]. Some of the actions of IL-10 can be explained by an inhibitory effect on the transcription factor nuclear factor- κ B (NF- κ B), but this does not account for all effects as IL-10 is very effective on inhibiting IL-5 transcription which is independent of NF- κ B^[13].

The immunoregulatory activity of IL-10 is based upon its ability to inhibit both cytokine synthesis and antigen presentation. IL-10 inhibits the synthesis of proinflammatory cytokines (IL-1 β , TNF- α , IL-6), and the Th2 cell-derived cytokines (IL-4 and IL-5)^[13]. IL-10 also inhibits chemokines such as monocyte inflammatory protein-1 α (MIP-1 α), RANTES, IL-8 and eotaxin^[14], as well as the expression of inflammatory enzymes inducible nitric oxide synthase (iNOS) and cyclooxygenase (COX-2) in macrophages, the proliferation of CD4⁺ T lymphocytes by inhibiting IL-2 release and reducing expression of major histocompatibility complex (MHC) class II molecules and the costimulatory molecules B7-1, B7-2, and low-affinity IgE receptors (CD23) in antigen-presenting cells, thus effectively blocking allergen presentation by mononuclear cells and dendritic cells to T cells. In addition, IL-10 also increases the expression of several anti-inflammatory proteins, including IL-1 receptor antagonist, soluble TNF- α receptor and tissue inhibitor of matrix metalloproteinases. Although many of the inhibitory effects of IL-10 on T lymphocytes are secondary to this reduction in monocyte-derived pro-inflammatory cytokines, it also has a direct regulatory effect on T-cell differentiation and proliferation by inhibiting IL-2 and IFN- γ release from activated T-cell clones^[15].

However, the biology of IL-10 is highly complex. In addition to the down-regulation of immunity, both human IL-10 and murine IL-10 exert immunostimulatory effects by up-regulating MHC class II expression on B lymphocytes, and inducing cytotoxic T-cell differentiation. To complicate the issue, there is strong homology in the complementary DNA of human and murine IL-10 with an open reading frame sequence in the Epstein-Barr virus (human herpes virus type 4) genome, termed viral IL-10. Whereas viral IL-10 shares many of the immunoregulatory properties of human IL-10, it lacks immunostimulatory effects.

IL-10 THERAPY FOR IBD

Recombinant IL-10

The therapeutic experience of IL-10 in animal models of colitis is very encouraging. *In vitro* studies have shown that exogenous IL-10 can down-regulate the enhanced pro-inflammatory cytokine release from lamina propria mononuclear cells isolated from patients with Crohn's disease. Early clinical studies in untreated, as well as steroid-refractory Crohn's disease

patients, suggested that IL-10 might have strong potential in the treatment of human diseases. Colombel *et al*^[16] performed a double blind controlled trial to evaluate the safety and tolerance of recombinant human interleukin 10 (IL-10, Tenovil) in subjects operated on for Crohn's disease. Tenovil treatment for 12 consecutive weeks in patients with Crohn's disease after intestinal resection was safe and well tolerated. No evidence of prevention of endoscopic recurrence of Crohn's disease by Tenovil was observed.

Unfortunately, this enthusiasm was dampened by the results of 2 multinational multicenter studies reporting the efficacy and safety of daily subcutaneous injections of recombinant human IL-10 (rhuIL-10) in patients with moderately active and steroid-refractory Crohn's disease^[17,18]. Fedorak *et al*^[17] reported a 24-week double-blind placebo controlled study of 95 patients with moderately active Crohn's disease randomized to receive subcutaneous rhuIL-10 at 1 of 4 doses (rhuIL-10: 1, 5, 10, or 20 μ g/kg) or placebo daily. After a 28-day treatment period, a modest response was seen in the group receiving the 5 μ g/kg dose, whereby 23.5% of patients ($n=17$) showed improvement compared with 0% of patients treated with placebo ($n=23$). Interestingly, higher doses were less effective, although there was no difference in reported adverse events between doses. During the course of a 20-week follow-up period, disease recurrence requiring therapeutic intervention occurred in 70% of placebo-treated patients compared to 55% of the rhuIL-10-treated group^[17].

In the study by Schreiber *et al*^[18] involving 329 therapy refractory patients with active Crohn's disease, no significant differences in the induction of clinical remission were seen between placebo and rhuIL-10 at any dose (1, 4, 8, and 20 μ g/kg), although clinical improvement was achieved in 46% of patients in the 8 μ g/kg group compared with 27% of patients receiving placebo ($P=0.03$). The authors also determined the nuclear levels of transcription factor NF- κ B p65 and cytoplasmic concentrations of its inhibitor I κ B α in ileocolonic biopsy specimens. They noticed significant differences between patients who responded to rhuIL-10 treatment and those who did not, implicating the inhibition of NF- κ B nuclear translocation as one possible mechanism of the action of this therapy^[18].

Recent studies linking high systemic concentrations of IL-10 with headache, fever^[19], and anemia^[20] have further aroused the enthusiasm for IL-10 as a therapeutic drug in treatment of IBD. Indeed, the biology of IL-10 is complex. In addition to its effects in down-regulating pro-inflammatory events, IL-10 has been shown to exert immunostimulatory effects by up-regulating MHC II expression on B lymphocytes and inducing cytotoxic T-cell differentiation. Clinical data support these immunostimulatory effects of IL-10 at high systemic doses. Tilg *et al*^[19] reported that patients with Crohn's disease receiving rhIL-10 at high doses experienced a significant increase in serum neopterin and phytohaemagglutinin (PHA) induced IFN- γ production from whole blood cells. This phenomenon may be responsible for the lack of efficacy of high doses of IL-10 in the treatment of Crohn's disease^[19]. In fact, the emerging picture regarding the *in vivo* effects of IL-10 is one of both the anti- and pro-inflammatory effects, depending on the local concentrations of IL-10 achieved, the types of antigens present in the microenvironment, and the activation state of the immune cells in the vicinity. It is possible that high systemic doses of IL-10 alter the balance between its immunoregulatory and immunostimulatory effects, which would explain the bell-shaped curve in therapeutic efficacy reported in the clinical trials. In addition, it is entirely possible that the pharmacodynamics of daily systemic IL-10 administration does not allow for efficient delivery of the cytokine to the local sites of inflammation. The serum half-life of IL-10 is between 1.1 and 2.6 hours, thus, the cytokine may be cleared before

reaching its target.

Treatment by *lactococcus lactis* secreting IL-10

IBD in humans responds to high dose of intravenous interleukin 10, but this cannot be administered orally because stomach acid destroys it. Recently, studies have been published that looked at alternative methods of delivery of IL-10. The first study used the genetically engineered bacterium, *Lactococcus lactis* (*L. lactis*), as a delivery vehicle for IL-10. Steidler *et al*^[21] hypothesised that an oral delivery system that effectively bypassed the stomach might provide a treatment which would cut the dose of IL-10 required and also reduce the risk of systemic side effects. Steidler and his colleagues^[21] have engineered a non-pathogenic bacterium that produces interleukin 10, an anti-inflammatory cytokine that reduces inflammatory colitis. They then established two different mice models of inflammatory bowel disease. In the first model chronic colitis was induced by feeding dextran sulphate sodium to the mice over several weeks. When the recombinant bacteria were introduced into the mice stomachs, they survived the acid environment and released interleukin 10 in the colon. The second mouse model had its interleukin 10 gene knocked out. The resultant mice were shown to develop IBD spontaneously within 8 weeks of life. When the team administered the genetically engineered *L. lactis* to these mice at 3 weeks of age, colitis did not occur in the first place. They showed that daily intragastric administration of IL-10-secreting *L. lactis* caused a 50% reduction in colitis in mice treated with dextran sulfate sodium and prevented the onset of colitis in IL-10(-/-) mice. High serum concentrations of interleukin 10 were not found, despite good uptake by inflamed cells of the gut mucosa. This approach may lead to better methods for cost-effective and long-term management of IBD in humans. Because the genetically engineered bacterium survives stomach acid, the cytokine can be delivered directly to the inflammatory target in the colon. This could reduce the dose needed and any systemic effects.

However, the release of such genetically modified organisms through clinical use raises safety concerns. Steidler *et al*^[22] replaced the thymidylate synthase gene *thyA* of *L. lactis* with a synthetic human IL10 gene to address this problem. This *thyA*-hIL10⁺ *L. lactis* strain produced human IL-10(hIL-10), and when deprived of thymidine or thymine, its viability dropped by several orders of magnitude, essentially preventing its accumulation in the environment. The biological containment system and the bacterium's capacity of secreting hIL-10 were validated *in vivo* in pigs. This approach is a promising one for transgene containment because, in the unlikely event that the engineered *L. lactis* strains acquired an intact *thyA* gene from a donor such as *L. lactis* subsp. *cremoris*, the transgene would be eliminated from the genome.

Two technical hitches must be ironed out, however, before human trials can be considered. Human interleukin 10 is slightly different from murine interleukin 10, so the *L. lactis* has to be re-engineered. The second obstacle is that human bile is stronger than mouse bile and is likely to kill the bacteria as they pass through the stomach and duodenum^[23].

Gelatine microspheres containing interleukin-10

IL-10 is an anti-inflammatory cytokine that suppresses the T helper 1 immune response and down-regulates macrophages and monocytes. The therapeutic effect of systemic administration of IL-10 for patients with IBD, however, has not been satisfactory. Several studies have indicated that active monocytes, such as macrophages and T cells, play an important role in the pathogenesis of chronic human IBD, although the etiology remains unclear. Manipulation of these cells appears essential for the treatment of patients with IBD. Recently,

considerable attention has been paid to the use of polymer microspheres for the sustained release of various drugs and the targeting of therapeutic agents to their sites of action.

Nakase *et al*^[24,25] developed gelatine microspheres(GM) containing IL-10(GM-IL-10), which can be released sustainably to a local site without losing bioactivity. They administered these microspheres to IL-10 knocked out mice rectally to investigate whether this treatment could ameliorate colitis. Colonic inflammation in mice treated with GM-IL-10 was remarkably reduced compared to those treated with IL-10 alone. Macroscopic and microscopic examination revealed marked improvement of colitis in IL-10(-/-) mice treated with GM-IL-10. mRNA expression of IL-12 in Mac-1-positive cells in GM-IL-10-treated mice was significantly decreased compared with that in the mice treated with IL-10 alone. CD40 expression in Mac-1-positive cells in GM-IL-10-treated mice was decreased more prominently than that in mice treated with IL-10 alone. The therapeutic effects of GM-IL-10 were associated with decreased expression of IL-12 mRNA and down-regulation of CD40 expression in Mac-1-positive cells. Additionally, intestinal administration of these microspheres significantly improved colitis with a decrease in histological score, myeloperoxidase activity, and nitric oxide production compared with those treated with free agents. Gene expressions of TNF- α , IL-1 β , and IFN- γ were down-regulated in treated animals. Serum IL-10 levels and systemic macrophages were unchanged after treatment^[26].

These data suggest that local macrophages in the intestine play a critical role in the initiation of chronic colitis in the animal model of IBD. A drug delivery system using these microspheres containing immunomodulatory IL-10(GM-IL-10) might be useful for treatment of patients with IBD.

Gene therapy

IL-10 is an endogenous anti-inflammatory and immunomodulatory cytokine that has been shown to prevent inflammation and injury in several animal studies, however clinical IL-10 treatment remains insufficient because of difficulties in the route of IL-10 administration and its biological half-life. It may be possible to use replication-deficient adenoviral vectors to deliver the IL-10 gene directly to gastrointestinal epithelial cells. This would lead to localized high level IL-10 release for a short duration that is determined by the lifetime of the infected cells. IL-10 adenoviral gene therapy has proved very successful in murine models of rheumatoid arthritis^[27], a condition with many immunological similarities to Crohn's disease. Previous studies have demonstrated that adenoviral vectors, when delivered by rectal infusion, could infect intestinal epithelial cells^[28]. This approach may be limited by the host anti-adenoviral immune response, that has limited gene expression and prevented re-treatment with other adenoviral vectors^[29]. However, there is evidence that the delivery of immunoregulatory genes, such as IL-10, would diminish both the cell-mediated and humoral anti-adenoviral responses^[30,31].

Barbara *et al*^[32] reported that gene transfer was achieved by intraperitoneal injection of non-replicating human type 5 adenovirus bearing IL-10 gene, either 24 hours before or one hour after intrarectal administration of dinitrobenzene sulphonic acid in rats. Colonic damage and inflammation were assessed macroscopically and by measuring the myeloperoxidase activity and leukotriene B4 concentrations. Gene transfer increased IL-10 protein in serum for up to six days. IL-10 gene transfer prior to colitis improved colitis macroscopically and histologically, and significantly reduced colonic myeloperoxidase activity and leukotriene B4 concentrations. In contrast, IL-10 gene transfer after the onset of colitis had no beneficial effect. Lindsay *et al*^[33] showed that local adenoviral vectors encoding IL-10 (AdvmuIL-10) reverse

colitis in IL-10^{-/-} mice without systemic effects seen after intravenous administration.

Enhanced expression of MAdCAM-1 (mucosal addressin cell adhesion molecule-1) is associated with the onset and progression of IBD. Sasaki *et al.*^[34] reported transfection of the IL-10 vector into endothelial cell cultures significantly reduced TNF- α induction, MAdCAM-1 dependent lymphocyte adhesion (compared to non-transfected cells). IL-10 transfected endothelial cells expressed less than half (46 \pm 6.6%) of the MAdCAM-1 induced by TNF- α (set as 100%) in non-transfected (control) cells.

These results suggest that gene therapy strategies using plasmid IL-10 vectors or an adenovirus-IL-10 construct may prove to be a potent approach to the treatment of chronic inflammatory diseases such as Crohn's disease.

Combining regulatory T cells and IL-10

T cells, and in particular, regulatory T (Treg) cells, play a pivotal role in the control of intestinal inflammation^[35,36]. Regulatory cells lacking anti-inflammatory cytokine IL-10 were unable to inhibit IBD, showing that IL-10 was required for the protective effects of lymphocytes in this setting^[37].

van Montfrans *et al.*^[38,39] presented a novel method of IL-10 delivery to intestinal mucosal tissue by the use of transduced T cells. In these studies, the authors demonstrated that T lymphocytes could be engineered by retrovirus construct transduction to express high levels of IL-10 upon activation. With the goal of providing long-term therapy for Crohn's disease, peripheral blood mononuclear cells were obtained from healthy adults and transduced with a retroviral vector containing IL-10 and green fluorescent protein (GFP). These CD4⁺ T lymphocytes responded to CD3/CD28 stimulation with a 6-fold increase in IL-10 production that was shown to be biologically active. Transduced cells had high expressions of the mucosal integrin α 4 β 7, and displayed efficient binding to MAdCAM-1 expressing cells *in vivo*, suggesting that they would home to gut mucosa. Importantly, albeit *in vitro*, cells remained stably transfected for up to 4 months. In the classic CD45RB^{high} model, these IL-10 transduced CD4⁺ cells were able to effectively prevent the development of colitis, even when given up 14 days after the transfer of the CD45RB^{high} cells. Although circulating levels of IL-10 were not detectable, IL-10-GFP encoding messenger RNA was detected in colons of mice 15 weeks after cell transfer, and IL-10 was detected in the intestinal draining lymph nodes, spleen, and colon, indicating that the IL-10-GFP transduced CD4⁺ cells persisted *in vivo* and migrated into the large intestine. The mice receiving IL-10 transduced CD4⁺ cells exhibited a decrease in the production of TNF- α in the colon and a decreased production of IFN- γ and/or TNF- α in the intestinal draining lymph nodes. These results indicate that the transferred CD4⁺ cells are stimulated *in vivo* and therapeutically effective.

One of the advantages of using T cells as delivery vehicles is the likelihood that the cytokine of interest, in this case, IL-10, would primarily be released only on activation in local sites of inflammation, which would avoid the side effects known to be associated with high systemic levels and may further induce the development of immune-suppressor Treg cells in the area of inflammation. Secondly, the use of *ex vivo* transduction methodology would prevent systemic exposure to the retroviral vector, but still ensure sustained gene expression. However, the question remains, will even local delivery of IL-10 be effective in patients with IBD? IL-10 certainly exhibits potent inhibitory effect on the activation and effector functions of T cells, monocytes, and dendritic cells, all of which are key players in intestinal inflammation. However, the colon from a patient with Crohn's disease already secreted higher levels of IL-10 compared with control colons^[40] and mononuclear cells

isolated from the ileum of patients with Crohn's disease appeared to be nonresponsive to IL-10^[41]. These findings suggest that even if IL-10 is delivered directly to the intestinal mucosa, it may not be therapeutic in Crohn's disease. This is mirrored by effects both in the IL-10 gene-deficient mouse chronic colitis model and in the dinitrobenzene sulphonic acute model of colitis^[42] where IL-10 is able to prevent the development of colitis if given before inflammation develops, but is ineffective if given either exogenously or via gene transfer, once inflammation has become established. However, although IL-10 therapy may be ineffectual in treating active diseases, there may still exist a role for such therapy as maintenance treatment in Crohn's disease. Low ileal IL-10 concentrations have been shown to predict relapse after ileocecal resection^[43]. In addition, it may be that only certain subgroups of Crohn's disease patients respond to IL-10 therapy, whether it is delivered systemically or locally. It is clear that even among patients with similar clinical presentations, there exists a large diversity of patterns of immune responses to environmental and bacterial antigens^[44]. It is not known how patients with these types of immune reactivities respond to different therapies.

CONCLUSION AND PERSPECTIVES

IL-10 is a pivotal cytokine in the control of intestinal inflammation. Several clinical trials^[45] have demonstrated that daily systemic rhuIL-10 injections were safe and well tolerated with modest efficacy in Crohn's disease, but clinical trials with rhuIL-10 in Crohn's disease were disappointing, although some patients showed healing of intestinal mucosa. With the administered dose of IL-10 in the clinical trials, the ultimate local IL-10 concentrations in the intestine could be too low to result in downregulation of inflammation. Furthermore, higher doses of systemically administered IL-10 (which were also used in the clinical trials) might be detrimental rather than helpful^[46]. But it is possible that response to IL-10 is limited to a subgroup of patients, and perhaps delivering the IL-10 in a more sustained and focused manner would prove to be effective. These may be the several reasons why this is not the end of the road for rhuIL-10 therapy in Crohn's disease^[29]. Recently, some novel alternative approaches, including the use of genetically modified *Lactococcus lactis*, gelatine microsphere containing IL-10, adenoviral vectors encoding IL-10 and combining regulatory T cells, may ensure that delivery of IL-10 is indeed local, tissue-specific, and therapeutic. These therapeutic approaches caused a significant reduction in intestinal inflammation in different mouse models, and they might be useful for treatment of human IBD. However, there is still a long way to go until these approaches can be evaluated in clinical studies.

New mammalian genes that encode IL-10-related cytokines have been described as the result of experiments using cDNA subtraction cloning focusing on melanocyte differentiation (*IL24*)^[47], virus-induced T-cell transformation (*IL26*)^[48] or IL-9-mediated gene induction (*IL22*)^[49]. The sequencing and annotation of the human genome could lead to the identification of five additional IFN- or IL-10-related genes^[50-53]: *IL19*, *IL20*, *IL28A* (also known as *IFN12*), *IL28B* (also known as *IFN13*) and *IL29* (also known as *IFN11*). Similar to IL-10, these IL-10-related cytokines are α -helical proteins with similar cysteine localizations, whose amino acid sequences are about 20-30% identical. IL-19, IL-20, IL-22, IL-24, IL-26, IL-28A, IL-28B and IL-29 are grouped together on the basis of structural homologies, indicating that these genes are derived from common ancestors^[54]. All these new IL-10 supfamily member cytokines are strongly involved in immune regulation and inflammatory response, further studies will provide a better understanding of potential therapeutic utilities, some of them

may reduce adverse side effects and/or increase the efficacy typically seen in IL-10 therapy for IBD in the future.

REFERENCES

- Rampton DS, Phil D. New treatments for inflammatory bowel disease. *World J Gastroenterol* 1998; **4**: 369-376
- Sandborn WJ, Targan SR. Biologic therapy of inflammatory bowel disease. *Gastroenterology* 2002; **122**: 1592-1608
- Strober W, Fuss IJ, Blumberg RS. Immunology of mucosal models of inflammation. *Ann Rev Immunol* 2002; **20**: 495-549
- Landers CJ, Cohavy O, Misra R, Yang H, Lin Y, Braun J, Targan SR. Selected loss of tolerance evidenced by Crohn's disease-associated immune responses to auto and microbial antigens. *Gastroenterology* 2002; **123**: 689-699
- Madsen K. Combining T cells and IL-10: A new therapy for Crohn's disease? *Gastroenterology* 2002; **123**: 2140-2144
- Das KM, Farag SA. Current medical therapy of inflammatory bowel disease. *World J Gastroenterol* 2000; **6**: 483-489
- Ishizuka K, Sugimura K, Homma T, Matsuzawa J, Mochizuki T, Kobayashi M, Suzuki K, Otsuka K, Tashiro K, Yamaguchi O, Asakura H. Influence of interleukin-10 on the interleukin-1 receptor antagonist/interleukin-1 beta ratio in the colonic mucosa of ulcerative colitis. *Digestion* 2001; **63**: 22-27
- Rennick DM, Fort MM. Lessons from genetically engineered animal models. XII. IL-10-deficient (IL-10^{-/-}) mice and intestinal inflammation. *Am J Physiol Gastrointest Liver Physiol* 2000; **278**: G829-833
- Asadullah K, Sterry W, Volk HD. Interleukin-10 Therapy—Review of a New Approach. *Pharmacol Rev* 2003; **55**: 241-269
- Donnelly RP, Dickensheets H, Finbloom DS. The interleukin-10 signal transduction pathway and regulation of gene expression in mononuclear phagocytes. *J Interferon Cytokine Res* 1999; **19**: 563-573
- Reboul J, Gardiner K, Monneron D, Uze G, Lutfalla G. Comparative genomic analysis of the interferon/interleukin-10 receptor gene cluster. *Genome Res* 1999; **9**: 242-250
- Riley JK, Takeda K, Akira S, Schreiber RD. Interleukin-10 receptor signaling through the JAK-STAT pathway. Requirement for two distinct receptor-derived signals for anti-inflammatory action. *J Biol Chem* 1999; **274**: 16513-16521
- Staples KJ, Bergmann M, Barnes PJ, Newton R. Stimulus-specific inhibition of IL-5 by cAMP-elevating agents and IL-10 reveals differential mechanisms of action. *Biochem Biophys Res Commun* 2000; **273**: 811-815
- Chung KF, Patel HJ, Fadlon EJ, Rousell J, Haddad EB, Jose PJ, Mitchell J, Belvisi M. Induction of eotaxin expression and release from human airway smooth muscle cells by IL-1 β and TNF- α : effects of IL-10 and corticosteroids. *Br J Pharmacol* 1999; **127**: 1145-1150
- Ebert EC. IL-10 enhances IL-2-induced proliferation and cytotoxicity by human intestinal lymphocytes. *Clin Exp Immunol* 2000; **119**: 426-432
- Colombel JF, Rutgeerts P, Malchow H, Jacyna M, Nielsen OH, Rask-Madsen J, Van Deventer S, Ferguson A, Desreumaux P, Forbes A, Geboes K, Melani L, Cohard M. Interleukin 10 (Tenovil) in the prevention of postoperative recurrence of Crohn's disease. *Gut* 2001; **49**: 42-46
- Fedorak RN, Gangl A, Elson CO, Rutgeerts P, Schreiber S, Wild G, Hanaver SB, Kilian A, Cohard M, Le Beaut A, Feagan B. Recombinant human interleukin 10 in the treatment of patients with mild to moderately active Crohn's disease. *Gastroenterology* 2000; **119**: 1473-1482
- Schreiber S, Fedorak RN, Nielsen OG, Wild G, Williams CN, Nikolaus S, Jacyna M, Lashner BA, Gangl A, Rutgeerts P, Isaacs K, van Deventer SJ, Koningsberger JC, Cohard M, Le Beaut A, Hanaver SB. Safety and efficacy of recombinant human interleukin 10 in chronic active Crohn's disease. *Gastroenterology* 2000; **119**: 1461-1472
- Tilg H, van Montfrans C, van den Ende A, Kaser A, van Deventer SJ, Schreiber S, Gregor M, Ludwiczek O, Rutgeerts P, Gasche C, Koningsberger JC, Abreu L, Kuhn I, Cohard M, Le Beaut A, Grnt P, Weiss G. Treatment of Crohn's disease with recombinant human interleukin 10 induces the proinflammatory cytokine interferon gamma. *Gut* 2002; **50**: 191-195
- Tilg H, Ulmer H, Kaser A, Weiss G. Role of IL-10 for induction of anemia during inflammation. *J Immunol* 2002; **169**: 2204-2209
- Steidler L, Hans W, Schotte L, Neiryck S, Obermeier F, Falk W, Fiers W, Remaut E. Treatment of murine colitis by Lactococcus lactis secreting interleukin-10. *Science* 2000; **289**: 1352-1355
- Steidler L, Neiryck S, Huyghebaert N, Snoeck V, Vermeire A, Goddeeris B, Cox E, Remon JP, Remaut E. Biological containment of genetically modified Lactococcus lactis for intestinal delivery of human interleukin 10. *Nat Biotechnol* 2003; **21**: 785-789
- Michie C. Germ therapy with IL-10 to treat inflammatory bowel diseases. *Mol Med Today* 2000; **6**: 416
- Nakase H, Okazaki K, Tabata Y, Ozeki M, Watanabe N, Ohana M, Uose S, Uchida K, Nishi T, Mastuura M, Tamaki H, Itoh T, Kawanami C, Chiba T. New cytokine delivery system using gelatin microspheres containing interleukin-10 for experimental inflammatory bowel disease. *J Pharmacol Exp Ther* 2002; **301**: 59-65
- Nakase H, Okazaki K, Tabata Y, Chiba T. Biodegradable microspheres targeting mucosal immune-regulating cells: new approach for treatment of inflammatory bowel disease. *J Gastroenterol* 2003; **38**: 59-62
- Okazaki K, Nakase H, Watanabe N, Tabata Y, Ikada Y, Chiba T. Intestinal drug delivery systems with biodegradable microspheres targeting mucosal immune-regulating cells for chronic inflammatory colitis. *J Gastroenterol* 2002; **37**: 44-52
- Whalen JD, Lechman EL, Carlos CA, Weiss K, Kovessi I, Glorioso JC, Robbins PD, Evans CH. Adenoviral transfer of the viral IL-10 gene periarticularly to mouse paws suppresses development of collagen-induced arthritis in both injected and uninjected paws. *J Immunol* 1999; **162**: 3625-3632
- Wirtz S, Galle PR, Neurath MF. Efficient gene delivery to the inflamed colon by local administration of recombinant adenoviruses with normal or modified fibre structure. *Gut* 1999; **44**: 800-807
- Lindsay JO, Hodgson H. The immunoregulatory cytokine interleukin-10—a therapy for Crohn's disease? *Aliment Pharmacol Ther* 2001; **15**: 1709-1716
- Minter RM, Rectenwald JE, Fukuzuka K, Tannahill CL, La Face D, Tsai V, Ahmed I, Hutchins E, Moyer R, Copeland EM 3rd, Moldawer LL. TNF-alpha receptor signaling and IL-10 gene therapy regulate the innate and humoral immune responses to recombinant adenovirus in the lung. *J Immunol* 2000; **164**: 443-451
- Chirmule N, Truneh A, Haecker SE, Tazelaar J, Gao G, Raper SE, Hughes JV, Wilson JM. Repeated administration of adenoviral vectors in lungs of human CD4 transgenic mice treated with a nondepleting CD4 antibody. *J Immunol* 1999; **163**: 448-455
- Barbara G, Xing Z, Hogaboam CM, Gauldie J, Collins SM. Interleukin 10 gene transfer prevents experimental colitis in rats. *Gut* 2000; **46**: 344-349
- Lindsay JO, Ciesielski CJ, Scheinin T, Brennan FM, Hodgson HJ. Local delivery of adenoviral vectors encoding murine interleukin 10 induces colonic interleukin 10 production and is therapeutic for murine colitis. *Gut* 2003; **52**: 363-369
- Sasaki M, Jordan P, Houghton J, Meng X, Itoh M, Joh T, Alexander JS. Transfection of IL-10 expression vectors into endothelial cultures attenuates alpha4beta7-dependent lymphocyte adhesion mediated by MAdCAM-1. *BMC Gastroenterol* 2003; **3**: 3
- Singh B, Read S, Asseman C, Malmstrom V, Mottet C, Stephens LA, Stepankova R, Tlaskalova H, Powrie F. Control of intestinal inflammation by regulatory T cells. *Immunol Rev* 2001; **182**: 190-200
- Roncarolo MG, Bacchetta R, Bordignon C, Narula S, Levings MK. Type 1 T regulatory cells. *Immunol Rev* 2001; **182**: 68-79
- Groux H, Powrie F. Regulatory T cells and inflammatory bowel disease. *Immunol Today* 1999; **20**: 442-445
- Van Montfrans C, Hooijberg E, Rodriguez Pena M, de Jong E, Spits H, te Velde A, van Deventer SJH. Generation of regulatory gut-homing human T lymphocytes using *ex vivo* interleukin 10 gene transfer. *Gastroenterology* 2002; **123**: 1877-1888
- Van Montfrans C, Rodriguez Pena M, Pronk I, ten Kate FJW, te Velde AA, van Deventer SJH. Prevention of colitis by interleukin-10 transduced T lymphocytes in the transfer model. *Gastroenterology* 2002; **123**: 1865-1876
- Lindsay JO, Feldmann M, Hodgson H, Brennan F. The immunoregulatory role of interleukin-10 in Crohn's disease (CD)

- cell cultures. *Gastroenterology* 2000; **118**: A110
- 41 **Colpaert S**, Vanstraelen K, Liu Z, Penninckx F, Geboes K, Rutgeerts P, Ceuppens J. Decreased lamina propria effector cell responsiveness to interleukin-10 in ileal Crohn's disease. *Clin Immunol* 2002; **102**: 68-76
- 42 **Barbara G**, Xing Z, Hogaboam CM, Gaultie J, Collins SM. Interleukin 10 gene transfer prevents experimental colitis in rats. *Gut* 2000; **46**: 344-349
- 43 **Meresse B**, Rutgeerts P, Malchow H, Dubucquoi S, Dessaint JP, Cohard M, Colombel JF, Desreumaux P. Low ileal interleukin 10 concentrations are predictive of endoscopic recurrence in patients with Crohn's disease. *Gut* 2002; **50**: 25-28
- 44 **Landers CJ**, Cohavy O, Misra R, Yang H, Lin Y, Braun J, Targan SR. Selected loss of tolerance evidenced by Crohn's disease-associated immune responses to auto and microbial antigens. *Gastroenterology* 2002; **123**: 689-699
- 45 **Bickston SJ**, Cominelli F. Recombinant interleukin 10 for the treatment of active Crohn's disease: lessons in biologic therapy. *Gastroenterology* 2000; **119**: 1781-1783
- 46 **Herfarth H**, Scholmerich J. IL-10 therapy in Crohn's disease: at the crossroads. Treatment of Crohn's disease with the anti-inflammatory cytokine interleukin 10. *Gut* 2002; **50**: 146-147
- 47 **Jiang H**, Lin JJ, Su ZZ, Goldstein NI, Fisher PB. Subtraction hybridization identifies a novel melanoma differentiation associated gene, mda-7, modulated during human melanoma differentiation, growth and progression. *Oncogene* 1995; **11**: 2477-2486
- 48 **Knappe A**, Hor S, Wittmann S, Fickenscher H. Induction of a novel cellular homolog of interleukin-10, AK155, by transformation of T lymphocytes with herpesvirus saimiri. *J Virol* 2000; **74**: 3881-3887
- 49 **Dumoutier L**, Louahed J, Renaud JC. Cloning and characterization of IL-10-related T cell-derived inducible factor (IL-TIF), a novel cytokine structurally related to IL-10 and inducible by IL-9. *J Immunol* 2000; **164**: 1814-1819
- 50 **Gallagher G**, Dickensheets H, Eskdale J, Izotova LS, Mirochnitchenko OV, Peat JD, Vazquez N, Pestka S, Donnelly RP, Kotenko SV. Cloning, expression and initial characterization of interleukin-19 (IL-19), a novel homologue of human interleukin-10 (IL-10). *Genes Immun* 2000; **1**: 442-450
- 51 **Blumberg H**, Conklin D, Xu WF, Grossmann A, Brender T, Carollo S, Eagan M, Foster D, Haldeman BA, Hammond A, Haugen H, Jelinek L, Kelly JD, Madden K, Maurer MF, Parrish-Novak J, Prunkard D, Sexson S, Sprecher C, Waggie K, West J, Whitmore TE, Yao L, Kuechle MK, Dale BA, Chandrasekhar YA. Interleukin 20: discovery, receptor identification, and role in epidermal function. *Cell* 2001; **104**: 9-19
- 52 **Sheppard P**, Kindsvogel W, Xu W, Henderson K, Schlutsmeyer S, Whitmore TE, Kuestner R, Garrigues U, Birks C, Roraback J, Ostrand C, Dong D, Shin J, Presnell S, Fox B, Haldeman B, Cooper E, Taft D, Gilbert T, Grant FJ, Tackett M, Krivan W, McKnight G, Clegg C, Foster D, Klucher KM. IL-28, IL-29 and their class II cytokine receptor IL-28R. *Nature Immunol* 2003; **4**: 63-68
- 53 **Kotenko SV**, Gallagher G, Baurin VV, Lewis-Antes A, Shen M, Shah NK, Langer JA, Sheikh F, Dickensheets H, Donnelly RP. IFN- λ s mediate antiviral protection through a distinct class II cytokine receptor complex. *Nature Immunol* 2003; **4**: 69-77
- 54 **Renaud JC**. Class II cytokine receptors and their ligands: key antiviral and inflammatory modulators. *Nat Rev Immunol* 2003; **3**: 667-676

Edited by Wang XL Proofread by Zhu LH

Long-term effect on carcinoma of esophagus of distal subtotal gastrectomy

Yu-Ping Chen, Jie-Sheng Yang, Di-Tian Liu, Yu-Quan Chen, Wei-Ping Yang

Yu-Ping Chen, Jie-Sheng Yang, Di-Tian Liu, Yu-Quan Chen, Wei-Ping Yang, Department of Thoracic Surgery, Tumor Hospital of Shantou University Medical College, Shantou 515031, Guangdong Province, China

Correspondence to: Dr. Yu-Ping Chen, Department of Thoracic Surgery, Tumor Hospital of Shantou University Medical College, Shantou 515031, Guangdong Province, China. chenyp@pub.shantou.gd.cn

Telephone: +86-754-8630899 **Fax:** +86-754-8630899

Received: 2003-05-13 **Accepted:** 2003-06-02

Abstract

AIM: To investigate the surgical treatment and long-term survival for patients with carcinoma of esophagus after distal subtotal gastrectomy.

METHODS: Resections of the tumor through left thoracotomy were performed in 85 patients with esophageal carcinoma following distal subtotal gastrectomy. The procedure involved preserving the left short gastric artery and transporting the residual stomach, the spleen and tail of the pancreas into the left thoracic cavity, and using the residual stomach to reconstruct the alimentary tract.

RESULTS: The resectable rate was 91.8%, complication rate 10.3%, and no death occurred in the postoperative period. The 1-, 3-, 5-, and 10-year survival rates were 85.7%, 50.7%, 30.6% and 18.8%, respectively.

CONCLUSION: Surgical resection is the optimal management method for the patients with esophageal carcinoma after distal subtotal gastrectomy. The reconstruction of digestive tract using anastomosis of the esophagus and the residual stomach is not only simple but also can achieve a better curative effect, promoting the digestive function and improving the quality of life.

Chen YP, Yang JS, Liu DT, Chen YQ, Yang WP. Long-term effect on carcinoma of esophagus of distal subtotal gastrectomy. *World J Gastroenterol* 2004; 10(5): 626-629 <http://www.wjgnet.com/1007-9327/10/626.asp>

INTRODUCTION

The primary management of esophageal carcinoma is surgical resection, and the stomach is the organ most often chosen for substitution following removal of esophagus for carcinoma. However, following the resection of esophageal carcinoma after distal subtotal gastrectomy, the replacement of esophagus mostly selected other organs, such as jejunum or colon^[1-11]. Since we first applied this new technique to use the residual stomach in patients all with previous distal subtotal gastrectomy in 1982^[12,13], we have treated 85 patients by such approach, and will report it as follows.

MATERIALS AND METHODS

Clinical data

There were 74 men and 11 women with age ranging from 34

to 78 years (mean 60.3 years). The interval between the time of subtotal gastrectomy and the time when the patients were diagnosed having carcinoma of esophagus ranged from 7 to 29 years, averaging 15 years. According to the procedures of subtotal gastrectomy, two cases were classified as Billroth I type, 83 cases Billroth II type, including 27 cases undergoing gastrectomy posterior to colon, and 58 cases anterior to colon. The digestive functions in all of the patients were approximately normal. All the patients presented with the symptoms of dysphagia to some degree with only 42.4% (36/85) being able to take semi-fluid diet. The average body weight of the patients was 47.7±10.2 kg. With regard to the classification of Performance Status, 30.6% (26/85) patients belonged to class 0-1, and 69.4% (59/85) to class 2-4.

In terms of the location of the tumor, 4 cases were localized in upper thoracic esophagus, 62 cases in mid thoracic, and 19 cases in lower thoracic. With regard to gross type, 60 patients belonged to medullary type, 15 ulcerative type, six constrictive type, three fungating type and one intraluminal type. All of cases received barium meal examination of gastrointestinal tract to measure the maximal diameter of residual stomach that was from the fundus to the gastrojejunal anastomosis, and no lesion was found in the residual stomach. The diameter ranged from 5 cm to 9.2 cm, mean 7.9 cm. Forty-three cases in this group were further examined by fiber-gastroscopy, which revealed nothing pathological in their residual stomachs.

All the patients underwent the resection of involved portion esophagus through left thoracotomy under the intratracheal anesthesia, except for 7 cases being found to have unresectable tumors, in which 5 cases had the local tumors infiltrating the aortic arch or / and bronchus, and two cases were found to be accompanied with metastasis of liver and extensive spread of intra-abdominal cavity.

Seventy-eight cases underwent the resection of the carcinoma of esophagus with a resectability rate of 91.8% (78/85), including 64 cases for radical resection and 14 cases for palliative resection. As for length of the involved segment of esophagus, 21 cases were shorter than 3 cm, 17 cases ranged from 3-5 cm, and 40 cases longer than 5 cm. The maximal diameters of residual stomachs measured from the fundus to the gastrojejunal anastomosis, ranged from 6 cm to 11.3 cm, mean 9.1 cm which was in contrast to X-ray examination. According to the location of anastomosis sites, 5 cases were localized in neck, 51 above aortic arch, and 22 below aortic arch. Sixty-five patients were anastomosed by handwork, 13 by mechanical anastomat, including 10 above aortic arch and 3 below aortic arch. During the operation, a silica-gel catheter with a metal guiding core was inserted into the jejunum through nostril for 30 cases^[14]. Those patients were fed with mixed milk or nutritional fluid through the nasal feeding catheter one day after operation. The patients had a meal 5-10 d following operation (mean 7 d). The span of hospitalization ranged from 14 to 52 d (mean 14.6 d).

Procedure of operation

Our approach was through a left thoracotomy incision. The tumor was examined and if it appeared to be resectable, the left diaphragm was opened and the exploration of abdominal

cavity was done. After examining the operative condition of previous subtotal gastrectomy, the spleen, splenic hilus and pancreatic tail were dissociated from the back of peritoneum. Meanwhile, two to four short gastric blood vessels should be preserved to provide adequate blood supply for the residual stomach. The residual stomach, afferent and efferent loops of jejunum were mobilized from peripheral cohesion, and the previous gastrojejunal anastomosis was brought into the left thorax, the afferent loop of jejunum close to gastrojejunal anastomosis was transected and the gastric end was closed. If the part of gastrojejunal anastomosis was removed at the same time, the length of the residual stomach may be prolonged (Figure 1: C). The afferent loop is rejoined to the efferent loop 30 cm below the original gastrojejunostomy (Roux-en-Y method, Figure 2: AA'). The cardia was transected and closed (if mechanical approach was used, the cardia was not closed temporarily, Figure 1: D). The residual stomach, gastrojejunal anastomosis, efferent of jejunum, spleen, tail of pancreas were all transposed into the left thoracic cavity. The esophagus was mobilized and the upper end of esophagus resected 5 cm above the tumor as described in Sweet's esophago-gastrostomy (Figure 2: BB'). If the staple was used, the esophagus was anastomosed to the fundus of the substitution through the cardiac, and the end of cardiac was shut soon after. The splenic ligament was fixed firmly to the thoracic wall to reduce the tension on the esophagogastric anastomosis. If the anastomosis was performed in neck, the fundus of the residual stomach could be brought up into the neck through thoracic cavity or the bed of esophagus. The approach of the operation is represented diagrammatically in Figures 1 and 2. Preoperative and postoperative barium meal examinations, postoperative roentgenogram of chest and field of operation in one of the patients are shown in Figures 3-7.

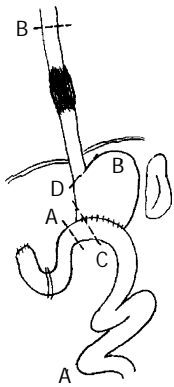


Figure 1 Resection range. **Figure 2** Postoperative situation.

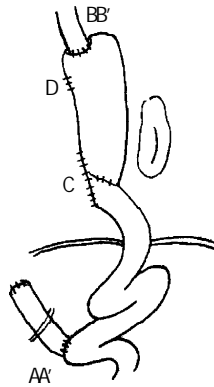


Figure 3 Preoperative barium meal examination, showing mid-thoracic esophageal tumor.



Figure 4 Preoperative barium meal examination, showing residual stomach.

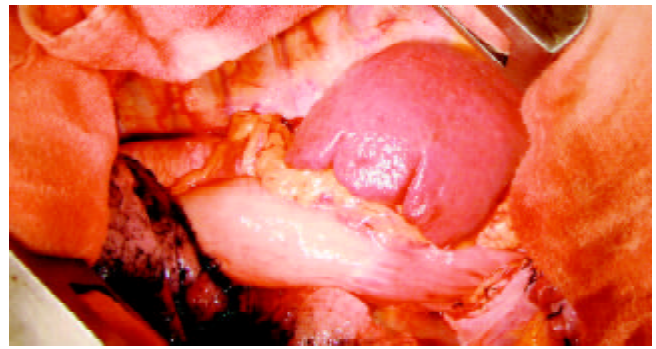


Figure 5 Field of operation, showing the spleen in the left thoracic cavity.



Figure 6 Postoperative roentgenogram of chest, showing the spleen shadow in the left thoracic cavity.

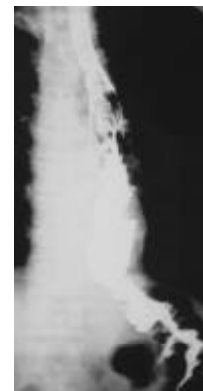


Figure 7 Postoperative barium meal examination, showing the esophagogastric anastomosis above the aortic arch, the residual stomach with previous gastrointestinal anastomosis, and the Roux-en-Y anastomosis.

Follow-up and statistical analysis

All the patients were followed up after operation. The patients failed to be followed up were deemed as death according to the last time they could be contacted. The survival rate was calculated on the basis of Kaplan-Meier procedure by statistical software SPSS10.0. The condition of eating, the body weight and the Performance Status for the patients recruited in our study 3 months after the operation. Enumeration data and measurement data were analyzed by χ^2 and t test, respectively.

RESULTS

Seventy-eight patients received resection of the tumor, including 24 cases having grade I of squamous carcinoma, 47 cases having grade II of squamous carcinoma, 4 cases grade III of squamous carcinoma, 2 cases adenocarcinoma and 1 case

carcinosarcoma. There were two cases having positive resection margins. With regard to lymph node status, 34 patients were complicated with metastasis of lymph node, and 43 patients without. According to UICC1997 PTNM stage, 5 patients were classified as stage I, 30 stage II, and 43 stage III. The complication rate following operation was 10.3% (8/78), with two cases suffering from arrhythmia, two cases having pneumonia and four cases having anastomotic leakage. All these patients with complications were cured through conservative management without operation death. The follow-up rate was 91.0% (71/78), six patients lost contact. The 1, 3, 5, and 10yr survival rate were 85.7%, 50.7%, 30.6% and 18.8%, respectively (Figure 8). The patients undergoing resection could take semi-fluid diet, accounting for 92.3% (72/78). Among all the patients, 84.7% (72/85) could have 300±500 mL volume of semi-fluid diet. The mean body mass was 49.8±8.9 kg. Compared with the previous body mass, 41.0% (32/78) patients got a body weight gain after operation. In term of the grade of Performance Status, 72.9% (62/85) patients had grade 0-1, and 27.1% (23/85) grades 2-4. Apart from the body mass, the difference between the index of quality of life before operation and the comparative index after operation was statistically significant ($P<0.05$).

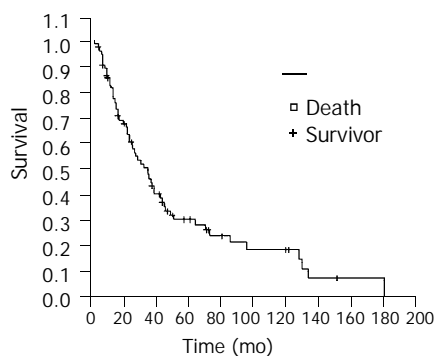


Figure 8 Kaplan-Meier survival curve.

DISCUSSION

Cancer of esophagus in Chaoshan region is prevalent with a high incidence, so are the gastroduodenal diseases, especially the peptic ulcer. Therefore, there are some patients with esophageal carcinoma after subtotal gastrectomy in this area. The incidence rate of these patients was 2.3% (85/3632) compared with the patients with esophageal carcinoma treated surgically in our hospital in the same period, which demonstrates the management of these patients should also be emphasized. The average interval between gastrectomy and diagnosis of esophageal carcinoma was 15 years. The mean age of the patients was 60.3 years, with no significant difference compared with other patients suffering from esophageal carcinoma without subtotal gastrectomy. So it may be suggested the development of carcinoma of esophagus is not obviously correlated with the history of surgical operation of stomach. The relationship between esophageal carcinoma and previous gastrectomy for benign ulcer disease are still not clear^[9,10,15-19].

As for the influence of previous operation, the colon or jejunum is the most popular choice as a substitution in such patients. This approach is complicated and can greatly affect the postoperative quality of life^[13,20,21]. For this reason, some patients were not accessible to resection, but were treated by radiotherapy. When the demand of the resection of esophageal carcinoma was met, the procedure of using the residual stomach to reconstruct the digestive tract, is the best choice, which not only facilitates the recovery of digestive function following operation, but also improves the quality of life in patients with

esophageal carcinoma after previous subtotal gastrectomy. In the process of this procedure, the residual stomach must have sufficient length for lifting, and good blood supply. The blood supply of the residual stomach originated from the short artery. Transferring spleen, tail of pancreas to thoracic cavity can provide the residual stomach with good blood supply, and benefit the lifting length of it. Amputating at the jejunal afferent loop near anastomosis, and making the jejunal Roux-Y anastomosis, fully dissociating the previous operative cohesion could also prolong the lifting length and decrease the lifting tension of the residual stomach. After being fully dissociated, the residual stomach can be lifted up by about 20 cm. Four cases were complicated with anastomotic leakage in the group, including 3 cases with thoracic leakage^[13] occurring during the early application of this technique. The causes of the thoracic leakage might be related to the local infection and suturing skill. The cause of the other case with anastomotic leakage in neck probably was connected with the tension of the residual stomach. Recently, we replaced manual manipulation with mechanical anastomosis, using staple to close the cardiac and the lesser curvature of stomach. This is better for the extension of the residual stomach, reducing the traction and tension of anastomosis. At the early period after operation, the patients were offered nasal feeding nutrition, which was conducive to the rehabilitation and reduction of complications for patients after resection.

So far, there has been no clear report on the benefit of this procedure, which preserves the residual stomach and anastomoses it to esophagus, in terms of the long-term effect and quality of life for the patients with esophageal carcinoma after subtotal gastrectomy^[21-29]. Compared with the management of the other patients with esophageal carcinoma in corresponding period, the difference between the means of operation and the findings of pathology in this group was not significant. The 5- and 10-year survival rates were 30.6% and 18.8% respectively. In comparison of the long-term survival rate of our group and those of the other big groups^[10,30-33], no significant difference could be found. All these demonstrate that such an approach can achieve a good efficacy. The patients were satisfied with their quality of life, and the majority of them could have semi-fluid diet. Over 50% of them had a body mass gain. The grade of Performance Status of them also improved greatly. In conclusion, the above evidences further confirm that in the management of the patients with carcinoma of esophagus after previous subtotal gastrectomy, the technique, which used the residual stomach to reconstruct the alimentary tract, not only accomplished a rather good long-term survival rate, but also improved the quality of patients' life. So it is a simple operative approach with few trauma and good results.

REFERENCES

- Xie ZL**, Zhu KS, Liu SY, Zhang LD. Surgical Treatment of esophageal carcinoma in gastrectomized patients. *Zhongguo Zhongliu Linchuang* 1998; **25**: 570-572
- Zhang YM**, Chi QM, Li ZM, Zhang BJ, Yang RS, Chen JC, Zhang LM, Li DT, Gao HJ. Surgical Treatment of esophageal carcinoma and cardiac carcinoma after gastrectomy: a report of 24 cases. *Zhongliu Fangzhi Zazhi* 1999; **6**: 188-189
- Wei JY**, Chen BJ, Sun M. Surgical mode of esophageal and cardiac carcinoma after gastrectomy. *Jiangshu Yiyao* 1999; **25**: 742-744
- Fu CG**, Gao HC, Cai YJ, Kang JR. Surgical Treatment of esophageal and cardiac cancer after gastrectomy: report of 22 cases. *Fujian Yiyao Zazhi* 2000; **22**: 10-11
- Jia P**, Lin HX. Reconstruction of esophagus with colon by anterior sterna for esophageal cancer after gastrectomy: report of 12 cases. *Xiandai Zhenduan Yu Zhiliao* 1998; **9**: 295
- Xu ZF**, Sun YC, Da ZW, Zhao XW, Chen HQ. Surgical Treatment of primary cardiac and esophageal carcinoma of remnant

- stomach. *Jiefangjun Yixue Zazhi* 1997; **22**: 167-168
- 7 **Ping YM**, Yan JS, Du XQ. Clinical application and technical problems of colonic interposition for esophageal substitution. *Zhonghua Waikē Zazhi* 1994; **32**: 755-756
 - 8 **Takemura M**, Higashino M, Osugi H, Tokuhara T, Kaseno S, Kinoshita H. Surgical treatment of esophageal cancer in four patients after gastrectomy for gastric cancer. *Nippon Kyobu Geka Gakkai Zasshi* 1996; **44**: 89-94
 - 9 **Mafune K**, Tanaka Y, Ma YY, Takubo K. Synchronous cancers of the esophagus and the ampulla of Vater after distal gastrectomy: successful removal of the esophagus, gastric remnant, duodenum, and pancreatic head. *J Surg Oncol* 1995; **60**: 277-281
 - 10 **Tachibana M**, Abe S, Yoshimura H, Suzuki K, Matsuura H, Nagasue N, Nakamura T. Squamous cell carcinoma of the esophagus after partial gastrectomy. *Dysphagia* 1995; **10**: 49-52
 - 11 **Kato H**, Tachimori Y, Watanabe H. Surgical treatment for thoracic esophageal carcinoma in patients after gastrectomy. *J Surg Oncol* 1992; **51**: 94-99
 - 12 **Lu SJ**, Chen JQ, Chen YQ, Yang JS. Surgical operation of esophageal carcinoma after subtotal gastrectomy: esophagogastrostomy. *Aizheng* 1986; **5**: 41-44
 - 13 **Lu SJ**, Chen BX. Operative technique for carcinoma of the esophagus after distal subtotal gastrectomy: a new method using the residual stomach to reconstruct the alimentary tract. *Aust N Z J Surg* 1990; **60**: 719-722
 - 14 **Yang JS**, Yang WP, Chen YP, Chen YQ, Yang XH. Clinical application of silica-gel catheter with a metal guiding core in 43 severe patients. *Zhongguo Weizhongbing Jijiu Yixue* 1995; **7**: 242-243
 - 15 **Hsu NY**, Chen CY, Chen JT, Hsu CP. Oesophageal squamous cell carcinoma after gastrectomy for benign ulcer disease. *Scand J Thorac Cardiovasc Surg* 1996; **30**: 29-33
 - 16 **Caygill CP**, Hill MJ, Kirkham JS, Northfield TC. Oesophageal cancer in gastric surgery patients. *Ital J Gastroenterol* 1993; **25**: 168-170
 - 17 **Caygill CP**, Hill MJ. Malignancy following surgery for benign peptic disease: a review. *Ital J Gastroenterol* 1992; **24**: 218-224
 - 18 **Maeta M**, Koga S, Shimizu T, Matsui K. Possible association between gastrectomy and subsequent development of esophageal cancer. *J Surg Oncol* 1990; **44**: 20-24
 - 19 **Lundegardh G**, Adami HO, Helmick C, Zack M. Risk of cancer following partial gastrectomy for benign ulcer disease. *Br J Surg* 1994; **81**: 1164-1167
 - 20 **Deshmane VH**, Sharma S, Shinde SR, Vyas JJ. Functional results following esophagogastrectomy for carcinoma of the esophagus. *J Surg Oncol* 1992; **50**: 153-155
 - 21 **Guo QX**, Xu JH, Lin JQ, Zheng JF. Surgical Treatment of esophageal carcinoma in patients who had had partial gastrectomy: a report of 30 cases. *Zhongguo Zhongliu Linchuang* 1998; **25**: 573-575
 - 22 **Shu ZD**, Guo XY, Tu YR, Li X, Lin M, Wang Y. Surgical Treatment of the esophageal carcinoma after subtotal gastrectomy: (report of 18 cases). *Zhongguo Shiyong Waikē Zazhi* 2000; **20**: 159-160
 - 23 **Xu M**, Zhang SL, Zhou Y. Improving surgical mode for the carcinoma of mid-lower thoracic esophagus after gastrectomy. *Zhonghua Xiongxinxueguan Waikē Zazhi* 1998; **14**: 265
 - 24 **Wu XY**, Zhang XH, Yin FZ, Lu HS, Guan GX. Clinical study of surgical treatment of esophageal cancer after gastrectomy. *Zhongliu* 1998; **18**: 158-160
 - 25 **Chen J**, Cheng KL, He YG. Treatment of esophageal cancer in post-subtotal gastrectomy with esophagogastrostomy. *Linchuang Waikē Zazhi* 1998; **6**: 25-26
 - 26 **Zhang YJ**, Zhang L. Again Operation of esophageal and cardiac cancer after gastrectomy. *Zhonghua Xiongxinxueguan Waikē Zazhi* 1997; **13**: 234-235
 - 27 **Wang JS**, Feng LG, Wang WD, Yang L. Again Operation for cardiac and esophageal carcinoma after gastrectomy. *Tongji Yike Daxue Xuebao* 1994; **23**: 420-422
 - 28 **Song QQ**, Zeng L, Ge D, Chou DH. Surgical Treatment of esophageal and cardiac cancer after gastrectomy. *Shiyong Zhongliu Zazhi* 2001; **16**: 132-133
 - 29 **Huang HR**, Huang Y. Surgical treatment for patients with esophageal cancer after gastrectomy. *Xin Yixue* 2003; **34**: 498-499
 - 30 **Zhang DW**, Cheng GY, Huang GJ, Zhang RG, Liu XY, Mao YS, Wang YG, Chen SJ, Zhang LZ, Wang LJ, Zhang DC, Yang L, Meng PJ, Sun KL. Operable squamous esophageal cancer: current results from the East. *World J Surg* 1994; **18**: 347-354
 - 31 **Shao LF**. Long-term results of surgical resection of early esophageal and cardiac carcinomas. *Zhonghua Waikē Zazhi* 1993; **31**: 131-133
 - 32 **Shao LF**, Chen YH, Gao ZR, Wei GQ, Xu JL, Chen MY, Cheng JH. Surgical treatment of carcinoma of esophagus and gastric cardia: a 34-year investigation. *Chine Germ J Clinical Oncol* 2002; **1**: 61-63
 - 33 **Huang YT**, Luo YG. Management of esophageal cancer: what progress has been made? *Zhonghua Weichang Waikē Zazhi* 2001; **4**: 133-141

Edited by Ma JY Proofread by Zhu LH

Antitumor effects of vaccine consisting of dendritic cells pulsed with tumor RNA from gastric cancer

Bing-Ya Liu, Xue-Hua Chen, Qin-Long Gu, Jian-Fang Li, Hao-Ran Yin, Zheng-Gang Zhu, Yan-Zhen Lin

Bing-Ya Liu, Xue-Hua Chen, Qin-Long Gu, Jian-Fang Li, Hao-Ran Yin, Zheng-Gang Zhu, Yan-Zhen Lin, Department of Surgery, Shanghai Institute of Digestive Surgery, Ruijin Hospital, Shanghai Second Medical University, Shanghai 200025, China

Supported by National Natural Science Foundation of China, No. 30170915, Health Ministry of China, No. 9802292, and Shanghai Medical Development Foundation from the Health Bureau of Shanghai, No.983008

Correspondence to: Bing-Ya Liu, Ph.D., Department of Surgery, Shanghai Institute of Digestive Surgery, Ruijin Hospital, Shanghai Second Medical University, Shanghai 200025, China. digsurgliu@netscape.net

Telephone: +86-21-64674654 **Fax:** +86-21-64373909

Received: 2003-08-23 **Accepted:** 2003-10-07

Abstract

AIM: To investigate the immunotherapeutic potential of vaccine consisting of dendritic cells (DCs) pulsed with total RNA from MFC gastric cancer cells.

METHODS: DCs were prepared from the spleens of strain 615 mice by magnetic cell sorting (MACS). After culture for 24 h, DCs were pulsed with total RNA from MFC gastric cancer cells. Mice of one group were immunized with tumor RNA pulsed DC (RNA/DC) at the dosage of 1×10^6 on d 14 and 7 by s.c. inoculation before tumor implantation. Mice of another group were immunized with unpulsed DC (UDC) at the same dosage on days as the RNA/DC group. The third group of control mice was untreated. On d 0, all the mice were challenged with s.c. injections of 5×10^5 MFC gastric cancer cells. After inoculation, the mice were monitored closely with respect to tumor growth. Activities of NK cells in PBL and splenocytes and CTL were tested.

RESULTS: On d 21 after tumor cell inoculation, the mice of control group manifested the largest tumors with volume at a mean of 2.6323 ± 1.1435 cm³, followed by the UDC and RNA/DC groups with mean volumes at 0.7536 ± 0.3659 cm³ and 0.3688 ± 0.6571 cm³, respectively. The activities of NK cells in PBL and splenocytes in RNA/DC group were 66.2% and 65.4%, respectively, higher than that in the control group. The tumor specific CTL activity in RNA/DC group was 49.5%, higher than that in the control group.

CONCLUSION: The tumor vaccine with DCs pulsed with total RNA from gastric cancer cells possesses the ability to stimulate tumor specific CTL activity and to establish anti-tumor immunity when administered *in vivo*.

Liu BY, Chen XH, Gu QL, Li JF, Yin HR, Zhu ZG, Lin YZ. Antitumor effects of vaccine consisting of dendritic cells pulsed with tumor RNA from gastric cancer. *World J Gastroenterol* 2004; 10(5): 630-633

<http://www.wjgnet.com/1007-9327/10/630.asp>

INTRODUCTION

T cells, in particular CD8⁺ cytotoxic T lymphocytes (CTLs),

are regarded as the principal effectors of anti-tumor immunity. Several studies have demonstrated that tumor-specific CTL can be induced to recognize peptide epitopes presented on the tumor cell surface in the context of MHC class I molecules. Tumors, however, have evolved various mechanisms to escape from host immune surveillance, such as loss of class I or antigen variants, secretion of immuno-suppressive agents, or development of antigen-specific T cell clonally anergy due to lack of co-stimulation^[1].

The dendritic cell (DC) system of antigen-presenting cells (APCs), is the initiator and modulator of immune response^[2]. DCs are efficient stimulators of B and T lymphocytes. DCs have been known to be highly specialized antigen-presenting cells and principal activators of resting or naive T cells *in vitro* and *in vivo*, capable of efficiently transporting antigens^[3].

Immature DCs are capable of capturing and processing antigens extensively, they are also able to internalize apoptotic cells by binding to them via adhesion molecules^[4]. After the uptake and processing of antigens, DCs leave peripheral tissues and migrate to lymphoid organs in order to present antigens to T lymphocytes. In lymph nodes, DCs form clusters with T lymphocytes by means of various adhesion molecules, in particular CD54(ICAM-1), CD102(ICAM-3) and CD58 (LFA-3), that are highly expressed by activated DCs^[5]. The DC/T cell interaction is stabilized by the specific ligation of T cell receptors (TCR) of the MHC-peptide complex, which delivers the first activation signal to T lymphocytes. The second costimulatory signal is absolutely necessary to allow T cell activation and proliferation. This signal is mediated by the interaction of CD80(B7-1) and CD86(B7-2), both of which present on DC, with T cell CD28. Expression of a large amount of MHC costimulatory molecules and production of IL-12 by mature DCs turn them into very potent professional APCs^[6]. DCs pulsed with tumor antigen can induce specific CTL activity^[7].

The aim of the present study was to investigate the ability of DC pulsed with tumor RNA to stimulate specific CTL reaction and the potential usefulness of DC-based vaccines for the treatment of cancer patients.

MATERIALS AND METHODS

Mice and cell line

Seven to eight wk-old strain 615 mice (H-2K^k) used in these experiments, were obtained from the Chinese Academy of Medical Sciences (Beijing, China). The murine gastric carcinoma cell line MFC derived from strain 615 mouse was provided by the Chinese Academy of Medical Sciences. MFC was cultured in MPRI-1640 medium containing 100 g/L FCS.

Isolation of dendritic cells from mouse spleen

Spleen cells were prepared and treated with collagenase D. Splenocytes were labeled with mouse CD11c⁺ DC MicroBeads (MACS, Miltenyi Biotec) according to the manufacturer's manual. In brief, 10^8 splenocytes were resuspended in 400 μ L buffer and 100 μ L of MACS CD11c MicroBeads was added. After thoroughly mixed, the splenocytes were incubated for

15 min at 6–12 °C, followed by a wash with 10–20× labeling volume of buffer. Cells were resuspended in 500 µL of buffer and applied onto the MS⁺/MS⁺ column to allow removal of the negative cells. Three rinses with 500 µL of buffer were performed prior to removal of the column from the separator. The column was placed in a collection tube, and 1 ml of buffer was flushed into the column to secure the positive cells. The positive cells were cultured in IMDM containing 200 mL/L FCS, 100 ng/mL IL-4, 100 ng/mL GM-CSF, 10 ng/mL TNF- α for 24 h, then examined by scanning electron microscope and flow cytometry.

Preparation of tumor total RNA

Tumor total RNA was isolated from actively growing tissue culture cells, 1×10⁷ MFC murine gastric cancer cells were lysed in 1 mL of Trizol reagent (Life Technologies) prepared according to the protocol provided by the manufacturer. One mL of Trizol reagent was added to 1×10⁷ of MFC cells which were well mixed well prior to incubation for 5 min at room temperature. Then 0.2 mL of chloroform was added and the mixture was thoroughly mixed and incubated for 3 min at room temperature. After centrifugation of 12 000 g for 15 min at 4 °C, contents were transferred in the aqueous phase to a fresh tube, then 500 µL of isopropyl alcohol was added and mixed well, followed by incubation at room temperature for 10 min and centrifuged at 12 000 g for 10 min at 4 °C. The RNA pellet was washed with 1 mL of 750 mL/L ethanol, and redissolved in RNase free water.

Pulsing DCs with tumor RNA

The procedure used for pulsing DCs with tumor RNA was described by Boszkowski^[8]. In brief, DCs were washed twice in Opti-MEM medium (GIBCO BRL). Cells were resuspended in Opti-MEM medium at 2–5×10⁶ cells/mL and transferred into 15 mL polypropylene tubes (Falcon). The cationic lipid, DOTAP (Boehringer Mannheim), was used to deliver RNA into the cells, and 25 µg of total RNA in 500 µL Opti-MEM and 50 µg of DOTAP in 500 µL Opti-MEM were mixed in 12×75 mm polystyrene tubes at room temperature for 20 min. The complex was added to the DCs and incubated at 37 °C for 2–4 h.

Immunization of mice using tumor RNA pulsed DCs vaccine and tumor challenge

Tumor RNA pulsed DCs (RNA/DC) and unpulsed DCs (UDC) were collected, washed twice with PBS and then resuspended in PBS. Mice from the respective treatment groups were immunized with these preparations. Each mouse received the designated dose of 1×10⁶ DCs s.c with an intervening period of 7 d before administration of the second dose. The mice untreated were used as control. Twelve mice were in RNA/DC group, 10 mice in UDC group, and 12 mice in control group.

Seven days after vaccination with DCs for the second and last time, each mouse in the RNA/DC group received inoculation of 5×10⁵ MFC stomach cancer cells subcutaneously. The animals were closely monitored until the first palpable tumor appeared. Thereafter, two-dimensional tumor measurements were made using calipers, the measurements were recorded every 3–4 d.

Cytotoxicity and cytokine analysis

Three weeks after tumor challenge, all the mice were sacrificed. Their spleens were removed and placed in PBS. The splenocytes were depleted of red blood cells through incubation in 8.4 g/L ammonium chloride for 10 min at 37 °C. The samples were then washed twice with PBS. The cells obtained were resuspended with RPMI-1640 containing 100 g/L FCS, 2 β -

mercaptoethanol and 10 u/mL IL-2. Splenocytes were stimulated with irradiated MFC gastric cancer cells (5 000 rads) in the ratio of 10:1 (E:T). The samples were then cultured for 5 days and CTLs from each culture were tested. Cell mediated lysis was confirmed *in vitro* using standard chromium (⁵¹Cr)-release assay.

When the mice were sacrificed, p40 subunits of IL-12 in serum were measured using standard ELISA (R & D).

RESULTS

DCs phenotype

DCs were cultured in IMDM containing 200 g/L FCS, 100 ng/mL IL-4, 100 ng/mL GM-CSF, 10 ng/mL TNF- α for 24 h after sorted by mouse CD11C⁺ DC MicroBeads. DCs phenotypes were detected by flow cytometry with H-2KK, I-EK, CD80, and CD 86 (Table 1).

Table 1 DCs phenotypes before and after culture

	Before culture (%)	After culture (%)
H-2K ^K	92.1	91.6
I-E ^K	28.1	59.2
CD80	21.0	76.4
CD86	23.1	61.3

Induction of host protective immunity against tumor by RNA pulsed DCs

To determine whether RNA pulsed DC could induce host protective immunity against MFC gastric cancer, strain 615 mice were immunized subcutaneously with RNA pulsed DCs or unpulsed DCs. Seven days after immunization, the mice were inoculated subcutaneously with 5×10⁵ MFC murine gastric cancer cells. The results (Figure 1) showed that the mice in the control group (control mice) were all tumor positive on d 7, while the mice immunized with RNA pulsed DCs demonstrated a significant delay in tumor development (7 vs 11 d). RNA pulsed DC immunization reduced tumor incidence significantly. In the RNA/DC group, 41.7% of the mice (5/12) were free from tumor; in the UDC group, 80% of the mice (8/10) developed tumors, and all the mice (12/12) developed tumor in control group on 21 d after tumor cell inoculation. On d 21 after tumor cell inoculation, the tumor volume of the control group attained a mean of 2.6323±1.1435 cm³, followed by the UDC and RNA/DC groups with mean volumes of 0.7536±0.3659 cm³ and 0.3688±0.6571 cm³, respectively (Figure 1).

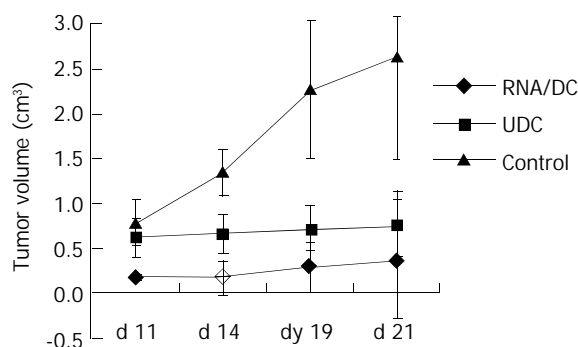


Figure 1 Tumor growth curve. Control group mice (n=12) were inoculated s.c with 5×10⁵ MFC gastric cancer cells without any immunization. UDC group mice (n=10) were immunized twice with unpulsed DCs followed by inoculation s.c with 5×10⁵ MFC gastric cancer cells. RNA/DC group mice (n=12) were immunized twice with RNA pulsed DCs followed by inoculation s.c with 5×10⁵ MFC gastric cancer cells.

Induction of tumor specific CTL cytotoxicity by RNA pulsed DCs

Four weeks after immunization, splenocytes were restimulated *in vitro* with irradiated MFC murine gastric cancer cells for cytotoxic T lymphocyte (CTL) propagation. The results demonstrated that tumor RNA pulsed DCs induced strong tumor specific CTL production. Immunization with MFC tumor RNA pulsed DCs induced stronger lysis of MFC (Figure 2). NK cell activity in PBL or in splenocytes was examined after the mice were sacrificed, revealing that the greatest NK cell activity was seen in the RNA/DC group.

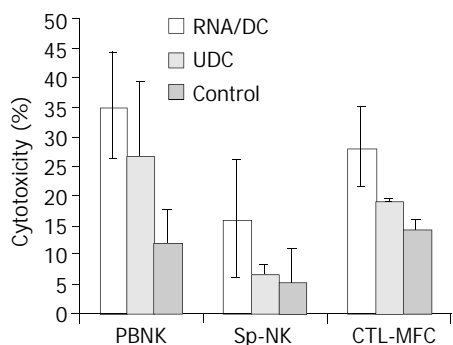


Figure 2 Cytotoxicity of NK cells and CTL. PBNK: NK cell activity in PBL, Sp-NK: NK cell activity in splenocytes, CTL-MFC: CTL activity to lyses MFC murine gastric cancer cells.

Serum IL-12 level

Three weeks after tumor challenge, IL-12 in serum was detected by ELISA. The results showed that the serum IL-12 level was the highest in the RNA/DC group among the three groups (Figure 3).

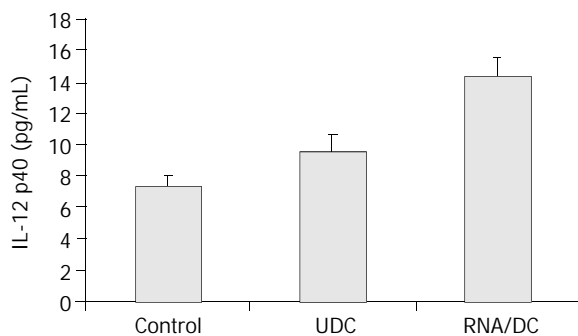


Figure 3 Serum IL-12 p40 levels in three groups of mice three weeks after tumor challenge.

DISCUSSION

In recent years, DCs have been found to play an important role in the rejection of tumors by the immune system. Their infiltration of tumors has been associated with an improved prognosis for many neoplasms^[9,10].

A number of tumor antigens recognized by CD8+ CTL have been identified^[11]. These defined antigens could simply be added as 9-11 mer HLA-I-restricted peptides to mature DCs^[12]. So, the use of peptide-pulsed DC can obtain clearly effective results, but it requires prior knowledge of patients' HLA types and the sequence of the relevant peptide epitopes. It has been suggested that the use of longer peptides or whole proteins, which are not directly present but are endocytosed and processed, is a better way to generate a fully competent DC vaccine since it allows selection by the APC of the optimal 9-mer peptide for presentation^[13]. After cloning, these tumor

antigens can also be used as cDNA in appropriate vectors to load DCs. But there are three major restrictions when defined tumor antigen is used. First, effective TSA or TAA is not identified in a large number of cancers, especially in gastric cancer. Second, it is clear that immunotherapy approaches directing against a unique antigen favor the selection of a tumor mutant that has selectively lost its ability to present efficiently to the defined antigen^[14]. Third, the acquisition of antigen-specific CTL *in vitro* is not a guarantee of the development of a curative immune response *in vivo*.

To bypass these disadvantages, several alternative methodologies have been developed. Unfractionated MHC-I-presented peptides could be eluted from tumor cells and loaded onto DC^[11]. DCs could also be pulsed with whole tumor antigens, such as cell lysates^[15], cell extracts^[16], apoptotic cells^[4,17], total RNA or mRNA^[7]. The method of fusing tumor cells with DCs has also been explored^[18,19]. The recent demonstration of cell-contact generated by short-term coculture of DC with tumor cells without cell fusion could result in a potent immunogen and was particularly relevant^[20]. DCs pulsed with tumor RNA may thus be a potential effective means to induce host T cell-mediated anti-tumor responses. Boczkowski *et al.* have recently demonstrated that vaccination with tumor RNA pulsed DCs could elicit T cell protective immunity against tumor challenge and induce immune rejection of established tumors^[8].

Gastric cancer is one of the tumors with very high heterogeneity. Host immune status in patients with gastric cancer is usually poor. Up to the present, immunotherapy for gastric cancer has not been clearly effective. The use of DC-based tumor vaccine can provide a glimmer of hope for patients with gastric cancer. In this experiment, we used tumor total RNA as tumor whole antigen to pulse DCs. All the antigens were processed and selectively presented to T cells by DCs. The results following the use of tumor total RNA pulsed DCs as vaccine, indeed, induced anti-tumor immune responses by stimulating NK cells and tumor-specific CTL activity in the mouse.

For clinical trials of DC-based vaccine for cancer, other matters must be considered. The first is the source of DCs for clinical use. The second is the choice of tumor antigens and method for antigen loading of DCs. Third, the DC dose-response relationship should be determined using individual cell preparation methods. Finally, the optimal route and frequency of administration need to be determined.

ACKNOWLEDGMENT

We want to thank Dr. Dong-Qing Zhang, Shanghai Institute of Immunology for his good advice, and Yi Zhang, research assistant, for her work and Dr. Ming-Jun Zhang for his help in animal experimentation.

REFERENCES

- Zitvogel L**, Mayordomo JI, Tjandrawan T, Deleo AB, Clarke MR, Lotze MT, Storkus WJ. Therapy of murine tumors with tumor peptide-pulsed dendritic cells: dependence on T cells, B7 costimulation, and T helper cell 1-associated cytokines. *J Exp Med* 1996; **183**: 87-97
- Banchereau J**, Steinman RM. Dendritic cells and the control of immunity. *Nature* 1998; **392**: 245-252
- Constant S**, Sant' Angelo D, Pasqualini T, Taylor T, Levin D, Flavell R, Bottomly K. Peptide and protein antigens require distinct antigen-presenting cell subsets for the priming of CD4+ T cells. *J Immunol* 1995; **154**: 4915-4923
- Albert ML**, Pearce SF, Francisco LM, Sauter B, Roy P, Silverstein RL, Bhardwaj N. Immature dendritic cells phagocytose apoptotic cells via alphavbeta5 and CD36, and cross-present antigens to cytotoxic T lymphocytes. *J Exp Med* 1998; **188**: 1359-1368

- 5 **Scheeren RA**, Koopman G, Van der Baan S, Meijer CJ, Pals ST. Adhesion receptors involved in clustering of blood dendritic cells and T lymphocytes. *Eur J Immunol* 1991; **21**: 1101-1105
- 6 **Tarte K**, Klein B. Dendritic cell-based vaccine: a promising approach for cancer immunotherapy. *Leukemia* 1999; **13**: 653-663
- 7 **Zhang JK**, Li J, Chen HB, Sun JL, Qu YJ, Lu JJ. Antitumor activities of human dendritic cells derived from peripheral and cord blood. *World J Gastroenterol* 2002; **8**: 87-90
- 8 **Boczkowski D**, Nair SK, Snyder D, Gilboa E. Dendritic cells pulsed with RNA are potent antigen-presenting cells *in vitro* and *in vivo*. *J Exp Med* 1996; **184**: 465-472
- 9 **Ishigami S**, Aikou T, Natsugoe S, Hokita S, Iwashige H, Tokushige M, Sonoda S. Prognostic value of HLA-DR expression and dendritic cell infiltration in gastric cancer. *Oncology* 1998; **55**: 65-69
- 10 **Saito H**, Tsujitani S, Ikeguchi M, Maeta M, Kaibara N. Relationship between the expression of vascular endothelial growth factor and the density of dendritic cells in gastric adenocarcinoma tissue. *Br J Cancer* 1998; **78**: 1573-1577
- 11 **Boon T**, Van der Bruggen P. Human tumor antigens recognized by T lymphocytes. *J Exp Med* 1996; **183**: 725-729
- 12 **Tsai V**, Southwood S, Sidney J, Sakaguchi K, Kawakami Y, Appella E, Sette A, Celis E. Identification of subdominant CTL epitopes of the GP100 melanoma-associated tumor antigen by primary *in vitro* immunization with peptide-pulsed dendritic cells. *J Immunol* 1997; **158**: 1796-1802
- 13 **Nieda M**, Nicol A, Kikuchi A, Kashiwase K, Taylor K, Suzuki K, Tadokoro K, Juji T. Dendritic cells stimulate the expansion of bcr-abl specific CD8+ T cells with cytotoxic activity against leukemic cells from patients with chronic myeloid leukemia. *Blood* 1998; **91**: 977-983
- 14 **Ikeda H**, Lethe B, Lehmann F, van Baren N, Baurain JF, de Smet C, Chambost H, Vitale M, Moretta A, Boon T, Coulie PG. Characterization of an antigen that is recognized on a melanoma showing partial HLA loss by CTL expressing an NK inhibitory receptor. *Immunity* 1997; **6**: 199-208
- 15 **Tang ZH**, Qiu WH, Wu GS, Yang XP, Zou SQ, Qiu FZ. The immunotherapeutic effect of dendritic cells vaccine modified with interleukin-18 gene and tumor cell lysate on mice with pancreatic carcinoma. *World J Gastroenterol* 2002; **8**: 908-912
- 16 **Asavaroengchai W**, Kotera Y, Mule JJ. Tumor lysate-pulsed dendritic cells can elicit an effective antitumor immune response during early lymphoid recovery. *Proc Natl Acad Sci U S A* 2002; **99**: 931-936
- 17 **Albert ML**, Sauter B, Bhardwaj N. Dendritic cells acquire antigen from apoptotic cells and induce class I-restricted CTLs. *Nature* 1998; **392**: 86-89
- 18 **Zhang JK**, Li J, Zhang J, Chen HB, Chen SB. Antitumor immunopreventive and immunotherapeutic effect in mice induced by hybrid vaccine of dendritic cells and hepatocarcinoma *in vivo*. *World J Gastroenterol* 2003; **9**: 479-484
- 19 **Zhang J**, Zhang JK, Zhou SH, Chen HB. Effect of a cancer vaccine prepared by fusions of hepatocarcinoma cells with dendritic cells. *World J Gastroenterol* 2001; **7**: 690-694
- 20 **Celluzzi CM**, Falo LD Jr. Physical interaction between dendritic cells and tumor cells results in an immunogen that induces protective and therapeutic tumor rejection. *J Immunol* 1998; **160**: 3081-3085

Edited by Wang XL

Maspin expression and its clinicopathological significance in tumorigenesis and progression of gastric cancer

Meng-Chun Wang, Yan-Min Yang, Xiao-Han Li, Fang Dong, Yan Li

Meng-Chun Wang, Yan-Min Yang, Yan Li, Department of Gastroenterology, The Second Affiliated Hospital of China Medical University, Shenyang 110004, Liaoning Province, China
Xiao-Han Li, Fang Dong, Department of Pathology, The Second Affiliated Hospital of China Medical University, Shenyang 110004, Liaoning Province, China

Correspondence to: Meng-Chun Wang, Department of Gastroenterology, The Second Affiliated Hospital of China Medical University, Shenyang 110004, Liaoning Province, China. mengchunwang@hotmail.com

Telephone: +86-24-83956947

Received: 2003-06-16 **Accepted:** 2003-08-25

Abstract

AIM: To investigate maspin expression in tumorigenesis and progression of gastric cancer and to explore its relevant molecular mechanisms.

METHODS: Formalin-fixed and paraffin-embedded tissues from normal mucosa ($n=182$), dysplasia ($n=69$), cancer ($n=113$) of the stomach were studied for maspin expression by immunohistochemistry. Microvessel density (MVD) in gastric cancer was labeled using anti-CD34 antibody. Maspin expression was compared with clinical parameters and MVD of tumors. Caspase-3 expression was also detected in gastric carcinoma by immunohistochemistry. The relationship between Caspase-3 and maspin expression was concerned as well.

RESULTS: The positive rates of maspin expression were 79.8% (145/182), 75.4% (52/69) and 50.4% (57/113) in normal mucosa, dysplasia and cancer of the stomach, respectively. Cancer less frequently expressed maspin than normal mucosa and dysplasia ($P<0.05$). Maspin expression showed a significantly negative association with invasive depth, metastasis, Lauren's and Nakamura's classification ($P<0.05$), but not with tumor size, Borrmann's classification, growth pattern or TNM staging ($P>0.05$). The positive rate of Caspase-3 was significantly lower in gastric cancer than in normal gastric mucosa ($P<0.05$, 32.7% vs 50.4%). It was noteworthy that maspin expression was negatively correlated with MVD, but positively correlated with expression of Caspase-3 in gastric cancer ($P<0.05$).

CONCLUSION: Down-regulated maspin expression is a late molecular event in gastric carcinogenesis. Reduced expression of maspin contributes to progression of gastric cancer probably by inhibiting cell adhesion, enhancing cell mobility, decreasing cell apoptosis and facilitating angiogenesis. Additionally altered expression of maspin underlies the molecular mechanism of differentiation of gastric cancer and supports the different histogenetic pathways of intestinal and diffuse gastric cancers. Maspin expression can be considered as an effective and objective marker to reveal biological behaviors of gastric cancer.

Wang MC, Yang YM, Li XH, Dong F, Li Y. Maspin expression and its clinicopathological significance in tumorigenesis and

progression of gastric cancer. *World J Gastroenterol* 2004; 10(5): 634-637

<http://www.wjgnet.com/1007-9327/10/634.asp>

INTRODUCTION

Mammary serine protease inhibitor (maspin) was identified by subtractive hybridization as a candidate tumor suppressor protein in normal mammary epithelial cells^[1]. Maspin gene maps to human chromosome 18q21.3-q23, whose cDNA consists of 2 584 nucleotides encoding for a 42 ku peptide^[2]. A number of findings support its inhibitory effects on tumors. Levels of maspin expression showed an inverse correlation with progression of malignancies. Mammary carcinoma cells transfected with maspin showed a reduction of tumor growth and metastasis in nude mice, the addition of recombinant maspin decreased the migration potential of breast and prostate cancer cells across a reconstituted basement membrane. More recently, maspin has been shown to inhibit angiogenesis by blocking *in vitro* migration of vascular endothelial cells and by *in vivo* inhibition of rat cornea neovascularization^[1-8]. It has been documented that maspin transgene expression in mouse mammary gland inhibited Simian virus 40 (SV40) large T-antigen induced breast carcinogenesis and was correlated with increased apoptosis of mammary gland cells^[9].

Gastric cancer is one of the commonest malignancies in China, and even in the world. However, the molecular aspects of carcinogenesis and progression of gastric cancer remain elusive^[10-19]. The purposes of this study were to examine maspin expression in normal gastric mucosa, gastric dysplasia, gastric cancer, and to compare its expression with clinicopathological features of gastric cancer, and to analyze the correlation of maspin expression with Caspase-3 expression and MVD in gastric cancer.

MATERIALS AND METHODS

Patients and samples

Normal mucosa ($n=182$), dysplasia ($n=69$), cancer ($n=113$) of the stomach were collected from the Second Affiliated Hospital of China Medical University between Sept. 1996 and Feb. 2002. All tissues were fixed in 40 g/L formaldehyde, embedded in paraffin and incised into 4 μ m sections. These sections were stained by hematoxylin-and-eosin method to confirm their histological diagnosis and other microscopic characteristics. All patients did not undergo chemotherapy and radiotherapy before operation.

Evaluation of clinicopathological parameters of gastric cancer

Clinicopathological staging for each gastric carcinoma was evaluated according to the TNM system. Gross appearance of the tumors was described according to Borrmann's classification. Histomorphological architecture of the tumor samples was expressed according to Lauren's and Nakamura's classifications. Growth patterns of gastric cancer were classified into mass-,

nest-, or diffuse- type. Furthermore, tumor diameter, invasive depth and metastasis were determined.

Immunohistochemistry

Representative and consecutive sections were studied with streptavidin-biotin-peroxidase immunohistochemistry (SABC kit from Boster Biotech.). Anti-maspin, anti-Caspase-3 and anti-CD34 antibodies were purchased from Novocastra, Zhongshan (China) and DAKO respectively. All procedures were implemented according to the instructions of the product. For negative controls, sections were processed as above but treated with PBS (0.01 mol/L, pH7.4) instead of primary antibodies.

Evaluation of maspin and Caspase-3 immunostaining

The immunoreactivity to maspin and Caspase-3 was localized in cytoplasm. One hundred cells were selected and counted from 5 representative fields of each section by two independent observers. The positive percentage of counted cells was graded semi-quantitatively into one of the four-tier scoring system: negative(-), 5%; weakly positive (+), 5-25%; moderately positive(++), 25-50%; and strongly positive(+++), 50%.

Microvessel density counting

CD34 antibodies were distributed in cell membranes and cytoplasm of vascular endothelial cells. Modified Weidner's method was used to calculate the microvessel density, which was described as follows. Microvessels in tumor were considered as hot points in vessel counts. Any brown staining endothelial cell or endothelial cell cluster was regarded as a single, countable microvessel. Observers selected such five areas and counted individual microvessels at 400 \times magnification (*i.e.* 40 \times objective lens and 10 \times ocular lens, 0.1885 mm² per field).

Statistical analysis

Statistical evaluation was performed using *chi*-square test to differentiate the rates between different groups, using Spearman correlation test to analyze the rank data, and using one-way ANOVA to differentiate means of different groups. $P < 0.05$ was considered as statistically significant. SPSS 10.0 software was employed to analyze all data.

RESULTS

Maspin expression in normal mucosa, dysplasia, and cancer of the stomach

Figures 1A-D show the positive immunoreactivity to maspin in cytoplasm of epithelial, dysplasia and cancer cells of the stomach. As summarized in Table 1, the positive rates of maspin expression were 79.8% (145/182), 75.4% (52/69), and 50.4% (57/113) in normal mucosa, dysplasia and cancer of gastric cancer, respectively. Normal mucosa and dysplasia more frequently expressed maspin than cancer ($P < 0.05$).

Table 1 Maspin expression in normal mucosa, dysplasia, and primary cancer of the stomach

Groups	n	Maspin expression			
		-	++	+++	%
Normal mucosa	182	37	145		79.8 ^b
Dysplasia	69	17	52		75.4 ^d
Primary cancer	113	56	57		50.4

Compared with primary cancer ^b $P = 0.000$ ($\chi^2 = 27.589$, Pearson' $r = 0.306$), ^d $P = 0.000$ ($\chi^2 = 11.075$, Pearson' $r = 0.247$).

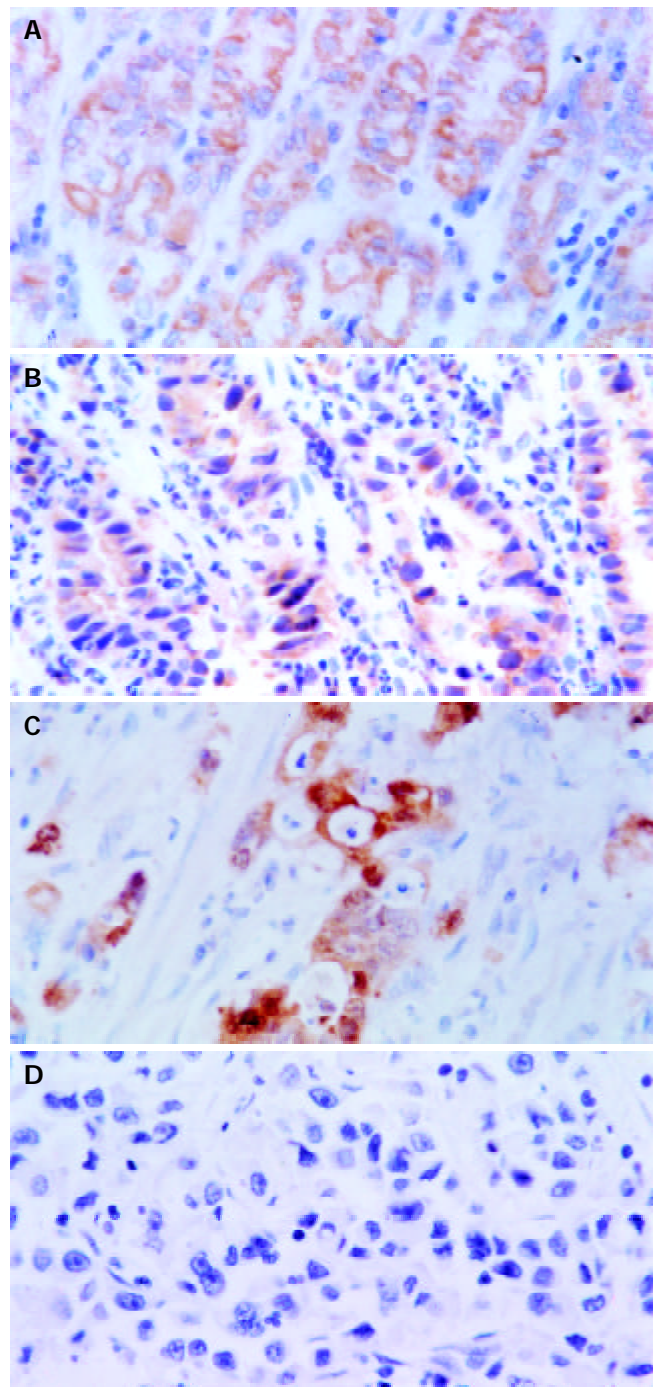


Figure 1 A: Localization of maspin in cytoplasm, and strong expression in gastric epithelial cells (SABC, $\times 400$), B: Strong immunoreactivity of gastric dysplastic cells to maspin (SABC, $\times 400$), C: Strong immunostaining of maspin in gastric papillary adenocarcinoma cells (SABC, $\times 400$), D: Negative expression of maspin in poorly-differentiated gastric adenocarcinoma cells (SABC, $\times 400$).

Relationship between maspin expression and clinicopathological features of gastric cancer

Table 2 shows that maspin expression had a significantly negative association with invasive depth, metastasis, Lauren's and histological classifications ($P < 0.05$), but not with tumor size, Borrmann's classification, growth pattern or TNM staging ($P > 0.05$).

Relationship between maspin and Caspase-3 expression, MVD in gastric cancer

The positive rate of Caspase-3 expression was lower in gastric

cancer than in normal gastric mucosa ($P<0.05$, 32.7% vs 50.4%). It was noticeable that maspin expression was positively correlated with Caspase-3 expression, but negatively with MVD in gastric cancer ($P<0.05$) (Tables 2-3, Figures 2,3).

Table 2 Relationship between maspin expression and clinicopathological features of gastric cancer

Clinicopathological features	n	Maspin expression					rs	P value
		-	+	++	+++	%		
Tumor size							0.000	0.999
<4 cm	47	22	13	7	5	53.2		
≥4 cm	66	34	11	15	6	48.5		
Borrmann's classification							0.014	0.896
I, II	28	12	9	5	2	57.1		
III, IV	59	30	10	13	6	49.2		
Invasive depth							0.280	0.003
Above submucosa	26	10	4	6	6	61.5		
Muscularis propria	34	12	11	7	4	64.7		
Below subserosa	53	34	9	9	1	35.8		
Metastasis							0.208	0.027
-	75	31	18	19	7	58.7		
+	38	25	6	3	4	34.2		
TNM staging							0.004	0.967
O, I	46	22	11	10	3	52.2		
II, III, IV	67	34	13	12	8	49.3		
Growth pattern							0.032	0.767
Mass	23	13	4	5	1	43.5		
Nest	30	11	6	8	5	63.3		
Diffuse	34	18	9	5	2	47.1		
Lauren's classification							0.228	0.015
Intestinal	36	12	8	11	5	66.7		
Diffuse	57	33	12	8	4	42.1		
Mixed	20	11	4	3	2	45.0		
Nakamura's classification							0.212	0.024
Differentiated	53	20	14	12	7	62.3		
Undifferentiated	60	36	10	1	4	10.0		
Caspase-3 expression							0.246	0.009
-	78	44	17	12	5	56.4		
+~+++	35	12	7	10	6	65.7		

Table 3 Relationship between maspin expression and MVD in primary gastric cancer

Maspin expression	n	MVD (mean±SD)	F value	P value
-	56	51.72±26.87	4.911	0.029
+~++++	57	41.70±20.92		
Total	113	46.67±24.47		

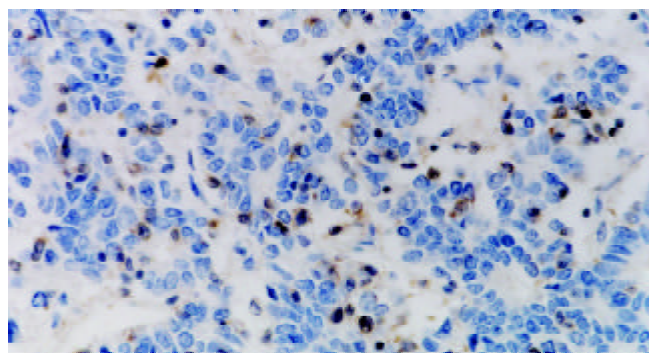


Figure 2 Negatively immunostaining of Caspase-3 in poorly-differentiated gastric adenocarcinoma cells and positive expression in infiltrating lymphocytes (SABC, ×400).

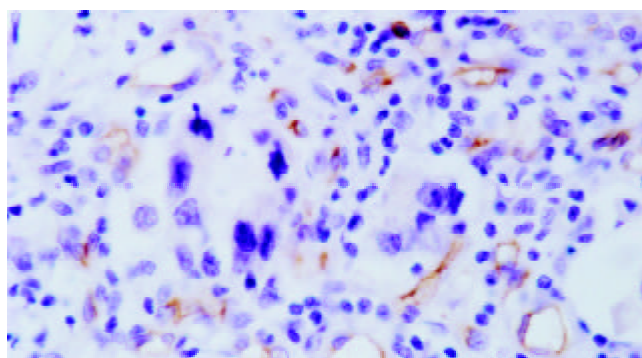


Figure 3 Localization of CD34 antigens in cell membranes and cytoplasm of vascular endothelial cells (SABC, ×400).

DISCUSSION

Carcinogenesis and progression of malignancies are a complicated multistage process that requires the coordination of multiple genes, including oncogenes and tumor suppressor genes. Genomic instability is one of the driving forces for tumor development. Among all genetic alterations, inactivation of metastasis suppressor genes has been found to be an important factor because of their contribution to malignant change of normal cells and metastasis of tumor cells^[20,21].

It is known that maspin is highly expressed in various kinds of normal cells and lowly expressed in cancer cells. Our data showed that maspin expression was gradually reduced from normal mucosa, through dysplasia to cancer of the stomach. The positive rate of maspin expression was lower in gastric cancer than in normal gastric mucosa and gastric dysplasia with no significant difference in the latter two. These results suggested that reduced maspin expression contributed to malignant change of gastric epithelial cells. The down-regulated expression of maspin could be considered as a late molecular event of gastric carcinogenesis. Previous reports indicated that DNA methylation, histone deacetylation or LOH was partially responsible for the silencing of maspin gene expression^[22-24]. Decreased expression of maspin might be attributable to these genetic alterations in gastric carcinogenesis as mentioned above.

Our study showed that maspin expression was negatively associated with invasion and metastasis of tumors, suggesting its inhibitory effects on progression of gastric cancer. Biliran *et al*^[25] found that maspin could specifically inhibit cell surface-associated urokinase-type plasminogen activator and fibrinogen-bound tissue-type plasminogen activator, which was correlated with significantly decreased cell invasion potential and motility *in vitro*. Blacque *et al*^[26] reported that interaction between recombinant maspin and some collagens might contribute to cell adhesion, cell migration and angiogenesis. Seftor *et al*^[27] demonstrated that maspin was able to regulate integrin expression, indicating that maspin could reduce the invasive phenotype of cancer cells by altering their integrin profile. These findings suggested that maspin expression could inhibit tumor progression *in vivo*, likely through a combination of increased cell adhesion, decreased angiogenesis, and inhibition of tumor cell migration.

Additionally, it was found that undifferentiated gastric carcinomas had a lower expression of maspin as compared with the differentiated ones, suggesting that down-regulated expression of maspin was closely associated with the differentiation of gastric cancer. Diffuse-type gastric cancers had less expression of maspin as compared with the intestinal-type ones. It supported that there were different tumorigenic pathways between diffuse-type and intestinal-type gastric carcinomas. Diffuse-type gastric cancer, the main part of which was undifferentiated

carcinoma, displayed a diffusely invasive growth pattern. It is possible that down-regulation of maspin expression could influence mobility and adhesion of cancer cells.

Our study also showed a negative correlation between maspin expression and MVD in gastric cancer. Song *et al.*^[28] found that maspin-positive colonic adenocarcinomas showed less MVD than maspin-negative ones. Zhang *et al.*^[8] reported that maspin might act directly on vascular endothelial cells to stop their migration towards basic fibroblast growth factor and vascular endothelial growth factor and to limit mitogenesis and tube formation, which could dramatically reduce tumor-associated MVD. These *in vivo* and *in vitro* data suggest that the tumor suppressor activity of maspin may depend in large part on its ability to inhibit angiogenesis and raise the possibility that maspin and similar serpins may be excellent targets for the development of drugs that modulate angiogenesis.

Furthermore, it was found that Caspase-3 expression was increased in gastric cancer with maspin positively expressed. Jiang *et al.*^[29] reported that endogenous maspin expression could enhance staurosporine-induced apoptosis of carcinoma cells as judged by the increased fragmentation of DNA, increased proteolytic inactivation of poly-[ADP-ribose]-polymerase, as well as the increased activation of Caspase-8 and Caspase-3. Li *et al.*^[30] showed that apoptosis induced by manganese-containing superoxide dismutase was associated with elevated maspin expression level. These results indicated that it was possible that maspin expression might inhibit progression of gastric cancer by inducing apoptosis.

In summary, down-regulated maspin expression is a late molecular event in gastric carcinogenesis. Reduced expression of maspin can contribute to progression of gastric cancer by inhibiting cell adhesion, enhancing cell mobility, decreasing cell apoptosis and facilitating angiogenesis. Additionally altered expression of maspin underlies the molecular mechanism of differentiation of gastric cancer and supports the different histogenetic pathways of intestinal and diffuse gastric cancers. Maspin expression can be considered as an effective marker to reveal biological behaviors of gastric cancer.

REFERENCES

- 1 **Maass N**, Hojo T, Zhang M, Sager R, Jonat W, Nagasaki K. Maspin—a novel protease inhibitor with tumor-suppressing activity in breast cancer. *Acta Oncol* 2000; **39**: 931-934
- 2 **Reis-Filho JS**, Torio B, Albergaria A, Schmitt FC. Maspin expression in normal skin and usual cutaneous carcinomas. *Virchows Arch* 2002; **441**: 551-558
- 3 **Kim DH**, Yoon DS, Dooley WC, Nam ES, Ryu JW, Jung KC, Park HR, Sohn JH, Shin HS, Park YE. Association of maspin expression with the high histological grade and lymphocyte-rich stroma in early-stage breast cancer. *Histopathology* 2003; **42**: 37-42
- 4 **Odero-Marah VA**, Khalkhali-Ellis Z, Schneider GB, Seftor EA, Seftor RE, Koland JG, Hendrix MJ. Tyrosine phosphorylation of maspin in normal mammary epithelia and breast cancer cells. *Biochem Biophys Res Commun* 2002; **295**: 800-805
- 5 **Zou Z**, Zhang W, Young D, Gleave MG, Rennie P, Connell T, Connelly R, Moul J, Srivastava S, Sesterhenn I. Maspin expression profile in human prostate cancer (CaP) and *in vitro* induction of Maspin expression by androgen ablation. *Clin Cancer Res* 2002; **8**: 1172-1177
- 6 **Shi HY**, Liang R, Templeton NS, Zhang M. Inhibition of breast tumor progression by systemic delivery of the maspin gene in a syngeneic tumor model. *Mol Ther* 2002; **5**: 755-761
- 7 **Streuli CH**. Maspin is a tumour suppressor that inhibits breast cancer tumour metastasis *in vivo*. *Breast Cancer Res* 2002; **4**: 137-140
- 8 **Zhang M**, Volpert O, Shi YH, Bouck N. Maspin is an angiogenesis inhibitor. *Nat Med* 2000; **6**: 196-199
- 9 **Zhang M**, Shi Y, Magit D, Furth PA, Sager R. Reduced mammary tumor progression in WAP-TAG/WAP-maspin bitransgenic mice. *Oncogene* 2000; **19**: 6053-6058
- 10 **Yin T**, Ji XL, Shen MS. Relationship between lymph node sinuses with blood and lymphatic metastasis of gastric cancer. *World J Gastroenterol* 2003; **9**: 40-43
- 11 **Yang L**, Kuang LG, Zheng HC, Li JY, Wu DY, Zhang SM, Xin Y. PTEN encoding product: a marker for tumorigenesis and progression of gastric carcinoma. *World J Gastroenterol* 2003; **9**: 35-39
- 12 **Jiang YA**, Zhang YY, Luo HS, Xing SF. Mast cell density and the context of clinicopathological parameters and expression of p185, estrogen receptor, and proliferating cell nuclear antigen in gastric carcinoma. *World J Gastroenterol* 2002; **8**: 1005-1008
- 13 **Zhang H**, Wu J, Meng L, Shou CC. Expression of vascular endothelial growth factor and its receptors KDR and Flt-1 in gastric cancer cells. *World J Gastroenterol* 2002; **8**: 994-998
- 14 **Zhou YN**, Xu CP, Han B, Li M, Qiao L, Fang DC, Yang JM. Expression of E-cadherin and beta-catenin in gastric carcinoma and its correlation with the clinicopathological features and patient survival. *World J Gastroenterol* 2002; **8**: 987-993
- 15 **Fang DC**, Luo YH, Yang SM, Li XA, Ling XL, Fang L. Mutation analysis of APC gene in gastric cancer with microsatellite instability. *World J Gastroenterol* 2002; **8**: 787-791
- 16 **Song ZJ**, Gong P, Wu YE. Relationship between the expression of iNOS, VEGF, tumor angiogenesis and gastric cancer. *World J Gastroenterol* 2002; **8**: 591-595
- 17 **Yao XX**, Yin L, Sun ZC. The expression of hTERT mRNA and cellular immunity in gastric cancer and precancerosis. *World J Gastroenterol* 2002; **8**: 586-590
- 18 **Niu WX**, Qin XY, Liu H, Wang CP. Clinicopathological analysis of patients with gastric cancer in 1200 cases. *World J Gastroenterol* 2001; **7**: 281-284
- 19 **Xin Y**, Li XL, Wang YP, Zhang SM, Zheng HC, Wu DY, Zhang YC. Relationship between phenotypes of cell-function differentiation and pathobiological behavior of gastric carcinomas. *World J Gastroenterol* 2001; **7**: 53-59
- 20 **Jaeger EB**, Samant RS, Rinker-Schaeffer CW. Metastasis suppression in prostate cancer. *Cancer Metastasis Rev* 2001; **20**: 279-286
- 21 **Debies MT**, Welch DR. Genetic basis of human breast cancer metastasis. *J Mammary Gland Biol Neoplasia* 2001; **6**: 441-451
- 22 **Maass N**, Biallek M, Rosel F, Schem C, Ohike N, Zhang M, Jonat W, Nagasaki K. Hypermethylation and histone deacetylation lead to silencing of the maspin gene in human breast cancer. *Biochem Biophys Res Commun* 2002; **297**: 125-128
- 23 **Spring P**, Nakashima T, Frederick M, Henderson Y, Clayman G. Identification and cDNA cloning of headpin, a novel differentially expressed serpin that maps to chromosome 18q. *Biochem Biophys Res Commun* 1999; **264**: 299-304
- 24 **Domann FE**, Rice JC, Hendrix MJ, Futscher BW. Epigenetic silencing of maspin gene expression in human breast cancers. *Int J Cancer* 2000; **85**: 805-810
- 25 **Biliran H Jr**, Sheng S. Pleiotrophic inhibition of pericellular urokinase-type plasminogen activator system by endogenous tumor suppressive maspin. *Cancer Res* 2001; **61**: 8676-8682
- 26 **Blacque OE**, Worrall DM. Evidence for a direct interaction between the tumor suppressor serpin, maspin, and types I and III collagen. *J Biol Chem* 2002; **277**: 10783-10788
- 27 **Seftor RE**, Seftor EA, Sheng S, Pemberton PA, Sager R, Hendrix MJ. Maspin suppresses the invasive phenotype of human breast carcinoma. *Cancer Res* 1998; **58**: 5681-5685
- 28 **Song SY**, Lee SK, Kim DH, Son HJ, Kim HJ, Lim YJ, Lee WY, Chun HK, Rhee JC. Expression of maspin in colon cancers: its relationship with p53 expression and microvessel density. *Dig Dis Sci* 2002; **47**: 1831-1835
- 29 **Jiang N**, Meng Y, Zhang S, Mensah-Osman E, Sheng S. Maspin sensitizes breast carcinoma cells to induced apoptosis. *Oncogene* 2002; **21**: 4089-4098
- 30 **Li JJ**, Colburn NH, Oberley LW. Maspin gene expression in tumor suppression induced by overexpressing manganese-containing superoxide dismutase cDNA in human breast cancer cells. *Carcinogenesis* 1998; **19**: 833-839

Modulation of human telomerase reverse transcriptase in hepatocellular carcinoma

Cheng-Jueng Chen, Satoru Kyo, Yao-Chi Liu, Yeung-Leung Cheng, Chung-Bao Hsieh, De-Chuan Chan, Jyh-Cherng Yu, Horng-Jyh Harn

Cheng-Jueng Chen, Yao-Chi Liu, Chung-Bao Hsieh, De-Chuan Chan, Jyh-Cherng Yu, Division of General Surgery, Department of Surgery, Tri-Service General Hospital, Taipei, Taiwan, China
Yeung-Leung Cheng, Division of Thoracic Surgery, Department of Surgery, Tri-Service General Hospital, Taipei, Taiwan, China
Satoru Kyo, Department of Obstetrics and Gynecology, Kanazawa University, Kanazawa, Japan

Horng-Jyh Harn, Division of Molecular Medicine, Department of Pathology, Buddhist Tzu-Chi General Hospital, Tzu-Chi University, Hua-Lien, Taiwan, China

Correspondence to: Horng-Jyh Harn, MD, PhD, Division of Molecular Medicine, Department of Pathology, Buddhist Tzu-Chi General Hospital, 707, Section 3, Chung-Yang Rd., 970 Hua-Lien, Taiwan, China. duke@tzuchi.com.tw

Telephone: +886-2-87927191 **Fax:** +886-2-87927372

Received: 2003-10-08 **Accepted:** 2003-12-16

Abstract

AIM: Most cancer cells acquire immortal capability by telomerase activation. The human telomerase reverse transcriptase gene (*hTERT*) is considered to be the major determinant of the enzymatic activity of human telomerase, and the *hTERT* promoter contains several c-Myc binding sites that mediate *hTERT* transcriptional activation. Few studies have examined the role of *hTERT* in hepatocarcinogenesis, and the relationship between c-Myc and telomerase in human hepatocellular carcinoma tissue is unknown.

METHODS: We measured *hTERT* mRNA levels and c-Myc oncoprotein expression in 57 patients with hepatocellular carcinoma using *in situ* hybridization and immunohistochemistry, respectively. The transcription regulation of *hTERT* was evaluated by transient transfection of pGL3-1375 into the human hepatocellular carcinoma cell line J5. To determine the relationship between c-Myc and the *hTERT* promoter, a 1375-bp DNA fragment encompassing the promoter was placed upstream of the luciferase reporter gene and transiently transfected into the cell line. Two additional *hTERT* promoter constructs (-776 and -100 bp region) and an *hTERT* promoter-LUC construct containing 2 c-Myc mutations (pGL3-181 MycMT) were also used for luciferase assays.

RESULTS: In 30 of 57 cases (52%), *hTERT* mRNA expression was associated with c-Myc protein expression. However, 16 of 57 cases (28%) showed strong *hTERT* mRNA detection without c-Myc protein expression, and 11 cases (19%) showed weak *hTERT* mRNA expression and strong c-Myc expression. Although luciferase activity was decreased between upstream 1375 bp and 776 bp, there was no significant difference between upstream 776 bp and 100 bp. Finally, there was no significant decrease in activity after transfection of the *hTERT* promoter-LUC construct.

CONCLUSION: The results indicate that c-Myc does not play a major role in gene regulation of the catalytic subunit of telomerase (*hTERT*) in human hepatocellular carcinoma.

Other regulatory elements or epigenetic phenomena should be further investigated to understand *hTERT* gene regulation in human hepatocellular carcinoma.

Chen CJ, Kyo S, Liu YC, Cheng YL, Hsieh CB, Chan DC, Yu JC, Harn HJ. Modulation of human telomerase reverse transcriptase in hepatocellular carcinoma. *World J Gastroenterol* 2004; 10(5): 638-642

<http://www.wjgnet.com/1007-9327/10/638.asp>

INTRODUCTION

Telomerase is a ribonucleoprotein enzyme that synthesizes G-rich telomeric repeats using its complementary RNA sequence as a template^[1,2]. Telomerase is expressed in most human cancers and immortal cell lines but is inactive in normal somatic cell lines or tissue^[3-5]. Recent reports support the concept that activation of telomerase may be an important and obligate step in the development of most malignant tumors^[6,7], including human hepatocellular carcinoma (HCC)^[8]. The human telomerase catalytic subunit (*hTERT*) has been shown to be a rate-limiting determinant of the enzymatic activity of human telomerase^[9,10]. Takakura *et al* identified the proximal 181-bp core promoter region essential for transactivation of *hTERT*^[11]. Their findings suggest that *hTERT* expression is strictly regulated at the transcription machinery, and that the proximal core promoter containing an E-box which binds to Myc/Max, as well as the 3' -region containing the GC-box which binds to Sp1, is required for transactivation of *hTERT*^[12]. Their findings further indicate that c-Myc and Sp1 cooperatively function as the major determinants of *hTERT* expression, and that the switching functions of Myc/Max and Mad/Max might also play roles in telomerase regulation. Wang *et al* added further support that Myc induce telomerase both in normal human mammary epithelial cells and in normal human diploid fibroblasts by introducing HPV-16, E6 protein into these cells^[13]. Their findings suggest that the ability of c-Myc to activate telomerase may contribute to its ability to promote tumor formation. Further, telomerase activity in estrogen receptor-positive MCF-7 cells was upregulated by treatment with 17 β -estradiol^[14]. Kyo *et al* reported that estrogen activated c-Myc expression in MCF-7 cells, and that E-boxes in the *hTERT* promoter that bind to c-Myc/max played additional roles in estrogen-induced transactivation of *hTERT*.

By using TRAP assay, we previously measured telomerase activity in surgically resected specimens from 25 cases of hepatocellular and adjacent healthy tissues^[15]. Telomerase activity was detected in 21 of the 25 HCC specimens from 25 different cases. This telomerase activity was correlated with human telomerase reverse transcriptase (*hTERT*) mRNA isoform expression but was poorly related to c-Myc expression in the hepatoma cell line J5^[16]. However, the role of c-Myc in *hTERT* expression in HCC remains unresolved.

In this study, we explored the relationship between *hTERT* mRNA regulation and c-Myc expression by RNA *in situ* hybridization and immunohistochemistry stain, respectively. The methods of *in situ* hybridization and immunohistochemistry

are semiquantitative and can determine localization. In addition, to determine the cis-elements essential for transcriptional activation of *hTERT*, luciferase assays were performed with reporter plasmids with serial deletions or mutation of the core promoter using hepatoma cell line J5. The results provide evidence for a role of c-Myc in the regulation of *hTERT* in hepatoma cells.

MATERIALS AND METHODS

Cell lines

All culture media including fetal bovine serum were purchased from Gibco Laboratories (Grand Island, NY). L-glutamine and penicillin/streptomycin were obtained from Sigma (St. Louis, MO).

WI38 cells (normal human fibroblasts) were obtained from the American Type Culture Collection and grown in DMEM containing 2 mmol/L L-glutamine, 50 U/mL penicillin, 50 mg streptomycin, and 100 mL/L fetal bovine serum. J5^[16] was maintained in RPMI 1640 medium containing 3 g/L L-glutamine and penicillin/streptomycin. All cell lines were cultivated in an atmosphere of 50 mL/L CO₂ at 37 °C.

Preparation of RNA probes

Total RNA was obtained from the HT29 cells (ATCC, Rockville, MD) by addition of TRIZOL reagent (Life Technologies, Rockville, MD) according to the manufacturer's instructions.

Ten micrograms of total RNA were used as a template for cDNA synthesis with Moloney murine leukemia virus (M-MTV) reverse transcriptase and oligo (dT)₁₂₋₁₈ (SUPERScript Preamplification System, Life Technologies). Subsequently, the forward primer 5'-CGG AAG AGT GTC TGG AGC AA-3' and the reverse primer 5'-GGA TGA AGC GGA GTC TGG-3' were designed for amplification of a 145-bp segment of *hTERT* spanning from nucleotide position 1 784 to 1 928 (GenBank accessory No. AF015950). Thirty-five PCR cycles were performed. For each cycle, the sample was denatured at 94 °C for 30 s, annealed at 55 °C for 60 s, and extended at 72 °C for 60 s. A 10 µL sample from 100 µL PCR solution was fractionated by electrophoresis on 20 g/L agarose gel. Subsequently, the PCR product was eluted from the agarose gel and subcloned into the pCRII-TOPO vector (Invitrogen, Carlsbad, CA), generating the construct-designated pCRII/*hTERT*-145.

The sense and antisense riboprobes were synthesized from *Bam* HI- and *Eco* RV-linearized pCRII/*hTERT*-145 according to the manufacturer's instructions using T7 and SP6 RNA polymerase, respectively, and labeled with digoxigenin-UTP (DIG RNA Labeling Kit, SP6/T7, Roche Molecular Biochemicals, Mannheim, Germany). Moreover, the housekeeping gene *GAPDH* was used to confirm the presence of intact RNA within the slides from each sample used for ISH.

RNA in situ hybridization

Formalin-fixed, paraffin-embedded tissue sections (4-µm thick) were deparaffinized with two 10 min washes with xylene and a graded series of alcohols for 3 min each. The deparaffinized tissues were then pretreated with 20 µg/mL proteinase K (Sigma) and 40 µg/mL pronase (Roche Molecular Biochemicals) at room temperature for 30 min. The tissues were then fixed with 40 g/L paraformaldehyde (Sigma) in phosphate-buffered saline at room temperature for 10 min and then acetylated with 2.5 mL/L acetic anhydride in 0.1 mmol/L triethanolamine-HCl (pH 8.0) at room temperature for 10 min.

Prehybridization was carried out in hybridization solution containing 500 g/L deionized formamide (Merck, Darmstadt, Germany), 5× SSC (1× SSC=150 mmol/L NaCl, 15 mmol/L sodium citrate, pH 7.2), 1 g/L N-lauroylsarcosine 2 g/L sodium dodecylsulfate, 20 mL/L blocking solution (DIG wash and block buffer set, Roche Molecular Biochemicals) and 250 µg/mL sonicated salmon sperm DNA (Invitrogen) at 50 °C for 1 h.

The slides were then incubated in a moist chamber at 50 °C for 16 h with the hybridization solution containing 0.1 to 0.5 µg/mL digoxigenin-labeled RNA probe. The slides were subsequently washed twice with 50% formamide-2× SSC at 50 °C for 30 min, twice with 2× SSC at room temperature for 15 min, and twice with 0.2× SSC at room temperature for 15 min. The slides were then equilibrated with 1× washing solution for 2 min and incubated with 10 mL/L blocking solution (DIG wash and block buffer set, Roche Molecular Biochemicals) for 10 min.

The tissues were incubated with a sheep monoclonal antidigoxigenin antibody (Roche Molecular Biochemicals) diluted 1:100 in 10 mL/L blocking solution at room temperature for 2 h. After washed three times with 1× washing solution (Roche Molecular Biochemicals), the color reaction was carried out by incubation with 1× nitroblue tetrazolium (NBT)/5-bromo-4-chloro-3-indolyl phosphate solution (Roche Molecular Biochemicals) at room temperature overnight. The slides were then counterstained with nuclear fast red for 5 min and then mounted with Crystal Mounting reagent (DAKO, Glostrup, Denmark).

Two independent observers evaluated the signal intensity of *hTERT* expression, which was semiquantitated as strong, moderate, weak, or no staining. Sense and antisense probes were applied to paired serial slides, and the noncoding strand detected by sense probes was used as a negative control.

Immunohistochemistry

Immunohistochemical staining was performed to determine the expression of c-Myc. The immunostaining procedure was performed using the labeled streptavidin-biotin method (LASB-2 Kit, DAKO). Briefly, the tissue was placed in a boiling citrate buffer (pH 6; ChemMate™, DAKO) twice for 5 min in a microwave oven at 750 W after deparaffinization and rehydration, as previously described. Quenching of the endogenous peroxidase activity by incubation with 30 mL/L hydrogen peroxide for 10 min at room temperature was followed by incubation with mouse monoclonal antibody NCL-cMYC (Clone 9E11, Novocastra Laboratories Ltd., Newcastle-upon-Tyne, UK) diluted 1:200 at room temperature for 2 h. After washed with Tris-buffered saline containing 1 g/L Tween-20, the specimens were sequentially incubated for 10 to 30 min with biotinylated anti-mouse immunoglobulins and peroxidase-labeled streptavidin. Staining was performed after 10 min of incubation with a freshly prepared substrate-chromogen solution containing 3% 3-amino-9-ethylcarbazole and hydrogen peroxide. Finally, the slides were lightly counterstained with hematoxylin, washed with water and then mounted. Two independent observers assessed the sections. Because the extent of c-Myc labeling index was heterogeneous, the scoring system included both the staining intensity and the percentage of stained cells^[17]. Staining intensity was graded as no staining (0), weak (1), moderate (2), or strong (3). The percentage of tumor cells with c-Myc staining was scored as follows: 1, <5%; 2, 5-20%; 3, 21-50%; 4, >50%. The multiplication values were then grouped into 4 scores as 0 (multiplication values 0, 1), 1 (multiplication values 2, 3), 2 (multiplication values 4, 6), or 3 (multiplication values 8, 9, 12).

PCR amplification and mutation screening of *hTERT* promoter

One microliter of genomic DNA was obtained as DNA template for use in PCR amplification of the *hTERT* promoter. The forward primer 5'-CCC ACG CGT GCA TTC GTG GTG CCC GGA GC-3' and the reverse primer 5'-CCC AGA TCT ATC GCG GGG GTG GCC GGG GCC AGG-3' were designed on the basis of a published *hTERT* promoter sequence^[11]. The PCR product was amplified in the presence of 1 µmol primers with Taq DNA polymerase (Takara Shuzo Company, Shiga, Japan) for 35 cycles of 1 min at 95 °C, 1 min at 56 °C, and 1 min at 72 °C. DNA sequencing using the reverse primer was

performed directly from the gel-purified PCR product or individual PCR product subcloned into the pCRII-TOPO vector. The analysis of the DNA sequences was compared with the wild-type sequence.

Construction of luciferase reporter gene plasmids

A P-3996 construct containing 3 996 bp of sequences upstream of the ATG (with A being position 1) plus exon 1 (219 bp), intron 1 (104 bp), and 37 bp of exon 2 of *hTERT* was used (a kind gift from Silvia Bacchetti, Department of Pathology and Molecular Medicine, McMaster University, Canada)^[18]. Various lengths of DNA fragments upstream of the initiating ATG codon were PCR amplified and inserted into luciferase reporter vector pGL3-Basic, a promoter- and enhancerless vector (Promega, Madison, WI) in sense orientation relative to the luciferase coding sequence at *Mlu*I and *Bgl*III sites. The sequences of primers were as follows: pGL3-1375-forward: 5' -CCCACGCGTAGACAATTCACAAACACAGC-3', pGL3-776-forward: 5' -CCCACGCGTGCCAGCAGGAGCCGCTGGCT-3', pGL3-100-forward: 5' -CCCACGCGTCCGCGCGGACCCCGCCCGT-3' and reverse (common): 5' -CCCAGATCTATCGCGGGGGTGGCCGGGGC CAGGGCTTC-3' with the PCR condition supported by Satoru Kyo (Department of Obstetrics and Gynecology, Kanazawa University, School of Medicine, Ishikawa, Japan)^[11]. The PCR product was amplified in the presence of 1 μ L primers with TaKaRa Taq DNA polymerase (Takara Shuzo Company, Shiga, Japan) for 30 cycles of 30 s at 96 °C, 45 s at 62 °C, and 7 min at 72 °C, and 30 min at 72 °C. The products were confirmed to have correct sequences by nucleotide sequencing, and their quantity and quality were routinely checked by agarose gel

electrophoresis. All plasmid DNAs were purified with the QIAquick gel extraction kit (QIAGEN, Hilden, Germany).

Transfection luciferase assay

Transient transfection of luciferase reporter plasmids was performed using LipofectAMINE 2000 (LF2000, Invitrogen), according to the protocol recommended by the manufacturer. In brief, 5×10^4 cells were seeded on 24-well plates, cultured overnight, and exposed to transfection mixtures containing 2 mg luciferase reporter plasmids for 4 h at 37 °C. Then, 0.5 ml growth media was added and cells were harvested 48 h after transfection. Luciferase assays were performed with the dual-luciferase reporter assay system (Promega) according to the manufacturer's protocols. The pGL3-control plasmid (1 mg/well, Promega) was also transfected into each cell line for better comparison among cell lines with different transfection efficiencies. The pRL-SV40 (1 ng/well, Promega) containing the *Renilla reniformis* luciferase gene was cotransfected with the *hTERT* promoter-luciferase constructs (1 mg/well) for normalization of the luciferase activity in each transfection. The MLX microtiter plate luminometer (Dynex Technologies, Chantilly, VA) was used to detect luciferase activity. All experiments were performed at least 3 times in each plasmid and represented the average relative luciferase activity.

Statistical analysis

To evaluate the relationships among paired groups, the Fisher exact test was performed using SPSS 10.0 software. Additionally, the correlation of paired groups was analyzed using chi-square test with the SPSS program. A *P* value ≤ 0.05 was considered statistically significant.

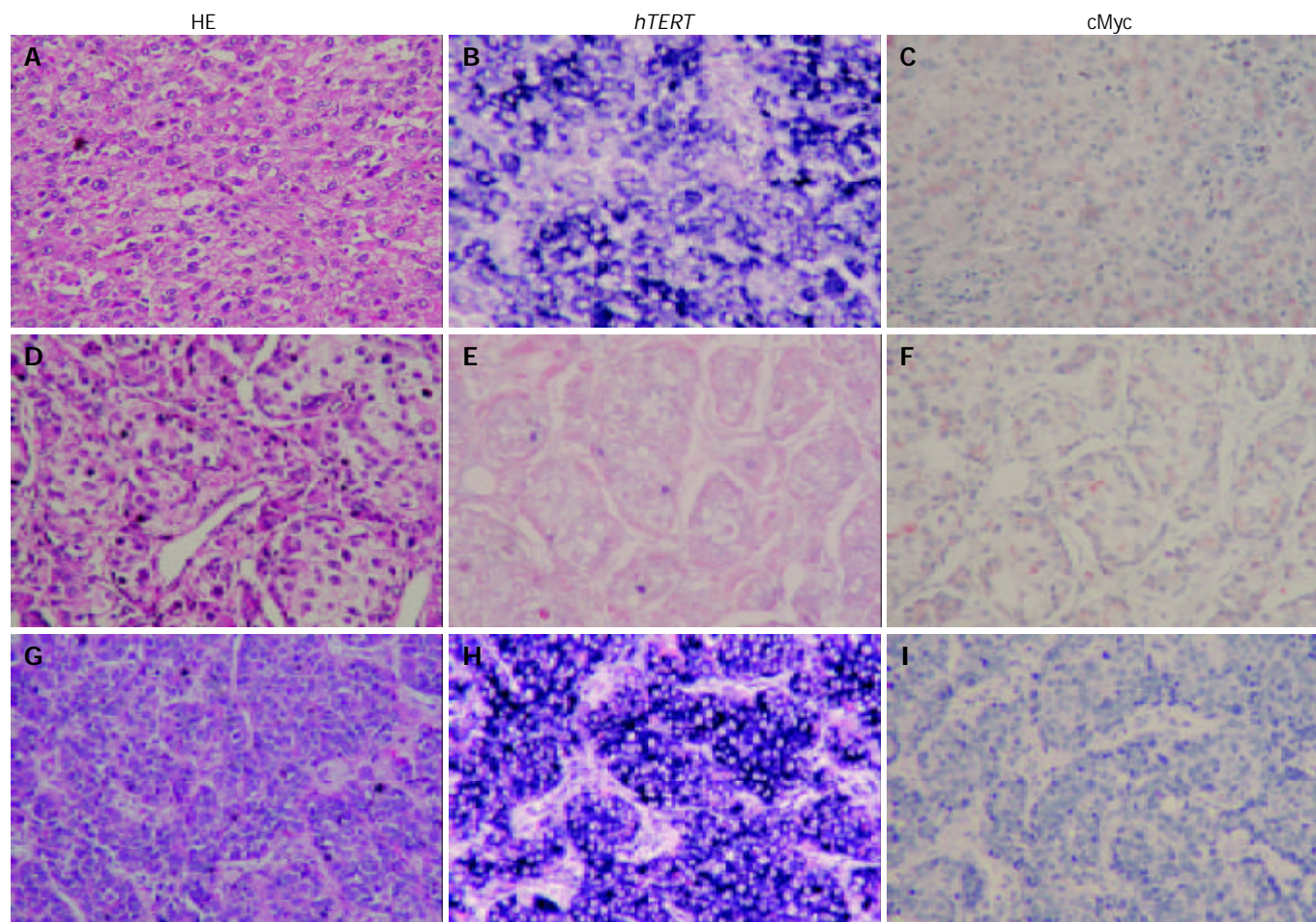


Figure 1 Corresponding distribution of *hTERT* signals and c-Myc staining in HCC tissue detected by HE staining (A, D, and G); *in situ* hybridization (*hTERT* positive, B and H; *hTERT* negative, E); and immunohistochemistry (c-Myc positive, C and F; c-Myc negative, I).

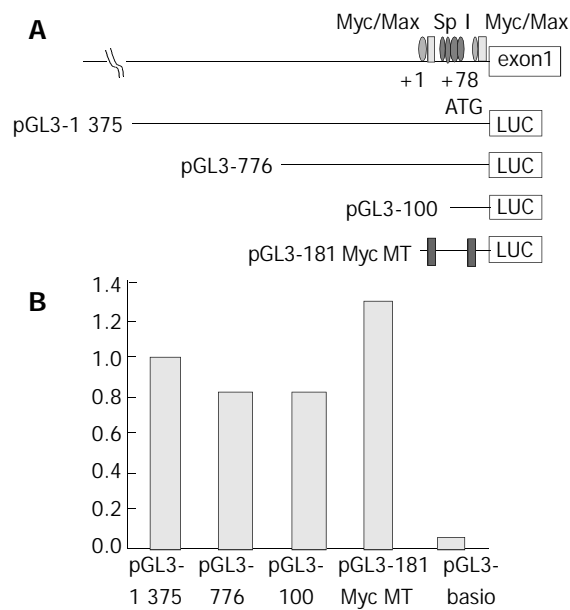


Figure 2 A: Schematic diagram of LUC reporter plasmids. Promoter fragments of decreasing size from the 5' end (1 375 bp, 776 bp, 100 bp and Myc double deletion mutant *hTERT*-promoter reporter plasmids of 181 bp) upstream of the initiating ATG were inserted into luciferase (*LUC*) reporter vector pGL3-Basic in sense orientation. +1, the transcription start site. Binding sites for c-Myc/Max and Sp1 are shown. B: Transcription activation of *hTERT* promoter. Data represent normalized relative luciferase fold activity compared with the promoterless pGL3 basic plasmid.

RESULTS

To investigate *hTERT* expression in HCC tissue, *in situ* hybridization was applied. Immunohistochemistry stain was used to observe c-Myc expression and its relationship with *hTERT* mRNA. Forty-seven of 57 cases showed weak to strong *hTERT* mRNA expression. The expression of *hTERT* mRNA was not related to tumor differentiation ($P < 0.815$) (Table 1). Forty-three of 57 cases showed c-Myc expression without tumor differentiation ($P < 0.348$) (Table 2).

Table 1 Comparison of *hTERT* expression and HCC differentiation

Differentiation	<i>hTERT</i> expression				Number
	None	Weak	Moderate	Strong	
Strong	1	2	2	7	12
Moderate	7	3	4	14	28
Weak	2	4	3	8	17
Number	10	9	9	29	57

Table 2 Comparison of c-Myc expression and HCC differentiation

Differentiation	c-Myc expression				Number
	0	1	2	3	
Strong	3	0	2	7	12
Moderate	5	7	7	9	28
Weak	6	3	2	6	17
Number	14	10	11	22	57

Thirty of 57 cases (52%) of *hTERT* mRNA expression were associated with c-Myc protein expression (30/57). However, 16 of 57 cases (28%) showed strong *hTERT* mRNA detection

with no Myc protein expression, whereas 11 of 57 cases (19%) showed weak *hTERT* mRNA expression with strong c-Myc detection ($P < 0.079$) (Figure 1).

Three different-length DNA fragments (-1 375, -776, and -100 bp) encompassing the *hTERT* promoter were placed upstream of the luciferase reporter gene, as was an *hTERT* promoter-Luc construct containing 2 c-Myc mutations (pGL-181 MycMT, a gift from Kyo *et al.*). All constructs were transiently transfected into HCC cell line J5 for luciferase study. Luciferase activity decreased between upstream 1 375 and 776 bp, but there was no significant difference of luciferase activity between upstream 776 and 100 bp or the 2 c-Myc mutations (Figure 2).

DISCUSSION

In a previous report, we demonstrated that telomerase activity in the HCC cell line J5 was not related to c-Myc expression^[16]. To our knowledge, this is the first study to determine the role of c-Myc in *hTERT* HCC. According to *in situ* hybridization and immunohistochemistry analysis, only half of *hTERT* mRNA expression co-occurred with c-Myc protein expression. Twenty-eight percent of HCC tissue samples had strong *hTERT* mRNA detection with no or weak c-Myc protein expression, 19% of HCC tissue samples had no or weak *hTERT* mRNA expression with strong c-Myc expression. However, several studies reported that Myc expression could transactivate *hTERT* via 2 E-boxes in cooperation with Sp1 motif^[12]. One of our constructs (a gift from Kyo), which encompassed 4 Sp1 and 2 c-Myc mutations, showed a high luciferase activity in the HCC cell line.

In contrast to the data of Kyo *et al.*^[14], pGL3-181MycMT, a double c-Myc mutant, compared with wild type pGL3-181, exhibited a 50% decreased luciferase activity when transfected to the MCF-7 breast cell line. These results implicate that c-Myc is a positive regulator of *hTERT*, though other yet undetermined regulatory elements of *hTERT* in HCC may exist. For example, hepatitis B virus pre-S2/S gene has been found to be a cis-activator of the *hTERT* promoter^[19]. By transfection of *HBx* gene into the HepG2 cell line, the activity of telomerase and apoptosis were decreased^[20]. Further investigation of non-c-Myc regulatory proteins in hepatoma is required in the future.

In our 16 HCC tissue specimens and 1 J5 cell line, *hTERT* promoter cis-element sequencing was performed. There was a polymorphism site (A transversion to T) just 3 bp away from the distal E-box, which might have affected the binding affinity of c-Myc^[21]. This effect might explain why two E-box mutations still had a high telomerase activity. However, more evidence is required in support of this polymorphism nucleotide in 2 E-box mutation construct.

Furthermore, the presence of a large CpG island with a dense CG-rich content implicates that DNA methylation and chromatin structure may play a role in the regulation of *hTERT* expression. Devereux *et al.* demonstrated that the promoter of one *hTERT*-negative fibroblast cell line, SUSM-1, was methylated at all sites examined^[22]. Treatment of SUM-1 cells with the demethylating agent induced the cells to express *hTERT*, suggesting a potential role for DNA methylation in negative regulation. This epigenetic mechanism could explain why 19% of HCC samples showed strong c-Myc detection with no or weak *hTERT* mRNA expression. The role of GC island methylation in the regulation of *hTERT* expression merits further study.

In the Kyo *et al.* report, the cis-acting effect of E-boxes and the Myc or Max requirement for transactivation varied among different cell types^[12]. Deletion and mutation of the E-box resulted in significant loss of transcriptional activity in C33A cells, but not in SiHa cells. In C33A cells, expression of

Myc and Max had only marginal effects on transactivation. This diversity among different cell lineages suggests a varied role of c-Myc in *hTERT* gene regulation. The data also indicate that there are multiple levels of regulation of *hTERT* activity in human neoplasm.

In summary, in the present hepatoma tissue study, 50% of hepatomas showed c-Myc overexpression with *hTERT* transcript upregulation. Other regulator elements and epigenetic mechanisms may be involved in *hTERT* transcript regulation. The proximal c-Myc motif plays a minor role in *hTERT* gene regulation. The results of immunohistochemistry and promoter-constructed luciferase analyses suggest that, in HCC, *hTERT* regulation is not restricted to c-Myc and involves other mechanisms.

REFERENCES

- Moyzis RK**, Buckingham JM, Cram LS, Dani M, Deaven LL, Jones MD, Meyne J, Ratliff RL, Wu JR. A highly conserved repetitive DNA sequence, (TTAGGG)_n, present at the telomeres of human chromosomes. *Proc Natl Acad Sci U S A* 1988; **85**: 6622-6626
- Shippen-Lentz D**, Blackburn EH. Functional evidence for an RNA template in telomerase. *Science* 1990; **247**: 546-552
- Counter CM**, Hirte HW, Bacchetti S, Harley CB. Telomerase activity in human ovarian carcinoma. *Proc Natl Acad Sci U S A* 1994; **91**: 2900-2904
- Kim NW**, Piatyszek MA, Prowse KR, Harley CB, West MD, Ho PL, Coviello GM, Wright WE, Weinrich SL, Shay JW. Specific association of human telomerase activity with immortal cells and cancer. *Science* 1994; **266**: 2011-2015
- Shay JW**, Bacchetti S. A survey of telomerase activity in human cancer. *Eur J Cancer* 1997; **33**: 787-791
- Chadeneau C**, Hay K, Hirte HW, Gallinger S, Bacchetti S. Telomerase activity associated with acquisition of malignancy in human colorectal cancer. *Cancer Res* 1995; **55**: 2533-2536
- Zhan WH**, Ma JP, Peng JS, Gao JS, Cai SR, Wang JP, Zheng ZQ, Wang L. Telomerase activity in gastric cancer and its clinical implications. *World J Gastroenterol* 1999; **5**: 316-319
- Tahara H**, Nakanishi T, Kitamoto M, Nakashio R, Shay JW, Tahara E, Kajiyama G, Ide T. Telomerase activity in human liver tissues: comparison between chronic liver disease and hepatocellular carcinomas. *Cancer Res* 1995; **55**: 2734-2736
- Counter CM**, Meyerson M, Eaton EN, Ellisen LW, Caddle SD, Haber DA, Weinberg RA. Telomerase activity is restored in human cells by ectopic expression of hTERT (hEST2), the catalytic subunit of telomerase. *Oncogene* 1998; **16**: 1217-1222
- Kim HR**, Christensen R, Park NH, Sapp P, Kang MK, Park NH. Elevated expression of hTERT is associated with dysplastic cell transformation during human oral carcinogenesis *in situ*. *Clin Cancer Res* 2001; **7**: 3079-3086
- Takakura M**, Kyo S, Kanaya T, Hirano H, Takeda J, Yutsudo M, Inoue M. Cloning of human telomerase catalytic subunit (hTERT) gene promoter and identification of proximal core promoter sequences essential for transcriptional activation in immortalized and cancer cells. *Cancer Res* 1999; **59**: 551-557
- Kyo S**, Takakura M, Taira T, Kanaya T, Itoh H, Yutsudo M, Ariga H, Inoue M. Sp1 cooperates with c-Myc to activate transcription of the human telomerase reverse transcriptase gene (hTERT). *Nucleic Acids Res* 2000; **28**: 669-677
- Wang J**, Xie LY, Allan S, Beach D, Hannon GJ. Myc activates telomerase. *Genes Dev* 1998; **12**: 1769-1774
- Kyo S**, Takakura M, Kanaya T, Zhuo W, Fujimoto K, Nishio Y, Orimo A, Inoue M. Estrogen activates telomerase. *Cancer Res* 1999; **59**: 5917-5921
- Hsieh HF**, Harn HJ, Chiu SC, Liu YC, Lui WY, Ho LI. Telomerase activity correlates with cell cycle regulators in human hepatocellular carcinoma. *Liver* 2000; **20**: 143-151
- Chen CJ**, Tsai NM, Liu YC, Ho LI, Hsieh HF, Yen CY, Harn HJ. Telomerase activity in human hepatocellular carcinoma: parallel correlation with human telomerase reverse transcriptase (hTERT) mRNA isoform expression but not with cell cycle modulators or c-Myc expression. *Eur J Surg Oncol* 2002; **28**: 225-234
- Brabletz T**, Herrmann K, Jung A, Faller G, Kirchner T. Expression of nuclear beta-catenin and c-myc is correlated with tumor size but not with proliferative activity of colorectal adenomas. *Am J Pathol* 2000; **156**: 865-870
- Cong YS**, Wen J, Bacchetti S. The human telomerase catalytic subunit hTERT: organization of the gene and characterization of the promoter. *Hum Mol Genet* 1999; **8**: 137-142
- Horikawa I**, Barrett JC. Cis-Activation of the human telomerase gene (hTERT) by the hepatitis B virus genome. *J Natl Cancer Inst* 2001; **93**: 1171-1173
- Zhou W**, Shen Q, Gu B, Ren H, Zhang D. Effects of hepatitis B virus X gene on apoptosis and the activity of telomerase in HepG (2) cells. *Zhonghua Ganzangbing Zazhi* 2000; **8**: 212-214
- O'Hagan RC**, Schreiber-Agus N, Chen K, David G, Engelman JA, Schwab R, Alland L, Thomson C, Ronning DR, Sacchettini JC, Meltzer P, DePinho RA. Gene-target recognition among members of the myc superfamily and implications for oncogenesis. *Nat Genet* 2000; **24**: 113-119
- Devereux TR**, Horikawa I, Anna CH, Annab LA, Afshari CA, Barrett JC. DNA methylation analysis of the promoter region of the human telomerase reverse transcriptase (hTERT) gene. *Cancer Res* 1999; **59**: 6087-6090

Edited by Wang XL Proofread by Zhu LH

Prognostic significance of preoperative circulating vascular endothelial growth factor messenger RNA expression in resectable hepatocellular carcinoma: A prospective study

Kuo-Shyang Jeng, I-Shyan Sheen, Yi-Ching Wang, Shu-Ling Gu, Chien-Ming Chu, Shou-Chuan Shih, Po-Chuan Wang, Wen-Hsing Chang, Horng-Yuan Wang

Kuo-Shyang Jeng, Department of Surgery, Mackay Memorial Hospital, Taipei, Taiwan, China

I-Shyan Sheen, Liver Research Unit, Chang Gung Memorial Hospital, Taipei, Taiwan, China

Yi-Ching Wang, Shu-Ling Gu, Chien-Ming Chu, Medical Research, Mackay Memorial Hospital, Taipei, Taiwan, China

Kuo-Shyang Jeng, Mackay Junior School of Nursing, Taipei, Taiwan, China

Shou-Chuan Shih, Po-Chuan Wang, Wen-Hsing Chang, Horng-Yuan Wang, Department of Internal Medicine, Mackay Memorial Hospital, Taipei, Taiwan, China

Correspondence to: I-Shyan Sheen, M.D., Liver Research Unit, Chang Gung Memorial Hospital, No. 199, Tung-Hwa North Road, Taipei, Taiwan, China. issheen.jks@msa.hinet.net

Telephone: +886-3-3281200 Ext 8102 **Fax:** +886-2-27065704

Received: 2003-10-15 **Accepted:** 2003-12-15

Abstract

AIM: To investigate the prognostic value of vascular endothelial growth factor messenger RNA (VEGF mRNA) in the peripheral blood (PB) of patients with hepatocellular carcinoma (HCC) undergoing curative resection.

METHODS: Using a reverse-transcription polymerase chain reaction (RT-PCR)-based assay, VEGF mRNA in the PB was determined prospectively in 50 controls and in 50 consecutive patients undergoing curative resection for HCC.

RESULTS: Among the isoforms of VEGF mRNA, VEGF₁₆₅ and VEGF₁₂₁ were expressed. By multivariate analysis, a higher level of VEGF₁₆₅ in preoperative PB correlated with a risk of HCC recurrence with borderline significance ($P=0.050$) and significantly with recurrence-related mortality ($P=0.048$); while VEGF₁₂₁ did not. Other significant predictors of HCC recurrence included cellular dedifferentiation ($P=0.033$), an absent or incomplete capsule ($P=0.020$), vascular permeation ($P=0.018$), and daughter nodules ($P=0.006$). The other significant parameter of recurrence related mortality was cellular dedifferentiation ($P=0.053$). The level of circulating VEGF mRNA, however, did not significantly correlate with tumor size, cellular differentiation, capsule, daughter nodules, vascular permeation, necrosis and hemorrhage of tumors.

CONCLUSION: The preoperative level of circulating VEGF mRNA, especially isoform VEGF₁₆₅, plays a significant role in the prediction of postoperative recurrence of HCC.

Jeng KS, Sheen IS, Wang YC, Gu SL, Chu CM, Shih SC, Wang PC, Chang WH, Wang HY. Prognostic significance of preoperative circulating vascular endothelial growth factor messenger RNA expression in resectable hepatocellular carcinoma: A prospective study. *World J Gastroenterol* 2004; 10(5): 643-648

<http://www.wjgnet.com/1007-9327/10/643.asp>

INTRODUCTION

Angiogenesis, known to be essential for the survival, growth, invasion, and metastasis of tumor cells, is a complex multistep process. There are extracellular matrix remodeling and binding of angiogenic factors to specific endothelial cell (EC) receptors, leading to EC proliferation, invasion of the basement membrane, migration, differentiation, and formation of new capillary tubes. Anastomosis of these new vessels develops into a vascular network^[1,2].

Several factors with angiogenic activity have been identified, but one of the most potent, direct acting and specific is vascular endothelial growth factor (VEGF), also known as vascular permeability factor and vasculotropin^[3].

Hepatocellular carcinoma (HCC), a leading cause of death in Taiwan and many Asian countries, is a highly vascular tumor dependent on neovascularization. Some authors have reported markedly elevated VEGF protein levels in HCC patients with remote metastases compared with those without metastasis, suggesting that VEGF may be a marker for metastasis in HCC^[4-6]. Most such studies, however, depended on enzyme immunoassay to determine VEGF protein concentrations. To our knowledge, little is known about the prognostic significance of VEGF mRNA expression in the prediction of postresection recurrence of HCC. We conducted this prospective study to investigate the correlation between preoperative VEGF mRNA expression in peripheral blood (PB) and postoperative recurrence of HCC.

MATERIALS AND METHODS

Study population

From July 2001 to April 2003, 50 patients (31 men and 19 women, with a mean age of 56.2 ± 13.3 yr) of 58 consecutive patients with HCC undergoing curative hepatectomy were enrolled in this prospective study. Patients who had previously had a hepatectomy or preoperative neoadjuvant ethanol injection or hepatic arterial chemoembolization (TACE) were excluded. The surgical procedures performed included 38 major resections (8 extended right lobectomies, 10 right lobectomies, 8 left lobectomies and 12 two-segmentectomies) and 12 minor resections (10 segmentectomies, 1 subsegmentectomy, and 1 wedge resection). A control group including 30 healthy volunteers without liver disease (15 men, 15 women, mean age 40 yr) and 20 patients with chronic liver disease but without evidence of HCC also gave PB samples.

PB samples for the detection of VEGF mRNA were obtained by forearm venipuncture one day prior to surgery from all 50 patients. After discharge, the patients were assessed regularly to detect tumor recurrence with abdominal ultrasonography (every 2-3 mo during the first 5 yr, then every 4-6 mo thereafter), serum alpha fetoprotein (AFP) and liver biochemistry (every 2 mo during the first 2 yr, then every 4 mo during the following 3 yr, and every 6 mo thereafter), abdominal computed tomography (CT) (every 6 mo during the first 5 yr, then annually), and chest X-ray and bone scans

(every 6 mo). Hepatic arteriography was obtained if the other studies suggested possible cancer recurrence. Detection of tumor on any imaging study was defined as recurrence.

Clinicopathological parameters analyzed included sex (male vs female), age, the presence of liver cirrhosis, hepatitis B virus (HBV) infection (hepatitis B surface antigen), hepatitis C virus (HCV) infection (anti-hepatitis C virus antibody), serum AFP level (<20 ng/mL vs 20 to 1 000 ng/mL vs >1 000 ng/mL), cirrhosis, Child-Pugh class of liver functional reserve (A vs B), tumor size (<3 cm vs 3 to 10 cm vs >10 cm), tumor encapsulation (complete vs incomplete or absent), presence of daughter nodules, vascular permeation (including vascular invasion and/or tumor thrombi in either the portal or hepatic vein), and cell differentiation grade (Edmondson and Steiner grades I to IV).

Detection of VEGF mRNA

Ethylenediamine tetraacetic acid (EDTA)-treated whole blood was centrifuged and the plasma fraction removed. The cellular fraction was enriched for mononuclear cells or possible tumor cells according to the method described by Oppenheim. Nucleated cells were isolated from peripheral blood using tetradecyltrimethyl-ammonium bromide. Total cellular RNA was then extracted with PUREscript RNA Isolation Kits TRI-Zol (Life Technologies Inc., Gaithersburg, USA). cDNA was synthesized from 5 µg of the mRNA. The reverse transcription reaction solution contained 6 µL of 5×first strand buffer, 10 mmol/L dithiothreitol, 125 mmol/L each of dCTP, dATP, dGTP and dTTP, 0.3 µg of random hexamers, and 200 units of Superscriptase II Moloney murine leukemia virus reverse transcriptase (Life Technologies Inc.). The RNA solution was incubated at 95 °C for 10 min, quickly chilled on ice, then mixed with the reverse transcription reaction solution (total volume 20 µL), and incubated at 37 °C for 60 min. The sequences of the sense primers were 5' -AGTGTGTGCCCACTGAGGA-3' (VEGF) and 5' -AGTCAACGGATTTGGTCGTA-3' (GAPDH) and those of the antisense primers were 5' -AGTCAACGGATTTGGTCGTA-3' (VEGF) and 5' -GGAACATGTAAACCATGTAG-3' (GAPDH). The first polymerase chain reaction (RT-PCR) solution contained 5 µL of the synthesized cDNA solution, 10 µL of 10× polymerase reaction buffer, 500 mol/L each of dCTP, dATP, dGTP and dTTP, 15 pmol of each external primer (EX-sense and EX-antisense), 4 units of Thermus Brockiamus Prozyme DNA polymerase (PROtech Technology Ent. Co., Ltd. Taipei, Taiwan), and water. The PCR cycles were: denaturing at 94 °C for 1 min, annealing at 52 °C for 1 min, and primer extension at 72 °C for 1 min. The cycles were repeated 40 times. The PCR product was reamplified with internal primers for nested PCR to obtain a higher sensitivity. The first and second PCR components were the same, but for the primer pairs (IN-sense and IN-antisense), the final product was electrophoresed on 20g/L agarose gel and stained with ethidium bromide. Four different isoforms of human VEGF were identified, arising from alternative splicing of the primary transcript of a single gene. The majority were VEGF₁₂₁ (165 bp) and VEGF₁₆₅ (297 bp). The percentage intensity of the VEGF PCR fragment for each liver was relative to a GAPDH PCR fragment (122 bp). The intensity of bands was measured using Fujifilm Science Lab 98 (Image Gauge V3.12). The sensitivity of our assay was assessed using human hepatocytes.

A HepG2 (hepatoblastoma) cell line served as a positive control for VEGF mRNA expression. For negative controls, we used EDTA-treated water (filtered and vaporized).

Statistical analysis

A statistical software (SPSS for Windows, version 8.0, Chicago, Illinois) was employed, with Student's *t*-test used to analyze

continuous variables and a chi-square or Fisher's exact test for categorical variables. Factors relating to the presence of postoperative hAFP mRNA in peripheral blood were analyzed by stepwise logistic regression. A Cox proportional hazards model was used for multivariate stepwise analysis to identify significant factors for predicting recurrence and mortality. Significance was taken as a *P* value <0.05.

RESULTS

RT-PCR analysis of VEGF transcript in peripheral blood

VEGF mRNA was expressed in the peripheral blood of 10 (VEGF₁₆₅ in 4 and VEGF₁₂₁ in 10) of 50 control patients (10/50, 20%). In the HCC group, isoform VEGF₁₆₅ was detected in 40 patients (80%) (with a concentration ranging from 0.198 to 0.7190) and isoform VEGF₁₂₁ in all 50 patients (100%) (concentration ranging from 0.2958 to 1.0356).

We did not detect isoforms VEGF₁₈₉ and/or VEGF₂₀₆ in either study or control patients

Table 1 Demographic, clinical and tumor variables of patients with HCC undergoing curative resection (*n*=50)

Variables	No. of patients (%)
Age (mean, years)	56.2±13
Male	31 (62)
Child- Pugh's class A	43 (86)
Serum AFP <20 ng/mL	16 (32)
20-10 ³ ng/mL	18 (36)
>10 ³ ng/mL	14 (28)
HBsAg (+)	36 (72)
Anti-HCV (+)	13 (26)
Size of HCC <3 cm	12 (24)
3-10 cm	13(26)
>10 cm	25(50)
Cirrhosis	40(80)
Edmondson-Steiner's Grade I	4 (8)
Grade II	12 (24)
Grade III	18 (36)
Grade IV	16 (32)
Complete capsule	19 (38)
Vascular permeation	29 (58)
Daughter nodules	31 (62)
Tumor necrosis	33(66)
Tumor hemorrhage	29(58)

AFP: serum alpha fetoprotein; HBsAg (+): positive hepatitis B surface antigen; Anti-HCV(+): positive hepatitis C virus antibody; Edmondson Steiner grade: differentiation grade.

Correlation of VEGF mRNA expression and tumor recurrence

Sixteen patients (32%) had clinically detectable recurrence during the follow up period (median 1.5 yr, range 1 to 2.5 yr), of whom 7 died. A high preoperative level of isoform VEGF₁₆₅ mRNA correlated significantly with tumor recurrence both univariately (*P*=0.021) and multivariately (*P*=0.050). Isoform VEGF₁₂₁ levels had no such correlation. By multivariate analysis, other significant predictors of recurrence included poor cellular differentiation (*P*=0.033), less encapsulation (*P*=0.020), more vascular permeation (*P*=0.018) and the presence of daughter nodules (*P*=0.006) (Table 2).

Correlation of VEGF mRNA expression and recurrence-related death

The preoperative level of isoform VEGF₁₆₅ in PB significantly correlated with death from recurrence both univariately

($P < 0.001$) and multivariately ($P = 0.048$). By multivariate analysis, a greater degree of vascular permeation significantly correlated with mortality ($P = 0.045$), and poor cellular differentiation approached significance ($P = 0.053$) (Table 3).

Table 2 Predictors of HCC recurrence

Variable	P values	
	UV	MV
Sex	0.895	-
Age	0.279	-
Size (<3 cm, >10 cm)	0.415	-
Liver cirrhosis	0.510	-
Child-Pugh class	0.528	-
Serum AFP	0.744	-
HBsAg (+)	0.280	-
Anti-HCV (+)	0.481	-
Edmondson Steiner grade	0.0005	0.033
Capsule	<0.0001	0.020
Vascular permeation	<0.0001	0.018
Daughter nodules	<0.0001	0.006
Tumor necrosis	0.344	-
Tumor hemorrhage	0.812	-
Serum VEGF ₁₆₅ mRNA	0.0206	0.050
Serum VEGF ₁₂₁ mRNA	0.520	-

UV: univariate analysis; MV: multivariate analysis; AFP: serum alpha fetoprotein; HBsAg(+): positive hepatitis B surface antigen; Anti-HCV(+): positive hepatitis C virus antibody; Edmondson Steiner grade: differentiation grade I, II vs III, IV; n.s: not significant.

Table 3 Correlation between clinical and tumor variables and recurrence-related mortality

Variables	P values	
	UV	MV
Sex	0.510	-
Age	0.440	-
Size (<3 cm, >10 cm)	0.519	-
Liver cirrhosis	0.510	-
Child-Pugh class	0.548	-
HBsAg (+)	0.351	-
Anti-HCV (+)	0.521	-
Edmondson Steiner grade	<0.001	0.053
Capsule	0.033	n.s.
Vascular permeation	<0.001	0.045
Daughter nodules	0.016	n.s.
Tumor necrosis	0.373	-
Tumor hemorrhage	0.306	-
Serum VEGF ₁₆₅ mRNA	<0.001	0.048
Serum VEGF ₁₂₁ mRNA	0.763	-

UV: univariate analysis; MV: multivariate analysis; AFP: serum alpha fetoprotein; HBsAg (+): positive hepatitis B surface antigen; Anti-HCV(+): positive hepatitis C virus antibody; Edmondson Steiner grade: differentiation grade I, II vs III, IV; n.s: not significant.

Correlation between VEGF mRNA expression and clinical and histopathologic features

There was no significant association between either isoform of VEGF mRNA and gender, age, serum AFP level, chronic HBV or HCV carriage, tumor size, coexisting cirrhosis, cellular differentiation, capsule, vascular permeation, daughter nodules, tumor necrosis, or tumor hemorrhage (all $P > 0.05$).

DISCUSSION

Our study showed that a higher value of circulating VEGF mRNA isoform ₁₆₅ before curative resection of HCC was significantly associated with an increased risk of postoperative recurrence and disease mortality. The presence of preoperative VEGF mRNA isoform ₁₂₁ was not significantly predictive of outcomes.

The active form of VEGF was a homodimeric cytokine with molecular weight of 34-46 ku, the variation in size was due to alternative exon splicing which produces four different isoforms of 121, 165, 189 and 206 amino acids (monomeric size). The last three of those had heparin binding activity^[15]. Different cancers have different expression of the isoforms. The majority of HCC could express an abundance of VEGF ₁₂₁ and VEGF ₁₆₅^[4,7,8]. Further analysis by Ferrara indicated that VEGF₁₆₅ was the predominantly expressed form in human cDNA libraries as well as in most normal cells and tissues^[8].

Several studies have revealed that the serum VEGF level is of value for predicting disease progression and prognosis in cancers of different origins, including the breast, gastrointestinal organs, kidney, urothelium, ovary, lung, and lymphoma^[9-18]. However, the serum level of VEGF, which is what most other investigators have measured, might be influenced by other factors such as platelet number, associated liver cirrhosis, or coexisting infection^[19-22]. For accurate measurement, citrated plasma processed within 1 h of venipuncture is better than serum.

Measuring VEGF in HCC tissue has the disadvantage of not being available until after a biopsy or resection has been done. The majority of angiogenic factors are soluble, diffusible peptides. Hence, the circulating level of angiogenic factors theoretically reflects the angiogenic activity of the tumor. Compared with expression in tumor tissue, the advantage of the measurement of circulating VEGF expression is that it can be performed without tissue specimens and repeated serially. Jinno *et al.*, believed that circulating VEGF might be derived mainly from a large burden of tumor cells, but also partly from platelets activated by vascular invasion of HCC cells^[20].

We chose to measure circulating mRNA expression of VEGF rather than the protein itself. According to El-Assal's study, the level of VEGF mRNA did not always correlate with the protein concentration^[23]. Immunohistochemistry could not distinguish small amounts of protein, which may partly explain the discrepancy in protein and mRNA levels.

An additional question is whether the value of circulating VEGF (either protein or mRNA) corresponds with VEGF mRNA in HCC tissue. Tokunaga noted that the circulating VEGF mRNA isoform pattern in colon cancer was not always significantly correlated with the gene expression level. The release of VEGF mRNA might be influenced by some cells other than HCC cells^[24]. Warren found VEGF mRNA in hepatocytes and some Kupffer cells^[25]. According to Banks, the presence of mRNA for VEGF was also described in T lymphocytes, CD34* cells, and monocytes^[19,21].

There are considerable discrepancies among reports about the clinical significance of VEGF expression in HCC^[20,26-34]. The high recurrence rate after resection has been found to be the main determinant for the poor outcome of HCC^[35-37]. Tumor invasiveness variables correlating with recurrence include high serum AFP, hepatitis, vascular permeation, the grade of cellular differentiation, infiltration or absence of capsule, tumor size, coexisting cirrhosis, the presence of daughter nodules, and multiple lesions. Therefore, a number of studies have been done to see if VEGF correlated with any or all of those factors.

Zhou showed that high VEGF expression in HCC was associated with portal vein tumor thrombosis^[28]. Li reported that VEGF mRNA in HCC correlated significantly with portal

vein emboli, poorly encapsulated tumors, and microvascular density in HCC tissues^[27]. Chow found that VEGF expression was significantly associated with the PCNA index and sonographic evidence of portal vein tumor thrombosis but not with the liver biochemical profile, tumor volume, gender, severity of liver disease, or tumor grading^[26].

One possible explanation for the discrepancies may be the assessment of tumors of different sizes and etiologies. The number of study patients is another possible factor. Because most of the reported investigations were performed in small series, we used 50 patients which seemed an adequate sample size compared with other studies. It is also likely that the effect of VEGF on angiogenesis depends on not only tumor cell expression of VEGF, but also on the VEGF receptors in endothelial cells.

Some have reported a correlation between increased plasma VEGF protein level in HCC patients and tumor size, number, portal vein emboli, poorly encapsulated tumors, microscopic venous invasion, metastasis, and recurrence. Yamamoto found there was a positive correlation between the increment of intratumoral MVD and serum VEGF concentrations^[38].

According to our study, a higher expression of circulating VEGF mRNA was significantly correlated with tumor recurrence and recurrence-related mortality but not with the other accepted measures of invasiveness. Circulating VEGF mRNA thus appears to be an independent risk factor of postoperative recurrence. There are several possible explanations for this dissociation.

Some studies have found that the histologic grade of HCC was associated with VEGF expression in noncancerous liver cells, suggesting a complex regulatory mechanism for circulating VEGF in liver disease. Coexisting liver cirrhosis might influence VEGF expression^[22,23]. About 80% of our study patients had cirrhosis. Some investigators have found that VEGF expression was significantly higher in cirrhotic livers than in noncirrhotic livers. Furthermore, it has been shown that cirrhosis itself was associated with increased angiogenic activity. El-Assal *et al* observed that cirrhotic livers had significantly higher VEGF expressions than noncirrhotic livers, suggesting that VEGF might be associated with angiogenesis in cirrhosis^[23]. In addition, some suggested a possible involvement of VEGF in angiogenesis of the cirrhotic liver but not in angiogenesis of HCC. Akiyoshi suggested that a low serum VEGF level in liver cirrhosis might reflect the degree of liver dysfunction and might be associated with the grade of hepatocyte regeneration^[22], VEGF levels were decreased with the worsening of the Child-Pugh score. However, most of our patients were Child-Pugh class A, and their resectable lesions, were unlike those studied by Akiyoshi.

The stage of cancer might influence the VEGF expression^[38-41]. Chao showed that a lower range of circulating VEGF levels in patients with early-stage HCC overlapped considerably with those in normal controls or in patients with chronic hepatitis or cirrhosis^[30]. Therefore, serum VEGF is probably not useful for early detection of HCC. In contrast, a large quantity of VEGF may be released by the large load of HCC cells in advanced disease (stage VI B). Because plasma VEGF level is significantly higher in stage IVB than in stage IVA, other mechanisms may be responsible, such as agglutination and activation of platelets caused by vascular invasion and circulating tumor cells. It may thus be the platelets rather than or in addition to HCC cells that are responsible for the release of VEGF into circulation. Our patients did not have such an advanced disease.

The relation between tumor size and VEGF mRNA expression might be complex and dynamic because of different vascular growth patterns^[5,34,42-44]. In small hypervascular HCCs, approximately 1.0 cm in diameter in those that grow with a pattern of vessel replacement, artery-like vessels are not well

developed. Capillarization of the blood spaces is present but in an incomplete form, and portal tracts often appear within cancerous nodules. These HCCs are thought to receive a predominantly portal blood supply. As tumor size increases, portal tracts decrease in number, and artery-like vessels gradually increase in number and size. Well-differentiated HCCs measuring 1.0 to 1.5 cm in diameter are in a transitional stage from portal to arterial blood supply, with the reduction in portal flow preceding the increase in arterial flow. Therefore, blood flow in HCC at this point would be low. This may be the reason why many well-differentiated HCCs are not detected on angiography, with hypervascularity seen until nodules become larger than 2 cm in diameter.

VEGF positivity may therefore gradually decrease with increasing tumor size. According to Yamaguchi, 36.8% of nodules larger than 3.0 cm were VEGF-negative^[34]. El-Assal showed that, contrary to the usual angiographic findings, HCCs larger than 5 cm in diameter were not more vascular than smaller tumors and were less vascular than medium-sized lesions^[23]. However, it has been reported that the intercapillary distance increased as the tumors size or weight increased, which may be caused by the significantly different rates of endothelial (50 to 60 h) and neoplastic cell (22 h) turnover.

These complicated changes in vascularity may account for the disparate results among reported studies. Suzuki reported that VEGF mRNA levels were not correlated with the vascularity of HCCs as seen on angiography^[4]. On the contrary, Mise *et al.* showed that the degree of VEGF mRNA expression was significantly correlated with the intensity of tumor staining in angiograms ($P < 0.01$)^[5]. Some have reported higher VEGF expression in small-size and well-differentiated HCCs and suggested that VEGF played its most important role in a relatively early stage of angiogenesis. In general, advanced HCCs are mainly supplied with arterial blood, and arterial angiography may reveal hypervascularity. Serum VEGF concentrations have been reported to be significantly higher in advanced stage rather than in early stage of breast and gastric cancer^[9,13,14].

Neovascularization appears to be one of the crucial steps in a tumor's transition from a small, harmless cluster of mutated cells to a large, malignant growth, capable of spreading to other organs throughout the body. Because of the complex nature of the angiogenic process, however, it seems that VEGF expression is not the sole contributor to angiogenesis in HCC. Other factors involved in this process may include TGF- β , TNF- α , IL-8, *etc.*

It has been reported recently that VEGF mRNA expression was readily induced by hypoxia or ischemia. This is why we excluded patients who received preoperative TACE, in order to avoid ischemia-induced changes in VEGF expression.

Although tumor necrosis was present in 66% of our study patients (Table 1), circulating VEGF mRNA did not statistically correlate with it. We also did not find any correlation with fibrous capsule or septum formation, in contrast to the findings of Inoue *et al.*^[12]. The origin of the capsule and fibrous septa in HCC is unclear. Nakashima *et al* suggested the possibility of fibrogenesis at the interface of two tumor nodules of different properties, a process requiring fibrin deposition in the initial stage^[45]. Some authors stated that a capsule or septa was formed when the HCC nodule grew to 1.5 cm or larger. It has been suggested that capsule formation is a result of compression and collagenization of the adjacent stroma. However, this mechanism has been doubted, since the tumor size did not correlate with the thickness of the capsule or the incidence of its formation. This suggests that capsules are formed by active fibrosis rather than by tumor compression on the adjacent stroma.

According to our study, circulating VEGF mRNA did not significantly correlate with the grade of cellular differentiation.

We attributed this to the possibility of different histological grades coexisting in HCC tissues. Yamaguchi examined VEGF expression immunohistochemically in HCC of various histological grades and sizes^[34]. In tumors composed of a single histological grade, VEGF expression was the highest in well-differentiated, followed by moderately differentiated, and then poorly differentiated HCC. In tumors consisting of cancerous tissues of two different histological grades, the expression was less intense in the higher-grade HCC component. VEGF was also expressed in the surrounding HCC tissues in which inflammatory cell infiltration was apparent. Based on these findings, VEGF expression in HCC tissues was thought to be partly related to the histological grade but other cytokines and growth factors could also cooperatively act to enhance or influence VEGF expressions in HCC.

Solid tumors such as HCC are composed of two distinct compartments, namely the malignant cells themselves and the vascular and connective tissue stroma. The stroma provides the vascular supply that tumors require for obtaining nutrients, gas exchange, and waste disposal. Fibrin serves as a provisional stroma that is gradually replaced by granulation tissue and then by mature stroma. Human HCC is commonly surrounded by a fibrous capsule with an abundant extracellular matrix, even in the early stage. It is possible that VEGF also plays a certain role in the stimulation of regional development of the stroma in HCC.

Angiogenesis also appears to be involved in the invasion of tumors into the surrounding tissues, because this invasion requires concomitant neovascularization through the sprouting of endothelial cells in the extracellular matrix. It has been reported that VEGF induced both urokinase-type and tissue-type plasmin in endothelial cells. These are the key proteases involved in the degradation of the extracellular matrix. Thus VEGF may promote the process of vascular invasion by HCC cells.

Some authors suggested that VEGF mRNA expression in PB, which correlates well with the shift of VEGF mRNA in liver tissue, was strongly related to the development of HCC, including the progression from preneoplastic to neoplastic tissue and the potential of post-resection recurrence, the invasiveness of HCC, and poor survival^[42-44]. Some stated that serum VEGF was a predictor of invasion and metastasis of HCC and a potential biomarker of metastatic recurrence after curative resection^[20].

Surgery remains the best potentially curative treatment for patients with HCC. High recurrence rate limits the long term survival. Examination of preoperative VEGF mRNA in PB expression may give us information about high risk of postoperative recurrence. Addition of neoadjuvant or antiangiogenic therapy before or after surgery may be considered for such patients. Furthermore, the serial measurement of circulating VEGF mRNA during postoperative follow-up to monitor the effect of therapy or the development of recurrence needs further investigation.

From this prospective study, we suggest that circulating VEGF mRNA expression, especially isoform VEGF₁₆₅, may play a significant role in the prediction of postresection recurrence of HCC.

ACKNOWLEDGEMENT

This study was supported by grants from the Department of Medical Research, Mackay Memorial Hospital, Taiwan (MMH 9237).

REFERENCES

- Folkman J.** Endothelial cells and angiogenic growth factors in cancer growth and metastasis. *Cancer Metastasis Rev* 1990; **9**: 171-174
- Zetter BR.** Angiogenesis and tumor metastasis. *Annu Rev Med* 1998; **49**: 407-424
- Dvorak HF,** Brown LF, Detmar M, Dvorak AM. Vascular permeability factor/vascular endothelial growth factor, microvascular hyperpermeability, and angiogenesis. *Am J Pathol* 1995; **146**: 1029-1039
- Suzuki K,** Hayashi N, Miyamoto Y, Yamamoto M, Ohkawa K, Ito Y, Sasaki Y, Yamaguchi Y, Nakase H, Noda K, Enomoto N, Arai K, Yamada Y, Yoshihara H, Tujimura T, Kawano K, Yoshikawa K, Kamada T. Expression of vascular permeability factor/vascular endothelial growth factor in human hepatocellular carcinoma. *Cancer Res* 1996; **56**: 3004-3009
- Mise M,** Arai S, Higashitani H, Furutani M, Niwano M, Harada T, Ishigami S, Toda Y, Nakayama H, Fukumoto M, Fujita J, Imamura M. Clinical significance of vascular endothelial growth factor and basic fibroblast growth factor gene expression in liver tumor. *Hepatology* 1996; **23**: 455-464
- Miura H,** Miyazaki T, Kuroda M, Oka T, Machinami R, Kodama T, Shibuya M, Makuuchi M, Yazaki Y, Ohnishi S. Increased expression of vascular endothelial growth factor in human hepatocellular carcinoma. *J Hepatol* 1997; **27**: 854-861
- Houck KA,** Ferrara N, Winer J, Cachianes G, Li B, Leung DW. The vascular endothelial growth factor family: identification of a fourth molecular species and characterization molecular species and characterization of alternative splicing of RNA. *Mol Endocrinol* 1991; **5**: 1806-1814
- Ferrara N,** Houck K, Jakeman L, Leung DW. Molecular and biological properties of the vascular endothelial growth factor family of proteins. *Endocrinol Rev* 1992; **13**: 18-32
- Brown LF,** Berse B, Jackman RW, Tognazzi K, Guidi AJ, Dvorak HF, Senger DR, Connolly JL, Schnitt SJ. Expression of vascular endothelial permeability factor (vascular endothelial growth factor) and its receptors in breast cancer. *Hum Pathol* 1995; **26**: 86-91
- Anan K,** Morisaki T, Katano M, Ikubo A, Kitsuki H, Uchiyama A, Kuroki S, Tanaka M, Torisu M. Vascular endothelial growth factor and platelet-derived growth factor are potential angiogenic and metastatic factors in human breast cancer. *Surgery* 1996; **119**: 333-339
- Takahashi Y,** Kitadai Y, Bucana CD, Cleary KR, Ellis LM. Expression of vascular endothelial growth factor and its receptor, KDR, correlates with vascularity, metastasis, and proliferation of human colon cancer. *Cancer Res* 1995; **55**: 3964-3968
- Inoue K,** Ozeki Y, Suganuma T, Sugiura Y, Tanaka S. Vascular endothelial growth factor expression in primary esophageal squamous cell carcinoma: association with angiogenesis and tumor progression. *Cancer* 1997; **79**: 206-213
- Brown LF,** Berse B, Jackman RW, Tognazzi K, Manseau EJ, Senger DR, Dvorak HF. Expression of vascular permeability factor (vascular endothelial growth factor) and its receptor in adenocarcinomas of the gastrointestinal tract. *Cancer Res* 1993; **53**: 4727-4735
- Maeda K,** Chung YS, Ogawa Y, Takatsuka S, Kang SM, Ogawa M, Sawada T, Sowa M. Prognostic value of vascular endothelial growth factor expression in gastric carcinoma. *Cancer* 1996; **77**: 858-863
- Salven P,** Ruotsalainen T, Mattson K, Joensuu H. High pre-treatment serum level of vascular endothelial growth factor (VEGF) is associated with poor outcome in small-cell lung cancer. *Int J Cancer* 1998; **79**: 144-146
- Miyake H,** Hara I, Yamanaka K, Gohji K, Arakawa S, Kamidono S. Elevation of serum level of vascular endothelial growth factor as new predictor of recurrence and disease progression in patients with superficial urothelial cancer. *Urology* 1999; **53**: 302-307
- Tempfer C,** Obrmair A, Hefler L, Haeusler G, Gitsch G, Kainz C. Vascular endothelial growth factor serum concentrations in ovarian cancer. *Obstet Gynecol* 1998; **92**: 360-363
- Salven P,** Teerenhovi L, Joensuu H. A high pretreatment serum vascular endothelial growth factor concentration is associated with poor outcome in non-Hodgkin's lymphoma. *Blood* 1997; **90**: 3167-3172
- Banks RE,** Forbes MA, Kinsey SE. Release of the angiogenic cytokine vascular endothelial growth factor (VEGF) from platelets: bearing human hepatocellular carcinoma. *J Cancer Res Clin Oncol* 1997; **123**: 383-387
- Jin-no K,** Tanimizu M, Hyodo I, Nishikawa Y, Hosokawa Y, Doi T, Endo H, Yamashita T, Okada Y. Circulating vascular endot-

- helial growth factor (VEGF) is a possible tumor marker for metastasis in human hepatocellular carcinoma. *J Gastroenterol* 1998; **33**: 376-382
- 21 **Banks RE**, Forbes MA, Kinsey SE, Stanley A, Ingham E, Walters C, Selby PJ. Release of the angiogenic cytokine vascular endothelial growth factor (VEGF) from platelets: significance for VEGF measurements and cancer biology. *Br J Cancer* 1998; **77**: 956-964
- 22 **Akiyoshi F**, Sata M, Suzaki H, Uchimura Y, Mitsuyama K, Matsuo K, Tanikawa K. Serum vascular endothelial growth factor levels in various liver diseases. *Dig Dis Sci* 1998; **43**: 41-45
- 23 **El-Assal ON**, Yamanoi A, Soda Y, Yamaguchi M, Igarashi M, Yamamoto A, Nabika T, Nagasue N. Clinical significance of microvessel density and vascular endothelial growth factor expression in hepatocellular carcinoma and surrounding liver: possible involvement of vascular endothelial growth factor in the angiogenesis of cirrhotic liver. *Hepatology* 1998; **27**: 1554-1562
- 24 **Tokunaga T**, Oshika Y, Abe Y, Ozeki Y, Sadehiro S, Kijima H, Tsuchida T, Yamazaki H, Ueyama Y, Tamaoki N, Nakamura M. Vascular endothelial growth factor (VEGF) mRNA isoform expression pattern is correlated with liver metastasis and poor prognosis in colon cancer. *Br J Cancer* 1998; **77**: 998-1002
- 25 **Warren RS**, Yuan H, Matli MR, Gillett NA, Ferrara N. Regulation by vascular endothelial growth factor of human colon cancer tumorigenesis in a mouse model of experimental liver metastasis. *J Clin Invest* 1995; **95**: 1789-1797
- 26 **Chow NH**, Hsu PI, Lin XZ, Yang HB, Chan SH, Cheng KS, Huang SM, Su JJ. Expression of vascular endothelial growth factor in normal liver and hepatocellular carcinoma: an immunohistochemical study. *Hum Pathol* 1997; **28**: 698-703
- 27 **Li XM**, Tang ZY, Zhou G, Lui YK, Ye SL. Significance of vascular endothelial growth factor mRNA expression in invasion and metastasis of hepatocellular carcinoma. *J Exp Clin Cancer Res* 1998; **17**: 13-17
- 28 **Zhou J**, Tang ZY, Fan J, Wu ZQ, Li XM, Liu YK, Liu F, Sun HC, Ye SL. Expression of platelet-derived endothelial cell growth factor and vascular endothelial growth factor in hepatocellular carcinoma and portal vein tumor thrombus. *J Cancer Res Clin Oncol* 2000; **126**: 57-61
- 29 **Qin LX**, Tang ZY. The prognostic molecular markers in hepatocellular carcinoma. *World J Gastroenterol* 2002; **8**: 385-392
- 30 **Chao Y**, Li CP, Chau GY, Chen CP, King KL, Lui WY, Yen SH, Chang FY, Chan WK, Lee SD. Prognostic significance of vascular endothelial growth factor, basic fibroblast growth factor, and angiogenin in patients with resectable hepatocellular carcinoma after surgery. *Ann Surg Oncol* 2003; **10**: 355-362
- 31 **Miura H**, Miyazaki T, Kuroda M, Oka T, Machinami R, Kodama T, Shibuya M, Makuuchi M, Yazaki Y, Ohnishi S. Increased expression of vascular endothelial growth factor in human hepatocellular carcinoma. *J Hepatol* 1997; **27**: 854-861
- 32 **Torimura T**, Sata M, Ueno T, Kin M, Tsuji R, Suzaku K, Hashimoto O, Sugawara H, Tanikawa K. Increased expression of vascular endothelial growth factor is associated with tumor progression in hepatocellular carcinoma. *Hum Pathol* 1998; **29**: 986-991
- 33 **Motoo Y**, Sawabu N, Nakanuma Y. Expression of epidermal growth factor and fibroblast growth factor in human hepatocellular carcinoma: an immunohistochemical study. *Liver* 1991; **11**: 272-277
- 34 **Yamaguchi R**, Yano H, Iemura A, Ogasawara S, Haramaki M, Kojiro M. Expression of vascular endothelial growth factor in human hepatocellular carcinoma. *Hepatology* 1998; **28**: 68-77
- 35 **Poon RT**, Fan ST, Lo CM, Liu CL, Wong J. Intrahepatic recurrence after curative resection of hepatocellular carcinoma. Long-term results of treatment and prognostic factors. *Ann Surg* 1999; **229**: 216-222
- 36 **Jeng KS**, Sheen IS, Chen BF, Wu JY. Is the p53 gene mutation of prognostic value in hepatocellular carcinoma after resection? *Arch Surg* 2000; **135**: 1329-1333
- 37 **Ng IO**, Lai EC, Fan ST, Ng MM, So MK. Prognostic significance of pathologic features of hepatocellular carcinoma. *Cancer* 1995; **76**: 2443-2448
- 38 **Yamamoto Y**, Toi M, Kondo S, Matsumoto T, Suzuki H, Kitamura M, Tsuruta K, Taniguchi T, Okamoto A, Mori T, Yoshida M, Ikeda T, Tominaga T. Concentration of vascular endothelial growth factor in the sera of normal controls and cancer patients. *Clin Cancer Res* 1996; **2**: 821-826
- 39 **Dirix LY**, Vermeulen PB, Pawinski A, Prove A, Benoy I, De Pooter C, Martin M, Van Oosterom AT. Elevated levels of the angiogenic cytokines basic fibroblast growth factor and vascular endothelial growth factor in sera of cancer patients. *Br J Cancer* 1997; **76**: 238-243
- 40 **Salven P**, Manpaa H, Orpana A, Alitalo K, Joensuu H. Serum vascular endothelial growth factor is often elevated in disseminated cancer. *Clin Cancer Res* 1997; **3**: 647-651
- 41 **Kraft A**, Weindel K, Ochs A, Marth C, Zmija J, Schumacher P, Unger C, Marme D, Gastl G. Vascular endothelial growth factor in the sera and effusions of patients with malignant and nonmalignant disease. *Cancer* 1999; **85**: 178-187
- 42 **Yoshiji H**, Kuriyama S, Yoshii J, Yamazaki M, Kikukawa M, Tsujinoue H, Nakatani T, Fukui H. Vascular endothelial growth factor tightly regulates *in vivo* development of murine hepatocellular carcinoma cells. *Hepatology* 1998; **28**: 1489-1496
- 43 **Sakamoto M**, Ino Y, Fujii T, Hirohashi S. Phenotype changes in tumor vessels associated with the progression of hepatocellular carcinoma. *Jpn J Clin Oncol* 1993; **23**: 98-104
- 44 **Terada T**, Nakanuma Y. Arterial elements and perisinusoidal cells in borderline hepatocellular nodules and small hepatocellular carcinomas. *Histopathology* 1995; **27**: 333-339
- 45 **Nakashima O**. Pathological diagnosis of hepatocellular carcinoma. *Nippon Rinsho* 2001; **59**(Suppl 6): 333-341

Salvage therapy for hepatocellular carcinoma with thalidomide

Tsang-En Wang, Chin-Roa Kao, Shee-Chan Lin, Wen-Hsiung Chang, Cheng-Hsin Chu, Johson Lin, Ruey-Kuen Hsieh

Tsang-En Wang, Chin-Roa Kao, Shee-Chan Lin, Wen-Hsiung Chang, Cheng-Hsin Chu, Gastroenterology Section, Department of Internal Medicine, Mackay Memorial Hospital, Taipei, Taiwan, China
Johson Lin, Ruey-Kuen Hsieh, Oncology Section, Department of Internal Medicine, Mackay Memorial Hospital, Taipei, Taiwan, China
Correspondence to: Dr. Tsang-En Wang, Gastroenterology Section, Department of Internal Medicine, Mackay Memorial Hospital and Mackay Junior College of Nursing, No.92 Section 2, Chang-San North Road, Taipei, Taiwan, China. tewang@ms2.mmh.org.tw
Telephone: +886-2-25433535 **Fax:** +886-2-27752142
Received: 2003-09-09 **Accepted:** 2003-11-06

Abstract

AIM: To evaluate the clinical benefit of thalidomide in patients with advanced hepatocellular carcinoma (hepatoma).

METHODS: From March 2000 to July 2002, patients who had advanced hepatocellular carcinoma and failed to or were unsuited for aggressive treatment, were enrolled and took thalidomide 150 to 300 mg/d. All cases were followed till April 2003. Data collection included viral hepatitis, grade of cirrhosis, total dosage of thalidomide, side effect, stage of hepatoma by Okuda and CLIP classification, and prognosis. The subjects were divided into A and B groups, depending on 5 000 mg dosage of thalidomide. Survival time of all cases and in the two subgroups was evaluated.

RESULTS: Ninety-nine patients with hepatoma were enrolled, 81 men and 18 females with median age 58 ± 14.1 years. Eighty-six percent had viral hepatitis and one case was alcoholism. Hepatoma was diagnosed with histology, alpha-fetoprotein (aFP) > 400 ng/mL, or image examination, there were 30, 33 and 36 cases respectively. At the time of thalidomide therapy, more than 81% had cirrhotic status. Twenty-two patients were in group A (< 5 000 mg) with median survival time about 25 days, for 77 cases in group B (≥ 5 000 mg) the median survival time was about 109 days. Six subjects had partial response. Most adverse effects were skin rash, neuropathy, somnolence, and constipation.

CONCLUSION: Several patients responded to thalidomide therapy. As a single drug therapy, thalidomide might not have good therapeutic effect for all cases, but a small ratio of patients had exciting response, the resistance or tumor escape would develop after long-term use. Up to now, no defined facts could be used to predict response. The effect of thalidomide on hepatoma might be associated with the dosage. As salvage therapy, thalidomide has its value. Combination or adjuvant therapy will be the next trial.

Wang TE, Kao CR, Lin SC, Chang WH, Chu CH, Lin J, Hsieh RK. Salvage therapy for hepatocellular carcinoma with thalidomide. *World J Gastroenterol* 2004; 10(5): 649-653
<http://www.wjgnet.com/1007-9327/10/649.asp>

INTRODUCTION

Hepatocellular carcinoma (hepatoma) is a major cause of death in the world, especially in the endemic areas of viral hepatitis

B and C, such as Taiwan, China. Taiwan is a high prevalence area of hepatocellular carcinoma, more than 6 900 people died of hepatocellular carcinomas at Taiwan in 2002. Although the incidence rate of small hepatoma was increased in the last few years, but most patients had severe liver cirrhosis that made them lose the opportunities to receive curative therapy. Therapy of hepatocellular carcinoma in chronic liver disease patients is challenging also. Local treatments, such as surgical resection, ethanol intratumor injection, ablation with high frequency, or transhepatic artery embolization have been improved, but these procedure might cause new problems and the curative and survival rates of these patients are still low^[1]. The average survival time is shorter than 6 months if metastasis occur. However, to seek new effective therapy for hepatoma, to prolong the patient life or improve their life quality with later stage of hepatoma are major issues at Taiwan.

Anti-angiogenesis is a new concept for cancer therapy, in the 1970's, Dr Folkman launched out the theory^[2]. Neoplasm's growth depends on angiogenesis, angiogenesis inhibitors could block the process and treat neoplasm, especially vascularized ones. Many antiangiogenic agents are developed and some are going in clinical trials. Thalidomide is one of them and has been studied for its anti-angiogenic activity in last several years.

Hepatoma is a hypervascular tumor that has been proved by angiography and histology. For this reason, antiangiogenesis therapy may be effective for hepatoma. Up to now, few papers described the antiangiogenesis therapy for hepatoma. The first success case of hepatoma treated with thalidomide, was reported in 2000. A 67-year-old man had a 6 cm large tumor. Unfortunately, the tumor continued to grow after 5FU and interferon therapy, chemoembolization and chemotherapy. Thalidomide therapy was used. The tumor was shrunk, aFP was diminished, and the patient was alive in 2000^[3]. Henceforward, some might had exciting results, some were disappointed, Although a few patients would get benefit from thalidomide therapy^[4-8]. No final conclusion was made. In this study, we report our experience in using thalidomide as a salvage drug for the patients with hepatoma, who were unsuitable for other managements.

MATERIALS AND METHODS

One hundred and six patients with hepatocellular carcinoma were entered into the study between Mar 2000 and July 2002. A diagnosis of hepatoma was made by histopathology, alpha fetoprotein (AFP) more than 400 ng/mL or image plus clinical manifestation. All of them were poor candidates for more aggressive treatment. Those patients were required to receive a risk-benefit counseling, to sign an informed-consent agreement, to use forms of birth control. The Institutional Ethics Committee of the Mackay Memorial Hospital and Department of Public Health in Taiwan approved the study protocol and the informed consent form.

They were given oral thalidomide table, containing 50 mg (Taiwan Tung Yang Biopharm Co. Ltd), at a dosage of 150 to 300 mg/day according to clinical reactions and adverse effects for a variable period. The drug was given 2 dosages in the morning and bedtime. The subjects were followed to April 2003. Ninety-nine patients were evaluated.

Depending the total dosage used, the patients were divided into two subgroups, group A took thalidomide less 100 tablets

(5 000 mg), and group B had more than 100 tablets. Data collected included viral hepatitis, grade of cirrhosis, total dosage of thalidomide, side effect, stage of hepatoma by Okuda and CLIP classification^[9], and prognosis. The trial was prompted by the observation of response and survival times in all case and in the two subgroups. Survival time was calculated with SPSS 10 software and observation time interval was one week.

RESULTS

General data

Ninety-nine patients were valuable for evaluation (Table 1). The ratio of men and women was 81:18. The median age of the patients was 58 years (range, 21-86 years, S=14.1 years). Fifty-eight patients were chronic hepatitis B, 22 patients had hepatitis C, and five patients were infected with viral hepatitis B and C. Six cases were confirmed with non-B and non-C hepatitis. Seven cases had an underminted condition. One was alcoholic cirrhosis without viral hepatitis. Among them, another 12 patients had alcohol consumption. At the time of hepatoma diagnosed, 81% (80 cases) of the patients had cirrhosis diagnosed with histology or image studies, 14 cases had chronic parenchyma disease, and only 5 patients had normal texture of liver. The hepatoma diagnosis was dependent on either histopathology, aFP >400 ng/mL or image and clinical manifestations. There were 33, 30 and 36 cases respectively. They were followed up, with median follow-up time about 6 months (average 177 days) to April 2003 in this study. Group A had 22 patients and group B had 77 patients.

Table 1 Description of cases

Age (yr)	
Median	58±14.1
Range	21-86
Sex	
Male	81
Female	18
Modality of diagnosis	
Cytological/histological	33
Imaging + AFP > 400 ng/mL	30
Imaging + AFP < 400 ng/mL or unknown	36
Cirrhosis	
Absent	5
Present	80
Chronic parenchymal d's	14
Causes of liver disease	
Hepatitis B	58
Hepatitis C	22
Hepatitis B +C	5
Non B and Non C	6
Alcoholic	1
Child-Pugh stage (unknown = 2)	
A	43
B	33
C	21
AFP (ng/mL) (unknown =10)	
10 <	17
11-400	33
400	39
Portal vein thrombosis (unknown=3)	
No	46
Yes	50
Pre Thalidomide Treatment (unknown=7)	
No	30
Yes	72
Surgery	11
PEI	16
TACE	49
Radiation	6
Chemotherapy	3

Laboratory data

The pretreatment median platelet count was $187 \times 10^3/\text{mm}^3$, leukocyte count was about $6\,820/\text{mm}^3$. Analyzed the liver function by Child's classification, 43, 33 and 21 patients belong to grades A, B and C, respectively. Two cases were unclassified at the beginning of medication because of incomplete data record. Both of them were grade A when hepatoma was diagnosed. One had bone and lung metastasis and one was followed up at other hospital. Fifty-two percent of the patients had alpha-fetoprotein level more than 400 ng/mL. According to hepatoma stage Okuda (Table 2) and CLIP (Table 3), the numbers of patients and survival time in the both groups are shown in Table 4 and Table 5. There were no confirmed complete responses. Although no scheduled image evaluation was done, six patients having partial response were observed, yielding a rate of 7% at least. Four responded patients had a high serum aFP initially, which was decreased after treatment.

Table 2 Okuda staging for HCC

Point	0	1
Size of tumor	<50% of liver	> 50 %
Ascites	No	Yes
Albumin	>=3	<3
Bilirubin	<3	>=3
Stage I: 0	II: 1 or 2	III: 3 or 4

Table 3 CLIP scoring system

Scores Variables	0	1	2
Child-pugh stage	A	B	C
Tumor morphology	Uninodular and extension <=50%	Multinodular and extension <=50%	Massive or extension > 50%
AFP	<400	>=400	
Portal vein thrombosis	No	Yes	

Table 4 Hepatocellular carcinoma stage and survival time, Okuda stage and survival time

Group		Stage			MSD
		I	II	III	
A (n=19)	Case No.	5	9	5	
	Survival days	161	26.8	10.5	25.2
B (n=76)	Case No.	19	41	16	
	Survival days	171.5	136.5	47.3	108.5

MSD: medium survival day.

Table 5 Hepatocellular carcinoma stage and survival time, CLIP classification and survival time

Group		Score						
		0	1	2	3	4	5	6
A (n=20)	Case	0	2	2	2	8	5	1
	Survival days	220.5	49	42	35	12.3	11	
B (n=76)	Case	1	8	20	20	15	9	3
	Survival days	>345	301	150.5	106.8	96.2	59.5	19.3

Response and survival

Overall, the median survival time was about 80 days to Apr 2003. Twenty-one of 22 patients in group A had expired, only one survived to Dec 2000 then lost follow-up. The median survival time in group A was 25 days. Most of them had a

poor condition for aggressive treatment and died due to liver function decompensation. Thirty-six percent patients of group A has Child-pugh's grade C, compared only 16% in group B. One third patients died with hepatic failure and 4 patients died with massive esophageal varices bleeding in group A. Fifty percent cases had multiple lesions in liver or distal metastasis. Some of them liked to try TAE again and other alternative therapies. One patient had grade 3 dermatologic toxicity. These were major causes the withdrawal of thalidomide. Seventy-seven patients were group B, 61 patients died, and 16 patients experienced disease progression or partial responses. The median overall survival time in group B was 108.5 days.

Toxicity

The most common treatment-related toxic effects were skin itching, rash and urticaria. Twenty patients were relieved by antihistamine, two patients with severe dermatitis prompted discontinuation of thalidomide treatment. Other adverse effects included neuropathy, somnolence, and constipation and six had it with others side effect, such as gastrointestinal symptom. Most of them took laxative, therefore the rate of constipation was not real. Toxicity of thalidomide in our patients was tolerable.

Table 6 Response rate of hepatoma treated with thalidomide

	Tumor response		Stabilization rate		
	N	CR/PR	SD	PD	(PR + SD)
Patt <i>et al.</i> '00 ^[6]	21	0/1	11	9	12 (57%)
Chen <i>et al.</i> '00 ^[8]	42	0/2	15	25	17 (43%)
Kong <i>et al.</i> '01 ^[5]	11	0/1	4	6	5 (45%)
Lin <i>et al.</i> '02 ^[4]	27	0/1	1	25	2 (8%)
Schwartz <i>et al.</i> '02 ^[7]	20	1/1	7	11	9 (45%)
Total	121	1/6	38	76	45 (37%)
Wang <i>et al.</i> '03	99	0/6	Survival 16 upto Apr 31 '03		

CR: complete response, PR: partial response, SD: stable disease, PD: Progressive disease.

DISCUSSION

Thalidomide was developed in the 1950's and originally marketed as a sedative but was withdrawn after its teratogenic effects were recognized in 1964. FDA approved thalidomide for erythema nodosum leprosum in 1999, which stimulated new interests^[10]. Thalidomide has been shown to be effective in treating cutaneous lupus erythematosus, idiopathic oral and oropharyngeal aphthous ulceration in HIV-1 positive patients. It has subsequently been used in the treatment of graft versus host disease, rheumatoid arthritis, inflammatory bowel disease, and the malignancy diseases in phase II or phase III, such as multiple myeloma, renal cell carcinoma, prostate cancer, breast cancer, ovary cancer, *etc.* The effects may come from its potent inhibitor of angiogenesis and immune response-modifying properties, which are essential to many physiologic and pathologic pathways. Thalidomide could inhibit the production of tumor necrosis factor-alpha^[11,12] and alter multiple cytokines. Several other immunomodulatory effects have been reported, such as down-regulation of T-lymphocyte surface molecules, inhibition of lymphocyte proliferative responses to alloantigens and mitogens, and lowering of CD4:CD8 peripheral T-lymphocyte ratios^[13,14]. It could induce a shift from T helper cell type 1(Th1) to Th2 T-cell responses and modify various cell surface receptors^[15].

Hepatoma is a hypervascular tumor, blood support comes from new branch vessels of hepatic artery. Presumably, chemoembolization intercept the vessels has become one of

standard treatments for hepatoma. We can speculate that anti-angiogenetic agents can inhibit hepatoma growth, such as thalidomide. Thalidomide was believed to be species-specific antiangiogenesis drug^[16,17]. That is the most likely reason for its reported effectiveness against some solid tumors involving neoformation of blood vessels in early days. In addition, angiogenesis inhibitor TNP-470 can inhibit both the growth of primary tumors and the formation of liver metastases from gastric and colon cancer xenografts in nude mice. In a rat hepatoma model, it also enhanced apoptosis in hepatic metastases and improved survival^[18]. Again, inhibition of tumor necrosis factor-alpha (TNF-alpha) is one important action of thalidomide, which could be used to treat human hepatoma.

To treat hepatoma with thalidomide will be feasible. Some papers have actually discussed this issue since 1999, most were reported with case studies or in academic meetings^[4-8] (Table 6). The complete response was rare, partial response rate was 5% to 10%, stable disease was about 37%, the variant was depending on the duration of observation, cancer stage of patients and definition of stability. In our study, no patient had complete remission, the initial partial response was 7%.

The effect of thalidomide on cancer is still mysterious. We surmised that interaction between the drug, patient immunity and heterogeneous cancer was very complex. The impact factors of response are multiple. However, there are some other antitumor mechanisms in addition to antiangiogenesis and TNF suppression. For example, degradation of tumor necrosis factor-alpha mRNA in human monocytes was modulated by thalidomide^[12]. On the contrary, TNF-alpha production in IL-1beta-stimulated or PMA-stimulated hepatocyte cultures was not altered following the addition of thalidomide^[19]. Thalidomide can augment natural killer cell cytotoxicity. The number of NK cells increased in multiple myeloma after medication, but only those patients who responded to treatment showed an increase in the percentage of NK cells. Thalidomide for multiple myeloma might trigger the NK cells^[20]. Same phenomena might occur in hepatoma. The exact mechanism of thalidomide is not fully clear, lot of effect wait to discover.

Why thalidomide for hepatoma does not work as a targeted therapy? Hepatoma was heterogeneous in genotype and phenotype^[21]. Animal experiments showed that angioarchitecture and blood flow velocity in liver cancer were heterogeneous^[22]. Adhesion molecular, E-cadherin, revealed various expressions among tumor samples^[23]. These could explain why not all the solid tumors or patients had no response to thalidomide therapy, even in treatment of hepatoma. Although a few hepatomas had very good response to thalidomide beyond expectancy. At present, we still lack a landmark to select the suitable patients and specific parameters to predict the response to thalidomide treatment. Host may be another important factor affecting the response to thalidomide. All these need more researches to answer.

It seems that thalidomide may offer hepatocellular carcinoma stabilization, but has no significant antitumor activity. Most papers discussed the rate of response only. The survival time may be one of the major destinations in clinical trails of thalidomide therapy. A few phase I and II studies showed survival times slightly increased in hepatoma patient, but the survival time of those patients was also unpredictable and thalidomide did not significantly prolong the life of all patients. Our patients survived average of 25 and 108 days in groups A and B, respectively. The survival time appeared shorter than reported^[9,24]. We thought the time was calculated from the day of thalidomide therapy, not the day of hepatoma diagnosed. In group A, the general condition of them was poor, they seemed not get any benefit from thalidomide therapy. All the response cases in our study were belong to group B with a large total dosage. Chen found the average survival time in patients with responded or stable disease was 269 days,

significantly longer than 74 days in the patients with progression^[8]. Neben Kai reported the cumulative 3-month dosage was the remaining factor for overall survival rate in treating multiple myeloma^[25]. At the same time, that might occur in HCC and the anticancer effect of thalidomide was associated with cell cycle and total dosage, as other chemotherapy. So, thalidomide might not be suitable for patients with too terminal status because they do not have chance to take enough dosage of thalidomide. It is the issue to be studied.

Besides, this study might have a worth finding. We usually think there is no drug resistance to antiangiogenic therapy, but it did occur. We revealed a case with high aFP and lung metastasis had a good response. His serum level of aFP dropped and lung lesions became small and disappeared after thalidomide therapy. Unfortunately, the aFP increased again and lung lesion regrew after 9 months thalidomide continuous therapy. That means the resistant may develop if patients take thalidomide for enough long time. These need more case observations to confirm.

However, patients with hepatoma at later stage do not have time to wait for a new therapy. Most hepatomas develop in patients with cirrhosis. In this study, the ratio of cirrhosis was more than 80%. Lot of patients are poor candidates for aggressive treatment. Moreover, the prognosis of patients with metastatic or refractory HCC was very poor, to cure the patients was almost impossible. The aim of therapy was to improve their life quality and prolong their survival time^[26]. Overall, as a single medication, thalidomide has the response rate about 5 to 10%.

At one time, thalidomide was notorious for its side effect that has been under control in last few years. Phocomelia is the most severe adverse effect that did not cause any problem in patients with hepatoma. The other adverse effects were sedation, constipation, and skin rash in our study. These effects were usually dose-related and mild, and could be treated except few patients who must discontinue medication. Peripheral axonal sensory neuropathy caused by thalidomide appeared only after a large dose accumulation. In our study, even at the later stage of cirrhosis, only few patients discontinued thalidomide. Another unusual adverse effect of thalidomide is vascular thrombosis. Deep venous thrombosis may occur, especially in patients with multiple myeloma and renal cell carcinoma, but has not seen in patients with hepatoma. Our results showed that thalidomide was tolerated in cirrhotic patients with hepatoma. Thalidomide is convenient for oral intake. It can be used as a salvage therapy before more powerful antiangiogenetics or other combined or adjuvant methods are developed. Several pilot studies have been on going^[27], such as combination therapy of thalidomide plus interferon alfa in phase II^[28]. A combination of capecitabine and thalidomide, celecoxib and escalating doses of thalidomide in patients with unresectable HCC revealed few response patients^[29,30].

In conclusions, thalidomide is a drug with multifunctions, may be useful in some of patients with advanced hepatocellular carcinoma and it produces durable stability disease in approximately one third of patients, with a partial response rate not beyond 10%. Most side effects of thalidomide are minimal, it could be administered to patients with even significant liver cirrhosis and poor candidates for other therapies. However, thalidomide as a single drug formula for hepatoma is no so good, resistance will be appear after long-term use. If it is used as a salvage therapy in patients with hepatoma, some patients get benefit^[27]. A controlled trial of thalidomide in selected patients with cirrhosis and hepatoma is warranted. The combination therapy with other drugs or adjuvant therapy in different stage hepatoma will be the next step studies. Thalidomide analogues have been under investigation. Hopefully, this will be the beginning of the development of a

new therapeutic modality for hepatoma.

REFERENCES

- 1 **Lin SC**, Shih SC, Kao CR, Chou SY. Transcatheter arterial embolization treatment in patients with hepatocellular carcinoma and risk of pulmonary metastasis. *World J Gastroenterol* 2003; **9**: 1208-1211
- 2 **Folkman J**, Watson K, Ingber D, Hanahan D. Induction of angiogenesis during the transition from hyperplasia to neoplasia. *Nature* 1989; **339**: 58-61
- 3 **Patt YZ**, Hassan MM, Lozano RD, Ellis LM, Peterson JA, Waugh KA. Durable clinical response of refractory hepatocellular carcinoma to orally administered thalidomide. *Am J Clin Oncol* 2000; **23**: 319-321
- 4 **Lin AY**, Brophy N, Fisher GA, So S, Biggs C, Yock T, Levitt L. Phase II study of thalidomide in patients (pts) with unresectable hepatocellular carcinoma (HCC). *Proc Am Soc Clin Oncol* 2002; **21**: p97b abstr:2202
- 5 **Kong HL**, Boyer MJ, Lim R, Clarke S, Milward JM, Wong E. Phase II trial of thalidomide in unresectable hepatocellular carcinoma (HCC)-a cancer therapeutics group (CTRG) study. *Proc Am Soc Clin Oncol* 2001; **20**: p133b, abstr: 2282
- 6 **Patt YZ**, Hassan MM, Lozano RD, Zeldis JB, Schnirer I, Frome A, Abbruzzese J, Wolff R, Brwom T, Lee E, Charnsangavej C. Phase II trial of thalidomide for treatment of nonresectable hepatocellular carcinoma. *Proc Am Soc Clin Oncol* 2000; **14**(Suppl 12, abstr): 1035
- 7 **Schwartz JD**, Sung Max W, Lehrer D, Goldenberg A, Muggia F, Volm M. Thalidomide for unresectable hepatocellular cancer (HCC) with optional interferon- γ upon disease progression. *Proc Am Soc Clin Oncol* 2002 abstr: 1847
- 8 **Jacqueline WP**, Chen LT. Thalidomide and hepatoma. NHRI-AACR Joint Conference 2001 abstr: 653. (The Fifth Taiwan Cancer Clinical Research Organization Cooperative Annual Conference and Cross-Strait Anti-Cancer Pharmaceuticals Research and Development Conference.) <http://tpmd.nhri.org.tw/~scba/php-bin/scba2001/abstract/abs653.htm>
- 9 **The Cancer of the Liver Italian Program (CLIP) Investigators**. Prospective validation of the CLIP Score: a new prognostic system for patients with cirrhosis and hepatocellular carcinoma. *Hepatology* 2000; **31**: 840-845
- 10 **Cori V**. Preparing for thalidomide's comeback. *Ann Internl Med* 1997; **127**: 951-952
- 11 **Calabrese L**, Fleischer AB. Thalidomide current and potential clinical applications. *Am J Med* 2000; **108**: 487-495
- 12 **Moriera AL**, Sampaio EP, Zmuidzinas A, Frindt P, Smith KA, Kaplan G. Thalidomide exerts its inhibitory action on tumor necrosis factor [alpha] by enhancing mRNA degradation. *J Exp Med* 1993; **177**: 1675-1680
- 13 **Gad SM**, Shannon EJ, Krotoski WA, Hastings RC. Thalidomide induces imbalances in T-lymphocyte subpopulations in the circulating blood of healthy males. *Lepr Rev* 1985; **56**: 35-39
- 14 **Haslett PA**, Corral LG, Albert M, Kaplan G. Thalidomide costimulates primary human T lymphocytes, preferentially inducing proliferation, cytokine production, and cytotoxic responses in the CD8+subset. *J Exp Med* 1998; **187**: 1885-1892
- 15 **Verbon A**, Juffermans NP, Speelman P, van Deventer SJ, ten Berge IJ, Guchelaar HJ, van der Poll T. A single oral dose of thalidomide enhances the capacity of lymphocytes to secrete gamma interferon in healthy humans. *Antimicrob Agents Chemother* 2000; **44**: 2286-2290
- 16 **Bauer KS**, Dixon SC, Figg WD. Inhibition of angiogenesis by thalidomide requires metabolic activation, which is species-dependent. *Biochem Pharmacol* 1998; **55**: 1827-1834
- 17 **D'Amato RJ**, Loughnan MS, Flynn E, Folkman J. Thalidomide is an inhibitor of angiogenesis. *Proc Natl Acad Sci U S A* 1994; **91**: 4082-4085
- 18 **Konno H**. Antitumor effect of angiogenesis inhibitor TNP-470 on human digestive organ malignancy. *Cancer Chemother Pharmacol* 1999; **43**(Suppl): S85-89
- 19 **Wordemann M**, Fandrey J, Jelkmann W. Tumor necrosis factor-alpha production by human hepatoma cell lines is resistant to drugs that are inhibitory to macrophages. *J Interferon Cytokine*

- Res 1998; **18**: 1069-1075
- 20 **Davies FE**, Raje N, Hideshima T, Lentzsch S, Young G, Tai YT, Lin B, Podar K, Gupta D, Chauhan D, Treon SP, Richardson PG, Schlossman RL, Morgan GJ, Muller GW, Stirling DI, Anderson KC. Thalidomide and immunomodulatory derivatives augment natural killer cell cytotoxicity in multiple myeloma. *Blood* 2001; **98**: 210-216
- 21 **Hui AM**, Kawasaki S, Imamura H, Miyagawa S, Ishii K, Katsuyama T, Makuuchi M. Heterogeneity of DNA content in multiple synchronous hepatocellular carcinomas. *Br J Cancer* 1997; **76**: 335-339
- 22 **Maksan SM**, Paulo H, Ryschich E, Kuntz C, Gebhard MM, Klar E, Schmidt J. *In vivo* assessment of angioarchitecture and microcirculation in experimental liver cancer: a new model in rats. *Dig Dis Sci* 2003; **48**: 279-290
- 23 **Wei Y**, Van Nhieu JT, Prigent S, Srivatanakul P, Tiollais P, Buendia MA. Altered expression of E-cadherin in hepatocellular carcinoma: correlations with genetic alterations, beta-catenin expression, and clinical features. *Hepatology* 2002; **36**: 692-701
- 24 **Okuda K**, Ohtsuki T, Obata H, Tomimatsu M, Okazaki N, Hasegawa H, Nakajima Y, Ohnishi K. Nature history of hepatocellular carcinoma and prognosis in relation to treatment - study of 850 patients. *Cancer* 1985; **56**: 918-928
- 25 **Neben K**, Moehler T, Benner A, Kraemer A, Egerer G, Ho AD, Goldschmidt H. Dose-dependent effect of thalidomide on overall survival in relapsed multiple myeloma. *Clin Cancer Res* 2002; **8**: 3377-3382
- 26 **Feun LG**, Marini A, Molina E, O' Brien C, Schiff E, Jeffers L, Savaraj N. Thalidomide as palliative care for patients with unresectable hepatocellular carcinoma. *Proc Am Soc Clin Oncol* 2003; abstr: 865
- 27 **von Moos R**, Stolz R, Cerny T, Gillessen S. Thalidomide; from tragedy to promise. *Swiss Med WKLY* 2003; **133**: 77-87
- 28 **Schwartz JD**, Lehrer D, Mandeli J, Goldenberg A, Sung M, Volm M. Thalidomide in hepatocellular cancer (HCC) with optional interferon- upon progression. *Proc Am Soc Clin Oncol* 2003; abstr: 1210
- 29 **Chun HG**, Waheed F, Iqbal A, Wolf DC, Li Z, Kempin SJ. A combination of capecitabine and thalidomide in patients with unresectable, recurrent or metastatic hepatocellular carcinoma. *Proc Am Soc Clin Oncol* 2003; Abstr: 1407
- 30 **Chen CS**, Hillebrand D, Hill K, Lilly M. A pilot study of celecoxib combined with escalating doses of thalidomide for treatment of unresectable hepatocellular carcinoma (HCC). *Proc Am Soc Clin Oncol* 2002; abstr: 2350

Edited by Wang XL **Proofread by** Xu FM

Anti-liver cancer activity of TNF-related apoptosis-inducing ligand gene and its bystander effects

Chao He, Wei-Feng Lao, Xiao-Tong Hu, Xiang-Ming Xu, Jing Xu, Bing-Liang Fang

Chao He, Wei-Feng Lao, Xiao-Tong Hu, Jing Xu, Sir Run Run Shaw Hospital, College of Medicine, Zhejiang University, Hangzhou 310016, Zhejiang Province, China

Xiang-Ming Xu, First Affiliated Hospital, College of Medicine, Zhejiang University, Hangzhou 310003, Zhejiang Province, China

Bing-Liang Fang, Department of Thoracic and Cardiovascular Surgery, M.D. Anderson Cancer Center, Huston, 77030, USA

Supported by the National Natural Science Foundation of China, No. 30271467

Correspondence to: Dr. Chao He, Department of Oncology, Sir Run Run Shaw Hospital, College of Medicine, Zhejiang University, Hangzhou 310016, Zhejiang Province, China. drhe@zju.edu.cn

Telephone: +86-571-86048962 **Fax:** +86-571-86993719

Received: 2003-03-20 **Accepted:** 2003-06-02

Abstract

AIM: To observe the anti-liver cancer activity of tumor necrosis factor-related apoptosis-inducing ligand (TRAIL) gene and its bystander effects on hepatocellular carcinoma (HCC) cell line SMMC7721.

METHODS: Full-length cDNA of human TRAIL was transferred into SMMC7721 cells with a binary adenoviral vector system. Polymerase-chain reaction following reverse transcription (RT-PCR) was used to determine the expression of TRAIL gene. Effects of the transfected gene on proliferation of SMMC7721 cells were measured by MTT assay. Its influence on apoptosis was demonstrated by fluorescence-activated cell sorting (FACS). The bystander effect was observed by co-culturing the SMMC7721 cells with and without the transfected TRAIL gene at different ratios, and the culture medium supernatant from the transfected cells was also examined for its influence on SMMC7721 cells.

RESULTS: The growth-inhibition rate and apoptotic cell fraction in the cells transfected with the TRAIL gene, Bax gene or only LacZ gene were 91.2%, 48.0%, 28.8% and 29.1%, 12.5%, 6.6%, respectively. The growth-inhibition rate of transfection with these three sequences in normal human fibroblasts was 6.1%, 45.5% and 7.6%, respectively, indicating a discriminative inhibition of TRAIL transfection on the cancer cells. In the co-culturing test, addition of the transfected TRAIL to SMMC7721 cells in proportions of 5%, 25%, 50%, 75% and 100%, resulted in a growth-inhibition of 15.9%, 67%, 80.2%, 86.4% and 87.7%, respectively. We failed to observe a significant growth-inhibition effect of the culture medium supernatant on SMMC7721 cells.

CONCLUSION: TRAIL gene transferred by a binary adenoviral vector system can inhibit proliferation of SMMC7721 cells and induce their apoptosis. A bystander effect was observed, which seemed not to be mediated by soluble factors.

He C, Lao WF, Hu XT, Xu XM, Xu J, Fang BL. Anti-liver cancer activity of TNF-related apoptosis-inducing ligand gene and its bystander effects. *World J Gastroenterol* 2004; 10(5): 654-659 <http://www.wjgnet.com/1007-9327/10/654.asp>

INTRODUCTION

TRAIL, first identified by searching an expressed sequence tag (EST) database with a conserved sequence contained in many tumor necrosis factor (TNF) family members, appears to induce apoptotic cell death only in tumorigenic or transformed cells and not in most of normal cells^[1,2]. TRAIL has five receptors, including two death receptors DR4 and DR5, two decoy receptors DcR1 and DcR2, one soluble receptor osteoprotegerin. TRAIL is expressed constitutively in many normal tissues, which suggests that normal cells contain mechanisms that protect them from apoptosis induced by TRAIL. One explanation reported was that the decoy receptors DcR1 and DcR2 and another receptor osteoprotegerin could compete with DR4 and DR5 for TRAIL binding^[3,4]. Furthermore, TRAIL has a synergistic effect with chemotherapeutic drugs to kill tumor cells and cause substantial tumor regression^[5-7]. Much evidence have shown that repeated intravenous injection of a recombinant, biologically active TRAIL protein could induce tumor cell apoptosis, suppress tumor progression, and improve the survival of animals bearing solid tumors without any detectable toxicity in nonhuman primates^[5,8]. Therefore, it appears that TRAIL may act as a potent anticancer agent. Furthermore, TRAIL can elicit apoptotic bystander effects on malignant cells. However, few researches of anti-liver cancer activity and bystander effects of TRAIL have been carried out up to date. Here, we first transferred human TRAIL gene to liver cancer cell line SMMC7721 with a binary adenoviral vector system, and assessed the anti-liver cancer activity of TRAIL gene and explored its bystander effects. In addition, we also assessed the toxicity of TRAIL to normal human fibroblasts (NHFB).

MATERIALS AND METHODS

Cell lines and culture conditions

Human embryonal kidney cells transformed by introducing sheared fragments of Ad5 DNA (293 cell) and human liver cancer cell line SMMC7721 were obtained from the Key Laboratory of Infective Diseases under Ministry of Public Health (Zhejiang University), normal human fibroblasts (NHFB) from normal human bone marrow were cultured; Cells were grown in RPMI 1640 medium supplemented with 10% fetal calf serum (NHFB with 20% fetal calf serum) in a 5% CO₂ atmosphere at 37 °C.

Adenoviral vectors

Adenoviral vectors Ad/GT-Bax, Ad/GT-LacZ and Ad/PGK-GV16 were constructed as described previously^[9,10]. Ad/GT-TRAIL, an adenoviral vector expressing TRAIL, was also constructed as described previously^[9]. Amplification, titration, and quality analysis of all of the vectors were performed as described previously^[9,10]. The titer determined by the absorbency of dissociated viruses at A_{260 nm} (one A_{260 nm} unit=10¹² viral particles/ml) was used in the study, whereas the titers determined by plaque assay were used as additive information.

Transgene expression of TRAIL

As determined in preliminary experiments, cells were

coinfecting with Ad/GT-TRAIL or Ad/GT-LacZ and Ad/PGK-GV16 at a ratio of 1:1. The optimal MOI was determined by infecting each cell line with Ad/GT-LacZ + Ad/PGK-GV16 and the expression of β -galactosidase was assessed via X-gal staining. The MOI that resulted in >80% of blue stained cells were used in this experiment. These MOI were 1000 particles for SMMC7721 and NHFB. Unless otherwise specified, Ad/GT-LacZ and Ad/PGK-GV16 were used as the vector control for Ad/GT-TRAIL and Ad/PGK-GV16. Ad/GT-Bax and Ad/PGK-GV16 were used as the positive control. Cells treated with PBS only were used as a blank control.

1×10^6 SMMC7721 cells were plated on 6-well plates and infected with Ad/GT-TRAIL+ Ad/PGK-GV16 or Ad/GT-LacZ + Ad/PGK-GV16. Forty-eight hours after infection, the cells were harvested and washed in PBS. RNA was extracted from the cells using Trizol reagent (Life Technology Inc.) and reversely transcribed to cDNA. The PCR conditions for cDNA amplification were 35 cycles of at 95 °C for 45 s, at 58 °C for 45 s, at 72 °C for 45 s, forward primer: 5' -AGA CCT GCG TGC TGA TCG TG-3', and reverse primer: 5' -TTA TTT TGC GGC CCA GAG CC-3'. The PCR products were separated in a 10g/L agarose gel and visualized by ethidium bromide staining.

Cell viability

Cell viability was assessed using MTT assay (Amresco) according to the manufacturer's protocol. The 5×10^3 SMMC7721 and NHFB cells were inoculated in to 96-well plates, with 3 parallel teams. Twenty-four hours after inoculation, the cells were infected with Ad/GT-TRAIL+ Ad/PGK-GV16, Ad/GT-Bax+ Ad/PGK-GV16, Ad/GT-LacZ + Ad/PGK-GV16 at MOI of 1000, and treated with PBS. At the 1st, 3rd and 5th day after infection, the cells were incubated with 5mL/L MTT for 4 h. Then the medium was removed and 150 μ l of sterilized DMSO solution was added, followed by incubation at 37 °C for 4 h. The absorbance of the reaction solution at 490 nm was measured. These data were used to make growth curves. The cell growth inhibition rate was (1-absorbance of experimental group/absorbance of control group) $\times 100\%$.

Apoptosis

Cell apoptosis was assessed by observing morphology and using the Annexin Vkit (Immunotech, Annexin-FITC) according to the manufacturer's protocol. The 5×10^4 SMMC7721 cells were inoculated in to 6-well plates. Twenty-four hours after inoculation, the cells were infected with adenoviruses at MOI of 1000. Then the cell morphology was observed with a reversed microscope every day. On the 4th day, the cells were harvested by trypsinization, washed in PBS and labeled with ANNEXIN V and propidium iodide (PI) according to the manufacturer's protocol. Finally, they were subjected to flow cytometry to determine the extent of cell death.

Bystander effects

Bystander effects of the TRAIL gene were assayed by MTT as follows: 5×10^4 SMMC7721 cells were washed in PBS and plated on 80-mm dishes, cultured with fresh RPMI 1640. Twenty-four hours later, the cells were infected with adenoviruses at MOI of 1000. Another 24 h after infection, the cells were harvested as the transferred SMMC7721 cells (SMMC7721/TRAIL cells). SMMC7721/TRAIL and SMMC7721 cells were suspended in 2×10^4 /ml of RPMI 1640 medium. SMMC7721/TRAIL and SMMC7721 cells were mixed with different ratios, SMMC7721/TRAIL cells accounted for 0, 5%, 25%, 50%, 75% and 100%, respectively.

Mixed cells (1×10^4) were inoculated in to 96-well plates with 3 parallel teams each ratio. Four days later the cell viability was determined by MTT assay.

Mechanism of bystander effects

In this study we tried to discover the effect of soluble factors on bystander effects of TRAIL. The 1×10^6 SMMC7721 cells were washed in PBS and plated on 80-mm dishes, cultured with fresh RPMI 1640. Twenty-four hours later, the cells were infected with Ad/GT-TRAIL+ Ad/PGK-GV16, and then cultured for another 24 h. Finally, the dishes were sent to be centrifuged and the medium was collected. This medium was filtrated with a 0.22 μ m filter membrane. Other dishes of non-infected SMMC7721 cells were cultured with this filtrated medium. We made the RPMI 1640 medium as blank control and Ad/GT-TRAIL+ Ad/PGK-GV16 as positive control. Four days later, the cell viability was assessed with MTT assay.

Statistical analysis

Statistical analysis was performed with SPSS 10.0, the cells viability and the cell apoptosis ratio were determined by paired *t*-test. Statistical significance was set when $P < 0.05$.

RESULTS

Virus titers

The titers of viruses determined by A_{260} were 1×10^{10} particles/mL.

Transgene expression of TRAIL

The expression of TRAIL gene with this system was confirmed *in vitro* in human liver cancer cell line SMMC7721 by RT-PCR. Treatment of cells with Ad/GT-TRAIL+ Ad/PGK-GV16 resulted in a strong TRAIL-specific band, whereas infection with control vectors resulted in undetectable expression (Figure 1). It indicated that TRAIL gene was transferred into the SMMC7721 cells and the binary adenoviral vectors were effective.

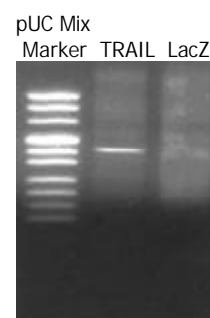


Figure 1 Expression of TRAIL tested with RT-PCR assay.

Cell viability

In cultured SMMC7721 cells, the cell viability (MTT) study showed a significant difference in cell killing effects between lines responsive to treatment with TRAIL-expression vectors versus control vectors, blank controls, even positive controls (Table 1, Figure 2). In cultured NHFB cells, the cell viability study showed a significant difference in cell killing only between TRAIL-expression vectors and Bax-expression vectors (Table 2, Figure 3). These results demonstrated that treatment with TRAIL gene could effectively elicit cell killing in cultured human liver cancer cells but not in normal human fibroblasts. TRAIL gene was more effective than Bax gene in killing cultured human liver cancer cells. Bax gene was obviously toxic to normal human fibroblasts.

Table 1 Cell growth-inhibition of SMMC7721 cells

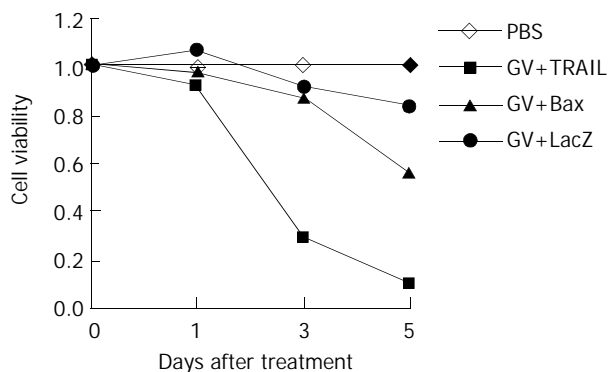
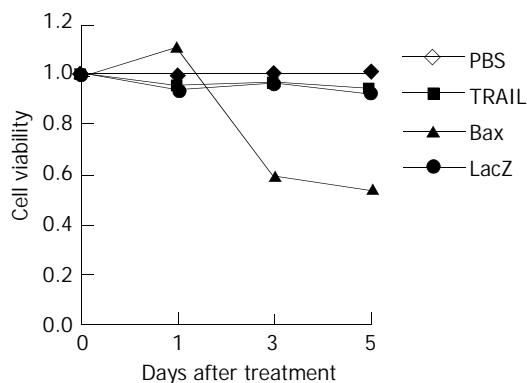
Groups	OD(mean±SD)	Cell growth-inhibition rate (%)
PBS	1.25±0.20	0
TRAIL	0.11±0.02 ^{ac}	91.2
Bax	0.65±0.13 ^a	48.0
LacZ	0.89±0.04	28.8

^a $P < 0.05$ vs PBS, ^c $P < 0.05$ vs Bax.

Table 2 Cell growth-inhibition of NHFB cells

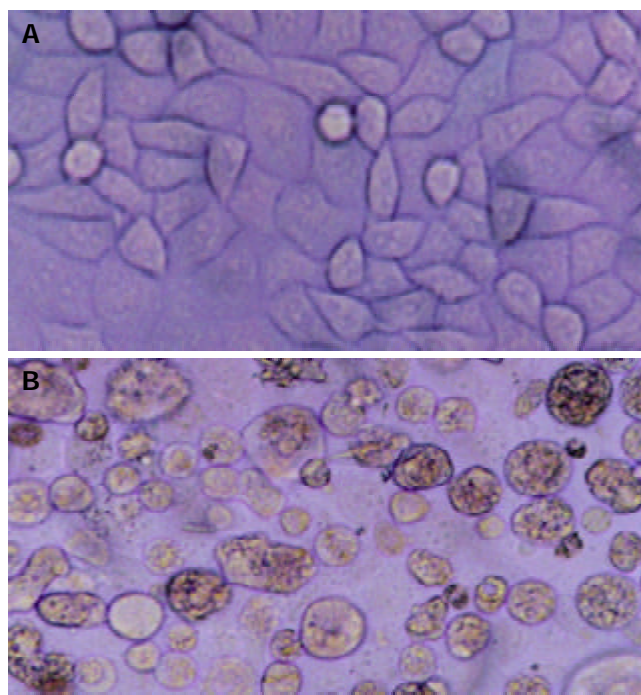
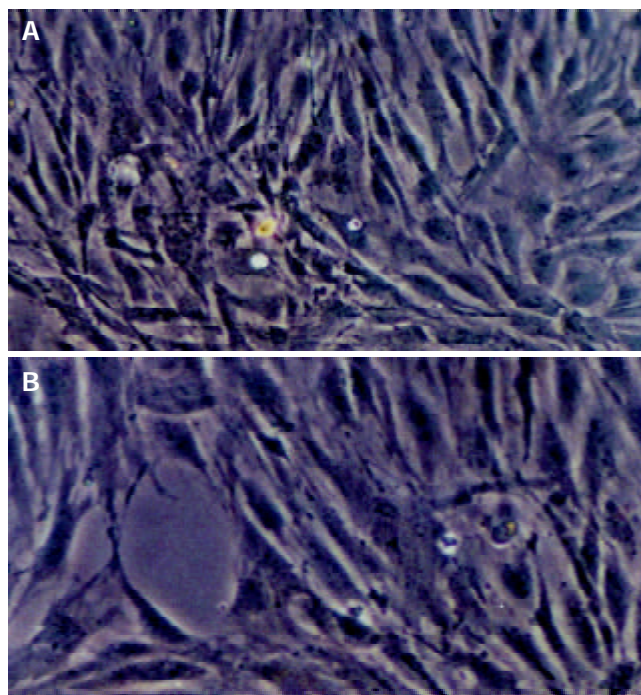
Groups	OD(mean±SD)	Cell growth-inhibition rate (%)
PBS	0.66±0.02	0
TRAIL	0.62±0.02 ^c	6.1
Bax	0.36±0.02 ^a	45.5
LacZ	0.61±0.03	7.6

^a $P < 0.05$ vs PBS, ^c $P < 0.05$ vs Bax.

**Figure 2** Viability of SMMC7721 cells.**Figure 3** Viability of NHFB cells.

Apoptosis

Morphologic changes of SMMC7721 cells showed cell apoptosis in cells treated with TRAIL gene versus PBS (Figure 4). NHFB cells treated with TRAIL gene and PBS showed no obvious difference in morphology (Figure 5). Assessed by FCM, the apoptosis of SMMC7721 cells infected with TRAIL gene, Bax gene, LacZ gene and treated with PBS was 29.07%, 12.53%, 6.58%, and 2.94%, respectively. There were significant differences between SMMC7721 cells treated with TRAIL gene and Bax gene, LacZ gene and PBS (Table 3, Figure 6). It indicated that TRAIL gene had a great ability to induce apoptosis of human liver cancer cells. It was also shown that TRAIL gene was more effective than Bax gene in inducing apoptosis of human liver cancer cells.

**Figure 4** SMMC7721 cells. A: uninfected with Ad/GT-TRAIL+Ad/PGK-GV16, B: infected with Ad/GT-TRAIL+Ad/PGK-GV16.**Figure 5** NHFB cells. A: uninfected with Ad/GT-TRAIL+Ad/PGK-GV16, B: infected with Ad/GT-TRAIL+Ad/PGK-GV16.

Bystander effects

The results of MTT assay showed that when transduced SMMC7721/TRAIL cells accounted for 5%, 25%, 50%, 75% and 100% of all cells, 4 days later 15.9%, 67.0%, 80.2%, 86.4%, 87.7% of all cells were killed (Table 4). It showed that partial untransfected cells were killed by bystander effects of TRAIL gene.

Moreover, we found that bystander effects could not be transferred by the medium leached transduced cell components. The viability of SMMC7721 cells cultured with the medium leached transduced cell components was 96%, similar to that

cultured with fresh RPMI 1640 (which was set to be 100%). There were no significant differences between them ($P>0.05$, Table 5).

Table 3 Percentage of apoptotic SMMC7721 cells

Groups	Percentage of apoptotic cells (%), mean \pm SD
TRAIL	29.07 \pm 4.96 ^{ace}
Bax	12.53 \pm 1.23 ^{ae}
LacZ	6.58 \pm 0.49 ^{ac}
PBS	2.94 \pm 0.63 ^{ce}

^a $P<0.05$ vs PBS, ^c $P<0.05$ vs Bax, ^e $P<0.05$ vs LacZ.

Table 4 Bystander effects of TRAIL on SMMC7721 cells

Percentage of SMMC7721/TRAIL(%)	OD (mean \pm SD)	Cell growth-inhibition rate (%)
0	0.693 \pm 0.028	0
5	0.583 \pm 0.036	15.9
25	0.228 \pm 0.014	67.0
50	0.137 \pm 0.019	80.2
75	0.094 \pm 0.009	86.4
100	0.084 \pm 0.010	87.7

Table 5 Percentage of apoptotic SMMC7721 cells

Groups	OD (mean \pm SD)	Cell growth-inhibition rate (%)
PBS	0.846 \pm 0.016	0
Cultured medium	0.794 \pm 0.027	4.0
TRAIL	0.108 \pm 0.010 ^a	87.5

^a $P<0.05$ vs PBS.

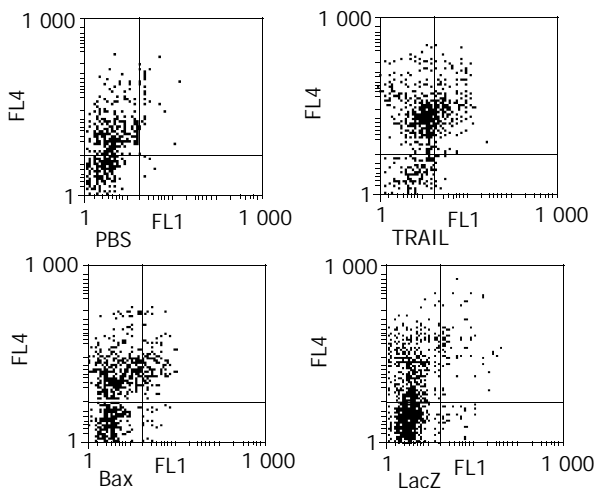


Figure 6 SMMC7721 cell apoptosis.

DISCUSSION

Liver cancer is one of the most malignant cancers with poor prognosis, and about two thirds of patients have been in China^[11]. Though many therapeutic methods have been available to its treatment, no one showed a more notable effect than operation. However, the patients who could be radically operated were less than 15%^[11]. It is now considered that apoptosis plays an important role in tumorigenesis, and at the same time inducing apoptosis of malignant cells has been prevailing in tumor therapy. There have been clinical reports of primary hepatocellular carcinoma treated with wild-type

p53 gene^[12].

TRAIL has become an attractive molecule for the treatment of cancer because it could kill tumor cells^[5,8]. Studies of recombinant TRAIL protein have revealed that the extracellular portion of TRAIL molecule was sufficient for its antitumor activity but its homotrimerization was necessary for TRAIL protein to retain this activity^[5,8], suggesting that the conformational structure of TRAIL is crucial for interaction with its receptors. In this study, we studied whether TRAIL gene could be directly transferred into tumor cells, and whether the expression of biologically active molecules could effectively kill human liver cancer cell lines rather than normal human cells *in vitro*, and whether the bystander effect exists during the process of killing.

It has been reported that a variety of malignant tumors, such as breast carcinoma^[13], thyroid carcinoma^[14], melanoma^[15], glioma^[16], multiple myeloma^[17,18], colon carcinoma^[19] and pancreatic carcinoma^[20,21] were all sensitive to TRAIL, but few reports related to liver cancers were available. In this study, binary adenoviral vectors were used to introduce the therapeutic genes into liver cancer cell line SMMC7721 and normal human fibroblasts (NHBF) to evaluate their anti-tumor activity, toxicity and bystander effects.

It was difficult to design an adenoviral vector to transexpress proapoptotic genes because of their high proapoptotic activity and toxicity on packaging 293 cells. Arai *et al.*^[22] reported that they constructed an adenovirus vector containing Fas-L gene, but it required packaging 293 cells bearing resistance to Fas-L or was decorated with Caspase depressor. Okuyama *et al.*^[23] designed another system to achieve the transexpression of proapoptotic genes but it was too complicated. We constructed a binary adenovirus vector system, which showed that TRAIL gene had a strong proapoptotic activity on packaging 293 cells. On the other hand this system could augment transgene expressions via a GAL4 gene regulatory system. In brief, we constructed two mated vectors, Ad/PGK-GV16 and Ad/GT-TRAIL, the promoter GT was a synthetic promoter consisting of five GAL4-binding sites and a TATA box, which had a very low transcriptional activity *in vitro* and *in vivo* when it was placed in an adenoviral backbone. But the transgene activity could be substantially induced *in vitro* and *in vivo* by administering this construct in combination with an adenoviral vector (Ad/PGK-GV16) expressing a GT transactivator, the GAL4-VP16 fusion protein^[24,25]. A weak promoter PGK would drive expression of the GAL4/VP16 fusion protein (GV16), which in turn would transactivate a minimal synthetic promoter, GAL4/TATA (GT), upstream of a transgene. It has been reported that this system used in CEA-positive cells treated with Ad/CEA-GV16+Ad/GT-LacZ versus Ad/CEA-LacZ had a 20- to 100- fold increase in transgene expression^[24]. We determined the ratio of two vectors as 1:1 via X-gal staining with LacZ gene expression. The binary adenoviral vector system was effective for expressing high-level products of the proapoptotic gene. This has been confirmed in Bax gene study^[5,26], therefore, Bax gene was used as a positive control in our study. We detected the transgene expression of TRAIL gene by RT-PCR and the result showed quite positive. Another result was that proapoptotic genes TRAIL and Bax had a high toxicity to liver cancer cells while LacZ did not by using this system.

TRAIL demonstrated its antitumor activity in a variety of tumors^[1,2,5], although different tumors might vary in their sensitivity. This phenomenon was observed in this study as before^[27]. SMMC7721 cells showed 29% of apoptosis. In comparison with other cell lines we tested before, HT29 had 24.6% of apoptosis^[28], DLD-1, H460 and A549 had 77%, 26% and 43.5% of apoptosis^[27], respectively. The mechanism underlying the differential sensitivity of malignant cells to

TRAIL treatment, as well as the differential killing of normal cells versus malignant cells, remain to be delineated. It could be partially explained by the presence of multiple receptors for TRAIL that functioned as either death-inducing or decoy receptors^[4,29,30]. Some groups have proposed that expression of decoy receptors confer resistance to normal tissues^[29,30], others have suggested that the level of intracellular Caspase/apoptosis inhibitors including FLIP and Bcl-X_L might result in resistance^[15,31,32]. Oppositely, some other studies considered that the levels of DR4, DR5, and DcR1 could not explain this phenomenon^[7,15,27,31]. Accordingly, we hold that the presence of decoy receptors is not the exclusive reason for different sensitivity of different cells. Recently, it was reported that a combined treatment with certain chemotherapy reagents could sensitize resistance to TRAIL-induced apoptosis^[5,6,33]. But one of these reports also mentioned that normal cells could be sensitized to TRAIL-inducing apoptosis^[7], suggesting that such a combination treatment may also increase toxicity.

Our study revealed that treatment with TRAIL gene was nontoxic to normal human fibroblasts cultured *in vitro*. This result was consistent with previous reports^[5,8,27]. Recently it was reported that human hepatocytes were very sensitive to apoptosis induced by recombinant TRAIL protein^[34]. But the toxicity could arise from histamine or/and leucine taken in combination with recombinant TRAIL protein^[35,36]. Another report showed that Z-LEHD-FMK, one of the Caspase inhibitors, could protect hepatocytes from apoptosis induced by TRAIL, but TRAIL gene could induce apoptosis of malignant cells^[37]. Now, we can transfer transgenes directly into target cells by target techniques, such as tumor specific promoter hTERT^[38], to reduce the toxicity to normal cells.

One of the bottlenecks of gene therapy for malignant tumors is the low transgene efficiency. It is difficult to transfer target genes into each tumor cell. Investigators have attempted to circumvent this limitation by exploiting what was called the bystander effects based on the transfer of vector transgene products from infected to uninfected cells. Though the existence of bystander effects could not increase the transgene efficiency, it could enhance the cell killing capability. Theoretically, treatment with TRAIL may elicit bystander effects either through interaction of cell surface TRAIL molecules with receptors on the neighboring cells or through the action of soluble TRAIL from TRAIL-expression cells. It has been reported that TRAIL gene could exert proapoptotic bystander effects on cancer cells^[27,39] as we demonstrated.

TRAIL is a type II membranous protein, it is speculated that membrane-bound TRAIL can be cleaved and then turned into a soluble form. Both membrane-bound TRAIL and soluble TRAIL could rapidly induce apoptosis in a wide variety of tumor cell lines via interaction with the death receptors DR4 and DR5^[40,41]. Nevertheless, in our study, the cell killing effects of TRAIL gene were not transferable with the medium of TRAIL-expressing cell cultures. This result suggested that the proapoptotic activity of TRAIL gene was mainly elicited via membrane-bound TRAIL. The soluble factors contributed little to antitumor activity and to the bystander effects of TRAIL gene. One explanation is that the effects of soluble TRAIL may be dose-dependent. In previous reports, the cell killing activity of recombinant soluble TRAIL was demonstrated, but the effect was elicited by high doses of TRAIL. They could not be achieved by spontaneous cleavage of TRAIL from cultured cells.

In conclusion, we found that TRAIL gene was more effective than Bax gene in killing liver cancer cells with bystander effects TRAIL had no toxicity to normal cells. These results suggest that TRAIL gene is more effective as a therapeutic gene of malignant tumors than Bax gene.

More researches should be carried out to reveal the anti-

liver cancer activity and bystander effects of TRAIL *in vivo*. It is possible that TRAIL gene will be used in clinical practices as new promoters and neoteric transgene vector systems are developed.

REFERENCES

- 1 **Wiley SR**, Schooley K, Smolak PJ, Din WS, Huang CP, Nicholl JK, Sutherland GR, Smith TD, Rauch C, Smith CA. Identification and characterization of a new member of the TNF family that induces apoptosis. *Immunity* 1995; **3**: 673-682
- 2 **Pitti RM**, Marsters SA, Ruppert S, Donahue CJ, Moore A, Ashkenazi A. Induction of apoptosis by Apo-2 ligand, a new member of the tumor necrosis factor cytokine family. *J Biol Chem* 1996; **271**: 12687-12690
- 3 **Ashkenazi A**, Dixit VM. Apoptosis control by death and decoy receptors. *Curr Opin Cell Biol* 1999; **11**: 255-260
- 4 **Griffith TS**, Lynch DH. TRAIL: a molecule with multiple receptors and control mechanism. *Curr Opin Immunol* 1998; **10**: 559-563
- 5 **Ashkenazi A**, Pai RC, Fong S, Leung S, Lawrence DA, Marsters SA, Blackie C, Chang L, McMurtrey AE, Hebert A, DeForge L, Koumenis IL, Lewis D, Harris L, Bussiere J, Koeppen H, Shahrokhi Z, Schwall RH. Safety and antitumor activity of recombinant soluble Apo2 ligand. *J Clin Invest* 1999; **104**: 155-162
- 6 **Lacour S**, Micheau O, Hammann A, Drouineaud V, Tschopp J, Solary E, Dimanche-Boitrel MT. Chemotherapy enhances TNF-related apoptosis-inducing ligand DISC assembly in HT29 human colon cancer cells. *Oncogene* 2003; **22**: 1807-1816
- 7 **Keane MM**, Ettenberg SA, Nau MM, Russell EK, Lipkowitz S. Chemotherapy augments TRAIL-induced apoptosis in breast cell line. *Cancer Res* 1999; **59**: 734-741
- 8 **Walczak H**, Miller RE, Ariail K, Gliniak B, Griffith TS, Kubin M, Chin W, Jones J, Woodward A, Le T, Smith C, Smolak P, Goodwin RG, Rauch CT, Schuh JC, Lynch DH. Tumoricidal activity of tumor necrosis factor-related apoptosis-inducing ligand *in vivo*. *Nat Med* 1999; **5**: 157-163
- 9 **Fang BL**, Ji L, Bouvet M, Roth JA. Evaluation of GAL4/TATA *in vivo* induction of transgene expression by adenovirally mediated gene codelivery. *J Biol Chem* 1998; **273**: 4972-4975
- 10 **Kagawa S**, Gu J, Swisher SG, Lin J, Roth JA, Lai D, Stephens LC, Fang B. Antitumor effect of adenovirus-mediated Bax gene transfer on p53-sensitive and p53-resistant cancer lines. *Cancer Res* 2000; **60**: 1157-1161
- 11 **Wu MC**. Clinical research advances in primary liver cancer. *World J Gastroenterol* 1998; **4**: 471-474
- 12 **Habib NA**, Ding SF, Masry R, Mitry RR, Honda K, Michail NE, Dalla Serra G, Izzi G, Greco L, Bassyouni M, el-Toukhy M, Abdel-Gaffar Y. Preliminary report: the short term effects of direct p53 DNA injection in primary hepatocellular carcinomas. *Cancer Detect Prev* 1996; **20**: 103-107
- 13 **Lin T**, Huang X, Gu J, Zhang L, Roth JA, Xiong M, Curley SA, Yu Y, Hunt KK, Fang B. Long-term tumor-free survival from treatment with the GFP-TRAIL fusion gene expressed from the hTERT promoter in breast cancer cells. *Oncogene* 2002; **21**: 8020-8028
- 14 **Ahmad M**, Shi Y. TRAIL-inducing apoptosis of thyroid cancer cells: potential for therapeutic intervention. *Oncogene* 2000; **19**: 3363-3371
- 15 **Griffith TS**, Chin WA, Jackson GC, Lynch DH, Kubin MZ. Intracellular regulation of TRAIL-induced apoptosis in human melanoma cells. *J Immunol* 1998; **161**: 2833-2840
- 16 **Knight MJ**, Riffkin CD, Muscat AM, Ashley DM, Hawkins CJ. Analysis of FasL and TRAIL induced apoptosis pathways in glioma cells. *Oncogene* 2001; **20**: 5789-5798
- 17 **Lincz LF**, Yeh TX, Spencer A. TRAIL-induced eradication of primary tumour cells from multiple myeloma patient bone marrows is not related to TRAIL receptor expression or prior chemotherapy. *Leukemia* 2001; **15**: 1650-1657
- 18 **Chen Q**, Gong B, Mahmoud-Ahmed AS, Zhou A, Hsi ED, Hussein M, Almasan A. Apo2L/TRAIL and Bcl-2-related proteins regulate type I interferon-induced apoptosis in multiple myeloma. *Blood* 2001; **98**: 2183-2192
- 19 **Burns TF**, El-Deiry WS. Identification of inhibitors of TRAIL-induced death (ITIDs) in the TRAIL-sensitive colon carcinoma

- cell line SW480 using a genetic approach. *J Biol Chem* 2001; **276**: 37879-37886
- 20 **Trauzold A**, Wermann H, Arlt A, Schutze S, Schafer H, Oestern S, Roder C, Ungefroren H, Lampe E, Heinrich M, Walczak H, Kalthoff H. CD95 and TRAIL receptor-mediated activation of protein kinase C and NF-kappaB contributes to apoptosis resistance in ductal pancreatic adenocarcinoma cells. *Oncogene* 2001; **20**: 4258-4269
- 21 **Ibrahim SM**, Ringel J, Schmidt C, Ringel B, Muller P, Koczan D, Thiesen HJ, Lohr M. Pancreatic adenocarcinoma cell lines show variable susceptibility to TRAIL-mediated cell death. *Pancreas* 2001; **23**: 72-79
- 22 **Arai H**, Gordon D, Nabel EG, Nabel GJ. Gene transfer of Fas ligand induces tumor regression *in vivo*. *Proc Natl Acad Sci U S A* 1997; **94**: 13862-13867
- 23 **Okuyama T**, Fujino M, Li XK, Funeshima N, Kosuga M, Saito I, Suzuki S, Yamada M. Efficient Fas-ligand gene expression in rodent liver after intravenous injection of a recombinant adenovirus by the use of a Cre-mediated switching system. *Gene Ther* 1998; **5**: 1047-1053
- 24 **Koch PE**, Guo ZS, Kagawa S, Gu J, Roth RA, Fang B. Augmenting transgene expression from carcinoembryonic antigen (CEA) promoter via a GAL4 gene regulatory system. *Mol Ther* 2001; **3**: 278-283
- 25 **Pan G**, Ni J, Yu G, Wei YF, Dixit VM. TRUNDD, a new member of the TRAIL receptor family that antagonizes TRAIL signaling. *FEBS Lett* 1998; **424**: 41-45
- 26 **He C**, Xu XM, Hu XT, Fang BL. Experimental study of effects of bax gene on human colorectal cancer cell line HT-29. *Zhonghua Xiaohua Zazhi* 2002; **22**: 535-538
- 27 **Kagawa S**, He C, Gu J, Koch P, Rha SJ, Roth JA, Curley SA, Stephens LC, Fang B. Antitumor activity and bystander effects of the tumor necrosis factor-related apoptosis-inducing ligand (TRAIL) gene. *Cancer Res* 2001; **61**: 3330-3338
- 28 **Xu XM**, He C, Hu XT, Fang BL. Tumor necrosis factor-related apoptosis-inducing ligand gene on human colorectal cancer cell line HT29. *World J Gastroenterol* 2003; **9**: 965-969
- 29 **Pan G**, Ni J, Wei YF, Yu G, Gentz R, Dixit VM. An antagonist decoy receptor and a death domain-containing receptor for TRAIL. *Science* 1997; **277**: 815-818
- 30 **Sheridan JP**, Masters SA, Pitti RM, Gurney A, Skubatch M, Baldwin D, Ramakrishnan L, Grey CL, Baker K, Wood WI, Goddard AD, Godowski P, Ashkenazi A. Control of TRAIL-induced apoptosis by a family of signaling and decoy receptors. *Science* 1997; **277**: 818-821
- 31 **Leverkus M**, Neumann M, Mengling T, Rauch CT, Brocker EB, Krammer PH, Walczak H. Regulation of tumor necrosis factor-related apoptosis-inducing ligand sensitivity in primary and transformed human keratinocytes. *Cancer Res* 2000; **60**: 553-559
- 32 **Marsters SA**, Pitti RM, Donahue CJ, Ruppert S, Bauer KD, Ashkenazi A. Activation of apoptosis by Apo-2 ligand is independent of FADD but blocked by CrmA. *Curr Biol* 1996; **6**: 750-752
- 33 **Wu XX**, Kakehi Y, Mizutani Y, Nishiyama H, Kamoto T, Megumi Y, Ito N, Ogawa O. Enhancement of TRAIL/Apo2L-mediated apoptosis by adriamycin through inducing DR4 and DR5 in renal cell carcinoma cells. *Int J Cancer* 2003; **104**: 409-417
- 34 **Jo M**, Kim TH, Seol DW, Esplen JE, Dorko K, Billiar TR, Strom SC. Apoptosis induced in normal human hepatocytes by tumor necrosis factor-related apoptosis-inducing ligand. *Nat Med* 2000; **6**: 564-567
- 35 **Lawrence D**, Shahrokh Z, Marsters S, Achilles K, Shih D, Mounho B, Hillan K, Totpal K, DeForge L, Schow P, Hooley J, Sherwood S, Pai R, Leung S, Khan L, Gliniak B, Bussiere J, Smith CA, Strom SS, Kelley S, Fox JA, Thomas D, Ashkenazi A. Differential hepatocyte toxicity of recombinant Apo2L/TRAIL versions. *Nature Med* 2001; **7**: 383-385
- 36 **Qin JZ**, Chau BN, Bonish B, Nickoloff BJ. Avoiding premature apoptosis of normal epidermal cells. *Nature Med* 2001; **7**: 385-386
- 37 **Ozoren N**, Kim K, Burns TF, Dicker DT, Moscioni AD, El-Deiry WS. The caspase-9 inhibitor Z-LEDH-FMK protects human liver cells while permitting death of cancer cells exposed to tumor necrosis factor-related apoptosis-inducing ligand. *Cancer Res* 2000; **60**: 6259-6265
- 38 **Nakamura TM**, Morin GB, Chapman KB, Weinrich SL, Andrews WH, Lingner J, Harley CB, Cech TR. Telomerase catalytic subunit homologs from fission yeast and human. *Science* 1997; **277**: 955-959
- 39 **Griffith TS**, Anderson RD, Davidson BL, Williams RD, Ratliff TL. Adenoviral-mediated transfer of the TNF-related apoptosis-inducing ligand/Apo-2 ligand gene induces tumor cell apoptosis. *J Immunol* 2000; **165**: 2886-2894
- 40 **Pan G**, O'Rourke K, Chinnaiyan AM, Gentz R, Ebner R, Ni J, Dixit VM. The receptor for the cytotoxic ligand TRAIL. *Science* 1997; **276**: 111-113
- 41 **Walczak H**, Degli-Esposti MA, Johnson RS, Smolak PJ, Waugh JY, Boiani N, Timour MS, Gerhart MJ, Schooley KA, Smith CA, Goodwin RG, Rauch CT. TRAIL-R2: a novel apoptosis-mediating receptor for TRAIL. *EMBO J* 1997; **16**: 5386-5397

Edited by Wang XL Proofread by Zhu LH

Preparation and characteristics of DNA-nanoparticles targeting to hepatocarcinoma cells

Qin He, Ji Liu, Xun Sun, Zhi-Rong Zhang

Qin He, Xun Sun, Zhi-Rong Zhang, West China School of Pharmacy, Sichuan University, Chengdu 610041, Sichuan Province, China

Ji Liu, West China School of Preclinical and Forensic Medicine, Sichuan University, Chengdu 610041, Sichuan Province, China

Correspondence to: Dr. Qin He, West China School of Pharmacy, Sichuan University, Chengdu 610041, Sichuan Province, China. qinhe317@vip.sina.com

Telephone: +86-28-85502532

Received: 2003-09-18 **Accepted:** 2003-11-19

Abstract

AIM: To prepare thymidine kinase gene (TK gene) nanoparticles and to investigate the expression of TK gene.

METHODS: Poly(D,L-lactic-co-glycolic acid) (PLGA), a biodegradable and biocompatible polymer, was used to prepare recombinant plasmid P^{EGFP-AFP} nanoparticles by a double-emulsion evaporation technique. Characteristics of the nanoparticles were investigated in this study, including morphology, entrapment efficiency, and tissue distribution. The expression of TK gene was also investigated by MTT assay, by which the viable cells were determined after the addition of ganciclovir (GCV). The enhanced green fluorescent protein (EGFP) expression in human hepatocellular carcinoma SMMC-7721 cells and normal parenchymal Chang liver cells were assessed by flow cytometry.

RESULTS: The prepared plasmid-nanoparticles had regular spherical surface and narrow particle size span with a mean diameter of 72±12 nm. The mean entrapment efficiency was 91.25%. A total of 80.14% DNA was found to be localized in the livers after 1-h injection with ³²P-DNA-PLGA nanoparticles in mouse caudal vein. The expression of DNA encapsulated in nanoparticles was much higher than that in naked DNA, and human hepatocellular carcinoma SMMC-7721 cells were more sensitive to GCV than human normal parenchymal Chang liver cells.

CONCLUSION: The enhanced transfection efficiency and stronger ability to protect plasmid DNA from being degraded by nucleases are due to nanoparticles encapsulation.

He Q, Liu J, Sun X, Zhang ZR. Preparation and characteristics of DNA-nanoparticles targeting to hepatocarcinoma cells. *World J Gastroenterol* 2004; 10(5): 660-663
<http://www.wjgnet.com/1007-9327/10/660.asp>

INTRODUCTION

In recent years, the gene delivery system has attracted much attention^[1-3]. However, safe and efficient gene delivery remains a crucial barrier to successful gene therapy. Viral and retroviral vectors have been the most efficient and commonly used delivery modalities for *in vivo* gene transfer, but viral vector may provoke mutagenesis and carcinogenesis. Repeated administration of a viral vector induces an immune response

which abolishes the transgene expression^[4-7]. The non-viral delivery system has the potential to be non-immunogenic and stable *in vivo*^[8-11]. Encapsulation of DNA in biodegradable polymer potentially offers a way to protect DNA from degradation and to control DNA release^[12,13], and many examples of DNA incorporated in synthetic polymers have been developed in the micron scale. Recently, some studies have shown that intracellular biodistribution of particles with diameter less than 100 nm can be achieved^[14].

Among all the present gene therapeutic protocols, combination of the administration of GCV with transfecting thymidine kinase gene of *Herpes simplex virus* (HSV-TK) into tumor cells is rather practical and potential in intra-tumoral gene therapy. The TK genes in the tumor cells can induce the metabolism of antitumor prodrug GCV into cytotoxic parent drug, which can cause the suicide of cells. This protocol presents good potential in intra-tumoral gene therapy^[15,16]. However, common TK genes (naked genes) do not have the abilities to target to specific organs and tissues, which can be harmful to the normal cells and tissues. In addition, they are easily degraded by nucleases *in vivo*.

To solve the problems mentioned above, a recombinant plasmid P^{EGFP-TKAFP} was constructed, which can be specifically expressed in hepatocellular carcinoma cells. Furthermore, the plasmid was encapsulated in a biodegradable and biocompatible PLGA polymer to protect plasmid DNA from being digested by nucleases. The following characteristics of the nanoparticles were investigated, including *in vitro* anti-nuclease ability, tissue distribution in mice and the gene expression in hepatocellular carcinoma cells and normal parenchymal cells *in vitro*.

MATERIALS AND METHODS

Materials

Poly(D,L-lactic-co-glycolic acid) (PLGA; lactic-glycolic acid ratio: 75:25, $M_n=30\ 000$, batch number: 020112) was purchased from Chengdu Institute of Organic Chemistry, Chinese Academy of Science. Recombinant plasmid P^{EGFP-TKAFP} was a gift from Dr. Liu Ji (Sichuan University). Human hepatocellular carcinoma SMMC-7721 cells^[17] and normal parenchymal Chang liver cells^[18] were provided by Shanghai Institute of Cell Biology, Chinese Academy of Science. DNase I was purchased from Chengdu Huamei Biochemicals Cooperation (Sichuan Province, China). Kunming mice, weighted 18-22 g, were provided by Experimental Animal Center of Sichuan University.

Methods

Nanoparticles preparation A double-emulsion evaporation technique^[19] was used to prepare the nanoparticles. Briefly, plasmid DNA (200 µg) in 100 µL Tris-EDTA (TE) buffer was emulsified in 1 mL methylene chloride solution containing 100 mg of PLGA using a probe sonicator for 5 s. Polyvinyl alcohol (2 mL) was added to the primary emulsion and sonicated for another 5 s to form a double emulsion. The emulsion was added into the same concentration of polyvinyl alcohol and agitated by a magnetic stirrer for 3 h at room

temperature to remove methylene chloride.

Particle size and morphology analysis The PLGA nanoparticles were sized by laser diffractometry using a Malvern 2 000 laser sizer. The morphology was observed by the scanning electron microscope (JEM-100SX, Akishima, Japan). The samples were placed on to special copper grids and then stained with 20 mL/L phosphato-tungstic acid prior to visualization.

Entrapment ratio analysis The entrapment ratio was determined by measuring the total amount of added DNA and that of DNA being not encapsulated. In detail, colloid solution of DNA-PLGA nanoparticles was centrifuged at 45 000 *g* for 1 h. Then, the concentration of DNA in the supernatant was assessed by fluorescence spectrophotometry after stained with ethidium bromide. The exciting and emission wavelengths were 546 nm and 590 nm, respectively. The entrapment rate (ER) was calculated as follows: $ER (\%) = \frac{DNA_{added} - DNA_{in\ the\ supernatant}}{DNA_{added}} \times 100\%$

Protection from DNase The PLGA nanoparticles were incubated with DNase I (0.1 unit) at 37 °C in a shaking water bath. The nanoparticles were collected by centrifugation after 4, 8, and 16 h incubation, and then chloroform was added to solubilize the nanoparticles. An equal volume of PBS solution was added, and the mixture was rotated end-over-end to facilitate the extraction of DNA from the organic phase into the aqueous phase. The samples were then centrifuged at 15 000 *g* for 15 min. The resulted supernatant was transferred to another tube and DNA was precipitated with the addition of isopropanol. Precipitate was obtained after centrifugation at 5 000 r/min for 15 min. Then, the resulted pellet was rinsed with 700 mL/L ethanol and resuspended in sterile TE buffer. The purified DNA was analyzed by gel electrophoresis.

Tissue distribution One hundred Kunming mice weighed 18–22 g were randomly divided into 10 test groups and 10 control groups with 5 in each group. The nanoparticles of ³²P-DNA-PLGA at a dose of 10 µL/g was intravenously administered to each mouse in test groups, and ³²P-DNA at the same dose was intravenously administered in control groups. At predetermined intervals, mice were sacrificed for blood collection. Then, heart, livers, spleen, lungs, and kidneys were removed from mice. The radioactivity of each organ was measured by a liquid scintillation analyzer.

The cpm_t was the total value of cpm in each organ (cpm_t) at a certain time point. The ratio of $cpm_t/cpm_i \times 100\%$ represented the relative content of DNA in viscera and blood.

MFI assay Human hepatocellular carcinoma SMMC-7721 cells and normal parenchymal Chang liver cells (5×10^5) were cultured in the DMEM medium containing 100 mL/L fetal bovine serum (FBS) in 12-well plates. The cells were transfected with plasmid DNA or nanoparticles containing DNA, and maintained at 37 °C in an incubator at a 50 mL/L CO₂ humidified atmosphere. After incubation for 12 h, the medium was removed and replaced with fresh DMEM containing 100 mL/L FBS for further 48 h incubation. The mean fluorescence intensity (MFI) of the cells was measured by flow cytometry.

Cytotoxicity assay Cells were cultured in the same way as the MFI assay. After incubation for 12 h, the medium was removed, replaced with DMEM containing 100 mL/L FBS, and incubated with 0.1, 1, or 10 µg/mL GCV. The cytotoxicity of GCV was detected by MTT assay.

RESULTS

Size and morphology

The resulted plasmid-nanoparticles had regular spherical surface (Figure 1) and a narrow size distribution with a mean diameter of 72 ± 12 nm.

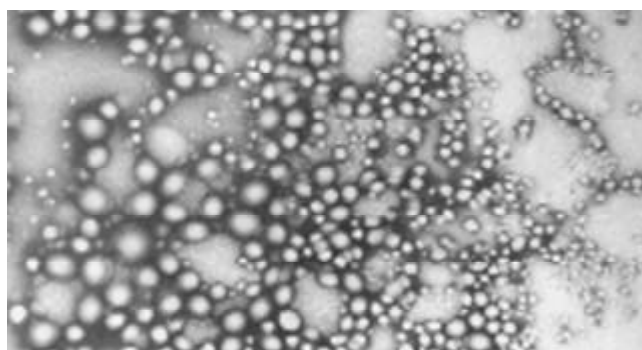


Figure 1 Transmission electron microphotography of TK-PLGA nanoparticles.

Entrapment efficiency

The mean entrapment efficiency was 91.25%, which was rather high in the nanoparticles preparation with PLGA as a carrier.

Protection from DNase

Plasmid DNA encapsulated in nanoparticles remained intact in the presence of DNase I for up to 16 h incubation. On the other hand, control plasmid DNA was completely digested within 1 h incubation with the equal amount of DNase I. This result demonstrated that PLGA nanoparticles could protect encapsulated plasmid DNA from nuclease digestion (Figure 2).

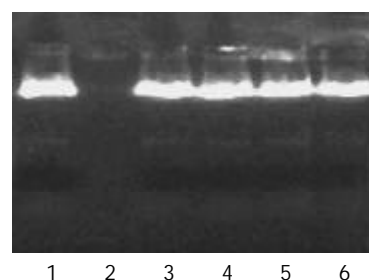


Figure 2 Agarose gel electrophoresis of DNA extracted from nanoparticles after treatment with sonication and DNase I. Lane 1 represented untreated control plasmid DNA, lane 2 represented plasmid DNA incubated with DNase I at 37 °C for 1 h, and lane 3, 4, 5, 6 indicated DNA extracted from PLGA nanoparticles incubated with DNase I at 37 °C for 0, 4, 8, or 16 h, respectively.

Measurement of DNA in blood and viscera of mice

The tissue distribution of DNA-PLGA nanoparticles was investigated by the technique of gamma scintigraphy. The results showed that 1 h after injection with ³²P-DNA-PLGA nanoparticles in mouse caudal vein, the ratio of radioactivity in livers against total radioactivity was more than 80%, which was 1.5-fold of that after injection with ³²P-DNA alone (Table 1 and Table 2).

Cytotoxicity assay and MFI assay

The EGFP expression in human hepatocellular carcinoma SMMC-7721 cells and normal parenchymal Chang liver cells were assessed by flow cytometry. The expression of TK gene was also investigated by MTT assay, by which the viable cells were quantitated after the addition of parent drug GCV. The results showed that the EGFP and TK expression in human hepatocellular carcinoma SMMC-7721 cells was much higher than that in human normal parenchymal Chang liver cells ($P < 0.05$) (Table 3). It also showed that plasmid DNA encapsulated in nanoparticles could enhance the expression of TK or EGFP gene compared with naked plasmid DNA ($P < 0.05$) (Table 4).

Table 1 Distribution (%) of ³²P-DNA in mice after intravenous administration of ³²P-DNA (n=5)

Time	Heart	Liver	Spleen	Lung	Kidney	Blood
5 min	3.14±0.60	36.67±2.65	3.56±1.58	16.32±0.79	23.52±1.48	16.79±1.62
15 min	3.15±0.97	41.26±2.89	5.25±0.86	14.16±0.99	20.61±1.62	15.57±1.58
30 min	6.94±1.57	52.59±4.02	10.46±0.75	7.95±0.58	13.10±0.85	2.95±0.65
1 h	6.11±1.95	54.62±3.12	14.85±1.23	7.82±0.67	13.50±0.94	3.10±0.78
2 h	4.56±1.01	51.34±2.88	14.93±0.68	9.65±1.41	15.03±1.34	4.49±0.28
6 h	5.12±0.79	48.66±1.87	13.15±0.84	9.66±1.27	18.26±1.58	5.15±1.67
12 h	5.48±0.99	44.52±2.02	11.32±1.33	11.36±1.34	21.83±2.54	5.49±0.58
24 h	3.93±0.65	43.31±1.67	11.48±1.11	10.12±0.64	25.01±3.12	6.16±0.94
48 h	3.43±0.84	36.75±1.65	11.56±0.82	13.36±1.60	28.52±2.15	6.38±0.83
72 h	4.52±0.77	34.48±1.85	12.03±1.73	13.88±1.63	28.31±3.01	6.78±0.91

Table 2 Distribution (%) of ³²P-DNA in mice after intravenous administration of ³²P-DNA-PLGA nanoparticles (n=5)

Time	Heart	Liver	Spleen	Lung	Kidney	Blood
5 min	2.22±0.51	57.32±2.36	2.96±0.69	8.29±1.33	16.58±2.02	12.63±1.24
15 min	3.52±0.64	69.69±3.32	3.19±0.58	5.77±0.55	13.87±0.99	3.96±0.36
30 min	2.38±0.67	73.37±3.62	7.55±1.03	3.64±0.41	11.28±1.28	1.78±0.65
1 h	2.08±0.54	80.14±4.56	3.37±0.67	3.08±0.62	9.34±0.68	1.99±0.54
2 h	2.59±0.28	78.45±4.02	3.73±0.76	5.35±0.58	8.36±0.94	1.47±0.23
6 h	3.18±0.60	75.03±3.69	7.38±1.03	3.74±0.39	9.61±0.96	1.06±0.24
12 h	2.21±0.51	69.34±3.96	6.17±1.24	7.88±0.64	10.17±1.04	4.22±0.32
24 h	1.94±0.32	65.59±3.25	6.46±1.04	7.95±0.57	12.10±1.23	5.96±0.59
48 h	2.21±0.29	61.18±2.69	7.01±0.48	9.27±0.71	12.87±0.86	6.46±0.86
72 h	2.51±0.37	60.56±2.98	6.45±0.69	9.98±0.65	13.54±1.11	6.96±0.75

Table 3 Inhibition ratio of different concentrations of GCV on SMMC-7721 and Chang liver cells

GCV (μg/mL)	SMMC-7721		Chang liver	
	DNA	NP	DNA	NP
1	2.0	6.6 ^a	1.2	3.7
10	3.0	10.0 ^a	2.8	5.8

^aP<0.05 vs Chang liver NP group; NP: nanoparticles.

Table 4 Mean fluorescence intensity in SMMC-7721 and Chang liver cells

Cell	MFI	
	DNA	NP
SMMC-7721	0.6±0.1 ^a	2.1±0.3 ^c
Chang liver	0.6±0.2	0.7±0.2

^aP<0.05 vs NP group; ^cP<0.05 vs Chang liver NP group; NP: nanoparticles.

DISCUSSION

Recombinant plasmid pEGFP-AFP was constructed, which could be specifically expressed in hepatocellular carcinoma cells because of alpha-fetoprotein-albumin (AFP-alb) promoter^[20-27]. Meanwhile, EGFP as the reporter gene of plasmid DNA, can be assessed by confocal laser scanning microscopy and flow cytometry^[28-32]. A polymer, PLGA, was selected due to its biocompatible and biodegradable properties, which was already approved for *in vivo* applications^[33-39]. Non-toxicity of the carrier may permit repeated administration of the nanoparticles to compensate for transient gene expression.

Our results showed that plasmid DNA could be encapsulated in PLGA nanoparticles without compromising its structural and functional integrity. Additionally, PLGA nanoparticles

could protect plasmids from nuclease degradation, and therefore offer an effective approach for gene delivery *in vivo*. However, the relatively low transfection efficiency was obtained in comparison with viral vector, which still remains to be a problem.

The DNA nanoparticles probably permeate the cells through endocytotic mechanism due to their small size and negative charged surface^[40]. The encapsulation of plasmid DNA in cationic liposomes offers another choice to be protected from DNases. However, cationic liposomes may be toxic to cells due to an excess of positive charge^[41,42], and can be easily influenced by the substances in plasma. In recent years, nanoparticles attract more and more attention because of many advantages, including high stability at room temperature, favorable safety, the ability to deliver plasmid DNA at a controllable rate, and easy adaptability. Unlike most viral vector, there is no limit on the size of plasmids encapsulated into the nanoparticles^[43,44].

REFERENCES

- 1 **Wiethoff CM**, Middaugh CR. Barriers to nonviral gene delivery. *J Pharm Sci* 2003; **92**: 203-217
- 2 **Guo SY**, Gu QL, Zhu ZG, Hong HQ, Lin YZ. TK gene combined with mIL-2 and mGM-CSF genes in treatment of gastric cancer. *World J Gastroenterol* 2003; **9**: 233-237
- 3 **Mhashilkar A**, Chada S, Roth JA, Ramesh R. Gene therapy. Therapeutic approaches and implications. *Biotechnol Adv* 2001; **19**: 279-297
- 4 **Liu F**, Huang L. Development of non-viral vectors for systemic gene delivery. *J Control Release* 2002; **78**: 259-266
- 5 **Corsi K**, Chellat F, Yahia L, Fernandes JC. Mesenchymal stem cells, MG63 and HEK293 transfection using chitosan-DNA nanoparticles. *Biomaterials* 2003; **24**: 1255-1264
- 6 **Brown MD**, Schatzlein AG, Uchegbu IF. Gene delivery with synthetic (non viral) carriers. *Int J Pharm* 2001; **229**: 1-21
- 7 **Kirchis R**, Wightman L, Wagner E. Design and gene delivery activity of modified polyethylenimines. *Adv Drug Deliv Rev* 2001; **53**: 341-358

- 8 **Hashida M**, Nishikawa M, Yamashita F, Takakura Y. Cell-specific delivery of genes with glycosylated carriers. *Adv Drug Deliv Rev* 2001; **52**: 187-196
- 9 **Kamiya H**, Tsuchiya H, Yamazaki J, Harashima H. Intracellular trafficking and transgene expression of viral and non-viral gene vectors. *Adv Drug Deliv Rev* 2001; **52**: 153-164
- 10 **Zhdanov RI**, Podobed OV, Vlassov VV. Cationic lipid-DNA complexes-lipoplexes-for gene transfer and therapy. *Bioelectrochemistry* 2002; **58**: 53-64
- 11 **Oku N**, Yamazaki Y, Matsuura M, Sugiyama M, Hasegawa M, Nango M. A novel non-viral gene transfer system, polycation liposomes. *Adv Drug Deliv Rev* 2001; **52**: 209-218
- 12 **Crommelin DJ**, Storm G, Jiskoot W, Stenekes R, Mastrobattista E, Hennink W. Nanotechnological approaches for the delivery of macromolecules. *J Control Release* 2003; **87**: 81-88
- 13 **Guang Liu W**, De Yao K. Chitosan and its derivatives- a promising non-viral vector for gene transfection. *J Control Release* 2002; **83**: 1-11
- 14 **Hirosue S**, Muller BG, Mulligan RC, Langer R. Plasmid DNA encapsulation and release from solvent diffusion nanospheres. *J Control Release* 2001; **70**: 231-242
- 15 **Singh S**, Cunningham C, Buchanan A, Jolly D, Nemunaitis J. Toxicity assessment of intratumoral injection of the herpes simplex type I thymidine kinase gene delivered by retrovirus in patients with refractory cancer. *Mol Ther* 2001; **4**: 157-160
- 16 **Vlachaki MT**, Chhikara M, Aguilar L, Zhu X, Chiu KJ, Woo S, Teh BS, Thompson TC, Butler EB, Aguilar-Cordova E. Enhanced therapeutic effect of multiple injections of HSV-TK +GCV gene therapy in combination with ionizing radiation in a mouse mammary tumor model. *Int J Radiat Oncol Biol Phys* 2001; **51**: 1008-1017
- 17 **Dong RC**, Zhou RH, Lu FD, Tao WZ. Primary study on the establishment of Human hepatocellular carcinoma cell line SMMC-7721 and its biological characteristics. *Dier Junyi Daxue Xuebao* 1980; **1**: 5-9
- 18 **Chang RS**. Continuous subcultivation of epithelial-like cells from normal human tissues. *Proc Soc Exp Biol Med* 1954; **87**: 440-443
- 19 **Prabha S**, Zhou WZ, Panyam J, Labhasetwar V. Size-dependency of nanoparticle-mediated gene transfection: studies with fractionated nanoparticles. *Int J Pharm* 2002; **244**: 105-115
- 20 **Sa Cunha A**, Bonte E, Dubois S, Chretien Y, Eraiser T, Degott C, Brechot C, Tran PL. Inhibition of rat hepatocellular carcinoma tumor growth after multiple infusions of recombinant Ad.AFPtk followed by ganciclovir treatment. *J Hepatol* 2002; **37**: 222-230
- 21 **Li MS**, Li PF, He SP, Du GG, Li G. The promoting molecular mechanism of alpha-fetoprotein on the growth of human hepatoma Bel 7402 cell line. *World J Gastroenterol* 2002; **8**: 469-475
- 22 **Cao G**, Kuriyama S, Gao J, Nakatani T, Chen Q, Yoshiji H, Zhao L, Kojima H, Dong Y, Fukui H, Hou J. Gene therapy for hepatocellular carcinoma based on tumour-selective suicide gene expression using the alpha-fetoprotein (AFP) enhancer and a house-keeping gene promoter. *Eur J Cancer* 2001; **37**: 140-147
- 23 **Kim J**, Lee B, Kim JS, Yun CO, Kim JH, Lee YJ, Joo CH, Lee H. Antitumoral effects of recombinant adenovirus YKL-1001, conditionally replicating in alpha-fetoprotein-producing human liver cancer cells. *Cancer Lett* 2002; **180**: 23-32
- 24 **Ishikawa H**, Nakata K, Mawatari F, Ueki T, Tsuruta S, Ido A, Nakao K, Kato Y, Ishii N, Eguchi K. Retrovirus-mediated gene therapy for hepatocellular carcinoma with reversely oriented therapeutic gene expression regulated by alpha-fetoprotein enhancer/promoter. *Biochem Biophys Res Commun* 2001; **287**: 1034-1040
- 25 **Takahashi M**, Sato T, Sagawa T, Lu Y, Sato Y, Lyama S, Yamada Y, Fukaura J, Takahashi S, Miyanishi K, Yamashita T, Sasaki K, Kogawa K, Hamada H, Kato J, Niitsu Y. E1B-55K-deleted adenovirus expressing E1A-13S by AFP-enhancer/promoter is capable of highly specific replication in AFP-producing hepatocellular carcinoma and eradication of established tumor. *Mol Ther* 2002; **5**(5 Pt 1): 627-634
- 26 **Ye X**, Liang M, Meng X, Ren X, Chen H, Li ZY, Ni S, Lieber A, Hu F. Insulation from viral transcriptional regulatory elements enables improvement to hepatoma-specific gene expression from adenovirus vectors. *Biochem Biophys Res Commun* 2003; **307**: 759-764
- 27 **Lu SY**, Sui YF, Li ZS, Pan CE, Ye J, Wang WY. Construction of a regulable gene therapy vector targeting for hepatocellular carcinoma. *World J Gastroenterol* 2003; **9**: 688-691
- 28 **Kantakamalaku W**, Jaroenpool J, Pattanapanyasat K. A novel enhanced green fluorescent protein (EGFP)-K562 flow cytometric method for measuring natural killer (NK) cell cytotoxic activity. *J Immunol Methods* 2003; **272**: 189-197
- 29 **Bi JX**, Wirth M, Beer C, Kim EJ, Gu MB, Zeng AP. Dynamic characterization of recombinant Chinese hamster ovary cells containing an inducible c-fos promoter GFP expression system as a biomarker. *J Biotechnol* 2002; **93**: 231-242
- 30 **Henry SC**, Schmader K, Brown TT, Miller SE, Howell DN, Daley GG, Hamilton JD. Enhanced green fluorescent protein as a marker for localizing murine cytomegalovirus in acute and latent infection. *J Virol Methods* 2000; **89**: 61-73
- 31 **Jakobs S**, Subramaniam V, Schonle A, Jovin TM, Hell SW. EFGP and DsRed expressing cultures of *Escherichia coli* imaged by confocal, two-photon and fluorescence lifetime microscopy. *FEBS Lett* 2000; **479**: 131-135
- 32 **Hanson P**, Mathews V, Marrus SH, Graubert TA. Enhanced green fluorescent protein targeted to the Sca-1 (Ly-6A) locus in transgenic mice results in efficient marking of hematopoietic stem cells *in vivo*. *Exp Hematol* 2003; **31**: 159-167
- 33 **Yamaguchi Y**, Takenaga M, Kitagawa A, Ogawa Y, Mizushima Y, Igarashi R. Insulin-loaded biodegradable PLGA microcapsules: initial burst release controlled by hydrophilic additives. *J Control Release* 2002; **81**: 235-249
- 34 **Perez-Rodriguez C**, Montano N, Gonzalez K, Griebenow K. Stabilization of α -chymotrypsin at the CH₂Cl₂/water interface and upon water-in-oil-in-water encapsulation in PLGA microspheres. *J Control Release* 2003; **89**: 71-85
- 35 **Dorta MJ**, Santovena A, Llabres M, Farina JB. Potential applications of PLGA film-implants in modulating *in vitro* drugs release. *Int J Pharm* 2002; **248**: 149-156
- 36 **Lu L**, Yaszemski MJ, Mikos AG. Retinal pigment epithelium engineering using synthetic biodegradable polymers. *Biomaterials* 2001; **22**: 3345-3355
- 37 **Jain RA**, Rhodes CT, Railkar AM, Malick AW, Shah NH. Controlled release of drugs from injectable *in situ* formed biodegradable PLGA microspheres: effect of various formulation variables. *Eur J Pharm Biopharm* 2000; **50**: 257-262
- 38 **Panyam J**, Labhasetwar V. Biodegradable nanoparticles for drug and gene delivery to cells and tissue. *Adv Drug Deliv Rev* 2003; **55**: 329-347
- 39 **Vila A**, Sanchez A, Tobio M, Calvo P, Alonso MJ. Design of biodegradable particles for protein delivery. *J Control Release* 2002; **78**: 15-24
- 40 **Garcia-Chaumont C**, Seksek O, Grzybowska J, Borowski E, Bolard J. Delivery systems for antisense oligonucleotides. *Pharmacol Ther* 2000; **87**: 255-277
- 41 **Han SO**, Mahato RI, Kim SW. Water-soluble lipopolymer for gene delivery. *Bioconjug Chem* 2001; **12**: 337-345
- 42 **Pouton CW**, Seymour LW. Key issues in non-viral gene delivery. *Adv Drug Deliv Rev* 2001; **46**: 187-203
- 43 **del Barrio GG**, Novo FJ, Irache JM. Loading of plasmid DNA into PLGA microparticles using TROMS (Total Recirculation One-Machine System): evaluation of its integrity and controlled release properties. *J Control Release* 2003; **86**: 123-130
- 44 **Davis ME**. Non-viral gene delivery systems. *Curr Opin Biotechnol* 2002; **13**: 128-131

Inhibitor RNA blocks the protein translation mediated by hepatitis C virus internal ribosome entry site *in vivo*

Xue-Song Liang, Jian-Qi Lian, Yong-Xing Zhou, Mo-Bin Wan

Xue-Song Liang, Mo-Bin Wan, Department of Infectious Diseases, Changhai Hospital, Second Military Medical University, Shanghai, China

Jian-Qi Lian, Yong-Xing Zhou, Department of Infectious Diseases, Tangdu Hospital, Fourth Military Medical University, Xi'an 710038, Shaanxi Province, China

Supported by the National Natural Science Foundation of China, No. 30000147

Co-correspondents: Xue-Song Liang and Jian-Qi Lian

Correspondence to: Dr. Xue-Song Liang, Department of Infectious Diseases, Changhai Hospital, Second Military Medical University, Shanghai, China. liangxuesong2000@163.com

Telephone: +86-21-25072109

Received: 2003-08-08 **Accepted:** 2003-10-07

Abstract

AIM: To investigate the inhibitory effect of hepatitis C virus internal ribosome entry site (HCV IRES) specific inhibitor RNA (IRNA) on gene expression mediated by HCV IRES *in vivo*.

METHODS: By using G418 screening system, hepatoma cells constitutively expressing IRNA or mutant IRNA (mIRNA) were established and characterized, and HCV replicons containing the 5' untranslated region (5' UTR) were constructed by using the same method. Cotransfection of pCMVNCRLuc containing HCV 5' UTR-luc fusion genes and eukaryotic vector of IRNA into human hepatic carcinoma cells (HepG2) was performed and the eukaryotic expression plasmid of IRNA was transfected transiently into HCV replicons. pCMVNCRLuc or pCDNA-luc was cotransfected with pSV40- β Gal into IRNA expressing hepatoma cells by using lipofectamine 2000 *in vitro*. Then the reporting gene expression level was examined at 48 h after transfection by using a luminometer and the expressing level of HCV C antigen was analysed with a confocal microscope.

RESULTS: Transient expression of IRES specific IRNA could significantly inhibit the expression of reporter gene and viral antigen mediated by HCV IRES by 50% to 90% *in vivo*, but mIRNA lost its inhibitory activity completely. The luciferase gene expression mediated by HCV IRES was blocked in the HHCC constitutively expressing IRNA. At 48 h after transfection, the expression level of reporter gene decreased by 20%, but cap-dependent luciferase gene expression was not affected. IRNA could inhibit the HCV replicon expression 24 h after transfection and the highest inhibitory activity was 80% by 72 h, and the inhibitory activity was not increased until 7d after transfection.

CONCLUSION: IRNA can inhibit HCV IRES mediated gene expression *in vivo*.

Liang XS, Lian JQ, Zhou YX, Wan MB. Inhibitor RNA blocks the protein translation mediated by hepatitis C virus internal ribosome entry site *in vivo*. *World J Gastroenterol* 2004; 10 (5): 664-667

<http://www.wjgnet.com/1007-9327/10/664.asp>

INTRODUCTION

Hepatitis C virus (HCV) is the primary causative agent of parenterally transmitted non-A, non-B hepatitis and affects a significant part of the world population. HCV infection frequency leads to chronic hepatitis, cirrhosis of the liver, and hepatocellular carcinoma. The genome of HCV is a single-stranded, plus-polarity RNA. The 5' untranslated region (UTR) of HCV RNA is approximately 340 nt long, and contains multiple AUG codons. The 5' UTR is highly conserved among different strains of HCV. Nucleotides 40 to 370 of the 5' UTR of HCV have been shown to contain an internal ribosome entry site (IRES)^[1-3]. The presence and stability of IRES play an important role in virus life cycle, so the region has become the target of antiviral gene therapy^[4-16]. Coward and Dasgupta found that gene expression mediated by polio virus (PV) IRES was inhibited by one 60 nt long RNA which is called inhibitor RNA (IRNA). Because HCV and PV IRES elements bound to similar polypeptides^[16-20], it was reasoned that IRNA might also interfere with HCV IRES-mediated translation. Using transient transfection of hepatoma cells and a hepatoma cell line constitutively expressing IRNA, we demonstrated specific inhibition of HCV IRES-mediated translation by IRNA *in vivo*.

MATERIALS AND METHODS

Materials

Vectors pcRz-IRNA and pcRz-mIRNA were constructed by our laboratory, which introduced the sequences of 5' and 3' *cis*-self cleavage ribozyme into both sides of IRNA or mIRNA sequence^[21]. pCMVNCRLuc contain full sequence of HCV 5' UTR and 66 nt core gene, and was fused with luciferase gene (generous gift of professor Alt). pcHCVluc was constructed by our laboratory containing full sequence of HCV 5' UTR and partial sequence of core region, and could express in cells stably.

Methods

Cell culture Human hepatocarcinoma cell (HHCC) HepG2 was grown in RPMI1640 medium supplemented with 100 mL/L newborn calf serum.

Plasmid construction By using subcloning methods, IRNA and mIRNA sequence were cloned into the pcDNA3 vector, yielding pcRz-IRNA and pcRz-mIRNA which introduced the ribozyme sequence over both sides of IRNA and mIRNA to generate the correct side of IRNA and mIRNA^[16]. In brief, by using PCR methods the sequences of target RNA were generated from pGRz-IRNA or pGRz-mIRNA which was constructed by our laboratory. Then the PCR product was cloned into the *Bam*HI-*Apa*I sites of the pcDNA3 vector.

Establishment of stable hepatoma cell line expressing IRNA or cloning HCV replicon Plasmids pcRz-IRNA, pcRz-mIRNA, pcDNA3 and pcHCVluc were transfected into HHCC respectively by using Lipofectamine 2000 reagent (GIBCO) and screened for neomycin resistance with 300 μ g/mL of geneticin (G418) (Invitrogen) per milliliter for 4 weeks. The antibiotic-resistant cell clones were harvested and further screened by dilution titer.

Detection of IRNA in cell lines IRNA or miRNA expression in the cells was measured by isolating total RNA from these cells and IRNA or miRNA were detected by reverse transcriptase (RT)-mediated PCR (RT-PCR) by using IRNA or miRNA specific oligonucleotide primers. One to 2 μg of total RNA isolated from the IRNA or miRNA expressing cells, and 2 μg total RNA from HHCC control cells were reversely transcribed by murine leukemia virus RT using random hexamer primers in 20 μL reaction mixture according to the TaKaRa RNA PCR kit protocol. Twenty pmol of each primer (corresponding to 5' nt 1 to 20 and 3' nt 1 to 20 of the IRNA or miRNA sequence) was used to amplify the 60-nt fragment in 100 μL PCR reaction. The cycling parameters were as follows: denaturation at, 95 $^{\circ}\text{C}$ for 1 min, annealing at, 65 $^{\circ}\text{C}$ for 1 min, extension at, 72 $^{\circ}\text{C}$ for 1 min, a total of 50 cycles, then total extension at, 72 $^{\circ}\text{C}$ for 10 min. Twenty microliters of each reaction product were loaded onto 20 g/L gel and visualized by ethidium bromide staining.

Detection of HCV core protein expression in HHCC HCV core protein was detected by using indirect immune fluorescence method. HCV replicon cells were plated on a cover glass and fixed with pure ethanol for 10 min. Monoclonal antibody of HCV core protein was properly diluted (1:100) and covered on the glass with HCV replicon cells for 1 h at 37 $^{\circ}\text{C}$, and then the glass was washed 3 times with PBS (10 min each). Then FITC labeled second antibody was covered on the glass at 37 $^{\circ}\text{C}$ for 1 h and the glass was washed 3 times again with PBS. At last the cells were examined by using fluorescence microscopy or laser confocal microscopy.

DNA transfection For each transfection assay, 1×10^6 HHCC cells in 30-mm-diameter plates were transfected with 15 μL of lipofectin (GIBCO) and 2 to 5 μg of plasmid DNA. At 16 h post transfection, cell lysates were prepared according to the luciferase assay kit protocol (Promega) and assayed for both β -galactosidase (β -Gal) and luciferase expression.

RESULTS

Inhibitor effect of IRNA transient expression on HCV IRES-mediated translation

To test the possibility that IRNA interfered with HCV IRES-mediated translation, human hepatocellular carcinoma cells (HepG2) were transiently cotransfected with three plasmids: a reporter gene expressing luciferase programmed by the HCV IRES element (pCMVNCRLuc), pSV- β -galactosidase to measure transfection efficiency, and the plasmid expressing IRNA (pcRz-IRNA). All transfections were done in triplicate and contained equal amounts of the luciferase reporter and β -Gal plasmid. Increasing concentrations of plasmid pcRz-IRNA were used in various reactions, and the total amount of DNA in each reaction was kept constant by addition of an appropriate amount of a nonspecific DNA (pcDNA3). Following transfection, luciferase activity was measured in cell extracts at 48 h. At the lowest concentration of the IRNA plasmid, inhibition of luciferase activity from plasmid pCMVNCRLuc was approximately 50% compared to the control. However, at the highest concentration, 92% of luciferase activity was inhibited. Translation of luciferase from

a control plasmid (pCDNA-luc) without HCV IRES was not significantly inhibited by IRNA, ($P > 0.05$, Table 1).

In order to determine the inhibitor effect of IRNA on HCV IRES-mediated translation further, the HHCCs were transfected with pCMVNCRLuc or cotransfected with pcRz-IRNA and pCMVNCRLuc. Following transfection, the HCV core protein programmed by HCV IRES was detected by using laser confocal microscopy. HCV core protein could express efficiently in the HHCC cells as shown in Figure 1. But IRNA plasmid cotransfection could inhibit HCV core protein expression. The pels density of HCV core protein was different between the two groups (58.05 ± 42.24 vs 15.56 ± 8.54). The inhibitory rate was plotted by $1 - \text{pels density of IRNA transfection group} / \text{pels density of control} \times 100\%$.

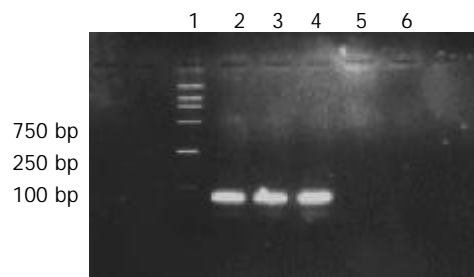


Figure 1 Stable expression of IRNA and miRNA in HHCC cells. 1: DL2000 DNA marker; 2, 3: IRNA RT-PCR; 4: miRNA RT-PCR; 5: IRNA PCR.

Construction of hepatoma cell line expressing IRNA or miRNA

To determine the long-term effect of RNA expression in HepG2, the cell line constitutionally expressing IRNA was generated by using a pcDNA-based vector as described in Material and Methods. In order to obtain both the correct and stable sites of the expressed IRNA, ribozyme sequences were introduced into both sides of IRNA and miRNA. IRNA or miRNA was examined by RT-PCR using appropriate primers. IRNA and miRNA were expressed stably in the stable cell lines as shown in Figure 2.

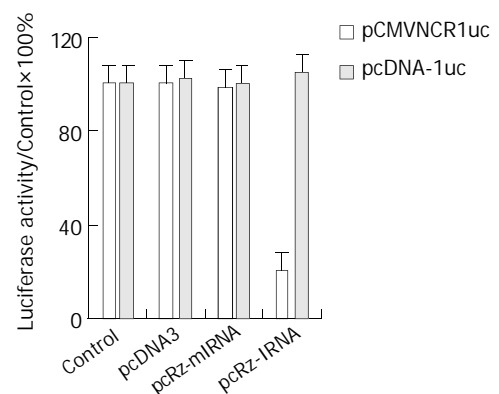


Figure 2 Inhibitory effect of IRNA on luciferase expression mediated by different mechanism.

Table 1 Inhibitory effect of IRNA on HCV IRES mediated gene translation

Sample pcRz-IRNA μg	Activity of luciferase programmed by cap-dependent mechanism (IU/U)	Activity of luciferase programmed by HCV IRES (IU/U)	Inhibitory rate (%)	
			pcDNA-luc	pCMVNCRLuc
0	55.5 ± 3.11	52.49 ± 2.31		
2	60.1 ± 2.31	27.0 ± 0.740	0	50
4	58.3 ± 1.89	14.7 ± 0.380	0	72
6	52.4 ± 2.12	4.03 ± 0.120	4	92

HCV IRES-mediated gene expression in IRNA expressing HepG2 cells

IRNA or miRNA expressing HepG2 cells and empty vector pcDNA3 expressing cells or control cells were cotransfected with pCMVNCRLuc and transfection efficiency control plasmid pSV- β -Gal. At 48 h post-transfection cell extracts were used to measure the activities of both luciferase and β -galactosidase. The result was plotted as percent of control after normalized for β -Gal activity and protein concentration. The pcRz-IRNA cells showed approximately 80% inhibition of luciferase activity compared to the control. Both pcRz-miRNA cells and pcDNA3 cells showed less than 5% inhibition activity. No significant inhibition of cap-dependent translation from the pCDNA-luc construct was observed in cell lines expressing IRNA, ($P=0.05$, Figure 3).

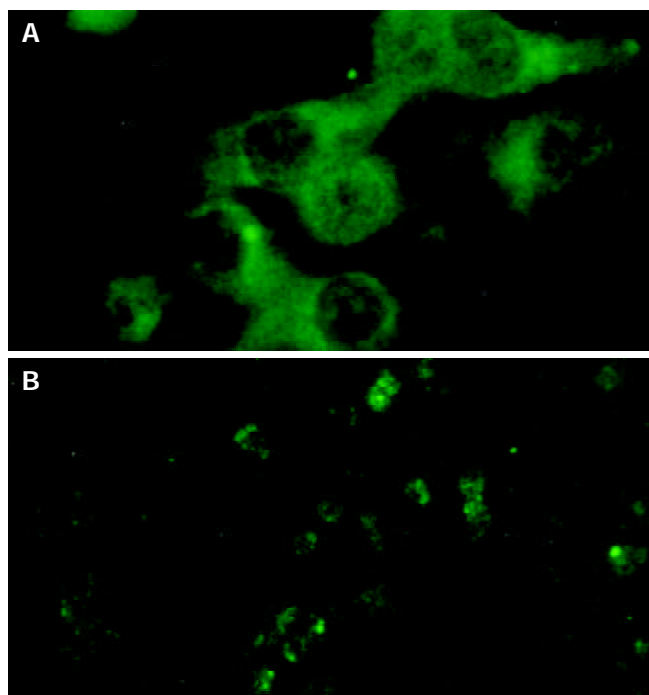


Figure 3 Inhibitory effect of IRNA on HCV Core expression mediated by HCV IRES(A: 40 \times 10 vs B: 25 \times 10). A: HCV Core protein of pCMVNCRLuc transfection group, B: HCV Core protein of pcRz-IRNA and pCMVNCRLuc cotransfection group.

Construction of HCV replicon containing HCV IRES

The results demonstrated that HCV core programmed by HCV IRES was positive in about 90% of HHCC cells (Figure 4).

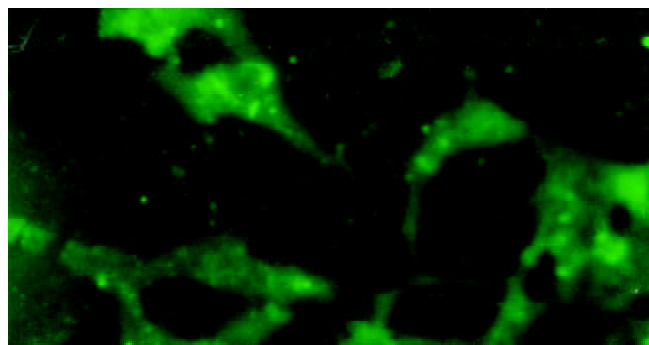


Figure 4 Detection of HCV core protein in HHCC lines stably expressing pcHCV Cluc (25 \times 10).

Interference of IRNA with HCV replicon translation

To confirm the result obtained in IRNA expressing cells, HCV

replicon containing HCV IRES was transfected with IRNA expressing plasmid, and luciferase activity was determined at different time following transfection. The result was that at 24 h HCV IRES-mediated luciferase gene translation decreases by 15% compared to the control HHCC cells, and along with time extending, the inhibitory effect of IRNA on HCV IRES-mediated luciferase gene translation increased and reached 80% at 72 h. On d 7, the inhibitory effect was still 80%. But miRNA and nonspecific short RNA did not show any inhibitory effect on HCV IRES-mediated gene translation (Figure 5).

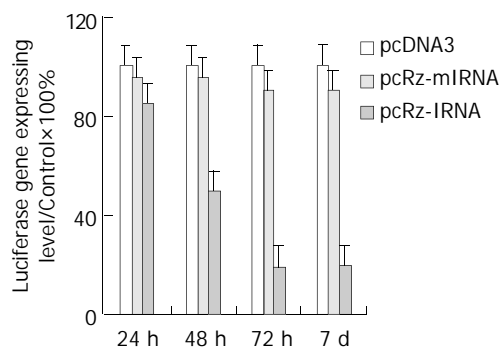


Figure 5 Interference of IRNA with HCV replicon translation.

DISCUSSION

IRES-dependent protein translation mechanism was first discovered in picornaviruses, including PV, rhinovirus and hepatitis A virus, as well as certain flaviviruses, such as hepatitis C virus^[23-28]. Although there is very little sequence homology between these different IRES elements, structural similarity does appear to exist. In fact, in order to keep the activity of IRES, it was more important to maintain the secondary structure than to maintain the integrality of certain genome sequences^[1-3,7,8]. IRES is the key structure for some viral RNA replication, so it has become the target for antiviral infection. We have constructed the self-cleavage plasmid of IRNA, and affirmed that IRNA can inhibit IRES-dependent protein translation *in vitro*^[22]. In order to further confirm the effect of long-term expressing IRNA on cellular protein and viral protein translation, we established a HHCC line stably expressing IRNA, and confirmed that long-term expressing IRNA could significantly inhibit IRES mediated protein translation compared to the control cells and miRNA expressing cells. Das *et al* prepared the human hepatoma (Huh-7) cell lines expressing IRNA by using the similar methods. They found that HCV IRES-mediated cap-independent translation was markedly inhibited in cells constitutively expressing IRNA compared to control hepatoma cells^[29].

Alt *et al* designed the vector pCMVNCRLuc fusing the luciferase gene to HCV core gene 66 nt site, and the gene expression was mediated by HCV 5' UTR, so we could determine the inhibitor effect of new strategies on HCV 5' UTR by examining the activity of luciferase. In this study, three plasmids pCMVNCRLuc, pcRz-IRNA expressing IRNA and transfection efficiency control plasmid pSV- β Gal were cotransfected into HHCC cells and luciferase activity (light units) was expressed as percentage of the control after normalized for β gal activity. When the effect of transfection efficiency and transient expression efficiency were excluded, the results of this study showed that IRNA could specifically inhibit HCV IRES mediated gene expression *in vivo*. The results of our study suggested that HCV 5' UTR-mediated translation was specifically inhibited by IRNA transient expression in hepatoma cells (50% to 92%), whereas cap-dependent translation of luciferase from the control plasmid

lack of HCV IRES element was not significantly affected by IRNA. To confirm the result obtained by using transient transfection, the vector containing HCV IRES was transfected into human hepatoma cells expressing IRNA constitutively and the results demonstrated that stably expressing IRNA could inhibit HCV IRES-mediated translation. By using a bicistronic construct containing CAT and luciferase genes flanked by the HCV 5' UTR Das *et al* found that IRNA could significantly inhibit HCV IRES-mediated gene expression *in vitro*. Further, they studied the IRNA effect *in vivo* and obtained the similar result to our study^[29,30].

In order to determine the IRNA inhibitor effect *in vivo* further, we used the HCV replicon containing the full length of HCV 5' UTR to investigate the IRNA activity; the results demonstrated that IRNA could inhibit HCV 5' UTR mediated gene expression *in vivo*, but IRNA could not completely block HCV 5' UTR mediated gene expression.

To rule out the nonspecific effect of nonspecific short RNA regimen on HCV IRES-mediated gene expression, plasmids pCDNA3 and pCMVNCRLuc were cotransfected into human hepatoma cells and the results showed that nonspecific RNA regimen didn't have the inhibitor effect on HCV IRES-mediated translation.

In summary, IRNA can significantly inhibit HCV IRES-mediated translation.

REFERENCES

- Friebe P**, Lohmann V, Krieger N, Bartenschlager R. Sequences in the 5' nontranslated region of hepatitis C virus required for RNA replication. *J Virol* 2001; **75**: 12047-12057
- Jubin R**. Hepatitis C IRES: translating translation into a therapeutic target. *Curr Opin Mol Ther* 2001; **3**: 278-287
- Reusken CB**, Dalebout TJ, Eerligh P, Bredenbeek PJ, Spaan WJ. Analysis of hepatitis C virus/classical swine fever virus chimeric 5' NTRs: sequences within the hepatitis C virus IRES are required for viral RNA replication. *J Gen Virol* 2003; **84**(Pt 7): 1761-1769
- Klinck R**, Westhof E, Walker S, Afshar M, Collier A, Aboul-Ela F. A potential RNA drug target in the hepatitis C virus internal ribosomal entry site. *RNA* 2000; **6**: 1423-1431
- Wang W**, Preville P, Morin N, Mounir S, Cai W, Siddiqui MA. Hepatitis C viral IRES inhibition by phenazine and phenazine-like molecules. *Bioorg Med Chem Lett* 2000; **10**: 1151-1154
- Shimazaki T**, Honda M, Kaneko S, Kobayashi K. Inhibition of internal ribosomal entry site-directed translation of HCV by recombinant IFN- α correlates with a reduced La protein. *Hepatology* 2002; **35**: 199-208
- Gallego J**, Varani G. The hepatitis C virus internal ribosome-entry site: a new target for antiviral research. *Biochem Soc Trans* 2002; **30**: 140-145
- Vyas J**, Elia A, Clemens MJ. Inhibition of the protein kinase PKR by the internal ribosome entry site of hepatitis C virus genomic RNA. *RNA* 2003; **9**: 858-870
- Kikuchi K**, Umehara T, Fukuda K, Hwang J, Kuno A, Hasegawa T, Nishikawa S. RNA aptamers targeted to domain II of hepatitis C virus IRES that bind to its apical loop region. *J Biochem* 2003; **133**: 263-270
- Liang XS**, Lian JQ, Zhou YX, Nie QH, Hao CQ. A small yeast RNA inhibits HCV IRES mediated translation and inhibits replication of poliovirus *in vivo*. *World J Gastroenterol* 2003; **9**: 1008-1013
- He Y**, Yan W, Coito C, Li Y, Gale M Jr, Katze MG. The regulation of hepatitis C virus (HCV) internal ribosome-entry site-mediated translation by HCV replicons and nonstructural proteins. *J Gen Virol* 2003; **84**(Pt 3): 535-543
- Otto GA**, Lukavsky PJ, Lancaster AM, Sarnow P, Puglisi JD. Ribosomal proteins mediate the hepatitis C virus IRES-HeLa 40S interaction. *RNA* 2002; **8**: 913-923
- Das S**, Ott M, Yamane A, Venkatesan A, Gupta S, Dasgupta A. Inhibition of internal entry site (IRES)-mediated translation by a small yeast RNA: a novel strategy to block hepatitis C virus protein synthesis. *Front Biosci* 1998; **3**: D1241-1252
- Das S**, Coward P, Dasgupta A. A small yeast RNA selectively inhibits internal initiation of translation programmed by poliovirus RNA: specific interaction with cellular proteins that bind to the viral 5' untranslated region. *J Virol* 1994; **68**: 7200-7211
- Kikuchi K**, Umehara T, Fukuda K, Hwang J, Kuno A, Hasegawa T, Nishikawa S. Structure-inhibition analysis of RNA aptamers that bind to HCV IRES. *Nucleic Acids Res Suppl* 2003; **3**: 291-292
- Liang X**, Zhou Y, Lian J, Nie Q, Jia Z. Effect of inhibitor RNA on intracellular inhibition of viral gene expression in 5' noncoding region of hepatitis C virus. *Zhonghua Nei Ke Za Zhi* 2002; **41**: 660-662
- Das S**, Kenan DJ, Bocskai D, Keene JD, Dasgupta A. Sequences within a small yeast RNA required for inhibition of internal initiation of translation: interaction with La and other cellular proteins influences its inhibitory activity. *J Virol* 1996; **70**: 1624-1632
- Isoyama T**, Kamoshita N, Yasui K, Iwai A, Shiroki K, Toyoda H, Yamada A, Takasaki Y, Nomoto A. Lower concentration of La protein required for internal ribosome entry on hepatitis C virus RNA than on poliovirus RNA. *J Gen Virol* 1999; **80**(Pt 9): 2319-2327
- Gamarnik AV**, Andino R. Interactions of viral protein 3CD and poly(rC) binding protein with the 5' untranslated region of the poliovirus genome. *J Virol* 2000; **74**: 2219-2226
- Ray PS**, Das S. La autoantigen is required for the internal ribosome entry site-mediated translation of Coxsackievirus B3 RNA. *Nucleic Acids Res* 2002; **30**: 4500-4508
- Ali N**, Pruijn GJ, Kenan DJ, Keene JD, Siddiqui A. Human La antigen is required for the hepatitis C virus internal ribosome entry site-mediated translation. *J Biol Chem* 2000; **275**: 27531-27540
- Liang XS**, Zhou YX, Lian JQ, Hao CQ, Wang LX. Structure modeling and construction recombinant plasmid of HCV IRES specific inhibitor RNA (IRNA). *J Med Post* 2002; **15**: 189-192
- Jin J**, Yang JY, Liu J, Kong YY, Wang Y, Li GD. DNA immunization with fusion genes encoding different regions of hepatitis C virus E2 fused to the gene for hepatitis B surface antigen elicits immune responses to both HCV and HBV. *World J Gastroenterol* 2002; **8**: 505-510
- Woitats RP**, Petersen U, Moshage D, Brackmann HH, Matz B, Sauerbruch T, Spengler U. HCV-specific cytokine induction in monocytes of patients with different outcomes of hepatitis C. *World J Gastroenterol* 2002; **8**: 562-566
- Yu YC**, Mao Q, Gu CH, Li QF, Wang YM. Activity of HDV ribozymes to trans-cleave HCV RNA. *World J Gastroenterol* 2002; **8**: 694-698
- Tang BZ**, Zhuang L, You J, Zhang HB, Zhang L. Seven-years follow-up on trial of Interferon alpha in patients with HCV RNA positive chronic hepatitis C. *World J Gastroenterol* 2000; **6**: 68
- Li LF**, Zhou Y, Xia S, Zhao LL, Wang ZX, Wang CQ. The epidemiologic feature of HCV prevalence in Fujian. *World J Gastroenterol* 2000; **6**: 80
- Kato J**, Kato N, Moriyama M, Goto T, Taniguchi H, Shiratori Y, Omata M. Interferons specifically suppress the translation from the internal ribosome entry site of hepatitis C virus through a double-stranded RNA-activated protein kinase-independent pathway. *J Infect Dis* 2002; **186**: 155-163
- Das S**, Kenan DJ, Bocskai D, Keene JD, Dasgupta A. Sequences within a small yeast RNA required for inhibition of initiation of translation: interaction with La and other cellular proteins influences its inhibitory activity. *J Virol* 1996; **70**: 1624-1632
- Venkatesan A**, Das S, Dasgupta A. Structure and function of a small RNA that selectively inhibits internal ribosome entry site-mediated translation. *Nucleic Acids Res* 1999; **27**: 563-572

Low eradication rate of *Helicobacter pylori* with triple 7-14 days and quadruple therapy in Turkey

Yuksel Gumurdulu, Ender Serin, Birol Özer, Fazilet Kayaselcuk, Kursat Ozsahin, Arif Mansur Cosar, Murat Gursoy, Gurden Gur, Ugur Yilmaz, Sedat Boyacioglu

Yuksel Gumurdulu, Ender Serin, Birol Özer, Arif Mansur Cosar, Faculty of Medicine, Baskent University, Department of Gastroenterology, Adana Teaching and Medical Research Center, Adana, Turkey

Fazilet Kayaselcuk, Department of Pathology, Adana Teaching and Medical Research Center, Adana, Turkey

Kursat Ozsahin, Department of Family Physician, Adana Teaching and Medical Research Center, Adana, Turkey

Murat Gursoy, Gurden Gur, Ugur Yilmaz, Sedat Boyacioglu, Faculty of Medicine, Baskent University, Department of Gastroenterology, Ankara Hospital, Ankara, Turkey

Correspondence to: Yuksel Gumurdulu, MD, Ba^o kent Üniversitesi Tıp Fakültesi, Adana Uygulama ve Ara^o tırma Merkezi, Dadalođlu Mahallesi, 39 Sokak, No: 6, 01250 Adana, Turkey. yukselgumurdulu@hotmail.com

Telephone: +90-322-3272727 **Fax:** +90-322-3271273

Received: 2003-10-08 **Accepted:** 2003-11-12

Abstract

AIM: The eradication rate of *Helicobacter pylori* (*H pylori*) shows variation among countries and regimens of treatment. We aimed to study the eradication rates of different regimens in our region and some factors affecting the rate of eradication.

METHODS: One hundred and sixty-four *H pylori* positive patients (68 males, 96 females; mean age: 48±12 years) with duodenal or gastric ulcer without a smoking history were included in the study. The patients were divided into three groups according to the treatment regimens. Omeprazole 20 mg, clarithromycin 500 mg, amoxicillin 1 g were given twice daily for 1 week (Group I) and 2 weeks (Group II). Patients in Group III received bismuth subsitrate 300 mg, tetracycline 500 mg and metronidazole 500 mg four times daily in addition to Omeprazole 20 mg twice daily. Two biopsies each before and after treatment were obtained from antrum and corpus, and histopathologically evaluated. Eradication was assumed to be successful if no *H pylorus* was detected from four biopsy specimens taken after treatment. The effects of factors like age, sex, *H pylori* density on antrum and corpus before treatment, the total *H pylori* density, and the inflammation scores on the rate of *H pylori* eradication were evaluated.

RESULTS: The overall eradication rate was 42%. The rates in groups II and III were statistically higher than that in group I ($P<0.05$). The rates of eradication were 24.5%, 40.7% and 61.5% in groups I, II and III, respectively. The eradication rate was negatively related to either corpus *H pylori* density or total *H pylori* density ($P<0.05$). The median age was older in the group in which the eradication failed in comparison to that with successful eradication (55 yr vs 39 yr, $P<0.001$). No correlation between sex and *H pylori* eradication was found.

CONCLUSION: Our rates of eradication were significantly lower when compared to those reported in literature. We

believe that advanced age and high *H pylori* density are negative predictive factors for the rate of *H pylori* eradication.

Gumurdulu Y, Serin E, Özer B, Kayaselcuk F, Ozsahin K, Cosar AM, Gursoy M, Gur G, Yilmaz U, Boyacioglu S. Low eradication rate of *Helicobacter pylori* with triple 7-14 days and quadruple therapy in Turkey. *World J Gastroenterol* 2004; 10(5): 668-671 <http://www.wjgnet.com/1007-9327/10/668.asp>

INTRODUCTION

Eradication treatment for *H pylori* infection has been generally accepted since the relation between *H pylori* and peptic ulcer disease was established^[1,2]. Furthermore, this treatment approach has gained importance since the eradication of *H pylori* was found to reduce the recurrence of duodenal and gastric ulcer^[3,4]. The eradication rate of *H pylori* has reached high levels with combined use of antibiotics and proton pump inhibitors (PPIs), being 60-90% in Turkey^[5]. Different treatment protocols have been used for *H pylori* eradication. The rate of *H pylori* eradication was higher than 85% with the combination of drugs consisting of two antibiotics and a PPI^[6]. We aimed to study the rates of *H pylori* eradication in Cukurova region with regard to different treatment regimens and the effects of patient age, sex, and *H pylori* density on *H pylori* eradication rates.

MATERIALS AND METHODS

One hundred and 64 patients (68 males, 96 females; mean age 48±12 yr, range 17-78 yr) with gastric or duodenal ulcer and *H pylori* detected at endoscopy were included in the study. Two biopsies from antrum and two from corpus were taken. *H pylori* density and gastric inflammation in both antrum and corpus were assessed based on Sydney classification (normal=0, mild=1, moderate=2, marked=3)^[7]. The patients were randomly divided into three groups and each group was treated with one of the protocols as follows. Group I received Omeprazole (O) 20 mg, Clarithromycin (C) 500 mg, amoxicillin (A) 1 000 mg, twice daily for 7 d. Group II received the same drugs as in group I for 14 d. Group III received Omeprazole 20 mg twice daily, Bismute subsitrate (BS) 300 mg 4 times daily, tetracycline (T) 500 mg 4 times daily, metronidazole (M) 500 mg 4 times daily for 10 d. There were 53, 59 and 52 patients in the 3 groups, respectively. Antibiotics, PPIs, and H₂ receptor blockers were used for at least one month. Smoking, pregnancy and lactation, past history of gastric surgery, renal or liver failure, diabetes mellitus and irregular use of drugs in the eradication regimens were accepted as exclusion criteria. Endoscopy was repeated and two biopsies each from corpus and antrum were obtained after 45-60 d of treatment. Eradication was accepted to be successful if *H pylori* were not found in any of the 4 samples. Total bacterial density was calculated semi quantitatively by addition of antrum and corpus *H pylori* density^[8]. None of the patients had atrophy in histologic evaluation. The relations of *H pylori* densities in

different locations before treatment, age, and sex with the rate of *H pylori* eradication were analyzed.

Statistical analysis

Data were expressed as medians with interquartiles. Mann-Whitney-*U* test or χ^2 test was used to assess significant differences between values in various groups of patients. $P < 0.05$ was considered statistically significant. Data were analyzed using the SPSS for Windows (version 9.05; SPSS, Inc., Chicago, Illinois, USA).

RESULTS

Out of 164 patients who completed the study, 69 (42%) had eradication of *H pylori* infection, and 151 (91.4%) showed ulcer healing. Eradication could not be achieved in 10 of 13 patients without ulcer healing. The eradication rate in group I, II, and III was 24.5% (13/53), 40.6% (24/59), and 61.5% (32/52), respectively. The rate of eradication in group III was higher than group I and II ($P < 0.03$). There was a difference between groups I and II, which did not reach statistical significance ($P = 0.07$). The ulcer cure was 45/53, 55/59, and 51/52, respectively in the 3 groups. *H pylori* density in antrum before treatment or severity of inflammation was not statistically related to its eradication. Corpus and total *H pylori* densities were higher in patients who failed the eradication treatment when compared to those who showed successful eradication ($P < 0.01$ and $P < 0.05$, respectively for corpus and total densities) (Table 1). The median patient age was higher in the group in which eradication failed. (55 vs 39 yrs, $P < 0.001$). The distribution of age, sex and *H pylori* density of corpus in the patient groups were summarized in Table 2.

Table 1 Rates of *H pylori* eradication and ulcer healing in various treatment regimens

Group	n	Age	F/M	Eradication (%)	Ülcer healing ^d (%)
I	53	49±12	30/23	13 (24.5) ^{a,b}	45 (84.9)
II	59	48±11	35/24	24 (40.7) ^c	55 (93.2)
III	52	45±12	31/21	32 (61.5)	51 (98)
Total	164	48±12	96/68	69 (42)	151(92.1)

^a $P = 0.07$ vs Group II; ^b $P < 0.01$ vs Group III; ^c $P < 0.03$ vs Group III; ^d $P = N.S.$ among the three groups.

DISCUSSION

The discovery of *H pylori* by Marshall and Warren has been considered as a revolution^[9]. As the role of this microorganism in gastric pathologies is fully understood, the treatment principles of some of the gastro-duodenal lesions have been changed^[10].

Nowadays, *H pylori*-positive peptic ulcer disease is accepted as an infectious process, and combination of drugs,

including the same antibiotics were used in all of the treatment protocols^[11-13]. No standard therapy for *H pylori* eradication has been underlined. An ideal *H pylori* treatment must be safe, cheap, easy and tolerable with more than an 80% eradication rate and must have a low rate of antibiotic resistance^[14,15].

PPIs are commonly used in the combined regimens as a result of significant *in vivo* and *in vitro* effects on *H pylori*. Many treatment regimens including PPIs were still hard to eradicate *H pylori*^[16-19].

In Europe and in the USA despite resistance to metronidazole, clarithromycin, and tetracycline was 30-40%, 2-10% and <1%, respectively, the eradication rate of the combined treatment with clarithromycin, PPI and amoxicillin or metronidazole for 7-14 d was 87-100% in metronidazole sensitive group and 57-88% in metronidazole resistant group. In 10-12 d of PPI-A-C regimens, 88-96% eradication rate was maintained in clarithromycin sensitive group and 50% in the resistant group. These findings showed the importance of antibiotic resistance in unsuccessful eradication trials^[20]. Several studies, in which the antibiotic resistance was analyzed as one of the independent parameters that can be predictors of eradication failure, supported the same suggestion^[21-23]. In Turkey, Boyanova *et al* found the resistance to M 37.9%, to C 9.5%, and to A 0.9%, respectively. The double drug resistance (M+C) was 6.1%^[24]. In a former study we found C and M resistance rates were 5.2% (1/19) and 36.8% (7/19) in a group of 19 patients (data unpublished). These observations suggested that antibiotic resistance could not explain completely the low eradication rate as we observed in the present study. The resistance in our patients was similar to that detected in the Western world whereas the rate of eradication was markedly lower when compared to Western population.

The effect of combination therapies on *H pylori* eradication rates varied according to the differences in treatment duration. Some studies which showed that 14 d trials were more successful than 7 d trials, whereas other studies showed no difference. In our study the rate of *H pylori* eradication was higher in prolonged treatment but did not reach any statistical significance^[25].

The reported higher rates of *H pylori* eradication with either OCA or OCM combination in early studies in our country as compared to recent ones suggested the development of resistance was due to irregular and unsubscribed use of antibiotics in our population^[17]. The possible differences in the production process of drugs by various manufacturers may play a role in the bioavailability of active compounds. We could not find any study regarding to this issue. However, Kim *et al.* from South Korea have found similar benefits in *H pylori* eradication rate of three drug combinations with two different Omeprazole preparations^[26]. If similar studies can be made for antibiotics, questions on this matter can be answered.

Patient incompliance to treatment is another factor contributing to eradication failure. Graham *et al* have found that the eradication rate was about 96% in patients who used

Table 2 The distribution of age, sex and *H pylori* density of corpus in the patient groups

Group	Eradicated				Non-eradicated			
	n	Age ^a	F/M	Density	n	Age ^a	F/M	Density
I	13	35.3 ± 11.7 ^a	9/4	1.31 ± 0.95 ^b	40	54.0 ± 9.1 ^a	21/19	2.17 ± 0.87 ^b
II	24	40.04 ± 9.3 ^a	13/11	1.92 ± 0.8 ^b	35	54.94 ± 8.8 ^a	21/14	2.37 ± 0.77 ^b
III	32	40.03 ± 11.6 ^a	20/12	1.91 ± 0.69 ^b	20	55.15 ± 9.0 ^a	12/8	2.35 ± 0.75 ^b
Total	69	39.14 ± 10.9 ^a	42/27	1.8 ± 0.83 ^b	95	54.61 ± 8.9 ^a	54/41	2.28 ± 0.79 ^b

^a $P < 0.001$, vs noneradicated in each group for age, ^b $P < 0.05$, vs noneradicated in each group for *H pylori* corpus density.

60% or more of their drugs and 69% in those who used less than 60% of drugs^[27]. We tried to eliminate this factor via good questioning and follow-up throughout the study. Patient incompliance did not seem to be a determinant factor for *H pylori* eradication failure in our study.

The response to combination of four drugs was around 87-100% in several studies. Nelson *et al.* found that the ulcer cure and eradication rate of *H pylori* with BSOMT in a 2 d and 7 d regimen were 95.7% and 76.1%, and 98% and 100%, respectively^[11]. In studies using BSTMO combination, the eradication rate of *H pylori* was 96% in the metronidazole sensitive group and 82% in the metronidazole resistant group^[28]. The rate of *H pylori* eradication with the same protocol in our study was much lower compared to previous trials, but significantly higher than two other protocols we used. This shows the necessity for studying some geographic factors.

Smoking; one of the parameters of antibiotic resistance in literature, was restrained during the inclusion phase of this study. We studied two other factors associated with *H pylori* eradication failure, namely the grade of *H pylori* density and gastritis. Our findings suggested that the eradication was more difficult in patients who had high total or corpus *H pylori* density. Georgopoulos *et al* found no relation between eradication and *H pylori* density or the severity of gastritis^[21]. Yang *et al* reported a lower total bacterial density in the eradicated group^[8]. In our study corpus and total (sum of *H pylori* density in antrum and corpus) *H pylori* densities were higher in patients with eradication failure compared to the successfully eradicated group. Consequently, the factors affecting *H pylori* density can be expected to affect the eradication rate. Some studies on this issue showed that some factors related with host or bacteria could affect *H pylori* density in gastric mucosa^[21,29-31].

The patients' lifetime exposure to several kinds of antibiotics could cause resistance and this might partly explain the difference noted in the age groups with respect to *H pylori* eradication rate^[32].

Another factor that can contribute to the resistance to antibiotic treatment is intracellular settling of bacteria. The examples of this fact were some chronic infections such as tuberculosis and brucellosis for which a long term use of antibiotics was required^[33,34]. The difficulty in eradication treatment of *H pylori* may in part be due to intracellular location of these bacteria since *H pylori* has been shown to penetrate into cells in cell cultures^[35]. This suggestion was firmly supported when 14 d regimens were shown to be more effective than 7 d regimens as reported in this and previous studies.

The rate of eradication we encountered was significantly lower than those in literature, which suggests further studies concerning the mechanisms underlying the eradication failure in our community should be designed.

REFERENCES

- Ikeda S**, Tamamuro T, Hamashima C, Asaka M. Evaluation of the cost-effectiveness of *Helicobacter pylori* eradication triple therapy vs conventional therapy for ulcers in Japan. *Aliment Pharmacol Ther* 2001; **15**: 1777-1785
- Malfertheiner P**, Megraud F, O' Morain C, Hungin AP, Jones R, Axon A, Graham DY, Tytgat G. Current concepts in the management of *Helicobacter pylori* infection—the Maastricht 2-2000 Consensus Report. *Aliment Pharmacol Ther* 2002; **16**: 167-180
- Marzio L**, Cellini L, Angelucci D. Triple therapy for 7 days vs. triple therapy for 7 days plus omeprazole for 21 days in treatment of active duodenal ulcer with *Helicobacter pylori* infection. A double blind placebo controlled trial. *Dig Liver Dis* 2003; **35**: 20-23
- Leodolter A**, Kulig M, Brasch H, Meyer-Sabellek W, Willich SN, Malfertheiner P. A meta-analysis comparing eradication, healing and relapse rates in patients with *Helicobacter pylori*-associated gastric or duodenal ulcer. *Aliment Pharmacol Ther* 2001; **15**: 1949-1958
- Tytgat GN**. Review article: treatments that impact favourably upon the eradication of *Helicobacter pylori* and ulcer recurrence. *Aliment Pharmacol Ther* 1994; **8**: 359-368
- Bhasin DK**, Sharma BC, Ray P, Pathak CM, Singh K. Comparison of Seven and Fourteen Days of Lansaprazole, Claritromycin and amoxicillin Therapy for Eradication of *Helicobacter pylori*: A Report from India. *Helicobacter* 2000; **5**: 84-87
- Dixon MF**, Genta RM, Yardley JH, Correa P. Classification and Grading of Gastritis. The Updated Sydney system. *Am J Surg Pathol* 1996; **20**: 1161-1181
- Yang HB**, Sheu BS, Su IJ, Chien CH, Lin XZ. Clinical Application of Gastric Histology to Monitor Treatment of Dual Therapy in *H pylori* Eradication. *Dig Dis Sci* 1997; **42**: 1835-1840
- Unidentified curved bacilli on gastric epithelium in active chronic gastritis. *Lancet* 1983; **1**: 1273-1275
- World Health Organization**. International agency for research on cancer. Infection with *Helicobacter pylori*. Schistosomes, Liver flukes and *Helicobacter pylori*. Lyon: IARC 1994: 172-202
- Hopkins RJ**, Girardi LS, Turney EA. Relationship between *Helicobacter pylori* eradication and reduced duodenal and gastric ulcer recurrence: a review. *Gastroenterology* 1996; **110**: 1244-1252
- Peitz U**, Hackelsberger A, Malfertheiner P. A practical approach to patients with refractory *Helicobacter pylori* infection, or who are re-infected after standart therapy. *Drugs* 1999; **57**: 905-920
- Marshall BJ**, Warren JR. Unidentified curved bacilli in the stomach of patients with gastritis and peptic ulceration. *Lancet* 1984; **16**: 1311-1315
- Working Party of the european Helicobacter pylori study group**. Guidelines for clinical trials in *Helicobacter pylori* infection. *Gut* 1997; **41**(Suppl 2): S1-9
- Soll AH**. Consensus conference. Medical treatment of peptic ulcer disease. Practice guidelines. Practice Parameters Committee of the American College of Gastroenterology. *JAMA* 1996; **275**: 622-628
- Taskin V**, Özyilkan E, Aydın A, Çetin F, Eskiođlu E, Köseođlu T. Can resistant *Helicobacter pylori* infection be estimated histologically: Effects of gastric histology on eradication rates of *Helicobacter pylori* infection. *The Turk J Gastroenterol* 2001; **12**: 126-129
- Aydın A**, Ersöz G, Tunçyürek M, Cavusoglu H. One-week triple therapies for *Helicobacter pylori* eradication. *The Turk J Gastroenterol* 1998; **9**: 40-45
- Iwahi T**, Satoh H, Nakao M, Iwasaki T, Yamazaki T, Kubo K, Tamura T, Imada A. Lansaprazole, a novel benzimidazole proton pump inhibitor, and its related compounds have selective activity against *Helicobacter pylori*. *Antim Agents Chem* 1991; **35**: 490-496
- Hunt RH**. pH and *H pylori*-gastric acid secretion and *Helicobacter pylori*. Implications for ulcer healing and eradication of the organism. *Am J Gastroenterol* 1993; **88**: 481-483
- Glupczynski Y**. Antimicrobial resistance in *Helicobacter pylori*: a global overview. *Acta Gastroenterol Belg* 1998; **61**: 357-366
- Georgopoulos SD**, Ladas SD, Karatapanis S, Mentis A, Spiliadi C, Artikis V, Raptis SA. Factors that may Affect Treatment Outcome of Triple *Helicobacter pylori* Eradication Therapy with Omeprazole, Amoxicillin, and Clarithromycin. *Dig Dis Sci* 2000; **45**: 63-67
- Huang JQ**, Hunt RH. Treatment after failure: the problem of 'non-responders'. *Gut* 1999; **45**(Suppl1): 140-144
- Kim JJ**, Reddy R, Lee M, Kim JG, El-Zaatari FA, Osato MS, Graham DY, Kwon DH. Analysis of metronidazole, claritromycin and tetracycline resistance of *Helicobacter pylori* isolated from Korea. *J Antim Chem* 2001; **47**: 459-461
- Boyanova L**, Mentis A, Gubina M, Rozynek E, Gosciniak G, Kalenic S, Goral V, Kupcinskas L, Kantarceken B, Aydın A, Archimandritis A, Dzierzanowska D, Vcev A, Ivanova K, Marina M, Mitov I, Petrov P, Ozden A, Popova M. The status of antimicrobial resistance of *Helicobacter pylori* in eastern Europe. *Clin Microbiol Infect* 2002; **8**: 388-396
- Forne M**, Viver JM, Esteve M, Fernandez-Banares F, Lite J, Espinos JC, Quintana S, Salas A, Garau J. Randomize clinical trial comparing two one week triple therapy regimens for the eradication of *Helicobacter pylori* infection and duodenal ulcer healing. *Am J Gastroenterol* 1998; **93**: 35-38

- 26 **Kim HS**, Lee DK, Kim KH, Jeong YS, Kim JW, Seo JI, Baik SK, Kwon SO, Cho MY. Comparison of the efficacy and safety of different formulations of omeprazole-based triple therapies in the treatment of *Helicobacter pylori*-positive peptic ulcer. *J Gastroenterol* 2001; **36**: 96-102
- 27 **Graham DY**, Lew GM, Malaty HM, Evans DG, Evans DJ Jr, Klein PD, Alpert LC, Genta RM. Factors influencing eradication of *Helicobacter pylori* with triple therapy. *Gastroenterology* 1992; **102**: 493-496
- 28 **Kung NN**, Sung JJ, Yuen NW, Ng PW, Wong KC, Chung EC, Lim BH, Choi CH, Li TH, Ma HC, Kwok SP. Anti-*Helicobacter pylori* Treatment in Bleeding Ulcers: Randomized Controlled Trial Comparing 2-day versus 7-Day bismuth Quadruple Therapy. *Am J Gastroenterol* 1997; **92**: 438-441
- 29 **Megraud F**. Resistance of *Helicobacter pylori* to antibiotics: the main limitation of current proton-pump inhibitor triple therapy. *Eur J Gastroenterol Hepatol* 1999; **11**: (Suppl 2): S35-37
- 30 **Kamada T**, Haruma K, Komoto K, Mihara M, Chen X, Yoshihara M, Sumii K, Kajiyama G, Tahara K, Kawamura YM. Effect of smoking and histological gastritis severity on the rate of *H pylori* eradication with omeprazole, amoxicillin, and clarithromycin. *Helicobacter* 1999; **4**: 204-210
- 31 **Russo A**, Maconi G, Spinelli P, Felice GD, Eboli M, Andreola S, Ravagnani F, Settesoldi D, Ferrari D, Lombardo C, Bertario L. Effect of lifestyle, smoking, and diet on development of intestinal metaplasia in *H pylori*-positive subject. *Am J Gastroenterol* 2001; **96**: 1402-1408
- 32 **Huang JQ**, Hunt RH. Review: eradication of *Helicobacter pylori*. Problems and recommendations. *J Gastroenterol Hepatol* 1997; **12**: 590-598
- 33 **Raviglione MC**, O'Brien RJ. Tuberculosis. in Fauci A.S.ed. *Harrison's principles of internal medicine*. **14th** ed. New York: McGraw-Hill Co 1998: 1004-1014
- 34 **Madkour M**. Brucellosis in Fauci A.S.ed. *Harrison's principles of internal medicine*. **14th** ed. New York: McGraw-Hill co 1998: 1004-1014
- 35 **Bjorkholm B**, Zhukhovitsky V, Lofman C, Hulten K, Enroth H, Block M, Rigo R, Falk P, Engstrand L. *Helicobacter pylori* entry into human gastric epithelial cells: A potential determinant of virulence, persistence, and treatment failures. *Helicobacter* 2000; **5**: 148-154

Edited by Wang XL Proofread by Zhu LH

Relationship of gastric *Helicobacter pylori* infection to Barrett's esophagus and gastro-esophageal reflux disease in Chinese

Jun Zhang, Xiao-Li Chen, Kang-Min Wang, Xiao-Dan Guo, Ai-Li Zuo, Jun Gong

Jun Zhang, Jun Gong, Ai-Li Zuo, Xiao-Dan Guo, Department of Gastroenterology, Second Hospital, Xi'an Jiaotong University, Xi'an 710004, Shaanxi Province, China

Xiao-Li Chen, Kang-Min Wang, Department of Pathology, Second Hospital of Xi'an Jiaotong University, Xi'an 710004, Shaanxi Province, China

Correspondence to: Dr. Jun Zhang, Department of Gastroenterology, Second Hospital, Xi'an Jiaotong University, Xi'an 710004, Shaanxi Province, China. jun3z@163.com

Telephone: +86-29-7678009

Received: 2003-09-06 **Accepted:** 2003-10-27

Abstract

AIM: To evaluate the relationship of *Helicobacter pylori* infection to reflux esophagitis (RE), Barrett's esophagus (BE) and gastric intestinal metaplasia (IM).

METHODS: RE, BE and gastric IM were determined by upper endoscopy. Patients were divided into 2 groups; those with squamocolumnar junction (SCJ) beyond gastroesophageal junction (GEJ) ≥ 3 cm (group A), and those with SCJ beyond GEJ < 3 cm (group B). Biopsy specimens were obtained endoscopically from just below the SCJ, gastric antrum along the greater and lesser curvature. Pathological changes and *H pylori* infection were determined by HE staining, Alcian blue staining and Giemsa staining.

RESULTS: The prevalence of *H pylori* infection was 46.93%. There was no difference in the prevalence between males and females. The prevalence of *H pylori* infection decreased stepwise significantly from RE grade I to III. There was no difference in the prevalence between the two groups, and between long-segment and short-segment BE. In distal stomach, prevalence of *H pylori* infection was significantly higher in patients with IM than those without IM.

CONCLUSION: There is a protective role of *H pylori* infection to GERD. There may be no relationship between *H pylori* infection of stomach and BE. *H pylori* infection is associated with the development of IM in the distal stomach.

Zhang J, Chen XL, Wang KM, Guo XD, Zuo AL, Gong J. Relationship of gastric *Helicobacter pylori* infection to Barrett's esophagus and gastro-esophageal reflux disease in Chinese. *World J Gastroenterol* 2004; 10(5): 672-675

<http://www.wjgnet.com/1007-9327/10/672.asp>

INTRODUCTION

The incidence of adenocarcinoma in the esophagus and gastroesophageal junction (GEJ) is increasing, whereas the incidence of distal gastric cancer is falling for the two decades in North America, Europe, Japan and China. In China, the incidence of adenocarcinoma at the GEJ is increasing even more significantly^[1-3].

The adenocarcinomas at the esophagus and GEJ differ

from those in the stomach^[4]. They share epidemiological characteristics with each other, and often originate from segments of Barrett's esophagus (BE). It has therefore been proposed that both of them can be called "esophagocardia adenocarcinoma"^[5]. BE is a well-defined premalignant condition for esophageal adenocarcinoma and most of adenocarcinomas at GEJ^[6,7]. Neoplastic progression of BE has been shown to involve multiple steps with intestinal metaplasia and dysplasia serving as histopathologic markers^[5]. It is considered that the absence of specialized intestinal metaplasia in many patients with adenocarcinoma at the GEJ may be due to the complete replacement of the metaplastic epithelium by the tumor, and in these tumors, IM usually is confined to ultrashort segments that may easily be overgrown by the tumor^[8].

Gastro-esophageal reflux disease (GERD) can give rise to BE, and reflux symptoms are important indicators that a patient is at risk of having Barrett's metaplasia. Recently, interest has focused on the relationship between *H pylori* infection and GERD as well as BE, but controversial findings have been obtained. Several retrospective studies have examined the association of Barrett's adenocarcinoma with gastric *H pylori* infection, yielding discordant results. It has been known that the prevalence of *H pylori* infection in China is high. It is necessary to clarify whether *H pylori* infection is the causally associated with BE or whether it has a protective effect on BE. In addition, further investigations are also required to clarify the relationship between *H pylori* infection and GERD. Therefore, the aim of this prospective study was to evaluate the relationship between gastric *H pylori* infection and reflux esophagitis (RE), BE, and gastric IM in China.

MATERIALS AND METHODS

Patients

Consecutive patients undergoing esophagogastroendoscopy at Second Hospital, Xi'an Jiaotong University, Xi'an, China from August 1, 2000 to the end of August 1, 2001 were included in the study. Exclusion criteria included previous gastric or esophagus resection, contraindication to performing biopsies, prior history of *H pylori* eradication therapy, and/or use of bismuth-containing compounds or antibiotics within the previous 4 weeks. The study was approved by the Ethics Committee of the hospital, and informed consents were obtained from all patients before entry.

Endoscopy and biopsy

Endoscopy was performed in a standardized manner by experienced endoscopists. The appearance of the squamocolumnar junction (SCJ) was carefully studied in the prograde view after insufflation of air and after retroversion in the stomach. According to the length from the GEJ to SCJ, patients were divided into two groups; those with velvety red gastric-like mucosa lining the distal esophagus for 3 cm or over (group A) and those with velvety red gastric-like mucosa lining the distal esophagus for less than 3 cm (group B). Endoscopic esophagitis was graded as I, mucosal erythema; II, non-circumferential mucosal breaks or erosions; III,

circumferential erosion or ulcer.

Four-quadrant biopsies were taken from the area immediately distal to the SCJ. Additional targeted biopsies were also taken from erosions, nodules or ulcers. For assessment of *H pylori* status biopsies were taken from antral greater curvature (two), and lesser curvature (two).

Biopsy specimens were fixed in 40 g/L buffered formaldehyde, embedded in paraffin, serially sectioned, and then stained with hematoxylin and eosin. BE was defined as the presence of distended, barrel-shaped goblet cells, indicative of intestinal metaplasia^[6,31,32], which was further confirmed by staining with Alcian blue pH 2.5.

In addition, BE was divided into long-segment Barrett's esophagus (LSBE, the segments of IM more than or equal to 3 cm in length) and short-segment Barrett's esophagus (SSBE, the segment of IM less than 3 cm in length).

The presence of gastric *H pylori* infection was defined when one or more of Giemsa-stained gastric biopsy specimens demonstrated typical *H pylori*-like organisms.

The gastric IM was defined by the presence of barrel-shaped goblet cells.

Statistical analysis

Statistical analyses were performed using the χ^2 test.

RESULTS

Altogether, 391 patients were recruited. Of these patients, 253 had esophageal disorders; 103 with RE (39 grade I, 35 grade II and 29 grade III), 120 with BE (26 LSBE and 94 SSBE), 12 with dysplasia (seven low-grade and five high-grade), 17 with adenocarcinoma at the GEJ and one with adenocarcinoma at lower esophagus (Table 1). Males were more likely to have esophageal disorders than females. The average age ranged from 52.41 to 62.64 years old, with and increased progressively from RE→BE→LGD→HGD→adenocarcinoma.

Table 1 Clinic features of study population

	No.	Mean age (yr)	Male: Female
No. Of patients	391	52.41	211:180
RE I	39	52.12	26:13
II	35	53.67	26:9
III	29	55.56	24:5
BE SSBE	94	54.71	62:32
LSBE	26	58.66	20:6
Low-grade dysplasia	7	59.57	5:2
High-grade dysplasia	5	62.00	3:2
Adenocarcinoma at GEJ	17	62.64	14:3

Status of *H pylori* infection was available for 375 patients. The prevalence of *H pylori* infection was 46.93% (176/375). There was no significant difference in the prevalence between males and females (males, 48.71% and females, 45.00%) ($P>0.05$) (Table 2). The prevalence of *H pylori* infection in Group A was 41.84% (41/98), which was slightly lower than that 48.73% (135/277) in group B ($P>0.05$). The prevalence of *H pylori* infection decreased stepwise significantly from RE Grade I (51.72%), grade II (28.57%) to grade III (20.68%) ($P<0.05$) (Table 2).

The prevalence of IM in group A (LSBE) (26.53%) was slightly lower than that in group B (SSBE) (33.94%) ($P>0.05$). In groups A and B the prevalence of *H pylori* infection (46.15% and 51.06%, respectively) in patients with IM was slightly higher than that (40.27% and 47.54%, respectively) in those without IM (both $P>0.05$) (Table 3). The prevalence of *H pylori* infection of LSBE (46.15%) is slightly lower than that of SSBE

(51.06%) ($P>0.05$). However, in the distal stomach, the prevalence of *H pylori* infection in patients with IM (56.29%) was significantly higher than that in those without IM (37.89%) ($P<0.05$) (Table 3).

Table 2 Comparisons of *H pylori* status among patients with sex, length of SCJ, grade of RE

	No.	Hp* (%)	Hp (%)	P
No. Of patients	375	176 (46.93)	199 (53.06)	
Male: Female	195:180	95: 81	100:99	0.534
Group A	98	41 (41.84)	57 (58.16)	0.239
Group B	277	135 (48.73)	142 (51.26)	
RE I	29	15 (51.72)	14 (48.28)	0.032
II	35	10 (28.57)	25 (41.43)	
III	29	6 (20.68)	23 (79.31)	

Table 3 Comparisons of *H pylori* status between patients with IM in LSBE, SSBE and distal stomach

IM	Group A		Group B		Distal stomach	
	+ (%)	- (%)	+ (%)	- (%)	+ (%)	- (%)
HP+	12 (46.15)	29 (40.27)	48 (51.06)	87 (47.54)	76 (56.29)	97 (37.89)
HP-	14 (53.84)	43 (59.72)	46 (48.93)	96 (52.45)	59 (43.70)	159 (62.11)
Total	26	72	94	183	135	256

Comparison of *H pylori* status between LSBE (IM+ in group A) and SSBE (IM+ in group B), $P=0.658$, ($\chi^2=0.196$); Comparison of *H pylori* status between IM "+" and IM "-" in group A, $P=0.603$, ($\chi^2=0.271$); Comparison of *H pylori* status between IM "+" and IM "-" in group B, $P=0.579$, ($\chi^2=0.308$); Comparison of *H pylori* status between IM "+" and IM "-" in distal stomach, $P=0.000$, ($\chi^2=12.14$).

DISCUSSION

Since the isolation of *H pylori* from gastric mucosa by Warren and Marshall in 1983, there has been renewed interest in a possible bacterial cause of upper gastrointestinal diseases^[9]. *H pylori* is now widely accepted as a major cause of antral gastritis and peptic ulcer disease^[10,11]. Epidemiological evidence for an association with gastric carcinoma has also been reported^[12,13]. In addition, gastric mucosa-associated lymphoid tissue (MALT) lymphoma has been linked to *H pylori* infection^[14,15]. The relationship of *H pylori* to GERD and BE is less clear. Some groups have reported a lower prevalence of *H pylori* infection in individuals with GERD, and have postulated that infection may reduce the risk of reflux esophagitis^[16-18]. However, other epidemiological studies have found little or no association between *H pylori* infection and GERD^[19-21]. With regard to Barrett's esophagus the majority of studies have found no association with *H pylori* infection^[22,23]. However, there is also evidence to the contrary^[18]. Our prospective study tried to evaluate the relation between gastric *H pylori* infection and RE, BE, and gastric IM in Chinese.

H pylori infection can be diagnosed by a variety of noninvasive or invasive tests. Histological examination with special staining of gastric biopsy specimens is accepted as the gold standard for *H pylori* diagnosis^[24,25]. Gastric antrum is the most common place for *H pylori* colonization^[26,27]. Modified Giemsa staining, which has been shown to have a high specificity and sensitivity^[25,28], was used to detect *H pylori* status in this study.

In early studies, BE was defined as the presence of specialized IM in a columnar-lined mucosa encompassing more than 3 cm proximal to GEJ or a LSBE^[29]. Any columnar-lined mucosa less than 3 cm above the GEJ was thought to be a

normal variant. However studies over the past years have indicated that there is a spectrum of involvement that includes the distal 3 cm of esophagus or a SSBE^[30,31]. What is important is the presence of IM relating to adenocarcinoma. It has been shown that a patient with LSBE has a higher risk to develop dysplasia or cancer^[32]. It also has been shown that the development of LSBE is more closely related to gastroesophageal reflux^[33]. Therefore, in our study, patients were divided into two groups; those with a velvety red gastric-like mucosa lining the distal esophagus for 3 cm or over and those with a velvety red gastric-like mucosa lining the distal esophagus for less than 3 cm. Because esophageal hiatal hernia is often complicated by GERD and BE, many researchers think that to define an esophageal hiatal hernia, the presence of a velvety red gastric-like mucosa lining the distal esophagus for 2 cm should be considered as normal. In our study, therefore, we referred to this definition; the length from the GEJ to SCJ for esophageal hiatal hernia reduced 2 cm^[34,35].

Altogether, 391 patients were evaluated over the course of the study (Table 1). The presence of IM was confirmed in 26 cases of the 98 patients suspected of having LSBE, and in 94 cases of the 277 patients suspected of having SSBE. Seven BE cases with dysplasia, 103 RE and 17 adenocarcinoma at GEJ were diagnosed. The average age of patients increased gradually with the sequence of RE, BE, LGD, HGD and adenocarcinoma at GEJ from 52.41 to 62.64 years old. Males were more likely to have the diseases. Cameron *et al* reported that the age after 40 had a high incidence of BE, and development of adenocarcinoma from BE required about 20 years^[36].

Of the entire study population, 375 subjects received histological examination for *H pylori* infection, with a prevalence of *H pylori* infection of 46.93%. There was no significant difference between males and females. These results are similar to the report by Hui *et al* about *H pylori* infection in the same area of China^[37].

The first change in BE, is the replacement of the normal stratified epithelium with metaplastic columnar epithelium in the distal esophagus, making the SCJ rising upward above the GEJ. It is accepted that BE is an acquired condition, and is related to gastro-esophageal reflux. An excellent overview and hypothesis detailing the role of *H pylori* infection in the pathogenesis of duodenal ulcer, gastric cancer, and GERD has been given by Graham and Yamaoka^[38,39]. *H pylori* infection has been shown to decrease acid secretion in patients with body-predominant *H pylori* colonization^[40]. With less acid production, the offensive potency of the refluxate may be reduced. An additional mechanism could be neutralization of acid by ammonia produced by *H pylori*, with subsequent reduction in intragastric acid load and in the reflux of acid into the esophagus, as proposed by Bercik *et al*^[41]. Ammonia may also promote protective adaptation of the esophageal mucosa^[42]. So, if *H pylori* infection can decrease the offensive potency of the refluxate, we could infer indirectly whether *H pylori* infection has the protective effect in GERD and BE by comparing the RE grade and the prevalence of *H pylori* infection in different length from the GEJ to the SCJ (*i.e.* between group A and group B). In our study there was no significant difference in the prevalence of *H pylori* infection between group A (41.84%) and group B 48.73%. Furthermore, the prevalence of *H pylori* infection decreased stepwise significantly from RE Grade I (51.72%), grade II (28.57%) to grade III (20.68%) ($P=0.032$). These findings suggest that there is no relationship between gastric *H pylori* infection and GERD, although gastric *H pylori* infection had an apparent protective effect against the progression of GERD.

Barrett's metaplasia is precancerous lesion of esophageal adenocarcinoma and most of adenocarcinoma at the GEJ. Progression from metaplasia, LGD, HGD to invasive cancer

occurs in a stepwise process. It is unquestionably BE, especially LSBE, is linked with gastroesophageal reflux. Our study shows that *H pylori* infection has the protective effect in GERD. But how about BE? The present study demonstrated that there was no significant difference in IM prevalence between group A and group B. Marian *et al* reported that the prevalence of LSBE was higher than that of SSBE and the prevalence of IM is directly proportional to the length of column-lined esophagus^[33]. This finding, which is different from ours, may explain the reason why the incidence of esophageal adenocarcinoma is on the increase in North America and Europe. However, in our study, the prevalence of SSBE was higher than that of LSBE, which may explain the reason why the incidence of adenocarcinoma at the GEJ is more common than that at the esophagus in China. There was no significant difference in the prevalence of *H pylori* infection between patients with and without IM in both group A and group B. Similarly, there was no significant difference in the prevalence of *H pylori* infection between LSBE and SSBE. However, in distal stomach, the prevalence of *H pylori* infection in patients with IM (56.29%) is much higher than that in those without IM (37.89%) ($P<0.001$), which is in agreement with previous observations^[22,23,43]. It is suggested that *H pylori* infection is associated with IM in the distal stomach, but may have no protective effect in BE. The distal gastric IM is thought to be less dangerous to progress to gastric carcinoma, and thus it is not suggested to supervise routinely the patients with distal gastric IM^[44]. However, patients with BE has an overrated risk, about 30 to 125 times to progress to adenocarcinoma than patients without BE^[45, 46].

In conclusion, *H pylori* infection may have a protective role in GERD. There is no relationship between gastric *H pylori* infection and BE. *H pylori* infection is associated with IM in the distal stomach.

REFERENCES

- 1 **Devesa SS**, Blot WJ, Fraumeni JF Jr. Changing patterns in the incidence of esophageal and gastric carcinoma in the United States. *Cancer* 1998; **83**: 2049-2053
- 2 **Blot WJ**, Devesa SS, Kneller RW, Fraumeni JF Jr. Rising incidence of adenocarcinoma of the esophagus and gastric cardia. *JAMA* 1991; **265**: 1287-1289
- 3 **Zhou Q**, Wang LD. Biological characteristics of cardiac cancer. *Huaren Xiaohua Zazhi* 1998; **6**: 636-637
- 4 **Ruol A**, Parenti A, Zaninotto G, Merigliano S, Costantini M, Cagol M, Alfieri R, Bonavina L, Peracchia A, Ancona E. Intestinal metaplasia is the probable common precursor of adenocarcinoma in Barrett esophagus and adenocarcinoma of the gastric cardia. *Cancer* 2000; **88**: 2520-2528
- 5 **Rabinovitch PS**, Reid BJ, Haggitt RC, Norwood TH, Rubin CE. Progression to cancer in Barrett's esophagus is associated with genomic instability. *Lab Invest* 1989; **60**: 65-71
- 6 **Weston AP**, Krmpotich PT, Cherian R, Dixon A, Topalovski M. Prospective evaluation of intestinal metaplasia and dysplasia within the cardia of patients with Barrett's esophagus. *Dig Dis Sci* 1997; **42**: 597-602
- 7 **Cameron AJ**, Lomboy CT, Pera M, Carpenter HA. Adenocarcinoma of the esophagogastric junction and Barrett's esophagus. *Gastroenterology* 1995; **109**: 1541-1546
- 8 **Clark GW**, Smyrk TC, Burdiles P, Hoeft SF, Peters JH, Kiyabu M, Hinder RA, Bremner CG, DeMeester TR. Is Barrett's metaplasia the source of adenocarcinomas of the cardia? *Arch Surg* 1994; **129**: 609-614
- 9 **Warren JR**, Marshall BJ. Unidentified curved bacilli on gastric epithelium in active chronic gastritis. *Lancet* 1983; **1**: 1273-1275
- 10 **Marshall BJ**, Warren JR. Unidentified curved bacilli in the stomach of patients with gastritis and peptic ulceration. *Lancet* 1984; **16**: 1311-1315
- 11 **Rauws EA**, Langenberg W, Houthoff HJ, Zanen HC, Tytgat GN. Campylobacter pyloridis-associated chronic active antral gastritis. A prospective study of its prevalence and the effects of

- antibacterial and antiulcer treatment. *Gastroenterology* 1988; **94**: 33-40
- 12 **Parsonnet J**, Friedman GD, Vandersteen DP, Chang Y, Vogelstein JH, Orentreich N, Sibley RK. *Helicobacter pylori* infection and the risk of gastric carcinoma. *N Engl J Med* 1991; **325**: 1127-1131
 - 13 **Nomura A**, Stemmermann GN, Chyou PH, Kato I, Perez-Perez GI, Blaser MJ. *Helicobacter pylori* infection and gastric carcinoma among Japanese Americans in Hawaii. *N Engl J Med* 1991; **325**: 1132-1136
 - 14 **Isaacson PG**. Gastrointestinal lymphoma. *Hum Pathol* 1994; **25**: 1020-1029
 - 15 **Sigal SH**, Saul SH, Auerbach HE, Raffensperger E, Kant JA, Brooks JJ. Gastric small lymphocytic proliferation with immunoglobulin gene rearrangement in pseudolymphoma versus lymphoma. *Gastroenterology* 1989; **97**: 195-201
 - 16 **Werdmuller BF**, Loffeld RJ. *Helicobacter pylori* infection has no role in the pathogenesis of reflux esophagitis. *Dig Dis Sci* 1997; **42**: 103-105
 - 17 **Koike T**, Ohara S, Sekine H, Iijima K, Kato K, Toyota T, Shimosegawa T. Increased gastric acid secretion after *Helicobacter pylori* eradication may be a factor for developing reflux oesophagitis. *Aliment Pharmacol Ther* 2001; **15**: 813-820
 - 18 **Weston AP**, Badr AS, Topalovski M, Cherian R, Dixon A, Hassanein RS. Prospective evaluation of the prevalence of gastric *Helicobacter pylori* infection in patients with GERD, Barrett's esophagus, Barrett's dysplasia, and Barrett's adenocarcinoma. *Am J Gastroenterol* 2000; **95**: 387-394
 - 19 **Walker SJ**, Birch PJ, Stewart M, Stoddard CJ, Hart CA, Day DW. Patterns of colonisation of *Campylobacter pylori* in the oesophagus, stomach and duodenum. *Gut* 1989; **30**: 1334-1338
 - 20 **Newton M**, Bryan R, Burnham WR, Kamm MA. Evaluation of *Helicobacter pylori* in reflux oesophagitis and Barrett's oesophagus. *Gut* 1997; **40**: 9-13
 - 21 **Befrits R**, Granstrom M, Rylander M, Rubio C. *Helicobacter pylori* in 205 consecutive endoscopy patients. *Scand J Infect Dis* 1993; **25**: 189-191
 - 22 **Talley NJ**, Cameron AJ, Shorter RG, Zinsmeister AR, Phillips SF. *Campylobacter pylori* and Barrett's esophagus. *Mayo Clin Proc* 1988; **63**: 1176-1180
 - 23 **Abbas Z**, Hussainy AS, Ibrahim F, Jafri SM, Shaikh H, Khan AH. Barrett's esophagus and *H pylori*. *J Gastroenterol Hepatol* 1995; **10**: 331-333
 - 24 **Genta RM**, Graham DY. Comparison of biopsy sites for the histopathologic diagnosis of *Helicobacter pylori*: a topographic study of *H pylori* density and distribution. *Gastrointest Endosc* 1994; **40**: 342-345
 - 25 **El-Zimaity HM**, al-Assi MT, Genta RM, Graham DY. Confirmation of successful therapy of *H pylori* infection: number and sites of biopsies or a rapid urease test. *Am J Gastroenterol* 1995; **90**: 1962-1964
 - 26 **Bayerdorffer E**, Lehn N, Hatz R, Mannes GA, Oertel H, Sauerbruch T, Stolte M. Difference in expression of *Helicobacter pylori* gastritis in antrum and body. *Gastroenterology* 1992; **102**: 1575-1582
 - 27 **Bayerdorffer E**, Oertel H, Lehn N, Kasper G, Mannes GA, Sauerbruch T, Stolte M. Topographic association between active gastritis and *Campylobacter pylori* colonisation. *J Clin Pathol* 1989; **42**: 834-839
 - 28 **Brown KE**, Peura DA. Diagnosis of *Helicobacter pylori* infection. *Gastroenterol Clin North Am* 1993; **22**: 105-115
 - 29 **Skinner DB**, Walther BC, Riddell RH, Schmidt H, Iacone C, DeMeester TR. Barrett's esophagus. Comparison of benign and malignant cases. *Ann Surg* 1983; **198**: 554-565
 - 30 **Spechler SJ**, Zeroogian JM, Antonioli DA, Wang HH, Goyal RK. Prevalence of metaplasia at the gastro-oesophageal junction. *Lancet* 1994; **344**: 1533-1536
 - 31 **Weston AP**, Krmpotich P, Makdisi WF, Cherian R, Dixon A, McGregor DH, Banerjee SK. Short segment Barrett's esophagus: clinical and histologic features associated endoscopic findings and association with gastric intestinal metaplasia. *Am J Gastroenterol* 1996; **91**: 981-986
 - 32 **Menke-Pluymers MB**, Hop WC, Dees J, van Blankenstein M, Tilanus HW. Risk factors for the development of an adenocarcinoma in columnar-lined (Barrett) esophagus. The rotterdam esophageal tumor study group. *Cancer* 1993; **72**: 1155-1158
 - 33 **Csendes A**, Maluenda F, Braghetto I, Csendes P, Henriquez A, Quesada MS. Location of the lower oesophageal sphincter and the spumous columnar mucosal junction in 109 healthy controls and 778 patients with different degrees of endoscopic oesophagitis. *Gut* 1993; **34**: 21-27
 - 34 **Tytgat GN**, Hameeteman W, Onstenk R, Schotborg R. The spectrum of columnar-lined esophagus-Barrett's esophagus. *Endoscopy* 1989; **21**: 177-185
 - 35 **Voutilainen M**, Farkkila M, Mecklin JP, Juhola M, Sipponen P. Classical Barrett esophagus contrasted with Barrett-type epithelium at normal-appearing esophagogastric junction. Central finland endoscopy study group. *Scand J Gastroenterol* 2000; **35**: 2-9
 - 36 **Cameron AJ**. Epidemiologic studies and the development of Barrett's esophagus. *Endoscopy* 1993; **25**: 635-636
 - 37 **Hui YP**, Liu Y, Li YH, Ma FC, Wang YM. The relationship between *H pylori* and chronic gastritis. *J Fourth Mil Med Univ* 2001; **22**: 574-575
 - 38 **Graham DY**. *Helicobacter pylori* infection in the pathogenesis of duodenal ulcer and gastric cancer: a model. *Gastroenterology* 1997; **113**: 1983-1991
 - 39 **Graham DY**, Yamaoka Y. *H pylori* and cagA: relationships with gastric cancer, duodenal ulcer, and reflux esophagitis and its complications. *Helicobacter* 1998; **3**: 145-151
 - 40 **Stolte M**, Stadelmann O, Bethke B, Burkard G. Relationships between the degrees of *Helicobacter pylori* colonization and the degree and activity of gastritis, surface epithelial degeneration and mucus secretion. *Z Gastroenterol* 1995; **33**: 89-93
 - 41 **Bercik P**, Verolu E, Armstrong D. Reflux esophagitis and *H pylori*. *Gastroenterology* 1997; **113**: 2020-2021
 - 42 **Labenz J**, Malfertheiner P. *Helicobacter pylori* in gastrooesophageal reflux disease: causal agent, independent or protective factor? *Gut* 1997; **41**: 277-280
 - 43 **Spechler SJ**. The role of gastric carditis in metaplasia and neoplasia at the gastrooesophageal junction. *Gastroenterology* 1999; **117**: 218-228
 - 44 **Provenzale D**, Kemp JA, Arora S, Wong JB. A guide for surveillance of patients with Barrett's esophagus. *Am J Gastroenterol* 1994; **89**: 670-680
 - 45 **Spechler SJ**, Robbins AH, Rubins HB, Vincent ME, Heeren T, Doos WG, Colton T, Schimmel EM. Adenocarcinoma and Barrett's esophagus: an overrated risk? *Gastroenterology* 1984; **87**: 927-933
 - 46 **Williamson WA**, Ellis FH Jr, Gibb SP, Shahian DM, Aretz HT, Heatley GJ, Watkins E Jr. Barrett's esophagus. Prevalence and incidence of adenocarcinoma. *Arch Intern Med* 1991; **151**: 2212-2216

Is the vascular endothelial growth factor messenger RNA expression in resectable hepatocellular carcinoma of prognostic value after resection?

Kuo-Shyang Jeng, I-Shyan Sheen, Yi-Ching Wang, Shu-Ling Gu, Chien-Ming Chu, Shou-Chuan Shih, Po-Chuan Wang, Wen-Hsing Chang, Horng-Yuan Wang

Kuo-Shyang Jeng, Department of Surgery, Mackay Memorial Hospital, Taipei, Taiwan, China

I-Shyan Sheen, Liver Research Unit, Chang Gung Memorial Hospital, Taipei, Taiwan, China

Yi-Ching Wang, Shu-Ling Gu, Chien-Ming Chu, Medical Research, Mackay Memorial Hospital, Mackay Junior School of Nursing, Taipei, Taiwan, China

Shou-Chuan Shih, Po-Chuan Wang, Wen-Hsing Chang, Horng-Yuan Wang, Department of Internal Medicine, Mackay Memorial Hospital, Taipei, Taiwan, China

Correspondence to: I-Shyan Sheen, M.D., Liver Research Unit, Chang Gung Memorial Hospital, No. 199, Tung-Hwa North Road Taipei, Taiwan, China. issheen.jks@msa.hinet.net

Telephone: +886-3-3281200 Ext 8102 **Fax:** +886-2-27065704

Received: 2003-10-31 **Accepted:** 2003-12-15

Abstract

AIM: To study whether vascular endothelial growth factor messenger RNA (VEGF mRNA) in the hepatocellular carcinoma (HCC) tissues obtained after curative resection has a prognostic value.

METHODS: Using a reverse-transcription polymerase chain reaction (RT-PCR)-based assay, VEGF mRNA was determined prospectively in liver tissues of 50 controls and in HCC tissues of 50 consecutive patients undergoing curative resection for HCC.

RESULTS: Among the isoforms of VEGF mRNA, VEGF₁₆₅ and VEGF₁₂₁ were expressed. By multivariate analysis, a higher level of VEGF₁₆₅ in HCC tissue correlated with a significant risk of HCC recurrence ($P=0.038$) and significantly with recurrence-related mortality ($P=0.045$); while VEGF₁₂₁ did not. Other significant predictors of HCC recurrence included cellular dedifferentiation ($P=0.033$), an absent or incomplete capsule ($P=0.020$), vascular permeation ($P=0.018$), and daughter nodules ($P=0.006$). The other significant variables of recurrence related mortality consisted of vascular permeation ($P=0.045$), and cellular dedifferentiation ($P=0.053$). The level of VEGF mRNA in HCC tissues, however, did not significantly correlate with tumor size, cellular differentiation, capsule, daughter nodules, vascular permeation, necrosis and hemorrhage of tumors.

CONCLUSION: The expression of VEGF mRNA, especially isoform VEGF₁₆₅, in HCC tissues, may play a significant and independent role in the prediction of postoperative recurrence of HCC.

Jeng KS, Sheen IS, Wang YC, Gu SL, Chu CM, Shih SC, Wang PC, Chang WH, Wang HY. Is the vascular endothelial growth factor messenger RNA expression in resectable hepatocellular carcinoma of prognostic value after resection? *World J Gastroenterol* 2004; 10(5): 676-681

<http://www.wjgnet.com/1007-9327/10/676.asp>

INTRODUCTION

Angiogenesis, the establishment of a neovascular blood supply from preexisting blood vessels, known to be essential for the survival, growth, invasion, and metastasis of tumor cells, is a complex multistep process. The process may include the extracellular matrix remodeling and the binding of angiogenic factors to specific endothelial cell (EC) receptors, leading to EC proliferation, invasion of the basement membrane, migration, differentiation, and formation of new capillary tubes and developing into a vascular network^[1-10].

One of the most potent, direct acting, and specific factors with angiogenic activity is vascular endothelial growth factor (VEGF)^[11,12].

Hepatocellular carcinoma (HCC), a leading cause of death in Taiwan and many Asian countries, is a highly vascular tumor dependent on neovascularization. Some authors have suggested that VEGF may be a marker for metastasis in HCC because they found markedly elevated VEGF protein levels in HCC patients with remote metastases compared with those without metastasis^[13-15]. However, most such studies determined VEGF protein concentrations by enzyme immunoassay. To our knowledge, in the prediction of postresection recurrence, little is known about the prognostic significance of VEGF mRNA expression in tumor tissues. We conducted this prospective study to investigate the correlation between VEGF mRNA expression in HCC tissues and postoperative recurrence of HCC.

MATERIALS AND METHODS

Study population

Fifty patients (31 men and 19 women, with a mean age of 56.2 ± 13.3 yr) of 58 consecutive patients with HCC undergoing curative hepatectomy from July 2001 to April 2003, were enrolled in this prospective study. Patients who had previously had a hepatectomy or preoperative neoadjuvant ethanol injection or hepatic arterial chemoembolization (TACE) were excluded. Surgical procedures performed included 38 major resections (8 extended right lobectomies, 10 right lobectomies, 8 left lobectomies and 12 two-segmentectomies) and 12 minor resections (10 segmentectomies, 1 subsegmentectomies, and 1 wedge resection). HCC tissues were obtained from all 50 patients after resection. A control group including 10 healthy volunteers without liver disease (5 men, 5 women, mean age 40 yr) and 20 patients with chronic liver disease but without evidence of HCC also received liver biopsy during laparotomy on them for other reasons. All these HCC tissues and liver biopsy tissues (from control group patients) were examined for VEGF mRNA.

After discharge, the patients were assessed regularly to detect tumor recurrence with abdominal ultrasonography (every 2-3 mo during the first 5 yr, then every 4-6 mo thereafter), serum alpha fetoprotein (AFP) and liver biochemistry (every 2 mo during the first 2 yr, then every 4 mo during the following

3 yr, and every 6 mo thereafter), abdominal computed tomography (CT) (every 6 mo during the first 5 yr, then annually), and chest X-ray and bone scans (every 6 mo). Hepatic arteriography was obtained if the other studies suggested possible cancer recurrence. Detection of tumor on any imaging study was defined as clinical recurrence.

Clinicopathological variables analyzed included age, sex (male *vs* female), the presence of liver cirrhosis, Child-Pugh class of liver functional reserve (A *vs* B), hepatitis B virus (HBV) infection (hepatitis B surface antigen), hepatitis C virus (HCV) infection (anti-hepatitis C virus antibody), serum AFP level (<20 ng/mL *vs* 20 to 1 000 ng/mL *vs* >1 000 ng/mL), tumor size (<3 cm *vs* 3 to 10 cm *vs* >10 cm), tumor encapsulation (complete *vs* incomplete or absent), presence of daughter nodules, vascular permeation (including vascular invasion and/or tumor thrombi in either the portal or hepatic vein), and cell differentiation grade (Edmondson and Steiner grades I to IV).

Detection of VEGF mRNA

It included extraction of RNA, reverse transcription and amplification of cDNA of VEGF and GAPDH by PCR.

VEGF mRNA of liver tissue

Extraction of RNA We homogenized resected tissues completely in 1 mL of RNA-*bee*TM, and added 0.2 mL chloroform and shaken vigorously for 15-30 s. We stored the sample on ice for 5 min and centrifuged at 12 000 *g* for 15 min. We transferred the supernatant to a new 1.5 mL eppendorf tube and precipitated it with 0.5 mL of isopropanol. Precipitation could be as short as 5 min at 4 °C. We centrifuged it at 12 000 *g* for 5 min at 4 °C. We removed the supernatant and washed the RNA pellet with 1 mL of 750 mL/L ethanol, it dislodged the pellet from the slide of the tube by shaking. We centrifuged at 7 500 *g* for 5 min at 4 °C and carefully removed ethanol. We removed the supernate and dissolved RNA in DEPC-H₂O (usually between 50-100 µL) and store at -80 °C.

Reverse transcription We heated the RNA sample at 55 °C for 10 minutes and chilled it on ice. We added the following components: (1) 4 µL 5×RT buffer containing 50 mmol/L Tris-HCl (pH 8.3), 75 mmol/L KCl, 3 mmol/L MgCl₂ and 10 mmol/L DTT(dithiothreitol), (2) 3 µL 10 mmol/L dNTP, (3) 1.6 µL Oligo-d(T)₁₈ and 0.4 µL random hexamers (N)6 (1 µg/µL), (4) 0.5 uL RNase inhibitor (40 units/µL), (5) 3 µL 25 mmol/L MnCl₂, (6) 6 µL RNA in DEPC-H₂O, (7) 0.5 µL DEPC-H₂O. We incubated it at 70 °C for 2 minutes, chilled it to 23 °C to anneal primers to RNA. We added 1 µL of M-MLV RTase (moloney murine leukemia virus reverse transcriptase, 200 units/µL, Promega). We incubated it for 8 min at 23 °C followed by 60 min at 40 °C. We heated the reaction at 94 °C for 5 min, chilled it on ice and stored cDNA at -20 °C.

Amplification of cDNA of VEGF and GAPDH by PCR The sequences of the sense primers were 5' -AGTGTGTGCCCA CTGAGGA-3' (VEGF) and 5' -AGTCAACGGATTTGGT CGTA-3' (GAPDH) and those of the antisense primers were 5' -AGTCAACGGATTTGGTTCGTA-3' (VEGF) and 5' -GGAACATGTAAACCATGTAG-3' (GAPDH). The first polymerase chain reaction (RT-PCR) solution contained 5 µL of the synthesized cDNA solution, 10 µL of 10× polymerase reaction buffer, 500 moi/L each of dCTP, dATP, dGTP and dTTP, 15 pmol of each external primer (EX-sense and EX-antisense), 4 units of Thermus Brockiamus Prozyme DNA polymerase (PROtech Technology Ent. Co., Ltd. Taipei, Taiwan) and water. The PCR cycles were denaturing at 94 °C for 1 min, annealing at 52 °C for 1 min, and primer extension at 72 °C for 1 min. The cycles were repeated 40 times. The PCR product was reamplified with internal primers for nested PCR to obtain a higher sensitivity. The first and second PCR components were the same, but for the primer pairs (IN-sense

and IN-antisense), the final product was electrophoresed on 20g/L agarose gel and stained with ethidium bromide. Four different isoforms of human VEGF were identified, arising from alternative splicing of the primary transcript of a single gene. The majority were VEGF₁₂₁ (165 bp) and VEGF₁₆₅ (297 bp). The percentage intensity of the VEGF PCR fragment for each liver was relative to a GAPDH PCR fragment (122 bp). The intensity of bands was measured using Fujifilm Science Lab 98 (Image Gauge V3.12). The sensitivity of our assay was assessed using human hepatocytes.

A hepatoblastoma cell line (HepG2) served as a positive control for VEGF mRNA expression. For negative controls, we used EDTA-treated water (filtered and vaporized).

Statistical analysis

A statistical software (SPSS for Windows, version 8.0, Chicago, Illinois) was employed, with Student's *t*-test used to analyze continuous variables and a chi-square or Fisher's exact test for categorical variables. Parameters relating to the presence of postoperative hAFP mRNA in peripheral blood were analyzed by stepwise logistic regression. A Cox proportional hazards model was used for multivariate stepwise analysis to identify the significant variables for predicting recurrence and mortality. Significance was taken as a *P* value <0.05.

RESULTS

RT-PCR analysis of VEGF transcript in liver tissues

VEGF mRNA was expressed in the liver tissues of 10 (VEGF₁₆₅ in 10 and VEGF₁₂₁ in 6) out of 30 control patients. In the HCC group, isoform VEGF₁₆₅ was detected in all the 50 patients (100%) (with a concentration ranging from 0.1860 to 0.7240) and isoform VEGF₁₂₁ in 40 patients (80%) (with a concentration ranging from 0.2849 to 1.0298).

We did not detect isoforms VEGF₁₈₉ and/or VEGF₂₀₆ in either HCC tissues or control liver tissues.

Table 1 Demographic, clinical and tumor variables of patients with HCC undergoing curative resection (*n*=50)

Variables	No. of patients (%)
Age (mean, years)	56.2±13
Male	31 (62)
Cirrhosis	40 (80)
Child- Pugh' s class A	43 (86)
Serum AFP <20 ng/mL	16 (32)
20-10 ³ ng/mL	18 (36)
>10 ³ ng/mL	14 (28)
HBsAg (+)	36 (72)
Anti-HCV (+)	13 (26)
Size of HCC <3 cm	12 (24)
3-10 cm	13 (26)
>10 cm	25 (50)
Edmondson-Steiner' s Grade I	4 (8)
Grade II	12 (24)
Grade III	18 (36)
Grade IV	16 (32)
Absent or incomplete capsule	31 (62)
Vascular permeation	29 (58)
Daughter nodules	31 (62)
Tumor necrosis	33 (66)
Tumor hemorrhage	29 (58)

AFP: serum alpha fetoprotein, HBsAg (+): positive hepatitis B surface antigen, Anti-HCV(+): positive hepatitis C virus antibody, Edmondson Steiner grade: differentiation grade.

Correlation of VEGF mRNA expression and clinical recurrence

During the follow up period (median 1.5 yr, range 1 to 2.5 yr), 16 patients (32%) had clinically detectable recurrence, of whom 7 died. A higher level of isoform VEGF₁₆₅ mRNA in HCC tissue correlated significantly with clinical recurrence both univariately ($P=0.022$) and multivariately, ($P=0.038$). Isoform VEGF₁₂₁ levels had no such correlation. By multivariate analysis, other significant predictors of recurrence included poor cellular differentiation ($P=0.033$), less encapsulation ($P=0.020$), more vascular permeation ($P=0.018$) and the presence of daughter nodules ($P=0.006$) (Table 2).

Table 2 Predictors of HCC recurrence

Variable	P values	
	UV	MV
Sex	0.895	-
Age	0.279	-
Size(<3 cm, >10 cm)	0.415	-
Liver cirrhosis	0.510	-
Child-Pugh class	0.528	-
Serum AFP	0.744	-
HBsAg (+)	0.280	-
Anti-HCV (+)	0.481	-
Edmondson Steiner grade	0.0005	0.033
Capsule	<0.0001	0.020
Vascular permeation	<0.0001	0.018
Daughter nodules	<0.0001	0.006
Tumor necrosis	0.344	-
Tumor hemorrhage	0.812	-
Tissue VEGF ₁₆₅ mRNA	0.022	0.038
Tissue VEGF ₁₂₁ mRNA	0.622	-

UV: univariate analysis, MV: multivariate analysis, AFP: serum alpha fetoprotein, HBsAg(+): positive hepatitis B surface antigen, Anti-HCV(+): positive hepatitis C virus antibody, Edmondson Steiner grade: differentiation grades I, II vs III, IV, n.s: not significant.

Table 3 Correlation between clinical and tumor variables and recurrence-related mortality

Parameters	P values	
	UV	MV
Sex	0.510	-
Age	0.440	-
Size (<3 cm, >10 cm)	0.519	-
Liver cirrhosis	0.510	-
Child-Pugh class	0.548	-
HBsAg (+)	0.351	-
Anti-HCV (+)	0.521	-
Edmondson Steiner grade	<0.001	0.053
Capsule	0.033	n.s.
Vascular permeation	<0.001	0.045
Daughter nodules	0.016	n.s.
Tumor necrosis	0.373	-
Tumor hemorrhage	0.306	-
Tissue VEGF ₁₆₅ mRNA	0.018	0.045
Tissue VEGF ₁₂₁ mRNA	0.744	-

UV: univariate analysis, MV: multivariate analysis, AFP: serum alpha fetoprotein, HBsAg (+): positive hepatitis B surface antigen, Anti-HCV(+): positive hepatitis C virus antibody, Edmondson Steiner grade: differentiation grades I, II vs III, IV, n.s: not significant.

Correlation of VEGF mRNA expression and recurrence-related death

The level of isoform VEGF₁₆₅ in HCC tissue significantly correlated with death due to recurrence both univariately ($P=0.018$) and multivariately ($P=0.045$). By multivariate analysis, a greater degree of vascular permeation significantly correlated with mortality ($P=0.045$), and poor cellular differentiation approached significance ($P=0.053$)(Table 3).

Correlation between VEGF mRNA expression in HCC tissues and clinical and histopathologic features

There was no significant association between isoform of VEGF mRNA and gender, age, serum AFP level, chronic HBV or HCV carriage, tumor size, coexisting cirrhosis, cellular differentiation, capsule, vascular permeation, daughter nodules, tumor necrosis, or tumor hemorrhage ($P>0.05$).

DISCUSSION

Our study revealed that a higher value of VEGF mRNA isoform₁₆₅ in resected HCC tissues was significantly associated with an increased risk of postoperative recurrence and disease mortality. The value of VEGF mRNA isoform₁₂₁ in HCC tissues was not significantly predictive of the outcome.

VEGF is also known as a vascular permeability factor and vasculotropin. Its active form is a homodimeric cytokine with molecular weight 34-46 ku. The variation in size due to alternative exon splicing might produce four different isoforms of 121, 165, 189 and 206 amino acids (monomeric size). The last had heparin binding activity^[11,12]. Different cancers might have different expression of the isoforms. The majority of HCC expressed an abundance of VEGF₁₂₁ and VEGF₁₆₅^[13-15]. According to Ferrara's finding, VEGF₁₆₅ was the predominantly expressed form in human cDNA libraries as well as in most normal cells and tissues^[12].

Some authors have shown that the VEGF level in serum or in tissue is of value for predicting disease progression and prognosis in different cancers, such as the gastrointestinal origins, breast, lung, urothelium, ovary, and lymphoma^[16-26]. Compared with expression in tumor tissue, the advantage of measurement of serum VEGF level is that it can be performed without tissue specimens and repeated, but it may be influenced by some factors such as coexisting liver cirrhosis, associated infection and platelet activation^[27-32].

In addition, the expression of VEGF mRNA in serum might not always correlate significantly with the gene expression level of tumors^[33]. Therefore, we used liver tissue instead of serum in this study. Warren found VEGF mRNA in hepatocytes and in some Kupffer cells^[34]. However, release of VEGF mRNA might also be influenced by some cells other than HCC cells^[34]. The presence of mRNA for VEGF has also been described in T lymphocytes, CD34* cells, and monocytes^[27, 30].

For more accuracy, we chose to measure mRNA expression of VEGF in liver tissue rather than the protein itself. The level of VEGF mRNA did not always correlate with the protein concentration^[32]. Immunohistochemistry could not distinguish small amounts of protein, which may partly explain the discrepancy in protein and mRNA levels.

The high recurrence rate after resection is the main determinant for the poor outcome of HCC^[35-40]. Tumor invasiveness variables correlated with recurrence include high serum AFP, hepatitis, vascular permeation, grade of cellular differentiation, infiltration or absence of capsule, tumor size, coexisting cirrhosis, presence of daughter nodules, and multiple lesions. Therefore, a number of studies have been done to see if VEGF correlated with any or all of those factors.

Among reports about the clinical significance of VEGF

expression in HCC, there are considerable discrepancies^[13-15,28,41-48]. Li found that VEGF mRNA in HCC correlated significantly with portal vein emboli, poorly encapsulated tumors, and microvascular density in HCC tissues^[42]. Zhou reported that high VEGF expression in HCC was associated with portal vein tumor thrombosis^[43]. Chow showed that VEGF expression was significantly associated with portal vein tumor thrombosis (sonographic evidence) but not with liver function, tumor volume, gender, severity of liver disease, or tumor grading^[41]. In addition, the correlation between increased VEGF protein level in HCC and tumor size, number, microscopic venous invasion, metastasis, and recurrence has also been reported.

However, according to our study, a higher expression of VEGF mRNA was significantly correlated with tumor recurrence and recurrence-related mortality but not with the other parameters of tumor invasiveness. VEGF mRNA in HCC tissue thus appears to be an independent risk factor of postoperative recurrence. There are several possible explanations for this dissociation.

The number of study patients is one possible factor. Because most of the reported investigations were performed in small series, the 50 patients we used seemed a more adequate sample size compared with other studies. Another possible explanation for the discrepancies may be the assessment of tumors of different sizes and etiologies.

The relation between tumor size and VEGF mRNA expression might be complex and dynamic because of different vascular growth patterns^[14,48-52]. If HCCs are about 1.0 cm in diameter, artery-like vessels are not well developed. Capillarization of the blood spaces is present but incomplete, and portal tracts may appear within cancerous nodules. These HCCs are thought to receive a predominantly portal blood supply. As tumor size increases, portal tracts decrease in number, and artery-like vessels gradually increase in number and size. Well-differentiated HCCs measuring 1.0 to 1.5 cm in diameter are in a transitional stage from portal to arterial blood supply, with reduction in portal flow prior to the increase in arterial flow. Therefore, blood flow in HCC at this point would be low and may not be detected on angiography. Hypervascularity becomes easily seen when nodules are larger than 2 cm in diameter. However, with increasing tumor size, VEGF positivity may gradually decrease. According to Yamaguchi, 36.8% of nodules larger than 3.0 cm were VEGF-negative^[48]. El-Assal showed that, HCCs larger than 5 cm in diameter were less vascular than smaller or medium-sized lesions^[32]. However, it has been reported that the intercapillary distance increased as the tumor size or weight increased, caused by the significantly different rates of turnover of endothelial cells and neoplastic cells. These complicated changes in vascularity may account for the disparate results among reported studies.

Suzuki reported that VEGF mRNA levels were not correlated with the vascularity of HCCs as seen on angiography^[13]. On the contrary, Mise *et al* showed that the degree of VEGF mRNA expression was significantly correlated with the intensity of tumor staining in angiograms ($P < 0.01$)^[14]. Because of the complex nature of the angiogenic process, however, it seems that VEGF expression is not the sole contributor to angiogenesis in HCC. Other factors involved in this process may include TGF- β , TNF- α , IL-8, *etc.*

The stage of cancer might also influence VEGF expression^[53-55]. VEGF concentrations have been reported to be significantly higher in advanced rather than early stages of breast, colon and gastric cancer^[16-18,21]. Chao showed that a lower range of VEGF levels in patients with early-stage HCC overlapped considerably with those of normal controls or patients with chronic hepatitis or cirrhosis^[45].

Coexisting liver cirrhosis may influence VEGF expression.

About 80% of our study patients had cirrhosis. Some investigators have found that VEGF expression was significantly higher in cirrhotic liver than in noncirrhotic liver. Furthermore, it has been shown that cirrhosis itself was associated with increased angiogenic activity. According to El-Assal, cirrhotic livers had significantly higher VEGF expressions than noncirrhotic livers^[32]. In addition, some suggested a possible involvement of VEGF in angiogenesis of cirrhotic liver but not in angiogenesis of HCC^[31,32]. Akiyoshi suggested that a low serum VEGF level in liver cirrhosis might reflect the degree of liver dysfunction and be associated with the grade of hepatocyte regeneration and VEGF levels decreased with the worsening of Child-Pugh score^[31]. Whereas, most of our patients belonged to Child-Pugh class A, with resectable lesions, unlike those studied by Akiyoshi.

According to the cell differentiation, the regulation of VEGF may be complex. In our study, VEGF mRNA did not significantly correlate with the grade of cell differentiation. We attribute this to the possibility of different histological grades coexisting in some HCC tissues. Yamaguchi examined VEGF expression immunohistochemically in HCC with various histological grades and sizes^[48]. In tumors composed of a single histological grade, VEGF expression was the highest in well-differentiated, followed by moderately differentiated, and then poorly differentiated HCC. In tumors consisting of cancerous tissues of two different histological grades, the expression was less intense in the higher-grade HCC component. VEGF was also expressed in the surrounding HCC tissues in which inflammatory cell infiltration was apparent. Based on these findings, VEGF expression in HCC tissues was thought to be partly related to the histological grade, but other cytokines and growth factors could also cooperatively act to enhance or influence VEGF expressions in HCC.

We also found no correlation between VEGF and the absence or presence of fibrous capsule or septum formation, which was in contrast to the findings of Suzuki *et al*^[13]. The origin of the capsule and fibrous septa in HCC is unclear. Nakashima *et al* suggested the possibility of fibrogenesis at the interface of two tumor nodules with different properties, a process requiring fibrin deposition in the initial stage when the HCC nodule grows to 1.5 cm or larger^[52]. However, this mechanism has been doubted, since the tumor size did not correlate with the thickness of the capsule or the incidence of its formation.

In our study, a higher level of VEGF mRNA in tumor tissue correlated with more postresection recurrences. We attribute it to two possible mechanisms. One is that the higher angiogenesis may have more invasive nature of cancer to spread into the surrounding tissues. This invasion requires concomitant neovascularization through the sprouting of endothelial cells in extracellular matrix. It has been reported that VEGF could induce both urokinase-type and tissue-type plasmin in endothelial cell, which are the key protease involved in the degradation of the extracellular matrix. The other mechanism is that a shift of VEGF mRNA occurred in liver tissue, which is strongly related to the development of HCC. The progression from preneoplastic to neoplastic tissue would contribute to recurrence.

Surgery remains the potentially curative treatment for patients with HCC. High recurrence rate limits the long term survival. Examination of VEGF mRNA expression in resected HCC tissue may give us information on the risk of postoperative recurrence. Addition of neoadjuvant antiangiogenic therapy after surgery may be considered for such patients. Furthermore, serial measurement of circulating VEGF mRNA during postoperative follow-up to monitor the effect of therapy or the development of recurrence should be further investigated^[56,57].

In conclusion, expression of VEGF, especially isoform

VEGF₁₆₅, in HCC tissues may play a significant role in the prediction of postresection recurrence of HCC.

ACKNOWLEDGEMENT

This study was supported by grants from the Department of Medical Research, Mackay Memorial Hospital, Taiwan (MMH 9237).

REFERENCES

- Zetter BR.** Angiogenesis and tumor metastasis. *Annu Rev Med* 1998; **49**: 407-424
- Skobe M, Rockwell P, Goldstein N, Vosseler S, Fusenig NE.** Halting angiogenesis suppresses carcinoma cell invasion. *Nat Med* 1997; **3**: 1222-1227
- Marme D.** Tumor angiogenesis: the pivotal role of vascular endothelial growth factor. *World J Urol* 1996; **14**: 166-174
- Folkman J.** Angiogenesis in cancer, vascular, rheumatoid and other disease. *Nat Med* 1995; **1**: 27-31
- Folkman J.** Endothelial cells and angiogenic growth factors in cancer growth and metastasis. *Cancer Metastasis Rev* 1990; **9**: 171-174
- Liotta LA, Steeg PS, Stetler-Stevenson WG.** Cancer metastasis and angiogenesis: an imbalance of positive and negative regulation. *Cell* 1991; **64**: 327-336
- Fidler IJ, Ellis LM.** The implications of angiogenesis for the biology and therapy of cancer metastasis. *Cell* 1994; **79**: 185-188
- Hanahan D, Folkman J.** Patterns and emerging mechanisms of the angiogenic switch during tumorigenesis. *Cell* 1996; **86**: 353-364
- Fox SB, Gatter KC, Harrist AL.** Tumour angiogenesis. *J Pathol* 1996; **179**: 232-237
- Dvorak HF, Brown LF, Detmar M, Dvorak AM.** Vascular permeability factor/vascular endothelial growth factor, microvascular hyperpermeability, and angiogenesis. *Am J Pathol* 1995; **146**: 1029-1039
- Houck KA, Ferrara N, Winer J, Cachianes G, Li B, Leung DW.** The vascular endothelial growth factor family: identification of a fourth molecular species and characterization molecular species and characterization of alternative splicing of RNA. *Mol Endocrinol* 1991; **5**: 1806-1814
- Ferrara N, Houck K, Jakeman L, Leung DW.** Molecular and biological properties of the vascular endothelial growth factor family of proteins. *Endocrinol Rev* 1992; **13**: 18-32
- Suzuki K, Hayashi N, Miyamoto Y, Yamamoto M, Ohkawa K, Ito Y, Sasaki Y, Yamaguchi Y, Nakase H, Noda K, Enomoto N, Arai K, Yamada Y, Yoshihara H, Tujimura T, Kawano K, Yoshikawa K, Kamada T.** Expression of vascular permeability factor/vascular endothelial growth factor in human hepatocellular carcinoma. *Cancer Res* 1996; **56**: 3004-3009
- Mise M, Arai S, Higashitani H, Furutani M, Niwano M, Harada T, Ishigami S, Toda Y, Nakayama H, Fukumoto M, Fujita J, Imamura M.** Clinical significance of vascular endothelial growth factor and basic fibroblast growth factor gene expression in liver tumor. *Hepatology* 1996; **23**: 455-464
- Miura H, Miyazaki T, Kuroda M, Oka T, Machinami R, Kodama T, Shibuya M, Makuuchi M, Yazaki Y, Ohnishi S.** Increased expression of vascular endothelial growth factor in human hepatocellular carcinoma. *J Hepatol* 1997; **27**: 854-861
- Brown LF, Berse B, Jackman RW, Tognazzi K, Guidi AJ, Dvorak HF, Senger DR, Connolly JL, Schnitt SJ.** Expression of vascular endothelial permeability factor (vascular endothelial growth factor) and its receptors in breast cancer. *Hum Pathol* 1995; **26**: 86-91
- Anan K, Morisaki T, Katano M, Ikubo A, Kitsuki H, Uchiyama A, Kuroki S, Tanaka M, Torisu M.** Vascular endothelial growth factor and platelet-derived growth factor are potential angiogenic and metastatic factors in human breast cancer. *Surgery* 1996; **119**: 333-339
- Takahashi Y, Kitadai Y, Bucana CD, Cleary KR, Ellis LM.** Expression of vascular endothelial growth factor and its receptor, KDR, correlates with vascularity, metastasis, and proliferation of human colon cancer. *Cancer Res* 1995; **55**: 3964-3968
- Inoue K, Ozeki Y, Suganuma T, Sugiura Y, Tanaka S.** Vascular endothelial growth factor expression in primary esophageal squamous cell carcinoma: association with angiogenesis and tumor progression. *Cancer* 1997; **79**: 206-213
- Brown LF, Berse B, Jackman RW, Tognazzi K, Manseau EJ, Senger DR, Dvorak HF.** Expression of vascular permeability factor (vascular endothelial growth factor) and its receptor in adenocarcinomas of the gastrointestinal tract. *Cancer Res* 1993; **53**: 4727-4735
- Maeda K, Chung YS, Ogawa Y, Takatsuka S, Kang SM, Ogawa M, Sawada T, Sowa M.** Prognostic value of vascular endothelial growth factor expression in gastric carcinoma. *Cancer* 1996; **77**: 858-863
- Imoto H, Osaki T, Taga S, Ohgami A, Ichiyoshi Y, Yasumoto K.** Vascular endothelial growth factor expression in non-small-cell lung cancer: prognostic significance in squamous cell carcinoma. *J Thorac Cardiovasc Surg* 1998; **115**: 1007-1014
- Salven P, Ruotsalainen T, Mattson K, Joensuu H.** High pre-treatment serum level of vascular endothelial growth factor (VEGF) is associated with poor outcome in small-cell lung cancer. *Int J Cancer* 1998; **79**: 144-146
- Miyake H, Hara I, Yamanaka K, Gohji K, Arakawa S, Kamidono S.** Elevation of serum level of vascular endothelial growth factor as a new predictor of recurrence and disease progression in patients with superficial urothelial cancer. *Urology* 1999; **53**: 302-307
- Tempfer C, Obrmair A, Hefler L, Haeusler G, Gitsch G, Kainz C.** Vascular endothelial growth factor serum concentrations in ovarian cancer. *Obstet Gynecol* 1998; **92**: 360-363
- Salven P, Teerenhovi L, Joensuu H.** A high pretreatment serum vascular endothelial growth factor concentration is associated with poor outcome in non-Hodgkin's lymphoma. *Blood* 1997; **90**: 3167-3172
- Banks RE, Forbes MA, Kinsey SE, Stanley A, Ingham E, Walters C, Selby PJ.** Release of the angiogenic cytokine vascular endothelial growth factor (VEGF) from platelets: bearing human hepatocellular carcinoma. *Br J Cancer* 1998; **77**: 956-964
- Jinno K, Tanimizu M, Hyodo I, Nishikawa Y, Hosokawa Y, Doi T, Endo H, Yamashita T, Okada Y.** Circulating vascular endothelial growth factor (VEGF) is a possible tumor marker for metastasis in human hepatocellular carcinoma. *J Gastroenterol* 1998; **33**: 376-382
- Wartiovaara U, Salven P, Mikkola H, Lassila R, Kaukonen J, Joukov V, Orpana A, Ristimaki A, Heikinheimo M, Joensuu H, Alitalo K, Palotie A.** Peripheral blood platelets express VEGF-C and VEGF which are released during platelet activation. *Thromb Haemost* 1998; **80**: 171-175
- Banks RE, Forbes MA, Kinsey SE, Stanley A, Ingham E, Walters C, Selby PJ.** Release of the angiogenic cytokine vascular endothelial growth factor (VEGF) from platelets: significance for VEGF measurements and cancer biology. *Br J Cancer* 1998; **77**: 956-964
- Akiyoshi F, Sata M, Suzaki H, Uchimura Y, Mitsuyama K, Matsuo K, Tanikawa K.** Serum vascular endothelial growth factor levels in various liver diseases. *Dig Dis Sci* 1998; **43**: 41-45
- El-Assal ON, Yamanoi A, Soda Y, Yamaguchi M, Igarashi M, Yamamoto A, Nabika T, Nagasue N.** Clinical significance of microvessel density and vascular endothelial growth factor expression in hepatocellular carcinoma and surrounding liver: possible involvement of vascular endothelial growth factor in the angiogenesis of cirrhotic liver. *Hepatology* 1998; **27**: 1554-1562
- Tokunaga T, Oshika Y, Abe Y, Ozeki Y, Sadehiro S, Kijima H, Tsuchida T, Yamazaki H, Ueyama Y, Tamaoki N, Nakamura M.** Vascular endothelial growth factor (VEGF) mRNA isoform expression pattern is correlated with liver metastasis and poor prognosis in colon cancer. *Br J Cancer* 1998; **77**: 998-1002
- Warren RS, Yuan H, Matli MR, Gillett NA, Ferrara N.** Regulation by vascular endothelial growth factor of human colon cancer tumorigenesis in a mouse model of experimental liver metastasis. *J Clin Invest* 1995; **95**: 1789-1797
- Poon RT, Fan ST, Lo CM, Liu CL, Wong J.** Intrahepatic recurrence after curative resection of hepatocellular carcinoma. Long-term results of treatment and prognostic factors. *Ann Surg* 1999; **229**: 216-222
- Jeng KS, Chen BF, Lin HJ.** En bloc resection for extensive hepatocellular carcinoma. Is it advisable? *World J Surg* 1994; **18**: 834-849
- Jeng KS, Sheen IS, Chen BF, Wu JY.** Is the p53 gene mutation of prognostic value in hepatocellular carcinoma after resection? *Arch Surg* 2000; **135**: 1329-1333
- Yamamoto J, Kosuge T, Takayama T, Shimada K, Yamasaki S,**

- Ozaki H, Yamaguchi N, Makuuchi M. Recurrence of hepatocellular carcinoma after surgery. *Br J Surg* 1996; **83**: 1219-1222
- 39 **Jeng JS**, Sheen IS, Tsai YC. Gamma glutamyl transpeptidase messenger RNA may serve as a diagnostic aid in hepatocellular carcinoma. *Br J Surg* 2001; **88**: 986-987
- 40 **Ng IO**, Lai EC, Fan ST, Ng MM, So MK. Prognostic significance of pathologic features of hepatocellular carcinoma. A multivariate analysis of 278 patients. *Cancer* 1995; **76**: 2443-2448
- 41 **Chow NH**, Hsu PI, Lin XZ, Yang HB, Chan SH, Cheng KS, Huang SM, Su JJ. Expression of vascular endothelial growth factor in normal liver and hepatocellular carcinoma: an immunohistochemical study. *Hum Pathol* 1997; **28**: 698-703
- 42 **Li XM**, Tang ZY, Zhou G, Lui YK, Ye SL. Significance of vascular endothelial growth factor mRNA expression in invasion and metastasis of hepatocellular carcinoma. *J Exp Clin Cancer Res* 1998; **17**: 13-17
- 43 **Zhou J**, Tang ZY, Fan J, Wu ZQ, Li XM, Liu YK, Liu F, Sun HC, Ye SL. Expression of platelet-derived endothelial cell growth factor and vascular endothelial growth factor in hepatocellular carcinoma and portal vein tumor thrombus. *J Cancer Res Clin Oncol* 2000; **126**: 57-61
- 44 **Qin LX**, Tang ZY. The prognostic molecular markers in hepatocellular carcinoma. *World J Gastroenterol* 2002; **8**: 385-392
- 45 **Chao Y**, Li CP, Chau GY, Chen CP, King KL, Lui WY, Yen SH, Chang FY, Chan WK, Lee SD. Prognostic significance of vascular endothelial growth factor, basic fibroblast growth factor, and angiogenin in patients with resectable hepatocellular carcinoma after surgery. *Ann Surg Oncol* 2003; **10**: 355-362
- 46 **Torimura T**, Sata M, Ueno T, Kin M, Tsuji R, Suzaku K, Hashimoto O, Sugawara H, Tanikawa K. Increased expression of vascular endothelial growth factor is associated with tumor progression in hepatocellular carcinoma. *Hum Pathol* 1998; **29**: 986-991
- 47 **Motou Y**, Sawabu N, Nakanuma Y. Expression of epidermal growth factor and fibroblast growth factor in human hepatocellular carcinoma: an immunohistochemical study. *Liver* 1991; **11**: 272-277
- 48 **Yamaguchi R**, Yano H, Iemura A, Ogasawara S, Haramaki M, Kojiro M. Expression of vascular endothelial growth factor in human hepatocellular carcinoma. *Hepatology* 1998; **28**: 68-77
- 49 **Yoshiji H**, Kuriyama S, Yoshii J, Yamazaki M, Kikukawa M, Tsujinoue H, Nakatani T, Fukui H. Vascular endothelial growth factor tightly regulates *in vivo* development of murine hepatocellular carcinoma cells. *Hepatology* 1998; **28**: 1489-1496
- 50 **Sakamoto M**, Ino Y, Fujii T, Hirohashi S. Phenotype changes in tumor vessels associated with the progression of hepatocellular carcinoma. *Jpn J Clin Oncol* 1993; **23**: 98-104
- 51 **Terada T**, Nakanuma Y. Arterial elements and perisinusoidal cells in borderline hepatocellular nodules and small hepatocellular carcinomas. *Histopathology* 1995; **27**: 333-339
- 52 **Nakashima O**. Pathological diagnosis of hepatocellular carcinoma. *Nippon Rinsho* 2001; **59**(Suppl 6): 333-341
- 53 **Dirix LY**, Vermeulen PB, Pawinski A, Prove A, Benoy I, De Pooter C, Martin M, Van Oosterom AT. Elevated levels of the angiogenic cytokines basic fibroblast growth factor and vascular endothelial growth factor in sera of cancer patients. *Br J Cancer* 1997; **76**: 238-243
- 54 **Salven P**, Manpaa H, Orpana A, Alitalo K, Joensuu H. Serum vascular endothelial growth factor is often elevated in disseminated cancer. *Clin Cancer Res* 1997; **3**: 647-651
- 55 **Kraft A**, Weindel K, Ochs A, Marth C, Zmija J, Schumacher P, Unger C, Marme D, Gastl G. Vascular endothelial growth factor in the sera and effusions of patients with malignant and nonmalignant disease. *Cancer* 1999; **85**: 178-187
- 56 **Baccala AA**, Zhong H, Clift SM, Nelson WG, Marshall FF, Passe TJ, Gambill NB, Simons JW. Serum vascular endothelial growth factor is a candidate biomarker of metastatic tumor response to *ex vivo* gene therapy of renal cell cancer. *Urology* 1998; **51**: 327-332
- 57 **Denekamp J**. Angiogenesis, neovascular proliferation and vascular pathophysiology as targets for cancer therapy. *Br J Radiol* 1993; **66**: 186-196

Edited by Wang XL Proofread by Zhu LH

Mechanisms of acupuncture and moxibustion in regulation of epithelial cell apoptosis in rat ulcerative colitis

Huan-Gan Wu, Xiao Gong, Li-Qing Yao, Wei Zhang, Yin Shi, Hui-Rong Liu, Ye-Jing Gong, Li-Bin Zhou, Yi Zhu

Huan-Gan Wu, Xiao Gong, Wei Zhang, Yin Shi, Hui-Rong Liu, Ye-Jing Gong, Yi Zhu, Shanghai Institute of Acupuncture-Moxibustion and Meridians, Shanghai 200030, China; Shanghai Research Center of Acupuncture and Meridian, Shanghai 201200, China
Li-Qing Yao, Zhongshan Hospital Fudan University, Shanghai 200032, China

Li-Bin Zhou, RuiJin Hospital Shanghai Institute of Endocrinology, Shanghai 200025, China

Supported by the National Natural Science Foundation of China, No. 30200368 and Shanghai Commission of Science and Technology, No. 02DZ19150-3 and key program of Shanghai and State Administration of Traditional Chinese Medicine of China

Correspondence to: Professor Huan-Gan Wu, Shanghai Institute of Acupuncture-Moxibustion and Meridians, Shanghai 200030, China. wuhuangan@citiz.net

Telephone: +86-21-54592009/64383910

Received: 2003-07-15 **Accepted:** 2003-08-16

Abstract

AIM: To investigate the effect of acupuncture and moxibustion on epithelial cell apoptosis and expression of Bcl-2, Bax, fas and FasL proteins in rat ulcerative colitis.

METHODS: A rat model of ulcerative colitis was established by immunological methods and local stimulation. All rats were randomly divided into model control group (MC), electro-acupuncture group (EA), herbs-partition moxibustion group (HPM). Normal rats were used as normal control group (NC). Epithelial cell apoptosis and expression of Bcl-2, Bax, fas and FasL proteins were detected by TUNEL and immunohistochemical method respectively.

RESULTS: The number of epithelial cell apoptosis in MC was significantly higher than that in NC, and was markedly decreased after the treatment with herbs-partition moxibustion or electro-acupuncture. The expression of Bcl-2, Bax, fas and FasL in colonic epithelial cells in MC was higher than that in NC, and was markedly down-regulated by herbs-partition moxibustion or electro-acupuncture treatment.

CONCLUSION: The pathogenesis of ulcerative colitis in rats involves abnormality of apoptosis. Acupuncture and moxibustion can regulate the expression of Bcl-2, Bax, fas and FasL proteins and inhibit the apoptosis of epithelial cells of ulcerative colitis in rats by Bcl-2/Bax, fas/FasL pathways.

Wu HG, Gong X, Yao LQ, Zhang W, Shi Y, Liu HR, Gong YJ, Zhou LB, Zhu Y. Mechanisms of acupuncture and moxibustion in regulation of epithelial cell apoptosis in rat ulcerative colitis. *World J Gastroenterol* 2004; 10(5): 682-688

<http://www.wjgnet.com/1007-9327/10/682.asp>

INTRODUCTION

Ulcerative colitis (UC) is a non-specific inflammatory intestinal disease. The pathogenesis of ulcerative colitis involves abnormality of apoptosis which is affected by a variety of

factors^[1-3]. At present, increasing evidence suggests that acceleration of apoptosis of epithelial cells and inhibition of apoptosis of inflammatory cells (such as neutrophil) are closely associated with colonic tissue injury and immunological abnormality in ulcerative colitis.

Apoptosis is determined by the relative expression of serial genes involved in the regulation of apoptosis. Fas/FasL is one of the important pathways of epithelial cell apoptosis in UC. In tissues of UC, the number of FasL positive cells is significantly increased, resulting in apoptosis. FasL expression increases in the focal region of active UC, which directly promotes apoptosis of Fas expressing colonic epithelium. The apoptosis promoting gene bax also plays an important role in apoptosis. The ratio of bax/bcl-2 determines whether apoptosis occurs or not. Excessive expression of bax promotes apoptosis.

In the present study, a rat model of UC was established by immunological method and local stimulation. After the treatment with electro-acupuncture and herbs-partition moxibustion, the number of colonic epithelial cell apoptosis and the expression of Bcl-2/Bax and Fas/FasL proteins were detected by TUNEL and immunohistochemistry respectively for elucidating the mechanism of acupuncture and moxibustion underlying colonic epithelial cell apoptosis in rat UC.

MATERIALS AND METHODS

Experimental animals and materials

Two hundred male SD rats (weighting 200±20 g) were provided by Experimental Animal Center of Shanghai University of TCM. TUNEL kits was purchased from Boehringer Mannheim (Germany). Bax, Bcl-2 and FasL kits were from Dako (Denmark). Fas was from Santa-cruz (USA).

Methods

Animal model and therapeutic methods Establishment of animal model: According to Experimental Methodology of Pharmacology^[4], UC rat model was established by immunological method and local stimulation. Colonic mucosa was prepared from human fresh surgical colonic specimens, homogenized by adding appropriate amount of normal saline and centrifuged for 30 min at 3 000 r/min. The supernatant was removed for the measurement of protein concentration and then mixed with Freund adjuvant. The antigen fluid was first injected into the plantar pedis of the model group rats, then into the plantar pedis, dorsum, inguen and abdominal cavity (no Freund adjuvant in the last injection) on the tenth, seventeenth, twenty-fourth and thirty-first day respectively. When a certain titer of serum anti-colonic antibody was reached, 3 mL 3% formalin and 2 mL antigen fluid (no Freund adjuvant) were administered by enema successively. The rats in NC were administrated with normal saline as the same procedure of MC.

Treatment: After the ulcerative colitis rat model was built, the animals were randomly divided into model control group (MC 8), electro-acupuncture group (EA 8), herbs-partition moxibustion group (HPM 8) and normal control group (NC 6). HPM: Moxa cones made of refined mugwort floss were placed on the medicinal formula (medicinal formula dispensing: *Radix Aconiti praeparata*, *cortex Cinnamomi*, et al) for Qihai (RN

6) and Tianshu (ST 25, bilateral) and ignited. Two moxa cones were used for each treatment once a day and 14 times as a course. EA: Tianshu (bilateral) and Qihai were acupunctured and then stimulated by intermittent pulse with 2HZ frequency, 4 mA intensity for 20 minutes once a day and 14 times as a course.

After treatment, four group rats were killed simultaneously. The distal 6 cm long colons were dissected and reserved in formaldehyde solution.

TUNEL analysis Formalin fixed specimens were embedded in paraffin using standard procedures. Deparaffinised and rehydrated sections were immersed in 3mL/L H₂O₂ for 30 min at room temperature and digested with proteinase K for 20 min at 37 °C. The sections were immersed in 1g/L Triton-100 and then incubated with TUNEL mixture for 1 hour at room temperature, with streptavidin-HRP(1:400) for 30 min at 37 °C. The sections were stained with 0.4g/L DAB and treated with 3mL/L H₂O₂ for 10 min and with hematoxylin for 1 min. The results were observed with light microscopy. Positive reaction was shown by brown color. The apoptotic cells were counted as the mean of cells in 3 visual fields of one section. The data were analysed by *q* test, using statistical package SPSS.

Immunohistochemistry Formalin fixed specimens were embedded in paraffin using standard procedures. Sections attached on carry sheet glass were autoclaved at 58 °C for 24 h. Deparaffinised and rehydrated sections were immersed in 10mL/L H₂O₂ for 20 min and washed three times, each time for 3 min with PBS. Sections were preincubated with 10mL/L normal goat anti rabbit serum for 20 min at room temperature and then incubated with the first antibodies diluted for 18 h at 4 °C and Envision reagent for 30 min at 37 °C. Sections were stained by 0.4g/L DAB with 0.3mL/L H₂O₂ for 8 min and hematoxylin for 30 s. The results were observed under light microscope.

Positive specimens were used as positive controls. The result of PBS instead of the first antibody was used as negative control. The positive reactions showed brown particles. The positive cells expressing Bcl-2, Bax, fas and FasL were counted as the mean of cells in 3 visual fields of one section. The data were analysed by *q* test, using statistical package SPSS.

RESULTS

The effect of acupuncture and moxibustion on epithelial cell apoptosis in UC rats is shown in Table 1 and Figure 1(A-D).

Table 1 Results of epithelial cell apoptosis in different groups

Group	<i>n</i>	Number of apoptotic cells (mean±SD)
NC	6	20.61±1.99
MC	8	66.21±8.51 ^b
HPM	8	33.58±3.59 ^{bd}
EA	8	34.29±2.70 ^{bd}

^b*P*<0.01 vs NC; ^d*P*<0.01 vs MC.

Table 1 shows that the number of epithelial cell apoptosis in MC was significantly increased compared with that of NC (*P*<0.01). The number of epithelial cell apoptosis in EA and HPM was remarkably decreased compared with that of MC (*P*<0.01), but was not as low as that of NC (*P*<0.01).

The effect of acupuncture and moxibustion on Bax expression in colonic epithelia of UC rats is shown in Table 2 and Figure 2(A-D)

Table 2 Bax expression in colonic epithelia of different groups (mean±SD)

Group	<i>n</i>	Area of expression	Intensity of expression
NC	6	35 905.06±2 987.97	0.1683±0.0105
MC	8	52 451.13±3 174.10 ^b	0.2558±0.0142 ^b
HPM	8	39 561.50±1 382.94 ^d	0.1900±0.0047 ^d
EA	8	38 477.79±3 309.19 ^d	0.1796±0.0117 ^d

^b*P*<0.01 vs NC; ^d*P*<0.01 vs MC.

Table 2 shows that the area and intensity of Bax expression in the colonic epithelia of MC were significantly increased compared with that of NC (*P*<0.01). The area and intensity

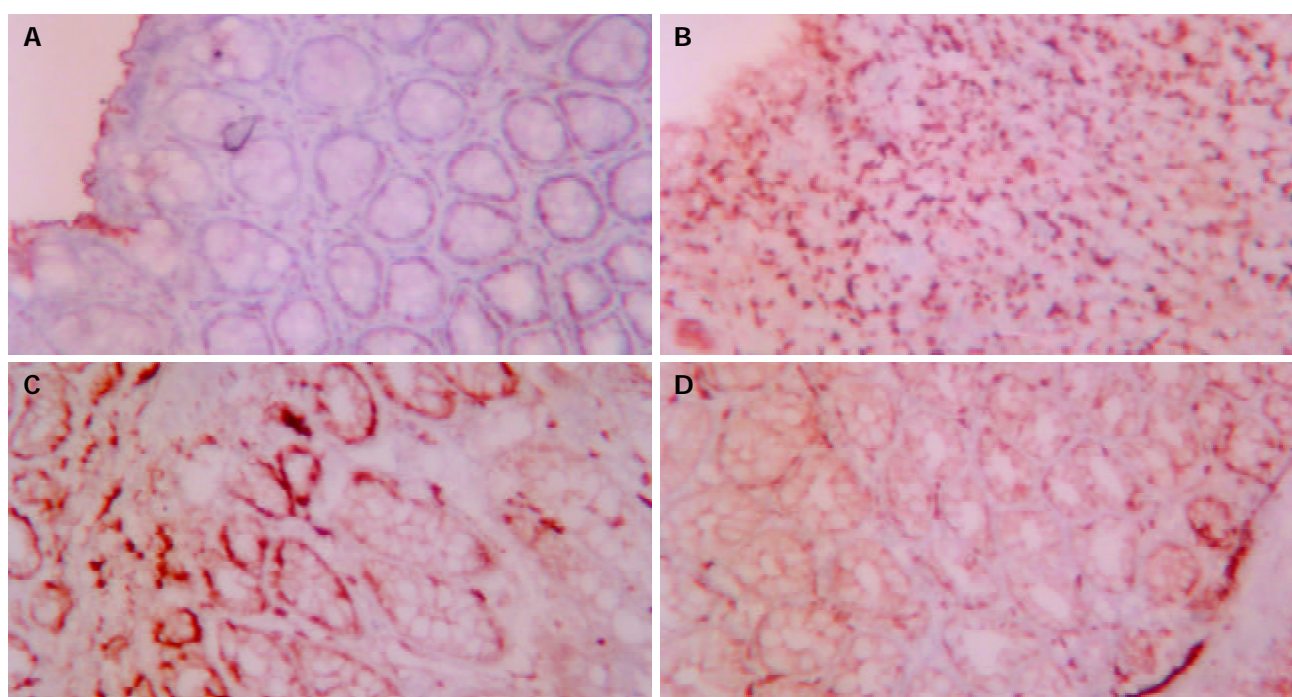


Figure 1 A: Epithelial cell apoptosis in NC ×200, B: Epithelial cell apoptosis in MC ×200, C: Epithelial cell apoptosis in EA ×200, D: Epithelial cell apoptosis in HPM ×200.

of Bax expression in the colonic epithelia of PHM and EA were markedly decreased compared with that of MC, but showed no significant difference when compared with that of NC.

The effect of acupuncture and moxibustion on Bcl-2 expression in the colonic epithelium of UC rats is shown in Table 3 and Figure 3(A-D)

Table 3 shows that the area and intensity of Bcl-2 expression in the colonic epithelia of MC were significantly increased compared with that of NC ($P < 0.01$). The area and intensity of Bcl-2 expression in the colonic epithelia of PHM and EA were

markedly decreased compared with that of MC, but which were not as low as that of NC.

The effect of acupuncture and moxibustion on Fas expression in the colonic epithelium of UC rats is shown in Table 4 and Figure 4(A-D)

Table 4 shows that the area and intensity of Fas expression in the colonic epithelia of MC were significantly increased compared with that of NC ($P < 0.01$). The area and intensity of Fas expression in the colonic epithelia of PHM and EA were markedly decreased compared with that of MC ($P < 0.01$), but still had a significant difference compared with that of NC ($P < 0.05$).

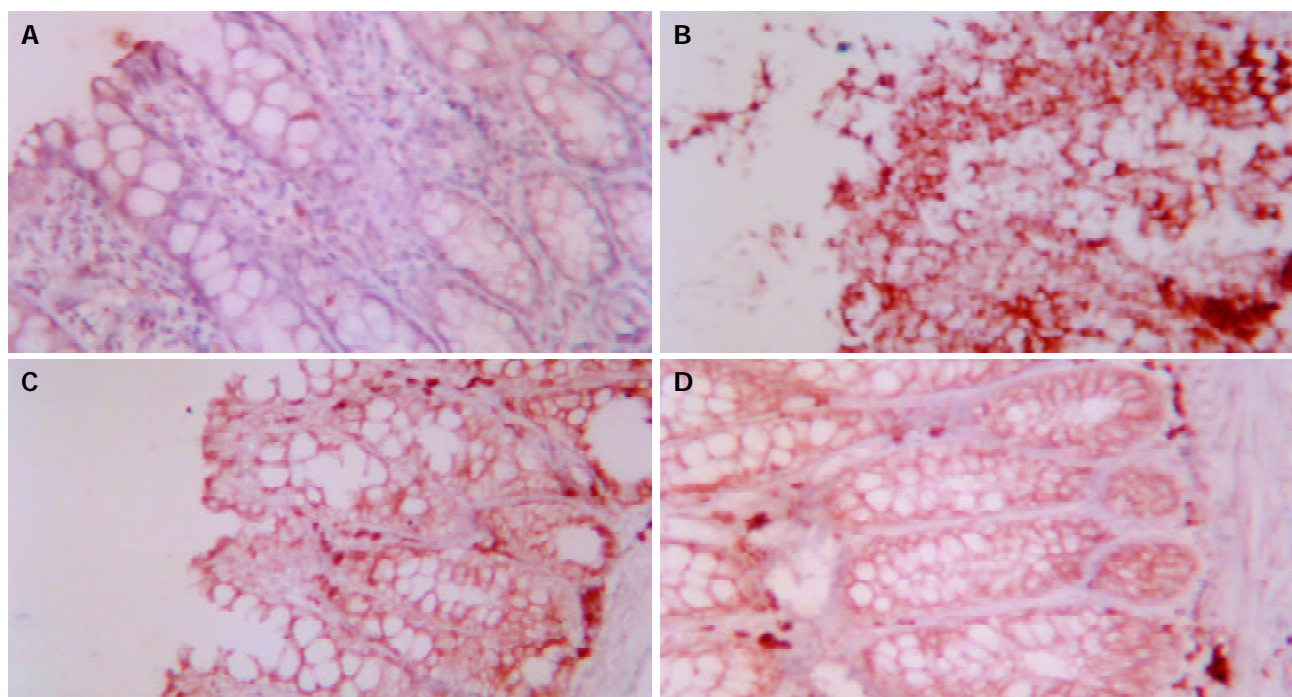


Figure 2 A: Bax expression in colonic epithelia of NC $\times 200$, B: Bax expression in colonic epithelia of MC $\times 200$, C: Bax expression in colonic epithelia of EA $\times 200$, D: Bax expression in colonic epithelia of HPM $\times 200$.

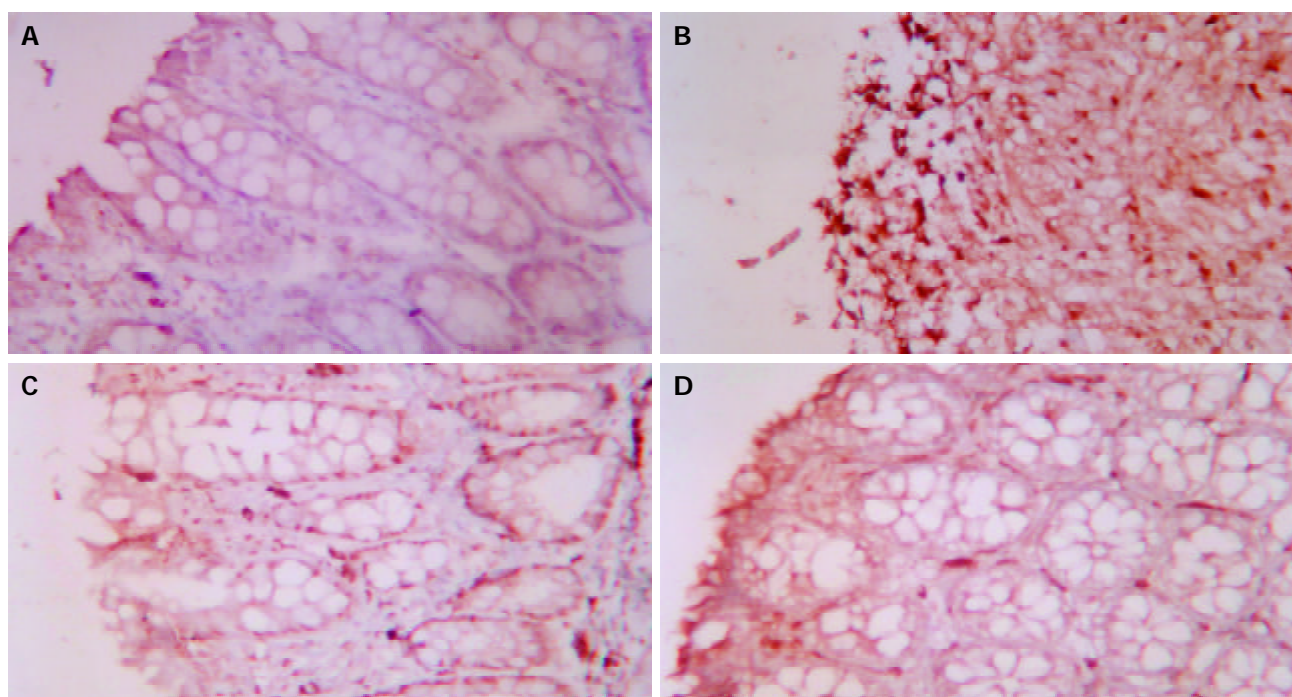


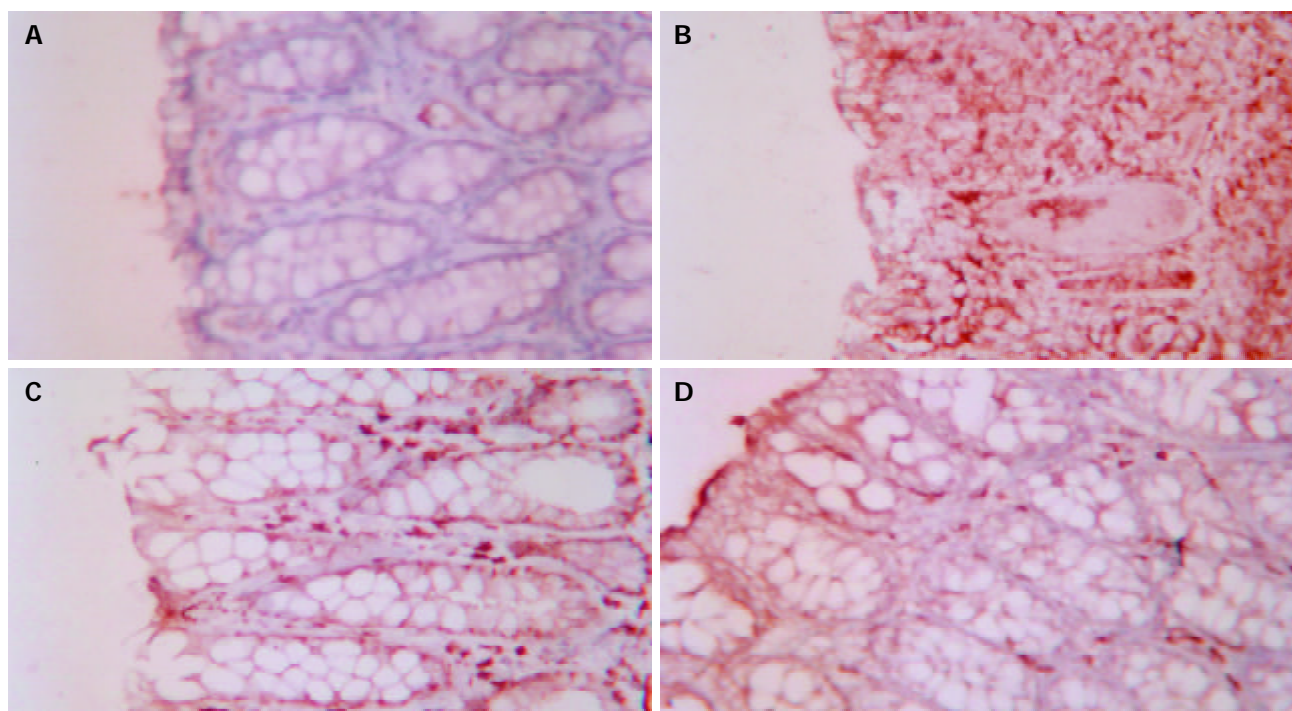
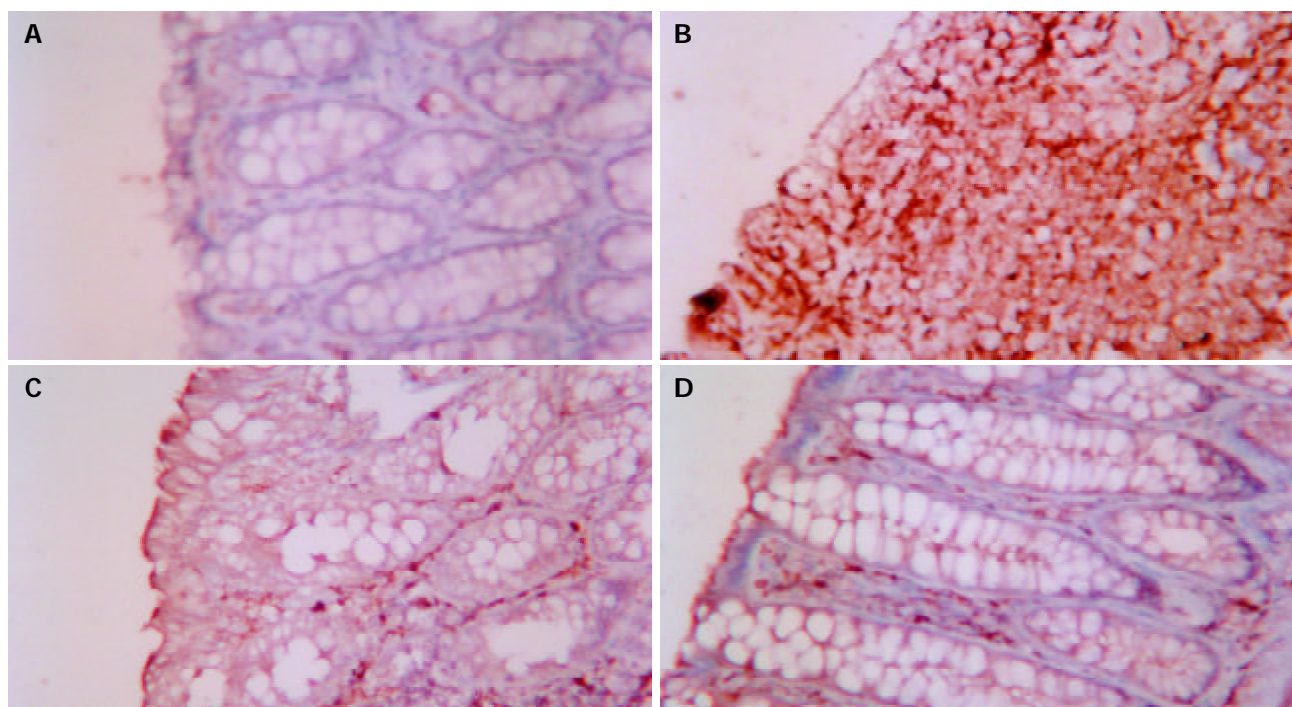
Figure 3 A: Bcl-2 expression in colonic epithelia of NC $\times 200$, B: Bcl-2 expression in colonic epithelia of MC $\times 200$, C: Bcl-2 expression in colonic epithelia of EA $\times 200$, D: Bcl-2 expression in colonic epithelia of HPM $\times 200$.

Table 3 Bcl-2 expression in colonic epithelia of different groups (mean±SD)

Group	n	Area of expression (μm ²)	Intensity of expression
NC	6	30 863.61±2 273.44	0.1539±0.0114
MC	8	44 757.67±28.1.53 ^b	0.2242±0.0196 ^b
HPM	8	40 061.63±4 937.84 ^{be}	0.1979±0.0177 ^{bd}
EA	8	39 219.04±3 449.84 ^{db}	0.1875±0.0133 ^{bd}

^b*P*<0.01 vs NC; ^d*P*<0.01 vs MC; ^e*P*<0.05 vs MC.**Table 4** Fas expression in colonic epithelia of different groups (mean±SD)

Group	n	Area of expression (μm ²)	Intensity of expression
NC	6	33 764.67±4 422.37	0.1722±0.0153
MC	8	50 262.08±4 780.34 ^b	0.2500±0.0212 ^b
HPM	8	37 992.29±3 239.23 ^{de}	0.1825±0.0200 ^d
EA	8	38 913.21±4 669.80 ^{de}	0.1850±0.0138 ^d

^b*P*<0.01 vs NC; ^d*P*<0.01 vs MC; ^e*P*<0.05 vs NC.**Figure 4** A: Fas expression in colonic epithelia of NC ×200, B: Fas expression in colonic epithelia of MC ×200, C: Fas expression in colonic epithelia of EA ×200, D: Fas expression in colonic epithelia of HPM ×200.**Figure 5** A: FasL expression in colonic epithelia of NC ×200, B: FasL expression in colonic epithelia of MC ×200, 5: FasL expression in colonic epithelia of EA ×200, D: FasL expression in colonic epithelia of HPM ×200.

The effect of acupuncture and moxibustion on FasL expression in the colonic epithelium of UC rats is shown in Table 5 and Figure 5(A-D)

Table 5 FasL expression in colonic epithelia of different groups (mean±SD)

Group	n	Area of expression (μm ²)	Intensity of expression
NC	6	33 063.56±3 347.24	0.1561±0.0080
MC	8	44 566.58±4 637.23 ^b	0.2600±0.0105 ^b
HPM	8	38 825.58±2 495.51 ^{bd}	0.1838±0.0156 ^{bd}
EA	8	38 553.29±3 489.38 ^{bd}	0.1850±0.0108 ^{bd}

^bP<0.01 vs NC; ^dP<0.01 vs MC.

Table 5 shows that the area and intensity of FasL expression in the colonic epithelia of MC were significantly increased compared with that of NC (P<0.01). The area and intensity of FasL expression in the colonic epithelia of PHM and EA were markedly decreased compared with that of MC (P<0.01), which had a significant difference compared with that of NC (P<0.01).

DISCUSSION

UC is a non-specific inflammatory intestinal disease. The incidence of UC in our country has an increasing trend yearly. The pathogenesis of ulcerative colitis in rats involved in the abnormality of apoptosis^[5-8]. Increasing evidence showed that acceleration of epithelial cell apoptosis and inhibition of inflammatory cell apoptosis were closely associated with colonic tissue injury and immunological abnormality in ulcerative colitis^[9-11].

Studies showed that cell proliferation, differentiation and apoptosis of epithelial cells in intestines mucosa were a dynamic equilibrium process, and neonate epithelial cells migration along crypt villi from pit cells became mature villous epithelial cells. In physiological condition, apoptosis only occurred on superficial epithelial cells of intestine. In pathologic status, this sequence was destructive. For example, at the area of active inflammation, the apoptotic rate of neonate epithelial cells is accelerated and pit cells were superproliferative^[12-14]. This alteration would lead to destruction of epithelial barrier of colon and imbalance of intestinal function of absorption and excretion.

Apoptosis is a procedure of death adjusted by a flock of apoptotic genes, the cell apoptosis was determined by the relative gene expression level of a series of apoptosis genes^[15-17]. The bcl-2 gene kindred is an important apoptosis adjusting gene, the position of Bcl-2 protein is at mitochondrial membrane, endoplasmic reticulum and nuclear membrane. As it could prolong the life of cells, it has been generally accepted as an antiapoptosis gene^[18-23]. Bax is a new member of bcl-2 gene kindred, it could form a dimer with bcl-2 to inhibit its function^[24-27]. The relative expression ratio of bcl-2 and bax determines whether apoptosis happens in cells or not. When expression of bax gained advantage, apoptosis would occur and when the expression of bcl-2 gained advantage, the cells would continue to exist^[28-32]. Many studies have shown that abnormal apoptosis in ulcerative colitis could be affected by many agents^[33-36].

This study showed that persistent inflammation resulted in the abnormal increase of epithelial cell apoptosis in UC rats. Meanwhile, the area and intensity of Bcl-2 and Bax expression in colonic epithelia of MC were significantly increased compared with that of NC, suggesting that epithelial cell apoptosis is abnormally active. The upregulation of Bcl-2 and Bax expression in colonic epithelia increased the number of

apoptotic cells, which might be one of the important mechanisms of colonic pathological changes in UC. After the treatment with electro-acupuncture and herbs-partition moxibustion, the ulceration of colonic tissues in both groups was markedly improved and the tissue structure was well restored. The number of apoptotic cells in colonic tissues in EA and HPM was significantly decreased compared with that of NC. The area and intensity of Bcl-2 and Bax expression in colonic epithelia of PHM and EA were markedly decreased compared with that of MC. Especially, Bax expression was much downregulated. The above results showed that electro-acupuncture and herbs-partition moxibustion could inhibit colonic epithelial cell apoptosis of UC rats by decreasing Bcl-2 and Bax expression. The extent of Bcl-2 and Bax expression in colonic epithelia of UC rats downregulated by acupuncture and herbs-partition moxibustion was different, thus the relative ratio of Bcl-2 and Bax expression in colonic epithelia was changed due to the inhibition of the abnormal increase of epithelial cell apoptosis in UC. The above results showed that down-regulation of the inflammatory reaction of colonic epithelia in UC rats, inhibition of the injurious effect of a variety of proinflammatory cytokines on colonic tissues, decrease of Bcl-2 and Bax expression of epithelial cells and regulation of the relative ratio of Bcl-2 and Bax expression could change the active state of colonic epithelial cell apoptosis due to its decrease. This is one of the important mechanisms of acupuncture and moxibustion in regulating apoptosis and treating UC.

Many studies^[37-39] have shown Fas/FasL is an important pathway of epithelial cell apoptosis in UC. Fas is also named Apo-1 or CD95, belongs to tumour necrosis factor receptor (TNFR) kindred, it has comprehensive expressions in various histocytes and can bind anti-Fas antibody or FasL to change the constitution of cell surface. So it can transmit signals in cells to switch on apoptosis mechanism, leading to apoptosis of cells that express Fas. The function of Fas/FasL is to maintain immune stability of body and balance of body's apoptosis^[40-44]. Normally colonic epithelium could express Fas, and a small quantity of cells could express FasL in the site where the number of apoptosis cells was markedly increased. When UC occurred, because of stimulation by inflammation, the increase of FasL expression would cause apoptosis^[45,46]. The high expression of FasL in active UC could cause apoptosis of cells expressing Fas^[47-49], this would accelerate migration and activity of neutrophils and lymphocytes, causing progressive mucosal lesion of UC^[50-52]. Therefore, the study of epithelial cell apoptosis may develop a new effective therapeutic approach to UC.

The study showed that the area and intensity of Fas and FasL expression in colonic epithelia of MC were significantly increased compared with that of NC as apoptosis increased, suggesting that the high expression of Fas and FasL plays an important role in epithelial cell apoptosis in UC. After the treatment with electro-acupuncture and herbs-partition moxibustion, Fas and FasL expressions in colonic epithelia of both groups were markedly downregulated compared with MC, and the number of apoptosis cells was also decreased. The above results showed that regulating the abnormal expression of Fas and FasL in colonic tissues of UC rats and decreasing its epithelial cell apoptosis might be one of the important mechanisms of acupuncture and moxibustion in treating UC. Our previous study showed that acupuncture and moxibustion could markedly inhibit the expression of proinflammatory cytokines such as IL-1β and IL-6^[53-56]. It is suggested that acupuncture and moxibustion can regulate Fas and FasL expression in colonic tissues of UC rats, and may be associated with the inhibition of the activation of macrophages in colonic epithelia and decrease of the expression of proinflammatory cytokines such as IL-1β and IL-6. Further activation of

macrophages in the blocked initial cascade reaction of inflammation and immunity in colonic epithelia can be effectively controlled. Stimulation of inflammatory cytokines on colonic tissues is relieved and stability of immunological function in UC rats is restored.

REFERENCES

- Xia B**, Shivananda S, Zhang GS, Yi JY, Crusius JBA, Peña AS. Inflammatory bowel disease in Hubei Province of China. *China Natl J New Gastroenterol* 1997; **3**: 119-120
- Xia B**, Guo HJ, Crusius JBA, Deng CS, Meuwissen SGM, Peña AS. *In vitro* production of TNF- α , IL-6 and sIL-2R in Chinese patients with ulcerative colitis. *World J Gastroenterol* 1998; **4**: 252-255
- Hu QY**, Hu XY, Jiang Y. Clinical investigation of ulcerative colitis patients treated by integrated traditional Chinese and Western medicine. *World J Gastroenterol* 1998; **4**(Suppl 2): 93-94
- Xu SY**, Bian RL, Chen X. Experimental methodology of pharmacology. *Beijing: People's Health Publishing House* 1982: 892
- Seidelin JB**, Nielsen OH. Apoptosis in chronic inflammatory bowel disease. The importance for pathogenesis and treatment. *Ugeskr Laeger* 2003; **165**: 790-792
- Sasaki S**, Yoneyama H, Suzuki K, Suriki H, Aiba T, Watanabe S, Kawauchi Y, Kawachi H, Shimizu F, Matsushima K, Asakura H, Narumi S. Blockade of CXCL10 protects mice from acute colitis and enhances crypt cell survival. *Eur J Immunol* 2002; **32**: 3197-3205
- Vetuschi A**, Latella G, Sferra R, Caprilli R, Gaudio E. Increased proliferation and apoptosis of colonic epithelial cells in dextran sulfate sodium-induced colitis in rats. *Dig Dis Sci* 2002; **47**: 1447-1457
- Sipos F**, Molnar B, Zagoni T, Tulassay Z. Changes in cell kinetics and clinical course in inflammatory bowel diseases. *Orv Hetil* 2002; **143**: 1175-1181
- Buttke TM**, Sandstrom PA. Oxidative stress as a mediator of apoptosis. *Immunol Today* 1994; **15**: 7-10
- Arai N**, Mitomi H, Ohtani Y, Igarashi M, Kakita A, Okayasu I. Enhanced epithelial cell turnover associated with p53 accumulation and high p21WAF/CIP1 expression in ulcerative colitis. *Mod Pathol* 1999; **12**: 604-611
- Bu P**, Keshavarzian A, Stone DD, Liu J, Le PT, Fisher S, Qiao L. Apoptosis: one of the mechanisms that maintains unresponsiveness of the intestinal mucosal immune system. *J Immunol* 2001; **166**: 6399-6403
- Sasaki S**, Yoneyama H, Suzuki K, Suriki H, Aiba T, Watanabe S, Kawauchi Y, Kawachi H, Shimizu F, Matsushima K, Asakura H, Narumi S. Blockade of CXCL10 protects mice from acute colitis and enhances crypt cell survival. *Eur J Immunol* 2002; **32**: 3197-3205
- Dieckgraefe BK**, Crimmins DL, Landt V, Houchen C, Anant S, Porche-Sorbet R, Ladenson JH. Expression of the regenerating gene family in inflammatory bowel disease mucosa: Reg Ialpha upregulation, processing, and anti apoptotic activity. *J Investig Med* 2002; **50**: 421-434
- Ruemmele FM**, Seidman EG. Cytokine-intestinal epithelial cell interactions: implications for immune mediated bowel disorders. *Zhonghua Minguo Xiaoei Keyi Xuehui Zazhi* 1998; **39**: 1-8
- Huang XM**. Bcl-2 with its protein and regulation of apoptosis. *Foreign Med Sci Sec Mol Biol* 1997; **19**: 16-19
- Wu K**, Zhao Y. Investigation progres of apoptosis. *Foreign Med Sci Sec Mol Biol* 2001; **24**: 134-136
- Mercer WE**, Shields MT, Lin D, Appella E, Ullrich SJ. Growth suppression induced by wild-type p53 protein is accompanied by selective down-regulation of proliferating cell nuclear antigen expression. *Proc Natl Acad Sci U S A* 1991; **88**: 1958-1962
- Ohman L**, Franzen L, Rudolph U, Birnbaumer L, Hornquist EH. Regression of Peyer's patches in G alpha i2 deficient mice prior to colitis is associated with reduced expression of Bcl-2 and increased apoptosis. *Gut* 2002; **51**: 392-397
- Yan J**, Ouyang Q, Liu WP, Li GD, Li FY. Apoptosis and proliferation of epithelial cells in ulcerative colitis. *Zhonghua Xiaohua Neijing Zazhi* 2001; **18**: 161-163
- Jiang XL**, Quan QZ, Sun ZQ, Wang YJ, Qi F, Wang D, Zhang XL. The expression of apoptosis adjust protein of ulcerative colitis patient's lymphocyte. *Shijie Huaren Xiaohua Zazhi* 1999; **7**: 903-904
- Mayer B**, Oberbauer R. Mitochondrial regulation of apoptosis. *News Physiol Sci* 2003; **18**: 89-94
- Buduneli E**, Genel F, Atilla G, Kutukculer N. Evaluation of p53, bcl-2, and interleukin-15 levels in gingival crevicular fluid of cyclosporin A-treated patients. *J Periodontol* 2003; **74**: 506-511
- Sohn SK**, Jung JT, Kim DH, Kim JG, Kwak EK, Park T, Shin DG, Sohn KR, Lee KB. Prognostic significance of bcl-2, bax, and p53 expression in diffuse large B-cell lymphoma. *Am J Hematol* 2003; **73**: 101-107
- Chiu CT**, Yeh TS, Hsu JC, Chen MF. Expression of Bcl-2 family modulated through p53-dependent pathway in human hepatocellular carcinoma. *Dig Dis Sci* 2003; **48**: 670-676
- Korkolopoulou P**, Lazaris ACH, Konstantinidou AE, Kavantzias N, Patsouris E, Christodoulou P, Thomas-Tsagli E, Davaris P. Differential expression of bcl-2 family proteins in bladder carcinomas. Relationship with apoptotic rate and survival. *Eur Urol* 2002; **41**: 274-283
- Scorrano L**, Korsmeyer SJ. Mechanisms of cytochrome c release by proapoptotic BCL-2 family members. *Biochem Biophys Res Commun* 2003; **304**: 437-444
- Oltvai ZN**, Milliman CL, Korsmeyer SJ. Bcl-2 heterodimerizes *in vivo* with a conserved homolog, Bax, that accelerates programmed cell death. *Cell* 1993; **74**: 609-619
- Korkolopoulou P**, Oates J, Kittas C, Crocker J. p53, c-myc, p62 and proliferating cell nuclear antigen (PCNA) expression in non-Hodgkin's lymphomas. *J Clin Pathol* 1994; **47**: 9-14
- Iimura M**, Nakamura T, Shinozaki S, Iizuka B, Inoue Y, Suzuki S, Hayashi N. Bax is downregulated in inflamed colonic mucosa of ulcerative colitis. *Gut* 2000; **47**: 228-235
- Mueller E**, Vieth M, Stolte M, Mueller J. The differentiation of true adenomas from colitis-associated dysplasia in ulcerative colitis: a comparative immunohistochemical study. *Hum Pathol* 1999; **30**: 898-905
- Ina K**, Itoh J, Fukushima K, Kusugami K, Yamaguchi T, Kyokane K, Imada A, Binion DG, Musso A, West GA, Dobrea GM, McCormick TS, Lapetina EG, Levine AD, Ottaway CA, Fiocchi C. Resistance of Crohn's disease T cells to multiple apoptotic signals is associated with a Bcl-2/Bax mucosal imbalance. *J Immunol* 1999; **163**: 1081-1090
- Kraus MD**, Shahsafaei A, Antin J, Odze RD. Relationship of Bcl-2 expression with apoptosis and proliferation in colonic graft versus host disease. *Hum Pathol* 1998; **29**: 869-875
- Ilyas M**, Tomlinson IP, Hanby AM, Yao T, Bodmer WF, Talbot IC. Bcl-2 expression in colorectal tumors: evidence of different pathways in sporadic and ulcerative-colitis-associated carcinomas. *Am J Pathol* 1996; **149**: 1719-1726
- Itoh J**, de La Motte C, Strong SA, Levine AD, Fiocchi C. Decreased Bax expression by mucosal T cells favours resistance to apoptosis in Crohn's disease. *Gut* 2001; **49**: 35-41
- Cui YF**, Xia GW, Fu XB, Yang H, Peng RY, Zhang Y, Gu QY, Gao YB, Cui XM, Hu WH. Relationship between expression of Bax and Bcl-2 proteins and apoptosis in radiation compound wound healing of rats. *Chin J Traumatol* 2003; **6**: 135-138
- Nagata S**, Golstein P. The Fas death factor. *Science* 1995; **267**: 1449-1456
- Strater J**, Wellisch I, Riedl S, Walczak H, Koretz K, Tandara A, Krammer PH, Moller P. CD95 (APO-1/Fas)-mediated apoptosis in colon epithelial cells: a possible role in ulcerative colitis. *Gastroenterology* 1997; **113**: 160-167
- Iwamoto M**, Koji T, Makiyama K, Kobayashi N, Nakane PK. Apoptosis of crypt epithelial cells in ulcerative colitis. *J Pathol* 1996; **180**: 152-159
- Iwamoto M**, Makiyama K, Koji T, Kohno S, Nakane PK. Expression of Fas and Fas-ligand in epithelium of ulcerative colitis. *Nippon Rinsho* 1996; **54**: 1970-1974
- Mountz JD**, Zhou T, Su X, Wu J, Cheng J. The role of programmed cell death as an emerging new concept for the pathogenesis of autoimmune diseases. *Clin Immunol Immunopathol* 1996; **80**(3 Pt 2): S2-14
- Nagata S**. Fas and Fas ligand: a death factor and its receptor. *Adv Immunol* 1994; **57**: 129-144
- Yukawa M**, Iizuka M, Horie Y, Yoneyama K, Shirasaka T, Ito

- H, Komatsu M, Fukushima T, Watanabe S. Systemic and local evidence of increased Fas-mediated apoptosis in ulcerative colitis. *Int J Colorectal Dis* 2002; **17**: 70-76
- 43 **Coffey JC**, Bennett MW, Wang JH, O'Connell J, Neary P, Shanahan F, Redmond HP, Kirwan WO. Upregulation of Fas-Fas-L (CD95/CD95L)-mediated epithelial apoptosis—a putative role in pouchitis? *J Surg Res* 2001; **98**: 27-32
- 44 **Iwamoto M**, Makiyama K, Koji T, Kohno S, Nakane PK. Expression of Fas and Fas-ligand in epithelium of ulcerative colitis. *Nippon Rinsho* 1996; **54**: 1970-1974
- 45 **Moller P**, von Reyher U, Leithauser F, Strater J. CD95 (APO-1/Fas) and CD95-ligand (CD95L). Implications of these apoptosis mediating receptor/ligand systems in the pathogenesis of autoimmune diseases. *Verh Dtsch Ges Pathol* 1996; **80**: 12-22
- 46 **Wu HG**, Zhou LB, Shi DR, Liu SM, Liu HR, Zhang BM, Chen HP, Zhang LS. Morphological study on colonic pathology in ulcerative colitis treated by moxibustion. *World J Gastroenterol* 2000; **9**: 861-865
- 47 **Tsukada Y**, Nakamura T, Iimura M, Iizuka BE, Hayashi N. Cytokine profile in colonic mucosa of ulcerative colitis correlates with disease activity and response to granulocytapheresis. *Am J Gastroenterol* 2002; **97**: 2820-2828
- 48 **Banks C**, Bateman A, Payne R, Johnson P, Sheron N. Chemokine expression in IBD. Mucosal chemokine expression is unselectively increased in both ulcerative colitis and Crohn's disease. *J Pathol* 2003; **199**: 28-35
- 49 **Brown KA**, Back SJ, Ruchelli ED, Markowitz J, Mascarenhas M, Verma R, Piccoli DA, Baldassano RN. Lamina propria and circulating interleukin-6 in newly diagnosed pediatric inflammatory bowel disease patients. *Am J Gastroenterol* 2002; **97**: 2603-2608
- 50 **Ueyamam H**, Kiyohara T, Sawada N, Isozaki K, Kitamura S, Kondo S, Miyagawa J, Kanayama S, Shinomura Y, Ishikawa H, Ohtani T, Nezu R, Nagata S, Matsuzawa Y. High Fas ligand expression on lymphocytes in lesions of ulcerative colitis. *Gut* 1998; **43**: 48-55
- 51 **Strater J**, Wellisch I, Riedl S, Walczak H, Koretz K, Tandara A, Krammer PH, Moller P. CD95(APO-1/Fas)-mediated apoptosis in colon epithelial cells: a possible role in ulcerative colitis. *Gastroenterology* 1997; **113**: 160-167
- 52 **Suzuki A**, Sugimura K, Ohtsuka K, Hasegawa K, Suzuki K, Ishizuka K, Mochizuki T, Honma T, Narisawa R, Asakura H. Fas/Fas ligand expression and characteristics of primed CD45RO+ T cells in the inflamed mucosa of ulcerative colitis. *Scand J Gastroenterol* 2000; **35**: 1278-1283
- 53 **Wu HG**, Chen HP, Shi Z, Hua XG, Zhao C. Clinical study of the treatment of chronic ulcerative colitis with moxibustion. *Int J Clin Acupunct* 1999; **1**: 26-28
- 54 **Wu HG**, Shi Z, Zhou LB, Pan YY, Tan WL. Acupuncture and moxibustion's effect on cytokine of ulcerative colitis rat. *Int J Clin Acupunct* 2000; **3**: 43-48
- 55 **Wu HG**, Zhou LB, Huang C, Pan YY, Chen HP, Shi Z, Hua XG. Gene expression of cytokines in acupuncture and moxibustion treatment for ulcerative colitis in rats. *Huaren Xiaohua Zazhi* 1998; **6**: 853-855
- 56 **Wu HG**, Chen HP, Zhou LB, Pan YY, Huang C, Shi Z. molecule mechanism of acupuncture and moxibustion's therapy effect on ulcerative colitis rat. *Shanghai Zhenjiu Zazhi* 1998; **17**: 30

Edited by Wang XL

Effects of tumor necrosis factor, endothelin and nitric oxide on hyperdynamic circulation of rats with acute and chronic portal hypertension

Ji-Jian Wang, Gen-Wu Gao, Ren-Zhong Gao, Chang-An Liu, Xiong Ding, Zhen-Xiang Yao

Ji-Jian Wang, Gen-Wu Gao, Chang-An Liu, Xiong Ding, Department of General Surgery, Second Affiliated Hospital of Chongqing University of Medical Sciences, Chongqing 400010, China

Ren-Zhong Gao, Department of Emergency, Maroondah Hospital, Melbourne, Australia

Zhen-Xiang Yao, Department of General Surgery, First Affiliated Hospital of Chongqing University of Medical Sciences, Chongqing 400016, China

Supported by Science Foundation of Chongqing Health Bureau, No. 97-09

Correspondence to: Ji-Jian Wang, Department of General Surgery, Second Affiliated Hospital of Chongqing University of Medical Sciences, 74 Linjing Road, Chongqing 400010, China. wangjijian11@hotmail.com

Telephone: +86-23-67764551 **Fax:** +86-23-67652167

Received: 2002-10-30 **Accepted:** 2002-11-25

Abstract

AIM: To evaluate the effect of tumor necrosis factor (TNF), endothelin (ET) and nitric oxide (NO) on hyperdynamic circulation (HC) of rats with acute and chronic portal hypertension (PHT).

METHODS: Chronic portal hypertension was induced in Wistar rats by injection of carbon tetrachloride. After two weeks of cirrhosis formation, L-NMMA (25 mg/kg) was injected into one group of cirrhotic rats via femoral vein and the experiment was begun immediately. Another group of cirrhotic rats was injected with anti-rat TNF α (300 mg/kg) via abdominal cavity twice within 48 h and the experiment was performed 24 h after the second injection. The blood concentrations of TNF α , ET-1 and NO in portal vein and the nitric oxide synthase (NOS) activity in hepatic tissue were determined pre-and post-injection of anti-rat TNF α or L-NMMA. Stroke volume (SV), cardiac output (CO), portal pressure (PP), superior mesenteric artery blood flow (SMA flow) and iliac artery blood flow (IAflow) were measured simultaneously. Acute portal hypertension was established in Wistar rats by partial portal-vein ligation (PVL). The parameters mentioned above were determined at 0.5 h, 24 h, 48 h, 72 h and 120 h after PVL. After the formation of stable PHT, the PVL rats were injected with anti-rat TNF α or L-NMMA according to different groups, the parameters mentioned above were also determined.

RESULTS: In cirrhotic rats, the blood levels of TNF α , NO in portal vein and the liver NOS activity were significantly increased ($P < 0.05$) while the blood level of ET-1 was not statistically different ($P > 0.05$) from the control animals (477.67 \pm 83.81 pg/mL vs 48.87 \pm 32.79 pg/mL, 278.41 \pm 20.11 μ mol/L vs 113.28 \pm 14.51 μ mol/L, 1.81 \pm 0.06 u/mg·prot vs 0.87 \pm 0.03 u/mg·prot and 14.33 \pm 4.42 pg/mL vs 8.72 \pm 0.79 pg/mL, respectively). After injection of anti-rat TNF α , the blood level of TNF α was lower than that in controls (15.17 \pm 18.79 pg/mL vs 48.87 \pm 32.79 pg/mL). The blood level

of NO and the liver NOS activity were significantly decreased, but still higher than those of the controls. The blood level of ET-1 was not significantly changed. PP, SV, CO, SMAflow and IAflow were ameliorated. After injection of L-NMMA, the blood level of NO and the liver NOS activity were recovered to those of the controls. PP and CO were also recovered to those of the controls. SV, SMAflow and IAflow were ameliorated. In PVL rats, the blood levels of TNF α , NO in portal vein and the liver NOS activity were gradually increased and reached the highest levels at 48 h after PVL. The blood level of ET-1 among different staged animals was not significantly different from the control animals. PP among different staged animals (2.4 \pm 0.18 kPa at 0.5 h, 1.56 \pm 0.08 kPa at 24 h, 1.74 \pm 0.1 kPa at 48 h, 2.38 \pm 0.05 kPa at 72 h, 2.39 \pm 0.16 kPa at 120 h) was significantly higher than that in controls (0.9 \pm 0.16 kPa). After injection of anti-rat TNF α in 72 h PVL rats, the blood level of TNF α was lower than that in controls (14 \pm 14 pg/mL vs 48.87 \pm 32.79 pg/mL). The blood level of NO and the liver NOS activity were significantly decreased, but still higher than those of the controls. The blood level of ET-1 was not significantly changed. PP was decreased from 2.38 \pm 0.05 kPa to 1.68 \pm 0.12 kPa, but significantly higher than that in controls. SV, CO, SMAflow and IAflow were ameliorated. After injection of L-NMMA in 72 h PVL rats, the blood level of NO and the liver NOS activity were recovered to those of the controls. PP, SV, CO, SMAflow and IAflow were also recovered to those of the controls.

CONCLUSION: NO plays a critical role in the development and maintenance of HC in acute PHT and is a key factor for maintenance of HC in chronic PHT. TNF α may not participate in the hemodynamic changes of HC directly, while play an indirect role by inducing the production of NO through activating NOS. No evidence that circulating ET-1 plays a role in both models of portal hypertension has been found.

Wang JJ, Gao GW, Gao RZ, Liu CA, Ding X, Yao ZX. Effects of tumor necrosis factor, endothelin and nitric oxide on hyperdynamic circulation of rats with acute and chronic portal hypertension. *World J Gastroenterol* 2004; 10(5): 689-693
<http://www.wjgnet.com/1007-9327/10/689.asp>

INTRODUCTION

Associated with hyperdynamic circulatory syndrome (HCS), the portal hypertension (PHT) is characterized by systemic vasodilatation, increase of plasma volume, cardiac output and regional blood flow^[1-8]. Although it is most likely initiated by vasodilatation resulted from an increase of vasodilator activity^[9], the etiology of HCS is still controversial. Two potent vasodilators, endogenous nitric oxide (NO) and tumor necrosis factor (TNF) may play important roles in the pathogenesis of hemodynamic changes of PHT^[1,10]. As a powerful vasoconstrictor, endothelin (ET) could influence the

pathogenesis of hemodynamic changes of PHT as well^[5,11-15]. Since ET has contradictory effect on blood vessels in comparison with the former two, it is hard to imagine that they synergistically take part in the hemodynamic changes. It is thus necessary to find out what kind of role the three factors play in the pathogenesis of HCS, respectively.

MATERIALS AND METHODS

Reagents

Carbon tetrachloride was purchased from Chongqing Chemical Reagents Factory (Chongqing, China). A rabbit anti-rat TNF α antibody was purchased from PharMingen Company (USA). N^G-methyl-L-arginine (L-NMMA) and endothelin EIA kit were purchased from Cayman Company (USA). Rat TNF α ELISA kit was purchased from Endogen Company (USA). NO and NOS determining kits were purchased from Nanjing Jiancheng Bioengineering Institute (Nanjing, China).

Animal model of acute PHT (aPHT)

Partial portal vein ligation (PVL) was performed to establish the aPHT model as described previously^[10]. In brief, male Wistar rats (220-280 g, offered by the Animal Center of Chongqing University of Medical Sciences) had free access to water and standard rat chow. After fasted overnight, the rats were anesthetized with pentobarbital intra- abdominally at a dose of 60 mg/kg. The portal vein was isolated and two ligatures were placed around both the portal vein and a 16-gauge blunt-end needle. One ligature was placed 1 mm distal to the bifurcation of portal vein and the other ligature was placed 1-2 mm to the input point of splenic vein. The needle was ligated together with the portal vein and immediately removed to allow the portal vein to expand to the limit imposed by the ligature. The abdomen was closed. In sham-operated rats, surgery consisted of dissection and visual inspection of the portal vein without ligation.

Animal model of chronic PHT (cPHT)

Carbon tetrachloride induced cirrhosis was made as the cPHT model. Male Wistar rats (150-200 g, provided by the Animal Center of Chongqing University of Medical Sciences) had free access to standard rat chow and 100mL/L alcohol. Cirrhosis model was established by injection with 600mL/L carbon tetrachloride mixed with paraffin liquid subcutaneously at a dose of 0.3 mL/100g at the lateral abdomen of both sides, twice a week for 17 times. The rats were allowed to stabilize for 2 weeks.

Determination of hemodynamic indexes

Stroke volume (SV) and cardiac output (CO) Ultrasonic probe of HEWLETT PACKARD 5500 type ultrasonic instrument (USA) was placed on the parasternum of rats at the left ventricle long axis and mitral valve level and then exchanged by M type ultrasonic image. The inner computer system of this instrument would calculate and display the data we needed.

Superior mesenteric artery (SMA) and iliac artery (IA) blood flow SMA and IA were isolated and embraced by a cuff of electromagnetic flowmeter (NIHON KH DEN, Japan) respectively. Its blood flow was determined while blood passed a photoelectric sensor.

Portal pressure (PP) and right atrial pressure (RAP) A 7 gauge needle was penetrated into portal vein in the direction of liver and a catheter was inserted through the internal jugular vein into the right atrium and connected to a pressure transducer respectively. PP and RAP were recorded with a four-channel physiometer (NIHON KOHDEN, Japan).

Mean arterial pressure (MAP) Rat's tail was placed in a photoelectric channel and MAP was determined with an RBP-1 type blood pressometer.

Calculation of superior mesenteric artery vascular resistance (VR_{SMA}) and iliac artery vascular resistance (VR_{IA}) VR_{SMA} and VR_{IA} were calculated according to the following formula reported by Colombato *et al*^[16].

$$VR_{SMA}(\text{kPa}/\text{L}\cdot\text{min}) = \frac{MAP-PP}{SMA-flow}$$

$$VR_{IA}(\text{kPa}\cdot/\text{L}\cdot\text{min}) = \frac{MAP-RAP}{IA-flow}$$

Serum levels of TNF α , ET-1 and NO and hepatic activity of NOS

Blood was obtained from the portal vein at the time of sacrifice. Hepatic tissue was obtained from the left lobe of rat's liver. Serum level of TNF α was measured by ELISA according to the manufacturer's instructions (PharMingen Co., USA). Serum samples were analyzed for ET-1 content by EIA according to the manufacturer's instructions (Cayman Co., USA). Serum samples and hepatic tissues were analyzed for NO content and NOS activity according to the manufacturer's instructions by Nanjing Jiancheng Bioengineering Institute (Nanjing, China).

Experimental protocol

The rats involved in this experiment were divided into experimental group, treated group and control group. Fifty aPHT(PVL) rats were divided into five staged subgroups (0.5 h, 24 h, 48 h, 72 h and 120 h after PVL, 10 rats each group) and 10 cPHT rats were used as the experimental group. Twenty cPHT rats and 20 aPHT rats were divided into two groups (10 rats each group) respectively as the treatment group, and the method of treatment was as following. Ten cPHT rats were injected with anti-rat TNF α twice within 48 h and the experiment was performed 24 h after the second injection and 10 aPHT rats were injected with anti-rat TNF α at 0.5 h and 48 h after PVL respectively and the experiment was performed at 72 h after PVL (one dose of 300 μ g/kg, via intra-abdominal cavity). The other 10 aPHT rats and 10 cPHT rats were injected with L-NMMA (25 mg/kg) through femoral vein 72 h after PVL and the experiment was performed immediately. Ten normal rats and 10 sham operated rats were used as the cPHT and the aPHT control groups respectively. The following parameters were determined, namely the hemodynamic indexes, serum levels of TNF α , ET-1 and NO, hepatic NOS activity.

Statistical analysis

Data were expressed as mean \pm SD and analysis of variance was performed using SPSS 8.0 software. Differences between groups were analyzed using *t*-test. One-way analysis of variance was used for multiple comparisons, and Newman-Keuls test was used for intra-group comparisons. *P*<0.05 was considered statistically significant.

RESULTS

Hemodynamic change

In PVL rats, SV, CO, PP, SMAflow and IAflow were significantly increased from 0.16 \pm 0.04 mL/s, 0.058 \pm 0.008 L/min, 0.9 \pm 0.16 kPa, 8.24 \pm 1.16 ml \cdot min⁻¹ and 10 \pm 0.89 ml \cdot min⁻¹ to 0.27 \pm 0.02 mL/s, 0.113 \pm 0.004 L/min, 1.74 \pm 0.1 kPa, 17.58 \pm 0.7 mL/min and 20.42 \pm 1.07 mL/min respectively at 48 h after PVL (*P*<0.05). VR_{SMA} and VR_{IA} were significantly decreased from 15.57 \pm 2.75 kPaL/min and 13.58 \pm 2.19 kPaL/min to 5.96 \pm 0.35 kPaL/min and 5.62 \pm 0.33 kPaL/min respectively at 48 h after PVL (*P*<0.05).

These hemodynamic variables no matter increased or decreased, all reached a maximal level at 72 h after PVL ($P<0.05$) and did not change thereafter ($P>0.05$). In cirrhotic rats, SV, CO, PP, SMAflow and IAflow were significantly increased from 0.162 ± 0.04 mL/s, 0.058 ± 0.017 L/min, 0.91 ± 0.16 kPa, 8.42 ± 1.16 mL/min and 10 ± 0.89 mL/min to 0.59 ± 0.06 mL/s, 0.159 ± 0.031 L/min, 2.26 ± 0.39 kPa, 27 ± 3.19 mL/min and 27.33 ± 1.21 mL/min respectively at the time of cirrhosis formation ($P<0.05$). VR_{SMA} and VR_{IA} were significantly decreased from 15.57 ± 2.74 kPaL/min and 13.58 ± 2.19 kPaL/min to 4.07 ± 0.43 kPaL/min and 4.44 ± 0.13 kPaL/min respectively at the time of cirrhosis formation ($P<0.05$).

Alteration of serum TNF α , ET-1 and NO and hepatic NOS activity

Serum TNF α and NO levels and NOS activity were significantly increased at 24 h compared with those of control ($P<0.05$) and reached a maximal level at 48 h after PVL and did not change thereafter. An increase of serum ET-1 levels was also observed at different time points post PVL, however, all of them did not reach the significant level as compared with control ($P>0.05$). The serum TNF α and NO levels were significantly increased compared with control in cirrhotic rats ($P<0.05$) and their increment was markedly greater than those rats 48 h after PVL ($P<0.05$). The NOS activity was also markedly increased ($P<0.05$) and the serum ET-1 level was slightly increased, but did not reach the significant level ($P>0.05$) compared with control in cirrhotic rats (Table 1).

Effects of anti-rat TNF α and L-NMMA on serum TNF α , ET-1 and NO and hepatic NOS

The serum level of TNF α was markedly decreased and lower than that of controls in both rat models, and the serum level of NO and hepatic NOS activity were significantly decreased,

but still markedly greater than those of controls. Injection of anti-rat TNF α had no effect on the level of ET-1. The serum level of NO and hepatic NOS activity were significantly decreased to the levels of the controls in both rat models after injection of L-NMMA (Table 2).

Table 1 Serum levels of TNF α , ET-1 and NO and hepatic NOS activities in PVL and cPHT rats

Groups	TNF α (pg/min)	ET-1 (pg/min)	NO (μ mol/L)	NOS (u/mg·prot)
Control	48.67 \pm 32.79	8.72 \pm 0.79	113 \pm 15	0.9 \pm 0.03
aPHT				
PVL0.5 h	50 \pm 15	13.4 \pm 2.6	128.64 \pm 18.29	0.86 \pm 0.14
PVL24 h	328 \pm 100 ^{ac}	12.8 \pm 5.7	169.40 \pm 21.07 ^{ac}	1.45 \pm 0.17 ^{ac}
PVL48 h	428 \pm 69 ^a	13.5 \pm 2.6	223.71 \pm 35.44 ^a	1.7 \pm 0.12 ^a
PVL72 h	416 \pm 48 ^a	13.1 \pm 3.2	215.49 \pm 12.75 ^a	1.67 \pm 0.16 ^a
PVL120 h	425 \pm 49 ^a	13.4 \pm 3.5	225.36 \pm 18.66 ^a	1.7 \pm 0.12 ^a
cPHT	477.67 \pm 83.81 ^{ae}	14.33 \pm 4.42	278.41 \pm 20.11 ^{ae}	1.81 \pm 0.06 ^a

^a $P<0.05$ vs control, ^c $P<0.05$ PVL 24 h group compared with PVL 48 h, 72 h, 120 h and cPHT groups respectively, ^e $P<0.05$ cPHT group compared with PVL 48 h, 72 h, 120 h groups respectively.

Effects of anti-rat TNF α and L-NMMA on hemodynamic variables

In both rat models, SV, CO, PP, SMAflow and IAflow were significantly decreased, but were still markedly higher than those of the controls. However, VR_{SMA} and VR_{IA} were significantly increased but still markedly lower than those of the controls after injection of anti-rat TNF α . In PVL rats, SV, CO, PP, SMAflow, IAflow, VR_{SMA} and VR_{IA} were all recovered to the levels of the controls after injection of L-NMMA. In cPHT rats, CO and PP were exclusively recovered to the levels of controls. SV, SMAflow, IAflow, VR_{SMA} and VR_{IA} were markedly increased or decreased, but still significantly different from those of the controls after injection of L-NMMA (Table 3).

Table 2 Effects of anti-rat TNF α and L-NMMA on levels of TNF α , ET-1 and hepatic NO and NOS activity in PVL and cPHT rats

Groups	TNF α (pg/mL)	ET-1 (pg/mL)	NO (μ mol/L)	NOS (u/mg·prot)
Control	48.67 \pm 32.29	8.72 \pm 0.79	113 \pm 15	0.9 \pm 0.03
cPHT	477.67 \pm 83.8 ^{ac}	14.33 \pm 4.42	278.41 \pm 20.11 ^{ac}	1.81 \pm 0.06 ^{ac}
cPHT+anti-rat TNF α	15.17 \pm 18.79 ^a	14.33 \pm 4.42	190.61 \pm 10.9 ^a	1.39 \pm 0.04 ^a
cPHT+L-NMMA	–	–	119.18 \pm 11.51 ^e	4.92 \pm 0.03 ^e
PVL72 h	416 \pm 48 ^{ag}	13.1 \pm 3.2	215.49 \pm 12.75 ^{ag}	1.67 \pm 0.16 ^{ag}
PVL72 h+anti-rat TNF α	14 \pm 14 ^a	13.5 \pm 2.6	178.59 \pm 14.61 ^a	1.34 \pm 0.09 ^a
PVL72 h+L-NMMA	–	–	104.61 \pm 18 ⁱ	0.95 \pm 0.08 ⁱ

^a $P<0.05$ vs control, ^c $P<0.05$ cPHT group compared with cPHT+anti-rat TNF α and cPHT+L-NMMA groups respectively, ^e $P<0.05$ cPHT+anti-rat TNF α compared with cPHT+L-NMMA groups, ^g $P<0.05$ PVL72 h group compared with PVL72 h+anti-rat TNF α and PVL72 h+L-NMMA groups respectively, ⁱ $P<0.05$ PVL72 h+anti-rat TNF α compared with PVL72 h+L-NMMA.

Table 3 Effects of anti-rat TNF α and L-NMMA on hemodynamic variables

Groups	SV (mL/s)	CO (L/min)	PP (kPa)	SMAflow (mL/min)	IAflow (mL/min)	VR_{SMA} (kPa/L·min)	VR_{IA} (kPa/L·min)
Control	0.162 \pm 0.04	0.05 \pm 0.017	0.91 \pm 0.16	8.42 \pm 1.16	10 \pm 0.89	15.57 \pm 2.74	13.58 \pm 2.19
cPHT	0.59 \pm 0.06 ^{ac}	0.159 \pm 0.031 ^{ac}	2.26 \pm 0.34 ^{ac}	27 \pm 3.19 ^{ac}	27.33 \pm 1.21 ^{ac}	4.07 \pm 0.43 ^{ac}	4.44 \pm 0.51 ^{ac}
cPHT+anti-rat TNF α	0.39 \pm 0.08 ^a	0.138 \pm 0.029 ^a	1.53 \pm 0.13 ^a	20.75 \pm 1.92 ^a	24.15 \pm 1.67 ^a	5.56 \pm 0.59 ^a	5.21 \pm 0.51 ^a
cPHT+L-NMMA	0.32 \pm 0.02 ^a	0.076 \pm 0.005 ^e	1.12 \pm 0.08 ^e	12.75 \pm 0.82 ^{ac}	16.08 \pm 0.74 ^{ae}	10.13 \pm 0.26 ^{ac}	8.84 \pm 0.66 ^{ae}
PVL72 h	0.42 \pm 0.03 ^{ag}	0.143 \pm 0.029 ^{ag}	2.38 \pm 0.05 ^{ag}	23.27 \pm 1.52 ^{ag}	25.43 \pm 1.44 ^{ag}	4.44 \pm 0.28 ^{ag}	4.54 \pm 0.32 ^{ag}
PVL72 h+anti-rat TNF α	0.33 \pm 0.02 ^a	0.127 \pm 0.008 ^a	1.68 \pm 0.12 ^a	19.3 \pm 1.1 ^a	20.7 \pm 2 ^a	5.9 \pm 0.1 ^a	6.0 \pm 0.5 ^a
PVL72 h+L-NMMA	0.24 \pm 0.04 ⁱ	0.072 \pm 0.013 ⁱ	0.85 \pm 0.15 ⁱ	9.82 \pm 0.96 ⁱ	10.77 \pm 1.11 ⁱ	12.58 \pm 0.93 ⁱ	12.42 \pm 0.99 ⁱ

^a $P<0.05$ vs control, ^c $P<0.05$ cPHT group compared with cPHT+anti-rat TNF α and cPHT+L-NMMA groups respectively, ^e $P<0.05$ cPHT+anti-rat TNF α compared with cPHT+L-NMMA groups, ^g $P<0.05$ PVL 72 h group compared with PVL 72 h+anti-rat TNF α and PVL 72 h+L-NMMA groups respectively, ⁱ $P<0.05$ PVL 72 h+anti-rat TNF α compared with PVL 72 h+L-NMMA.

DISCUSSION

In our study, HCS was observed in rats with acute and chronic PHT, and characterized by the increase of SV, CO, regional blood flow and PP, as well as the decrease of peripheral and splanchnic vascular resistance. This agreed with a lot of literature^[1-8]. Lopez-Talavera *et al*^[9,10] studied the correlation between hemodynamic changes and TNF α on days 5, 13 and 14 after PVL, and found that TNF α might play a role in HCS of portal hypertension. In this study, we found that the serum level of TNF α in portal vein was markedly increased at 24 h, reached a peak at 48 h and maintained stable thereafter in PVL rats. Whereas, the obvious hemodynamic changes occurred at 48 h and HCS was induced at 72 h, about 24 h later than the obvious increase in TNF α level. The serum level of TNF α was much more higher in cPHT rats than that in rats 48 h after PVL. There was no obvious difference between the hemodynamic indexes of both groups. Therefore, we speculated that TNF α might play a role in the early stage of HCS, and that overproduction of TNF α might have a mild effect on hemodynamic changes. In the anti-rat TNF α experiment, we found that the serum level of TNF α was lower than that of the controls and the effect of TNF α was completely inhibited by the injected anti-rat TNF α . Although the hemodynamics was significantly changed, it still had a remarkable difference in comparison with the controls. In other words, HCS was improved and a new HCS balanced on a lower basis formed. At the same time, the NO levels and hepatic NOS activity in rats with hepatic cirrhosis and PVL were decreased by 20-25% and 15-30%, respectively. Kaviani *et al*^[17] revealed that after gastric strips from PVL rats were incubated with TNF α neutralizing antibody, inducible NOS mRNA expression was significantly decreased by 40%, 70%, and 80% after 1, 2, and 6 h. This suggested that the vasoactive effect of TNF α itself on the development and formation of HCS in portal hypertension was little, and that corresponding hemodynamic changes after injection of TNF α antibody were due to the elimination of TNF α activation on NOS and the decreased production of NO. This conclusion disagreed with the report of Lopez-Talavera *et al*^[9] that anti-rat TNF α treatment of rats after PVL significantly inhibited hyperdynamic circulation and reduced portal pressure. It was also inconsistent with the report of Munoz *et al*^[18]. In their experiment, anti-TNF α polyclonal antibodies were injected into rats before and 4 days after portal vein stenosis (PVS) (short-term inhibition) and at 24 h and 4, 7, 10 d after PVS (long-term inhibition). After a short-term inhibition or a long-term inhibition, portal pressure kept unchanged. Tabrizchi^[19] found that cardiac output, blood pressure and mean circulatory filling pressure were significantly reduced, but the arterial resistance increased following treatment with TNF α in anaesthetized rats. This, obviously, did not accord with the features of HCS at PHT, and also suggested that TNF α did not directly take part in the hemodynamic changes at PHT.

In our study, we found the serum NO level and hepatic NOS activity in the two animal models with portal hypertension were decreased by 20-25% and 15-30% respectively after injection of anti-rat TNF α antibody. This suggested that the increase of serum NO level was stimulated by the combination of TNF α and other media such as IL-6 and INF α , *etc.*, which agreed with what was reported^[10,20,21]. Wiest *et al*^[21] reported that upregulation of eNOS release and increase of NO by SMA endothelium occurred before the development of hyperdynamic splanchnic circulation, suggesting a primary role of NO in the pathogenesis of arterial vasodilatation. But the results reported by Albornoz *et al*^[22] disagreed with those of ours. Their results showed that dexamethasone (an inhibitor of the expression of the iNOS) administration did not modify

systemic and splanchnic hemodynamic parameters in endotoxemic cirrhotic rats and suggested that stimulation of iNOS might not play a role in increasing NO production in portal hypertension. We found that the NO level in portal vein and the liver NOS activity were significantly decreased to the level of controls by injecting L-NMMA in cirrhotic rats and in rats 72 h after PVL. In PVL rats, the hemodynamics was recovered to the controls. In cirrhotic rats, the PP was also recovered to the control. But the SV was still significantly greater than that of control and the systemic vasodilatation was not recovered to the state of control. These results suggested that NO played a critical role in the development and maintenance of HCS in acute PHT and was a key factor in maintenance of HCS in chronic PHT. This conclusion was consistent with those of most authors^[1,5-7,23-26]. In patients with chronic portal vein hypertension, since the tissue structure of vascular wall was changed due to the long term dilatation of systemic blood vessels, the dilated blood vessels would be hard to recover, even if the effect of vasodilators had been completely eliminated.

Elevated ET-1 level in blood and its active role in portal hypertension in cirrhotic patients and a variety of animal models have been reported by many authors^[13-16,27-29]. Nevertheless, Poo *et al*^[30] reported that the liver paracrine ET system did not play a major role in the pathogenesis of portal hypertension, but took part in the development of liver fibrogenesis. Varagic *et al*^[31] reported that circulating endothelin-1 did not play a role in spontaneously hypertensive rats. In this study, the blood level of ET-1 in portal vein was mildly increased but not significantly higher in comparison with the controls in cirrhotic and PVL rats. This finding suggested that ET-1 might not play a role in the development of hemodynamic abnormalities in PHT. It might keep the tension of blood vessels and antagonize the effect of vasodilators. Therefore, ET-1 may have a regulating effect on the vasodilatation and vascular refilling. Our finding was consistent with Poo *et al*^[30], but inconsistent with the other authors^[12-15,27-29].

Based on the result of a combination study of TNF α , NO and ET, we draw a conclusion that TNF α may not directly participate in the hemodynamic changes of HCS, while exert an indirect effect by inducing the production of NO. NO is the primary factor for forming and maintaining HCS at PHT. ET does not directly take part in the hemodynamic changes of PHT either, while keeps the tension of blood vessel and prevents it from overdilating under the effect of vasodilatation factors.

REFERENCES

- Huang YQ, Xiao SD, Zhang DZ, Mo JZ. Nitric oxide synthase distribution in esophageal mucosa and hemodynamic changes in rats with cirrhosis. *World J Gastroenterol* 1999; **5**: 213-216
- Trevisani F, Sica G, Mainqua P, Santese G, Notariis SD, Caraceni P, Domenicali M, Zaca F, Grazi GL, Mazziotti A, Cavallari A, Bernardi M. Autonomic dysfunction and hyperdynamic circulation in cirrhosis with ascites. *Hepatology* 1999; **30**: 1387-1392
- Zhu JY, Leng XS, Wang D, Du RY. Effects of somatostatin on splanchnic hemodynamics in cirrhotic patients with portal hypertension. *World J Gastroenterol* 2000; **6**: 143-144
- Lebrec D, Moreau R. Pathogenesis of portal hypertension. *Eur J Gastroenterol Hepatol* 2001; **13**: 309-311
- Tsugawa K, Hashizume M, Migou S, Kishihara F, Kawnaka H, Tomikawa M, Tanoue K, Sugimachi K. Role of nitric oxide and endothelin-1 in a portal hypertensive rat model. *Scand J Gastroenterol* 2000; **35**: 1097-1105
- Howe LM, Boothe DM, Slater MR, Boothe HW, Wilkie S. Nitric oxide generation in a rat model of acute portal hypertension. *Am J Vet Res* 2000; **61**: 1173-1177
- Bi XJ, Chen MH, Wang JH, Chen J. Effect of endotoxin on portal hemodynamic in rats. *World J Gastroenterol* 2002; **8**: 528-530

- 8 **Moller S**, Bendtsen F, Henriksen JH. Splanchnic and systemic hemodynamic derangement in decompensated cirrhosis. *Can J Gastroenterol* 2001; **15**: 94-106
- 9 **Lopez-Talavera JC**, Merrill WW, Groszmann RJ. Tumor necrosis factor α : a major contributor to the hyperdynamic circulation in prehepatic portal-hypertensive rats. *Gastroenterology* 1995; **108**: 761-767
- 10 **Lopez-Talavera JC**, Cadelina G, Olchowski J, Merrill W, Groszmann RJ. Thalidomide inhibits tumor necrosis factor α , decreases nitric oxide synthesis, and ameliorates the hyperdynamic circulatory syndrome in portal-hypertensive rats. *Hepatology* 1996; **23**: 1616-1621
- 11 **Liu F**, Li JX, Li CM, Leng XS. Plasma endothelin in patients with endotoxemia and dynamic comparison between vasoconstrictor and vasodilator in cirrhotic patients. *World J Gastroenterol* 2001; **7**: 126-127
- 12 **Chan CC**, Wang SS, Lee FY, Chang FY, Lin HC, Chu CJ, Chen CT, Huang HC, Lee SD. Endothelin-1 induces vasoconstriction on portal-systemic collaterals of portal hypertensive rats. *Hepatology* 2001; **33**: 816-820
- 13 **Nagasue N**, Dhra DK, Yamanoi A, Emi Y, Udagawa J, Yamamoto A, Tachibana M, Kubota H, Kohno H, Harada T. Production and release of endothelin-1 from the gut and spleen in portal hypertension due to cirrhosis. *Hepatology* 2000; **31**: 1107-1114
- 14 **Gottardi AD**, Shaw S, Sagesser H, Reichen J. Type A, but not type B, endothelin receptor antagonists significantly decrease portal pressure in portal hypertensive rats. *J Hepatol* 2000; **33**: 733-737
- 15 **Yokoyama Y**, Wawrzyniak A, Baveja R, Sonin N, Clemens MG, Zhang JX. Altered endothelin receptor expression in prehepatic portal hypertension predisposes the liver to microcirculatory dysfunction in rats. *J Hepatol* 2001; **35**: 29-36
- 16 **Colombato LA**, Albillos A, Groszmann RJ. Temporal relationship of peripheral vasodilatation, plasma volume expansion and the hyperdynamic circulatory state in portal-hypertensive rats. *Hepatology* 1991; **15**: 323-328
- 17 **Kaviani A**, Ohta M, Itani R, Sander F, Tarnawski AS, Sarfeh II. Tumor necrosis factor-alpha regulates inducible nitric oxide synthase gene expression in the portal hypertensive gastric mucosa of the rat. *J Gastrointest Surg* 1997; **1**: 371-376
- 18 **Munoz J**, Albillos A, Perez-Paramo M, Rossi I, Alvarez-Mon M. Factors mediating the hemodynamic effects of tumor necrosis factor-alpha in portal hypertensive rats. *Am J Physiol* 1999; **276**(3 Pt 1): G687-693
- 19 **Tabrizchi R**. The influence of tumour necrosis factor-alpha on the cardiovascular system of anaesthetized rats. *Naunyn Schmiedebergs Arch Pharmacol* 2001; **363**: 307-321
- 20 **Zhang GL**, Wang YH, Teng HL, Lin ZB. Effects of aminoguanidine on nitric oxide production induced by inflammatory cytokines and endotoxin in cultured rat hepatocytes. *World J Gastroenterol* 2001; **7**: 331-334
- 21 **Wiest R**, Shah V, Sessa WC, Groszmann RJ. NO overproduction by eNOS precedes hyperdynamic splanchnic circulation in portal hypertensive rats. *Am J Physiol* 1999; **276**(4 Pt 1): G1043-1051
- 22 **Albormoz L**, Bandi JC, de las Heras M, Mastai R. Dexamethasone, an inhibitor of the expression of inducible nitric oxide synthase, does not modify the hyperdynamic state in cirrhotic rats. *Medicina* 2000; **60**: 477-481
- 23 **Chen YM**, Qian ZM, Zhang J, Chang YZ, Duan XL. Distribution of constitutive nitric oxide synthase in the jejunum of adult rat. *World J Gastroenterol* 2002; **8**: 537-539
- 24 **Wolfard A**, Kaszaki J, Szabo C, Balogh Z, Nagy S. Effects of selective nitric oxide synthase inhibition in hyperdynamic endotoxemia in dogs. *Eur Surg Res* 1999; **31**: 314-323
- 25 **Pateron D**, Tazi KA, Sogni P, Heller J, Chagneau C, Poirel O, Philippe M, Moreau R, Lebrec D. Role of aortic nitric oxide synthase 3(eNOS) in the systemic vasodilation of portal hypertension. *Gastroenterology* 2000; **119**: 196-200
- 26 **Villa GL**, Barletta G, Pantaleo P, Bene RD, Vizzutti F, Vecchiarino S, Masini E, Perfetto F, Tarquini R, Gentilini P, Laffi G. Hemodynamic, renal, and endocrine effects of acute inhibition of nitric oxide synthase in compensated cirrhosis. *Hepatology* 2001; **34**: 19-27
- 27 **Kojima H**, Yamao J, Tsujimoto T, Uemura M, Takaya A, Fukui H. Mixed endothelin receptor antagonist, SB209670, decreases portal pressure in biliary cirrhotic rats *in vivo* by reducing portal venous system resistance. *J Hepatol* 2000; **32**: 43-50
- 28 **Kojima H**, Sakurai S, Kuriyama S, Yoshiji H, Imazu H, Uemura M, Nakatani Y, Yamao J, Fukui H. Endothelin-1 plays a major role in portal hypertension of biliary cirrhotic rats through endothelin receptor subtype B together with subtype A *in vivo*. *J Hepatol* 2001; **34**: 805-811
- 29 **Taddei S**, Virdis A, Ghiadoni L, Salvetti A. Vascular effects of endothelin-1 in essential hypertension: relationship with cyclooxygenase-derived endothelium-dependent contracting factors and nitric oxide. *J Cardiovasc Pharmacol* 2000; **35**(4 Suppl 2): S37-40
- 30 **Poo JL**, Jimenez W, Maria Munoz R, Bosch-Marce M, Bordas N, Morales-Ruis M, Perez M, Deulofeu R, Sole M, Arroyo V, Rodes J. Chronic blockade of endothelin receptors in cirrhotic rats: hepatic and hemodynamic effects. *Gastroenterology* 1999; **116**: 161-167
- 31 **Varagic J**, Jerkic M, Jovicic D, Nastic-Miric D, Adanja-Grujic G, Markovic-Lipkovski J, Lackovic V, Radujkovic-Kuburovic G, Kentera D. Regional hemodynamics after chronic nitric oxide inhibition in spontaneously hypertensive rats. *Am J Med Sci* 2000; **320**: 171-176

Protective effect of taurine on hypochlorous acid toxicity to nuclear nucleoside triphosphatase in isolated nuclei from rat liver

Ju-Xiang Li, Yong-Zheng Pang, Chao-Shu Tang, Zai-Quan Li

Ju-Xiang Li, Department of Physiology and Pathophysiology, Health Science Center, Peking University, Beijing 100083, China

Yong-Zheng Pang, Chao-Shu Tang, Institute of Cardiovascular Research, First Hospital, Peking University, Beijing 100034, China

Zai-Quan Li, Department of Biochemistry and Molecular Biology, Health Science Center, Peking University, Beijing 100083, China

Supported by the Major State Basic Research Development Program of People's Republic of China, No. G2000056905 and the National Natural Science Foundation of China, No. 30070308

Correspondence to: Zai-Quan Li, Department of Biochemistry and Molecular Biology, Health Science Center, Peking University, Beijing 100083, China. lizaiquan@bjmu.edu.cn

Telephone: +86-10-82801631 **Fax:** +86-10-66176255

Received: 2003-06-21 **Accepted:** 2003-08-16

Abstract

AIM: Taurine has been shown to be an effective scavenger of hypochlorous acid (HOCl). The role of HOCl is well established in tissue damage associated with inflammation and injury. In the present study, the effect of HOCl on nuclear nucleoside triphosphatase of hepatocytes and the ability of taurine to prevent this effect were investigated.

METHODS: Isolated hepatic nuclei from rat liver were exposed to HOCl with or without taurine. The NTPase activity on nuclear envelope was assayed using ATP and GTP as substrates, respectively.

RESULTS: The first series of experiments evaluated the toxicity of HOCl and the efficacy of taurine to protect NTPase. HOCl at 10^{-9} - 5×10^{-6} mol/L reduced nuclear NTPase activities in a concentration dependent manner (ATP and GTP as substrates) ($P < 0.01$). HOCl at 10^{-6} mol/L reduced the NTPase activity by 65% (ATP as substrate) and 76% (GTP as substrate). Taurine (10^{-7} to 10^{-4} mol/L) was tested for protection against HOCl at 10^{-6} mol/L and the nuclei treated with 5×10^{-4} mol/L taurine exhibited only 20% and 12% reduction in NTPase activities compared to untreated controls. A second study was performed comparing taurine to glutathione (GSH). GSH and HOCl at 10^{-6} mol/L exhibited 46% and 67.4% reduction in NTPase activities compared with control. GSH (10^{-4} mol/L) which was incubated with the nuclei and HOCl still exhibited 44.2% and 44.8% reduction in NTPase activities of untreated control. Taurine with HOCl only exhibited 15.2% and 17.1% reduction in NTPase activities, which provided more powerful protection against HOCl than GSH. The third experiment was undertaken to evaluate the specificity of taurine against HOCl. Incubation of rat hepatic nuclei with $\text{Fe}^{3+}/\text{H}_2\text{O}_2$ (1 m mol/L vs 5μ mol/L) resulted in a decrease in nuclear NTPase activities ($P < 0.01$). When hepatic nuclei were incubated with Tau (10^{-4} mol/L) and $\text{Fe}^{3+}/\text{H}_2\text{O}_2$ (1 m mol/L vs 5μ mol/L), nuclear NTPase activities were only slightly increased as compared with that of incubation with $\text{Fe}^{3+}/\text{H}_2\text{O}_2$ alone. However, GSH failed to alter the NTPase activities induced by $\text{Fe}^{3+}/\text{H}_2\text{O}_2$.

CONCLUSION: The present findings indicate that HOCl

can act as an inhibitor of nuclear NTPase. Taurine can antagonistically reduce the toxicity of HOCl to NTPase.

Li JX, Pang YZ, Tang CS, Li ZQ. Protective effect of taurine on hypochlorous acid toxicity to nuclear nucleoside triphosphatase in isolated nuclei from rat liver. *World J Gastroenterol* 2004; 10(5): 694-698

<http://www.wjgnet.com/1007-9327/10/694.asp>

INTRODUCTION

The mechanism of mRNA transport involves two major steps: the recognition of RNA molecules to be transported and their transfer through the nuclear pore. The latter step is an important rate-limiting step in protein expression^[1]. The nucleocytoplasmic transport of mRNA is an energy-consuming process. The energy requirement is associated with the functioning of a nucleoside triphosphatase (NTPase). The nuclear NTPase activity exhibits a broad substrate specificity toward nucleotides and divalent metal cations^[2,3]. The recent data demonstrated that the activity of the NTPase was strikingly inhibited by cholesterol oxidase treatment, which indicated that oxidation of nuclear membrane cholesterol could inhibit NTPase activity^[4]. These results have implications for mRNA flux across the nuclear membrane during conditions where lipid peroxidation may be expected.

Hypochlorous acid (HOCl) is a major oxidant produced by neutrophils and monocytes, via the myeloperoxidase-catalyzed oxidation of chloride by hydrogen peroxide^[5]. HOCl is a potent oxidant capable of damaging host tissue during inflammation. The strong oxidizing species HOCl plays a highly significant role in the bactericidal function of the neutrophil. However, inappropriate and/or excessive activation of neutrophils leads to oxidative stress and collateral damage to surrounding tissues. Cysteine and methionine residues in proteins and reduced glutathione (GSH) appear to be the main targets for HOCl^[6], thereby altering the structure and function of proteins and lowering antioxidant status in the cell. In the literature, taurine, a 2-amino ethanesulfonic acid, is characterized as an antioxidant, a membrane protector, or a regulator of calcium ion homeostasis. It is the major free intracellular amino acid that presents in many tissues^[7,8] and possibly acts physiologically as a trap for HOCl^[8]. In the present study, we explored the possible action of HOCl on hepatic nuclear NTPase activity and the protective effect of taurine on the changes of NTPase activity induced by HOCl.

MATERIALS AND METHODS

Materials

Male Sprague-Dawley (SD) rats were supplied by the Animal Center, Health-Science Center, Peking University. Taurine and GSH were purchased from Sigma Chemical Co (St. Louis, MO, USA). The term HOCl was used to cover the equilibrium mixture with OCl⁻ present at neutral pH. The following reagents were freshly prepared. Phenylmethylsulfonyl fluoride (PMSF), sodium salt of nucleotides (ATP and GTP); DS/PMSF buffer

(mmol/L): 250 sucrose, 50 Tris/HCl pH 7.4, 5 MgCl₂, 1 PMSF; STM/ Buffer (mmol/L): 2 100 sucrose, 50 Tris/HCl pH 7.4, 5 MgCl₂, 1 PMSF, 1 EDTA, 1 DTT, and 1 μmol/L leupeptin. All the reagents were analytically pure.

Isolation of rat hepatocytes

Rat hepatocytes were isolated according to Berry and Friend methods^[9]. Briefly, under anesthesia with urethane (1 g/kg *i.p.*), male SD rats (220–250 g) were in situ liver-perfused at 37 °C via portal vein, with Ca²⁺-free Hanks' solution containing 5 mg/L collagenase and 1 mg·L⁻¹ hyaluronidase bubbling of 950 ml/L O₂-50 ml/L CO₂. After 20 min perfusion, the liver was removed, transferred to a beaker containing 200 mL of enzyme medium, broken up with a blunt spatula, and shaken at 37 °C for 15 min in an atmosphere of air. The suspension was filtered through nylon mesh and the cells were separated from debris by centrifuging at 50 g for 2 min. The cells were resuspended in Hanks' solution at 4 °C. Cell viability tested by trypan blue exclusion was higher than 90%.

Isolation and characterization of hepatic nuclei

Isolation of rat liver nuclei was performed according to the method described by Kaufmann *et al.*^[10] with modification. Suspended cells were homogenized in Teflon (10 strokes), sedimented at 800 *r/min* for 10 min. The nuclei were suspended in DS/PMSF buffer, layered over cushions of this buffer, and sedimented at 70 000 *g* for 60 min. Isolated nuclei were resuspended in STM/PMSF buffer, again layered over cushions of DS/PMSF buffer, and sedimented at 70 000 *g* for 30 min. The final pellet was resuspended with STM/PMSF to 1 mg protein/mL, and stored at -70 °C.

Nuclear membrane NADH pyrophosphorylase activity and microsome- NADPH cytochrome-C reductase activity were determined to test the purification of the freshly isolated hepatocyte nuclei.

Protocol for treatment of isolated nuclei with hypochlorous acid and taurine

Isolated purified nuclei (0.25 mL) were incubated with different chemicals (dissolved in 0.25 mL) for 10 min at 30 °C. The reaction was stopped by cold (4 °C) centrifugation on microcentrifuge for 2 min, and the nuclei pellet was washed once and then resuspended in STM/PMSF to obtain a final protein concentration of 1 mg/mL.

Protocol 1: incubation with buffer alone (control) and sodium hypochlorite (10⁻⁹ to 5×10⁻⁶ mol/L), respectively. Protocol 2: Incubation with buffer alone (control), taurine (10⁻⁶, 10⁻⁵ and 10⁻⁴ mol/L), sodium hypochlorite (10⁻⁶ mol/L), sodium hypochlorite (10⁻⁶ mol/L) plus taurine (10⁻⁷ to 10⁻⁴ mol/L), respectively. Protocol 3: Incubation with sodium hypochlorite (10⁻⁶ mol/L), sodium hypochlorite (10⁻⁶ mol/L) plus glutathione (GSH, 10⁻⁶ to 10⁻⁴ mol/L), respectively. Protocol 4: Incubation with buffer alone (control), taurine (10⁻⁴ mol/L), GSH (10⁻⁴ mol/L), H₂O₂/FeSO₄ (1 mmol/L/5 μmol/L), H₂O₂/FeSO₄ (1 mmol/L/5 μmol/L) plus taurine (10⁻⁶ to 10⁻⁴ mol/L), H₂O₂/FeSO₄ (1 mmol/L/5 μmol/L) plus GSH (10⁻⁶ to 10⁻⁴ mol/L), respectively.

Assay of nuclear NTPase activity

NTPase activity was assayed as described by Tiffany^[11] and Ramjiawan^[12] with modification. Nuclear suspension (1 μg protein/μL) was preincubated for 10 min at 30 °C. Addition of 1.0 mmol/L ATP or 1.0 mmol/L GTP initiated the reaction. Ten minutes after 30 °C-incubation, the reaction was stopped by addition of 100g/L SDS and placing the test tube on ice bath, and inorganic phosphate was measured according to the method of Raess^[13], which was expressed as nmol/mgPr per 10 min.

Preliminary experiments showed a linear relationship of NTPase activity with incubation time of nucleoside triphosphate within 30 min. The values were normalized to protein content.

Data analysis

Separated six experiments were performed in duplicate. All results were expressed as mean±SD. Statistical analysis of the data was performed using one-way analysis of variance followed by Student-Newman-Keuls tests. *P*<0.05 was accepted as statistically significant.

RESULTS

Characterization of hepatic nuclei

The level of NADH pyrophosphorylase activity (as marker enzyme for nuclear envelope) in prepared nuclei from rat hepatocytes was 7-fold that in homogenate of whole cells (25.77±1.26 vs 3.68±0.27 nmol/mg Pr per min, *P*<0.01), but NADPH cytochrome C reductase activity (marker enzyme for microsome) was only 28% of that in hepatocytes homogenate (2.88±0.22 vs 10.27±0.87 nmol/mg Pr per min, *P*<0.01). While the activity of mannose-6-phosphatase existing in both microsomes and nuclei, was 4–5 times that in cell homogenate (412±22 vs 91±6 nmol/mg Pr per min, *P*<0.01). It showed that the isolated hepatic nuclear fraction was of high purity and little contaminated by other organelles.

Inhibitory effect on hepatic nuclear NTPase of hypochlorous acid

HOCl (at mol/L: 10⁻⁹-5×10⁻⁶) could significantly depress NTPase activity of hepatic nuclei in a concentration- dependent manner, regardless ATP or GTP as a substrate (Figure 1). After incubation of hepatic nuclei with 5×10⁻⁶ mol·L⁻¹ HOCl, the hepatic nuclear NTPase activities were decreased by 70.0% (ATP as substrate) and by 76.3% (GTP as substrate), compared with those of control groups (both *P* values less than 0.01) respectively.

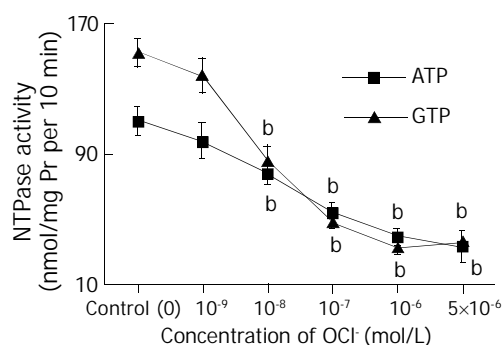


Figure 1 Inhibitory effect of hypochlorous acid on hepatic nuclear NTPase activity. ATP and GTP were used as reaction substrates, respectively. Mean±SD, *n*=6. ^a*P*<0.05, ^b*P*<0.01 compared with control.

Effects of taurine on hepatic nuclear NTPase activity

The effect of taurine on NTPase activity is shown in Table 1. After incubation of hepatic nuclei with different concentrations of taurine (10⁻⁶, 10⁻⁵ and 10⁻⁴ mol/L), the NTPase activities on nuclear envelope were increased in a concentration-dependant fashion, either using ATP or GTP as a substrate (all *P* values <0.05 as compared with those of controls). When taurine was at 10⁻⁴ mol/L, the NTPase activities were increased by 18.1% (ATP as substrate) and 27.3% (GTP as substrate), respectively. All *P* values were less than 0.01 as compared with those of their controls.

Table 1 Effects of taurine on hepatic nuclear NTPase activity

Groups	NTPase activity (nmol/mg Pr per 10 min)	
	ATP as substrate	GTP as substrate
Control	127±7	150±9
Taurine 10 ⁻⁶ mol/L	136±9 (+7.1%)	168±10(+12.0%) ^a
Taurine 10 ⁻⁵ mol/L	148±7 (+16.5%) ^b	179±11(+19.3%) ^b
Taurine 10 ⁻⁴ mol/L	150±8 (+18.1%) ^b	191±12 (±27.3%) ^b

ATP and GTP were used as reaction substrates, respectively. The increases of the enzyme activities are indicated in parentheses as percentage of the control. Mean±SD, *n*=6. ^a*P*<0.05, ^b*P*<0.01 compared with control.

Effect of taurine on OCl⁻-induced inhibition of hepatic nuclear NTPase activity

The abilities of HOCl to depress NTPase were confirmed by detecting NTPase activities. Incubation of hepatic nuclei with HOCl at 10⁻⁶ mol·L⁻¹ resulted in an obviously lower nuclear NTPase activity than that with buffer alone. The hepatic nuclear NTPase activities were decreased by 65.4% (ATP as substrate) and by 76.0% (GTP as substrate), compared with the control groups respectively (*P*<0.01).

The reduction of NTPase activities induced by HOCl was antagonized by taurine (as shown in Figure 2), even at a very low concentration (10⁻⁶ mol/L) (ATP and GTP as substrates). The antagonistic effect of taurine on HOCl was in a concentration dependent manner. When the nuclei were incubated with HOCl (10⁻⁶ mol/L) and taurine (5×10⁻⁴ mol/L), the NTPase activity reached 80.3% (ATP as substrate) and 88.7% of control group (GTP as substrate), respectively (all *P* values less than 0.01).

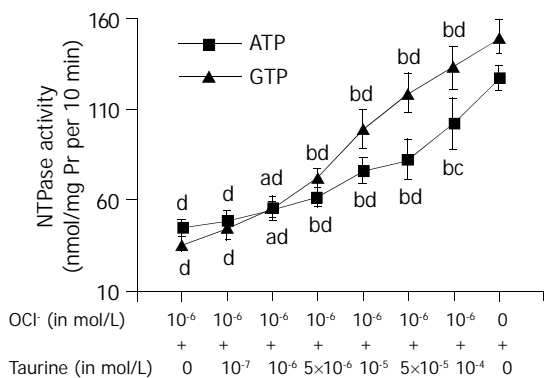


Figure 2 Effect of taurine on OCl⁻-induced inhibition of NTPase activity in hepatic nuclei. ATP and GTP were used as reaction substrates, respectively. Mean±SD, *n*=6. ^a*P*<0.05, ^b*P*<0.01 compared with OCl⁻ (10⁻⁶ mol/L) group. ^c*P*<0.05, ^d*P*<0.01 compared with control.

Effect of glutathione on OCl⁻-induced inhibition of hepatic nuclear NTPase activity

Incubation of hepatic nuclei with HOCl at 10⁻⁶ mol/L resulted in an obviously lower nuclear NTPase activity. The hepatic nuclear NTPase activities were decreased by 51.2% (ATP as substrate) and by 101.3% (GTP as substrate), compared with the control groups respectively (*P*<0.01). The reduction of NTPase activities induced by HOCl was antagonized by taurine (10⁻⁴ mol/L, ATP and GTP as substrates). Incubation of taurine increased the NTPase activity by 92.6% (ATP as substrate) and 154% (GTP as substrate) compared with HOCl incubation (as shown in Figure 3). GSH incubation attenuated the depressive effect of HOCl in a concentration-dependent manner. When the nuclei were incubated with HOCl (10⁻⁴ mol/L

and GSH (10⁻⁴ mol/L), the NTPase activity was increased by 27% (ATP as substrate) and 38.5% (GTP as substrate) of HOCl incubation group, respectively (all *P* values less than 0.01). It was showed that the effect of GSH on HOCl-induced depression of NTPase was smaller than that of taurine (*F* value: 5.3, *P*<0.01).

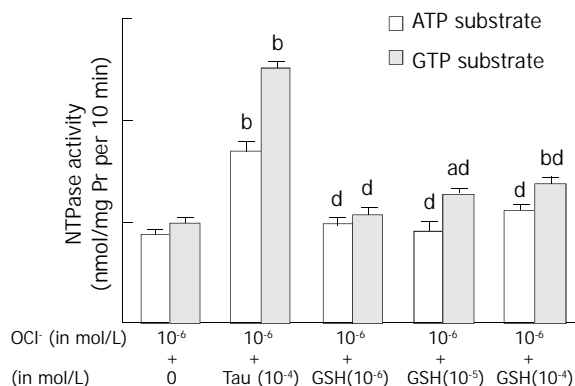


Figure 3 Effects of glutathione on OCl⁻-induced inhibition of NTPase activity in hepatic nuclei. ATP and GTP were used as reaction substrates, respectively. Mean±SD, *n*=6. ^b*P*<0.01 compared with control group (OCl⁻ 10⁻⁶ mol/L). ^a*P*<0.05, ^c*P*<0.01 compared with (10⁻⁶ mol/L OCl⁻+10⁻⁴ mol/L taurine).

Effect of taurine and GSH on ·OH-induced inhibition of hepatic nuclear NTPase activity

The ability of the Fe³⁺-H₂O₂ system to produce ·OH was confirmed by detecting NTPase activities. Incubation of hepatic nuclei with Fe³⁺-H₂O₂ at 1 m mol/L/5 μ mol/L resulted in a lower nuclear NTPase activity as compared with buffer alone. The NTPase activities on nuclear envelopes were decreased by 70% (ATP as substrate) and by 76.7% (GTP as substrate), compared with control group respectively (Table 2).

The reduction of NTPase activities induced by Fe³⁺-H₂O₂ was antagonized by taurine. When taurine was at 10⁻⁴ mol/L (ATP as substrate), the decreases of NTPase activities induced by Fe³⁺-H₂O₂ (1 m mol/L/5 μ mol/L) were slightly reversed (from 29.8±8.2 to 46.5±8.7, *P*<0.05). Whereas, GSH, at all concentrations used in our experiment, had no significant effect on Fe³⁺-H₂O₂-induced depression of NTPase activity (Table 2).

Table 2 Effect of taurine and glutathione on ·OH-induced inhibition of NTPase activity in hepatic nuclei

Groups	NTPase activity (nmol/mg Pr per 10 min)	
	ATP as substrate	GTP as substrate
Control	100.0±9.9	151.8±9.9
Tau (10 ⁻⁴ mol/L)	138±14.6	175.5±5.9
GSH (10 ⁻⁴ mol/L)	95±12.2	150.0±9.8
·OH	29.8±8.2 ^b	35.3±7.8 ^b
·OH+Tau (10 ⁻⁶ mol/L)	35.6±6.1	36.2±8.8
·OH+Tau (10 ⁻⁵ mol/L)	40.8±8.8	32.7±7.3
·OH+Tau (10 ⁻⁴ mol/L)	46.5±8.7 ^a	43.3±7.2
·OH+GSH (10 ⁻⁶ mol/L)	32.0±8.2	43.2±11.8
·OH+GSH (10 ⁻⁵ mol/L)	32.1±9.7	41.2±9.6
·OH+GSH (10 ⁻⁴ mol/L)	44.3±6.2	39.8±5.9

ATP and GTP were used as reaction substrates, respectively. ·OH was produced by Fenton chemistry (Fe³⁺-H₂O₂: 1 m mol/L/5 μ mol/L). Mean±SD, *n*=6. Tau: taurine, GSH: glutathione. ^b*P*<0.01 compared with control group (OCl⁻ 10⁻⁶ mol·L⁻¹). ^a*P*<0.05 compared with ·OH (Fe³⁺-H₂O₂: 1 mmol/L/5 μ mol/L) group.

DISCUSSION

Nuclear NTPase, a nuclear membrane-associated enzyme, provides energy for poly (A)⁺mRNA export through the nuclear pore. Many factors may play a modulatory role in NTPase activity. Extracellular biological active molecules, such as insulin, epidermal growth factor and nuclear membrane cholesterol, could affect NTPase activities through the individual cellular signal transduction system^[14]. In addition, oxygen derived free radicals of nuclear membrane cholesterol could inhibit nucleoside triphosphatase activity^[4]. Thus, export of poly (A) mRNA from the nucleus via the nuclear pore complex was influenced, which plays a crucial role in protein synthesis^[1-3, 14].

In this present study using nuclei purified from rat hepatocytes, HOCl was confirmed to be a very efficient inhibitor of nuclear NTPase activity. Hepatic nuclear NTPase activity was depressed by incubation of hepatic nuclei with HOCl in a concentration dependent manner, regardless of using ATP or GTP as substrate. It was suggested that NTPase was one of the favorite targets of HOCl. The inhibition of this enzyme might probably be caused by oxidation of an amino acid critical for enzyme function. It is difficult to determine the exact concentration of HOCl that can be reached *in vivo* since it is formed locally and HOCl is very reactive. Concentrations of the drugs in the present study were not quite inadequately used. In our experiments, taurine and GSH were present which might repair the oxidative damage to the NTPase. Therefore the inhibition of nuclear NTPase activity *in vitro* was reversible. Furthermore, taurine has been found to be an activator for nuclear NTPase, since it could stimulate hepatic nuclear NTPase activity in a concentration dependent manner. Taurine and thiol group-containing compounds could play a protecting role during inflammatory processes.

The mechanisms of the effect of HOCl were not concerned in the present studies. It has been shown that HOCl is highly reactive with a wide range of biological molecules^[15,16]. Of these, thiols are among the most reactive and crucial targets for oxidation in a cell. The deleterious effects of HOCl could be prevented by incubating the nuclei with thiol group-containing compounds as glutathione in the present study. This was in perfect agreement with Pullar *et al*^[6] who reported that HOCl could react rapidly with thiol groups. The initial product of oxidation of thios by HOCl was sulfenyl chloride^[17]. It could react with additional thiols to give disulfide^[17]. Oxidation of sulfhydryl groups in proteins might affect their functional properties. Formation of protein disulfides, mixed disulfides with GSH, or sulfinic acids could result in changes in enzymatic activity, conformation or affinity toward other molecules. Such changes could contribute to the cell damage caused by oxidative stress^[18].

As an antioxidant, taurine could effectively antagonize the toxic effect of HOCl on NTPase. However, the mechanism of this effect remains unclear. More recent information has revealed that taurine could interact with peroxide anions to form stable products TauCl^[8]. The latter was the product formed through the sequestration of taurine with HOCl and has been found to be an exceptionally stable and long-lived compound with cytoprotective properties due to its ability to preserve cellular function in response to physiologic stress^[7]. In the present study, taurine greatly inhibited the suppression of hepatic nuclear NTPase activity induced by OCl⁻, indicating the important protective role of taurine against OCl⁻ attack.

It has been found that oxygen free radical species such as H₂O₂ and O₂ are produced in mammalian cells during normal aerobic metabolism^[19,20]. However, O₂ or H₂O₂ dose not directly act under physiologically relevant conditions. It has been proposed that much of the toxicity of these species in living

organisms be due to the iron-dependent generation of ·OH, and /or other powerful oxidants, by Fenton chemistry^[21]. Once it oxidizes Fe²⁺, the reactive ·OH is produced. Incubation of hepatic nuclei with Fe³⁺-H₂O₂ in the present study resulted in the decrease of NTPase activities in a concentration dependent manner both using ATP and GTP as substrates, which was coincident with that of Ramjiawan's work^[4]. The results of this *in vitro* study demonstrated that neither taurine nor GSH could directly prevent the reduction of nuclear NTPase activity caused by the ·OH producing Fe³⁺/H₂O₂ system, even if very high concentrations of them (10⁻⁴ mol·L⁻¹) were used regardless of using ATP or GTP as substrate. These results therefore suggested that taurine could protect NTPase from HOCl specifically.

It has been found that HOCl is produced under aerobic and pathophysiological conditions such as oxidative stress and inflammation^[22]. Under most circumstances, HOCl is likely to be the major strong oxidant produced by neutrophils, and contributors to oxidative damages associated with a variety of diseases in which inflammatory cells participate^[23]. Impairment of NTPase on hepatic nuclei by HOCl might result in default of RNA nucleocytoplasmic transport. Taurine could antagonize the toxic effect of HOCl on NTPase. This observation could be a part of the global machinery, which acts as a cytoprotective factor in liver inflammation and oxygen stress.

In summary, our results showed that HOCl could cause a decrease in nuclear NTPase activities, which was most likely the result of decreased breakdown of NTPase. This pointed toward HOCl as an inhibitor of this enzyme. Nuclear NTPase can be effectively protected by taurine against HOCl driven oxidative injury, a consequence of direct drug scavenging capacity towards HOCl. Interaction of taurine with HOCl can also protect nuclear NTPase activity. Therefore, taurine treatment would have a beneficial effect on some diseases relating to protein synthesis.

REFERENCES

- 1 **Izaurralde E**, Mattaj IW. RNA export. *Cell* 1995; **81**: 153-159
- 2 **Tomassoni ML**, Amori D, Magni MV. Changes of nuclear membrane lipid composition affect RNA nucleocytoplasmic transport. *Biochem Biophys Res Commun* 1999; **258**: 476-481
- 3 **Agutter PS**. Influence of nucleotides, cations and nucleoside triphosphatase inhibitors on the release of ribonucleic acid from isolated rat liver nuclei. *Biochem J* 1980; **188**: 91-97
- 4 **Ramjiawan B**, Czubryt MP, Massaelli H, Gilchrist JS, Pierce GN. Oxidation of nuclear membrane cholesterol inhibits nucleoside triphosphatase activity. *Free Radic Biol Med* 1997; **23**: 556-562
- 5 **Winterbourn CC**, Vissers MC, Kettle AJ. Myeloperoxidase. *Curr Opin Hematol* 2000; **7**: 53-58
- 6 **Pullar JM**, Winterbourn CC, Vissers MC. Loss of GSH and thiol enzymes in endothelial cells exposed to sublethal concentrations of hypochlorous acid. *Am J Physiol* 1999; **277**(4 Pt 2): H1505-1512
- 7 **Lourenco R**, Camilo ME. Taurine: a conditionally essential amino acid in humans? An overview in health and disease. *Nutr Hosp* 2002; **17**: 262-270
- 8 **Huxtable RJ**. Physiological actions of taurine. *Physiol Rev* 1992; **72**: 101-163
- 9 **Berry MN**, Friend DS. High-yield preparation of isolated rat liver parenchymal cells. *J Cell Biol* 1969; **43**: 506-520
- 10 **Kaufmann SH**, Gibson W, Shaper JH. Characterization of the major polypeptides of the rat liver nuclear envelope. *J Biol Chem* 1983; **258**: 2710-2719
- 11 **Tiffany BR**, White BC, Krause GS. Nuclear-envelope nucleoside triphosphatase kinetics and mRNA transport following brain ischemia and reperfusion. *Ann Emerg Med* 1995; **25**: 809-817
- 12 **Ramjiawan B**, Czubryt MP, Gilchrist JS, Pierce GN. Nuclear membrane cholesterol can modulate nuclear nucleoside triphosphatase

- activity. *J Cell Biochem* 1996; **63**: 442-452
- 13 **Racess BU**, Vincenzi FF. A semi-automated method for the determination of multiple membrane ATPase activities. *J Pharmacol Methods* 1980; **4**: 273-283
- 14 **Schroder HC**, Wenger R, Ugarkovic D, Friese K, Bachmann M, Muller WE. Differential effect of insulin and epidermal growth factor on the mRNA translocation system and transport of specific poly (A+) mRNA and poly (A-) mRNA in isolated nuclei. *Biochemistry* 1990; **29**: 2368-2378
- 15 **Prutz WA**. Hypochlorous acid interactions with thiols, nucleotides, DNA, and other biological substrates. *Arch Biochem Biophys* 1996; **332**: 110-120
- 16 **Prutz WA**, Kissner R, Koppenol WH, Ruegger H. On the irreversible destruction of reduced nicotinamide nucleotides by hypohalous acids. *Arch Biochem Biophys* 2000; **380**: 181-191
- 17 **Peskin AV**, Winterbourn CC. Kinetics of the reactions of hypochlorous acid and amino acid chloramines with thiols, methionine, and ascorbate. *Free Radic Biol Med* 2001; **30**: 572-579
- 18 **Sen CK**, Packer L. Antioxidant and redox regulation of gene transcription. *FASEB J* 1996; **10**: 709-720
- 19 **Jaeschke H**. Mechanisms of oxidant stress-induced acute tissue injury. *Proc Soc Exp Biol Med* 1995; **209**: 104-111
- 20 **Simpkins CO**. Metallothionein in human disease. *Cell Mol Biol* 2000; **46**: 465-488
- 21 **Halliwell B**, Gutteridge JM. Role of free radicals and catalytic metal ions in human disease: an overview. *Methods Enzymol* 1990; **186**: 1-85
- 22 **Bomzon A**, Ljubuncic P. Oxidative stress and vascular smooth muscle cell function in liver disease. *Pharmacol Ther* 2001; **89**: 295-308
- 23 **Winterbourn CC**, Kettle AJ. Biomarkers of myeloperoxidase-derived hypochlorous acid. *Free Radic Biol Med* 2000; **29**: 403-409

Edited by Wang XL Proofread by Zhu LH

Primary hepatocyte culture in collagen gel mixture and collagen sandwich

Ying-Jie Wang, Hong-Ling Liu, Hai-Tao Guo, Hong-Wei Wen, Jun Liu

Ying-Jie Wang, Hong-Ling Liu, Hai-Tao Guo, Hong-Wei Wen, Jun Liu, Institute of Infectious Diseases, Southwest Hospital, Third Military Medical University, Chongqing 400038, China
Supported by the National Natural Science Foundation of China, No. 30027001

Correspondence to: Dr. Ying-Jie Wang, Institute of Infectious Diseases, Southwest Hospital, Third Military Medical University, Chongqing 400038, China. wangyj103@263.net
Telephone: +86-23-68754479-8062
Received: 2003-08-05 **Accepted:** 2003-09-24

Abstract

AIM: To explore the methods of hepatocytes culture in a collagen gel mixture or between double layers of collagen sandwich configuration and to examine the functional and cytomorphological characteristics of cultured hepatocytes.

METHODS: A two-step collagenase perfusion technique was used to isolate the hepatocytes from Wistar rats or newborn Chinese experimental piglets. The isolated hepatocytes were cultured in a collagen gel mixture or between double layers of collagen sandwich configuration respectively. The former was that rat hepatocytes were mixed with type I rat tail collagen solution till gelled, and the medium was added onto the gel. The latter was that swine hepatocytes were seeded on a plate precoated with collagen gel for 24 h, then another layer of collagen gel was overlaid, resulting in a sandwich configuration. The cytomorphological characteristics, albumin secretion, and LDH-release of the hepatocytes cultured in these two models were examined.

RESULTS: Freshly isolated rat hepatocytes were successfully mixed and fixed in collagen gel, and cultured in the gel condition. During the culture period, the urea synthesized and secreted by rat hepatocytes was detected throughout the period. Likewise, newborn experimental piglet hepatocytes were successfully fixed between the double layers of collagen gel, forming a sandwich configuration. Within a week of culture, the albumin secreted by swine hepatocytes was detected by SDS/PAGE analysis. The typical cytomorphological characteristics of the hepatocytes cultured by the above two culture models were found under a phase-contrast microscope. There was little LDH-release during the culture period.

CONCLUSION: Both collagen gel mixture and double layers of collagen sandwich configuration can provide cultural conditions much closer to *in vivo* environment, and are helpful for maintaining specific hepatic functions and cytomorphological characteristics. A collagen gel mixture culture may be more eligible for the study of bioartificial livers.

Wang YJ, Liu HL, Guo HT, Wen HW, Liu J. Primary hepatocyte culture in collagen gel mixture and collagen sandwich. *World J Gastroenterol* 2004; 10(5): 699-702
<http://www.wjgnet.com/1007-9327/10/699.asp>

INTRODUCTION

Isolated and cultured hepatocytes *in vitro* are an important tool for hepatic disease study, and have been extensively used in basic researches of liver disease, pathophysiology, pharmacology and other related subjects^[1-5]. Furthermore, they are a core material of bioartificial liver system which has been developed rapidly in recent years^[6-10]. However, normal culture condition of hepatocytes *in vitro* differs greatly from the environment *in vivo*, and is difficult to maintain the physiological function of hepatocytes, leading to restriction of their extensive uses. Along with the advances in the research of bioartificial liver support system and its related fields, a highly active hepatocyte culture system is urgently required to meet the quality requirement of cultured hepatocytes in these studies^[11-15].

It has been discovered that collagen is one kind of important matrix of hepatocytic basal membrane. Type I rat tail collagen is usually used as a coated material for hepatocyte culture. It promotes attachment and growth of hepatocytes. The effect of culture is much better than that without collagen coating, indicating that collagen matrix might be an important condition for long-term hepatocyte culture^[16-18]. Based on this idea, we performed the collagen mixture culture for rat hepatocytes and the collagen sandwich culture for new-born Chinese experimental piglet hepatocytes, in order to improve the effect of hepatocyte culture, and provide experimental data for bioartificial liver.

MATERIALS AND METHODS

Animal

Wistar rats (both sexes, less than one month old) and newborn Chinese experimental piglets (both sexes, one week old) were provided by the Experimental Animal Center, Third Military Medical University. All studies were performed with the approval of Experimental Animal Committee in our university. The animals were fed under standard conditions and fasted for 4 h before the experiment.

Reagents

Type IV collagenase, type I mouse collagen (collagen VII) and epidermal growth factor (EGF) were purchased from Sigma. DMEM medium, RPMI1640 medium and FBS were from Gibco. Acrylamide, N,N'-methylene-bis-acrylamide, sodium dodecyl sulfate (SDS), Coomassie blue were from Shengong Biothech Company (Shanghai, China).

Cell isolation

Hepatocytes were harvested using a two-step collagenase perfusion technique described previously^[19,20]. Briefly, an animal was anesthetized by pentobarbital sodium (30 mg/kg), followed by sterilizing the skin, opening the abdomen, exposing the portal vein, and heparin sodium (100-150 u) was injected into the portal vein. When the liver was isolated at liver hilus, it was first perfused with calcium and magnesium-free Hank's buffer at 80-100 mL/min for 10-15 min. The liver was then perfused with 0.5g/L collagenase solution at 50-70 mL/min for

10 min. The two perfusion systems were kept at 37-38 °C. After perfusion, the liver capsule was incised. The thick fibrous connective tissue was discarded, and cell suspensions were harvested. The cell suspensions were further digested at 37 °C for 10-15 min in case. When RPMI 1640 medium was used for cessation of digestion, the released cells were filtered through three-layer sterilized gauze and washed via three centrifugations (50 g). The hepatocyte viability greater than 95% as determined by trypan blue exclusion was used for culture.

Collagen mixture gel culture

The collagen mixture consisted of a 4:1 ratio of rats tail collagen and 4× DMEM brought to a pH of 7.2 using 1mol/L NaOH. 1×10^6 isolated rat hepatocytes were mixed with collagen solution and plated in a flask. The height of hepatocyte-collagen mixture was 0.3-0.4 cm. The mixture was incubated in a 37 °C incubator for 2 h until the collagen mixture was gelled, resulting in hepatocyte-collagen mixture gel. After washed 2-3 times with PBS, RPMI1640 medium containing 100mL/L FBS and EFG was added and the cells were cultured in normal conditions. The medium was changed daily and the culture was over on day 9. The normal single layer culture was used as control, the seeding density and medium were the same as collagen gel mixture culture.

Collagen sandwich culture

The collagen solution was prepared as described above, and coated on a 6-well plate. Collagen solution (1.2 mL) was added into each well and incubated in a 37 °C incubator for 2 h until the collagen was gelled. Freshly isolated hepatocytes (10^6) were plated on a 6-well plate precoated with collagen gel and cultured with serum free RPMI 1640. After 24 h, the culture medium was replaced by 1.2 mL/well collagen solution, and incubated in an incubator for 1 h until the collagen was fixed. The hepatocytes were cultured under the above conditions. The medium was changed daily and the culture was over on day 7.

Morphological and functional observations of cultured hepatocytes

Supernatant of the medium was collected every day during the rat hepatocytes-collagen gel culture, and BUN was measured using a biochemical autoanalyzer (Model 7020, Hitach Co., Tokyo, Japan). Twenty-five µl of the supernatant of serum free medium with piglet hepatocyte sandwich culture was harvested on days 1, 2, 5, and 7 respectively, and separated on a 120 g/L SDS-PAGE, resulting in porcine albumin bands. The gel was stained with 5g/L Coomassie blue, and the images were analyzed with the gel documentation-analyzing systems (Gel Doc™ 2000, Bio-Rad, USA). LDH-release in the supernatants of the two kinds of hepatocyte culture media was analyzed by ultraviolet dynamic method. Morphological changes of hepatocytes in both collagen gel mixture and sandwich cultures were observed under a phase-contrast microscope.

RESULTS

Morphology of rat hepatocytes cultured in collagen gel mixture
When freshly isolated hepatocytes were mixed with collagen and seeded on the culture plate, spherical hepatocytes were mixed in a slightly transparent collagen solution. When the collagen solution was gelled, the hepatocytes were uniformly fixed within. After cultured for 24 h, most hepatocytes remained spherical in shape with part of the cells transformed into polygonal shape. The majority of hepatocytes adhered to each other presenting a fascicular growth (Figure 1). After cultured for 48 h, the majority of hepatocytes reconstructed their cellular polarity presenting a typical and even polygonal

morphology. Binuclei were observed in the majority of hepatocytes, the hepatic plate structure was gradually formed, and the boundary between hepatocytes was perfectly clear and bright, illustrating the formation and participation of bile canaliculi (Figure 2). Such cytomorphological characteristics remained till the end of culture. The rat hepatocytes via an ordinary single layer culture quickly sank and attached to the bottom of culture plate after seeding. Their cytomorphology changed from freshly isolated spherical morphology to a monolayer flat polygon. The cells became flat 48-72 h later and gradually lost their typical polygonal characteristic, and eventually, the hepatocytes were in conjunction with each other and grew in patches.

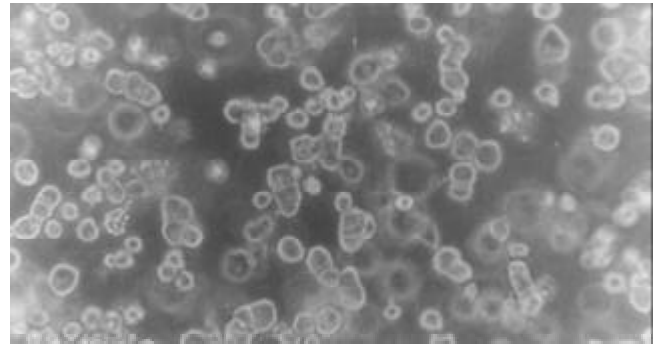


Figure 1 Morphology of rat hepatocytes in collagen gel mixture culture at 24 h (phase-contrast microscope ×200).

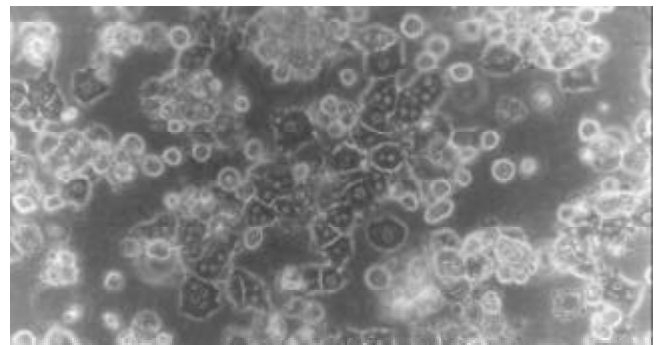


Figure 2 Morphology of rat hepatocytes in collagen gel mixture culture at 72 h (phase-contrast microscope ×200).

Morphological changes of hepatocytes cultured in sandwich configurations

After freshly isolated piglet hepatocytes were seeded on a single layer of collagen gel, the hepatocytes soon attached to the culture plates and their spherical morphology changed quickly to polygonal morphology. After 4 h of culture, the hepatocytes exhibited colonial and fascicular growth, showing typical, uniform polygonal morphology (Figure 3).

Twenty-four hours after overlaying the upper-layer of the gel, the cells still remained polygonal in shape. Over the culture period, polygonal characteristics were much more typical, and showed unique nuclei, most of which were binuclei. Another unique appearance was that the cellular border was clear and bright among the cells, indicating formation of bile canaliculi. The reconstructed hepatocytes had a cellular polarity and a plate-like structure, and maintained their characteristics till the end of culture (Figure 4).

Urea synthesis by rat hepatocytes cultured in collagen gel mixture

Figure 5 shows the BUN level in supernatant of the medium

by dynamic measurement. The BUN level in collagen gel mixture culture group was higher than that in the normal culture group throughout the period, and was significantly higher on d 3, 4, 5, 7 and 8 ($n=5$, $P<0.05$).

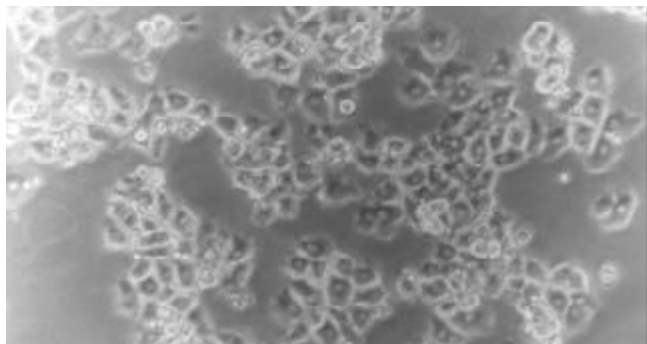


Figure 3 Morphology of piglet hepatocytes cultured on a single layer of collagen gel at 4 h (phase-contrast microscope $\times 200$).

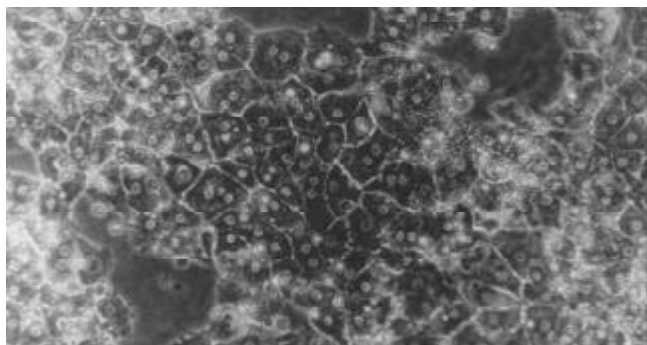


Figure 4 Morphology of piglet hepatocytes cultured in sandwich configurations on d 5 (phase-contrast microscope $\times 200$).

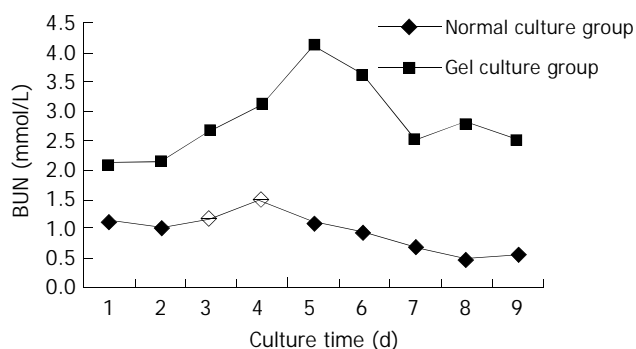


Figure 5 BUN level in supernatant of medium.

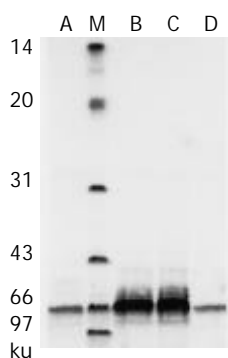


Figure 6 Albumin secretion in cultured piglet hepatocytes by SDS-PAGE analysis. M: Low-range protein molecular weight markers; lanes A, B, C, D are culture media on days 1, 3, 5, 7.

Albumin secretion of piglet hepatocytes

Porcine albumin released from piglet hepatocytes was detected by SDS-PAGE during the procedure of sandwich culture and high rates of urea biosynthesis were maintained throughout this period (Figure 6).

LDH-release

The amount of LDH released from hepatocytes cultured in collagen gel was detected to be an average of 106 ± 17.4 U/L by dynamic measurement in supernatant of the medium. The amount of LDH in supernatant of the medium with sandwich culture fluctuated between 24.8-58.6 U/L, and was not significantly different ($P>0.05$) at various batches. LDH release was declined both in collagen gel mixture and in sandwich culture and remained at a similar low level towards the end of culture.

DISCUSSION

Along with the improvement in the techniques of enzyme-digested hepatocyte isolation in recent years, hepatocyte culture has been applied extensively. However, since the complexity of liver structure and function as well as the existence of specificity of hepatocytes *in vivo*, isolating hepatocytes *in vitro* requires very strict conditions. Monolayer attachment culture model is not suitable for hepatocytes *in vivo*, it only meets the general experimental requirements so far. In order to overcome this difficulty, enormous researches have been carried out to improve the media, supplements, growth factors, matrix or culture methods in hepatocyte culture. A series of methods have been developed, such as specified medium, addition of trace elements, transferrin, insulin, HGF, EGF, coated specific matrix, and the use of microcarrier as well as mixed culture^[21-28]. However, a mature technique meeting the specific requirements of research in bioartificial liver supporting system requires a large scale of high density, high activity, and long-term hepatocyte culture. This has not been developed so far. Therefore, the exploration of hepatocyte culture with high activity becomes an important subject in this research field.

It is known that normal hepatocytes appear as a three dimensional structure arranged in the liver lobules. There exists a complicated connection between hepatocytes, parenchymal-nonparenchymal cells, and hepatocytes-extracellular matrix. Among them, the matrix has been found to play an important role in maintaining hepatocytic functions. A large number of researches have shown that using collagen to fix hepatocytes in the manner of sandwich configuration could create a matrix environment close to that *in vivo*, and availed thus, hepatocytes of growth and their specific function. In this study, freshly isolated hepatocytes from newborn Chinese experimental piglets were cultured between double layers of collagen sandwich configuration, and the hepatocytes were found to have good functions of protein secretion and maintained their cytomorphological characteristics with little LDH-leakage. This illustrated that double layers of collagen sandwich configuration could provide a fairly good cultural and growth condition to piglet hepatocytes with high activity. Even though the double layers of collagen sandwich configuration technique could be used in highly active hepatocyte culture, it is still a monolayer attachment culture, the liver plate so formed is still unlike the normal three dimensional structure of hepatocytes *in vivo*, and also lacks connections with other kinds of cells in the liver. In addition, the cell density is not high, and operation is not convenient, requiring digestion twice. Thereby, the double layers of collagen sandwich technique might not be suitable for the study of bioartificial liver supporting system and hepatocyte transplantation.

Collagen gel mixture is a novel gel immobilizing technique. In this method, the hepatocytes, collagen and medium are mixed and gelled after seeding. The medium was added on its top. Our study showed that rat hepatocytes cultured by such a method could uniformly mix in collagen gel, showing high-density and a three dimensional structural characteristic. During the culture period, the urea synthesizing ability of rat hepatocytes cultured by collagen gel mixture was obviously superior to that of hepatocytes cultured ordinarily and the LDH-release reflecting the hepatocyte activity was close to that of hepatocytes cultured ordinarily. This illustrated that collagen gel mixture could provide fine hepatocytes culture and growth with high density and high activity. The greatest advantage of this culture method is that the structure of cultured hepatocytes is closer to the normal three dimensional hepatocyte structure *in vivo* with the characteristics of high density and more extensive connections between hepatocytes and other cells. Therefore, collagen gel mixture immobilization may become one of the effective methods for hepatocytes culture in the bioartificial liver supporting system.

REFERENCES

- Low-Baselli A**, Hufnagl K, Parzefall W, Schulte-Hermann R, Grasl-Kraupp B. Initiated rat hepatocytes in primary culture: a novel tool to study alterations in growth control during the first stage of carcinogenesis. *Carcinogenesis* 2000; **21**: 79-86
- Hoebe KH**, Witkamp RF, Fink-Gremmels J, Van Miert AS, Monshouwer M. Direct cell-to-cell contact between Kupffer cells and hepatocytes augments endotoxin-induced hepatic injury. *Am J Physiol Gastrointest Liver Physiol* 2001; **280**: G720-728
- Yao XX**, Tang YW, Yao DM, Xiu HM. Effects of Yigan Decoction on proliferation and apoptosis of hepatic stellate cells. *World J Gastroenterol* 2002; **8**: 511-514
- Delmas J**, Schorr O, Jamard C, Gibbs C, Trepo C, Hantz O, Zoulim F. Inhibitory effect of adefovir on viral DNA synthesis and covalently closed circular DNA formation in duck hepatitis B virus-infected hepatocytes *in vivo* and *in vitro*. *Antimicrob Agents Chemother* 2002; **46**: 425-433
- Martin-Aragon S**, de las Heras B, Sanchez-Reus MI, Benedi J. Pharmacological modification of endogenous antioxidant enzymes by ursolic acid on tetrachloride-induced liver damage in rats and primary cultures of rat hepatocytes. *Exp Toxicol Pathol* 2001; **53**: 199-206
- Donato MT**, Castell JV, Gomez-Lechon MJ. Characterization of drug metabolizing activities in pig hepatocytes for use in bioartificial liver devices: comparison with other hepatic cellular models. *J Hepatol* 1999; **31**: 542-549
- Gerlach JC**, Zeilinger K, Sauer IM, Mieder T, Naumann G, Grunwald A, Pless G, Holland G, Mas A, Vienken J, Neuhaus P. Extracorporeal liver support: porcine or human cell based systems? *Int J Artif Organs* 2002; **25**: 1013-1018
- Sauer IM**, Zeilinger K, Obermayer N, Pless G, Grunwald A, Pascher A, Mieder T, Roth S, Goetz M, Kardassis D, Mas A, Neuhaus P, Gerlach JC. Primary human liver cells as source for modular extracorporeal liver support—a preliminary report. *Int J Artif Organs* 2002; **25**: 1001-1005
- Morsiani E**, Brogli M, Galavotti D, Pazzi P, Puviani AC, Azzena GF. Biologic liver support: optimal cell source and mass. *Int J Artif Organs* 2002; **25**: 985-993
- Vilei MT**, Granato A, Ferrareso C, Neri D, Carraro P, Gerunda G, Muraca M. Comparison of pig, human and rat hepatocytes as a source of liver specific metabolic functions in culture systems—implications for use in bioartificial liver devices. *Int J Artif Organs* 2001; **24**: 392-396
- Linti C**, Zipfel A, Schenk M, Dauner M, Doser M, Viebahn R, Becker HD, Planck H. Cultivation of porcine hepatocytes in polyurethane nonwovens as part of a biohybrid liver support system. *Int J Artif Organs* 2002; **25**: 994-1000
- Jasmund I**, Langsch A, Simmoteit R, Bader A. Cultivation of primary porcine hepatocytes in an OXY-HFB for use as a bioartificial liver device. *Biotechnol Prog* 2002; **18**: 839-846
- Nakazawa K**, Ijima H, Fukuda J, Sakiyama R, Yamashita Y, Shimada M, Shirabe K, Tsujita E, Sugimachi K, Funatsu K. Development of a hybrid artificial liver using polyurethane foam/hepatocyte spheroid culture in a preclinical pig experiment. *Int J Artif Organs* 2002; **25**: 51-60
- Yamashita Y**, Shimada M, Tsujita E, Tanaka S, Ijima H, Nakazawa K, Sakiyama R, Fukuda J, Ueda T, Funatsu K, Sugimachi K. Polyurethane foam/spheroid culture system using human hepatoblastoma cell line (Hep G2) as a possible new hybrid artificial liver. *Cell Transplant* 2001; **10**: 717-722
- Yamashita Y**, Shimada M, Tsujita E, Rikimaru T, Ijima H, Nakazawa K, Sakiyama R, Fukuda J, Funatsu K, Sugimachi K. The efficacy of nafamostat mesilate on the performance of a hybrid-artificial liver using a polyurethane foam/porcine hepatocyte spheroid culture system in human plasma. *Int J Artif Organs* 2001; **24**: 34-40
- Nagaki M**, Miki K, Kim YI, Ishiyama H, Hirahara I, Takahashi H, Sugiyama A, Muto Y, Moriwaki H. Development and characterization of a hybrid bioartificial liver using primary hepatocytes entrapped in a basement membrane matrix. *Dig Dis Sci* 2001; **46**: 1046-1056
- Luttringer O**, Theil FP, Lave T, Wernli-Kuratli K, Guentert TW, de Saizieu A. Influence of isolation procedure, extracellular matrix and dexamethasone on the regulation of membrane transporters gene expression in rat hepatocytes. *Biochem Pharmacol* 2002; **64**: 1637-1650
- Hong JT**, Glauert HP. Effect of extracellular matrix on the expression of peroxisome proliferation associated genes in cultured rat hepatocytes. *Toxicol In Vitro* 2000; **14**: 177-184
- Wang YJ**, Li MD, Wang YM, Chen GZ, Lu GD, Tan ZX. Effect of extracorporeal bioartificial liver support system on fulminant hepatic failure rabbits. *World J Gastroenterol* 2000; **6**: 252-254
- Wang YJ**, Li MD, Wang YM, Nie QH, Chen GZ. Experimental study of bioartificial liver with cultured human liver cells. *World J Gastroenterol* 1999; **5**: 135-137
- Zeilinger K**, Sauer IM, Pless G, Strobel C, Rudzitis J, Wang A, Nussler AK, Grebe A, Mao L, Auth SH, Unger J, Neuhaus P, Gerlach JC. Three-dimensional co-culture of primary human liver cells in bioreactors for *in vitro* drug studies: effects of the initial cell quality on the long-term maintenance of hepatocyte-specific functions. *Altern Lab Anim* 2002; **30**: 525-538
- Sakai Y**, Jiang J, Kojima N, Kinoshita T, Miyajima A. Enhanced *in vitro* maturation of fetal mouse liver cells with oncostatin M, nicotinamide, and dimethyl sulfoxide. *Cell Transplant* 2002; **11**: 435-441
- Klein H**, Ullmann S, Drenckhan M, Grimmsmann T, Unthan-Fechner K, Probst I. Differential modulation of insulin actions by dexamethasone: studies in primary cultures of adult rat hepatocytes. *J Hepatol* 2002; **37**: 432-440
- Yamashita Y**, Shimada M, Tsujita E, Shirabe K, Ijima H, Nakazawa K, Sakiyama R, Fukuda J, Funatsu K, Sugimachi K. High metabolic function of primary human and porcine hepatocytes in a polyurethane foam/spheroid culture system in plasma from patients with fulminant hepatic failure. *Cell Transplant* 2002; **11**: 379-384
- Katsura N**, Ikai I, Mitaka T, Shiotani T, Yamanokuchi S, Sugimoto S, Kanazawa A, Terajima H, Mochizuki Y, Yamaoka Y. Long-term culture of primary human hepatocytes with preservation of proliferative capacity and differentiated functions. *J Surg Res* 2002; **106**: 115-123
- Kamiya A**, Kojima N, Kinoshita T, Sakai Y, Miyajima A. Maturation of fetal hepatocytes *in vitro* by extracellular matrices and oncostatin M: induction of tryptophan oxygenase. *Hepatology* 2002; **35**: 1351-1359
- Wang YJ**, Li MD, Wang YM, Ding J, Nie QH. Simplified isolation and spheroidal aggregate culture of rat hepatocytes. *World J Gastroenterol* 1998; **4**: 74-76
- Washizu J**, Berthiaume F, Chan C, Tompkins RG, Toner M, Yarmush ML. Optimization of rat hepatocyte culture in citrated human plasma. *J Surg Res* 2000; **93**: 237-246

Therapeutic effects and molecular mechanisms of anti-fibrosis herbs and selenium on rats with hepatic fibrosis

Yu-Tong He, Dian-Wu Liu, Li-Yu Ding, Qing Li, Yong-Hong Xiao

Yu-Tong He, Dian-Wu Liu, Li-Yu Ding, Qing Li, Yong-Hong Xiao, Department of Epidemiology, Hebei Medical University, Shijiazhuang 050017, Hebei Province, China

Supported by the Natural Science Foundation of Hebei Province, No. 302489

Correspondence to: Dr. Dian-Wu Liu, Department of Epidemiology, Hebei Medical University, Shijiazhuang 050017, Hebei Province, China. liudianw@hebmu.edu.cn

Telephone: +86-311-6265601 **Fax:** +86-311-6265531

Received: 2003-06-05 **Accepted:** 2003-10-12

Abstract

AIM: To study the therapeutic effects of anti-fibrosis herbs and selenium on hepatic fibrosis induced by carbon tetrachloride (CCl₄) in rats and the underlying molecular mechanisms.

METHODS: Fifty-three Wistar rats were randomly divided into: normal control group, model control group, colchicine group, anti-fibrosis herbs group (AF group) and anti-fibrosis herbs plus selenium group (AS group). The last four groups were administered with CCl₄ at the beginning of experiment to induce hepatic fibrosis. Then colchicine, anti-fibrosis herbs and selenium were used to treat them. The normal control group and the model control group were given normal saline at the same time. At the end of the 6th week, rats in each group were sacrificed. Blood and tissue specimens were taken. Serum indicators (ALT, AST, HA, LN) were determined and histopathological changes were graded. Lymphocyte CD₄ and CD₈ were examined by flow cytometry. Expression of TGF- β ₁ and NF- κ B was detected by immunohistochemistry and expression of TGF- β ₁ mRNA was detected by semi-quantified RT-PCR.

RESULTS: Histological grading showed much a smaller degree of hepatic fibrogenesis in AS group and AF group than that in colchicine group and model control group. The serum content of ALT, AST, HA and LN in AF group and AS group were significantly lower than that in colchicine group (ALT: 65.8 \pm 26.5, 67.3 \pm 18.4 and 96.2 \pm 20.9 in AF, AS and colchicine groups respectively; AST: 150.8 \pm 34.0, 154.6 \pm 27.3 and 215.8 \pm 24.6 respectively; HA: 228 \pm 83, 216 \pm 58 and 416 \pm 135 respectively; LN: 85.9 \pm 15.0, 80.6 \pm 18.6 and 106.3 \pm 14.2 respectively) (P <0.05). The level of CD₄ and CD₄/CD₈ ratio in AF group and AS group was significantly higher than those in colchicine group (CD₄: 50.8 \pm 3.8, 52.6 \pm 3.4 and 40.2 \pm 2.1 in AF, AS and colchicine groups respectively; CD₄/CD₈ ratio: 1.45, 1.46 and 1.26, respectively) (P <0.05). The expression level of NF- κ B and TGF- β ₁ in the liver tissues of AF and AS treatment groups was markedly decreased compared with that in colchicine group, and TGF- β ₁ mRNA was also markedly decreased (1.07 \pm 0.31 and 0.98 \pm 0.14 vs 2.34 \pm 0.43, P <0.05).

CONCLUSION: Anti-fibrosis herbs and selenium have beneficial effects on hepatic fibrosis in rats by enhancing immunity and inhibiting NF- κ B and TGF- β ₁ expressions.

He YT, Liu DW, Ding LY, Li Q, Xiao YH. Therapeutic effects and molecular mechanisms of anti-fibrosis herbs and selenium on rats with hepatic fibrosis. *World J Gastroenterol* 2004; 10(5): 703-706

<http://www.wjgnet.com/1007-9327/10/703.asp>

INTRODUCTION

Hepatic fibrosis is a common pathological process of chronic hepatic disease, leading to the development of irreversible cirrhosis^[1-3]. The incidence of hepatitis is high in China^[4-8]. If treated properly at fibrosis stage, cirrhosis could be prevented^[9]. However, there are no effective antifibrosis drugs to date. Chinese herbs, which are well known for their long history of proven therapy of various diseases with low cost and few side effects, have particular potentials in the treatment of hepatic fibrosis^[10-18]. In addition, some studies have indicated that selenium is closely related to the inhibition of hepatic fibrosis^[19,20]. In the present study, we first established a rat model of chronic liver injury - hepatic fibrosis-cirrhosis and then tested the therapeutic effects of Chinese herbs and selenium on hepatic fibrosis. An array of indexes in proteins and mRNA levels were evaluated in order to understand the mechanism underlying the effects observed.

MATERIALS AND METHODS

Reagents

TGF- β ₁ mRNA primers were purchased from Sangon Biological Technology Company, China. Anti-TGF- β ₁ monoclonal antibody and anti-NF- κ B polyclonal antibody were purchased from Santa Cruz Biological Technology Company, USA. Streptomycin avidin peroxidase immunohistochemistry kit for immunohistochemistry and RNA isolation kit were purchased from Boster Biological Technology Ltd, China. Anti-CD₄ and CD₈ polyclonal antibodies were purchased from Caltag Biological Technology Company, USA. Serum activities of aspartate aminotransferase (AST) and alanine aminotransferase (ALT) were determined by the Laboratory Department of 4th affiliated hospital, Hebei Medical University, China. Serum hyaluronic acid (HA) and laminin (LN) concentrations were measured radioimmunologically using a commercial kit (Shanghai Navy Medical Institute, China).

Preparation of Chinese herbs

The anti-fibrosis herbs included *Salvia miltiorrhiza*, *Sparganium stoloniferum*, *Angelica sinensis*, *Amyda sinensis*, *Curcuma aromatica*, *Carex phacota*. These were purchased from Shijiazhuang Lerentang Pharmacy, China. The herbs were boiled with water and extracted by alcohol: put 95% alcohol in liquid of anti-fibrosis herbs, mixed the alcohol and herbs, filtrate the protein and amyllum, then heat the liquid at 90-95 °C to evaporate the remained alcohol.

Establishment of animal model

Wistar rats, half males-half females, weighing 180-200 g were obtained from Experimental Animal Center of Hebei Medical

University, China. The rats were housed 5 heads per cage and subjected to 12 h-d/12 h-night cycle with free access to basic food and water. All animals were treated humanely according to the national guideline for the care of animals in the country.

Hepatic fibrosis was induced in rats by carbon tetrachloride (CCl₄). Wister rats were randomly assigned to normal control group (10), model control group (13), Colchicine group (10), anti-fibrosis herbs group (AF group, 10) and anti-fibrosis herbs plus selenium group (AS group, 10). On the first day of experiment, the rats in model group, colchicine group, AF group and AS group were given hypodermic injection of bean oil solution containing 400g/L CCl₄ (0.5 mL/100 g body mass), followed by injection of the same solution (0.3 mL/100 g body mass) every 4 d. The rats in normal control group received hypodermic injection of bean oil at the same dose and frequency. Fourteen times after CCl₄ administration, 3 rats in model control group were sacrificed to evaluate the liver histological change, which indicated the development of chronic hepatitis. Then colchicine group was given colchicine orally at a dose of 0.01 mg/100 g body weight daily, AF group was given anti-fibrosis herbs (2.11 g/mL) orally at a dose of 0.5 mL/100 g body mass daily, AS group was given orally anti-fibrosis herbs containing sodium selenite (Na₂SeO₃·5H₂O) at 3 µg/mL daily. Normal control group was given saline orally at a dose of 0.5 mL/100 g body mass daily. All the administrations lasted for 6 weeks.

Collection of specimens

At the end of the 6th week of the administration, rats in each group were sacrificed by amobarbital sodium anesthesia. Midline laparotomy was performed. Livers and thymus were excised and blood was collected through cardiopuncture.

Histological grading

Liver tissues were fixed in formalin and embedded in paraffin. Hematoxylin and eosin (HE) staining and Masson staining were performed according to the standard procedure. Histological grade of chronic hepatic fibrosis was determined by a semi-quantitative method based on the criteria described below: grade 0: normal liver, grade 1: few collagen fibrils extended from the central vein and portal tract, grade 2: collagen fibrils extension was apparent but had not yet encompassed the whole lobule, grade 3: collagen fibrils extended into and encompassed the whole lobule, grade 4: diffuse extension of collagen fibrils and pseudo-lobule formed.

Two pathologists who had no knowledge of their sources and each other's assessment examined the stained slide independently.

Flow cytometry of CD₄ and CD₈ positive cells

Sample fluorescence staining was performed using indirect immunofluorescence labeling method. Sample cells were washed in 10 mL Na-azide-PBS and centrifuged. Primary mAb to human CD₄ and CD₈ was added to each tube. The tube was vortexed and incubated at 37 °C for 30 min, 10 mL azide-PBS was added for inactivation and the cells were centrifuged. The supernatant was sucked away. The second antibody of FITC-IgG was added to each tube. The tube was vortexed and incubated in the dark at 37 °C for 30 min. 10 mL azide-PBS was added for inactivation and the cells were centrifuged. The samples were stored at 4 °C in the dark for FACS analysis. The primary antibody and secondary antibody were replaced by 30g/L BSA in azide-PBS as negative controls, the primary antibody was replaced by 30g/L BSA in azide-PBS as the second antibody control. The stained samples were analyzed in a FACS 420 flow cytometer (FACS 420 Fluorescence Activated Cell Sorting, Becton, Dickinson, Sunnyvale, California, USA.) The

light source was a 2W argon ion laser using a wave-length of 488 nm. The working power was 300 mW. Single parameter was measured respectively. Usually, 10 000 cells for each sample were analyzed. The analytic data were processed with a HP-Consort 30 computer. The coefficient of variation of the instrument was adjusted within 5% using PI staining chicken red blood cells.

Immunohistochemistry

Liver samples were formalin-fixed, paraffin-embedded and sectioned serially at 5 µm thickness. Immunohistochemistry was performed as described in streptomycin avidin peroxidase immunohistochemistry kit (Boster). The sections were treated with 30mL/L H₂O₂ methanol at room temperature for 10 min and then washed with PBS for 5 min. After antigen retrieval, nonspecific binding sites were blocked by normal non-immune goat serum. The sections were incubated with primary antibody overnight at 4 °C, secondary antibody at 37 °C for 30 min, and avidin peroxidase at 37 °C for 20 min, followed by DAB visualization. After several washings, the sections were counterstained with hematoxylin. Negative control slides were treated with PBS.

Semi-quantitative PCR

Total RNA was extracted using an RNA isolation kit, and quantity and quality of the RNA extracted were measured on a spectrophotometer. Purified RNA 2 µg and primer Oligo (dT) were used for reverse transcription (Promega). 5 µL reverse transcription template was used for amplification through PCR. The primers were: TGF-β₁, 113 bp: forward: 5' -AGGGCTACCATGCCACTTC-3', reverse: 5' -GCGGCACGCAGCACGGTGAT-3', GAPDH, 299 bp: forward: 5' -GTGAAGGTCTGGAGTCAACG-3', reverse: 5' -GGTGAAGACGCCAGTGGACTC-3'. Amplification conditions included initial denaturation for 5 minutes at 94 °C, 30 cycles of amplification with denaturation at 94 °C for 45 seconds, annealing at 61 °C for 45 s, and extension at 72 °C for 1 min. PCR products were analyzed by agarose gel electrophoresis (15 g/L) and visualized by ethidium bromide staining and ultraviolet illumination. Expression of each TGF-β₁ was scanned by a computer. The obtained values were related to housekeeping gene GAPDH, and the resulting relative ratios were analyzed statistically.

Statistical analysis

Data were analyzed with SPSS software. Quantitative data were presented as mean±SD and compared using one way ANOVA procedure. Frequency data were compared using Ridit procedure.

RESULTS

Anti-fibrosis herbs and anti-fibrosis herbs plus selenium treatment suppressed fibril deposition in and ameliorated liver function of hepatic fibrosis

Specimens from normal control group showed normal structures. Specimens from model control group showed apparent formation of fibrotic septa, encompassing regenerated hepatocytes into pseudo-lobules. Regenerated hepatocytes underwent severe lipid degeneration. Specimens from AF and AS groups showed only mild fibrogenesis without pseudo-lobule formation. Statistical analysis presented significant differences between either AF group or AS group and model control group in histological gradings, indicating that fibrogenesis in both AS and AF groups was much less severe than that in colchicine group and model control group (Table 1).

Serum content of ALT, AST, HA and LN in AF group and AS group was slightly higher than that of normal control

group, but significantly lower than that in model control group ($P<0.05$). Serum content of ALT, AST, HA and LN in AF group and AS group was also lower than that in colchicine group ($P<0.05$). These data confirmed the histological findings that anti-fibrosis herbs and anti-fibrosis herbs plus selenium could inhibit hepatic fibrogenesis and ameliorate liver function (Table 2).

Table 1 Histological grading of hepatic fibrosis

Group	Grade 0	Grade I	Grade II	Grade III	Grade IV
Normal	10	0	0	0	0
Model	0	0	0	0	8 ^c
Colchicine	0	1	3	4	1 ^c
AF	4	3	1	1	0 ^a
AS	3	3	2	1	0 ^{ac}

^a $P<0.05$, vs colchicine group; ^c $P<0.05$, vs normal control group.

Table 2 Serum content of ALT, AST, HA and LN

Group	ALT (u/L)	AST(u/L)	HA(μg/L)	LN (μg/L)
Normal	52.5±9.2 ^a	137.8±18.7 ^a	178±58 ^a	59.8±21.8 ^a
Model	165.6±32.7 ^{acc}	257.4±22.6 ^c	550±68 ^c	130.0±30.5 ^c
Colchicine	96.2±20.9 ^c	215.8±24.6 ^c	416±135 ^c	106.3±14.2 ^c
AF	65.8±26.5 ^a	150.8±34.0 ^a	228±83 ^{ac}	85.9±15.0 ^c
AS	67.3±18.4 ^a	154.6±27.3 ^a	216±58 ^{ac}	80.6±18.6 ^c

^a $P<0.05$, vs colchicine group; ^c $P<0.05$, vs normal control group; ^e $P>0.05$, vs control group.

Anti-fibrosis herbs and anti-fibrosis herbs plus selenium treatment enhanced immunity of rats with hepatic fibrosis

The percentage of CD₄ and CD₈ and the ratio of CD₄ to CD₈ were significantly lower in model control group than that in normal control group. Both AF group and AS group showed a lower percentage of CD₄ and a lower ratio of CD₄ to CD₈ than normal control group. However, these values were significantly higher than those in colchicine group, suggesting that anti-fibrosis herbs and anti-fibrosis herbs plus selenium could enhance the immunity of rats with hepatic fibrosis (Table 3).

Table 3 Content of CD₄ and CD₈ in thymus

Group	Rats	CD ₄ (%)	CD ₈ (%)	CD ₄ /CD ₈
Normal	10	54.1±1.4 ^a	34.1±1.2	1.58
Model	8	40.2±2.1 ^c	31.7±1.3	1.26 ^c
Colchicine	9	42.1±2.0 ^c	32.1±0.9	1.31 ^c
AF	9	50.8±3.8 ^a	34.8±2.1	1.45
AS	9	52.6±3.4 ^a	35.9±2.2	1.46

^a $P<0.05$, vs Colchicine group; ^c $P<0.05$, vs normal control group.

Anti-fibrosis herbs and anti-fibrosis herbs plus selenium treatment reduced TGF-β₁ expression

Positive staining of TGF-β₁ was found at central vein and Disse's areas but not at hepatocytes on sections of normal controls, whereas on sections of model control group, the positive staining was seen at interstitial cells, inflammatory cells, impaired hepatocytes as well as normal hepatocytes. Fibrotic septa were only slightly stained.

Compared with model control group, the staining index of TGF-β₁ in AF and AS groups was markedly decreased ($P<0.05$ in both groups). TGF-β₁ mRNA was detected in normal rat liver, but the expression level was increased significantly in

model control group. Compared with colchicine group, TGF-β₁ level in AF and AS groups was markedly decreased ($P<0.05$, Table 4). Thus, the data at both transcript and protein levels suggested that anti-fibrosis herbs and anti-fibrosis herbs plus selenium could reduce TGF-β₁ expression in hepatic fibrosis.

Table 4 Level of TGF-β₁ mRNA in relation to GAPDH

Group	Rats	Ratio
Normal	10	0.57±0.11
Model	8	2.34±0.43 ^c
Colchicine	9	1.88±0.21 ^c
AF	9	1.07±0.31 ^a
AS	9	0.98±0.21 ^a

^a $P<0.05$, vs Colchicine group; ^c $P<0.05$, vs normal control group.

Anti-fibrosis herbs and anti-fibrosis herbs plus selenium treatment reduced NF-κB expression

Positive staining of NF-κB was not found on sections of normal control group. In model control group, NF-κB was extensively expressed in nuclei of hepatocellular cells. The cells positive for NF-κB were diffusely distributed. After treatment with anti-fibrosis herbs and anti-fibrosis herbs plus selenium, the level of NF-κB staining decreased markedly.

DISCUSSION

Hepatic fibrosis is a common pathological process of chronic hepatic disease, resulting in development of irreversible cirrhosis in patients. In recent years, the mechanism of development of hepatic fibrosis has been partly disclosed^[2,4,5]. If treated properly at fibrosis stage, cirrhosis could be prevented. The present study demonstrated that administration of anti-fibrosis herbs and selenium was effective in treating hepatic fibrosis in rats based on both histological examination and functional analysis. The underlying therapeutic mechanism may involve enhanced immunity and down regulation of the expression of NF-κB and TGF-β₁.

There are various kinds of chronic liver injuries all over the world, causing great affliction to patients. The incidence of hepatitis in China is high. Searches for effective ways to inhibit fibrogenesis and to prevent the development of cirrhosis are of great significance. Although many agents were tested, there have been no satisfactory agents with ascertained effectiveness and few side effects. Colchicine has been commonly used for anti-fibrosis^[21], but its side effect is high and its clinical use is, therefore, limited. Chinese herbs, well known for their wide range of effectiveness and low prices and few side effects, have particular potentials in the treatment of hepatic fibrosis. In this study anti-fibrosis herb treatment for chronic liver injury in rats, prevented hepatic fibrosis from developing of cirrhosis was shown by histological grading. HA and LN have been found to be good serum markers of hepatic fibrogenesis^[22]. We showed that the serum content of HA and LN in AF group and AS group dropped markedly when compared with colchicine group, indicating that anti-fibrosis herb could prevent hepatic fibrogenesis. Anti-fibrosis herb could also enhance the immunity of the body by increasing the percentage of CD₄ and the ratio of CD₄ to CD₈ in AF group, especially in AS group, compared with that in colchicine group.

To understand the mechanism, we evaluated the effect of anti-fibrosis herb treatment on the expression of TGFβ₁ at both the protein and mRNA levels as TGFβ₁ has been considered to be the key cytokine in acceleration of the cirrhotic procession and over expression of this cytokine was closely associated with fibrogenesis in many ways^[23-27]. Our results showed that

both TGF β ₁ and its mRNA expression decreased significantly in AF group and AS group compared with those in control groups, indicating that anti-fibrosis herb down-regulated the expression of this cytokine, which may have contributed to the reduction of fibrosis.

NF- κ B is known to be a family of dimeric transcription factors. It was ubiquitously expressed in non-B cells as an inactive form sequestered in cytoplasm by binding to specific inhibitory proteins termed I- κ B^[28-32]. When cells were stimulated by inducing agents, the I- κ B became phosphorylated, ubiquitinated, and degraded. Degradation of I- κ B could free NF- κ B, which was then translocated into the nucleus, where it activate transcription^[33-35]. NF- κ B/Rel has been shown to be implicated in the inflammatory response and synthesis of adhesion molecules. Furthermore, NF- κ B has been found to be related to cell proliferation and transformation^[36]. Down-regulation of NF- κ B/Rel activity could decrease the transcription of TGF β ₁ to reduce the liver injury.

REFERENCES

- 1 **Missale G**, Ferrari C, Fiaccadori F. Cytokine mediators in acute inflammation and chronic course of viral hepatitis. *Ann Ital Med Int* 1995; **10**: 14-18
- 2 **Wang YJ**, Sun ZQ. Advance in cytology and molecular biology investigation in liver fibrosis. *Xin Xiaohua Bingxue Zazhi* 1994; **2**: 244-246
- 3 **Wang FS**, Wu ZZ. Current situation in studies of gene therapy for liver cirrhosis and liver fibrosis. *Shijie Huaren Xiaohua Zazhi* 2000; **8**: 371-373
- 4 **Zhu YH**, Hu DR, Nie QH, Liu GD, Tan ZX. Study on activation and c-fos, c-jun expression of *in vitro* cultured human hepatic stellate cells. *Shijie Huaren Xiaohua Zazhi* 2000; **8**: 299-302
- 5 **Du WD**, Zhang YE, Zhai WR, Zhou XM. Dynamic changes of type I, III and IV collagen synthesis and distribution of collagen-producing cells in carbon tetrachloride-induced rat liver fibrosis. *World J Gastroenterol* 1999; **5**: 397-403
- 6 **Huang ZG**, Zhai WR, Zhang YE, Zhang XR. Study of heteroserum-induced rat liver fibrosis model and its mechanism. *World J Gastroenterol* 1998; **4**: 206-209
- 7 **Jia JB**, Han DW, Xu RL, Gao F, Zhao LF, Zhao YC, Yan JP, Ma XH. Effect of endotoxin on fibronectin synthesis of rat primary cultured hepatocytes. *World J Gastroenterol* 1998; **4**: 329-331
- 8 **Cheng ML**, Wu YY, Huang KF, Luo TY, Ding YS, Lu YY, Liu RC, Wu J. Clinical study on the treatment of liver fibrosis due to hepatitis B by IFN- α ₁ and traditional medicine preparation. *World J Gastroenterol* 1999; **5**: 267-269
- 9 **Riley TR 3rd**, Bhatti AM. Preventive strategies in chronic liver disease: part II. Cirrhosis. *Am Fam Physician* 2001; **64**: 1735-1740
- 10 **Liu YK**, Shen W. Inhibitive effect of cordyceps sinensis on experimental hepatic fibrosis and its possible mechanism. *World J Gastroenterol* 2003; **9**: 529-533
- 11 **Ma X**, Qiu DK, Xu J, Zeng MD. Effects of Cordyceps polysaccharides in patients with chronic hepatitis C. *Huaren Xiaohua Zazhi* 1998; **6**: 582-584
- 12 **Yang Q**, Yan YC, Gao YX. Inhibitory effect of Quxianruangan Capsulae on liver fibrosis in rats and chronic hepatitis patients. *Shijie Huaren Xiaohua Zazhi* 2001; **9**: 1246-1249
- 13 **You H**, Wang B, Wang T. Proliferation and apoptosis of hepatic stellate cells and effects of compound 861 on liver fibrosis. *Zhonghua Ganzangbing Zazhi* 2000; **8**: 78-80
- 14 **Nan JX**, Park EJ, Kim YC, Ko G, Sohn DH. Scutellaria baicalensis inhibits liver fibrosis induced by bile duct ligation or carbon tetrachloride in rats. *J Pharm Pharmacol* 2002; **54**: 555-563
- 15 **Wang QC**, Shen DL, Zhang CD, Xu LZ, Nie QH, Xie YM, Zhou YX. Effect of Rangansuopiwan in expression of tissue inhibitor of metalloproteinase-1/2 in rat liver fibrosis. *Shijie Huaren Xiaohua Zazhi* 2001; **9**: 379-382
- 16 **Shen M**, Qiu DK, Chen Y, Xiong WJ. Effects of recombinant augmenter of liver regeneration protein, danshen and oxymatrine on rat fibroblasts. *Shijie Huaren Xiaohua Zazhi* 2001; **9**: 1129-1133
- 17 **Wang XL**, Liu P, Liu CH, Liu C. Effects of coordination of FZHY decoction on functions of hepatocytes and hepatic satellite cells. *Shijie Huaren Xiaohua Zazhi* 1999; **7**: 663-665
- 18 **Yao XX**, Tang YW, Yao DM, Xiu HM. Effect of yigan decoction on the expression of type I, III collagen proteins in experimental hepatic fibrosis in rats. *Shijie Huaren Xiaohua Zazhi* 2001; **9**: 263-267
- 19 **Hang M**, Song G, Minuk GY. Effects of hepatic stimulator substance, herbal medicine, Selenium/Vitamin E, and ciproloxacin on cirrhosis in the rat. *Gastroenterology* 1996; **110**: 1150-1155
- 20 **Buljbcac M**, Roimic Z, Vuclic B. Serum selenium concentration in patients with liver cirrhosis hepatocellular carcinoma. *Acta Med Crearice* 1996; **50**: 11-15
- 21 **Weng HL**, Cai WM, Liu RH. Animal experiment and clinical study of effect of gamma interferon on hepatic fibrosis. *World J Gastroenterol* 2001; **7**: 42-48
- 22 **Li BS**, Wang J, Zhen YJ, Liu JX, Wei MX, Sun SQ, Wang SQ. Experimental study on serum fibrosis markers and liver tissue pathology and hepatic fibrosis in immuno-damaged rats. *Shijie Huaren Xiaohua Zazhi* 1999; **7**: 1031-1034
- 23 **Bissell DM**. Chronic liver injury, TGF-beta, and cancer. *Exp Mol Med* 2001; **33**: 179-190
- 24 **Friedman SL**. Cytokines and fibrogenesis. *Semin Liver Dis* 1999; **19**: 129-140
- 25 **Chen WX**, Li YM, Yu CH, Cai WM, Zheng M, Chen F. Quantitative analysis of transforming growth factor beta 1 mRNA in patients with alcoholic liver disease. *World J Gastroenterol* 2002; **8**: 379-381
- 26 **Gressner AM**, Weiskirchen R, Breitkopf K, Dooley S. Roles of TGF-beta in hepatic fibrosis. *Front Biosci* 2002; **7**: d793-807
- 27 **Lewindon PJ**, Pereira TN, Hoskins AC, Bridle KR, Williamson RM, Shepherd RW, Ramm GA. The role of hepatic stellate cells and transforming growth factor-beta (1) in cystic fibrosis liver disease. *Am J Pathol* 2002; **160**: 1705-1715
- 28 **Beraud C**, Henzel WJ, Baeuerle PA. Involvement of regulatory and catalytic subunits of phosphoinositide 3-kinase in NF- κ B activation. *Proc Natl Acad Sci U S A* 1999; **96**: 429-434
- 29 **Regnier CH**, Song HY, Gao X, Goeddel DV, Cao Z, Rothe M. Identification and characterization of an I κ B kinase. *Cell* 1997; **90**: 373-383
- 30 **Zandi E**, Karin M. Bridging the gap: composition, regulation, and physiological function of the I κ B kinase complex. *Mol Cell Biom* 1999; **19**: 4547-4551
- 31 **May MJ**, Ghosh S. I κ B kinases: Kinsmen with different crafts. *Science* 1999; **284**: 271-273
- 32 **Baeuerle PA**. I κ B-NF- κ B structures: at the interface of inflammation control. *Cell* 1999; **95**: 729-731
- 33 **Baeuerle PA**, Henkel T. Function and activation of NF- κ B in the immune system. *Annu Rev Immunol* 1994; **12**: 141-179
- 34 **Ozes ON**, Mayo LD, Gustin JA, Pfeffer SR, Pfeffer LM, Donner DB. NF- κ B activation by tumour necrosis factor requires the Akt serine-threonine kinase. *Nature* 1999; **401**: 83-85
- 35 **Romashkova JA**, Makarov SS. NF- κ B is a target of AKT in anti-apoptotic PDGF signalling. *Nature* 1999; **401**: 86-90
- 36 **Hinz M**, Krappmann D, Eichten A, Scheiderei C, Strauss M. NF- κ B function in growth control: regulation of cyclin D1 expression and G0-G1-to-S-phase transition. *Mol Cell Biol* 1999; **19**: 2690-2698

Population based study of noncardiac chest pain in southern Chinese: Prevalence, psychosocial factors and health care utilization

Wai Man Wong, Kwok Fai Lam, Cecilia Cheng, Wai Mo Hui, Harry Hua-Xiang Xia, Kam Chuen Lai, Wayne H.C. Hu, Jia Qing Huang, Cindy L.K. Lam, Chi Kuen Chan, Annie O.O. Chan, Shiu Kum Lam, Benjamin Chun-Yu Wong

Wai Man Wong, Wai Mo Hui, Harry Hua-Xiang Xia, Kam Chuen Lai, Wayne H.C. Hu, Jia Qing Huang, Cindy L.K. Lam, Chi Kuen Chan, Annie O.O. Chan, Shiu Kum Lam, Benjamin Chun-Yu Wong, Department of Medicine, The University of Hong Kong, Hong Kong SAR, China

Kwok Fai Lam, Department of Statistics and Actuarial Science, The University of Hong Kong, Hong Kong, China

Cecilia Cheng, Division of Social Science, Hong Kong University of Science and Technology, Hong Kong SAR, China

Supported by the Competitive Earmarked Research Grant HKU 7487/03M of the Hong Kong Research Grant Council, the Simon K. Y. Lee Gastroenterology Fund of the University of Hong Kong and the Hong Kong Society of Gastroenterology

Correspondence to: Dr. Benjamin Chun-Yu Wong, Department of Medicine, University of Hong Kong, Queen Mary Hospital, Pokfulam Road, Hong Kong, China. bcywong@hku.hk

Telephone: +852-2855-4541 **Fax:** +852-2872-5828

Received: 2003-09-15 **Accepted:** 2003-10-20

Abstract

AIM: Population-based assessment of noncardiac chest pain (NCCP) is lacking. The aim of this study was to evaluate the prevalence, psychosocial factors and health seeking behaviour of NCCP in southern Chinese.

METHODS: A total of 2 209 ethnic Hong Kong Chinese households were recruited to participate in a telephone survey to study the epidemiology of NCCP using the Rose angina questionnaire, a validated gastroesophageal reflux disease (GERD) questionnaire and the hospital anxiety-depression scale. NCCP was defined as non-exertional chest pain according to the Rose angina questionnaire and had not been diagnosed as ischaemic heart diseases by a physician.

RESULTS: Chest pain over the past year was present in 454 subjects (20.6%, 95% CI 19-22), while NCCP was present in 307 subjects (13.9%, 95% CI 13-15). GERD was present in 51% of subjects with NCCP and 34% had consulted a physician for chest pain. Subjects with NCCP had a significantly higher anxiety ($P<0.001$) and depression score ($P=0.007$), and required more days off ($P=0.021$) than subjects with no chest pain. By multiple logistic regression analysis, female gender (OR 1.9, 95% CI 1.1-3.2), presence of GERD (OR 2.8, 95% CI 1.6-4.8), and social life being affected by NCCP (OR 6.9, 95% CI 3.3-15.9) were independent factors associated with health seeking behaviour in southern Chinese with NCCP.

CONCLUSION: NCCP is a common problem in southern Chinese and associated with anxiety and depression. Female gender, GERD and social life affected by chest pain were associated with health care utilization in subjects with NCCP.

Wong WM, Lam KF, Cheng C, Hui WM, Xia HHX, Lai KC, Hu

WHC, Huang JQ, Lam CLK, Chan CK, Chan AOO, Lam SK, Wong BCY. Population based study of noncardiac chest pain in southern Chinese: Prevalence, psychosocial factors and health care utilization. *World J Gastroenterol* 2004; 10(5): 707-712
<http://www.wjgnet.com/1007-9327/10/707.asp>

INTRODUCTION

Noncardiac chest pain (NCCP) is a common problem and affects 23% of the U.S. population^[1]. It is a benign condition with an estimated 10 year mortality of less than 1%^[2]. However, the associated morbidity, as a result of inability to work and health care utilization, is enormous^[3]. Population-based data of NCCP in Asia are lacking^[4,5]. Furthermore, the effects of co-existing anxiety and depression on health care utilization in subjects with NCCP are unknown in Chinese. Various studies have shown an increased psychological morbidity in patients attending specialist clinics for functional gastrointestinal diseases^[6-10]. This may be due to a causative effect of psychological factors on gastrointestinal symptoms, or the psychological morbidity may be a result of the functional gastrointestinal disease. Alternatively, psychological factors may influence health-seeking behaviour, and patients with co-morbid anxiety or depression may be more likely to seek medical consultation. Thus the aims of this study were to determine the population prevalence of NCCP, the effects of co-existing anxiety and depression and the health seeking behaviour of Chinese subjects with NCCP.

MATERIALS AND METHODS

Data collection

The telephone interview was conducted over a period of two weeks by a professional team of trained telephone interviewers from the Social Sciences Research Centre, the University of Hong Kong in November 2002. The interviewers went through intense training on the delivery of questionnaire to ensure uniformity and the questions to be understood. Random telephone numbers were generated by computer and dialed automatically. Only numbers corresponding to ethnic Chinese households were used in the study. Office numbers, facsimile machines, and non-Chinese households were excluded. Upon identification of target households, the interviewer asked to speak to the household member with the most recent birthday. This aimed to provide randomization among different members of the household. Baseline demographic data, education, occupation and income were assessed, followed by a translated version of the Rose Angina questionnaire^[11], a validated GERD questionnaire^[12], a validated translated version of the hospital anxiety depression scale^[13-15] and assessment of medical care utilization and impact of the disease on social activity as described below. Overall, 3605 ethnic Chinese households were contacted by telephone. The interview was completed in

2 209 subjects (response rate=61.3%, mean age=40.3±14, 58% female). The demographic characteristics of the study subjects were comparable to the census data of Hong Kong in 2001^[16]. This study was approved by the ethics committee of the University of Hong Kong.

Sample size

A previous study demonstrated that the prevalence of NCCP was approximately 23% in Minnesota, USA^[1]. To provide a 95% confidence interval ±2% and a meaningful comparison between health care seekers and non-health care seekers, we estimated a sample size of around 2000 of successful cases.

Questionnaire

The Rose angina questionnaire is a standardized method of measuring angina and myocardial infarction in population surveys and has been validated in different ethnic groups^[17-26]. 'Definite' angina was defined as chest pain that limits exertion (walking uphill or hurry, or walking at an ordinary pace on the level), is situated over the sternum or in the left chest and left arm, and is relieved within 10 min by rest^[11]. 'Possible' angina was defined as chest pain that limits exertion and other criteria for definite angina not fulfilled. NCCP was defined as non-exertional chest pain according to the Rose angina questionnaire and had not been diagnosed as ischaemic heart diseases by a physician^[27]. Musculoskeletal-like chest pain was defined as chest pain that worsens on breathing, movement or the presence of chest wall tenderness. The duration and characteristics of the chest pain were recorded. In the development of the Chinese version of the questionnaire, the original instrument was translated, back translated and tested for reproducibility in a sample of thirty patients attending the gastrointestinal clinic. The intraclass correlation coefficient of the translated questionnaire was 0.91. Furthermore, we tested the Rose angina questionnaire in a pilot of 50 patients with known coronary heart diseases proven by coronary angiography and 100 healthy controls. The sensitivity and specificity determined by the pilot study was 68% and 95% for the diagnosis of ischemic heart disease respectively.

Gastrointestinal symptoms were assessed by a translated Chinese version of a validated GERD questionnaire^[12]. The GERD questionnaire examined the symptoms of heartburn, acid regurgitation, dyspepsia, dysphagia, globus, odynophagia, hoarseness of voice, chronic cough, asthma and pneumonia in details. In addition, past medical history, medication use, past history of esophageal, gastric, cardiac or pulmonary disease; smoking, alcohol intake, and the intake of tea and coffee were assessed. Part of the results on GERD had been presented elsewhere^[28]. The severity and frequency of chest pain and other gastrointestinal symptoms were graded on a five-point Likert scale as follows: 1 (none- no symptoms / none in the past year), 2 (mild- symptoms can be easily ignored / less than once per mo), 3 (moderate- awareness of symptoms but easily tolerated / >= once per month), 4 (severe- symptoms sufficient to cause an interference with normal activities / >= once weekly) and 5 (incapacitating- incapacitating symptoms with an inability to perform daily activities or require day-off / >= once daily)^[29]. GERD was defined as heartburn and/or acid regurgitation over the past year, which has been shown to be specific for the diagnosis of GERD^[30, 31]. Patients who had used non-steroidal anti-inflammatory drugs (NSAIDs) / aspirin for at least 3 d at any dosage within 3 mo prior to the survey were considered to be NSAIDs / aspirin users^[32]. Anxiety and depression were assessed by the hospital anxiety and depression scale^[13]. The Chinese version of this questionnaire has previously been validated^[14, 15] which consists of 7 questions on anxiety and 7 questions on depression.

Medical care utilization

Medical care utilization of subjects with NCCP was classified into categories including the use of over-the-counter medication, community based medicine, accident and emergency department and admission to hospital. Impact of disease was measured by the proportion of subjects requiring days-off work due to gastrointestinal complaints, and whether subjects reported an adverse effect of the chest pain on their normal social life (social life being affected), *i.e.* symptoms sufficient to cause an interference with normal daily and social activity.

Statistical analysis

Univariate analysis was performed by Student's *t* test for continuous variables and by chi-square test for categorical variables to assess the risk factors associated with NCCP. Multiple logistic regression analysis with sex and age adjustment was then performed to determine the risk factors associated with NCCP. Furthermore, a multiple logistic regression model was designed to determine the factors (severity and frequency of chest pain, presence of heartburn and/or acid regurgitation over the past year, gender, age, educational level (primary school or below, secondary or matriculation and tertiary), occupation (3 levels), anxiety and depression scores and social life being affected by chest pain) associated with health seeking behaviour in NCCP. To find the best model, a backward elimination stepwise procedure was carried out in a way that the factor would be eliminated from the analysis if the corresponding *P* value was greater than 0.2, in order not to miss out too much information in view of the small sample size. A *P* value of 0.05 or less was considered statistically significant and all reported *P* values were 2 sided.

RESULTS

Cardiac chest pain

Chest pain over the past year was present in 454 subjects (20.6%, 95% CI 19-22), of which 147 (6.7%) had 'possible' angina by the Rose angina questionnaire and/or ischaemic heart diseases diagnosed by a physician^[11, 27].

Noncardiac chest pain

NCCP over the past year was present in 307 subjects (13.9%, 95% CI 13-15). The demographic characteristics of subjects with NCCP, cardiac chest pain or no chest pain are given in Table 1. The prevalence of NCCP was higher in men than in women (16.6% vs 11.9%, *P*=0.002). Subjects with NCCP were significantly younger than subjects with no chest pain. However, for subjects with cardiac chest pain, the prevalence was similar between men and women (7.5% vs 8%, *P*=0.68) and the mean age was similar to subjects with no chest pain. Aspirin usage was significantly higher in subjects with cardiac chest pain than in subjects with no chest pain (20.6% vs 7.7%, *P*<0.001). NSAIDs usage was significantly higher in subjects with either NCCP or cardiac chest pain than in subjects with no chest pain. Cigarette and coffee consumption were the highest in subjects with NCCP, while alcohol consumption was similar between subjects with NCCP and subjects with cardiac chest pain. The education level and socioeconomic status were similar in subjects with NCCP, cardiac chest pain or no chest pain (Table 1). The median duration of NCCP was 24 mo (range 0.1 to 360 mo). Most (96%) subjects with NCCP had mild to moderate chest pain over the central chest area (50%) (Table 2). The frequency of chest pain was less than once per mo in three quarters of the subjects. Of the 307 subjects with NCCP, 155 (50.5%) could be classified as having GERD, while 79 (25.7%) had musculoskeletal-like chest pain. But GERD and musculoskeletal-like chest pain were overlapped

in 15.6% (48/307) of subjects. The gender difference in NCCP between men and women persisted after exclusion of subjects with musculoskeletal-like chest pain (13.1% vs 8.5%, $P=0.001$). Figure 1 shows the age and sex- prevalence rates of NCCP and musculoskeletal-like chest pain over the past year. For men with NCCP over the past year, the prevalence was the highest in 18-24 age group, less common in 25-54 age group and increased again after the age of 55 (Figure 1). In contrast, the prevalence of NCCP in women was almost constant from age 18 to 44, and then dropped gradually with age. The overall prevalence of musculoskeletal-like chest pain was similar between men and women (4.2% vs 4.0%, $P=NS$), but men aged 18-24 had a higher prevalence when compared to women of similar age (7.9% vs 2.6%, $P=0.034$).

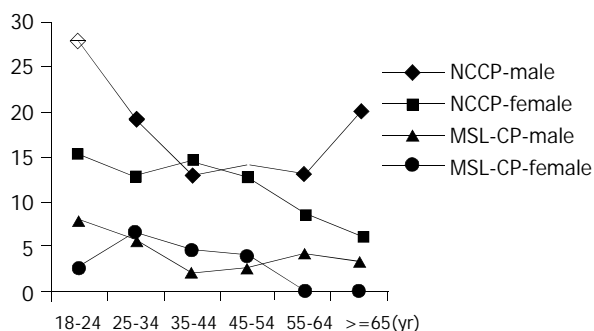


Figure 1 Age and sex-specific prevalence rates (per 100) of noncardiac chest pain (NCCP) and musculoskeletal-like chest pain (MSL-CP) over the past year.

Table 1 Demographic data of study subjects ($n=2209$)

	^a NCCP ($n=307$)	^a Cardiac chest pain ($n=147$)	^a No chest pain ($n=1755$)
Mean age	38±14 ^c	42±14	41±14
Gender (M/F)	156/151 ^c	58/89	723/1032
Smoking (%)	20.6	16.7	16.0
Alcohol (%)	10.2 ^d	10.9	6.8
Aspirin user (%)	11.2	20.6 ^b	7.7
NSAID user (%)	11.6 ^c	13.9 ^b	6.0
Coffee (%)	22.7	14.0	18.7
Education (%)			
Primary or below	37 (13)	28 (21)	290 (18)
Secondary or matriculation	171 (61)	88 (65)	920 (57)
Tertiary	72 (26)	20 (15)	392 (25)
Total	280 (100)	136 (100)	1602 (100)
Monthly income in US\$ (%)			
None	90 (33)	60 (44)	539 (35)
1280 or below	78 (29)	34 (25)	364 (24)
1280 – 1920	39 (14)	22 (16)	254 (16)
1920 – 3200	40 (15)	10 (7)	228 (15)
>3200	25 (9)	10 (7)	160 (10)
Total	272 (100)	136 (100)	1545 (100)
Occupation (%)			
Professional and managerial	45 (16)	17 (13)	262 (16)
Technical worker and craftsmen	37 (13)	14 (10)	175 (11)
Clerical work	29 (10)	16 (12)	243 (15)
Service and sales	32 (12)	11 (8)	157 (10)
Agriculture and others	18 (7)	8 (6)	87 (6)
Non-technical worker	8 (3)	4 (3)	33 (2)
Others (students, housewife, retired and unemployed)	109 (39)	66 (49)	637 (40)
Total	278 (100)	136 (100)	1594 (100)

^aThe total in each individual cell may be smaller because of subject refusal, ^b $P<0.001$ when compared to subjects with no chest pain, ^c $P<0.01$ when compared to subjects with no chest pain, ^d $P<0.05$ when compared to subjects with no chest pain.

Risk factors for NCCP

By univariate analysis, NCCP was associated with heartburn and/or acid regurgitation, globus, dyspepsia, feeling of acidity in stomach, alcohol and NSAID usage but not with dysphagia, odynophagia, chronic cough, hoarseness of voice, asthma, pneumonia, history of smoking, aspirin usage and coffee intake (Tables 1 and 3). By multiple logistic regression analysis, heartburn and/or acid regurgitation (OR 2.3, 95% CI 1.7-3.1), globus (OR 1.9, 95% CI 1.3-2.8), and NSAIDs use (OR 1.9, 95% CI 1.2-2.9) were independent risk factors associated with NCCP.

Table 2 Prevalence rates and characteristics of chest pain in studied population

	Male ($n=938$)	Female ($n=1271$)	Total ($n=2209$)
Chest pain over the past year (%)	213 (22.7)	241 (19.0)	454 (20.6)
Possible angina by Rose questionnaire or ischaemic heart disease diagnosed by physicians (%)	57 (6.1)	90 (7.1)	147 (6.7)
Noncardiac chest pain-NCCP (%)	156 (16.6)	151 (11.9)	307 (13.9)
NCCP severity (%)			
Mild	69	66	67
Moderate	27	32	29
Severe or incapacitated	4	3	4
NCCP frequency (%)			
< once / month	75	76	76
≥ once / month	22	19	21
> once / weekly	3	4	4
NCCP location			
Central	46	55	50
Left	44	37	41
Right	10	8	9

Table 3 Association of non-cardiac chest pain with other GERD symptoms over the past year

	NCCP ($n=307$)	No chest pain ($n=1755$)	OR (95% CI)
Heartburn and/or acid regurgitation (%)	50.5 ^a	23.2	3.4 (2.6-4.3)
Dysphagia (%)	4.1	2.8	1.5 (0.8-2.8)
Odynophagia (%)	7.1	5.8	1.2 (0.8-2.0)
Globus (%)	15.9 ^a	5.3	3.4 (2.3-4.9)
Dyspepsia (%)	21.8 ^b	14.0	1.7 (1.3-2.3)
Feeling of acidity in stomach (%)	31.3 ^a	16.5	2.3 (1.8-3.0)
Chronic cough (%)	8.3	5.0	1.7 (1.1-2.7)
Hoarseness of voice (%)	6.3	5.5	1.2 (0.7-1.9)
Asthma (%)	4.2	2.5	1.7 (0.9-3.3)
Pneumonia (%)	0.7	0.5	1.5 (0.3-6.9)

^a $P<0.001$ when compared to subjects with no chest pain, ^b $P<0.01$ when compared to subjects with no chest pain.

Health care utilization, days off work and effects of NCCP on social life

Thirty-nine percent of subjects with NCCP over the past year used one or more forms of treatment for their problems. Among the 307 subjects with NCCP over the past year, 14 (5%) purchased over the counter medication, 85 (28%) visited an outpatient clinic; 10 (3%) visited the accident and emergency department, and 11 (4%) were admitted to regional hospitals for further management. NCCP over the past year was significantly correlated with increased health care utilization ($P<0.001$, OR 3.2, 95% CI 2.4-4.3). A significantly higher proportion of health

seekers with NCCP had moderate to severe chest pain when compared to non-health seekers (39% vs 27%, $P=0.025$) (Table 4). However, the proportion of subjects with at least monthly chest pain (28% vs 22% $P=0.265$) was similar between health seekers and non-health seekers. GERD (heartburn and/or acid regurgitation) over the past year was more prevalent in NCCP health seekers than in NCCP non-health seekers (67.5% vs 40.1%, $P<0.001$). A significantly higher proportion of subjects with NCCP reported their social life was affected by the chest pain (17% vs 9%, $P<0.001$, OR 1.9, 95% CI 1.4-2.5) and required days-off (17% vs 12%, $P=0.021$, OR 1.4, 95% CI 1.1-1.9) when compared to subjects with no chest pain.

Anxiety and depression score

Subjects with NCCP symptoms over the past year had higher average anxiety (5.5 vs 4.1, $P<0.001$) and depression (4.4 vs 3.8, $P=0.007$) scores when compared to subjects with no chest pain. However, for subjects with NCCP symptoms, the mean anxiety score and the mean depression score were similar between NCCP subjects who had sought any medical consultation and those who had not (Table 4).

Table 4 Comparison between subjects with noncardiac chest pain over the past year who did and did not seek health care

	NCCP health care seekers (n=131)	NCCP non-health care seekers (n=176)
Mean age \pm SD	39 \pm 14	36 \pm 14
Female (%)	57.5 ^a	42.8
Chest pain severity moderate or worse (%)	39.2 ^a	26.5
Chest pain once a month or more (%)	27.5	21.7
Chest pain requiring days-off	35.3 ^b	3.1
Presence of GERD (heartburn and/or acid regurgitation) (%)	67.5 ^b	40.1
Social life being affected	31.4 ^b	6.2
Mean anxiety score	5.8	5.3
Mean depression score	4.7	4.2

^a $P<0.05$ when compared to non-health seekers, ^b $P<0.001$ when compared to non-health seekers.

Determinants of health care utilization in NCCP

By multiple logistic regression analysis, female gender (OR 1.9, 95% CI 1.1-3.2, $P=0.023$), the presence of GERD (heartburn and/or acid regurgitation) symptoms over the past year (OR 2.8, 95% CI 1.6-4.8, $P<0.001$) and social life being affected by chest pain (OR 6.9, 95% CI 3.3-15.9, $P<0.001$) were independent factors associated with health seeking behaviour of subjects with NCCP.

DISCUSSION

The epidemiology of NCCP is scanty in the literature and most studies are not population-based. Locke *et al* reported a prevalence of 23% in a semi-rural US population^[1]. However, chest pain (including both exertional and non-exertional chest pain) with no past history of heart disease was the criteria for the diagnosis of NCCP in the study. Using Rose angina criteria, a population-based study in Mexican American and non-Hispanic white found a prevalence of 30% for chest pain thought not angina^[33]. A UK study reported a population prevalence of 24% (Rose angina questionnaire) in 7754 subjects from 24 towns of Britain for "other chest pain"^[23]. Recently, a population survey performed in Australia, using a similar definition of NCCP, reported a prevalence of 33% in

672 residents of Penrith^[34]. The only independent factor for NCCP was the frequency of heartburn. No particular factor for health seeking behaviour was identified. The criteria of NCCP in our study were similar to the Australian study, but we found a considerably lower prevalence of NCCP (14%) when compared to the Western population. The exact reason is unknown but may be related to the lower prevalence of GERD (both erosive esophagitis and non-erosive reflux disease) in the Chinese population^[28,32], as GERD is the most common etiology of NCCP. The gender, age distribution and socio-economic status closely resembled those of the census data of Hong Kong in 2001, suggesting our data are highly representative^[16]. Fifty-one percent of subjects with NCCP could be classified as having GERD in our study, suggesting an esophageal cause of the chest pain. Interestingly, both musculoskeletal-like chest pain and GERD were overlapped in 16% of subjects, indicating the difficulty in establishing the etiology of chest pain through a questionnaire. Furthermore, we were not able to exclude panic attacks without proper psychiatric assessment. Nevertheless, we could still obtain useful data about the impact of chest pain of presumably 'noncardiac' in origin in the Chinese community. The prevalence of NCCP was unexpectedly high in young men. It could be partially explained by the higher proportion of young men with musculoskeletal-like chest pain when compared to women of similar age. Further endoscopic and physiological studies are warranted to investigate the exact causes of chest pain in these subjects.

By multiple logistic regression analysis, the presence of heartburn and/or acid regurgitation, globus and NSAIDs intake were independent risk factors for NCCP. The symptoms of GERD and globus suggested an esophageal origin of the chest pain, but the positive association of NSAIDs intake with NCCP was interesting. It is unknown whether these subjects took NSAIDs for the symptomatic relief of chest pain or NSAID intake indirectly linked to esophageal chest pain as a result of erosive damage to the esophageal mucosa^[35-38]. Furthermore, it has been shown that subjects receiving 1 500 mg aspirin per day had higher gastric mechanosensory thresholds^[39]. Those who failed to increase sensory thresholds were associated with dyspepsia. Similar mechanism may operate to account for the positive association between NSAIDs and NCCP as a result of abnormal visceral perception.

In the United States, it has been estimated that US\$8 billion was spent annually for the initial care of patients who were suspected to have an acute coronary syndrome, but subsequently found not to have coronary artery disease^[3]. The socio-economic effects were reflected by the higher proportion of NCCP subjects requiring days-off work and reporting an adverse effect of the illnesses on their social life when compared to subjects with no chest pain. It also concurred with our previous findings that quality of life assessment by SF-36 was significantly lower in patients with NCCP than in healthy controls^[40].

Few studies have assessed the factors associated with health care utilization in NCCP. In the Australian study mentioned above, no particular factor was found to be associated with health seeking behaviour. We found that the presence of heartburn and/or acid regurgitation were important in motivating health seeking behaviour of subjects with NCCP. Furthermore, female gender was more commonly associated with health care utilization in subjects with NCCP. Despite the higher prevalence of NCCP in men in our study, women were more likely to seek medical attention and correlated with the findings of female predominance in previous non-population based studies^[41,42]. We did not find any effect of anxiety and depression on health care utilization, but subjects feeling their social life affected by chest pain were more likely

to seek help.

The major limitation of this study was the diagnosis of NCCP through a questionnaire. In clinical practice, diagnosis of NCCP requires full cardiology evaluation. However, criteria like Rome II are not available for noncardiac chest pain^[43], but rather for a sub-group of patient population only (chest pain of presumed esophageal origin). It has been shown in prospective studies that 'possible' angina or exertional chest pain was equally reliable for the prediction of future ischemic events, in both men and women^[23,26]. Furthermore, self-reported history of doctor-diagnosis of angina has been shown to be a valid measure of angina in population-based studies^[27]. Although the sensitivity of Rose angina questionnaire is variable, it is highly specific for the diagnosis of angina^[17-26]. In our pilot study, we found that the translated Chinese version of the Rose angina questionnaire had a sensitivity and specificity of 68% and 95%. We used the combination of 'possible angina' and history of ischemic heart disease diagnosed by a physician for the diagnosis of cardiac chest pain, hoping that it would reduce the number of unrecognized ischemic heart disease in this study. Furthermore, it is unpractical to perform exercise testing or coronary angiograms in all subjects with chest pain in the setting of a population-based study.

In conclusion, NCCP is a common problem in Chinese and associated with anxiety and depression. Female gender, the presence of GERD symptoms over the past year and social life affected by chest pain are independent factors associated with health care utilization in Chinese.

ACKNOWLEDGEMENTS

The authors would like to thank the Social Science Research Centre of the University of Hong Kong for coordinating and conducting the telephone interview.

REFERENCES

- 1 **Locke GR 3rd**, Talley NJ, Fett SL, Zinsmeister AR, Melton LJ 3rd. Prevalence and clinical spectrum of gastroesophageal reflux: a population-based study in Olmsted County, Minnesota. *Gastroenterology* 1997; **112**: 1448-1456
- 2 **Chambers J**, Bass C. Chest pain with normal coronary anatomy: a review of natural history and possible etiologic factors. *Progr Cardiovasc Dis* 1990; **33**: 161-184
- 3 **Eslick GD**, Coulshed DS, Talley NJ. The burden of noncardiac chest pain. *Aliment Pharmacol Ther* 2002; **16**: 1217-1223
- 4 **Goh KL**, Chang CS, Fock KM, Ke M, Park HJ, Lam SK. Gastroesophageal reflux disease in Asia. *J Gastroenterol Hepatol* 2000; **15**: 230-238
- 5 **Wong WM**, Cheng C, Hui WM, Lam SK. Noncardiac chest pain. *Medical Progress* 2003; **30**: 15-21
- 6 **Talley NJ**, Fung LH, Gilligan IJ, McNeil D, Piper DW. Association of anxiety, neuroticism, and depression with dyspepsia of unknown cause. A case-control study. *Gastroenterology* 1986; **90**: 886-892
- 7 **Talley NJ**, Jones M, Piper DW. Psychosocial and childhood factors in essential dyspepsia. A case-control study. *Scand J Gastroenterol* 1988; **23**: 341-346
- 8 **Langeluddecke P**, Goulston K, Tennant C. Psychological factors in dyspepsia of unknown cause: a comparison with peptic ulcer disease. *J Psychosom Res* 1990; **34**: 215-222
- 9 **Harris A**, Martin BJ. Increased abdominal pain during final examinations. *Dig Dis Sci* 1994; **39**: 104-108
- 10 **Hui WM**, Shiu LP, Lam SK. The perception of life events and daily stress in nonulcer dyspepsia. *Am J Gastroenterol* 1991; **86**: 292-296
- 11 **Rose G**. The diagnosis of ischaemic heart pain and intermittent claudication in field surveys. *Bull World Health Organ* 1962; **27**: 645-658
- 12 **Locke GR**, Talley NJ, Weaver AL, Zinsmeister AR. A new questionnaire for gastroesophageal reflux disease. *Mayo Clin Proc* 1994; **69**: 539-547
- 13 **Zigmond AS**, Snaith RP. The hospital anxiety and depression scale. *Acta Psychiatr Scand* 1983; **67**: 361-370
- 14 **Leung CM**, Ho S, Kan CS, Hung CH, Chen CN. Evaluation of the Chinese version of the Hospital Anxiety and Depression Scale. A cross-cultural perspective. *Int J Psychosom* 1993; **40**: 29-34
- 15 **Lam CL**, Pan PC, Chan AW, Chan SY, Munro C. Can the Hospital Anxiety and Depression (HAD) Scale be used on Chinese elderly in general practice? *Fam Pract* 1995; **12**: 149-154
- 16 **Hong Kong Census 2001**. Census and Statistics Department, Hong Kong
- 17 **Rose GA**, Ahmeteli M, Checcacci L, Fidanza F, Glazunov I, De Haas J, Horstmann P, Kornitzer MD, Meloni C, Menotti A, van der Sande D, de Soto-Hartgrink MK, Pisa Z, Thomsen B. Ischaemic heart disease in middle-aged men. Prevalence comparisons in Europe. *Bull World Health Organ* 1968; **38**: 885-895
- 18 **Marmot MG**, Syme SL, Kagan A, Kato H, Cohen JB, Belsky J. Epidemiologic studies of coronary heart disease and stroke in Japanese men living in Japan, Hawaii and California: prevalence of coronary and hypertensive heart disease and associated risk factors. *Am J Epidemiol* 1975; **102**: 514-525
- 19 **Erikssen J**, Forfang K, Storstein O. Angina pectoris in presumably healthy middle-aged men. Validation of two questionnaire methods in making the diagnosis of angina pectoris. *Eur J Cardiol* 1977; **6**: 285-298
- 20 **Krogh V**, Trevisan M, Panico S, Farinara E, Mancini M, Menotti A, Ricci G. Prevalence and correlates of angina pectoris in the Italian nine communities study. Research Group ATS-RF2 of the Italian National Research Council. *Epidemiology* 1991; **2**: 26-32
- 21 **Kutty VR**, Balakrishnan KG, Jayasree AK, Thomas J. Prevalence of coronary heart disease in the rural population of Thiruvananthapuram district, Kerala, India. *Int J Cardiol* 1993; **39**: 59-70
- 22 **Singh RB**, Sharma JP, Rastogi V, Raghuvanshi RS, Moshiri M, Verma SP, Janus ED. Prevalence of coronary artery disease and coronary risk factors in rural and urban populations of north India. *Eur Heart J* 1997; **18**: 1728-1735
- 23 **Lampe FC**, Whincup PH, Wannamethee SG, Ebrahim S, Walker M, Shaper AG. Chest pain on questionnaire and prediction of major ischaemic heart disease events in men. *Eur Heart J* 1998; **19**: 63-73
- 24 **Udol K**, Mahanonda N. Comparison of the Thai version of the Rose questionnaire for angina pectoris with the exercise treadmill test. *J Med Assoc Thai* 2000; **83**: 514-522
- 25 **Fischbacher CM**, Bhopal R, Unwin N, White M, Alberti KG. The performance of the Rose angina questionnaire in South Asian and European origin populations: a comparative study in Newcastle, UK. *Int J Epidemiol* 2001; **30**: 1009-1016
- 26 **Hart CL**, Watt GC, Davey Smith G, Gillis CR, Hawthorne VM. Pre-existing ischaemic heart disease and ischaemic heart disease mortality in women compared with men. *Int J Epidemiol* 1997; **26**: 508-515
- 27 **Lampe FC**, Walker M, Lennon LT, Whincup PH, Ebrahim S. Validity of a self-reported history of doctor-diagnosed angina. *J Clin Epidemiol* 1999; **52**: 73-81
- 28 **Wong WM**, Lai KC, Lam KF, Hui WM, Hu WHC, Lam CLK, Xia HHX, Huang JQ, Chan CK, Lam SK, Wong BCY. Prevalence, clinical spectrum and health care utilisation of gastroesophageal reflux disease in Chinese population: a population-based study. *Gastroenterology* 2003; **124**(Suppl 1): A167
- 29 **Wong WM**, Lam KF, Lai KC, Hui WM, Hu WH, Lam CL, Wong NY, Xia HHX, Huang JQ, Chan AO, Lam SK, Wong BC. Validated symptoms questionnaire (Chinese-GERDQ) for the diagnosis of gastroesophageal reflux disease in Chinese population. *Aliment Pharmacol Ther* 2003; **17**: 1407-1413
- 30 **Klauser AG**, Schindlbeck NE, Muller-Lissner SA. Symptoms in gastroesophageal reflux disease. *Lancet* 1990; **335**: 205-208
- 31 **Dent J**, Brun J, Fendrick AM, Fennerty MB, Janssens J, Kahrilas PJ, Lauritsen K, Reynolds JC, Shaw M, Talley NJ. An evidence-based appraisal of reflux disease management-the Genval Workshop Report. *Gut* 1999; **44**(Suppl 2): S1-S16
- 32 **Wong WM**, Lam SK, Hui WM, Lai KC, Chan CK, Hu WH, Xia HHX, Hui CK, Yuen MF, Chan AO, Wong BC. Long-term pro-

- spective follow-up of endoscopic oesophagitis in southern Chinese – prevalence and spectrum of the disease. *Aliment Pharmacol Ther* 2002; **16**: 2037-2042
- 33 **Mitchell BD**, Hazuda HP, Haffner SM, Patterson JK, Stern MP. High prevalence of angina pectoris in Mexican-American men. A population with reduced risk of myocardial infarction. *Ann Epidemiol* 1991; **1**: 415-426
- 34 **Eslick GD**, Jones MP, Talley NJ. Non-cardiac chest pain: prevalence, risk factors, impact and consulting - a population-based study. *Aliment Pharmacol Ther* 2003; **17**: 1115-1124
- 35 **Wilkins WE**, Ridley MG, Pozniak AL. Benign stricture of the esophagus: role of non-steroidal anti-inflammatory drugs. *Gut* 1984; **25**: 478-480
- 36 **Semble EL**, Wu WC, Castell DO. Nonsteroidal antiinflammatory drugs and esophageal injury. *Semin Arthritis Rheum* 1989; **19**: 99-109
- 37 **El-Serag HB**, Sonnenberg A. Association of esophagitis and esophageal strictures with diseases treated with nonsteroidal anti-inflammatory drugs. *Am J Gastroenterol* 1997; **92**: 52-56
- 38 **Avidan B**, Sonnenberg A, Schnell TG, Sontag SJ. Risk factors for erosive reflux oesophagitis: a case-control study. *Am J Gastroenterol* 2001; **96**: 41-46
- 39 **Holtmann G**, Gschossmann J, Buenger L, Gerken G, Talley NJ. Do changes in visceral sensory function determine the development of dyspepsia during treatment with aspirin? *Gastroenterology* 2002; **123**: 1451-1458
- 40 **Wong WM**, Lai KC, Lau CP, Hu WH, Chen WH, Wong BC, Hui WM, Wong YH, Xia HHX, Lam SK. Upper gastrointestinal evaluation of Chinese patients with non-cardiac chest pain. *Aliment Pharmacol Ther* 2002; **16**: 465-471
- 41 **Billing E**, Hjerdahl P, Rehnqvist N. Psychosocial variables in female vs male patients with stable angina pectoris and matched healthy controls. *Eur Heart J* 1997; **18**: 911-918
- 42 **Kirchgatterer A**, Weber T, Auer J, Wimmer L, Mayr H, Maurer E, Eber B. Analysis of referral diagnoses of patients with normal coronary angiogram. *Wien Klin Wochenschr* 1999; **111**: 434-438
- 43 **Clouse RE**, Richter JE, Heading RC, Janssens J, Wilson JA. Functional esophageal disorders. *Gut* 1999; **45**(Suppl 2): II31-36

Edited by Wang XL Proofread by Zhu LH

An extended assessment of bowel habits in a general population

Gabrio Bassotti, Massimo Bellini, Filippo Pucciani, Renato Bocchini, Antonio Bove, Pietro Alduini, Edda Battaglia, Paolo Bruzzi, Italian Constipation Study Group

Gabrio Bassotti, Sezione di Gastroenterologia ed Epatologia, Dipartimento di Medicina Clinica e Sperimentale, Università di Perugia
Massimo Bellini, Pietro Alduini, Sezione di Gastroenterologia, Dipartimento di Medicina Interna, Università di Pisa

Filippo Pucciani, Clinica Chirurgica Generale e Discipline Chirurgiche, Università di Firenze

Renato Bocchini, UO di Medicina Polispecialistica, Azienda Sanitaria Locale, Cesena

Antonio Bove, UO di Gastroenterologia ed Endoscopia Digestiva, Azienda Ospedaliera "A. Cardarelli", Napoli

Edda Battaglia, Dipartimento di Fisiopatologia Clinica, Università di Torino

Paolo Bruzzi, Struttura Complessa di Epidemiologia Clinica, IST Genova, Italy

Italian Constipation Study Group (the list of all participating members of the Italian Constipation Study Group is given at the end of the paper)

Correspondence to: Dr. Gabrio Bassotti, Strada del Cimitero, 2/a, 06131 San Marco (Perugia), Italy. gabassot@tin.it

Telephone: +39-75-5847570

Received: 2003-09-15 **Accepted:** 2003-11-06

Abstract

AIM: Bowel habits are difficult to study, and most data on defecatory behaviour in the general population have been obtained on the basis of recalled interview. The objective assessment of this physiological function and its pathological aspects continues to pose a difficult challenge. The aim of this prospective study was to objectively assess the bowel habits and related aspects in a large sample drawn from the general population.

METHODS: Over a two-month period 488 subjects were prospectively recruited from the general population and asked to compile a daily diary on their bowel habits and associated signs and symptoms (the latter according to Rome II criteria). A total of 298 (61%) participants returned a correctly compiled record, so that data for more than 8 000 patient-days were available for statistical analysis.

RESULTS: The average defecatory frequency was once per day (range of 0.25-3.25) and was similar between males and females. However, higher frequencies of straining at stool ($P=0.001$), a feeling of incomplete emptying and/or difficult evacuation ($P=0.0001$), and manual manoeuvres to facilitate defecation ($P=0.046$) were reported by females as compared to males.

CONCLUSION: This study represents one of the first attempts to objectively and prospectively assess bowel habits in a sample of the general population over a relatively long period of time. The variables we analyzed are coherent with the criteria commonly used for the clinical assessment of functional constipation, and can provide a useful adjunct for a better evaluation of constipated patients.

Bassotti G, Bellini M, Pucciani F, Bocchini R, Bove A, Alduini P, Battaglia E, Bruzzi P, Italian Constipation Study Group. An extended assessment of bowel habits in a general population. *World J Gastroenterol* 2004; 10(5): 713-716
<http://www.wjgnet.com/1007-9327/10/713.asp>

INTRODUCTION

Bowel habits are a difficult function to study objectively because of their highly private nature and negative associations. Therefore, it is not surprising that they represent one of the least understood aspects of human behaviour^[1]. In the past, most knowledge of bowel habits was drawn from limited data on small groups of subjects (nurses, jail prisoners, elderly people, students)^[2-5]. More recently, studies aimed generically at investigating functional gastrointestinal disorders^[6-10] have yielded data on large numbers of subjects by means of telephone interviews or mailed questionnaires^[11-14]. However, these studies and other reports have all been retrospective in nature and based on the subjects' assertions regarding their recent bowel function^[11,15,16]. More objective investigations have assessed small groups of subjects for limited periods of time (e.g. one week)^[17].

Prospective studies on bowel habits conducted over an adequate period of time in the general population are still lacking. The aim of our prospective study was to objectively assess the frequency and characteristics of defecation in a sample of the general population over a longer period of time.

MATERIALS AND METHODS

During a two-month period a questionnaire was consecutively distributed to 488 relatives or friends of patients attending the outpatient gastrointestinal clinic in six centres located in different regions of Italy (two in the north, two in the centre, and two in the south). A total of 259 women and 229 men received the form. To obtain the most objective possible data on bowel habits, the questionnaire took the form of a diary covering a period of 4 wk in which "yes-no" responses were to be given daily to six questions (Table 1). Drawing upon the Rome II criteria for functional constipation^[18], data on the following symptoms and signs were recorded each day, namely number of bowel movements, straining during bowel movements, feeling of incomplete emptying and/or difficult evacuation, manual manoeuvres to facilitate defecation, lumpy or hard stools. In addition, the use of laxatives was recorded.

The questionnaires were anonymous, and the only personal information the participants were required to give was their age and sex. All subjects received an exhaustive explanation about the aim of the study and the structure of the questionnaire.

Each centre received approval from the local ethics committee, the written consent of all subjects was obtained after they had been given a complete explanation of the aims of the study and the nature of the questionnaire, and the study was conducted in accordance with the Helsinki Declaration (Edinburgh revision, 2000).

For each subject, an overall score for each variable was computed as follows. The average number of bowel movements per day was obtained by taking the total number of defecations reported by the participants and divided by the total number of days in the study period (i.e., 28). The frequency in the use of laxatives was computed in the same way. The frequency of the four variables associated with defecation (straining, feeling of incomplete evacuation, need of manual help, lumpy/hard stools) was evaluated as the ratio between the total number of episodes recorded by the individual and the total number of bowel movements during the study period.

Table 1 Four-week daily diary (Patients giving yes-no responses and number of bowel movements/day were recorded)

Questions	Time						
	Monday	Tuesday	Wednesday	Thursday	Friday	Saturday	Sunday
FIRST WEEK							
Bowel movements (number/day)							
Straining at defecation							
Feeling of incomplete defecation and/or difficult evacuation							
Manual manoeuvres							
Lumpy or hard stools							
Use of laxatives							
SECOND WEEK							
Bowel movements (number/day)							
Straining at defecation							
Feeling of incomplete defecation and/or difficult evacuation							
Manual manoeuvres							
Lumpy or hard stools							
Use of laxatives							
THIRD WEEK							
Bowel movements (number/day)							
Straining at defecation							
Feeling of incomplete defecation and/or difficult evacuation							
Manual manoeuvres							
Lumpy or hard stools							
Use of laxatives							
FOURTH WEEK							
Bowel movements (number/day)							
Straining at defecation							
Feeling of incomplete defecation and/or difficult evacuation							
Manual manoeuvres							
Lumpy or hard stools							
Use of laxatives							

Statistical evaluation

All group means and standard deviations (SD) were calculated by averaging the individual scores. Comparisons among groups were carried out using the chi-square test or non-parametric tests. Correlations between pairs of variables were assessed by means of the non-parametric Spearman's correlation coefficient. *P* values <0.05 were chosen for rejection of the null hypothesis. Data are presented as mean±SD.

RESULTS

A total of 298 adult subjects (163 women (54.7%), mean age 42.5±15.5 yr and 135 men (45.3%), mean age 42.4±15.9 yr) returned the completed questionnaire. The mean response rate was 61.1 % (females 62.9 %; males 58.9 %, n.s.). Therefore, data for 8 344 d were available for statistical analysis.

The distribution of the participating subjects by age and sex is shown in Table 2. Table 3 reports the frequency of defecation, expressed as the average number of evacuations per day, the frequency of pathological features and sensations at defecation, and the use of laxatives per day. Overall, the frequency of bowel movements averaged one per day (range 0.25-3.25), and was similar between males and females. No significant intra-personal variation in the parameters under examination was detected over the four-week period. Higher frequencies of straining at stool (*P*=0.001), feeling of incomplete emptying and/or difficult evacuation (*P*=0.0001),

and manual manoeuvres to facilitate defecation (*P*=0.046) were reported by females as compared to males.

Table 2 Distribution for age and sex of population under investigation

years	Women	Men	Total
<20	3 (1.8)	3 (2.2)	6 (2)
21-30	32 (19.6)	39 (28.9)	71 (23.8)
31-40	59 (36.2)	32 (23.7)	91 (30.5)
41-50	22 (13.5)	21 (15.6)	43 (14.4)
51-60	21 (12.9)	20 (14.8)	41 (13.8)
61-70	19 (11.7)	13 (9.6)	32 (10.7)
>70	7 (4.3)	7 (5.2)	14 (4.7)

Table 4 shows the correlations between pairs of defecatory variables. Bowel movement frequency was negatively correlated with other features of defecation and the use of laxatives. Straining, a sensation of incomplete/difficult evacuation, manual manoeuvres, lumpy/hard stools and the use of laxatives were positively correlated with each other.

Concerning the relative weights of the single variables, it might be noted that 15 (5%) subjects showed a low frequency (<3/wk) of defecations, 35 (11.7%) straining during >¼ defecations, 32 (10.7%) incomplete/difficult evacuation during >¼ defecations, 2 (0.7%) manual manoeuvres during >¼ defecations, and 18 (6%) lumpy/hard stools during ¼ defecations.

Table 3 Defecatory frequency and defecation-related variables in our population sample (data are expressed as mean±SD)

Sex	No. of defecations/day	Straining at stool/defecation	Feeling of incomplete emptying/defecation	Manual help for evacuation/defecation	Lumpy/hard stools/defecation	Use of laxatives/day
Total	1.00±0.4	0.06±0.1	0.06±0.15	0.0090±0.07	0.07±0.2	0.07±0.2
Men	1.03±0.34	0.05±0.13	0.03±0.09	0.0008±0.001	0.06±0.2	0.02±0.1
Women	0.97±0.4	0.12±0.21	0.09±0.2	0.0170±0.09	0.08±0.2	0.09±0.2
<i>P</i> (between sexes)	n.s.	0.001	0.0001	0.046	n.s.	0.001

Table 4 Correlations among bowel habits

	Bowel mov/day	Straining	Incomplete/difficult evacuation	Manual manoeuvres	Lumpy/hard stools	Laxatives
Bowel movements (per day)	1	-0.365 ^a	-0.246 ^b	-0.123 ^b	-0.218 ^b	-0.356 ^b
Straining		1	0.562 ^b	0.293 ^b	0.592 ^b	0.416 ^b
Incomplete/difficult evacuation			1	0.327 ^b	0.558 ^b	0.273 ^b
Manual manoeuvres				1	0.303 ^b	0.233 ^b
Lumpy/hard stools					1	0.300 ^b
Laxatives						1

^b*P*<0.01.

DISCUSSION

Most studies on bowel habits have been based on phone interviews and on the assumption that people would report accurately, but there has been good evidence that bowel movement frequency might be misreported^[19,20]. Indeed, it is very difficult to remember and report accurately one's bowel habits over recent months in a 20 min interview. Studies have shown marked discrepancies between recalled data and data that was recorded daily^[19,21,22]. Moreover, people without a telephone or who were not at home when contact was attempted would be excluded from any given survey^[23]. Another source of bias was the possibility that symptomatic individuals would be more keen to complete the survey process than asymptomatic subjects, which might lead to an overestimation of the frequency of symptoms.

Validated and universally accepted criteria are definitely needed if functional bowel disorders are to become a formally recognized disease entity by physicians, patients, and society^[24].

In order to circumvent some of the methodological biases discussed above, for this study a questionnaire designed to elicit the most objective possible data on individual bowel habits was drawn up. With this instrument bowel movement frequency, and sensations and characteristics related to each bowel movement were prospectively recorded by nearly 300 subjects on a daily basis for 4 wk. Moreover, to obtain a geographically representative sample of our population, participants were recruited from different parts of the country.

It may be stressed that the 61% response rate could be considered relatively high, given the nature of the data being sought. Studies employing telephone interviews or mailed questionnaires have yielded a response rate ranging from 19% to 80%. We believe that our high response rate can be attributed to the simplicity of the questionnaire (which examined only six items) and its complete anonymity. A daily dial-in service might have been more reliable, but this is costly to implement and potentially dependent on the socio-cultural environment in which the study is conducted.

It must be pointed out that due to the recruiting procedure used, the individuals who participated in this study were not selected with respect to factors such as social status, education, occupation and, possibly, the prevalence and type of bowel habits reported. However, they were prospectively recruited and not selected based on the basis of factors such as the presence/absence of pathological symptoms. Nevertheless, in light of the high participation rate, it seems reasonable to

postulate that the results of this study provide an acceptable approximation of the prevalence and type of symptoms in a general sample of Italian adults.

We are certain of our findings to be underlined. Firstly, there was a relatively large variation in bowel movement frequency, with an average of one per day, but a range of one evacuation every 4 d to about 3 bowel movements per day, with no differences in distribution between the sexes. It might also be noted that 5% of the participants reported less than 3 evacuations/week. Secondly, the number of subjects who reported abnormal features during >1/4 defecations was low, in particular, the incidence of manual manoeuvres to facilitate defecation was almost nil (0.7%). However, these variables showed a positive correlation with one another. Thirdly, the prevalence of defecation-related variables (except for the presence of lumpy/hard stools) was significantly different between the sexes, with a higher frequency in women, and interestingly, all of these are variables related with pelvic floor function. The use of laxatives was also rare (5% of the population sample), but much (*P*=0.0001) more frequent among women.

The variables analysed in this study could be helpful in the clinical assessment of functional constipation. Our data furthermore suggest that different symptoms and signs should be attributed to different weights in the evaluation of constipation scores^[25,26]. For instance, a value of less than one defecation per week or the use of manual manoeuvres to facilitate defecation could represent clinically important indications for the diagnosis of constipation.

In conclusion, this study represents one of the first attempts to prospectively assess bowel habits in a general population sample over a long period of time. Further studies in "normal" subjects will obviously be needed to confirm these observations.

The following researchers of the Italian Constipation Study (ICS) Group participated in the study: Bassotti G, Chistolini F, Morelli A (Perugia); Bellini M, Alduini P, Mammìni C, Rappelli L, Costa F, Stasi C, Mumolo MG, Berni I, Giorgetti S, Marchi S (Pisa); Pucciani F, Iozzi L, Cianchi F, Cortesini C (Firenze); Bocchini R, Cimatti M, Fornasari L, Montaletti I, Pazzi P (Cesena/Forlì); Bove A, Balzano A (Napoli); Battaglia E, Dughera L, Emanuelli G (Torino); Bruzzi P (Genova).

REFERENCES

- 1 **Heaton KW**, Radvan J, Cripps H, Mountford RA, Braddon FE, Hughes AO. Defecation frequency and timing, and stool form in the general population: a prospective study. *Gut* 1992; **33**: 818-824

- 2 **Hardy TL.** Order and disorder in the large intestine. *Lancet* 1945; **i**: 519-524
- 3 **Rendtorff RC.** Kashgarian M. Stool patterns of healthy adult males. *Dis Colon Rectum* 1967; **10**: 222-228
- 4 **Milne JS.** Williamson J. Bowel habit in older people. *Gerontol Clin* 1972; **14**: 56-60
- 5 **Sandler RS,** Drossman DA. Bowel habits in apparently healthy young adults not seeking health care. *Dig Dis Sci* 1987; **32**: 841-845
- 6 **Everhart JE,** Go VLW, Johannes RS, Fitzsimmons SC, Roth HP, White LR. A longitudinal survey of self-reported bowel habits in the United States. *Dig Dis Sci* 1989; **34**: 1153-1162
- 7 **Drossman DA,** Li Z, Andruzzi E, Temple RD, Talley NJ, Thompson WG, Whitehead WE, Janssens J, Funch-Jensen P, Corazziari EUS. Householder survey of functional gastrointestinal disorders. Prevalence, sociodemography and health impact. *Dig Dis Sci* 1993; **38**: 1569-1580
- 8 **Talley NJ,** Weaver AL, Zinsmeister AR, Melton LJ. Functional constipation, and outlet delay. A population-based study. *Gastroenterology* 1993; **105**: 781-790
- 9 **Stewart WF,** Liberman JN, Sandler RS, Woods MS, Stemhagen A, Chee E, Lipton RB, Farup CE. Epidemiology of constipation (EPOC) study in the United States: relation of clinical subtypes to sociodemographic features. *Am J Gastroenterol* 1999; **94**: 3530-3540
- 10 **Pare P,** Ferrazzi S, Thompson WG, Irvine EJ, Rance L. An epidemiological survey of constipation in Canada: definitions, rates, demographics, and predictors of health care seeking. *Am J Gastroenterol* 2001; **96**: 3130-3137
- 11 **Chen LY,** Ho KY, Phua KH. Normal bowel habits and prevalence of functional bowel disorders in Singaporean adults-findings from a community based study in Bishan. *Singapore Med J* 2000; **41**: 255-258
- 12 **Boekema PJ,** van Dam van Isselt EF, Bots ML, Smout AJ. Functional bowel symptoms in a general Dutch population and associations with common stimulants. *Neth J Med* 2001; **59**: 23-30
- 13 **Icks A,** Haastert B, Enck P, Rathmann W, Giani G. Prevalence of functional bowel disorders and related health care seeking: a population-based study. *Z Gastroenterol* 2002; **40**: 177-183
- 14 **Walter S,** Hallbook O, Gotthard R, Bengmark M, Sjodahl R. A population-based study on bowel habits in a Swedish community: prevalence of faecal incontinence and constipation. *Scand J Gastroenterol* 2002; **37**: 911-916
- 15 **Levy N,** Stermer E, Steiner Z, Epstein L, Tamir A. Bowel habits in Israel. A cohort study. *J Clin Gastroenterol* 1993; **16**: 295-299
- 16 **Olubuyide IO,** Olawuyi F, Fasanmade AA. Frequency of defaecation and stool consistency in Nigerian students. *J Trop Med Hyg* 1995; **98**: 228-232
- 17 **Aichbichler BW,** Wenzl HH, Santa Ana CA, Porter JL, Schiller LR, Fordtran JS. A comparison of stool characteristics from normal and constipated people. *Dig Dis Sci* 1998; **43**: 2353-2362
- 18 **Thompson WG,** Longstreth GF, Drossman DA, Heaton KW, Irvine EJ, Müller-Lissner SA. Functional bowel disorders and functional abdominal pain. *Gut* 1999; **45** (Suppl 2): II43-II47
- 19 **Drossman DA,** Sandler RS, McKee DC, Lovitz AJ. Bowel patterns among subjects not seeking health care. Use of a questionnaire to identify a population with bowel dysfunction. *Gastroenterology* 1982; **83**: 529-534
- 20 **Manning AP,** Wyman JB, Heaton KW. How trustworthy are bowel histories? Comparison of recalled and recorded information. *BMJ* 1976; **3**: 213-214
- 21 **Whitehead WE,** Drinkwater D, Cheskin LJ, Heller BR, Schuster MM. Constipation in the elderly living at home. Definition, prevalence and relationship to lifestyle and health status. *J Am Geriatr Soc* 1989; **37**: 423-429
- 22 **Ashraf W,** Park F, Lof J, Quigley EM. An examination of the reliability of reported stool frequency in the diagnosis of idiopathic constipation. *Am J Gastroenterol* 1996; **91**: 26-32
- 23 **Thompson WG,** Irvine EJ, Pare P, Ferrazzi S, Rance L. Functional gastrointestinal disorders in Canada. First population-based survey using Rome II criteria with suggestions for improving the questionnaire. *Dig Dis Sci* 2002; **47**: 225-235
- 24 **Drossman DA.** The Rome criteria process: diagnosis and legitimation of irritable bowel syndrome. *Am J Gastroenterol* 1999; **94**: 2803-2807
- 25 **Thompson WG.** And the Working Team for functional bowel disorders. Functional bowel disorders and functional abdominal pain. In Drossman DA, Richter JE, Talley NJ, Thompson WG, Corazziari E, Whitehead WE, eds. The functional gastrointestinal disorders. Diagnosis, pathophysiology, and treatment. *Little Brown and Company Boston* 1994: 115-173
- 26 **Whitehead WE,** Bassotti G, Palsson O, Taub E, Cook EC, Drossman DA. Factor analysis of bowel symptoms in U.S. and Italian populations. *Dig Liver Dis* 2003; **35**: 774-783

Edited by Wang XL Proofread by Zhu LH

Association of *FAS* (*TNFRSF6*)-670 gene polymorphism with villous atrophy in coeliac disease

Jing Wu, BZ Alizadeh, TV Veen, JWR Meijer, CJJ Mulder, AS Peña

Jing Wu, BZ Alizadeh, TV Veen, AS Peña, Laboratory of Immunogenetics and Department of Gastroenterology, VU University Medical Centre, Amsterdam, PO Box 7057, 1007 MB Amsterdam, The Netherlands

JWR Meijer, CJJ Mulder, Departments of Pathology and Hepatogastroenterology, Rijnstate Hospital, Arnhem, The Netherlands

CJJ Mulder, Head of Department of Gastroenterology, VU University Medical Center, P.O. Box 7057, 1007 MB Amsterdam, Netherlands

Jing Wu, Department of Gastroenterology, Jiangsu Provincial Hospital of Traditional Chinese Medicine, 210029 Nanjing, Jiangsu Province, China

BZ Alizadeh, Genetic Epidemiology Unit, Department of Epidemiology and Biostatistics and Department of Clinical Genetics, Erasmus Medical Centre, Rotterdam, The Netherlands

TV Veen, Department of Neurology, VU University Medical Centre, Amsterdam, PO Box 7057, 1007 MB Amsterdam, The Netherlands

Supported by the Chinese Scholarship Council, No. 98932034

Correspondence to: Professor A.S. Peña, MD, PhD, FRCP, VU University Medical Centre, Department of Gastroenterology, Laboratory of Immunogenetics, P.O. Box 7057, 1007 MB Amsterdam, The Netherlands. as.pena@vumc.nl

Telephone: +31-20-4448416 **Fax:** +31-20-4448418

Received: 2003-07-17 **Accepted:** 2003-10-07

Abstract

AIM: To investigate the association of *FAS* gene polymorphism with coeliac disease (CD) development.

METHODS: *FAS-G670A* gene polymorphism, located in a gamma interferon activation site, was studied in 146 unrelated CD patients and 203 healthy ethnically matched controls. The restriction fragment length polymorphism (RFLP) method was used to identify *FAS-G670A* gene polymorphism.

RESULTS: No significant difference was found in genotype frequency between CD cases and controls. In controls, however, the frequency of the *GG* genotype was significantly higher in women (26.5%) than in men (12.8%) ($OR=2.44$, 95% CI 1.15-5.20, $P=0.020$) and it was also higher in men with CD than controls ($OR=2.60$, 95% CI 0.96-7.05, $P=0.061$). The *GG* genotype frequency was significantly higher in patients with most severe villous atrophy (Marsh IIIc lesions) ($OR=3.74$, 95% CI 1.19-11.82, $P=0.025$). A significantly less proportion of men suffered from Marsh IIIc lesions than women ($OR=0.20$, 95% CI 0.06-0.68, $P=0.01$). The risk of having severe villous atrophy increased with the additive effect of the *G* allele in women ($P=0.027$ for trend, age and gender adjusted).

CONCLUSION: *FAS-G670A* gene polymorphism is associated with the severity of villous atrophy in CD. Female gender is also associated with the severity of villous atrophy.

Wu J, Alizadeh BZ, Veen TV, Meijer JWR, Mulder CJJ, Peña AS. Association of *FAS* (*TNFRSF6*)-670 gene polymorphism with villous atrophy in coeliac disease. *World J Gastroenterol* 2004; 10(5): 717-720

<http://www.wjgnet.com/1007-9327/10/717.asp>

INTRODUCTION

The pathogenesis of coeliac disease (CD) is unclear. Although the majority of CD patients are HLA-DQ2 or DQ8 positive, only a small percentage of HLA-DQ2 and DQ8 carriers in the healthy European population develop CD^[1]. Human genome screening of CD patients and their families support the polygenic inheritance of the disease^[2]. Different genes are involved in the disease susceptibility or in determining clinical course and severity of the lesion^[3]. Ciccocioppo *et al*^[4] reported the significant correlation between the degree of villous atrophy (VA) and the level of enterocyte apoptosis. *FAS* (*TNFRSF6*) expression increased in the abnormal segment of small intestine in CD^[4,5]. Therefore, the epithelial *FAS* engagement might contribute to the development of villous atrophy^[4,5]. We studied the association between the *FAS-G670A* gene polymorphism with the severity of VA and the disease susceptibility in a cohort of untreated Caucasian CD patients at the time of presentation and ethnically matched healthy controls.

MATERIALS AND METHODS

Subjects

Before treatment, 146 unrelated CD patients were classified according to modified Marsh classification. Their diagnoses were confirmed only if patients responded to gluten-free diet both clinically and histologically^[6], and 203 healthy ethnically matched controls were enrolled in this study.

Methods

Villous atrophy classification The histological features were classified according to the modified Marsh classification^[7]. In the original classification, Marsh described subtotal villous atrophy as a destructive lesion and called it the Marsh III lesion. In our study, to assess the severity of the histological features, we classified the Marsh III type lesion into 3 subgroups^[8]. Briefly, in all subgroups, histological lesions had the significant intraepithelial lymphocytosis (>30 lymphocytes per 100 epithelial cells). The architectural changes permitted classifying the lesion into three subtypes with increasing severity. They were designated as Marsh IIIa (partial VA) when the villous-crypt ratio was less than 1/1, Marsh IIIb (subtotal VA) when there were still recognizable villi in an otherwise flat mucosa, and Marsh IIIc (total VA) when there was nearly complete absence of villi.

Typing *FAS-G670A* polymorphism PCR amplification and genotype analysis for *FAS-G670A* were performed according to previously published methods^[9]. In brief, genomic DNA was extracted from peripheral blood using a standard proteinase K digestion and phenol/chloroform extraction method and mouthwash method^[10]. The *FAS-G670A* polymorphism was typed as described previously by Huang *et al*^[9] with the following minor modifications. PCR: 5 min at 95 °C, 30 cycles of 30 s at 95 °C, 30 s at 62 °C, and 1 min at 72 °C, followed by a final extension for 7 min at 72 °C. Primer sequences were 5'-CTA CCT AAG AGC TAT CTA CCG TTC-3' and 5'-GGC TGT CCA TGT TGT GGC TGC-3'. The 332 bp PCR product

was digested with *MvaI* for 5 h at 37 °C. Allele G yielded three fragments of 99 bp, 189 bp, and 44 bp, whereas allele A yielded two fragments of 99 bp and 233 bp. Digested fragments were separated on 30g/L agarose gels and visualized after ethidium bromide staining (Figure 1).

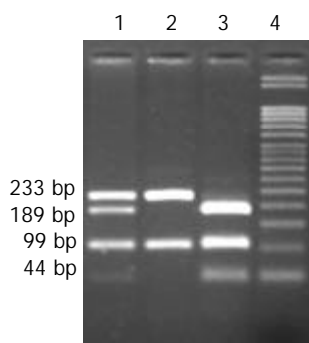


Figure 1 1: GA genotype, 2: AA genotype, 3: GG genotype, 4: 50 bp DNA marker distinguished alleles G (189 bp) and A (233 bp).

Statistical analysis

Hardy–Weinberg equilibrium test was carried out by using statistical software for linkage analysis^[11]. χ^2 statistics and Fisher's exact test were used for comparisons of frequencies. The subjects were classified according to the number of G alleles that they inherited, such as 0 for subjects who were carriers for A allele of *FAS-G670A*, *i.e.* AA genotype, 1 for those who were carriers of 1 copy of G allele, *i.e.* AG genotype and 2 for subjects who inherited 2 copies of G allele, *i.e.* GG genotype. Logistic regression was used to fit statistical models to predict the association of *FAS-G670A* polymorphism with the severity of villous atrophy or with susceptibility to CD. All the statistical models were adjusted for age (years) and gender. Associations are expressed as odd ratios (OR) with 95% confidence interval (95% CI). Estimation of 95% CI was based on Wald's method. A two tailed *P* value <0.05 was considered as significant. Statistical analysis was performed with SPSS version 10.07 for windows software.

Table 1 Characteristics and genotype frequencies of *FAS-G670A* in untreated CD with villous atrophy

	CD (n=146)	Controls (n=203)	OR ¹ (95%CI)	OR ² (95% CI)	OR ³ (95% CI)
Age (mean±SD) yr.	38.7±20.0	39.1±11.9			
Gender (F/M)	113/33	117/86			
GG genotype (F/M)	25/9	31/11	1.08 (0.64-1.82)	2.44 (1.15-5.20)	0.75 (0.31-1.82)
GA genotype (F/M)	60/15	66/49	0.79 (0.51-1.22)	0.99 (0.57-1.75)	1.37 (0.63-2.99)
AA genotype(F/M)	28/9	20/26	1.30 (0.78-2.16)	0.46 (0.24-0.91)	0.88 (0.37-2.11)

F, women; M, men, OR¹, age and gender adjusted, CD vs controls, OR², age adjusted, F vs M in healthy controls, OR³, age adjusted, F vs M in CD.

Table 2 Association of severity of villous atrophy with *FAS-G670A* polymorphism in untreated CD

Marsh	Genotype analysis			Allelic analysis			
	GG genotype F/M	GA genotype F/M	AA genotype F/M	OR ¹ (95% CI)	G allele (%)	A allele (%)	OR ² (95% CI)
IIIa (%)	3/3 (15.0)	17/6 (57.5)	6/5 (27.5)	Reference	35 (44.0)	45 (56.0)	Reference
IIIb (%)	9/5 (21.5)	25/7 (49.2)	15/4 (29.2)	1.63 (0.56-4.76)	60 (46.0)	70 (54.0)	1.10 (0.63-1.93)
IIIc (%)	13/1 (34.1) ³	18/2 (48.8)	7/0 (17.1)	3.74 (1.19-11.82)	48 (58.5)	34 (41.5)	1.81 (0.97-3.38)

F, women; M, men, OR¹, adjusted, for GG genotype frequency; ³*P*=0.025, OR², adjusted, for G allele frequency.

RESULTS

Susceptibility of CD

The characteristics of study participants are shown in Table 1. The genotype frequencies were in Hardy–Weinberg equilibrium proportions in patients and controls. There was no significant difference in genotype distributions between patients and controls (Table 1). In men, the frequency of GG genotype was higher in cases (27.3%) compared to that of controls (12.8%), yielding to OR of 2.60, 95% CI 0.96-7.05, *P*=0.061. The GG genotype was significantly (*P*=0.020) higher in women (26.5%) compared with men (12.8%) in healthy control.

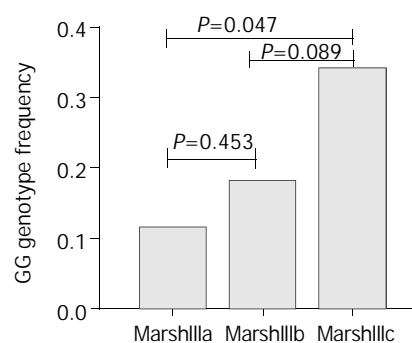


Figure 2 Trend for GG genotype frequency in different severity of villous atrophy in untreated CD women, *P*=0.027, adjusted for age.

Association of villous atrophy

In cases, men had a significantly lower frequency of Marsh IIIc compared to women (OR=0.20, 95% CI 0.06-0.68, *P*=0.01). Genotype and allele frequencies in Marsh III subgroups are presented in Table 2. There was a significant (*P*=0.025) difference of GG genotype frequency between Marsh IIIc which had the most severe form of the disease and Marsh IIIa (OR=3.74, 95% CI 1.19-11.82). In chromosomal analysis, we found a borderline significant association between G allele and Marsh IIIc villous atrophy (OR=1.81, 95% CI 0.97-3.38, Table 2). However, in women, G allele was significantly associated with this subgroup (OR=1.75, 95% CI 1.00-3.06, *P*=0.048).

The severity of VA increased additively with increasing number of G alleles in women ($P_{\text{for trend}}=0.027$) (Figure 2).

DISCUSSION

We found a significant association between the *FAS*-670 GG genotype and the severity of celiac disease, particularly in women. However, we did not find significant differences in genotype frequencies between controls and CD patients. This suggested that the *FAS* gene was not a susceptible gene for this disease. The fact that genotype frequencies of patients and controls were in Hardy Weinberg equilibrium confirmed the validity of the typing of the results. The intestinal pathological diagnosis was confirmed by two independent pathologists. Therefore our data suggested an association of *FAS*-G670A polymorphism with the severity of CD.

Since this polymorphism of the *FAS* gene (*TNFRSF6*) is located in the promoter region, it may affect the level of transcription of the *FAS* protein. Previous work suggested that the substitution of G to A in the position -670 (TTCCAG G/A AA) would change the gamma interferon activation site (GAS) (TTCnnnGAA)^[12-14]. This site was involved in interferon gamma and interferon alpha signalling^[15]. GAS elements are known to bind to homodimers of a phosphorylated form of the 91-kDa transcription factor, STAT1. Interferon gamma could cause tyrosine phosphorylation of STAT1 by the interferon gamma receptor-associated Janus kinases 1 and 2. Subsequently, phosphorylated STAT1 formed homodimers and translocated into the nucleus where it induced transcription of GAS-containing genes^[16]. *FAS* was significantly upregulated by interferon gamma according to several reports^[17-19]. Xu *et al.*^[20] and De Saint Jean *et al.*^[21] have implicated STAT1 in this upregulation effect of interferon gamma. We therefore postulate that *FAS*-670G variant containing the GAS (TTCCAGGAA) could be affected by interferon gamma production and increase the transcription of *Fas*. This may result in different degree of apoptosis in CD with different degrees of VA. Our data confirmed that the risk of having severe villous atrophy increased additively with the number of G alleles. The GG homozygote was strongly correlated to the severity of VA in CD. Intermediated by GAS, both interferon gamma and *Fas* might play an important role in the pathogenesis of villous atrophy. This was in agreement with previous reports showing that mucosal gluten exposure elicited a high level interferon gamma expression in CD^[22]. Interferon gamma could increase *FAS*-induced apoptosis of human intestinal epithelial cells in a dose-dependent manner^[23].

Considering the previous reports^[24-26], we hypothesize that *FAS*-G670A is functional and further functional tests are necessary. The *FAS*-G670A gene polymorphism contributes to the determination of the severity of small intestinal lesions and opens a new area of research that may help understand the heterogeneity of this disease. Our findings were in the same line of a recent genome-wide family-based linkage study of CD that found a potential susceptible locus at 10q23.1^[27] close to the cytogenetic region (10q23.31) of the *FAS* (*TNFRSF6*) gene^[28]. These results may also explain why the different genome-wide studies of families with multiple cases of CD had not uniformly found a similar lod score at chromosome 10q23, since the proportion of patients with severe villous atrophy might differ from each other in those studies.

Our data also showed a gender difference in relation to the severity of VA and in the genotype distribution of *FAS*-G670A. Even though there was no difference of GG genotype frequency in women and men among the cases, men had a significantly less proportion of Marsh IIIc VA than women. This might be due to the different immune responses between men and women. Women were more likely to develop Th1 response

(secreting higher amounts of IL-2, interferon gamma, and TNF-beta than men)^[29]. In summary, our findings suggest that increased expression of *FAS* in villous atrophy is in part genetically regulated and the *FAS* gene plays a significant role.

ACKNOWLEDGEMENTS

The authors would like to express thanks to JBA Crusius PhD, A. Zwiers MSc and Ms. M Demirkaya for their laboratory support, and Ms. L Atjak for her secretarial assistance.

REFERENCES

- Schuppan D.** Current concepts of celiac disease pathogenesis. *Gastroenterology* 2000; **119**: 234-242
- King AL, Ciclitira PJ.** Celiac disease: strongly heritable, oligogenic, but genetically complex. *Mol Genet Metab* 2000; **71**: 70-75
- Fraser JS, Ciclitira PJ.** Pathogenesis of coeliac disease: implications for treatment. *World J Gastroenterol* 2001; **7**: 772-776
- Ciccocioppo R, Di Sabatino A, Parroni R, Muzi P, D' Alo S, Ventura T, Pistoia MA, Cifone MG, Corazza GR.** Increased enterocyte apoptosis and Fas-Fas ligand system in celiac disease. *Am J Clin Pathol* 2001; **115**: 494-503
- Maiuri L, Ciacci C, Raia V, Vacca L, Ricciardelli I, Raimondi F, Auricchio S, Quarantino S, Londei M.** FAS engagement drives apoptosis of enterocytes of coeliac patients. *Gut* 2001; **48**: 418-424
- Revised criteria for diagnosis of coeliac disease.** Report of Working Group of European Society of Paediatric Gastroenterology and Nutrition. *Arch Dis Child* 1990; **65**: 909-911
- Marsh MN.** Gluten, major histocompatibility complex, and the small intestine. A molecular and immunobiologic approach to the spectrum of gluten sensitivity ('celiac sprue'). *Gastroenterology* 1992; **102**: 330-354
- Rostami K, Kerckhaert J, Tiemessen R, von Blomberg BM, Meijer JW, Mulder CJ.** Sensitivity of antiendomysium and antigliadin antibodies in untreated celiac disease: disappointing in clinical practice. *Am J Gastroenterol* 1999; **94**: 888-894
- Huang QR, Morris D, Manolios N.** Identification and characterization of polymorphisms in the promoter region of the human Apo-1/Fas (CD95) gene. *Mol Immunol* 1997; **34**: 577-582
- Laine ML, Farre MA, Crusius JB, van Winkelhoff AJ, Pena AS.** The mouthwash: a non-invasive sampling method to study cytokine gene polymorphisms. *J Periodontol* 2000; **71**: 1315-1318
- Ott J.** Utility programs for analysis of genetic linkage; Program HWE; 1988; URL: <http://www.hgmp.mrc.ac.uk/Registered/Help/linkutil/>
- Decker T, Kovarik P, Meinke A.** GAS elements: a few nucleotides with a major impact on cytokine-induced gene expression. *J Interferon Cytokine Res* 1997; **17**: 121-134
- Chatterjee-Kishore M, Wright KL, Ting JP, Stark GR.** How Stat1 mediates constitutive gene expression: a complex of unphosphorylated Stat1 and IRF1 supports transcription of the LMP2 gene. *EMBO J* 2000; **19**: 4111-4122
- Bauvois B, Djavaheri-Mergny M, Rouillard D, Dumont J, Wietzerbin J.** Regulation of CD26/DPPIV gene expression by interferons and retinoic acid in tumor B cells. *Oncogene* 2000; **19**: 265-272
- Shuai K.** Interferon-activated signal transduction to the nucleus. *Curr Opin Cell Biol* 1994; **6**: 253-259
- Gao J, Morrison DC, Parmely TJ, Russell SW, Murphy WJ.** An interferon-gamma-activated site (GAS) is necessary for full expression of the mouse iNOS gene in response to interferon-gamma and lipopolysaccharide. *J Biol Chem* 1997; **272**: 1226-1230
- Schwartzberg LS, Petak I, Stewart C, Turner PK, Ashley J, Tillman DM, Douglas L, Tan M, Billups C, Mihalik R, Weir A, Tauer K, Shope S, Houghton JA.** Modulation of the Fas signaling pathway by IFN-gamma in therapy of colon cancer: phase I trial and correlative studies of IFN-gamma, 5-fluorouracil, and leucovorin. *Clin Cancer Res* 2002; **8**: 2488-2498
- Dai C, Krantz SB.** Interferon gamma induces upregulation and activation of caspases 1, 3, and 8 to produce apoptosis in human erythroid progenitor cells. *Blood* 1999; **93**: 3309-3316
- Pouly S, Becher B, Blain M, Antel JP.** Interferon-gamma modu-

- lates human oligodendrocyte susceptibility to Fas-mediated apoptosis. *J Neuropathol Exp Neurol* 2000; **59**: 280-286
- 20 **Xu X**, Fu XY, Plate J, Chong AS. IFN-gamma induces cell growth inhibition by Fas-mediated apoptosis: requirement of STAT1 protein for up-regulation of Fas and FasL expression. *Cancer Res* 1998; **58**: 2832-2837
- 21 **De Saint Jean M**, Brignole F, Feldmann G, Goguel A, Baudouin C. Interferon-gamma induces apoptosis and expression of inflammation-related proteins in Chang conjunctival cells. *Invest Ophthalmol Vis Sci* 1999; **40**: 2199-2212
- 22 **Nilsen EM**, Jahnsen FL, Lundin KE, Johansen FE, Fausa O, Sollid LM, Jahnsen J, Scott H, Brandtzaeg P. Gluten induces an intestinal cytokine response strongly dominated by interferon gamma in patients with celiac disease. *Gastroenterology* 1998; **115**: 551-563
- 23 **Ruemmele FM**, Russo P, Beaulieu J, Dionne S, Levy E, Lentze MJ, Seidman EG. Susceptibility to FAS-induced apoptosis in human nontumoral enterocytes: role of costimulatory factors. *J Cell Physiol* 1999; **181**: 45-54
- 24 **Huang QR**, Danis V, Lassere M, Edmonds J, Manolios N. Evaluation of a new Apo-1/Fas promoter polymorphism in rheumatoid arthritis and systemic lupus erythematosus patients. *Rheumatology* 1999; **38**: 645-651
- 25 **Feuk L**, Prince JA, Breen G, Emahazion T, Carothers A, St Clair D, Brookes AJ. Apolipoprotein-E dependent role for the FAS receptor in early onset Alzheimer's disease: finding of a positive association for a polymorphism in the TNFRSF6 gene. *Hum Genet* 2000; **107**: 391-396
- 26 **Bolstad AI**, Wargelius A, Nakken B, Haga HJ, Jonsson R. Fas and Fas ligand gene polymorphisms in primary Sjogren's syndrome. *J Rheumatol* 2000; **27**: 2397-2405
- 27 **King AL**, Yiannakou JY, Brett PM, Curtis D, Morris MA, Dearlove AM, Rhodes M, Rosen-Bronson S, Mathew C, Ellis HJ, Ciclitira PJ. A genome-wide family-based linkage study of coeliac disease. *Ann Hum Genet* 2000; **64**(Pt 6): 479-490
- 28 <http://genome.ucsc.edu/>, Assembly Human April 2003
- 29 **Whitacre CC**, Reingold SC, O'Looney PA. A gender gap in autoimmunity. *Science* 1999; **283**: 1277-1278

Edited by Gupat MK and Wang XL

Gallbladder contractility and volume characteristics in gallstone dyspepsia

De-Chuan Chan, Tzu-Ming Chang, Cheng-Jueng Chen, Teng-Wei Chen, Jyh-Cherng Yu, Yao-Chi Liu

De-Chuan Chan, Cheng-Jueng Chen, Teng-Wei Chen, Jyh-Cherng Yu, Yao-Chi Liu, Division of General Surgery, Department of Surgery, Tri-Service General Hospital, National Defense Medical Center, Taipei, Taiwan, China

Tzu-Ming Chang, Department of Surgery, Shalu Tungs' Memorial Hospital, Tai-Chung, Taiwan, China

Correspondence to: Yao-Chi Liu, MD, Division of General Surgery, Department of Surgery, Tri-Service General Hospital, 325 Section 2, Cheng-Kung Road, Neihu 114, Taipei, Taiwan, China. chrischan1168@yahoo.com.tw

Telephone: +886-2-87927191 **Fax:** +886-2-87927372

Received: 2003-10-08 **Accepted:** 2003-12-30

Abstract

AIM: It is difficult to differentiate gallstone dyspepsia and functional dyspepsia by clinical symptoms and signs. We hypothesized that gallstone dyspepsia was related to abnormal gallbladder motility. We aimed to differentiate gallstone dyspepsia from functional dyspepsia by measuring gallbladder motility.

METHODS: We measured gallbladder volume changes in response to gastric distension (saline 500 mL) and fatty meal in 10 normal volunteers (controls) and 62 patients with gallstones and dyspepsia before cholecystectomy. Forty cholecystectomized patients were symptom free or had improvement (group I), while the remaining 22 patients had persistent dyspepsia (group II). Gallbladder volume change and ejection fraction were analyzed and compared among the three groups.

RESULTS: In group I, there were significant decreases in gallbladder volumes 5-25 min after gastric distension, compared to fasting volumes. Compared to normal volunteers and group II, group I had significantly decreased gallbladder volumes 10-20 min after drinking 500 mL of normal saline and 10 to 50 min after eating fatty meal.

CONCLUSION: Our results support the hypothesis that increased gallbladder contraction after gastric distension or fatty meal may be related to dyspeptic symptoms in uncomplicated gallstone disease. These findings may be useful in differentiating functional dyspepsia from gallstone dyspepsia, patients with the latter disease may benefit from laparoscopic cholecystectomy.

Chan DC, Chang TM, Chen CJ, Chen TW, Yu JC, Liu YC. Gallbladder contractility and volume characteristics in gallstone dyspepsia. *World J Gastroenterol* 2004; 10(5): 721-724

<http://www.wjgnet.com/1007-9327/10/721.asp>

INTRODUCTION

Laparoscopic cholecystectomy is the choice of treatment for symptomatic gallstone disease and is performed with increasing frequency. It is clear that gallstone patients with complications

(acute cholecystitis, gallstone pancreatitis or jaundice) or severe biliary pain should undergo cholecystectomy. Conversely, for asymptomatic gallstone disease, no treatment should be done. Nonetheless, some patients with uncomplicated gallstone disease, once termed gallstone dyspepsia^[1], suffer from mild abdominal symptoms, such as postprandial flatulence, bloating, nausea and belching. Most of these patients also undergo laparoscopic cholecystectomy, but about 20-30% of these cholecystectomized patients still complain of abdominal symptoms after surgery. These symptoms may be associated with preoperatively undiagnosed functional gut disease unrelated to gallstones^[2-4]. In order to avoid unnecessary cholecystectomies, it is important to ascertain preoperatively that these mild symptoms of gallstone patients with dyspepsia are really caused by gallstones. New diagnostic methods to predict which patients will benefit from cholecystectomy are therefore necessary.

Gallstone dyspepsia and functional dyspepsia have coexisting symptoms and it is difficult to differentiate from each other based on the dyspeptic symptoms^[5-7]. Despite numerous studies, the mechanism of gallstone dyspepsia has not been completely explained^[8-10]. In the past, the majority of literature focused on the pathogenesis of gallstone formation. It is postulated that two distinct subgroups of gallstone patients can be identified with regard to gallbladder emptying, including "normal contractors" and "pathologic contractors" or "strong contractors" and "weak contractors"^[11-14]. Therefore, we hypothesize that in these patients, gallstone dyspepsia may result from abnormal gallbladder motor activity stimulated by gastric distension or fatty meals. In this study, we investigated the difference in gallbladder contractility in response to gastric distension and fatty meals in healthy volunteers and patients with gallstones and dyspepsia. If so, preoperative assessment of gallbladder contractility with ultrasonography would contribute to better outcomes of cholecystectomy.

MATERIALS AND METHODS

Gallbladder volume was assessed in 72 subjects, including 10 healthy controls and 62 gallstone patients with symptoms of dyspepsia. None of the gallstone patients had past or present signs of complicated gallstone diseases, such as acute cholecystitis, biliary pancreatitis, jaundice or severe biliary pain. Panendoscopy and abdominal ultrasound were done to exclude esophagitis, peptic ulcer, pancreatitis or other organic diseases in all gallstone patients. After an overnight fast, the fasting gallbladder volume was measured ultrasonographically three times within 5 min, with the subjects lying supine or turned partially on their sides. The gallbladder volume was estimated using a real-time ultrasound system (MK-500, ATL, Bothell, WA) with a 3.5-MHz transducer. The largest longitudinal and transverse gallbladder images were recorded. The gallbladder volume was calculated using the computerized sum-of-cylinders method as described by Hopman *et al*^[15]. Then, the gallbladder volume was again measured after the patient drank 500 mL of normal saline at room temperature within a 2-min period. Measurement was made at 5 min

intervals for the first 30 min, then at 10 min intervals between 30 to 90 min after drinking. On the next day, we serially measured gallbladder volumes after the patients ate a fatty meal (fried egg cake) containing protein 9.32 g, fat 20.3 g and carbohydrate 14.4 g, 277.58 Kcal, followed by 100 mL of water. After the measurements, the gallstone patients with dyspepsia underwent laparoscopic cholecystectomy and were monitored in the outpatient department at least for 1 yr after surgery. These patients were allocated to 2 groups according to cholecystectomy outcomes. Forty patients (group I) were symptom free or had improved symptoms after cholecystectomy. Twenty-two patients (group II) complained of persistent dyspepsia after cholecystectomy, with the same symptoms as their preoperative symptoms. Thereafter, we analyzed and compared the differences among the three patient groups (groups I, II and controls) for fasting gallbladder volume, volume changes and ejection fraction in response to gastric distension and fatty meal.

The fasting gallbladder volume was calculated as the mean of three values before meal intake. The postprandial gallbladder volume was expressed as a percentage of the fasting volume. Results are expressed as mean±SE. Statistical analyses were performed using Statistical Package for the Social Sciences (SPSS) software. Comparisons among the three groups were analyzed using the χ^2 test. Differences between means were considered significant at $P<0.05$.

RESULTS

Patient characteristics are shown in Table 1. The fasting gallbladder volume tended to be larger in the two groups of patients with gallstones than in healthy volunteers during either test (Table 1).

Table 1 Characteristics of subjects (χ^2 test)

	Normal (n=10)	Group I (n=40)	Group II (n=22)	P value
Age, (yr)	61.2±12.3	59.5±15.1	62.5±13.4	NS
Sex (M:F)	4:6	14:26	9:13	NS
Weight (kg)	60.9±5.7	59.8±13.8	57.6±9.8	NS
BMI	27.8±3.8	24.8±4.7	24.4±5.7	NS
Fasting gallbladder volume (mL)	26.3±7.4	32.6±14.1	33.9±10.7	<0.05

BMI, body mass index. $P<0.05$ was considered statistically significant.

In normal volunteers and group II gallstone patients after drinking 500 mL normal saline, the gallbladder volume did not significantly change from the basal fasting level throughout the 90-min observation period (Figure 1). In contrast, in group I patients, within 5 to 25 min after drinking 500 mL of normal saline, there was a significant decrease in the gallbladder volume from the basal fasting volume ($P<0.05$) (Figure 1). The gallbladder volume change (10-20 min) in group I patients was significantly larger than that in healthy volunteers and group II patients ($P<0.05$) (Figure 1).

After the fatty meal, there were significant decreases in gallbladder volume in healthy volunteers and the two groups of gallstone patients throughout the 90-min study period (Figure 2). Group I patients had larger gallbladder volume changes ($P<0.05$) than the other two groups during the early phase (10-50 min) of testing, the lowest residual volume was detected at the 40th min. We also found that the gallbladder volume change was significantly smaller ($P<0.05$) in group II during the early phase (10-40 min) than in healthy volunteers in

response to fatty meal (Figure 2). The ejection fraction was significantly greater ($P<0.05$) in group I than the other two groups 10-50 min after the fatty meal (Figure 3).

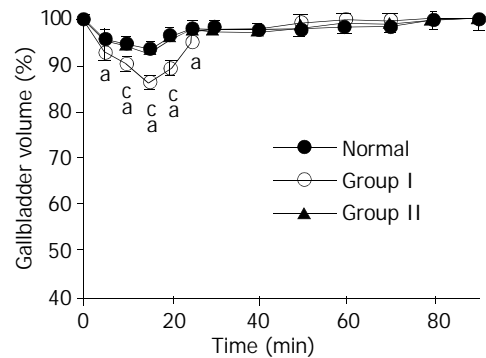


Figure 1 Gallbladder volume change after ingestion of 500 mL of normal saline (N.S.) in healthy volunteers (normal controls, $n=10$), group I (symptom free or symptom improved after cholecystectomy) ($n=40$) and group II (persistent dyspepsia after cholecystectomy) ($n=22$) gallstone patients. Values are mean±SE (χ^2 test). ^a $P<0.05$: significant volume change from fasting gallbladder volume. ^c $P<0.05$: significant difference among three groups (group I vs normal group and group II patients).

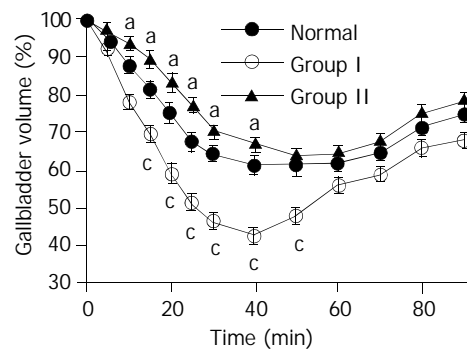


Figure 2 Gallbladder volume change after fatty meal in healthy volunteers (normal, $n=10$), group I (symptom free or symptom improved after cholecystectomy) ($n=40$) and group II (persistent dyspepsia after cholecystectomy) ($n=22$) gallstone patients. Values are mean±SE (χ^2 test). ^a $P<0.05$: significant difference between normal group and group II. ^c $P<0.05$: significant differences among three groups (group I vs normals and group II patients).

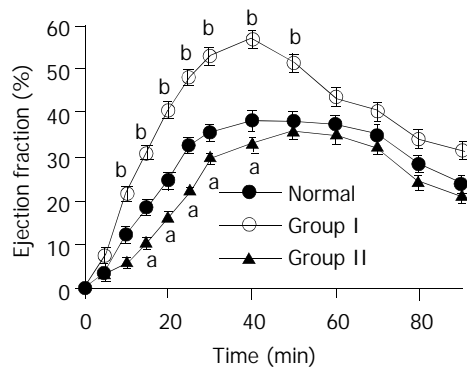


Figure 3 Ejection fraction of gallbladder in healthy volunteers and gallstone patients after oral fatty meal. Values are mean±SE (χ^2 test). ^a $P<0.05$: significant difference between group II (persistent dyspepsia after cholecystectomy) and normal group. ^b $P<0.05$: significant differences among three groups (group I vs normal group and group II).

DISCUSSION

It is clear that complicated gallstone diseases, such as acute cholecystitis, obstructive jaundice, gallstone pancreatitis and severe biliary pain, are good indications for cholecystectomy. With the technical improvements in laparoscopic surgery, many patients with uncomplicated gallstone disease termed gallstone dyspepsia underwent laparoscopic cholecystectomy for only mild gastrointestinal symptoms such as postprandial flatulence, bloating or belching. However, the benefit of cholecystectomy for gallstone patients with dyspepsia has remained debatable^[16]. Only about one half of patients were symptom free after cholecystectomy^[17,18]. About 20-30% of cholecystectomized patients still complained of dyspepsia, which might have been associated with preoperatively undiagnosed functional gut diseases unrelated to gallstones^[2-4]. Because gallstone dyspepsia and functional dyspepsia had coexisting symptoms, it is difficult to differentiate them based on dyspeptic symptoms^[5]. In order to avoid unnecessary cholecystectomies, it is important to ascertain preoperatively that the symptoms of gallstone patients with dyspepsia are truly caused by gallstones.

Even with numerous studies, the mechanisms underlying gallstone dyspepsia could not be completely explained^[8-10]. Some investigators believed that dyspepsia was associated with functional gut diseases such as antroduodenal reflux and irritable bowel syndrome, rather than with gallstone disease^[19,20]. However, Johnson^[21] suggested that an association existed between flatulent dyspepsia and gallbladder disease, although it had no direct relationship. In the past, the majority of literature focused on the pathogenesis of gallstone formation rather than on the association of gallbladder motility and clinical symptoms. Using different techniques, investigators showed decreased^[10-12], normal^[22] or even increased^[23] gallbladder contractility compared to normal controls. Moreover, it has been postulated that two distinct subgroups of gallstone patients could be identified with regard to gallbladder emptying, including strong and weak contractors^[24,25]. Perhaps the mild abdominal symptoms were related to abnormal gallbladder motility. We identified two distinct groups of patients with gallstones and dyspepsia in terms of gallbladder contractility.

In our study, patients with gallstones and dyspepsia had significantly larger fasting gallbladder volumes, which were similar to a previous report^[26]. The symptoms experienced in gallstone patients were traditionally believed to arise from gallbladder spasm, and normal gallbladder contractility was thought to be a prerequisite for the development of symptoms. Heaton reported that gallstones were prone to cause symptoms in younger patients and cited the explanation that younger people perhaps had stronger gallbladder contractions^[27]. We also found that group I patients had larger gallbladder volume changes and stronger gallbladder contractions during the early phase of observation in response to 500 mL of normal saline and fatty meals, although there was no significant difference in age among them. We found that in group I patients, symptoms improved after cholecystectomy, that is, patients who had stronger gallbladder contractions in response to gastric distension and fatty meal benefited from cholecystectomy. However, group II patients with impaired gallbladder contractility did not benefit from cholecystectomy because their symptoms were perhaps unrelated to gallbladder motility.

In 1979 Debas *et al* found that antral distension initiated a cholinergic pyloro-cholecystic reflex causing gallbladder contraction in dogs^[28]. Intact vagus nerves and cholinergic pathways were required for this reflex. Vagal stimulation via mechanoreceptors in the stomach initiated gallbladder contraction independently of meal composition^[29]. Yamamura *et al* found that gastric distension following ingestion of

400 mL of water induced a maximum gallbladder evacuation of 25%, compared with a maximum gallbladder contraction of 44% after ingestion of fatty meal in humans^[30]. However, in our study, the gallbladder response to gastric distension following ingestion of 500 mL of normal saline in healthy volunteers and group II gallstone patients was not significantly different from fasting gallbladder volumes. In group I gallstone dyspepsia patients, after drinking 500 mL of normal saline, the lowest gallbladder residual volume (13%) occurred at 15 min, with progressive recovery to the fasting volume thereafter. This saline water induced gallbladder early net emptying most prominently between 5 and 25 min in group I patients. In contrast, after fatty meal, there were significant decreases in gallbladder volumes both in healthy volunteers and the two groups of gallstone patients throughout the study period. The group I gallstone patients had the largest gallbladder volume change at the 40th min of the study. The ejection fraction was significantly increased in group I patients compared to the other two groups 10-50 min after fatty meal, but not thereafter.

Our study showed that gallbladders of group I gallstone dyspepsia patients had greater motility than those of normal individuals and group II patients in response to both gastric distension and fatty meal, which is important for elucidating the pathophysiology of gallstone dyspepsia. To our knowledge, these findings have not been previously reported. The greater motility might have been caused by hypersensitivity of the gallbladder wall to neural stimuli and hormone or by increased serum hormone levels in patients with gallstone dyspepsia. We do not know if gallbladder hypermotility precedes the development of gallstones, accompanies their development or is a relatively late sequel of their appearance. The finding that not all gallstone patients have gallbladder hypermotility also suggests there may be mechanisms for hypermotility other than the gallstones themselves. The primary mechanism is still debated and may indeed differ among individual patients. The gallbladder hypermotility phenomenon requires further studies.

In our study, more patients (34%) did not benefit from cholecystectomy than those in other studies (20-30%). We consider that the difference in the study populations may explain this phenomenon. Previous studies included more patients with acute cholecystitis or severe biliary pain who are better candidates for cholecystectomy^[2-4]. The patients in our study were selected because of their relatively mild symptoms of postprandial distress without fever, chills, transient jaundice or severe biliary pain. This is one reason that might explain why others reported better cholecystectomy results.

Most studies of gallbladder motility in the presence of gallstones have shown impaired gallbladder contractility. Thus, our findings have also been noted by others^[22-25]. Our study indicated that increased gallbladder contraction was the prerequisite for the development of dyspepsia symptoms. Previous studies included more asymptomatic patients with decreased gallbladder contractions in response to gastric distension and fatty meals.

Increased gallbladder contractility in patients with gallstone dyspepsia may be useful in identifying patients with atypical mild symptoms or possibly with early acalculous cholecystitis. The studies we conducted were noninvasive, inexpensive and within the capability of conducting ultrasonography in modern hospitals. The findings of promptly increased gallbladder contractility in response to intake of 500 mL of normal saline and fatty meal may lend support to including gallbladder contractility studies as part of the dyspepsia differential diagnosis.

Postprandial gallbladder volume changes and relative ejection fraction, determined sonographically, seem to be able to discriminate gallstone dyspepsia from functional dyspepsia.

In clinical practice, this type of diagnostic study may help to determine the appropriate treatment for gallstone patients with dyspepsia.

REFERENCES

- 1 **Barbara L**, Camilleri M, Corinaldesi R. Definition and investigation of dyspepsia. Consensus of an international ad hoc working party. *Dig Dis Sci* 1989; **34**: 1272-1276
- 2 **Ure BM**, Troidl H, Spangenberg. Long-term result after laparoscopic cholecystectomy. *Br J Surg* 1995; **82**: 267-270
- 3 **Borly L**, Anderson IB, Bardram L. Preoperative prediction model of outcome after cholecystectomy for symptomatic gallstones. *Scand J Gastroenterol* 1999; **34**: 1144-1152
- 4 **Gui GP**, Cheruvu CV, West N. Is cholecystectomy effective treatment for symptomatic gallstones? Clinical outcome after long-term follow up. *Ann R Coll Surg Engl* 1998; **80**: 25-32
- 5 **Muszynski J**, Sieminska J, Zagorowicz. Comparison of clinical features of cholecystolithiasis and functional dyspepsia. *Med Sci Monit* 2000; **6**: 330-335
- 6 **Heikkinen M**, Pikkarainen P, Takala J, Rasanen H, Julkunen R. Etiology of dyspepsia: four hundred unselected consecutive patients in general practice. *Scand J Gastroenterol* 1995; **30**: 519-523
- 7 **Koch M**, Caparso G. Functional dyspepsia: how could a biliary dyspepsia sub-group be recognized? A methodological approach. *Ita J Gastroenterol* 1996; **28**: 261-268
- 8 **Crean GP**, Holden RJ, Knill-Jones RP. A database on dyspepsia. *Gut* 1994; **35**: 191-202
- 9 **Kang JY**, Yap I, Gwee KA. The pattern of functional and organic disorders in an Asian gastroenterological clinic. *J Gastroenterol Hepatol* 1994; **9**: 124-127
- 10 **Berstad A**, Hausken T, Gilja OH. Imaging studies in dyspepsia. *Eur J Surg Suppl* 1998; **582**: 42-49
- 11 **Pomeranz IS**, Shaffer EA. Abnormal gallbladder emptying in a subgroup of patients with gallstones. *Gastroenterology* 1985; **88**: 787-791
- 12 **Fan Y**, Dou YL, Dai XZ. Gallbladder hypokinesia in patients with functional dyspepsia. *Chin Nat J New Gastroenterol* 1996; **2**(Suppl 1): 114
- 13 **Thompson JC**, Fried GM, Ogden WD. Correlation between release of cholecystokinin and contraction of the gallbladder in patients with gallstones. *Ann Surg* 1982; **195**: 670-676
- 14 **Zhu XG**, Greeley GH, Newman J. Correlation of in vitro measurement of contractility of the gallbladder with *in vivo* ultrasonographic findings in patients with gallstones. *Surg Gynaecol Obstet* 1985; **161**: 470-472
- 15 **Hopman WP**, Brouwer WF, Rosenbusch G. A computerized method for rapid quantification of gall bladder volume from real-time sonograms. *Radiology* 1985; **154**: 236-237
- 16 **Paul A**, Troidl H, Gay K. Dyspepsia and food intolerance in symptomatic gallstone disease. Does cholecystectomy help? *Chirurg* 1991; **62**: 462-466
- 17 **Ros E**, Zambon D. Postcholecystectomy symptoms > a prospective study of gallstone patients before and two years after surgery. *Gut* 1987; **28**: 1500-1504
- 18 **Johnson AG**. Cholecystectomy and gallstone dyspepsia-clinical and physiological study of a symptom complex. *Ann Royal Coll Surg Engl* 1975; **56**: 69-80
- 19 **Egbert AM**. Gallstone symptoms. Myth and reality. *Postgrad Med* 1991; **90**: 119-126
- 20 **Talley NJ**. Gallstones and upper abdominal discomfort. Innocent bystander or a cause of dyspepsia? *J Clin Gastroenterol* 1995; **20**: 182-183
- 21 **Howard PJ**, Murphy GM, Dowling RH. Gallbladder emptying patterns in response to a normal meal in healthy subjects and patients with gallstones: ultrasound study. *Gut* 1991; **32**: 1406-1411
- 22 **Fisher RS**, Stelzer F, Rock E. Abnormal gallbladder emptying in patients with gallstones. *Dig Dis Sci* 1982; **27**: 1019-1024
- 23 **Shaffer EA**, McOrmond P, Duggan H. Quantitative cholecintigraphy: assessment of gallbladder filling and emptying and duodenogastric reflux. *Gastroenterology* 1980; **79**: 899-906
- 24 **Van Berge Henegouwen GP**, Hofman AF. Nocturnal gallbladder storage and emptying in gallstone patients and healthy subjects. *Gastroenterology* 1978; **75**: 879-885
- 25 **Maudgal DP**, Kupfer RM, Zentler-Munro PL. Postprandial gallbladder emptying in patients with gallstones. *BMJ* 1980; **280**: 141-143
- 26 **van Erpecum KJ**, van Berg Henegouwen GP, Stolk MFG. Fast-ing gallbladder volume, postprandial emptying and cholecysto-kinin release in gallstone patients and normal subjects. *J Hepatol* 1992; **14**: 194-202
- 27 **Heaton KW**, Braddon FE, Mountford RA. Symptomatic and silent gall stones in community. *Gut* 1991; **32**: 316-332
- 28 **Debas HT**, Yamagishi T. Evidence for a pyloro-cholecytic reflex for gallbladder contraction. *Ann Surg* 1979; **190**: 170-175
- 29 **Froehlich F**, Gonvers JJ, Fried M. Role of nutrient fat and chole-cystokinin in regulation of gallbladder emptying in man. *Dig Dis Sci* 1995; **40**: 529-533
- 30 **Yamamura T**, Takahashi T, Kusunoki M. Gallbladder dynamics and plasma cholecystokinin responses after meals, oral water, or sham feeding in healthy subjects. *Am J Med Sci* 1988; **295**: 102-107

Edited by Wang XL Proofread by Zhu LH

Relationship between inducible nitric oxide synthase expression and angiogenesis in primary gallbladder carcinoma tissue

Xin-Jie Niu, Zuo-Ren Wang, Sheng-Li Wu, Zhi-Min Geng, Yun-Feng Zhang, Xing-Lei Qing

Xin-Jie Niu, Zuo-Ren Wang, Sheng-Li Wu, Zhi-Min Geng, Yun-Feng Zhang, Xing-Lei Qing, Department of Hepatobiliary Surgery, First Hospital of Xi'an Jiaotong University, Xi'an 710061, Shaanxi Province, China

Correspondence to: Dr. Xin-Jie Niu, Department of Hepatobiliary Surgery, First Hospital of Xi'an Jiaotong University, Xi'an 710061, Shaanxi Province, China. niuxinjie@email.com

Telephone: +86-29-85324009 **Fax:** +86-29-85324009

Received: 2003-05-11 **Accepted:** 2003-06-07

Abstract

AIM: To explore the relationship between angiogenesis and biological behaviors of primary gallbladder carcinoma (PGBC), the relationship between the expression of inducible nitric oxide synthase (iNOS) and biological behaviors of PGBC and its relationship with the expression of iNOS and angiogenesis of PGBC.

METHODS: The expression of iNOS and micro-vessel density (MVD) were assessed by immunohistochemical method and image analysis system in 40 specimens of PGBC and in 8 specimens of normal gallbladder. The immunostaining results and related clinicopathologic materials were analyzed by statistical methods.

RESULTS: MVD in PGBC was significantly higher than that in normal gallbladder tissue (46 ± 14 vs 14 ± 6 , $P < 0.05$), and was not related with age, gender, tumor size and histological type. MVD of poorly and undifferentiated tumor tissues was higher than that of moderately-differentiated and well-differentiated tumor tissues (52 ± 9 vs 43 ± 9 vs 33 ± 6 , $P < 0.01$). MVD of Nevin IV and V stages was higher than that of Nevin I, II and III stages (52 ± 8 vs 37 ± 13 , $P < 0.01$). MVD of cases with lymphatic or liver metastasis was significantly higher than that without liver metastasis (55 ± 6 vs 42 ± 10 , $P < 0.05$) or lymphatic metastasis (53 ± 8 vs 38 ± 8 , $P < 0.01$). The positive level index (PLI) of iNOS in PGBC was 0.435 ± 0.134 , and was not related with age, gender, tumor size, histological type, differentiation and clinical stage of PGBC. The PLI of iNOS in cases with lymphatic metastasis was higher than that without lymphatic metastasis (0.573 ± 0.078 vs 0.367 ± 0.064 , $P < 0.01$). The PLI of iNOS in cases with liver metastasis was higher than that without liver metastasis (0.533 ± 0.067 vs 0.424 ± 0.084 , $P < 0.05$). There was a significant correlation between PLI of iNOS and MVD in PGBC ($P < 0.05$).

CONCLUSION: Angiogenesis of PGBC is significantly related to the biological behaviors of PGBC. The expression of iNOS is related to the biological behaviors of PGBC. The detection of MVD and the expression of iNOS in PGBC can be used as parameters to determine the degree of malignancy and prognosis.

Niu XJ, Wang ZR, Wu SL, Geng ZM, Zhang YF, Qing XL. Relationship between inducible nitric oxide synthase expression and angiogenesis in primary gallbladder carcinoma tissue. *World J Gastroenterol* 2004; 10(5): 725-728

<http://www.wjgnet.com/1007-9327/10/725.asp>

INTRODUCTION

PGBC is a kind of malignant neoplasm with poor prognosis, and accounts for 1.5% of digestive carcinomas^[1]. It is difficult to be diagnosed in its early stage. Recent studies have shown its morbidity is gradually increasing^[2]. Tumor growth is a multistage process and tumor angiogenesis is one of the key steps in tumor growth, infiltration and metastasis. In many tumors, the expression of iNOS is strong^[3]. NO is synthesized from the amino acid L-arginine by iNOS and has many biological functions closely related with carcinogenesis and development of carcinomas, especially with tumor angiogenesis^[4]. At present, the study about angiogenesis of PGBC is few and the relationship between angiogenesis and iNOS of PGBC has not been reported. In the present study the expressions of iNOS and MVD of 40 PGBCs and 8 normal gallbladders were investigated by immunohistochemistry and image analysis methods. The clinicopathologic indexes, the relationship between expression of iNOS and angiogenesis of PGBC and significance of the expression of iNOS were discussed.

MATERIALS AND METHODS

Pathological materials

Forty specimens of PGBC were collected between 1996 and 2002 in the Department of Hepatobiliary Surgery, First Hospital of Xi'an Jiaotong University. No treatment was given before operation. Specimens were fixed with formaldehyde and embedded with paraffin. The histological grading of tumor was done on hematoxylin-eosin stained sections. There were 11 males and 29 females, their mean age of patients was 59 years old. Among the 35 adenocarcinomas, 31 belonged to differentiated adenocarcinomas, 2 mucinous adenocarcinomas and 2 undifferentiated adenocarcinomas. There were 2 adenosquamous carcinomas, 1 adenoacanthoma, 1 sarcoma carcinoma and 1 neuroendocrine carcinoma. Eighteen tumours had a size ≥ 3 cm, 22 had a size < 3 cm. Seven were well differentiated carcinomas, 14 moderately differentiated, 16 poorly differentiated and 3 undifferentiated. Twenty cases had metastases in lymph nodes, 11 in liver. Eight normal gallbladders were studied as control.

Immunohistochemistry

Tissue samples were fixed in 10g/L neutral-buffered formaldehyde, embedded in paraffin, sectioned (4 μ m thick), and deparaffinized. Slides were immersed first in 3 mL/L H_2O_2 at room temperature for 10 min to get rid of the activity of endogenous peroxidase. Then slides were digested with 1 g/L trypsin for 10 min. The slides were washed with distilled water, soaked in PBS for 5 min, then put into microwave at 95 °C for 8 min to repair the antigen. Then slides were immersed in goat serum (1.5%) at room temperature for 40 min to block endogenous nonspecific binding sites. Immunostaining was performed with the primary rabbit polyclonal IgG specific for iNOS (dilution, 1:50; Santa Cruz Biotechnology, USA) at room temperature for 2 h. The primary rabbit polyclonal IgG specific for factor VIII-related antigen (dilution, 1:100; Sigma Biotechnology, USA) was used. Then a biotinylated secondary antirabbit antibody

(BOSHIDE Biotechnology, Wuhan, China) diluted 1:200 in PBS was applied on the sections for 20 min, followed by the streptavidin-biotin-peroxidase complex (dilution, 1:200; BOSHIDE Biotechnology, Wuhan, China) for 20 min. The color was developed by diaminobenzidine (DAB). The sections were counter-stained with hematoxylin, dehydrated, made transparent, covered and observed. Primary antibody replaced by PBS was used as a negative control. For positive controls, hemangioma was stained for factor VIII-related antigen and gastric carcinoma for iNOS.

Determination of iNOS

Under light microscope the positive cells were stained as brownish yellow in cytoplasm. Determination of iNOS was performed by an image analysis system (IBAS System, Kontron Eledtronik, Germany). According to guide system set operation was made for determination of optical density. The average optical density (AOD) of 100-200 iNOS positive cells was randomly measured with $\times 20$ objective, and the average percentage of positive cells (APCP) was obtained by measuring positive cells and total tumor cells in random 10 high power fields (HPFs) with $\times 40$ objective. The positive level index (PLI) was calculated according to the following formula: $PLI = APCP \times AOD$.

Quantification of angiogenesis

Determination of MVD was based upon the method reported by Marrogi *et al*^[6]. An all-round observation was first made with $\times 10$ objective, then five areas with the highest density of micro-vessels (hot spots) were selected, and the amount of micro-vessels was counted with $\times 20$ objective (any endothelial cell or endothelial cluster close to tumor cells and connective tissue around tumor cells, which was stained brownish yellow were considered as a single, countable micro-vessel). MVD was counted from an average of five HPFs with $\times 20$ objective (Figure 1).

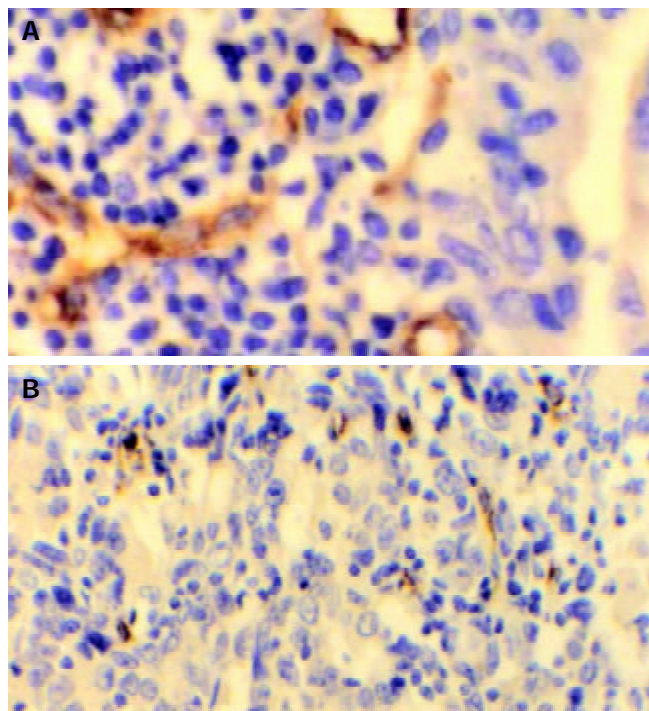


Figure 1 Distribution of MVD in PGBC tissue, SABC $\times 200$. A: high MVD, B: low MVD.

Statistical analysis

SPSS for Windows (10.0 edition) was used for statistical analysis. All data were expressed as mean \pm SD. Statistical

differences were evaluated using the unpaired *t* test, *F* test and *q* test. Analysis of linear correlation was used to discuss the relationship between expressions of iNOS and MVD. A *P* value less than 0.05 was considered statistically significant.

RESULTS

MVD and PGBC

Through the stains by polyclonal IgG specific for factor VIII-related antigen, micro-vessels could be identified. The distribution of micro-vessels in PGBC was not even, which was irregular in morphology and differed greatly in quantity (Figure 1). MVD was the highest at the margin of tumor tissues. MVD (46 ± 14) in PGBC was significantly higher than that (14 ± 6) in normal gallbladder tissue ($P < 0.05$). MVD in PGBC was not related with age, gender, tumor size and histological type. MVD in poorly and undifferentiated tumor tissues was higher than that of moderately differentiated and well-differentiated tumor tissues ($P < 0.01$). MVD of Nevin IV and V stages was higher than that of Nevin I, II and III stages ($P < 0.01$). MVD of cases with lymphatic or liver metastasis was significantly higher than that without liver metastasis ($P < 0.05$) or lymphatic metastasis ($P < 0.01$, Table 1).

iNOS and PGBC

The expression of iNOS in normal gallbladder epithelial cells was negative and occasionally positive in stromal cells. In tissue of PGBC, iNOS was mainly expressed in cytoplasm and few in inflammatory cells around the tumor cells (Figure 2). The PLI of iNOS in 40 PGBCs was 0.435 ± 0.134 . It was not related with age, gender, tumor size, histological type, differentiation and clinical stage of PGBC. The PLI of iNOS in cases with lymphatic metastasis was higher than that without lymphatic metastasis ($P < 0.01$). The PLI of iNOS in cases with liver metastasis was higher than that without liver metastasis ($P < 0.05$, Table 1).

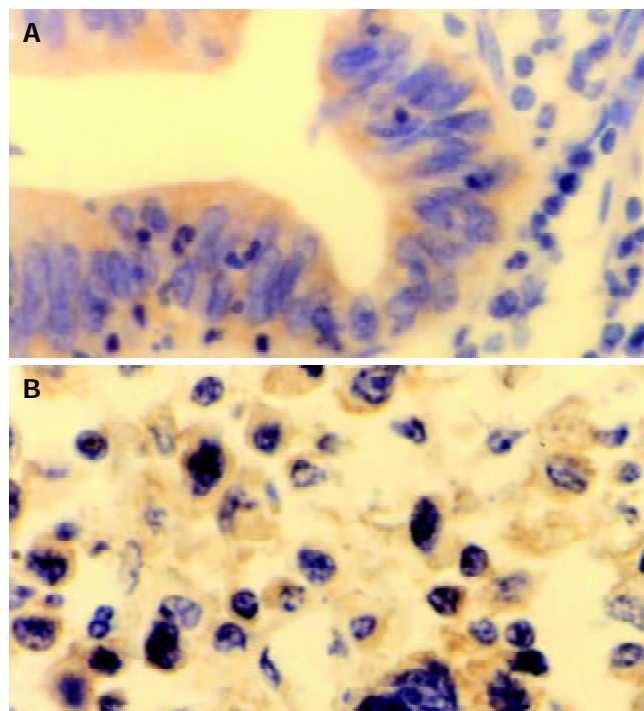


Figure 2 Positive expression of iNOS in PGBC tissues SABC $\times 400$. A: well-differentiated, B: poorly-differentiated.

iNOS and angiogenesis of PGBC

By serial analysis of sections, high MVD was observed in

areas of high iNOS expression. Linear correlation analysis showed that PLI of iNOS was positively correlated with MVD ($r=0.4021$, $P<0.05$). This demonstrated that expression of iNOS could influence MVD and blood supply of tumor.

Table 1 Relationship between MVD, PLI and clinicopathologic indexes

Group	n	MVD	PLI
Age <58yr	17	43±14	0.340±0.048
≥58yr	23	45±11	0.371±0.061
Male	11	46±11	0.376±0.056
Female	29	44±11	0.421±0.073
Size ≥3 cm	18	42±11	0.365±0.077
<3 cm	22	46±10	0.434±0.097
Adenocarcinoma	35	45±12	0.473±0.086
Adeno-squamous carcinoma	2	41±3	0.391±0.131
Others	3	47±6	0.447±0.025
Differentiation well	7	33±6	0.397±0.089
Moderate	14	43±9 ^a	0.413±0.072
Poor & Non	19	52±9 ^{ac}	0.453±0.113
Nevin stages I, II, III	18	37±13	0.410±0.092
IV, V	22	52±8 ^b	0.459±0.088
Lymphatic Metastasis +	20	53±8	0.573±0.078
-	20	38±8 ^d	0.367±0.064 ^f
Liver Metastasis +	11	55±6	0.533±0.067
-	29	42±10 ^e	0.424±0.084 ^g

^a $P<0.05$, vs Well. ^c $P<0.05$, vs Moderate. ^b $P<0.01$, vs I, II, III Stages. ^{d,f} $P<0.01$, vs Positive. ^{e,g} $P<0.05$, vs Positive.

DISCUSSION

The formation of new blood vessels known as angiogenesis induced by tumor cells is a critical determinant of tumor progression^[5-10]. Unlike normal blood vessels, tumor blood vessels are not mature vessels which are chaotic, irregular and leaky. Studies showed that proliferation, infiltration and metastasis of solid tumor were closely related with tumor angiogenesis^[11-16]. In our study we found that the distribution of micro-vessels in PGBC was not even, but irregular in morphology and its quantity differed greatly. MVD was the highest at the margin of tumor tissues. In tumor tissues MVD was higher than that in normal tissues. Our study showed that MVD in PGBC was significantly higher than that in normal gallbladder tissue. Research on mammary cancer showed that MVD was increased in patients with distant metastasis compared with those without distant metastasis^[17]. The risk of metastasis would increase by 159% per increase of 10 micro-vessels^[18]. This study found that MVD in cases with lymphatic or liver metastasis was significantly higher than that without liver or lymphatic metastasis, which was consistent with other researchers^[19-22]. It is generally believed that invasion of tumor cells from tumor tissue with rich vasculature increases and the risk of lymphatic metastasis is increased by invasion of veno-lymphatic anastomosis and lymphatic vessels accompanying blood capillaries.

Calcium-independent iNOS was expressed in macrophages, neutrophils, hepatocytes, cardiac myocytes, chondrocytes, and many other cell types^[23-26]. It was mainly induced by cytokines and could generate locally high concentrations of NO for a prolonged period of time and play a variety of regulatory functions *in vivo*^[27,28]. In many studies, iNOS positivity was predominantly found in tumor cells^[29,30], but in another study a relatively high iNOS immunoreactivity was noted in stromal cells^[31]. Our study showed that in PGBC iNOS was mainly expressed in cytoplasm of tumor cells and in few inflammatory

cells around the tumor cells. Vakkala *et al.*^[32] showed that iNOS positivity was observed in mammary cancer cells in 46.5% *in situ* carcinomas and 58.8% invasive carcinomas. Expression of iNOS was related with differentiation of carcinomas *in situ*. In this study PLI of iNOS was not related to age, gender, tumor size, histological type, differentiation and clinical stage of PGBC. The PLI of iNOS in cases with lymphatic metastasis was higher than that without lymphatic metastasis and the PLI of iNOS in cases with liver metastasis was higher than that without liver metastasis. The effects of NO could be tumor promoting or tumor suppressing. High concentrations of NO (umol/L) could be cytotoxic, whereas low concentration (nmol/g or pmol/g) might even protect some cell types from damage and apoptosis^[33]. During the initiation of tumor growth, natural killer cells and macrophages could kill tumor cells by a NO-mediated mechanism^[34]. However, NO might also suppress antitumor effect, promote tumor angiogenesis and blood flow in tumor neovasculature, and enhance tumor growth, invasion, and metastasis^[35]. Jenkins *et al.*^[36] engineered gene of iNOS into adenocarcinoma cell line DLD-1 to get iNOS-19 subclone which generated NO continuously, and found that in nude mice tumors from iNOS-19 subclone cells grew faster than those derived from wild-type cells and were much markedly vascularized and had a stronger ability to invade. Our conclusion is that NO produced by iNOS in PGBC is in low concentration and can promote tumor angiogenesis, invasion and metastasis of PGBC.

REFERENCES

- 1 **Ishikawa T**, Horimi T, Shima Y, Okabayashi T, Nishioka Y, Hamada M, Ichikawa J, Tsuji A, Takamatsu M, Morita S. Evaluation of aggressive surgical treatment for advanced carcinoma of the gallbladder. *J Hepatobiliary Pancreat Surg* 2003; **10**: 233-238
- 2 **Yamamoto T**, Uki K, Takeuchi K, Nagashima N, Honjo H, Sakurai N, Okuda C, Watanabe G, Mori M, Kuyama Y. Early gallbladder carcinoma associated with primary sclerosing cholangitis and ulcerative colitis. *J Gastroenterol* 2003; **38**: 704-706
- 3 **Kvasnicka T**. NO (nitric oxide) and its significance in regulation of vascular homeostasis. *Vnitr Lek* 2003; **49**: 291-296
- 4 **Esken FA**. Angiogenesis inhibitors in clinical development; where are we now and where are we going? *Br J Cancer* 2004; **90**: 1-7
- 5 **Detmar M**. Tumor angiogenesis. *J Invest Dermatol Symp Proc* 2000; **5**: 20-23
- 6 **Marrogi AJ**, Travis WD, Welsh JA, Khan MA, Rahim H, Tazelaar H, Pairolero P, Trastek V, Jett J, Caporaso NE, Liotta LA, Harris CC. Nitric oxide synthase, cyclooxygenase 2, and vascular endothelial growth factor in the angiogenesis of non-small cell lung carcinoma. *Clin Cancer Res* 2000; **6**: 4739-4744
- 7 **Gupta MK**, Qin RY. Mechanism and its regulation of tumor-induced angiogenesis. *World J Gastroenterol* 2003; **9**: 1144-1155
- 8 **Abdulkadir SA**, Carvalho GF, Kaleem Z, Kisiel W, Humphrey PA, Catalona WJ, Mibrandt J. Tissue factor expression and angiogenesis in human prostate carcinoma. *Hum Pathol* 2000; **31**: 443-447
- 9 **Forootan SS**, Ke Y, Jones AS, Helliwell TR. Basic fibroblast growth factor and angiogenesis in squamous carcinoma of the tongue. *Oral Oncol* 2000; **36**: 437-443
- 10 **Yoshikawa T**, Yanoma S, Tsuburaya A, Kobayashi O, Sairenji M, Motohashi H, Noguchi Y. Angiogenesis inhibitor, TNP-470, suppresses growth of peritoneal disseminating foci. *Hepatogastroenterology* 2000; **47**: 298-302
- 11 **Erenoglu C**, Akin ML, Uluutku H, Tezcan L, Yildirim S, Batkin A. Angiogenesis predicts poor prognosis in gastric carcinoma. *Dig Surg* 2000; **17**: 581-586
- 12 **Shimoyama S**, Kaminishi M. Increased angiogenin expression in gastric cancer correlated with cancer progression. *J Cancer Res Clin Oncol* 2000; **126**: 468-474
- 13 **Xiong B**, Gong LL, Zhang F, Hu MB, Yuan HY. TGF β 1 expression and angiogenesis in colorectal cancer tissue. *World J Gastroenterol* 2002; **8**: 496-498
- 14 **Gu ZP**, Wang YJ, Li JG, Zhou YA. VEGF165 antisense RNA sup-

- presses oncogenic properties of human esophageal squamous cell carcinoma. *World J Gastroenterol* 2002; **8**: 44-48
- 15 **Li HX**, Chang XM, Song ZJ, He SX. Correlation between expression of cyclooxygenase-2 and angiogenesis in human gastric adenocarcinoma. *World J Gastroenterol* 2003; **9**: 674-677
- 16 **Coomber BL**, Yu JL, Fathers KE, Plumb C, Rak JW. Angiogenesis and the role of epigenetics in metastasis. *Clin Exp Metastasis* 2003; **20**: 215-227
- 17 **Toivonen P**, Makitie T, Kujala E, Kivela T. Microcirculation and tumor-infiltrating macrophages in choroidal and ciliary body melanoma and corresponding metastases. *Invest Ophthalmol Vis Sci* 2004; **45**: 1-6
- 18 **Wong YK**, Liu CJ, Kwan PC, Chao SY. Microvascular density and vascular endothelial growth factor immunoreactivity as predictors of regional lymph node metastasis from betel-associated oral squamous cell carcinoma. *J Oral Maxillofac Surg* 2003; **61**: 1257-1262
- 19 **Sugawara Y**, Makuuchi M, Harihara Y, Noie T, Inoue K, Kubota K, Takayama T. Tumor angiogenesis in gallbladder carcinoma. *Hepatogastroenterology* 1999; **46**: 1682-1686
- 20 **Nakashima T**, Kondoh S, Kitoh H, Ozawa H, Okita S, Harada T, Shiraiishi K, Ryozaawa S, Okita K. Vascular endothelial growth factor-C expression in human gallbladder cancer and its relationship to lymph node metastasis. *Int J Mol Med* 2003; **11**: 33-39
- 21 **Giatromanolaki A**, Sivridis E, Simopoulos C, Polychronidis A, Gatter KC, Harris AL, Koukourakis MI. Thymidine phosphorylase expression in gallbladder adenocarcinomas. *Int J Surg Pathol* 2002; **10**: 181-188
- 22 **Giatromanolaki A**, Sivridis E, Koukourakis MI, Polychronidis A, Simopoulos C. Prognostic role of angiogenesis in operable carcinoma of the gallbladder. *Am J Clin Oncol* 2002; **25**: 38-41
- 23 **Hunter RP**. Nitric oxide, inducible nitric oxide synthase and inflammation in veterinary medicine. *Anim Health Res Rev* 2002; **3**: 119-133
- 24 **Ortiz PA**, Garvin JL. Cardiovascular and renal control in NOS-deficient mouse models. *Am J Physiol Regul Integr Comp Physiol* 2003; **284**: R628-638
- 25 **Qin JM**, Zhang YD. Intestinal expressions of eNOSmRNA and iNOSmRNA in rats with acute liver failure. *World J Gastroenterol* 2001; **7**: 652-656
- 26 **Dong WG**, Mei Q, Yu JP, Xu JM, Xiang L, Xu Y. Effects of melatonin on the expression of iNOS and COX-2 in rat models of colitis. *World J Gastroenterol* 2003; **9**: 1307-1311
- 27 **Beauregard C**, Brandt PC, Chiou GC. Induction of nitric oxide synthase and over-production of nitric oxide by interleukin-1beta in cultured lacrimal gland acinar cells. *Exp Eye Res* 2003; **77**: 109-114
- 28 **Zhou JL**, Jin GH, Yi YL, Zhang JL, Huang XL. Role of nitric oxide and peroxynitrite anion in lung injury induced by intestinal ischemia-reperfusion in rats. *World J Gastroenterol* 2003; **9**: 1318-1322
- 29 **Lala PK**, Orucevic A. Role of nitric oxide in tumor progression: lessons from experimental tumors. *Cancer Metastasis Rev* 1998; **17**: 91-106
- 30 **Kojima M**, Morisaki T, Tsukahara Y, Uchiyama A, Matsunari Y, Mibu R, Tanaka M. Nitric oxide synthase expression and nitric oxide production in human colon carcinoma tissue. *J Surg Oncol* 1999; **70**: 222-229
- 31 **Aaltoma SH**, Lipponen PK, Kosma VM. Inducible nitric oxide synthase (iNOS) expression and its prognostic value in prostate cancer. *Anticancer Res* 2001; **21**: 3101-3106
- 32 **Vakkala M**, Kahlos K, Lakari E, Paakko P, Kinnula V, Soini Y. Inducible nitric oxide synthase expression, apoptosis, and angiogenesis in *in situ* and invasive breast carcinoma. *Clin Cancer Res* 2000; **6**: 2408-2416
- 33 **Ambis S**, Hussain SP, Harris CC. Interactive effects of nitric oxide and the p53 tumor suppressor gene in carcinogenesis and tumor progression. *FASEB J* 1997; **11**: 443-448
- 34 **Wink DA**, Vodovotz Y, Laval J, Laval F, Dewhirst MW, Mitchell JB. The multifaceted roles of nitric oxide in cancer. *Carcinogenesis* 1998; **19**: 711-721
- 35 **Song ZJ**, Gong P, Wu YE. Relationship between the expression of iNOS, VEGF, tumor angiogenesis and gastric cancer. *World J Gastroenterol* 2002; **8**: 591-595
- 36 **Jenkins DC**, Charles IG, Thomsen LL, Moss DW, Holmes LS, Baylis SA, Rhodes P, Westmore K, Emson PC, Moncada S. Roles of nitric oxide in tumor growth. *Proc Natl Acad Sci U S A* 1995; **92**: 4392-4396

Edited by Xu JY and Wang XL

Effects of low molecular weight heparin on platelet surface P-selectin expression and serum interleukin-8 production in rats with trinitrobenzene sulphonic acid-induced colitis

Bing Xia, Hong Han, Ke-Jian Zhang, Jin Li, Guang-Song Guo, Ling-Ling Gong, Xian-Chang Zeng, Jun-Yan Liu

Bing Xia, Hong Han, Ke-Jian Zhang, Jin Li, Xian-Chang Zeng, Department of Internal Medicine, Zhongnan Hospital, Wuhan University, Wuhan 430071, Hubei Province, China

Guang-Song Guo, Ling-Ling Gong, Department of Pathology, Zhongnan Hospital, Wuhan University, Wuhan 430071, Hubei Province, China

Jun-Yan Liu, Department of Immunology, Medical School, Wuhan University, Wuhan 430071, Hubei Province, China

Supported by the Hubei Provincial Natural Science Foundation, No. 2000J047

Correspondence to: Professor Bing Xia, Department of Internal Medicine, Zhongnan Hospital, Wuhan University, Wuhan 430071, Hubei Province, China. bingxia@public.wh.hb.cn

Telephone: +86-27-67812985 **Fax:** +86-27-87307622

Received: 2003-07-10 **Accepted:** 2003-08-18

Abstract

AIM: To observe the effects of low molecular weight heparin (LMWH) on platelet surface P-selectin expression and serum interleukin-8 production in rats with trinitrobenzene sulphonic acid (TNBS) induced colitis.

METHODS: Colitis was induced in female Sprague-Dawley rats by colonic administration of 2, 4, 6-TNBS. LMWH, a dalteparin (150 U/kg, 300 U/kg) was subcutaneously administered one hour before induction of colitis and went on once a day for 6 days. Then a half dose was given for the next 7 days. Control animals received the same volume of normal saline once a day for 14 days after treated by TNBS. Animals were sacrificed at 24 h, days 7 and 14 after induction of colitis. The colon was excised for the evaluation of macroscopic and histological findings and TNF- α immunohistochemical assay. Platelet surface P-selectin expression was determined by radioimmunoassay and serum IL-8 production was assayed by ELISA method.

RESULTS: LMWH treatment in a dose of 300 U/kg for 14 days significantly improved colonic inflammation by histological examination. Serum IL-8 production in the 300 U/kg treatment group was more significantly decreased at day 14 than that at 24 h ($P < 0.05$). However, platelet surface P-selectin expression and TNF- α staining in colonic tissue were not significantly different among the three groups.

CONCLUSION: LMWH has an anti-inflammatory effect on TNBS induced colitis in rats. The effect is possibly related to inhibition of proinflammatory cytokine IL-8, but not involved platelet surface P-selectin expression.

Xia B, Han H, Zhang KJ, Li J, Guo GS, Gong LL, Zeng XC, Liu JY. Effects of low molecular weight heparin on platelet surface P-selectin expression and serum interleukin-8 production in rats with trinitrobenzene sulphonic acid-induced colitis. *World J Gastroenterol* 2004; 10(5): 729-732
<http://www.wjgnet.com/1007-9327/10/729.asp>

INTRODUCTION

Inflammatory bowel disease (IBD) includes ulcerative colitis (UC) and Crohn's disease (CD), both of which are chronic non-specific intestinal inflammation with unknown etiology. Several studies have shown that IBD exists a hypercoagulant state in active period of the disease and may have microvascular thrombosis in the wall of intestine^[1-8]. An abnormal platelet activity has been reported in patients with UC and CD, and plays an important role in inflammation aggravation^[9-12]. P-selectin is a membrane glycoprotein, which is expressed on activated platelets and endothelial cells, promotes leukocyte adhesion and migration as well as inflammatory cytokine production. IL-8 is a key proinflammatory cytokine and its production is increased in activated platelets. An up-regulation of platelet IL-8 receptors in patients with IBD has been reported^[11].

Heparin is a glycoaminoglycan formed by sulphated disaccharides and varies in the length of polymeric units and therefore has different molecular weights. Low molecular weight heparin (LMWH) is made by partial hydrolysis or enzymatic degradation of unfractionated heparin. Heparin and LMWH prevent the process of blood coagulation and have a natural anti-thrombin effect. In recent years several studies have shown that heparin and LMWH have an obvious anti-inflammatory activity in addition to its traditional anticoagulant effects^[9,13,14]. In animal model heparin disaccharides inhibited TNF- α production by macrophages and decreased immune inflammation^[15]. Heparin accelerated the healing process of mucosa in colitis in several clinical studies and had anti-inflammatory effects^[16-21]. Therefore, administration of heparin can afford both anti-inflammatory and anticoagulant effects. The mechanisms of anti-inflammation of heparin are unknown. The limited studies demonstrated that it was possibly associated with the increase of several growth factors and the decrease of nitric oxide synthesis (NOS) and myeloperoxidase^[9,13,14,22,23]. The effects of heparin on platelet surface P-selectin and IL-8 have not been studied. The present study was designed to observe the effects of LMWH on platelet surface P-selectin expression, serum IL-8 production, and TNF- α expression in mucosa of rats with trinitrobenzene sulphonic acid (TNBS)-induced colitis, and to clarify the anti-inflammatory mechanisms of LMWH in the treatment of colitis.

MATERIALS AND METHODS

Animals

Female Sprague-Dawley rats weighing 200-250 g were used in the study. The animals were fasted for 24 h before the experiment and allowed food and water *ad libitum* after induction of colitis. The study was approved by the Ethic Committee of Wuhan University Medical School.

Induction of TNBS-induced colitis

Colitis was induced by a method of hapten-induced colonic inflammation as previously described^[24]. Rats were anaesthetized by intraperitoneal administration of 100g/L urethane. A small

volume of 2, 4, 6-TNBS (Sigma Company) was dissolved in 50% ethanol to a final concentration of 100 mg/mL, and 0.3 mL of TNBS solution was intracolonicly administrated with a polypropylene catheter by inserting 8 cm via the anal canal. Rats in a group were given 150 U/kg LMWH (dalteparin made by Pharmacia & Upjohn Company) subcutaneously 1 h before induction of colitis, and went on once a day for 6 d. Then a half dose of LMWH was given for the next 7 d. Treatment of the LMWH 300 U/kg group was the same as the 150 U/kg group, but the dose of LMWH was as high as 300 U/kg. Control animals received the same volume of normal saline once a day instead of LMWH after treated by TNBS.

Animals in each group were sacrificed at 24 h, d 7 and 14 after induction of colitis. The colon was isolated and a segment of colon was excised for the evaluation of macroscopic and histological findings and also for TNF- α immunohistochemical assay. A blood sample was drawn from heart of the rats for determination of platelet surface P-selectin and serum IL-8 before the rats were sacrificed.

Macroscopic evaluation of colonic damage

Macroscopic evaluation of colonic damage was conducted by two authors (HH, LLG) and mucosal hyperemia, ulcers, inflammatory exudation and bleeding were recorded. The most damaged site of the colon was chosen as the part for histological studies. For control group the colon at 8 cm above anus was excised for histological studies.

Histological studies of colonic damage

For histological examination, formalin-fixed tissues were embedded in paraffin and 5 μ m -thick sections were stained with hematoxylin and eosin, and evaluated under light microscope by a pathologist (GSG) blinded to the experimental protocol. Colonic damage was assessed by the grades described by Fedorak *et al*^[25]. Mucosal ulceration: 0: no-ulceration; 1: focal ulceration; 2: multifocal-ulceration; 3: diffuse ulceration. Depth of injury was graded as follows: 0: no injury; 1: mucosal involvement only; 2: mucosal and submucosal involvement; 3: transmural involvement. The ulceration and depth of injury grades were scored and put together as a result ranging between the minimum of 0 and maximum of 6.

Determination of platelet surface P-selectin molecules

Platelet surface P-selectin molecules were detected by radioimmunoassay. The kit was purchased from the Institute of Thrombosis and Homeostasis of Suzhou University, China. Briefly, 2 mL of anti-coagulated blood was taken from the heart of rats and platelets were counted under microscope. The blood was fixed by 2g/L glutaraldehyde in PBS solution at room temperature for 30 min and stored at 4 $^{\circ}$ C for determination of platelet surface P-selectin. The fixed blood with 2.5×10^6 platelets was divided into 3 tubes and washed with 1 mL of 0.01mol/L PBS, pH 7.4, per tube and centrifuged at 2 500 rpm for 10 min. Supernatants were removed. 50 μ L of SZ-51mab labeled with 125 I was added into the reaction tubes and mixed fully. 15 μ L of SZ-51mab without 125 I was added into control tubes. Each tube was incubated at 37 $^{\circ}$ C, washed 3 times with PBS, and centrifuged at 3 000 r/min for 10 min. Cpm of precipitations in each tube was measured by a γ reader.

Determination of serum IL-8 production

Serum IL-8 production was assayed by ELISA sandwich method. The IL-8 ELISA kit was purchased from the Institute of Immunology of the Fourth Military Medical University, China. Briefly, 96-well plates were precoated with monoclonal antibody specific to human IL-8. Serum samples, negative control and diluted IL-8 standard markers were added into the

plates. The serum samples were detected according to the procedures described in the protocol. A_{410} value was read by the ELISA reader.

Determination of TNF- α in colonic mucosa

Expression of TNF- α in colonic mucosa was assessed by immunohistochemistry. The reagents of TNF- α were purchased from Beijing Zhongshan Biotechnology, China. Positive expression of TNF- α was brown deposited granules in the plasma of neutrophils, monocytes and lymphocytes. The grades of expression of TNF- α in mucosa were classified as follows: 0: no staining; 1: a few maple granules, or a few fine brown granules, not exceeding the 1/4 total area of cytoplasm; 2: uniformity maple in the whole cytoplasm or wide brown granules in the cytoplasm, not exceeding the 1/2 area of cytoplasm; 3: the cytoplasm was full of brown granules with a lower density; 4: the total cytoplasm was full of crassitude dark brown granules, and covered whole nuclei of the cell. One hundred cells were counted under oil microscope, positive cells were recorded and positive cell rate was calculated. The scores of expression of TNF- α were calculated by sum of each grade multiplying its positive cell rate.

Statistical analysis

Data were expressed as mean \pm SD. Data in different groups were analyzed by ANOVA and post multiple tests (Tukey-Kramer or Student-Newman-Keuls). A *P* value less than 0.05 was considered statistically significant.

RESULTS

Macroscopic evaluation of TNBS-induced colitis

Control animals subjected to intracolonic administration of TNBS in 500ml/l ethanol showed colonic mucosal injury with ulceration. Signs of the mucosal damage were monitored for 14 d. As early as 24 h after TNBS treatment, colonic mucosa was shown to have hyperemia, congestion, erosion, hemorrhagic ulcerations in the injured site. The damage was still maintained at d 7 and appeared to be multiple ulcerations and partial epithelial necrosis. On d 14, the colonic ulceration still existed. In both doses of LMWH treated groups, mucosal hyperemia, congestion and ulcerations in the injured site were slighter than those in control group. However, mucosal hemorrhage in both LMWH treated groups was severer than that in control group at 24 h, but was resolved on d 7 and 14, respectively.

Histological examination of TNBS-induced colitis

In control group a large number of neutrophils, monocytes and eosinophils infiltrated in mucosa and submucosa at 24 h and the damage reached peak on d 7. As shown in Table 1, the histological grades according to Fedorak *et al*^[25] were greatly higher on d 7 compared with those at 24 h (*P*<0.01). On d 14, the damage of colon was mild, but still had ulceration, chronic inflammatory cell infiltration, vesiculitis and granulation tissue formation. In contrast, in both 150 U/kg and 300 U/kg LMWH treated groups colonic damage was mild. Table 1 shows that the histological injury grades in the 300 U/kg LMWH group were decreased at 24 h and on d 7 after treatment, and much obviously on day 14 compared with the control group (*P*<0.01).

Expression of TNF- α in colonic mucosa of TNBS-induced colitis

As shown in Table 2, the scores of expression of TNF- α in mucosa were greatly higher in the first 24 h and decreased on d 7 and 14 after induction of colitis, but there were no

significant differences among the three groups except a difference at 24 h between 300 U/kg LMWH treatment group and 150 U/kg LMWH treatment group.

Table 1 Effect of low molecular weight heparin (dalteparin) in Fedorak grades on mucosa of TNBS-induced colitis in rats

	n	24 h	Day 7	Day 14
Control group	5	1.33±0.54	4.33±0.81 ^b	3.67±2.13
150 U/kg LMWH group	4	1.00±0.00	3.33±2.08	1.67±1.15
300 U/kg LMWH group	5	0.57±0.33	2.00±1.33	0.66±0.32 ^d

^b*P*<0.01 vs control group at 24 h; ^d*P*<0.01 vs control group on day 14.

Table 2 Effect of low molecular weight heparin (dalteparin) on scores of mucosal TNF- α expression in rats with TNBS-induced colitis

	n	24 h	d 7	d 14
Control group	5	217±44 ^a	48±11	50±18
150 U/kg LMWH group	4	264±42 ^a	46±21	48±16
300 U/kg LMWH group	5	198±38 ^{ab}	26±18	16±8

^a*P*<0.001 vs control group on day 7 and 14; ^b*P*<0.05 vs 150 U/kg group at 24 h.

Platelet surface P-selectin expression and serum interleukin 8 production

Expression of platelet surface P-selectin was increased on d 7 and 14 in all three groups as shown in Table 3, but reached a significant level only in control group. There were no significant differences among these three groups at the three time points, 24 h, d 7 and 14. Production of serum interleukin 8 was higher at 24 h in the three groups, but significantly decreased on day 14 compared with that at 24 h in 300 U/kg LMWH treated group as shown in Table 4.

Table 3 Effects of low molecular weight heparin (dalteparin) on platelet surface P-selectin expression (moleculars/per platelet) in rats with TNBS-induced colitis

	n	24 h	d 7	d 14
Control group	5	177.50±88.60	657.23±300.90 ^a	767.50±359.11 ^b
150 U/kg LMWH group	4	193.67±59.98	521.95±200.10	534.61±16.13
300 U/kg LMWH group	5	211.72±72.23	598.23±233.70	653.90±286.70

^a*P*<0.05 vs control group at 24 h; ^b*P*<0.01 vs control group at 24 h.

Table 4 Effects of low molecular weight heparin (dalteparin) on production of serum IL-8 (pg/ml) in rats with TNBS-induced colitis

	n	24 h	d 7	d 14
Control group	5	7.50±3.50	4.51±2.59	4.53±3.37
150 U/kg LMWH group	4	8.38±4.01	5.04±2.01	4.44±2.88
300 U/kg LMWH group	5	8.11±3.87	3.09±1.28	2.06±1.03 ^a

^a*P*<0.05 vs 300 U/kg LMWH group at 24 h.

DISCUSSION

In this study we observed an anti-inflammatory effect of LMWH (dalteparin) in rats with TNBS-induced colitis. This effect was demonstrated by improvement of colonic inflammation with

macroscopic and histological alterations in a dose of 300 U/kg of heparin treatment for 14 d. The result was similar to that of Fries *et al*^[26], in which they showed that heparin could prevent TNBS-induced colitis, but steroids could not. Our data showed that serum IL-8 production in 300 U/kg LMWH treated group was significantly lower on d 14 than that at 24 h, but we did not find this variation in other groups. Expression of platelet surface P-selectin in control group was significantly increased consecutively at 24 h, d 7 and 14, but expression of platelet surface P-selectin did not increase in LMWH treatment group. We also did not find differences of expression of TNF- α in colonic mucosa between LMWH treatment group and control group. Our results suggested that LMWH (dalteparin) in a high dose had anti-inflammatory effects. The effects were possibly related to the decrease of proinflammatory cytokine IL-8, but not related to platelet surface P-selectin.

We observed dose and time-dependent effects of LMWH in rats with TNBS-induced colitis. Three hundreds U/kg LMWH treatment group showed more histological improvement of colitis, lower TNF- α expression in mucosa and serum IL-8 production than 150 U/kg LMWH treated group. With a continuing LMWH treatment these effects were gradually demonstrated on d 7 and 14. Our result was slightly different from that of Dotan *et al*^[18]. They showed that a single dose of 80 μ g/kg of LMWH (enoxaparin) was more optimal for amelioration of dinitrobenzene sulphonic acid- and iodoacetamide-induced colitis in rats than a dose of 200 μ g/kg and 40 μ g/kg of enoxaparin. The mechanism is not known, but may be related to optimal interactions between LMWH fragments and their receptors.

Chowers *et al*^[27] found that disaccharides derived from heparin sulfate and heparin could suppress IL-8 and IL-1 β production in intestinal epithelial cells *in vivo*. Our result was similar to that of the treatment of LMWH (dalteparin), serum IL-8 was much decreased. Salas *et al*^[28] also showed that heparin pretreatment significantly attenuated leukocyte rolling, adhesion, and migration *ex vivo* but did not affect the expression of cell adhesion molecules or vascular permeability elicited by TNF- α . The effects of heparin involved attenuation of a CD11b dependent adherent mechanism. Nelson *et al*^[29] found that *in vitro* heparin tetrasaccharides reduced binding of neutrophils to COS cells expressing P-selectin but not to COS cells expressing E-selectin.

As for the side effects of heparin in the treatment of IBD, intestinal bleeding was mentioned in several studies^[30]. Our study also showed more severe intestinal bleeding in LMWH treatment group than in control group at 24 h by macroscopic and histological observations. Thus, we should be cautious of using LMWH for clinical treatment of IBD.

In conclusion, our data indicate that LMWH has an anti-inflammatory effect in TNBS-induced colitis. The mechanism is possibly related to inhibition of proinflammatory cytokine, IL-8, but not to platelet surface P-selectin production.

REFERENCES

- 1 **Musio F**, Older SA, Jenkins T, Gregorie EM. Case report: cerebral venous thrombosis as a manifestation of acute ulcerative colitis. *Am J Med Sci* 1993; **305**: 28-35
- 2 **Thornton M**, Solomon MJ. Crohn's disease: in defense of a microvascular aetiology. *Int J Colorectal Dis* 2002; **17**: 287-297
- 3 **Mutlu B**, Ermeydan CM, Enc F, Fotbolcu H, Demirkol O, Bayrak F, Basaran Y. Acute myocardial infarction in a young woman with severe ulcerative colitis. *Int J Cardiol* 2002; **83**: 183-185
- 4 **Srivastava AK**, Khanna N, Sardana V, Gaekwad S, Prasad K, Behari M. Cerebral venous thrombosis in ulcerative colitis. *Neuro India* 2002; **50**: 215-217
- 5 **Crowe A**, Taffinder N, Layer GT, Irvine A, Nicholls RJ. Portal vein thrombosis in a complicated case of Crohn's disease. *Postgrad*

- Med J* 1992; **68**: 291-293
- 6 **Nguyen LT**, Laberge JM, Guttman FM, Albert D. Spontaneous deep vein thrombosis in childhood and adolescence. *J Pediatr Surg* 1986; **21**: 640-643
- 7 **Braverman D**, Bogoch A. Arterial thrombosis in ulcerative colitis. *Am J Dig Dis* 1978; **23**: 1148-1150
- 8 **Ryan FP**, Timperley WR, Preston FE, Holdsworth CD. Cerebral involvement with disseminated intravascular coagulation in intestinal disease. *J Clin Pathol* 1977; **30**: 551-555
- 9 **Mannaioni PF**, Di Bello MG, Masini E. Platelets and inflammation: role of platelet-derived growth factor, adhesion molecules and histamine. *Inflamm Res* 1997; **46**: 4-18
- 10 **Collins CE**, Cahill MR, Newland AC, Rampton DS. Platelets circulate in an activated state in inflammatory bowel disease. *Gastroenterology* 1994; **106**: 840-845
- 11 **Schaufelberger HD**, Uhr MR, McGuckin C, Logan RP, Misiewicz JJ, Gordon-Smith EC, Beglinger C. Platelets in ulcerative colitis and Crohn's disease express functional interleukin-1 and interleukin-8 receptors. *Eur J Clin Invest* 1994; **24**: 656-663
- 12 **Collins CE**, Rampton DS. Review article: platelets in inflammatory bowel disease—pathogenetic role and therapeutic implications. *Aliment Pharmacol Ther* 1997; **11**: 237-247
- 13 **Levine A**, Kenet G, Bruck R, Avni Y, Avinoach I, Aeed H, Matas Z, David M, Yayon A. Effect of heparin on tissue binding activity of fibroblast growth factor and heparin-binding epidermal growth factor in experimental colitis in rats. *Pediatr Res* 2002; **51**: 635-640
- 14 **Tyrrell DJ**, Horne AP, Holme KR, Preuss JM, Page CP. Heparin in inflammation: potential therapeutic applications beyond anticoagulation. *Adv Pharmacol* 1999; **46**: 151-208
- 15 **Cahalon L**, Lider O, Schor H, Avron A, Gilat D, Hershkovich R, Margalit R, Eshel A, Shoseyev O, Cohen IR. Heparin disaccharides inhibit tumor necrosis factor-alpha production by macrophages and arrest immune inflammation in rodents. *Int Immunol* 1997; **9**: 1517-1522
- 16 **Vrij AA**, Jansen JM, Schoon EJ, de Bruine A, Hemker HC, Stockbrugger RW. Low molecular weight heparin treatment in steroid refractory ulcerative colitis: clinical outcome and influence on mucosal capillary thrombi. *Scand J Gastroenterol Suppl* 2001; **234**: 41-47
- 17 **Dotan I**, Hallak A, Arber N, Santo M, Alexandrowitz A, Knaani Y, Hershkovich R, Brazowski E, Halpern Z. Low-dose low-molecular weight heparin (enoxaparin) is effective as adjuvant treatment in active ulcerative colitis: an open trial. *Dig Dis Sci* 2001; **46**: 2239-2244
- 18 **Dotan I**, Hershkovich R, Karmeli F, Brazowski E, Peled Y, Rachmilewitz D, Halpern Z. Heparin and low-molecular-weight heparin (enoxaparin) significantly ameliorate experimental colitis in rats. *Aliment Pharmacol Ther* 2001; **15**: 1687-1697
- 19 **Torkvist L**, Thorlacius H, Sjoqvist U, Bohman L, Lapidus A, Flood L, Agren B, Raud J, Lofberg R. Low molecular weight heparin as adjuvant therapy in active ulcerative colitis. *Aliment Pharmacol Ther* 1999; **13**: 1323-1328
- 20 **Folwaczny C**, Wiebecke B, Loeschke K. Unfractionated heparin in the therapy of patients with highly active inflammatory bowel disease. *Am J Gastroenterol* 1999; **94**: 1551-1555
- 21 **Evans RC**, Wong VS, Morris AI, Rhodes JM. Treatment of corticosteroid-resistant ulcerative colitis with heparin—a report of 16 cases. *Aliment Pharmacol Ther* 1997; **11**: 1037-1040
- 22 **Michell NP**, Lalor P, Langman MJ. Heparin therapy for ulcerative colitis? Effects and mechanisms. *Eur J Gastroenterol Hepatol* 2001; **13**: 449-456
- 23 **Papa A**, Danese S, Gasbarrini A, Gasbarrini G. Review article: potential therapeutic applications and mechanisms of action of heparin in inflammatory bowel disease. *Aliment Pharmacol Ther* 2000; **14**: 1403-1409
- 24 **Morris GP**, Beck PL, Herridge MS, Depew WT, Szewczuk MR, Wallace JL. Hapten-induced model of chronic inflammation and ulceration in the rat colon. *Gastroenterology* 1989; **96**: 795-803
- 25 **Fedorak RN**, Empey LR, MacArthur C, Jewell LD. Misoprostol provides a colonic mucosal protective effect during acetic acid-induced colitis in rats. *Gastroenterology* 1990; **98**: 615-625
- 26 **Fries W**, Pagiaro E, Canova E, Carraro P, Gasparini G, Pommeri F, Martin A, Carlotto C, Mazzon E, Sturniolo GC, Longo G. The effect of heparin on trinitrobenzene sulphonic acid-induced colitis in the rat. *Aliment Pharmacol Ther* 1998; **12**: 229-236
- 27 **Chowers Y**, Lider O, Schor H, Barshack I, Tal R, Ariel A, Bar-Meir S, Cohen IR, Cahalon L. Disaccharides derived from heparin or heparan sulfate regulate IL-8 and IL-1 beta secretion by intestinal epithelial cells. *Gastroenterology* 2001; **120**: 449-459
- 28 **Salas A**, Sans M, Soriano A, Reverter JC, Anderson DC, Pique JM, Panes J. Heparin attenuates TNF-alpha induced inflammatory response through a CD11b dependent mechanism. *Gut* 2000; **47**: 88-96
- 29 **Nelson RM**, Cecconi O, Roberts WG, Aruffo A, Linhardt RJ, Bevilacqua MP. Heparin oligosaccharides bind L- and P-selectin and inhibit acute inflammation. *Blood* 1993; **82**: 3253-3258
- 30 **Panes J**, Esteve M, Cabre E, Hinojosa J, Andreu M, Sans M, Fernandez-Banares F, Feu F, Gassull MA, Pique JM. Comparison of heparin and steroids in the treatment of moderate and severe ulcerative colitis. *Gastroenterology* 2000; **119**: 903-908

Edited by Zhang JZ and Wang XL

Effect of *in vitro* interferon-beta administration on hepatitis C virus in peripheral blood mononuclear cells as a predictive marker of clinical response to interferon treatment for chronic hepatitis C

Kaori Mochizuki, Tatehiro Kagawa, Shinji Takashimizu, Kazuya Kawazoe, Sei-Ichiro Kojima, Naruhiko Nagata, Atsushi Nakano, Yasuhiro Nishizaki, Koichi Shiraishi, Masaru Itakura, Norihito Watanabe, Tetsuya Mine, Shohei Matsuzaki

Kaori Mochizuki, Tatehiro Kagawa, Shinji Takashimizu, Kazuya Kawazoe, Sei-Ichiro Kojima, Naruhiko Nagata, Atsushi Nakano, Yasuhiro Nishizaki, Koichi Shiraishi, Masaru Itakura, Norihito Watanabe, Tetsuya Mine, Shohei Matsuzaki, Department of Internal Medicine, Division of Gastroenterology, Tokai University School of Medicine, Bohseidai, Isehara 259-1193, Japan

Correspondence to: Dr. Tatehiro Kagawa, Department of Internal Medicine, Division of Gastroenterology, Tokai University School of Medicine, Bohseidai, Isehara 259-1193, Japan. kagawa@is.icc.u-tokai.ac.jp

Telephone: +81-463-93-1121

Received: 2003-10-08 **Accepted:** 2003-12-30

Abstract

AIM: To test whether *in vitro* incubation of peripheral blood mononuclear cells (PBMC) with interferon (IFN) could efficiently decrease hepatitis C virus-RNA (HCV-RNA) amount and to analyze whether this effect was associated with clinical response to IFN.

METHODS: Twenty-seven patients with histologically proven chronic hepatitis C were given intravenous administration of 6 million units (MU) IFN- β daily for 6 weeks followed by three times weekly for 20 weeks. PBMC collected before IFN therapy were incubated with IFN- β and HCV-RNA in PBMC was semi-quantitatively determined.

RESULTS: Twenty-five patients completed IFN therapy. Eight patients (32%) had sustained loss of serum HCV-RNA with normal serum ALT levels after IFN therapy (complete responders). HCV-RNA in PBMC was detected in all patients, whereas it was not detected in PBMC from healthy subjects. *In vitro* administration of IFN- β decreased the amount of HCV-RNA in PBMC in 18 patients (72%). Eight of these patients obtained complete response. On the other hand, none of the patients whose HCV-RNA in PBMC did not decrease by IFN- β was complete responders. Multiple logistic regression analysis revealed that the decrease of HCV-RNA amount in PBMC by IFN- β was the only independent predictor for complete response ($P < 0.05$).

CONCLUSION: The effect of *in vitro* IFN- β on HCV in PBMC reflects clinical response and would be taken into account as a predictive marker of IFN therapy for chronic hepatitis C.

Mochizuki K, Kagawa T, Takashimizu S, Kawazoe K, Kojima SI, Nagata N, Nakano A, Nishizaki Y, Shiraishi K, Itakura M, Watanabe N, Mine T, Matsuzaki S. Effect of *in vitro* interferon-beta administration on hepatitis C virus in peripheral blood mononuclear cells as a predictive marker of clinical response to interferon treatment for chronic hepatitis C. *World J Gastroenterol* 2004; 10(5): 733-736
<http://www.wjgnet.com/1007-9327/10/733.asp>

INTRODUCTION

Interferon (IFN) is effective in the treatment of chronic hepatitis C. However, the efficacy of IFN is limited and approximately 20% of patients obtain sustained virological response^[1,2]. Even the combination therapy with IFN and ribavirin induces it in 30% to 40% of patients^[3-5]. Because IFN is expensive and also has potentially severe adverse effects, it is important to discriminate which patient is responsive to IFN before starting therapy. The low amount of serum hepatitis C virus (HCV)-RNA, viral genotypes other than 1b and the absence of cirrhosis are associated with favorable response^[1]. However, accurate prediction is still difficult before IFN treatment and more sensitive markers related to good response are required.

HCV is a hepatotropic virus, but was reported to exist in peripheral blood mononuclear cells (PBMC)^[6-8]. The existence of minus strand HCV-RNA^[7,9] suggests the proliferation of HCV in PBMC. Both *in vivo* and *in vitro* administration of IFN induce antiviral enzymes such as 2',5'-oligoadenylate synthetase (2-5AS) in PBMC as well as in liver^[10,11]. We hypothesized that *in vitro* administration of IFN might exert antiviral effect on HCV proliferating in PBMC. We tested whether *in vitro* incubation of PBMC with IFN could efficiently decrease HCV-RNA amount and also analyzed whether this effect was associated with clinical response to IFN.

MATERIALS AND METHODS

Patients and study design

Twenty-seven patients with chronic hepatitis C were enrolled into this study. Criteria for enrollment were elevation of serum ALT levels, positivity for anti-HCV antibody and serum HCV-RNA, presence of histologically proven chronic hepatitis, and absence of other chronic liver diseases such as autoimmune hepatitis, primary biliary cirrhosis, hemochromatosis, Wilson's disease. Liver histology was obtained from all patients before IFN treatment and evaluated for staging of fibrosis and grade of activity according to the METAVIR scoring system^[12,13]. They were given intravenous administration of 6 million units (MU) IFN- β (Feron, Toray Pharmaceuticals, Tokyo, Japan) daily for 6 weeks followed by three times weekly for 20 weeks. Informed consent was obtained from all patients.

The effect of IFN was defined as complete response (CR): sustained loss of serum HCV-RNA and normal ALT levels, partial response (PR): disappearance of serum HCV-RNA at the end of treatment and reappearance after treatment, and no response (NR): positive serum HCV-RNA at the end of treatment.

Serum viral load was defined by multicyclic reverse transcription (RT)-polymerase chain reaction (PCR) method^[14,15] and patients were categorized into 2 groups, namely high: $\geq 10^8$ copies/ml, and low: $< 10^8$ copies/ml. HCV genotyping was performed with type-specific primers^[16].

Effect of IFN- β on PBMC

Twenty ml of peripheral blood was drawn before IFN

treatment. PBMC were separated by gradient centrifugation and washed with phosphate-buffered saline (PBS) seven times. After this procedure the supernatants were negative for HCV-RNA even after two-step PCR as described below. PBMC were suspended in RPMI-1640 medium supplemented with fetal bovine serum (IWAKI, Tokyo, Japan) at a concentration of 2×10^6 cells/mL, plated on a 24-well plate (IWAKI), and cultured at 37 °C in a humidified atmosphere with 50 mL/L CO₂ in the absence or presence of IFN- β at a concentration of 100 IU/L. After incubation for 72 h PBMC were washed five times with PBS followed by RNA extraction with guanidium thiocyanate. Total RNA was reversely transcribed into cDNA in a 40 μ L reaction mixture containing 100 pmoles antisense primer (5' -AACACTACTCGGCTAGCAGT-3') and 200 units of SuperScript II reverse transcriptase (Invitrogen Japan, Tokyo, Japan). The amplification of cDNA was performed for 35 cycles in four temperature steps (at 94 °C for 2 min, 37 °C for 2 min, 55 °C for 2 min and 72 °C for 3 min) in a 100 μ L reaction mixture containing the template, 1 unit of Taq polymerase (Perkin Elmer, Norwalk, CT), 20 pmol of each outer primer, 2.5 nmol of each deoxyribonucleotide triphosphates, 10 mmol/L Tris HCl, pH 8.3, 50 mmol/L KCl and 0.15 mmol/L MgCl₂. After the first PCR, 10 μ L of the PCR product was subjected to a second PCR amplification using the inner primer pair under the same conditions as described for the first PCR. Primers were designed from the sequence of 5' non-coding region, an outer primer pair of 242-base span: sense (5' -ACTCCACCATAGATCATCCC-3') and antisense (5' -AACACTACTCGGCTAGCAGT-3') and an inner primer pair of 145-base span: sense (5' -TTCACGCAGAAAAGCGTCTAG-3') and antisense (5' -GTTGATCCAA-GAAAGGACCC-3'). PCR products were analyzed by gel-electrophoresis. The amount of HCV-RNA in PBMC was determined semi-quantitatively as 2+: positive after first PCR; 1+: negative after first PCR and positive after second PCR; and -: negative after first and second PCR. PBMC from 5 healthy subjects were also examined for the presence of HCV-RNA.

Statistical analysis

Categorical variables were analyzed by the chi-square test. Continuous numeric variables were examined by the Student's *t*-test (two-tail). Multiple logistic regression analysis was preformed by SPSS for Macintosh to identify independent predictors for CR.

RESULTS

Response to IFN treatment (Table 1)

Twenty-five of 27 patients completed IFN treatment. One discontinued IFN because of retinal hemorrhage, the other could not visit our hospital due to moving. All patients had fever, general fatigue or myalgia. However, no severe adverse effects were seen. Eight patients (32%) maintained normal serum ALT levels with negative serum HCV-RNA after IFN treatment, resulting in CR. Ten patients (40%) were negative for HCV-RNA at the end of treatment but relapsed after the discontinuation of IFN (PR). The other 7 patients (28%) were still positive for HCV-RNA at the end of IFN treatment (NR). The distribution of gender, age and serum ALT levels was not significantly different among three groups. Neither grade of activity nor staging of fibrosis in liver histology was different. Low serum viral load and genotypes other than 1b were associated with favorable response ($P < 0.05$).

HCV-RNA in PBMC (Table 2)

We analyzed the presence of HCV-RNA in PBMC by two-step RT-PCR. All patients were positive for HCV-RNA in PBMC, whereas none of the healthy subjects was positive.

Three patients (12%) revealed 1+; 2 with low serum viral load and 1 with high viral load. The other 22 patients (88%) resulted in 2+. The amount of HCV-RNA in PBMC before the addition of IFN- β was not related to clinical response to IFN.

Table 1 Demographic characteristics and clinical response

Variable	NR ^a (n=7)	PR (n=10)	CR (n=8)	P value
Sex (F:M)	4:3	8:2	6:2	NS
Age (mean \pm SD)	57.2 \pm 6.7	51.4 \pm 7.2	44.4 \pm 15.7	NS
Serum ALT levels (mean \pm SD)	68.5 \pm 39.5	95.4 \pm 67.9	90.9 \pm 40.1	NS
Liver histology				
Activity index				
A1	4	3	1	
A2	2	6	7	NS
A3	1	1	0	
Fibrosis index				
F1	3	5	5	
F2	3	3	2	NS
F3	1	2	1	
Serum viral load ^b				
Low	1	6	6	<0.05
High	6	4	2	
Genotype				
1b	6	7	2	<0.05
Others	1	3	6	

^aComplete response (CR): sustained loss of serum HCV-RNA and normal ALT levels, partial response (PR): disappearance of serum HCV-RNA at the end of treatment and reappearance after treatment, and no response (NR): positive serum HCV-RNA at the end of treatment. ^bhigh: $\geq 10^8$ copies/mL, low: $< 10^8$ copies/mL.

Table 2 Viral load in PBMC and clinical response

Variable	NR ^a (n=7)	PR (n=10)	CR (n=8)	P value
Viral load ^b (pretreatment)				
-	0	0	0	
1+	0	2	1	NS
2+	7	8	7	
Decrease of HCV-RNA by IFN- β ^c				
Yes	1	9	8	<0.05
No	6	1	0	

^aComplete response (CR): sustained loss of serum HCV-RNA and normal ALT levels, partial response (PR): disappearance of serum HCV-RNA at the end of treatment and reappearance after treatment, and no response (NR): positive serum HCV-RNA at the end of treatment. ^bThe amount of HCV-RNA in PBMC was determined semi-quantitatively as follows; 2+: positive after first PCR, 1+: negative after first PCR and positive after second PCR, and -: negative after first and second PCR. ^cHCV-RNA amount in PBMC was semi-quantitatively determined before and after incubation with IFN- β (100 IU/L).

We studied the effect of *in vitro* administration of IFN- β on HCV in PBMC. We used 100 IU/L as a concentration of IFN- β because preliminary experiments revealed that 10 IU/L of IFN- β was insufficient to decrease HCV-RNA in PBMC and that 1 000 IU/L of IFN- β did not have more effects than 100 IU/L of IFN- β (data not shown). After incubation with IFN- β the HCV-RNA amount in PBMC decreased in 18 patients (72%), 7 patients: 2+ to -; 8 patients: 2+ to 1+; and 3 patients: 1+ to -. Whereas no decrease was observed in the other 7 patients (28%). Incubation without IFN- β did not lead

to decrease in the amount of HCV-RNA (data not shown), suggesting that this decrease was attributable to the antiviral effect of IFN- β .

We analyzed the relationship between the effect of IFN- β on HCV in PBMC and clinical response. Patients with HCV-RNA decrease were significantly associated with better clinical response, 8 (44%) and 9 patients (50%) obtained CR and PR, respectively. On the other hand, 6 of 7 patients (86%) whose HCV-RNA amount did not decrease by IFN resulted in NR. Multiple logistic regression analysis revealed that the decrease in HCV-RNA amount in PBMC was the only independent predictor for CR ($P < 0.05$).

DISCUSSION

In our study 8 patients (32%) obtained CR. IFN- β therapy was as effective as IFN- α in the treatment of chronic hepatitis C as already reported^[17-19]. In one patient (4%) IFN treatment was discontinued due to retinal hemorrhage, which was the only major adverse effect observed in this study. Retinopathy was one of the common adverse effects of IFN^[20,21]. Low serum viral load and viral genotypes other than 1b were associated with good clinical response in consistent with other studies using IFN- α ^[22-25].

We could detect HCV-RNA in PBMC before IFN therapy in all cases. HCV-RNA was not found in PBMC from healthy subjects, suggesting that the technique we used was specific for HCV. Several studies demonstrated the presence of HCV-RNA in PBMC^[26-30], although the positive rate was variable from 25% to 100%. The *in vitro* administration of IFN- β decreased HCV-RNA in PBMC in 72% patients. Because incubation with medium alone did not affect HCV-RNA amount, this decrease would be attributable to IFN's antiviral effect. In fact Pawlotsky *et al* reported that 2-5AS activity in PBMC from patients with chronic hepatitis C was augmented by incubation with IFN^[10]. Furthermore a preliminary experiment showed that *in vitro* addition of IFN at a concentration of 1 000 IU/mL reduced the HCV-RNA amount in PBMC^[30]. In our study 7 patients (28%) maintained the same amount of HCV-RNA in PBMC even after incubation with IFN. It should be noted that none of these patients was complete responders. The reason why IFN could not decrease HCV-RNA in these patients is unclear. One possibility is that IFN could not induce antiviral enzymes such as 2-5AS. In this case the breakdown of IFN-induced antiviral system might be responsible. A more likely explanation is that HCV strains in these patients were resistant to antiviral enzymes. Some strains such as those with mutations in NS5A region^[31] are refractory to IFN.

Clinical outcome was significantly different between those with decreased HCV-RNA amount in PBMC and those without. Multivariate analysis demonstrated the decrease of HCV-RNA amount in PBMC by IFN as the only independent predictive factor for CR. These data suggest that the effect of *in vitro* IFN- β on HCV-RNA in PBMC reflects clinical response and would be taken into account as a predictive marker of IFN therapy for chronic hepatitis C.

REFERENCES

- 1 **Hoofnagle JH**, di Bisceglie AM. The treatment of chronic viral hepatitis. *N Engl J Med* 1997; **336**: 347-356
- 2 **Poynard T**, Bedossa P, Chevallier M, Mathurin P, Lemonnier C, Trepo C, Couzigou P, Payen JL, Sajus M, Costa JM. A comparison of three interferon alfa-2b regimens for the long-term treatment of chronic non-A, non-B hepatitis. Multicenter Study Group. *N Engl J Med* 1995; **332**: 1457-1462
- 3 **McHutchison JG**, Gordon SC, Schiff ER, Shiffman ML, Lee WM, Rustgi VK, Goodman ZD, Ling MH, Cort S, Albrecht JK. Interferon alfa-2b alone or in combination with ribavirin as initial treatment for chronic hepatitis C. Hepatitis Interventional Therapy Group. *N Engl J Med* 1998; **339**: 1485-1492
- 4 **Davis GL**, Esteban-Mur R, Rustgi V, Hoefs J, Gordon SC, Trepo C, Shiffman ML, Zeuzem S, Craxi A, Ling MH, Albrecht J. Interferon alfa-2b alone or in combination with ribavirin for the treatment of relapse of chronic hepatitis C. International Hepatitis Interventional Therapy Group. *N Engl J Med* 1998; **339**: 1493-1499
- 5 **Di Bisceglie AM**, McHutchison J, Rice CM. New therapeutic strategies for hepatitis C. *Hepatology* 2002; **35**: 224-231
- 6 **Chang TT**, Young KC, Yang YJ, Lei HY, Wu HL. Hepatitis C virus RNA in peripheral blood mononuclear cells: comparing acute and chronic hepatitis C virus infection. *Hepatology* 1996; **23**: 977-981
- 7 **Lerat H**, Berby F, Trabaud MA, Vidalin O, Major M, Trepo C, Inchauspe G. Specific detection of hepatitis C virus minus strand RNA in hematopoietic cells. *J Clin Invest* 1996; **97**: 845-851
- 8 **Rodriguez-Inigo E**, Casqueiro M, Navas S, Bartolome J, Pardo M, Carreno V. Fluorescent "in situ" hybridization of hepatitis C virus RNA in peripheral blood mononuclear cells from patients with chronic hepatitis C. *J Med Virol* 2000; **60**: 269-274
- 9 **Willems M**, Peerlinck K, Moshage H, Deleu I, Van den Eynde C, Vermeylen J, Yap SH. Hepatitis C virus RNAs in plasma and in peripheral blood mononuclear cells of hemophiliacs with chronic hepatitis C: evidence for viral replication in peripheral blood mononuclear cells. *J Med Virol* 1994; **42**: 272-278
- 10 **Pawlotsky JM**, Hovanessian A, Roudot-Thoraval F, Lebon P, Robert N, Bouvier M, Babany G, Duval J, Dhumeaux D. Activity of the interferon-induced 2' ,5' -oligoadenylate synthetase in patients with chronic hepatitis C. *J Interferon Cytokine Res* 1995; **15**: 857-862
- 11 **Grandier D**, Sangfelt O, Skoog L, Hansson J. *In vivo* induction of the interferon-stimulated protein 2' 5' -oligoadenylate synthetase in tumor and peripheral blood cells during IFN-alpha treatment of metastatic melanoma. *J Interferon Cytokine Res* 1998; **18**: 691-695
- 12 **The French METAVIR Cooperative Study Group**. Intraobserver and interobserver variations in liver biopsy interpretation in patients with chronic hepatitis C. *Hepatology* 1994; **20**: 15-20
- 13 **Bedossa P**, Poynard T. An algorithm for the grading of activity in chronic hepatitis C. The METAVIR Cooperative Study Group. *Hepatology* 1996; **24**: 289-293
- 14 **Ishiyama N**, Katayama K, Ishimi N, Takahashi S, Igarashi H, Nakajima H, Andoh T, Saito S, Aoyagi T. Measurement of copy-number of hepatitis C virus by multicyclic RT-PCR. *Nippon Shokakibyo Gakkai Zasshi* 1992; **89**: 1396
- 15 **Ishiyama N**, Katayama K, Ishimi N, Takahashi S, Igarashi H, Nakajima H, Saito S, Aoyagi T, Andoh T, Oya A. Quantitative detection of hepatitis C virus RNA by multicyclic RT-PCR. *Int Hepatol Com* 1993; **1**: 72-79
- 16 **Okamoto H**, Sugiyama Y, Okada S, Kurai K, Akahane Y, Sugai Y, Tanaka T, Sato K, Tsuda F, Miyakawa Y. Typing hepatitis C virus by polymerase chain reaction with type-specific primers: application to clinical surveys and tracing infectious sources. *J Gen Virol* 1992; **73**(Pt 3): 673-679
- 17 **Asahina Y**, Izumi N, Uchihara M, Noguchi O, Tsuchiya K, Hamano K, Kanazawa N, Itakura J, Miyake S, Sakai T. A potent antiviral effect on hepatitis C viral dynamics in serum and peripheral blood mononuclear cells during combination therapy with high-dose daily interferon alfa plus ribavirin and intravenous twice-daily treatment with interferon beta. *Hepatology* 2001; **34**: 377-384
- 18 **Furusyo N**, Hayashi J, Ohmiya M, Sawayama Y, Kawakami Y, Ariyama I, Kinukawa N, Kashiwagi S. Differences between interferon-alpha and -beta treatment for patients with chronic hepatitis C virus infection. *Dig Dis Sci* 1999; **44**: 608-617
- 19 **Kobayashi Y**, Watanabe S, Konishi M, Yokoi M, Kakehashi R, Kaito M, Kondo M, Hayashi Y, Jomori T, Suzuki S. Quantitation and typing of serum hepatitis C virus RNA in patients with chronic hepatitis C treated with interferon-beta. *Hepatology* 1993; **18**: 1319-1325
- 20 **Hayasaka S**, Nagaki Y, Matsumoto M, Sato S. Interferon associated retinopathy. *Br J Ophthalmol* 1998; **82**: 323-325
- 21 **Tsolakos A**, Zalatio N. Hepatitis C: a review of diagnosis,

- management, and ocular complications from treatment. *Optometry* 2003; **74**: 517-523
- 22 **Chemello L**, Bonetti P, Cavalletto L, Talato F, Donadon V, Casarin P, Belussi F, Frezza M, Noventa F, Pontisso P. Randomized trial comparing three different regimens of alpha-2a-interferon in chronic hepatitis C. The TriVeneto Viral Hepatitis Group. *Hepatology* 1995; **22**: 700-706
- 23 **Tsubota A**, Chayama K, Ikeda K, Yasuji A, Koida I, Saitoh S, Hashimoto M, Iwasaki S, Kobayashi M, Hiromitsu K. Factors predictive of response to interferon-alpha therapy in hepatitis C virus infection. *Hepatology* 1994; **19**: 1088-1094
- 24 **Martinot-Peignoux M**, Marcellin P, Pouteau M, Castelnau C, Boyer N, Poliquin M, Degott C, Descombes I, Le Breton V, Milotova V. Pretreatment serum hepatitis C virus RNA levels and hepatitis C virus genotype are the main and independent prognostic factors of sustained response to interferon alfa therapy in chronic hepatitis C. *Hepatology* 1995; **22**: 1050-1056
- 25 **Nousbaum JB**, Pol S, Nalpas B, Landais P, Berthelot P, Brechot C. Hepatitis C virus type 1b (II) infection in France and Italy. Collaborative Study Group. *Ann Intern Med* 1995; **122**: 161-168
- 26 **Trimoulet P**, Bernard PH, de Ledinghen V, Oui B, Chene G, Saint-Marc Girardin MF, Dantin S, Couzigou P, Fleury H. Quantitation of hepatitis C virus RNA in plasma and peripheral blood mononuclear cells of patients with chronic hepatitis treated with interferon-alpha. *Dig Dis Sci* 2000; **45**: 175-181
- 27 **Kao JH**, Chen PJ, Lai MY, Wang TH, Chen DS. Positive and negative strand of hepatitis C virus RNA sequences in peripheral blood mononuclear cells in patients with chronic hepatitis C: no correlation with viral genotypes 1b, 2a, and 2b. *J Med Virol* 1997; **52**: 270-274
- 28 **Ounanian A**, Gueddah N, Rolachon A, Thelu MA, Zarski JP, Seigneurin JM. Hepatitis C virus RNA in plasma and blood mononuclear cells in patients with chronic hepatitis C treated with alpha-interferon. *J Med Virol* 1995; **45**: 141-145
- 29 **Taliani G**, Badolato C, Lecce R, Poliandri G, Bozza A, Duca F, Pasquazzi C, Clementi C, Furlan C, De Bac C. Hepatitis C virus RNA in peripheral blood mononuclear cells: relation with response to interferon treatment. *J Med Virol* 1995; **47**: 16-22
- 30 **Martin J**, Navas S, Fernandez M, Rico M, Pardo M, Quiroga JA, Zahm F, Carreno V. *In vitro* effect of amantadine and interferon alpha-2a on hepatitis C virus markers in cultured peripheral blood mononuclear cells from hepatitis C virus-infected patients. *Antiviral Res* 1999; **42**: 59-70
- 31 **Enomoto N**, Sakuma I, Asahina Y, Kurosaki M, Murakami T, Yamamoto C, Ogura Y, Izumi N, Marumo F, Sato C. Mutations in the nonstructural protein 5A gene and response to interferon in patients with chronic hepatitis C virus 1b infection. *N Engl J Med* 1996; **334**: 77-81

Edited by Wang XL Proofread by Zhu LH

Factors related to lymph node metastasis and surgical strategy used to treat early gastric carcinoma

Dong Yi Kim, Jae Kyoon Joo, Seong Yeob Ryu, Young Jin Kim, Shin Kon Kim

Dong Yi Kim, Jae Kyoon Joo, Seong Yeob Ryu, Young Jin Kim, Shin Kon Kim, Division of Gastroenterologic Surgery, Department of Surgery, Chonnam National University Medical School, Gwangju, Korea

Correspondence to: Dr. Dong Yi Kim, Division of Gastroenterologic Surgery, Department of Surgery, Chonnam National University Hospital, 8, Hakdong, Dongku, Gwangju, 501-757, Korea. dockim@chonnam.ac.kr

Telephone: +82-62-220-6450 **Fax:** +82-62-227-1635

Received: 2003-10-29 **Accepted:** 2003-12-16

Abstract

AIM: The prognosis of early gastric carcinoma (EGC) is generally excellent after surgery. The presence or absence of lymph node metastasis in EGC is an important prognostic factor. The survival and recurrence rates of node-negative EGC are much better than those of node-positive EGC. This study examined the factors related to lymph node metastasis in EGC to determine the appropriate treatment for EGC.

METHODS: We investigated 748 patients with EGC who underwent surgery between January 1985 and December 1999 at the Division of Gastroenterologic Surgery, Department of Surgery, Chonnam National University Hospital. Several clinicopathologic factors were investigated to analyze their relationship to lymph node metastasis: age, sex, tumor location, tumor size, gross type, histologic type, depth of invasion, extent of lymph node dissection, type of operation, and DNA ploidy.

RESULTS: Lymph node metastases were found in 75 patients (10.0%). Univariate analysis showed that male sex, tumor size larger than 2.0 cm, submucosal invasion of tumor, histologic differentiation, and DNA ploidy pattern were risk factors for regional lymph node metastasis in EGC patients. However, a multivariate analysis showed that three risk factors were associated with lymph node metastasis: large tumor size, undifferentiated histologic type and submucosal invasion. No statistical relationship was found for age, sex, tumor location, gross type, or DNA ploidy in multivariate analysis. The 5-year survival rate was 94.2% for those without lymph node metastasis and 87.3% for those with lymph node metastasis, and the difference was significant ($P < 0.05$).

CONCLUSION: In patients with EGC, the survival rate of patients with positive lymph nodes is significantly worse than that of patients with no lymph node metastasis. Therefore, a standard D2 lymphadenectomy should be performed in patients at high risk of lymph node metastasis: large tumor size, undifferentiated histologic type and submucosal invasion.

Kim DY, Joo JK, Ryu SY, Kim YJ, Kim SK. Factors related to lymph node metastasis and surgical strategy used to treat early gastric carcinoma. *World J Gastroenterol* 2004; 10(5): 737-740
<http://www.wjgnet.com/1007-9327/10/737.asp>

INTRODUCTION

Early gastric carcinoma (EGC) is defined as a lesion confined to the mucosa or submucosa of the stomach with or without lymph node metastasis^[1]. The incidence of lymph node metastasis differs in mucosal and submucosal gastric carcinomas. When invasion extends to the submucosal layer, the incidence of lymph node metastasis increases^[2] and submucosal gastric carcinoma is reported to have a poorer prognosis than mucosal gastric carcinoma^[3].

We analyzed data from 673 patients with node-negative EGC, and 75 patients with node-positive EGC who had been surgically treated, to evaluate the clinicopathologic factors related to lymph node metastasis in EGC and to determine the appropriate treatment criteria for patients with EGC.

MATERIALS AND METHODS

Between 1985 and 1999, 748 Korean patients with EGC underwent surgery at the Division of Gastroenterologic Surgery, Department of Surgery, Chonnam National University Hospital. Of these, 75 patients (10.0%) were found to have lymph node metastasis.

Medical records were reviewed, and data were abstracted for the following factors: clinical findings, tumor size, tumor location, gross appearance, histologic grade, lymph node involvement, operation type, DNA ploidy pattern, and 5-year survival rate.

The clinical features of the 673 patients with node-negative EGC, and the 75 patients with node-positive EGC were compared. Curative resections were defined as histologic or relative curative resections according to the criteria of the Japanese Research Society for Gastric Cancer^[4]. The data were analyzed statistically using a chi-square test and an unpaired Student's *t*-test. Overall survival rates were calculated using the Kaplan-Meier method. Multivariate analysis was performed using the Cox proportional hazards model with the program SPSS 11.0 to test the variables associated with lymph node metastasis in EGC. A *P* value < 0.05 was considered statistically significant.

RESULTS

Of the 2 767 patients with gastric carcinoma who underwent surgery in our hospital over the 15-year period, 748 patients (27.0%) were diagnosed as EGC. The incidence of node-positive EGC was 10.0% (75/748) in this study group.

Table 1 describes the clinicopathologic findings in the 673 patients with node-negative EGC, and the 75 patients with node-positive EGC. There was no statistically significant difference between the ages of patients with and without lymph node metastasis. Of the 75 patients with lymph node metastasis, 41 (54.7%) were males and 34 (45.3%) were females. There were 453 males (67.3%) and 220 females (32.7%) in the group of 673 patients with node-negative EGC. There were more males than females in each group and the gender ratio was statistically significant ($P < 0.05$). The mean tumor size of patients with node-positive EGC (3.1 cm) was larger than that of patients with node-negative EGC (2.2 cm), and the difference was statistically significant ($P < 0.01$). Lymph node metastasis was

present in only 10 patients (13.3%) with a tumor <2.0 cm in size. Of these 75 patients with node-positive EGC, 65 patients (86.7%) were found to have a tumor \geq 2.0 cm in size ($P<0.01$). Most gastric carcinomas were located in the lower portion of the stomach, in both node-negative (445 cases, 66.1%) and node-positive EGC patients (55 cases, 73.3%), but the differences in location were not significant. There was no correlation between lymph node metastasis and macroscopic appearance of the tumor. Based on the degree of anaplasia, 10 (13.3%) patients with node-positive EGC had well-differentiated, 14 (18.7%) had moderately differentiated, 45 (60.0%) had poorly differentiated, and 3 (4.0%) had mucinous adenocarcinomas ($P<0.01$). The submucosal invasion was found more frequently in patients with node-positive EGC (81.3%) than in those with node-negative EGC (46.1%, $P<0.01$). Distant metastasis was found in one patient with node-negative EGC. There was no significant difference between node-negative and node-positive EGC patients in the operative type. The curative resection rate for patients with node-negative EGC was similar to that for patients with node-positive EGC (99.7% vs 97.3%).

Table 1 Clinicopathologic findings in patients with early gastric carcinoma with and without lymph node metastasis

	Node-negative <i>n</i> =673, (%)	Node-positive <i>n</i> =75, (%)	<i>P</i> value
Age (mean, yr)	55.7±10.7	57.9±10.7	NS
Gender			<0.05
Male	453 (67.3)	41 (54.7)	
Female	220 (32.7)	34 (45.3)	
Age (yr)			NS
≤ 40	71 (10.5)	5 (6.7)	
> 40	602 (89.5)	70 (93.3)	
Tumor size (mean, cm)	2.2±1.45	3.1±1.89	<0.01
< 2	434 (64.5)	10 (13.3)	<0.01
2-3	141 (21.0)	24 (32.0)	
> 3	98 (14.5)	41 (54.7)	
Tumor location			NS
Upper	28 (4.2)	2 (2.7)	
Middle	200 (29.7)	18 (24.0)	
Lower	445 (66.1)	55 (73.3)	
Macroscopic appearance			NS
Protruded	208 (30.9)	21 (28.0)	
Depressed	417 (62.0)	50 (66.7)	
Mixed	48 (7.1)	4 (5.3)	
Stage			<0.01
Ia	672 (99.9)		
Ib		65 (86.7)	
II		6 (8.0)	
IV	1 (0.1)	4 (5.3)	
Histologic type			<0.01
Differentiated	348 (51.7)	24 (32.0)	
Undifferentiated	325 (48.3)	51 (68.0)	
Depth of invasion			<0.01
Mucosa	363 (53.9)	14 (18.7)	
Submucosa	310 (46.1)	61 (81.3)	
Operative type			NS
Total gastrectomy	62 (9.2)	8 (10.7)	
Proximal gastrectomy	4 (0.6)		
Distal gastrectomy	583 (86.8)	65 (86.7)	
Others	24 (3.4)	2 (2.7)	
Lymph node dissection			<0.01
D1	144 (21.4)	8 (10.7)	
D2	484 (71.9)	50 (66.7)	
≥D3	45 (6.7)	17 (22.7)	
Curability			NS
Curative	671 (99.7)	73 (97.3)	
Non-curative	2 (0.3)	2 (2.7)	

NS, not significant.

Univariate analysis showed that male sex, tumor size, depth of invasion, undifferentiated type, and aneuploid pattern were significant factors associated with lymph node metastasis in EGC (Tables 1 and 2).

Table 2 Lymph node metastasis according to DNA ploidy pattern (*n*=238)

DNA ploidy	Node-negative (%)	Node-positive (%)	<i>P</i> value
Aneuploid	80 (38.5)	17 (56.7)	<0.05
Diploid	128 (61.5)	13 (43.3)	

Table 3 Logistic regression analysis for variables associated with lymph node metastasis in early gastric carcinoma

Variables	Risk ratio	95% CI	<i>P</i> value
Age	1.040	0.996-1.021	0.50
Gender	1.022	0.884-1.121	0.183
Tumor size	1.342	1.134-1.642	0.003
Gross appearance	1.124	0.987-1.342	0.384
Histologic type	0.948	0.737-1.221	0.009
Depth of invasion	1.241	0.949-1.369	<0.001
Tumor location	0.963	0.822-1.522	0.09
DNA ploidy	0.876	0.744-1.675	0.06

CI, confidence interval.

All of the factors listed in Tables 1 and 2 were examined using a logistic regression analysis. The independent risk factors for lymph node metastasis were larger tumor size, undifferentiated type, and submucosal invasion (Table 3).

The postoperative survival rate of the patients without lymph node metastasis was compared with that obtained from those with lymph node metastasis. The 5-year survival rates were 94.2% for those without lymph node metastasis and 87.3% for those with lymph node metastasis, and the difference was significant ($P<0.05$, Figure 1).

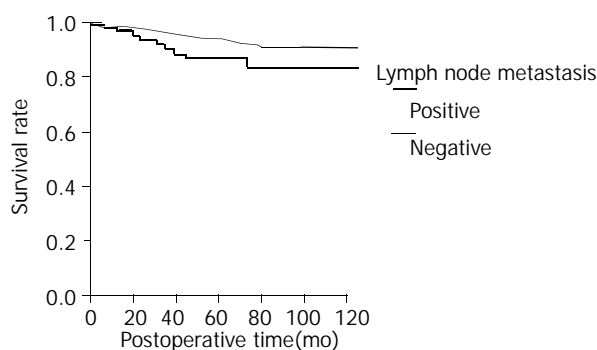


Figure 1 Survival curves according to lymph node metastasis. The early gastric carcinoma patients without lymph node metastasis showed a better survival rate than early gastric carcinoma patients with lymph node metastasis (94.2% vs 87.3%, $P<0.05$).

DISCUSSION

Early gastric carcinoma (EGC) has been defined as gastric carcinoma in which invasion is confined to the mucosa or submucosa, regardless of lymph node metastasis^[1]. The incidence of EGC has increased due to the advances in technical developments regarding both radiological modalities and endoscopy^[5]. In our department, 27.0% of the patients had EGC, a rate similar to the 20-40% range previously reported^[6]. The prognosis of EGC after curative resection was favorable,

with a 5-year survival rate exceeding 90%^[6-8]. Moreover, the survival and recurrence rates of node-negative EGC were much better than those of node-positive EGC^[7,8].

The reported incidence of lymph node metastasis in EGC was 2-4% in mucosal carcinoma^[9-11], but increased to 15-25% in submucosal carcinoma^[12]. Here, we found a 3.7% incidence of lymph node metastasis in mucosal carcinoma and a 16.4% incidence in submucosal carcinoma. The incidence of lymph node metastasis was similar to those in mucosal carcinoma reported by Yamao *et al*^[9] and Tsujitani *et al*^[10], and lower in submucosal carcinoma reported by other investigators^[13,14]. Some investigators have reported that submucosal invasion is one of the predictive risk factors for lymph node metastasis in EGC patients^[8,15,16]. Shimada *et al* reported that the number of metastatic lymph nodes occurring in patients with gastric carcinoma was correlated with the survival rate^[6]. EGC patients with lymph node metastasis had a lower survival rate than patients without lymph node metastasis. Of note, they suggested that the involvement of three or more lymph nodes could predict a poor prognosis in submucosal gastric carcinoma. Seto *et al*^[17] reported a 5-year survival of 74% in patients with more than 4 positive lymph nodes. Folli *et al*^[11] also reported a lower 5-year survival, especially for patients who presented more than 3 metastatic lymph nodes.

The presence of lymph node metastasis in EGC worsened the prognosis, as reported by some investigators^[8,13] and as observed in this study (87.3% vs 94.2%). Nio *et al*^[18] reported that the 5-year survival of EGC was 93% for N1 patients and 68.4% for N2 patients. Miwa *et al*^[15] observed similar results. When EGC was subdivided into mucosal and submucosal carcinomas, the survival rate for mucosal carcinoma was significantly better than that for submucosal carcinoma^[19] because the former had a lower incidence of lymph node metastasis. Nevertheless, submucosal invasion could not always predict a poor prognosis, the survival rates in patients with submucosal carcinoma were the same as those in patients with mucosal carcinoma^[20]. In our study, the incidence of lymph node metastasis from submucosal carcinoma (16.4%) was significantly higher than that from mucosal carcinoma (3.7%). However, the 5-year survival rate for patients with submucosal carcinoma (88.6%) did not differ from that for patients with mucosal carcinoma (95.2%), because the curative resection rate was high for both submucosal (97.3%) and mucosal (99.7%) carcinomas. We performed gastrectomy with D2 lymphadenectomy for most patients with submucosal gastric carcinoma. Furthermore, some investigators^[12,21] have recommended that a standard D2 lymphadenectomy is essential, even in cases of mucosal carcinoma.

Lymphadenectomy, a prognostic factor that can be influenced by the surgeon, improves the survival rate in gastric carcinoma, although there has been no extensive prospective randomized trial. Viste *et al*^[22] reported that the survival of patients who underwent extensive lymph node dissection was higher than that of patients without dissection. Furthermore, lymph node recurrence has been attributed to inadequate lymph node dissection. We found that in patients with submucosal gastric carcinoma, the survival rate with positive lymph nodes was significantly poorer than that with no lymph node metastasis (87.3% vs 94.2%, $P < 0.05$). Therefore, we recommend gastrectomy with D2 lymphadenectomy as the appropriate operative procedure for patients with submucosal carcinoma of the stomach.

There have been several attempts to identify risk factors predicting lymph node metastasis. Maehara *et al*^[6] found that the risk factors for lymph node metastasis in EGC patients were large tumor, lymphatic involvement, and submucosal invasion. Yamao *et al*^[9] also reported that lymphatic invasion, histologic type, and large tumor size were independent risk

factors for lymph node metastasis in patients with intramucosal EGC. Abe *et al*^[23] reported that submucosal invasion, female sex, large tumor size, and lymphatic vessel involvement were significantly and independently related to the presence of lymph node metastasis in depressed EGC. Baba *et al*^[24] reported that there was no metastasis in lesions less than 1 cm in diameter, but the incidence of positive nodes increased with the size of the primary lesion. Wu *et al*^[25] reported that poor differentiation, submucosal invasion and large tumor size were independent risk factors for lymph node metastasis in early gastric cancer. Macroscopic classification was not correlated with lymph node metastasis. Sasaki *et al*^[26] reported that DNA aneuploidy was a useful indicator of lymph node metastasis in EGC patients. We studied the DNA ploidy pattern in 238 patients with EGC and found that there was a correlation between lymph node metastasis and DNA ploidy pattern in univariate analysis. But we found there was no correlation between lymph node metastasis and DNA ploidy pattern in multivariate analysis (Table 3). In our study, the univariate analysis showed that lymph node metastasis in EGC patients was associated with male sex, large tumor size, submucosal invasion, and undifferentiated histologic grade, while the multivariate analysis showed that metastasis was associated with large tumor size, undifferentiated type and submucosal invasion (Table 3).

In conclusion, this study suggests that tumor size, depth of tumor invasion and undifferentiated histologic grade are risk factors for lymph node metastasis in EGC. Therefore, standard D2 lymphadenectomy should be performed in patients with these high-risk factors.

REFERENCES

- 1 **Kajitani T.** The general rules for the gastric cancer study in surgery and pathology. Part I. Clinical classification. *Jpn J Surg* 1981; **11**: 127-139
- 2 **Inoue K,** Tobe T, Kan N, Nio Y, Sakai M, Takekuchi E, Sugiyama T. Problems in the definition and treatment of early gastric cancer. *Br J Surg* 1991; **78**: 818-821
- 3 **Hioki K,** Nakane Y, Yamamoto M. Surgical strategy for early gastric cancer. *Br J Surg* 1990; **77**: 1330-1334
- 4 **Japanese Research Society for Gastric Cancer.** The general rules for the gastric cancer study in surgery and pathology. 12th ed. Tokyo: Kanahara Shuppan 1993
- 5 **Hisamichi S,** Sugawara N. Mass screening for gastric cancer by X-ray examination. *Jpn J Clin Oncol* 1984; **14**: 211-223
- 6 **Maehara Y,** Okuyama T, Oshiro T, Baba H, Anai H, Akazawa K, Sugimachi K. Early carcinoma of the stomach. *Surg Gynecol Obstet* 1993; **177**: 593-597
- 7 **Sano T,** Kobori O, Muto T. Lymph node metastasis from early gastric cancer: endoscopic resection of tumour. *Br J Surg* 1992; **79**: 241-244
- 8 **Maehara Y,** Orita H, Okuyama T, Moriguchi S, Tsujitani S, Korenaga D, Sugimachi K. Predictors of lymph node metastasis in early gastric cancer. *Br J Surg* 1992; **79**: 245-247
- 9 **Yamao T,** Shirao K, Ono H, Kondo H, Saito D, Yamaguchi H. Risk factors for lymph node metastasis from intramucosal gastric carcinoma. *Cancer* 1996; **77**: 602-606
- 10 **Tsujitani S,** Oka S, Saito H, Kondo A, Ikeguchi M, Maeta M, Kaibara N. Less invasive surgery for early gastric cancer based on the low probability of lymph node metastasis. *Surgery* 1999; **125**: 148-154
- 11 **Folli S,** Morgagni P, Roviello F, De Manzoni G, Marrelli D, Saragoni L, Di Leo A, Gaudio M, Nanni O, Carli A, Cordiano C, Dell' Amore D, Vio A. Risk factors for lymph node metastases and their prognostic significance in early gastric cancer (EGC) for the Italian Research Group for Gastric Cancer (IRGGC). *Jpn J Clin Oncol* 2001; **31**: 495-499
- 12 **Sowa M,** Kato Y, Nishimura M, Kubo T, Maekawa H, Umeyama K. Surgical approach to early gastric cancer with lymph node metastasis. *World J Surg* 1989; **13**: 630-636
- 13 **Kitamura K,** Yamaguchi T, Taniguchi H, Hagiwara A, Sawai K,

- Takahashi T. Analysis of lymph node metastasis in early gastric cancer: Rationale of limited surgery. *J Surg Oncol* 1997; **64**: 42-47
- 14 **Kurihara N**, Kubota T, Otani Y, Ohgami M, Kumai K, Sugiura H, Kitajima M. Lymph node metastasis of early gastric cancer with submucosal invasion. *Br J Surg* 1998; **85**: 835-839
- 15 **Mita T**, Shimoda T. Risk factors for lymph node metastasis of submucosal invasive differentiated type gastric carcinoma: clinical significance of histological heterogeneity. *J Gastroenterol* 2001; **36**: 661-668
- 16 **Shimada S**, Yagi Y, Honmyo U, Shiomori K, Yoshida N, Ogawa M. Involvement of three or more lymph nodes predicts poor prognosis in submucosal gastric carcinoma. *Gastric Cancer* 2001; **4**: 54-59
- 17 **Seto Y**, Nagawa H, Muto T. Impact of lymph node metastasis on survival with early gastric cancer. *World J Surg* 1997; **21**: 186-190
- 18 **Nio Y**, Tsubono M, Kawabata K, Masai Y, Hayashi H, Meyer C. Comparison of surgical curves of gastric cancer patients after surgery according to the UICC stage classification and General Rules for Gastric Cancer Study by the Japanese Research Society for gastric cancer. *Ann Surg* 1993; **218**: 47-53
- 19 **Moreaux J**, Bougaran J. Early gastric cancer: a 25-year surgical experience. *Ann Surg* 1993; **217**: 347-355
- 20 **Yasuna O**, Hayashi S. Factors influencing the postoperative course 113 patients with early gastric cancer. *Jpn J Clin Oncol* 1986; **16**: 325-334
- 21 **Ichikura T**, Uefuji K, Tomimatsu S, Okusa Y, Yahara T, Tamakuma S. Surgical strategy for patients with gastric carcinoma with submucosal invasion. *Cancer* 1995; **76**: 935-940
- 22 **Viste A**, Svanes K, Janssen CW, Maartmann-Moh H, Soreide O. Prognostic importance of radical lymphadenectomy in curative resections for gastric cancer. *Eur J Surg* 1994; **160**: 497-502
- 23 **Abe N**, Watanabe T, Suzuki K, Machida M, Toda H, Nakaya Y, Masaki T, Mori T, Sugiyama M, Atomi Y. Risk factors predictive of lymph node metastasis in depressed early gastric cancer. *Am J Surg* 2002; **183**: 168-172
- 24 **Baba H**, Maehara Y, Okuyama T, Orita H, Anai H, Akazawa K, Sugimachi K. Lymph node metastasis and macroscopic features in early gastric cancer. *Hepatogastroenterology* 1994; **41**: 380-383
- 25 **Wu CY**, Chen JT, Chen GH, Yeh HZ. Lymph node metastasis in early gastric cancer: a clinicopathological analysis. *Hepatogastroenterology* 2002; **49**: 1465-1468
- 26 **Sasaki O**, Kido K, Nagahama S. DNA ploidy, Ki-67 and p53 as indicators of lymph node metastasis in early gastric cancer. *Anal Quant Cytol Histol* 1999; **21**: 85-88

Edited by Wang XL Proofread by Zhu LH

Effect of human milk and colostrum on *Entamoeba histolytica*

Ciler Akisu, Umit Aksoy, Hasan Cetin, Sebnem Ustun, Mete Akisu

Ciler Akisu, Umit Aksoy, Department of Parasitology, School of Medicine, Dokuz Eylul University, 35340, Inciralti, Izmir, Turkey

Hasan Cetin, Mete Akisu, Department of Pediatrics, School of Medicine, Ege University, 35100, Bornova, Izmir, Turkey

Sebnem Ustun, Department of Gastroenterology, School of Medicine, Ege University, 35100, Izmir, Turkey

Correspondence to: Ciler Akisu, MD, Department of Parasitology, School of Medicine, Dokuz Eylul University, 35340 Inciralti-Izmir, Turkey. ciler.akisu@deu.edu.tr

Telephone: +90-232-412 45 40 **Fax:** +90-232-259 05 41

Received: 2003-10-15 **Accepted:** 2003-12-16

Abstract

AIM: Many defense factors of the mother's colostrum or milk protect infants from intestinal, respiratory and systemic infections. In the present study, we investigated the effect of colostrum and mature human milk on *E. histolytica* parasites *in vitro*.

METHODS: Samples of human milk were collected from 5 healthy lactating mothers. The medium with human milk at concentrations of 2%, 5% and 10% was obtained.

RESULTS: The lethal effect of *E. histolytica* on the medium supplemented with different concentrations of both colostrum and mature human milk was significant during the first 30 min. We also detected that the results of colostrum and mature human milk were similar. No statistically significant differences were found between same concentrations of colostrum and mature human milk at the same times.

CONCLUSION: Colostrum and mature human milk have significant lethal effect on *E. histolytica* and protect against its infection in breast fed children.

Akisu C, Aksoy U, Cetin H, Ustun S, Akisu M. Effect of human milk and colostrum on *Entamoeba histolytica*. *World J Gastroenterol* 2004; 10(5): 741-742

<http://www.wjgnet.com/1007-9327/10/741.asp>

INTRODUCTION

Entamoeba histolytica has a worldwide distribution with a high prevalence in areas with poor hygiene, overcrowding, and low socioeconomic conditions. When ingested, cyst passes through the stomach and excyst in the distal part of the small intestine and colon. *E. histolytica* generally lives in the lumen of the large intestine of man. The emerging trophozoites live in the lumen of the bowel close to the mucosa, where they feed by phagocytosis on particulate matter and bacteria and by pinocytosis on liquid nutrients. As such, they may invade the gut wall and produce ulceration and subsequent dysentery. The parasite may be transported by the blood to extraintestinal locations, such as the liver, lungs, and brain^[1-3].

The role of breast milk ingestion in passive and active protection of infants is very important. Some reports showed that the incidence of intestinal and systemic *E. histolytica* infections was decreased in human breast milk fed infants.

This protective effect has been attributed to the anti-infective and anti-inflammatory properties of human breast milk^[4,5].

The aim of the present study was to investigate the effects of colostrum and mature human milk on *E. histolytica*. Human colostrum or mature milk, if effective in producing lethal effect on *E. histolytica*, could be useful in preventing infections caused by infected water and food in breast-fed children.

MATERIALS AND METHODS

E. histolytica fresh clinical isolate was obtained from a patient with acute amebiasis. The isolate was cultivated in Robinson medium^[6].

Fresh human milk was collected from 5 healthy lactating mothers with no clinical evidence of infection or inflammation, who voluntarily donated up to 10 mL of milk and colostrum samples, with their informed consent, by breast pump (Ameda Egnell SMB Pump, Switzerland), in Ege University Hospital, Izmir, Turkey. None of these mothers received hormones or antibiotics during the postpartum period. Colostrum and mature human milk were obtained during the first 3 d of lactation and the 3rd wk of lactation, respectively. All samples were collected from mothers between 9 and 12 a.m., just before they began to nurse their babies. The colostrum and mature human milk samples were rapidly centrifuged for 15 min at 1 000 g. The fresh clear middle layer was collected and immediately frozen (-70 °C) until the study^[7].

Culture methods and evaluation of amoeba-cidal activity

The trophozoites were adapted by three successive subcultures at 36±0.5 °C. At the end of the period amoebae reached logarithmic growth phase. Trophozoites were chilled for 10 min in an ice water bath, then vigorously shaken to detach amoebae adherent to the walls of the tube. The culture tubes were centrifuged for 2 min (500 r/min) and supernatant was discarded. Once their content was homogenized by repeated inversion. They were counted with a haemocytometer and then 20×10⁴ amoebae/mL were transferred to fresh medium. Five tubes including 5 mL medium were prepared for each group. Then, colostrum and mature human milk were added in medium at different concentrations (2%, 5% and 10%). Tubes were incubated at 36±0.5 °C for 30, 60, 120, 180 and 240 min respectively. At the end of incubation, only motile parasites were counted with a haemocytometer^[8]. All experiments were done in triplicate and repeated at least twice.

Statistical analysis

All values were given as mean±SD. To determine the statistical significance of the difference between study groups, we used nonparametric tests, Kruskal-Wallis analysis of variance and Mann-Whitney test. *P* value less than 0.05 was considered significant.

RESULTS

In the study, we analyzed the lethal effect of colostrum and mature human milk at three different concentrations on *E. histolytica*. The number of living parasite was recorded at the different incubation periods. The results of this experiment showed that the best lethal effect (50% killing) was obtained from all samples

during the first 30 min exposure. We have also observed that there was no living parasite at the end of 12 h incubation.

A significant lethal effect of different concentrations of colostrum on *E. histolytica* was observed during 30 min and 180 min exposure ($P < 0.001$) (Figure 1). However, no statistically significant differences were shown between them ($P > 0.05$).

When the lethal effect of mature human milk at different concentrations on *E. histolytica* was compared with each other, the difference was statistically significant during 30 min and 180 min exposure ($P < 0.001$) (Figure 2). There was no statistically significant difference between 30 and 180 min exposure ($P > 0.005$).

The results of colostrum and mature human milk were similar. Colostrum did not prove to be very superior to mature human milk. No statistically significant differences were found between same concentrations of colostrum and mature human milk at 30, 60, 120, 180, and 240 min exposure.

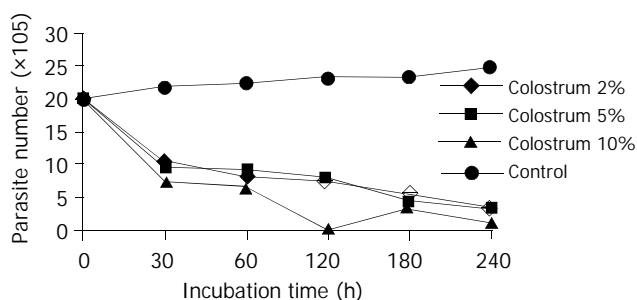


Figure 1 Lethal effect of colostrum at various concentrations on *E. histolytica*.

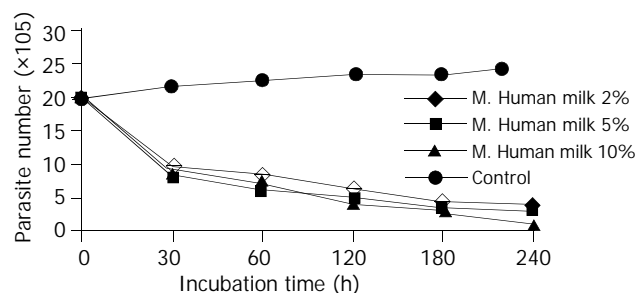


Figure 2 Lethal effect of mature human milk at various concentrations on *E. histolytica*.

DISCUSSION

Colostrum and mature human milk may play a protective role in breast-fed children exposed to some parasites (such as *G. intestinalis*). Both contain considerable amounts of immunoglobulins, mainly the secretory immunoglobulin A (sIgA) type that may play a role in such protection. It has been shown that such immunoglobulins have antibody specificities, which reflect antigenic stimuli in the intestinal tract^[9,10].

The demonstration of antibodies in breast milk may have epidemiological significance in population studies. Antibodies of the IgA class were found in serum and colostrum of parturient women in an endemic area of amebiasis^[11]. Grundy *et al*^[12] demonstrated sIgA antibodies to *E. histolytica* in milk (31%) and serum (14%) of mothers living in Kenya. They suggested that serum antibodies indicated past or present invasive amebiasis, milk antibodies were more likely to present intestinal infection in endemic areas. Anti-Eh sIgA antibody titers were significantly increased in colostrum samples of mothers of newborn children with diarrhea^[13]. The infants,

mostly uninfected, were found to have *E. histolytica* cysts in small numbers (2/1 200 samples), despite the high prevalence of *E. histolytica* in their mothers^[14].

Human milk cells (macrophages, lymphocytes, neutrophils) and antibodies could protect intestinal mucosa, remain active in the neonatal intestine and possibly migrate to other tissues^[5]. Colostral macrophages might be cytotoxic to trophozoites of *E. histolytica*. This has been shown by direct microscopy^[7]. It was proposed that colostral macrophages might interrupt colonization and subsequent invasion in infants who were breast-fed. Although there are many epidemiological studies in endemic areas, studies about colostrum and mature human milk *in vitro* are limited. Gillin *et al* reported that 90% of *E. histolytica* were killed in approximately 3 h with 1% milk. But we could not find any publications containing colostrum and mature human milk together *in vitro*. We established that *E. histolytica* was killed by exposure to colostrum and mature human milk *in vitro*. IgA and lactoferrin amounts in colostrum were richer than mature human milk. However, we obtained similar results from both of them. Fifty percent of *E. histolytica* were killed by all dilutions of both secretions during a 30 min exposure. Thus, the lethal effect did not depend on the amounts of various protectable milk components. Similarly, some studies showed that the lethal effect of sIgA on some parasites did not depend on the amount of sIgA.

In this study, we showed that colostrum and mature human milk had direct lethal effect on *E. histolytica* *in vitro*. Therefore, when trophozoites that emerge from cysts in the small intestine are exposed to colostrum and mature human milk, they may be killed. Thus, breast fed children have a lower rate of amebiasis than nonbreast fed children.

REFERENCES

- 1 **Ravdin JI**. Amebiasis. *Clin Infect Dis* 1995; **20**: 1453-1464
- 2 **Proctor EM**. Laboratory diagnosis of amebiasis. *Clin Lab Med* 1991; **11**: 829-859
- 3 **Stanley SL Jr**. Amoebiasis. *Lancet* 2003; **22**: 1025-1034
- 4 **Chierici R**. Antimicrobial actions of lactoferrin. *Adv Nutr Res* 2001; **10**: 247-269
- 5 **Xanthou M**, Bines J, Walker WA. Human milk and intestinal host defense in newborns: an update. *Adv Pediatr* 1995; **42**: 171-208
- 6 **Clark CG**, Diamond LS. Methods for cultivation of luminal parasitic protists of clinical importance. *Clin Microbiol Rev* 2002; **15**: 329-341
- 7 **Acosta-Altamirano G**, Rocha-Ramirez LM, Reyes-Montes R, Cote V, Santos JI. Anti-amoebic properties of human colostrum. *Adv Exp Med Biol* 1987; **216B**: 1347-1352
- 8 **Chavez-Duenas L**, Gomez-Dominguez R, Lopez-Revilla R. Effects of Panmede and various horse serum concentrations on the axenic cultivation of *Entamoeba histolytica* strains in TPS-1 medium. *Parasitol Res* 1989; **76**: 50-54
- 9 **Hanson LA**, Korotkova M. The role of breastfeeding in prevention of neonatal infection. *Semin Neonatol* 2002; **7**: 275-281
- 10 **Ogra PL**, Losonsky GA, Fishaut M. Colostrum-derived immunity and maternal-neonatal interaction. *Ann N Y Acad Sci* 1983; **409**: 82-95
- 11 **Berber AC**, Escobar A, Zamora M, Acosta G. Identification of *Entamoeba histolytica* antigens recognized by IgA class human antibodies in sera and colostrum of puerperal women using immunoblotting techniques. *Arch Invest Med* 1990; **21**(Suppl 1):97-101
- 12 **Grundy MS**, Cartwright-Taylor L, Lundin L, Thors C, Huld G. Antibodies against *Entamoeba histolytica* in human milk and serum in Kenya. *Clin Microbiol* 1983; **17**: 753-758
- 13 **Lopez Revilla R**, Navarro-Garcia F, Valadez-Sanchez M, Lopez Vidal Y, Calva Mercado J. Dot-enzyme-linked immunosorbent assay (Dot-ELISA) of anti-*Entamoeba histolytica* antibodies in human serum and colostrum. *Arch Invest Med* 1991; **22**: 249-253
- 14 **Islam A**, Stoll BJ, Ljungstrom I, Biswas J, Nazrul H, Huld G. The prevalence of *Entamoeba histolytica* in lactating women and in their infants in Bangladesh. *Trans R Soc Trop Med Hyg* 1988; **82**: 99-103

Detection of K-ras gene mutation in fecal samples from elderly large intestinal cancer patients and its diagnostic significance

Jun Wan, Zi-Qi Zhang, Wei-Di You, Hua-Kui Sun, Jian-Ping Zhang, Ya-Hong Wang, Yong-He Fu

Jun Wan, Zi-Qi Zhang, Wei-Di You, Hua-Kui Sun, Jian-Ping Zhang, Ya-Hong Wang, Yong-He Fu, Department of Geriatric Gastroenterology, General Hospital of the Chinese PLA, Beijing 100853, China

Correspondence to: Jun Wan, Department of Geriatric Gastroenterology, South Building of General Hospital of the Chinese PLA, Beijing, China. wanjun@301hospital.com.cn

Telephone: +86-10-66937622

Received: 2003-11-04 **Accepted:** 2003-12-29

Abstract

AIM: To study the diagnostic significance of K-ras gene mutations in fecal samples from elderly patients with large intestinal cancer.

METHODS: DNA was extracted in the fecal and tissue samples from 23 large intestinal cancer patients, 20 colonic adenomatoid polypus patients and 20 healthy subjects. The K-ras gene mutations at the first and second bases of codon 12 were detected by the allele specific mismatch method.

RESULTS: The K-ras gene mutation was 56.52%(13/23) in the large intestinal cancer patients, which was notably higher than that in the normal subjects whose K-ras gene mutation was 5%(1/20) ($\chi^2=12.93$, $P<0.001$). There was no significant difference in comparison with that of colonic adenomatoid polypus patients whose K-ras gene mutation was 30%(6/12) ($\chi^2=3.05$, $P>0.05$). The K-ras gene mutation at the second base of codon 12 was 92.13%(12/13) in the large intestinal cancer patients. There was no significant difference between the detection rate of K-ras gene mutation in the fecal and tissue samples ($\chi^2=9.35$, $P<0.01$).

CONCLUSION: Our results indicate that detection of the K-ras gene mutations in fecal samples provides a non-invasive diagnostic method for the elderly large intestinal cancer patients. Its significance in the early diagnosis of large intestinal cancer awaits further studies.

Wan J, Zhang ZQ, You WD, Sun HK, Zhang JP, Wang YH, Fu YH. Detection of K-ras gene mutation in fecal samples from elderly large intestinal cancer patients and its diagnostic significance. *World J Gastroenterol* 2004; 10(5): 743-746
<http://www.wjgnet.com/1007-9327/10/743.asp>

INTRODUCTION

Large intestinal cancer is one of the common malignant tumors in China. Its incidence has been increasing in the elderly, and its death rate is approximately 60% in large intestinal cancer patients over 60 years old. In China, large intestinal cancer is often resulted from the malignancy of colonic adenomas, because the incidence of large intestinal polypus is high in the elderly. It was reported that the detectable rate of large intestinal polypus and adenomatoid polypus was as high as 62.1% and 67.9%, respectively^[1]. Therefore, early detection of cancerous

adenomas is of great significance in decreasing the incidence and death rate of large intestinal cancer. At present, colonoscopy is the most ideal diagnostic method for large intestinal cancer^[2,3], the reported detectable rate of early large intestinal cancer was 36.5% in the elderly^[1]. Since colonoscopy is an invasive method and the examined subjects would have some suffering, it has therefore become a topic of general interest to find a non-invasive diagnostic method for large intestinal cancer patients^[4-10]. The K-ras gene mutations in fecal samples from the elderly were detected by the allele specific mismatch method, and its diagnostic significance in the large intestinal cancer patients was discussed.

MATERIALS AND METHODS

Reagents

Taq DNA polymerase, dNTPS, DNA fragments, agarose, DNA extraction kits were the products of Promega (Madison, USA). Proteinase K was the product of Merck.

Specimens

The patients enrolled in this study were 23 cases of large intestinal cancer (19 males, 4 females, averaging 68.8 years), 20 cases of colonic adenomatoid polypus and 20 healthy subjects. Their diagnoses were confirmed by endoscopy and biopsy. Of the 23 cases of large intestinal cancer, 5 had well differentiated adenocarcinomas, 10 had moderately differentiated adenocarcinomas, 6 had poorly differentiated adenocarcinomas, and 2 had mucinous adenocarcinomas. The fecal samples were collected from the above patients before undergoing surgery and stored at -30 °C.

DNA extraction

DNA was extracted from the fecal samples using the DNA extraction kits. The fecal samples were processed according to the following procedures: 100-200 g of the fecal samples was diluted in 500 μ L of phosphate buffered saline (PBS), pH7.5, and homogenized for 2 min at 1 000 r/min. Then, 500 μ L supernatant after the addition of 50 μ L hydrolytic buffer was homogenized for 5 min, and centrifuged at 6 000 r/min for 2 min. The precipitate was placed into 500 μ L cleaning solution and centrifuged at 6 000 r/min for 2 min. After washed twice and addition of 50 μ L lysate and covered by paraffin oil, the precipitate was boiled for 5 min, centrifuged at 13 000 g for 10 min and stored at -30 °C before it was used. The DNA in the 16 cancer tissue samples was extracted by proteinase K (10 g/L, thermostatic water bath at 37 °C for 24 h), and purified by phenol-chloro-isopentanol extraction, and dissolved in TE buffer after ethanol precipitation for use.

PCR reaction

The oligonucleotide primer was synthesized by the Oligo 1000DNA synthesizer (Beckman). The DNA amplification PCR reaction was carried out in a total volume of 50 μ L buffer containing 5 μ L of diluted DNA templates, 10 mmol/L Tris-HCl (pH8.8), 1.5 mmol/L MgCl₂, 1g/L Triton X-100, 200 mmol/L dNTPs, 50 pmol/L of each primer and 1U of Taq DNA

polymerase. The PCR conditions were as follows: denaturing at 95 °C for 1 min, annealing at 55 °C for 1 min, extension at 72 °C for 3 min. The amplification was performed for 30 cycles. L14841 and H15149 are the primers specific for human cytochrome B gene, COI and ND2 are the primers specific for human mitochondrial cytochrome oxidase COI subunit. These primers were also used in the detection of K-ras gene mutations.

The point mutation at the first and second bases of codon 12 of the K-ras gene was detected by the allele specific mismatch method^[11]. The amplification PCR reaction was performed for 45 cycles in a total volume of 50 µL of buffer, but the conditions were slightly modified as the follows: denaturing at 95 °C for 1 min, annealing at 58 °C for 2 min, extension at 72 °C for 1 min. The A set and B set primers were used to detect the presence of K-ras gene mutations at the first and second bases of codon 12. Besides one general primer found in the 2 groups, both Ag and Bc primers were specific for the wild-type K-ras gene. The other primers were used to amplify various mutations of the K-ras gene. The control bands of DNA fragments from the corresponding tumors were validated using an ultraviolet detector after the PCR products were analyzed on a 30g/L agarose gel and visualized by ethidium bromide staining.

The nucleotide sequences of human cytochrome B gene primers and human mitochondrial cytochrome oxidase COI subunits used in the amplification reactions were as follows: L14841: 5' AAAAAGCTTCCATCCAACATCTCAGCATGATGAAA3', H15 149: 5' AACTGCAGCCCCCTCAGAATGATATTTGTCCTCA3', COI: 5' ACGATGTCTAGTGATGAGTTTGC-TA3', ND2: 5' ACGCCTAATCTACTCCACCTCAATC 3'.

A 300-bp PCR amplification product was detected using L14841 and H15149, and a 1 400 bp PCR amplification product was detected using COI and ND2. The K-ras gene mutation detected at the first base of codon 12 using the A set primers included K-ras A: 5' CAGAGAAACCTTTATCTG 3', K-ras Aa: 5' TGGTAGTTGGAGCTA 3'. K-ras Ac, K-ras Ag and K-ras At differed from K-ras Aa in the last nucleotide, which was replaced by C, G and T respectively^[11], and produced a 146 bp DNA amplification fragment.

The K-ras gene mutations detected using the B set primers at the second base of codon 12 included K-ras B: 5' GTACTGGTGGAGTATTT3' and K-ras Ba: 5' ACTCTTGCCTACGCCAA3'. K-ras Bc, K-ras Bg and K-ras Bt differed from K-ras Ba in the last 3' nucleotide, which was replaced by C, G and T respectively^[11], and generated a 161 bp DNA amplification fragment.

RESULTS

Sequence of specific human DNA in fecal extraction

The DNA of human cytochrome B gene (a 300 bp amplification fragment) and human mitochondrial cytochrome oxidase COI (a 1 400 bp amplification fragment) in the extraction of 10 fecal samples was amplified using the pair of L14841 and H15149 primers and the pair of COI and ND2 primers. A 300 bp and a 1 400 bp electrophoretic bands were observed in 9 fecal samples after the PCR products were analyzed on a 15g/L agarose gel and visualized by ethidium bromide staining.

Consistency of K-ras gene mutations in fecal and tissue samples

The K-ras gene mutations in the fecal and tissue samples of 16 large intestinal cancer patients were detected. Of the 16 large intestinal cancer patients, 9 had identical K-ras gene mutation detected both in fecal and tissue samples, none had K-ras gene mutation detected both in fecal and tissue samples, and only 2 had K-ras gene mutation in tissue samples. The consistency test showed that the K-ras gene mutations in fecal and tissue samples were well correlated ($\chi^2=9.35$, $P<0.01$).

K-ras gene mutation in fecal samples

The K-ras gene mutation was detected in the fecal samples from 23 large intestinal cancer patients. The K-ras gene mutation rate was 56.25% (13/23), which was significantly higher than that (5%, 1/20) in the healthy subjects ($\chi^2=12.93$, $P<0.001$). There was no significant difference in comparison with that (30%, 6/20) of colonic adenomatoid polypi ($\chi^2=3.05$, $P>0.05$). The K-ras gene mutation rate was 40% (2/5), 60% (6/10), 66.67% (4/6), and 50% (1/2) in the well, moderately and poorly differentiated adenomas and mucinous adenomas, respectively. The K-ras gene mutation was detected in 2 patients with cancerous colonic adenomatoid polypus, its mutation rate was 30% (6/20) in the fecal samples from colonic adenomatoid polypus patients, which was significantly higher than that in the healthy subjects ($\chi^2=4.33$, $P<0.05$). The mutation rate of K-ras gene was 23.08% (3/13), 40% (2/5), and 50% (1/2) in the polypi with a diameter less than 1 cm, a diameter of 1-2 cm, a diameter larger than 2 cm, respectively. Among the 13 large intestinal cancer patients, the K-ras gene mutation was detected at the second base of codon 12 in 12 patients (92.31%), GGT was mutated into GAT and GTT in 9 and 3 patients, respectively. The K-ras gene mutation site was observed at the first base of codon 12 in 1 patient, whose GGT was mutated into GTT.

DISCUSSION

A healthy adult excretes approximately 10^{10} epithelial cells every day. A large number of tumor cells will renew and exfoliate into the intestinal cavity of colonic cancer patients every day. A certain amount of DNA can maintain its stability due to the resistance of intestinal tumor cells to various degradation enzymes or due to the impairment of apoptotic mechanism of tumor cells^[12]. Based on the above findings, Sidransky *et al*^[13] detected the K-ras gene mutation in the fecal samples from early large intestinal cancer patients in 1992, and found the K-ras gene mutation in the fecal and tissue samples from tumor patients. Since then, several scholars have carried out some similar studies^[11,14-16]. However, their research findings have not been popularized and applied due to low PCR amplification rate of DNA in fecal samples. We used the conventional phenol-chloroform extraction method to extract DNA in 10 fecal samples. The PCR amplification product was observed only in 3 faecal samples using the primers specific for mitochondrial DNA of human eukaryotic cells. Then, the PCR amplification reaction was performed in the DNA extraction kits, the amplification rate was as high as 90% (9/10) when the DNA extraction kits used in the detection of DNA in fecal samples were washed twice in hydrolysate to remove the hybrid proteins. In the experiment, we found that the number of templates had a certain effect on the PCR amplification reaction, and could dilute the extract stock to some extent. The results indicated that the amplification rate increased with increase of dilution strength, suggesting that the amount of DNA was quite suitable to its amplification. The effect of some PCR inhibitors present in the PCR amplification reaction was significantly reduced due to the increase of dilution strength. Berndt *et al*^[17] held that these PCR inhibitors were the bile salts and bilirubin present in the fecal samples. Villa *et al*^[14] recovered the purified DNA using purification columns after the absorbent was added to the extract from the fecal samples, and found that the amplification rate was significantly increased, but the cost was rather high. In our experiment, the amplification rate was increased when the DNA extract was approximately diluted, which simplified the procedures of DNA preparation and reduced the cost. However, as the amount of templates in the DNA extract stock from the fecal samples was uncertain, its dilution factor exerted an effect on the DNA

amplification stability. Therefore, the fecal samples with a poor amplification result should be amplified again after the dilution factor of the extract stock was adjusted. This would no doubt increase the cost and time in detecting some fecal samples. In the present study, we detected the K-ras gene mutation in tissue and fecal samples from 16 large intestinal cancer patients, and achieved a rather good consistency ($P < 0.01$), indicating that detection of the K-ras gene mutation could reflect the presence of its mutation in the tissues. Since it is much easier to obtain tissue samples than fecal samples in clinic, this method will make it clinically possible to screen colorectal cancer.

Researches showed that the K-ras gene mutation in oncogenes was most frequently found in large intestinal cancer, accounting for 40-50%^[18-20]. Smith-Ravin *et al.*^[11] detected the K-ras gene mutation in the fecal samples from large intestinal cancer patients using the allele specific mismatch method, and found that the mutation rate was 50%. Xiao *et al.*^[21] detected the K-ras gene mutation in the fecal samples from large intestinal cancer patients using PCR-RFLP, and found the mutation rate was 36.4%. In our study, the detection rate of K-ras gene mutation was 56.25% and 5% in the fecal samples from large intestinal cancer patients and healthy subjects, respectively. There was a very significant difference between the two groups ($P < 0.001$), but there was no significant difference in comparison with that of colonic adenomatoid polypus patients ($P > 0.05$), suggesting that adenomatoid polypus, a precancerous lesion of large intestinal cancer, is closely related with the development of colonic cancer. According to the literature reports, 90% of large intestinal cancers were resulted from large intestinal adenomatoid polypi. Therefore, early detection and resection of large intestinal adenomatoid polypi could greatly reduce the incidence of large intestinal cancer^[2,22]. However, the diagnostic significance of large intestinal cancer at its early stages should be further studied in a larger number of large intestinal cancer patients. Many researchers^[23-29] held that the mutation rate of K-ras gene in colonic adenomas would increase with the growth of adenomas. In our study, among the two cases of adenomas with a diameter larger than 2 cm, the K-ras gene mutation was detected in one case, and was also detected in the 2 cases after their colonic adenomatoid polypi were found to be cancerous. This was consistent with the K-ras gene mutation found at the early stages of large intestinal cancer reported both in Chinese and foreign literature. Further researches showed that the K-ras gene mutation was usually resulted from the mutation of GGT to GAT of its codon 12, and 84% K-ras gene mutations were observed at the second base of codon 12. In our study, the mutation site of K-ras gene was observed at the second base of codon 12, accounting for 92.31% (12/13), 69.23% of which was resulted from the mutation of GGT to GAT, and 23.08% was resulted from the mutation of GGT to GTT. This was consistent with that reported in the literature^[11,30,31].

The non-invasive method for the detection of K-ras gene mutation in fecal samples reported in this paper is simple to operate and the samples are easy to collect. Its preliminary application in clinic has shown that it is of significance in the diagnosis of elderly large intestinal cancer patients, and can be used in combination with colonoscopy to screen the high risk population for colorectal cancer. It should be further improved because its PCR reaction time is long, which leads to the prolonged detection and is disadvantageous to the detection of large samples.

REFERENCES

- 1 **Wan J**, Zhang ZQ, Zhu C, Wang MW, Zhao DH, Fu YH, Zhang JP, Wang YH, Wu BY. Colonoscopic screening and follow-up for colorectal cancer in the elderly. *World J Gastroenterol* 2002; **8**: 267-269
- 2 **Pignone M**, Rich M, Teutsch SM, Berg AO, Lohr KN. Screening for colorectal cancer in adults at average risk: a summary of the evidence for the U.S. Preventive Services Task Force. *Ann Intern Med* 2002; **137**: 132-141
- 3 **Xiang DN**, Xiang P, Zheng SB, Cao XY, Wang GS. Diagnostic value of colonofibroscopy in 1507 elderly patients of lower gastrointestinal bleeding. *Laonian Yixue Yu Baojian* 2002; **8**: 35-36
- 4 **Atkin W**. Options for screening for colorectal cancer. *Scand J Gastroenterol Suppl* 2003; **237**: 13-16
- 5 **Meng W**, Li SR, Li L. Effect of the combined sequent program for screening colorectal carcinoma. *Linchuang Xiaohuabin Zazhi* 2000; **11**: 157-158
- 6 **Lou CY**, Li SY, Zhu XG. The detection of the rearrangements of bcl-2 gene in the cancer tissues and stool of the patients with colorectal carcinoma by semi-nest PCR. *Zhonghua Shiyian Waikexue* 1999; **16**: 197-198
- 7 **Fan RY**, Li SR, Wu ZT. The detection of K-ras mutations in stools and tissue samples from patients with colorectal cancer. *Zhonghua Xiaohua Zazhi* 2001; **21**: 445-446
- 8 **Fan RY**, Li SR, Wu X, Wu ZT, Chen ZM, Deng YJ, Cao JB, Zhang HG. The expression of P53 in shedding cells from patients with colorectal cancer. *Shijie Huaren Xiaohua Zazhi* 2000; **8**: 814-815
- 9 **Mandel JS**, Church TR, Bond JH, Ederer F, Geisser MS, Mongin SJ, Snover DC, Schuman LM. The effect of fecal occult-blood screening on the incidence of colorectal cancer. *N Engl J Med* 2000; **343**: 1603-1607
- 10 **Ito S**, Hibi K, Nakayama H, Kodera Y, Ito K, Akiyama S, Nakao A. Detection of tumor DNA in serum of colorectal cancer patients. *Jpn J Cancer Res* 2002; **93**: 1266-1269
- 11 **Smith-Ravin J**, England J, Talbot IC, Bodmer W. Detection of c-Ki-ras mutations in faecal samples from sporadic colorectal cancer patients. *Gut* 1995; **36**: 81-86
- 12 **Ratto C**, Flamini G, Sofo L, Nucera P, Ippoliti M, Curigliano G, Ferretti G, Sgambato A, Merico M, Doglietto GB, Cittadini A, Crucitti F. Detection of oncogene mutation from neoplastic colonic cells exfoliated in feces. *Dis Colon Rectum* 1996; **39**: 1238-1244
- 13 **Sidransky D**, Tokino T, Hamilton SR, Kinzler KW, Levin B, Frost P, Vogelstein B. Identification of ras oncogene mutations in the stool of patients with curable colorectal tumors. *Science* 1992; **256**: 102-105
- 14 **Villa E**, Dugani A, Rebecchi AM, Vignoli A, Grottola A, Buttafoco P, Losi L, Perini M, Trande P, Merighi A, Lerose R, Manenti F. Identification of subjects at risk for colorectal carcinoma through a test based on K-ras determination in the stool. *Gastroenterology* 1996; **110**: 1346-1353
- 15 **Tagore KS**, Lawson MJ, Yucaitis JA, Gage R, Orr T, Shuber AP, Ross ME. Sensitivity and specificity of a stool DNA multitarget assay panel for the detection of advanced colorectal neoplasia. *Clin Colorectal Cancer* 2003; **3**: 47-53
- 16 **Ito Y**, Kobayashi S, Taniguchi T, Kainuma O, Hara T, Ochiai T. Frequent detection of K-ras mutation in stool samples of colorectal carcinoma patients after improved DNA extraction: comparison with tissue samples. *Int J Oncol* 2002; **20**: 1263-1268
- 17 **Berndt C**, Haubold K, Wenger F, Brux B, Muller J, Bendzko P, Hillebrand T, Kottgen E, Zanow J. K-ras mutations in stools and tissue samples from patients with malignant and nonmalignant pancreatic diseases. *Clin Chem* 1998; **44**: 2103-2107
- 18 **Okulczyk B**, Piotrowski Z, Kovalchuk O, Niklinski J, Chyczewski L. Evaluation of K-RAS gene in colorectal cancer. *Folia Histochem Cytobiol* 2003; **41**: 97-100
- 19 **van Engeland M**, Roemen GM, Brink M, Pachen MM, Weijenberg MP, de-Bruine AP, Arends JW, van den Brandt PA, de Goeij AF, Herman JG. K-ras mutations and RASSF1A promoter methylation in colorectal cancer. *Oncogene* 2002; **21**: 3792-3795
- 20 **Kislitsin D**, Lerner A, Rennert G, Lev Z. K-ras mutations in sporadic colorectal tumors in Israel: unusual high frequency of codon 13 mutations and evidence for nonhomogeneous representation of mutation subtypes. *Dig Dis Sci* 2002; **47**: 1073-1079
- 21 **Xiao SX**, Xu AM, Wang DB, Wu L, Liu HP, Zeng B. The detection of codon 12 mutations of K-ras gene in feces by nested PCR-RFLP. *Zhongguo Shengwu Zhipin Zazhi* 1998; **11**: 103-105

- 22 **Hermesen M**, Postma C, Baak J, Weiss M, Rapallo A, Sciotto A, Roemen G, Arends JW, Williams R, Giaretti W, De Goeij A, Meijer G. Colorectal adenoma to carcinoma progression follows multiple pathways of chromosomal instability. *Gastroenterology* 2002; **123**: 1109-1119
- 23 **Scott N**, Bell SM, Sagar P, Blair GE, Dixon MF, Quirke P. p53 expression and K-ras mutation in colorectal adenomas. *Gut* 1993; **34**: 62162-62164
- 24 **Blum HE**. Colorectal cancer: future population screening for early colorectal cancer. *Eur J Cancer* 1995; **31A**: 1369-1672
- 25 **Hosaka S**, Aoki Y, Akamatsu T, Nakamura N, Hosaka N, Kiyosawa K. Detection of genetic alterations in the p53 suppressor gene and the K-ras oncogene among different grades of dysplasia in patients with colorectal adenomas. *Cancer* 2002; **94**: 219-227
- 26 **Rashid A**, Houlihan PS, Booker S, Petersen GM, Giardiello FM, Hamilton SR. Phenotypic and molecular characteristics of hyperplastic polyposis. *Gastroenterology* 2000; **119**: 323-332
- 27 **Lamlum H**, Papadopoulou A, Ilyas M, Rowan A, Gillet C, Hanby A, Talbot I, Bodmer W, Tomlinson I. APC mutations are sufficient for the growth of early colorectal adenomas. *Proc Natl Acad Sci U S A* 2000; **97**: 2225-2228
- 28 **Rashid A**, Zahurak M, Goodman SN, Hamilton SR. Genetic epidemiology of mutated K-ras proto-oncogene, altered suppressor genes, and microsatellite instability in colorectal adenomas. *Gut* 1999; **44**: 826-833
- 29 **Glarakis IS**, Savva S, Spandidos DA. Activation of the ras genes in malignant and premalignant colorectal tumors. *Oncol Rep* 1998; **5**: 1451-1454
- 30 **Nishikawa T**, Maemura K, Hirata I, Matsuse R, Morikawa H, Toshina K, Murano M, Hashimoto K, Nakagawa Y, Saitoh O, Uchida K, Katsu K. A simple method of detecting K-ras point mutations in stool samples for colorectal cancer screening using one-step polymerase chain reaction/restriction fragment length polymorphism analysis. *Clin Chim Acta* 2002; **318**: 107-112
- 31 **Prix L**, Uciechowski P, Bockmann B, Giesing M, Schuetz AJ. Diagnostic biochip array for fast and sensitive detection of K-ras mutations in stool. *Clin Chem* 2002; **48**: 428-435

Edited by Wang XL Proofread by Zhu LH

Clinical evaluation of four one-week triple therapy regimens in eradicating *Helicobacter pylori* infection

Chuan-Yong Guo, Yun-Bin Wu, Heng-Lu Liu, Jian-Ye Wu, Min-Zhang Zhong

Chuan-Yong Guo, Yun-Bin Wu, Heng-Lu Liu, Jian-Ye Wu, Min-Zhang Zhong, Department of Gastroenterology, Tielu hospital of Tongji University, Shanghai 200072, China

Correspondence to: Dr. Chuan-Yong Guo, Department of Gastroenterology, Tielu Hospital of Tongji University, Shanghai 200072, China. guochuanyong@hotmail.com

Telephone: +86-21-56779971 **Fax:** +86-21-66303983

Received: 2003-06-04 **Accepted:** 2003-07-24

Abstract

AIM: To evaluate clinical efficacy of four one-week triple therapies in eradicating *Helicobacter pylori* infection.

METHODS: In this clinical trial, 132 patients with duodenal ulcer and chronic gastritis were randomly divided into four groups, and received treatment with OAC (omeprazole 20 mg + amoxicillin 1 000 mg + clarithromycin 250 mg), OFC (omeprazole 20 mg + furazolidone 100 mg + clarithromycin 250 mg), OFA (omeprazole 20 mg + furazolidone 100 mg + amoxicillin 1 000 mg) and OMC (omeprazole 20 mg + metronidazole 200 mg + clarithromycin 250 mg), respectively. Each drug was taken twice daily for one week. The ¹³C urea breath test was carried out 4-8 weeks after treatment to determine the success of *H pylori* eradication.

RESULTS: A total of 127 patients completed the treatment. The eradication rate for *H pylori* infection was 90.3%, 90.9%, 70.9% and 65.6%, respectively in OAC, OFC OMC and OFA groups.

CONCLUSION: A high eradication rate can be achieved with one-week OAC or OFC triple therapy. Thus, one-week triple therapies with OAC and OFC are recommended for Chinese patients with duodenal ulcers and chronic gastritis.

Guo CY, Wu YB, Liu HL, Wu JY, Zhong MZ. Clinical evaluation of four one-week triple therapy regimens in eradicating *Helicobacter pylori* infection. *World J Gastroenterol* 2004; 10(5): 747-749
<http://www.wjgnet.com/1007-9327/10/747.asp>

INTRODUCTION

Eradication of *Helicobacter pylori* infection has become a wide clinical practice for *H pylori* related diseases such as peptic ulcers, and considerable clinical efficacy has been achieved over the past two decades^[1-6]. However, many short-term (one week) triple therapy regimens include metronidazole and suffer from the problem of metronidazole resistance, which could significantly decrease clinical efficacy^[7-11]. Therefore, it is a very important issue to search for anti-*H pylori* regimens that are highly effective in eradicating *H pylori* infection but without drug resistance^[12]. The aim of the present study was to evaluate the clinical efficacy of four short-term triple therapy regimens with clarithromycin.

MATERIALS AND METHODS

Selection of patients

Criteria of selection (1) Those aged 18-70 years. (2) Those with duodenal ulcer (DU) or chronic gastritis (CG) confirmed by gastroscopy. (3) Those who were positive for *H pylori* by a rapid urease test (RUT) and positive by serology, silver or Giemsa staining and histological examination.

Criteria of exclusion (1) Patients who had gastric ulcer or severe gastroesophageal reflux disease, and those who had gastric operation history, hemolytic anemia or family history of hemolytic anemia. (2) Patients who were in lactation or pregnancy. (3) Patients who had combined severe diseases of other system that might affect the medical evaluation of this study. (4) Patients who took the drugs included in this study over the past month. (5) Patients who was allergic to the drugs included in this study.

Methods

Drugs Omeprazole (20 mg/cap, Changzhou fourth Pharmaceutical Factory), clarithromycin (250 mg/tab, Hangzhou Chinese-American Eastchina Pharmaceutical Co. Ltd), furazolidone (100 mg/tab, Guangdong Jiangmen Pharmaceutical Factory), metronidazole (200 mg/tab, Shanghai Ensai Pharmaceutical Co. Ltd) and amoxicillin (250 mg/cap, Kunming Baker Norton Pharmaceutical Co. Ltd) were used.

Regimens Patients were randomly divided into four groups, and receive treatment with OAC (omeprazole 20 mg + amoxicillin 1 000 mg + clarithromycin 250 mg), OFC (omeprazole 20 mg + furazolidone 100 mg + clarithromycin 250 mg), OMC (omeprazole 20 mg + metronidazole 200 mg + clarithromycin 250 mg) and OFA (omeprazole 20 mg + furazolidone 100 mg + amoxicillin 1 000 mg), respectively. Each group took the drugs twice a day for 7 d.

Procedures At the entry, clinical symptoms, demographic data and medical history were recorded, and gastroscopy was performed to establish the endoscopic diagnosis and status of *H pylori* infection. During the gastroscopy examination, four biopsy specimens were taken from stomach: one for a rapid urease test (RUT), one for silver or modified Giemsa staining, and two for histological examination. Serum anti-*H pylori* IgG antibodies were also detected. The patients who were intensive positive by the RUT (positive in five minutes) were initially considered to be qualified for the study. Only those patients who were also positive by serology, *H pylori* staining and histological examination were included in the clinical trial. Patients were followed up on the eighth day to check clinical symptoms, side effects and compliance. A ¹³C urea breath test was carried out 4-8 wk after completion of the therapy.

Definition of *H pylori* eradication *H pylori* eradication was defined when the ¹³C urea breath test was negative 4-8 weeks after completion of anti-*H pylori* therapy.

Statistical analysis

H pylori eradication rate was the main analytic target. Total eradication rate and its 95% confidence interval of each regimen was calculated and analyzed by intention-to-treat

analysis (ITT) and per protocol (PP), respectively. The significance in the difference of eradication rate between various regimens was tested by Fisher exact probability and Chi-square test. The possible factors affecting eradication rate was analyzed in a logistic regression model. The difference in the incidence of side effects of each regimen was tested by Fisher exact probability test.

RESULTS

Demographic and clinical data

Of the 132 patients enrolled in the study, 127 (96.2%) completed the treatment and five (3.8%) dropped off. The demographic data and the proportion of DU and CG were not significantly different among the groups (Table 1).

Table 1 Comparison between patient age gender and endoscopic diagnostic results of each group

Group	n	Male/Female	Age (years)	DU/CG
OAC	33	20/13	43.5(18-70)	18/15
OFC	33	19/14	40.8(20-70)	17/16
OMC	33	21/12	41.6(19-69)	18/15
OFA	33	20/13	41.2(20-70)	19/14
Total	132	80/52	42.0(18-70)	72/64

H pylori eradication rates

H pylori eradication rates were significantly different in patients receiving OAC and OFC than in those receiving OMC and OFA ($P < 0.05$) (Tables 2 and 3). In the logistic regression model including treatment regimen, age, sex and endoscopes diagnosis, treatment regimens were identified as an independent factor responsible for the difference in the eradication rate (Table 3).

Table 2 H pylori eradication rate in each group

Group	n	Per protocol		Intent to treat		
		Eradication rate (%)	Confidence interval (95%)	n	Eradication rate (%)	Confidence interval (95%)
OAC	31	90.3	79.8-95.6	33	84.9	80.1-92.3
OFC	33	90.9	78.5-97.3	33	90.9	79.6-95.4
OMC	31	70.9	64.0-81.7	33	66.7	62.5-76.7
OFA	32	65.6	59.9-72.2	33	63.6	60.2-71.6
Total	127	79.5	72.4-82.5	33	76.5	70.5-81.8

Table 3 H pylori eradication rate in each group in relation to endoscopic diagnosis

Group	Duodenal ulcer		Chronic gastritis	
	n	Eradication rate (%)	n	Eradication rate (%)
OAC	17	88.2	14	92.9
OFC	17	94.1	16	87.5
OMC	16	68.8	15	73.3
OFA	19	57.9	13	76.9
Total	69	76.8	58	82.8

Incidence of side effects

The incidence of side effects varied among the treatment regimens (Table 4). All of side effects were slight. A compliance of >90% was achieved for all the patients who completed the study.

Table 4 Incidence of side effects in each group

Side effects	Incidence of side effects in each group patients (%)				Total (n=127)
	OAC (n=31)	OFC (n=33)	OMC (n=31)	OFA (n=32)	
Gastroenteric reactions	6.45	9.09	12.9	9.38	9.45
Skin eruption	6.45	0	3.23	6.25	3.94
Headache	6.45	6.06	3.23	0	4.72
Glossitis	0	0	3.23	0	0.79
Weakness	0	0	3.23	0	0.79
Fever	0	3.03	0	0	0.79
Somnolence	3.23	0	3.23	0	1.57

DISCUSSION

In 1990, the 14-d bismuth triple therapy was recommended in the Ninth World Gastroenterology Conference in Sydney. Due to its high incidence of side effects (high than 30%) and poor compliance, this regimen has been replaced with other short-term 7-day triple therapy regimens that are more efficient and had fewer and milder side effects^[13-19]. These new regimens include OMC 250 and OAC 500, which achieved H pylori eradication rates of more than 90% in the MACH-1 study^[20-26]. However, the eradication rates with those regimens decreased due to emergence of metronidazole resistance in H pylori over the past few years. It has been reported that prevalence of metronidazole resistant H pylori strains has increased to more than 70% in China and other countries^[27-31]. This accounts for the failure of H pylori eradication with metronidazole triple therapy.

With the wide application of anti-H pylori therapy and antibiotic abuse, drug resistance in H pylori has become an increasingly serious problem and a main reason of poor curative effect. At present^[30,31], the resistance to clarithromycin in H pylori is diverse in the world. South-north difference existed such as the drugs used to treat other infection before (mainly respiratory infection). There are significant difference in the prevalence of metronidazole resistance between developed and developing countries. High prevalence of metronidazole resistance mainly relates to the wide application in parasite infection, dental infection and gynecological diseases in developing countries. Now there is a tendency that metronidazole resistance in H pylori is increasing in the developed countries, probably due to the application of anti-H pylori therapy. In spite of wide application of treatment with amoxicillin, amoxicillin resistance in H pylori was rare.

In order to overcome the problem of metronidazole resistance and to compare the clinical efficacy of triple therapy regimens containing clarithromycin, we carried out this study. We achieved relatively high eradication rates for the clarithromycin-containing regimens OAC and OFC (90.3% and 90.9%, respectively). On the other hand, the eradication rate was relatively low for the metronidazole-containing regimen OMC and OFA. Taken together, we conclude that OAC and OFC are efficient regimens in eradicating H pylori infection. Since the cost of furazolidone in OFC regimen is cheap and the H pylori eradication rate of OFC regimen is high, we recommend that this regimen be one of choices for H pylori eradication.

REFERENCES

- 1 **Marzio L**, Cellini L, Angelucci D. Triple therapy for 7 days vs triple therapy for 7 days plus omeprazole for 21 days in treatment of active duodenal ulcer with *Helicobacter pylori* infection. A double blind placebo controlled trial. *Dig Liver Dis* 2003; **35**: 20-23

- 2 **Sargyn M**, Uygur-Bayramicli O, Sargyn H, Orbay E, Yavuzer D, Yayla A. Type 2 diabetes mellitus affects eradication rate of *Helicobacter pylori*. *World J Gastroenterol* 2003; **9**: 1126-1128
- 3 **Yamada T**, Miwa H, Fujino T, Hirai S, Yokoyama T, Sato N. Improvement of Gastric Atrophy After *Helicobacter pylori* Eradication Therapy. *J Clin Gastroenterol* 2003; **36**: 405-410
- 4 **Li S**, Lu AP, Zhang L, Li YD. Anti-*Helicobacter pylori* immunoglobulin G (IgG) and IgA antibody responses and the value of clinical presentations in diagnosis of *H pylori* infection in patients with precancerous lesions. *World J Gastroenterol* 2003; **9**: 755-758
- 5 **Konturek SJ**, Brzozowski T, Konturek PC, Kwiecien S, Karczewska E, Drozdowicz D, Stachura J, Hahn EG. *Helicobacter pylori* infection delays healing of ischaemia-reperfusion induced gastric ulcerations: new animal model for studying pathogenesis and therapy of *H pylori* infection. *Eur J Gastroenterol Hepatol* 2000; **12**: 1299-1313
- 6 **Goh KL**. Update on the management of *Helicobacter pylori* infection, including drug-resistant organisms. *J Gastroenterol Hepatol* 2002; **17**: 482-487
- 7 **Wolle K**, Leodolter A, Malfertheiner P, Konig W. Antibiotic susceptibility of *Helicobacter pylori* in Germany: stable primary resistance from 1995 to 2000. *J Med Microbiol* 2002; **51**: 705-709
- 8 **Bruley Des Varannes S**. How to treat after *Helicobacter pylori* eradication failure? *Gastroenterol Clin Biol* 2003; **27**: 478-483
- 9 **Hua JS**, Bow H, Zheng PY, Khay-Guan Y. Prevalence of primary *Helicobacter pylori* resistance to metronidazole and clarithromycin in Singapore. *World J Gastroenterol* 2000; **6**: 119-121
- 10 **Yeh YC**, Chang KC, Yang JC, Fang CT, Wang JT. Association of metronidazole resistance and natural competence in *Helicobacter pylori*. *Antimicrob Agents Chemother* 2002; **46**: 1564-1567
- 11 **Latham SR**, Labigne A, Jenks PJ. Production of the RdxA protein in metronidazole -susceptible and -resistant isolates of *Helicobacter pylori* cultured from treated mice. *J Antimicrob Chemother* 2002; **49**: 675-678
- 12 **Ivashkin VT**, Lapina TL, Bondarenko OY, Sklanskaya OA, Grigoriev PY, Vasiliev YV, Yakovenko EP, Gulyaev PV, Fedchenko VI. Azithromycin in a triple therapy for *H pylori* eradication in active duodenal ulcer. *World J Gastroenterol* 2002; **8**: 879-882
- 13 **Marais A**, Bilardi C, Cantet F, Mendz GL, Megraud F. Characterization of the genes rdxA and frxA involved in metronidazole resistance in *Helicobacter pylori*. *Res Microbiol* 2003; **154**: 137-144
- 14 **O' Morain C**, Borody T, Farley A, De Boer WA, Dallaire C, Schuman R, Piotrowski J, Fallone CA, Tytgat G, Megraud F, Spenard J. International multicentre study. Efficacy and safety of single-triple capsules of bismuth biskalcitrate, metronidazole and tetracycline, given with omeprazole, for the eradication of *Helicobacter pylori*: an international multicentre study. *Aliment Pharmacol Ther* 2003; **17**: 415-420
- 15 **Houben MH**, van de Beek D, Hensen EF, de Craen AJ, van 't Hoff BW, Tytgat GN. *Helicobacter pylori* eradication therapy in The Netherlands. *Scand J Gastroenterol Suppl* 1999; **230**: 17-22
- 16 **Wong BC**, Wang WH, Berg DE, Fung FM, Wong KW, Wong WM, Lai KC, Cho CH, Hui WM, Lam SK. High prevalence of mixed infections by *Helicobacter pylori* in Hong Kong: metronidazole sensitivity and overall genotype. *Aliment Pharmacol Ther* 2001; **15**: 493-503
- 17 **Qasim A**, O' Morain CA. Review article: treatment of *Helicobacter pylori* infection and factors influencing eradication. *Aliment Pharmacol Ther* 2002; **16**: 24-30
- 18 **Wong BC**, Wong WM, Yee YK, Hung WK, Yip AW, Szeto ML, Li KF, Lau P, Fung FM, Tong TS, Lai KC, Hu WH, Yuen MF, Hui CK, Lam SK. Rabepazole-based 3-day and 7-day triple therapy vs omeprazole-based 7-day triple therapy for the treatment of *Helicobacter pylori* infection. *Aliment Pharmacol Ther* 2001; **15**: 1959-1965
- 19 **Choi IJ**, Jung HC, Choi KW, Kim JH, Ahn DS, Yang US, Rew JS, Lee SI, Rhee JC, Chung IS, Chung JM, Hong WS. Efficacy of low-dose clarithromycin triple therapy and tinidazole-containing triple therapy for *Helicobacter pylori* eradication. *Aliment Pharmacol Ther* 2002; **16**: 145-151
- 20 **Lind T**, Veldhuyzen van Zanten S, Unge P, Spiller R, Bayerdorffer E, O' Morain C, Bardhan KD, Bradette M, Chiba N, Wrangstadh M, Cederberg C, Idstrom JP. Eradication of *Helicobacter pylori* using one-week triple therapies combining omeprazole with two antimicrobials: the MACH I Study. *Helicobacter* 1996; **1**: 138-144
- 21 **Zanten SJ**, Bradette M, Farley A, Leddin D, Lind T, Unge P, Bayerdorffer E, Spiller RC, O' Morain C, Sipponen P, Wrangstadh M, Zeijlon L, Sinclair P. The DU-MACH study: eradication of *Helicobacter pylori* and ulcer healing in patients with acute duodenal ulcer using omeprazole based triple therapy. *Aliment Pharmacol Ther* 1999; **13**: 289-295
- 22 **Sung JJ**, Chan FK, Wu JC, Leung WK, Suen R, Ling TK, Lee YT, Cheng AF, Chung SC. One-week ranitidine bismuth citrate in combinations with metronidazole, amoxicillin and clarithromycin in the treatment of *Helicobacter pylori* infection: the RBC-MACH study. *Aliment Pharmacol Ther* 1999; **13**: 1079-1084
- 23 **Malfertheiner P**, Bayerdorffer E, Dietsch U, Gil J, Lind T, Misiuna P, O' Morain C, Sipponen P, Spiller RC, Stasiewicz J, Treichel H, Ujjasz L, Unge P, Zanten SJ, Zeijlon L. The GU-MACH study: the effect of 1-week omeprazole triple therapy on *Helicobacter pylori* infection in patients with gastric ulcer. *Aliment Pharmacol Ther* 1999; **13**: 703-712
- 24 **Unge P**. The OAC and OMC options. *Eur J Gastroenterol Hepatol* 1999; **11**: 23-24
- 25 **Spiller RC**. Is there any difference in *Helicobacter pylori* eradication rates in patients with active peptic ulcer, inactive peptic ulcer and functional dyspepsia? *Eur J Gastroenterol Hepatol* 1999; **11**: 43-45
- 26 **Megraud F**, Lehn N, Lind T, Bayerdorffer E, O' Morain C, Spiller R, Unge P, van Zanten SV, Wrangstadh M, Burman CF. Antimicrobial susceptibility testing of *Helicobacter pylori* in a large multicenter trial: the MACH 2 study. *Antimicrob Agents Chemother* 1999; **43**: 2747-2752
- 27 **Jenks PJ**, Edwards DI. Metronidazole resistance in *Helicobacter pylori*. *Int J Antimicrob Agents* 2002; **19**: 1-7
- 28 **Calvet X**, Ducons J, Guardiola J, Tito L, Andreu V, Bory F, Guirao R. One-week triple vs quadruple therapy for *Helicobacter pylori* infection-a randomized trial. *Aliment Pharmacol Ther* 2002; **16**: 1261-1267
- 29 **Owen RJ**, Ferrus M, Gibson J. Amplified fragment length polymorphism genotyping of metronidazole-resistant *Helicobacter pylori* infecting dyspeptics in England. *Clin Microbiol Infect* 2001; **7**: 244-253
- 30 **Yakoob J**, Fan X, Hu G, Liu L, Zhang Z. Antibiotic susceptibility of *Helicobacter pylori* in the Chinese population. *J Gastroenterol Hepatol* 2001; **16**: 981-992
- 31 **Isakov V**, Domareva I, Koudryavtseva L, Maev I, Ganskaya Z. Furazolidone-based triple 'rescue therapy' vs quadruple 'rescue therapy' for the eradication of *Helicobacter pylori* resistant to metronidazole. *Aliment Pharmacol Ther* 2002; **16**: 1277-1282

Pathobiological behavior and molecular mechanism of signet ring cell carcinoma and mucinous adenocarcinoma of the stomach: A comparative study

Xue-Fei Yang, Lin Yang, Xiao-Yun Mao, Dong-Ying Wu, Su-Min Zhang, Yan Xin

Xue-Fei Yang, Xiao-Yun Mao, Dong-Ying Wu, Su-Min Zhang, Yan Xin, The Fourth Laboratory, Cancer Institute, The First Affiliated Hospital of China Medical University, Shenyang 110001, Liaoning Province, China

Lin Yang, Department of Pathology, Cancer Hospital, Chinese Academy of Medical Sciences, Beijing 100021, China

Supported by the National Natural Science Foundation of China, No.30070845 and No.30371607

Correspondence to: Professor Yan Xin, The Fourth Laboratory, Cancer Institute, The First Affiliated Hospital of China Medical University, Shenyang 110001, Liaoning Province, China. yxin@mail.cmu.edu.cn

Telephone: +86-24-23256666 Ext 6351 **Fax:** +86-24-23253443

Received: 2003-09-09 **Accepted:** 2003-10-22

Abstract

AIM: To elucidate the distinctive pathobiological behavior between signet ring cell carcinoma (SRC) and mucinous adenocarcinoma of the stomach.

METHODS: Based on the histological growth patterns and cell-functional differentiation classifications of stomach carcinoma, we conducted a series of comparative studies. All paraffin-embedded and frozen blocks were collected from the files of Cancer Institute of China Medical University. On the basis of histopathological observation, we applied enzymatic and mucous histochemistry, immunohistochemistry, flow cytometry (FCM) and molecular biology to compare these two categories of gastric cancers in terms of the DNA ploidy, proliferative kinetics, the expression of gastric carcinoma associated gene product and instabilities of mitochondrial DNA (mtDNA).

RESULTS: Gastric SRC was commonly seen in females below 45 years, mostly presenting diffuse growth and ovary or uterine cervix metastasis. The majority of SRC were absorptive and mucus-producing functional differentiation type (AMPFDT), which growth relied on estrogen. Meanwhile, stomach mucinous adenocarcinomas were mostly observed in males over 50 years, prone to massive growth or nest growth and extensive peritoneal infiltration, showing two categories of cell-functional differentiation types: AMPFDT and mucus-secreting functional differentiation type (MSFDT). Expressions of ER, enzyme c-PDE and 67kDaLN-R in SRC were evidently higher than that in mucinous adenocarcinoma, while expressions of LN, CN-IV, CD44v6, and PTEN protein were obviously lower in SRC than that in mucinous adenocarcinoma ($P < 0.05$). There was no statistic significance in VEGF, ECD and instabilities of mtDNA ($P > 0.05$) between the above two gastric carcinomas.

CONCLUSION: Though SRC and mucinous adenocarcinoma were both characterized by abundant mucus-secretion, they were quite different in morphology, ultrastructure, cell-functional differentiation and protein expression, indicating different mechanisms of carcinogenesis. We concluded that

combining histological growth patterns, cell-functional differentiation types with tumor related markers might be significant in early diagnosis and prognosis assessment for SRC and mucinous adenocarcinoma of the stomach.

Yang XF, Yang L, Mao XY, Wu DY, Zhang SM, Xin Y. Pathobiological behavior and molecular mechanism of signet ring cell carcinoma and mucinous adenocarcinoma of the stomach: A comparative study. *World J Gastroenterol* 2004; 10(5): 750-754

<http://www.wjgnet.com/1007-9327/10/750.asp>

INTRODUCTION

SRC and mucinous adenocarcinoma of the stomach were generally confounded as “mucoïd carcinoma” until 1964 when Zhang *et al* proposed that the so-called “mucoïd carcinoma” included two categories that presented different growth patterns. “Mucoïd carcinoma” was finally divided into mucinous adenocarcinoma and SRC in WHO’s histological classification of the stomach in 1974. At that time, it remained unclear of the different biological behaviors and metastatic or infiltrative characteristics of these two stomach carcinomas.

From 1962, Cancer Institute of China Medical University began a series of studies on histological growth patterns, cell-functional phenotype classifications and infiltrative, metastatic patterns of stomach carcinoma, and a series of comparative studies on SRC and mucinous adenocarcinoma of the stomach were also carried out the following 40 years. We classified functional differentiation types of gastric cancer by histopathological observation, enzymatic and mucous histochemistry, and detected the expressions of related genes with the help of biological techniques. Different biological behaviors of local infiltration and metastasis of SRC and mucinous adenocarcinoma were investigated at morphological, functional and protein levels.

MATERIALS AND METHODS

All paraffin-embedded and frozen blocks were collected from the files of Cancer Institute of China Medical University. On the basis of histopathological observation, AKP, ACP and LAP were detected by enzymatic histochemistry and various kinds of mucin were detected by mucous histochemistry in order to propose a new cell-functional classification of gastric carcinomas. We observed the expression of ER, cPDE, laminin (LN) and its receptor 67kuN-R, collagen-IV (CN-IV), CD44v6, VEGF, ECD and PTEN proteins by immunohistochemistry, the variation of DNA ploidy, proliferative kinetics by flow cytometry (FCM), and three adjacent regions of mtDNA (D-loop, tRNA^{phe} and 12S rRNA) were detected for instabilities via PCR amplification followed by direct DNA sequencing and dHPLC. All procedures were done according to references^[1-11].

RESULTS

SRC and mucinous adenocarcinoma were found quite different

in pathological morphology, functional differentiation phenotypes, molecular pathology mechanisms and prognosis as follows.

Morphologic observation

The different growth patterns of mucinous adenocarcinoma and SRC were firstly proposed, following the histological growth classifications of the stomach in 1964. The former presented nest or massive growth, which cancer cells produced and secreted abundant mucus-like substance and then hoarded in the cancerous nest; while the latter presented signet ring cells, widely infiltrated in the stomach wall, accompanied by the formation of "migratory cancerous embolus of lymphatic vessel". SRC had specific cytogenetics: cancer cells were separate, and presented irregular amebocyte shape. Image of ameboidism was often observed emigrating from lymphatic vessel especially in loose part of the stomach (subserosa and submucosa), which suggested the characteristic of widespread growth and invasion. This image was not shown in mucinous adenocarcinoma of nest or massive growth. Meanwhile, the mesenchymal reaction was also quite different between the above two stomach carcinomas: cancerous foci of mucinous adenocarcinoma was mainly unwrapped by collagen fibers, and the argyrophilia fibers were thick and intensive to bundles, surrounding the outside of the cancerous foci; some transition to collagen fibers and even basement membrane-like structures were shown. There were such lymphoid cells and macrophages as inflammatory reaction in adjacent cancerous foci. However, mesenchyma of SRC was loose and in edema, and argyrophilia fibers were reticularly loose, which suggested that the host

immunological reaction was weaker than that of the mucinous adenocarcinoma and coincident with its diffusely infiltrating growth pattern.

Functional differentiation vs invasion and metastatic characteristics

Functional differentiation investigation showed that more than 80.0% of SRC showed AMPFDT: SRC cells not only produced mucus, but also expressed intestinal enzymes of absorption cell markers (AKP and LAP), ACP, and estrogen receptor (ER) in most cancer cells.

Mucinous adenocarcinoma showed specific functional differentiation: 55.3%(21/38) of them showed single MSFDT; 44.7%(17/38) were AMPFDT. The latter was similar to SRC in biological characteristics, while the former did not express intestinal enzymes of absorption cell markers or ER (Table 1).

Tumor related markers

Expressions of ER, enzyme c-PDE and 67kuN-R were evidently higher in SRC than in mucinous adenocarcinoma, while expressions of LN, CN-IV, CD44v6, and PTEN protein were obviously lower in SRC than those in mucinous adenocarcinoma ($P<0.05$). There was no statistic significance in VEGF, ECD and instabilities of mtDNA ($P>0.05$) between the two gastric carcinomas. In SRC, DNA ploidy was different at different pathologic stages: the elevated contents of DNA, polyploid and heteroploid were often seen in early SRC; while the content of DNA was lower and diploid or subdiploid were often presented in advanced SRC. Polyploid and heteroploid were often observed in mucinous adenocarcinoma (Table 1).

Table 1 The comparison of pathobiologic characteristics between SRC and mucinous adenocarcinoma

Pathobiologic characteristics	SRC (AMPFDT)	Mucinous adenocarcinoma	
		AMPFDT	MSFDT
Onset age	Mostly below 50	Same as the left	Mostly over 50 ^[1,2]
Sex	more in female	Same as the left	More in male ^[1,2]
Infiltrative depth	16.7% (2/12) passing through the serosa		70.0% (7/10) passing through the serosa ^[1,2]
Growth pattern	Diffuse growth 100.0%(12/12)		Diffuse growth 40.0%(4/10), massive growth 60.0%(6/10) ^[1,2]
Metastasis rate of lymph node	66.7% (8/12)		80.0%(8/10) ^[1,2]
Distant metastasis	Often to ovary and uterus, sometimes to bones, marrow, bladder, blepharon or skin of lower extremities	Same as the left	Prone to peritoneal extensive infiltration ^[1,2]
Tumor related markers			
ER	Positive rate 75.0%(9/12)		Positive rate 10.0%(1/10) ^[1,2]
c-PDE	Positive rate 80.0%(4/5)		Positive rate 20.0%(1/5) ^[3]
LN	Few, positive rate 25.0%(2/8)		BM*-like line structure was seen frequently, positive rate 83.3%(5/6) ^[4]
67KDa LN-R	Positive rate 75.0%(15/20)		Positive rate 25.0%(1/4) ^[5]
Collagen IV	CN-IV positive fragments or particles only, positive rate 87.5%(7/8)		BM*-like line structure was seen frequently
CD ₄₄ V ₆	Positive rate 11.8%(2/17)		Positive rate 100.0%(6/6) ^[4]
PTEN	Low expression (25.0%, 7/21)		Positive rate 62.5%(5/8) ^[6]
VEGF	Positive rate 90.0%(9/10)		High expression (60.0%) 6/10 ^[8]
ECD	Negative expression 85.0% (17/20)		Positive rate 100.0%(7/7) ^[7]
DNA ploidy	Polyloid and heteroploid were often seen in early stage, while diploid and hypodiploid were often seen in advanced stage		Negative rate 75.0%(3/4) ^[9]
mtDNA variation	66.7%(2/3), para-cancerous tissue 33.3%(1/3)		Polyloid and heteroploid were often observed ^[10]
D-loop region	33.3%(1/3)		66.7%(2/3), para-cancerous tissue 66.7%(2/3)
12S rRNA	33.3%(1/3)		66.7%(2/3) ^[11]
Ultrastructure	More mucous secretion. Few desmosome junctions and gap junctions between cells.		Plenty of mucous secretion. Several desmosome junctions and gap junctions between cells
5 year survival rate	15.9%		19.4%

*Basement membrane.

DISCUSSION

The survival rate of both SRC and mucinous adenocarcinoma was extremely low. According to the National Cooperation Group of Stomach Carcinoma, the 5-year survival rate of SRC and mucinous adenocarcinoma of the stomach was only 15.9% and 19.4% respectively mainly because most clinical cases of SRC or mucinous adenocarcinomas were moderate to advanced cancer accompanied with extensive infiltration and metastasis. Metastasis, especially unmanageable metastasis to the remote important viscera was the primary cause of patients' death. Research findings of more than 40 years revealed different infiltrative and metastatic mechanisms of SRC and mucinous adenocarcinoma at morphological, functional and protein levels, based on histological growth patterns and cell functional differentiation phenotypes.

The structural basis of different growth patterns of SRC and mucinous adenocarcinoma was demonstrated by electron microscopic observation and mucus histochemistry by Wang *et al* (Cell Biology Institute of China Medical University) and other Chinese scholars^[12]. Under electron microscope, SRC was lack of free ribosomes but rich in rough endoplasmic reticulum (RER), lysosomes, mucus granules, and Golgi complex presented cystiform dilatation, which suggested SRC cells had a strong capability of protein and mucus synthesis. In addition, there were few microvilli on the surface of SRC cell membrane, desmosome junction and gap junction ultimately vanished, the interspaces of cancer cells were enlarged, which suggested that adhesive ability of cancer cells decreased and detachment was easy among cells. Histochemical observation found that these changes were accompanied by releasing of multiple sialomucin, sulfuric acid mucopolysaccharide (AMP), and polysaccharide hydrolases such as acid phosphatase (ACP). These characteristics contributed to the potential of dissolving surrounding tissues, and strong infiltration and metastasis. Nevertheless, cancer cells of mucinous adenocarcinoma were rich in free ribosomes, with scattered RER, and fewer Golgi complex and lysosomes than that of SRC. Further, different from SRC, microvilli and part of desmosome junction and gap junction were shown on the surface of cell membrane. All above characteristics suggested mucinous adenocarcinoma had a stronger adhesive ability than SRC, which partly explained their different growth patterns.

In 1979, Zhang *et al* firstly reported that diffusely growing SRC could show retrograde metastasis from the stomach to cervix and parametrium via "migratory cancerous embolus"^[13], which raised two questions at the same time: Why was it often seen that SRC or poorly differentiated adenocarcinoma and undifferentiated carcinoma containing signet ring cell metastasized to cervix and parametrium, but it was rarely seen in mucinous adenocarcinoma? Was there any difference in cell-functional differentiation and associated molecular pathological characteristics apart from morphologic differences?

The authors detected cell-functional differentiation of gastric cancer cells by enzymatic, mucus histochemistry and immunohistochemistry, proposed a new concept of cell-functional classification of stomach carcinoma, and found that the carcinoma of different functional types were quite different in local infiltration and metastasis to remote viscera^[1,2]. Based on this study, we extensively investigated the hypostases of different biological behaviors of the above two carcinomas^[2]. According to cell-functional differentiation of cancer cells, more than 80.0% of SRC showed AMPFDT, which suggested it was a specific carcinoma cell type with disturbed cell-functional differentiation, possessing both absorptive and mucus-producing functions, and its growth and infiltration relied on ER. SRC not only produced mucus, but also expressed small intestine absorptive cell marker enzymes and ACP. Mucus-producing functional differentiation and the release

of ACP in SRC contributed to hydrolyze mesenchyma surrounding the cancerous foci and invade into normal tissue; and absorptive functional differentiation contributed to absorb nutrition from the host, which accelerated its malignant proliferation. SRC cells customarily expressed ER, which suggested that its growth relied on the existence of estrogen. The reason why SRC was often observed in the female of the premenopause and prone to metastasize to ovary or uterine cervix was its high affinity to organs with a high level of estrogen such as ovary. During the metastasis from the stomach to ovary, "ER (on cancer cells)-estrogen (in the ovary)" affinity linkage might play an important role. Our results suggested that under the prerequisite of hematogenous metastasis, lymphatic metastasis or implantation metastasis to the ovary or cervix, cancer cells with high activities of ER had specific affinity and adaptability to organs rich in estrogen and thus could easily metastasize to the ovary or cervix^[2].

Mucinous adenocarcinoma exhibited two functional classifications as AMPFDT and MSFDT. The biological behaviors and part of molecular pathological characteristics of the former were similar to that of SRC; but the latter did not express small intestine absorptive cell marker enzymes, which disabled its absorptive activity, decreased absorption of enough nutrition and restrained the growth and spread. It was probably one reason why mucinous adenocarcinoma was prone to massive or nest growth, and thus exhibited better prognosis than SRC. These two functional classifications of mucinous adenocarcinoma were quite different in onset age, serosa infiltration, dependence on estrogen (ER expression), *etc.* It was suggested that mucinous adenocarcinoma had the heterogeneity both in cell-functional differentiation and biological feature. So special attention should be paid to cell-functional differentiation characteristics in judging malignant biological behaviors and metastatic patterns of mucinous adenocarcinoma.

In order to explore the difference of molecular mechanisms between the above two gastric carcinomas, we also designed a series of molecular pathological markers ranging from cell proliferation and differentiation, extracellular matrix, tumor angiogenesis, tumor suppressor genes, *ect.* Cyclic nucleotide acid phosphodiesterase (cPDE) is a key enzyme degrading cyclic adenosine phosphate (cAMP) and cyclic guanosine phosphate (cGMP), thereby influencing cell proliferation and differentiation. This study revealed that SRC exhibited higher activities of cAMP-PDE and cGMP-PDE than mucinous adenocarcinoma, and it was concluded that SRC cells had stronger abilities of synthesizing and secreting cPDE than mucinous adenocarcinoma. And cAMP-PDE was a reliable enzymatic marker to estimate malignant degree and prognosis of the above two gastric carcinomas^[3]. LN was the main ingredient of basement membrane. The studies found stomach cancer cells could not only destroy basement membrane but also unceasingly synthesize the ingredient of its basement membrane. Mucinous adenocarcinoma cells had the capacity of synthesizing, and excreting LN out of the cells, which formed a line-like structure similar to basement membrane. This might be one of the reasons why mucinous adenocarcinoma often grew in a nest or massive shape. SRC synthesized very few LN and there were only a few LN particles in extracellular matrix. This might be related to some characteristics of SRC, such as infiltrative growth and high invasiveness^[4]. The quantity and expression intensity of 67KDa LN-R influenced the infiltrative migration of malignant tumor cells. Acting as a kind of LN receptor, 67KDa LN-R usually was involved in the identification of ECM and information convection. Increased expression of 67KDa LN-R in tumor cells would benefit adhesiveness and infiltration. Among the different histological types of gastric cancer, the expression of 67KDa LN-R was

highest in SRC (75.0%, 15/20), and lowest in mucinous adenocarcinoma (25.0%, 1/4), which might be in relation to their different abilities of infiltration and metastasis^[5]. The change of LN expression level was closely correlated to the pathological behaviors of gastric cancer, and could be used as an objective marker to assess the growth ability and the tendency of hematogenous metastasis between the above two gastric cancers. CN-IV was expressed in the above two gastric cancers, but the expression pattern was quite different^[4]. In mucinous adenocarcinoma, the basement membrane-like structure containing CN-IV was seen clearly. However, only linear fragments or positive particles containing CN-IV were seen in SRC. The findings suggested that the above two gastric cancers had different capacities of synthesizing and secreting CN-IV hydrolase. CN-IV hydrolase was strong in the interstitial of SRC, and hydrolyzed CN-IV into discontinuous fragments or particles, which led to the infiltrative growth of cancer cells. The expression of CN-IV in gastric cancer presented negative correlation with its infiltrative growth ability, and could be used as one of the markers to evaluate the poor prognosis of the above two gastric cancers^[4].

CD44v6 took part in specific adhesion processes between cells or cells and matrix. Our results^[6,14] showed CD44v6 had a close relation to metastatic potential of gastric cancer cells and the poor prognosis of patients. It was found that the protein expression of CD44v6 was quite higher in mucinous adenocarcinoma than in SRC. This was probably due to the crypt formation and nest or massive growth pattern of mucinous adenocarcinoma. VEGF is correlated with tumor angiogenesis. A lot of evidence showed that VEGF greatly increased the probability of tumor metastasis by accelerating blood vessel growth. But between the above two gastric cancers, the difference of VEGF expression was not significant^[7]. Up to now, PTEN/MMAC1/TEP1 gene is the first tumor suppressor gene that was proved to have phosphatase activity. Using immunohistochemistry, we found the expression of PTEN protein in SRC was significantly lower than in mucinous adenocarcinoma. The expression of PTEN protein presented negative correlation with gastric cancer's pathological grade and prognosis, which indicated that PTEN gene mutation or inactivation might be one of the reasons for the poorer prognosis of SRC compared with mucinous adenocarcinoma^[8]. ECD is a kind of transmembrane glycoprotein, which induced the adhesion of homogenous cells. The dysfunction of ECD made the adhesion of homogenous cells impossible. Thus, cancer cells tended to separate from each other and metastasize. ECD presented negative expression in 85% (17/20) of SRC and 75% (3/4) of mucinous adenocarcinoma. So ECD could be used as one of the markers to evaluate the poor prognosis of the above two gastric cancers^[9].

There were some studies on tumor related markers from other aspects about the above two gastric cancers. For example, the expression of GST- π was lower in SRC (50.0%, 4/8) than that in mucinous adenocarcinoma (66.7%, 6/9), and it was related to differentiation degree of cancer cells. The expression of GST- π in well differentiated cells was higher, and it was closely correlated with carcinogenesis and progress of gastric cancer, but there was no significance^[15]. S-Tn antigen is a prosoma of saliva acidulated T antigen, and belongs to the embryo or differentiated antigen. It might take part in the early malignant transformation of gastric cancer. It has been reported that the expression of S-Tn antigen in SRC was highest among different histological types of gastric cancers^[16], while the mechanism is still unknown.

DNA aneuploidy of tumor cells is one of its malignant characteristics. DNA aneuploidy of gastric cancer is closely related to the remote organic metastasis, especially to the hematogenous metastasis^[10]. There were a lot of polyploid and

heteroploid cells in early SRC, while most of advanced SRC showed diploid or hypodiploid cells. It suggested that the reduction of DNA content in advanced SRC cells was probably related to the accumulation and crushing of mucus. SRC had the tendency to infiltrate into submucosa in early stage, and this behavior was related to the DNA heteroploidy of cancer cells. Detection of DNA ploidy, especially early detection would help to estimate the malignant level and poor prognosis of the above two gastric cancers.

Recently, researchers have paid more attention to the relationship between the damage of mtDNA and carcinogenesis. mtDNA is a 16 569-bp double stranded, closed circular molecule, which encodes polypeptides participating in oxidative phosphorylation and synthesis of ATP. Compared to nuclear DNA, mtDNA is more susceptible to damage, because of the lack of protective action by histones and the limited capacity of damage repairing system as in yeast and most nuclear genomes. Mitochondrial D-loop and hypervariable region suffered the attack of ROS easily. Chomyn *et al* considered that mtDNA was not necessary to the start-up of necrosis, but it influenced the speed of necrosis because the decrease or damage of mtDNA would result in the increase of ROS^[17]. Our study found that there was no statistic significance in instabilities in D-loop region between gastric cancerous and para-cancerous tissues. There was a significant correlation between differentiation degree of gastric cancer and variant frequencies of 12S rRNA-tRNA^{phe}. The poorly differentiated gastric cancers were more prone to 12S rRNA-tRNA^{phe} variations. But there was no significance between SRC and mucinous adenocarcinoma^[11]. This result needs to be proved by larger sample studies. The relationship between mtDNA and gastric cancer would further be clarified.

There were several molecular biology studies about gastric SRC and mucinous adenocarcinoma. MSI is a frequent genetic change in gastric cancer. Up to now, the average rate of MSI was 33.9% among 29 sites that have been detected, and phenotypes of MSI were different in gastric cancers due to their different pathological types^[18,19]. MSI-positive frequency of SRC was significantly higher than mucinous adenocarcinoma of the stomach, which indicated that the occurrence and progress of the above two gastric cancers probably had different molecular mechanisms. Loss of heterozygous (LOH) is one of MSI phenotypes. The fractional allelic loss (FAL) (the odds of LOH positive marker number and MSI marker number) was related to infiltrative ability of gastric cancer cells and different growth patterns of gastric cancer. Our studies suggested that there might be different allelic deletion between SRC and mucinous adenocarcinoma, which might clarify that the different heredity phenotypes and biological behaviors of the above two gastric cancers were closely correlated with MSI and LOH. We plan on marking MSI and screening LOH site so as to discover minimal deletion fragment nearby these sites by molecular biology and LCM technique. This would lead us to detect some unknown TSGs and study the molecular biological mechanisms of different biological behaviors of the above two gastric cancers.

In conclusion, from the view of histological growth patterns and cell-functional differentiation types of gastric cancer, we investigated various kinds of pathobiological behaviors of gastric SRC and mucinous adenocarcinoma. On the basis of this, we studied on tumor related markers for early diagnosis and prognosis evaluation of gastric cancer, so to instruct clinical surgical treatment scientifically and effectively, and improve survival rate and survival quality. In our cancer institute, the 5 year survival rate of gastric cancer has risen from 19.6% to 58.5%, approaching international advanced level^[20]. Along with the preliminary accomplishment of human genome project, the studies on tumor genomics are advancing with

every passing day. A lot of tumor related genes will be found, and their roles need to be clarified in occurrence, progress and prognosis of the above two gastric cancers. Meanwhile, little literature has been reported on the morphogenetic or histogenetic mechanisms and early diagnostic markers of gastric SRC and mucinous adenocarcinoma, and there is still much dispute in this field. All these problems need further research.

REFERENCES

- Xin Y**, Li XL, Wang YP, Zhang SM, Zheng HC, Wu DY, Zhang YC. Relationship between phenotypes of cell-function differentiation and pathobiological behavior of gastric carcinomas. *World J Gastroenterol* 2001; **7**: 53-59
- Xin Y**, Zhao FK, Wu DY, Wang YP, Zhang YC. Comparative study of the pathobiological behavior in mucinous adenocarcinoma and signet ring cell carcinoma of the stomach. *Zhongguo Yike Daxue Xuebao* 1996; **25**: 441-443
- Xin Y**, Zhao FK, Wu DY, Zhang YC. Comparative study of cyclic nucleotide phosphodiesterases and marker enzymes of small intestinal absorptive cell in gastric cancer tissue. *Zhongguo Yike Daxue Xuebao* 1991; **20**: 333-337
- Zhao FK**, Zhang SM, Wang YP, Xu L, Wu DY, Xin Y. Relationship between the expression of collagen IV and laminin and the pathobiological behavior of gastric carcinomas. *Zhongguo Yike Daxue Xuebao* 1998; **27**(Suppl): 6-8
- Li XL**, Wang YP, Wu DY, Zhang SM, Xin Y. Expression of PTEN-encoding product, ECD and 67KDa laminin receptor and invasion and metastasis of gastric carcinomas. *Zhonghua Yixue Zazhi* 2003; **83**: 599-601
- Xin Y**, Zhao FK, Zhang SM, Wu DY, Wang YP, Xu L. Relationship between CD44v6 expression and prognosis in gastric carcinoma patients. *Shijie Huaren Xiaohua Zazhi* 1999; **7**: 210-214
- Wang YP**, Chen Y, Yang L, Wu DY, Zhang SM, Kuang LG, Sun HW, Zheng HC, Xin Y. Expression of VEGF in gastric carcinoma and its clinical significance. *Zhongguo Yike Daxue Xuebao* 2003; **32**: 184-186
- Zheng HC**, Chen Y, Kuang LG, Yang L, Li JY, Wu DY, Zhang SM, Xin Y. Expression of PTEN-encoding product in different stages of carcinogenesis and progression of gastric carcinoma. *Zhonghua Zhongliu Zazhi* 2003; **25**: 13-16
- Li XL**, Yang XF, Wu DY, Zhang SM, Xin Y. ECD and expression of PTEN gene an invasion and metastasis of gastric carcinomas. *Zhongguo Zhongliu Linchuang* 2003; **30**: 349-352
- Xu L**, Zhang SM, Wang YP, Zhao FK, Wu DY, Xin Y. Relationship between DNA ploidy, expression of ki-67 antigen and gastric cancer metastasis. *World J Gastroenterol* 1999; **5**: 10-11
- Han CB**, Li F, Zhao YJ, Ma JM, Wu DY, Zhang YK, Xin Y. Variations of mitochondrial D-loop region plus downstream gene 1 2S rRNA-tRNA^{phe} and gastric carcinomas. *World J Gastroenterol* 2003; **9**: 1925-1929
- Zhu SY**, Tang XP, Zhang PY. Ultrastructure observation of angiogenesis and microvessel density in the signet ring cell carcinoma of stomach. *Dianzi Xianwei Xuebao* 2002; **21**: 900-902
- Zhang YC**, Zhang PF, Wei YH. Metastatic carcinoma of the cervix uteri from the gastrointestinal tract. *Gynecol Oncol* 1983; **15**: 287-290
- Xin Y**, Wang YP, Zhang SM, Wu DY, Xu L, Zhang YC. Relationship between CD44v6 expression and metastatic potential and prognosis in gastric carcinoma. *Chin Med Sci J* 2000; **15**: 128
- Lin LX**, Jiang HC, Zhu AL, Qi SY. The expression of GST- π and P-gp in gastric carcinoma. *Zhongguo Zhongliu Linchuang Yu Kangfu* 2000; **7**: 23-24
- Qiao SX**, Wang WH, Yuan M, Tan SQ. The expression of S-Tn antigen in the tissues of gastric cancer and precancerous lesions. *Zhonghua Putong Waikexue Zazhi* 2000; **15**: 358-360
- Chomyn A**, Attardi G. mtDNA mutations in aging and apoptosis. *Biochem Biophys Res Commun* 2003; **304**: 519-529
- Kim KM**, Kwon MS, Hong SJ, Min KO, Seo EJ, Lee KY, Choi SW, Rhyu MG. Genetic classification of intestinal-type and diffuse-type gastric cancers based on chromosomal loss and microsatellite instability. *Virchows Arch* 2003; **443**: 491-500
- Wang Y**, Ke Y, Ning T, Feng L, Lu G, Liu W, E Z. Studies of microsatellite instability in Chinese gastric cancer tissues. *Zhonghua Yixue Yichuanxue Zazhi* 1998; **15**: 155-157
- Zhang WF**, Zhang YC, Chen JQ. *Gastric Carcinoma*. 2nd edition. Shanghai: *Shanghai Kexue Jishu Chubanshe* 2001: 264-265

Edited by Zhu LH Proofread by Xu FM

Preventive effect of Ganfujian granule on experimental hepatocarcinoma in rats

Yan Qian, Chang-Quan Ling

Yan Qian, Department of Traditional Chinese Medicine, General Hospital of PLA, Beijing 100853, China

Chang-Quan Ling, Department of Traditional Chinese Medicine, Changhai Hospital, Second Military Medical University, Shanghai 200433, China

Correspondence to: Yan Qian, Department of Traditional Chinese Medicine, General Hospital of PLA, Beijing 100853, China. qianxdcn@yahoo.com

Telephone: +86-10-66937093

Received: 2003-06-21 **Accepted:** 2003-08-18

Abstract

AIM: To investigate the inhibitory effect of dietary and medicinal formula Ganfujian granule on diethylnitrosamine (DEN)-induced hepatocarcinoma in rats.

METHODS: Male SD rats had free access to water containing 0.1 g/L DEN for 16 weeks, during which the rats fed with standard diet or administration of Ganfujian granule (30.4 g/Kg in diet). At weeks 4, 8, 12 and 16 of hepatocarcinogenesis 5 rats of each group were sacrificed, and at week 20 another 30 rats were sacrificed from each group. The end point for survival observation was at week 28. Immunohistochemistry methods were used to examine the effect of Ganfujian granule on the process of hepatocarcinogenesis including proliferation of hepatocytes and cell cycle modulation.

RESULTS: Ganfujian granule could reduce and delay the incidence of hepatocarcinoma in rats and prolong the survival of animals. In addition, Ganfujian granule had a marked inhibitory effect on high expression of cyclin dependent kinase (CDK4) during the whole process of hepatocarcinogenesis and cyclin D1 at week 16 and the number of proliferating cell nuclear antigen (PCNA) positive cells in different stages of hepatocarcinogenesis.

CONCLUSION: Ganfujian granule can reduce and delay the incidence of hepatocarcinoma in rats by exerting direct or indirect effects on cell cycle and inhibiting uncontrolled proliferation of hepatocytes.

Qian Y, Ling CQ. Preventive effect of Ganfujian granule on experimental hepatocarcinoma in rats. *World J Gastroenterol* 2004; 10(5): 755-757

<http://www.wjgnet.com/1007-9327/10/755.asp>

INTRODUCTION

Liver cancer is one of the common malignancies in the world, especially in Asia and Africa. Despite many advances in the treatment of this disease in recent decades, its long-term therapeutic outcome remains poor and prognosis is devastating. Prevention seems to be the best strategy in lowering the present prevalence of the disease. Much work has been done in the prevention of liver cancer, including monitoring of high risk populations (residents in areas of high incidence, cirrhosis of

various causes and patients with chronic hepatitis)^[1,2], extensive immunization to prevent HBV infection^[3], and use of interferon to alleviate HCV infection, both providing hope of lowering or delaying the complication of hepatic cirrhosis or progression to liver cancer in chronic hepatitis patients^[4]. More and more efforts have been made in search of natural materials and foods as a means of chemical prevention of liver cancer^[5]. Characterized by low toxicity and effectiveness, traditional Chinese herbs have aroused more interest in the prevention of tumors^[6]. Ganfujian granule is an oral granule consisting of dietary and medicinal Chinese herbs for preventing liver cancer, developed by our laboratory based on the basic traditional Chinese medicine (TCM) theories of “invigorating spleen and soothing liver” as the key principle in combination with our clinical experience in preventing and treating liver cancer. Our previous experiments have demonstrated that Ganfujian granule can effectively prevent the formation of liver preneoplastic lesions^[7]. In the present study we attempted to observe the effect of Ganfujian granule on DEN induced liver cancer in rats and to explore the potential preventive mechanism from the perspective of modulation of proliferation of hepatocytes.

MATERIALS AND METHODS

Materials

Male SD rats (160-180 g in body mass) were obtained from the Animal Center of the Second Military Medical University of Shanghai. DEN and 2-bromo-3'-deoxyuridine (BrdU) marker were from Sigma, CDK4 sheep monoclonal antibody and cyclin D1 monoclonal antibody were from Santa Cruz, PCNA and BrdU test kit from DAKO.

Methods

Animal model The rats had free access to food and water throughout the study. The basal diet was a standard diet. The Ganfujian granule-containing diets were prepared by mixing 3.04% Ganfujian granule with the standard diet (the Ganfujian granule amount for the rats was converted from the kg body mass daily for adults). After a 5 d acclimatization period, 165 rats were assigned into group I (carcinogen-exposed control) and group II (Ganfujian granule treatment). Fresh sterile water was used to prepare DEN solution of 100 µg/mL concentration, to which the rats had free access. The rats in group I were fed with basal diet and those in group II with Ganfujian granule containing diet. At wk 16 DEN water was discontinued and the food for the animals in group II was changed into basal diet. Five rats from each group were sacrificed at wk 4, 8, 12 and 16 of DEN hepatocarcinogenesis. Livers of the rats were resected, cut into 3 mm slices and fixed. Another 30 rats from each group were sacrificed at wk 20 to observe incidence rate of liver cancer. The remaining animals were raised continuously to observe survival. The end point of observation was at wk 28.

Immunohistochemical staining The liver tissues were fixed in 40g/L buffered formaldehyde and processed for embedding in paraffin, cut into 4 µm thick slices, deparaffinized with

xylene and washed with alcohol, and then processed for immunohistochemistry by using a streptavidin-biotin-peroxidase complex methods. Cyclin D1 rat monoclonal antibody, CDK4 rabbit polyclonal antibody and PCNA rat monoclonal antibody were used as primary antibodies. As controls, known positive tissue sections were used, and for negative controls exposure to the primary antibody was omitted.

To determine labeling index (LI), 5 rats from each group at wk 20 received intraperitoneal injections of 2-bromo-3'-deoxyuridine (BrdU) 35 mg/kg body mass 1 h before death. BrdU incorporation into nuclei was determined immunohistochemically with a 'BrdU test kit'.

Analysis and quantification of staining results

Staining of cyclin D1 and CDK4 foci in liver tissue section was analyzed and quantified using an image analyzer (HPIAS-1000 highly clear color pathological graph analysis system). With the gray scale unified, five different fields were selected for each section to conduct automatic measurement by selecting the mean gray scale as the index of measurement, $\times 400$. The system uses 256 as the maximal gray of white and 0 as the minimal gray of black. The smaller the mean gray scale, the higher the positive reaction. The brownish yellow particles and dark blue particles covering the nuclei represented the positive signal of PCNA and BrdU respectively. The number of positive liver cells was counted. Ten un-overlapped high power fields ($\times 40$) of the same transmigration were used for counting the positive and negative cells (100 cells).

Statistical analysis

Data relative to tumor incidence were analyzed by Fisher's exact test. Survival functions were analyzed by the log-rank analysis. The differences between groups were analyzed by Student's *t* test, and the two-tailed statistical significance was determined. The statistical calculations were carried out by SPSS and NIOSA software packages.

RESULTS

General effects of ganfujian granule

The liver surface of rats in the group I grew coarse gradually between 4-8 wk of DEN hepatocarcinogenesis, on which small granules of local focus were seen. Light microscopy showed that liver cells became degenerative and locally necrotic. Cirrhosis was evidently seen in 40% at wk 12, and at wk 16, cirrhosis was seen in all the rats (100%). More and larger nodules were seen on the liver surface, the liver became smaller, and deranged pseudobulbi of different sizes were seen histologically. Early cancer change was seen in 20% rats. At wk 20, all the 30 rats (100%) developed hepatocarcinoma. Liver impairment of group II was milder than that of group I at various stages of hepatocarcinogenesis. No cirrhosis was seen at wk 12, 60% developed cirrhosis at wk 16, but no cancerous change was observed, and at wk 20, 24 of the 30 rats (80%) developed liver cancer. Fisher's exact test analysis showed that the incidence rate of liver cancer between the two groups was significant ($P < 0.05$). Using 28 wk as the end point of observation, the longest survival of rats in group I was 20 wk, and 28 wk in group II. Log-rank test showed that survival of rats in group II was longer than rats in group I, and risk of death in group I was lower than that in group II ($P < 0.05$, Figure 1).

Changes in expression of PCNA and BrdU

The number of PCNA positive hepatocytes increased gradually with progression of hepatocarcinogenesis at the early stage, and showed a tendency of sharp increase after 12 wk. Two-

tailed *t* test showed that the number of PCNA positive hepatocytes of group II was lower than that of group I, and the difference between two groups was evident between 12 and 20 wk ($P < 0.05$), (Table 1). The number of BrdU positively labeled hepatocytes was also smaller in group II at wk 20 of hepatocarcinogenesis (28.80 ± 0.65 vs 45.71 ± 1.90 , $P < 0.05$).

Table 1 Effect of Ganfujian granule on positive expression of PCNA during hepatocarcinogenesis ($n=5$, mean \pm SD)

Group	4 wk	8 wk	12 wk	16 wk	20 wk
Control	15.22 \pm 3.28	21.50 \pm 3.04	21.06 \pm 0.32	31.10 \pm 7.06	41.77 \pm 1.01
Treatment	10.88 \pm 3.22	12.20 \pm 1.87	6.38 \pm 0.18 ^a	10.11 \pm 0.78 ^a	16.14 \pm 0.43 ^a

^a $P < 0.05$ vs control.

Effects of Ganfujian granule on expression tendency of cell-cycle modulators

The gray scale of positively stained cyclin D1 of hepatocytes in rats treated with DEN decreased continuously, that is, positive expression of cyclin D1 showed an increasing tendency, reaching the peak at wk 16-20 of hepatocarcinogenesis. Positive expression of CDK4 reached the peak at wk 8, decreased gradually afterwards, and rose again gradually at wk 20. Linear regression correlation analysis showed that there was no significant correlation between two modulators ($P > 0.05$). Positive expression of CDK4 in group II was significantly lower than that in group I during different stages of hepatocarcinogenesis ($P < 0.05$) and the expression of cyclin D1 was significantly lower at wk 12 and 20 ($P < 0.05$), (Figure 2).

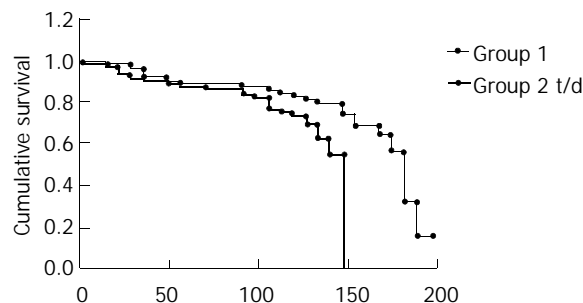


Figure 1 Survival of rats in two groups.

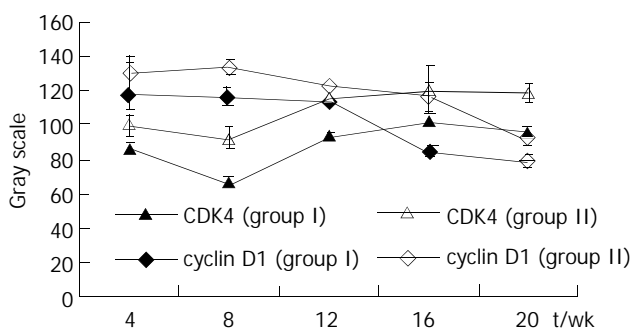


Figure 2 Expression of cyclin D1 and CDK4 during hepatocarcinogenesis in two groups of rat's liver.

DISCUSSION

Carcinogenesis is a multi-stage process characterized by continuous change in specific heredity and phenotype. The whole process of carcinogenesis is accompanied by subsequent activation of a group of protooncogenes and inactivation of

cancer suppressor genes, leading to continuous accumulation of uncontrolled proliferation of cells^[8]. Therefore, the liver backgrounds such as nodular cirrhosis and viral hepatitis, and abnormal expression of related genes and proteins play crucial roles in the process of carcinogenesis. In our model of using DEN as the chemical carcinogen, the rat liver underwent different stages of inflammatory change, cirrhosis, carcinogenesis and progression. The incidence rate of liver cancer was 100%. Almost all these liver cancers developed on the basis of cirrhosis. This process might imitate the pathogenesis of human liver cancer to some extent^[9,10]. Therefore, our model provides necessary evidence for dynamic observation of the whole process of hepatocarcinogenetic evolution from cancer initiation to malignant transformation based on the change of cell proliferation modulations.

Ganfujian granule is composed of dietary and medicinal Chinese herbs including Chinese yam (*Rhizoma Dioscoreae*), hawthorn fruit (*Fructus Crataegi*) and Chinese date (*Fructus Ziziphi Jujubae*). It is atoxic for long-term use. As a basic formula, it has achieved good therapeutic effects in clinical treatment of liver diseases. In the present study, we observed its effect on DEN induced liver cancer in rats and found that in group I 100% of these rats presented with nodular cirrhosis at wk 16, of which 20% were accompanied by early cancer change at wk 20, all rats developed liver cancer. The longest survival of rats was 20 wk. In group II, cirrhosis was found in 60% rats at wk 16, liver cancer was found in 80% at wk 20. The longest survival of rats was 28 wk. Statistical results showed that Ganfujian granule reduced and delayed the occurrence of liver cancer in rats and prolonged survival of these animals.

Abnormal proliferation of cells is the main feature of carcinogenesis, and therefore exploration of drugs that can affect malignant proliferation of liver cells is of primary importance in chemical prevention of liver cancer. PCNA, a polypeptide chain derived and purified from the cell nucleus, is directly involved in DNA replication. It has been found that the content and positive expression of PCNA were a common index for proliferation of hepatocytes at late G1 stage and early S stage^[11]. As BrdU may seep into cells during DNA synthesis, it can be used to reflect the number of S stage cells. Both PCNA and BrdU are good indexes reflecting proliferation of cells. The positive expression of two proteins was mainly found in the pre-cancerous proliferation focus and cancerous liver tissue during DEN induced hepatocarcinogenesis^[9]. Their high expression suggested that the ability of cell proliferation became stronger, and this was closely related to malignant cell proliferation and carcinogenesis^[12,13]. In the early stage of our experimental model, PCNA positive hepatocytes increased gradually and this increasing tendency became more evident between 12 and 20 wk (the period during which cirrhosis-liver cancer formed). The inhibitory effect of Ganfujian granule on PCNA positive cells was most prominent during this period. In addition, Ganfujian granule also reduced the number of BrdU positively labeled cells at wk 20, suggesting that Ganfujian granule had the action to suppress malignant proliferation of hepatocytes in experimental liver cancer.

The events of cell cycle are normally controlled by the clock within the cell, which is reflected by periodic activation of cyclin D/CDK complex. Irregular regulation may lead to abnormal cleavage of cells and is closely related to malignant transformation of cells^[12-15]. In our experiment, we found that positive expression of cyclin D1 tended to increase gradually during DEN induced hepatocarcinogenesis, reaching the peak

at the end stage of carcinogenesis. On the other hand, positive expression of CDK4 was active during the early stage of carcinogenesis, became weaker during the middle stage, and rose gradually in the late stage. In group II, positive expression of CDK4 at various stages of carcinogenesis and that of cyclin D1 at wk 16 were significantly lower than those in group I. These findings indicate that DEN induced hepatocarcinogenesis was accompanied by continuous accumulation of cell cycle positive modulators such as cyclin D and CDK, leading to disturbance of cell cycle and uncontrolled proliferation. Ganfujian granule can suppress over-expression of these modulators, regulate the process of cell cycle and capture over-proliferation of hepatocytes that escape the G1-S check-point so as to suppress uncontrolled proliferation and hepatocarcinogenesis.

Based on the results from our experiment, it is concluded that the dietary and medicinal formula Ganfujian granule is able to reduce and delay the occurrence of liver cancer by affecting the abnormal expression of multiple proteins related to cell proliferation cycle at different stages of hepatocarcinogenesis. As a liver cancer chemical preventive agent, clinical application of Ganfujian granule is promising.

REFERENCES

- 1 **Lemoine A**, Azoulay D, Jezequel M, Debuire B. Hepatocellular carcinoma. *Pathol Biol* 1999; **47**: 903-910
- 2 **Wang QH**, Liu XF. Study on monitoring of high risk populations of liver cancer. *Guowai Yixue Zhongliu Fence* 2002; **29**: 449-451
- 3 **Chang MH**, Chen DS. Prospects for hepatitis B virus eradication and control of hepatocellular carcinoma. *Baillieres Best Pract Res Clin Gastroenterol* 1999; **13**: 511-517
- 4 **Baffis V**, Shrier I, Sherker AH, Szilagyi A. Use of interferon for prevention of hepatocellular carcinoma in cirrhotic patients with hepatitis B or hepatitis C virus infection. *Ann Intern Med* 1999; **131**: 696-701
- 5 **Young KJ**, Lee PN. Intervention studies on cancer. *Eur J Cancer Prev* 1999; **8**: 91-103
- 6 **Li ZQ**. Traditional Chinese medicine for primary liver cancer. *World J Gastroenterol* 1998; **4**: 360-364
- 7 **Qian Y**, Ling CQ, Yu CQ, Pan RP, Zhang YN, Wang YZ. Obstructive effect of three traditional Chinese prescriptions on liver preneoplastic lesion in rats. *Disi Junyi Daxue Xuebao* 1999; **20**: 916-918
- 8 **Wei W**, Gong JP, Qiu FZ. Relationship between cell proliferation and apoptosis during the normal and abnormal liver tissue proliferation. *Zhonghua Shiyian Waikexue Zazhi* 2001; **18**: 156-158
- 9 **Zhang XL**, Shi JQ, Bian XW. Quantitative study on morphologic features and proliferative activity during DEN induced hepatocarcinogenesis in rats. *Disi Junyi Daxue Xuebao* 2001; **23**: 304-307
- 10 **Ling CQ**, Qian Y, Zhao JA, Jin Y. Expression of c-myc IGF-II gene and CyclinD1 protein in experimental hepatocarcinoma. *Shijie Huaren Xiaohua Zazhi* 2001; **9**: 1452-1453
- 11 **Lu S**, Zhan AH, Huang XX, Ren YJ. Expression and significance of proliferating cell nuclear antigen in resistance of lithium carbonate to Aflatoxin B1 induced hepatocarcinogenesis in rats. *Aibian Jibian Tubian* 2002; **14**: 84-86
- 12 **Kui Y**, Lin C, Wu W. Relationship between several important modulators of cell cycle G1-S check point and tumor. *Guowai Yixue Fenzi Shengwuxue Fence* 1998; **20**: 10-13
- 13 **Liu LX**, Jiang HC, Zhu AL, Wang XQ, Zhu J. Cell cycle and growth regulators gene expression in liver cancer tissues and adjacent normal tissues. *Zhonghua Shiyian Waikexue Zazhi* 2001; **18**: 123-126
- 14 **Yuan JH**, Zhong RP, Zhong RG, Guo LX, Wang XW, Luo D, Xie Y, Xie H. Growth-inhibiting effects of taxol on human liver cancer *in vitro* and in nude mice. *World J Gastroenterol* 2000; **6**: 210-215
- 15 **Yang LJ**, Si XH. Expression and significance of cyclin D1 in human hepatocellular carcinoma. *Shiyong Zhongliuxue Zazhi* 2000; **15**: 124-126

Definitive palliation for neoplastic colonic obstruction using enteral stents: Personal case-series with literature review

Giuseppe Piccinni, Anna Angrisano, Mario Testini, G. Martino Bonomo

Giuseppe Piccinni, Anna Angrisano, Mario Testini, G. Martino Bonomo, Section of General Surgery, Vascular Surgery and Clinical Oncology, Department of Applications in Surgery of Innovative Technologies, University of Bari- School of Medicine - Bari, Italy
Correspondence to: Giuseppe Piccinni M.D., Sezione di Chirurgia Generale, Vascolare ed Oncologia Clinica, Dipartimento per le Applicazioni in Chirurgia delle Tecnologie Innovative Università di Bari, Policlinico, Piazza G. Cesare 11, 70124, Bari, Italy. beppopiccinni@tin.it
Telephone: +39-080-5478856 **Fax:** +39-080-5478749
Received: 2003-10-27 **Accepted:** 2003-12-24

Abstract

Acute colonic obstruction due to malignancies is an emergency that requires surgical treatment. Elderly patients or inoperable tumors require intestinal decompression that is a simple colostomy in almost all cases. This "manoeuvre" leads the patient to a percentage of mortality/morbidity and to a bad quality of life due to acceptance of stoma. The introduction of enteral metal stent inserted endoscopically has, in our opinion, provided a new way to obtaining the definitive palliation of inoperable colo-rectal cancer with a simple method. We reported our case-series and we analyzed the current literature and costs of treatments.

Piccinni G, Angrisano A, Testini M, Bonomo GM. Definitive palliation for neoplastic colonic obstruction using enteral stents: Personal case-series with literature review. *World J Gastroenterol* 2004; 10(5): 758-764

<http://www.wjgnet.com/1007-9327/10/758.asp>

INTRODUCTION

Curative resection of colorectal cancer is not feasible in more than 25% of patients presenting obstruction due to extensive local tumor infiltration, distant metastases, or severe comorbidities.

In the treatment of patients with inoperable malignant obstruction, maintenance of gastrointestinal luminal patency is of paramount importance, and in view of this palliative cures are challenging.

Surgical treatment still remains the optimal treatment for high-risk patients with large bowel obstruction, although morbidity and mortality rates are relatively high. Moreover, surgical decompression with a palliative colostomy may be a major source of morbidity, and increase the time of hospitalization, need for further medical care, and reduces quality of life. In the last decade the health care industry has introduced really sophisticated visceral prosthesis. In recent years we have been challenged in stenting occlusive colo-rectal cancer bridging patients from emergency to elective surgery. With this work we reported our experience in treating inoperable colonic neoplastic obstruction, proposing definitive palliation for both obstructive symptoms and continuous oral intake, positioning enteral stents. This endoscopic treatment, in high-risk or inoperable patients, can avoid surgical approach with colostomy, greatly enhancing the quality of life.

Evaluation of the outcome of this treatment cannot ignore cost analysis that appears favorable in our and other opened experiences.

CASE SERIES

A retrospective review performed on 4 patients presenting incomplete colonic obstruction secondary to left-side colon cancer received a colonic stent at our institution between June 2000 and July 2003.

Clinical and radiographic criteria for patient eligibility to this treatment included (a) symptoms of obstruction with constipation for a period longer than 48 h, abdominal distension, nausea, vomiting, or abdominal pain, and (b) conventional radiologic evidence of colon-rectal obstruction (confirmed by abdominal computed tomography).

We excluded patients if they manifested clinical evidence of bowel perforation and free intraperitoneal air on abdominal radiograph, peritonitis, massive gastrointestinal bleeding, a fixed rectal mass.

All patients underwent baseline endoscopic evaluation for delineation of tumor length and demarcation. In all cases, histopathologic findings from biopsy revealed adenocarcinoma. After adequate explanation regarding discouraging complications (including difficulty of insertion because of propagation of the tumor, possible perforation on insertion and expansion of the stent, stent migration and tumor ingrowth), informed consent was given by each patient and family.

Case 1

In July 2000 a 90-year-old man came to our department because of rectal bleeding, appearing 1 mo before, and ileus symptoms. At admission the physical examination demonstrated abdomen distension and a rectal mass on finger exploration. Laboratory tests revealed an anaemic condition alone. American Society of Anesthesiologists (ASA) status was III. Then the patient underwent nasogastric decompression and received intravenous fluid supplements. CT of the abdomen and pelvis showed a rectal mass involving the whole wall thickness. Colonoscopy identified a substenotic rectal mass, measuring 4 cm in length, 8 cm away from the dentate line, which was dilated with a TTS-balloon (BE-6 OLYMPUS - Europe, Amburg, Germany). We decided to stent the lesion and opted for this kind of temporary treatment because of stent supply times. Balloon dilation showed an improvement of abdominal symptoms with gas and liquid stools transit. In the meantime we supported the patient with a liquid diet and total parenteral nutrition. Small enemas were also administered. On d 10 after admission, we inserted a Wallstent prosthesis (Schneider, Bulach, Switzerland) measuring 9 cm in length and 22 mm in diameter. The patient's symptoms improved immediately after stent placement with passage of stools and flatus from the anus. He died 6 mo after stent placement due to progression of the initial disease without constipation symptoms or signs.

Case 2

In July 2002 a 75-year-old man was admitted complaining of

abdominal pain and constipation for 3 d. Family history was positive for familiarity with neoplastic colonic disease (one sister had died). Past history: in 1984 radical cystectomy with urostomy for bladder carcinoma, chronic renal failure, in 1994 surgical clearing for choledocholithiasis, cerebral ischaemia and outcomes of lacunar encephalopathy, left hemiparesis, sclero-hypertensive cardiomyopathy, ventricular extrasystoles. In the last 6 mo, a body mass loss of 10 kg and poor appetite were noted. The patient had also been suffering from hypogastric pain for a month. For this reason, on 27 of July 2002 he underwent colonoscopy that revealed a circular stenosis 75 cm away from the anal verge, in the distal transverse colon (near splenic flexure) line, and unable to get through. Biopsy of this tissue demonstrated a histopathological finding of a well-differentiated adenocarcinoma. On August 28, 2002 he was referred to our institution because of ileus symptoms.

At physical examination, his abdomen was markedly distended. Laboratory tests disclosed hyper blood urea and hyper-creatinine level, malnutrition with a total protein level of 5.4 g/dL (normal value 6.4-8.3 g/dL), a white blood cell count of 8,500/mm³ (with normal differential cell and platelet counts), a hemoglobin level of 12 g/dL, a hematocrit of 36%. The ASA status was IV.

Plain abdominal Rx at admission showed fluid line. He was then subjected to total parenteral nutrition and a nasogastric tube to reduce gastrointestinal pressure. On the following days, ileus was temporally improved, on September 4, he underwent definitive colonic decompression using a Wallstent (Boston Scientific Microvasive, Minnesota, USA) measuring 9 cm in length and 22 mm in diameter (Figure 1). After one year he is still alive, follow-up control was scheduled for the 30th 2003.

Case 3

An 85-year-old woman was admitted to our department in October 2002 suffering from rectal bleeding first noted the year before. On admission the patient was diagnosed with ileus symptoms due to ulcerated, exophytic substenotic recto-sigmoid neoplasm, 5 cm long starting 14 cm from the anal verge as a result of colonoscopic examination. Laboratory studies disclosed malnutrition (total protein level of 5.6 g/dL) and anaemia (hemoglobin level of 10.7 g/dL, hematocrit of 33.5%). ASA status was IV. Plain computed tomography revealed tumor shadow of the sigmoid and the cephalic side of the colon was markedly dilated with fluid collection. Swelling of intraperitoneal lymph nodes and an abundant bilateral pleural effusion were also noted. We inserted a Precision Ultraflex prosthesis (Boston Scientific Microvasive, Minnesota, USA), measuring 9 cm in length and 25 mm in diameter. We obtained immediate recovery of colonic transit (Figure 2). She was discharged after 2 d and died after 45 d.

Case 4

A 61-year-old woman, without any medical history, had its beginning in March 2003, when she noted relapsing episodes/events of sub-occlusion and a body mass loss of 10 kg. At hematologic examinations, carcino-embryonic antigen and carbohydrate antigen 19-9 levels were significantly elevated at 8 000 ng/mL and over 10 000 U/mL, respectively. Plain computed tomography performed on May 29 showed multiple liver metastases, ascites and peritoneal carcinomatosis. Colonoscopic examination showed a circular stenosis at the sigmoid. Histopathological findings demonstrated adenocarcinoma. Initial support therapy was sought at a medical institute and then she was referred to ours for the required treatment. ASA-status was IV. A water-soluble contrast-media enema performed just after the colonoscope introduction, demonstrated a 3 cm

long stenosis. A Precision Ultraflex stent, measuring 9 cm in length and 25 mm in diameter, was selected and positioned. The day after stent insertion, we saw a full canalization. The patient was discharged on the 3rd hospital day and she is still alive (end of follow-up: August 2003).

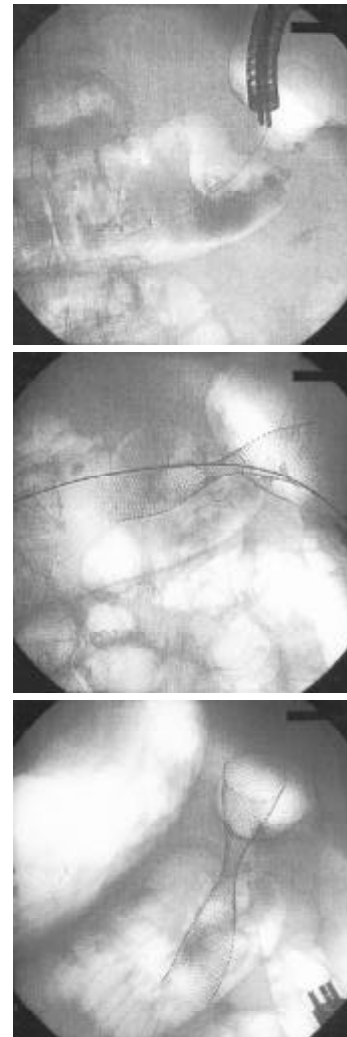


Figure 1 Radiologic sequence of stenting procedure in left transverse colon.



Figure 2 Endoscopic view of Wallstent positioned in the sigmoid colon with recovery of intestinal transit.

Before stent placement, all the patients underwent one or more colonic enemas, depending on the site of obstruction for cleaning the colon below the stricture. The patients were placed in the supine position only using a suitable combination of intravenous medication appropriate for a colonoscopic procedure as sedation and analgesia. There was no routine

administration of antibiotics. Vital signs (pulse rate and oxygen saturation) were monitored continuously.

As regards the stent placement technique used, once the colonoscope was inserted, a water-soluble contrast media was injected for careful assessment of the length and the morphology of the stricture by fluoroscopy. Then, an Amplatz superstiff guidewire (Boston Scientific Microvasive, Minnesota, USA) was inserted through the colonoscope channel and advanced as far as possible into the proximal bowel, and kept *in situ*. The instrument was then removed and reinserted adjacent to the wire. The stent was then deployed over the guidewire and across the stenosis. Using fluoroscopy, the stent was placed with each end equidistant from the tumor margins except for the first case. Deployment was performed under fluoroscopic and endoscopic guidance. Finally, endoscopic and X-ray images were used to assess the accuracy of the stent position.

Dedicated enteral stents were used (Enteral Wallstent/Precision Ultraflex endoprotheses). We chose enteral stents about 5 cm longer than the stricture, 1 or 2 cm of the stent to extend beyond both ends of the tumor.

We did not dilate the strictures before stent placement, except for the first patient, because neoplasms were not totally obstructing, but it should be remembered that this procedure could increase the risk of colonic perforation.

To determine the stent position and the relief of colonic obstruction until the patients were discharged, a conventional radiograph of the abdomen was obtained and changes in bowel gas patterns were analyzed within 24 h of stent placement and each subsequent day thereafter.

All patients tolerated the procedures well, which were technically successful.

There were no immediate technical complications associated with stent placement, and no perforation, major bleeding, or death related to endoscopic procedure. Each of the patient's symptoms improved immediately after stent placement with passage of stools and flatus from the anus. Initially the patients were able to take at least liquids, later they assumed a low-residue diet. The only delayed complication was dislodgment of 1 stent (25%) after one month.

The average survival time was 22.5 wk, and ranged from 6 to 48 wk. Two patients were alive at the end of the study period, two died because of the natural disease history. No patients showed clinical symptoms of obstruction at the time of death or termination of the study, all tolerated oral semi-solid feedings.

DISCUSSION

Malignancy is the major cause (85%) of acute colonic obstruction (ACO) and 10-30% of patients with colonic cancer had a large-bowel intestinal occlusion at presentation^[1-3].

Therefore, not surprisingly, ACO is considered as a surgical emergency, traditionally treated with surgical intervention that, though effective, was associated with high morbidity (10-36%) and mortality (6-30%) rates^[4].

Emergency surgery, mainly in acutely ill patients, often results in a diverting colostomy alone, which may be associated with a morbidity rate of 20-40% and a mortality rate of more than 10%^[5].

Indeed, many of these patients have already reached an advanced stage of the disease at the time of diagnosis. For patients with advanced tumors no longer resectable, widespread metastatic disease, peritoneal carcinomatosis, unfortunately the only therapeutic options have been palliative, with colostomy being the only reasonable and often unavoidable surgical option^[6]. Besides, many of these patients were elderly (up to 50% between 70 and 89 years old) and instable because of

significant co-morbidities, all this made them of high surgical risk^[7-9]. Moreover this treatment option entailed a significant decrease in quality of life, with major psychological repercussions^[10]. In addition, this unfortunate group of patients had short life expectancies (mean survival of patients who had hepatic metastases at the time of surgery was only 4.5 mo)^[11] and it was of paramount importance to keep them out of hospital. So, it is therefore preferable to seek more comfortable therapeutic approaches.

The primary goal of a non-surgical approach for treating ACO is to avoid the need of emergency surgical treatment in non stabilized patients. Such non-surgical alternatives to colostomy as balloon dilation^[12] and ablative methods (cryotherapy, electrocoagulation, laser photocoagulation)^[13,14], have been used in inoperable patients or with unresectable tumors. Laser therapy (LT) has gained considerable support by virtue of reports of its high initial success in luminal diameter increasing. Nd:Yag laser therapy was considered the treatment of choice for endoscopic palliation of advanced rectal carcinoma. In 1986 Mathus-Vliegen reported a success rate of 85-95% (5, 15). The drawbacks of LT were expensive equipment, time consuming sessions, lack of immediate relief of symptoms, need for repeated sessions to maintain patency, needs to repeat sessions, even every 5 to 9 wk^[12,16,17], significant (13%)^[18,19] risk of major complications like stenosis, perforation^[20], fistula (3.2%), abscess (1.7%) and bleeding (4.1%), as published by Gevers *et al*^[21].

In conclusion, LT is affected by such shortcomings as the need to be repeated periodically to maintain patency and limited applicability restricted solely to selected patients^[22] with tumors in distal locations.

In recent years, enteral stenting has emerged as an effective alternative to the surgical approach. However, the concept of colonic decompression using "stent" in obstructing colonic tumors, in the absence of peritonitis^[23], is not new. Initial reports were published in the early 1990s with some promising results but containing only a handful of patients, Lelcuk in 1986^[24] and Keen^[25] in 1992 passed a nasogastric tube respectively through the tumor to relieve obstruction. In 1991 the first report describing use of a metal stent in the rectum was published by Dohmoto^[26]. The following year, in a small series of four and two patients respectively, Spinelli in 1992^[27] and Itabashi in 1993^[28] confirmed the feasibility of inserting self-expanding metal stents for immediate relief of acute colonic obstruction due to rectal malignant tumors. In 1998 De Gregorio^[29] published a large multicenter retrospective study (24 pts) evaluating the success of the placement of colorectal stents for palliation, reporting a 100% technical success and a 96% clinical improvement. Using various kinds of stent, in 25 patients, Baron's group^[30] had less impressive results. They failed to put in the stents in 6% of their patients because of technical problems and only 85% of their stented patients had relief from obstruction.

The question as to which strictures by site are amenable to colonic endoluminal stenting (CELS) is not well addressed in literature by many authors. Similarly their description of the sites of lesions they have stented is unclear. The most commonly reported cases of CELS in literature were of lesions within the rectum and rectosigmoid, which was unsurprising as 70% of the obstructing colonic strictures were located in the left colon^[1,31].

While the initial series excluded patients thought to have lesions located in difficult anatomical positions^[32]. To date location has not appeared to be a limitation for CELS^[30,33,34], neither did the length of the tumor. If the lesion was not successfully or totally covered by the stent, an additional stent could be placed.

Distal extent of disease does not limit suitability for

stenting, although lesions less than 5 cm from the anal verge (dentate line) might be inappropriate^[35,36] and difficult to palliate with a metal stent, because of perianal trauma occurring due to stent irritation^[37]. Despite the recent advances in stent technology, the search for the ideal enteral stent has not stopped. Enteral stents should be flexible enough to allow placement but should remain in position once deployed^[38].

Initially since dedicated colonic stents were not available, a variety of stents originally designed for use elsewhere were used, as reported in literature studies, including the preferred enteral Wallstent®^[39-41]. Others were Endocoil® (Euromed Inc), esophageal nitinol Strecker stent, Gianturco self-expanding Z-stent, Ultraflex® Instent Esophacoil®^[28,30,34,39,40,42-45]. There was no noticeable difference in the outcomes using any of the above stents.

Metallic stents are of two types, expandable or self-expanding (so-called self-expanding metal stents, or SEMS). Because of their flexibility SEMS are easier to deploy than rigid tubes and allow peristalsis to continue, but they usually have a narrow lumen and are prone to tumor ingrowth. Some of these mesh type stents have been coated with polyurethane or other materials to prevent occlusion by tumor although this may increase the likelihood of dislocation. Covered stents have the advantage of resisting tumor ingrowth but tend to be less stable and more rigid, they require a larger delivery system, and are more likely to migrate. They are thus more difficult to deploy at distant locations through a tortuous delivery path^[46]. Uncovered stents are more flexible, and at least one can be passed through the working channel of an endoscope. However, when used for long-term palliation of malignant obstruction, they are subjected to tumor ingrowth and resultant obstruction. Most authors now use SEMS made of nitinol, a nickel/titanium alloy, which has <<shape memory>> meaning that once deployed, it adopts a preformed shape, an advantage over expandable systems that require dilation. Stent technology is currently evolving rapidly, and devices are now being developed specifically for colorectal applications.

The mean technical success, defined as successful stent placement and deployment, ranged from 64% (40) and 100%^[32,28,39,47]. Failure to stent deployment was usually a result of inability to pass a guide wire through a lesion, other reasons for technical failure, apart from tight or tortuous stenosis through which the guide wire could not be passed^[30,34,40,44,45] included insufficient length of the stent to span the entire stricture, inadequate introducer lengths^[30,44], floppy introducer system and incorrect deployment of the stent (42). A higher rate of successful stent placement could be achieved with more distal lesions. The most proximally placed stents described in literature till now have been in the right and proximal transverse colon^[30,34].

The stent placement procedure is generally painless and neither anesthesia nor analgesia is provided. It was frequently sufficient to provide a suitable combination of intravenous medication for a simple colonoscopy procedure^[9,17]. Clinical success, that is relief of obstructive symptoms, defined as colonic decompression within 96 h without endoscopic or surgical reintervention after stent placement (this time interval was chosen because it was integral to the definition used in nearly all the papers reviewed) has been reported in 75-96%^[2,23,30].

Stent placement complications were common to many authors, distinguishing the early from late ones. In previously published series^[9,29,34,45,48] the complication rate has been reported to range from 14% to 42%, most complication being minor. In the literature surveyed these were successfully managed with medical or supportive treatment in the majority of cases. Less seen complications included minor rectal bleeding, anorectal pain, temporary incontinence (11%)^[42], fecal impaction (8%)^[40] and severe tenesmus. Rectal bleeding

(0-100%) was usually hemodynamically insignificant and self-limited. It could result from mucosal irritation, pressure necrosis of the stent in the colonic mucosa, or friability of the tumor itself^[49]. Anorectal pain (5-100%) might occur and was usually mild and transient, lasting for only 3-5 days, it was easily controlled by analgesia^[39,45,49]. Severe tenesmus occurred during the first 48 hours and might be controlled with non-steroid anti-inflammatory drugs. It seemed to be related to insertion of the stent in a lower portion of the rectum^[50]. However, Camuñez^[51] described a patient who was readmitted twice because of persistent analgesic therapy, and was offered a colostomy which ultimately was refused.

Stent migration, restenosis, and perforation were the major complications encountered with colonic stent placement. Stent dislocation (0-44%) and obstruction (0-33%) were reported as the most common major complications described, but are not usually serious. Stent migration has been reported to occur in as many as 40% of cases and was usually detected on follow-up radiographs within 1 week of insertion. Camuñez^[22] believed the cause of stent migration was shrinkage of the tumours as a result of adjuvant chemotherapy. Generally, it appeared that predisposing factors included inappropriate stent selection as covered stent or those with too narrow diameter (with weak radial expansive strength), colonic angulation and post-operative chemotherapy or radiation therapy^[38,49,52]. Consequently, specific monitoring to check for possible reduction in tumor size and assess the advisability of stent extraction, is recommendable in patients receiving adjuvant therapy. When stent migration occurred, the stent might generally be passed spontaneously or require endoscopic removal and redeployment^[49]. Some stents which became dislocated and were expelled did not necessarily require replacement, since bowel function was adequately maintained.

Restenosis has been reported in up to 25% of cases and was usually due to malpositioning of the stent, as well as impaction with stool or food matter (it has been recommended that patients with colorectal stent ingest a low-residue diet and use stool softeners to lessen the likelihood of stent obstruction)^[38,53] but especially tumor ingrowth. Stent obstruction was usually amenable to a variety of nonoperative measures such as further coaxial restenting^[30] and laser therapy^[42]. However it would be interesting to point out that in Dohmoto's study 15% of patients needed a palliative colostomy to treat stent occlusion related to tumor ingrowth.

Restenosis due to tumor overgrowth (extension of tumor above or below the stent) could also be treated with a second stent. It could be best prevented by deploying the original stent 2-3 cm above or below the lesion when possible.

The most serious and potentially devastating complication of colonic stent placement was colonic perforation, reported in 0-16% of cases^[49,54,55]. Perforation can be either early or late, it should be suspected in patients who complain of abdominal pain during or immediately after the stenting procedure. Colonic perforation may have different causes, related either to the method itself or to the stent. One of the major causes is excessive balloon dilation of the stricture, causing full-thickness tear of the mucosa. Baron *et al.*^[30] reported colonic perforation in four patients, associated with balloon dilation of the stricture at the time of stent placement in three of the patients. Without balloon dilation, perforation rate might fall below 5%. Therefore, this practice is no longer recommended^[56], and stents are allowed to slowly self-expand.

Fortunately, it is possible to achieve stent placement even in patients with tight strictures without employing dilatation when modern stents are used. In addition, as perforation is more likely to occur during guidewire manipulation, the introduction of a wide range of soft-tipped guide-wires may contribute further to prevention of perforation. In the experience

of many authors^[34,44,22] perforation due to manipulation of guidewires and catheters has been asymptomatic, and it has been possible to complete the procedure in all cases. Late perforation could occur (though it is rare) due to pressure necrosis and erosion through the colon. Histologically, the side of the cancerous lesion compressed by the stent was thin and consisted of a serosal layer alone. Granulomatous change was detected histologically in normal mucosa that was in contact with the metallic stent. These histological changes were caused by direct compression or ischemic damage due to the self-expanding stent. Therefore, if SEMS is inserted in patients with complete obstruction due to advanced carcinoma infiltrating the serosa, Kusayanagi's experience suggests that a risk of perforation might develop approximately 2 months later^[49,57]. Several authors concluded that the possibility of colonic perforation as a potential complication must be kept constantly in mind and that consequently close clinical observation was required particularly in the days immediately following stent placement^[22].

Because of the continual changes in design, it is difficult to compare complication rates among different kinds of stent. However, some general conclusion may be drawn. The decreasing diameters of delivery systems make perforation a rare occurrence, and it is generally related to pre-stenting treatments.

Indeed, certain authors, prior to stent placement, pretreated the neoplastic strictures endoscopically first to canalize an obstruction using laser therapy^[17,48], argon plasma or coagulation, others used mechanical dilatation with endoluminal balloon catheters^[30,41]. Nevertheless, the added efficacy of these approaches is unproven, and certainly they increase the risk.

Patients stented for palliation usually underwent clinical follow-up, conventional abdominal radiographs were obtained at monthly intervals. Period of patency was defined as the period from stent placement to the recurrence of symptoms of obstruction in clinically successful cases^[58]. No absolute data exist on the mean time to occlusion of stents, also because this procedure has been carried out in a small total number of patients in the same short follow-up periods. Hence, assessment of stent patency and long-term behavior are difficult to define and data coming from literature are wide-ranging. Thus, according to Baron^[30], stent duration ranged from 2 to 64 wk (mean 17.3 wk). Kusayanagi's data^[57] was also in this range. According to him the mean time before re-obstruction was approximately 10 wk and the median follow-up for Repici^[59] was 21 wk (range 1-46). Moreover, no recurrence of obstruction was observed during the follow-up period. For Camuñez^[51] follow-up lasted an average of 138±93 d (range: 36-334 d), and the estimated primary stent patency rate was 91% at 3 and 6 mo. Even for mortality rate existing data in literature are controversial. For some authors^[17,60] no deaths have been reported directly attributable to the stenting procedure, on the contrary, Spinelli^[48] had a mortality rate of 3%.

Until now we have seen that, when LBO due to cancer has progressed beyond the stage of any curable intervention, there are only two options to relieve the obstruction by colostomy or by use of a stent, since both are capable of relieving acute obstruction and stenting clearly offers a preferable quality of life. Another important issue to consider is their cost, considering the fact that the principal cost determinants for the stenting option was the cost of the stent itself and the duration of in-hospital treatment^[61,62]. Few publications examined the cost impact of stenting compared to surgical decompression. One study^[34], concerning the cost of the stenting procedure compared with a control group undergoing only surgical treatment for malignant colorectal obstruction, showed that the overall cost of treating the stented group was 19.7% lower. According to Zollikofer's data^[63], a British

study^[64], comparing the cost of management by stenting 16 patients with acute large bowel obstruction with 10 unselected patients previously managed by surgical decompression, estimated that the cost of a palliative care was less than half of that of a surgically decompressed case. These cost savings were due mainly to the shorter hospital stay associated with stenting. Other factors were fewer surgical procedures, reduced operating time and fewer days in intensive care room. On the other hand, these data have much more relevance considering that the often hidden cost of stoma care in the community cannot be overlooked, about Euro 100 per mo is required for disposable stoma bags for each patient.

CONCLUSION

Malignant neoplasm of the left colon and rectum may lead to bowel obstruction in 10% to 30% of cases. Acute malignant obstruction of the large bowel is considered as a surgical emergency. Controversy currently exists as to optimal approach among surgical and nonoperative techniques in the case of patients with unresectable cancer or with a high ASA-grade. Physicians are often faced with the dilemma of finding the right balance between the need for timely aggressive intervention and the patient's underlying debilitated state. Recently several reports have indicated that, to reestablish luminal patency, the use of a stent may be a valid alternative to traditional surgical approach often consisting of a definitive colostomy. This treatment option entails serious disadvantages, namely substantial morbidity, and an obvious decrease in quality of the remaining life, with important psychological repercussions. The stent insertion is a combined endoscopic-radiologic technique that enables decompression of acute colonic obstruction with immediate restoration of bowel function, allowing all the pathophysiologic changes of obstruction to reverse. This procedure is feasible and successful in fully relieving the obstruction in almost all cases. Neither balloon dilation nor laser therapy is universally recommended prior to colorectal stenting to canalize a neoplastic obstruction, because of unproven efficacy and certainly increased risk.

We believe that the advantages of minimally invasive management of malignant acute large bowel obstruction are of particular and clear interest for geriatric population, because many of them often are not particularly good surgical candidates and so they are not suitable for definitive curative surgery.

In our experience there is evidence that is possible to stent a tumor in more proximal difficult tract like the left transverse colon near the splenic flexure. In the future stent technology and design will continue to evolve with the aim of improving safety parameters. In addition to this, the suggestion that stents impregnated with chemotherapeutic agents or composed by radioactive wire, may also help the tumor growth control, represents a very exciting area of interest.

Surgeons should become familiar with this technique, since it offers an alternative to surgical therapy for patients in critical general conditions, improving their quality of life and reducing the costs of the whole treatment. Therefore, we recommend that enteral stenting be considered as an alternative to traditional surgical therapy for definitive palliation in patients with malignant enteral obstruction.

ACKNOWLEDGMENTS

The authors gratefully acknowledge the assistance of Professor Malcolm Clark in the preparation of the English manuscript.

REFERENCES

- 1 Deans GT, Krukowski ZH, Irwin ST. Malignant obstruction of

- the left colon. *Br J Surg* 1994; **81**: 1270-1276
- 2 **Khot UP**, Lang AW, Murali K, Parker MC. Systematic review of the efficacy and safety of colorectal stents. *Br J Surg* 2002; **89**: 1096-1102
 - 3 **Nicholl MB**, Shilyansky J, Ota DM. Current management of malignant large-bowel obstruction. *Contempor Surg* 2002; **58**: 396-400
 - 4 **Riedl S**, Wiebelt H, Bergmann U, Hermanek P Jr. Postoperative complications and fatalities in surgical therapy of colon carcinoma. Results of the German multicenter study by the colorectal carcinoma study group. *Chirurg* 1995; **66**: 597-606
 - 5 **Dohmoto M**, Hunerbein M, Schlag PM. Palliative endoscopic therapy of rectal carcinoma. *Eur J Cancer* 1996; **32A**: 25-29
 - 6 **Phillips RK**, Hittinger R, Fry JS, Fielding LP. Malignant large bowel obstruction. *Br J Surg* 1985; **72**: 296-302
 - 7 **Anderson JH**, Hole D, McArdle CS. Elective versus emergency surgery for patients with colorectal cancer. *Br J Surg* 1992; **79**: 706-709
 - 8 **Scott-Conner CE**, Scher KS. Implications of emergency operations on the colon. *Am J Surg* 1987; **153**: 535-540
 - 9 **Mainar A**, De Gregorio MA, Ariza MA, Tejero E, Tobio R, Alfonso E, Pinto I, Herrera M, Fernández JA. Acute colorectal obstruction: treatment with self-expandable metallic stents before scheduled surgery—results of a multicenter study. *Radiology* 1999; **210**: 65-69
 - 10 **Nugent KP**, Daniels P, Stewart B, Patankar R, Johnson CD. Quality of life in stoma patients. *Dis Colon Rectum* 1999; **42**: 1569-1574
 - 11 **Bengtsson G**, Carlsson G, Hafstrom L, Jonsson PE. Natural history of patients with untreated liver metastases from colorectal cancer. *Am J Surg* 1981; **141**: 586-589
 - 12 **Oz MC**, Forde KA. Endoscopic alternatives in the management of colonic strictures. *Surgery* 1990; **108**: 513-519
 - 13 **Hoekstra HJ**, Verschueren RC, Oldhoff J, van der Ploeg E. Palliative and curative electrocoagulation for rectal cancer. Experience and results. *Cancer* 1985; **55**: 210-213
 - 14 **Spinelli P**, Dal Fante M, Meroni E. Traitement endoscopique au laser des tumeurs colo-rectales. *Acta Endosc* 1987; **17**: 157-168
 - 15 **Mathus-Vliegen EM**, Tytgat GN. Laser photocoagulation in the palliation of colorectal malignancies. *Cancer* 1986; **57**: 2212-2216
 - 16 **Dauphine CE**, Tan P, Beart RW Jr, Vukasin P, Cohen H, Corman ML. Placement of self-expanding metal stents for acute malignant large-bowel obstruction: a collective review. *Ann Surg Oncol* 2002; **9**: 574-579
 - 17 **Harris GJ**, Senagore AJ, Lavery IC, Fazio VW. The management of neoplastic colorectal obstruction with colonic endoluminal stenting devices. *Am J Surg* 2001; **181**: 499-506
 - 18 **Russin DJ**, Kaplan SR, Goldberg RI, Barkin JS. Neodymium-YAG laser. A new palliative tool in the treatment of colorectal cancer. *Arch Surg* 1986; **121**: 1399-1403
 - 19 **Wodnicki H**, Goldberg R, Kaplan S, Yahr WZ, Kreiger B, Russin D. The laser: an alternative for palliative treatment of obstructing intraluminal lesions. *Am Surg* 1988; **54**: 227-230
 - 20 **Mathus-Vliegen EM**, Tytgat GN. Analysis of failures and complications of neodymium: YAG laser photocoagulation in gastrointestinal tract tumors. A retrospective survey of 18 years' experience. *Endoscopy* 1990; **22**: 17-23
 - 21 **Gevers AM**, Macken E, Hiele M, Rutgeerts P. Endoscopic laser therapy for palliation of patients with distal colorectal carcinoma: analysis of factors influencing long-term outcome. *Gastrointest Endosc* 2000; **51**: 580-585
 - 22 **Camunez F**, Echenagusia A, Simo G, Turegano F, Vazquez J, Barreiro-Meiro I. Malignant colorectal obstruction treated by means of self-expanding metallic stents: effectiveness before surgery and in palliation. *Radiology* 2000; **216**: 492-497
 - 23 **Tamin WZ**, Ghellai A, Counihan TC, Swanson RS, Colby JM, Sweeney WB. Experience with endoluminal colonic wall stents for the management of large bowel obstruction for benign and malignant disease. *Arch Surg* 2000; **135**: 434-438
 - 24 **Lelcuk S**, Ratan J, Klausner JM, Skornick Y, Merhav A, Rozin RR. Endoscopic decompression of acute colonic obstruction. Avoiding staged surgery. *Ann Surg* 1986; **203**: 292-294
 - 25 **Keen RR**, Orsay CP. Rectosigmoid stent for obstructing colonic neoplasms. *Dis Colon Rectum* 1992; **35**: 912-913
 - 26 **Dohmoto M**, Rupp KD, Hohlbach G. Endoscopically-implanted prosthesis in rectal carcinoma. *Dtsch Med Wochenschr* 1990; **115**: 915
 - 27 **Spinelli P**, Dal Fante M, Mancini A. Self-expanding mesh stent for endoscopic palliation of rectal obstructing tumors: a preliminary report. *Surg Endosc* 1992; **6**: 72-74
 - 28 **Itabashi M**, Hamano K, Kameoka S, Asahina K. Self-expanding stainless steel stent application in rectosigmoid stricture. *Dis Colon Rectum* 1993; **36**: 508-511
 - 29 **De Gregorio MA**, Mainar A, Tejero E, Tobio R, Alfonso E, Pinto I, Fernandez R, Herrera M, Fernandez JA. Acute colorectal obstruction: stent placement for palliative treatment—results of a multicenter study. *Radiology* 1998; **209**: 117-120
 - 30 **Baron TH**, Dean PA, Yates MR 3rd, Canon C, Koehler RE. Expandable metal stents for the treatment of colonic obstruction: techniques and outcomes. *Gastrointest Endosc* 1998; **47**: 277-286
 - 31 **Gukovsky-Reicher S**, Lin RM, Sial S, Garrett B, Wu D, Lee T, Lee H, Arnell T, Stamos MJ, Eysselein VE. Self-expandable metal stent in palliation of malignant gastrointestinal obstruction: review of the current literature data and 5-year experience at Harbor-UCLA Medical Center. *Medscape General Medicine* 2003; **5**(1). Available from: URL: <http://www.medscape.com/viewarticle/444668>. Posted 01/10/2003
 - 32 **Dohmoto M**, Hunerbein M, Schlag PM. Application of rectal stents for palliation of obstructing rectosigmoid cancer. *Surg Endosc* 1997; **11**: 758-761
 - 33 **Obayashi M**, Katube T, Shimizu N, Kotani J, Takano Y, Amano R, Yanagawa K, Nishimori T, Sawa Y, Matsumoto T, Arakawa T. Endoscopic placement of metallic stent for colonic stricture resulting from carcinoma located at the splenic flexure. *Dig Endosc* 2002; **14**: 123-127
 - 34 **Binkert CA**, Ledermann H, Jost R, Saurenmann P, Decurtins M, Zollikofer CL. Acute colonic obstruction: clinical aspects and cost-effectiveness of preoperative and palliative treatment with self-expanding metallic stents – a preliminary report. *Radiology* 1998; **206**: 199-204
 - 35 **Paul Diaz L**, Pinto Pabon I, Fernandez lobato R, Montes Lopez C. Palliative treatment of malignant colorectal strictures with metallic stents. *Cardiovasc Intervent Radiol* 1999; **22**: 29-36
 - 36 **Rupp KD**, Dohmoto M, Meffert R, Holzgreve A, Hohlbach G. Cancer of the rectum-palliative endoscopic treatment. *Eur J Surg Oncol* 1995; **21**: 644-647
 - 37 **Mergener K**, Kozarek RA. Stenting of the gastrointestinal tract. *Dig Dis* 2002; **20**: 173-181
 - 38 **Mauro MA**, Koehler RE, Baron TH. Advances in gastrointestinal intervention: the treatment of gastroduodenal and colorectal obstructions with metallic stents. *Radiology* 2000; **215**: 659-669
 - 39 **Tejero E**, Fernandez-Lobato R, Mainar A, Montes C, Pinto I, Fernandez L, Jorge E, Lozano R. Initial results of a new procedure for treatment of malignant obstruction of the left colon. *Dis Colon Rectum* 1997; **40**: 432-436
 - 40 **Turegano-Fuentes F**, Echenagusia-Belda A, Simo-Muerza G, Camunez F, Munoz-Jimenez F, Del Valle Hernandez E, Quintans-Rodriguez A. Transanal self-expanding metal stents as an alternative to palliative colostomy in selected patients with malignant obstruction of the left colon. *Br J Surg* 1998; **85**: 232-235
 - 41 **Feretis C**, Benakis P, Dimopoulos C, Georgopoulos K, Manouras A, Apostolidis N. Palliation of large-bowel obstruction due to recurrent rectosigmoid tumor using self-expandable endoprostheses. *Endoscopy* 1996; **28**: 319-322
 - 42 **Spinelli P**, Dal Fante M, Mancini A. Rectal metal stents for palliation of colorectal malignant stenosis. *Bildgebung* 1993; **60**(Suppl 1): 48-50
 - 43 **Mainar A**, Tejero E, Maynar M, Ferral H, Castaneda-Zuniga W. Colorectal obstruction: treatment with metallic stents. *Radiology* 1996; **198**: 761-764
 - 44 **Saida Y**, Sumiyama Y, Nagao J, Takase M. Stent endoprosthesis for obstructing colorectal cancers. *Dis Colon Rectum* 1996; **39**: 552-555
 - 45 **Choo IW**, Do YS, Suh SW, Chun HK, Choo SW, Park HS, Kang SK, Kim SK. Malignant colorectal obstruction: treatment with a flexible covered stent. *Radiology* 1998; **206**: 415-421
 - 46 **Adam A**, Morgan R, Ellul J, Mason RC. A new design of the esophageal wallstent endoprosthesis resistant to distal migration. *Am J Roentgenol* 1998; **170**: 1477-1481
 - 47 **Chevallier P**, Baque P, Benchimol D, Bernard J, Souci J, Chevallier A, Bourgeon A, Padovani B. Treatment of colorectal obstruction

- with self-expanding metallic stents under fluoroscopic guidance. *J Radiol* 2002; **83**(4 Pt 1): 473-477
- 48 **Spinelli P**, Mancini A. Use of self-expanding metal stents for palliation of rectosigmoid cancer. *Gastrointest Endosc* 2001; **53**: 203-206
- 49 **Lo SK**. Metallic stenting for colorectal obstruction. *Gastrointest Endosc Clin N Am* 1999; **9**: 459-477
- 50 **Coco C**, Cogliandolo S, Riccioni ME, Ciletti S, Marino-Cosentino L, Coppola R, Picciocchi A. Use of a self-expanding stent in the palliation of rectal cancer recurrences. A report of three cases. *Surg Endosc* 2000; **14**: 708-711
- 51 **Camunez F**, Echenagusia A, Simo G, Turegano F, Vazquez J, Barreiro-Meiro I. Malignant colorectal obstruction treated by means of self-expanding metallic stents: effectiveness before surgery and in palliation. *Radiology* 2000; **216**: 492-497
- 52 **Chong LW**, Sun CK, Yang KC. Application of the self-expandable metallic stent for palliation of obstructing rectosigmoid cancer: report of a case. *J Intern Med Taiwan* 2002; **13**: 293-299
- 53 **Baron TH**. Expandable metal stents for the treatment of cancerous obstruction of the gastrointestinal tract. *N Engl J Med* 2001; **344**: 1681-1687
- 54 **Morino M**, Bertello A, Garbarini A, Rozzio G, Repici A. Malignant colonic obstruction managed by endoscopic stent decompression followed by laparoscopic resections. *Surg Endosc* 2002; **16**: 1483-1487
- 55 **McGrath K**. Clinical applications for expandable metal stents in the lumen of the gastrointestinal tract. *MedGenMed* **3**, 2001 [formerly published in *Medscape Gastroenterology eJournal* 3 (3), 2001]. Available at: <http://www.medscape.com/viewarticle/407972>
- 56 **Ely CA**, Arregui ME. The use of enteral stents in colonic and gastric outlet obstruction. *Surg Endosc* 2003; **17**: 89-94
- 57 **Kusayanagi S**, Kaneko K, Yamamura F, Hirakawa M, Miyasaka N, Konishi K, Kurahashi T, Yoshikawa N, Tsunoda A, Kusano M, Mitamura K. Histological findings after placement of a self-expanding stent in rectal carcinoma with complete obstruction - case report. *Hepatogastroenterology* 2002; **49**: 412-415
- 58 **Kang SG**, Jung GS, Cho SG, Kim JG, Oh JH, Song HY, Kim ES. The efficacy of metallic stent placement in the treatment of colorectal obstruction. *Korean J Radiol* 2002; **3**: 79-86
- 59 **Repici A**, Reggio D, De Angelis C, Barletti C, Marchesa P, Musso A, Carucci P, Debernardi W, Falco M, Rizzetto M, Saracco G. Covered metal stents for management of inoperable malignant colorectal strictures. *Gastrointest Endosc* 2000; **52**: 735-740
- 60 **Law WL**, Chu KW, Ho JW, Tung HM, Law SY, Chu KM. Self-expanding metallic stent in the treatment of colonic obstruction caused by advanced malignancies. *Dis Colon Rectum* 2000; **43**: 1522-1527
- 61 **Arnell T**, Stamos MJ, Takahashi P, Ojha S, Sze G, Eysselein V. Colonic stents in colorectal obstruction. *Am Surg* 1998; **64**: 986-988
- 62 **McGregor M**. The Technology Assessment Unit (TAU) of the McGill University Health Centre (MUHC). Should the MUHC approve the use of colorectal stents? Available from: https://upload.mcgill.ca/tau/stents_colorectal_Feb_2003
- 63 **Zollikofer CL**, Jost R, Schoch E, Decurtins M. Gastrointestinal stenting. *Eur Radiol* 2000; **10**: 329-341
- 64 **Osman HS**, Rashid HI, Sathananthan N, Parker NC. The cost effectiveness of self-expanding metal stents in the management of malignant left-sided large bowel obstruction. *Colorectal Disease* 2000; **2**: 233-237

Edited by Wang XL Proofread by Zhu LH

Successful treatment with rifampin for fulminant antibiotics-associated colitis in a patient with non-Hodgkin's lymphoma

Kenichi Nomura, Yosuke Matsumoto, Naohisa Yoshida, Sawako Taji, Naoki Wakabayashi, Shoji Mitsufuji, Shigeo Horiike, Masuji Morita, Takeshi Okanoue, Masafumi Taniwaki

Kenichi Nomura, Yosuke Matsumoto, Shigeo Horiike, Molecular Hematology and Oncology, Kyoto Prefectural University of Medicine Graduate School of Medical Science, Kyoto, Japan

Naohisa Yoshida, Sawako Taji, Naoki Wakabayashi, Shoji Mitsufuji, Takeshi Okanoue, Molecular Gastroenterology and Hepatology, Kyoto Prefectural University of Medicine Graduate School of Medical Science, Kyoto, Japan

Masuji Morita, School of Nursing, Kyoto Prefectural University of Medicine Graduate School of Medical Science, Kyoto, Japan

Masafumi Taniwaki, Clinical Molecular Genetics and Laboratory Medicine, Kyoto Prefectural University of Medicine Graduate School of Medical Science, Kyoto, Japan

Correspondence to: Kenichi Nomura, M.D. Ph.D., Molecular Hematology and Oncology, Kyoto Prefectural University of Medicine Graduate School of Medical Science, Kawaramachi-Hirokoji, Kamigyo-ku, Kyoto, 602-0841, Japan. nomuken@sun.kpu-m.ac.jp
Telephone: +81-75-251-5521 **Fax:** +81-75-251-0710

Received: 2003-11-12 **Accepted:** 2003-12-16

Abstract

A 74-year-old man was admitted to the hospital because of chemotherapy for relapsed non-Hodgkin's lymphoma (NHL). The patient became febrile and experienced diarrhea after chemotherapy. Although ceftazidime and amikacin sulfate were administered as empiric therapy, diarrhea was continued. After several days, stool cytotoxin assay for *Clostridium difficile* (*C. difficile*) was positive and he was diagnosed as having antibiotics-associated colitis (AAC). Although antibiotics were discontinued and both oral vancomycin and metronidazole were administered, disease was not improved. To rule out the presence of an additional cause of diarrhea, colon fiberoptic examination was performed. It revealed multiple deep ulcerative lesions at right side colon, surface erosive and minute erosive lesions in all continuous colon. Pseudomembranes were not seen. These findings are compatible with AAC without pseudomembranes. There are no reports that the rifampin is effective on refractory AAC. However, we administered oral rifampin for the current patient. The reasons are 1) conventional antibiotics were not effective, 2) rifampin has excellent *in vitro* activity against *C. difficile*, and 3) the efficacy of rifampin on relapsing colitis due to *C. difficile* is established. After administration of rifampin, fever alleviated and diarrhea was improved. Because AAC may result in significant mortality, patients with refractory or fulminant AAC should be treated with oral rifampin from outset.

Nomura K, Matsumoto Y, Yoshida N, Taji S, Wakabayashi N, Mitsufuji S, Horiike S, Morita M, Okanoue T, Taniwaki M. Successful treatment with rifampin for fulminant antibiotics-associated colitis in a patient with non-Hodgkin's lymphoma. *World J Gastroenterol* 2004; 10(5): 765-766
<http://www.wjgnet.com/1007-9327/10/765.asp>

INTRODUCTION

Antibiotics-associated colitis (AAC) due to *Clostridium difficile*

(*C. difficile*) is a nosocomial infection that may result in significant morbidity and mortality. AAC is capable of causing toxigenic colitis in susceptible patients such as those receiving chemotherapy. Approximately, 50% cases having endoscopic evidence of pseudomembranous colitis revealed exudative and punctate raised plaques with slip areas. The remainder had milder degrees of colitis without pseudomembranes^[1,2]. The clinical features of AAC without pseudomembranes are thought to be similar to those seen with pseudomembranes colitis, but of less severity^[3,4]. Patients with mild colitis are improved only by discontinuation of antibiotics. However, most patients are now treated with vancomycin (VCM) or metronidazole capable of eradicating *C. difficile* infection because of high mortality from AAC. The typical response to VCM therapy is improvement in diarrhea within a few days.

The recommendation is not established for patients with fulminant AAC. Colectomy may be life-saving in patients with severe AAC who fail to respond to antibiotic therapy. However, the surgical mortality is approximately 50%^[5].

We described a refractory patient having AAC without pseudomembranes. This patient was refractory to metronidazole and VCM. We administered oral rifampin for the current patient and he gained improvement. This is the first report that rifampin is effective for refractory or fulminant AAC.

CASE REPORT

A 74-year-old man was admitted to our hospital in May 2002 because of chemotherapy for relapsed non-Hodgkin's lymphoma. He presented a huge mass of NHL at lumber. He was treated with 3 courses of VeMP combination chemotherapy^[6]. After the first VeMP chemotherapy, he complained of diarrhea. Fosfomycin calcium (FOM) was administered and diarrhea was stopped. There was no side effect during the second course of VeMP chemotherapy. During the third chemotherapy, he became febrile without diarrhea, we administered ceftazidime (CAZ) and amikacin sulfate (AMK) as empiric therapy. Fever alleviated immediately. Considering the high frequencies of relapse in patients treated with VeMP, we stopped VeMP therapy and started CHOP therapy (cyclophosphamide, adriamycin, vincristine, and prednisolone) on 6 August. Because the patient became febrile and experienced diarrhea from d 4, we administered lactomin. On d 8, the patient developed massive watery diarrhea (over 1 500 mL/d) with exacerbation of fever, respiratory distress and marked hypovolemia. Ultrasound examination revealed massive ascites and pleural effusion. Although bolus methylprednisolone was administered promptly and CAZ and AMK as empiric therapy, the patient remained febrile and watery green diarrhea was not controlled. Salmonella, Shigella, campylobacter, cryptosporidium, fecal viruses and parasites were negative in repeated stool cultures. Because *C. difficile* toxin was detected using an enzyme immunoassay (Meridian Diagnostics, Inc., Cincinnati, OH, USA) in stools on day 13, the patient was diagnosed as having AAC. Although CAZ and AMK were stopped and oral VCM and metronidazole 250 mg

daily were started concomitantly, symptom did not improve. Colonoscopic examination revealed multiple deep ulcerative lesions at right side colon, surface erosive and minute erosive lesions in all continuous colon. Pseudomembranes were not seen. Biopsy reveals an outpouring of fibrin, mucus, and inflammatory cells from a microulceration of the surface epithelium. These findings are compatible with AAC without pseudomembranes. Because VCM and metronidazole were not effective, the enteral use of rifampin 600 mg twice daily was started on d 23. In the following several days, fever alleviated and diarrhea was improved (Figure 1).

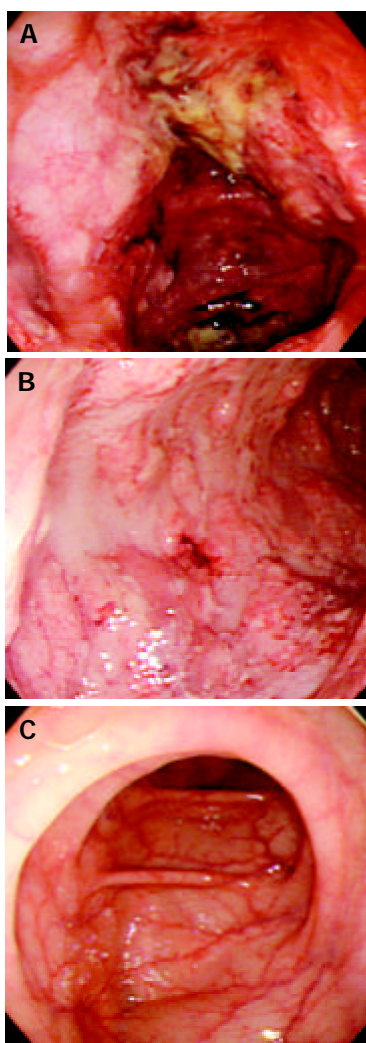


Figure 1 A: Multiple deep ulcerative lesions at right side colon, B: Surface erosive and minute erosive lesions in all continuous colon, C: After administration of rifampin.

DISCUSSION

We described a patient having refractory AAC without pseudomembranes. The current patient presented severe

watery diarrhea, malaise, fever, leukocytosis and dehydration. Administration of VCM and metronidazole was not effective. Some treatment regimens as the second therapy for refractory AAC have been tried, but none has been completely effective in randomized clinical trials. Although there have been some reports of the efficacy of oral teicoplanin for the treatment of antibiotics-associated colitis^[7,8], oral teicoplanin is not available in Japan. Colectomy was not required, because the current patient had a substantial comorbid disease and was extremely ill.

Rifampin had excellent *in vitro* activity against *C. difficile* with minimum inhibitory concentrations averaging $<0.2 \mu\text{g/mL}$ ^[9,10] and the efficacy of rifampin on relapsing colitis due to *C. difficile* was established^[11]. Thus, we administered rifampin 600 mg twice daily. Diarrhea and abdominal pain resolved promptly. Although there are no reports that rifampin is a useful agent for refractory and severe AAC, patients should be treated with oral rifampin from the outset.

REFERENCES

- 1 **Lishman AH**, Al-Jumaili IJ, Record CO. Spectrum of antibiotic-associated diarrhoea. *Gut* 1981; **22**: 34-37
- 2 **Bergstein JM**, Kramer A, Wittman DH, Aprahamian C, Quebbeman EJ. Pseudomembranous colitis: how useful is endoscopy? *Surg Endosc* 1990; **4**: 217-219
- 3 **Totten MA**, Gregg JA, Fremont-Smith P, Legg M. Clinical and pathological spectrum of antibiotic-associated colitis. *Am J Gastroenterol* 1978; **69**(3 Pt 1): 311-319
- 4 **Gerding DN**, Olson MM, Peterson LR, Teasley DG, Gebhard RL, Schwartz ML, Lee JT Jr. Clostridium difficile-associated diarrhea and colitis in adults. A prospective case-controlled epidemiologic study. *Arch Intern Med* 1986; **146**: 95-100
- 5 **Klingler PJ**, Metzger PP, Seelig MH, Pettit PD, Knudsen JM, Alvarez SA. Clostridium difficile infection: risk factors, medical and surgical management. *Dig Dis* 2000; **18**: 147-160
- 6 **Santini G**, Contu A, Porcellini A, Chisesi T, Coser P, Congiu AM, Morandi S, Manna A, Schintu GM, Quanini R, Rancan L, Miglio L, Damasio E, Rizzoli V. Mitoxantrone alone or in combination chemotherapy (VeMP) as second-line treatment in relapsed or refractory poor-prognosis non-Hodgkin's lymphoma. A report of the Non-Hodgkin's Lymphoma Co-operative Study Group (NHLCSG). *Haematologica* 1991; **76**: 485-490
- 7 **de Lalla F**, Privitera G, Rinaldi E, Ortisi G, Santoro D, Rizzardini G. Treatment of Clostridium difficile-associated disease with teicoplanin. *Antimicrob Agents Chemother* 1989; **33**: 1125-1127
- 8 **Wenisch C**, Parschalk B, Hasenhundl M, Hirschl AM, Graninger W. Comparison of vancomycin, teicoplanin, metronidazole, and fusidic acid for the treatment of Clostridium difficile-associated diarrhea. *Clin Infect Dis* 1996; **22**: 813-818
- 9 **O'Connor RP**, Silva J Jr, Fekety R. Rifampicin and antibiotic-associated colitis. *Lancet* 1981; **1**: 499
- 10 **Ripa S**, Mignini F, Prenna M, Falcioni E. *In vitro* antibacterial activity of rifaximin against Clostridium difficile, Campylobacter jejuni and Yersinia spp. *Drugs Exp Clin Res* 1987; **13**: 483-488
- 11 **Buggy BP**, Fekety R, Silva J Jr. Therapy of relapsing Clostridium difficile-associated diarrhea and colitis with the combination of vancomycin and rifampin. *J Clin Gastroenterol* 1987; **9**: 155-159

Recurrent inflammatory fibroid polyp of cardia: A case report

Krzysztof Zinkiewicz, Witold Zgodziński, Andrzej D¹ browski, Justyna Szumi³ o, Grzegorz Ąwik, Grzegorz Wallner

Krzysztof Zinkiewicz, Witold Zgodziński, Andrzej D¹ browski, Grzegorz Ąwik, Grzegorz Wallner, 2nd Department of General Surgery, Skubiszewski Medical University of Lublin, Staszica 16, 20-081, Lublin, Poland

Justyna Szumi³ o, Department of Human Pathology, Skubiszewski Medical University of Lublin, Jaczewskiego 8, 20-950, Lublin, Poland

Correspondence to: Krzysztof Zinkiewicz, MD, 2nd Department of General Surgery, Skubiszewski Medical University of Lublin, Staszica 16, 20-081, Lublin, Poland. kzinek@yahoo.com

Telephone: +4881-53-241-27 **Fax:** +4881-53-288-10

Received: 2003-11-04 **Accepted:** 2003-12-24

Abstract

Inflammatory fibroid polyp is one of the chronic inflammatory diseases in the digestive tract, which often mimics the submucosal tumor. Precise diagnosis is possible after removal of the detected lesion. Endoscopic removal is recommended as a safe and efficient method of the treatment. In this report the authors present a case of inflammatory fibroid polyp located in the cardia, which has been removed endoscopically. Twelve months later, recurrence of the lesion was noted and the patient was referred to surgical resection.

Zinkiewicz K, Zgodziński W, D¹ browski A, Szumi³ o J, Ąwik G, Wallner G. Recurrent inflammatory fibroid polyp of cardia: A case report. *World J Gastroenterol* 2004; 10(5): 767-768
<http://www.wjgnet.com/1007-9327/10/767.asp>

INTRODUCTION

Inflammatory fibroid polyp (IFP) in the digestive tract is one of the chronic inflammatory diseases, which most often is located in the stomach. Precise diagnosis of IFP remains difficult because available methods such as barium swallow or even endoscopy with endoscopic ultrasonography (EUS) provide only nonspecific, insufficient information. Some cases of IFP can macroscopically mimic gastric cancer^[1,2]. Hence, it is most important to exclude malignancy by histology on the detected lesion. In the case of submucosal lesions, standard biopsies are insufficient in obtaining adequate diagnostic tissue. Then endoscopic tumor excision or polypectomy is recommended. However the curative significance of endoscopic treatment in patients with IFP is still under discussion. We would like to report a rare case of IFP, localized within the esophago-gastric junction, which recurred 12 mo after endoscopic removal.

CASE REPORT

A 48-year-old male with symptoms of dysphagia for solids and epigastric pain of moderate intensity, lasting for 3 weeks, was admitted to the hospital. No weight loss was noted. The patient had no history of any other diseases including parasites and allergies. No abnormalities were found upon physical examination and laboratory results (hematology, serum biochemistry, urine analysis) were within normal ranges. Gastrofiberoscopy revealed an elevated, round, polypoid tumor, 15×20 mm with small ulceration in the center filled

with necrotic tissue (Figures 1, 2). The tumor was located exactly within the esophagogastric junction and significantly reduced the lumen of the cardia. The surface of the lesion was covered with hypertrophic mucosus. On retroflexion, the tumor was entirely within the confines of the stomach, suggesting the possibility of complete endoscopic excision (Figure 3). EUS showed a low echoic but rather homogenous tumor which did not invade the muscular layer. No other pathologies in the upper part of gastrointestinal tract were found. Endoscopic biopsies showed normal mucosa and attention was directed to endoscopic removal. Macroscopically radical endoscopic excision of the tumor, completed with argon plasma coagulation of its basement was performed under general anesthesia, and removed lesion was investigated by pathologists. Histological examination revealed a superficially ulcerated and well-circumscribed but nonencapsulated submucosal tumor, which extended partly into the cardiac mucosa. The tumor was composed of fibrous tissue with abundant small blood vessels and numerous eosinophils admixed with plasma cells and lymphocytes (Figure 4A,B). The lymphoid aggregates were also occasionally seen within the tumor and in adjacent tissues (Figure 4B). The inflammatory fibroid polyp was diagnosed. One day after the endoscopic procedure, the patient was discharged from the hospital with no postoperative complications noted.

Twelve months after the treatment, the patient was admitted to the hospital with the same symptoms as previously. Gastrofiberoscopy revealed the presence of the tumor in the cardia with an endoscopic appearance mostly as described above. The recurrent tumor was larger, 25×39 mm as shown on barium contrast radiography, and was more proximally located. In light of these findings the patient was referred to surgical treatment. Proximal gastrectomy with local lymphadenectomy, via laparotomy and distal esophagectomy via right thoracotomy with esophago-gastrostomy within the posterior mediastine were performed. Histological appearance of the recurrent tumor was identical with the first one. Postoperative course was uneventful and the patient was discharged 15 d after surgery. No significant changes within 4-mo follow-up were observed. Follow-up fiberoscopy performed 3 mo after the surgery showed no pathological signs within the esophago-gastrostomy.



Figure 1 Endoscopic view of inflammatory fibroid polyp (IFP) located in cardia. An elevated, round, polypoid tumor can be seen.



Figure 2 Inflammatory fibroid polyp of cardia. A small ulceration can be seen in the center of the lesion filled with necrotic tissue.



Figure 3 Retroflexion of endoscope. The tumor is indented into the stomach.

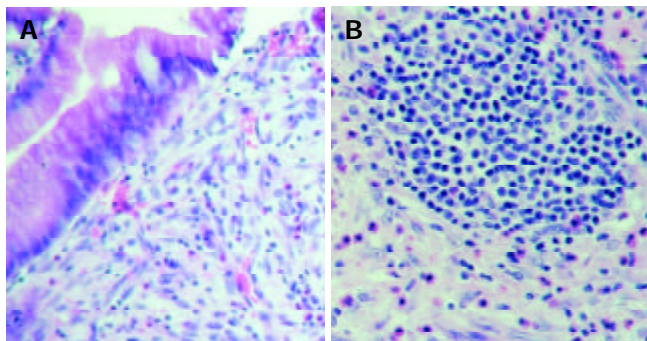


Figure 4 Histologic appearance of primary inflammatory fibroid polyp of cardia. A superficially ulcerated tumor can be observed involving cardiac mucosa and submucosa, and consists of fibrovascular tissue as well as numerous eosinophils admixed with plasma cells and lymphocytes. (HE; A: magn. $\times 100$; B: magn. $\times 200$).

DISCUSSION

In 1953 Helwig and Rainer proposed the term of inflammatory fibroid polyp for eosinophilic granuloma of the stomach which presently is generally accepted^[3]. IFP arises from submucosa of the gastrointestinal tract. It consists of loose connective tissue with a rich vasculature and abundant fibrous component. Usually the lesion was sessile or polypoid with ulceration of the overlying mucosa^[4]. IFP was mainly located in the pyloric region of the stomach, less frequent in the ileum, and only occasionally in the colon or esophagus^[4-6]. Small lesion is usually asymptomatic until pyloric stenosis or small bowel obstruction occurs. In the case described in the present report, a relatively small IFP was detected due to symptoms of

dysphagia. Its localization in the esophago-gastric junction has not been reported previously. Although IFP was nonneoplastic in nature^[4,6], its cause remains unclear. Fibroblastic^[4] or vascular origin of IFP^[7] has been considered. Eosinophilic infiltration which sometimes may occur as a submucosal tumor was also related to parasitic infections such as gastric anisakiasis^[8,9].

However, endoscopists should always suspect submucosal mesenchymal tumors of being gastrointestinal stromal tumor (GIST), leiomyoma or leiomyosarcoma especially when tumor macroscopically mimics a malignant lesion. Biopsy specimens using standard forceps may not be adequate for histological diagnosis when tumor is covered with normal mucosa. Then endoscopic excision/polypectomy preceded with EUS should be the best diagnostic method. There were some reports concerning the curative role of endoscopic removal of IFP^[10-12]. However, our results indicate the possibility of local recurrence of IFP after endoscopic treatment. Thus we recommend endoscopic removal as the most valuable diagnostic method for providing the specimens to accurate histological assessment. It may be reserved as the curative procedure in elderly and high-risk patients as has been proposed previously^[11] and should be repeated if necessary. Elevation of the tumor after submucosal saline or xylocaine injection can be helpful in making decision of endoscopic removal, and may indicate the possibility of complete, radical dissection. In other cases, minimal invasive surgery, *i.e.* laparoscopic resection, may be considered. To date only a single report has been available about recurrent eosinophilic granuloma of the ileum in a 2-year-old child^[13].

REFERENCES

- 1 **Yoh H**, Natsugoe S, Ohsako T, Yamada K, Suenaga T, Hokita S, Ohi H, Nishimata Y, Nishimata H, Aikou T. Eosinophilic granuloma of the stomach mimicking gastric cancer, report of a case. *Hepatogastroenterology* 2001; **48**: 606-608
- 2 **Premaratna R**, Saparamadu A, Samarasekera DN, Warren BF, Jewell DP, de Silva HJ. Eosinophilic granulomatous vasculitis mimicking a gastric neoplasm. *Histopathology* 1999; **35**: 479-481
- 3 **Helwig EB**, Ranier A. Inflammatory fibroid polyps of the stomach. *Surg Gynecol Obstet* 1953; **96**: 355-367
- 4 **Johnstone JM**, Morson BC. Inflammatory fibroid polyp of the gastrointestinal tract. *Histopathology* 1978; **2**: 349-361
- 5 **Samter TG**, Alstott DF, Kurlander GJ. Inflammatory fibroid polyps of the gastrointestinal tract. A report of 3 cases, 2 occurring in children. *Am J Clin Pathol* 1966; **45**: 420-436
- 6 **Shimer GR**, Helwig EB. Inflammatory fibroid polyps of the intestine. *Am J Clin Pathol* 1984; **81**: 708-714
- 7 **Pack GT**. Unusual tumors of the stomach. *Ann N Y Acad Sci* 1964; **114**: 985-1011
- 8 **Sakai K**, Ohtani A, Muta H, Tominaga K, Chijiwa Y, Hiroshige K, Fujishima H, Ohkubo A, Misawa T, Nawata H. Endoscopic ultrasonography findings in acute gastric anisakiasis. *Am J Gastroenterol* 1992; **87**: 1618-1623
- 9 **Takeuchi K**, Hanai H, Iida T, Suzuki S, Isobe S. A bleeding gastric ulcer on a vanishing tumor caused by anisakiasis. *Gastrointest Endosc* 2000; **52**: 549-551
- 10 **Tada S**, Iida M, Yao T, Matsui T, Kuwano Y, Hasuda S, Fujishima M. Endoscopic removal of inflammatory fibroid polyps of the stomach. *Am J Gastroenterol* 1991; **86**: 1247-1250
- 11 **Eugene C**, Penalba C, Gompel H, Bergue A, Felsenheld C, Fingerhut A, Quevauvilliers J. Gastric eosinophilic granuloma: value of endoscopic polypectomy. Apropos of 2 cases. *Sem Hop* 1983; **59**: 2249-2250
- 12 **Matsushita M**, Hajiro K, Okazaki K, Takakuwa H. Endoscopic features of gastric inflammatory fibroid polyps. *Am J Gastroenterol* 1996; **91**: 1595-1598
- 13 **McGreevy P**, Doberneck RC, McLeay JM, Miller FA. Recurrent eosinophilic infiltrate (granuloma) of the ileum causing intussusception in a two-year-old child. *Surgery* 1967; **61**: 280-284

Endoscopic retrieval of multiple fragmented gastric bamboo chopsticks by using a flexible overtube

Jia-Jang Chang, Cho-Li Yen

Jia-Jang Chang, Cho-Li Yen, Department of Hepatogastroenterology, Chang Gung Memorial Hospital, Keelung, Taiwan, China

Correspondence to: Cho-Li Yen, M.D. Department of Hepatogastroenterology, Chang Gung Memorial Hospital, Keelung, 222, Mai Chin Road, Keelung, Taiwan, 204, China. g15539@cgmh.org.tw

Telephone: +886-2-24313131~2627 **Fax:** +886-2-24335342

Received: 2003-10-20 **Accepted:** 2003-12-24

Abstract

This is a rare case of a patient with mental disorder, who ingested nineteen pieces of fragmented bamboo chopsticks. We managed the multiple gastric foreign bodies with a sclerotherapy overtube, and these multiple fragmented bamboo chopsticks were retrieved successfully using the endoscopic method. There were only multiple erosions with hemorrhage over the mucosa of fundus and body of stomach, no fragments adhered or perforated through the gastric wall. The mucosa of esophagus was intact. The patient tolerated the procedure well and without any major complications. Multiple sharp elongated gastric foreign bodies can be successfully and safely retrieved by using protective sheath of oropharynx without assistance with laparoscopy or surgical intervention. This renders an option for the endoscopists to manage multiple elongated gastric foreign bodies.

Chang JJ, Yen CL. Endoscopic retrieval of multiple fragmented gastric bamboo chopsticks by using a flexible overtube. *World J Gastroenterol* 2004; 10(5): 769-770

<http://www.wjgnet.com/1007-9327/10/769.asp>

INTRODUCTION

Foreign body ingestion is a common problem in the emergency department. Most ingestions may be accidental, but may also be a result of contributory factors as mental disorder, bulimia, alcohol consumption, and prison inmates^[1]. When foreign bodies are ingested, they will usually pass spontaneously through the whole alimentary tract and out to the feces. The risk of perforation of gastrointestinal tract is only 1%^[2]. Ten to twenty percent of the objects will have to be removed endoscopically, about 1% will require surgery^[1]. However, sharp and pointed foreign bodies, as well as elongated materials in the stomach, can be very challenging and difficult to manage by endoscopy. Long and sharp foreign bodies should be removed immediately before they pass from the stomach to the intestine, as 15% to 35% of them will cause intestinal perforation^[3]. Elongated materials such as toothbrushes, toothpicks, and bones are the most common foreign bodies in the stomach that require surgery for their removal^[4,5]. Here, we report a rare case of a patient with mental disorder, who ingested nineteen pieces of fragmented chopsticks. The problem was treated successfully using the endoscopic method.

CASE REPORT

The case of a 24 year-old man had a history of substance

dependence. He had used amphetamine for years, intermittently in the first three years and thereafter nearly everyday. As he developed a physical tolerance to amphetamine, he then turned to alcohol abuse. He was admitted to a psychiatry ward because of his drug and alcohol addictions. Two weeks after he was discharged from the psychiatry ward, he stayed at home doing nothing and continued alcohol abuse. His mother described his behavior as being mood swinging from depression to mania. He suffered from insomnia, having had hot temper, restlessness, to being bed-ridden and mental disturbed. He was forced by his mother to admit to a daytime psychiatric ward again for substance dependence. After admission, he committed to suicide by swallowing fragmented bamboo chopsticks. His roommate found that he swallowed small pieces of chopsticks and complained of epigastric pain 4 d after admission. The nurse was notified and called the doctor to check him up. As the patient stated that he began to swallow in fragmented bamboo chopsticks piece by piece at meals 4 d before. On physical examination, his abdomen was found to be soft, but he had tenderness over the epigastric area, and he produced a normally active bowel sound. A plain abdomen radiography did not show foreign body. An upper gastrointestinal panendoscopy was performed on March 14, 2000 to ascertain if he had indeed ingested chopsticks. In the left lateral decubitus position, the patient was given local anesthetic. Afterward, he was given intravenous hyoscine-N-butylbromide (20 mg) and sedated with intravenous midazolam (5 mg). There were food residues mixed with plenty of fragmented bamboo chopsticks with one or two sharp ends in the fundus and body of the stomach (Figure 1). We placed a "flexible overtube" (Sumitomo®, Japan) through the mouth to esophagus and used Dormia basket to grasp the blunt end of fragmented bamboo chopsticks out of the overtube. The blunt ends were grasped tightly at the uppermost part, and withdrawn through the esophago-cardiac junction without any difficulty. Small fragments could be easily and repeatedly passed through the esophagus into the channel of the overtube, whereas the larger fragments (more than 10 cm long) stuck at the oropharynx where the angle is almost rectangular (Figure 2). To remove the long fragments we withdrew the gastroscope together with the overtube. Since five of the fragments were more than 10 cm, we repeated this operation 5 times. Sumitomo® overtube which is quite flexible and elastic could be passed through the oropharynx to the esophagus repeatedly and easily without causing injury to the esophagus. The fragmented chopsticks were mixed with food debris, making blunt ends difficult to be found and grasped. It took 2 h to accomplish the procedure. In all, a total of nineteen fragmented bamboo chopsticks were retrieved (Figure 3). After removal of the fragmented bamboo chopsticks, the esophagus and stomach were thoroughly examined. There were multiple erosions and hemorrhage spots over the mucosa of the fundus and the body, fortunately no fragment pieced through the gastric wall. The mucosa of esophagus was intact. The patient was observed for 2 d, he had no complaint except mild epigastric pain that could be controlled by antacids. He was referred for psychiatric evaluation and discharged uneventfully.



Figure 1 Plenty of fragmented bamboo chopsticks mixed with food debris in fundus and body of stomach.

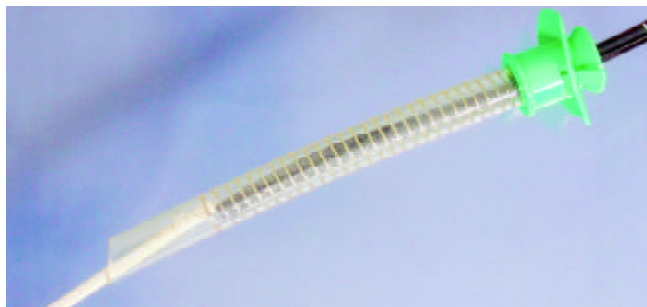


Figure 2 Impaction of a large piece of fragmented bamboo chopsticks (more than 10 cm long) impacted in channel of Sumitomo sclerotherapy overtube (Simulate picture).



Figure 3 Retrieval of nineteen fragmented bamboo chopsticks.

DISCUSSION

About 80% to 90% of small indigestible objects that entered the stomach could eventually pass through the intestinal tract. However, sharp foreign bodies might lodge in the esophagus and lead to esophageal perforation, retroesophageal abscess, mediastinitis, and esophagoaortic fistulae^[4]. It was very difficult to remove sharp and pointed foreign bodies, as well as elongated objects in the gastrointestinal tract by endoscopic management and they have become a technical challenge^[5]. Objects that are longer than six centimeters are difficult to pass through the duodenal sweep. If the objects are greater than two centimeter in diameter, they may not pass through the pylorus. Ingested objects longer than six centimeters in children or 13 centimeters in adults should be promptly removed endoscopically due to the high incidence of penetration and entrapment in the bowel^[6]. Up to 15% to 35% of sharp and pointed foreign bodies ingested would penetrate the wall of the gastrointestinal tract^[3]. Indicating that when a sharp or pointed foreign body is found in the stomach or duodenum during an endoscopic evaluation, emergent endoscopic removal of the foreign body is mandatory, even if the patient is asymptomatic.

Adults ingesting pointed objects are mostly prisoners or psychiatric patients, and carried a higher complication rate and surgical rate than when that of accidental ingestion. In the review of Gracia *et al.*, there were 22 deliberate ingestors, five of whom had complications of perforation. There was also a high rate of endoscopic failure, up to 80%^[7]. Bamboo chopsticks are commonly used in China and Far Eastern Asia. In this present case, the young psychiatric patient swallowed fragmented bamboo chopsticks to attract attention of others.

We have tried using the Dormia basket to hold the blunt ends of the fragments and remove them piece by piece, but we failed to remove them because the long bamboo chopsticks would get trapped at the oropharynx. Sometimes the grip of the Dormia basket would be lost when it passed the oropharynx. The endoscopy overtube technique is especially useful in extracting multiple foreign bodies at one time. It could facilitate rapid reinsertion of the endoscope after each retrieval and protect the esophageal mucosa as well as cricopharyngeus muscles from injury^[8,9]. Werth *et al.* used a protective Terblanche sclerotherapy overtube to remove multiple gastric foreign bodies^[10]. Yong *et al.* removed a dinner fork from the stomach by using a double snare method to align the axis of the objects and facilitate its withdrawal^[11]. Wishner *et al.* recommended laparoscopy assisted removal via gastrostomy to remove a swallowed toothbrush^[12].

In this case, there were multiple fragmented bamboo chopsticks with various lengths. They measured up to 10 cm each with a sharp broken end. The long chopstick could only be retrieved along with the overtube, because the long chopstick and Dormia Basket could have entrapped in the inner channel of the overtube at the oropharynx level. As a result, repeated intubations of the overtube were necessary. Fortunately, these gastric foreign bodies were successfully and safely retrieved without assistance with laparoscopy or surgical intervention. Therefore, we recommend using repeated insertion of Sumitomo® sclerotherapy overtube, which is flexible and easy to pass through the oropharynx, to extract the ingested sharp foreign bodies. The maneuver is safe although time-consuming. This renders an option for endoscopists to manage multiple elongated and pointed gastric foreign bodies.

REFERENCES

- 1 **Webb WA.** Management of foreign bodies of the upper gastrointestinal tract. *Gastrointest Endosc* 1995; **41**: 39-51
- 2 **Carp L.** Foreign bodies in the intestine. *Ann Surg* 1927; **85**: 575-591
- 3 **Rosch W, Classen M.** Fibroendoscopic foreign body removal from the upper gastrointestinal tract. *Endoscopy* 1972; **4**: 193-197
- 4 **Nandi P, Ong GB.** Foreign bodies in the esophagus: review of 2394 cases. *Br J Surg* 1978; **65**: 5-9
- 5 **Stack LB, Munter DW.** Foreign bodies in the gastrointestinal tract. *Emerg Med Clin North Am* 1996; **14**: 493-521
- 6 **Brady PG.** Esophageal foreign bodies. *Gastroenterol Clin North Am* 1991; **20**: 691-701
- 7 **Gracia C, Frey CF, Bodai BI.** Diagnosis and management of ingested foreign body: a ten-year experience. *Am Emerg Med* 1984; **13**: 30-34
- 8 **Rogers BH, Kot C, Meiri S.** An overtube for the flexible fibroptic esophagogastroduodenoscopy. *Gastrointest Endosc* 1982; **28**: 256
- 9 **Spurling TJ, Zaloga GP, Richter JE.** Fiberoendoscopic removal of a gastric foreign body with overtube technique. *Gastrointest Endosc* 1983; **29**: 226-227
- 10 **Werth RW, Edwards C, Jennings WC.** A safe and quick method for endoscopic retrieval of multiple gastric foreign bodies using a protective sheath. *Surg Gynecol Obstetrics* 1990; **171**: 419-420
- 11 **Yong PTL, Teh CH, Look M, Wee SB, Tan JCH, Chew SP, Low CH.** Removal of a dinner fork from the stomach by double snare endoscopic extraction. *Hong Kong Med J* 2000; **6**: 319-12
- 12 **Wishner JD, Rogers AM.** Laparoscopic removal of a swallowed toothbrush. *Surgical Endoscopy* 1997; **11**: 472-473

Downregulation of retinoic acid receptor-*b*₂ expression is linked to aberrant methylation in esophageal squamous cell carcinoma cell lines

Zhong-Min Liu, Fang Ding, Ming-Zhou Guo, Li-Yong Zhang, Min Wu, Zhi-Hua Liu

Zhong-Min Liu, Fang Ding, Li-Yong Zhang, Min Wu, Zhi-Hua Liu, National Laboratory of Molecular Oncology, Cancer Institute, Peking Union Medical College and Chinese Academy of Medical Sciences, Beijing, China

Ming-Zhou Guo, Division of Tumor Biology, Department of Oncology, The Sidney Kimmel Comprehensive Cancer Center at Johns Hopkins, Baltimore, MD, USA

Supported by China Key Program on Basic Research, G1998051021, the Chinese Hi-tech R&D program, 2001AA231041, and National Science Foundation of China, 30170519

Correspondence to: Zhi-Hua Liu, Professor, National Laboratory of Molecular Oncology, Cancer Institute, Peking Union Medical College and Chinese Academy of Medical Sciences, Beijing 100021, China. liuzh@pubem.cicams.ac.cn

Telephone: +86-10-67723789 **Fax:** +86-10-67723789

Received: 2003-12-10 **Accepted:** 2004-01-08

Abstract

AIM: To study the role of hypermethylation in the loss of retinoic acid receptor *b*₂ (*RARB*₂) in esophageal squamous cell carcinoma (ESCC).

METHODS: The role of hypermethylation in *RARB*₂ gene silencing in 6 ESCC cell lines was determined by methylation-specific PCR (MSP), and its methylation status was compared with *RARB*₂ mRNA expression by RT-PCR. The MSP results were confirmed by bisulfite sequencing of *RARB*₂ promoter regions.

RESULTS: Methylation was detected in 4 of the 6 cell lines, and the expression of *RARB*₂ was markedly downregulated in 3 of the 4 methylated cell lines. The expression of *RARB*₂ was restored in one *RARB*₂-downregulated cell line with the partial demethylation of promoter region of *RARB*₂ after 5-aza-2'-deoxycytidine (5-aza-dc) treatment.

CONCLUSION: The methylation of the 5' region may play an important role in the downregulation of *RARB*₂ in some ESCC cell lines, suggesting that multiple mechanisms contribute to the loss of *RARB*₂ expression in ESCC cell lines. This study may have clinical applications for treatment and prevention of ESCC.

Liu ZM, Ding F, Guo MZ, Zhang LY, Wu M, Liu ZH. Downregulation of retinoic acid receptor-*b*₂ expression is linked to aberrant methylation in esophageal squamous cell carcinoma cell lines. *World J Gastroenterol* 2004; 10(6): 771-775
<http://www.wjgnet.com/1007-9327/10/771.asp>

INTRODUCTION

Retinoids, the important factors in modulating cell growth, differentiation, apoptosis and suppressing carcinogenesis *in vitro* and *in vivo*, are a group of natural and synthetic vitamin

A analogs. In many animal models, such as cancers of skin, lung, prostate and esophagus, retinoids could suppress or reverse epithelial carcinogenesis^[1]. The effects of retinoids are mainly mediated through two classes of nuclear receptors: the retinoic acid receptors (RARs) and retinoid X receptors (RXRs) which belong to a steroid/thyroid hormone-receptor superfamily. Each of them is composed of 3 subtypes (α , β and γ), of which *RARB* is expressed as three isoforms: *b*₁, *b*₂ and *b*₄^[2]. Most human cells express *RARB*₂ as the major isoform. Many studies have confirmed that altered expression or function of the retinoid receptors may be related to malignant transformation of human cells^[3,4].

*RARB*₂ was decreased in many tumors, including lung carcinoma, breast cancer and esophageal cancers^[5-7]. A study of esophageal cancer demonstrated that loss of *RARB* expression was an early event associated with esophageal carcinogenesis and the status of squamous differentiation^[6], however the mechanisms underlying the inactivation of *RARB*₂ expression in cancer, especially the esophageal cancer, have not been well known yet. In breast cancer, no mutation or polymorphism was detected within the *BRARE* promoter, which was located in the promoter regions of target genes, and the lack of correlation between *RARB*₂ expression and LOH at chromosome 3p24 was demonstrated in esophageal cancer^[8,9]. The *RARB*₂ promoter was characterized by an island, which was located in the 5' -untranslated region, and increasing data showed that aberrant methylation of the CpG islands in tumors was associated with transcriptional repression of tumor suppressor genes, such as *p*16 in esophageal cancer^[10]. To clarify the epigenetic mechanism of *RARB*₂ loss or reduction in ESCC cell lines, we analyzed the methylation status of the *RARB*₂ promoter region by MSP assay and bisulfite sequencing. Our results indicated that downregulation of *RARB*₂ expression was associated with the aberrant methylation of the CpG islands in some ESCC cell lines, but not in others.

MATERIALS AND METHODS

Reagents and chemicals

5-aza-dc (Sigma, St. Louis, MO) was dissolved in pure ethanol at a stock concentration of 2 mM, and stored in aliquots at -70 °C.

ESCC cell cultures and treatments

Six cell lines were used in this study: KYSE180, KYSE410, KYSE450, KYSE510, COLO680N, and TE12 were purchased from DSMZ (Deutsche Sammlung von Mikroorganismen und Zellkulturen GmbH). Each of the cell lines was cultured in either 90% RPMI 1640 medium (Invitrogen, Carlsbad, CA) or 45% RPMI 1640/45% Ham's F-12 medium (Invitrogen) with 100 mL/L fetal bovine serum at 37 °C containing 50 mL/LCO₂. In the demethylation experiment, the cells with lower *RARB*₂ expression were treated with 5-aza-dc at a final concentration of 5 μ mol/L for 96 h. The growth medium with or without the drug was changed every 24 h.

DNA preparation

The esophageal cell cultures were digested with trypsin-EDTA before collection. Genomic DNA from cell lines was extracted by proteinase-K digestion and phenol/chloroform extraction as described previously^[11]. DNA was dissolved in TE buffer and stored at -20 °C.

RNA isolation and semi-quantitative RT-PCR

Total RNAs were isolated from ESCC cell lines with Trizol reagent (Invitrogen) according to the manufactures' instructions. RNA quality was assessed with agarose gel electrophoresis and spectrophotometric analysis. Ten µg of total RNA of each sample was treated with 2 µL DNase I (10 units/µL, Promega, Madison, WI), 1 µL LRNasin (40 units/µL, Promega) at 37 °C for 15 min to remove contaminated DNA. First strand cDNA was reversely transcribed from 5 µg of total RNAs using SuperScript™ first-strand synthesis system for RT-PCR II kit (Invitrogen) at 42 °C for 80 min and 0.5-1 µL aliquots of the cDNA was then subjected to RT-PCR. The primers used for the amplification of *RARB2* were as follows: sense 5' - ATCGATGCCAATACTGTCTGA-3', antisense 5' - GACTCGATGGTCAGCACTG-3'^[8]. As, *GAPDH* was used as an internal control to ensure quality and quantity of cDNA for each RT-PCR. A product with 241 bp was generated, and PCR products were analyzed on 20g/L agarose gels. The PCR assay for each sample was repeated at least twice.

Methylation-specific PCR

Bisulfite modification of genomic DNA from primary esophageal cancer cell lines was carried out essentially as described previously^[12]. Briefly, 2 µg of genomic DNA was denatured with freshly prepared NaOH (final concentration 0.3 mol/L) for 15 min in a 37 °C water bath, 30 µL of freshly prepared 10 mmol/L hydroquinone (Sigma) and 520 µL of freshly prepared 3.6 mol/L sodium bisulfite (Sigma) at pH 5 were added and mixed. The samples were then incubated under mineral oil for 16 h at 50 °C. The modified DNA was purified with a Wizard DNA clean-up system (Promega). After purification, the samples were treated with NaOH (0.3 M) for 15 min at 37 °C. The DNA was ethanol-precipitated and re-suspended in water for MSP analysis.

The bisulfite-induced changes affecting unmethylated (U) and methylated (M) alleles were detected by nested PCR. The primers for the first round PCR were as follows: sense 5' - AAGTGAGTTGTTTAGAGGTAGGAGGG3', and antisense 5' - CCTATAATTAATCCAAATAATCATTACC-3'^[13]. The amplification was performed under the following modified conditions: pre-denaturation at 95 °C for 5 min; 35 amplification cycles (denature at 95 °C for 15 s; annealing at 53 °C for 15 s; and extension at 72 °C for 30 s) and final extension at 72 °C for 5 min for the first round of PCR. The PCR products were diluted (1:10 dilution) and used in the second round of PCR with the primers: forward 5' -TTGAGAATGTGAGTGATTTGA-3', reverse 5' -AACCAATCCAACCAAAACAA-3' for the unmethylated sequence; and forward 5' -TCGAGAACGCGAGCGATTTCG-3', reverse 5' -GACCAATCCAACCGAAA-CGA-3' for the methylated sequences^[14]. The amplification was performed under following conditions: pre-denaturation at 95 °C for 5 min; 35 amplification cycles (denature at 95 °C for 15 s; annealing at 52 °C for 15 s; and extension at 72 °C for 15 s for U-primers) and pre-denaturation at 95 °C for 5 min; 20 amplification cycles (denature at 95 °C for 15 s; annealing at 62 °C for 15 s; and extension at 72 °C for 15 s M-primers). DNA from normal lymphocytes was used as negative control for methylated alleles, and placental DNA treated *in vitro* with SssI methyltransferase (New England Biolabs, Beverly, MA) was used as positive control for methylated genes. The product of

146 bp was generated, and the PCR products were analyzed on 25g/L agarose gels and photographed. The controls without DNA were performed in each set of PCR, and MSP assay for each sample was repeated at least twice.

Bisulfite sequencing

The PCR products amplified with primers specific either for the methylated or for the unmethylated DNA were purified and cloned into the pMD-T vector (Takara, Dalian, China) according to the manufacture's protocol. Recombinants were transformed into *Escherichia coli*. Plasmid DNA was isolated and integrated PCR fragments were verified by enzyme digestion and PCR. The cloned PCR fragments were further analyzed by automated sequencing (Bioasia, Shanghai, China).

RESULTS

Expression of *RARB2* in ESCC cell lines

The expression of the *RARB2* mRNA was detected in the six ESCC cell lines by RT-PCR. Figure 1 shows representative examples of RT-PCR and MSP results. Markedly downregulation of *RARB2* expression was observed in the cell lines KYSE410, KYSE510 and COLO680N as shown in Figure 1A.

Methylation analysis of the *RARB2* promoter region

Using MSP method, both the methylated and unmethylated alleles were found in the four cell lines except KYSE180 and TE12 in which only the unmethylated alleles were present (Figure 1B). The quantitation of the unmethylated or the methylated products varied in different cell lines. To confirm the reliability of the nested MSP method, PCR products amplified with primers specific either for the methylated (cell lines KYSE410) or for the unmethylated (cell line KYSE180) DNA were cloned and sequenced. Bisulfite sequencing of 4 individual clones of PCR products from cell line KYSE180 revealed no methylation of CpGs within the promoter region, whereas the methylated products showed dense methylation within the CpG islands in cell line KYSE410 (Figure 2).

Association between *RARB2* promoter methylation and downregulation of its expression in ESCC cell lines

The reduction of *RARB2* mRNA expression was observed in three of the four cell lines that had partially methylated alleles, however the another one cell line showed strong *RARB2* gene expression, which suggesting that the aberrant methylation might play other roles except leading to gene silencing.

Restoration of *RARB2* expression after 5-aza-dc treatment

To confirm whether *RARB2* promoter methylation could be further linked to downregulation of its expression, the cancer cell lines which showed evidently decreased expression of *RARB2* and cell line KYSE180 without methylated alleles were treated with the demethylating agent (5-aza-dc). To determine the effects of demethylating agent, we analyzed the methylation status in KYSE410 cells after 5-aza-dc treatment, and partial demethylation was detected by MSP as shown in Figure 3A. In addition, the MSP product was still observed after treatment because 5-aza-dc only inhibited methylation of newly synthesized DNA. The level of *RARB2* mRNA was not changed in cell line KYSE180 before and after demethylating treatment. Among the three cell lines where *RARB2* genes were methylated, the treatment led to up-regulation of *RARB2* mRNA expression only in cell line KYSE410 (Figure 3B). The other two cell lines showed no detectable re-expression of *RARB2* mRNA after 5-aza-dc treatment (data not shown). These data indicated that *RARB2* promoter methylation was closely associated with downregulation of *RARB2* expression in some ESCC cell lines.

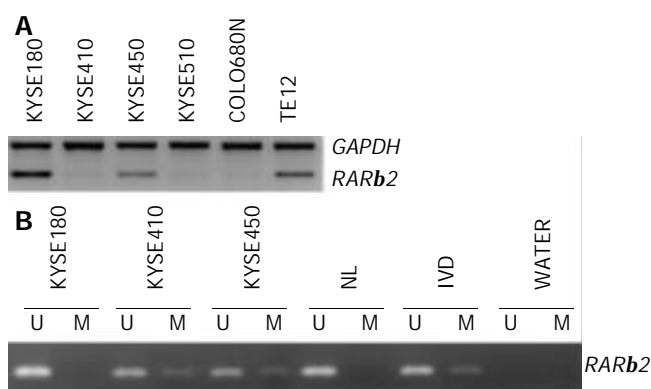


Figure 1 *RARB2* expression and methylation in ESCC cell lines. A: RT-PCR analysis of *RARB2* expression, *GAPDH* was used as internal control. B: MSP analysis of *RARB2* promoter methylation status, (U) lanes and (M) lanes represent amplification of unmethylated and methylated alleles, respectively. *In vitro* methylated DNA (IVD) and normal human peripheral lymphocytes (NL) serve as positive and negative methylation controls, respectively.

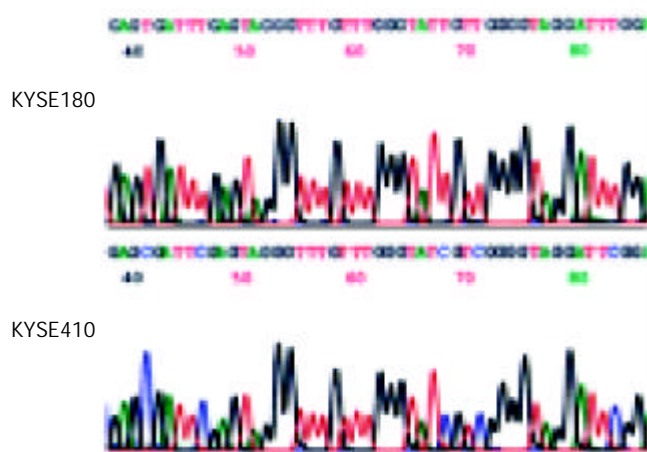


Figure 2 Sodium bisulfite sequencing of *RARB2* in the cell lines that were found to include only unmethylated alleles (cell line KYSE180) or partial methylated alleles (cell line KYSE410) by MSP.

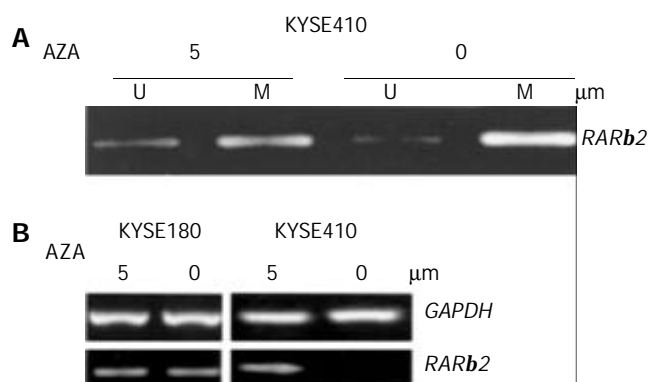


Figure 3 Treatment with the indicated concentrations of 5-aza-dc induced demethylation and *RARB2* mRNA expression in ESCC cell lines. A: MSP analysis shows partial demethylation of the *RARB2* promoter region after 5-aza-dc treatment. B: RT-PCR analysis of *RARB2* mRNA expression before and after 5-aza-dc treatment in cell lines that were found to have either positive (cell line KYSE180) or reduced (cell line KYSE410) baseline *RARB2* expression, *GAPDH* was used as internal control.

DISCUSSION

There were two major *RARB2* antineoplastic mechanisms in breast cancer cell lines, which were RA-dependent and RA-independent apoptosis^[15,16], however little was known how *RARB2* performed its anticancer activity. A growing evidence indicated that *RARB2* was required for the growth inhibitory action of RA. In *RARB2*-negative cancer cells, RA-induced growth inhibition and decreased tumorigenicity could be restored by expression of *RARB2*; on the contrary, in *RARB2*-positive cancer cells, RA effects could be abolished by inhibition of *RARB2* expression^[17-19]. Another study indicated that not only expression but also up-regulation of *RARB* was linked to retinoid sensitivity in esophageal cancer cell lines^[20], and our previous study also suggested that RA resistance in EC109 cells paralleled with the loss of *RARB2* inducibility^[21]. A clinical trial using N-4-(ethoxycarbophenyl) retinamide, a synthetic retinoid, demonstrated that cancer incidence among the treatment groups with severe esophageal dysplasia was decreased by 43.2% compared with the placebo group^[22], whereas this was not the case for recent clinical trials of 13-cis retinoic acid in the treatment of advanced esophageal cancer patients, for which an explanation was that the loss of *RARB* expression could lead to the resistance to treatment with 13-cis RA in esophageal cancer^[23,24]. Recent study suggested that hypermethylation of *RARB* might play an important role in the early stage of esophageal squamous cell carcinogenesis^[25]. However, the mechanisms of *RARB2* suppression remained largely unknown in esophageal cancer.

Genetic and epigenetic mechanisms may be involved in progressive decrease in *RARB2* mRNA expression during esophageal carcinogenesis. *RARB* was localized on chromosome 3p24, and LOH occurred frequently on chromosome arm 3p in many cancers, including esophageal cancer^[2]. However, no correlation was observed between the expression of *RARB* and the LOH on chromosome 3p24 in ESCC; moreover, no mutations or other genetic alterations were found in different cell lines without *RARB2* mRNA expression^[9,26,27]. Thus, other mechanisms for *RARB2* suppression should be considered. DNA methylation, which led to the inactivation of all kinds of essential genes, such as *HLA class I*, *E-cadherin*, *FHIT* and *p16*, was an important mechanism for gene silencing or suppressing in ESCC^[10,28-30]. In addition, Arapshian *et al.*^[31] concluded that methylation of the RARE region might be particularly important in *RARB2* suppression. Data presented in this report demonstrated that epigenetic silencing of the *RARB2* gene promoter might be an important event, and that downregulation of *RARB2* expression was closely associated with *RARB2* gene promoter methylation in some ESCC cell lines. In our study, of the three *RARB2*-downregulated cell lines, only the one poorly differentiated cell line showed evidently re-expression of *RARB2* with the partial demethylation of its promoter region, indicating that repression was, at least in part, mediated by methylation in the poorly differentiated cell lines, and multiple mechanisms were involved in the gene silencing in the other two cell lines. Our results suggested that a relationship between methylation status and decreased *RARB2* expression only existed in some differentiated ESCC cell lines or ESCC. Previous study has demonstrated that for breast carcinoma a relationship between methylation status and decreased *RARB2* expression in breast cancer was found only in invasive grade II lesions^[13]. There was mounting evidence that suggested epigenetic modifications might be a mechanism responsible for the lack of *RARB2* expression in many epithelial cancers or cancer cell lines, such as breast cancer, colon cancer and prostate cancer^[8,13,32,33]. Taken together the further analysis of the cytogenetic data of the cell lines, we found that there was

no deletion in 3p in the cell line exhibiting re-expression of *RARB2*. We therefore speculate that methylation may be at least one of the major mechanisms resulting in loss of *RARB2* expression in such cell lines. It has been reported that in ESCC cell lines without any structural alteration, hypermethylation at CpG sites was the important mechanism for transcription inactivation of the *FHIT* gene^[30]. Given that the *RARB2* gene is recognized as a putative tumor suppressor gene, restoration of its function may have implications for both cancer therapy and prevention.

Notably, demethylation could only lead to the restoration of *RARB2* expression in 1/3 ESCC cell lines without 3p deletion, but not in the other cell lines with 3p deletion, indicating that there were other mechanisms, such as deletion, involved in the loss of *RARB2* expression in ESCC cell lines. It was reported that differential function of coactivators and corepressors might determine the level of *RARB* induction that might mediate retinoid action in colon cancer cells^[34]. In lung cancer cell lines, loss of *RARB* gene expression was linked to aberrant histone H3 acetylation, so the aberrant acetylation status might have effects on *RARB2* expression^[35]. In addition, orphan receptor COUP-TF have been identified to play a key role in modulating *RARB* expression and retinoid sensitivity in cancer cells^[36]. Thus, multiple mechanisms may contribute to the loss of *RARB2*.

In conclusion, this study not only shows a high frequency of methylation of *RARB2* promoter region but also provides the first evidence that downregulation of *RARB2* is closely associated with DNA methylation in ESCC cell lines. These findings will be helpful to further understand the mechanisms underlying tumor progression in ESCC, and subsequently improve the prevention and treatment.

REFERENCES

- 1 **Evans TR**, Kaye SB. Retinoids: present role and future potential. *Br J Cancer* 1999; **80**: 1-8
- 2 **Chambon P**. A decade of molecular biology of retinoic acid receptors. *FASEB J* 1996; **10**: 940-954
- 3 **Collins SJ**, Robertson KA, Mueller L. Retinoic acid-induced granulocytic differentiation of HL-60 myeloid leukemia cells is mediated directly through the retinoic acid receptor (RAR-alpha). *Mol Cell Biol* 1990; **10**: 2154-2163
- 4 **Xu XC**, Lotan R. Aberrant expression and function of retinoic acid receptors in cancer. In Nau H, Blaner WS, editors. *Handbook of experimental pharmacology: retinoids*. Berlin: Springer-Verlag 1999: p323-324
- 5 **Picard E**, Seguin C, Monhoven N, Rochette-Egly C, Siat J, Borrelly J, Martinet Y, Martinet N, Vignaud JM. Expression of retinoic acid receptor genes and proteins in non-small-cell lung cancer. *J Natl Cancer Inst* 1999; **91**: 1059-1066
- 6 **Qiu H**, Zhang W, El-Naggar AK, Lippman SM, Lin P, Lotan R, Xu XC. Loss of retinoic acid receptor-beta expression is an early event during esophageal carcinogenesis. *Am J Pathol* 1999; **155**: 1519-1523
- 7 **Xu XC**, Sneige N, Liu X, Nandagiri R, Lee JJ, Lukmanji F, Hortobagyi G, Lippman SM, Dhingra K, Lotan R. Progressive decrease in nuclear retinoic acid receptor beta messenger RNA level during breast carcinogenesis. *Cancer Res* 1997; **57**: 4992-4996
- 8 **Yang Q**, Mori I, Shan L, Nakamura M, Nakamura Y, Utsunomiya H, Yoshimura G, Suzuma T, Tamaki T, Umemura T, Sakurai T, Kakudo K. Biallelic inactivation of retinoic acid receptor beta2 gene by epigenetic change in breast cancer. *Am J Pathol* 2001; **158**: 299-303
- 9 **Qiu H**, Lotan R, Lippman SM, Xu XC. Lack of correlation between expression of retinoic acid receptor-beta and loss of heterozygosity on chromosome band 3p24 in esophageal cancer. *Genes Chromosomes Cancer* 2000; **28**: 196-202
- 10 **Tanaka H**, Shimada Y, Imamura M, Shibagaki I, Ishizaki K. Multiple types of aberrations in the p16 (INK4a) and the p15 (INK4b) genes in 30 esophageal squamous-cell-carcinoma cell lines. *Int J Cancer* 1997; **70**: 437-442
- 11 **Sambrook J**, Fritsch EF, Maniatis T. Molecular cloning: a laboratory manual. *Cold Spring Harbor Laboratory Press*, NY (1989)
- 12 **Herman JG**, Graff JR, Myohanen S, Nelkin BD, Baylin SB. Methylation-specific PCR: a novel PCR assay for methylation status of CpG islands. *Proc Natl Acad Sci U S A* 1996; **93**: 9821-9826
- 13 **Widschwendter M**, Berger J, Hermann M, Muller HM, Amberger A, Zeschnigk M, Widschwendter A, Abendstein B, Zeimet AG, Daxenbichler G, Marth C. Methylation and silencing of the retinoic acid receptor-beta2 gene in breast cancer. *J Natl Cancer Inst* 2000; **92**: 826-832
- 14 **Ivanova T**, Petrenko A, Gritsko T, Vinokourova S, Eshilev E, Kobzeva V, Kisseljov F, Kisseljova N. Methylation and silencing of the retinoic acid receptor-beta 2 gene in cervical cancer. *BMC Cancer* 2002; **2**: 4
- 15 **Lin F**, Xiao D, Kolluri SK, Zhang X. Unique anti-activator protein-1 activity of retinoic acid receptor beta. *Cancer Res* 2000; **60**: 3271-3280
- 16 **Liu Y**, Lee MO, Wang HG, Li Y, Hashimoto Y, Klaus M, Reed JC, Zhang X. Retinoic acid receptor beta mediates the growth-inhibitory effect of retinoic acid by promoting apoptosis in human breast cancer cells. *Mol Cell Biol* 1996; **16**: 1138-1149
- 17 **Faria TN**, Mendelsohn C, Chambon P, Gudas LJ. The targeted disruption of both alleles of RARbeta(2) in F9 cells results in the loss of retinoic acid-associated growth arrest. *J Biol Chem* 1999; **274**: 26783-26788
- 18 **Houle B**, Rochette-Egly C, Bradley WE. Tumor-suppressive effect of the retinoic acid receptor beta in human epidermoid lung cancer cells. *Proc Natl Acad Sci U S A* 1993; **90**: 985-989
- 19 **Si SP**, Lee X, Tsou HC, Buchsbaum R, Tibaduiza E, Peacocke M. RAR beta 2-mediated growth inhibition in HeLa cells. *Exp Cell Res* 1996; **223**: 102-111
- 20 **Xu XC**, Liu X, Tahara E, Lippman SM, Lotan R. Expression and up-regulation of retinoic acid receptor-beta is associated with retinoid sensitivity and colony formation in esophageal cancer cell lines. *Cancer Res* 1999; **59**: 2477-2483
- 21 **Liu G**, Wu M, Levi G, Ferrari N. Inhibition of cancer cell growth by all-trans retinoic acid and its analog N-(4-hydroxyphenyl) retinamide: a possible mechanism of action via regulation of retinoid receptors expression. *Int J Cancer* 1998; **78**: 248-254
- 22 **Han J**. Highlights of the cancer chemoprevention studies in China. *Prev Med* 1993; **22**: 712-722
- 23 **Roth AD**, Morant R, Alberto P. High dose etretinate and interferon-alpha-a phase I study in squamous cell carcinomas and transitional cell carcinomas. *Acta Oncol* 1999; **38**: 613-617
- 24 **Slabber CF**, Falkson G, Burger W, Schoeman L. 13-Cis-retinoic acid and interferon alpha-2a in patients with advanced esophageal cancer: a phase II trial. *Invest New Drugs* 1996; **14**: 391-394
- 25 **Kuroki T**, Trapasso F, Yendamuri S, Matsuyama A, Alder H, Mori M, Croce CM. Allele loss and promoter hypermethylation of VHL, RAR-beta, RASSF1A, and FHIT tumor suppressor genes on chromosome 3p in esophageal squamous cell carcinoma. *Cancer Res* 2003; **63**: 3724-3728
- 26 **Bartsch D**, Boye B, Baust C, zur Hausen H, Schwarz E. Retinoic acid-mediated repression of human papillomavirus 18 transcription and different ligand regulation of the retinoic acid receptor beta gene in non-tumorigenic and tumorigenic HeLa hybrid cells. *EMBO J* 1992; **11**: 2283-2291
- 27 **Hu L**, Crowe DL, Rheinwald JG, Chambon P, Gudas LJ. Abnormal expression of retinoic acid receptors and keratin 19 by human oral and epidermal squamous cell carcinoma cell lines. *Cancer Res* 1991; **51**: 3972-3981
- 28 **Nie Y**, Yang G, Song Y, Zhao X, So C, Liao J, Wang LD, Yang CS. DNA hypermethylation is a mechanism for loss of expression of the HLA class I genes in human esophageal squamous cell carcinomas. *Carcinogenesis* 2001; **22**: 1615-1623

- 29 **Si HX**, Tsao SW, Lam KY, Srivastava G, Liu Y, Wong YC, Shen ZY, Cheung AL. E-cadherin expression is commonly downregulated by CpG island hypermethylation in esophageal carcinoma cells. *Cancer Lett* 2001; **173**: 71-78
- 30 **Tanaka H**, Shimada Y, Harada H, Shinoda M, Hatooka S, Imamura M, Ishizaki K. Methylation of the 5' CpG island of the FHIT gene is closely associated with transcriptional inactivation in esophageal squamous cell carcinomas. *Cancer Res* 1998; **58**: 3429-3434
- 31 **Arapshian A**, Kuppumbatti YS, Mira-y-Lopez R. Methylation of conserved CpG sites neighboring the beta retinoic acid response element may mediate retinoic acid receptor beta gene silencing in MCF-7 breast cancer cells. *Oncogene* 2000; **19**: 4066-4070
- 32 **Cote S**, Sinnett D, Momparler RL. Demethylation by 5-aza-2'-deoxycytidine of specific 5-methylcytosine sites in the promoter region of the retinoic acid receptor beta gene in human colon carcinoma cells. *Anticancer Drugs* 1998; **9**: 743-750
- 33 **Nakayama T**, Watanabe M, Yamanaka M, Hirokawa Y, Suzuki H, Ito H, Yatani R, Shiraishi T. The role of epigenetic modifications in retinoic acid receptor beta2 gene expression in human prostate cancers. *Lab Invest* 2001; **81**: 1049-1057
- 34 **Lee MO**, Kang HJ. Role of coactivators and corepressors in the induction of the *RAR* beta gene in human colon cancer cells. *Biol Pharm Bull* 2002; **25**: 1298-1302
- 35 **Suh YA**, Lee HY, Virmani A, Wong J, Mann KK, Miller WH Jr, Gazdar A, Kurie JM. Loss of retinoic acid receptor beta gene expression is linked to aberrant histone H3 acetylation in lung cancer cell lines. *Cancer Res* 2002; **62**: 3945-3949
- 36 **Lin B**, Chen GQ, Xiao D, Kolluri SK, Cao X, Su H, Zhang XK. Orphan receptor COUP-TF is required for induction of retinoic acid receptor beta, growth inhibition, and apoptosis by retinoic acid in cancer cells. *Mol Cell Biol* 2000; **20**: 957-970

Edited by Gupta MK **Proofread by** Xu FM

Expression of heparanase gene, CD44v6, MMP-7 and *nm23* protein and their relationship with the invasion and metastasis of gastric carcinomas

Jun-Qiang Chen, Wen-Hua Zhan, Yu-Long He, Jun-Sheng Peng, Jian-Ping Wang, Shi-Rong Cai, Jin-Ping Ma

Jun-Qiang Chen, Wen-Hua Zhan, Yu-Long He, Jun-Sheng Peng, Jian-Ping Wang, Shi-Rong Cai, Jin-Ping Ma, Department of Gastrointestinal Surgery, The First Affiliated Hospital, Sun Yat-sen University, Guangzhou 510080, Guangdong Province, China
Supported by the National Natural Science Foundation of China, No. 30271276

Correspondence to: Dr. Wen-Hua Zhan, Department of Gastrointestinal Surgery, the First Affiliated Hospital, Sun Yat-sen University, Guangzhou 510080, Guangdong Province, China. wzwk@gzsums.edu.cn
Telephone: +86-20-87755766 Ext 8211 **Fax:** +86-20-87335945
Received: 2003-11-17 **Accepted:** 2003-12-16

Abstract

AIM: To explore the expression of heparanase gene, CD44v6, MMP-7 and *nm23* proteins in human gastric carcinoma as well as their relationship with the clinicopathological factors.

METHODS: Reverse transcription polymerase chain reaction (RT-PCR) was used to measure the expressions of heparanase mRNA in 43 human gastric carcinomas and 10 adjacent normal gastric tissues. Streptavidin-peroxidase (S-P) two step method was used to measure the immunohistochemical expression of CD44v6, MMP-7 and *nm23* protein in 43 human gastric carcinomas.

RESULTS: The expression of heparanase gene was positive in 29 cases of gastric cancer with a positive rate of 67.4%, which was significantly higher than those in adjacent normal gastric tissues ($P < 0.05$). The heparanase mRNA expression was significantly related to advanced stage of disease, serosal infiltration, lymph node metastasis and size of tumors ($P < 0.05$), but not related to tumor location, gross and histological types of the cancer, peritoneal dissemination and liver metastasis ($P > 0.05$). The positive rate of CD44v6, *nm23* and MMP-7 proteins was 76.7%, 37.2% and 60.5%, respectively. The CD44v6 protein expression was significantly related to serosal infiltration, lymph node metastasis and TNM stage of disease ($P < 0.05$). The *nm23* protein expression was significantly related to the tumor gross appearance, lymph node and peritoneal metastasis ($P < 0.05$). The MMP-7 protein expression was significantly related to serosal infiltration and TNM stage of disease ($P < 0.05$). In an attempt to measure the association between these agents, we found that the expression of heparanase mRNA had significantly negative correlation with the expression of CD44v6 and MMP-7 protein ($P < 0.05$), the expression of MMP-7 protein had significantly positive correlation with the expression of CD44v6 protein ($r = 0.568$, $P < 0.05$), the expression of MMP-7 protein had no correlation with the expression of *nm23* protein ($P > 0.05$), and the expression of *nm23* protein had no correlation with the expression of CD44v6 protein ($P > 0.05$).

CONCLUSION: Despite their different mechanisms of action, heparanase, CD44v6 and *nm23* may play important roles in the invasive infiltration and lymph node metastasis

in gastric carcinomas. Instead of metastatic spreading, MMP-7 may be just related to the invasion of gastric carcinomas. However, co-detection of these factors may be important to predict metastatic spreading in such patients.

Chen JQ, Zhan WH, He YL, Peng JS, Wang JP, Cai SR, Ma JP. Expression of heparanase gene, CD44v6, MMP-7 and *nm23* protein and their relationship with the invasion and metastasis of gastric carcinomas. *World J Gastroenterol* 2004; 10(6): 776-782
<http://www.wjgnet.com/1007-9327/10/776.asp>

INTRODUCTION

Invasion and metastasis of gastric carcinomas involve many processes including adherence, degradation, motility, and angiogenesis and escaping from immune surveillance. However, the penetration through the barrier formed by the basement membrane (BM) and extracellular matrix (ECM) is critical for invasion and metastasis of cancerous cells. This barrier is mainly composed of structural proteins and glycosaminoglycans. The former mainly includes collagen, laminin and fibronectin, whereas the latter chiefly consists of heparan sulfate proteoglycans (HSPGs) which is formed by a core protein and several covalent-binding heparan sulfate (HS) side chains. In the past decade, the damage of structural proteins has been considered to be a critical step for tumors' invasion and metastasis^[1-3]. Previous researches mostly focused on property of some enzymes such as matrix metalloproteinases (MMPs) which use structural proteins as substrates. However, we should never neglect the effect of hydrolytic enzymes which use HSPGs as substrates, as well as their roles in degrading the BM and ECM. Heparanase is an endoglycosidase cloned out by Vlodaysky *et al* in 1999, which degrades the HS chain of HSPGs^[1,2]. Recently, protein or messenger RNA (mRNA) expression of heparanase has been identified in various cancer cells, and the overexpression of heparanase protein or mRNA in tumour cells has been reported to correlate with the metastatic potential of tumour cells *in vitro* and *in vivo* as well as with poor prognosis^[4-7]. However its role in gastric carcinomas is still not clearly clarified. In the present study, the expression of heparanase mRNA in gastric carcinomas and its correlation with clinicopathological features were investigated.

nm23, a metastasis suppressor gene, was reported to be associated with the tumor invasion and metastasis^[8,9]. CD44v6, a highly glycosylated cell surface protein, was reported to be involved in cell-cell and cell-matrix interactions and thought to take part in cell motility, tumor growth, and invasion^[10]. MMP-7, a member of matrix metalloproteinases family, was reported to play an important role in the degradation of connective tissue which is associated with the development of tumor metastases^[11]. However, their roles in gastric carcinomas have not been clearly illustrated. In current study, CD44v6, *nm23* and MMP-7 protein expression in gastric carcinomas and their relationship with each other were also investigated.

MATERIALS AND METHODS

Patients

Between Oct 2002 and May 2003, 43 patients with gastric carcinoma underwent radical gastrectomy (D2 or D3), as subtotal or total gastrectomy in the Department of Gastrointestinal Surgery at the First Affiliated Hospital of Sun Yat-sen University. The age and sex of the patients, as well as the location, macroscopic type, histological grade, stage and depth of the invasion of the tumor, histological lymph node metastasis, and type of surgical procedures were retrieved from the patients' records. Pathological diagnosis and classifications were done according to the UICC standard published in 1997. Histological grouping based on UICC TNM classification was confirmed by histological examination.

mRNA extraction

The gastric tissues were obtained from those duly informed patients whose consents were obtained for the use of their subsequent resected tissues. The present study conformed to regulations of the Ethic Committee of the First Affiliated Hospital of Sun Yat-sen University. Tissue samples of approximately 1 g were collected immediately after each gastrectomy. Non-cancerous gastric tissues were obtained from regions distant from the tumours. Half of the both cancerous and non-cancerous tissues were fixed in 40g/L buffered formaldehyde and embedded in paraffin. Sections (4 mm thick) were prepared with haematoxylin-eosin staining for histopathological diagnosis and with immunohistochemical staining. The other half of the tissues was stored in RNAlater (Sigma, USA) at 4 °C overnight, then transferred to a clean freezing tube and stored at -80 °C for mRNA extraction. Before starting the study, histopathological examination had confirmed that no cancerous cells had contaminated the non-cancerous gastric tissues. Total RNA from tissues was isolated using RNeasy Mini Kits (Qiagen, USA) according to the manufacturer's protocol. Complementary DNA (cDNA) was synthesized from 2 µg of total RNA in a 25 µL reaction mixture. The 25 µL reaction mixture contained 2 µg RNA solution, 1 µL oligo d(T)18 (0.5 µg/µL), 1 µL M-MLV reverse transcriptase (Promega, USA), 1 µL RNasin ribonuclease inhibitor (Promega, USA) and 2 µL dNTP. The integrity of RNA was checked electrophoretically and quantified spectrophotometrically.

Real-time reverse transcription^[6,12,13]

The following primers such as forward primer 5' -TTC GAT CCC AAG AAG GAA TCA AC-3' and reverse primer 5' -GTA GTG ATG CCA TGT AAC TGA ATC-3' were used for heparanase. The PCR reaction was run for 40 cycles under the following conditions: denaturation at 94 °C for 3 min, denaturation at 94 °C for another 30 s, annealing at 50 °C for 30 s and extension at 72 °C for 1 min with an extra 10-min extension for the last cycle. We determined the nucleotide sequence of this PCR product and confirmed that it was identical to the expected fragment of cDNA of heparanase. Glyceraldehyde-3-phosphate dehydrogenase (GAPDH) transcripts were monitored as a control to quantify the transcripts of the genes in each sample. GAPDH-specific sequences were amplified using the forward primer 5' -CAG GGG GGA GCC AAA AGG-3', reverse primer 5' -GGC AGT GGG GAC ACG GAA-3', which yielded a 378-bp product. After completion of these amplification cycles, 10 µL of each PCR product was electrophoresed at 50-80V for 30-40 minutes on a 10g/L agarose gel in Tris boric acid EDTA buffer together with 100 bp DNA ladder marker (TaKaRa Biotechnology(Dalian) Co.,Ltd) and was stained with ethidium bromide.

Immunohistochemistry

Streptavidin-peroxidase (S-P) two step method was used for

the immunohistochemical detection of CD44v6, *nm23* and MMP-7 proteins. Immunohistochemical detection of CD44v6, *nm23* and MMP-7 was performed with monoclonal antibodies (Maixin Biological, Fuzhou, China) against CD44v6, MMP-7 and *nm23*/NDP kinase.

The sections were first washed for 3 min with phosphate buffered saline (PBS) 3 times and then blocked with a solution of 30mL/L hydrogen peroxide in ethanol for 10 min at room temperature. After that they were immersed in 30mL/L normal horse serum for 10 min also at room temperature. Primary antibodies to CD44v6, *nm23* and MMP-7 were incubated for 1 h at room temperature. The ultrasensitive S-P kit (Maixin Biological, Fuzhou, China) was used to detect the resulting immune complex. The procedures of blocking, linkage, and labeling of binding reaction were carried out according to manufacturer's instructions. The peroxidase activity was visualized by DAB kit (Maixin Biological, Fuzhou, China), the sections were finally counterstained with hematoxylin and the negative control was processed by incubation with non-immune rabbit IgG in substitution for the primary antibody.

To evaluate the expression of CD44v6, only cell membrane staining equivalent to normal control was considered positive, while for *nm23* and MMP-7, only cytoplasmic staining equivalent to normal control was considered positive. Slides were examined and scored by two pathologists ignorant of the clinical details. Those slides exhibiting diffuse immunostaining or presenting more than 50% of tumor cells were classified as (++), more than 10% but less than 50% as (+) and those with immunoreactivity less than 10% were classified as (-). (+) and (++) were combined together as positive cases for statistical analysis.

Statistics

Statistical analyses were done with the SPSS 10.0 for Windows program. Frequency tables were analyzed with the Pearson Chi-square test or Fisher's exact test. The relationships between heparanase and *nm23* and CD44v6 and MMP-7 in gastric tumor tissues were evaluated statistically using the Kendall rank correlation test. Statistical differences with *P* values less than 0.05 by two-tailed tests were considered significant.

RESULTS

Clinical findings

The subjects included 26 men and 17 women. Their average age at the time of surgery was 58.5±13.4 years (ranging from 29 to 86 years). Ten cases of gastric cancer located at the upper third of the stomach, 7 at the middle third and 26 at the lower third. Of these 43 patients, 3 had peritoneal metastasis, 2 had liver metastasis, 35 had serosal invasion, and 27 had lymph node metastasis. Histopathological diagnoses of the patients were made according to the guidelines for classification of the primary gastric cancer. Thirty patients were classified as adenocarcinoma, 5 as mucinous carcinoma and 8 as signet-ring cell carcinoma. For histological differentiation, 4 were well differentiated, 10 were moderate differentiated and 29 were poorly differentiated. For TNM staging, 6 patients belonged to stage I, 8 belonged to stage II, 13 belonged to stage III, and 16 belonged to stage IV. None of the patients had received preoperative chemotherapy.

Relationship between heparanase gene expression and clinicopathological features in gastric carcinomas

The expression of heparanase mRNA was positive in 29 cases of gastric cancer with a positive rate of 67.4%. While its expression rate in the 10 cases of non-cancerous gastric tissues

was 10.0% (1 case). The difference was statistically significant ($P < 0.05$) (Figure 1).

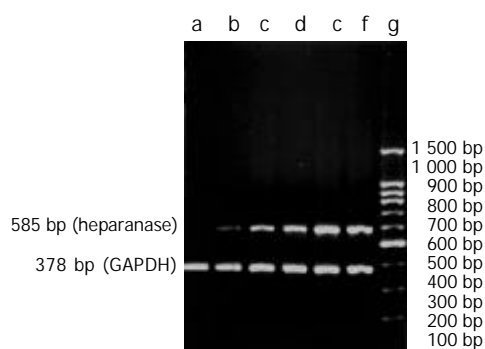


Figure 1 Expression of heparanase mRNA in gastric carcinomas. a: non-cancerous tissue, b-f: cancerous tissue, g: marker (100 bp DNA ladder marker).

From Table 1, we could find that the mRNA expression of heparanase was not correlated with tumor location, gross appearance, histological characteristics, peritoneal dissemination and liver metastasis ($P > 0.05$). It was correlated with tumor size, serosal infiltration, lymph node metastasis, distant metastasis and TNM staging of gastric carcinomas ($P < 0.05$). In 14 cases of negative expression of heparanase mRNA, only 5 cases had lymph node metastasis. However, in 29 cases of positive expression of heparanase mRNA, twenty-two had lymph node metastasis, among which N₁ was in 11 cases, N₂ in 3 cases and N₃ in 8 cases. The difference between these two groups was statistically significant ($P < 0.05$).

Relationship between CD44v6, nm23 and mmp-7 protein expression and clinicopathological features in gastric carcinomas

The expression of CD44v6 protein was positive in 33 cases of gastric cancer with a positive rate of 76.7% and the intensity of its immunoreactivity in cancer tissue was scored as (+) in 27

Table 1 Relationship between clinicopathological features and heparanase mRNA expression and CD44v6, nm23 and MMP-7 protein expression in primary gastric carcinomas

Clinicopathological features	Number of patients											
	Heparanase			CD44v6			nm23			MMP-7		
	(+)	(-)	<i>P</i> value	(+)	(-)	<i>P</i> value	(+)	(-)	<i>P</i> value	(+)	(-)	<i>P</i> value
Gender			0.307			0.481			0.280			0.415
Female	13	4		12	5		8	9		9	8	
Male	16	10		21	5		8	18		17	9	
Tumor location			0.216			0.346			0.903			0.804
Upper third	9	1		9	1		4	6		6	4	
Middle third	4	3		6	1		3	4		5	2	
Lower third	16	10		18	8		9	17		15	11	
Gross type			0.242			0.325			0.025			0.121
Borrmann I	1	0		1	0		0	1		1	0	
Borrmann II	4	5		5	4		7	2		5	4	
Borrmann III	21	9		25	5		9	21		20	10	
Borrmann IV	3	0		2	1		0	3		0	3	
Histologic type			0.671			0.297			0.444			0.325
Adenocarcinoma	19	11		23	7		13	17		20	10	
Mucinous carcinoma	4	1		5	0		1	4		3	2	
Signet-ring cell carcinoma	6	2		5	3		2	6		3	5	
Peritoneal metastasis			0.539			1.000			0.045			0.266
Absent	26	14		30	10		13	27		23	17	
Present	3	0		3	0		3	0		3	0	
Liver metastasis			1.000			1.000			0.133			0.511
Absent	27	14		31	10		14	27		24	17	
Present	2	0		2	0		2	0		2	0	
Histologic differentiation			1.000			0.704			0.888			0.101
Well/moderate	9	5		10	4		5	9		6	8	
Poorly	20	9		23	6		11	18		20	9	
Serosal invasion			0.009			0.010			0.101			0.042
Absent	2	6		3	5		5	3		2	6	
Present	27	8		30	5		11	24		24	11	
Lymph node metastasis			0.018			0.024			0.008			0.084
Absent	7	9		9	7		10	6		7	9	
Present	22	5		24	3		6	21		19	8	
Distant metastasis			0.039			0.656			0.125			1.000
Absent	21	14		26	9		11	24		21	14	
Present	8	0		7	1		5	3		5	3	
TNM stage			0.001			0.001			0.228			0.021
I-II	4	10		6	8		7	7		5	9	
III-IV	25	4		27	2		9	20		21	8	

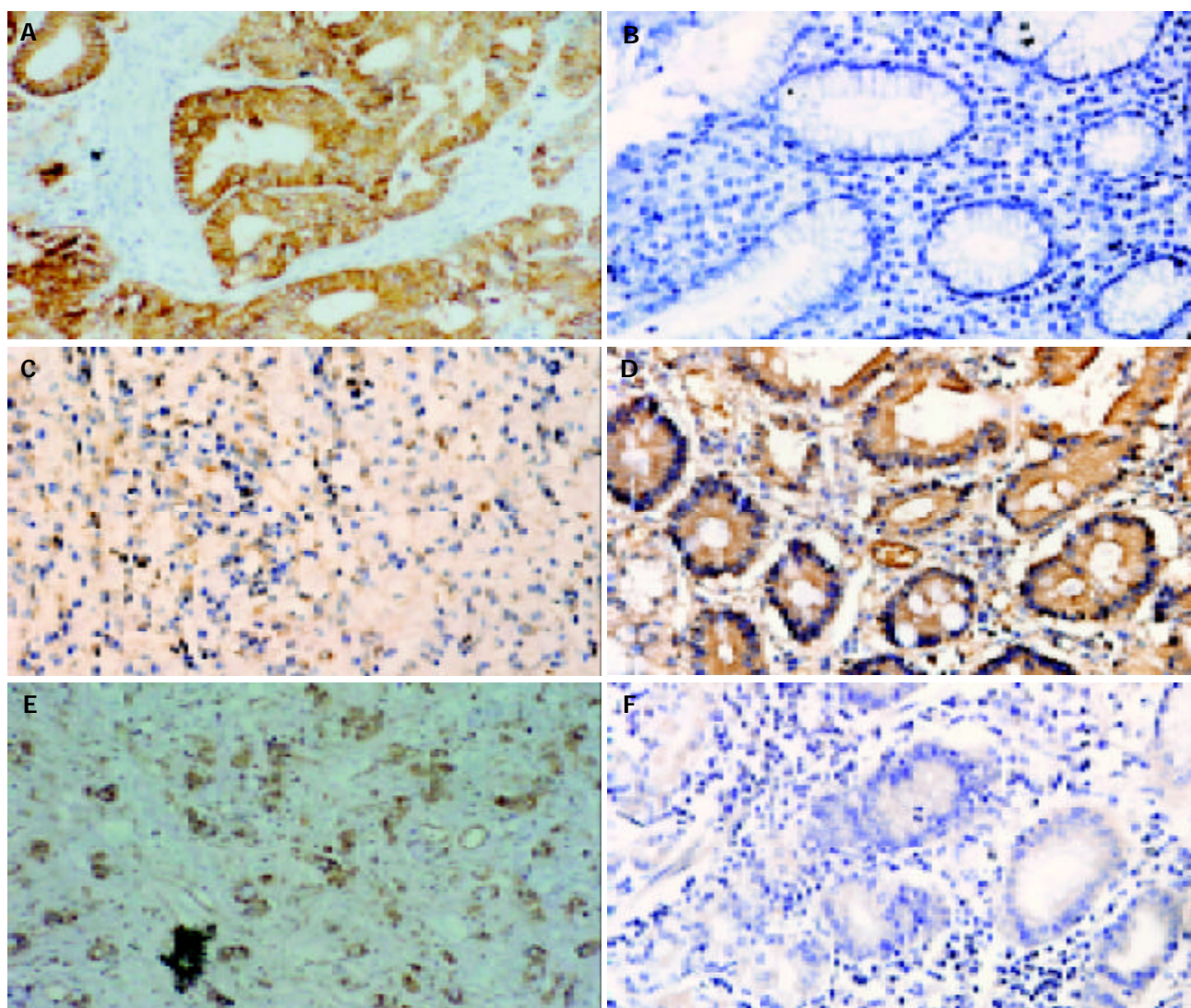


Figure 2 Expression of CD44v6, *nm23* and MMP-7 protein in gastric carcinomas and non-cancerous gastric tissues. A: gastric carcinoma stained for CD44v6($\times 400$), B: non-cancerous gastric tissue stained for CD44v6($\times 400$), C: gastric carcinoma stained for *nm23* ($\times 400$), D: non-cancerous gastric tissue stained for *nm23* ($\times 400$), E: gastric carcinoma stained for MMP-7 ($\times 400$), F: non-cancerous gastric tissue stained for MMP-7 ($\times 400$).

patients and (++) in 6 patients. The expression of *nm23* protein was positive in 16 cases of gastric cancer with a positive rate of 37.2% and the intensity of its immunoreactivity in cancer tissue was scored as (+) in 10 patients and (++) in 6 patients. The expression of MMP-7 protein was positive in 26 cases of gastric cancer with a positive rate of 60.5% and the intensity of its immunoreactivity in cancer tissue was scored as (+) in 20 patients and (++) in 6 patients (Figure 2).

The expression of CD44v6 protein was significantly correlated with lymph node metastasis, TNM staging and serosal infiltration ($P < 0.05$). The expression of *nm23* protein was significantly correlated with the tumor gross appearance, peritoneal metastasis and lymph node metastasis ($P < 0.05$). The expression of MMP-7 protein was significantly correlated with serosal invasion and TNM staging (Table 1).

Correlation between heparanase mRNA expression and CD44v6, *nm23* and MMP-7 protein expression

The expression of heparanase mRNA had significant negative correlation with the expression of CD44v6 and MMP-7 protein ($P < 0.05$) (Table 2). The expression of MMP-7 protein had significant positive correlation with the expression of CD44v6 protein ($\gamma = 0.568$, $P < 0.01$). The expression of MMP-7 protein had no correlation with the expression of *nm23* protein ($P > 0.05$).

The expression of *nm23* protein had no correlation with the expression of CD44v6 protein ($P > 0.05$).

Table 2 Correlation between the expression of heparanase mRNA and the expression of CD44v6, *nm23* and MMP-7 protein

Items	Number of cases	Heparanase (+)	Correlation coefficient	<i>P</i> value
CD44v6			-0.440	0.004
(-)	10	3		
(+)	33	26		
<i>Nm23</i>			-0.021	0.889
(-)	27	18		
(+)	16	11		
MMP-7			-0.352	0.023
(-)	17	8		
(+)	26	21		

DISCUSSION

In normal human tissues, heparanase mRNA is chiefly distributed in placenta and lymphatic tissues. Contrarily in the connective tissues and most of the epithelial cell, its expression is rare or even absent^[1-3]. Vlodayvsky *et al.*^[1] confirmed that

heparanase could promote the metastasis of tumor by gene transfection experiments. They transfected non-metastatic Eb cells with a full-length human heparanase cDNA using a pcDNA3 expression plasmid. As a result, the transfected cells expressed high levels of heparanase mRNA and high heparanase activity. Ninety percent of the DBA/2 mice injected with heparanase-transfected Eb cells died by d 34, whereas 60% of the mice inoculated with mock-transfected cells were alive at that time. The livers of mice inoculated with heparanase-transfected cells were infiltrated with numerous Eb lymphoma cells. In contrast, metastatic lesions could not be detected by gross examination in the liver of the mice with mock-transfected and control Eb cells. Few or no lymphoma cells infiltrated the liver tissue. Furthermore, transient transfection of the heparanase gene into B16-F1 mouse melanoma cells with low metastatic potential followed by intravenous inoculation resulted in a 400-500% increase in lung metastases. All these implied that heparanase might play an important role in tumor invasion and metastasis.

In the present study, the positive rate of heparanase mRNA expression in gastric carcinomas (67.4%) was significantly higher than that of non-cancerous gastric tissues (10%) ($P < 0.05$). Heparanase mRNA tended to express more in those patients with serosal invasion, lymph node metastasis, advanced stage of diseases, distant metastasis and larger size of tumors ($P < 0.05$). The results indicated that heparanase mRNA was closely related with the clinicopathological features that reflected the invasion and metastatic potential and prognosis. Up to now, invasion depth, lymph node metastasis or distant metastasis and TNM stage were considered to be the prognostic factors for gastric carcinomas^[14,15]. That heparanase mRNA expression statistically related with these factors implied that the invasion and metastasis induced by heparanase might indicate a poor prognosis of the gastric carcinomas. This needs to be confirmed by further survival analysis.

According to the researches on other kinds of carcinomas, the mechanisms by which heparanase accelerates invasion and metastasis can be summarized as the following two points. First, heparanase is responsible for degrading HSPGs side chain HS which is the chief component of the BM and ECM but not degraded by MMPs. Second, the degradation of HSPGs by heparanase leads to the release of various growth factors and cytokines trapped in HSPGs which regulate the angiogenesis, tissue repair, inflammation and lipid metabolism^[12,16,17]. In our study, we observed that heparanase mRNA expression often occurred in patients with serosal infiltration and advanced stage of disease, which might imply the important role of heparanase in damaging and penetrating the BM in gastric carcinomas.

The metastasis in gastric carcinomas occurs not only through lymphatic and hematogenous ways but also by direct infiltration. It is still unknown of the definite roles of heparanase in the metastasis of gastric carcinomas. We found none of the patients with liver metastasis expressed heparanase mRNA, while those with lymph node metastasis were significantly related with the expression of heparanase mRNA ($P < 0.05$). We supposed that heparanase was involved in lymphatic metastasis of gastric carcinomas instead of hematogenous metastasis. To draw a further conclusion, larger sample investigations on gastric carcinoma are needed, since the cases with liver metastasis in our study were few. However, Endo *et al.*^[12] found there was no correlation between heparanase expression and lymph node metastasis in gastric carcinomas. In their study, 65%(20/31) patients with positive expression of heparanase mRNA had venous metastasis, compared with 47%(15/32) in negative mRNA expression. They thought heparanase was involved in hematogenous metastasis of gastric carcinomas instead of lymphatic metastasis.

The *nm23* was the first identified metastasis suppressor

gene. In 1988, Steeg *et al.*^[18] discovered murine *nm23* cDNA by using differential colony hybridization between murine K-1735 melanoma cell lines that varied in metastatic potential *in vivo*. They found that the *nm23* mRNA levels of two low metastatic potential cell lines were quantitatively higher than that of five related but highly metastatic cell lines. Later, the examination of protein levels exhibited a similar pattern^[19]. This discovery aroused much interest in the role of *nm23* in progression of carcinomas. Up to now, eight members of the human *nm23* family have been reported and are found in multiple subcellular compartments. Homologs in other species are known as nucleoside diphosphate kinases (NDP kinase or ndpk) or, in *Drosophila*, as abnormal wing discs (awd)^[20]. Two highly homologous genes have been described so far, both located at the long arm of chromosome 17, coding for the 18.5 and 17 kD proteins *nm23-H1* and *nm23-H2*, respectively. The *nm23-H1* and *nm23-H2* gene products have been shown to be identical to human nucleoside diphosphate (NDP) kinases A and B^[19]. *nm23* has been considered as an antimetastatic gene for most malignancies, but the role of *nm23* gene in gastric carcinomas is still not completely known.

In our study, we found that *nm23* had a significant association with lymph node metastasis and peritoneal dissemination. In 27 patients with lymph node metastasis 21 were *nm23* negative, while in 16 patients without lymph node metastasis only 6 were *nm23* negative. The difference was statistically significant ($P < 0.01$). In 40 patients without peritoneal metastasis, 27 were *nm23* negative, but in 3 patients with peritoneal metastasis all were *nm23* positive. The difference was also statistically significant ($P < 0.05$). It indicates that *nm23* suppresses lymphatic metastasis and peritoneal metastasis in gastric carcinomas. Our study also demonstrated that decreased expression of *nm23* was related to tumor's gross type. Other researches showed similar results and proposed *nm23* was related to 5 year survival of the patients^[21]. However Yoo *et al.*^[22] found there was no significant difference in 5-year survival rates between patients with *nm23*-positive and *nm23*-negative tumors ($P > 0.05$) and denied *nm23* to be a predictor of outcome of patients with gastric carcinomas.

CD44 is a highly glycosylated cell surface protein. In normal tissues, CD44 is expressed in a variety of epithelial and mesenchymal cells, as well as in blood cells and glial cells of the central nervous system^[10,23]. Tremendous interest in CD44 was generated when Gunthert and colleagues conferred metastatic potential on a non-metastatic cell line by transfecting a variant of CD44^[23,24]. CD44 has two isoforms, one has been termed CD44 standard (CD44s) and the other CD44 variant (CD44v). The mRNA of CD44s contains no variant exons, while CD44v may contain one or more variant regions, such as CD44v6 or CD44v3-v7. CD44v6 now is considered to be involved in cell-cell and cell-matrix interactions and take part in cell motility, tumour growth, invasion and metastasis^[10,23,25].

Our results demonstrated that CD44v6 was significantly related to lymph node metastasis, serosal invasion and TNM stage. Twenty-four out of 27 patients with lymph node metastases were CD44v6 positive, while 9 out of 16 patients without lymph node metastasis were CD44v6 positive. The difference was statistically significant ($P < 0.05$). Twenty-seven out of 29 stage III and IV patients were CD44v6 positive but only 6 out of 14 stage I and II patients were CD44v6 positive. Their difference was also statistically significant ($P < 0.05$). These indicated that CD44v6 might be a useful predictor of lymph node metastasis in gastric carcinomas. Joo *et al.*^[26,27] obtained almost the same results as ours. But Yamaguchi *et al.*^[28] tended to consider CD44v6 protein to have an important role in hematogenous metastasis of gastric carcinomas.

MMPs are a family of zinc-dependent endoproteinases whose enzymatic activity is directed against components of

the ECM. Up to now, 24 different vertebrate MMPs have been identified, of which 23 are found in humans. On the basis of substrate specificity, sequence similarity, and domain organization, vertebrate MMPs can be divided into six groups: collagenases; gelatinases; stromelysins; membrane-type MMPs; matrilysins and other MMPs. MMP-7 is also called matrilysin^[29,30]. The mechanism of MMP-7 in gastric carcinomas is still unclear. Our study demonstrated that only serosal invasion and advanced stage of disease were closely related to MMP-7 protein expression and it had no correlation with other clinicopathological features. In 26 MMP-7 positive cases, 24 cases had serosal invasion while for 17 MMP-7 negative cases, only 11 cases had serosal invasion ($P < 0.05$). Yonemura *et al.*^[31] found MMP-7 had not only significant positive correlation with serosal involvement but also with lymph node metastasis, poor differentiation and peritoneal dissemination. Patients with MMP-7-positive tumor had significantly poorer survival and more frequently died of peritoneal recurrence than did those with MMP-7-negative tumors. So MMP-7 was considered to be a good indicator of peritoneal dissemination. This was confirmed later by the study using MMP-7-specific antisense oligonucleotide which could inhibit peritoneal dissemination in human gastric cancer^[32]. However, our study did not show any correlation between MMP-7 expression and peritoneal metastasis.

According to the studies on other kinds of carcinomas, MMPs facilitate tumor cell invasion and metastasis by at least three distinct mechanisms. First, proteinase removes physical barriers to invasion through degradation of ECM macromolecules such as collagens, laminins, and proteoglycans. Second, MMPs have the ability to modulate cell adhesion. Finally, MMPs may act on ECM components or other proteins to unknown hidden biologic activities^[11]. Liu *et al.*^[33] investigated immunohistochemically MMP-7 expression in 214 gastric carcinomas and found MMP-7-positive tumor cells were preferentially found in deeply invading nests, especially at the invasive front. The mean MMP-7 labeling index (LI) at the invasive front was significantly higher in tumors invading or penetrating the muscularis propria and in stages II - IV than within the submucosal layer and in stage I, respectively ($P < 0.001$). Our study also showed serosal invasion and advanced stage of disease were closely related to MMP-7 protein expression. Liu *et al.*^[34] also found Ki-67 antigen, an indicator of cell proliferation, was absent in MMP-7 positive tumor cells and vice versa and concluded that MMP-7 expression was related inversely with proliferative activity of tumor cells. So it could be deduced that MMP-7 might participate in the penetration of BM and ECM in gastric carcinomas instead of promoting cell proliferation. Recently, two studies demonstrated that MMP-7 upregulation was closely related with the *H. pylori* cag pathogenicity island and this implied a certain role of MMP-7 in carcinogenesis of gastric carcinomas^[35,36].

Invasion and metastasis of gastric carcinomas are a multistep process. As far as we know, the relationship between heparanase, CD44v6, *nm23* and MMP-7 has not been reported. In our study, we found the expression of heparanase mRNA had significant negative correlation with the expression of CD44v6 and MMP-7 protein. Although heparanase and MMPs both acted on BM and ECM, their substrates were different. Heparanase mainly used HS as substrate while MMPs mainly used structural proteins as substrates. This might account for the negative correlation between the expression of heparanase mRNA and MMP-7 protein. But what exactly caused this is worthy of further studying. That the expression of MMP-7 protein had significant positive correlation with the expression of CD44v6 protein further confirmed that MMPs have the ability to modulate cell adhesion. Why there was no correlation

between the expression of MMP-7 and *nm23* protein? Might it be caused by their different mechanisms? Further studies will be needed to elucidate their relationship in tumors.

REFERENCES

- Vlodavsky I**, Friedmann Y, Elkin M, Aingorn H, Atzmon R, Ishai-Michaeli R, Bitan M, Pappo O, Peretz T, Michal I, Spector L, Pecker I. Mammalian heparanase: gene cloning, expression and function in tumor progression and metastasis. *Nat Med* 1999; **5**: 793-802
- Hulett MD**, Freeman C, Hamdorf BJ, Baker RT, Harris MJ, Parish CR. Cloning of mammalian heparanase, an important enzyme in tumor invasion and metastasis. *Nat Med* 1999; **5**: 803-809
- Parish CR**, Freeman C, Hulett MD. Heparanase: a key enzyme involved in cell invasion. *Biochim Biophys Acta* 2001; **1471**: 99-108
- Kuniyasu H**, Chihara Y, Kubozoe T, Takahashi T. Co-expression of CD44v3 and heparanase is correlated with metastasis of human colon cancer. *Int J Mol Med* 2002; **10**: 333-337
- Kim AW**, Xu X, Hollinger EF, Gattuso P, Godellas CV, Prinz RA. Human heparanase-1 gene expression in pancreatic adenocarcinoma. *J Gastrointest Surg* 2002; **6**: 167-172
- Rohloff J**, Zinke J, Schoppmeyer K, Tannapfel A, Witzigmann H, Mossner J, Wittekind C, Caca K. Heparanase expression is a prognostic indicator for postoperative survival in pancreatic adenocarcinoma. *Br J Cancer* 2002; **86**: 1270-1275
- Uno F**, Fujiwara T, Takata Y, Ohtani S, Katsuda K, Takaoka M, Ohkawa T, Naomoto Y, Nakajima M, Tanaka N. Antisense-mediated suppression of human heparanase gene expression inhibits pleural dissemination of human cancer cells. *Cancer Res* 2001; **61**: 7855-7860
- Ouatas T**, Salerno M, Palmieri D, Steeg PS. Basic and translational advances in cancer metastasis: Nm23. *J Bioenerg Biomembr* 2003; **35**: 73-79
- Wang YK**, Ji XL, Ma NX. *nm23* expression in gastric carcinoma and its relationship with lymphoproliferation. *World J Gastroenterol* 1999; **5**: 87-89
- Jothy S**. CD44 and its partners in metastasis. *Clin Exp Metastasis* 2003; **20**: 195-201
- Kleiner DE**, Stetler-Stevenson WG. Matrix metalloproteinases and metastasis. *Cancer Chemother Pharmacol* 1999; **43**(Suppl): S42-51
- Endo K**, Maejara U, Baba H, Tokunaga E, Koga T, Ikeda Y, Toh Y, Kohno S, Okamura T, Nakajima M, Sugimachi K. Heparanase gene expression and metastatic potential in human gastric cancer. *Anticancer Res* 2001; **21**: 3365-3369
- El-Assal ON**, Yamanoi A, Ono T, Kohno H, Nagasue N. The clinicopathological significance of heparanase and basic fibroblast growth factor expressions in hepatocellular carcinoma. *Clin Cancer Res* 2001; **7**: 1299-1305
- Shiraishi N**, Inomata M, Osawa N, Yasuda K, Adachi Y, Kitano S. Early and late recurrence after gastrectomy for gastric carcinoma. Univariate and multivariate analysis. *Cancer* 2000; **89**: 255-261
- Borie F**, Millat B, Fingerhut A, Hay JM, Fagniez PL, Saxce B. Lymphatic involvement in early gastric cancer: prevalence and prognosis in France. *Arch Surg* 2000; **135**: 1218-1223
- Marchetti D**, Li J, Shen R. Astrocytes contribute to the brain-metastatic specificity of melanoma cells by producing heparanase. *Cancer Res* 2000; **60**: 4767-4770
- Myler HA**, West JL. Heparanase and platelet factor-4 induce smooth muscle cell proliferation and migration via bFGF release from the ECM. *J Biochem* 2002; **131**: 913-922
- Steeg PS**, Bevilacqua G, Kopper L, Thorgerirsson UP, Talmadge JE, Liotta LA, Sobel ME. Evidence for a novel gene associated with low tumor metastatic potential. *J Natl Cancer Inst* 1988; **80**: 200-204
- Salerno M**, Ouatas T, Palmieri D, Steeg PS. Inhibition of signal transduction by the *nm23* metastasis suppressor: possible mechanisms. *Clin Exp Metastasis* 2003; **20**: 3-10
- Lacombe ML**, Milon L, Munier A, Mehus JG, Lambeth DO. The human *nm23*/nucleoside diphosphate kinases. *J Bioenerg Biomembr* 2000; **32**: 247-258
- Nesi G**, Palli D, Pernice LM, Saieva C, Paglierani M, Kroning

- KC, Catarzi S, Rubio CA, Amorosi A. Expression of nm23 gene in gastric cancer is associated with a poor 5-year survival. *Anticancer Res* 2001; **21**: 3643-3649
- 22 **Yoo CH**, Noh SH, Kim H, Lee HY, Min JS. Prognostic significance of CD44 and nm23 expression in patients with stage II and stage IIIA gastric carcinoma. *J Surg Oncol* 1999; **71**: 22-28
- 23 **Ponta H**, Sherman L, Herrlich PA. CD44: from adhesion molecules to signalling regulators. *Nat Rev Mol Cell Biol* 2003; **4**: 33-45
- 24 **Gunthert U**, Hofmann M, Rudy W, Reber S, Zoller M, Haussmann I, Matzku S, Wenzel A, Ponta H, Herrlich P. A new variant of glycoprotein in CD44 confers metastatic potential to rat carcinoma cells. *Cell* 1991; **65**: 13-24
- 25 **Zhang JC**, Wang ZR, Cheng YJ, Yang DZ, Shi JS, Liang AL, Liu NN, Wang XM. Expression of proliferating cell nuclear antigen and CD44 variant exon 6 in primary tumors and corresponding lymph node metastases of colorectal carcinoma with Dukes' stage C or D. *World J Gastroenterol* 2003; **9**: 1482-1486
- 26 **Joo M**, Lee HK, Kang YK. Expression of E-cadherin, beta-catenin, CD44s and CD44v6 in gastric adenocarcinoma: relationship with lymph node metastasis. *Anticancer Res* 2003; **23**: 1581-1588
- 27 **Xin Y**, Grace A, Gallagher MM, Curran BT, Leader MB, Kay EW. CD44v6 in gastric carcinoma: a marker of tumor progression. *Appl Immunohistochem Mol Morphol* 2001; **9**: 138-142
- 28 **Yamaguchi A**, Goi T, Yu J, Hirose Y, Ishida M, Iida A, Kimura T, Takeuchi K, Katayama K, Hirose K. Expression of CD44v6 in advanced gastric cancer and its relationship to hematogenous metastasis and long-term prognosis. *J Surg Oncol* 2002; **79**: 230-235
- 29 **Visse R**, Nagase H. Matrix metalloproteinases and tissue inhibitors of metalloproteinases: structure, function, and biochemistry. *Circ Res* 2003; **92**: 827-839
- 30 **Stamenkovic I**. Matrix metalloproteinases in tumor invasion and metastasis. *Semin Cancer Biol* 2000; **10**: 415-433
- 31 **Yonemura Y**, Endou Y, Fujita H, Fushida S, Bandou E, Taniguchi K, Miwa K, Sugiyama K, Sasaki T. Role of MMP-7 in the formation of peritoneal dissemination in gastric cancer. *Gastric Cancer* 2000; **3**: 63-70
- 32 **Yonemura Y**, Endo Y, Fujita H, Kimura K, Sugiyama K, Momiyama N, Shimada H, Sasaki T. Inhibition of peritoneal dissemination in human gastric cancer by MMP-7-specific antisense oligonucleotide. *J Exp Clin Cancer Res* 2001; **20**: 205-212
- 33 **Liu XP**, Kawauchi S, Oga A, Tsushimi K, Tsushimi M, Furuya T, Sasaki K. Prognostic significance of matrix metalloproteinase-7 (MMP-7) expression at the invasive front in gastric carcinoma. *Jpn J Cancer Res* 2002; **93**: 291-295
- 34 **Liu XP**, Oga A, Suehiro Y, Furuya T, Kawauchi S, Sasaki K. Inverse relationship between matrilysin expression and proliferative activity of cells in advanced gastric carcinoma. *Hum Pathol* 2002; **33**: 741-747
- 35 **Bebb JR**, Letley DP, Thomas RJ, Aviles F, Collins HM, Watson SA, Hand NM, Zaitoun A, Atherton JC. *Helicobacter pylori* upregulates matrilysin (MMP-7) in epithelial cells *in vivo* and *in vitro* in a Cag dependent manner. *Gut* 2003; **52**: 1408-1413
- 36 **Crawford HC**, Krishna US, Israel DA, Matrisian LM, Washington MK, Peek RM Jr. *Helicobacter pylori* strain-selective induction of matrix metalloproteinase-7 *in vitro* and within gastric mucosa. *Gastroenterology* 2003; **125**: 1125-1136

Edited by Zhu LH Proofread by Xu FM

Expression of vascular endothelial growth factor C and chemokine receptor CCR7 in gastric carcinoma and their values in predicting lymph node metastasis

Chao Yan, Zheng-Gang Zhu, Ying-Yan Yu, Jun Ji, Yi Zhang, Yu-Bao Ji, Min Yan, Jun Chen, Bing-Ya Liu, Hao-Ran Yin, Yan-Zhen Lin

Chao Yan, Zheng-Gang Zhu, Ying-Yan Yu, Jun Ji, Yi Zhang, Yu-Bao Ji, Min Yan, Jun Chen, Bing-Ya Liu, Hao-Ran Yin, Yan-Zhen Lin, Department of General Surgery, Ruijin Hospital, Shanghai Second Medical University, Shanghai Institute of Digestive Surgery, Shanghai 200025, China

Correspondence to: Dr. Zheng-Gang Zhu, Shanghai Institute of Digestive Surgery, Ruijin Hospital, Shanghai Second Medical University, 197 Ruijin Road II, Shanghai 200025, China. digsurg@online.sh.cn

Telephone: +86-21-64373909 **Fax:** +86-21-64373909

Received: 2003-10-20 **Accepted:** 2003-12-08

Abstract

AIM: To study the expression of vascular endothelial growth factor C (VEGF-C) and chemokine receptor CCR7 in gastric carcinoma and to investigate their associations with lymph node metastasis of gastric carcinoma and their values in predicting lymph node metastasis.

METHODS: The expression of VEGF-C and CCR7 in gastric carcinoma tissues obtained from 118 patients who underwent curative gastrectomy was examined by immunohistochemistry. Among these patients, 39 patients underwent multi-slice spiral CT (MSCT) examination.

RESULTS: VEGF-C and CCR7 were positively expressed in 52.5 and 53.4% of patients. VEGF-C expression was more frequently found in tumors with lymph node metastasis than those without it ($P < 0.001$). VEGF-C expression was also closely related to lymphatic invasion ($P < 0.001$), vascular invasion ($P < 0.01$), and TNM stage ($P < 0.001$). However, there was no significant correlation between VEGF-C expression and age at surgery, gender, tumor size, tumor location, Lauren classification, and depth of invasion. CCR7 expression was significantly higher in patients with lymph node metastasis compared with those without lymph node metastasis ($P < 0.001$) and was also associated with tumor size ($P < 0.01$), depth of invasion ($P < 0.001$), lymphatic invasion ($P < 0.001$), and TNM stage ($P < 0.001$). However, the presence of CCR7 had no correlation to age at surgery, gender, tumor location, Lauren classification, and vascular invasion. Among the 39 patients who underwent MSCT examination, only CCR7 expression was related to lymph node metastasis determined by MSCT ($P < 0.05$). In the current retrospective study, the sensitivity, specificity, positive predictive value (PPV), negative predictive value (NPV), and accuracy of VEGF-C and CCR7 expression in the diagnosis of lymph node metastasis for patients with gastric carcinoma were 73.8%, 70.2%, 72.6%, 71.4% and 72.0%, and 82.0%, 77.2%, 79.4%, 80.0% and 79.7%, respectively. After subdivision according to the combination of VEGF-C and CCR7 expression, receiver operating characteristic (ROC) analysis showed that the accuracy of the combined examination of VEGF-C and CCR7 expression in predicting

lymph node metastasis was relatively high (area under ROC curve [Az]=0.83).

CONCLUSION: The expression of VEGF-C and CCR7 is related to lymph node metastasis of gastric carcinoma and both of them may become new targets for the treatment of gastric carcinoma. Furthermore, the combined examination of VEGF-C and CCR7 expression in endoscopic biopsy specimens may be useful in predicting lymph node metastasis of gastric carcinoma and deciding the extent of surgical lymph node resection.

Yan C, Zhu ZG, Yu YY, Ji J, Zhang Y, Ji YB, Yan M, Chen J, Liu BY, Yin HR, Lin YZ. Expression of vascular endothelial growth factor C and chemokine receptor CCR7 in gastric carcinoma and their values in predicting lymph node metastasis. *World J Gastroenterol* 2004; 10(6): 783-790

<http://www.wjgnet.com/1007-9327/10/783.asp>

INTRODUCTION

Lymph node metastasis is an important prognostic factor for patients with gastric carcinoma^[1-4]. In spite of this, the function of intratumor lymphatic vessels in lymph node metastasis of gastric carcinoma is unclear. Recently, the molecular pathway that signals for lymphangiogenesis and relatively specific markers for lymphatic endothelium have been described allowing analyses of tumor lymphangiogenesis to be performed^[5-8]. Many experimental studies indicated that lymphangiogenic factors (VEGF-C and VEGF-D) could stimulate lymphangiogenesis in tumors by binding to their receptors (VEGFR-3) on the lymphatic endothelial cells and inducing proliferation and growth of new lymphatic capillaries, then enhance the incidence of lymph node metastasis in animal models^[9-12]. A recent study by Orlandini *et al.*^[13] demonstrated that β -catenin was a negative regulator of VEGF-D mRNA stability, therefore VEGF-D expression might only be responsible for the nodal metastatic behavior in tumors that have lost or reduced expression of β -catenin. In addition, there was apparent discrepancy of VEGF-D expression in tumors reported by different authors^[14-18]. Thus, here we only investigate the role of VEGF-C in promoting lymph node metastasis in gastric carcinoma.

It has long been unclear as to why particular cancers preferentially metastasize to certain sites. However, a recent report by Muller *et al.*^[19] provided evidence for preferential homing of breast cancer to metastatic sites. The findings indicated that the chemokine receptors CXCR4 and CCR7 were found on breast cancer cells and their ligands were highly expressed at sites associated with breast cancer metastases. In addition, both CCL19 and CCL21 (chemokines, ligands of CCR7) are highly expressed in lymph nodes, therefore the migration of tumor cells positive for CCR7 towards lymph nodes may share many similarities with leukocyte trafficking,

which is critically regulated by chemokines and their receptors^[20]. A recent study by Takanami *et al.*^[20] has demonstrated that CCR7 was related to the development of lymph node metastasis in nonsmall cell lung cancers. Here, we aim to explore the association of CCR7 expression with lymph node metastasis in gastric carcinoma. Furthermore, activation of lymphatics by VEGF-C may promote production of chemoattractants such as CCL21 by lymphatic endothelial cells and thereby facilitate tumor cell positive for CCR7 expression entry into lymphatics^[21], so the other aim of this study is to investigate the value of the combined examination of VEGF-C and CCR7 expression in predicting lymph node metastasis of gastric carcinoma.

MATERIALS AND METHODS

Patients and tumor samples

One hundred and eighteen patients, who had undergone curative gastrectomy for gastric carcinoma between 2001 and 2002 in the Department of General Surgery, Ruijin Hospital affiliated to Shanghai Second Medical University, Shanghai, China, were enrolled in this study. All of the resected primary tumors and regional lymph nodes were histologically examined by hematoxylin and eosin staining according to the TNM classification. Among these patients, 39 cases preoperatively underwent MSCT examination by using the method previously reported^[22].

Immunohistochemical staining

Formalin-fixed and paraffin-embedded sections of tumor tissue obtained from resected stomach were cut 4 μ m thick, dewaxed in xylene and rehydrated in graded alcohol, then immersed in 30 mL/L hydrogen peroxide in methanol for 30 min to inhibit endogenous peroxidase activity. The sections were boiled in EDTA (0.01 mol/L, pH 8.0) for 20 min for antigen retrieval. After being rinsed in phosphate-buffered saline (PBS), the sections for CCR7 staining were treated sequentially with avidin and biotin (Biotin blocking system) (Dako) to block the endogenous biotin-like molecules. Then, all sections were incubated with normal goat serum for 10 min for blocking nonspecific reaction. The sections were then incubated with primary antibody at 37 °C in humid chambers for 1 h. The rabbit anti-human VEGF-C polyclonal antibody (Zymed) was at a 1:100 dilution, and the mouse anti-human CCR7 monoclonal antibody (BD PharMingen) was at a 1:300 dilution. After washing 3 times with PBS, the sections for CCR7 staining were then incubated for 10 min at room temperature with biotinylated secondary antibody (goat anti-mouse IgM) and streptavidin conjugated to horseradish peroxidase, respectively, whereas the sections for VEGF-C staining were reacted with EnVision plus (Dako) for 30 min at room temperature. After being rinsed 3 times with PBS, the sections were incubated with 3, 3'-diaminobenzidine tetrahydrochloride (DAB) (Dako), then rinsed with distilled water, counterstained with haematoxylin, dehydrated with alcohol and xylene, and mounted routinely. Negative controls were performed in all cases by omitting the first antibody.

Evaluation of immunohistochemical staining

Two pathologists evaluated and interpreted the results of immunohistochemical staining, without knowledge of the clinical data of each patient. The immunohistochemical expression of VEGF-C was defined as positive if distinct staining was observed in at least 30% of tumor cells^[23]. CCR7 expression in the cancer tissue was classified as positive if more than 10% tumor cells were immunoreactive. Very faint or equivocal immunoreaction was ignored.

Evaluation of lymph node status by MSCT

Two radiologists prospectively analyzed the CT images. Lymph nodes were considered involved when the short-axis diameter was more than 6 mm for the perigastric lymph nodes and more than 8 mm for the extraperigastric lymph nodes^[24]. The preoperative N staging obtained by MSCT was compared with the pathological findings according to the TNM classification (UICC).

Statistical analysis

Statistical analyses were performed using the χ^2 test and ROC analysis. $P < 0.05$ was considered statistically significant. All the statistical analyses were performed using SAS 6.04 software.

RESULTS

Expression of VEGF-C and CCR7 in gastric carcinoma and adjacent normal mucosa

In adjacent normal gastric mucosa, no or faint cytoplasmic staining of VEGF-C was seen in the parietal cells, but almost all epithelial cells were negative. Moderate to strong staining of VEGF-C protein was identified in the cytoplasm of immunoreactive cancer cells (Figure 1). Furthermore, in a few cases, some stromal cells were also positive for VEGF-C. The percentage of patients positive for VEGF-C was 52.5% (62/118). In adjacent normal gastric mucosa, no or very weak staining of CCR7 was also found, whereas moderate to strong staining of CCR7 was found mainly in cell membrane and/or cytoplasm of immunoreactive cancer cells as well as a few lymphocytes (Figure 2). The percentage of patients positive for CCR7 was 53.4% (63/118). Among these samples, there were 2 specimens with 1 metastatic lymph node adjacent to the primary tumor. It turned out that not only the primary tumors but also the metastatic lymph nodes were positive for both VEGF-C and CCR7 expression in both cases (Figures 3 and 4).

Association of VEGF-C and CCR7 expression with clinicopathological features

The correlation between VEGF-C and CCR7 expression and clinicopathological factors is summarized in Table 1. VEGF-C expression was more frequently found in tumors with lymph node metastasis than those without it ($P < 0.001$). VEGF-C expression was also closely related to lymphatic invasion ($P < 0.001$), vascular invasion ($P < 0.01$), and TNM stage ($P < 0.001$). However, there was no significant correlation between VEGF-C expression and age at surgery, gender, tumor size, tumor location, Lauren classification, and depth of invasion. The CCR7 expression was significantly higher in patients with lymph node metastasis compared with those without lymph node metastasis ($P < 0.001$) and was also associated with tumor size ($P < 0.01$), depth of invasion ($P < 0.001$), lymphatic invasion ($P < 0.001$), and TNM stage ($P < 0.001$). However, the presence of CCR7 had no correlation to age at surgery, gender, tumor location, Lauren classification, and vascular invasion.

Relationship between expression of VEGF-C and CCR7 and lymph node metastasis of gastric carcinoma determined by MSCT

As shown in Table 2, among the 39 patients who underwent MSCT examination, CCR7 expression was related to lymph node metastasis determined by MSCT ($P < 0.05$), whereas there was no significant correlation between VEGF-C expression and lymph node metastasis determined by MSCT (Figures 5-7). However, both VEGF-C and CCR7 expression were closely

related to lymph node metastasis determined by pathological examination ($P < 0.01$). In addition, the accuracy of MSCT in determining the N stage was 69.2% (27/39) (Table 3). Findings at MSCT were concordant with pathological findings in 15 of 20 N_0 tumors (75.0%), 5 of 10 N_1 tumors (50.0%), and 7 of 9 N_2 tumors (77.8%), respectively. The sensitivity, specificity, PPV, NPV, and accuracy of MSCT in predicting lymph node metastasis were 84.2% (16/19), 75.0% (15/20), 76.2% (16/21), 83.3% (15/18), and 79.5% (31/39). However, the sensitivity, specificity, PPV, NPV, and accuracy of VEGF-C and CCR7 expression in the diagnosis of lymph node metastasis for patients with gastric carcinoma were 68.4% (13/19), 75.0% (15/20), 72.2% (13/18), 71.4% (15/21) and 71.8% (28/39), and 73.7% (14/19), 75.0% (15/20), 73.7% (14/19), 75.0% (15/20) and 74.4% (29/39), respectively (Table 2).

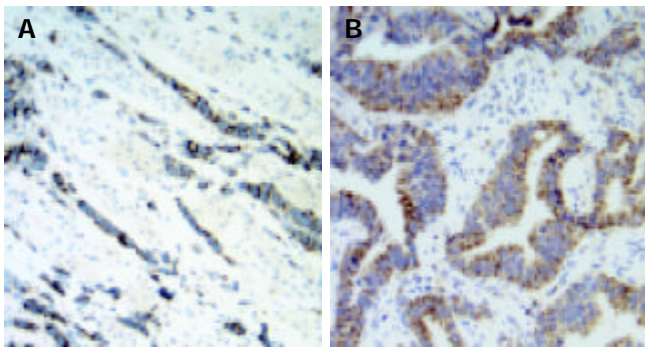


Figure 1 Expression of VEGF-C was observed mainly in the cytoplasm of gastric carcinoma cells (original magnification $\times 200$). A: diffuse gastric carcinoma; B: intestinal gastric carcinoma.

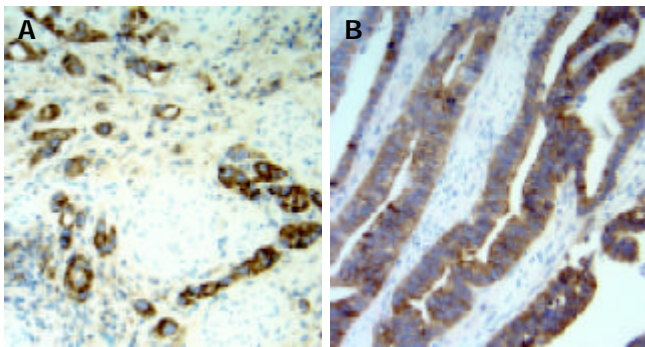


Figure 2 Expression of CCR7 was observed mainly in the cytoplasm and membrane of gastric carcinoma cells (original magnification $\times 200$). A: diffuse gastric carcinoma; B: intestinal gastric carcinoma.

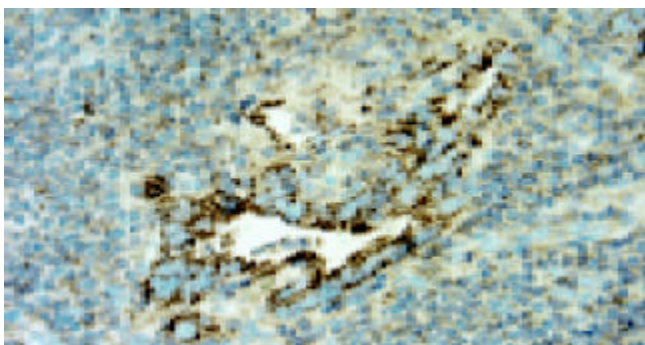


Figure 3 Expression of VEGF-C was observed mainly in gastric carcinoma cells in metastatic lymph node (original magnification $\times 400$).

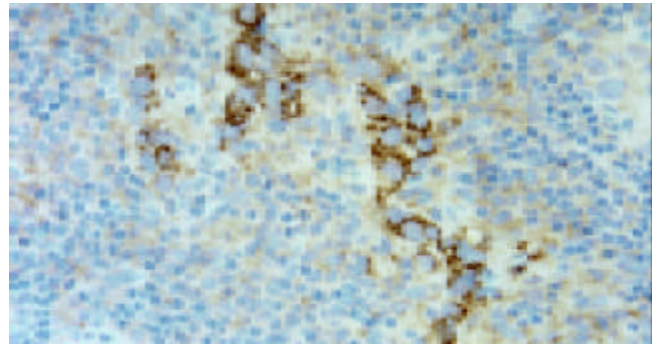


Figure 4 Expression of CCR7 was observed mainly in gastric carcinoma cells in metastatic lymph node (original magnification $\times 400$).

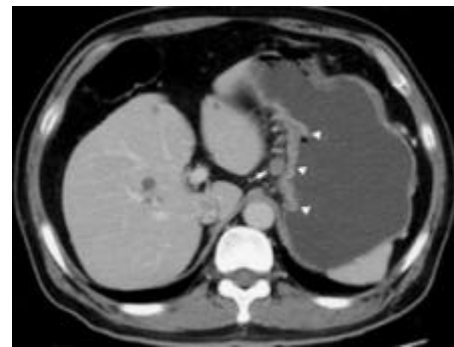


Figure 5 CT scan shows a metastatic lymph node (confirmed by pathologic examination) (arrow) 10 mm in short-axis diameter, which is adjacent to the primary lesion of gastric carcinoma (arrowhead).

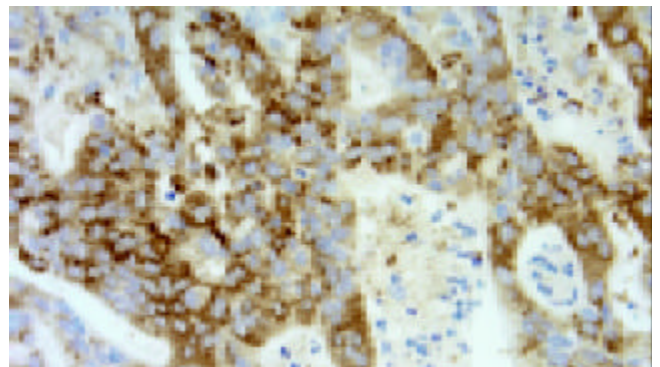


Figure 6 The same patient as Figure 5, expression of CCR7 was observed in the cytoplasm and membrane of gastric carcinoma cells (original magnification $\times 400$).

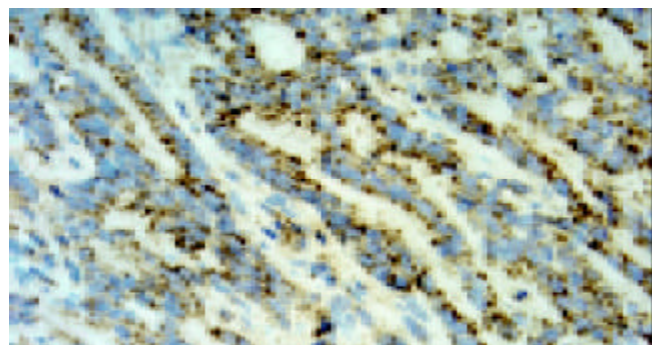


Figure 7 The same patient as Figure 5, expression of VEGF-C was observed in the cytoplasm of gastric carcinoma cells (original magnification $\times 400$).

Table 1 Relationship between expression of VEGF-C and CCR7 and clinicopathologic parameters in patients with gastric carcinoma

	No. of patients	Expression of VEGF-C		P value	Expression of CCR7		P value
		Positive	Negative		Positive	Negative	
Age				NS*			NS
<61 years	46	21	25		23	23	
≥61 years	72	41	31		40	32	
Gender				NS			NS
Male	71	38	33		39	32	
Female	47	24	23		24	23	
Tumor size				NS			<0.01
<5 cm	53	23	30		21	32	
≥5 cm	65	39	26		42	23	
Tumor location				NS			NS
Lower third (L)	81	40	41		44	37	
Middle third (M)	21	12	9		11	10	
Upper third (U)	16	10	6		8	8	
Lauren classification				NS			NS
Intestinal	53	24	29		25	28	
Diffuse	53	30	23		32	21	
Mixed	12	8	4		6	6	
Depth of invasion				NS			<0.001
T1/2	24	9	15		5	19	
T3/4	94	53	41		58	36	
Lymph node metastasis				<0.001			<0.001
Positive	61	45	16		50	11	
Negative	57	17	40		13	44	
Lymphatic invasion				<0.001			<0.001
Positive	68	48	20		51	17	
Negative	50	14	36		12	38	
Vascular invasion				<0.01			NS
Positive	35	25	10		20	15	
Negative	83	37	46		43	40	
Stage				<0.001			<0.001
I, II	55	19	36		13	42	
III, IV	63	43	20		50	13	

*NS, not significant.

Table 2 Correlation between expression of VEGF-C and CCR7 and lymph node metastasis determined by MSCT and pathological examination

	No. of patients	Expression of VEGF-C		P value	Expression of CCR7		P value
		Positive	Negative		Positive	Negative	
Lymph node metastasis ¹				NS ³			<0.05
Positive	21	12	9		14	7	
Negative	18	6	12		5	13	
Lymph node metastasis ²				<0.01			<0.01
Positive	19	13	6		14	5	
Negative	20	5	15		5	15	

¹Lymph node metastasis determined by MSCT; ²Lymph node metastasis determined by pathological examination; ³NS, not significant.**Table 3** Comparison of MSCT and pathological diagnosis of N stage

Pathologic N stage	No. of patients	N stage determined by MSCT		
		N ₀	N ₁	N ₂
N ₀	20	15 ¹	2	3
N ₁	10	2	5 ¹	3
N ₂	9	1	1	7 ¹

¹MSCT findings were concordant with pathological findings.**Table 4** Relationship between expression of VEGF-C and CCR7 after the subdivision and lymph node metastasis

Lymph node metastasis	No. of patients	Expression of VEGF-C and CCR7			
		CCR7(+) and VEGF-C(+)	CCR7(+) and VEGF-C(-)	CCR7(-) and VEGF-C(+)	CCR7(-) and VEGF-C(-)
Positive	61	41	9	4	7
Negative	57	7	6	10	34

Value of the combined examination of VEGF-C and CCR7 expression in predicting lymph node metastasis

As shown in Table 1, in the current retrospective study, the sensitivity, specificity, PPV, NPV, and accuracy of VEGF-C and CCR7 expression in the diagnosis of lymph node metastasis for patients with gastric carcinoma were 73.8% (45/61), 70.2% (40/57), 72.6% (45/62), 71.4% (40/56) and 72.0% (85/118), and 82.0% (50/61), 77.2% (44/57), 79.4% (50/63), 80.0% (44/55) and 79.7% (94/118), respectively. To further investigate the value of the combined examination of VEGF-C and CCR7 expression in predicting lymph node metastasis, we divided patients into four groups: group A, CCR7(+) and VEGF-C(+); group B, CCR7(+) and VEGF-C(-); group C, CCR7(-) and VEGF-C(+); group D, CCR7(-) and VEGF-C(-). In groups A, B, C, and D, the percentage of patients with lymph node metastasis was 85.4% (41/48), 60.0% (9/15), 28.6% (4/14), and 17.1% (7/41), respectively (Table 4). In addition, ROC analysis showed that the accuracy of the combined examination of VEGF-C and CCR7 expression in predicting lymph node metastasis was relatively high (area under ROC curve [Az]= 0.83) (Figure 8). When the patients with positive expression of both VEGF-C and CCR7 were regarded as those with lymph node metastasis, the PPV in the diagnosis of lymph node metastasis reached to 85.4% (41/48). In addition, when the patients with negative expression of both VEGF-C and CCR7 were regarded as those without lymph node metastasis, the NPV reached to 82.9% (34/41).

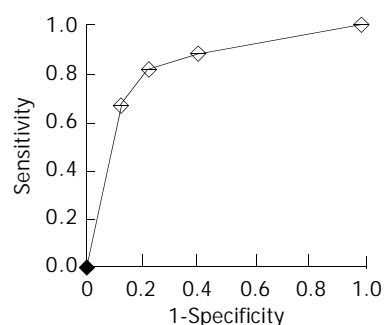


Figure 8 ROC curve generated from the combination of VEGF-C and CCR7 expression shows area under curve to be 0.83.

DISCUSSION

Tumor cells can disseminate within the body by a number of mechanisms, such as direct invasion of surrounding tissues, lymphatic spread and hematogenous spread. The role of angiogenesis involving blood vessels in facilitating the growth and hematogenic spread of solid tumors has been well established. The ability of tumor cells to induce angiogenesis is considered a prerequisite for tumor growth, invasion, and successful metastasis, and the angiogenic switch is recognized as one of the key events in tumorigenesis^[25-30]. In contrast, studies of the lymphatic system have been hindered by the lack of specific markers for tumor-associated lymphatic vessels and growth factors that control lymphatic development and lymphatic vessel growth (lymphangiogenesis), although the importance of the lymphatic system as a pathway for lymph node metastasis has been well recognized. In the past few years, with the identification of proteins such as hyaluronan receptor LYVE-1^[31], prox-1^[7], podoplanin^[32], and desmoplakin^[33] specifically expressed on lymphatic vessels and the discovery of molecules (VEGF-C and VEGF-D) that can drive lymphatic vessel growth, occurrence of tumor lymphangiogenesis and its correlation with lymph node metastasis has been proved in animal models and clinicopathological studies.

Nine recently reported animal studies have provided the first direct *in vivo* evidence that tumours are able not only to induce lymphangiogenesis but also to enhance lymph node metastasis^[8-12,34-37]. Yanai *et al*^[37] constructed a VEGF-C transfectant (AZ-VEGF-C) from the AZ521 human gastric carcinoma cell line, which ordinarily shows little nodal metastatic potential and little VEGF-C expression. They orthotopically implanted transfected tumor cells into the stomachs of nude mice. The number of mice developing lymph node metastases and the number of lymph node metastases per mouse with nodal metastases were higher than with implants of mock-transfected control cells. In addition, the number of vessels stained for VEGFR-3 in tumors and surrounding tissues was higher for AZ-VEGF-C than for controls. Furthermore, recent studies in human head and neck cancer^[38,39] and melanoma^[40] have demonstrated the existence of proliferating intratumoral lymphatic vessels. Clinical studies using the RT-PCR, *in situ* hybridization, and/or immunohistochemistry have revealed significant associations between lymph node metastasis and VEGF-C or VEGF-D expression in human primary tumors of the breast, colon, rectum, prostate, testis, esophagus, stomach, thyroid, lung, pleura, head-and-neck squamous cells, uterine cervix, and endometrium^[41]. Because of the reasons above-mentioned, we only investigated the VEGF-C expression in gastric carcinoma.

The findings of the current study demonstrated a positive correlation of VEGF-C expression with both lymph node metastasis and lymphatic invasion in gastric carcinoma. Our results were consistent with those of previous reports^[23,42-47]. A study by Yanai *et al*^[37] indicated that VEGF-C was a specific lymphangiogenic growth factor with an important role in lymph node metastasis of gastric carcinoma in an animal model. In addition, the studies by Yonemura *et al*^[42,43] showed that VEGF-C mRNA level was closely related to VEGFR-3 mRNA level and the number of VEGFR-3-positive lymphatic vessels in human gastric carcinoma. Thus, VEGF-C may stimulate lymphangiogenesis in gastric carcinoma by binding to their receptors (VEGFR-3) on the lymphatic endothelial cells and inducing proliferation and growth of new lymphatic capillaries, then enhance the incidence of lymph node metastasis in gastric carcinoma. However, our present study showed that VEGF-C expression was closely related to lymph node metastasis determined by pathological examination, but not by MSCT examination, although the accuracy of MSCT in the diagnosis of the lymph node metastasis for 39 patients with gastric carcinoma reached to 79.5%. Nevertheless, Hashimoto *et al*^[48] demonstrated that VEGF-C mRNA expression was correlated with lymph node metastasis diagnosed by magnetic resonance (MR) imaging in cervical cancer. So further study must be made. Furthermore, our present study showed that the VEGF-C expression was correlated with vascular invasion in gastric carcinoma. Other investigators^[42,45] also found a positive correlation between VEGF-C expression and vascular invasion in gastric carcinoma. In addition, a study by Amioka *et al*^[23] showed that VEGF-C expression in tumor cells was closely related to the microvessel density (MVD) in gastric carcinoma. As we all know, VEGF-C is a ligand for VEGFR-2 and VEGFR-3. VEGFR-2 is mainly expressed on vascular endothelial cells. However, VEGF-C displays greater affinity for VEGFR-3 than VEGFR-2, and only the mature 21-kDa form of VEGF-C can bind to VEGFR-2^[36]. As a result, VEGF-C may also be correlated with angiogenesis in gastric carcinoma, but the activity of tumor angiogenesis by VEGF-C may be weak. Further study is needed to investigate the biological effect of VEGF-C on angiogenesis in gastric carcinoma.

Chemokines are chemoattractant cytokines that bind to specific G-protein-coupled receptors on target cells; these target cells follow chemokine concentration gradients into selected

tissues. Through their interactions with target cells, these small proteins induce cytoskeletal rearrangement and directional migration. Chemokines are involved in physiologic and pathologic regulation of leukocyte trafficking^[44]. Recent studies showed that chemokine receptor CCR7 was expressed in the tumor cells of breast cancer^[19], nonsmall cell lung cancer^[20], esophageal squamous cell carcinoma^[49], and gastric carcinoma^[50]. In addition, both CCL21 and CCL19 (chemokines, ligands of CCR7) show most abundant expression in lymph nodes. CCL21 is expressed in the high endothelial venules of lymph nodes and in the T-cell zone of lymph nodes. CCL19 is expressed predominantly by stromal cells within the T-cell zones of lymph nodes^[19]. Previous studies showed that lymphatic endothelial cells also produced CCL21^[51, 52]. *In vitro* experiments showed that actin polymerization and pseudopodia formation, which were needed for the invasion of malignant cells into tissues and for efficient metastasis, could be induced by CCL21 and CCL19 in tumor cells with CCR7 expression^[19, 49, 50]. Thus, the migration of tumor cells positive for CCR7 towards lymph nodes may share many similarities with leukocyte trafficking. In addition, CCR7 may help retain tumor cells in the lymph nodes where the CCR7 ligands are rich.

Wiley *et al.*^[53] examined the role of CCR7 in regional lymph node metastasis in a murine melanoma model. They transduced a murine melanoma cell line, B16, with CCR7 and, surprisingly, transduction with this single gene was sufficient to substantially increase the metastasis to draining lymph nodes of B16 cells, which otherwise have a low propensity to spread, and metastasis was completely blocked by adding neutralizing anti-CCL21 antibodies. In the model used by Wiley *et al.*, transduced cells were injected subcutaneously, thus mimicking lymphgenic metastasis of melanoma cells from the skin. Of interest, intravenous application of CCR7-transduced B16 melanoma cells did not show increased spread of the tumor cells to lung or peripheral lymph nodes. In clinicopathologic studies, a positive correlation of CCR7 expression with lymphatic invasion and lymph node metastasis has been found in nonsmall cell lung cancer^[20], esophageal squamous cell carcinoma^[49], and gastric carcinoma^[50]. Here we investigate the role of chemokine receptor CCR7 in directional migration of gastric carcinoma cells towards lymph nodes.

The findings of the current study demonstrated that the CCR7 expression in the cytoplasm and / or member of gastric carcinoma cells was closely correlated with lymphatic invasion, lymph node metastasis, and TNM stage, but was not correlated with vascular invasion. Our findings were consistent with those reported by Mashino *et al.*^[50]. In addition, the study by Mashino *et al.*^[50] showed that CCR7 expression was closely related to histological classification, whereas the current study showed that there was no significant correlation between CCR7 expression and Lauren classification. The main reason for this discrepancy was that there was no significant correlation between Lauren classification and lymph node metastasis among the 118 patients, although the incidence of lymph node metastasis in diffuse gastric carcinoma (50.9%) was higher than that in intestinal gastric carcinoma (45.3%). Furthermore, the current study showed that the CCR7 expression was closely correlated with lymph node metastasis determined not only by pathological examination but also by MSCT examination.

Many factors affect prognosis in patients with gastric carcinoma, including tumor size, lymph node metastasis, depth of tumor invasion, distant metastasis, histological classification, and surgery performed. Of these, lymph node metastasis is one of the most important factors. Therefore, preoperative evaluation of lymph node status is essential. With the development of endoscopic or laparoscopic resection of small, localized gastric carcinoma, the pretherapeutic evaluation of

lymph node metastasis has become more important. For preoperative N staging, endoscopic ultrasonography (EUS), CT, and MR imaging have been used^[4, 54-58]. However, the paraaortal and celiacal regions are often beyond the scope of the EUS^[55], and comparative studies demonstrated that the accuracy of CT in N staging was higher than that of MR imaging^[57, 58]. Therefore, among these three methods, CT may be superior to EUS and MR imaging in predicting lymph node status for patients with gastric carcinoma. In the current study, the accuracy of MSCT in N staging was 69.2%. Notably, the accuracy of MSCT in predicting lymph node metastasis reached to 79.5%, and the sensitivity and specificity was 84.2% and 75.0%, respectively. However, although spiral CT could detect lymph nodes small than 5 mm and the sensitivity for detecting metastasis-positive nodes was remarkably higher than that for detecting metastasis-negative nodes^[59], both overstaging and downstaging still existed because lymph node size was not a reliable indicator for lymph node metastasis of gastric carcinoma^[60]. Furthermore, Maruyama computer program can also be used to predict lymph node metastasis for patients with gastric carcinoma. Analysis of eight prognostic parameters such as gender, age, macroscopic type, location, position, diameter, histological classification, and depth of invasion using this computer program can gain the information on the expected frequency of metastasis in the 16 lymph node stations of each patient with gastric carcinoma^[61, 62]. However, to date, the prospective study for evaluating the accuracy of this computer program has not been reported. Two retrospective studies^[61, 62] showed that the accuracy of Maruyama computer program in predicting lymph node metastasis was relatively high, but the specificity was too low. In addition, only clinicopathologic parameters were included in this computer program, whereas the molecular biologic features of gastric carcinoma were neglected.

Recently, a study using the microarray technology showed that lymph node metastasis of gastric carcinoma could be precisely predicted from the view of molecular biologic features. In this study, investigators developed an equation to achieve a scoring parameter for the prediction of lymph node metastasis on the basis of 12 genes with statistically significant differences in expression between node-positive and node-negative tumors. In the prospective study, the lymph node status of all nine test cases was correctly predicted^[63]. In the current retrospective study, the sensitivity, specificity, PPV, NPV, and accuracy of VEGF-C and CCR7 expression in the diagnosis of lymph node metastasis for patients with gastric carcinoma were 73.8%, 70.2%, 72.6%, 71.4% and 72.0%, and 82.0%, 77.2%, 79.4%, 80.0% and 79.7%, respectively. Especially when the combined examination of VEGF-C and CCR7 expression was performed, the PPV and NPV reached to 85.4% and 82.9%, respectively. However, the PPV and NPV of MSCT in predicting lymph node metastasis was only 76.2% and 83.3%, respectively, among 39 patients. In addition, successful lymph node metastasis requires a complex series of related steps, such as detachment of cancer cells, invasion into the lymphatic vessels, transfer within the lymphatic vessels, embedding in the lymph nodes and proliferation in the lymph nodes. Therefore, lymphangiogenesis and directional migration of gastric carcinoma cells towards lymph nodes may only be two main steps involved in lymph node metastasis. Thus, we hypothesize that an equation established on the basis of many factors involved in the metastasis-associated steps can predict the lymph node status for patients with gastric carcinoma more accurately, especially when it is combined with Maruyama computer program and MSCT.

In conclusion, the current study demonstrates that expression of VEGF-C and CCR7 is related to lymph node metastasis of gastric carcinoma and both of them may become

new targets for the treatment of gastric carcinoma. Furthermore, the combined examination of VEGF-C and CCR7 expression in endoscopic biopsy specimens may be useful in predicting lymph node metastasis of gastric carcinoma and deciding the extent of surgical lymph node resection.

REFERENCES

- Zheng HC**, Li YL, Sun JM, Yang XF, Li XH, Jiang WG, Zhang YC, Xin Y. Growth, invasion, metastasis, differentiation, angiogenesis and apoptosis of gastric cancer regulated by expression of PTEN encoding products. *World J Gastroenterol* 2003; **9**: 1662-1666
- Ding YB**, Chen GY, Xia JG, Zang XW, Yang HY, Yang L. Association of VCAM-1 overexpression with oncogenesis, tumor angiogenesis and metastasis of gastric carcinoma. *World J Gastroenterol* 2003; **9**: 1409-1414
- Zhou YN**, Xu CP, Han B, Li M, Qiao L, Fang DC, Yang JM. Expression of E-cadherin and beta-catenin in gastric carcinoma and its correlation with the clinicopathological features and patient survival. *World J Gastroenterol* 2002; **8**: 987-993
- Yan C**, Zhu ZG, Zhu Q, Yan M, Chen J, Liu BY, Yin HR, Lin YZ. A preliminary study of endoscopic ultrasonography in the pre-operative staging of early gastric carcinoma. *Zhonghua Zhongliu Zazhi* 2003; **25**: 390-393
- Joukov V**, Pajusola K, Kaipainen A, Chilov D, Lahtinen I, Kukk E, Saksela O, Kalkkinen N, Alitalo K. A novel vascular endothelial growth factor, VEGF-C, is a ligand for the Flt4 (VEGFR-3) and KDR (VEGFR-2) receptor tyrosine kinases. *EMBO J* 1996; **15**: 290-298
- Achen MG**, Jeltsch M, Kukk E, Makinen T, Vitali A, Wilks AF, Alitalo K, Stacker SA. Vascular endothelial growth factor D (VEGF-D) is a ligand for the tyrosine kinase VEGF receptor 2 (Flk1) and VEGF receptor 3 (Flt4). *Proc Natl Acad Sci U S A* 1998; **95**: 548-553
- Wigle JT**, Harvey N, Detmar M, Lagutina I, Grosveld G, Gunn MD, Jackson DG, Oliver G. An essential role for Prox1 in the induction of the lymphatic endothelial cell phenotype. *EMBO J* 2002; **21**: 1505-1513
- Padera TP**, Kadambi A, di Tomaso E, Carreira CM, Brown EB, Boucher Y, Choi NC, Mathisen D, Wain J, Mark EJ, Munn LL, Jain RK. Lymphatic metastasis in the absence of functional intratumor lymphatics. *Science* 2002; **296**: 1883-1886
- Karpanen T**, Egeblad M, Karkkainen MJ, Kubo H, Yla-Herttuala S, Jaattela M, Alitalo K. Vascular endothelial growth factor C promotes tumor lymphangiogenesis and intralymphatic tumor growth. *Cancer Res* 2001; **61**: 1786-1790
- Mattila MM**, Ruohola JK, Karpanen T, Jackson DG, Alitalo K, Harkonen PL. VEGF-C induced lymphangiogenesis is associated with lymph node metastasis in orthotopic MCF-7 tumors. *Int J Cancer* 2002; **98**: 946-951
- Stacker SA**, Caesar C, Baldwin ME, Thornton GE, Williams RA, Prevo R, Jackson DG, Nishikawa S, Kubo H, Achen MG. VEGF-D promotes the metastatic spread of tumor cells via the lymphatics. *Nat Med* 2001; **7**: 151-152
- Skobe M**, Hawighorst T, Jackson DG, Prevo R, Janes L, Velasco P, Riccardi L, Alitalo K, Claffey K, Detmar M. Induction of tumor lymphangiogenesis by VEGF-C promotes breast cancer metastasis. *Nat Med* 2001; **7**: 192-198
- Orlandini M**, Semboloni S, Oliviero S. Beta-catenin inversely regulates VEGF-D mRNA stability. *J Biol Chem* 2003; **278**: 44650-44656
- Funaki H**, Nishimura G, Harada S, Ninomiya I, Terada I, Fushida S, Tani T, Fujimura T, Kayahara M, Shimizu K, Ohta T, Miwa K. Expression of vascular endothelial growth factor D is associated with lymph node metastasis in human colorectal carcinoma. *Oncology* 2003; **64**: 416-422
- Kawakami M**, Furuhashi T, Kimura Y, Yamaguchi K, Hata F, Sasaki K, Hirata K. Expression analysis of vascular endothelial growth factors and their relationships to lymph node metastasis in human colorectal cancer. *J Exp Clin Cancer Res* 2003; **22**: 229-237
- White JD**, Hewett PW, Kosuge D, McCulloch T, Enholm BC, Carmichael J, Murray JC. Vascular endothelial growth factor -D expression is an independent prognostic marker for survival in colorectal carcinoma. *Cancer Res* 2002; **62**: 1669-1675
- Hanrahan V**, Currie MJ, Gunningham SP, Morrin HR, Scott PA, Robinson BA, Fox SB. The angiogenic switch for vascular endothelial growth factor (VEGF)-A, VEGF-B, VEGF-C, and VEGF-D in the adenoma-carcinoma sequence during colorectal cancer progression. *J Pathol* 2003; **200**: 183-194
- Yokoyama Y**, Charnock-Jones DS, Licence D, Yanaihara A, Hastings JM, Holland CM, Emoto M, Sakamoto A, Sakamoto T, Maruyama H, Sato S, Mizunuma H, Smith SK. Expression of vascular endothelial growth factor (VEGF)-D and its receptor, VEGF receptor 3, as a prognostic factor in endometrial carcinoma. *Clin Cancer Res* 2003; **9**: 1361-1369
- Muller A**, Homey B, Soto H, Ge N, Catron D, Buchanan ME, McClanahan T, Murphy E, Yuan W, Wagner SN, Barrera JL, Mohar A, Verastegui E, Zlotnik A. Involvement of chemokine receptors in breast cancer metastasis. *Nature* 2001; **410**: 50-56
- Takanami I**. Overexpression of CCR7 mRNA in nonsmall cell lung cancer: correlation with lymph node metastasis. *Int J Cancer* 2003; **105**: 186-189
- Cassella M**, Skobe M. Lymphatic vessel activation in cancer. *Ann NY Acad Sci* 2002; **979**: 120-130
- Takao M**, Fukuda T, Iwanaga S, Hayashi K, Kusano H, Okudaira S. Gastric cancer: evaluation of triphasic spiral CT and radiologic-pathologic correlation. *J Comput Assist Tomogr* 1998; **22**: 288-294
- Amioka T**, Kitadai Y, Tanaka S, Haruma K, Yoshihara M, Yasui W, Chayama K. Vascular endothelial growth factor-C expression predicts lymph node metastasis of human gastric carcinomas invading the submucosa. *Eur J Cancer* 2002; **38**: 1413-1419
- D'Elia F**, Zingarelli A, Palli D, Grani M. Hydro-dynamic CT pre-operative staging of gastric cancer: correlation with pathological findings. A prospective study of 107 cases. *Eur Radiol* 2000; **10**: 1877-1885
- Wang ZQ**, Li JS, Lu GM, Zhang XH, Chen ZQ, Meng K. Correlation of CT enhancement, tumor angiogenesis and pathologic grading of pancreatic carcinoma. *World J Gastroenterol* 2003; **9**: 2100-2104
- Du JR**, Jiang Y, Zhang YM, Fu H. Vascular endothelial growth factor and microvascular density in esophageal and gastric carcinomas. *World J Gastroenterol* 2003; **9**: 1604-1606
- Shi H**, Xu JM, Hu NZ, Xie HJ. Prognostic significance of expression of cyclooxygenase-2 and vascular endothelial growth factor in human gastric carcinoma. *World J Gastroenterol* 2003; **9**: 1421-1426
- Xiong B**, Sun TJ, Yuan HY, Hu MB, Hu WD, Cheng FL. Cyclooxygenase-2 expression and angiogenesis in colorectal cancer. *World J Gastroenterol* 2003; **9**: 1237-1240
- Zheng S**, Han MY, Xiao ZX, Peng JP, Dong Q. Clinical significance of vascular endothelial growth factor expression and neovascularization in colorectal carcinoma. *World J Gastroenterol* 2003; **9**: 1227-1230
- Gupta MK**, Qin RY. Mechanism and its regulation of tumor-induced angiogenesis. *World J Gastroenterol* 2003; **9**: 1144-1155
- Banerji S**, Ni J, Wang SX, Clasper S, Su J, Tammi R, Jones M, Jackson DG. LYVE-1, a new homologue of the CD44 glycoprotein, is a lymph-specific receptor for hyaluronan. *J Cell Biol* 1999; **144**: 789-801
- Sedivy R**, Beck-Mannagetta J, Haverkamp C, Battistutti W, Honigschnabl S. Expression of vascular endothelial growth factor-C correlates with the lymphatic microvessel density and the nodal status in oral squamous cell cancer. *J Oral Pathol Med* 2003; **32**: 455-460
- Ebata N**, Nodasaka Y, Sawa Y, Yamaoka Y, Makino S, Totsuka Y, Yoshida S. Desmoplakin as a specific marker of lymphatic vessels. *Microvasc Res* 2001; **61**: 40-48
- Mandriota SJ**, Jussila L, Jeltsch M, Compagni A, Baetens D, Prevo R, Banerji S, Huarte J, Montesano R, Jackson DG, Orci L, Alitalo K, Christofori G, Pepper MS. Vascular endothelial growth factor-C-mediated lymphangiogenesis promotes tumor metastasis. *EMBO J* 2001; **20**: 672-682
- He Y**, Kozaki K, Karpanen T, Koshikawa K, Yla-Herttuala S, Takahashi T, Alitalo K. Suppression of tumor lymphangiogenesis and lymph node metastasis by blocking vascular endothelial growth factor receptor 3 signaling. *J Natl Cancer Inst* 2002; **94**: 819-825
- Skobe M**, Hamberg LM, Hawighorst T, Schirner M, Wolf GL, Alitalo K, Detmar M. Concurrent induction of lymphangiogenesis,

- angiogenesis, and macrophage recruitment by vascular endothelial growth factor-C in melanoma. *Am J Pathol* 2001; **159**: 893-903
- 37 **Yanai Y**, Furuhashi T, Kimura Y, Yamaguchi K, Yasoshima T, Mitaka T, Mochizuki Y, Hirata K. Vascular endothelial growth factor C promotes human gastric carcinoma lymph node metastasis in mice. *J Exp Clin Cancer Res* 2001; **20**: 419-428
- 38 **Beasley NJ**, Prevo R, Banerji S, Leek RD, Moore J, van Trappen P, Cox G, Harris AL, Jackson DG. Intratumoral lymphangiogenesis and lymph node metastasis in head and neck cancer. *Cancer Res* 2002; **62**: 1315-1320
- 39 **Maula SM**, Luukka M, Grenman R, Jackson D, Jalkanen S, Ristamaki R. Intratumoral lymphatics are essential for the metastatic spread and prognosis in squamous cell carcinomas of the head and neck region. *Cancer Res* 2003; **63**: 1920-1926
- 40 **Straume O**, Jackson DG, Akslen LA. Independent prognostic impact of lymphatic vessel density and presence of low-grade lymphangiogenesis in cutaneous melanoma. *Clin Cancer Res* 2003; **9**: 250-256
- 41 **Nathanson SD**. Insights into the mechanisms of lymph node metastasis. *Cancer* 2003; **98**: 413-423
- 42 **Yonemura Y**, Endo Y, Fujita H, Fushida S, Ninomiya I, Bandou E, Taniguchi K, Miwa K, Ohoyama S, Sugiyama K, Sasaki T. Role of vascular endothelial growth factor C expression in the development of lymph node metastasis in gastric cancer. *Clin Cancer Res* 1999; **5**: 1823-1829
- 43 **Yonemura Y**, Fushida S, Bando E, Kinoshita K, Miwa K, Endo Y, Sugiyama K, Partanen T, Yamamoto H, Sasaki T. Lymphangiogenesis and the vascular endothelial growth factor receptor (VEGFR)-3 in gastric cancer. *Eur J Cancer* 2001; **37**: 918-923
- 44 **Kabashima A**, Maehara Y, Kakeji Y, Sugimachi K. Overexpression of vascular endothelial growth factor C is related to lymphogenous metastasis in early gastric carcinoma. *Oncology* 2001; **60**: 146-150
- 45 **Ichikura T**, Tomimatsu S, Ohkura E, Mochizuki H. Prognostic significance of the expression of vascular endothelial growth factor (VEGF) and VEGF-C in gastric carcinoma. *J Surg Oncol* 2001; **78**: 132-137
- 46 **Takahashi A**, Kono K, Itakura J, Amemiya H, Feng Tang R, Iizuka H, Fujii H, Matsumoto Y. Correlation of vascular endothelial growth factor-C expression with tumor-infiltrating dendritic cells in gastric cancer. *Oncology* 2002; **62**: 121-127
- 47 **Ishikawa M**, Kitayama J, Kazama S, Nagawa H. Expression of vascular endothelial growth factor C and D (VEGF-C and -D) is an important risk factor for lymphatic metastasis in undifferentiated early gastric carcinoma. *Jpn J Clin Oncol* 2003; **33**: 21-27
- 48 **Hashimoto I**, Kodama J, Seki N, Hongo A, Yoshinouchi M, Okuda H, Kudo T. Vascular endothelial growth factor-C expression and its relationship to pelvic lymph node status in invasive cervical cancer. *Br J Cancer* 2001; **85**: 93-97
- 49 **Ding Y**, Shimada Y, Maeda M, Kawabe A, Kaganai J, Komoto I, Hashimoto Y, Miyake M, Hashida H, Imamura M. Association of CC chemokine receptor 7 with lymph node metastasis of esophageal squamous cell carcinoma. *Clin Cancer Res* 2003; **9**: 3406-3412
- 50 **Mashino K**, Sadanaga N, Yamaguchi H, Tanaka F, Ohta M, Shibuta K, Inoue H, Mori M. Expression of chemokine receptor CCR7 is associated with lymph node metastasis of gastric carcinoma. *Cancer Res* 2002; **62**: 2937-2941
- 51 **Gunn MD**, Tangemann K, Tam C, Cyster JG, Rosen SD, Williams LT. A chemokine expressed in lymphoid high endothelial venules promotes the adhesion and chemotaxis of naive T lymphocytes. *Proc Natl Acad Sci U S A* 1998; **95**: 258-263
- 52 **Saeki H**, Moore AM, Brown MJ, Hwang ST. Cutting edge: secondary lymphoid-tissue chemokine (SLC) and CC chemokine receptor 7 (CCR7) participate in the emigration pathway of mature dendritic cells from the skin to regional lymph nodes. *J Immunol* 1999; **162**: 2472-2475
- 53 **Wiley HE**, Gonzalez EB, Maki W, Wu MT, Hwang ST. Expression of CC chemokine receptor-7 and regional lymph node metastasis of B16 murine melanoma. *J Natl Cancer Inst* 2001; **93**: 1638-1643
- 54 **Xi WD**, Zhao C, Ren GS. Endoscopic ultrasonography in preoperative staging of gastric cancer: determination of tumor invasion depth, nodal involvement and surgical resectability. *World J Gastroenterol* 2003; **9**: 254-257
- 55 **Willis S**, Truong S, Gribnitz S, Fass J, Schumpelick V. Endoscopic ultrasonography in the preoperative staging of gastric cancer: accuracy and impact on surgical therapy. *Surg Endosc* 2000; **14**: 951-954
- 56 **Chen F**, Ni YC, Zheng KE, Ju SH, Sun J, Ou XL, Xu MH, Zhang H, Marchal G. Spiral CT in gastric carcinoma: Comparison with barium study, fiberoptic gastroscopy and histopathology. *World J Gastroenterol* 2003; **9**: 1404-1408
- 57 **Kim AY**, Han JK, Seong CK, Kim TK, Choi BI. MRI in staging advanced gastric cancer: is it useful compared with spiral CT? *J Comput Assist Tomogr* 2000; **24**: 389-394
- 58 **Sohn KM**, Lee JM, Lee SY, Ahn BY, Park SM, Kim KM. Comparing MR imaging and CT in the staging of gastric carcinoma. *Am J Roentgenol* 2000; **174**: 1551-1557
- 59 **Fukuya T**, Honda H, Hayashi T, Kaneko K, Tateshi Y, Ro T, Maehara Y, Tanaka M, Tsuneyoshi M, Masuda K. Lymph-node metastases: efficacy for detection with helical CT in patients with gastric cancer. *Radiology* 1995; **197**: 705-711
- 60 **Monig SP**, Zirbes TK, Schroder W, Baldus SE, Lindemann DG, Dienes HP, Holscher AH. Staging of gastric cancer: correlation of lymph node size and metastatic infiltration. *Am J Roentgenol* 1999; **173**: 365-367
- 61 **Bollschweiler E**, Boettcher K, Hoelscher AH, Sasako M, Kinoshita T, Maruyama K, Siewert JR. Preoperative assessment of lymph node metastases in patients with gastric cancer: evaluation of the Maruyama computer program. *Br J Surg* 1992; **79**: 156-160
- 62 **Guadagni S**, de Manzoni G, Catarci M, Valenti M, Amicucci G, De Bernardinis G, Cordiano C, Carboni M, Maruyama K. Evaluation of the Maruyama computer program accuracy for preoperative estimation of lymph node metastases from gastric cancer. *World J Surg* 2000; **24**: 1550-1558
- 63 **Hasegawa S**, Furukawa Y, Li M, Satoh S, Kato T, Watanabe T, Katagiri T, Tsunoda T, Yamaoka Y, Nakamura Y. Genome-wide analysis of gene expression in intestinal-type gastric cancers using a complementary DNA microarray representing 23040 genes. *Cancer Res* 2002; **62**: 7012-7017

Coexpression of cholecystokinin-B/gastrin receptor and gastrin gene in human gastric tissues and gastric cancer cell line

Jian-Jiang Zhou, Man-Ling Chen, Qun-Zhou Zhang, Jian-Kun Hu, Wen-Ling Wang

Jian-Jiang Zhou, Man-Ling Chen, Department of Biochemistry and Molecular Biology, School of Basic Medical Sciences, Sichuan University, Chengdu 610041, Sichuan Province, China

Qun-Zhou Zhang, Oral & Maxillofacial Department, Charles R. Drew University of Medicine and Science, Los Angeles, CA 90059, USA

Jian-Kun Hu, Department of Surgery, West China Medical School, Sichuan University, Chengdu 610041, Sichuan Province, China

Wen-Ling Wang, Department of Oncology, Affiliated Hospital of Guiyang Medical College, Guiyang 550001, Guizhou Province, China

Correspondence to: Professor Man-Ling Chen, Department of Biochemistry and Molecular Biology, School of Basic Medical Sciences, West China Medical Center, Sichuan University, Chengdu 610041, Sichuan Province, China. zjjdjb@hotmail.com

Telephone: +86-28-85501254

Received: 2003-08-11 **Accepted:** 2003-10-22

Abstract

AIM: To compare the expression patterns of cholecystokinin-B (CCK-B)/gastrin receptor genes in matched human gastric carcinoma and adjacent non-neoplastic mucosa of patients with gastric cancer, inflammatory gastric mucosa from patients with gastritis, normal stomachs from 2 autopsied patients and a gastric carcinoma cell line (SGC-7901), and to explore their relationship with progression to malignancy of human gastric carcinomas.

METHODS: RT-PCR and sequencing were employed to detect the mRNA expression levels of CCK-B receptor and gastrin gene in specimens from 30 patients with gastric carcinoma and healthy bordering non-cancerous mucosa, 10 gastritis patients and normal stomachs from 2 autopsied patients as well as SGC-7901. The results were semi-quantified by normalizing it to the mRNA level of β -actin gene using Lab Image software. The sequences were analyzed by BLAST program.

RESULTS: CCK-B receptor transcripts were detected in all of human gastric tissues in this study, including normal, inflammatory and malignant tissues and SGC-7901. However, the expression levels of CCK-B receptor in normal gastric tissues were higher than those in other groups ($P < 0.05$), and its expressions did not correlate with the differentiation and metastasis of gastric cancer ($P > 0.05$). On the other hand, gastrin mRNA was detected in SGC-7901 and in specimens obtained from gastric cancer patients (22/30) but not in other gastric tissues, and its expression was highly correlated with the metastases of gastric cancer ($P < 0.05$).

CONCLUSION: Human gastric carcinomas and gastric cancer cell line SGC-7901 cells coexpress CCK-B receptor and gastrin mRNA. Gastrin/CCK-B receptor autocrine or paracrine pathway may possibly play an important role in the progression of gastric cancer.

Zhou JJ, Chen ML, Zhang QZ, Hu JK, Wang WL. Coexpression of cholecystokinin-B/gastrin receptor and gastrin gene in human gastric tissues and gastric cancer cell line. *World J Gastroenterol* 2004; 10(6): 791-794

<http://www.wjgnet.com/1007-9327/10/791.asp>

INTRODUCTION

Human beings have developed highly efficient cell-cell communication to integrate and coordinate the proliferation of individual cell types, among which growth factors and hormones play a pivotal role. Gastrointestinal peptides, including gastrin and cholecystokinin (CCK), are a structurally diverse group of molecular messengers that play an important role in the control of appetite and hormonal secretion. Gastrin is secreted by gastrin (G) cells located in the antral part of the stomach, and identified as the circulating hormone responsible for stimulation of acid secretion from the parietal cells. It stimulates gastric enterochromaffin-like (ECL) cells to release histamine, which in turn increases acid secretion via histamine H_2 -receptors in parietal cells^[1-3]. Recently, it has been demonstrated that gastrin plays a significant role in the proliferation and differentiation of gastric and intestinal epithelial cells^[4-6].

Previous studies have shown that hormones and receptors are key molecules in regulating cell growth, differentiation and apoptosis^[7]. Cholecystokinin-B (CCK-B)/gastrin receptor belongs to the seven transmembrane G-protein-coupled receptor superfamily and is mainly expressed in parietal cells and ECL cells of gastrointestinal tract. It has been reported that CCK-B receptor on the basolateral cell membrane domain was immunoreactive and showed high-affinity binding sites for gastrin^[8]. It has been widely accepted that gastrin, a trophic factor, promotes growth of cancer cells both *in vitro* and *in vivo* through CCK-B receptors, and that expressions of gastrin gene and CCK-B receptor are closely related to the development, progression and invasion of cancer cells, in particular, colorectal and pancreatic cancers^[9,10]. Taken together, we propose that gastrin/CCK-B receptors may play an important role in the development and progression of gastric cancers. To test this viewpoint, we detected the levels of gastrin and CCK-B mRNA transcripts in human gastric cancer cell line SGC-7901 and in gastric tissues including gastric cancers and their corresponding normal mucosa tissues, gastritis and normal autopsied stomach specimens.

MATERIALS AND METHODS

Gastric tissues

Thirty gastric cancer specimens (including 12 moderate and 18 low differentiation adenocarcinomas, 22 with and 8 without local lymph node metastases) and surrounding non-tumour mucosa surgically resected from gastric corpus were confirmed histopathologically. Two normal autopsied gastric mucosa specimens were authorized by the Pathology Department of West China Medical School of Sichuan University. Ten gastritis specimens from gastroscopic examination were histopathologically confirmed by Pathology Department of Guiyang Medical College. Tissue samples were immediately stored in RNA protection solution (Omega).

Cell culture

SGC-7901 cells were cultured in RPMI 1640 medium supplemented with 100 mL/L newborn calf serum, 100 units/mL penicillin, and 100 μ g/mL streptomycin in a humidified environment of 50 mL/L CO_2 in air at 37 °C.

Table 1 PCR primers

Gene	Primers	Sequences	Base pairs	GenBank accession number
CCK-B/gas- trin receptor	Sense (545-566)	5'-CGGACTACTCATGGTGCCCTAC-3'	316	L08112.1
	Antisense (861-842)	5'-GCCAACCGCGCCAGTCTCAG-3'		
Gastrin	Sense (166-189)	5'-TAGGTACAGGGGCCAACAA-3'	266	NM-000805
	Antisense (431-413)	5'-GGGGACAGGGCTGAAGTG-3'		
β -actin	Sense (320-340)	5'-TGGAGAAAATCTGGCACCAC-3'	190	BC016045
	Antisense (509-489)	5'-GAGGCGTACAGGGATAGCAC-3'		

CCK-B: cholecystokinin-B.

Reverse transcription

Total RNA was extracted from gastric samples or 10^6 cells using TRIzol (Invitrogen) reagent according to the manufacturer's recommendations. Five microgramme of total RNA was used as a template for the first-strand cDNA synthesis when the reaction mixture consisted of 120 units of MMLV (Maloney murine leukemia virus) reverse transcriptase, 5 μ mol/L random hexamer oligonucleotide primer, 10 mmol/L dithioerythritol, 2 mmol/L dNTP, and 1 \times first-strand buffer in a total volume of 20 μ L. RNA was denatured at 65 $^{\circ}$ C for 15 min and immediately chilled on ice, and then incubated for 10 min at room temperature before reverse transcriptase was added. The reverse transcription was performed for 60 min at 37 $^{\circ}$ C and terminated by heating to 95 $^{\circ}$ C for 10 min.

PCR analysis of CCK-B receptor and gastrin

The primers used for PCR amplification in the study are listed in Table 1. Two microliter of reverse transcripts was amplified by PCR in a total volume of 50 μ L containing 0.1 μ mol/L oligonucleotide primers for CCK-B receptor or gastrin and β -actin, respectively, 250 μ mol/L dNTP, 2 mmol/L $MgCl_2$, and 1 \times PCR buffer. cDNAs were denatured for 5 min at 95 $^{\circ}$ C before 2.5 units *Taq* DNA polymerase was added. The conditions of touch-down PCR were at 94 $^{\circ}$ C for 45 s, at 68-62 $^{\circ}$ C for 1 min for CCK-B receptor or at 60-55 $^{\circ}$ C for 1 min for gastrin with decreasing 1 $^{\circ}$ C per cycle at beginning, and at 72 $^{\circ}$ C for 1 min for 35 cycles. PCR products were visualized by agarose gel electrophoresis and ethidium bromide staining.

Semi-quantitative analysis of CCK-B/gastrin receptor gene expression

PCR was performed simultaneously by adding the specific primers for both CCK-B/gastrin receptor and β -actin in a single reaction system after reverse transcription. PCR products were separated by 15 g/L agarose gel and the results of electrophoresis were photographed. The level of CCK-B/gastrin receptor mRNA expression vs β -actin was semi-quantified by Lab image software and the data were expressed as mean \pm SD and followed statistical analysis through one-way ANOVA, Student-Newman-Keuls multiple comparisons and independent-samples *t* test by SPSS 10.0. Statistical significance was assumed when $P < 0.05$.

Sequencing

The PCR products of CCK-B/gastrin receptor amplified from the gastric tissues were separately purified by a gel extraction kit, and sequenced by an ABI sequencing machine. The sequences were compared with the GenBank database using BLAST analysis.

RESULTS

Expression of CCK-B receptor gene in human gastric tissues and SGC-7901 cells

CCK-B receptor expression was indicated by the presence of

a 316-bp PCR product, and the gastrin gene expression yielded a 266-bp PCR product while the β -actin mRNA as an internal control revealed a 190-bp product on agarose gel. Figure 1 shows the expression of CCK-B/gastrin receptor detected in all specimens taken from normal, inflammatory, cancerous gastric tissues and SGC-7901 cells.

Then, all of the samples were further divided into three groups including normal (surrounding healthy and autopsied gastric tissues, $n=32$), inflammatory ($n=10$) and malignant groups ($n=30$) which were subdivided into the local lymph node metastases ($n=22$) and non-metastases ($n=8$) groups, or moderate (12) and low (18) differentiation adenocarcinoma groups. Data were analyzed by one-way ANOVA. As shown in Figure 2, the expression level of CCK-B receptor mRNA in surrounding healthy gastric tissues is significantly higher than that in neoplastic and inflammatory tissues ($P < 0.05$) while there are neither significant differences between metastases and non-metastases groups nor between groups with different differentiations ($P > 0.05$).

Gastrin gene expression in human gastric cancer tissues and SGC-7901 cells

Gastrin mRNA was detected on both SGC-7901 cells and gastric cancer specimens (22/30), among which 86.4% (19/22) with local lymph node metastases, and 10.0% (3/30) without metastases. The positive expression rate of gastrin mRNA in metastatic cases was significantly higher than that in lymph node metastasis-negative cases ($P < 0.05$). Gastrin mRNA was detected in 9 out of 12 gastric adenocarcinoma specimens with moderate differentiation and in 13 out of 18 cancerous specimens with poor differentiation. Statistical analyses showed no significant difference between the poor and moderate differentiation groups ($P > 0.05$). Surprisingly, gastrin mRNA transcripts were detected neither in normal gastric tissues nor in inflammatory ones (Figure 1).

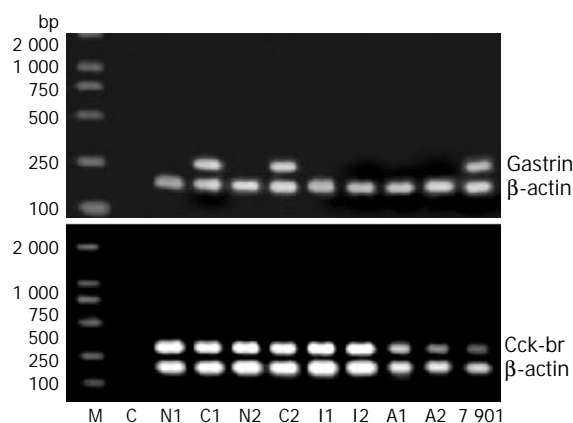


Figure 1 Expression of CCK-B receptor (below) and gastrin (above) mRNA in human gastric tissues and gastric cancer cell line. Total RNA extracted from matched tumor (C1, C2) and non-neoplastic (N1, N2) gastric tissues of patients with gastric

gastric carcinomas. However, human tumor cells can express different CCK-B receptor subtypes and different bioactive forms of gastrin amidated and non-amidated, and that complex networks may exist among these components. More studies are needed for their roles in the development of human gastric carcinomas.

REFERENCES

- Dockray GJ.** Gastrin and gastric epithelial physiology. *J Physiol* 1999; **518**(Pt 2): 315-324
- Sun FP,** Song YG. G and D cells in rat antral mucosa: An immunoelectron microscopic study. *World J Gastroenterol* 2003; **9**: 2768-2771
- Li YY.** Mechanisms for regulation of gastrin and somatostatin release from isolated rat stomach during gastric distention. *World J Gastroenterol* 2003; **9**: 129-133
- Rozengurt E,** Walsh JH. Gastrin, CCK, Signaling, and Cancer. *Annu Rev Physiol* 2001; **63**: 49-76
- Zhang ZL,** Chen WW. Proliferation of intestinal crypt cells by gastrin-induced ornithine decarboxylase. *World J Gastroenterol* 2002; **8**: 183-187
- Wang Z,** Chen WW, Li RL, Wen B, Sun JB. Effect of gastrin on differentiation of rat intestinal epithelial cells *in vitro*. *World J Gastroenterol* 2003; **9**: 1786-1790
- Konturek PC,** Kania J, Kukharsky V, Ocker S, Hahn EG, Konturek SJ. Influence of gastrin on the expression of cyclooxygenase-2, hepatocyte growth factor and apoptosis-related proteins in gastric epithelial cells. *J Physiol Pharmacol* 2003; **54**: 17-32
- Kulaksiz H,** Arnold R, Goke B, Maronde E, Meyer M, Fahrenholz F, Forssmann WG, Eissele R. Expression and cell-specific localization of the cholecystokinin B/gastrin receptor in the human stomach. *Cell Tissue Res* 2000; **299**: 289-298
- Watson SA,** Morris TM, McWilliams DF, Harris J, Evans S, Smith A, Clarke PA. Potential role of endocrine gastrin in the colonic adenoma carcinoma sequence. *Br J Cancer* 2002; **87**: 567-573
- Clerc P,** Leung-Theung-Long S, Wang TC, Dockray GJ, Bouisson M, Delisle MB, Vaysse N, Pradayrol L, Fourmy D, Dufresne M. Expression of CCK2 receptors in the murine pancreas: proliferation, transdifferentiation of acinar cells, and neoplasia. *Gastroenterology* 2002; **122**: 428-437
- Pagliocca A,** Wroblewski LE, Ashcroft FJ, Noble PJ, Dockray GJ, Varro A. Stimulation of the gastrin-cholecystokinin(B) receptor promotes branching morphogenesis in gastric AGS cells. *Am J Physiol Gastrointest Liver Physiol* 2002; **283**: G292-299
- Xie B,** He SW, Wang XD. Effect of gastrin on protein kinase C and its subtype in human colon cancer cell line SW480. *World J Gastroenterol* 2000; **6**: 304-306
- Yen TW,** Sandgren EP, Liggitt HD, Palmiter RD, Zhou W, Hinds TR, Grippo PJ, McDonald JM, Robinson LM, Bell RH Jr. The gastrin receptor promotes pancreatic growth in transgenic mice. *Pancreas* 2002; **24**: 121-129
- Lefranc F,** Chaboteaux C, Belot N, Brotchi J, Salmon I, Kiss R. Determination of RNA expression for cholecystokinin/gastrin receptors (CCKA, CCKB and CCKC) in human tumors of the central and peripheral nervous system. *Int J Oncol* 2003; **22**: 213-219
- Blaker M,** de Weerth A, Tometten M, Schulz M, Hoppner W, Arlt D, Hoang-Vu C, Dralle H, Terpe H, Jonas L, von Schrenck T. Expression of the cholecystokinin 2-receptor in normal human thyroid gland and medullary thyroid carcinoma. *Eur J Endocrinol* 2002; **146**: 89-96
- Moody TW,** Jensen RT. CI-988 inhibits growth of small cell lung cancer cells. *J Pharmacol Exp Ther* 2001; **299**: 1154-1160
- Wang XJ,** Ma QJ, Lai DN, Li CJ, Li JM, Wu YZ, Wang Q. Gastrin receptor antagonist combined with cytosine deaminase suicide gene therapy enhances killing of colorectal carcinoma. *Shijie Huaren Xiaohua Zazhi* 2003; **11**: 1385-1388
- Reubi JC,** Waser B, Gugger M, Friess H, Kleeff J, Kaye H, Buchler MW, Laissue JA. Distribution of CCK1 and CCK2 receptors in normal and diseased human pancreatic tissue. *Gastroenterology* 2003; **125**: 98-106
- Rozengurt E.** Autocrine loops, signal transduction, and cell cycle abnormalities in the molecular biology of lung cancer. *Curr Opin Oncol* 1999; **11**: 116-122
- Cong B,** Li SJ, Ling YL, Yao YX, Gu ZY, Wang JX, You HY. Expression and cell-specific localization of cholecystokinin receptors in rat lung. *World J Gastroenterol* 2003; **9**: 1273-1277
- Henwood M,** Clarke PA, Smith AM, Watson SA. Expression of gastrin in developing gastric adenocarcinoma. *Br J Surg* 2001; **88**: 564-568
- Baldwin GS,** Shulkes A. Gastrin, gastrin receptors and colorectal carcinoma. *Gut* 1998; **42**: 581-584
- He SW,** Shen KQ, He YJ, Xie B, Zhao YM. Regulatory effect and mechanism of gastrin and its antagonists on colorectal carcinoma. *World J Gastroenterol* 1999; **5**: 408-416
- Seva C,** Dickinson CJ, Yamada T. Growth-promoting effects of glycine-extended progastrin. *Science* 1994; **265**: 410-412
- Hellmich MR,** Rui XL, Hellmich HL, Fleming RY, Evers BM, Townsend CM. Human colorectal cancers express a constitutively active cholecystokinin-B/gastrin receptor that stimulates cell growth. *J Biol Chem* 2000; **275**: 32122-32128
- Gales C,** Sanchez D, Poirot M, Pyronnet S, Buscail L, Cussac D, Pradayrol L, Fourmy D, Silvente-Poirot S. High tumorigenic potential of a constitutively active mutant of the cholecystokinin 2 receptor. *Oncogene* 2003; **22**: 6081-6089
- Ding WQ,** Kuntz SM, Miller LJ. A misspliced form of the cholecystokinin-B/gastrin receptor in pancreatic carcinoma: role of reduced cellular U2AF35 and a suboptimal 3-splicing site leading to retention of the fourth intron. *Cancer Res* 2002; **62**: 947-952
- Smith JS,** Verderame MF, McLaughlin P, Martenisi M, Ballard E, Zagon I. Characterization of the CCK-C(cancer) receptor in human pancreatic cancer. *Int J Mol Med* 2002; **10**: 689-694
- Konturek PC,** Bielanski W, Konturek SJ, Hartwich A, Pierzchalski P, Gonciarz M, Marlicz K, Starzynska T, Zuchowicz M, Darasz Z, Gotze JP, Rehfeld J, Hahn EG. Progastrin and cyclooxygenase-2 in colorectal cancer. *Dig Dis Sci* 2002; **47**: 1984-1991
- Kermorgant S,** Lehy T. Glycine-extended gastrin promotes the invasiveness of human colon cancer cells. *Biochem Biophys Res Commun* 2001; **285**: 136-141
- Kelly A,** Hollande F, Shulkes A, Baldwin GS. Expression of progastrin-derived peptides and gastrin receptors in a panel of gastrointestinal carcinoma cell lines. *J Gastroenterol Hepatol* 1998; **13**: 208-214
- Jensen RT.** Involvement of cholecystokinin/gastrin-related peptides and their receptors in clinical gastrointestinal disorders. *Pharmacol Toxicol* 2002; **91**: 333-350

Edited by Chen WW and Wang XL Proofread by Xu FM

Effect of mitogen-activated protein kinase signal transduction pathway on multidrug resistance induced by vincristine in gastric cancer cell line MGC803

Bo Chen, Feng Jin, Ping Lu, Xiang-Lan Lu, Ping-Ping Wang, Yun-Peng Liu, Fan Yao, Shu-Bao Wang

Bo Chen, Feng Jin, Ping Lu, Fan Yao, Shu-Bao Wang, Department of Surgical Oncology, the First Affiliated Hospital, China Medical University, Shenyang 110001, Liaoning Province, China

Xiang-Lan Lu, Ping-Ping Wang, Institute of Hematology, the First Affiliated Hospital, China Medical University, Shenyang 110001, Liaoning Province, China

Yun-Peng Liu, Department of Medical Oncology, the First Affiliated Hospital, China Medical University, Shenyang 110001, Liaoning Province, China

Correspondence to: Bo Chen, Department of Surgical Oncology, the First Affiliated Hospital, China Medical University, Shenyang 110001, Liaoning Province, China. chbyxl@163.com

Telephone: +86-24-23256666 to 6227

Received: 2003-08-28 **Accepted:** 2003-11-06

Abstract

AIM: To investigate the correlation between mitogen-activated protein kinase (MAPK) signal transduction pathway and multidrug resistance (MDR) in MGC803 cells.

METHODS: Western blot was used to analyze the expression of MDR associated gene in transient vincristine (VCR) induced MGC803 cells, which were treated with or without the specific inhibitor of MAPK, PD098059. Morphologic analysis of the cells treated by VCR with or without PD098059 was determined by Wright-Giemsa staining. The cell cycle analysis was performed by using flow cytometric assay and the drug sensitivity of MGC803 cells which were exposed to VCR with or without PD098059 was tested by using MTT assay.

RESULTS: Transient exposure to VCR induced P-gp but not MRP1 or GST- π expression in MGC803 cells and the expression of P-gp was inhibited by PD098059. Apoptotic bodies were found in the cells treated with VCR or VCR+PD098059. FCM results indicated that more MGC803 cells showed apoptotic phenotype when treated by VCR and PD098059 (rate: 31.23%) than treated by VCR only (rate: 18.42%) ($P < 0.05$). The IC_{50} ($284 \pm 13.2 \mu\text{g/L}$) of MGC803 cells pretreated with VCR was 2.24-fold as that of negative control group ($127 \pm 17.6 \mu\text{g/L}$) and 1.48-fold as that of the group treated with PD098059 ($191 \pm 27.9 \mu\text{g/L}$).

CONCLUSION: This study shows that the expression of P-gp can be induced by transient exposure to VCR and this induction can be prevented by PD098059, which can block the activity of MAPK. MAPK signal transduction pathway may play some roles in modulating MDR1 expression in gastric cancer.

Chen B, Jin F, Lu P, Lu XL, Wang PP, Liu YP, Yao F, Wang SB. Effect of mitogen-activated protein kinase signal transduction pathway on multidrug resistance induced by vincristine in gastric cancer cell line MGC803. *World J Gastroenterol* 2004; 10(6): 795-799

<http://www.wjgnet.com/1007-9327/10/795.asp>

INTRODUCTION

Multidrug resistance (MDR) is a major factor in the failure of many forms of chemotherapy^[1-4]. Several different molecular mechanisms will switch on in MDR cells, the most investigated mechanisms with known clinical significance are: (1) activation of transmembrane proteins effluxing different chemical substance from the cells, including mainly P-glycoprotein (P-gp) encoded by MDR1 and multidrug resistance related protein (MRP); (2) activation of the enzymes of the glutathione detoxification system (especially GST- π); (3) alteration of the genes and proteins involved in the control of apoptosis (especially p53 and Bcl-2)^[5-14]. MDR associated genes are expressed in a large proportion of human tumors, and its expression in several different forms of cancer was shown to be associated with a lack of response to combination chemotherapy. MDR1 expression is usually low or undetectable prior to treatment, but it is frequently increased during the progression of the disease and, most noticeably, after chemotherapy^[15-20]. The increased expression of MDR1 mRNA can be found in some drug-sensitive cancer cells by transient exposure to different chemotherapeutic drugs^[21-24].

The signal transduction pathway of the mitogen-activated protein kinase (MAPK) plays a critical role in cell proliferation, differentiation and apoptosis. The ERK1/2 (Ras/Raf-1/MEK1/2/ERK1/2) signal transduction pathway is a subfamily of MAPK. The expression of MDR and the activation of MAPK are increased in cancer cells after treatment with various therapeutic drugs. The selective inhibitor of MEK1/2, PD098058, has been shown to significantly reverse the drug resistance of drug resistant cell line L1210/VCR^[25]. The mechanism is unclear. Whether MAPK plays a role in MDR, and whether the alteration of MEK can regulate the expression of MDR need to be elucidated.

Our study was to observe the expressions of associated genes of MDR of human gastric cancer cell line MGC803 by their transient exposure to vincristine (VCR) and the effect on MDR by the specific inhibitor of MEK1/2, PD098059.

MATERIALS AND METHODS

Reagents

Human gastric cancer cell line MGC803 was obtained from Tumor Research Institute (China Medical University, Shenyang). RPMI1640 medium was the product of Gibco (USA). Chemical drug vincristine was purchased from Hualian Co. (Shanghai, China). PD098059 was the product of Promega (USA). Rabbit anti-human P-gp, MRP1, GST- π polyclonal antibody were products of Oncogen (USA). Alkaline phosphatase-conjugated goat anti-rabbit IgG was purchased from Zhongshan Co. (Beijing).

Morphological analysis of cells

After treated with VCR ($20 \mu\text{g/L}$) or VCR ($20 \mu\text{g/L}$)+PD098059 ($10 \mu\text{mol/L}$) for 24 h, 48 h, MGC803 cells were analyzed by wright-Giemsa staining, and the morphology of cells was examined under optic microscope.

Cell cycle analysis

MGC803 cells ($1 \times 10^8/L$) were seeded into 12-well plates and cultured in 1 mL RPIM medium. After cultured for 4 h, cells were treated with VCR (20 $\mu\text{g/L}$), PD098059 (10 $\mu\text{mol/L}$) or VCR (20 $\mu\text{g/L}$) + PD098059 (10 $\mu\text{mol/L}$) for 24 h, 48 h, 96 h. Cells were harvested and washed with ice-cold PBS twice, centrifuged (120 \times g, 5 min) and supplemented with ice-cold 70 mL/L ethanol overnight. Cells were treated with RNase (200 mg/L) at 37 °C for 1 h after washed with ice-cold PBS twice, then centrifuged (120 g, 5 min), treated with PI (20 mg/L) for 30 min in dark room at 4 °C. Cell cycle was analyzed by flow cytometer and CELLQuest software.

MTT assay of drug sensitivity

Cells ($1 \times 10^8/L$) pretreated with VCR (20 $\mu\text{g/L}$) for 72 h were plated into 96-well plates and cultured in 100 μL RPMI medium. After cultured for 4 h, cells were divided into two groups: one group was treated with various concentrations of VCR (1 $\mu\text{g/L}$, 10 $\mu\text{g/L}$, 100 $\mu\text{g/L}$, 1 000 $\mu\text{g/L}$), the other group was treated with a fixed concentration of PD098059 (10 $\mu\text{mol/L}$) and various concentration of VCR (1 $\mu\text{g/L}$, 10 $\mu\text{g/L}$, 100 $\mu\text{g/L}$, 1 000 $\mu\text{g/L}$). The untreated MGC803 was treated with various concentration of VCR (1 $\mu\text{g/L}$, 10 $\mu\text{g/L}$, 100 $\mu\text{g/L}$, 1 000 $\mu\text{g/L}$) as negative control group. After treated for 72 h, 20 μL of 5 g/L MTT [3-(4,4-dimethylthiazol-2-yl)2,5-diphenylterazolium bromide] in PBS was added to each well, incubated for 4 h at 37 °C and the formed formazan crystals were dissolved in 100 μL of DMSO. The absorbance was recorded at 570 nm on a microplate reader (BIORAD). Drug sensitivity is expressed as IC_{50} for cells, which the concentration of drugs that caused a 50% reduction in the at 570 nm relative to untreated cells (controls).

Western blot analysis

MGC803 cells were harvested after treated with VCR (20 $\mu\text{g/L}$) or VCR (20 $\mu\text{g/L}$) + PD098059 (10 $\mu\text{mol/L}$) for 24, 48, 72 h. A total of 2×10^7 cells were lysed in 200 μL RIPA buffer containing phenylmethyl fluoride (PMSF, 100 mg/L), Aprotinin (2 mg/L), 50 mmol/L TrisCl pH 7.4, 150 mmol/L NaCl, 1 g/L SDS, 10 g/L Triton-100, 1 mmol/L EDTA pH 8.0. Protein samples were sonicated on ice, lysed for 40 min at 4 °C, then centrifuged (15 400 g, 20 min) at 4 °C. The supernatant was transferred to a new tip on ice and then the amount of the protein calculated. Protein samples were separated by sodium dodecyl sulfate polyacrylamide gel electrophoresis (SDSPAGE), transferred to a PVDF membrane. The membrane was incubated in a blocking solution containing 50 g/L fat free milk powder for 1 h, then probed with rabbit anti-human P-gp polyclonal antibody overnight, and incubated with alkaline phosphatase-conjugated goat anti-rabbit IgG for 2 h. The membrane was then stained by blue tetrazolium (NBT) and 5'-bromo-4-chloro-3-indolylphosphate (BCIP) solution. The integrated density value (IDV) was analyzed by Fluorchem software.

Statistical analysis

Data were analyzed by chi square test. $P < 0.05$ was considered as significant.

RESULTS

Apoptosis of cells treated with VCR and PD098059

The apoptotic bodies were observed in the MGC803 cells after treated with VCR (20 $\mu\text{g/L}$) or VCR (20 $\mu\text{g/L}$) + PD098059 (10 $\mu\text{mol/L}$) for 48 h (Figure 1A, B, C).

The apoptosis of MGC803 cells was detected by flow cytometric analysis. The rate of apoptotic cells treated with VCR for 72 h was 18.41%, and that treated with VCR and

PD098059 for 72 h was 35.61%. There was a significant difference between them ($P < 0.05$). The apoptotic rates of MGC803 cells untreated and treated with PD098059 only were 8.46% and 6.26%. There was no significant difference between them ($P > 0.05$) (Figure 2).

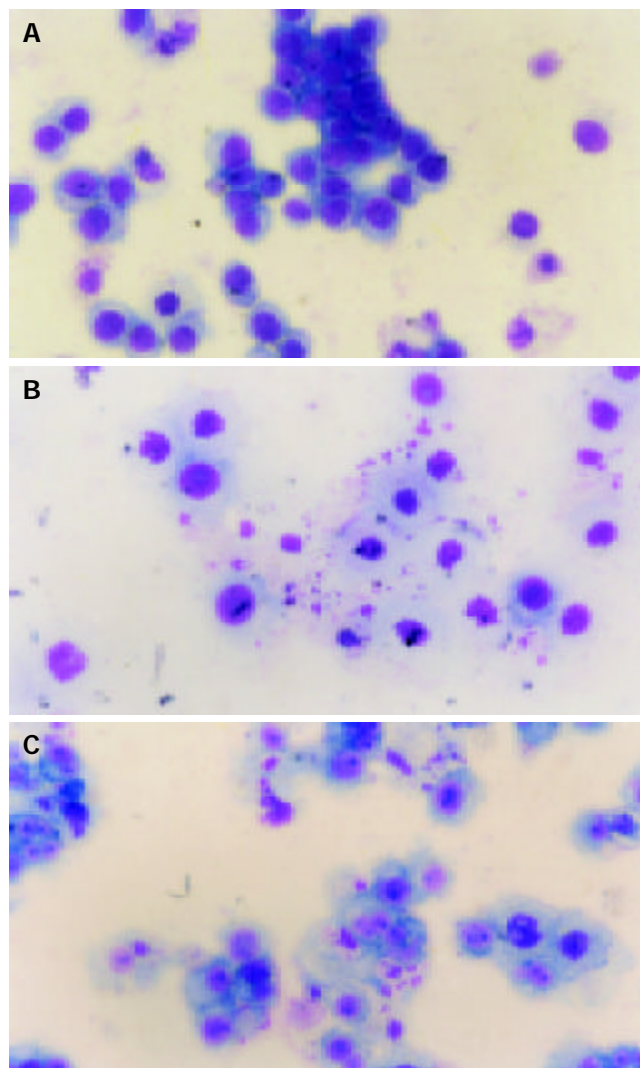


Figure 1 A: Untreated MGC803 Cells (apoptotic bodies could not be found), B: MGC803 cells treated with VCR 48 h (apoptotic bodies could be found), C: MGC803 cells treated with VCR+PD098059 48 h (apoptotic bodies could be found).

Drug sensitivity of cells treated with VCR and PD098059

The IC_{50} of MGC803 pretreated with VCR for 72 h followed by treatment with various concentrations of VCR was $284 \pm 13.2 \mu\text{g/L}$. It was 2.24-fold as that of negative control group ($127 \pm 17.6 \mu\text{g/L}$), and 1.48-fold as those of cells treated with various concentrations of VCR ($191 \pm 27.9 \mu\text{g/L}$). And, the concentration of PD098059 was fixed. It showed that the drug-resistance of MGC803 pretreated with VCR was increased and PD098059 could reverse the drug resistance induced by VCR partially.

Expression of MDR1, MRP1 and GST-p

Western blot was used to detect the expression of MDR associated genes. The expression of P-gp in MGC803 cells gradually increased after treated with VCR for 24-72 h (Table 1, Figure 3). But the expression of MRP1 and GST- π did not increase significantly (Table 1, Figure 3). The expression of P-gp was inhibited when MGC803 cells were treated with VCR and PD098059 for 24-72 h (Table 1, Figure 3).

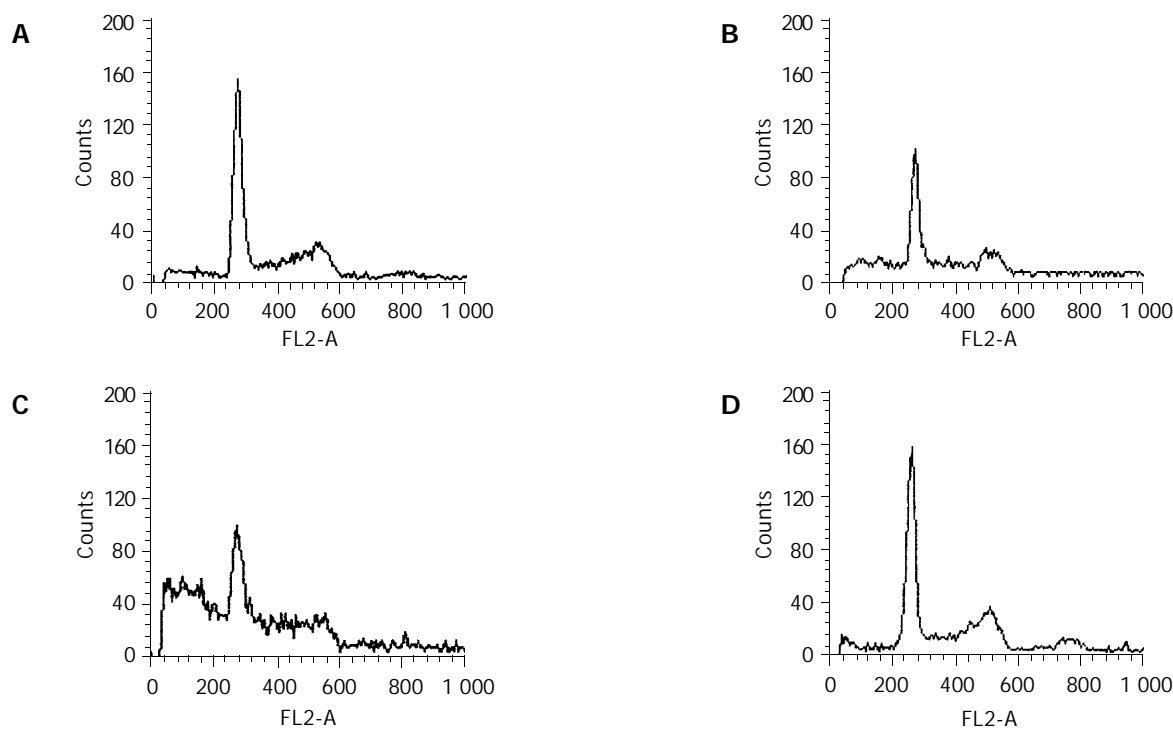


Figure 2 Cell cycle analysis of MGC803. A: Untreated MGC803 cells at 72 h (G_0G_1 : 48.20%; G_2M : 28.18%, S: 14.16%, apoptosis: 8.46%), B: MGC803 cells treated with VCR (20 ng/mL) after 72 h (G_0G_1 : 37.62%; G_2M : 20.05%, S: 24.92%, apoptosis: 18.41%), C: MGC803 cells treated with VCR (20 ng/mL) +PD098059 (10 nmol/mL) after 72 h (G_0G_1 : 32.53%; G_2M : 13.91%, S: 18.95%, apoptosis: 35.61%), D: MGC803 cells treated with PD098059 (10 nmol/mL) only after 72 h (G_0G_1 : 49.27%; G_2M : 27.56%, S: 16.91%, apoptosis: 6.26%).

Table 1 IDV of expression of MDR associated gene

Group	VCR (MDR1)	VCR (MRP1)	VCR (GST- π)	VCR+PD098059 (MDR1)
Untreated MGC803 cells	116 \pm 7.5	38 \pm 14.5	122 \pm 16	54 \pm 9.5
Positive control	192 \pm 8.6	64 \pm 13.2	144 \pm 21	105 \pm 9.5
24 h	159 \pm 9.5	34 \pm 9.3	123 \pm 19.5	63 \pm 16.7
48 h	172 \pm 7.6	30 \pm 11.5	110 \pm 15.6	64 \pm 21.1
72 h	196 \pm 15.1	33 \pm 15.5	110 \pm 13.6	58 \pm 9.5

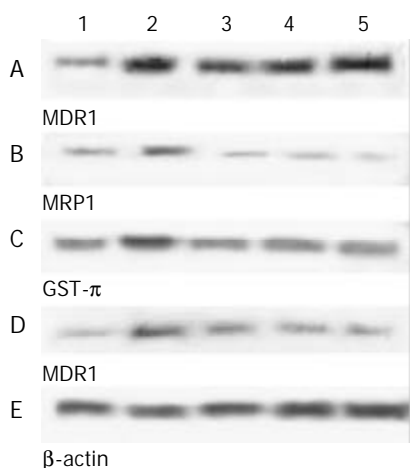


Figure 3 The expression of associated gene of MDR in MGC803 cells treated with VCR or VCR+PD098059 24h-72 h. A: The expression of MDR1 of MGC803 cells treated with VCR increased. B,C: The expression of MRP1 and GST- π of MGC803 cells treated with VCR did not increase. D: The expression of MDR1 was inhibited when MGC803 cells treated with VCR and PD098059. E: The protein level of β -actin was detected to assess the loading amount in each well in SDS-PAGE. Lane 1, untreated cells; Lane 2, positive control cells; Lane 3, cells treated for 24 h; Lane 4, cells treated 48 h; Lane 5, cells treated for 72 h.

DISCUSSION

Different tumors are different in sensitivity to chemotherapeutic drugs, and drug resistance can be induced by chemotherapy. The failure of cancer chemotherapy is mainly due to the overexpression of associated genes of MDR. Cytotoxic drug resistant cell lines have been induced after long-term exposure to gradient concentrations of cytotoxic drugs. Whether the expression of MDR could be induced by transient exposure to chemotherapeutic drugs has aroused. Chaudhary *et al* have found that the expressions of MDR1 mRNA in drug sensitive leukemia cell line K562 increased by short-term exposure to different chemotherapeutic drugs^[21]. Schondorf *et al* also found that MDR1-mRNA was detectable in each cell line when short-term cultures of 6 established ovarian cancer cell lines were exposed to one of three anticancer drugs at concentrations equivalent to the clinically achievable plasma peak concentration. The method described here was easy to perform and could be of striking value in predicting the development of tumor chemoresistance^[24]. Our results of western blot showed that the expression of P-gp in MGC803 cells increased significantly but the expressions of MRP1 and GST- π did not increase after induction by VCR for 72 h and the MTT assay showed that the drug resistance of MGC803 cells pretreated with VCR was 2.24-fold as that of untreated MGC803 cells. It suggested that the expression of MDR1 in MGC803 cells could be induced after transient exposure to VCR.

Mitogen-activated protein kinases (MAPKs), found in all eukaryotes, are common participants in signal transduction pathway from the membrane to the nucleus, and play an important role in cell proliferation, differentiation and apoptosis^[26-28]. The mammalian MAPK family includes ERK1/2, JNK/SAPKs, ERK4 and *etc.* ERK1/2 is the most important subgroup among them. ERK1/2 signal transduction pathways contain at least three protein kinases. They are Raf-1, MAPK/ERK kinases1/2(MEK1/2) and ERK1/2. Raf-1 is activated by Ras, then phosphorylates two residues, either serine or threonine, to activate MEK1/2^[29,30]. MEK1/2 activates ERK1/ERK2 by

phosphorylating a tyrosine and a threonine residues^[31].

Signal transduction pathways play critical roles in pathogenesis and progress of tumor. The activation of MAPK and expression of MDR can be induced by anti-cancer drugs^[32]. But the relation between them is not clear. Kisucka *et al* found PD098059 significantly reduced the survival of murine vincristine resistant L1210/VCR cells with a decrease of LC₅₀ to vincristine from 2.65 mmol/L to 0.67 mmol/L. The result of the study demonstrated that the inhibitor of MEK1/2 signaling pathway was a reversal agent of VCR resistance in L1210/VCR cells, but the precise mechanism of PD098059 in modulation of MDR is not resolved yet, and the role of ERK-mediated phosphorylation cascade could be considered^[25]. Ding *et al* found that PD098059 re-sensitized the Taxol resistant human ovarian cancer cell line A1847/TX at least 20-fold, but when MDR1 cDNA was stably expressed in the wild-type cell line to generate a highly Taxol-resistant sub-line, 1847/MDR5, MAPK kinases again became activated. This result demonstrated that the increased activity of the signaling pathway in the Taxol-resistant lines was directly attributable to MDR1 overexpression and was not due to the effects of Taxol itself, and that MAPK regulated the expression of MDR1^[33]. It has been found that the expression of MDR1 can block apoptosis induced by the Fas ligand cascade. Expression of MDR1 resulted in a decrease in the rate of production of active caspase 3, a key effector caspase in the apoptotic cascade, upon Fas ligation^[11]. The ERK1/2 pathway has also been shown to inhibit caspase-3 activation^[34]. Another possibility is that MDR1 may have additional physiological functions, for instance, MDR1 induces novel Na⁺ and Cl⁻ dependent pathway for transmembrane H⁺ efflux that results in intracellular alkalization^[35]. Apoptosis induced by chemotherapeutic drugs is prevented by intracellular acidification and the induction of apoptotic events such as DNA laddering can be inhibited by increasing the intracellular pH in this manner. In a recent study, Wittstein *et al* demonstrated that inhibition of the ERK1/2 pathway using PD098059 resulted in re-alkalinisation of vascular endothelial cells in perfusion experiments^[36]. Thus alterations in cellular pH may provide the stimulus for a variety of signaling pathways and responses mediated by both MDR and ERK1/2. The relation between MAPK and MDR1 is not clear yet. MAPK signal pathway may combine with other different mechanisms to modulate the expression of MDR1. Our study showed that PD098059 could reduce the drug resistance and enhance the killing action of VCR, and rates of apoptosis of MGC803 cells which were treated with VCR only increased from 18.41% to 35.61% when treated with PD098059 and VCR. It showed that PD098059 could reverse the drug resistance partially by reducing the IC₅₀ of MGC803 cells pretreated by VCR from (287±13.2) µg/L to (191±27.9) µg/L. At the same time, the expression of P-gp was inhibited by PD098059. It was suggested that when MGC803 cells were treated with VCR, the stimulation may be transduced by activation of MAPK signaling pathway to MDR1 gene and the expression of MDR1 increased. As a result, VCR was transported out of cells and multidrug resistance developed. The inhibitor of MEK1/2, PD098059 could reduce the expression of *mdr1* and drug resistance of cells exposed to VCR by blocking the ERK1/2 signal transduction pathway. The precise mechanism between MDR1 and MAPK signal transduction pathway needs further study.

REFERENCES

- Zhang LJ, Chen KN, Xu GW, Xing HP, Shi XT. Congenital expression of *mdr-1* gene in tissues of carcinoma and its relation with pathomorphology and prognosis. *World J Gastroenterol* 1999; **5**: 53-56
- Thottassery JV, Zambetti GP, Arimori K, Schuetz EG, Schuetz JD. p53-dependent regulation of MDR1 gene expression causes selective resistance to chemotherapeutic agents. *Proc Natl Acad Sci U S A* 1997; **94**: 11037-11042
- Nagata J, Kijima H, Hatanaka H, Asai S, Miyachi H, Abe Y, Yamazaki H, Nakamura M, Watanabe N, Mine T, Kondo T, Scanlon KJ, Ueyama Y. Reversal of drug resistance using hammerhead ribozymes against multidrug resistance-associated protein and multidrug resistance 1 gene. *Int J Oncol* 2002; **21**: 1021-1026
- Lage H, Perltz C, Abele R, Tampe R, Dietel M, Schandendorf D, Sinha P. Enhanced expression of human ABC-transporter tap is associated with cellular resistance to mitoxantrone. *FEBS Lett* 2001; **503**: 179-184
- Zhan M, Yu D, Lang A, Li L, Pollock RE. Wild type p53 sensitizes soft tissue sarcoma cells to doxorubicin by down-regulating multidrug resistance-1 expression. *Cancer* 2001; **92**: 1556-1566
- Liu B, Staren E, Iwamura T, Appert H, Howard J. Effects of Taxotere on invasive potential and multidrug resistance phenotype in pancreatic carcinoma cell line SUIT-2. *World J Gastroenterol* 2001; **7**: 143-148
- Stavrovskaya AA. Cellular mechanisms of multidrug resistance of tumor cells. *Biochemistry* 2000; **65**: 95-106
- van Brussel JP, van Steenbrugge GJ, Romijn JC, Schroder FH, Mickisch GH. Chemosensitivity of prostate cancer cell lines and expression of multidrug resistance-related proteins. *Eur J Cancer* 1999; **35**: 664-671
- Ruefli AA, Smyth MJ, Johnstone RW. HMBA induces activation of a caspase-independent cell death pathway to overcome P-glycoprotein-mediated multidrug resistance. *Blood* 2000; **95**: 2378-2385
- Bohacova V, Kvackajova J, Barancik M, Drobna Z, Breier A. Glutathione S-transferase does not play a role in multidrug resistance of L1210/VCR cell line. *Physiol Res* 2000; **49**: 447-453
- Smyth MJ, Krasovskis E, Sutton VR, Johnstone RW. The drug efflux protein, P-glycoprotein, additionally protects drug-resistant tumor cells from multiple forms of caspase-dependent apoptosis. *Proc Natl Acad Sci U S A* 1998; **95**: 7024-7029
- Naito S, Yokomizo A, Koga H. Mechanisms of drug resistance in chemotherapy for urogenital carcinoma. *Int J Urol* 1999; **6**: 427-439
- Warr JR, Bamford A, Quinn DM. The preferential induction of apoptosis in multidrug-resistance KB cells by 5-fluorouracil. *Cancer Lett* 2002; **175**: 39-44
- Roepe PD. PH and multidrug resistance. *Novartis Found Symp* 2001; **240**: 232-247
- Holzmayr TA, Hilsenbeck S, Von Hoff DD, Roninson IB. Clinical correlates of MDR1 (P-glycoprotein) gene expression in ovarian and small-cell lung carcinomas. *J Natl Cancer Inst* 1992; **84**: 1486-1491
- Chan HS, Thorer PS, Haddad G, Ling V. Immunohistochemical detection of P-glycoprotein: Prognostic correlation in soft tissue sarcoma of childhood. *J Clin Oncol* 1990; **8**: 689-704
- Tseng CP, Cheng AJ, Chang JT, Tseng CH, Wang HM, Liao CT, Chen IH, Tseng KC. Quantitative analysis of multidrug-resistance *mdr1* gene expression in head and neck cancer by real-time RT-PCR. *Jpn J Cancer Res* 2002; **93**: 1230-1236
- Schondorf T, Kurbacher CM, Gohring UJ, Benz C, Becker M, Sartorius J, Kolhagen H, Mallman P, Neumann R. Induction of MDR1-gene expression by antineoplastic agents in ovarian cancer cell lines. *Anticancer Res* 2002; **22**: 2199-2203
- Kato A, Miyazaki M, Ambiru S, Yoshitomi H, Ito H, Nakagawa K, Shimizu H, Yokosuka O, Nakajima N. Multidrug resistance gene (MDR-1) expression as a useful prognostic factor in patients with human hepatocellular carcinoma after surgical resection. *J Surg Oncol* 2001; **78**: 110-115
- Sonneveld P. Multidrug resistance in haematological malignancies. *J Intern Med* 2000; **247**: 521-534
- Chaudhary PM, Roninson IB. Induction of multidrug resistance in human cells by transient exposure to different chemotherapeutic drugs. *J Natl Cancer Inst* 1993; **85**: 632-639
- Zhang P, Wang D, Zheng G. Induction of multidrug resistance in Tca8113 cells by transient exposure to different chemotherapeutic drugs. *Huaxi Kouqiang Yixue Zazhi* 2003; **21**: 70-73
- Brugger D, Brischwein K, Liu C, Bader P, Niethammer D, Gekeler V, Beck JF. Induction of drug resistance and protein kinase C genes in A2780 ovarian cancer cells after incubation with antine-

- oplastic agents at sublethal concentrations. *Anticancer Res* 2002; **22**: 4229-4232
- 24 **Schondorf T**, Neumann R, Benz C, Becker M, Riffelmann M, Gohring UJ, Sartorius J, von Konig CH, Breidenbach M, Valter MM, Hoopmann M, Di Nicolantonio F, Kurbacher CM. Cisplatin, doxorubicin and paclitaxel induce mdr1 gene transcription in ovarian cancer cell lines. *Recent Results Cancer Res* 2003; **161**: 111-116
- 25 **Kisucka J**, Barancik M, Bohacova V, Breier A. Reversal effect of specific inhibitors of extracellular-signal regulated protein kinase pathway on P-glycoprotein mediated vincristine resistance of L1210 cells. *Gen Physiol Biophys* 2001; **20**: 439-444
- 26 **Lewis TS**, Shapiro PS, Ahn NG. Signal transduction through MAP kinase cascades. *Adv Cancer Res* 1998; **74**: 49-139
- 27 **Karin M**. Mitogen-activated protein kinase cascades as regulators of stress responses. *Ann N Y Acad Sci* 1998; **851**: 139-146
- 28 **Evans DR**, Hemmings BA. Signal transduction. What goes up must come down. *Nature* 1998; **394**: 23-24
- 29 **Chen J**, Fujii K, Zhang L, Roberts T, Fu H. Raf-1 promotes cell survival by antagonizing apoptosis signal-regulating kinase 1 through a MEK-ERK independent mechanism. *Proc Natl Acad Sci U S A* 2001; **98**: 7783-7788
- 30 **Busca R**, Abbe P, Mantoux F, Aberdam E, Peyssonnaud C, Eychene A, Ortonne JP, Ballotti R. Ras mediates the cAMP-dependent activation of extracellular signal-regulated kinases (ERKs) in melanocytes. *EMBO J* 2000; **19**: 2900-2910
- 31 **Payne DM**, Rossomando AJ, Martino P, Erickson AK, Her JH, Shabanowitz J, Hunt DF, Weber MJ, Sturgill TW. Identification of the regulatory phosphorylation sites in pp42/mitogen-activated protein kinase (MAP kinase). *EMBO J* 1991; **10**: 885-892
- 32 **Dent P**, Jarvis WD, Birrer MJ, Fisher PB, Schmidt-Ullrich RK, Grant S. The roles of signaling by the p42/p44 mitogen-activated protein (MAP) kinase pathway; a potential route to radio- and chemo-sensitization of tumor cells resulting in the induction of apoptosis and loss of clonogenicity. *Leukemia* 1998; **12**: 1843-1850
- 33 **Ding S**, Chamberlain M, McLaren A, Goh L, Duncan I, Wolf CR. Cross-talk between signalling pathways and the multidrug resistant protein MDR-1. *Br J Cancer* 2001; **85**: 1175-1184
- 34 **Kim MS**, So HS, Park JS, Lee KM, Moon BS, Lee HS, Kim TY, Moon SK, Park R. Hwansodan protects PC12 cells against serum-deprivation-induced apoptosis via a mechanism involving Ras and mitogen-activated protein (MAP) kinase pathway. *Gen Pharmacol* 2000; **34**: 227-235
- 35 **Fritz F**, Howard EM, Hoffman MM, Roepe PD. Evidence for altered ion transport in *Saccharomyces cerevisiae* overexpressing human MDR1 protein. *Biochemistry* 1999; **38**: 4214-4226
- 36 **Wittstein IS**, Qiu W, Ziegelstein RC, Hu Q, Kass DA. Opposite effects of pressurized steady versus pulsatile perfusion on vascular endothelial cell cytosolic pH: role of tyrosine kinase and mitogen-activated protein kinase signaling. *Circ Res* 2000; **86**: 1230-1236

Edited by Zhu LH Proofread by Xu FM

Mitochondrial microsatellite instability in gastric cancer and its precancerous lesions

Xian-Long Ling, Dian-Chun Fang, Rong-Quan Wang, Shi-Ming Yang, Li Fang

Xian-Long Ling, Dian-Chun Fang, Rong-Quan Wang, Shi-Ming Yang, Li Fang, Department of Gastroenterology, Southwest Hospital, Third Military Medical University, Chongqing 400038, China

Supported by the National Natural Science Foundation of China, No. 30070043, and Scientific Research Project of Chinese PLA during the 10th Five-year plan period, No. 01Z075

Correspondence to: Dian-Chun Fang, M.D., Ph.D. Southwest Hospital, Third Military Medical University, Chongqing 400038, China. fangdianchun@hotmail.com

Telephone: +86-23-68754624 **Fax:** +86-23-68754124

Received: 2003-08-26 **Accepted:** 2003-09-18

Abstract

AIM: To evaluate the role of mitochondrial microsatellite instability (mtMSI) in gastric carcinogenesis.

METHODS: MtMSI was measured with PCR-single strand conformation polymorphism (PCR-SSCP) in 68 cases of advanced gastric cancer, 40 cases of chronic gastritis, 30 cases of intestinal metaplasia and 20 cases of dysplasia.

RESULTS: MtMSI was observed in 12.5% (5 of 40) of chronic gastritis, 20.0% (6 of 30) of intestinal metaplasia, 25.0% (5 of 20) of dysplasia and 38.2% (26 of 68) of gastric cancer. These findings showed a sequential accumulation of mtMSI in the histological progression from chronic gastritis to gastric cancer. An association of mtMSI with intestinal histological type and distal location was found ($P=0.001$ and $P=0.002$), whereas no significant correlation was found between mtMSI and age at diagnosis, sex, tumor size, depth of invasion, lymph node spread and clinical stages ($P>0.05$).

CONCLUSION: MtMSI may play an early and important role in the gastric carcinogenesis pathway, especially in the intestinal type and distal gastric cancer.

Ling XL, Fang DC, Wang RQ, Yang SM, Fang L. Mitochondrial microsatellite instability in gastric cancer and its precancerous lesions. *World J Gastroenterol* 2004; 10(6): 800-803

<http://www.wjgnet.com/1007-9327/10/800.asp>

INTRODUCTION

The mechanisms of carcinogenesis in the gastric mucosa remain unclear. Genetic instability is strongly involved in neoplastic transformation and progression^[1-7]. In gastrointestinal carcinomas, such genetic instability may be classified into two different forms in which hypermutability occurs either due to chromosomal instability or due to microsatellite instability (MSI)^[8-11]. MSI represents an important form of genomic instability associated with defective DNA mismatch repair in tumors. Although the MSI in nuclear DNA (nMSI) of gastric cancer has been established, little attention was paid to the MSI in mitochondrial DNA (mtMSI) in this cancer. In the present study, we analysed the mtMSI in gastric cancer and its premalignant lesions to elucidate whether

mtMSI led to the progression from chronic gastritis to gastric cancer, via intestinal metaplasia and dysplasia.

MATERIALS AND METHODS

Tissue samples

Forty cases of chronic gastritis, 30 cases of intestinal metaplasia and 20 cases of dysplasia obtained from patients undergoing upper endoscopy for dyspepsia and 68 cases of surgically resected gastric cancer tissues were studied. Tissues from non-tumor or non-inflammatory gastric mucosa, showing no dysplasia or metaplasia, were used as a control in analysis of mtMSI. Hematoxylin-eosin (HE) staining was used for the histopathological diagnosis, evaluation and grading of gastritis, atrophy, intestinal metaplasia, dysplasia and cancer. Genomic DNA was isolated by standard proteinase-K digestion and phenol-chloroform extraction protocols. None of the patients with gastric cancer included in the present series had received chemotherapy or radiation therapy before operation.

mtMSI detection

PCR-single strand conformation polymorphism (PCR-SSCP) was performed to amplify the microsatellite sequence of mtDNA using published primers^[18]. The primer consisted of 2 D-loop regions and 5 coding regions (Table 1). The reaction conditions and procedures were similar to those reported by Hebrano *et al*^[12].

Each PCR was digested by appropriate restriction enzymes and electrophoresed at 300 V at 22 °C for 2 h on a 75g/L polyacrylamide gel containing 50 mmol/L boric acid, 1 mmol/L EDTA and 25g/L glycerol. After silver staining, PCR products that showed mobility shifts were directly sequenced using an appropriate internal primer and analyzed using the 373A automated DNA sequencer (Perkin Elmer Cetus). All analyses were repeated twice to rule out PCR artifacts.

Table 1 Sequences of primer for PCR analysis

Repeat sequence	mtDNA region	Position	Annealing (°C)	Primer (5'-3')
(C) _n	270-425	D-loop	58	TCCACACAGACATCAATAACA AAAGTGCATACCGCCAAAAG
(CA) _n	467-556	D-loop	55	CCCATACTACTAATCTCATCAA TTTGTTGGTTCGGGGTATG
(C) ₆	3 529-3 617	ND1	55	CCGACCTTAGCTCTCACCAT AATAGGAGGCTAGGTTGAG
(A) ₇	4 555-4 644	ND2	55	CCTGAGTAGGCCTAGAAATAAA ACTTGATGGCAGCTTCTGTG
(T) ₇	9 431-9 526	COIII	55	CCAAAAGGCCTTCGATACG GCTAGGCTGGAGTGTAATA
(C) ₆ and (A) ₈	12 360-12 465	ND5	55	CACCCTAACCCCTGACTTCC GGTGGATCGACAATGGATT
(CCT) ₃ and (AGC) ₃	12 940-13 032	ND5	55	GCCCTTCTAAACGCTAATCC TCAGGGGTGGAGACCTAATT

Statistical analysis

Chi-square test with Yates' correction was used. A P value <0.05 was considered statistically significant.

RESULTS

Sixty-eight gastric cancer samples and 90 benign gastric mucosal lesions were screened for mtMSI at seven repeat sites using the PCR-RFLP method. Figure 1 exhibits a representative mobility-shift band compared with normal counterpart. mtMSI was observed in 26 out of 68 cases (38.2%) of gastric cancer, 5 out of 40 cases (12.5%) of chronic gastritis, 6 out of 30 cases (20%) of intestinal metaplasia, and 5 out of 20 cases (25.0%) of dysplasia (Table 2).

The clinicopathological characteristics of mtMSI-positive cases were compared with those of cases that were mtMSI-negative (Table 3). An association of mtMSI with intestinal histological type and distal location was found ($P=0.001$ and $P=0.002$), whereas no significant correlation was found between mtMSI and age at diagnosis, sex, tumor size, depth of invasion, lymph node spread and clinical stages ($P>0.05$).

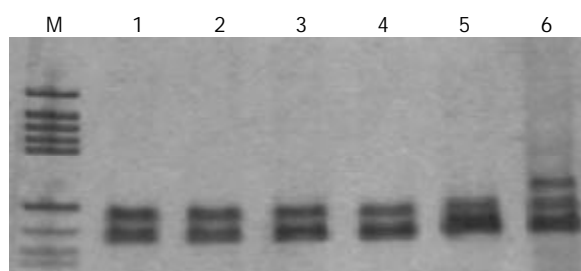


Figure 1 Detection of mitochondrial DNA microsatellite instability in gastric cancer by PCR-single strand conformation polymorphism. Lane 6 indicates conformational variants associated with mitochondrial DNA microsatellite instability.

Table 2 mtMSI in gastric cancer and its precursor

	<i>n</i>	mtMSI(%)
Chronic gastritis	40	5(12.5)
Intestinal metaplasia	30	6(20.0)
Dysplasia	20	5(25.0)
Gastric cancer	68	26(38.2)

Table 3 Characteristics of 68 gastric cancer patients

Characteristic	<i>n</i>	mtMSI-positive	tMSI-negative
Age			
<40 years	15	5	10
>40 years	53	21	32
Sex			
Male	42	15	27
Female	26	11	15
Size			
<5 cm	38	14	24
>5 cm	30	12	18
Histological type			
Intestinal	41	22 ^b	19
Diffuse	27	4	23
Tumor location			
Distal	45	23 ^c	22
Proximal	23	3	20
Invasion			
Within the wall	33	12	21
Invading serosa	35	14	21
Lymph node spread			
Absent	30	11	19
Present	38	15	23

^b $P=0.001$ vs the groups of diffuse type and ^c $P=0.002$ vs the groups of proximal location.

DISCUSSION

Carcinogenesis is a long-term, multistep process driven by multiple genetic and epigenetic changes in susceptible cells, which gain a selective growth advantage and undergo clonal expansion. Genetic instability is an important factor in the rapid accumulation of these genetic changes. Much attention has been directed to the genetic events in nDNA, such as activation of oncogenes, inactivation of tumor suppressor genes, and defects of mismatched DNA repair genes^[13,14]. However, several aspects in the process of carcinogenesis are still unclear. It has been shown that somatic mutations in mtDNA were detected in various human tumors^[15-18]. In addition, microsatellite instability has also been shown in mtDNA of colorectal and gastric carcinomas^[18-20]. Further studies demonstrated that repeated mononucleotide alteration, missense mutation, and small deletion in NADH dehydrogenase genes and alteration in polycytidine (C)*n* tract in the D-loop region of mtDNA could occur in colorectal carcinomas^[18]. These results imply that mtMSI of colorectal carcinomas may likely result from certain deficiencies in DNA repair. Therefore, it has been proposed that somatic mutations and mtMSI play a role in tumorigenesis and development of cancer^[21,22]. To study the role of mtMSI in gastric carcinogenesis, we analyzed 68 cases of gastric cancer using seven microsatellite markers known to be altered in gastrointestinal carcinomas. MtMSI was found in 38.2% of patients with gastric cancer, implying that mtMSI may play an important role in the occurrence of a part of gastric cancers.

The majority of gastric carcinomas, particularly the "intestinal" type, which is most common in populations at high risk, were preceded by a precancerous stage, characterized by the following sequential steps, namely chronic gastritis, intestinal metaplasia, and dysplasia^[23,24]. Although numerous cytogenetic and molecular genetic studies have been performed on gastric adenocarcinomas, fundamental data pertaining to precursor lesions which could substantially clarify our understanding of the tumorigenesis in gastric mucosa are not available. This is the first study to examine the frequency of mtMSI in intestinal metaplasia and dysplasia, two premalignant lesions of gastric cancer in individuals without gastric cancer. If mtMSI plays an early and significant role in gastric carcinogenesis, one might expect to find mtMSI in metaplastic and dysplasia tissues before the development of cancer. In this study, mtMSI was detected in 12.5% of chronic gastritis, 20.0% of intestinal metaplasia, and 38.2% of gastric cancer tissues examined. These findings showed a sequential accumulation of mtMSI in the histological progression from chronic gastritis to cancer via intestinal metaplasia and dysplasia, suggesting an early and important role of mtMSI in the gastric carcinogenesis pathway, and they may define a subset of individuals susceptible to gastric cancer.

Cancers from different mutational pathways are thought to have different clinical features. nMSI+ gastric cancer was characterized by older age, antral location, intestinal type, lower prevalence of lymph node metastasis, and a lower pTNM stage^[25,26]. However, the clinicopathologic characteristics of mtMSI+ gastric cancers remain unclear. In the current study, we did not find an obvious relationship between mtMSI and tumor size, depth of invasion, node metastasis or clinical stages, indicating a limited role of mtMSI in predicting the prognosis of gastric carcinomas. Gastric carcinomas can be divided into "intestinal" type and "diffuse" type. A distinct genetic pathway has been found in gastric carcinogenesis of different histological subtypes and their tumor progression^[27-29]. Increased beta-catenin mRNA levels and mutational alterations of APC and beta-catenin gene were present in intestinal type gastric cancer^[30,31], whereas epigenetic inactivation of E-cadherin via promoter hypermethylation might be an early critical event

in the development of undifferentiated tumors^[32-35]. In this study, a marked difference in mtMSI was noted in gastric cancer. MtMSI was much more frequent in intestinal-type gastric cancers as compared with diffuse-type gastric cancer, suggesting that mtMSI is a predisposing event in intestinal type of gastric cancer. In contrast to mtMSI-negative gastric cancer, mtMSI-positive gastric tumors tended to exhibit a predominant distal location, similar to nMSI-positive gastric tumors.

The mechanisms underlying mtMSI in gastric mucosa remain unclear. In gastric mucosa, reactive oxygen species (ROS) are commonly released in inflamed gastric mucosa as a result of infection with *Helicobacter pylori* (*H pylori*), especially CagA+ strains, and they might be responsible for mtMSI-positive gastric cancer^[36-38]. Mitochondrial genome was particularly susceptible to oxidative damage and mutation because of the high rate of ROS generation and inefficient DNA repair system in the organelle^[39,40]. ROS and defective DNA repair were the two causes of increased damage proposed to explain mtMSI in *H pylori*-associated gastric cancer^[41-43]. A possibly important role of *H pylori* in the development of mtMSI-positive gastric cancer needed to be further studied.

Although gastric cancer is a common disease, molecular markers for its early diagnosis are lacking. Mitochondrial DNA mutations occurred in a wide variety of cancers and might be useful in the detection of cancer^[44]. Indeed, some authors have implied that mitochondrial genome instability is so common and the enrichment of mutations in cancer is so significant that some mutations probably confer a selective or replicative advantage to those cells that have acquired such mutations^[21]. Others have suggested that mtDNA mutations may enhance the toxicity of anti-cancer treatments^[45-48]. Thus, the existence of mtDNA mutations in cancer may impact diagnosis and treatment and may be important in understanding the progression of some cancers. Given the early involvement of mtMSI in the multistep gastric carcinogenesis model, detection of mtMSI could serve as a surrogate marker for the risk of gastric cancer development^[49]. It might help to identify high-risk patient, by determining mtMSI of preneoplastic lesions, such that close monitoring or potential intervention can be performed. Because the majority of patients with intestinal metaplasia and dysplasia will not progress to cancer and only a proportion of these patients harbor mtMSI, it is conceivable that patients with intestinal metaplasia and dysplasia displaying mtMSI are at greater risk of developing gastric cancer than those without mtMSI.

In conclusion, a high frequency of mtMSI can be found in gastric cancer and its premalignant lesions. Taking into consideration of the progressive increase in mtMSI frequency from premalignant to malignant lesions, our results suggest the early involvement and continuous accumulation of mtMSI in gastric cells that have entered the multistep gastric carcinogenesis pathway. The role of mtMSI in premalignant gastric lesions as a surrogate marker of the risk of gastric cancer development warrants further investigation.

REFERENCES

- Lengauer C**, Kinzler KW, Vogelstein B. Genetic instability in colorectal cancers. *Nature* 1997; **386**:623-627
- Thibodeau SN**, Bren G, Schaid D. Microsatellite instability in cancer of the proximal colon. *Science* 1993; **260**: 816-819
- Ionov Y**, Peinado MA, Malkhosyan S, Shibata D, Perucho M. Ubiquitous somatic mutations in simple repeated sequences reveal a new mechanism for colonic carcinogenesis. *Nature* 1993; **363**: 558-561
- Vogelstein B**, Fearon ER, Hamilton SR, Kern SE, Preisinger AC, Leppert M, Nakamura Y, White R, Smits AM, Bos JL. Genetic alterations during colorectal-tumor development. *N Engl J Med* 1988; **319**: 525-532
- Fearon ER**, Vogelstein B. A genetic model for colorectal tumorigenesis. *Cell* 1990; **61**: 759-767
- Jen J**, Kim H, Piantadosi S, Liu ZF, Levitt RC, Sistonen P, Kinzler KW, Vogelstein B, Hamilton SR. Allelic loss of chromosome 18q and prognosis in colorectal cancer. *N Engl J Med* 1994; **331**: 213-221
- White RL**. Tumor suppressing pathways. *Cell* 1998; **92**: 591-592
- Fang DC**, Jass JR, Wang DX, Zhou XD, Luo YH, Young J. Infrequent loss of heterozygosity of APC/MCC and DCC genes in gastric cancer showing DNA microsatellite instability. *J Clin Pathol* 1999; **52**: 504-508
- Fang DC**, Yang SM, Zhou XD, Wang DX, Luo YH. Telomere erosion is independent of microsatellite instability but related to loss of heterozygosity in gastric cancer. *World J Gastroenterol* 2001; **7**: 522-526
- Martins C**, Kedda MA, Kew MC. Characterization of six tumor suppressor genes and microsatellite instability in hepatocellular carcinoma in southern African blacks. *World J Gastroenterol* 1999; **5**: 470-476
- Wu BP**, Zhang YL, Zhou DY, Gao CF, Lai ZS. Microsatellite instability, MMR gene expression and proliferation kinetics in colorectal cancer with familial predisposition. *World J Gastroenterol* 2000; **6**: 902-905
- Habano W**, Nakamura S, Sugai T. Microsatellite instability in the mitochondrial DNA of colorectal carcinomas: evidence for mismatch repair systems in mitochondrial genome. *Oncogene* 1998; **17**: 1931-1937
- Fang DC**, Wang RQ, Yang SM, Yang JM, Liu HF, Peng GY, Xiao TL, Luo YH. Mutation and methylation of hMLH1 in gastric carcinomas with microsatellite instability. *World J Gastroenterol* 2003; **9**: 655-659
- Fang DC**, Luo YH, Yang SM, Li XA, Ling XL, Fang L. Mutation analysis of APC gene in gastric cancer with microsatellite instability. *World J Gastroenterol* 2002; **8**: 787-791
- Fliiss MS**, Usadel H, Caballero OL, Wu L, Buta MR, Eleff SM, Jen J, Sidransky D. Facile detection of mitochondrial DNA mutations in tumors and bodily fluids. *Science* 2000; **287**: 2017-2019
- Richard SM**, Bailliet G, Paez GL, Bianchi MS, Peltomaki P, Bianchi NO. Nuclear and mitochondrial genome instability in human breast cancer. *Cancer Res* 2000; **60**: 4231-4237
- Yeh JJ**, Lunetta KL, van Orsouw NJ, Moore FD Jr, Mutter GL, Vijg J, Dahia PL, Eng C. Somatic mitochondrial DNA (mtDNA) mutations in papillary thyroid carcinomas and differential mtDNA sequence variants in cases with thyroid tumours. *Oncogene* 2000; **19**: 2060-2066
- Habano W**, Sugai T, Yoshida T, Nakamura S. Mitochondrial gene mutation, but not large-scale deletion, is a feature of colorectal carcinomas with mitochondrial microsatellite instability. *Int J Cancer* 1999; **83**: 625-629
- Habano W**, Sugai T, Nakamura SI, Uesugi N, Yoshida T, Sasou S. Microsatellite instability and mutation of mitochondrial and nuclear DNA in gastric carcinoma. *Gastroenterology* 2000; **118**: 835-841
- Maximo V**, Soares P, Seruca R, Rocha AS, Castro P, Sobrinho-Simoes M. Microsatellite instability, mitochondrial DNA large deletions, and mitochondrial DNA mutations in gastric carcinoma. *Genes Chromosomes Cancer* 2001; **32**: 136-143
- Hochhauser D**. Relevance of mitochondrial DNA in cancer. *Lancet* 2000; **356**: 181-182
- Liu MR**, Pan KF, Li ZF, Wang Y, Deng DJ, Zhang L, Lu YY. Rapid screening mitochondrial DNA mutation by using denaturing high-performance liquid chromatography. *World J Gastroenterol* 2002; **8**: 426-430
- Correa P**, Shiao YH. Phenotypic and genotypic events in gastric carcinogenesis. *Cancer Res* 1994; **54**(7 Suppl): 1941s-1943s
- Leung WK**, Kim JJ, Kim JG, Graham DY, Sepulveda AR. Microsatellite instability in gastric intestinal metaplasia in patients with and without gastric cancer. *Am J Pathol* 2000; **156**: 537-543
- Wu MS**, Lee CW, Shun CT, Wang HP, Lee WJ, Chang MC, Sheu JC, Lin JT. Distinct clinicopathologic and genetic profiles in sporadic gastric cancer with different mutator phenotypes. *Genes Chromosomes Cancer* 2000; **27**: 403-411
- Wu MS**, Chang MC, Huang SP, Tseng CC, Sheu JC, Lin YW, Shun CT, Lin MT, Lin JT. Correlation of histologic subtypes and replication error phenotype with comparative genomic hybrid-

- ization in gastric cancer. *Genes Chromosomes Cancer* 2001; **30**: 80-86
- 27 **Wu MS**, Shun CT, Wang HP, Sheu JC, Lee WJ, Wang TH, Lin JT. Genetic alterations in gastric cancer: relation to histological subtypes, tumor stage, and *Helicobacter pylori* infection. *Gastroenterology* 1997; **112**: 1457-1465
- 28 **Endoh Y**, Sakata K, Tamura G, Ohmura K, Ajioka Y, Watanabe H, Motoyama T. Cellular phenotypes of differentiated-type adenocarcinomas and precancerous lesions of the stomach are dependent on the genetic pathways. *J Pathol* 2000; **191**: 257-263
- 29 **Ohmura K**, Tamura G, Endoh Y, Sakata K, Takahashi T, Motoyama T. Microsatellite alterations in differentiated-type adenocarcinomas and precancerous lesions of the stomach with special reference to cellular phenotype. *Hum Pathol* 2000; **31**: 1031-1035
- 30 **Ebert MP**, Fei G, Kahmann S, Muller O, Yu J, Sung JJ, Malfetheriner P. Increased beta-catenin mRNA levels and mutational alterations of the APC and beta-catenin gene are present in intestinal-type gastric cancer. *Carcinogenesis* 2002; **23**: 87-91
- 31 **Park WS**, Oh RR, Park JY, Lee SH, Shin MS, Kim YS, Kim SY, Lee HK, Kim PJ, Oh ST, Yoo NJ, Lee JY. Frequent somatic mutations of the beta-catenin gene in intestinal-type gastric cancer. *Cancer Res* 1999; **59**: 4257-4260
- 32 **Tamura G**, Sato K, Akiyama S, Tsuchiya T, Endoh Y, Usuba O, Kimura W, Nishizuka S, Motoyama T. Molecular characterization of undifferentiated-type gastric carcinoma. *Lab Invest* 2001; **81**: 593-598
- 33 **Becker KF**, Atkinson MJ, Reich U, Becker I, Nekarda H, Siewert JR, Hofler H. E-cadherin gene mutations provide clues to diffuse type gastric carcinomas. *Cancer Res* 1994; **54**: 3845-3852
- 34 **Ascano JJ**, Frierson H Jr, Moskaluk CA, Harper JC, Roviello F, Jackson CE, El-Rifai W, Vindigni C, Tosi P, Powell SM. Inactivation of the E-cadherin gene in sporadic diffuse-type gastric cancer. *Mod Pathol* 2001; **14**: 942-949
- 35 **Machado JC**, Oliveira C, Carvalho R, Soares P, Bex G, Caldas C, Seruca R, Carneiro F, Sobrinho-Simoes M. E-cadherin gene (CDH1) promoter methylation as the second hit in sporadic diffuse gastric carcinoma. *Oncogene* 2001; **20**: 1525-1528
- 36 **Wu AH**, Crabtree JE, Bernstein L, Hawtin P, Cockburn M, Tseng CC, Forman D. Role of *Helicobacter pylori* CagA+ strains and risk of adenocarcinoma of the stomach and esophagus. *Int J Cancer* 2003; **103**: 815-821
- 37 **Farinati F**, Cardin R, Degan P, Ruggie M, Mario FD, Bonvicini P, Naccarato R. Oxidative DNA damage accumulation in gastric carcinogenesis. *Gut* 1998; **42**: 351-356
- 38 **Drake IM**, Mapstone NP, Schorah CJ, White KL, Chalmers DM, Dixon MF, Axon AT. Reactive oxygen species activity and lipid peroxidation in *Helicobacter pylori* associated gastritis: relation to gastric mucosal ascorbic acid concentrations and effect of *H pylori* eradication. *Gut* 1998; **42**: 768-771
- 39 **Yakes FM**, Van Houten B. Mitochondrial DNA damage is more extensive and persists longer than nuclear DNA damage in human cells following oxidative stress. *Proc Natl Acad Sci U S A* 1997; **94**: 514-519
- 40 **Li JM**, Cai Q, Zhou H, Xiao GX. Effects of hydrogen peroxide on mitochondrial gene expression of intestinal epithelial cells. *World J Gastroenterol* 2002; **8**: 1117-1122
- 41 **Bagchi D**, McGinn TR, Ye X, Bagchi M, Krohn RL, Chatterjee A, Stohs SJ. *Helicobacter pylori*-induced oxidative stress and DNA damage in a primary culture of human gastric mucosal cells. *Dig Dis Sci* 2002; **47**: 1405-1412
- 42 **Shimoyama T**, Fukuda S, Liu Q, Nakaji S, Fukuda Y, Sugawara K. Production of chemokines and reactive oxygen species by human neutrophils stimulated by *Helicobacter pylori*. *Helicobacter* 2002; **7**: 170-174
- 43 **Bohr VA**, Stevnsner T, de Souza-Pinto NC. Mitochondrial DNA repair of oxidative damage in mammalian cells. *Gene* 2002; **286**: 127-134
- 44 **Bianchi NO**, Bianchi MS, Richard SM. Mitochondrial genome instability in human cancers. *Mutat Res* 2001; **488**: 9-23
- 45 **Shen ZY**, Shen J, Li QS, Chen CY, Chen JY, Zeng Y. Morphological and functional changes of mitochondria in apoptotic esophageal carcinoma cells induced by arsenic trioxide. *World J Gastroenterol* 2002; **8**: 31-35
- 46 **Peters U**, Preisler-Adams S, Lanvers-Kaminsky C, Jurgens H, Lamprecht-Dinnesen A. Sequence variations of mitochondrial DNA and individual sensitivity to the ototoxic effect of cisplatin. *Anticancer Res* 2003; **23**: 1249-1255
- 47 **Carew JS**, Zhou Y, Albitar M, Carew JD, Keating MJ, Huang P. Mitochondrial DNA mutations in primary leukemia cells after chemotherapy: clinical significance and therapeutic implications. *Leukemia* 2003; **17**: 1437-1447
- 48 **Wardell TM**, Ferguson E, Chinnery PF, Borthwick GM, Taylor RW, Jackson G, Craft A, Lightowlers RN, Howell N, Turnbull DM. Changes in the human mitochondrial genome after treatment of malignant disease. *Mutat Res* 2003; **525**: 19-27
- 49 **Hiyama T**, Tanaka S, Shima H, Kose K, Kitadai Y, Ito M, Sumii M, Yoshihara M, Shimamoto F, Haruma K, Chayama K. Somatic mutation of mitochondrial DNA in *Helicobacter pylori*-associated chronic gastritis in patients with and without gastric cancer. *Int J Mol Med* 2003; **12**: 169-174

Edited by Zhang JZ and Wang XL Proofread by Xu FM

Detection of micrometastasis of gastric carcinoma in peripheral blood circulation

Xi-Mei Chen, Guo-Yu Chen, Zhi-Rong Wang, Feng-Shang Zhu, Xiao-Lei Wang, Xia Zhang

Xi-Mei Chen, Guo-Yu Chen, Zhi-Rong Wang, Feng-Shang Zhu, Xiao-Lei Wang, Xia Zhang, Department of Gastroenterology, Tongji Hospital of Tongji University, Shanghai 200065, China

Correspondence to: Dr. Guo-Yu Chen, Department of Endoscopy, Tongji Hospital of Tongji University, 200065, Shanghai, China. cguoyu@yahoo.com.cn

Telephone: +86-21-56051080-2102

Received: 2003-07-17 **Accepted:** 2003-08-25

Abstract

AIM: To detect the micrometastasis of gastric carcinoma in peripheral blood circulation using immunomagnetic beads sorting technique and RT-PCR technique, and to discuss its significance and the difference between the two methods.

METHODS: Density gradient centrifugation was used to isolate mononuclear cells from peripheral blood, immunomagnetic beads sorting technique and RT-PCR technique were used to detect the disseminated carcinoma cells. HE, immunocytochemical and immunofluorescence staining were also used to identify the characteristics of the cells separated with immunomagnetic beads sorting technique.

RESULTS: Cells expressing cytokeratin were separated and enriched from the peripheral blood specimens of patients suffering from gastric carcinoma or chronic gastritis. After HE staining, two kinds of cells with little cytoplasm were found. Majority of these cells had small and round nuclei, even chromatin and the thickness of nuclear membrane was normal. Immunohistochemical staining indicated that there were CD34 and CD45 expression on the cell membrane of this kind of cells and these cells also showed expressed human telomerase reverse transcriptase by immunofluorescence staining, but the expression of carcinoembryonic antigen was absent. So, these cells might hematopoiesis precursors. Another kind of cells had larger and abnormal nuclei with thicker nuclear membranes. Massed chromatin and poly-nucleoli were found in the nuclei. These cells expressed human telomerase reverse transcriptase and carcinoembryonic antigen, but CD34 and CD45 were not found on the cell membrane. So, these cells were considered as gastric carcinoma cells escaping from the original focuses and existing in the peripheral blood circulation. Carcinoma cells were found in 25 of 60(41.7%) specimens of peripheral blood from patients with gastric carcinoma, while there were no such cells separated from the blood specimens of chronic gastritis patients. The difference of positive rates of disseminated carcinoma cells between two groups was markedly significant ($P < 0.005$). The expressions of CK20 mRNA in peripheral blood specimens were examined with RT-PCR. CK20 mRNA was detected from 32 of 60(53.3%) peripheral blood specimens in the group of gastric carcinoma patients, while none of the specimens from patients suffering from chronic gastritis had CK20 mRNA. Significant difference was also found between two groups ($P < 0.005$). Statistic analyses also showed that there was a significant difference

between the positive rates of two methods in detecting the disseminated carcinoma cells from the peripheral blood circulation of gastric carcinoma patients ($P < 0.05$).

CONCLUSION: The results demonstrated that there were disseminated carcinoma cells in the peripheral blood circulation of some patients with gastric carcinoma. Disseminated carcinoma cells can be detected from the peripheral blood samples with immunomagnetic beads sorting technique and RT-PCR technique. The positive rate of RT-PCR technique is higher than that of immunomagnetic beads sorting technique in detecting micrometastasis.

Chen XM, Chen GY, Wang ZR, Zhu FS, Wang XL, Zhang X. Detection of micrometastasis of gastric carcinoma in peripheral blood circulation. *World J Gastroenterol* 2004; 10(6): 804-808
<http://www.wjgnet.com/1007-9327/10/804.asp>

INTRODUCTION

Gastric carcinoma is one of the most common causes of cancer mortality in China and is responsible for approximately 160 000 deaths annually. The disease is often advanced at first presentation, and only 30-40% patients undergoing surgery have a curative resection. Metastasis and relapse are the common reasons leading to death of patients^[1-6]. During the development of malignant neoplasm of non-hematopoietic system, a few of tumor cells escape from the original focus and disseminated into the lymph system, blood circulation, bone marrow, liver, kidney and other organs, which is called micrometastasis. It cannot be detected by any routine biochemical and histopathological assays or any graphical methods such as X-ray, CT, MRI, etc.^[7-11]. At the same time, the patients have not any obvious symptoms. Minute focus would grow rapidly and develop to metastasis and relapse. So, to develop an efficient diagnostic method for the detection of micrometastasis is of great clinical significance^[12-14]. In this study, immunomagnetic beads sorting technique and RT-PCR technique were used to detect the micrometastatic carcinoma cells in peripheral blood circulation of patients suffering from gastric carcinoma; HE staining was utilized to observe the cells' morphology changes; immunocytochemical staining and immunofluorescence staining were also used to identify the characteristics of the cells separated by immunomagnetic beads sorting technique. The significance of the micrometastatic carcinoma cell detection and the difference between the two methods were also discussed.

MATERIALS AND METHODS

Specimens

Eighty specimens of peripheral blood from sixty advanced gastric cancer patients and twenty chronic gastritis patients were collected from the Department of Endoscopy of the Tongji Hospital of Tongji University. The final diagnoses of these patients were determined pathologically. The blood specimens were anti-coagulated with heparin (5 U/mL).

Separation of mononuclear cells

We carefully layered a maximum of diluted whole blood with Hank's solution over 10 mL Ficoll-Paque and centrifuged for 25 min at 2 400 r/min at room temperature, aspirated the mononuclear cells located at the plasma-Ficoll-Paque interface. We then washed the mononuclear cells once by 10 mL Hank's solution and centrifuged them at 600 r/min for 10 min.

Immunomagnetic beads separation

MACS carcinoma cell enrichment and detection kits were purchased from Miltenyi Biotech, the beads were coated with cytokeratin7 (CK7) and cytokeratin 8 (CK8). The mononuclear cells were diluted with 10 mL Dilution-Buffer and 1.3 mL MACS CellPerm Solution for 5 min. After incubated with 1.3 mL MACS CellFix solution for 30 min, the solution was centrifuged at 2 000 rpm for 10 min. Then, the sediment was mixed with 7.5 mL MACS CellStain solution and centrifuged, these two procedures were repeated again. The sediment acquired was incubated with 50 μ L MACS CellStain solution, 50 μ L FcR blocking reagent and 50 μ L MACS cytokeratin microbeads for 45 min, and after that, the mixture was centrifuged at 2 000 rpm for 5 min. The sediment was diluted with 500 μ L dilution buffer and flew through the MACS column in magnetic field. The column was washed with 500 μ L Dilution Buffer apart from magnetic field. The solution obtained included CK⁺ cells and was smeared on slides. The slides were fixed with acetone and stained with HE.

Immunocytochemical detection of CD34 and CD45 expressions in CK⁺ cells

Immunohistochemical detection of CD34 and CD45 expressions was performed through a two-step procedure and the kits were purchased from Immunotech Co.

Immunofluorescence detection for hTERT and CEA expression in CK⁺ cells

Immunofluorescence detection of human telomerase reverse transcriptase (hTERT) and carcinoembryonic antigen (CEA) expression was operated through two-step procedure and the kits were purchased from Sigma Co.

RT-PCR

Total RNA was extracted with Trizol (Gibco. Co) and resuspended in sterile RNase-free water for storage at -70 °C. RT-PCR analysis was performed as follows. RNA was incubated at 60 °C for 10 min and chilled to 4 °C immediately before being reverse transcribed. Reverse transcription of 1 μ g total RNA using antisense primers was performed in a volume of 20 μ L for 40 min at 65 °C, containing 200 U MMLV reverse transcriptase, 1 \times buffer RT, 1 MU/L RNasin, 2.0 mmol/L dNTP and 0.2 μ mol/L oligo (dT) as a primer (All primers were synthesized by Life Technology, Shanghai). The primers of CK20 and β -actin were as follows: CK20 (485 bp) upstream primer: 5' AAG GCT CTG GGA GGT GCG TCT C3', downstream primer: 5' CAG TGT TGC CCA GAT GCT TGT G3'; β -actin (317 bp) upstream primer: 5' ATC ATG TTT GAG ACC A3', downstream primer: 5' CAT CTC TTG CTC GAA GTC CA3' [15]. The samples were heated to 94 °C for 5 min to terminate the reverse transcription reaction. The amplification reaction mixture consisted of 10 \times buffer 5 μ L, 0.2 mmol/L dATP, dGTP, dCTP and dTTP respectively, 2.5 U TaqDNA polymerase, and 0.2 μ mol/L each of sense and antisense primers including CK20 and β -actin respectively in a final volume of 50 μ L. The reaction mixture was first heated at 94 °C for 5 min and amplification was carried out for 35 cycles at 94 °C for 1 min, at 58 °C for 1 min, at 72 °C for 1 min, followed by an incubation at 72 °C for 10 min. A volume of

10 μ L RT-PCR products was added in 20 g/L agarose gel containing 0.5 mg/L EB and visualized with UV illumination after electrophoresis.

Statistic analysis

Experimental results were analyzed with Chi-square tests and $P < 0.05$ was accepted as the level of significance.

RESULTS

Detection of micrometastasis by immunomagnetic sorting technique

After immunomagnetic separation, CK⁺ cells were separated in all of the peripheral blood specimens from gastric carcinoma and chronic gastritis patients. There were two kinds of cells on the slides after HE staining. Because of the application of CellPerm solution, the cytoplasm of these cells decreased obviously. One kind of these cells had small and round nuclei, even chromatin and the thickness of nuclear membrane was normal. The other kind of cells had larger nuclei, which had abnormal forms and thicker membrane. Massed chromatin and more than one nuclei could also be found in this kind of cells.

Immunocytochemical and immunofluorescence staining

Immunohistochemical staining showed that there were CD34 (Figure 1) and CD45 (Figure 2) expressions on the cell membranes of the first kind of cells and these cells also had positive expressions of hTERT (Figure 3) after immunofluorescence staining, but the expression of CEA was negative. So this kind of cells might be hematopoiesis precursors (Figure 4)^[17-20]. The other kind of cells had positive hTERT and CEA (Figure 5) expressions after immunohistochemical staining, but expression of CD34 and CD45 was absent. According to the morphology and the outcome of immunohistochemical and immunofluorescence staining, these cells were considered as the disseminated carcinoma cells escaped from the primary neoplasm focus (Figure 6)^[17,21-23]. The first kind of cells was found on all slides, while the other kind of cells was only found on the slides from some gastric carcinoma patients (25/60), the positive rate was about 41.7% (Table 1). There was a significant difference between two groups ($P < 0.005$).

Detection of micrometastasis by RT-PCR technique

CK20 mRNA was detected in 32 blood specimens from gastric carcinoma patients; the positive rate was 53.3% (Figure 7). While no CK20 mRNA was detected from the blood specimens of patients with chronic gastritis. There was a significant difference between these positive rates ($P < 0.005$, Table 2).

Table 1 Comparison of tumor cells detected with immunomagnetic beads technique

Patients	+	-	Total	%
Gastric carcinoma	25	35	60	41.7
Chronic gastritis	0	20	20	0.0
Total	25	55	80	41.7

$\chi^2=10.26$, $P < 0.005$.

Table 2 Comparison of tumor cells detected with RT-PCR

Patients	+	-	Total	%
Gastric carcinoma	32	28	60	53.3
Chronic gastritis	0	20	20	0.0
Total	32	48	80	53.3

$\chi^2=15.63$, $P < 0.005$.



Figure 1 Immunohistochemical staining showed that there was CD34 expression on the membranes of the cells, these cells had small and round nuclei, even chromatin and the thickness of nuclear membrane was normal (amplification $\times 1\ 000$).



Figure 2 Immunohistochemical staining showed that there was CD45 expression on the membranes of the cells, these cells had small and round nuclei, even chromatin and the thickness of nuclear membrane was normal (amplification $\times 1\ 000$).

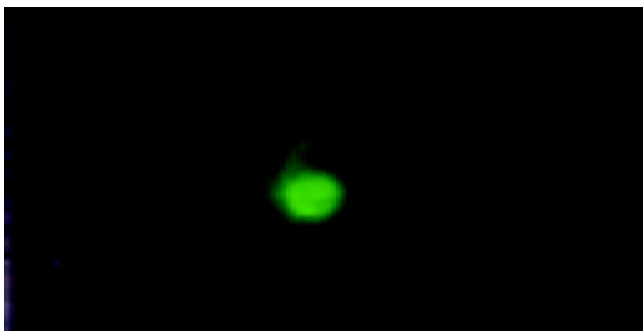


Figure 3 Immunofluorescence staining the cells, which had small and round nuclei, even chromatin and the thickness of nuclear membrane was normal (amplification $\times 200$), had positive expressions of hTERT.

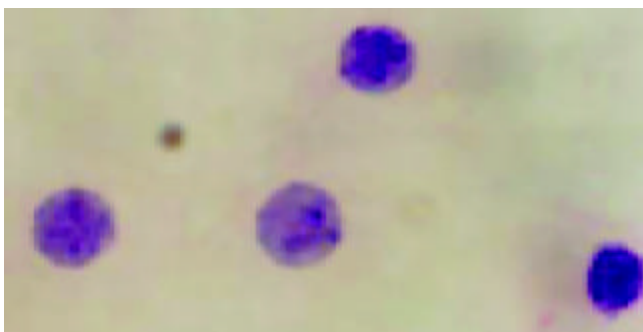


Figure 4 The cells, which had small and round nuclei, even chromatin and the thickness of nuclear membrane was normal (HE staining, amplification $\times 1\ 000$), might be hematopoiesis precursors.

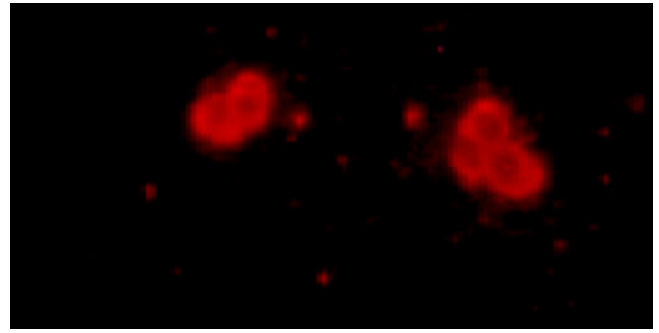


Figure 5 The cells, which had larger nuclei, abnormal forms and thicker membrane, and massed chromatin and more than one nuclei could also be found in this kind of cells, had positive expression of CEA (Immunofluorescence staining, amplification $\times 200$).

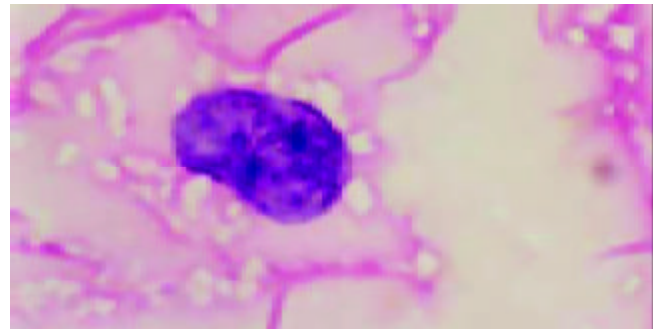


Figure 6 The cells, which had larger nuclei, abnormal forms and thicker membrane, and massed chromatin and more than one nuclei could also be found in this kind of cells, had positive expressions of CEA and hTERT, and negative expressions of CD34 and CD45, were considered as the disseminated carcinoma cells escaped from the primary neoplasm focus (HE staining, amplification $\times 1\ 000$).

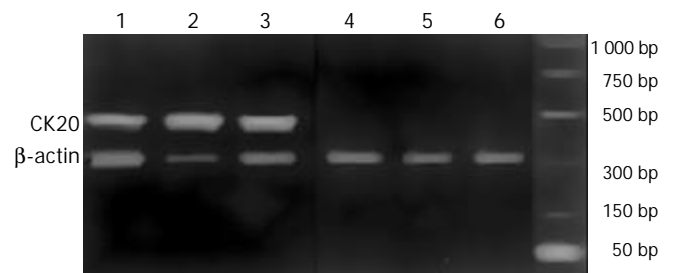


Figure 7 RT-PCR for CK20 and β -actin. M: Marker; Lanes1-4 blood from gastric cancer; Lanes5-6 blood from chronic gastritis.

Difference between positive rates of these two methods

Statistic analysis indicated that the difference between the positive rates of these two methods which were used to detect the disseminated carcinoma cells was significant ($P < 0.05$, Table 3), that is to say the positive rate of RT-PCR was higher than that of immunomagnetic bead separation technique.

Table 3 Comparison of positive rates between two methods

RT-PCR	Immunomagnetic bead separation		Total
	+	-	
+	25	7	32
-	0	28	28
Total	25	35	60

$\chi^2 = 5.14, P < 0.05$.

DISCUSSION

The first reporter of micrometastasis is Ashworth who claimed that he had found cells similar to tumor cells from the peripheral blood circulation of a carcinoma patient in 1869. After that more than twenty methods have been used to detect micrometastasis on about 5 000 patients. But the latest researches indicated that those so called tumor cells were components of hematopoietic tissues, especially prokaryotic cells^[24,25].

In this study, immunomagnetic beads sorting technique and RT-PCR technique were used to detect the micrometastatic gastric carcinoma cells from peripheral blood circulation and the difference of these two methods was also discussed. There are many components in peripheral blood. It has been found that tumor cells had the similar density with mononuclear cells and they located in the same layer after density gradient centrifugation^[26,27]. So we removed about 90% hemocytes from blood specimens with Ficoll's solution and mononuclear cells mixed with carcinoma cells were enriched. Because gastric carcinoma is derived from epithelial tissue, so carcinoma cells could express CK, a particular component of epithelial tissue^[28,29]. To separate micrometastatic gastric carcinoma cells expressing CK, immunomagnetic beads coated with anti-CK7 and anti-CK8 antibodies were used to incubate or those mononuclear cells that had been reacted with MACS CellPerm. Anti-CK7 and anti-CK8 antibodies combined with CK in the plasma of carcinoma cells by antigen-antibody reaction. So, the cells expressing CK combined with magnetic beads and detained in the magnetic field. To define the origin and characteristics of these cells, HE, immunocytochemical and immunofluorescence staining were performed. Two kinds of cells were separated after staining. Majority of these cells had small and round nucleus, and their chromatins were even. These cells' nuclear membranes had normal thickness and expressed CD34 and CD45. They also expressed hTERT, but no CEA. Normally, CD34 and CD45 in hematopoiesis precursors, could also express hTERT^[30-32]. So, these cells might be hematopoietic precursors. Minority of these cells had larger and abnormal forms of nuclei that had thicker nuclear membrane. Massive chromatins could be observed in these cells. These cells expressed hTERT and CEA, but the expressions of CD34 and CD45 were absent on the membrane of cells. Usually, hTERT and CEA could be found in tumor cells and CEA was a marker of carcinoma derived from digestive tract^[33-35], so these cells were gastric carcinoma cells escaped from the primary focuses and existed in peripheral blood circulation. This kind of cells was detected from 25 of 60 patients suffering from gastric carcinoma, while no cells were acquired from chronic gastritis patients.

CK is a component of cell skeleton and distributes in cells deriving from ectoderm. CK20, a member of this family has been found to have a stricter selectivity to epithelial tissue^[28,36]. CK8 and CK9 mRNA could be detected in blood circulation with nested RT-PCR in healthy subjects, but CK20 mRNA could not be detected^[37]. In this study, anti-CK7 and anti-CK8 but not anti-CK20 antibodies were coated on the beads, this should take responsibility for the separation of those hematopoietic precursors in the process of immunomagnetic beads sorting. If the immunomagnetic beads were coated with CK20, cells derived from epithelial tissue would be separated from hemocytes. These cells should be gastric carcinoma cells escaped from primary gastric carcinoma focus. Traditional methods for detecting disseminated tumor cells such as cell morphology, flowcytometer and cytogenetics were not so sensitive^[38-40]. It has been found that immunomagnetic beads sorting technique has a high sensitivity to 1/10⁵^[41], but it has a complicated procedure and a high cost and is not so practical in clinical application. In recent years, convenient RT-PCR was invented and it has a high efficiency in detecting the

micrometastasis of peripheral blood circulation, bone marrow, lymph tract and peritoneal cavity. It could detect one tumor cell diluted with one-milliliter body fluid or one gram tissue and it has been presently regarded as the most effective method to detect the disseminated carcinoma cells^[42].

In this study, RT-PCR was also used to detect micrometastatic gastric carcinoma cells. According to the researches of Soeth and Burchill^[15,37], CK20 was selected as the target gene for amplification. Because of the RNase existing in blood circulation, mRNA free to live cells would be decomposed rapidly. This means that there were live cells expressing CK20 mRNA existing in blood specimens when CK20 mRNA was detected from the peripheral blood circulation of patients. On the other hand, hemocytes came from mesoderm and there were no epithelial cells in blood circulation. So, when CK20 was amplified from blood circulation, there must be tumor cells in the specimen. If the specimen was extracted from a gastric carcinoma patient, the tumor cells might be gastric carcinoma cells. In this study, CK20 mRNA was detected from 32 of 60 specimens extracted from gastric carcinoma patients, but not from patients with chronic gastritis. This also confirmed that there were carcinoma cells in the peripheral blood circulation of gastric carcinoma patients.

Statistical analysis also indicated that the positive rate of detection of disseminated carcinoma cells with RT-PCR technique was higher than that with immunomagnetic beads sorting technique. This might be related with the high sensitivity of RT-PCR, which cell morphology and immunocytochemistry could not possess^[43,44]. On the other hand, it is cheaper in detecting disseminated carcinoma cells with RT-PCR than immunomagnetic beads sorting technique, so it is more worthy of clinical practice. Immunomagnetic beads sorting technique could directly separate micrometastatic carcinoma cells with high behaviors of metastasis. Those tumor cells separated with immunomagnetic beads sorting technique could be cultured and the characteristics of the cells could be determined, so it is more valuable for further research^[45].

In conclusion, our results indicate that there are micrometastatic carcinoma cells in the peripheral blood circulation of patients suffering from gastric carcinoma. Immunomagnetic beads sorting technique and RT-PCR technique can detect the disseminated carcinoma cells in the peripheral blood circulation. RT-PCR technique has a higher positive rate and a lower cost than immunomagnetic beads sorting technique, so it is worthy of clinical practice. Immunomagnetic beads sorting technique can directly separate carcinoma cells, so this method is more valuable for research work.

REFERENCES

- Zhou Y**, Gao SS, Li YX, Fan ZM, Zhao X, Qi YJ, Wei JP, Zou JX, Liu G, Jiao LH, Bai YM, Wang LD. Tumor suppressor gene p16 and Rb expression in gastric cardia precancerous lesions from subjects at a high incidence area in northern China. *World J Gastroenterol* 2002; **8**: 423-425
- Cai L**, Yu SZ, Zhan ZF. Cytochrome p450 2E1 genetic polymorphism and gastric cancer in Changle, Fujian Province. *World J Gastroenterol* 2001; **7**: 792-795
- Su M**, Lu SM, Tian DP, Zhao H, Li XY, Li DR, Zheng ZC. Relationship between ABO blood groups and carcinoma of esophagus and cardia in Chaoshan inhabitants of China. *World J Gastroenterol* 2001; **7**: 657-661
- Cai L**, Yu SZ, Zhang ZF. Glutathione S-transferases M1, T1 genotypes and the risk of gastric cancer: A case-control study. *World J Gastroenterol* 2001; **7**: 506-509
- Xin Y**, Li XL, Wang YP, Zhang SM, Zheng HC, Wu DY, Zhang YC. Relationship between phenotypes of cell- function differentiation and pathobiological behavior of gastric carcinomas. *World J Gastroenterol* 2001; **7**: 53-59
- Wang RT**, Wang T, Chen K, Wang JY, Zhang JP, Lin SR, Zhu

- YM, Zhang WM, Cao YX, Zhu CW, Yu H, Cong YJ, Zheng S, Wu BQ. *Helicobacter pylori* infection and gastric cancer: evidence from a retrospective cohort study and nested case-control study in China. *World J Gastroenterol* 2002; **8**: 1103-1107
- 7 **Yin T**, Ji XL, Shen MS. Relationship between lymph node sinuses with blood and lymphatic metastasis of gastric cancer. *World J Gastroenterol* 2003; **9**: 40-43
- 8 **Zhou YN**, Xu CP, Han B, Li M, Qiao L, Fang DC, Yang JM. Expression of E-cadherin and beta-catenin in gastric carcinoma and its correlation with the clinicopathological features and patient survival. *World J Gastroenterol* 2002; **8**: 987-993
- 9 **Culp LA**, Lin W, Kleinman NR, O' Connor KL, Lechner R. Earliest steps in primary tumor formation and micrometastasis resolved with histochemical markers of gene-tagged tumor cells. *J Histochem Cytochem* 1998; **46**: 557-568
- 10 **Funke I**, Schraut W. Meta-analyses of studies on bone marrow micrometastases: an independent prognostic impact remains to be substantiated. *J Clin Oncol* 1998; **16**: 557-566
- 11 **Timar J**, Csuka O, Orosz Z, Jeney A, Kopper L. Molecular pathology of tumor metastasis. *Pathol Oncol Res* 2002; **8**: 204-219
- 12 **Schleiermacher G**, Peter M, Oberlin O, Philip T, Rubie H, Mechinaud F, Sommelet-Olive D, Landman-Parker J, Bours D, Michon J, Delattre O. Increased risk of systemic relapses associated with bone marrow micrometastasis and circulating tumor cells in localized ewing tumor. *J Clin Oncol* 2003; **21**: 85-91
- 13 **Kakeji Y**, Maehara Y, Shibahara K, Hasuda S, Tokunaga E, Oki E, Sugimachi K. Clinical significance of micrometastasis in bone marrow of patients with gastric cancer and its relation to angiogenesis. *Gastric Cancer* 1999; **2**: 46-51
- 14 **Zhao A**, Li J, Sun W. Detection and significance of lymph node micrometastases in patients with histologically node-negative gastric carcinoma. *Zhonghua Zhongliu Zazhi* 2000; **22**: 222-224
- 15 **Soeth E**, Roder C, Juhl H, Kruger U, Kremer B, Kalthoff H. The detection of disseminated tumor cells in bone marrow from colorectal-cancer patients by a cytokeratin-20-specific nested reverse-transcriptase-polymerase-chain reaction is related to the stage of disease. *Int J Cancer* 1996; **69**: 278-282
- 16 **Van der Velde-Zimmermann D**, Roijers JF, Bouwens-Rombouts A, De Weger RA, De Graaf PW, Tilanus MG, Van den Tweel JG. Molecular test for the detection of tumor cells in blood and sentinel nodes of melanoma patients. *Am J Pathol* 1996; **149**: 759-764
- 17 **Cima F**, Matozzo V, Marin MG, Ballarin L. Haemocytes of the clam *Tapes philippinarum* (Adams & Reeve, 1850): morphofunctional characterisation. *Fish Shellfish Immunol* 2000; **10**: 677-693
- 18 **Kruger W**, Datta C, Badbaran A, Togel F, Gutensohn K, Carrero I, Kroger N, Janicke F, Zander AR. Immunomagnetic tumor cell selection-implications for the detection of disseminated cancer cells. *Transfusion* 2000; **40**: 1489-1493
- 19 **Xing J**, Zhan WB, Zhou L. Endoenzymes associated with haemocyte types in the scallop (*Chlamys farreri*). *Fish Shellfish Immunol* 2002; **13**: 271-278
- 20 **Anggraeni MS**, Owens L. The haemocytic origin of lymphoid organ spheroid cells in the penaeid prawn *Penaeus monodon*. *Dis Aquat Organ* 2000; **40**: 85-92
- 21 **Oertel J**, Huhn D. Immunocytochemical methods in haematology and oncology. *J Cancer Res Clin Oncol* 2000; **126**: 425-440
- 22 **Hu XC**, Wang Y, Shi DR, Loo TY, Chow LW. Immunomagnetic tumor cell enrichment is promising in detecting circulating breast cancer cells. *Oncology* 2003; **64**: 160-165
- 23 **Benez A**, Geiselhart A, Handgretinger R, Schiebel U, Fierlbeck G. Detection of circulating melanoma cells by immunomagnetic cell sorting. *J Clin Lab Anal* 1999; **13**: 229-233
- 24 **Noack F**, Schmitt M, Bauer J, Helmecke D, Kruger W, Thorban S, Sandherr M, Kuhn W, Graeff H, Harbeck N. A new approach to phenotyping disseminated tumor cells: methodological advances and clinical implications. *Int J Biol Markers* 2000; **15**: 100-104
- 25 **Woitats RP**, Petersen U, Moshage D, Brackmann HH, Matz B, Sauerbruch T, Spengler U. HCV-specific cytokine induction in monocytes of patients with different outcomes of hepatitis C. *World J Gastroenterol* 2002; **8**: 562-566
- 26 **Meier V**, Mihm S, Braun Wietzke P, Ramadori G. HCV-RNA positivity in peripheral blood mononuclear cells of patients with chronic HCV infection: does it really mean viral replication? *World J Gastroenterol* 2001; **7**: 228-234
- 27 **Su Q**, Fu Y, Liu YF, Zhang W, Liu J, Wang CM. Laminin induces the expression of cytokeratin 19 in hepatocellular carcinoma cells growing in culture. *World J Gastroenterol* 2003; **9**: 921-929
- 28 **Natsugoe S**, Nakashima S, Matsumoto M, Nakajo A, Miyazono F, Kijima F, Ishigami S, Aridome K, Hokita S, Baba M, Takao S, Aikou T. Para-aortic lymph node micrometastasis and tumor cell microinvolvement in advanced gastric carcinoma. *Gastric Cancer* 1999; **2**: 179-185
- 29 **Song ZJ**, Gong P, Wu YE. Relationship between the expression of iNOS, VEGF, tumor angiogenesis and gastric cancer. *World J Gastroenterol* 2002; **8**: 591-595
- 30 **Li HX**, Chang XM, Song ZJ, He SX. Correlation between expression of cyclooxygenase-2 and angiogenesis in human gastric adenocarcinoma. *World J Gastroenterol* 2003; **9**: 674-677
- 31 **Yao XX**, Yin L, Sun ZC. The expression of hTERT mRNA and cellular immunity in gastric cancer and precancerosis. *World J Gastroenterol* 2002; **8**: 586-590
- 32 **Shen ZY**, Xu LY, Li EM, Cai WJ, Chen MH, Shen J, Zeng Y. Telomere and telomerase in the initial stage of immortalization of esophageal epithelial cell. *World J Gastroenterol* 2002; **8**: 357-362
- 33 **Hu JK**, Chen ZX, Zhou ZG, Zhang B, Tian J, Chen JP, Wang L, Wang CH, Chen HY, Li YP. Intravenous chemotherapy for resected gastric cancer: meta-analysis of randomized controlled trials. *World J Gastroenterol* 2002; **8**: 1023-1028
- 34 **Cui JH**, Krueger U, Henne-Bruns D, Kremer B, Kalthoff H. Orthotopic transplantation model of human gastrointestinal cancer and detection of micrometastases. *World J Gastroenterol* 2001; **7**: 381-386
- 35 **Chausovsky G**, Luchansky M, Figier A, Shapiro J, Gottfried M, Novis B, Bogelman G, Zemer R, Zimlichman S, Klein A. Expression of cytokeratin 20 in the blood of patients with disseminated carcinoma of the pancreas, colon, stomach, and lung. *Cancer* 1999; **86**: 2398-2405
- 36 **Burchill SA**, Selby PJ. Molecular detection of low-level disease in patients with cancer. *J Pathol* 2000; **190**: 6-14
- 37 **Huang MS**, Wang TJ, Liang CL, Huang HM, Yang IC, Yi-Jan H, Hsiao M. Establishment of fluorescent lung carcinoma metastasis model and its real-time microscopic detection in SCID mice. *Clin Exp Metastasis* 2002; **19**: 359-368
- 38 **Su LD**, Lowe L, Bradford CR, Yahanda AI, Johnson TM, Sondak VK. Immunostaining for cytokeratin 20 improves detection of micrometastatic Merkel cell carcinoma in sentinel lymph nodes. *J Am Acad Dermatol* 2002; **46**: 661-666
- 39 **Leers MP**, Schoffelen RH, Hoop JG, Theunissen PH, Oosterhuis JW, vd Bijl H, Rahmy A, Tan W, Nap M. Multiparameter flow cytometry as a tool for the detection of micrometastatic tumour cells in the sentinel lymph node procedure of patients with breast cancer. *J Clin Pathol* 2002; **55**: 359-366
- 40 **Burkhardt O**, Merker HJ. Phagocytosis of immunobeads by CD8 positive lymphocytes during magnetic cell sorting. *Ann Anat* 2002; **184**: 55-60
- 41 **Sakakura C**, Hagiwara A, Shirasu M, Yasuoka R, Fujita Y, Nakanishi M, Aragane H, Masuda K, Shimomura K, Abe T, Yamagishi H. Polymerase chain reaction for detection of carcinoembryonic antigen-expressing tumor cells on milky spots of the greater omentum in gastric cancer patients: a pilot study. *Int J Cancer* 2001; **95**: 286-289
- 42 **Okada Y**, Fujiwara Y, Yamamoto H, Sugita Y, Yasuda T, Doki Y, Tamura S, Yano M, Shiozaki H, Matsuura N, Monden M. Genetic detection of lymph node micrometastases in patients with gastric carcinoma by multiple-marker reverse transcriptase-polymerase chain reaction assay. *Cancer* 2001; **92**: 2056-2064
- 43 **Lin JC**, Chen KY, Wang WY, Jan JS, Liang WM, Wei YH. Evaluation of cytokeratin-19 mRNA as a tumor marker in the peripheral blood of nasopharyngeal carcinoma patients receiving concurrent chemoradiotherapy. *Int J Cancer* 2002; **97**: 548-553
- 44 **Ghossein RA**, Osman I, Bhattacharya S, Ferrara J, Fazzari M, Cordon-cardo C, Scher HI. Detection of prostatic specific membrane antigen messenger RNA using immunobead reverse transcriptase polymerase chain reaction. *Diagn Mol Pathol* 1999; **8**: 59-65
- 45 **Luers GH**, Hartig R, Mohr H, Hausmann M, Fahimi HD, Cremer C, Volkl A. Immunolocalization of highly purified peroxisomes using magnetic beads and continuous immunomagnetic sorting. *Electrophoresis* 1998; **19**: 1205-1210

Effects of PI3K and p42/p44 MAPK on overexpression of vascular endothelial growth factor in hepatocellular carcinoma

Geng-Wen Huang, Lian-Yue Yang, Wei-Qun Lu

Geng-Wen Huang, Lian-Yue Yang, Wei-Qun Lu, Department of Surgery and Liver Cancer Laboratory, Xiangya Hospital, Central South University, Changsha 410008, Hunan Province, China

Supported by the grant from National Key Technologies R and D Program, No.2001BA703B04 and the grant from Hunan Province Developing Planning Committee, No.2001-907

Correspondence to: Lian-Yue Yang, MD, Department of Surgery and Liver Cancer Laboratory, Xiangya Hospital, Central South University, Changsha 410008, Hunan Province, China. lianyueyang@hotmail.com

Telephone: +86-731-4327326

Received: 2003-11-18 **Accepted:** 2003-12-08

Abstract

AIM: To study the relationship between hypoxia or epidermal growth factor (EGF) and the overexpression of vascular endothelial growth factor (VEGF) in hepatocellular carcinoma (HCC) and the signal transduction pathway of the transcription of VEGF in hepatoma cells.

METHODS: Cobalt chloride and recombinant human EGF were used to stimulate the hepatoma cell lines HepG₂. VEGF mRNA was detected by using of semi-quantitative polymerase chain reaction (RT-PCR). Specific inhibitors of phosphatidylinositol 3-kinase (PI3K) and p42/p44 mitogen activated protein kinase (MAPK) were used to observe the effects of the two kinases on the regulation of the transcription of VEGF in hepatoma cells.

RESULTS: The expression of VEGF mRNA in HepG₂ cells cultured in serum-free medium was 0.117. However, 100 μmol/L cobalt chloride for 24 h increased the expression of VEGF mRNA and VEGF mRNA increased gradually with the increase of the concentration and duration of cobalt chloride. Also, 25 ng/mL recombinant human EGF stimulated the expression of VEGF in HepG₂ cells and the expression increased with the increase of EGF concentration. 5 μmol/L LY294002 inhibited the expression of VEGF stimulated by cobalt chloride or recombinant human EGF and the inhibition decreased step by step with increase of the concentration of LY294002. But even 20 μmol/L LY294002 could not completely block the expression of VEGF. In contrast, PD98059 had no inhibitory effects on the transcription of VEGF stimulated by cobalt chloride or recombinant human EGF.

CONCLUSION: The overexpression of VEGF in HCC could be promoted by hypoxia and EGF expression in HCC. The signal transduction pathway of VEGF transcription in HepG₂ cells may be through PI3K pathway, but not through p42/p44 MAPK pathway.

Huang GW, Yang LY, Lu WQ. Effects of PI3K and p42/p44 MAPK on overexpression of vascular endothelial growth factor in hepatocellular carcinoma. *World J Gastroenterol* 2004; 10 (6): 809-812

<http://www.wjgnet.com/1007-9327/10/809.asp>

INTRODUCTION

Hepatocellular carcinoma (HCC) is one of the most common cancers in China. Owing to the improvement of surgical technique and early diagnostic methods, the resection rate of HCC has increased. However, the postoperative relapse rate remains high, which has become one of the main obstacles to the therapy of HCC. The mechanisms leading to the relapse are still unclear. Much effort has been done to make it clear. Recently, neovascularization, commonly observed in HCC, has been suggested to play important roles in the relapse of HCC^[1-3]. Vascular endothelial growth factor (VEGF) is one of the most potent proangiogenic agents to date. It is confirmed that there is overexpression of VEGF in HCC tissue. However, the mechanisms of VEGF overexpression in HCC are still unclear.

Phosphatidylinositol 3-kinase (PI3K) is a kind of lipid kinase which generates specific inositol lipids that are implicated in many cellular processes, such as cell growth, proliferation, survival, differentiation and cytoskeletal changes^[4,5]. MAP kinases are a family of serine/threonine kinases activated through a signaling pathway triggered by numerous agonists such as growth factors, hormones, lymphokines, extracellular matrix components, tumor promoters and stress factors^[6]. It has become clear that MAPKs regulate almost all cellular processes, from gene expression to cell death. Recently, both PI3K and p42/p44MAPK pathways have been both found to play important roles in the regulation of angiogenesis^[7-9].

The objective of the current study was to investigate the mechanisms leading to the overexpression of VEGF in HCC *in vitro* and the possible roles of PI3K and p42/p44 MAPK in the regulation of VEGF transcription in hepatoma cells.

MATERIALS AND METHODS

Cell culture

The HepG₂ cells (a hepatocellular carcinoma cell line), provided by the Center of Cell Culture in Xiangya Medical College, were cultured in DMEM supplemented with 100 mL/L fetal bovine serum (FBS) and incubated at 37 °C in a 50 mL/L CO₂ atmosphere. The cells were cultured overnight in DMEM without FBS before intervention.

Reagents

Hypoxia-inducer cobalt chloride (Sigma) and recombinant human epidermal growth factor (rhEGF, Promega) were used to stimulate the cells. Before stimulation, LY294002 (Promega) and PD98059 (Promega) were used to pretreat the cells to test the function of PI3K and p42/p44 MAPK, respectively.

Treatment procedures and drugs

Seven groups included: 1. no stimulation group (NS); 2. cobalt chloride group (CC), 100-400 μmol/Lcobalt chloride stimulated the cells for 3-24 h; 3. EGF group (EGF), 25-200 ng/mL rhEGF stimulated the cells for 24 h; 4. cobalt chloride plus LY294002 group (CCL), 5-20 μmol/LLY294002 stimulated the cells 30 min before cobalt chloride treatment; 5. EGF plus LY294002 group

(EL), 5-20 $\mu\text{mol/L}$ LY294002 stimulated the cells 30 min before rhEGF stimulation; 6. cobalt chloride plus PD98059 group (CCP), 25-100 $\mu\text{mol/L}$ PD98059 stimulated the cells 30 min before cobalt chloride treatment; 7. EGF plus PD98059 group (EP), 25-100 $\mu\text{mol/L}$ PD98059 stimulated the cells 30 min before rhEGF treatment.

Reverse transcription-polymerase chain reaction (RT-PCR)

After incubation for a given duration, the cells were harvested and the total RNA was extracted by using the TRIZOL Reagent (GIBCO BRL., USA). One microgram of RNA was reversely transcribed into cDNA in 20 μL reverse transcriptional system containing 50 mmol/L Tris-HCl, 75 mmol/L KCl, 3 mmol/L MgCl_2 , 0.5 μg oligo-dT primer, 0.5 mmol/L deoxynucleotide triphosphate (dNTP), 20U RNasin and 200 U murine Moloney leukemia virus (M-MLV) reverse transcriptase (Promega Corp., Madison, WI), at 37 $^\circ\text{C}$ for 1 h. After reverse transcription, 5 μL of product was added to PCR buffer containing 10 mmol/L Tris-HCl, 1.5 mmol/L MgCl_2 , 50 mmol/L KCl, 1 g/L Triton-X-100, 0.2 $\mu\text{mol/L}$ forward primer, 0.2 $\mu\text{mol/L}$ reverse primer, 200 $\mu\text{mol/L}$ dNTP and 2.5U DNA polymerase (SANGON, SHANGHAI). The PCR was performed in a DNA thermal cycler (Perkin Elmer, USA) with a program of denaturing at 94 $^\circ\text{C}$ for 5 min; denaturing at 94 $^\circ\text{C}$ for 30 s, annealing at 55 $^\circ\text{C}$ for 30 s, extension at 72 $^\circ\text{C}$ for 1 min, the amplification was carried out for 30 cycles. The reaction was stopped in a final extension at 72 $^\circ\text{C}$ for 5 min. The forward and reverse primers for human VEGF and beta actin were purchased from SANGON (SHANGHAI) and their nucleotide sequences were listed below: VEGF: forward primer: 5' -TTGCTGCTCTACCTCCAC-3'; reverse primer: 5' -AATGCTTTCTCCGCTCTG-3' beta actin: forward primer: 5' -ACACTGTGCCCATCTAGGAGG-3'; reverse primer: 5' -AGGGGCCGGACTCGTCATACT-3'. The sizes of PCR products were: 417 bp for VEGF, 680 bp for beta actin, respectively.

PCR products were loaded on a 20 g/L agarose gel with ethidium bromide, and band intensity was quantified by photo image analyzer (Stratagene Eagleeye II). The ratio of band intensity of the sample to the internal standard was calculated in the four reactions that contained significant amounts of both sample and standard, which stood for the amount of expression of VEGF mRNA.

Immunocytochemistry

The cells were fixed in cool acetone and sections were stained for VEGF based on streptavidin-biotin-horseradish peroxidase complex formation mentioned before^[10]. In brief, the slides were treated with target retrieval solution. Monoclonal anti-VEGF antibody JH121 (200 $\mu\text{g/mL}$, NEOMARKERS, USA) was used at a dilution of 1:50. The peroxidase reaction was developed using diaminobenzidine and slides were washed. Nuclei were lightly counterstained with hematoxylin. Negative controls were performed using PBS instead of the monoclonal antibody. Two investigators independently evaluated the results of immunocytochemistry.

Statistical analysis

ANOVA was used appropriately. For the test, a *P* value of less than 0.05 was considered as significant. All statistics were calculated through SPSS 10.0 software.

RESULTS

The effects of cobalt chloride and rhEGF on the expression of VEGF mRNA in HepG₂ cells

The amount of expression of VEGF mRNA in HepG₂ cells cultured in DMEM without FBS was 0.117. With the increase

of the concentration of cobalt chloride, the expression of VEGF mRNA increased ($P < 0.05$) (Figure 1). And also with the increase of the duration of cobalt chloride stimulation, the expression of VEGF mRNA also increased. rhEGF also stimulated the expression of VEGF mRNA in HepG₂ cells in a dependant manner of concentration and duration (Figure 2).

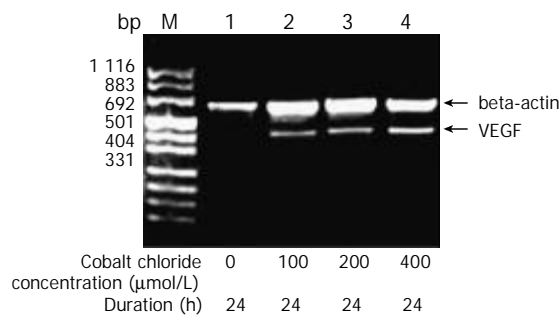


Figure 1 Cobalt chloride stimulated the expression of VEGF mRNA in HepG₂ cells in a concentration-dependant manner.

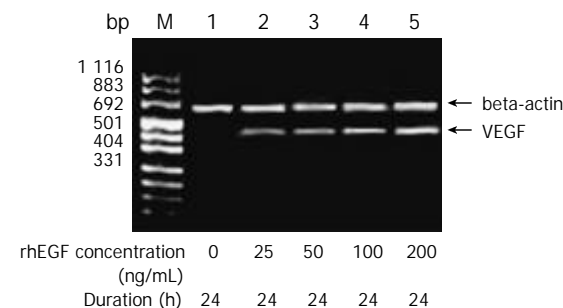


Figure 2 rhEGF stimulated the expression of VEGF mRNA in HepG₂ cells in a concentration-dependant manner.

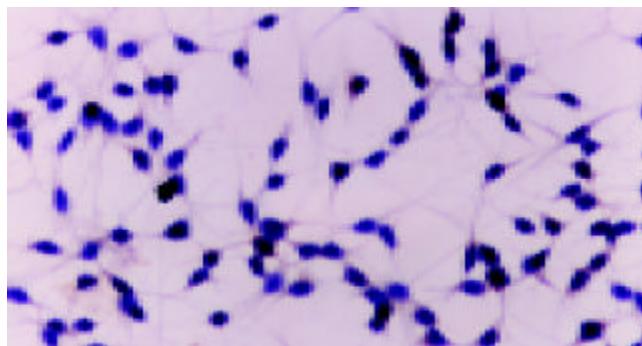


Figure 3 Negative expression of VEGF protein in HepG₂ cells cultured in DMEM without serum. Immunocytochemistry $\times 400$.

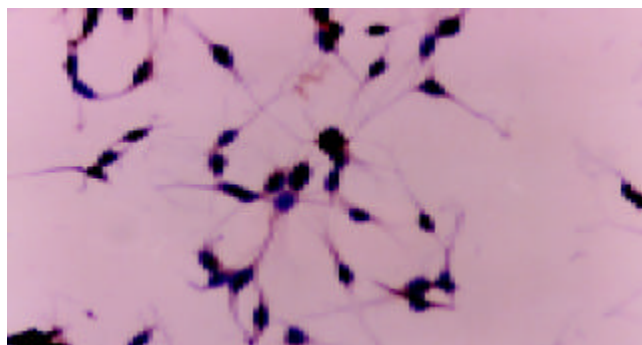


Figure 4 Expression of VEGF protein in HepG₂ cells stimulated by cobalt chloride (400 $\mu\text{mol/L}$, 24 h) immunocytochemistry $\times 400$.

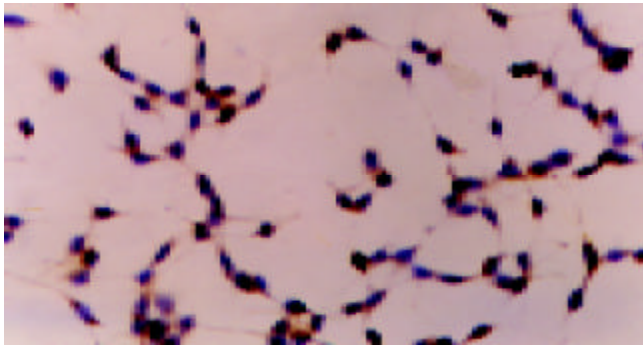


Figure 5 Expression of VEGF protein in HepG₂ cells stimulated by rhEGF(25 ng/mL, 24 h) immunocytochemistry ×400.

The effects of cobalt chloride and rhEGF on the expression of VEGF protein in HepG₂ cells

There was no positive staining in HepG₂ cells cultured in DMEM without FBS. Cobalt chloride or rhEGF stimulated the expression of VEGF protein in the cytoplasm of HepG₂ cells (Figure 3-5), which demonstrated the results of RT-PCR.

Effects of LY294002 or PD98059 on VEGF transcription stimulated by cobalt chloride or rhEGF in HepG₂ cells

A 5 μmol/L LY294002 inhibited the expression of VEGF stimulated by cobalt chloride or recombinant human EGF and the inhibition decreased step by step with increase of the concentration of LY294002 ($P < 0.05$). But even 20 μmol/L LY294002 did not completely block the expression of VEGF mRNA (Figure 6). In contrast, PD98059 had no inhibitory effects on the transcription of VEGF stimulated by cobalt chloride or recombinant human EGF ($P > 0.05$) (Figure 7).

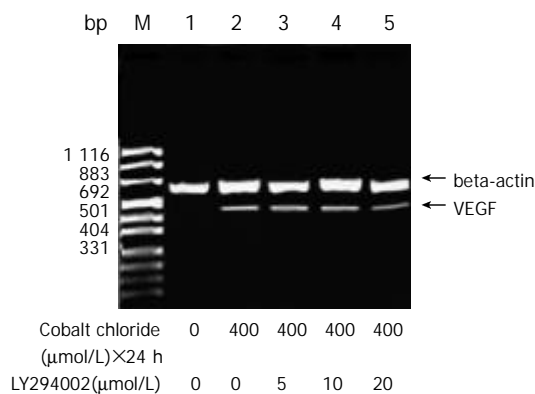


Figure 6 LY294002 inhibited the expression of VEGF mRNA in HepG₂ cells stimulated by cobalt chloride.

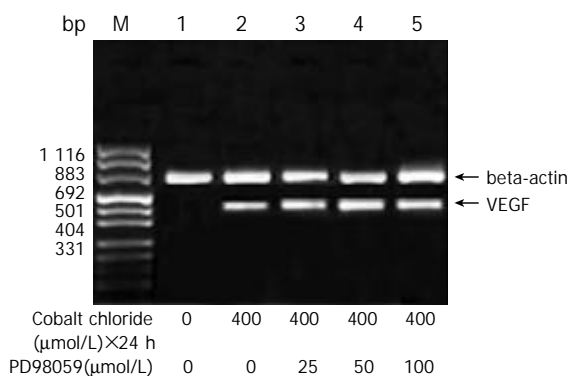


Figure 7 PD98059 had no effect on the expression of VEGF mRNA in HepG₂ cells stimulated by cobalt chloride.

DISCUSSION

Neovascularization was essential for tumour growth and metastasis^[1-3]. The mechanisms underlying the neovascularization in malignancies have been the “hot spot” in the cancer research. VEGF is one of the growth factors proven to be specific and critical for blood vessel formation. In clinical experiment, we have demonstrated that there is VEGF overexpression in HCC and the level of VEGF expression in HCC is correlated not only with microvessel invasion of cancer cells, but also with the survival^[11]. So it is very important to make clear the mechanisms and signal transduction pathways that control the VEGF expression in HCC. This would help us find new targets to prevent the neovascularization in HCC so as to preclude the relapse and metastasis of HCC.

Hypoxia, one of the fundamental characteristics of the tumour microenvironment, was demonstrated to be involved in the progression and metastasis of malignancy^[12-16]. In the current study, we have shown that hypoxia-inducer cobalt chloride could induce the expression of VEGF in HepG₂ cells in a concentration and duration-dependant manner. We have also shown that rhEGF could stimulate the expression of VEGF in HepG₂ cells in the same manner. As a result, we could draw a conclusion that both hypoxia and EGF might be the fundamental stimulators of VEGF overexpression in HepG₂ cells.

Phosphatidylinositol 3-kinase (PI3K) was a kind of lipid kinase^[17-21]. The lipid product of PI3K, phosphatidylinositol-3,4,5-trisphosphate (PIP₃), recruited a subset of signaling proteins with pleckstrin homology (PH) domains to the membrane, where they were activated. These proteins included protein serine-threonine kinases (Akt and PDK1), protein tyrosine kinases (Tec family), exchange factors for GTP-binding proteins (Grp1 and Rac exchange factors), and adaptor proteins (GAB-1). Ultimately, these proteins initiated complex sets of events that controlled protein synthesis, actin polymerization, cell survival, and cell cycle entry.

Recently, PI3K has been demonstrated to be involved in the regulation of the transcription of VEGF in certain types of cells. Overexpression of VEGF mRNA has been found in endothelial cells in which the PI3K pathway has been activated^[22]. LY294002, the specific inhibitor of PI3K, could inhibit the expression of VEGF in endothelial cells. In addition, PI3K was found to be involved in the regulation of VEGF transcription in cancer cells. In the prostate cancer cell line, LY294002 could completely block the expression of VEGF^[23]. Maity *et al* also demonstrated PI3K was essential in the regulation of VEGF transcription in glioma cell line U87MG^[24]. In the current study, we have shown that LY294002 inhibit VEGF transcription stimulated by cobalt chloride or rhEGF in a concentration and duration dependant manner. To our knowledge we demonstrated for the first time that PI3K was involved in the regulation of the signal transduction pathway of VEGF transcription in the hepatoma cells. At the same time, we observed that even 20 μmol/L LY294002 could not block the VEGF mRNA expression completely, which was likened to the results of Zhong^[23] and Maity^[24]. So there was PI3K-independent pathway in the regulation of VEGF transcription in HepG₂ cells.

MAPKs were important signal transducing enzymes, unique to eukaryotes, that were involved in many facets of cellular regulation, such as gene expression, cellular proliferation and programmed cell death^[25-27]. Recently, MAPKs has been shown to be involved in the regulation of neovascularization. Rak *et al* have shown that in the Ras-transforming mouse fibroblast cell line 3T3RAS, VEGF expression was not blocked by LY294002, but by PD98059, the specific inhibitor of p42/p44 MAPK^[28]. This result suggested that p42/p44 MAPK was involved in the regulation of VEGF transcription in 3T3RAS cells. In the current study, we did not observe PD98059 could

preclude VEGF transcription in HepG₂ cells, which indicated p42/p44 MAPK was not involved in the regulation of VEGF transcription in HepG₂ cells.

In conclusion, hypoxia and EGF were two stimulators to the VEGF overexpression in hepatoma cells. VEGF transcription might be regulated by PI3K pathway and other PI3K-independent pathway, but not by p42/p44 MAPK pathway.

REFERENCES

- Folkman J.** Seminars in medicine of the beth israsl hospital, bos clinical applications of research on angiogenesis. *N Eng J Med* 1995; **333**: 1757-1763
- Carmeliet P, Jain RK.** Angiogenesis in cancer and other diseases. *Nature* 2000; **407**: 249-257
- Yancopoulos GD, Davis S, Gale NW, Rudge JS, Wiegand SJ, Holash J.** Vascular-specific growth factors and blood vessel formation. *Nature* 2000; **407**: 242-248
- Sotsios Y, Ward SG.** Phosphoinositide 3-kinase: a key biochemical signal for cell migration in response to chemokines. *Immunol Rev* 2000; **177**: 217-235
- Roymans D, Slegers H.** Phosphatidylinositol 3-kinases in tumor progression. *Eur J Biochem* 2001; **268**: 487-498
- Chang L, Karin M.** Mammalian MAP kinase signalling cascades. *Nature* 2001; **410**: 37-40
- Dimmeler S, Zeiher AM.** Akt takes center stage in angiogenesis signaling. *Circ Res* 2000; **86**: 4-5
- Jiang BH, Zheng JZ, Aoki M, Vogt PK.** Phosphatidylinositol 3-kinase signaling mediates angiogenesis and expression of vascular endothelial growth factor in endothelial cells. *Proc Natl Acad Sci U S A* 2000; **97**: 1749-1753
- Berra E, Milanini J, Richard DE, Le Gall M, Vinals F, Gothie E, Roux D, Pages G, Pouyssegur J.** Signaling angiogenesis via p42/p44 MAP kinase and hypoxia. *Biochem Pharmacol* 2000; **60**: 1171-1178
- Huang GW, Yang LY.** Metallothionein expression in hepatocellular carcinoma. *World J Gastroenterol* 2002; **8**: 650-653
- Huang GW, Yang LY, Lu XS, Liu HL, Yang JQ, Yang ZL.** Expression of hypoxia-inducible factor 1 alpha in hepatocellular carcinoma and the impact on neovascularization. *Zhonghua Xiaohua Zazhi* 2002; **22**: 627-628
- Huang GW, Yang LY.** Molecular mechanisms of hypoxia-induced malignant transformation. *Shijie Huaren Xiaohua Zazhi* 2001; **9**: 1300-1304
- Huang GW, Yang LY.** Hypoxic signal transduction pathway in malignancy. *Shijie Huaren Xiaohua Zazhi* 2002; **10**: 1441-1444
- Sutherland RM.** Tumor hypoxia and gene expression-implications for malignant progression and therapy. *Acta Oncol* 1998; **37**: 567-574
- Dachs GU, Tozer GM.** Hypoxia modulated gene expression: angiogenesis, metastasis and therapeutic exploitation. *Eur J Cancer* 2000; **36**: 1649-1660
- Wykoff CC, Beasley NJ, Watson PH, Turner KJ, Pastorek J, Sibtain A, Wilson GD, Turley H, Talks KL, Maxwell PH, Pugh CW, Ratcliffe PJ, Harris AL.** Hypoxia-inducible expression of tumor-associated carbonic anhydrases. *Cancer Res* 2000; **60**: 7075-7083
- Cantley LC.** The phosphoinositide 3-kinase pathway. *Science* 2002; **296**: 1655-1657
- Dhawan P, Singh AB, Ellis DL, Richmond A.** Constitutive activation of Akt/protein kinase B in melanoma leads to up-regulation of nuclear factor-kappaB and tumor progression. *Cancer Res* 2002; **62**: 7335-7342
- Romieu-Mourez R, Landesman-Bollag E, Seldin DC, Sonenshein GE.** Protein kinase CK2 promotes aberrant activation of nuclear factor-kappaB, transformed phenotype, and survival of breast cancer cells. *Cancer Res* 2002; **62**: 6770-6778
- Narita Y, Nagane M, Mishima K, Huang HJ, Furnari FB, Cavenee WK.** Mutant epidermal growth factor receptor signaling down-regulates p27 through activation of the phosphatidylinositol 3-kinase/Akt pathway in glioblastomas. *Cancer Res* 2002; **62**: 6764-6769
- Neri LM, Borgatti P, Capitani S, Martelli AM.** The nuclear phosphoinositide 3-kinase/AKT pathway: a new second messenger system. *Biochim Biophys Acta* 2002; **1584**: 73-80
- Wang D, Huang HJ, Kazlarskas A, Cavenee WK.** Induction of vascular endothelial growth factor expression in endothelial cells by platelet-derived growth factor through the activation of phosphatidylinositol 3-kinase. *Cancer Res* 1999; **59**: 1464-1472
- Zhong H, Chiles K, Feldser D, Laughner E, Hanrahan C, Georgescu MM, Simons JW, Semenza GL.** Modulation of hypoxia-inducible factor 1 α expression by the epidermal growth factor/phosphatidylinositol 3-kinase/PTEN/AKT/FRAP pathway in human prostate cancer cells: implications for tumor angiogenesis and therapeutics. *Cancer Res* 2000; **60**: 1541-1545
- Maity A, Pore N, Lee J, Solomon D, O'Rourke DM.** Epidermal growth factor receptor transcriptionally up-regulates vascular endothelial growth factor expression in human glioblastoma cells via a pathway involving phosphatidylinositol 3'-kinase and distinct from that induced by hypoxia. *Cancer Res* 2000; **60**: 5879-5886
- Johnson GL, Lapadat R.** Mitogen-activated protein kinase pathways mediated by ERK, JNK, and p38 protein kinases. *Science* 2002; **298**: 1911-1912
- Chen G, Goeddel DV.** TNF-R1 signaling: a beautiful pathway. *Science* 2002; **296**: 1634-1635
- Ling MT, Wang X, Ouyang XS, Lee TK, Fan TY, Xu K, Tsao SW, Wong YC.** Activation of MAPK signaling pathway is essential for Id-1 induced serum independent prostate cancer cell growth. *Oncogene* 2002; **21**: 8498-8505
- Rak J, Mitsuhashi Y, Sheehan C, Tamir A, Vitoria-Petit A, Filmus J, Mansour SJ, Ahn NG, Kerbel RS.** Oncogenes and tumor angiogenesis: differential modes of vascular endothelial growth factor up-regulation in ras-transformed epithelial cells and fibroblasts. *Cancer Res* 2000; **60**: 490-498

Edited by Hu DK and Xu FM

Vascular endothelial growth factor antisense oligodeoxynucleotides with lipiodol in arterial embolization of liver cancer in rats

Han-Ping Wu, Gan-Sheng Feng, Hui-Min Liang, Chuan-Sheng Zheng, Xin Li

Han-Ping Wu, Gan-Sheng Feng, Hui-Min Liang, Chuan-Sheng Zheng, Xin Li, Department of Interventional Radiology, Union Hospital, Tongji Medical College, Huazhong University of Science and Technology, Wuhan 430022, Hubei Province, China
Supported by the National Natural Science Foundation of China, No. 39770839

Correspondence to: Dr. Han-Ping Wu, Department of Interventional Radiology, Union Hospital, Tongji Medical College, Huazhong University of Science and Technology, Wuhan 430022, Hubei Province, China. shhwph@public.wh.hb.cn
Telephone: +86-27-85726432 **Fax:** +86-27-85727002
Received: 2003-07-17 **Accepted:** 2003-07-30

Abstract

AIM: Transcatheter arterial embolization (TAE) of the hepatic artery has been accepted as an effective treatment for unresectable hepatocellular carcinoma (HCC). However, embolized vessel recanalization and collateral circulation formation are the main factors of HCC growth and recurrence and metastasis after TAE. Vascular endothelial growth factor (VEGF) plays an important role in tumor angiogenesis. This study was to explore the inhibitory effect of VEGF antisense oligodeoxynucleotides (ODNs) on VEGF expression in cultured Walker-256 cells and to observe the anti-tumor effect of intra-arterial infusion of antisense ODNs mixed with lipiodol on rat liver cancer.

METHODS: VEGF antisense ODNs and sense ODNs were added to the media of non-serum cultured Walker-256 cells. Forty-eight hours later, VEGF concentrations of supernatants were detected by ELISA. Endothelial cell line ECV-304 cells were cultured in the supernatants. Seventy-two hours later, growth of ECV-304 cells was analyzed by MTT method. Thirty Walker-256 cell implanted rat liver tumor models were divided into 3 groups. 0.2 mL lipiodol (LP group, $n=10$), 3OD antisense ODNs mixed with 0.2 mL lipiodol (LP+ODNs group, $n=10$) and 0.2 mL normal saline (control group, $n=10$) were infused into the hepatic artery. Volumes of tumors were measured by MRI before and 7 d after the treatment. VEGF mRNA in cancerous and peri-cancerous tissues was detected by RT-PCR. Microvessel density (MVD) and VEGF expression were observed by immunohistochemistry.

RESULTS: Antisense ODNs inhibited Walker-256 cells' VEGF expression. The tumor growth rate was significantly lower in LP+ODNs group than that in LP and control groups ($140.1\pm33.8\%$, $177.9\pm64.9\%$ and $403.9\pm69.4\%$ respectively, $F=60.019$, $P<0.01$). VEGF mRNAs in cancerous and peri-cancerous tissues were expressed highest in LP group and lowest in LP+ODNs group. The VEGF positive rates showed no significant difference among LP, control and LP+ODNs groups (90%, 70% and 50%, $H=3.731$, $P>0.05$). The MVD in LP+ODNs group (53.1 ± 18.4) was significantly less than that in control group (73.2 ± 20.4) and LP group (80.3 ± 18.5) ($F=5.44$, $P<0.05$).

CONCLUSION: VEGF antisense ODNs can inhibit VEGF

expression of Walker-256 cells. It may be an antiangiogenesis therapy agent for malignant tumors. VEGF antisense ODNs mixed with lipiodol embolizing liver cancer is better in inhibiting liver cancer growth, VEGF expression and microvessel density than lipiodol alone.

Wu HP, Feng GS, Liang HM, Zheng CS, Li X. Vascular endothelial growth factor antisense oligodeoxynucleotides with lipiodol in arterial embolization of liver cancer in rats. *World J Gastroenterol* 2004; 10(6): 813-818
<http://www.wjgnet.com/1007-9327/10/813.asp>

INTRODUCTION

Hepatocellular carcinoma (HCC) is one of the most common malignant tumors in human beings^[1,2]. In China, HCC is responsible for 130 000 deaths every year and the second cause of cancer deaths^[3]. Surgical resection is still the only potentially curative treatment for HCC, particularly for small HCC^[3,4]. To date, the resection rate for HCC is unfortunately less than 30%^[3,5,6]. Since HCC's blood supply is derived almost exclusively from hepatic arteries, transcatheter arterial embolization (TAE) of the hepatic artery has been accepted as an effective treatment for unresectable HCC^[5-10]. Although embolic materials and technique have been improved during the last decade, the outcome of TAE is not satisfactory. It hardly leads to tumor necrosis totally. The 3-year survival rate is about 14-35%^[11-14]. Recanalization of the embolized vessel and collateral circulation formation, which are related with tumor angiogenesis, are the main factors of HCC growth, recurrence and metastasis after TAE^[15,16]. In TAE, HCC cells undergo coagulative necrosis, a pathologic feature of anoxia. Anoxia and hypoxic liver injury are caused by the absolute and relative deficiency of oxygen, respectively. It is well known that hypoxia tension is a key factor of the gene expression of angiogenic factors such as VEGF, acidic and basic fibroblast growth factors (FGF), platelet derived growth factor (PDGF). These factors could promote tumor angiogenesis, growth, recurrence and metastasis^[17,18]. It is possible that in addition to elimination of cancer cells, TAE may play a role in enhancing some cells' malignant potency and ability to escape anoxia and ischemia after treatment.

VEGF is a key mediator of pathological angiogenesis. Many researchers found that it overexpressed in many solid tumor tissues including HCC, and was associated with tumor growth, recurrence, metastasis and patient's prognosis^[19-23]. It has been reported that preoperative TAE enhanced VEGF expression in both HCC cells and non-carcinoma liver cells. Antisense RNA could inhibit and block gene expression effectively^[24-26]. In this study, we devised antisense ODNs specific to VEGF mRNA, and observed their inhibitory effects on VEGF expression in Walker-256 cell lines *in vitro*, and the anti-tumor effect of them mixed with lipiodol arterial embolization on Walker-256 cell transplanted rat liver cancer models.

MATERIALS AND METHODS

Cell culture

Walker 256 carcinosarcoma cells were purchased from China

Center for Type Culture Collection. After recovery, the cells were inoculated in the abdominal cavity of male pathogen-free Wistar rats, weighing 100-120 g (supplied by Department of Experimental Animal, Tongji Medical College). Three days later, cancerous ascites was aspirated and cultured in RPMI-1640 containing 50 mL/L fetal calf serum (FCS) (Gibco, Grand Island, NY) and equilibrated with 950 mL/L air and 50 mL/L CO₂. Cells were passaged every 2 d. The cells at passage 3 were used for experiments.

Oligodeoxynucleotides (ODNs)

Phosphorothioate ODNs were synthesized by Shanghai Sangon Biological Engineering Technology and Service Co., LTD. The sequences of ODNs were designed as follows: antisense ODNs: 5' -GCA GTA GCT GCG CTG ATA GCG C-3', complementary to the linkage area of VEGF exon 2 and exon 3; sense ODNs: 5' -GCA CTA TCA GCG CAG CTA CTG C-3', equivalent to the linkage area of VEGF exon 2 and exon 3.

Cell proliferation studies

Walker-256 carcinosarcoma cells were planted into a 24-well plate at 1×10^5 /well (1 mL/well) and cultured in non-serum medium. Ten μ L of 0.25, 0.5, 1.0, 2.0 μ mol/L antisense ODNs and sense ODNs was added to the media every 24 h. Ten μ L of non-serum medium was added to the blank control wells. Forty-eight hours later, the supernatant fluids were collected. The concentration of VEGF was measured by ELISA. Two hundred μ L of supernatant fluids was added triplicate to a 96-well plate to culture ECV-304 cells (endothelial cell line, purchased from China Center for Type Culture Collection, 1×10^4 /well), equilibrated with 950 mL/L air and 50 mL/L CO₂. Seventy-two hours later, ECV-304 cells were collected. MTT method was used to detect the growth of ECV-304 cells.

Tumor model and treatment schedule

Walker-256 carcinosarcoma cells were inoculated subcutaneously in the right flank of rats with 10^7 tumor cells in approximately 0.1 mL of cell suspension. Tumors were palpable 7 d after transplantation. Fresh tumor tissues were isolated and cut into 1 mm³ size. Following midline laparotomy, the Walker 256 carcinosarcoma tissue pieces were implanted into the left hepatic lobe of rats. Seven days later, after anesthesia and laparotomy, the gastroduodenal artery was retrograde catheterized with a Portex PE10 tube (inner diameter 0.28 mm, external diameter 0.61 mm, Neolab, Germany) under a binocular operative microscope (Suzhou Medical Instruments Factory, Jiangsu, China) and infused embolic materials to perform TAE. The common hepatic artery and right hepatic artery were temporarily ligated during infusion. Thirty tumor-bearing rats were randomly divided into 3 groups, 10 rats each. LP group: the hepatic arteries were embolized with 0.2 mL lipiodol (Lipiodol Ultra-Fluid; Andre Guerbet, Aulnay-Sous-Bois, France), LP+ODNs group: the hepatic arteries were embolized with 3OD antisense ODNs mixed with 0.2 mL lipiodol, control group: 0.2 mL normal saline was infused into hepatic arteries. Then the gastroduodenal artery was ligated and the abdominal cavity was closed.

MR scans were performed on 1.5-Tesla system (Magnetom Vision, Siemens, Germany) supplemented by a cervical coil before and 7 d after TAE. T1-weighted (TR/TE, 450/12 ms) and T2-weighted (TR/TE, 2800/96 ms) transverse SE images (slice thickness 2 mm) were acquired using acquisition times of 7:25 and 6:16 min, respectively. Tumor volume was determined from MR measurements of the largest and smallest diameters and calculated according to the following formula: Tumor volume (mm³, V) = largest diameter (mm) \times [smallest diameter (mm)]²/2. The tumor growth rate = $V_{\text{post}}/V_{\text{pre}} \times 100\%$.

The rats were sacrificed 7 d after TAE. Liver cancerous and peri-cancerous tissues were dissected. Some of them were frozen at -70 °C for RNA isolation. The reminders were fixed in 40g/L formaldehyde, dehydrated and embedded in paraffin. Five- μ m sections were stained with hematoxylin-eosin for light microscopy and measurement of the degree of tumor necrosis.

RNA isolation and RT-PCR analysis

Total RNA was extracted from liver cancerous and peri-cancerous tissues using the TRIzol reagent (Gibco). Reverse transcription of 5 μ g total RNA was performed in a volume of 20 μ L for 60 min at 37 °C, containing AMV 5U, Oligo dT 0.050 μ g, RNasin 20 U, 10 mmol/L dNTP 2 μ L. The samples were heated to 95 °C for 5 min to terminate the reverse transcription reaction. By using a Perkin-Elmer DNA thermocycler 2 400 (Perkin-Elmer, Norwalk, CT), 2 μ L cDNA mixture obtained from the reverse transcription reaction was then amplified for VEGF and G₃PDH. G₃PDH was used as a housekeeping gene and amplified with VEGF as control. The amplification reaction mixture consisted of 10 \times buffer 2.5 μ L, 5 mmol/L dNTP 0.5 μ L, 25 mmol/L MgCl₂ 1.5 μ L, 10 pmol/L each of sense and antisense primers, Taqase 5U. The reaction mixture was first heated at 95 °C for 5 min and amplification was carried out for 35 cycles at 94 °C for 30 s, at 60 °C for 30 s, and at 72 °C for 30 s, followed by incubation for 10 min at 72 °C. The PCR primers used were: VEGF, sense 5' -GAA GTG GTG AAG TTC ATG GAT GTC-3' and antisense 5' -CGA TCG TTC TGT ATC AGT CTT TCC-3'; G₃PDH, sense 5' -TCC CTC AAG ATT GTC AGC AA-3' and antisense 5' -AGA TCC ACA ACG GAT ACA TT-3'. The length of PCR products for VEGF and G₃PDH was 394 bp and 309 bp. PCR products were checked with 15 g/L agarose gel electrophoresis stained with ethidium bromide.

Immunohistochemical analysis

Five micron paraffin-embedded tissue sections were deparaffinized and rehydrated. Rabbit anti-mouse vWF, VEGF monoclonal antibody and SABC kit were provided by Beijing Zhongshan Biological Technology Co., Ltd. Immunohistochemical studies were performed by SABC methods according to the manufacturer's instructions. VEGF staining was evaluated semiquantitatively on the basis of the percentage of positive cells, and classified as follows: diffusely positive (+++) when positive cells accounted for more than 50% of the total cells, moderately positive (++) when positive cells were 16-50%, weakly positive (+) when positive cells accounted for 5-15%, and negative (-) when positive cells accounted for less than 5%. For MVD determination, 5 areas were randomly selected and counted at a magnification of 200. Briefly, the stained sections were screened at a magnification of 40 under a light microscope to identify 3 regions of the section with the highest microvessel density. Microvessels were counted in these areas at a magnification of 200, and the average number of microvessels was recorded.

Statistical analysis

Experimental results were analyzed with analysis of variance (ANOVA) and Kruskal-Wallis rank test. The difference between 2 groups was analyzed by SNK-*q* and Dunn test respectively. Statistical significance was determined at $P < 0.05$.

RESULTS

VEGF concentration in supernatant of walker-256 cells

After incubated with walker-256 cells for 48 h, antisense ODNs decreased the concentration of VEGF in the supernatant of walker-256 cells in a dose-dependent manner, whereas no significant changes were seen in sense ODNs (Table 1).

Table 1 Concentration of VEGF in supernatant of Walker-256 cells (pg/ml)(mean±SD)

Group	0.25 μmol/L	0.5 μmol/L	1.0 μmol/L	2.0 μmol/L
Antisense ODNs	84.2±2.2	79.2±2.6	74.4±2.1	65.2±2.0
Sense ODNs	89.2±1.9	90.4±2.6	88.2±1.9	88.6±2.5
Control	90.2±1.9	90.8±1.8	89.4±2.1	90.4±1.7
F values	7.877	23.132	49.906	133.636
P values	0.021 ¹	0.002 ¹	0.000 ¹	0.000 ¹

¹SNK-*q* test: The difference between sense ODNs and control groups was not statistically significant.

Cell proliferation study

The supernatants of Walker-256 cells that were incubated with antisense ODNs could inhibit the growth of ECV-304 cells in a dose-dependent manner. No significant effects were seen in those incubated with sense ODNs (Table 2).

Table 2 Inhibitory effect of supernatants of Walker-256 cells cultured with ODNs on ECV-304 proliferation (OD) (mean±SD)

Group	0.25 μmol/L	0.5 μmol/L	1.0 μmol/L	2.0 μmol/L
Antisense ODNs	0.339±0.012	0.332±0.006	0.327±0.008	0.321±0.019
Sense ODNs	0.345±0.021	0.348±0.014	0.336±0.022	0.359±0.014
Control	0.357±0.010	0.359±0.008	0.356±0.005	0.360±0.009
F values	2.477	5.573	12.931	7.296
P values	0.164	0.043 ¹	0.007 ¹	0.025 ¹

¹SNK-*q* test: The difference between sense ODNs and control groups was not statistically significant.

Tumor growth and histopathological findings

Seven days after implantation, the tumor was located in the left lobe of liver as a solitary mass. There was no statistical difference between the volumes of tumors in control group, LP group and LP+ODNs group (212.3±117.5 mm³, 174.6±106.5 mm³, 173.9±91.8 mm³ respectively) before TAE treatment. Seven days after the treatment, all tumors grew. The volumes and growth rates in LP group (286.0±186.4 mm³, 177.9±64.9%, respectively) and LP+ODNs group (337.6±98.1 mm³, 140.1±33.8%, respectively) were significantly less than those in control group (823.3±426.1 mm³, 403.9±69.4%, respectively, *P*<0.01) (Table 3).

Table 3 Volumes and growth rates of transplanted liver tumors (mean±SD)

Group	Volume of pre-TAE(mm ³)	Volume of post-TAE(mm ³)	Growth rate (%)
Control	212.3±117.5	823.3±426.1	403.9±69.4
LP	174.6±106.5	286.0±186.4	177.9±64.9
LP+ODNs	173.9±91.8	337.6±98.1	140.1±33.8
F values	0.432	14.319	60.019
P values	0.653	0.000 ¹	0.000

¹SNK-*q* test: The difference between antisense LP and LP+ODNs groups was not statistically significant.

Hematoxylin-eosin (H & E) stained sections of the liver specimens showed a poorly differentiated carcinoma, which was spherical or ovoid in shape. Tumor cells arranged in irregular nests and signs of malignancy including hyperchromatosis, polymorphism and numerous mitoses were detected. The mass had a sharp demarcation from the surrounding normal hepatic parenchyma, its capsules were thin and composed of collagen fibers, which were caused by the

compression of the tumor. The tumor showed inhomogeneous signs of hypervascularization consisting mainly of small arteries and capillaries. Seven days after therapy, spotty and scattered necrosis were seen in all cases of control group (Figure 1A). Satellite nodules could be seen in some tumors. In LP group, the necrotic area was increased. Many patched necrotic zones were seen in tumor tissues (Figure 1B). In LP+ODNs group, the tumor necrotic area was much wider. It showed a big area of central necrosis. The residual tumors could be seen only in the margin of tumor (Figure 1C).

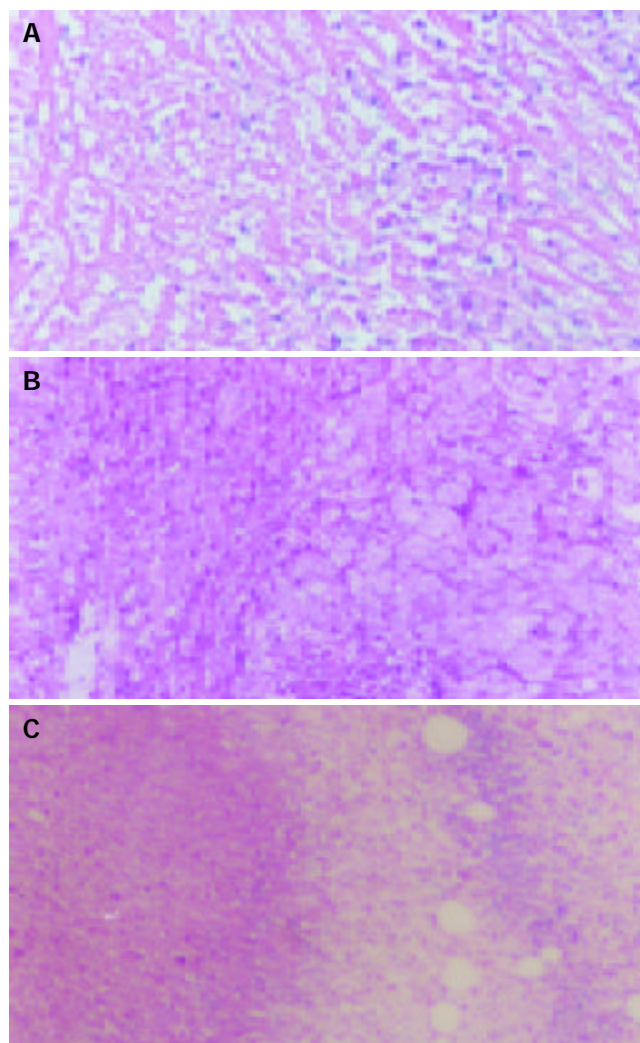


Figure 1 Pathological changes of tumor tissues 7 d after TAE. A: Control group showing spotty and scattered necrosis. B: LP group showing many patched necrotic zones. C: LP+ODNs group showing big areas of central necrosis. Hematoxylin-eosin ×40.

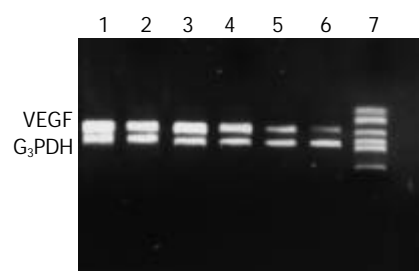


Figure 2 RT-PCR analysis of VEGF mRNA level in cancerous and peri-cancerous tissues using G₃PDH as internal control. Control group: 1 tumor, 2 peri-tumor. LP group: 3 tumor, 4 peri-tumor. LP+ODNs group: 5 tumor, 6 peri-tumor, 7 marker.

RT-PCR analysis of VEGF mRNA expression

VEGF mRNA expression was detected in cancerous and peri-cancerous tissues. The expression level in cancerous tissue was higher than that in peri-cancerous tissues. The VEGF mRNA levels in cancerous and peri-cancerous tissues in LP group were higher than those in control group, and those in LP+ODNs group were lower than those in control and LP groups (Figure 2).

Table 4 Expression of VEGF and MVD by immunohistochemical staining ($n=10$)

Group	MVD (mean±SD)	VEGF				Positive rate (%)
		+++	++	+	-	
Control	73.2±20.4	3	2	2	3	70
LP	80.3±18.5	3	4	2	1	90
LP+ODNs	53.1±18.4	1	2	2	5	50
Test values	$F=5.440$					$H=3.731$
P values	0.010 ¹					0.1545

¹SNK- q test: The difference between LP and control groups was not statistically significant.

Immunohistochemical analysis of VEGF protein expression and MVD

VEGF immunoreactivity was observed mainly in the cytoplasm of tumor cells, and also frequently in hepatic cells in peri-cancerous tissues. The distribution of strong VEGF-staining zones and microvessels was mainly in the survival nidui and margins of the tumor. The positive rate of VEGF in LP group, control group and LP+ODNs group was 90%, 70% and 50% respectively, and the difference was not statistically significant

($P=0.065$) (Table 4, Figure 3). The MVD in LP+ODNs group ($53.1±18.4$) was significantly less than that in control group ($73.2±20.4$) and LP group ($80.3±18.5$). Although the MVD in control group and LP group showed no significant difference, but abundant tumor vessels were seen in residual nidui in LP group (Table 4, Figure 4).

DISCUSSION

Many authors have reported the effects of TAE on VEGF expression of HCC. An *et al*^[27] found that preoperative TAE enhanced VEGF expression in both HCC cells and non-carcinoma liver cells. Kobayashi *et al*^[28] reported that the frequency of Bcl-2 positive cells was higher in HCCs undergone TAE than that in HCCs not undergone TAE, and the immunohistochemical staining intensity for VEGF was higher in Bcl-2 positive than in Bcl-2 negative area. Suzuki *et al*^[29] reported that the serum levels of VEGF in HCC patients increased significantly 7 d after TAE. Guo *et al*^[30] reported that blockage of hepatic arterial blood supply resulted in decreased blood perfusion and increased expression of metastasis-associated genes VEGF and MMP-1 of transplanted liver cancer in rats. The results in this study showed that VEGF mRNA and protein had an increasing tendency after TAE. These findings suggested that TAE could enhance the expression of VEGF in HCC cells. The rationale is based on the following points: TAE was hard to lead to total tumor necrosis and to make the tumor tissue anoxia further. Hypoxia induced transcription of VEGF mRNA was mediated by the binding of hypoxia-inducible factor 1 (HIF-1) to an HIF-1 binding site located in the VEGF promoter^[31-33]. VEGF plays an important role in each stage of tumor angiogenesis. The overexpression of VEGF in cancerous and peri-cancerous tissues of HCC could certainly promote tumor

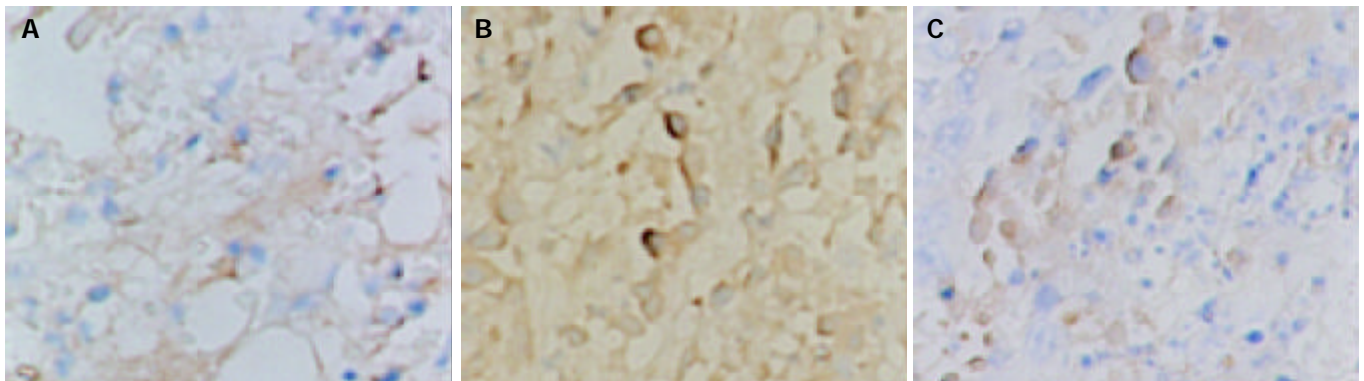


Figure 3 Immunohistochemical staining of VEGF in tumor tissues 7 d after TAE, showing strong expression in LP group and low expression in LP+ODNs group. A: Control group, B: LP group, C: LP+ODNs group. SABC×200.

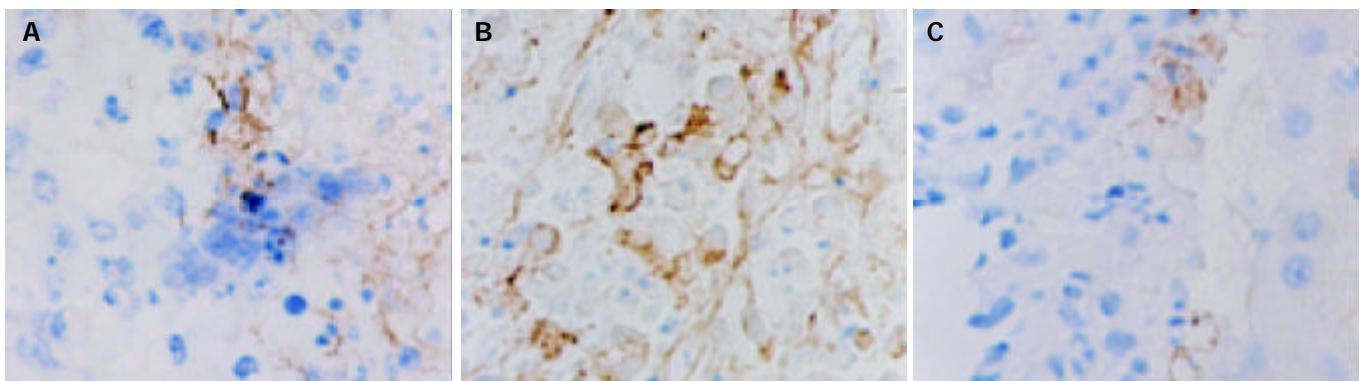


Figure 4 Immunohistochemical staining of vWF in tumor tissues 7 d after TAE, showing plenty of microvessels in LP group and a few microvessels in LP+ODNs group. A: Control group, B: LP group, C: LP+ODNs group. SABC×200.

angiogenesis and collateral vessels formation, and enhance the possibility of recurrence and metastasis^[34-37]. In this study, although we found that the MVD in LP group was higher than that in control group, but the difference was not significant and abundant tumor vessels were seen in residual tumor in LP group. It must be due to tumor angiogenesis enhancement caused by VEGF overexpression after TAE. In clinical setting, we also found that the collateral vessels were increased with the time of increased TAE. These vessels are very small and hard to catheterize, resulting in the embolized HCC tissue receiving blood and escaping from anoxia stress. Some HCC vessels not embolized completely would grow acceleratedly and were prone to recurrence and metastasis. So it is very important to reduce VEGF expression and collateral vessel formation after TAE.

Antisense ODNs have shown great efficacy in selective inhibition of gene expression. They are designed and synthesized artificially, and can enter cells directly to hybridize with complementary mRNA and decrease protein expression. They have been used as an important tool to inhibit the expression of oncogenes and/or growth factors and some of them have been used as drugs in tumor gene therapies^[38-41]. In this study, antisense ODNs were designed to complement the region between exon 2 and exon 3 of VEGF gene. They could inhibit 4 kinds of VEGF molecules' expression^[42,43]. To enforce their stability, ODNs were modified by phosphorothioate. Our previous study showed fluorescence labeled ODNs could transfect Walker-256 cells and keep in them for about 48 h (in press). The *in vitro* experimental results in this study showed that VEGF antisense ODNs could decrease VEGF expression of cultured Walker-256 cells in a dose-dependent manner. Similar effect has been reported on other tumor cell lines^[41,44-46]. In *in vivo* study, we also found that VEGF antisense ODNs could inhibit VEGF expression of liver tumor tissues after TAE, reduce tumor MVD and growth rate in walker-256 cell transplanted rat liver cancer models. These imply that VEGF antisense ODNs could be used as an antiangiogenesis agent to inhibit HCC' s overexpression and collateral vessel formation after TAE.

Intravenous injection is the routine means for phosphorothioate ODNs in clinical administration. However, intravenous infusion is not an ideal route for VEGF antisense ODNs in HCC treatment. First, it has a very short lifetime after injection into animal bodies. To enhance the target cell transfection rate and therapeutic effect, it is needed to increase the dose of antisense ODNs. A higher dose of ODNs may result in more side effects such as dose-dependent hypotension, complement activation, and transient prolongation of thromboplastin time^[47-50]. Second, systemic administration of VEGF antisense ODNs might inhibit physiological angiogenesis, such as wound healing, menstruation. In this study, we mixed antisense ODNs with lipiodol and used them as an embolic agent in liver tumor TAE therapy. To infuse the agents into the left hepatic artery (the tumor was planted in the left lobe of the rat liver) and to make each tumor receive the same amount of agents, we catheterized the gastroduodenal artery retrograde and ligated the common hepatic artery and right hepatic artery temporarily during infusion. The results showed that antisense ODNs mixed with lipiodol was better in inhibiting tumor growth rate, VEGF expression and MVD than lipiodol alone. These indicated that antisense ODNs used in combination with lipiodol and transcatheter artery embolization were the ideal route in HCC treatment. The rationale is based on the following points. The blood supply of HCC is mainly from hepatic artery. ODNs hepatic artery infusion could increase the concentration in tumor tissue and reduce the dosage and systemic side-effects. When injected to the hepatic artery, lipiodol could stay in tumor tissue for a long time (several months), and could even be

absorbed by tumor cells^[51,52]. When mixed with lipiodol, the latter could act as a carrier, ODNs would give off slowly from it. It would prolong the contact time of ODNs and tumor cells, which is very important to increase the transfect rate. Our previous *in vivo* experimental study showed that fluorescence labeled ODNs could stay in tumor tissue for about 6 d when used in combination with lipiodol hepatic artery embolization on Walker-256 cell transplanted rat liver cancer models (in press). This is why the long-term inhibitory effect on VEGF expression and MVD was achieved in this study.

In conclusion, TAE can increase the formation of microvessels in residual tumor tissues. VEGF plays an important role in liver cancer angiogenesis and collateral vascular formation after TAE treatment. VEGF antisense ODNs are able to inhibit tumor cells' VEGF expression. VEGF antisense ODNs can inhibit the residual tumor angiogenesis and growth and reduce the possibility of metastasis and recurrence. The combination of TAE and VEGF antisense ODNs will be a hopeful strategy for HCC treatment.

REFERENCES

- 1 **Pisani P**, Parkin DM, Bray FI, Ferlay J. Estimates of the world-wide mortality from 25 cancers in 1990. *Int J Cancer* 1999; **83**: 18-29
- 2 **Akriviadis EA**, Llovet JM, Efreimidis SC, Shouval D, Canelo R, Ringes B, Meyers WC. Hepatocellular carcinoma. *Br J Surg* 1998; **85**: 1319-1331
- 3 **Tang ZY**. Hepatocellular carcinoma-cause, treatment and metastasis. *World J Gastroenterol* 2001; **7**: 445-454
- 4 **Yuen MF**, Cheng CC, Laufer JJ, Lam SK, Ooi CG, Lai CL. Early detection of hepatocellular carcinoma increases the chance of treatment: Hong Kong experience. *Hepatology* 2000; **31**: 330-335
- 5 **Acunas B**, Rozanes I. Hepatocellular carcinoma: treatment with transcatheter arterial chemoembolization. *Eur J Radiol* 1999; **32**: 86-89
- 6 **Rose DM**, Chapman WC, Brockenbrough AT, Wright JK, Rose AT, Meranze S, Mazer M, Blair T, Blanke CD, Debelak JP, Pinson CW. Transcatheter arterial chemoembolization as primary treatment for hepatocellular carcinoma. *Am J Surg* 1999; **177**: 405-410
- 7 **Zangos S**, Gille T, Eichler K, Engelmann K, Woitaschek D, Balzer JO, Mack MG, Thalhammer A, Vogl TJ. Transarterial chemoembolization in hepatocellular carcinomas: technique, indications, results. *Radiologe* 2001; **41**: 906-914
- 8 **Livraghi T**. Treatment of hepatocellular carcinoma by interventional methods. *Eur Radiol* 2001; **11**: 2207-2219
- 9 **Poon RT**, Ngan H, Lo CM, Liu CL, Fan ST, Wong J. Transarterial chemoembolization for inoperable hepatocellular carcinoma and postresection intrahepatic recurrence. *J Surg Oncol* 2000; **73**: 109-114
- 10 **Camma C**, Schepis F, Orlando A, Albanese M, Shahied L, Trevisani F, Andreone P, Craxi A, Cottone M. Transarterial chemoembolization for unresectable hepatocellular carcinoma: meta-analysis of randomized controlled trials. *Radiology* 2002; **224**: 47-54
- 11 **Loewe C**, Cejna M, Schoder M, Thurnher MM, Lammer J, Thurnher SA. Arterial embolization of unresectable hepatocellular carcinoma with use of cyanoacrylate and lipiodol. *J Vasc Interv Radiol* 2002; **13**: 61-69
- 12 **Zheng C**, Feng G, Liang H. Bletilla striata as a vascular embolizing agent in interventional treatment of primary hepatic carcinoma. *Chin Med J* 1998; **111**: 1060-1063
- 13 **Li X**, Hu G, Liu P. Segmental embolization by ethanol iodized oil emulsion for hepatocellular carcinoma. *J Tongji Med Univ* 1999; **19**: 135-140
- 14 **Li L**, Wu PH, Li JQ, Zhang WZ, Lin HG, Zhang YQ. Segmental transcatheter arterial embolization for primary hepatocellular carcinoma. *World J Gastroenterol* 1998; **4**: 511-512
- 15 **Tian JM**, Wang F, Ye H, Wang ZT, Sun F, Liu Q, Yang JJ, Cheng D. Classification study of arterial blood supply of hepatic cancer: regular, variant and parasitic blood supply. *Linchuang Fangshexue Zazhi* 1997; **16**: 40-43
- 16 **Li HP**, Cao J, Wang XY, Luo JQ. Effect of hepatic artery

- chemoembolization in patients with primary liver carcinoma and analysis of factors affecting the prognosis. *Linchuang Fangshexue Zazhi* 2001; **20**: 66-69
- 17 **Carmeliet P**, Jain RK. Angiogenesis in cancer and other disease. *Nature* 2000; **407**: 249-257
- 18 **Battegay EJ**. Angiogenesis: mechanistic insights, neovascular diseases, and therapeutic prospects. *J Mol Med* 1995; **73**: 333-346
- 19 **Ferrara N**. Role of vascular endothelial growth factor in the regulation of angiogenesis. *Kidney Int* 1999; **56**: 794-814
- 20 **Ferrara N**. Molecular and biological properties of vascular endothelial growth factor. *J Mol Med* 1999; **77**: 527-543
- 21 **Zheng S**, Han MY, Xiao ZX, Peng JP, Dong Q. Clinical significance of vascular endothelial growth factor expression and neovascularization in colorectal carcinoma. *World J Gastroenterol* 2003; **9**: 1227-1230
- 22 **Tao HQ**, Qin LF, Lin YZ, Wang RN. Expression of vascular endothelial growth factor and its prognostic significance in gastric carcinoma. *China Natl J New Gastroenterol* 1996; **2**: 128-130
- 23 **Jiang YF**, Yang ZH, Hu JQ. Recurrence or metastasis of HCC: predictors, early detection and experimental antiangiogenic therapy. *World J Gastroenterol* 2000; **6**: 61-65
- 24 **Narayanan R**, Akhtar S. Antisense therapy. *Curr Opin Oncol* 1996; **8**: 509-515
- 25 **Gu ZP**, Wang YJ, Li JG, Zhou YA. VEGF₁₆₅ antisense RNA suppresses oncogenic properties of human esophageal squamous cell carcinoma. *World J Gastroenterol* 2002; **8**: 44-48
- 26 **Tang YC**, Li Y, Qian GX. Reduction of tumorigenicity of SMMC-7721 hepatoma cells by vascular endothelial growth factor antisense gene therapy. *World J Gastroenterol* 2001; **7**: 22-27
- 27 **An FQ**, Matsuda M, Fujii H. Expression of vascular endothelial growth factor in surgical specimens of hepatocellular carcinoma. *J Cancer Res Clin Oncol* 2000; **126**: 153-160
- 28 **Kobayashi N**, Ishii M, Ueno Y, Kisara N, Chida N, Iwasaki T, Toyota T. Co-expression of Bcl-2 protein and vascular endothelial growth factor in hepatocellular carcinomas treated by chemoembolization. *Liver* 1999; **19**: 25-31
- 29 **Suzuki H**, Mori M, Kawaguchi C, Adachi M, Miura S, Ishii H. Serum vascular endothelial growth factor in the course of transcatheter arterial embolization of hepatocellular carcinoma. *Int J Oncol* 1999; **14**: 1087-1090
- 30 **Guo WJ**, Li J, Ling WL, Bai YR, Zhang WZ, Cheng YF, Gu WH, Zhuang JY. Influence of hepatic arterial blockage on blood perfusion and VEGF, MMP-1 expression of implanted liver cancer in rats. *World J Gastroenterol* 2002; **8**: 476-479
- 31 **Nomura M**, Yamagishi S, Harada S, Hayashi Y, Yamashita T, Yamashita J, Yamamoto H. Possible participation of autocrine and paracrine vascular endothelial growth factors in hypoxia-induced proliferation of endothelial cells and pericytes. *J Biol Chem* 1995; **270**: 28316-28324
- 32 **Sivridis E**, Giatromanolaki A, Gatter KC, Harris AL, Koukourakis MI. Tumor and Angiogenesis Research Group. Association of hypoxia-inducible factors 1alpha and 2alpha with activated angiogenic pathways and prognosis in patients with endometrial carcinoma. *Cancer* 2002; **95**: 1055-1063
- 33 **Buchler P**, Reber HA, Buchler M, Shrinkante S, Buchler MW, Friess H, Semenza GL, Hines OJ. Hypoxia-inducible factor 1 regulates vascular endothelial growth factor expression in human pancreatic cancer. *Pancreas* 2003; **26**: 56-64
- 34 **Carmeliet P**, Collen D. Vascular development and disorders: molecular analysis and pathogenic insights. *Kidney Int* 1998; **53**: 1519-1549
- 35 **Poon RT**, Ng IO, Lau C, Zhu LX, Yu WC, Lo CM, Fan ST, Wong J. Serum vascular endothelial growth factor predicts venous invasion in hepatocellular carcinoma: a prospective study. *Ann Surg* 2001; **233**: 227-235
- 36 **Qin LX**, Tang ZY. The prognostic molecular markers in hepatocellular carcinoma. *World J Gastroenterol* 2002; **8**: 385-392
- 37 **Meng C**, Chen X. Association of VEGF, uPA, ICAM-1 and PCNA expression with metastasis and recurrence in hepatocellular carcinoma. *Zhonghua Waike Zazhi* 2002; **40**: 673-675
- 38 **Oza AM**, Elit L, Swenerton K, Faught W, Ghatage P, Carey M, McIntosh L, Dorr A, Holmlund JT, Eisenhauer E. Phase II study of CGP 69846A (ISIS 5132) in recurrent epithelial ovarian cancer: an NCIC clinical trials group study (NCIC IND.116). *Gynecol Oncol* 2003; **89**: 129-133
- 39 **Taylor AH**, al-Azzawi F, Pringle JH, Bell SC. Inhibition of endometrial carcinoma cell growth using antisense estrogen receptor oligodeoxyribonucleotides. *Anticancer Res* 2002; **22**: 3993-4003
- 40 **Yacyshyn BR**, Barish C, Goff J, Dalke D, Gaspari M, Yu R, Tami J, Dorr FA, Sewell KL. Dose ranging pharmacokinetic trial of high-dose alicaforsen (intercellular adhesion molecule-1 antisense oligodeoxynucleotide) (ISIS 2302) in active Crohn's disease. *Aliment Pharmacol Ther* 2002; **16**: 1761-1770
- 41 **Robinson GS**, Pierce EA, Rook SL, Foley E, Webb R, Smith LE. Oligodeoxynucleotides inhibit retinal neovascularization in a murine model of proliferative retinopathy. *Proc Natl Acad Sci USA* 1996; **93**: 4851-4856
- 42 **Tischer E**, Mitchell R, Hartman T, Silva M, Gospodarowicz D, Fiddes JC, Abraham JA. The human gene for vascular endothelial growth factor: Multiple protein forms are encoded through alternative exon splicing. *J Biol Chem* 1991; **266**: 11947-11954
- 43 **Park JE**, Keller GA, Ferrara N. The vascular endothelial growth factor (VEGF) isoforms: differential deposition into the subepithelial extracellular matrix and bioactivity of extracellular matrix-bound VEGF. *Mol Biol Cell* 1993; **4**: 1317-1326
- 44 **Dong F**, Jin YX. Inhibition of angiogenesis with antisense ODN of VEGF. *Chin J Oncol* 1997; **19**: 264-266
- 45 **Chen YF**, Sun HW, Zou Q, Zou SQ. Inhibition of growth of human cholangiocarcinoma in nude mice by vascular endothelial growth factor antisense phosphorothioate oligodeoxynucleotides. *Zhonghua Shiyian Waike Zazhi* 2000; **17**: 22-23
- 46 **Shi W**, Siemann DW. Inhibition of renal cell carcinoma angiogenesis and growth by antisense oligonucleotides targeting vascular endothelial growth factor. *Br J Cancer* 2002; **87**: 119-126
- 47 **Iversen PL**, Copple BL, Tewary HK. Pharmacology and toxicology of phosphorothioate oligonucleotides in the mouse, rat, monkey and man. *Toxicol Lett* 1995; **82**: 425-430
- 48 **Leeds JM**, Henry SP, Bistner S, Scherrill S, Williams K, Levin AA. Pharmacokinetics of an antisense oligonucleotide injected intravitreally in monkeys. *Drug Metab Dispos* 1998; **26**: 670-675
- 49 **Tolcher AW**, Reyno L, Venner PM, Ernst SD, Moore M, Geary RS, Chi K, Hall S, Walsh W, Dorr A, Eisenhauer E. A randomized phase II and pharmacokinetic study of the antisense oligonucleotides ISIS 3521 and ISIS 5132 in patients with hormone-refractory prostate cancer. *Clin Cancer Res* 2002; **8**: 2530-2535
- 50 **Webb MS**, Tortora N, Cremese M, Kozłowska H, Blaquiére M, Devine DV, Kornbrust DJ. Toxicity and toxicokinetics of a phosphorothioate oligonucleotide against the c-myc oncogene in cynomolgus monkeys. *Antisense Nucleic Acid Drug Dev* 2001; **11**: 155-163
- 51 **Han GH**, Guo QL, Huang GS, Guo YL. Distribution of lipiodol in hepatocellular carcinoma after hepatic arterial injection and its significance. *Zhonghua Fangshexue Zazhi* 1993; **27**: 828-831
- 52 **Kan Z**, Sato M, Ivancev K, Uchida B, Hedgpeth P, Lunderquist A, Rosch J, Yamada R. Distribution and effect of iodized poppyseed oil in the liver after hepatic artery embolization: experimental study in several animal species. *Radiology* 1993; **186**: 861-866

Alpha-fetoprotein stimulated the expression of some oncogenes in human hepatocellular carcinoma Bel 7402 cells

Meng-Sen Li, Ping-Feng Li, Qian Chen, Guo-Guang Du, Gang Li

Meng-Sen Li, Qian Chen, Department of Biochemistry, Hainan Medical College, Haikou 571101, China

Ping-Feng Li, Guo-Guang Du, Gang Li, Department of Biochemistry and Molecular Biology, Health Science Center, Peking University, Beijing 100083, China

Supported by the National Natural Science Foundation of China, No. 30260117, Natural Science Foundation of Hainan Province, No. 30315 and the Nursery Foundation of Hainan Medical College, No. 200202

Correspondence to: Dr. Meng-Sen Li, Department of Biochemistry, Hainan Medical College, Haikou 571101, China. mengsenli@163.com

Telephone: +86-898-66893779

Received: 2003-09-18 **Accepted:** 2003-11-15

Abstract

AIM: To investigate the molecular mechanism of alpha-fetoprotein (AFP) on regulating the proliferation of human hepatocellular carcinoma cells.

METHODS: Alpha-fetoprotein purified from human umbilical blood was added to cultured human hepatocellular carcinoma Bel 7402 cells *in vitro* for various treatment periods. The expression of *c-fos*, *c-jun*, and *N-ras* mRNA involved in proliferation and differentiation of cells was analyzed by Northern blot, and the expression of mutative p53 and p21^{ras} proteins was determined by Western blot.

RESULTS: The results showed that AFP (20 mg/L) stimulated mRNA expression of these oncogenes in Bel 7402 cells. The expression of *c-fos* mRNA increased by 51.1%, 60.9%, 96.0%, and 25.5% at 2, 6, 12, and 24 h, respectively. The expression of *c-jun* and *N-ras* mRNA reached to the maximum which increased by 81.3% and 59.9% as compared with the control after 6 h and 24 h incubation with AFP, respectively. Western blot assay also demonstrated that AFP promoted the expression of mutative p53 and p21^{ras} proteins, and the increased rate of those proteins was 13.0%, 39.9%, and 70.9%, as well as 35.2%, 102.6%, and 46.8% at 6, 12, and 24 h, respectively, as compared with the control. Both human serum albumin (the same dosage as AFP) and monoclonal anti-AFP antibody failed to stimulate the expression of these oncogenes, but anti-AFP antibody could block the functions of AFP.

CONCLUSION: The data indicate that AFP can stimulate the expression of some oncogenes to enhance the proliferation of human hepatocellular carcinoma Bel 7402 cells.

Li MS, Li PF, Chen Q, Du GG, Li G. Alpha-fetoprotein stimulated the expression of some oncogenes in human hepatocellular carcinoma Bel 7402 cells. *World J Gastroenterol* 2004; 10(6): 819-824

<http://www.wjgnet.com/1007-9327/10/819.asp>

INTRODUCTION

Alpha-fetoprotein is the major serum protein in human

embryos, and is synthesized by embryonic liver and yolk sac. During the embryonic growth course, AFP expresses much more (3 g/L), and falls to the adult level (0.02×10^{-3} g/L) after one-year birth. Although many investigations for the function of AFP had been carried out, the biological role of AFP is still a riddle so far. Because the composition and the sequence of the amino acid residues of AFP were very similar to those of human serum albumin, thus, people always think that the function of AFP just like human serum albumin, which functions to transport materials and stabilize blood colloid osmotic pressure in the life course of the fetus. However, the concentration of serum AFP increases apparently with liver cancer or liver optimum regeneration in humans. AFP always accompanies with the growth of liver cells, and it is possible that AFP may be related to the proliferation of tumor or fetal cells. Some investigations had showed that AFP could be individually synergy with other growth factors to promote the growth of many tumor or normal cells^[1-6]. Alpha-fetoprotein (MW 69 ku) is a kind of biomacromolecules, and it is impossible to directly permeate the cells to regulate cell proliferation. We previously found that AFP could enhance growth of human hepatocellular carcinoma Bel 7402 and NIH3T3 cells, and there were two typical receptors of AFP existed on the membranes of these cells^[7,8]. However, it has not been reported in former investigations how AFP influences the expression of oncogenes which are mediated by AFP receptors to regulate growth of human hepatocellular carcinoma cells. This study used human hepatocellular carcinoma Bel 7402 cell line, which is closely related to AFP, to observe mRNA expression of the oncogene *c-fos*, *c-jun*, and *N-ras*, and protein expression of mutative p53 and p21^{ras}, which are correlated with cell proliferation, after treated with AFP. Additionally, the study explored some molecular mechanisms for AFP-mediated growth of human hepatocellular carcinoma cells.

MATERIALS AND METHODS

Materials

Human hepatocellular carcinoma Bel 7402 cells, crude AFP, and monoclonal anti-AFP antibody were provided by Endocrine Research Group of the Department of Biochemistry and Molecular Biology, Health Science Center, Peking University; RPMI 1640 medium was purchased from GIBCO; Fetal calf serum (FCS) was from the Blood Research Institute of Chinese Medicine Science Academy (Tianjin, China); Human serum albumin (HSA) and MOPS were purchased from Sigma Company; Diethyl pyrocarbonate (DEPC), sodium dodecyl sulfate (SDS), agarose, and Tris were obtained from Bio-Rad Company; Total RNA extraction kit was purchased from Promega Company; α -³²P-dCTP was bought from YaHui Biology Engineer Company (Beijing, China); *N-ras*, *c-fos*, *c-jun*, and β -actin cDNA probes were from the Department of Endocrinology, Northwestern University (Chicago); Random primer labeling kit was the product of Takara company (Japan); Salmon sperm DNA, fraction V of bovine serum albumin (BSA), and Ficoll-400 were bought from the Jingke Chemical

Reagents Company (Beijing, China); Monoclonal antibodies for mutative p53 and p21^{ras} were from NEOMARKERS Company.

Methods

Purification of human AFP Human AFP was prepared by the method as described elsewhere^[9]. Briefly, human cord blood AFP was precipitated by ammonium sulfate and passed through an anti-AFP antibody affinity chromatography column. The AFP-positive fractions were collected and concentrated. The purity of prepared AFP was 92.7% determined by SDS-polyacrylamide gel electrophoresis (SDS-PAGE). The protein was stored at -80 °C until analysis.

Cells culture Human hepatocellular carcinoma Bel 7402 cells (1.5×10^4 /mL) were cultured in RPMI 1640 medium supplemented with 100 mL/L FCS at 37 °C in a humidified atmosphere of 50 mL/L CO₂. The cultured medium was changed after 24 h.

RNA isolation and Northern blot analysis The cells were treated with AFP (20 mg/L), HSA (20 mg/L), anti-AFP antibody (40 mg/L), or AFP (20 mg/L) + anti-AFP antibody (40 mg/L) for 2, 6, 12, and 24 h, respectively. Total cellular RNA was isolated from Bel 7402 cells using a TRIzol reagent kit (Promega, Madison, WI) according to the manufacturer's protocol. Then, RNA was quantitated by the absorbance at 260 nm, and RNA (10-20 µg/lane) was fractionated by electrophoresis through 10 g/L formaldehyde agarose gel. The fractionated RNA was transferred in 20×SSC buffer to the nitrocellulose membrane (Millipore Corporation, Bedford, MA) using the standard procedure^[10]. These membranes were hybridized with α-³²P labeled probe, and washed using the standard protocol. The membranes were then exposed to the X-ray film at -80 °C.

Purification of protein and Western blot analysis The cells were treated with AFP (20 mg/L), HSA (20 mg/L), anti-AFP antibody (40 mg/L), or AFP (20 mg/L) + anti-AFP antibody (40 mg/L) for 6, 12, and 24 h, respectively. After washed three times with PBS (pH 7.4, 0.15 mol/L), the cells were lysed in 10 µL of lysis buffer containing 2 mL/L Triton X-100, 500 mmol/L NaCl, 500 mmol/L sucrose, 1 mmol/L EDTA, 0.15 mmol/L spermine, 0.5 mmol/L spermidine, 10 mmol/L HEPES (pH 8.0), 200 µmol/L phenylmethylsulfonyl fluoride, 2 mg/L leupeptin, 2 mg/L pepstatin, 24 000 IU/L aprotinin, and 7 mmol/L β-mercaptoethanol. Proteins (40 µg) were subjected to SDS-PAGE, and transferred to the PVDF membrane for immunodetection. The SDS-PAGE molecular weight markers (Bio-Rad) verified the correct location of the visualized bands. The membranes were blocked with 50 mL/L nonfat milk in PBS-Tween, probed with anti-p53 or anti-p21 antibody, and followed by secondary antibody (goat anti-mouse IgG-alkaline phosphatase). Immunoreactive proteins were detected using a color develop system (NBT/BCIP) by the standard procedure^[10].

RESULTS

Expression of *c-fos* mRNA

Northern blot analysis demonstrated the overexpression of *c-fos* mRNA in Bel 7402 cells after treated with AFP for 2, 6, and 12 h. The data showed that AFP (20 mg/L) treated for 2 h significantly increased the expression of *c-fos* mRNA in Bel 7402 cells by 51.1% compared with the control group. The expression of *c-fos* mRNA continuously increased by 60.9% and 96.0% when treated with AFP for 6 h and 12 h, respectively, and declined thereafter to 25.5% increase at 24 h, compared with control group (Figure 1). However, HSA at the same dosage (20 mg/L) as AFP and anti-AFP antibody (40 mg/L)

had no significant influence on the expression of *c-fos* mRNA in Bel 7402 cells. Anti-AFP antibody partially blocked an increase in the expression of *c-fos* mRNA by AFP (Figure 2).

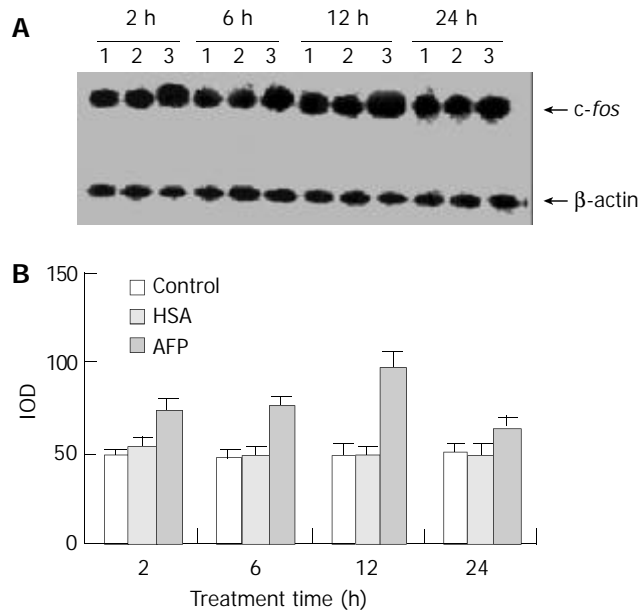


Figure 1 Effects of AFP (20 mg/L) or HSA (20 mg/L) on the expression of *c-fos* mRNA in human hepatocellular carcinoma Bel 7402 cells analyzed by Northern blot. The cells were incubated with AFP or HSA for 2, 6, 12, and 24 h, respectively. A: Autoradiogram of Northern blot. Lane 1: control group; Lane 2: HSA treated group; Lane 3: AFP treated group. B: Densitometric intensity of absorbance (IOD) of *c-fos* mRNA expression in Bel 7402 cells. The data were selected from 3 independent experiments.

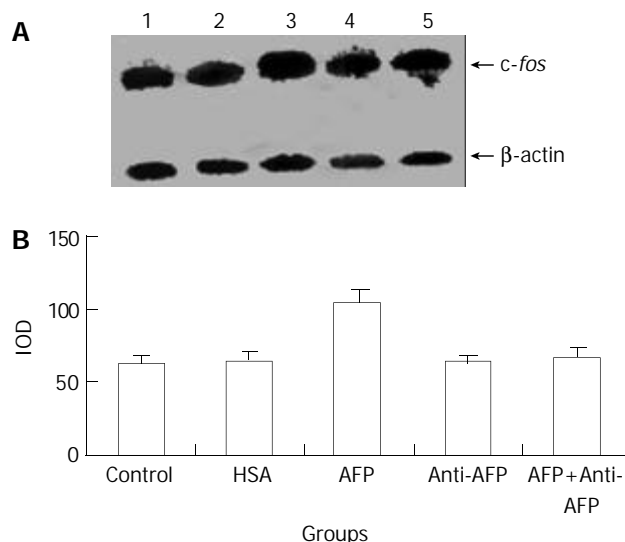


Figure 2 Effects of AFP (20 mg/L), HSA (20 mg/L), anti-AFP antibody (40 mg/L), and AFP (20 mg/L) + anti-AFP antibody (40 mg/L) on *c-fos* mRNA expression in human hepatocellular carcinoma Bel 7402 cells analyzed by Northern blot after 2 h treatment. A: Autoradiogram of Northern blot. Lane 1: control group; Lane 2: HSA treated group; Lane 3: AFP treated group; Lane 4: anti-AFP antibody treated group; Lane 5: AFP + anti-AFP antibody treated group. B: Densitometric intensity of absorbance (IOD) of *c-fos* mRNA expression in Bel 7402 cells. The data were selected from 3 independent experiments.

Expression of *c-jun* mRNA

AFP (20 mg/L) had no significant influence on the expression

of *c-jun* mRNA in human hepatocellular carcinoma cells when treated for 2 h, but when treated for 6 h the expression of *c-jun* mRNA increased obviously, the increase rate was 81.3%, but when treated for 24 h, increased rate fell to 14.6% as compared with the control group (Figure 3). However, HSA (20 mg/L) at the same dosage as AFP and anti-AFP antibody (40 mg/L) had no significant influence on the expression of *c-jun* mRNA in Bel 7402 cells. Anti-AFP antibody partially inhibited an increase in the expression of *c-jun* mRNA by AFP (Figure 4).

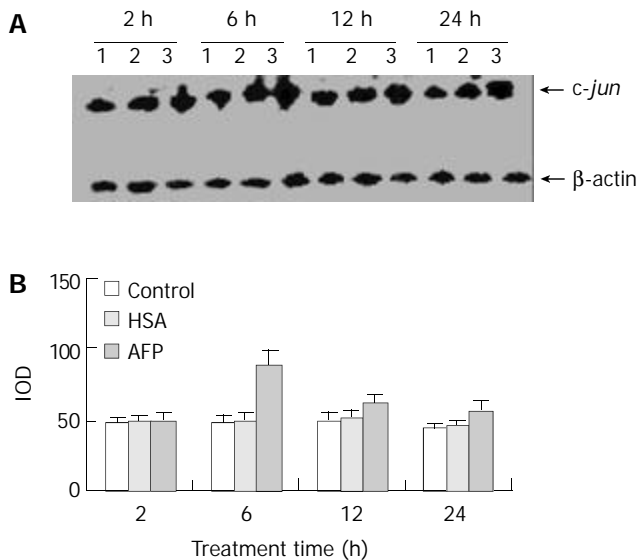


Figure 3 Effects of AFP (20 mg/L) or HSA (20 mg/L) on the expression of *c-jun* mRNA in human hepatocellular carcinoma Bel 7402 cells analyzed by Northern blot. The cells were incubated with AFP or HSA for 2, 6, 12, and 24 h, respectively. A: Autoradiogram of Northern blot. Lane 1: control group; Lane 2: HSA treated group; Lane 3: AFP treated group. B: Densitometric intensity of absorbance (IOD) of *c-jun* mRNA expression in Bel 7402 cells. The data were selected from 3 similar experiments.

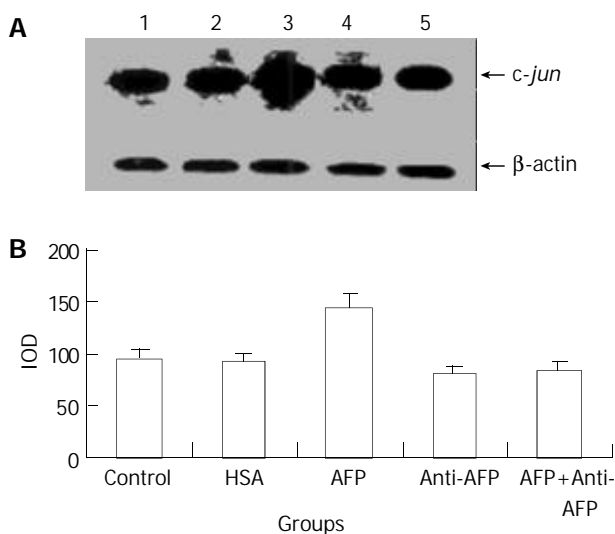


Figure 4 Effects of AFP (20 mg/L), HSA (20 mg/L), anti-AFP antibody (40 mg/L), and AFP (20 mg/L) + anti-AFP antibody (40 mg/L) on the expression of *c-jun* mRNA in human hepatocellular carcinoma Bel 7402 cells analyzed by Northern blot after 6 h treatment. A: Autoradiogram of Northern blot. Lane 1: control group; Lane 2: HSA treated group; Lane 3: AFP treated group; Lane 4: anti-AFP antibody treated group; Lane 5: AFP + anti-AFP antibody treated group. B: Densitometric

intensity of absorbance (IOD) of *c-jun* mRNA expression in Bel 7402 cells. The data were selected from 3 independent experiments.

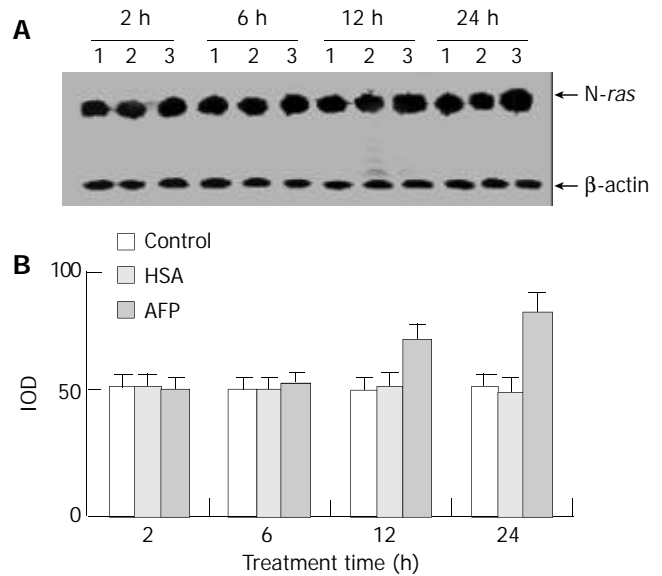


Figure 5 The effects of AFP (20 mg/L) or HSA (20 mg/L) on the expression *N-ras* mRNA in human hepatocellular carcinoma Bel 7402 cells analyzed by Northern blot. The cells were incubated with AFP or HSA for 2, 6, 12, and 24 h, respectively. A: Autoradiogram of Northern blot. Lane 1: control group; Lane 2: HSA treated group; Lane 3: AFP treated group. B: Densitometric intensity of absorbance (IOD) of *N-ras* mRNA expression in Bel 7402 cells. The data were selected from 3 similar experiments.

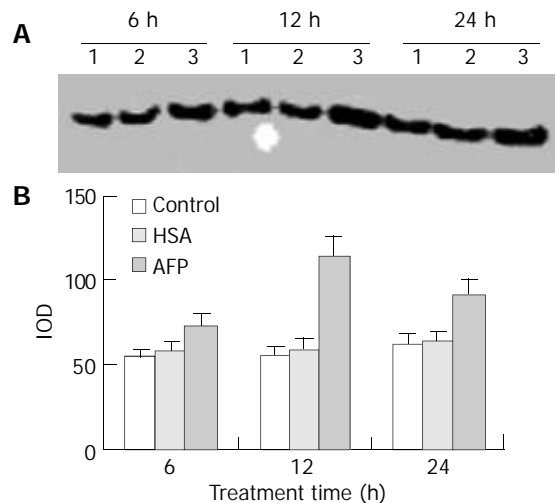


Figure 6 Effects of AFP (20 mg/L) or HSA (20 mg/L) on the expression of p21^{ras} in Bel 7402 cells analyzed by Western blot. The cells were incubated with AFP or HSA for 6, 12, and 24 h, respectively. A: Western blot analysis. Lane 1: control group; Lane 2: HSA treated group; Lane 3: AFP treated group. B: Densitometric intensity of absorbance (IOD) of p21^{ras} protein. The data were selected from 3 similar experiments.

Expression of *N-ras* mRNA

Northern blot analysis showed that AFP (20 mg/L) had no significant influence on the expression of *N-ras* mRNA in Bel 7402 cells when treated for 2 h and 6 h, but *N-ras* mRNA was overexpressed when treated with AFP (20 mg/L) for 12 h and 24 h. The increased ratios were 22.6% (12 h) and 59.9% (24 h), respectively, compared with the control group, and HSA (20 mg/L) did not significantly affect the expression of *N-ras* mRNA (Figure 5).

Expression of p21^{ras} protein

Western blot analysis demonstrated that AFP significantly enhanced the expression of p21^{ras} protein in Bel 7402 cells by 35.2%, 102.6%, and 46.8% at 6, 12, and 24 h, respectively, compared with the control group. However, HSA (20 mg/L) did not influence the expression of p21^{ras} protein (Figure 6).

Expression of mutative p53 protein

The data showed that AFP significantly influenced the expression of mutative p53 protein in Bel 7402 cells by 13.4%, 39.9%, and 70.6% at 6, 12, and 24 h, respectively, compared with the control group. However, HSA (20 mg/L) did not affect the expression of mutative p53 protein (Figure 7).

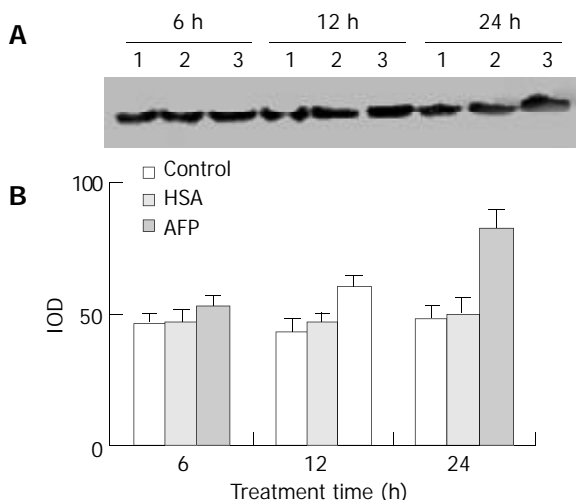


Figure 7 Effects of AFP (20 mg/L) or HSA (20 mg/L) on the expression of mutative p53 protein in Bel 7402 cells analyzed by Western blot. The cells were treated with AFP or HSA for 6, 12, and 24 h, respectively. A: Western blot analysis. Lane 1: control group; Lane 2: HSA treated group; Lane 3: AFP treated group. B: Densitometric intensity of absorbance (IOD) of p53 protein. The data were selected from 3 similar experiments.

DISCUSSION

Many investigations have shown that AFP receptors exist on the membrane of various tumor cells^[5,7,8,11-13], and play an important role in regulating growth of the cells^[7,8,14]. The receptor may mediate intercellular signal transduction which influences the expression of genes related to proliferation, and the expression of these genes is the most direct factor that controls cell cycle. Our results showed that AFP stimulated the expression of *c-fos*, *c-jun*, and *N-ras* mRNA in hepatocellular carcinoma Bel 7402 cells. Both *c-fos* and *c-jun* have the characteristics of early response genes. When treated with AFP, the two oncogenes in Bel 7402 cells express promptly, thereafter the expression of these oncogenes dramatically declines. Previous researches had showed that AFP promoted the proliferation^[1-6] and some oncogene expression of many tumor cells^[15,16]. Cell growth was regulated by various factors, in which, some oncogene coding proteins have an important function in modulating growth and differentiation of the cells. *c-fos* and *c-jun* are the immediate early genes (IEG) with the characteristics of early response gene. When Bel 7402 cells were treated with AFP, the expression of these oncogenes had the characteristics of dynamics, which was independent on the translation of RNA. Additionally, IEG coding regulated-proteins can control the expression of some later response genes through the activation of nuclear transcription factors. Furthermore, *c-Fos* and *c-Jun* proteins can interact with each other to form a heterodimer (*Fos-Jun*) called AP-1 (activator

protein-1). The dimer has leucine zipper structure, which has stronger binding affinity to DNA, and is the third messenger of signal transduction. The AP-1 protein is a nuclear transcription factor, which can regulate gene transcription by binding to a gene transcription-regulated element, and can increase transcriptional activation of downstream target genes. A previous study showed that the transcriptional properties of AP-1 depended on the site of cAMP-response elements to influence the expression of growth-related genes in hepatocellular carcinoma^[17]. Therefore, we thought that AFP regulated cell cycle of Bel 7402 cells, which was related to the expression of early-response genes. Our result also showed that AFP promoted the expression of *N-ras* in Bel 7402 cells. The *N-ras* gene is closely related to cell proliferation, and p21^{ras}, the *N-ras* coding protein, is an important intermediate of tyrosine-protein kinase (TPK) signal pathway in the cells to regulate growth-related gene expression. Therefore, we suggested that AFP could affect signal transduction to regulate growth of Bel 7402 cells probably through stimulating the expression of *N-ras*.

The wild type p53 is a very important tumor suppressor gene to inhibit proliferation of tumor cells. Some studies had showed that hepatocellular carcinoma was closely related to abnormal expression of p53 gene^[18,19]. Additionally, p53 and beta-catenin mutation rates were inversely correlated in hepatocellular carcinoma^[20]. The inactivation of p53 was an important cause of aberrant accumulation of beta-catenin, which was involved in both cell-cell interactions and wnt pathway-dependent cell fate determination in many cancer cells^[20]. A previous study found that p53 mutation was correlated significantly with invasiveness including vascular permeation of hepatocellular carcinoma cells, and p53 mutation in the primary lesion was useful as an indicator of the biological behavior of recurrent hepatocellular carcinoma^[21]. It showed that mutative p53 protein played a critical role in cell proliferation of hepatocellular carcinoma. The p53 gene could influence AFP expression to regulate the biological behavior of tumor cells^[22,23]. Our data had showed that AFP could enhance the expression of mutative p53 protein. When p53 gene is mutated, it can not suppress the growth of tumor cells, on the contrary, it possesses the functions of oncogenes. There are two types of mutative p53 genes in tumor cells, one of the mutative p53 genes can restrain the growth-suppressing activity of wild type p53 gene, then display apparently its negative regulation; the other type of mutative p53 genes can cooperate with *ras* gene to actuate cell transformation, and then become a dominant oncogene, which promotes the growth of tumor cells. Because *Ras* protein is an important intermediate in TPK signal transduction pathway, we analyzed the expression of *N-ras* mRNA, and then further detected its protein in this study. The results showed that AFP promoted the expression of p21^{ras} protein in Bel 7402 cells. The functions of p21^{ras} protein are similar to those of guanylate binding protein, and it can phosphorylate the intermediate in the downstream of TPK signal pathway to activate mitogen-activated protein kinase (MAPK) and to participate in intercellular signal transduction. The p21^{ras} protein can transduce the signal from TPK to threonine/serine protein kinase chain through Ras-Raf-MAPK signal pathway. These responses further activate some transcription factors which promote gene expression to enhance the growth of various cells. Our results demonstrated that AFP increased the expression of p21^{ras}. Therefore, we speculated that AFP affected the expression of p53 and p21^{ras} proteins through AFP receptor-mediated signal transduction pathway to accelerate the proliferation of Bel 7402 cells. Similar to the findings in this study, our previous study found that AFP enhanced the growth of HeLa and NIH3T3 cells through stimulating the expression of some oncogenes^[8,15,16], suggesting

that AFP might unselectively regulate proliferation of tumor cells in different tissues and species.

The mechanism for growth-promoting activity of AFP is still unclear. It has been known for a long time that AFP has the ability to transport the substances essential for cell proliferation to enter the cells. Studies have indicated that AFP is an important protein in the embryos to regulate growth of the fetus^[24], and required for female fertility, but not essential for embryonic development^[25]. Up to date, it is not clear whether the biological function of AFP is involved in regulating cell proliferation. Some studies indicated that AFP inhibited immune response to promote the growth of tumor cells *in vivo*^[26,27]. Escaping from the surveillance of immune system was the primary cause for malignant growth of tumor cells. Hepatocellular carcinoma cells can escape from the surveillance of immune system through altering the expression of tumor necrosis factor-related apoptosis-inducing ligand (TRAIL) receptors^[28], which can sustain the growth of tumor cells *in vivo*. However, our *in vitro* study could not establish the immune response without immune factors to affect the expression of the oncogenes in Bel 7402 cells. Therefore, it could not explain that AFP inhibited immune response to affect cell growth. Because AFP is a macromolecule, it is impossible to enter the cells through the cell membrane directly. Although AFP can transport some substances required for cell proliferation, it is not enough to completely support cell proliferation. Many studies found that AFP receptors existed on the membrane surface of various tumor cells, and mediated signal transduction to regulate the expression of the genes. The expression of these genes was the ultimate determination factor in regulating cell growth. Our results showed that AFP had the ability to stimulate the expression of the oncogenes *c-fos*, *c-jun*, and *N-ras* in Bel 7402 cells, and the response of these genes to AFP was various. Both the expression of *c-fos* and *c-jun* responded early, whereas the expression of *N-ras* and mutative p53 gene responded thereafter. Some oncogenes such as p53 and ras are important prognostic molecular markers in human hepatocellular carcinoma^[29]. According to previous studies^[5,7,8] and our results, we considered that the action of AFP was via TPK signal transduction pathway to stimulate the expression of some oncogenes which could regulate the growth of tumor cells. Many investigations had showed that the expression of some oncogenes was up-regulated in hepatocellular carcinoma, and some factors such as integrin gene, p28/gankyrin, and HLA class I could influence cell proliferation of hepatocellular carcinoma^[30-32]. However, some studies had shown that treatment of tumor cells *in vitro* with high dosage of AFP (1-10 $\mu\text{mol/L}$) significantly suppressed the growth of tumor cells, because AFP positively regulated cytochrome c-mediated caspase activation, apoptosome complex formation, and low-dose cytochrome c-mediated signals^[33,34]. The mechanisms for how AFP regulates the expression of these genes and signal transduction, and why it is not essential for embryonic development^[24], although it promotes the growth of some tumor cells^[1-8] remain to be studied.

A previous study showed that AFP could coordinate other growth factors existed in HSA and serum to promote the growth of porcine granulosa cells, and AFP could function to modulate growth factor-mediated cell proliferation during development and neoplasia^[4]. To further verify the up-regulation of these oncogenes was mediated by AFP, this study used HSA as a negative control due to similar amino acid sequences of AFP as HSA. The results showed that HSA or anti-AFP antibody did not stimulate the expression of these genes in Bel 7402 cells, but anti-AFP antibody efficiently blocked the function of AFP, which can be explained that AFP specifically stimulated the expression of these oncogenes in human hepatocellular carcinoma Bel 7402 cells.

REFERENCES

- 1 **Dudich E**, Semonkova L, Gorbatova E, Dudich I, Khromykh L, Tatulov E, Grechko G, Sukhikh G. Growth-regulative activity of human alpha-fetoprotein for different types of tumor and normal cells. *Tumour Biol* 1998; **19**: 30-40
- 2 **Wang XW**, Xie H. Alpha-fetoprotein enhances the proliferation of human hepatoma cells *in vitro*. *Life Sci* 1999; **64**: 17-23
- 3 **Wang XW**, Xu B. Stimulation of tumor-cell growth by alpha-fetoprotein. *Int J Cancer* 1998; **75**: 596-599
- 4 **Keel BA**, Eddy KB, Cho S, May JV. Synergistic action of purified alpha-fetoprotein and growth factors on the proliferation of porcine granulosa cells in monolayer culture. *Endocrinology* 1991; **129**: 217-225
- 5 **Li MS**, Li PF, Zhou AR, Li G, Du GG. Growth factor like activity of alpha-fetoprotein in human hepatoma cell line, Bel7402 and HeLa cell (abstract). *Endo 2000 the Endocrine Society 82nd Annual Meeting, Toronto, Canada* 2000: 143
- 6 **Nunez EA**. Biological role of alpha-fetoprotein in the endocrinological field: data and hypothesis. *Tumour Biol* 1994; **15**: 63-72
- 7 **Li MS**, Li PF, He SP, Du GG, Li G. The promoting molecular mechanism of alpha-fetoprotein on the growth of human hepatoma Bel7402 cell line. *World J Gastroenterol* 2002; **8**: 469-475
- 8 **Li MS**, Li PF, Yang FY, He SF, Du GG, Li G. The intracellular mechanism of alpha-fetoprotein promoting the proliferation of NIH 3T3 cells. *Cell Res* 2002; **12**: 151-156
- 9 **Yamada T**, Kakinoki M, Totsuka K, Ashida Y, Nishizono K, Tsuchiya R, Kobayashi K. Purification of canine alpha-fetoprotein and alpha-fetoprotein values in dogs. *Vet Immunol Immunopathol* 1995; **47**: 25-33
- 10 **Sambrook J**, Fritsch EF, Maniatis T. Molecular cloning: A laboratory manual, 2nd ed. New York: Cold Spring Harbor Laboratory Press 1989: 888-897
- 11 **Esteban C**, Geuskens M, Uriel J. Activation of an alpha-fetoprotein (AFP)/receptor autocrine loop in HT-29 human colon carcinoma cells. *Int J Cancer* 1991; **49**: 425-430
- 12 **Villacampa MJ**, Moro R, Naval J, Faily-Crepin C, Lempereur F, Uriel J. Alpha-fetoprotein receptors in a human breast cancer cell line. *Biochem Biophys Res Commun* 1984; **122**: 1322-1327
- 13 **Naval J**, Villacampa MJ, Goguel AF, Uriel J. Cell-type-specific receptor for alpha-fetoprotein in mouse T-lymphoma cell line. *Proc Natl Acad Sci U S A* 1985; **82**: 3301-3305
- 14 **Laderoute MP**, Pilarski LM. The inhibition of apoptosis by alpha-fetoprotein (AFP) and the role of AFP receptors in anti-cellular senescence. *Anticancer Res* 1994; **14**(6B): 2429-2438
- 15 **Li MS**, Li PF, Du GG, Li G. The enhancement effects of alpha-fetoprotein on the expression of *N-ras* and p53 and p21^{ras} in HeLa cells. *Chin J Biochem Mol Biol* 2002; **18**: 750-754
- 16 **Li MS**, Li PF, Li G, Du GG. Enhancement of proliferation of HeLa cells by the α -fetoprotein. *Shengwu Huaxue Yu Shengwu Wuli Xuebao* 2002; **34**: 769-774
- 17 **Guberman AS**, Scassa ME, Giono LE, Varone CL, Canepa ET. Inhibitory effect of AP-1 complex on 5-aminolevulinic synthase gene expression through sequestration of cAMP-response element protein (CRE)-binding protein (CBP) coactivator. *J Biol Chem* 2003; **278**: 2317-2326
- 18 **Caruso ML**, Valentini AM. Overexpression of p53 in a large series of patients with hepatocellular carcinoma: a clinicopathological correlation. *Anticancer Res* 1999; **19**(5B): 3853-3856
- 19 **Zhang XW**, Xu B. Differential regulation of P53, c-Myc, Bcl-2, Bax and AFP protein expression, and caspase activity during 10-hydroxycamptothecin-induced apoptosis in Hep G2 cells. *Anticancer Drugs* 2000; **11**: 747-756
- 20 **Cagatay T**, Ozturk M. P53 mutation as a source of aberrant beta-catenin accumulation in cancer cells. *Oncogene* 2002; **21**: 7971-7980
- 21 **Sheen IS**, Jeng KS, Wu JY. Is p53 gene mutation an indicator of biological behaviors of recurrence of hepatocellular carcinoma? *World J Gastroenterol* 2003; **9**: 1202-1207
- 22 **Ogden SK**, Lee KC, Wernke-Dollries K, Stratton SA, Aronow B, Barton MC. p53 targets chromatin structure alteration to repress alpha-fetoprotein gene expression. *J Biol Chem* 2001; **276**: 42057-42062
- 23 **Lee KC**, Crowe AJ, Barton MC. p53-mediated repression of alpha-fetoprotein gene expression by specific DNA binding. *Mol*

- Cell Biol* 1999; **19**: 1279-1288
- 24 **Mazure NM**, Chauvet C, Bois-Joyeux B, Bernard MA, Nacer-Cherif H, Danan JL. Repression of alpha-fetoprotein gene expression under hypoxic conditions in human hepatoma cells: characterization of a negative hypoxia response element that mediates opposite effects of hypoxia inducible factor-1 and c-Myc. *Cancer Res* 2002; **62**: 1158-1165
- 25 **Gabant P**, Forrester L, Nichols J, Van Reeth T, De Mees C, Pajack B, Watt A, Smits A, Alexandre H, Szpirer C, Szpirer J. Alpha-fetoprotein, the major fetal serum protein, is not essential for embryonic development but is required for female fertility. *Proc Natl Acad Sci U S A* 2002; **99**: 12865-12870
- 26 **Semeniuk DJ**, Boismenu R, Tam J, Weissenhofer W, Murgita RA. Evidence that immunosuppression is an intrinsic property of the alpha-fetoprotein molecule. *Adv Exp Med Biol* 1995; **383**: 255-269
- 27 **Gotsman I**, Israeli D, Alper R, Rabbani E, Engelhardt D, Ilan Y. Induction of immune tolerance toward tumor-associated enables growth of human hepatoma in mice. *Int J Cancer* 2002; **97**: 52-57
- 28 **Chen XP**, He SQ, Wang HP, Zhao YZ, Zhang WG. Expression of TNF-related apoptosis-inducing Ligand receptors and anti-tumor effects of TNF-related apoptosis-inducing Ligand in human hepatocellular carcinoma. *World J Gastroenterol* 2003; **9**: 2433-2440
- 29 **Qin LX**, Tang ZY. The prognostic molecular markers in hepatocellular carcinoma. *World J Gastroenterol* 2002; **8**: 385-392
- 30 **Liu LX**, Jiang HC, Liu ZH, Zhou J, Zhang WH, Zhu AL, Wang XQ, Wu M. Intergrin gene expression profiles of human hepatocellular carcinoma. *World J Gastroenterol* 2002; **8**: 631-637
- 31 **Fu XY**, Wang HY, Tan L, Liu SQ, Cao HF, Wu MC. Overexpression of p28/gankyrin in human hepatocellular carcinoma and its clinical significance. *World J Gastroenterol* 2002; **8**: 638-643
- 32 **Huang J**, Cai MY, Wei DP. HLA class I expression in primary hepatocellular carcinoma. *World J Gastroenterol* 2002; **8**: 654-657
- 33 **Dudich E**, Semenkova L, Dudich I, Gorbatova E, Tochtamisheva N, Tatulov E, Nikolaeva M, Sukhikh G. Alpha-fetoprotein causes apoptosis in tumor cells via a pathway independent of CD95, TNFR1 and TNFR2 through activation of caspase-3-like proteases. *Eur J Biochem* 1999; **266**: 750-761
- 34 **Semenkova L**, Dudich E, Dudich I, Tokhtamisheva N, Tatulov E, Okruzhnov Y, Garcia-Foncillas J, Palop-Cubillo JA, Korpela T. Alpha-fetoprotein positively regulates cytochrome c-mediated caspase activation and apoptosome complex formation. *Eur J Biochem* 2003; **270**: 4388-4399

Edited by Chao CJ Proofread by Xu FM

Comparison of long-term effects between intra-arterially delivered ethanol and Gelfoam for the treatment of severe arterioportal shunt in patients with hepatocellular carcinoma

Ming-Sheng Huang, Qu Lin, Zai-Bo Jiang, Kang-Shun Zhu, Shou-Hai Guan, Zheng-Ran Li, Hong Shan

Ming-Sheng Huang, Zai-Bo Jiang, Kang-Shun Zhu, Shou-Hai Guan, Zheng-Ran Li, Hong Shan, Department of Radiology, The 3rd Affiliated Hospital of Sun Yat-sen University, Guangzhou 51000, Guangdong Province, China

Qu Lin, Department of Internal Medicine, The 3rd Affiliated Hospital of Sun Yat-sen University, Guangzhou 51000, Guangdong Province, China

Correspondence to: Professor Hong Shan, Department of Radiology, The 3rd Affiliated Hospital of Sun Yat-sen University, 600 Tianhe Road Guangzhou, 510630 China. gzshsums@public.guangzhou.gd.cn

Telephone: +86-20-85516867-2316 **Fax:** +86-20-87580725

Received: 2003-11-12 **Accepted:** 2003-12-16

Abstract

AIM: To evaluate long-term effect of ethanol embolization for the treatment of hepatocellular carcinoma (HCC) with severe hepatic arterioportal shunt (APS), compared with Gelfoam embolization.

METHODS: Sixty-four patients (ethanol group) and 33 patients (Gelfoam group) with HCC and APS were respectively treated with ethanol and Gelfoam for APS before the routine interventional treatment for the tumor. Frequency of recanalization of shunt, complete occlusion of the shunt, side effects, complications, and survival rates were analyzed between the two groups.

RESULTS: The occlusion rate of APS after initial treatment in ethanol group was 70.3%(45/64), and recanalization rate of 1 month after embolization was 17.8%(8/45), and complete occlusion rate was 82.8%(53/64). Those in Gelfoam group were 63.6%(21/33), 85.7%(18/21), and 18.2%(6/33). There were significant differences in recanalization rate and complete occlusion rate between the two groups ($P<0.05$). The survival rates in ethanol group were 78% at 6 months, 49% at 12 months, 25% at 24 months, whereas those in Gelfoam group were 58% at 6 months, 23% at 12 months, 15% at 24 months. The ethanol group showed significantly better survival than Gelfoam group ($P<0.05$). In the ethanol group, there was a significant prolongation of survival in patients with monofocal HCC ($P<0.05$) and Child class A ($P<0.05$). There were no significant differences in survival rate in the Gelfoam group with regard to the number of tumor and Child class ($P>0.05$). The incidence rate of abdominal pain during procedure in ethanol group was 82.8%. There was no significant difference in postembolization syndromes between two groups. Procedure-related hepatic failure did not occur in ethanol group.

CONCLUSION: Ethanol embolization for patients with HCC and severe APS is efficacious and safe, and may contribute to prolongation of the life span versus Gelfoam embolization.

Huang MS, Lin Q, Jiang ZB, Zhu KS, Guan SH, Li ZR, Shan H. Comparison of long-term effects between intra-arterially

delivered ethanol and Gelfoam for the treatment of severe arterioportal shunt in patients with hepatocellular carcinoma. *World J Gastroenterol* 2004; 10(6): 825-829

<http://www.wjgnet.com/1007-9327/10/825.asp>

INTRODUCTION

Hepatocellular carcinoma is frequently associated with arterioportal shunts. Kido and Ngan *et al*^[1,2] reported that APS in HCC occurred in 60%, and Okuda *et al*^[3] reported that severe APS of main or right or left portal veins occurred in 30% of patients with HCC. Severe APS led to life threatening conditions (*e.g.*, esophageal varices, ascites and hepatic encephalopathy) as a result of portal regurgitation or portal hypertension^[4-7]. To improve portal hypertension caused by severe APS in patients with HCC, APS needs to be treated. To date, Gelfoam and steel coil are the most commonly used embolic materials^[8-10]. However, any long-term effect of embolization of APS with steel coil or Gelfoam on survival have not been proved, although they produced a good short-term effect as reported^[8-10]. It has been a hot issue how to choose an ideal embolic material to occlude APS. In this study, we used ethanol as the embolic material to treat the APS before the routine interventional treatment for 64 patients. The purpose of this study was to evaluate the long-term effect of the transcatheter arterial embolization (TAE) of APS with new embolic material in patients with HCC and APS, in comparison with the most commonly used material: Gelfoam.

MATERIALS AND METHODS

Patients

Among 596 patients with HCC treated with transcatheter arterial chemoembolization (TACE) or transcatheter arterial infusion chemotherapy (TAI) at the 3rd Affiliated Hospital of Sun Yat-sen University from February 1999 to March 2003, 161(27%) patients with severe APS were identified by digital subtraction angiography (DSA). We excluded patients with Child class C disease and patients who underwent the treatment of surgical resection, percutaneous local ethanol injection, microwave coagulation, or systemic chemotherapy throughout the study period. According to the exclusive criteria, 64 of 161 patients were excluded from this study. Ninety-seven patients were enrolled in our study (78 men and 19 women, ranging from 21 to 78 years of age; mean age, 57.9). All the patients were treated with TAI or TACE after undergoing embolization of APS.

Written informed consent was obtained from the patients involved in this study. We divided the patients into 2 groups: ethanol group, in which APS was treated with ethanol for 64 patients from April 2000 to March 2003, and Gelfoam group, in which APS was treated with gelatin sponge particles for 33 patients from February 1999 to March 2000. The clinical characteristics of two therapeutic groups were illustrated in Table 1. Although this was a retrospective nonrandomized

study, there were no significant differences between two groups in background factors (Table 1).

Table 1 Clinicopathologic characteristics of patients with HCC and APS

Characteristics	Ethanol group (n=64)	Gelfoam group (n=33)	P value
Age (y)	56.4±21.4	52.3±26.6	0.42
Sex (M/F)	52/12	25/7	0.72
Child classification			
Child class A	35(55%)	20(61%)	
Child class B	29(45%)	13(39%)	0.56
Serum total bilirubin (mg/ml)	1.6±1.5	2.0±1.8	0.31
Serum albumin (g/dl)	3.6±0.8	3.4±1.1	0.30
Number of tumors			
1	15(23%)	11(33%)	
2-3	19(30%)	8(24%)	
≥4, diffuse	30(47%)	14(43%)	0.32

Treatments

Firstly, arteriography of hepatic common artery was performed to visualize the arterial vascularization of the liver and to identify the location, severity and direction of vessels of APS. Secondly, a 3-F microcatheter was superselectively inserted into the dominant artery of APS through a 5-F catheter. The embolic material was injected to occlude APS. All diagnostic studies and treatments of APS were performed during the same procedure.

Ethanol group: 2-3 mL absolute ethanol was injected slowly and gently at the rate of about 1 mL/min after 2 mL 10g/L lidocaine was injected through catheter. About 5-10 min later, a repeated DSA was performed to evaluate the occlusive extent of APS. If persistence of APS was shown, another 2-3 mL ethanol was injected repeatedly until the occlusion of APS was confirmed with angiography.

Gelfoam group: Gelatin sponge particles (size, 1 mm×1 mm×1 mm) were mixed with contrast media (Iopamilon, Schering, Berlin, Germany) and were injected with 1-mL tuberculin syringe under fluoroscopic monitoring until a slow flow or stasis of APS was demonstrated. Then arteriography was done again to confirm the occlusion of APS. If APS could not be occluded with Gelatin sponge particles (size, 1 mm×1 mm×1 mm) and microcatheter, a 4F Rösch hepatic catheter or 4F cobra catheter would replace the 3-F microcatheter and be inserted into or by the way of the feeding artery of shunt. Then several large pieces of Gelfoam (beyond 1×1×1 mm) were used to occlude the shunt.

After embolization of APS, the routine interventional therapy was done for the tumor, as reported^[11-15]. After catheter was inserted into feeding artery of tumour, pirarubicin (THP)/lipiodol(LPD) emulsion was injected through catheter for the patients without tumour thrombus in main portal vein. THP/LPD was prepared with the following procedure. THP (60-80 mg) was dissolved in 3-10 mL of 50 g/L glucose and then mixed with 3-10 mL LPD at a 1:1 ratio repeating approximately 10 times. Then gelatin sponges embolization of feeding artery was performed. We only injected pirarubicin (60-80 mg) which was dissolved in 100 mL of 50g/L glucose for the patients with tumour thrombus in main portal vein.

Criteria for evaluating embolic effect

Recanalization of APS was defined as APS was shown again at arterial phase of DSA 1 month postprocedure in the patients who had the complete occlusion of shunt after initial treatment. Complete occlusion of APS was defined as APS was not demonstrated in DSA for 2 times consecutively.

Follow-up protocol

All patients were followed up by means of spiral CT scan of liver and laboratory tests such as concentrations of α -fetoprotein, liver function before and after treatment. Change of APS was evaluated with DSA which was performed 1 and 2 mo after initial treatment. Then all patients should be followed up every 2-3 mo. When elevation of tumor markers (α -fetoprotein), persistence of APS or recurrence of tumor were observed, patients were readmitted for angiography and treatment as before.

Statistical analysis

The cumulative proportional survival rates were calculated according to the Kaplan-Meier method. The starting point was defined as the day of initial treatment. The significance of differences between background clinical characteristics of the patients groups (ethanol and Gelfoam) was assessed with the χ^2 test and Student's *t* test. The significance of difference in survival rates between patients was evaluated by the generalized Wilcoxon test. Values of $P < 0.05$ were considered significant.

RESULTS

Results of occlusion of APS

In the ethanol group, APS was occluded completely at the initial treatment in 45(70.3%) patients. Among them, recanalization of APS 1 month post-procedure was shown in 8(17.8%). There were 30(46.9%) patients with APS 1 month after initial treatment, which included incomplete occlusion of APS in the initial treatment, recanalizational and newly occurred APS. Of them APSs were occluded completely after a second treatment in 16 patients. The rate of complete occlusion of APS in ethanol group was 82.8%(53/64) totally (Figures 1A-F).

In the Gelfoam group, 21(63.6%) patients had the complete occlusion of APS in the initial treatment. Recanalization of APS occurred in 18(85.7%) patients of them 1 mo after initial treatment. Thirty (90.6%) patients were with APS 1 mo after initial treatment, which consisted of incomplete occlusion of APS in the initial treatment, recanalizational and newly occurred APS. In 3 patients of them, APS were occluded completely after another treatment. The complete occlusion rate of APS in Gelfoam group was 18.2%(6/33) totally.

The recanalization rate of APS in ethanol group was lower than that in Gelfoam group ($\chi^2=24.91$, $P < 0.05$), and the complete occlusion rate of APS in ethanol group was higher than that in Gelfoam group ($\chi^2=32.06$, $P < 0.05$).

Survival

The survival rate in the ethanol group were 78% at 6 mo, 49% at 12 mo, and 25% at 24 mo. The median survival was 11 mo. By comparison, the survival rates in the Gelfoam group were 58% at 6 mo, 29% at 12 mo, 15% at 24 mo, and the median survival was 7 mo. The survival rates in the ethanol group were significantly higher than those in the Gelfoam group ($P < 0.05$) (Figure 2).

In the ethanol group, the survival rates of patients with single HCC nodule were 92% at 6 mo, 70% at 12 mo, and 55% at 24 mo. The survival rates of patients with two or three HCC nodules were 73% at 6 mo, 55% at 12 mo and 22% at 24 mo. The survival rates of patients with multiple HCC nodules or diffuse HCC were 68% at 6 mo, 33% at 12 mo and 15% at 24 mo. The survival rates of patients with monofocal HCC were significantly higher than those of patients with multifocal HCC ($P < 0.05$) (Figure 3). The survival rates of patients of Child class A were 91% at 6 mo, 60% at 12 mo, and 38% at 24 mo. The survival rates of patients of Child class B were 62% at 6 mo, 35% at 12 mo and 13% at 24 mo. The survival rates of patients of Child class A were higher than those of patients of Child class B ($P < 0.05$) (Figure 4).

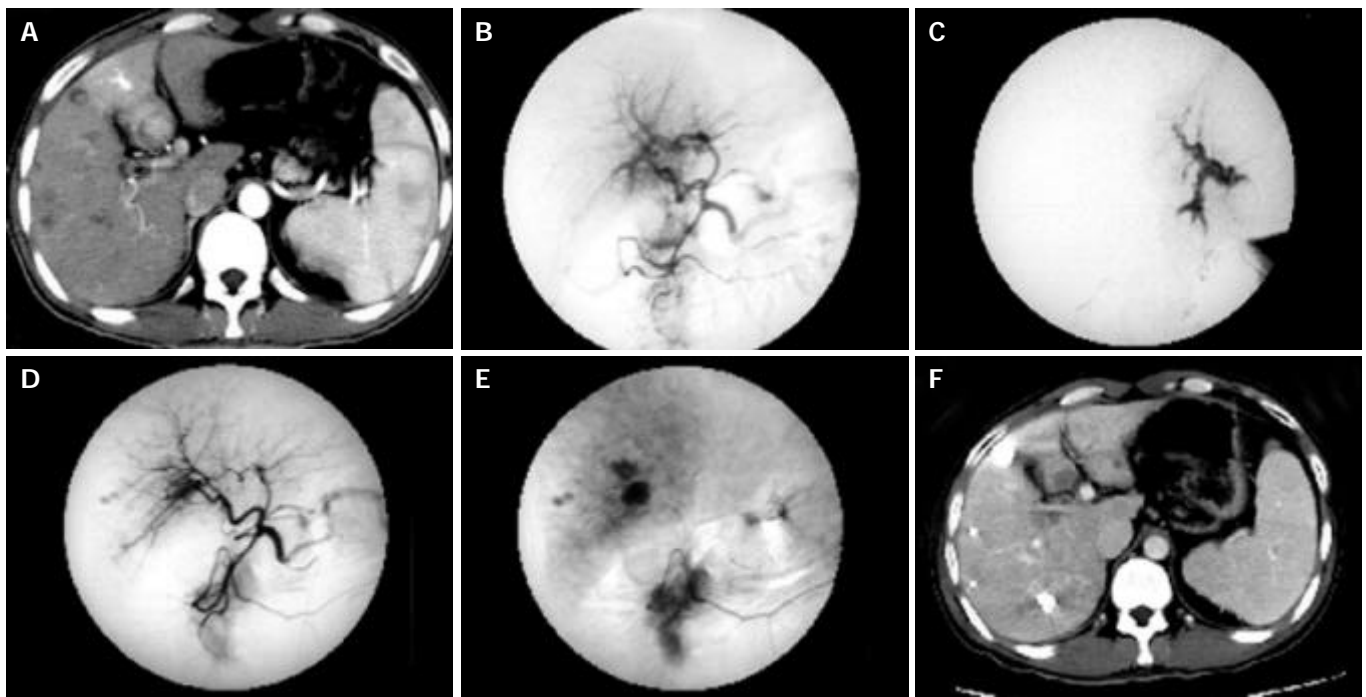


Figure 1 Multiple HCC nodules in a 34-year-old patient. A: CT image obtained during the arterial phase showed the predominant enhancement of the medial segment of left lobe and the enhancement of left portal branches, which represent APS. B: Hepatic arteriogram demonstrated the arterioportal shunt. C: The microcatheter was inserted into the feeding artery of APS. DSA showed the strong or fast blood flow of APS. D-E: Hepatic arteriogram showed that the arterioportal shunt was no longer visible after embolization with a microcoil and ethanol. F: Follow-up CT scan showed lipiodol accumulation in multiple HCC nodules, and liver necrosis was not seen in the distribution of the hepatic artery which had been treated with ethanol.

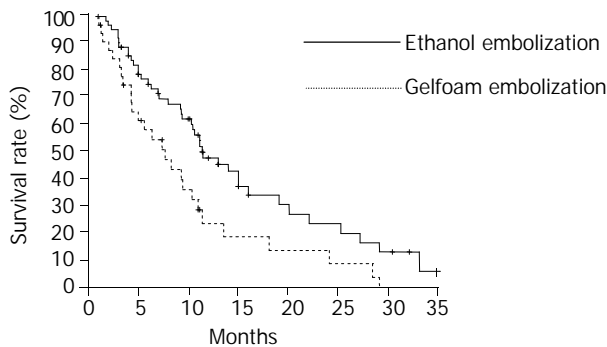


Figure 2 Cumulative survival curves for patients with HCC and APS in two therapeutic groups are shown. The survival rates for patients in the ethanol group were significantly higher than those in the Gelfoam group ($P<0.05$).

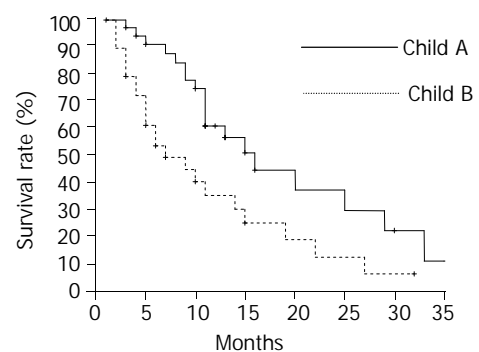


Figure 4 Cumulative survival curves for patients with HCC and APS according to the Child class were shown in ethanol group. The survival rates of patients of Child class A were higher than those of Child class B ($P<0.05$).

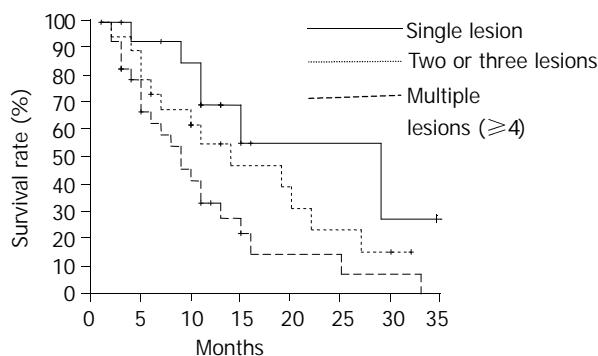


Figure 3 Cumulative survival curves for patients with HCC and APS in relation to number of tumors are shown in ethanol group. The survival rates of patients with monofocal HCC and APS were significantly higher than those of patients with multifocal HCC and APS (single lesion vs two or three lesions, $P<0.05$; two or three lesions vs four or more lesions, $P<0.05$).

In the Gelfoam group, the survival rates of patients with single HCC nodule were 62% at 6 mo, 38% at 12 mo, and 19% at 24 mo. The survival rates of patients with two or three HCC nodules were 61% at 6 mo, 26% at 12 mo and 12% at 24 mo. The survival rates of patients with multiple HCC nodules or diffuse HCC were 60% at 6 mo, 28% at 12 mo and 0 at 24 mo. The survival rates of patients of Child class A were 60% at 6 mo, 25% at 12 mo, and 18% at 24 mo. The survival rates of patients of Child class B were 68% at 6 mo, 30% at 12 mo and 15% at 24 mo. There were no significant differences in survival rates with regard to the number of tumor, and Child class ($P>0.05$).

Side effects and complications

In the ethanol group, a short-period intense abdominal pain occurred in 53(82.8%) patients during the process of ethanol injection, and mild abdominal pain in 9(14.1%) patients, and indolence in 2(3.1%) patients. Postembolization syndromes (such as nausea, vomiting, fever, and abdominal pain) occurred

in 50(78.1%) patients in ethanol group, and 30(90.9%) patients in Gelfoam group. There was no significant difference between the 2 groups ($\chi^2=1.66$, $P>0.05$). No patient died of procedure-related hepatic failure. In ethanol group, all feeding artery remained patent in the follow-up DSA arteriograms, and liver necrosis in the distribution of the hepatic artery which had been treated with ethanol was not seen in all patients according to the follow-up CT scans.

DISCUSSION

Hepatocellular carcinoma is frequently associated with arterioportal shunts. In our series, severe APSs were verified in 27% of patients with HCC by DSA. Severe APS leads to or aggravates portal hypertension which leads to life-threatening conditions such as esophageal varices, refractory ascites, refractory diarrhea and hepatic encephalopathy^[4-7,16,17]. Additionally, severe APSs have an influence on the performance of TAI or TACE for the treatment of HCC^[18]. The persistence of APS may possibly result in the poor prognosis of HCC. For the reasons as above, severe APS needs to be treated effectively.

Many embolic materials have been used to treat APS in patients with HCC^[8,9,19-23]. Of those Gelfoam and steel coil were the most commonly used. Clark^[9] and Tarazov^[8] reported that Gelfoam and steel coil emboli for the treatment of APS could not prolong the survival of patients with HCC, although they had a good short-term effect on the control of gastric bleeding and ascites. Those effects may be attributable to certain actions of those embolic materials. Firstly, Gelfoam embolization was likely to result in inadvertent embolization, and cause the occlusion of feeding artery of tumor, which would influence the procedure of TAI or TACE for the treatment of tumor. Secondly, the recanalization of APS occurred easily as a result of the development of collateral vessels and the absorption of Gelfoam two to four weeks after embolization. In our study, the recanalization rate of APS was 85.7% 1 month after embolization with Gelfoam. Similarly, the embolization with steel coil also produced the recanalization of APS as a result of the development of collateral anastomoses^[8].

Ethanol is a liquid embolic agent that causes immediate vascular sclerosis and occlusion by a combination of direct toxic effect on the vascular wall and clumping of damaged erythrocytes and denatured proteins^[24-26]. It has been used widely in the treatment of renal cell carcinoma, esophageal varices, and arteriovenous malformations^[24-35]. Similar to the treatment of arteriovenous malformation, injecting ethanol into APS results in clot formation, denudes the endothelium and causes embolization by penetrating into the capillaries. As an embolic material, ethanol is superior to Gelfoam in the treatment of APS. First, ethanol can pass to and occlude the capillaries and veins of shunt, and does not lead to the occlusion of feeding artery of tumor. Thus it produces a more complete occlusion of APS than Gelfoam. Second, ethanol is a kind of long-acting embolic material, and it rarely develops the collateral anastomoses after embolization with ethanol. It has a low recanalization rate of APS. Third, ethanol also has a direct tumoricidal effect. Our results showed the recanalization rate of APS 1 month after embolization with ethanol was 17.8%, and complete occlusion rate was 82.8%, which were better than those of Gelfoam group ($P<0.05$).

Furuse *et al*^[10] reported that the survival rate of patients with HCC and APS after steel coil embolization were 45% at 6 mo, 12% at 12 mo, and 6% at 2 yr, and it could not prolong the survival of patient with HCC after the treatment of APS. However, Liu *et al*^[36] reported that the survivals of HCC patients without APS were higher than those of patients with APS. It indicated that the persistence of APS was an important

prognostic factor. In our study, the complete occlusion rate of shunt in ethanol group was higher than that in Gelfoam group ($P<0.05$). The survival rate of patients in the ethanol group was 78% at 6 mo, 49% at 12 mo, 25% at 24 mo, which were higher than those of Gelfoam group ($P<0.05$). Our results suggest that the embolization of APS with ethanol provides a survival advantage over that with gelfoam in patient with HCC. In addition, there was a significant prolongation of survival in patients with monofocal HCC and Child class A in ethanol group ($P<0.05$). However, there were no significant differences in survival rates in Gelfoam group with regard to the differences in the number of tumor and Child class ($P>0.05$). It was suggested that the survival rate was also related to the stage and invasive extent of tumor, and general state of patients. On the other hand, the persistence of severe APS was the important factor which influenced the survival of patient with HCC and APS.

The most common complication of embolization of APS with ethanol was abdominal pain caused by destruction of the vascular endothelium when ethanol was injected^[24,25]. The incidence was 82.8% in our study. It could be alleviated immediately when we stopped injecting ethanol. There was no severe complication related to ethanol embolization. In our study, liver necrosis was not seen in the distribution of the hepatic artery which had been treated with ethanol in the follow-up CT scans. The postembolization syndromes were related to the specific treatment of tumor, and there was no significant difference between the two groups.

In conclusion, ethanol embolization for patients with HCC and severe APS is efficacious and safe, and may contribute to prolongation of the life span versus Gelfoam embolization.

ACKNOWLEDGMENTS

We thank David A. Kumpe, MD, from the Health Sciences Center, University of Colorado Derver, USA, for his assistance in revising the manuscript.

REFERENCES

- 1 **Kido C**, Sasaki T, Kaneko M. Angiography of primary liver cancer. *Am J Roentgenol Radium Ther Nacl Med* 1971; **113**: 70-81
- 2 **Ngan H**, Peh WC. Arteriovenous shunting in hepatocellular carcinoma: its prevalence and clinical significance. *Clin Radiol* 1997; **52**: 36-40
- 3 **Okuda K**, Musha H, Yamasaki T, Kubo Y, Shimokawa Y, Nagasaki Y, Sawa Y, Jinnouchi S, Kaneko T, Obata H, Hisamitsu T, Motoike Y, Okazaki N, Kojiro M, Sakamoto K, Nakashima T. Angiographic demonstration of intrahepatic arterio-portal anastomoses in hepatocellular carcinoma. *Radiology* 1977; **122**: 53-58
- 4 **Lazaridis KN**, Kamath PS. Images in hepatology. Arterio-portal fistula causing recurrent variceal bleeding. *J Hepatol* 1998; **29**: 142
- 5 **Choi BI**, Lee KH, Han JK, Lee JM. Hepatic arterioportal shunts: dynamic CT and MR features. *Korean J Radiol* 2002; **3**: 1-15
- 6 **Yu JS**, Rofsky NM. Magnetic resonance imaging of arterioportal shunts in the liver. *Top Magn Reson Imaging* 2002; **13**: 165-176
- 7 **Okuyama M**, Fujiwara Y, Hayakawa T, Shiba M, Watanabe T, Tominaga K, Tamori A, Oshitani N, Higuchi K, Matsumoto T, Nakamura K, Wakasa K, Hirohashi K, Ashida S, Shuin T, Arakawa T. Esophagogastric varices due to arterioportal shunt in a serous cystadenoma of the pancreas in von Hippel-Lindau disease. *Dig Dis Sci* 2003; **48**: 1948-1954
- 8 **Tarazov PG**. Intrahepatic arterioportal fistulae: role of transcatheter embolization. *Cardiovasc Intervent Radiol* 1993; **16**: 368-373
- 9 **Clark RA**, Frey RT, Colley DP, Eiseman WR. Transcatheter embolization of hepatic arteriovenous fistulas for control of hemobilia. *Gastrointest Radiol* 1981; **6**: 353-356
- 10 **Furuse J**, Iwasaki M, Yoshino M, Konishi M, Kawano N, Kinoshita T, Ryu M, Satake M, Moriyama N. Hepatocellular car-

- cinoma with portal vein tumor thrombus: embolization of arterioportal shunts. *Radiology* 1997; **204**: 787-790
- 11 **Ueno K**, Miyazono N, Inoue H, Nishida H, Kanetsuki I, Nakajo M. Transcatheter arterial chemoembolization therapy using iodized oil for patients with unresectable hepatocellular carcinoma: evaluation of three kinds of regimens and analysis of prognostic factors. *Cancer* 2000; **88**: 1574-1581
 - 12 **Favoulet P**, Cercueil JP, Faure P, Osmak L, Isambert N, Beltramo JL, Cognet F, Krause D, Bedenne L, Chauffert B. Increased cytotoxicity and stability of Lipiodol-pirarubicin emulsion compared to classical doxorubicin-Lipiodol: potential advantage for chemoembolization of unresectable hepatocellular carcinoma. *Anticancer Drugs* 2001; **12**: 801-806
 - 13 **Fan J**, Wu ZQ, Tang ZY, Zhou J, Qiu SJ, Ma ZC, Zhou XD, Ye SL. Multimodality treatment in hepatocellular carcinoma patients with tumor thrombi in portal vein. *World J Gastroenterol* 2001; **7**: 28-32
 - 14 **Chen MS**, Li JQ, Zhang YQ, Lu LX, Zhang WZ, Yuan YF, Guo YP, Lin XJ, Li GH. High-dose iodized oil transcatheter arterial chemoembolization for patients with large hepatocellular carcinoma. *World J Gastroenterol* 2002; **8**: 74-78
 - 15 **Lin SC**, Shih SC, Kao CR, Chou SY. Transcatheter arterial embolization treatment in patients with hepatocellular carcinoma and risk of pulmonary metastasis. *World J Gastroenterol* 2003; **9**: 1208-1211
 - 16 **Morse SS**, Sniderman KW, Galloway S, Rapoport S, Ross GR, Glickman MG. Hepatoma, arterioportal shunting, and hyperkinetic portal hypertension: therapeutic embolization. *Radiology* 1985; **155**: 77-82
 - 17 **Velazquez RF**, Rodriguez M, Navascues CA, Linares A, Perez R, Sotorrios NG, Martinez I, Rodrigo L. Prospective analysis of risk factors for hepatocellular carcinoma in patients with liver cirrhosis. *Hepatology* 2003; **37**: 520-527
 - 18 **Ueno K**, Miyazono N, Inoue H, Nishida H, Kanetsuki I, Nakajo M. Transcatheter arterial chemoembolization therapy using iodized oil for patients with unresectable hepatocellular carcinoma: evaluation of three kinds of regimens and analysis of prognostic factors. *Cancer* 2000; **88**: 1574-1581
 - 19 **Applbaum YN**, Renner JW. Steel coil embolization of hepatoportal fistulae. *Cardiovasc Intervent Radiol* 1987; **10**: 75-79
 - 20 **Yamagami T**, Nakamura T, Nishimura T. Portal hypertension secondary to spontaneous arterio-portal venous fistulas: transcatheter arterial embolization with n-butyl cyanoacrylate and microcoils. *Cardiovasc Intervent Radiol* 2000; **23**: 400-402
 - 21 **Orons PD**, Zajko AB, Jungrels CA. Arterioportal fistula causing portal hypertension and variceal bleeding: treatment with a detachable balloon. *J Vasc Interv Radiol* 1994; **5**: 373-376
 - 22 **Raghuram L**, Korah IP, Jaya V, Athyal RP, Thomas A, Thomas G. Coil embolization of a solitary congenital intrahepatic hepatoportal fistula. *Abdom Imaging* 2001; **26**: 194-196
 - 23 **Akpek S**, Ilgit ET, Cekirge S, Yucel C. High-flow arterioportal fistula: treatment with detachable balloon occlusion. *Abdom Imaging* 2001; **26**: 277-280
 - 24 **Guan SH**, Shan H, Jiang ZB, Huang MS, Zhu KS, Li ZR, Meng XC. Transmicrocatheter local injection of ethanol to treat hepatocellular carcinoma with high flow arteriovenous shunts. *Zhonghua Fangshexue Zazhi* 2002; **36**: 997-1000
 - 25 **Luo PF**, Chen XM, Zhang LM, Zhou ZJ, Fu L, Wei ZH. The management of arteriovenous shunting in hepatocellular carcinoma. *Zhonghua Fangshexue Zazhi* 2002; **36**: 114-117
 - 26 **Wang SP**, Xu WD, Huo F, Chen GZ. The clinical significance of intrahepatic arteriovenous shunt in patients with hepatic carcinoma. *Zhonghua Putong Waikexue Zazhi* 2003; **18**: 84-86
 - 27 **Lee BB**, Bergan JJ. Advanced management of congenital vascular malformations: a multidisciplinary approach. *Cardiovasc Surg* 2002; **10**: 523-533
 - 28 **De Baere T**, Lagrange C, Kuoch V, Morice P, Court B, Roche A. Transcatheter ethanol renal ablation in 20 patients with persistent urine leaks: an alternative to surgical nephrectomy. *J Urol* 2000; **164**: 1148-1152
 - 29 **Lee W**, Kim TS, Chung JW, Han JK, Kim SH, Park JH. Renal angiomyolipoma: embolotherapy with a mixture of alcohol and iodized oil. *J Vasc Interv Radiol* 1998; **9**: 255-261
 - 30 **Shimamura T**, Nakajima Y, Une Y, Namieno T, Ogasawara K, Yamashita K, Haneda T, Nakanishi K, Kimura J, Matsushita M, Sato N, Uchino J. Efficacy and safety of preoperative percutaneous transhepatic portal embolization with absolute ethanol: a clinical study. *Surgery* 1997; **121**: 135-141
 - 31 **Saitoh H**, Hayakawa K, Nishimura K, Kubo S, Hida S. Long-term results of ethanol embolization of renal cell carcinoma. *Radiat Med* 1997; **15**: 99-102
 - 32 **Gong GQ**, Wang XL, Wang JH, Yan ZP, Cheng JM, Qian S, Chen Y. Percutaneous transsplenic embolization of esophageal and gastro-fundal varices in 18 patients. *World J Gastroenterol* 2001; **7**: 880-883
 - 33 **Lu MD**, Chen JW, Xie XY, Liang LJ, Huang JF. Portal vein embolization by fine needle ethanol injection: experimental and clinical studies. *World J Gastroenterol* 1999; **5**: 506-510
 - 34 **Okano H**, Shiraki K, Inoue H, Kawakita T, Deguchi M, Sugimoto K, Sakai T, Ohmori S, Murata K, Nakano T. Long-term follow-up of patients with liver cirrhosis after endoscopic esophageal varices ligation therapy: comparison with ethanol injection therapy. *Hepatogastroenterology* 2003; **50**: 2013-2016
 - 35 **Ghoshal UC**, Dhar K, Chaudhuri S, Pal BB, Pal AK, Banerjee PK. Esophageal motility changes after endoscopic intravariceal sclerotherapy with absolute alcohol. *Dis Esophagus* 2000; **13**: 148-151
 - 36 **Liu Q**, Tian JM, Jia YC, Wang ZT, Ye H, Yang JJ, Sun F, Lin L, He J. Interventional therapies and analysis of prognostic in hepatocellular carcinoma with tumor thrombus of main portal vein. *Zhonghua Fangshexue Zazhi* 1999; **33**: 538-541

Expression of transforming growth factor- α and hepatitis B surface antigen in human hepatocellular carcinoma tissues and its significance

Jing Zhang, Wen-Liang Wang, Qing Li, Qing Qiao

Jing Zhang, Wen-Liang Wang, Qing Li, Department of Pathology, Xijing Hospital, Fourth Military Medical University, Xi'an 710033, Shaanxi Province, China

Qing Qiao, Department of General Surgery, Tangdu Hospital, Fourth Military Medical University, Xi'an 710038, Shaanxi Province, China
Correspondence to: Jing Zhang, Department of Pathology, Xijing Hospital, Fourth Military Medical University, Xi'an 710033, Shaanxi Province, China. jzhang@fmmu.edu.cn

Telephone: +86-29-83375497 **Fax:** +86-29-83375497

Received: 2003-12-19 **Accepted:** 2004-01-08

Abstract

AIM: To evaluate the expression of transforming growth factor- α (TGF- α) and hepatitis B surface antigen (HBsAg) in human hepatocellular carcinoma (HCC) tissues and its significance.

METHODS: Seventy specimens of HCC tissues were detected by immunohistochemical method. Five specimens of normal human liver tissues were used as control.

RESULTS: The TGF- α positive expression rates in HCC and its surrounding tissues were 74.3%(52/70) and 88.1%(52/59), respectively. TGF- α positive granules were mainly in the cytoplasm and fewer existed on the karyotheca. The TGF- α positive expressing rate in well differentiated HCC was significantly higher than that in moderately and poorly differentiated HCC ($P < 0.05$). The TGF- α positive expression also was observed in intrahepatic bile ducts (part of those were hyperplastic ducts). The HBsAg positive expression rates in HCC and its surrounding tissues were 21.4%(15/70) and 79.7%(47/59), respectively. HBsAg positive granules were in the cytoplasm, inclusion and on the karyotheca. There was a prominent positive correlation between TGF- α and HBsAg expression in HCC surrounding tissues ($P < 0.05$, $\gamma = 0.34$). TGF- α was usually existed with HBsAg in regenerated and/or dysplastic liver cells. In the five normal liver tissues, TGF- α and HBsAg were not detectable in hepatocytes and bile ducts.

CONCLUSION: Hepatitis B virus infection is closely related with hepatocarcinogenesis. The overexpression of TGF- α in the liver seems to be associated with the regeneration of hepatocytes injured by HBsAg. The continued expression of TGF- α might lead to dysplasia of liver cells and development of HCC. Furthermore, TGF- α might play a role in morphogenesis and regeneration of intrahepatic bile ducts.

Zhang J, Wang WL, Li Q, Qiao Q. Expression of transforming growth factor- α and hepatitis B surface antigen in human hepatocellular carcinoma tissues and its significance. *World J Gastroenterol* 2004; 10(6): 830-833

<http://www.wjgnet.com/1007-9327/10/830.asp>

INTRODUCTION

Hepatocellular carcinoma (HCC) is a common malignant tumor in China with poor prognosis^[1-8]. Substantial evidences have supported the concept that hepatitis B virus (HBV) infection is a causative factor for HCC^[9-12]. The idiographic mechanisms of HBV in hepatocarcinogenesis had not been clearly defined yet. Transforming growth factor- α (TGF- α) is a multi-peptide, which can promote cellular proliferation and transformation^[13-15]. The normal hepatocytes almost had no expression of TGF- α mRNA except the epitheliums of bile ducts in human normal liver tissues^[16]. It was also thought to be an autocrine regulator of normal growth and regeneration in the rat liver. There was also a close relationship between TGF- α and hepatocarcinogenesis^[17-19]. In order to find the relationship between TGF- α and HBV infection in hepatocarcinogenesis, the expression of TGF- α and HBsAg in HCC tissues was studied by immunohistochemical method. Such studies have been rarely reported in China.

MATERIALS AND METHODS

Specimens

Tissue samples were obtained from seventy cases of HCC in Xijing Hospital from January 1988 to January 1995. Among them, fifty-nine cases of HCC had surrounding tissues. Five cases of normal human liver tissues were obtained from autopsy (excluding liver disease). All specimens were fixed in 40 g/L methanal solution, embedded in wax, and cut into 5 μ m thick serial sections.

Reagents and methods

Mouse anti-human TGF- α was purchased from Santa Cruze, UAS. Mouse anti-human HBsAg and SABC kit were purchased from Wuhan Boster Co. Ltd. The expression of TGF- α and HBsAg was detected by SABC immunohistochemical method. In the control group, the primary antibody was substituted by PBS or normal mouse serum. All paraffin embedded sections were deparaffinized and rehydrated, and pretreated for 20 min at 75 °C in a microwave oven. After being treated with 1 mL/L H₂O₂ for 30 min to block the endogenous peroxidase, the sections were incubated with 20 mL/L fetal calf serum for 30 min to reduce nonspecific binding. Then the primary HBsAg and TGF- α antibodies were applied to the sections and incubated at 4 °C overnight. The sections were subsequently incubated with goat anti mouse IgG at 37 °C for 30 min, followed by incubation with SABC at 37 °C for 30 min, and stained with DAB-H₂O₂ for 5-10 min and counterstained with hematoxylin. Results estimation: the specimens with no positive cells or positive cells <10% were negative (-); with light brownish yellow cells or positive cells between 10-50% were weakly positive (\pm); with deep brownish yellow cells or positive cells >50% were positive (+).

Statistical analysis

Chi-square test was used to analyse the results. The expression of TGF- α and HBsAg were compared by analysis of coherence.

RESULTS

The expression of TGF- α and HBsAg in HCC

The TGF- α positive expression rates in HCC and its surrounding tissues were 74.3% (52/70) and 88.1% (52/59), respectively. The positive cells mainly existed diffusely and fewer existed in foci. The positive stainings were like brown-yellow granules, and were mainly located in the cytoplasm and/or fewer located on the karyotheca (Figure 1). There was a prominent difference in TGF- α distribution between HCC and its surrounding tissues ($\chi^2=3.93$, $P<0.05$). The TGF- α positive expression rate in well differentiated HCC was significantly higher than that in moderately and poorly differentiated HCC ($\chi^2=9.11$, $P<0.05$, Table 1). TGF- α positive expression also was observed in intrahepatic bile ducts (part of those were hyperplastic ducts). In the five cases of normal liver tissues, TGF- α was undetectable in hepatocytes and bile ducts.

Table 1 TGF- α expression in different HCC differentiation

Differentiation	<i>n</i>	Positive cases	Positive rate (%)
Well	15	15	100.0
Moderately	48	34	70.8
Poorly	7	3	42.9

The HBsAg positive expression rates in HCC and its surrounding tissues were 21.4% (15/70) and 79.7% (47/59), respectively. The positive cells mainly existed diffusely and fewer existed in foci. The positive stainings were like brown-yellow granules or floccules. They were located in the cytoplasm, inclusion and on the karyotheca (Figure 2). There was a prominent difference in HBsAg distribution between HCC and its surrounding tissues ($\chi^2=43.5$, $P<0.05$). HBsAg expression was negative in the five cases of normal liver tissues.

The PBS blank controls and normal mouse serum substituted controls were negative for immunohistochemical staining.

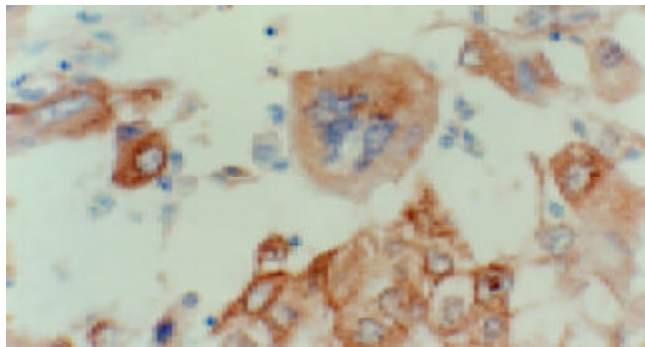


Figure 1 TGF- α positive stainings as brownish yellow granules in the cytoplasm of HCC tumor cells. SABC $\times 400$.

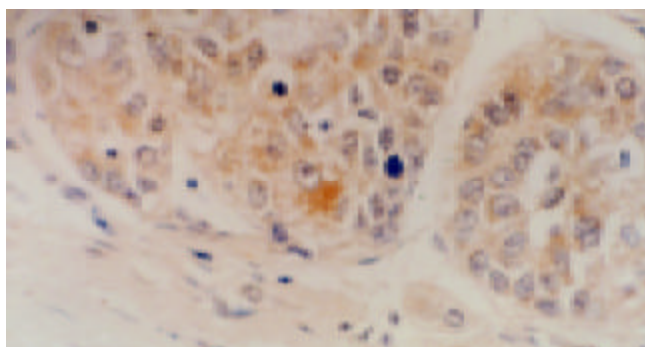


Figure 2 HBsAg positive stainings as brownish yellow granules in the cytoplasm of HCC tumor cells. SABC $\times 400$.

Relationship between TGF- α and HBsAg expression

There was not a prominent correlation between TGF- α and HBsAg expression in HCC tissues, but there was a prominent positive correlation between TGF- α and HBsAg expression in HCC surrounding tissues ($P<0.05$, $\gamma=0.34$, Table 2). TGF- α was usually existed with HBsAg in regenerated and/or dysplastic liver cells. These cells had increscent or double nucleus, prominent or anomalous nucleolus, high ratio of nucleus/ cytoplasm, *etc.* (Figures 3 and 4).

Table 2 Relation between TGF- α and HBsAg expression in HCC surrounding tissues

TGF- α	<i>n</i>	HBsAg	
		+	-
+	52	44	8
-	7	3	4
Total	59	47	12

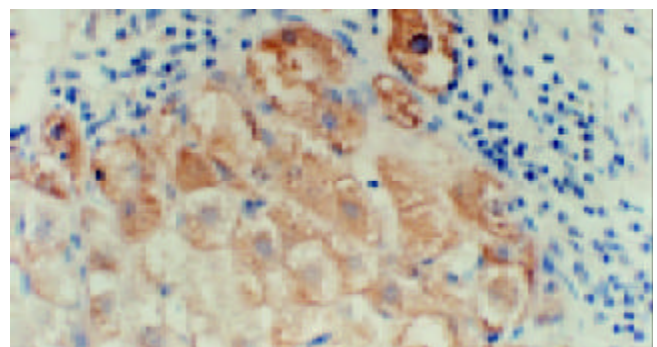


Figure 3 Location of immunohistochemical staining of TGF- α expression in regenerated and/or dysplastic liver cells. SABC $\times 400$.

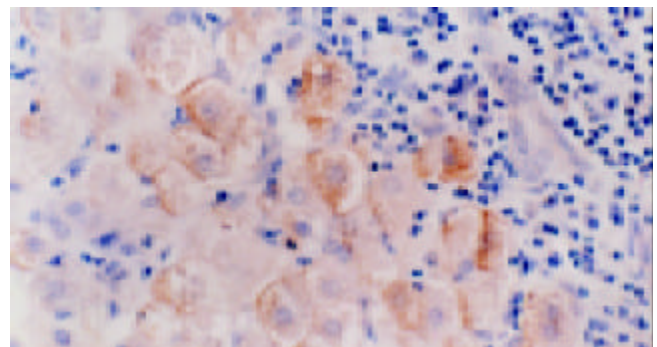


Figure 4 Location of immunohistochemical staining of HBsAg expression in regenerated and/or dysplastic liver cells. SABC $\times 400$.

DISCUSSION

TGF- α was found in culture medium of fibroblasts transformed by some retroviruses in 1970s and nominated because of its ability to transform and induce the renal fibroblasts to proliferate. It is composed of 50 amino acid residues, with a 30% to 40% amino acid homology to epidermal growth factor (EGF), and binds the EGF receptor in the cellular membrane^[20]. TGF- α was secreted by many transformed cells and involved in embryonic development. In human cancers, studies showed that TGF- α could serve as a tumor marker and as a marker for the malignant potential of a tumor^[21]. Thus far, the types of carcinomas with which abnormal TGF- α expression has been associated include liver^[22], gastrointestinal^[23], breast^[24], skin^[25], lung^[26], brain^[27] and ovarian cancers^[28]. TGF- α might play a role in the processes involved with tumor initiation and

growth. In cell lines, TGF- α has been found to be associated with autocrine and/or paracrine types of cellular growth initiation and with increased levels of oncogene expression^[29,30]. It could promote the hepatocellular proliferation, differentiation, regeneration and tumor cell growth^[31]. Transgenic mice that overexpressed TGF- α developed liver tumors between 12 and 15 months of age^[22]. In our study, we found the TGF- α expression in the HCC and its surrounding tissues was significantly higher than that of normal liver tissues. The positive rate of TGF- α expression in well differentiated HCC was higher than that in moderately and poorly differentiated HCC. These may suggest the involvement of TGF- α in cellular transformation and provide a supporting evidence for the autocrine stimulation model. Increased expression of TGF- α might be the events of human primary hepatocarcinogenesis. In the later stages of HCC, there might be the other factors responsible for decreasing expression of TGF- α . Furthermore, we also found that intrahepatic bile ducts (part of these were hyperplasia ducts) were stained positive for TGF- α , suggesting that TGF- α might play a role in morphogenesis and regeneration of intrahepatic bile ducts.

Up to now, the close relationship among hepatitis B virus, liver cirrhosis and HCC has been approved^[32], but the mechanisms have not been clearly defined yet. One hypothesis is that chronic HBV infection caused prolonged liver cellular injury, inflammation and cellular death. The hepatic regeneration after liver necrosis, along with DNA damage from genotoxic agents generated during the inflammatory response, was thought to increase the risk of HCC development^[33]. Because of HBV replication in liver cells, HBV major envelope protein, HBsAg was often overexpressed. It accumulated to toxic levels in the endoplasmic reticulum of hepatocytes. This could lead to the chronic injury of hepatocytes, inflammation and cellular death by immune reaction^[34]. In our study, we found the positive expression rate of HBsAg in the HCC surrounding tissues was higher than that of HCC tissues. There was a prominent difference in HBsAg distribution between the HCC and its surrounding tissues ($\chi^2=43.5$, $P<0.05$). This suggested HBsAg might have more closely involved in hepatic cells injury than in hepatocarcinogenesis.

TGF- α is a potent mitogen for hepatocytes. It can induce hepatocytes to proliferate. Though we did not find the correlation between TGF- α and HBsAg in the HCC tissues, we found there was a prominent positive correlation between TGF- α and HBsAg in the HCC surrounding tissues. They were usually existed in regenerated and/or dysplastic liver cells. These cells had increscent or double nucleus, prominent or anomalous nucleolus and high ratio of nucleus/cytoplasm, etc. These data suggest that TGF- α overexpression in the liver seems to be associated with the hepatocellular regeneration injured by HBsAg. HBsAg may up-regulate the expression of TGF- α . Continued overexpression of TGF- α could lead to hepatocellular proliferation and dysplasia. These might have contributed to hepatocarcinogenesis and HCC growth.

REFERENCES

- Zhao H**, Zhou KR, Yan FH. Role of multiphase scans by multirow-detector helical CT in detecting small hepatocellular carcinoma. *World J Gastroenterol* 2003; **9**: 2198-2201
- Li QL**, Wang WL, Zhang XH, Yan W. Expression of hsMAD₂ in human hepatocellular carcinoma and its significance. *Shijie Huaren Xiaohua Zazhi* 2003; **11**: 1326-1328
- Ge NL**, Ye SL, Zheng N, Sun RX, Liu YK, Tang ZY. Prevention of hepatocellular carcinoma in mice by IL-2 and B7-1 genes co-transfected liver cancer cell vaccines. *World J Gastroenterol* 2003; **9**: 2182-2185
- Wang W**, Yang LY, Yang ZL, Huang GW, Lu WQ. Expression and significance of RhoC gene in hepatocellular carcinoma. *World J Gastroenterol* 2003; **9**: 1950-1953
- Jin ZY**, Cheng RX, Zheng CL, Zheng H. Expression of PTTG and *c-myc* gene in human primary hepatocellular carcinoma. *Shijie Huaren Xiaohua Zazhi* 2003; **11**: 1677-1681
- Qian J**, Feng GS, Vogl T. Combined interventional therapies of hepatocellular carcinoma. *World J Gastroenterol* 2003; **9**: 1885-1891
- Huang J**, Cai MY, Wei DP. HLA class I expression in primary hepatocellular carcinoma. *World J Gastroenterol* 2002; **8**: 654-657
- Hsu CY**, Chu CH, Lin SC, Yang FS, Yang TL, Chang KM. Concomitant hepatocellular adenoma and adenomatous hyperplasia in a patient without cirrhosis. *World J Gastroenterol* 2003; **9**: 627-630
- Ma CH**, Sun WS, Tian PK, Gao LF, Liu SX, Wang XY, Zhang LN, Cao YL, Han LH, Liang XH. A novel HBV antisense RNA gene delivery system targeting hepatocellular carcinoma. *World J Gastroenterol* 2003; **9**: 463-467
- Shen LJ**, Zhang HX, Zhang ZJ, Li JY, Chen MQ, Yang WB, Huang R. Detection of HBV, PCNA and GST- π in hepatocellular carcinoma and chronic liver diseases. *World J Gastroenterol* 2003; **9**: 459-462
- Dai ZY**, Xu QH, Li G, Ma HH, Tang ZH, Shu X, Yao JL. Study on X gene mutation of hepatitis B virus from patients with hepatocellular carcinoma. *Shijie Huaren Xiaohua Zazhi* 2003; **11**: 1349-1352
- Tang ZY**. Hepatocellular carcinoma—cause, treatment and metastasis. *World J Gastroenterol* 2001; **7**: 445-454
- Awwad RA**, Sergina N, Yang H, Ziober B, Willson JK, Zborowska E, Humphrey LE, Fan R, Ko TC, Brattain MG, Howell GM. The role of transforming growth factor alpha in determining growth factor independence. *Cancer Res* 2003; **63**: 4731-4738
- Ciana P**, Ghisletti S, Mussi P, Eberini I, Vegeto E, Maggi A. Estrogen receptor alpha, a molecular switch converting transforming growth factor-alpha-mediated proliferation into differentiation in neuroblastoma cells. *J Biol Chem* 2003; **278**: 31737-31744
- Grasl-Kraupp B**, Schausberger E, Hufnagl K, Gerner C, Low-Baselli A, Rossmanith W, Parzefall W, Schulte-Hermann R. A novel mechanism for mitogenic signaling via pro-transforming growth factor alpha within hepatocyte nuclei. *Hepatology* 2002; **35**: 1372-1380
- Derynck R**, Goeddel DV, Ullrich A, Gutterman JU, Williams RD, Bringman TS, Berger WH. Synthesis of messenger RNAs for transforming growth factors alpha and beta and the epidermal growth factor receptor by human tumors. *Cancer Res* 1987; **47**: 707-712
- Thorgeirsson SS**, Grisham JW. Molecular pathogenesis of human hepatocellular carcinoma. *Nat Genet* 2002; **31**: 339-346
- Matsumoto T**, Takagi H, Mori M. Androgen dependency of hepatocarcinogenesis in TGFalpha transgenic mice. *Liver* 2000; **20**: 228-233
- Jo M**, Stolz DB, Esplen JE, Dorko K, Michalopoulos GK, Strom SC. Cross-talk between epidermal growth factor receptor and c-Met signal pathways in transformed cells. *J Biol Chem* 2000; **275**: 8806-8811
- Todaro GJ**, Fryling C, De Larco JE. Transforming growth factors produced by certain human tumor cells: polypeptides that interact with epidermal growth factor receptors. *Proc Natl Acad Sci U S A* 1980; **77**: 5258-5262
- Grigioni WF**. Relevance of biologic markers in colorectal carcinoma: a comparative study of a broad panel. *Cancer* 2002; **94**: 647-657
- Vail ME**, Pierce RH, Fausto N. Bcl-2 delays and alters hepatic carcinogenesis induced by transforming growth factor alpha. *Cancer Res* 2001; **61**: 594-601
- Sawhney RS**, Sharma B, Humphrey LE, Brattain MG. Integrin alpha2 and extracellular signal-regulated kinase are functionally linked in highly malignant autocrine transforming growth factor-alpha-driven colon cancer cells. *J Biol Chem* 2003; **278**: 19861-19869
- More E**, Fellner T, Doppelmayr H, Hauser-Kronberger C, Dandachi N, Obrist P, Sandhofer F, Paulweber B. Activation of the MAP kinase pathway induces chicken ovalbumin upstream promoter-transcription factor II (COUP-TFII) expression in human breast cancer cell lines. *J Endocrinol* 2003; **176**: 83-94

- 25 **Wu M**, Putti TC, Bhuiya TA. Comparative study in the expression of p53, EGFR, TGF- α , and cyclinD1 in verrucous carcinoma, verrucous hyperplasia, and squamous cell carcinoma of head and neck region. *Appl Immunohistochem Mol Morphol* 2002; **10**: 351-356
- 26 **Piyathilake CJ**, Frost AR, Manne U, Weiss H, Bell WC, Heimburger DC, Grizzle WE. Differential expression of growth factors in squamous cell carcinoma and precancerous lesions of the lung. *Clin Cancer Res* 2002; **8**: 734-744
- 27 **Zhou R**, Skalli O. Identification of cadherin-11 down-regulation as a common response of astrocytoma cells to transforming growth factor- α . *Differentiation* 2000; **66**: 165-172
- 28 **Doraiswamy V**, Parrott JA, Skinner MK. Expression and action of transforming growth factor alpha in normal ovarian surface epithelium and ovarian cancer. *Biol Reprod* 2000; **63**: 789-796
- 29 **Masuda M**, Suzui M, Lim JT, Deguchi A, Soh JW, Weinstein IB. Epigallocatechin-3-gallate decreases VEGF production in head and neck and breast carcinoma cells by inhibiting EGFR-related pathways of signal transduction. *J Exp Ther Oncol* 2002; **2**: 350-359
- 30 **Wong YC**, Wang YZ. Growth factors and epithelial-stromal interactions in prostate cancer development. *Int Rev Cytol* 2000; **199**: 65-116
- 31 **Sohda T**, Iwata K, Tsutsu N, Kamimura S, Shijo H, Sakisaka S. Increased expression of transforming growth factor- α in a patient with recurrent hepatocellular carcinoma following partial hepatectomy. *Pathology* 2001; **33**: 511-514
- 32 **Yuen MF**, Lai CL. Specific considerations in the design of hepatitis B virus clinical studies in the far East. *Methods Mol Med* 2004; **96**: 457-464
- 33 **Jakubczak JL**, Chisari FV, Merlino G. Synergy between transforming growth factor alpha and hepatitis B virus surface antigen in hepatocellular proliferation and carcinogenesis. *Cancer Res* 1997; **57**: 3606-3611
- 34 **Chisari FV**, Klopchin K, Moriyama T, Pasquinelli C, Dunsford HA, Sell S, Pinkert CA, Brinster RL, Palmiter RD. Molecular pathogenesis of hepatocellular carcinoma in hepatitis B virus transgenic mice. *Cell* 1989; **59**: 1145-1156

Edited by Gupta MK **Proofread by** Xu FM

Somatic mutations of APC gene in carcinomas from hereditary non-polyposis colorectal cancer patients

Jian Huang, Shu Zheng, Shen-Hang Jin, Su-Zhan Zhang

Jian Huang, Shu Zheng, Su-Zhan Zhang, Department of Oncology, Second Affiliated Hospital, Zhejiang University School of Medicine, Hangzhou 310009, Zhejiang Province, China

Shen-Hang Jin, Zhejiang University School of Medicine, Hangzhou 310009, Zhejiang Province, China

Supported by the National Natural Science Foundation of China, No. 39600055, Research for Returned Chinese Visiting Scholars from Abroad, Chinese Ministry of Education and Research of Provincial Education Ministry

Correspondence to: Dr. Jian Huang, Department of Oncology, Second Affiliated Hospital, Zhejiang University School of Medicine, Hangzhou 310009, Zhejiang Province, China. hjys@zju.edu.cn

Telephone: +86-571-87784556 **Fax:** +86-571-87784556

Received: 2003-06-16 **Accepted:** 2003-09-01

Abstract

AIM: To investigate the mutational features of adenomatous polyposis coli (APC) gene and its possible arising mechanism in hereditary non-polyposis colorectal cancers (HNPCC).

METHODS: PCR-based *In Vitro* Synthesized Protein Test (IVSP) assay and sequencing analysis were used to confirm somatic mutations of whole APC gene in 19 HNPCC cases.

RESULTS: Eleven cases with 13 mutations were determined to harbor APC mutations. The prevalence of APC mutation was 58%(11/19). The mutations consisted of 9 frameshift and 4 nonsense ones, indicating that there were more frameshift mutations (69%). The frameshift mutations all exhibited deletion or insertion of 1-2 bp and most of them (7/9) happened at simple nucleotide repeat sequences, particularly within (A)_n tracts (5/9). All point mutations presented C-to-T transitions at CpG sites.

CONCLUSION: Mutations of APC gene were detected in more than half of HNPCC, indicating that its mutation was a common molecular event and might play an important role in the tumorigenesis of HNPCC. Locations of frameshift mutations at simple nucleotide repeat sequences and point mutations at CpG sites suggested that many mutations probably derived from endogenous processes including mismatch repair (MMR) deficiency. Defective MMR might affect the nature of APC mutations in HNPCC and likely occur earlier than APC mutational inactivation in some patients.

Huang J, Zheng S, Jin SH, Zhang SZ. Somatic mutations of APC gene in carcinomas from hereditary non-polyposis colorectal cancer patients. *World J Gastroenterol* 2004; 10(6): 834-836 <http://www.wjgnet.com/1007-9327/10/834.asp>

INTRODUCTION

Familial colorectal cancer (CRC) can be mainly divided into 2 distinct classes, hereditary non-polyposis colorectal cancers (HNPCC) and familial adenomatous polyposis (FAP). HNPCC is an autosomal dominant inherited disease characterized by an increased predisposition to colorectal and some extracolonic

cancers and presents with particular clinicopathological and molecular features^[1]. Affected individuals often carry germline alterations at mismatch repair (MMR) genes, such as hMsh2, hMlh1, hPsm1 and hPsm2, which lead to microsatellite instability (MSI) and replication errors (RER). FAP is caused by the germline mutation of tumor suppressor gene APC and manifested by the development of hundreds of colorectal adenomas, some of which will inevitably undergo malignant transformations if not removed. APC mutations can be detected in both FAP and non-FAP tumors including HNPCC and sporadic colorectal ones, somatic mutation of which is a common defect in sporadic colorectal tumor and FAP, both sharing similar mutational spectra and distribution^[2,3-5]. It is accepted that adenoma-carcinoma sequence of CRC was initiated by APC mutation in majority of non-HNPCC^[2,6]. Adenoma in HNPCC featured aggressiveness and followed by an alternative and rapidly evolving pathway. There was evidence that HNPCC lacked loss of heterozygosity (LOH) of APC gene, being quite different from FAP^[7]. It showed that all adenomas from *Min* mice demonstrated LOH, had significantly less numbers of somatic APC mutations compared with those from Msh2 deficient *Min* (*Apc*^{+/+}-*Msh2*^{-/-}), which had a 2-fold higher rate of somatic *Apc* mutations (10/adenoma) than the non-neoplastic intestinal mucosa (5/sample), and did not demonstrate LOH. The results proved that somatic APC mutation rather than LOH, was a likely mechanism in the development of adenomas in *Apc*^{+/+}-*Msh2*^{-/-} mice^[8].

Studies also revealed^[9,10] that APC gene might play a role in chromosomal segregation, with mutations in APC disrupting this function and causing chromosomal (or karyotypic) instability (CIN). MSI and CIN were two different forms of genetic instability occurring in CRC. In MI⁺ sporadic and HNPCC tumors, defective repair of mismatched bases resulted in an increased mutation rate at the nucleotide level and consequent widespread MSI with diploidy while a large fraction of others had CIN, leading to an abnormal chromosome number (aneuploidy). In HNPCC, mutations of APC, p53 and K-ras-2 genes and LOH of tumor-suppressor genes were significantly less frequent ($P=0.03$ or 0.0006), but transforming growth factor beta type II receptor mutation was significantly more frequent ($P=0.000001$) than those in non-HNPCC^[7]. Summarized data from Jass^[11] supported that the frequency of APC mutation was significantly lower in MSI-H colorectal tumors (39%, 36/92) and HNPCC (44%, 21/48) than in MSI-L (51%, 18/35) and MSS (58%, 241/417). However, the situation was quite different for 5q LOH in MSI-H tumors (3%;1/32) and HNPCC (10%;1/10), which were significantly less than MSI-L (47%;17/49) and MSS (57%;113/199). This suggested that MSI instead of APC mutation probably conferred a growth advantage in the context of early tumorigenesis of HNPCC and MSI-H tumors. Here we focused on APC gene to analyze its mutational frequency and features in carcinomas from HNPCC, which would be helpful to understand the effect of MMR deficiency on APC mutation in the early stage of carcinogenesis.

Based on the fact that both somatic and germline mutations of APC gene were dispersed throughout the 5' half of the sequence, vast majority of which were premature ones and led to truncated proteins^[3-5]. A Coupled *In Vitro* Synthesized

Protein Test (IVSP) was therefore used to selectively and rapidly detect any mutations leading to stop codons^[12-14]. The assay was proved very efficient and only a small proportion of nontruncating APC mutations like missense mutations were reported to be missed^[15]. The study aimed at exploring the possible arising mechanism of somatic APC mutation and its role through investigating frequency and mutational features of the gene in HNPCC.

MATERIALS AND METHODS

Sample collection and DNA extraction

HNPCC was determined according to ICG criteria based on the family history^[16], fresh tumor samples of the patients were from resected and histologically verified colorectal carcinomas. Genomic DNA and RNA of tumors and matched normal-looking colonic mucosa were isolated by standard procedures. Nineteen samples were collected from paired carcinomas and adjacent normal tissues in HNPCC patients.

Determination of APC mutation

Whole APC gene with at least 15 exons (8.5Kb) was divided into 5 overlapping segments (seg.), Exon 1-14 was defined as seg. 1 and exon 15 amplified with four overlapping segments as seg. 2-5. The RT-PCR primer-pair sequence for seg. 1 and PCR primer-pairs for seg. 2-5 was similar to those reported^[12,13,15]. IVSP assay, which selectively detected truncating mutations, was used to screen mutations of whole APC gene segment by segment. All samples showing producible truncated protein bands were sequenced using Sequenase 2 (United States Biochemical) with ³⁵S-labeled dATP, dried sequence gels were exposed to XAR (Kodak) film at room temperature overnight.

Table 1 Spectra of APC mutations in carcinomas from HNPCC patients

Tumor ID	APC nt change	Codon	Target sequence
Point mutations			
T27	C>T	332	CpG
T533	C>T	1 338	CpG
K1, C×7*	C>T	1 450	CpG
Frameshift mutations			
C×7*	1 bp ins	847	TCTCaAAAAAGAT
C086*	1 bp ins	941	TCGGaAAAATTCA
K40	1 bp ins	1 454	CCTaAAAAATAAA
22	1 bp ins	1 554	GCAGaAAAAACTAT
Cx10	1 bp ins	1 935	TTTCCCCaAGTCA
K10	1 bp del	907	TCTgGGTCT
C086*	2 bp del	1 464	AAGAGAGagAGTGG
K39	2 bp del	799	GATtaTGTT
T10	1 bp del	1 416	AGTGGcATTATA

Note: ID means tumor identification; nt stands for nucleotide; '>' for transition or transversion; each tumor with more than 2 mutations marked by *; del for deletion; ins for insertion; small letter for nucleotide frameshift.

RESULTS

Spectra of APC mutations in HNPCC are listed in Table 1. Screening for truncating APC mutations was carried out using IVSP assay in carcinomas from 19 HNPCC cases. There were altogether 11 mutated cases with 13 mutations confirmed in the study, all of which were only found in the tumor tissues, indicating the somatic nature of mutation. The prevalence of APC mutation in HNPCC was 58% (11/19). Exhibiting mutations consisted of 9 frameshift ones and 4 nonsense, indicating the existence of more frameshift mutations. All of

frameshift mutations were deletion or insertion of 1-2 bp and most of them (7/9) happened at simple nucleotide repeat sequences, particularly within (A)_n tracts (5/9). Repeat number (n) of mononucleotide A ranged from 2 to 7. All of four detected point mutations presented C-to-T transitions at CpG sites in the study. Distributions of mutations were uneven and with no hot spot but hot region. Eight (61.5%) of thirteen mutations were located in the segment 3 (codon 1099-1701) and half of them in the mutation cluster region (codon 1286-1513).

DISCUSSION

Colorectal cancer is the fourth leading cause of cancer deaths and tends to increase in China, especially in big cities like Shanghai. The basic mechanism of reducing the mortality remains elusive and poses a big challenge for clinicians and researchers.

HNPCC is one of the most common inherited cancer syndromes, accounting for approximately 4-6% of all CRCs. It is characterized by defective MMR, which results in MSI and manifests hypermutable phenotype^[17,18]. In our study, MSI was defined in all but one (T16) of HNPCC cases (data not shown).

In contrast to FAP, HNPCC was usually not associated with LOH of APC allele and therefore not develop extensive polyposis but multiple primary cancers. MMR gene responsible for HNPCC functioned as caretaker and indirectly inhibited the promotion of tumor growth, defective MMR was considered to be primary event because of its occurrence throughout the adenomas in HNPCC^[19,20]. It had been reported that CRC with and without MSI involved different genes including APC^[21]. APC gene, a FAP causing gene, was proven to be rate-limiting for tumor initiation and functioned as housekeeper of cellular proliferation. APC mutation provided cells with a selective advantage without known effect on the mutation rate, it suggested that both APC and MMR genes played an important role in the early carcinogenesis of familial CRC. Accumulating evidence actually revealed that the sequence of alteration of cancer genes in MMR deficient tumor was somewhat different from non-HNPCC^[7,21]. The study was to investigate the mutational features of housekeeping gene APC and its potential arising mechanism in carcinomas with deficiency of caretaking gene MMR, in order to evaluate the role of APC gene alteration in HNPCC.

There were 11 (58%) of the 19 HNPCC carcinomas exhibiting APC somatic mutations, which was a bit higher than that (50%) reported in a series of Japanese HNPCC adenomas^[22] and somewhat lower than that (67%) in sporadic CRC^[4,5]. The result implied that inactivation of APC gene also played an important role in the tumorigenesis of HNPCC. But there was evidence that the frequency of APC gene mutation in HNPCC was likely less than that in non-HNPCC (21% vs >70%; $P < 0.05$)^[23].

Analysis of the spectra of APC mutations revealed that APC frameshift mutations were more frequent than point ones in HNPCC (69.3% vs 30.7%; $P < 0.05$). As with frameshift mutations, most of them (67%) occurred in the simple repeat sequences (microsatellite) of the APC coding regions, particularly at (A)_n tracts (56%), which was consistent with the effect of mismatch repair deficiency on mutations of other target genes containing short repeated sequences in the coding regions^[24]. It suggested that MMR deficiency might be one of the important pathway leading to inactivation of its tumor suppressor ability by altering microsatellite of the APC coding regions. Animal studies further supported the notion that APC mutations in Msh6(-/-)Apc1638N mice consisted predominantly of base substitutions (93%) creating stop codons, however, in Msh3(-/-)Msh6(-/-)Apc1638N tumors, a mixture of base substitutions (46%) and frameshifts (54%) was observed, indicating that Msh3 could suppress frameshift mutations of Apc gene in Msh6(-/-)Apc1638N mice^[25]. The observation demonstrated that type of APC mutation was closely related

to the function of specific MMR gene while in *Mlh1*^{-/-} *Apc*^{1638N} animals, the prevailing mechanism of APC mutation in tumors was altered from allelic loss to intragenic mutation as a result of *Mlh1* deficiency, the observed mutations were more frameshifts (73%) than base substitutions (27%), most frameshifts were located within dinucleotide repeats^[26]. We therefore hypothesized that defective MMR might precede APC mutation in some HNPCC cases whereas for those frameshifts not showing microsatellite alterations, the initiation mechanism for these tumors was not clear yet and proposed to be similar to that for sporadic CRCs^[23,5,12], which meant that APC mutation, rather than genomic instability, might be the initiating event in tumorigenesis.

With respect to point mutations of APC gene, they were all non-sense mutations and with pathogenic nature because of the generation of stop codons. All these mutations in the study presented C-to-T transitions and affected *Cog* dinucleotides, suggesting that they probably derived from endogenous processes due to spontaneous deaminations of 5-methylcytosine. Further studies were therefore necessary to clarify the origin and relationship between endogenous and exogenous processes of APC mutations in CRC tumorigenesis.

In HNPCC cases without detected APC mutations, it was still of great importance to determine methylated status of APC gene or mutation of other genes like β -catenin, although more sensitive methods needed to be developed or used. Yamamoto reported that DNA methylation of APC was higher in HNPCC than in sporadic CRC with MSI-H (53% vs 35%)^[27]. Miyaki observed that a notable frequency of β -catenin gene mutation (43%) was found to occur in HNPCC and detected in tumors without APC mutations^[23]. These data suggested that activation of the β -catenin -Tcf signaling pathway, through either β -catenin mutation or silence (methylation) of APC, might also contribute to part of HNPCC colorectal carcinogenesis.

In conclusion, inactivation of APC gene played an important role in the tumorigenesis of HNPCC; Most of APC mutations probably derived from endogenous processes including MMR deficiency and presented some mutational features. Defective MMR might occur earlier than APC mutation in some patients with HNPCC.

REFERENCES

- Lynch HT**, Smyrk T. Hereditary nonpolyposis colorectal cancer (Lynch syndrome). An updated review. *Cancer* 1996; **78**: 1149-1167
- Powell SM**, Zilz N, Beazer-Barclay Y, Bryan TM, Hamilton SR, Thibodeau SN, Vogelstein B, Kinzler KW. APC mutations occur early during colorectal tumorigenesis. *Nature* 1992; **359**: 235-237
- Gryfe R**, Swallow C, Bapat B, Redston M, Gallinger S, Couture J. Molecular biology of colorectal cancer. *Curr Probl Cancer* 1997; **21**: 233-300
- Huang J**, Zheng S, Jin SH. APC mutation analysis in sporadic colorectal cancer. *Zhonghua Zhongliu Zazhi* 1996; **18**: 415-418
- Nagase H**, Kakamura Y. Mutations of the APC (adenomatous polyposis coli). *Hum Mutat* 1993; **2**: 425-434
- Jen J**, Powell SM, Papadopoulos N, Smith KJ, Hamilton SR, Vogelstein B, Kinzler KW. Molecular determinants of dysplasia in colorectal lesions. *Cancer Res* 1994; **54**: 5523-5526
- Konishi M**, Kikuchi-Yanoshita R, Tanaka K, Muraoka M, Onda A, Okumura Y, Kishi N, Iwama T, Mori T, Koike M, Ushio K, Chiba M, Nomizu S, Konishi F, Utsunomiya J, Miyaki M. Molecular nature of colon tumors in hereditary nonpolyposis colon cancer, familial polyposis and sporadic colon cancer. *Gastroenterology* 1996; **111**: 307-317
- Sohn KJ**, Choi M, Song J, Chan S, Medline A, Gallinger S, Kim YI. Msh2 deficiency enhances somatic Apc and p53 mutations in *Apc*^{+/-} *Msh2*^{-/-} mice. *Carcinogenesis* 2003; **24**: 217-224
- Fodde R**, Kuipers J, Rosenberg C, Smits R, Kielman M, Gaspar C, van Es JH, Breukel C, Wiegant J, Giles RH, Clevers H. Mutations in the APC tumour suppressor gene cause chromosomal instability. *Nat Cell Biol* 2001; **3**: 433-438
- Kaplan KB**, Burds AA, Swedlow JR, Bekir SS, Sorger PK, Nathke IS. A role for the Adenomatous Polyposis Coli protein in chromosome segregation. *Nat Cell Biol* 2001; **3**: 429-432
- Jass JR**, Young J, Leggett BA. Evolution of colorectal cancer: change of pace and change of direction. *J Gastroenterol Hepatol* 2002; **17**: 17-26
- Powell SM**, Petersen GM, Krush AJ, Booker S, Jen J, Giardiello FM, Hamilton SR, Vogelstein B, Kinzler KW. Molecular diagnosis of familial adenomatous polyposis. *N Eng J Med* 1993; **329**: 1982-1987
- van der Luijt R**, Khan PM, Vasen H, van Leeuwen C, Tops C, Roest P, den Dunnen J, Fodde R. Rapid detection of translation-termination mutations at the adenomatous polyposis coli (APC) gene by direct protein truncation test. *Genomics* 1994; **20**: 1-4
- Huang J**, Zheng S, Wu JM, Cai XH. Rapid detection of APC gene mutations in colorectal tumors using IVSP assay. *Zhonghua Yixue Yichuanxue Zazhi* 1997; **14**: 134-137
- Heinimann K**, Thompson A, Locher A, Furlanetto T, Bader E, Wolf A, Meier R, Walter K, Bauerfeind P, Marra G, Muller H, Foerzler D, Dobbie Z. Nontruncating APC germ-line mutations and mismatch repair deficiency play a minor role in APC mutation-negative polyposis. *Cancer Res* 2001; **61**: 7616-7622
- Vasen HF**, Mecklin JP, Khan PM, Lynch HT. The international collaborative group on hereditary nonpolyposis colorectal cancer (ICG-HNPCC). *Dis Colon Rectum* 1991; **34**: 424-425
- Fishel R**, Kolodner RD. Identification of Mismatch repair genes and their role in the development of cancer. *Curr Opin Genet Dev* 1995; **5**: 382-395
- Loeb LA**. A mutator phenotype in cancer. *Cancer Res* 2001; **61**: 3230-3239
- Jass JR**, Iino H, Ruzskiewicz A, Painter D, Solomon MJ, Koorey DJ, Cohn D, Furlong KL, Walsh MD, Palazzo J, Edmonston TB, Fishel R, Young J, Leggett BA. Neoplastic progression occurs through mutator pathways in hyperplastic polyposis of the colorectum. *Gut* 2000; **47**: 43-49
- Iino H**, Simms L, Young J, Arnold J, Winship IM, Webb SI, Furlong KL, Leggett B, Jass JR. DNA microsatellite instability and mismatch repair protein loss in adenomas presenting in hereditary polyposis colorectal cancer. *Gut* 2000; **47**: 37-42
- Salahshor S**, Kressner U, Pahlman L, Glimelius B, Lindmark G, Lindblom A. Colorectal cancer with and without microsatellite instability involves different genes. *Genes Chromosomes Cancer* 1999; **26**: 247-252
- Yoshimitsu A**, Hiromi N, Kenji Osmar Y, Tadashi N, Yasuhito Y. β -Catenin and adenomatous polyposis coli (APC) mutations in adenomas from hereditary non-polyposis colorectal cancer patients. *Cancer Lett* 2000; **157**: 185-191
- Miyaki M**, Iijima T, Kimura J, Yasuno M, Mori T, Hayashi Y, Koike M, Shitara N, Iwama T, Kuroki T. Frequent mutation of beta-catenin and APC genes in primary colorectal tumors from patients with hereditary nonpolyposis colorectal cancer. *Cancer Res* 1999; **59**: 4506-4509
- Johannsdottir JT**, Jonasson JG, Bergthorsson JT, Amundadottir LT, Magnusson J, Egilsson V, Ingvarsson S. The effect of mismatch repair deficiency on tumorigenesis; microsatellite instability affecting genes containing short repeated sequences. *Int J Oncol* 2000; **16**: 133-139
- Kuraguchi M**, Yang K, Wong E, Avdievich E, Fan K, Kolodner RD, Lipkin M, Brown AM, Kucherlapati R, Edelman W. The distinct spectra of tumor-associated Apc mutations in mismatch repair-deficient *Apc*^{1638N} mice define the roles of MSH3 and MSH6 in DNA repair and intestinal tumorigenesis. *Cancer Res* 2001; **61**: 7934-7942
- Kuraguchi M**, Edelman W, Yang K, Lipkin M, Kucherlapati R, Brown AM. Tumor-associated Apc mutations in *Mlh1*^{-/-} *Apc*^{1638N} mice reveal a mutational signature of *Mlh1* deficiency. *Oncogene* 2000; **19**: 5755-5763
- Yamamoto H**, Min Y, Itoh F, Imsumran A, Horiuchi S, Yoshida M, Iku S, Fukushima H, Imai K. Differential involvement of the hypermethylator phenotype in hereditary and sporadic colorectal cancers with high-frequency microsatellite instability. *Genes Chromosomes Cancer* 2002; **33**: 322-325

Assessment of resin perfusion in hepatic failure *in vitro* and *in vivo*

Ying-Jie Wang, Ze-Wen Wang, Bing-Wei Luo, Hong-Ling Liu, Hong-Wei Wen

Ying-Jie Wang, Ze-Wen Wang, Bing-Wei Luo, Hong-Ling Liu, Hong-Wei Wen, Institute of Infectious Diseases, Southwest Hospital, Third Military Medical University, Chongqing 400038, China
Supported by the National Natural Science Foundation of China, No. 30027001

Correspondence to: Dr. Ying-Jie Wang, Institute of Infectious Diseases, Southwest Hospital, Third Military Medical University, Chongqing 400038, China. wangyj103@263.net

Telephone: +86-23-68754479-8062

Received: 2003-08-05 **Accepted:** 2003-09-18

Abstract

AIM: To observe the adsorbent effect of resin on endotoxin, cytokine, bilirubin in plasma of patients with hepatic failure and to determine the resin perfusion as an artificial liver support system in the treatment of hepatic failure.

METHODS: One thousand milliliters of discarded plasma was collected from each of 6 severe hepatitis patients treated with plasma exchange. The plasma was passed through a resin perfusion equipment for 1-2 h via extracorporeal circulation, and then absorbent indicators of transaminase, bilirubin, blood ammonia, endotoxin and cytokines were examined. In the meantime, study of *in vivo* resin plasma perfusion was performed on 7 severe hepatitis patients to compare the changes of endotoxin and cytokines in blood before and after perfusion.

RESULTS: The levels of total bilirubin, endotoxin, interleukin 1 β and TNF- α in plasma were significantly decreased after *in vitro* resin plasma perfusion. The levels of interleukin 1 β , TNF- α and endotoxin in blood were also evidently declined after *in vivo* resin plasma perfusion. Nevertheless, no obvious changes in IL-6, creatinine (Cr) and urea nitrogen (UN), blood ammonia and electrolytes were found both *in vitro* and *in vivo*.

CONCLUSION: Bilirubin, endotoxin and cytokines in plasma of patients with hepatic failure can be effectively adsorbed by resin *in vitro*. Most cytokines and endotoxin in plasma can also be effectively removed by resin *in vivo*. It demonstrates that resin perfusion may have good treatment efficacy on hepatic failure and can be expected to slow down the progression of hepatic failure.

Wang YJ, Wang ZW, Luo BW, Liu HL, Wen HW. Assessment of resin perfusion in hepatic failure *in vitro* and *in vivo*. *World J Gastroenterol* 2004; 10(6): 837-840

<http://www.wjgnet.com/1007-9327/10/837.asp>

INTRODUCTION

In the research field of artificial liver, blood perfusion, blood filtration, plasma exchange techniques and methods are called non-biological artificial liver^[1-3]. They are based on the mechanical mechanism of blood purification to remove toxins in body to achieve the treatment goal for hepatic failure^[4-11]. New-style resin blood perfusion is mostly used in toxicosis rescue and uremia, etc in clinic, but was rarely reported in the

treatment of hepatic failure. Since endotoxin and cytokine play a pivotal role in the pathogenesis of hepatic failure in severe hepatitis^[12-16], it has become an important issue whether resin blood perfusion can effectively remove endotoxin and cytokine in body. Therefore, we examined the effect of a non-bioartificial liver with resin plasma perfusion on the plasma endotoxin and cytokine removal in patients with severe hepatitis to determine and assess the curative effect of resin plasma perfusion in the treatment of severe hepatitis.

MATERIALS AND METHODS

Subjects

Thirteen subjects with severe viral hepatitis (female 1, male 12, aged 28 to 57 years with a mean of 41.3 years) were enrolled in this study. All subjects belonged to chronic severe hepatitis caused by HBV infection according to the diagnostic criteria described in the Viral Hepatitis Protection and Cure Guideline established on a national conference. Of these patients, 8 were in middle stage, 5 in final stage, complication of encephalopathy, spontaneous peritonitis and hepatorenal syndrome was found in 11, 5 and 3, respectively.

Experimental protocol *in vitro*

One thousand milliliters of discarded plasma was collected from each of 6 severe hepatitis patients treated with plasma exchange, and mimic blood perfusion was performed in 3 h. The resin perfusion device (Lizhu Bio-material Company, Zhuhai, China) and tubes were filled with 500 mL of 50 g/L glucose injection, then rinsed with 3 000 mL of normal saline containing 80 mg heparin from bottom to top at 50-100 mL/min. In the mean time, perfusion device was tapped by hand and rotated to exclude bubbles and particles. Plasma perfusion was performed for 1-2 h (average 1.7 h) and the velocity of plasma cycling through the perfusion device was at 80-120 ml/min. Plasma before and after circulation was collected, sealed and stored at -40 °C. All the procedures, such as plasma collection, perfusion *in vitro* and sample harvesting used aseptic technique, syringe, cycling tubes and frozen tubes were radiated by ⁶⁰Co to remove pyrogen.

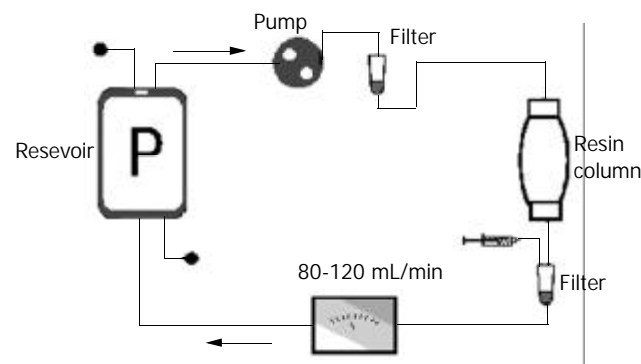


Figure 1 Schematic diagrams of resin perfusion *in vitro*.

Experimental protocol *in vivo*

Resin plasma perfusion was performed in 7 patients with severe hepatitis. Temporal artery-vein circuit was established by

insertion of femoral and pectoral venous cannulas. The patients were heparinized based on individual conditions. The first dose was 1-1.5 mg/kg, then 0.1 mg/kg each 30 min was added. The patients' blood was introduced to a plasma separator (Fresenius Medical Care, Bad Homblurg, GER) at 100-120 mL/min for separation of plasma from the whole blood. The separated plasma was absorbed by the resin perfusion device, then mixed with separated blood cells, and returned to patients. The perfusion was maintained for 1-2 h (average 1.6 h) (Figure 2). The plasma before and after perfusion was collected and stored as the above methods.

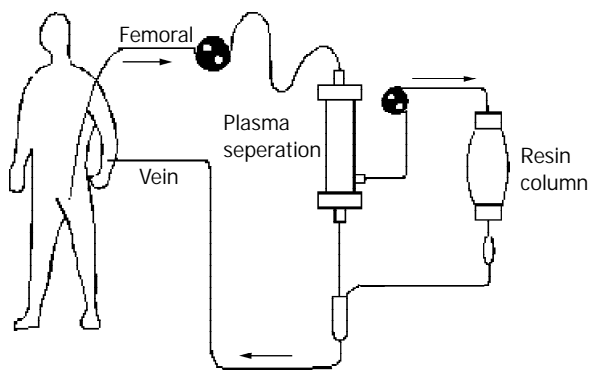


Figure 2 Circuit diagrams of plasma perfusion.

Biochemical estimations and cytokines detection

Plasma aminotransferase, total bilirubin (TB), total bile acid (TBA), electrolyte, UN and Cr were measured using a biochemical autoanalyzer (Hitach Co., Tokyo, Japan). Blood ammonia was measured by a blood ammonia detector (Shiga Co., Tokyo, Japan). Endotoxin was measured by using a limulus test kit according to the manufacturer's instructions (Yihua Medical Technology Co., Shanghai, China). The level of IL-1 β and TNF- α was measured by using a radio immunoassay (RIA) kit according to manufacturer's instructions (Department of Radio Immunoassay, PLA General Hospital Technical Development Center). IL-6 level was measured by using an ELISA kit according to manufacturer's instructions (Shengxiong Medical Technology Co., Shanghai, China).

Statistical analysis

All results were expressed as mean \pm SD. Comparisons between the groups and the same group before and after perfusion were analyzed by Student's *t* test.

RESULTS

Changes in transaminase and bilirubin

After resin perfusion device was used to absorb plasma of the patients with severe hepatitis *in vitro*, transaminase, TB and TBA were all declined with a statistically significant difference in TB, DB and IB before and after resin perfusion (*t* value was 2.081, 2.048, and 2.086 respectively, $P < 0.05$).

Table 1 Comparison of transaminase, TB and TBA before and after *in vitro* resin perfusion (mean \pm SD)

	Before absorption	After absorption
ALT(IU/L)	74.17 \pm 49.68	47.83 \pm 22.33
AST(IU/L)	88.83 \pm 45.58	58.33 \pm 44.64
TB(μ mol/L)	518.8 \pm 180.27	356.13 \pm 162.87 ^a
TBA(μ mol/L)	157.17 \pm 53.53	131.67 \pm 34.95

^a $P < 0.05$, vs before absorption.

TBA was markedly declined in patients with *in vivo* resin plasma perfusion with a significant difference ($P < 0.01$). Nevertheless, transaminase and TB had no marked change before and after absorption (Table 2).

Table 2 Comparison of transaminase, TB, and TBA before and after *in vivo* resin perfusion (mean \pm SD)

	Before absorption	After absorption
ALT(IU/L)	270.03 \pm 355.54	288.38 \pm 314.58
AST(IU/L)	252.50 \pm 391.51	224.88 \pm 356.79
TB(μ mol/L)	519.66 \pm 209.00	460.80 \pm 165.99
TBA(μ mol/L)	194.88 \pm 47.32	166.75 \pm 48.98 ^b

^b $P < 0.01$ vs before absorption.

Comparison of electrolytes and renal function

The electrolytes – K, Na, Cl, Ca, Mg, and P after absorption had no significant changes compared to those before absorption. UN and Cr were declined after absorption with no statistical significance compared to those before absorption with UN value of 6.79 \pm 4.14 mmol/L before absorption and 6.42 \pm 3.39 mmol/L after absorption, and Cr value of 135.67 \pm 30.77 μ mol/L before absorption and 121.85 \pm 20.40 μ mol/L after absorption.

Blood ammonia

After *in vitro* resin absorption, blood ammonia in plasma was not markedly decreased (98.17 \pm 20.60 μ mol/L and 91.50 \pm 18.84 μ mol/L). Similar to the result of *in vitro*, blood ammonia had no significant difference before and after *in vivo* resin plasma perfusion (48.25 \pm 8.63 μ mol/L and 46.75 \pm 9.44 μ mol/L).

Level of LPS and cytokines

The level of LPS was markedly decreased after *in vitro* absorption ($t = 6.604$, $P < 0.01$). The changes in TNF- α and IL-1 β had a statistical significance (*t* was 2.876 and 3.673 respectively, $P < 0.05$). IL-6 had no significant change before and after *in vitro* resin absorption (Table 3).

Table 3 Level of LPS and cytokines before and after *in vitro* resin absorption (mean \pm SD)

	Before absorption	After absorption
LPS (ng/L)	60.35 \pm 8.58	32.75 \pm 10.14 ^a
TNF- α (ng/L)	1.49 \pm 1.06	1.04 \pm 0.91 ^b
IL-1 β (ng/L)	2.61 \pm 1.42	1.68 \pm 0.92 ^b
IL-6(ng/L)	100.07 \pm 10.99	87.64 \pm 12.27

^a $P < 0.05$, ^b $P < 0.01$ vs before absorption.

The plasma endotoxin was markedly decreased after *in vivo* resin plasma perfusion ($t = 5.233$, $P < 0.001$). TNF- α and IL-1 β also changed significantly (*t* value was 3.474 and 4.869 respectively, $P < 0.01$) with declined levels of 16.3% and 37.1% respectively. IL-6 had no evident change before and after *in vivo* plasma perfusion (Table 4).

Table 4 Level of LPS and cytokines before and after *in vivo* resin absorption (mean \pm SD)

	Per- perfusion	Post- perfusion
LPS(ng/L)	58.64 \pm 11.03	36.13 \pm 5.24 ^a
TNF- α (ng/L)	2.28 \pm 0.89	1.69 \pm 0.76 ^a
IL-1 β (ng/L)	1.98 \pm 0.82	1.24 \pm 0.88 ^a
IL-6(ng/L)	88.41 \pm 24.96	84.85 \pm 16.55

^a $P < 0.01$ vs before absorption.

DISCUSSION

Blood perfusion is a commonly used method for blood purification^[17-20]. Activated charcoal representing perfusion equipment is most widely applied in the clinical treatment for drug toxicosis, uremia and liver coma and a good result has been obtained^[21,22]. However, the shape of activated charcoal particles is irregular and their mechanical strength is inferior, thus particles are easily broken. If a broken particle directly contacts with blood, it will cause hemolysis and microvessel occlusion. Therefore, activated charcoal must be encapsulated before use. Synthetic resin is another kind of medical absorbent material with macropore high molecular polymers belonging to neutral macropore resin that absorbs substances via Vander Val gravitation. Its absorbent ability has been found to be characterized by a fast absorbent speed, high mechanical strength, relative absorbent specificity mainly absorbing the substances with a molecular weight of 500- 5 000 Da and showing an outstanding absorbent ability to those toxins which can bind to proteins closely or are highly fat-soluble^[23,24].

In the experiment of resin blood perfusion *in vitro*, we found that the resin blood perfusion device was able to effectively absorb transaminase and bilirubin but weakly affect kidney function and blood ammonia, considering that it absorbed medium molecules not small molecules. It illustrated the resin blood perfusion could improve the hepatic function in patients with severe hepatitis. In the meantime, it did not cause electrolyte imbalance and disturbance in the internal environment. Therefore, resin blood perfusion can be used as an artificial liver support system in the treatment of severe hepatitis.

Current studies considered that the pathogenesis of severe hepatitis was the superposition of virus-caused primary immunopathological damage and cytokine-induced secondary damage^[25-27]. When liver barrier function was impaired, endotoxaemia would occur. Endotoxins stimulated the mononuclear phagocyte system inside and outside the liver, and thus, enormous cytokines were released. Furthermore, this cytokine-induced secondary hepatocellular damage played an important role in the course of hepatitis. Hereby, cytokine removal was good for alleviating liver damage, reducing leukoplania and thrombocyte aggregates, maintaining internal environmental equilibrium, and sequentially slowing down or even reversing the progression of disease and improving prognosis^[28-30].

Along with the development in molecular biology, research of antagonists for various cytokines has been launched, for example, monoclonal antibody, receptor antibody, soluble antibody. However, their clinical application is not ideal. In recent years, more and more researchers have began to use blood purification to remove cytokines^[31-33]. At present, it is still disputable whether blood purification can effectively remove cytokines^[34,35]. Some researchers held that leucocytes could be activated by passing through the device during blood perfusion to cause the releasing of cytokines. In addition, it has been found the molecular weight of cytokines is relatively high, and cytokines are mostly bound to proteins in plasma, the half-life of cytokines is short and they are produced and metabolized quickly. Therefore, it would be hard to remove them via blood purification^[36].

In this study, after plasma perfusion treatment for severe hepatitis, both TNF- α and IL-1 β in plasma were significantly decreased, illustrating that plasma perfusion was an effective method for cytokine removal. The change of IL-6 was not significant, because IL-6 might be produced too fast, or it related to different absorbent efficacy of the perfusion device to various cytokines.

In conclusion, resin can effectively absorb bilirubin, LPS, TNF- α and IL-1 β *in vitro*, and LPS, TNF- α and IL-1 β can be

significantly decreased in resin plasma perfusion *in vivo*, resin perfusion has good curative effects on severe hepatitis with hepatic failure.

REFERENCES

- 1 **Dowling DJ**, Mutimer DJ. Artificial liver support in acute liver failure. *Eur J Gastroenterol Hepatol* 1999; **11**: 991-996
- 2 **Kjaergard LL**, Liu J, Als-Nielsen B, Gluud C. Artificial and bioartificial support systems for acute and acute-on-chronic liver failure: a systematic review. *JAMA* 2003; **289**: 217-222
- 3 **Stockmann HBAC**, Hiemstra CA, Marquet RL, IJzermans JNM. Extracorporeal perfusion for the treatment of acute liver failure. *Ann Surg* 2000; **231**: 460-470
- 4 **Borra M**, Galavotti D, Bellini C, Fumi L, Morsiani E, Bellini G. Advanced technology for extracorporeal liver support system devices. *Int J Artif Organs* 2002; **25**: 939-949
- 5 **Bertani H**, Gelmini R, Del Buono MG, De Maria N, Girardis M, Solfrini V, Villa E. Literature overview on artificial liver support in fulminant hepatic failure: a methodological approach. *Int J Artif Organs* 2002; **25**: 903-910
- 6 **Oda S**, Hirasawa H, Shiga H, Nakanishi K, Matsuda K, Nakamura M. Continuous hemofiltration/hemodiafiltration in critical care. *Ther Apher* 2002; **6**: 193-198
- 7 **Ash SR**, Caldwell CA, Singer GG, Lowell JA, Howard TK, Rustgi VK. Treatment of acetaminophen-induced hepatitis and fulminant hepatic failure with extracorporeal sorbent-based devices. *Adv Ren Replace Ther* 2002; **9**: 42-53
- 8 **Clemmesen JO**, Kondrup J, Nielsen LB, Larsen FS, Ott P. Effects of high-volume plasmapheresis on ammonia, urea, and amino acids in patients with acute liver failure. *Am J Gastroenterol* 2001; **96**: 1217-1223
- 9 **Steczko J**, Bax KC, Ash SR. Effect of hemodiabsorption and sorbent-based pheresis on amino acid levels in hepatic failure. *Int J Artif Organs* 2000; **23**: 375-388
- 10 **Hughes RD**. Review of methods to remove protein-bound substances in liver failure. *Int J Artif Organs* 2002; **25**: 911-917
- 11 **Di Campi C**, Zileri Dal Verme L, Andrisani MC, Armuzzi A, Candelli M, Gaspari R, Gasbarrini A. Advances in extracorporeal detoxification by MARS dialysis in patients with liver failure. *Curr Med Chem* 2003; **10**: 341-348
- 12 **Shito M**, Balis UJ, Tompkins RG, Yarmush ML, Toner M. A fulminant hepatic failure model in the rat: involvement of interleukin-1 β and tumor necrosis factor- α . *Dig Dis Sci* 2001; **46**: 1700-1708
- 13 **Galun E**, Axelrod JH. The role of cytokines in liver failure and regeneration: potential new molecular therapies. *Biochim Biophys Acta* 2002; **1592**: 345-358
- 14 **Streetz K**, Leifeld L, Grundmann D, Ramakers J, Eckert K, Spengler U, Brenner D, Manns M, Trautwein C. Tumor necrosis factor alpha in the pathogenesis of human and murine fulminant hepatic failure. *Gastroenterology* 2000; **119**: 446-460
- 15 **Yumoto E**, Higashi T, Nouse K, Nakatsukasa H, Fujiwara K, Hanafusa T, Yumoto Y, Tanimoto T, Kurimoto M, Tanaka N, Tsuji T. Serum gamma-interferon-inducing factor (IL-18) and IL-10 levels in patients with acute hepatitis and fulminant hepatic failure. *J Gastroenterol Hepatol* 2002; **17**: 285-294
- 16 **Han DW**. Intestinal endotoxemia as a pathogenetic mechanism in liver failure. *World J Gastroenterol* 2002; **8**: 961-965
- 17 **Samatskaya VV**, Lindup WE, Walther P, Maslenny VN, Yushko LA, Sidorenko AS, Nikolaev AV, Nikolaev VG. Albumin, bilirubin, and activated carbon: new edges of an old triangle. *Artif Cell Blood Substit Immobil Biotechnol* 2002; **30**: 113-126
- 18 **Nakamura T**, Ushiyama C, Suzuki Y, Inoue T, Shoji H, Shimada N, Koide H. Combination therapy with polymyxin B-immobilized fibre haemoperfusion and teicoplanin for sepsis due to methicillin-resistant *Staphylococcus aureus*. *J Hosp Infect* 2003; **53**: 58-63
- 19 **Tsuchida K**, Takemoto Y, Sugimura K, Yoshimura R, Nakatani T. Direct hemoperfusion by using Lixelle column for the treatment of systemic inflammatory response syndrome. *Int J Mol Med* 2002; **10**: 485-488
- 20 **Sechser A**, Osorio J, Freise C, Osorio RW. Artificial liver support devices for fulminant liver failure. *Clin Liver Dis* 2001; **5**: 415-430

- 21 **Ash SR.** Extracorporeal blood detoxification by sorbents in treatment of hepatic encephalopathy. *Adv Ren Replace Ther* 2002; **9**: 3-18
- 22 **Kramer L,** Gendo A, Madl C, Ferrara I, Funk G, Schenk P, Sunder-Plassmann G, Horl WH. Biocompatibility of a cuprophane charcoal-based detoxification device in cirrhotic patients with hepatic encephalopathy. *Am J Kidney Dis* 2000; **36**: 1193-1200
- 23 **Musanje L,** Darvell BW. Polymerization of resin composite restorative materials: exposure reciprocity. *Dent Mater* 2003; **19**: 531-541
- 24 **Gode F,** Pehlivan E. A comparative study of two chelating ion-exchange resins for the removal of chromium(III) from aqueous solution. *J Hazard Mater* 2003; **100**: 231-243
- 25 **Endo Y,** Shibazaki M, Yamaguchi K, Kai K, Sugawara S, Takada H, Kikuchi H, Kumagai K. Enhancement by galactosamine of lipopolysaccharide(LPS)-induced tumour necrosis factor production and lethality: its suppression by LPS pretreatment. *Br J Pharmacol* 1999; **128**: 5-12
- 26 **Masai T,** Sawa Y, Ohtake S, Nishida T, Nishimura M, Fukushima N, Yamaguchi T, Matsuda H. Hepatic dysfunction after left ventricular mechanical assist in patients with end-stage heart failure: role of inflammatory response and hepatic microcirculation. *Ann Thorac Surg* 2002; **73**: 549-555
- 27 **Rahman T,** Hodgson H. Clinical management of acute hepatic failure. *Intensive Care Med* 2001; **27**: 467-476
- 28 **Stange J,** Mitzner SR, Klammt S, Freytag J, Peszynski P, Looock J, Hickstein H, Korten G, Schmidt R, Hentschel J, Schulz M, Löhr M, Liebe S, Schareck W, Hopt UT. Liver support by extracorporeal blood purification: a clinical observation. *Liver Transpl* 2000; **6**: 603-613
- 29 **Stange J,** Mitzner SR, Risler T, Erley CM, Lauchart W, Goehl H, Klammt S, Peszynski P, Freytag J, Hickstein H, Löhr M, Liebe S, Schareck W, Hopt UT, Schmidt R. Molecular adsorbent recycling system (MARS): clinical results of a new membrane-based blood purification system for bioartificial liver support. *Artif Organs* 1999; **23**: 319-330
- 30 **Nakae H,** Yonekawa C, Wada H, Asanuma Y, Sato T, Tanaka H. Effectiveness of combining plasma exchange and continuous hemodiafiltration (combined modality therapy in a parallel circuit) in the treatment of patients with acute hepatic failure. *Ther Apher* 2001; **5**: 471-475
- 31 **Nakamura T,** Ushiyama C, Suzuki S, Shimada N, Ebihara I, Suzaki M, Takahashi T, Koide H. Effect of plasma exchange on serum tissue inhibitor of metalloproteinase 1 and cytokine concentrations in patients with fulminant hepatitis. *Blood Purif* 2000; **18**: 50-54
- 32 **Nakae H,** Asanuma Y, Tajimi K. Cytokine removal by plasma exchange with continuous hemodiafiltration in critically ill patients. *Ther Apher* 2002; **6**: 419-424
- 33 **Ho DW,** Fan ST, To J, Woo YH, Zhang Z, Lau C, Wong J. Selective plasma filtration for treatment of fulminant hepatic failure induced by D-galactosamine in a pig model. *Gut* 2002; **50**: 869-876
- 34 **Ryan CJ,** Anilkumar T, Ben-Hamida AJ, Khorsandi SE, Aslam M, Pusey CD, Gaylor JD, Courtney JM. Multisorbent plasma perfusion in fulminant hepatic failure: effects of duration and frequency of treatment in rats with grade III hepatic coma. *Artif Organs* 2001; **25**: 109-118
- 35 **Nakae H,** Yonekawa T, Narita K, Endo S. Are proinflammatory cytokine concentrations reduced by plasma exchange in patients with severe acute hepatic failure? *Res Commun Mol Pathol Pharmacol* 2001; **109**: 65-72
- 36 **Iwai H,** Nagaki M, Naito T, Ishiki Y, Murakami N, Sugihara J, Muto Y, Moriwaki H. Removal of endotoxin and cytokines by plasma exchange in patients with acute hepatic failure. *Crit Care Med* 1998; **26**: 873-876

Edited by Zhang JZ and Wang XL Proofread by Xu FM

Establishment of mice model with human viral hepatitis B

Li-Fen Gao, Wen-Sheng Sun, Chun-Hong Ma, Su-Xia Liu, Xiao-Yan Wang, Li-Ning Zhang, Ying-Lin Cao, Fa-Liang Zhu, Yu-Gang Liu

Li-Fen Gao, Wen-Sheng Sun, Chun-Hong Ma, Su-Xia Liu, Xiao-Yan Wang, Li-Ning Zhang, Ying-Lin Cao, Fa-Liang Zhu, Yu-Gang Liu, Institute of Immunology, Medical College, Shandong University, Jinan 250012, Shandong Province, China

Supported by the National Natural Science Foundation of China, No.30070341, and the National Natural Science Foundation of China for Young Scholars Abroad, No.30128023

Correspondence to: Professor Wen-Sheng Sun, Institute of Immunology, Medical College, Shandong University, Jinan 250012, Shandong Province, China. sunwenshengsws@yahoo.com

Telephone: +86-531-8382038

Received: 2003-08-26 **Accepted:** 2003-10-07

Abstract

AIM: To establish a mice model of hepatitis B by using HBV-transgenic mice, and to transfer HBV-specific cytotoxic T lymphocytes (CTL) induced from syngeneic BALB/c mice immunized by a eukaryotic expression vector containing HBV complete genome DNA.

METHODS: HBV DNA was obtained from digested pBR322-2HBV and ligated with the vector pcDNA3. Recombinant pcDNA3-HBV was identified by restriction endonuclease assay and transfected into human hepatoma cell line HepG2 with lipofectin. ELISA was used to detect the expression of HBsAg in culture supernatant, and RT-PCR to determine the existence of HBV PreS1 mRNA. BALB/c mice were immunized with pcDNA3-HBV or pcDNA3 by intramuscular injection. ELISA was used to detect the expression of HBsAb in serum. MTT assay was used to measure non-specific or specific proliferation ability and specific killing activity of spleen lymphocytes. Lymphocytes from immunized mice were transferred into HBV-transgenic mice (2.5×10^7 per mouse). Forty-eight hours later, the level of serum protein and transaminase was detected with biochemical method, liver and kidney were sectioned and stained by HE to observe the pathological changes.

RESULTS: By enzyme digestion with *Eco* RI, *Xho* I and *Hind* III, the recombinant pcDNA3-HBV was verified to contain a single copy of HBV genome, which was inserted in the positive direction. HepG2 cells transfected with the recombinant could stably express PreS1 mRNA and HBsAg. After immunized by pcDNA3-HBV for 4 weeks, HBsAb was detected in the serum of BALB/c mice. The potential of spleen lymphocytes for both non-specific and specific proliferation and the specific killing activity against target cells were enhanced. The transgenic mice in model group had no significant changes in the level of serum protein but had an obvious increase of ALT and AST. The liver had obvious pathological changes, while the kidney had no evident damage.

CONCLUSION: A eukaryotic expression vector pcDNA3-HBV containing HBV complete genome is constructed successfully. HepG2 cells transfected with the recombinant can express PreS1 mRNA and HBsAg stably. Specific cellular

immune response can be induced in mice immunized by pcDNA3-HBV. A mice model of acute hepatitis with HBV has been established.

Gao LF, Sun WS, Ma CH, Liu SX, Wang XY, Zhang LN, Cao YL, Zhu FL, Liu YG. Establishment of mice model with human viral hepatitis B. *World J Gastroenterol* 2004; 10(6): 841-846

<http://www.wjgnet.com/1007-9327/10/841.asp>

INTRODUCTION

HBV infection is a worldwide problem that affects human health severely^[1-3]. No appropriate animal model is available till now because of the strict host specificity of HBV infection. At present, HBV transgenic animals could be obtained during embryonic period, which always induce immune tolerance to dominating HBV antigens^[4-6]. In addition, it has great difference in biological characteristics between duck hepatitis B virus and HBV. So it is imperative to establish a mice model that can simulate human viral hepatitis B precisely and is convenient for wider applications.

Both clinical researches and animal experiments suggest that the pathological changes are not caused by the virus directly, but are mediated by immunity^[7,8]. HBV specific CTL induced by HBV antigens can cause immune damage to the liver to clear the viruses and recruit non-specific inflammatory cells to local infection tissue simultaneously, thus aggravating hepatic injury^[9,10]. We planned to induce HBV specific CTL by gene immunity and to establish a mice model of hepatitis B by transferring CTLs to HBV-transgenic mice.

MATERIALS AND METHODS

Animals

SPF BALB/c mice were provided by the Laboratory Animal Center of Shandong University. HBV complete genome (ayw subtype) transgenic BALB/c mice with a high level of HBsAg, HBeAg and with HBV DNA positive in peripheral blood, were purchased from Transgenic Animal Central Laboratory, 458 Hospital of PLA, China.

Cell lines

Hepatocellular carcinoma cell line HepG2 was cultured and conserved in our laboratory. HepG2.2.15 cell line carrying four whole HBV genes can not only express HBsAg and HBeAg but also produce Dane's particles of HBV. SP2/0-HBV is a mouse myeloma cell line with pcDNA3-HBV stably transfected.

Plasmids

pBR322-2HBV was a recombinant plasmid with a double copy of HBV (ayw subtype) inserted into *Eco*RI restriction site of pBR322. Mammalian animal cell expression vector pcDNA3 was 5.4 kb in length. It has a CMV early promoter enhancer, multiple cloning sites (MCS) and neomycin resistant gene.

Construction of recombinant pcDNA3-HBV

Alkaline lysis method was used to extract large quantity of

pBR322-2HBV and pcDNA3 DNA respectively. Precipitation with polyethylene glycol was used to purify plasmid DNA, and biometer was used for quantitative analysis. pBR322-2HBV was digested with *EcoRI* and separated by 10 g/L agarose gel electrophoresis. The gel band containing 3.2 kb DNA was cut under UV light. HBV DNA was extracted using a DNA recovery kit. pcDNA3 was also digested by *EcoRI* and a 5.4 kb fragment was recovered with the same method. Ten microliter of HBV DNA and 2 μ L of pcDNA3-HBV (mol ratio 3:1) were mixed together with 2 μ L of T4 DNA ligase, 2 μ L of buffer and 2 μ L of sterile water. The mixture was placed overnight at 4 °C, and then the reaction was terminated. Ten microliter of ligated product was transformed to competent DH5 α , which was then transferred to a LB medium plate containing 60 μ g/mL of ampicillin and incubated overnight at 37 °C.

Identification of recombinant pcDNA3-HBV

Antibiotic selection and restriction endonuclease assay were used to screen and identify positive clones. A positive clone was selected randomly and amplified for recombinant plasmid DNA. Then the recombinant DNA was digested by *EcoRI*, *XhoI* and *HindIII*, respectively. The digestion system was 20 μ L, including 1 μ L DNA, 1 μ L endonuclease, 2 μ L 10 \times buffer and 16 μ L sterile water, and incubated for 3 hours at 37 °C. The correctness of ligation was further identified by 10 g/L agarose gel electrophoresis.

pcDNA3-HBV transfected to HepG2 cell with lipofectin

HepG2 cells during logarithmic period were digested by trypsinization and diluted to 4 \times 10⁵/mL. Then the cells were plated to 24-well plates with 0.5 mL per well (cell count 2 \times 10⁵) and cultured for 24 h for transfection next day, when 80-90% of the cells were fused. One μ g purified pcDNA3-HBV plasmid DNA was transfected to the prepared HepG2 cells using lipofectin reagent. After transfection, HepG2 cells were screened by G418 resistance and routinely cultured. The culture supernatant was collected periodically to detect HBV antigens. The selected positive clone was named as HepG2.02G.

HbsAg detection

Concentration of HBsAg in culture supernatant of transfected cells was detected by ELISA. Critical value (cutoff) = 2.1 \times N, in which N is the average OD of negative control, and S is the OD of sample. The sample was positive when S/N \geq 2.1, otherwise negative.

Extraction of total RNA

HepG2.02G, HepG2.2.15, and HepG2 cells in logarithmic period were harvested, each of 1 \times 10⁶ cells, was rinsed by 0.01 mol/L PBS once and centrifuged at 1 000 rpm for 5 min. The precipitate was used for total RNA extraction according to the protocol of TRIZOL kit.

Primer design and synthesis

According to the sequence of HBV S1 (subtype ayw) described by GenBank, primers were designed to amplify HBV PreS1 gene. PCR product would be 625 bp. β -actin served as control, with a PCR product 366 bp in length. The sequences of the primers were: PreS1 forward: 5' - GCTCTAGACACCAAATGCCCTA-3', reverse: 5' - GCTCTAGAGAATCCCAGAGG-3', β -actin forward: 5' - ACACTGTGCCCATCTACGAGGGC-3', reverse: 5' - ATGATGGAGTTGAAGGTAGTT TCG TGG AT-3'. These oligonucleotide primers were synthesized by Shanghai Sangon Biological Engineering Technology and Service Co. Ltd.

Amplification of PreS1 mRNA

Reverse transcription was performed with 1 μ g of total RNA

to obtain cDNA as the template. PCR was carried out in 25 μ L volume with 1 μ L RT-PCR product, 2.5 μ L 10 \times PCR buffer, 0.3 μ L Mg²⁺, 5 nmol/L of dNTP, 3 U *Taq* polymerase and 10 nmol/L of primers (forward and reverse). The reaction conditions were pre-denatured at 94 °C for 3 min, 30 cycles (denatured at 94 °C for 1 min, annealed at 50 °C for 1 min and extended at 72 °C for 1 min), followed by a final extension at 72 °C for 5 min. Ten microliter of the PCR product then underwent 2% agarose gel electrophoresis at 70 V for 30 min. HepG2 cells were used as negative control, while HepG2.2.15 as positive.

Scheme for mice immunization with pcDNA3-HBV or pcDNA3

The purified pcDNA3-HBV DNA was diluted with sterile NS to the concentration of 1 000 μ g/mL and preserved at -20 °C. Twelve male BALB/c mice were randomly divided into 2 groups, 6 mice each. One was experimental group (Exp), which was injected 50 μ L 250 g/L sucrose intramuscularly to both sides of anterior tibial muscle, 50 μ L pcDNA3-HBV (100 μ L per mouse) was injected at the same site 20 min later. Another was the control group (Ctrl), the same quantity of pcDNA3 was injected as negative control. The immunization was intensified once 2 to 3 wk.

HbsAb detection in serum of mice immunized with pcDNA3-HBV

Blood samples were collected by cutting tails of the mice at wk 2, 4, 8 and 10, respectively. Serum was separated and HBsAb was detected by double-antibody sandwich ELISA.

Measurement of proliferation reaction of spleen lymphocytes of mice immunized by pcDNA3-HBV or pcDNA3

Mice spleen cells were prepared routinely (cell density adjusted to 5 \times 10⁶/mL) and plated to 96-well plates (100 μ L per well). The supernatant of HepG2.2.15 (containing a high level of HBsAg), PHA (eventual concentration 25 μ g/mL) or ConA (eventual concentration 10 μ g/mL) was added to 3 wells, respectively. MTT assay was performed after the cells were cultured at 37 °C for 68 h. Proliferation rate was calculated as: (OD of stimulatory - OD of non-stimulatory) / OD of non-stimulatory \times 100%.

Measurement of specific killing activity of spleen lymphocytes of mice immunized by pcDNA3-HBV or pcDNA3

Mice spleen cells were plated to 96-well plates, mixed with SP2/0-HBV cells (effector/target ratio 50:1). Control groups were designed and each group had 3 wells. MTT assay was performed after the cells were cultured for 72 h. Killing rate of CTLs was calculated as: [1 - (OD of effector and target cells - OD of effector cells) / OD of target cells] \times 100%.

Establishment of animal model

Transgenic mice were divided into 3 groups (6 mice each): Model, negative control and blank control. Mice in model or negative control group were injected with spleen lymphocytes of mice immunized by pcDNA3-HBV (HBsAb positive) or pcDNA3 respectively. Mice in blank control group were injected with NS, 0.5 mL each mouse. Spleen lymphocytes were adjusted to 5.0 \times 10⁷/mL using NS and injected to transgenic mice through caudal vein (2.5 \times 10⁷ lymphocytes, 0.5 mL per mouse).

Identification of animal model

After 48 h, the transgenic mice were killed and their venous blood was collected. Serum total protein, albumin, globulin, ALT and AST were detected. Liver and kidney were fixed with 100 g/L formaldehyde, embedded, sliced and stained with HE to observe inflammation and immune-pathological changes with a microscope.

Statistical analysis

All data were shown as mean±SD. Significant levels of differences between values were analyzed using the Chi-square test and Student's *t* test. Statistically significant *P* value was defined as <0.05.

RESULTS

Restriction digestion results of pBR322-2HBV and pcDNA3

Extracted plasmid DNA had a high purity ($OD_{260/280}=1.6-1.8$). After pBR322-2HBV was digested by *EcoRI*, 2 bands were obtained at about 4.3 kb and 3.2 kb in size (Figure 1). pcDNA3 was linear after digestion, and a band at 5.4 kb proved it was completely digested (Figure 2).

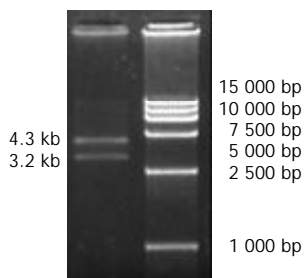


Figure 1 Enzymatic digestion of pBR322-2HBV by *EcoRI*.

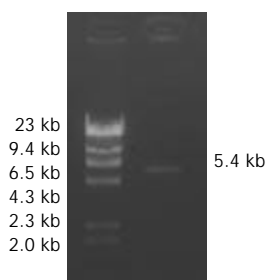


Figure 2 Enzymatic digestion of pcDNA3 by *EcoRI*.

Identification of recombinant pcDNA3-HBV

A high purity of the extracted 2 kinds of DNA was certified by electrophoresis. The recombinant pcDNA3-HBV was digested by *EcoRI* and the product underwent electrophoresis. Only a band of 5.4 kb indicated that the transformed plasmid was pcDNA3 without exogenous genes, while 2 bands at 5.4 kb and 3.2 kb indicated successful ligation (Figure 3). pcDNA3-HBV was digested by *HindIII*, and the product of 8.6 kb in size indicated that the recombinant pcDNA3-HBV contained a single HBV gene. pcDNA3-HBV was digested by *XhoI*, and the products of 3.1 kb and 5.5 kb showed that HBV was inserted at the correct direction (Figure 4).

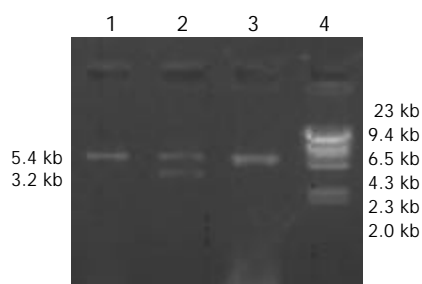


Figure 3 Analysis of ligation of HBV and pcDNA3. 1, 3: pcDNA3 vector, 2: pcDNA3-HBV (5.4 kb+3.2 kb), 4: DNA marker (λ DNA/*HindIII*).

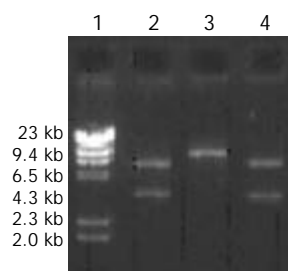


Figure 4 Digestive identification of recombinant plasmid pcDNA3-HBV. 1: DNA marker (λ DNA/*HindIII*), 2: *XhoI* digestion (3.1 kb+5.5 kb), 3: *Hind III* digestion (8.6 kb), 4: *EcoRI* digestion (5.4 kb+3.2 kb).

HBsAg expression in supernatant of HepG2.02G cell culture

HBsAg in supernatant could be detected on day 15, and expressed stably after 40 d (S/N=48).

PreS1 mRNA expression in HepG2.02G

A specific band at 625 bp demonstrated that HBV could efficiently replicate and transcript in human hepatocellular carcinoma cells, as shown in Figure 5.

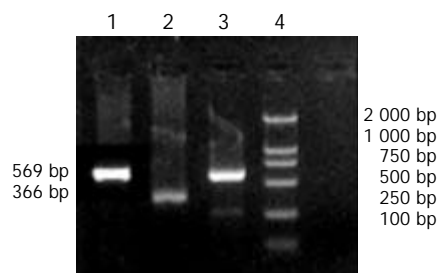


Figure 5 Expression of preS1 mRNA by RT-PCR. 1: HepG2.2.15 (positive control); 2: β -actin; 3: HepG2.02G; 4: DNA marker (DL2 000); 5: HepG2 (negative control).

HBsAb level in serum of mice immunized by pcDNA3-HBV

pcDNA3-HBV immunized mice had specific immune response at the 4th week (S/N=19). Antibody expression reached the highest level at the 8th week and this level lasted to the 10th week.

Proliferation reaction of spleen lymphocytes of mice immunized by pcDNA3-HBV or pcDNA3

As illustrated in Table 1, the non-specific proliferation ability of spleen lymphocytes of mice immunized by pcDNA3-HBV to both PHA and ConA was enhanced as compared with that of pcDNA3 ($P<0.05$), and the specific proliferation ability to supernatant of HepG2.2.15 was also promoted ($P<0.01$).

Table 1 Spleen lymphocyte proliferation of immunized mice (%)

Group	PHA (25 μ g/mL)	ConA (10 μ g/mL)	HepG2.2.15 media (1:1)
Exp	52.9±3.7	80.9±8.3	33.8±3.2
Ctrl	32.6±2.4 ^a	61.6±4.5 ^a	4.1±0.5 ^b

^a $P<0.05$ vs Exp, ^b $P<0.01$ vs Exp.

Specific killing activity of spleen lymphocytes of mice immunized by pcDNA3-HBV or pcDNA3

MTT assay showed that the killing activity of spleen lymphocytes of mice immunized by pcDNA3 against SP2/0 and SP2/0-HBV had no significant difference ($P>0.05$), but that of mice immunized by pcDNA3-HBV to SP2/0-HBV was

distinctly enhanced as compared to SP2/0 ($P < 0.01$). Results are shown in Table 2.

Table 2 Specific killing activity of mice spleen lymphocytes (% , mean \pm SD)

Group	SP2/0	SP2/0-HBV
Exp	14.3 \pm 3.4 ¹	51.5 \pm 9.8 ^b
Ctrl	20.8 \pm 4.6 ²	24.5 \pm 3.7 ³

^b $P < 0.01$ vs 1, 2, 3.

Identification of mice model of hepatitis B

The mice in each group had no significant changes in the level of serum protein compared with the blank control group ($P > 0.05$). The serum ALT and AST of transgenic mice in blank and negative control groups were normal (0-40 U/L), while they (ALT 232 \pm 14 U/L, AST 315 \pm 21 U/L) were much higher in the model group than in the control group ($P < 0.01$). The hepatic cords of mice in the blank control group had a radiated structure surrounding the central vein, the hepatic lobule had a clear structure with cells tightly connected. The hepatic cells

had large and round nuclei, with obvious nucleoli and abundant symmetrical cytoplasm. There was no inflammatory cell infiltration in the portal area with a clear structure (Figure 6A). Mice in negative control group had sporadic acidophilic changes of hepatic cells, without inflammatory cell infiltration (Figure 6B). In the model group, hepatic cells of transgenic mice had diffuse ballooning degeneration, cytoplasmic loosening, acidophilic changes, appearance of acidophilic body, spotty necrosis of hepatic tissue and obvious infiltration of inflammatory cells in the portal area (Figure 7). However, mice in the model group had no obvious inflammation and structure damage of the kidney.

DISCUSSION

The host variety of HBV infection is limited. At present, the animal models for HBV research included chimpanzee^[11], Tupaia Glis^[12] and other hepadnaviridae virus infected animals^[13]. Although duck hepatitis B virus (DHBV) has been found to be similar to HBV in mechanism of pathogenesis, ducks infected with DHBV did not develop hepatic cirrhosis and hepatocellular carcinoma because DHBV lacks X gene^[14]. Mice

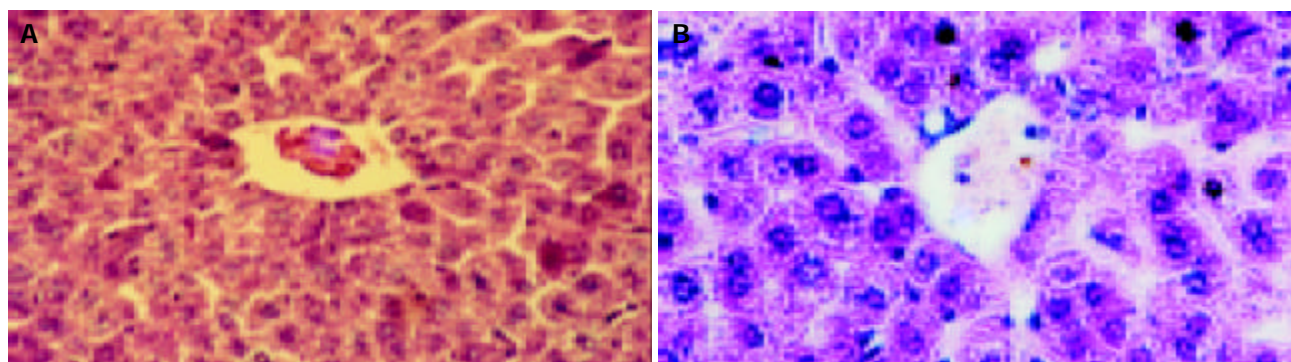


Figure 6 Liver structure of mice by HE-staining ($\times 200$). A: Liver structure of mice in blank control group, B: Liver structure of mice in negative control group.

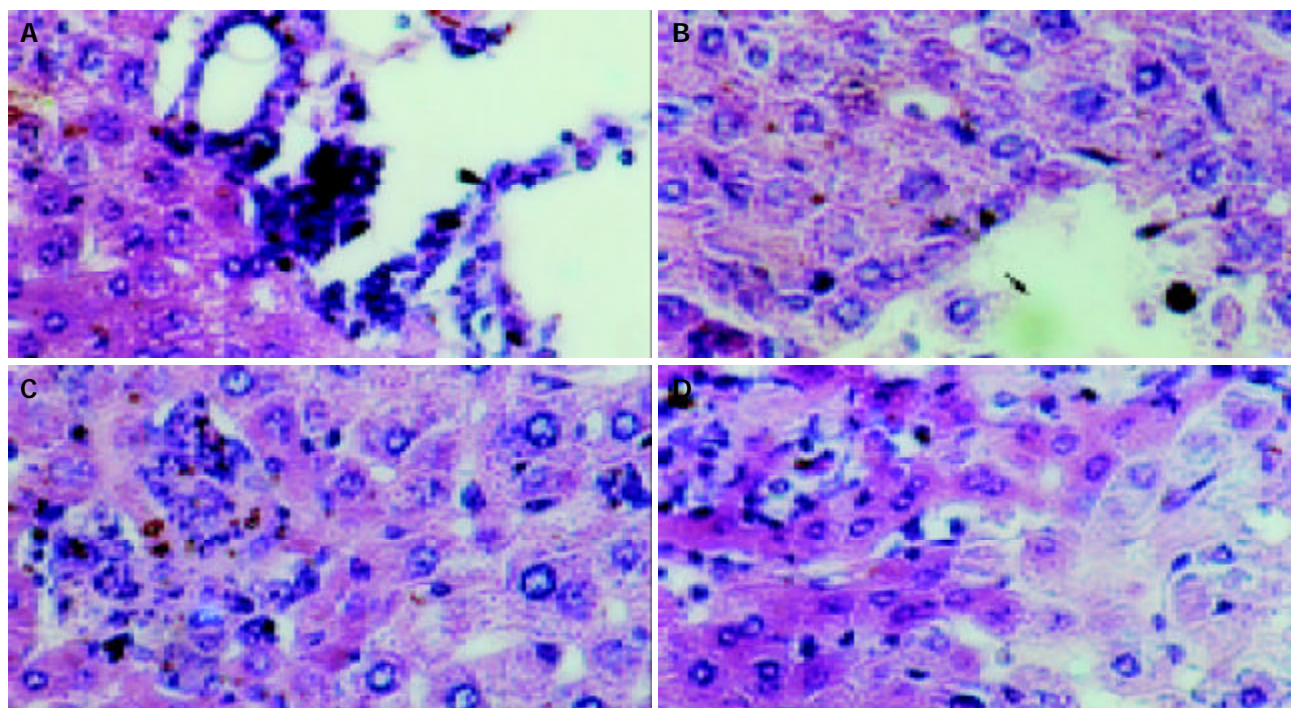


Figure 7 Pathological changes of mouse liver with acute hepatitis in model group (HE, $\times 200$). A: Infiltration of inflammatory cells in the portal area, B: Local necrosis as arrow indicated, C: Obvious infiltration of inflammatory cells and eosinophilic changes, D: Cytoplasmic loosening of liver cells.

had low susceptibility to HBV, but HBV could replicate in transgenic mice^[15]. Two research groups established the transgenic mice which could produce HBV envelopes or HBsAg particles in 1985^[16,17]. A high level of HBsAg in circulatory blood could be detected, but no hepatitis was observed in the transgenic mice. The mechanisms of HBV pathogenesis was not caused by virus directly, but closely related to T lymphocyte activation, as demonstrated both *in vitro* and *in vivo*^[18,19]. Ando *et al*^[20] induced a fulminant hepatitis mice model by transferring HBsAg-specific CTLs to HBsAg-transgenic mice, in which there was no human hepatitis B virus. To establish a mice model of human viral hepatitis B by using HBV complete genome transgenic mice with virus replication *in vivo*, we constructed a new eukaryotic expression vector containing HBV complete genome and produced HBV-specific CTLs for adoptive transfer by immunizing non-transgenic syngeneic mice with the recombinant.

HBV complete genome DNA was obtained from *EcoRI* digested pBR322-2HBV and ligated with the vector pcDNA3 which was also digested by *EcoRI*, thus constructing the recombinant pcDNA3-HBV. pcDNA3 is a eukaryotic expression vector. MCS contains the restriction sites of *EcoRI*, *XhoI* and *HindIII*. CMV promoter can express efficiently in many kinds of cells. The immunostimulatory sequences (ISS) of pcDNA3 can not only activate B lymphocytes to produce antibodies, but also stimulate lymphocytes to secrete IL-12, IFN- γ and IL-6. IL-12 and IFN- γ could foster Th1 responses and enhance cell-mediated immunity, while IL-6 could further promote B lymphocyte activation and antibody secretion and also enhance cell-mediated immunity as its primary role^[21,22]. So this vector is a better alternative for gene immunity. The recombinant was constructed by inserting the HBV complete genome to *EcoRI* sites of pcDNA3, with *HindIII* site upstream of *EcoRI* in MCS of pcDNA3 and no *HindIII* site in HBV genes. A single *XhoI* site was at 180 bp upstream of HBV gene. According to these characteristics, restriction endonuclease assay was used to verify whether pcDNA3-HBV contained a complete HBV gene with correct direction. In order to verify the expression of the recombinant in mammal cells, pcDNA3-HBV was transfected into HepG2 cells with lipofectin. Positive clones were selected by G418 resistance. A high level of HBsAg was detected in culture supernatant and HBV PreS1 mRNA expression was proved by RT-PCR. These results could demonstrate that HBV can stably replicate, transcript and express in transfected host cells.

The molecular mechanisms of hepatic cell death and viral clearance during HBV infection have not been illuminated clearly yet. Studies *in vitro* and *in vivo* indicated that hepatic injury caused by HBV infection was immunity mediated^[23-25]. It is considered at present that CTL was the dominate effector molecule during viral clearance, and CTL inducement was the precondition^[26-28]. To simulate human hepatitis after natural HBV infection, we chose HBV complete genome transgenic BALB/c mice as the experimental model. Syngeneic BALB/c mice were undertaken gene immunity by a self-constructed HBV complete genome expression vector to induce HBV specific CTLs. Mice models of viral hepatitis B were established after transgenic mice administrated CTLs with different schemes.

There were two reasons to adopt gene immunity method. First, HBV complete genome recombinant of ayw subtype was constructed because of the transgenic mice containing HBV of the same subtype, while the main component of the present gene vaccines was HBsAg with no definite subtype. Second, generally speaking, humoral immunity could be induced by protein antigens, while cell mediated immunity could be induced by gene immunization^[29-31]. There were several ways of gene transfer for gene immunity, which would influence

immune effect and even determine the type of immunity. Skeletal muscle has been found to be the exclusive tissue that can efficiently ingest and express foreign genes, especially for plasmid DNA^[32,33]. Because of its simpleness and convenience, it has become the dominant method for immunity. After immunized by pcDNA3-HBV once 2-3 wk, HBsAb was detected in the serum of BALB/c mice at the 4th wk. Pretreatment with 250g/L sucrose improved immune effect and induced HBV specific CTLs with a high activity.

The liver would have the most severe pathological changes in viral hepatitis B. The essential changes included degeneration and necrosis of hepatic cells, inflammatory cell infiltration, regeneration of hepatic cells, hyperplasia of fibrous tissue, and increase of serum transaminase^[34,35]. HBV specific CTLs produced by immunized mice were transferred into HBV-transgenic mice. Forty-eight hours later, normal serum protein content and a high level of serum AST and ALT were detected both in negative and blank control groups. The liver stained by HE in the model group showed typical pathological changes of acute viral hepatitis B, while no pathological damage was found in the negative control group. The kidney had no pathological changes in all groups. Acute hepatitis model of mice with HBV complete genome has been established successfully by the above research project, which could mimic human hepatitis B much better because of viral replication and HBV antigens expression in the model. This study would provide a new way for anti-HBV drug screening and mechanism investigation of liver injury due to HBV infection.

REFERENCES

- 1 **Ryu WS.** Molecular aspects of hepatitis B viral infection and the viral carcinogenesis. *J Biochem Mol Biol* 2003; **36**: 138-143
- 2 **Ke WM, Ye YN, Huang S.** Discriminant function for prognostic indexes and probability of death in chronic severe hepatitis B. *J Gastroenterol* 2003; **38**: 861-864
- 3 **Rabe C, Pilz T, Klostermann C, Berna M, Schild HH, Sauerbruch T, Caselmann WH.** Clinical characteristics and outcome of a cohort of 101 patients with hepatocellular carcinoma. *World J Gastroenterol* 2001; **7**: 208-215
- 4 **Wu JM, Lin JS, Chen BT, Zheng XM, Zhao HB, Liang KH.** Establishment and identification of highly expressing and replicating hepatitis B virus genome transgenic mouse models. *Zhonghua Ganzangbing Zazhi* 2003; **11**: 338-340
- 5 **Wieland SF, Vega RG, Muller R, Evans CF, Hilbush B, Guidotti LG, Sutcliffe JG, Schultz PG, Chisari FV.** Searching for interferon-induced genes that inhibit hepatitis B virus replication in transgenic mouse hepatocytes. *J Virol* 2003; **77**: 1227-1236
- 6 **Kimura K, Kakimi K, Wieland S, Guidotti LG, Chisari FV.** Interleukin-18 inhibits hepatitis B virus replication in the livers of transgenic mice. *J Virol* 2002; **76**: 10702-10707
- 7 **Sureau C, Romet-Lemonne JL, Mullins JI, Essex M.** Production of hepatitis B virus by a differentiated human hepatoma cell line after transfection with cloned circular HBV DNA. *Cell* 1986; **47**: 37-47
- 8 **Marinos G, Torre F, Chokshi S, Hussain M, Clarke BE, Rowlands DJ, Eddleston AL, Naoumov NV, Williams R.** Induction of T-helper cell response to hepatitis B: A major factor in activation of the host immune response to the hepatitis B virus. *Heptology* 1995; **22**: 1040-1049
- 9 **Guidotti LG.** The role of cytotoxic T cells and cytokines in the control of hepatitis B virus infection. *Vaccine* 2002; **20**: A80-82
- 10 **Liu DX.** A new hypothesis of pathogenetic mechanism of viral hepatitis B and C. *Med Hypotheses* 2001; **56**: 405-408
- 11 **Sun J, Hou JL, Xiao L, Wang ZH, Luo KX.** Analysis of three lamivudine-resistant HBV mutants with the method of restriction enzyme digestion and its application. *Zhonghua Shiyuan He Linchuang Bingdu Xue Zazhi* 2003; **17**: 18-20
- 12 **Muchmore EA.** Chimpanzee models for human disease and immunobiology. *Immunol Rev* 2001; **183**: 86-93
- 13 **Cooper A, Paran N, Shaul Y.** The earliest steps in hepatitis B virus infection. *Biochim Biophys Acta* 2003; **1614**: 89-96

- 14 **Chang SF**, Netter HJ, Hildt E, Schuster R, Schaefer S, Hsu YC, Rang A, Will H. Duck hepatitis B virus expresses a regulatory HBx-like protein from a hidden open reading frame. *J Virol* 2001; **75**: 161-170
- 15 **Raney AK**, Eggers CM, Kline EF, Guidotti LG, Pontoglio M, Yaniv M, McLachlan A. Nuclear covalently closed circular viral genomic DNA in the liver of hepatocyte nuclear factor 1 alpha-null hepatitis B virus transgenic mice. *J Virol* 2001; **75**: 2900-2911
- 16 **Babinet C**, Farza H, Morello D, Hadchouel M, Pourcel C. Specific expression of hepatitis B surface antigen (HBsAg) in transgenic mice. *Science* 1985; **230**: 1160-1163
- 17 **Chisari FV**, Pinkert CA, Milich DR, Filippi P, McLachlan A, Palmiter RD, Brinster RL. A transgenic mouse model of the chronic hepatitis B surface antigen carrier state. *Science* 1985; **230**: 1157-1160
- 18 **Guidotti LG**, Matzke B, Schaller H, Chisari FV. High level hepatitis B virus replication in transgenic mice. *J Virol* 1995; **69**: 6158-6169
- 19 **Kao JH**, Chen PJ, Lai MY, Chen DS. Basal core promoter mutations of hepatitis B virus increase the risk of hepatocellular carcinoma in hepatitis B carriers. *Gastroenterology* 2003; **124**: 327-334
- 20 **Ando K**, Moriyama T, Guidotti LG, Wirth S, Schreiber RD, Schlicht HJ, Huang SN, Chisari FV. Mechanisms of class I restricted immunopathology. A transgenic mouse model of fulminant hepatitis. *J Exp Med* 1993; **178**: 1541-1554
- 21 **Roman M**, Martin-Orozco E, Goodman JS, Nguyen MD, Sato Y, Ronaghy A, Kornbluth RS, Richman DD, Carson DA, Raz E. Immunostimulatory DNA sequences function as T-helper-1-promoting adjuvants. *Nat Med* 1997; **3**: 849-854
- 22 **Klinman DM**, Yamshchikov G, Ishigatsubo Y. Contribution of CpG motifs to the immunogenicity of DNA vaccines. *J Immunol* 1997; **158**: 3635-3639
- 23 **Moriyama T**, Guillhot S, Klopchin K, Moss B, Pinkert CA, Palmiter RD, Brinster RL, Kanagawa O, Chisari FV. Immunobiology and pathogenesis of hepatocellular injury in hepatitis B virus transgenic mice. *Science* 1990; **248**: 361-364
- 24 **Tang TJ**, Kwekkeboom J, Iaman JD, Niesters HG, Zondervan PE, De Man RA, Schalm SW, Janssen HL. The role of intrahepatic immune effector cells in inflammatory liver injury and viral control during chronic hepatitis B infection. *J Viral Hepat* 2003; **10**: 159-167
- 25 **Kasahara S**, Ando K, Saito K, Sekikawa K, Ito H, Ishikawa T, Ohnishi H, Seishima M, Kakumu S, Moriwaki H. Lack of tumor necrosis factor alpha induces impaired proliferation of hepatitis B virus-specific cytotoxic T lymphocytes. *J Virol* 2003; **77**: 2469-2476
- 26 **Sobao Y**, Sugi K, Tomiyama H, Saito S, Fujiyama S, Morimoto M, Hasuike S, Tsubouchi H, Tanaka K, Takiguchi M. Identification of hepatitis B virus-specific CTL epitopes presented by HLA-A*2402, the most common HLA class I allele in East Asia. *J Hepatol* 2001; **34**: 922-929
- 27 **Roh S**, Lee YK, Ahn BY, Kim K, Moon A. Induction of CTL responses and identification of a novel epitope of hepatitis B virus surface antigens in C57BL/6 mice immunized with recombinant vaccinia viruses. *Virus Res* 2001; **73**: 17-26
- 28 **Street M**, Herd K, Londono P, Doan T, Dougan G, Kast WM, Tindle RW. Differences in the effectiveness of delivery of B- and CTL-epitopes incorporated into the hepatitis B core antigen (HBcAg) c/e1-region. *Arch Virol* 1999; **144**: 1323-1343
- 29 **Prugnaud JL**. DNA vaccines. *Ann Pharm Fr* 2003; **61**: 219-233
- 30 **Wang J**, Murakami T, Yoshida S, Matsuoka H, Ishii A, Tanaka T, Tobita K, Ohtsuki M, Nakagawa H, Kusama M, Kobayashi E. Predominant cell-mediated immunity in the oral mucosa: gene gun-based vaccination against infectious diseases. *J Dermatol Sci* 2003; **31**: 203-210
- 31 **Isaguliant MG**, Petrakova NV, Mokhonov VV, Pokrovskaya K, Suzdaltzeva YG, Krivonos AV, Zaberezhny AD, Garaev MM, Smirnov VD, Nordenfelt E. DNA immunization efficiently targets conserved functional domains of protease and ATPase/helicase of nonstructural 3 protein (NS3) of human hepatitis C virus. *Immunol Lett* 2003; **88**: 1-13
- 32 **Wolff JA**, Malone RW, Williams P, Chong W, Acsadi G, Jani A, Felgner PL. Direct gene transfer into mouse muscle *in vivo*. *Science* 1990; **247**(4949 Pt 1): 1465-1468
- 33 **Corr M**, von Damm A, Lee DJ, Tighe H. *In vivo* priming by DNA injection occurs predominantly by antigen transfer. *J Immunol* 1999; **163**: 4721-4727
- 34 **Myers RP**, Tainturier MH, Ratzliff V, Piton A, Thibault V, Imbert-Bismut F, Messous D, Charlotte F, Di Martino V, Benhamou Y, Poinard T. Prediction of liver histological lesions with biochemical markers in patients with chronic hepatitis B. *J Hepatol* 2003; **39**: 222-230
- 35 **Wang FS**. Current status and prospects of studies on human genetic alleles associated with hepatitis B virus infection. *World J Gastroenterol* 2003; **9**: 641-644

Edited by Zhang JZ and Wang XL Proofread by Xu FM

Sequence evolution of putative cytotoxic T cell epitopes in NS3 region of hepatitis C virus

Hua-Zhang Guo, Ying Yin, Wen-Liang Wang, Chuan-Shan Zhang, Tao Wang, Zhe Wang, Jing Zhang, Hong Cheng, Hai-Tao Wang

Hua-Zhang Guo, Wen-Liang Wang, Chuan-Shan Zhang, Tao Wang, Zhe Wang, Jing Zhang, Hong Cheng, Department of Pathology, Xijing Hospital, Fourth Military Medical University, Xi'an 710033, Shaanxi Province, China

Ying Yin, Department of Clinical Laboratories, Xijing Hospital, Fourth Military Medical University, Xi'an 710033, Shaanxi Province, China

Hai-Tao Wang, Institute of Microbiology and Epidemiology, Academy of Military Medical Sciences, Beijing 100071, China

Correspondence to: Wen-Liang Wang, Department of Pathology, Xijing Hospital, Fourth Military Medical University, Xi'an 710033, Shaanxi Province, China. wliwang@fmmu.edu.cn

Telephone: +86-29-3374595 **Fax:** +86-29-3284284

Received: 2003-10-20 **Accepted:** 2003-12-16

Abstract

AIM: Quasispecies of hepatitis C virus (HCV) are the foundation for rapid sequence evolution of HCV to evade immune surveillance of hosts. The consensus sequence evolution of a segment of HCV NS3 region, which encompasses putative cytotoxic T cell epitopes, was evaluated.

METHODS: Three male patients, infected with HCV through multiple transfusions, were identified from clinical symptoms and monitored by aminotransferase for 60 months. Blood samples taken at months 0, 32, and 60 were used for viral RNA extraction. A segment of HCV NS3 region was amplified from the RNA extraction by RT-PCR and subjected to subcloning and sequencing. HLA types of these three patients were determined using complement-dependent microlymphocytotoxic assay. CTL epitopes were predicted using MHC binding motifs.

RESULTS: No patient had clinical symptoms or elevation of aspartate/alanine aminotransferase. Two patients showed positive HCV PCR results at all 3 time points. The other one showed a positive HCV PCR result only at month 0. A reported HLA-A2-restricted CTL epitope had no alteration in the HLA-A2-negative carrier over 60 months. In the HLA-A2-positive individuals, all the sequences from 0 month 0 showed an amber mutation on the initial codon of the epitope. Most changes of consensus sequences in the same patient occurred on predicted cytotoxic T cell epitopes.

CONCLUSION: Amber mutation and changes of consensus sequence in HCV NS3 region may be related to viral immune escape.

Guo HZ, Yin Y, Wang WL, Zhang CS, Wang T, Wang Z, Zhang J, Cheng H, Wang HT. Sequence evolution of putative cytotoxic T cell epitopes in NS3 region of hepatitis C virus. *World J Gastroenterol* 2004; 10(6): 847-851

<http://www.wjgnet.com/1007-9327/10/847.asp>

INTRODUCTION

Hepatitis C virus (HCV) is one of the main pathogens of

transfusion-associated hepatitis. After acute transfusion-associated HCV infection, about 70-80% of the patients may progress to chronicity. Although many patients with chronic hepatitis C have no symptoms, cirrhosis may develop in 20% within 10 to 20 years after acute infection. The risk for hepatocellular carcinoma is increased in patients with chronic hepatitis C and almost exclusively in patients with cirrhosis^[1-15].

HCV is a linear, single-stranded positive-sense, 9400-nucleotide RNA virus. HCV constitutes its own genus in the family *Flaviviridae*. The HCV genome contains a single large open reading frame that codes for a virus polyprotein of approximately 3000 amino acids. Due to the high mutation rate of RNA dependent RNA polymerase, there are genotype and quasispecies diversity of HCV^[16-19]. The high mutation rate may interfere with effective immunity and cause the progression to chronicity^[20, 21].

Of the components of adaptive immunity, cytotoxic T cells play an important role in eliminating intracellular infections^[22]. They recognize body cells infected with viruses by detecting peptide fragments derived from viruses bound to MHC class I molecules on the infected body cells. Then, they kill the infected cells before viral replications complete. In this study, 3 patients with transfusion-associated hepatitis C were followed-up for 60 mo to evaluate the evolution of cytotoxic T cell epitopes in the HCV NS3 region.

MATERIALS AND METHODS

Patients

Patients C, Z and W, being 43, 48 and 49 years old Chinese males, were infected with HCV through multiple transfusions. They were followed-up for 60 mo after identification. During the follow-up period, no elevation of aspartate/alanine aminotransferase was found. Their peripheral blood was collected at mo 0 (the time of identification), 32 and 60, and stored at -70 °C. Patients C and Z were positive for HCV RNA. Patient W was positive for HCV RNA only in the blood sample taken at mo 0 and consistently negative after that.

HLA typing

HLA types of the three patients were assessed by using the Tasaki HLA class I dry tissue typing tray (One Lambda, Canoga Park, CA). Briefly, blood samples were drawn and lymphocytes were isolated immediately. After antibody and 2×10^6 lymphocytes were mixed in each well, 1 μ L of complement was added into each well to incubate at room temperature for 1 hour. After incubation, the cells were stained with eosin and fixed with formaldehyde. Positive (dead) lymphocytes appeared dark and non-refractiles with eosin dye.

RNA extraction and RT-PCR

Single step guanidine thiocyanate-chloroform method^[23] was used to extract HCV RNA from 50 μ L of plasma. RNA extracted was reverse-transcribed using random primers. Nested PCR (primers see Table 1) was used to amplify the HCV NS3 region that spanned a reported cytotoxic T cell

epitope (-KLVALGINAV-)^[24], which is HLA-A2-restricted. The first round PCR was run for 35 cycles with denaturing at 94 °C for 1 min, annealing at 53 °C for 1 min, and elongating at 72 °C for 1 min. The second round of PCR was run for 35 cycles with denaturing at 94 °C for 1 min, annealing at 60 °C for 1 min, and elongating at 72 °C for 1 min.

Cloning and sequencing of amplified segment of HCV NS3

PCR products were subcloned into M13mp19 phage. For each blood sample, 5 clones were selected and amplified. The single strand DNA produced by the M13mp19 phage was purified by QIAprep Spin 13 kit (Qiagen, Valencia, CA) and sequenced using sequence version 2.0 sequencing kit (USB, Cleveland, OH).

Sequence analysis

DNA sequences were translated and aligned. Consensus sequence was produced for every 5 clones of each blood sample. Cytotoxic T cell epitopes for each consensus sequence were predicted based on the HLA type of the patients and MHC molecule binding motifs^[25].

RESULTS

HLA types

Patient C was (A11, 30; B13, -; Bw4, -). Patient Z was [A2, 11; B60 (40), 70; Bw6, -]. Patient W was [A2, 11; B40, 55 (22); Bw6, -].

Nucleotide sequences of HCV

Five clones of NS3 sequences were ascertained for each blood sample. Since all the blood samples of patients C and Z were positive for HCV RNA, 15 sequences were obtained from each one of them. Due to the negative result of HCV RNA in the later 2 blood samples in patient W, only 5 cDNA sequences

were obtained. The GenBank accession numbers for all the sequences are in Table 2. The translated amino acid sequences are aligned in Figure 1.

Table 2 Assigned accession number for each nucleotide sequence of three patients

Time point measured	Patient W	Patient C	Patient Z
0 mo	AF051270	AF051261	AF051270
	AF051270	AF051261	AF051270
	AF051271	AF051261	AF051270
	AF051272	AF051260	AF051270
	AF051273	AF051259	AF051270
32 th mo	NA	AF051254	AF051265
		AF051255	AF051266
		AF051256	AF051267
		AF051257	AF051268
		AF051258	AF051269
60 th mo	NA	AF051253	AF051262
		AF051253	AF051262
		AF051253	AF051263
		AF051253	AF051263
		AF051253	AF051264

NA: not applicable as the sample was PCR negative for HCV RNA.

Sequence variation on reported cytotoxic T cell epitope

Our consensus sequences showed (K/*)LSSLGLNAV (*: stop codon) on the site of the reported HLA-A2-restricted cytotoxic T cell epitope^[24]. In patient C, who was not HLA-A2-restricted, all the 15 sequences were KLSSLGLNAV. In patient W, who was HLA-A2-restricted, all the 5 sequences showed a stop codon at the beginning of this peptide (four sequences showed

Table 1 Oligonucleotides used to amplify the NS3 region*

	Primer sequences	Strand	Nucleotide position in HCV genome
First round primers (5' -3')	CCCCATCAC(A/G)TACTC(C/T)ACCTA	+	4 197
	ACA(C/T)GT(A/G)TT(G/A)CAGTC(T/G)ATCAC	-	4 681
Second round primers (5' -3')	CGAGGATCCGTCCT(T/G)GACCAAGC(A/G)GAGAC	+	4 315
	GCAACTGCAGCT(G/A)G(T/A)(C/T)GG(G/T)ATGAC(A/G)GACAC	-	4 597

*Degenerate primers were used to cover the variable HCV genomes.

Table 3 Predicted CTL epitopes by MHC binding peptide motifs while incorporating persistent substitutions

Patient	HLA subtype	MHC binding peptide motif ^[38, 39]	Genome position	Predicted epitope	Time point measured
C	A11	X[MLIVSATGNCDF]XXXXXX[KRHY]	1 349	ATPPGSITVPH*	0 mo
			1 378	ATPPGSVTVPH*	32 th , 60 th mo
				KAIPIEAIR	0 mo
Z	A11	X[MLIVSATGNCDF]XXXXXX[KRHY]		KAIPIEAIK	32 th , 60 th mo
				PIEAIKGGGR	0 mo
				PIEAIKGGGR	32 th , 60 th mo
	A2	X[LMIVAT]XXXXXX[LVIAMT]	1 347	ATATPPGSV	0 mo
			1 348	ATATPPGSI	32 th , 60 th mo
			1 349	TATPPGSVT	0 mo
	TATPPGSIT	32 th , 60 th mo			
	ATPPGSVTV	0 mo			
	ATPPGSITV	32 th , 60 th mo			

*These two peptides fitted the MHC binding motif because proline and glycine residues allowed flexibility which made the peptides accommodate to the motif by kinking in the peptide backbone^[40].

*LSSLGLNAV and one sequence showed *LSPLGLNAV). In patient Z, who was also HLA-A2-restricted, all the sequences from 0-mo showed the stop codon at the beginning of the epitope (*LSSLGLNAV), nine sequences from blood samples at mo 32 and 60 showed KLSSLGLNAV, one sequence from blood sample at mo 32 showed KLSSLGLKPV.

Sequence variation on predicted cytotoxic T cell epitopes

Using MHC binding motifs to predict cytotoxic T cell epitopes, we found that most sites which showed changes of consensus sequences between successive blood samples were on the predicted cytotoxic T cell epitopes (Table 3).

DISCUSSION

Due to errors of the RNA-dependent RNA polymerase, RNA genomes had a relatively high mutation rate^[25,26]. RNA viruses evolve as complex distributions of mutants termed viral quasispecies. These coexisting mutant genomes always have a consensus or master sequence. Despite the potentially high mutation rate and variability of RNA viruses, changes in the consensus sequence of a viral population would occur only if some selection mechanism acted on the population and caused a shift in the population equilibrium^[27]. Immune response of the host can influence the distribution between different viral variants and will consequently cause a change in the consensus

Patient W

0 mo
 1340 1350 1360 1370 1380 1390 1400 1410 1420
 Consensus AGARLVVLTATATPPGSVTVPHPNIQEVGLSNTGEIPFYGKAIP IEA IKGGRHLIFCHSKKKCDELA A*LSSLGLNAVAYYRGLD
 Clone 1
 Clone 2
 Clone 3
 Clone 4P.....
 Clone 5P.....

Patient Z

0 mo
 1340 1350 1360 1370 1380 1390 1400 1410 1420
 Consensus AGARLVVLTATATPPGSVTVPHPNIQEVGLSNTGEIPFYGKAIP IEA IKGGRHLIFCHSKKKCDELA A*LSSLGLNAVAYYRGLD
 Clone 1
 Clone 2
 Clone 3
 Clone 4
 Clone 5

32th mo

1340 1350 1360 1370 1380 1390 1400 1410 1420
 Consensus AGARLVVLTATATPPGSITVPHPNIQEVALSNTGEIPFYGKAIP IEA IRGGRHLIFCHSKKKCDELA AKLSSLGLNAVAYYRGLD
 Clone 1
 Clone 2
 Clone 3
 Clone 4P.....
 Clone 5K.....

60th mo

1340 1350 1360 1370 1380 1390 1400 1410 1420
 Consensus AGARLVVLTATATPPGSITVPHPNIQEVALSNTGEIPFYGKAIP IEA IRGGRHLIFCHSKKKCDELA AKLSSLGLNAVAYYRGLD
 Clone 1
 Clone 2
 Clone 3
 Clone 4
 Clone 5KP.....

Patient C

0 mo
 1340 1350 1360 1370 1380 1390 1400 1410 1420
 Consensus AGARLVVLTATATPPGSITVPHPNIQEVALSNTGEIPFYGKAIP IEA IKGGRHLIFCHSKKKCDELA AKLSSLGLNAVAYYRGLD
 Clone 1
 Clone 2
 Clone 3
 Clone 4R.....
 Clone 5

32th mo

1340 1350 1360 1370 1380 1390 1400 1410 1420
 Consensus AGARLVVLTATATPPGSVTVPHPNIQEVALSNTGEIPFYGKAIP IEA IKGGRHLIFCHSKKKCDELA AKLSSLGLNAVAYYRGLD
 Clone 1
 Clone 2
 Clone 3
 Clone 4
 Clone 5T.....

60th mo

1340 1350 1360 1370 1380 1390 1400 1410 1420
 Consensus AGARLVVLTATATPPGSVTVPHPNIQEVALSNTGEIPFYGKAIP IEA IKGGRHLIFCHSKKKCDELA AKLSSLGLNAVAYYRGLD
 Clone 1
 Clone 2
 Clone 3
 Clone 4
 Clone 5

Figure 1 Alignment of HCV amino acid sequences from three patients. Consensus sequences were given for the 5 sequences from the same blood sample.

sequence. A cellular immune-driven selection pressure has been demonstrated by the existence of HCV escape mutants in relation to cytotoxic T cell epitopes^[28]. In the HCV-infected human, the NS3 protein seems to be fairly immunogenic. T cell activation in response to NS3 has been detected in a number of studies of patients with acute or chronic HCV infection^[24, 29]. It was proposed that a strong *in vitro* T cell reaction to NS3 correlated with clearance of acute HCV infection whereas a less vigorous, or absent, NS3-specific T cell reactivity was observed in those who progressed to chronicity^[30]. Thus, in this study, we chose a segment of HCV NS3 region as our focus on sequence evolution.

T lymphocytes recognize their antigens in context of MHC-encoded molecules, a phenomenon called MHC restriction. Our sequence segment encompassed a cytotoxic T cell epitope, which was restricted by HLA-A2 and reported by Rehmann *et al*^[24]. In patients with HLA-A2 allele, their viral consensus sequences showed stop codons at the initial part of this epitope. On the contrary, in patients without HLA-A2 allele, their viral consensus sequences did not show the stop codon. Normally, stop codons are generated by random non-sense mutations in RNA virus and they are expected to occur randomly throughout the entire coding region. Viruses with stop codon in the open reading frame have been found to be defective viruses which usually make a small fraction of the RNA virus quasispecies^[31,32]. Here, stop codons were unusually concentrated at the beginning of the reported epitope, in the sequences of patients with HLA-A2 allele, suggesting that they are specifically selected by some pressure, probably by cytotoxic T cells. We would suppose that HCV specific and HLA-A2-restricted cytotoxic T cells, which recognize and kill the infected hepatocytes to prevent replication and proliferation of the viruses, were generated in patients W and Z. Under this immune pressure, viral quasispecies in these two patients would have shifted toward a new equilibrium to avoid the immune attack. In patients W and Z, the defective viruses, which did not express the reported cytotoxic T cell epitope, dominated the viral quasispecies at month 0. This may reflect the strong immune pressure at that time. Thirty-two months later, in patient W, the viruses were cleared and the patient was recovered. In patient Z, the viruses were not cleared at month 32 or 60, suggesting that the viral quasispecies escaped from the immune pressure and survived.

Cytotoxic T cells could recognize peptides loaded on the MHC class I molecules^[33]. The solution of the crystal structure of MHC class I molecules could reveal peptide-binding groove made up by $\alpha 1$ and $\alpha 2$ domains of heavy chains^[34,35]. Naturally occurring processed peptides have been isolated from purified MHC class I molecules. Analyzing their sequences revealed the presence of simple amino acid sequence motifs that were specific to particular allelic forms of class I molecules^[36]. Based on the sequence motifs, we found that most sites, with changes of the consensus sequences, were on the putative cytotoxic T cell epitopes in the corresponding patients, implying the possible underlying immune impetus for sequence evolution.

In summary, by molecular sequencing, the quasispecies nature and sequence evolution of HCV NS3 region can be revealed. By HLA typing and epitope prediction, the non-sense mutation and changes of consensus sequences might be the result of immune pressure. This study has paved the way for further cytotoxicity assay^[37] to confirm the possible immune target sites of HCV.

REFERENCES

- National Institutes of Health Consensus Development Conference Panel statement: management of hepatitis C. *Hepatology* 1997; **26**(3 Suppl): 2S-10S
- Maier I, Wu GY. Hepatitis C and HIV co-infection: a review. *World J Gastroenterol* 2002; **8**: 577-579
- Meier V, Mihm S, Braun Wietzke P, Ramadori G. HCV-RNA positivity in peripheral blood mononuclear cells of patients with chronic HCV infection: does it really mean viral replication? *World J Gastroenterol* 2001; **7**: 228-234
- Chen MY, Huang ZQ, Chen LZ, Gao YB, Peng RY, Wang DW. Detection of hepatitis C virus NS5 protein and genome in Chinese carcinoma of the extrahepatic bile duct and its significance. *World J Gastroenterol* 2000; **6**: 800-804
- He QQ, Cheng RX, Sun Y, Feng DY, Chen ZC, Zheng H. Hepatocyte transformation and tumor development induced by hepatitis C virus NS3 c-terminal deleted protein. *World J Gastroenterol* 2003; **9**: 474-478
- Li K, Wang L, Cheng J, Lu YY, Zhang LX, Mu JS, Hong Y, Liu Y, Duan HJ, Wang G, Li L, Chen JM. Interaction between hepatitis C virus core protein and translin protein—a possible molecular mechanism for hepatocellular carcinoma and lymphoma caused by hepatitis C virus. *World J Gastroenterol* 2003; **9**: 300-303
- Worman HJ, Lin F. Molecular biology of liver disorders: the hepatitis C virus and molecular targets for drug development. *World J Gastroenterol* 2000; **6**: 465-469
- Nelson DR, Marousis CG, Davis GL, Rice CM, Wong J, Houghton M, Lau JY. The role of hepatitis C virus-specific cytotoxic T lymphocytes in chronic hepatitis C. *J Immunol* 1997; **158**: 1473-1481
- Assy N, Minuk G. A comparison between previous and present histologic assessments of chronic hepatitis C viral infections in humans. *World J Gastroenterol* 1999; **5**: 107-110
- Caselmans WH, Serwe M, Lehmann T, Ludwig J, Sproat BS, Engels JW. Design, delivery and efficacy testing of therapeutic nucleic acids used to inhibit hepatitis C virus gene expression *in vitro* and *in vivo*. *World J Gastroenterol* 2000; **6**: 626-629
- Chen LK, Hwang SJ, Tsai ST, Luo JC, Lee SD, Chang FY. Glucose intolerance in Chinese patients with chronic hepatitis C. *World J Gastroenterol* 2003; **9**: 505-508
- Fan XG, Tang FQ, Ou ZM, Zhang JX, Liu GC, Hu GL. Lymphoproliferative response to hepatitis C virus (HCV) antigens in patients with chronic HCV infection. *Shijie Huaren Xiaohua Zazhi* 1999; **7**: 1038-1040
- Song ZQ, Hao F, Zhang J, Gu CH. Detection of antibodies against hypervariable region 1 in sera from patients with hepatitis C. *Shijie Huaren Xiaohua Zazhi* 1999; **7**: 666-668
- Wu HB, Li ZW, Li Y. Clinical significance of detection of positive and negative strands of HCV RNA in peripheral blood mononuclear cells. *Shijie Huaren Xiaohua Zazhi* 1999; **7**: 220-221
- Zhou YX, Feng ZH, Jia ZS, Lian JQ, Li JG, Li WB. A study of gene immunization with recombinant expression plasmid of hepatitis C virus core antigen. *Shijie Huaren Xiaohua Zazhi* 1998; **6**: 966-968
- Major ME, Feinstone SM. The molecular virology of hepatitis C. *Hepatology* 1997; **25**: 1527-1538
- Chen S, Wang YM. Genetic evolution of structural region of hepatitis C virus in primary infection. *World J Gastroenterol* 2002; **8**: 686-693
- Flichman D, Kott V, Sookoian S, Campos R. Acute hepatitis C in a chronically HIV-infected patient: Evolution of different viral genomic regions. *World J Gastroenterol* 2003; **9**: 1496-1500
- Chen YD, Liu MY, Yu WL, Li JQ, Dai Q, Zhou ZQ, Tsiminetzky SG. Mix-infections with different genotypes of HCV and with HCV plus other hepatitis viruses in patients with hepatitis C in China. *World J Gastroenterol* 2003; **9**: 984-992
- Weiner AJ, Geysen HM, Christopherson C, Hall JE, Mason TJ, Saracco G, Bonino F, Crawford K, Marion CD, Crawford KA. Evidence for immune selection of hepatitis C virus (HCV) putative envelope glycoprotein variants: potential role in chronic HCV infections. *Proc Natl Acad Sci U S A* 1992; **89**: 3468-3472
- Rehmann B, Chang KM, McHutchison JG, Kokka R, Houghton M, Chisari FV. Quantitative analysis of the peripheral blood cytotoxic T lymphocyte response in patients with chronic hepatitis C virus infection. *J Clin Invest* 1996; **98**: 1432-1440
- Li CP, Wang KX, Wang J, Pan BR. mL-2R, T cell subsets & hepatitis C. *World J Gastroenterol* 2002; **8**: 298-300
- Chomczynski P, Sacchi N. Single-step method of RNA isolation by acid guanidinium thiocyanate-phenol-chloroform extraction.

- Anal Biochem* 1987; **162**: 156-159
- 24 **Rehermann B**, Chang KM, McHutchinson J, Kokka R, Houghton M, Rice CM, Chisari FV. Differential cytotoxic T-lymphocyte responsiveness to the hepatitis B and C viruses in chronically infected patients. *J Virol* 1996; **70**: 7092-7102
- 25 **Guo H**, Wang W, Wang T. An application of T cell epitope prediction computer program in the study of HCV adaptive immune responses. *Disi Junyi Daxue Xuebao* 1999; **20**: 845-848
- 26 **Huang F**, Zhao GZ, Li Y. HCV genotypes in hepatitis C patients and their clinical significances. *World J Gastroenterol* 1999; **5**: 547-549
- 27 **Elena SF**, Miralles R, Cuevas JM, Turner PE, Moya A. The two faces of mutation: extinction and adaptation in RNA viruses. *IUBMB Life* 2000; **49**: 5-9
- 28 **Wodarz D**. Hepatitis C virus dynamics and pathology: the role of CTL and antibody responses. *J Gen Virol* 2003; **84**(Pt 7): 1743-1750
- 29 **Encke J**, zu Putlitz J, Geissler M, Wands JR. Genetic immunization generates cellular and humoral immune responses against the nonstructural proteins of the hepatitis C virus in a murine model. *J Immunol* 1998; **161**: 4917-4923
- 30 **Wertheimer AM**, Miner C, Lewinsohn DM, Sasaki AW, Kaufman E, Rosen HR. Novel CD4+ and CD8+ T-cell determinants within the NS3 protein in subjects with spontaneously resolved HCV infection. *Hepatology* 2003; **37**: 577-589
- 31 **Martell M**, Esteban JI, Quer J, Genesca J, Weiner A, Esteban R, Guardia J, Gomez J. Hepatitis C virus (HCV) circulates as a population of different but closely related genomes: quasispecies nature of HCV genome distribution. *J Virol* 1992; **66**: 3225-3229
- 32 **Higashi Y**, Kakumu S, Yoshioka K, Wakita T, Mizokami M, Ohba K, Ito Y, Ishikawa T, Takayanagi M, Nagai Y. Dynamics of genome change in the E2/NS1 region of hepatitis C virus *in vivo*. *Virology* 1993; **197**: 659-668
- 33 **Androlewicz MJ**. Peptide generation in the major histocompatibility complex class I antigen processing and presentation pathway. *Curr Opin Hematol* 2001; **8**: 12-16
- 34 **Khan AR**, Baker BM, Ghosh P, Biddison WE, Wiley DC. The structure and stability of an HLA-A*0201/octameric tax peptide complex with an empty conserved peptide-N-terminal binding site. *J Immunol* 2000; **164**: 6398-6405
- 35 **Sliz P**, Michielin O, Cerottini JC, Luescher I, Romero P, Karplus M, Wiley DC. Crystal structures of two closely related but antigenically distinct HLA-A2/melanocyte-melanoma tumor-antigen peptide complexes. *J Immunol* 2001; **167**: 3276-3284
- 36 **Davenport MP**, Smith KJ, Barouch D, Reid SW, Bodnar WM, Willis AC, Hunt DF, Hill AV. HLA class I binding motifs derived from random peptide libraries differ at the COOH terminus from those of eluted peptides. *J Exp Med* 1997; **185**: 367-371
- 37 **Zhou HC**, Xu DZ, Wang XP, Zhang JX, Huang Y, Yan YP, Zhu Y, Jin BQ. Identification of the epitopes on HCV core protein recognized by HLA-A2 restricted cytotoxic T lymphocytes. *World J Gastroenterol* 2001; **7**: 583-586
- 38 **Reche PA**, Glutting JP, Reinherz EL. Prediction of MHC class I binding peptides using profile motifs. *Hum Immunol* 2002; **63**: 701-709
- 39 **Rammensee H**, Bachmann J, Emmerich NP, Bachor OA, Stevanovic S. SYFPEITHI: database for MHC ligands and peptide motifs. *Immunogenetics* 1999; **50**: 213-219
- 40 **Guo HC**, Jardetzky TS, Garrett TP, Lane WS, Strominger JL, Wiley DC. Different length peptides bind to HLA-Aw68 similarly at their ends but bulge out in the middle. *Nature* 1992; **360**: 364-366

Edited by Chen WW and Wang XL Proofread by Xu FM

Establishment of *Helicobacter pylori* infection model in Mongolian gerbils

Jie Yan, Yi-Hui Luo, Ya-Fei Mao

Jie Yan, Yi-Hui Luo, Ya-Fei Mao, Department of Medical Microbiology and Parasitology, College of Medical Science, Zhejiang University, Hangzhou 310031, China

Supported by the Excellent Young Teacher Fund of Chinese Education Ministry and the General Research Plan of the Science and Technology Department of Zhejiang Province, No. 001110438

Correspondence to: Jie Yan, Department of Medical Microbiology and Parasitology, College of Medical Science, Zhejiang University, 353 Yan an Road, Hangzhou 310031, Zhejiang Province, China. yanchen@mail.hz.zj.cn

Telephone: +86-571-87217385 **Fax:** +86-571-87217044

Received: 2003-09-15 **Accepted:** 2003-11-13

Abstract

AIM: To establish a stable and reliable model of *Helicobacter pylori* infection model in Mongolian gerbils and to observe pathological changes in gastric mucosa in infected animals.

METHODS: Mongolian gerbils were randomly divided into 18 groups; 6 groups were infected with *H pylori* clinical strain Y06 ($n=6$, groups Y), 6 groups were infected with *H pylori* strain NCTC11637 ($n=6$, groups N), and 6 uninfected groups as negative controls ($n=4$, groups C). *H pylori* suspensions at the concentrations of 2×10^8 and 2×10^9 CFU/mL of strain NCTC11637 and strain Y06 were prepared. The animals in three groups N and in three groups Y were orally challenged once with 0.5 mL of the low concentration of the bacterial suspension. The animals in another three groups N and in another three groups Y were orally challenged with 0.5 mL of the high concentration of the bacterial suspension for 3 times at the intervals of 24 h, respectively. For the negative controls, the animals in six groups C were orally given with the same volume of Brucella broth at the corresponding inoculating time. The animals were killed after 2nd, 4th and 6th week after the last challenge and the gastric mucosal specimens were taken for urease test, bacterial isolation, pathological and immunohistochemical examinations.

RESULTS: Positive isolation rates of *H pylori* in the animals of groups Y at the 2nd, 4th and 6th week after one challenge were 0%, 16.7% and 66.7%, while in the animals of groups N were 0%, 0% and 16.7%, respectively. Positive isolation rates of *H pylori* in the animals of groups Y at the 2nd, 4th and 6th week after three challenges were 66.7%, 100% and 100%, while in the animals of groups N were 66.7%, 66.7% and 100%, respectively. In animals with positive isolation of *H pylori*, the bacterium was found to colonized on the surface of gastric mucosal cells and in the gastric pits, and the gastric mucosal lamina propria was infiltrated with inflammatory cells.

CONCLUSION: By using *H pylori* suspension at high concentration of 2×10^9 CFU/mL for multiple times, the orally challenged Mongolian gerbils can be used as a stable and reliable *H pylori* infection model. The 2 strains of *H pylori* can colonize in gastric mucosa of the infected animals and

cause mild inflammation reaction.

Yan J, Luo YH, Mao YF. Establishment of *Helicobacter pylori* infection model in Mongolian gerbils. *World J Gastroenterol* 2004; 10(6): 852-855

<http://www.wjgnet.com/1007-9327/10/852.asp>

INTRODUCTION

Helicobacter pylori, a microaerophilic, spiral and Gram-negative bacillus, is recognized as an important pathogen causing human gastritis and peptic ulcer and a high risk factor for gastric carcinoma^[1,2]. In China, chronic gastritis and peptic ulcer are two of the most common digestive diseases, and gastric cancer is one of the malignant tumors with high morbidities^[3-34]. An ideal public measure to prevent and control these *H pylori* infection-associated diseases may be a vaccine that could induce strong humoral and cellular immune responses. However, no commercial *H pylori* vaccine is available so far, and the development of *H pylori* vaccine by using genetic engineering techniques is being active^[35-39]. A stable and reliable *H pylori* infection animal model would be necessary for evaluating vaccine efficacy and helpful for understanding the pathological mechanism of the organism. Therapeutic drugs for *H pylori* eradication differ from those for many other bacteria such as using metronidazole^[40,41]. Therefore, *H pylori* infection animal models would contribute to screen new drugs against *H pylori*. In recent published data, Mongolian gerbils have been considered as ideal animals to establish infection model by using internationally collected *H pylori* strains^[42-44]. In this study, we used a clinical *H pylori* isolate named Y06 to establish a stable and reliable infection model in Mongolian gerbils. The colonization sites of *H pylori* and pathological changes in gastric mucosa of the animals were also observed.

MATERIALS AND METHODS

H pylori strains

A clinical strain of *H pylori* named Y06 was isolated from a patient with gastric ulcer. This strain was identified based on their characteristic morphology by Gram staining under microscope, and positive for urease and oxidase activities, further confirmed by slide agglutination test using commercial rabbit antiserum against whole cell of *H pylori* (DAKO). A reference *H pylori* strain, NCTC11637, was used as an infection control. The two strains were subcultured in Columbia agar (bioMérieux) containing 80 mL/L sheep blood under microaerobic conditions containing 100 mL/L CO₂, 50 mL/L O₂ and 850 mL/L N₂.

Animals

Eight-week-old specific pathogen-free male Mongolian gerbils with body mass of 75 ± 5 g were provided by Experimental Animal Center, Zhejiang Academy of Medical Sciences. These gerbils were randomly divided into eighteen groups: six groups infected with the clinical strain Y06 (groups Y, $n=6$ in each group), six groups infected with the reference *H pylori* strain NCTC11637

(groups N, $n=6$ in each group) and six groups as negative controls (groups C, $n=4$ in each group).

Dosages and pathway of inoculation

Bacterial cells grown on the 2 strains on Columbia agar for 3–5 d were collected and diluted to the final concentrations of 2×10^8 CFU/mL and 2×10^9 CFU/mL, respectively, by using Brucella broth (bioMérieux). Each Mongolian gerbils in 3 groups Y and 3 groups N were orally challenged with 0.5 mL of 2×10^8 CFU/mL *H pylori* suspension, while the animals in another 3 groups Y and 3 groups N were attacked with 0.5 mL of 2×10^9 CFU/mL *H pylori* suspension through the same pathway. For the negative controls, the animals in 6 groups C were orally given with 0.5 mL of Brucella broth. Each animal in the groups was given with the different concentrations of *H pylori* suspensions or Brucella broth, respectively, as the described above for 3 times at an interval of 24 h. The animals were deprived of food but offered with water for 12 h before the challenge, and supplied with food and water after 4 h of *H pylori* inoculation.

Isolation and identification of *H pylori*

Six animals in group Y, 6 in group N and 4 animals in group C were killed, respectively, at 2, 4 and 6 wk after the last challenge. Two gastric mucosal specimens at the adjacent position were taken from antrum and corpus, respectively. One of the specimens was used for *H pylori* isolation, and the others were fixed with 40 g/L formaldehyde solution. The colonies on Columbia plates were identified by microscopy after Gram-staining, assays for urease and oxidase activities and slide agglutination test using the commercial *H pylori*-specific antiserum. The bacterium was defined to be *H pylori* if it was Gram-negative with arc shape or “seagull-like”, positive for the two enzymes and immune agglutination.

Pathological and immunohistochemical examinations

The gastric mucosal specimens fixed with formaldehyde were pathologically examined after embedding, section and haematoxylin-eosin (HE) staining. *H pylori* in gastric mucosal specimens were detected by the immunohistochemical method using a commercial rabbit anti-*H pylori* antibody and goat anti-rabbit HRP-labeled IgG antibody (Jackson Immunoresearch).

RESULTS

Infection of Mongolian gerbils with *H pylori* strains

The results of *H pylori* isolation from gastric mucosal specimens of Mongolian gerbils are shown in Table 1.

Table 1 The detection results of *H pylori* isolated from gastric mucosa of experimental infected Mongolian gerbils

Group	Detection time (wk)	Infection rate (%) (positive/total cases)	
		1×10^8 CFU (1 challenge)	1×10^9 CFU (3 challenges)
Y	2	0(0/6)	66.7(4/6)
N	2	0(0/6)	66.7(4/6)
C	2	0(0/4)	0(0/4)
Y	4	16.7(1/6)	100(6/6)
N	4	0(0/6)	66.7(4/6)
C	4	0(0/4)	0(0/4)
Y	6	66.7(4/6)	100(6/6)
N	6	16.7(1/6)	100(6/6)
C	6	0(0/4)	0(0/4)

Y, groups infected with strain Y06; N, groups infected with strain NCTC11637; C, negative controls.

Pathological and immunohistochemical findings

In animals with positive *H pylori* isolation, the organisms were found to colonize the surface of gastric mucosa and the gastric pits (Figure 1). In the presence of *H pylori* infection, infiltration of chronic inflammatory cells in the lamina propria and erosions on the surface of gastric mucosa were observed (Figure 2).

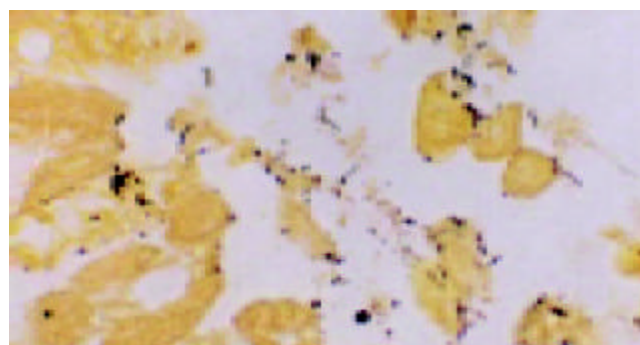


Figure 1 The *H pylori* bodies located on the surface of gastric mucosal cells and in gastric pits ($\times 1000$).

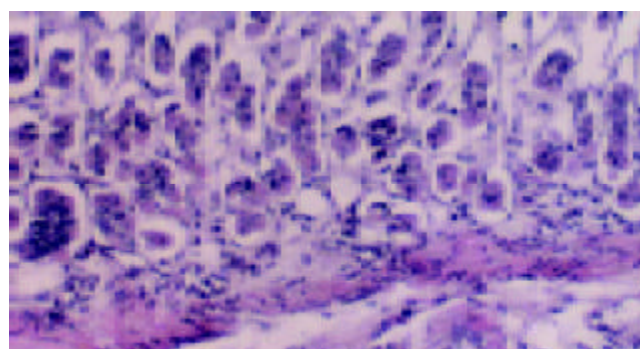


Figure 2 The infiltrated chronic inflammatory cells in the gastric mucosal lamina propria of the specimens with positive *H pylori* isolation ($\times 400$).

DISCUSSION

In previous published data, animals for establishment of *H pylori* infection models included guinea pigs, rats, nude mice, chimpanzee *etc.*^[45–48]. These animal models have many disadvantages such as low infection rates, instability, immunodeficiency and high costs. In 1997, Lee *et al* successfully established an animal model infected with a *H pylori* strain named as SS1 in C₅₇BL/6 and BalB/c mice^[48]. This animal model showed a high frequency and stability for *H pylori* infection. However, strain SS1 is a mutant of *H pylori* and its virulence is considerably low. Recently, Mongolian gerbils, which has distinct advantages such as high frequency and stability of infection, large colonization of *H pylori*, longer living suitable for study with long period of time and pathological changes similar to those observed in human with chronic gastritis, have become the predominant animals for preparing *H pylori* infection model^[42–44]. In 1999, Chi *et al* established a stable model of *H pylori* infection in Mongolian gerbils, which was orally pretreated with alcohol^[49]. Therefore, Mongolian gerbils are regarded as an ideal animal for *H pylori* infection models.

Previous studies have shown that infection model in Mongolian gerbils by oral challenge once with *H pylori* suspension at the concentration of 1×10^8 CFU of *H pylori* is stable^[42–44]. In the present study, *H pylori* was undetectable in the gastric mucosa from Mongolian gerbils at 2 wk after challenge once with 1×10^8 CFU of the bacterium. Furthermore,

the infection rates at 6 wk after one challenge by *H pylori* strain Y06 and strain NCTC11637 were only 66.7% and 16.7%, respectively. On contrast, by using three oral challenges at the dosage of 1×10^9 CFU, *H pylori* colonization rates in the gastric mucosa at 2 and 6 wk after challenge by *H pylori* strain Y06 or strain NCTC11637 were both 66.7% and 100%, respectively, which indicates that multiple challenges with a high concentration of *H pylori* contribute to the increased infection rates.

The infection rates of *H pylori* strain Y06 and strain NCTC11637 in Mongolian gerbils were 100% and 66.7% at 4 wk for 3 challenges using the low concentration of bacterial suspension, and 16.7% and 0% at 4 wk and 66.7% and 16.7% at 6 wk after one challenge using the high concentration. *H pylori* strain Y06, a fresh clinical isolate, seems to be more virulent than strain NCTC11637 and more beneficial for establishing *H pylori* infection model in Mongolian gerbils with a higher infection rate in a shorter period of time.

H pylori was found on the surface of gastric mucosa and in the gastric pits of Mongolian gerbils when infection was established. The observations that there were erosions of mucosal surface and infiltration of chronic inflammatory cells in the lamina propria of gastric mucosa of *H pylori* infected Mongolian gerbils indicates that the two tested *H pylori* strains are able to colonize gastric mucosa of Mongolian gerbils and cause chronic inflammation and gastric erosions.

REFERENCES

- 1 **Frenck RW Jr**, Clemens J. *Helicobacter* in the developing world. *Microbes Infect* 2003; **5**: 705-713
- 2 **Sharma P**, Vakil N. Review article: *Helicobacter pylori* and reflux disease. *Aliment Pharmacol Ther* 2003; **17**: 297-305
- 3 **Zhang Z**, Yuan Y, Gao H, Dong M, Wang L, Gong YH. Apoptosis, proliferation and p53 gene expression of *H pylori* associated gastric epithelial lesions. *World J Gastroenterol* 2001; **7**: 779-782
- 4 **Lu XL**, Qian KD, Tang XQ, Zhu YL, Du Q. Detection of *H pylori* DNA in gastric epithelial cells by in situ hybridization. *World J Gastroenterol* 2002; **8**: 305-307
- 5 **Yao YL**, Xu B, Song YG, Zhang WD. Overexpression of cyclin E in Mongolian gerbil with *Helicobacter pylori*-induced gastric precancerosis. *World J Gastroenterol* 2002; **8**: 60-63
- 6 **Guo DL**, Dong M, Wang L, Sun LP, Yuan Y. Expression of gastric cancer-associated MG7 antigen in gastric cancer, precancerous lesions and *H pylori*-associated gastric diseases. *World J Gastroenterol* 2002; **8**: 1009-1013
- 7 **Peng ZS**, Liang ZC, Liu MC, Ouyang NT. Studies on gastric epithelial cell proliferation and apoptosis in Hp associated gastric ulcer. *Shijie Huaren Xiaohua Zazhi* 1999; **7**: 218-219
- 8 **Hiyama T**, Haruma K, Kitadai Y, Miyamoto M, Tanaka S, Yoshihara M, Sumii K, Shimamoto F, Kajiyama G. B-cell monoclonality in *Helicobacter pylori*-associated chronic atrophic gastritis. *Virchows Arch* 2001; **483**: 232-237
- 9 **Xia HHX**. Association between *Helicobacter pylori* and gastric cancer: current knowledge and future research. *World J Gastroenterol* 1998; **4**: 93-96
- 10 **Quan J**, Fan XG. Progress in experimental research of *Helicobacter pylori* infection and gastric carcinoma. *Shijie Huaren Xiaohua Zazhi* 1999; **7**: 1068-1069
- 11 **Liu HF**, Liu WW, Fang DC. Study of the relationship between apoptosis and proliferation in gastric carcinoma and its precancerous lesion. *Shijie Huaren Xiaohua Zazhi* 1999; **7**: 649-651
- 12 **Zhu ZH**, Xia ZS, He SG. The effects of ATRA and 5Fu on telomerase activity and cell growth of gastric cancer cells *in vitro*. *Shijie Huaren Xiaohua Zazhi* 2000; **8**: 669-673
- 13 **Tu SP**, Zhong J, Tan JH, Jiang XH, Qiao MM, Wu YX, Jiang SH. Induction of apoptosis by arsenic trioxide and hydroxy camptothecin in gastric cancer cells *in vitro*. *World J Gastroenterol* 2000; **6**: 532-539
- 14 **Cai L**, Yu SZ, Zhang ZF. *Helicobacter pylori* infection and risk of gastric cancer in Changle County, Fujian Province, China. *World J Gastroenterol* 2000; **6**: 374-376
- 15 **Yao XX**, Yin L, Zhang JY, Bai WY, Li YM, Sun ZC. Htert expression and cellular immunity in gastric cancer and precancerosis. *Shijie Huaren Xiaohua Zazhi* 2001; **9**: 508-512
- 16 **Xu AG**, Li SG, Liu JH, Gan AH. Function of apoptosis and expression of the proteins Bcl-2, p53 and C-myc in the development of gastric cancer. *World J Gastroenterol* 2001; **7**: 403-406
- 17 **Wang X**, Lan M, Shi YQ, Lu J, Zhong YX, Wu HP, Zai HH, Ding J, Wu KC, Pan BR, Jin JP, Fan DM. Differential display of vincristine-resistance-related genes in gastric cancer SGC7901 cell. *World J Gastroenterol* 2002; **8**: 54-59
- 18 **Liu JR**, Li BX, Chen BQ, Han XH, Xue YB, Yang YM, Zheng YM, Liu RH. Effect of cis-9, trans-11-conjugated linoleic acid on cell cycle of gastric adenocarcinoma cell line (SGC-7901). *World J Gastroenterol* 2002; **8**: 224-229
- 19 **Cai L**, Yu SZ. A molecular epidemiologic study on gastric cancer in Changle, Fujian Province. *Shijie Huaren Xiaohua Zazhi* 1999; **7**: 652-655
- 20 **Gao GL**, Yang Y, Yang SF, Ren CW. Relationship between proliferation of vascular endothelial cells and gastric cancer. *Shijie Huaren Xiaohua Zazhi* 2000; **8**: 282-284
- 21 **Xue XC**, Fang GE, Hua JD. Gastric cancer and apoptosis. *Shijie Huaren Xiaohua Zazhi* 1999; **7**: 359-361
- 22 **Niu WX**, Qin XY, Liu H, Wang CP. Clinicopathological analysis of patients with gastric cancer in 1200 cases. *World J Gastroenterol* 2001; **7**: 281-284
- 23 **Li XY**, Wei PK. Diagnosis of stomach cancer by serum tumor markers. *Shijie Huaren Xiaohua Zazhi* 2001; **9**: 568-570
- 24 **Fang DC**, Yang SM, Zhou XD, Wang DX, Luo YH. Telomere erosion is independent of microsatellite instability but related to loss of heterozygosity in gastric cancer. *World J Gastroenterol* 2001; **7**: 522-526
- 25 **Morgner A**, Miehke S, Stolte M, Neubauer A, Alpen B, Thiede C, Klann H, Hierlmeier FX, Ell C, Ehninger G, Bayerdorffer E. Development of early gastric cancer 4 and 5 years after complete remission of *Helicobacter pylori* associated gastric low-grade marginal zone B-cell lymphoma of MALT type. *World J Gastroenterol* 2001; **7**: 248-253
- 26 **Deng DJ**. Progress of gastric cancer etiology: n-nitrosamides in the 1990s. *World J Gastroenterol* 2000; **6**: 613-618
- 27 **Liu ZM**, Shou NH, Jiang XH. Expression of lung resistance protein in patients with gastric carcinoma and its clinical significance. *World J Gastroenterol* 2000; **6**: 433-434
- 28 **Guo CQ**, Wang YP, Liu GY, Ma SW, Ding GY, Li JC. Study on *Helicobacter pylori* infection and p53, c-erbB-2 gene expression in carcinogenesis of gastric mucosa. *Shijie Huaren Xiaohua Zazhi* 1999; **7**: 313-315
- 29 **Cai L**, Yu SZ, Ye WM, Yi YN. Fish sauce and gastric cancer: an ecological study in Fujian Province, China. *World J Gastroenterol* 2000; **6**: 671-675
- 30 **Xue FB**, Xu YY, Wan Y, Pan BR, Ren J, Fan DM. Association of *H pylori* infection with gastric carcinoma: a Meta analysis. *World J Gastroenterol* 2001; **7**: 801-804
- 31 **Wang RT**, Wang T, Chen K, Wang JY, Zhang JP, Lin SR, Zhu YM, Zhang WM, Cao YX, Zhu CW, Yu H, Cong YJ, Zheng S, Wu BQ. *Helicobacter pylori* infection and gastric cancer: evidence from a retrospective cohort study and nested case-control study in China. *World J Gastroenterol* 2002; **8**: 1103-1107
- 32 **Hua JS**. Effect of Hp: cell proliferation and apoptosis on stomach cancer. *Shijie Huaren Xiaohua Zazhi* 1999; **7**: 647-648
- 33 **Liu DH**, Zhang XY, Fan DM, Huang YX, Zhang JS, Huang WQ, Zhang YQ, Huang QS, Ma WY, Chai YB, Jin M. Expression of vascular endothelial growth factor and its role in oncogenesis of human gastric carcinoma. *World J Gastroenterol* 2001; **7**: 500-505
- 34 **Cao WX**, Ou JM, Fei XF, Zhu ZG, Yin HR, Yan M, Lin YZ. Methionine-dependence and combination chemotherapy on human gastric cancer cells *in vitro*. *World J Gastroenterol* 2002; **8**: 230-232
- 35 **Mao YF**, Yan J, Li LW, Li SP. Construction of *hpaA* gene from a clinical isolate of *Helicobacter pylori* and identification of fusion protein. *World J Gastroenterol* 2003; **9**: 1529-1536
- 36 **Ruggiero P**, Peppoloni S, Rappuoli R, Del Giudice G. The quest for a vaccine against *Helicobacter pylori*: how to move from mouse to man? *Microbes Infect* 2003; **5**: 749-756

- 37 **Garhart CA**, Nedrud JG, Heinzl FP, Sigmund NE, Czinn SJ. Vaccine-induced protection against *Helicobacter pylori* in mice lacking both antibodies and interleukin-4. *Infect Immun* 2003; **71**: 3628-3633
- 38 **Garhart CA**, Heinzl FP, Czinn SJ, Nedrud JG. Vaccine-induced reduction of *Helicobacter pylori* colonization in mice is interleukin-12 dependent but gamma interferon and inducible nitric oxide synthase independent. *Infect Immun* 2003; **71**: 910-921
- 39 **Pantheil K**, Faller G, Haas R. Colonization of C57BL/6J and BALB/c wild-type and knockout mice with *Helicobacter pylori*: effect of vaccination and implications for innate and acquired immunity. *Infect Immun* 2003; **71**: 794-800
- 40 **Sheu BS**, Huang JJ, Yang HB, Huang AH, Wu JJ. The selection of triple therapy for *Helicobacter pylori* eradication in chronic renal insufficiency. *Aliment Pharmacol Ther* 2003; **17**: 1283-1290
- 41 **Marais A**, Bilardi C, Cantet F, Mendz GL, Megraud F. Characterization of the genes rdxA and frxA involved in metronidazole resistance in *Helicobacter pylori*. *Res Microbiol* 2003; **154**: 137-144
- 42 **Ohkusa T**, Okayasu I, Miwa H, Ohtaka K, Endo S, Sato N. *Helicobacter pylori* infection induces duodenitis and superficial duodenal ulcer in Mongolian gerbils. *Gut* 2003; **52**: 797-803
- 43 **Sugiyama T**, Hige S, Asaka M. Development of an *H pylori*-infected animal model and gastric cancer: recent progress and issues. *J Gastroenterol* 2002; **37**(Suppl 13): 6-9
- 44 **Wang J**, Court M, Jeremy AH, Aboshkiwa MA, Robinson PA, Crabtree JE. Infection of Mongolian gerbils with Chinese *Helicobacter pylori* strains. *FEMS Immunol Med Microbiol* 2003; **36**: 207-213
- 45 **Fujioka T**, Murakami K, Kodama M, Kagawa J, Okimoto T, Sato R. *Helicobacter pylori* and gastric carcinoma—from the view point of animal model. *Keio J Med* 2002; **51**(Suppl 2): 69-73
- 46 **Eaton KA**, Kersulyte D, Mefford M, Danon SJ, Krakowka S, Berg DE. Role of *Helicobacter pylori* cag region genes in colonization and gastritis in two animal models. *Infect Immun* 2001; **69**: 2902-2908
- 47 **Keenan JI**, Rijpkema SG, Durrani Z, Roake JA. Differences in immunogenicity and protection in mice and guinea pigs following intranasal immunization with *Helicobacter pylori* outer membrane antigens. *FEMS Immunol Med Microbio* 2003; **36**: 199-205
- 48 **Lee A**, O'Rourke J, De Ungria MC, Robertson B, Daskalopoulos G, Dixon MF. A standardized mouse model of *Helicobacter pylori* infection: introducing the Sydney strain. *Gastroenterology* 1997; **112**: 1386-1397
- 49 **Chi J**, Fu BY, Nakajima, Hattori, Kushima. Establishment of Mongolian gerbil animal model infected with *Hp* infection and change of inflammation and proliferation before and after *Hp* eradication. *Shijie Huaren Xiaohua Zazhi* 1999; **7**: 557-560

Edited by Xia HHX and Xu FM

Effects of non-starch polysaccharides enzymes on pancreatic and small intestinal digestive enzyme activities in piglet fed diets containing high amounts of barley

Wei-Fen Li, Jie Feng, Zi-Rong Xu, Cai-Mei Yang

Wei-Fen Li, Jie Feng, Zi-Rong Xu, Cai-Mei Yang, Animal Science College, Zhejiang University, The Key Laboratory of Molecular Animal Nutrition, Ministry of Education, Hangzhou, 310029, Zhejiang Province, China

Supported by the National Natural Science Foundation of China, No. 30000118

Correspondence to: Jie Feng, Animal Science College, Zhejiang University, 268 Kaixuan Road, Hangzhou, 310029, Zhejiang Province, China. fengj@zju.edu.cn

Telephone: +86-571-86986127 **Fax:** +86-571-86091820

Received: 2003-09-18 **Accepted:** 2003-11-13

Abstract

AIM: To investigate effects of non-starch polysaccharides(NSP) enzymes on pancreatic and small intestinal digestive enzyme activities in piglet fed diets containing high amounts of barley.

METHODS: Sixty crossbred piglets averaging 13.5 kg were randomly assigned to two treatment groups with three replications (pens) based on sex and mass. Each group was fed on the diet based on barley with or without added NSP enzymes (0.15%) for a 40-d period. At the end of the experiment the pigs were weighed. Three piglets of each group were chosen and slaughtered. Pancreas, digesta from the distal end of the duodenum and jejunal mucosa were collected for determination. Activities of the digestive enzymes trypsin, chymotrypsin, amylase and lipase were determined in the small intestinal sections as well as in homogenates of pancreatic tissue. Maltase, sucrase, lactase and γ -glutamyl transpeptidase (γ -GT) activities were analyzed in jejunal mucosa.

RESULTS: Supplementation with NSP enzymes improved growth performance of piglets. It showed that NSP enzymes had no effect on digestive enzyme activities in pancreas, but decreased the activities of proteolytic enzyme, trypsin, amylase and lipase in duodenal contents by 57.56%, 76.08%, 69.03% and 40.22% ($P < 0.05$) compared with control, and increased γ -GT activities in jejunal mucosa by 118.75% ($P < 0.05$).

CONCLUSION: Supplementation with NSP enzymes in barley based diets could improve piglets' growth performance, decrease activities of proteolytic enzyme, trypsin, amylase and lipase in duodenal contents and increase γ -GT activities in jejunal mucosa.

Li WF, Feng J, Xu ZR, Yang CM. Effects of non-starch polysaccharides enzymes on pancreatic and small intestinal digestive enzyme activities in piglet fed diets containing high amounts of barley. *World J Gastroenterol* 2004; 10(6): 856-859
<http://www.wjgnet.com/1007-9327/10/856.asp>

INTRODUCTION

Barley is one of the major energy sources of swine diets in

many parts of the world. But anti-nutritive factors in barley limit its use in feed industry^[1]. The predominant anti-nutritive factor is non-starch polysaccharides (NSP), including β -glucan ((1-3), (1-4)- β -D-glucan)^[2,3] and arabinoxylan^[4]. The β -glucan and pentosan content in whole barley grain was 4.2% and 6.6%, being 1.8% and 1.4% in endosperm^[5]. The major nutrients in barley, starch and protein, are enclosed within endosperm cell walls, which consist mainly of mix-linked β -glucan and arabinoxylan^[6]. Pigs, especially piglets, do not produce enzymes that can degrade the cell wall and NSP in barley. So β -glucan and arabinoxylan in barley may interfere with digestion and absorption of nutrients^[7], even the production of digestive enzymes^[8,9].

Studies have shown that mix-linked β -glucan and arabinoxylan are easily hydrolyzed by β -glucanases and xylanases respectively. Addition of cell wall degrading enzymes *in vitro* increased the release of proteins and non-starch carbohydrate in barley^[10]. Supplementation of exogenous NSP enzymes to piglet diets can increase the digestibility of barley and pigs' growth^[11-13]. This has been attributed mainly to the breakdown of endosperm cell wall components, resulting in more complete digestion of starch and protein in the small intestine. But there is little information on the effect of β -glucanases and xylanases supplementation on digestive enzyme activities in barley-based diets for piglets.

The aim of the present study was to investigate the effect of supplementation of NSP enzymes on pancreatic and small intestine digestive enzyme activities in piglets fed diets containing high amounts of barley.

MATERIALS AND METHODS

Animals, diets and enzyme complex

Sixty crossbred (Duroc \times Landrace \times Jiaying) piglets averaging 13.5 kg were randomly assigned to two treatment groups with three replications (pens) based on sex and mass. Each group was fed on one of the two experimental diets for 40 d. As shown in Table 1, pigs received the same basal diet based on barley-soybean meal and NSP enzymes were added to the basal diet respectively at 0% and 0.15% of the diet at the expense of barley. To accustom pigs to the diets, all pigs were allowed access to the basal diet on alternate days for 7 d prior to commencement of the experiment. The diets and water were offered ad libitum throughout the experiment. Pigs were weighed individually and feed consumption per pen was measured weekly. Growth performance results as average daily gain (ADG), average daily feed intake (ADFI), feed gain ratio (FGR) were collected for all pigs for the experimental period. At the end of feeding trial, three pigs from each treatment (one pig per pen) were slaughtered under general anaesthesia. The pigs were then immediately eviscerated to collect intestinal samples. NSP enzymes complex was supplied by Primal Co. Ltd., BIOTEC, Finland, which contained 10 000 U/g β -glucanase (E.C.3.2.1.6) and 80 000 U/g xylanase (E.C.3.2.1.8).

Table 1 Formula and chemical composition of the basal diet

Ingredients (%)	Percentage
Barley	79.0
Soybean meal (dehulled, solvent)	11.0
Fishmeal	4.0
Yeast meal	2.0
Limestone	1.0
Dicalcium phosphate	1.2
Sodium chloride	0.3
L-Lysine-HCl (78%)	0.2
Vitamin-mineral premix ¹	1.3
Analyzed chemical composition (% as feed)	
Digestible energy(Kcal/kg) ²	2960
Crude protein	18.28
Crude fat	1.70
Crude fiber	5.26
Calcium	1.11
Phosphorus	0.48

¹The vitamin/mineral premix provided (per kg feed): 2 000 IU vitamin A, 200 IU vitamin D₃, 20 mg vitamin E, 1 mg vitamin K, 1 mg thiamine, 3 mg riboflavin, 10 mg d-pantothenic acid, 0.5 mg folic acid, 1 mg pyridoxine, 20 mg niacin, 10 µg cobalamin, 500 mg choline chloride, 0.1 mg biotin, 0.2 mg Se, 0.2 mg I, 80 mg Fe, 5 mg Cu, 2 mg Mn, and 80 mg Zn. ²Digestible energy was based on calculated values.

Sampling procedure

The contents taken from the small intestine were digesta from the distal end of the duodenum to the ileo-cecal junction. Digesta samples were collected by massaging the tract from both ends. The digesta samples were stored immediately at -20 °C until use. Enzyme activity analyses of the samples obtained from the small intestine were performed on freeze-dried material, which was extracted with 1 mmol/L HCl (50 mg lyophilized digesta in 1 mL 1 mmol/L HCl) for 1 h at 4 °C followed by centrifugation (3 000 r/min). The supernatants were then collected for analysis of protease, trypsin, chymotrypsin, amylase and lipase activities.

The pancreas from slaughtered pigs was homogenized in ice-cold 0.2 mol/L Tris-HCl buffer containing 0.05 mol/L NaCl. The homogenate was centrifuged at 3 000 r/min for 15 min at 4 °C and the supernatant was saved. Protease, chymotrypsin, amylase and lipase activities were determined.

Jejunum mucosa was homogenized in 4.0 mL distilled-water and kept at 4 °C for 24 h followed by 10 min centrifugation (3 000 r/min). The supernatants were then collected for analysis of maltase, sucrase, lactase and γ -glutamyl transpeptidase (γ -GT) activities.

Digestive enzyme assay

Protease activity was analyzed using the method of Iwamori *et al.* (1997)^[14] Chymotrypsin (EC 3.4.21.1) was determined according to Erlanger *et al.*^[15] using glutaryl-L-phenylalanine-p-nitroanilid (GPNA) as substrate. Amylase (EC 3.2.1.1) activity was determined using a kit (No.700) from Sigma Chemical Company (Sigma Chemical Co., St. Louis, MO 63178-9916) and lipase (EC 3.1.1.3) by a pH-stat titration method using tributyrin as substrate according to Erlanson-Albertsson *et al.*^[16]. The activities of protease, trypsin, chymotrypsin, amylase, and lipase are expressed as unit (U) which is defined as the amount of enzyme that hydrolyses 1 µmol of substrate per min. Maltase, sucrase, lactase and γ -GT activities were analyzed using the modified method of Dahlqvist^[17]. The activities of maltase, sucrase, lactase and

γ -GT are expressed as unit (U) which is defined as the amount of enzyme that hydrolyses 10 µmol of substrate per min.

Statistical analysis

One way analysis of variance was performed using the General Linear Model (GLM) Procedure of SAS^[18]. Differences among means were tested using Duncan's multiple range test. A significant level of 0.05 was used.

RESULTS

Growth performance

Growth performance of pigs fed NSP enzymes is presented in Table 2. As compared to control, supplementation with 1.5 g/L NSP enzymes significantly improved average daily gain (ADG), average daily feed intake (ADFI) and feed conversion ratio (FCR) by 6.22% ($P<0.01$), 2.14% ($P<0.05$) and 3.69% ($P<0.05$) respectively.

Table 2 Growth performance of piglets fed diets based on barley with and without NSP enzymes

	Dietary NSP enzymes level (%)	
	0	0.15
Initial mass(kg)	13.91±0.25	14.01±0.17
Final mass(kg)	33.95±0.38 ^a	35.35±0.40 ^c
Average daily gain (g)	501.16±16.18 ^a	532.34±6.88 ^c
Average daily feed intake (g)	1 224.00±3.62 ^a	1 250.15±7.27 ^c
Feed/Gain ratio	2.44±0.03 ^a	2.35±0.02 ^c

Values are presented as mean±SD; $n=30$ for average daily gain (ADG), $n=3$ for average daily feed intake (ADFI) and feed/gain ratio per treatment. Means in a row with different letters differ significantly, $P<0.05$.

Pancreatic digestive enzyme activities

The results of the effects of NSP enzymes on the digestive enzyme activities in the pancreas of piglets are shown in Table 3. Supplementation with 1.5 g/L NSP enzymes had no significant effect on the activities of protease, chymotrypsin, amylase and lipase in pancreas.

Table 3 Effects of NSP enzymes on the digestive enzyme activities (U/g pancreas) in the pancreas of piglets

	Dietary NSP enzymes level (%)	
	0	0.15
Protease	160.50±17.49	188.86±63.93
Chymotrypsin	1.09±0.28	0.99±0.19
Trypsin	32.14±21.96	27.25±6.79
Amylase	3 009.40±157.19	2 957.02±302.35
Lipase	89.08±13.86	92.15±13.86

Values are presented as mean±SD; $n=3$ per treatment.

Duodenal digestive enzyme activities

Effects of NSP enzymes on duodenal digestive activities are presented in Table 4. NSP enzymes affected duodenal digestive activities significantly. Compared with the control, protease, trypsin, amylase and lipase activities were decreased by 57.56%, 76.08%, 69.03% and 40.22% ($P<0.05$) respectively.

Jejunal digestive enzyme activities

The activities of digestive enzyme in jejunal mucosa are shown in Table 5. Supplementation with 1.5g/LNSP enzymes had no effect on maltase, sucrase, lactase activities, but increased γ -GT activities by 118.75% ($P<0.05$) compared with the control.

Table 4 Effects of NSP enzymes on the digestive enzyme activities (U/mg protein) in the small intestinal contents of piglets

	Dietary NSP enzymes level (%)	
	0	0.15
Protease	60.04±12.86 ^a	25.48±4.98 ^c
Trypsin	37.21±11.47 ^a	8.90±3.72 ^c
Amylase	3 600.45±155.68 ^a	1 115.16±93.32 ^c
Lipase	68.68±11.93 ^a	41.06±6.81 ^c

Values are presented as mean±SD; *n*=3 per treatment. Means in a row with different letters differ significantly, *P*<0.05.

Table 5 Effects of NSP enzymes on the digestive enzyme activities (U/mg) in jejunal mucosa of piglets

	Dietary NSP enzymes level (%)	
	0	0.15
Maltase	28.49±6.45	29.89±10.017
Sucrase	8.13±0.62	8.92±2.16
Lactase	1.22±0.75	1.72±0.97
γ-Glutamyl transpeptidase	0.16±0.05 ^c	0.35±0.13 ^a

Values are presented as mean±SD; *n*=3 per treatment. Means in a row with different letters differ significantly, *P*<0.05.

DISCUSSION

Numerous researchers have reported increased growth and improved feed conversion ratio as a consequence of NSP enzymes inclusion in animal diets based on barley, especially for poultry^[19-22]. Effects of exogenous enzymes on growth performance for swine have been variable. Inbarr *et al*^[11] reported that barley-based diets supplementation with NSP enzymes increased average daily gain and feed conversion ratio of weaned piglets significantly (*P*<0.05). Yin *et al* (2001)^[23] showed that β-glucanases and xylanase improved growth performance and feed gain ratio when piglets were fed with barley based diets. Lindberg *et al*^[24] found enzymes (including β-glucanases, xylanases and cellulase) could enhance growth performance especially body mass gain of piglets when fed with diets based on barley. However, negative results were also reported. Baas^[25] found there was no effect of β-glucanases on growth performance of finishing swine. But most experiments indicated that NSP had positive effects on growth performance for young pigs. Our study verified this point. Increase of digestibility of nutrients is the main reason for this phenomenon. The inconsistent effects between the experiments may result from different stage of pigs and/or formula of diets used.

Endogenous enzyme is very important for digestibility of nutrients. Increasing gut viscosity due to viscous polysaccharides has been shown to increase the output of pancreatic juice and enzyme activities in rats^[9]. However, Mosenthin *et al*^[26] and Zebrowska and Low^[27] observed no change in the secretion of enzymes from the exocrine pancreas when feeding pigs on diets containing different levels of dietary fibre. Makkink *et al*^[28] showed that trypsin and chymotrypsin activity depended on dietary protein source. However, in the present experiment the protein source was the same as in all other diets which may explain why no differences in enzyme activities were observed. The activities of the pancreatic enzymes in the present study were not changed with the enzyme supplementation. This indicated that the synthesis of pancreatic enzymes was unaffected by these factors.

The present study also showed that NSP enzymes decreased the activities of protease, chymotrypsin, amylase and lipase significantly in digesta from the distal end of the duodenum.

Almirall *et al*^[29] observed that supplementation with β-glucanases increased trypsin, amylase and lipase obviously in chyme of chicken. Jensen^[30] found that when pigs were fed barley based diets supplemented with NSP enzymes, chymotrypsin activity was enhanced sharply. Ikegami *et al* (1990) reported that soluble NSP could increase the activities of lipase, amylase and chymotrypsin in rat gut^[9]. Our results are different from the studies mentioned above, but are consistent with the results reported by Inbarr^[11]. Inbarr found exogenous NSP enzymes decreased the activities of endogenous enzymes and he thought NSP enzymes might provide a situation appropriate for endogenous enzyme action. But this may result from the fact that NSP enzymes degrade β-glucan and arabinoxylan in endosperm cell wall and decrease the viscosity of digesta in small intestine. Viscosity may act as a barrier to prevent contact of digestive enzymes with their substrates, thickening of the unstirred layer of mucosa and prevention of micelle formation required for absorption of lipids^[31]. This process makes the endogenous enzymes to approach substrate easily and work more efficiently.

γ-GT is the key enzyme for amino acids absorption. The present study showed that supplementation with NSP enzymes increased γ-GT activities in jejunal mucosa when piglets were fed barley based diets. The results may indicate that NSP enzymes improves digestibility of the nutrients and supplies more substrates for these endogenous enzymes to act on, which then feedback on the secretion of the enzymes.

REFERENCES

- 1 **Bhatty RS**. The potential of hull-less Barley - A Review. *Cereal Chem* 1986; **63**: 97-103
- 2 **White WB**, Bird HR, Sunde ML, Prentice N, Burger WC, Marlett JA. The viscosity interaction of barley beta-glucan with *Trichoderma viride* cellulase in the chick intestine. *Poult Sci* 1981; **60**: 1043-1048
- 3 **Hesselman K**, Aman P. The effect of β-glucanase on the utilization of starch and nitrogen by broiler chickens fed on barley of low- or high- viscosity. *Anim Feed Sci Technol* 1986; **15**: 83-93
- 4 **Fleury MD**, Edney MJ, Campbell LD, Crow GH. Total, water-soluble and acid-soluble arabinoxylans in western Canadian barleys. *Can J Plant Sci* 1997; **77**: 191-196
- 5 **Henry RJ**. A comparison of the non-starch carbohydrates in cereal grains. *J Sci Food Agric* 1985; **36**: 1243-1253
- 6 **Chesson A**. Feed enzymes. *Anim Feed Sci Technol* 1993; **45**: 65-79
- 7 **Campbell GL**, Rossnagel BG, Classen HL, Thacker PA. Genotypic and environmental differences in extract viscosity of barley and their relationship to its nutritive value for broiler chickens. *Anim Feed Sci Technol* 1989; **26**: 221-230
- 8 **Graham H**, Löwgren W, Pettersson D, Åman P. Effect of enzyme supplementation on digestion of a barley/pollard-based pig diet. *Nutr Reports Inter* 1988; **38**: 1073-1079
- 9 **Ikegami S**, Tsuchihashi F, Harada H, Tsuchihashi N, Nishide E, Innami S. Effect of viscous indigestible polysaccharides on pancreatic-biliary secretion and digestive organs in rats. *J Nutr* 1990; **120**: 353-360
- 10 **Boisen S**, Fernández JA. Prediction of the total tract digestibility of energy in feedstuffs and pig diets by *in vitro* analyses. *Anim Feed Sci Technol* 1997; **68**: 277-286
- 11 **Inbarr J**, Schmitz M, Ahrens F. Effect of adding fiber and starch degrading enzymes to a barley/wheat based diet on performance and nutrient digestibility in different segments of the small intestine of early weaned pigs. *Anim Feed Sci Technol* 1993; **44**: 113-127
- 12 **Li S**, Sauer WC, Mosenthin R, Kerr B. Effect of beta-glucanase supplementation of cereal-based diets for starter pigs on the apparent digestibilities of dry matter, crude protein and energy. *Anim Feed Sci Technol* 1996; **59**: 223-231
- 13 **Li S**, Sauer WC, Huang SX, Gabert VM. Effect of beta-glucanase supplementation to hullless barley- or wheat-soybean meal diets on the digestibilities of energy, protein, beta- glucans, and amino acids in young pigs. *J Anim Sci* 1996; **74**: 1649-1656
- 14 **Iwamori M**, Iwamori Y, Ito N. Sulfated lipids as inhibitors of

- pancreatic trypsin and chymotrypsin in epithelium of the mammalian digestive tract. *Biochem Biophys Res Commun* 1997; **237**: 262-265
- 15 **Erlanger BF**, Edel F, Cooper AG. The action of chymotrypsin on two new chromogenic substrates. *Arch Biochem Biophys* 1966; **115**: 206-210
- 16 **Erlanson-Albertsson C**, Larsson A, Duan R. Secretion of pancreatic lipase and colipase from rat pancreas. *Pancreas* 1987; **2**: 531-535
- 17 **Dahlqvist A**. Method for assay of intestinal disaccharides. *Anal Biochem* 1964; **7**: 18-25
- 18 **SAS**. 1991. SAS User's Guide Version 6.03. *SAS Institute, Cary, NC*
- 19 **Krogdahl A**, Sell JL. Influence of age on lipase, amylase and protease activities in pancreatic tissue and intestinal contents of young turkeys. *Poult Sci* 1989; **68**: 1561-1568
- 20 **Almirall M**, Francesch M, Perez-Vendrell AM, Brufau J, Esteve-Garcia E. The differences in intestinal viscosity produced by barley and β -glucanase alter digesta enzyme activities and ileal nutrient digestibilities more in broiler chicks than in cocks. *J Nutr* 1995; **125**: 947-955
- 21 **Yin YL**, Baidoo SK, Boychuk JLL. Effect of enzyme supplementation on the performance of broilers fed maize, wheat, barley or micronized dehulled barley diets. *J Anim Feed Sci* 2000; **9**: 493-504
- 22 **Jamroz D**, Jakobsen K, Bach Knudsen KE, Wiliczkiewicz A, Orda J. Digestibility and energy value of non-starch polysaccharides in young chickens, ducks and geese, fed diets containing high amounts of barley. *Comp Biochem Physiol A Mol Integr Physiol* 2002; **131**: 657-668
- 23 **Yin YL**, Baidoo SK, Schulze H, Simmins PH. Effects of supplementing diets containing hullless barley varieties having different levels of non-starch polysaccharides with β -glucanases and xylanase on the physiological status of the gastrointestinal tract and nutrient digestibility of weaned pigs. *Livestock Prod Sci* 2001; **71**: 97-107
- 24 **Lindberg JE**, Arvidsson A, Wang J. Influence of naked barley cultivar with normal, amylose-rich or amylopectin-rich starch and enzyme supplementation on digestibility and piglet performance. *Anim Feed Sci Technol* 2003; **104**: 121-131
- 25 **Baas TC**, Thacker PA. Impact of gastric pH on dietary enzyme activity and survivability in swine fed β -glucanase supplemented diets. *Can J Anim Sci* 1996; **76**: 245-252
- 26 **Mosenthin R**, Sauer WC, Ahrens F. Dietary pectin's effect on ileal and fecal amino acid digestibility and exocrine pancreatic secretions in growing pigs. *J Nutr* 1994; **124**: 1222-1229
- 27 **Zebrowska T**, Low AG. The influence of diets based on whole wheat, wheat flour and wheat bran on exocrine pancreatic secretion in pigs. *J Nutr* 1987; **117**: 1212-1216
- 28 **Makkink CA**, Negulescu GP, Qin G, Verstegen MW. Effect of dietary protein source on feed intake, growth, pancreatic enzyme activities and jejunal morphology in newly-weaned piglets. *Br J Nutr* 1994; **72**: 353-368
- 29 **Almirall M**, Esteve-Garcia E. *In vitro* stability of a β -glucanase preparation from *Trichoderma longibrachiatum* and its effect in a barley based diet fed to broiler chicks. *Anim Feed Sci Technol* 1995; **54**: 149-158
- 30 **Jensen MS**, Thaela MJ, Pierzynowski SG, Jakobsen K. Exocrine pancreatic secretion in young pigs fed barley-based diets supplemented with β -glucanase. *J Anim Physiol A Anim Nutr* 1996; **75**: 231-241
- 31 **Wang L**, Newman RK, Newman CW, Hofer PJ. Barley beta-glucans alter intestinal viscosity and reduce plasma cholesterol concentrations in chicks. *J Nutr* 1992; **122**: 2292-2297

Edited by Zhu LH and Xu FM

Effects of daidzein on estrogen-receptor-positive and negative pancreatic cancer cells *in vitro*

Jun-Ming Guo, Bing-Xiu Xiao, De-Jian Dai, Qiong Liu, Hong-Hui Ma

Jun-Ming Guo, Bing-Xiu Xiao, Qiong Liu, School of Medicine, Ningbo University, Ningbo 315211, Zhejiang Province, China

De-Jian Dai, Second Affiliated Hospital of Medical College, Zhejiang University, Huangzhou 310009, Zhejiang Province, China

Hong-Hui Ma, School of Life Science and Bioengineering, Ningbo University, Ningbo 315211, Zhejiang Province, China

Supported by Scientific Research Fund of Zhejiang Provincial Education Department, No.20010217

Correspondence to: Dr. Jun-Ming Guo, School of Medicine, Ningbo University, Ningbo 315211, Zhejiang Province, China. junmingguo@yahoo.com

Telephone: +86-574-87600758 **Fax:** +86-574-87608638

Received: 2003-08-26 **Accepted:** 2003-09-18

Abstract

AIM: To study the effects of daidzein on human pancreatic cancer cells *in vitro*.

METHODS: Human estrogen-receptor (ER)-positive pancreatic cancer cells MiaPaCa-2 and ER-negative pancreatic cancer cells PANC-1 were treated by 0.1 $\mu\text{mol/L}$, 1 $\mu\text{mol/L}$, 10 $\mu\text{mol/L}$, 25 $\mu\text{mol/L}$, 50 $\mu\text{mol/L}$, 75 $\mu\text{mol/L}$ and 100 $\mu\text{mol/L}$ of daidzein, respectively. Its antiproliferative effect was studied by MTT assay.

RESULTS: Daidzein inhibited the growth of MiaPaCa-2 and PANC-1 cells at the concentrations from 0.1 $\mu\text{mol/L}$ to 100 $\mu\text{mol/L}$. A dose- and time-dependent manner was found. The IC_{50} of daidzein on MiaPaCa-2 and PANC-1 cells was 45 $\mu\text{mol/L}$ and 75 $\mu\text{mol/L}$, respectively. After MiaPaCa-2 cells were treated by daidzein for 3 d and at the concentrations more than IC_{50} , the inhibitory manner was identical and the inhibition appeared a saturation phenomenon, but the inhibitory manner of daidzein on PANC-1 cells was different from that of MiaPaCa-2 cells.

CONCLUSION: Daidzein has antiproliferative effects on human estrogen-receptor-positive and negative pancreatic cancer cells, but their mechanisms may be different.

Guo JM, Xiao BX, Dai DJ, Liu Q, Ma HH. Effects of daidzein on estrogen-receptor-positive and negative pancreatic cancer cells *in vitro*. *World J Gastroenterol* 2004; 10(6): 860-863
<http://www.wjgnet.com/1007-9327/10/860.asp>

INTRODUCTION

Phytoestrogens are natural compounds, which exhibit estrogen-like activities. They have been thought to have a preventive effect against a wide range of human conditions, including breast cancer, bowel cancer, prostate cancer, colon cancer and other cancers, cardiovascular diseases, brain function, alcohol abuse, osteoporosis and menopausal symptoms^[1-4]. There are three main classes of phytoestrogens, namely isoflavones, coumestans, and lignans^[5]. They are widely distributed in soybeans, oil seeds, and vegetables. Soy contains a number of

isoflavones (such as genistein, genistin, daidzein, and biochanin A), which are found to have potential anticancer properties^[6]. Interestingly, phytoestrogens can not only inhibit the growth of estrogen-receptor (ER)-dependent cancer cells, but also the growth of ER-independent cancer cells^[7]. The mechanisms of their anticancer effects include induction of apoptosis, alterations of cell cycle distribution, *etc.*^[8,9].

The morbidity of pancreatic carcinoma has taken an upward trend all over the world. In Occidental countries, the morbidity of pancreatic carcinoma has increased by 3 to 7 times in nearly thirty years, and pancreatic carcinoma has become one of the ten commonest malignant tumors^[10]. Only 15% of patients with pancreatic cancer could undergo resection and the overall 5-year survival rate was about 10%^[11]. In recent years, many advances in the diagnosis and treatment (including surgical and adjuvant treatment) of pancreatic cancer have been achieved^[12-14].

Estrogen receptor has been found in many cases of pancreatic tumor tissues and antiestrogen therapy has benefit to some patients with pancreatic cancers^[15,16]. There is evidence to support the hypothesis that the increased incidence of pancreatic cancer in Western communities might be related to the relatively low dietary content and protective role of naturally occurring plant hormones and related compounds^[17]. Generally speaking, treatment of pancreatic cancer is still a serious challenge to us^[10]. The key problem is to seek novel diagnostic methods, effective adjunctive therapy and the mechanism of pathogenesis and progression of pancreatic cancer. Pancreatic cancer is often detected in its late stages. As a result, it is very important to develop new potential chemopreventive and anticancer reagents for pancreatic cancer, especially those from nature. The effects of daidzein, one of the rich compounds in Eastern countries' traditional diet, on human pancreatic cancer cells are unclear. In this study, we observed the effects of daidzein on the growth of human pancreatic cancer cells *in vitro*.

MATERIALS AND METHODS

Materials

Daidzein was purchased from Sigma Chemical Co. (St. Louis, MO) and dissolved in dimethylsulfoxide (DMSO). 3-(4,5-dimethylthiazol-2-yl)-2,5-diphenyl tetrazolium bromide (MTT) was from Sigma. RPMI-1640 medium was from Life Technologies (Grand Island, NY). Human pancreatic cancer cell lines MiaPaCa-2 and PANC-1 were obtained from Department of General and Gastroenterological Surgery, Osaka Medical College, Takatsuki City, Japan.

Cell culture and treatment

Cells were cultured in plastic flasks or multi-well plates at 37 °C in a humidified atmosphere of 50 ml/L CO₂ and 950 ml/L air with RPMI-1640 medium containing 100 ml/L fetal calf serum, 50 000 U/L penicillin and 50 mg/L streptomycin. The medium was changed every other day. Exponentially growing cells were used in experiments. For quantitative assays of proliferation, 1×10⁴ MiaPaCa-2 or PANC-1 cells were seeded in 96-well

plates in regular growth medium. Twenty-four hours later, cells were incubated in the medium with test compounds or 1 ml/L DMSO (as control). There were 7 test groups. Their concentrations of daidzein were 0.1 $\mu\text{mol/L}$, 1 $\mu\text{mol/L}$, 10 $\mu\text{mol/L}$, 25 $\mu\text{mol/L}$, 50 $\mu\text{mol/L}$, 75 $\mu\text{mol/L}$ and 100 $\mu\text{mol/L}$, respectively. After cells were treated for 1 d, 2 d, 3 d, 4 d, 5 d and 6 d, the growth of cells was monitored by MTT assay.

MTT assay

Sets of 12 wells were used for each dose and control in this assay. When the growth time reached, 30 μL MTT solution (2 g/L in PBS) was added into each well of a 96-well plate. After cells were treated for 4 h at 37 $^{\circ}\text{C}$, the medium was removed and then 150 μL DMSO was added into each well to solubilize formazan. After that, the microplate was shaken on a rotary platform for 10 min. Finally, absorbance was measured at 550 nm with a Wellscan (Labsystems, USA). The inhibitive rate (%) = $(A_{\text{control}} - A_{\text{experiment}}) / A_{\text{control}} \times 100\%$.

Statistics

Statistical analysis was performed using SPSS software 10.0. Student's *t*-test was used to make a statistical comparison between groups. The level of significance was set at $P < 0.05$.

RESULTS

Morphologic change of the cells

The effects of daidzein on the growth of pancreatic cancer MiaPaCa-2 and PANC-1 cells were tested over a range of concentrations from 0.1 $\mu\text{mol/L}$ to 100 $\mu\text{mol/L}$. The changes of configuration and number were observed under a microscope (Figures 1, 2). Both pancreatic cancer cells treated by daidzein grew slower than control (Figures 1, 2). The higher the concentration of daidzein, the less the number of cells.

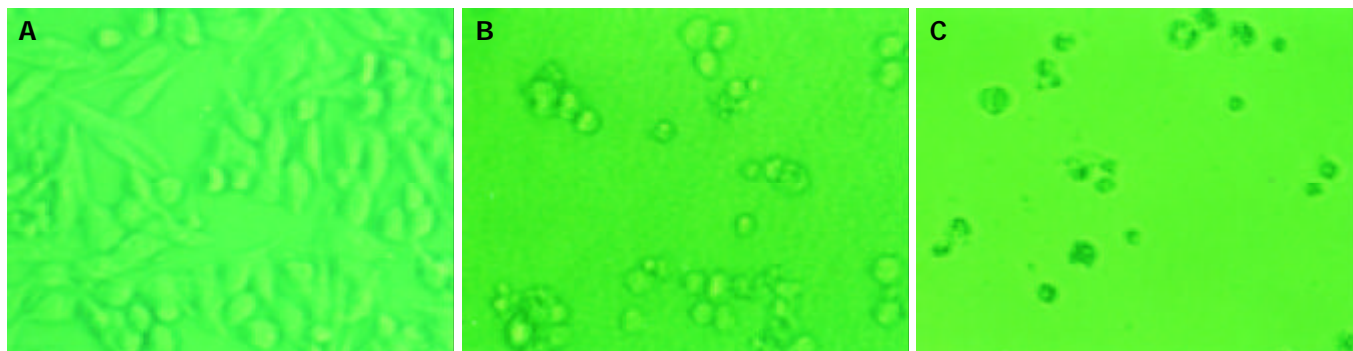


Figure 1 Morphologic changes of MiaPaCa-2 cells treated by daidzein. A: Control, B: Cells treated by 10 $\mu\text{mol/L}$ of daidzein for 3 d, C: Cells treated by 75 $\mu\text{mol/L}$ of daidzein for 3 d ($\times 200$).

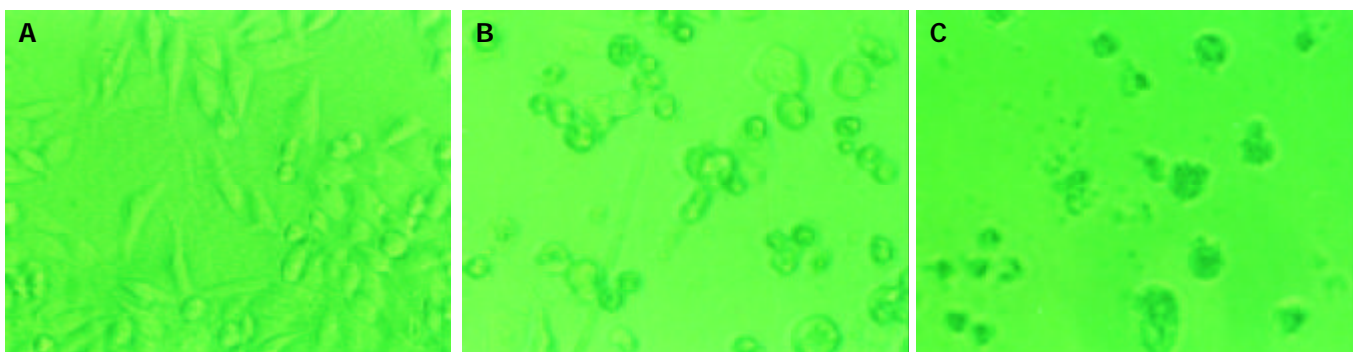


Figure 2 Morphologic changes of PANC-1 cells treated by daidzein. A: Control, B: Cells treated by 10 $\mu\text{mol/L}$ of daidzein for 3 d, C: Cells treated by 75 $\mu\text{mol/L}$ of daidzein for 3 d ($\times 200$).

Inhibitory effect of daidzein on estrogen-receptor-positive pancreatic cancer cells

Estrogen-receptor-positive MiaPaCa-2 cells were treated by various concentrations of daidzein for 1 d to 6 d. At the concentrations from 0.1 $\mu\text{mol/L}$ to 100 $\mu\text{mol/L}$, especially at 50 $\mu\text{mol/L}$, 75 $\mu\text{mol/L}$, and 100 $\mu\text{mol/L}$, daidzein inhibited the growth of cells ($P < 0.01$) in a time-dependent manner (Figure 3). When cells were treated for 3 d, 50% inhibitory rate might be reached. The IC_{50} was 45 $\mu\text{mol/L}$. At the concentrations of more than IC_{50} , the inhibitory patterns were identical ($P > 0.05$, Figure 3).

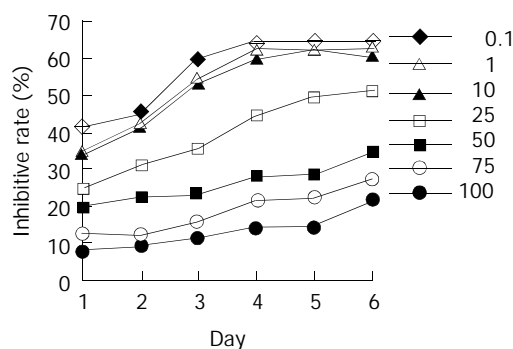


Figure 3 Inhibitory effects of daidzein on growth of estrogen-receptor-positive pancreatic cancer MiaPaCa-2 cells. 0.1 $\mu\text{mol/L}$, 1 $\mu\text{mol/L}$, 10 $\mu\text{mol/L}$, 25 $\mu\text{mol/L}$, 50 $\mu\text{mol/L}$, 75 $\mu\text{mol/L}$ and 100 $\mu\text{mol/L}$ of daidzein were used, respectively.

Inhibitory effect of daidzein on estrogen-receptor-negative pancreatic cancer cells

ER-negative pancreatic cancer PANC-1 cells were treated by daidzein. A dose-dependent effect was observed (Figure 4; 10 $\mu\text{mol/L}$, 25 $\mu\text{mol/L}$, 50 $\mu\text{mol/L}$ and 75 $\mu\text{mol/L}$, $P < 0.05$;

100 $\mu\text{mol/L}$, $P < 0.01$). When cells were treated for 2 d, 50% inhibitory rate might be observed. The IC_{50} was 80 $\mu\text{mol/L}$ on day 2 and 75 $\mu\text{mol/L}$ on day 3.

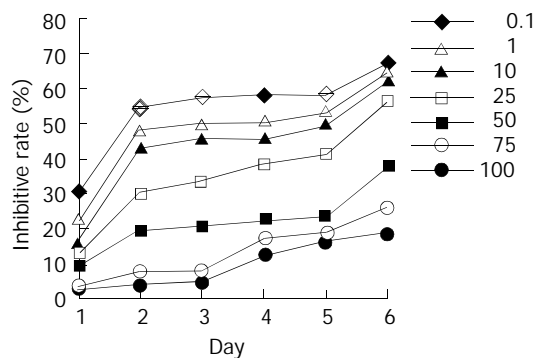


Figure 4 Inhibitory effects of daidzein on growth of estrogen-receptor-negative pancreatic cancer PANC-1 cells. 0.1 $\mu\text{mol/L}$, 1 $\mu\text{mol/L}$, 10 $\mu\text{mol/L}$, 25 $\mu\text{mol/L}$, 50 $\mu\text{mol/L}$, 75 $\mu\text{mol/L}$ and 100 $\mu\text{mol/L}$ of daidzein were used, respectively.

DISCUSSION

There has been an increase in the incidence of pancreatic cancer recent years^[18-21]. The pattern of its increase had some similarities to the high incidence of breast cancer in women and prostate cancer in men in Western communities^[17]. Typical Western diets have a low content of natural plant hormones, phytoestrogens, which are beneficial to our health^[1-6]. They exerted their anticancer effects by their specific bi-effects, estrogenic and antiestrogenic properties^[22-24]. On the one hand, they acted as antiestrogens by competing with endogenous estrogens for receptor binding sites, and decrease the promoting effects of high levels of endogenous estrogens^[25]. On the other hand, they could inhibit the activities of tyrosine protein kinase, DNA topoisomerase, angiogenesis and antioxidant^[26-29].

Hormone products were related to the pathological behaviors of several carcinomas (including colorectal carcinoma, gastric carcinoma, pancreatic carcinoma, etc.) and might help to predict the prognosis and effectiveness of endocrine therapy for some kinds of carcinomas^[30-32]. As to pancreatic carcinoma, there were indications of possible effects of sex hormones^[33]. The pancreatic cell lines, MiaPaCa-2 and PANC-1, used in our study were ER positive and negative cells, respectively^[34,35]. We found that daidzein inhibited the growth of both ER positive and negative pancreatic cancer cells. However, their inhibitory patterns were different. For ER-positive cells, MiaPaCa-2, when the concentrations of daidzein were higher than the level of IC_{50} , the inhibitory effect would not significantly increase. It indicated that its antiproliferative effect was exerted by binding to ER and appeared a saturation phenomenon. For PANC-1, an ER-negative cell, the saturation phenomenon was not found and the inhibition was in a dose-dependent manner. Its IC_{50} was higher than that of MiaPaCa-2, indicating that for the chemoprevention of ER-negative pancreatic cancer, high concentrations of daidzein should be used.

The antiestrogen reagent, tamoxifen was a choice of hormonal therapy for pancreatic cancer^[16,33]. The favorable response to this therapy and survival of patients were dependent on whether the patients' tumor cells were estrogen receptor positive or not^[16]. The presence or absence of estrogen receptors was also important in determining the effects of phytoestrogens on pancreatic cancer cells. A report used four kinds of phytoestrogens to study human pancreatic cancer cells showed that equol and coumestrol had anticarcinogenic effects on human ER positive pancreatic cancer Su86.86 cells. However,

they stimulated the growth of human ER negative pancreatic cancer HPAF-11 cells, genistein stimulated the growth of HPAF-11 cells but had little effect on Su86.86 cells. Another phytoestrogen, biochanin A, inhibited the growth of both Su86.86 cells and HPAF-11 cells^[36]. Our results showed that daidzein, another main phytoestrogen, had inhibitory effects on both ER positive and negative pancreatic cancer cells. As phytoestrogens are a large group of compounds, the possibility of gender differences in response to these reagents may be important in determining their ability to act as chemoprotective reagents for pancreatic cancer.

REFERENCES

- Bingham SA, Atkinson C, Liggins J, Bluck L, Coward A. Phytoestrogens: where are we now? *Br J Nutr* 1998; **79**: 393-406
- Yamamoto S, Sobue T, Kobayashi M, Sasaki S, Tsugane S. Japan Public Health Center-Based Prospective Study on Cancer Cardiovascular Diseases Group. Soy, soflavones, and breast cancer risk in Japan. *J Natl Cancer Inst* 2003; **95**: 906-913
- Adlercreutz H. Phyto-oestrogens and cancer. *Lancet Oncol* 2002; **3**: 364-373
- Morrissey C, Watson RW. Phytoestrogens and prostate cancer. *Curr Drug Targets* 2003; **4**: 231-241
- Peeters PH, Keinan-Boker L, van der Schouw YT, Grobbee DE. Phytoestrogens and breast cancer risk. Review of the epidemiological evidence. *Breast Cancer Res Treat* 2003; **77**: 171-183
- Zhou JR, Mukherjee P, Gugger ET, Tanaka T, Blackburn GL, Clinton SK. Inhibition of murine bladder tumorigenesis by soy isoflavones via alterations in the cell cycle, apoptosis, and angiogenesis. *Cancer Res* 1998; **58**: 5231-5238
- Maggiolini M, Bonfiglio D, Marsico S, Panno ML, Cenni B, Picard D, Ando S. Estrogen receptor alpha mediates the proliferative but not the cytotoxic dose-dependent effects of two major phytoestrogens on human breast cancer cells. *Mol Pharmacol* 2001; **60**: 595-602
- Yanagihara K, Ito A, Toge T, Numoto M. Antiproliferative effects of isoflavones on human cancer cell lines established from the gastrointestinal tract. *Cancer Res* 1993; **53**: 5815-5821
- Su SJ, Yeh TM, Lei HY, Chow NH. The potential of soybean foods as a chemoprevention approach for human urinary tract cancer. *Clin Cancer Res* 2000; **6**: 230-236
- Tan ZJ, Hu XG, Cao GS, Tang Y. Analysis of gene expression profile of pancreatic carcinoma using cDNA microarray. *World J Gastroenterol* 2003; **9**: 818-823
- Li YJ, Ji XR. Relationship between expression of E-cadherin-catenin complex and clinicopathologic characteristics of pancreatic cancer. *World J Gastroenterol* 2003; **9**: 368-372
- Zheng M, Liu LX, Zhu AL, Qi SY, Jiang HC, Xiao ZY. K-ras gene mutation in the diagnosis of ultrasound guided fine-needle biopsy of pancreatic masses. *World J Gastroenterol* 2003; **9**: 188-191
- Shankar A, Russell RC. Recent advances in the surgical treatment of pancreatic cancer. *World J Gastroenterol* 2001; **7**: 622-626
- Ghaneh P, Slavin J, Sutton R, Hartley M, Neoptolemos JP. Adjuvant therapy in pancreatic cancer. *World J Gastroenterol* 2001; **7**: 482-489
- Singh S, Baker PR, Poulson R, Wright NA, Sheppard MC, Langman MJ, Neoptolemos JP. Expression of oestrogen receptor and oestrogen-inducible genes in pancreatic cancer. *Br J Surg* 1997; **84**: 1085-1089
- Horimi T, Takasaki M, Toki A, Nishimura W, Morita S. The beneficial effect of tamoxifen therapy in patients with resected adenocarcinoma of the pancreas. *Hepatogastroenterology* 1996; **43**: 1225-1229
- Stephens FO. The increased incidence of cancer of the pancreas: is there a missing dietary factor? Can it be reversed? *Aust N Z J Surg* 1999; **69**: 331-335
- Xu HB, Zhang YJ, Wei WJ, Li WM, Tu XQ. Pancreatic tumor: DSA diagnosis and treatment. *World J Gastroenterol* 1998; **4**: 80-81
- Zhao XY, Yu SY, Da SP, Bai L, Guo XZ, Dai XJ, Wang YM. A clinical evaluation of serological diagnosis for pancreatic cancer. *World J Gastroenterol* 1998; **4**: 147-149
- Guo XZ, Friess H, Shao XD, Liu MP, Xia YT, Xu JH, Buchler MW.

- KAI1 gene is differently expressed in papillary and pancreatic cancer: influence on metastasis. *World J Gastroenterol* 2000; **6**: 866-871
- 21 **Yue H**, Na YL, Feng XL, Ma SR, Song FL, Yang B. Expression of p57kip2, Rb protein and PCNA and their relationships with clinicopathology in human pancreatic cancer. *World J Gastroenterol* 2003; **9**: 377-380
- 22 **So FV**, Guthrie N, Chambers AF, Carroll KK. Inhibition of proliferation of estrogen receptor-positive MCF-7 human breast cancer cells by flavonoids in the presence and absence of excess estrogen. *Cancer Lett* 1997; **112**: 127-133
- 23 **Shao ZM**, Alpaugh ML, Fontana JA, Barsky SH. Genistein inhibits proliferation similarly in estrogen receptor-positive and negative human breast carcinoma cell lines characterized by P21WAF1/CIP1 induction, G2/M arrest, and apoptosis. *J Cell Biochem* 1998; **69**: 44-54
- 24 **Hopert AC**, Beyer A, Frank K, Strunck E, Wunsche W, Vollmer G. Characterization of estrogenicity of phytoestrogens in an endometrial-derived experimental model. *Environ Health Perspect* 1998; **106**: 581-586
- 25 **Scambia G**, Ranelletti FO, Panici PB, Piantelli M, De Vincenzo R, Ferrandina G, Bonanno G, Capelli A, Mancuso S. Quercetin induces type-II estrogen-binding sites in estrogen-receptor-negative (MDA-MB231) and estrogen-receptor-positive (MCF-7) human breast-cancer cell lines. *Int J Cancer* 1993; **54**: 462-466
- 26 **Robinson MJ**, Corbett AH, Osheroff N. Effects of topoisomerase II-targeted drugs on enzyme-mediated DNA cleavage and ATP hydrolysis: evidence for distinct drug interaction domains on topoisomerase II. *Biochemistry* 1993; **32**: 3638-3643
- 27 **Spinozzi F**, Pagliacci MC, Migliorati G, Moraca R, Grignani F, Riccardi C, Nicoletti I. The natural tyrosine kinase inhibitor genistein produces cell cycle arrest and apoptosis in Jurkat T-leukemia cells. *Leuk Res* 1994; **18**: 431-439
- 28 **Fotsis T**, Pepper M, Adlercreutz H, Fleischmann G, Hase T, Montesano R, Schweigerer L. Genistein, a dietary-derived inhibitor of *in vitro* angiogenesis. *Proc Natl Acad Sci U S A* 1993; **90**: 2690-2694
- 29 **Wei H**, Wei L, Frenkel K, Bowen R, Barnes S. Inhibition of tumor promoter-induced hydrogen peroxide formation *in vitro* and *in vivo* by genistein. *Nutr Cancer* 1993; **20**: 1-12
- 30 **Xin Y**, Li XL, Wang YP, Zhang SM, Zheng HC, Wu DY, Zhang YC. Relationship between phenotypes of cell-function differentiation and pathobiological behavior of gastric carcinomas. *World J Gastroenterol* 2001; **7**: 53-59
- 31 **Zhao XH**, Gu SZ, Liu SX, Pan BR. Expression of estrogen receptor and estrogen receptor messenger RNA in gastric carcinoma tissues. *World J Gastroenterol* 2003; **9**: 665-669
- 32 **Yao GY**, Zhou JL, Lai MD, Chen XQ, Chen PH. Neuroendocrine markers in adenocarcinomas: an investigation of 356 cases. *World J Gastroenterol* 2003; **9**: 858-861
- 33 **Theve NO**, Pousette A, Carlstrom K. Adenocarcinoma of the pancreas—a hormone sensitive tumor? A preliminary report on Nolvadex treatment. *Clin Oncol* 1983; **9**: 193-197
- 34 **Kuramoto M**, Yamashita J, Ogawa M. Tissue-type plasminogen activator predicts endocrine responsiveness of human pancreatic carcinoma cells. *Cancer* 1995; **75**: 1263-1272
- 35 **Abe M**, Yamashita J, Ogawa M. Medroxyprogesterone acetate inhibits human pancreatic carcinoma cell growth by inducing apoptosis in association with Bcl-2 phosphorylation. *Cancer* 2000; **88**: 2000-2009
- 36 **Lyn-Cook BD**, Stottman HL, Yan Y, Blann E, Kadlubar FF, Hammons GJ. The effects of phytoestrogens on human pancreatic tumor cells *in vitro*. *Cancer Lett* 1999; **142**: 111-119

Edited by Zhang JZ and Wang XL Proofread by Xu FM

Intravenous administration of glutathione protects parenchymal and non-parenchymal liver cells against reperfusion injury following rat liver transplantation

Rolf J. Schauer, Sinan Kalmuk, Alexander L. Gerbes, Rosemarie Leiderer, Herbert Meissner, Friedrich W. Schildberg, Konrad Messmer, Manfred Bilzer

Rolf J. Schauer, Sinan Kalmuk, Friedrich W. Schildberg, Surgical Department, Klinikum Grosshadern, Ludwig-Maximilians-University of Munich, Germany

Alexander L. Gerbes, Manfred Bilzer, Department of Medicine II, Klinikum Grosshadern, Ludwig-Maximilians-University of Munich, Germany

Rosemarie Leiderer, Konrad Messmer, Institute for Surgical Research, Klinikum Grosshadern, Ludwig-Maximilians-University of Munich, Germany

Herbert Meissner, Institute of Pathology, Klinikum Grosshadern, Ludwig-Maximilians-University of Munich, Germany

Supported in part by a grant from the Friedrich-Baur Stiftung, the Muenchener Medizinische Wochenschrift (MMW) and the Deutsche Forschungsgemeinschaft (DFG Scha 857/1-1; DFG Ge 576/24-1)

Correspondence to: Dr. Rolf J. Schauer, Surgical Department, University Hospital Klinikum Grosshadern, Marchioninistr. 15, 81377 Munich, Germany. schauer@gch.med.uni-muenchen.de

Telephone: +49-89-7095-3560 **Fax:** +49-89-7095-8894

Received: 2004-01-10 **Accepted:** 2004-02-28

Abstract

AIM: To investigate the effects of intravenous administration of the antioxidant glutathione (GSH) on reperfusion injury following liver transplantation.

METHODS: Livers of male Lewis rats were transplanted after 24 h of hypothermic preservation in University of Wisconsin solution in a syngeneic setting. During a 2-h reperfusion period either saline (controls, $n=8$) or GSH (50 or 100 $\mu\text{mol}/(\text{h}\cdot\text{kg})$, $n=5$ each) was continuously administered via the jugular vein.

RESULTS: Two hours after starting reperfusion plasma ALT increased to $1\,457\pm 281$ U/L (mean \pm SE) in controls but to only 908 ± 187 U/L ($P<0.05$) in animals treated with 100 μmol GSH/(h·kg). No protection was conveyed by 50 μmol GSH/(h·kg). Cytoprotection was confirmed by morphological findings on electron microscopy: GSH treatment prevented detachment of sinusoidal endothelial cells (SEC) as well as loss of microvilli and mitochondrial swelling of hepatocytes. Accordingly, postischemic bile flow increased 2-fold. Intravital fluorescence microscopy revealed a nearly complete restoration of sinusoidal blood flow and a significant reduction of leukocyte adherence to sinusoids and postsinusoidal venules. Following infusion of 50 μmol and 100 μmol GSH/(h·kg), plasma GSH increased to 65 ± 7 mol/L and 97 ± 18 mol/L, but to only 20 ± 3 mol/L in untreated recipients. Furthermore, plasma glutathione disulfide (GSSG) increased to 7.5 ± 1.0 mol/L in animals treated with 100 $\mu\text{mol}/(\text{h}\cdot\text{kg})$ GSH but did not raise levels of untreated controls (1.8 ± 0.5 mol/L) following infusion of 50 μmol GSH/(h·kg) (2.2 ± 0.2 mol/L).

CONCLUSION: Plasma GSH levels above a critical level may act as a "sink" for ROS produced in the hepatic vasculature

during reperfusion of liver grafts. Therefore, GSH can be considered a candidate antioxidant for the prevention of reperfusion injury after liver transplantation, in particular since it has a low toxicity in humans.

Schauer RJ, Kalmuk S, Gerbes AL, Leiderer R, Meissner H, Schildberg FW, Messmer K, Bilzer M. Intravenous administration of glutathione protects parenchymal and non-parenchymal liver cells against reperfusion injury following rat liver transplantation. *World J Gastroenterol* 2004; 10(6): 864-870

<http://www.wjgnet.com/1007-9327/10/864.asp>

INTRODUCTION

A decade after the introduction of the University of Wisconsin (UW) solution for cold preservation of solid organs, hepatic preservation and reperfusion injury is still a serious problem which contributes to primary nonfunction and dysfunction of the liver allograft^[1-3]. Years of research in liver preservation have established the superiority of the UW formulation over other solutions. Although hepatocytes and sinusoidal endothelial cells are injured during cold preservation in UW solution they remain alive even after periods of ischemia well beyond the limit of organ viability^[2-4]. Hepatocyte and SEC death occurs rapidly on oxygenated reperfusion^[2,4] and the extent of SEC death has been shown to be a critical factor influencing graft survival in various animal models^[5-7]. However, therapeutic strategies which reduce reperfusion injury to hepatocytes and SEC during liver transplantation remain to be established.

There is substantial evidence that activation of Kupffer cells (KC), the generation of reactive oxygen species (ROS) and disturbance of the hepatic microcirculation contribute to reperfusion injury^[8-11]. During the reperfusion, activated KC produce mediators of inflammation, including tumor necrosis factor α , interleukins and chemokines, and release ROS into the sinusoidal space^[3,8]. The resulting vascular oxidant stress has been discovered as potential mechanism of vasoconstriction and leukocyte adherence in the liver^[12-16]. This may lead to disturbance of the hepatic microcirculation, ultimately resulting in hypoxic cell injury. Furthermore, KC-derived ROS could activate redox-sensitive transcription factors such as nuclear factor (NF)- κ B and activator protein-1 (AP-1) in endothelial cells and hepatocytes, thereby activating proinflammatory genes and adding to the hepatic damage^[17,18].

Thus, ROS can be considered as signal molecules which trigger several pivotal mechanisms of reperfusion injury. A large number of investigations using antioxidant interventions support this hypothesis^[10]. However, the clinical relevance of many antioxidants is limited by side-effects or high cost which may explain the lack of established antioxidative interventions to prevent hepatic reperfusion injury^[3]. Therefore, recent studies investigated the therapeutic potential of the endogenous

antioxidant *glutathione* (GSH), in particular since it has a low toxicity in humans^[19]. Furthermore, GSH is able to react spontaneously with nearly all oxidants formed during inflammation, which results in the formation of oxidized glutathione (GSSG)^[20-22]. Previous studies demonstrated that GSH released through the GSH transporter of hepatocytes may act as an endogenous defense system against KC – and leukocyte – derived ROS, thus protecting the hepatic vasculature from damage by inflammatory cells^[8]. Therefore, interventions increasing plasma GSH levels should confer protection against reperfusion injury. Accordingly, treatment of cold preserved livers with GSH upon reperfusion prevented damage to hepatocytes in the model of isolated rat liver perfusion^[23]. These *in vitro* findings suggest that GSH, as a candidate drug, could prevent reperfusion injury of the liver allograft. Consequently, future studies need to be directed toward characterization of the protective potential of GSH treatment *in vivo* which may have important implications for an application in the clinical setting.

Therefore, the purpose of this study was to investigate whether intravenous administration of GSH protects the rat liver against reperfusion injury during liver transplantation. In particular, the aims of the current study are: (1) to investigate effects of intravenously applied GSH on hepatocyte and SEC damage; (2) to examine the effect of GSH treatment on disturbances of the hepatic microcirculation, and (3) to determine the functional significance of changes of the extracellular antioxidant capacity.

MATERIALS AND METHODS

Animals and preparation

Syngeneic, male Lewis rats (donors: 207±12 g; recipients: 276±18 g body mass) were purchased from Charles River Wiga, Sulzfeld, Germany and housed in a temperature- and humidity-controlled room under a constant 12-h light/dark cycle. Animals had free access to water and rat chow (standard diet, Altromin, Germany). All experiments were performed with rats fasted 12 h prior to donor and recipient operations. All studies were performed with the permission of the government authorities and in accordance with the German Legislation on Laboratory Animal Experiments.

Donor and recipient operations were performed under spontaneous ether inhalation. The left carotid artery was cannulated with a polyethylene catheter for continuous monitoring of the mean arterial blood pressure and heart rate during the operation. Another catheter was inserted into the jugular vein for substitution of plasma volume and injection of fluorescent compounds as well as for continuous infusion of glutathione during reperfusion. Body temperature was kept between 36.5 °C and 37.5 °C by means of a heating pad. Donor livers were preserved by retrograde aortal flush with 10 mL UW-solution and stored at 4 °C for 24 h. Prior to the implantation procedure, the livers were rinsed with warm Ringer's lactate solution (10 mL) via the portal vein at a hydrostatic pressure of 10 cm H₂O. Orthotopic liver transplantation was performed using a modified cuff technique^[24]. Differing from the original technique, grafted livers were rearterialized and simultaneously reperfused through the portal vein and hepatic artery^[25]. Portal clamping time was less than 20 min in all experiments.

The common bile duct of the graft was cannulated with a PE-tube and bile was collected in Eppendorf cups. Plasma samples (500 µL) were obtained in the recipient before hepatectomy and 60 and 120 min after reperfusion of the transplanted liver. The volume of the blood drawn was replaced by saline. Five minutes after starting reperfusion, all rats received 0.5 mL of albumin (5%) and 0.5 mL sodium bicarbonate in order to maintain blood pressure and physiological pH. To

avoid major fluid loss and drying of the liver, possibly affecting microhemodynamics the abdominal cavity was covered with Saran wrap throughout the operation. After 120 min of reperfusion, experiments were terminated and the liver weight was determined.

Experimental groups

Two intervention groups ($n=5$ each) were compared with the control group ($n=8$). In control animals, saline was infused intravenously (2 mL/h) during reperfusion of the grafted liver, starting 20 min before declamping of the portal vein and hepatic artery. In contrast, intervention groups received GSH via the jugular vein, starting 20 min prior to reperfusion until the end of the two hour reperfusion period (total infusion time 140 min). GSH (Tationil 600[®], Roche Pharmaceuticals/Italy) was administered at 50 or 100 µmol/(h·kg) ($n=5$ each) by continuous infusion (2 mL/h) of stock solutions (0.24 mol/L and 0.48 mol/L), using a micro-infusion pump (SP100i, WPI, Aston, UK). Two sham groups underwent laparotomy and intravital microscopy without hepatic ischemia in the absence ($n=6$) or presence of intravenous GSH infusion (100 µmol GSH/(h·kg), $n=5$) for 140 min.

In-vivo fluorescence microscopy (IVM)

In vivo fluorescence microscopic studies were performed 30 min after revascularization under stable hemodynamic conditions, using a modified Leitz-Orthoplan microscope combined with epi-illumination technique^[26,27]. For assessment of microvascular liver perfusion and leukocyte-endothelial interaction the left liver lobe was exteriorized on a stage. For visualization of microcirculatory disturbances, sodium fluorescein (1 µmol/kg; Merck AG, Darmstadt, Germany) and rhodamin 6G (0.1 µmol/kg; Merck AG, Darmstadt, Germany) were injected intravenously for fluorescent staining of hepatocytes (negative contrast for plasma) and leukocytes, respectively. Quantification of microhemodynamic parameters was performed offline by frame-to-frame analysis of the videotaped images in a blinded fashion. Lobular perfusion and leukocyte adherence were analyzed by scanning a region of 10 randomly selected acinar areas and postsinusoidal venules, respectively. *Non – perfused sinusoids* were estimated by counting the number of continuously perfused and non - perfused sinusoids and were expressed as the percentage of all sinusoids visible in a pre-defined area. *Permanent adherence (sticking) of leukocytes to the sinusoidal endothelium* was quantified by counting the number of permanently attached leukocytes (at least for 20 s) within the 3 different segments of sinusoids. *Leukocyte sticking in postsinusoidal venules* was determined by the quantity of leukocytes attached for at least 20 s to the surface of postsinusoidal venules. Furthermore, *temporary adherence of leukocytes (rolling)* was assessed as the number of transiently attached leukocytes along the endothelial surface of postsinusoidal venules during an observation period of 20 s.

Determination of Kupffer cell function

KC function was assessed by determination of their particle phagocytosis as described earlier^[28,29]. At the end of IVM analysis, plain fluorescent latex beads in isotonic saline solution were injected as bolus (3×10^8 /kg) through the carotid catheter (diameter 1.1 µm, Polysciences Inc., Warrington, PA, USA). Phagocytic activity was then analyzed successively during the first 5 min after injection in 10 randomly selected liver lobules in each experiment. Adherence of latex particles was quantified by counting the number of beads moving in sinusoids as a percentage of all beads visible in the field during an observation period of 10 s. Beads in presinusoidal and postsinusoidal venules were not included in analysis.

Analytical methods

Blood samples of 500 μL were collected for determination of total glutathione (sum of GSH and GSSG) and GSSG. For GSSG analysis, an aliquot (200 μL) of blood was mixed immediately with 200 μL of 10 mmol/L N-ethylmaleimide (NEM) in 100 mmol/L phosphate buffer (pH 6.5) containing 17.5 mmol/L EDTA^[30]. The remaining blood was centrifuged at full speed for 1 min. An aliquot (100 μL) of plasma was pipetted into 100 μL sulfosalicylic acid (5%) for determination of total glutathione. To separate GSSG from NEM and NEM-GSH adducts, an aliquot of NEM treated plasma was passed through a Sep-Pak_{C18} cartridge (Waters, Framingham, MA, USA) followed by 1 mL of 100 mmol/L phosphate buffer (pH 7.5). GSSG in the eluates and total glutathione in acidified plasma samples was determined by an enzymatic test as described previously^[31]. GSH plasma concentrations were calculated as the difference between total glutathione and GSSG.

Serum aminotransferases

Serum aminotransferases were used as established markers of hepatic injury. Aspartate aminotransferase (AST) and alanine aminotransferase (ALT) were measured 2 h after reperfusion using a serum multiple analyzer (Hitachi 917, Roche Germany).

Transmission electron microscopy

At the end of the experiments, perfusion-fixation of hepatic tissue was performed using a 50 g/L glutaraldehyde/40 g/L paraformaldehyde mixture in phosphate buffer (pH 7.4) via the hepatic artery at a constant pressure of approximately 80 mmHg. Specimens were cut from both the right and left liver lobes and blocks were diced into 1 mm cubes. Samples were stored in fixative for 2 to 3 d prior to further processing. Specimens were postfixed with osmium tetroxide, dehydrated in graded alcohol and embedded in Epon 812. Ultrathin sections were cut and contrasted with uranyl acetate and lead citrate for electron microscopy^[11].

Statistical analysis

All data are expressed as mean \pm SE. Statistical differences between groups were calculated using paired or unpaired Student's *t* test for randomly distributed data and the Mann-Whitney *U* test for nonparametric data following analysis of variance (ANOVA). Differences were considered significant at $P < 0.05$.

RESULTS

Cell injury and liver function after liver transplantation

Injury of parenchymal and non-parenchymal liver cells after liver transplantation was assessed by the release of ALT and AST as well as by electron microscopic analysis at 120 min of reperfusion. Parenchymal cell damage in untreated animals was indicated by a 25- and 40-fold increase of ALT and AST serum levels, respectively, when compared with sham-operated animals (Figure 1). Continuous intravenous administration of 100 μmol GSH/(h \cdot kg) during reperfusion significantly ($P < 0.05$) reduced ALT and AST levels by almost 40% whereas infusion of 50 μmol GSH/(h \cdot kg) had no effect (Figure 1).

Transmission electron microphotographs of the untreated liver grafts after 120 min of reperfusion showed alterations of hepatocytes, including cell edema, a substantial loss of microvilli and generalized swelling of mitochondria (Figure 2A,B). Furthermore, non-parenchymal injury was evident by various degrees of SEC-detachment from the perisinusoidal matrix plate or even complete loss of the sinusoidal endothelial lining (Figure 2 A,B). Consequently, the space of Dissé was

enlarged in control livers. In contrast, treatment of animals with 100 μmol /(h \cdot kg) GSH was effective in protecting hepatocytes with only minimal loss of microvilli of normally shaped parenchymal cells and only sporadic mitochondrial swelling. Moreover, GSH prevented SEC detachment, thus resulting in normal spaces of Dissé (Figure 2 C,D).

Function of liver allografts was estimated by recovery of bile flow. Bile flow of sham-operated animals remained constant during the observation period of 150 min and was comparable to bile flow rates of donor livers before ischemia (Figure 3). After transplantation of control livers, bile flow returned to only 45% of baseline values. Intravenous infusion of 50 μmol GSH/(h \cdot kg) had no effect on the postischemic bile flow whereas 100 μmol GSH/(h \cdot kg) significantly ($P < 0.05$) increased bile flow during the complete reperfusion period (Figure 3).

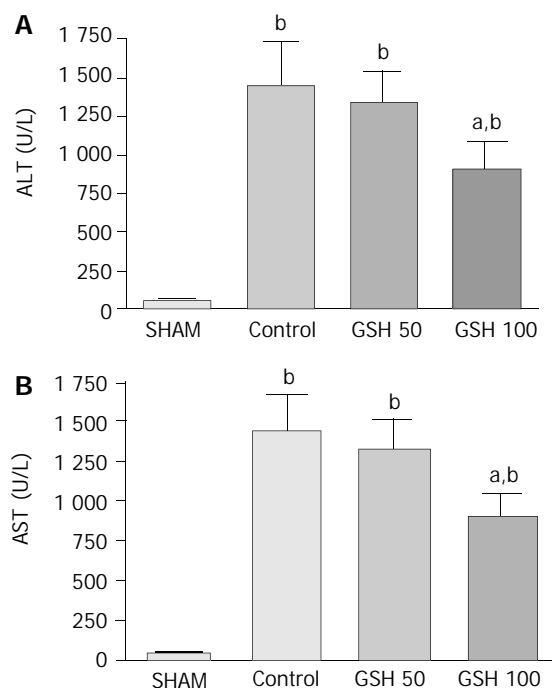


Figure 1 ALT (A) and AST (B) plasma levels after liver transplantation. Livers preserved for 24 h in UW solution at +4 °C before transplantation. Compared to untreated livers ($n=8$) administration of 100 μmol GSH/(h \cdot kg) ($n=5$), but not of 50 μmol GSH/(h \cdot kg) ($n=5$), resulted in a significant decrease of plasma ALT and AST levels at 2 h of reperfusion. Results are mean \pm SE. ^b $P < 0.001$ vs sham-operated animals ($n=5$); ^a $P < 0.05$ vs untreated livers.

Kupffer cell function after liver transplantation

Latex particle phagocytosis by KC reflects their function under various conditions. In agreement with earlier observations, rapid clearance of intra-arterially administered fluorescent latex particles was observed in sham-operated animals. Five minutes after injection only 8.1 \pm 2.5% particles were freely movable in the sinusoids. This rate was not influenced by liver transplantation as indicated by 11.2 \pm 1.0% of all visible beads, freely movable in the sinusoids of untreated animals. Neither GSH treatment with 50 μmol /(h \cdot kg) nor with 100 μmol /(h \cdot kg) affected phagocytosis of latex particles, resulting in 12.0 \pm 1.1% and 10.5 \pm 2.0% of beads moving in sinusoids at 5 min upon bolus injection, respectively. Since KC represents approximately 90% of the phagocytic capacity in the liver, these results suggest unaltered KC function after reperfusion of untreated and GSH-treated liver grafts.

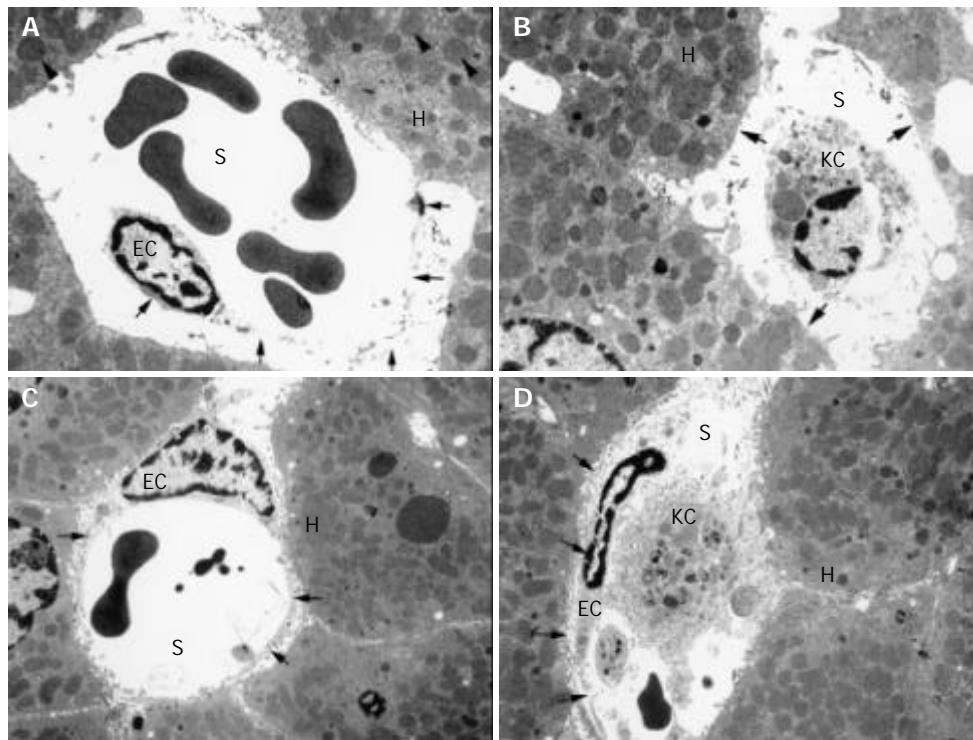


Figure 2 Transmission electron microphotographs of untreated and GSH- treated liver allografts. Arrow-heads indicate mitochondrial swelling of hepatocytes in untreated livers (A) which was almost absent in allografts treated with 100 $\mu\text{mol}/(\text{h}\cdot\text{kg})$ during reperfusion (C). Arrows demonstrate the loss of hepatocyte microvilli in untreated controls (B) whereas GSH administration preserved microvilli in nearly all hepatocyte membranes (D). As indicated by open arrows detachment of SEC (A) as well as its complete loss (B) was evident in untreated livers. GSH- treatment preserved sinusoidal endothelial lining with a normal space of Dissé (C,D). Letters indicate: H, hepatocyte; KC, Kupffer cell; EC, endothelial cell; S, sinusoidal lumen. Bars represent either 1.7 μm (B) or 2.5 μm (A,C,D).

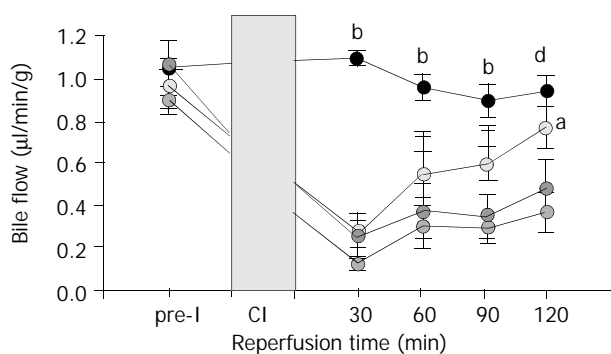


Figure 3 Effect of GSH treatment on bile flow after liver transplantation. Animals were treated with 50 $\mu\text{mol}/(\text{h}\cdot\text{kg})$ GSH (○, $n=5$) or 100 $\mu\text{mol}/(\text{h}\cdot\text{kg})$ GSH (◐, $n=5$) and compared with untreated controls (●, $n=8$) and a sham- operated group (●, $n=5$). Results are mean \pm SE. ^b $P<0.001$ vs untreated or GSH- treated livers; ^d $P<0.01$ vs 100 $\mu\text{mol}/(\text{h}\cdot\text{kg})$ GSH; ^a $P<0.05$ vs untreated controls.

Effect of GSH treatment on the microcirculation of liver allografts

Compared with sham-operated animals, substantial disturbances of the microcirculation were observed in untreated liver allografts (Figure 4). Thirty minutes after starting reperfusion almost 25% of the sinusoids were not perfused. Intravenous infusion of 50 as well as 100 $\mu\text{mol}/(\text{h}\cdot\text{kg})$ prevented this no – reflow phenomenon, thereby improving hepatic perfusion (Figure 4 A).

Furthermore, intravital microscopy revealed considerable leukocyte sticking within sinusoids and postsinusoidal venules in untreated liver allografts (Figure 4 B,C). A significant

reduction ($P<0.001$) of stagnant leukocytes in sinusoids was found in both treatment groups (Figure 4 B). Comparable to acinar leukocyte sticking, permanent adherence of leukocytes to postsinusoidal venules was reduced by 57% and 69% ($P<0.001$) when animals received 50 or 100 $\mu\text{mol}/(\text{h}\cdot\text{kg})$, respectively (Figure 4 C). Temporary adherence of leukocytes (rolling) in postsinusoidal venules is supposed to be the initiating event in the sequence to permanent adherence to the vascular endothelium. However rolling of leukocytes was slightly increased by GSH treatment (Figure 4E).

Effect of intravenous GSH infusion on plasma GSH and GSSG levels

Sixty minutes after starting reperfusion plasma GSH levels of untreated animals increased 2-fold when compared to sham-operated animals (Figure 5). This was accompanied by a 3-fold increase of plasma GSSG (Figure 5). Infusion of 50 $\mu\text{mol}/(\text{h}\cdot\text{kg})$ GSH resulted in a 6-fold increase of plasma GSH whereas GSSG did not exceed levels of untreated controls. In contrast, 100 $\mu\text{mol}/(\text{h}\cdot\text{kg})$ elevated plasma GSH as well as GSSG by up to 9-fold above values obtained in the sham-group (Figure 5). Moreover, plasma GSSG increased to significant higher levels when compared with untreated or GSH – treated (50 $\mu\text{mol}/(\text{h}\cdot\text{kg})$) animals. In order to estimate the role of spontaneous oxidation of intravenously applied GSH a second group of sham-operated animals was treated with 100 $\mu\text{mol}/(\text{h}\cdot\text{kg})$ GSH. This resulted in marked increase of plasma GSH to 93 ± 10 mol/L which was similar to that observed in liver allografts (7.5 \pm 1.8 mol/L). However, plasma GSSG increased to only 3.0 ± 0.9 in contrast to 7.5 ± 0.9 mol/L in GSH- treated liver allografts. These findings clearly indicate enhanced oxidation of intravenously applied GSH at the cytoprotective dose of 100 $\mu\text{mol}/(\text{h}\cdot\text{kg})$.

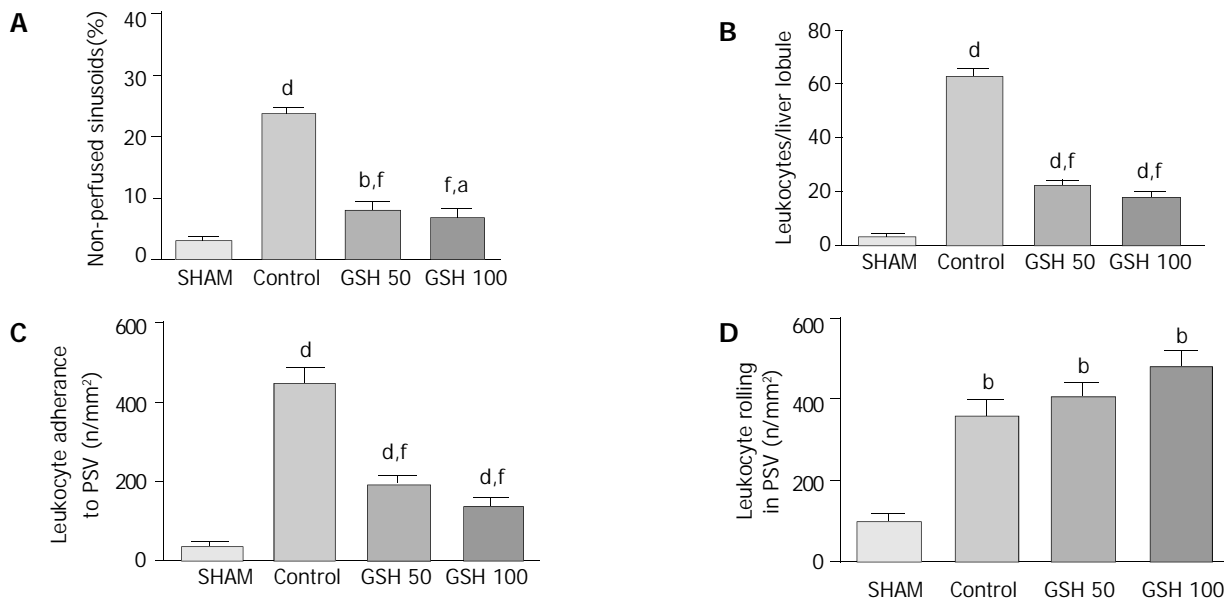


Figure 4 Impact of GSH treatment on the hepatic microcirculation after liver transplantation. Data from *in vivo* microscopy were obtained 30 min after starting reperfusion comparing untreated controls ($n=8$) with GSH-treated allografts (50 $\mu\text{mol}/(\text{h}\cdot\text{kg})$ and 100 $\mu\text{mol}/(\text{h}\cdot\text{kg})$; each $n=5$) as well as to a sham group ($n=5$). (A) Acinar perfusion failure is indicated as the percentage of non-perfused sinusoids (no reflow). (B) Leukocyte-adhesion (sticking) to sinusoids and (C) to postsinusoidal venules. (D) Temporary attachment of leukocytes (rolling) to the endothelium of postsinusoidal venules (PSV). Results are mean \pm SE. ^a $P<0.05$, ^d $P<0.01$ and ^b $P<0.001$ vs sham group. ^f $P<0.001$ vs control group.

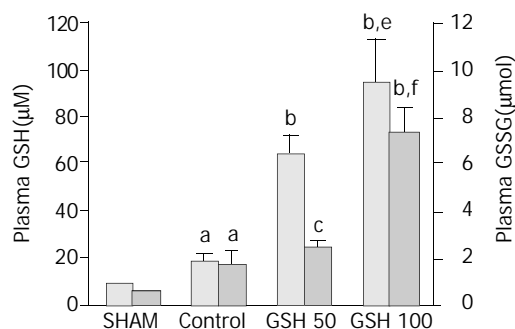


Figure 5 Plasma GSH- and GSSG concentrations following liver transplantation. Compared to sham-operated animals ($n=5$) a significant increase of reduced and oxidized glutathione was determined upon reperfusion of untreated grafts ($n=8$). Intravenous infusion of GSH at rates of 50 $\mu\text{mol}/(\text{h}\cdot\text{kg})$ ($n=5$) and 100 $\mu\text{mol}/(\text{h}\cdot\text{kg})$ ($n=5$) resulted in a dose-dependent increase of plasma GSH concentrations. The corresponding GSSG levels showed only a slight increase after administration of 50 μmol GSH/ $(\text{h}\cdot\text{kg})$, but increased markedly following infusion of 100 μmol GSH/ $(\text{h}\cdot\text{kg})$. Mean \pm SE. ^a $P<0.05$ vs sham; ^b $P<0.001$ and ^c $P<0.05$ vs control group; ^e $P<0.05$ vs GSH 50 and ^f $P<0.01$ vs GSH 50.

DISCUSSION

Recently, we have found that treatment of cold preserved livers with GSH upon reperfusion prevented reperfusion injury in the model of isolated rat liver perfusion^[23]. Due to several limitations of this experimental model, such as the absence of plasma antioxidants and the lack of leukocytes^[32,33], the potential protective effect of GSH treatment during liver transplantation remained to be defined. We also found that intravenous GSH treatment during liver transplantation prevents reperfusion injury of the liver allograft.

We obtained the following main results: (1) increase of the vascular antioxidant capacity by intravenous infusion of GSH causes a significant reduction of injury to hepatocytes and SEC as well as of (2) microcirculatory disturbances in liver allografts, and (3) Administration of GSH does not affect

KC function but enhances detoxification of KC-derived ROS as indicated by a marked increase of plasma GSSG.

Prevention of reperfusion injury to liver allografts by GSH

Intravenous administration of GSH at a dose of 100 $\mu\text{mol}/(\text{h}\cdot\text{kg})$ during the reperfusion phase of liver transplantation significantly reduced ALT and AST release by approximately 40% indicating the protection of the liver allografts. This contention is supported by distinct signs of parenchymal and non-parenchymal cell injury under electron microscopy already after 2 h of re-establishing blood flow. Untreated livers showed a complete detachment of SEC from the perisinusoidal matrix which in part determines graft viability^[4-7]. In contrast, detachment of SEC was dramatically attenuated in GSH-treated livers, indicating preservation of the sinusoidal architecture. Furthermore, GSH treatment markedly reduced mitochondrial swelling and the loss of microvilli in hepatocytes. These cytoprotective effects were accompanied by a marked improvement of postischemic liver function as assessed by a 2.5-fold increase of bile flow. Because postischemic GSH treatment can only protect cells which are not already seriously damaged before the onset of reperfusion, our results clearly demonstrate prevention of reperfusion injury to parenchymal and non-parenchymal liver cells by GSH.

Prevention of reperfusion injury by GSH depended on the GSH dose: 100 $\mu\text{mol}/(\text{h}\cdot\text{kg})$ but not 50 $\mu\text{mol}/(\text{h}\cdot\text{kg})$ showed protection. Based on steady state GSH plasma concentrations following GSH infusion, a concentration of approximately 100 $\mu\text{mol}/\text{L}$ appears to be pivotal for cytoprotection. In view of these findings, GSH seems as ideal and presumably safe candidate drug for prevention of reperfusion injury of the liver allograft since plasma GSH levels up to 500 $\mu\text{mol}/\text{L}$ showed no toxicity in humans^[19].

Mechanisms of GSH-mediated protection

Effect on Kupffer cell function There is extensive experimental evidence for KC activation as a central pathomechanism of reperfusion injury of the liver after warm or cold ischemia^[8,9]. To assess KC function we used the tool of intravital microscopic

analysis of latex particle phagocytosis^[28,29]. In agreement with earlier studies^[29] particle phagocytosis was not affected by cold preservation indicating functionally intact Kupffer cells in liver allografts. Furthermore, clearance of latex particles was not affected by postschismic administration of GSH. These results argue against a suppression of KC function as a potential protective mechanism of GSH action. Thus, potential hazards of other protective approaches interfering with vital host-defense function of KC (*e.g.* calcium channel blocker, KC-depleting agents,^[18,34,35]) would be avoided by GSH treatment. **Detoxification of ROS in the hepatic vasculature** Intravenous administration of GSH results in the degradation of GSH to its amino acids which are the again available for GSH synthesis in various organs including the liver^[36]. However several studies demonstrated no relevant increase of the hepatic GSH content 2 h after starting high-dose GSH infusion^[22,23]. These findings suggest that GSH effects are related rather to the increase in the extracellular antioxidant capacity than to influences on intracellular GSH. In line with this interpretation we obtained evidence for an extracellular mechanism of GSH-mediated cytoprotection.

The increase in plasma GSSG observed during reperfusion of untreated and GSH-treated livers was associated with a marked increase in plasma GSH. This parallel increase in GSH and GSSG suggests that GSSG resulted from extracellular oxidation rather than from intrahepatic generation of GSSG^[37,38]. Accordingly, previous studies with the blood – free perfused rat liver found only a very small release of GSSG into the perfusate during reperfusion^[39]. Furthermore, there was no evidence for a relevant increase of intracellular GSSG formation^[8,39]. Thus, plasma GSSG formation observed during reperfusion of liver allografts is likely to take place extracellularly. This could be due to spontaneous as well as reactive oxygen species-related oxidation of GSH. The results of the present study argue against a predominant role for spontaneous GSH oxidation. First, intravenous infusion of 50 $\mu\text{mol GSH}/(\text{h} \cdot \text{kg})$ during reperfusion of liver allografts resulted in a several fold increase of plasma GSH whereas plasma GSSG did not exceed the levels of untreated controls. Second, a comparable increase of plasma GSH was observed when sham-operated or transplanted animals were treated with 100 $\mu\text{mol GSH}/(\text{h} \cdot \text{kg})$. In contrast, a 2.5-fold higher increase of plasma GSSG was determined in transplanted rats. This difference clearly indicates that spontaneous oxidation of intravenously applied GSH contributes only in part to the increase in plasma GSSG. Based on these findings oxidation of GSH by ROS appears as a major determinant of plasma GSSG formation following liver transplantation. Consequently, the marked increase of plasma GSSG during infusion of the protective GSH dose of 100 $\mu\text{mol}/(\text{h} \cdot \text{kg})$ most likely reflects an enhanced detoxification of ROS in the hepatic vasculature.

Activated KC have been identified as potential source of extracellular ROS formation and GSH oxidation during reperfusion after warm hepatic ischemia^[8,40]. Accordingly, there was no evidence for plasma GSSG formation during reperfusion of KC-depleted liver allografts^[41]. These findings suggest that intravenously applied GSH protects liver allografts against the vascular oxidant stress produced by KC during reperfusion. This interpretation is further substantiated by the observation that externally added GSH and catalase protected leukocyte- free perfused rat livers against oxidant cell injury following selective KC activation^[42,43]. In this experimental model cytoprotection was achieved by vascular GSH concentrations of 100 mol/L, but not by 50 mol/L. The same vascular concentrations of GSH were achieved in the present study. Again, protection of liver allografts was only evident at plasma GSH concentrations of approximately 100 mol/L and was associated with a considerable extra-formation of plasma GSSG. These findings suggest that plasma GSH above a critical level may act as a “sink“

for ROS produced by KC during reperfusion. This could be due to non-enzymatic reactions between GSH and various ROS which strongly depend on the GSH concentration^[29,44,45].

Prevention of microcirculatory perfusion failure and SEC injury GSH of both doses remarkably improved the hepatic microcirculation. In particular, the number of perfused sinusoids increased to that observed in non-ischemic livers indicating prevention of the no-reflow phenomenon. This could be related to the counteraction of ROS-mediated mechanisms of vasoconstriction and leukocyte adherence to sinusoids and postsinusoidal venules^[12-16]. In accordance with the proposed stepwise process of leukocyte-endothelial interaction from leukocyte rolling as an initial event to permanent attachment of leukocytes as the second step^[46], our results indicate GSH as an inhibitor of the second step: treatment with GSH prevented sticking but slightly increased the rolling of leukocytes. Similar effects can be achieved by the administration of superoxide dismutase^[12,13,16], suggesting superoxide anion ($\text{O}_2^{\cdot -}$) as the contributing mediator of leukocyte adherence. Therefore, it seems likely that GSH prevents leukocyte adherence through reaction with $\text{O}_2^{\cdot -}$ or inhibition of $\text{O}_2^{\cdot -}$ - mediated mechanisms of leukocyte adherence. Protection of leukocyte adherence by 50 $\mu\text{mol GSH}/(\text{h} \cdot \text{kg})$ without evidence for additional GSSG formation does not argue against this concept because the reaction of GSH with $\text{O}_2^{\cdot -}$ can result in the formation of glutathione sulfonate^[44].

However, the antioxidative potential of GSH does not rule out beneficial effects through non-antioxidative properties. Accumulating evidence indicates that detachment of SEC from the perisinusoidal matrix plate represents a critical component of preservation injury and postschismic microcirculatory failure^[5,47,48]. It has been proposed that SEC damage occurs independent of ROS formation because several antioxidants failed to prevent SEC injury in the liver allograft^[6]. SEC detachment is caused by various matrix metalloproteinases (MMPs) released into the extracellular compartment during cold liver preservation. In the present study attachment of SEC to their matrix was impressively preserved by GSH and could contribute to the improvement of the hepatic microcirculation. Recent experiments demonstrated the inhibition of MMPs by GSH *in vitro*. These findings suggest that MMPs were possible targets of GSH in liver allografts but this requires further investigations.

In summary, the present study demonstrates a dose-dependent prevention of reperfusion injury in rat liver allografts by postschismic intravenous administration of GSH. Treatment of recipient animals with GSH prevented reperfusion injury to SEC as well as to hepatocytes, markedly improved the hepatic microcirculation and preserved postschismic liver function. GSH-mediated protection of liver allografts was associated with an increased formation of plasma GSSG providing evidence for an accelerated detoxification of ROS by intravenously applied GSH. Therefore, intravenous administration of GSH appears to be a candidate therapy for the prevention of ROS-related reperfusion injury after liver transplantation, in particular since it has a low toxicity in humans and seems cost-effective.

ACKNOWLEDGMENTS

The excellent technical assistance of Ms I. Liss is gratefully appreciated. Presented in abstract form at the 50th annual meeting of the American Association for the Study of Liver Diseases (AASLD), 1999, Dallas.

REFERENCES

- 1 **Clavien PA**, Harvey PRC, Strasberg SM. Preservation and reperfusion injuries in liver allografts. *Transplantation* 1992; **53**: 957-978
- 2 **Lemasters JJ**, Thurman RG. Reperfusion injury after liver preservation for transplantation. *Annu Rev Pharmacol Toxicol* 1997;

- 37: 327-338
- 3 **Bilzer M**, Gerbes AL. Preservation injury of the liver: mechanisms and novel therapeutic strategies. *J Hepatol* 2000; **32**: 508-515
- 4 **Clavien PA**. Sinusoidal endothelial cell injury during hepatic preservation and reperfusion. *Hepatology* 1998; **28**: 281-285
- 5 **McKeown CMB**, Edwards V, Phillips MJ, Harvey PRC, Petrunka CN, Strasberg SM. Sinusoidal lining cell damage: the critical injury in cold preservation of liver allografts in the rat. *Transplantation* 1988; **46**: 178-191
- 6 **Caldwell-Kenkel JC**, Thurman RG, Lemasters JJ. Selective loss of nonparenchymal cell viability after cold ischemic storage of rat livers. *Transplantation* 1988; **45**: 834-837
- 7 **Gao W**, Bentley R, Madden JF, Clavien PA. Apoptosis of sinusoidal endothelial cells is a critical mechanism of preservation injury in rat liver transplantation. *Hepatology* 1998; **27**: 1652-1660
- 8 **Jaeschke H**, Farhood A. Neutrophil and Kupffer cell-induced oxidant stress and ischemia-reperfusion injury in rat liver. *Am J Physiol* 1991; **260**: G355-G362
- 9 **Brass CA**, Roberts TG. Hepatic free radical production after cold storage: Kupffer cell-dependent and -independent mechanisms in rats. *Gastroenterology* 1995; **108**: 1167-1175
- 10 **Jaeschke H**. Reactive oxygen and ischemia/reperfusion injury of the liver. *Chem Biol Interact* 1991; **79**: 115-136
- 11 **Vollmar B**, Glasz J, Leiderer R, Post S, Menger MD. Hepatic microcirculatory perfusion failure is a determinant of liver dysfunction in warm ischemia-reperfusion. *Am J Pathol* 1994; **145**: 1421-1431
- 12 **Koo A**, Komatsu H, Tao G, Inoue M, Guth PH, Kaplowitz N. Contribution of no-reflow phenomenon to hepatic injury after ischemia-reperfusion: evidence for a role for superoxide anion. *Hepatology* 1992; **15**: 507-514
- 13 **Marzi I**, Knee J, Buhren V, Menger MD, Trentz O. Reduction by superoxide dismutase of leukocyte - endothelial adherence after liver transplantation. *Surgery* 1992; **111**: 90-97
- 14 **Bilzer M**, Gerbes AL. Prolonged modulation of the hepatic circulation by Kupffer cell-derived reactive oxygen species. In Cells of the hepatic sinusoid (eds. E. Wisse, D.L. Knook, C. Balabaud), Vol. 6., Leiden, Netherlands: Kupffer Cell Foundation 1996; pp. 200-201
- 15 **Shibuya H**, Ohkohchi N, Seya K, Satomi S. Kupffer cells generate superoxide anions and modulate reperfusion injury in rat livers after cold preservation. *Hepatology* 1997; **25**: 356-360
- 16 **Kondo T**, Terajima H, Todoroki T, Hirano T, Ito Y, Usia T, Messmer K. Prevention of hepatic ischemia-reperfusion injury by SOD-DIVEMA conjugate. *J Surg Res* 1999; **85**: 26-36
- 17 **Essani NA**, McGuire GM, Manning AM, Jaeschke H. Endotoxin-induced activation of the nuclear transcription factor kB in in hepatocytes, Kupffer cells and endothelial cells *in vivo*. *J Immunol* 1996; **156**: 2956-2963
- 18 **Essani NA**, Fischer MA, Jaeschke H. Inhibition of NF- κ B activation by dimethyl sulfoxide correlates with suppression of TNF α formation, reduced ICAM-1 gene transcription, and protection against endotoxin-induced liver injury. *Shock* 1997; **7**: 90-96
- 19 **Aebi S**, Assereto R, Lauterburg BH. High-dose intravenous glutathione in man. Pharmacokinetics and effects on cyst(e)ine in plasma and urine. *Eur J Clin Invest* 1991; **21**: 103-110
- 20 **Bilzer M**, Lauterburg BH. Glutathione metabolism in activated human neutrophils: Stimulation of glutathione synthesis and consumption of glutathione by reactive oxygen species. *Eur J Clin Invest* 1991; **21**: 316-322
- 21 **Bilzer M**, Lauterburg BH. Effects of hypochlorous acid and chloramines on vascular resistance, cell integrity, and biliary glutathione disulfide in the perfused rat liver: modulation by glutathione. *J Hepatol* 1991; **13**: 84-89
- 22 **Liu P**, Fisher MA, Farhood A, Smith CY, Jaeschke H. Beneficial effects of extracellular glutathione against endotoxin-induced liver injury during ischemia and reperfusion. *Circ Shock* 1994; **43**: 64-70
- 23 **Bilzer M**, Paumgartner G, Gerbes AL. Glutathione protects the rat liver against reperfusion injury after hypothermic preservation. *Gastroenterology* 1999; **117**: 200-210
- 24 **Kamada N**, Calne RY. Orthotopic liver transplantation in the rat. Technique using cuff for portal vein anastomosis and biliary drainage. *Transplantation* 1979; **28**: 47-56
- 25 **Post S**, Menger MD, Rentsch M, Gonzalez AP, Herfarth C, Messmer K. The impact of arterialization on hepatic microcirculation and leukocyte accumulation after liver transplantation in the rat. *Transplantation* 1992; **54**: 789-794
- 26 **Vollmar B**, Richter S, Menger MD. Leukocyte stasis in hepatic sinusoids. *Am J Physiol* 1996; **270**: G798-G803
- 27 **Menger MD**, Marzi I, Messmer K. *In vivo* fluorescence microscopy for quantitative analysis of the hepatic microcirculation in hamsters and rats. *Eur Surg Res* 1991; **23**: 158-169
- 28 **Bloch EH**, McCuskey RS. Biodynamics of phagocytosis: an analysis of the dynamics of phagocytosis in the liver by *in vivo* microscopy. In Kupffer cells and other liver sinusoidal cells (eds. E. Wisse, D.L. Knook), Amsterdam: Elsevier Science Publishers 1977; pp. 21-32
- 29 **Post S**, Gonzalez AP, Palma P, Rentsch M, Stiehl A, Menger MD. Assessment of hepatic phagocytic activity by *in vivo* microscopy after liver transplantation in the rat. *Hepatology* 1992; **16**: 803-809
- 30 **Jaeschke H**, Mitchell JR. Use of isolated perfused organs in hypoxia and ischemia / reperfusion oxidant stress. *Methods Enzymol* 1990; **186**: 752-759
- 31 **Tietze F**. Enzymatic method for quantitative determination of nanogram amounts of total and oxidized glutathione. *Ann Biochem* 1969; **27**: 502-522
- 32 **Gores GJ**, Kost LJ, LaRusso NF. The isolated perfused rat liver: conceptual and practical considerations. *Hepatology* 1986; **6**: 511-517
- 33 **Halliwell B**, Gutteridge MC. The antioxidants of human extracellular fluids. *Arch Biochem Biophys* 1990; **280**: 1-8
- 34 **Marzi I**, Walcher F, Buhren V. Macrophage activation and leukocyte adhesion after liver transplantation. *Am J Physiol* 1993; **265**: G172-G177
- 35 **Post S**, Palma P, Rentsch M, Gonzalez AP, Menger MD. Differential impact of Carolina Rinse and University of Wisconsin solutions on microcirculation, leukocyte adhesion, Kupffer cell activity and biliary excretion after liver transplantation. *Hepatology* 1993; **18**: 1490-1497
- 36 **Aebi S**, Lauterburg BH. Divergent effects of intravenous GSH and cysteine on renal and hepatic GSH. *Am J Physiol* 1992; **263**: R348-R352
- 37 **Adams JD**, Lauterburg BH, Mitchell JR. Plasma glutathione and glutathione disulfide in the rat: regulation and response to oxidant stress. *J Pharmacol Exp Therapeutics* 1983; **227**: 749-754
- 38 **Lauterburg BH**, Smith CV, Hughes H, Mitchell JR. Biliary excretion of glutathione and glutathione disulfide in the rat. *J Clin Invest* 1984; **73**: 124-133
- 39 **Jaeschke H**, Smith CV, Mitchell JR. Reactive oxygen species and ischemia-reflow injury in isolated perfused rat liver. *J Clin Invest* 1988; **81**: 1240-1246
- 40 **Jaeschke H**, Bautista AP, Spolarics Z, Spitzer JJ. Superoxide generation by Kupffer cells and priming of neutrophils during reperfusion after hepatic ischemia. *Free Radic Res Commun* 1991; **15**: 277-284
- 41 **Schauer R**, Bilzer M, Kalmuk S, Gerbes AL, Leiderer R, Schildberg FW, Messmer K. Microcirculatory failure after rat liver transplantation is related to Kupffer cell- derived oxidant stress but not involved in early graft dysfunction. *Transplantation* 2001; **72**: 1692-1699
- 42 **Baron A**, Gerbes AL, Bilzer M. Prevention of Kupffer cell- induced injury in rat liver by glutathione. *Hepatology* 1999; **30**: 226A
- 43 **Bilzer M**, Jaeschke H, Vollmar AM, Paumgartner G, Gerbes AL. Prevention of Kupffer cell-induced injury in rat liver by atrial natriuretic peptide (ANP): A novel endogenous defense mechanism against oxidant injury. *Am J Physiol* 1999; **276**: G1137-G1144
- 44 **Wefers H**, Sies H. Oxidation of glutathione by the superoxide radical to the disulfide and the sulfonate yielding singlet oxygen. *Eur J Biochem* 1983; **137**: 29-36
- 45 **Winterbourn CC**, Metodiewa D. The reaction of superoxide with reduced glutathione. *Arch Biochem Biophys* 1994; **314**: 284-290
- 46 **Hernandez LA**, Grisham MB, Twhogig B, Arfors KE, Harlan JM, Granger DN. Role of neutrophils in ischemia-reperfusion-induced microvascular injury. *Am J Physiol* 1987; **253**: H699-H703
- 47 **Clavien PA**, Harvey PRC, Sanabria JR, Cywes R, Levy GA, Strasberg SM. Lymphocyte adherence in the reperfused liver allograft. Mechanisms and effects. *Hepatology* 1993; **17**: 131-142
- 48 **Takey Y**, Marzi I, Gao W, Gores GJ, Lemasters JJ, Thurman RG. Leukocyte adhesion and cell death following orthotopic liver transplantation in the rat. *Transplantation* 1991; **51**: 959-965

Protective effect of exogenous adenosine triphosphate on hypothermically preserved rat liver

Xiao-Dong Tan, Hiroshi Egami, Feng-Shan Wang, Michio Ogawa

Xiao-Dong Tan, Hiroshi Egami, Feng-Shan Wang, Michio Ogawa,
Department of Surgery II, Kumamoto University Medical School,
Kumamoto 860-8556, Japan

Correspondence to: Dr. Xiao-Dong Tan, Department of Surgery II,
Kumamoto University Medical School. Honjo 1-1-1, Kumamoto 860-
8556, Japan. tanxd@hotmail.com

Telephone: +81-96-3735211 **Fax:** +81-96-371-4378

Received: 2003-10-15 **Accepted:** 2003-11-20

Abstract

AIM: To clarify the protective effect of exogenous adenosine triphosphate (ATP) on hypothermically preserved rat livers.

METHODS: Establishment of continuous hypothermic machine perfusion model, detection of nucleotides in hepatocytes with HPLC, measurement of activities of LDH and AST in the perfusate, observation of histopathological changes in different experiment groups, and autoradiography were carried out to reveal the underlying mechanism of the protective effect of ATP.

RESULTS: The intracellular levels of ATP and EC decreased rapidly after hypothermic preservation in control group, while a higher ATP and EC level, and a slower decreasing rate were observed when ATP-MgCl₂ was added to the perfusate ($P < 0.01$). As compared with the control group, the activities of LDH and AST in the ATP-MgCl₂ group were lower ($P < 0.05$). Furthermore, more severe hepatocyte damage and neutrophil infiltration were observed in the control group. Radioactive [α -³²P] ATP entered the hypothermically preserved rat hepatocytes.

CONCLUSION: Exogenous ATP has a protective effect on rat livers during hypothermic preservation. However, Mg²⁺ is indispensable, addition of ATP alone produces no protective effect. The underlying mechanism may be that exogenous ATP enters the hypothermically preserved rat liver cells.

Tan XD, Egami H, Wang FS, Ogawa M. Protective effect of exogenous adenosine triphosphate on hypothermically preserved rat liver. *World J Gastroenterol* 2004; 10(6): 871-874
<http://www.wjgnet.com/1007-9327/10/871.asp>

INTRODUCTION

Improving the quality of cold stored organs and prolonging the effective preservation time are the pivotal contents in the investigation of hypothermic preservation of transplant grafts. Several investigators have reported that the intracellular level of adenosine triphosphate (ATP) in cold stored organs was closely correlated with the viability of transplant grafts^[1-3]. Bowers reported that ATP level in cold stored pretransplant organs was a sensitive parameter for examining the activities of cold stored organs^[4]. Therefore, providing direct energy substrate ATP to cold stored organs^[5], should be a simple and effective method to sustain the high level of intracellular ATP.

However, thus far, whether exogenous ATP could enter cells or not is controversial^[6-9]. Furthermore, there were few reports which elucidated the protective effect of ATP on cold stored transplant grafts. In this study, a continuously hypothermic machine perfusion model of rat liver was applied to reveal the protective effect of ATP on cold stored rat livers and its mechanism.

MATERIALS AND METHODS

Experimental animals

Wistar rats weighing 180-220 g, both male and female, were randomly used..

Experiment groups and protocol

Cold storage study on rat livers The rats mentioned above were divided into 3 groups at random, group A (containing neither ATP nor MgCl₂ in the perfusate), group B (containing 5 mmol/L ATP but no MgCl₂ in the perfusate), group C (containing either ATP or MgCl₂ in the perfusate), respectively. There were 6 rats in each group. The rat liver was weighed immediately after resection by the method described previously^[10-12], then these grafts were put into the modified Hoffmann perfusate^[13] (0-4 °C) for 30 min (Table 1). Finally, the livers were preserved in a hypothermic preservation incubator by continuously hypothermic preservation perfusion model (Figure 1). The perfusate temperature was 6-8 °C^[14], perfusion speed was 0.1 mL/(min.g)^[14], the total volume of perfusate was 120 mL.

Autoradiography study Six rats were chosen randomly, the livers were resected with the same method. One mCi [α -³²P] ATP, 5 mmol MgCl₂, 200 μ L and 40 U phenol kinase were added into 1 L perfusate, and the same liver preservation method was applied.

Table 1 Components of perfusate

Composition	Concentration
Hydroxyethyl starch	50 g/L
Calcium gluconate	80 mmol/L
Raffinose	10 mmol/L
KH ₂ PO ₄	25 mmol/L
Hydroxyethyl piperazine	10 mmol/L
Dexamethasone	12 mg/L
Penicillin	2×10 ⁵ units/L
Insulin	100 units/L
¹ MgCl ₂	5 mmol/L
¹ ATP	5 mmol/L

The pH value was modulated to 7.35 with NaOH, and the osmotic pressure was 300-320 mOsm/L; ¹Addition of MgCl₂ and ATP was dependent on the different groups.

Biochemical detection

Detection of energy status in cold stored rat livers The rat liver samples were used to detect the intracellular ATP, ADP, AMP, TAN and EC at 0, 1, 2, 6, 12, 24 and 36 h after

preservation by HPLC method^[15] ($TAN=ATP+ADP+AMP$, $EC=[ATP+0.5ADP]/TAN$)^[16]. One milliliter of perfusate was taken to detect the LDH and AST activities^[17,18] at 6, 12, 24 and 36 h respectively after preservation.

Histological and morphological findings Paraffin sections of HE staining were made after 24 h preservation of the rat livers^[19], and observed by a light microscope.

Autoradiography of [α -³²P] ATP The rat liver samples were made into paraffin sections of HE staining after 4-h preservation. Moreover, whether ATP entered the cells of cold stored rat livers or not was examined by autoradiography of [α -³²P] ATP^[20].

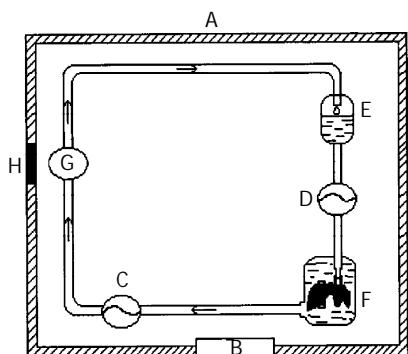


Figure 1 Preservation of continuously hypothermic machine perfusion. A: Organ hypothermic preservation box, B: Temperature displayer, C: Perfusion pump, D: Perfusion pump, (Displaying the perfusion pressure), E: Perfusate container, F: Organ preservation container, G: pH displayer, H: Entry of wire, (Being sealed while preservation).

Statistical analysis

The average values were presented as mean \pm SD, *t*-test was applied and $P<0.05$ was considered to be statistically significant.

RESULTS

Energy status in cold stored rat livers (mmol/g wet liver)

In group A, following the prolongation of preservation time, the ATP and EC levels in rat liver cells were significantly decreased. The ATP and EC levels were also rapidly decreased in group B, there was no statistical difference between these two groups ($P>0.05$). However, the ATP and EC levels were slowly decreased in group C ($P<0.01$, Table 2).

LDH and AST activities in hypothermic preservation perfusate

LDH and AST activities in the perfusate were increased in groups A and B, there was no significant difference between two groups ($P>0.05$). On the other hand, compared with those in groups A and B, the relevant activities were slowly increased in group C ($P<0.05$, Table 3).

Histological and morphological findings after 24-h hypothermic perfusion preservation

In group A (Figure 2), the hepatocytes were obviously swollen, cytosol and part of nucleus were faintly stained. Part of the endothelial cells entered the hepatosinus.

In group B (Figure 3), the hepatocytes were also expanded, cytosol was faintly stained. Some nuclei were strongly stained. Some endothelial cells entering the hepatosinus were also found.

In group C (Figure 4), the hepatocytes were lightly expanded. There was no apparent bubble in cytosol, and the morphology of nucleus was normal. The endothelial cells of hepatosinus were continuous.

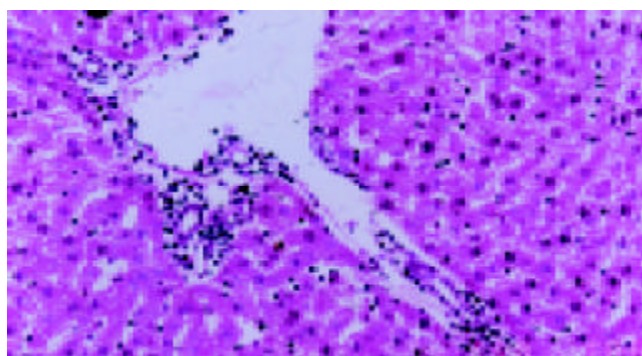


Figure 2 Histological and morphological findings in hypothermically preserved hepatocytes. Group A: 24-h preservation, HE staining 100 \times .

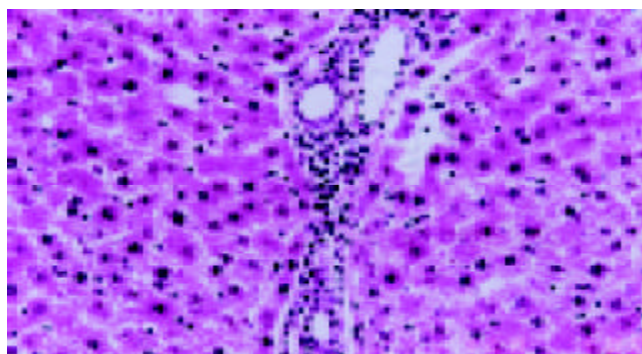


Figure 3 Histological and morphological findings in hypothermically preserved hepatocytes. Group B: 24-h preservation, HE staining 100 \times .

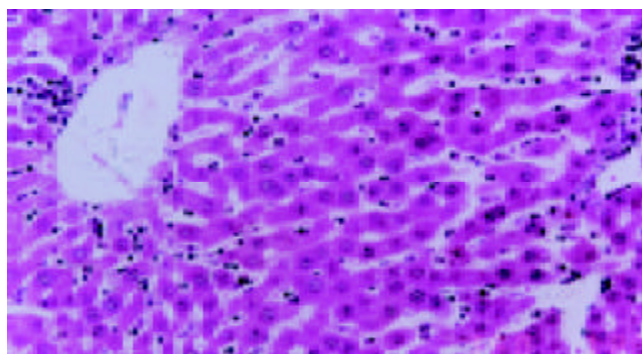


Figure 4 Histological and morphological findings in hypothermically preserved hepatocytes. Group C: 24-h preservation, HE staining 100 \times .

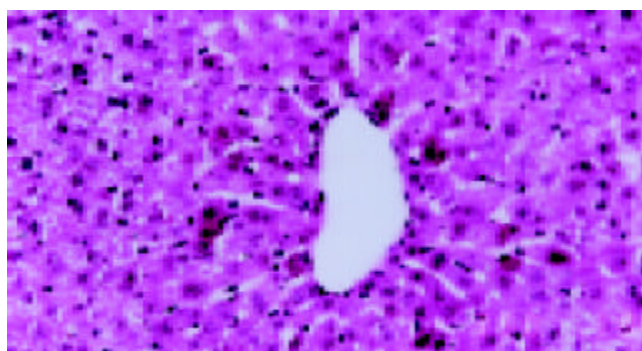


Figure 5 Autoradiography of [α -³²P] ATP in hypothermically preserved hepatocytes. Black spots in hepatocytes are the autoradiographies of [α -³²P] ATP, 4-h preservation, HE staining 100 \times .

Table 2 Energy status in hypothermically preserved rat livers ($n=6$, mean \pm SD)

	ATP ($\mu\text{mol/g}$ wet liver)			EC		
	Group A	Group B	Group C	Group A	Group B	Group C
0 h	2.760 \pm 0.302	2.760 \pm 0.302	2.760 \pm 0.302	0.871 \pm 0.093	0.871 \pm 0.093	0.871 \pm 0.093
1 h	2.337 \pm 0.202	2.263 \pm 0.282	2.514 \pm 0.298	0.803 \pm 0.090	0.789 \pm 0.083	0.791 \pm 0.083
2 h	1.914 \pm 0.209	1.971 \pm 0.205	2.391 \pm 0.276 ^a	0.741 \pm 0.082	0.736 \pm 0.082	0.743 \pm 0.079
6 h	1.509 \pm 0.211	1.506 \pm 0.180	2.523 \pm 0.269 ^b	0.653 \pm 0.071	0.645 \pm 0.068	0.695 \pm 0.071 ^a
12 h	1.145 \pm 0.177	1.136 \pm 0.150	2.715 \pm 0.298 ^b	0.543 \pm 0.063	0.537 \pm 0.060	0.660 \pm 0.070 ^b
24 h	0.755 \pm 0.082	0.842 \pm 0.088	2.547 \pm 0.279 ^b	0.380 \pm 0.045	0.406 \pm 0.045	0.601 \pm 0.068 ^b
36 h	0.603 \pm 0.065	0.706 \pm 0.080	1.782 \pm 0.200 ^b	0.316 \pm 0.040	0.348 \pm 0.042	0.471 \pm 0.051 ^b

^a $P<0.05$, ^b $P<0.01$ vs group A.

Table 3 Activities of AST and LDH in perfusate (IU/L.g liver) ($n=6$, mean \pm SD)

	6 h		12 h		24 h		36 h	
	LDH	AST	LDH	AST	LDH	AST	LDH	AST
Group A	80.2 \pm 3.8	4.6 \pm 0.6	112.7 \pm 4.1	8.9 \pm 0.9	188.4 \pm 5.1	15.6 \pm 1.4	452.2 \pm 7.4	20.1 \pm 1.7
Group B	76.4 \pm 4.2	4.8 \pm 0.5	123.8 \pm 3.6	8.2 \pm 0.8	170.1 \pm 6.2	14.1 \pm 1.7	423.7 \pm 6.5	18.7 \pm 2.2
Group C	9.3 \pm 1.8 ^a	1.2 \pm 0.4 ^a	26.7 \pm 2.3 ^a	2.4 \pm 0.5 ^a	42.6 \pm 3.5 ^a	4.4 \pm 0.6 ^a	90.1 \pm 6.2 ^a	6.3 \pm 0.8 ^a

^a $P<0.05$ vs group A.

Autoradiography of [α -³²P] ATP

Numerous silver spots of [α -³²P] ATP were found to be limited within the rat hepatocytes, while no silver spots were found in the hepatosinus and central vein (Figure 5). This observation demonstrated that [α -³²P] ATP entered the cold stored rat hepatocytes.

DISCUSSION

Protective effects of exogenous ATP on hypothermically preserved rat livers

Up to now, some reports have revealed that ATP-MgCl₂ had a protective effect on the therapy of hemorrhagic shock^[7,21], but reports revealing the protective effect of ATP-MgCl₂ on hypothermically preserved transplant organs were few^[22]. The results of this study demonstrated that the intracellular level of ATP in the group containing no ATP-MgCl₂ or the group containing ATP alone decreased rapidly after hypothermic preservation. Simultaneously, the release of intracellular enzymes was increased, indicating severe damages of the membrane functions. Moreover, significant swelling of the hepatocytes and obvious infiltration of neutrophils were found histologically. On the contrary, the intracellular ATP level in the group containing ATP-MgCl₂ was almost maintained at the normal level for quite a long time, and decreased much slower after hypothermic preservation. Furthermore, because of the protective effect of ATP on cell membranes^[23,24], the metabolic function of hepatocytes was restored, and the release of intracellular enzymes (LDH and AST) was significantly inhibited. The histological observations also showed that the swelling of hepatocytes was milder than that in groups B and C. These results suggested that ATP-MgCl₂ could directly provide the energy or energy substrates for intracellular Na⁺-K⁺ ATPase as well as Ca²⁺-ATPase to remain the extracellular and intracellular ion balance^[25-29], and lighten the intracellular acidosis and cell swelling^[21,23]. In addition, ATP-MgCl₂ also had effects on the amelioration of microcirculation, restoration of membrane voltage, restoration of normal membrane permeability and improvement of cellular functions^[30,31].

Together, ATP showed protective effects on cold stored rat livers, and it might be a synthetical effect of multiple actions.

Mechanism of protective effect of ATP on hypothermically preserved rat livers

ATP had a very strong effect on vascular expansion^[7], but our current study demonstrated that exogenous ATP protected cold stored rat livers not through vascular expansion.

If ATP-MgCl₂ protected the cold stored rat livers through vascular expansion, then addition of ATP alone to the perfusate should also exhibit a protective effect. But no protective effect was observed by the addition of ATP alone in our study (Data not shown). Moreover, addition of MgCl₂ alone to the perfusate also showed no protective effect^[21]. Addition of ADP-MgCl₂ complex, which has a more effective action of vascular expansion, showed no protective effect as ATP-MgCl₂ (Data not shown). An even more important finding was that, ATP-MgCl₂ could enter cold stored rat liver cells in our study. This also directly confirmed that exogenous ATP-MgCl₂ could protect cold stored rat livers through the intracellular mechanism. By our knowledge, no report has revealed that exogenous ATP could enter hepatocytes through the membrane, and the mechanism is still unclear. We suspect that the possible pathway might be considered as followings. First, as ATP is a large biomolecule, the membrane is impermeable to it under normal status. But the permeability is increased to ATP due to the activation of some membrane carrier proteins by hypothermia and anoxia. Second, ATP enters hepatocytes through the disrupted hepatocyte membrane. In addition, how does ATP play the protective effect after entering the cells is still poorly understood.

Taken together, these results indicate that exogenous ATP-MgCl₂ could protect cold stored livers through an intracellular rather than an extracellular mechanism.

Participation of Mg²⁺ in protection of cold stored rat livers by exogenous ATP

As we know, ATP could form chelate with other extracellular bivalent cations (Ca²⁺, Sr²⁺, Mg²⁺, *etc.*). However, addition of ATP-MgCl₂ complex could inhibit the dephosphorylation and deamino action of ATP, suppress the extracellular hydrolysis of ATP, and prevent the different dynamic effects by interaction of ATP and other extracellular cations^[32]. The other possible reason may be that participation of Mg²⁺ may be required while

ATP goes through the cell membrane. The carrier protein has been found on the intima of mitochondria. The functional mechanism was found to be: $\text{ATP-Mg}^{2+}_{\text{out}} + \text{HPO}_4^{2-}_{\text{in}} \rightleftharpoons \text{ATP-Mg}^{2+}_{\text{in}} + \text{HPO}_4^{2-}_{\text{out}}$ ^[33]. Further investigation is needed to confirm whether there is such a carrier protein on the outside membrane of hepatocytes or not, and whether ATP enters hepatocytes by interaction with Mg^{2+} or not. In addition, there is also the possibility that, as a co-factor of many intracellular functions, Mg^{2+} could participate in a diverse of ATP dependent intracellular actions, such as $\text{Na}^+ - \text{K}^+$ ATPase, $\text{Ca}^{2+} - \text{ATPase}$, and glycolysis^[34].

In summary, the results of the current study suggest that exogenous ATP could protect cold stored rat livers by entering hepatocytes. ATP-MgCl_2 should be a pivotal component in the hypothermic preservation solution. Further study is required to clarify the protective mechanism of ATP on cold stored organs, which may contribute to the development of hypothermic preservation solution.

REFERENCES

- 1 **Marubayashi S**, Takenaka M, Dohi K, Ezaki H, Kawasaki T. Adenosine nucleotide metabolism during hepatic ischemia and subsequent blood reflow periods and its relation to organ viability. *Transplantation* 1980; **30**: 294-296
- 2 **Lanir A**, Jenkins RL, Caldwell C, Lee RG, Khettry U, Clouse ME. Hepatic transplantation survival: correlation with adenine nucleotide level in donor liver. *Hepatology* 1988; **8**: 471-475
- 3 **Takesue M**, Maruyama M, Shibata N, Kunieda T, Okitsu T, Sakaguchi M, Totsugawa T, Kosaka Y, Arata A, Ikeda H, Matsuoka J, Oyama T, Kodama M, Ohmoto K, Yamamoto S, Kurabayashi Y, Yamamoto I, Tanaka N, Kobayashi N. Maintenance of cold-preserved porcine hepatocyte function with UW solution and ascorbic acid-2 glucoside. *Cell Transplant* 2003; **12**: 599-606
- 4 **Bowers JL**, Teramoto K, Khettry U, Clouse ME. ³¹P NMR assessment of orthotopic rat liver transplantation viability. The effect of warm ischemia. *Transplantation* 1992; **54**: 604-609
- 5 **Wu XT**, Li JS, Zhao XF, Zhuang W, Feng XL. Modified techniques of heterotopic total small intestinal transplantation in rats. *World J Gastroenterol* 2002; **8**: 758-762
- 6 **Glynn IM**. Membrane adenosine triphosphate and cation transport. *Br Med Bull* 1968; **24**: 165-169
- 7 **Chaudry IH**, Baue AE. Further evidence for ATP uptake by rat tissues. *Biochim Biophys Acta* 1980; **628**: 336-342
- 8 **Chaudry IH**, Sayeed MM, Baue AE. Evidence for enhanced uptake of ATP by liver and kidney in hemorrhagic shock. *Am J Physiol* 1977; **233**: R83-R88
- 9 **Forrester T**. An estimate of adenosine triphosphate release into the venous effluent from exercising human forearm muscle. *J Physiol* 1972; **224**: 611-628
- 10 **Miyata M**, Fischer JH, Fuhs M, Isselhard W, Kasai Y. A simple method for orthotopic liver transplantation in the rat cuff technique for three vascular anastomoses. *Transplantation* 1980; **30**: 335-338
- 11 **Kobayashi E**, Kamada N, Goto S, Miyata M. Protocol for the technique of orthotopic liver transplantation in the rat. *Micorsurgery* 1993; **14**: 541-546
- 12 **Jiang Y**, Gu XP, Qiu YD, Sun XM, Chen LL, Zhang LH, Ding YT. Ischemic preconditioning decreases C-X-C chemokine expression and neutrophil accumulation early after liver transplantation in rats. *World J Gastroenterol* 2003; **9**: 2025-2029
- 13 **Hoffmann RM**, Southard JH, Lutz M, Mackety A, Belzor FO. Synthetic Perfusate for Kidney Preservation. Its use in 72-hour preservation of dog kidneys. *Arch Surg* 1983; **118**:919-921
- 14 **Tamaki T**, Kamada N, Wight DG, Pegg DE. Successful 48-hour preservation of the rat liver by continuous hypothermic perfusion with haemaccel-isotonic citrate solution. *Transplantation* 1987; **43**: 468-471
- 15 **Li YS**, Li JS, Li N, Jiang ZW, Zhao YZ, LI NY, Liu FN. Evaluation of various solutions for small bowel graft preservation. *World J Gastroenterol* 1998; **4**: 140-143
- 16 **Cheng XD**, Jiang XC, Liu YB, Peng CH, Xu B, Peng SY. Effect of ischemic preconditioning on P-selectin expression in hepatocytes of rats with cirrhotic ischemia-reperfusion injury. *World J Gastroenterol* 2003; **9**: 2289-2292
- 17 **Sun B**, Jiang HC, Piao DX, Qian HQ, Zhang L. Effects of cold preservation and warm reperfusion on rat fatty liver. *World J Gastroenterol* 2000; **6**: 271-274
- 18 **Zhu XH**, Qiu YD, Shen H, Shi MK, Ding YT. Effect of matrine on Kupffer cell activation in cold ischemia reperfusion injury of rat liver. *World J Gastroenterol* 2002; **8**: 1112-1116
- 19 **Yang YL**, Dou KF, Li KZ. Influence of intrauterine injection of rat fetal hepatocytes on rejection of rat liver transplantation. *World J Gastroenterol* 2003; **9**: 137-140
- 20 **Pimlott SL**, Piggott M, Owens J, Greally E, Court JA, Jaros E, Perry RH, Perry EK, Wyper D. Nicotinic Acetylcholine Receptor Distribution in Alzheimer's Disease, Dementia with Lewy Bodies, Parkinson's Disease, and Vascular Dementia: *In Vitro* Binding Study Using 5-[(125)I]-A-85380. *Neuropsychopharmacology* 2004; **29**: 108-116
- 21 **Ohkawa M**, Clemens MG, Chaudry IH. Studies on the mechanism of beneficial effects of ATP-MgCl_2 following hepatic ischemia. *Am J Physiol* 1983; **244**: R695-702
- 22 **Lytton B**, Vaisbort VB, Glazier WB, Chaudry IH, Baue AE. Improved renal function using adenosine triphosphate-magnesium chloride in preservation of canine kidneys subjected to warm ischemia. *Transplantation* 1981; **31**: 187-189
- 23 **Hayashi H**, Chaudry IH, Clemens MG, Hull MJ, Baue AE. Reoxygenation injury in isolated hepatocytes: effect of extracellular ATP on cation homeostasis. *Am J Physiol* 1986; **250** (4 Pt 2): R573-579
- 24 **Stanca C**, Jung D, Meier PJ, Kullak-Ublick GA. Hepatocellular transport proteins and their role in liver disease. *World J Gastroenterol* 2001; **7**: 157-169
- 25 **Tanioka Y**, Kuroda Y, Kim Y, Matsumoto S, Suzuki Y, Ku Y, Fujita H, Saitoh Y. The effect of ouabain (inhibitor of an ATP-dependent Na^+ / K^+ pump) on the pancreas graft during preservation by the two-layer method. *Transplantation* 1996; **62**: 1730-1734
- 26 **Southard JH**, van Gulik TM, Ametani MS, Vreugdenhil PK, Lindell SL, Pienaar BL, Belzer FO. Important components of the UW solution. *Transplantation* 1990; **49**: 251-257
- 27 **Neveux N**, De Bandt JP, Fattal E, Hannoun L, Poupon R, Chaumeil JC, Delattre J, Cynober LA. Cold preservation injury in rat liver: effect of liposomally-entrapped adenosine triphosphate. *J Hepatol* 2000; **33**: 68-75
- 28 **Janicki PK**, Wise PE, Belous AE, Pinson CW. Interspecies differences in hepatic $\text{Ca}^{2+} - \text{ATPase}$ activity and the effect of cold preservation on porcine liver $\text{Ca}^{2+} - \text{ATPase}$ function. *Liver Transpl* 2001; **7**: 132-139
- 29 **Belous A**, Knox C, Nicoud IB, Pierce J, Anderson C, Pinson CW, Chari RS. Reversed activity of mitochondrial adenine nucleotide translocator in ischemia-reperfusion. *Transplantation* 2003; **27**: 1717-1723
- 30 **Chaudry IH**. Cellular mechanisms in shock and ischemia and their correction. *Am J Physiol* 1983; **245**: R117-134
- 31 **Mahmoud MS**, Wang P, Chaudry IH. Salutary effects of ATP-MgCl_2 on altered hepatocyte signal transduction after hemorrhagic shock. *Am J Physiol* 1997; **272**(6 Pt 1): G1347-1354
- 32 **Hirasawa H**, Chaudry IH, Baue AE. Improved hepatic function and survival with adenosine triphosphate-magnesium chloride after hepatic ischemia. *Surgery* 1978; **83**: 655-662
- 33 **Joyal J L**, Aprille J R. The ATP-Mg/Pi carrier of rat liver mitochondria catalyzes a divalent electroneutral exchange. *J Biol Chem* 1992; **267**: 19198-19203
- 34 **Zakaria M**, Brown PR. High performance liquid column chromatography of nucleotides, nucleosides and bases. *J Chromatogr* 1981; **226**: 267-290

Levels of vasoactive intestinal peptide, cholecystokinin and calcitonin gene-related peptide in plasma and jejunum of rats following traumatic brain injury and underlying significance in gastrointestinal dysfunction

Chun-Hua Hang, Ji-Xin Shi, Jie-Shou Li, Wei Wu, Wei-Qin Li, Hong-Xia Yin

Chun-Hua Hang, Ji-Xin Shi, Wei Wu, Hong-Xia Yin, Department of Neurosurgery, Jinling Hospital, School of Medicine, Nanjing University, Nanjing 210002, Jiangsu Province, China

Jie-Shou Li, Wei-Qin Li, Research Institute of General Surgery, Jinling Hospital, School of Medicine, Nanjing University, Nanjing 210002, Jiangsu Province, China

Supported by the Scientific Research Foundation of the Chinese PLA Key Medical Programs during the 10th Five-Year Plan Period, No. 01Z011

Correspondence to: Dr. Chun-Hua Hang, Department of Neurosurgery, Jinling Hospital, 305 East Zhongshan Road, Nanjing 210002, Jiangsu Province, China. hang1965@public1.ptt.js.cn

Telephone: +86-25-80860010 **Fax:** +86-25-84810987

Received: 2003-10-31 **Accepted:** 2003-12-16

Abstract

AIM: To study the alterations of brain-gut peptides following traumatic brain injury (TBI) and to explore the underlying significance of these peptides in the complicated gastrointestinal dysfunction.

METHODS: Rat models of focal traumatic brain injury were established by impact insult method, and divided into 6 groups (6 rats each group) including control group with sham operation and TBI groups at postinjury 3, 12, 24, 72 h, and d 7. Blood and proximal jejunum samples were taken at time point of each group and gross observations of gastrointestinal pathology were recorded simultaneously. The levels of vasoactive intestinal peptide (VIP) in plasma, calcitonin gene-related peptide (CGRP) and cholecystokinin (CCK) in both plasma and jejunum were measured by enzyme immunoassay (EIA). Radioimmunoassay (RIA) was used to determine the levels of VIP in jejunum.

RESULTS: Gastric distension, delayed gastric emptying and intestinal dilatation with a large amount of yellowish effusion and thin edematous wall were found in TBI rats through 12 h and 72 h, which peaked at postinjury 72 h. As compared with that of control group (247.8±29.5 ng/L), plasma VIP levels were significantly decreased at postinjury 3, 12 and 24 h (106.7±34.1 ng/L, 148.7±22.8 ng/L, 132.8±21.6 ng/L, respectively), but significantly increased at 72 h (405.0±29.8 ng/L) and markedly declined on d 7 (130.7±19.3 ng/L). However, Plasma levels CCK and CGRP were significantly increased through 3 h and 7 d following TBI (126-691% increases), with the peak at 72 h. Compared with control (VIP, 13.6±1.4 ng/g; CGRP, 70.6±17.7 ng/g); VIP and CGRP levels in jejunum were significantly increased at 3 h after TBI (VIP, 35.4±5.0 ng/g; CGRP, 103.8±22.1 ng/g), and declined gradually at 12 h and 24 h (VIP, 16.5±1.8 ng/g, 5.5±1.4 ng/g; CGRP, 34.9±9.7 ng/g, 18.5±7.7 ng/g), but were significantly increased again at 72 h (VIP, 48.7±9.5 ng/g; CGRP, 142.1±24.3 ng/g), then declined in various

degrees on d 7 (VIP, 3.8±1.1 ng/g; CGRP, 102.5±18.1 ng/g). The CCK levels in jejunum were found to change in a similar trend as that in plasma with the concentrations of CCK significantly increased following TBI (99-517% increases) and peaked at 72 h.

CONCLUSION: Traumatic brain injury can lead to significant changes of brain-gut peptides in both plasma and small intestine, which may be involved in the pathogenesis of complicated gastrointestinal dysfunction.

Hang CH, Shi JX, Li JS, Wu W, Li WQ, Yin HX. Levels of vasoactive intestinal peptide, cholecystokinin and calcitonin gene-related peptide in plasma and jejunum of rats following traumatic brain injury and underlying significance in gastrointestinal dysfunction. *World J Gastroenterol* 2004; 10(6): 875-880

<http://www.wjgnet.com/1007-9327/10/875.asp>

INTRODUCTION

Gastrointestinal dysfunction occurs frequently in patients with traumatic brain injury (TBI)^[1-3]. More than 50% patients with severe head injuries do not tolerate enteral feedings^[4]. This intolerance is manifested by vomiting, abdominal distention, delayed gastric emptying^[5,6], esophageal reflux^[7] and decreased intestinal peristalsis^[8], indicating that gastrointestinal dysfunction is a common phenomenon following TBI. The association of severity of brain injury with the intolerance of enteral feeding suggests a strong link between the central nervous system and the nonfunctioning gut. However, the precise mechanism of gastrointestinal dysfunction following TBI has not been reported to date and remains to be interpreted.

Gastrointestinal motility is mainly regulated by two factors including humoral hormones and nervous transmitters from both central nervous system and peripheral enteric nervous system^[9]. Brain-gut peptides possess two functions as mentioned above, *e.g.*, exerting action on gastrointestinal motility via both endocrine hormones and peptidergic transmitters. These peptides also play their roles in modulation of the gastrointestinal motility through central nervous system, which is a part of brain-gut interaction^[10]. Recent studies have indicated that some disorders of gastrointestinal motility following sepsis^[11-13], trauma^[14], surgery^[15-17], chronic stress^[18] and experimental spleen deficiency^[19] are related to brain-gut peptides, such as cholecystokinin (CCK), vasoactive intestinal peptide (VIP), calcitonin gene-related peptide (CGRP), neuropeptide Y (NPY) and substance P (SP), suggesting that brain-gut peptides are important mediators in the regulation of gastrointestinal motility^[20-22]. Until now, no study has been made to investigate the relationship between brain-gut peptides and gastrointestinal dysmotility following TBI. Therefore, we hypothesized that TBI could induce marked alterations of

brain-gut peptides in both plasma and gut, which could be involved in the pathogenesis of complicated gastrointestinal dysfunction.

Brain-gut peptides as modulatory mediators appear to be major components of bodily integration and have important regulatory actions on physiological function of gastrointestinal tract. Increasing studies have demonstrated that VIP^[14,17,19,23], CCK^[12,20,21] and CGRP^[11,15,16,24] play important protective role in regulation of blood flow, cell differentiation, immune function and secretion of digestive glands. On the other hand, they have an adverse effect on the gut motility^[11-19]. It is also well known that VIP, CCK and CGRP are located in both central nervous system (CNS) and peripheral enteric nervous system, and mainly exert inhibitory action on gut motility^[16-21,24]. Several kinds of stress, such as trauma, cold, restraint and pain, can induce the release of these brain-gut peptides from CNS and enteric nerve^[14,18], and the alterations of relevant receptors in the gut^[19] to induce the gastrointestinal dysmotility. However, it is unknown how these peptides change and what the underlying significance of these changes is in the gastrointestinal dysmotility following TBI. Further insights into the alterations of brain-gut peptides following TBI may provide new therapeutic opportunities for the gastrointestinal dysfunction complicating head trauma. In current study, rat models of TBI were made to measure the alterations of VIP, CCK and CGRP in both plasma and jejunum and to investigate the underlying role of brain-gut peptides in gastrointestinal dysfunction.

MATERIALS AND METHODS

Rat models of TBI

Male Wistar rats, weighing from 220 to 250 g, were purchased from Animal Center of Chinese Academy of Science, Shanghai, China. The rats were fed rodent chow with free access to tap water and housed in temperature- and humidity-controlled animal quarters with 12 h light/dark cycle. All procedures were approved by the Institutional Animal Care Committee.

The rats were randomly divided into six groups (6 rats/group) including control group with right parietal bone window alone and no brain injury, and TBI groups at h 3, 12, 24 and 72, and day 7, respectively. Following intraperitoneal anesthesia with urethane (1 000 mg/kg), animal head was fixed in the stereotactic device. A right parietal bone window of 5 mm in diameter was made under aseptic conditions with dental drill just behind cranial coronal suture and beside midline. The dura was kept intact. Right parietal brain contusion was adopted from the impact method described by Feeney *et al.*^[25] and severe traumatic brain injury was made by dropping weight with impact diameter of 4 mm, depth of 5 mm and total impact energy of 1 000 g·cm. The control animals were killed for sample collection at 72 h, and TBI group rats were decapitated at corresponding time point. Blood samples were obtained by right ventricle puncture and centrifuged with the plasma stored at -40 °C for further analysis. A segment of the jejunum 15 cm distal to Treitz ligament was taken, rinsed and weighed, then were put into a tube with 1 mL saline water. The tube was plunged into vigorous boiling water and boiled for 3 min, and then all layers of jejunum sample and 0.5 mL of 1 mol/L glacial acetic acid were added to a homogenizer to be homogenized for 10 min. The 0.5 mL of 1 mol/L NaOH was mixed with the homogenized sample. After centrifugation at 3 000 r/min for 5 min at low temperature, the supernatant was collected and stored at -40 °C until assay of brain-gut peptides.

Assay analysis of VIP, CCK and CGRP in plasma

The concentrations of VIP, CCK and CGRP in plasma samples were measured by enzyme immunoassay (EIA) with commercially available kits according to the manufacturer's

instructions. Peptides [VIP (S-80039), CCK (S-80013-B), α -CGRP (S-80011-R)] were purchased from AOR Diagnostics, USA. The minimum detectable concentration for VIP, CCK and α -CGRP was 0.06-0.08 ng/L of sample with intra- and inter-assay variation less than 6% and 15% respectively. There was 25% cross-reaction with β -CGRP.

Assay analysis of VIP, CCK and CGRP in jejunum samples

VIP levels in jejunum were determined by radioimmunoassay (RIA) with the kit purchased from Beijing Huayin Biotechnology Institute, China. The concentrations of CCK and CGRP in all layers of jejunum were measured by EIA as mentioned above. The protein concentration of jejunum samples was determined by using a bicinchoninic acid assay kit with bovine serum albumin as the standard (Pierce Biochemicals, Rockford, IL).

Statistical analysis

Software SPSS 11.0 was used in the statistical analysis. Parameters were expressed as mean \pm SD, and compared using one-way ANOVA analysis of variance, followed by Tukey test. Statistical significance was determined at $P < 0.05$.

RESULTS

Gross observations of gastrointestinal pathology

Gastrointestinal tract was found to be nearly normal in rats of control group and TBI 3 hour group (Figure 1A). In TBI groups at 12, 24 and 72 h postinjury, gastric distention and intestinal dilatation with a large amount of yellowish effusion existing within intestinal cavity were found, and intestinal wall became thinner and edematous (Figures 1B and 1C), suggesting that delayed gastric emptying and paralytic ileus occurred following TBI. The above mentioned pathological changes culminated at 72 h following TBI. On d 7 postinjury, small intestine was found to become thin and slender, suggesting that an atrophy in the gut occurred (Figure 1D).

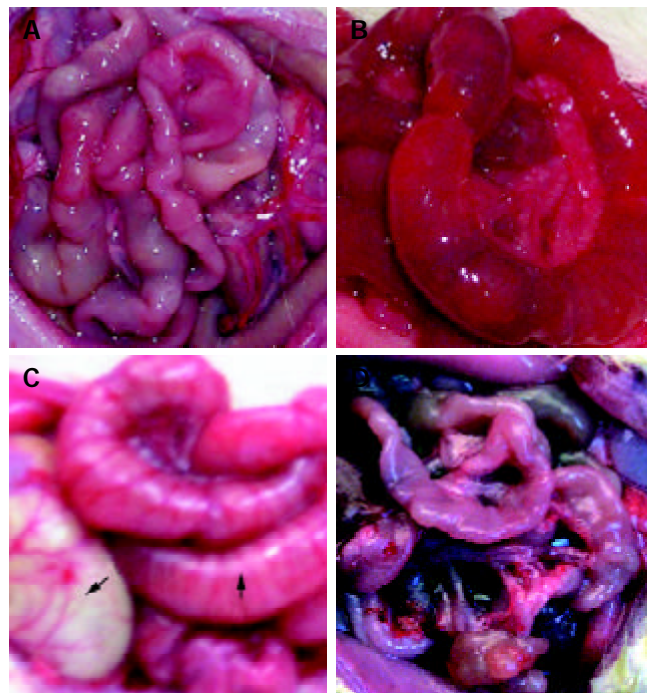


Figure 1 Gross observation of intestinal pathology was shown as A, B, C and D. A: nearly normal morphology at TBI 3 h; B: intestinal dilation with large amount of yellowish effusion and thin edematous wall at 72 h following TBI; C: gastrointestinal distention at 72 h following TBI, stomach indicated by solid arrow and intestine by blank arrow; D: gastrointestinal atrophy on day 7 following TBI.

Levels of VIP, CCK and CGRP in plasma

As compared with that of control group (247.8±29.5 ng/L), plasma VIP levels were significantly decreased at 3, 12 and 24 h postinjury (106.7±34.1 ng/L, 148.7±22.8 ng/L, 132.8±21.6 ng/L, respectively), but significantly increased at 72 h (405.0±29.8 ng/L) and declined markedly on d 7 (130.7±19.3 ng/L) (Figure 2). However, Plasma levels CCK and CGRP were significantly increased through 3 h and 7 d following TBI (126-691% increases), with the peak at 72 h (Figures 3 and 4).

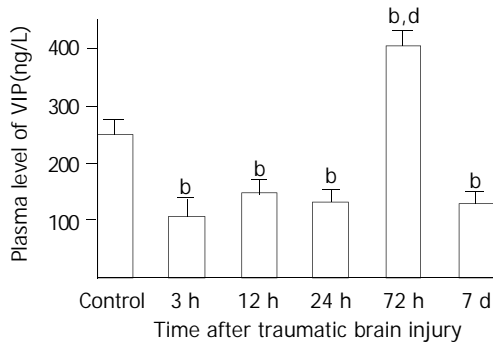


Figure 2 Alteration of VIP in plasma after TBI. Compared with control, plasma level of VIP was significantly decreased at 3, 12 and 24 h postinjury, but was significantly increased at 72 h, then declined to a low level on d 7 with the value similar to that of groups of 3 h, 12 h and 24 h. ^b*P*<0.01 vs control; ^d*P*<0.01 vs 3 h, 12 h, 24 h and 7 d.

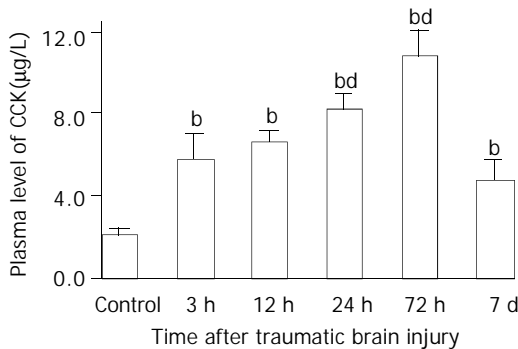


Figure 3 Alteration of CCK in plasma after TBI. Compared with control, plasma level of CCK was significantly increased postinjury, and peaked at 72 h, then declined to some degree on d 7, but was still significantly higher than that of control. ^b*P*<0.01 vs control; ^d*P*<0.01 vs 3 h. Mean±SD of 6 animals, control: 2.1±0.3 µg/L, 3 h: 5.8±1.2 µg/L, 12 h: 6.7±0.5 µg/L, 24 h: 8.3±0.7 µg/L, 72 h: 10.8±1.2 µg/L, 7 d: 4.8±0.9 µg/L.

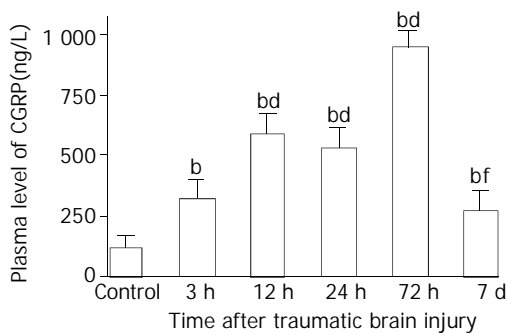


Figure 4 Alteration of CGRP in plasma after TBI. Compared with control, plasma level of CGRP was significantly increased postinjury, and peaked at 72 h, then declined obviously on d 7 with the value still significantly higher than that of control. ^b*P*<0.01 vs control; ^d*P*<0.01 vs 3 h; ⁱ*P*<0.01 vs 12 h, 24 h and 72 h.

Mean±SD of 6 animals, control: 120.8±47.7 ng/L, 3 h: 323.8±75.9 ng/L, 12 h: 596.7±82.7 ng/L, 24 h: 536.0±77.2 ng/L, 72 h: 955.0±63.0 ng/L, 7 d: 273.3±83.8 ng/L.

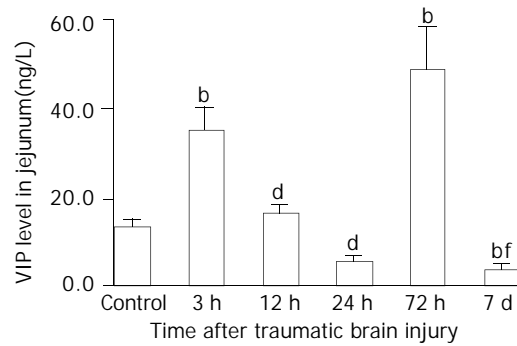


Figure 5 Alteration of VIP levels in all layers of jejunum after TBI. Compared with control, the level of VIP was significantly increased at 3 h following TBI, then declined markedly at 12 h and 24 h, and was significantly increased again at 72 h, but was at its lowest level on day 7 postinjury. ^b*P*<0.01 vs control; ^d*P*<0.01 vs 3 h; ⁱ*P*<0.01 vs 3 h and 12 h.

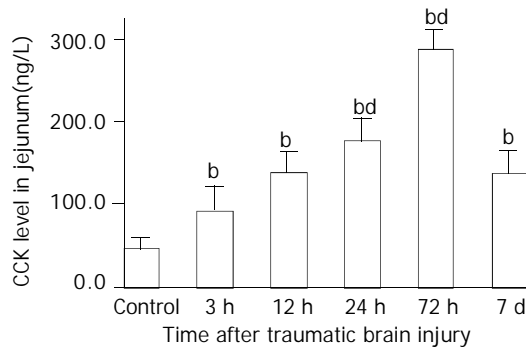


Figure 6 Alteration of CCK levels in all layers of jejunum after TBI. The level of CCK was significantly increased after TBI as compared with that of control, and peaked at 72 h postinjury, then declined to some degree but was still significantly higher than that of control on d 7. ^b*P*<0.01 vs control; ^d*P*<0.01 vs 3 h. Mean±SD of 6 animals, control: 46.5±13.9 ng/g, 3 h: 92.6±28.7 ng/g, 12 h: 139.8±24.7 ng/g, 24 h: 178.5±25.8 ng/g, 72 h: 286.8±25.9 ng/g, 7 d: 137.8±27.3 ng/g.

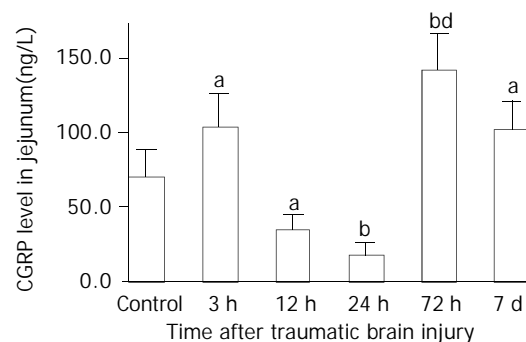


Figure 7 Alteration of CGRP levels in all layers of jejunum after TBI. Compared with control group, the level of CGRP was significantly increased at 3 h, then declined significantly at 12 h and 24 h, and significantly increased again at 72 h postinjury, then declined on d 7, but was still significantly higher than that of control. ^a*P*<0.05 vs control; ^b*P*<0.01 vs control; ^d*P*<0.01 vs 3 h, 12 h, 24 h and 7 d.

Levels of VIP, CCK and CGRP in jejunum

As compared with that of control group (VIP, 13.6±1.4 ng/g;

CGRP, 70.6 ± 17.7 ng/g), VIP and CGRP levels in jejunum were increased significantly at 3 h after TBI (VIP, 35.4 ± 5.0 ng/g; CGRP, 103.8 ± 22.1 ng/g, $P < 0.01$), then declined gradually at 12 h and 24 h (VIP, 16.5 ± 1.8 ng/g, 5.5 ± 1.4 ng/g; CGRP, 34.9 ± 9.7 ng/g, 18.5 ± 7.7 ng/g), but were significantly increased again at 72 h postinjury (VIP, 48.7 ± 9.5 ng/g; CGRP, 142.1 ± 24.3 ng/g, $P < 0.01$). The VIP level declined to a significantly low level on d 7 (3.8 ± 1.1 ng/g) (Figure 5), otherwise, CGRP declined to the level close to that of TBI 3 h group (102.5 ± 18.1 ng/g) (Figure 7). The CCK levels in jejunum were found to change in a similar trend as that in plasma with the concentrations of CCK significantly increased (99-517% increases) from 3 h to 7 d following TBI and peaked at 72 h (Figure 6).

DISCUSSION

TBI is a critically ill condition resulting in metabolic and immune alterations, inflammatory response and disturbance of gastrointestinal peptides via hypothalamo-pituitary-adrenal axis and brain-gut axis^[10,26]. Therefore, TBI can lead to disturbance of peptidergic mediators as a result of systemic stress with the same mechanism as occurred in trauma, sepsis, surgery and burns^[11-17]. Brain-gut peptides possess many biological functions such as dilating vessels, improving focal blood flow perfusion, regulating immune action and relaxing smooth muscle of trachea^[13,27,28]. The present study shows that brain-gut peptides VIP, CCK and CGRP change significantly following TBI in both plasma and jejunum, behave in different manner and partly adapt to the systemic pathophysiological needs. Our data suggest that levels of CCK in plasma and jejunum tissue change in parallel and increase gradually following TBI, with a maximum at 72 h postinjury. By contrast, VIP and CGRP levels in plasma and in jejunum tissue show non-parallel fluctuations. Nevertheless, concentrations of all neurohormonal mediators peak at 72 h postinjury, which coincides with the maximal morphological alterations occurring in the gut following TBI^[29]. High level of VIP, CCK and CGRP in plasma implies a large amount of release of these peptides into circulation from nerve ending due to systemic stress. Decreased VIP and CGRP level in plasma and/or jejunum may be related to the low synthesis, depletion of secretion, more binding to the relevant receptors, reduced tissue perfusion of blood flow and cell edema.

On the other hand, obvious alterations of VIP, CCK and CGRP may play an important role in gastrointestinal dysmotility induced by TBI, mainly because brain-gut peptides involved in the endocrine and enteric nervous systems as well as in the central nervous system are the important factors in the regulation of gastrointestinal motility through pathways of endocrine, paracrine or neurocrine. CCK exerts action mainly via endocrine, otherwise, VIP and CGRP mainly via neurocrine^[9]. Mechanic and chemical stimuli which induce peptide release from the epithelial endocrine cells are the earliest step in the initiation of peristaltic activities. The dorsal vagal complex (DVC), located in the medulla of brainstem, constitutes the basic neural circuit of vago-vagal reflex control of gastrointestinal motility^[9]. Several gut peptides act on the DVC to modify the vagal cholinergic reflexes directly (VIP and CGRP) or indirectly via the afferent fibers in the peripheral (CCK). The DVC is also a primary site of action of many neuropeptides in mediating gastrointestinal motor activities (TRH and NPY). More and more evidences have shown that there is a complicated bidirectional inter-relationship between nervous system and gastrointestinal tract^[30]. Gastrointestinal signals produced during chronic stress and colitis can be transmitted into central nervous system (CNS) and influence the function of the latter. In turn, CNS can modulate the electrical activity of gastrointestinal tract, as occurred in TBI.

VIP is a 28 amino acid neurotransmitter peptide that is widely distributed, particularly in the central and peripheral nervous systems, with a broad spectrum of biological actions mediated by stimulation of parasympathetic nerves coinciding with tissue responses. VIP is one of main inhibitory nervous transmitters located in the gut, which induces relaxation of intestinal smooth muscle and sphincters, dilation of peripheral blood vessels and inhibition of gastric acid secretion. Additionally, *in vivo* studies showed VIP could protect lung, retina, heart, kidney and stomach from the harmful effects of inflammation, ischemia-reperfusion injury and glutamate-induced cell death^[27,31]. It also increases survival rate of animals exposed to severe septic and hemorrhagic shock^[32]. VIP is a nonadrenergic noncholinergic nervous transmitter, and exerts inhibitory action on gastrointestinal motility through its binding to the relevant receptors located in gastrointestinal tract and subsequent activation of cyclic AMP-dependent protein kinase. VIP neurons occupy 40% of submucosal neurons of rat small intestine^[33]. In the intestine, VIP markedly stimulates intestinal secretion of electrolytes and hence of water. The results of this study showed that VIP level in both plasma and jejunum was increased significantly at 72 h following TBI. Increased concentrations of VIP in plasma and jejunum might be responsible for the intestinal dilation and large amounts of intra-intestinal effusion as shown in Figure 1 B and C. From 12 h to 24 h following TBI, VIP concentrations in both plasma and jejunum were decreased significantly due to binding to receptors and low synthesis, which was partially responsible for the acute gastrointestinal mucosal damage induced by ischemia.

CCK is involved in the endocrine cells in the upper small intestine, principally acting to stimulate gallbladder contractions^[34] and pancreatic secretion^[35], and to delay gastric emptying after meals^[26]. Evidence has shown that CCK, stimulated by nutrients, is a physiological mediator which inhibits gastric emptying and subsequently suppresses food intake^[26]. CCK mainly reduces the tone of lower esophageal sphincter, inhibits the peristalsis of proximal duodenum and promotes the peristalsis of distal duodenum and jejunum via activation of Ca^{2+} -dependent protein kinase. Previous studies have demonstrated that CCK could increase the mean contractile amplitude of antral circular muscle, motility index of pyloric circular muscle and the resting tension of fundus^[21,24,36,37]. Therefore, CCK possesses both excitatory and inhibitory action on contractile activity of different regions of stomach. Since systemic administration of CCK increases vagal afferent activity^[27] and this effect is blocked by the disruption of vagal capsaicin-sensitive afferent fibers, it has been suggested that CCK acts on the vagal afferent neurons and induces gastric relaxation^[28] and CCK-A receptor mediates this action^[30,38]. CCK exerts an inhibitory function on the colonic motility, which is mediated by CCK-A receptors^[39]. Besides the effects of CCK on the digestive tract, other biological actions of this peptide have been observed, such as appetite inhibition^[40], prevention of LPS-induced decrease of blood pressure and attenuation of LPS-induced increase of proinflammatory cytokines (TNF- α , IL-1 β and IL-6) *in vivo*^[12]. The current study showed that the levels of CCK in both plasma and jejunum were increased significantly following TBI, suggesting that CCK may play an important role in protection of splanchnic functions. Conversely, increased concentrations of CCK in plasma and jejunum might be highly responsible for the gastric emptying dysfunction^[20,41-44] and esophageal reflux which usually occur after head trauma^[1,6,7] through the mechanism as mentioned above. Gastric distention was found in rats at 12, 24 and 72 h following TBI, as shown in Figure 1, possibly due to the inhibitory action of persistently high CCK concentrations on the stomach contraction.

CGRP is a 37 amino acid neurotransmitter peptide that is widely distributed in the central and peripheral nervous

systems^[11,28,45], particularly in the viscera and vascular adventitia. It can also be synthesized and released by lymphocytes in rats^[46]. CGRP in blood mainly comes from the gut and vessels. CGRP may be released extensively from the nerve ending around vessels into circulation through organ stimuli such as endotoxin, inflammatory mediators, stress and intestinal ischemia-reperfusion injury in the rat^[11,13,47]. Endotoxemia, inflammatory cytokines and other kinds of stress can also stimulate the synthesis of CGRP in spinal dorsal root ganglia neurons (DRG). Therefore, TBI can also induce the extensive release of CGRP into plasma and synthesis of CGRP in jejunum as demonstrated in this study. CGRP possesses extensive biological functions such as cardiogenic effect, dilating vessels and regulating immune system^[11]. It has been previously shown that CGRP is one of the important mediators involved in the pathogenesis of infection, hemorrhage and trauma, and also is one of the mediators for the interactions of neural-immune systems. Recently, the involvement of CGRP in abdominal surgery-induced inhibition of gastric and colonic motility has been reported^[15]. The postoperative gastric ileus is mediated by CGRP released from spinal afferent neurons in the celiac and superior mesenteric ganglia as part of an extra-spinal gastrointestinal inhibitory reflex pathways^[15,16]. This study demonstrated that the CGRP concentration in plasma was increased persistently after TBI. Increased level of CGRP in plasma following TBI may contribute to the decreased tone of lower esophageal sphincter, delayed gastric emptying and paralytic ileus of small intestine. Decreased concentrations of CGRP in jejunum may be responsible for the ischemic damage of gut mucosa. The mechanism of CGRP inhibiting gastrointestinal motility includes: (1) CGRP is released into local gut tissue or circulation, and then binds to the relevant receptors located on the surface of gastrointestinal smooth muscle to exert inhibitory action; (2) CGRP, acting as a part of inhibitory spinal reflex, is released into local gut induced by all kinds of stress factors to activate spinal afferent nerve fibers, leading to decreased gastrointestinal motility^[15]; (3) CGRP can promote the release of substance P which partly mediate postoperative intestinal ileus^[17]; (4) CGRP interacts with the receptors on surface of D cells to induce the release of somatostatin, inhibiting gastrointestinal motility; (5) CGRP may slow the transmit of cholinergic nerve fibers of enteric nervous system to inhibit gastrointestinal peristalsis.

It is concluded that the concentrations of VIP, CCK and CGRP in both plasma and jejunum change significantly following TBI. All these data imply that alterations of these peptide concentrations in plasma and gut may be involved in the pathogenesis of gastrointestinal dysfunction after traumatic brain injury. Increased CCK level might be responsible for the delayed gastric emptying, otherwise, VIP and CGRP might be responsible for the paralytic dilation of small intestine and large amounts of intra-intestinal effusion.

ACKNOWLEDGEMENT

We would like to thank Dr. Gen-Bao Feng and Zhong-Shu Zhang for their technical assistance.

REFERENCES

- Jackson MD**, Davidoff G. Gastroparesis following traumatic brain injury and response to metoclopramide therapy. *Arch Phys Med Rehabil* 1989; **70**: 553-555
- Pilitsis JG**, Rengachary SS. Complications of head injury. *Neurol Res* 2001; **23**: 227-236
- Brown TH**, Davidson PF, Larson GM. Acute gastritis occurring within 24 hours of severe head injury. *Gastrointest Endosc* 1989; **35**: 37-40
- Norton JA**, Ott LG, McClain C, Adams L, Dempsey RJ, Haack D, Tibbs PA, Young AB. Intolerance to enteral feeding in the brain-injured patient. *J Neurosurg* 1988; **68**: 62-66
- Mackay LE**, Morgan AS, Bernstein BA. Factors affecting oral feeding with severe traumatic brain injury. *J Head Trauma Rehabil* 1999; **14**: 435-447
- Kao CH**, ChangLai SP, Chieng PU, Yen TC. Gastric emptying in head-injured patients. *Am J Gastroenterol* 1998; **93**: 1108-1112
- Saxe JM**, Ledgerwood AM, Lucas CE, Lucas WF. Lower esophageal sphincter dysfunction precludes safe gastric feeding after head injury. *J Trauma* 1994; **37**: 581-584
- Pedoto MJ**, O'Dell MW, Thrun M, Hollifield D. Superior mesenteric artery syndrome in traumatic brain injury: two cases. *Arch Phys Med Rehabil* 1995; **76**: 871-875
- Rogers RC**, McTigue DM, Hermann GE. Vagal control of digestion: modulation by central neural and peripheral endocrine factors. *Neurosci Biobehav Rev* 1996; **20**: 57-66
- Gue M**, Bueno L. Brain-gut interaction. *Semin Neurol* 1996; **16**: 235-243
- Joyce CD**, Fiscus RR, Wang X, Dries DJ, Morris RC, Prinz RA. Calcitonin gene-related peptide levels are elevated in patients with sepsis. *Surgery* 1990; **108**: 1097-1101
- Ling YL**, Meng AH, Zhao XY, Shan BE, Zhang JL, Zhang XP. Effect of cholecystokinin on cytokines during endotoxic shock in rats. *World J Gastroenterol* 2001; **7**: 667-671
- Wang X**, Jones SB, Zhou Z, Han C, Fiscus RR. Calcitonin gene-related peptide (CGRP) and neuropeptide Y (NPY) levels are elevated in plasma and decreased in vena cava during endotoxin shock in the rat. *Circ Shock* 1992; **36**: 21-30
- Onuoha G**, Alpar K, Jones I. Vasoactive intestinal peptide and nitric oxide in the acute phase following burns and trauma. *Burns* 2001; **27**: 17-21
- Zittel TT**, Lloyd KC, Rothenhofer I, Wong H, Walsh JH, Raybould HE. Calcitonin gene-related peptide and spinal afferents partly mediate postoperative colonic ileus in the rat. *Surgery* 1998; **123**: 518-527
- Zittel TT**, Reddy SN, Plourde V, Raybould HE. Role of spinal afferents and calcitonin gene-related peptide in the postoperative gastric ileus in anesthetized rats. *Ann Surg* 1994; **219**: 79-87
- Espat NJ**, Cheng G, Kelley MC, Vogel SB, Sninsky CA, Hocking MP. Vasoactive intestinal peptide and substance P receptor antagonists improve postoperative ileus. *J Surg Res* 1995; **58**: 719-723
- Chen ZY**, Yan MX, Xiang BK, Zhan HW. Alterations of gut hormones of blood and colonic mucosa in rats with chronic stress. *Shijie Huaren Xiaohua Zazhi* 2001; **9**: 59-61
- Li LS**, Qu RY, Wang W, Guo H. Significance of changes of gastrointestinal peptides in blood and ileum of experimental spleen deficiency rats. *World J Gastroenterol* 2003; **9**: 553-556
- Higham A**, Vaillant C, Yegen B, Thompson DG, Dockray GJ. Relation between cholecystokinin and antral innervation in the control of gastric emptying in the rat. *Gut* 1997; **41**: 24-32
- Li W**, Zheng TZ, Qu SY. Effect of cholecystokinin and secretin on contractile activity of isolated gastric muscle strips in guinea pigs. *World J Gastroenterol* 2000; **6**: 93-95
- Yao YL**, Xu B, Zhang WD, Song YG. Gastrin, somatostatin, and experimental disturbance of the gastrointestinal tract in rats. *World J Gastroenterol* 2001; **7**: 399-402
- Pincus DW**, DiCicco-Bloom EM, Black IB. Vasoactive intestinal peptide regulates mitosis, differentiation and survival of cultured sympathetic neuroblasts. *Nature* 1990; **343**: 564-567
- Maggi CA**, Giuliani S, Zagorodnyuk V. Calcitonin gene-related peptide (CGRP) in the circular muscle of guinea-pig colon: role as inhibitory transmitter and mechanisms of relaxation. *Regul Pept* 1996; **61**: 27-36
- Feeney DM**, Boyeson MG, Linn RT, Murray HM, Dail WG. Responses to cortical injury: I. Methodology and local effects of contusions in the rat. *Brain Res* 1981; **211**: 67-77
- Grundy PL**, Harbuz MS, Jessop DS, Lightman SL, Sharples PM. The hypothalamo-pituitary-adrenal axis response to experimental traumatic brain injury. *J Neurotrauma* 2001; **18**: 1373-1381
- Tuncel N**, Erkasap N, Sahinturk V, Ak DD, Tuncel M. The protective effect of vasoactive intestinal peptide (VIP) on stress-induced gastric ulceration in rats. *Ann N Y Acad Sci* 1998; **865**:

- 309-322
- 28 **Melagros L**, Ghatei MA, Bloom SR. Release of vasodilator, but not vasoconstrictor, neuropeptides and of enteroglucagon by intestinal ischemia/reperfusion in the rat. *Gut* 1994; **35**: 1701-1706
- 29 **Hang CH**, Shi JX, Li JS, Wu W, Yin HX. Alterations of intestinal mucosa structure and barrier function following traumatic brain injury in rats. *World J Gastroenterol* 2003; **9**: 2776-2781
- 30 **Wang X**, Wang BR, Zhang XJ, Xu Z, Ding YQ, Ju G. Evidences for vagus nerve in maintenance of immune balance and transmission of immune information from gut to brain in STM-infected rats. *World J Gastroenterol* 2002; **8**: 540-545
- 31 **Said SI**, Dickman KG. Pathways of inflammation and cell death in the lung: modulation by vasoactive intestinal peptide. *Regul Pept* 2000; **93**: 21-29
- 32 **Delgado M**, Martinez C, Pozo D, Calvo JR, Leceta J, Ganea D, Gomariz RP. Vasoactive intestinal peptide (VIP) and pituitary adenylate cyclase-activation polypeptide (PACAP) protect mice from lethal endotoxemia on through the inhibition of TNF-alpha and IL-6. *J Immunol* 1999; **162**: 1200-1205
- 33 **Pataky DM**, Curtis SB, Buchan AM. The co-localization of neuropeptides in the submucosa of the small intestine of normal Wistar and non-diabetic BB rats. *Neuroscience* 1990; **36**: 247-254
- 34 **Pendleton RG**, Bendesky RJ, Schaffer L, Nolan TE, Gould RJ, Clineschmidt BV. Roles of endogenous cholecystokinin in biliary, pancreatic and gastric function: studies with L-364, 718, a specific cholecystokinin receptor antagonist. *J Pharmacol Exp Ther* 1987; **241**: 110-116
- 35 **Li Y**, Owyang C. Vagal afferent pathway mediates physiological action of cholecystokinin on pancreatic enzyme secretion. *J Clin Invest* 1993; **92**: 418-424
- 36 **Grider JR**, Makhoulouf GM. Regional and cellular heterogeneity of cholecystokinin receptors mediating muscle contraction in the gut. *Gastroenterology* 1987; **92**: 175-180
- 37 **Gerner T**. Pressure responses to OP-CCK compared to CCK-PZ in the antrum and fundus of isolated guinea-pig stomachs. *Scand J Gastroenterol* 1979; **14**: 73-77
- 38 **Xu MY**, Lu HM, Wang SZ, Shi WY, Wang XC, Yang DX, Yang CX, Yang LZ. Effect of devazepide reversed antagonism of CCK-8 against morphine on electrical and mechanical activities of rat duodenum *in vitro*. *World J Gastroenterol* 1998; **4**: 524-526
- 39 **Hayashi K**, Kishimoto S, Kannbe M. Endogenous CCK inhibits colonic contractions in unrestrained conscious rats. *Regul Pept* 1997; **72**: 131-137
- 40 **Du YP**, Zhang YP, Wang SC, Shi J, Wu SH. Function and regulation of cholecystokinin octapeptide, β -endorphin and gastrin in anorexic infantile rats treated with ErBao Granules. *World J Gastroenterol* 2001; **7**: 275-280
- 41 **Forster ER**, Green M, Elliot M, Bremner A, Dockray GJ. Gastric emptying in rats: role of afferent neurons and cholecystokinin. *Am J Physiol* 1990; **258**(4 Pt 1): G552-G556
- 42 **Grundy D**, Bagaev V, Hillsley K. Inhibition of gastric mechanoreceptor discharge by cholecystokinin in the rat. *Am J Physiol* 1995; **268**(2 Pt 1): G355-G360
- 43 **Schwartz GJ**, Moran TH, White WO, Ladenheim EE. Relationships between gastric motility and gastric vagal afferent responses to CCK and GRP in rats differ. *Am J Physiol* 1997; **272**(6 Pt 2): R1726-R1733
- 44 **Shoji E**, Okumura T, Onodera S, Takahashi N, Harada K, Kohgo Y. Gastric emptying in OLETF rats not expressing CCK-A receptor gene. *Dig Dis Sci* 1997; **42**: 915-919
- 45 **Varro A**, Green T, Holmes S, Dockray GJ. Calcitonin gene-related peptide in visceral afferent nerve fibres: quantification by radioimmunoassay and determination of axonal transport rates. *Neuroscience* 1988; **26**: 927-932
- 46 **Wang X**, Xing L, Xing Y, Tang Y, Han C. Identification and characterization of immunoreactive calcitonin gene-related peptide from lymphocytes of the rat. *J Neuroimmunol* 1999; **94**: 95-102
- 47 **Wang X**, Wu Z, Tang Y, Fiscus RR, Han C. Rapid nitric oxide- and prostaglandin-dependent release of calcitonin gene-related peptide (CGRP) triggered by endotoxin in rat mesenteric arterial bed. *Br J Pharmacol* 1996; **118**: 2164-2170

Edited by Zhu LH and Xu FM

Detection of point mutation in K-ras oncogene at codon 12 in pancreatic diseases

Yue-Xin Ren, Guo-Ming Xu, Zhao-Shen Li, Yu-Gang Song

Yue-Xin Ren, Yu-Gang Song, Department of Gastroenterology, Nanfang Hospital, First Military Medical University, Guangzhou 510515, Guangdong Province, China

Guo-Ming Xu, Zhao-Shen Li, Department of Gastroenterology, Changhai Hospital, Second Military Medical University, Shanghai 200433, China

Supported by the Technology Committee of Shanghai, NO.994119044

Correspondence to: Dr Yue-Xin Ren, Department of Gastroenterology, Nanfang Hospital, First Military Medical University, Guangzhou 510515, China. yzxu@fimmu.com

Telephone: +86-21-61641544

Received: 2003-08-26 **Accepted:** 2003-10-22

Abstract

AIM: To investigate frequency and clinical significance of K-ras mutations in pancreatic diseases and to identify its diagnostic values in pancreatic carcinoma.

METHODS: 117 ductal lesions were identified in the available sections from pancreatic resection specimens of pancreatic ductal adenocarcinoma, comprising 24 pancreatic ductal adenocarcinoma, 19 peritumoral ductal atypical hyperplasia, 58 peritumoral ductal hyperplasia and 19 normal duct at the tumor free resection margin. 24 ductal lesions were got from 24 chronic pancreatitis. DNA was extracted. Codon 12 K-ras mutations were examined using the two-step polymerase chain reaction (PCR) combined with restriction enzyme digestion, followed by nonradioisotopic single-strand conformation polymorphism (SSCP) analysis and by means of automated DNA sequencing.

RESULTS: K-ras mutation rate of the pancreatic carcinoma was 79%(19/24) which was significantly higher than that in the chronic pancreatitis 33%(8/24) ($P<0.01$). It was also found that K-ras mutation rate was progressively increased from normal duct at the tumor free resection margin, peritumoral ductal hyperplasia, peritumoral ductal atypical hyperplasia to pancreatic ductal adenocarcinoma. The mutation pattern of K-ras 12 codon of chronic pancreatitis was GGT→GAT, GGT and CGT, which is identical to that in pancreatic carcinoma.

CONCLUSION: K-ras mutation may play a role in the malignant transformation of pancreatic ductal cell. K-ras mutation was not specific enough to diagnose pancreatic carcinoma.

Ren YX, Xu GM, Li ZS, Song YG. Detection of point mutation in K-ras oncogene at codon 12 in pancreatic diseases. *World J Gastroenterol* 2004; 10(6): 881-884

http://www.wjgnet.com/1007-9327/10/881.asp

INTRODUCTION

Despite considerable development in sophisticated imaging techniques and cytological examination, an early diagnosis of pancreatic neoplasm is rare. Furthermore, surgical therapy for pancreatic cancer is frequently not curative, most often as a

consequence of this tumor's propensity to metastasize. Only in a minority of cases is the diagnosis made at a very early stage, when curative surgery might significantly ameliorate the 5-year survival rate^[1-3]. Therefore, a better understanding of the molecular basis of transformation into malignant tumor may contribute to the establishment of new criteria for diagnosis, prognosis and treatment of human neoplasms. K-ras mutation at codon 12 is one of the most common mutational events in the carcinogenesis of human malignancies^[4]. It occurs mainly in mucin-producing adenocarcinomas^[5]. The highest incidence of K-ras mutation has been found in ductal adenocarcinoma of the pancreas, in which it ranged from 70% to 100%^[6,7]. Because K-ras has been found in very small incidental carcinomas, which were diagnosed only at autopsy^[8], as well as in intraductal portions of ductal carcinomas, it is considered as an initial event in carcinoma development. This may make it a good tool for detecting pancreatic carcinomas at an early stage^[9,10]. However, Yanagisawa *et al.*^[11] showed that K-ras mutations also occur in hyperplastic ductal lesions in pancreas that do not harbor any malignancy. Therefore the K-ras mutation cannot be used as a marker of pancreatic ductal adenocarcinoma. However, this also suggests that ductal lesions, even without dysplasia, may be the forerunners of ductal adenocarcinoma. This assumption also was fostered by the early observation that some of the described ductal lesions frequently are associated with ductal adenocarcinoma. Several studies generally have confirmed the results of Yanagisawa *et al.*, whereas others failed to detect K-ras mutations in nondysplastic epithelium. To address these issues we analyzed 117 ductal lesions for K-ras mutations.

MATERIALS AND METHODS

Tissue selection

The tissues used in this study were derived from patients who underwent partial duodenopancreatectomy for ductal adenocarcinoma of the pancreas and chronic pancreatitis. The basis for selection was the availability of suitable paraffin blocks (blocks age <5 years). 117 ductal lesions were identified in the available sections from pancreatic resection specimens of 24 pancreatic ductal adenocarcinoma, comprising 24 pancreatic ductal adenocarcinoma, 19 peritumoral ductal atypical hyperplasia, 58 peritumoral ductal hyperplasia and 19 normal duct at the tumor free resection margin. 24 ductal lesions were obtained from 24 patients of chronic pancreatitis. 7 surgical specimens of normal pancreas from patients with widely invasive gastric and colonic carcinoma in whom the tumor had not invaded the pancreas and who did not have pancreatic carcinoma or pancreatitis were examined. Multiple 5- and 10- μ m sections were cut from each block and floated onto glass slides. Hematoxylin and eosin staining was performed on 5- μ m sections from each paraffin block. The blade was replaced after each block was cut to prevent carryover of DNA between sections. Pancreatic carcinoma cell line Patu-8988 was obtained from Doctor Elsasser Philips of University of Germany.

DNA extraction

A boiling method of DNA extraction was employed similar to

that previously described by Shibata^[12]. Tissue sections were deparaffinized and digested with a proteinase K digestion buffer (50 mmol/L Tris-HCL, pH 8.5, with 250 µg/mL proteinase K overnight at 55 °C). The tissue was then boiled for 10 min and centrifuged. DNA was quantitated using a spectrophotometer.

Enriched PCR amplification

The first PCR- mediated amplifications were performed as described previously with minor modifications^[13] and produced a 157-base pair fragment that contain K-ras codon 12. Aliquots of the first PCR product were digested with BstN1 (Biolab) at 60 °C for 2 h under the conditions recommended by the supplier. After boiling the mixture for 5 min to inhibit the enzymatic activity, 1/100 volume of the PCR product was subjected to the second PCR under the same conditions but using a different primer set, which flanked internal sequences of 135 bp DNA fragments. The amplified fragments were directly subjected to SSCP. The oligonucleotide primers were purchased from Sangon Co. (Shanghai, China). The sequences of oligonucleotide primers were as follows: 5' ACT GAA TAT AAA CTT GTG GTA GTT GGA CCT 3' (forward primer for first and second PCR); 5' TCA AAG AAT GGT CCT GGA CC 3' (reverse primer for first PCR); 5' TAA TAT GTC GAC TAA AAC AAG ATT TAC CTC 3' (reverse primer for second PCR).

Nonradioisotopic SSCP analysis

Nonradioisotopic SSCP Analyses were performed as described previously, with minor modification^[13]. After denaturation at 100 °C for 5 min, a 10 µL sample was applied and resolved by 120 g/L polyacrylamide gel electrophoresis at 35 V for 21 h at 4 °C. The gels were silver-stained. Each sample was analyzed by SSCP repeatedly to confirm its accuracy.

Direct sequencing of the amplified PCR product

For sequencing the deviant homoduplex bands were cut out of the gel, the DNA eluted by soaking in TE, reamplified, and TA cloned in the pUCm-T vector. Sequencing was performed on an ABI PRISM 377 automated sequencer.

Statistical analysis

A statistical analysis was performed using the chisquare test, the Fisher' s exact test and Student *t* test with SPSS.

RESULTS

Detection of K-ras point mutation by nonradioisotopic SSCP analysis and direct sequencing of PCR product

To estimate the sensitivity of this analysis, 1 µg of the DNA extracted from normal peripheral blood lymphocytes and a pancreatic carcinoma cell line were subjected to PCR. Figure 1 shows the electrophoretic profiles of amplified DNA fragments by SSCP. The positive percentage of K-ras mutation of the pancreatic carcinoma was 79% (19/24) which was significantly higher than that in the chronic pancreatitis 33% (8/24) (*P*<0.01). It was also found that K-ras mutation rate was progressively increased from normal duct at the tumor free resection margin, peritumoral ductal hyperplasia, peritumoral ductal atypical hyperplasia to pancreatic ductal adenocarcinoma (Table 1).

The nucleotide sequences of K-ras mutation showed the following transitions: GGT to GAT, GGT to GTT, and GGT to CGT. (Table 2).

Relationship between K-ras gene mutation and location, histological grade and clinical stage of tumors

The diagnostic accuracy of K-ras mutations in pancreatic

carcinoma relative to the location, histological grade and clinical stage of the tumor is summarized in Table 3. There are no apparent correlation between the location, histological grade, clinical stage of the tumor and the presence of K-ras gene mutations.

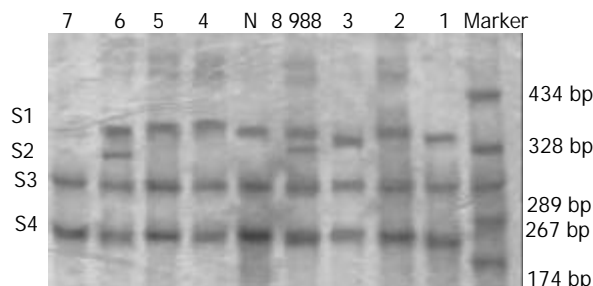


Figure 1 Detection of point mutations of the K-ras oncogene in pancreatic diseases. Lane N, healthy control subject DNA from normal peripheral blood lymphocytes. Lane 8988, pancreatic carcinoma cell line Patu-8988 DNA with confirmed mutant K-ras. Lane 6, patients with pancreatic carcinoma with mutant K-ras. Lane 7, normal pancreatic tissue. Lane 1, 3, 4, patients with chronic pancreatitis with mutant K-ras. Lane 2, 5, patients with chronic pancreatitis with wild type K-ras.

Table 1 Relative frequency of K-ras mutation in ductal lesions with pancreatic diseases

Ductal lesion	n	K-ras (-)	K-ras (+)	Positive percentage (%)
Pancreatic ductal adenocarcinoma	24	5	19	79.2
Peritumoral ductal atypical hyperplasia	19	15	14	73.6
Peritumoral ductal hyperplasia	58	38	20	34.5
Normal duct at the tumor free resection margin	16	16	0	0
Chronic pancreatitis	24	16	8	33.3
Normal pancreas	7	7	0	0

Table 2 K-ras mutation pattern of ductal lesions and the corresponding primary pancreatic carcinoma

Ductal lesion	Nucleotide sequence of K-ras12 codon		
	GAT	GTT	CGT
Pancreatic ductal adenocarcinoma	8	4	7
Peritumoral ductal atypical hyperplasia	7	2	3
Peritumoral ductal hyperplasia	10	3	7
Chronic pancreatitis	4	2	2

Table 3 Relationship between K-ras gene mutation and location, histological grade and clinical stage of pancreatic carcinomas

Pathologic factor	n	Positive rate (%)
Tumor location		
Head	18	55.6
Tail/Corpus	6	66.7
Histological grade		
G1	6	66.7
G2	10	50
G3	8	62.5
Clinical stage		
I	1	100
II	3	66.7
III	9	66.7
IV	11	45.5

Clinical and morphologic data on 24 patients with chronic pancreatitis

The occurrence of mutations was unrelated to clinical and morphologic indexes. The difference was not statistically significant (Student *t* test) (Table 4).

Table 4 Clinical and morphologic data on 24 patients with chronic pancreatitis

	K-ras positive cases (n=8)	K-ras negative cases (n=16)
Mean age of patients (yrs)	39.9±15.5(19-68)	51±14.9(23-67)
Gender ratio (M:F)	6:2	10:6
Mean duration of CP (yrs)	6.7±3.2(2-27)	5.7±4.5(3-25)
Mass-CP of pancreatic head	5 cases	10 cases
Weight loss (>10 kg)	3 cases	7 cases
Diabetes (insulin dependent)	4 cases	7 cases
Nicotine(>20 cigarettes/day, >5 yrs)	5 cases	8 cases

CP: chronic pancreatitis.

DISCUSSION

Pancreatic ductal carcinoma is known to have the highest K-ras mutation rate among all tumors. The codon 12 of this gene is affected in 80-100% of the cases. Mutated K-ras also has been found in ductal lesions such as mucinous cell hypertrophy and ductal papillary hyperplasia; therefore these lesions have been regarded as precursor lesions of carcinoma^[11]. However, this assumption is based on rather contradictory results, with K-ras mutation rates in ductal lesions ranging from 0-94%^[14]. The discrepancies between the results of the various studies are based on the wide range of investigated cases, the selection of lesion types, and PCR employed.

Matsubayashi *et al.*^[15] analyzed 317 carcinoma-associated ductal lesions, 39% were positive for K-ras mutations. Moskaluk *et al.*^[14] focused on atypical papillary hyperplasia and found K-ras mutations in 75% of their samples. Both study groups used a detection method (nested PCR-RLFP) with a sensitivity of 5%. But SSCP analysis is one of the simplest and most sensitive methods for detection of mutations based on PCR technology^[16-18]. Since its first report, the SSCP analysis has been widely used to detect mutations in genes responsible for various hereditary diseases and somatic mutations of oncogenes. In an earlier study, Lemoine *et al.*^[19] found no mutations in cases of ductal hyperplasia, but they did find mutation in all severely dysplastic lesions that they regarded as intraductal extensions of the associated ductal adenocarcinoma. It appears that their method, which was based on slot-blot analysis, was not sensitive enough to detect K-ras mutations in nondysplastic ductal lesions.

Chronic pancreatitis, regardless of its etiology, is considered a risk factor for the development of pancreatic ductal adenocarcinoma^[20]. The risk seems to increase with the duration of CP. Some histological studies have searched for possible carcinoma precursor lesions in this disease. Cylwik *et al.*^[21] reported severe dysplasia in 8.6% of 70 resection specimens from patients with CP; advanced fibrosis was associated with dysplasia in 65%. Because of these results, they concluded that surgical removal of the pancreas should be recommended. We cannot confirm these data. We were unable to identify any severe dysplasia carcinoma in situ changes in 24 resection specimens from patients with CP and varying duration of the disease.

K-ras mutation is considered an early event in the tumorigenesis of pancreatic carcinomas. In our study the positive percentage of K-ras mutation of the pancreatic carcinoma was 79%(19/24) which was significantly higher than

that in the chronic pancreatitis 33%(8/24) ($P<0.01$). It was also found that K-ras mutation rate was progressively increased from normal duct at the tumor free resection margin, peritumoral ductal hyperplasia, peritumoral ductal atypical hyperplasia to pancreatic ductal adenocarcinoma. It appeared that the locations, histological grade, clinical stage of pancreatic carcinomas were all not related to the presence of K-ras mutations. The occurrence of K-ras mutations was not associated with the duration of CP and also not with mass-CP of pancreatic head. Rivera *et al.*^[22] reported K-ras mutations in 2 of 11 cases and Yanagisawa *et al.*^[11] even 62.5% mutations in 10 of 16 lesions from 10 cases. K-ras mutations were not detected by Kubrusly *et al.*^[23]. Their negative results probably were due to the comparatively insensitive PCR method and the tissues they selected for investigation. To summarize, when sensitive enough methods are applied, K-ras mutation frequently can be detected in nondysplastic ductal epithelium of patients with CP. Berger *et al.*^[24] reported a clear correlation between K-ras mutations and the nicotine history of their patients. In our study, the relationship was unclear. Therefore, nicotine seems to be a major factor in the induction of the mutation but does not inevitably induce it.

The relation between CP and pancreatic adenocarcinoma remains difficult to explain. Continuous epithelial regeneration and proliferation are thought to promote carcinogenesis in many organs. In our study, the incidence of the ductal lesions and K-ras mutations did not increase with the duration of CP. It therefore seems that hyperplastic ductal changes and K-ras mutations will not inevitably lead to the development of ductal adenocarcinoma.

Future prospective studies should be performed to get a well documented long term follow-up of K-ras positive cases to elucidate the role of K-ras mutations in pancreatic carcinogenesis in CP patients. In addition, other mutations, such as those of the p16, DPC4, and BRCA2 genes or promoter methylation of tumor suppressor, which evidently play role in a linear tumor progression model of pancreatic carcinoma, also should be looked for in lesions that might be responsible for the presumed pancreatic carcinoma sequence in chronic pancreatitis^[25-30].

REFERENCES

- 1 **Postier RG.** Past, present, and future of pancreatic surgery. *Am J Surg* 2001; **182**: 547-551
- 2 **Beger HG,** Gansauge F, Leder G. Pancreatic cancer: who benefits from curative resection? *Can J Gastroenterol* 2002; **16**: 117-120
- 3 **Shankar A,** Russell RC. Recent advances in the surgical treatment of pancreatic cancer. *World J Gastroenterol* 2001; **7**: 622-626
- 4 **Barbacid M.** Ras oncogenes: their role in neoplasia. *Eur J Clin Invest* 1990; **20**: 225-235
- 5 **Bos JL.** Ras oncogenes in human cancer: a review. *Cancer Res* 1989; **49**: 4682-4689
- 6 **Grunewald K,** Lyons J, Frohlich A, Feichtinger H, Weger RA, Schwab G, Janssen JW, Bartram CR. High frequency of Ki-ras codon 12 mutations in pancreatic adenocarcinomas. *Int J Cancer* 1989; **43**: 1037-1041
- 7 **Hruban RH,** van Mansfield AD, Offerhaus GJ, van Weering DH, Allison DC, Goodman SN, Kensler TW, Bose KK, Cameron JL, Bos JL. K-ras oncogene activation in adenocarcinoma of the human pancreas. A study of 82 carcinomas using a combination of mutant-enriched polymerase chain reaction analysis and allele-specific oligonucleotide hybridization. *Am J Pathol* 1993; **143**: 545-554
- 8 **Kimura W,** Morikane K, Esaki Y, Chan WC, Pour PM. Histologic and biologic patterns of microscopic pancreatic ductal adenocarcinomas detected incidentally at autopsy. *Cancer* 1998; **82**: 1839-1849
- 9 **Miki H,** Matsumoto S, Harada H, Mori S, Haba R, Ochi K, Kobayashi S, Ohmori M. Detection of c-Ki-ras point mutation

- from pancreatic juice. A useful diagnostic approach for pancreatic carcinoma. *Int J Pancreatol* 1993; **14**: 145-148
- 10 **Iguchi H**, Sugano K, Fukayama N, Ohkura H, Sadamoto K, Ohkoshi K, Seo Y, Tomoda H, Funakoshi A, Wakasugi H. Analysis of Ki-ras codon 12 mutations in the duodenal juice of patients with pancreatic cancer. *Gastroenterology* 1996; **110**: 221-226
- 11 **Yanagisawa A**, Ohtake K, Ohashi K, Hori M, Kitagawa T, Sugano H, Kato Y. Frequent c-Ki-ras oncogene activation in mucous cell hyperplasias of pancreas suffering from chronic inflammation. *Cancer Res* 1993; **53**: 953-956
- 12 **Shibata D**. Extraction of DNA from paraffin-embedded tissue for analysis by polymerase chain reaction: new tricks from an old friend. *Hum Pathol* 1994; **25**: 561-563
- 13 **Kahn SM**, Jiang W, Culbertson TA, Weinstein IB, Williams GM, Tomita N, Ronai Z. Rapid and sensitive nonradioactive detection of mutant K-ras genes via 'enriched' PCR amplification. *Oncogene* 1991; **6**: 1079-1083
- 14 **Moskaluk CA**, Hruban RH, Kern SE. p16 and K-ras gene mutations in the intraductal precursors of human pancreatic adenocarcinoma. *Cancer Res* 1997; **57**: 2140-2143
- 15 **Matsubayashi H**, Watanabe H, Nishikura K, Ajioka Y, Kijima H, Saito T. Determination of pancreatic ductal carcinoma histogenesis by analysis of mucous quality and K-ras mutation. *Cancer* 1998; **82**: 651-660
- 16 **Hayashi K**. PCR-SSCP: a method for detection of mutations. *Genet Anal Tech Appl* 1992; **9**: 73-79
- 17 **Hayashi K**, Yandell DW. How sensitive is PCR-SSCP? *Hum Mutat* 1993; **2**: 338-346
- 18 **Hayashi K**. Recent enhancements in SSCP. *Genet Anal* 1999; **14**: 193-196
- 19 **Lemoine NR**, Jain S, Hughes CM, Staddon SL, Maillet B, Hall PA, Kloppel G. Ki-ras oncogene activation in preinvasive pancreatic cancer. *Gastroenterology* 1992; **102**: 230-236
- 20 **Lowenfels AB**, Maisonneuve P, Cavallini G, Ammann RW, Lankisch PG, Andersen JR, Dimagno EP, Andren-Sandberg A, Domellof L. Pancreatitis and the risk of pancreatic cancer. International Pancreatitis Study Group. *N Engl J Med* 1993; **328**: 1433-1437
- 21 **Cylwik B**, Nowak HF, Puchalski Z, Barczyk J. Epithelial anomalies in chronic pancreatitis as a risk factor of pancreatic cancer. *Hepatogastroenterology* 1998; **45**: 528-532
- 22 **Rivera JA**, Rall CJ, Graeme-Cook F, Fernandez-del Castillo C, Shu P, Lakey N, Tepper R, Rattner DW, Warshaw AL, Rustgi AK. Analysis of K-ras oncogene mutations in chronic pancreatitis with ductal hyperplasia. *Surgery* 1997; **121**: 42-49
- 23 **Kubrusly MS**, Cunha JE, Bacchella T, Abdo EE, Jukemura J, Penteado S, Morioka CY, de Souza LJ, Machado MC. Detection of K-ras point mutation at codon 12 in pancreatic diseases: a study in a Brazilian casuistic. *JOP* 2002; **3**: 144-151
- 24 **Berger DH**, Chang H, Wood M, Huang L, Heath CW, Lehman T, Ruggeri BA. Mutational activation of K-ras in nonneoplastic exocrine pancreatic lesions in relation to cigarette smoking status. *Cancer* 1999; **85**: 326-332
- 25 **Moore PS**, Sipos B, Orlandini S, Sorio C, Real FX, Lemoine NR, Gress T, Bassi C, Kloppel G, Kalthoff H, Ungefroren H, Lohr M, Scarpa A. Genetic profile of 22 pancreatic carcinoma cell lines. Analysis of K-ras, p53, p16 and DPC4/Smad4. *Virchows Arch* 2001; **439**: 798-802
- 26 **Klump B**, Hsieh CJ, Nehls O, Dette S, Holzmann K, Kiesslich R, Jung M, Sinn U, Ortner M, Porschen R, Gregor M. Methylation status of p14ARF and p16INK4a as detected in pancreatic secretions. *Pancreatol* 2002; **2**: 17-25
- 27 **Fukushima N**, Walter KM, Uek T, Sato N, Matsubayashi H, Cameron JL, Hruban RH, Canto M, Yeo CJ, Goggins M. Diagnosing pancreatic cancer using methylation specific PCR analysis of pancreatic juice. *Cancer Biol Ther* 2003; **2**: 78-83
- 28 **Fukushima N**, Sato N, Ueki T, Rosty C, Walter KM, Wilentz RE, Yeo CJ, Hruban RH, Goggins M. Aberrant methylation of preproenkephalin and p16 genes in pancreatic intraepithelial neoplasia and pancreatic ductal adenocarcinoma. *Am J Pathol* 2002; **160**: 1573-1581
- 29 **Ohtsubo K**, Watanabe H, Yamaguchi Y, Hu YX, Motoo Y, Okai T, Sawabu N. Abnormalities of tumor suppressor gene p16 in pancreatic carcinoma: immunohistochemical and genetic findings compared with clinicopathological parameters. *J Gastroenterol* 2003; **38**: 663-671
- 30 **House MG**, Guo M, Iacobuzio-Donahue C, Herman JG. Molecular progression of promoter methylation in intraductal papillary mucinous neoplasms (IPMN) of the pancreas. *Carcinogenesis* 2003; **24**: 193-198

Edited by Xu JY Proofread by Xu FM

Effect of local CTLA4Ig gene transfection on acute rejection of small bowel allografts in rats

Yi-Fang Wang, Ai-Gang Xu, Yi-Bing Hua, Wen-Xi Wu

Yi-Fang Wang, Ai-Gang Xu, Yi-Bing Hua, Wen-Xi Wu, Department of Gastrointestinal Surgery, the First Affiliated Hospital of Nanjing Medical University, Nanjing 210029, Jiangsu Province, China
Supported by the Innovative Foundation of Nanjing Medical University, N0.200106

Correspondence to: Wen-Xi Wu, Department of Gastrointestinal Surgery, the First Affiliated Hospital of Nanjing Medical University, Nanjing 210029, Jiangsu Province, China. wuwenxi@yahoo.com
Telephone: +86-25-3718836-6828

Received: 2003-10-08 **Accepted:** 2003-12-16

Abstract

AIM: To evaluate the local expression of CTLA4Ig gene in small bowels and its effect on preventing acute rejection of the small bowel allografts.

METHODS: Groups of Wistar rats underwent heterotopic small bowel transplantation from SD rats. The recipients were randomly divided into experimental group (allografts were transfected with CTLA4Ig gene) and control group (non CTLA4Ig gene transfected). In the experimental group, the donor small bowels were perfused *ex vivo* with CTLA4Ig cDNA packaged with lipofectin vector via intra-superior mesenteric artery before transplantation, and the CTLA4Ig expression in the small bowel grafts post-transplantation was assessed by immunohistology. On d 3, 7 and 10 post-transplantation, the allografts in each group were harvested for the examination of histology and detection of apoptosis.

RESULTS: Small bowel allografts treated with CTLA4Ig cDNA showed abundant CTLA4Ig expression after transplantation. Acute rejection of grade I on d 7 and grade II on d 10 after transplantation was noticed in the control allografts, and a dramatically increased number of apoptotic enterocytes in parallel to the progressive rejection could be recognized. In contrast, the allografts treated with CTLA4Ig cDNA showed nonspecific histological changes and only a few apoptotic enterocytes were found after transplantation.

CONCLUSION: Local CTLA4Ig gene transfection of small bowel allograft is feasible, and the local CTLA4Ig expression in the allograft can prevent acute rejection after transplantation.

Wang YF, Xu AG, Hua YB, Wu WX. Effect of local CTLA4Ig gene transfection on acute rejection of small bowel allografts in rats. *World J Gastroenterol* 2004; 10(6): 885-888
<http://www.wjgnet.com/1007-9327/10/885.asp>

INTRODUCTION

CTLA4Ig is a soluble recombinant fusion protein constructed with an extracellular domain of mouse CTLA4 and Fc portion of human IgG. This protein binds to the mouse and rat B7-1/2 molecules, and blocks the co-stimulatory signals from antigen processing cell (APC) to antigen specific T cell. Treatment with CTLA4Ig gene transfection has been shown to prolong

graft survival in mouse and rat heart, liver, pancreatic islet, kidney and lung transplantations and to induce donor-specific tolerance in some of these cases^[1-7].

There are two methods of gene transduction: systemic administration (*ie.* intravenous injection) and local transfection of allograft. Gene transfer of sequences coding for soluble immunosuppressive molecules into transplanted organs aims to create a local microenvironment directly modulating the activation state of immune cells responsible for graft rejection^[8]. Therefore, when compared with systemic administration, local and continuous production of biologically active compounds might increase their bioavailability and allow a more effective treatment. Furthermore, cells not involved in the rejection process could be spared, and side effects or generalized immunosuppression may thus be avoided.

Intra-graft expression of CTLA4Ig by gene transfection at the time of transplantation can successfully prolong survival of several grafts^[9-12]. Nevertheless, study of CTLA4Ig expression within the small bowel allograft has not been reported. In the present study, we transfected gene by *ex vivo* intra-superior mesenteric artery infusion of mCTLA4Ig cDNA packaged with lipofectin vector before transplantation, evaluated the local expression of CTLA4Ig gene and its effect on preventing acute rejection of small bowel allografts in rats.

MATERIALS AND METHODS

Animals and transplantation

Inbred male SD and Wistar rats weighing 250 to 300 g were used as donors and recipients, respectively. All rats were obtained from the Animal Center of Nanjing Medical University.

After fasting for 24 h, donors and recipients were anesthetized with an intraperitoneal injection of pentobarbital (50 mg/kg). The vasculature of the donor small bowel was perfused with 10 mL heparinized saline solution at 4 °C. A segment of 20 cm small bowel with portal vein and superior mesenteric artery attached to a cuff of aorta were removed. The lumen of the donor small bowel perfused with 20 mL pure saline solution at 4 °C. The small bowel graft was transplanted with an end-to-side anastomosis of the cuff of aorta and portal vein of the graft to the infrarenal aorta and infrarenal vena cava (Figure 1). After revascularization of the graft, the oral end and the anal end of the small bowel graft were constructed as a stoma respectively through the right abdominal wall of the recipient. All animals had free access to water within 24 h after transplantation. Starting from postoperative d 1, they received standard rat chow.

Experimental groups

Animals were placed into two groups: One group of recipients did not receive treatment (control group, *n*=21), and the other group of recipients received CTLA4Ig gene transfection (experimental group, *n*=21).

Delivery of mCTLA4Ig to small intestine

The plasmid of AAVmCTLA4Ig was a kind gift of Professor I. Anegon (INSERM U437, Nants, France). DOTAP:Chole (*in vivo* GenSHUTTLE, Qbiogene) was used as the vector.

The AAVmCTLA4Ig was mixed with DOTAP:Chole at room temperature for 15 min to create the DNA-lipid complex. The final concentration of DNA in the complex was 0.5 $\mu\text{g}/\mu\text{L}$. Before cold preservation, the small bowel graft was irrigated with cold saline and then 50 μL lipid (control group) or 50 μL DNA-lipid complex (experimental group) was delivered into the superior mesenteric artery by slow infusion over 5-10 min. After 1.5 h of cold preservation, the superior mesenteric artery of small bowel was reperused with 5 mL cold saline for 10 min before transplantation.



Figure 1 Heterotopic small bowel transplantation in the rat. The vasculature of the graft has been anastomosed. RSB: recipient's small bowel. TSB: transplanted small bowel.

Graft histology, apoptosis detection and immunohistology

Three, seven and ten days after transplantation, 7 rats were killed in each group. Samples of the small bowel allografts were obtained. One half was fixed in paraformaldehyde for histology examination and cell apoptosis detection. Another half was preserved in nitrogen liquid for immunohistology.

For histology, sections from paraffin embedded blocks were stained with hematoxylin-eosin (H&E). Kuusanmaki's protocol^[13] served as basis for the grading of acute graft rejection and determination of diagnostic categories.

Apoptosis was detected on sections from paraffin-embedded blocks by the terminal deoxynucleotidyl transferase (TdTase) mediated d-UTP-biotin nick end labeling (TUNEL) technique^[14-17]. Apoptosis assay with a detection kit from Boehringer (Mannheim, Germany), conformed to the manufacturer's protocol strictly except that the sections were finally counterstained with methylgreen (Vector Laboratories). The nuclei of apoptotic cells were stained brown as detected under light microscope, and the number of apoptotic cells was determined by counting labeled enterocytes in 10 randomly chosen high-power fields^[18].

Immunohistology was performed in cryostat sections. To detect CTLA4Ig in tissues, sections were subsequently incubated (60 min) with hamster anti-murine CTLA4 mAb (UC-4F10-11, BD Biosciences). Tissues probed with the mAb were then incubated with a biotin-conjugated mouse IgG-adsorbed anti-hamster IgG Ab (60 min; G70-204 & G94-56, BD Biosciences), followed by HRP-conjugated streptavidin (45 min; Woburn MA) and DAB substrate, and sections were counterstained with hematoxylin.

Statistical analysis

Data were expressed as mean \pm SD and Student's *t* test was used. Significant difference was assumed when $P < 0.05$.

RESULTS

Immunohistology

The CTLA4Ig expression of implanted small bowels was detected by immunohistology, and the small bowel grafts transduced with CTLA4Ig showed the presence of abundant

labeling in mesenteric vascular walls, muscularis, submucosa and villus. Higher densities of CTLA4Ig were detected in grafts sampled at early time points, and persistent expression of CTLA4Ig was confirmed within 10 d after transplantation (Figure 2: A, B, C). As anticipated, there was no detectable expression of CTLA4Ig in the control small intestines (Figure 2: D).

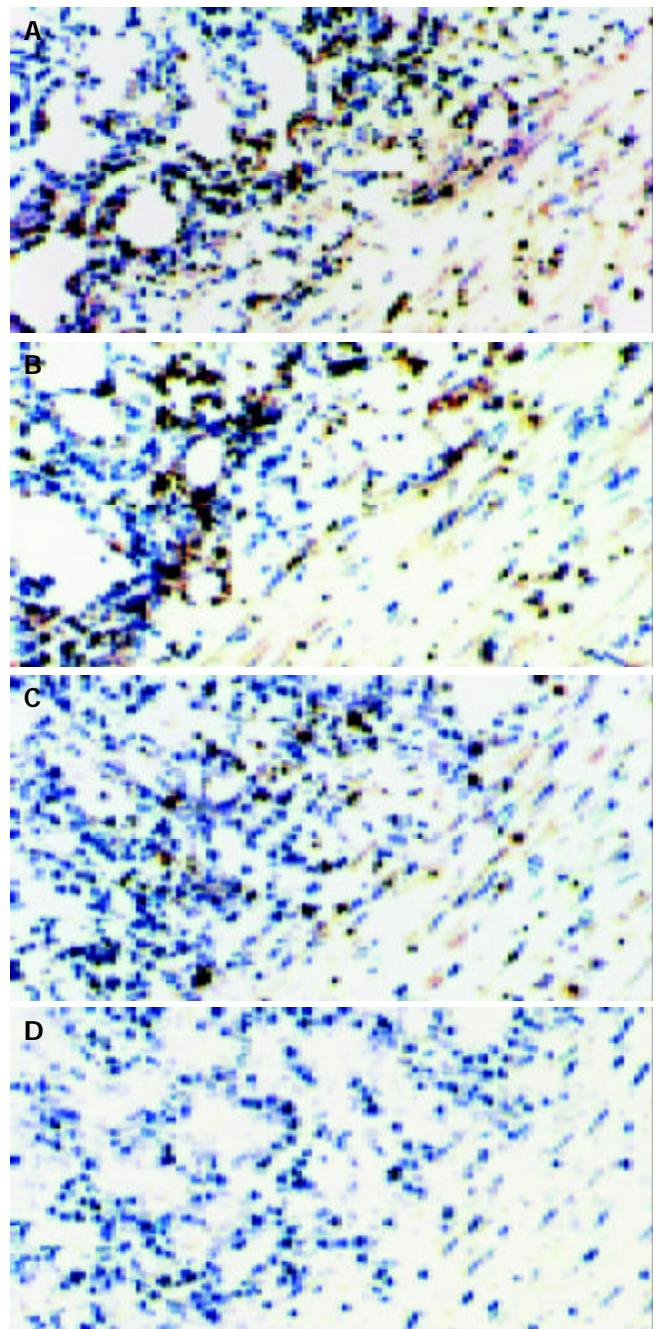


Figure 2 Presence of CTLA4Ig in the small bowel allografts. CTLA4Ig was stained as the brown granules. A, B, C represent the cryostat sections of CTLA4Ig gene transfected grafts on d 3, 7, 10 after transplantation, respectively. D represent the cryostat sections of non-CTLA4Ig gene transfected grafts, expression of CTLA4Ig was not detected. [original magnification $\times 200$].

Morphological findings

In the control group, on d 3 after transplantation, only nonspecific changes were noted. Focal mesenteric inflammation, mild endothelial vacuolization, and minimal swelling and desquamation of enterocytes were observed in allografts, and a relatively normal villiform mucosal structure was retained. On d 7, a widespread inflammatory infiltrate in the mesentery, with moderate invasion of the intestinal wall,

villous blunting and part of the crypt destruction, was noticed in allografts. In addition, endothelial swelling and proliferation with intimal thickening were found in small mesenteric arteries and arterioles. On d 10, a pronounced mesenteric infiltrate with severe invasion of the intestinal wall was found in allografts. Endothelial proliferation with intimal thickening resulted in luminal obliteration. Furthermore, moderate to extreme enterocystic necrosis could be recognized as erosions and focal ulcerations. However, the allografts treated with CTLA4Ig gene transfection showed nearly normal mucosal structure, slight cell infiltration and minimal swelling and desquamation of enterocytes on d 3, 7 and 10 post-transplantation.

Detection of apoptotic enterocytes by TUNEL

Apoptotic cells were detected mainly in the crypts. On d 3 after transplantation, a small number of labeled enterocytes were observed both in control (5.3 ± 1.5 , $n=7$) and experimental (5.8 ± 1.8 , $n=7$) groups. There was no significant difference in the number of apoptotic enterocytes between the two groups. On d 7, the number of labeled enterocytes increased dramatically (61.7 ± 2.8 , $n=7$) and reached a higher level on d 10 (101 ± 6.1 , $n=7$) in control group after transplantation (Figure 3: A1, B1, C1), whereas an increasing number of labeled nuclei could not be recognized in experimental group on d 7 (3.4 ± 1.0 , $n=7$) and on d 10 (3.6 ± 1.3 , $n=7$) after transplantation (Figure 3: A2, B2, C2). The difference in the number of apoptotic enterocytes in allografts between control and experimental groups on d 7 and 10 was extremely significant ($^bP < 0.0005$, $t=41.2876$ on day 7 and $^dP < 0.005$, $t=39.2437$ on d 10).

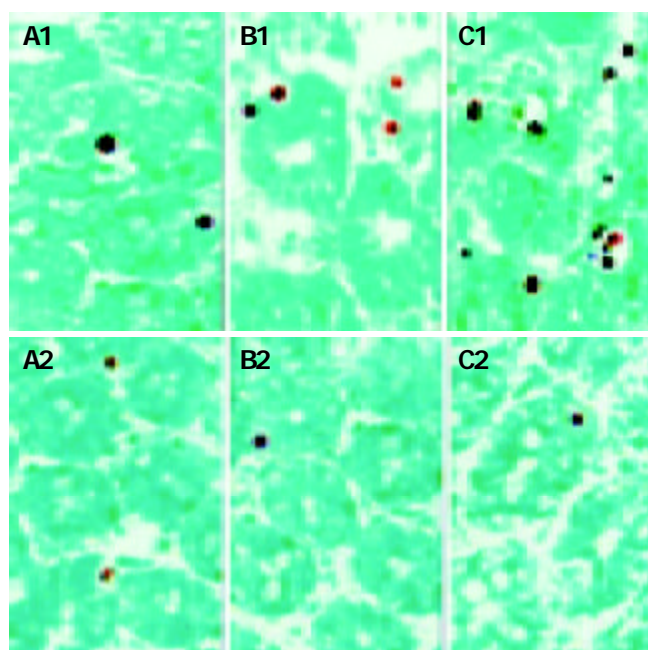


Figure 3 Apoptotic crypt cells in the small bowel allografts. A1, B1, C1 represent the tissue sections of non-CTLA4Ig gene transfected grafts obtained on d 3, 7, 10 after transplantation, respectively. A2, B2, C2 represent the tissue sections of CTLA4Ig gene transfected grafts obtained on d 3, 7, 10 after transplantation, respectively. [original magnification $\times 400$].

DISCUSSION

Small bowel transplantation has emerged as a life-saving therapy for patients with irreversible intestinal failure and is now a routine therapeutic tool at some transplant centers^[19,20]. Nevertheless, graft rejection is still the major obstacle to the transplantation^[21-23]. Blockade of the B7/CD28 co-stimulation signal by systemic transfer of CTLA4Ig gene through

intravenous infusion of AdCTLA4Ig has been shown to prolong small intestinal graft survival^[24]. However, different from heart, liver, kidney and other organs, the small bowel is unique among vascularized organ grafts with rich lymphoid components and large amounts of bacteria, severe infection as well as rejection occurs easier after transplantation. Local CTLA4Ig gene transfection of small bowel allograft could be the ideal therapeutic strategy of anti-rejection. It allows inhibition of the recipient's rejection response, while maintaining the recipient's efficient peripheral immune function (not suppressing the antibacterial response). The local transfection of CTLA4Ig gene has been successfully achieved in rat heart, liver, kidney, islet and lung allografts^[9-12], but it has not been studied in the small bowel transplantation. In the present study, we perfused CTLA4Ig cDNA packaged with lipofectin vector via intra-superior mesenteric artery into the small bowels. By immunohistology, there were a large amount of CTLA4Ig expression in the small bowel allografts on days 3, 7 and 10 after transplantation. The result suggests that local CTLA4Ig gene transfection of small bowel allograft is feasible.

In non-CTLA4Ig gene transfected small bowel allografts, a histological change of progressive acute allograft rejection could be recognized. Although the allografts did not show any specific morphological changes on d 3, acute allograft rejection of grade I on d 7 and grade II on d 10 after transplantation was noticed. In contrast, no evidence of acute rejection was observed in CTLA4Ig gene transfected allografts on d 3, 7 and 10 after transplantation. These data indicate that local CTLA4Ig expression in small bowel allografts can prevent acute rejection after transplantation. The protection of local CTLA4Ig expression in small bowel allografts from acute rejection may be because of the inhibition of expansion of alloantigen-induced T cell priming. The local transfection of CTLA4Ig can block B7 ligand expression on the surface of intragraft APCs, and thus blocking B7/CD28 co-stimulatory pathway. In the absence of B7/CD28 co-stimulatory signal, the interaction of T cell with the alloantigen commonly produces T cell anergy^[25-29].

Apoptosis is a DNA-dependent cell death mechanism, which occurs under physiological and pathological conditions. In organ transplantation, apoptosis is an important biochemical indicator of allograft rejection^[14-17]. In the process of allograft rejection, the target cells damage is mainly mediated by cytotoxic T lymphocytes through the perforin-dependent granule-exocytosis pathway and the Fas/Fas ligand (FasL) pathway^[30-32]. Both perforin- and Fas-mediated pathways of cytotoxicity can result in target cell apoptosis. Numerous reports have demonstrated up-regulation of transcripts for perforin, granzyme B, and FasL during allograft rejection^[33-36]. In the present study, TUNEL illustrated a few apoptotic enterocytes on d 3 and showed a dramatically increased number of apoptotic enterocytes on d 7 and 10 after transplantation in non-CTLA4Ig gene transfected small bowel allografts. This result demonstrates the existence of acute rejection after transplantation. Nevertheless, in CTLA4Ig gene transfected small bowel allografts, a few apoptotic crypt cells was observed on days 3, but the number of apoptotic enterocytes did not increase on d 7 and 10 after transplantation. It indicates that the apoptosis in small bowel allografts can be prevented by local CTLA4Ig gene transfection, and the cytotoxic roles of infiltrated T lymphocytes and the acute rejection after transplantation can be prevented by CTLA4Ig expression in the allografts. The few apoptosis in allografts on d 3 was likely caused by cold preservation damage and posts ischemic reperfusion damage^[37-39].

In conclusion, local CTLA4Ig gene transfection of small bowel allograft can be achieved by perfusing CTLA4Ig cDNA packaged with lipofectin vector via intra-superior mesenteric artery into the small bowels, and the local CTLA4Ig expression in the allograft can prevent acute rejection after transplantation.

ACKNOWLEDGMENT

The authors are grateful to Professor I. Anegon (INSERM U437, Nantes, France) for the kind gift of the AAVmCTLA4IgG plasmid, and thank Professor Xirong Guo (Experimental Research Center of Nanjing Medical University) for the experimental help.

REFERENCES

- 1 **Laumonier T**, Potiron N, Boeffard F, Chagneau C, Brouard S, Guillot C, Soullou JP, Anegon I, Le Mauff B. CTLA4Ig adenoviral gene transfer induces long-term islet rat allograft survival, without tolerance, after systemic but not local intragraft expression. *Hum Gene Ther* 2003; **14**: 561-575
- 2 **Kosuge H**, Suzuki J, Gotoh R, Koga N, Ito H, Inobe M, Uede T. Induction of immunologic tolerance to cardiac allograft by simultaneous blockade of inducible co-stimulator and cytotoxic T-lymphocyte antigen 4 pathway. *Transplantation* 2003; **75**: 1374-1379
- 3 **Shiraishi T**, Yasunami Y, Takehara M, Uede T, Kawahara K, Shirakusa T. Prevention of acute lung allograft rejection in rat by CTLA4Ig. *Am J Transplant* 2002; **2**: 223-228
- 4 **Kita Y**, Nogimura H, Ida M, Kageyama Y, Ohi S, Ito Y, Matsushita K, Takahashi T, Suzuki K, Kazui T, Hayashi S, Li XK, Suzuki S. Effects of adenoviral vectors containing CTLA4Ig-gene in rat heterotopic lung implants. *Transplant Proc* 2002; **34**: 1434-1436
- 5 **Yanagida N**, Nomura M, Yamashita K, Takehara M, Murakami M, Echizenya H, Konishi K, Kitagawa N, Furukawa H, Uede T, Todo S. Tolerance induction by a single donor pretreatment with the adenovirus vector encoding CTLA4Ig gene in rat orthotopic liver transplantation. *Transplant Proc* 2001; **33**: 573-574
- 6 **Shindo J**. Effect of CTLA4Ig gene transfer with adenovirus vector on allogeneic renal graft survival in the rat. *Hokkaido Igaku Zasshi* 2001; **76**: 251-256
- 7 **Iwasaki N**, Gohda T, Yoshioka C, Murakami M, Inobe M, Minami A, Uede T. Feasibility of immunosuppression in composite tissue allografts by systemic administration of CTLA4Ig. *Transplantation* 2002; **73**: 334-340
- 8 **Guillot C**, Menoret S, Guillonneau C, Braudeau C, Castro MG, Lowenstein P, Anegon I. Active suppression of allogeneic proliferative responses by dendritic cells after induction of long-term allograft survival by CTLA4Ig. *Blood* 2003; **101**: 3325-3333
- 9 **Kita Y**, Li XK, Nogimura H, Ida M, Kageyama Y, Ohi S, Suzuki K, Kazui T, Suzuki S. Prolonged graft survival induced by CTLA4Ig gene transfection in rat lung allografting. *Transplant Proc* 2003; **35**: 456-457
- 10 **Umeda Y**, Iwata H, Yoshikawa S, Matsuno Y, Marui T, Nitta T, Idia Y, Takagi H, Mori Y, Miyazaki J, Kosugi A, Hirose H. Gene gun-mediated CTLA4Ig-gene transfer for modification of allogeneic cardiac grafts. *Transplant Proc* 2002; **34**: 2622-2623
- 11 **Cheung ST**, Tsui TY, Wang WL, Yang ZF, Wong SY, Ip YC, Luk J, Fan ST. Liver as an ideal target for gene therapy: expression of CTLA4Ig by retroviral gene transfer. *J Gastroenterol Hepatol* 2002; **17**: 1008-1014
- 12 **Benigni A**, Tomasoni S, Remuzzi G. Impediments to successful gene transfer to the kidney in the context of transplantation and how to overcome them. *Kidney Int* 2002; **61**(Suppl 1): 115-119
- 13 **Kuusanmaki P**, Halttunen J, Paavonen T, Pakarinen M, Luukkonen P, Hayry P. Acute rejection of porcine small bowel allograft. An extended histological scoring system. *Transplantation* 1994; **58**: 757-763
- 14 **Wu MY**, Liang YR, Wu XY, Zhuang CX. Relationship between Egr-1 gene expression and apoptosis in esophageal carcinoma and precancerous lesions. *World J Gastroenterol* 2002; **8**: 971-975
- 15 **Sun P**, Ren XD, Zhang HW, Li XH, Cai SH, Ye KH, Li XK. Serum from rabbit orally administered cobra venom inhibits growth of implanted hepatocellular carcinoma cells in mice. *World J Gastroenterol* 2003; **9**: 2441-2444
- 16 **Huang ZH**, Fan YF, Xia H, Feng HM, Tang FX. Effects of TNP-470 on proliferation and apoptosis in human colon cancer xenografts in nude mice. *World J Gastroenterol* 2003; **9**: 281-283
- 17 **Zhao AG**, Zhao HL, Jin XJ, Yang JK, Tang LD. Effects of Chinese Jianpi herbs on cell apoptosis and related gene expression in human gastric cancer grafted onto nude mice. *World J Gastroenterol* 2002; **8**: 792-796
- 18 **Fayyazi A**, Schlemminger R, Gieseler R, Peters JH, Radzun HJ. Apoptosis in the small intestinal allograft of the rat. *Transplantation* 1997; **63**: 947-951
- 19 **Platell CF**, Coster J, McCauley RD, Hall JC. The management of patients with the short bowel syndrome. *World J Gastroenterol* 2002; **8**: 13-20
- 20 **Kato T**, Ruiz P, Thompson JF, Eskind LB, Wepler D, Khan FA, Pinna AD, Nery JR, Tzakis AG. Intestinal and multivisceral transplantation. *World J Surg* 2002; **26**: 226-237
- 21 **Ding J**, Guo CC, Li CN, Sun AH, Guo XG, Miao JY, Pan BR. Postoperative endoscopic surveillance of human living-donor small bowel transplantation. *World J Gastroenterol* 2003; **9**: 595-598
- 22 **Zhang WJ**, Liu DG, Ye QF, Sha B, Zhen FJ, Guo H, Xia SS. Combined small bowel and reduced auxiliary liver transplantation: case report. *World J Gastroenterol* 2002; **8**: 956-960
- 23 **Ghanekar A**, Grant D. Small bowel transplantation. *Curr Opin Crit Care* 2001; **7**: 133-137
- 24 **Echizenya H**, Yamashita K, Takehara M, Konishi K, Nomura M, Yanagida N, Kitagawa N, Kobayashi T, Furukawa H, Inobe M, Uede T, Todo S. Adenovirus-mediated CTLA4-IgG gene therapy in orthotopic small intestinal transplantation in rats. *Transplant Proc* 2001; **33**: 183-184
- 25 **Vasilevko V**, Ghochikyan A, Sadzikava N, Petrushina I, Tran M, Cohen EP, Kessler PJ, Cribbs DH, Nicolson GL, Agadjanyan MG. Immunization with a vaccine that combines the expression of MUC1 and B7 co-stimulatory molecules prolongs the survival of mice and delays the appearance of mouse mammary tumors. *Clin Exp Metastasis* 2003; **20**: 489-498
- 26 **Chung JB**, Wells AD, Adler S, Jacob A, Turka LA, Monroe JG. Incomplete activation of CD4 T cells by antigen-presenting transitional immature B cells: implications for peripheral B and T cell responsiveness. *J Immunol* 2003; **171**: 1758-1767
- 27 **Elhalel MD**, Huang JH, Schmidt W, Rachmilewitz J, Tykocinski ML. CTLA-4, FasL induces alloantigen-specific hyporesponsiveness. *J Immunol* 2003; **170**: 5842-5850
- 28 **Arpinati M**, Terragna C, Chirumbolo G, Rizzi S, Urbini B, Re F, Tura S, Baccarani M, Rondelli D. Human CD34(+) blood cells induce T-cell unresponsiveness to specific alloantigens only under costimulatory blockade. *Exp Hematol* 2003; **31**: 31-38
- 29 **Appleman LJ**, Boussiotis VA. T cell anergy and costimulation. *Immunol Rev* 2003; **192**: 161-180
- 30 **Mandrup-Poulsen T**. Beta cell death and protection. *Ann N Y Acad Sci* 2003; **1005**: 32-42
- 31 **Abrahams VM**, Straszewski-Chavez SL, Guller S, Mor G. First trimester trophoblast cells secrete Fas ligand which induces immune cell apoptosis. *Mol Hum Reprod* 2004; **10**: 55-63
- 32 **Catalfamo M**, Henkart PA. Perforin and the granule exocytosis cytotoxicity pathway. *Curr Opin Immunol* 2003; **15**: 522-527
- 33 **D'Errico A**, Corti B, Pinna AD, Altimari A, Gruppioni E, Gabusi E, Fiorentino M, Bagni A, Grigioni WF. Granzyme B and perforin as predictive markers for acute rejection in human intestinal transplantation. *Transplant Proc* 2003; **35**: 3061-3065
- 34 **Liang LW**, Zhang Q, Gjertson D, Gritsch HA, Reed EF. Non-invasive immune monitoring of perforin/granzyme B in peripheral blood may predict renal allograft rejection. *Hum Immunol* 2003; **64**(10 Suppl): S32
- 35 **Simon T**, Opelz G, Wiesel M, Ott RC, Susal C. Serial peripheral blood perforin and granzyme B gene expression measurements for prediction of acute rejection in kidney graft recipients. *Am J Transplant* 2003; **3**: 1121-1127
- 36 **Zhang SG**, Wu MC, Tan JW, Chen H, Yang JM, Qian QJ. Expression of perforin and granzyme B mRNA in judgement of immunosuppressive effect in rat liver transplantation. *World J Gastroenterol* 1999; **5**: 217-220
- 37 **Wang SF**, Li GW. Early protective effect of ischemic preconditioning on small intestinal graft in rats. *World J Gastroenterol* 2003; **9**: 1866-1870
- 38 **Ma K**, Yu Y, Bu XM, Li YJ, Dai XW, Wang L, Dai Y, Zhao HY, Yang XH. Prevention of grafted liver from reperfusion injury. *World J Gastroenterol* 2001; **7**: 572-574
- 39 **Zhu XH**, Qiu YD, Shen H, Shi MK, Ding YT. Effect of matrine on Kupffer cell activation in cold ischemia reperfusion injury of rat liver. *World J Gastroenterol* 2002; **8**: 1112-1116

Effects of cholesterol on proliferation and functional protein expression in rabbit bile duct fibroblasts

Bao-Ying Chen, Jing-Guo Wei, Yao-Cheng Wang, Jun Yu, Ji-Xian Qian, Yan-Ming Chen, Jing Xu

Bao-Ying Chen, Jing-Guo Wei, Yao-Cheng Wang, Department of Radiology, Tangdu Hospital, Fourth Military Medical University, Xi' an 710038, Shannxi Province, China

Jun Yu, Yan-Ming Chen, Department of Physiology, Fourth Military Medical University, Xi' an 710032, Shannxi Province, China

Ji-Xian Qian, Department of Orthopaedics, Tangdu Hospital, Fourth Military Medical University, Xi' an 710038, Shannxi Province, China

Jing Xu, Cell Engineering Research Center, Fourth Military Medical University, Xi' an 710032, Shannxi Province, China

Correspondence to: Jing-Guo Wei, Department of Radiology, Tangdu Hospital, Fourth Military Medical University, Xi' an 710038, Shannxi Province, China. chenby@fmmu.edu.cn

Telephone: +86-29-3377163 **Fax:** +86-29-3377163

Received: 2003-12-17 **Accepted:** 2004-01-08

Abstract

AIM: To investigate the effect of cholesterol (Ch) on the growth and functional protein expression of rabbit bile duct fibroblasts.

METHODS: The cultured bile duct fibroblasts were divided randomly into two groups: the control group and the experiment group (fibroblasts were incubated respectively with 0.6 g/L Ch for 12, 24, 36 and 48 h). The growth and DNA synthesis of bile duct fibroblasts were measured by the means of ³H-TdR incorporation. The total protein content of fibroblast was measured by BSA protein assay reagent kit, then the expression of α -actin was analyzed semi-quantitatively by Western blot.

RESULTS: After treatment with 0.6 g/L Ch for 12, 24, 36 and 48 h, the values of ³H-TdR incorporation of bile duct fibroblasts were respectively 3.1 ± 0.39 , 3.8 ± 0.37 , 4.6 ± 0.48 and 5.2 ± 0.56 mBq/cell, and the values of the corresponding control groups were 3.0 ± 0.33 , 3.2 ± 0.39 , 3.7 ± 0.49 and 4.3 ± 0.43 mBq/cell. After comparing the values of experiment groups and their corresponding control groups, it was found that the ³H-TdR incorporation of bile duct fibroblasts after treatment with 0.6 g/L Ch for 24, 36 and 48 h were significantly increased ($P<0.05$, $P<0.01$, $P<0.01$), while the ³H-TdR incorporation of 12-h group was not different statistically from its control group. Ch had no obvious effect on the total protein content of fibroblasts. After incubated with 0.6 g/L Ch for 12, 24, 36 and 48 h, the total protein content of each experiment group was not altered markedly compared with its corresponding control group. The values of experiment groups were 0.246 ± 0.051 , 0.280 ± 0.049 , 0.263 ± 0.044 and 0.275 ± 0.056 ng/cell, and those of corresponding control groups were 0.253 ± 0.048 , 0.270 ± 0.042 , 0.258 ± 0.050 and 0.270 ± 0.045 ng/cell. Western blot analysis revealed that the α -actin expression in fibroblasts affected by Ch for 12 and 24 h was not markedly changed compared with their corresponding control groups ($P>0.05$), the values of total gray scale of 12- and 24-h groups were $1\ 748\pm 185$ and $1\ 756\pm 173$, respectively. But after stimulation with Ch for 36 h, the total gray scale of fibroblasts ($1\ 923\pm 204$) was significantly higher than that of

control group ($1\ 734\pm 197$). When the time of Ch treatment was lengthened to 48 h, the α -actin expression was markedly elevated, the total gray scale was $2\ 189\pm 231$ ($P<0.01$ vs control group).

CONCLUSION: Moderately concentrated Ch can promote the proliferation of bile duct fibroblasts at early stage. With the prolongation of Ch treatment, the α -actin expression of fibroblasts was also increased, but the hypertrophy of fibroblasts was not observed.

Chen BY, Wei JG, Wang YC, Yu J, Qian JX, Chen YM, Xu J. Effects of cholesterol on proliferation and functional protein expression in rabbit bile duct fibroblasts. *World J Gastroenterol* 2004; 10(6): 889-893

<http://www.wjgnet.com/1007-9327/10/889.asp>

INTRODUCTION

The disorder of cholesterol metabolism is an important cause of biliary diseases. Previous studies suggest that cholesterol can change the motility of cholecyst^[1,2] and decrease gallbladder contraction^[3-7] in the patients with cholesterol calculus and in the animals with hypercholesterolemia. Weak contraction of gallbladder may be a reason of cholesterol calculus^[8-12]. Researchers consider that cholesterol metabolism disorder has an effect on the structure and function of bile duct and sphincter of bile duct (SBD)^[13-16]. We have found that cholesterol liposome (CL) affected not only the configuration and quantity of cytoskeleton in rabbit SBD smooth muscle cells, but also the proliferation of cells^[17,18]. There are many fibroblasts in biliary system except that SBD is formed mainly with smooth muscle cells^[19-22]. In our previous experiment, we observed that middle concentration Ch could accelerate the proliferation of bile duct fibroblasts and result in the changes of phenotype^[23,24]. Fibroblasts displayed some characteristics of myofibroblasts or smooth muscle cells^[23,24]. In order to lucubrate the reactivity of bile duct fibroblasts to Ch and the role of fibroblasts on the configuration variation of bile duct and SBD, the effects of Ch on bile duct fibroblasts at different time point were studied and the relation between the effects of Ch and time was analyzed in this study.

MATERIALS AND METHODS

Materials

New Zealand rabbits aged 1 month were provided by the Animal Center of the Fourth Military Medical University. Trysin (Gibco, Paisley, Renfrewshire, UK), Dulbecco's modified eagles medium (DMEM) (Gibco, Paisley, Renfrewshire, UK), fetal calf serum (Qinghu Institute of Foetus Bovine Utilization in Jinhua Zhejiang), water soluble cholesterol (Sigma, St. Louis, USA), antibody of vimentin, α -actin and desmin (DakoCytomation, Glostrup, Denmark), ABC immunohistochemical kit (Shaanxi Biotech. Co., Xi' an, China), IMT-2 inverted biological microscope (Olympus

Corporation, Japan), YJ-875 Itra-clean operating boar (Suhang Experimental Animal Technology Development Co), LD4-2 centrifugal machine (Beijing Medical Centrifugal Machine Factory), and BCA protein assay reagent kit (Pierce Chemical Company, Rockford, USA) were commercially obtained.

Dispensing of main reagent

Ch was diluted to 0.6 g/L with DMEM before experiment. DMEM was dispensed according to the description. Fetal calf serum was inactivated for 30 min at 56 °C, and was stored at -20 °C. Trypsin was made into 2.5 g/L solution with PBS (0.01 mol/L, pH 7.4) and stored at 4 °C. TBST was prepared by mixing 10 mL of Tri-Cl, 8.78 g of NaCl, 500 µL of Tween-20, and adding distilled water up to 1L.

Primary culture of rabbit bile duct fibroblasts

Bile ducts of New Zealand rabbits were dissociated by the means of aseptic technique and broken by shears. The tissue was digested to become single cell suspension by trypsin (1.25 g/L). Cells were washed and resuspended with DMEM (containing 100 mL/L fetal calf serum) and incubated at room temperature for 75-90 min. Then the cells were collected and transferred into culture bottles. The cells of 2nd-4th passages were used for experiments.

Identification of rabbit bile duct fibroblasts

Three glass cover slips (18 mm×18 mm) were placed into 6 cm diameter culture dishes, and then cell suspension was added and incubated at room temperature for 48 h. The slips covered with cells were washed twice with PBS (pH 7.4). Some slips were fixed by cold acetone for 15 min at 4 °C and used for HE staining, another three slips were fixed by citromint (40 g/L) for immunohistochemical ABC staining to exam vimentin and desmin expression.

[³H] Thymidine incorporation

Bile duct fibroblasts were planted in 96-well plates. Sub-confluent cells were cultured without serum for 24 h, then treated respectively by 0.6 g/L Ch for 12, 24, 36 and 48 h and pulsed with 18.5 kBq of [³H] thymidine for 4 h. The control group cells were incubated with DMEM containing 20 mL/L fetal calf serum instead of Ch. The radioactivity of each group was counted by Beckman LS6500 counter.

Assay of total protein content

The cells of each group were trypsinized and counted. Cells were centrifugated at 1 000 r/min for 5 min at 4 °C, washed twice with ice-cold PBS and lysed in ice-cold lysis buffer for 30-60 min. The lysates were centrifugated at 12 000 g for 5 min at 4 °C and supernatant was transferred into new Eppendorf tubes. The standard curve was drawn according to the description of BCA protein assay reagent kit, and then the total protein content per cell was measured and converted.

Western blot analysis

Loading buffer was added to each lysate, which was subsequently boiled for 10 min. Equal amounts (10 µg) of cell extracts were separated by 100 g/L SDS-PAGE and transferred to nitrocellulose membrane. The membrane was blocked for one h at room temperature in 50 g/L skim milk and probed with α-actin antibody for one h. The membrane was washed three times with PBS-T and incubated for one h with secondary antibody. After washing the membrane with PBS-T for several times, the protein reactive to the primary antibody were visualized by electrochemiluminescence (ECL) detection, and semi-quantitatively analyzed by Kodak digital science 1D software.

Statistical analyses

Results were presented as mean±SD. Significance was determined by Student's *t* test or one-way ANOVA. *P*<0.05 was considered statistically significant.

RESULTS

Cultured rabbit bile duct fibroblasts

Under phase-contrast microscope, the cultured rabbit bile duct fibroblasts showed shuttle-shaped or multiangular. Their cytoplasm was clear and nucleus was large and ellipse, and their nucleoli were obvious. The isolated bile duct fibroblasts were free of smooth muscle cell contamination because they presented positive staining with vimentin and negative staining with desmin by the means of immunocytochemical ABC staining.

³H-TdR incorporation of bile duct fibroblasts

Following incubation with 0.6 g/L Ch for 12, 24, 36 and 48 h, the values of ³H-TdR incorporation of bile duct fibroblasts were respectively 3.1±0.39, 3.8±0.37, 4.6±0.48 and 5.2±0.56 mBq/cell, and those of the corresponding control groups were 3.0±0.33, 3.2±0.39, 3.7±0.49 and 4.3±0.43 mBq/cell. After comparing the values of experiment groups and their corresponding control groups, we found that the ³H-TdR incorporation of bile duct fibroblasts after treatment with 0.6 g/L Ch for 24, 36 and 48 h were significantly increased (*P*<0.05, *P*<0.01, *P*<0.01), while the ³H-TdR incorporation of the 12 h group was not statistically significant as compared with the control group (Figure 1).

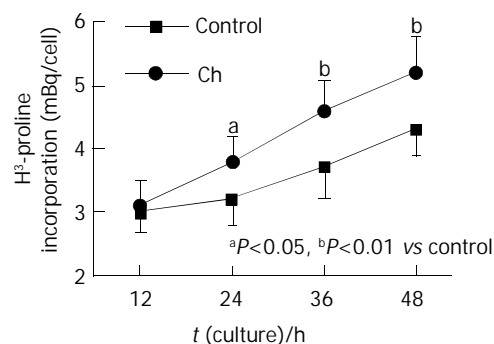


Figure 1 Effects of cholesterol on the H³-TdR incorporation of bile duct fibroblasts.

Total protein content of bile duct fibroblasts

Ch has little effect on the total protein content of fibroblasts. After being incubated with 0.6 g/L Ch for 12, 24, 36 and 48 h, the total protein content of each experiment group was not altered markedly compared with its corresponding control group. The values of experiment groups were 0.246±0.051, 0.280±0.049, 0.263±0.044 and 0.275±0.056 ng/cell, and those of corresponding control groups were 0.253±0.048, 0.270±0.042, 0.258±0.050 and 0.270±0.045 ng/cell (Figure 2).

α-actin expression of bile duct fibroblasts

Western blot analysis revealed that the α-actin expression of fibroblasts affected by Ch for 12 h and 24 h was not markedly changed compared with their corresponding control groups, the values of total gray scale of the 12 h and 24 h groups were 1 748±185 and 1 756±173 respectively, but after stimulation with Ch for 36 h, the total gray scale of fibroblasts (1 923±204) was significantly higher than that of control group (1 734±197). When the time of Ch treatment was lengthened to 48 h, the α-actin expression was markedly elevated, and the total gray

scale was $2\ 189\pm 231$ ($P<0.01$ vs control group) (Figure 3, Table 1).

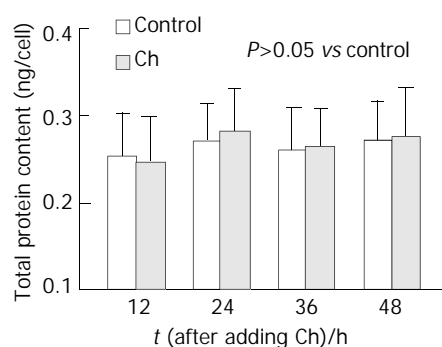
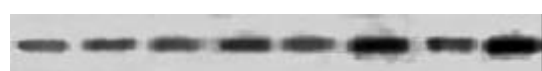


Figure 2 Effects of cholesterol on total protein content of bile duct fibroblasts.



Ch	-	+	-	+	-	+	-	+
t/h	12		24		36		48	

Figure 3 The expression of α -actin in bile duct fibroblasts detected by Western blot.

Table 1 Effects of cholesterol on the expression of α -actin in bile duct fibroblasts (mean \pm SD gray scale)

t/h	Control	Ch
12	1 723 \pm 192	1 748 \pm 185
24	1 719 \pm 138	1 756 \pm 173
36	1 734 \pm 197	1 923 \pm 204 ^a
48	1 746 \pm 164	2 189 \pm 231 ^b

^a $P<0.05$, ^b $P<0.01$, vs Control.

DISCUSSION

Fibroblasts are derived from mesenchymal cell of embryo period. During the process of wound healing, fibroblasts can proliferate greatly by mitoses, and also synthesize and excrete collagen fibers and matrix components^[25-29]. With the stimulation of trauma and other agents, some mature fibroblasts could change into infantile fibroblasts and their function could be recovered^[30,31]. Cardiac fibroblasts are able to secrete biological active substances, which facilitate the growth of myocardial cells^[32,33], suggesting that cardiac fibroblasts must play an important role in the normal growth of heart and its pathologic remodeling^[34,35]. Hypoxia could, mediated by pulmonary arterial endothelial cells (PAECs), induce phenotype alteration of human embryonic lung fibroblasts, transforming to smooth muscle cell-like cells, suggesting that the transformation of human embryonic lung fibroblasts might be one of the reasons for nonmuscular lung arteriole to become muscular arteriole^[36-38]. Silent fibroblasts in the border of wound can differentiate to contraction phenotype and have the special expression of α -SM actin. The cells are considered as myofibroblasts which can cause contraction of granulation tissue^[39,40]. It is thus clear that fibroblasts can take part in many kinds of physiological and pathologic responses and they have important effects on the occurrence and development of diseases.

Biliary system is the unique passage of bile ejection,

especially its terminal sphincter, SBD. Biliary system can modulate bile ejection and maintain normal pressure of biliary system^[41,42]. The coordination of its anatomic structure and function makes it not only prevent regurgitation of duodenal fluid but also modulate and stabilize the pressure of bile duct^[42-44]. So the structural remodeling of biliary system, especially the structural change and dysfunction of SBD, might be one of basic reasons of biliary system diseases occurrence. There are a lot of fibroblasts in bile duct system. In previous study, we have found that the middle concentration Ch can promote the proliferation of bile duct fibroblasts and make them present some phenotypic characteristics of muscle cell^[23,24]. But at present, it is still unclear what are the exact effects of cholesterol on bile duct fibroblasts and how fibroblasts are revolved in remodeling of biliary system, especially what roles fibroblasts play in the remodeling of SBD. In order to lucubrate the problem, we observed the effects of Ch on the proliferation and functional protein expression of bile duct fibroblasts at different times and analyzed the relation between the effects of Ch and time.

³H-TdR, prosoma of DNA synthesis, can incorporate into DNA synthesis. So the radioactivity intensity of cells can reflect DNA metabolism and proliferation of cells. It has been demonstrated that middle concentration Ch can accelerate the proliferation of bile duct fibroblasts^[23]. But the relation between Ch effects and time is still unknown. In the present study, our focal point is to observe how the Ch effects on fibroblasts alter with the changes of incubation time. Our results show that the DNA synthesis and proliferation of bile duct fibroblasts are elevated after incubated with moderately concentrated Ch for 24 h, and the effect becomes more significant gradually with the elongation of Ch treatment.

In the research of cardiovascular disease, it has been found that the proliferation and hypertrophy of cardiac fibroblasts participate in the cardiac remodeling^[34,35]. In the process of estrogen-induced uterine enlargement, there are not only the hyperplasia of uterine smooth muscle cell and epithelial cell but also augmentation of size of cells. Chronic enteritis is linked with hypertrophy of intestinal smooth muscle cells^[45-47]. From the phenomena mentioned above, we conjecture whether Ch can not only accelerate the proliferation of bile duct fibroblasts but also cause hypertrophy of fibroblasts. According to our result, the total protein content of bile duct fibroblasts was not altered after fibroblasts were treated with Ch, indicating that Ch might not significantly facilitate the hypertrophy of bile duct fibroblasts although it could promote the proliferation of fibroblasts greatly.

In our previous experiment, we detected that middle concentration Ch could increase α -actin expression of bile duct fibroblasts, and we also observed that bile duct fibroblasts showed some characteristics of muscle cells, which suggested that Ch might lead to the phenotypic variation of fibroblasts^[24]. In present study, we aim to observe the time effects of Ch on fibroblasts by the means of Western blot. It has been demonstrated that α -actin expression in bile duct fibroblasts begins to increase after incubated with Ch for 36 h, and the effect becomes more significant after 48 h. From the results above, we can easily find that the proliferation of bile duct fibroblasts is enhanced after Ch treatment for 24 h, however, it is not until Ch incubation for 36 h that the α -actin expression in bile duct fibroblasts begins to ascend. It indicates that the short-term effects of Ch are mainly to promote the proliferation of bile duct fibroblasts, and by the prolongation of Ch treatment time, Ch can also alter the functional protein expression of fibroblasts. Ch has no obvious effect on the total protein content of bile duct fibroblasts, nevertheless, it can enhance α -actin expression in fibroblasts. It suggests that Ch can only result in the changes of some special protein

expression instead of causing the hypertrophy of bile duct fibroblasts. The protein, α -actin, is an important functional protein existing in myofibroblasts and smooth muscle cells^[48,49]. So we can realize that Ch accelerates the proliferation of bile duct fibroblasts, and what is most important is that Ch can induce bile duct fibroblasts to possess some phenotypic characteristics of muscle cell.

By studying the anatomy of SBD, people found that the length of SBD is 5-15 mm without accordant result and the data fluctuates in a wide range. It has not been lucubrated whether it is only attributed to the congenital diversity of individual or it is the result of SBD remodeling induced by some postnatal factors. Wei *et al.*^[21] have found that gallbladder-derived abdominal pain after cholecystectomy, recurrent bile calculus and cholangiectasis have significant correlation with too lengthy of SBD (≥ 10 mm). It has also been manifested that most of the patients whose SBD length exceeds 10 mm are often accompanied by SBD motor dysfunction^[50]. Combining our present outcome, we suspect that some postnatal factors may result in constitution alteration of SBD, including the changes of length. The proliferation of fibroblasts, especially their phenotype transformation, may play an important role during the constitution changes of bile duct and SBD.

In conclusion, cholesterol does activate bile duct fibroblasts at the early stage, facilitating the proliferation of fibroblasts, and it can also induce the phenotype transformation of fibroblasts following the elongation of Ch treatment time. The alteration of fibroblasts might participate in the configuration remodeling of biliary system, especially the reconstitution of SBD. Gradually the function of bile duct system becomes abnormal and ultimately biliary system diseases occur. But the change *in vivo* is affected by multiple factors and is a multistage procedure. *In vitro* experiments can not absolutely reflect the conditions *in vivo*. So our experiment provides a clue to research the occurrence, development and treatment of biliary system diseases, but the certain role of bile duct fibroblasts and the certain mechanisms are still open to be elucidated.

REFERENCES

- 1 **Li XP**, Ouyang KQ, Cai SX. The regulation of bile secretion and education. *Shijie Huaren Xiaohua Zazhi* 2001; **9**: 1066-1070
- 2 **Wei JG**, Wang YC, Du F, Yu HJ. Dynamic and ultrastructural study of sphincter of Oddi in early-stage cholelithiasis in rabbits with hypercholesterolemia. *World J Gastroenterol* 2000; **6**: 102-106
- 3 **Lammert F**, Sudfeld S, Busch N, Matern S. Cholesterol crystal binding of biliary immunoglobulin A: visualization by fluorescence light microscopy. *World J Gastroenterol* 2001; **7**: 198-202
- 4 **Lui P**, Chen DF. The separation and primary culture of canine gallbladder epithelium. *Shijie Huaren Xiaohua Zazhi* 2001; **9**: 99-100
- 5 **Zapata R**, Severin C, Manriquez M, Valdivieso V. Gallbladder motility and lithogenesis in obese patients during diet-induced weight loss. *Dig Dis Sci* 2000; **45**: 421-428
- 6 **Greaves RR**, O'Donnell LJ, Farthing MJ. Differential effect of prostaglandins on gallstone-free and gallstone-containing human gallbladder. *Dig Dis Sci* 2000; **45**: 2376-2381
- 7 **Buhman KK**, Accad M, Novak S, Choi RS, Wong JS, Hamilton RL, Turley S, Farese RV Jr. Resistance to diet-induced hypercholesterolemia and gallstone formation in ACAT2-deficient mice. *Nat Med* 2000; **6**: 1341-1347
- 8 **Gustafsson U**, Sahlin S, Einarsson C. High level of deoxycholic acid in human bile does not promote cholesterol gallstone formation. *World J Gastroenterol* 2003; **9**: 1576-1579
- 9 **Bogdarin IuA**, Kozlov DV. Correction of lipid metabolism in rabbits with experimental cholelithiasis. *Vopr Med Khim* 2002; **48**: 368-372
- 10 **Quallich LG**, Stern MA, Rich M, Chey WD, Barnett JL, Elta GH. Bile duct crystals do not contribute to sphincter of Oddi dysfunction. *Gastrointest Endosc* 2002; **55**: 163-166
- 11 **Masclée AA**, Vu MK. Gallbladder motility in inflammatory bowel diseases. *Dig Liver Dis* 2003; **35**(Suppl 3): S35-S38
- 12 **Pallotta N**. Ultrasonography in the assessment of gallbladder motor activity. *Dig Liver Dis* 2003; **35**(Suppl 3): S67-S69
- 13 **Rhee JY**, Elta GH. The relationship of bile duct crystals to sphincter of Oddi dysfunction. *Curr Gastroenterol Rep* 2003; **5**: 160-163
- 14 **Kohut M**, Nowak A, Nowakowska-Duiawa E, Marek T. Presence and density of common bile duct microlithiasis in acute biliary pancreatitis. *World J Gastroenterol* 2002; **8**: 558-561
- 15 **Zanlungo S**, Nervi F. The molecular and metabolic basis of biliary cholesterol secretion and gallstone disease. *Front Biosci* 2003; **8**: S1166-S1174
- 16 **Toouli J**. Biliary dyskinesia. *Curr Treat Options Gastroenterol* 2002; **5**: 285-291
- 17 **Wang XJ**, Wei JG, Wang CM, Wang YC, Wu QZ, Xu JK, Yang XX. Effect of cholesterol liposomes on calcium mobilization in muscle cells from the rabbit sphincter of Oddi. *World J Gastroenterol* 2002; **8**: 144-149
- 18 **Wang XJ**, Wei JG, Wang YC, Xu JK, Wu QZ, Wu DC, Yang XX. Effect of cholesterol liposome on contractility of rabbit Oddi's sphincter smooth muscle cells. *Shijie Huaren Xiaohua Zazhi* 2000; **8**: 633-637
- 19 **Corazziari E**. Sphincter of Oddi dysfunction. *Dig Liver Dis* 2003; **35**(Suppl 3): S26-S29
- 20 **Avisse C**, Flament JB, Delattre JF. Ampulla of Vater. Anatomic, embryologic, and surgical aspects. *Surg Clin North Am* 2000; **80**: 201-212
- 21 **Wei JG**, Wang YC, Liang GM, Wang W, Chen BY, Xu JK, Song LJ. The study between the dynamics and the X-ray anatomy and regularizing effect of gallbladder on bile duct sphincter of the dog. *World J Gastroenterol* 2003; **9**: 1014-1019
- 22 **Savrasov VM**. Functional radiographic anatomy of the terminal sphincter duct of the biliary pancreatic system. *Eksp Klin Gastroenterol* 2002; **6**: 81-82
- 23 **Chen BY**, Wei JG, Wang YC, Yang XX, Qian JX, Yu J, Chen ZN, Xu J, Wu DC. Effects of cholesterol on the proliferation of cultured rabbit bile duct fibroblasts. *Shijie Huaren Xiaohua Zazhi* 2002; **10**: 566-570
- 24 **Chen BY**, Wei JG, Wang YC, Wang CM, Yu J, Yang XX. Effects of cholesterol on the phenotype of rabbit bile duct fibroblasts. *World J Gastroenterol* 2003; **9**: 351-355
- 25 **Laplante AF**, Germain L, Auger FA, Moulin V. Mechanisms of wound reepithelialization: hints from a tissue-engineered reconstructed skin to long-standing questions. *FASEB J* 2001; **15**: 2377-2389
- 26 **Jun JB**, Kuechle M, Harlan JM, Elkon KB. Fibroblast and endothelial apoptosis in systemic sclerosis. *Curr Opin Rheumatol* 2003; **15**: 756-760
- 27 **Gabbiani G**. The myofibroblast in wound healing and fibrocontractive diseases. *J Pathol* 2003; **200**: 500-503
- 28 **Phan SH**. Fibroblast phenotypes in pulmonary fibrosis. *Am J Respir Cell Mol Biol* 2003; **29**(3 Suppl): S87-92
- 29 **Tejoro-Trujeque R**. How do fibroblasts interact with the extracellular matrix in wound contraction? *J Wound Care* 2001; **10**: 237-242
- 30 **Hinz B**, Gabbiani G. Cell-matrix and cell-cell contacts of myofibroblasts: role in connective tissue remodeling. *Thromb Haemost* 2003; **90**: 993-1002
- 31 **Bisson MA**, McGrouther DA, Mudera V, Grobelaar AO. The different characteristics of Dupuytren's disease fibroblasts derived from either nodule or cord: expression of alpha-smooth muscle actin and the response to stimulation by TGF-beta1. *J Hand Surg* 2003; **28**: 351-356
- 32 **Piper C**, Schultheiss HP, Akdemir D, Rudolf J, Horstkotte D, Pauschinger M. Remodeling of the cardiac extracellular matrix differs between volume- and pressure-overloaded ventricles and is specific for each heart valve lesion. *J Heart Valve Dis* 2003; **12**: 592-600
- 33 **Jugdutt BI**. Remodeling of the myocardium and potential targets in the collagen degradation and synthesis pathways. *Curr Drug Targets Cardiovasc Haematol Disord* 2003; **3**: 1-30
- 34 **Yang F**, Liu YH, Yang XP, Xu J, Kapke A, Carretero OA. Myocardial infarction and cardiac remodeling in mice. *Exp Physiol* 2002; **87**: 547-555
- 35 **Manabe I**, Shindo T, Nagai R. Gene expression in fibroblasts and fibrosis: involvement in cardiac hypertrophy. *Circ Res* 2002; **91**: 1103-1113

- 36 **Papakonstantinou E**, Aletras AJ, Roth M, Tamm M, Karakiulakis G. Hypoxia modulates the effects of transforming growth factor-beta isoforms on matrix-formation by primary human lung fibroblasts. *Cytokine* 2003; **24**: 25-35
- 37 **Das M**, Dempsey EC, Reeves JT, Stenmark KR. Selective expansion of fibroblast subpopulations from pulmonary artery adventitia in response to hypoxia. *Am J Physiol Lung Cell Mol Physiol* 2002; **282**: L976-986
- 38 **Bogatkevich GS**, Tourkina E, Abrams CS, Harley RA, Silver RM, Ludwicka-Bradley A. Contractile activity and smooth muscle alpha-actin organization in thrombin-induced human lung myofibroblasts. *Am J Physiol Lung Cell Mol Physiol* 2003; **285**: L334-343
- 39 **Eyden B**. Electron microscopy in the study of myofibroblastic lesions. *Semin Diagn Pathol* 2003; **20**: 13-24
- 40 **Ehrllich HP**, Diez T. Role for gap junctional intercellular communications in wound repair. *Wound Repair Regen* 2003; **11**: 481-489
- 41 **Li XP**, Mao XZ. Effect of estrogen, cholic acid loading and bile draining on hepatobiliary functions in rats. *Shijie Huaren Xiaohua Zazhi* 2000; **8**: 1009-1012
- 42 **Zhu XF**, Chen GH, He XS, Lu MQ, Wang GD, Cai CJ, Yang Y, Huang JF. Liver transplantation and artificial liver support in fulminant hepatic failure. *World J Gastroenterol* 2001; **7**: 566-568
- 43 **He XS**, Huang JF, Liang LJ, Lu MD, Cao XH. Surgical resection for hepato portal bile duct cancer. *World J Gastroenterol* 1999; **5**: 128-131
- 44 **Yang HM**, Wu J, Li JY, Zhou JL, He LJ, Xu XF. Optic properties of bile liquid crystals in human body. *World J Gastroenterol* 2000; **6**: 248-251
- 45 **Diana A**, Pietra M, Guglielmini C, Boari A, Bettini G, Cipone M. Ultrasonographic and pathologic features of intestinal smooth muscle hypertrophy in four cats. *Vet Radiol Ultrasound* 2003; **44**: 566-569
- 46 **Cheng AC**, Wang MS, Chen XY, Guo YF, Liu ZY, Fang PF. Pathogenic and pathological characteristic of new type gosling viral enteritis first observed in China. *World J Gastroenterol* 2001; **7**: 678-684
- 47 **Bettini G**, Muracchini M, Della Salda L, Preziosi R, Morini M, Guglielmini C, Sanguinetti V, Marcato PS. Hypertrophy of intestinal smooth muscle in cats. *Res Vet Sci* 2003; **75**: 43-53
- 48 **Gunst SJ**, Tang DD, Opazo Saez A. Cytoskeletal remodeling of the airway smooth muscle cell: a mechanism for adaptation to mechanical forces in the lung. *Respir Physiol Neurobiol* 2003; **137**: 151-168
- 49 **Schelling JR**, Sinha S, Konieczkowski M, Sedor JR. Myofibroblast differentiation: plasma membrane microdomains and cell phenotype. *Exp Nephrol* 2002; **10**: 313-319
- 50 **Prajapati DN**, Hogan WJ. Sphincter of Oddi dysfunction and other functional biliary disorders: evaluation and treatment. *Gastroenterol Clin North Am* 2003; **32**: 601-618

Edited by Gupta MK and Xu FM

Fenofibrate for patients with asymptomatic primary biliary cirrhosis

Kazufumi Dohmen, Toshihiko Mizuta, Makoto Nakamuta, Naoya Shimohashi, Hiromi Ishibashi, Kyosuke Yamamoto

Kazufumi Dohmen, Department of Internal Medicine, Okabe Hospital, Japan

Hiromi Ishibashi, Department of Clinical Research Center, National Nagasaki Medical Center, Japan

Toshihiko Mizuta, Kyosuke Yamamoto, Department of Internal Medicine, Saga Medical School, Japan

Makoto Nakamuta, Department of Medicine and Bioregulatory Science, Graduate School of Medical Sciences, Kyushu University, Japan

Naoya Shimohashi, Department of Internal Medicine, Fukuoka City Hospital, Japan

Correspondence to: Dr. Kazufumi Dohmen, Department of Internal Medicine, Okabe Hospital, 1-2-1 Myojinzaka Umi-machi Kasuyagan Fukuoka 811-2122 Japan. dohmenk@par.odn.ne.jp

Telephone: +81-92-932-0025 **Fax:** +81-92-933-7253

Received: 2003-11-17 **Accepted:** 2004-01-18

Abstract

AIM: Primary biliary cirrhosis (PBC) is a chronic, cholestatic disease of autoimmune etiology, the histology of which shows a destruction of the intrahepatic bile duct and portal inflammation. Ursodeoxycholic acid (UDCA) is now used as a first-line drug for asymptomatic PBC (aPBC) because it is reported that UDCA decreases mortality and prolongs the time of liver transplantation. However, only 20-30% of patients respond fully to UDCA. Recently, lipoprotein-lowering agents have been found to be effective for PBC. The aim of this study was to examine the safety and efficacy of fenofibrate, a member of the fibrate class of hypolipidemic and anti-inflammatory agent via peroxysome proliferator-activated receptor α , in patients with aPBC.

METHODS: Fenofibrate was administered for twelve weeks in nine patients with aPBC who failed to respond to UDCA. UDCA was used along with fenofibrate during the study. The data from aPBC patients were analyzed to assess the biochemical effect of fenofibrate during the study.

RESULTS: The serum levels of alkaline phosphatase (ALP) (285 ± 114.8 IU/L) and immunoglobulin M (IgM) (255.8 ± 85.9 mg/dl) significantly decreased to 186.9 ± 76.2 IU/L and 192.9 ± 67.5 mg/dL respectively, after fenofibrate treatment in patients with aPBC ($P < 0.05$). Moreover, the titer of antimitochondrial antibody (AMA) also decreased in 4 of 9 patients with aPBC. No adverse reactions were observed in any patients.

CONCLUSION: Fenofibrate appears to be significantly effective in treating patients with aPBC who respond incompletely to UDCA alone. Although the mechanism of fenofibrate on aPBC has not yet been fully clarified, combination therapy using fenofibrate and UDCA might be related to the anti-immunological effects, such as the suppression of AMA production as well as its anti-inflammatory effect.

Dohmen K, Mizuta T, Nakamuta M, Shimohashi N, Ishibashi H, Yamamoto K. Fenofibrate for patients with asymptomatic primary biliary cirrhosis. *World J Gastroenterol* 2004; 10(6): 894-898 <http://www.wjgnet.com/1007-9327/10/894.asp>

INTRODUCTION

Primary biliary cirrhosis (PBC) is a chronic, cholestatic liver disease characterized by inflammation and progressive destruction of interlobular bile ducts, eventually leading to cholestasis, biliary cirrhosis and finally hepatic failure. The etiology of PBC is attributed to autoimmunity mainly due to the association with autoantibodies such as antimitochondrial antibodies (AMA), which present in 95% of PBC patients, and an increased level of immunoglobulin M (IgM). Regarding this therapy, orthotopic liver transplantation is selected for PBC patients with liver failure and intractable pruritus, while ursodeoxycholic acid (UDCA) has been widely used as a first-line drug for asymptomatic PBC (aPBC) to slow the disease progression^[1-3]. Although the biochemical data of the liver functions tend to normalize in 20-30% of patients with aPBC who are administered UDCA, the rest of the patients often progress to cirrhosis^[4,5]. Therefore, there is a need for a more effective treatment^[6].

PBC is often associated with lipoprotein abnormalities such as an elevation of serum cholesterol concentration^[7]. Recently, several studies focusing on lipoprotein-lowering drugs for PBC have been reported^[8-15]. Simvastatin, an HMG-CoA reductase inhibitor, was proven to be useful as a modulator of cholestasis and an immune response in PBC^[8]. Bezafibrate, a hypolipidemic agent, was also effective in PBC patients who failed to respond to UDCA^[9-15]. The mechanism of action of bezafibrate is believed to be the anti-inflammatory effects via peroxysome proliferator-activated receptor α (PPAR α), a member of the nuclear hormone receptor superfamily, and the expression of multiple drug resistance gene-3, both of which ameliorate hepatobiliary inflammation in PBC^[11,16-18]. Fenofibrate is a member of fibrate class agents as bezafibrate and works as a ligand of PPAR α , showing a potent triglyceride-lowering effect. Fenofibrate treatment for PBC has been addressed in very few studies^[19], including our previous abstracts which we presented at conferences^[20,21]. The effect of fenofibrate on PBC therefore has to be clarified and is currently being evaluated.

For this purpose, we studied the efficacy of fenofibrate on nine patients with aPBC who responded insufficiently to monotherapy of UDCA.

MATERIALS AND METHODS

Patients and regimen

Nine patients with aPBC consisting of 2 males and 7 females were included in the prospective study. Ages were 50.3 ± 11.7 (mean \pm SD) yr ranging from 34 to 69 yr, and mean body mass 57.9 ± 5.6 (mean \pm SD) kg ranging from 50.0 to 64.6 kg. They were diagnosed to have aPBC according to laboratory and/or histological findings. All patients were negative both for anti-hepatitis C virus antibody and for hepatitis B surface antigen. All 9 patients with aPBC exhibited a poor therapeutic response to UDCA of 600 mg/d for 6 mo or more. Fenofibrate of 100 mg/d was administered for 4 patients (less than 60 kg in body mass) and of 150 mg for 5 patients (60 kg or more in body mass) for at least 12 wk. The study was approved by the local ethics committee, and informed consent was obtained from each patient included in the study.

Laboratory examination

During the study, any changes in dietary therapy were prohibited. In order to determine the drug compliance and safety, all patients were required to visit the hospital every 2 wk, and the serum blood chemistry including apolipoprotein was examined every 4 wk. Serum concentrations of total bilirubin, immunoglobulins G and M (IgG, IgM) as well as aspartate aminotransferase (AST), alanine aminotransferase (ALT), alkaline phosphatase (ALP) and gamma-glutamyltransferase (γ GTP) were determined before the fenofibrate treatment as well after the treatment of 12 wk by routine laboratory procedures. AMA titers were measured using indirect immunofluorescence based on stomach/kidney frozen sections. Blood was sampled early in the morning during fasting, and a medical laboratory (SRL Co., Tokyo) centrally controlled the measurements up to 12 wk after the start of administration.

Statistical analysis

Differences in the means and proportions were evaluated by Chi-square test and Student's *t*-test. Baseline variables were assessed in the study, including AST, ALT, ALP, γ GTP, apolipoproteins, IgG, IgM and AMA titers. *P* value less than 0.05 was considered statistically significant.

RESULTS

Effect of fenofibrate on laboratory findings for hepatobiliary system and serum lipids

Table 1 and Figure 1 show the enzymatic changes in the hepatobiliary system identified up to 12 wk after the start of the combination therapy of fenofibrate and UDCA. The mean ALP value of 285.0 IU/L prior to fenofibrate therapy decreased to 186.9 IU/L at wk 12 after the initiation of the therapy, thus showing a statistically significant difference. The serum γ -GTP concentration also decreased after 12 wk of fenofibrate and UDCA treatment compared to that at initiation, although the difference was not statistically significant. The serum concentrations of AST and ALT did not change statistically regarding those obtained prior to and after 12 wk of treatment. The serum concentration of IgM of 255.8 mg/dL prior to the treatment was significantly reduced to 192.9 mg/dL at wk 12, whereas the concentration of IgG did not decrease. Regarding the titer of AMA, a reduction was identified in 4 of the 9 patients based on that obtained prior to and after 12 wk of treatment. As shown in Figure 2, the AMA titer of 320 decreased to 40, 320 to 80, 80 to 20 and 40 to 20 in 4 of 9 patients, respectively. The titers of AMA in the rest 5 patients remained unchanged. The serum levels of ALP of 571 IU/L and IgM of 236 mg/dL decreased to 306 IU/L and 154 mg/dL, respectively, in a patient whose AMA titer decreased from more than 320 to 40. Likewise, those of 276 and 159 decreased to 285 and 102 in a patient whose AMA titer decreased from more than 320 to 80, those of 215 and 375 decreased to 107 and 241 in a patient whose AMA titer decreased from 80 to 20, and those of 191 and 240 decreased to 114 and 180 in a patient whose AMA titer decreased from 80 to 20, respectively. Interestingly, all the four cases who showed a reduction of the AMA titer were females.

Table 2 shows the changes in serum lipids and apoprotein levels in all 9 patients. The concentrations of apo A-II (median value: 31.6 mg/dL) and apo C-II (median value: 3.9 mg/dL) increased statistically to 44.1 mg/dL and 4.5 mg/dL during fenofibrate therapy ($P < 0.005$), respectively. The concentrations of total cholesterol (TC), triglyceride (TG), low density lipoprotein-cholesterol (LDL-C) and Apo B lipoprotein tended to decrease while the high density lipoprotein-cholesterol (HDL-C), apo A-I and apo E levels tended to increase. However, the difference was not statistically significant.

Table 1 Change in concentrations of laboratory data (mean \pm SD)

Laboratory Variable	Before therapy	4 wk	8 wk	12 wk
AST (IU/L)	29.9 \pm 8.1	50.0 \pm 36.3	46.6 \pm 24.9	46.9 \pm 28.3
ALT (IU/L)	31.1 \pm 13.2	48.6 \pm 35.2	57.0 \pm 38.9	48.4 \pm 42.5
ALP (IU/L)	285.0 \pm 114.8	238.5 \pm 88.4	200.6 \pm 76.7 ^a	186.9 \pm 76.2 ^a
γ -GTP (IU/L)	149.6 \pm 143.0	147.0 \pm 178.6	128.8 \pm 128.1	125.2 \pm 110.3
LDH (IU/L)	311.2 \pm 46.7	318.4 \pm 44.8	320.1 \pm 59.9	324.6 \pm 59.2
TB (mg/dl)	0.7 \pm 0.7	0.4 \pm 0.2	0.6 \pm 0.4	0.6 \pm 0.5
IgG (mg/dl)	1 431.4 \pm 285.3	-	-	1 415.0 \pm 316.1
IgM (mg/dl)	255.8 \pm 85.9	-	-	192.9 \pm 67.5 ^a

^a $P < 0.05$ (baseline-matched *t*-test) vs the serum concentrations prior to the treatment.

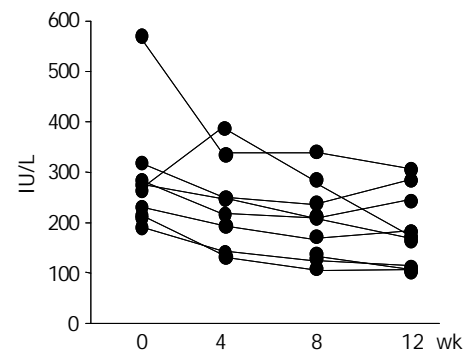


Figure 1 Change in the serum alkaline phosphatase levels during fenofibrate treatment.

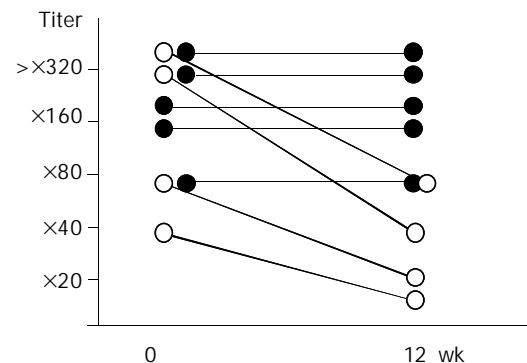


Figure 2 Change in antimitochondria antibody titers before and after fenofibrate treatment.

Table 2 Change in concentrations of serum lipids and apoproteins

Variables	Before	4 wk	8 wk	12 wk
TC (mg/dL)	206.3 \pm 26.5	186.3 \pm 22.9	189.9 \pm 27.7 ^a	192.1 \pm 30.1
TG (mg/dL)	126.0 \pm 50.1	119.5 \pm 76.2	102.8 \pm 52.3	103.6 \pm 53.0
HDL-C (mg/dL)	63.6 \pm 11.3	63.8 \pm 14.0	68.8 \pm 12.6	69.3 \pm 13.1
LDL-C (mg/dL)	115.7 \pm 22.1	99.3 \pm 29.3	105.6 \pm 28.0	105.2 \pm 25.1
Apo A-I (mg/dL)	159.0 \pm 17.9	154.7 \pm 19.4	158.3 \pm 17.9	172.1 \pm 24.3
Apo A-II (mg/dL)	31.6 \pm 6.5	39.5 \pm 7.0 ^a	40.7 \pm 4.6 ^a	44.1 \pm 4.9 ^a
Apo B (mg/dL)	95.1 \pm 22.9	84.1 \pm 31.4	81.0 \pm 26.5	84.1 \pm 23.1
Apo C-II (mg/dL)	3.9 \pm 1.7	4.6 \pm 2.0 ^a	4.2 \pm 1.6	4.5 \pm 1.5 ^a
Apo C-III (mg/dL)	9.7 \pm 3.8	9.5 \pm 4.2	8.9 \pm 2.9	9.8 \pm 3.6
Apo E (mg/dL)	4.3 \pm 1.0	4.3 \pm 0.8	4.4 \pm 0.8	4.6 \pm 0.9

TC: total cholesterol, TG: triglyceride, HDL-C: HDL-cholesterol, LDL-C: LDL-cholesterol, Apo: apoprotein. ^a $P < 0.05$ (baseline-matched *t*-test) vs the serum concentrations prior to the treatment.

Rate of change of each variable between AMA-reduced group and AMA-unchanged group

The rate of change of each variable between the AMA-reduced group and the AMA-unchanged group was compared before and after the combination therapy of fenofibrate and UDCA. As shown in Table 3, the IgM concentrations dropped to $35.4 \pm 0.6\%$ in the AMA-reduced group and $7.1 \pm 1.8\%$ in the AMA-unchanged group, showing a statistically significance between the two groups. Interestingly, however, the values of ALP, γ GTP and apo A-II dropped at a similar rate in two groups.

Table 3 Rate of change in the valuables between AMA-reduced group and AMA-unchanged group

Factors	AMA-reduced group	AMA-unchanged group	t-test
ALT (IU/L)	61.6 ± 124.8^1	52.0 ± 109.2	0.905
ALP (IU/L)	-33.4 ± 24.8	-33.8 ± 16.0	0.978
γ -GTP (IU/L)	-2.8 ± 73.4	-5.3 ± 39.8	0.950
IgM (mg/dL)	-35.4 ± 0.6	-7.1 ± 11.8	0.010
Apo A-II (mg/dL)	52.0 ± 17.3	37.4 ± 38.6	0.573
Apo C-II (mg/dL)	29.5 ± 13.8	10.6 ± 10.1	0.089

¹Changing rate (%) (mean \pm SD).

Adverse effects

In all the nine patients, no subjective symptoms such as systemic malaise, anoxia, were observed. No deterioration of the liver function tests was identified in any cases as shown in Table 1. The blood urea nitrogen and creatinine levels did not change either after fenofibrate administration.

DISCUSSION

Primary biliary cirrhosis presents as a chronic cholestatic disease involving predominantly middle-aged women with a very frequent association with AMA. In addition, PBC has been found to be often associated with other autoimmune diseases^[22-27]. Therefore, PBC is thought to be an autoimmune disease and most therapies have thus been directed at altering the immune response. So far, the use of corticosteroid, azathioprine, cyclosporine^[28], D-penicillamine^[29], methotrexate^[30,31], colchicines^[31,32] has been studied for patients with PBC.

However, none of these drugs appeared to offer any significant benefits while they tended to induce adverse effects such as osteoporosis, or pulmonary toxicity^[24]. Recently UDCA appeared to be a drug which most effectively treated patients with PBC^[1-3] through cytoprotective and choleric effects and alterations in the bile pool by competition for uptake by ileal bile acid receptors. However, a considerable number of patients with PBC still clinically respond insufficiently to UDCA alone, and now a new problem has emerged concerning which agent should be used for these patients.

Several clinical studies on lipoprotein-lowering agents such as simvastatin^[8] and bezafibrate^[9-15] for PBC patients who failed to respond to UDCA have so far been conducted, and the results have been found to be of value. In addition, fenofibrate, a member of such fibrate class agents as bezafibrate, has recently been found to be an expected agent for PBC because of its stronger activity of an anti-inflammatory effect via PPAR α ^[33], and more potentiality in reducing TG and LDL-C levels^[34] than that of bezafibrate. Early attempts of the apoprotein-lowering agents focused on treating concomitant conditions of hypertriglycemia or hypercholesterolemia. Therefore, we conducted a study on the efficacy of fenofibrate in nine patients with aPBC.

Indeed, serum concentrations of TC and TG decreased and the concentration of HDL-C increased in all the 9 patients with aPBC, however, these changes were not statistically significant. As for apoprotein, apo AII and apo C II, which are major protein constituents of HDL, were significantly increased in the study. As a result, lipoprotein, an indicator for the risk of developing atherosclerotic disease was improved after fenofibrate treatment in PBC patients in our study^[7,35].

Fenofibrate has been shown to regulate the expression of various kinds of lipids and proteins, and cell proliferation through the activation of PPAR α ^[36,37]. However, apart from the lipoprotein-lowering effect, its pleiotropic effects have recently received much attention ranging from inhibited production of interleukin (IL)-1, IL-6, IL-1- and IL-6-induced prostaglandin E2 as well as cyclooxygenase (COX)-2 expression to the induction of apo A-II through the inhibition of the nuclear factor (NF)- κ B signalling by activation of PPAR α ^[38,39]. Furthermore, fenofibrate could inhibit the expression of intercellular adhesion molecule (ICAM)-1 and vascular cell adhesion molecule (VCAM)-1, which play a role in the adhesion of monocytes through apo A-II induction or NF- κ B inhibition

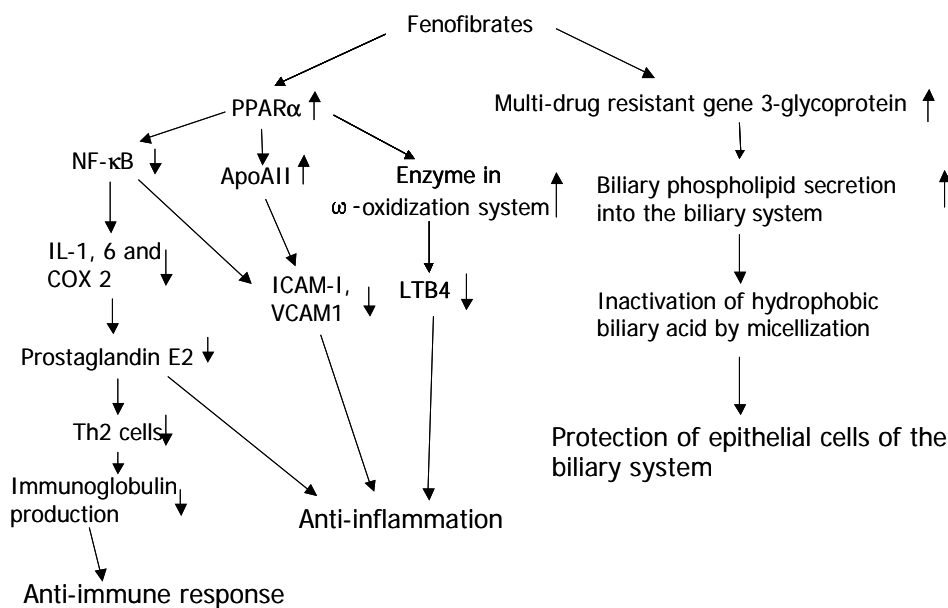


Figure 3 Possible mechanisms of action for fibrates on PBC.

[40]. These findings suggest that fenofibrate can inhibit not only the lipid metabolism but also the inflammatory reaction through PPAR α . It is therefore likely that the PPAR α activation-mediated anti-inflammatory effects of fenofibrate, such as the inhibited expression of NF- κ B, IL-1, IL-6, COX-2 and prostaglandin E2 might contribute to an improvement of PBC. Apo A-II could inhibit the expression of such adhesion molecules as ICAM-1 and VCAM-1 which are believed to be progression factors in cases of PBC, because adhesion molecules induce lymphocytes into epithelial cells of hepatobiliary ducts. From another point of view, as reported by Iwasaki *et al* [11], improvement of PBC might also occur because the canalicular phospholipid translocator, encoded by multi-drug resistant gene-3 (MDR3) expressed by bezafibrate administration, was exclusively present on the canalicular membrane, increases the secretion of biliary phospholipids and inactivating hydrophobic bile acid by micellization to protect hepatocytes and epithelial cells of bile ducts [18] (Figure 3). Thus, MDR3 messenger RNA and the canalicular phospholipid translocator (MDR3-P glycoprotein) of fibrates are strictly PPAR α dependent. Although the different sensitivities to PPAR α between fenofibrate and bezafibrate have not yet been clarified, a possible reason is that fenofibrate could selectively act on PPAR α only, while bezafibrate could act on PPAR α , γ as well as δ [33].

The emerging question is whether fenofibrate's anti-immunological effect is truly mediated via PPAR α or its receptor-independent anti-inflammatory effects. Our results demonstrated that fenofibrate did not only improve dyslipoproteinemia but also significantly reduce serum ALP and IgM levels. It was of great interest that a reduction of AMA titer was also observed in 4 of 9 patients. The immunological response of PBC patients to fenofibrate therapy thus raises another question, namely, how is the AMA production regulated by PPAR α in PBC? Is the AMA production interrelated in the inflammation or lipid synthesis? Kurihara *et al* reported 5 cases of aPBC who responded to the combination therapy of bezafibrate and UDCA [9], however, the AMA titer remained unchanged in all cases. Nevertheless, there was a reduction of IgM as well as ALP, γ GTP and TC. Similarly, Iwasaki *et al* described that IgM decreased significantly, but the AMA titers were not affected in all 5 PBC patients treated with bezafibrate [11]. In contrast, Fukuo *et al* showed 6 cases of aPBC who responded to bezafibrate with a decreased AMA titer [10]. Nakai *et al* did not analyze the AMA titer among 23 patients with PBC treated with a combination therapy of bezafibrate and UDCA, while they confirmed a decrease in the IgM concentration [12]. Although no relationship between IgM concentration and AMA titer was observed in these papers, our study demonstrated that IgM concentration closely correlated with the reduction of AMA titer, whereas the decrease of ALP and γ -GTP levels was not correlated with the AMA reduction. Interestingly, immunoglobulins, the secretory products of stimulated B lymphocytes, were characteristically elevated, with a distinct focus on IgM in PBC. One possibility to explain the reduction of IgM by fenofibrate treatment for PBC is that the decreased production of prostaglandin E2 via PPAR α suppressed the Th2 lymphocytes that induce B cells, thus leading to the reduced production of immunoglobulin [41]. However, our study showed that fenofibrate treatment for PBC resulted in a decrease in IgM level, while IgG level was unchanged. Fenofibrate may also possess an additional or synergistic potential for lowering IgM levels as observed in the ALP and γ GTP levels. The exact cause of hyperglobulinemia in PBC, however, remains to be elucidated.

Regarding the adverse effect of fenofibrate, diabetes arteriosclerosis intervention study (DAIS) showed that micronized fenofibrate at 200 mg (equivalent to 300 mg of the

standard formulation) was administered for 3 yr to type 2 diabetic patients in order to observe its inhibitory effect on the progression of coronary arterial stenosis. As a result, no difference in the safety between fenofibrate and placebo was observed [42]. In addition, studies of human first-generation cultured cells and HepG2 cells suggested that serum aminotransferase levels were transiently elevated and then normalized or returned to pretreatment levels [43]. The increase in the aminotransferase level after treatment with fenofibrate was not considered to be clinically significant. As fenofibrate could activate the aminotransferase gene expression, thus leading to a mild and transient elevation of aminotransferase through mechanisms of PPAR α involving increased levels of reactive oxygen species and intracellular glutathion depletion, thus leading to mitochondrial dysfunction and perturbation of intracellular Ca⁺⁺ homeostasis and also to cell death [43,44]. A dosage of 100 mg or 150 mg per day of fenofibrate in the 9 patients studied, which is half the commonly administered dose, was thus administered to poor responders to UDCA, and a blood examination was performed every 2 wk. No adverse effect was observed either clinically or biochemically in all the 9 patients in our study.

Administration of fenofibrate in combination with UDCA was safe and useful for patients with aPBC. This finding confirms our belief that fenofibrate's beneficial effects are mediated only through its lipoprotein-lowering effect. The mechanism underlying the long term efficacy of fenofibrate for symptomatic PBC remains to be elucidated [15]. The expansive array of ligands, target genes, and metabolic processes regulated by nuclear receptors such as PPAR α , β , γ within hepatocytes, and ever-changing internal milieu, has made a completely comprehensive regulatory scheme virtually impossible to depict graphically [44]. Nuclear receptors-regulated gene products may create or disable a protein ligand or regulate the import or export of another nuclear receptor, which might be related to the production of IgM or AMA. There are likely many more mechanisms of action for fenofibrate on PBC still awaiting further discovery.

In conclusion, fenofibrate can be well tolerated by all patients with aPBC, while it has no remarkable side effects. This agent is beneficial for the treatment of aPBC. However, further studies are needed to elucidate the effect of fenofibrate on PBC and to determine its long-term biochemical and histological efficacy.

REFERENCES

- 1 **Poupon RE**, Poupon R, Balkau B. Ursodiol for the long-term treatment of primary biliary cirrhosis. *N Eng J Med* 1994; **330**: 1342-1347
- 2 **Poupon R**, Poupon RE. Treatment of primary biliary cirrhosis. *Bailliere's Clin Gastroenterol* 2000; **14**: 615-628
- 3 **Combes B**, Carithers RL, Maddrey WC, Lin D, McDonald MF, Wheeler DE, Eigenbrodt EH, Munoz SJ, Rubin R, Garcia-Tsao G, Bonner GF, West AB, Boyer J, Luketic VA, Shiffman ML, Mills AS, Peters MG, White HM, Zetterman RK, Rossi SS, Hofman AF, Markin RS. A randomized, double-blind, placebo-controlled trial of ursodeoxycholic acid in primary biliary cirrhosis. *Hepatology* 1995; **22**: 759-766
- 4 **Jorgensen RA**, Dickson ER, Hofmann AF, Rossi SS, Lindor KD. Characterisation of patients with a complete biochemical response to ursodeoxycholic acid. *Gut* 1995; **36**: 935-938
- 5 **Leuschner M**, Dietrich CF, You T, Seidl C, Raedle J, Herrmann G, Ackermann H, Leuschner U. Characterization of patients with primary biliary cirrhosis responding to long term ursodeoxycholic acid treatment. *Gut* 2000; **46**: 121-126
- 6 **Levy C**, Lindor KD. Current management of primary biliary cirrhosis and primary sclerosing cholangitis. *J Hepatol* 2003; **38**: S24-S37
- 7 **Jahn CE**, Schaefer EJ, Taam LA, Hoofnagle JH, Lindgren FT,

- Albers JJ, Jones EA, Brewer Jr B. Lipoprotein abnormalities in primary biliary cirrhosis. Association with hepatic lipase inhibition as well as altered cholesterol esterification. *Gastroenterology* 1985; **89**: 1266-1278
- 8 **Ritzel U**, Leonhardt U, Nather M, Schafer G, Armstrong VW, Ramadori G. Simvastatin in primary biliary cirrhosis: effects on serum lipids and distinct disease markers. *J Hepatol* 2002; **36**: 454-458
- 9 **Kurihara T**, Yanagisawa A, Kitamura Y, Itabashi K, Arita Y, Tsuchiya M, Akimoto M, Ishiguro H, Hashimoto H, Maeda A, Shigemoto M, Yamashita K, Yokoyama I. Effect of bezafibrate in patients with PBC. *Rhinsho Iyaku* 1997; **13**: 4255-4258
- 10 **Fukuo Y**, Tada N, Yamamoto K. Study of efficacy of bezafibrate for PBC. *Rinsho Seijinkyu* 1999; **29**: 1367-1372
- 11 **Iwasaki S**, Tsuda K, Ueta H, Aono R, Ono M, Saibara T, Maeda T, Onishi S. Bezafibrate may have a beneficial effect in pre-cirrhotic primary biliary cirrhosis. *Hepatol Res* 1999; **16**: 12-18
- 12 **Nakai S**, Masaki T, Kurokohchi K, Deguchi A, Nishioka M. Combination therapy of bezafibrate and ursodeoxycholic acid in primary biliary cirrhosis: a preliminary study. *Am J Gastroenterol* 2000; **95**: 326-327
- 13 **Miyaguchi S**, Ebinuma H, Imaeda H, Nitta Y, Watanabe T, Saito H, Ishii H. A novel treatment for refractory primary biliary cirrhosis? *Hepatogastroenterology* 2000; **47**: 1518-1521
- 14 **Kurihara T**, Niimi A, Maeda A, Shigemoto M, Yamashita K. Bezafibrate in the treatment of primary biliary cirrhosis: Comparison with ursodeoxycholic acid. *Am J Gastroenterol* 2000; **95**: 2990-2992
- 15 **Yano K**, Kato H, Morita S, Takahara O, Ishibashi H, Furukawa R. Is bezafibrate histologically effective for primary biliary cirrhosis? *Am J Gastroenterol* 2002; **97**: 1075-1077
- 16 **Krey G**, Braissant O, L'Horset F, Kalkhoven E, Perroud M, Parker MG, Wahli W. Fatty acid, eicosanoids, and hypolipidemic agents identified as ligands of peroxisome proliferator-activated receptors by coactivator-dependent receptor ligand assay. *Mol Endocrinol* 1997; **11**: 779-791
- 17 **Devchand PR**, Keller H, Peters JM, Vazquez M, Gonzalez FJ, Wahli W. The PPAR α -leukotriene B₄ pathway to inflammation control. *Nature* 1996; **384**: 39-43
- 18 **Chianale J**, Vollrath V, Wielandt AM, Amigo L, Rigotti A, Nervi F, Gonzalez S, Andrade L, Pizarro M, Accatino L. Fibrates induce *mdr2* gene expression and biliary phospholipid secretion in the mouse. *Biochem J* 1996; **314**: 781-786
- 19 **Ohira H**, Sato Y, Ueno T, Sata M. Fenofibrate treatment in patients with primary biliary cirrhosis. *Am J Gastroenterol* 2002; **97**: 2147-2149
- 20 **Mizuta T**, Dohmen K, Nakamuta M, Shimohashi N, Yamamoto K. Study of efficacy of fenofibrate on primary biliary cirrhosis poorly responded to ursodeoxycholic acid. *Acta Hepatol Jpn* 2001; **42** (Suppl 1): A294
- 21 **Dohmen K**, Mizuta T, Nakamuta M, Shimohashi N, Ishibashi H, Yamamoto K. Fenofibrate for patients with asymptomatic primary biliary cirrhosis. *Hepatology* 2003; **38**(Suppl 1): 518A
- 22 **Culp KS**, Fleming CR, Duffy J, Baldus WP, Dickson ER. Autoimmune associations in primary biliary cirrhosis. *Mayo Clin Proc* 1982; **57**: 365-370
- 23 **Harada N**, Dohmen K, Itoh H, Ohshima T, Yamamoto H, Nagano M, Iwata Y, Hachisuka K, Ishibashi H. Sibling cases of primary biliary cirrhosis associated with polymyositis, vasculitis and Hashimoto's thyroiditis. *Internal Med* 1992; **31**: 289-293
- 24 **Lindor KD**, Dickson ER. Primary biliary cirrhosis. In Schiff's Diseases of the Liver, Eighth ed. *Lippin Cott Raevan Publishers, Philadelphia* 1999: 679-692
- 25 **Shimoda S**, Nakamura M, Shigematsu H, Tanimoto H, Gushima H, Gershwin ME, Ishibashi H. Mimicry peptides of human PDC-E2, 163-176, the immunodominant T-cell epitope of primary biliary cirrhosis. *Hepatology* 2000; **31**: 1212-1216
- 26 **Dohmen K**. Primary biliary cirrhosis and pernicious anemia. *J Gastroenterol Hepatol* 2001; **16**: 1316-1318
- 27 **Dohmen K**, Shigematsu H, Miyamoto Y, Yamasaki F, Irie K, Ishibashi H. Atrophic corpus gastritis and *Helicobacter pylori* infection in primary biliary cirrhosis. *Dig Dig Sci* 2002; **47**: 162-169
- 28 **Wiesner RH**, Ludwig J, Lindor KD, Jorgensen RA, Baldus WP, Hombueger HA, Dickson ER. A controlled trial of cyclosporine in the treatment of primary biliary cirrhosis. *N Engl J Med* 1990; **322**: 1419-1424
- 29 **Dickson ER**, Fleming TR, Wiesner RH, Baldus WP, Fleming CR, Ludwig J, McCall JT. Trial of penicillamine in advanced primary biliary cirrhosis. *N Engl J Med* 1985; **312**: 1011-1015
- 30 **Bach N**, Bodian C, Bodenheimer H, Croen E, Berk PD, Thung SN, Lindor KD, Therneau T, Schaffner F. Methotrexate therapy for primary biliary cirrhosis. *Am J Gastroenterol* 2003; **98**: 187-193
- 31 **Kaplan MM**, Schmid C, Provenzale D, Sharma A, Dickstein G, McKusick A. A prospective trial of colchicines and methotrexate in the treatment of primary biliary cirrhosis. *Gastroenterology* 1999; **117**: 1173-1180
- 32 **Lee YM**, Kaplan MM. Efficacy of colchicine in patients with primary biliary cirrhosis poorly responsive to ursodiol and methotrexate. *Am J Gastroenterol* 2003; **98**: 205-208
- 33 **Willson TM**, Brown PJ, Sternbach DD, Henke BR. The PPARs: From orphan receptors to drug discovery. *J Med Chem* 2000; **43**: 527-550
- 34 **Hata Y**, Goto Y, Itakura H, Nakaya N, Saito Y. Clinical evaluation of fenofibrate (GRS-001) on hyperlipidemia -Double-blind study with bezafibrate. *Ronen Igaku* 1995; **33**: 765-822
- 35 **Longo M**, Crosignani A, Battezzati PM, Squarcia Giussani C, Invernizzi P, Zuin IM, Podda M. Hyperlipidaemic state and cardiovascular risk in primary biliary cirrhosis. *Gut* 2002; **51**: 265-269
- 36 **Gebel T**, Arand M, Oesch F. Induction of the peroxisome proliferator activated receptor by fenofibrate in rat liver. *FEBS Lett* 1992; **309**: 37-40
- 37 **Schoonjans K**, Staels B, Auwerx J. Role of the peroxisome proliferator-activated receptor (PPAR) in mediating the effects of fibrates and fatty acids on gene expression. *J Lipid Res* 1996; **37**: 907-925
- 38 **Vu-Dac N**, Schoonjans K, Kosykh V, Dallongeville J, Fruchart JC, Staels B, Auwerx J. Fibrates increase human apolipoprotein A-II expression through activation of the peroxisome proliferator-activated receptor. *J Clin Invest* 1995; **96**: 741-750
- 39 **Staels B**, Koenig W, Habib A, Merval R, Lebret M, Torra IP, Delerive P, Fadel A, Chinetti G, Fruchart JC, Najib J, Maclout J, Tedgui A. Activation of human aortic smooth-muscle cells is inhibited by PPAR α but not by PPAR γ activators. *Nature* 1998; **393**: 790-793
- 40 **Marx N**, Sukhova GK, Collins T, Libby P, Plutzky J. PPAR α activators inhibit cytokine-induced vascular cell adhesion molecule-1 expression in human endothelial cells. *Circulation* 1999; **99**: 3125-3131
- 41 **Betz M**, Fox BS. Prostaglandin E2 inhibits production of Th1 lymphokines but not of Th2 lymphokines. *J Immunol* 1991; **146**: 108-113
- 42 **Diabetes Arteriosclerosis Intervention Study Investigators**. Effect of fenofibrate on progression of coronary-artery disease in type 2 diabetes: the Diabetes Arteriosclerosis Intervention Study, a randomized study. *Lancet* 2001; **357**: 905-910
- 43 **Edgar AD**, Tomkiewicz C, Costet P, Legendre C, Aggerbeck M, Bouguet J, Staels B, Guyomard C, Pneau T, Barouki R. Fenofibrate modifiers transaminase gene expression via a peroxisome proliferator activated receptor α -dependent pathway. *Toxicol Lett* 1998; **98**: 13-23
- 44 **Jiao HL**, Zhao BL. Cytotoxic effect of peroxisome proliferator fenofibrate on human HepG2 hepatoma cell line and relevant mechanisms. *Toxicol Appl Pharmacol* 2002; **185**: 172-179
- 45 **Karpen SJ**. Nuclear receptor regulation of hepatic function. *J Hepatol* 2002; **36**: 832-850

Clinical features and risk factors of patients with fatty liver in Guangzhou area

Qi-Kui Chen, Hai-Ying Chen, Kai-Hong Huang, Ying-Qiang Zhong, Ji-Ao Han, Zhao-Hua Zhu, Xiao-Dong Zhou

Qi-Kui Chen, Kai-Hong Huang, Ying-Qiang Zhong, Ji-Ao Han, Zhao-Hua Zhu, Department of Gastroenterology, The Second Affiliated Hospital, Sun Yat-Sen University, Guangzhou 510120, Guangdong Province, China

Hai-Ying Chen, Department of Gastroenterology, The People's Hospital of Zhongshan City, Zhongshan, 528400, Guangdong Province, China
Xiao-Dong Zhou, The Medical Research Center, The Second Affiliated Hospital, Sun Yat-Sen University, Guangzhou 510120, Guangdong Province, China

Supported by the National Natural Science Foundation of China, No.30270371

Correspondence to: Dr. Qi-Kui Chen, Department of Gastroenterology, The Second Affiliated Hospital, Sun Yat-Sen University, 107 West Yanjiang Road, Guangzhou 510120, Guangdong Province, China. qkchen@21cn.com

Telephone: +86-20-81332598 **Fax:** +86-20-81332244

Received: 2003-10-31 **Accepted:** 2003-12-22

Abstract

AIM: There is still no accepted conclusion regarding the clinical features and related risk factors of patients with fatty liver. The large-scale clinical studies have not carried out yet in Guangzhou area. The aim of the present study was to investigate the clinical features and related risk factors of patients with fatty liver in Guangzhou area.

METHODS: A total of 413 cases with fatty liver were enrolled in the study from January 1998 to May 2002. Retrospective case-control study was used to evaluate the clinical features and related risk factors of fatty liver with logistic regression.

RESULTS: Obesity (*OR*: 21.204), alcohol abuse (*OR*: 18.601), type 2 diabetes mellitus (*OR*: 4.461), serum triglyceride (TG) (*OR*: 3.916), serum low-density lipoprotein cholesterol (LDL-C) (*OR*: 1.840) and fasting plasma glucose (FPG) (*OR*: 1.535) were positively correlated to the formation of the fatty liver. The levels of serum alanine aminotransferase (ALT) and gamma-glutamyltransferase (GGT) increased mildly in the patients with fatty liver and were often less than 2-fold of the normal limit. The higher abnormalities of aspartate aminotransferase (AST) levels (42.9%) with AST/ALT more than 2 (17.9%) were found in patients with alcoholic fatty liver (AFL) than those with nonalcoholic fatty liver (NAFL) (16.9% and 5.0% respectively). The elevation of serum TG, cholesterol (CHOL), LDL-C was more common in patients with NAFL than with AFL.

CONCLUSION: Obesity, alcohol abuse, type 2 diabetes mellitus and hyperlipidemia may be independent risk factors of fatty liver. The mildly abnormal hepatic functions can be found in patients with fatty liver. More obvious damages of liver function with AST/ALT usually more than 2 were noted in patients with AFL.

Chen QK, Chen HY, Huang KH, Zhong YQ, Han JA, Zhu ZH, Zhou XD. Clinical features and risk factors of patients with fatty liver in Guangzhou area. *World J Gastroenterol* 2004; 10(6): 899-902
<http://www.wjgnet.com/1007-9327/10/899.asp>

INTRODUCTION

Fatty liver is a condition of hepatic steatosis caused by many risk factors and may progress to liver fibrosis and cirrhosis. Generally, the diagnosis of fatty liver should be based on the history, clinical manifestation, laboratory investigation and medical imaging. Liver biopsy should be taken if necessary. After to know the possible related risk factors of fatty liver existed in the history, the abnormal degree of the biochemical and imaging features can provide a clue for early diagnosis. Although the related risk factors and laboratory features have already been reported, there is still no well-accepted conclusion^[1-3]. The large-scale clinical studies have not carried yet in Guangzhou area, southern China^[4].

Retrospective case-control study was used to analyze fatty liver. The age, gender, obesity, type 2 diabetes mellitus, hyperlipidemia, alcohol abuse, smoking, and history of drugs or toxins and so on were recorded to evaluate the effects of these variables on fatty liver and investigate the related risk factors. The liver function and other serum biochemical levels were compared to find out the difference of laboratory abnormalities, so that they could provide a scientific foundation for the diagnosis, prevention and treatment of fatty liver.

MATERIALS AND METHODS

Clinical data

The data of 413 cases of fatty liver in this hospital from January 1998 to May 2002 were collected. Fatty liver was diagnosed according as the standard by Chinese Association of Medicine and Sherlock^[5-7]. The 200 cases without fatty liver during the same period were selected randomly as control. Age, gender, serum lipids, fasting plasma glucose (FPG), obesity (body mass index, BMI ≥ 25), alcohol abuse, smoking, type 2 diabetes mellitus, history of drugs and toxins, hepatitis virus infection (HCV and HBV), pregnancy, jejunum-ileal bypass surgery and total parenteral nutrition were recorded in fatty liver group and non fatty liver group respectively.

The laboratory data of serum triglyceride (TG), cholesterol (CHOL), high-density lipoprotein cholesterol (HDL-C), low-density lipoprotein cholesterol (LDL-C), apolipoprotein AI (Apo AI), apolipoprotein B (Apo B), uric acid (UA), aspartate aminotransferase (AST), alanine aminotransferase (ALT), the ratio of AST/ALT, albumin (ALB), globin (GLB), ratio of A/G, gamma-glutamyltransferase (GGT) and total bilirubin were collected in two groups respectively. The serum biochemical indexes were examined by an autoanalyzer based on a standard protocol.

Statistical analysis

All data analysis was performed with EXCEL 97 and SPSS 10.0/PC statistical package. A *P* value less than 0.05 (2-tailed) was considered to be statistically significant. The frequency was compared using Chi-squared (χ^2) test. The univariate and multivariate stepwise logistic regression was used to select the independent variables. Data with normal distribution were expressed as mean \pm SD. The differences between groups were analyzed for statistical significance using Student's *t* test. Data

with abnormal distribution were expressed as median and interquartile range.

RESULTS

General condition

Among 413 fatty liver cases, the gender ratio (M/F) was 1.02:1. The age ranged from 8 to 83 years. The median age was 57 years. No significant differences in age and gender were found between the fatty liver group and non-fatty liver group. The possible causes of fatty liver are showed in Table 1.

Table 1 Possible causes of fatty liver and its comparison with non-fatty liver group (%)

Factors	Fatty liver group (n=413)	Non-fatty liver group (n=200)
Alcohol abuse	51(12.4) ^b	7(3.5)
Obesity	244(59.1) ^b	17(8.5)
Type 2 diabetes mellitus	206(49.9) ^b	15(7.5)
Hyperlipidemia	276(66.8) ^b	63(31.5)
Hypertriglyceridemia	92(22.3) ^b	17(8.5)
Hypercholesterolemia	64(15.5)	35(17.5)
Mixed Hyperlipidemia	120(29.1) ^b	11(5.5)
HBV infection	50(12.1)	31(15.5)
HCV infection	34(8.2)	10(5.0)
History of drugs and toxins	6(1.5)	2(1.0)

^b*P*<0.001, vs Non-fatty liver group.

Analysis of independent risk factors of patients with fatty liver

Analysis of univariate logistic regression was performed among 20 variables, such as age, gender, obesity, alcohol abuse, smoking, type 2 diabetes mellitus, TG, CHOL, HDL-C, LDL-C, Apo AI, Apo B, FPG, HCV and HBV infection, history of drugs and toxins, pregnancy, jejunum-ileal bypass surgery and total parenteral nutrition. TG, CHOL, HDL-C, LDL-C, Apo B, FPG, obesity, alcohol abuse, smoking, type 2 diabetes mellitus were positively correlated to fatty liver respectively (odds rate, *OR*>1, *P*<0.05), while Apo AI was negatively correlated to it (*OR*<1, *P*<0.05). Multivariate stepwise logistic regression was used to select the variables independently associated with fatty liver. Obesity, alcohol abuse, type 2 diabetes mellitus, TG, LDL-C and FPG were entered the model of logistic regression as the independent risk factors of fatty liver. In contrast, Apo B was negatively correlated to it (Table 2).

Table 2 Multivariate stepwise logistic regression

Variables	β	SE	OR	95%CI	P-value
Obesity	3.054	0.354	21.204	10.539-42.429	0.000
Alcohol abuse	2.923	0.509	18.601	6.585-50.432	0.000
Type 2 diabetes mellitus	1.495	0.354	4.461	2.228-8.952	0.022
TG	1.365	0.268	3.916	2.316-6.621	0.000
LDL-C	0.610	0.184	1.840	1.283-2.640	0.001
FPG	0.429	0.094	1.535	1.278-1.846	0.000
Apo B	-1.590	0.530	0.204	0.072-0.576	0.003

β : partial regression coefficient; SE: standard error of partial regression coefficient; OR: odds ratio; CI: confidence interval.

Abnormal liver function in patients with fatty liver

Using χ^2 test, the abnormal frequencies of ALT, AST/ALT and GGT showed significant differences between the patients with and without fatty liver (Table 3).

Comparison of serum biochemical features between alcoholic fatty liver (AFL) group and nonalcoholic fatty liver (NAFL) group

The abnormal frequencies of serum TG, CHOL, LDL-C and ApoB were higher in NAFL group than those in AFL group. The proportion of HDL-C \leq 1.0, AST \geq 40 and AST/ALT \geq 2 were higher in patients with AFL than with NAFL (Table 4).

Table 3 Abnormal liver function in the patients with fatty liver and non-fatty liver (%)

Liver function	Fatty liver group (n=413)	Non-fatty liver group (n=200)
AST (\geq 40 U)	85(20.6)	38(19.0)
(40-80 U)	65(15.7)	26(13.0)
(\geq 80 U)	20(4.8)	12(6.0)
ALT (\geq 40 U)	129(31.2) ^a	37(18.5)
(40-80 U)	84(20.3) ^a	26(13.0)
(\geq 80 U)	45(10.9) ^a	11(5.5)
AST/ALT (<1)	161(39.0) ^a	28(14.0)
(\geq 2)	23(5.6) ^a	54(27.0)
ALB (\leq 35 g/L)	16(3.9)	15(7.5)
GLB (\geq 30 g/L)	42(10.2)	29(14.5)
A/G (\leq 1.5)	84(20.3)	47(23.5)
GGT (\geq 50 U/L)	145(35.1) ^a	46(23.0)
TBIL (\geq 17.1 μ mol/L)	75(18.2)	39(19.5)

^a*P*<0.05, vs Non-fatty liver group.

Table 4 Comparison of laboratory abnormalities among AFL, NAFL and control groups (%)

Biochemical Index	AFL group (n=28)	NAFL group (n=301)	Control group (n=163)
TG (\geq 1.7 mmol/L)	2(7.1) ^a	169(56.2) ^c	27(17.7)
CHOL (\geq 5.2 mmol/L)	2(7.1) ^a	148(49.2) ^c	35(22.9)
HDL-C (\leq 1.0 mmol/L)	9(32.1) ^a	35(11.6)	27(17.7)
LDL-C (\geq 2.6 mmol/L)	12(42.9) ^a	214(71.1)	97(63.4)
Apo AI (\leq 1.2 mmol/L)	13(46.4)	118(39.2)	45(29.4)
Apo B (\geq 1.1 mmol/L)	4(14.3) ^{ac}	149(49.5) ^e	53(34.6)
UA (\geq 452 mg/dL)	5(17.9)	89(29.6) ^e	18(11.8)
AST (\geq 40 U)	12(42.9) ^{ac}	51(16.9)	24(15.7)
ALT (\geq 40 U)	10(35.7) ^c	87(28.9) ^e	26(17.0)
AST/ALT (<1)	11(39.3) ^c	168(55.8) ^e	31(20.3)
(\geq 2)	5(17.9) ^a	15(5.0) ^e	40(26.1)
ALB (\leq 35 g/L)	3(10.7)	9(3.0)	7(4.6)
GLB (\geq 30 g/L)	3(10.7)	32(10.6)	20(13.1)
A/G (\leq 1.5)	7(25.0)	64(21.3)	31(20.3)
GGT (\geq 50 U/L)	10(35.7)	95(31.6) ^e	30(19.6)
TBIL (\geq 17.1 μ mol/L)	6(21.4)	50(16.6)	30(19.6)

^a*P*<0.05, vs NAFL group; ^c*P*<0.05, vs control group; ^e*P*<0.05, vs control group.

DISCUSSION

In recent years, the prevalence of fatty liver is constantly increasing along with the improvement of life-style, the change of dietetic structure, the aged population and the application of new diagnostic technique. The incidence of fatty liver in 3432 Japanese adults thorough medical examination was 21.8%^[2]. In China, fatty liver affected 10.2% of cadres in Nanjing^[8] with 11.4% of male and 6.8% of female. There were no data to show the prevalence of fatty liver in the southern China. Because of distinct life-style and climate feature in Guangzhou, the pattern

of fatty liver could be different from other area. Among 413 patients with fatty liver, the gender ratio (M/F) was 1.02:1. The age ranged widely. The median age was 57 years.

Fatty liver may be an independent disease, but more generally, it is a lesion of the liver in certain systemic diseases. Fatty liver may be caused by many diseases and risk factors, and can progress from mild steatohepatitis to severe fibrosis and cirrhosis^[9]. The etiological prevention is very important because of the lack of effective therapy. Although the etiology of hepatic steatosis is explored extensively, the complicated and multi-factor pathogenesis make it remain poorly understood. The possible related risk factors include: alcohol abuse, diabetes mellitus, obesity, hyperlipidemia, drugs and toxins, hepatitis virus infection (especially HCV), rapid weight loss, jejunio-ileal bypass surgery, total parenteral nutrition, pregnancy and so on^[10-16].

413 patients with fatty liver were diagnosed mainly according to the history, clinical manifestations, laboratory and ultrasound examination. Liver biopsy was the best method of diagnosing fatty liver. But it was difficult to carry out in large sample of populations. This was the possible limitations of the study.

Our data from 413 patients with fatty liver showed that obesity, alcohol abuse, type 2 diabetes mellitus, hyperlipidemia and elevation of fasting plasma were independent risk factors confirmed by a multivariate logistic analysis. These correlations were similar to the researches at home and abroad^[3,4]. It suggested that the pathogenesis of fatty liver in southern China might have a similar pattern to other area in China and abroad.

Obesity was easily accompanied with fatty liver^[17]. The percentage of the obese patients with fatty liver (59.1%) was significantly higher than controls (8.5%). Obesity is a very common phenomenon in the developed countries. 60-100% patients of non-alcoholic steatohepatitis (NASH) were proved to have obesity^[18]. This situation was also found in developing country, especially in China. According to the data in 11 provinces/autonomous regions/municipalities of China from July 1995 to July 1997, the prevalence rate of overweight and obesity among 42 751 Chinese adults aged 20-74 years were 21.51% and 2.92% respectively^[19]. There were about 200-300 million of overweight and 30-40 million of obese populations in China. With the odds ratio of 21.204, obesity was a predictor of fatty liver. The practice of prevention for overweight and obesity was very important for control of fatty liver.

Alcohol liver disease was the major medical complications of alcohol abuse. Alcohol abuse was one of the major causes of fatty liver and cirrhosis in the Western countries. At least 80% of heavy drinkers developed fatty liver, 10-35% of alcoholic hepatitis, and approximately 10% cirrhosis^[20]. Alcohol drinkers were not as common in southern China as in northern China^[19]. Based on our data, there were only 12.4% patients with alcohol abuse and 6.8% of them with alcoholic fatty liver among 413 patients with fatty liver according to diagnostic standard of China in 2002. But, the proportion of alcoholic abuse was still higher in patients with fatty liver than those without fatty liver. Alcoholic abuse contributed to a risk factor of fatty liver.

Type 2 diabetes mellitus usually accompanied insulin resistance^[12,21]. Both peripheral and hepatic insulin resistance were present in almost all patients with nonalcoholic fatty liver disease, irrespective of the coexistence of related risk factors^[21]. Above findings, together with the associated hyperlipidemia, obesity, hypertension and hyperuricemia, were considered as the manifestations of the metabolic syndrome that was associated with insulin resistance^[22,23]. In this study, either type 2 diabetes or elevation of fasting plasma glucose was related to fatty liver. It suggested that insulin resistance might be a risk factor of fatty liver.

The role of serum lipids in fatty liver remained controversial^[16,24]. Some researches showed that the effects of hyperlipidemia on fatty liver were complicated and difficult to be disassociated with obesity and type 2 diabetes mellitus. Among the 413 patients with fatty liver, the total incidence of hyperlipidemia was 66.8%, which consisted of 22.3% of hypertriglyceridemia, 15.5% of hypercholesterolemia and 29.1% of mixed hyperlipidemia. TG and LDL-C were independent risk factors and ApoB was a protective factor confirmed by multivariate logistic analysis. TG and LDL-C stimulated the proliferation and collagen synthesis of hepatic stellate (HSC) and increased deposition of extracellular matrix (ECM) in the liver by means of lipid peroxidation^[25,26]. This process was relative to hepatic fibrosis and effected prognosis of patients with fatty liver.

The correlation between hepatitis virus infection (especially HCV) and hepatic steatosis was found^[27]. Although the incidence of chronic HBV and HCV infection in China remained the highest proportion in the world, there was no significant difference in the incidence of HBV or HCV infection between patients with and without fatty liver. The infection of HBV and HCV was excluded from the model of multivariate stepwise logistic regression.

The clinical and laboratory features varied greatly with different causes and degree of hepatic steatosis in patients with fatty liver^[28]. The elevation of serum TG, CHOL and LDL-C was more common in patients with NAFL than those with AFL. Most patients with fatty liver had no obvious symptoms and signs of liver disease at the time of diagnosis. But a higher proportion of patients with cryptogenic cirrhosis shared many of the clinical and demographic features of patients with fatty liver. NASH played an under-recognized role in many patients with cryptogenic cirrhosis^[29]. Mild elevation usually less than 2 folds of the normal limit of serum ALT and GGT was showed in this investigation. The mitochondria was the most likely source of the reactive oxygen species (ROS) leading to lipid peroxidation in patients with fatty liver^[30]. AST, a mitochondrial enzyme, was more easily affected by ethanol^[31]. Among the abnormal hepatic functions, the higher AST levels with AST/ALT more than 2 were found in those with AFL. The increases of serum lipids and AST/ALT ratio might be useful in differentiating NAFL from AFL.

ACKNOWLEDGMENTS

We greatly thank Dr. Jie Yan from the Department of Medical Statistics of Sun Yat-Sen University for statistical analysis.

REFERENCES

- 1 **Angulo P.** Nonalcoholic fatty liver disease. *N Engl J Med* 2002; **346**: 1221-1231
- 2 **Omagari K,** Kadokawa Y, Masuda J, Egawa I, Sawa T, Hazama H, Ohba K, Isomoto H, Mizuta Y, Hayashida K, Murase K, Kadota T, Murata I, Kohno S. Fatty liver in non-alcoholic non-overweight Japanese adults: incidence and clinical characteristics. *J Gastroenterol Hepatol* 2002; **17**: 1098-1105
- 3 **Angulo P,** Lindor KD. Non-alcoholic fatty liver disease. *J Gastroenterol Hepatol* 2002; **17**: S187-190
- 4 **Fan JG.** Studies on fatty liver in China. *Shijie Huaren Xiaohua Zazhi* 2001; **9**: 6-10
- 5 **Sherlock S,** Dooley J. Diseases of the liver and biliary system. 10ed. Oxford: *Blackwell Sci Pub* 1997: 427-433
- 6 **Fatty Liver and Alcoholic Liver Disease Study Group of Chinese Liver Disease Association.** Diagnostic criteria of nonalcoholic fatty liver disease. *Zhonghua Ganzhangbing Zazhi* 2003; **11**: 71
- 7 **Fatty Liver and Alcoholic Liver Disease Study Group of Chinese Liver Disease Association.** Diagnostic criteria of alcoholic fatty liver disease. *Zhonghua Ganzhangbing Zazhi* 2003; **11**: 72
- 8 **Wang H,** Chen J. Epidemiological studies of fatty livers. *Xin*

- Xiaohuabingxue Zazhi* 1997; **5**: 100-101
- 9 **Bacon BR**, Farahvash MJ, Janney CG, Neuschwander-Tetri BA. Nonalcoholic steatohepatitis: An expanded clinical entity. *Gastroenterology* 1994; **107**: 1103-1109
- 10 **James O**, Day C. Non-alcoholic steatohepatitis: another disease of affluence. *Lancet* 1999; **353**: 1634-1636
- 11 **Pares A**, Tresserras R, Nurez L, Cerralbo M, Plana P, Pujol FJ, Massip J, Caballeria L, Bru C, Caballeria J, Vidal J, Salleras L, Rodes J. Prevalence and factors associated to the presence of fatty liver in apparently healthy adult men. *Med Clin* 2000; **114**: 561-565
- 12 **Marchesini G**, Brizi M, Morselli-Labate AM, Bianchi G, Bugianesi E, McCullough AJ, Forlani G, Melchionda N. Association of non-alcoholic fatty liver disease with insulin resistance. *Am J Med* 1999; **107**: 450-455
- 13 **Falchuk KR**, Fiske SC, Haggitt RC, Federman M, Trey C. Pericentral hepatic fibrosis and intracellular hyaline in diabetes mellitus. *Gastroenterology* 1980; **78**: 535-541
- 14 **Rinella ME**, Alonso E, Rao S, Whittington P, Fryer J, Abecassis M, Superina R, Flamm SL, Blei AT. Body mass index as a predictor of hepatic steatosis in living liver donors. *Liver Transpl* 2001; **7**: 409-414
- 15 **Powell EE**, Cooksley WG, Hanson R, Searle J, Halliday JW, Powell LW. The natural history of nonalcoholic steatohepatitis: a follow-up study of forty-two patients for up to 21 years. *Hepatology* 1990; **11**: 74-80
- 16 **Assy N**, Kaita K, Mymin D, Levy C, Rosser B, Minuk G. Fatty infiltration of liver in hyperlipidemic patients. *Dig Dis Sci* 2000; **45**: 1929-1934
- 17 **Gray DS**. Diagnosis and prevalence of obesity. *Med Clin North Am* 1989; **73**: 1-13
- 18 **Sheth SG**, Gordon FD, Chopra S. Nonalcoholic steatohepatitis. *Ann Intern Med* 1997; **126**: 137-145
- 19 **Wang WJ**, Wang KA, Li TL, Xiang HD, Ma LM, Fu ZY, Chen JS, Liu ZY, Bai J, Fong JG, Jin SX, Li YQ, Qing NL, Chen H. A study on the epidemiological characteristics of obesity in Chinese Adults. *Zhonghua Liuxingbingxue Zazhi* 2001; **22**: 129-132
- 20 **Walsh K**, Alexander G. Alcoholic liver disease. *Postgrad Med J* 2000; **76**: 280-286
- 21 **Marceau P**, Biron S, Hould FS, Marceau S, Simard S, Thung SN, Kral JG. Liver pathology and the metabolic syndrome X in severe obesity. *J Clin Endocrinol Metab* 1999; **84**: 1513-1517
- 22 **Marchesini G**, Brizi M, Bianchi G, Tomassetti S, Bugianesi E, Lenzi M, McCullough AJ, Natale S, Forlani G, Melchionda N. Nonalcoholic fatty liver disease: a feature of the metabolic syndrome. *Diabetes* 2001; **50**: 1844-1850
- 23 **Luyckx FH**, Lefebvre PJ, Scheen AJ. Non-alcoholic steatohepatitis: association with obesity and insulin resistance, and influence of weight loss. *Diabetes Metab* 2000; **26**: 98-106
- 24 **Neuschwander-Tetri BA**, Bacon BR. Nonalcoholic steatohepatitis. *Med Clin North Am* 1996; **80**: 1147-1166
- 25 **Lu LG**, Zeng MD, Li JQ, Hua J, Fan JG, Fan ZP, Oiu DK. Effect of lipid on proliferation and activation of rat hepatic stellate cells (I). *World J Gastroenterol* 1998; **4**: 497-499
- 26 **Lu LG**, Zeng MD, Li JQ, Hua J, Fan JG, Oiu DK. Study on the role of free fatty acids in proliferation of rat hepatic stellate cells (II). *World J Gastroenterol* 1998; **4**: 500-502
- 27 **Rubbia-Brandt L**, Leandro G, Spahr L, Giostra E, Quadri R, Male PJ, Negro F. Liver steatosis in chronic hepatitis C: a morphological sign suggesting infection with HCV genotype 3. *Histopathology* 2001; **39**: 119-124
- 28 **Itoh S**, Yougel T, Kawagoe K. Comparison between nonalcoholic steatohepatitis and alcoholic hepatitis. *Am J Gastroenterol* 1987; **82**: 650-654
- 29 **Caldwell SH**, Oelsner DH, Iezzoni JC, Hespenheide EE, Battle EH, Driscoll CJ. Cryptogenic cirrhosis: clinical characterization and risk factors for underlying disease. *Hepatology* 1999; **29**: 664-669
- 30 **Day CP**. Non-alcoholic steatohepatitis (NASH): where are we now and where are we going? *Gut* 2002; **50**: 585-588
- 31 **French SW**. Mechanisms of alcoholic liver injury. *Can J Gastroenterol* 2000; **14**: 327-332

Disseminated tumor cells homing into rats' liver: A new possible mechanism of HCC recurrence

Qi-Gen Li, Guang-Shun Yang, Qing Yang, Li-Xin Wei, Ning Yang, Xue-Ping Zhou, Feng-Qi Jia

Qi-Gen Li, Guang-Shun Yang, Qing Yang, Li-Xin Wei, Ning Yang, Xue-Ping Zhou, Feng-Qi Jia, Eastern Hepatobiliary Surgery Hospital, Second Military Medical University, Shanghai 200438, China
Supported by the National Natural Science Foundation of China, No. 39870752

Correspondence to: Dr. Guang-Shun Yang, Eastern Hepatobiliary Surgery Hospital, Second Military Medical University, Shanghai 200438, China. guangshun@smmu.edu.cn

Telephone: +86-21-25070803

Received: 2003-03-02 **Accepted:** 2003-05-21

Abstract

AIM: To detect the origin of hepatocellular carcinoma (HCC) recurring and attempt to propose a new recurrent mechanism.

METHODS: Orthotopic liver allotransplantation was performed on male rats with HCC- induced by diethylnitrosamine using female donors. Metastatic tumors in transplanted livers were obtained. A DNA probe that exhibits specificity for the rat Y chromosome was generated by using a set of primers specific to murine *sry* gene. *In situ* hybridization (ISH) for Y chromosome was used to detect the origin of HCC recurring. Male HCC tissue was designed to be positive control. ISH on female tissue and using non-labeled with DIG probe was thought to be negative control.

RESULTS: Positive marks were seen through ISH for Y chromosome in recurrent tumor tissue and positive control. No signal was detected in both negative controls.

CONCLUSION: Recurrent HCC after liver transplantation originated from disseminated tumor cells in recipients. Extrahepatic cells homing into liver may be a new HCC recurrence mechanism. Likewise, it implicates that this mechanism is responsible for HCC recurring after hepatectomy.

Li QG, Yang GS, Yang Q, Wei LX, Yang N, Zhou XP, Jia FQ. Disseminated tumor cells homing into rats' liver: A new possible mechanism of HCC recurrence. *World J Gastroenterol* 2004; 10(6): 903-905

<http://www.wjgnet.com/1007-9327/10/903.asp>

INTRODUCTION

The poor outcomes of patients with hepatocellular carcinoma (HCC) are mainly resulted from high postoperative recurrence rate with 65% after radical resection versus 58% after liver transplantation^[1,2]. Over the past decades, many investigations using clinicopathological and molecular biological methods have showed that there existed two HCC recurrent mechanisms of intrahepatic metastasis (IM) and multicentric occurrence (MO)^[3-5]. However, the both mechanisms are very reluctant to elucidate the HCC recurrence following liver transplantation in rigidly selected patients. Therefore, we refer a hypothesis that recurrent HCC in transplanted liver is likely to originate from extrahepatic tumor cells in recipient if de novo

carcinogenesis is excluded. Likewise, disseminated tumor cells possibly go back to remnant liver after hepatectomy.

We have established an animal model of liver transplantation for HCC in rats. Male rat liver with HCC induced by diethylnitrosamine (DENa) was replaced by allograft from normal syngenic female animal. Recurrent tumors from male recipient of female liver were analyzed using *in situ* hybridization (ISH) for the Y chromosome to indicate cells origins. On the basis of our investigation and other supportive literatures, we make an attempt to propose a new possible mechanism of HCC recurrence.

MATERIALS AND METHODS

Orthotopic liver transplantation (OLT) for HCC-induced in gender discordant rats

Ninety-eight inbred seven-week-old male SD rats, weight ranged from 100 g to 120 g, were purchased from PEAK Company in Shanghai with the approval of Shanghai Animal Committee. HCC was induced by oral administration of 100 ppm DENa (Sigma Company, USA) water solution. OLT for HCC was performed according to Kamada cuff techniques^[6] on male rats with HCC and donor livers were from normal syngenic female SD rats with weight ranged from 250 g to 300 g. No immunosuppressant was postoperatively administered. Explanted livers were examined pathologically. The recurrent tumors in the transplants may be explored through laparotomy before the recipients' death. Harvested specimens were preserved at -70 °C.

Using ISH to detect the Y chromosomes in recurrent HCC cells^[7,8]

Male rat genomic DNA was purified from 300 µL blood sample using Wizard Genomic DNA Purification Kit (Promega). *sry* gene specific primer, of which the sequences are 5' -CAGAGATCAGCAAGCAGCTG-3' and 5' -TGCAGCTCTACTCCAGTCTTG-3', was synthesized by Shengong Biochemical Incorporation in Shanghai. 0.1 µg of the genomic DNA as template, *sry* gene was amplified by PCR. The reaction was comprised of 35 cycles of 5 min at 94 °C, 0.5 min at 60 °C, 1 min at 72 °C. PCR products were analyzed on 15 g/L agarose gel and then purified with QIAquick Gel Extraction Kit (Qiagen). Target gene was labeled according to the instruction of DIG High Prime DNA Labeling and Detection Starter Kit II (Roche).

Male SD rat HCC tissue confirmed by pathology was designed to be positive control. ISH on female SD rat liver tissue and using non-labeled with DIG probe was thought to be negative control. ISH efficacy would be verified by the both controls.

Frozen tissue sections (5 µm in thickness) were fixed on the slides treated by 40g/L polyformaldehyde. Slides were washed in PBS (PH7.4) for 5 min (2 times), 3g/L Triton X-100/PBS for 10 min, and PBS (PH7.4) for 5 min (2 times). Tissue was digested with pepsin 2 µg/mL for 15 min at 37 °C, and then washed in PBS for 5 min and rinsed in 4×sodium saline citrate (SSC) for 2 min at room temperature. Slides were

denatured with 50% formamide in 2×SSC for 15 min at room temperature, then dehydrated and air dried. Probe for Y chromosome (10 ng/μL) was denatured for 5 min at 75 °C, added to the denatured tissue, coverslipped and incubated in a humid chamber overnight at 42 °C. Slides were then washed in 2×SSC for 10 min (2 times), 1×SSC for 10 for min (2 times), 0.1×SSC 10 for min (3 times), and in buffer1 (Tris-HCl, PH7.5, 100 mmol/L; NaCl 150 mmol/L) for 5 min. Anti-DiG-Ap (1:500 dilution) was added to tissues and incubated for 2 h at 43 °C. Slides were washed in buffer1 for 5 min (2 times) and buffer 2 (Tris-HCl, PH9.5, 100 mmol/L; NaCl 100 mmol/L, MgCl₂ 50 mmol/L) for 10 min. And then slides were transferred to NBT/BCIP solution to be stained for more than 2 h, and rinsed with distilled water. Tissue sections were mounted and evaluated by light microscopy.

RESULTS

HCC recurrence was found in 6 transplants from 98 transplanted rats. Of them, 3 grafts were discarded because the recipients have been dead when laparotomy. Thirteen lesions were obtained in other three available transplants, confirmed to HCC by pathological examination. These specimens were preserved at -70 °C as a bank for further utilization.

HCC cells carrying a positive reaction product (blue staining) were seen in control male rats. No signal was detected in the controls of female liver and system using non-labeled probe. Control trials showed that the *sry* gene specific probe was efficient.

Positive staining was seen in frozen sections of the 3 recurrent transplants. Typically, the probe was successfully hybridized with target gene on tumor cells, whereas failed to on para-tumor tissues. The capsule, aimed at by arrow, definitely parts the recurrent tumor from the recipient liver parenchyma under 10×10 magnification (Figure 1).

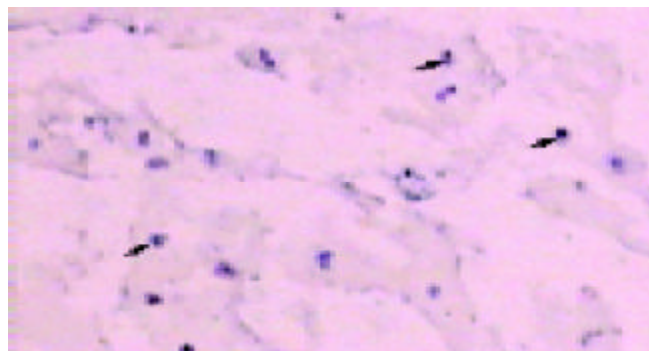


Figure 1 The blue blots under the purple background indicated Y chromosomes in these nuclei of recurrent tumor cells with 10×10 magnification microscope. The capsule definitely parted the recurrent tumor tissue from the recipient liver parenchyma. No positive signals were found out in the para-tumor tissue.

DISCUSSION

Liver transplantation for HCC in rats provides an excellent animal model to carcinogenesis investigation^[9]. Intrahepatic tumors and underlying lesions are removed completely, and then some interventional trials could be executed etiologically. In our experiments, no immunosuppressants were administered because rejective reaction was weak in allotransplantation on syngenic SD rats. The promotion of immunosuppressants to tumor growth can be excluded. However, it remains indefinite that induction of HCC existed in recipients after the withdrawal of DENA^[10]. There were two possible mechanisms of tumor recurring with the inclusion of disseminated tumor cells homing

into implanted liver and sequential contribution of DENA. Therefore, a marker is a key to discriminate between the two possibilities.

Cellular markers have been obtained through varieties of strategies such as transgenic animal, retroviral transduction. But these strategies are very complicated and low efficient. Discordant gender transplants offer the benefit of having 100% of the cells marked, as opposed to retroviral transduction, where at best only 5-10% of the cells are marked^[11]. In our experience, Y chromosome, uniquely existed in male cell, was initially acted as a marker with which male and female tissues were differentiated. Y chromosome-specific probe was successfully hybridized with *sry* gene of which multiple copies facilitated this hybridization^[7]. This *in situ* hybridization system was proved to be reliable by positive and negative control we designed. Our results therefore indicated that the origin of recurrent HCC in female liver was from disseminated tumor cells in male recipient. We personally define this phenomenon that extrahepatic tumor cells go back to liver as "homing".

Other studies could support the homing hypothesis we proposed. (1). Alpha-fetoprotein (AFP) messenger RNA (mRNA) has been proposed as a marker of HCC cells disseminated into the circulation. Multiple molecular methods, such as nested and semi-quantitative retro-transcription polymerase chains reaction (RT-PCR), have been utilized to detect AFP mRNA in order to confirm the presence of hematogenous HCC cells. This marker expression in peripheral blood of patients with HCC indicates the existence of tumor cells, although it remains controversial that AFP mRNA is taken as an evidence of HCC recurrence^[12-14]. (2). The homing of both lymphocytes and malignant hematic cells has been acknowledged^[15,16]. Involved adhesion molecules that mediate their migration also contribute to invasiveness of liver cancer^[16]. (3). Metastasis is the result of multiple sequential steps and is a highly organized, nonrandom, and organ-selective process^[17]. A group of biological molecules is collectively responsible for determining whether tumor cells can progress from a single malignant cell to a metastatic disease^[17]. But metastatic cells eventually colonize a particular organ that provides an optimal microenvironment^[18,19]. It therefore is warranted that transplanted liver or regenerating liver after resection may be a particularly fertile ground for extrahepatic HCC cells to proliferate.

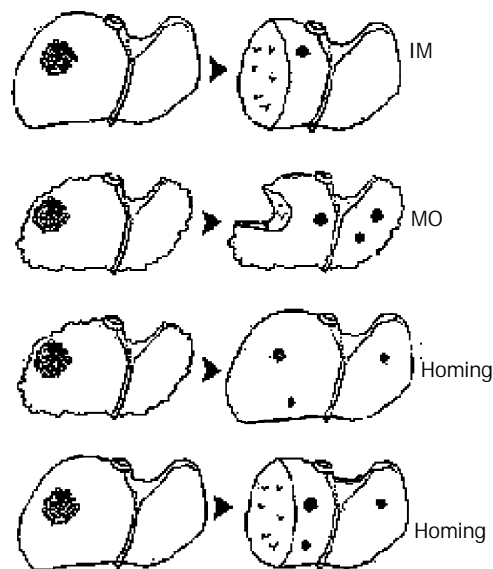


Figure 2 It is acknowledged that there exist two HCC recurring mechanisms of intrahepatic metastasis through portal venous system and multicentric occurrence from cirrhotic nodules. These extrahepatic cells homing into liver may be a

new mechanism after liver transplantation. Likewise, it implicates that this mechanism is responsible for HCC recurrence after hepatectomy.

On the basis of this experiment, we concluded that recurrent HCC after liver transplantation originated from the disseminated tumor cells. These extrahepatic cells homing into liver may be a new HCC recurrence mechanism. Likewise, it implicates that this new mechanism is responsible for HCC recurrence after hepatectomy besides MO and IM (Figure 2). But our experiment, to some extent, was to describe a homing phenomenon. Its real mechanism needs to be further investigated by molecular biology.

REFERENCES

- Schlitt HJ**, Neipp M, Weimann A, Oldhafer KJ, Schmoll E, Boeker K, Nashan B, Kubicka S, Maschek H, Tusch G, Raab R, Ringe B, Manns MP, Pichlmayr R. Survival and recurrence after hepatic resection of 386 consecutive patients with hepatocellular carcinoma. *J Am Coll Surg* 2000; **191**: 381-388
- Schlitt HJ**, Neipp M, Weimann A. Recurrence patterns of hepatocellular and fibrolamellar carcinoma after liver transplantation. *J Clin Oncol* 1999; **17**: 324-331
- Nakashima O**, Kojiro M. Recurrence of hepatocellular carcinoma: multicentric occurrence or intrahepatic metastasis? A viewpoint in terms of pathology. *J Hepatobiliary Pancreat Surg* 2001; **8**: 404-409
- Poon RT**, Fan ST, Ng IO, Lo CM, Liu CL, Wong J. Different risk factors and prognosis for early and late intrahepatic recurrence after resection of hepatocellular carcinoma. *Cancer* 2000; **89**: 500-507
- Kumada T**, Nakano S, Takeda I, Sugiyama K, Osada T, Kiriyama S, Sone Y, Toyoda H, Shimada S, Takahashi M, Sassa T. Patterns of recurrence after initial treatment in patients with small hepatocellular carcinoma. *Hepatology* 1997; **25**: 87-92
- Goto S**, Kamada N, Delriviere L, Kobayashi E, Lord R, Ware F, Hara Y, Edwards-Smith C, Shimizu Y, Vari F. Orthotopic liver retransplantation in rats. *Microsurgery* 1995; **16**: 167-170
- An J**, Beauchemin N, Albanese J, Abney TO, Sullivan AK. Use of a rat cDNA probe specific for the Y chromosome to detect male-derived cells. *J Androl* 1997; **18**: 289-293
- Theise ND**, Nimmakayalu M, Gardner R, Illei PB, Morgan G, Teperman L, Henegariu O, Krause DS. Liver from bone marrow in humans. *Hepatology* 2000; **32**: 11-15
- Schotman SN**, Schraa EO, Marquet RL, Zondervan PE, Ijzermans JN. Hepatocellular carcinoma and liver transplantation: an animal model. *Transpl Int* 1998; **11**: 201-205
- Curtis C**, Terry W, Pamela D. Diethylnitrosamine-induced hepatocarcinogenesis in rats: a theoretical study. *Toxicol Appl Pharmacol* 1991; **109**: 289-304
- Eckert JW**, Buerkle CJ, Major AM, Finegold MJ, Brandt ML. *In situ* hybridization utilizing a Y chromosome DNA probe. *Transplantation* 1995; **59**: 109-111
- Gross-Goupil M**, Saffroy R, Azoulay D, Precetti S, Emile JF, Delvart V, Tindiliere F, Laurent A, Bellin MF, Bismuth H, Debuire B, Lemoine A. Real-time quantification of AFP mRNA to assess hematogenous dissemination after transarterial chemoembolization of hepatocellular carcinoma. *Ann Surg* 2003; **238**: 241-248
- Ijichi M**, Takayama T, Matsumura M, Shiratori Y, Omata M, Makuuchi M. alpha-Fetoprotein mRNA in the circulation as a predictor of postsurgical recurrence of hepatocellular carcinoma: a prospective study. *Hepatology* 2002; **35**: 853-860
- Wong IH**, Yeo W, Leung T, Lau WY, Johnson PJ. Hematogenous dissemination of hepatocytes and tumor cells after surgical resection of hepatocellular carcinoma: a quantitative analysis. *Clin Cancer Res* 1999; **5**: 4021-4027
- Wiedle G**, Dunon D, Imhof BA. Current concepts in lymphocyte homing and recirculation. *Crit Rev Clin Lab Sci* 2001; **38**: 1-31
- Aziz KA**, Till KJ, Zuzel M, Cawley JC. Involvement of CD44-hyaluronan interaction in malignant cell homing and fibronectin synthesis in hairy cell leukemia. *Blood* 2000; **96**: 3161-3167
- Sun JJ**, Zhou XD, Liu YK, Tang ZY, Feng JX, Zhou G, Xue Q, Chen J. Invasion and metastasis of liver cancer: expression of intercellular adhesion molecule 1. *J Cancer Res Clin Oncol* 1999; **125**: 28-34
- Ji XN**, Ye SL, Li Y, Tian B, Chen J, Gao DM, Chen J, Bao WH, Liu YK, Tang ZY. Contributions of lung tissue extracts to invasion and migration of human hepatocellular carcinoma cells with various metastatic potentials. *J Cancer Res Clin Oncol* 2003; **129**: 556-564
- Fidler IJ**. Seed and soil revisited: contribution of the organ microenvironment to cancer metastasis. *Surg Oncol Clin N Am* 2001; **10**: 257-269

Edited by Ma JY and Xu FM

Risk factors influencing recurrence following resection of pancreatic head cancer

De-Qing Mu, Shu-You Peng, Guo-Feng Wang

De-Qing Mu, Shu-You Peng, Department of Surgery, the Second Affiliated Hospital, Medical College of Zhejiang University, Hangzhou 310009, Zhejiang Province, China

Guo-Feng Wang, Department of Pathology, the Second Affiliated Hospital, Medical College of Zhejiang University, Hangzhou 310009, Zhejiang Province, China

Correspondence to: Dr De-Qing Mu, Department of Surgery, the Second Affiliated Hospital, Medical College of Zhejiang University, Hangzhou 310009 Zhejiang Province, China. samier-1969@163.com

Telephone: +86-571-87783762

Received: 2003-06-10 **Accepted:** 2003-09-01

Abstract

AIM: Whether operative procedure is a risk factor influencing recurrence following resection of carcinoma in the head of pancreas or not remains controversies. In this text we compared the recurrence rate of two operative procedure: the Whipple procedure and extended radical operation, and inquired into the factors influencing recurrence after radical resection.

METHODS: From January 1995 to December 1998, 35 cases of carcinoma of pancreas underwent the Whipple operadure, 21 patients received the Extended radical operation. All patients were followed up for more than 3 years. Prognostic factors included operative procedure, size of tumor, lymph node, interstitial invasion.

RESULTS: Deaths duo to recurrence within 3 years after operation were studied. The death rate was 51.4% in the Whipple procedure and 42.9% in the Extended radical operative procedure. There was a significant difference between the two groups. Recurrence occurred in 75% patients with tumor large than 4 cm, in 87.5% patients with lymph node involvement, and in 50% patients with the presence of interstitial invasion.

CONCLUSION: Tumor exceeding 4 cm, lymph node involvement, and presence of interstitial invasion are high risk factors of recurrence after Whipple's procedure and extended radical operation.

Mu DQ, Peng SY, Wang GF. Risk factors influencing recurrence following resection of pancreatic head cancer. *World J Gastroenterol* 2004; 10(6): 906-909
<http://www.wjgnet.com/1007-9327/10/906.asp>

INTRODUCTION

Recurrence of pancreatic cancer is common after operation. Intraabdominal recurrence ranged 38% to 86%^[1-3]. Factors influencing recurrence in some studies included lymph node metastasis^[4,5], tumor size^[5,6], and tumor in surgical resection^[5-7]. In the present study we retrospectively analysis 56 patients with carcinoma located in pancreatic head after operation in our department of surgery, The aim was to find the factors

influencing recurrence following surgical resection for patients with pancreatic cancer hoping to improve the therapeutic results of carcinoma in the head of pancreas.

MATERIALS AND METHODS

Materials

Fifty six curative surgical resections were performed for pancreatic cancer in our department of surgery between January 1995 and December 1998. The patients did not receive any anticancer therapy before or after surgery.

Methods

Our radical procedures employed for carcinoma of pancreas was the Whipple operation in 35 cases, male/female ratio was 2.2:1(24/11), patients with an average of age were (57.3±4.6) years. According to the General Rules for Cancer of the Pancreas (4th edition, 1996), lymphatic clearance was limited to the regional lymph nodes immediately adjacent to the pancreatic head (D1⁻). In the pancreas, the line of resection was on the left border of the superior mesenteric vein. Extended radical operation (D2⁺) was performed in the other 21 cases, the male/female ratio was 2.5:1(15/6) with an average of age 58.9±5.1 years (Figure 1A and B). On the basis of n1 and n2 group and neighboring connective tissue clearance, the n3 group lymph nodes and soft tissues were properly cleared, nerve-plexus dissection around the retroperitoneum in 13 cases. Resection and reconstruction of the portal -vein system were performed in 6 cases, the line of resection of the pancreas was 1-2 cm outside the left border of the aorta.

The resected specimens were fixed in 40g/L formaldehyde solution, and sliced into 5 μm sections. Histologic sections were stained with hematoxylin and eosin. We measure the maximum size of the tumor, metastasis in lymph nodes, and determined whether tumors extended directly beyond the posterior confines of the pancreas. The maximum tumor sizes were classified into four grades: 0<t1≤2 cm, 2.0<t2≤4.0 cm (t2), 4.0<t3≤6.0 cm, and t4>6.0 cm. The lymph node involvement were graded into n0, n1, n2, and n3 according to the General Rules for Pancreatic Cancer Study (4th edition, 1996) proposed by the Japanese Pancreatic Society. The primary group included N₀₆: infrapyloric, N₀₈: anterosuperior nodes along the common hepatic artery, N_{012inferior}: inferior nodes along the proper hepatic artery, along the bile duct, and along the posterior to the portal vein, N₀₁₃: posterior surface of the head of pancreas, N₀₁: origins of the superior mesenteric artery, the inferior pancreaticoduodenal artery, and the middle colic artery along the first jejunal branch, and the the superior mesenteric vein, N₀₁₇: on the anterior surface of the head of pancreas. The second group included (N2): N₀₉: around the celiac artery, N₀₁₁: along the splenic artery, N_{012superior}: superior nodes along the proper hepatic artery, the bile duct, superior to the portal vein, around the cystic duct, N₀₁₆: paraabdominal aorta. The third group (N3) included N₀₃: lessur curvature, N₀₄: greater curvature, N₀₅: suprapyloric, N₀₇: left gastric artery. Retroperitoneal invasion was classified into two grades Rp (+) and Rp(-) on the basis of whether the tumors extended directly beyond the posterior confines of the pancreas.

After surgery, all patients were followed up by serial determinations of plasma carcinoembryonic antigen (CEA), CA19-9, ultrasonograms and computed tomograms (CT) to determine whether and where cancer recurrence developed. The mode of clinical recurrence was classified into four types: hepatic metastasis (H), retroperitoneal recurrence (R), peritoneal dissemination (P), and distant metastasis (M). Retroperitoneal recurrence was divided into two subtypes: (1) local retroperitoneal recurrence was defined as infiltration of nerves, lymphatic vessels, and connective soft tissue, and (2) lymph node metastasis (LN).

The cumulative recurrence rate was analysed by using a χ^2 test. *P* value less than 0.05 was considered statistically significant.

RESULTS

No operative death occurred within 1 mo after excision. The follow-up period was more than 3 years for all patients of the two groups. In D1⁻ group, 6 cases were lost to be followed, 7 cases died of other diseases unrelated to cancer within three years, the remaining 22 patients died of recurrence, of which 18 patients was dead within 3 years. In D2⁺ group, 2 patients were lost to be followed, 3 patients died of other diseases within

3 years, the remaining 9 patients died of recurrence within 3 years. The 3 years cumulative rate of death duo to recurrence was 51.4% in D1⁻ group and 42.9% in D2⁺ group, there was a significant difference between the 2 groups (*P*<0.05). The histopathological backgrounds in patients who died of recurrence are showed in Table 1.

Recurrent styles

In D1⁻ group at least more than 2 recurrent sites could be found. Eighteen patients had retroperitoneal recurrence, among them 7 patients were complicated with peritoneal dissemination, 2 patients were complicated with liver metastasis, and 1 patient was complicated with extroabdomen metastasis. In D2⁺ group, the major recurrent styles of were as fellows: hepatic metastasis alone or in combination with retroperitoneal recurrence (*n*=5), peritoneal dissemination alone or combined with abdomen lymph node enlargement (*n*=4), or combined with other organ out of abdomen cavity metastasis (*n*=1).

Histopathological diagnosis

The distribution of cases was histopathologically (Figure 2) based on 3 factors: maximum tumor size, lymph node involvement, and interstitial invasion (Table 2).

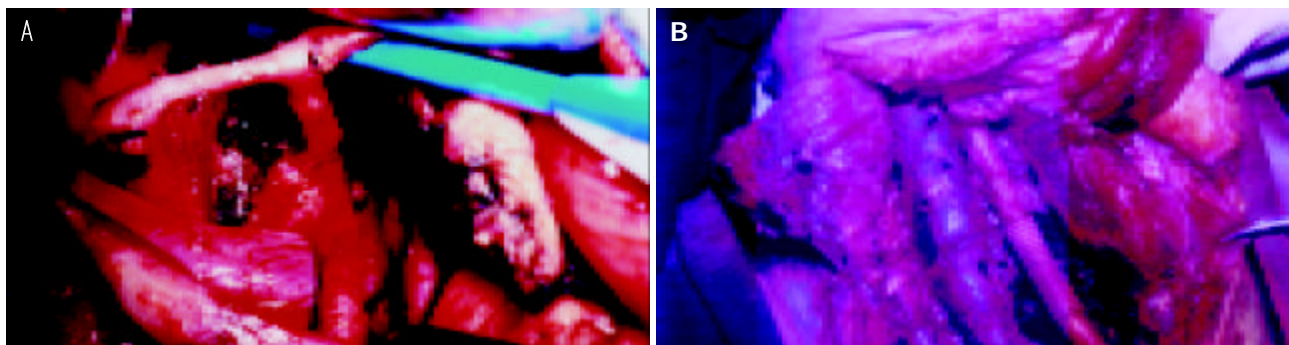


Figure 1 A: Ranges of lymphatic and neighboring connective tissue dissection n1, n2, and part of n3 group nodes were cleared with neighboring connective tissue, B: lymph node dissection around aorta, inferior vein, resection and reconstruction portal vein.

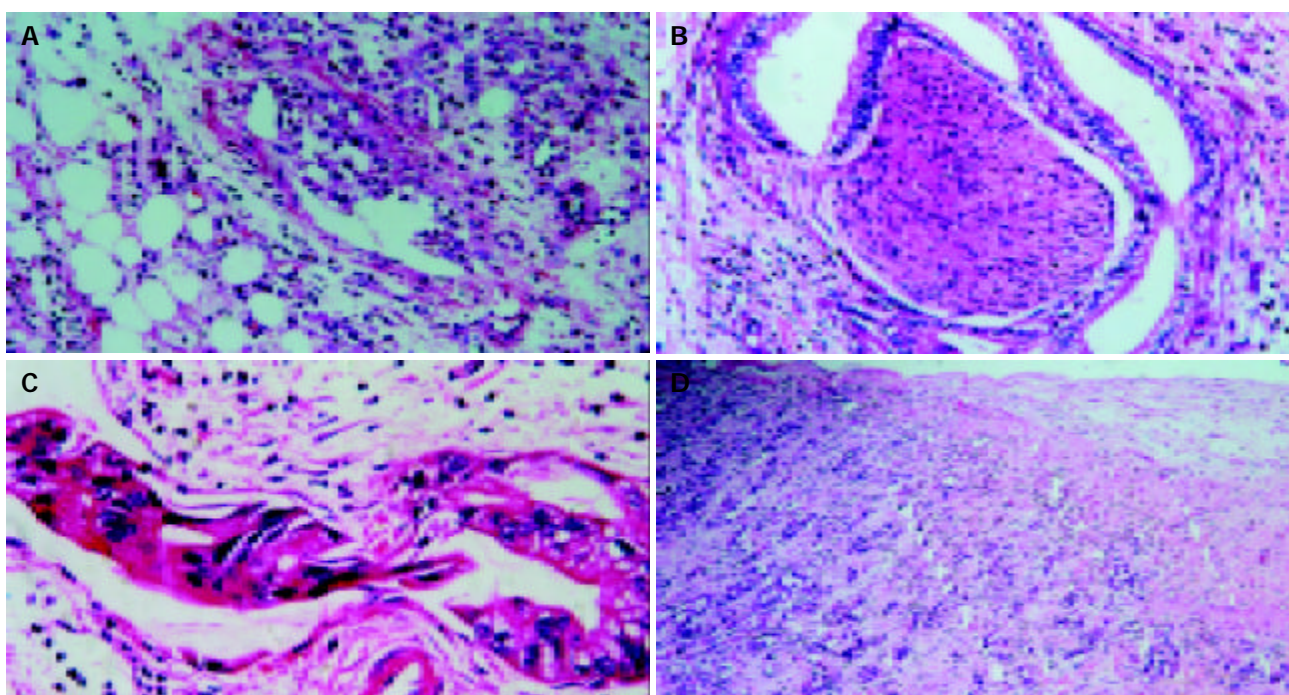


Figure 2 A: peritoneal dissemination, B: nerve invasion, C: cancer thrombus in lymphatic vessel, D: portal venous wall invasion. (HE original magnification $\times 200$).

Table 1 Histopathological findings in patients died of Recurrence

Operative procedure (No. of patients)	Maximum size				Nodal involvement				Interstitial invasion	
	t1	t2	t3	t4	n0	n1	n2	n3	Ii (-)	Ii (+)
D1-	1/5	7/16	10/14	-	3/9	15/26	-	-	6/13	12/22
D2+	0/4	3/9	3/5	3/3	0/6	2/7	4/5	3/3	1/5	8/16

Table 2 Comparison of tumor Size, nodal involvement and interstitial invasion between two groups

Operative procedure (No. of patients)	Maximum size				Nodal involvement				Interstitial invasion	
	t1	t2	t3	t4	n0	n1	n2	n3	Ii (-)	Ii (+)
D1-	5	16	14	-	9	26			13	22
D2+	4	9	5	3	6	7	5*	3**	2	19

*5 is positive also in n1, **3 is also positive in n1, and n2.

In D2⁺ group, tumors were less than 2 cm in diameter (4 cases), one case had lymph-node metastasis, and 2 lymph node vessels and perineural invasion respectively. In t2 group, 77.8% (7/9) of cases was associated with lymph-vessel invasion. Perineural invasion was present in 88.9% (8/9) of the tumor, and loose connective tissue invasion occurred in 55.6% (5/9). Tumors larger than 4.1 cm were all associated with lymph-vessel, perineural, and loose connective tissue invasion. Metastatic rate of lymph node was 69.2% (n=15). Lymph node metastatic rate was 69.2% (n=15). Rates of histologically proved metastasis to individual lymph nodes observed in our series were as follows: N1: N₀₆: 23.8% (n=5), N₀₈: 14.4% (n=3), N_{012inferior}: 33.3% (n=7), N₀₁₃: 33.3% (n=7), N₀₁₄: 28.6% (n=6), N₀₁₇: 33.3% (n=7); N2: N₀₉: 14.4% (n=3), N₀₁₁: 19.1% (n=4), N_{012superior}: 23.8% (n=5), N₀₁₆: 23.8% (n=5); N3: N₀₃: 0%, N₀₄: 0%, N₀₅: 14.4% (n=3), N₀₇: 13.3% (n=2). In tumors with negative lymph nodes, 5/6 had lymph-vessel invasion, and 4/6 had perineural invasion. The tumors with nodal involvement were all associated with lymph-vessel, perineural, and loose connective tissue invasion.

DISCUSSION

Argument existed about whether operative procedure on the risk factors influencing recurrence or not^[8-11]. Factors that influence the recurrent rate after resection were the absence of lymph node involvement^[12,13], and retroperitoneal invasion^[14], and microscopic curative resection^[12,14]. Such a procedure is also called Ro surgery. In our current study we confirmed that D2⁺ procedure could decrease recurrence in comparison with D1-. In D2⁺ group we found there exists wide extension of nodal involvement, and 'interstitial invasion' required careful dissection. D1- procedure only provided simple lymphadenectomy limited to the region of the head of pancreas without resection of surrounding connective tissues, and dissection of the second and tertiary group lymph node was inadequate for the purpose of lymphatic clearance. Theoretically D2⁺ procedure could achieve a microscopic curative resection^[15,16]. Macroscopic curative resection has been proven to be microscopic noncurative resection by precise serial section analysis. Even the patients with microscopic curative resection had a surgical margin of only a few millimeters away from tumor^[17], that could not assure avoidance of future metastasis. Only in those with small (t1/t2), noninvasive lesions or slight retroperitoneal invasion, could D2⁺ actually decrease recurrence. In those with t3/t4 tumors, even after extended lymphatic and soft tissue dissection that goes beyond the regional lymph-node stations, D2⁺ procedure still has a higher recurrence.

The rate of recurrence in patients with t1 and t2 tumors generally was lower than that in those with t3 and t4 tumors

after D2⁺ procedure. The collective recurrence rate in t3 and t4 tumors was 75% (6 of 8). Tumors larger than 4.1 cm were all associated with lymph-vessel and perineural invasions. Therefore, our conclusion is that the larger the tumor the more extensive infiltration within interstitial invasion and nodal involvement, or the higher the recurrent risk, this is in accord with that reported in the literature^[18-21].

In comparison with D1-, D2⁺ procedure decreased recurrence in n0 and n1 group. There was a close relation between lymph node involvement and 'interstitial invasion'. Positive lymph node was often accompanied by lymph vessels invasion. Even if in pNo stage, lymph vessels invasion was present in 64% of the cases^[19]. Lymph vessel invasion might imply lymphatic metastasis before cancer cells flowed into lymph nodes. If nodal involvement was found in n1 region, microinvasion had already occurred in the n2 region^[22]. If n2 and n3 groups were invaded, the chance of distant recurrence was much increased.

Our study confirmed that pancreatic cancer tended to be accompanied by 'interstitial invasion' and positive of 'interstitial invasion' was a factor influencing recurrence. The so-called 'interstitial invasion' includes lymph vessel, nerves, and loose connective tissue invasions. The recurrence rate in patients with or without 'interstitial invasion' was 50% and 20%, respectively. The significance of nerve invasion has been annotated by other researchers^[23-25]. Peritoneal dissemination after excision could not be treated by surgery alone, because cancer cells either as single cells or cell clumps were randomly allocated on the large area of loose connective tissue of the peritoneum^[26]. About 40% of patients had small distant metastases. Such metastases were typical 1-2 mm nodules located on the surface of the peritoneum^[27]. So far as peritoneal dissemination concerned, there is no effective treatment. Even extensive lymph node dissection and resection of surrounding connective tissues and major vessels combined with radiotherapy and chemotherapy could not assure avoidance of recurrence up to now^[28-30].

In summary, the long term survival following resection depends on decrease of recurrence. Therefore rationally standardized operative procedure with due attention to factors of recurrence may help improve the long term survival of pancreatic cancer patients.

REFERENCES

- 1 Nitecki SS, Sarr MG, Colby TV, van Heerden JA. Long-term survival after resection for ductal adenocarcinoma of the pancreas. Is it really improving? *Ann Surg* 1995; **221**: 59-66
- 2 Griffin JF, Smalley SR, Jewell W, Paradelo JC, Raymond RD, Hassanein RE, Evans RG. Patterns of failure after curative

- resection of pancreatic carcinoma. *Cancer* 1990; **66**: 56-61
- 3 **Westerdahl J**, Andren-Sandberg A, Ihse I. Recurrence of exocrine pancreatic cancer- local or hepatic? *Hepatogastroenterology* 1993; **40**: 384-387
 - 4 **Meyer W**, Jurowich C, Reichel M, Steinhauser B, Wunsch PH, Gebhardt C. Pathomorphological and histological prognostic factors in curatively resected ductal adenocarcinoma of the pancreas. *Surg Today* 2000; **30**: 582-587
 - 5 **Benassai G**, Mastroianni M, Quarto G, Gappiello A, Giani U, Mosella G. Survival after pancreaticoduodenectomy for ductal adenocarcinoma of the head of the pancreas. *Chir Ital* 2000; **52**: 263-270
 - 6 **Yamaguchi K**, Mizumoto K, Noshiro H, Sugitani A, Shimizu S, Chijiwa K, Tanaka M. Pancreatic carcinoma: <or = 2 cm versus> 2 cm in size. *Int Surg* 1999; **84**: 213-219
 - 7 **van Geenen RC**, van Gulik TM, Offerhaus GJ, de Wit LT, Busch OR, Obertop H, Gouma DJ. Survival after pancreaticoduodenectomy for periampullary adenocarcinoma: an update. *Eur J Surg Oncol* 2001; **27**: 549-557
 - 8 **Iacono C**, Facci E, Bortolasi L, Zamboni G, Scarpa A, Talamini G, Prati G, Nifosi F, Serio G. Intermediate results of extended pancreaticoduodenectomy. Verona experience. *J Hepatobiliary Pancreat Surg* 1999; **6**: 74-78
 - 9 **Tsiotos GG**, Farnell MB, Sarr MG. Are the results of pancreatectomy for pancreatic cancer improving? *World J Surg* 1999; **23**: 913-919
 - 10 **Pedrazzoli S**, Pasquali C, Sperti C. General aspects of surgical treatment of pancreatic cancer. *Dig Surg* 1999; **16**: 265-275
 - 11 **Benassai G**, Mastroianni M, Mosella F, Mosella G. Significance of lymph node metastases in the surgical management of pancreatic head carcinoma. *J Exp Clin Cancer Res* 1999; **18**: 23-28
 - 12 **Yeo CJ**, Cameron JL, Sohn TA, Lillemoe KD, Pitt HA, Talamini MA, Hruban RH, Ord SE, Sauter PK, Coleman J, Zahurak ML, Grochow LB, Abrams RA. Six hundred fifty consecutive pancreaticoduodenectomies in the 1990s: Pathology, complications, and outcomes. *Ann Surg* 1997; **226**: 248-257
 - 13 **Nagakawa T**, Nagamori M, Futakami F, Tsukioka Y, Kayahara M, Ohta T, Ueno K, Miyazaki I. Results of extensive surgery for pancreatic carcinoma. *Cancer* 1996; **77**: 640-645
 - 14 **Nakao A**, Harada A, Nonami T, Kaneko T, Takagi H. Clinical significance of carcinoma invasion of the extrapancreatic nerve plexus in pancreatic cancer. *Pancreas* 1996; **12**: 357-361
 - 15 **Nakao A**, Kaneko T, Takeda S, Inoue S, Harada A, Nomoto S, Ekmel T, Yamashita K, Hatsuno T. The role of extended radical operation for pancreatic cancer. *Hepatogastroenterology* 2001; **48**: 949-952
 - 16 **Imamura M**, Hosotani R, Kogire M. Rationale of the so-called extended resection for pancreatic invasive ductal carcinoma. *Digestion* 1999; **60** (Suppl 1): 126-129
 - 17 **Kayahara M**, Nagakawa T, Ueno K, Ohta T, Takeda T, Miyazaki I. An evaluation of radical resection for pancreatic cancer based on the mode of recurrence as determined by autopsy and diagnostic imaging. *Cancer* 1993; **172**: 2118-2123
 - 18 **Nagai H**, Kuroda A, Morioka Y. Lymphatic and local spread of T1 and T2 pancreatic cancer. A study of autopsy material. *Ann Surg* 1986; **204**: 65-71
 - 19 **Gebhardt C**, Meyer W, Reichel M, Wunsch PH. Prognostic factors in the operative treatment of ductal pancreatic carcinoma. *Langenbecks Arch Surg* 2000; **385**: 14-20
 - 20 **Takao S**, Shinchi H, Sha K, Natsugoe S, Maenohara S, Suenaga T, Nishimata Y, Aikou T. Clinical and biological features of T1 ductal adenocarcinoma of the pancreas. *Hepatogastroenterology* 1999; **46**: 498-503
 - 21 **Benassai G**, Mastroianni M, Quarto G, Gappiello A, Giani U, Forestieri P, Mazzeo F. Factors influencing survival after resection for ductal adenocarcinoma of the head of the pancreas. *J Surg Oncol* 2000; **73**: 212-218
 - 22 **Ishikawa O**, Ohhigashi H, Sasaki Y, Kabuto T, Fukuda I, Furukawa H, Imaoka S, Iwanaga T. Practical usefulness of lymphatic and connective tissue clearance for the carcinoma of the pancreas head. *Ann Surg* 1998; **208**: 215-220
 - 23 **Ozaki H**, Hiraoka T, Mizumoto R, Matsuno S, Matsumoto Y, Nakayama T, Tsunoda T, Suzuki T, Monden M, Saitoh Y, Yamauchi H, Ogata Y. The prognostic significance of lymph node metastasis and intrapancreatic perineural invasion in pancreatic cancer after curative resection. *Surg Today* 1999; **29**: 16-22
 - 24 **Dang C**, Qin Z, Ji Z, Li Y, Zhao J, Takashi E, Naito Z, Yokoyama M, Asono G. Morphological characteristics and clinical significance of nerve distribution in pancreatic cancers. *Nippon Ika Daigaku Zasshi* 1997; **64**: 526-531
 - 25 **Takahashi S**, Hasebe T, Oda T, Sasaki S, Kinoshita T, Konishi M, Ueda T, Ochiai T, Ochiai A. Extra-tumor perineural invasion predicts postoperative development of peritoneal dissemination in pancreatic ductal adenocarcinoma. *Anticancer Res* 2001; **21**(2B): 1407-1412
 - 26 **Hiraoka T**, Uchino R, Kanemitsu K, Toyonaga M, Saitoh N, Nakamura I, Tashiro S, Miyauchi Y. Combination of intraoperative radiation with resection of cancer of the pancreas. *Int J Pancreatol* 1990; **7**: 201-207
 - 27 **Warshaw AL**, Tepper JE, Shipley WU. Laparoscopy in the staging and planning of therapy for pancreatic cancer. *Am J Surg* 1986; **151**: 76-80
 - 28 **Cellini N**, Trodella L, Valentini V, Doglietto GB, Morganti AG, Ziccarelli P, Alfieri S, Bossola M, Brizi MG, Crucitti F. Radiotherapy, local control and survival in carcinomas of the exocrine pancreas. *Rays* 1998; **23**: 528-534
 - 29 **Alfieri S**, Morganti AG, Di Giorgio A, Valentini V, Bossola M, Trodella L, Cellini N, Doglietto GB. Improved survival and local control after intraoperative radiation therapy and postoperative radiotherapy: a multivariate analysis of 46 patients undergoing surgery for pancreatic head cancer. *Arch Surg* 2001; **136**: 343-347
 - 30 **Foo ML**, Gunderson LL, Nagorney DM, McIlrath DC, van Heerden JA, Robinow JS, Kvols LK, Garton GR, Martenson DJ, Cha SS. Patterns of failure in grossly resected pancreatic ductal adenocarcinoma treated with adjuvant irradiation +/- 5 fluorouracil. *Int J Radiat Oncol Biol Phys* 1993; **26**: 483-489

Efficacy and safety of lamivudine treatment for chronic hepatitis B in pregnancy

Guan-Guan Su, Kong-Han Pan, Nian-Feng Zhao, Su-Hua Fang, Dan-Hong Yang, Yong Zhou

Guan-Guan Su, Kong-Han Pan, Su-Hua Fang, Dan-Hong Yang, Yong Zhou, Department of Infection, Sir Run Run Shaw Hospital affiliated to Zhejiang University, Hangzhou, 310016, Zhejiang Province, China

Nian-Feng Zhao, First Hospital affiliated to Zhejiang University, Hangzhou, 310007, Zhejiang Province, China

Correspondence to: Dr. Guan-Guan Su, Department of Infection, Sir Run Run Shaw Hospital Affiliated to Zhejiang University, Hangzhou, 310016, Zhejiang Province, China. pankonghan@medmail.com.cn

Telephone: +86-571-86090073-6013 **Fax:** +86-571-86032877

Received: 2003-08-02 **Accepted:** 2003-09-24

Abstract

AIM: To evaluate the efficacy and safety of lamivudine treatment of chronic hepatitis B disease in pregnancy.

METHODS: The study group was comprised of 38 chronic HBV patients who were diagnosed pregnant during lamivudine treatment and voluntary to continue the same therapy. The control group was from documented patient data in the literatures. We compared the following parameters with those of a control group: anti-HBV efficacy, complications of pregnancy (abortion, preterm birth, neonatal asphyxia, fetal death, and congenital anomaly), incidence of HBV-positive babies and developmental anomalies in pregnant women treated with lamivudine.

RESULTS: The blocking rate of lamivudine treatment was significantly higher than that of active vaccine immunization for babies with double-positive (HBsAg/HBeAg) mothers with 30-30-10 µg doses of vaccine (74.07%) and with 30-20-10 µg (64.87%). The natural vertical HBV transmission from mother to infant of "double-positive" mothers was 100% (10/10). No pregnancy complication was noted during the observation period, but in the control group the incidences of pregnancy complication were 16.67% (abortion), 43.02% (preterm), 15.62% (neonatal asphyxia), and 4.49% (fetal death), 10.0% (congenital anomaly). No HBV-positive newborn was detected and no developmental anomaly was found in the study group.

CONCLUSION: Lamivudine is helpful to prevent maternal-infant HBV transmission and may reduce the complications of HBV-infected pregnant patients.

Su GG, Pan KH, Zhao NF, Fang SH, Yang DH, Zhou Y. Efficacy and safety of lamivudine treatment for chronic hepatitis B in pregnancy. *World J Gastroenterol* 2004; 10(6): 910-912
<http://www.wjgnet.com/1007-9327/10/910.asp>

INTRODUCTION

Throughout the world, over 300 million people have chronic hepatitis B virus (HBV) infection, and more than 75 percent of those affected are of Asian origin^[1]. Chronic HBV infection causes cirrhosis, liver cancer, and death^[2,3]. The disease is

endemic in Africa and Asia, where the virus is transmitted from mother to newborn or between close contacts in early childhood^[4-6].

Chronically infected persons with viral replication are at the highest risk for progressive liver disease^[7]. In China, chronic HBV infection is a common clinical occurrence in pregnancy as well as a potentially serious condition^[8]. In pregnant patients the complications of HBV occur more frequently and with a higher mortality^[9]. Also vertical transmission of HBV to the infant is common^[4,5]. Perinatal transmission of HBV is the most important cause of chronic HBV infection and remains one serious problem despite passive immunization (hepatitis B immune globulin at birth) and active immunization (hepatitis B vaccination according to the standard 3-dose schedule). In different studies high maternal HBV DNA levels were associated with a vaccination breakthrough^[10,11]. Recently nucleoside analogues have been used to prevent mother-to-infant transmission of HIV-1^[12]. In that setting, lamivudine given during the last weeks of pregnancy in HIV-1 and HBV positive women appeared to be safe^[12-15]. Following a similar rationale, there was a clinical trial about the use of lamivudine, a potent inhibitor of HBV replication, in pregnant women with high HBV viral loads in highly endemic countries^[16].

However, few data are available regarding the efficacy and safety of lamivudine treatment for chronic HBV from the early phase of pregnancy. Pharmaceutical inserts regarding lamivudine indicate it is of "uncertain safety" during pregnancy. In this retrospective analysis, we evaluated 38 cases of chronic HBV pregnant patients treated with lamivudine from the early phase of pregnancy for pregnancy-related complications and congenital anomalies.

MATERIALS AND METHODS

Patients

Forty-two chronic HBV-infected women were found to be pregnant during lamivudine treatment and presented to the physician between 2-3 mo of gestation. Then they were enrolled in the study. During the study, one patient chose to terminate her pregnancy, two stopped lamivudine therapy, and one was lost to follow-up. Thus the final study consisted of 38 pregnant patients who continued lamivudine therapy. The pretreatment diagnosis of HBV was based on National Prevention and Treatment Profiles of Viral Hepatitis (2000)^[17] criteria with the following criteria: detectable HBsAg and HBeAg/HBeAb in serum, detectable serum HBV DNA, and elevated alanine aminotransferase (ALT) levels (more than 3-4 times normal level). Patients were excluded if they had hepatitis C or D infection. Patients had not received any other antiviral drugs in the preceding 6 mo. All patients were warned about that studies in rabbits had demonstrated lamivudine to result in fetal demise. However, it was also explained that the dosages used in animal studies were nearly 60 times higher than those used in humans (private communication).

Currently there is a clinical trial in Asia evaluating lamivudine use perinatally in mothers with high HBV viral

loads with the goal to reduce vertical HBV transmission to the infants^[13]. The patients who earlier stopped lamivudine often experienced significant clinical deterioration. Thus overall we felt it appropriate to consider continuing lamivudine therapy. HBV infection in pregnant women was more serious than in non-pregnant women^[9]. All the above were informed to any pregnant patients with HBV infection. Decision was made by patient herself on whether to terminate lamivudine treatment or not.

The data of complications of HBV hepatitis and HBV-positive babies were based on Prevention and Treatment of Viral Hepatitis study edited by Gao^[19]. Lamivudine safety profile was obtained from international studies^[13-15,18].

Regimen and parameters

Pregnant women with chronic HBV infection were treated with lamivudine. The dosage, course, efficacy evaluation, follow-up, measures to deal with resistant mutation were based on the Guideline for Lamivudine Clinical Use (2000)^[20] and Expert Consensus on Lamivudine Clinical Use (2001)^[21]. Complications of pregnancy included abortion, preterm birth, neonatal asphyxia, fetal death, and congenital anomaly^[19]. Regular ultrasonic examination was carried out to monitor the safety of the fetus. All newborns were given the standard passive-active immunization or actively immunized at birth. Twelve babies were tested of HVB DNA (PCR), HBsAg, HBeAg, anti-HBs, anti-HBe, anti-HBc at birth before HBIG administration (T₀) and at the 6th mo (T₆) and the 12th mo (T₁₂) after birth. The percentage of HBV-positive babies was calculated. The health status and development of babies were assessed by the local children healthcare institution. All children were followed-up and documented.

RESULTS

Antiviral efficacy

HBV-DNA was converted to negative in 35 patients (92.11%) of the study group. HBeAg was converted to negative in 12 patients (31.58%). The rate of HBeAg seroconversion (loss of HBeAg or development of antibody to HBeAg) was 26.32% (10/38). The normalization rate of ALT was 73.68% (28/38). The rate of resistant mutation was 11.43% (4/35). Lamivudine efficacy was similar to other reports in the international medical literatures^[13-15]. ALT normalization may have been confounded by hepatic injury of pregnancy. Thus the complete efficacy of lamivudine was difficult to assess.

Incidence of HBV-positive baby (Table 1)

Twelve maternal-baby pairs were evaluated for HBV markers (HBsAg, HBeAg, anti-HBs, and anti-HBe, anti-HBc) before and after delivery. All 12 mothers were double positive (HBsAg/HBeAg) before lamivudine treatment. Although the HBV-DNA parameters of all 12 mothers were converted to negative prepartum, 8 mothers remained HBeAg-positive, 1 HBeAg negative, and 3 reached seroconversion. Of the 8 mothers who were HBeAg-positive at childbirth, 3 babies were HBsAg-positive at birth (T₀), but turned negative at T₆ and T₁₂ postpartum. The other babies were all HBsAg-negative during 12 months of follow-up. Thus after one year, 100% of the babies were HBsAg-negative. But in control group, the blocking rates of active vaccine immunization for babies with double-positive (HBsAg/HBeAg) mothers were 74.07% with 30-30-10 µg doses of vaccine and 64.87% with 30-20-10 µg. The natural vertical HBV transmission from mother (double-positive) to infant was 100% (10/10)^[19]. The prevention of HBV maternal-infant transmission was very significant in lamivudine-treated mothers.

Table 1 Blocking of maternal transmission in HBsAg and HBeAg double-positive mothers^[19]

	n	HBsAg(+)			HBV-DNA(+)	Blocking rate
		T ₀	T ₆	T ₁₂		
Lamivudine treatment	12	3	0	0	0	100.00
Vaccine 30-30-10 µg	81		21	21	21	74.07
Vaccine 30-20-10 µg	37		13	13	13	64.87
Natural transmission	10		10	10	10	0.00

Complications of pregnancy (Table 2)

The infants of lamivudine-treated mothers were delivered at full term without any complication. The incidence of pregnancy complication was lower in the study group than in the control group of pregnant mothers with chronic HBV^[19].

Table 2 Complications of pregnancy in different groups^[19]

	Abortion (%)	Preterm (%)	Neonatal asphyxia (%)	Fetal death (%)	Congenital anomaly (%)
Lamivudin	0/38	0/38	0/38	0/38	0/38
Control	16.67 (1/6)	43.02 (37/86)	15.62 (14/89)	4.49 (4/89)	10 (1/10)

Control of viral hepatitis activity (Table 3)

Although three out of 38 patients in the study group did not convert to HBV-DNA-negative within one year, ALT normalized in all three patients. Ten patients in the study group converted to HBV-DNA-negative, but their ALT remained abnormal. They were included in the pregnancy liver injury group. Six patients were HBeAg-negative, and four patients had seroconversion for HBeAb. A resistant HBV mutant emerged in four cases though their ALT remained normal. Thus overall hepatitis activity was controlled in all the study patients (100%). In the two patients who quitted lamivudine after the consultation, active hepatitis recurred within 6 months. Honkoop *et al* reported that the incidence of "lamivudine withdrawal hepatitis" was 17% (7/41)^[22]. Hepatitis activity was better controlled in lamivudine treatment group than in the group who quitted lamivudine therapy (Table 3).

Table 3 Control of hepatitis activity^[22]

	n	Active hepatitis (%)
Lamivudine treatment during pregnancy	38	0 (0.00)
Stop lamivudine while pregnant	2	2 (100.00)
Stop lamivudine	41	7 (17.07)

Infant development and health

Community maternal-child health clinics failed to detect any unfavorable outcome related to the infant's health and development.

DISCUSSION

It has been well-known that the pregnant women chronically infected with HBV have more complications and a higher mortality during pregnancy^[5,8,9]. Lamivudine has been found to be an effective treatment strategy for chronic HBV^[15]. However, its use is not recommended during pregnancy especially during the first trimester because animal studies have demonstrated lethal effects on the rabbit fetus (private communication). In our study 38 pregnant women with chronic HBV infection continued lamivudine therapy during the entire pregnancy. Their decision to continue its therapy was voluntary

after informed consent. They were all provided with information about the drug benefits and risks. Our results indicated lamivudine therapy not only provided a protective effect against maternal-infant HBV transmission, but decreased the likelihood of active HBV infection in the mother. Further complications were minimal compared with the control group. These results should be presented to a mother contemplating continuation of lamivudine therapy during pregnancy.

Pregnancy complications are likely caused by the activity of hepatitis B virus in mothers with chronic HBV infections. The rate of vertical maternal-infant HBV transmission was 90-100% in mothers who were double positive for both HBsAg and HBeAg^[19]. It is probable that such a high transmission rate has been led by the high viral load^[10,11]. The data in our study indicated lamivudine was able to neutralize hepatitis activity and reduction in the viral load might result in fewer pregnancy complications and prevent maternal-infant HBV transmission. This benefit may well outweigh the risk of lamivudine's early toxic effects on the infant during the first trimester. Lamivudine has been found belonging to the L-form enantiomorph nucleotide analogue which is negatively selective for the human nucleotide^[15]. Toxicity was detected only at very high dosages of 1 000 times higher than the recommended human dosages. The dosage used in animals was 60 times greater than that used in human (private communication). Thus currently recommended lamivudine dosages for human may represent little risk to the pregnant mother.

However, there are several concerns about our current study. First, our study was not designed as a randomized-placebo-controlled study, thus any improvement in the study group could be due to such confounding factors as "self-selection" bias, or observer bias. Second, the study group was small and thus might lack power to distinguish a true difference between the treated group and the control group. However, we do consider the study to be of value in raising the question of benefit of lamivudine treatment of chronic HBV in pregnancy. Further studies, especially larger well-designed placebo-controlled studies are needed to confirm a true beneficial effect of lamivudine therapy for chronic HBV infection in pregnancy.

REFERENCES

- 1 **Maynard JE**. Hepatitis B: global importance and need for control. *Vaccine* 1990; **8**: S18-20
- 2 **Liaw YF**, Tai DI, Chu CM, Chen TJ. The development of cirrhosis in patients with chronic type B hepatitis: a prospective study. *Hepatology* 1988; **8**: 493-496
- 3 **Chang MH**, Chen CJ, Lai MS, Hsu HM, Wu TC, Kong MS, Liang DC, Shau WY, Chen DS. Universal hepatitis B vaccination in Taiwan and the incidence of hepatocellular carcinoma in children. Taiwan Childhood Hepatoma Study Group. *N Engl J Med* 1997; **336**: 1855-1859
- 4 **Stevens CE**, Neurath RA, Beasley RP, Szmuness W. HBeAg and anti-HBe detection by radioimmunoassay: correlation with vertical transmission of hepatitis B virus in Taiwan. *J Med Virol* 1979; **3**: 237-241
- 5 **Xu ZY**, Liu CB, Francis DP, Purcell RH, Gun ZL, Duan SC, Chen RJ, Margolis HS, Huang CH, Maynard JE. Prevention of perina-

- 6 **tal acquisition of hepatitis B virus carriage using vaccine: preliminary report of a randomized, double-blind placebo-controlled and comparative trial. *Pediatrics* 1985; **76**: 13-18**
- 7 **Beasley RP**, Hwang LY. Postnatal infectivity of hepatitis B surface antigen-carrier mothers. *J Infect Dis* 1983; **147**: 185-190
- 8 **de Jongh FE**, Janssen HL, de Man RA, Hop WC, Schalm SW, van Blankenstein M. Survival and prognostic indicators in hepatitis B surface antigen-positive cirrhosis of the liver. *Gastroenterology* 1992; **103**: 1630-1635
- 9 **Yang H**, Chen R, Li Z, Zhou G, Zhao Y, Cui D, Li S, Han C, Yang L. Analysis of fetal distress in pregnancy with hepatitis B virus infection. *Zhonghua Fuchanke Zazhi* 2002; **37**: 211-213
- 10 **Khuroo MS**, Kamili S. Aetiology, clinical course and outcome of sporadic acute viral hepatitis in pregnancy. *J Viral Hepat* 2003; **10**: 61-69
- 11 **Ip HM**, Lelie PN, Wong VC, Kuhns MC, Reesink HW. Prevention of hepatitis B virus carrier state in infants according to maternal serum levels of HBV DNA. *Lancet* 1989; **1**: 406-410
- 12 **del Canho R**, Grosheide PM, Mazel JA, Heijtkink RA, Hop WC, Gerards LJ, de Gast GC, Fetter WP, Zwijneberg J, Schalm SW. Ten-year neonatal hepatitis B vaccination program, The Netherlands, 1982-1992: Protective efficacy and long-term immunogenicity. *Vaccine* 1997; **15**: 1624-1630
- 13 **Faucher P**, Batallan A, Bastian H, Matheron S, Morau G, Madelenat P, Benifla JL. Management of pregnant women infected with HIV at Bichat Hospital between 1990 and 1998: analysis of 202 pregnancies. *Gynecol Obstet Fertil* 2001; **29**: 211-225
- 14 **van Zonneveld M**, van Nunen AB, Niesters HG, de Man RA, Schalm SW, Janssen HL. Lamivudine treatment during pregnancy to prevent perinatal transmission of hepatitis B virus infection. *J Viral Hepat* 2003; **10**: 294-297
- 15 **Moodley J**, Moodley D, Pillay K, Coovadia H, Saba J, van Leeuwen R, Goodwin C, Harrigan PR, Moore KH, Stone C, Plumb R, Johnson MA. Pharmacokinetics and antiretroviral activity of lamivudine alone or when coadministered with zidovudine in human immunodeficiency virus type 1-infected pregnant women and their offspring. *J Infect Dis* 1998; **178**: 1327-1333
- 16 **Johnson MA**, Moore KH, Yuen GJ, Bye A, Pakes GE. Clinical pharmacokinetics of lamivudine. *Clin Pharmacokinet* 1999; **36**: 41-66
- 17 **Van Nunen AB**, de Man RA, Heijtkink RA, Niesters HG, Schalm SW. Lamivudine in the last 4 weeks of pregnancy to prevent perinatal transmission in highly viremic chronic hepatitis B patients. *J Hepatol* 2000; **32**: 1040-1041
- 18 **Branch society of Infectious Disease and Parasitology and Branch society of Hepatology of Chinese Medical Association**. National Prevention and Treatment Profiles of Viral Hepatitis (2000). *Zhonghua Chuanranbing Zazhi* 2001; **19**: 56-62
- 19 **Lai CL**, Chien RN, Leung NW, Chang TT, Guan R, Tai DI, Ng KY, Wu PC, Dent JC, Barber J, Stephenson SL, Gray DF. A one-year trial of lamivudine for chronic hepatitis B. Asia Hepatitis Lamivudine Study Group. *N Engl J Med* 1998; **339**: 61-68
- 20 **Gao SZ**. Research on prevention and treatment of viral hepatitis. *Beijing: Beijing pub* 1993: 38-46, 286-291
- 21 **Expert team for lamivudine clinical use**. The year 2000 guideline for lamivudine clinical use. *Zhonghua Ganzangbing Zazhi* 2000; **8**: 249-250
- 22 **Expert team for lamivudine clinical use**. Expert consensus on lamivudine clinical use (2001). *Zhonghua Ganzangbing Zazhi* 2002; **10**: 157-158
- 23 **Honkoop P**, de Man RA, Niesters HG, Zondervan PE, Schalm SW. Acute exacerbation of chronic hepatitis B virus infection after withdrawal of lamivudine therapy. *Hepatology* 2000; **32**: 635-639

Edited by Gupta MK and Wang XL Proofread by Xu FM

Clinical value of *Helicobacter pylori* stool antigen test, ImmunoCard STAT HpSA, for detecting *H pylori* infection

Yi-Hui Li, Hong Guo, Peng-Bin Zhang, Xiao-Yan Zhao, Si-Ping Da

Yi-Hui Li, Hong Guo, Peng-Bin Zhang, Xiao-Yan Zhao, Si-Ping Da, Department of Gastroenterology, Xinqiao Hospital, Third Military Medical University, Chongqing 400037, China

Correspondence to: Hong Guo, Department of Gastroenterology, Xinqiao Hospital, Third Military Medical University, Chongqing 400037, China. haoguo11@yahoo.com

Telephone: +86-23-68755604

Received: 2003-08-23 **Accepted:** 2003-10-12

Abstract

AIM: To evaluate the reliability of the *Helicobacter pylori* stool antigen test, ImmunoCard STAT HpSA, for detecting *H pylori* infection.

METHODS: Stool specimens were collected from 53 patients who received upper endoscopy examination due to gastrointestinal symptoms. ImmunoCard STAT HpSA was used to detect *H pylori* stool antigens. *H pylori* infection was detected based on three different tests: the urease test, Warthin-Starry staining and culture. *H pylori* status was defined as positive when both the urease test and histology or culture alone was positive.

RESULTS: Sensitivity, specificity, positive predictive and negative predictive values and the total accuracy of ImmunoCard STAT HpSA for the diagnosis of *H pylori* infection were 92.6% (25/27), 88.5% (23/26), 89.3% (25/28), 92% (23/25) and 90.6% (48/53), respectively.

CONCLUSION: The stool antigen test, ImmunoCard STAT HpSA, is a simple noninvasive and accurate test for the diagnosis of *H pylori* infection.

Li YH, Guo H, Zhang PB, Zhao XY, Da SP. Clinical value of *Helicobacter pylori* stool antigen test, ImmunoCard STAT HpSA, for detecting *H pylori* infection. *World J Gastroenterol* 2004; 10(6): 913-914

<http://www.wjgnet.com/1007-9327/10/913.asp>

INTRODUCTION

Helicobacter pylori infection is a major cause of chronic gastritis and peptic ulcer, and is associated with gastric cancer and gastric MALT lymphoma^[1-4]. There are several methods of diagnosing *H pylori* infection including invasive procedures using mucosa biopsies taken during endoscopy (mainly culture, histology and the rapid urease test) and noninvasive procedures (mainly ¹³C or ¹⁴C urea breath tests (UBTs) and serological tests). But invasive procedures suffer from biopsies and endoscopy, and the UBTs require expensive equipment or is harmful to patients. Because *H pylori* antibody titers fall very slowly even after successful eradication, tests lack of specificity and sensitivity^[5-9]. Recently, the *H pylori* stool antigen (HpSA) test has been put in the market as another noninvasive technique^[10-13], but has rarely validated in China^[14]. The aim of this study is to evaluate the

clinical value of a new test, ImmunoCard STAT HpSA, for the diagnosis of *H pylori* infection.

MATERIALS AND METHODS

Patients

A total of 56 patients (33 males and 23 females, average age 43.7 years old) participated in this study. Chronic gastritis and peptic ulcer were endoscopically diagnosed in 47 and 9 patients, respectively. Patients treated with antibiotics, bismuth, or proton pump inhibitors within 4 weeks preceding the study were excluded.

Methods

Invasive tests using mucosal biopsies including culture, histology (Warthin-Starry staining) and the rapid urease test (RUT) were used to establish the "gold standard", in order to evaluate the accuracy of the new stool antigen test, ImmunoCard STAT HpSA.

Mucosal biopsies for detecting Hp

During upper endoscopy, three gastric biopsies were taken. One biopsy was used for RUT and the remaining two were used for Warthin-Starry staining and culture. The gold standard for the presence of *H pylori* infection was defined when both RUT and Warthin-Starry staining or culture alone was positive. The absence of *H pylori* infection required all three tests to be negative.

ImmunoCard STAT HpSA

On the same day of endoscopy, patients collected stool into an air tight container. The stool assay was performed using the same test series of the ImmunoCard STAT HpSA (Meridian Diagnostics, Inc, USA). A small portion (5-6 mm diameter) of stool specimen was transferred into the sample diluent vial using the applicator stick, vortexed for 15 s, and then 4 drops were dispensed into the round window at the lower end of the device. The results were read 5 min later. Positive and negative results were judged as recommended by the manufactures. The endoscopy-based tests and HpSA test were carried out by different people with double blind procedures.

Statistical analysis

Sensitivity, specificity, PPV, NPV and accuracy of the kit were calculated according to the gold standard.

RESULTS

Altogether, 53 patients were enrolled and tested by ImmunoCard STAT HpSA and the endoscopy-based tests. *H pylori* infection was present in 27 patients as determined by the gold standard. The HpSA test produced positive and negative results in 28 and 25 patients, respectively. Compared with the gold standard, the HpSA was inaccurate in five patients (three false positive, and two false negative), giving a sensitivity, specificity, positive predictive and negative predictive values and total accuracy of the ImmunoCard STAT HpSA of 92.6% (25/27), 88.5% (23/26), 89.3% (25/28), 92% (23/25) and 90.6% (48/53), respectively (Table 1).

Table 1 Performance of the ImmunoCard STAT HpSA test in the detection of *H pylori* infection, according to the biopsy-based gold standard

ImmunoCard STAT HpSA	Gold standard		Total
	Positive	Negative	
Positive	25	3	28
Negative	2	23	25
Total	27	26	53

DISCUSSION

A variety of highly sensitive and specific tests are available to diagnose *H pylori* infection. Invasive tests using mucosal biopsies taken during endoscopy might lead to cross infection. In addition, some patients refuse to undergo endoscopy, especially after eradication therapy, due to its invasive nature. Fortunately, there are several noninvasive tests including ^{13}C or ^{14}C urea breath tests (UBT) and serological tests. The UBT tests are currently proven to have high sensitivity and specificity, and considered to be the optimal test for monitoring *H pylori* eradication therapy. However, ^{13}C -UBT needs special equipment and is expensive, and ^{14}C -UBT requires a radioactive isotope, and cannot be used for children and pregnant women. As a result, UBTs are not widely available. Therefore, it is necessary to find a new, easy, cheaper and accurate noninvasive test.

Gastric epithelial cells renew once in one to three days, and are output in feces with *H pylori*, which can be detected by polyclonal capture anti-*H pylori* antibodies. The HpSA was reported in America Gastroenterology Week in 1997, and put in the market by Meridian Company in the same year, with the name Premier Platinum HpSA. Premier Platinum HpSA is a microplate enzyme-immunoassay for the qualitative detection of *H pylori* antigens in human stool, and was approved by FDA to be used in clinic in 1998. The HpSA test has been widely evaluated around the world, with a weighted mean sensitivity and specificity of 90-98%, respectively^[13,15,16]. The HpSA test is a cheap and useful method for the diagnosis of *H pylori* infection before and after eradication therapy^[17,18]. It is an accurate test in all age groups of children too^[19]. However, Peitz *et al* reported that the diagnostic accuracy, in particular the sensitivity, of the HpSA stool test was reduced by upper gastrointestinal bleeding, and a negative test result should be confirmed by a further diagnostic method^[20,21]. Although the HpSA test seems to be less accurate than the UBT, both UBT and stool antigen tests are reliable noninvasive tests for monitoring the efficacy of *H pylori* eradication therapy.

A novel easier stool antigen test named ImmunoCard STAT HpSA has recently been put in the market by Meridian Company. This test was first reported to have a sensitivity of 96.1% and specificity of 90.6% at Gastrointestinal Pathology and *Helicobacter* Conference in 2002 in Athens, but have not been reported since. In the present study, we conclude that the ImmunoCard STAT HpSA test has a diagnostic value comparable to the gold standard in detecting *H pylori*. The sensitivity and specificity of the ImmunoCard STAT HpSA for the diagnosis of *H pylori* infection were 92.6% and 88.5%, respectively, with an accuracy of 90.6%. Because it is easy and convenient to perform, the ImmunoCard STAT HpSA could be used at many situations, especially for children, pregnant women, old people and others who are not suitable for endoscopy. The ImmunoCard STAT HpSA is an ideal test for the diagnosis of *H pylori* infection in clinical practice.

REFERENCES

1 **Hobsley M**, Tovey FI. *Helicobacter pylori*: the primary cause of

- duodenal ulceration or a secondary infection? *World J Gastroenterol* 2001; **7**: 149-151
- 2 **Xia HHX**. Association between *Helicobacter pylori* and gastric cancer: current knowledge and future research. *World J Gastroenterol* 1998; **4**: 93-96
- 3 **Wang KX**, Wang XF, Peng JL, Cui YB, Wang J, Li CP. Detection of serum anti-*Helicobacter pylori* immunoglobulin G in patients with different digestive malignant tumors. *World J Gastroenterol* 2003; **9**: 2501-2504
- 4 **Wang RT**, Wang T, Chen K, Wang JY, Zhang JP, Lin SR, Zhu YM, Zhang WM, Cao YX, Zhu CW, Yu H, Cong YJ, Zheng S, Wu BQ. *Helicobacter pylori* infection and gastric cancer: evidence from a retrospective cohort study and nested case-control study in China. *World J Gastroenterol* 2002; **8**: 1103-1107
- 5 **Wang XZ**, Li D. The serodiagnosis of *Helicobacter pylori*. *Shijie Huaren Xiaohua Zazhi* 2000; **8**: 550-551
- 6 **Sun T**, Ye JX, Ma GX, Cui LH, Liu CQ, Pu J, Fu SF, Jiang Y. Using ^{13}C -urea breath test to diagnose *Helicobacter pylori* infection. *Shijie Huaren Xiaohua Zazhi* 2000; **8**: 270
- 7 **Li ZJ**, Jiang T, Zhou WM. The value of detecting *Helicobacter pylori* antibody in saliva by enzyme-linked immuno-sorbent assay. *Shijie Huaren Xiaohua Zazhi* 2000; **8**: 241-242
- 8 **Wang CD**, Lu XQ. Clinical application of *Helicobacter pylori* urea breath test. *Shijie Huaren Xiaohua Zazhi* 2000; **8**: 789-792
- 9 **Huang Y**, Xu LN. The dependent test of *Helicobacter pylori* urea enzyme. *Shijie Huaren Xiaohua Zazhi* 2000; **8**: 549-550
- 10 **Makrithathis A**, Pasching E, Schutze K, Wimmer M, Rotter ML, Hirschl AM. Detection of *Helicobacter pylori* in stool specimens by PCR and antigen enzyme immunoassay. *J Clin Microbiol* 1998; **36**: 2772-2774
- 11 **Vaira D**, Malfertheiner P, Megraud F, Axon AT, Deltenre M, Hirschl AM, Gasbarrini G, O' Morain C, Garcia JM, Quina M, Tytgat GN. Diagnosis of *Helicobacter pylori* infection with a new non-invasive antigen-based assay. HpSA European study group. *Lancet* 1999; **354**: 30-33
- 12 **Fanti L**, Mezzi G, Cavallero A, Gesu G, Bonato C, Masci E. A new simple immunoassay for detecting *Helicobacter pylori* infection: antigen in stool specimens. *Digestion* 1999; **60**: 456-460
- 13 **Metz DC**. Stool testing for *Helicobacter pylori* infection: yet another noninvasive alternation. *Am J Gastroenterol* 2000; **95**: 546-548
- 14 **Liu X**, Zhi M, Dong L, Chang BX. The evaluation of *Helicobacter pylori* stool antigen test. *Shijie Huaren Xiaohua Zazhi* 2002; **10**: 726-728
- 15 **Monteiro L**, de Mascarel A, Sarrasqueta AM, Bergey B, Barberis C, Talby P, Roux D, Shouler L, Goldfain D, Lamouliatte H, Megraud F. Diagnosis of *Helicobacter pylori* infection: noninvasive methods compared to invasive methods and evaluation of two new tests. *Am J Gastroenterol* 2001; **96**: 353-358
- 16 **Manes G**, Balzano A, Iaquinto G, Ricci C, Piccirillo MM, Giardullo N, Todisco A, Lioniello M, Vaira D. Accuracy of the stool antigen test in the diagnosis of *Helicobacter pylori* infection before treatment and in patients on omeprazole therapy. *Aliment Pharmacol Ther* 2001; **15**: 73-79
- 17 **Aksoy DY**, Aybar M, Ozaslan E, Kav T, Engin D, Ercis S, Altinok G, Hascelik G, Uzunalimoglu B, Arslan S. Evaluation of the *Helicobacter pylori* stool antigen test (HpSA) for the detection of *Helicobacter pylori* infection and comparison with other methods. *Hepatogastroenterology* 2003; **50**: 1047-1049
- 18 **Tanaka A**, Watanabe K, Tokunaga K, Hoshiya S, Imase K, Sugano H, Shingaki M, Kai A, Itoh T, Ishida H, Takahashi S. Evaluation of *Helicobacter pylori* stool antigen test before and after eradication therapy. *J Gastroenterol Hepatol* 2003; **18**: 732-738
- 19 **Kato S**, Ozawa K, Okuda M, Fujisawa T, Kagimoto S, Konno M, Maisawa S, Iinuma K. Accuracy of the stool antigen test for the diagnosis of childhood *Helicobacter pylori* infection: a multicenter Japanese study. *Am J Gastroenterol* 2003; **98**: 296-300
- 20 **Peitz U**, Leodolter A, Kahl S, Agha-Amiri K, Wex T, Wolle K, Gunther T, Steinbrink B, Malfertheiner P. Antigen stool test for assessment of *Helicobacter pylori* infection in patients with upper gastrointestinal bleeding. *Aliment Pharmacol Ther* 2003; **17**: 1075-1084
- 21 **van Leerdam ME**, van der Ende A, ten Kate FJ, Rauws EA, Tytgat GN. Lack of accuracy of the noninvasive *Helicobacter pylori* stool antigen test in patients with gastroduodenal ulcer bleeding. *Am J Gastroenterol* 2003; **98**: 798-801

Functional hepatic flow in patients with liver cirrhosis

Zheng Pan, Xing-Jiang Wu, Jie-Shou Li, Fang-Nan Liu, Wei-Su Li, Jian-Ming Han

Zheng Pan, Xing-Jiang Wu, Jie-Shou Li, Fang-Nan Liu, Wei-Su Li, Jian-Ming Han, Research Institute of General Surgery, Nanjing General Hospital of Nanjing Command/Clinical School of Medical College of Nanjing University, Nanjing 210002, Jiangsu Province, China

Correspondence to: Zheng Pan, Research Institute of General Surgery, Nanjing General Hospital of Nanjing Command, No.305, Eastern Road of Zhongshan, Nanjing 210002, Jiangsu Province, China. pz2233@sina.com

Telephone: +86-25-80860065 **Fax:** +86-25-84803956

Received: 2003-07-12 **Accepted:** 2003-10-07

Abstract

AIM: To evaluate hepatic reserve function by investigating the change of functional hepatic flow and total hepatic flow in cirrhotic patients with portal hypertension.

METHODS: HPLC method was employed for the determination of concentration of D-sorbitol in human plasma and urine. The functional hepatic flow (FHF) and total hepatic flow (THF) were determined by means of modified hepatic clearance of D-sorbitol combined with duplex doppler color sonography in 20 patients with cirrhosis and 10 healthy volunteers.

RESULTS: FHF, evaluated by means of the D-sorbitol clearance, was significantly reduced in patients with cirrhosis in comparison to controls (764.74 ± 167.91 vs $1\ 195.04 \pm 242.97$ mL/min, $P < 0.01$). While THF was significantly increased in patients with cirrhosis in comparison to controls ($1\ 605.23 \pm 279.99$ vs $1\ 256.12 \pm 198.34$ mL/min, $P < 0.01$). Portal blood flow and hepatic artery flow all were increased in cirrhosis compared to controls ($P < 0.05$ and $P < 0.01$). D-sorbitol total clearance was significantly reduced in cirrhosis compared to control ($P < 0.01$), while D-sorbitol renal clearance was significantly increased in cirrhosis ($P < 0.05$). In controls FHF was similar to THF ($1\ 195.05 \pm 242.97$ vs $1\ 256.12 \pm 198.34$ mL/min, $P = 0.636$), while FHF was significantly reduced compared with THF in cirrhosis (764.74 ± 167.91 vs $1\ 605.23 \pm 279.99$ mL/min, $P < 0.01$).

CONCLUSION: Our method that combined modified hepatic clearance of D-sorbitol with duplex doppler color sonography is effective in the measurement of FHF and THF. FHF can be used to estimate hepatic reserve function.

Pan Z, Wu XJ, Li JS, Liu FN, Li WS, Han JM. Functional hepatic flow in patients with liver cirrhosis. *World J Gastroenterol* 2004; 10(6): 915-918
<http://www.wjgnet.com/1007-9327/10/915.asp>

INTRODUCTION

The management of portal hypertension in patients with liver cirrhosis is still a therapeutic challenge^[1]. Liver failure and variceal bleeding are the chiefly causes that lead to death in cirrhosis. Now surgical devascularization and shunting play an important role in treatment of portal hypertension. Though operation is useful in controlling variceal bleeding, the mortality of operation is very high. Some cirrhotic patients

can not bear the strike of operation and anaesthesia because of inadequate hepatic reserve function. So the evaluation of hepatic reserve function preoperatively is very important, in addition to proper perioperative management. At present the evaluation of clinical severity of cirrhosis is mostly based on the Child-Pugh score. However, such an approach can not directly provide reliable quantitative evaluations of the integrity and functional reserve of the hepatic parenchyma because the parameters are not very specific and test sensitivity is sometimes too low to detect mild liver alteration^[2]. Recently several studies^[3-10] have considered that hepatic clearance of D-sorbitol was a valid procedure in determination of FHF, by which hepatic reserve function could be estimated. The aim of this study was to measure THF and FHF of control subjects and patients with cirrhosis by means of duplex doppler color sonography combined with modified hepatic clearance of D-sorbitol and then to evaluate the hepatic reserve function.

MATERIALS AND METHODS

Patients

This study was carried out on 20 patients with cirrhosis and portal hypertension. The diagnosis of cirrhosis was established by liver biopsy intraoperatively. Fourteen patients with cirrhosis were males and six were females. They ranged in age from 35 to 73 years. The etiology of the disease was virus-related in 19 cases and drug-induced in the remaining one. The exclusion criteria were: patients with a variceal bleeding in the previous four weeks; those on portal-pressure-lowering drugs; those with portal and splenic vein thrombosis; those with severe ascites.

Ten subjects that without any clinical or laboratory evidence of liver disease served as controls. They were matched with the patients with cirrhosis for sex, age and body surface area. All patients gave their informed consent before participation in this study, which was performed according to the Helsinki Declaration.

Measurement of THF

Duplex doppler measurements of the portal vein and common hepatic artery were obtained using a real-time electronic sector scanner and a pulsed doppler unit.

All the patients and controls were kept fasting overnight prior to the procedure. They were examined in the supine position and were asked to hold their breath during the doppler recording. The portal vein was scanned longitudinally, and the sample volume was positioned in the middle of the portal trunk. The hepatic artery measurements were taken where a straight stretch ran parallel to the portal vein, some centimeters away from the coeliac axis. Care was taken to maintain the angle at below 55°. Portal vein and hepatic artery flow were determined by multiplying the mean blood velocity (V_{mean}) by the sectional area (πr^2). Total hepatic flow was calculated as the sum of portal flow and hepatic artery flow.

Measurement of FHF

All tests were carried out at rest after an overnight fast. The sterile pyrogen-free 5% water solution of D-sorbitol (Fluka,

US) was intravenously infused at a constant rate of 50 mg/min. The steady-state regimen would be achieved after 2-h of continuous infusion^[11]. Three blood samples were taken from peripheral vein at about 15-min intervals between 135 and 165 min after the start of the infusion. Urine samples were spontaneously collected for a 1-h period between 120 and 180 min during the infusion. FHF was determined on the basis of the hepatic clearance of SOR, as previously described by Molino^[8].

Analyses

Blood and urine samples were centrifuged at 2 500 r/min for 15 min and the supernatants were stored at -40 °C until analysis. All samples were thawed before concentration measurement, then deproteinized by means of super-filter.

HPLC method was employed for the determination of concentration of D-sorbitol in human plasma and urine. The HPLC system (Waters) consisted of a pump, an injector and a fluorescence-detection (4210). The extracts of samples were chromatographed on a CORGEL-87P column that was kept at 85 °C and monitored by fluorescence-detection. The mobile phase was H₂O at a flow-rate of 1.0 mL/min. All data were treated according to the formula described by Molino^[8].

Statistical analysis

All the data are expressed as mean±SD. The statistical analyses were performed by means of two-sample *t*-test and paired *t*-test.

RESULTS

The results are shown in the Table 1. All the tests were performed on 20 patients with cirrhosis and 10 healthy controls and all subjects tolerated the procedure without complications or side effects. As expected, FHF, evaluated by means of the D-sorbitol clearance, was significantly reduced in patients with cirrhosis in comparison to controls (764.74±167.91 vs 1 195.05±242.97 mL/min, *P*<0.01). While THF was significantly increased in patients with cirrhosis in comparison to controls (1 605.23±279.99 vs 1 256.12±198.34 mL/min, *P*<0.01).

Portal blood flow and hepatic artery flow were increased in cirrhosis compared to controls (*P*<0.05 and *P*<0.01). D-sorbitol total clearance was significantly reduced in cirrhosis compared to control, while D-sorbitol renal clearance was significantly increased in cirrhosis (*P*<0.01).

In controls FHF and THF were similar (1 195.05±242.97 vs 1 256.12±198.34 mL/min, *P*=0.636), while FHF was significantly reduced compared to THF in cirrhosis (764.74±167.91 vs 1 605.23±279.99 mL/min, *P*<0.01).

DISCUSSION

Liver cirrhosis is the final pathologic and clinical expression of a wide variety of chronic liver diseases. The commonest causes of cirrhosis are chronic hepatitis B or C virus infection (nearly 90% of the total cases of cirrhosis in China). Pathophysiologically, the clinical manifestation of liver cirrhosis arises from the occurrence of two major events: hepatocellular insufficiency and portal hypertension^[12]. In cirrhosis, portal hypertension develops as a result of an increased sinusoidal or post-sinusoidal portal resistance to blood flow, due to the loss of normal hepatic architecture and collagenization of the space of Disse^[13,14]. The major pathophysiologic consequences of portal hypertension include portal-systemic collaterals formation, ascites and splenomegaly. The gastric and esophageal varices constitute the major cause of life-threatening digestive tract bleeding in cirrhosis. Now surgical devascularization and shunting play an important role in management of the complications of portal hypertension. Though operation is effective in controlling bleeding, the mortality of operation is still higher as some patients can not bear the strike of operation and anaesthesia due to inadequate hepatic reserve function. Recently some study discovered that the patients whose liver volume was decreased by 40% and the hepatic clearance of D-sorbitol was below 600 mL/min would have a higher incidence of postoperative complication^[15]. Therefore it is of much importance to evaluate the hepatic reserve function preoperatively for the selection of operation approaches and the timing of operation.

FHF may be defined as the blood perfusing the liver that makes contact with functioning hepatocytes. The most widely used procedures to assess FHF are based on the clearance technique. But the test compound must not be eliminated by any organ other than the liver, must not re-enter the circulation once it has been eliminated, and has relatively high hepatic intrinsic clearance. To date, no compound has fulfilled these requirements completely. D-sorbitol, a naturally occurring polyol with prevailing hepatic metabolism, is almost completely extracted by the liver during the first-pass, and extrahepatic elimination is negligible^[16]. Reproducible first-order kinetics and flow-dependent principle were demonstrated for D-sorbitol in previous studies^[2,10,11,17]. D-sorbitol had an exceptionally high extraction ratio in the normal liver (approaching 100%)^[16,17], even in the presence of a severely impaired liver function, so we might consider that hepatic clearance of D-sorbitol very closely approximates total hepatic flow. While in cirrhosis, the hepatic clearance of D-sorbitol is less than total hepatic flow due to intrahepatic shunting. The

Table 1 Results of Duplex doppler and D-sorbitol clearance in 20 patients with liver cirrhosis and 10 healthy controls

	Controls	Cirrhosis	<i>P</i>
Portal blood flow (mL/min)	960.35±220.86	1 181.10±279.79	<0.05
Hepatic artery flow (mL/min)	295.77±82.59	424.13±116.89	<0.01
Total hepatic flow (THF) (mL/min)	1 256.12±198.34	1 605.23±279.99	<0.01
THF per kg b.w. (mL/min)	20.14±3.51	25.12±4.40	<0.01
D-sorbitol concentration in blood (mg/dl)	4.15±0.81	6.05±1.22	<0.01
D-sorbitol total clearance (mL/min)	1 246.72±242.59	857.22±167.61	<0.01
D-sorbitol urinary elimination rate (mg/min)	2.16±1.0	5.58±2.76	<0.01
D-sorbitol renal clearance (mL/min)	51.67±19.96	92.48±48.66	<0.05
Functional hepatic flow(FHF) (mL/min)	1 195.05±242.97	764.74±167.91	<0.01
FHF per kg b.w. (mL/min)	19.18±4.28	12.07±2.40	<0.01

The data are expressed as mean±SD.

difference between THF and FHF can be assumed to be a parameter reflecting intrahepatic shunting.

Generally THF was measured by means of the hepatic extraction of D-sorbitol and indocyanine green, according to the Fick's principle^[4,10]. But the procedure, which needs hepatic vein catheterization is invasive and difficult to popularize. In addition, direct measurements of total hepatic flow through the hepatic artery and the portal vein have been achieved with electromagnetic flow probes or laser doppler flow meter^[18]. But the technique is applicable only during surgical procedures, which severely limits its usefulness. Recently the technique of duplex doppler color sonography has been gaining increasing popularity in the measurement of hepatic blood flow and found to be a safe, reproducible, noninvasive and fairly accurate method^[19-22].

There are still large variabilities in determination of FHF and THF by means of hepatic clearance of D-sorbitol and duplex doppler color sonography because of limitation of techniques and operations. To the former, the measurement of concentration of D-sorbitol is difficult. A small error of D-sorbitol concentration will lead to a large variability of final outcome. The concentration of D-sorbitol in plasma and urine used to be determined by an enzymatic-spectrophotometric method. It needs an enzymatic oxidation and deoxidization reaction since there is no absorption of ultraviolet for D-sorbitol. The concentration of D-sorbitol is determined indirectly following the measurement of fluorescence intensity of NADH1 that produced in reaction. While the attenuation of fluorescence and the incompleteness of reaction will result in certainty errors. To minimize these errors, we first established the method that measured the concentration of D-sorbitol by the use of HPLC and made the standard concentration curve. The data obtained in our study are in agreement with previous observations^[2,3,9]. Moreover, there is smaller standard error than that of other studies due to absence of extremely big or small data. In the latter, the errors stem from uncertainty in the measurement of blood velocity, vessel caliber and the possible non-circular shape of the cross-sectional area of the vessel. To minimize these errors, the examination was always performed by the same investigator, who had more than 5 years' experience in doppler examination of deep vessels and was unaware of the clinical diagnosis of the subject, and following strict guidelines during the operation.

The results of our study showed that THF was similar to FHF in controls (1 256.12±198.34 vs 1 195.05±242.97 mL/min, $P=0.636$), which support the measurement of FHF and THF by non-invasive techniques. However, since D-sorbitol hepatic extraction was never completed, the FHF slightly underestimated THF in controls. In cirrhosis, the FHF was significantly decreased, while doppler-assessed THF was increased, indicating that a part of the portal flow was diverted through intrahepatic shunts or a substantial impairment of the functional integrity of hepatocytes^[23]. In this case simultaneous assessment of these two non-invasive parameters could be useful to quantify functional shunting in cirrhosis. As expected, portal vein and hepatic artery blood flow were increased in cirrhosis in comparison to controls respectively, suggesting a hyperkinetic systemic circulation with a high cardiac output and decreased total peripheral vascular resistance. Though the THF was preserved or increased, the FHF was still reduced. This is thought to be due to reduced FHF and a compensatory increase in THF to maintain hepatic perfusion. In addition, we measured the FHF and THF in six patients with liver cirrhosis before and after transjugular intrahepatic portosystemic shunt (TIPS). We discovered that the THF measured one week after TIPS was more than that of before TIPS, while FHF was reduced significantly in all subjects. It may be considered that the reduction of portal vein pressure and increase in

portosystemic shunting caused by TIPS are associated with the reduction of hepatic perfusion, which can partly explain the high incidence of hepatic encephalopathy in patients with liver cirrhosis^[24-26].

REFERENCES

- 1 **Seewald S**, Seitz U, Yang AM, Soehendra N. Variceal bleeding and portal hypertension: still a therapeutic challenge? *Endoscopy* 2001; **33**: 126-139
- 2 **Garello E**, Battista S, Bar F, Niro GA, Cappello N, Rizzetto M, Molino G. Evaluation of hepatic function in liver cirrhosis: clinical utility of galactose elimination capacity, hepatic clearance of D-sorbitol, and laboratory investigations. *Dig Dis Sci* 1999; **44**: 782-788
- 3 **Zoli M**, Magalotti D, Bianchi G, Ghigi G, Orlandini C, Grimaldi M, Marchesini G, Pisi E. Functional hepatic flow and Doppler-assessed total hepatic flow in control subjects and in patients with cirrhosis. *J Hepatol* 1995; **23**: 129-134
- 4 **Molino G**, Avagnina P, Ballare M, Torchio M, Niro AG, Aurucci PE, Grosso M, Fava C. Combined evaluation of total and functional liver plasma flows and intrahepatic shunting. *Dig Dis Sci* 1991; **36**: 1189-1196
- 5 **Molino G**, Battista S, Bar F, Garello E, Avagnina P, Grosso M, Spalluto E. Determination of functional portal-systemic shunting in patients submitted to hepatic angiography. *Liver* 1996; **16**: 347-352
- 6 **Ott P**, Clemmesen O, Keiding S. Interpretation of simultaneous measurements of hepatic extraction fractions of indocyanine green and sorbitol: evidence of hepatic shunts and capillarization? *Dig Dis Sci* 2000; **45**: 359-365
- 7 **Bar F**, Battista S, Garello E, Grosso M, Spalluto F, Zanon E, Torchio M, Molino G. Short-term effects of transjugular intrahepatic portosystemic shunt (TIPS) on functional liver plasma flow in patients with advanced cirrhosis. *Liver* 1998; **18**: 245-250
- 8 **Molino G**, Avagnina P, Belforte G, Bircher J. Assessment of the hepatic circulation in humans: new concepts based on evidence derived from a D-sorbitol clearance method. *J Lab Clin Med* 1998; **131**: 393-405
- 9 **Fabbi A**, Magalotti D, Brizi M, Bianchi G, Zoli M, Marchesini G. Prostaglandin E1 infusion and functional hepatic flow in control subjects and in patients with cirrhosis. *Dig Dis Sci* 1999; **44**: 377-384
- 10 **Clemmesen JO**, Tygstrup N, Ott P. Hepatic plasma flow estimated according to Fick's principle in patients with hepatic encephalopathy: evaluation of indocyanine green and D-sorbitol as test substances. *Hepatology* 1998; **27**: 666-673
- 11 **Molino G**, Avagnina P, Garrone C, Sansoe G, Degerfeld MM, Peretti P, Tinivella M, Bianco S. Time-dependent modifications of splanchnic circulation in female pigs submitted to end-to-side portacaval anastomosis. *Dig Dis Sci* 2001; **46**: 489-494
- 12 **Bilbao JI**, Quiroga J, Herrero JJ, Benito A. Transjugular intrahepatic portosystemic shunt (TIPS): current status and future possibilities. *Cardiovasc Intervent Radiol* 2002; **25**: 251-269
- 13 **Liu YK**, Shen W. Inhibitive effect of cordyceps sinensis on experimental hepatic fibrosis and its possible mechanism. *World J Gastroenterol* 2003; **9**: 529-533
- 14 **Wang XB**, Liu P, Lu X, Liu CH, Hu YY, Gu HT, Liu C. Dynamic changes of pressure of portal vein in development of liver fibrosis induced by dimethylnitrosamine in rats. *Shijie Huaren Xiaohua Zazhi* 2002; **10**: 401-405
- 15 **Li YM**, Lv F, Xu X, Ji H, Gao WT, Lei TJ, Ren GB, Bai ZL, Li Q. Evaluation of liver functional reserve by combining D-sorbitol clearance rate and CT measured liver volume. *World J Gastroenterol* 2003; **9**: 2092-2095
- 16 **Burggraaf J**, Schoemaker RC, Lentjes EG, Cohen AF. Sorbitol as a marker for drug-induced decreases of variable duration in liver blood flow in healthy volunteers. *Eur J Pharm Sci* 2000; **12**: 133-139
- 17 **Bar F**, Battista S, Bucchi MC, Zanon C, Grosso M, Alabiso O, Miraglia S, Cappello N, Gariboldi A, Molino G. Sorbitol removal by the metastatic liver: a predictor of systemic toxicity of intra-arterial chemotherapy in patients with liver metastases. *J Hepatol*

- 1999; **30**: 1112-1118
- 18 **Tomoda F**, Yamanaka N, Furukawa K, Kawamura E, Tanaka T, Ichikawa N, Kuroda N, Okamoto E. Contribution of the portal flow on hepatic tissue perfusion increases in reduced hepatic vascular bed. *Hepato Res* 2000; **17**: 212-222
- 19 **Chawla Y**, Santa N, Dhiman RK, Dilawari JB. Portal hemodynamics by duplex Doppler sonography in different grades of cirrhosis. *Dig Dis Sci* 1998; **43**: 354-357
- 20 **Walsh KM**, Leen E, MacSween RN, Morris AJ. Hepatic blood flow changes in chronic hepatitis C measured by duplex Doppler color sonography: relationship to histological features. *Dig Dis Sci* 1998; **43**: 2584-2590
- 21 **Merkel C**, Sacerdoti D, Bolognesi M, Bombonato G, Gatta A. Doppler sonography and hepatic vein catheterization in portal hypertension: assessment of agreement in evaluating severity and response to treatment. *J Hepatol* 1998; **28**: 622-630
- 22 **Bolognesi M**, Sacerdoti D, Merkel C, Bombonato G, Gatta A. Noninvasive grading of the severity of portal hypertension in cirrhotic patients by echo-color-Doppler. *Ultrasound Med Biol* 2001; **27**: 901-907
- 23 **Molino G**, Bar F, Battista S, Torchio M, Niro AG, Garello E, Avagnina P, Fava C, Grosso M, Spalluto F. Arterial-venous shunting in liver cirrhosis. *Dig Dis Sci* 1998; **43**: 51-55
- 24 **Riggio O**, Merli M, Pedretti G, Servi R, Meddi P, Lionetti R, Rossi P, Bezzi M, Salvatori F, Ugolotti U, Fiaccadori F, Capocaccia L. Hepatic encephalopathy after transjugular intrahepatic portosystemic shunt. Incidence and risk factors. *Dig Dis Sci* 1996; **41**: 578-584
- 25 **Sanyal AJ**, Freedman AM, Shiffman ML, Purdum PP 3rd, Luketic VA, Cheatham AK. Portosystemic encephalopathy after transjugular intrahepatic portosystemic shunt: results of a prospective controlled study. *Hepatology* 1994; **20**(1 Pt 1): 46-55
- 26 **Jalan R**, Gooday R, O'Carroll R, Redhead DN, Elton RA, Hayes PC. A prospective evaluation of changes in neuropsychological and liver function tests following transjugular intrahepatic portosystemic shunt. *J Hepatol* 1995; **23**: 697-705

Edited by Zhu LH Proofread by Xu FM

Clinical characteristics and management of patients with early acute severe pancreatitis: Experience from a medical center in China

Hou-Quan Tao, Jing-Xia Zhang, Shou-Chun Zou

Hou-Quan Tao, Jing-Xia Zhang, Shou-Chun Zou, Department of Surgery, Zhejiang Provincial Peoples' Hospital, Hangzhou 310014, Zhejiang Province, China

Correspondence to: Dr. Hou-Quan Tao, Department of Surgery, Zhejiang Provincial Peoples' Hospital, Hangzhou 310014, Zhejiang Province, China. houquantao@yahoo.com

Telephone: +86-571-85239988

Received: 2003-10-10 **Accepted:** 2003-11-13

Abstract

AIM: To study clinical characteristics and management of patients with early severe acute pancreatitis (ESAP).

METHODS: Data of 297 patients with severe acute pancreatitis (SAP) admitted to our hospital within 72 h after onset of symptoms from January 1991 to June 2003 were reviewed for the occurrence and development of early severe acute pancreatitis (ESAP). ESAP was defined as presence of organ dysfunction within 72 h after onset of symptoms. Sixty-nine patients had ESAP, 228 patients without organ dysfunction within 72 h after onset of symptoms had SAP. The clinical characteristics, incidence of organ dysfunction during hospitalization and prognosis between ESAP and SAP were compared.

RESULTS: Impairment degree of pancreas (Balthazar CT class) in ESAP was more serious than that in SAP (5.31 ± 0.68 vs 3.68 ± 0.29 , $P < 0.01$). ESAP had a higher mortality than SAP (43.4% vs 2.6%, $P < 0.01$), and a higher incidence of hypoxemia (85.5% vs 25%, $P < 0.01$), pancreas infection (15.9% vs 7.5%, $P < 0.05$), abdominal compartment syndrome (ACS) (78.3% vs 23.2%, $P < 0.01$) and multiple organ dysfunction syndrome (MODS) (78.3% vs 10.1%, $P < 0.01$). In multiple logistic regression analysis, the main predisposing factors to ESAP were higher APACHE II score, Balthazar CT class, MODS and hypoxemia.

CONCLUSION: ESAP is characterised by MODS, severe pathological changes of pancreas, early hypoxemia and abdominal compartment syndrome. Given the poor prognosis of ESAP, these patients should be treated in specialized intensive care units with special measures such as close supervision, fluid resuscitation, improvement of hypoxemia, reduction of pancreatic secretion, elimination of inflammatory mediators, prevention and treatment of pancreatic infections.

Tao HQ, Zhang JX, Zou SC. Clinical characteristics and management of patients with early acute severe pancreatitis: Experience from a medical center in China. *World J Gastroenterol* 2004; 10(6): 919-921

<http://www.wjgnet.com/1007-9327/10/919.asp>

INTRODUCTION

Despite considerable improvement in the treatment of severe acute pancreatitis (SAP), the mortality of the disease still ranges

between 15-25%^[1-3]. Multiple organ dysfunction syndrome (MODS)^[4-7], the extent of necrotic pancreatic parenchyma and the presence of bacterial infection have been identified as major determinants for death^[8,9]. A number of such patients developed pancreatitis-associated intractable organ failure during the early course of SAP, and no effective treatment methods were available, the mortality was up to 40-60%^[3,10,11]. For the purpose of assessing the clinical course and management of these specific severe pancreatitis, we defined these severe acute pancreatitis with presence of organ dysfunction within 72 h after onset of symptoms as early severe acute pancreatitis (ESAP)^[12]. In this paper, we analyzed the clinical features of 69 cases of ESAP and discussed the key of ESAP management.

MATERIALS AND METHODS

Clinical data

From January 1991 to June 2003, a total of 297 patients with SAP were treated in our hospital, including 140 males and 157 females (average age 58.53, from 15 to 79 years). Among them 69 cases were with organ dysfunction within 72 h after onset of symptoms, and 228 cases without organ dysfunction.

SAP and organ dysfunction definitions were adopted from the Atlanta Classification System for SAP^[13]. All patients received standardized intensive care treatment as the following: (1) Supportive care including maintaining circulation volume, nutritional supplements, prophylactic antibiotics for pancreatic infection, oxygen supplementation, and mechanical ventilation, as well as monitoring for respiratory, cardiovascular and renal insufficiency and correcting them early. (2) To 'rest the pancreas' by fasting with nasogastric drainage to remove gastric secretions and by using anticholinergic agents or H₂-blocking agents and somatostatin to inhibit pancreatic secretion. (3) Multiple measures were taken early for accelerating the recovery of gastrointestinal function. (4) Infectious necrosis of pancreas was identified by dynamic contrast-enhanced CT. (5) Oddi's sphincterotomy and nasobiliary drainage were performed for biliary pancreatitis accompanied by bile duct obstruction. (6) Surgical treatment (necrosectomy with drainage and continuous postoperative lavage of the lesser sac) was performed if infected pancreatic necrosis was identified or if the patient did not respond to maximal intensive care treatment over a period of more than 72 h.

Patients were divided into two sub-groups: ESAP with organ dysfunction and SAP without organ dysfunction within 72 h after onset of symptoms. APACHEII score, Balthazar CT class, number of organ dysfunction and rate of pancreatic infection in both groups were analyzed retrospectively.

Statistical analysis

Measurement data was expressed as mean±SD, the difference between the groups was analyzed with Student's *t* test. Quantitative data was analyzed with Chi-square test. To identify the risk factors for ESAP, multiple logistic regression analysis with backward elimination was used. The level of significance was $P < 0.05$.

RESULTS

ESAP characteristic

Data of 297 SAP are given in Table 1. The mean time between onset of symptoms and hospital admission was 25.64 h. Mortality of ESAP was higher than that of SAP, early death rate (within 1 wk) was 53.3% (16/30) in ESAP and 33.3% (2/6) in SAP respectively. Pulmonary failure was the most frequent organ dysfunction in ESAP. Compared with SAP group, the different types of organ dysfunction were observed more frequently in the ESAP group. The hospital course of patients with ESAP was characterized by a high incidence of progressive MODS (Table 2).

Table 1 Comparison of clinical characteristics between ESAP and SAP

Factor	ESAP group	SAP group
Age (year)	58.95±5.51 ^a	60.12±5.16
Sex (M/F)	38/31 ^a	102/126
Hours between onset and admission	24.72±5.21 ^a	26.04±4.03
APACHE II at admission	16.6±0.72 ^b	9.4±0.45
Impairment degree of pancreas (Balthazar CT class)	5.31±0.68 ^b	3.68±0.29
Hypoxemia (%)	59(85.5) ^b	57(25)
ACS (%)	54(78.3) ^b	53(23.2)
Fever (T>38.5 °C)(%)	38(55.1) ^b	55(24.1)
Pancreas infection (%)	11(15.9) ^a	17(7.5)
Other infections (%)	40(57.9) ^b	41(17.9)
Non-effective after 48 h	42(60.8) ^b	27(11.8)
ICU treatment (%)		
Surgical treatment (%)	18(26.1) ^b	15(6.5)
Death (%)	30(43.4) ^b	6(2.6)
Death within 3 d	7	1
Death within 1 wk	16	2
Death after 1 wk	14	4
Mean hospitalization (d)	44.72±42.15 ¹	21.26±23.66

¹P>0.05, ^aP<0.05, ^bP<0.01, vs SAP group, ACS: abdominal compartment syndrome.

Table 2 Incidence of organ dysfunction during hospitalization in patients with ESAP and SAP (%)

Factor	ESAP group	SAP group
Single organ dysfunction	15(21.7) ^a	25(10.9)
MODS	54(78.3) ^b	20(10.1)
Pulmonary insufficiency	59(85.5) ^b	27(11.8)
Hepatic dysfunction	14(20.3) ^b	17(7.5)
Renal insufficiency	28(40.6) ^b	9(3.9)
GI dysfunction	24(34.8) ^b	16(7.0)
Shock	29(42.0) ^b	10(4.4)

^aP<0.05, ^bP<0.01, vs SAP group.

Table 3 Features of victim in ESAP group

Factor	Death group (n=30)	Cure group (n=39)
Numbers of organ dysfunction	3.33±0.25 ^b	2.27±0.21
APACHE II score	16.1±1.12 ^b	14.2±1.09
Balthazar CT class	5.69±0.62 ^b	4.47±0.43
Hypoxemia (%)	30(100) ^b	27(69.2)
Abdominal compartment syndrome (%)	27(90) ^b	22(56.4)
Pancreas infection (%)	8(26.7) ¹	4(10.3)
Other infections (%)	16(53.3) ¹	24(61.5)

¹P>0.05, ^bP<0.01, vs cure group.

Features of victim in ESAP

Table 3 shows the features of death cases of ESAP. Multiple logistic regression analysis with backward elimination revealed that hypoxemia, higher APACHE II score, MODS and the extent of pancreatic necrosis were high risks for ESAP death.

DISCUSSION

With the advance in SAP study over the years, that the occurrence of early organ dysfunction is correlated with cascade response which gives rise to inflammatory mediators such as cytokine has been recognized gradually^[14-16]. The effect of cytokine on the early stage of SAP should be emphasized. In fact, ESAP, a special critical type of SAP, is manifested as sharp changes during the early stage of SAP of non-stable vital signs and early organ dysfunction. Isenmann and Beger reported a group of SAP cases admitted to hospital within 72 h after onset of abdominal pain with organ dysfunction, which was defined as ESAP, and the mortality rate was up to 42%^[12]. According to McKay's data^[11], 40% of all death occurred within 3 d in SAP. In our data, the mortality rate was 23.3% (7/30) in ESAP group within 3 d and 53.3% (16/30) within 1 week. This indicated that ESAP was the higher risk group of acute pancreatitis death. Therefore it is very important to understand the characteristics of ESAP, which were mainly summarized as: a short disease course with progressive multiple organ dysfunction; early hypoxemia; a higher incidence of abdominal compartment syndrome; a higher incidence of infected pancreatic necrosis; and higher CT score of pancreatic changes. ESAP is a critical type of SAP with a high early mortality rate and poor prognosis. High-risk factors of mortality in ESAP group are early hypoxemia and multiple organs dysfunction.

Because there is an extremely high risk of progressive MODS, as well as an extremely high mortality rate in ESAP, ESAP patients should receive maximal intensive care treatment for organ dysfunction. First of all, our data showed that hypoxemia occurred in 85.5% ESAP. For correcting hypoxemia, all patients were given positive end-expiratory pressure (PEEP) early. Respirator respiration through tracheal intubation should be used if hypoxemia can not be improved after 4-6 h. The principle of respirator use is 'to use early and to stop early', the oxygen concentration should be lower than 40%. The most important change of respiration system is ARDS. Pulmonary infection may be present due to ARDS, and even pulmonary infection may become the main reason for deterioration in ESAP. Monitoring of occurrence and progression of ARDS should be emphasized. Secondly, abdominal compartment syndrome (ACS) will be established if intra-abdominal pressure is higher than 15 mmHg (2kPa) with low cardiac output and progressive oliguria, and hypoxia occurred even if the airway peak value is normal or higher. Our result showed that higher pressure of abdominal cavity was presented in 78.3% ESAP. Higher pressure of abdominal cavity may damage the function of lung, heart, kidney and liver, inducing or exacerbating organ dysfunction. Abdominal decompression is the only way treating ACS. ACS can be divided into two types: one is present as ascites, peritoneal lavage or drainage can not only reduce the higher intra-abdominal pressure by using laparoscope but can also reduce systemic inflammation by diluting and draining abdominal exudates which contained pancreatic juice and cytokines. Another type of ACS is the result of enteroparalysis and gastrointestinal (GI) pneumatosis. Recovery of GI function is very important. We usually use purgative agents such as magnesium sulfate or Dahuang decoction (TCM) for accelerating GI function. These agents can promote GI peristalsis, decrease the intra-abdominal pressure, combat bacteria infection, protect the barrier function of GI tract, decrease translocation of bacterial and endotoxin and accelerate

the ascites absorption. Also, magnesium sulfate can reduce the opportunity of bacterial infection by promoting bile excretion and pancreatic juice excretion. Additionally, Pixiao can draw ascites out of peritoneal cavity. Our results indicated that the earlier the ACS was relieved, the better the prognosis was. Thirdly, most ESAP cases had systemic inflammatory response syndrome (SIRS), which is the result of interaction of multiple inflammatory cytokines and has no specific therapeutic treatment modality. Hemofiltration has the effect of stabilizing hemodynamic and homeostasis, cleaning excess inflammatory factors such as cytokines, improving the function of heart, lung and kidney, and reducing the degree of illness^[17-20]. We treated 25 ESAP patients with SIRS by hemofiltration at the early stage and obtained satisfactory (Data not shown). Fourthly, our data showed that the prognosis of early non-organ dysfunction group was satisfactory based on the same treatment principle and the mortality rate was just 2.6%. In the absence of evidence for pancreatic necrosis, SAP should be treated by non-surgical treatment if the condition is stable^[21-25]. Owing to the unstable condition in ESAP, the mortality rate may increase because of operation^[26]. Surgical treatment would be considered when: (1) Higher intra-abdominal pressure is not resolved or ascites is increased after 8-12 h' therapy. (2) Dynamic CT examination indicates the evidence of severe pancreatic lesion or inflammatory necrosis. As conventional operation may make patient's condition worse at this stage, we proposed the method with minimal interruptions on body function such as peritoneal lavage under laparoscope, posterior peritoneal or paracolic sulci drainage to avoid systemic circulation or metabolism disturbances. The emphasis of surgery is peritoneal drainage and relief of intraabdominal pressure. Our data indicated that the outcome was better than simple conservation group and the mortality rate was reduced. Fifthly, prophylactic antibiotic was used early. All patients were given antibiotics once SAP was diagnosed. Antibiotics which can pass the blood-pancreas barrier and have effect on normal gut bacteria were first of choice. In general, Tienam or third generation cephalosporin with flagyl was applied. Sometimes, antibiotic was given by using arterial catheterization so that the pancreas could encounter higher drug concentration. Sixthly, low molecular weight heparin and Alprostadil can improve the microcirculation in pancreas^[27,28]. We usually used these agents early. Lastly, nutritional support should be applied under the circumstance of stable systemic condition^[29,30]. In general, we used parenteral nutrition (PN) at early stage. Enteral nutrition (EN) was used through jejunum once gut function recovered. EN can maintain gut mucosa barrier function, prevent or reverse the damage of gut mucosa barrier.

As our knowledge about the pathogenesis of systemic complications of ESAP is limited, patients with early organ dysfunction still remain a serious problem. The mechanism of ESAP and effective therapy still pose a challenge for future study.

REFERENCES

- Bradley EL 3rd. A fifteen year experience with open drainage for infected pancreatic necrosis. *Surg Gynecol Obstet* 1993; **177**: 215-222
- Tsiotos GG, Luque-de Leon E, Soreide JA, Bannon MP, Zietlow SP, Baerga-Varela Y, Sarr MG. Management of necrotizing pancreatitis by repeated operative necrosectomy using a zipper technique. *Am J Surg* 1998; **175**: 91-98
- Beger HG, Isenmann R. Surgical management of necrotizing pancreatitis. *Surg Clin North Am* 1999; **79**: 783-800
- de Beaux AC, Palmer KR, Carter DC. Factors influencing morbidity and mortality in acute pancreatitis; an analysis of 279 cases. *Gut* 1995; **37**: 121-126
- Tenner S, Sica G, Hughes M, Noordhoek E, Feng S, Zinner M, Banks PA. Relationship of necrosis to organ failure in severe acute pancreatitis. *Gastroenterology* 1997; **113**: 899-903
- Neoptolemos JP, Raraty M, Finch M, Sutton R. Acute pancreatitis: the substantial human and financial costs. *Gut* 1998; **42**: 886-891
- Buter A, Imrie CW, Carter CR, Evans S, McKay CJ. Dynamic nature of early organ dysfunction determines outcome in acute pancreatitis. *Br J Surg* 2002; **89**: 298-302
- Isenmann R, Rau B, Beger HG. Bacterial infection and extent of necrosis are determinants of organ failure in patients with acute necrotizing pancreatitis. *Br J Surg* 1999; **86**: 1020-1024
- Takeda K, Matsuno S, Sunamura M, Kobari M. Surgical aspects and management of acute necrotizing pancreatitis: recent results of a cooperative national survey in Japan. *Pancreas* 1998; **16**: 316-322
- Bosscha K, Hulstaert PF, Hennipman A, Visser MR, Gooszen HG, van Vroonhoven TJ, vd Werken C. Fulminant acute pancreatitis and infected necrosis: results of open management of the abdomen and "planned" reoperations. *J Am Coll Surg* 1998; **18**: 255-262
- McKay CJ, Evans S, Sinclair M, Carter CR, Imrie CW. High early mortality rate from acute pancreatitis in Scotland, 1984-1995. *Br J Surg* 1999; **86**: 1302-1305
- Isenmann R, Rau B, Beger HG. Early severe acute pancreatitis: characteristics of a new subgroup. *Pancreas* 2001; **22**: 274-278
- Bradley EL 3rd. A clinically based classification system for acute pancreatitis. *Ann Chir* 1993; **47**: 537-541
- Norman J. The role of cytokines in the pathogenesis of acute pancreatitis. *Am J Surg* 1998; **17**: 76-83
- Osman MO, Gesser B, Mortensen JT, Matsushima K, Jensen SL, Larsen CG. Profiles of pro-inflammatory cytokines in the serum of rabbits after experimentally induced acute pancreatitis. *Cytokine* 2002; **17**: 53-59
- Frossard JL. Pathophysiology of acute pancreatitis: a multistep disease. *Acta Gastroenterol Belg* 2003; **66**: 166-173
- Oda S, Hirasawa H, Shiga H, Nakanishi K, Matsuda K. Continuous hemofiltration/hemodiafiltration in critical care. *Ther Apher* 2002; **6**: 193-198
- Pupelis G, Austrums E, Snippe K. Blood purification methods for treatment of organ failure in patients with severe pancreatitis. *Zentralbl Chir* 2001; **126**: 780-784
- Xie HL, Ji DX, Gong DH, Liu Y, Xu B, Zhou H, Liu ZH, Li LS, Li WQ, Quan ZF, Li JS. Continuous veno venous hemofiltration in treatment of acute necrotizing pancreatitis. *Chin Med J* 2003; **116**: 549-553
- Wang H, Li WQ, Zhou W, Li N, Li JS. Clinical effects of continuous high volume hemofiltration in severe acute pancreatitis complicated with multiple organ dysfunction syndrome. *World J Gastroenterol* 2003; **9**: 2096-2099
- Mier J, Leon EL, Castillo A, Robledo F, Blanco R. Early versus late necrosectomy in severe necrotizing pancreatitis. *Am J Surg* 1997; **173**: 71-75
- Hartwig W, Maksan SM, Foitzik T, Schmidt J, Herfarth C, Klar E. Reduction in mortality with delayed surgical therapy of severe pancreatitis. *J Gastrointest Surg* 2002; **6**: 481-487
- Silverman WB. Medical and endoscopic treatment of acute pancreatitis. *Curr Treat Options Gastroenterol* 2003; **6**: 381-387
- Werner J, Uhl W, Buchler MW. Surgical treatment of acute pancreatitis. *Curr Treat Options Gastroenterol* 2003; **6**: 359-367
- Slavin J, Ghaneh P, Sutton R, Hartley M, Rowlands P, Garvey C, Hughes M, Neoptolemos J. Management of necrotizing pancreatitis. *World J Gastroenterol* 2001; **7**: 476-481
- Dugernier T, Reynaert M, Laterre PF. Early multi-system organ failure associated with acute pancreatitis: a plea for a conservative therapeutic strategy. *Acta Gastroenterol Belg* 2003; **66**: 177-183
- Sunamura M, Yamauchi J, Shibuya K, Chen HM, Ding L, Takeda K, Kodari M, Matsuno S. Pancreatic microcirculation in acute pancreatitis. *J Hepatobil Pancreat Surg* 1998; **5**: 62-68
- Zhou ZG, Chen YD. Influencing factors of pancreatic microcirculatory impairment in acute pancreatitis. *World J Gastroenterol* 2002; **8**: 406-412
- Zhao G, Wang CY, Wang F, Xiong JX. Clinical study on nutrition support in patients with severe acute pancreatitis. *World J Gastroenterol* 2003; **9**: 2105-2108
- Tu WF, Li JS, Zhu WM, Li ZD, Liu FN, Chen YM, Xu JG, Shao HF, Xiao GX, Li A. Influence of Glutamine and caecostomy/colonic irrigation on gut bacterial/endotoxin translocation in acute severe pancreatitis in pigs. *Shijie Huaren Xiaohuua Zazhi* 1999; **7**: 135-138

Relationship between plasma D-dimer levels and clinicopathologic parameters in resectable colorectal cancer patients

Gang Xu, Ya-Li Zhang, Wen Huang

Gang Xu, Ya-Li Zhang, Wen Huang, Institute of Gastroenterology, First Military Medical University, Guangzhou 510515, Guangdong Province, China

Correspondence to: Gang Xu, Institute of Gastroenterology, First Military Medical University, Guangzhou 510515, Guangdong Province, China. tianzr@sdu.edu.cn

Telephone: +86-20-85141544

Received: 2001-10-12 **Accepted:** 2001-11-27

Abstract

AIM: To assess the clinical significance of the D-dimer levels and the relationship between plasma D-dimer levels and clinicopathologic parameters in operable colorectal cancer patients.

METHODS: The plasma levels of D-dimer were measured pre- and postoperatively in 35 patients with colorectal cancer, and 30 healthy subjects served as controls by the method of quantitative enzyme-linked immunosorbent assay (ELISA).

RESULTS: The mean preoperative plasma levels of D-dimer in the patients with colorectal cancer (1.06 ± 0.24 mg/L) were significantly higher than those of controls (0.33 ± 0.12 mg/L, $P < 0.01$). The D-dimer levels were remarkably elevated on the 1st day after operation (1.22 ± 0.55 mg/L, $P < 0.01$). On the 3rd day the level of D-dimer began to stepwise descend and on the 14th day nearly returned to control level. The preoperative levels of D-dimer were significantly correlated with the lymph node metastasis and Dukes stage but had no association with tumor location and the degree of differentiation. A stepwise increase in the mean D-dimer levels was found with increase of the tumor stage.

CONCLUSION: Hypercoagulation and higher fibrinolytic activities occur in patients with colorectal cancer. The operative trauma could enhance the fibrinolysis in the patients with colorectal cancer. The measurement of preoperative D-dimer levels is considered to be useful for predicting lymph node metastasis and stage of colorectal cancer.

Xu G, Zhang YL, Huang W. Relationship between plasma D-dimer levels and clinicopathologic parameters in resectable colorectal cancer patients. *World J Gastroenterol* 2004; 10 (6): 922-923

<http://www.wjgnet.com/1007-9327/10/922.asp>

INTRODUCTION

Activation of coagulation and fibrinolysis is known to be frequently associated with malignancy, although the mechanism involved has not been fully clarified. The extent of such activation has been reported to correlate with tumor stage and prognosis in some malignancies, including

colorectal cancer^[1-3]. D-dimer is a stable end-product of fibrin degradation and levels of D-dimer are elevated by enhanced fibrin formation and fibrinolysis. It is a marker of hypercoagulable stage. D-dimer levels are elevated in the plasma of various solid tumor patients^[4,5]. The present study was to assess the clinical significance of the D-dimer levels and the relationship between plasma D-dimer levels and clinicopathologic findings in pre and post operative patients with colorectal cancer.

MATERIALS AND METHODS

Patients

Thirty-five patients with colorectal cancer were investigated. There were 21 males and 14 females, with a median age of 52 years, ranging from 32 to 75 years. Patients with cerebrovascular and diabetes were excluded. Meanwhile, 30 healthy subjects served as controls (17 males and 13 females, median age 56 years, ranging from 33 to 86 years).

Measurement of plasma D-dimer

Five milliliter of whole blood was drawn from antecubital vein of patients on the day prior to operation and on the 1st, 3rd, 7th, 14th postoperative days, using 3.8g sodium citrate collection tube. All samples were centrifuged within 4 h of veinpuncture, the plasma components were pipetted off and placed in plastic tubes. Centrifuged plasma was stored at -80°C until assay. Meanwhile 30 samples of healthy subjects served as controls. Plasma D-dimer levels were determined by quantitative enzyme-linked immunosorbent assay (ELISA).

Statistical analysis

Statistical analysis of mean value of D-dimer levels was made by Student's *t* test and Student Newman-keuls' *s* test. $P < 0.05$ was considered to be significant.

RESULTS

Relationship between plasma D-dimer levels and clinicopathologic parameters

The D-dimer levels of colorectal cancer patients with positive lymph nodes were significantly higher than that of negative lymph nodes (0.94 ± 0.26 vs 1.15 ± 0.12 , $P < 0.01$, Table 1). A stepwise increase in the mean D-dimer levels was found with the increase of tumor clinical stage. There was no association between D-dimer levels and tumor location or degree of the differentiation.

Pre- and postoperative plasma D-dimer levels in colorectal cancer patients

The mean plasma levels of D-dimer in the patients with colorectal cancer were significantly higher than that of the controls ($P < 0.01$, Table 1). It was also observed that D-dimer levels were remarkably elevated on the 1st day after the operation ($P < 0.01$). On the 3rd day after operation the D-dimer levels began to stepwise descend and on the 14th day almost returned to control ($P > 0.05$).

Table 1 Relationship between plasma D-dimer levels (mean±SD) and clinicopathology variables

Course (d)	Clinicopathology		n	D-dimer (mg/L)
Preoperation	Location	Colon	14	1.06±0.24 ^b
		Rectum	21	1.11±0.16
	Differentiation	Well	13	1.03±0.25
		Moderate	16	1.01±0.28
		Poor	6	1.02±0.31
	Lymph node	Negative	15	1.08±0.14
		Positive	15	0.94±0.26
	Metastasis	Positive	20	1.15±0.12 ^a
		Dukes stage	A + B	15
	Postoperation	1	C	15
D			5	1.29±0.11 ^d
3			35	1.22±0.55 ^b
			35	0.82±0.49 ^{bc}
7			30	0.67±0.41 ^{bf}
			17	0.46±0.17 ^f
14			30	0.33±0.12
		Control		30

^bP<0.01 vs control; ^aP<0.05 vs negative; ^cP<0.05, ^dP<0.01 vs Dukes A+B; ^eP<0.05, ^fP<0.01 vs preoperation.

DISCUSSION

Both experimental and clinical data have shown that coagulation disorders are common in patients with cancer although clinical symptoms may occur rarely. Recent reports showed hypercoagulable state in cancer patients and the plasma D-dimer levels were increased in these patients^[4,5]. The process of metastasis involves multiple tumor-host interactions. To survive, metastatic cancer cells must leave the primary tumor, migrate into the lymphovascular system and establish a new blood supply at their metastatic site^[6-8]. Fibrin remodeling is almost certainly involved in all steps of metastasis and has been proved to play a crucial role in new vessel formation^[9-11]. Our study showed that the preoperative D-dimer levels were higher and correlated with the tumor lymph node metastasis. It confirmed that unregulated fibrinolytic activities in colorectal cancer and increased levels of fibrinolytic activities in metastasis of colorectal cancer. The reason may be that cancer cells appear to be capable of both thrombin formation and induction of fibrin degradation because cancer cells tend to adhere to, aggregate, necrose, which could induce monocytes and endothelioid cells to release many clotting factors^[12,13]. Studies suggested that higher D-dimer levels could induce the secretion of interleukin-1, urokinase-type plasminogen activator (u-PA) and plasminogen activator inhibitor-2 in a human promonocytic leukemia cell line. u-PA is the predictive marker in many malignant tumors and may play an important role in the invasive cancer^[14-16]. The prethrombotic state (depicted by a prolongation of PT and increase of D-dimer) is confirmed to be an aggravating condition in cancers. Studies suggesting an attempt to reverse possible haemostatic abnormalities with the use of anticoagulants have been justified. Thus anticoagulant treatment may have a positive influence on colorectal cancer therapy.

We found that D-dimer levels were remarkably elevated on the 1st day after the operation. On the 3rd day after operation the D-dimer levels began to stepwise descend and on the 14th day returned to control. The remarkable increase in D-dimer levels occurring in patients indicated that patients undergoing surgery were at high risks for the occurrence of a thromboembolic event. Thus D-dimer could be used for estimating individual risk of thromboembolism and prophylactic treatment in these patients. Oya *et al* had obtained the same results. In addition,

we found the D-dimer levels of colorectal cancer patients with positive lymph nodes were significantly higher than that of negative lymph nodes. A stepwise increase in the mean D-dimer levels was found with the increase of tumor clinical stage. The measurement of preoperative D-dimer levels is considered to be useful for predicting lymph node metastasis and clinical stage of colorectal cancer.

REFERENCES

- Kalweit GA**, Feindt P, Micek M, Gams E, Hellstern P. Markers of activated hemostasis and fibrinolysis in patients with pulmonary malignancies: comparison of plasma levels in central venous and pulmonary venous blood. *Thromb Res* 2000; **97**: 105-111
- Tanabe K**, Terada Y, Shibutani T, Kunitada S, Kondo T. A specific inhibitor of factor Xa, DX-9065a, exerts effective protection against experimental tumor induced disseminated intravascular coagulation in rats. *Thromb Res* 1999; **96**: 135-143
- Oya M**, Akiyama Y, Okuyama T, Ishikawa H. High preoperative plasma D-dimer level is associated with advanced tumor stage and short survival after curative resection in patients with colorectal cancer. *Jpn J Clin Oncol* 2001; **31**: 388-394
- Blackwell K**, Haroon Z, Broadwater G, Berry D, Harris L, Iglehart JD, Dewhirst M, Greenberg C. Plasma D-dimer levels in operable breast cancer patients correlate with clinical stage and axillary lymph node status. *J Clin Oncol* 2000; **18**: 600-608
- Kobayashi T**, Gabazza EC, Taguchi O, Risteli J, Risteli L, Kobayashi H, Yasui H, Yuda H, Sakai T, Kaneda M, Adachi Y. Type I collagen metabolites as tumor markers in patients with lung carcinoma. *Cancer* 1999; **85**: 1951-1957
- Hou L**, Li Y, Jia YH, Wang B, Xin Y, Ling MY, Lü S. Molecular mechanism about lymphogenous metastasis of hepatocarcinoma cells in mice. *World J Gastroenterol* 2001; **7**: 532-536
- Takes RP**, Baatenburg-de-Jong RJ, Wjffels K, Schuurin E, Litvinov SV, Hermans J, van-Krieken JH. Expression of genetic markers in lymph node metastases compared with their primary tumours in head and neck cancer. *J Pathol* 2001; **194**: 298-302
- Sun HC**, Li XM, Xue Q, Chen J, Gao DM, Tang ZY. Study of angiogenesis induced by metastatic and non-metastatic liver cancer by corneal micropocket model in nude mice. *World J Gastroenterol* 1999; **5**: 116-118
- Xu G**, Tian KL, Liu GP, Zhong XJ, Tang SL, Sun YP. Clinical significance of plasma D-dimer and von Willebrand factor levels in patients with ulcer colitis. *World J Gastroenterol* 2002; **8**: 575-576
- Simpson-Haidaris PJ**, Rybarczyk B. Tumors and fibrinogen. The role of fibrinogen as an extracellular matrix protein. *Ann N Y Acad Sci* 2001; **936**: 406-425
- Shoji M**, Hancock WW, Abe K, Micko C, Casper KA, Baine RM, Wilcox JN, Danave I, Dillehay DL, Matthews E, Contrino J, Morrissey JH, Gordon S, Edgington TS, Kudryk B, Kreutzer DL, Rickles FR. Activation of coagulation and angiogenesis in cancer: immunohistochemical localization in situ of clotting proteins and vascular endothelial growth factor in human cancer. *Am J Pathol* 1998; **152**: 399-411
- Ornstein DL**, Zacharski LR. Treatment of cancer with anticoagulants: rationale in the treatment of melanoma. *Int J Hematol* 2001; **73**: 157-161
- Chiarugi V**, Ruggiero M, Magnelli L. Molecular polarity in endothelial cells and tumor-induced angiogenesis. *Oncol Res* 2000; **12**: 1-4
- Delebecq TJ**, Porte H, Zerimech F, Copin MC, Gouyer V, Dacquembonne E, Balduyck M, Wurtz A, Huet G. Overexpression level of stromelysin 3 is related to the lymph node involvement in non-small cell lung cancer. *Clin Cancer Res* 2000; **6**: 1086-1092
- Vasse M**, Thibout D, Paysant J, Legrand E, Soria C, Crepin M. Decrease of breast cancer cell invasiveness by sodium phenylacetate (NaPa) is associated with an increased expression of adhesive molecules. *Br J Cancer* 2001; **84**: 802-807
- Kitange G**, Tsunoda K, Anda T, Nakamura S, Yasunaga A, Naito S, Shibata S. Immunohistochemical expression of Ets-1 transcription factor and the urokinase-type plasminogen activator is correlated with the malignant and invasive potential in meningiomas. *Cancer* 2000; **89**: 2292-2300

DC-SIGN: Binding receptor for HCV?

Zhi-Hua Feng, Quan-Chu Wang, Qing-He Nie, Zhan-Sheng Jia, Yong-Xin Zhou

Zhi-Hua Feng, Quan-Chu Wang, Qing-He Nie, Zhan-Sheng Jia, Yong-Xin Zhou, The Center of Diagnosis and Treatment for Infectious Diseases of PLA, Tangdu Hospital, Fourth Military Medical University, Xi'an 710038, Shaanxi Province, China

Supported by the National Natural Science Foundation of China, No. 30170822

Correspondence to: Professor Zhi-Hua Feng, The Center of Diagnosis and Treatment for Infectious Diseases of PLA, Tangdu Hospital, Fourth Military Medical University, Xi'an 710038, Shaanxi Province, China. fengzh@fmmu.edu.cn

Telephone: +86-29-3377752 **Fax:** +86-29-3535377

Received: 2003-06-04 **Accepted:** 2003-12-06

Abstract

DC-SIGN, a dendritic Cell-specific adhesion receptor and a type II transmembrane mannose-binding C-type lectin, is very important in the function of DC, both in mediating naive T cell interactions through ICAM-3 and as a rolling receptor that mediates the DC-specific ICAM-2-dependent migration processes. It can be used by viral and bacterial pathogens including Human Immunodeficiency Virus (HIV), HCV, Ebola Virus, CMV and Mycobacterium tuberculosis to facilitate infection. Both DC-SIGN and DC-SIGNR can act either in *cis*, by concentrating virus on target cells, or in *trans*, by transmission of bound virus to a target cell expressing appropriate entry receptors. Recent work showed that DC-SIGN are high-affinity binding receptors for HCV. Besides playing a role in entry into DC, HCV E2 interaction with DC-SIGN might also be detrimental for the interaction of DC with T cells during antigen presentation. The clinical strategies that target DC-SIGN may be successful in restricting HCV dissemination and pathogenesis as well as directing the migration of DCs to manipulate appropriate immune responses in autoimmunity and tumorigenic situations.

Feng ZH, Wang QC, Nie QH, Jia ZS, Zhou YX. DC-SIGN: Binding receptor for HCV? *World J Gastroenterol* 2004; 10(7): 925-929 <http://www.wjgnet.com/1007-9327/10/925.asp>

INTRODUCTION

Dendritic cells and Langerhans cells are specialized for the recognition of pathogens and have a pivotal role in the control of immunity^[1-7]. Recently, several C-type lectin and lectin-like receptors (DC-SIGN and DC-SIGNR) have been characterized that they are expressed abundantly on the surface of these professional antigen-presenting cells, which not only serve as antigen receptors but also regulate the migration of dendritic cells and their interaction with lymphocytes. DC-SIGN was originally defined as an intercellular adhesion molecule-3 (ICAM-3) receptor supporting DC-mediated T-cell proliferation and binding and presentation of HIV-1 virions through gp120. DC-SIGNR or L-SIGN is a homologue of DC-SIGN and expressed in lymph nodes and by liver sinusoidal endothelial cells. L-SIGN has the same ligand-binding specificities as DC-SIGN, but is not produced by DCs or LCs. Furthermore, a series of DC-SIGN-like transcripts are predicted to encode other membrane-associated and soluble isoforms. The DC-

SIGN and L-SIGN genes, map to chromosome 19p13 adjacent to the type II C-type lectins CD23 (Fc_E receptor II) and activation marker CD69. DC-SIGN and L-SIGN can bind mannose residues of viral glycoproteins through a C-terminal carbohydrate recognition domain (CRD)^[8].

Hepatitis C virus (HCV) is the major causative agent of non-A, non-B hepatitis throughout the world with more than 170 million people infected. The majority of infected patients are unable to clear the virus and many develop chronic liver disease, cirrhosis and hepatocellular carcinoma. Replication of the HCV genome could be demonstrated *in vivo* and *in vitro* in liver hepatocytes and hematopoietic cells including dendritic cells and B cells. However, the molecular mechanism by which the virus targets to these sites of replication, notably in the liver, is not known. Regarding the interaction with DC-SIGN it has been shown that this lectin facilitates virus entry into DC in *cis* by enhancing attachment of HCV, as well as HIV, Ebola Virus, Cytomegalovirus, and Dengue Virus to the cell, thereby increasing the likelihood of interaction with specific entry receptors^[9-17].

TROJAN HORSES: DUAL ROLES FOR DC-SIGN

DCs from different anatomical sites express distinct arrays of alternative HIV receptors. Some of these subsets could represent good gatekeepers, whereas others may be "Trojan horses" that carry HIV into the lymph node^[18]. Our understanding of the role of DC-SIGN has become more complicated with the discovery of other functions. First, DC-SIGN binds ICAM-2, an integrin expressed on the endothelia of blood vessels and high endothelial vessels. DC-SIGN-ICAM-2 interactions help mediate tethering and transendothelial migration of DCs and may be critical for permitting DCs or their precursors to migrate towards inflammation in peripheral tissue or to enter lymph nodes^[19-22]. Second, DC-SIGN initiates interactions with naïve T cells through contact with a third ligand, ICAM-3, which is believed to stabilize DC-T cell membrane contacts and enable efficient T cell receptor engagement. Finally, DC-SIGN can internalize soluble antigen ligands, resulting in processing and presentation of antigenic peptides to T cells^[23-27].

All of the above functions are consistent with a general model in which DCs in mucosa encounter HIV-1, internalize particles *via* DC-SIGN and become "Trojan horses", traveling to lymph nodes to release infectious particles into the midst of activated T cells. The concept that DC-SIGN is the primary receptor mediating this sequence of events came mostly from studies of DCs derived *in vitro* from monocytes. To address this problem, Turville *et al*^[28] isolated resident DC subsets from skin, tonsils and blood and analyzed DC-SIGN expression and the gp120 binding capacity of these cell types directly *ex vivo*. Their results showed DC-SIGN has been detected on immature DCs in the lamina propria of mucosal tissues as well as on macrophages in decidua and placenta. DC-SIGN supports tethering and rolling of DC-SIGN-positive cells on the vascular ligand ICAM-2 under shear flow. The DC-SIGN-ICAM-2 interaction regulates chemokine induced transmigration of DCs across both resting and activated endothelium. Thus, DC-SIGN is central to the unusual trafficking capacity of DCs, further supported by the expression of DC-SIGN on precursors in blood and on immature and mature DCs in both peripheral

and lymphoid tissues. DC-SIGN- and DC-SIGNR-gp120 interactions represent a potential target for anti-HIV therapy aimed at disrupting the DC-virus interaction at primary sites of infection, in order to lower the efficiency of T cell infection. Lastly, these studies^[29-31] suggest that the interaction of DC-SIGN and DC-SIGNR with endogenous ligands may not be restricted to ICAMs that have been studied to date, but may include other cell surface or soluble glycoproteins with appropriately displayed high mannose oligosaccharides. The mechanism of DC SIGN-mediated *trans*-infection is not completely understood, but it involves the internalization of HIV particles into an early endosome, where they appear to undergo pH-dependent changes that make them more infectious. When DCs contact CD4⁺ T cells, virus is released and T cells become infected. Evidence is accumulating that DC-SIGN may also facilitate infection in *cis*. *Cis* infection occurs when virus directly infects the DC-SIGN-expressing cell. Because DC-SIGN also binds HIV-2 and SIV, it has been dubbed the “universal receptor” for primate lentiviruses. All of the above functions are consistent with a general model in which DCs in mucosa encounter HIV-1, internalize particles *via* DC-SIGN and become “Trojan horses”, traveling to lymph nodes to release infectious particles into the midst of activated T cells. Another example is *M. tuberculosis*. Dendritic cells (DCs) are important mediators of immune responses against *M. tuberculosis*. The interaction of mycobacteria with DC-SIGN also results in production of IL-10, which can modify the immune response, and might promote survival of mycobacteria. These results^[11] indicate that *M. tuberculosis* infects DCs and interferes with DC-mediated immune responses by targeting DC-SIGN. So, DC-SIGN is a Trojan horse for *M. tuberculosis* as has been shown previously for HIV-1.

DC-SIGN also binds HIV gp120 to facilitate HIV transmission from DCs to T cells. Engering *et al*^[32] showed DC-SIGN underwent rapid ligand-specific internalization to deliver its cargo to the acidic late endosome-lysosome compartments, where subsequent antigen-processing and presentation to T cells could occur. Internalization of soluble DC-SIGN ligands triggered antigen-specific T cell activation^[33,34]. Importantly, such ligand internalization points to a mechanism by which HIV may cloak itself for delivery to T cell-rich areas in peripheral lymphoid tissues. There was high expression of DC-SIGN on MDDCs and in gp120 binding assays, DC-SIGN mediated all gp120 binding on MDDC. Recently Pohlmann *et al*^[35] discovered DC-SIGNR, which can also act as a similar HIV ‘trans-infection,’ receptor in a 293T transfectant background. Furthermore, DC-SIGNR is expressed predominantly in the liver and lymph node tissue and MDDCs do not appear to express this receptor at high levels, suggesting it has a less important role in HIV binding. Therefore in addition to DC-SIGN, CD4, MMR, and as yet unknown trypsin resistant DC-SIGN and, possibly, DC-SIGNR, on DCs seems likely to have the capacity to bind gp120. This work supports intraepithelial DC as the first target for HIV but the original SIV tracking work suggested deeper tissue DC within the lamina propria were the first to be infected. Trauma during sexual transmission or genital ulceration would favour the latter. These data suggest that skin and probably other tissue DCs bind gp120 and/or HIV via both DC-SIGN and CD4/CCR5. HIV gp120 saccharide-DC-SIGN binding may provide constant high affinity virion binding to DC for any HIV strain, facilitating subsequent CD4/chemokine receptor binding and fusion. Therefore DC-SIGN may enhance DC infection and mucosal transmission. Furthermore mucosal DCs may provide the selection event which results in the predominance of R5 isolates^[36].

Two papers in <<Immunity>> show that the HIV-1 protein Nef up-regulates DC-SIGN expression on DCs and that binding

of DC-SIGN mediates internalization of virus particles into a non-lysosomal compartment, which enhances infectivity. The study from Sol-Foulon *et al*^[37] examined the role of HIV-1 Nef in viral infectivity. DC-SIGN was found to be upregulated at the surface of infected cells. Up-regulation was dependent on Nef, given that DCs infected with Nef-deficient virus showed DC-SIGN staining patterns similar to uninfected cells. Two putative internalization signals - a tyrosine-based motif and a dileucine motif - are located in the cytoplasmic tail of DC-SIGN. The role of these motifs was examined using DC-SIGN-negative HeLa cells transfected with plasmids encoding DC-SIGN or Nef, or both. HeLa cells expressing wild-type DC-SIGN had very little surface expression but a high rate of endocytosis. By contrast, dileucine mutants of DC-SIGN showed high levels of surface expression with little or no internalization. Co-transfection with wild-type DC-SIGN and Nef resulted in stable expression of DC-SIGN at the plasma membrane. These results show that Nef up-regulates DC-SIGN surface expression by preventing internalization, which enhances the ability of DCs to form clusters with lymphocytes and facilitates viral transmission. The study from Baribaud *et al*^[36] focused on the role of DC-SIGN in internalization and infectivity of HIV-1. DC-SIGN was shown to mediate the internalization of gp120 in a monocyte cell line transduced with a DC-SIGN-encoding virus. Fluorescence confocal microscopy showed that whole viral particles could be internalized by human DCs. After 45 min, most of the viral particles were localized in a non-lysosomal compartment, and these could be transmitted to a second target cell. Low pH in this compartment was important for maintenance of infectivity, given that neutralization of pH abolished the ability of DC-SIGN-positive cells to enhance infection of T cells. Although several questions - such as how HIV returns to the cell surface and what regulates this process - remain to be answered, this new work has implications for our understanding of HIV pathogenesis. Finally, DC-SIGN is up-regulated on monocytes exposed to inflammatory cytokines or undergoing differentiation into DCs, which suggests that expression on cells can be modulated by the microenvironment^[38-41]. More definitive experiments will be required to determine actual amounts of expression in the blood and lymph nodes of both healthy and HIV-infected subjects. They suggest that DC-SIGN-mediated *cis*-infection of DCs could play a key role in viral dissemination^[42-46]. This diversity may pose additional challenges for those who wish to block HIV infection by targeting DC-SIGN.

BINDING RECEPTORS FOR HCV

HCV is a small, enveloped, plus-strand RNA virus belonging to the family flaviviridae and genus hepacivirus. The HCV RNA genome is 9 600 nucleotides in length and encodes a single polypeptide that is post-translationally cleaved into up to 10 polypeptides including three structural proteins (core, E1 and E2), located at the N-terminus, and five nonstructural proteins. Shortly after translocation into the endoplasmic reticulum (ER), oligosaccharidetransferase catalyzes addition of Glc3Man9GlcNAc2 complexes at up to 6 (E1) and 11 (E2) Nglycosylation sites. Glucose residues are removed by glucosidases I and II and correctly folded proteins are released from ER chaperones calnexin and calreticulin. The transmembrane domains of E1 and E2 are responsible for both heterodimerization and retention of the glycoproteins in a high mannose EndoH sensitive glycoform in the ER. By analogy to other flaviviruses it is assumed that HCV capsids bud from the cytoplasm into the ER and that enveloped particles follow the secretion pathway through the Golgi. However, attempts to produce secreted HCV particles *in vitro* have not been successful so far and it is not known if E1 and E2 on mature

infectious virions possess a high-mannose, complex or mixed glycosylation.

Since the genomic sequence of HCV was determined, significant progress has been made towards understanding the functions of the HCV-encoded proteins, despite the lack of an efficient *in-vitro* replication system or convenient small-animal model. The identity of the receptor for HCV remains elusive, however. Several receptors have been proposed that could play a role in HCV entry into hepatocytes. Low-density lipoprotein receptor, CD81 and GAGs may all act as receptors for HCV, either sequentially or by different viral quasispecies. The low density lipoprotein (LDL) receptor (LDLR) has been shown to mediate HCV internalization via binding to virus associated LDL particles. A second putative HCV receptor, the tetraspanin CD81, has been identified as a high affinity binding receptor for soluble recombinant E2 from HCV genotype 1a. CD81 and LDLR are expressed in most cell types and thus not likely account for the hepatic tropism of the virus. Recent work using pseudotyped VSV bearing E1 or E2 chimeric molecules showed that entry of the E1 pseudotype can be inhibited by recombinant LDLr, whereas the E2 pseudotype is more sensitive to inhibition by recombinant CD81 or heparin. These results suggest that E1 and E2 may be responsible for interactions with different cellular molecules. It is also conceivable that additional, yet unidentified, cellular proteins are involved in viral binding and entry. Intriguingly, the reports of HCV-RNA associated with PBMC suggest that HCV infection may not be restricted to hepatocytes. Thus, separate reservoirs of virus may exist, and HCV may use different receptors to access these different cell types. The lack of an efficient cell culture model has precluded functional confirmation of these receptor candidates at the level of virus entry. Recently Lozach *et al*^[9] found that DC-SIGN and L-SIGN are two novel HCV envelope binding receptors and the HCV envelope glycoprotein E2 binds DC-SIGN and L-SIGN through high-mannose N-glycans. Competing ligands such as mannan and an antibody directed against the carbohydrate recognition domains (CRD) abrogated binding. The highest affinity is seen for plasma membrane expressed DC-SIGN and L-SIGN. These results indicate that several high-mannose N-glycans in a structurally defined cluster on E2 bind to several subunits of the oligomeric lectin CRD. Its localization on the endothelium lining hepatic sinusoids makes it an interesting candidate for the capture of HCV. Productive infection of endothelial cells by HCV has not been demonstrated, but L-SIGN could be responsible for the transmission of bound virus to neighbouring hepatocytes. This kind of mechanism of *trans*-enhancement has been demonstrated more than a decade ago for HIV transmission from DC to T cells and can be attributed to DC-SIGN. In the case of HCV, it is tempting to speculate that subsequent to interaction with L-SIGN on endothelial cells, the virus could be transmitted to hepatocytes where it uses a specific receptor for entry. In conclusion, the results show that HCV envelope glycoprotein E2 strongly binds to oligomeric C-type lectins in a high-mannose N-glycan dependent fashion. High affinity interaction of viral glycoproteins with lectins might represent a strategy by which enveloped viruses target to the site of replication and represents an interesting novel target for antiviral drug development.

In another, Pohlmann *et al*^[47] found that soluble versions of the hepatitis C virus (HCV) E2 glycoprotein and retrovirus pseudotypes expressing chimeric forms of both HCV E1 and E2 glycoproteins bound efficiently to DC-SIGN and DC-SIGNR expressed on cell lines and primary human endothelial cells but not to other C-type lectins tested. Soluble E2 bound to immature and mature human monocyte-derived dendritic cells (MDDCs). Binding of E2 to immature MDDCs was dependent on DC-SIGN interactions, while binding to mature

MDDCs was partly independent of DC-SIGN, suggesting that other cell surface molecules may mediate HCV glycoprotein interactions. HCV interactions with DC-SIGN and DC-SIGNR may contribute to the establishment or persistence of infection both by the capture and delivery of virus to the liver and by modulating dendritic cell function^[48].

QUESTIONS TO BE ANSWERED

DC-SIGN and DC-SIGNR are two closely related membrane-associated C-type lectins that bind human immunodeficiency virus (HIV) envelope glycoprotein with high affinity. Binding of HIV to cells expressing DC-SIGN or DC-SIGNR can enhance the efficiency of infection of cells coexpressing the specific HIV receptors^[49-51]. DC-SIGN is expressed on some dendritic cells, while DC-SIGNR is localized to certain endothelial cell populations, including hepatic sinusoidal endothelial cells. The pattern of cellular expression of DC-SIGN is somewhat controversial. The term "DC-specific" DC-SIGN is also expressed on brain microvascular endothelial cells, certain tissue macrophages, can be induced on monocyte-derived macrophages under certain conditions and can even be found on rare CD14⁺ cells, resembling monocytes in blood^[52-55]. Pathogenic microbes have evolved means to bypass these sentinels^[56-67]. For example, human immunodeficiency virus binds to DC-SIGN and hides directly beneath the cell surface until the DC encounters a T cell, that which the virus can then infect. The measles virus seems to induce death and/or fusion of the DC, thereby preventing immune responses. Wu *et al*^[68] demonstrated that Dengue virus (DV), an RNA virus with a peculiar pathogenesis, preferentially targets DCs. They have demonstrated that immature monocyte-derived DCs, generated *in vitro*, were 10-fold more permissive for DV infection than either monocytes or macrophages. Several avenues are now open for investigation. How does the infection affect DCs function and the ensuing T-cell responses? Although the authors did not explore the effects of DV on DCs, a block in LC function could explain the lack of cytotoxic T-lymphocyte immunity in response to Dengue infection. Would the targeting of different DC subsets explain why some patients develop protective immunity whereas others develop non-protective responses? Indeed, targeting of interstitial DCs could skew the immune responses toward the production of DV-specific antibodies, which may result in enhanced viral load through increased entry into macrophages. Another important question is which of the DC-specific molecules DV uses as a receptor for entry. Answering this could provide a target for the design of an anti-DV compound. Furthermore, receptor polymorphisms might explain why some patients mount protective immunity whereas others do not. Finally, would the targeting of appropriate DC subset permit us to develop a successful vaccine? All these questions represent exciting areas of experimentation and are likely to keep the DC experts busy and DC researchers eager to follow their work^[69-71].

REFERENCES

- 1 **Xu MQ**, Yao ZX. Functional changes of dendritic cells derived from allogeneic partial liver graft undergoing acute rejection in rats. *World J Gastroenterol* 2003; **9**: 141-147
- 2 **Chen HB**, Zhang JK, Huang ZL, Sun JL, Zhou YQ. Effects of cytokines on dendritic cells against human hepatoma cell line. *Shijie Huaren Xiaohua Zazhi* 1999; **7**: 191-193
- 3 **Zhang JK**, Chen HB, Sun JL, Zhou YQ. Effect of dendritic cells on LPAK cells induced at different times in killing hepatoma cells. *Shijie Huaren Xiaohua Zazhi* 1999; **7**: 673-675
- 4 **Zhang J**, Zhang JK, Zhuo SH, Chen HB. Effect of a cancer vaccine prepared by fusions of hepatocarcinoma cells with dendritic cells. *World J Gastroenterol* 2001; **7**: 690-694

- 5 **Luo ZB**, Luo YH, Lu R, Jin HY, Zhang PB, Xu CP. Immunohistochemical study on dendritic cells in gastric mucosa of patients with gastric cancer and precancerous lesions. *Shijie Huaren Xiaohua Zazhi* 2000; **8**: 400-402
- 6 **Li MS**, Yuan AL, Zhang WD, Chen XQ, Zhang YL, Zhou DY. Functional changes of dendritic cells derived from PBMC of patients with colorectal neoplasms. *Shijie Huaren Xiaohua Zazhi* 1999; **7**: 429
- 7 **Xing LH**, Wang FS, Liou MX, Zhu CL. Dendritic cells and liver diseases. *Shijie Huaren Xiaohua Zazhi* 2000; **8**: 1276-1279
- 8 **Appelmelk BJ**, Van Die I, Van Vliet SJ, Vandenbroucke-Grauls CM, Geijtenbeek TB, Van Kooyk Y. Cutting edge: carbohydrate profiling identifies new pathogens that interact with dendritic cell-specific ICAM-3-grabbing nonintegrin on dendritic cells. *J Immunol* 2003; **170**: 1635-1639
- 9 **Lozach PY**, Lortat-Jacob H, de Lacroix de Lavalette A, Staropoli I, Foug S, Amara A, Houles C, Fieschi F, Schwartz O, Virelizier JL, Arenzana-Seisdedos F, Altmeyer R. DC-SIGN and L-SIGN are high affinity binding receptors for hepatitis C Virus glycoprotein E2. *J Biol Chem* 2003; **278**: 20358-20366
- 10 **Soilleux EJ**, Coleman N. Transplacental transmission of HIV: a potential role for HIV binding lectins. *Int J Biochem Cell Biol* 2003; **35**: 283-287
- 11 **Tailleux L**, Schwartz O, Herrmann JL, Pivert E, Jackson M, Amara A, Legres L, Dreher D, Nicod LP, Gluckman JC, Lagrange PH, Gicquel B, Neyrolles O. DC-SIGN is the major Mycobacterium tuberculosis receptor on human dendritic cells. *J Exp Med* 2003; **197**: 121-127
- 12 **Geijtenbeek TB**, Van Vliet SJ, Koppel EA, Sanchez-Hernandez M, Vandenbroucke-Grauls CM, Appelmelk B, Van Kooyk Y. Mycobacteria target DC-SIGN to suppress dendritic cell function. *J Exp Med* 2003; **197**: 7-17
- 13 **Kaufmann SH**, Schaible UE. A dangerous liaison between two major killers: Mycobacterium tuberculosis and HIV target dendritic cells through DC-SIGN. *J Exp Med* 2003; **197**: 1-5
- 14 **Simmons G**, Reeves JD, Grogan CC, Vandenbergh LH, Baribaud F, Whitbeck JC, Burke E, Buchmeier MJ, Soilleux EJ, Riley JL, Doms RW, Bates P, Pohlmann S. DC-SIGN and DC-SIGNR bind ebola glycoproteins and enhance infection of macrophages and endothelial cells. *Virology* 2003; **305**: 115-123
- 15 **Lin G**, Simmons G, Pohlmann S, Baribaud F, Ni H, Leslie GJ, Haggarty BS, Bates P, Weissman D, Hoxie JA, Doms RW. Differential N-linked glycosylation of human immunodeficiency virus and Ebola virus envelope glycoproteins modulates interactions with DC-SIGN and DC-SIGNR. *J Virol* 2003; **77**: 1337-1346
- 16 **Maeda N**, Nigou J, Herrmann JL, Jackson M, Amara A, Lagrange PH, Puzo G, Gicquel B, Neyrolles O. The cell surface receptor DC-SIGN discriminates between Mycobacterium species through selective recognition of the mannose caps on lipoarabinomannan. *J Biol Chem* 2003; **278**: 5513-5516
- 17 **Bashirova AA**, Wu L, Cheng J, Martin TD, Martin MP, Benveniste RE, Lifson JD, Kewal Ramani VN, Hughes A, Carrington M. Novel member of the CD209 (DC-SIGN) gene family in primates. *J Virol* 2003; **77**: 217-227
- 18 **Pohlmann S**, Doms RW. Evaluation of current approaches to inhibit HIV entry. *Curr Drug Targets Infect Disord* 2002; **2**: 9-16
- 19 **Wang QC**, Feng ZH, Zhou YX, Nie QH, Hao CQ, Wang JP. Comparative research of dendritic cells cultured from mice bone marrow with different ways. *Shijie Huaren Xiaohua Zazhi* 2003; **11**: 219-223
- 20 **Xing LH**, Wang FS, Liu MX, Zhu CL, Li HW, Lei ZY, Wang HF. Dendritic cells cultured from PBMC of patients with chronic hepatitis B viral. *Shijie Huaren Xiaohua Zazhi* 2001; **9**: 591-593
- 21 **Li MS**, Yuan AL, Zhang WD, Chen XQ, Tian XH, Piao YJ. Immune response induced by dendritic cells induce apoptosis and inhibit proliferation of tumor cells. *Shijie Huaren Xiaohua Zazhi* 2000; **8**: 56-58
- 22 **Li MS**, Yuan AL, Zhang WD. Low immune function of peripheral blood dendritic cells in hepatocarcinoma patients. *Shijie Huaren Xiaohua Zazhi* 1998; **6**: 240-241
- 23 **Halary F**, Amara A, Lortat-Jacob H, Messerle M, Delaunay T, Houles C, Fieschi F, Arenzana-Seisdedos F, Moreau JF, Dechanet-Merville J. Human cytomegalovirus binding to DC-SIGN is required for dendritic cell infection and target cell trans-infection. *Immunity* 2002; **17**: 653-664
- 24 **Yu Kimata MT**, Cella M, Biggins JE, Rorex C, White R, Hicks S, Wilson JM, Patel PG, Allan JS, Colonna M, Kimata JT. Capture and transfer of simian immunodeficiency virus by macaque dendritic cells is enhanced by DC-SIGN. *J Virol* 2002; **76**: 11827-11836
- 25 **Steinman RM**. DC-SIGN: a guide to some mysteries of dendritic cells. *Cell* 2000; **100**: 491-494
- 26 **Schwartz AJ**, Alvarez X, Lackner AA. Distribution and immunophenotype of DC-SIGN-expressing cells in SIV-infected and uninfected macaques. *AIDS Res Hum Retroviruses* 2002; **18**: 1021-1029
- 27 **Feinberg H**, Mitchell DA, Drickamer K, Weis WI. Structural basis for selective recognition of oligosaccharides by DC-SIGN and DC-SIGNR. *Science* 2001; **294**: 2163-2166
- 28 **Turville SG**, Cameron PU, Handley A, Lin G, Pohlmann S, Doms RW, Cunningham AL. Diversity of receptors binding HIV on dendritic cell subsets. *Nat Immunol* 2002; **3**: 975-983
- 29 **Kavanagh DG**, Bhardwaj N. A division of labor: DC subsets and HIV receptor diversity. *Nat Immunol* 2002; **3**: 891-893
- 30 **Geijtenbeek TB**, Groot PC, Nolte MA, van Vliet SJ, Gangaram-Panday ST, van Duijnhoven GC, Kraal G, van Oosterhout AJ, van Kooyk Y. Marginal zone macrophages express a murine homologue of DC-SIGN that captures blood-borne antigens *in vivo*. *Blood* 2002; **100**: 2908-2916
- 31 **Li MS**, Yuan AL, Zhang WD, Liu SD, Lu AM, Zhou DY. Dendritic cells *in vitro* induce efficient and special anti-tumor immune response. *Shijie Huaren Xiaohua Zazhi* 1999; **7**: 161-163
- 32 **Engering A**, Geijtenbeek TB, van Vliet SJ, Wijers M, van Liempt E, Demarex N, Lanzavecchia A, Franssen J, Figdor CG, Piguet V, van Kooyk Y. The dendritic cell-specific adhesion receptor DC-SIGN internalizes antigen for presentation to T cells. *J Immunol* 2002; **168**: 2118-2126
- 33 **Liu JR**, Zhang LT, Li T, Zhao YL, Zhang CY, Chen JS, Zhang NS, Qian YZ, Wu FX, Tang K, Tang ZH. Dendritic cells induce efficient and special anti-gastric tumor immune response. *Shijie Huaren Xiaohua Zazhi* 2002; **10**: 467-469
- 34 **van Kooyk Y**, Geijtenbeek TB. A novel adhesion pathway that regulates dendritic cell trafficking and T cell interactions. *Immunol Rev* 2002; **186**: 47-56
- 35 **Pohlmann S**, Baribaud F, Lee B, Leslie GJ, Sanchez MD, Hiebenthal-Millow K, Munch J, Kirchhoff F, Doms RW. DC-SIGN interactions with human immunodeficiency virus type 1 and 2 and simian immunodeficiency virus. *J Virol* 2001; **75**: 4664-4672
- 36 **Baribaud F**, Doms RW, Pohlmann S. The role of DC-SIGN and DC-SIGNR in HIV and Ebola virus infection: can potential therapeutics block virus transmission and dissemination? *Expert Opin Ther Targets* 2002; **6**: 423-431
- 37 **Sol-Foulon N**, Moris A, Nobile C, Boccaccio C, Engering A, Abastado JP, Heard JM, van Kooyk Y, Schwartz O. HIV-1 Nef-induced upregulation of DC-SIGN in dendritic cells promotes lymphocyte clustering and viral spread. *Immunity* 2002; **16**: 145-155
- 38 **Piguet V**, Blauvelt A. Essential roles for dendritic cells in the pathogenesis and potential treatment of HIV disease. *J Invest Dermatol* 2002; **119**: 365-369
- 39 **Baribaud F**, Pohlmann S, Leslie G, Mortari F, Doms RW. Quantitative expression and virus transmission analysis of DC-SIGN on monocyte-derived dendritic cells. *J Virol* 2002; **76**: 9135-9142
- 40 **Colmenares M**, Puig-Kroger A, Pello OM, Corbi AL, Rivas L. Dendritic cell (DC)-specific intercellular adhesion molecule 3 (ICAM-3)-grabbing nonintegrin (DC-SIGN, CD209), a C-type surface lectin in human DCs, is a receptor for Leishmania amastigotes. *J Biol Chem* 2002; **277**: 36766-36769
- 41 **Akiyama Y**, Maruyama K, Nara N, Hojo T, Cheng JY, Mori T, Wiltrout RH, Yamaguchi K. Antitumor effects induced by dendritic cell-based immunotherapy against established pancreatic cancer in hamsters. *Cancer Lett* 2002; **184**: 37-47
- 42 **Alvarez CP**, Lasala F, Carrillo J, Muniz O, Corbi AL, Delgado R. C-type lectins DC-SIGN and L-SIGN mediate cellular entry by Ebola virus in cis and in trans. *J Virol* 2002; **76**: 6841-6844
- 43 **Geijtenbeek TB**, Engering A, Van Kooyk Y. DC-SIGN, a C-type lectin on dendritic cells that unveils many aspects of dendritic cell biology. *J Leukoc Biol* 2002; **71**: 921-931
- 44 **Lore K**, Sonnerborg A, Brostrom C, Goh LE, Perrin L, McDade H, Stellbrink HJ, Gazzard B, Weber R, Napolitano LA, van Kooyk Y, Andersson J. Accumulation of DC-SIGN+CD40+ dendritic cells with reduced CD80 and CD86 expression in lymphoid tissue

- during acute HIV-1 infection. *AIDS* 2002; **16**: 683-692
- 45 **Relloso M**, Puig-Kroger A, Pello OM, Rodriguez-Fernandez JL, de la Rosa G, Longo N, Navarro J, Munoz-Fernandez MA, Sanchez-Mateos P, Corbi AL. DC-SIGN (CD209) expression is IL-4 dependent and is negatively regulated by IFN, TGF-beta, and anti-inflammatory agents. *J Immunol* 2002; **168**: 2634-2643
- 46 **Jameson B**, Baribaud F, Pohlmann S, Ghavimi D, Mortari F, Doms RW, Iwasaki A. Expression of DC-SIGN by dendritic cells of intestinal and genital mucosae in humans and rhesus macaques. *J Virol* 2002; **76**: 1866-1875
- 47 **Pohlmann S**, Zhang J, Baribaud F, Chen Z, Leslie GJ, Lin G, Granelli-Piperno A, Doms RW, Rice CM, McKeating JA. Hepatitis C virus glycoproteins interact with DC-SIGN and DC-SIGNR. *J Virol* 2003; **77**: 4070-4080
- 48 **Coombs BK**, Mahony JB. Dendritic cell discoveries provide new insight into the cellular immunobiology of DNA vaccines. *Immunol Lett* 2001; **78**: 103-111
- 49 **Geijtenbeek TB**, Koopman G, van Duijnhoven GC, van Vliet SJ, van Schijndel AC, Engering A, Heeney JL, van Kooyk Y. Rhesus macaque and chimpanzee DC-SIGN act as HIV/SIV gp120 trans-receptors, similar to human DC-SIGN. *Immunol Lett* 2001; **79**: 101-107
- 50 **Bleijs DA**, Geijtenbeek TB, Figdor CG, van Kooyk Y. DC-SIGN and LFA-1: a battle for ligand. *Trends Immunol* 2001; **22**: 457-463
- 51 **Patterson S**, Rae A, Hockey N, Gilmour J, Gotch F. Plasmacytoid dendritic cells are highly susceptible to human immunodeficiency virus type 1 infection and release infectious virus. *J Virol* 2001; **75**: 6710-6713
- 52 **Mitchell DA**, Fadden AJ, Drickamer K. A novel mechanism of carbohydrate recognition by the C-type lectins DC-SIGN and DC-SIGNR. Subunit organization and binding to multivalent ligands. *J Biol Chem* 2001; **276**: 28939-28945
- 53 **Mummidi S**, Catano G, Lam L, Hoefle A, Telles V, Begum K, Jimenez F, Ahuja SS, Ahuja SK. Extensive repertoire of membrane-bound and soluble dendritic cell-specific ICAM-3-grabbing nonintegrin 1 (DC-SIGN1) and DC-SIGN2 isoforms. Inter-individual variation in expression of DC-SIGN transcripts. *J Biol Chem* 2001; **276**: 33196-33212
- 54 **Geijtenbeek TB**, van Vliet SJ, van Duijnhoven GC, Figdor CG, van Kooyk Y. DC-SIGN, a dendritic cell-specific HIV-1 receptor present in placenta that infects T cells in trans—a review. *Placenta* 2001; **22**(Suppl A): S19-23
- 55 **Zhang J**, Zhang JK, Zhuo SH, Chen HB. Effect of a cancer vaccine prepared by fusions of hepatocarcinoma cells with dendritic cells. *World J Gastroenterol* 2001; **7**: 690-694
- 56 **Geijtenbeek TB**, Krooshoop DJ, Bleijs DA, van Vliet SJ, van Duijnhoven GC, Grabovsky V, Alon R, Figdor CG, van Kooyk Y. DC-SIGN-ICAM-2 interaction mediates dendritic cell trafficking. *Nat Immunol* 2000; **1**: 353-357
- 57 **Bashirova AA**, Geijtenbeek TB, van Duijnhoven GC, van Vliet SJ, Eilering JB, Martin MP, Wu L, Martin TD, Viebig N, Knolle PA, KewalRamani VN, van Kooyk Y, Carrington M. A dendritic cell-specific intercellular adhesion molecule 3-grabbing nonintegrin (DC-SIGN)-related protein is highly expressed on human liver sinusoidal endothelial cells and promotes HIV-1 infection. *J Exp Med* 2001; **193**: 671-678
- 58 **Pohlmann S**, Soilleux EJ, Baribaud F, Leslie GJ, Morris LS, Trowsdale J, Lee B, Coleman N, Doms RW. DC-SIGNR, a DC-SIGN homologue expressed in endothelial cells, binds to human and simian immunodeficiency viruses and activates infection in trans. *Proc Natl Acad Sci U S A* 2001; **98**: 2670-2675
- 59 **Geijtenbeek TB**, Kwon DS, Torensma R, van Vliet SJ, van Duijnhoven GC, Middel J, Cornelissen IL, Nottet HS, Kewal Ramani VN, Littman DR, Figdor CG, van Kooyk Y. DC-SIGN, a dendritic cell-specific HIV-1-binding protein that enhances trans-infection of T cells. *Cell* 2000; **100**: 587-597
- 60 **Zhang JK**, Li J, Zhang J, Chen HB, Chen SB. Antitumor immunopreventive and immunotherapeutic effect in mice induced by hybrid vaccine of dendritic cells and hepatocarcinoma *in vivo*. *World J Gastroenterol* 2003; **9**: 479-484
- 61 **Wang FS**, Xing LH, Liu MX, Zhu CL, Liu HG, Wang HF, Lei ZY. Dysfunction of peripheral blood dendritic cells from patients with chronic hepatitis B virus infection. *World J Gastroenterol* 2001; **7**: 537-541
- 62 **Tang ZH**, Qiu WH, Wu GS, Yang XP, Zou SQ, Qiu FZ. The immunotherapeutic effect of dendritic cells vaccine modified with interleukin-18 gene and tumor cell lysate on mice with pancreatic carcinoma. *World J Gastroenterol* 2002; **8**: 908-912
- 63 **Zhang JK**, Li J, Chen HB, Sun JL, Qu YJ, Lu JJ. Antitumor activities of human dendritic cells derived from peripheral and cord blood. *World J Gastroenterol* 2002; **8**: 87-90
- 64 **Tailleux L**, Schwartz O, Herrmann JL, Pivert E, Jackson M, Amara A, Legres L, Dreher D, Nicod LP, Gluckman JC, Lagrange PH, Gicquel B, Neyrolles O. DC-SIGN is the major Mycobacterium tuberculosis receptor on human dendritic cells. *J Exp Med* 2003; **197**: 121-127
- 65 **Simmons G**, Reeves JD, Grogan CC, Vandenberghe LH, Baribaud F, Whitbeck JC, Burke E, Buchmeier MJ, Soilleux EJ, Riley JL, Doms RW, Bates P, Pohlmann S. DC-SIGN and DC-SIGNR bind ebola glycoproteins and enhance infection of macrophages and endothelial cells. *Virology* 2003; **305**: 115-123
- 66 **Lint M**, Quinn ER, Levy S. In search of hepatitis C virus receptor (s). *Clin Liver Dis* 2001; **5**: 873-893
- 67 **Pohlmann S**, Zhang J, Baribaud F, Chen Z, Leslie GJ, Lin G, Granelli-Piperno A, Doms RW, Rice CM, McKeating JA. Hepatitis C Virus Glycoproteins Interact with DC-SIGN and DC-SIGNR. *J Virol* 2003; **77**: 4070-4080
- 68 **Wu SJ**, Grouard-Vogel G, Sun W, Mascola JR, Brachtel E, Putvatana R, Louder MK, Filgueira L, Marovich MA, Wong HK, Blauvelt A, Murphy GS, Robb ML, Innes BL, Bix DL, Hayes CG, Frankel SS. Human skin Langerhans cells are targets of dengue virus infection. *Nat Med* 2000; **6**: 816-820
- 69 **Kwon DS**, Gregorio G, Bittan N, Hendrickson WA, Littman DR. DC-SIGN-mediated internalization of HIV is required for trans-enhancement of T cell infection. *Immunity* 2002; **16**: 135-144
- 70 **Li MS**, Yuan AL, Zhang WD, Chen XQ, Tian XH, Piao YJ. Immune response induced by dendritic cells induce apoptosis and inhibit proliferation of tumor cells. *Shijie Huaren Xiaohua Zazhi* 2000; **8**: 56-58
- 71 **Soilleux EJ**. DC-SIGN (dendritic cell-specific ICAM-grabbing non-integrin) and DC-SIGN-related (DC-SIGNR): friend or foe? *Clin Sci* 2003; **104**: 437-446

Intestinal failure: Pathophysiological elements and clinical diseases

Lian-An Ding, Jie-Shou Li

Lian-An Ding, Department of General Surgery, Affiliated Hospital of Qingdao University Medical School, 16 Jiangsu Road, Qingdao 266003, Shandong Province, China

Jie-Shou Li, Research Institute of General Surgery, Clinical College of Nanjing University Medical School, 305 East Zhongshan Road, Nanjing 210002, Jiangsu Province, China

Correspondence to: Lian-An Ding, Associate Professor, Medical School of Qingdao University, 266003 Qingdao, Shandong Province, China. dlahaolq@hotmail.com

Telephone: +86-532-2712851 **Fax:** +86-532-2911840

Received: 2003-11-22 **Accepted:** 2003-12-16

Abstract

There are two main functions of gastrointestinal tract, digestion and absorption, and barrier function. The latter has an important defensive effect, which keeps the body away from the invading and damaging of bacteria and endotoxin. It maintains the systemic homeostasis. Intestinal dysfunction would happen when body suffers from diseases or harmful stimulations. The lesser dysfunction of GI tract manifests only disorder of digestion and absorption, whereas the more serious intestinal disorders would harm the intestinal protective mechanism, or intestinal barrier function, and bacterial/endotoxin translocation, of intestinal failure (IF) would ensue. This review discussed the theory of the intestinal failure, aiming at attracting recognition and valuable comments by clinicians.

Ding LA, Li JS. Intestinal failure: Pathophysiological elements and clinical diseases. *World J Gastroenterol* 2004; 10(7): 930-933
<http://www.wjgnet.com/1007-9327/10/930.asp>

INTRODUCTION

It is traditionally considered that the gut is quiescent in diseases. That is why the GI tract is not paid much attention and protected like other organs as heart, lungs and kidneys by ICU doctors. It is considered that the metabolism of the body takes place mainly in liver. Because of the advancements in research and surgical technology, issues in gastrointestinal metabolism, nourishment, anatomy, physiology and the like have been further understood. It is very important for functions of GI tract when body suffers from hunger and stress. It bears not only digesting and absorbing nutrients, but also supplying and modulating systemic immunity. Moreover, the GI tract can prevent germs and toxin from entering into the body (so-called barrier function). Capability in GI tract sometimes determines the recovery or deterioration of a disease. It is of traditional nutrition support that makes the intestinal mucous membrane in hunger and that would aggravate the intestinal dysfunction, or accelerate the occurrence of the intestinal failure. The further study and recognition of gut physiological function and pathophysiology hence, is of initial importance to gastroenterologists^[1-3].

RECOGNITION OF GI TRACT FUNCTION

There are unusual structures for GI tract: villus, microvillus,

crypt and tight junction. Small holes (about 0.4-0.7 nm in radius) bestrew the epithelial surface of the GI tract. The epithelial cells of small intestine is one of the tissues that most rapidly grow and metabolise in the body. It renews in 2-5 d for a cycle. The circular folds, villi and microvilli expand the absorptive area of small intestine to hundreds times of its primary area, reaching to 600 m²[4-6]. Modern technology reveals that GI tract has following actions or functions except for digestion and absorption.

Gut is the primary one of four bacterial reservoirs in the body

There is a homeostasis between intestinal epithelium, total system and the flora in the bowel. Bacteria generally divide once every 20 min, but they only reproduce 4 to 5 generations within the bowel lumen. Once the balance destroyed, intestinal failure follows, bacteria translocation and morbidity would ensue. The upper GI tract and proximal jejunum are considered aseptic in general, because the number of bacteria in these sites is smaller or approximately equals to 10³[7-11]. Table 1 lists the normal flora in the bowel^[7].

Table 1 Normal Flora in Humans' GI Tract

	Stomach	Jejunum	Ileum	Feces
Total bacterial count	0-10 ³	0-10 ⁵	10 ³ -10 ⁷	10 ¹⁰ -10 ¹²
Aerobic facultative or anaerobic bacteria				
Enterobacteria	0-10 ²	0-10 ³	10 ² -10 ⁶	10 ⁴ -10 ¹⁰
Streptococci	0-10 ³	0-10 ⁴	10 ² -10 ⁶	10 ⁵ -10 ¹⁰
Staphylococci	0-10 ²	0-10 ³	10 ² -10 ⁵	10 ⁴ -10 ⁷
Lactobacilli	0-10 ³	0-10 ⁴	10 ² -10 ⁵	10 ⁶ -10 ¹⁰
Fungi	0-10 ²	0-10 ²	10 ² -10 ³	10 ² -10 ⁶
Anaerobic bacteria	0	0	0	0
Bacteroids	Rare	0-10 ²	10 ³ -10 ⁷	10 ¹⁰ -10 ¹²
Bifidobacteria	Rare	0-10 ³	10 ³ -10 ⁵	10 ⁸ -10 ¹²
Gram-positive cocci ¹	Rare	0-10 ³	10 ² -10 ⁵	10 ⁸ -10 ¹¹
Clostridia	Rare	Rare	10 ² -10 ⁴	10 ⁶ -10 ¹¹
Eubacteria	Rare	Rare	Rare	10 ⁹ -10 ¹²

¹Includes peptostreptococcus and peptococcus.

Secretion and absorption of digestive juice

Secretions of gastrointestinal fluid during 24 h vary in different site or segments. They are: saliva, 500 mL, gastric juice, 1 000-2 000 mL, bile, 800 mL and pancreatic juice, 700 mL daily. Chyme in upper segment of jejunum (200 cm lower from duodenum-jejunal flexure) can be diluted into 5 to 8 times more than that of ingested amount. That is why stoma in proximal jejunum and the higher intestinal fistula could cause severely lose of water, electrolytes and nutrients^[1].

Immunological Functions

GI tract is the largest immune organ in the body. The mucosal immune system is made up of gut-associated lymphoid tissue (GALT), which contains 10¹⁰ cells/m and accounts for 80% of the total body immunocytes^[12].

Absorption function of different intestinal segments

Stomach and duodenum do not nearly absorb any nutrients.

The upper jejunum (a segment in 200 cm long distal from Treitz's ligament), absorbs carbohydrates, protein and most of water soluble vitamins, whereas the fat absorption needs a longer segment of jejunum. The ending segment of ileum contributes to absorption of vitB12 and re-absorption of bile-salts for circulation of intestine-liver. Right half of colon is in charge of absorption water and inorganic salts; and left half of colon, in charge of storage and excreting feces. Adaptation and compensation happens in structure and function of the rest small intestines and colons after resection of most parts of small intestine^[1].

A specific mechanism for nutrients absorption

Nutriments that all the organs and tissues needed in the body are supplied solely by arteries, but the intestinal mucous epithelia has a completely different mode of nutrient uptake. It receives 30% of nutrients from the artery and takes in the other 70% from the contents within the lumen directly. That is why total parenteral nutrition (TPN) could result in an atrophy of intestinal mucosa^[10,11].

INTESTINAL BARRIER FUNCTION

Conception of gut barrier and bacterial/endotoxin translocation

In normal situations the GI tract can only absorb the needed nutrients selectively. It is the largest reservoir of germs in the body and contains about 10^{12} of bacteria, occupying about 1/3 of dry weight of feces^[7]. Such an astronomical figures of bacteria produces a great quantity of toxin, which was not taken in by the intestine because of presence of the mucosal barrier function and hence no sickness was resulted by the toxin. Generally, the intestinal mucosa barrier is consisted of three parts: mechanical, biological and immune barriers. Any etiological factors that impair these barriers would cause bacterial/endotoxin translocation (a phenomenon that bacteria/endotoxin gets across the gut barrier and enter into blood and other aseptic tissues)^[13,14].

Mechanical Barrier

It consist of closed-lining intestinal epithelial cells^[5,6]. Many harmful factors and diseases could destroy this structure, such as intestinal obstruction, haemorrhagic and necrotic enteritis, chemotherapy, radiotherapy, using some medicines (for example, anti-inflammatory drugs of non-steroids) for a longer time and shock^[11,15].

Structure of intestinal mechanical barrier

It is constituted by intestinal epithelial cells and the tight-junction between enterocytes^[5,6]. The enterocyte apical membrane is interspersed with water-filled pores (<0.8 nm in radius), which permit the permeation of non-lipid polar molecules. The tight junction between enterocytes constitutes only a small proportion (<5%) of the total surface area of the intestinal epithelium, which is about 0.95 nm in radius and permits transition of larger molecules. The dual saccharides test for measuring intestinal permeability is devised according to this structure^[5].

Immune barrier

It is composed of intra-epithelial secreting IgA, intra-mucosal lymphocytes, Payer's nodules and mesenteric lymph nodes. It is also called the GALT^[12]. Any factors that destroy the body's immunity, such as protein malnutrition, leukemia, systemic chemotherapy and HIV infection, would damage the barrier^[9,16].

Biological barrier

It is made up of normal inhabitant flora in GI tract, and hence the colonization resistance comes into being^[7,17]. It is an effect

of the flora that prevents the external or harmful bacteria from colonizing in the bowel because of the intrinsic flora holding the surface of intestinal mucosa. The colonization resistance would be destroyed by the alterations of inhabitant bacteria in the bowel. These diseases are bacterial enteritis, ileus (bacterial overbreeding), antibiotic enteritis (double infection), and so on^[1,18].

Micro-ecological equilibrium

There is a micro-ecological balance between bacteria in bowel with intestinal mucosal epithelia and the body system (the intestinal flora would colonizes for a postnatal infant in a few days). Any alterations in each of these three aspects would impair the balance and lead to sickness. Such cases are the impairment of systemic immunity (damage of immune barrier), destruction of intestinal mucosal structure(damage of mechanical barrier), and overgrowth of bacteria in the bowel (damage of biological barrier)^[1,17].

GASTROINTESTINAL TRACT IS A CENTRAL ORGAN FOR SURGICAL STRESS

Developments in different disciplines since the middle of last century have led to our current understanding and treatment of intestinal failure. This owes to the advances in 3 aspects: First, the application to both normal subjects and those with intestinal resection of new laboratory techniques, has advanced understanding of small intestinal function; Second, the scope of surgical treatments has extended to more complex operations on the intestine so that intestinal failure occurs more frequently and is often more severe; Third, clinical necessity has stimulated the application of innovative techniques to treat the condition in the short- or long-term^[1].

Clinical phenomena

(1) No matter what the cause is for critically-illed patients, infection would happen during the course of disease, and is one of the main causes of death. The mostly infected bacteria are normal intestinal flora. (2) Although isolated in aseptic wards for patients with transplantation of bone marrow, leukemia, and severe burns, they still had a high morbidity of infection. The pathogens cultured were mainly those of normal intestinal inhabitants. (3) Treatments with intravenous antibiotics and selected digestive decontamination therapy to these patients could markedly reduce the morbidity of infection. (4) Treatment with antibiotics excessively would cause a "double infection"^[1,18].

Animal experiments

(1) Enterocytes and colon cells proliferate rapidly (the enterocyte renew once in 5-7 d), and cover a broad area of intestinal inner surface. So metabolism and energy need for them are high. Windmueller *et al.*^[19] investigated the metabolism of mucosal epithelia with an isolated, vascularly perfused preparation of rat intestine. They discovered that small intestine extracted large amounts of glutamine as energy fuel when fed enterally miscellaneous nutriments quantitatively. The mucosal enterocyte converts most of the glutamine into metabolites of ammonia, alanine, citrulline. The epithelium metabolize the ketones (β -hydroxybutyrate, acetoacetate and acetone) as fuel, and colon combust short chain fatty acids. (2) It has been discovered through immunologic research that there are a great deal of intraepithelial lymphocytes, Peyer's nodules, secreted IgAs, lymphatic follicles and mesenteric lymph nodes (named as GALT- Gut associated lymphatic tissue) in gut. When stimulated by stresses, an intense immunologic responses in them would happen^[1,12]. (3) Phenomena revealed by experiments that phagocytosis of intestinal mucous epithelium and bacteria gain

access to blood stream and other tissues across the epithelia (so-called bacterial translocation) explain the existence of mucosal barrier of the gut^[18,20]. (4) Animals with intestines resected had a better resistance to trauma and strike than that of not resected when given equal parenteral nutrition. They had lived for a longer time and had a low morbidity of infection (such as Hammer-Hodges test that blocks the upper mesenteric artery temporarily so as to induce a lethal endotoxin shock in rabbits)^[21]. (5) Specific pathogen-free and gnotobiotic animals tolerate well to harmful stimulations and have lower morbidity of infection than that of ordinary animals.

Based on researches and advances we mentioned above, especially developments in medical sciences of last century, Wilmore^[17] suggested in 1988 that 'gut is a central organ after surgical stress'. The main contents of the hypothesis are as follows: The breakage of gut barrier occurs in patients after injury, multiorgan system failure, or severe burns and in persons with cancer after undergoing chemotherapy or bone marrow transplantation, which results in the entrance of bacteria and endotoxin into the blood stream and other tissues across the mucous epithelium from the gut. The cytokines produced by the reticular-endothelial system when body suffers from invasions of bacteria and endotoxin would stimulate pituitary-adrenal gland axis, and hence stress responses ensue. There are active metabolic effects for GI tract, especially when stimulated by stresses.

CONCEPTS OF INTESTINAL FAILURE

Historical retrospect

In the beginning of last century, Dr. Metchnikoff, the father of hypothesis of phagocytosis suggested that the entrance of microbes and associated toxin from the bowel into the body was an important cause of early death^[1]. In 1970's, the theory of multiple organs failure for death was put forward, underlying the facts that many critical-ill patients die of organs failure. But the concept have not given the course of evolving and transforming of a disease, whereas it just told a clinical phenomenon of a terminal patient^[22]. This is less helpful to treatments for patients by doctors. The studies in animal experiment and clinical investigation on physiology and pathophysiology of gastrointestinal tract have been increasingly reported since 1980s^[20,23-26]. The concept of multi-organs dysfunction syndrome (MODS) and systemic inflammatory response syndrome (SIRS) were raised since 1990s, and recognition in essence of inflammation, infestation and of the gut functions, and re-defining on them was made at the same time^[27-29]. All these have established a steady foundation for hypothesis of intestinal failure, which is a magnitude in gastroenterology, critical care medicine and infection-immunology *etc*^[1].

Definition of intestinal failure

The term 'intestinal failure' was first used by Irving and colleagues in the title of a paper published in 1980^[30]. The following year, a book chapter by Flamming and Remington^[1] gave the first definition as a 'reduction in functioning gut mass below the minimal amount necessary for adequate digestion and absorption of nutrients'. Now the viewpoint is further advanced. It widens the concept that 'reduced gastrointestinal absorption to the extent that macronutrient and/or fluid supplements are required', which includes the need for enteral or parenteral supplements to maintain a normal nutritional state. Malnutrition and/or dehydration would happen if supplements are not given or compensation does not work during the time^[31]. Comparative to description on functional failure of heart, lungs, brain and kidneys, it is no doubtful that the concept emphasized the equal importance of GI tract as other vital organs during the course of diseases.

CLASSIFICATION AND TREATMENTS OF INTESTINAL FAILURE^[1]

Staging of intestinal failure

Acute intestinal failure It is divided into reversible (in 6 mo) and causative surgical factors (such as percutaneous fistula, ileus), and those of internal medicine (such as chemotherapy or enteritis caused by acute radioactive injury, or infectious enteritis including HIV infection).

Chronic intestinal failure It results from following diseases: gastrointestinal resections (such as short bowel syndrome and gastrectomy), intestinal bypass operations (such as surgery for obesity treatment), and dysfunction of small intestine (such as pseudo-ileus, chronic enteritis - Crohn's and radioactive, microvilus atrophic or autoimmune enteropathy). Total or subtotal gastrectomy with a remnant of gastrointestinal disorders often needs nutrients complements and also belongs to intestinal failure.

Grading of intestinal failure

The severity of intestinal failure can be graded as follows according to the method by which macronutrients/fluid are given.

Severe intestinal failure Parenteral nutrition and/or parenteral saline are required because health cannot be sustained by exposing the small bowel mucosa to more, continuous or altered nutrients and/or electrolytes.

Moderate intestinal failure An enteral tube is used for the administration of macronutrients and/or a glucose/saline solution.

Mild intestinal failure Dietary adjustments, oral nutrients and/or a glucose/saline solution (or sodium chloride supplements) are needed.

A patient may change, due to compensatory mechanisms, from severe to mild IF with time. For example, a patient who has had a massive small intestinal resection, and in whom intestinal adaptation has occurred, may with careful dietary advice and appropriate drug therapy be able to stop parenteral nutrition (such as the intestinal rehabilitation therapy in short bowel syndrome).

COMMON DISEASES UNDERLYING IF

Acute IF

The usual conditions that cause an IF are as follows: (1) inflammatory diseases: in their attacks of Crohn's disease and ulcerous colonitis, especially in cases with surgical complications; (2) peptic ulcer; (3) pancreatitis; (4) mesenteric vascular disease; (5) malignancy; (6) external intestinal fistula; (7) cases receiving chemotherapy and transplantation of bone marrow; (8) AIDs; (9) others: such as acute ileus, gastric paralysis, inflammatory intestinal obstruction, severe intestinal infections (for example, shigellosis, cholera), external abdominal trauma (blunt or sharp and viscera rupture).

Chronic IF

(1) pseudo-intestinal obstruction; (2) radioactive enteritis; (3) post-gastrectomy; (4) short bowel syndrome; (5) post-surgery for obesity; (6) others: such as constipation resulting from various etiological factors.

The concept of IF presented above involves miscellaneous diseases and it seems confused because of that the meaning of the word 'failure' is different in Chinese from the English original word. It describes a broad functional status of an organ from dysfunction to complete loss of function in English meaning, whereas the word 'failure' denotes the function of an organ being severely injured or complete lost in Chinese. The gut has two functions: digestion and absorption, and barrier function. Therefore, we comprehend that the IF contains two implications: gastrointestinal dysfunction when there is only disorder of

digestion and absorption, whereas it would be named as IF when there is a disorder of barrier function. The former presents a less sick situation clinically and recovers easily, and the latter is complicated by critical illness or manifestations of severe enteropathy and has a high morbidity and mortality because of bacterial/endotoxin translocation. The suggested classification seems more reasonable, practical and directive.

EPILOGUE

Theory of IF is a great advancement in clinical medicine, especially in gastroenterology. It comes from developments and researches in the disciplines of critical care medicine, immunology in infection, clinical nutrition support and others. It also profits from developments in modern surgical technology and its clinical application. The IF theory has a significant guiding role to gastroenterologists. We should pay attention to the capability of GI tract in diseases and do not neglect protecting the barrier function of GI tract in clinical practice.

REFERENCES

- 1 **Nightignale J.** *Intestinal Failure*, London: Greenwich Medical Media Limited 2001: pp1-177
- 2 **Li JS.** *Clinical enteral and parenteral nutrition support*. Beijing: People's Military Surgeon Press 1993: pp9-10
- 3 **Li JS.** Enhancing studies to dysfunctions of gut barrier. *Chin Med J* 1999; **79**: 581
- 4 **Klein S,** Alpers DH, Grand RJ, Levin MS, Lin HC, Mansbach CM, Burant C, Reeds P, Rombeau JL. Advances in nutrition and gastroenterology: summary of the 1997 A.S.P.E.N. Research Workshop. *J Parenter Enteral Nutr* 1998; **22**: 3-13
- 5 **Travis S,** Menzies I. Intestinal permeability: functional assessment and significance. *Clin Sci* 1992; **82**: 471-488
- 6 **Daugherty AL,** Mrsny RJ. Regulation of the intestinal epithelial paracellular barrier. *PSTT* 1999; **2**: 281-287
- 7 **Simon GL,** Gorbach SL. Intestinal Flora in Health and Disease. *Gastroenterology* 1984; **86**: 174-193
- 8 **Sugiura T,** Tashiro T, Yamamori H, Takagi K, Hayashi N, Itabashi T, Toyoda Y, Sano W, Nitta H, Hirano J, Nakajima N, Ito I. Effects of total parenteral nutrition on endotoxin translocation and extent of the stress response in burned rats. *Nutrition* 1999; **15**: 570-575
- 9 **van der Hulst RR,** von Meyenfeldt MF, van Kreel BK, Thunnissen FB, Brummer RJ, Arends JW, Soeters PB. Gut permeability, intestinal morphology, and nutritional depletion. *Nutrition* 1998; **14**: 1-6
- 10 **Hulsewe KW,** van Acker BA, von Meyenfeldt MF, Soeters PB. Nutritional depletion and dietary manipulation: effects on the immune response. *World J Surg* 1999; **23**: 536-544
- 11 **Nakasaki H,** Mitomi T, Tajima T, Ohnishi N, Fuji K. Gut bacterial translocation during total parenteral nutrition in experimental rats and its countermeasure. *Am J Surg* 1998; **175**: 38-43
- 12 **Brandtzaeg P,** Halstensen TS, Kett K, Krajci P, Kvale D, Rognum TO, Scott H, Sollid LM. Immunobiology and Immunopathology of Human Gut Mucosa: Humoral Immunity and Intraepithelial Lymphocytes. *Gastroenterology* 1989; **97**: 1562-1584
- 13 **MacFie J.** Enteral Versus Parenteral Nutrition: The Significance of Bacterial Translocation and Gut-Barrier Function. *Nutrition* 2000; **16**: 606-611
- 14 **Van Deventer SJ,** Ten Cate JW, Tytgat GN. Intestinal endotoxemia: clinical significance. *Gastroenterology* 1988; **94**: 825-831
- 15 **Küçükaydin M,** Kocaoğlu C, Köçdak F, Konaş O. Detection of intestinal bacterial translocation in subclinical ischemia-reperfusion using the polymerase chain reaction technique. *J Pediatr Surg* 2000; **35**: 41-43
- 16 **Marshall JC,** Christou NV, Meakins JL. Small-bowel bacterial overgrowth and systemic immunosuppression in experimental peritonitis. *Surgery* 1988; **104**: 404-411
- 17 **Wilmore DW,** Smith RJ, O'Dwyer ST, Jacobs DO, Ziegler TR, Wang XD. The gut: A central organ after surgical stress. *Surgery* 1988; **104**: 917-923
- 18 **Berg RD.** Bacterial translocation from the gastrointestinal tract. *Trends In Microbiol* 1995; **3**: 149-154
- 19 **Windmueller HG,** Spaeth AE. The Journal of Biological Chemistry, Volume 249, 1974: Uptake and metabolism of plasma glutamine by the small intestine. *Nutr Rev* 1990; **48**: 310-312
- 20 **MacFie J,** O'Boyle C, Mitchell CJ, Buckley PM, Johnstone D, Sudworth P. Gut origin of sepsis: a prospective study investigating associations between bacterial translocation, gastric microflora, and septic morbidity. *Gut* 1999; **45**: 223-228
- 21 **Hammer-Hodges D,** Woodruff P, Cuevas P, Kaufman A, Fine J. Role of the intrainestinal gram-negative bacterial flora in response to major injury. *Surg Gynecol Obstet* 1974; **138**: 599-603
- 22 **Carrico CJ,** Meakins JL, Marshall JC, Fry D, Maier RV. Multiple-Organ-Failure Syndrome. *Arch Surg* 1986; **121**: 196-208
- 23 **Bengmark S,** Gianotti L. Nutritional support to prevent and treat multiple organ failure. *World J Surg* 1996; **20**: 474-481
- 24 **Bjarnason I,** Hayllar J, Smethurst P, Price A, Gumpel MJ. Metronidazole reduces intestinal inflammation and blood loss in Non-steroidal anti-inflammatory drug induced enteropathy. *Gut* 1992; **33**: 1204-1208
- 25 **Allison MC,** Howatson AG, Torrance CJ, Lee FD, Russell RI. Gastrointestinal damage associated with the use of nonsteroidal antiinflammatory drugs. *N Engl J Med* 1992; **327**: 749-753
- 26 **Swank GM,** Deitch EA. Role of the gut in multiple organ failure: bacterial translocation and permeability changes. *World J Surg* 1996; **20**: 411-417
- 27 **Wichterman KA,** Baue AE, Chaudry IH. Sepsis and septic shock—a review of laboratory models and a proposal. *J Surg Res* 1980; **29**: 189-201
- 28 **Fish RE,** Spitzer JA. Continuous infusion of endotoxin from an osmotic pump in the conscious unrestrained rat: a unique model. *Cir Shock* 1984; **12**: 135-149
- 29 **Schmidt H,** Secchi A, Wellmann R, Bach A, Böhner H, Gebhard MM, Martin E. Effect of endotoxemia on intestinal villus microcirculation in rats. *J Surg Res* 1996; **61**: 521-526
- 30 **Milewski PJ,** Gross E, Holbrook I, Clarke C, Turnberg LA, Irving MH. Parenteral nutrition at home in management of intestinal failure. *Br Med J* 1980; **280**: 1356-1357
- 31 **Byrne TA,** Morrissey TB, Nattakom TV, Ziegler TR, Wilmore DW. Growth hormone, glutamine, and a modified diet enhance nutrient absorption in patients with severe short bowel syndrome. *J Parenter Enteral Nutr* 1995; **19**: 296-302

Edited by Zhang JZ and Xu FM

Study on immune function of dendritic cells in patients with esophageal carcinoma

Shen-Ren Chen, Yi-Ping Luo, Jin-Kun Zhang, Wei Yang, Zhi-Chao Zhen, Lin-Xin Chen, Wei Zhang

Shen-Ren Chen, Yi-Ping Luo, Wei Yang, Zhi-Chao Zhen, Lin-Xin Chen, Wei Zhang, The Second University Hospital, Shantou University Medical College, Shantou 515041, Guangdong Province, China

Jin-Kun Zhang, Cancer Pathology Laboratory, Shantou University Medical College, Shantou 515031, Guangdong Province, China

Supported by Natural Science Foundation of the Higher Education Office of Guangdong Province, No. 0144

Correspondence to: Professor Shen-Ren Chen, The Second University Hospital of Shantou University Medical College, Dongsha Northern Road, Shantou 515041, Guangdong Province, China. chen-shenren@163.com

Telephone: +86-754-8355431 **Fax:** +86-754-8346543

Received: 2003-08-23 **Accepted:** 2003-10-22

Abstract

AIM: To investigate the immune function of dendritic cells from both peripheral blood and operated tissues of esophageal carcinoma patients in order to find the relationship between the immune function of dendritic cells and the pathogenesis of esophageal carcinoma.

METHODS: The expression of CD83, CD80, and CD86 on the surface of dendritic cells cultured from the peripheral blood of patients was detected compared with that from health donors using flow cytometry. The ability of dendritic cells to induce T lymphocyte proliferation was evaluated by a liquid scintillation counter. The expression of CD80, CD86, CD83, and S-100 proteins was assessed in esophageal carcinoma tissues using immunohistochemical method.

RESULTS: Compared with those from healthy donors, dendritic cells cultured from the peripheral blood of patients expressed lower CD80 and CD86. Furthermore, the ability of dendritic cells in patients to induce T lymphocyte proliferation was significantly lower than that of the control group. Compared with the control group, the positive expression ratio and frequencies of CD80, CD86, and S-100 in esophageal carcinoma tissues were significantly down regulated. The expression of CD83 was up-regulated in the pericancerous tissues, but no expression was found in the cancerous nodules.

CONCLUSION: The impaired immune function and the decreased number of dendritic cells cause pathogenesis and progression of esophageal carcinoma.

Chen SR, Luo YP, Zhang JK, Yang W, Zhen ZC, Chen LX, Zhang W. Study on immune function of dendritic cells in patients with esophageal carcinoma. *World J Gastroenterol* 2004; 10(7): 934-939

<http://www.wjgnet.com/1007-9327/10/934.asp>

INTRODUCTION

Esophageal carcinoma (EC) is one of the top ten frequently occurred malignant cancers, particularly common in China. Our

palace - Chaoshan area, located in the Eastern Guangdong, China, is one of the areas of high-incidence EC with morbidity of 197.82/10⁵ and 81.32/10⁵ world-standardized populations for males and females, respectively^[1,2]. Squamous cell carcinoma has been the more common cell-type of EC, accounting for almost 90%. Now the therapy including surgery, chemotherapy, radiation, or a combination for EC is only to palliate the symptoms. However, a 5-year survival rate in patients with esophageal carcinoma is less than 10%^[3]. Novel treatment options of EC are urgently needed. Indeed, tumor immunotherapy has evolved specifically to offer several attractive potential advantages. It is strictly autologous with very few side effects. Additionally, once the immune response has started, its efficacy is independent on the localization, type, and proliferative state of tumor cells^[4,5].

The aim of tumor immunotherapy is to activate our own immune system to fight the existing tumor. The majority of experimental systems clearly demonstrate that tumor cells are largely defended by CD4⁺, CD8⁺ T lymphocytes, or NK cells^[6-8]. Lymphocyte T and possibly NK cells, however, require to be activated by antigen-presenting cells (APCs). The dendritic cells (DCs) are one of the most potent APCs *in vivo* and play crucial roles in the enhancement or regulation of cell-mediated immune reactions^[9-11]. Since DCs strongly express various costimulatory and/or adhesion molecules, they can activate even naive T cells in a primary response. The DCs-based approach has been used to establish treatments for several malignant diseases, including B cell lymphoma and melanoma^[12-14]. However, the immune functions of DCs are occasionally suppressed under some tumor-bearing states. Thus, the functions of DCs must be assessed in relation to the disease status to further apply DCs as an immunotherapeutic tool. In this study, we detected the expression of CD83, CD80, and CD86 molecules on the surface of DCs cultured from the peripheral blood of patients and healthy donors, and the ability to induce T lymphocyte proliferation. Furthermore immunohistochemical method was used to assess the expression of CD80, CD86, CD83, and S-100 proteins in esophageal carcinoma tissues to find the relationships between the immune function of DCs and the pathogenesis and progression of esophageal carcinoma.

MATERIALS AND METHODS

Materials

Ten Patients with EC were enrolled in this study. All patients were diagnosed by clinical criteria and confirmed by appropriate histological findings (hematoxylin and eosin staining). To assess the DC function of EC patients, 10 age-matched healthy individuals were assigned as controls.

Methods

Esophageal tissue specimens Esophageal tissue specimens were obtained during operation. All patients attended the Second Affiliated Hospital of Shantou University Medical College (Shantou, China) between 2001 and 2002. All samples were fixed in 40 g/L buffered formaldehyde, embedded in paraffin, and cut into 5 μ m section. Thirty patients with esophageal carcinoma (aged 58-76 yr) were diagnosed by clinical criteria

and confirmed by appropriate histological findings (hematoxylin and eosin staining). We took specimens from the esophageal carcinoma tissue (ECT), pericancerous tissue (PCT), and tissue far away from the esophageal carcinoma tissues about 8 cm as the normal esophageal tissue (NET). At the time of surgery, all patients were free from any other tumor therapy.

Generation of DCs from peripheral blood mononuclear cells

The DCs were generated from peripheral blood mononuclear cells (PBMNC) according to the methods described by Zhu *et al.*^[15-19]. The PBMNC were collected from venous blood by Ficoll-Hypaque density-gradient centrifugation. After the PBMNC were suspended in DCs culture medium (RPMI 1640 supplemented with 100 mL/L fetal calf serum, 50 U/mL penicillin, 2 mmol/L L-glutamine, and 50 μ mol/L 2-mercaptoethanol), they were placed at 10 mL polystyrene culture plates and stored at 37 °C for 2 h. After incubation, nonadherent cells were removed by gently pipetting with warm RPMI 1640. Adherent cells were supplied with DCs medium containing 800 U/mL of recombinant human GM-CSF and 500 U/mL of recombinant human IL-4, and cultured for 7 d at 37 °C under 50 mL/L CO₂. Cells were referred fresh medium containing 800 U/mL of GM-CSF and 500 U/mL of IL-4 every 2 d. After 7 d, the cultures developed an adherent monolayer and clusters of DCs colonies (Figure 1). The DCs yield was defined as the percentage of the obtained DCs numbers to the PBMNC numbers used as the source.

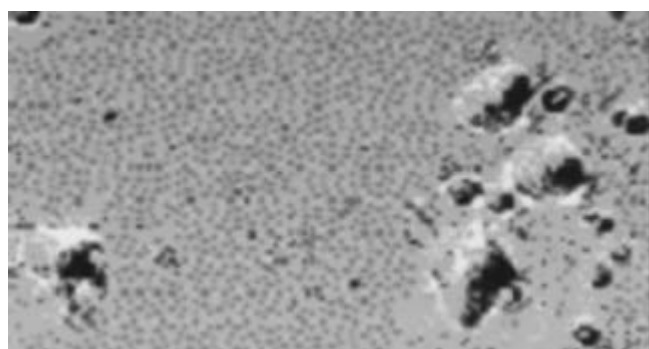


Figure 1 Typical appearance of DC cultures on 7 d.

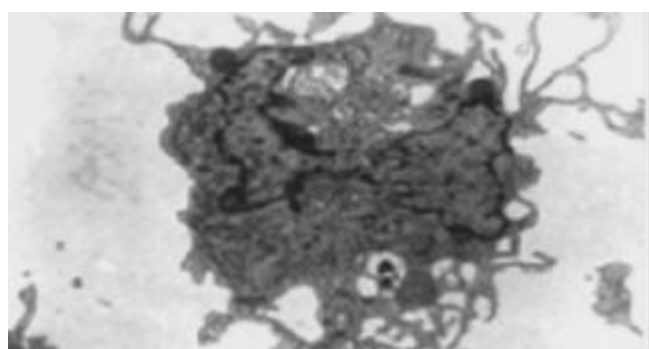


Figure 2 Transmission electron microscopy ($\times 8000$).

Electron microscopy

The nonadherent cells were aspirated, washed in PBS, pelleted, and fixed for 30 min in 30 g/L glutaraldehyde in 0.1 mol/L phosphate buffer (pH 7.35). After washing, the cells were postfixated for 1 h in 10 g/L buffered osmium tetroxide, washed once in phosphate buffer and 3 times in water, and stained with 5 mL/L aqueous uranyl acetate for 1 h. After dehydration through a series of ethanol dilutions, the cells were pelleted, and embedded in 1:1 Poly/Bed. Thin sections were cut with Diatome diamond knife, mounted 200 mesh nickel grids, and poststained with 50 mL/L methanolic uranyl acetate. Samples were viewed on a Philips 400 transmission electron microscope (Figure 2).

Mixed lymphocyte reaction

To evaluate the allostimulatory capacity of DCs, mixed lymphocyte reaction (MLR) was performed. To compare the function between DCs from EC patients (EC-DCs) and those from donors (N-DCs), allogeneic lymphocytes were obtained from the same healthy volunteer. The PBMNC were suspended in DC culture medium and incubated at 37 °C under 50 mL/L CO₂ for 1 h, non-adherent cells were gathered as T cells (TCs). After DCs were treated with 50 μ g/mL of mitomycin C for 45 min at 37 °C, they were suspended in DC medium and placed at 1×10^2 – 2×10^4 /well on 96-well flat-bottom culture plates. The TCs were mixed with DCs at 2×10^5 /well and cultured for 96 h at 37 °C, 50 mL/L CO₂. During the last 16 h of incubation, pulse labeling was done with 2.0 μ Ci/well of [³H] thymidine (MSI, Beijing, China). Assays were performed in triplicate. On day 4, the cells were harvested, and the amounts of [³H] thymidine incorporated to responder cells were counted with a beta counter. The ratio of MLR was determined by the ratios of cpm between EC-DC and N-DC in the presence of the same reagents at a TCs/DCs ratio of 10 to 1.

Flow cytometric analysis

After 7 d of culture, DCs were harvested, and their surface molecule expression was analyzed using FACS (Becton Dickinson Immunocytometry Systems, San Jose, CA). In each step of the staining, 5×10^4 cells were stored with specific antibodies (Abs) for 30 min at 4 °C in 50 μ L of PBS containing 20 mL/L of bovine serum albumin and 1 mL/L of sodium azide. For the staining of mouse monoclonal anti-human CD80, CD83, or CD86 (PharMingen, San Diego, CA), fluorescein isothiocyanate (FITC)-conjugated goat monoclonal anti-mouse IgG was used according to the procedure of indirect immunofluorescence staining. Isotypic Ab (purified mouse IgG) was substituted for specific Abs to obtain a negative control. After staining, all cells were fixed with 10 mL/L paraformaldehyde (Sigma), and analyzed with the FACStarP1 (Becton Dickinson) using a single argon laser. For the comparison of CD83 and costimulators, the mean fluorescence intensity of stained DCs (MFIs) and that of controls (MFic) was measured using a Consort 30 software program (Becton Dickinson). The degree of surface molecule expression was estimated as the ratio of MFIs to MFic (MFIs/MFic) and expressed as the net fluorescence intensity (NFI). All samples were assayed in duplicate.

Immunohistochemical staining of CD80, CD86, and S100 proteins

Immunohistochemical staining was performed. Rabbit anti-human monoclonal antibodies to CD80, CD86 and S100 proteins (PharMingen International) were used as primary antibodies (Ab1). The antigen-Ab1 complex was then incubated with biotinylated secondary antibody followed by horseradish peroxidase-avidin. Staining procedure was done according to the introduction of the agent box, SP method. A known sample from a patient with breast cancer was used as a positive control, and the staining for negative controls was followed the method described above, except for incubation with PBS instead of the primary antibody. Colorization was performed by diaminobenzidine (DAB)-hydrogen peroxide as a chromogen.

Immunohistochemical staining of CD83 The staining of CD83 was performed with some modifications, according to a previously described method^[19]. Formalin-fixed, paraffin-embedded specimens were washed three times in PBS and treated with pepsin (5 mg/mL in 0.01 mol/L HCl, Zhongshan, Beijing, China) for 20 min at 37 °C before staining for CD83. The specimens were then treated with normal goat serum for 20 min to block non-specific binding. The monoclonal antibody with appropriate dilution was then added. Tissue sections were treated with 0.3 mL/L methanol-hydrogen peroxide to inactivate endogenous peroxidase. The sections then were reincubated

with biotinylated goat anti-mouse immunoglobulin at room temperature for 1 h. After a wash in PBS, sections were soaked in alkaline phosphatase-conjugated streptavidin, washed, and New Fuchsin was used as a chromogen. A known sample from patients with primary biliary cirrhosis was used as a positive control. The staining of negative controls was performed using PBS instead of primary antibody.

Enumeration of positive staining cells The numbers of CD80-, CD86-, S100-, and CD83-positive cells in the whole specimen were determined. The prevalence of CD80, CD86, and S100 protein-positive cells were shown as the ratio of a total 100 infiltrating cells. The prevalence of CD83 positive cells was shown as total numbers of cells/specimen.

Statistical analysis

The data were expressed as mean±SD. The statistical analyses were done by unpaired and paired *t*-tests, when indicated. Mann-Whitney's U-test and the Wilcoxon rank-sum test were also used when unpaired and paired *t*-tests were not indicated, respectively. *P*-values less than 0.05 were considered to indicate statistical significance. Statistical calculations were performed using the SPSS 10.0 statistical program.

RESULTS

Phenotypic analysis of DC

After 7 d of culture under GM-CSF and IL-4, the cells from patients or volunteers exhibited DC morphology with veiled process and dendrites. Through the observation from transmission electron microscopy, the cell surface was irregular but lacked the discrete microvilli and ruffles (Figures 1, 2). The cells were free polysomes and ribosomes, and lysosomes were scanty. These results showed that the generated cells from both patients and donors were morphological and compatible with DCs. The expression of CD80 and CD86 in EC patients was weaker than that in volunteers, but not the expression of CD83 was not different between EC patients and volunteers (Table 1 and Figure 3). The yield of DCs was not different between patients and donors (5±3% vs 5±1%).

Low mixed lymphocyte reaction in DCs generated from EC patients

In MLRs, the degree of T cell proliferation from EC-DCs was

significantly lower than that from N-DCs. The reduced allogeneic response from EC-DCs was confirmed with the comparison of the cpm at a TCs/DCs ratio of 10 to 1 with large numbers of subjects (*P*<0.01) (Table 1). Since the responders were identical in each series of the comparisons, the difference in TCs proliferation mainly depended on the DCs difference.

Table 1 Antigen presentation and ability to induce T lymphocyte proliferation on DCs in peripheral blood from donors and EC patients (% mean±SD)

Group	CD80	CD86	CD83	MLR (cpm)
Donor	61.41±7.47	37.28±6.75	5.18±1.59	20 000±3 000
Patient	41.76±7.35 ^b	29.68±7.32 ^b	4.44±1.17	10 000±2 000 ^b

^b*P*<0.01 vs donor group.

Lower expression of CD80 and CD86 in EC patients

The expression of CD80 and CD86 could be detected in the nucleus and cytoplasm but not on the cell membrane for all the specimens. The expression of CD80 and CD86 in the nucleus was found randomly. The expression in the cytoplasm was located in the necrotic area and around with infiltrated lymphocytes (Figure 4A, B, C, D). The prevalence of positive expression of CD80 and CD86 was lower in ECT than that in NET (*P*<0.01), but there was no significant difference between PCT and NET (Table 2).

Table 2 Positive staining of CD80, CD86, and S100 proteins in esophageal tissues

Group	Tissue	<i>n</i>	Prevalence	Frequency (%)
CD80	ECT	30	8 (26.7%) ^b	24.37±4.87 ^b
CD80	NET	30	18 (60%)	46.25±14.04
CD86	ECT	30	12 (40%)	20.37±4.89 ^a
CD86	NET	30	13 (43.3%)	26.87±5.89
S-100	ECT	30	30 (100%)	56.32±6.25 ^b
S-100	NET	30	30 (100%)	72.45±12.34

^a*P*<0.05 vs NET group; ^b*P*<0.01 vs NET group. ECT: esophageal carcinoma tissue, NET: normal esophageal tissue.

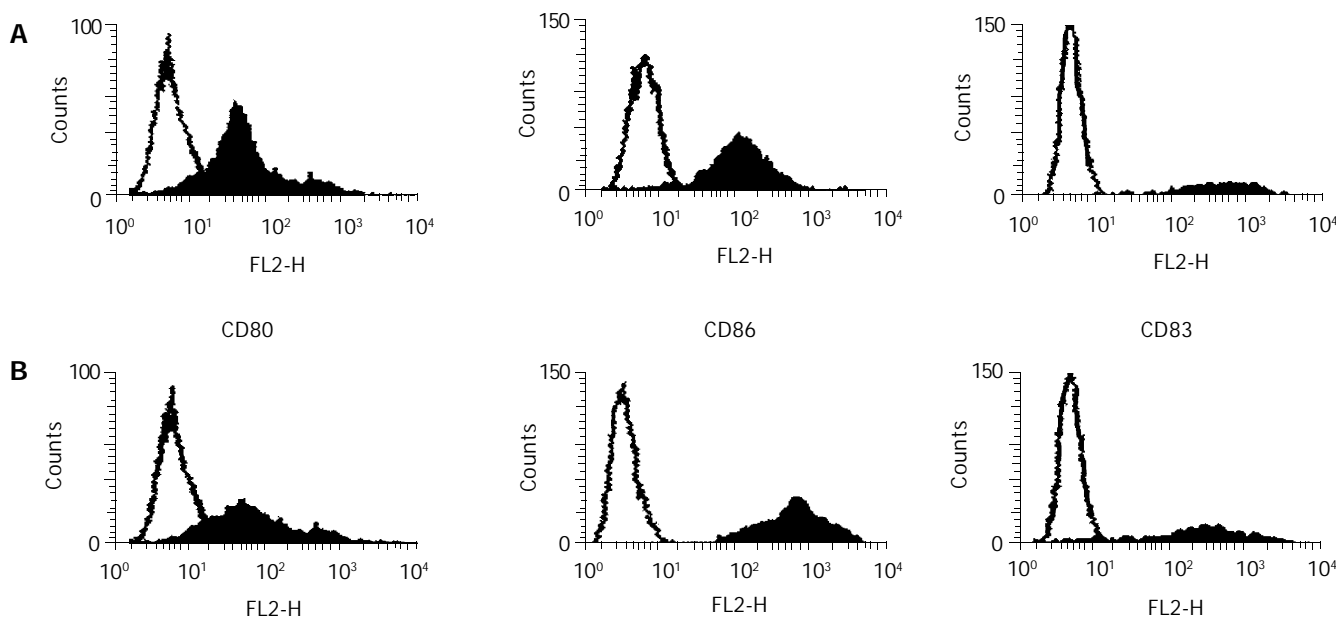


Figure 3 Surface phenotype of DCs on d 7 of culture. Flow cytometric analyses of surface molecules in DC generated from PBMNC obtained from a healthy volunteer (A) or an EC patient (B). Representative results of one of the subjects are shown.

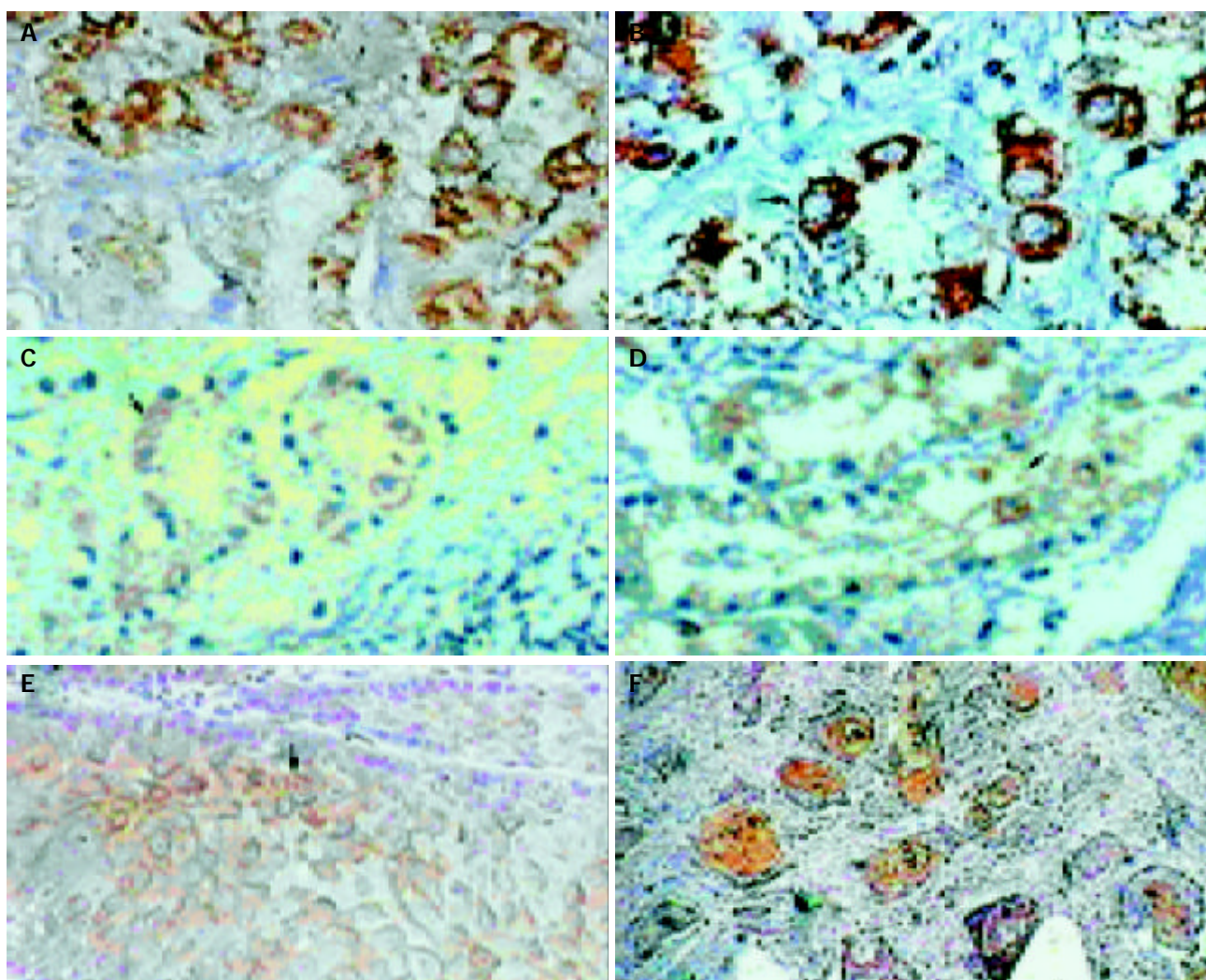


Figure 4 A: Positive expression of CD80 in NET (SP method, DAB, $\times 400$), B: Positive expression of CD80 in ECT (SP method, DAB, $\times 400$), C: Positive expression of CD86 in NET (SP method, DAB, $\times 400$), D: Positive expression of CD86 in ECT (SP method, DAB, $\times 400$), E: Positive expression of S100 protein in NET (SP method, DAB, $\times 400$), F: Positive expression of S100 protein in ECT (SP method, DAB, $\times 400$).

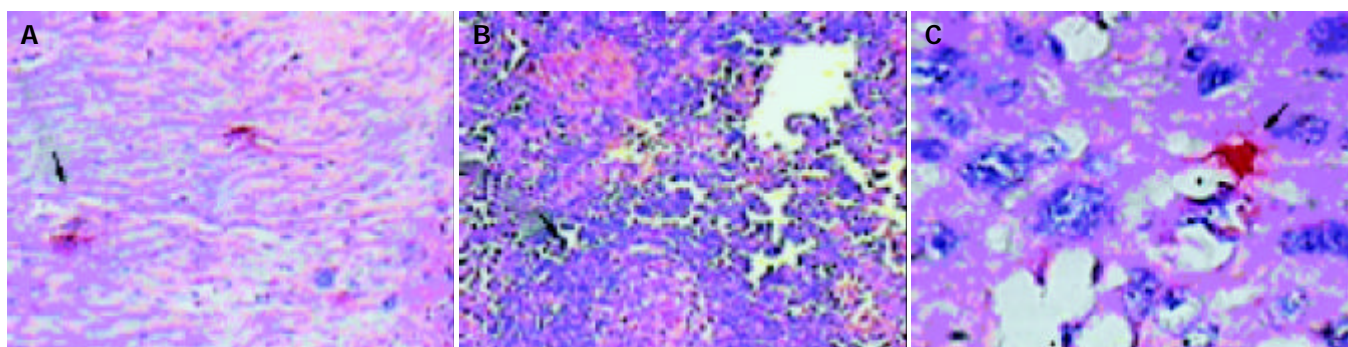


Figure 5 A: Positive expression of CD83 in PCT (New Fuchsin, $\times 100$), B: No CD83-positive cells in cancer nodules (New Fuchsin, $\times 100$), C: Positive expression of CD83 in ECT (New Fuchsin, $\times 400$).

Table 3 Expression of CD83 in esophageal tissues

Group	n	Prevalence (%)	Frequency (%)
ECT	30	10 (33.3) ^a	7.82 \pm 6.69 ^a
PCT	30	18 (60)	23.34 \pm 19.7

^a $P < 0.05$ vs PCT group. ECT: esophageal carcinoma tissue, PCT: pericancerous tissue.

Lower expression of S-100 in EC patients

The S100 protein-positive cells were diffusely detected in

infiltrating cells of esophageal mucous membrane and epithelium tissues. In ECT, they were localized in cancer cells and cancer nodules; only little could be detected in the tissues away from cancer tissues (Figure 4E, F). Contrast to NET, ECT expressed lower S100-positive cells ($P < 0.05$) (Table 2).

Expression of CD83-positive cells

The CD83-positive cells were detected in infiltrating cells in PCT. The NET did not show any positive staining for CD83. In ECT, CD83-positive cells could only be dispersedly detected surround cancer nodules, but there were no CD83-positive

activated DCs in cancer nodules (Figure 5A, B, C). Contrast to PCT, ECT expressed lower CD83-positive cells ($P < 0.05$) (Table 3).

DISCUSSION

To activate naive T cells, DCs can uptake, process, and present antigens via their MHC molecules. In addition, T cell activation requires engagement of costimulatory receptors on the T cells. The DCs are at the center of the developing tumor-specific immune response, and are involved both in the initiation of tumor-specific immunity and the generation of immune effector functions. Many observations have suggested that DCs in tumors are functionally impaired^[19-24].

In this study, we compared the functions of DCs generated from EC patients with those from healthy volunteers. Our results showed that the allogeneic MLR from EC-DCs was lower than that from N-DCs. With regard to the APC dysfunction in EC-DCs, the decreased expression of costimulators might be involved. Among the examined costimulators, lower expression of CD80 and CD86 was found in EC-DCs. The importance of the CD80/CD86-CD28 system in T cell responses has been well demonstrated^[10,20,21,29].

The CD80 and CD86, members of the immunoglobulin super gene family, are encoded by separate genes and provide costimulatory function for APC-dependent T-cell activation both *in vivo* and *in vitro*^[25-28]. A previous study reported that most tumor tissues, like those from the nonhematopoietic origin, did not express costimulatory molecules, which would render T cells unresponsive for the specific antigens^[20]. Recent studies demonstrated that B7 expression of tumor cells resulted in increased tumor immunogenicity, enhanced generation of allogeneic and antitumor reactive CTL. The decrease, abrogation or loss of CD80 and CD86 were detected both from EC-DCs and specimens from EC patients in this study, which might have profound implications for the down-regulation of the immune system and for enhancing the progression of esophageal carcinoma.

Furthermore, both the expression of CD80 and CD86 in EC sections could only be detected in the nucleus and cytoplasm but not on the cell membrane, suggesting the impaired transmembrane transduction of CD80 and CD86 molecules. This interesting phenomena was similar to the B7 molecule expression in renal carcinoma and hepatocarcinoma^[29,30].

The lower frequency of S100-positive cells in EC indicated the less DCs during esophageal carcinogenesis. However, the S100 protein family contains 21 members, and so far the physiological implication of its function is confusing^[19]. Therefore, the significance of positive S100 protein is not clearly known.

Because CD83-positive DCs could not be detected in most of the normal esophagus, their existence in the tissues from EC patients indicated the maturation and activation of immature DCs. Alternatively, it was also possible that the activated CD83-positive DCs infiltrated into the esophagus in EC patients through the circulation in spite of having almost similar frequencies of CD83-positive DCs in peripheral blood from both healthy donors and EC patients. Most strikingly, all CD83-positive DCs were localized in the pericancerous tissues, and there were no CD83-positive DCs in any cancer nodules.

What is the significance of absence of activated DCs in cancer nodules from patients with EC? Activated DCs present the antigenic epitope to T cells and induce its activation, which are the most strong inducers for IL-12 and specific cytotoxic T lymphocytes during carcinogenesis^[31,32]. In the absence of activated DCs in cancer nodules, normal immune surveillance against EC may be hampered due to defective production of tumor-specific lymphocytes. Again, tumor-specific lymphocytes would not be able to function and survive in the absence of activated DCs.

In summary, the impaired immune functions of DCs in patients with EC, including lower amount of DCs, decreased expression of CD80/86, minimally activated DCs, and complete absence of activated DCs in cancer nodules, are correlated to the pathogenesis and progression of EC.

REFERENCES

- 1 **Simchuk EJ**, Alderson D. Oesophageal surgery. *World J Gastroenterol* 2001; **7**: 760-765
- 2 **Dan HL**, Bai Y, Meng H, Song CL, Zhang J, Zhang Y, Wan LC, Zhang YL, Zhang ZS, Zhou DY. A new three-layer-funnel-shaped esophagogastric anastomosis for surgical treatment of esophageal carcinoma. *World J Gastroenterol* 2003; **9**: 22-25
- 3 **Zhou J**, Zhao LQ, Xiong MM, Wang XQ, Yang GR, Qiu ZL, Wu M, Liu ZH. Gene expression profiles at different stages of human esophageal squamous cell carcinoma. *World J Gastroenterol* 2003; **9**: 9-15
- 4 **Liu XJ**, Wang BM. Biotherapy of esophageal carcinoma. *Shijie Huaren Xiaohua Zazhi* 2000; **8**: 1027-1029
- 5 **Chen KN**, Xu GW. Diagnosis and therapy of esophageal carcinoma. *Shijie Huaren Xiaohua Zazhi* 2000; **8**: 196-202
- 6 **Zhang J**, Zhang JK, Zhuo SH, Chen HB. Effect of a cancer vaccine prepared by fusions of hepatocarcinoma cells with dendritic cells. *World J Gastroenterol* 2001; **7**: 690-694
- 7 **Wykes M**, Macpherson G. Dendritic cell-B-cell interaction: dendritic cells provide B cells with CD40-independent proliferation signals and CD40-dependent survival signals. *Immunology* 2000; **100**: 1-3
- 8 **Tascon RE**, Soares CS, Ragno S, Stavropoulos E, Hirst EMA, Colston MJ. Mycobacterium tuberculosis-activated dendritic cells induce protective immunity in mice. *Immunology* 2000; **99**: 473-480
- 9 **Aiba S**, Manome H, Yoshino Y, Tagami H. *In vitro* treatment of human transforming growth factor- β_1 -treated monocyte derived dendritic cells with haptens can induce the phenotypic and functional changes similar to epidermal Langerhans cells in the initiation phase of allergic contact sensitivity reaction. *Immunology* 2000; **101**: 68-75
- 10 **Mogi S**, Sakurai J, Kohsaka T, Enomoto S, Yagita H, Okumura K, Azuma M. Tumour rejection by gene transfer of 4-1BB ligand into a CD80+ murine squamous cell carcinoma and the requirements of co-stimulatory molecules on tumor and host cells. *Immunology* 2000; **101**: 541-547
- 11 **Li MS**, Yuan AL, Zhang WD, Chen XQ, Tian XH, Piao YJ. Immune response induced by dendritic cells induce apoptosis and inhibit proliferation of tumor cells. *Shijie Huaren Xiaohua Zazhi* 2000; **8**: 56-58
- 12 **Sun JL**, Zhang JK, Chen JD, Chen HB, Qiu YQ, Chen JX. *In vitro* study on the morphology of human blood dendritic cells and LPAK cells inducing apoptosis of the hepatoma cells line. *Chin Med J* 2001; **114**: 600-605
- 13 **Li MS**, Yuan AL. Study about immunology function of dendritic cells from liver patients. *Chin Oncology* 1998; **8**: 85-87
- 14 **Yu JW**, Wang GQ, Lu SL. Study of immune function of peripheral blood dendritic cells from chronic hepatitis B patients. *Chin Infer Dis* 2001; **19**: 144-147
- 15 **Zhu XJ**, Cao XT, Yu YZ, Chen GY, Wan T, Ma SH, Tang H, Zhang WP. Generation of dendritic cells from human peripheral blood. *Chin J Cancer Biother* 1997; **4**: 302-306
- 16 **Wang YD**, Xie W, Qiu YH, Gu ZJ, Zhang XG. The study of dendritic cells induced by cytokines from different adherent cells *in vitro*. *Shanghai Immunol J* 2000; **20**: 140-144
- 17 **Li YQ**, Zeng BH. *In vitro* culture and anti-cancer immunity of dendritic cells. *Chin J Cancer Prev Treat* 2001; **8**: 78-80
- 18 **Lutz MB**, Kukutsch N, Ogilvie AL, Rossner S, Koch F, Romani N, Schuler G. An advanced culture method for generating large quantities of highly pure dendritic cells from mouse bone marrow. *J Immunol Methods* 1999; **223**: 77-92
- 19 **Chen S**, Akbar SM, Tanimoto K, Ninomiya T, Iuchi H, Michitaka K, Horiike N, Onji M. Absence of CD83-positive mature and activated dendritic cells at cancer nodules from patients with hepatocellular carcinoma: relevance to hepatocarcinogenesis. *Cancer Lett* 2000; **148**: 49-57

- 20 **Woods GM**, Doherty KV, Malley RC, Rist MJ, Muller HK. Carcinogen-modified dendritic cells induce immunosuppression by incomplete T-cell activation resulting from impaired antigen uptake and reduced CD86 expression. *Immunology* 2000; **99**: 16-22
- 21 **Avigan D**. Dendritic cells: development, function and potential use for cancer immunotherapy. *Blood Rev* 1999; **13**: 51-64
- 22 **Zhang JK**, Sun JL, Chen HB, Zeng Y, Qu YJ. Influence of granulocyte-macrophage colony-stimulating factor and tumor necrosis factor on anti-hepatoma activities of human dendritic cells. *World J Gastroenterol* 2000; **6**: 718-720
- 23 **Zhang JK**, Li J, Chen HB, Sun JL, Qu YJ, Lu JJ. Antitumor activities of human dendritic cells derived from peripheral and cord blood. *World J Gastroenterol* 2002; **8**: 87-90
- 24 **Li MS**, Yuan AL, Zhang WD, Chen XQ, Zhang YL, Zhou DY. Study on immune function of dendritic cells in patients with colorectal neoplasms. *Shijie Huaren Xiaohua Zazhi* 1999; **7**: 429
- 25 **Zhang JW**, Xu J, Jia SS. Infiltration of dendritic cells into cervical lymph nodes in laryngeal carcinoma. *Chin J Otolaryngol* 2000; **35**: 472-474
- 26 **Zhang XZ**, An HL, Zhang XB. Immunohistochemical study of S-100 protein-positive dendritic cells in esophageal carcinoma. *J Xi'an Med Univ* 1998; **19**: 215-218
- 27 **Ito T**, Amakawa R, Inaba M, Ikehara S, Inaba K, Fukuhara S. Differential regulation of human blood dendritic cell subsets by IFNs. *Immunology* 2001; **104**: 2961-2969
- 28 **Xing LH**, Wang FS, Liu MX, Zhu CL. Dendritic cells and liver diseases. *Shijie Huaren Xiaohua Zazhi* 2000; **8**: 1276-1279
- 29 **Zai SH**, Liu JB, Zhu P, Wang YH. The expression of CD80 and CD86 in hepatocarcinoma and cirrhosis tissues. *J Fourth Mil Med Univ* 2001; **21**: 26-27
- 30 **Wang HL**, Xiu AP, Tan SF, Wu J, Xie H, Xiao J. The expression of CD80 and CD86 in renal carcinoma. *Anat Res* 2001; **23**: 88-90
- 31 **Fan P**, Wu ZY, Wang S. An investigation on the phenotype of cultured dendritic cells from the peripheral blood of patients with breast cancer. *J NanJing Med Univ* 2002; **16**: 115-118
- 32 **Hao MW**, Liang YR, Liu YF, Liu L, Wu MY, Yang HX. Transcription factor EGR-1 inhibits growth of hepatocellular carcinoma and esophageal carcinoma cell lines. *World J Gastroenterol* 2002; **8**: 203-207

Edited by Chao JCJ and Xu FM

Genetic susceptibility and environmental factors of esophageal cancer in Xi'an

An-Hui Wang, Chang-Sheng Sun, Liang-Shou Li, Jiu-Yi Huang, Qing-Shu Chen, De-Zhong Xu

An-Hui Wang, Chang-Sheng Sun, Liang-Shou Li, Jiu-Yi Huang, De-Zhong Xu, Department of Epidemiology, Faculty of Preventive Medicine, Fourth Military Medical University, Xi'an 710033, Shanxi Province, China

Qing-Shu Chen, Department of Thoracic Surgery, Tangdu Hospital, Fourth Military Medical University, Xi'an 710038, Shanxi Province, China

Supported by the National Natural Science Foundation of China, No.39670651

Correspondence to: Dr. An-Hui Wang, Department of Epidemiology, Faculty of Preventive Medicine, Fourth Military Medical University, Xi'an 710033, Shanxi Province, China. wanganhui@hotmail.com

Telephone: +86-29-3374871

Received: 2002-07-18 **Accepted:** 2003-04-01

Abstract

AIM: To analyse the role of genetic susceptibility and environmental factors in the process of esophageal cancer (EC) formation in Xi'an, China.

METHODS: A hospital based case-control study, combined with molecular epidemiological method, was carried out. A total of 127 EC cases and 101 controls were interviewed with questionnaires containing demographic items, habit of tobacco smoking, alcohol drinking, and family history of EC. Polymorphism of CYP1A1 and GSTM1 of 127 EC cases and 101 controls were detected by PCR method. The interactions between genetic susceptibility and environmental factors were also discussed.

RESULTS: Tobacco smoking, alcohol drinking and a family history of EC were risk factors for EC with an OR of 2.04 (95% CI 1.15-3.60), 3.45(95% CI 1.74-6.91), 3.14 (95% CI 1.28-7.94), respectively. Individuals carrying CYP1A1 Val/Val genotype compared to those with CYP1A1 Ile/Ile genotype had an increased risk for EC (OR 3.35, 95% CI 1.49-7.61). GSTM1 deletion genotype was a risk factor for EC (OR1.81, 95% CI 1.03-3.18). Gene-environment interaction analysis showed that CYP1A1 Val/Val genotype, GSTM1 deletion genotype had synergetic interactions with tobacco smoking, alcohol drinking and family history of EC.

CONCLUSION: Tobacco smoking, alcohol drinking and a family history of EC are risk factors for EC. CYP1A1 Val/Val and GSTM1 deletion genotypes are genetic susceptibility biomarkers for EC. There are synergic interactions between genetic susceptibility and environmental factors.

Wang AH, Sun CS, Li LS, Huang JY, Chen QS, Xu DZ. Genetic susceptibility and environmental factors of esophageal cancer in Xi'an. *World J Gastroenterol* 2004; 10(7): 940-944
<http://www.wjgnet.com/1007-9327/10/940.asp>

INTRODUCTION

China is a country with high incidence and mortality rate of EC. Risks for EC vary in different countries or different places^[1-6].

Studies have shown that tobacco smoking, alcohol drinking^[7-13], nutrition factors (fruit and vegetable consumption), life style, virus infection, heredity or exposure to nitro amines, fungi or AFB1 may be involved in the process of EC^[1,3,14-24]. In China, the risks for EC were different among areas with different incidences^[1-5,17,19,25,26]. The mortality rate of EC is about 24 per 100 000 in Xi'an, and it ranks first of all cancer mortalities. Previous studies showed that tobacco smoking and a family history of EC were risk factors for EC in Xi'an^[2,27,28].

Environmental risks and genetic susceptibility may play the main role in the process of EC^[2,27-37]. Susceptibility and environmental carcinogens exposure are indispensable factors for EC^[25,28,37]. To explore the bio-basis of genetic susceptibility to EC in Xi'an, we carried out a hospital based case-control study to analyze the role of tobacco smoking, alcohol drinking, family history of cancer, family history of EC, CYP1A1, and GSTM1 gene polymorphism in the process of EC, and possible susceptibility-environmental risk interaction.

MATERIALS AND METHODS

Selection of patients and controls

Cases of esophageal cancer (confirmed by pathological diagnosis) came from inpatients of Tangdu Hospital, during Dec 1999 to May 2000. Controls were randomly selected from non-cancer inpatients from different wards of the same hospital during the same period. Both cases and controls were confined to Xi'an area residents.

Data collection

Trained interviewers using a structured questionnaire interviewed cases and controls in the hospital. The questionnaire contained information of residence, occupation, tobacco smoking habit, alcohol intake, family history of EC, etc. Tobacco smoking was defined as smoking at least one cigarette per day and persisting for more than one year. Alcohol intake was defined as drinking at least twice a week with more than 50 gram every time and persisting for more than one year. Totally 127 cases (male 97, female 30) and 101(male 78, female 23) controls were included. Blood samples were also collected for extraction of DNA genome. All blood samples were stored at -70 °C before DNA extraction.

Detection of polymorphism of CYP1A1 and GSTM1 by PCR methods

DNA genomes were extracted from blood clots by proteinase K digestion, hydroxybenzene, and chloroform method. Polymerase chain reaction (PCR) was used to identify their CYP1A1 and GSTM1 polymorphisms.

Primers for GSTM1(P1: 5'-GTA CCC TAC TTG ATT GAT GGG-3'; P2: 5'-CTG GAT TGT AGC AGA TCA TGC-3') and CYP1A1 (P3: 5'-CGG AAG TGT ATC GGT GAG ACC A-3', P4: 5'-CGG AAG TGT ATC GGT GAG ACC G-3'; P5: 5'-GTA GAC AGA GTC TAG GCC TCA-3') were synthesized by Shengong Bio-technology Company of Shanghai. PCR condition for GSTM1: 50 μL solution containing 10×buffer 5 μL, Mg²⁺ 2 μL, P1,P2 1 μL, template

DNA1.5 μ L, dNTPs 1 μ L and *Taq* DNA polymerase 3u. PCR consisted of denaturation first at 94 $^{\circ}$ C for 10 min, followed by addition of *Taq* DNA polymerase, and then at 94 $^{\circ}$ C for 1 min, at 60 $^{\circ}$ C for 1 min, at 72 $^{\circ}$ C for 1 min with 30 cycles. After 20 g/L agar was used for electrophoresis, PCR products were observed under violet light. GSTM1 genotype was characterized by 273 bp fragment, while GSTM1 deletion genotype had no fragment.

Two pairs of primers were used to detect the polymorphism of CYP1A1 (7th exon). For each DNA sample two sets of PCR were carried out using P3, P5 (marked as tube A) and P4, P5 (marked as tube B) respectively. PCR conditions for tube A and tube B were the same: 50 μ L solution containing 10 \times buffer 5 μ L, Mg²⁺ 2 μ L, P3, P5 (or P4, P5) 1 μ L, template DNA1.5 μ L, dNTPs 1 μ L and *Taq* DNA polymerase 3u. PCR was carried out at 94 $^{\circ}$ C for 10 min, followed by at 94 $^{\circ}$ C for 1 min, at 55 $^{\circ}$ C for 1 min, at 72 $^{\circ}$ C for 1 min, for a total of 35 cycles, at last extension at 72 $^{\circ}$ C for 10 min. After 20 g/L agar was used for electrophoresis, PCR products were observed under the violet light. If only tube A had the specific fragment (200 bp), the DNA was regarded as CYP1A1 *Ile/Ile* genotype (pure wild genotype). If only tube B had the positive fragment, CYP1A1 *Val/Val* genotype (pure mutation) was considered, and CYP1A1 *Ile/Val* genotype was identified when both tube A and tube B had the fragment.

Quality control

DNA extraction and PCR were conducted in different times and places. The genotypes of DNA samples were identified

blindly. Controls were set up within every PCR operation as blank control (without DNA template), positive control and negative control and when any one of these controls failed, PCR needed to be re-conducted.

Statistical analysis

Data were checked and input into the computer. The values of chi-square, odds ratio (OR) and OR 95% CI (confidence interval) were calculated. And interactions between genetic susceptibility-environmental factors were also estimated.

RESULTS

Test of comparability between cases and controls showed that the age and gender in cases and controls were comparable.

Risk factors for EC

Tobacco smoking, alcohol drinking, a family history of EC, GSTM1 deletion genotype and CYP1A1 genotype (*Val/Val*) were risk factors of EC (Table 1).

Analysis of genetic susceptibility-environmental factor interaction

GSTM1 deletion genotype had synergic interactions with tobacco smoking, alcohol drinking and family history of EC (Tables 2,3,4).

CYP1A1 *Val/Val* genotype had synergic interactions with tobacco smoking, alcohol drinking, and family history of esophageal cancer (Tables 5, 6, 7).

Table 1 Risk factors for esophageal cancer

Risk factors		Case	Control	OR	OR95%CI	χ^2	P
Tobacco smoking	Yes	70	38	2.04	1.15-3.60	6.88	0.009
	No	59	63				
Alcohol drinking	Yes	50	16	3.45	1.74-6.91	15.08	0.000
	No	77	85				
FHEC	Yes	27	8	3.14	1.28-7.94	7.67	0.006
	No	100	93				
GSTM1	Deletion	74	44	1.81	1.03-3.18	4.85	0.028
	Existed	53	57				
CYP1A1	<i>Ile/Ile</i>	21	31	1.00			
	<i>Ile/Val</i>	56	48	1.72	0.83-3.58	2.50	0.114
	<i>Val/Val</i>	50	22	3.35	1.49-7.61	10.33	0.001

FHEC: family history of esophageal cancer.

Table 2 Synergic interactions of tobacco smoking and GSTM1 deletion genotype

Tobacco smoking	GSTM1 deletion	Case	Control	OR	OR95%CI	χ^2	P
No	No	24	37	1.00			
No	Yes	33	26	2.96	0.89-4.33	3.28	0.07
Yes	No	29	20	2.24	0.97-5.19	4.24	0.04
Yes	Yes	41	18	3.51	1.55-8.05	10.89	0.001

SIA=3.51/(2.24+1.96-1.00)=1.10. SIA: Synergic index of addition.

Table 3 Synergic interactions of alcohol drinking and GSTM1 deletion genotype

Alcohol drinking	GSTM1 deletion	Case	Control	OR	OR95%CI	χ^2	P
No	No	35	48				
No	Yes	42	37	1.56	0.80-3.04	1.95	0.16
Yes	No	18	9	2.74	1.01-7.55	4.85	0.03
Yes	Yes	32	7	6.27	2.30-17.72	16.91	0.00

SIM=6.27/(1.56 \times 2.74)=1.47 SIM: Synergic index of multiplication.

Table 4 Synergic interaction of GSTM1 deletion genotype and family history of esophageal cancer

ECFH	GSTM1deletion	Case	Control	OR	OR95%CI	χ^2	P
No	No	44	53	1.00			
No	Yes	56	40	1.69	0.92-3.11	3.24	0.07
Yes	No	9	4	2.71	0.69-12.76	2.59	0.11
Yes	Yes	18	4	5.42	1.60-23.34	9.47	0.00

SIM=5.42/(1.69×2.71)=1.18.

Table 5 Interaction of tobacco smoking and CYP1A1 Val/Val genotype

Smoking	CYP1A1 (Val/Val)	Case	Control	OR	OR95%CI	χ^2	P
No	No	33	47	1.00			
No	Yes	24	16	2.14	0.92-4.99	3.73	0.05
Yes	No	44	32	1.96	0.99-3.90	4.29	0.04
Yes	Yes	26	6	6.17	2.14-20.10	14.54	0.00

SIM=6.17/(2.14×1.96)=1.47.

Table 6 Interaction of alcohol drinking and CYP1A1 Val/Val genotype

Alcohol drinking	CYP1A1 Val/Val	Case	Control	OR	OR95%CI	χ^2	P
No	No	50	67	1.00			
No	Yes	27	18	2.01	0.94-3.43	3.86	0.05
Yes	No	27	12	3.02	1.31-7.03	8.16	0.00
Yes	Yes	23	4	7.71	2.39-32.16	15.71	0.00

SIM=7.71/(2.01×3.02)=1.27.

Table 7 Interaction of CYP1A1 Val/Val genotype and a family history of esophageal cancer

ECFH	CYP1A1 Val/Val	Case	Control	OR	OR95%CI	χ^2	P
No	No	65	74	1.00			
No	Yes	35	19	2.10	1.04-4.24	5.05	0.03
Yes	No	12	5	2.73	0.84-10.38	3.42	0.06
Yes	Yes	15	3	5.69	1.50-31.72	8.47	0.00

SIA=5.69/(2.73+2.10-1.00)=1.49.

DISCUSSION

Under similar environmental carcinogens exposure, different individuals respond to environmental exposures differently. The different liability to cancer was called genetic susceptibility to cancer. Genetic susceptibility can affect in every step of carcinogenesis, including modifying the effect of environmental carcinogens^[29,38-44]. Oncogenes and tumor suppressor genes can also affect individual's susceptibility to cancer^[34-36,45]. Cancer susceptibility genes include type I, type II metabolism enzyme genes, DNA repair gene and those affecting cell proliferation rate. In recent years the evidence has been accumulated to support the hypothesis that cancer susceptibility genes may be of importance in determining individual susceptibility to cancer^[43,46-59].

EC is a multi-factor determined disease, including environmental risk factors and genetic factors. In recent years, more and more researchers considered environmental and genetic susceptibility factors and their interactions in evaluating the risks of cancer^[2,18,53,60-63]. Investigations showed the mortality rate of EC in Shanxi province was not decreased during the latest 20 years, and risk factors for EC in Xi'an city were discussed in several researches^[2,27,28,33]. In the present hospital based case-control study, it was revealed that tobacco smoking was a risk factor, and also had interactions with GSTM1 deletion genotype and CYP1A1 Val/Val genotype.

Aroma hydrocarbons (AHs) in tobacco smoking are pro-carcinogens. They need to be activated to reactive electrophilic forms by type I metabolic enzymes (CYP450s), then initiate cell carcinogenesis. On the other hand, the reactive electrophilic forms of carcinogen can be detoxified and excreted by type II

metabolic enzymes such as GSTM1. Although theoretically the increase of activity of type I metabolic enzymes and/or decrease of activity of type II metabolic enzymes can increase the risk for cancer, there were different results in different studies^[43,44,47,50-52,64-69]. Our results showed that individuals carrying GSTM1 deletion genotype or/and CYP1A1 Val/Val genotype had increased risks for EC.

P450 CYP1A1 gene product metabolizes pro-carcinogens. There are three kinds of polymorphism of CYP1A1: *Msp*I site, 7th exon (Ile-Val) and AA polymorphism. CYP1A1 Ile-Val polymorphism is caused by a base difference (A or G) at 4 889 of 7th exon. The transition of A to G results changing of amino acid from isoleucine to valine at 462^[14], thus forming three kinds of genotypes: homozygote wild genotype (*Ile/Ile*), mutation genotype (*Val/Val*) and heterozygote *Ile/Val* genotype. Researches showed CYP1A1 *Val/Val* genotype had a higher ability to activate pro-carcinogen than CYP1A1 *Ile/Ile* genotype. PAH-DNA adducts in leukocytes were higher in heavy smoking population with CYP1A1 *Val/Val* genotype than those with CYP1A1 *Ile/Val* or *Ile/Ile* genotype.

The associations between CYP1A1 genotype and susceptibility to cancers were varied^[39-42,47,70]. Data from Guangdong province of China showed that *Msp*I C correlated with lung cancer susceptibility in no-smoking populations^[65]. In studies in Shanghai and Haerbin, no significant relationship was discovered between CYP1A1 (*Ile-Val*) polymorphism and lung cancer susceptibility in non-smoking female patients^[64]. CYP1A1 *Val/Val* genotype in white population only appeared about 3.2-5%, while in Japanese it was about 19.8%, in Chinese

22.3%. Our study showed that CYP1A1 *Val/Val* genotype was a genetic susceptibility risk factor for EC (OR 3.35, 95% CI 1.49-7.61). CYP1A1 *Val/Val* genotype had synergic interactions with tobacco smoking, alcohol drinking, and a family history of esophageal cancer.

GSTM1 can detoxify a number of reactive electrophilic compound substances, including the carcinogens PAHs. In individuals with GSTM1 deletion genotype, the ability of detoxifying the carcinogens decreased. Individuals with GSTM1 deletion could have increased risk of cancers^[29,53,56]. In China there were similar researches on GSTM1 deletion genotype and the risks of lung cancer (OR=2.56)^[66], and stomach cancer (OR 1.90, 95%CI 1.01-3.56)^[67]. It was reported that in Henan province, a high incidence area of EC in China, GSTM1 deletion genotype did not show significant relation with EC susceptibility^[25]. Results in our study indicated GSTM1 deletion genotype was a genetic susceptibility risk factor for EC (OR1.81, 95% CI 1.03-3.18), which interacted synergistically with tobacco smoking, alcohol drinking and family history of esophageal cancer.

In summary, we found that tobacco smoking, alcohol drinking, and a family history of EC were risk factors for EC in Xi' an area. CYP1A1 *Val/Val* genotype, GSTM1 deletion genotype were genetic susceptibility risk factors for EC. Gene-environment interaction analysis showed that CYP1A1 *Val/Val* genotype, GSTM1 deletion genotype synergetically interacted with tobacco smoking, alcohol intake, and family history of EC. Gene-gene interaction analysis did not show synergistic interaction between CYP1A1 mutation genotype and GSTM1 deletion genotype, although individuals carrying these two genotypes had increased risks for EC.

REFERENCES

- Zhang W**, Bailey-Wilson JE, Li W, Wang X, Zhang C, Mao X, Liu Z, Zhou C, Wu M. Segregation analysis of esophageal cancer in a moderately high-incidence area of northern China. *Am J Hum Genet* 2000; **67**: 110-119
- Li LS**, Sun CS, Zhang XL, Qiao GB, Xu DZ, Han CL, Yang WX, Chang GS, Yan MX, Wang Y, Zhang HY. A comparative molecular epidemiological study on esophageal cancer between Xi' an and Lichou. *Jiefangjun Yufangyixue Zazhi* 1999; **17**: 255-259
- Zhou XG**, Watanabe S. Factor analysis of digestive cancer mortality and food consumption in 65 Chinese countries. *J Epidemiol* 1999; **9**: 275-284
- Wang LD**, Zou JX, Hong JY, Zhou Q, Deng CJ, Xie DW, Holly C. Identification of a novel genetic polymorphism of human O-6-alkylguanine-DNA alkyltransferase in patients with esophagus cancer. *Huaren Xiaohua Zazhi* 1998; **6**: 560-463
- Lu JB**, Lian SY, Sun XB, Zhang ZX, Dai DX, Li BW, Cheng LP, Wei JR, Duan WJ. A case-control study on the risk factors of esophageal cancer in Linzhou. *Zhonghua Liuxingbingxue Zazhi* 2000; **21**: 434-436
- Li WD**, Wang XQ, Zhang CL, Han XY, Chen DQ, Zhang T, Pan XF, Jia YT, Mao XZ, Zhang R. Esophageal carcinoma in part of population of Yangquan city. *Zhonghua Yixue Zazhi* 1998; **78**: 203-206
- Castellsague X**, Munoz N, De Stefani E, Victora CG, Quintana MJ, Castelletto R, Rolon PA. Smoking and drinking cessation and risk of esophageal cancer (Spain). *Cancer Causes Control* 2000; **11**: 813-818
- Lagrgren J**, Bergstron R, Lindgren A, Nyren O. The role of tobacco, snuff and alcohol use in the aetiology of cancer of the oesophagus and gastric cardia. *Int J Cancer* 2000; **85**: 340-346
- Launoy G**, Mila C, Faivre J, Pienkowski P, Gignoux M. Tobacco type and risk of squamous cell cancer of the oesophagus in males: a French multicentre case-control study. *Int J Epidemiol* 2000; **29**: 36-42
- Talamini G**, Capelli P, Zamboni G, Mastromauro M, Pasetto M, Castagnini A, Angelini G, Bassi C, Scarpa A. Alcohol, smoking and papillomavirus infection as risk for esophageal squamous-cell papilloma and esophageal squamous-cell carcinoma in Italy. *Int J Cancer* 2000; **86**: 874-878
- Castellsague X**, Munzo N, De Stefani E, Victora CG, Castelletto R, Rolon PA, Quintana MJ. Independent and joint effects of tobacco smoking and alcohol drinking on the risk of esophageal cancer in men and women. *Int J Cancer* 1999; **82**: 657-664
- Castellsague X**, Munoz N, De Stefani E, Victora CG, Castelletto R, Rolon PA. Influence of mate drinking, hot beverages and diet on esophageal cancer risk in South America. *Int J Cancer* 2000; **88**: 658-664
- Gallus S**, Bosetti C, Franceschi S, Levi F, Simonato L, Negri E, La Vecchia C. Oesophageal cancer in women: tobacco, alcohol, nutritional and hormonal factors. *Br J Cancer* 2001; **85**: 341-345
- Dhillon PK**, Farrow DC, Vaughan TL, Chow WH, Risch HA, Gammon MD, Mayne ST, Stanford JL, Schoenberg JB, Ahsan H, Dubrow R, West AB, Rotterdam H, Blot WJ, Fraumeni JF Jr. Family history of cancer and risk of esophageal and gastric cancers in the United States. *Int J Cancer* 2001; **93**: 148-152
- Nayar D**, Kapil U, Joshi YK, Sundaram KR, Srivastava SP, Shukla NK, Tandon RK. Nutritional risk factors in esophageal cancer. *J Assoc Physicians India* 2000; **48**: 781-787
- Chang F**, Syrjanen S, Shen Q, Cintorriano M, Santopietro R, Tosi P, Syrjanen K. Evaluation of HPV, CMV, HSV and EBV in esophageal squamous cell carcinomas from a high-incidence area of china. *Anticancer Res* 2000; **20**: 3935-3940
- Li T**, Lu ZM, Chen KN, Guo M, Xing HP, Mei Q, Yang HH, Lechner JF, Ke Y. Human papillomavirus type 16 is an important infectious factor in the high incidence of esophageal cancer in Anyang area of China. *Carcinogenesis* 2001; **22**: 929-934
- Shi QL**, Xu DZ, Sun CS, Li LS. Study on family aggregation of esophageal cancer in Linzhou city. *Zhonghua Yufang Yixue Zazhi* 2000; **34**: 269-270
- Shen YP**, Gao YT, Dai Q, Hu X, Xu TL, Xiang YB, Tang ZL, Li WL. A case-control study on esophageal cancer in Huaian city, Jiangu province(I):role of the cigarette smoking and alcohol drinking. *Zhongliu* 1999; **19**: 363-367
- Lagergren J**, Ye W, Lindgren A, Nyren O. Heredity and risk of cancer of the esophagus and GASTRIC cardia. *Cancer Epidemiol Biomarkers Prev* 2000; **9**: 7557-7560
- Chen H**, Ward MH, Graubard BI, Heineman EF, Markin RM, Potischman NA, Russell RM, Weisenburger DD, Tucker KL. Dietary patterns and adenocarcinoma of the esophagus and distal stomach. *Am J Clin Nutr* 2002; **75**: 137-144
- Phukan RK**, Ali MS, Chetia CK, Mahanta J. Betel nut and tobacco chewing; potential risk factors of cancer of oesophagus in Assam, India. *Br J Cancer* 2001; **85**: 661-667
- Ke L**, Yu P, Zhang ZX. Novel epidemiologic evidence for the association between fermented fish sauce and esophageal cancer in South China. *Int J Cancer* 2002; **99**: 424-426
- Terry P**, Lagergren J, Hansen H, Wolk A, Nyren O. Fruit and vegetable consumption in the prevention of oesophageal and cardia cancers. *Eur J Cancer Prev* 2001; **10**: 365-369
- Lin DX**, Tang YM, Lu SX, Kadlubar FF. Glutathione S-transferase M1, T1 genotypes and risks of esophageal cancer: a case-control study. *Zhonghu Liuxingbing Zazhi* 1998; **19**: 195-199
- Gao YT**, Den J, Xiang YB, Ruan ZX, Wang ZX, Hu BY, Guo MR, Ten WK, Han JJ, Zhang YS. Smoking, related cancers, and other diseases in Shanghai: A 10-year prospective study. *Zhonghua Yufang Yixue Zazhi* 1999; **33**: 5-8
- Zhang HY**, Sun CS, Li LS, Yan MX. Cytochrome P450A1 and the genetic susceptibility to esophageal carcinoma. *Zhonghua Yufang Yixue Zazhi* 2000; **34**: 69-71
- Wang AH**, Zhang HY, Wang Y, Yan MX, Sun CS, Li LS, Huang JY, Cheng QS, Zhu YF. Molecular epidemiological study on esophageal cancer in Xi' an. *Disi Junyi Daxue Xuebao* 2001; **22**: 61-63
- Tan W**, Song N, Wang GQ, Liu Q, Tang HJ, Kadlubar FF, Lin DX. Impact of genetic polymorphisms in cytochrome P450 2E1 and glutathione S-transferases M1, T1, and P1 on susceptibility to esophageal cancer among high-risk individuals in China. *Cancer Epidemiol Biomarkers Prev* 2000; **9**: 551-556
- Hu N**, Huang J, Emmert-buck MR, Tang ZZ, Roth MJ, Wang C, Dawsey SM, Li WJ, Wang QH, Han XY, Ding T, Giffen C, Goldstein AM, Taylor PR. Frequent inactivation of the TP53 gene in esophageal squamous cell carcinoma from a high-risk population in China. *Clin Cancer Res* 2001; **7**: 883-891
- Taniere P**, Martel-Planche G, Casson A, Montesano R, Chanvitan A, Hainaut P. TP53 mutations and MDM2 gene amplification in squamous-cell carcinomas of the esophagus in south Thailand. *Int J Cancer* 2000; **88**: 223-227

- 32 **Ryan BM**, McManus R, Daly JS, Carton E, Keeling PW, Reynolds JV, Kelleher D. A common p73 polymorphism is associated with a reduced incidence of oesophageal carcinoma. *Br J Cancer* 2001; **85**: 1499-1503
- 33 **Wang AH**, Sun CS, Li LS, Huang JY, Chen QS. Relationship of tobacco smoking CYP1A1 GSTM1 gene polymorphism and esophageal cancer in Xi'an. *World J Gastroenterol* 2002; **8**: 49-53
- 34 **Saeki H**, Ohno S, Miyazaki M, Araki K, Egashira A, Kawaguchi H, Watanabe M, Morita M, Sugimachi K. p53 protein accumulation in multiple esophageal squamous cell carcinoma: relationship to risk factors. *Oncology* 2002; **62**: 175-179
- 35 **Fujiki T**, Haraoka S, Yoshioka S, Ohshima K, Iwashita A, Kikuchi M. p53 Gene mutation and genetic instability in superficial multifocal esophageal squamous cell carcinoma. *Int J Oncol* 2002; **20**: 669-679
- 36 **Kato H**, Yoshikawa M, Miyazaki T, Nakajima M, Fukai Y, Tajima K, Masuda N, Tsukada K, Fukuda T, Nakajima T, Kuwano H. Expression of p53 protein related to smoking and alcoholic beverage drinking habits in patients with esophageal cancers. *Cancer Lett* 2001; **167**: 65-72
- 37 **Mizobuchi S**, Furihata M, Sonobe H, Ohtsuki Y, Ishikawa T, Murakami H, Kurabayashi A, Ogoshi S, Sasaguri S. Association between p53 immunostaining and cigarette smoking in squamous cell carcinoma of the esophagus. *Jpn J Clin Oncol* 2000; **30**: 423-428
- 38 **van Lieshout EM**, Roelofs HM, Dekker S, Mulder CJ, Wobbes T, Jansen JB, Peters WH. Polymorphic expression of the glutathione S-transferase P1 gene and its susceptibility to Barrett's esophagus and esophageal carcinoma. *Cancer Res* 1999; **59**: 586-589
- 39 **Roth MJ**, Dawsey SM, Wang G, Tangrea JA, Zhou B, Ratnasinghe D, Woodson KG, Olivero OA, Poirier MC, Frye BL, Taylor PR, Weston A. Association between GSTM1*0 and squamous dysplasia of the esophagus in the high risk region of Linxian, China. *Cancer Lett* 2000; **156**: 73-81
- 40 **Morita S**, Yano M, Tsujinaka T, Akiyama Y, Taniguchi M, Kaneko K, Miki H, Fujii T, Yoshino K, Kusuoka H, Monden M. Genetic polymorphisms of drug-metabolizing enzymes and susceptibility to head-and-neck squamous-cell carcinoma. *Int J Cancer* 1999; **80**: 685-688
- 41 **Butler WJ**, Ryan P, Roberts-Thomson IC. Metabolic genotypes and risk for colorectal cancer. *J Gastroenterol Hepatol* 2001; **16**: 631-635
- 42 **Rojas M**, Cascorbi I, Alexandrov K, Kriek E, Auburtin G, Mayer L, Kopp-Schneider A, Roots I, Bartsch H. Modulation of benzo[a]pyrene diol-epoxide-DNA adduct levels in human white blood cells by CYP1A1, GSTM1 and GSTT1 polymorphism. *Carcinogenesis* 2000; **21**: 35-41
- 43 **Tanimoto K**, Hayashi S, Yoshiga K, Ichikawa T. Polymorphisms of the CYP1A1 and GSTM1 gene involved in oral squamous cell carcinoma in association with a cigarette dose. *Oral Oncol* 1999; **35**: 191-196
- 44 **Sato M**, Sato T, Izumo T, Amagasa T. Genetic polymorphism of drug-metabolizing enzymes and susceptibility to oral cancer. *Carcinogenesis* 1999; **20**: 1927-1931
- 45 **Kumimoto H**, Hamajima N, Nishizawa K, Nishimoto Y, Matsuo K, Harada H, Shinoda M, Hatooka S, Ishizaki K. Different susceptibility of each L-myc genotype to esophageal cancer risk factors. *Jpn J Cancer Res* 2001; **92**: 735-739
- 46 **Xing D**, Tan W, Song N, Lin D. Genetic polymorphism in hOGG1 and susceptibility to esophageal cancer in Chinese. *Zhonghuayixue Yichuanxue Zazhi* 2000; **17**: 377-380
- 47 **Chen S**, Xue K, Xu L, Ma G, Wu J. Polymorphisms of the CYP1A1 and GSTM1 genes in relation to individual susceptibility to lung carcinoma in Chinese population. *Mutat Res* 2001; **458**: 41-47
- 48 **Song C**, Xing D, Tan W, Wei Q, Lin D. Methylenetetrahydrofolate reductase polymorphisms increase risk of esophageal squamous cell carcinoma in a Chinese population. *Cancer Res* 2001; **61**: 3272-3275
- 49 **Lee JM**, Lee YC, Yang SY, Yang PW, Luh SP, Lee CJ, Chen CJ, Wu MT. Genetic polymorphisms of XRCC1 and risk of the esophageal cancer. *Int J Cancer* 2001; **95**: 240-246
- 50 **Chao YC**, Wang LS, Hsieh TY, Chu CW, Chang FY, Chu HC. Chinese alcoholic patients with esophageal cancer are genetically different from alcoholics with acute pancreatitis and liver cirrhosis. *Am J Gastroenterol* 2000; **95**: 2958-2964
- 51 **Sato M**, Sato T, Izumo T, Amagasa T. Genetically high susceptibility to oral squamous cell carcinoma in terms of combined genotyping of CYP1A1 and GSTM1 genes. *Oral Oncol* 2000; **36**: 267-271
- 52 **Gsur A**, Haidinger G, Hollaus P, Herbacek I, Madersbacher S, Trieb K, Pridun N, Mohn-Staudner A, Vetter N, Vutuc C, Micksche M. Genetic polymorphisms of CYP1A1 and GSTM1 and lung cancer risk. *Anticancer Res* 2001; **21**: 2237-2242
- 53 **Dong CH**, Yu SZ, Zhao DM, Hu Y. Association of polymorphisms of glutathione S transferase M1 and T1 genotypes with elevated aflatoxin and increased risk of primary liver cancer. *Huaren Xiaohua Zazhi* 1998; **6**: 463-466
- 54 **Bian JC**, Shen FM, Shen L, Wang TR, Wang XH, Chen GC, Wang JB. Susceptibility to hepatocellular carcinoma associated with null genotypes of GSTM1 and GSTT1. *World J Gastroenterol* 2000; **6**: 228-230
- 55 **Cai L**, Yu SZ, Zhang ZF. Glutathione S-transferase M1, T1 genotypes and the risk of gastric cancer: a case-control study. *World J Gastroenterol* 2001; **7**: 506-509
- 56 **Cai L**, Yu SZ. A molecular epidemiologic study on gastric cancer in Changde, Fujian province. *Shijie Huaren Xiaohua Zazhi* 1999; **7**: 652-655
- 57 **Tan W**, Chen GF, Xing DY, Song CY, Kadlubar FF, Lin DX. Frequency of CYP2A6 gene deletion and its relation to risk of lung and esophageal cancer in the Chinese population. *Int J Cancer* 2001; **95**: 96-101
- 58 **Shibuta J**, Eto T, Kataoka A, Inoue H, Ueo H, Suzuki T, Barnard GF, Mori M. Genetic polymorphism of N-acetyltransferase 2 in patients with esophageal cancer. *Am J Gastroenterol* 2001; **96**: 3419-3424
- 59 **Matsuo K**, Hamajima N, Shinoda M, Hatooka S, Inoue M, Takezaki T, Tajima K. Gene-environment interaction between an aldehyde dehydrogenase-2 (ALDH2) polymorphism and alcohol consumption for the risk of esophageal cancer. *Carcinogenesis* 2001; **22**: 913-916
- 60 **Lee JM**, Lee YC, Yang SY, Shi WL, Lee CJ, Luh SP, Chen CJ, Hsieh CY, Wu MT. Genetic polymorphisms of p53 and GSTP1, but not NAT2, are associated with susceptibility to squamous-cell carcinoma of the esophagus. *Int J Cancer* 2000; **89**: 458-464
- 61 **Bartsch H**, Nair U, Risch A, Rojas M, Wikman H, Alexandrov K. Genetic polymorphism of CYP genes, alone or in combination, as a risk modifier of tobacco-related cancers. *Cancer Epidemiol Biomarkers Prev* 2000; **9**: 3-28
- 62 **Butkiewicz D**, Cole KJ, Phillips DH, Harris CC, Chorazy M. GSTM1, GSTP1, CYP1A1 and CYP2D6 polymorphisms in lung cancer patients from an environmentally polluted region of Poland: correlation with lung DNA adduct levels. *Eur J Cancer Prev* 1999; **8**: 315-323
- 63 **Liu G**, Zhou Q, Wang LD, Hong JY, Deng CJ, Wang YY, Zou JX. Blood clot as a DNA source for studying genetic polymorphism of human carcinogen-metabolizing enzymes. *World J Gastroenterol* 1998; **4**: 108-109
- 64 **Qu YH**, Shi YB, Peter S, Zhong LJ, Sun L, Sun XW, Cheng JR, Lin YJ, Xian YB, Dai XD, Gao YT. The genotypes of cytochrome P4501A1 and GST M1 in non-smoking female lung cancer. *Zhongliu* 1998; **18**: 80-82
- 65 **Hu YL**, Zhang Q. Genetic Polymorphisms of CYP1A1 and susceptibility of lung cancer. *Zhonghua Yixue Yichuanxue Zazhi* 1999; **16**: 26-28
- 66 **Gao J**, Ren CL, Zhang Q. CYP2D6 and GSTM1 genetic polymorphism and lung cancer susceptibility. *Zhonghua Zhongliu Zazhi* 1998; **20**: 185-186
- 67 **Cai L**, Yu SZ. Preliminary studies on cytochrome P4502E1 and Glutathione S-transferase M1 polymorphisms and susceptibility to gastric cancer. *Zhongguo Gonggong Weisheng* 1999; **15**: 895-897
- 68 **Olshan AF**, Mark CW, Mary AW, Douglas AB. GSTM1, GSTT1, GSTP1, CYP1A1 and NAT1 Polymorphisms, Tobacco use, and the risk of head and neck cancer. *Cancer Epidemiol Biomarkers Prve* 2000; **9**: 185-191
- 69 **London SJ**, Yuan JM, Coetzee GA, Gao YT, Ross RK, Yu MC. CYP1A1 1462V genetic polymorphism and lung cancer risk in a cohort of men in Shanghai, China. *Cancer Epidemiol Biomarkers Prev* 2000; **9**: 987-991
- 70 **Murata M**, Watanabe M, Yamanaka M, Kubota Y, Ito H, Nagao M, Katoh T, Kamataki T, Kawamura J, Yatani R, Shiraiishi T. Genetic polymorphisms in cytochrome P450 (CYP) 1A1, CYP1A2, CYP2E1, glutathione S-transferase (GST) M1 and GSTT1 and susceptibility to prostate cancer in the Japanese population. *Cancer Lett* 2001; **165**: 171-177

Effects of vitamin E succinate on the expression of Fas and PCNA proteins in human gastric carcinoma cells and its clinical significance

Kun Wu, Lan Zhao, Yao Li, Yu-Juan Shan, Li-Jie Wu

Kun Wu, Lan Zhao, Yao Li, Yu-Juan Shan, Li-Jie Wu, Department of Nutrition and Food Hygiene, School of Public Health, Harbin Medical University, Harbin 150001, Heilongjiang Province, China
Supported by the National Nature Science Foundation of China, No. 39970647

Correspondence to: Professor Kun Wu, Department of Nutrition and Food Hygiene, School of Public Health, Harbin Medical University, Harbin 150001, Heilongjiang Province, China. wukun@ems.hrbmu.edu.cn
Telephone: +86-451-3648665 **Fax:** +86-451-3648617
Received: 2003-06-06 **Accepted:** 2003-07-30

Abstract

AIM: To investigate the effects of vitamin E succinate (VES) on the expression of Fas and PCNA proteins as well as its clinical significance in human gastric carcinoma, and to explore the mechanism of VES-induced inhibition of gastric carcinoma cell growth.

METHODS: Immunohistochemical methods were used to detect Fas and PCNA expression both in human gastric cancer SGC-7901 cells treated with VES at different doses and in human gastric carcinoma tissues.

RESULTS: After the SGC-7901 cells were treated with VES at 5, 10, 20 mg/L for 48 h, the positive rates of Fas expression were 16%, 27% and 48%, respectively, significantly increased compared to that of control group ($P < 0.05$); while the positive rates of PCNA expression in groups treated with different doses of VES were 20%, 18% and 7%, respectively, which were significantly decreased compared to that of the control group ($P < 0.05$). In human gastric carcinoma tissues, the Fas positive expression rate was 42.4% (25/59), which declined with the decrease in the degree of tumor differentiation ($P < 0.05$) and with the existence of lymph node metastasis ($P < 0.001$). While the PCNA positive expression rate was 91.5% (54/59), no relationship was observed between PCNA expression and clinicopathologic parameters.

CONCLUSION: VES inhibited the growth of gastric cancer cells by inducing Fas expression and inhibiting PCNA expression. It is, therefore, considered that the expression of Fas and PCNA genes, through tumor cell apoptosis and proliferation, respectively, may be useful as a clinical predictive index in the application of VES to gastric carcinoma therapy, where as Fas may be of more value than PCNA.

Wu K, Zhao L, Li Y, Shan YJ, Wu LJ. Effects of vitamin E succinate on the expression of Fas and PCNA proteins in human gastric carcinoma cells and its clinical significance. *World J Gastroenterol* 2004; 10(7): 945-949

<http://www.wjgnet.com/1007-9327/10/945.asp>

INTRODUCTION

RRR- α -tocopheryl succinate (vitamin E succinate, VES), a derivative of natural vitamin E, has been shown to be a potent

growth inhibitor of many kinds of cancer cell types such as human monocytic leukemia cell^[1], murine B16 melanoma cell^[2,3], human prostate cancer cell^[4], human breast cancer cell^[5,6] and murine EL-4 thymic lymphoma cell^[7,8]. Characterization of cellular processes involved in VES antiproliferative effects have shown that VES inhibits tumor cell growth by a variety of mechanisms, including cell cycle blockage^[9,10], DNA synthesis arrest^[11], induction of differentiation^[12-14], and triggering of apoptosis^[15-19]. Meanwhile, VES is also noteworthy because of its non-toxic and non-inhibitory effects on normal cell types^[20], indicating that VES can be used as a chemopreventive/chemotherapeutic agent against tumors.

Gastric cancer is one of the most common malignant tumors in China^[21-29]. Our previous studies found that VES could inhibit human gastric cancer SGC-7901 cell growth by blocking cell cycle, arresting DNA synthesis and triggering apoptosis^[30-32]. In addition, our *in vivo* research demonstrated that VES inhibited benzo (a) pyrene (B (a) P)-induced forestomach carcinogenesis in female mice^[33]. In this study, the expression of Fas and PCNA both in SGC-7901 cells treated with VES and in human gastric carcinoma tissues was investigated further for its clinical significance. It may provide reference indices for VES application in clinical therapy.

MATERIALS AND METHODS

Cell culture and treatment

Human gastric cancer cell lines SGC-7901 were maintained in RPMI 1640 medium supplemented with 100 mL/L fetal calf serum (FCS), 100 kU/L penicillin, 100 mg/L streptomycin and 2 mmol/L L-glutamine, incubated in a humidified atmosphere containing 50 mL/L CO₂ at 37 °C. The SGC-7901 cells were collected after incubation for 48 h in the presence of VES at 5, 10 and 20 mg/L and of ethanol at 1 mL/L as the control group (VES was dissolved in absolute ethanol and diluted in RPMI 1640 complete condition media correspondingly to a final concentration of VES and 1 mL/L ethanol). The cells were then fixed in 40 g/L formaldehyde and embedded in paraffin.

Clinical materials

Fifty-nine paraffin-embedded specimens of gastric cancer were obtained from the pathological laboratory of the First Affiliated Hospital of Harbin Medical University. These specimens were from resections of gastric cancer in this hospital from 1991 to 2001. Of these, 35 were from males, and 24 from females and the age of the patients varied from 31 to 77 years. These specimens had been histologically classified in which 7 were highly to moderately differentiated adenocarcinomas, 52 were poorly differentiated. Thirty-three tumors had invaded the serosa by histology, and 22 cases had local lymph node metastasis.

Reagents and methods

VES was purchased from Sigma Co. Ltd. RPMI 1640 medium was obtained from Gibco BRL. Antibodies against either PCNA or Fas and SP immunohistochemical reagent kit were purchased from Beijing Zhongshan Biotechnology Co. Ltd.

Serial sections of 4 μ m thick were sliced from each of the

cell and clinical tissue blocks. These were deparaffinized and rehydrated, and immersed in 30 mL/L H_2O_2 for 10 min to remove the endogenous peroxidase activity. The sections were further incubated with 100 mL/L normal goat serum for 1 h to reduce nonspecific binding. They were, then, incubated with either primary Fas or PCNA antibody at 4 °C for 12-16 h. All sections were washed in phosphate buffer solution (PBS) (0.01 mol/L, pH7.2). Afterwards, they were sequentially incubated with biotin conjugated secondary antibody, and avidin biotin enzyme reagent. Staining was done by first immersing the slides in 3, 3'-diaminobenzidine tetrahydrochloride (DAB). All slides were counterstained with haematoxylin/methyl-green, dehydrated and mounted. PBS substituted for the primary antibody was used as the negative control. For the slides initially incubated with primary Fas antibody, if the proportion of positively stained cells was more than 10%, it was considered as a Fas positive sample. For the slides initially incubated with primary PCNA antibody, if the proportion of positively stained cells as more than 50%, it was considered as a PCNA positive sample.

Statistics

The data of Fas and PCNA expression were analyzed by *t*-test. Correlations between Fas and PCNA expression and clinicopathologic parameters were examined using χ^2 test. $P < 0.05$ was considered to be statistically significant.

RESULTS

The effect of VES on Fas expression in SGC-7901 cells

The Fas positive expression appeared as brown granules located in the membrane and cytoplasm, and the cell nucleus appeared green after counterstaining with methyl green (Figure 1). After the SGC-7901 cells were treated with VES at 5, 10, 20 mg/L and ethanol at 1 mL/L for 48 h, the Fas positive rates were 16%, 27%, 48% and 10%, respectively (Figure 3). The positive rates for the VES treated groups at different doses were significantly increased compared to that of the control group ($P < 0.05$), with an evident dose-effect relationship.

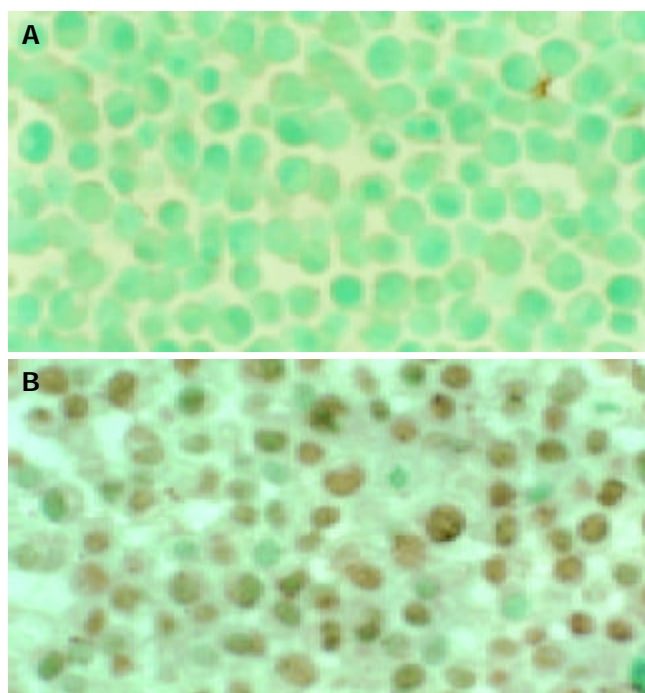


Figure 1 Effects of VES on the expression of Fas protein in SGC-7901 cells. A: control group ($\times 200$), B: 20 mg/L VES treated for 48 h ($\times 200$).

Effects of VES on PCNA expression in SGC-7901 cells

In contrast to Fas positive expression, the positive PCNA brown stained granules were in the nucleus, while the negative cell nucleus appeared blue after counterstaining with hematoxylin (Figure 2). PCNA positive expression rates, when the cells were treated with VES at 5, 10, 20 mg/L for 48 h were 20%, 18% and 7%, respectively (Figure 3), and in the control group 28%. The positive rates of the cells treated with VES at different doses were significantly decreased compared to that of the control group ($P < 0.05$), with an evident dose-effect relationship.

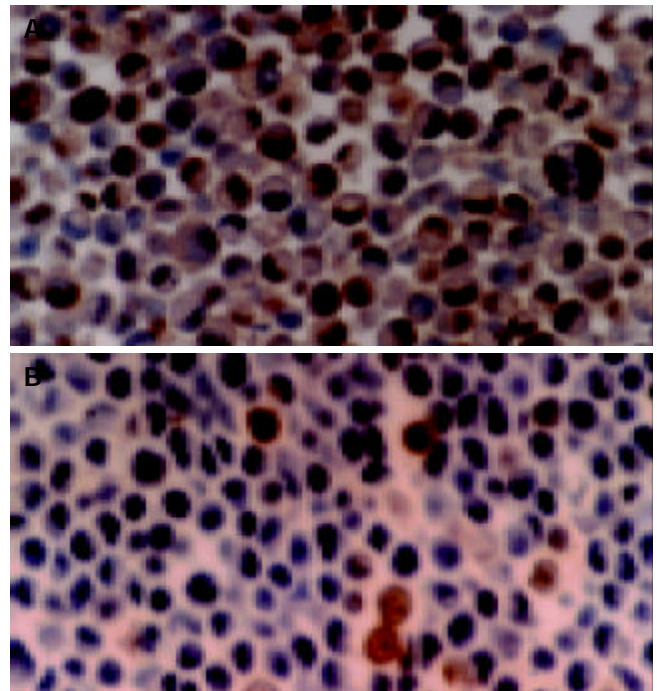


Figure 2 Effects of VES on the expression of PCNA protein in SGC-7901 cells. A: control group ($\times 200$), B: 20 mg/L VES treated for 48 h ($\times 200$).

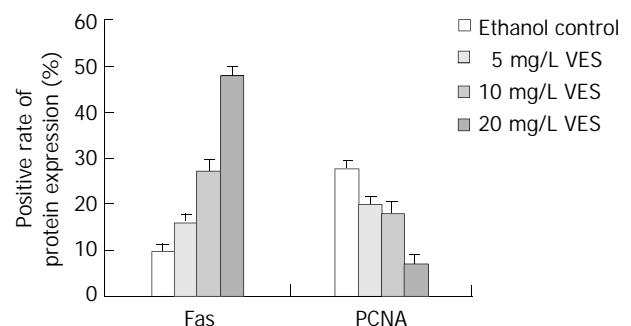


Figure 3 Effects of VES on the expression of Fas and PCNA proteins at different doses.

Expression of Fas in clinical pathological tissues of gastric carcinoma

As shown in Figure 4A, the expression of Fas protein in normal gastric tissues was stronger, for there were many brown stained granules in the membrane and cytoplasm of both glandular and interstitial cells. In the gastric carcinoma tissues, the Fas expression was decreased (Figure 4B) or even negative, the Fas positive rate was only 42.4% (25/59).

Expression of PCNA in clinical pathological tissue of gastric carcinoma

There were brown stained granules located in the nuclei of

PCNA positive cells, while the negative cell nucleus appeared blue after counterstaining with hematoxylin (Figure 5). The positive expression rate of PCNA in normal gastric tissues was not high; the stained cell rate was 49.6%. The stained cell rate in gastric carcinoma tissues was between 33-99%, and the PCNA positive rate was 91.5% (54/59).

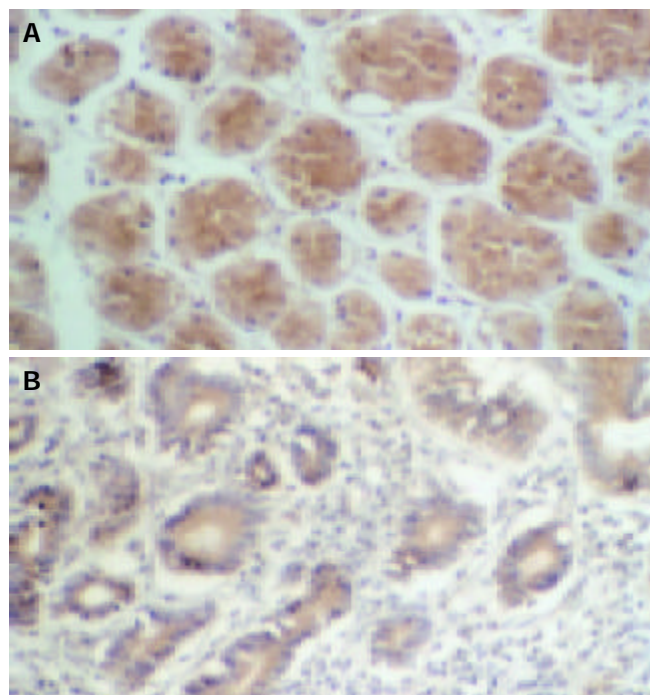


Figure 4 Expression of Fas protein in human normal gastric tissues and gastric carcinoma tissues. A: normal gastric tissue ($\times 200$), B: gastric carcinoma tissue ($\times 200$).

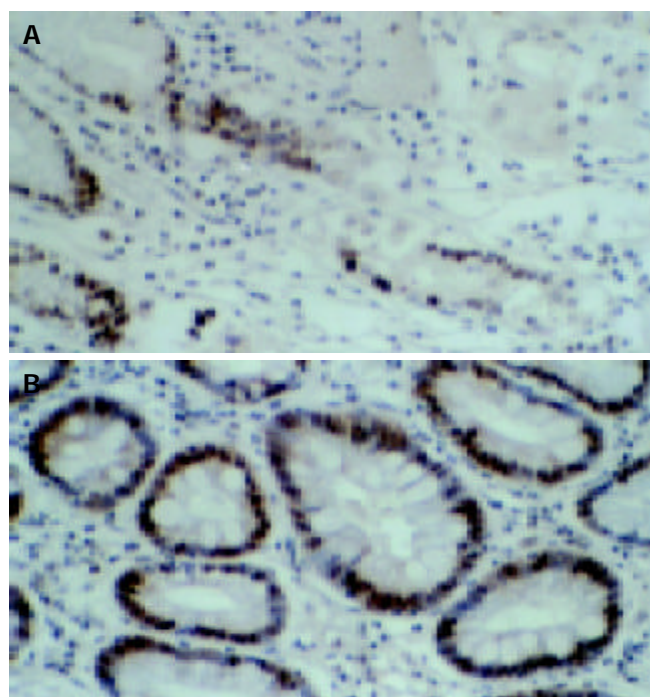


Figure 5 Expression of PCNA protein in human normal gastric tissues and gastric carcinoma tissues. A: normal gastric tissue ($\times 200$), B: gastric carcinoma tissue ($\times 200$).

Correlation of clinicopathological parameters with expression of Fas and PCNA in gastric carcinoma tissues

As shown in Table 1, the rates of Fas and PCNA protein

expression were not correlated with either the patient's age or sex ($P > 0.05$). The immunoreactivity of Fas was significantly associated with tumor differentiation and lymph node metastasis. Among the 59 cases of gastric carcinoma, Fas positive expression rate in the 7 well-differentiated tissues (85.7%) was obviously higher than that in the 52 cases that were poorly differentiated tissues (36.5%) ($P < 0.05$). The Fas positive expression rate in the group with lymph node metastasis was 13.6% (3/11), lower than in that without lymph node metastasis ($P < 0.01$). PCNA positive expression was not associated with clinicopathologic parameters ($P > 0.05$).

Table 1 Correlation of clinical pathological parameters with expression of Fas and PCNA in clinical gastric carcinoma tissues

Pathologic parameters	n	Fas expression		PCNA expression	
		+	(%)	+	(%)
Age (yr)					
≤45	11	4	(36.3)	11	(100)
>45	48	21	(43.7)	43	(89.5)
Sex					
Male	35	17	(48.5)	30	(85.7)
Female	24	8	(33.3)	24	(100)
Tumor differentiation					
Well-moderate	7	6	(85.7)	5	(71.4)
Poor	52	19	(36.5) ^a	49	(94.2)
Tumor invasion					
Muscularis	26	14	(53.8)	24	(92.3)
Serosa	33	11	(33.3)	30	(90.9)
Node metastasis					
(+)	22	3	(13.6)	22	(100)
(-)	37	22	(59.6) ^b	32	(99.8)

^a $P < 0.05$, ^b $P < 0.01$.

DISCUSSION

The mechanisms of VES-induced inhibition of tumor cell growth have been a topic of great interest. Turley *et al.*^[34] observed that the expression of Fas, a cell surface receptor, was increased after treatment of breast cancer cells with VES. They also observed that VES-induced apoptosis in breast cancer cells was inhibited when using Fas neutralizing antibody or transfecting Fas antisense oligonucleotides to cancer cells. Since then, other studies have shown that Fas-mediated apoptosis may be another important pathway by which VES inhibits tumor cell growth^[35-37].

Fas/APO-1, a 45 ku type I transmembrane protein, belongs to the nerve growth factor (NGF)/tumor necrosis factor (TNF) receptor superfamily. As a member of the five death domain-containing receptors, Fas initiates a signal-transduction cascade leading to programmed cell death^[38-46]. In recent studies, Fas protein expression has been identified in various organs. It was reported that Fas antigen expression could be related to lymph node status and clinical stages in cancer patients. The rate of Fas antigen expression was significantly higher in gastric carcinoma tissues without lymph node metastasis than in those with lymph node metastasis, and also higher in clinical stages I and II than in clinical stages III and IV of gastric carcinoma. Moreover, the prognosis of patients with negative expression of Fas was worse^[47,48]. In this study, we determined the Fas expression both in SGC-7901 cells treated with VES and in human gastric carcinoma tissues. The data showed that after 48 h of VES treatment, the expression of Fas protein was evidently increased with a marked dose-dependent relationship compared to that of the control group, indicating that Fas signal

pathway was involved in VES-triggered apoptosis. In addition, the expression of Fas protein in gastric carcinoma tissue was depressed with the decrease of tumor differentiation degree and with the existence of lymph node metastasis. These results are in accordance with the reports mentioned earlier. It suggested that Fas protein expression may be one of indices to predict prognosis of patients with gastric carcinoma, thus establishing a theoretical foundation for using Fas protein expression to assess the effect and prognosis of VES application in clinic therapy.

PCNA functions as a cofactor for DNA polymerase δ . It is associated with DNA repair in both S phase and DNA synthesis phase. As an index of cellular proliferative status, PCNA was determined in various lesions. The overexpression of PCNA with high frequency was usually used as a reliable marker for assessment of tumor progression, premalignant evolution and clinical prognosis of patients with various malignancies^[49-59]. Our *in vitro* results showed that VES at different doses could decrease the PCNA expression in SGC-7901 cells to different degrees, indicating that the inhibition of the growth of human gastric carcinoma by VES might be associated with its depression of PCNA protein, decrease in DNA-polymerase δ activity and interference of DNA synthesis. Additionally, the expression of PCNA in clinical gastric carcinoma tissue was higher than that in normal gastric tissues, but we failed to demonstrate the correlation between PCNA expression and clinicopathological parameters in gastric carcinoma in this study, which was conflicted with the reports about PCNA expression in gastric carcinoma^[60,61] and the reports that PCNA could be an effective indicator of prognosis for tumor. Based on the *in vitro* results that VES has effects on PCNA expression in gastric carcinoma cells in our study and the reports we have mentioned, we presumed that the conflicting results in our study might be related to fewer cases we have collected, such as only seven cases of highly-moderately differentiated carcinoma.

With the progress of tumor research, it has been realized that the tumorigenesis is a result of imbalance between cell proliferation and apoptosis. On the one hand, cells proliferate massively; on the other hand, cellular apoptosis is inhibited. Fas and PCNA are the two genes closely related to apoptosis and proliferation. Our study indicates that both of them play important roles in the inhibitory effects of VES on gastric carcinoma cells *in vitro*. But for evaluating the effect of VES on gastric carcinoma tissue, Fas, as an effective predicting index for VES application to gastric carcinoma therapy may be of more value than PCNA.

ACKNOWLEDGEMENTS

We thank Dr. Love (University of Calgary, Canada) for his comments on the manuscript.

REFERENCES

- 1 **Fariss MW**, Fortuna MB, Everett CK, Smith JD, Trent DF, Djuric Z. The selective antiproliferation effects of α -tocopheryl hemisuccinate and cholesteryl hemisuccinate on murine leukemia cells result from the action of the intact compounds. *Cancer Res* 1994; **54**: 3346-3357
- 2 **Ottino P**, Duncan JR. Effect of alpha-tocopherol succinate on free radical and lipid peroxidation levels in BL6 melanoma cells. *Free Radic Biol Med* 1997; **22**: 1145-1151
- 3 **Prasad KN**, Edwards-Prasad J. Effects of tocopherol (vitamin E) acid succinate on morphological alterations and growth inhibition in melanoma cells in culture. *Cancer Res* 1982; **42**: 550-555
- 4 **Zhang Y**, Ni J, Messing EM, Chang E, Yang CR, Yeh S. Vitamin E succinate inhibits the function of androgen receptor and the expression of prostate-specific antigen in prostate cancer cells. *Proc Natl Acad Sci U S A* 2002; **99**: 7408-7413
- 5 **Turley JM**, Ruscetti FW, Kim SJ, Fu T, Gou FV, Birchenall-Roberts MC. Vitamin E succinate inhibits proliferation of BT-20 human breast cancer cells: increased binding of cyclin A negatively regulates E2F transactivation activity. *Cancer Res* 1997; **57**: 2668-2675
- 6 **Malafa MP**, Neitzel LT. Vitamin E succinate promotes breast cancer tumor dormancy. *J Surg Res* 2000; **93**: 163-170
- 7 **Kline K**, Sanders BG. RRR- α -tocopheryl succinate inhibition of lectin-induced T cell proliferation. *Nutr Cancer* 1993; **19**: 241-252
- 8 **Yu W**, Sanders BG, Kline K. Modulation of murine EL-4 thymic lymphoma cell proliferation and cytokine production by Vitamin E succinate. *Nutr Cancer* 1996; **25**: 137-149
- 9 **Kline K**, Yu WP, Zhao BH, Israel K, Charpentier A, Simmons-Menchaca M, Sanders BG. Vitamin E Succinate: Mechanisms of action as tumor cell growth inhibitor. In: *Nutrients in Cancer Prevention and Treatment*. Prasad KN, Santamaria L, Williams RM (eds). Totowa, NY: Humana Press Inc 1995: 39-56
- 10 **Kline K**, Yu WP, Sanders BG. Vitamin E: Mechanisms of Action as Tumor Cell Growth Inhibitors. *Cancer and Nutrition*. Prasad KN, Cole WC (Eds). IOS Press 1998: 37-53
- 11 **Yu W**, Sanders BG, Kline K. RRR-alpha-tocopheryl succinate inhibits EL4 thymic lymphoma cell growth by inducing apoptosis and DNA synthesis arrest. *Nutr Cancer* 1997; **27**: 92-101
- 12 **Kim SJ**, Bang OS, Lee YS, Kang SS. Production of inducible nitric oxide is required for monocytic differentiation of U937 cells induced by vitamin E-succinate. *J Cell Sci* 1998; **111**(Pt 3): 435-441
- 13 **You H**, Yu W, Munoz-Medellin D, Brown PH, Sanders BG, Kline K. Role of extracellular signal-regulated kinase pathway in RRR-alpha-tocopheryl succinate-induced differentiation of human MDA-MB-435 breast cancer cells. *Mol Carcinog* 2002; **33**: 228-236
- 14 **Israel K**, Sanders BG, Kline K. RRR- α -tocopheryl succinate inhibits the proliferation of human prostatic tumor cells with defective cell cycle /differentiation pathways. *Nutr Cancer* 1995; **24**: 161-169
- 15 **Yu W**, Liao QY, Hantash FM, Sanders BG, Kline K. Activation of extracellular signal-regulated kinase and c-Jun-NH(2)-terminal kinase but not p38 mitogen-activated protein kinases is required for RRR-alpha-tocopheryl succinate-induced apoptosis of human breast cancer cells. *Cancer Res* 2001; **61**: 6569-6576
- 16 **Neuzil J**, Weber T, Schroder A, Lu M, Ostermann G, Gellert N, Mayne GC, Olejnicka B, Negre-Salvayre A, Sticha M, Coffey RJ, Weber C. Induction of cancer cell apoptosis by alpha-tocopheryl succinate: molecular pathways and structural requirements. *FASEB J* 2001; **15**: 403-415
- 17 **Weber T**, Lu M, Andera L, Lahm H, Gellert N, Fariss MW, Korinek V, Sattler W, Ucker DS, Terman A, Schroder A, Erl W, Brunk UT, Coffey RJ, Weber C, Neuzil J. Vitamin E succinate is a potent novel antineoplastic agent with high selectivity and cooperativity with tumor necrosis factor-related apoptosis-inducing ligand (Apo2 ligand) *in vivo*. *Clin Cancer Res* 2002; **8**: 863-869
- 18 **Yu W**, Simmons-Menchaca M, You H, Brown P, Birrer MJ, Sanders BG, Kline K. RRR- α -tocopheryl succinate induction of prolonged activation of c-jun amino-terminal kinase and c-jun during induction of apoptosis in human MDA-MB-435 breast cancer cells. *Mol Carcinog* 1998; **22**: 247-257
- 19 **Neuzil J**, Weber T, Gellert N, Weber C. Selective cancer cell killing by alpha-tocopheryl succinate. *Br J Cancer* 2001; **84**: 87-89
- 20 **Hua JS**. Effect of Hp: cell proliferation and apoptosis on stomach cancer. *Shijie Huaren Xiaohua Zazhi* 1999; **7**: 647-648
- 21 **Zhu ZH**, Xia ZS, He SG. The effects of ATRA and 5-Fu on telomerase activity and cell growth of gastric cancer cells *in vitro*. *Shijie Huaren Xiaohua Zazhi* 2000; **8**: 669-673
- 22 **Xia JZ**, Zhu ZG, Liu BY, Yan M, Yin HR. Significance of immunohistochemically demonstrated micrometastases to lymph nodes in gastric carcinomas. *Shijie Huaren Xiaohua Zazhi* 2000; **8**: 1113-1116
- 23 **Tu SP**, Zhong J, Tan JH, Jiang XH, Qiao MM, Wu YX, Jiang SH. Induction of apoptosis by arsenic trioxide and hydroxy camptothecin in gastric cancer cells *in vitro*. *World J Gastroenterol* 2000; **6**: 532-539
- 24 **Cai L**, Yu SZ, Zhang ZF. *Helicobacter pylori* infection and risk of gastric cancer in Changle County, Fujian Province, China. *World J Gastroenterol* 2000; **6**: 374-376
- 25 **Yao XX**, Yin L, Zhang JY, Bai WY, Li YM, Sun ZC. hTERT expression and cellular immunity in gastric cancer and precancerosis. *Shijie Huaren Xiaohua Zazhi* 2001; **9**: 508-512

- 26 **Xu AG**, Li SG, Liu JH, Gan AH. Function of apoptosis and expression of the proteins Bcl-2, p53 and C-myc in the development of gastric cancer. *World J Gastroenterol* 2001; **7**: 403-406
- 27 **Liu DH**, Zhang XY, Fan DM, Huang YX, Zhang JS, Huang WQ, Zhang YQ, Huang QS, Ma WY, Chai YB, Jin M. Expression of vascular endothelial growth factor and its role in oncogenesis of human gastric carcinoma. *World J Gastroenterol* 2001; **7**: 500-505
- 28 **Wang X**, Lan M, Shi YQ, Lu J, Zhong YX, Wu HP, Zai HH, Ding J, Wu KC, Pan BR, Jin JP, Fan DM. Differential display of vincristine-resistance-related genes in gastric cancer SGC7901 cell. *World J Gastroenterol* 2002; **8**: 54-59
- 29 **Cao WX**, Ou JM, Fei XF, Zhu ZG, Yin HR, Yan M, Lin YZ. Methionine-dependence and combination chemotherapy on human gastric cancer cells *in vitro*. *World J Gastroenterol* 2002; **8**: 230-232
- 30 **Wu K**, Liu BH, Zhao DY, Zhao Y. Effect of vitamin E succinate on expression of TGF- β 1, c-Jun and JNK1 in human gastric cancer SGC-7901 cells. *World J Gastroenterol* 2001; **7**: 83-87
- 31 **Wu K**, Zhao Y, Liu BH, Li Y, Liu F, Guo J, Yu WP. RRR- α -tocopherol succinate inhibits human gastric cancer SGC-7901 cell growth by inducing apoptosis and DNA synthesis arrest. *World J Gastroenterol* 2002; **8**: 26-30
- 32 **Zhao Y**, Wu K, Xia W, Shan YJ, Wu LJ, Yu WP. The effects of vitamin E succinate on the expression of c-jun gene and protein in human gastric cancer SGC-7901 cells. *World J Gastroenterol* 2002; **8**: 782-786
- 33 **Wu K**, Shan YJ, Zhao Y, Yu JW, Liu BH. Inhibitory effects of RRR- α -tocopherol succinate on benzo(a)pyrene (B(a)P)-induced forestomach carcinogenesis in female mice. *World J Gastroenterol* 2001; **7**: 60-65
- 34 **Turley JM**, Fu T, Ruscetti FW, Mikovits JA, Bertolette DC 3rd, Birchenall-Roberts MC. Vitamin E succinate induces Fas-mediated apoptosis in estrogen receptor-negative human breast cancer cells. *Cancer Res* 1997; **57**: 881-890
- 35 **Yu W**, Israel K, Liao QY, Aldaz CM, Sanders BG, Kline K. Vitamin E succinate (VES) induces Fas sensitivity in human breast cancer cells: role for M, 43 000 Fas in VES-triggered apoptosis. *Cancer Res* 1999; **59**: 953-961
- 36 **Israel K**, Yu W, Sanders BG, Kline K. Vitamin E succinate induces apoptosis in human prostate cancer cells: role for Fas in vitamin E succinate-triggered apoptosis. *Nutr Cancer* 2000; **36**: 90-100
- 37 **Wu K**, Li Y, Zhao Y, Shan YJ, Xia W, Yu WP, Zhao L. Roles of Fas signaling pathway in vitamin E succinate-induced apoptosis in human gastric cancer SGC-7901 cells. *World J Gastroenterol* 2002; **8**: 982-986
- 38 **Salih HR**, Starling GC, Knauff M, Llewellyn MB, Davis PM, Pitts WJ, Aruffo A, Kiener PA. Retinoic acid and vitamin E modulate expression and release of CD178 in carcinoma cells: consequences for induction of apoptosis in CD95-sensitive cells. *Exp Cell Res* 2001; **270**: 248-258
- 39 **Rubio CA**, Jacobsson B. The Fas-FasL system and colorectal tumours. *J Clin Pathol* 2002; **55**: 559-560
- 40 **Peng ZH**, Xing TH, Qiu GQ, Tang HM. Relationship between Fas/FasL expression and apoptosis of colon adenocarcinoma cell lines. *World J Gastroenterol* 2001; **7**: 88-92
- 41 **Geng YJ**. Molecular signal transduction in vascular cell apoptosis. *Cell Res* 2001; **11**: 253-264
- 42 **Li ZY**, Zou SQ. Fas counterattack in cholangiocarcinoma: a mechanism for immune evasion in human hilar cholangiocarcinomas. *World J Gastroenterol* 2001; **7**: 860-863
- 43 **Wajant H**. The Fas signaling pathway: more than a paradigm. *Science* 2002; **296**: 1635-1636
- 44 **Hou L**, Li Y, Jia YH, Wang B, Xin Y, Ling MY, Lu S. Molecular mechanism about lymphogenous metastasis of hepatocarcinoma cells in mice. *World J Gastroenterol* 2001; **7**: 532-536
- 45 **Yin F**, Shi YQ, Zhao WP, Xiao B, Miao JY, Fan DM. Suppression of P-gp induced multiple drug resistance in a drug resistant gastric cancer cell line by overexpression of Fas. *World J Gastroenterol* 2000; **6**: 664-670
- 46 **Xiao B**, Shi YQ, Zhao YQ, You H, Wang ZY, Liu XL, Yin F, Qiao TD, Fan DM. Transduction of Fas gene or Bcl-2 antisense RNA sensitizes cultured drug resistant gastric cancer cells to chemotherapeutic drugs. *World J Gastroenterol* 1998; **4**: 421-425
- 47 **Reimer T**, Koczan D, Muller H, Friese K, Thiesen HJ, Gerber B. Tumour Fas ligand: Fas ratio greater than 1 is an independent marker of relative resistance to tamoxifen therapy in hormone receptor positive breast cancer. *Breast Cancer Res* 2002; **4**: R9
- 48 **Liu HF**, Liu WW, Fang DC, Liu FX, He GY. Clinical significance of Fas antigen expression in gastric carcinoma. *World J Gastroenterol* 1999; **5**: 90-91
- 49 **Zhang W**, Meng R, Fu C, Yu D. Gene expression significance of beta-catenin, p53 and PCNA in PJS polyposis. *Zhonghua Waikexue* 2002; **40**: 104-106
- 50 **Lin GY**, Chen ZL, Lu CM, Li Y, Ping XJ, Huang R. Immunohistochemical study on p53, H-rasp21, c-erbB-2 protein and PCNA expression in HCC tissues of Han and minority ethnic patients. *World J Gastroenterol* 2000; **6**: 234-238
- 51 **Li JQ**, Zhang CQ, Feng KT. PCNA, P53 protein and prognosis in primary liver cancer. *China Natl J New Gastroenterol* 1996; **2**: 220-222
- 52 **Wang YK**, Ji XL, Gu YG, Zhang SC, Xiao JH. P53 and PCNA expression in glandular dilatation of gastric mucosa. *China Natl J New Gastroenterol* 1996; **2**: 106-108
- 53 **Qin LX**, Tang ZY. The prognostic molecular markers in hepatocellular carcinoma. *World J Gastroenterol* 2002; **8**: 385-392
- 54 **Shen LJ**, Zhang HX, Zhang ZJ, Li JY, Chen MQ, Yang WB, Huang R. Detection of HBV, PCNA and GST-pi in hepatocellular carcinoma and chronic liver diseases. *World J Gastroenterol* 2003; **9**: 459-462
- 55 **Yue H**, Na YL, Feng XL, Ma SR, Song FL, Yang B. Expression of p57kip2, Rb protein and PCNA and their relationships with clinicopathology in human pancreatic cancer. *World J Gastroenterol* 2003; **9**: 377-380
- 56 **Huang ZH**, Fan YF, Xia H, Feng HM, Tang FX. Effects of TNP-470 on proliferation and apoptosis in human colon cancer xenografts in nude mice. *World J Gastroenterol* 2003; **9**: 281-283
- 57 **Chen H**, Wang LD, Guo M, Gao SG, Guo HQ, Fan ZM, Li JL. Alterations of p53 and PCNA in cancer and adjacent tissues from concurrent carcinomas of the esophagus and gastric cardia in the same patient in Linzhou, a high incidence area for esophageal cancer in northern China. *World J Gastroenterol* 2003; **9**: 16-21
- 58 **Ouyang GL**, Li QF, Peng XX, Liu QR, Hong SG. Effects of tachyplesin on proliferation and differentiation of human hepatocellular carcinoma SMMC-7721 cells. *World J Gastroenterol* 2002; **8**: 1053-1058
- 59 **Jia XD**, Han C. Chemoprevention of tea on colorectal cancer induced by dimethylhydrazine in Wistar rats. *World J Gastroenterol* 2000; **6**: 699-703
- 60 **Liu WZ**, Zheng X, Shi Y, Dong QJ, Xiao SD. Effect of *Helicobacter pylori* infection on gastric epithelial proliferation in progression from normal mucosa to gastric carcinoma. *World J Gastroenterol* 1998; **4**: 246-248
- 61 **Elpek GO**, Gelen T, Aksoy NH, Karpuzoglu T, Keles N. Microvessel count, proliferating cell nuclear antigen and Ki-67 indices in gastric adenocarcinoma. *Pathol Oncol Res* 2000; **6**: 59-64

Effect of O-4-ethoxyl-butyl-berbamine in combination with pegylated liposomal doxorubicin on advanced hepatoma in mice

Bai-Jun Fang, Mei-Li Yu, Shao-Guang Yang, Lian-Ming Liao, Jie-Wen Liu, Robert -C-H Zhao

Bai-Jun Fang, Mei-Li Yu, Shao-Guang Yang, Lian-Ming Liao, Jie-Wen Liu, Robert -C-H Zhao, Sino-American Collaborative Laboratory, Stat Key Laboratory of Experimental Haematology, Institute of Haematology and Blood Disease Hospital, and Tissue Engineering Center, Chinese Academy of Medical Sciences, Tianjin 300020, China

Supported by Tianjin Natural Foundation of Sciences, No. 941409017 and the Minister of Public Health of China, No. 94-2-024

Correspondence to: Robert Chun-Hua Zhao, Professor of State Key Laboratory of Experimental Haematology, Institute of Hematology and Blood Disease Hospital, and Tissue Engineering Center, Chinese Academy of Medical Sciences, Tianjin 300020, China. chunhuaz@public.tpt.tj.cn

Telephone: +86-22-27210060 **Fax:** +86-22-27210060

Received: 2003-05-12 **Accepted:** 2003-06-27

Abstract

AIM: To study the synergistic effects of calmodulin (CaM) antagonist O-4-ethoxyl-butyl-berbamine (EBB) and pegylated liposomal doxorubicin (PLD) on hepatoma-22 (H₂₂) *in vivo*.

METHODS: Hepatoma model was established in 50 Balb/c mice by inoculating H₂₂ cells (2.5×10⁶) subcutaneously into the right backs of the mice. These mice were divided into 5 groups, and treated with saline only, PLD only, doxorubicin (Dox) only, PLD plus EBB and Dox plus EBB, respectively. In the treatment groups, mice were given 5 intravenous of PLD or Dox on days 0, 3, 6, 9 and 12. The first dosage of PLD or Dox was 4.5 mg/kg, the other 4 injections was 1 mg/kg. EBB (5 mg/kg) was coadministered with PLD or Dox in the corresponding groups. The effect of drugs on the life spans of hepatoma-bearing mice and tumor response to the drugs were recorded. Dox levels in the hepatoma cells were measured by a fluorescence assay. Light microscopy was performed to determine the histopathological changes in the major organs of these tumor-bearing mice. The MTT method was used to analyze the effect of Dox or PLD alone, Dox in combination with EBB, or PLD in combination with EBB on the growth of H₂₂ cells in an *in vitro* experiment.

RESULTS: EBB (5 mg/kg) significantly augmented the antitumor activity of Dox or PLD, remarkably prolonged the median survival time. The median survival time was 18.2 d for control group, but 89.2 d for PLD+EBB group and 70.1 d for Dox+EBB group, respectively. However, Dox alone did not show any remarkable antitumor activity, and the median survival time was just 29.7 d. Addition of EBB to Dox or PLD significantly increased the level of Dox in H₂₂ cells *in vivo*. Moreover, EBB diminished liver toxicity of Dox and PLD. *In vitro*, EBB reduced the IC₅₀ value of Dox or PLD on H₂₂ cells from 0.050±0.006 mg/L and 0.054±0.004 mg/L to 0.012±0.002 mg/L and 0.013±0.002 mg/L, respectively (*P*<0.01).

CONCLUSION: EBB and liposomization could improve the therapeutic efficacy of Dox in liver cancer, while decreasing its liver toxicity.

Fang BJ, Yu ML, Yang SG, Liao LM, Liu JW, Zhao RCH. Effect of O-4-ethoxyl-butyl-berbamine in combination with pegylated liposomal doxorubicin on advanced hepatoma in mice. *World J Gastroenterol* 2004; 10(7): 950-953

<http://www.wjgnet.com/1007-9327/10/950.asp>

INTRODUCTION

O-4-ethoxyl-butyl-berbamine (EBB)^[1,2], a new derivative of bisbenzylisoquinoline, is one of the most powerful and specific calmodulin (CaM) antagonist with almost no cytotoxicity on normal cells. Its IC₅₀ value is 100 times lower than that of tetrandrine and in the same grade with R2457. Previous studies have shown that EBB has a strong inhibitory effect on the proliferation of hepatoma cells, and can prolong the life span of tumor-bearing mice. EBB augments the antitumor activity of 5-FU^[2], restores abnormal CaM content in major organs of tumor-bearing mice^[3] and improves their immunofunction^[4]. Therefore, EBB may have a synergistic effect with chemotherapeutic drugs and alleviate their organ toxicity clinically.

Doxorubicin (Dox) is a widely used anti-tumor agent. However, systemic treatment with Dox is complicated by its dose limiting toxicity, even at relatively low concentrations, as well as its rapid plasma clearance and distribution to non-relevant tissues^[5-10]. Pegylated liposomal doxorubicin (PLD) not only increases concentration of Dox in tumor and thus enhances its antitumor activity, but also has lower toxicity to the cardiac muscle compared with Dox alone^[7,11-15]. In this study, we adopted two strategies to enhance the anti-tumor activity and lower the cytotoxicity of Dox: Dox was administered in liposome form and in combination with EBB.

MATERIALS AND METHODS

Reagents

EBB was kindly provided by Dr. Xu YH (Institute of Molecular Biology, Nankai University, China). Hydrogenated egg phosphatidylcholine (HEPC) was kindly supplied by Lipod (Ludwigshafen, Germany). Polyethylene glycol-distearoyl phosphatidylethanolamine (PEG-DSPE) was purchased from Pharmachemie (Haarlem, the Netherlands). PLD (stabilized long circulating liposomes, Dox-HEPC-SLL) with an average diameter of 80 nm was prepared as described earlier^[16].

Animals and tumor model

Age- and sex-matched Balb/c mice (weighting 18-22 g) from the Animal Breeding Center of Peking University (Beijing, China) were used. H₂₂ cells in 0.2 mL (2.5×10⁶) were inoculated subcutaneously into the right backs of the mice. Tumor became apparent about 7 d after the inoculation, and the mice died approximately 18 d later without treatment.

Treatment protocol

On d 7 after inoculation, tumor-bearing mice were randomly divided into 5 groups. Control group received only saline. PLD or Dox group received 4.5 mg/kg PLD or Dox *i.v.* on the first

day, followed by 4 dosages of 1 mg/kg PLD or Dox in 3-d intervals. PLD+EBB or Dox+EBB group was treated in the same way, except that EBB (5 mg/kg, toxicity-free dosage)^[2] was coadministered. All these dosages could be well tolerated by mice (Dr. Yang SG, unpublished observations).

Assessment of tumor response

Tumor growth was recorded before and after the treatment by caliper measurements, and tumor size was calculated using the formula $0.4 \times (A^2 \times B)$ (where B represents the largest diameter and A the diameter perpendicular to B). Tumor response was also assessed by the life span of mice.

Tumor response rate was assessed on d 0 and 10 after commencement of the treatment as follows: progressive disease (PD) = increase in tumor size above 25%, no change (NC) = tumor size equal to that at the beginning of treatment (at a range of -25% and +25%), partial remission (PR) = decrease in tumor size between -25% and -90%, and complete remission (CR) = decrease in tumor size between -90% and -100%.

Drug levels in tumor tissue^[17]

Seven days after inoculation, Dox (10 mg/kg) or PLD (equal to 10 mg/kg Dox) alone, or each of them in combination with EBB (5 mg/kg) was injected *i.v.* After 1, 18, and 36 h, the mice were anesthetized with pentobarbital. Tumors were excised immediately after being perfused with saline. Tissues were homogenized and subjected to acidic isopropanol extraction, and Dox level was measured by a Perkin-Elmer Model MPF44 spectrofluorometer using an excitation wave at 490 nm and the emission wave at 590 nm. Fluorescence intensity was translated to μg or ng of Dox equivalents using a standard curve of Dox.

Histological examinations

One of the major objectives of these studies was to assess whether the treatment with Dox or PLD in combination with EBB would result in any significant alleviation of their tissue damages. Light microscopy was performed to determine the histological changes in organs from tumor-bearing mice treated with saline and drugs. Mice were sacrificed by cervical dislocation on d 20. The liver, spleen, kidney, lung, and heart were moved and fixed in formalin solution and cut into 4 μm thick sections. The tissue sections were hematoxylin-eosin stained and accessed by conventional histological criteria.

Determination of anti-tumor activity in vitro

H₂₂ cells were cultured at the concentration of 1×10^7 cells/L in 24-well plates in RPMI1640 culture medium containing 100 mL/L heat-inactivated fetal calf serum, 100 U penicillin, and 1 000 U streptomycin at 37 °C, 50 mL/L CO₂. Dox (0.01-0.20 mg/L) or PLD (0.01-0.20 mg/L) alone, Dox (0.01-0.20 mg/L) + EBB (1.17 mg/L, the IC₅₀)^[2], or PLD (0.01-0.20 mg/L) + EBB (1.17 mg/L, the IC₅₀) were added. Cells were harvested 72 h later, and 50 μL of MTT reagent was added to each well followed by 4 h incubation at room temperature. Absorbance was measured at 540 nm. Four replicate experiments were performed, and IC₅₀ values were calculated.

Statistical analysis

SPSS9.0 for Windows 98 statistic software was used for data analysis. A P -value less than 0.05 was considered statistically significant.

RESULTS

Antitumor activity of DOX or PLD in combination with EBB

Intravenous administration of 5 injections of Dox or PLD in

combination with EBB (5 mg/kg) strongly inhibited the growth of tumor, and resulted in tumor regression in some mice. The median survival time was 89.2 d in PLD+EBB group and 70.1 d in Dox+EBB group, respectively, significantly longer than that of control group (18.2 d) and Dox group (29.7 d) (Figure 1, Table 1).

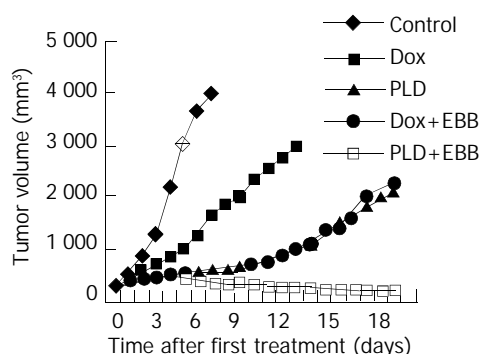


Figure 1 Antitumor activity of Dox or PLD alone or in combination with EBB in mice with hepatoma.

Table 1 Tumor response and survival time of hepatoma-bearing mice after systemic treatment with Dox or PLD alone or in combination with EBB

Group	Tumor response ¹					Mean survival time (d)
	PD	NC	PR	CR	(PR+CR)%	
Dox (n=10)	10				0	29.7±8.2 ^a
Dox+EBB (n=10)	5	2	3		30	70.1±8.3 ^{ac}
PLD (n=10)	6	2	2		20	67.2±9.1 ^{ac}
PLD+EBB (n=12)	2	1	6	3	75	89.2±13.2 ^{abg}
Controls (n=8)	8				0	18.2±2.7

¹Tumor response was scored on d 0 and d 10 after start of treatment. ^a $P < 0.05$ compared with control group; ^c $P < 0.05$ compared with Dox alone; ^e $P < 0.05$ compared with Dox+EBB; ^g $P < 0.05$ compared with PLD alone.

Drug concentrations in tumor tissues

The Dox levels in subcutaneous hepatoma were significantly increased by EBB in both Dox+EBB and PLD+EBB groups ($P < 0.01$) (Figure 2).

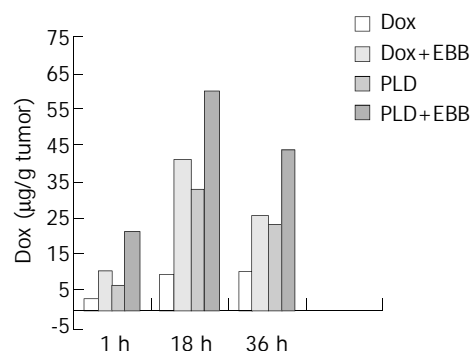


Figure 2 Dox concentrations in tumor tissues from mice after *i.v.* injection of Dox (10 mg/kg) or PLD (equal to 10 mg/kg Dox) in combination with EBB (5 mg/kg).

Histopathological changes

Severe histological changes were found in the liver of Dox group as compared to both Dox+EBB and PLD+EBB groups. Briefly, compared with control mice (Figure 3A), Dox-treated mice showed diffuse fatty degeneration and necrotic changes

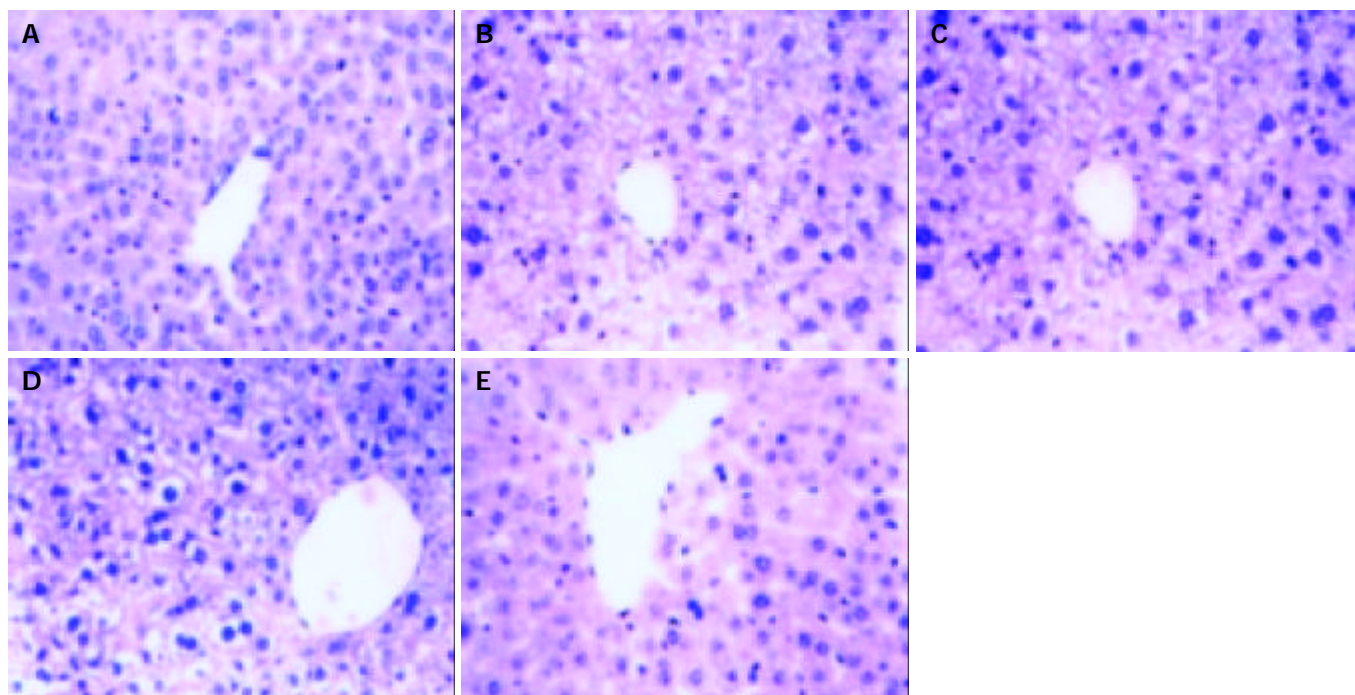


Figure 3 Histopathological changes in livers of tumor-bearing mice treated with saline (A), Dox (B), Dox+EBB (C), PLD (D) or PLD+EBB (E). (Original magnification, $\times 200$).

in the liver (Figure 3B). Livers from Dox+EBB-treated and PLD-treated mice showed similar change, but all were milder than Dox-treated mice (Figure 3C, D). Livers from PLD+EBB-treated mice showed very mild or even undetectable changes (Figure 3E). Severe histological damage was observed in the spleens from all drug-treated mice (data not shown). However, there were no significant abnormalities in the hearts, lungs, and kidneys from all animals (data not shown).

Synergetic effect of EBB with Dox or PLD *in vitro*

The *in vitro* experiment confirmed that EBB (1.17 mg/L, the IC_{50}) augmented the cytotoxicity of Dox and PLD, and reduced the IC_{50} of Dox or PLD on H₂₂ cells from 0.050 ± 0.006 mg/L and 0.054 ± 0.004 mg/L to 0.0120 ± 0.002 mg/L and 0.0130 ± 0.002 mg/L, respectively ($P < 0.01$, Figure 4).

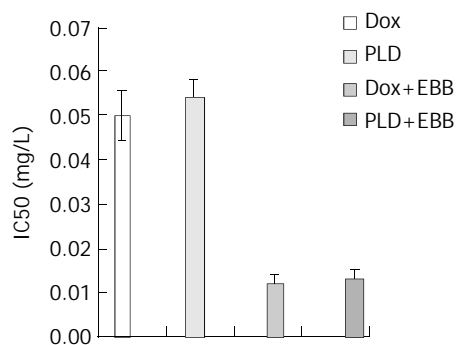


Figure 4 IC_{50} value of Dox or PLD alone or in combination with EBB.

DISCUSSION

Liposomes are attractive drug carriers for intravenous use because of their biocompatibility and versatility of formulation. As witnessed by publications, liposomes can be used for the delivery of cytotoxic drugs, antifungal agents, and biological response modifiers in humans. Phase I and some Phase II studies with liposomal doxorubicin have been reported. However,

the rapid and dominant uptake of these liposomes by the reticuloendothelial system affects its distribution in tumor^[18-20]. We have previously reported that encapsulation of Dox in long-circulating, pegylated liposomes could dramatically improve its mean residence time in serum^[16]. In the present study, we demonstrated the ability of sonicated liposomes to deliver DOX into H₂₂ cells. This may account for the increased antitumor effect of liposome-entrapped Dox observed in the model of hepatoma.

CaM is a ubiquitous calcium-binding protein that is responsible for many intracellular actions of calcium^[21-30]. Lot of evidences suggest that CaM not only plays an important role in the proliferation of normal cells, but also is related to hepatoma growth^[2,31]. In fact, an increased concentration of CaM has been demonstrated in malignant tissues and transformed cell lines^[32,33], and the correlation between inhibition of cell growth and antagonism of CaM has been observed^[21,34]. EBB, one of the strongest and most specific CaM antagonists with almost no cytotoxicity on normal cells, could decrease the amount of CaM in hepatoma cells and block the proliferation of hepatoma cells at G₂/M phase^[2].

In the present study, we demonstrated for the first time that EBB could strongly enhance the antitumor activity of liposomal doxorubicin. *In vitro*, EBB reduced the IC_{50} value of both Dox and PLD in inhibiting H₂₂ cells. *In vivo*, EBB enhanced accumulation of Dox in tumor tissue. There are at least three possible mechanisms underlying these effects. First, EBB could significantly enhance intracellular accumulation of Dox. Secondly, EBB could decrease the CaM content in cytoplasm, resulting in the inhibition of hepatoma cell growth^[2]. The third is that EBB upregulated the expression of wild-type p53 gene^[2], which is an antioncogene.

In terms of histological damage in the livers of the tumor-bearing mice, the present study showed that the changes were milder in mice treated with Dox+EBB and PLD+EBB than in mice treated with Dox or PLD alone. Unfortunately, severe histological damage was observed in the spleens of all experimental animals treated with drugs (data not shown). The reasons for these remain to be further investigated.

In conclusion, although Dox is extremely toxic when used

systemically, encapsulation of Dox in pegylated liposomes allows effective treatment of hepatoma when used in combination with EBB without potential hazards. In our model, administration of PLD resulted in a better tumor response compared with free Dox, and addition of EBB to PLD regimen resulted in a strongly enhanced synergistic tumor response. Therefore, in combination with EBB, the dosage of PLD can be reduced without loss of its antitumor activity, but with a decrease in cytotoxicity.

REFERENCES

- Zhang JH**, Geng ZH, Duan JY, Chen JT, He H, Huang JY. Calmodulin antagonist-effect of berbamine and its derivatives on the cytotoxicity of normal cells. *Xibao Shengwuxue Zazhi* 1997; **19**: 76-79
- Liu J**, Qi S, Zhu H, Zhang J, Li Z, Wang T. The effect of calmodulin antagonist berbamine derivative-EBB on hepatoma *in vitro* and *vivo*. *Chin Med J* 2002; **115**: 759-762
- Zhang JH**, Mao QL, Xu NH, Du XM, Shan T, Chen JT. Effect of calmodulin antagonist on calmodulin content in organs of mice bearing tumor. *Nankai Daxue Xuebao* 1998; **31**: 72-77
- Zhang JH**, Mao QL, Xu NH, Chen JT. Effect of berbamine derivative (EBB) on anticancer and immune function of tumor-bearing mice. *Zhongcaoyao* 1998; **29**: 243-246
- Koh E**, Ueda Y, Nakamura T, Kobayashi A, Katsuta S, Takahashi H. Apoptosis in young rats with adriamycin-induced cardiomyopathy-comparison with pirarubicin, a new anthracycline derivative. *Pediatr Res* 2002; **51**: 256-259
- Forrest GL**, Gonzalez B, Tseng W, Li X, Mann J. Human carbonyl reductase overexpression in the heart advances the development of doxorubicin-induced cardiotoxicity in transgenic mice. *Cancer Res* 2000; **60**: 5158-5164
- Working PK**, Newman MS, Sullivan T, Yarrington J. Reduction of the cardiotoxicity of doxorubicin in rabbits and dogs by encapsulation in long-circulating, pegylated liposomes. *J Pharmacol Exp Ther* 1999; **289**: 1128-1133
- Pacher P**, Liaudet L, Bai P, Virag L, Mabley JG, Hasko G, Szabo C. Activation of poly (ADP-ribose) polymerase contributes to development of doxorubicin-induced heart failure. *J Pharmacol Exp Ther* 2002; **300**: 862-867
- Lim HJ**, Masin D, McIntosh NL, Madden TD, Bally MB. Role of drug release and liposome-mediated drug delivery in governing the therapeutic activity of liposomal mitoxantrone used to treat human A431 and LS180 solid tumors. *J Pharmacol Exp Ther* 2000; **292**: 337-345
- Weinstein DM**, Mihm MJ, Bauer JA. Cardiac peroxynitrite formation and left ventricular dysfunction following doxorubicin treatment in mice. *J Pharmacol Exp Ther* 2000; **294**: 396-401
- Cabanes A**, Even-Chen S, Zimberoff J, Barenholz Y, Kedar E, Gabizon A. Enhancement of antitumor activity of polyethylene glycol-coated liposomal doxorubicin with soluble and liposomal interleukin 2. *Clin Cancer Res* 1999; **5**: 687-693
- Lyass O**, Hubert A, Gabizon AA. Phase I study of doxil-cisplatin combination chemotherapy in patients with advanced malignancies. *Clin Cancer Res* 2001; **7**: 3040-3046
- Gabizon AA**. Stealth Liposomes and tumor targeting: one step further in the quest for the magic bullet. *Clin Cancer Res* 2001; **7**: 223-225
- Marina NM**, Cochrane D, Harney E, Zomorodi K, Blaney S, Winick N, Bernstein M, Link MP. Dose escalation and pharmacokinetics of pegylated liposomal doxorubicin (Doxil) in children with solid tumors: a pediatric oncology group study. *Clin Cancer Res* 2002; **8**: 413-418
- Wang GW**, Kang YJ. Inhibition of doxorubicin toxicity in cultured neonatal mouse cardiomyocytes with elevated metallothionein levels. *J Pharmacol Exp Ther* 1999; **288**: 938-944
- Wang L**, Hou BG, Hou XP, Yu ML, Yang JS. Effects of different phospholipids on the stabilities of doxorubicin liposomes *in vitro* and *in vivo*. *Yaoxue Xuebao* 2001; **36**: 444-447
- Hong RL**, Huang CJ, Tseng YL, Pang VF, Chen ST, Liu JJ, Chang FH. Direct comparison of liposomal doxorubicin with or without polyethylene glycol coating in C-26 tumor-bearing mice: is surface coating with polyethylene glycol beneficial? *Clin Cancer Res* 1999; **5**: 3645-3652
- Laverman P**, Carstens MG, Boerman OC, Dams ET, Oyen WJ, van Rooijen N, Corstens FH, Storm G. Factors affecting the accelerated blood clearance of polyethylene glycol-liposomes upon repeated injection. *J Pharmacol Exp Ther* 2001; **298**: 607-612
- Laverman P**, Brouwers AH, Dams ET, Oyen WJ, Storm G, van Rooijen N, Corstens FH, Boerman OC. Preclinical and Clinical evidence for disappearance of long-circulating characteristics of polyethylene glycol liposomes at low lipid dose. *J Pharmacol Exp Ther* 2000; **293**: 996-1001
- Dams ET**, Laverman P, Oyen WJ, Storm G, Scherphof GL, van Der Meer JW, Corstens FH, Boerman OC. Accelerated blood clearance and altered biodistribution of repeated injections of sterically stabilized liposomes. *J Pharmacol Exp Ther* 2000; **292**: 1071-1079
- Liao B**, Paschal BM, Luby-Phelps K. Mechanism of Ca²⁺-dependent nuclear accumulation of calmodulin. *Proc Natl Acad Sci U S A* 1999; **96**: 6217-6222
- Wang J**, Zhou Y, Wen H, Levitan IB. Simultaneous binding of two protein kinases to a calcium-dependent potassium channel. *J Neurosci* 1999; **19**: RC4
- Desrivieres S**, Cooke FT, Morales-Johansson H, Parker PJ, Hall MN. Calmodulin controls organization of the actin cytoskeleton via regulation of phosphatidylinositol (4,5)-bisphosphate synthesis in *Saccharomyces cerevisiae*. *Biochem J* 2002; **366**(Pt 3): 945-951
- Szymanski PT**, Szymanska G, Goyal RK. Differences in calmodulin and calmodulin-binding proteins in phasic and tonic smooth muscles. *Am J Physiol Cell Physiol* 2002; **282**: C94-C104
- Li Z**, Joyal JL, Sacks DB. Calmodulin enhances the stability of the estrogen receptor. *J Biol Chem* 2001; **276**: 17354-17360
- DeMaria CD**, Soong TW, Alseikhan BA, Alvania RS, Yue DT. Calmodulin bifurcates the local Ca²⁺ signal that modulates P/Q-type Ca²⁺ channels. *Nature* 2001; **41**: 484-489
- Zuhlke RD**, Pitt GS, Deisseroth K, Tsien RW, Reuter H. Calmodulin supports both inactivation and facilitation of L-type calcium channels. *Nature* 1999; **399**: 159-162
- Gillespie PG**, Cyr JL. Calmodulin binding to recombinant myosin-1c and myosin-1c IQ peptides. *BMC Biochem* 2002; **3**: 31
- Mateer SC**, McDaniel AE, Nicolas V, Habermacher GM, Lin MJ, Cromer DA, King ME, Bloom GS. The mechanism for regulation of the F-actin binding activity of IQGAP1 by calcium/calmodulin. *J Biol Chem* 2002; **277**: 12324-12333
- Briggs MW**, Li Z, Sacks DB. IQGAP1-mediated stimulation of transcriptional co-activation by beta-catenin is modulated by calmodulin. *J Biol Chem* 2002; **277**: 7453-7465
- Wu BW**, Wu Y, Wang JL, Lin JS, Yuan SY, Li A, Cui WR. Study on the mechanism of epidermal growth factor-induced proliferation of hepatoma cells. *World J Gastroenterol* 2003; **9**: 271-275
- McGinnis KM**, Shariat-Madar Z, Gnegy ME. Cytosolic calmodulin is increased in SK-N-SH human neuroblastoma cells due to release of calcium from intracellular stores. *J Neurochem* 1998; **70**: 139-146
- Liu J**, Sun L, Wang Q, Zheng H, Wong L. Effects of 17 beta-estradiol on intracellular free calcium, inositol-1,4,5-trisphosphate and calmodulin in human osteoblast-like osteosarcoma cell line TE85. *Zhongguo Yixue Kexueyuan Xuebao* 1999; **21**: 105-110
- Shin SY**, Kim SY, Kim JH, Min DS, Ko J, Kang UG, Kwon TK, Han MY, Kim YH, Lee YH. Induction of early growth response-1 gene expression by calmodulin antagonist trifluoperazine through the activation of Elk-1 in human fibrosarcoma HT1080 cells. *J Biol Chem* 2001; **276**: 7797-7805

Growth arrest and apoptosis of human hepatocellular carcinoma cells induced by hexamethylene bisacetamide

Gao-Liang Ouyang, Qiu-Feng Cai, Min Liu, Rui-Chuan Chen, Zhi Huang, Rui-Sheng Jiang, Fu Chen, Shui-Gen Hong, Shi-Deng Bao

Gao-Liang Ouyang, Qiu-Feng Cai, Min Liu, Zhi Huang, Rui-Sheng Jiang, Shui-Gen Hong, Shi-Deng Bao, Key Laboratory of China Education Ministry for Cell Biology and Tumor Cell Engineering, Laboratory of Cell Biology, School of Life Sciences, Xiamen University, Xiamen 361005, Fujian Province, China

Rui-Chuan Chen, Fu Chen, Cancer Research Center, School of Life Sciences, Xiamen University, Xiamen 361005, Fujian Province, China

Supported by the National Natural Science Foundation of China, No. 30170463 and Science Research Foundation of Xiamen University and Natural Science Foundation of Fujian Province, No. C0210005

Correspondence to: Professor Shi-Deng Bao, Key Laboratory of China Education Ministry for Cell Biology and Tumor Cell Engineering, School of Life Sciences, Xiamen University, Xiamen 361005, Fujian Province, China. sdbao26@yahoo.com

Telephone: +86-592-2186091 **Fax:** +86-592-2188101

Received: 2003-08-23 **Accepted:** 2003-10-07

Abstract

AIM: To investigate the cellular effects of hybrid polar compound hexamethylene bisacetamide (HMBA) on the growth and apoptosis of human hepatocellular carcinoma cells and to provide the molecular mechanism for potential application of HMBA in the treatment of liver cancer.

METHODS: Effects of HMBA on the growth of human hepatocellular carcinoma SMMC-7721 cells were assayed by MTT chromometry. Apoptosis induced by HMBA was detected by phase-contrast microscopy, flow cytometry, propidium iodide staining and immunocytochemical analysis.

RESULTS: The growth of SMMC-7721 cells was significantly inhibited by HMBA, and the growth inhibitory rate was 51.1%, 62.6%, 68.7% and 73.9% respectively after treatment with 5.0, 7.5, 10.0 and 12.5 mmol/L of HMBA. In the cells treated with 10 mmol/L of HMBA for 72 h, the population of cells at sub-G₁ phase significantly increased, and the apoptotic bodies and condensed nuclei were detected. Moreover, treatment of SMMC-7721 cells with 10 mmol/L of HMBA down-regulated the expression of Bcl-2 anti-apoptotic protein, while slightly up-regulated the level of pro-apoptotic protein Bax.

CONCLUSION: Treatment with 10.0 mmol/L of HMBA can significantly inhibit the growth and induce apoptosis of human hepatocellular carcinoma SMMC-7721 cells by decreasing the ratio of Bcl-2 to Bax.

Ouyang GL, Cai QF, Liu M, Chen RC, Huang Z, Jiang RS, Chen F, Hong SG, Bao SD. Growth arrest and apoptosis of human hepatocellular carcinoma cells induced by hexamethylene bisacetamide. *World J Gastroenterol* 2004; 10(7): 954-958 <http://www.wjgnet.com/1007-9327/10/954.asp>

INTRODUCTION

Hepatocellular carcinoma (HCC) is one of the most common malignancies worldwide and accounts for as many as one million deaths annually^[1]. HCC is a leading cause for cancer-related deaths of adults in Asia and sub-Saharan^[2,3]. In China, the mortality rate of HCC ranks first in rural areas and second in cities^[4,5]. The main environmental risk factors identified to be closely associated with hepatocellular carcinoma incidences are hepatitis B virus (HBV) and hepatitis C virus (HCV) infections, which account for more than 80% of HCC cases worldwide. Other agents that also play an important role in HCC development include aflatoxin B1 (AFB1) exposure, heavy alcohol consumption and cigarette smoking^[3,6]. However, the cellular and molecular mechanism underlying HCC development remains poorly understood. HCC is still one of the worst malignant diseases without an effective treatment. Therefore, it is critical to search for novel chemotherapeutic agents that can inhibit the growth or induce the apoptosis of hepatocellular carcinoma cells.

Hybrid polar compounds are potent inducers of cell differentiation for a wide variety of tumor cells^[7]. Hexamethylene bisacetamide (HMBA), a prototype of hybrid polar compounds, has been used to induce terminal differentiation in a number of leukemic and solid tumor cell lines^[8-12]. In the previous reports^[13,14], we have shown that HMBA at a low concentration induced differentiation of human hepatocellular carcinoma SMMC-7721 cells, a cell line that has been previously used as an appropriate cell model *in vitro* to study the cellular mechanism of HCC development^[15-22]. However, whether HMBA at a higher concentration can induce apoptosis of hepatocellular carcinoma cells has not been determined yet. Here we reported the effects of HMBA on the growth and apoptosis of human hepatocellular carcinoma SMMC-7721 cells. We revealed that treatment with 10.0 mmol/L of HMBA significantly inhibited the growth and induced apoptosis of SMMC-7721 cells by down-regulating the Bcl-2/Bax ratio.

MATERIALS AND METHODS

Materials

Hexamethylene bisacetamide (HMBA), [3-(4,5)-dimethylthiazol-2-yl]-2,5-diphenyltetrazolium bromide (MTT), dimethyl sulphoxide (DMSO) and propidium iodide (PI) were purchased from Sigma. DMEM was obtained from Invitrogen Inc. Fetal bovine serum was supplied by Si-Ji-Qing Biotechnology Co. (Hangzhou, China). Mouse anti-human Bcl-2 and Bax monoclonal antibodies were obtained from Santa Cruz Biotechnology. SP detection kit and DAB kit were purchased from Beijing Zhongshan Biotechnology Co.

Cell culture

SMMC-7721 cell line was obtained from the Institute of Biochemistry and Cell Biology, Shanghai Institute of Biological Sciences, Chinese Academy of Sciences. Cells were maintained in DMEM supplemented with 100 mL/L heat-inactivated fetal

bovine serum, 100 units/mL of penicillin and 100 mg/L of streptomycin at 37 °C with 50 mL/L CO₂ in atmosphere.

MTT assay

SMMC-7721 cells were seeded in 96-well plates at a density of 7×10^3 cells/well. After 24 h, the cells were treated with different concentrations of HMBA for different times. One hundred μ L MTT (250 mg/mL) was added to the cells per well. The plate was incubated for 4 h at 37 °C until purple formazan crystal developed. Then MTT-containing medium was removed and 200 μ L DMSO solution (containing 900 mL/L DMSO and 100 mL/L 0.1 mol/L of glycine-NaOH) was added to each well and incubated at room temperature for 30 min. The absorbance at 570 nm was read and four wells were examined with an ELISA plate reader (Bio-Rad) for each treatment.

Phase-contrast microscopy

SMMC-7721 cells and the cells treated with 10 mmol/L of HMBA for 72 h on 6-well plates were examined under phase-contrast microscopy (Leica DM IRB).

Flow cytometry assay and fluorescence microscopy

SMMC-7721 cells untreated and treated with 10 mmol/L of HMBA for 72 h were assayed for DNA content using the propidium iodide staining method and subsequent flow cytometry analysis. Briefly, the cells (generally 2×10^6) were collected, rinsed in PBS, resuspended and fixed in 70% ethanol at 4 °C overnight. The fixed cells were pelleted, resuspended in PBS, and incubated in 100 mg/L of RNase A at 37 °C for 30 min and in 50 mg/L of propidium iodide at 4 °C for 30 min in the dark. Cell cycle distribution at different phase was analyzed with FACScan flow cytometry (Becton Dickinson). More than 10 000 events were acquired for analysis. The nuclear morphology of the stained cells was also observed under fluorescence microscope (Leica DM IRB).

Immunocytochemical analysis

SMMC-7721 cells untreated and treated with 10 mmol/L of HMBA were cultured on coverslips in a 6-well plate. After 72 h, the cells growing on coverslips were fixed with cold acetone for 10 min, rinsed twice in PBS for 10 min. Endogenous peroxidases were inactivated by immersing the sections in 3% hydrogen peroxide for 10 min, washed with distilled water and PBS for 15 min, blocked with 100 mL/L normal goat serum for 10 min to reduce the non-specific binding, and incubated with monoclonal mouse anti-human Bcl-2, Bax antibodies (1:200) at 4 °C overnight. After incubation, the cells on coverslips were incubated with biotinylated anti-mouse IgG at 37 °C for 10 min, rinsed twice in PBS for 15 min, and then incubated in streptavidin-peroxidase at 37 °C for 10 min. The chromogenic reaction was developed with diaminobenzidine (DAB). Negative controls were incubated in the absence of primary antibodies.

Statistical analysis

Data of MTT assay were expressed as mean \pm SD. Difference between means was analyzed using Student's *t*-test, $P < 0.05$ was considered statistically significant.

RESULTS

Effects of HMBA on growth of SMMC-7721 cells

To address whether HMBA affected the growth of hepatocellular carcinoma cells, SMMC-7721 cells were treated with different concentrations of HMBA and then examined by MTT dye reduction assay. As is shown in Table 1, HMBA significantly inhibited the growth of hepatocellular carcinoma cells at concentrations of 5.0, 7.5, 10.0 and 12.5 mmol/L, and the growth inhibitory rate on SMMC-7721 cells at the 72 h was 51.1%, 62.6%, 68.7% and 73.9%, respectively ($P < 0.05$).

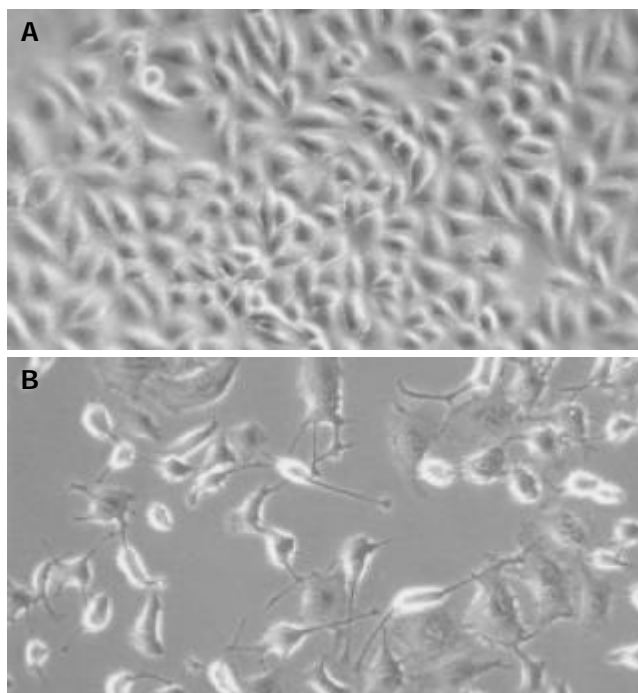


Figure 1 Detection of cell morphology by phase-contrast microscopy ($\times 200$). A: SMMC-7721 cells, B: SMMC-7721 cells treated with 10 mmol/L of HMBA for 72 h.

Apoptosis of SMMC-7721 cells induced by HMBA

In the previous reports, we have revealed that treatment with 5 mmol/L of HMBA induced differentiation of SMMC-7721. In this study, we found that treatment with 10 mmol/L of HMBA caused more dramatic changes of cellular morphology of SMMC-7721 cells (Figure 1). To test whether HMBA-mediated growth inhibition and morphological alteration of hepatocellular carcinoma cells were associated with the induction of apoptosis,

Table 1 Growth inhibition of SMMC-7721 cells by HMBA

Concentration (mmol/L)	24 h treatment		48 h treatment		72 h treatment	
	A_{570}	I R (%)	A_{570}	I R (%)	A_{570}	I R (%)
0	0.201 \pm 0.029	/	0.409 \pm 0.064	/	0.788 \pm 0.037	/
5.0	0.155 \pm 0.009	22.9	0.238 \pm 0.031	41.8	0.385 \pm 0.033	51.1
7.5	0.154 \pm 0.011	23.4	0.216 \pm 0.046	47.2	0.295 \pm 0.031	62.6
10.0	0.146 \pm 0.013	27.4	0.209 \pm 0.020	48.9	0.247 \pm 0.019	68.7
12.5	0.133 \pm 0.021	33.8	0.195 \pm 0.024	52.3	0.206 \pm 0.021	73.9

I R: Inhibitory rate.

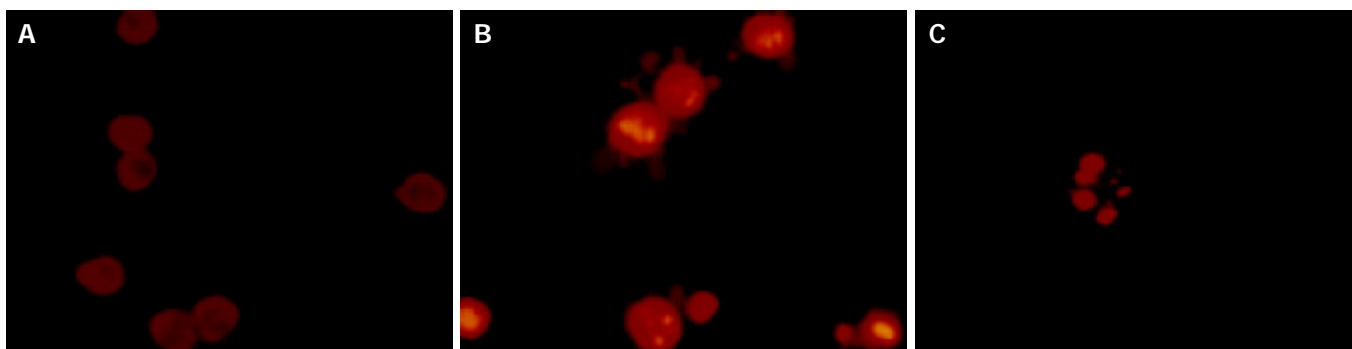


Figure 2 Detection of apoptotic morphology in SMMC-7721 cells treated with 10 mmol/L of HMBA for 72 h ($\times 400$). SMMC-7721 cells displayed fragmented nuclei and apoptotic bodies (B, C) after treatment with 10 mmol/L of HMBA for 72 h, while the untreated cells did not show these apoptotic characteristics (A).

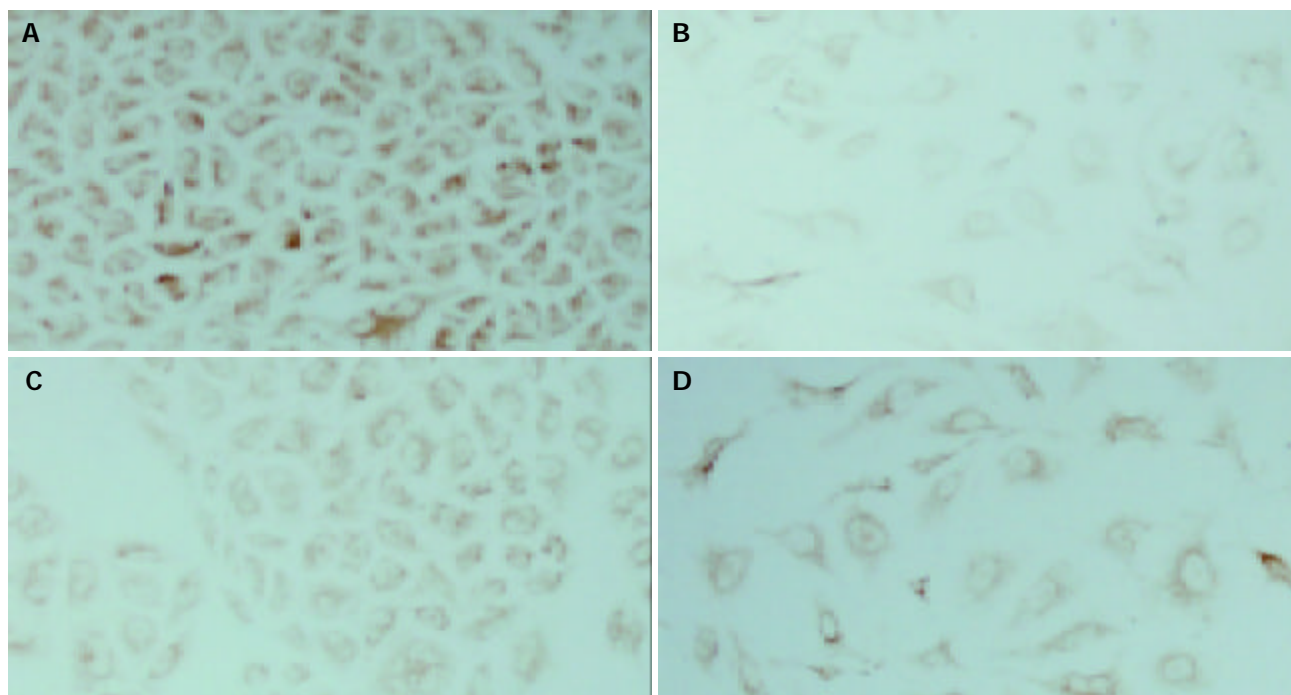


Figure 3 Immunocytochemical analysis of Bcl-2 and Bax expression in SMMC-7721 cells treated with 10 mmol/L of HMBA for 72 h ($\times 200$). A: The high level of Bcl-2 protein in SMMC-7721 cells, B: The decreased level of Bcl-2 protein in the cells treated with 10 mmol/L of HMBA, C: The low level of Bax protein in SMMC-7721 cells, D: The slightly increased level of Bax protein in the cells treated with 10 mmol/L of HMBA.

SMMC-7721 cells were cultured in the presence of 10 mmol/L of HMBA for 72 h, stained with propidium iodide and then cellular morphology was examined. A significant population of cells treated with 10 mmol/L of HMBA displayed the features of apoptosis, such as fragmented nuclei and apoptotic bodies (Figure 2). In addition, in the untreated control cells, only 2.74% cells were found in sub- G_1 phase, but in the cells treated with 10 mmol/L of HMBA for 24, 48 and 72 h, 5.49%, 7.31% and 21.6% cells were found in sub- G_1 phase respectively, indicating that HMBA treatment at a high concentration could significantly induce apoptosis of SMMC-7721 hepatocellular carcinoma cells.

Effects of HMBA on expression of Bcl-2 and Bax in SMMC-7721 cells

To elucidate the mechanism by which HMBA induces apoptotic cell death of SMMC-7721 cells, we analyzed the expression of two critical apoptosis-associated proteins, Bcl-2 and Bax, which are known to regulate the cell death/survival in opposite manners. As is shown in Figure 3, Bcl-2 protein level was significantly decreased while Bax protein level was slightly

increased in the cells treated with 10 mmol/L of HMBA for 72 h. This result suggested that HMBA could induce apoptosis of SMMC-7721 cells by down-regulating the ratio of Bcl-2 to Bax.

DISCUSSION

Dysregulations of cell proliferation, differentiation and apoptosis are hallmarks of cancer cells^[23]. It is possible that these malignant features could be altered by many differentiation inducers such as hybrid polar compound HMBA. Considerable progress has been made toward elucidating the mechanism by which HMBA induces terminal differentiation of cancer cells. In recent year, some reports showed that HMBA induced apoptosis on a number of cancer cells^[24-28], which appeared characteristics of cell shrinkage, chromatin condensation, DNA fragmentation and membrane blebbing^[29,30].

In the present study, we investigated the cellular effects of HMBA on the growth and apoptosis of human hepatocellular carcinoma SMMC-7721 cells. Our data demonstrated that HMBA could effectively inhibit the growth of SMMC-7721 cells in a dose- and time-dependent manner. A significant

portion of the cells treated with 10 mmol/L of HMBA for 72 h displayed the classical hallmarks of apoptosis with typical condensed nuclei and apoptotic bodies. In addition, as was shown in the previous reports^[13,14], HMBA at 5 mmol/L concentration could arrest most of SMMC-7721 cells in G₀/G₁ phase and induce differentiation but not apoptosis. Our present results indicated that HMBA at 10 mmol/L concentration could not only inhibit cell proliferation and induce cell terminal differentiation, but also significantly induce apoptosis in human hepatocellular carcinoma SMMC-7721 cells.

To investigate the mechanism by which HMBA induces cellular apoptosis, we studied the effects of HMBA on apoptotic regulatory proteins in SMMC-7721 cells. Numerous molecular entities have been shown to regulate the apoptosis. Among these, the Bcl-2 family of proteins is well known for its regulatory role during apoptosis, and the interaction between anti-apoptotic and pro-apoptotic members of the family, such as between Bcl-2 and Bax, seemed to be crucial for regulation of this process^[31-33]. Bcl-2, originally described as a proto-oncogene, is known as a cell death inhibitor that is regulated by its interaction with pro-apoptotic factors such as Bax family. Bax, one of the pro-apoptotic proteins, could counteract the anti-apoptotic effects of Bcl-2 by forming a heterodimer with Bcl-2^[34]. In fact, the ratio of Bcl-2 to Bax, rather than the levels of individual proteins, has been considered to be critical in determining the survival or death of cells^[35-38]. A number of studies have revealed that apoptosis induced by many agents is mediated through a decrease of the Bcl-2/Bax ratio^[39-43]. Our results also showed that HMBA could reduce the ratio of Bcl-2 to Bax, indicating that the decreased ratio of Bcl-2 to Bax caused by HMBA treatment might trigger apoptosis of SMMC-7721 cells.

In conclusion, HMBA as a potent inducer can effectively inhibit the proliferation of human hepatocellular carcinoma cells at a low concentration and induce cellular apoptosis at a higher concentration. HMBA induces cell apoptosis of human hepatocellular carcinoma cells by decreasing the ratio of Bcl-2 to Bax.

REFERENCES

- Varela M**, Sala M, Llovet JM, Bruix J. Treatment of hepatocellular carcinoma: is there an optimal strategy? *Cancer Treat Rev* 2003; **29**: 99-104
- Kew MC**. Epidemiology of hepatocellular carcinoma. *Toxicology* 2002; **181-182**: 35-38
- Chen CJ**, Yu MW, Liaw YF. Epidemiological characteristics and risk factors of hepatocellular carcinoma. *J Gastroenterol Hepatol* 1997; **12**: S294-308
- Wu MC**. Clinical research advances in primary liver cancer. *World J Gastroenterol* 1998; **4**: 471-474
- Zeng ZC**, Jiang GL, Wang GM, Tang ZY, Curran WJ, Iliakis G. DNA-PKcs subunits in radiosensitization by hyperthermia on hepatocellular carcinoma hepG2 cell line. *World J Gastroenterol* 2002; **8**: 797-803
- Yu MC**, Yuan JM, Govindarajan S, Ross RK. Epidemiology of hepatocellular carcinoma. *Can J Gastroenterol* 2000; **14**: 703-709
- Herrero R**, Moncelli MR, Guidelli R, Carla M, Arcangeli A, Olivotto M. Hybrid polar compounds produce a positive shift in the surface dipole potential of self-assembled phospholipid monolayers. *Biochim Biophys Acta* 2000; **1466**: 278-288
- Rifkind RA**, Richon VM, Marks PA. Induced differentiation, the cell cycle, and the treatment of cancer. *Pharmacol Ther* 1996; **69**: 97-102
- Leszczyniecka M**, Roberts T, Dent P, Grant S, Fisher PB. Differentiation therapy of human cancer: basic science and clinical applications. *Pharmacol Ther* 2001; **90**: 105-156
- Guilbaud NF**, Gas N, Dupont MA, Valette A. Effects of differentiation-inducing agents on maturation of human MCF-7 breast cancer cells. *J Cell Physiol* 1990; **145**: 162-172
- Marks PA**, Richon VM, Kiyokawa H, Rifkind RA. Inducing differentiation of transformed cells with hybrid polar compounds: a cell cycle-dependent process. *Proc Natl Acad Sci U S A* 1994; **91**: 10251-10254
- Li XN**, Du ZW, Huang Q. Modulation effects of hexamethylene bisacetamide on growth and differentiation of cultured human malignant glioma cells. *J Neurosurg* 1996; **84**: 831-838
- Ouyang GL**, Li QF, Peng XX, Hong SG. Differentiation of human hepatocarcinoma SMMC-7721 cells induced by HMBA. *Shiyan Shengwu Xuebao* 2001; **34**: 269-273
- Ouyang GL**, Li QF, Peng XX, Hong SG. Effects of HMBA on the expression of cell-cycle-associated genes in human hepatocarcinoma SMMC-7721 cells. *Shiyan Shengwu Xuebao* 2002; **35**: 173-178
- Ren JG**, Zheng RL, Shi YM, Gong B, Li JF. Apoptosis, redifferentiation and arresting proliferation simultaneously triggered by oxidative stress in human hepatoma cells. *Cell Biol Int* 1998; **22**: 41-49
- Li J**, Huang CY, Zheng RL, Cui KR, Li JF. Hydrogen peroxide induces apoptosis in human hepatoma cells and alters cell redox status. *Cell Biol Int* 2000; **24**: 9-23
- Yuan JH**, Wang XW, Luo D, Xie Y, Xie H. Anti-hepatoma activity of taxol *in vitro*. *Acta Pharmacol Sin* 2000; **21**: 450-454
- Zhang SW**, Lin WS, Ying XL, Zhu D, Guo MY, Gu JX. Effect of suppression of TGF- β 1 expression on cell-cycle and gene expression of β -1, 4-galactosyltransferase 1 in human hepatocarcinoma cells. *Biochem Biophys Res Commun* 2000; **273**: 833-838
- Chan EW**, Cheng SC, Sin FW, Xie Y. Triptolide induced cytotoxic effects on human promyelocytic leukemia, T cell lymphoma and human hepatocellular carcinoma cell lines. *Toxicol Lett* 2001; **122**: 81-87
- Ouyang GL**, Li QF, Peng XX, Liu QR, Hong SG. Effects of tachyplesin on proliferation and differentiation of human hepatocellular carcinoma SMMC-7721 cells. *World J Gastroenterol* 2002; **8**: 1053-1058
- Chen RC**, Su JH, Ouyang GL, Cai KX, Li JQ, Xie XG. Induction of differentiation in human hepatocarcinoma cells by isoverbascoside. *Planta Med* 2002; **68**: 370-372
- Geng CX**, Zeng ZC, Wang JY. Docetaxel inhibits SMMC-7721 human hepatocellular carcinoma cells growth and induces apoptosis. *World J Gastroenterol* 2003; **9**: 696-700
- Hanahan D**, Weinberg RA. The hallmarks of cancer. *Cell* 2000; **100**: 57-70
- Siegel DS**, Zhang X, Feinman R, Teitz T, Zelenetz A, Richon VM, Rifkind RA, Marks PA, Michaeli J. Hexamethylene bisacetamide induces programmed cell death (apoptosis) and down-regulates BCL-2 expression in human myeloma cells. *Proc Natl Acad Sci U S A* 1998; **95**: 162-166
- Hyman T**, Rothmann C, Heller A, Malik Z, Salzberg S. Structural characterization of erythroid and megakaryocytic differentiation in Friend erythroleukemia cells. *Exp Hematol* 2001; **29**: 563-571
- Shelly LL**, Fuchs C, Miele L. Notch-1 inhibits apoptosis in murine erythroleukemia cells and is necessary for differentiation induced by hybrid polar compounds. *J Cell Biochem* 1999; **73**: 164-175
- Ruefli AA**, Smyth MJ, Johnstone RW. HMBA induces activation of a caspase-independent cell death pathway to overcome P-glycoprotein-mediated multidrug resistance. *Blood* 2000; **95**: 2378-2385
- Zhang Z**, Liong EC, Lau TY, Leung KM, Fung PC, Tipoe GL. Induction of apoptosis by hexamethylene bisacetamide is p53-dependent associated with telomerase activity but not with terminal differentiation. *Int J Oncol* 2000; **16**: 887-892
- Liu JR**, Chen BQ, Yang YM, Wang XL, Yue YB, Zheng YM, Liu RH. Effect of apoptosis on gastric adenocarcinoma cell line SGC-7901 induced by cis-9, trans-11-conjugated linoleic acid. *World J Gastroenterol* 2002; **8**: 999-1004
- Kroemer G**, Dallaporta B, Resche-Rigon M. The mitochondrial death/life regulator in apoptosis and necrosis. *Annu Rev Physiol* 1998; **60**: 619-642
- Chao DT**, Korsmeyer SJ. BCL-2 family: regulators of cell death. *Annu Rev Immunol* 1998; **16**: 395-419

- 32 **Kluck RM**, Bossy-Wetzel E, Green DR, Newmeyer DD. The release of cytochrome C from mitochondria: a primary site for Bcl-2 regulation of apoptosis. *Science* 1997; **275**: 1132-1136
- 33 **Evan G**, Littlewood T. A matter of life and cell death. *Science* 1998; **281**: 1317-1322
- 34 **Kobayashi T**, Ruan S, Clodi K, Kliche KO, Shiku H, Andreeff M, Zhang W. Overexpression of Bax gene sensitizes K562 erythroleukemia cells to apoptosis induced by selective chemotherapeutic agents. *Oncogene* 1998; **16**: 1587-1591
- 35 **Oltvai ZN**, Milliman CL, Korsmeyer SJ. Bcl-2 heterodimerizes *in vivo* with a conserved homolog, Bax, that accelerates programmed cell death. *Cell* 1993; **74**: 609-619
- 36 **Oltvai ZN**, Korsmeyer SJ. Checkpoints of dueling dimers foil death wishes. *Cell* 1994; **79**: 189-192
- 37 **Reed JC**. Bcl-2 family proteins. *Oncogene* 1998; **17**: 3225-3236
- 38 **Fukamachi Y**, Karasaki Y, Sugiura T, Itoh H, Abe T, Yamamura K, Higashi K. Zinc suppresses apoptosis of U937 cells induced by hydrogen peroxide through an increase of the Bcl-2/Bax ratio. *Biochem Biophys Res Commun* 1998; **246**: 364-369
- 39 **Panaretakis T**, Pokrovskaja K, Shoshan MC, Grander D. Interferon-alpha-induced apoptosis in U266 cells is associated with activation of the proapoptotic Bcl-2 family members Bak and Bax. *Oncogene* 2003; **22**: 4543-4556
- 40 **Yan J**, Xu YH. Tributyrin inhibits human gastric cancer SGC-7901 cell growth by inducing apoptosis and DNA synthesis arrest. *World J Gastroenterol* 2003; **9**: 660-664
- 41 **Zhou HB**, Zhu JR. Paclitaxel induces apoptosis in human gastric carcinoma cells. *World J Gastroenterol* 2003; **9**: 442-445
- 42 **Aranha O**, Grignon R, Fernandes N, McDonnell TJ, Wood DP Jr, Sarkar FH. Suppression of human prostate cancer cell growth by ciprofloxacin is associated with cell cycle arrest and apoptosis. *Int J Oncol* 2003; **22**: 787-794
- 43 **Pettersson F**, Dagleish AG, Bissonnette RP, Colston KW. Retinoids cause apoptosis in pancreatic cancer cells via activation of RAR-gamma and altered expression of Bcl-2/Bax. *Br J Cancer* 2002; **87**: 555-561

Edited by Zhang JZ and Wang XL **Proofread by** Xu FM

Transfection and expression of hepatitis B virus x gene and its effect on apoptosis in HL-7702 cells

Hong-Ying Chen, Nan-Hong Tang, Xiu-Jin Li, Sheng-Jun Zhang, Zhi-Xin Chen, Xiao-Zhong Wang

Hong-Ying Chen, Sheng-Jun Zhang, Zhi-Xin Chen, Xiao-Zhong Wang, Department of Gastroenterology, Union Hospital, Fujian Medical University, Fuzhou 350001, Fujian Province, China
Nan-Hong Tang, Xiu-Jin Li, Department of Hepato-biliary, Union Hospital, Fujian Medical University, Fuzhou 350001, Fujian Province, China

Supported by Science and Technology Issue of Fujian Province, No. 99-Z-162

Correspondence to: Dr. Xiao-Zhong Wang, Department of Gastroenterology, Union Hospital, Fujian Medical University, Fuzhou 350001, Fujian Province, China. drwangxz@pub6.fz.fj.cn

Telephone: +86-591-3357896-8482

Received: 2003-12-28 **Accepted:** 2004-01-08

Abstract

AIM: To investigate the effects of hepatitis B virus x gene and its protein product HBxAg on apoptosis in hepatocyte line HL-7702.

METHODS: The reconstituted plasmid pcDNA3-x was established through recombination DNA technique; pcDNA3-X was transfected into HL-7702 cells by lipid-mediated transfection. Positive clones were screened by G418, and HL-7702/HBx cells were analysed by the RT-PCR to confirm the steady expression of X gene in HL-7702 cells. The apoptosis rate in HL-7702 cells was determined by flow cytometry, TUNEL technology, electronic microscope. At the mean time, pcDNA3-X was transfected transiently into HL-7702 cells, and total RNA from HL-7702 cells was extracted 24, 48, 72, 96 and 120 h after the transient transfection, and semi-quantitative analysis was performed by RT-PCR to detect the expression of HBV X gene. Furthermore, apoptosis rate in HL-7702 cells was determined by flow cytometry analysis at the different times.

RESULTS: RT-PCR analysis showed that HBV X gene could be expressed stably in HL-7702 cells. Both flow cytometry and TUNEL technology revealed that the apoptosis rates of HL-7702/HBx cells were much higher than those of HL-7702/pcDNA3 and HL-7702 cells. Furthermore, the apoptotic phenomena and apoptotic body were observed in HL-7702/HBx cells under electronic microscope, but not in HL-7702/pcDNA3 and HL-7702 cells. In the experiment of transient transfection, RT-PCR reveals that X gene was expressed most at 72 h after transfection; and the apoptosis rate reached the highest at the same time. After that, the apoptosis rate was reduced with the decrease of the X gene expression.

CONCLUSION: HBV X gene and X protein can promote the apoptosis in hepatocyte. And there exist a quantity-effect relationship between the X gene expression and apoptosis rate in hepatocyte.

Chen HY, Tang NH, Li XJ, Zhang SJ, Chen ZX, Wang XZ. Transfection and expression of hepatitis B virus x gene and its effect on apoptosis in HL-7702 cells. *World J Gastroenterol* 2004; 10(7): 959-964

<http://www.wjgnet.com/1007-9327/10/959.asp>

INTRODUCTION

Chronic Hepatitis B virus (HBV) infection is associated with a high incidence of liver disease, including hepatitis and hepatocellular carcinoma (HCC)^[1-3]. Based on epidemiologic studies involving chronic HBV infection, it is estimated that the relative risk of developing HCC for HBV carriers may be 100- to 200-fold higher than that for non-carriers^[4].

HBV genome has four open reading frames (ORFs), including envelope genes coding region (*pre-s1*, *pre-s2* and *s* gene coding region), precore (*pc*) gene and core (*c*) gene coding region, polymerase (*p*) gene coding region, X gene coding region. X gene is the smallest open reading frame of HBV. X gene codes for a 16.5-ku protein (X protein, HBx), which is made of 154 amino acids. HBx is a multifunctional viral regulator that modulates transcription, cell responses to genotoxic stress, protein degradation, and signaling pathways^[5]. Besides, it may affect DNA repair, cell cycle control, and apoptosis^[6-9].

To explore the effect of HBV X gene and its protein product on apoptosis, we transfected X gene into hepatocyte line HL-7702, and observed its role on cell apoptosis by flow cytometry, TUNEL technology and electronic microscope.

MATERIALS AND METHODS

Biological and chemical materials

Restriction *end* onucleases, T4 DNA ligase, reverse transcription system, G418 and Transfast transfection reagent were obtained from Promega Biotech (USA). Vector pUCmT was purchased from Shanghai Sangon Co. (China). RNA isolation kit was from Jingmei Biotech Co. (China). TUNEL reagent was obtained from Beijing Zhongshan Co. (China). The plasmid pcDNA3 was from Invitrogen Co. (USA).

Construction of HBx expression vector

The HBV X DNA fragment was amplified by polymerase chain reaction (PCR) using the HBV carrier's serum as a template. The sequences of primers for the PCR were as follows: 5' - ATGCAAGCTTATGGCTGCTAGGCTGTACTG-3' and 5' - TGCGAATTCTTAGGCAGAGGTGAAAAAGTTG-3'. The PCR was carried out as follows: pre-denaturation at 95 °C for 5 min, 30 amplification cycles (denaturation at 94 °C for 45 s, annealing at 61 °C for 35 s, and extension at 72 °C for 1 min). After the PCR product was added an A-tailing, it was connected with vector pUCmT to construct the middle vector pUCmT-X. According to the sequencing result of pUCmT, the positive clone was selected to extract plasmid. Then the plasmid was digested with *Eco*R I and *Hind* III and ligated into pcDNA3 to establish the reconstituted plasmid pcDNA3-X, which was confirmed by restriction *end* onucleases digestion and direct DNA sequencing.

Steady expression of HBx and apoptosis analysis

Cell culture and DNA transfection HL-7702 cells were cultured in RPMI 1640 supplemented with 200 mL/L FBS. The cells in logarithmic growth were separately transfected with pcDNA3-X and pcDNA3 plasmids, by lipid-mediated transfection using Transfast transfection reagent with a total of 2 µg of DNA per well in a 6-well plate. G418 was added to

select the resistant clones after 48 h. After 2-wk selection, positive clones that were named HL-7702/HBx and HL-7702/pcDNA3 were isolated and further expanded.

RT-PCR analysis Total RNA was extracted separately from the cells of each group (HL-7702/HBx, HL-7702/pcDNA3, HL-7702) with RNA isolation kit, and RT-PCR was carried out. Using 5 μ L of RT product as template, X gene and β -actin were amplified together by PCR. The sequence of X gene primers for RT-PCR were as described above. The primers of β -actin were: 5'-GGCATCGTGATGGACTCCG-3' and 5'-GCTGGAAGGTGGACAGCGA-3'. PCR was carried out as follows: Pre-denaturation for 5 min at 95 $^{\circ}$ C; 32 amplification cycles (denaturation at 94 $^{\circ}$ C for 35 s, annealing at 65 $^{\circ}$ C for 35 s, and extension at 72 $^{\circ}$ C for 1 min).

Flow cytometric analysis The cells of three groups were harvested with trypsin, resuspended in PBS (1×10^6 cells/mL), and analyzed for cell apoptosis rate by flow cytometry.

TUNEL technology The cells of three groups were separately seeded into the wells of 96-well plate. When cells nearly full confluent, they were fixed for 1 h at 37 $^{\circ}$ C. TUNEL assay was performed following the manufacturer's instructions. Finally, the cells were analyzed under a microscope. The apoptosis cells which had blue-black nucleus were counted among 3 000 cells.

Electronic microscope observation A total of 1×10^6 cells of HL-7702/HBx or HL-7702/pcDNA3 or HL-7702 were digested, centrifuged, fixed and analyzed for cell apoptosis under an electronic microscope.

Instantaneous expression of HBx and apoptosis analysis

Instantaneous transfection HL-7702 cells were cultured in RPMI 1640 supplemented with 200 mL/L FBS. The cells in logarithmic growth were separately transfected with pcDNA3-X and pcDNA3 plasmids with Transfast transfection reagent with a total of 2 μ g of DNA per well in a 6-well plate.

RT-PCR semi-quantitative analysis At the time of 24, 48, 72, 96, 120 h of post-transfection, RNA from the cells of 3 groups were separately extracted and transcribed reversely to cDNA. The RT reaction contained 2.5 μ g RNA, 2 μ L of 10 \times buffer, 4 μ L of MgCl₂, 2 μ L of dNTP (10 mmol/L), 0.5 μ L of RNasin, 0.6 μ L AMV (24 U/ μ L). A 20 μ L total RT reaction

volume was obtained by adding sterile water, and RT was carried out at 42 $^{\circ}$ C for 1 h and 95 $^{\circ}$ C for 5 min. Then using 5 μ L RT product as template, X gene and β -actin were amplified together by PCR as described above. The semi-quantitative analysis for the expression of HBV X gene was performed through the luminosity contrast between X gene and β -actin at the different time under ultraviolet ray. This experiment was repeated under the same conditions 3 times.

Flow cytometric analysis At the 5 different times, the cells of 3 groups were harvested by trypsinization, resuspended in PBS (1×10^6 cells/mL), and analyzed for cell apoptosis by flow cytometry.

RESULTS

pcDNA3-X vector construction

A 465 bp HBV X gene was amplified from HBV genomic DNA and subcloned into the expression vector pcDNA3, with which the pcDNA3-X was constructed. The sequence of X gene in the plasmid was coincident with that reported before as identified by restriction endonucleases digestion (Figure 1) and confirmed by DNA direct sequencing (Figure 2).

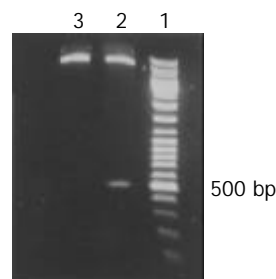


Figure 1 The reconstituted plasmid pcDNA3-X confirmed by restriction endonucleases digestion. Lane 1: 1 Kb DNA ladder; Lane 2: digestion product of pcDNA3-X; Lane 3: digestion product of pcDNA3.

Steady expression of HBx gene in HL-7702 cells

After pcDNA3-X plasmids were transfected into HL-7702

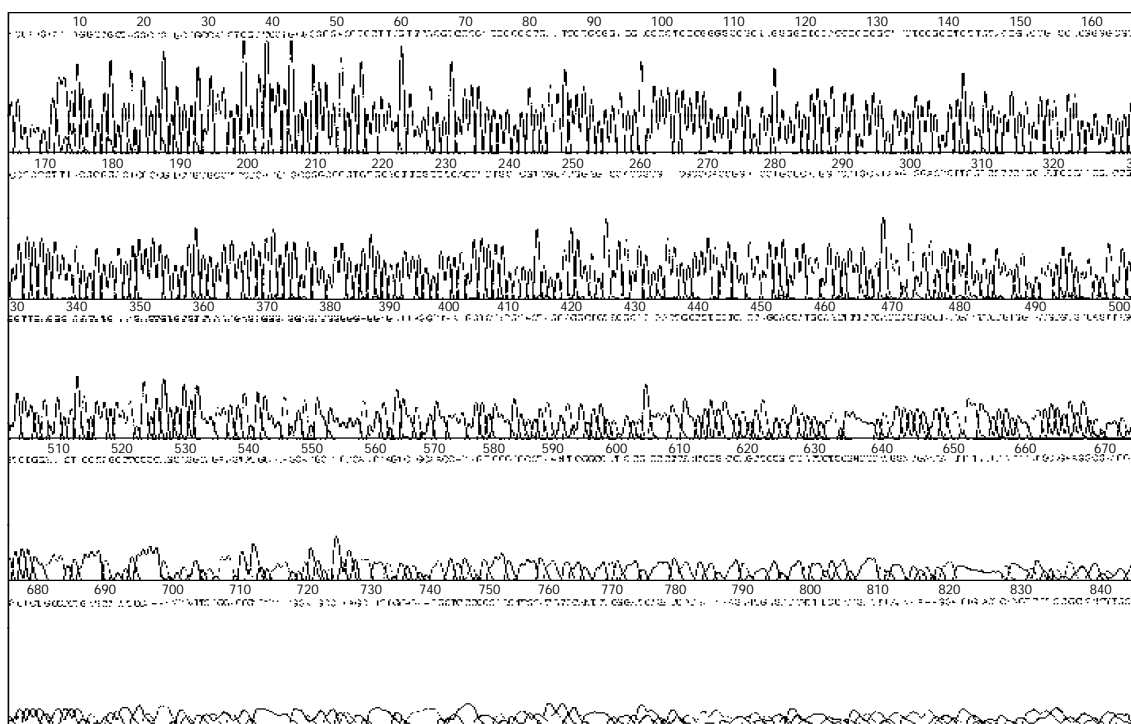


Figure 2 The direct sequencing result of pcDNA3-X (HBV X gene was inserted from 10th bp to 474th bp).

cells, the cells were isolated by G418 selection. HBV X mRNA was detected in HL-7702/HBx cells by RT-PCR which suggested that pcDNA3-X plasmids were expressed steadily in eukaryotic cells (Figure 3).



Figure 3 Detection of HBV X gene expression in transfected HL-7702 cells by RT-PCR. 1: 100 bp DNA ladder; 2: HL-7702/HBx cells; 3: HL-7702/PcDNA3 cells; 4: HL-7702 cells.

Effects of HBx steady expression on cell apoptosis

Flow cytometric analysis The apoptosis rate of HL-7702/HBx cells was 23%, while no apoptosis of cells was found in the HL-7702/pcDNA3 and HL-7702 cells (Figure 4).

TUNEL analysis Of 3000 HL-7702/HBx cells counted, 589 cells underwent apoptotic cell death, while in the HL-7702/pcDNA3 and HL-7702 cells only 36 and 29 cells underwent apoptotic cell death, respectively. Apoptosis was significantly increased in HL-7702/HBx cells compared with the other two groups (using SAS software, χ^2 test: $P_1, P_2 < 0.01$, Figure 5).

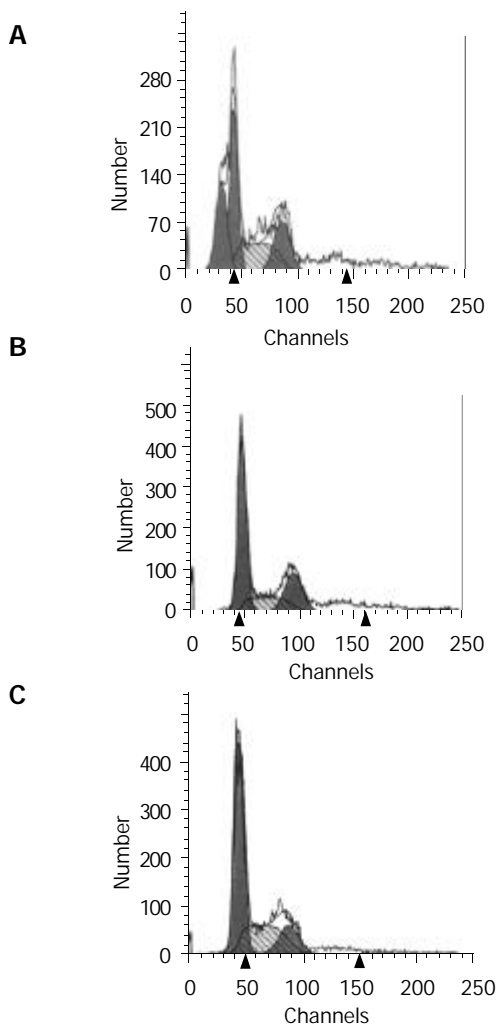


Figure 4 Flow cytometric analysis of apoptosis of HL-7702 cells. A: HL-7702/HBx cells; B: HL-7702/pcDNA3 cells; C: HL-7702 cells.

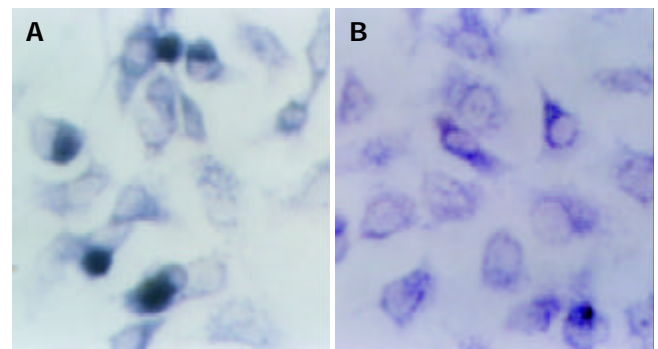


Figure 5 TUNEL analysis of apoptosis of HL-7702 cells. A: HL-7702/HBx cells ($\times 400$). The cells showing blue-dark nuclear staining were apoptotic cells. B: HL-7702/PcDNA3 cells ($\times 400$), no apoptotic cells were seen.

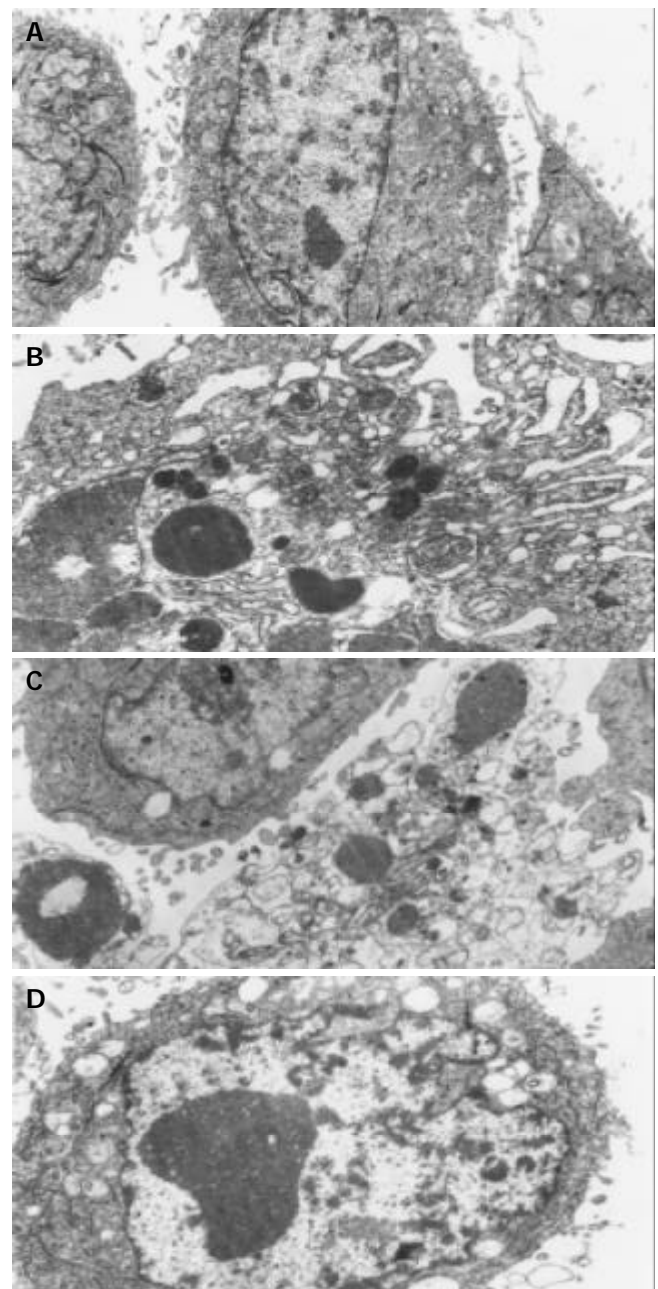


Figure 6 Cell apoptosis observed under electronic microscope. A: HL-7702/pcDNA3 cells ($\times 4\ 800$). B: Typical apoptosis were found in HL-7702/HBx cells ($\times 6\ 000$). C: apoptotic body was found in HL-7702/HBx cells ($\times 4\ 800$). D: assemblage of heterochromatin and edema of mitochondria were found in HL-7702/HBx cells ($\times 4\ 800$).

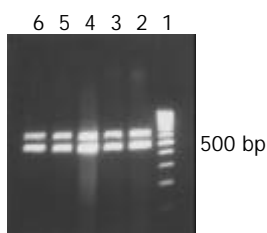


Figure 7 Semi-quantitative analysis of instantaneous expression of X gene by RT-PCR. Lane 1: 100 bp ladder; Lane 2: 24 h after transfection; Lane 3: 48 h after transfection; Lane 4: 72 h after transfection; Lane 5: 96 h after transfection; Lane 6: 120 h after transfection.

Electronic microscope analysis Under electronic microscope, typical apoptosis phenomena were found in HL-7702/HBx cells: the outward appearance of cells look like plum blossom; the membrane existed entirely; stainable feature concentrate into blocks and break down; the decreased density of cytoplasm; endoplasmic reticulum looked like bubbles (Figure 6B). And apoptotic body (Figure 6C), assemblage of heterochromatin and edema of mitochondria (Figure 6D) were found in some apoptotic cells, While none of apoptotic phenomena were observed in the HL-7702/PcDNA3 and HL-7702 cells (Figure 6A).

Effects of HBx instantaneous expression on cell apoptosis

RT-PCR semi-quantitative analysis The result of RT-PCR can be seen in Figure 7. The luminosity contrasts between X gene and β -actin at the different times is described in Table 1. The results suggest that HBV X gene was expressed the first day after transfection, and most strongly expressed 72 h after transfection. After that, the expression of HBV X gene decreased with time.

Table 1 The luminosity contrasts between X gene and β -actin at the different times

The time after transfection(h)	First time	Second time	Third time	Average
24	1.3234	1.2823	1.3333	1.3130
48	1.2396	1.3433	1.3568	1.3132
72	1.5884	1.6212	1.6345	1.6147
96	1.2814	1.3612	1.3245	1.3224
120	1.3224	1.3041	1.3012	1.3092

Flow cytometric analysis As shown in Figure 8A-E, the apoptosis phenomena were observed the first day after transfection, and reach the highest at 72 h, then dropped again.

The link between apoptosis rate and X gene expression A two-axis broken line graph was drawn in order to determine the association between HBV X gene expression and cell apoptosis rate (Figure 9).

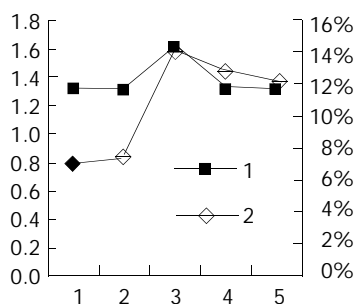


Figure 9 A two-axis broken line graph. The abscissa represents the days after transfection, and the two axis of ordinate are the relative figure of X gene expression and apoptosis rate: 1: X gene expression; 2: apoptosis rate.

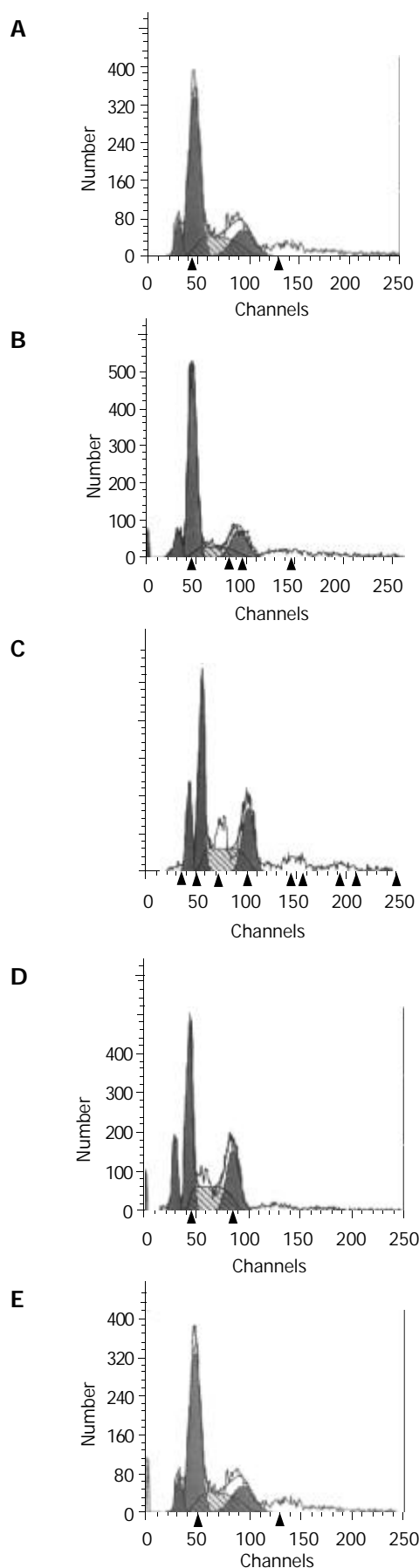


Figure 8 Flow cytometric analysis of apoptosis of HL-7702 after transient transfected with HBV X gene. A: 24 h after transfection (the apoptosis rate is 7.17%); B: 48 h after transfection (the apoptosis rate is 7.40%); C: 72 h after transfection (the apoptosis rate is 14.13%); D: 96 h after transfection (the apoptosis rate is 12.77%); E: 120 h after transfection (the apoptosis rate is 12.11%).

DISCUSSION

The HBx protein is a small polypeptide encoded by mammalian hepadnaviruses that is essential for viral infectivity and is thought to play a role in development of hepatocellular carcinoma during chronic hepatitis B virus infection^[10]. It is known to be a transactivator of transcriptional elements that regulates the expression of a variety of genes associated with the growth, differentiation, survival and the apoptosis of cells. However, the role of the hepatitis B virus protein HBx in liver cell proliferation and apoptosis remains controversial. A number of studies have revealed that HBx protein exerts dual activity on cell apoptosis^[11].

On one hand, HBx protein can block apoptosis through the following ways: (1) upregulates the activity of NF-kappa B^[12] and activates NF-kappa B to translocate into nuclei of hepatocellular carcinoma cells^[13,14]; (2) upregulates the expression of FasL in hepatoma cells, which contribute to tumor escape from immune surveillance of the body^[15,16]; (3) abrogates Bcl-2-mediated protection against Fas apoptosis in the liver^[17]; (4) decreases the expression of Bid^[18]; (5) inhibits caspase 3 activity^[19]; (6) inhibits transforming growth factor beta-induced apoptosis through the activation of phosphatidylinositol 3-kinase pathway^[20].

On the other hand, increasing evidence here suggested that HBx may exert a proapoptotic effect on hepatocytes and in the liver of HBx transgenic mice^[9,21-31]. HBx protein has been shown to induce or sensitize cells to apoptotic killing by proapoptotic stimuli, such as etoposide and tumor necrosis factor α ^[24,25,32,33]. Terradillos *et al* reported that HBx induced apoptosis in a p53-independent manner^[23], but Chirillo *et al* reported p53-dependent apoptotic killing of cells by HBx^[26]. However, a recent study could not substantiate that HBx has any detectable effect on p53 activity or location^[34]. In addition, HBx can also lead to several activities, including stimulation of Ras, activation of Src kinases, transcriptional activation of myc genes, constitutive activation of JNKs, and loss of cell cycle checkpoint controls, thereby leading to cell apoptosis^[9]. Moreover, HBx could interact with mitochondria, cause loss of mitochondrial membrane potential^[35] and mitochondrial aggregation at the nuclear periphery^[31], leading to cell death.

The dual activity of HBx protein on cell death suggests that the expression of HBx gene and its physiological role in viral pathogenesis are not simple and might be tightly regulated^[11]. It seems that HBx may have evolved strategies to block and/or induce apoptosis depending on the cellular environment^[24] and infection stage. Thus, HBx protein may play an opposite role in the different cellular environments and different infection stages.

Here, we constructed the HL-7702/HBx cells which could express HBV X gene steadily and found that X gene able to promote cell apoptosis. In addition, a dose-dependent apoptotic function of HBx was demonstrated in transient transfections of liver cell lines. There existed quantity-effect relationship between the X gene expression and apoptosis rate, suggesting that the more X gene expression, the higher apoptosis rate in liver cells.

However, the precise role of HBx-mediated apoptosis is still unknown. It has been proposed that induction of apoptosis by HBx can actually facilitate propagation of viral infection by permitting efficient particle release from cells while minimizing the antiviral inflammatory response^[9]. Alternatively, it is also possible that stimulation of apoptosis by HBx might promote release of hepatocyte growth factors, enhancing regenerative responses and increasing the level of uninfected hepatocytes for new infection, ultimately leading to liver cell transformation^[9,12,24]. And the apoptotic effects of HBx by naturally occurring mutations might render the hepatocytes susceptible to uncontrolled growth and contribute to multistep

hepatocarcinogenesis associated with HBV-infection. Further study is required to explore the mechanisms and roles of HBx-mediated apoptosis.

REFERENCES

- 1 **Chisari FV**, Ferrari C. Hepatitis B virus immunopathogenesis. *Annu Rev Immunol* 1995; **13**: 29-60
- 2 **Chisari FV**. ROUS-Whipple Award Lecture. Viruses, immunity, and cancer: lessons from hepatitis B. *Am J Pathol* 2000; **156**: 1117-1132
- 3 **Montalto G**, Cervello M, Giannitrapani L, Dantona F, Terranova A, Castagnetta LA. Epidemiology, risk factors, and natural history of hepatocellular carcinoma. *Ann N Y Acad Sci* 2002; **963**: 13-20
- 4 **Xiong J**, Yao YC, Zi XY, Li JX, Wang XM, Ye XT, Zhao SM, Yan YB, Yu HY, Hu YP. Expression of hepatitis B virus X protein in transgenic mice. *World J Gastroenterol* 2003; **9**: 112-116
- 5 **Murakami S**. Hepatitis B virus X protein: a multifunctional viral regulator. *J Gastroenterol* 2001; **36**: 651-660
- 6 **Koike K**, Moriya K, Yotsuyanagi H, Iino S, Kurokawa K. Induction of cell cycle progression by hepatitis B virus HBx gene expression in quiescent mouse fibroblasts. *J Clin Invest* 1994; **94**: 44-49
- 7 **Benn J**, Schneider RJ. Hepatitis B virus HBx protein deregulates cell cycle checkpoint controls. *Proc Natl Acad Sci U S A* 1995; **92**: 11215-11219
- 8 **Shih WL**, Kuo ML, Chuang SE, Cheng AL, Doong SL. Hepatitis B virus X protein inhibits transforming growth factor-beta-induced apoptosis through the activation of phosphatidylinositol 3-kinase pathway. *J Biol Chem* 2000; **275**: 25858-25864
- 9 **Su F**, Theodosis CN, Schneider RJ. Role of NK-kappaB and myc proteins in apoptosis induced by hepatitis B virus HBx protein. *J Virol* 2001; **75**: 215-225
- 10 **Wang XZ**, Jiang XR, Chen XC, Chen ZX, Li D, Lin JY, Tao QM. Seek protein which can interact with hepatitis B virus X protein from human liver cDNA library by yeast two-hybrid system. *World J Gastroenterol* 2002; **8**: 95-98
- 11 **Jin YM**, Yun C, Park C, Wang HJ, Cho H. Expression of hepatitis B Virus X protein is closely correlated with the high periportal inflammatory activity of liver diseases. *J Viral Hepat* 2001; **8**: 322-330
- 12 **Su F**, Schneider RJ. Hepatitis B virus HBx protein activates transcription factor NF-kappaB by acting on multiple cytoplasmic inhibitors of rel-related proteins. *J Virol* 1996; **70**: 4558-4566
- 13 **Guo SP**, Wang WL, Zhai YQ, Zhao YL. Expression of nuclear factor-kappa B in hepatocellular carcinoma and its relation with the X protein of hepatitis B virus. *World J Gastroenterol* 2001; **7**: 340-344
- 14 **Madden CR**, Slagle BL. Stimulation of cellular proliferation by hepatitis B virus X protein. *Dis Markers* 2001; **17**: 153-157
- 15 **Shin EC**, Shin JS, Park JH, Kim H, Kim SJ. Express of fas ligand in human hepatoma cell lines: role of hepatitis-B virus X (HBx) in induction of Fas ligand. *Int J Cancer* 1999; **82**: 587-591
- 16 **Wang XZ**, Chen XC, Chen YX, Zhang LJ, Li D, Chen FL, Chen ZX, Chen HY, Tao QM. Overexpression of HBxAg in hepatocellular carcinoma and its relationship with Fas/FasL system. *World J Gastroenterol* 2003; **9**: 2671-2675
- 17 **Terradillos O**, de La Coste A, Pollicino T, Neuveut C, Sitterlin D, Lecoerur H, Gougeon ML, Kahn A, Buendia MA. The hepatitis B virus X protein abrogates Bcl-2-mediated protection against Fas apoptosis in the liver. *Oncogene* 2002; **21**: 377-386
- 18 **Chen GG**, Lai PB, Chan PK, Chak EC, Yip JH, Ho RL, Leung BC, Lau WY. Decreased expression of Bid in human hepatocellular carcinoma is related to hepatitis B virus X protein. *Eur J Cancer* 2001; **37**: 1695-1702
- 19 **Gottlob K**, Fulco M, Levrero M, Graessmann A. The hepatitis B virus HBx protein inhibits caspase 3 activity. *J Biol Chem* 1998; **273**: 33347-33353
- 20 **Shih WL**, Kuo ML, Chuang SE, Cheng AL, Doong SL. Hepatitis B virus X protein inhibits transforming growth factor-beta-induced apoptosis through the activation of phosphatidylinositol 3-kinase pathway. *J Biol Chem* 2000; **275**: 25858-25864
- 21 **Sirma H**, Giannini C, Poussin K, Paterlini P, Kremesdorf D, Brechot

- C. Hepatitis B virus, X mutants, present in hepatocellular carcinoma tissue abrogate both the antiproliferative and transactivation effects of HBx. *Oncogene* 1999; **18**: 4848-4859
- 22 **Bergametti F**, Prigent S, Lubet B, Benoit A, Tiollais P, Sarasin A, Transy C. The proapoptotic effect of hepatitis B virus HBx protein correlates with its transactivation activity in stably transfected cell lines. *Oncogene* 1999; **18**: 2860-2871
- 23 **Terradillos O**, Pollicino T, Lecoeur H, Tripodi M, Gougeon ML, Tiollais P, Buendia MA. p53-independent apoptotic effects of the hepatitis B virus HBx protein *in vivo* and *in vitro*. *Oncogene* 1998; **17**: 2115-2123
- 24 **Kim H**, Lee H, Yun Y. X-gene product of hepatitis B virus induces apoptosis in liver cells. *J Biol Chem* 1998; **273**: 381-385
- 25 **Su F**, Schneider RJ. Hepatitis B virus HBx protein sensitizes cells to apoptotic killing by tumor necrosis factor α . *Proc Natl Acad Sci U S A* 1997; **94**: 8744-8749
- 26 **Chirillo P**, Pagano S, Natoli G, Puri PL, Burgio VL, Balsano C, Levrero M. The hepatitis B virus X gene induces p53-mediated programmed cell death. *Proc Natl Acad Sci U S A* 1997; **94**: 8162-8167
- 27 **Koike K**, Moriya K, Yotsuyanagi H, Shintani Y, Fujie H, Tsutsumi T, Kimura S. Compensatory apoptosis in preneoplastic liver of a transgenic mouse model for viral hepatocarcinogenesis. *Cancer Lett* 1998; **134**: 181-186
- 28 **Schuster R**, Gerlich WH, Schaefer S. Induction of apoptosis by the transactivating domains of the hepatitis B virus X gene leads to suppression of oncogenic transformation of primary rat embryo fibroblasts. *Oncogene* 2000; **19**: 1173-1180
- 29 **Kim YC**, Song KS, Yoon G, Nam MJ, Ryu WS. Activated ras oncogene collaborates with HBx gene of hepatitis B virus to transform cells by suppressing HBx-mediated apoptosis. *Oncogene* 2001; **20**: 16-23
- 30 **Tu H**, Bonura C, Giannini C, Mouly H, Soussan P, Kew M, Paterlini-Brechot P, Brechot C, Kremsdorf D. Biological impact of natural COOH-terminal deletions of hepatitis B virus X protein in hepatocellular carcinoma tissues. *Cancer Res* 2001; **61**: 7803-7810
- 31 **Takada S**, Shirakata Y, Kaneniwa N, Koike K. Association of hepatitis B virus X protein with mitochondria causes mitochondrial aggregation at the nuclear periphery, leading to cell death. *Oncogene* 1999; **18**: 6965-6973
- 32 **Bergametti F**, Prigent S, Lubet B, Benoit A, Tiollais P, Sarasin A, Transy C. The proapoptotic effect of hepatitis B virus HBx protein correlates with its transactivation activity in stably transfected cell lines. *Oncogene* 1999; **18**: 2860-2871
- 33 **Pollicino T**, Terradillos O, Lecoeur H, Gougeon ML, Buendia MA. Pro-apoptotic effect of the hepatitis B virus X gene. *Biomed Pharmacother* 1998; **52**: 363-368
- 34 **Su Q**, Schroder CH, Otto G, Bannasch P. Overexpression of p53 protein is not directly related to hepatitis B x protein expression and is associated with neoplastic progression in hepatocellular carcinomas rather than hepatic preneoplasia. *Mutat Res* 2000; **462**: 365-380
- 35 **Shirakata Y**, Koike K. Hepatitis B virus X protein induces cell death by causing loss of mitochondrial membrane potential. *J Biol Chem* 2003; **278**: 22071-22078

Edited by Gupta MK and Xu FM

Resistance index in differential diagnosis of liver lesions by color doppler ultrasonography

Yan Wang, Wen-Ping Wang, Hong Ding, Bei-Jian Huang, Feng Mao, Zhi-Zhang Xu

Yan Wang, Wen-Ping Wang, Hong Ding, Bei-Jian Huang, Feng Mao, Zhi-Zhang Xu, Department of Ultrasound, Zhongshan Hospital of Shanghai Fudan University, Shanghai 200032, China

Correspondence to: Yan Wang, Department of Function, the Second Affiliated Hospital of Hebei Medical University, Shijiazhuang 050000, Hebei Province, China

Received: 2003-06-10 **Accepted:** 2003-08-16

Abstract

AIM: To investigate the specific value of resistance index (RI) in color Doppler ultrasonography in the diagnosis of focal hepatic lesions.

METHODS: Eight hundred patients with 893 hepatic solid lesions were studied with color Doppler flow imaging (CDFI) and pulsed Doppler, including 644 malignant cases (596 primary malignant liver tumors, and 48 metastatic liver tumors), 156 benign cases. All were confirmed by operation and pathology.

RESULTS: The detection rate of arterial flow in malignant tumors was 92%, and 52% in benign lesions. Doppler spectrum analysis showed that the resistance index in primary malignant tumors was 0.75 ± 0.12 , 0.73 ± 0.09 in metastatic tumors, and was below 0.6 in benign lesions. The difference was significant ($P < 0.001$). This difference was related with its histopathologic structure.

CONCLUSION: The arterial flow with $RI \geq 0.6$ identified by CDFI within the liver lesion can be regarded as a criterion of malignant tumors, $RI < 0.6$ can be regarded as benign disorders. RI is useful in differential diagnosis of liver neoplasms.

Wang Y, Wang WP, Ding H, Huang BJ, Mao F, Xu ZZ. Resistance index in differential diagnosis of liver lesions by color doppler ultrasonography. *World J Gastroenterol* 2004; 10(7): 965-967 <http://www.wjgnet.com/1007-9327/10/965.asp>

INTRODUCTION

Extensive use of high resolution ultrasonography has led to the detection of a large number of small focal lesions in general practice. However, differential diagnosis of benign and malignant liver lesions may be difficult, even with clinical, biochemical data, and imaging techniques^[1,2]. Color Doppler flow imaging can provide information on blood flow, which is useful in the differential diagnosis of liver tumors^[3]. Our study was to develop a standard protocol of color Doppler ultrasound for liver tumor vascularization and to assess resistance index (RI) in the differential diagnosis of liver lesions.

MATERIALS AND METHODS

Materials

From 1992 to 2001, 800 patients with 893 hepatic solid lesions were studied (643 males, 157 females), their age ranged from 14-101 years (mean 50 years). The lesions included 644

malignancies (596 primary malignant liver tumors, and 48 metastatic liver tumors) and 156 benignancies. Primary malignant liver tumors included 564 hepatocellular carcinomas, 7 cholangiocarcinomas, and 12 mixed hepatocellular cholangiocarcinomas, 13 others. The benign lesions included 62 hepatic cavernous hemangiomas, 36 focal nodular hyperplasias, 14 hepatic angiomyolipomas, 11 inflammatory pseudotumors of liver, 11 cirrhotic nodules, 5 hepatic tuberculosis, 3 hepatic adenomas, 3 liver abscesses, 2 liver lipomas, 9 others. The lesion size ranged from 6-180 mm in diameter. The histological distribution and tumor size are shown in Table 1.

Table 1 Histopathological type and tumor size distribution of liver tumors

Histological type	Size (mm)			
	n (lesions)	<30	30-60	>60
Primary malignant tumor	596(651)	232	255	164
Metastatic tumor	48(57)	15	25	17
Hemangioma	62(86)	25	33	28
Fucal nodual hyperplasia	36(36)	19	16	1
Inflammatory pseudotumor	11(11)	6	5	
Angiomyolipoma	14(17)	3	10	4
Cirrhotic nodules	11(11)	9	2	
Tuberculosis	5(6)	4	2	
Adenoma	3(4)	1		3
Abscess	3(3)	1	2	
Lipoma	2(2)	1		1
Others	9(9)	2	5	2
Total	800(893)	316	357	220

Methods

For ultrasonic evaluation of hepatic lesions, high-resolution ultrasonography equipment Acuson 128/XP10.USA.) with a 3.5MHz vector transducer was used. To minimize the splanchnic vasomotor influences, all patients were fasted overnight before sonographic evaluation. After the morphological characteristics of the lesions were assessed by B mode, Color Doppler ultrasound was used to determine the distribution, intra-and/or peritumoral vessels, and pulsed Doppler was used to point the interested lesions. Echogenicity and vascularity of the lesions were determined by using a magnification mode (Res) that not only provided simple geometric magnification but also improved the spatial resolution in the area of interest.

To visualize the blood flow, standard color Doppler sonography was used for each lesion, and pulsed Doppler was optimized to detect the low flow components by diminishing pulse repetition frequencies, usually down to 500Hz and adapting frequency filters. The color gain was manipulated until noise began to exceed the homogeneous single color background of color Doppler scans. Within the lesions, pulsed Doppler samples were assessed whenever possible on the basis of pulsatile flow. Vascularity could be arterial or venous. At least three measurements of resistance index (RI) of intratumoral and peritumoral arterial blood flow would be the last mean value. Only those showing the highest SPV values obtained with pulsed Doppler were taken into account. For statistical analysis, one-way ANOVA and χ^2 test were used.

RESULTS

The 893 lesions were manifested as hyperechoic, hypoechoic or isoechoic masses with distinct or indistinct margins. In the real time ultrasonography, intra-and/or perilesional blood flow signals presented as pulsed or continuous activity, slow blood flow showed a single color, and fast flow showed mixed color signals. The pulsating wave of arterial flow in malignant tumors, appeared as linear color signals or branching, whereas in benign tumors, a constant spectrum of venous flow was shown as dots or patches.

Intratumoral and peritumoral arterial flow signals were obtained in 92% of the malignant tumors, and in 52% of benign lesions ($P < 0.01$). The detection rate of intratumoral and peritumoral arterial flow was 92.3% in primary malignant liver tumors, 87.7% in metastatic liver tumors, and 33.7% in hemangiomas. The detection rates of intratumoral and peritumoral arterial flow in different lesions are shown in Figure 1. The detection rates of intratumoral and peritumoral arterial flow signals in malignant tumors, including primary or metastatic tumors were much higher than those in benign tumors, except angiomyolipomas and focal nodular hyperplasias. Then RI was more helpful in differentiating the lesions having more arterial flow signals.

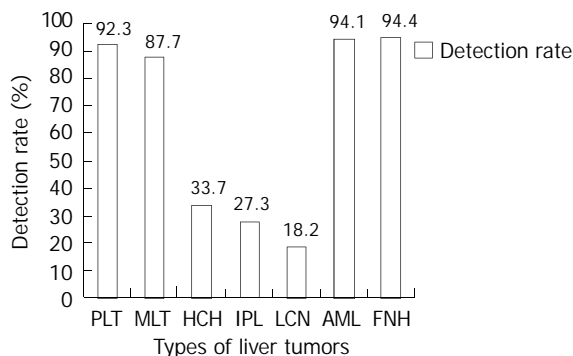


Figure 1 Detection rates of arterial blood flow in different types of liver tumors. PLT-primary liver tumor, MLT-metastatic liver tumor, HCH-hepatic cavernous hemangioma, IPL-inflammatory pseudotumor of liver, LCN-liver cirrhotic node, AML-angiomyolipoma, FNH-focal nodular hyperplasia.

The average value of RI in primary malignant liver tumors was 0.75 ± 0.12 and 0.73 ± 0.09 in metastatic tumors (the difference was not statistically significant, and so was it in different histologic types). It was significantly higher than that in benign ones. RI of hemangiomas was 0.55 ± 0.08 . The values of RI in different histological lesions are shown in Table 2. There were significant differences between malignant and benign tumors.

In our study we also found that the detection rates of intratumoral and/or peritumoral arterial flow signals and the value of RI in spectral analysis tended to be related to the tumor size, as arterial flow was easily detected in ≥ 2 cm lesions. The higher RI was mainly observed in smaller malignant tumors, but it decreased in larger tumors. The detection rates of arterial flow and the value of RI of vascular primary liver tumor (PLT) stratified by tumor size are shown in Table 3.

In our series, there were 50 lesions of PLT with no arterial flow signals. Most of them were hyperechoic masses, the size of 28 lesions was smaller than 30 mm. In 19 cases the position of the lesions was deeply located in the right posterior lobe. Eleven lesions near the diaphragm were interfered with the lung gas. Ten cases were in the left lateral lobe, 4 cases in the left medium lobe, 3 cases near the inferior vena cava (IVC), with interference of the heart beat. One case was necrosis, 2 cases were unable to control breath.

Table 2 RI in different histopathological lesions (mean \pm SD)

Histopathological type	RI range	RI means
Primary malignant tumor	0.34-1.0	0.75 ± 0.12^b
Metastatic tumor	0.57-1.0	0.73 ± 0.09^b
Hemangioma	0.45-0.77	0.55 ± 0.08
Focal nodular hyperplasia	0.41-0.79	0.58 ± 0.10
Angiomyolipoma	0.38-0.71	0.52 ± 0.14
Cirrhotic nodules	0.57-0.59	0.58 ± 0.01
Inflammatory pseudotumor	0.49-0.55	0.54 ± 0.05

^b $P < 0.001$ vs different groups.

Table 3 Detection rates of arterial flow and RI in primary liver malignant tumors, stratified by tumor size (mean \pm SD)

Diameter	<30(mm)	30-60(mm)	>60(mm)	P
Detection rates (%)	87.93 ^b (204/232)	93.3 ^b (238/255)	97 ^b (159/164)	<0.01
RI	0.77 ± 0.12^a	0.76 ± 0.11^a	0.71 ± 0.12^a	<0.05

^a $P < 0.05$, vs RI different datum groups, ^b $P < 0.01$ vs different rate groups.

DISCUSSION

The type of blood flow signal (arterial or venous) and its distribution detected by color and pulsed Doppler is more helpful in differential diagnosis. Our study showed that the presence of both intra-and peritumoral arterial flow was strongly suggestive of malignancy, whereas the presence of intratumoral venous flow was remarkably suggestive of benignancy^[4-7]. Intratumoral and peritumoral arterial flow signals were obtained in 92% of malignant tumors, but only in 52% of benign lesions. In the present study, with improvement of the equipment, we also found some arterial flow in some of the benign lesions, such as focal nodular hyperplasia (FNH) and angiomyolipoma (AML). How to differentiate them from malignant tumors remains a question. In our study, RI was more useful, combination of the type of signals and RI could significantly increase the accuracy of diagnosis. In 1997, Gonzalez-Anon *et al*^[8] evaluated these aspects and the distribution of tumoral vessels, and concluded that the type of signals (arterial or venous) and its distribution detected by color and pulsed Doppler was more helpful than the assessment of quantitative spectral parameters obtained by pulsed Doppler. Some researchers attempted to characterize tumors by quantitative spectral criteria only, and found that systolic peak velocity (SPV) was above 70 cm/s in 12 hepatocarcinomas in their series, the velocities differed significantly from those found in metastases and hemangiomas. Numata *et al*^[9] found that the mean of SPV in hepatocarcinomas was significantly higher than that of metastases, and hemangiomas. They also correlated the findings by Doppler angiography and hepatic pathology in both experimental animals and human beings, the high velocities of systolic peak was related with the presence of arterial venous shunts and the low resistant spectra were associated with vascular channels in the absence of muscle layer^[10]. Since then, many attempts have been made to assess the usefulness of Doppler in the study of liver tumors^[11]. Someda, *et al*^[12] found that the arteries supplying HCCs had lower PI and higher PSV. Some investigators found a remarkable overlap between the spectral values of metastases and primary carcinomas. Kamalov *et al*^[13] studied 128 lesions of primary and metastatic liver tumors, and found that the velocity and RI had no significance in differential diagnosis of tumors. In our experience, the value of SPV could usually be affected by the Doppler angle, but in most cases, the course

of tumor vessels could not be determined. So the mean of SPV varied greatly, and high SPV usually presented in larger tumors, and was not significant in the differentiation of small lesions. RI (resistance index=(Vsp-Ved)/Vsp) presents the resistance of distal vessels. It is not influenced by the Doppler angle. In 1991, Xu *et al* and Wang *et al* studied the value of RI in differentiation of liver tumors, and concluded that RI>0.5 was usually observed in malignant tumors, and RI<0.5 was found in the hemangiomas^[14,15]. In our further study, the statistical analysis of 800 patients also showed that RI in malignant tumors was significantly higher than that in benign tumors. The average value of RI in primary liver malignant tumors was 0.75±0.12, and 0.73±0.09 in metastatic tumors. They were much higher than that of benignancies. Pulsed Doppler spectrum analysis showed that the lesions without any signal during diastole or with diastolic reversal spectrum were all malignant. The mean value of RI in hemangiomas was 0.55±0.08. Furthermore, the larger the tumor size was, the more the arterial flow could be visualized. The detection rates of intratumoral and/or peritumoral arterial flow signals and the value of RI in spectral analysis tended to be related to the tumor size. High RI was mainly observed in smaller malignant nodules, but it decreased in larger malignant tumors. It is conceivable that several factors are involved such as histological pattern, pseudocapsular growth type, and absence of necrotic areas. These would contribute to the increase of vascular impedance in small tumors. Some angioarchitectural features may also contribute to the explanation of the peculiar hemodynamic pattern observed. The nodule comprises exclusively arterial tumoral vessels, and hepatocytes are arranged in trabeculae of varying thickness that may compress the interposed vascular space, producing multiple “stenoses”. Furthermore, the presence of pseudocapsules and cirrhotic parenchymas that usually surround HCCs might affect the venous outflow by compression of peritumoral portal branches. But in larger tumors (diameter>6 cm) with formation of A-V shunt and destruction of pseudocapsules, the value of RI tended to be lower.

In our series, combination of color Doppler flow imaging and RI was more helpful in differentiating malignant from benign tumors. Some of FNH, AML usually had more arterial flow just like malignant tumors, but they showed peculiar angioarchitectural features. FNH was characterized pathologically by cholangiolar proliferation associated with hyperplastic hepatocytes, blood vessels and fibrosis. AML was characterized pathologically by vessels with a thick muscle layer, showing more arterial flow signals like “blood ball”. They often showed high peak velocity and low impedance, RI was usually <0.6. In the other aspect, RI was more useful to differentiate some benign lesions with less blood flow such as inflammatory pseudotumors of liver and cirrhotic nodules. Inflammatory pseudotumors of liver had no blood flow or less peritumoral flow signals with RI<0.6. Cirrhotic nodules usually had venous intratumoral flow or less peritumor flow with RI<0.6.

The factors affecting RI in the diagnosis of liver lesions include: (1) sensitivity of the equipment. The difference in findings of flow is presumably due to the sensitivity of the equipment used for Doppler frequency shifts. Thus even lower and finer blood flows can probably be visualized if newer instruments are developed. (2) Management of the equipment. To visualize blood flow, pulsed Doppler is optimized to detect even low flow components by deminishing pulse repetition frequencies, usually down to 500Hz and adapting frequency filters. (3) Color imaging of blood flow is insufficient when the tumor is located deep within in the liver. (4) Tumor size. It is difficult to visualize when tumor size is less than 2 cm with deep location or near the diaphragm. (5) Cirrhotic parenchyma of the liver usually causes acoustic attenuation. (6) The angle of Doppler can affect the sensitivity of CDFI.

We should notice that the lesion without blood flow signals is presumably due to the angioarchitectural features or the above factors. In our series, most of malignant tumors without blood flow were usually smaller than 3 cm, and deeply located in the right posterior lobe of the liver or near the diaphragm, or located in the left lateral lobe with interference of the lung gas and the heart beating.

In conclusion, the type of flow signals (arterial and/or venous) and its distribution in CDFI and pulsed Doppler are helpful in differentiating benign from malignant lesions. The presence of intratumoral venous flow is strongly suggestive of benign tumors. When intra-and/or peritumoral arterial blood flow is found, RI<0.6 would strongly suggest a benign tumor. Simultaneous occurrence of both intra-and peritumoral arterial flow and RI≥0.6 would strongly suggest malignancies. So that combined studies of the type of intra-and peritumoral flow signals in CDFI and the parameter of RI would be more helpful in differential diagnosis of benign and malignant liver tumors.

REFERENCES

- 1 **Furuse J**, Iwasaki M, Yoshino M, Konishi M, Kawano N, Kinoshita T, Ryu M. Evaluation of blood flow signal in small hepatic nodules by color Doppler ultrasonography. *Jpn J Clin Oncol* 1996; **26**: 335-340
- 2 **Perkins AB**, Imam K, Smith WJ, Cronan JJ. Color and power Doppler sonography of liver hemangiomas: a dream unfulfilled? *J Clin Ultrasound* 2000; **28**: 159-165
- 3 **Tanaka S**, Kitamura T, Fujita M, Nakanishi K, Okuda S. Color Doppler flow imaging of liver tumors. *Am J Roentgenol* 1990; **154**: 509-514
- 4 **Ralls PW**, Johnson MB, Lee KP, Radin DR, Halls J. Color Doppler sonography in hepatocellular carcinoma. *Am J Physiol Imaging* 1991; **6**: 57-61
- 5 **Srivastava DN**, Mahajan A, Berry M, Sharma MP. Color Doppler flow imaging of focal hepatic lesions. *Australas Radiol* 2000; **44**: 285-289
- 6 **Tang J**. Color Doppler flow imaging and duplex Doppler in the examination of primary liver cancer. *Zhonghua Zhongliu Zazhi* 1992; **14**: 138-140
- 7 **Nino-Murcia M**, Ralls PW, Jeffrey RB Jr, Johnson M. Color flow Doppler characterization of focal hepatic lesions. *Am J Roentgenol* 1992; **159**: 1195-1197
- 8 **Gonzalez-Anon M**, Cervera-Deval J, Garcia-Vila JH, Bordon-Ferre F, Ambit-Capdevila S, Piqueras-Olmeda R, Jornet-Fayos J, Gil-Sanchez S, Marco-Domenech SF, Cortes-Vizcaino V. Characterization of solid liver lesions with color and pulsed Doppler imaging. *Abdom Imaging* 1999; **24**: 137-143
- 9 **Numata K**, Tanaka K, Kiba T, Morimoto M, Arata S, Kondo M, Sekihara H. Use of hepatic tumor index on color Doppler sonography for differentiating large hepatic tumors. *Am J Roentgenol* 1997; **168**: 991-995
- 10 **Numata K**, Tanaka K, Mitsui K, Morimoto M, Inoue S, Yonezawa H. Flow characteristics of hepatic tumors at color Doppler sonography: correlation with arteriographic findings. *Am J Roentgenol* 1993; **160**: 515-521
- 11 **Uggowitzer M**, Kugler C, Machan L, Groll R, Stauber R, Mischinger HJ, Ratschek M, Fortter R. Power Doppler imaging and evaluation of the resistive index in focal nodular hyperplasia of the liver. *Abdom Imaging* 1997; **22**: 268-273
- 12 **Someda H**, Moriyasu F, Hamato N, Fujimoto M, Okuma M. Change in hepatic arterial hemodynamics induced by hepatocellular carcinoma detected with Doppler sonography. *J Clin Ultrasound* 1997; **25**: 359-365
- 13 **Kamalov IR**, Sandrikov VA, Gautier SV, Tsrulnikova OM, Skipenko OG. The significance of color velocity and spectral Doppler ultrasound in the differentiation of liver tumors. *Eur J Ultrasound* 1998; **7**: 101-108
- 14 **Wang WP**, Xu ZZ, Shen SC. Combined color Doppler and pulsed Doppler in the diagnosis of small hepatocellular carcinomas. *Zhonghua Waike Zazhi* 1994; **32**: 474-476
- 15 **Xu ZZ**, Wang WP. Application of ultrasonic Doppler in the diagnosis of the hepatic solid space-occupying lesions. *Zhonghua Wuli Yixue Zazhi* 1991; **13**: 65-69

Effect of SEN virus coinfection on outcome of lamivudine therapy in patients with hepatitis B

Dong Xu, De-Ying Tian, Zhen-Gang Zhang, Hong-Yun Chen, Pei-Hui Song

Dong Xu, De-Ying Tian, Zhen-Gang Zhang, Hong-Yun Chen, Pei-Hui Song, Department of Infectious Diseases, Tongji Hospital, Tongji Medical College, Huazhong University of Science and Technology, Wuhan 430030, Hubei Province, China

Supported by the Science and Technology Commission Foundation of Hubei Province, No. 2002AA301C32

Correspondence to: Dr. De-Ying Tian, Department of Infectious Diseases, Tongji Hospital, Tongji Medical College, Huazhong University of Science and Technology, Jiefang Street 1095, Wuhan 430030, Hubei Province, China. xudongtj@tom.com

Telephone: +86-27-83662815 **Fax:** +86-27-83613408

Received: 2003-06-06 **Accepted:** 2003-07-30

Abstract

AIM: Interactions between hepatitis B virus (HBV) and other viral hepatitis infections are well known, whether the newly discovered SEN virus (SENV) has any effect on lamivudine antiHBV activity is unclear. Our aim was to clarify the effect on treatment outcome of coinfection with SENV virus in patients with hepatitis B during lamivudine therapy.

METHODS: Nested polymerase chain reaction (PCR) amplification was used to detect SENV-D and SENV-H strains in serum from 45 patients with chronic hepatitis B treated with lamivudine 100 mg daily for 12 mo. HBV DNA load was detected with fluorescence quantitative PCR (FQ-PCR) and YMDD (tyrosine, methionine, aspartate, aspartate) motif mutation of HBV DNA was investigated with cDNA microarray.

RESULTS: SENV DNA was detected in 5 of 45(11.1%) cases after 12 mo they received lamivudine treatment. SENV-D and SENV-H were 4.4% and 6.7% respectively. HBV DNA failed to respond to lamivudine therapy in 4 of 5 SENV coinfecting patients while only 10 of 40 patients became SENV positive and the difference was statistically significant. Response of ALT and HBeAg to lamivudine had no significant difference between coinfection patients and single HBV infection ones.

CONCLUSION: Coinfection with SEN virus in chronic hepatitis B patients may adversely affect the outcome of lamivudine treatment.

Xu D, Tian DY, Zhang ZG, Chen HY, Song PH. Effect of SEN virus coinfection on outcome of lamivudine therapy in patients with hepatitis B. *World J Gastroenterol* 2004; 10(7): 968-971 <http://www.wjgnet.com/1007-9327/10/968.asp>

INTRODUCTION

A new DNA virus with approximately 3 800 nucleotides, referred to as SEN virus (SENV), has been isolated in blood of a human immunodeficiency virus (HIV)-infected injection drug user (IDU)^[1,2]. Phylogenetic analysis showed that 8 strains of SENV were members of the circoviridae family, a group of

small, single-strand, nonenveloped circular DNA virus that includes TT virus (TTV), TUS01, SANBAN and YONBAN^[3-6]. Although structurally similar to TTV, SENV has less than 55% sequence homology and less than 37% amino acid homology with the TTV prototype^[2]. A strong association between two SENV variants (SENV-D and SENV-H) infections and transfusion-associated non-A to E hepatitis has been reported^[7]. SENV-D and SENV-H have been extensively studied, they were found to be present in approximately 2% of Americans and 20% of Japanese blood donors, and could be readily transmitted by blood transfusion and other common parenteral routes^[8]. However, the association of SENV infection with liver cell damage remains controversial^[9]. Furthermore, several recent studies have shown that persons with SENV-D/H infection alone or coinfecting with HBV or HCV had no evidence of liver disease^[10-14].

Chronic liver diseases are common in China, most of them can be attributed to infection with hepatitis B virus (HBV) or hepatitis C virus (HCV)^[15-21]. Although GB virus and TT virus (TTV) have been claimed to be prevalent in chronic liver disease patients in our previous study and other researches, most studies have indicated that neither virus causes liver diseases^[22-25]. Taking advantage of the frequency of SENV-D/H coinfection in cases of chronic hepatitis and transient elevations of alanine aminotransferase observed in babies following transmission of SENV from mothers^[8,26], the preliminary observation of clinical relevance of SENV infection alone or in combination with HBV or HCV infection needs to be independently confirmed in larger numbers of patients and in different areas.

A research letter appeared in *Lancet* by Basil Rigas and colleagues suggests that coinfection with SEN virus in hepatitis C patients (HC) may adversely affect the outcome of antiviral therapy with interferon and ribavirin^[27]. On the contrary, another result indicated coinfection with SENV did not affect the clinical/pathological features of chronic hepatitis C and response to combination therapy^[28]. These conflicting interpretations may reflect the difference in patient selection and sample size. Since coinfection of hepatitis B virus (HBV) and SEN virus is common^[10,26], the precise role of SEN virus in chronic hepatitis B patients remains to be determined. Our aim was to provide the initial the evidence whether SENV coinfection affected the outcome of lamivudine therapy in patients with hepatitis B.

MATERIALS AND METHODS

Subjects

From Sept 2001 to July 2002, serum samples were obtained from 45 patients treated with lamivudine 100 mg daily in Hubei province. All patients were excluded infection of hepatitis viruses A, C, D, E, and TTV, HGV, HIV. These serum samples were stored at -70 °C. Hepatitis B virus infection was confirmed by enzyme-linked immunosorbent assay (ELISA, second-generation). Commercially available ELISAs were used for immunoglobulin M (IgM) antibodies to hepatitis A virus, hepatitis B surface antigen (HBsAg) and e antigen (HBeAg), antibodies to hepatitis B core antigen (HBcAb) and e antigen

(HBeAb), hepatitis D virus, hepatitis E virus TTV, HGV and HIV. Serum HBV DNA levels was quantified using the hepatitis virus B nucleic acid amplification fluorescence Kit according to manufactures instructions (DA AN Gene Co. Ltd, Zhongshan University). The detection limit of this assay is 10^3 copies/ml^[29].

Detection of SEN-V DNA by polymerase chain reaction

DNA was extracted from 50 µL of serum using Acupure DNA/RNA kit (Inc Biotronics, USA). PCR amplification was performed using primers specific for ORF1 region. Two common external primers were used. They were sense primer: 5' -TACCCCAACGACCAACTACGC-3', antisense primer: 5' -GTTTGTGGTGAGCAGAACGGAA-3'. Inner primers for SENV-D were sense primer: 5' -TAAGCAGCCCTAACAC TCATCCA-3', antisense primer: 5' -CAGTTGACCGCAAAG TTACAAG-3'. Inner primers for SENV-H were sense primer: 5' -ATACTTTGGCTGCACCTTCTG-3', antisense primer: 5' -CCAACTGACTAGGGGAACCTTA-3'. The first-round PCR amplification was carried out in a volume of 30 µL including 3 µL of DNA extraction product, 1×PCR buffer (Promega), 1.5 mmol/L MgCl₂, 100 pmoles of each sense and antisense external primers, 20 mmol/L each dNTP and 1U Taq DNA polymerase (Promega). PCR was performed for 30 cycles at 94 °C for 45 s, at 55 °C for 45 s, at 72 °C for 50 s. Two microliter of the first PCR product was subjected to a second amplification for 30 cycles under the same condition as for the first PCR, using sense and antisense inner primers. The amplified products were visualized by 20 g/L agarose gel electrophoresis and ethidium bromide stained. The amplified DNA was directly sequenced by the BigDye terminator kit (Bioasia Biotechnology Ltd) using the ABI 377 sequencer.

DNA microarray analysis

HBV YMDD mutation chip was provided by Shanghai Institute of Microsystem and Information Technology and Ruixin Biotechnology Ltd. The probes on the chip were labeled with digoxigenin-dUTP for color detection with NBT/BCIP. HBV DNA extracted from 50 µL of serum was amplified with PCR. The PCR products were denatured respectively in a 95 °C bath for 5 min, then added on the chip. They were hybridized in a sealed chamber at 42 °C for 30 min and washed in turn with solutions of 2×SSC + 2 g/L SDS, 0.1×SSC + 2 g/L SDS and 1 g/L SSC for 10 min each, then dried at room temperature. The hybridization was detected with anti-digoxigenin-AP Fab fragments and visualized with the colorimetric substrate NBT/BCIP.

Data statistics

Data were analyzed by Fisher's exact test, χ^2 test with Yate's correction, or Student's *t* test. A *P* value <0.05 was considered statistically significant.

RESULTS

Prevalence of SENV-DNA

SENV DNA was detected in 5 of 45 patients (11.1%) with chronic hepatitis B after 12 mo they received lamivudine treatment. Of the 5 patients with SENV coinfection, 2 (4.4%) were infected with SENV-D and 3 (6.7%) with SENV-H.

Association of SENV with severity of liver disease

Of the 45 patients received lamivudine treatment 100 mg daily, 1 had abnormal serum alanine transaminase (ALT) (>45 IU/L) among 5 cases of SENV infection and 8 had no SENV infection among 40 cases of SENV infection. The ALT level between patients with and without SENV coinfection was

not statistically significant (42.0±19.9 U/L vs 39.2±35.8 U/L, *t*=0.174, *P*=0.863) (Table 1).

Table 1 Association of SENV with severity of liver disease

	Normal ALT (n)	Abnormal ALT (n)	Total
SENV DNA P	4	1	5
SENV DNA N	32	8	40

Abbreviations: *P*, positive; *N*, negative.

Association of SENV with HBeAg response to lamivudine treatment

None of the 5 patients coinfecting with SENV had HBeAg seroconversion or HBeAg loss, and 4 of 40 patients without SENV coinfection had HBeAg seroconversion or HBeAg loss. There was no significant difference between patients with SENV infection and those without SENV coinfection in HBeAg seroconversion ($\chi^2=0.549$, *P*=0.459).

Table 2 Association of SENV with HBeAg response to lamivudine treatment

	HBeAg P (n)	HBeAg N (n)	Total
SENV-DNA P	5	0	5
SENV-DNA N	36	4	40

Abbreviations: *P*, positive; *N*, negative.

Association of SENV with HBV DNA response to lamivudine treatment

Only one of the 5 patients coinfecting with SENV responded to lamivudine treatment in terms of HBV DNA, while 30 of the 40 patients infected with HBV alone responded to the treatment of lamivudine. The difference was statistically significant ($\chi^2=3.97$, *P*=0.046). Although the baseline mean of serum HBV DNA level in the patients coinfecting with SENV was higher than that in those without SENV infection (5.50±0.47 vs 4.98±0.75), the difference was not statistically significant (*t*=1.246, *P*=0.236).

Table 3 Effect of lamivudine treatment on patients with SENV coinfection

	HBV DNA positive patients (n)	Mean Log ₁₀ HBV DNA (copies/mL)	HBV DNA negative patients(n)
SENV DNA Positive	4	5.50±0.47	1
SENV DNA Negative	10	4.98±0.75	30

Abbreviations: *P*, positive; *N*, negative.

Table 4 Clinical features of 5 patients with SENV infection

Patient	Sex (M/F)	Age (yr)	ALT (IU/L)	HBeAg	HBV DNA	YMDD motif
SENV-D1	M	24	25	P	P	YMDD
SENV-D2	M	34	96	P	P	YIDD
SENV-H1	M	27	38	P	P	YMDD
SENV-H2	M	29	17	P	N	
SENV-H3	M	19	29	P	P	YVDD

Abbreviations: *P*, positive; *N*, negative; *M*, male.

Clinical features of 5 patients with SENV infection

Of the 14 HBV DNA positive patients, 2 had YMDD mutation in 4 patients with SENV coinfection and 5 had YMDD

mutation in 10 patients with HBV infection alone. One was YIDD mutant and the other was YVDD mutant in 4 coinfecting patients, 3 were YVDD mutants and 2 were YIDD mutants in 10 HBV infected alone patients. Lamivudine resistant mutation (YMDD mutate to YIDD or YVDD) had no significant difference in SENV coinfecting group and HBV infected alone group ($\chi^2=0.35$, $P=0.72$).

DISCUSSION

Recent studies indicated that SENV-D/H infections occurred more often in high-risk groups (54-90%), patients with chronic hepatitis B (41%), HBV-related hepatocellular carcinoma (HCC) (54%), chronic hepatitis C (67%), and HCV-related HCC (76%) than in healthy adults (15%)^[10]. Although most subjects with SENV-D/H infection alone had no hepatitis or mild hepatitis^[13,30-32], an association of SENV-D/H with transfusion-associated hepatitis has been reported^[7]. Whether SENV-D/H serves as causative agents of non-A and non-E hepatitis remains controversial^[7,12,30].

Coinfection with HBV and hepatitis D virus has been reported to be associated with severe and rapidly progressive liver diseases^[33]. The clinical manifestations of patients with HBV/HCV coinfection seemed mild and occult. Additionally, it was shown that HBV could inhibit HCV replication, but no evidence that HCV could suppress HBV replication was found in the data^[34]. In contrast, another study showed that acute superinfection in patients with chronic hepatitis might increase the risk of severe hepatitis, suggesting that HBV as a newcomer might suppress pre-existing HCV^[35]. Together with the earlier observation that acute HCV superinfection suppressed pre-existing HBV, it seemed that the time or sequence of infection was a factor influencing the outcome of viral interactions. Newly published issue indicated that infections with HCV plus other hepatitis viruses might exacerbate the pathological lesion of the liver^[36]. Interactions between two specific viruses need to be determined. Our data showed the ALT level (42.0 ± 19.9 U/L vs 39.2 ± 35.8 U/L) between patients with or without SENV coinfection was not statistically significant, so did HBeAg response to lamivudine antiviral treatment. These data suggested that SENV had limited or no hepatic pathogenicity, which was consistent with the previous observation that the vast majority of SENV-infected hemodialysis patients did not develop hepatitis^[37].

The clinical relevance of SENV infection alone or in combination with HBV remains controversial. Whether SENV affects other virus replication needs to be determined. In our study, the baseline mean of serum HBV DNA level in the patients coinfecting with SENV was higher than that in those without SENV infection (5.50 ± 0.47 vs 4.98 ± 0.75), the difference was not statistically significant. However, the lamivudine antiviral response rate of HBV DNA was lower in patients coinfecting with SENV infection than those without (20% vs 75%), and the result indicated that coinfection with SEN virus in chronic hepatitis B patients might adversely affect the outcome of lamivudine treatment. In patients with chronic hepatitis C infection after interferon plus ribavirin therapy in another study, serum HCV level in patients coinfecting with SENV was not significantly lower than that in patients without SENV infection, but HCV genotype 2a was more often found among patients with HCV and SENV coinfection than among those with HCV infection alone, suggesting that there was a specific link between SENV and HCV genotype 2a^[28].

Recent registration of lamivudine, a dideoxycytidine analogue that inhibits HBV reverse transcriptases, has provided new perspectives for the treatment of chronic HBV infection^[38,39]. Mutation of methionine to valine or isoleucine at the YMDD motif of HBV reverse transcriptase has been shown to be

responsible for lamivudine resistance in HBV^[40,41]. HBV precore stop mutant was increased in the first stage following acute superinfection of HCV and then decreased in the later stage^[42]. The observation raised the possibility of a limit relation of HBV mutant to coinfecting virus in different stages of coinfection. Whether YMDD mutant has an association with SENV coinfection is unknown. No significant association was observed between SENV and HBV YMDD mutations during lamivudine treatment in our present study.

Coinfection with SENV might adversely affect the outcome of lamivudine treatment. It is not surprising that infection of the liver with more than one virus might render it resistant to antiviral therapy. Indeed, coinfection with HBV, either HDV or HIV, could predict the unfavourable outcome of antiviral treatment compared with those infected with HBV only^[43], but TTV coinfection did not influence the outcome of long-term lamivudine therapy on hepatitis B^[44], so did interferon therapy on chronic hepatitis B or C^[45]. Thus, further studies need to address this important and interesting issue.

In summary, coinfection with SENV in chronic hepatitis B in Wuhan area might adversely affect the outcome of lamivudine treatment. SENV should be detected when HBV DNA fails to respond to lamivudine treatment for HBV infected patients.

ACKNOWLEDGEMENTS

We thank Dr. Chen-Hui Huang, Third Hospital, Zhongshan University for providing SEN virus primers, Drs. Yu-Hu Song and Hao-Yi Yang, Tongji Hospital, Tongji Medical College, Huazhong University of Science and Technology.

REFERENCES

- 1 **Tanaka Y**, Primi D, Wang RY, Umemura T, Yeo AE, Mizokami M, Alter HJ, Shih JW. Genomic and molecular evolutionary analysis of a newly identified infectious agent (SEN virus) and its relationship to the TT virus family. *J Infect Dis* 2001; **183**: 359-367
- 2 **Fiordalisi G**, Bonelli M, Olivero P, Primi D, Vaglini L, Mattioli S, Bonelli F, Dal CA, Mantero GL, Sottini A. Identification of SENV genotypes. International patent number WO0028039 (international application published under the patent cooperation treaty). Internet address: <http://epcspacenet.com/>
- 3 **Nishizawa T**, Okamoto H, Konishi K, Yoshizawa H, Miyakawa Y, Mayumi M. A novel DNA virus (TTV) associated with elevated transaminase levels in posttransfusion hepatitis of unknown etiology. *Biochem Biophys Res Commun* 1997; **241**: 92-97
- 4 **Okamoto H**, Takahashi M, Nishizawa T, Ukita M, Fukuda M, Tsuda F, Miyakawa Y, Mayumi M. Marked genomic heterogeneity and frequent mixed infection of TT virus demonstrated by PCR with primers from coding and noncoding regions. *Virology* 1999; **259**: 428-436
- 5 **Hijikata M**, Takahashi K, Mishiro S. Complete circular DNA genome of a TT virus variant (isolate name SANBAN) and 44 partial ORF2 sequences implicating a great degree of diversity beyond genotypes. *Virology* 1999; **260**: 17-22
- 6 **Takahashi K**, Hijikata M, Samokhvalov EI, Mishiro S. Full or near full length nucleotide sequences of TT virus variants (Types SANBAN and YONBAN) and the TT virus-like mini virus. *Intervirology* 2000; **43**: 119-123
- 7 **Umemura T**, Yeo AE, Sottini A, Moratto D, Tanaka Y, Wang RY, Shih JW, Donahue P, Primi D, Alter HJ. SEN virus infection and its relationship to transfusion-associated hepatitis. *Hepatology* 2001; **33**: 1303-1311
- 8 **Pirovano S**, Bellinzoni M, Ballerini C, Cariani E, Duse M, Albertini A, Imberti L. Transmission of SEN virus from mothers to their babies. *J Med Virol* 2002; **66**: 421-427
- 9 **Wilson LE**, Umemura T, Astemborski J, Ray SC, Alter HJ, Strathdee SA, Vlahov D, Thomas DL. Dynamics of SEN virus infection among injection drug users. *J Infect Dis* 2001; **184**: 1315-1319
- 10 **Kao JH**, Chen W, Chen PJ, Lai MY, Chen DS. Prevalence and implication of a newly identified infectious agent (SEN virus) in Taiwan. *J Infect Dis* 2002; **185**: 389-392

- 11 **Yoshida EM**, Buczkowski AK, Giulivi A, Zou S, Forrester LA. A cross-sectional study of SEN virus in liver transplant recipients. *Liver Transpl* 2001; **7**: 521-525
- 12 **Shibata M**, Wang RY, Yoshida M, Shih JW, Alter HJ, Mitamura K. The presence of a newly identified infectious agent (SEN virus) in patients with liver diseases and in blood donors in Japan. *J Infect Dis* 2001; **184**: 400-404
- 13 **Mikuni M**, Moriyama M, Tanaka N, Abe K, Arakawa Y. SEN virus infection does not affect the progression of non-A to -E liver disease. *J Med Virol* 2002; **67**: 624-629
- 14 **Yoshida H**, Kato N, Shiratori Y, Shao R, Wang Y, Shiina S, Omata M. Weak association between SEN virus viremia and liver disease. *J Clin Microbiol* 2002; **40**: 3140-3145
- 15 **Fan CL**, Wei L, Jiang D, Chen HS, Gao Y, Li RB, Wang Y. Spontaneous viral clearance after 6-21 years of hepatitis B and C viruses coinfection in high HBV endemic area. *World J Gastroenterol* 2003; **9**: 2012-2016
- 16 **Wang FS**. Current status and prospects of studies on human genetic alleles associated with hepatitis B virus infection. *World J Gastroenterol* 2003; **9**: 641-644
- 17 **Hou CS**, Wang GQ, Lu SL, Yue B, Li MR, Wang XY, Yu JW. Role of activation-induced cell death in pathogenesis of patients with chronic hepatitis B. *World J Gastroenterol* 2003; **9**: 2356-2358
- 18 **Qin LX**, Tang ZY. The prognostic significance of clinical and pathological features in hepatocellular carcinoma. *World J Gastroenterol* 2002; **8**: 193-199
- 19 **He QQ**, Cheng RX, Sun Y, Feng DY, Chen ZC, Zheng H. Hepatocyte transformation and tumor development induced by hepatitis C virus NS3 c-terminal deleted protein. *World J Gastroenterol* 2003; **9**: 474-478
- 20 **Li K**, Wang L, Cheng J, Lu YY, Zhang LX, Mu JS, Hong Y, Liu Y, Duan HJ, Wang G, Li L, Chen JM. Interaction between hepatitis C virus core protein and translin protein—a possible molecular mechanism for hepatocellular carcinoma and lymphoma caused by hepatitis C virus. *World J Gastroenterol* 2003; **9**: 300-303
- 21 **Wu CH**, Ouyang EC, Walton C, Promrat K, Forouhar F, Wu GY. Hepatitis B virus infection of transplanted human hepatocytes causes a biochemical and histological hepatitis in immunocompetent rats. *World J Gastroenterol* 2003; **9**: 978-983
- 22 **Tian DY**, Yang DF, Xia NS, Zhang ZG, Lei HB, Huang YC. The serological prevalence and risk factor analysis of hepatitis G virus infection in Hubei Province of China. *World J Gastroenterol* 2000; **6**: 585-587
- 23 **Jeon MJ**, Shin JH, Suh SP, Lim YC, Ryang DW. TT virus and hepatitis G virus infections in Korean blood donors and patients with chronic liver disease. *World J Gastroenterol* 2003; **9**: 741-744
- 24 **Hu ZJ**, Lang ZW, Zhou YS, Yan HP, Huang DZ, Chen WR, Luo ZX. Clinicopathological study on TTV infection in hepatitis of unknown etiology. *World J Gastroenterol* 2002; **8**: 288-293
- 25 **Zhu WF**, Yin LM, Li P, Huang J, Zhuang H. Pathogenicity of GB virus C on virus hepatitis and hemodialysis patients. *World J Gastroenterol* 2003; **9**: 1739-1742
- 26 **Chemini I**, Parana R, Trepo C. A new viral agent, SEN virus (SENV), has been detected in patients from several countries: the pathogenic role of SENV in coinfections with hepatitis B virus or hepatitis C virus should be investigated. *J Infect Dis* 2002; **185**: 710
- 27 **Rigas B**, Hasan I, Rehman R, Donahue P, Wittkowski KM, Lebovics E. Effect on treatment outcome of coinfection with SEN viruses in patients with hepatitis C. *Lancet* 2001; **358**: 1961-1962
- 28 **Kao JH**, Chen W, Chen PJ, Lai MY, Chen DS. SEN virus infection in patients with chronic hepatitis C: preferential coinfection with hepatitis C genotype 2a and no effect on response to therapy with interferon plus ribavirin. *J Infect Dis* 2003; **187**: 307-310
- 29 **Li G**, Shu X, Ma HH, Chen W, Chen WS, Chen Q, Jiang YS, Yao JL. Detection of HBV, HCV and HBV YMDD mutants by DNA microarray. *Shijie Huaren Xiaohua Zazhi* 2003; **11**: 178-181
- 30 **Wong SG**, Primi D, Kojima H, Sottini A, Giulivi A, Zhang M, Uhanova J, Minuk GY. Insights into SEN virus prevalence, transmission, and treatment in community-based persons and patients with liver disease referred to a liver disease unit. *Clin Infect Dis* 2002; **35**: 789-795
- 31 **Tangkijvanich P**, Theamboonlers A, Sriponthong M, Thong-Ngam D, Kullavanijaya P, Poovorawan Y. SEN virus infection in patients with chronic liver disease and hepatocellular carcinoma in Thailand. *J Gastroenterol* 2003; **38**: 142-148
- 32 **Kobayashi N**, Tanaka E, Umemura T, Matsumoto A, Iijima T, Higuchi M, Hora K, Kiyosawa K. Clinical significance of SEN virus infection in patients on maintenance haemodialysis. *Nephrol Dial Transplant* 2003; **18**: 348-352
- 33 **Jardi R**, Rodriguez F, Buti M, Costa X, Cotrina M, Galimany R, Esteban R, Guardia J. Role of hepatitis B, C, and D viruses in dual and triple infection: influence of viral genotypes and hepatitis B precore and basal core promoter mutations on viral replicative interference. *Hepatology* 2001; **34**: 404-410
- 34 **Fan CL**, Wei L, Jiang D, Chen HS, Gao Y, Li RB, Fei R, Ji Y, Zhu L, Wang Y. Clinical and virological course of dual infection by hepatitis B and C viruses in China. *Zhonghua Yixue Zazhi* 2003; **83**: 1214-1218
- 35 **Liaw YF**, Yeh CT, Tsai SL. Impact of acute hepatitis B virus superinfection on chronic hepatitis C virus infection. *Am J Gastroenterol* 2000; **95**: 2978-2980
- 36 **Chen YD**, Liu MY, Yu WL, Li JQ, Dai Q, Zhou ZQ, Tisminetzky SG. Mix-infections with different genotypes of HCV and with HCV plus other hepatitis viruses in patients with hepatitis C in China. *World J Gastroenterol* 2003; **9**: 984-992
- 37 **Schroter M**, Laufs R, Zollner B, Knodler B, Schafer P, Feucht HH. A novel DNA virus (SEN) among patients on maintenance hemodialysis: prevalence and clinical importance. *J Clin Virol* 2003; **27**: 69-73
- 38 **Chang CN**, Skalski V, Zhou JH, Cheng YC. Biochemical pharmacology of (+)- and (-)-2', 3' -dideoxy-3' -thiacytidine as anti-hepatitis B virus agents. *J Biol Chem* 1992; **267**: 22414-22420
- 39 **Jaboli MF**, Fabbri C, Liva S, Azzaroli F, Nigro G, Giovanelli S, Ferrara F, Miracolo A, Marchetto S, Montagnani M, Colecchia A, Festi D, Reggiani LB, Roda E, Mazzella G. Long-term alpha interferon and lamivudine combination therapy in non-responder patients with anti-HBe-positive chronic hepatitis B: Results of an open, controlled trial. *World J Gastroenterol* 2003; **9**: 1491-1495
- 40 **Tipples GA**, Ma MM, Fischer KP, Bain VG, Kneteman NM, Tyrrell DL. Mutation in HBV RNA-dependent DNA polymerase confers resistance to lamivudine *in vivo*. *Hepatology* 1996; **24**: 714-717
- 41 **Bai YJ**, Zhao JR, Lv GT, Zhang WH, Wang Y, Yan XJ. Rapid and high throughput detection of HBV YMDD mutants with fluorescence polarization. *World J Gastroenterol* 2003; **9**: 2344-2347
- 42 **Yeh CT**, Chu CM, Liaw YF. Progression of the proportion of hepatitis B virus precore stop mutant following acute superinfection of hepatitis C. *J Gastroenterol Hepatol* 1998; **13**: 131-136
- 43 **Torresi J**, Locarnini S. Antiviral chemotherapy for the treatment of hepatitis B virus infections. *Gastroenterology* 2000; **118**: S83-103
- 44 **Garcia JM**, Marugan RB, Garcia GM, Lindeman MLM, Abete JF, del Campo Terron S. TT virus infection in patients with chronic hepatitis B and response of TTV to lamivudine. *World J Gastroenterol* 2003; **9**: 1261-1264
- 45 **Lai YC**, Hu RT, Yang SS, Wu CH. Coinfection of TT virus and response to interferon therapy in patients with chronic hepatitis B or C. *World J Gastroenterol* 2002; **8**: 567-570

Sequential changes of serum ferritin levels and their clinical significance in lamivudine-treated patients with chronic viral hepatitis B

Zheng-Wen Liu, Qun-Ying Han, Ni Zhang, Wen Kang

Zheng-Wen Liu, Qun-Ying Han, Ni Zhang, Wen Kang,
Department of Infectious Diseases, First Hospital, Xi'an Jiaotong University, Xi'an, 710061, Shaanxi Province, China

Supported by Key Programs on Science and Technology of Shaanxi Province, No.2000K14-G16

Correspondence to: Zheng-Wen Liu, Department of Infectious Diseases, First Hospital, Xi'an Jiaotong University, Xi'an, 710061, Shaanxi Province, China. zhengwenl@sohu.com

Telephone: +86-29-5324066 **Fax:** +86-29-5226360

Received: 2003-10-24 **Accepted:** 2003-12-08

Abstract

AIM: To study the sequential changes of serum ferritin levels in lamivudine-treated patients with chronic viral hepatitis B and the clinical implications.

METHODS: Thirty-eight patients with chronic viral hepatitis B were prospectively studied during their treatment with lamivudine. Each patient received 100 mg oral lamivudine daily for 12 mo, and was observed and tested for blood biochemistry and hepatitis B virus (HBV) DNA levels and serum ferritin levels at baseline and at 3, 6 and 12 mo during the treatment. Serum HBV DNA levels were quantitatively determined using fluorescent quantitative polymerase chain reaction (FQ-PCR), and serum ferritin levels were measured by radioimmunoassay. The sequential changes of serum ferritin levels and their relationships with virological, serological and biochemical responses in the patients were analyzed.

RESULTS: All the patients had a baseline HBV DNA level higher than 1×10^7 copies/L as determined by FQ-PCR and positive HBsAg and HBeAg and abnormal ALT levels. At the end of the 12-mo treatment, 19 of the 38 (50.00%) patients had undetectable serum HBV DNA levels by FQ-PCR, and 12 (31.58%) became negative for serum HBeAg and 10 (26.32%) had seroconversion from HBeAg to HBeAb. Nineteen out of the 38 (50.00%) patients had biochemically normal ALT levels after 12-mo lamivudine treatment. Sequential determination showed that lamivudine treatment significantly reduced ferritin levels in chronic hepatitis B patients. When the patients were divided into different groups according to their post-treatment virological, serological and biochemical responses for analysis of the sequential changes of ferritin levels, it was found that the decrease of ferritin levels in HBV DNA-negative group was significantly more obvious than that in HBV DNA-positive group at 6 mo during the treatment ($P=0.013$). Consecutive comparisons showed that ferritin levels at 3 mo of treatment were obviously decreased as compared with the baseline levels ($P<0.05$) in HBeAg-negative group, and the decrease of serum ferritin levels in patients with normalized ALT was more significant than that in patients with abnormal ALT at the end of the 12-mo treatment ($P=0.048$).

CONCLUSION: Lamivudine treatment can reduce the serum

ferritin levels in chronic viral hepatitis B patients and decreases of ferritin levels can be more significant in patients exhibiting virological, serological and biochemical responses, indicating that dynamic observation of serum ferritin levels in patients with chronic viral hepatitis B during lamivudine treatment might be helpful for monitoring and predicting patients' responses to the therapy.

Liu ZW, Han QY, Zhang N, Kang W. Sequential changes of serum ferritin levels and their clinical significance in lamivudine-treated patients with chronic viral hepatitis B. *World J Gastroenterol* 2004; 10(7): 972-976

<http://www.wjgnet.com/1007-9327/10/972.asp>

INTRODUCTION

Hepatitis B virus (HBV) is one of the major causes of liver diseases worldwide, which may progress into cirrhosis and hepatocellular carcinoma^[1-5]. It is thus important to implement anti-viral therapy against chronic hepatitis B to minimize the liver damage^[6]. Studies suggest that around half of all patients with chronic HBV infection respond to a 6- to 12-mo course of interferon (IFN) therapy, which may induce the elimination of serum hepatitis B viral DNA (HBV DNA) and hepatitis B e antigen (HBeAg), as well as normalization of serum alanine aminotransferase (ALT) activity. However, the response rate is still low and relapse occurs in about half of the responders^[6-12]. Lamivudine has become a recent interest in the treatment of chronic viral hepatitis B^[13-20] and it is suggested that high levels of pretreatment ALT and low levels of HBV DNA are predictive of response^[8,21-23]. However, other predictors of response to lamivudine therapy are unclear. Studies indicated that serum ferritin levels could be used to assess the degree of hepatocyte lesion in chronic viral hepatitis B^[24-31], but the role of serum ferritin determination in the treatment of viral hepatitis B with lamivudine remains uncertain. We therefore conducted the present study to investigate the possible role of sequential determination of serum ferritin levels in patients treated with lamivudine to explore the clinical implications.

MATERIALS AND METHODS

Patients and treatment

We prospectively studied 38 chronic hepatitis B patients with a complete clinical record, including 28 male and 10 female patients aged between 13 and 59 years (mean 29.32 ± 10.97 years), and none of the patients received interferon or other anti-viral therapy 6 mo before this study. Chronic hepatitis B was defined as positive hepatitis B surface antigen (HBsAg), positive HBeAg, detectable HBV DNA and abnormal serum ALT levels (normal <40 IU/L) for more than 6 mo. All patients had at least three documented occasions of serum ALT levels higher than the upper normal limit measured at intervals of one mo, within 6 mo prior to the enrollment. Alcoholics and intravenous drug users or homosexual persons and patients

with use of hepatotoxic drugs, herbal medicine or immunosuppressive therapy within the past 6 mo were excluded, and none of the patients had decompensated liver function, cirrhosis, chronic renal failure, clotting abnormalities, hemophiliacs, serious neurological disorders, obesity, chronic viral hepatitis C or delta, human immunodeficiency virus (HIV) infection, autoimmune disease (anti-nuclear antibody titer $>1:40$), and/or inheritable disorders such as hemochromatosis, alpha-1-antitrypsin deficiency or Wilson's disease. All patients with peripheral white blood cells $<4\,000$ per mm^3 and platelet $<80\,000$ per mm^3 were also excluded. Serum HBV DNA levels were quantitatively determined using hepatitis B virus fluorescence polymerase chain reaction (FQ-PCR) diagnostic kit manufactured by Daan Gene Corporation Limited of Zhongshan University (Shenzhen, China) according to the instruction. The lowest detectable HBV DNA level of FQ-PCR was 10^4 copies/mL. Serum ferritin levels were determined using a commercially available radioimmunoassay kit manufactured by China Atomic Energy Research Institute (Beijing, China). The reference values for normal serum ferritin level are 20-140 $\mu\text{g/L}$ and 16-132 $\mu\text{g/L}$ for male and female, respectively.

All patients received 100 mg oral lamivudine daily for 12 mo, and were observed and tested for blood biochemistry, HBV DNA levels, serological markers of HBV infection and serum ferritin levels at baseline and at 3, 6 and 12 mo during the treatment. Absence of serum HBV DNA and HBeAg, HBeAg seroconversion to HBeAb and normalization of serum ALT levels were assessed for the efficacy of treatment. Informed consent was obtained from all the patients before treatment.

Statistical analysis

Data in the text and tables are expressed as mean \pm SD and were analyzed with SPSS software. Statistical analysis was performed using two-tailed Fisher's exact test, two-tailed Student's *t* test and Chi-square test where appropriate. A *P* value less than 0.05 was considered statistically significant.

RESULTS

Sequential changes of serum ferritin levels during treatment

All of the 38 patients completed the 12-mo treatment. When all the patients were analyzed for the changes of serum ferritin levels, it was shown that their serum ferritin levels gradually decreased as lamivudine treatment prolonged (Figure 1). Serum ALT and aspartate aminotransferase (AST) levels declined in correlation with the serum ferritin levels. Serum ferritin levels were significantly decreased within 6 mo of lamivudine treatment (baseline *vs* mo 3, $P=0.018$; mo 3 *vs* mo 6, $P=0.027$) and stabilized thereafter (mo 6 *vs* mo 12, $P=0.593$).

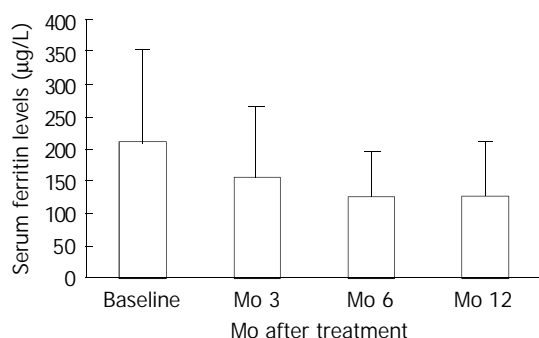


Figure 1 Sequential changes and comparisons of serum ferritin levels ($\mu\text{g/L}$) at different time points during lamivudine treatment.

Relationships between sequential changes of serum ferritin levels and virological responses to treatment

At the end of 12-mo treatment, 19 of the 38 (50.00%) patients had undetectable serum HBV DNA levels and another half of the patients still had detectable HBV DNA by FQ-PCR. The ferritin levels and their sequential changes were analyzed between these two groups. The ages (28.58 ± 11.47 years *vs* 30.05 ± 10.71 years) and HBV DNA levels at baseline [$(6.3\pm 8.6)\times 10^8$ copies/mL *vs* $(7.1\pm 6.1)\times 10^8$ copies/mL] between two groups had no statistical difference. The mean baseline ALT and AST levels in the HBV DNA-negative group (141.68 ± 105.99 IU/L and 101.00 ± 71.85 IU/L, respectively) were higher than those in HBV DNA-positive group (99.94 ± 73.00 IU/L and 63.80 ± 37.99 IU/L, respectively), but not statistically different ($P=0.166$ and $P=0.054$, respectively) between two groups. The mean baseline ferritin levels between two groups were not statistically different (Table 1). After initiation of lamivudine treatment, serum ferritin levels were decreased in both HBV DNA-negative and -positive groups, but the decrease in the former group was more apparent, with a statistically significant difference at mo 6 ($P=0.013$, Table 1). Interestingly, the percentage of female patients was higher in HBV DNA-negative group than in HBV DNA-positive group (10/19 *vs* 0/19, $P<0.01$).

In HBV DNA-negative group, consecutive comparisons of the ferritin levels within this group showed that the mean ferritin level at mo 3 of treatment was significantly decreased as compared with the baseline level ($P<0.01$), and the level at mo 6 was not obviously decreased compared with that at mo 3 ($P=0.140$), as with the comparison between the level at mo 12 and at mo 6 ($P=0.866$). In HBV DNA-positive group, consecutive comparisons showed no significant decreases in ferritin levels when compared in the same way as in HBV DNA-negative group ($P=0.825$, $P=0.110$ and $P=0.349$, respectively, Table 1).

Relationships between sequential changes of serum ferritin levels and serological responses to treatment

Of the 38 patients, 12 (31.58%) were negative for serum HBeAg and 26 positive for serum HBeAg at the end of the 12-mo treatment. The ferritin levels and their changes were analyzed between these two groups. The gender (female/total, 4/12 *vs* 6/26), ages (28.33 ± 12.67 years *vs* 29.77 ± 10.33 years), baseline ALT (116.25 ± 70.58 *vs* 122.92 ± 101.88 IU/L), AST (91.92 ± 59.13 *vs* 78.00 ± 60.67 IU/L), ferritin (Table 2) and HBV DNA levels [$(8.85\pm 9.83)\times 10^8$ copies/mL *vs* $(5.67\pm 5.92)\times 10^8$ copies/mL] between two groups had no statistical difference. The comparisons of serum ferritin levels between the 2 groups showed no significant difference at any time point (Table 2).

Consecutive comparisons of ferritin levels within the two groups showed that, in HBeAg-negative group, ferritin level at mo 3 of treatment was obviously decreased as compared with the baseline levels ($P<0.05$), and the levels at mo 6 and 12 of treatment were not significantly decreased when compared with the level at month 3 ($P=0.261$) and mo 6 ($P=0.373$), respectively. In HBeAg-positive group, ferritin levels were not obviously decreased when compared in the same way as in HBeAg-negative group ($P=0.228$, $P=0.051$ and $P=0.834$, respectively, Table 2).

Of the 38 patients treated, 10 (26.32%) had a seroconversion from HBeAg to HBeAb while 28 had not at the end of 12-mo treatment. The ferritin levels and their changes were also analyzed between these 2 groups of patients. The ages (29.77 ± 10.33 years *vs* 28.33 ± 12.67 years), ratio of female patients (3/10 *vs* 7/28) and baseline ALT (116.10 ± 76.55 *vs* 122.50 ± 98.43 IU/L), AST (96.50 ± 64.12 *vs* 77.36 ± 58.49 IU/L), ferritin (Table 3) and HBV DNA levels [$(10.2\pm 1.03)\times 10^8$ copies/mL *vs* $(5.52\pm 5.77)\times 10^8$ copies/mL] between the 2

groups were comparable. Statistically, no significant differences in serum ferritin levels between two groups were found at any time points although the decreases of ferritin levels in HBeAb-positive group after the initiation of treatment were more apparent than those in HBeAb-negative group (Table 3).

In HBeAb-positive group, consecutive comparisons of the ferritin levels showed that ferritin level at mo 3 of treatment was not obviously decreased as compared with the baseline level ($P=0.077$), and the levels at mo 6 and 12 of treatment were not obviously decreased compared with those at mo 3 ($P=0.303$) and 6 ($P=0.370$), respectively. In HBeAb-negative group, consecutive comparisons showed that the ferritin level at mo 6 was statistically decreased when compared with that at mo 3 ($P=0.041$), while the ferritin levels at mo 3 and mo 12 of treatment were not decreased as compared with those at baseline ($P=0.121$) and mo 6 ($P=0.836$), respectively (Table 3).

Relationships between sequential changes of serum ferritin levels and biochemical responses to treatment

Nineteen out of the 38 (50.00%) patients had biochemically normal ALT levels and another half of the patients still had elevated ALT levels at mo 12 of treatment. The ferritin levels and their changes were analyzed between these 2 groups of patients. The ages (29.16 ± 11.71 years vs 29.47 ± 10.49 years), ratio of female patients (5/19 vs 5/19) and baseline ALT (139.58 ± 112.45 vs 102.05 ± 63.98 IU/L), AST (94.58 ± 77.00 vs 70.21 ± 33.07 IU/L), and ferritin (Table 4) and HBV DNA levels [$(7.34\pm 9.12)\times 10^8$ copies/mL vs $(6.14\pm 5.31)\times 10^8$ copies/mL]

between two groups were comparable. It was shown that the decrease of serum ferritin levels in patients with normalized ALT was more significant than that in those with abnormal ALT at mo 12 of treatment ($P=0.048$, Table 4).

In both groups, consecutive comparisons showed that the ferritin levels at mo 3, 6 and 12 of treatment were not significantly decreased when compared with those at baseline, mo 3 and 6 ($P=0.120$, $P=0.145$ and $P=0.108$ in patients with normalized ALT and $P=0.062$, $P=0.088$ and $P=0.720$ in those with still elevated ALT), respectively, although the ferritin levels at mo 12 were significantly decreased compared with the baseline levels in both groups ($P=0.008$ and $P=0.020$, respectively. Table 4).

DISCUSSION

Elimination of HBeAg could significantly improve the clinical outcome and survival in chronic hepatitis B patients^[5-7]. A 6- to 12-mo course of IFN therapy could induce the elimination of serum HBV DNA and HBeAg, as well as normalization of serum ALT activity in about half of patients with chronic HBV infection at the end of treatment^[6-8]. The usage of immune modulators, as the currently available thymosin- $\alpha 1$, seemed effective in part of patients^[32,33]. However, the response rate was still low and relapse occurred in a high proportion of responders. Lamivudine has been increasingly administered to chronic viral hepatitis B patients in recent years and had a reportedly response with HBeAg seroconversion in about (15-30)% of patients after 1 to 2 years of therapy^[13-20].

Table 1 Sequential changes and comparisons of serum ferritin levels ($\mu\text{g/L}$) at different time points during lamivudine treatment between patients negative and positive for HBV DNA at end of treatment

Group	Baseline	Months after treatment		
		3	6	12
HBV DNA (-) group ($n=19$)	231.20 \pm 182.50	130.51 \pm 110.21	96.25 \pm 68.03	110.78 \pm 83.37
HBV DNA (+) group ($n=19$)	187.42 \pm 103.60	182.44 \pm 107.15	154.92 \pm 66.62	141.28 \pm 86.48
<i>P</i> values	0.371	0.150	0.013	0.283

Table 2 Sequential changes and comparisons of serum ferritin levels ($\mu\text{g/L}$) at different time points during lamivudine treatment in HBeAg-negative and -positive groups at end of treatment

Group	Baseline	Months after treatment		
		3	6	12
HBeAg (-) group ($n=12$)	250.16 \pm 190.78	135.72 \pm 138.33	106.13 \pm 74.10	97.80 \pm 76.96
HBeAg (+) group ($n=26$)	190.45 \pm 123.50	166.05 \pm 96.51	135.31 \pm 71.60	140.18 \pm 87.40
<i>P</i> values	0.336	0.439	0.262	0.160

Table 3 Sequential changes and comparisons of serum ferritin levels ($\mu\text{g/L}$) at different time points during lamivudine treatment in HBeAb-negative and -positive groups at end of treatment

Group	Baseline	Months after treatment		
		3	6	12
HBeAb (+) group ($n=10$)	249.19 \pm 176.48	147.33 \pm 147.60	114.47 \pm 76.62	104.41 \pm 78.60
HBeAb (-) group ($n=28$)	195.07 \pm 137.31	159.74 \pm 96.94	129.85 \pm 72.26	134.61 \pm 87.51
<i>P</i> values	0.328	0.765	0.577	0.346

Table 4 Sequential changes and comparisons of serum ferritin levels ($\mu\text{g/L}$) at different time points during lamivudine treatment in patients with normalized serum ALT and those with abnormal ALT at end of treatment

Group	Baseline	Months after treatment		
		3	6	12
ALT normal group ($n=19$)	198.40 \pm 161.58	139.39 \pm 111.38	112.35 \pm 57.51	99.19 \pm 60.52
ALT elevated group ($n=19$)	220.22 \pm 136.72	173.56 \pm 109.68	140.37 \pm 86.07	155.21 \pm 98.94
<i>P</i> value	0.656	0.347	0.266	0.048

In this study, 19 of the 38 patients (50.00%) had undetectable serum HBV DNA levels after the 12-mo treatment, suggesting the potent inhibition of HBV replication in patients with chronic hepatitis B. In 12 of the 38 (31.58%) patients, their serum HBeAg became negative and 10 (26.32%) had HBeAg seroconversion to HBeAb at the end of treatment, indicating that lamivudine treatment can enhance the elimination of HBeAg and its seroconversion to HBeAb in chronic hepatitis B patients through the inhibition of HBV replication. Biochemically, 19 (50.00%) of the 38 patients had normalized ALT levels after lamivudine treatment, indicating that lamivudine treatment can also improve the biochemical abnormalities in the patients. The HBeAg seroconversion rate in the patients in this study was in accordance with other reports^[13-20]. It can be obviously seen from our results and other reports that the response rate is still not satisfactory and further studies on new regimens, including lamivudine in combination with IFN and other agents, are needed^[23,34-41].

The relationship between iron metabolism and liver diseases has long been a focus of study. More than two decades ago, it was found that a high serum ferritin level prior to HBV infection might increase the likelihood of persistent infection^[24]. Correlations between an increase of both AST and ALT and a higher level of ferritin in patients with chronic hepatitis C and B and alcoholic hepatitis were also documented by previous observations^[31]. Furthermore, Serum ferritin was significantly higher in cirrhotic patients in comparison to patients with chronic viral hepatitis and highly elevated ferritin levels were observed in hepatocellular carcinoma (HCC) patients^[25-31]. Clinical observations also indicated that desferrioxamine infusion to achieve a normal serum ferritin level could enhance the likelihood of response by a chronic hepatitis B patient to IFN therapy^[42].

The precise mechanisms associated with elevated ferritin levels in chronic hepatitis and other acute and chronic liver diseases have not been fully clarified. Firstly, it is implicated that HBV might infect the liver cells and then actively replicate with the propensity for increasing ferritin synthesis, resulting in increased liver iron storage^[24,25]. The iron overload may enhance the hepatocyte damage induced by HBV. Secondly, serum AST activities correlated with serum ferritin levels in patients with liver disease and the severer the hepatocyte damage is, the higher the serum ferritin and serum iron are, which seems more obvious in fulminant hepatitis and liver cirrhosis. It is therefore suggested that ferritin and iron levels would increase in serum because of their release from hepatocellular storage in association with necrosis^[29-31]. Thirdly, it was also indicated that tumor cells might produce ferritin^[27], and lastly, iron-induced oxidative stress, in addition to iron storage and hepatocyte damage, has been believed to be another cause of increased serum ferritin levels in chronic liver diseases^[43]. Our observations on the sequential changes of serum ferritin levels showed that the antiviral treatment with lamivudine could reduce the ferritin levels in patients with chronic hepatitis B and the decrease in HBV DNA-negative group at the end of 12-mo treatment could be more profound than that in HBV DNA-positive group, supporting the notion that virus replication could stimulate ferritin synthesis^[24,25]. Our sequential determination also showed that the ferritin level in patients with normalized ALT at the end of treatment decreased more apparently than that in patients with abnormal ALT, and the decrease in ferritin levels paralleled that in ALT and AST levels, indicating that the improvement of necroinflammatory damage of hepatocytes also contributes to the decline of ferritin levels. In addition, the virological response in patients was associated with early decrease of ferritin levels while the biochemical response appeared to be associated with relatively gradual decreases of ferritin levels, indicating that the early decrease of ferritin levels might result mainly from the

inhibition of HBV replication in hepatocytes and the reduction of ferritin synthesis while the subsequent changes might result from the improvement of necroinflammatory damage of liver tissues and the reduction of ferritin release from hepatocytes.

Many factors may affect the response to antiviral treatment for chronic hepatitis B and it was indicated that serum ferritin levels could be used for predicting the response to IFN treatment in patients with chronic hepatitis B. Interferon- α treatment of chronic hepatitis B showed that ferritin levels correlated well with the type of IFN response, as the serum ferritin level increased, the response rate to IFN declined. Serum ferritin level appeared to influence the type of IFN response achieved^[8]. Observations in children with chronic hepatitis B found that in the group of patients with detectable seroconversion in the HBe system resulting from interferon- α therapy, lower serum levels of iron and ferritin could be present^[44]. Therefore, to detect serum markers of iron metabolism was believed to be helpful for evaluating the curative effect and prognosis of hepatitis B^[30]. So far, although it is suggested that higher levels of pretreatment ALT and lower levels of pretreatment HBV DNA levels were predictors of response^[21-23], no data are currently available to address the value of serum ferritin detection in patients with chronic hepatitis B treated with lamivudine.

Our observation was focused mainly on serum ferritin levels with regard to their sequential changes and their relationships with the virological, serological and biochemical responses to lamivudine treatment in chronic hepatitis B patients. We found that lamivudine treatment could reduce serum ferritin levels in chronic hepatitis B patients and the effect was more significant during the first 6 mo of treatment. As the ages, gender, baseline ALT, AST and HBV DNA levels between the groups were comparable, our determination and analysis showed that statistically significant decreases of ferritin levels occurred in virologically and biochemically responding groups but not in nonresponding groups although female patients appeared to be more likely to have viral response. The decreases of ferritin levels in serologically responding groups (elimination of HBeAg and HBeAg seroconversion to HBeAb) were also more obvious than those in serologically nonresponding groups although they were not statistically significant between the two groups. Furthermore, we found that the decreases of serum ferritin levels paralleled the declines of serum ALT and AST levels during lamivudine treatment. Therefore, it indicates that sequential determination of serum ferritin levels, rather than only the detection of pretherapy ferritin levels, in chronic hepatitis B patients treated with lamivudine is helpful for monitoring and predicting the responses to treatment.

Contrary to other observations^[22,23], we did not observe any statistical differences in the baseline ALT, AST and HBV DNA levels between any responding and nonresponding groups although, generally speaking, pretherapy ALT and AST levels in responding groups appeared to be higher than those in nonresponding groups. As the number of patients we observed in this study was relatively small, large-scale observations on the response predicting and monitoring factors in relation to lamivudine treatment are needed.

In conclusion, lamivudine treatment for patients with chronic hepatitis B can decrease serum ferritin levels, and the decreases are more profound in virologically and biochemically responsive patients. It is suggested that sequential determination of serum ferritin levels, rather than only the baseline ferritin levels, in patients with chronic hepatitis B may be useful for monitoring and predicting the virological and biochemical responses to the treatment of lamivudine.

REFERENCES

- 1 **Margolis HS**, Alter MJ, Hadler SC. Hepatitis B: evolving epidemiology and implications for control. *Semin Liver Dis* 1991; **11**: 84-92

- 2 **Sherlock S**. Viruses and hepatocellular carcinoma. *Gut* 1994; **35**: 828-832
- 3 **Yip D**, Findlay M, Boyer M, Tattersall MH. Hepatocellular carcinoma in central Sydney: a 10-year review of patients seen in a medical oncology department. *World J Gastroenterol* 1999; **5**: 483-487
- 4 **Tang ZY**. Hepatocellular carcinoma-cause, treatment and metastasis. *World J Gastroenterol* 2001; **7**: 445-454
- 5 **Liaw YF**, Tai DI, Chu CM, Chen TJ. The development of cirrhosis in patients with chronic type B hepatitis: a prospective study. *Hepatology* 1988; **8**: 493-496
- 6 **Hoofnagle JH**, di Bisceglie AM. The treatment of chronic viral hepatitis. *N Engl J Med* 1997; **336**: 347-356
- 7 **Carreno V**, Bartolome J, Castillo I. Long-term effect of interferon therapy in chronic hepatitis B. *J Hepatol* 1994; **20**: 431-435
- 8 **Bayraktar Y**, Koseoglu T, Temizer A, Kayhan B, Van Thiel DH, Uzunalimoglu B. Relationship between the serum alanine aminotransferase level at the end of interferon treatment and histologic changes in wild-type and precore mutant hepatitis B virus infections. *J Viral Hepat* 1996; **3**: 137-142
- 9 **Tine F**, Liberati A, Craxi A, Almasio P, Pagliaro L. Interferon treatment in patients with chronic hepatitis B: a meta-analysis of the published literature. *J Hepatol* 1993; **8**: 154-162
- 10 **Di Bisceglie AM**. Long-term outcome of interferon-alpha therapy for chronic hepatitis B. *J Hepatol* 1995; **22**(1 Suppl): 65-67
- 11 **Lau DT**, Everhart J, Kleiner DE, Park Y, Vergalla J, Schmid P, Hoofnagle JH. Long-term follow-up of patients with chronic hepatitis B treated with interferon alfa. *Gastroenterology* 1997; **113**: 1660-1667
- 12 **Han HL**, Lang ZW. Changes in serum and histology of patients with chronic hepatitis B after interferon alpha-2b treatment. *World J Gastroenterol* 2003; **9**: 117-121
- 13 **Dienstag JL**, Perrillo RP, Schiff ER, Bartholomew M, Vicary C, Rubin M. A preliminary trial of lamivudine for chronic hepatitis B infection. *N Engl J Med* 1995; **333**: 1657-1661
- 14 **Schalm SW**, de Man RA, Heijtkink RA, Niesters HG. New nucleoside analogues for chronic hepatitis B. *J Hepatol* 1995; **22**(1 Suppl): 52-56
- 15 **Lai CL**, Chien RN, Leung NW, Chang TT, Guan R, Tai DI, Ng KY, Wu PC, Dent JC, Barber J, Stephenson SL, Gray DF. A one-year trial of lamivudine for chronic hepatitis B. Asia Hepatitis Lamivudine Study Group. *N Engl J Med* 1998; **339**: 61-68
- 16 **Lau DT**, Khokhar MF, Doo E, Ghany MG, Herion D, Park Y, Kleiner DE, Schmid P, Condreay LD, Gauthier J, Kuhns MC, Liang TJ, Hoofnagle JH. Long-term therapy of chronic hepatitis B with lamivudine. *Hepatology* 2000; **32**(4 Pt 1): 828-834
- 17 **Song BC**, Suh DJ, Lee HC, Chung YH, Lee YS. Hepatitis B e antigen seroconversion after lamivudine therapy is not durable in patients with chronic hepatitis B in Korea. *Hepatology* 2000; **32**(4 Pt 1): 803-806
- 18 **Yang SS**, Hsu CT, Hu JT, Lai YC, Wu CH. Lamivudine does not increase the efficacy of interferon in the treatment of mutant type chronic viral hepatitis B. *World J Gastroenterol* 2002; **8**: 868-871
- 19 **Dienstag JL**, Schiff ER, Wright TL, Perrillo RP, Hann HW, Goodman Z, Crowther L, Condreay LD, Woessner M, Rubin M, Brown NA. Lamivudine as initial treatment for chronic hepatitis B in the United States. *N Engl J Med* 1999; **341**: 1256-1263
- 20 **Liaw YF**, Leung NW, Chang TT, Guan R, Tai DI, Ng KY, Chien RN, Dent J, Roman L, Edmundson S, Lai CL. Effects of extended lamivudine therapy in Asian patients with chronic hepatitis B. Asia Hepatitis Lamivudine Study Group. *Gastroenterology* 2000; **119**: 172-180
- 21 **Brook MG**, Karayiannis P, Thomas HC. Which patients with chronic hepatitis B virus infection will respond to alpha-interferon therapy? A statistical analysis of predictive factors. *Hepatology* 1989; **10**: 761-763
- 22 **Chien RN**, Liaw YF, Atkins M. Pretherapy alanine transaminase level as a determinant for hepatitis B e antigen seroconversion during lamivudine therapy in patients with chronic hepatitis B. Asian Hepatitis Lamivudine Trial Group. *Hepatology* 1999; **30**: 770-774
- 23 **Schalm SW**, Heathcote J, Cianciara J, Farrell G, Sherman M, Willems B, Dhillion A, Moorat A, Barber J, Gray DF. Lamivudine and alpha interferon combination treatment of patients with chronic hepatitis B infection: a randomised trial. *Gut* 2000; **46**: 562-568
- 24 **Lustbader ED**, Hann HW, Blumberg BS. Serum ferritin as a predictor of host response to hepatitis B virus infection. *Science* 1983; **220**: 423-425
- 25 **Cohen C**, Berson SD, Shulman G, Budgeon LR. Liver iron stores and hepatitis B antigen status. *Cancer* 1985; **56**: 2201-2204
- 26 **Hengeveld P**, Zuyderhoudt FM, Jobsis AC, van Gool J. Some aspects of iron metabolism during acute viral hepatitis. *Hepatogastroenterology* 1982; **29**: 138-141
- 27 **Zhou XD**, DeTolla L, Custer RP, London WT. Iron, ferritin, hepatitis B surface and core antigens in the livers of Chinese patients with hepatocellular carcinoma. *Cancer* 1987; **59**: 1430-1437
- 28 **Hann HW**, Kim CY, London WT, Blumberg BS. Increased serum ferritin in chronic liver disease: a risk factor for primary hepatocellular carcinoma. *Int J Cancer* 1989; **43**: 376-379
- 29 **Di Bisceglie AM**, Axiotis CA, Hoofnagle JH, Bacon BR. Measurements of iron status in patients with chronic hepatitis. *Gastroenterology* 1992; **102**: 2108-2113
- 30 **Cao Z**, Bai Y, Yang X, Liu J, Li B, Li F. Study of iron metabolism abnormality in the hepatocyte damage of hepatitis B. *Zhonghua Ganzhangbing Zazhi* 2001; **9**: 37-39
- 31 **Jurczyk K**, Wawrzynowicz-Syczewska M, Boron-Kaczmarek A, Sych Z. Serum iron parameters in patients with alcoholic and chronic cirrhosis and hepatitis. *Med Sci Monit* 2001; **7**: 962-965
- 32 **You J**, Zhuang L, Tang BZ, Yang WB, Ding SY, Li W, Wu RX, Zhang HL, Zhang YM, Yan SM, Zhang L. A randomized controlled clinical trial on the treatment of Thymosin-a1 versus interferon-alpha in patients with hepatitis B. *World J Gastroenterol* 2001; **7**: 411-414
- 33 **Zhuang L**, You J, Tang BZ, Ding SY, Yan KH, Peng D, Zhang YM, Zhang L. Preliminary results of Thymosin-a1 versus interferon-alpha treatment in patients with HBeAg negative and serum HBV DNA positive chronic hepatitis B. *World J Gastroenterol* 2001; **7**: 407-410
- 34 **Terrault NA**. Combined interferon and lamivudine therapy: is this the treatment of choice for patients with chronic hepatitis B virus infection? *Hepatology* 2000; **32**: 675-677
- 35 **Farrell G**. Hepatitis B e antigen seroconversion: effects of lamivudine alone or in combination with interferon alpha. *J Med Virol* 2000; **61**: 374-379
- 36 **Jaboli MF**, Fabbri C, Liva S, Azzaroli F, Nigro G, Giovanelli S, Ferrara F, Miracolo A, Marchetto S, Montagnani M, Colecchia A, Festi D, Reggiani LB, Roda E, Mazzella G. Long-term alpha interferon and lamivudine combination therapy in non-responder patients with anti-HBe-positive chronic hepatitis B: Results of an open, controlled trial. *World J Gastroenterol* 2003; **9**: 1491-1495
- 37 **Liu P**, Hu YY, Liu C, Zhu DY, Xue HM, Xu ZQ, Xu LM, Liu CH, Gu HT, Zhang ZQ. Clinical observation of salvianolic acid B in treatment of liver fibrosis in chronic hepatitis B. *World J Gastroenterol* 2002; **8**: 679-685
- 38 **Chen XS**, Wang GJ, Cai X, Yu HY, Hu YP. Inhibition of hepatitis B virus by oxymatrine *in vivo*. *World J Gastroenterol* 2001; **7**: 49-52
- 39 **Weng HL**, Cai WM, Liu RH. Animal experiment and clinical study of effect of gamma-interferon on hepatic fibrosis. *World J Gastroenterol* 2001; **7**: 42-48
- 40 **Wu JM**, Lin JS, Xie N, Liang KH. Inhibition of hepatitis B virus by a novel L-nucleoside, β -L-D4A and related analogues. *World J Gastroenterol* 2003; **9**: 1840-1843
- 41 **Cheng ML**, Wu YY, Huang KF, Luo TY, Ding YS, Lu YY, Liu RC, Wu J. Clinical study on the treatment of liver fibrosis due to hepatitis B by IFN- α_1 and traditional medicine preparation. *World J Gastroenterol* 1999; **5**: 267-269
- 42 **Bayraktar Y**, Saglam F, Temizer A, Uzunalimodlu B, van Thiel DH. The effect of interferon and desferrioxamine on serum ferritin and hepatic iron concentrations in chronic hepatitis B. *Hepatogastroenterology* 1998; **45**: 2322-2327
- 43 **Sumida Y**, Nakashima T, Yoh T, Kakisaka Y, Nakajima Y, Ishikawa H, Mitsuyoshi H, Okanoue T, Nakamura H, Yodoi J. Serum thioredoxin elucidates the significance of serum ferritin as a marker of oxidative stress in chronic liver diseases. *Liver* 2001; **21**: 295-299
- 44 **Chrobot A**, Chrobot AM, Szaflarska-Szczepanik A. Assessment of iron metabolism in children with chronic hepatitis B - prognostic factor in interferon alpha therapy. *Med Sci Monit* 2002; **8**: CR269-273

Construction of prokaryotic expression system of *ureB* gene from a clinical *Helicobacter pylori* strain and identification of the recombinant protein immunity

Ya-Fei Mao, Jie Yan

Ya-Fei Mao, Jie Yan, Department of Medical Microbiology and Parasitology, College of Medical Science, Zhejiang University, Hangzhou 310031, Zhejiang Province, China

Supported by the Excellent Young Teacher Fund of Chinese Education Ministry and the General Science and Technology Research Plan of Zhejiang Province, No. 001110438

Correspondence to: Jie Yan, Department of Medical Microbiology and Parasitology, College of Medical Science, Zhejiang University, 353 Yanan Road, Hangzhou 310031, Zhejiang Province, China. yanchen@mail.hz.zj.cn

Telephone: +86-571-87217385 **Fax:** +86-571-87217044

Received: 2003-10-08 **Accepted:** 2003-12-06

Abstract

AIM: To clone *ureB* gene from a clinical isolate of *Helicobacter pylori* and construct a prokaryotic expression system of the gene and identify immunity of the expressed recombinant protein.

METHODS: *ureB* gene from a clinical *H pylori* strain Y06 was amplified by the high fidelity polymerase chain reaction technique. The target DNA fragment amplified from *ureB* gene was sequenced after T-A cloning. Prokaryotic recombinant expression vector pET32a inserted with *ureB* gene (pET32a-*ureB*) was constructed. The expression of recombinant UreB protein (rUreB) in *E. coli* BL21DE3 induced by isopropylthio- β -D-galactoside (IPTG) at different concentrations was examined by SDS-PAGE. Western blot using commercial antibodies against whole cell of *H pylori* and an immunodiffusion assay using a self-prepared rabbit anti-rUreB antibody were applied to determine immunity of the target recombinant protein. ELISA was used to detect the antibody against rUreB in sera of 125 *H pylori* infected patients and to examine rUreB expression in 109 *H pylori* isolates.

RESULTS: In comparison with the reported corresponding sequences, the nucleotide sequence homology of the cloned *ureB* gene was from 96.88-97.82% while the homology of its putative amino acid sequence was as high as 99.65-99.82%. The rUreB output expressed by pET32a-*ureB*-BL21DE3 was approximate 30% of the total bacterial proteins. rUreB specifically combined with the commercial antibodies against whole cell of *H pylori* and strongly induced rabbits to produce antibody with a 1:8 immunodiffusion titer after the animals were immunized with the recombinant protein. Serum samples from all *H pylori* infected patients were positive for UreB antibody and UreB expression were detectable in all tested *H pylori* isolates.

CONCLUSION: A prokaryotic expression system with high expression efficiency of *H pylori ureB* gene was successfully established. The expressed rUreB showed qualified immunoreactivity and antigenicity. High frequencies of UreB

expression in different *H pylori* isolates and specific antibody against *UreB* in sera of *H pylori* infected patients indicate that *UreB* is an excellent antigen candidate for developing *H pylori* vaccine.

Mao YF, Yan J. Construction of prokaryotic expression system of *ureB* gene from a clinical *Helicobacter pylori* strain and identification of the recombinant protein immunity. *World J Gastroenterol* 2004; 10(7): 977-984

<http://www.wjgnet.com/1007-9327/10/977.asp>

INTRODUCTION

In China, chronic gastritis and peptic ulcer are two most common gastric diseases, and gastric cancer is one of the malignant tumors with high mortalities and morbidities^[1-34]. *Helicobacter pylori*, a microaerophilic, spiral and Gram-negative bacterium, is recognized as a human-specific gastric pathogen that colonizes the stomachs of at least half of the world's populations^[35]. Most infected individuals are asymptomatic. However, in some subjects, *H pylori* infection causes acute/chronic gastritis or peptic ulceration. Furthermore, the infection is also a high risk factor for the development of gastric adenocarcinoma, mucosa-associated lymphoid tissue (MALT) lymphoma and primary gastric non-Hodgkin's lymphoma^[36-43]. Recently, direct evidence that *H pylori* causes gastric carcinoma in an animal model has been reported^[44-46]. Immunization against the bacterium represents a cost-effective strategy to prevent *H pylori*-associated peptic ulcer disease and to reduce the incidence of global gastric cancer^[47]. The selection of antigenic targets is critical in the design of *H pylori* vaccine. So far, no vaccine preventing *H pylori* infection was commercially available. Almost all *H pylori* strains produce a special urease decomposing urea and forming ammonia, which is harmful to gastric mucosa. Moreover, a high pH value is benefit for organisms to colonize the stomach. Urease is composed of 4 subunits, A, B, C and D. The subunit B (UreB), a peptide with 569 amino acid residuals encoded by *ureB* gene, has been demonstrated to show the strongest antigenicity and protection among all known *H pylori* proteins^[48-50]. Furthermore, almost all *H pylori* isolates have *ureB* gene and express UreB protein, and their nucleotide and putative amino acid sequence homologies are as high as approximate 95%^[51-53]. These data strongly indicate that UreB is a potential antigen candidate for *H pylori* vaccine. In this study, a recombinant prokaryotic vector responsible for the recombinant UreB protein (rUreB) expression was constructed. Immunogenicity and immunoreactivity of rUreB were further examined. Furthermore, rUreB was used as an antigen in ELISA to detect specific antibody in sera from *H pylori* infected patients, and rabbit anti-rUreB serum was prepared to examine the UreB expression in different *H pylori* isolates. The results of this study will supply further experimental foundation for the development of *H pylori* vaccine.

MATERIALS AND METHODS

Materials

A clinical strain of *H pylori*, provisionally named Y06, which was well-characterized by the Department of Medical Microbiology and Parasitology, College of Medical Science, Zhejiang University, was used in this study. A plasmid pET32a (Novagen, Madison, USA) and *E. coli* BL21 DE3 (Novagen, Madison, USA) were used as the expression vector and host cell, respectively. Primers for polymerase chain reaction (PCR) amplification were synthesized by BioAsia (Shanghai, China). A Taq-plus high fidelity PCR kit and restriction endonucleases were purchased from TaKaRa (Dalian, China). The T-A Cloning kit and sequencing service were provided by BBST (Shanghai, China). DAKO (Glostrup, Denmark) and Jackson ImmunoResearch (West Grove, USA) supplied rabbit antiserum against whole cell of *H pylori*, HRP-labeling sheep anti-rabbit IgG and anti-human IgG antibodies, respectively. Agents for *H pylori* isolation and identification were purchased from bioMérieux (Marcy l'Étoile, France). Overall, 126 patients (86 males and 40 females; age range: from 6-78 yr; mean age: 40.5 yr) who were referred for upper endoscopy from 4 different hospitals in Hangzhou during the period between December 2001 and June 2002 and had *H pylori* isolated from gastric mucosa were included in the study. All patients gave a written informed content. Of the 126 patients, 68 were endoscopically diagnosed as having chronic gastritis (CG, 48 superficial, 10 active and 10 atrophic gastritis), and 58 as having peptic ulcer disease (PUD, 12 gastric, 40 duodenal, and 6 gastric and duodenal ulcer). None of the patients had taken nonsteroidal anti-inflammatory drugs, antacids and antibiotics during the 2-wk before seeking medical advice. At the same time, serum specimens were also collected from these patients.

Isolation and identification of *H pylori*

Each gastric biopsy taken during endoscopy was homogenized with a tissue grinder and then inoculated on Columbia agar plates supplemented with 80 mL/L sheep blood, 5 g/L cyclodextrin, 5 mg/L trimethoprim, 10 mg/L vancomycin, 2.5 mg/L amphotericin B and 2 500 U/L cefsulodin. The plates were incubated at 37 °C under microaerobic conditions (50 mL/LO₂, 100 mL/LCO₂ and 850 mL/LN₂) for 3 to 5 d. A bacterial isolate was identified as *H pylori* according to typical Gram stain morphology, biochemical tests positive for urease and oxidase, and agglutination with the commercial rabbit antibodies against whole cell of *H pylori*. One of the isolated strains, named as Y06 that had typical characteristics of *H pylori*, was selected for further experiments.

Preparation of DNA template

Genomic DNA of *H pylori* strain Y06 was prepared by the routine phenol-chloroform method and DNase-free RNase treatment. The obtained DNA was dissolved in TE buffer, and its concentration and purity were determined by ultraviolet spectrophotometry^[54].

Polymerase Chain Reaction

Primers were designed to amplify the whole sequence of *ureB* gene from strain Y06 based on the published sequences and reading frames^[51-53]. The sequences of *ureB* sense primer with an endonuclease site of EcoRV and antisense primer with an endonuclease site of *XhoI* were 5'-GGAGATATCATGATTAGCAGAAAAG AATATGTTTC-3' and 5'-GGACTCGAGCTAGAAAATGCTAAAGATTTGTGC-3', respectively. Total volume per PCR was 100 µL containing 2.5 mol/L each dNTP, 250 nmol/L each of the 2 primers, 15 mol/L MgCl₂, 3.0 U Taq-plus polymerase, 100 ng DNA template and

1×PCR buffer (pH8.3). The parameters for PCR were 94 °C for 5 min, ×1; 94 °C for 30 s, 56 °C for 30 s, 72 °C for 120 s, ×10; 94 °C for 30 s, 56 °C for 30 s, 72 °C for 130 s (10 s addition for each of the following cycles), ×20; and then 72 °C for 12 min, ×1. The results of PCR were observed under UV light after electrophoresis in 10 g/L agarose, pre-stained with ethidium bromide. The expected size of target amplification fragment was 1 704 bp.

Cloning and sequencing

The target amplification DNA fragment from *ureB* gene was cloned into pUCm-T vector (pUCm-T-*ureB*) by using the T-A Cloning kit according to the manufacturer's instruction. The recombinant plasmid was amplified in *E. coli* strain DH5α and then extracted by Sambrook's method^[54]. A professional company (BBST) was responsible for nucleotide sequence analysis of the inserted fragment. Two *E. coli* DH5α strains containing pUCm-T-*ureB* and expression vector pET32a, respectively, were subcultured in LB medium. Then the plasmids were extracted^[54] and digested with *EcoRV* and *XhoI*, respectively. The *ureB* target fragments and pET32a were recovered for ligation. The recombinant expression vector pET32a-*ureB* was transformed into *E. coli* BL21DE3, which was named as pET32a-*ureB*-BL21DE3. The target *ureB* gene fragment inserted in pET32a plasmid was sequenced again.

Expression and identification of the fusion protein

pET32a-*ureB*-BL21DE3 was rotatively cultured in LB medium at 37 °C and induced by isopropylthio-β-D-galactoside (IPTG) at different concentrations of 1.0, 0.5 and 0.1 mmol/L. The supernatant and precipitate were separated by centrifugation after the bacterial pallet was ultrasonically broken (300 V, 5 s×3). The molecular mass and output of rUreB were measured by SDS-PAGE. The expressed rUreB was collected by Ni-NTA affinity chromatography. The commercial rabbit antiserum against whole cell of *H pylori* and HRP-labeling sheep anti-rabbit IgG were used as the first and second antibodies, respectively, to determine the immunoreactivity of rUreB by Western blot. Rabbits were immunized with rUreB to prepare the antiserum, and an immunodiffusion assay was applied to determine the antigenicity of rUreB.

ELISA

By using rUreB as antigen at the coated concentration of 20 µg/mL, a patient serum sample (1:400 dilution) as the first antibody and HRP-labeling sheep anti-human IgG (1:4 000 dilution) as the second antibody, the specific antibody against UreB in sera from the 126 patients infected with *H pylori* were detected by ELISA. The result of ELISA for a patient's serum sample was considered as positive if the *A* value at 490 nm (*A*₄₉₀) was over the mean plus 3 SD of 6 negative serum samples^[55]. UreB expression in *H pylori* isolates was examined by ELISA using the ultrasonic supernatant of each isolate (50 µg/mL) as a coated protein antigen, the self-prepared rabbit anti-rUreB serum (1:2 000 dilution) as the first antibody and HRP-labeling sheep anti-rabbit IgG (1:3 000 dilution) as the second antibody. The result of ELISA for a *H pylori* ultrasonic supernatant sample was considered as positive if its *A*₄₉₀ value was over the mean plus 3 SD of 6 ultrasonic supernatant samples at the same protein concentration of *E. coli* ATCC 25922^[55].

Data analysis

The nucleotide sequences of the cloned *ureB* gene inserted in the two recombinant plasmid vectors were compared for homology with the 3 published *ureB* gene sequences (NC000915, M60398, X57132, AB032429)^[51-53] by using a molecular biological analysis soft ware.

RESULTS

PCR

The target fragment of *ureB* gene with the expected size amplified from DNA template of *H pylori* strain Y06 is shown in Figure 1.

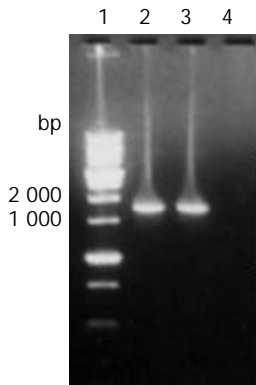


Figure 1 The target fragment of *ureB* gene amplified from *H pylori* strain Y06 DNA. Lane 1, 1 kb DNA marker (BBST); lanes 2 and 3, the target amplification fragment of *ureB* gene from genomic DNA of *H pylori* strain Y06; lane 4: blank control.

Nucleotide sequence analysis

The nucleotide sequences of *ureB* gene in *pUCm-T-ureB* and *pET32a-ureB* were completely same. The homologies of the nucleotide and putative amino acid sequences of the cloned *ureB* gene compared with the published *ureB* gene sequences^[51-53] were from 96.88% to 97.82% and from 99.65% to 99.82%, respectively (Figures 2 and 3).

Expression of the target fusion protein

IPTG at concentrations of 1.0, 0.5 and 0.1 mmol/L efficiently induced the expression of rUreB in the pET32a-ureB-BL21DE3 system. The product of rUreB was mainly presented in ultrasonic precipitates and the output was approximate 30% of the total bacterial proteins (Figure 4).

Immunoreactivity and antigenicity of rUreB

The commercial rabbit antibodies against the whole cell of *H pylori* combined with rUreB as confirmed by Western blot (Figure 5), and the titer demonstrated by immunodiffusion assay between rUreB and self-prepared rabbit anti-rUreB serum was 1:8.

ELISA

Since the mean±SD of A₄₉₀ values of the 6 negative serum

```
(1)1   ATGAAAAAGATTAGCAGAAAAGAATATGTTTCTATGTATGGCCCTACTACAGGCGATAAA
(2)1   .....
(3)1   .....
(4)1   ATG.....T.....

(1)61  GTGAGATTGGGCGATACAGACTTGATCGCTGAAGTAGAACATGACTACACCATTATGGC
(2)61  .....
(3)61  .....
(4)61  .....

(1)121 GAAGAGCTTAAATTCGGTGGCGGTAACCCCTGAGAGAAGGCATGAGCCAATCCAACAAC
(2)121 .....
(3)121 .....CC.....T.....T.....T.....
(4)121 .....G..TT...G.....

(1)181 CCTAGCAAAGAAGAATTGGATCTAATCATCACTAACGCTTTAATCGTGGATTACACCGGT
(2)181 .....G.....T...T.....
(3)181 .....C...T.....G.....
(4)181 .....C...T.....

(1)241 ATTTATAAAGCGGATATTGGTATTAAAGATGGCAAAATCGCTGGCATTGGTAAAGGCGGT
(2)241 .....
(3)241 .....
(4)241 .....C.....

(1)301 AACAAAGACATGCAAGATGGCGTTAAAAACAATCTTAGCGTAGGTCCTGCTACTGAAGCC
(2)301 .....
(3)301 .....G.....
(4)301 .....G.....

(1)361 TTAGCCGGTGAAGGTTTGATCGTAACTGCTGGTGGTATTGACACACACATCCACTTCATT
(2)361 .....G.....
(3)361 .....C.....
(4)361 .....T.....C.....C.....

(1)421 TCACCCCAACAAATCCCTACAGCTTTTGCAAGCGGTGTAACAACCATGATTGGTGGCGGA
(2)421 .....T...
(3)421 ..C.....G.....
(4)421 ..C.....

(1)481 ACTGGTCCTGCTGATGGCACTAATGCGACTACTATCACTCCAGGCAGAAGAAATTTAAAA
(2)481 ..C.....
(3)481 .....C.....C..A..C.....
(4)481 .....C..A..C.....C.....

(1)541 TGGATGCTCAGAGCGGCTGAAGAATATTCTATGAACTTAGGTTTCTTGGCTAAAGGTAAC
(2)541 .....T.....
(3)541 .....
(4)541 .....C.....A.....
```

(1)601 GCTTCTAACGACGCGAGCTTAGCCGATCAAATTGAAGCTGGTGCATTGGCTTTAAAATC
(2)601T.....C.....T
(3)601T..T.....C.....
(4)601 A.....T.....C.....T.....

(1)661 CACGAAGACTGGGGCACCCTCTTCTGCAATCAATCATGCGTTAGATGTTGCAGACAAA
(2)661G.....
(3)661T.....A..A.....
(4)661A..A.....G.....

(1)721 TACGATGTGCAAGTCGCTATCCACACAGACACTTTGAATGAAGCCGGTTGCGTGGGAAGAC
(2)721T..A.....
(3)721T..A.....
(4)721T..A.....

(1)781 ACTATGGCAGCTATTGCCGGACGCACTATGCACACTTTCCACACTGAAGGTGCTGGCGGC
(2)781T.....T.....C.....
(3)781C.....T.....
(4)781C.....C.....T.....

(1)841 GGACACGCTCCTGATATTATTAAAGTAGCTGGTGAACACAACATTCTTCCCCTTCCACT
(2)841C.....
(3)841C.....G.....
(4)841G..C..C.....G.....

(1)901 AACCCCACTATCCCTTTCCTACTGTGAATACAGAAGCAGAACACATGGACATGCTTATGGTG
(2)901C.....C.....G.....
(3)901
(4)901
(5)901

(1)961 TGCCACCCTTGATAAAAAGCATTAAAGAAGATGTTTCAGTTCGCTGATTCAAGGATCCGC
(2)961
(3)961
(4)961

(1)1021 CCTCAAACCATGCGGCTGAAGACACTTTGCATGACATGGGGATTTTCTCAATCACCAGC
(2)1021T.....
(3)1021T..T.....
(4)1021T.....C.....T..T.....

(1)1081 TCTGACTCTCAAGCTATGGGTCGTGTGGGTGAAGTTATCACTAGAACTGGCAAACAGCT
(2)1081G.....C.....
(3)1081C.....
(4)1081

(1)1141 GACAAAAACAAAAAGAATTGGCCGCTTGAAAGAAGAAAAAGGCGATAACGACAACCTTC
(2)1141G.....
(3)1141
(4)1141

(1)1201 AGGATCAAACGCTACTTGTCTAAATACACCATTAACCCAGCGATCGCTCATGGGATTAGC
(2)1201
(3)1201
(4)1201

(1)1261 GAGTATGTAGTTCTGTAGAAGTGGGCAAAGTGGCTGACTTGGTATTGTGGAGTCCCAGCA
(2)1261A.....A...
(3)1261A.....A...
(4)1261A.....

(1)1321 TTCTTTGGCGTAAAACCAACATGATCATCAAAGCGGGTTCATTGCGTTGAGTCAAATG
(2)1321G.....A.....A..C.....
(3)1321G.....T.....A.....
(4)1321G.....A.....

(1)1381 GGTGACGCGAACGCTTCTATCCCTACCCACAACCAGTTTATTACAGAGAAATGTTTCGCT
(2)1381 ..C..T.....G.....
(3)1381 ..C..T.....
(4)1381 ..C..T.....

(1)1441 CATCATGGTAAAGCCAAATACGATGCAAACATCACTTTTGTGTCTCAAGCGGCTTATGAC
(2)1441T.....
(3)1441A..C.....A.....
(4)1441

```

(1)1501 AAAGGCATTAAAGAAGAATTAGGGCTTGAAAGACAAGTGTGCGGTAAAAAATTGCAGA
(2)1501 .....A.....
(3)1501 .....
(4)1501 .....

(1)1561 AACATCACTAAAAAGACATGCAATTCAACGACACTACCGCTCACATTGAAGTCAATCCT
(2)1561 ..T.....T.....
(3)1561 .....
(4)1561 .....

(1)1621 GAAACTTACCATGTGTTTCGTGGATGGCAAAGAAGTAACTTCTAAACCAGCCAATAAAGTG
(2)1621 .....
(3)1621 .....C.....
(4)1621 .....C.....

(1)1681 AGCTTGGCGCAACTCTTTAGCATTCTTAG
(2)1681 .....
(3)1681 .....
(4)1681 .....A.....

```

Figure 2 Homology comparison of the cloned and reported *H pylori ureB* nucleotide sequences.(1)-(3): the reported sequences from GenBank (No. NC000915, strain 26695; No. M60398, X57132; No. AB032429); (4): the sequencing result of *H pylori* strain Y06 *ureB* gene. Underlined areas indicate the positions of primer sequences.

```

[1]1  MKKISRKEYVSMYGPTTGDKVRLGDTDLIAEVEHDYTIYGEELKFGGGKTLREGMSQSNN
[2]1  .....
[3]1  .....
[4]1  //M.....

[1]61  PSKEELDLIITNALIVDYTGIIYKADIGIKDGKIAGIGKGGNKMDQGVKNNLSVGPATEA
[2]61  .....
[3]61  .....
[4]61  .....

[1]121 LAGEGLIVTAGGIDTHIHFISPOQIPTAFASGVTTMIGGGTGPADGTNATTITPGRRLK
[2]121 .....
[3]121 .....
[4]121 .....

[1]181 WMLRAAEEYSMNLGFLAKGNASNDASLADQIEAGAIGFKIHEDWGTTPSAINHALDVADK
[2]181 .....
[3]181 .....
[4]181 .....

[1]241 YDVQVAIHDTLNEAGCVEDTMAAIAGRTMHTFHTEGAGGGHAPDIKVVAGEHNILPAST
[2]241 .....
[3]241 .....
[4]241 .....

[1]301 NPTIPFTVNTAEHMDMLMVCHHLDKSIKEDVQFADSRIRPQTIAAEDTLHDMGIFSITS
[2]301 .....
[3]301 .....
[4]301 .....

[1]361 SDSQAMGRVGEVITRTWQTADKNKKEFGRLKEEKGDNDNFRIKRYLSKYTINPAIAHGIS
[2]361 .....
[3]361 .....
[4]361 .....

[1]421 EYVGSVEVGKVADLVLWSPAFFGVKPNMIKGGFIALSQMGDANASIPTPQPVVYREMFA
[2]421 .....
[3]421 .....
[4]421 .....

[1]481 HHGKAKYDANITFVSQAAYDKGIKEELGLERQVLPVKNCRNITKKDMQFNDTTAHIEVNP
[2]481 .....
[3]481 .....
[4]481 .....

[1]541 ETYHVFVDGKEVTSKPANKVSLAQLFSIF
[2]541 .....
[3]541 .....T.....
[4]541 .....

```

Figure 3 Homology comparison of the putative amino acid sequences of the cloned and reported *H pylori ureB* gene. [1]-[3]: the reported sequences from GenBank (No. NC000915, strain 26695; No. M60398, X57132; No. AB032429); [4]: the putative amino acid sequence of the cloned *H pylori* strain Y06 *ureB* gene.

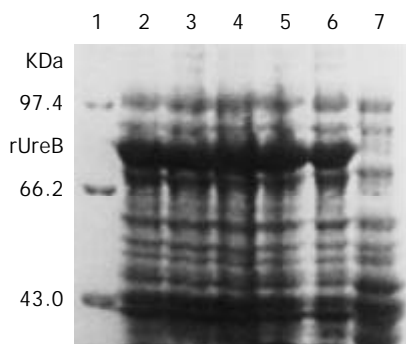


Figure 4 Expression of *rUreB* induced by IPTG at different concentrations. Lane 1, molecular mass marker; lanes 2-4, IPTG at 1.0, 0.5, and 0.1 mmol/L, respectively; lanes 5 and 6, bacterial precipitate and supernatant with IPTG at 1 mmol/L, respectively; lane 7, control.

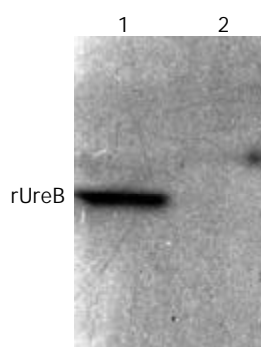


Figure 5 Western blot result of commercial rabbit antibodies against the whole cell of *H. pylori* and *rUreB*. Lane 1, *rUreB*; lane 2, blank.

samples was 0.173 ± 0.025 , the positive reference value for the specific antibody detection in patients' sera was 0.248. According to the reference value, 100% (125/125, one serum sample was contaminated) of the tested patients' serum samples were positive for antibody against *rUreB* with an A_{490} value range of 0.27-1.97. Since the mean \pm SD of A_{490} of the 6 negative bacterial controls was 0.170 ± 0.026 , the positive reference value was 0.248 for *UreB* detection in *H. pylori* isolates. According to the reference value, 100% (109/109, the other 17 isolates could not be revived from -70°C) of the tested *H. pylori* isolates were positive for *rUreB* epitopes with an A_{490} value range of 0.47-1.93.

DISCUSSION

Amoxicillin and metronidazole, used as routinely therapeutic antibiotics in a triple therapy, effectively eradicate *H. pylori* infection *in vivo*^[56-58]. However, there are problems such as side effects, emergence of drug resistance and re-infection after withdrawal of antibiotics, etc. It is generally considered that inoculation with *H. pylori* vaccine is of value in prevention and control of *H. pylori* infection. Previous studies have demonstrated that inoculation with sonic-broken *H. pylori* resist the challenge of live *H. pylori* and even eliminate existing infection of *H. pylori* in animal models. But high nutrition requirements, poor growth after several passages, easy contamination during cultivation and difficulty in bacterial conservation make whole cell vaccine of *H. pylori* impracticable. Genetic engineering vaccine seems to be a possible pathway for developing *H. pylori* vaccine. *UreB*, used as a candidate antigen for *H. pylori* genetic engineering vaccine, has advantages of high sequence conservation, a high frequency of distribution and large expression in different isolates, strong

antigenicity due to its big molecular mass, granular structure and exposure on the surface of bacteria^[59,60].

In the present study, a prokaryotic expression system of *rUreB* was constructed. In comparison with the three published *ureB* gene sequences^[51-53], high homologies of 96.88-97.82% and 99.65-99.82% of the nucleotide and putative amino acid sequences of the cloned *ureB* gene from the *H. pylori* strain Y06, respectively, were found, whereas homologies were 96.78-97.83% and 99.82-100%, respectively, among the *ureB* genes from the 3 *H. pylori* strains. These data indicate that the mutation level of *ureB* gene from different *H. pylori* strains is considerably low.

The results of SDS-PAGE performed in this study demonstrate that the constructed prokaryotic expression system pET32a-*ureB*-BL21DE3 efficiently produces *rUreB* even at the concentration of IPTG as low as 0.1 mmol/L. *rUreB* mainly is presented in the form of dissoluble inclusion body and appears in the supernatant of culture only in a small amount. The output of *rUreB* is relatively high (approximately 30% of the total bacterial proteins), which is beneficial to industrial production.

Western blot assay performed in this study confirms that the commercial rabbit antiserum against whole cell of *H. pylori* recognizes and combines to *rUreB*, indicating a high immunoreactivity of the recombinant protein. The immunodiffusion assay also demonstrates that *rUreB* efficiently induces rabbit to produce specific antibody with a higher titer, exhibiting a favorable antigenicity of the recombinant protein.

The findings by ELISA that all the tested *H. pylori* isolates expressed *UreB* and all the tested sera from *H. pylori* infected patients were positive for *UreB*-specific antibody indicate the universal existence of *UreB* in *H. pylori* strains and a high frequency of *UreB*-specific antibody in human, which supports application of *rUreB* as an antigen for the development of *H. pylori* vaccine.

ACKNOWLEDGEMENTS

We are grateful to the people's Hospital of Zhejiang, the First Affiliated Hospital of Zhejiang University, the Second Affiliated Hospital of Zhejiang University and the Affiliated Run Run Shaw Hospital of Zhejiang University in Hangzhou for kindly providing gastric biopsies in this study.

REFERENCES

- 1 **Ye GA**, Zhang WD, Liu LM, Shi L, Xu ZM, Chen Y, Zhou DY. *Helicobacter pylori vacA* gene polymorphism and chronic gastritis. *Shijie Huaren Xiaohua Zazhi* 2001; **9**: 593-595
- 2 **Lu SY**, Pan XZ, Peng XW, Shi ZL. Effect of Hp infection on gastric epithelial cell kinetics in stomach diseases. *Shijie Huaren Xiaohua Zazhi* 1999; **7**: 760-762
- 3 **Zhang Z**, Yuan Y, Gao H, Dong M, Wang L, Gong YH. Apoptosis, proliferation and p53 gene expression of *H. pylori* associated gastric epithelial lesions. *World J Gastroenterol* 2001; **7**: 779-782
- 4 **Lu XL**, Qian KD, Tang XQ, Zhu YL, Du Q. Detection of *H. pylori* DNA in gastric epithelial cells by *in situ* hybridization. *World J Gastroenterol* 2002; **8**: 305-307
- 5 **Yao YL**, Xu B, Song YG, Zhang WD. Overexpression of cyclin E in Mongolian gerbil with *Helicobacter pylori*-induced gastric precancerosis. *World J Gastroenterol* 2002; **8**: 60-63
- 6 **Guo DL**, Dong M, Wang L, Sun LP, Yuan Y. Expression of gastric cancer-associated MG7 antigen in gastric cancer, precancerous lesions and *H. pylori*-associated gastric diseases. *World J Gastroenterol* 2002; **8**: 1009-1013
- 7 **Peng ZS**, Liang ZC, Liu MC, Ouyang NT. Studies on gastric epithelial cell proliferation and apoptosis in Hp associated gastric ulcer. *Shijie Huaren Xiaohua Zazhi* 1999; **7**: 218-219
- 8 **Hiyama T**, Haruma K, Kitadai Y, Miyamoto M, Tanaka S, Yoshihara M, Sumii K, Shimamoto F, Kajiyama G. B-cell

- monoclonality in *Helicobacter pylori*-associated chronic atrophic gastritis. *Virchows Arch* 2001; **483**: 232-237
- 9 **Xia HHX**. Association between *Helicobacter pylori* and gastric cancer: current knowledge and future research. *World J Gastroenterol* 1998; **4**: 93-96
 - 10 **Quan J**, Fan XG. Progress in experimental research of *Helicobacter pylori* infection and gastric carcinoma. *Shijie Huaren Xiaohua Zazhi* 1999; **7**: 1068-1069
 - 11 **Liu HF**, Liu WW, Fang DC. Study of the relationship between apoptosis and proliferation in gastric carcinoma and its precancerous lesion. *Shijie Huaren Xiaohua Zazhi* 1999; **7**: 649-651
 - 12 **Zhu ZH**, Xia ZS, He SG. The effects of ATRA and 5-Fu on telomerase activity and cell growth of gastric cancer cells *in vitro*. *Shijie Huaren Xiaohua Zazhi* 2000; **8**: 669-673
 - 13 **Tu SP**, Zhong J, Tan JH, Jiang XH, Qiao MM, Wu YX, Jiang SH. Induction of apoptosis by arsenic trioxide and hydroxy camptothecin in gastric cancer cells *in vitro*. *World J Gastroenterol* 2000; **6**: 532-539
 - 14 **Cai L**, Yu SZ, Zhang ZF. *Helicobacter pylori* infection and risk of gastric cancer in Changle County, Fujian Province, China. *World J Gastroenterol* 2000; **6**: 374-376
 - 15 **Yao XX**, Yin L, Zhang JY, Bai WY, Li YM, Sun ZC. HTERT expression and cellular immunity in gastric cancer and precancerosis. *Shijie Huaren Xiaohua Zazhi* 2001; **9**: 508-512
 - 16 **Xu AG**, Li SG, Liu JH, Gan AH. Function of apoptosis and expression of the proteins Bcl-2, p53 and C-myc in the development of gastric cancer. *World J Gastroenterol* 2001; **7**: 403-406
 - 17 **Wang X**, Lan M, Shi YQ, Lu J, Zhong YX, Wu HP, Zai HH, Ding J, Wu KC, Pan BR, Jin JP, Fan DM. Differential display of vincristine-resistance-related gene in gastric cancer SGC7901 cell. *World J Gastroenterol* 2002; **8**: 54-59
 - 18 **Liu JR**, Li BX, Chen BQ, Han XH, Xue YB, Yang YM, Zheng YM, Liu RH. Effect of cis-9, trans-11-conjugated linoleic acid on cell cycle of gastric adenocarcinoma cell line (SGC-7901). *World J Gastroenterol* 2002; **8**: 224-229
 - 19 **Cai L**, Yu SZ. A molecular epidemiologic study on gastric cancer in Changle, Fujian Province. *Shijie Huaren Xiaohua Zazhi* 1999; **7**: 652-655
 - 20 **Gao GL**, Yang Y, Yang SF, Ren CW. Relationship between proliferation of vascular endothelial cells and gastric cancer. *Shijie Huaren Xiaohua Zazhi* 2000; **8**: 282-284
 - 21 **Xue XC**, Fang GE, Hua JD. Gastric cancer and apoptosis. *Shijie Huaren Xiaohua Zazhi* 1999; **7**: 359-361
 - 22 **Niu WX**, Qin XY, Liu H, Wang CP. Clinicopathological analysis of patients with gastric cancer in 1 200 cases. *World J Gastroenterol* 2001; **7**: 281-284
 - 23 **Li XY**, Wei PK. Diagnosis of stomach cancer by serum tumor markers. *Shijie Huaren Xiaohua Zazhi* 2001; **9**: 568-570
 - 24 **Fang DC**, Yang SM, Zhou XD, Wang DX, Luo YH. Telomere erosion is independent of microsatellite instability but related to loss of heterozygosity in gastric cancer. *World J Gastroenterol* 2001; **7**: 522-526
 - 25 **Morgner A**, Miehke S, Stolte M, Neubauer A, Alpen B, Thiede C, Klann H, Hierlmeier FX, Ell C, Ehninger G, Bayerdorffer E. Development of early gastric cancer 4 and 5 years after complete remission of *Helicobacter pylori*-associated gastric low-grade marginal zone B-cell lymphoma of MALT type. *World J Gastroenterol* 2001; **7**: 248-253
 - 26 **Deng DJ**. Progress of gastric cancer etiology: N-nitrosamides in the 1990s. *World J Gastroenterol* 2000; **6**: 613-618
 - 27 **Liu ZM**, Shou NH, Jiang XH. Expression of lung resistance protein in patients with gastric carcinoma and its clinical significance. *World J Gastroenterol* 2000; **6**: 433-434
 - 28 **Guo CQ**, Wang YP, Liu GY, Ma SW, Ding GY, Li JC. Study on *Helicobacter pylori* infection and p53, c-erbB-2 gene expression in carcinogenesis of gastric mucosa. *Shijie Huaren Xiaohua Zazhi* 1999; **7**: 313-315
 - 29 **Cai L**, Yu SZ, Ye WM, Yi YN. Fish sauce and gastric cancer: an ecological study in Fujian Province, China. *World J Gastroenterol* 2000; **6**: 671-675
 - 30 **Xue FB**, Xu YY, Wan Y, Pan BR, Ren J, Fan DM. Association of *H pylori* infection with gastric carcinoma: a Meta analysis. *World J Gastroenterol* 2001; **7**: 801-804
 - 31 **Wang RT**, Wang T, Chen K, Wang JY, Zhang JP, Lin SR, Zhu YM, Zhang WM, Cao YX, Zhu CW, Yu H, Cong YJ, Zheng S, Wu BQ. *Helicobacter pylori* infection and gastric cancer: evidence from a retrospective cohort study and nested case-control study in China. *World J Gastroenterol* 2002; **8**: 1103-1107
 - 32 **Hua JS**. Effect of *Hp*: cell proliferation and apoptosis on stomach cancer. *Shijie Huaren Xiaohua Zazhi* 1999; **7**: 647-648
 - 33 **Liu DH**, Zhang XY, Fan DM, Huang YX, Zhang JS, Huang WQ, Zhang YQ, Huang QS, Ma WY, Chai YB, Jin M. Expression of vascular endothelial growth factor and its role in oncogenesis of human gastric carcinoma. *World J Gastroenterol* 2001; **7**: 500-505
 - 34 **Cao WX**, Ou JM, Fei XF, Zhu ZG, Yin HR, Yan M, Lin YZ. Methionine-dependence and combination chemotherapy on human gastric cancer cells *in vitro*. *World J Gastroenterol* 2002; **8**: 230-232
 - 35 **Michetti P**, Kreiss C, Kotloff K, Porta N, Blanco JL, Bachmann D, Herranz M, Saldinger PF, Corthesy-Theulaz I, Losonsky G, Nichols R, Simon J, Stolte M, Ackerman S, Monath TP, Blum AL. Oral immunization with urease and *Escherichia coli* heat-labile enterotoxin is safe and immunogenic in *Helicobacter pylori*-infected adults. *Gastroenterology* 1999; **116**: 804-812
 - 36 **Suganuma M**, Kurusu M, Okabe S, Sueoka N, Yoshida M, Wakatsuki Y, Fujiki H. *Helicobacter pylori* membrane protein 1: a new carcinogenic factor of *Helicobacter pylori*. *Cancer Res* 2001; **61**: 6356-6359
 - 37 **Nakamura S**, Matsumoto T, Suekane H, Takeshita M, Hizawa K, Kawasaki M, Yao T, Tsuneyoshi M, Iida M, Fujishima M. Predictive value of endoscopic ultrasonography for regression of gastric low grade and high grade MALT lymphomas after eradication of *Helicobacter pylori*. *Gut* 2001; **48**: 454-460
 - 38 **Uemura N**, Okamoto S, Yamamoto S, Matsumura N, Yamaguchi S, Yamakido M, Taniyama K, Sasaki N, Schlemper RJ. *Helicobacter pylori* infection and the development of gastric cancer. *N Engl J Med* 2001; **345**: 784-789
 - 39 **Morgner A**, Miehke S, Fischbach W, Schmitt W, Muller-Hermelink H, Greiner A, Thiede C, Schetelig J, Neubauer A, Stolte M, Ehninger G, Bayerdorffer E. Complete remission of primary high-grade B-cell gastric lymphoma after cure of *Helicobacter pylori* infection. *J Clin Oncol* 2001; **19**: 2041-2048
 - 40 **Kate V**, Ananthakrishnan N, Badrinath S. Effect of *Helicobacter pylori* eradication on the ulcer recurrence rate after simple closure of perforated duodenal ulcer: retrospective and prospective randomized controlled studies. *Br J Surg* 2001; **88**: 1054-1058
 - 41 **Zhuang XQ**, Lin SR. Progress in research on the relationship between *Hp* and stomach cancer. *Shijie Huaren Xiaohua Zazhi* 2000; **8**: 206-207
 - 42 **Gao HJ**, Yu LZ, Bai JF, Peng YS, Sun G, Zhao HL, Miu K, Lü XZ, Zhang XY, Zhao ZQ. Multiple genetic alterations and behavior of cellular biology in gastric cancer and other gastric mucosal lesions: *H pylori* infection, histological types and staging. *World J Gastroenterol* 2000; **6**: 848-854
 - 43 **Yao YL**, Zhang WD. Relation between *Helicobacter pylori* and gastric cancer. *Shijie Huaren Xiaohua Zazhi* 2001; **9**: 1045-1049
 - 44 **Goto T**, Nishizono A, Fujioka T, Ikewaki J, Mifune K, Nasu M. Local secretory immunoglobulin A and postimmunization gastritis correlate with protection against *Helicobacter pylori* infection after oral vaccination of mice. *Infect Immun* 1999; **67**: 2531-2539
 - 45 **Watanabe T**, Tada M, Nagai H, Sasaki S, Nakao M. *Helicobacter pylori* infection induces gastric cancer in mongolian gerbils. *Gastroenterology* 1998; **115**: 642-648
 - 46 **Honda S**, Fujioka T, Tokieda M, Satoh R, Nishizono A, Nasu M. Development of *Helicobacter pylori*-induced gastric carcinoma in Mongolian Gerbils. *Cancer Res* 1998; **58**: 4255-4259
 - 47 **Hatzifoti C**, Wren BW, Morrow JW. *Helicobacter pylori* vaccine strategies-triggering a gut reaction. *Immuno Today* 2000; **21**: 615-619
 - 48 **Rupnow MF**, Owens DK, Shachter R, Parsonnet J. *Helicobacter pylori* vaccine development and use: a cost-effectiveness analysis using the Institute of Medicine Methodology. *Helicobacter* 1999; **4**: 272-280
 - 49 **Corthesy-Theulaz I**, Porta N, Glauser M, Saraga E, Vaney AC, Haas R, Kraehenbuhl JP, Blum AL, Michetti P. Oral im-

- munization with *Helicobacter pylori* urease B subunit as a treatment against *Helicobacter* infection in mice. *Gastroenterology* 1995; **109**: 115-121
- 50 **Pappo J**, Thomas WD Jr, Kabok Z, Taylor NS, Murphy JC, Fox JG. Effect of oral immunization with recombinant urease on murine *Helicobacter felis* gastritis. *Infect Immun* 1995; **63**: 1246-1252
- 51 **Tomb JF**, White O, Kerlavage AR, Clayton RA, Sutton GG, Fleischmann RD, Ketchum KA, Klenk HP, Gill S, Dougherty BA, Nelson K, Quackenbush J, Zhou L, Kirkness EF, Peterson S, Loftus B, Richardson D, Dodson R, Khalak HG, Glodek A, McKenney K, Fitzgerald LM, Lee N, Adams MD, Venter JC. The complete genome sequence of the gastric pathogen *Helicobacter pylori*. *Nature* 1997; **388**: 539-547
- 52 **Akada JK**, Shirai M, Takeuchi H, Tsuda M, Nakazawa T. Identification of the urease operon in *Helicobacter pylori* and its control by mRNA decay in response to pH. *Mol Microbiol* 2000; **36**: 1071-1084
- 53 **Labigne A**, Cussac V, Courcoux P. Shuttle cloning and nucleotide sequences of *Helicobacter pylori* genes responsible for urease activity. *J Bacteriol* 1991; **173**: 1920-1931
- 54 **Sambrook J**, Fritsch EF, Maniatis T. Molecular Cloning, A Laboratory Manual [M]. 2nd edition. New York: Cold Spring Harbor Laboratory Press. 1989, pp1.21-1.52, 2.60-2.80, 7.3-7.35, 9.14-9.22
- 55 **Chen Y**, Wang J, Shi L. *In vitro* study of the biological activities and immunogenicity of recombinant adhesion of *Helicobacter pylori* rHpaA. *Zhonghua Yixue Zazhi* 2001; **81**: 276-279
- 56 **McMahon BJ**, Hennessy TW, Bensler JM, Bruden DL, Parkinson AJ, Morris JM, Reasonover AL, Hurlburt DA, Bruce MG, Sacco F, Butler JC. The relationship among previous antimicrobial use, antimicrobial resistance, and treatment outcomes for *Helicobacter pylori* infections. *Ann Intern Med* 2003; **139**: 463-469
- 57 **Wong WM**, Gu Q, Wang WH, Fung FM, Berg DE, Lai KC, Xia HH, Hu WH, Chan CK, Chan AO, Yuen MF, Hui CK, Lam SK, Wong BC. Effects of primary metronidazole and clarithromycin resistance to *Helicobacter pylori* on omeprazole, metronidazole, and clarithromycin triple-therapy regimen in a region with high rates of metronidazole resistance. *Clin Infect Dis* 2003; **37**: 882-889
- 58 **Chi CH**, Lin CY, Sheu BS, Yang HB, Huang AH, Wu JJ. Quadruple therapy containing amoxicillin and tetracycline is an effective regimen to rescue failed triple therapy by overcoming the antimicrobial resistance of *Helicobacter pylori*. *Aliment Pharmacol Ther* 2003; **18**: 347-353
- 59 **Dieterich C**, Bouzourene H, Blum AL, Corthesy-Theulaz IE. Urease-based mucosal immunization against *Helicobacter heilmannii* infection induces corpus atrophy in mice. *Infect Immun* 1999; **67**: 6206-6209
- 60 **Ernst JD**. Toward the development of antibacterial vaccines: report of a symposium and workshop. Organizing Committee. *Clin Infect Dis* 1999; **29**: 1295-1302

Edited by Xia HHX and Xu FM

Construction of a prokaryotic expression system of *vacA* gene and detection of *vacA* gene, VacA protein in *Helicobacter pylori* isolates and ant-VacA antibody in patients' sera

Jie Yan, Ya-Fei Mao

Jie Yan, Ya-Fei Mao, Department of Medical Microbiology and Parasitology, College of Medical Science, Zhejiang University, Hangzhou 310031, Zhejiang Province, China

Supported by the Excellent Young Teacher Fund of Chinese Education Ministry and the General Science and Technology Research Program of Zhejiang Province, No. 001110438

Correspondence to: Jie Yan, Department of Medical Microbiology and Parasitology, College of Medical Science, Zhejiang University, 353 Yan An Road, Hangzhou 310031, Zhejiang Province, China. yanchen@mail.hz.zj.cn

Telephone: +86-571-87217385 **Fax:** +86-571-87217044

Received: 2003-10-15 **Accepted:** 2003-12-06

Abstract

AIM: To construct a recombinant prokaryotic expression vector inserted with *Helicobacter pylori vacA* gene and identify the immunity of the expressed recombinant protein, and to determine prevalence of *vacA*-carrying/VacA expressing *H pylori* isolates and seroprevalence of specific anti-VacA antibody in *H pylori* infected patients.

METHODS: Polymerase chain reaction technique was used to amplify complete *vacA* gene of *H pylori* strain NCTC11637 and to detect *vacA* gene in 109 *H pylori* isolates. The amplification product of the complete *vacA* gene was sequenced after T-A cloning. A recombinant expression vector inserted with a complete *vacA* gene fragment, named as *pET32a-vacA*, was constructed. Expression of the target recombinant protein VacA (rVacA) was examined by SDS-PAGE. Western blot using commercial antibodies against whole cell of *H pylori* and an immunodiffusion assay using self-prepared rabbit anti-rVacA antibody were applied to determine immunoreaction and antigenicity of rVacA. Two ELISA methods were established to detect VacA expression in *H pylori* isolates and the specific anti-VacA antibody in sera from 125 patients infected with *H pylori*.

RESULTS: In comparison with the reported corresponding sequences, homologies of nucleotide and putative amino acid sequences of the cloned *vacA* gene were 99.82% and 100%, respectively. The constructed recombinant prokaryotic expression system efficiently produced rVacA. rVacA was able to combine with the commercial antibodies against whole cell of *H pylori* and to induce the immunized rabbit to produce specific antibody with an immunodiffusion titer of 1:4. All tested *H pylori* isolates carried *vacA* gene, but only 66.1% expressed VacA protein. Of the serum samples tested, 42.4% were positive for specific anti-VacA antibody.

CONCLUSION: A prokaryotic expression system of *H pylori vacA* gene was successfully constructed. The expressed rVacA can be used to detect specific anti-VacA antibody in human and to prepare antiserum in animals. The high frequency of *vacA* gene in *H pylori* isolates, but with a low frequency of VacA expression and specific anti-VacA antibody

in *H pylori* infected patients implies that VacA is not an ideal antigen for *H pylori* vaccine.

Yan J, Mao YF. Construction of a prokaryotic expression system of *vacA* gene and detection of *vacA* gene, VacA protein in *Helicobacter pylori* isolates and ant-VacA antibody in patients' sera. *World J Gastroenterol* 2004; 10(7): 985-990
<http://www.wjgnet.com/1007-9327/10/985.asp>

INTRODUCTION

In China, gastritis and peptic ulcer are two most prevalent gastric diseases, and gastric cancer is one of the malignant tumors with high morbidities^[1-34]. *Helicobacter pylori* is recognized as a human-specific gastric pathogen that colonizes the stomachs of at least half of the world's populations^[35]. Most infected individuals are asymptomatic. However, in some subjects, the infection causes acute/chronic gastritis or peptic ulceration, and plays an important role in the development of gastric adenocarcinoma, mucosa-associated lymphoid tissue (MALT) lymphoma and primary gastric non-Hodgkin's lymphoma^[36-43].

Vacuolating cytotoxin, an important pathogenic factor of *H pylori*, is able to cause vacuolar degeneration in epithelial cells such as HeLa and RK-13 cell lines^[44-46]. The gene of vacuolating cytotoxin has 3 864-3 888 bp in size containing a region for a signal peptide at the amino-end, a fragment with approximate 2 241 bp (*vacA*) and a region for a peptide at the carboxyl-end^[47]. The signal and C-end peptides are left in inner and outer membranes of *H pylori* during secreting the cytotoxin^[48]. VacA, responsible for the toxicity of vacuolating cytotoxin, is excreted out of the bacterium^[49]. In some of the previous studies, VacA was demonstrated as a fine antigen for *H pylori* vaccine^[50,51]. However, it has been reported that almost all *H pylori* strains carry *vacA* gene but VacA is detectable only in 50-60% of the strains^[52]. For a fine practical strategy of genetic engineering vaccine development, an antigen candidate must satisfy the requirements including exposure on the surface of bacterial body, universal distribution in different strains and strong antigenicity to induce a specific antibody. So it is a critical subject to determine VacA expression in different *H pylori* strains and the prevalence of specific anti-VacA antibody in infected individuals from various geographical areas. In this study, a recombinant expression plasmid containing complete *vacA* gene was constructed. By using ELISA, VacA expression in different *H pylori* isolates and seroprevalence of anti-VacA specific antibody from *H pylori* infected patients were determined.

MATERIALS AND METHODS

Materials

H pylori strain NCTC11637 was kept in our laboratory. Primers for polymerase chain reaction (PCR) amplification were synthesized by BioAsia (Shanghai, China). Taq-plus high fidelity

PCR kit and restriction endonucleases were purchased from TaKaRa (Dalian, China). The T-A Cloning kit and sequencing service were provided by BBST (Shanghai, China). A plasmid *pET32a* as an expression vector and *E. coli* BL21 DE3 as a host cell were provided by Novagen (Novagen, Madison, USA). Rabbit antiserum against whole cell of *H. pylori*, HRP-labeling sheep antisera against rabbit IgG and against human IgG were purchased from DAKO (Glostrup, Denmark) and Jackson ImmunoResearch (West Grove, USA), respectively. Overall, 156 patients who were referred for upper endoscopy at four hospitals in Hangzhou during November 2001 to February 2003 due to various gastroduodenal diseases and who had a positive urease test on gastric biopsy specimens and serum samples collected, were included in the study. Reagents used in isolation and identification of *H. pylori* were purchased from bioMérieux (Marcy l'Étoile, France).

Isolation and identification of *H. pylori*

Each biopsy specimen was homogenized with a tissue grinder and then inoculated on Columbia agar plates supplemented with 80 mL/L sheep blood, 5 g/L cyclodextrin, 5 mg/L trimethoprim, 10 mg/L vancomycin, 2.5 mg/L amphotericin B and 2 500 U/L cefsulodin. The plates were incubated at 37 °C under microaerobic conditions (50 mL/L O₂, 100 mL/L CO₂ and 850 mL/L N₂) for 3 to 5 d. A bacterial isolate was identified as *H. pylori* according to typical Gram staining morphology, biochemical tests positive for urease and oxidase, and slide agglutination with the commercial rabbit antibodies against whole cell of *H. pylori*. A total of 126(80.1%) *H. pylori* strains isolated from the 156 specimens were well-characterized.

Preparation of DNA template

Genomic DNA from each *H. pylori* strain was extracted by the conventional phenol-chloroform method and DNase-free RNase treatment. The obtained DNA was dissolved in TE buffer. Concentration and purity of the DNA preparations were determined by ultraviolet spectrophotometry^[53].

Polymerase chain reaction

Primers were designed to amplify complete *vacA* gene from *H. pylori* strain NCTC11637 based on the published data (GenBank accession No.: AF049653)^[54]. The sequences of sense primer with an endonuclease site of *EcoR* I and antisense primer with an endonuclease site of *Xho* I were 5'-GAGGAATTCATGGAAATACAACAAACACACCGC-3' and 5'-GGACTCGAGTTAATTGGTACCTGTAGAAACATTACC-3', respectively. The total volume per PCR was 100 µL containing 2.5 mol/L each dNTP, 250 nmol/L each of the 2 primers, 15 mol/L MgCl₂, 3.0 U Taq-plus polymerase, 100 ng DNA template and 1×PCR buffer (pH8.3). The parameters for PCR were 94 °C for 5 min, ×1; 94 °C for 30 s, 58 °C for 30 s, 72 °C for 120 s, ×10; 94 °C for 30 s, 58 °C for 30 s, 72 °C for 135 s (15 s addition for the each of the following cycles), ×15; and then 72 °C for 15 min, ×1.

The sequences of primers for detecting *vacA* gene in *H. pylori* isolates were 5'-TCAATATCAACAAGCTC-3' (sense), and 5'-CCGCATGCTTTAATGTC-3' (antisense)^[55]. The reagents and the concentrations, reaction volume and PCR parameters were the same as those for amplifying complete *vacA* gene, except primer difference, annealing temperature at 52 °C, extensive time for 60 s and 35 cycles.

The results of PCR were visualized under UV light after electrophoresis in 10 g/L agarose pre-stained with ethidium bromide. The expected sizes of the target amplification fragments with whole length of *vacA* gene for cloning and partial length of *vacA* gene for detection were 2 241 bp and 787 bp, respectively.

Cloning and sequencing

The target amplification fragment of complete *vacA* gene from *H. pylori* strain NCTC11637 was cloned into plasmid vector *pUCm-T* (*pUCm-T-vacA*) by using the T-A Cloning kit according to the manufacturer's instruction. The recombinant plasmid was amplified in *E. coli* DH5α and then extracted by Sambrook's method^[53]. A professional company (BBST) was responsible for nucleotide sequence analysis of the inserted fragment. Two plasmids, *pUCm-T-vacA* and *pET32a*, in 2 different strains of *E. coli* DH5α after amplified in LB medium were extracted and then digested with *EcoRI* and *Xho* I, respectively^[53]. The target fragments of *vacA* gene and *pET32a* were recovered and then ligated. The recombinant expression vector *pET32a-vacA* was transformed into *E. coli* BL21DE3, and the expression system was named as *pET32a-vacA-E. coliBL21DE3*. *vacA* gene inserted in *pET32a* plasmid was sequenced again.

Expression and identification of the target recombinant protein

pET32a-vacA-E. coliBL21DE3 was rotatively cultured in LB medium at 37 °C and induced by isopropylthio-β-D-galactoside (IPTG) at different concentrations of 1.0, 0.5 and 0.1 mmol/L. Supernatant and precipitate of the culture after incubation were separated by centrifugation and then the bacterial pallet was ultrasonically broken (300 V, 5 s×3). SDS-PAGE was used to measure the molecular weight and output of rVacA, and Ni-NTA affinity chromatography was applied to collect the recombinant protein. The commercial rabbit antiserum against whole cell of *H. pylori* and HRP-labeling sheep antiserum against rabbit IgG were respectively used as the first and second antibodies to determine the immunoreactivity of rVacA by Western blot. Rabbits were immunized with rVacA to prepare the antiserum. An immunodiffusion assay was performed to determine antigenicity of rVacA.

ELISA

By using rVacA as the coated antigen at concentration of 20 µg/mL, a patient serum sample (1:200 dilution) as the first antibody and HRP-labeling sheep antibody against human IgG (1:4 000 dilution) as the second antibody, antibody against VacA in sera of the 126 *H. pylori* infected patients were detected. The result of ELISA for a patient's serum sample was considered as positive if the value of optical density at 490 nm (A₄₉₀) was over the mean plus 3 SD of five different negative serum samples^[56]. VacA expression in clinical isolates of *H. pylori* was examined by using the ultrasonic supernatant of each isolate (50 µg/mL) as the coated antigen, the self-prepared rabbit anti-rVacA serum (1:2 000 dilution) as the first antibody and HRP-labeling sheep antibody against rabbit IgG (1:4 000 dilution) as the second antibody. The result of ELISA for a *H. pylori* ultrasonic supernatant sample was considered as positive if its OD₄₉₀ value was over the mean plus 3 SD of five separated *E. coli* ATCC 25922 ultrasonic supernatant samples at the same protein concentration^[56].

Data analysis

The nucleotide and putative amino acid sequences of the cloned *vacA* gene were compared for homology with the published corresponding sequences (GenBank accession No. AF049653)^[54].

RESULTS

PCR

All tested *H. pylori* isolates (109/109) were positive for *vacA* gene. The target amplification products with whole length of *vacA* gene from *H. pylori* strain NCTC11637 and with partial

fragment of *vacA* gene from *H pylori* isolate were shown in Figure 1, respectively.

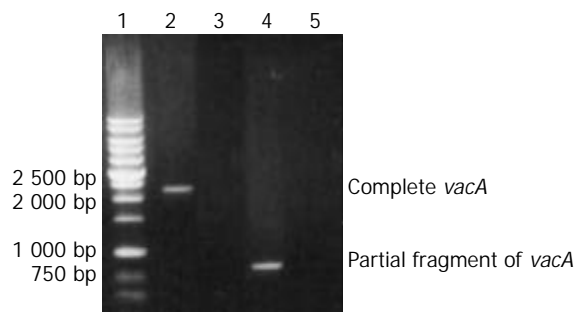


Figure 1 The target amplification products with whole length of *vacA* gene from *H pylori* strain NCTC11637 and partial fragment of *vacA* gene from a *H pylori* isolate. Lane 1, DNA marker; lane 2, an amplification fragment of complete *vacA* gene from *H pylori* strain NCTC11637; lane 4, an amplification fragment of partial *vacA* gene from a *H pylori* isolate; and lanes 3 and 5, blank controls.

Nucleotide sequence analysis

The nucleotide sequences of *vacA* gene in *pUCm-T-vacA* and *pET32a-vacA* were completely same. The nucleotide and putative amino acid sequences of the cloned *vacA* gene (Figure 2) showed 99.82% and 100% homologies, respectively, compared with the published sequence from *H pylori* strain NCTC11637 *vacA* gene (GenBank accession No.: AF049653)^[54].

Expression of the target recombinant protein

IPTG at concentrations of 1.0, 0.5 and 0.1 mmol/L efficiently induced the expression of rVacA in the *pET32a-vacA-E. coli BL21DE3* system. The expressed rVacA was mainly presented in ultrasonic precipitates, and the output was approximate 15% of the total bacterial proteins (Figure 3).

```

1  atggaaatacaacaacacaccgcaaaaatcaatcgcccttttggtttctcttgccttagta
1  M E I Q Q T H R K I N R P L V S L A L V
61  ggagcgttagtcagcatcacaccgcaacaaagtcatgcccgcctttttcacaaccgtgatc
21  G A L V S I T P Q Q S H A A F F T T V I
121  attccagccattggtgggggatCgctacagcgctgctgtaggaacgggtctcagggcctt
41  I P A I V G G I A T G A A V G T V S G L
181  cttAgctgggggctcaacaagccgaagaagccaataaaaccccagataaacccgataaa
61  L S W G L K Q A E E A N K T P D K P D K
241  gtttggcgattcaagcaggaagaggcttcaataatcttcctcacaaggaatacgcactta
81  V W R I Q A G K G F N N F P H K E Y D L
301  tacaaatcccttttatccagtaagattgatggaggctgggattgggggaatgccgctagg
101  Y K S L L S S K I D G G W D W G N A A R
361  cattattgggtcaaaggcgggcaatggaacaagcttgaagtggatatgaaagacgctgta
121  H Y W V K G G Q W N K L E V D M K D A V
421  gggacttataaactttcaggcctaataactttactgggtggggatttagatgtcaatag
141  G T Y K L S G L I N F T G G D L D V N M
481  caaaaagccactttgcgcttgggccaattcaatggcaattctttcacaagctataaggat
161  Q K A T L R L G Q F N G N S F T S Y K D
541  agTgctgatcgaccacgagagtggatttcaacgctaaaaatatcttaattgataatctt
181  S A D R T T R V D F N A K N I L I D N F
601  ttagaaatcaataatcgtgtgggttctggagccgggaggaaagccagctctacggtttta
201  L E I N N R V G S G A G R K A S S T V L
661  actttgcaagcttcagaagggatcactagcagtaaaaacgctgaaatctctttatgat
221  T L Q A S E G I T S S K N A E I S L Y D
    
```

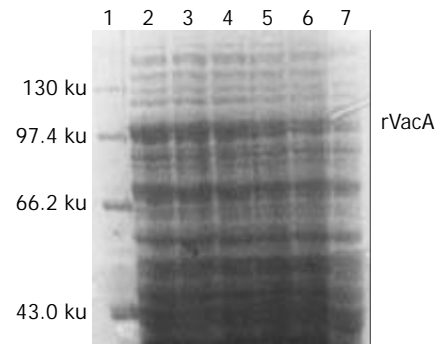


Figure 3 Expression of rVacA induced by IPTG at different concentrations. Lane 1, the protein marker; lanes 2-4, IPTG at 1.0, 0.5, 0.1 mmol/L respectively; lanes 5 and 6, bacterial precipitate and supernatant with IPTG at 0.5 mmol/L, respectively; and lane 7, the negative control.

Immunoreactivity and antigenicity of rVacA

The commercial rabbit antibodies against whole cell of *H pylori* combined with rVacA as confirmed by Western blot (Figure 4). The titer demonstrated by immunodiffusion assay between rVacA and rabbit anti-rVacA serum was 1:4.

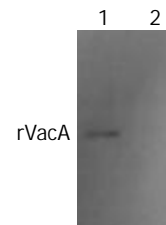


Figure 4 Western blot result of rabbit antibody against whole cell of *H pylori* and rVacA. Lane 1, rVacA expressed by *pET32a-vacA-E.coliBL21DE3*; and lane 2: negative control of *E.coliBL21DE3*.

721 ggtgccacgctcaatttggccttcaagcagtggttaaattaatgggtaatgtgtggatgggc
 241 G A T L N L A S S S V K L M G N V W M G
 781 cgtttgcaatacgtgggagcgtatctggccccttcatacagcagataaacacttcaaaa
 261 R L Q Y V G A Y L A P S Y S T I N T S K
 841 gtgacaggggaagtgaattttaaccatctcactgtgggcatcacaacgctgctcaagca
 281 V T G E V N F N H L T V G D H N A A Q A
 901 ggcatatcgctagtaacaagactcatattggcacattggatttgggcaaagcgcgggG
 301 G I I A S N K T H I G T L D L W Q S A G
 961 ctaaaccattatcgcccctccagaaggcggttataaggataaacctaaggataaacctagt
 321 L N I I A P P E G G Y K D K P K D K P S
 1021 aacaccagcgaataatgctaacaacaaccaacaaaacagcgctcaaaacaataataac
 341 N T T Q N N A N N N Q Q N S A Q N N N N
 1081 actcaggttattaaccacccaatagcgCgcaaaaaacagaaattcaaccacgcaagtc
 361 T Q V I N P P N S A Q K T E I Q P T Q V
 1141 attaatgggcttttggctgggtggcaagacacgggtggtcaatatcaaccgcatcaacact
 381 I N G P F A G G K D T V V N I N R I N T
 1201 aacgctgatggcacgattagagtgagggtataaagcttctcttaccaccaatgaggct
 401 N A D G T I R V G G Y K A S L T T N A A
 1261 catttgcatatcggcaaaggcggtatcaatctgtccaatcaagcgagcggcggttcttta
 421 H L H I G K G G I N L S N Q A S G R S L
 1321 ttggtggaaaatctaaccgggaatatcaccggtgatgggcctttaagagtgaataaccaa
 441 L V E N L T G N I T V D G P L R V N N Q
 1381 gtgggtggttatgctccttgaggatcaaacgcgaattttgagtttaaggctggcacggat
 461 V G G Y A L A G S N A N F E F K A G T D
 1441 accaaaaacggcacagccacttttaataacgatattagtttgggaagatttgtgaattta
 481 T K N G T A T F N N D I S L G R F V N L
 1501 aaagtggatgctcatacagctaattttaagggtattgatcgggtaatgggtggtttcaac
 501 K V D A H T A N F K G I D T G N G G F N
 1561 acctggatttttagtggcggttacagacaaagtcaatatcaacaagctcatcacagcttcc
 521 T L D F S G V T D K V N I N K L I T A S
 1621 actaatgtggccattaaaaacttcaacattaatgaattggtggttaagaccaatgggggtg
 541 T N V A I K N F N I N E L L V K T N G V
 1681 agtgtgggggaatacactcatttttagcgaagatataggcagtcattcgcgcatcaacacc
 561 S V G E Y T H F S E D I G S Q S R I N T
 1741 gtgcgttagaaaactggcactaggtcaatcttttctgggggtgtcaaatttaaaagcggc
 581 V R L E T G T R S I F S G G V K F K S G
 1801 gaaaaattggttatagatgagtttactatagcccttgggaatttttgacgctaggaat
 601 E K L V I D E F Y Y S P W N Y F D A R N
 1861 attaaaaatggtgaaatcaccagaaaattcgcttcttcaaccagaaaacccttggggc
 621 I K N V E I T R K F A S S T P E N P W G
 1921 acatcaaaaActcatgtttaataatctaaccctgggtcaaaatgcggtcatggactatagt
 641 T S K L M F N N L T L G Q N A V M D Y S
 1981 caattttcaaatttaaccattcaggggattttatcaacaatcaaggcactatcaactat
 661 Q F S N L T I Q G D F I N N Q G T I N Y
 2041 ctggtccgaggcgggaaagtggcaaccttaaatgtaggcaatgcagcagctatgatggtt
 681 L V R G G K V A T L N V G N A A A M M F
 2101 aataatgatatagacagcgcgaccggattttacaaccgctcatcaagattaacagcgcct
 701 N N D I D S A T G F Y K P L I K I N S A
 2161 caagatctcattaaaaatacagagcatgttttattgaaagcgaatcattgggtatggt
 721 Q D L I K N T E H V L L K A K I I G Y G
 2221 aatgtttctacaggtaccaattaa
 741 N V S T G T N *

Figure 2 Nucleotide and putative amino acid sequences of *vacA* gene from *H pylori* strain NCTC 11637. Note: Underlined areas indicate the position of primers; C, T, C and A are replaced by t, c, g and g in the nucleotide sequence from strain NCTC 11637, respectively, but the encoded amino acid residuals are not altered (are the changes correct?). “*” means stop codon.

ELISA

Since the mean±SD of A_{490} values of the five negative serum samples was 0.275±0.111 in the detection of specific antibodies in patients' sera, the positive reference value was 0.625. According to the reference value, 42.4% (53/125, one serum sample was contaminated) of the tested patients' serum samples were positive for antibody against rVacA with an A_{490} value range from 0.63-1.21. Since the mean±SD of A_{490} values of the five negative bacterial controls was 0.098±0.036 in the detection of VacA expression in *H pylori* isolates, the positive reference value was 0.205. According to the reference value, 66.1% (72/109, other 17 isolates could not be revived from -70 °C) of the tested *H pylori* isolates were positive for the epitope of rVacA with an A_{490} value range from 0.27-1.73.

DISCUSSION

Amoxcillin and metronidazole, used as routine therapeutic antibiotics in triple therapies, efficiently eradicate *H pylori* infection *in vivo*^[57-59]. However, there are problems such as side effects, emergence of drug resistance and re-infection after withdrawal of the antibiotics, etc. It is generally considered that *H pylori* vaccination is the optimal strategy for the prevention and control of *H pylori* infection.

VacA, confirmed as a unique *H pylori* exotoxin with strong antigenicity^[47,48], has been considered to be an antigen candidate in *H pylori* vaccine^[50,51]. However, the low prevalence (50-60%) of VacA expression in *H pylori* strains and rare data on specific antibody inducement after *H pylori* infection in human make this consideration difficult to test. Therefore, we constructed a prokaryotic expression system of *H pylori vacA* gene, used rVacA to detect anti-VacA antibody in *H pylori* infected patients and prepared rabbit anti-rVacA serum to determine VacA expression in *H pylori* isolates, in order to determine the potential of VacA as an antigen in *H pylori* vaccine development.

The present study demonstrated high homologies (99.82% and 100 %) of the nucleotide and putative amino acid sequences of the cloned *vacA* gene compared with the reported (GenBank accession No.: AF049653)^[54] and efficient expression of *pET32a-vacA-E. coliBL21DE3*, indicating the successful establishment of a prokaryotic expression system of this target gene. The high specificity, immunoreactivity and strong antigenicity of rVacA exhibited in this study are beneficial to establish ELISAs to detect VacA-specific antibody in *H pylori* infected patients and VacA expression in *H pylori* isolates.

All tested *H pylori* isolates were positive for *vacA* gene by PCR. However, expression of VacA, not like those of UreB and HpaA in our previous studies^[60], was detectable only in 66.1% of the tested *H pylori* isolates. The lower positive detection rate (42.4%) for VacA-specific antibody in sera of *H pylori* infected patients was also found. The fact that the prevalence of VacA expression is lower than that of *vacA* gene in *H pylori* strains suggests possible mutation of the gene^[44], and the even lower seroprevalence of specific anti-VacA antibody in infected patients is probably due to the defect of signal peptide in the protein^[61].

In conclusion, a prokaryotic expression system of *H pylori vacA* gene was successfully constructed. The expressed rVacA can be used to detect specific anti-VacA antibody in human and to prepare antiserum in animals. However, the evidence obtained from this study indicates a poor potential for VacA as an antigen in the development of *H pylori* vaccine. In addition, detection of specific anti-VacA antibody is not a reliable diagnostic indicator as to whether an individual is infected by *H pylori*.

ACKNOWLEDGEMENTS

We are grateful to the people's Hospital of Zhejiang, the First Affiliated Hospital of Zhejiang University, the Second

Affiliated Hospital of Zhejiang University and the Affiliated Run Run Shaw Hospital of Zhejiang University in Hangzhou for kindly providing gastric biopsies in this study.

REFERENCES

- 1 **Ye GA**, Zhang WD, Liu LM, Shi L, Xu ZM, Chen Y, Zhou DY. *Helicobacter pylori vacA* gene polymorphism and chronic gastritis. *Shijie Huaren Xiaohua Zazhi* 2001; **9**: 593-595
- 2 **Lu SY**, Pan XZ, Peng XW, Shi ZL. Effect of *Hp* infection on gastric epithelial cell kinetics in stomach diseases. *Shijie Huaren Xiaohua Zazhi* 1999; **7**: 760-762
- 3 **Zhang Z**, Yuan Y, Gao H, Dong M, Wang L, Gong YH. Apoptosis, proliferation and p53 gene expression of *H pylori* associated gastric epithelial lesions. *World J Gastroenterol* 2001; **7**: 779-782
- 4 **Lu XL**, Qian KD, Tang XQ, Zhu YL, Du Q. Detection of *H pylori* DNA in gastric epithelial cells by *in situ* hybridization. *World J Gastroenterol* 2002; **8**: 305-307
- 5 **Yao YL**, Xu B, Song YG, Zhang WD. Overexpression of cyclin E in Mongolian gerbil with *Helicobacter pylori*-induced gastric precancerosis. *World J Gastroenterol* 2002; **8**: 60-63
- 6 **Guo DL**, Dong M, Wang L, Sun LP, Yuan Y. Expression of gastric cancer-associated MG7 antigen in gastric cancer, precancerous lesions and *H pylori*-associated gastric diseases. *World J Gastroenterol* 2002; **8**: 1009-1013
- 7 **Peng ZS**, Liang ZC, Liu MC, Ouyang NT. Studies on gastric epithelial cell proliferation and apoptosis in *Hp* associated gastric ulcer. *Shijie Huaren Xiaohua Zazhi* 1999; **7**: 218-219
- 8 **Hiyama T**, Haruma K, Kitadai Y, Miyamoto M, Tanaka S, Yoshihara M, Sumii K, Shimamoto F, Kajiyama G. B-cell monoclonality in *Helicobacter pylori*-associated chronic atrophic gastritis. *Virchows Arch* 2001; **483**: 232-237
- 9 **Xia HHX**. Association between *Helicobacter pylori* and gastric cancer: current knowledge and future research. *World J Gastroenterol* 1998; **4**: 93-96
- 10 **Quan J**, Fan XG. Progress in experimental research of *Helicobacter pylori* infection and gastric carcinoma. *Shijie Huaren Xiaohua Zazhi* 1999; **7**: 1068-1069
- 11 **Liu HF**, Liu WW, Fang DC. Study of the relationship between apoptosis and proliferation in gastric carcinoma and its precancerous lesion. *Shijie Huaren Xiaohua Zazhi* 1999; **7**: 649-651
- 12 **Zhu ZH**, Xia ZS, He SG. The effects of ATRA and 5-Fu on telomerase activity and cell growth of gastric cancer cells *in vitro*. *Shijie Huaren Xiaohua Zazhi* 2000; **8**: 669-673
- 13 **Tu SP**, Zhong J, Tan JH, Jiang XH, Qiao MM, Wu YX, Jiang SH. Induction of apoptosis by arsenic trioxide and hydroxy camptothecin in gastric cancer cells *in vitro*. *World J Gastroenterol* 2000; **6**: 532-539
- 14 **Cai L**, Yu SZ, Zhang ZF. *Helicobacter pylori* infection and risk of gastric cancer in Changle County, Fujian Province, China. *World J Gastroenterol* 2000; **6**: 374-376
- 15 **Yao XX**, Yin L, Zhang JY, Bai WY, Li YM, Sun ZC. HTERT expression and cellular immunity in gastric cancer and precancerosis. *Shijie Huaren Xiaohua Zazhi* 2001; **9**: 508-512
- 16 **Xu AG**, Li SG, Liu JH, Gan AH. Function of apoptosis and expression of the proteins *Bcl-2*, *p53* and *C-myc* in the development of gastric cancer. *World J Gastroenterol* 2001; **7**: 403-406
- 17 **Wang X**, Lan M, Shi YQ, Lu J, Zhong YX, Wu HP, Zai HH, Ding J, Wu KC, Pan BR, Jin JP, Fan DM. Differential display of vincristine-resistance-related gene in gastric cancer SGC7901 cells. *World J Gastroenterol* 2002; **8**: 54-59
- 18 **Liu JR**, Li BX, Chen BQ, Han XH, Xue YB, Yang YM, Zheng YM, Liu RH. Effect of cis-9, trans-11-conjugated linoleic acid on cell cycle of gastric adenocarcinoma cell line (SGC-7901). *World J Gastroenterol* 2002; **8**: 224-229
- 19 **Cai L**, Yu SZ. A molecular epidemiologic study on gastric cancer in Changle, Fujian Province. *Shijie Huaren Xiaohua Zazhi* 1999; **7**: 652-655
- 20 **Gao GL**, Yang Y, Yang SF, Ren CW. Relationship between proliferation of vascular endothelial cells and gastric cancer. *Shijie Huaren Xiaohua Zazhi* 2000; **8**: 282-284
- 21 **Xue XC**, Fang GE, Hua JD. Gastric cancer and apoptosis. *Shijie Huaren Xiaohua Zazhi* 1999; **7**: 359-361
- 22 **Niu WX**, Qin XY, Liu H, Wang CP. Clinicopathological analysis of patients with gastric cancer in 1200 cases. *World J Gastroenterol*

- 2001; **7**: 281-284
- 23 **Li XY**, Wei PK. Diagnosis of stomach cancer by serum tumor markers. *Shijie Huaren Xiaohua Zazhi* 2001; **9**: 568-570
- 24 **Fang DC**, Yang SM, Zhou XD, Wang DX, Luo YH. Telomere erosion is independent of microsatellite instability but related to loss of heterozygosity in gastric cancer. *World J Gastroenterol* 2001; **7**: 522-526
- 25 **Morgner A**, Miehke S, Stolte M, Neubauer A, Alpen B, Thiede C, Klann H, Hiermeier FX, Ell C, Ehninger G, Bayerdorffer E. Development of early gastric cancer 4 and 5 years after complete remission of *Helicobacter pylori*-associated gastric low-grade marginal zone B-cell lymphoma of MALT type. *World J Gastroenterol* 2001; **7**: 248-253
- 26 **Deng DJ**. Progress of gastric cancer etiology: N-nitrosamides in the 1990s. *World J Gastroenterol* 2000; **6**: 613-618
- 27 **Liu ZM**, Shou NH, Jiang XH. Expression of lung resistance protein in patients with gastric carcinoma and its clinical significance. *World J Gastroenterol* 2000; **6**: 433-434
- 28 **Guo CQ**, Wang YP, Liu GY, Ma SW, Ding GY, Li JC. Study on *Helicobacter pylori* infection and p53, c-erbB-2 gene expression in carcinogenesis of gastric mucosa. *Shijie Huaren Xiaohua Zazhi* 1999; **7**: 313-315
- 29 **Cai L**, Yu SZ, Ye WM, Yi YN. Fish sauce and gastric cancer: an ecological study in Fujian Province, China. *World J Gastroenterol* 2000; **6**: 671-675
- 30 **Xue FB**, Xu YY, Wan Y, Pan BR, Ren J, Fan DM. Association of *H pylori* infection with gastric carcinoma: a Meta analysis. *World J Gastroenterol* 2001; **7**: 801-804
- 31 **Wang RT**, Wang T, Chen K, Wang JY, Zhang JP, Lin SR, Zhu YM, Zhang WM, Cao YX, Zhu CW, Yu H, Cong YI, Zheng S, Wu BQ. *Helicobacter pylori* infection and gastric cancer: evidence from a retrospective cohort study and nested case-control study in China. *World J Gastroenterol* 2002; **8**: 1103-1107
- 32 **Hua JS**. Effect of *Hp*: cell proliferation and apoptosis on stomach cancer. *Shijie Huaren Xiaohua Zazhi* 1999; **7**: 647-648
- 33 **Liu DH**, Zhang XY, Fan DM, Huang YX, Zhang JS, Huang WQ, Zhang YQ, Huang QS, Ma WY, Chai YB, Jin M. Expression of vascular endothelial growth factor and its role in oncogenesis of human gastric carcinoma. *World J Gastroenterol* 2001; **7**: 500-505
- 34 **Cao WX**, Ou JM, Fei XF, Zhu ZG, Yin HR, Yan M, Lin YZ. Methionine-dependence and combination chemotherapy on human gastric cancer cells *in vitro*. *World J Gastroenterol* 2002; **8**: 230-232
- 35 **Michetti P**, Kreiss C, Kotloff K, Porta N, Blanco JL, Bachmann D, Herranz M, Saldinger PF, Corthesy-Theulaz I, Losonsky G, Nichols R, Simon J, Stolte M, Ackerman S, Monath TP, Blum AL. Oral immunization with urease and *Escherichia coli* heat-labile enterotoxin is safe and immunogenic in *Helicobacter pylori*-infected adults. *Gastroenterology* 1999; **116**: 804-812
- 36 **Suganuma M**, Kurusu M, Okabe S, Sueoka N, Yoshida M, Wakatsuki Y, Fujiki H. *Helicobacter pylori* membrane protein 1: a new carcinogenic factor of *Helicobacter pylori*. *Cancer Res* 2001; **61**: 6356-6359
- 37 **Nakamura S**, Matsumoto T, Suekane H, Takeshita M, Hizawa K, Kawasaki M, Yao T, Tsuneyoshi M, Iida M, Fujishima M. Predictive value of endoscopic ultrasonography for regression of gastric low grade and high grade MALT lymphomas after eradication of *Helicobacter pylori*. *Gut* 2001; **48**: 454-460
- 38 **Uemura N**, Okamoto S, Yamamoto S, Matsumura N, Yamaguchi S, Yamakido M, Taniyama K, Sasaki N, Schlemper RJ. *Helicobacter pylori* infection and the development of gastric cancer. *N Engl J Med* 2001; **345**: 784-789
- 39 **Morgner A**, Miehke S, Fischbach W, Schmitt W, Muller-Hermelink H, Greiner A, Thiede C, Schetelig J, Neubauer A, Stolte M, Ehninger G, Bayerdorffer E. Complete remission of primary high-grade B-cell gastric lymphoma after cure of *Helicobacter pylori* infection. *J Clin Oncol* 2001; **19**: 2041-2048
- 40 **Kate V**, Ananthakrishnan N, Badrinath S. Effect of *Helicobacter pylori* eradication on the ulcer recurrence rate after simple closure of perforated duodenal ulcer: retrospective and prospective randomized controlled studies. *Br J Surg* 2001; **88**: 1054-1058
- 41 **Zhuang XQ**, Lin SR. Progress in research on the relationship between *Hp* and stomach cancer. *Shijie Huaren Xiaohua Zazhi* 2000; **8**: 206-207
- 42 **Gao HJ**, Yu LZ, Bai JF, Peng YS, Sun G, Zhao HL, Miu K, Lü XZ, Zhang XY, Zhao ZQ. Multiple genetic alterations and behavior of cellular biology in gastric cancer and other gastric mucosal lesions: *H pylori* infection, histological types and staging. *World J Gastroenterol* 2000; **6**: 848-854
- 43 **Yao YL**, Zhang WD. Relation between *Helicobacter pylori* and gastric cancer. *Shijie Huaren Xiaohua Zazhi* 2001; **9**: 1045-1049
- 44 **Atherton JC**, Cao P, Peek RM Jr, Tummuru MK, Blaser MJ, Cover TL. Mosaicism in vacuolating cytotoxin alleles of *Helicobacter pylori*. Association of specific *vacA* types with cytotoxin production and peptic ulceration. *J Biol Chem* 1995; **270**: 17771-17777
- 45 **Harris PR**, Cover TL, Crowe DR, Orenstein JM, Graham MF, Blaser MJ, Smith PD. *Helicobacter pylori* cytotoxin induces vacuolation of primary human mucosal epithelial cells. *Infect Immun* 1996; **64**: 4867-4871
- 46 **Pagliaccia C**, de Bernard M, Lupetti P, Ji X, Burrioni D, Cover TL, Papini E, Rappuoli R, Telford JL, Reyat JM. The m2 form of the *Helicobacter pylori* cytotoxin has cell type-specific vacuolating activity. *Proc Natl Acad Sci U S A* 1998; **95**: 10212-10217
- 47 **Phadnis SH**, Ilver D, Janzon L, Normark S, Westblom TU. Pathological significance and molecular characterization of the vacuolating toxin gene of *Helicobacter pylori*. *Infect Immun* 1994; **62**: 1557-1565
- 48 **Montecucco C**, Papini E, de Bernard M, Zoratti M. Molecular and cellular activities of *Helicobacter pylori* pathogenic factors. *FEBS Lett* 1999; **452**: 16-21
- 49 **Censini S**, Lange C, Xiang Z, Crabtree JE, Ghiara P, Borodovsky M, Rappuoli R, Covacci A. Cag, a pathogenicity island of *Helicobacter pylori*, encodes type I-specific and disease-associated virulence factors. *Proc Natl Acad Sci U S A* 1996; **93**: 14648-14653
- 50 **Marchetti M**, Arico B, Burrioni D, Figura N, Rappuoli R, Ghiara P. Development of a mouse model of *Helicobacter pylori* infection that mimics human disease. *Science* 1995; **267**: 1655-1658
- 51 **Prinz C**, Hafsi N, Voland P. *Helicobacter pylori* virulence factors and the host immune response: implications for therapeutic vaccination. *Trends Microbiol* 2003; **11**: 134-138
- 52 **Cover TL**, Blaser MJ. Purification and characterization of the vacuolating toxin from *Helicobacter pylori*. *J Biol Chem* 1992; **267**: 10570-10575
- 53 **Sambrook J**, Fritsch EF, Maniatis T. Molecular Cloning, A Laboratory Manual [M]. 2nd edition. New York: Cold Spring Harbor Laboratory Press. 1989, pp1.21-1.52, 2.60-2.80, 7.3-7.35, 9.14-9.22
- 54 **Ito Y**, Azuma T, Ito S, Suto H, Miyaji H, Yamazaki Y, Kohli Y, Kuriyama M. Full-length sequence analysis of the *vacA* gene from cytotoxic and noncytotoxic *Helicobacter pylori*. *J Infect Dis* 1998; **178**: 1391-1398
- 55 **Strobel S**, Bereswill S, Balig P, Allgaier P, Sonntag HG, Kist M. Identification and analysis of a new *vacA* genotype variant of *Helicobacter pylori* in different patient groups in Germany. *J Clin Microbiol* 1998; **36**: 1285-1289
- 56 **Chen Y**, Wang JD, Shi L. *In vitro* study of the biological activities and immunogenicity of recombinant adhesion of *Helicobacter pylori* rHpaA. *Zhonghua Yixue Zazhi* 2001; **81**: 276-279
- 57 **McMahon BJ**, Hennessy TW, Bensler JM, Bruden DL, Parkinson AJ, Morris JM, Reasonover AL, Hurlburt DA, Bruce MG, Sacco F, Butler JC. The relationship among previous antimicrobial use, antimicrobial resistance, and treatment outcomes for *Helicobacter pylori* infections. *Ann Intern Med* 2003; **139**: 463-469
- 58 **Wong WM**, Gu Q, Wang WH, Fung FM, Berg DE, Lai KC, Xia HH, Hu WH, Chan CK, Chan AO, Yuen MF, Hui CK, Lam SK, Wong BC. Effects of primary metronidazole and clarithromycin resistance to *Helicobacter pylori* on omeprazole, metronidazole, and clarithromycin triple-therapy regimen in a region with high rates of metronidazole resistance. *Clin Infect Dis* 2003; **37**: 882-889
- 59 **Chi CH**, Lin CY, Sheu BS, Yang HB, Huang AH, Wu JJ. Quadruple therapy containing amoxicillin and tetracycline is an effective regimen to rescue failed triple therapy by overcoming the antimicrobial resistance of *Helicobacter pylori*. *Aliment Pharmacol Ther* 2003; **18**: 347-353
- 60 **Mao YF**, Yan J, Li LW, Li SP. Construction of *hpaA* gene from a clinical isolate of *Helicobacter pylori* and identification of the fusion protein. *World J Gastroenterol* 2003; **9**: 1529-1535
- 61 **Kim N**, Weeks DL, Shin JM, Scott DR, Young MK, Sachs G. Proteins released by *Helicobacter pylori in vitro*. *J Bacteriol* 2002; **184**: 6155-6162

Pre-treatment urea breath test results predict the efficacy of *Helicobacter pylori* eradication therapy in patients with active duodenal ulcers

Yung-Chih Lai, Jyh-Chin Yang, Shih-Hung Huang

Yung-Chih Lai, Department of Internal Medicine, Cathay General Hospital, Taipei, Taiwan, China

Jyh-Chin Yang, Department of Internal Medicine, National Taiwan University Hospital, Taipei, Taiwan, China

Shih-Hung Huang, Department of Pathology, Cathay General Hospital, Taipei, Taiwan, China

Correspondence to: Yung-Chih Lai M.D. Department of Internal Medicine, Cathay General Hospital, 280 Jen-Ai Road, Section 4, Taipei 106, Taiwan, China. yungchihlai@hotmail.com

Telephone: +886-2-27082121 Ext. 3120 **Fax:** +886-2-27074949

Received: 2003-10-15 **Accepted:** 2003-12-01

Abstract

AIM: To evaluate the association of pre-treatment ¹³C-urea breath test (UBT) results with *H pylori* density and efficacy of eradication therapy in patients with active duodenal ulcers.

METHODS: One hundred and seventeen consecutive outpatients with active duodenal ulcer and *H pylori* infection were recruited. *H pylori* density was histologically graded according to the Sydney system. Each patient received lansoprazole (30 mg b.i.d.), clarithromycin (500 mg b.i.d.) and amoxicillin (1 g b.i.d.) for 1 week. According to pre-treatment UBT values, patients were allocated into low (<16%), intermediate (16-35%), and high (>35%) UBT groups.

RESULTS: A significant correlation was found between pre-treatment UBT results and *H pylori* density ($P<0.001$). *H pylori* eradication rates were 94.9%, 94.4% and 81.6% in the low, intermediate and high UBT groups, respectively (per protocol analysis, $P=0.11$). When patients were assigned into two groups (UBT results $\leq 35\%$ and $>35\%$), the eradication rates were 94.7% and 81.6%, respectively ($P=0.04$).

CONCLUSION: The intragastric bacterial load of *H pylori* can be evaluated by UBT, and high pre-treatment UBT results can predict an adverse outcome of eradication therapy.

Lai YC, Yang JC, Huang SH. Pre-treatment urea breath test results predict the efficacy of *Helicobacter pylori* eradication therapy in patients with active duodenal ulcers. *World J Gastroenterol* 2004; 10(7): 991-994

<http://www.wjgnet.com/1007-9327/10/991.asp>

INTRODUCTION

Helicobacter pylori can be identified in 90-95% of patients with duodenal ulcers and 60-80% of patients with gastric ulcers^[1]. Eradication of *H pylori* infection was reported to be able to change the natural history of peptic ulcer disease^[2-4]. Nowadays, *H pylori* has been regarded as the main cause of

chronic gastritis and peptic ulcer^[5, 6].

Eradication therapy for *H pylori* has developed rapidly in recent years. The global trend has now shifted to proton pump inhibitor (PPI)-based triple therapy (a PPI and two different antimicrobial agents)^[7], which can assure rapid symptom relief, improve ulcer healing, and reduce ulcer recurrence^[8,9]. However, treatment failure still occurs in some cases with this advanced PPI-based triple therapy. Patient compliance and antibiotic resistance are currently regarded as the major causes of eradication failure^[10]. In addition, several papers have also revealed that high pre-treatment ¹³C-urea breath test (UBT) results, suggestive of a high intragastric bacterial load, were an independent predictor of treatment failure^[10-12]. A high antral density of *H pylori* may be related to low eradication rate and increased rate of ulcer recurrence^[12-14]. The intragastric bacterial load could be another factor affecting the success of eradication therapy.

UBT is the noninvasive method of choice to determine *H pylori* status. It is easy to perform and reliable, with a high sensitivity and specificity^[15]. Furthermore, some authors have found that the results of UBT could be employed to semi-quantitatively assess both the intragastric bacterial load and the severity of gastritis^[12,16]. Therefore, we conducted this study to investigate the association of UBT results with *H pylori* density in the stomach and the efficacy of eradication therapy in patients with active duodenal ulcers.

MATERIALS AND METHODS

Patient recruitment

From January 2 000 to December 2 002, consecutive outpatients with endoscopically verified active duodenal ulcers (5 mm in diameter or larger) at Cathay General Hospital were enrolled for this study. All panendoscopic examinations were performed and interpreted by the same group of experienced endoscopists. We only selected patients with a positive diagnosis of *H pylori* infection proven by both histological examinations and UBT. To avoid interference in evaluating the status of *H pylori*, the following patients were initially excluded before endoscopy: those who had ingested bismuth, antibiotics, anti-secretory medication, or PPI during the 4 wk prior to beginning the study; those who used non-steroidal anti-inflammatory drug; those who were pregnant or immuno-compromised; and those who had a history of gastric surgery or a previous attempt to eradicate *H pylori*. Patients with coexisting gastric ulcers or gastric cancer were also excluded. All procedures were performed after obtaining informed consent from the patients.

The enrolled patients were all treated with the same regimen of 30 mg lansoprazole b.i.d. plus 500 mg clarithromycin b.i.d. and 1 g amoxicillin b.i.d. for the first 7 d and followed by 30 mg lansoprazole once daily for an additional 3 wk. After the completion of such therapy, neither PPI or anti-secretory H₂-blocker was used; only oral antacids were taken for symptomatic relief when necessary. The second endoscopic examination was scheduled 4 wk after the completion of therapy.

If the patient refused the second endoscopy, we arranged follow-up UBT only.

Histology

During the first endoscopic examination, three biopsies were taken from the gastric antrum (one near the incisura and the other two on the greater and lesser curvature, 2 cm within the pyloric ring)^[17]. On the follow-up endoscopic examination, two additional specimens were taken from the greater curvature of the gastric body due to the possibility of patchy distribution of *H pylori* after eradication therapy. We used an Olympus GIF-XQ 200 endoscope; the biopsy forceps were the FB 25-K type. Specimens were stained with hematoxylin-eosin and with a modified Giemsa stain. Then they were examined by an experienced histopathologist unaware of the patients' clinical diagnoses for the existence of *H pylori*. The version of the visual analogue scale in the updated Sydney system was used to grade the density of *H pylori* (4 grades: normal, no bacteria; mild, focally few bacteria; moderate, more bacteria in several areas; and marked, abundance of bacteria in most glands)^[18]. If the density varied, the highest grade of density in the specimens was selected.

Urea breath test (UBT)

UBTs were performed before the start of therapy (right away after the first endoscopy) and on two separate occasions, at 4 and 8 wk after the completion of therapy, respectively. The ¹³C-urea used was 100 mg of 99% ¹³C-labelled urea produced by the Institute of Nuclear Energy Research, Taiwan. Patients drank 100 mL of fresh milk as the test meal. The procedure was modified from the European standard protocol for the detection of *H pylori*^[19,20]. We chose 3 per mL for the cut-off level of the rise in the delta value of ¹³CO₂ at 15 min after the ingestion of ¹³C-urea. UBT was defined as positive when $\Delta \delta^{13}\text{CO}_2$ was above this value. By using this cut-off, the sensitivity and specificity of UBT are 97% and 95%, respectively^[20]. According to the pre-treatment UBT value, patients were allocated into low (<16%), intermediate (16-35%), and high (>35%) UBT groups^[12].

Eradication of *H pylori* infection was defined as negative results on both UBT and histology tests at 4 wk after the completion of therapy or negative results on two UBTs at both 4 and 8 wk after the completion of therapy^[21].

Statistical analysis

The qualitative data of patients were evaluated using chi-square or Fisher's exact test. ANOVA test was applied for the quantitative data. The relationship between the UBT results and *H pylori* density was assessed by Spearman's rank correlation test. The Kruskal-Wallis test was applied to detect the significant difference in UBT values among patients with different levels of *H pylori* density. Fisher's exact test was used to compare the eradication rates of *H pylori* infection in different UBT groups. The 95% confidence intervals (CI) were calculated. A *P* value of less than 0.05 was considered significant.

RESULTS

One hundred and twenty-three patients were initially considered eligible for the study, but 6 patients were later excluded due to negative results for *H pylori*. We thus enrolled 117 patients who fulfilled the inclusion criteria (intention-to-treat). Among them, 4 patients did not complete the study adequately because of not taking drugs regularly (2 cases) or taking disallowed medications (two cases). Therefore, a total of 113 patients were included for the per protocol analysis. Table 1 shows the

demographic and other baseline characteristics of the patients according to the levels of UBT results. None of the differences in variables was statistically significant.

Table 1 Clinical characteristics of patients

	UBT result (%)		
	Low (<16) n=39	Intermediate (16-35) n=36	High (>35) n=38
Gender			
Male	24	26	23
Female	15	10	15
Age (year)			
Mean±SD	45.1±10.6	44.6±12.8	47.0±13.2
Smoking			
Yes	20	20	22
No	19	16	16
Ulcer size			
<1 cm	35	32	34
1-2 cm	4	3	4
>2 cm	0	1	0
No. of ulcers			
One	37	33	35
Two	2	3	3

Correlation between *H pylori* density and UBT results

Levels of *H pylori* density, as assessed histologically, were compared with the UBT results in Figure 1. The median (P₇₅-P₂₅) UBT value in each group was 9.6 (13.2), 17.9 (26.9) and 33.2 (25.4), respectively (*P*<0.001). A significant correlation was found between the UBT result and *H pylori* density (*r*_s=0.47).

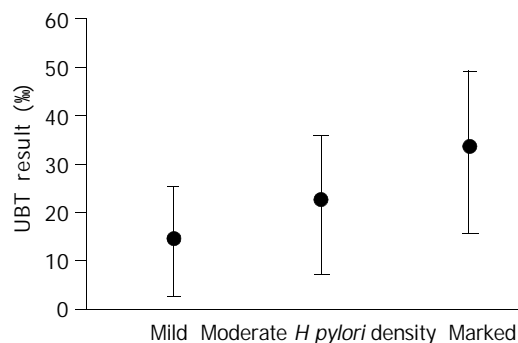


Figure 1 Relationship between UBT result and *Helicobacter pylori* density. *P*<0.001.

Table 2 Correlation between UBT results and eradication rates of *H pylori* infection

UBT result (%)	Eradication rate (95% CI)
Low (<16) n=39	94.9 (81.4-99.1%)
Intermediate (16-35) n=36	94.4 (79.9-99.0%)
Low+ Intermediate (n=75)	94.7 (86.2-98.3%)
High (>35) n=38	81.6 (65.1-91.7%) ^{1,2}

¹, comparison among low, intermediate and high UBT groups (three groups); *P*=0.11; ², comparison between low+intermediate and high UBT groups (two groups), *P*=0.04.

Eradication rates of *H pylori* infection and UBT results

The overall eradication rates were 87.2% (95% CI: 79.5-92.4%) in the intention-to-treat analysis and 90.3% (95% CI: 82.9-94.8%) in the per protocol analysis. Table 2 shows the eradication rates in the three UBT groups. Although there was a downward

trend in the eradication rate with an increase in the UBT results, the difference was not statistically significant ($P=0.11$). However, when the UBT results were allocated into only two groups ($\leq 35\%$ and $>35\%$), the difference in the eradication rates between the 2 groups became statistically significant ($P=0.04$) (Table 2). The higher UBT group had less eradication efficacy.

DISCUSSION

H pylori is now known to play the leading role in the pathogenesis of duodenal ulcer. Many reports have shown that eradication of *H pylori* not only aids ulcer healing but also prevents ulcer recurrence^[22]. Eradication of *H pylori* can cure duodenal ulcer disease, and has become a standard therapy for duodenal ulcer patients^[2,3,13].

The short-term (7 d) triple therapies including a PPI and two antibiotics (clarithromycin, and amoxicillin or a nitroimidazole compound) are currently considered as the firstline anti-*H pylori* regimens^[7]. Despite the high efficacy, treatment failure occurs in a proportion of patients, varying from 10% to 25%, in the first attempt to eradicate *H pylori*^[10]. Patient compliance and antibiotic resistance are regarded as the key factors affecting the outcome of treatment^[10,12]. However, several reports have also revealed that patients with higher intragastric *H pylori* loads had reduced eradication rates. This association was found in both bismuth- and PPI-based triple therapies^[10,12-14]. Thus, pre-treatment bacterial density has been used by some authors to predict the success of *H pylori* eradication in patients with duodenal ulcers^[13,14,23]. The relationship between the eradication efficacy and intragastric bacterial load supports the importance of bacterial density as a factor in the treatment of *H pylori* infection^[10,12-14].

UBT is the most useful noninvasive test for *H pylori*. The bacterium produces a powerful urease, which is the basis of UBT^[24]. Since the numerical results of UBT are a function of the total urease activity within the stomach, they might be a quantitative index of the density of gastric *H pylori* colonization. Many studies have reported inconsistent conclusions about the relationship between the UBT results and those of histology-based semi-quantitative measures of bacterial infection. Such inconsistencies may have arisen from inter-observer differences or inaccuracies in the estimation of bacterial density^[25]. Thus, UBT is best considered a qualitative test by some authors' opinions^[15]. However, in a recent study, Kobayashi *et al*^[26] used a sensitive real-time (TaqMan) polymerase chain reaction to estimate numbers of *H pylori* genomes in biopsy samples, and found that the numerical results of *H pylori* density correlated significantly with the values of UBT. So, they concluded the information from UBT was useful not only in identifying *H pylori* infection but also in indirectly assessing of the numbers of *H pylori* in the stomach. In our study, UBT results correlated with the density of *H pylori* in the stomach as well, although the number of cases was relatively small.

Higher intragastric bacterial loads, as semi-quantitatively assessed by UBT, are associated with lower eradication rates^[12-14]. Adopting the same cut-off value of δ UBT used by Perri *et al.*^[12], that is, $>35\%$ as an index of a high *H pylori* load, we confirmed the existence of an inverse relationship between successful eradication and intragastric bacterial load. Although we did not find a correlation between eradication efficacy and the UBT results when we allocated the patients into three UBT groups, statistically significant correlation was revealed when patients' UBT results were divided at 35% into 2 groups.

High UBT values may reflect high urease activity and indicate a high intragastric bacterial load. As observed in other infectious diseases, the bacterial load could be important in determining the outcome of eradication treatment^[11]. There are other factors than the number of *H pylori* which influence the

UBT results, including gastric emptying time, area of contact between the bacteria and the urea in the stomach, and differences in urease activity among *H pylori* strains^[15]. Levels of *H pylori* too low to be detected by histology are usually associated with a negative UBT. High urease activity implies a high density of *H pylori*. Between the two extremes, some authors have considered that the actual test results can tell the clinicians little except that the infection is present^[15]. When we wanted to use the results of UBT as a predictor of the efficacy of eradication therapy of *H pylori* infection, we had to set a high cut-off level to obtain statistical significance. Our result is consistent with previous reports which also revealed that high pre-treatment UBT results could be an independent predictor of eradication failure^[10-12].

Recognition of predictors for eradication therapy is helpful in clinical practice. Since high UBT results adversely influence the efficacy of eradication therapy, patients with high intragastric bacterial loads may benefit from an extension of treatment duration from 1 to 2 wk^[10]. Prolonging the duration of the standard triple therapy has been proposed to overcome the unfavorable effect caused by high *H pylori* density and proven to be effective^[10,12].

Most patients (113/117 cases, 96.6%) in this study had good drug compliance. However, bacterial culture and drug sensitivity test to assess the effect of antibiotic resistance were not performed. Thus, we cannot demonstrate the influence of drug resistance on eradication therapy. The culturing and susceptibility testing of *H pylori* are time-consuming, and they are not performed routinely in most countries^[27]. Our study may therefore provide an easy and practical option to disclose the pre-treatment predictor of eradication therapy when information on drug sensitivity is not available.

In conclusion, our findings reveal that the UBT results correlate with *H pylori* density in the stomach, and that high pre-treatment UBT results might adversely affect the success of eradication therapy in patients with active duodenal ulcers. Identifying patients with high bacterial loads before treatment and thus making adjustment in therapeutic regimens may further improve the efficacy of eradication therapy.

ACKNOWLEDGEMENTS

We would like to thank Mr. Shui-Cheng Lee (Institute of Nuclear Energy Research, Taiwan) for his help in the assessment of the urea breath test. This research was supported by a grant from Cathay General Hospital, Taiwan.

REFERENCES

- 1 **Hunt RH.** Peptic ulcer disease: defining the treatment strategies in the era of *Helicobacter pylori*. *Am J Gastroenterol* 1997; **92**(4 Suppl): 36S-43S
- 2 **Moss S, Calam J.** *Helicobacter pylori* and peptic ulcers: the present position. *Gut* 1992; **33**: 289-292
- 3 **Hunt RH.** pH and *Hp*-gastric acid secretion and *Helicobacter pylori*: implications for ulcer healing and eradication of the organism. *Am J Gastroenterol* 1993; **88**: 481-483
- 4 **Graham DY, Lew GM, Klein PD, Evans DG, Evans DJ Jr, Saeed ZA, Malaty HM.** Effect of treatment of *Helicobacter pylori* infection on the long-term recurrence of gastric or duodenal ulcer. A randomized, controlled study. *Ann Intern Med* 1992; **116**: 705-708
- 5 **Vandenplas Y.** *Helicobacter pylori* infection. *World J Gastroenterol* 2000; **6**: 20-31
- 6 **Wewer V, Andersen LP, Parregaard A, Gernow A, Hansen JP, Martzen P, Krasilnikoff PA.** Treatment of *Helicobacter pylori* in children with recurrent abdominal pain. *Helicobacter* 2001; **6**: 244-248
- 7 **Asaka M, Sugiyama T, Kato M, Satoh K, Kuwayama H, Fukuda Y, Fukuda Y, Fujioka T, Takemoto T, Kimura K, Shimoyama**

- T, Shimizu K, Kobayashi S. A multicenter, double-blind study on triple therapy with lansoprazole, amoxicillin and clarithromycin for eradication of *Helicobacter pylori* in Japanese peptic ulcer patients. *Helicobacter* 2001; **6**: 254-261
- 8 **Penston JG**. *Helicobacter pylori* eradication - understandable caution but no excuse for inertia. *Aliment Pharmacol Ther* 1994; **8**: 369-389
- 9 **Logan RP**, Bardhan KD, Celestin LR, Theodossi A, Palmer KR, Reed PI, Baron JH, Misiewicz JJ. Eradication of *Helicobacter pylori* and prevention of recurrence of duodenal ulcer: a randomized, double-blind, multi-centre trial of omeprazole with or without clarithromycin. *Aliment Pharmacol Ther* 1995; **9**: 417-423
- 10 **Maconi G**, Parente F, Russo A, Vago L, Imbesi V, Porro GB. Do some patients with *Helicobacter pylori* infection benefit from an extension to 2 weeks of a proton pump inhibitor-based triple eradication therapy? *Am J Gastroenterol* 2001; **96**: 359-366
- 11 **Perri F**, Villani MR, Festa V, Quitadamo M, Andriulli A. Predictors of failure of *Helicobacter pylori* eradication with the standard 'Maastricht triple therapy'. *Aliment Pharmacol Ther* 2001; **15**: 1023-1029
- 12 **Perri F**, Clemente R, Festa V, Quitadamo M, Conoscitore P, Niro G, Ghos Y, Rutgeerts P, Andriulli A. Relationship between the results of pre-treatment urea breath test and efficacy of eradication of *Helicobacter pylori* infection. *Ital J Gastroenterol Hepatol* 1998; **30**: 146-150
- 13 **Sheu BS**, Yang HB, Su JJ, Shiesh SC, Chi CH, Lin XZ. Bacterial density of *Helicobacter pylori* predicts the success of triple therapy in bleeding duodenal ulcer. *Gastrointest Endosc* 1996; **44**: 683-688
- 14 **Moshkowitz M**, Konikoff FM, Peled Y, Santo M, Hallak A, Bujanover Y, Tiomny E, Gilat T. High *Helicobacter pylori* numbers are associated with low eradication rate after triple therapy. *Gut* 1995; **36**: 845-847
- 15 **Graham DY**, Klein PD. Accurate diagnosis of *Helicobacter pylori*. 13C-urea breath test. *Gastroenterol Clin North Am* 2000; **29**: 885-893
- 16 **Labenz J**, Borsch G, Peitz U, Aygen S, Hennemann O, Tillenburg B, Becker T, Stolte M. Validity of a novel biopsy urease test (HUT) and a simplified ¹³C-urea breath test for diagnosis of *Helicobacter pylori* infection and estimation of the severity of gastritis. *Digestion* 1996; **57**: 391-397
- 17 **Genta RM**, Graham DY. Comparison of biopsy sites for the histopathologic diagnosis of *Helicobacter pylori*: a topographic study of *H pylori* density and distribution. *Gastrointest Endosc* 1994; **40**: 342-345
- 18 **Dixon MF**, Genta RM, Yardley JM, Correa P. Classification and grading of gastritis. The updated Sydney System. *Am J Surg Pathol* 1996; **20**: 1161-1181
- 19 **Logan RP**, Polson RJ, Misiewicz JJ, Rao G, Karim NQ, Newell D, Johnson P, Wadsworth J, Walker MM, Baron JH. Simplified single sample ¹³Carbon urea breath test for *Helicobacter pylori*: comparison with histology, culture, and ELISA serology. *Gut* 1991; **32**: 1461-1464
- 20 **Wang WM**, Lee SC, Ding HJ, Jan CM, Chen LT, Wu DC, Liu CS, Peng CF, Chen YW, Huang YF, Chen CY. Quantification of *Helicobacter pylori* infection: Simple and rapid ¹³C-urea breath test in Taiwan. *J Gastroenterol* 1998; **33**: 330-335
- 21 **Unge P**. The OAC and OMC options. *Eur J Gastroenterol Hepatol* 1999; **11**(Suppl 2): S9-S17
- 22 **Hosking SW**, Ling TK, Chung SC, Yung MY, Cheng AF, Sung JJ, Li AK. Duodenal ulcer healing by eradication of *Helicobacter pylori* without anti-acid treatment: randomised controlled trial. *Lancet* 1994; **343**: 508-510
- 23 **Lai YC**, Wang TH, Huang SH, Yang SS, Wu CH, Chen TK, Lee CL. Density of *Helicobacter pylori* may affect the efficacy of eradication therapy and ulcer healing in patients with active duodenal ulcers. *World J Gastroenterol* 2003; **9**: 1537-1540
- 24 **Atherton JC**, Spiller RC. The urea breath test for *Helicobacter pylori*. *Gut* 1994; **35**: 723-725
- 25 **el-Zimaity HM**, Graham DY, al-Assi MT, Malaty H, Karttunen TJ, Graham DP, Huberman RM, Genta RM. Interobserver variation in the histopathological assessment of *Helicobacter pylori* gastritis. *Hum Pathol* 1996; **27**: 35-41
- 26 **Kobayashi D**, Eishi Y, Ohkusa T, Ishige, Suzuki T, Minami J, Yamada T, Takizawa T, Koike M. Gastric mucosal density of *Helicobacter pylori* estimated by real-time PCR compared with results of urea breath test and histological grading. *J Med Microbiol* 2002; **51**: 305-311
- 27 **Lam SK**, Talley NJ. Report of the 1997 Asia Pacific Consensus Conference on the management of *Helicobacter pylori* infection. *J Gastroenterol Hepatol* 1998; **13**: 1-12

Edited by Xia HHX and Xu FM

Investigation of T-cell receptor- γ gene rearrangement in gastrointestinal lymphomas by PCR-SSCP analysis

Xi-Qun Han, Li He, Lan-Ying Shong, Hui-Yong Jiang, Mei-Gang Zhu, Tong Zhao

Xi-Qun Han, Li He, Lan-Ying Shong, Hui-Yong Jiang, Mei-Gang Zhu, Tong Zhao, Department of pathology, The First Military Medical University, Guangzhou 510515, Guangdong Province, China
Supported by Science and Technology Project of Guangzhou, No. 2002Z3-E4061; Science and Technology Project of Guangdong, No. B30101

Correspondence to: Professor Tong Zhao, Department of Pathology, the First Military Medical University, Guangzhou 510515, Guangdong Province, China. tongzhao@fimmu.com

Telephone: +86-20-61648228 **Fax:** +86-20-61363263

Received: 2004-01-02 **Accepted:** 2004-01-08

Abstract

AIM: To analyze the characterization of T-cell receptor- γ (TCR- γ) gene rearrangement in the gastrointestinal lymphomas and evaluate the value of PCR-SSCP analysis in gastrointestinal lymphomas investigation.

METHODS: TCR- γ gene rearrangement segments of gastrointestinal lymphomas were cloned and sequenced. Single clone plasmid and mixed clone pIsamids were subsequently submitted to PCR-SSCP analysis to investigate the relationship between the number of amplified clones and band patterns of the amplified products. The PCR products of TCR- γ gene rearrangement of 40 gastrointestinal lymphomas were electrophoresed on agarose gels and the positive cases on agarose gels were studied by SSCP analysis.

RESULTS: The sequencing showed that TCR- γ gene rearrangement of the gastrointestinal lymphomas included functional gene and pseudogene with extensive variety in the junctional regions. In SSCP analysis, the number of the single-stranded bands was about two times of the number of amplified clones, and double-stranded band became broad with the increased number of the amplified clones. Thirteen of the 25 B-cell gastrointestinal lymphomas and 14 of the 15 gastrointestinal T-cell lymphomas were positive detected on agarose gel electrophoresis. Of the positive cases detected by SSCP analysis, 3 B-cell lymphomas and 13 T-cell lymphomas showed positive bands. The other cases showed only smears. The rearranged pattern included 13 monoallelic gene rearrangements and 3 biallelic or oligoclonal gene rearrangements.

CONCLUSION: The pattern of TCR- γ gene rearrangement in gastrointestinal lymphomas are similar to that of the nodular lymphomas. PCR-SSCP analysis for TCR- γ gene rearrangement can be applied both for adjuvant diagnosis of gastrointestinal lymphomas and analysis of the gene rearrangement pattern. The ratio of TCR- γ gene rearrangements occurred in T-cell gastrointestinal lymphomas is significantly higher than that in B-cell gastrointestinal lymphomas. The gene rearrangement pattern involves monoallelic and biallelic (or oligoclonal) gene rearrangement.

Han XQ, He L, Shong LY, Jiang HY, Zhu MG, Zhao T. Investigation of T-cell receptor- γ gene rearrangement in gastrointestinal lymphomas by PCR-SSCP analysis. *World J Gastroenterol* 2004; 10(7): 995-999

<http://www.wjgnet.com/1007-9327/10/995.asp>

INTRODUCTION

Primary gastrointestinal lymphomas are the most common extranodal lymphomas and are almost exclusively of non-Hodgkin types^[1-3]. These lymphomas are biologically different from their nodal counterparts. Distinguishing the two phenotypes is of importance as the survival rates are different between T-cell and B-cell gastrointestinal lymphomas^[4-6]. As cytological features of gastrointestinal lymphomas are usually not specific, the combination with clinical, histological, immunophenotypic and molecular genetic studies is necessary to characterize these neoplasms^[7].

T-cell receptor (TCR) gene rearrangement provides a convenient genetic marker for demonstrating clonality in T-cell malignant neoplasm. Among the four TCR gene types, the TCR- γ gene rearrangement occurs in the early stage of cell differentiation and the rearrangement retains in both α β and γ δ phenotypic T cells along with the cell differentiation^[8]. Analysis of TCR- γ gene rearrangement is of practical value in determining the clonality of T-cell populations and for diagnosis T-cell malignant neoplasms^[9-11]. But the junctional diversity in TCR- γ gene rearrangement is limited compared with the other TCR or IgH gene rearrangement because of the fewer inserted nucleotides during the rearrangement, this lead the PCR products of TCR- γ gene rearrangement amplified by a consensus primers pair to be similar in length. The similarity may result in false clonal bands, when analyzed by standard gel electrophoresis methods that separate DNA molecules based solely on size^[12,13]. A high-resolution for the amplified products of TCR γ gene rearrangement is required.

Single-strand conformational polymorphism analysis (SSCP) separates different DNA molecules based on their single-strand secondary structure conformations under certain electrophoretic condition. DNA molecules with different conformations migrate different rates on polyacrylamide gel and therefore can be separated from each other^[14]. Besides gene point mutation analysis, SSCP analysis is also suitable for TCR- γ gene rearrangement study^[15].

In this study, we expected to analyze the characteristics of TCR- γ gene rearrangement and evaluate the practicability of PCR-SSCP for TCR- γ gene rearrangement in the diagnosis and analysis of gastrointestinal lymphomas.

MATERIALS AND METHODS

Clinical specimen

Specimens of the gastrointestinal lymphoma were obtained by biopsy and surgical resection between January 1997 to October 2002 in the department of pathology of the Nangfang Hospital of the First Military Medical University, the First Municipal Hospital of Guangzhou and the No. 157 Hospital of The People's

Liberation Army. Of the 40 patients, 9 had tumors located within stomach, 1 in duodenum, 1 in jejunum, 10 in ileum, 11 in ascending colon, 2 in transverse colon, 5 in descending colon and 1 in rectum. All cases were regarded gastrointestinal lymphomas because of absence of disease in other organs. The specimens were fixed in buffered formalin, embedded in paraffin and stained with haematoxylin-eosin (HE). Lineage was confirmed by staining with CD20 and CD79a for B-cells, and CD45RO and CD3 for T-cells. The 40 cases were retrospectively diagnosed according to the new WHO classification^[16]. Twenty-five of the 40 cases were confirmed B-cell lymphomas and 15 cases were confirmed T-cell lymphomas. A reactive lymph node and Jurkat cell line were considered as negative and positive control, respectively.

DNA extraction

The 7 μm thickness sections were cut with disposable blades, collected on glass slides, deparaffinized with xylene, washed with ethanol, and rehydrated in deionized water. The moist tissues of 0.5 cm \times 0.5 cm containing abundant malignant cells (according to HE) were scraped off the glass slides with a sterile blade, and collected in Eppendorf tube. Jurkat cells were collected and rinsed twice in PBS. A total of 50 μL digesting buffer containing 10 mmol/L Tris, 1 mmol/L EDTA, 10 g/L Tween 20, and 200 mg/mL proteinase K were added to the tubes. The digestion was performed at 37 $^{\circ}\text{C}$ for 16 h. Samples were then heated at 96 $^{\circ}\text{C}$ for 10 min to inactivate the enzyme, centrifuged, and the supernatant was used as template for PCR amplification.

PCR and agarose gel electrophoresis

The primers design was based on those used by Benhattar *et al.*^[13], spanning the rearranged V γ 1-8 and J1/2 region with the expected products ranging from 160 to 190 bp in length. The sequences of the primers were: TVG sense, 5' AGGGTTGTGTTGGAATCAGG3', and J1/2 antisense, 5' CCTGTGACAACAAGTGTGT3'. PCR amplification was performed in GeneAmp PCR system 9600 (Perkin Elmer, Norwalk, CT). The reaction mixture (30 μL) contained PCR buffer (50 mmol/L KCl, 10 mmol/L Tris-HCl, pH 8.3), 200 mmol/L each of dNTP, 1.5 mmol/L MgCl₂, 0.5 mmol/L of each primer, and 1.25 U of AmpliTaq (Perkin Elmer). A total of 300 ng of samples and cell line DNA (or 20 ng of plasmids) were used as templates, respectively. The PCR amplification cycles were designed to a decreasing annealing temperature similar to a touch-down PCR^[17]: 5 cycles consist of 94 $^{\circ}\text{C}$ for 45 s, 60 $^{\circ}\text{C}$ for 45 s, 72 $^{\circ}\text{C}$ for 30 s; the next 5 cycles consisted of 94 $^{\circ}\text{C}$ for 45 s, 56 $^{\circ}\text{C}$ for 45 s, 72 $^{\circ}\text{C}$ for 30 s; and the last 25 cycles consisted of 94 $^{\circ}\text{C}$ for 45 s, 56 $^{\circ}\text{C}$ for 45 s, 72 $^{\circ}\text{C}$ for 30 s. The reaction mixture was first incubated at 95 $^{\circ}\text{C}$ for 5 min to denature double-stranded DNA. Finally, an additional incubation for 10 min at 72 $^{\circ}\text{C}$ was performed to ensure full extension of the products. In all experiments, monoclonal (Jurkat cell lines) and polyclonal (reactive lymph node) controls were run in parallel with the test samples. Products were analyzed by electrophoresis on 20 g/L agarose gels stained with ethidium bromide, visualized and photographed on an UV transilluminator. SSCP analysis was performed only if a single band of the expected size was detected on the gel. DNA from each sample was amplified at least twice.

Cloning, sequencing and PCR amplifying for the plasmids inserted with TCR γ gene rearranged segment

A total of 100 μL PCR products of TCR- γ gene rearrangement from five T-cell gastrointestinal lymphomas was separately purified and ligated into pGEM-T Easy cloning vector (Promega Corporation, 2 800 Woods Hollow Road Madison WI 53711-

5399 USA). The recombinant vector DNA was then transformed into *Escherichia coli* JM109. The transformed bacteria solution was spread on selective LB-agar plate with X-gal, IPTG and ampicillin. After overnight incubation at 37 $^{\circ}\text{C}$, 2 to 3 white colonies (with DNA inserts in the plasmid) from each plate were selected randomly and cultured in LB medium containing ampicillin for 12 h at 37 $^{\circ}\text{C}$. Plasmid DNA was isolated from each culture following a standard protocol^[18] and dissolved in double distilled deionized water. Deoxyribonucleic acid sequencing of cloned PCR products was performed following the standard protocol^[19] involving the universal forward-sequencing primer M13 for pGEM-T vector. The concentration of the plasmids were adjusted to 20 ng/ μL . According to the sequencing results, 2, 3 and 4 plasmids with different inserted PCR products were mixed, respectively. Single and mixed plasmids were submitted as templates to PCR.

SSCP analysis

SSCP analysis was performed according to the Signoretti *et al.*^[15] with some alternation. Briefly, 6 μL of PCR products were mixed 1:1 with denaturing loading buffer (containing 95 g/L formamide, 0.5 g/L bromophenol blue, 2.5 g/L xylene cyanol and 20 mmol/L EDTA). The mixture was heated to 95 $^{\circ}\text{C}$ for 10 min, quickly chilled on ice for 1 min, and loaded on 120 g/L nondenaturing polyacrylamide (29:1 acrylamide/bisacrylamide) gel in Tris-borate-EDTA (1 \times TBE) buffer. The gel was electrophoresed at 120 (12 v/cm) volts for approximately 4 to 6 h at room temperature and subsequently stained with silver and photographed.

Statistical analysis

Comparisons between the 2 groups were performed by the chi-square test using SPSS 10.0 statistical software (SPSS Company, Chicago, Illinois, USA). *P* values < 0.05 in two-tailed were considered statistically significant.

RESULTS

Agarose gel electrophoresis analysis

PCR amplification for the TCR- γ rearranged gene showed single band of 160-190 bp in 93% (14/15) T-cell and 52% (13/25) B-cell gastrointestinal lymphomas on agarose gel electrophoresis. The positive rate was significantly higher in T-cell lymphomas (*P* < 0.05) than that in B-cell lymphomas. Both the reactive lymph node and the Jurkat cell line showed single band (Figure 1).

Analysis of the TCR- γ gene rearrangement by sequencing

Sequence of the clones were identified to the particular V γ (1-8) segment by internet (<http://www.ncbi.nlm.nih.gov/BLAST/Blast.cgi>) assisted comparison with published TCR- γ sequence (gi 28436398 ref NG_001336.2. Homo sapiens T cell receptor gamma locus (TRG@) on chromosome 7, Length=140728). The sequenced V γ segments were assigned to the member of the V γ (1-8) family that, by comparison, showed the highest degree of homology (95% to 100%). Most of the V γ (1-8) -J γ 1/2 combinations had the functional V γ genes: V3, V4, V5, V8. Of the 14 sequenced cases, only one case was pseudogene V γ 7. In the VJ junctional N regions, the deleted nucleotides ranged from 2 to 23 nucleotides with an average length of 9.38 \pm 6.42 bp, and the size of the inserted nucleotides ranged from 3 to 13 bp (average length, 7.38 \pm 2.98 bp). The TCR γ junctional regions showed considerable diversity with no two clones showing the same sequence. The size of the PCR products amplified by this primers combination ranged between 160-190 bp. The letters with delete lines represent the deleted nucleotides and the capital letters represent the inserted nucleotides during the rearrangement.

	V-region	N-region	J-region
(186 bp) V3.....	tctattactgtgccacctgggacaggCCTGGAgaattattataagaaactctttgg.....		J1/2
(185 bp)V4....	.attactgtgccacctgggatggGCCT gaattattataagaaactctttggc.....		I1/2
(185 bp) V5.....	.gtctattactgtgccacctgggaeaggTGGgaattattataagaaactcttt.....		I1/2
(188 bp)V5.....	.gtctattactgtgccacctgggacaggGGAGAGGgaattattataagaaactctt.....		I1/2
(164 bp) V7....	.ctgtgccacctgggaeaggTATTGGATTGgaattattataagaaactctttggca.....		J1/2
(164 bp) V8.....	tattactgtgccacctgggataggTCACGTTTTTGGGgaattattataagaaactctttg..		J1/2

PCR-SSCP analysis of plasmids inserted with TCR-g gene rearranged segments

During SSCP analysis and gel electrophoresis, the PCR products of plasmids inserted with TCR- γ gene rearranged segments showed discrete bands in all lanes, except lane 7 (Figure 2) with faint band, which might be due to the insufficient DNA product in lane 7. The fastest migrating band was double-stranded DNA, located in the zone ranging from 160-190 bp. Running above the double-stranded DNA were single-stranded bands. PCR products of one cloned plasmid showed two single-stranded bands. The bands patterns of different clones were different (Figure 1 lane 5, 6 and 8). PCR products of 2 mixed cloned plasmids showed one double-stranded band and 3 to 4 single-stranded bands (Figure 2 lane 1, 2, 3 and 4). PCR Products of 3 to 4 plasmids mixed together showed one broad double-stranded band and 6 to 8 single-stranded bands (Figure 3). Some faint single-stranded bands presented in the lanes were disregarded or interpreted with caution. Based on the results of these studies, two single-stranded bands (sometimes only one) represented the monoallelic gene rearrangement, and those with more than two single-stranded bands might be the biallelic or oligoclonal gene rearrangement.

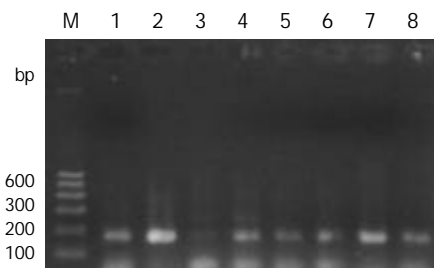


Figure 1 Agarose gel electrophoresis of the PCR products of TCR- γ gene rearrangement. M: DNA marker; Lane 1: reactive lymph node; lane 2: Jurkat cell line; lanes 3-8: gastrointestinal lymphomas.

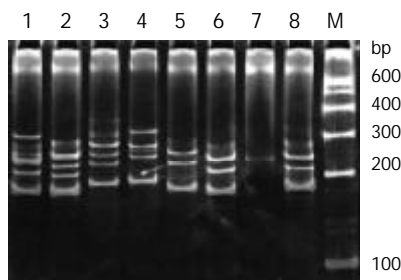


Figure 2 PCR-SSCP analysis of the plasmids inserted with TCR- γ gene rearranged segments. M: DNA marker; Lanes 1-4: two mixed plasmids amplified products showed one double-stranded band and three to four single-stranded bands; lanes 5-8: single plasmid PCR products showed one double-stranded band and two single-stranded bands (except lane 7).

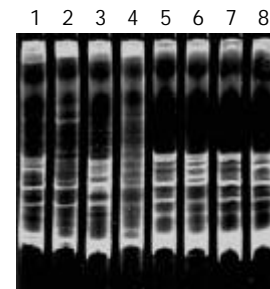


Figure 3 PCR-SSCP analysis of mixed plasmids inserted with TCR- γ gene rearranged segments. Lanes 1-4: PCR products of 3 mixed plasmids showed one double-stranded band and about five to six single-stranded bands; Lanes 5-8: PCR product of 4 mixed plasmids showed one double-stranded band and about six to eight single-stranded bands. The double-stranded bands were broader than that in the single or double plasmids amplified products.

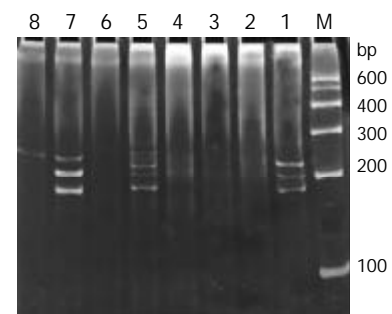


Figure 4 PCR-SSCP analysis of some gastrointestinal lymphomas. M: DNA marker; Lane 1: Jurkat cell line; lane 2: reactive lymph node; lanes 3-8: B-cell gastrointestinal lymphomas. Lane 5 had 4 single-stranded bands and lane 1, 7, 8 had one or two single-stranded bands. The other samples showed only smears with no predominant band.

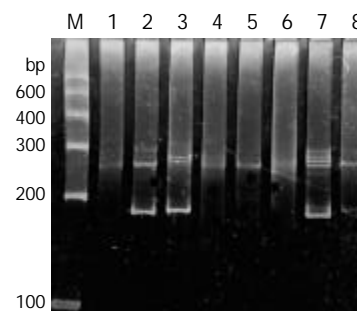


Figure 5 PCR-SSCP analysis of some T-cell gastrointestinal lymphomas. M: DNA marker; Lane 7 presented four single-stranded bands, and the others had one or two single-stranded bands. Four of the 8 samples were absent of the double-stranded bands probably due to insufficient PCR products.

PCR-SSCP analysis of the gastrointestinal lymphomas

Of the 29 samples submitted to SSCP analysis, 17 showed one or more discrete bands, including the Jurkat cell line, 3/13 B-cell gastrointestinal lymphomas (Figure 4) and 13/14 T-cell gastrointestinal lymphomas (Figure 5) confirmed by the HE and immunohistochemistry. The positive rate was significantly higher in T-cell lymphomas than that in B-cell lymphomas ($P < 0.01$). Less than half of the cases only showed the single-stranded bands, but not double-stranded bands. This might be due to insufficient quantity of PCR products. According to the numbers of the single-stranded bands of the 17 positive cases, 13 cases were monoallelic gene rearrangement, and 4 cases might be biallelic or oligoclonal gene rearrangements. The other 10 samples and reactive lymph node which were positive on the agarose gel electrophoresis yielded only smears with no obvious band. This patterns was the characteristic of rearranged TCR- γ V-J fragments amplified from polyclonal T-cell populations without a predominant.

DISCUSSION

Most T-cells express the $\alpha\beta$ T-cell phenotype and only a small population expresses $\gamma\delta$ TCR. The lineage is determined by the gene rearrangement and protein expression. γ -chain gene rearrangement generally takes place in the $\alpha\beta$ T-cell but not express a functional $\gamma\delta$ receptor^[12]. In addition, a fraction of B cells undergoes TCR- γ gene rearrangement, especially immature B cells (illegitimate gene rearrangement)^[20,21]. Furthermore, a T-cell lymphoma may aberrantly express the B-cell phenotype^[22]. In this study, the illegitimate TCR- γ gene rearrangement in B-cell gastrointestinal lymphomas was investigated, which showed about 12% (3/25) positive result. TCR-gamma gene rearrangement involves the recombination between one of the V region (V γ 1-8, V γ 9, V γ 10, V γ 11) and one of the J regions (J γ 1/2, J γ P1/2, J γ P)^[8]. In this study, we used only V γ 1-8 and J γ 1/2 consensus primers set to analyze the most common VJ gamma recombination. It is likely that using additional V and J region primers would have further increased the yield of positive results, but our study showed that this consensus primers combination seemed to be sufficient for the diagnosis of T-cell gastrointestinal lymphomas.

Cloning and sequencing are the precise but time and labour-consuming methods in the study of clonal gene rearrangement. Because of the admixture of reactive T-cells, at least 8 to 10 clones from each patient must be sequenced for the purpose of diagnosis, to confirm whether there are any two clones showing the same sequence^[21]. In this study, we intended to know the general aspects of the TCR- γ gene rearrangement in gastrointestinal lymphomas and to obtain the clonal rearranged gene segments. So, only 2 to 3 clones from each patient were sequenced, which were obviously inadequate for clonality judgement. The sequencing result showed that the TCR- γ junctional region (N region) presented considerable diversity with no two clones showing the same sequence. The junctional region differed in both sequence and size with the deleted and inserted nucleotides. The PCR products obtained by the consensus V $\gamma_{1-8}/J_{1/2}$ primers ranged from 160 to 190 base pairs. All these characteristics were similar to that of nodal lymphomas^[23]. The narrow size of the PCR products between different clones did not provide a means for distinguishing between monoclonal and polyclonal TCR junction by the conventional agarose gel electrophoresis^[13].

PCR-SSCP has been introduced to detect DNA mutation because it can resolve DNA molecules differing as little as a single base pairs substitution. The high sensitivity of PCR-SSCP makes it fit to tell apart the clonal from polyclonal gene rearrangement, and its simplicity makes it a good candidate for application in clinical laboratory tests^[15]. In the present study,

we would like to study whether the different band numbers observed on SSCP gel tell the different rearranged patterns apart in gastrointestinal lymphomas. The PCR products of single clone and mixed clones submitted to PCR-SSCP analysis showed that a consistent relationship existed between the number of single-stranded bands twice the numbers of clones amplified, which suggested that the number of single-stranded bands might estimate whether the samples were monoallelic or biallelic (oligoclonal) gene rearrangements. Two single-stranded bands (sometimes only one band) could definitely be regarded as monoallelic gene rearrangement. Three to four bands could be regarded as a clonal T-cell population with biallelic gene rearrangements or two clonal T-cells populations both with monoallelic gene rearrangements. Those with more than four single-stranded bands were most probably oligoclonal gene rearrangements^[24]. Owing to the high sensitivity and resolution of PCR-SSCP, multiple single-stranded bands must be interpreted with caution, and the PCR-SSCP analysis conditions must be optimized individually for a special pair of primers. The condition for the V $\gamma_{1-8}/J_{1/2}$ primers we used was optimized thoroughly before introducing to the study of gastrointestinal lymphomas.

Gastrointestinal lymphomas differ from their nodal counterpart in many aspects and are more likely to be misdiagnosed before surgical resections^[25]. The histological and cytological features may be more complex, with most having pleomorphic small, medium, large or anaplastic cell cytologic features and generally with a mixture of reactive cells. The immunophenotype is especially important for gastrointestinal lymphomas, as the prognosis for T-cell gastrointestinal lymphomas is poorer than that for B-cell type and more incline to perforation^[3]. It should be emphasized that gastrointestinal lymphomas must be defined by a combination of factors as not a single parameter is entirely specific.

The sensitivity and validity of TCR- γ gene rearrangement investigated by PCR-SSCP were compared with conventional histology and immunohistology. Of the 40 gastrointestinal lymphomas, 13 of the 15 T-cell lymphomas and 3 of the 25 B-cell lymphomas showed positive results. The high consistency indicates that PCR-SSCP analysis for the TCR- γ gene rearrangement study is an additional powerful tool for the diagnosis of T-cell gastrointestinal lymphomas.

Furthermore, the gene rearrangement pattern, which may be a prognostic factor, can be revealed by PCR-SSCP^[26]. Our study showed that 23.5% (4/17) of the positive cases were biallelic or oligoclonal gene rearrangements. PCR-SSCP gives reproducible band migration patterns for the same DNA molecules, therefore, this technique potentially can be used to compare multifocal lesion from a single patient or to compare a recurrent lesion with a primary one in a patient previously diagnosed with T-cell gastrointestinal lymphomas^[27].

REFERENCES

- 1 **Morton JE**, Leyland MJ, Vaughan Hudson G, Vaughan Hudson B, Anderson L, Bennett MH, MacLennan KA. Primary gastrointestinal non-Hodgkin's lymphoma: a review of 175 British National Lymphoma Investigation cases. *Br J Cancer* 1993; **67**: 776-782
- 2 **Kohno S**, Ohshima K, Yoneda S, Kodama T, Shirakusa T, Kikuchi M. Clinicopathological analysis of 143 primary malignant lymphomas in the small and large intestines based on the new WHO classification. *Histopathology* 2003; **43**: 135-143
- 3 **Lee SS**, Cho KJ, Kim CW, Kang YK. Clinicopathological analysis of 501 non-Hodgkin's lymphomas in Korea according to the revised European-American classification of lymphoid neoplasms. *Histopathology* 1999; **35**: 345-354
- 4 **Nakamura S**, Matsumoto T, Takeshita M, Kurahara K, Yao T, Tsuneyoshi M, Iida M, Fujishima M. A clinicopathologic study

- of primary small intestine lymphoma: prognostic significance of mucosa-associated lymphoid tissue-derived lymphoma. *Cancer* 2000; **88**: 286-294
- 5 **Zhang W**, Li G, Liu W, Ren X, Xu H. Analyzing of prognosis of intestinal T-cell lymphoma. *Zhonghua Binglixue Zazhi* 2002; **31**: 295-299
 - 6 **Sanchez-Bueno F**, Garcia-Marcilla JA, Alonso JD, Acosta J, Carrasco L, Pinero A, Parrilla P. Prognostic factors in primary gastrointestinal non-Hodgkin's lymphoma: a multivariate analysis of 76 cases. *Eur J Surg* 1998; **164**: 385-392
 - 7 **Kinney MC**. The role of morphologic features, phenotype, genotype, and anatomic site in defining extranodal T-cell or NK-cell neoplasms. *Am J Clin Pathol* 1999; **111**(1 Suppl 1): S104-118
 - 8 **Hodges E**, Krishna MT, Pickard C, Smith JL. Diagnostic role of tests for T cell receptor (TCR) genes. *J Clin Pathol* 2003; **56**: 1-11
 - 9 **Diss TC**, Watts M, Pan LX, Burke M, Linch D, Isaacson PG. The polymerase chain reaction in the demonstration of monoclonality in T cell lymphomas. *J Clin Pathol* 1995; **48**: 1045-1050
 - 10 **Sprouse JT**, Werling R, Hanke D, Lakey C, McDonnell L, Wood BL, Sabath DE. T-cell clonality determination using polymerase chain reaction (PCR) amplification of the T-cell receptor gamma-chain gene and capillary electrophoresis of fluorescently labeled PCR products. *Am J Clin Pathol* 2000; **113**: 838-850
 - 11 **Algara P**, Soria C, Martinez P, Sanchez L, Villuendas R, Garcia P, Lopez C, Orradre JL, Piris MA. Value of PCR detection of TCR gamma gene rearrangement in the diagnosis of cutaneous lymphocytic infiltrates. *Diagn Mol Pathol* 1994; **3**: 275-282
 - 12 **Macintyre EA**, Delabesse E. Molecular approaches to the diagnosis and evaluation of lymphoid malignancies. *Semin Hematol* 1999; **36**: 373-389
 - 13 **Benhattar J**, Delacretaz F, Martin P, Chaubert P, Costa J. Improved polymerase chain reaction detection of clonal T-cell lymphoid neoplasms. *Diagn Mol Pathol* 1995; **4**: 108-112
 - 14 **Orita M**, Iwahana H, Kanazawa H, Hayashi K, Sekiya T. Detection of polymorphisms of human DNA by gel electrophoresis as single-strand conformational polymorphisms. *Proc Natl Acad Sci U S A* 1989; **86**: 2766-2770
 - 15 **Signoretti S**, Murphy M, Cangi MG, Puddu P, Kadin ME, Loda M. Detection of clonal T-cell receptor gamma gene rearrangements in paraffin-embedded tissue by polymerase chain reaction and nonradioactive single-strand conformational polymorphism analysis. *Am J Pathol* 1999; **154**: 67-75
 - 16 **Harris NL**, Jaffe ES, Diebold J, Flandrin G, Muller-Hermelink HK, Vardiman J, Lister TA, Bloomfield CD. World Health Organization classification of neoplastic diseases of the hematopoietic and lymphoid tissues: report of the Clinical Advisory Committee meeting-Airlie House, Virginia, November 1997. *J Clin Oncol* 1999; **17**: 3835-3849
 - 17 **Ranheim EA**, Jones CD, Zehnder JL. Sensitive detection of clonal immunoglobulin rearrangements in frozen and paraffin embedded tissues by polymerase chain reaction heteroduplex analysis. *Diagn Mol Pathol* 2000; **9**: 177-183
 - 18 **Sambrook J**, Russel DW. Molecular cloning, a laboratory manual. 3rd ed. *Chinese edition: Sci Pub* 2002 (Translated from Cold Spring Harbor Laboratory Press 2001): 27-30
 - 19 **Sambrook J**, Russel DW. Molecular cloning, a laboratory manual. 3rd ed. *Chinese edition: Sci Pub* 2002 (Translated from Cold Spring Harbor Laboratory Press 2001): 1005-1010
 - 20 **Steenbergen EJ**, Verhagen OJ, van Leeuwen EF, van den Berg H, von dem Borne AE, van der Schoot CE. Frequent ongoing T-cell receptor rearrangements in childhood B-precursor acute lymphoblastic leukemia: implications for monitoring minimal residual disease. *Blood* 1995; **86**: 692-702
 - 21 **Chen Z**, Le Paslier D, Dausset J, Degos L, Flandrin G, Cohen D, Sigaux F. Human T cell gamma genes are frequently rearranged in B-lineage acute lymphoblastic leukemias but not in chronic B cell proliferations. *J Exp Med* 1987; **165**: 1000-1015
 - 22 **Yao X**, Teruya-Feldstein J, Raffeld M, Sorbara L, Jaffe ES. Peripheral T-cell lymphoma with aberrant expression of CD79a and CD20: a diagnostic pitfall. *Mod Pathol* 2001; **14**: 105-110
 - 23 **Kneba M**, Bolz I, Linke B, Bertram J, Rothaupt D, Hiddemann W. Characterization of clone-specific rearrangement T-cell receptor gamma-chain genes in lymphomas and leukemias by the polymerase chain reaction and DNA sequencing. *Blood* 1994; **84**: 574-581
 - 24 **Zhu P**, Wu S, Xue H, Lu Y, Wang L, Zhang Y, Yu J. Analysis of clonality of lymphocytic leukemia and lymphoma by T-cell receptor gene rearrangement. *Chin Med J* 1997; **110**: 607-611
 - 25 **Cheng AQ**, Luo EZ, Lu XY. 68 cases of primary malignant gastrointestinal lymphomas. *Shijie Huaren Xiaohua Zazhi* 2002; **8**: 240-241
 - 26 **Xu B**, Tian H, Zhou SY. Determination of clonal T cell receptor gene rearrangement in non-Hodgkin's lymphoma patients and its clinical significance. *Ai Zheng* 2003; **22**: 397-400
 - 27 **Crisi GM**, Emanuel JR, Johnson C, Crotty P, Costa J, Tallini G. Semireannealing, single-stranded conformational polymorphism: a novel and effective tool for the diagnosis of T-cell clonality. *Diagn Mol Pathol* 2002; **11**: 67-74

Edited by Gupta MK and Xu FM

Effect of cold-ischemia time on nuclear factor- κ B activation and inflammatory response in graft after orthotopic liver transplantation in rats

Xiao-Ping Gu, Yong Jiang, Fu-Tao Xu, Yu-Dong Qiu, Yi-Tao Ding

Xiao-Ping Gu, Fu-Tao Xu, Department of Anesthesiology, Gulou Hospital, Nanjing University Medical Center, Nanjing 210008, Jiangsu Province, China

Yong Jiang, Yu-Dong Qiu, Yi-Tao Ding, Department of Hepatobiliary Surgery, Gulou Hospital, Nanjing University Medical Center, Nanjing 210008, Jiangsu Province, China

Supported by the Education Foundation of Xuzhou Anesthesia Laboratory, Jiangsu, No.KJS02055

Correspondence to: Dr. Yi-Tao Ding, Department of Hepatobiliary Surgery, Drum Tower Hospital, Nanjing University Medical Center, Nanjing 210008, Jiangsu Province, China. yys982002@yahoo.com.cn

Telephone: +86-25-3304616 **Fax:** +86-25-3317016

Received: 2003-08-08 **Accepted:** 2003-10-07

Abstract

AIM: To study the mechanism and effect of nuclear factor- κ B (NF- κ B) activation and inflammatory response on the extended cold-preserved graft injury after orthotopic liver transplantation (OLT).

METHODS: OLT was performed in rats with varying time of cold ischemia grafts (6, 18 and 24 h in University Wisconsin solution at 4 °C). We determined the time of NF- κ B activation and expression of tumor necrosis factor- α (TNF- α), cytokine-inducible neutrophil chemoattractant (CINC), and intercellular adhesion molecule-1 (ICAM-1) within 6 h after reperfusion. Serum alarming aminotransferase (ALT), neutrophil sequestration, circulating neutrophil CD11b and L-selectin expression were also evaluated.

RESULTS: The accumulation of neutrophils in the graft was significantly increased in the 18 h and 24 h cold-ischemia groups within 0.5 h after reperfusion, compared with the 6 h group. But the strongly activated neutrophils was slightly increased at 2 h after reperfusion and remained at high levels 4 h after reperfusion, which was synchronized with the common situation of recipients after transplantation. Prolonged cold-preservation did not affect neutrophil accumulation and activation. NF- κ B activation preceded the expression of TNF- α , CINC, and ICAM-1 in the liver, which was significantly increased with prolonged cold preservation. In prolonged cold preserved grafts, prominently elevated NF- κ B activation occurred at 0.5 h and 1 h, compared with that at 2 h after reperfusion, which was consistent with greatly increased intrahepatic TNF- α response.

CONCLUSION: NF- κ B activation is correlated with the expression of TNF- α , CINC, and ICAM-1 *in vivo* in OLT rats. Extended cold preservation of grafts might up-regulate TNF- α , CINC, and ICAM-1 expression in the grafts, most probably through elevated NF- κ B activation, and might contribute to neutrophil infiltration in the grafts after reperfusion. Elevated NF- κ B activity is harmful to inflammatory response in the grafts, and inhibited NF- κ B activity might protect against early graft injury after liver transplantation.

Gu XP, Jiang Y, Xu FT, Qiu YD, Ding YT. Effect of cold-ischemia time on nuclear factor- κ B activation and inflammatory response in graft after orthotopic liver transplantation in rats. *World J Gastroenterol* 2004; 10(7): 1000-1004

<http://www.wjgnet.com/1007-9327/10/1000.asp>

INTRODUCTION

Liver transplantation has become an accepted therapy for end-stage liver diseases, but poor immediate graft function presents a persistent problem and contributes to mortality rates^[1-5]. The clinical incidence of primary graft nonfunction is strongly dependent on the duration of cold ischemia storage^[6]. It has become increasingly evident that reperfusion after ischemia is responsible for the majority of tissue injuries in liver transplantation^[5-7]. In addition, recent evidence confirms that liver ischemia-reperfusion injury is a result of the activation of inflammatory mediators in the early phase of reperfusion^[8-11].

Nuclear factor- κ B (NF- κ B) regulates the expression of many genes in which early response products are critical for the development of acute inflammation^[12-14]. But NF- κ B appears to have both beneficial and harmful effects on liver transplantation^[15]. It promotes liver regeneration and prevents apoptosis^[23-25], but may also contribute to the inflammatory response to ischemia/reperfusion. NF- κ B acts on target genes for proinflammatory cytokines, chemokines, and cell adhesion molecules, thus mediating inflammatory responses. In addition, products of the genes regulated by NF- κ B often cause the activation of NF- κ B, which creates a positive feedback loop that may amplify and perpetuate local inflammatory responses^[14]. But the exact role of NF- κ B activity in liver transplantation would depend on the regeneration and apoptosis or ischemia/reperfusion injury, which is the main factor leading to hepatocyte injury after transplantation. However, no definitive evidence has been found for the role of NF- κ B activation and inflammatory response after liver transplantation, especially in relation to cold-ischemia time.

In the current study, we investigated the importance of NF- κ B in a survival rat model of orthotopic liver transplantation. We determined the time of NF- κ B activation after OLT in relation to the expression of tumor necrosis factor (TNF- α), intercellular adhesion molecule (ICAM-1), and cytokine-induced neutrophil chemoattractant (CINC), as well as the recruitment and activation of neutrophils in the grafted livers, with varying cold ischemia time after liver transplantation, to determine whether prolonged cold ischemia time promoted NF- κ B activation and inflammatory response in the grafts after reperfusion.

MATERIALS AND METHODS

Experimental protocol

Male Wistar rats weighing 200-250 g were purchased from the Animal Experimental Center, Nanjing Military Command. Animals were allocated randomly to 3 groups ($n=30$ in each

group) according to the cold ischemia time for 6 h, 18 h, and 24 h. Liver harvesting and orthotopic transplantation were performed using the method described by Kamada and Calne^[16] with minor modifications^[17], and the hepatic artery was not reconstructed. The portal vein clamping time in the recipient varied from 18 to 20 min, implantation surgery required less than 50 min, all the procedures took about 60 min. No significant difference was seen in portal clamping time between groups. For the survival study, 8 rats in each group were examined. Animals that survived more than 7 d were considered survivors. The recipients were sacrificed at 0 h, 0.5 h, 1 h, 2 h, 4 h, and 6 h after reperfusion. Blood samples were collected from subhepatic vena cava to determine the serum levels of aspartate aminotransferase (ALT) and neutrophil activity at indicated time point. The median lobe of the liver was carefully excised at the designated time point and stored at -80 °C for analysis.

NF- κ B activity evaluation

Nuclear extracts were prepared using a nuclear extract kit (Active Motif) and p65/reIA subunit of NF- κ B was determined using a TransAM NF- κ B p65 kit (Active Motif) according to the manufacturer's protocols. The concentration of p65/reIA subunit in liver tissue homogenates was standardized as the total nuclear protein content in each specimen measured by the Pierce BCA protein assay reagent (Jiancheng, Nanjing, China). NF- κ B activity was expressed as p65/reIA subunit ug/mg total nuclear protein.

Measurement of TNF- α , CINC and ICAM-1

Hepatic levels of TNF- α , CINC and ICAM-1 were determined as previously described^[18]. In brief, the medial hepatic lobe was weighed and then homogenized in 5 mL of 0.1 mol/L phosphate buffer (pH 7.4) containing 0.5 g/L of sodium azide at 4 °C. Homogenate was first centrifuged at 2 000 g for 10 min to remove solid tissue debris. Supernatant was assayed using a rat ELISA system (Amersham, Buckinghamshire, UK). Concentration of antigens in liver tissue homogenates was standardized as the total protein content in each specimen measured by the Pierce BCA protein assay reagent. The results were expressed as pg/mg total protein.

Intrahepatic neutrophil accumulation assessment

Activity of MPO, an enzyme stored in the azurophilic granules of neutrophils, has been used as a well-established marker to determine tissue neutrophil sequestration^[19]. Frozen lungs were thawed and extracted for MPO, following the homogenization and sonication procedure as described in manufacturer's protocols (Jiancheng, Nanjing, China). MPO activity in the supernatant was measured and calculated from the absorbance (at 460 nm) changes resulting from decomposition of H₂O₂ in the presence of o-dianisidine and was expressed as units per milligram wet weight of tissue. To control intravascular leukocytosis, we calculated the ratio of MPO activity in tissue to WBC count in peripheral blood, and expressed it as MPO/WBC.

Circulating neutrophil activity analysis

Heparinized blood samples from each animal collected at each time point were prepared for flow cytometric analysis^[20]. For CD11b and L-selectin determination, 50 μ L of samples was incubated with 10 μ L of PE-labeled mouse anti-rat L-selectin antibody (Camarillo, CA) and 10 μ L of FITC-labeled mouse anti-rat CD11b antibody (Camarillo, CA) for 15 min, then 1 mL of FACS lysing solution (Becton Dickinson, San Jose, CA) was added 10 min, and then centrifuged at 1 500 g for 5 min. The cell pellets were washed, then resuspended in 500 μ L of PBS. The cells were read on a Becton-Dickinson FACS Calibur.

Statistical analysis

The data were expressed as mean \pm SD. Statistical analysis was performed using analysis of variance on SPSS software (version 11.0 for windows), evaluated by ANOVA, and followed by S-N-K multiple comparisons. A *P* value less than 0.05 was considered statistically significant.

RESULTS

Survival study

All recipients recovered from anesthesia within 15 min, no survivor died within 24 h after reperfusion and experienced massive ascites at the time of death in the absence of technical complication. Thus, the cause of death after reperfusion was considered to be the primary graft nonfunction (PGNF). In all groups, their conditions rapidly deteriorated within 2 h to 4 h after surgery. In the 6 h cold-ischemia group, the general situation was much better, all recipients survived (100%) for more than 7 d. In the 18 h cold-ischemia group, 5 of 8 recipients survived (62.5%) for more than 7 d. In the 24 h cold-ischemia group, no recipient survived (0%) for more than 7 d.

Evaluation of postransplantation liver function time

Serum ALT levels increased at 0.5 h after reperfusion, and remained greatly elevated throughout 6 h reperfusion, increased significantly in the 18 h and 24 h cold-preserved groups, as compared with those in the 6 h group during 6 hours' observation (Figure 1).

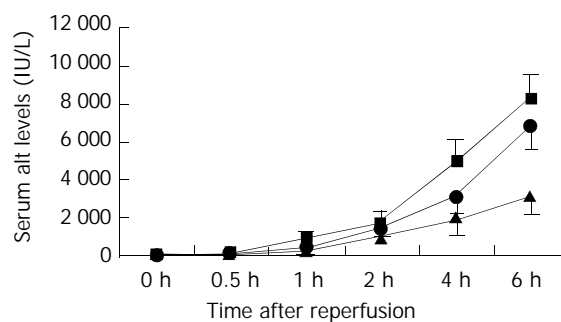


Figure 1 Changes in serum ALT levels after reperfusion. Serum ALT levels significantly increased in the 24 h (closed square) and 18 h (closed circle) cold-preserved groups, compared with the 6 h group (closed triangle) within 0.5 h after reperfusion (*P*<0.05, respectively). Results are mean \pm SD for each time point in each group (*n*=6).

NF- κ B activation time

The time of NF- κ B activity in liver tissue was established by evaluating p65/reIA subunit in nuclear extracts from the whole liver obtained at various time points. In three groups, the activity of NF- κ B in the preserved grafts increased slightly at 0.5 h after reperfusion, increased markedly at 2 h after reperfusion and decreased by 4 h (Figure 2). P65/reIA subunit significantly increased with prolonged cold preservation, especially at 0.5 h and 1 h after reperfusion. In the 24 h cold-preserved group, p65/reIA subunit increased to 3.2 fold of that in the 6 h cold-preserved group at 0.5 h after reperfusion. In the 24 h cold-preserved group, p65/reIA subunit increased to 1.7 fold of that in the 6 h cold-preserved group at 2 h after reperfusion. Furthermore, prolonged cold preservation had no effect on p65/reIA subunit at 0 h time point, but changed p65/reIA subunit level at 6 h after reperfusion, though it had no significant difference (Figure 2).

Inflammatory mediator expression time

We determined the time of OLT-induced TNF- α , CINC, and

ICAM-1 expression in the same tissues as used for NF- κ Bp65 transcription factor assay. Increases of TNF- α expression were maximal at 1 to 2 h after reperfusion, whereas CINC expression reached the peak at 4 h, and ICAM-1 expression peaked at 2 to 4 h (Figure 3). CINC and ICAM-1 were preceded by NF- κ B activation (peaked at 2 h after reperfusion). CINC and ICAM-1 expression, especially TNF- α , were significantly increased in the 18 h and 24 h cold-preserved groups compared with the 6 h cold-ischemia group. Prolonged cold preservation did not affect the time of inflammatory mediator response after OLT.

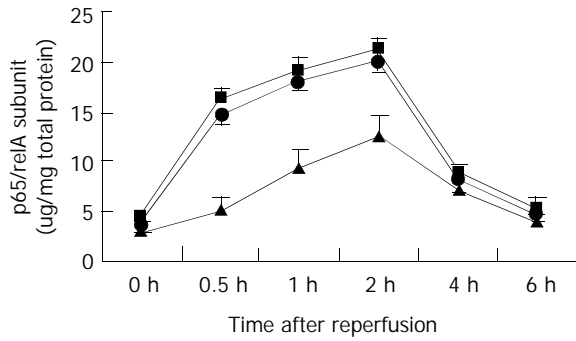


Figure 2 Changes in p65/relA subunit levels after reperfusion. P65/relA subunit levels significantly increased in the 24 h (closed square) and 18 h (closed circle) cold-preserved groups, compared with the 6 h group (closed triangle) at 0.5 h, 1 h, and 2 h after reperfusion ($P < 0.05$, respectively). Results are mean \pm SD for each time point in each group ($n = 6$).

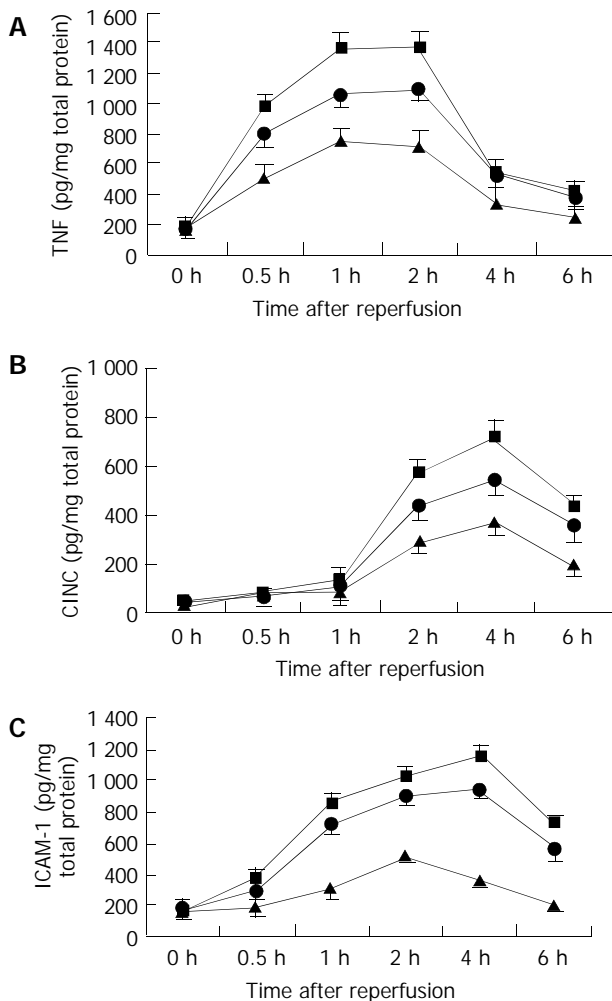


Figure 3 Changes in intrahepatic inflammatory mediator responses after reperfusion. A: TNF- α levels, B: CINC levels, C:

ICAM-1 levels. TNF- α levels significantly increased in the 24 h and 18 h groups 0.5 h after reperfusion, compared with the 6 h group ($P < 0.05$, respectively). CINC levels significantly increased in the 24 h and 18 h groups 2 h after reperfusion, compared with the 6 h group ($P < 0.05$, respectively). ICAM-1 levels significantly increased in the 24 h and 18 h cold-preserved groups 1 h after reperfusion, compared with the 6 h group ($P < 0.05$, respectively). Results are mean \pm SD for each time point in each group ($n = 6$). 6 h group—closed triangle, 24 h group—closed square, and 18 h group—closed circle.

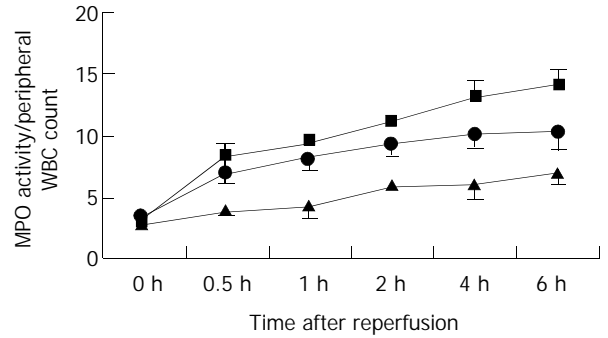


Figure 4 Changes in accumulation of neutrophils in the graft after reperfusion, as assessed by MPO/WBC. MPO/WBC in the 24 h (closed square) and 18 h (closed circle) cold-preserved groups increased significantly, compared with the 6 h group (closed triangle) within 0.5 h after reperfusion ($P < 0.05$, respectively). Results are mean \pm SD for each time point in each group ($n = 6$).

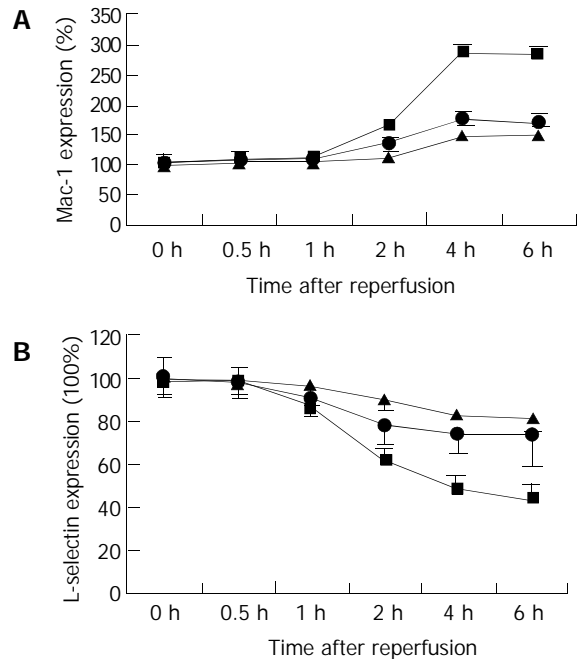


Figure 5 Changes in circulating neutrophil activity in the recipients after reperfusion, as assessed by CD11b and L-selectin expression. A: CD11b expression, B: L-selectin expression. CD11b expression elevated significantly in the 24 h (closed square) and 18 h (closed circle) groups, compared with the 6 h group (closed triangle) 2 h after reperfusion ($P < 0.05$, respectively). L-selectin shed significantly in the 24 h (closed square) and 18 h (closed circle) groups, compared with the 6 h group (closed triangle) 1 h after reperfusion ($P < 0.05$, respectively). Results are the mean \pm SD for each time point in each group ($n = 6$).

Neutrophils sequestration time in graft

We utilized the MPO biochemical assay to measure tissue

neutrophil infiltration over the course of reperfusion. In all recipients, MPO/WBC was significantly elevated within 30 min of reperfusion and remained at significantly elevated level 4 h after of reperfusion (Figure 4). Prolonged cold preservation promoted neutrophil accumulation.

Time of circulating neutrophil activity after reperfusion

Increased surface expression of Mac-1 (CD11b/CD18) is important to neutrophil adherence to parenchyma cells. CD11b content of circulating neutrophils was quantitatively evaluated by flow cytometric analysis at selected time points after the onset reperfusion (Figure 5). In the 24 h cold-preserved group, expression of Mac-1 at the control time point (0 h) showed low levels of CD11b (mean fluorescence intensity was 76.75 ± 19.15), which reached 131% at 2 h, and above the baseline levels of 227% at 4 h, and remained constantly elevated 6 h after reperfusion. Flow cytometric analysis of circulating neutrophils indicated that prolonged cold ischemia had no effect on the time of its CD11b expression, but increased the expression level. In the 6 h cold-preserved group, expression of Mac-1 reached 147% of baseline at 4 h after reperfusion. At the same time, L-selectin was shed, resulting in 41% loss of the adhesion molecules at 4 h in the 24 h cold-preserved group.

DISCUSSION

Graft injury after reperfusion has been one of the critical problems to be overcome in the field of organ transplantation^[1-7]. During recent years, many cellular and molecular events mediating graft inflammatory injury after OLT have been clarified^[8-11]. NF- κ B has been found to be an amplifying and perpetuating mechanism that can exaggerate the disease-specific inflammatory process through the coordinated activation of many inflammatory genes^[13,14,22]. However, there has not been definitive evidence of what a role it played in NF- κ B activation and inflammatory response in relation to graft injury and cold-preservation time after liver transplantation.

In this study, we extended our investigation on the pathogenesis of neutrophilic graft inflammation following rat orthotopic liver transplantation to assess the potential contribution of the transcription factor NF- κ B. Since transcription factors determine cellular phenotype by specifying protein production, it is particularly interesting to relate changes in activation of transcription factors such as NF- κ B, to the expression of specific proteins and evolution of biological relevant end points^[23]. We studied the expression of TNF- α , ICAM-1, and CINC because of their critical roles in the reperfusion-induced inflammatory response. In the rat model of orthotopic liver transplantation, we have shown a link between NF- κ B activation, intrahepatic TNF- α , CINC and ICAM-1 expression, neutrophilic inflammation, and graft injury. We further demonstrated that reperfusion-induced NF- κ B activation *in vivo* preceded the expression of TNF- α , CINC, and ICAM-1. In addition, we have shown that prolonged cold preservation would promote NF- κ B activation and inflammatory response in the graft. These observations support the hypothesis that elevated inflammatory response in the extended cold-preserved liver might be involved in NF- κ B activation and contribute to subsequent neutrophil-mediated tissue injury after liver transplantation.

In this study, the expression of CINC and ICAM-1 in the graft was at a detectable level even in nonreperfusion rats (0 h time point), suggesting that CINC and ICAM-1 proteins might be constitutively expressed in the liver. However, after cold ischemia/reperfusion, intrahepatic CINC and ICAM-1 increased with the duration of cold-ischemia. In contrast, intrahepatic TNF- α was not detectable before reperfusion,

implicating that TNF- α was an inducible chemokine in the liver. However, a significant increase of prominent up-regulation of intrahepatic TNF- α was found in the 24 h cold-preserved group, which was synchronized with early elevated NF- κ B activity. It is well known that Kupffer cells were primed for the release of TNF- α during cold-preservation, and then activated at the time of reperfusion^[26,28,29]. In addition, it has been previously reported that TNF- α producing activity of Kuffer cells increases with the duration of cold-ischemia *in vitro*^[27]. That is, the presence of primed Kupffer cells during the extended cold preservation might result in overresponse to early NF- κ B activity and excessive production of TNF- α in the initial phase of reperfusion.

In a rat model of warm hepatic ischemia, Jaeschke *et al.*, observed a biphasic pattern of reperfusion injury^[27-29]. During the initial hour after reperfusion, Kupffer cells became activated and were the predominant source of oxygen free radicals. Up to 24 h thereafter, increased hepatic accumulation of neutrophils occurred in parallel to the progression of reperfusion injury^[30]. In this study, neutrophils were sequestered earlier than warm ischemia, and increased significantly with prolonged cold-preservation. Neutrophil accumulation in the graft occurred within 0.5 h after reperfusion in the 24 h cold-preserved group, but early neutrophil accumulation was not synchronized with neutrophil activation, indicated by the high CD11b and low L-selectin expression. It was consistent with other studies that there was no rolling in sinusoids, and consequently selectin did not affect neutrophil accumulation in sinusoids^[30], and furthermore, antibodies against β_2 -integrins had no effect on the initial neutrophil sequestration^[31-33]. In addition, previous studies have shown that CD11b and L-selectin expressions were important to neutrophil-mediated tissue injury^[20,34]. It implied that in a rat model of OLT, neutrophil-induced graft injury occurred within 2 h after reperfusion in the 18 h and 24 h groups, but graft injury at 0.5 h and 1 h was not neutrophil-dependent.

In summary, in the present study, we have demonstrated that NF- κ B activation correlated with the expression of TNF- α , CINC, and ICAM-1 *in vivo* in the OLT model. Extended cold preservation might up-regulate TNF- α , CINC, and ICAM-1 expression in the graft, most probably through elevated NF- κ B activation, and might contribute to neutrophil recruitment in sinusoids and subsequent neutrophil-mediated graft injury after liver transplantation. Thus, this chain reaction might play an important role in the development of early graft dysfunction after liver transplantation. We believe that elevated NF- κ B activity is harmful to prolonged cold preservation, and inhibiting early NF- κ B activity might protect against early graft injury after liver transplantation.

ACKNOWLEDGEMENT

We thank Dr.Hao-Jun Chen, Gulou Hospital, Nanjing, for technical support of flow cytometric analysis.

REFERENCES

- 1 **Strasberg SM**, Howard TK, Molmenti EP, Hertl M. Selecting the donor liver: risk factors for poor function after orthotopic liver transplantation. *Hepatology* 1994; **20**(4 Pt 1): 829-838
- 2 **Ploeg RJ**, D' Alessandro AM, Knechtle SJ, Stegall MD, Pirsch JD, Hoffmann RM, Sasaki T, Sollinger HW, Belzer FO, Kalayoglu M. Risk factors for primary dysfunction after liver transplantation—a multivariate analysis. *Transplantation* 1993; **55**: 807-813
- 3 **Jaeschke H**. Preservation injury: mechanisms, prevention and consequences. *J Hepatol* 1996; **25**: 774-780
- 4 **Greig PD**, Woolf GM, Sinclair SB, Abecassis M, Strasberg SM, Taylor BR, Blendis LM, Superina RA, Glynn MF, Langer B. Treatment of primary liver graft nonfunction with prostaglandin E1.

- Transplantation* 1989; **48**: 447-453
- 5 **Clavien PA**, Harvey PR, Strasberg SM. Preservation and reperfusion injuries in liver allografts. An overview and synthesis of current studies. *Transplantation* 1992; **53**: 957-978
 - 6 **Furukawa H**, Todo S, Imventarza O, Casavilla A, Wu YM, Scotti-Foglieni C, Broznick B, Bryant J, Day R, Starzl TE. Effect of cold ischemia time on the early outcome of human hepatic allografts preserved with UW solution. *Transplantation* 1991; **51**: 1000-1004
 - 7 **Lemasters JJ**, Bunzendahl H, Thurman RG. Reperfusion injury to donor livers stored for transplantation. *Liver Transpl Surg* 1995; **1**: 124-138
 - 8 **Colletti LM**, Kunkel SL, Walz A, Burdick MD, Kunkel RG, Wilke CA, Strieter RM. Chemokine expression during hepatic ischemia/reperfusion-induced lung injury in the rat. The role of epithelial neutrophil activating protein. *J Clin Invest* 1995; **95**: 134-141
 - 9 **Colletti LM**, Cortis A, Lukacs N, Kunkel SL, Green M, Strieter RM. Tumor necrosis factor up-regulates intercellular adhesion molecule 1, which is important in the neutrophil-dependent lung and liver injury associated with hepatic ischemia and reperfusion in the rat. *Shock* 1998; **10**: 182-191
 - 10 **Farhood A**, McGuire GM, Manning AM, Miyasaka M, Smith CW, Jaeschke H. Intercellular adhesion molecule 1 (ICAM-1) expression and its role in neutrophil-induced ischemia-reperfusion injury in rat liver. *J Leukoc Biol* 1995; **57**: 368-374
 - 11 **Yadav SS**, Howell DN, Gao W, Steeber DA, Harland RC, Clavien PA. L-selectin and ICAM-1 mediate reperfusion injury and neutrophil adhesion in the warm ischemic mouse liver. *Am J Physiol* 1998; **275**(6 Pt 1): G1341-1352
 - 12 **Ghosh S**, May MJ, Kopp EB. NF- κ B and Rel proteins: Evolutionarily conserved mediators of immune responses. *Annu Rev Immunol* 1998; **16**: 225-260
 - 13 **Zwacka RM**, Zhang Y, Zhou W, Halldorson J, Engelhardt JF. Ischemia/reperfusion injury in the liver of BALB/c mice activates AP-1 and nuclear factor kappaB independently of IkappaB degradation. *Hepatology* 1998; **28**: 1022-1030
 - 14 **Lee JI**, Burckart GJ. Nuclear factor kappa B: important transcription factor and therapeutic target. *J Clin Pharmacol* 1998; **38**: 981-993
 - 15 **Lentsch AB**, Kato A, Yoshidome H, McMasters KM, Edwards MJ. Inflammatory mechanisms and therapeutic strategies for warm hepatic ischemia/reperfusion injury. *Hepatology* 2000; **32**: 169-173
 - 16 **Kamada N**, Calne RY. Orthotopic liver transplantation in the rat. Technique using cuff for portal vein anastomosis and biliary drainage. *Transplantation* 1979; **28**: 47-50
 - 17 **Jiang Y**, Gu XP, Qiu YD, Sun XM, Chen LL, Zhang LH, Ding YT. Ischemic preconditioning decreases C-X-C chemokine expression and neutrophil accumulation early after liver transplantation in rats. *World J Gastroenterol* 2003; **9**: 2025-2029
 - 18 **Chandrasekar B**, Streitman JE, Colston JT, Freeman GL. Inhibition of nuclear factor kappa B attenuates proinflammatory cytokine and inducible nitric-oxide synthase expression in postischemic myocardium. *Biochim Biophys Acta* 1998; **27**: 91-106
 - 19 **Schmekel B**, Karlsson SE, Linden M, Sundstrom C, Tegner H, Venge P. Myeloperoxidase in human lung lavage. I. A marker of local neutrophil activity. *Inflammation* 1990; **14**: 447-454
 - 20 **Vuorte J**, Jansson SE, Repo H. Standardization of a flow cytometric assay for phagocyte respiratory burst activity. *Scand J Immunol* 1996; **43**: 329-334
 - 21 **Jaeschke H**, Farhood A, Bautista AP, Spolarics Z, Spitzer JJ, Smith CW. Functional inactivation of neutrophils with a Mac-1 (CD11b/CD18) monoclonal antibody protects against ischemia-reperfusion injury in rat liver. *Hepatology* 1993; **17**: 915-923
 - 22 **Baeuerle PA**. IkappaB-NF-kappaB structures: at the interface of inflammation control. *Cell* 1998; **95**: 729-731
 - 23 **Kato A**, Edwards MJ, Lentsch AB. Gene deletion of NF-kappa B p50 does not alter the hepatic inflammatory response to ischemia/reperfusion. *J Hepatol* 2002; **37**: 48-55
 - 24 **Schoemaker MH**, Ros JE, Homan M, Trautwein C, Liston P, Poelstra K, van Goor H, Jansen PL, Moshage H. Cytokine regulation of pro- and anti-apoptotic genes in rat hepatocytes: NF-kappaB-regulated inhibitor of apoptosis protein 2 (cIAP2) prevents apoptosis. *J Hepatol* 2002; **36**: 742-750
 - 25 **Liu H**, Lo CR, Czaja MJ. NF-kappaB inhibition sensitizes hepatocytes to TNF-induced apoptosis through a sustained activation of JNK and c-Jun. *Hepatology* 2002; **35**: 772-778
 - 26 **Caldwell-Kenkel JC**, Currin RT, Tanaka Y, Thurman RG, Lemasters JJ. Kupffer cell activation and endothelial cell damage after storage of rat livers: effects of reperfusion. *Hepatology* 1991; **13**: 83-95
 - 27 **Arii S**, Monden K, Adachi Y, Zhang W, Higashitsuji H, Furutani M, Mise M, Fujita S, Nakamura T, Imamura M. Pathogenic role of Kupffer cell activation in the reperfusion injury of cold-preserved liver. *Transplantation* 1994; **58**: 1072-1077
 - 28 **Jaeschke H**, Farhood A, Bautista AP, Spolarics Z, Spitzer JJ. Complement activates Kupffer cells and neutrophils during reperfusion after hepatic ischemia. *Am J Physiol* 1993; **264**(4 Pt 1): G801-809
 - 29 **Jaeschke H**, Bautista AP, Spolarics Z, Spitzer JJ. Superoxide generation by neutrophils and Kupffer cells during *in vivo* reperfusion after hepatic ischemia in rat. *J Leukoc Biol* 1995; **52**: 377-382
 - 30 **Vollmar B**, Menger MD, Glasz J, Leiderer R, Messmer K. Impact of leukocyte-endothelial cell interaction in hepatic ischemia-reperfusion injury. *Am J Physiol* 1994; **267**(5 Pt 1): G786-793
 - 31 **Jaeschke H**. Cellular adhesion molecules: regulation and functional significance in the pathogenesis of liver diseases. *Am J Physiol* 1997; **273**(3 Pt 1): G602-611
 - 32 **Jaeschke H**, Smith CW. Cell adhesion and migration. III. Leukocyte adhesion and transmigration in the liver vasculature. *Am J Physiol* 1997; **273**(6 Pt 1): G1169-1173
 - 33 **Jaeschke H**, Farhood A, Fisher MA, Smith CW. Sequestration of neutrophils in the hepatic vasculature during endotoxemia is independent of beta 2 integrins and intercellular adhesion molecule-1. *Shock* 1996; **6**: 351-356
 - 34 **Lawson JA**, Burns AR, Farhood A, Lynn Bajt M, Collins RG, Smith CW, Jaeschke H. Pathophysiologic importance of E- and L-selectin for neutrophil-induced liver injury during endotoxemia in mice. *Hepatology* 2000; **32**: 990-998

Edited by Zhang JZ and Wang XL Proofread by Xu FM

Protective effects of rhubarb on experimental severe acute pancreatitis

Yu-Qing Zhao, Xiao-Hong Liu, Tetsuhide Ito, Jia-Ming Qian

Yu-Qing Zhao, Xiao-Hong Liu, Jia-Ming Qian, Department of Gastroenterology, Peking Union Medical College Hospital, Peking Union Medical College and Chinese Academy of Medical Science, Beijing 100730, China

Tetsuhide Ito, Pancreatic Diseases Branch, Department of Medicine and Bioregulatory Science, Graduate School of Medicine, Kyushu University, Fukuoka, Japan

Co-correspondents: Xiao-Hong Liu and Tetsuhide Ito

Correspondence to: Xiao-Hong Liu, MD and PhD, Department of Gastroenterology, Peking Union Medical College Hospital, Peking Union Medical College and Chinese Academy of Medical Science, Beijing 100730, China. xhliu41@medmail.com.cn

Telephone: +86-10-65295010

Received: 2003-10-10 **Accepted:** 2003-12-06

Abstract

AIM: To investigate the effects of rhubarb on severe acute pancreatitis (SAP) in rats.

METHODS: Severe acute pancreatitis was induced by two intraperitoneal injections of cerulein (40 µg/kg body weight) plus 5-h restraint water-immersion stress. Rhubarb (75-150 mg/kg) was orally fed before the first cerulein injection. The degree of pancreatic edema, serum amylase level, local pancreatic blood flow (PBF), and histological alterations were investigated. The effects of rhubarb on pancreatic exocrine secretion in this model were evaluated by comparing with those of somatostatin.

RESULTS: In the Cerulein+Stress group, severe edema and diffuse hemorrhage in the pancreas were observed, the pancreatic wet weight (11.60±0.61 g/Kg) and serum amylase (458 490±43 100 U/L) were markedly increased ($P<0.01$ vs control). In the rhubarb (150 mg/kg) treated rats, necrosis and polymorphonuclear neutrophil (PMN) infiltration in the pancreas were significantly reduced ($P<0.01$), and a marked decrease (50%) in serum amylase levels was also observed ($P<0.01$). PBF dropped to 38% (93±5 mL/min per 100 g) of the control in the Cerulein+Stress group and partly recovered in the Cerulein+Stress+Rhubarb 150 mg group (135±12 mL/min per 100 g) ($P<0.01$). The pancreatic exocrine function was impaired in the SAP rats. The amylase levels of pancreatic juice were reduced in the rats treated with rhubarb or somatostatin, comparing with that of untreated SAP group. The bicarbonate concentration of pancreatic juice was markedly elevated only in the rhubarb-treated group ($P<0.01$).

CONCLUSION: Rhubarb can exert protective effects on SAP, probably by inhibiting the inflammation of pancreas, improving pancreatic microcirculation, and altering exocrine secretion.

Zhao YQ, Liu XH, Ito T, Qian JM. Protective effects of rhubarb on experimental severe acute pancreatitis. *World J Gastroenterol* 2004; 10(7): 1005-1009
<http://www.wjgnet.com/1007-9327/10/1005.asp>

INTRODUCTION

Acute pancreatitis is a commonly occurring disease with self-limited course and uneventful recovery. But it can present as a severe form with significant morbidity and mortality. Up to now, the pathogenesis of acute pancreatitis still remains poorly understood and the treatment still remains nonspecific and primarily supportive. Rhubarb, a traditional Chinese herbal medicine, has been widely used in China for the treatment of many diseases. It has also been shown to have a good curative effect on acute pancreatitis in recent years^[1,2]. However, fewer experimental data are available to reveal its possible mechanisms. In the present study, we investigated the effects of rhubarb on severe acute pancreatitis (SAP) in rats, and tried to elucidate the possible mechanisms of its clinically well-known therapeutic effect.

MATERIALS AND METHODS

Materials

Cerulein was purchased from BACHEM Co., Ltd. (Switzerland). The tablets of rhubarb were kindly provided by professor Dong-Hai Jiao (Shanghai Xiangshan Chinese Medicine Hospital), which is the ethanol extract from crude rhubarb. The main chemical constituents of rhubarb tablets include emodin, aloe-emodin, rhein, d-catechin, and gallic acid. Sandostatin (somatostatin) is purchased from Novartis Pharma (Switzerland) and Secretin from Eisai Co., Ltd. (Japan). Male Sprague-Dawley rats (provided by the animal center of PUMC Hospital) weighing 350-450 g were used in these studies. They were fed standard laboratory chow and tap water *ad libitum* and housed in cages in a temperature-(22±2 °C) and humidity-(55±5%) controlled room, with a 12-h light cycle before experimentation.

Protocol I: effects of rhubarb on SAP

Animal models and experimental design SAP was induced by two intraperitoneal injections (*ip*) of cerulein (40 µg/kg body weight) at 1-hr interval and then the rats were immersed in 22 °C water to the level of the xiphoid in restraint cages for 5 h^[3] (stress). Rhubarb (75 or 150 mg/kg body weight) was orally administered (*po*) twice, 2 and 15 h before the first cerulein injection. The doses of rhubarb were selected according to our preliminary study. Experiments were performed 5 h after the first cerulein injection because previous data had shown that at that time cerulein-induced pancreatitis in the pancreas were the most severe^[4]. The time course of cerulein-induced pancreatitis had been confirmed in our early study^[5].

Thirty-four rats were randomly divided into five groups and treated as shown below: Control group: normal saline (NS) *po+ip*, without stress ($n=6$); Rhubarb group: rhubarb (150 mg/kg) *po+NS ip*, without stress ($n=6$); Cerulein+Stress group: NS *po+cerulein ip*, with stress ($n=9$); Cerulein+Stress+Rhubarb 75 mg group: rhubarb 75 mg/kg *po+cerulein ip*, with stress ($n=6$); Cerulein+Stress+Rhubarb 150 mg group: rhubarb 150 mg/kg *po+cerulein ip*, with stress ($n=7$).

Microcirculation in pancreas Local Pancreatic blood flow (PBF) was measured with a hydrogen gas clearance technique prior to sacrifice^[6,7]. All animals were anesthetized with an

intraperitoneal pentobarbital injection (40 mg/kg body weight). Body temperature was monitored by a rectal thermometer and kept at 36-37 °C with a heating lamp over the abdomen. The pancreas was exposed by laparotomy and then a urethane-coated platinum electrode, 80 µm in diameter with a 0.5 mm portion uncoated at its tip, was inserted into the pancreatic duct through an opening at proximal end of the duct and its tip was kept at 2.5 cm away from the duodenum. The incision was covered with a piece of wet gauze to avoid the loss of body warmth and fluid. The rats were then ventilated with 10% hydrogen in air through a nasal tube. Platinum catalyzes the oxidation of gaseous hydrogen to hydrogen ions. The process is accompanied by a release of electrons, which can be measured as current. For measuring the changing rate of the tissue hydrogen concentration, the blood flow can be determined and calculated by using the following formula: blood flow (mL/min/100 g pancreas)=100 (É.) 0.693/T_{1/2}. PBF value was directly provided using a MHG-D1 (Unique Medical Co., Tokyo, Japan) with a built-in computer.

Serum amylase level and pancreatic wet weight After measuring PBF, a blood sample was collected from the vena cava to determine serum amylase level by Phadebas amylase test^[8]. After decapitation, the pancreas was quickly removed, trimmed of fat and lymph nodes, and weighed to determine the severity of pancreatic edema, expressed as grams pancreatic wet weight per kilogram body weight.

Histologic examination A portion of the pancreatic tail from each rat was fixed in 40 g/L neutral-buffered formaldehyde, embedded in paraffin, and stained with hematoxylin and eosin. A blinded pathologist evaluated morphologic changes microscopically. Interstitial edema was scored as 0=absent, 1=expanded interlobular septa, 2=expanded intralobular septa, and 3= separated individual acini. Hemorrhage was evaluated as percentage involvement of the total pancreas: 0=absent, 1=1-10%, 2=11-50%, 3=more than 50%. Vacuolization and parenchymal necrosis were scored as percentage involvement of the examined area: 0=absent, 1=1-10%, 2=11-25%, 3=26-50%, and 4=more than 50%. Polymorphonuclear neutrophil (PMN) infiltration was scored as 0=absent, 1=less than 20 PMNs per intermediate-power field (IPF) (at×200 magnification), 2=20-50 PMNs per IPF, 3=more than 50 PMNs per IPF.

Protocol II: effects of rhubarb on pancreatic exocrine secretion in rats with SAP

Animal models and experimental design SAP was induced as mentioned in protocol I. Rhubarb (150 mg/kg) was orally administered twice at 2 and 15 h before the first cerulein injection. Sandostatin was subcutaneous injected (sc) from the leg three times at 30 min before, 1 h and 2.5 h after the first cerulein injection at a dose of 15 µg/kg 0.1 mL.

Thirty-six rats were randomly divided into six groups: Control group: NS *po+sc+ip*, without stress (*n*=6); Rhubarb group: rhubarb (150 mg/kg) *po+NS sc+ip*, without stress (*n*=6); Sandostatin group: NS *po+sandostatin sc+NS ip*, without stress

(*n*=6); Cerulein+Stress group: NS *po+sc+cerulein ip*, with stress (*n*=6); Cerulein+Stress+Rhubarb 150 mg group: rhubarb (150 mg/kg) *po+NS sc+cerulein ip*, with stress (*n*=6); Cerulein+Stress+Sandostatin group: NS *po+sandostatin sc+cerulein ip*, with stress (*n*=6).

Surgical Procedures Five hours after the initiation of the experiment, the rats were anesthetized and intravenously injected cerulein (0.25 µg/kg) and secretin (5 U/kg) respectively from the tail vein. A laparotomy was then performed through a midline incision, and the duodenal loop was identified. The main pancreatic duct was ligated proximal to the duodenal, and polyethylene tube (PE10) was inserted into the duct for draining pancreatic juice^[9]. Pancreatic juice was collected for 30 min. The protein content of pancreatic juice was quantitated by Follin's method. Amylase was assessed by Phadebas test and bicarbonate concentration by blood gas analyzer (ABL510, Denmark).

Statistics

All data were expressed as mean±SD. For continuous data, statistical analysis of data was accomplished by Student's *t*-test and analysis of variance (ANOVA). Histologic data were expressed as range of the scores and mean±SD and compared by means of nonparametric tests: the Mann-Whitney for two groups and the Kruskal-Wallis for multiple groups. *P*<0.05 was considered statistically significant.

RESULTS

Part I: protective effects of rhubarb on cerulein+stress-induced SAP in rats

Severe edema and diffused hemorrhage in the pancreas were observed macroscopically in the Cerulein+Stress group. Upon microscopic examination, edema, hemorrhage, focal acinar necrosis, conspicuous vacuolization, and PMN infiltration in the pancreas were observed also in the Cerulein+Stress group. In the Cerulein+Stress+Rhubarb (75 or 150 mg/kg) groups, the severities of pancreatitis were alleviated with reduced scores of histology (*P*<0.01, *P*<0.05). There was no significant change in edema between the groups (Table 1).

The data of pancreatic wet weight, serum amylase level, and PBF were shown in Table 2. There were no significant changes in the rats treated with rhubarb alone compared with the controls. The pancreatic wet weight and serum amylase level markedly increased in the Cerulein+Stress group. With the addition of rhubarb (150 mg/kg) to SAP model, a slight decrease in pancreatic wet weight from 11.60±0.61 g/kg to 10.65±0.77 g/kg (*P*>0.05) and an obvious reduction of 50% in serum amylase (*P*<0.01) was observed. PBF was 242±17 mL/min/100 g before the treatment. In the Cerulein+Stress group, it dropped to 93±5 mL/min/100 g (38% of the normal value) and partially recovered in the Cerulein+Stress+Rhubarb 150 mg group (135±12 mL/min per 100 g, 60% of the normal value, *P*<0.01 vs the SAP group).

Table 1 Effect of rhubarb on morphologic alterations in pancreas in rats with sever acute pancreatitis

Group	<i>n</i>	Edema	Hemorrhage	Vacuolization	Necrosis	PMN infiltration
Control	6	0	0	0	0	0
Rhubarb	6	0	0	0	0	0
Cerulein+Stress	9	2-3 (2.8±0.2)	2-3 (2.8±0.2)	2-3 (2.7±0.2)	2-3 (2.5±0.2)	2-3 (2.2±0.2)
Cerulein+Stress+Rhubarb 75 mg	6	3 (3.0±0)	1 (1.0±0)	2-3 (2.2±0.2)	1-2 (1.4±0.2)	1-2 (1.6±0.2)
Cerulein+Stress+Rhubarb 150 mg	7	2-3 (2.8±0.2)	1-2 (1.0±0.3) ^a	1-3 (1.8±0.3) ^a	1-2 (1.2±0.2) ^b	1-2 (1.8±0.2) ^b

Values are expressed as the range of the scores, with the mean±SD. The nonparametric test (Kruskal-Wallis method) showed ^a*P*<0.05, ^b*P*<0.01 vs Cn+St group; and no significant difference in edema.

Table 2 Effect of rhubarb on the changes of pancreatic wet weight, serum amylase activity, pancreatic blood flow

Group	<i>n</i>	Pancreatic wet weight (g/kg)	Serum amylase activity (U/L)	Pancreatic blood flow (mL/min/100 g)
Control	6	3.29±0.12	81 360±2 200	242±17
Rhubarb	6	3.34±0.14	85 370±2 910	238±18
Cerulein+Stress	9	11.60±0.61 ^b	458 490±43 100 ^b	93±5 ^b
Cerulein+Stress+Rhubarb 75 mg	6	10.99±0.91 ^b	321 710±89 800 ^b	113±12 ^a
Cerulein+Stress+Rhubarb 150 mg	7	10.65±0.77 ^b	298 650±36 450 ^{ad}	135±12 ^{ad}

^a*P*<0.05, ^b*P*<0.01 vs control group; ^c*P*<0.05, ^d*P*<0.01 vs Cn+St group.

Table 3 Effect of rhubarb and Sandostatin on the exocrine function of pancreatitis in rats

Group	<i>n</i>	Volume (μL/30 min)	Bicarbonate (mmol/L)	Protein (mg/mL)	Amylase (U/L)
Control	6	697.30±22.13	139.50±38.98	12.33±1.65	157 580±14 038
Rhubarb	6	704.58±29.52	108.00±38.31	12.87±2.52	154 000±18 717
Sandostatin	6	685.90±36.49	123.00±35.04	13.21±0.92	156 916±8 540
Cerulein +Stress	6	192.22±28.83 ^b	130.67±41.69	3.64±0.98 ^b	69 440±13 449 ^b
Rhubarb+Cerulein+Stress	6	177.33±46.70 ^b	403.00±68.59 ^{bd}	2.62±0.65 ^b	3 768±990 ^{bd}
Sandostatin+Cerulein+Stress	6	216.60±19.08 ^b	134.83±59.64	3.18±0.75 ^b	4 285±3 148 ^{bd}

^a*P*<0.05, ^b*P*<0.01 vs control group; ^c*P*<0.05, ^d*P*<0.01 vs Cn+St group.

Part II: the effects of rhubarb on pancreatic exocrine function in cerulein+stress-induced SAP

After pretreatment with rhubarb or somatostatin, total volume, amylase activity, protein content, and bicarbonate concentration of pancreatic juice in both Rhubarb group and Sandostatin group did not differ significantly from the controls (Table 3). Amylase activity in Cerulein+Stress group declined to 44%. In addition, the volume and protein output reduced significantly compared with that of the control group. No significant improvement was found in the volume and protein content of pancreatic juice in the Cerulein+Stress+Rhubarb group and the Cerulein+Stress+Sandostatin group compared with Cerulein+Stress group, whereas the amylase activity of pancreatic juice in the Cerulein+Stress+Rhubarb group and the Cerulein+Stress+Sandostatin group significantly decreased than that of the Cerulein+Stress group (*P*<0.01), and were 2.4% and 2.7% of the control respectively. Interestingly, the bicarbonate concentration of Cerulein+Stress+Rhubarb group increased to 403±69 mmol/L, which was three times of the control. This phenomenon could not be seen in Cerulein+Stress+Sandostatin group.

DISCUSSION

Severe acute pancreatitis still has a comparatively high mortality due to the systemic inflammatory response syndrome leading to multiple organ failure. Molecular and pathophysiologic investigations have allowed us to get more information about the events in the initiation and the natural course of acute pancreatitis, and subsequently to know more about how to deal with it. Despite considerable experimental efforts, the complexity in the evolution of acute pancreatitis is still far from being completely understood.

Since studies of acute human pancreatitis has many limitations due to its rapid and severe clinical course, so innovative therapeutic concepts should first be clarified in animal experiments. The cerulein model of experimental acute pancreatitis has become popular for the analysis of intracellular events in the early phase of pancreatitis. The major limitation of this non-invasive model is that it can only produce a mild, self-limited disorder. In order to establish a non-traumatic, easy to induce

and reproducible experimental model of clinical relevance, some researchers had modified the animal treatment protocols. It was revealed that early microcirculatory changes, included the increased permeability of endothelial lining and an accumulation of extravasated fluid in the perilobular space, would be more severe if cold stress was added to cerulein induced pancreatitis^[10]. Recently, Ding *et al.*^[11] had established a mouse model of severe acute pancreatitis by co-injection of cerulein and lipopolyascharide, which could produce the same pathological characteristics as those of severe acute pancreatitis in human. In our work, we have used a rat model, in which cerulein-induced mild acute pancreatitis could develop into severe acute pancreatitis under water-immersion stress^[12]. Cerulein can cause blocking of zymogen secretion, co-localization of zymogens and lysosome, and digestive enzyme activation. Water-immersion stress can stimulate sympathetic nerve system. In this model, multiple vasoconstrictive factors are released, which contribute to a reduction of pancreatic blood perfusion and tissue hypoxia or anoxia with the consequence of damages of microvascular endothelium. Moreover, an enhanced release of cytokines in turn precipitates the microcirculatory disorders. Our study had shown that cerulein plus water-immersion model evolved a highly reproducible form of pancreatitis that was characterized by hyperamylasemia, pancreatic hemorrhage and reduction of pancreatic blood flow.

The significance of disorders of the microcirculation with the consequence of tissue hypoxia or anoxia has been under consideration in the pathogenesis of acute pancreatitis for several decades^[13-15]. The hypothesis that the pathogenesis of acute pancreatitis involves ischemia - reperfusion-associated events has attracted new attention^[16,17]. The decreased pancreatic capillary blood flow, reduced functional capillary density, and irregular intermittent perfusion were observed in the specimens of cerulein-induced experimental acute pancreatitis^[18]. In addition, experimental studies have indicated that synthesis and release of pro-inflammatory cytokines such as TNFα, IL-1β^[19], and platelet activating factor (PAF)^[20,21], were responsible for local injury and systemic dispersion of the inflammation in the development of pancreatitis. There also had strong evidence that oxygen free radicals were closely associated with the severity of acute pancreatitis^[22,23]. Elucidation

of these mechanisms may lead to the possibility of specific therapies aimed at reducing microcirculatory disorders, interrupting the inflammatory process, and therefore preventing tissue injury in acute pancreatitis. Unfortunately, there is still no specific compound for treatment of severe acute pancreatitis other than supportive critical care today.

Rhubarb, a Chinese herbal medicine, has a very broad spectrum of biological activities and pharmacological functions. Rhubarb is used as a laxative, antiphlogistic, and homeostatic in the treatment of constipation, diarrhea, jaundice, and gastrointestinal hemorrhage, etc. Clinical studies have shown that rhubarb could improve the prognosis of patients with systemic inflammatory reaction syndrome (SIRS) by its antagonizing effect against inflammatory cytokines and complements^[24]. As reported by Chen *et al.*, rhubarb could reduce the leakage of oxygen radicals from the mitochondria of intestinal mucosa, exert protective effect on barrier of intestinal mucosa, and improve the gastrointestinal blood perfusion in shocked rats^[25-28]. It has also been shown that rhubarb was effective in alleviating the severity of early phase of acute pancreatitis, and preventing further complications at later stages^[2]. The sites of action could be related to its inhibition of pancreatic enzymic activities^[29]. In experimental pancreatitis the therapy of Tong Xia purgative method, in which rhubarb was the main compound, could alleviate the degree of lung injury mediated by TNF^[30]. Taken together, Chinese herbs have many pharmacological substances and therefore have multiple therapeutic effects on acute pancreatitis. This study has shown that administration of rhubarb resulted in a marked reduction of serum amylase activity, significant amelioration in the severity of SAP, and improvement of microcirculatory disturbances in pancreas. Rhubarb may play an important role in the regulation of local blood flow of pancreas by eliminating the oxygen free radicals, as well as inhibiting the release of cytokines.

Few studies have characterized the alteration in pancreatic exocrine function after the induction of experimental pancreatitis. Niederau *et al.*^[31] evaluated basal and stimulated pancreatic secretion *in vivo* and *in vitro* in four different models of acute pancreatitis. They found that a secretory blockade during pancreatitis was strikingly similar in all models, in particular the pancreatic secretory response to CCK. This secretory blockade might at least partly explain the failure to treat acute pancreatitis effectively by inhibition of secretion. Our preliminary experiment also showed a nearly complete blockade of pancreatic exocrine secretion in rats with SAP (data was not shown). We successfully obtained the pancreatic juice sample by co-injection with CCK analog and secretin at physiological dosage. This study demonstrated a significant reduction of the volume, amylase activity, and protein content of pancreatic juice in rats with SAP. After treatment with rhubarb, bicarbonate output was distinctively increased, which has yet unknown significance. Like secretin, rhubarb might stimulate flow of bicarbonate- and electrolyte-rich ductular secretion via cAMP, and then exert a protective effect on acute pancreatitis^[32], which requires further study.

Our present study showed that rhubarb with its natural complexity and typical prescription in combination exerted protective effects on SAP in rats, probably through improvement of pancreatic microcirculation, amelioration of inflammation, inhibition of pancreatic enzyme, and partial alteration of pancreatic exocrine.

ACKNOWLEDGMENT

This work was partly supported by grants from the Research on Specific Diseases, Intractable Diseases of the Pancreas, Health and Labour Sciences Research Grants, Japan. T.I.

(14570477) was supported by a grant from the Ministry of Education, Culture, Sports, Science, and Technology, Japan.

REFERENCES

- 1 **Zheng XL**, Wu XZ. A report of 100 cases of acute pancreatitis treated with Chinese and West medicine. *Zhongxiyi Jiehe Jifu Zhongtongxun* 1979; **1**: 14-17
- 2 **Jiao DH**, Shen XM, Jing BW. Clinical study of acute pancreatitis treated with a single recipe of rhubarb during the past 17 years. *Zhongyi Zazhi* 1994; **35**: 172-173
- 3 **Yamaguchi H**, Kimura T, Nawata H. Dose stress play a role in the development of severe pancreatitis in rats? *Gastroenterology* 1990; **98**: 1682-1688
- 4 **Yamaguchi H**, Kimura T, Mimura K, Nawata H. Activation of proteases in cerulein-induced pancreatitis. *Pancreas* 1989; **4**: 565-571
- 5 **Liu X**, Nakano I, Yamaguchi H, Ito T, Goto M, Koyanagi S, Kinjoh M, Nawata H. Protective effect of nitric oxide on the development of acute pancreatitis in rats. *Dig Dis Sci* 1995; **40**: 2162-2169
- 6 **Furukawa M**, Kimura T, Sumii T, Yamaguchi H, Nawata H. Role of local pancreatic blood flow in development of hemorrhagic pancreatitis induced by stress in rats. *Pancreas* 1993; **8**: 499-505
- 7 **Reber HA**, Karanjia ND, Alvarez C, Widdison AL, Leung FW, Ashley SW, Lutrin FJ. Pancreatic blood flow in cats with chronic pancreatitis. *Gastroenterology* 1992; **103**: 652-659
- 8 **Ceska M**, Birath K, Brown B. A new and rapid method for the clinical determination of α -amylase activities in human serum and urine. Optimal Conditions. *Clin Chim Acta* 1969; **26**: 437-444
- 9 **Tian R**, Zhou L. The effect of secretin, CCK-8 and insulin on pancreatic exocrine secretion in isolated rat pancreas. *Basic Medical Science Clinics* 1997; **17**: 353-357
- 10 **Chen HM**, Sunamura M, Shibuya K, Yamauchi JI, Sakai Y, Fukuyama S, Mikami Y, Takeda K, Matsuno S. Early microcirculatory derangement in mild and severe pancreatitis models in mice. *Surg Today* 2001; **31**: 634-642
- 11 **Ding SP**, Li JC, Jin C. A mouse model of severe acute pancreatitis induced with caerulein and lipopolysaccharide. *World J Gastroenterol* 2003; **9**: 584-589
- 12 **Bockman DE**. Microvasculature of the pancreas: Relation to pancreatitis. *Int J Pancreatol* 1992; **12**: 11-21
- 13 **Broe PJ**, Zuidema GD, Cameron JL. The role of ischemia in acute pancreatitis: studies with an isolated perfused canine pancreas. *Surgery* 1982; **91**: 377-382
- 14 **Pfeffer RB**, Lazzarini-Robertson A Jr, Safadi D, Mixer G Jr, Secoy CF, Hinton JW. Gradations of pancreatitis, edematous, through hemorrhagic, experimentally produced by controlled injection of microspheres into blood vessels in dogs. *Surgery* 1962; **51**: 764-769
- 15 **Slater DN**, Bardsley D, Mangnall Y, Smythe A, Fox M. Pancreatic ischaemia: sensitivity and reversibility of the changes. *Br J Exp Pathol* 1975; **56**: 530-536
- 16 **Menger MD**, Bonkhoff H, Vollmar B. Ischemia-reperfusion-induced pancreatic microvascular injury. An intravital fluorescence microscopic study rats. *Dig Dis Sci* 1996; **41**: 823-830
- 17 **Toyama MT**, Lewis MP, Kusske AM, Reber PU, Ashley SW, Reber HA. Ischaemia-reperfusion mechanisms in acute pancreatitis. *Scand J Gastroenterol Suppl* 1996; **31**: 20-23
- 18 **Zhou ZG**, Chen YD, Sun W, Chen Z. Pancreatic microcirculatory impairment in experimental acute pancreatitis in rats. *World J Gastroenterol* 2002; **8**: 933-936
- 19 **Gomez-Cambrotero LG**, Sabater L, Pereda J, Cassinello N, Camps B, Vina J, Sastre J. Role of cytokines and oxidative stress in the pathophysiology of acute pancreatitis: therapeutic implications. *Curr Drug Targets Inflamm Allergy* 2002; **1**: 393-403
- 20 **Zhao H**, Chen JW, Zhou YK, Zhou XF, Li PY. Influence of platelet activating factor on expression of adhesion molecules in experimental pancreatitis. *World J Gastroenterol* 2003; **9**: 338-341
- 21 **Konturek SJ**, Dembinski A, Konturek PJ, Warzecha Z, Jaworek J, Gustaw P, Tomaszewska R, Stachura J. Role of platelet activating factor in pathogenesis of acute pancreatitis in rats. *Gut*

- 1992; **33**: 1268-1274
- 22 **Sanfey H**, Bulkley GB, Cameron JL. The role of oxygen-derived free radicals in the pathogenesis of acute pancreatitis. *Ann Surg* 1984; **200**: 405-413
- 23 **Park BK**, Chung JB, Lee JH, Suh JH, Park SW, Song SY, Kim H, Kim KH, Kang JK. Role of oxygen free radicals in patients with acute pancreatitis. *World J Gastroenterol* 2003; **9**: 2266-2269
- 24 **Peng SM**, Wang SZ, Zhao JP. Effect of rhubarb on inflammatory cytokines and complements in patients with systemic inflammation reaction syndrome and its significance. *Zhongguo Zhongxiyi Jiehe Zazhi* 2002; **22**: 264-266
- 25 **Chen D**, Qiao L, Jing B. Effect of rhubarb on oxygen radicals leakage from mitochondria of intestinal mucosa in burned rats. *Zhongguo Zhongxiyi Jiehe Zazhi* 2000; **20**: 849-852
- 26 **Chen D**, Yang X, Jiang X. Clinical and experimental study on effect of rhubarb on gastrointestinal blood flow perfusion. *Zhongguo Zhongxiyi Jiehe Zazhi* 2000; **20**: 515-518
- 27 **Chen DC**, Jin BW, Zhang XY. Therapeutic effects of rhubarb on gastrointestinal failure. *China Natl J New Gastroenterol* 1996; **2**: 206-208
- 28 **Chen DC**, Yang XY, Zhang XY, Chen XY. Protective effect of rhubarb on barrier of intestinal mucosa. *China Natl J New Gastroenterol* 1997; **3**: 81-83
- 29 **Sun G**, Chen MZ, Pan GZ. An *in vitro* study of Qing-yi decoction NO. I on pancreatic enzyme activity and release. *Acta Academiae Medicinae Sinicae* 1985; **7**: 337-340
- 30 **Xia Q**, Jiang JM, Gong X, Chen GY, Li L, Huang ZW. Experimental study of Tong Xia purgative method in ameliorating lung injury in acute necrotizing pancreatitis. *World J Gastroenterol* 2000; **6**: 115-118
- 31 **Niederer C**, Niederer M, Luthen R, Strohmeyer G, Ferrell LD, Grendell JH. Pancreatic exocrine secretion in acute experimental pancreatitis. *Gastroenterology* 1990; **99**: 1120-1127
- 32 **Renner IG**, Wisner JR Jr, Lavigne BC. Partial restoration of pancreatic function by exogenous secretin in rats with ceruletide-induced acute pancreatitis. *Dig Dis Sci* 1986; **31**: 305-313

Edited by Xu JY Proofread by Xu FM

Cryopreservation and gel collagen culture of porcine hepatocytes

Hong-Ling Liu, Ying-Jie Wang, Hai-Tao Guo, Yu-Ming Wang, Jun Liu, Yue-Cheng Yu

Hong-Ling Liu, Ying-Jie Wang, Hai-Tao Guo, Yu-Ming Wang, Jun Liu, Yue-Cheng Yu, Research Institute of Infectious Diseases, Southwest Hospital, Third Military Medical University, Chongqing 400038, China
Hong-Ling Liu, Now in 302 Hospital of the PLA, Beijing 100039, China
Supported by the Natural Scientific Foundation of Nation, No. 30027001, and the National Excellent Doctor Special Foundation, No.199947

Correspondence to: Dr. Ying-Jie Wang, Research Institute of Infectious Diseases, Southwest Hospital, Third Military Medical University, Chongqing 400038, China. wangyj103@263.net

Telephone: +86-23-68754289

Received: 2003-10-27 **Accepted:** 2003-11-13

Abstract

AIM: To study the method of cryopreserving porcine hepatocytes and gel collagen culture measure after its cryopreservation.

METHODS: Hepatocytes, isolated from Chinese experimental suckling mini-pigs by two-step perfusion with collagenase using an extra corporeal perfusion apparatus, were cryopreserved with 50 mL/L to 200 mL/L DMSO in liquid nitrogen for 4 mo, then thawed and seeded in 1 or between 2 layers of gel collagen. The expression of porcine albumin message RNA, cellular morphology and content of aspartate aminotransferase (AST) and urea nitrogen (UN) were examined during culture in gel.

RESULTS: Viability of 150 mL/L DMSO group thawed hepatocytes was (83±4)%, but after purification, its viability was (90±5)%, attachment efficiency was (86±7)%, the viability of thawed hepatocytes was near to fresh cells. When the thawed hepatocytes were cultivated in gel collagen with culture medium adding epidermal growth factor, the hepatocytes grew in various administrative levels in mixed collagen gel, and bunched in the sandwich configuration cultures. For up to 10 days' culture, the typical cellular morphological characteristics of cultivated hepatocytes could be observed. The leakage of AST was lower during culture in gel than that in common culture. At the same time, the UN synthesized by cells cultivated in mixed gel collagen was higher than that in other groups.

CONCLUSION: Storage in liquid nitrogen can long keep hepatocytes' activities, the concentration of 150 mL/L DMSO is fit for porcine hepatocytes' cryopreservation. Thawed hepatocytes can be cultivated with collagenous matrix, which provides an environment that more closely resembles that *in vivo* and maintain the expression of certain liver-specific function of hepatocytes.

Liu HL, Wang YJ, Guo HT, Wang YM, Liu J, Yu YC. Cryopreservation and gel collagen culture of porcine hepatocytes. *World J Gastroenterol* 2004; 10(7): 1010-1014

<http://www.wjgnet.com/1007-9327/10/1010.asp>

INTRODUCTION

Bioartificial liver support systems (BALSS), which employ

freshly isolated primary hepatocytes, present severe logistic difficulties in the continuous supply of hepatocytes^[1-3]. Stored frozen hepatocytes that are thawed as required would solve this problem. Now, storing hepatocytes in liquid nitrogen was an important method to keep its biological abilities, suitable preserving measure can offer high vigorous hepatocytes for several researches. With the further development of related subjects, long-term preservation methods and active architecture of hepatocytes were needed badly to meet the immediate requirement of bioartificial liver and correlated researches^[4-7]. Cryopreservation of hepatocytes is essential for the emergent treatment of acute liver failure. Morsiani *et al* reported the clinical use of such thawed cells. These clinical reports certainly reflect the progress made to date in the isolation and handling of hepatocytes, and it is hoped this will lead to a wider use of cellular therapies in liver diseases^[8-13].

In order to find a suitable cryopreservation and culture measure, hepatocytes from newly born Chinese experimental mini-pigs were cryopreserved in -196 °C for 4 mo, then thawed hepatocytes were cultivated with mixed gel or sandwich gel collagen, and their morphology and biological functions were compared. So this study was to develop a cryopreservation protocol for long-time preparation of porcine hepatocytes, and to determine an optimal purification procedure and culture methods for thawed hepatocytes. At last it could provide important experimental data for the research of bioartificial liver and hepatocytes transplantation.

MATERIALS AND METHODS

Isolation of porcine hepatocytes

Pig hepatocytes were harvested from newly born Chinese experimental mini-pigs (Experimental Animal Center, Third Military Medical University) using the two-step collagenase perfusion method that was modified from the original methods developed by Seglen *et al*^[4,20-22]. Briefly, the animals were anesthetized with barbital (30 mg/kg, b.w, intraperitoneally) and their livers were removed. The liver was first perfused *in vitro* via the portal vein with warmed (37 °C) Ca²⁺ and Mg²⁺ free Hanks balanced salt solution at a flow rate of 20-30 mL/min for 10-15 mL/min, and then perfused with 0.5 g/L collagenase (Sigma, Type IV) in the same solution supplemented with 5 mM CaCl₂ and 50 mM HEPES. The reperfusion with collagenase solution lasted 20 min at a rate of 20 mL/min at 37 °C. After 10 min of incubation (37 °C) with gentle shaking, the cells suspension was filtered and centrifuged at 50 g, 3 min for 3 times. The viability of the isolated liver cells was determined using standard trypan blue exclusion, ranged from 89% to 98%^[14-18].

Cryopreservation of porcine hepatocytes

Isolated hepatocytes were slowly resuspended and gently mixed at 5×10⁹ cells/L concentration in different cryopreserving solution which consists of 200 mL/L fetal bovine serum (FBS) and 50 mL/L, 100 mL/L, 150 mL/L or 200 mL/L dimethyl sulphoxide (DMSO, Sigma, America), then placed hepatocytes in 1 mL freezing tube (AXYGEN, America), tagged and put into isopropanol. The concrete freezing procedure was: put in room temperature for 15 min; 4 °C for 20 min; -20 °C for 30 min;

and stayed overnight at -80°C , at last, liquid nitrogen for long-term preservation^[7,19-23].

Thawing and removal of DMSO

Four months later, the vials were removed from liquid nitrogen and rapidly thawed by immersion in a 37°C water bath. Immediately after thawing, dimethyl sulfoxide was removed by successive dilutions in 50 mL tubes, 20 mL of Leibowitz-15 medium containing 100 mL/L FBS was gently added to 1.0 mL of cell suspension at 3 min of intervals. The cells were washed three times by centrifugation for 3 minutes at 30 g and 4°C to remove cryoprotectant. Then hepatocytes pellet was resuspended in L-15 medium with 100 mL/L FBS. Cell viability was estimated by trypan blue dye exclusion. 1×10^6 thawed hepatocytes were centrifuged at 1 000 rpm for 10 min, the supernatants of medium discarded, pellet cells fixed by 30 mL/L glutaral and 10 mL/L OsO_4 etc, and hepatocytes' ultrastructure was observed through transmission electron microscope^[24,25].

Percoll purification of thawed hepatocytes

Working Percoll solution I was prepared by adding 1 part of 10 concentrated D-phosphate-buffered saline into 9 parts of Percoll. Then working Percoll solution II was consisted of 30 mL working Percoll solution I and phosphate-buffered saline. Hepatocytes purification was made by a procedure: to 10 mL of cell suspension, 25 mL of working Percoll solution II were added. The cells pellet was collected by centrifugation at 500 g during 3 min, resuspended, and purified hepatocytes were washed 3 times by centrifugation for 3 min at 30 g and 4°C .

Common, mixed collagen gel and sandwich configuration culture of thawed hepatocytes

Then hepatocytes were inoculated at 10^6 cell/ bottle in L-15 medium added by 100 mL/L FBS, 10 $\mu\text{L/L}$ glucagons, 200 U/L insulin and 20 ng/L epidermal growth factor (Sigma), as a control group and the medium was changed every day. The morphologies of hepatocytes were observed under inverted microscope, supernatants of culture cells was stored at -20°C for examination. Viability of cells was determined using standard trypan blue exclusion measure.

The collagen solution was prepared just before its use by mixing three parts of collagen type VII (Sigma) in one part of 4 \times Dulbecco's modified Eagle's medium (Gibco, America) without bicarbonate (pH 7.4), adjusting its pH to 7.20 with 1N NaOH. One million cells were mixed with 2 mL collagen solution and incubated in T-flasks (25cm²) at 37°C . When the mixed collagen matrix was fixed in an hour, the gel was washed slowly and medium was added, and hepatocytes were incubated at 37°C with 100 mL/L CO_2 900 mL/L humidity. The methods of culture and observation were the same to the control group^[26,27].

When thawed hepatocytes were cultivated in sandwich configuration, the collagen solution was prepared just as before, then T-flasks were coated with it and incubated one hour at 37°C . One million cells were cultivated with L-15 medium. Nonattached hepatocytes were washed after one hour; second layer of collagen solution was spread to sandwich the hepatocytes after 24 h. Thirty minutes later, sandwich configuration hepatocytes were formed^[28-30], and the methods of culture and observation were just performed as before.

Expression of porcine hepatocytes albumin message RNA

When hepatocytes were cultivated for one week, its total RNA were distilled by Tripure isolated reagent (the gel cultured hepatocytes were digested with 0.5 g/L pancreatin before distilled). The sequences of primers are designed in Table 1. "House-keeping gene" glyceraldehydes-3-phosphate dehydrogenase (G3PDH) gene was kept as inner standard^[31].

Table 1 Nucleotide sequences of primers and band sizes

Primers	Sequences (5' -3')	Band sizes
mRNA sense	CTTATTCAGGGGCTGTTC	324 bp
antisense	TCGTTTCTCTCAGGCTCTTCT	
G3PDH sense	CATCATCCCTGCTTCTACCC	160 bp
antisense	CCTGCTTACCACCTTTCTTG	

RNA was reverse transcribed using a one-step RT-PCR kit (Promga, America). For RT-PCR amplification, the standard RT-PCR program of one cycle of 48°C for 45 min and 94°C for 4 min, 35 cycles of 95°C for 1 min, 55°C for 1 min, and 72°C for 1 min and one cycle of 72°C for 7 min were applied. The products of RT-PCR were electrophoresised on 15 g/L agarose gel, and figures were gained on Gel-DocTM2000 (BIO-RAD, America). The densities of these straps were scanned, and the odds of every group's band/ corresponding G3PDH strap were seen as the expression of objective gene.

Aspartate aminotransferase (AST) and urea nitrogen (UN)

The level of AST and UN, in culture supernatants of the control group, mixed gel and sandwich configuration, were detected with biological analysis meter (HITACH. Japan)^[32].

Data statistics

The data was analysed by the duplication measurement analysis of variance or one-way analysis of variance on SPSS 11.0 software. Results were expressed on mean \pm standard deviation (mean \pm SD).

RESULTS

Survival rate and attaching efficiency of hepatocytes

Fresh isolated and cryopreserved/purified hepatocytes were assessed for viability and function by trypan blue dye exclusion. The yield of cells was 1.5 to 5×10^9 cells/liver. Cell viability was (91 \pm 4)%, and attachment efficiency of viable hepatocytes after 24 h culture was (89 \pm 5)%. After cryopreservation, the viabilities of 50 mL/L, 100 mL/L, 150 mL/L and 200 mL/L DMSO group of hepatocytes were in Table 2. However, when the 150 mL/L DMSO group thawed hepatocytes were purified by Percoll, its viability was (90 \pm 5)%, attachment efficiency was (86 \pm 7)%. The viability of thawed hepatocytes were near to fresh cells.

Table 2 Viability and 24 hours attaching efficiency of thawed hepatocytes (%)

Viability/group (mL/L)	50 DMSO	100 DMSO	150 DMSO	200 DMSO
Viability	51 \pm 3	71 \pm 4 ^a	83 \pm 4 ^c	79 \pm 5 ^c
Attaching efficiency	32 \pm 6	70 \pm 5 ^a	81 \pm 5 ^c	77 \pm 6 ^a

$n=5$, ^a $P<0.05$ vs 50 mL/L or 100 mL/L DMSO group, ^c $P<0.05$ vs 50 mL/L DMSO group.

In this table, we can see the viability of 100 mL/L DMSO group cells were much better than that of 50 mL/L and 100 mL/L DMSO groups ($P<0.05$), but there was no significant difference between the group of 150 mL/L DMSO and 200 mL/L DMSO ($P>0.05$).

Morphology of thawed hepatocytes

The ultrastructure of thawed hepatocytes in 150 mL/L DMSO group were kept well, number of mitochondria was normal, with slight swollen cristae, rough endoplasmic reticulum decreased, smooth endoplasmic reticulum and golgi apparatus increased,

chromatin in cell nucleus distributed normal (Figure 1A).

Thawed hepatocytes of 150 mL/L DMSO group attached to dishes within 4 h (Figure 1B). After 24 hours' culture, cells appeared polygonal, containing granular cytoplasm with one or two centrally located nuclei. Seven days later, they were more flattened and appeared bigger than 24 h cultured hepatocytes. Morphology and ultrastructure of other groups' hepatocytes were abnormal, thus the hepatocytes of 150 mL/L group were provided for gel collagen culture.

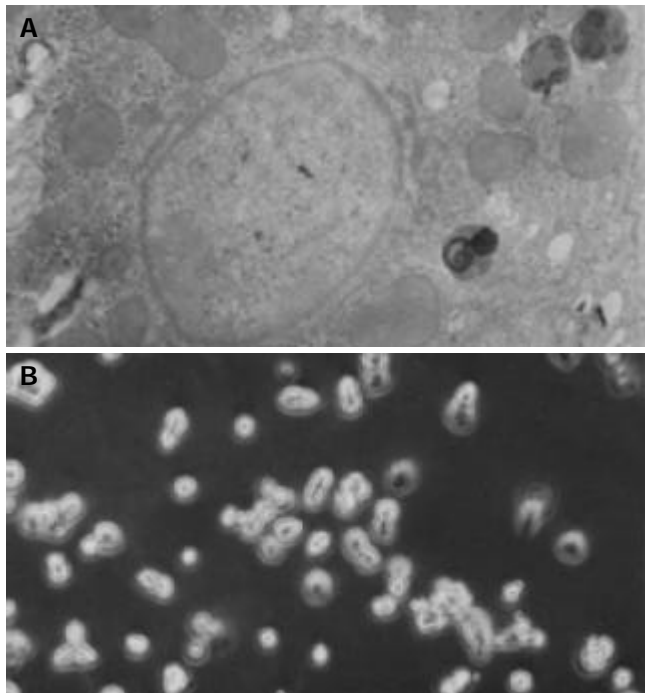


Figure 1 A: The thawed hepatocytes' ultrastructure after 4 mo cryopreservation, (TEM, $\times 4000$), B: The morphology of thawed hepatocytes after 4 h culture (PCM, $\times 200$).

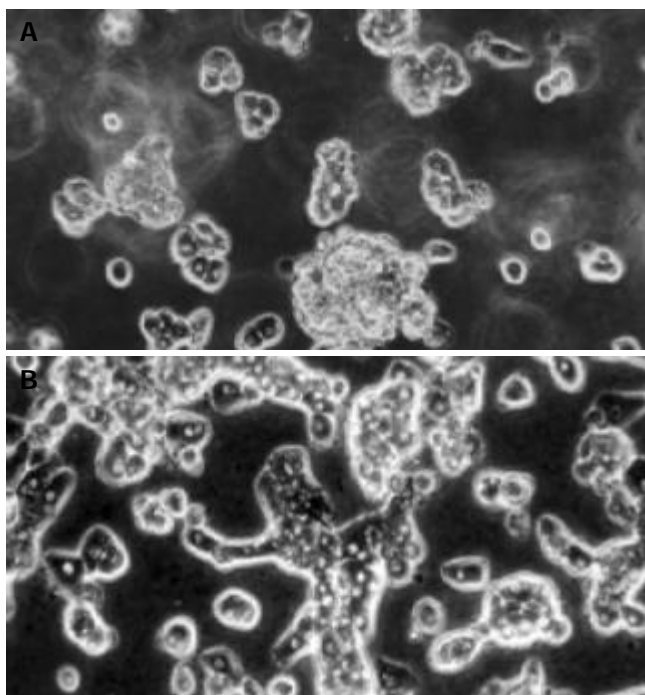


Figure 2 A: Morphology of thawed hepatocytes cultivated in mixed gel for 4 h (PCM, $\times 200$), B: Morphology of hepatocytes cultivated in sandwich configuration for 24 h (PCM, $\times 200$).

Morphology of mixed gelled cultivated pig hepatocytes

The hepatocytes kept their biological characters well after 150 mL/L DMSO cryopreservation. When the thawed hepatocytes were mixed in gel collagen and cultivated with medium adding epidermal growth factor, the hepatocytes grow in various administrative levels in collagen gel. For up to 7 days' culture, the typical cellular morphological characteristics of hepatocytes could be observed (Figure 2A).

Morphology of sandwich culture pig hepatocytes

Hepatocytes, cultivated for four hours in first layer gel, turned from pellet to polygon. When second layer gel collagen was added, hepatocytes cultured in collagen sandwich configuration had a cuboid, compact, bunched, and well-defined shape with a classical cobblestone appearance. In the seven-days' culture period, the hepatocytes maintained their typical morphological characteristics under phase contract microscope (Figure 2B).

Expression of albumin mRNA on thawed porcine hepatocytes

When the control group mixed gel collagen and sandwich configuration porcine hepatocytes were cultivated for seven days, they all kept expression of albumin message RNA using RT-PCR, but the level of mixed gel collagen group was higher than that of other group ($P < 0.05$), (Figure 3 and Table 3).

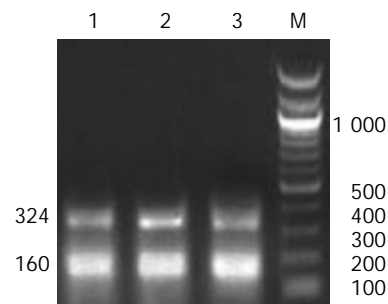


Figure 3 Expression of porcine albumin mRNA on culture hepatocytes after RT-PCR. M: DNA markers; lanes 1, 2 and 3 are control groups, mixed gel collagen and sandwich configuration.

Table 3 Change of albumin mRNA expression in culture pig hepatocytes (mean \pm SD)

Band density/group	Mixed gel group	Sandwich group	Control group
Mean rate of density	0.44 \pm 0.041 ^a	0.353 \pm 0.021 ^c	0.261 \pm 0.02

$n=3$, ^a $P < 0.05$ vs group of control or sandwich; ^c $P < 0.05$ vs control group.

Release of AST

The level of AST in common culture hepatocytes supernatant was very lower on day 1 to day 3, and ascended to the peak on day 7, which was marked higher than the group of mixed gel collagen or sandwich collagen ($P < 0.05$). The contents of AST in the group of gel collagen on culture 24 to 48 h were high, but they dropped at day 3 and kept at a lower level ($P > 0.05$), (Figure 4).

UN in culture supernatant

The levels of urea nitrogen synthesized by hepatocytes in three groups were different and changed. The content in common culture group decreased on day 5, and was lower than that of other groups on culture period ($P < 0.05$). Mixed gel group's level was higher than that of the sandwich, but they had no marked difference. ($P > 0.05$), (Figure 5).

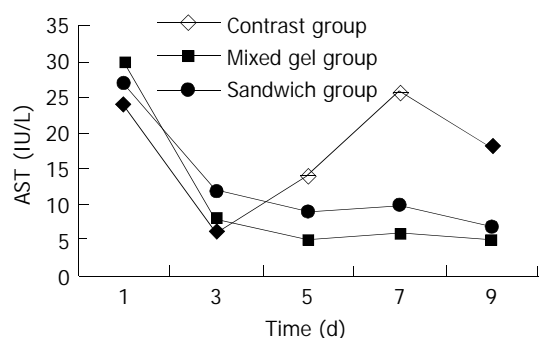


Figure 4 Content of AST on hepatocytes culture medium.

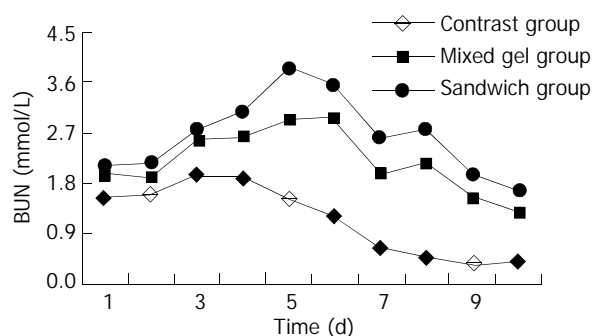


Figure 5 Content of urea nitrogen on hepatocytes culture medium.

DISCUSSION

Hepatocytes cryopreserved in liquid nitrogen were thought as only efficient measure to keep its ability currently^[33-36]. Shortage of hepatocytes necessitates the development of improved cryopreservation techniques for long-term storage of hepatocytes to make best use of available hepatocytes. The ultimate goal of any improved cryopreservation protocol is to minimize sudden intracellular formation of ice crystals that could result in ultrastructural damage, and thus maintains cell viability, attachment, and metabolic activity on thawing. Storage time of cryopreserved hepatocytes at temperatures -196°C may play an important role in the quality of thawed cells. Most of the available protocols use dimethyl sulfoxide in the cryopreservation medium^[19,37-39].

Successful cryopreservation of porcine hepatocytes would ensure the accessibility of cells for laboratory use, permit the standardisation of experiments, save lives of animals and lead to continuous supply of hepatocytes in BALSS treatment^[28,31]. Therefore, we sought the optimal procedure for cryopreservation of porcine hepatocytes for both laboratory and clinical purposes in this study. The protocol for cryopreservation of hepatocytes included the concentration of 150 mL/L DMSO, 200 mL/L fetal bovine serum and rapid thawing followed by slow dilution of DMSO to avoid osmotic shock. After 4 mo cryopreservation, the thawed cells were shown to have a reasonable level of cell viability, compared to freshly isolated hepatocytes. So the storage condition was proved to be suitable for long-time cryopreservation of pig hepatocytes. Our purification method using D-PBS and Percoll achieved a high cell recovery rate with satisfactory viability and function at high cell concentrations (5×10^9 cell/L), facilitating purification of hepatocytes in large quantities. We conclude that frozen/thawed/purified cells can possess satisfactory viability and function. Large-scale cryopreservation of porcine hepatocytes may provide an efficient alternative to freshly isolated porcine hepatocytes^[19, 40-42].

Proper cryopreservation measure can maintain porcine hepatocytes' abilities for a long time. However, if the thawed hepatocytes were cultivated in unfit conditions, it would not

meet the need of application in clinic and basic research. Therefore, the culture pattern of thawed hepatocytes also appeared very important. Traditional cell culture measure, which was common monolayer attaching incubation, was hard to simulate the circulation that hepatocytes grew *in vivo*, and were not suitable for BLASS^[43]. Collagen was a kind of matrix in common use to fix hepatocytes. Liver cells *in vivo* assume three-dimension configuration in a liver lobule, and there are complicated contacts among hepatocytes, liver non-parenchyma cells and cell matrix. Matrix is an important part of affecting hepatocytes function. Many researches showed that collagenous matrix could provides an environment that more closely resembles that *in vivo* and allows to maintain the expression of certain liver-specific function of hepatocytes^[44-47]. In this study, the hepatocytes keep their biological characters well after storage in liquid nitrogen for 4 mo. When the thawed hepatocytes were cultivated in gelled collagen with culture medium added by epidermal growth factor, the cells grow in various administrative levels in mixed collagen gel, and bunched in the collagen sandwich cultures. For up to 10 days' cultures, the typical cellular polygonal morphological characteristics of culture hepatocytes could be observed, and the bound between hepatocytes appear brightly and clearly; the leakage of aspartate aminotransferase was less and the level of urea nitrogen synthesized by hepatocytes was higher. Through sandwich culture can hold hepatocytes synthesizing and metabolizing abilities, the cultivated hepatocytes was also at monolayer attaching state, and do not have normal three-dimension construction *in vivo*, so it needs to be further ameliorated^[26,29,43].

In conclusion, through the study of many important factors in hypothermic preservation, we can optimize the hypothermic preservation protocols or cultivated conditions, and established a hepatocytes storage room. That will be helpful for the development of BAL and hepatocytes transplantation^[9,40,48].

REFERENCES

- 1 **Wang YJ**, Li MD, Wang YM, Nie QH, Chen GZ. Experimental study of bioartificial liver with cultured human liver cells. *World J Gastroenterol* 1999; **5**: 135-137
- 2 **Eguchi S**, Kamohara Y, Sugiyama N, Kawazoe Y, Kawashita Y, Tamura H, Morishita, M, Miyamoto S, Azuma T, Fujioka H, Furui J, Kanematsu T. Efficacy and current problems with a porcine hepatocyte-based bioartificial liver: light and shade. *Transplant Proc* 1999; **31**: 2014-2015
- 3 **Wu L**, Sun J, Qin G, Wang C, Woodman K, Koutalistras N, Horvat M, Sheil AGR. Cryopreserved porcine hepatocytes in a liver biodialysis system. *Transplant Proc* 2001; **33**: 1950-1951
- 4 **Sarkis R**, Honiger J, Chafai N, Baudrimont M, Sarkis K, Delelo R, Becquemont L, Benoist S, Balldur P, Capeau J, Nordlinger B. Semiautomatic macroencapsulation of fresh or cryopreserved porcine hepatocytes maintain their ability for treatment of acute liver failure. *Cell Transplant* 2001; **10**: 601-607
- 5 **Sarkis R**, Benoist S, Honiger J, Baudrimont M, Delelo R, Balladur P, Capeau J, Nordlinger B. Transplanted cryopreserved encapsulated porcine hepatocytes are as effective as fresh hepatocytes in preventing death from acute liver failure in rats. *Transplantation* 2000; **70**: 58-64
- 6 **Khalili TM**, Navarro A, Ting P, Kamohara Y, Arkadopoulos N, Solomon BA, DemetriouAA, Rozga J. Bioartificial liver treatment prolongs survival and lowers intracranial pressure in pigs with fulminant hepatic failure. *Artif Organs* 2001; **25**: 566-570
- 7 **Sarkis R**, Honiger J, Chafai N, Baudrimont M, Sarkis K, Delelo R, Becquemont L, Benoist S, Balladur P, Capeau J, Nordlinger B. Semiautomatic macroencapsulation of fresh or cryopreserved porcine hepatocytes maintain their ability for treatment of acute liver failure. *Cell Transplant* 2001; **10**: 601-607
- 8 **David P**, Alexandre E, Audet M, Chenard-Neu MP, Wolf P, Jaeck D, Azimzadeh A, Richert L. Engraftment and albumin production of intrasplenically transplanted rat hepatocytes (Sprague Dawley), freshly isolated versus cryopreserved, into Nagase analbuminemic rats (NAR). *Cell Transplant* 2001; **10**: 67-80
- 9 **Morsiani E**, Brogli M, Galavotti D, Bellini T, Ricci D, Pazzi P,

- Puviani AC. Long-term expression of highly differentiated functions by isolated porcine hepatocytes perfused in a radial-flow bioreactor. *Artif Organs* 2001; **25**: 740-748
- 10 **Morsiani E**, Pazzi P, Puviani AC, Brogli M, Valeri L, Gorini P, Scoletta P, Marangoni E, Ragazzi R, Azzena G, Frazzoli E, Di Luca D, Cassai E, Lombardi G, Cavallari A, Faenza S, Pasetto A, Girardis M, Jovine E, Pinna AD. Early experiences with a porcine hepatocyte-based bioartificial liver in acute hepatic failure patients. *Int J Artif Organs* 2002; **25**: 192-202
- 11 **Eguchi S**, Kawazoe Y, Sugiyama N, Kawashita Y, Fujioka H, Furui J, Sato M, Ishii T, Kanematsu T. Effects of recombinant human hepatocyte growth factor on the proliferation and function of porcine hepatocytes. *ASAIO J* 2000; **46**: 56-59
- 12 **Gao Y**, Xu XP, Hu HZ, Yang JZ. Cultivation of human liver cell lines with microcarriers acting as biological materials of bioartificial liver. *World J Gastroenterol* 1999; **5**: 221-224
- 13 **Alexandre E**, Viollon-Abadie C, David P, Gandillet A, Coassolo P, Heyd B, Mantion G, Wolf P, Bachellier P, Jaeck D, Richert L. Cryopreservation of adult human hepatocytes obtained from resected liver biopsies. *Cryobiology* 2002; **44**: 103-113
- 14 **Gao Y**, Hu HZ, Chen K, Yang JZ. Primary porcine hepatocytes with portal vein serum cultured on microcarriers or in spheroidal aggregates. *World J Gastroenterol* 2000; **6**: 365-370
- 15 **Matsushita T**, Yagi T, Hardin JA, Cragun JD, Crow FW, Bergen HR 3rd, Gores GJ, Nyberg SL. Apoptotic cell death and function of cryopreserved porcine hepatocytes in a bioartificial liver. *Cell Transplant* 2003; **12**: 109-121
- 16 **Funatsu K**, Ijima H, Nakazawa K, Yamashita Y, Shimada M, Sugimachi K. Hybrid artificial liver using hepatocyte organoid culture. *Artif Organs* 2001; **25**: 194-200
- 17 **Mitry RR**, Hughes RD, Dhawan A. Progress in human hepatocytes: isolation, culture & cryopreservation. *Semin Cell Dev Biol* 2002; **13**: 463-467
- 18 **Yao YQ**, Zhang DF, Huang AL, Luo Y, Zhang DZ, Wang B, Zhou WP, Ren H, Guo SH. Effects of electroporation on primary rat hepatocytes *in vitro*. *World J Gastroenterol* 2002; **8**: 893-896
- 19 **Guillouzo A**, Rialland L, Fautrel A, Guyomayd C. Survival and function of isolated hepatocytes after cryopreservation. *Chem Biol Interac* 1999; **121**: 7-16
- 20 **Yagi T**, Hardin JA, Valenzuela YM, Miyoshi H, Gores GJ, Nyberg SL. Caspase inhibition reduces apoptotic death of cryopreserved porcine hepatocytes. *Hepatology* 2001; **33**: 1432-1440
- 21 **Xue YL**, Zhao SF, Luo Y, Li XJ, Duan ZP, Chen XP, Li WG, Huang XQ, Li YL, Cui X, Zhong DG, Zhang ZY, Huang ZQ. TECA hybrid artificial liver support system in treatment of acute liver failure. *World J Gastroenterol* 2001; **7**: 826-829
- 22 **Darr TB**, Hubel A. Postthaw viability of precultured hepatocytes. *Cryobiology* 2001; **41**: 11-20
- 23 **Hubel A**, Conroy M, Darr TB. Influence of preculture on the prefreeze and postthaw characteristics of hepatocytes. *Biotechnol Bioeng* 2000-2001; **71**: 173-183
- 24 **Hengstler JG**, Utesch D, Steinberg P, Platt KL, Diener B, Ringel M, Swales N, Fischer T, Biefang K, Gerl M, Böttger T, Oesch F. Cryopreserved primary hepatocytes as a constantly available *in vitro* model for the evaluation of human and animal drug metabolism and enzyme induction. *Drug Metabolism Rev* 2000; **32**: 81-118
- 25 **Gerlach JC**, Zeilinger K, Sauer IM, Mieder T, Naumann G, Grunwald A, Pless G, Holland G, Mas A, Vienken J, Neuhaus P. Extracorporeal liver support: porcine or human cell based systems? *Int J Artif Organs* 2002; **25**: 1013-1018
- 26 **Kono Y**, Yang S, Roberts EA. Extended primary culture of human hepatocytes in a collagen gel sandwich system. *In Vitro Cell Dev Biol Anim* 1997; **33**: 467-472
- 27 **Lorenti A**, Barbich M, Hidalgo A, Hyon SH, Sorroche P, Guinle A, Schenone A, Chamoles N, Argibay P. Culture of porcine hepatocytes: the dogma of exogenous matrix revisited. *Artif Organs* 2001; **25**: 546-550
- 28 **Lau YY**, Sapidou E, Cui X, White RE, Cheng KC. Development of a novel *in vitro* model to predict hepatic clearance using fresh, cryopreserved, and sandwich-cultured hepatocytes. *Drug Metab Dispos* 2002; **30**: 1446-1454
- 29 **Weiss TS**, Jahn B, Cetto M, Jauch KW, Thasler WE. Collagen sandwich culture affects intracellular polyamine levels of human hepatocytes. *Cell Prolif* 2002; **35**: 257-267
- 30 **Hong JT**, Glauert HP. Effect of extracellular matrix on the expression of peroxisome proliferation associated genes in cultured rat hepatocytes. *Toxicol In Vitro* 2000; **14**: 177-184
- 31 **Benoist S**, Sarkis R, Chafai N, Barbu V, Honiger J, Lakehal F, Becquemont L, Baudrimont M, Capeau J, Housset C, Nordlinger B. Survival and differentiation of porcine hepatocytes encapsulated by semiautomatic device and allotransplanted in large number without immunosuppression. *J Hepatol* 2001; **35**: 208-216
- 32 **Vilei MT**, Granato A, Ferrareso C, Neri D, Carraro P, Gerunda G, Muraca M. Comparison of pig, human and rat hepatocytes as a source of liver specific metabolic functions in culture systems-implication for use in bioartificial liver devices. *Int J Artif Organs* 2001; **24**: 392-396
- 33 **Nagaki M**, Miki K, Kim YI, Ishiyama H, Hirahara I, Takahashi H, Sugiyama A, Muto Y, Moriwaki H. Development and characterization of a hybrid bioartificial liver using primary hepatocytes entrapped in a basement membrane matrix. *Dig Dis Sci* 2001; **46**: 1046-1056
- 34 **Enosawa S**, Miyashita T, Fujita Y, Suzuki S, Amemiya H, Omasa T, Hiramatsu S, Suga K, Matsumura T. *In vivo* estimation of bioartificial liver with recombinant HepG2 cells using pigs with ischemic liver failure. *Cell Transplant* 2001; **10**: 429-433
- 35 **Houle R**, Raoul J, Levesque JF, Pang KS, Nicoll-Griffith DA, Silva JM. Retention of transporter activities in cryopreserved, isolated rat hepatocytes. *Drug Metab Dispos* 2003; **31**: 447-451
- 36 **Tzanakakis ES**, Hess DJ, Sielaff TD, Hu WS. Extracorporeal tissue engineered liver-assist devices. *Annu Rev Biomed Eng* 2000; **2**: 607-632
- 37 **Baust JM**, Vogel MJ, Van Buskirk R, Baust JG. A molecular basis of cryopreservation failure and its modulation to improve cell survival. *Cell Transplant* 2001; **10**: 561-571
- 38 **Gao Y**, Hu HZ, Chen K, Yang JZ. Primary porcine hepatocytes with portal vein serum cultured on microcarriers or in spheroidal aggregates. *World J Gastroenterol* 2000; **6**: 365-370
- 39 **Secheser A**, Osorio J, Freise C, Osorio RW. Artificial liver support devices for fulminant liver failure. *Clin Liver Dis* 2001; **5**: 415-430
- 40 **Nyberg SL**, Hay EJ, Ramin KD, Rosen CB. Successful pregnancy after porcine bioartificial liver treatment and liver transplantation for fulminant hepatic failure. *Liver Transpl* 2002; **8**: 169-170
- 41 **Lorenti A**, Barbich M, Hidalgo A, Hyon SH, Sorroche P, Guinle A, Schenone A, Chamoles N, Argibay P. Culture of porcine hepatocytes: the dogma of exogenous matrix revisited. *Artif Organs* 2001; **25**: 546-550
- 42 **Sugimoto S**, Mitaka T, Ikeda S, Harada K, Ikai I, Yamaoka Y, Mochizuki Y. Morphological changes induced by extracellular matrix are correlated with maturation of rat small hepatocytes. *J Cell Biochem* 2002; **87**: 16-28
- 43 **De Smet K**, Cavin C, Vercrusysse A, Rogiers V. Collagen type I gel cultures of adult rat hepatocytes as a screening induction model for cytochrome P450-dependent enzymes. *Altern Lab Anim* 2001; **29**: 179-192
- 44 **Unger JK**, Catapano G, Horn NA, Schroers A, Gerlach JC, Rossaint R. Comparative analysis of metabolism of medium- and plasma perfused primary pig hepatocytes cultured around a 3-D membrane network. *Int J Artif Organs* 2000; **23**: 104-110
- 45 **Trehout D**, Desille M, Doan BT, Mahler S, Fremont B, Malledant Y, Campion JP, Desbois J, Beloeil JC, de Certaines J, Clement B. Follow-up by one- and two-dimensional NMR of plasma from pigs with ischemia-induced acute liver failure treated with a bioartificial liver. *NMR Biomed* 2002; **15**: 393-403
- 46 **Pahernik SA**, Thasler WE, Doser M, Gomez-Lechon MJ, Castell MJ, Planck H, Koebe HG. High density culturing of porcine hepatocytes immobilized on nonwoven polyurethane-based biomatrices. *Cell Tissues Organs* 2001; **168**: 170-177
- 47 **Haruyama T**, Ajioka I, Akaike T, Watanabe Y. Regulation and significance of hepatocyte-derived matrix metalloproteinases in liver remodeling. *Biochem Biophys Res Commun* 2000; **272**: 681-686
- 48 **Wang YJ**, Li MD, Wang YM, Chen GZ, Liu GD, Tan ZX. Effect of extracorporeal bioartificial liver support system on fulminant hepatic failure rabbits. *World J Gastroenterol* 2000; **6**: 252-254

Antiproliferative and proapoptotic effects of somatostatin on activated hepatic stellate cells

Qin Pan, Ding-Guo Li, Han-Ming Lu, Liang-Yong Lu, Yu-Qin Wang, Qin-Fang Xu

Qin Pan, Ding-Guo Li, Han-Ming Lu, Yu-Qin Wang, Qin-Fang Xu, Department of Gastroenterology, Xinhua Hospital, Shanghai Second Medical University, Shanghai 200092, China

Liang-Yong Lu, Research Center for Hepatic Diseases, Nanjing Military Command, Shanghai 200233, China

Supported by the Scientific Development Programs of Science and Technology Commission Foundation of Shanghai, No. 004119047

Correspondence to: Dr. Qin Pan, Department of Gastroenterology, Xinhua Hospital, 1665 KongJiang Rd., Shanghai 200092, China. fangchunhua@online.sh.cn

Telephone: +86-21-65790000-5319 **Fax:** +86-21-55571294

Received: 2003-07-17 **Accepted:** 2003-08-25

Abstract

AIM: To assess the effects of somatostatin on proliferation and apoptosis of activated rat hepatic stellate cells (HSCs).

METHODS: HSCs isolated from the livers of adult Sprague-Dawley rats (weighing 400-500 g) by *in situ* perfusion and purified by single-step density gradient centrifugation with Nycodenz, became activated after 10 days' cultivation. Then the apoptotic rate of HSCs treated with different doses of somatostatin for 72 h, was assayed by acridine orange/ethidium bromide fluorescent staining, terminal deoxynucleotidyl transferase-mediated dUTP nick end labeling, transmission electron microscopy and flow cytometry, while the proliferation of HSCs was measured by MTT assay. Furthermore, the mechanisms of somatostatin were investigated by cytodynamic analysis.

RESULTS: Somatostatin at the concentration of 10^{-6} - 10^{-9} mol/L could decrease the proliferative rate, and promote the apoptosis of activated rat HSCs in a dose-dependent way. Its action was most significant when the concentration reached 10^{-6} mol/L or 10^{-7} mol/L ($P < 0.05$ - 0.01). An obvious cell-cycle arrest (G_0/G_1 arrest) was the important way for somatostatin to exert its action.

CONCLUSION: Antiproliferative and proapoptotic effects of low-dose somatostatin on activated rat HSCs can be obtained. These findings reveal its potential antifibrotic action.

Pan Q, Li DG, Lu HM, Lu LY, Wang YQ, Xu QF. Antiproliferative and proapoptotic effects of somatostatin on activated hepatic stellate cells. *World J Gastroenterol* 2004; 10(7): 1015-1018
<http://www.wjgnet.com/1007-9327/10/1015.asp>

INTRODUCTION

Hepatic stellate cells (HSCs), critical mesenchymal cells in producing hepatic fibrosis and hepatic cirrhosis^[1-9], have been the major target of antifibrotic treatment for a long time, although success has been seldom achieved. Fortunately, progress in the research on inducing apoptosis of activated HSCs, together with inhibition of their proliferation, may provide us with a promising solution to fibrogenesis caused

by different kinds of chronic hepatic diseases.

Recent researches have revealed the apoptosis-inductive and proliferation-inhibitory effects of somatostatin on various cells. Furthermore, somatostatin also has an inhibitory effect on the secretion of some cytokines such as epidermal growth factor (EGF), transforming growth factor- α (TGF- α) and the like, which are essential for the activation of HSCs. Thus we attempted to investigate the effect of somatostatin on proliferation and apoptosis of HSCs and their possible therapeutic potential in hepatic fibrosis.

MATERIALS AND METHODS

Isolation, culture and identification of rat HSCs

Adult male Sprague-Dawley rats (400-500 g) were employed in the experiment. After anesthesia, *in situ* serial infusions were performed via the portal vein with D-Hank's solution and perfusion medium (Hank's medium containing 0.5 g/L collagenase IV and 1 g/L pronase E). Then the liver was broken into pieces and redigested with collagenase IV and DNase. Finally, HSCs were separated from the cell suspension by single-step density gradient centrifugation with 180 g/L Nycodenz (Sigma, USA). After cultured in Dulbecco's modified Eagle medium (DMEM) (Gibco, USA) containing 200 mL/L calf serum (Shishen, China), penicillin (100 IU/mL) and streptomycin (100 mg/mL), HSCs were inoculated into culture flasks and maintained at 37 °C in an atmosphere of 50 mL/L CO₂.

The percentage of freshly isolated living HSCs was up to 95% as defined by trypan blue staining (Sigma, USA), while their purity was over 90% when assessed by light microscopic appearance and their characteristic autofluorescence, which reflected the droplet of vitamin A in cytoplasm (at 325-328 nm). Immunocytochemical staining of desmin (Boster, China) and α -smooth muscle actin (α -SMA) (Boster, China), as well as myofibroblast-like phenotype showed the overall activation of almost all HSCs on the 10th day.

Determination of proliferation of activated HSCs

Exponentially growing activated first-passage-HSCs seeded in 96 well plates at 1×10^4 cells per well, were divided into six groups at random, namely the control group and five somatostatin-treatment groups of 10^{-6} mol/L, 10^{-7} mol/L, 10^{-8} mol/L, 10^{-9} mol/L and 10^{-10} mol/L. Six duplicate wells were arranged in each group. They were incubated at 37 °C in 50 mL/L CO₂ for five d, and then the following steps were taken. (a) Twenty microliters of MTT (5 mg/mL) was added to each well and incubated for four h. (b) The supernatant was aspirated and discarded. (c) One hundred microliters of DMSO was dropped into each well and the plate was agitated for a few min. (d) The optical density (OD) was analysed on an ELISA reader at a test wavelength of 490 nm and a reference wavelength of 620 nm. The inhibition rate (IR) of cell proliferation was calculated according to the following equation. $IR = [1 - (OD \text{ of somatostatin well} / OD \text{ of control well})] \times 100\%$.

Apoptotic analysis of activated HSCs

Activated first-passage HSCs during their logarithmic growth

period were inoculated on the surface of L-polylysine-covered-glass slides in six well plates. According to the same grouping method in the proliferation test, all these wells were divided into six groups for each item of experiment. The apoptotic rates of activated HSCs treated with different concentrations of somatostatin for 72 h, were measured by acridine orange (AO)/ethidium bromide (EB) fluorescent staining, terminal deoxynucleotidyl transferase-mediated dUTP nick end labeling (TUNEL), transmission electron microscopy and flow cytometry, respectively.

Firstly, HSC suspension was prepared via trypsinized method and modulated to a density of 0.5×10^6 cells/mL. Then it was mixed with AO/EB solution (PBS medium containing 0.1 mg/mL AO and 0.1 mg/mL EB) at a proportion of 25:1. Apoptotic cells among 300 randomly selected HSCs were distinguished under high power fluorescent microscope.

Secondly, HSCs fixed with 40 g/L polyformaldehyde were processed in accordance with the instructions of the TUNEL kit (Boster, China): (a) treatment by 30 mL/L H_2O_2 and pronase K successively, (b) reaction with the reactive mixture consisting of 1 μ L of TdT, 1 μ L of digoxin-labeled dUTP, 18 μ L of signal buffer and 20 μ L of signal medium, in a wet box at 37 °C overnight, (c) incubation with blocking medium, anti-digoxin-biotin and SABC sequentially, (d) exposure to DAB for coloration. Thereafter, twenty high power fields under the microscope in each glass slide were chosen at random and positive cells with brown nuclei were counted. Apoptosis Index (AI)=(apoptotic cells/total cells) \times 100%.

Thirdly, the following steps were taken for the digested HSCs: namely to rinse with PBS, to fix with cold ethanol at -20 °C, to incubate with 100 μ L 10 g/L RNase at 37 °C for 15 min, and to stain with propidium iodide (PI) for 30 min in darkness. Then the apoptotic rate and cell cycle could be obtained by flow cytometry.

Finally, HSCs in culture flask were fixed in 20 g/L glutaraldehyde, centrifuged, embedded in glass and sliced in series. HSC ultrastructure was observed by transmission electron microscopy.

Statistical analysis

Results were expressed as mean \pm SD. One way ANOVA and *t* test were applied for data analysis. *P* values less than 0.05 were considered statistically significant.

RESULTS

Effects of somatostatin on HSC proliferation

Data taken from colorimetric MTT assays showed that somatostatin (10^{-6} mol/L- 10^{-9} mol/L) could significantly inhibit the proliferation of activated HSCs in a dose-dependent way (Table 1). As compared with the control group, the inhibitory rates of somatostatin treatment groups rose up to 30.53% and 15.81% when the concentrations of somatostatin reached 10^{-6} mol/L and 10^{-7} mol/L, respectively. But no obvious effect was found in 10^{-10} mol/L somatostatin treatment group.

Table 1 Effects of somatostatin on HSC proliferation (mean \pm SD)

SST concentration (mol/L)	ODs	Inhibitory rates (%)
10^{-6}	0.19 \pm 0.03 ^b	30.53
10^{-7}	0.23 \pm 0.02 ^b	15.81
10^{-8}	0.25 \pm 0.03	7.77
10^{-9}	0.26 \pm 0.03	4.48
10^{-10}	0.27 \pm 0.04	0
0	0.27 \pm 0.04	0

^b*P*<0.01 vs control group.

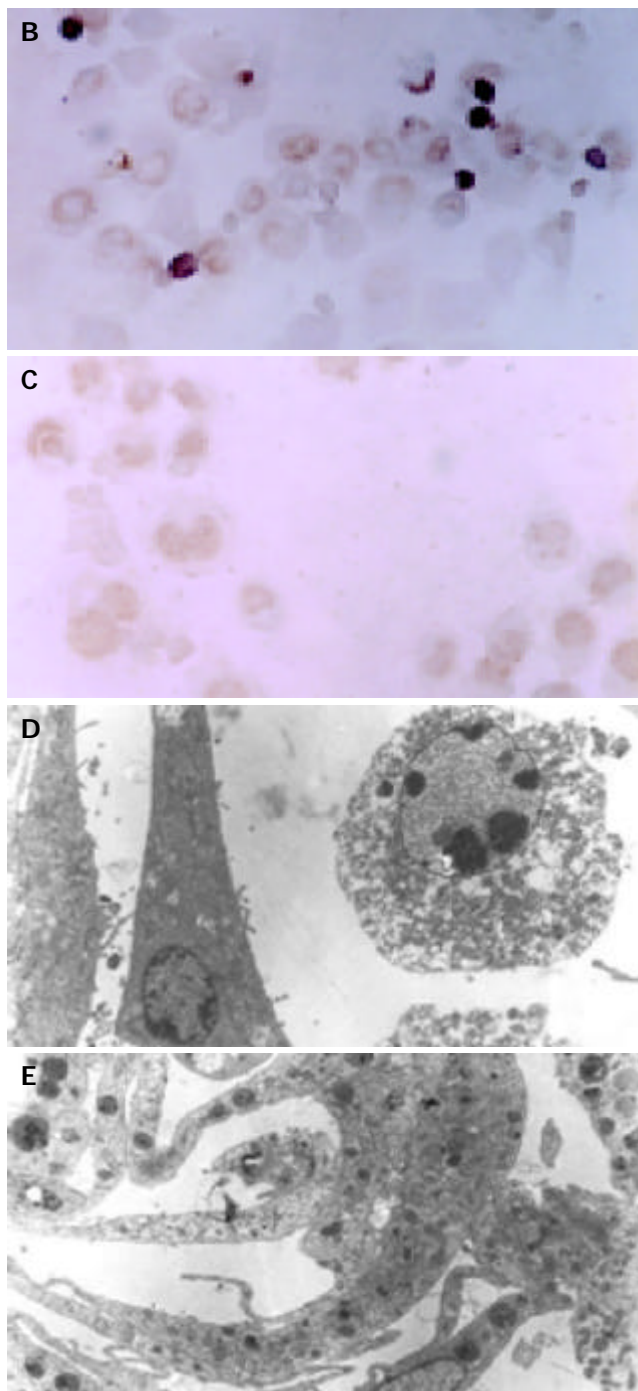
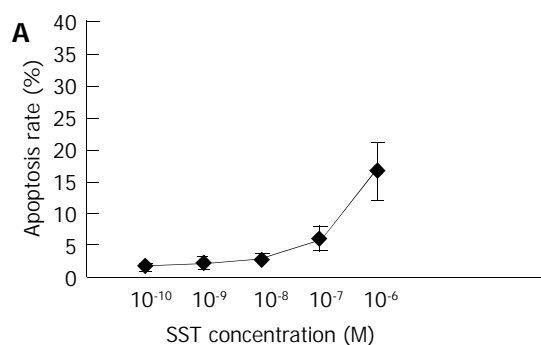


Figure 1 Effect of somatostatin on apoptosis of HSCs. A: Apoptosis rate of somatostatin-treated HSCs (fluorescent staining), B: Apoptosis of 10^{-6} M somatostatin-treated HSCs demonstrated by TUNEL (\times 400), C: Apoptosis could not be detected in normal HSCs by TUNEL (\times 400), D: Apoptosis of 10^{-6} M somatostatin-treated HSCs demonstrated by transmission electron microscopy (\times 8000). E: Apoptosis could not be detected in normal HSCs by transmission electron microscopy (\times 8000).

Apoptosis of HSCs examined by fluorescent staining

After 72 h' treatment, round-shaped HSCs with shrunk nuclei and conglomerated granules became visible in all somatostatin treatment groups. These HSCs underwent early apoptosis and displayed stronger green fluorescence. The experimental results showed that the higher the concentration of somatostatin, the stronger its proapoptotic action (Figure 1). The apoptosis-inductive effect of somatostatin reached its maximum at the concentration of 10^{-6} mol/L- 10^{-7} mol/L ($P<0.05$).

Apoptosis of HSC examined by flow cytometry

As detected by flow cytometry, somatostatin of different concentrations could dose-dependently promote apoptosis of activated HSCs. In 10^{-6} mol/L and 10^{-7} mol/L somatostatin treatment groups, the apoptotic rate was significantly higher than that in the control group ($P<0.01$) (Table 2).

Table 2 Effects of somatostatin on HSC apoptosis (mean±SD)

Somatostatin concentration (mol/L)	Apoptosis rate (%)
10^{-6}	16.54±4.59 ^b
10^{-7}	6.06±1.79 ^b
10^{-8}	2.81±0.72
10^{-9}	2.25±0.98
10^{-10}	1.55±0.64
0	1.53±1.19

^b $P<0.01$ vs control group.

Analysis of cytodynamics demonstrated that somatostatin could increase the percentage of HSCs in G_0/G_1 phase, and reduce it in S phase. However, there seemed to be no alternation in G_2/M phase. Experimental findings also made it clear that the percentage of somatostatin-treated HSCs was $93.14\pm6.69\%$ (10^{-6} mol/L) and $90.65\pm8.03\%$ (10^{-7} mol/L) in G_0/G_1 phase, and $78.48\pm4.43\%$ in control group respectively. Meanwhile, the percentage of somatostatin treated HSCs were $1.75\pm0.44\%$ (10^{-6} mol/L), $3.87\pm0.91\%$ (10^{-7} mol/L) in S phase, and $12.50\pm2.89\%$ in control group, respectively. The difference between somatostatin treatment groups and control group was statistically significant ($P<0.01-0.05$).

Apoptosis of HSC examined by TUNEL

The number of early apoptotic HSCs characterized by pyknosis of nuclear chromatin and condensation of cytoplasm, increased with somatostatin treatment in a dose-dependent manner (Figure 1). The apoptotic rates of different somatostatin treatment groups were $14.65\pm3.86\%$ (10^{-6} mol/L), $5.97\pm1.04\%$ (10^{-7} mol/L), $2.30\pm0.62\%$ (10^{-8} mol/L), $2.02\pm0.81\%$ (10^{-9} mol/L) and $1.65\pm0.88\%$ (10^{-10} mol/L), respectively. Statistical difference was found in the rates between two somatostatin treatment groups (10^{-6} mol/L, 10^{-7} mol/L) and the control group ($P<0.01$).

Apoptosis of HSC examined by transmission electron microscopy

Typical apoptotic HSCs could be identified under transmission electron microscope after treatment of somatostatin for 72 h. They were characterized by shrinkage of cells with vacuoles in cytoplasm, swelling of mitochondria, dilated endoplasmic reticulum, irregular nuclei and pyknosis and conglomeration of chromatin ranging along inside of the nuclear membrane (Figure 1).

DISCUSSION

Somatostatin, an important peptide for inhibiting cellular proliferation and differentiation, could slow down the growth

of various kinds of cells by blocking the synthesis and/or secretion of many important cytokines and hormones^[10-14]. On the other hand, extensive physiological effects of somatostatin and its analogues are mainly mediated by five subtypes of somatostatin receptors (SSTR), including SSTR₁, SSTR₂ (SSTR_{2a} and SSTR_{2b}), SSTR₃, SSTR₄ and SSTR₅. According to our knowledge, somatostatin-14 may be the main endogenous molecular form, although somatostatin-20, somatostatin-25 and somatostatin-28 also exist in the human body.

In recent years, researches have revealed the involvement of somatostatin and its receptors in the differentiation of HSC, *i.e.*, somatostatin-containing nerve fibers inside the liver lobule are in close contact with sinusoidal endothelium as well as HSC^[15]. In 2001 Reynaert *et al*^[16] demonstrated that HSCs expressed SSTR₁, SSTR₂ and SSTR₃ during their activation. Therefore, it is reasonable to deduce that somatostatin may play a negative regulatory role in the activation of HSCs via paracrine route. Except for its actions through SSTRs, somatostatin exerts inhibitory effect on the secretion of mitogens, including insulin-like growth factor (IGF), EGF and TGF- α , which are essential for the continuous activation of HSCs. In addition, somatostatin can even reverse the action of EGF on EGFR. So somatostatin may be quite a potent antifibrotic agent for liver cirrhosis.

Being consistent with the hypothesis, somatostatin shows an obvious inhibitory effect on the proliferation of activated HSCs in a dose-dependent way. Its pharmacological action is most significant when its concentration reaches 10^{-6} mol/L or 10^{-7} mol/L. Once somatostatin binds to SSTRs on HSCs, the occurrence of cytostatic effect is due to: (a) inhibition of adenylate cyclase activity through $G_{\alpha i}$, leading to a decrease in cAMP level in cells; (b) active induction of K^+ channel via $G_{\alpha s}$, whereas blockage of the voltage-operated Ca^{2+} channel through $G_{\alpha o}$ so as to reduce intracellular Ca^{2+} concentration; (c) inhibition of mitogen-activated protein kinase (MAPK)-dependent signal transduction pathway on the basis of protein tyrosine phosphatase (PTP) activation and aminodephosphorylation-induced deactivation of tyrosine kinase. Then the expression of *c-fos*, *c-jun* and *c-myc* was reduced significantly^[17,18]. As for the action of somatostatin on cytodynamics, G_0/G_1 arrest was observed in our study, which was in accordance with the result of Sharma *et al*^[19]. Cell-cycle-arrest may reflect the main mechanism of somatostatin.

In vivo and *in vitro* studies have illustrated that activated HSCs can be eliminated by different ways such as spontaneous apoptosis, stimulation of some membrane receptors, incubation with proapoptotic compounds^[20-28]. Activation of SSTR₃ by somatostatin may be relevant to this process. Binding of SSTR₃ and its natural or synthetic ligands can trigger intracellular acidification, and cause a selective activation of cation-insensitive acidic endonuclease through PTP. Then DNA fragmentation caused by acidic endonuclease stimulates the overexpression of bax and wild-type p53, resulting in apoptosis of HSCs. Additionally, dephosphorylation of serine in wild-type p53 has been found to be another pathway towards apoptosis^[29,30]. Our study has proved biochemically and ultrastructurally for the first time that somatostatin can dose-dependently promote the apoptosis of first-passage activated HSCs by fluorescent staining, TUNEL, flow cytometry and transmission electron microscopy. Furthermore, a significantly increased apoptosis rate could be obtained with low concentrations (10^{-6} mol/L- 10^{-7} mol/L) of somatostatin.

In conclusion, somatostatin at a low dose may exert antiproliferative and proapoptotic actions on activated HSCs. This result may provide a basis for utilizing somatostatin and even its analogues to protect people from hepatic fibrosis and to treat those suffering from it. However, the underlying mechanisms need to be further studied.

REFERENCES

- 1 **Liu WB**, Yang CQ, Jiang W, Wang YQ, Guo JS, He BM, Wang JY. Inhibition on the production of collagen type I, III of activated hepatic stellate cells by antisense TIMP-1 recombinant plasmid. *World J Gastroenterol* 2003; **9**: 316-319
- 2 **Wei HS**, Lu HM, Li DG, Zhan YT, Wang ZR, Huang X, Cheng JL, Xu QF. The regulatory role of AT 1 receptor on activated HSCs in hepatic fibrogenesis: effects of RAS inhibitors on hepatic fibrosis induced by CCl₄. *World J Gastroenterol* 2000; **6**: 824-828
- 3 **Li X**, Meng Y, Yang XS, Wu PS, Li SM, Lai WY. CYP11B2 expression in HSCs and its effect on hepatic fibrogenesis. *World J Gastroenterol* 2000; **6**: 885-887
- 4 **Liang ZW**, Zhang G, Wang TC. Extracellular signal-regulated kinase in liver fibrogenesis of rat. *Shijie Huaren Xiaohua Zazhi* 2003; **11**: 730-732
- 5 **Wang JY**, Zhang QS, Guo JS, Hu MY. Effects of glycyrrhetic acid on collagen metabolism of hepatic stellate cells at different stages of liver fibrosis in rats. *World J Gastroenterol* 2001; **7**: 115-119
- 6 **Chen PS**, Zhai WR, Zhou XM, Zhang JS, Zhang YE, Ling YQ, Gu YH. Effects of hypoxia, hyperoxia on the regulation of expression and activity of matrix metalloproteinase-2 in hepatic stellate cells. *World J Gastroenterol* 2001; **7**: 647-651
- 7 **Cheng ML**, Wu J, Wang HQ, Xue LM, Tan YZ, Ping L, Li CX, Huang NH, Yao YM, Ren LZ, Ye L, Li L, Jia ML. Effect of Maotai liquor in inducing metallothioneins and on hepatic stellate cells. *World J Gastroenterol* 2002; **8**: 520-523
- 8 **Liu XJ**, Yang L, Mao YQ, Wang Q, Huang MH, Wang YP, Wu HB. Effects of the tyrosine protein kinase inhibitor genistein on the proliferation, activation of cultured rat hepatic stellate cells. *World J Gastroenterol* 2002; **8**: 739-745
- 9 **Wang LT**, Zhang B, Chen JJ. Effect of anti-fibrosis compound on collagen expression of hepatic cells in experimental liver fibrosis of rats. *World J Gastroenterol* 2000; **6**: 877-880
- 10 **Xia D**, Zhao RQ, Wei XH, Xu QF, Chen J. Developmental patterns of GHR and SS mRNA expression in porcine gastric tissue. *World J Gastroenterol* 2003; **9**: 1058-1062
- 11 **Guo Y**, Guo X, Yao XX. Changes of gastrointestinal hormones in chronic atrophic gastritis and their clinical significance. *Shijie Huaren Xiaohua Zazhi* 2003; **11**: 531-534
- 12 **Yao YL**, Xu B, Zhang WD, Song YG. Gastrin, somatostatin, and experimental disturbance of the gastrointestinal tract in rats. *World J Gastroenterol* 2001; **7**: 399-402
- 13 **Sun FP**, Song YG, Cheng W, Zhao T, Yao YL. Gastrin, somatostatin, G and D cells of gastric ulcer in rats. *World J Gastroenterol* 2002; **8**: 375-378
- 14 **Li YY**. Mechanisms for regulation of gastrin and somatostatin release from isolated rat stomach during gastric distention. *World J Gastroenterol* 2003; **9**: 129-133
- 15 **Stoyanova II**, Gulubova MV. Immunocytochemical study on the liver innervation in patients with cirrhosis. *Acta Histochem* 2000; **102**: 391-402
- 16 **Reynaert H**, Vaeyens F, Qin H, Hellemans K, Chatterjee N, Winand D, Quartier E, Schuit F, Urbain D, Kumar U, Patel YC, Geerts A. Somatostatin suppresses endothelin-induced rat hepatic stellate cell contraction via somatostatin receptor subtype 1. *Gastroenterology* 2001; **121**: 915-930
- 17 **Ferjoux G**, Bousquet C, Cordelier P, Benali N, Lopez F, Rochaix P, Buscail L, Susini C. Signal transduction of somatostatin receptors negatively controlling cell proliferation. *J Physiol Paris* 2000; **94**: 205-210
- 18 **Feng DY**, Zheng H, Tan Y, Cheng RX. Effect of phosphorylation of MAPK and Stat3 and expression of *c-fos* and *c-jun* proteins on hepatocarcinogenesis and their clinical significance. *World J Gastroenterol* 2001; **7**: 33-36
- 19 **Sharma K**, Patel YC, Srikant CB. C-terminal region of human somatostatin receptor 5 is required for induction of Rb and G1 cell cycle arrest. *Mol Endocrinol* 1999; **13**: 82-90
- 20 **Zhao WX**, Zhao J, Liang CL, Zhao B, Pang RQ, Pan XH. Effect of caffeic acid phenethyl ester on proliferation and apoptosis of hepatic stellate cells *in vitro*. *World J Gastroenterol* 2003; **9**: 1278-1281
- 21 **Yao XX**, Tang YW, Yao DM, Xiu HM. Effects of Yigan Decoction on proliferation and apoptosis of hepatic stellate cells. *World J Gastroenterol* 2002; **8**: 511-514
- 22 **Zhang XL**, Liu L, Jiang HQ. Salvia miltiorrhiza monomer IH764-3 induces hepatic stellate cell apoptosis via caspase-3 activation. *World J Gastroenterol* 2002; **8**: 515-519
- 23 **Liu XJ**, Yang L, Wu HB, Qiang O, Huang MH, Wang YP. Apoptosis of rat hepatic stellate cells induced by anti-focal adhesion kinase antibody. *World J Gastroenterol* 2002; **8**: 734-738
- 24 **Issa R**, Williams E, Trim N, Kendall T, Arthur MJ, Reichen J, Benyon RC, Iredale JP. Apoptosis of hepatic stellate cells: involvement in resolution of biliary fibrosis and regulation by soluble growth factors. *Gut* 2001; **48**: 548-557
- 25 **Wright MC**, Issa R, Smart DE, Trim N, Murray GI, Primrose JN, Arthur MJ, Iredale JP, Mann DA. Gliotoxin stimulates the apoptosis of human and rat hepatic stellate cells and enhances the resolution of liver fibrosis in rats. *Gastroenterology* 2001; **121**: 685-698
- 26 **Fischer R**, Schmitt M, Bode JG, Haussinger D. Expression of the peripheral-type benzodiazepine receptor and apoptosis induction in hepatic stellate cells. *Gastroenterology* 2001; **120**: 1212-1226
- 27 **Trim N**, Morgan S, Evans M, Issa R, Fine D, Afford S, Wilkins B, Iredale J. Hepatic stellate cells express the low affinity nerve growth factor receptor p75 and undergo apoptosis in response to nerve growth factor stimulation. *Am J Pathol* 2000; **156**: 1235-1243
- 28 **Lang A**, Schoonhoven R, Tuvia S, Brenner DA, Rippe RA. Nuclear factor kappa B in proliferation, activation, and apoptosis in rat hepatic stellate cells. *J Hepatol* 2000; **33**: 49-58
- 29 **Liu D**, Martino G, Thangaraju M, Sharma M, Halwani F, Shen SH, Patel YC, Srikant CB. Caspase-8-mediated intracellular acidification precedes mitochondrial dysfunction in somatostatin-induced apoptosis. *J Biol Chem* 2000; **275**: 9244-9250
- 30 **Teijeiro R**, Rios R, Costoya JA, Castro R, Bello JL, Devesa J, Arce VM. Activation of human somatostatin receptor 2 promotes apoptosis through a mechanism that is independent from induction of p53. *Cell Physiol Biochem* 2002; **12**: 31-38

Edited by Zhu LH and Wang XL Proofread by Xu FM

Protein kinase C-dependent activation of P44/42 mitogen-activated protein kinase and heat shock protein 70 in signal transduction during hepatocyte ischemic preconditioning

Yi Gao, Yu-Qiang Shan, Ming-Xin Pan, Yu Wang, Li-Jun Tang, Hao Li, Zhi Zhang

Yi Gao, Yu-Qiang Shan, Ming-Xin Pan, Yu Wang, Li-Jun Tang, Hao Li, Zhi Zhang, Department of Hepatobiliary Surgery, Zhujiang Hospital, The First Military Medical University, Guangzhou 510282, Guangdong Province, China

Supported by the Natural Scientific Foundation of Guangdong Province in China, No.001086

Correspondence to: Dr. Yi Gao, Department of Hepatobiliary Surgery, Zhujiang Hospital, 253 Gongye Road, Guangzhou 510282, Guangdong Province, China. gaoyi6146@163.com

Telephone: +86-20-89839259

Received: 2003-11-18 **Accepted:** 2003-12-22

Abstract

AIM: To investigate the significance of protein kinase C (PKC), P44/42 mitogen-activated protein kinase (MAPKs) and heat shock protein (HSP)70 signal transduction during hepatocyte ischemic preconditioning.

METHODS: In this study we used an *in vitro* ischemic preconditioning (IP) model for hepatocytes and an *in vivo* model for rat liver to investigate the significance of protein kinase C (PKC), P44/42 mitogen-activated protein kinase (P44/42 MAPKs) and heat shock protein 70 (HSP70) signal transduction in IP. Through a normal liver cell hypoxic preconditioning (HP) model in which cultured normal liver cells were subjected to 3 cycles of 5 min of incubation under hypoxic conditions followed by 5 min of reoxygenation and subsequently exposed to hypoxia and reoxygenation for 6 h and 9 h respectively. PKC inhibitor, activator and MEK inhibitor were utilized to analyze the phosphorylation of PKC, the expression of P44/42 MAPKs and HSP70. Viability and cellular ultrastructure were also observed. By using rat liver as an *in vivo* model of liver preconditioning (3 cycles of 10-min occlusion and 10-min reperfusion), *in vivo* phosphorylation of PKC and P44/42MAPKs, HSP70 expression were further analyzed. AST/ALT concentration, cellular structure and ultrastructure were also observed. All the data were statistically analyzed.

RESULTS: Similar results were obtained in both *in vivo* and *in vitro* IP models. Compared with the control without IP (or HP), the phosphorylation of PKC and P44/42 MAPKs and the expression of HSP70 were obviously increased in IP (or HP) treated model in which cytoprotection could be found. The effects of preconditioning were mimicked by stimulating PKC with 4 β phorbol-12-myristate-13-acetate (PMA). Conversely, inhibiting PKC with chelerythrine abolished the protection given by preconditioning. PD98059, inhibitor of MEK (the upstream kinase of P44/42MAPKs), also reverted the cytoprotection exerted by preconditioning.

CONCLUSION: The results demonstrate that preconditioning induces a rapid activation of P44/42MAPKs and PKC activation plays a pivotal role in the activation of P44/42 MAPKs pathway

that participates in the preservation of liver cells. HSP expression is regulated by signals in PKC dependent P44/42 MAPKs pathway.

Gao Y, Shan YQ, Pan MX, Wang Y, Tang LJ, Li H, Zhang Z. Protein kinase C-dependent activation of P44/42 mitogen-activated protein kinase and heat shock protein 70 in signal transduction during hepatocyte ischemic preconditioning. *World J Gastroenterol* 2004; 10(7): 1019-1027

<http://www.wjgnet.com/1007-9327/10/1019.asp>

INTRODUCTION

The term ischemic preconditioning (IP) was first coined by Murry *et al.* to describe a phenomenon where brief periods of sublethal ischemia protected the heart against infarction caused by a subsequently more prolonged period of coronary artery occlusion^[1]. Preconditioning occurs in 2 phases: an early phase, also known as acute preconditioning, in which protection lasts up to 1-2 h following preconditioning, and a second phase, known as the second window of protection, in which protection reappears 24-72 h following preconditioning. Although a variety of mediators and effectors have been proposed to be essential for conferring preconditioning, including the adenosine receptor^[2], protein kinase C^[3], and the ATP-sensitive K⁺channel^[4]. The importance of PKC to ischemic preconditioning has been shown in a variety of studies in whole heart and isolated ventricular cardiocytes^[5]. Whereas it is widely accepted that PKC plays a pivotal role in ischemic preconditioning, the relevant downstream signaling molecules remain a topic of intense investigation and controversy.

Over the last few years, a number of studies in both whole hearts and isolated cardiomyocytes have described the activation of members of the MAPK family of signaling proteins during ischemia and ischemic reperfusion^[6,7]. All of the MAPKs are proline-directed, serine/threonine-protein kinases are activated by dual phosphorylation on tyrosine and threonine residues by upstream kinases. The family consists of 3 members, extracellular signal-regulated kinases 1 and 2 (ERK1/2; P44/42MAPKs), c-jun NH2-terminal kinases 1 and 2 (JNK1/2), P38MAPKs and ERK5/BMK1 (big mitogen-activated protein kinase, BMK1) which was found recently. ERK1/2 is predominantly activated by growth factors, and JNKs and P38MAPKs are generally activated by stresses such as ultraviolet light, inflammatory cytokines, heat shock, and ischemic reperfusion. Recent evidence implicates PKC is in the activation of 2 members of this kinase family, *i.e.*, the P44 and P42MAPKs^[8]. But whether PKC-dependent activation of P44/42 MAPKs in signal transduction pathways during hepatocyte ischemic preconditioning contributes to cytoprotective effect is largely unknown. Thus, in the present investigation we tested it by using an *in vitro* IP model for hepatocytes and an *in vivo* model for rat liver. Similar results were obtained both *in vivo* and *in vitro* IP models. The phosphorylation of PKC and P44/42 MAPKs was obviously increased in IP treated. The effects of

preconditioning were mimicked by stimulating PKC with 4 β phorbol-12-myristate 13-acetate (PMA). Conversely, inhibiting PKC with chelerythrine abolished the protection given by preconditioning. PD98059, an inhibitor of MEK (the upstream kinase of P44/42MAPKs), also reverted the cytoprotection exerted by preconditioning. This suggests that preconditioning induces a rapid activation of P44/42MAPKs and PKC activation plays a pivotal role in the activation of P44/42 MAPKs pathway that participates in the preservation of liver cells.

Although it has been reported that IP conveys protective signals to hepatocytes, few studies have been published on intracellular protective mechanism. It remains to be elucidated whether PKC-dependent P44/42MAPKs pathways are involved in the regulation of protective proteins, such as heat shock protein (HSP70). Some substantial literature describes the induction of HSP70 by ischemia^[9], the potential role of HSP70 in ischemic preconditioning^[10], and an inverse correlation between expression of HSP70 induced by ischemic or thermal preconditioning and infarct size in animal models^[11]. In addition, enhanced expression of HSP70 conveys a cytoprotective effect in cultured cells, including cardiac myocytes subjected to simulated ischemia^[12,13]. Specifically, overexpression of HSP70 in transgenic mice improves myocardial function^[14,15], preserves metabolic functional recovery, and reduces infarct size after ischemic preconditioning. Several recent studies suggest that PKC, a ubiquitous intracellular mediator, may play a role in mediating the protective effects of ischemic preconditioning while the activators such as PMA mimic the protective effect via phosphorylation of unknown effector protein. PKC plays a crucial role in the signal transduction for the activation of many cellular functions. Many transcription factors are known to be activated by various PKC subtypes^[16]. These include heat shock protein transcription factors (HSF). The synthesis of HSPs is mediated by the activation of heat shock gene transcription which is mediated by the binding of HSF to the heat shock element in the promoter region of HS genes. The gene knockout model of HSF1 *in vitro* demonstrated the essential requirement of this regulatory pathway in cellular protection^[17]. But whether P44/42 MAPKs signal pathways during hepatocyte ischemic preconditioning mediate the synthesis of protective protein (HSP70) remains elusive and represents an unresolved problem. In this study, we observed that HSP70 expression was increased in IP treated models, while it was inhibited by PKC inhibitor chelerythrine, the cytoprotective effect was reduced, but the activator of PKC (PMA) could induce the activation of PKC, HSP70 expression and cytoprotection apparently. Thus the data presented here suggested that PKC could regulate HSP70 expression directly or indirectly. While MEK inhibitor PD-98059 abolished the activation of P44 and P42 MAPKs. The synthesis of HSP70 was reduced and the protective effect of preconditioning was blocked. We propose that activation of P44 and P42 MAPKs correlates with the regulation of HSP70 expression.

MATERIALS AND METHODS

In vivo model

Nine to twelve-week male Sprague-Dawley rats weighing 220-230 g were obtained from the Animal Center of the First Military Medical University. Chelerythrine chloride (CHE) was purchased from Calbiochem Co. Phorbol 12-myristate 13-acetate (PMA) was obtained from Gibco/BRL Co. PD98059 was purchased from Sigma. All other chemicals in this study were of analytical reagent quality.

Grouping and experimental protocol Male Sprague-Dawley rats were fasted with free access to water 18 h before experiment. Animals were randomly divided into one of the 6 subgroups (6 rats in each group) and subjected to the following experimental

protocols. According to the method of Kobayashi *et al.*^[18], the model of rat local ischemic reperfusion was established. (1) Group C (control): The abdomen was opened by a midline incision and the liver hilus was exposed, but not occluded. (2) Group IR (ischemic reperfusion): All vessels (hepatic artery, portal vein, and bile duct) to the left and median liver lobes were occluded for 40 min with a vascular clamp. Thereafter the clamp was removed and blood flow was reperused for 3 h. Since blood vessels to the remaining parts of the liver were not occluded with this method, portal stasis could be avoided, which was of special relevance for circulatory stability in rats. The abdominal walls were closed during reperfusion. (3) Group IP (ischemic precondition): To induce ischemic preconditioning, mice underwent a sequence of three 10-min liver hilus occlusions separated by 10-min of reperfusion prior to the 40-min occlusion and 3 h reperfusion. (4) Group PMA (IR +PMA): PMA (4 μ g/kg^[19]) total volume 5 mL was slowly injected through dorsal veins of penis for 10 min, beginning 10 min before the start of ischemic reperfusion. (5) Group CHE (IP + chelerythrine chloride): Total volume of 5 mL chelerythrine chloride (5 mg/kg^[20]) was slowly injected through dorsal veins of penis for 10 min, 10 min before the start of ischemic preconditioning. (6) Group PD (IP + PD98059): Total volume of 5 mL PD98059 (5 mg/kg^[20]) was slowly injected through dorsal veins of penis over 10 min, 10 min before the start of ischemic preconditioning. The dose of PD98059 was shown to effectively block the activation of p44/p42MAPKs^[21].

Measurement of serum ALT and AST Three hours after the last reperfusion, the abdomen of each group was re-opened. Blood samples of infrahepatic vena cava were obtained and centrifuged to get serum in order to detect the concentration of ALT and AST.

PKC activity assay The rats were euthanized 3 h after the last reperfusion. 0.3 cm \times 0.3 cm \times 0.3 cm tissue samples from left liver lobe were rapidly removed. PKC activity assay kit was used. The tissue in 5 mL of cold extraction buffer was homogenized using a cold homogenizer then the lysate was centrifuged for 5 min at 4 $^{\circ}$ C, 14 000 g in a microcentrifuge and the supernatant was saved. The supernatant was passed over an 1-mL column of DEAE cellulose that was pre-equilibrated in extraction buffer and the column was washed with 5 mL of extraction buffer. The PKC-containing fraction was eluted using 5 mL of extraction buffer containing 200 mmol/L NaCl. Then enzyme sample, PKC coactivation buffer, PKC activation buffer, PKC biotinylated peptide substrate, and [γ -32P]ATP were mixed gently and incubated at 30 $^{\circ}$ C for 5 min. All samples were spotted on SAM2 membrane, and the washing and rinsing steps were followed. The SAM2 membrane was dried and placed into individual scintillation vials added with scintillation fluid and analysed using a phosphorimaging system.

Western blotting analysis of P44/42 MAPKs The rats were euthanized 3 h after the last reperfusion (a time point at which marked activation of P44/42 MAPKs begins^[21]). 0.3 cm \times 0.3 cm \times 0.3 cm tissue samples from left liver lobe were rapidly removed. P44/42 MAPKs test kit (New England Biolabs) was utilized.

Western blotting analysis of HSP70 The rats were euthanized 3 h after the last reperfusion and tissue samples were obtained as described above. When extracted from hepatocytes, protein samples were separated on 100 g/L SDS-polyacrylamide gel and transferred to nitrocellulose membranes. After membranes were transferred, they were blocked for 1 h with 50 mL/L nonfat milk in Tris-buffered saline. Membranes were incubated with murine monoclonal antibody to HSP70 overnight at 4 $^{\circ}$ C, washed 3 times for 5 min in TBST before addition of goat anti-mouse-HRP conjugated secondary antibody for 1 h at room temperature. Membranes were washed 3 times for 5 min with TBS, and peroxidase activity on the nitrocellulose sheet was visualized on X-ray film by means of the ECL Western blotting

detection system.

Changes of cellular structure and ultrastructure The rats were euthanized 3 h after the last reperfusion. 0.3 cm×0.3 cm×0.3 cm tissue samples from left liver lobe were also removed in order to observe the cellular structure and ultrastructure.

In vitro model

Liver cell line L02 was obtained from Shanghai Institute of Cell, (Academy of Medical Sciences of China). The necessary reagents and test kits were similar to *in vivo* setting.

Grouping and experimental protocol Cell viability, estimated at the beginning of the experiments, ranged between 90% to 95%. Hepatocytes were suspended in Krebs-Henseleit-Hepes (KHH)^[22] buffer containing 118 mmol/L NaCl, 4.7 mmol/L KCl, 1.2 mmol/L KH₂PO₄, 1.3 mmol/L CaCl₂, 25 mmol/L NaHCO₃, and 20 mmol/L Hepes at pH7.4. Hypoxic preconditioning was obtained by 3 cycles of 5 min of incubation at 37 °C in KHH buffer equilibrated with 900 mL/L N₂, 80 mL/L CO₂, 20 mL/L H₂ followed up by 5 min of reoxygenation obtained by fluxing the incubation flasks with 950 mL/L O₂, 50 mL/L CO₂ gas mixture. After reoxygenation, the cells were transferred in deoxygenated KHH buffer and further incubated at 37 °C in sealed bottles in a 900 mL/L N₂, 80 mL/L CO₂, 20 mL/L H₂ atmosphere for 6 h followed up by reoxygenation for 9 h. Nonpreconditioned cells were incubated in KHH buffer until the beginning of hypoxic treatment. Cells were randomly divided into one of the 6 subgroups and subjected to the following experimental protocols. (1) Group C (control): Untreated hepatocytes were incubated in 950 mL/L O₂, 50 mL/L CO₂ atmosphere. (2) Group HR (Hypoxia reoxygenation,HR): Untreated hepatocytes were incubated in 900 mL/L N₂, 80 mL/L CO₂, 20 mL/L H₂ atmosphere for 6 h followed up by reoxygenation for 9 h. (3) Group IP (hypoxic precondition, HP): preconditioned cells were incubated at 37 °C in sealed bottles in a 900 mL/L N₂, 80 mL/L CO₂, 20 mL/L H₂ atmosphere for 6 h followed up by reoxygenation for 9 h. (4) Group PMA (HR + PMA): Hepatocytes suspended in KHH medium were preincubated for 10 min at 37 °C with 150 nmol/L PMA^[23] and then subjected to hypoxic incubation for 6 h in sealed flasks in a 900 mL/L N₂, 80 mL/L CO₂, 20 mL/L H₂ atmosphere followed up by reoxygenation for 9 h. (5) Group CHE (HP + chelerythrine chloride): Hepatocytes suspended in KHH medium were pretreated with 50 mmol/L^[24] chelerythrine for 10 min before preconditioning. (6) Group PD (HP + PD98059): Hepatocytes were pretreated with 50 mmol/L^[21] PD98059 for 10 min before preconditioning.

Determination of cell viability Treated with the methods above, the cells of each group were incubated in KHH buffer containing 20 μL (4,5-dimethylthiazol-2-yl)-2,5-diphenyl-tetrazolium bromide (MTT) for 4 h at 37 °C in room air containing 50 mL/L CO₂. During this incubation tetrazolium component of the dye was reduced, in metabolically active cells, to a formazan dye. Thereafter the reaction was terminated by addition of 100 μL solubilization solution (ethanol) and the absorbance of the lysate was recorded at 570 nm using an ELISA reader.

PKC activity assay The protocol was the same as the above.

Western blotting analysis of P44/42 MAPKs The protocol was the same as the above.

Western blotting analysis of HSP70 The protocol was the same as the above.

Changes of cellular ultrastructure Having been treated with the methods above, the cellular ultrastructure of each group was observed.

Statistical analysis

Data were presented as mean±SD. Statistical comparisons were made by analysis of variance. When significant differences were observed, SNK-*q* test was used for multiple comparisons. Statistical significance was inferred at *P*<0.05.

RESULTS

Cytoprotective effects on hepatocytes induced by PC

The serum concentration of ALT and AST was increased and the cell viability was decreased significantly in group IR (HR) (*P*<0.01) compared with the control group. In contrast, compared with group IR (HR), the serum concentration of ALT and AST was reduced and the cell viability was increased markedly in group IP (HP) (*P*<0.01) (Tables 1, 3). In group C, cells had no apparent degeneration and necrosis where Kupffer cells did not proliferate markedly and the structure of portal area was not changed. Organellae were intact and mitochondria were lined up in order. In group IR, cells of lobules of liver were swollen and had hydropic degeneration where Kupffer cells proliferated significantly and had active phagocytosis. The spotty necrosis could be easily found. Portal area was enlarged and infiltrated with mononuclear cells. Hepatocytes were swollen and endothelial cells had malformation with mitochondria ballooned. Matrix was reduced, densely and floccularly degenerated. Bar was decreased and disarranged (Figures 3A, 6A). In group IP hepatocytes were slightly swollen and had no degeneration with no proliferation of Kupffer cells. Portal area was normal. Organellae were not swollen apparently with some neutrophils and lymphocytes infiltrated. Mitochondria were well distributed (Figures 3B, 6B). This indicated that PC could elicit the cytoprotective effects on hepatocytes subjected to a subsequent lethal ischemia reperfusion or hypoxia reoxygenation.

Table 1 Changes in serum concentration of ALT and AST (*n*=6, mean±SD)

Group	AST(U/L)	ALT(U/L)
C	99.3±13.2	61.90±12.1
IR	820.9±111.3 ^d	762.80±130.5 ^d
IP	407.7±73.7 ^b	281.00±35.6 ^b
IR+PMA	553.2±58.6 ^b	354.37±53 ^b
IP+PD	732.9±91.1 ^f	466.20±82.8 ^f
IP+CHE	678.6±136.5 ^f	645.61±90.4 ^f

^b*P*<0.01 versus group IR, ^d*P*<0.01 versus group C, ^f*P*<0.01 versus group IP.

Table 2 Changes in levels of phosphorylation activity of PKC in the liver (*n*=6, mean±SD)

Group	Phosphorylation activity of PKC (fmol/mg/min)
C	36.28±3.8
IR	42.78±2.22
IP	112.61±4.86 ^b
IP+CHE	34.07±2.77 ^d
IR+PMA	165.47±27.25 ^b

^b*P*<0.01 versus group IR, ^d*P*<0.01 versus group IP.

Effect of ischemic PC or hypoxic PC on PKC activity

Several studies performed in the heart implicated the activation of PKC as one of the key events in the development of ischemic PC^[25,26]. Similar results were obtained both *in vivo* and *in vitro* IP models. Compared with group IR (HR), the phosphorylation of PKC was obviously increased in group IP (HP) (Tables 2, 4) and the cytoprotective effect developed during ischemic PC (Tables 1, 3; Figures 3B, 6B). PMA, a well known activator of PKC, decreased cell killing by ischemia reperfusion or hypoxia reoxygenation (Tables 1, 3; Figures 3C, 6C). Conversely, PKC inhibitor chelerythrine reverted the effect of preconditioning on hepatocytes. Chelerythrine also abolished the protection against the damage caused by ischemia reperfusion or hypoxia

reoxygenation (Tables 1, 3; Figures 3D, 6D), suggesting that PKC might play a pivotal role in ischemic PC or hypoxic PC.

Table 3 Protection of hypoxic preconditioning against cytotoxicity caused by hypoxic hepatocyte incubation ($n=6$, mean \pm SD)

Group	Hepatocyte viability (%)
C	95 \pm 10.8
HR	35.57 \pm 3.99 ^b
HP	81.49 \pm 12.1 ^d
HR+PMA	75.29 \pm 11.9 ^d
HP+PD	51.03 \pm 9.09 ^f
HP+CHE	47.21 \pm 5.42 ^f

^b $P<0.01$ vs group C, ^d $P<0.01$ vs group HR, ^f $P<0.01$ vs group HP.

Table 4 Changes in PKC phosphorylation activity during hypoxia in control and preconditioned hepatocytes ($n=6$, mean \pm SD)

Group	Phosphorylation activity of PKC (fmol/mg/min)
C	32.67 \pm 5.11
HR	42.63 \pm 4.73
HP	109.42 \pm 16.09 ^b
HR+PMA	152.47 \pm 19.59 ^b
HP+CHE	65.28 \pm 5.36 ^d

^b $P<0.01$ vs group HR, ^d $P<0.01$ vs group IP.

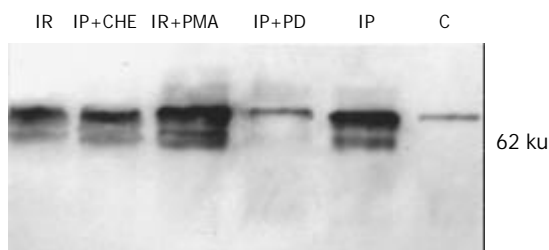


Figure 1 Expression of P44 and P42 MAPKs in rat liver.

Effect of ischemic PC or hypoxic PC on MAPK activity

Both *in vivo* and *in vitro* IP models, our results showed that hepatocyte lysates exhibited the sharp signal at 60 ku as detected by Western immunoblotting. Compared with group IR (HR), the expression of P44 and P42 MAPKs was markedly increased in group IP (HP) (Figures 1, 4), and the cytoprotective effect developed during ischemic PC (Tables 1, 3; Figures 3B, 6B). This result implied that the activation of P44 and P42 MAPKs was associated with the cytoprotection. The effect was abolished by the MEK inhibitor PD-98059. Compared with group IP (HP), the serum concentration of ALT and AST was increased and the cell viability was decreased significantly in group IP+PD ($P<0.01$). We observed that hepatocytes were swollen with mitochondria ballooned and Kupffer cells proliferated. The spotty necrosis was found. Portal area was slightly enlarged and a few mononuclear cells infiltrated (Figures 3E, 6E). The results indicated that P44 and P42 MAPKs as a major signal transduction molecule played an important role in cytoprotection during hepatocyte ischemic PC or hypoxic PC. To determine whether activation of P44/42 MAPKs during ischemic PC or hypoxic PC was dependent on PKC activation, we measured P44/42 MAPKs activity undergoing PC after pretreatment with chelerythrine (group IP or HP + CHE). Previous studies demonstrated that chelerythrine completely blocked the translocation of PKC and development of late PC in conscious rabbit model (39 rabbits). In the present study, we found that

chelerythrine completely blocked the activation of P44/42 MAPKs and cytoprotection, and the changes in serum concentration of ALT and AST, cell viability, cellular structure and ultrastructure were similar to those in group IR (HR) (Tables 1, 3; Figures 3D, 6D). PMA, an activator of PKC resulted in increased P44/42 MAPKs activity and mimicked the cytoprotection. The changes in serum concentration of ALT and AST, cell viability, cellular structure and ultrastructure were similar to those in group IP (HP) (Tables 1, 3; Figures 3C, 6C). These data demonstrated that the activation of P44 and P42 MAPKs during ischemic PC or hypoxic PC occurred via a PKC-dependent pathway.

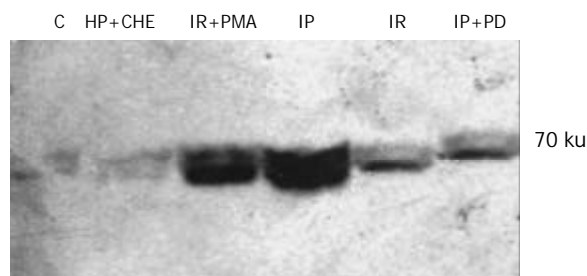


Figure 2 Expression of HSP70 in rat liver.

Effect of ischemic PC or hypoxic PC on HSP70 expression

The expression of HSP70 exhibited a sharp signal at 70 ku as detected by Western immunoblotting. Compared with group IR (HR), the expression of HSP70 was apparently increased in group IP (HP) (Figures 2, 5). In addition, IP conveyed a cytoprotective effect on hepatocytes suffering ischemia reperfusion or hypoxia reoxygenation (Tables 1, 3; Figures 3B, 6B). While PKC inhibitor chelerythrine and MEK inhibitor PD-98059 inhibited the protein expression, and the cytoprotective effect was reduced (Tables 1, 3; Figures 2, 5, 3D, 6D, 3E, 6E), but the activator of PKC (PMA) could induce HSP70 expression and cytoprotection apparently (Tables 1, 3; Figures 2, 5, 3C, 6C). Thus the data presented here suggested that expression of HSP70 had a cytoprotective effect on hepatocytes and PKC could regulate HSP70 expression directly or indirectly.

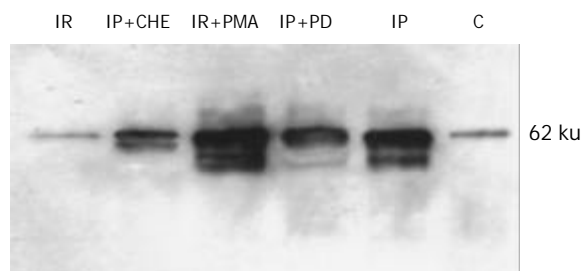


Figure 4 Expression of P44 and P42 MAPKs in isolated human hepatocytes.

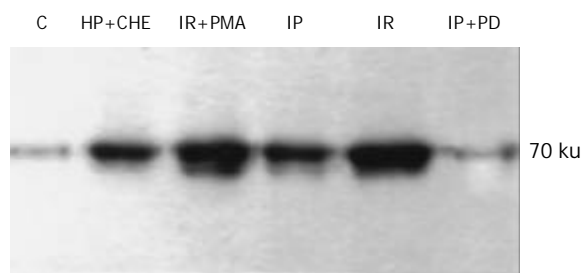
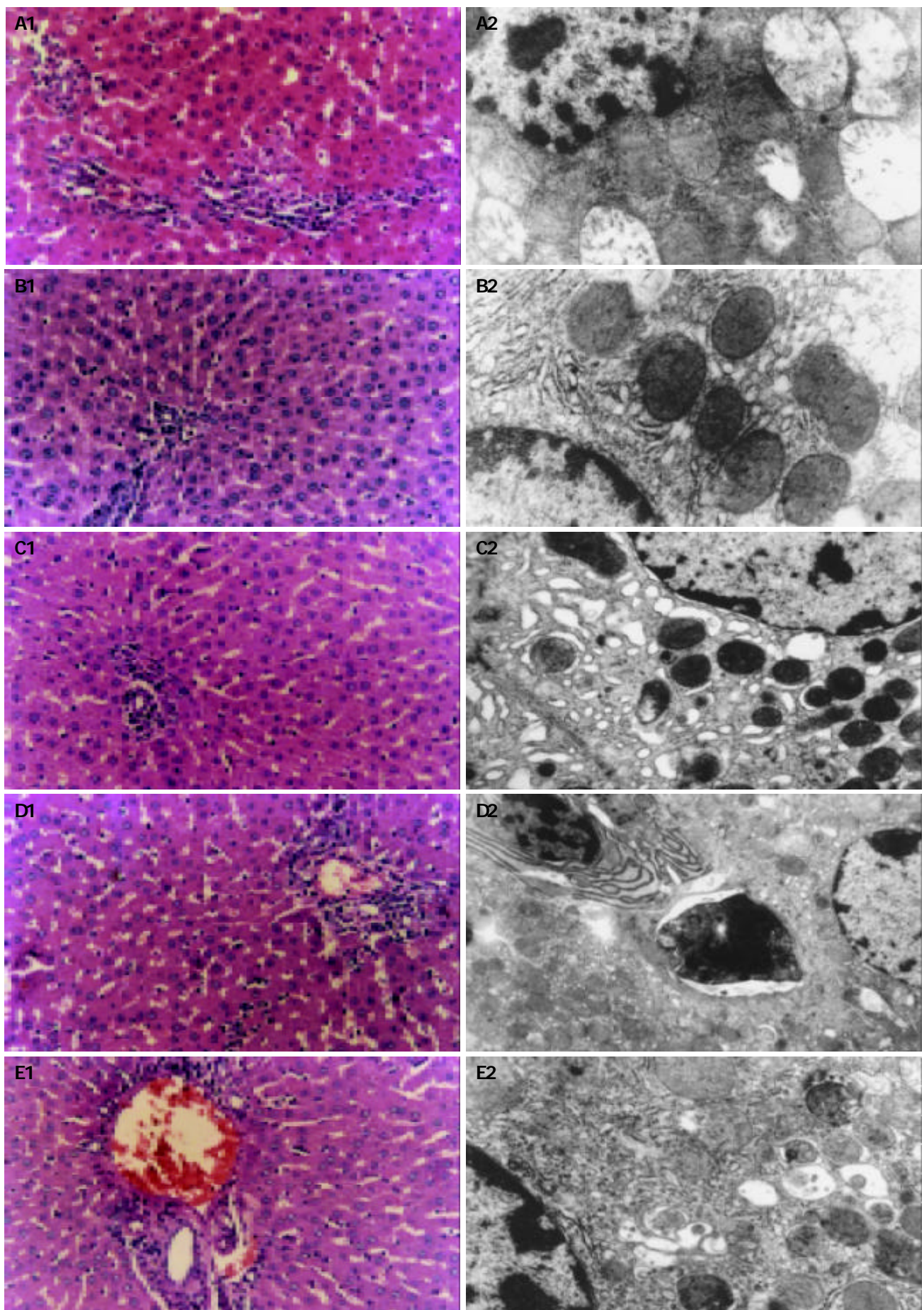


Figure 5 Expression of HSP70 in isolated human hepatocytes.



Figures 3 Changes of cellular structure and ultrastructure after treatment with IR, IP, IR+PMA, IP+CHE, and IP+PD98059. A1-2: Effect of ischemia and reperfusion on hepatocytes, B1-2: Cytoprotective effects of ischemia preconditioning, C1-2: Effects of ischemia preconditioning after stimulation of PKC with PMA, D1-2: Protective effect of ischemia preconditioning abolished by inhibition of PKC with chelerythrine, E1-2: Cytoprotective effect of ischemia preconditioning reverted by PD98059

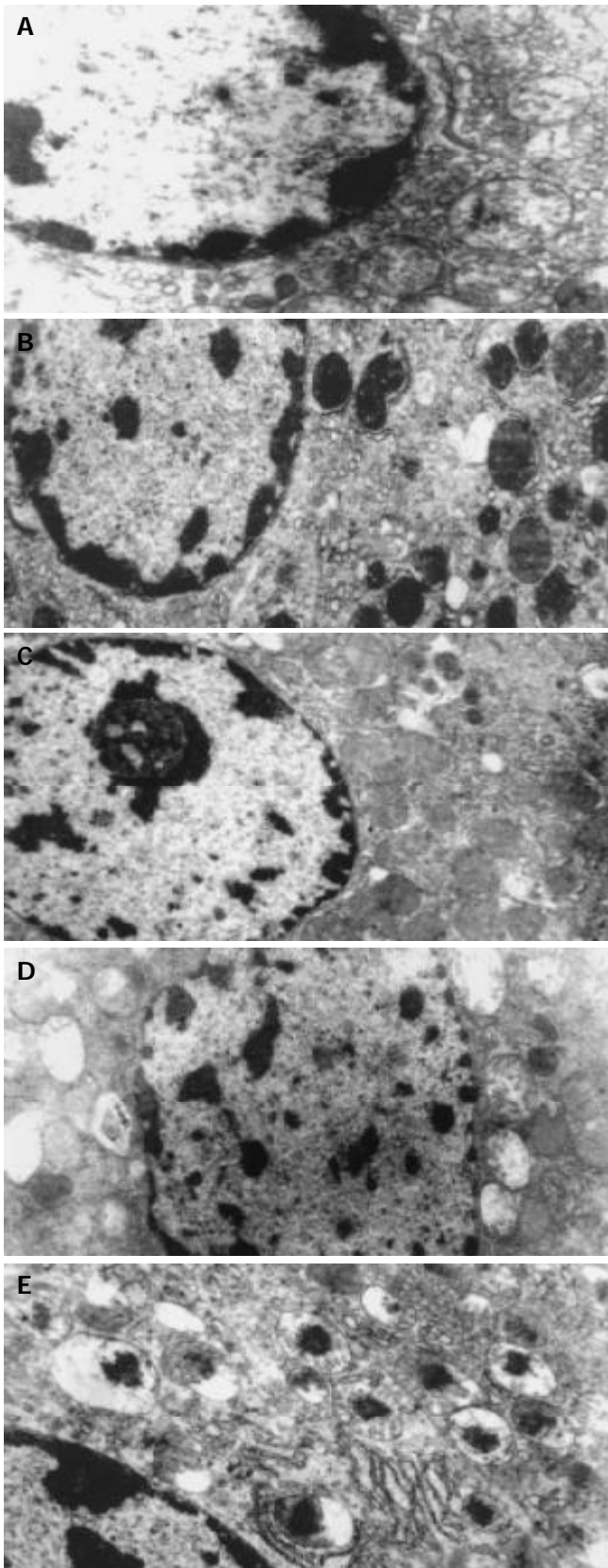


Figure 6 Changes of cellular ultrastructure after treatment with IR, IP, IR+PMA, IP+CHE, and IP+PD98059. A: Effect of hypoxia reoxygenation on hepatocytes, B: Cytoprotective effects of hypoxic preconditioning, C: Preconditioning effects mimicked by stimulation of PKC with PMA, D: Preconditioning protection abolished by inhibition of PKC with chelerythrine, E: Cytoprotection of preconditioning reverted by PD98059.

DISCUSSION

Ischemic preconditioning refers to the resistance to ischemic

injury acquired by tissues following one or more brief periods of ischemia followed by reperfusion. Ischemic preconditioning was first described in myocardium, but has been shown in several other organs, including the brain, skeletal muscles, and small intestine^[27-30]. Recent studies have shown that the same phenomenon could also be observed in the liver^[31]. Particularly, a 10-min interruption of liver blood supply in anesthetized rats followed by 10 min of reperfusion reduced the release of transaminases during a subsequent 90-min period of ischemia and 90 min of reperfusion^[32]. A similar effect has also been observed in steatotic liver after heat shock preconditioning^[33]. Furthermore, ischemic preconditioning before cold preservation of rat liver grafts increased the survival rate of rats receiving transplanted livers^[34]. The use of isolated hepatocyte suspensions has confirmed that the hepatoprotective action of liver preconditioning observed *in vivo* could be reproduced *in vitro*. In accordance with the *in vivo* experiment, hepatocyte preconditioning developed after a transient hypoxia lasting more than 5 min and not exceeding 10 min and reduced the cytotoxicity during a subsequently prolonged hypoxic incubation by about 40%. But the signal pathway that mediated the development of hepatocyte ischemic preconditioning or hypoxic preconditioning was also largely unknown^[35,36]. PKC-dependent activation of P44/42 MAPKs and HSP70 in signal transduction pathways during hepatocyte ischemic preconditioning or hypoxic preconditioning has not been reported.

There were several major findings in this study. First, ischemic PC or hypoxic PC had cytoprotective effects on hepatocytes subjected to a subsequent lethal ischemia reperfusion or hypoxia reoxygenation. Second, PKC appeared to play a pivotal role during hepatocyte ischemic PC. Third, the ischemic PC or hypoxic PC inducing activation of P44/42 MAPKs was completely abolished by the PKC inhibitor chelerythrine, indicating that the activation of P44/42 MAPKs is downstream of, and dependent on, PKC activation, and that P44/42 MAPKs may play a role in PKC mediated ischemic PC or hypoxic PC. Finally, protective proteins, such as HSP70, were induced by PC and regulated by signals in PKC dependent P44/42 MAPKs pathway.

The protective effect of ischemic preconditioning in myocardium involved the interstitial accumulation of endogenous mediators among which adenosine played a major role^[25]. Large quantities of adenosine were released within seconds from the beginning of myocardial ischemia. By interacting mainly with adenosine A1 receptors, adenosine mediated cardiocyte protection through the activation of a signaling pathway involving Gi-proteins, phospholipase C, diacylglycerol and PKC^[25]. Indeed, inhibiting PKC with polymyxin B, calphostin C, or chelerythrine could abolish the protective effect of myocardial ischemic preconditioning, whereas the stimulation of PKC by PMA or by diacylglycerol analogues significantly reduced the infarct size^[26]. The role of PKC was further supported by membrane translocation of the delta and epsilon PKC isoforms in isolated rat hearts exposed to preconditioning^[37]. We have observed that the cytoprotection exerted by preconditioning in the *in vivo* and *in vitro* setting was abolished by inhibiting PKC with chelerythrine. Moreover, PKC stimulation by PMA could reduce cell killing by ischemia reperfusion or hypoxia reoxygenation, mimicking the effect of preconditioning. This indicates that PKC activation might be involved in the signaling pathway responsible for the development of preconditioning in hepatocytes. Such a conclusion was consistent with a number of reports indicating that PKC stimulation was critical for the development of preconditioning in isolated rat, rabbit, and human cardiocytes^[38,39].

Previous studies have addressed the effect of ischemia on MAPK in *in vitro* models of global ischemia (isolated rat heart) and have yielded conflicting results. Maulik *et al.*^[40] showed

that 4 cycles of 5-min ischemia/10-min reperfusion caused a significant increase in total MAPK phosphorylation activity and in the activity of MAPK-activated protein kinase 2. Knight and Buxton^[41] reported that a single episode of ischemia ≤ 10 min followed by 15 min of reperfusion had no effect on total MAPK phosphorylation activity, a 15-min period of ischemia in itself had no effect but was associated with increased MAPK activity after 5-min reperfusion. The reason for these discrepancies is unclear. Maulik *et al.*^[40] Knight and Buxton^[41] determined total MAPK activity using a phosphorylation assay. To a certain extent, P38 MAPKs activity, or P44/42 MAPKs activity was not individually assessed. Saurin *et al.*^[42] reported that sustained P38 activation occurred during lethally simulated ischemia in cultured rat neonatal cardiocytes. This activation could be attenuated by cardioprotective treatments such as preconditioning and over expression of active PKC- δ ^[42]. Ping *et al.*^[43] demonstrated that P44/42 MAPKs were activated during preconditioning stimuli in both isolated rabbit cardiomyocytes and rabbit hearts. In the present study we examined P44/42 MAPKs and found that P44/42 MAPKs were activated during hepatocyte preconditioning stimuli in both *in vivo* and *in vitro* models. Furthermore, activation of P44/42 MAPKs was PKC dependent. Previous studies suggested that PKC activated MAPKs in neonatal cardiac cells^[44] and isolated hearts^[45]. Virtually no information is available whether PKC activates MAPKs during hepatocyte ischemic preconditioning *in vivo*. If so, whether, in the setting of ischemic PC, mobilization of PKC occurs in parallel to MAPK activation or is a distal event. The results both *in vivo* and *in vitro* models showed that P44/42 MAPKs expression was markedly increased and the cytoprotective effect developed during ischemic PC, implying that the activation of P44 and P42 MAPKs was associated with the cytoprotection. The effect was abolished by the MEK inhibitor PD-98059, indicating that P44/42 MAPKs as a major signal transduction molecule played an important role in cytoprotection during hepatocyte ischemic preconditioning or hypoxic preconditioning. The PC-induced activation of P44 and P42 MAPKs was completely abolished by the PKC inhibitor chelerythrine, and PMA, an activator of PKC resulted in increased P44/42 MAPKs activity and mimicked the cytoprotection. These data demonstrate three important points: (1) PKC plays an obligatory role in the stimulation of P44/42 MAPKs during ischemic PC; (2) PKC activation precedes MAPK activation in the cascade that leads to PC; (3) P44/42 MAPKs may play an important role in PKC-mediated ischemic PC. Because PKC activation was required for PC to develop^[46,47], P44/P42 MAPKs might be downstream phosphorylation targets of PKC and the PKC-induced signaling pathways that mediate ischemic PC or hypoxic PC.

Ping *et al.*^[43] indicated that PKC-dependent activation of P44/P42 MAPKs during hepatocyte preconditioning in both isolated rabbit cardiomyocytes and rabbit hearts produced a marked reduction in infarct size and the serum level of LDH, which had cardioprotective effects. Their results were coincident with what we presented. In preconditioned isolated rat hepatocytes, Carini *et al.*^[35] observed that interfering with P44 and P42 MAPKs activation using MEK inhibition PD98509 did not affect cytoprotection, whereas SB203580, a specific inhibition of P38 MAPKs completely abolished the effects of preconditioning. So they proposed that P44 and P42 MAPKs in signal transduction pathway was not responsible for the development of liver ischemic preconditioning. Their results were different from ours. The possible reasons might be as follows. (1) The experimental environment different *in vitro* IP model for hepatocyte and *in vivo* model for rat liver. *In vitro* experiment imitated the ischemia *in vivo* merely by depriving of the oxygen and blood serum, but it could not be mimicked completely. Ischemic preconditioning *in vivo* could be affected

by body temperature, homeostasis, anesthesia and some other factors. But in our experiment, both in the *in vivo* and *in vitro* setting, we got the same result. (2) By passing compensatory activation, cross talking existed in intracellular signal transduction pathways^[48], while P44 and P42 MAPKs signal transduction pathway was inhibited, which continued to convey the signals and induced the expression of cytoprotective proteins, such as P38MAPKs signal transduction pathway^[49]. (3) Different methods were used in ischemic preconditioning. Fryer *et al.*^[50] reported that multiple-cycle-induced IPC could activate more pathways than a single-cycle IPC stimulus and that this difference could be attributable to the recruitment of another PKC-independent signal transduction pathway. The major signal pathway eliciting the cytoprotection would change while using different IP method. Our results were in agreement with those results of Ping's group^[43] obtained in the rabbit heart also via repetitive IPC, but Carini *et al.*^[35] drew the different conclusion using a single IPC. (4) Dose and timing dependence. The activation of intracellular signal molecule was time dependent, and the reverse feedback regulation occurred at a time point. P44/42 MAPKs activity increased as early as 6 h following precondition, and peaked at 48 h. Preincubation with PD98059 (a selective MEK inhibitor) was associated with a dose-dependent inhibition which was statistically significant for concentrations higher than 10 $\mu\text{mol/L}$, and maximal at 100 $\mu\text{mol/L}$, and near-complete inhibition of activation of P44 and P42 MAPKs was observed with 50 $\mu\text{mol/L}$ PD98059^[21]. Referring to the time point of activation of P44/42 MAPKs and the dosage of PD98059, eventually we got the similar results^[43]. Carini *et al.*^[35] got various results by using different dosages of PD98059 (20 $\mu\text{mol/L}$) to treat hepatocytes and detect the effect of inhibition at different time points (after exposure to 90 min of hypoxia).

HSP is one of the most highly conserved proteins in existence, and has been found in every organism^[51]. These proteins are known to protect cells from the toxic effects of heat and other stresses and were synthesized quickly and intensely in response to stressors^[52]. Exactly how HSPs protect cells is unclear, however, several explanations have been offered. These include the renaturation of damaged proteins or facilitation of the folding and targeting of newly synthesized proteins to organelles^[52]. HSPs may also maintain newly synthesized proteins in a translocational configuration (linear or unfolded). Induction of heat shock protein has been shown to subsequently protect cells in signal transduction pathways in liver ischemic preconditioning^[53], but few studies have been published on intracellular protective mechanism. Whether PKC dependent P44/42 MAPKs pathways are involved in the regulation of protective proteins, such as HSP70 is largely unknown. Some substantial literature described the induction of HSP70 by ischemia^[21], the potential role of HSP70 in ischemic preconditioning^[24], and an inverse correlation between expression of HSP70 induced by ischemic or thermal preconditioning and infarct size in animal models^[25,26]. In addition, enhanced expression of HSP70 conveyed a cytoprotective effect in cultured cells, including cardiac myocytes subjected to simulated ischemia^[29,30]. Specifically, overexpression of HSP70 in transgenic mice could improve myocardial function^[32,33], preserve metabolic functional recovery, and reduce infarct size after ischemic preconditioning. Several recent studies suggested that PKC might play a role in mediating the protective effects of ischemic preconditioning while the activators such as PMA mimicked the protective effect via phosphorylation of unknown effector protein. PKC played a crucial role in the signal transduction for the activation of many cellular functions. Many transcription factors have been known to be activated by various PKC subtypes^[36]. These include heat shock protein transcription factors (HSF). The synthesis of HSPs is mediated by the activation of heat shock gene transcription which is mediated by

the binding of HSF to the heat shock element in the promoter region of HS genes. The gene knockout model of HSF1 *in vitro* demonstrated the essential requirement of this regulatory pathway in cellular protection^[37]. But whether P44/42 MAPKs signal pathways during hepatocyte ischemic preconditioning mediates the synthesis of HSP70 remains elusive and represents an unsolved problem. In this study, expression of HSP70 exhibited a sharp signal at 70 ku as detected by Western immunoblotting in both *in vivo* and *in vitro* models. HSP70 expression was increased in IP (HP) treated models which provided cytoprotective effect on hepatocytes suffering from ischemia reperfusion or hypoxia reoxygenation. While PKC inhibitor chelerythrine and MEK inhibitor PD-98059 inhibited the protein expression. The cytoprotective effect was reduced, but the activator of PKC (PMA) could induce HSP70 expression and cytoprotection apparently. Thus, HSP70 was recognized as molecular chaperones and could protect cells under the hazardous conditions such as ischemia reperfusion or hypoxia reoxygenation. It was induced by PC and regulated by signals in PKC dependent P44/42 MAPKs pathway.

In summary, PKC-dependent activation of P44/42 MAPKs and HSP70 in signal transduction pathways during hepatocyte ischemic preconditioning is an important part of endogenous protective mechanisms. PKC is upstream of P44/42 MAPKs, and PKC regulates the activation of P44 and P42 MAPKs positively. HSP expression is regulated by signals in P44/42 MAPKs pathway, but this passway is just one of the most important signal transduction pathways during liver ischemic preconditioning. PKC-dependent activation of MAPKs family such as p38MAPK, JNK and ERK5 can regulate HSP70 expression and deserve further study.

REFERENCES

- Murry CE**, Jennings RB, Reimer KA. Preconditioning with ischemia: a delay of lethal cell injury in ischemic myocardium. *Circulation* 1986; **74**: 1124-1136
- Baxter GF**, Marber MS, Patel VC, Yellon DM. Adenosine receptor involvement in a delayed phase of myocardial protection 24 h after ischemic preconditioning. *Circulation* 1994; **90**: 2993-3000
- Armstrong SC**, Hoover DB, Delacey MH, Ganote CE. Translocation of PKC, protein phosphatase inhibition and preconditioning of rabbit cardiomyocytes. *J Mol Cell Cardiol* 1996; **28**: 1479-1492
- Baines CP**, Liu GS, Birincioglu M, Critz SD, Cohen MV, Downey JM. Ischemic preconditioning depends on interaction between mitochondrial K_{ATP} channels and actin cytoskeleton. *Am J Physiol Heart Circ Physiol* 1999; **276**: H1361-H1368
- Goto M**, Liu Y, Yang XM, Ardell JL, Cohen MV, Downey JM. Role of bradykinin in protection of ischemic preconditioning in rabbit hearts. *Circ Res* 1995; **77**: 611-621
- Bogoyevitch MA**, Gillespie-Brown J, Ketterman AJ, Fuller SJ, Ben-Levy R, Ashworth A, Marshall CJ, Sugden PH. Stimulation of the stress-activated mitogen activated protein kinase subfamilies in perfused heart. *Circ Res* 1996; **79**: 162-173
- Mizukami Y**, Yoshida K. Mitogen-activated protein kinase translocates to the nucleus during ischemia and is activated during reperfusion. *Biochem J* 1997; **323**: 785-790
- Boulton TG**, Nye SH, Robbins DJ, Ip NY, Radziejewska E, Morgenbesser SD, DePinho RA, Panayotatos N, Cobb MH, Yancopoulos GD. ERKs: a family of protein-serine/threonine kinases that are activated and tyrosine phosphorylated in response to insulin and NGF. *Cell* 1991; **65**: 663-675
- Benjamin IJ**, Kroger B, Williams RS. Activation of the heat shock transcription factor by hypoxia in mammalian cells. *Proc Natl Acad Sci USA* 1990; **87**: 6263-6267
- Currie RW**, Karmazyn M, Kloc M, Mailer K. Heat-shock response is associated with enhanced postischemic ventricular recovery. *Circ Res* 1988; **63**: 543-549
- Donnelly TJ**, Sievers RE, Vissern FL, Welch WJ, Wolfe CL. Heat shock protein induction in rat hearts: a role for improved myocardial salvage after ischemia and reperfusion? *Circulation* 1992; **85**: 769-778
- Williams RS**, Thomas JA, Fina M, German Z, Benjamin IJ. Human heat shock protein 70 (hsp70) protects murine cells from injury during metabolic stress. *J Clin Invest* 1993; **92**: 503-508
- Mestrl R**, Chi SH, Sayen MR, O' Reilly K, Dillmann WH. Expression of inducible stress protein 70 in rat heart myogenic cells confers protection against simulated ischemia-induced injury. *J Clin Invest* 1994; **93**: 759-767
- Plumier JC**, Ross BM, Currie RW, Angelidis CE, Kazlaris H, Kollias G, Pagoulatos GN. Transgenic mice expressing the human heat shock protein 70 have improved post-ischemic myocardial recovery. *J Clin Invest* 1995; **95**: 1854-1860
- Marber MS**, Mestrl R, Chi SH, Sayen MR, Yellon DM, Dillmann WH. Overexpression of the rat inducible 70-kD heat stress protein in a transgenic mouse increases the resistance of the heart to ischemic injury. *J Clin Invest* 1995; **95**: 1446-1456
- Hug H**, Sarre TF. Protein kinase C isozymes: Divergence in signal transduction. *Biochem J* 1993; **291**: 329-343
- McMillan DR**, Xiao X, Shao L, Graves K, Benjamin IJ. Targeted disruption of heat shock transcription factor 1 abolishes thermotolerance and protection against heat-induced apoptosis. *J Biol Chem* 1998; **273**: 7523-7528
- Kobayashi H**, Nonami T, Kurokawa T, Sugiyama S, Ozawa T, Takagi H. Mechanism and prevention of ischemia-reperfusion induced liver injury in rats. *J Surg Res* 1991; **23**: 240-249
- Vogt AM**, Htun P, Arras M, Podzuweit T, Schaper W. Intramyocardial infusion of tool drugs for the sturdy of molecular mechanisms in ischemic preconditioning. *Basic Res Cardiol* 1996; **91**: 389-400
- Yamashita N**, Hoshida S, Nishida M, Igarashi J, Aoki K, Hori M, Kuzuya T, Tada M. Time course of tolerance to ischemia-reperfusion injury and induction of heat shock protein 72 by heat stress in the rat heart. *J Mol Cell Cardiol* 1997; **29**: 1815-1821
- Marra F**, Arrighi MC, Fazi M, Caligiuri A, Pinzani M, Romanelli RG, Efsen E, Laffi G, Gentilini P. Extracellular signal-regulated kinase activation differentially regulates platelet-derived growth factor's actions in hepatic stellate cells, and is induced by *in vivo* liver injury in the rat. *Hepatology* 1999; **30**: 951-958
- Carini R**, De Cesaris MG, Splendore R, Bagnati M, Albano E. Preconditioning reduced Na^+ accumulation and cell killing in isolated rat hepatocytes exposed to hypoxia. *Hepatology* 2000; **31**: 166-172
- Goldberg M**, Zhang HL, Steinberg SF. Hypoxia Alters the Subcellular Distribution of Protein Kinase C Isoforms in Neonatal Rat Ventricular Myocytes Michelle Goldberg. *J Clin Invest* 1997; **34**: 55-61
- Zhao J**, Renner O, Wightman L, Sugden PH, Stewart L, Miller AD, Latchman DS, Marber MS. The Expression of Constitutively Active Isoforms of Protein Kinase C to Investigate Preconditioning. *The J Biol Chem* 1998; **36**: 23072-23079
- Yellon DM**, Baxter GF, Garcia-Dorado D, Heusch G, Sumeray MS. Ischemic preconditioning: present position and future directions. *Cardiovasc Res* 1998; **37**: 21-33
- Simkhovich BZ**, Przyklenk K, Kloner RA. Pole of protein kinase C as a cellular mediator of ischemic preconditioning: a critical review. *Cardiovasc Res* 1998; **40**: 9-22
- Sun JZ**, Tang XL, Knowlton AA, Park SW, Qiu Y, Bolli R. Late preconditioning against myocardial stunning: an endogenous protective mechanism that confers resistance to postischemic dysfunction 24 hours after brief ischemia in conscious pigs. *J Clin Invest* 1995; **95**: 388-403
- Dana A**, Baxter GF, Walker JM, Yellon DM. Prolonging the delayed phase of myocardial protection: repetitive adenosine A1 receptor activation maintains rabbit myocardium in a preconditioned state. *J Am Coll Cardiol* 1998; **31**: 1142-1149
- Tang XL**, Takano H, Rizvi A, Turrens JF, Qiu Y, Wu WJ, Zhang Q, Bolli R. Oxidant species trigger late preconditioning against myocardial stunning in conscious rabbits. *Am J Physiol Heart Circ Physiol* 2002; **282**: H281-291
- Yamashita N**, Hoshida S, Taniguchi N, Kuzuya T, Hori M. Whole-body hyperthermia provides biphasic cardioprotection

- against ischemia/reperfusion injury in the rat. *Circulation* 1998; **98**: 1414-1421
- 31 **Chen XH**, Li ZZ, Bao MS. Ischemic preconditioning protects liver from ischemia-reperfusion injury in rats. *Xin Xiaohuabingxue Zazhi* 1997; **5**: 763-764
- 32 **Yoshizumi T**, Yanaga K, Soejima Y, Maeda T, Uchiyama H, Sugimachi K. Amelioration of the liver injury by ischemic preconditioning. *Br J Surg* 1998; **85**: 1636-1640
- 33 **Yamagami K**, Yamamoto Y, Kume M, Kimoto S, Yamamoto H, Ozaki N, Yamamoto M, Shimahara Y, Toyokuni S, Yamaoka Y. Heat shock preconditioning ameliorates liver injury following normothermic ischemia-reperfusion in steatotic rat livers. *J Surg Res* 1998; **79**: 47-53
- 34 **Yin DP**, Sankary HN, Chong AS, Ma LL, Shen J, Foster P, Williams JW. Protective effect of ischemic preconditioning on liver preservation reperfusion injury in rats. *Transplantation* 1998; **66**: 152-157
- 35 **Carini R**, De Cesaris MG, Splendore R, Vay D, Domenicotti C, Nitti MP, Paola D, Pronzato MA, Albano E. Signal pathway involved in the development of hypoxic preconditioning in rat hepatocytes. *Hepatology* 2001; **33**: 131-139
- 36 **Yamamoto Y**, Kume M, Yamaoka Y. Implications of heat shock proteins during liver surgery and liver perfusion. *Recent Results Cancer Res* 1998; **147**: 157-172
- 37 **Kawamura S**, Yoshida K, Miura T, Mizukami Y, Matsuzaki M. Ischemic preconditioning translocates PKC-delta and epsilon, which mediate functional protection in isolated rat heart. *Am J Physiol* 1998; **275**: H2266-H2271
- 38 **Rehring TF**, Shapiro JJ, Cain BS, Meldrum DR, Cleveland JC, Harken AH, Banerjee A. Mechanisms of pH preservation during global ischemia in preconditioned rat heart: role of PKC and NHE. *Am J Physiol* 1998; **275**: H805-H813
- 39 **Ladilov YV**, Balsler C, Piper HM. Protection of rat cardiomyocytes against simulated ischemia reperfusion by treatment with protein kinase C activator. *Circ Res* 1998; **82**: 451-457
- 40 **Maulik N**, Watanabe M, Zu YL, Huang CK, Cordis GA, Schley JA, Das DK. Ischemic PC triggers the activation of MAPKs and MAPKAP kinase2 in rat heart. *FEBS Lett* 1996; **396**: 233-237
- 41 **Knight RJ**, Buxton DB. Stimulation of c-Jun kinase and mitogen-activated protein kinase by ischemia and reperfusion in the perfused rat heart. *Biochem Biophys Res Commun* 1996; **218**: 83-88
- 42 **Saurin AT**, Martin JL, Heads RJ, Foley C, Mockridge JW, Wright MJ, Wang Y, Marber MS. The role of differential activation of P38MAPKs in preconditioned ventricular myocytes. *FASEB J* 2000; **14**: 2237-2246
- 43 **Ping P**, Zhang J, Cao X, Li RC, Kong D, Tang XL, Qiu Y, Manchikalapudi S, Auchampach JA, Black RG, Bolli R. PKC-dependent activation of p44/p42 MAPKs during myocardial ischemia-reperfusion in conscious rabbits. *Am J Physiol* 1999; **276**: H1468-1481
- 44 **Bogoyevitch MA**, Ketterman AJ, Sugden PH. Cellular stress differentially activate c-Jun N-terminal protein kinases and extracellular signal-regulated protein kinases in cultured ventricular myocytes. *J Biol Chem* 1995; **270**: 29710-29717
- 45 **Bogoyevitch MA**, Gillespie-Brown J, Ketterman AJ, Fuller SJ, Ben-Levy R, Ashworth A, Marshall CJ, Sugden PH. Stimulation of the stress-activated mitogen-activated protein kinase subfamilies in perfused heart: p38/RKMAPK and c-Jun N-terminal kinases are activated by ischemia reperfusion. *Circ Res* 1996; **79**: 162-173
- 46 **Baxter GF**, Goma FM, Yellon DM. Involvement of protein kinase C in the delayed cytoprotection following sublethal ischemia in rabbit myocardium. *Br J Pharmacol* 1995; **115**: 222-224
- 47 **Qiu Y**, Ping P, Tang XL, Manchikalapudi S, Rizvi A, Zhang J, Takano H, Wu WJ, Teschner S, Bolli R. Direct evidence that protein kinase C plays an essential role in the development of late preconditioning against myocardial stunning in conscious rabbits and that ϵ is the isoform involved. *J Clin Invest* 1998; **101**: 2182-2198
- 48 **Frost JA**, Steen H, Shapiro P, Lewis T, Ahn N, Shaw PE, Cobb MH. Cross-cascade activation of ERKs and ternary complex factors by Rho family proteins. *EMBO J* 1997; **16**: 6426-6438
- 49 **Shinmura K**, Tang XL, Wang Y, Xuan YT, Liu SQ, Takano H, Bhatnagar A, Bolli R. Cyclooxygenase-2 mediates the cardioprotective effects of the late phase of ischemic preconditioning in conscious rabbits. *Proc Natl Acad Sci U S A* 2000; **97**: 10197-10202
- 50 **Fryer RM**, Schultz JE, Hsu AK, Gross GJ. Importance of PKC and tyrosine kinase in single or multiple cycles of preconditioning in rat hearts. *Am J Physiol Heart Circ Physiol* 1999; **276**: H1229-H1235
- 51 **Hunt C**, Morimoto RI. Conserved features of eukaryotic HSP70 genes revealed by comparison with the nucleotide sequence of human HSP70. *Proc Natl Acad Sci U S A* 1985; **82**: 6455-6459
- 52 **Lindquist S**, Craig EA. The heat shock proteins. *Ann Rev Genet* 1988; **22**: 631-637
- 53 **Doi Y**, Hamazaki K, Yabuki M, Tanaka N, Utsumi K. Effect of HSP70 induced by warm ischemia to the liver on liver function after partial hepatectomy. *Hepatogastroenterology* 2001; **48**: 533-540

Edited by Wang XL and Zhang JZ Proofread by Xu FM

Ketamine suppresses intestinal NF-kappa B activation and proinflammatory cytokine in endotoxic rats

Jie Sun, Xiao-Dong Wang, Hong Liu, Jian-Guo Xu

Jie Sun, Jian-Guo Xu, Department of Anesthesiology, Jinling Hospital, College of Medicine, Nanjing University, Nanjing 210002, Jiangsu Province, China

Xiao-Dong Wang, Department of Surgery, Jinling Hospital, College of Medicine, Nanjing University, Nanjing 210002, Jiangsu Province, China

Hong Liu, Department of Chest Surgery, Jinling Hospital, College of Medicine, Nanjing University, Nanjing 210002, Jiangsu Province, China

Correspondence to: Professor Jian-Guo Xu, Department of Anesthesiology, Jinling Hospital 305 East Zhongshan Road, Nanjing 210002, Jiangsu Province, China. dgsunjie@hotmail.com

Telephone: +86-25-4806839 **Fax:** +86-25-4803956

Received: 2003-10-08 **Accepted:** 2003-12-16

Abstract

AIM: To investigate the protective effect of ketamine on the endotoxin-induced proinflammatory cytokines and NF-kappa B activation in the intestine.

METHODS: Adult male Wistar rats were randomly divided into 6 groups: (a) normal saline control, (b) challenged with endotoxin (5 mg/kg) and treated by saline, (c) challenged with endotoxin (5 mg/kg) and treated by ketamine (0.5 mg/kg), (d) challenged with endotoxin (5 mg/kg) and treated by ketamine (5 mg/kg), (e) challenged with endotoxin (5 mg/kg) and treated by ketamine (50 mg/kg), and (f) saline injected and treated by ketamine (50 mg/kg). After 1, 4 or 6 h, TNF- α and IL-6 mRNA were investigated in the tissues of the intestine (jejunum) by RT-PCR. TNF- α and IL-6 were measured by ELISA. We used electrophoretic mobility shift assay (EMSA) to investigate NF-kappa B activity in the intestine.

RESULTS: NF-kappa B activity, the expression of TNF- α and IL-6 were enhanced in the intestine by endotoxin. Ketamine at a dose of 0.5 mg/kg could suppress endotoxin-induced TNF- α mRNA and protein elevation and inhibit NF-kappa B activation in the intestine. However the least dosage of ketamine to inhibit IL-6 was 5 mg/kg in our experiment.

CONCLUSION: Ketamine can suppress endotoxin-induced production of proinflammatory cytokines such as TNF- α and IL-6 production in the intestine. This suppressive effect may act through inhibiting NF-kappa B.

Sun J, Wang XD, Liu H, Xu JG. Ketamine suppresses intestinal NF-kappa B activation and proinflammatory cytokine in endotoxic rats. *World J Gastroenterol* 2004; 10(7): 1028-1031
<http://www.wjgnet.com/1007-9327/10/1028.asp>

INTRODUCTION

Gram-negative bacteria caused sepsis remains an important cause of morbidity and mortality in septic and endotoxemic patients. Lipopolysaccharide (LPS), or endotoxin, a major component of the outer surface of Gram-negative bacteria, is a potent activator of cells of the immune and inflammatory systems, including macrophages, monocytes and endothelial

cells^[1], and contributes to the systemic changes seen in septic shock^[1-4]. The endotoxic shock syndrome is characterized by systemic inflammation, multiple organ damage, circulatory collapse and death^[1,2].

The important role of the intestinal mucosa in the inflammatory and metabolic responses to sepsis, severe injury and other critical illnesses has been increasingly recognized during the last decade. Thus, there is evidence that the gut mucosa becomes the site for production of various inflammatory cytokines^[5,6] and other yet unidentified substances that may influence not only the mucosa itself but also the function and integrity of remote organs and tissues^[7,8]. Indeed, the gut mucosa has been proposed to be the "motor" of multiple organ failure in critical illness^[9]. Besides, sepsis and severe injury are also associated with loss of mucosal integrity, resulting in increased permeability and bacterial translocation. These changes may accelerate the development of multiple organ failure^[10].

Ketamine, an intravenous anesthetic, has been advocated for anesthesia in septic or severely ill patients because of its cardiovascular stimulating effects^[11,12]. And several previous studies reported that ketamine could suppress LPS-induced tumor necrosis factor alpha (TNF- α) production in the serum and reduced mortality in carrageenan-sensitized endotoxin shock mice^[13,14]. However, few studies were undertaken to investigate the protective effect of ketamine on the inflammatory response in the intestine during septic shock *in vivo*. Since local produced cytokines were regarded as the contributing factors in tissue damage during sepsis^[15-17]. And nuclear factor kappa B (NF-kappa B) was verified to be an inducible transcription factor that was required for the transcription of some proinflammatory cytokines such as TNF- α , interleukin 6 and interleukin 8 (IL-6 and IL-8)^[18]. Our previous study indicated that ketamine could inhibit endotoxin induced NF-kappa B and TNF- α *in vitro*^[19]. Therefore, this study was to investigate whether ketamine could suppress endotoxin-induced NF-kappa B activation and proinflammatory cytokines in the intestine *in vivo* in order to define a possible mechanism of the anti-inflammatory effect of ketamine.

MATERIALS AND METHODS

Animals and treatment

Adult male Wistar rats (250-300 g body mass) used in this experiment were purchased from Shanghai Animal Center, Shanghai, China. The rats were exposed each day to 12 h of light and darkness respectively. The experimental protocol followed the institution's criteria for the care and use of laboratory animals in research. Further, all animals received humane care in compliance with Institutional Animal Care Committee.

Experimental protocol

The Wistar rat endotoxemia model was established by injection with a dose of LPS (5 mg/kg, *Escherichia coli* O111: B4) (Sigma Chemical Co., USA) via the tail vein. Then all animals were immediately treated with different doses of ketamine

(0.5, 5, 50 mg/kg) or normal saline (10 mL/kg) intraperitoneally (ip). Endotoxin and ketamine were diluted with normal saline at different concentrations so as to inject them into the rats at the same volume (10 mL/kg). After 1, 4 or 6 h, animals were killed, and tissues from the intestine was removed and kept in liquid nitrogen for later use. We used six rats in every time point of each group.

Electrophoretic mobility shift assay (EMSA)

Nuclear extracts of the intestine tissue was prepared by hypotonic lysis followed by high salt extraction^[20-22]. EMSA was performed using a commercial kit (Gel Shift Assay System; Promega, Madison, WI) as previously described. The NF-kappa B oligonucleotide probe, (5' -AGTTGAGGGGACT TTCCAGGC-3'), was end-labeled with [γ -³²P] ATP (Free Biotech, Beijing, China) with T4-polynucleotide kinase. Nuclear protein (80 μ g) was preincubated in 9 μ L of a binding buffer, consisting of 10 mmol/L Tris-Cl, pH 7.5, 1 mmol/L MgCl₂, 50 mmol/L NaCl, 0.5 mmol/L EDTA, 0.5 mmol/L DTT, 40 mL/L glycerol, and 0.05 g/L of poly-(deoxyinosinic deoxycytidylic acid) for 15 min at room temperature. After addition of the 1 μ L ³²P-labeled oligonucleotide probe, the incubation was continued for 30 min at room temperature. Reaction was stopped by adding 1 μ L of gel loading buffer, and the mixture was subjected to non-denaturing 40 g/L polyacrylamide gel electrophoresis in 0.5 \times TBE buffer. The gel was vacuum-dried and exposed to X-ray film (Fuji Hyperfilm) at -70 $^{\circ}$ C.

Reverse-transcription polymerase chain reaction (RT-PCR)

Total RNA was extracted with TriPure Isolation Reagent (Roche Molecular Biochemicals, Switzerland) and quantified by absorption at 260 nm. Reverse-transcription (RT) was implemented using Reverse Transcription System (Promega, WI, USA) according to the protocol. We used glyceraldehyde-3-phosphate dehydrogenase (GAPDH) as normalization control. The sequences of the primers were: TNF- α (sense) CACCACGCTCTTCTGTCTACTGAAC, (antisense) CCGGACTCCGTGATGTCTAAGTACT; IL-6 (sense) GACTGATGTTGTTGACAGCCACTGC, (antisense) TAGCC ACTCCTTCTGTGACTCTAACT; GAPDH (sense) CACGGCAAGTTCAATGGCACA, (antisense) GAATTGTGAGGGAGAGTGCTC. A total volume of 100 μ L reaction contained 2 μ L of RT product, 1.5 mmol/L MgCl₂, 2.5 U Taq DNA polymerase, 100 μ mol/L dNTP, 0.1 μ mol/L primer and 1 \times Taq DNA polymerase magnesium-free buffer (Promega, WI, USA). Then the reaction mixture was overlaid with two drops of mineral oil (Sigma Chemical Co., USA) and incubated in thermocycler (MiniCycler PTC 150, MJ Research Inc, USA) programmed to pre-denature at 95 $^{\circ}$ C for 2 min, denatured at 95 $^{\circ}$ C for 1 min, annealed at 60 $^{\circ}$ C for 1 min and extended at 72 $^{\circ}$ C for 2 min for a total of 30 cycles. The last cycle was followed by a final incubation at 72 $^{\circ}$ C for 5 min and cooled to 4 $^{\circ}$ C. The polymerase chain reaction products were 546 bp (TNF- α), 509 bp (IL-6) and 970 bp (GAPDH) respectively. Then they were electrophoresed on a 15 g/L agarose gel stained with ethidium bromide. The gel was captured as a digital image and analyzed using Scion Image software (Maryland, USA). Values in each sample were normalized with GAPDH control.

Enzyme-linked immunosorbent assay (ELISA)

TNF- α and IL-6 in the intestine were measured using commercially available enzyme-linked immunoassay kits (Diaclone USA for TNF- α ; Biosource USA for IL-6) according to the test protocol. Values were expressed as pg per milligram protein (pg/mg prot).

Statistics and presentation of data

Data were expressed as mean \pm SE. Statistical significance was determined by one-way ANOVA using SPSS 10.0. A value of $P < 0.05$ was considered significant.

RESULTS

NF-kappa B activation in the intestine

EMSA experiments were performed to examine the effect of ketamine on the activation of NF-kappa B induced by endotoxin. As shown in Figure 1, NF-kappa B activation in the intestine was increased after endotoxin challenge as compared with unstimulated group. The activity of NF-kappa B was in a time dependant manner after endotoxin injection. Ketamine inhibited NF-kappa B activation at three (0.5, 5, and 50 mg/kg) dosing levels ($P < 0.05$, as compared with endotoxin group) (Figure 1).

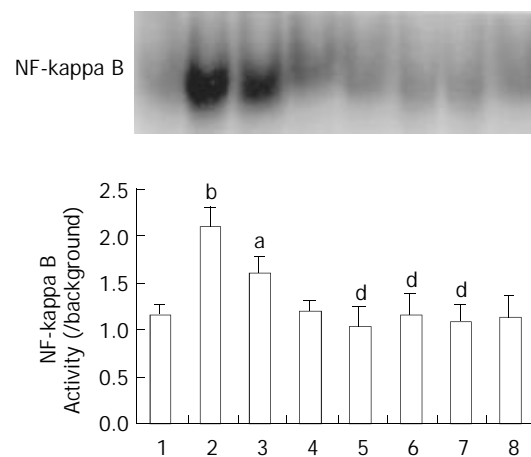


Figure 1 Activation of NF-kappa B in the intestine. Normal saline treatment (Lane 1). 1, 4, 6 h after endotoxin challenge (Lane 2, 3, 4), endotoxin plus ketamine (0.5, 5, 50 mg \cdot kg⁻¹) (Lane 5, 6, 7), ketamine only (50 mg \cdot kg⁻¹) (Lane 8) ^a $P < 0.05$ vs Lane 1; ^b $P < 0.01$ vs Lane 1; ^d $P < 0.01$ vs Lane 2.

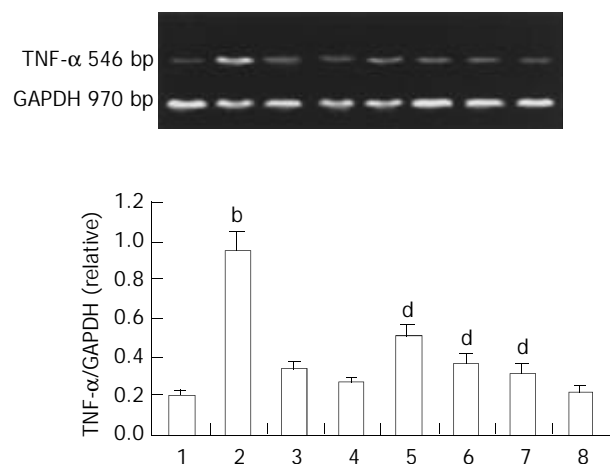


Figure 2 Expression of TNF- α in the intestine. Normal saline treatment (Lane 1). 1, 4, 6 h after endotoxin challenge (Lane 2, 3, 4), endotoxin plus ketamine (0.5, 5, 50 mg \cdot kg⁻¹) (Lane 5, 6, 7), ketamine only (50 mg \cdot kg⁻¹) (Lane 8); ^b $P < 0.01$ vs Lane 1; ^d $P < 0.01$ vs Lane 2.

TNF- α mRNA expression by endotoxin challenge and the protective effect of ketamine

TNF- α sustained a baseline level in normal rats. Endotoxin caused a transient elevation of TNF- α mRNA in the intestine. This activity increased with time reaching a maximum 1 h

after sepsis. Ketamine was administered intraperitoneally soon after endotoxin challenge. TNF- α gene expression was analyzed 1 h later since TNF- α could reach the maximum level about 1 h later. Ketamine suppressed TNF- α expression in a dose dependent manner. We found that ketamine at a dose of 0.5 mg/kg could suppress TNF- α expression significantly. This dosage was far below clinical anesthetic level (Figure 2).

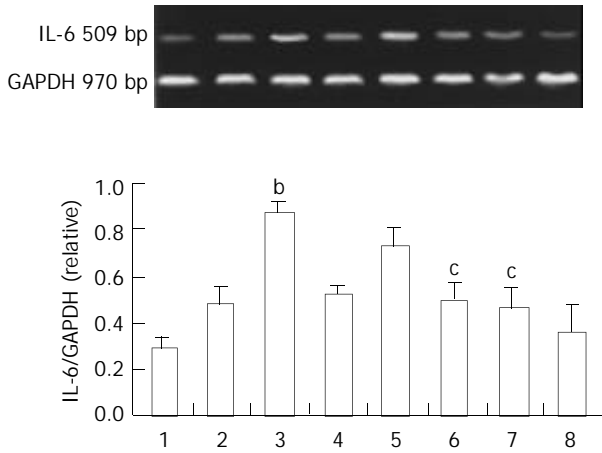


Figure 3 Expression of IL-6 in the intestine. Normal saline treatment (Lane 1). 1, 4, 6 h after endotoxin only (Lane 2, 3, 4), endotoxin plus ketamine (0.5, 5, 50 mg/kg) (Lane 5, 6, 7), ketamine only (50 mg/kg) (Lane 8); ^b $P < 0.01$ vs Lane 1; ^c $P < 0.05$ vs Lane 3.

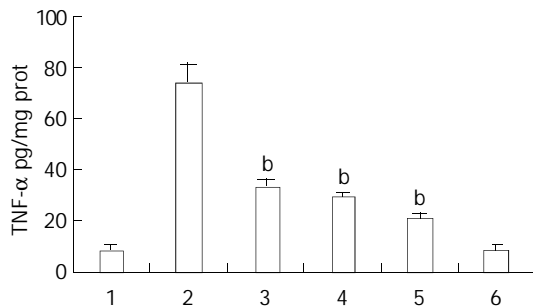


Figure 4 Protective effect of ketamine on the TNF- α production in the intestine. All of the values were obtained 1 h after sepsis. Lane 1 normal saline; Lane 2 endotoxin (5 mg/kg); Lane 3 endotoxin (5 mg/kg) plus ketamine (0.5 mg/kg); Lane 4 endotoxin (5 mg/kg) plus ketamine (5 mg/kg); Lane 5 endotoxin (5 mg/kg) plus ketamine (50 mg/kg); Lane 6 ketamine only (50 mg/kg) ^b $P < 0.01$ vs Lane 2.

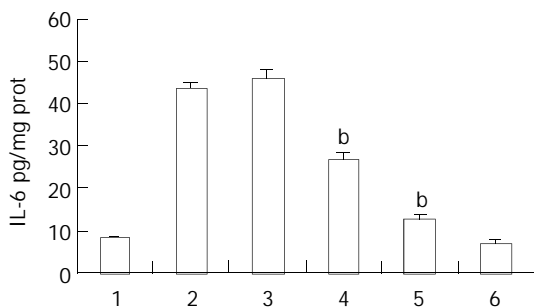


Figure 5 Protective effect of ketamine on the IL-6 production in the intestine. All of the values were obtained 4 h after sepsis. Lane 1 normal saline; Lane 2 endotoxin (5 mg/kg); Lane 3 endotoxin (5 mg/kg) plus ketamine (0.5 mg/kg); Lane 4 endotoxin (5 mg/kg) plus ketamine (5 mg/kg); Lane 5 endotoxin (5 mg/kg) plus ketamine (50 mg/kg); Lane 6 ketamine only (50 mg/kg) ^b $P < 0.01$ vs Lane 2.

IL-6 expression in intestine by endotoxin challenge and the protective effect of ketamine

The IL-6 expression of the small intestine is shown in Figure 3. Endotoxin also enhanced IL-6 expression in the intestine. However the peak time was 4 h after endotoxin challenge. We observed the protective effect of ketamine at this peak time. Ketamine suppressed IL-6 expression in a dose dependent manner. Unlike TNF- α , the minimal dosage at which ketamine could suppress IL-6 significantly was 5 mg/kg. This was within clinical anesthetic range (Figure 3).

Effect of ketamine on TNF-a and IL-6 production in intestine homogenates after endotoxin stimulation

Ketamine suppressed endotoxin-induced TNF- α and IL-6 production in a dose dependent manner. Ketamine beyond the concentration of 0.5 mg/kg could inhibit TNF- α production, however the minimal dosage at which ketamine suppressed IL-6 significantly was 5 mg/kg. This was within clinical anesthetic range (Figures 4 and 5).

DISCUSSION

Our laboratory and others have demonstrated that ketamine could suppress endotoxin-induced some proinflammatory cytokines *in vitro*^[23]. However it is to be determined in complex *in vivo* studies. We assessed the cytokines and transcriptional factor NF-kappa B in the intestine because of the important status of the intestine in sepsis or systemic inflammation reaction syndrome (SIRS). The intestine was not only the passive organs injured by sepsis but participation in the pathogenesis of SIRS^[5,6].

TNF- α is regarded as the most important proinflammatory cytokine, which is released early after an inflammatory stimulus^[24]. And IL-6, which is elevated after TNF- α , contributes to both morbidity and mortality in conditions of “uncontrolled” inflammation^[25]. Among the cytokines produced in the intestinal mucosa during inflammation, TNF- α and IL-6 are particularly important because of its multiple biological effects both in the intestine and in other organs and tissues. In this study, we demonstrated that ketamine suppressed both endotoxin-induced TNF- α and IL-6 expression and production in the intestine. TNF- α was the first cytokine expressed after endotoxin stimulation and later IL-6, which was consistent with several previous reports^[24,25]. Studies had demonstrated that ketamine could suppress endotoxin-induced cytokines *in vitro*. However, proinflammatory cytokines just like TNF- α and IL-6 were not merely stimulated by endotoxin *in vivo*. Therefore, our experimental protocol was more physiological and closer to clinical condition.

NF-kappa B is associated in the cytoplasm with its inhibitory subunit, inhibitory kappa B (I κ B), which prevents NF-kappa B from translocating into the nucleus. Endotoxin can induce the phosphorylation and degradation of I κ B. Many effector genes including those encoding cytokines (TNF- α and IL-6) are in turn regulated by NF-kappa B^[26]. To determine whether ketamine could inhibit NF-kappa B activation, we did EMSA to detect NF-kappa B activity in the intestine. We found a constitutive activation of NF-kappa B in intestine. Endotoxin could enhance NF-kappa B activation in the intestine and it was most significant 1 h later. Although we had previously demonstrated that ketamine could inhibit NF-kappa B activation in peripheral blood mononuclear cell (PBMC) after endotoxin challenge *in vitro*. It was to be studied whether ketamine had this effect *in vivo*. In our experiment, we found ketamine could inhibit NF-kappa B activation. However it was not in a dose dependent manner. We did not found any NF-kappa B activity changes in the group administered ketamine

(50 mg/kg) only, which excluded ketamine itself had any effect on NF-kappa B activity.

As the rats were not anesthetized during the whole experiment, we did not monitor the arterial pressure and pulse rate to confirm septic shock. Because the drug studied in our investigation was ketamine, just an anesthetic drug. To exclude any other anesthetic drug disturbance, we had to give up that monitoring. However, this septic model was successfully used in many other researches^[27-29]. In addition, we did find that the rats were dispirited with piloerection and diarrhea, which indicated the septic shock indirectly.

The dosage of ketamine used in this study was from 0.5 to 50 mg/kg, which covered the clinical range. Roytblat *et al.*^[30] reported that a single dose of ketamine 0.25 mg/kg administered before cardiopulmonary bypass suppressed the increase in serum IL-6 during and after coronary artery bypass surgery. However, other studies demonstrated such a small dose of ketamine did not suppress IL-6 production^[25]. The reason was not clear. In this study, only ketamine reaching a dose of 5 mg/kg could suppress IL-6 production in the intestine. There were perhaps some differences between human being and animals or between *in vitro* and *in vivo* studies. We found 0.5 mg/kg ketamine suppressed TNF- α production, which was in accordance with those *in vitro* studies^[25].

In conclusion, we demonstrated that ketamine could suppress endotoxin-induced TNF- α and IL-6 expression and production in the intestine. And this suppressive effect might act through inhibiting NF-kappa B. Further study is required to elucidate the mechanism of ketamine action.

ACKNOWLEDGEMENT

We thank Dr. Genbao Feng for his technical assistance.

REFERENCES

- 1 **Opal SM**, Cohen J. Clinical Gram-positive sepsis: does it fundamentally differ from Gram-negative bacterial sepsis? *Crit Care Med* 1999; **27**: 1608-1616
- 2 **Rietschel ET**, Brade H, Holst O, Brade L, Muller-Loennies S, Mamat U, Zahringer U, Beckmann F, Seydel U, Brandenburg K, Ulmer AJ, Mattern T, Heine H, Schletter J, Loppnow H, Schonbeck U, Flad HD, Hauschildt S, Schade UF, Di Padova F, Kusumoto S, Schumann RR. Bacterial endotoxin: chemical constitution, biological recognition, host response, and immunological detoxification. *Curr Topics Microbiol Immunol* 1996; **216**: 39-81
- 3 **Wenzel RP**, Pinsky MR, Ulevitch RJ, Young L. Current understanding of sepsis. *Clin Inf Dis* 1995; **22**: 407-412
- 4 **Huemann D**, Glauser MP, Calandra T. Molecular basis of host-pathogen interaction in septic shock. *Curr Opin Microbiol* 1998; **1**: 49-55
- 5 **Huang L**, Tan X, Crawford SE, Hsueh W. Platelet-activating factor and endotoxin induce tumor necrosis factor gene expression in rat intestine and liver. *Immunology* 1994; **83**: 65-69
- 6 **Meyer TA**, Wang J, Tiao GM, Ogle CK, Fischer JE, Hasselgren PO. Sepsis and endotoxemia stimulate interleukin-6 production. *Surgery* 1995; **118**: 336-342
- 7 **Magnotti LJ**, Xu DZ, Lu Q, Deitch EA. Gut-derived mesenteric lymph but not portal blood increases endothelial cell permeability and promotes lung injury after hemorrhagic shock. *Ann Surg* 1998; **228**: 518-527
- 8 **Sambol JT**, Xu DZ, Adams CA, Magnotti LJ, Deitch EA. Mesenteric lymph duct ligation provides long term protection against hemorrhagic shock-induced lung injury. *Shock* 2000; **14**: 416-419
- 9 **Langkamp-Henken B**, Donovan TB, Pate LM, Maul CD, Kudsk KA. Increased intestinal permeability following shock and penetrating trauma. *Crit Care Med* 1995; **23**: 660-664
- 10 **Swank GM**, Deitch EA. Role of the gut in multiple organ failure: bacterial translocation and permeability changes. *World J Surg* 1996; **21**: 411-417
- 11 **Lippmann M**, Appel PL, Mok MS, Shoemaker WC. Sequential cardiorespiratory patterns of anesthetic induction with ketamine in critically ill patients. *Crit Care Med* 1983; **11**: 730-734
- 12 **Yli-Hankala A**, Kirvela M, Randell T, Lindgren L. Ketamine anaesthesia in a patient with septic shock. *Acta Anaesthesiol Scand* 1992; **36**: 483-485
- 13 **Takenaka I**, Ogata M, Koga K, Matsumoto T, Shigematsu A. Ketamine suppresses endotoxin-induced tumor necrosis factor alpha production in mice. *Anesthesiology* 1994; **80**: 402-408
- 14 **Koga K**, Ogata M, Takenaka I, Matsumoto T, Shigematsu A. Ketamine suppresses tumor necrosis factor- α activity and mortality in carrageenan-sensitized endotoxin shock model. *Circ Shock* 1995; **44**: 160-168
- 15 **Cavaillon JM**, Munoz C, Fitting C, Misset B, Carlet J. Circulating cytokines: the tip of the iceberg? *Circ Shock* 1992; **38**: 145-152
- 16 **Beutler BA**, Milsark IW, Cerami A. Cachectin/tumor necrosis factor: production, distribution, and metabolic fate *in vivo*. *J Immunol* 1985; **135**: 3972-3977
- 17 **Keogh C**, Fong Y, Marano MA, Seniuk S, He W, Barber A, Minei JP, Felsen D, Lowry SF, Moldawer LL. Identification of a novel tumor necrosis factor alpha/cachectin from the livers of burned and infected rats. *Arch Surg* 1990; **125**: 79-84
- 18 **Baldwin AS Jr**. The NF- κ B and I κ B proteins: new discoveries and insights. *Ann Rev Immunol* 1996; **14**: 649-683
- 19 **Yu Y**, Zhou Z, Xu J, Liu Z, Wang Y. Ketamine reduces NF kappa B activation and TNF alpha production in rat mononuclear cells induced by lipopolysaccharide *in vitro*. *Ann Clin Lab Sci* 2002; **32**: 292-298
- 20 **Gong JP**, Liu CA, Wu CX, Li SW, Shi YJ, Li XH. Nuclear factor κ B activity in patients with acute severe cholangitis. *World J Gastroenterol* 2002; **8**: 346-349
- 21 **Zhou W**, Jiang ZW, Tian J, Jiang J, Li N, Li JS. Role of NF- κ B and cytokine in experimental cancer cachexia. *World J Gastroenterol* 2003; **9**: 1567-1570
- 22 **Liu Z**, Yu Y, Jiang Y, Li J. Growth hormone increases lung NF-kappaB activation and lung microvascular injury induced by lipopolysaccharide in rats. *Ann Clin Lab Sci* 2002; **32**: 164-170
- 23 **Kawasaki T**, Ogata M, Kawasaki C, Ogata J, Inoue Y, Shigematsu A. Ketamine suppresses proinflammatory cytokine production in human whole blood *in vitro*. *Anesth Analg* 1999; **89**: 665-669
- 24 **Hesse DG**, Tracey KJ, Fong Y, Manogue KR, Palladino MA Jr, Cerami A, Shires GT, Lowry SF. Cytokine appearance in human endotoxemia and primate bacteremia. *Surg Gynecol Obstet* 1988; **166**: 147-153
- 25 **Damas P**, Ledoux D, Nys M, Vrindts Y, Groote D, Franchimont P, Lamy M. Cytokine serum level during severe sepsis in human: IL-6 as a marker of severity. *Ann Surg* 1992; **215**: 356-362
- 26 **Bauerle PA**, Baltimore D. NF-kappa B: ten years after. *Cell* 1996; **87**: 13-20
- 27 **Arya R**, Grossie VB Jr, Weisbrodt NW, Lai M, Mailman D, Moody F. Temporal expression of tumor necrosis factor- α and nitric oxide synthase 2 in rat small intestine after endotoxin. *Dig Dis Sci* 2000; **45**: 744-749
- 28 **Secchi A**, Ortanderl JM, Schmidt W, Walther A, Gebhard MM, Martin E, Schmidt H. Effects of dobutamine and dopexamine on hepatic micro- and macrocirculation during experimental endotoxemia: an intravital microscopic study in the rat. *Crit Care Med* 2001; **29**: 597-600
- 29 **Taniguchi T**, Shibata K, Yamamoto K. Ketamine inhibits endotoxin-induced shock in Rats. *Anesthesiology* 2001; **95**: 928-932
- 30 **Roytblat L**, Talmor D, Rachinsky M, Greenberg L, Pekar A, Appelbaum A, Gurman GM, Shapira Y, Duvdenani A. Ketamine attenuates the interleukin-6 response after cardiopulmonary bypass. *Anesth Analg* 1998; **87**: 266-271

Protective effects of pentadecapeptide BPC 157 on gastric ulcer in rats

Xiao-Chang Xue, Yong-Jie Wu, Ming-Tang Gao, Wen-Guang Li, Ning Zhao, Zeng-Lu Wang, Chun-Jie Bao, Zhen Yan, Ying-Qi Zhang

Xiao-Chang Xue, Ning Zhao, Zeng-Lu Wang, Chun-Jie Bao, Zhen Yan, Ying-Qi Zhang, Biotechnology Centre, Fourth Military Medical University, Xi'an 710032, Shaanxi Province, China
Yong-Jie Wu, Ming-Tang Gao, Wen-Guang Li, Department of Pharmacology, Lanzhou Medical College, Lanzhou 730000, Gansu Province, China

Correspondence to: Dr. Ying-Qi Zhang, Biotechnology Centre, Fourth Military Medical University, 169 West Changle Road, Xi'an 710032, Shaanxi Province, China. xue_xiaochang@yahoo.com

Telephone: +86-29-3247213 **Fax:** +86-29-3224537

Received: 2003-07-12 **Accepted:** 2003-07-30

Abstract

AIM: To investigate the protective effects of gastric pentadecapeptide BPC 157 on acute and chronic gastric ulcers in rats and to compare the results in therapy of human gastric ulcers by different administration methods.

METHODS: Gastric pentadecapeptide BPC 157 was administered (initial single or continuous administration) into rats either intragastrically or intramuscularly before (induced acute gastric ulcer) or after (induced chronic gastric ulcer) the applications of inducing agents, and each animal was sacrificed to observe the protective effects of BPC 157 on gastric ulcers.

RESULTS: Both intramuscular (im) and intragastric (ig) administration of BPC 157 could apparently reduce the ulcer area and accelerate the healing of induced ulcer in different models and the effect of im administered BPC 157 was better than that of ig. The rats treated with higher dosages (400 ng/kg, 800 ng/kg) of BPC 157 (im and ig) showed significantly less lesion ($P < 0.01$ vs excipient or saline control), the inhibition ratio of ulcer formation varied between 45.7% and 65.6%, from all measurements except 400 ng/kg BPC 157 in pylorus ligation induced model ($P < 0.05$), in which the inhibition rate was 54.2%. When im administered (800 ng/kg BPC 157) in three models, the inhibition ratio of ulcer formation was 65.5%, 65.6% and 59.9%, respectively, which was better than that of famotidine (its inhibition rate was 60.8%, 57.2% and 34.3%, respectively). Continuous application of BPC 157 (in chronic acetate induced gastric ulcer) could accelerate rebuilding of glandular epithelium and formation of granulation tissue ($P < 0.05$ at 200 ng/kg and $P < 0.01$ at 400 ng/kg and 800 ng/kg vs excipient or saline control).

CONCLUSION: Both im and ig administered gastric pentadecapeptide BPC 157 can apparently ameliorate acute gastric ulcer in rats and antagonize the protracted effect of acetate challenge on chronic ulcer. The effect of im administration of BPC 157 is better than that of ig, and the effective dosage of the former is lower than that of the latter.

Xue XC, Wu YJ, Gao MT, Li WG, Zhao N, Wang ZL, Bao CJ,

Yan Z, Zhang YQ. Protective effects of pentadecapeptide BPC 157 on gastric ulcer in rats. *World J Gastroenterol* 2004; 10(7): 1032-1036

<http://www.wjgnet.com/1007-9327/10/1032.asp>

INTRODUCTION

Pentadecapeptide BPC 157 (M_r 1419), with the sequence Gly-Glu-Pro-Pro-Gly-Lys-Pro-Ala-Asp-Asp-Ala-Gly-Leu-Val, a 15-amino acid fragment of body protection compound (BPC) peptide in gastric juice^[1,2], is thought to be essential for BPC's activity and has been fully characterized and investigated. Although the detailed mechanism is poorly understood, BPC 157 appears to be beneficial to almost all organ systems in many species when very low dosages (mostly mg/kg and ng/kg) are used. It has many functions such as attenuating liver, lung, colon and gastric lesions^[3-13], displaying anti-anxiety and antidepressant effects^[14,15], improving angiogenesis and wound healing^[8,16,17], reversing MPTP-motor abnormalities in Parkinson's disease models^[11], having mucosal protective and anti-inflammatory effects^[10,18,19], particularly affecting dopamine systems^[20], and persistent activity^[6,21]. All these findings showed that BPC 157 could be a useful prototype of a new class of drugs and organ protective agents.

In this present we studied the protective effects of synthesized BPC 157 on acute and chronic gastric ulcers and also discussed the differences resulted from different administration methods.

MATERIALS AND METHODS

Materials

BPC 157 was synthesized and purified in our laboratory. Famotidine (Lot No. 970422) was provided by Changzhou Xinhua Industry General Company. Indomethacin was purchased from Lanzhou Pharmaceutical Factory. CIMAS8 true color image analyzer was from Beijing University of Aeronautics & Astronautics. WV-CP410 color camera was produced by Panasonic Electrical Company Limited.

Animals

A total of 330 male Wistar rats, weighing 200-240 g, were used for 3 different gastric ulcer models, namely indomethacin induced model, pylorus ligation induced model and acetate induced model. In each model, rats were randomly divided into 11 groups, of which 6 for intramuscular (im) administration and 5 for intragastric (ig) administration, 10 rats for each group.

Methods

Gastric pentadecapeptide BPC 157 was ig or im administered (1 mL/kg) at three different dosages (200, 400 and 800 ng/kg) in each model. Saline, excipient (mannitol) and famotidine were used as saline control, excipient control and positive control, respectively.

In model 1, the rats were fasted but with free access to water for 24 h, and then BPC 157 was given. Sixty minutes later

ulcer was induced by injection of indomethacin (33 mg/kg body mass). The rats were sacrificed 12 h later and both pylorus and cardia were ligated, followed by injection of 10 mL formaldehyde (40 g/L) into the stomach. Thirty minutes later, the stomach was cut and spread out and the area of the ulcer was measured.

In model 2, the rats were fasted for 54 h with free access to water before administrations of BPC 157. Famotidine and saline were given and pylorus ligation was performed by surgical procedure 60 min later. The rats were fasted for an additional period of 18 h and sacrificed and treated as in model 1.

In model 3 (chronic gastric ulcer model), the stomach was exposed under anesthesia followed by injection of 50 μ L acetate (300 mL/L) under the chorion after the rats were fasted with free access to water for 24 h. After injection of acetate, the rats were immediately treated with BPC 157 twice daily for 12 d. Twelve hours following the last treatment, the rats were sacrificed and the ulcer area, glandular epithelium rebuilding and granulation tissue thickness were investigated. The reepithelialization was reflected by the diameter of remnant ulcer and the thickness of granulation tissue was measured every 500 μ m.

RESULTS

Effects of BPC 157 on indomethacin induced gastric ulcer

BPC 157 could apparently inhibit the progression of indomethacin induced gastric ulcer. When im administered (400 ng/kg and 800 ng/kg), the protective effect of BPC 157 (the gastric ulcer area was 7.22 mm²) was better than that of famotidine (the ulcer area 8.20 mm²). While im and ig application had different effects, the former was better than the latter. The effective ($P < 0.01$ vs excipient control or saline control) dosage was different; im administration of 200 ng/kg BPC 157 was as effective as ig administration of 400 ng/kg of BPC 157 (Table 1, Figure 1).

Table 1 Effect of BPC 157 on indomethacin induced gastric ulcer formation ($n=10$)

Administration	Agents	Dosage (ng/kg)	Ulcer (mm ²)	Inhibition ratio(%)
im	Saline control	-	19.22±2.95	-
	Excipient control	-	20.90±7.55	-
	Famotidine	40 000	8.20±4.68	60.8 ^b
	BPC 157	200	9.71±5.00	53.5 ^b
	BPC 157	400	7.22±4.01	65.5 ^b
	BPC 157	800	7.22±4.64	65.5 ^b
ig	Saline control	-	20.18±8.50	-
	Famotidine	40 000	8.28±3.45	58.9 ^b
	BPC 157	200	13.56±6.79	32.8
	BPC 157	400	9.92±2.62	50.8 ^b
	BPC 157	800	9.75±5.25	51.7 ^b

^b $P < 0.01$ vs excipient control or saline control.

Effects of BPC 157 on pylorus ligation induced gastric ulcer

The effect of BPC 157 on pylorus ligation induced gastric ulcer was similar to that on indomethacin induced ulcer. When BPC 157 was im administered, it was effective ($P < 0.01$ vs excipient control) even at dosage of 200 ng/kg and the effects at dosages of 400 ng/kg and 800 ng/kg were better than that of famotidine. When BPC 157 was ig administered, the higher dosages showed significant effect compared with saline control ($P < 0.05$) and the lower dosage did not ($P > 0.05$) (Table 2, Figure 1).

Effects of BPC 157 on acetate induced gastric ulcer

In chronic acetate induced animal model, the lower dosage was effective ($P < 0.05$), and the higher dosages showed significant effects ($P < 0.01$) when compared with excipient control (im) or saline control (ig) (Table 3, Figure 1).

Table 2 Effect of BPC 157 on pylorus ligation induced gastric ulcer formation ($n=10$)

Administration	Agents	Dosage (ng/kg)	Ulcer (mm ²)	Inhibition ratio(%)
im	Saline control	-	131.2±58.1	-
	Excipient control	-	130.2±68.2	-
	Famotidine	40 000	55.7±46.7	57.2 ^b
	BPC 157	200	80.9±22.8	37.8 ^b
	BPC 157	400	47.6±27.8	63.5 ^b
	BPC 157	800	44.8±19.4	65.6 ^b
ig	Saline control	-	140.1±78.1	-
	Famotidine	40 000	34.1±33.1	75.7 ^b
	BPC 157	200	110.5±41.5	21.1
	BPC 157	400	64.1±35.4	54.2 ^a
	BPC 157	800	58.6±37.6	58.2 ^b

^a $P < 0.05$, ^b $P < 0.01$ vs excipient control (im) or saline control (ig).

Table 3 Effect of BPC 157 on acetate induced gastric ulcer area ($n=10$)

Administration	Agents	Dosage (ng/kg)	Ulcer (mm ²)	Inhibition ratio(%)
im	Saline control	-	13.66±4.10	-
	Excipient control	-	13.98±4.00	-
	Famotidine	40 000	9.18±3.04	34.3 ^a
	BPC 157	200	9.75±3.62	30.2 ^a
	BPC 157	400	6.81±3.67	51.3 ^b
	BPC 157	800	5.60±1.91	59.9 ^b
ig	Saline control	-	14.96±6.21	-
	Famotidine	40 000	3.20±1.54	78.6 ^b
	BPC 157	200	9.78±4.28	34.6 ^a
	BPC 157	400	8.13±2.84	45.7 ^b
	BPC 157	800	7.80±2.83	47.8 ^b

^a $P < 0.05$, ^b $P < 0.01$ vs excipient control (im) or saline control (ig).

BPC 157's effect on rebuilding of glandular epithelium and granulation tissue formation in chronic acetate induced gastric ulcer was also investigated. Table 4 shows that BPC 157, im and ig administered, had significant protective effects compared with controls ($P < 0.05$), and the effect of BPC 157 on the thickness of granulation tissue was more significant than that of famotidine ($P < 0.01$). The ulcer in rats treated at 800 ng/kg dosage of BPC 157 was almost healed and the granulation tissue became thick. In the control, putrescence and exudation were apparent, the ulcerous gap was large and the granulation tissue was very thin (Figure 2).

Table 4 Effects of BPC 157 on rebuilding of glandular epithelium and formation of granulation tissue in acetate induced chronic gastric ulcer ($n=10$)

Administration	Agent	Dosage (ng/kg)	Diameter of remnant ulcer (μ m)	Thickness of granulation tissue (μ m)
im	Saline control	-	3 928±636	718±165
	Excipient control	-	3 981±594	652±169
	Famotidine	40 000	3 175±577 ^b	768±268
	BPC 157	200	3 266±671 ^a	992±295 ^b
	BPC 157	400	2 658±744 ^b	1 018±202 ^b
	BPC 157	800	2 426±511 ^b	1 012±306 ^b
ig	Saline control	-	4 098±795	673±112
	Famotidine	40 000	1 772±458 ^b	805±100 ^a
	BPC 157	200	3 260±728 ^a	797±110 ^a
	BPC 157	400	2 972±564 ^b	837±114 ^b
	BPC 157	800	2 904±577 ^b	862±171 ^b

^a $P < 0.05$, ^b $P < 0.01$ vs excipient control (im) or saline control (ig).

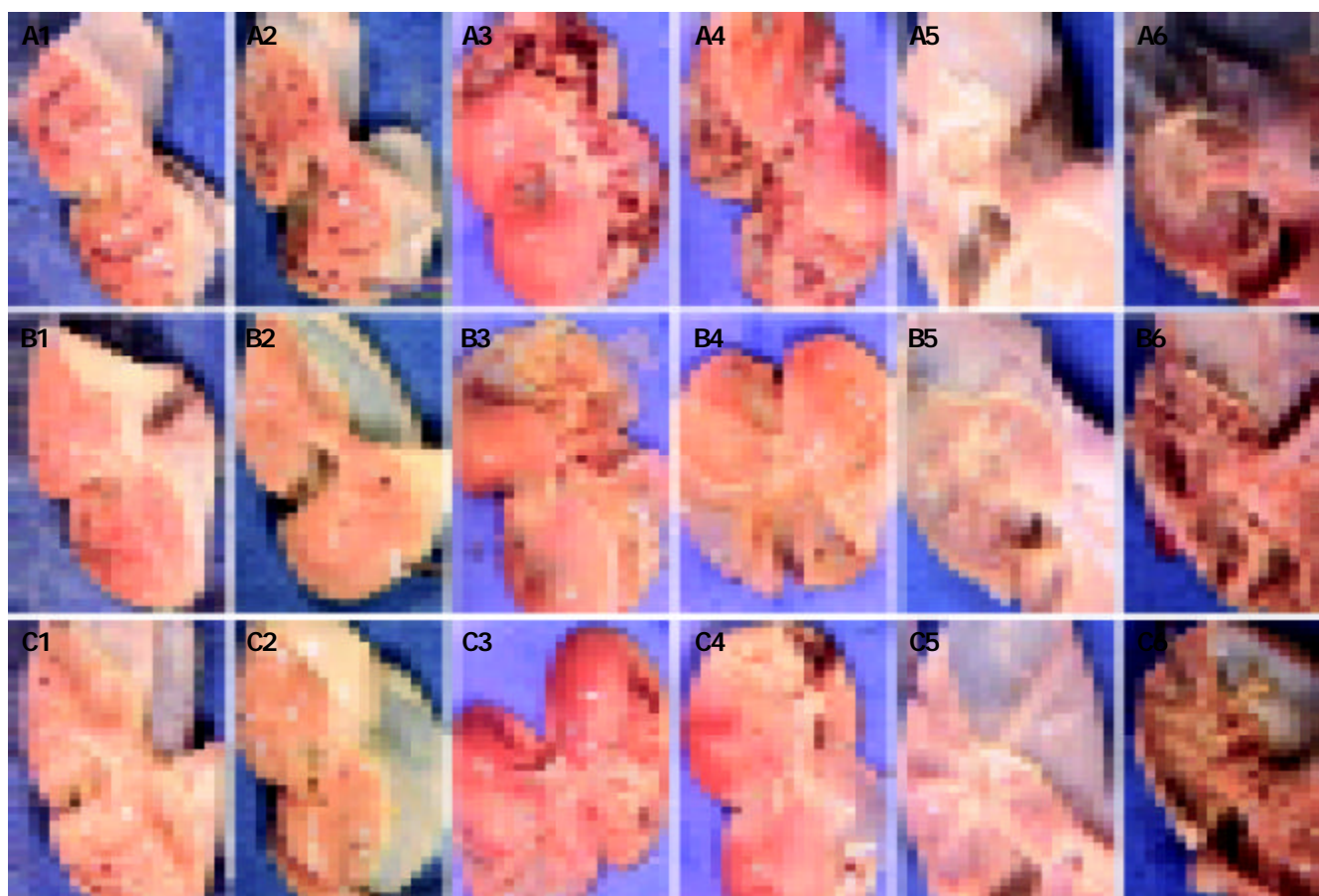


Figure 1 Effects of BPC 157 on gastric ulcers. An ($n=1-6$), Bn and Cn represent the excipient control (im) or saline control (ig) group, famotidine group and BPC 157 (800 ng/kg) group, respectively. Numbers 1-6 represent indomethacin induced model (im, ig), pylorus ligation model (im, ig) and acetate induced model (im, ig), respectively.

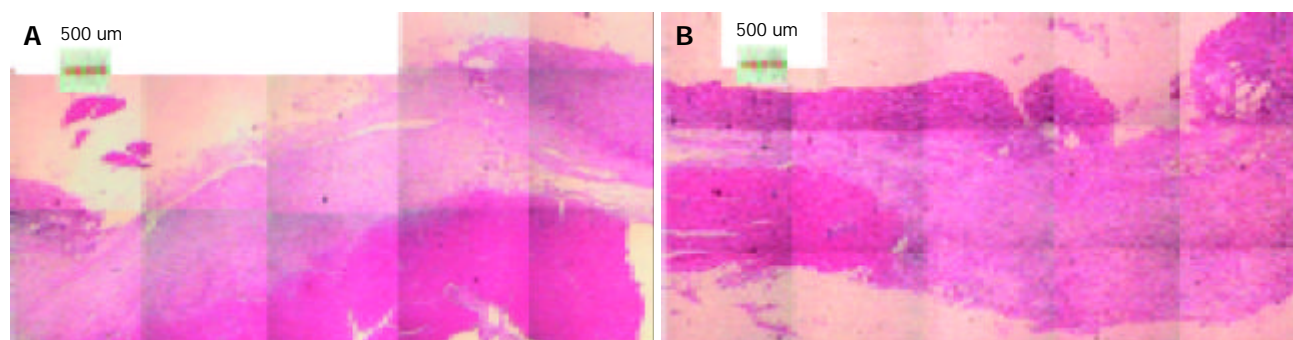


Figure 2 Effects of BPC 157 on regeneration of glandular epithelium and formation of granulation tissue in acetate induced chronic gastric ulcer. A, Saline control; B, BPC 157 (800 ng/kg) treated group.

DISCUSSION

Gastric pentadecapeptide BPC 157 is a widely studied molecule bearing cyto/organo- protective effects in many organs and can be administered in various ways. In the present study, we investigated the protective effects of chemically synthesized and purified BPC 157 on acute and chronic gastric ulcers in rats. The application way of the agent was also considered.

Generally, in acute and chronic induced gastric ulcers, im and ig administered gastric pentadecapeptide BPC 157 can prominently attenuate the syndrome in rats. When BPC 157 was im administered, the protective effect reached a statistical significance at a low dose (200 ng/kg) and the effect was better than that of famotidine, the positive control, at a higher dose (400 ng/kg or 800 ng/kg). When BPC 157 was ig administered, the effect was less than that when it was im administered, but better than that of saline controls. In the control, the ulcer area

was larger. What was more, the synthesized BPC 157 had a high bioactivity especially in pylorus ligation induced animal model. The effective dosage of famotidine (40 mg/kg) was 50 times that (800 ng/kg) of BPC 157. In acetate induced chronic gastric ulcer model, both famotidine and BPC 157 could apparently antagonize protracted acetate challenge by accelerating rebuilding of glandular epithelium and formation of granulation tissue. Although the protective effect of famotidine was as good as certain dosages of BPC 157, granulation tissue formation was far less than that of BPC 157, so BPC 157 may act at least to some extent in a different way from famotidine.

Although the function of BPC 157 has been fully elucidated, the detailed mechanism of BPC 157 is still poorly understood. Sikiric *et al.* found that gastric pentadecapeptide BPC 157 attenuated chronic amphetamine disturbances and the effect was present throughout the observation period at a statistically

significant level. So they believed that BPC 157 had a modulatory effect on dopamine system^[20]. In a haloperidol-induced gastric lesion model, both dopamine agonists (*i.e.*, bromocriptine, amantadine) and gastric pentadecapeptide BPC 157 could antagonize these lesions, but other antiulcer agents (atropine, pirenzepine, misoprostol, pantoprazole, lansoprazole, cimetidine and ranitidine) were not as effective^[10]. Besides, a particular interaction of BPC 157 with central dopamine system was also shown in other experimental models (*i.e.*, protection of stress ulcers). Likewise, a considerable number of evidence for interaction of gastric peptides with dopamine system has been found in gastric mucosal protection studies.

However, Sikiric *et al.* found that although the dopaminomimetics (bromocriptine, apomorphine and amphetamine) could apparently attenuate the otherwise consistent haloperidol or reserpine-gastric lesions when they were co-administered, their beneficial effects were absent in rats injured by haloperidol in combination with reserpine. On the other hand, BPC 157 was also effective. This result showed that BPC 157 might not act directly through dopamine system, but through a corresponding system parallel to dopamine system, and it might still function despite the extensive inhibition of endogenous dopamine system activity^[22]. Considering the indicated GABA (gamma-amino butyric acid)/dopamine system interactions, besides an anti-anxiety effect^[14], BPC 157 might act through GABA. Jelovac^[23] found that BPC 157 acted in favor of the natural homeostasis of the GABA receptor complex and of the GABAergic transmission, thus having a mechanism at least partly different from those involving diazepam tolerance/withdrawal.

With respect to the prolonged activity of BPC 157 and its surprisingly high activity (at ng level), it can be reasonably speculated that pentadecapeptide BPC 157 was most likely to act through the regulation of central nervous system (CNS) or some beneficial factors^[24-28], and then might activate a cascade network, but not directly act on the target tissue or cells. It was reported that the disordered ratio of G/D cells, which can secrete gastrointestinal hormones gastrin and somatostatin, could lead to gastrointestinal dysfunction in acetic acid induced gastric ulcer model^[29]. Maybe BPC 157 can antagonize the agents induced damage by modulating the number of G and D cells and maintaining the stable circumstances of stomach.

Although the mechanism of gastric ulcer has been studied for many years, the therapy of human gastric ulcer is still a hard nut to crack. Many substances have been investigated for the therapy of gastric ulcer, but few of them were found to be effective, some were bi-directional^[30]. It is well known that human gastric ulcer is characterized by relapse and difficulty in prevention. So, emphasis of treatment of peptic ulcer should be put on preventing relapse. Wang *et al.*^[31] found that traditional Chinese medicine Danshen (*Salvia miltiorrhiza*) was effective in promoting ulcer healing and preventing recurrence by strengthening gastric mucosal barrier and promoting gastric mucosal cell proliferation along the edge of the ulcer. The effect of BPC 157 on preventing gastric ulcer recurrence is under investigation.

In conclusion, BPC 157 is a potentially useful peptide and can be used in the treatment of human gastric ulcer. It may have other uses because of its multiple activity. Further studies on its mechanism are needed before we can benefit from this pentadecapeptide.

REFERENCES

- 1 **Sikiric P**, Petek M, Rucman R, Seiwerth S, Grabarevic Z, Rotkvic I, Jagic V, Turkovic B, Mildner B, Duvnjak M. The significance of the gastroprotective effect of body protection compound (BPC): modulation by different procedures. *Acta Physiol Hung* 1992; **80**: 89-98
- 2 **Sikiric P**, Petek M, Rucman R, Seiwerth S, Grabarevic Z, Rotkvic I, Turkovic B, Jagic V, Mildner B, Duvnjak M. A new gastric juice peptide, BPC. An overview of the stomach-stress-organoprotection hypothesis and beneficial effects of BPC. *J Physiol Paris* 1993; **87**: 313-327
- 3 **Prkacin I**, Separovic J, Aralica G, Perovic D, Gjurasin M, Lovric-Bencic M, Stancic-Rokotov D, Staresinic M, Anic T, Mikus D, Sikiric P, Seiwerth S, Mise S, Rotkvic I, Jagic V, Rucman R, Petek M, Turkovic B, Marovic A, Sebecic B, Boban-Blagaic A, Kocic N. Portal hypertension and liver lesions in chronically alcohol drinking rats prevented and reversed by stable gastric pentadecapeptide BPC 157 (PL-10, PLD-116), and propranolol, but not ranitidine. *J Physiol Paris* 2001; **95**: 315-324
- 4 **Stancic-Rokotov D**, Slobodnjak Z, Aralica J, Aralica G, Perovic D, Staresinic M, Gjurasin M, Anic T, Zoricic I, Buljat G, Prkacin I, Sikiric P, Seiwerth S, Rucman R, Petek M, Turkovic B, Kocic N, Jagic V, Boban-Blagaic A. Lung lesions and anti-ulcer agents beneficial effect: anti-ulcer agents pentadecapeptide BPC 157, ranitidine, omeprazole and atropine ameliorate lung lesion in rats. *J Physiol Paris* 2001; **95**: 303-308
- 5 **Stancic-Rokotov D**, Sikiric P, Seiwerth S, Slobodnjak Z, Aralica J, Aralica G, Perovic D, Anic T, Zoricic I, Buljat G, Prkacin I, Gjurasin M, Rucman R, Petek M, Turkovic B, Ivasovic Z, Jagic V, Staresinic M, Boban-Blagaic A. Ethanol gastric lesion aggravated by lung injury in rat. Therapy effect of antiulcer agents. *J Physiol Paris* 2001; **95**: 289-293
- 6 **Sikiric P**, Seiwerth S, Aralica G, Perovic D, Staresinic M, Anic T, Gjurasin M, Prkacin I, Separovic J, Stancic-Rokotov D, Lovric-Bencic M, Mikus D, Turkovic B, Rotkvic I, Mise S, Rucman R, Petek M, Ziger T, Sebecic B, Ivasovic Z, Jagic V, Komericki L, Balen I, Boban-Blagaic A, Sjekavica I. Therapy effect of antiulcer agents on new chronic cysteamine colon lesion in rat. *J Physiol Paris* 2001; **95**: 283-288
- 7 **Sikiric P**, Seiwerth S, Grabarevic Z, Balen I, Aralica G, Gjurasin M, Komericki L, Perovic D, Ziger T, Anic T, Prkacin I, Separovic J, Stancic-Rokotov D, Lovric-Bencic M, Mikus D, Staresinic M, Aralica J, DiBiaggio N, Simec Z, Turkovic B, Rotkvic I, Mise S, Rucman R, Petek M, Sebecic B, Ivasovic Z, Boban-Blagaic A, Sjekavica I. Cysteamine-colon and cysteamine-duodenum lesions in rats. Attenuation by gastric pentadecapeptide BPC 157, cimetidine, ranitidine, atropine, omeprazole, sulphasalazine and methylprednisolone. *J Physiol Paris* 2001; **95**: 261-270
- 8 **Mikus D**, Sikiric P, Seiwerth S, Petricevic A, Aralica G, Druzijancic N, Rucman R, Petek M, Pigac B, Perovic D, Kolombo M, Kocic N, Mikus S, Duplancic B, Fattorini I, Turkovic B, Rotkvic I, Mise S, Prkacin I, Konjevoda P, Stambuk N, Anic T. Pentadecapeptide BPC 157 cream improves burn-wound healing and attenuates burn-gastric lesions in mice. *Burns* 2001; **27**: 817-827
- 9 **Prkacin I**, Aralica G, Perovic D, Separovic J, Gjurasin M, Lovric-Bencic M, Stancic-Rokotov D, Ziger T, Anic T, Sikiric P, Seiwerth S, Staresinic M, Mise S, Rotkvic I, Jagic V, Rucman R, Petek M, Turkovic B, Marovic A, Sjekavica I, Sebecic B, Boban-Blagaic A, Ivasovic Z. Chronic cytoprotection: pentadecapeptide BPC 157, ranitidine and propranolol prevent, attenuate and reverse the gastric lesions appearance in chronic alcohol drinking rats. *J Physiol Paris* 2001; **95**: 295-301
- 10 **Bilic I**, Zoricic I, Anic T, Separovic J, Stancic-Rokotov D, Mikus D, Buljat G, Ivankovic D, Aralica G, Prkacin I, Perovic D, Mise S, Rotkvic I, Petek M, Rucman R, Seiwerth S, Sikiric P. Haloperidol-stomach lesions attenuation by pentadecapeptide BPC 157, omeprazole, bromocriptine, but not atropine, lansoprazole, pantoprazole, ranitidine, cimetidine and misoprostol in mice. *Life Sci* 2001; **68**: 1905-1912
- 11 **Sikiric P**, Marovic A, Matoz W, Anic T, Buljat G, Mikus D, Stancic-Rokotov D, Separovic J, Seiwerth S, Grabarevic Z, Rucman R, Petek M, Ziger T, Sebecic B, Zoricic I, Turkovic B, Aralica G, Perovic D, Duplancic B, Lovric-Bencic M, Rotkvic I, Mise S, Jagic V, Hahn V. A behavioural study of the effect of pentadecapeptide BPC 157 in Parkinson's disease models in mice and gastric lesions induced by 1-methyl-4-phenyl-1, 2, 3, 6-tetrahydropyridine. *J Physiol Paris* 1999; **93**: 505-512
- 12 **Petek M**, Sikiric P, Anic T, Buljat G, Separovic J, Stancic-Rokotov D, Seiwerth S, Grabarevic Z, Rucman R, Mikus D,

- Zoricic I, Prkacin I, Sebecic B, Ziger T, Coric V, Turkovic B, Aralica G, Rotkvic I, Mise S, Hahn V. Pentadecapeptide BPC 157 attenuates gastric lesions induced by alloxan in rats and mice. *J Physiol Paris* 1999; **93**: 501-504
- 13 **Sikiric P**, Seiwerth S, Grabarevic Z, Petek M, Rucman R, Turkovic B, Rotkvic I, Jagic V, Duvnjak M, Mise S. The beneficial effect of BPC 157, a 15 amino acid peptide BPC fragment, on gastric and duodenal lesions induced by restraint stress, cysteamine and 96% ethanol in rats. A comparative study with H2 receptor antagonists, dopamine promoters and gut peptides. *Life Sci* 1994; **54**: PL63-68
- 14 **Sikiric P**, Jelovac N, Jelovac-Gjeldum A, Dodig G, Staresinic M, Anic T, Zoricic I, Ferovic D, Aralica G, Buljat G, Prkacin I, Lovric-Bencic M, Separovic J, Seiwerth S, Rucman R, Petek M, Turkovic B, Ziger T. Anxiolytic effect of BPC-157, a gastric pentadecapeptide: shock probe/burying test and light/dark test. *Acta Pharmacol Sin* 2001; **22**: 225-230
- 15 **Sikiric P**, Separovic J, Buljat G, Anic T, Stancic-Rokotov D, Mikus D, Marovic A, Prkacin I, Duplancic B, Zoricic I, Aralica G, Lovric-Bencic M, Ziger T, Perovic D, Rotkvic I, Mise S, Hanzevacki M, Hahn V, Seiwerth S, Turkovic B, Grabarevic Z, Petek M, Rucman R. The antidepressant effect of an antiulcer pentadecapeptide BPC 157 in Porsolt's test and chronic unpredictable stress in rats. A comparison with antidepressants. *J Physiol Paris* 2000; **94**: 99-104
- 16 **Sikiric P**, Separovic J, Anic T, Buljat G, Mikus D, Seiwerth S, Grabarevic Z, Stancic-Rokotov D, Pigac B, Hanzevacki M, Marovic A, Rucman R, Petek M, Zoricic I, Ziger T, Aralica G, Konjevoda P, Prkacin I, Gjurasin M, Miklic P, Artukovic B, Tisljar M, Bratulic M, Mise S, Rotkvic I. The effect of pentadecapeptide BPC 157, H2-blockers, omeprazole and sucralfate on new vessels and new granulation tissue formation. *J Physiol Paris* 1999; **93**: 479-485
- 17 **Sebecic B**, Nikolic V, Sikiric P, Seiwerth S, Sosa T, Patrlj L, Grabarevic Z, Rucman R, Petek M, Konjevoda P, Jadrijevic S, Perovic D, Slaj M. Osteogenic effect of a gastric pentadecapeptide, BPC-157, on the healing of segmental bone defect in rabbits: a comparison with bone marrow and autologous cortical bone implantation. *Bone* 1999; **24**: 195-202
- 18 **Jelovac N**, Sikiric P, Rucman R, Petek M, Marovic A, Perovic D, Seiwerth S, Mise S, Turkovic B, Dodig G, Miklic P, Buljat G, Prkacin I. Pentadecapeptide BPC 157 attenuates disturbances induced by neuroleptics: the effect on catalepsy and gastric ulcers in mice and rats. *Eur J Pharmacol* 1999; **379**: 19-31
- 19 **Sikiric P**, Seiwerth S, Deskovic S, Grabarevic Z, Marovic A, Rucman R, Petek M, Konjevoda P, Jadrijevic S, Sosa T, Perovic D, Aralica G, Turkovic B. New model of cytoprotection/adaptive cytoprotection in rats: endogenous small irritants, antiulcer agents and indomethacin. *Eur J Pharmacol* 1999; **364**: 23-31
- 20 **Sikiric P**, Jelovac N, Jelovac-Gjeldum A, Dodig G, Staresinic M, Anic T, Zoricic I, Rak D, Perovic D, Aralica G, Buljat G, Prkacin I, Lovric-Bencic M, Separovic J, Seiwerth S, Rucman R, Petek M, Turkovic B, Ziger T, Boban-Blagaic A, Bedekovic V, Tonkic A, Babic S. Pentadecapeptide BPC 157 attenuates chronic amphetamine-induced behavior disturbances. *Acta Pharmacol Sin* 2002; **23**: 412-422
- 21 **Sikiric P**, Jadrijevic S, Seiwerth S, Sosa T, Deskovic S, Perovic D, Aralica G, Grabarevic Z, Rucman R, Petek M, Jagic V, Turkovic B, Ziger T, Rotkvic I, Mise S, Zoricic I, Sebecic B, Patrlj L, Kocman B, Sarlija M, Mikus D, Separovic J, Hanzevacki M, Gjurasin M, Miklic P. Long-lasting cytoprotection after pentadecapeptide BPC 157, ranitidine, sucralfate or cholestyramine application in reflux oesophagitis in rats. *J Physiol Paris* 1999; **93**: 467-477
- 22 **Sikiric P**, Separovic J, Buljat G, Anic T, Stancic-Rokotov D, Mikus D, Duplancic B, Marovic A, Zoricic I, Prkacin I, Lovric-Bencic M, Aralica G, Ziger T, Perovic D, Jelovac N, Dodig G, Rotkvic I, Mise S, Seiwerth S, Turkovic B, Grabarevic Z, Petek M, Rucman R. Gastric mucosal lesions induced by complete dopamine system failure in rats. The effects of dopamine agents, ranitidine, atropine, omeprazole and pentadecapeptide BPC 157. *J Physiol Paris* 2000; **94**: 105-110
- 23 **Jelovac N**, Sikiric P, Rucman R, Petek M, Perovic D, Marovic A, Anic T, Seiwerth S, Mise S, Pigac B, Duplancic B, Turkovic B, Dodig G, Prkacin I, Stancic-Rokotov D, Zoricic I, Aralica G, Sebecic B, Ziger T, Slobodnjak Z. The effect of a novel pentadecapeptide BPC 157 on development of tolerance and physical dependence following repeated administration of diazepam. *Chin J Physiol* 1999; **42**: 171-179
- 24 **Milani S**, Calabrò A. Role of growth factors and their receptors in gastric ulcer healing. *Microsc Res Tech* 2001; **53**: 360-371
- 25 **Ernst H**, Konturek PC, Hahn EG, Stosiek HP, Brzozowski T, Konturek SJ. Effect of local injection with basic fibroblast growth factor (bFGF) and neutralizing antibody to bFGF on gastric ulcer healing, gastric secretion, angiogenesis and gastric blood flow. *J Physiol Pharmacol* 2001; **52**: 377-390
- 26 **Szabo S**, Vincze A. Growth factors in ulcer healing: lessons from recent studies. *J Physiol Paris* 2000; **94**: 77-81
- 27 **He JH**, Luo HS. Expression of basic fibroblast growth factor (bFGF) in healing human gastric ulcer. *Shijie Huaren Xiaohua Zazhi* 2003; **11**: 61-64
- 28 **Jones MK**, Kawanaka H, Baatar D, Szabo IL, Tsugawa K, Pai R, Koh GY, Kim I, Sarfeh II, Tarnawski AS. Gene therapy for gastric ulcers with single local injection of naked DNA encoding VEGF and angiopoietin-1. *Gastroenterology* 2001; **121**: 1040-1047
- 29 **Sun FP**, Song YG, Cheng W, Zhao T, Yao YL. Gastrin, somatostatin, G and D cells of gastric ulcer in rats. *World J Gastroenterol* 2002; **8**: 375-378
- 30 **Shen XZ**. Effect of heme oxygenase inducer hemin on acetic acid-induced gastric ulcer formation in rats. *Shijie Huaren Xiaohua Zazhi* 2000; **8**: 1109-1112
- 31 **Wang GZ**, Ru X, Ding LH, Li HQ. Short term effect of *Salvia miltiorrhiza* in treating rat acetic acid chronic gastric ulcer and long term effect in preventing recurrence. *World J Gastroenterol* 1998; **4**: 169-170

Edited by Wang XL and Xu FM Proofread by Zhu LH

Ginkgo biloba extract reverses CCl₄-induced liver fibrosis in rats

Yan-Jun Luo, Jie-Ping Yu, Zhao-Hong Shi, Li Wang

Yan-Jun Luo, Jie-Ping Yu, Department of Gastroenterology, Hubei Renmin Hospital, Wuhan University, Wuhan 430060, Hubei Province, China

Zhao-Hong Shi, Department of Gastroenterology, Wuhan First Hospital, Wuhan 430036, Hubei Province, China

Li Wang, Department of Geriatrics, Wuhan General Hospital, Guangzhou Command of PLA, Wuhan 430070, Hubei Province, China

Correspondence to: Yan-Jun Luo, Department of Gastroenterology, Hubei Renmin Hospital, Wuhan University, Wuhan 430060, Hubei Province, China. lyj0019@sohu.com

Telephone: +86-27-88058274

Received: 2003-08-23 **Accepted:** 2003-10-22

Abstract

AIM: To study the reversing effect of Ginkgo biloba extract (GbE) on established liver fibrosis in rats.

METHODS: Following confirmation of CCl₄-induced liver fibrosis, GbE or saline was administered to the rats for 4 weeks. The remaining rats received neither CCl₄ nor GbE as normal control. The four groups were compared in terms of serum enzymes, tissue damage, expression of α SMA and tissue inhibitor-1 of metalloproteinase (TIMP-1) and metalloproteinase-1 (MMP-1).

RESULTS: Compared with saline-treated group, liver fibrosis rats treated with GbE had decreased serum total bilirubin ($P < 0.01$) and aminotransferase levels ($P < 0.01$) and increased levels of serum albumin ($P < 0.01$). Microscopic studies revealed that the livers of rats receiving GbE showed alleviation in fibrosis ($P < 0.05$) as well as expression of α SMA ($P < 0.01$). The liver collagen and reticulum contents were lower in rats treated with GbE than saline-treated group ($P < 0.01$). RT-PCR revealed that the level of TIMP-1 decreased while the level of MMP-1 increased in GbE group.

CONCLUSION: Administration of GbE improved CCl₄-induced liver fibrosis. It is possibly attributed to its effect of inhibiting the expression of TIMP-1 and promoting the apoptosis of hepatic stellate cells.

Luo YJ, Yu JP, Shi ZH, Wang L. Ginkgo biloba extract reverses CCl₄-induced liver fibrosis in rats. *World J Gastroenterol* 2004; 10(7): 1037-1042

<http://www.wjgnet.com/1007-9327/10/1037.asp>

INTRODUCTION

Hepatic fibrosis represents the response of the liver to diverse chronic insults such as parasitic disease, chronic viral infection (hepatitis B and C), immunologic attack (autoimmune hepatitis), hereditary metal overload, toxic damage, etc. Because of the worldwide prevalence of these insults, liver fibrosis is common and is associated with significant morbidity and mortality^[1-3]. Ginkgo biloba extract (GbE) is an extract from green leaves of the Ginkgo biloba tree. GbE has been shown to have an SOD-like activity and a hydroxyl radical scavenging activity^[4-10]. We have demonstrated that GbE concomitant administration to rats subjected to CCl₄-induced liver fibrosis resulted in a reliable

hepatoprotection against liver damage, as well as a curtailing process in the progression to liver fibrosis^[11]. Therefore, the aim of this study was to further evaluate the beneficial action of GbE in reversing a well-established liver fibrosis after 8 wk of administration.

MATERIALS AND METHODS

Animals and treatment

Twenty-four 2-month-old male inbred Wistar rats were purchased from the Experimental Animal Center of Wuhan University of Medical Science. Six normal rats were treated with neither CCl₄ nor GbE (group N). GbE was provided by Wuhan Wushi Pharmaceutical Company, China. (No 21003). GbE contains two groups of major components: flavonoid (>24%) and terpenoids (>6%). The GbE and double-distilled water were mixed to 0.1 mg/mL suspension and subjected to full vibration. Carbon tetrachloride (CCl₄) and liquid paraffin were purchased from Sigma Corporation, USA. CCl₄ was injected intraperitoneally at 0.15 mL per rat (diluted 1:1 in liquid paraffin) twice weekly for 8 wk to produce liver fibrosis. After completing the CCl₄ treatment, 3 d after withdrawal of the hepatotoxin, six rats were anaesthetized with ether (group C). One blood sample was taken and the plasma stored until analysis. After this, the animals were exsanguinated and the liver was quickly washed *in situ* with ice-cold isotonic saline, removed, weighed, and divided into two portions, one for histological study (immunohistochemical staining, HE, Gorden-Sweet and Masson staining), the other was immediately frozen in liquid nitrogen. Following establishment of CCl₄-induced liver fibrosis, GbE (200 mg/kg per day given orally daily with gavage) or saline was administered for 4 wk (group E and group Z, respectively). Three days after the last GbE administration, animals (groups N, E and Z) were anaesthetized with ether and kept at a constant temperature of 37.0±0.5°C. One blood sample was taken, centrifuged (3 000 rpm for 10 min), and the plasma stored until analysis. After this, the animals were exsanguinated and the liver was quickly washed *in situ* with ice-cold isotonic saline, removed, weighed, and divided into two portions, one was for histological study, the other immediately frozen in liquid nitrogen. Serum levels of TBIL, albumin and the activities of ALT and AST were determined by routine laboratory methods.

Animals were kept on standard rat chow with free access to tap water and received humane care in accordance with the animal care provisions, maintained in temperature- and humidity-controlled animal quarters under a 12 h light-dark cycle. The rats were weighed daily.

Histopathological examination

Liver tissue sections were fixed in 4 g/L formaldehyde saline and processed in paraffin wax. Sections from blocks were stained with hematoxylin-eosin (HE), reticulum (Gordon-Sweet staining) and Masson's Trichrome. Qualitative and quantitative histological analyses were performed blindly under a light microscope and computer image analysis system. The image intensity level was kept the same throughout the study. To quantify hepatic fibrosis, we used the Knodell index, scoring as the following: 0, absence of fibrosis; 1, portal fibrosis; 2, fibrous portal expansion; 3, bridging fibrosis (portal-portal or portal-central linkage); 4, cirrhosis. For each sample the

collagenous deposits at centrilobular field of the hepatic acinus, and at surrounding terminal hepatic veins were observed at 100× magnification. In order to avoid possible bias due to the sampling of the individual fields, for every specimen, we analyzed at least 5 fields each containing a centrilobular vein. The microscopic examinations were performed in a blind fashion. Actin, smooth muscle Ab-1 was from NeoMarkers and immunohistochemical streptavidin/peroxidase (SP) kit from Zhongshan Corporation. Immunohistochemistry of α SMA was performed using an indirect SP technique. At least 5 fields each containing a centrilobular vein were observed and the areas of positive hepatocytes were quantitated at 400×.

RT-PCR

Total RNA was extracted using Trizol (Biostar Biologic Technology Co. Ltd. USA.) according to the manufacturer's directions. Then total RNA was reverse transcribed into cDNA. PCR was performed using the following primer pairs: β -actin: sense 5' -ATC ATG TTT GAG ACC TTC AAC ACC-3', antisense 5' -CAT GGT GGT GCC GCC AGA CAG-3'; TIMP-1^[12]: sense 5' -ACA GCT TTC TGC AAC TCG-3', antisense 5' -CTA TAG GTC TTT ACG AAG GCC-3'. MMP-1^[12]: sense 5' -AGC TTG GCC ACT CGC TCG GTC TG-3', antisense 5' -GTC TCG GGA TGC ATG CTC GTA TGC-3'. The amplified products were electrophoresed on a 12 g/L agarose gel containing 0.5 μ g/mL ethidium bromide, and visualised under UV light.

RESULTS

Body, liver and spleen weight

Irritability, aggression, and weight loss were present predominantly in group C rats. Liver and body weight (LW and BW) of rats are presented in Table 1. No changes in body weight were observed in the rats of group Z and group E regardless of the treatment. Animals in group C showed an

evident hepato- and splenomegaly. GbE (group E) blocked the hepatosplenomegaly more significantly than saline (group Z).

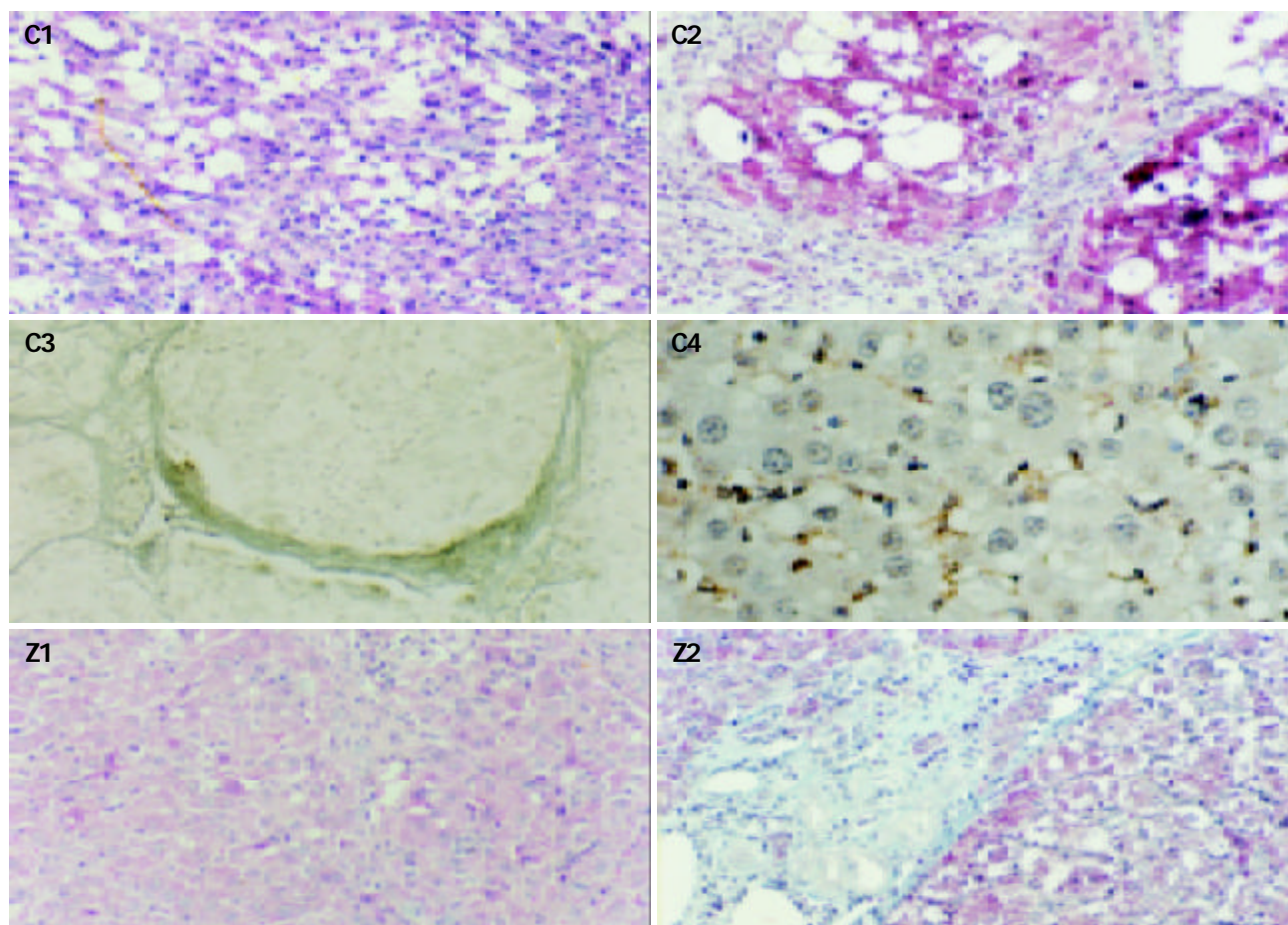
Table 1 Rat liver weight (LW), body weight (BW) and spleen weight (SW)

	BW (g)	LW (g)	LW/BW(%)	SW(g)	SW/BW (%)
C	297.0±39.6 ^d	14.6±3.0	4.9±0.7 ^c	1.5±0.2	0.5±0.06 ^d
E	343.3±25.7 ^b	9.6±4.2 ^{bc}	2.8±0.4 ^{bc}	1.0±0.1 ^{bd}	0.3±0.03 ^{bd}
Z	351.1±21.6 ^b	13.2±3.3	3.7±0.4 ^a	1.4±0.1	0.4±0.04 ^b
N	358.3±72.2 ^a	11.4±0.5 ^{ac}	3.2±0.1 ^{ad}	0.7±0.1 ^{bd}	0.2±0.02 ^{bd}

^a $P < 0.05$, ^b $P < 0.01$ vs C group; ^c $P < 0.05$, ^d $P < 0.01$ vs Z group.

Histopathology

The morphology of the rat livers was assessed by light microscopy and is presented in Table 2 and Figure 1. α SMA positive staining of immunohistochemistry was localized in the cytoplasm and membrane. Chronic administration of CCl₄ for 8 weeks induced liver fibrosis. The liver exhibited a marked increase in ECM content and displayed bundles of collagen surrounding the lobules, which resulted in large fibrous septa and distorted tissue architecture. These septa were populated by α SMA-positive cells. The liver damage varied from one area to another, and ranged from moderate fibrosis to cirrhosis. The degree of liver fibrosis was classified according to five stages in the development of fibrosis and the difference between group Z and E, group E and C was statistically significant (group Z vs group E, $q = 6.00$, $P < 0.01$; group E vs group C, $q = 9.46$, $P < 0.01$; group Z vs group N, $q = 6.74$, $P < 0.01$; group N vs group C, $q = 50.19$, $P < 0.01$; but group Z vs group C, $q = 2.29$, $P > 0.05$). In group Z, liver collagenous and reticulum proteins as well as expression of α SMA decreased. Microscopic studies revealed that the livers of rats receiving GbE showed decreases in fibrosis and the expression of α SMA was only surrounding blood vessels.



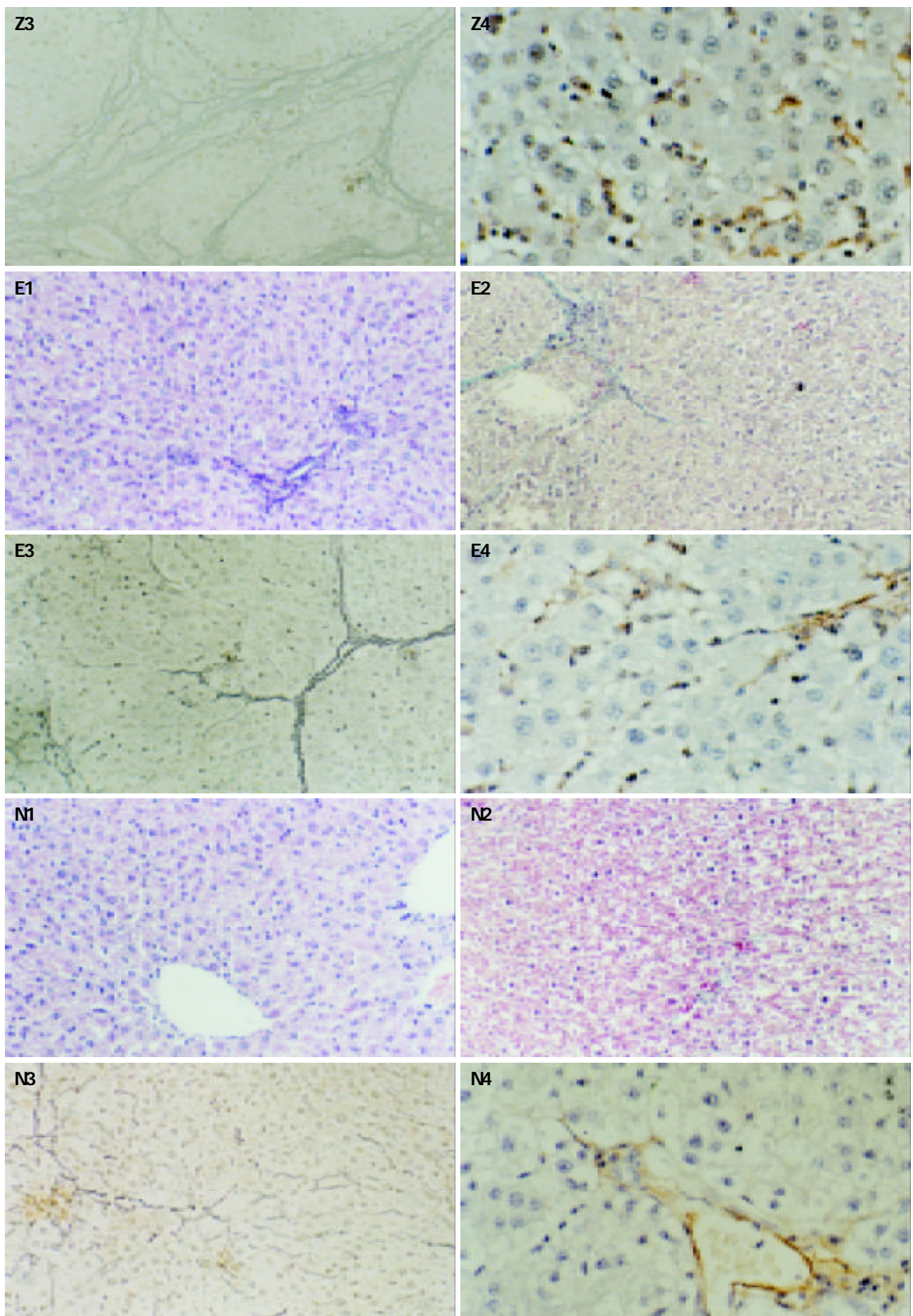


Figure 1 Histology of liver of normal rats (N) and rats treated with CCl_4 for 8 weeks (C) and then treated with saline (Z) or GbE (E) for 4 weeks. The samples were stained with HE (1), Masson (2), Reticulum staining (3) and immunohistochemistry of αSMA (4). (1)-(3) 100 \times , (4) 200 \times .

Table 2 Rat liver histopathology

	Liver fibrosis					Collagen (%)	Reticulum (%)	α SMA(+) (%)
	0	I	II	III	IV			
C	0	0	0	3	3	11.4 \pm 1.2 ^d	12.4 \pm 0.9 ^d	4.8 \pm 2.1 ^c
E	5	1	0	0	0	4.6 \pm 0.9 ^{bd}	4.0 \pm 1.1 ^{bd}	2.6 \pm 0.4 ^{bc}
Z	0	1	3	2	0	9.1 \pm 1.0 ^b	10.4 \pm 0.9 ^b	3.5 \pm 1.6 ^a
N	6	0	0	0	0	0.1 \pm 0.1 ^{bd}	1.0 \pm 0.3 ^{bd}	1.0 \pm 0.1 ^{bd}

^a P <0.05, ^b P <0.01 vs group C; ^c P <0.05, ^d P <0.01 vs group Z.

Liver function

Table 3 shows the serum parameters in the four groups of rats. Serum ALT, AST and TBIL concentrations in group C were all 1.3-fold more than that in group Z, and there was a more significant decrease in GbE group. GbE produced improvement both in markers of hepatocellular damage (AST and ALT) and in parameters that indicate synthetic activity (albumin). All the differences were statistically significant compared with group Z.

Table 3 Liver function parameters

	ALT (U/L)	AST (U/L)	Albumin (g/L)	TBIL (mg/L)
C	188.8 \pm 52.8	267.8 \pm 45.4 ^c	22.2 \pm 1.7 ^d	9.3 \pm 1.1 ^d
E	80.8 \pm 15.2 ^{bd}	108.1 \pm 23.4 ^{bd}	35.8 \pm 3.2 ^{bd}	5.6 \pm 0.9 ^{bd}
Z	143.1 \pm 35.0	211.6 \pm 53.1 ^a	28.7 \pm 1.9 ^b	7.0 \pm 0.8 ^b
N	43.4 \pm 7.7 ^{bd}	101.3 \pm 22.2 ^{bd}	36.3 \pm 1.3 ^{bd}	5.3 \pm 0.8 ^{bd}

^a P <0.05, ^b P <0.01 vs group C; ^c P <0.05, ^d P <0.01 vs group Z.

Expression of TIMP-1 and MMP-1

Remarkable TIMP-1 mRNA expression was observed in group C and TIMP-1 mRNA expression decreased in group Z. In groups E and N, RT-PCR analysis revealed very slight TIMP-1 mRNA expression (Figure 2). In groups C, Z and N, the expressions of MMP-1 were all slight while the expression in group E was remarkable.

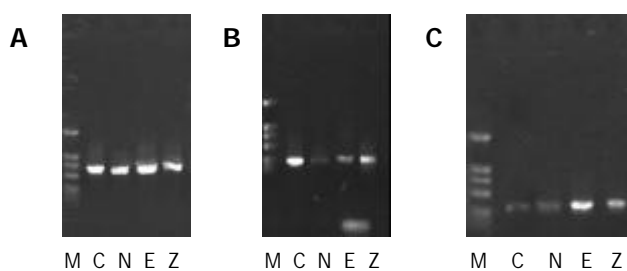


Figure 2 RT-PCR. M, 2 000 bp DNA marker, A. β -actin (556 bp), B. TIMP-1 (218 bp), C. MMP-1 (365 bp).

DISCUSSION

Incidence of liver fibrosis is growing as a result of the widespread occurrence of chronic hepatitis (predominantly type C). Cameron and Krunaratne first reported the reversibility of hepatic fibrosis after removal of the toxic agent CCl_4 in the CCl_4 -induced liver fibrosis model. Since then, fibrolysis after the removal of the causative agents has been observed in experimental models of fibrosis of various types^[13-20]. The reversibility of hepatic fibrosis has also been observed in alcoholic liver disease by clinicians. In this study, 4 wk after CCl_4 withdrawal, significant decreases in liver and spleen size as well as liver fibrosis state were recorded in the liver fibrosis rats treated with saline. But liver fibrosis is a complex process, and current therapies targeting at arresting or reversing liver fibrosis are largely ineffective and some has unacceptable

side effects in long-term therapy^[21-29]. For example, glucocorticosteroids, which have been shown to inhibit collagen synthesis in culture and in animal models, rarely suppressed fibrogenesis or prevented progression to liver fibrosis^[30]. In addition, long-term administration of glucocorticoids may cause serious adverse side effects, which that prevent their use as a general treatment of liver fibrosis. D-penicillamine, which blocks intra- and interchain crosslinking in the newly formed collagen molecules, was found to be ineffective on preventing the progression of hepatic fibrosis and was associated with a high incidence of serious side effects. Medicinally useful plants have made a significant contribution to current medical practice and traditional Chinese herbs are well known for their cheap prices and negligible side effects^[31-41]. GbE is a well-known and inexpensive herb that has been used to improve blood circulation without ill effects for centuries in traditional Chinese medicine. GbE contains two groups of major components: flavonoid glycosides and terpenoids. Furthermore, it has been recently reported that GbE has the property of inactivating oxo-ferryl radical species, which are more efficient oxidative agents than classical hydroxyl radicals^[3-8]. Li *et al.*^[41] demonstrated that procollagen II peptide, laminin, SOD and MDA were significantly decreased after GbE treatment in patients with chronic hepatitis B. In our previous study, the biochemical and histological protocol demonstrated that GbE^[12], administered at a safe dosage with minimal side effects, effectively prevented both the biochemical and histological changes associated with liver fibrosis in CCl_4 -injured rats.

The CCl_4 -treated rat is frequently used as an experimental model to study hepatic fibrosis. CCl_4 treatment generates free radicals that trigger a cascade of events resulting in hepatic fibrosis. In this study, when treated with CCl_4 twice weekly for 8 wk, the liver exhibited a marked increase in ECM content and displayed bundles of collagen surrounding the lobules leading to large fibrous septa and distorted tissue architecture. These septa were populated by α SMA-positive cells. All of these are characteristics of advanced fibrosis. In liver fibrosis rats, there was also evident liver dysfunction, as reflected by significantly decreased serum albumin and increased bilirubin contents. In addition, serum levels of ALT and AST were elevated.

When these animals received GbE, hepatomegaly was absent. A primary consideration in the assessment of the efficacy of a potential therapeutic agent for hepatic fibrosis is its effect on liver histology. Those livers from disease control (group C) had a high degree of fibrosis. Group Z had some improvement in histological scores compared to group C. GbE administration to liver fibrosis rats apparently accelerated the reversion of liver fibrosis and lowered the high levels of serum ALT and AST activity, indicating that GbE was also effective on reversing liver cirrhosis.

Hepatic fibrosis, regardless of the cause, is characterized by an increase in extracellular matrix (ECM) constituents. There is now overwhelming evidence suggesting that the hepatic stellate cells (HSC), lying in the space of Disse beneath the endothelial cell layer, are the principal cells involved in hepatic fibrogenesis. Thus, to prevent or reverse liver fibrosis depends greatly on controlling of HSC^[42-46]. These cells are usually quiescent, with a low proliferation rate. On activation, probably because of hepatocyte injury, they differentiate into myofibroblast-like cells, with a high proliferative capacity. It has been shown that activated HSCs constitute the source of various collagenases that are necessary for the ECM remodeling. In group C, large fibrous septa were populated by α SMA-positive cells. GbE given orally promoted the apoptosis of most of the HSC and only traces of α SMA-positive cells were detected. It suggests that GbE could enhance the apoptosis of HSC.

Matrix degradation occurs predominantly as a consequence of the action of a family of enzymes called matrix metalloproteinases (MMPs), and the expression of these enzymes are in turn inhibited by a family of TIMPs^[47-53]. To explore the way in which this herb results in a significant reduction in fibrosis, we investigated the effect of GbE treatment on the expression of genes known to have a role in hepatic fibrosis such as TIMP-1 and MMP-1 by reverse transcription-polymerase chain reaction (RT-PCR). In group Z, there was a rapid and significant decrease in the expression level of TIMP-1. We also systematically evaluated the mechanism of action of GbE at the molecular level by analyzing TIMP-1 transcript expression. GbE treatment was associated with an increased collagenolytic activity and a prompt normalization of liver levels of TIMP-1 and also caused a more marked reduction in the expression level of TIMP-1 transcript than group Z while increased the level of MMP-1. A lower expression of TIMP-1 indicated decreased hepatic fibrogenesis and might be an effect correlated with enhanced apoptosis in activated myofibroblast-like stellate cells. The expression levels of TIMP-1 in groups Z and E were lower than that in group C.

In summary, our results indicate that treatment with GbE after the establishment of CCl₄-induced hepatic fibrosis significantly reduces and even reverses the fibrosis in rats. This effect is related to an increased removal of deposited collagen, enhanced collagenolytic activity due to decreased TIMP-1 levels and enhanced apoptosis of HSC.

REFERENCES

- Shen L, Fan JG, Shao Y, Zeng MD, Wang JR, Luo GH, Li JQ, Chen SY. Prevalence of nonalcoholic fatty liver among administrative officers in Shanghai: an epidemiological survey. *World J Gastroenterol* 2003; **9**: 1106-1110
- Han DW. Intestinal endotoxemia as a pathogenetic mechanism in liver failure. *World J Gastroenterol* 2002; **8**: 961-965
- Chen WX, Li YM, Yu CH, Cai WM, Zheng M, Chen F. Quantitative analysis of transforming growth factor beta 1 mRNA in patients with alcoholic liver disease. *World J Gastroenterol* 2002; **8**: 379-381
- Wu Z, Smith JV, Paramasivam V, Butko P, Khan I, Cypser JR, Luo Y. Ginkgo biloba extract EGb 761 increases stress resistance and extends life span of *Caenorhabditis elegans*. *Cell Mol Biol* 2002; **48**: 725-731
- Gohil K, Packer L. Global gene expression analysis identifies cell and tissue specific actions of Ginkgo biloba extract, EGb 761. *Cell Mol Biol* 2002; **48**: 625-631
- Tang Y, Lou F, Wang J, Li Y, Zhuang S. Coumaroyl flavonol glycosides from the leaves of Ginkgo biloba. *Phytochemistry* 2001; **58**: 1251-1256
- Mazzanti G, Mascellino MT, Battinelli L, Coluccia D, Manganaro M, Saso L. Antimicrobial investigation of semipurified fractions of Ginkgo biloba leaves. *J Ethnopharmacol* 2000; **71**: 83-88
- Schindowski K, Leutner S, Kressmann S, Eckert A, Muller WE. Age-related increase of oxidative stress-induced apoptosis in mice prevention by Ginkgo biloba extract (EGb761). *J Neural Transm* 2001; **108**: 969-978
- McKenna DJ, Jones K, Hughes K. Efficacy, safety, and use of ginkgo biloba in clinical and preclinical applications. *Altern Ther Health Med* 2001; **7**: 70-86
- Diamond BJ, Shiflett SC, Feiwei N, Matheis RJ, Noskin O, Richards JA, Schoenberger NE. Ginkgo biloba extract: mechanisms and clinical indications. *Arch Phys Med Rehabil* 2000; **81**: 668-678
- Liu SQ, Yu JP, Ran ZX. Effect of Tanakan on liver fibrosis in rats. *Shiyong Yixue Zazhi* 2001; **18**: 574-576
- Phillips PA, McCarroll JA, Park S, Wu MJ, Pirola R, Korsten M, Wilson JS, Apte MV. Rat pancreatic stellate cells secrete matrix metalloproteinases: implications for extracellular matrix turnover. *Gut* 2003; **52**: 275-282
- Weng HL, Cai WM, Liu RH. Animal experiment and clinical study of effect of gamma-interferon on hepatic fibrosis. *World J Gastroenterol* 2001; **7**: 42-48
- Iredale JP, Benyon RC, Pickering J, McCullen M, Northrop M, Pawley S, Hovell C, Arthur MJ. Mechanisms of spontaneous resolution of rat liver fibrosis. Hepatic stellate cell apoptosis and reduced hepatic expression of metalloproteinase inhibitors. *J Clin Invest* 1998; **102**: 538-549
- Bruck R, Genina O, Aeed H, Alexiev R, Nagler A, Avni Y, Pines M. Halofuginone to prevent and treat thioacetamide-induced liver fibrosis in rats. *Hepatology* 2001; **33**: 379-386
- Wei HS, Li DG, Lu HM, Zhan YT, Wang ZR, Huang X, Zhang J, Cheng JL, Xu QF. Effects of AT1 receptor antagonist, losartan, on rat hepatic fibrosis induced by CCl₄. *World J Gastroenterol* 2000; **6**: 540-545
- Wang XZ, Chen ZX, Zhang LJ, Chen YX, Li D, Chen FL, Huang YH. Expression of insulin-like growth factor 1 and insulin-like growth factor 1 receptor and its intervention by interleukin-10 in experimental hepatic fibrosis. *World J Gastroenterol* 2003; **9**: 1287-1291
- Lin JS, Song YH, Kong XJ, Li B, Liu NZ, Wu XL, Jin YX. Preparation and identification of anti-transforming growth factor beta1 U1 small nuclear RNA chimeric ribozyme *in vitro*. *World J Gastroenterol* 2003; **9**: 572-577
- Han HL, Lang ZW. Changes in serum and histology of patients with chronic hepatitis B after interferon alpha-2b treatment. *World J Gastroenterol* 2003; **9**: 117-121
- Liu XJ, Yang L, Mao YQ, Wang Q, Huang MH, Wang YP, Wu HB. Effects of the tyrosine protein kinase inhibitor genistein on the proliferation, activation of cultured rat hepatic stellate cells. *World J Gastroenterol* 2002; **8**: 739-745
- Cheng ML, Wu YY, Huang KF, Luo TY, Ding YS, Lu YY, Liu RC, Wu J. Clinical study on the treatment of liver fibrosis due to hepatitis B by IFN-alpha(1) and traditional medicine preparation. *World J Gastroenterol* 1999; **5**: 267-269
- Xiong LJ, Zhu JF, Luo DD, Zen LL, Cai SQ. Effects of pentoxifylline on the hepatic content of TGF-beta1 and collagen in Schistosomiasis japonica mice with liver fibrosis. *World J Gastroenterol* 2003; **9**: 152-154
- Liu Y, Shimizu I, Omoya T, Ito S, Gu XS, Zuo J. Protective effect of estradiol on hepatocytic oxidative damage. *World J Gastroenterol* 2002; **8**: 363-366
- Xu JW, Gong J, Chang XM, Luo JY, Dong L, Hao ZM, Jia A, Xu GP. Estrogen reduces CCl₄-induced liver fibrosis in rats. *World J Gastroenterol* 2002; **8**: 883-887
- Ozars R, Tahan V, Aydin S, Uzun H, Kaya S, Senturk H. N-acetylcysteine attenuates alcohol-induced oxidative stress in rats. *World J Gastroenterol* 2003; **9**: 791-794
- Wang XZ, Zhang LJ, Li D, Huang YH, Chen ZX, Li B. Effects of transmitters and interleukin-10 on rat hepatic fibrosis induced by CCl₄. *World J Gastroenterol* 2003; **9**: 539-543
- Yao HW, Li J, Jin Y, Zhang YF, Li CY, Xu SY. Effect of leflunomide on immunological liver injury in mice. *World J Gastroenterol* 2003; **9**: 320-323
- Wang JY, Zhang QS, Guo JS, Hu MY. Effects of glycyrrhetic acid on collagen metabolism of hepatic stellate cells at different stages of liver fibrosis in rats. *World J Gastroenterol* 2001; **7**: 115-119
- Dai WJ, Jiang HC. Advances in gene therapy of liver cirrhosis: a review. *World J Gastroenterol* 2001; **7**: 1-8
- He rmandez-Munoz R, Diaz-Munoz M, Suarez-Cuenca JA, Trejo-Solis C, Lopez V, Sanchez-Sevilla L, Yanez L, De Sanchez VC. Adenosine reverses a preestablished CCl₄-induced micronodular cirrhosis through enhancing collagenolytic activity and stimulating hepatocyte cell proliferation in rats. *Hepatology* 2001; **34**: 677-687
- Shi J, Hao JH, Ren WH, Zhu JR. Effects of heparin on liver fibrosis in patients with chronic hepatitis B. *World J Gastroenterol* 2003; **9**: 1611-1614
- Gao ZL, Gu XH, Cheng FT, Jiang FH. Effect of Sea buckthorn on liver fibrosis: A clinical study. *World J Gastroenterol* 2003; **9**: 1615-1617
- Wu XL, Zeng WZ, Wang PL, Lei CT, Jiang MD, Chen XB, Zhang Y, Xu H, Wang Z. Effect of compound rhodiola sachalinensis A Bor on CCl₄-induced liver fibrosis in rats and

- its probable molecular mechanisms. *World J Gastroenterol* 2003; **9**: 1559-1562
- 34 **Liu YK**, Shen W. Inhibitive effect of cordyceps sinensis on experimental hepatic fibrosis and its possible mechanism. *World J Gastroenterol* 2003; **9**: 529-533
- 35 **Yao L**, Yao ZM, Yu T. Influence of BOL on hyaluronic acid, laminin and hyperplasia in hepatofibrotic rats. *World J Gastroenterol* 2001; **7**: 872-875
- 36 **Yao XX**, Tang YW, Yao DM, Xiu HM. Effects of Yigan Decoction on proliferation and apoptosis of hepatic stellate cells. *World J Gastroenterol* 2002; **8**: 511-514
- 37 **Liu P**, Hu YY, Liu C, Zhu DY, Xue HM, Xu ZQ, Xu LM, Liu CH, Gu HT, Zhang ZQ. Clinical observation of salvianolic acid B in treatment of liver fibrosis in chronic hepatitis B. *World J Gastroenterol* 2002; **8**: 679-685
- 38 **Tang WX**, Dan ZL, Yan HM, Wu CH, Zhang G, Liu M, Li Q, Li SB. Experimental study of effect of Ganyanping on fibrosis in rat livers. *World J Gastroenterol* 2003; **9**: 1292-1295
- 39 **Wu J**, Cheng ML, Zhang GH, Zhai RW, Huang NH, Li CX, Luo TY, Lu S, Yu ZQ, Yao YM, Zhang YY, Ren LZ, Ye L, Li L, Zhang HN. Epidemiological and histopathological study of relevance of Guizhou Maotai liquor and liver diseases. *World J Gastroenterol* 2002; **8**: 571-574
- 40 **Cheng ML**, Wu J, Wang HQ, Xue LM, Tan YZ, Ping L, Li CX, Huang NH, Yao YM, Ren LZ, Ye L, Li L, Jia ML. Effect of Maotai liquor in inducing metallothioneins and on hepatic stellate cells. *World J Gastroenterol* 2002; **8**: 520-523
- 41 **Li JC**, Ding SP, Xu J. Regulating effect of Chinese herbal medicine on the peritoneal lymphatic stomata in enhancing ascites absorption of experimental hepatofibrotic mice. *World J Gastroenterol* 2002; **8**: 333-337
- 42 **Liu CH**, Hu YY, Wang XL, Liu P, Xu LM. Effects of salvianolic acid-A on NIH/3T3 fibroblast proliferation, collagen synthesis and gene expression. *World J Gastroenterol* 2000; **6**: 361-364
- 43 **Du WD**, Zhang YE, Zhai WR, Zhou XM. Dynamic changes of type I, III and IV collagen synthesis and distribution of collagen-producing cells in carbon tetrachloride-induced rat liver fibrosis. *World J Gastroenterol* 1999; **5**: 397-403
- 44 **Zhang XL**, Liu L, Jiang HQ. Salvia miltiorrhiza monomer IH764-3 induces hepatic stellate cell apoptosis via caspase-3 activation. *World J Gastroenterol* 2002; **8**: 515-519
- 45 **Wei HS**, Lu HM, Li DG, Zhan YT, Wang ZR, Huang X, Cheng JL, Xu QF. The regulatory role of AT 1 receptor on activated HSCs in hepatic fibrogenesis: effects of RAS inhibitors on hepatic fibrosis induced by CCl(4). *World J Gastroenterol* 2000; **6**: 824-828
- 46 **Ikeda K**, Wakahara T, Wang YQ, Kadoya H, Kawada N, Kaneda K. *In vitro* migratory potential of rat quiescent hepatic stellate cells and its augmentation by cell activation. *Hepatology* 1999; **29**: 1760-1767
- 47 **Liu WB**, Yang CQ, Jiang W, Wang YQ, Guo JS, He BM, Wang JY. Inhibition on the production of collagen type I, III of activated hepatic stellate cells by antisense TIMP-1 recombinant plasmid. *World J Gastroenterol* 2003; **9**: 316-319
- 48 **Okazaki I**, Watanabe T, Hozawa S, Arai M, Maruyama K. Molecular mechanism of the reversibility of hepatic fibrosis: with special reference to the role of matrix metalloproteinases. *J Gastroenterol Hepatol* 2000; **15**(Suppl): D26-D32
- 49 **Wang JY**, Guo JS, Yang CQ. Expression of exogenous rat collagenase *in vitro* and in a rat model of liver fibrosis. *World J Gastroenterol* 2002; **8**: 901-907
- 50 **Wang LT**, Zhang B, Chen JJ. Effect of anti-fibrosis compound on collagen expression of hepatic cells in experimental liver fibrosis of rats. *World J Gastroenterol* 2000; **6**: 877-880
- 51 **Nie QH**, Cheng YQ, Xie YM, Zhou YX, Bai XG, Cao YZ. Methodologic research on TIMP-1, TIMP-2 detection as a new diagnostic index for hepatic fibrosis and its significance. *World J Gastroenterol* 2002; **8**: 282-287
- 52 **Nie QH**, Cheng YQ, Xie YM, Zhou YX, Cao YZ. Inhibiting effect of antisense oligonucleotides phosphorothioate on gene expression of TIMP-1 in rat liver fibrosis. *World J Gastroenterol* 2001; **7**: 363-369
- 53 **Liu HL**, Li XH, Wang DY, Yang SP. Matrix metalloproteinase-2 and tissue inhibitor of metalloproteinase-1 expression in fibrotic rat liver. *World J Gastroenterol* 2000; **6**: 881-884

Edited by Zhu LH Proofread by Xu FM

Antineoplastic effects of octreotide on human gallbladder cancer cells *in vitro*

Jing-Hua Wang, Quan-Tai Xing, Meng-Biao Yuan

Jing-Hua Wang, ICU of Beijing Hospital, Beijing 100730, China
Quan-Tai Xing, Meng-Biao Yuan, Department of Gastroenterology, Qilu Hospital of Shandong University, Jinan 250012, Shandong Province, China

Correspondence to: Dr. Jing-Hua Wang, ICU of Beijing Hospital, Beijing 100730, China. wjh6333@sina.com

Telephone: +86-10-65132266-6412

Received: 2003-10-31 **Accepted:** 2003-12-08

Abstract

AIM: To investigate whether octreotide can inhibit the growth of human gallbladder cancer cells *in vitro* and to elucidate the antineoplastic mechanism of octreotide in gallbladder cancer.

METHODS: A human gallbladder cancer cell line, GBC-SD, was cultured *in vitro*. The antiproliferative effects of octreotide were examined by means of an MTT assay and a colony forming ability assay. Morphological variation was investigated under scanning electron microscopy and transmission electron microscopy. Cell cycle analysis and apoptosis rate was evaluated by flow cytometry (FCM) after staining by propidium iodide. DNA fragmentation was assayed by agarose gel electrophoresis. Immunohistochemical staining was performed to evaluate the expressions of mutant-type *p53* and *bcl-2*.

RESULTS: The growth curve and colony forming ability assay showed significant inhibition of octreotide to the proliferation of GBC-SD cells in culture in a time- and dose-dependent manner. After exposure to octreotide, GBC-SD cells showed typically apoptotic characteristics, including morphological changes of chromatin condensation, vacuolar degeneration, nucleus fragmentation and apoptotic body formation. In FCM profile apoptotic cells showed increased sub-G₁ peaks in the octreotide group, significantly higher than the control group ($P=0.013$). There was also an augmentation in the cell proportion of G₀/G₁ phase ($P=0.015$), while the proportion of S phase and G₂/M phase remained unchanged ($P=0.057$ and $P=0.280$, respectively). DNA agarose gel electrophoresis displayed a ladder after exposure to 1 000 nmol/L octreotide. After being treated with octreotide, the expressions of both mutant-type *p53* and *bcl-2* decreased considering the percentage of positive cells ($P<0.05$).

CONCLUSION: Octreotide has a negative action to the proliferation of GBC-SD cells, and the mechanism may be related to cytostatic and cytotoxic effects. The reduction of mutant-type *p53* and *bcl-2* expressions may be associated with the apoptosis induced by octreotide.

Wang JH, Xing QT, Yuan MB. Antineoplastic effects of octreotide on human gallbladder cancer cells *in vitro*. *World J Gastroenterol* 2004; 10(7): 1043-1046

<http://www.wjgnet.com/1007-9327/10/1043.asp>

INTRODUCTION

Gallbladder cancer is the commonest tumor of the biliary system^[1]. Because of the absence of characteristic early symptoms, the majority of cases are diagnosed at a late stage when most patients already have occult or overt metastasis. As most gallbladder cancers are unresectable, the prognosis is dismal with the median survival time hardly exceeding 6-mo and 5-yr survival less than 5%. Due to the limited efficacy and considerable toxicity of conventional chemotherapy, novel cytotoxic agents and innovative noncytotoxic approaches are being developed. Amongst the various agents, our attention was being directed to somatostatin. Somatostatin and its analogs (SSTA) such as octreotide^[2] inhibit tumor cell growth *in vitro* and *in vivo*^[3,4]. Their effects are mediated by a family of G-protein-coupled receptors (SSTR₁₋₅) that can couple to diverse signal transduction pathways such as inhibition of adenylate cyclase and guanylate cyclase, modulation of ionic conductance channels, and protein dephosphorylation. There are both 'direct' mechanisms that are sequelae of binding of SSTA to somatostatin receptors present on neoplastic cells and 'indirect' mechanisms related to effects of SSTA on the host^[3] including antiangiogenic effect^[5] and inhibited secretion of tumor trophic factors or hormones such as insulin-like growth factor^[6]. Various tumors are inhibited by octreotide, but little is known about whether octreotide has any antineoplastic effects on human gallbladder cancers^[7].

MATERIALS AND METHODS

Materials

Octreotide was a generous gift from Jiuyuan Gene Engineering Co. (Hangzhou, China). RPMI 1640 medium was obtained from Gibco. Newborn bovine serum was supplied by Sijiqing Biotechnology Co. (Hangzhou, China). MTT and propidium iodide (PI) were from Sigma. DNA Extract kit was from Dingguo Biotechnology Co. (Beijing, China). Mouse anti-human P53 and Bcl-2 monoclonal antibodies were purchased from Santa Cruz. ABC kit was provided by Vector.

Methods

Cell culture Human gallbladder cancer line GBC-SD (obtained from Doctor Bo Liu in Department of Hepato-biliary Surgery, General Hospital of PLA) was cultured in RPMI 1640, supplemented with 100 mL/L heat-inactivated newborn bovine serum, 100 U/mL penicillin and 100 µg/mL streptomycin in a humidified atmosphere of 50 mL/L CO₂ at 37 °C.

MTT assay Equal numbers of cells were seeded into 96-well tissue culture plates. One day later, the cells were treated at different concentrations of octreotide. Cell viability was determined in 5 wells for each drug concentration using MMT assay 12, 24, 36, 48, 60 h later. Optical density was measured at 570 and 630 nm using a microplate reader. Growth curve was made according to the optical density.

Colony-forming ability after drug exposure Aliquots of about 1 000 dispersed cells were seeded into Petri dishes in triplicates and treated with octreotide of different concentrations 24 h later. Colonies consisting of more than 50 cells were scored

and the colony-forming rate was compared with that of untreated controls six days later.

Scanning electron microscopy (SEM) Cells grown on a small coverslip were prefixed with 25 mL/L glutaraldehyde, treated with OTO method, dehydrated in graded ethanol, critical point dried with CO₂ and gold coated. The specimens were examined with a JSM-T300 scanning electron microscope.

Transmission electron microscopy (TEM) Cell cultures to be analyzed by transmission electron microscopy were fixed in 25 mL/L glutaraldehyde in phosphate buffer and post fixed in 10 g/L osmium tetroxide, dehydrated in graded ethanol, embedded in an Epon 812 mixture, and sectioned on an ultramicrotome. After being stained with uranyl acetate and lead citrate, they were observed in a HITACHI H-800 electron microscope.

Agarose gel electrophoresis of DNA Cells treated with octreotide at 1 000 nmol/L for 72 h were collected, and DNA was extracted and analyzed in 10 g/L agarose gel for 1.5 h. After being stained with ethidium bromide solution for 10 to 15 min, the gel was viewed on a long wave UV transilluminator.

Flow cytometry assay (FCM) The cells subjected to treatment with octreotide were harvested, rinsed with PBS, resuspended and fixed in 700 mL/L ethanol at 4 °C overnight. The fixed cells were centrifuged, resuspended in 100 mg/L RNase A at 37 °C for 30 min and stained with PI at 4 °C for 30 min. FACS flow cytometer fluorescence intensity was measured by FACScan FCM and the DNA content in cells was analyzed by Modfit software. For each sample, 20 000 cells were measured.

Immunohistochemical analysis GBC-SD cells treated with octreotide for 24 h on coverslips were fixed with cold acetone for 5 min, rinsed in PBS for 5 min. Immunohistochemical staining proceeded according to kit instructions. Blank control, negative control (PBS substituting for primary antibodies) and positive control (paraffin section of human gastric cancer) were set up at the same time. Cells from at least 10 randomly selected fields (×400) were counted. The percentage of positive cells was calculated as (Number of positive cells/Total number in the same visual field)×100%.

Statistics

Data were analyzed employing the paired two-tailed Student *t* test and nonparameter analysis, and significance was assumed at $P<0.05$.

RESULTS

Effects of octreotide on the proliferation of GBC-SD cells

The growth curve (Figure 1) and colony forming ability assay (Table 1) showed significant inhibition of octreotide to the proliferation of GBC-SD cells in culture, inducing time- and dose-dependent effects.

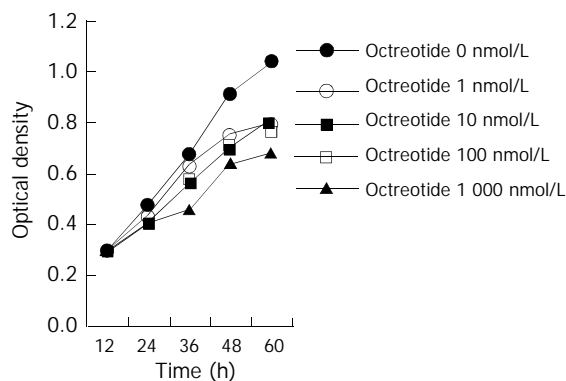


Figure 1 The inhibitory effect of octreotide on growth curve of GBC-SD. Each value was the mean of 5 duplicate wells.

Table 1 The inhibitory effect of octreotide on colony forming ability of GBC-SD (mean±SD,%)

Octreotide (nmol/L)	Colony forming rate
0	82.62±7.63
1	70.51±1.88 ^a
10	68.96±4.88 ^b
100	51.41±18.50 ^b
1000	27.48±2.68 ^d

^a $P<0.05$, ^b $P<0.01$, ^d $P<0.001$ vs the control group ($n=3$).

Effects of octreotide on the apoptosis and cell cycle of GBC-SD cells

After exposure to octreotide, some GBC-SD cells showed typically apoptotic morphology, including chromatin condensation, vacuolar degeneration, nucleus fragmentation and formation of apoptotic body, which could be seen under SEM and TEM (Figure 2 and Figure 3).

DNA of cells undergoing apoptosis usually displays a ladder in agarose gel electrophoresis. In the present study, a DNA ladder was characteristically identified in cells treated with 1 000 nmol/L of octreotide for 72 h as shown in Figure 4.

Usually, a reduced content in apoptotic cells under PI staining displays a 'sub-G₁' peak in FCM profile and apoptotic cells can be quantified in this way. As demonstrated in Table 2, GBC-SD cells exposed to octreotide showed increased sub-G₁ peaks, significantly higher than those of the control group ($P=0.013$). Compared with the control group, there was also an augmentation in the cell proportion of G₀/G₁ phase ($P=0.015$), while the proportion of S phase and G₂/M phase remained unchanged ($P=0.057$ and $P=0.280$, respectively). This indicated that octreotide could arrest the GBC-SD cells at G₀/G₁ phase.

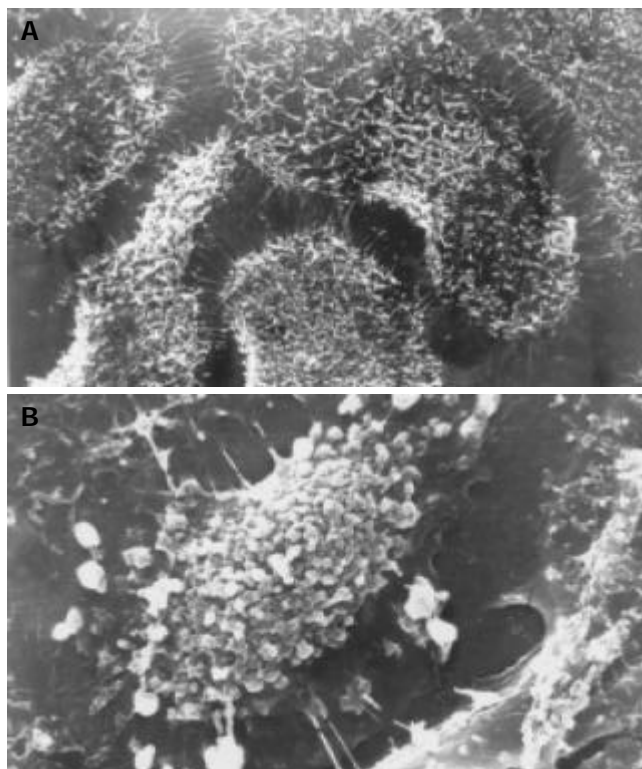


Figure 2 Apoptotic appearance of GBC-SD under SEM. A: control (1500×). B: after exposure to 1000 nmol/L octreotide for 72 h (3500×).

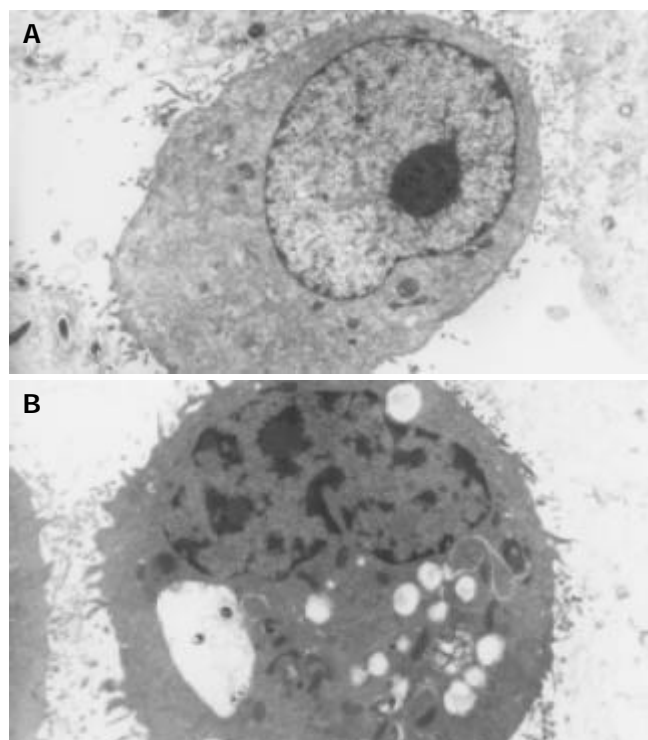


Figure 3 Apoptotic appearance of GBC-SD under TEM. A: control (5600 \times). B: after exposure to 1 000 nmol/L octreotide for 72 h (6400 \times).

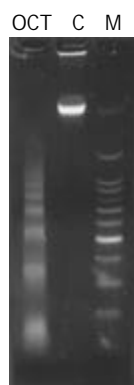


Figure 4 DNA ladder of GBC-SD after exposure to octreotide. M: marker. OCT: 1 000 nmol/L octreotide group. C: control group.

Table 2 Effects of octreotide on the cell cycle kinetics and apoptosis of GBC-SD cells (mean \pm SD, %)

Group	Apoptosis	G ₀ /G ₁	S	G ₂ /M
Control	0.49 \pm 0.21	57.47 \pm 6.69	32.40 \pm 4.86	10.13 \pm 5.99
Octreotide 1 000 nmol/L	22.05 \pm 8.09 ^a	71.08 \pm 4.58 ^a	22.72 \pm 6.68	6.20 \pm 2.84

^a $P < 0.05$ vs the control group ($n = 4$).

Table 3 Effects of octreotide on the *p53* and *bcl-2* expression of GBC-SD cells (mean \pm SD, %)

Group	Percentage of P53 protein positive	Percentage of Bcl-2 protein positive
Control	50.09 \pm 4.64	87.12 \pm 7.40
Octreotide 1 000 nmol/L	44.12 \pm 5.30 ^a	80.46 \pm 5.45 ^a

^a $P < 0.05$ vs the control group ($n = 10$).

Effects of octreotide on P53, Bcl-2 protein levels in GBC-SD cells

After being treated with octreotide, the expressions of both mutant-type *p53* and *bcl-2* decreased considering the percentage of positive cells ($P < 0.05$), as demonstrated in Table 3.

DISCUSSION

Somatostatin and SSTA show antineoplastic activity in a variety of experimental models *in vivo* and *in vitro*^[3,4]. There is considerable evidence for antineoplastic activity of SSTA for neoplasms of breast, prostate, pancreas, colon, stomach, liver, and other common solid tumors for which current treatments are inadequate^[8-18]. Some clinical trials employed octreotide in the treatment of human advanced tumors, showing increased survival, favorable toxicity profiles and improved life quality^[19,20]. Recent studies described some aspects of the molecular mechanisms underlying this antineoplastic activity^[21]. These researches suggest somatostatin and SSTA as drug candidates in oncology.

In this research we observed the effect of octreotide on the growth of GBC-SD cells in culture through two methods. Growth curve reflected group proliferative ability, while colony-forming assay reflected individual proliferative ability. Both methods showed significant inhibition of octreotide to the proliferation of GBC-SD cells, inducing time- and dose-dependent effects.

Over the past decade, a variety of studies revealed that somatostatin and SSTA mediated their action through both indirect and direct effects^[3]. In our *in vitro* experiments, only direct effect was concerned, including cytostatic and cytotoxic effects.

After exposure to octreotide, FCM demonstrated an increased number of GBC-SD cells at G₀/G₁ phase. In cholangiocarcinoma cells, the G₀/G₁ cycle arrest was also induced^[22]. This effect was attributed to the inhibition of signal transduction of some tumor trophic factors or hormones such as insulin and epidermal growth factor, which initiated tyrosine kinase pathway, activated the kinase cascade, increased the expression of cyclin, and promoted the cell cycle from G₁ to S phase^[23]. Some researches found octreotide activated SSTR on the membrane, down-regulated cyclin and up-regulated cyclin-dependent kinase inhibitor, thus leading to the inhibition of the mitogenic signal initiated by tyrosine kinase receptor family. Researchers reported specific phosphotyrosine phosphatases were required for maintaining high inhibitory levels of cyclin-dependent kinase inhibitor p27^{Kip1} and inactivating complex of cyclin E and cyclin dependent kinase 2^[23-26]. Another research reported octreotide-induced growth arrest was mediated by inhibition of phosphatidylinositol 3-kinase pathway and by enhanced expressions of p21^{Cip} and p27^{Kip1}^[27].

A variety of findings indicated that apoptosis could be induced in cancer cells by octreotide, which was implicated in its antineoplastic mechanism^[8,28]. In GBC-SD, spontaneous apoptosis was observed, showing an apoptosis rate varying from 0.21% to 0.69% in the control group and apoptosis could be induced by octreotide, displaying typical morphological changes, DNA ladder, and elevated sub-G₁ peaks in FCM profiles. Octreotide-inducing apoptosis was reported to be associated with tyrosine proteinphosphatase pathway, intracellular acidification, activation of endonuclease and modulation of some genes such as wide-type *p53*, *bax* and *bcl-2*^[28-31]. Sharma *et al* reported only SSTR3 mediated apoptosis, depending on the expression of wide-type *p53*^[29]. Recent studies demonstrated SSTR2 mediated apoptosis in human pancreatic cancer cells and HL60 cells expressing mutated *p53*^[32,33]. These results indicate that somatostatin can induce apoptosis by *p53*-dependent and *p53*-independent mechanisms^[26].

Two main signaling pathways initiate the apoptotic program in mammalian cells. The cell-extrinsic pathway triggers apoptosis in response to activation by their respective ligand of the tumor necrosis factor (TNF) family of death receptors, while the cell-intrinsic pathway triggers apoptosis in response to DNA damage, loss of survival factors, or other types of cell distress. Guillermet and colleagues reported SSTR2 affected both pathways^[32].

By means of immunohistochemical staining, we found high expressions of mutant-type *p53* and *bcl-2* in GBC-SD cells. In the process of octreotide-inducing apoptosis, expressions of both genes decreased. This suggests the down-regulation of both genes may be related to octreotide-inducing apoptosis.

In conclusion, we demonstrate that octreotide could inhibit proliferation *in vitro* in human gallbladder cancer cells, and speculate that cycle arrest and apoptotic induction might be involved in the mechanism.

REFERENCES

- Fong YM**, Kemeny N, Lawrence TS. Cancer of the liver and biliary tree In: Devita VT, Hellman S, Rosenberg S, eds. Cancer: principles and practice of oncology. 6th ed. Philadelphia: Lippincott Williams and Wilkins 2001: 1162-1203
- Lamberts SW**, van der Lely AJ, de Herder WW, Hofland LJ. Octreotide. *N Engl J Med* 1996; **334**: 246-254
- Pollak MN**, Schally AV. Mechanisms of antineoplastic action of somatostatin analogs. *Proc Soc Exp Biol Med* 1998; **217**: 143-152
- Scarpignato C**, Pelosini I. Somatostatin analogs for cancer treatment and diagnosis: an overview. *Chemotherapy* 2001; **47**(Suppl 2): 1-29
- Woltering EA**, Watson JC, Alperin-Lea RC, Sharma C, Keenan E, Kurozawa D, Barrie R. Somatostatin analogs: angiogenesis inhibitors with novel mechanisms of action. *Invest New Drugs* 1997; **15**: 77-86
- Khandwala HM**, McCutcheon IE, Flyvbjerg A, Friend KE. The effects of insulin-like growth factors on tumorigenesis and neoplastic growth. *Endocr Rev* 2000; **21**: 215-244
- Fiebiger WC**, Scheithauer W, Traub T, Kurtaran A, Gedlicka C, Kornek GV, Virgolini I, Raderer M. Absence of therapeutic efficacy of the somatostatin analogue lanreotide in advanced primary hepatic cholangiocellular cancer and adenocarcinoma of the gallbladder despite *in vivo* somatostatin-receptor expression. *Scand J Gastroenterol* 2002; **37**: 222-225
- Diaconu CC**, Szathmari M, Keri G, Venetianer A. Apoptosis is induced in both drug-sensitive and multidrug-resistant hepatoma cells by somatostatin analogue TT-232. *Br J Cancer* 1999; **80**: 1197-1203
- Raderer M**, Hejna MH, Muller C, Kornek GV, Kurtaran A, Virgolini I, Fiebiger W, Hamilton G, Scheithauer W. Treatment of hepatocellular cancer with the long acting somatostatin analog lanreotide *in vitro* and *in vivo*. *Int J Oncol* 2000; **16**: 1197-1201
- Gao S**, Yu BP, Li Y, Dong WG, Luo HS. Antiproliferative effect of octreotide on gastric cancer cells mediated by inhibition of Akt/PKB and telomerase. *World J Gastroenterol* 2003; **9**: 2362-2365
- Wang CH**, Tang CW, Liu CL, Tang LP. Inhibitory effect of octreotide on gastric cancer growth via MAPK pathway. *World J Gastroenterol* 2003; **9**: 1904-1908
- Wang XB**, Wang X, Zhang NZ. Inhibition of somatostatin analog Octreotide on human gastric cancer cell MKN45 growth *in vitro*. *Shijie Huaren Xiaohua Zazhi* 2002; **10**: 40-42
- Dolan JT**, Miltenburg DM, Granchi TS, Miller CC 3rd, Brunicardi FC. Treatment of metastatic breast cancer with somatostatin analogues—a meta-analysis. *Ann Surg Oncol* 2001; **8**: 227-233
- Tejeda M**, Gaal D, Barna K, Csuka O, Keri G. The antitumor activity of the somatostatin structural derivative (TT-232) on different human tumor xenografts. *Anticancer Res* 2003; **23**: 4061-4066
- Lee JU**, Hosotani R, Wada M, Doi R, Koshihara T, Fujimoto K, Miyamoto Y, Tsuji S, Nakajima S, Hirohashi M, Uehara T, Arano Y, Fujii N, Imamura M. Antiproliferative activity induced by the somatostatin analogue, TT-232, in human pancreatic cancer cells. *Eur J Cancer* 2002; **38**: 1526-1534
- Jia WD**, Xu GL, Xu RN, Sun HC, Wang L, Yu JH, Wang J, Li JS, Zhai ZM, Xue Q. Octreotide acts as an antitumor angiogenesis compound and suppresses tumor growth in nude mice bearing human hepatocellular carcinoma xenografts. *J Cancer Res Clin Oncol* 2003; **129**: 327-334
- Gonzalez-Barcena D**, Schally AV, Vadillo-Buenfil M, Cortez-Morales A, Hernandez LV, Cardenas-Cornejo I, Comaru-Schally AM. Response of patients with advanced prostatic cancer to administration of somatostatin analog RC-160 (vapreotide) at the time of relapse. *Prostate* 2003; **56**: 183-191
- He SW**, Shen KQ, He YJ, Xie B, Zhao YM. Regulatory effect and mechanism of gastrin and its antagonists on colorectal carcinoma. *World J Gastroenterol* 1999; **5**: 408-416
- Kouroumalis E**, Skordilis P, Thermos K, Vasilaki A, Moschandrea J, Manousos ON. Treatment of hepatocellular carcinoma with octreotide: a randomised controlled study. *Gut* 1998; **42**: 442-447
- Cascinu S**, Del Ferro E, Catalano G. A randomised trial of octreotide vs best supportive care only in advanced gastrointestinal cancer patients refractory to chemotherapy. *Br J Cancer* 1995; **71**: 97-101
- Bousquet C**, Puente E, Buscail L, Vaysse N, Susini C. Antiproliferative effect of somatostatin and analogs. *Chemotherapy* 2001; **47**(Suppl 2): 30-39
- Zhao B**, Zhao H, Zhao N, Zhu XG. Cholangiocarcinoma cells express somatostatin receptor subtype 2 and respond to octreotide treatment. *J Hepatobiliary Pancreat Surg* 2002; **9**: 497-502
- Pages P**, Benali N, Saint-Laurent N, Esteve JP, Schally AV, Tkaczuk J, Vaysse N, Susini C, Buscail L. sst2 somatostatin receptor mediates cell cycle arrest and induction of p27(Kip1). Evidence for the role of SHP-1. *J Biol Chem* 1999; **274**: 15186-15193
- Florio T**, Arena S, Thellung S, Iuliano R, Corsaro A, Massa A, Pattarozzi A, Bajetto A, Trapasso F, Fusco A, Schettini G. The activation of the phosphotyrosine phosphatase eta (r-PTP eta) is responsible for the somatostatin inhibition of PC C13 thyroid cell proliferation. *Mol Endocrinol* 2001; **15**: 1838-1852
- Lopez F**, Esteve JP, Buscail L, Delesque N, Saint-Laurent N, Theveniau M, Nahmias C, Vaysse N, Susini C. The tyrosine phosphatase SHP-1 associates with the sst2 somatostatin receptor and is an essential component of sst2-mediated inhibitory growth signaling. *J Biol Chem* 1997; **272**: 24448-24454
- Bousquet C**, Delesque N, Lopez F, Saint-Laurent N, Esteve JP, Bedecs K, Buscail L, Vaysse N, Susini C. sst2 somatostatin receptor mediates negative regulation of insulin receptor signaling through the tyrosine phosphatase SHP-1. *J Biol Chem* 1998; **273**: 7099-7106
- Charland S**, Boucher MJ, Houde M, Rivard N. Somatostatin inhibits Akt phosphorylation and cell cycle entry, but not p42/p44 mitogen-activated protein (MAP) kinase activation in normal and tumoral pancreatic acinar cells. *Endocrinology* 2001; **142**: 121-128
- Sharma K**, Srikant CB. Induction of wild-type p53, Bax, and acidic endonuclease during somatostatin-signaled apoptosis in MCF-7 human breast cancer cells. *Int J Cancer* 1998; **76**: 259-266
- Sharma K**, Patel YC, Srikant CB. Subtype-selective induction of wild-type p53 and apoptosis, but not cell cycle arrest, by human somatostatin receptor 3. *Mol Endocrinol* 1996; **10**: 1688-1696
- Sharma K**, Srikant CB. G protein coupled receptor signaled apoptosis is associated with activation of a cation insensitive acidic endonuclease and intracellular acidification. *Biochem Biophys Res Commun* 1998; **242**: 134-140
- Thangaraju M**, Sharma K, Liu D, Shen SH, Srikant CB. Interdependent regulation of intracellular acidification and SHP-1 in apoptosis. *Cancer Res* 1999; **59**: 1649-1654
- Guillermet J**, Saint-Laurent N, Rochaix P, Cuvillier O, Levade T, Schally AV, Pradayrol L, Buscail L, Susini C, Bousquet C. Somatostatin receptor subtype 2 sensitizes human pancreatic cancer cells to death ligand-induced apoptosis. *Proc Natl Acad Sci U S A* 2003; **100**: 155-160
- Teijeiro R**, Rios R, Costoya JA, Castro R, Bello JL, Devesa J, Arce VM. Activation of human somatostatin receptor 2 promotes apoptosis through a mechanism that is independent from induction of p53. *Cell Physiol Biochem* 2002; **12**: 31-38

Effects of PPAR γ agonist pioglitazone on rat hepatic fibrosis

Guang-Jin Yuan, Ming-Liang Zhang, Zuo-Jiong Gong

Guang-Jin Yuan, Zuo-Jiong Gong, Department of Infectious Diseases, Renmin Hospital of Wuhan University, Wuhan 430060, Hubei Province, China

Ming-Liang Zhang, Department of Gastroenterology, the Second Affiliated Hospital of Nanhua University, Hengyang 421001, Hunan Province, China

Correspondence to: Guang-Jin Yuan, Department of Infectious Diseases, Renmin Hospital of Wuhan University, Wuhan 430060, Hubei Province, China. guangjin_yuan@hotmail.com

Telephone: +86-27-88041919-8385 **Fax:** +86-27-88042292

Received: 2003-08-23 **Accepted:** 2003-11-06

Abstract

AIM: To investigate effects of pioglitazone on rat hepatic fibrosis and to explore its mechanism.

METHODS: Rat hepatic fibrosis was induced by carbon tetrachloride (CCl₄). Forty Sprague-Dawley rats were divided randomly into 4 groups: control, model, and two treatment (PI, PII) groups. Except for rats in control group, all rats were given subcutaneous injection of 400 mL/L CCl₄, twice a wk for 8 wk. Rats in PI and PII groups were also treated with pioglitazone of 3 mg/kg, daily via gastrogavage beginning on the 1st day and at the end of the 2nd week, administration of CCl₄ respectively. Liver functions (ALT, AST), serum fibrotic markers (HA, LN, PCIII) and hepatic hydroxyproline (HP) concentration were determined respectively. Histochemical staining of formalin-fixed liver sections with HE, Masson-Trichrome, and immunohistochemical staining for α -smooth muscle actin (α -SMA) were performed. Modified Knodell and Chevallier semi-quantitative scoring system (SSS) was used to evaluate necroinflammatory activity and fibrosis degree.

RESULTS: Compared with model group, pioglitazone significantly reduced the serum levels of ALT, AST, HA, LN and PCIII ($P < 0.05$ or < 0.01). The HP concentrations in PI (210.90 \pm 24.07 μ g/g), and PII (257.36 \pm 30.55 μ g/g) groups were also lower than those in model group (317.80 \pm 36.44 μ g/g) ($P < 0.01$). Histologic examination showed that PI and PII groups had milder hepatocellular degeneration, necrosis and infiltration of inflammatory cells, and thinner or less fibrotic septa than did model group. The scores for necroinflammation in PI (2.80 \pm 1.03), and PII (3.00 \pm 1.05) groups were significantly reduced as compared with model group (4.88 \pm 2.30) ($P < 0.05$ or < 0.01); the fibrosis scores in PI (3.40 \pm 1.65), and PII (4.60 \pm 1.35) groups were also markedly lower than those in model group (7.00 \pm 3.21) ($P < 0.05$ or < 0.01). Immunohistochemical staining showed that expression of α -SMA in PI and PII groups was ameliorated dramatically compared with model group.

CONCLUSION: PPAR γ agonist pioglitazone greatly retards the progression of rat hepatic fibrosis induced by CCl₄ through inhibition of HSC activation and amelioration of hepatocyte necroinflammation in rats.

Yuan GJ, Zhang ML, Gong ZJ. Effects of PPAR γ agonist

pioglitazone on rat hepatic fibrosis. *World J Gastroenterol* 2004; 10(7): 1047-1051

<http://www.wjgnet.com/1007-9327/10/1047.asp>

INTRODUCTION

Hepatic fibrosis is a common response to chronic liver injury of variable origins (e.g. viral, alcoholic, metabolic), which can lead to cirrhosis and ultimately, endstage liver failure and increased risk for hepatocellular carcinoma^[1-3]. It seems to be irreversible once liver cirrhosis has been developed^[4]. Therefore therapeutic intervention in the progression of hepatic fibrosis in the early stage plays an important role in the prevention of liver cirrhosis. However, until now no satisfactory antifibrotic agent is available.

Peroxisome proliferator-activated receptors (PPARs) are the members of a nuclear receptor superfamily, three isotypes of which have been identified: α , β (also called δ and NUC1) and γ . PPAR γ plays a pivotal role in the differentiation of adipocyte and metabolism of glucose and fatty acid^[5]. Some studies showed that PPAR γ is implicated in inducing differentiation or apoptosis of various human malignant cells^[6]. Agonists of PPAR γ include 15-deoxy- $\Delta^{12,14}$ -PGJ₂ (15 d-PGJ₂) and thiazolidinediones (TZDs), such as troglitazone, rosiglitazone, and pioglitazone, etc. TZDs are synthetic compounds with a high affinity to PPAR γ and a new class of oral antidiabetic drugs that act by improving insulin sensitivity. Rosiglitazone and pioglitazone have no obvious adverse effects and have been used in clinic^[7-10]. Recently, pioglitazone was reported to be able to prevent early-phase hepatic fibrogenesis induced by carbon tetrachloride (CCl₄) for 72 h^[11]. Galli *et al.* also demonstrated that oral administration of TZD (rosiglitazone and pioglitazone) can reduce extracellular matrix (ECM) deposition in both toxic and cholestatic models of liver fibrosis^[12]. In the present study, we investigated the effects of pioglitazone on rat hepatic fibrosis induced by CCl₄, and explored its mechanism.

MATERIALS AND METHODS

Animals

Forty adult male Sprague-Dawley rats, weighing 200-250 g, were purchased from Experimental Animal Department of Xiangya Medical School, Zhongnan University, Hunan Province. Rats were randomly divided into 4 groups including normal control, model and two treatment (PI, PII) groups. Except for control group, all rats were given subcutaneous injection of 400 mL/L CCl₄ (dissolved in castor oil) 3 mL/kg twice weekly for 8 wk, with the first dosage doubled. The control group received injection of castor oil vehicle of the same dosage twice weekly. Rats in PI and PII groups were also given pioglitazone (Beijing Taiyang Pharm. Co., Ltd.) of 3 mg/kg daily via gastrogavage beginning on the 1st day and at the end of the 2nd week, administration of CCl₄ respectively. Once per week, the animals were weighed and the dosages of CCl₄ and pioglitazone were adjusted. At the end of the 8-wk experimental period, all rats were sacrificed by bleeding from femoral arteries and veins. Blood and livers were collected for further examinations.

Serum assays

Alanine aminotransferase (ALT) and aspartate aminotransferase (AST) were measured by using a Hitachi Automatic Biochemical Analyzer. Serum fibrotic markers, such as hyaluronic acid (HA), laminin (LN) and type III procollagen (PCIII) were determined by a radioimmunological assay using a commercial kit (Shanghai Navy Medical Institute, China).

Hydroxyproline (HP) determination

Liver tissue (approximately 200 mg) was homogenized into powder and hydrolyzed in 5 mL of 6 mol/L HCl. Hepatic HP concentrations were measured according to manual description (Jiancheng Medical Institute, Nanjing, China).

Histopathological examination

Liver tissues were fixed in 40 g/L formaldehyde, embedded in paraffin and stained with hematoxylin-eosin (HE) and Masson's trichrome. Modified Knodell and Chevallier semi-quantitative scoring system (SSS)^[13] was used to evaluate necroinflammatory activity and fibrosis degree by an independent pathologist blindly.

α -Smooth muscle actin (α -SMA) immunohistochemical staining

Liver tissue sections were deparaffinized in xylene and rehydrated in alcohol gradually. Then the sections were incubated with a primary monoclonal mouse anti- α -SMA antibody (Boster, Wuhan, China) and a secondary biotin-conjugated goat anti-mouse IgG respectively. The positive stains were shown as a brown colour with a SABC technique.

Statistical analysis

Data were presented as mean \pm SD unless otherwise indicated. One-way analysis of variance (ANOVA) with LSD post-hoc comparison was used to test for differences in means of variables between groups. A *P* value <0.05 was considered statistically significant. All data were analyzed by SPSS10.0 software.

RESULTS

Histopathological alterations

At the end of the experiment, 2 rats in model group were dead because of infection at the site of injection, another 2 developed ascites. In treatment groups, no death or ascites occurred.

Control livers showed normal lobular architecture with central veins and radiating hepatic cords with irregular sinusoids, and a normal distribution of collagen with a variable amount in portal tracts and a thin rim around central veins (Figure 1). Livers in model group showed disorderly hepatocyte cords, severe fatty degeneration, spotty or focal necrosis and infiltration of inflammatory cells (Figure 2A), and collagen deposition extending from central veins or portal tracts, with thick or thin fibrotic septa and even pseudolobuli formation (Figure 2B). Treatment with pioglitazone in PI, PII groups resulted in apparent amelioration of hepatocyte degeneration, necrosis and infiltration of inflammatory cells (Figure 3), and marked reduction in collagen deposition with no obvious pseudolobuli formation (Figure 4). Scores of liver necroinflammation and fibrosis are shown in Table 1.

Effects of pioglitazone on liver functions and serum fibrotic markers

Serum ALT and AST levels in model group were significantly increased as compared with control group. But treatment with pioglitazone reduced the ALT, AST levels markedly compared

with model group and the effects in PI group were more obvious than those in PII group (Table 2). Serum levels of HA, LN and PCIII, the surrogate markers of liver fibrogenesis, were significantly higher in model group than those in control group. These markers were lowered markedly in treatment groups compared with model group (Table 3).

Table 1 Effects of pioglitazone on liver inflammation and fibrosis scores(mean \pm SD)

Group	<i>n</i>	Necroinflammatory scores	Fibrosis scores
Control	10	0	0
Model	8	4.88 \pm 2.30	7.00 \pm 3.21
PI	10	2.80 \pm 1.03 ^b	3.40 \pm 1.65 ^b
PII	10	3.00 \pm 1.05 ^a	4.60 \pm 1.35 ^a

^a*P*<0.05, ^b*P*<0.01 vs model group.

Table 2 Effects of pioglitazone on liver functions in fibrotic rats (mean \pm SD)

Group	<i>n</i>	ALT (U/L)	AST (U/L)
Control	10	41.09 \pm 6.58	136.34 \pm 31.23
Model	8	105.00 \pm 23.71 ^d	397.86 \pm 67.32 ^d
PI	10	58.64 \pm 11.40 ^b	259.58 \pm 45.89 ^b
PII	10	87.32 \pm 15.65 ^a	344.49 \pm 28.10 ^a

^a*P*<0.05, ^b*P*<0.01 vs model group; ^d*P*<0.001 vs control group.

Table 3 Effects of pioglitazone on serum fibrotic markers in fibrotic rats (mean \pm SD)

Group	<i>n</i>	HA (μ g/L)	LN (μ g/L)	PCIII (μ g/L)
Control	10	57.75 \pm 11.34	35.68 \pm 6.02	85.94 \pm 10.15
Model	8	167.64 \pm 19.46 ^d	74.35 \pm 12.45 ^d	178.93 \pm 7.42 ^d
PI	10	71.25 \pm 15.78 ^b	40.28 \pm 9.91 ^b	149.23 \pm 11.13 ^b
PII	10	103.64 \pm 27.55 ^b	56.62 \pm 8.95 ^b	161.30 \pm 9.22 ^a

^a*P*<0.05, ^b*P*<0.01 vs model group; ^d*P*<0.001 vs control group.

Effects of pioglitazone on liver HP contents

Liver HP concentrations in model group (317.80 \pm 36.44 μ g/g) were significantly increased as compared with control group (170.96 \pm 29.34 μ g/g) (*P*<0.001). Treatment with pioglitazone in PI (210.90 \pm 24.07 μ g/g), and PII (257.36 \pm 30.55 μ g/g) groups decreased HP concentrations markedly compared with model group.

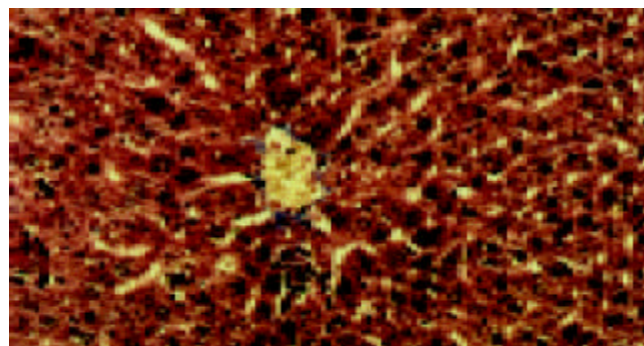


Figure 1 Liver tissue from control group showed normal lobular architecture and a normal distribution of collagen with a thin rim around central veins. Masson \times 200.

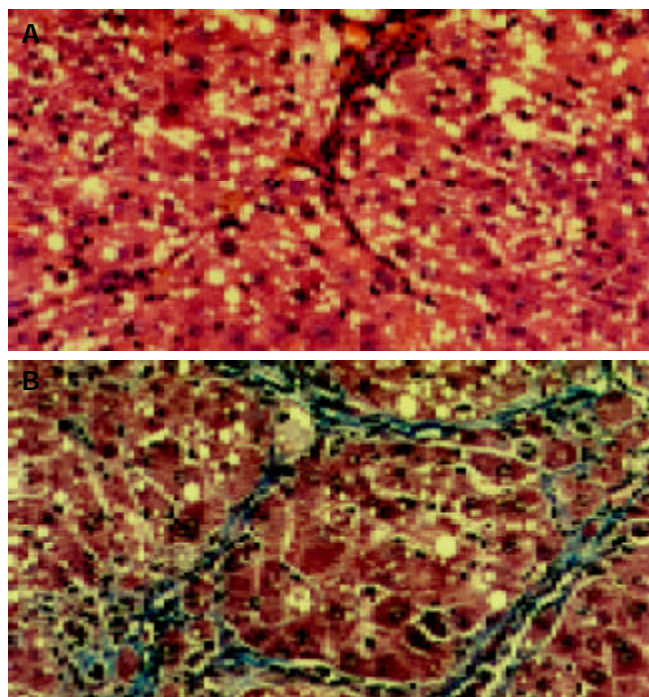


Figure 2 A: Liver tissue from model group showed disorderly hepatocyte cords, severe fatty degeneration, spotty or focal necrosis and infiltration of inflammatory cells. HE \times 200. B: Liver tissue from model group showed collagen deposition extending from central veins or portal tracts, with thick or thin fibrotic septa and pseudolobuli formation. Masson \times 200.

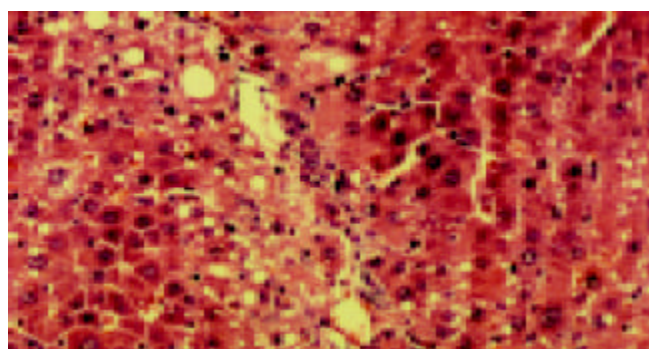


Figure 3 Liver tissue from PII group showed apparent amelioration of hepatocyte degeneration, necrosis and infiltration of inflammatory cells. HE \times 200.

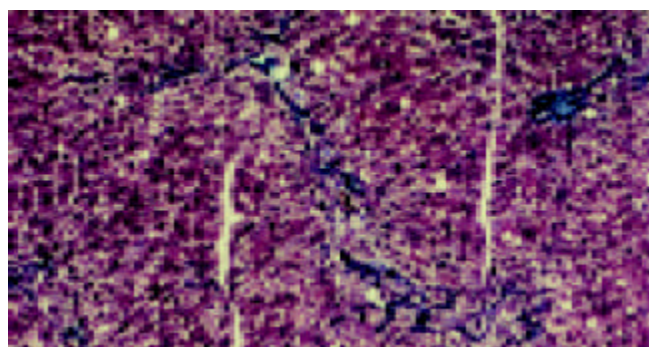


Figure 4 Liver tissue from PII group showed marked reduction in collagen deposition with no obvious pseudolobuli formation. Masson \times 100.

α -SMA immunohistochemical changes

α -SMA is a marker of hepatic stellate cells (HSC) activation. In

control livers, α -SMA was mainly expressed in vascular walls; but in model group, apart from vascular walls, α -SMA was strongly expressed in areas of centrilobular and periportal fibrotic bands. Compared with model group, treatment with pioglitazone dramatically reduced the expression of α -SMA in the livers. Besides the expression in vascular walls as in control group, there were only few mesenchymal cells expressing α -SMA around blood vessels in treatment groups.

DISCUSSION

Hepatic fibrosis is a reparative response to various chronic liver damage and activated hepatic stellate cells (HSCs) play a pivotal role in its pathogenesis^[14]. An abundance of evidence indicated that inhibition of HSCs activation may delay or reverse the progression of hepatic fibrosis^[15-17]. Recently, HSCs were reported to express PPAR γ which might be important in control of their activation state. Inhibition or inactivation of PPAR γ in HSCs may predispose to hepatic fibrosis. Miyahara *et al.* reported that PPAR γ mRNA level and its binding to PPAR-responsive element (PPRE) are reduced in HSCs from cholestatic liver fibrosis rats. Treatment of cultured-activated HSC with ligands for PPAR γ (15dPGJ₂ or BRL49653) inhibits DNA synthesis^[18]. Transfection experiments with a reporter gene ([PPRE]₃-tk-luciferase) also demonstrated a progressive reduction of PPAR transcriptional activity during plastic-induced HSC transdifferentiation. But cotransfection with human PPAR γ expression vector restored the reporter gene expression and inhibited cell proliferation in a dose-dependent manner in cultured HSCs^[19]. PPAR γ agonists also can inhibit HSC proliferation and chemotaxis induced by platelet-derived growth factors (PDGF), the effects of which are associated with inhibition of cell cycle progression beyond the G₁ phase^[19,20]. A latest study reported that curcumin, a potent antioxidant, inhibits proliferation of activated HSCs in cultures, which is involved in its induction of PPAR-gamma activation^[21]. HSCs are the main sources of excessive ECM production and deposition^[22]. Apart from inhibiting HSC proliferation and activation, PPAR γ ligands can inhibit collagen or fibronectin synthesis induced by transforming growth factor (TGF)- β 1 in HSC^[12,18]. Our experiments showed that α -SMA expression, a marker of activated HSC^[23], was reduced significantly in pioglitazone treatment groups compared with model group. The results demonstrated that pioglitazone could inhibit HSC proliferation and activation. Treatment with pioglitazone also resulted in significant decrease in levels of serum fibrotic markers and hepatic HP concentrations compared with model group. The antifibrotic effects were further confirmed by Masson's trichrome collagen staining, which showed that collagen deposition of liver tissues in treatment groups was markedly reduced as compared with model group and was associated with lower scores of fibrosis. Our results demonstrated that pioglitazone could also reduce ECM deposition in hepatic fibrosis rats induced by CCl₄. In PII group, pioglitazone was administered beginning at the end of the 2nd week of model establishment, at which time main microscopic changes in livers were hepatocellular degeneration, necrosis and slight collagen deposition^[24]. Studies showed that HSCs are activated and proliferate stably at the end of the 2nd week of model establishment^[25]. Our experiments found that pioglitazone administered beginning at that time could also inhibit the activated HSC proliferation and prevent the progression of hepatic fibrosis in rats.

Hepatic fibrogenesis is often associated with hepatocellular necrosis and inflammation accompanied by repair processes^[26,27]. Kupffer cells were shown to be a critical mediator of the inflammatory and fibrogenic responses during CCl₄-mediated

liver damages^[28]. Treatment with GdCl₃ or glycine that inactivated Kupffer cells, resulted in attenuation of CCl₄-induced hepatic fibrosis^[29], which proves that suppression of necroinflammation may be an effective antifibrotic treatment. Many studies showed that PPAR γ plays regulatory roles in inflammation and immunity^[30-32]. PPAR γ ligands can inhibit the activation of inflammatory response genes by antagonizing the AP-1, NF-kB and STAT signaling pathways^[33] and reduce proinflammatory cytokines (TNF- α , IL-1, IL-6, etc.) in various cell types (eg. macrophages)^[34]. Anti-inflammatory activities of some NSAIDs are associated with inhibition of cytokines production through PPAR γ activation^[34]. There are increasing reports suggesting that PPAR γ ligands can be used for treatment of chronic inflammatory diseases such as inflammatory bowel disease^[35], rheumatoid arthritis^[36] etc. Our experiments showed that treatment with pioglitazone in PI, PII groups ameliorated hepatocyte degeneration, necrosis and infiltration of inflammatory cells and reduced the scores of necroinflammation significantly compared with model group. Liver functions (ALT, AST) were also improved apparently. These results demonstrated that PPAR γ agonists also had anti-inflammatory effects, and subsequently retarded the progression of hepatic fibrosis in rats.

Thiazolidinediones are a new class of oral antidiabetic agents that sensitize insulin action and have no risk of hypoglycemic occurrence^[37]. Currently two TZDs, rosiglitazone and pioglitazone, have been approved by U.S. Food and Drug Administration (FDA) for treatment of type 2 diabetes. A wealth of clinical studies indicated that rosiglitazone and pioglitazone have no hepatotoxicity^[7-10]. Our experiments also showed that after administration with pioglitazone for 6 or 8 wk, no rats were observed to have hepatotoxicity; moreover, their liver functions (ALT, AST) were improved greatly compared with model rats.

In conclusion, pioglitazone, a PPAR γ ligand, greatly retards the progression of experimental hepatic fibrosis through inhibition of HSC activation and amelioration of hepatocyte necroinflammation in rats. Therefore, it is a potential new antifibrotic drug for clinical application.

ACKNOWLEDGMENTS

We are indebted to Prof. Zhou Xiu-tian from Department of Pathology, Nanhua University for his help with the pathological technique.

REFERENCES

- Miyazawa K, Moriyama M, Mikuni M, Matsumura H, Aoki H, Shimizu T, Yamagami H, Kaneko M, Shioda A, Tanaka N, Arakawa Y. Analysis of background factors and evaluation of a population at high risk of hepatocellular carcinoma. *Intervirology* 2003; **46**: 150-156
- Nagao Y, Fukuizumi K, Kumashiro R, Tanaka K, Sata M. The prognosis for life in an HCV hyperendemic area. *Gastroenterology* 2003; **125**: 628-629
- Rabe C, Pilz T, Klostermann C, Berna M, Schild HH, Sauerbruch T, Caselmann WH. Clinical characteristics and outcome of a cohort of 101 patients with hepatocellular carcinoma. *World J Gastroenterol* 2001; **7**: 208-215
- Lee HS, Huang GT, Chen CH, Chiou LL, Lee CC, Yang PM, Chen DS, Sheu JC. Less reversal of liver fibrosis after prolonged carbon tetrachloride injection. *Hepatogastroenterology* 2001; **48**: 1312-1315
- Everett L, Galli A, Crabb D. The role of hepatic peroxisome proliferator-activated receptors (PPARs) in health and disease. *Liver* 2000; **20**: 191-199
- Shimada T, Kojima K, Yoshiura K, Hiraishi H, Terano A. Characteristics of the peroxisome proliferator activated receptor gamma (PPARgamma) ligand induced apoptosis in colon cancer cells. *Gut* 2002; **50**: 658-664
- Lebovitz HE. Differentiating members of the thiazolidinedione class: a focus on safety. *Diabetes Metab Res Rev* 2002; **18**(Suppl 2): S23-29
- Sood V, Collieran K, Burge MR. Thiazolidinediones: a comparative review of approved uses. *Diabetes Technol Ther* 2000; **2**: 429-440
- Lebovitz HE, Kreider M, Freed MI. Evaluation of liver function in type 2 diabetic patients during clinical trials: evidence that rosiglitazone does not cause hepatic dysfunction. *Diabetes Care* 2002; **25**: 815-821
- Lawrence JM, Reckless JP. Pioglitazone. *Int J Clin Pract* 2000; **54**: 614-618
- Kon K, Ikejima K, Hirose M, Yoshikawa M, Enomoto N, Kitamura T, Takei Y, Sato N. Pioglitazone prevents early-phase hepatic fibrogenesis caused by carbon tetrachloride. *Biochem Biophys Res Commun* 2002; **291**: 55-61
- Galli A, Crabb DW, Ceni E, Salzano R, Mello T, Svegliati-Baroni G, Ridolfi F, Trozzi L, Surrenti C, Casini A. Antidiabetic thiazolidinediones inhibit collagen synthesis and hepatic stellate cell activation *in vivo* and *in vitro*. *Gastroenterology* 2002; **122**: 1924-1940
- Hepatic Fibrosis Study Group Of Chinese Liver Diseases Association. Consensus on evaluation of the diagnosis and efficacy of hepatic fibrosis. *Zhonghua Ganzangbing Zazhi* 2002; **10**: 327-328
- Safadi R, Friedman SL. Hepatic fibrosis—role of hepatic stellate cell activation. *Med Gen Med* 2002; **4**: 27
- Dai WJ, Jiang HC. Advances in gene therapy of liver cirrhosis: a review. *World J Gastroenterol* 2001; **7**: 1-8
- Wei HS, Lu HM, Li DG, Zhan YT, Wang ZR, Huang X, Cheng JL, Xu QF. The regulatory role of AT 1 receptor on activated HSCs in hepatic fibrogenesis: effects of RAS inhibitors on hepatic fibrosis induced by CCl₄. *World J Gastroenterol* 2000; **6**: 824-828
- Wu J, Zern MA. Hepatic stellate cells: a target for the treatment of liver fibrosis. *J Gastroenterol* 2000; **35**: 665-672
- Miyahara T, Schrum L, Rippe R, Xiong S, Yee HF Jr, Motomura K, Anania FA, Willson TM, Tsukamoto H. Peroxisome proliferator-activated receptors and hepatic stellate cell activation. *J Biol Chem* 2000; **275**: 35715-35722
- Galli A, Crabb D, Price D, Ceni E, Salzano R, Surrenti C, Casini A. Peroxisome proliferator-activated receptor gamma transcriptional regulation is involved in platelet-derived growth factor-induced proliferation of human hepatic stellate cells. *Hepatology* 2000; **31**: 101-108
- Marra F, Efsen E, Romanelli RG, Caligiuri A, Pastacaldi S, Batignani G, Bonacchi A, Caporale R, Laffi G, Pinzani M, Gentilini P. Ligands of peroxisome proliferator-activated receptor gamma modulate profibrogenic and proinflammatory actions in hepatic stellate cells. *Gastroenterology* 2000; **119**: 466-478
- Xu J, Fu Y, Chen A. Activation of peroxisome proliferator-activated receptor-gamma contributes to the inhibitory effects of curcumin on rat hepatic stellate cell growth. *Am J Physiol Gastrointest Liver Physiol* 2003; **285**: G20-30
- Liu WB, Yang CQ, Jiang W, Wang YQ, Guo JS, He BM, Wang JY. Inhibition on the production of collagen type I, III of activated hepatic stellate cells by antisense TIMP-1 recombinant plasmid. *World J Gastroenterol* 2003; **9**: 316-319
- Weng HL, Cai WM, Liu RH. Animal experiment and clinical study of effect of gamma-interferon on hepatic fibrosis. *World J Gastroenterol* 2001; **7**: 42-48
- Wang JY, Zhang QS, Guo JS, Hu MY. Effects of glycyrrhetic acid on collagen metabolism of hepatic stellate cells at different stages of liver fibrosis in rats. *World J Gastroenterol* 2001; **7**: 115-119
- Geerts A, Lazou JM, De Bleser P, Wisse E. Tissue distribution, quantitation and proliferation kinetics of fat-storing cells in carbon tetrachloride-injured rat liver. *Hepatology* 1991; **13**: 1193-1202
- Baroni GS, Pastorelli A, Manzin A, Benedetti A, Marucci L, Solforosi L, Di Sario A, Brunelli E, Orlandi F, Clementi M, Macarri G. Hepatic stellate cell activation and liver fibrosis are associated with necroinflammatory injury and Th1-like response

- in chronic hepatitis C. *Liver* 1999; **19**: 212-219
- 27 **Zheng RQ**, Wang QH, Lu MD, Xie SB, Ren J, Su ZZ, Cai YK, Yao JL. Liver fibrosis in chronic viral hepatitis: An ultrasonographic study. *World J Gastroenterol* 2003; **9**: 2484-2489
- 28 **Luckey SW**, Petersen DR. Activation of Kupffer cells during the course of carbon tetrachloride-induced liver injury and fibrosis in rats. *Exp Mol Pathol* 2001; **71**: 226-240
- 29 **Rivera CA**, Bradford BU, Hunt KJ, Adachi Y, Schrum LW, Koop DR, Burchardt ER, Rippe RA, Thurman RG. Attenuation of CCl₄-induced hepatic fibrosis by GdCl₃ treatment or dietary glycine. *Am J Physiol Gastrointest Liver Physiol* 2001; **281**: G200-207
- 30 **Daynes RA**, Jones DC. Emerging roles of PPARs in inflammation and immunity. *Nat Rev Immunol* 2002; **2**: 748-759
- 31 **Cabrero A**, Laguna JC, Vazquez M. Peroxisome proliferator-activated receptors and the control of inflammation. *Curr Drug Targets Inflamm Allergy* 2002; **1**: 243-248
- 32 **Nencioni A**, Wesselborg S, Brossart P. Role of peroxisome proliferator-activated receptor gamma and its ligands in the control of immune responses. *Crit Rev Immunol* 2003; **23**: 1-13
- 33 **Ricote M**, Li AC, Willson TM, Kelly CJ, Glass CK. The peroxisome proliferator-activated receptor-gamma is a negative regulator of macrophage activation. *Nature* 1998; **391**: 79-82
- 34 **Jiang C**, Ting AT, Seed B. PPAR-gamma agonists inhibit production of monocyte inflammatory cytokines. *Nature* 1998; **391**: 82-86
- 35 **Bull AW**. The role of peroxisome proliferator-activated receptor gamma in colon cancer and inflammatory bowel disease. *Arch Pathol Lab Med* 2003; **127**: 1121-1123
- 36 **Shiojiri T**, Wada K, Nakajima A, Katayama K, Shibuya A, Kudo C, Kadowaki T, Mayumi T, Yura Y, Kamisaki Y. PPAR gamma ligands inhibit nitrotyrosine formation and inflammatory mediator expressions in adjuvant-induced rheumatoid arthritis mice. *Eur J Pharmacol* 2002; **448**: 231-238
- 37 **Ikeda H**, Taketomi S, Sugiyama Y, Shimura Y, Sohda T, Meguro K, Fujita T. Effects of pioglitazone on glucose and lipid metabolism in normal and insulin resistant animals. *Arzneimittelforschung* 1990; **40**(2 Pt 1): 156-162

Edited by Zhu LH and Xu FM

Metabolic syndrome is directly associated with gamma glutamyl transpeptidase elevation in Japanese women

Hiroshi Sakugawa, Tomofumi Nakayoshi, Kasen Kobashigawa, Hiroki Nakasone, Yuko Kawakami, Tsuyoshi Yamashiro, Tatsuji Maeshiro, Ko Tomimori, Satoru Miyagi, Fukunori Kinjo, Atsushi Saito

Hiroshi Sakugawa, Tomofumi Nakayoshi, Kasen Kobashigawa, Hiroki Nakasone, Yuko Kawakami, Tsuyoshi Yamashiro, Tatsuji Maeshiro, Ko Tomimori, Satoru Miyagi, Fukunori Kinjo, Atsushi Saito, First Department of Internal Medicine, Faculty of Medicine, School of Medicine, University of the Ryukyus, Okinawa, Japan
Correspondence to: Hiroshi Sakugawa, M.D., First Department of Internal Medicine, University Hospital, Faculty of Medicine, University of the Ryukyus, 207 Uehara, Okinawa, 903-0125, Japan. b987607@med.u-ryukyu.ac.jp
Telephone: +98-895-1144 **Fax:** +98-895-1414
Received: 2003-09-23 **Accepted:** 2003-12-19

Abstract

AIM: This study aimed to determine whether metabolic syndrome is directly or indirectly, through fatty liver, associated with elevated gamma-glutamyl transpeptidase (GGT) levels in Japanese women.

METHODS: From 4 366 women who received their annual health check-up, 4 211 women were selected for analysis. All 4 211 women were negative for both hepatitis B surface antigen and antibody to hepatitis C virus. Clinical and biochemical variables were examined by using univariate and multivariate analysis.

RESULTS: A raised GGT level (>68 IU/L) was seen in 258 (6.1%) of the 4 211 women. In univariate analysis, all variables examined (age, body mass index, blood pressure, hemoglobin concentration, fasting blood glucose, glycosylated hemoglobin A1c, cholesterol, triglyceride, and uric acid) were associated with the elevated GGT level, whereas in multivariate analysis, four variables (age 50 yr, hemoglobin 14 g/dL, triglyceride 150 mg/dL, and presence of diabetes) were significantly and independently associated with raised GGT level. Clinical variables predicting the presence of ultrasonographic evidence of fatty liver were also examined by multivariate analysis; four variables were associated with the presence of fatty liver: BMI 25 kg/m², hemoglobin 14 g/dL, triglyceride 150 mg/dL, and uric acid 7 mg/dL. There was no significant association between the raised GGT level and the presence of fatty liver. Hypertriglyceridemia was significantly and independently associated with both the raised GGT level and the presence of fatty liver.

CONCLUSION: Metabolic syndrome seemed to be directly, not indirectly through fatty liver, associated with the raised GGT level in Japanese women.

Sakugawa H, Nakayoshi T, Kobashigawa K, Nakasone H, Kawakami Y, Yamashiro T, Maeshiro T, Tomimori K, Miyagi S, Kinjo F, Saito A. Metabolic syndrome is directly associated with gamma glutamyl transpeptidase elevation in Japanese women. *World J Gastroenterol* 2004; 10(7): 1052-1055
<http://www.wjgnet.com/1007-9327/10/1052.asp>

INTRODUCTION

The prevalence of overweight persons is increasing in developed and developing countries^[1-3]. Obesity is strongly associated with insulin resistance^[4-6], which is known to be associated with an elevated gamma-glutamyl transpeptidase (GGT) level^[7,8]. However, the mechanism of the relationship between insulin resistance and GGT elevation has not yet been clarified. Metabolic syndrome is associated with insulin resistant status^[4-6], and is increasing recently in Japan together with an increase in the prevalence of obesity^[2]. It is well known that insulin resistance is associated with fatty liver^[9,10]. Furthermore, fatty liver is associated with elevated GGT levels^[8]. Hence, the following question emerged: is insulin resistant status directly or indirectly, through fatty liver, associated with GGT elevation? Few population-based studies have been performed on the association between raised GGT level and metabolic syndrome^[7,8]. Moreover, these studies usually dealt with men^[8, 11]. It is well known that GGT elevation is frequently induced by habitual alcohol intake and drinkers are more frequently included among men than women. Most raised GGT levels seen in ordinary women are not caused by alcohol, because women with a history of regular alcohol intake in Japan are rare^[12]. However, nonalcoholic steatohepatitis (NASH), a severe form of nonalcoholic fatty liver disease, is known to be associated with female gender, metabolic syndrome, and raised GGT level^[10]. Hence, a general population study on the association of raised GGT level with risk factors of metabolic syndrome among women is urgently needed.

The aim of this study was to determine whether metabolic syndrome is directly or indirectly, through fatty liver, associated with GTP elevation in Japanese women.

MATERIALS AND METHODS

Subjects

From January 2000 to December 2000, 4 366 women received their annual health check-up at the Okinawa General Health Service Association. They were all Japanese aged between 21 and 88 years: 87% were 40 years of age or older.

Methods

For all women, the body mass index (BMI; kg/m²) was calculated. Obesity was defined as BMI 25 kg/m² as recommended by the Japan Society for Obesity^[13].

Laboratory tests included peripheral blood cell counts, liver function tests (aspartate aminotransferase (AST), alanine aminotransferase (ALT), GGT, alkaline phosphatase (ALP), fasting glucose, cholesterol and triglyceride levels, uric acid, glycosylated hemoglobin A1c (HbA1c), hepatitis B surface antigen (HBsAg), and antibody to hepatitis C virus (anti-HCV).

Blood samples were obtained in the morning after an overnight fast. Standard liver tests were performed on a multichannel autoanalyzer (Hitachi 7250). HBsAg was measured by a commercially available enzyme immunoassay (Enzygnost, Berling, Germany). Anti-HCV was tested by a

second generation enzyme immunoassay (Ortho Diagnostics, Raritan, NJ).

Diagnosis of fatty liver was made using ultrasound according to Saverymuttu *et al*¹⁴. The criterion for fatty liver was hyperechoic liver tissue with fine, tightly packed echoes. The degree of fatty change was assessed by the fall in echo amplitude with depth, increasing discrepancy of echo amplitude between liver and kidney, and loss of echoes from the wall of the portal veins.

The presence of diabetes mellitus was defined as fasting blood glucose 126 mg/dL and/or HbA1c 6.1^{15,16}. The presence of high blood pressure was defined as systolic blood pressure 140 mmHg and/or diastolic blood pressure 90 mmHg.

The main endpoint was the identification of the presence or absence of an elevated GGT level combined with clinically associated variables: age, BMI, hypertension, hemoglobin, total cholesterol, triglyceride, uric acid, diabetes mellitus, and fatty liver. All variables were included in a multivariate forward stepwise logistic regression analysis to find the independent predictors of the presence of an elevated GGT level.

Statistical analysis

The continuous variables were compared between the women with and without an elevated GGT level using the 2-tailed Student's *t* test. Correlation among these variables was analyzed by Pearson's correlation coefficient. Categorical variables were compared with Fisher's exact test. Multivariate analysis was tested using forward stepwise logistic regression analysis. The SPSS statistical software was used for statistical analysis. A *P* value less than 0.05 was considered statistically significant.

RESULTS

Among 4 366 women who received a health check-up, 141 were positive for HBsAg and 14 were positive for anti-HCV (None was positive for both HBsAg and anti-HCV). Persons with either HBsAg or anti-HCV were excluded from this study; the data of the remaining 4 211 women was used for the analysis.

Factors correlated with GGT elevation

Univariate analysis Of the 4 211 women without hepatitis virus markers, 258(6.1%) showed an elevated GGT level (>68 IU/L, reference range: 10-68 IU/L). In comparison, the frequency of raised GGT level in 6 620 male health check-up participants (all were negative for both HBsAg and anti-HCV) was 30.2%. When classified into two categories (normal or abnormal, present or absent, above or below), several variables were associated with GGT elevation (Table 1).

Fatty liver was detected in 391(9.3%) of the 4 211 women by using ultrasound. Among the 391 women with fatty liver and 3 820 women without fatty liver, correlations of the GGT level with several quantitative variables were assessed. Among the women with fatty liver, age and BMI were not correlated with the GGT level, whereas all variables examined were correlated well with the GGT level in the women without fatty liver. The GGT level was strongly correlated with both AST and ALT, and the correlations were both stronger than that between GGT and ALP (Table 2).

When the women were divided into 2 groups according to the presence or absence of an elevated triglyceride level, the frequency of GGT elevation did not differ between the women with and without fatty liver. However, the mean GGT level in the women with fatty liver was significantly higher than that in the women without fatty liver (Table 3).

Multivariate analysis In multiple regression analysis, all

independent variables but age were correlated with the GGT level. Although fatty liver was associated with GGT level, the association was weaker than those between the GGT level and the other independent variables (Table 4).

Table 1 Univariate analysis of the association between GGT elevation and different variables

Variable	Category	<i>n</i>	GGT>68 IU/L (%)	<i>P</i>
Age	50	2 342	181 (7.7)	<0.0001
	<50	1 869	77 (4.1)	
BMI	25	1 206	105 (8.7)	<0.0001
	<25	3 005	153 (5.1)	
Blood pressure	High	563	45 (8.0)	0.047
	Normal	3 648	213 (5.8)	
Hemoglobin (g/dL)	14	1 153	110 (9.5)	<0.0001
	<14	3 058	148 (4.8)	
Cholesterol (mg/dL)	220	1 408	122 (8.7)	<0.0001
	<220	2 803	136 (4.9)	
Triglyceride (mg/dL)	150	667	89 (13.3)	<0.0001
	<150	3 544	169 (4.8)	
Uric acid (mg/dL)	7.0	154	16 (10.4)	0.025
	<7.0	4 057	242 (6.0)	
Diabetes	Present	186	32 (17.2)	<0.0001
	Absent	4 025	226 (5.6)	
Fatty liver	Present	391	36 (9.2)	0.008
	Absent	3 820	222 (5.8)	

Table 2 Coefficients between GGT and several variables in women with and without fatty Liver (Pearson's correlation analysis)

Variable	Women with fatty liver (<i>n</i> =391)	<i>P</i> value	Women without fatty liver (<i>n</i> =3 820)	<i>P</i> value
Age	-0.035	0.485	0.091	<0.001
BMI	0.022	0.670	0.164	<0.001
SBP	0.078	0.122	0.131	<0.001
DBP	0.101	0.046	0.123	<0.001
Hemoglobin (g/dL)	0.140	0.006	0.100	<0.001
Blood sugar	0.129	0.011	0.195	<0.001
HbA1c (mg/dL)	0.108	0.032	0.186	<0.001
Total cholesterol (mg/dL)	0.187	<0.001	0.134	<0.001
Triglyceride (mg/dL)	0.226	<0.001	0.208	<0.001
AST (IU/L)	0.411	<0.001	0.455	<0.001
ALT (IU/L)	0.464	<0.001	0.524	<0.001
ALP (IU/L)	0.272	<0.001	0.363	<0.001
Uric acid (mg/dL)	0.188	<0.001	0.178	<0.001

SBP, systolic blood pressure; DBP, diastolic blood pressure.

Table 3 Relationship between GGT and fatty liver in women with and without elevated triglyceride (TG) Level

	GGT>68 IU/L (%)	Mean of GGT (Geometric mean±SD)
Women with elevated TG level (<i>n</i> =667)	89 (13.5)	32.4±1.9
With fatty liver (<i>n</i> =137)	22 (16.1)	38.9±1.8
Without fatty liver (<i>n</i> =530)	67 (12.6)	30.9±1.9 ^b
Women with normal TG level (<i>n</i> =3 544)	169 (4.8)	22.4±1.7
With fatty liver (<i>n</i> =254)	14 (5.5)	28.2±1.7
Without fatty liver (<i>n</i> =3 290)	155 (4.7)	22.4±1.7 ^b

^b*P*<0.001 when compared between with and without fatty liver.

Table 4 Multiple regression analysis of association between logarithmically transformed GGT level and independent variables

Variable	Regression coefficient	T value	P value
Age	-0.0007	-1.77	0.076
BMI	0.0058	4.82	<0.001
SBP	0.0007	3.36	0.001
Hemoglobin	0.0112	3.64	<0.001
Total cholesterol	0.0004	3.20	0.001
Triglyceride ^a	0.2160	11.38	<0.0001
Uric acid	0.0300	8.23	<0.0001
Diabetes	0.1140	6.45	<0.0001
Fatty liver	0.0340	2.60	0.009
R ²	0.1630		

a, logarithmically transformed triglyceride level.

Table 5 Factors contributing to elevated GGT level in women (n=4 211)

	Odds ratio	95% CI	P
Age 50 years	1.4	1.1-1.9	0.016
Hemoglobin 14 g/dL	1.6	1.3-2.1	<0.0001
Triglyceride 150 mg/dL	2.3	1.7-3.1	<0.0001
Diabetes	2.2	1.5-3.4	<0.0001

Table 6 Factors contributing to fatty liver in women (n=4 211)

	Odds ratio	95% CI	P
BMI 25 kg/m ²	3.3	2.8-3.9	<0.0001
Hemoglobin 14 g/dL	1.6	1.2-2.0	<0.0001
Triglyceride 150 mg/dL	2.3	1.8-2.9	<0.0001
Uric acid 7.0 mg/dL	1.9	1.2-2.8	0.003

Although all variables were associated with GGT elevation in univariate analysis (Table 1), the stepwise logistic regression analysis indicated that four variables (age 50 years, hemoglobin 14 g/dL, triglyceride 150 mg/dL, and presence of diabetes) were significantly and independently associated with GGT elevation (Table 4). The presence of fatty liver was not independently associated with GGT elevation. In the women with fatty liver (n=391), only two variables, triglyceride 150 mg/dL and presence of diabetes, were significantly and independently associated with elevated GGT level (P=0.003 and P=0.023, respectively).

Clinical variables predicting the presence of ultrasonographic evidence of fatty liver were also examined by stepwise logistic regression analysis. In all women, four variables were independently associated with the presence of fatty liver: BMI 25 (P<0.0001), hemoglobin 14 g/dL (P=0.002), triglyceride 150 mg/dL (P<0.0001), and uric acid 7.0 mg/dL (P<0.0001). The elevated GGT level was not independently correlated with fatty liver.

DISCUSSION

GGT is one of the biliary enzymes, and is synthesized in epithelial cells of the intrahepatic bile duct^[17]. A raised GGT level is usually seen in association with cholestasis and liver cell necrosis^[17]. Although GGT is a biliary enzyme, the levels in this study were more strongly associated with transaminase levels, which are associated with liver cell necrosis, as compared with ALP.

Recently, an association between GGT and metabolic syndrome: hypertension^[8], dyslipidemia^[7], diabetes mellitus^[11],

has been reported. The mechanism of the association was still unknown, but one of the likely mechanisms proposed is that GGT is associated with fatty liver, which is also related to hepatic insulin resistance leading to insulin resistance syndrome^[11].

In this study, the serum GGT level was correlated with metabolic syndrome (hypertension, diabetes mellitus, and dyslipidemia) and risk factors for metabolic syndrome (age, BMI, blood glucose level, and uric acid concentration) in the univariate analysis, whereas, in the multivariate analysis, only four variables were independently associated with the raised GGT level: age 50 yr, hemoglobin 14 g/dL, triglyceride 150 mg/dL, and presence of diabetes mellitus. Age 50 yr was one of the factors independently associated with GGT elevation, but the association was not seen in the multiple regression analysis. The reason for this discrepancy may be the unique distribution of the age-related prevalence of GGT elevation. The abnormally raised GGT level was most frequently seen in the women of 50-59 years of age.

A relationship between the ultrasonographic evidence of fatty liver and raised GGT level was seen in the univariate analysis, but the relationship was not observed in the multivariate analysis. The triglyceride level was strongly correlated with GGT level and also well associated with fatty liver. The association between the elevated GGT level and fatty liver might be influenced by the strong association between triglyceride and GGT and fatty liver. When the women were divided into two groups according to presence or absence of raised triglyceride level, the frequency of GGT elevation did not differ between the women with and without fatty liver. However, the mean GGT level in the women with fatty liver was significantly higher than that in the women without fatty liver, indicating the positive correlation between GGT level and fatty liver within its normal range.

Both hypertriglyceridemia and diabetes mellitus were independently associated with GGT elevation. Triglyceride level and diabetes mellitus are known to be strongly associated with insulin level and are included in metabolic syndrome^[8,18]. Moreover, hyperinsulinemia was reported to be associated with raised GGT level^[7]. Raised GGT level is associated with insulin resistance, which is related to an increase in oxidative stress, which leads to liver cell necrosis by stimulating inflammatory cytokines^[10]. Fatty liver may not always mediate between insulin resistance and raised GGT levels. For example, diabetes mellitus is the representative condition of the sequelae of insulin resistance and independently associated with raised GGT level, but many diabetic persons do not have fatty liver.

In this study, GGT was correlated with an elevated hemoglobin level. Insulin resistance status increases delivery of free fatty acids to the liver^[10], which leads to the formation of free radicals^[10]. Formation of free radicals is also induced by iron overload^[19], which is associated with insulin resistance^[20,21]. Liver iron concentration is correlated with serum ferritin levels and peripheral hemoglobin concentration^[21,22]. Obesity, which is linked with an elevated hemoglobin level, is associated with arterial hypoxemia, which may result from reduced pulmonary function^[23,24]. Sleep apnea syndrome is frequently seen in obese persons^[25,26], and is associated with hypoxemia and elevated levels of hemoglobin.

The serum GGT level is a well known indicator of excess alcohol intake. GGT is also raised in patients with various liver diseases: fatty liver, chronic viral hepatitis, drug-induced liver injury and primary biliary cirrhosis (PBC). These liver diseases are usually asymptomatic, and can be included in general-population studies^[27]. Patients with chronic viral hepatitis were supposed to be excluded from this study because all women included in this study were negative for both HBsAg and anti-HCV. However, we did not take a history regarding past or current medication, nor did we examine anti-mitochondrial

antibody. Hence, our study population might contain patients with subclinical drug-induced liver injury and those with asymptomatic PBC. Nevertheless, the influence of the presence of these liver diseases might be small because of the rarity of these liver diseases in a population-based study.

In this study, we enrolled only women, but the annual health check-ups include many men. General population studies from Japan showed that 73% of males having health check-ups drank alcohol and that 12.5% of them drank more than 453 mL/wk^[8,10]. Obtaining information on alcohol intake from family members who are in close contact with each other is difficult in population-based studies. We therefore excluded male health check-up participants from this study to minimize the possibility of including alcohol-related liver disease. Most female health check-up participants had no regular alcohol intake. We previously interviewed 140 female health check-up participants who had an elevated GGT level and only two (1.4%) of them had a history of regular alcohol intake. The subjects of this study may have included some women with a history of regular alcohol intake, but the influence of alcohol might be quite small and might not affect the whole data.

In conclusion, GGT elevation was independently associated with hypertriglyceridemia and diabetes mellitus but not associated with the ultrasonographic evidence of fatty liver. Metabolic syndrome seemed to be directly, not indirectly through fatty liver, associated with the raised GGT level in Japanese women.

ACKNOWLEDGEMENT

We are grateful to Dr. Kozen Kinjo and other staff members in the Okinawa General Health Service Association for their kind cooperation.

REFERENCES

- Kuczmarski RJ**, Carroll MD, Flegal KM, Troiano RP. Varying body mass index cutoff points to describe overweight prevalence among U.S. adults. *NHANES III (1988-1994) Obes Res* 1997; **5**: 542-558
- Hamaguchi K**, Sakata T. Epidemiology of obesity. *Kan Tan Sui* 2001; **42**: 9-18
- Kopelman PG**. Obesity as a medical problem. *Nature* 2000; **404**: 635-643
- De Fronzo RA**, Ferrannini E. Insulin resistance. A multifaceted syndrome responsible for NIDDM, obesity, hypertension, dyslipidemia, and atherosclerotic cardiovascular disease. *Diabetes Care* 1991; **14**: 173-194
- Moller DE**, Flier JS. Insulin resistance. Mechanism, syndromes, and implications. *N Engl J Med* 1991; **325**: 938-948
- Kissebah AH**, Krakower GR. Regional adiposity and morbidity. *Physiol Rev* 1994; **74**: 761-811
- Rantala AO**, Lilja M, Kauma H, Savolainen MJ, Reunanen A, Kesaniemi YA. Gamma-glutamyl transpeptidase and the metabolic syndrome. *J Intern Med* 2000; **248**: 230-238
- Ikai E**, Ishizaki M, Suzuki Y, Ishida M, Noborizaka Y, Yamada Y. Association between hepatic steatosis, insulin resistance and hyperinsulinaemia as related to hypertension in alcohol consumers and obese people. *J Hum Hypertens* 1995; **9**: 101-105
- Shen L**, Fan JG, Shao Y, Zeng MD, Wang JR, Luo GH, Li JQ, Chen SY. Prevalence of nonalcoholic fatty liver among administrative officers in Shanghai: an epidemiological survey. *World J Gastroenterol* 2003; **9**: 1106-1110
- Harrison SA**, Kadakia S, Lang KA, Schenker S. Nonalcoholic steatohepatitis: what we know in the new millennium. *Am J Gastroenterol* 2002; **97**: 2714-2724
- Perry LJ**, Wannamethee SG, Shaper AG. Prospective study of serum γ -glutamyltransferase and risk of NIDDM. *Diabetes Care* 1998; **21**: 732-737
- Nomura H**, Kashiwagi S, Hayashi J, Kajiyama W, Tani S, Goto M. Prevalence of fatty liver in a general population of Okinawa, Japan. *Jpn J Med* 1988; **27**: 142-149
- Yoshiike N**, Matsumura Y, Zaman MM, Yamaguchi M. Descriptive epidemiology of body mass index in Japanese adults in a representative sample from the National Nutrition Survey 1990-1994. *Int J Obes Relat Metab Disord* 1998; **22**: 684-687
- Saverymuttu SH**, Joseph AEA, Maxwell JD. Ultrasound scanning in the detection of hepatic fibrosis and steatosis. *Br Med J* 1986; **292**: 13-15
- The committee of Japan Diabetes Society for the Diagnostic Criteria of Diabetes Mellitus**. Report of the committee of Japan Diabetes Society on the classification and Diagnostic Criteria of Diabetes Mellitus. *J Jpn Diabetes Soc* 1999; **42**: 385-404
- Takahashi Y**, Noda M, Tsugane S, Kuzuya T, Ito C, Kadowaki T. Prevalence of diabetes estimated by plasma glucose criteria combined with standardized measurement of HbA1c among health checkup participants on Miyako island, Japan. *Diabetes Care* 2000; **23**: 1092-1096
- Nemesanszky E**, Lott JA. Gamma-glutamyltransferase and its isoenzymes: progress and problems. *Clin Chem* 1985; **31**: 797-803
- Perry LJ**, Wannamethee G, Whincup PH. Serum insulin and incident coronary heart disease in middle-aged British men. *Am J Epidemiol* 1996; **144**: 224-234
- Bacon B**, O' Neill R, Britton R. Hepatic mitochondrial energy production in rats with chronic iron overload. *Gastroenterology* 1993; **105**: 1134-1140
- Mendler MH**, Turlin B, Moirand R, Jouanolle AM, Sapey T, Guyader D, LeGall JY, Brissot P, David V, Deugnier Y. Insulin resistance-associated hepatic iron overload. *Gastroenterology* 1999; **117**: 1155-1163
- Fargion S**, Mattioli M, Fracanzani AL, Sampietro M, Tavazzi D, Fociani P, Taioli E, Valenti L, Fiorelli G. Hyperferritinemia, iron overload, and multiple metabolic alterations identify patients at risk for nonalcoholic steatohepatitis. *Am J Gastroenterol* 2001; **96**: 2448-2455
- Bonkovsky HL**, Banner BF, Rothman AL. Iron and chronic viral hepatitis. *Hepatology* 1997; **25**: 759-768
- Luce JM**. Respiratory complication of obesity. *Chest* 1980; **78**: 626-631
- Ray C**, Sue DY, Bray G, Hansen JE, Wasserman K. Effects of obesity on respiratory function. *Am Res Respir Dis* 1983; **128**: 501-550
- Messinezy M**, Pearson TC. A retrospective study of apparent and relative polycythemia: associated factors and early outcome. *Clin Lab Haemat* 1990; **12**: 121-129
- Coughlin S**, Calverley P, Wilding J. Sleep disordered breathing - a new component of syndrome X. *Obes Rev* 2001; **2**: 267-274
- Inoue K**, Hirohata J, Nakano T, Seki T, Sasaki H, Higuchi K, Ohta Y, Onji M, Muto Y, Moriwaki H. Prediction of primary biliary cirrhosis in Japan. *Liver* 1995; **15**: 70-77

Edited by Zhu LH and Xu FM

Subepithelial basement membrane thickness in patients with normal colonic mucosal appearance in colonoscopy: Results from southern Turkey

Fazilet Kayaselcuk, Ender Serin, Yüksel Gumurdulu, Birol Ozer, Ilhan Tuncer, Sedat Boyacioglu

Fazilet Kayaselcuk, Ilhan Tuncer, Department of Pathology, Adana Teaching and Medical Research Center, Baskent University, Turkey

Ender Serin, Yüksel Gumurdulu, Birol Ozer, Department of Gastroenterology, Adana Teaching and Medical Research Center, Baskent University, Turkey

Sedat Boyacioglu, Department of Gastroenterology, Baskent University Ankara Hospital, Ankara Turkey

Correspondence to: Fazilet Kayaselcuk, Baskent Universitesi, Tıp Fakültesi, Adana Hastanesi, Dadaloglu mah. Serinevler 39 sok. Yuregir/Adana, Turkey. faziletks@baskent-adn.edu.tr

Telephone: +90-322-3272727 **Fax:** +90-322-3271276

Received: 2003-02-25 **Accepted:** 2003-03-15

Abstract

AIM: Our aims were to determine the normal limits of subepithelial basement membrane (SEBM) thickness in order to more accurately diagnose collagenous colitis in the population from southern Turkey and to investigate into links between SEBM thickness and age, and sex.

METHODS: The study included 100 patients (mean age 50.0±13.3 years; male, 34; female, 66) with miscellaneous gastrointestinal symptoms, and normal colonic mucosal appearance in colonoscopic evaluation. Biopsies were taken from five different regions of the colon. SEBM was measured with a calibrated eyepiece on specimens prepared with specific stains for collagen. Intensity of inflammatory cells was graded semiquantitatively. Differences in SEBM thickness among the different colon regions, and relationships between SEBM thickness and age, sex, and density of inflammatory cells were statistically evaluated.

RESULTS: The cecum and rectum showed the largest amounts of infiltrate. None of the specimens showed histologic findings of collagenous colitis. The SEBM thicknesses measured for each case ranged from 3-20 µm. The biggest thickness was observed in rectal mucosa (median value: 10 µm). Cecum and ascending colon showed similar SEBM thickness (median value: 5 µm). SEBM thickness was not correlated with patient age or sex, but was positively correlated with the intensity of inflammatory cells in each colon segment.

CONCLUSION: In this patient group from southern Turkey, SEBM was thickest in the rectum. Our results indicate that, in this population, SEBM thickness is not correlated with age or sex, but is positively correlated with severity of inflammation. The findings also support the concept that measuring SEBM thickness at one segment in the colon is inadequate and may be misleading.

Kayaselcuk F, Serin E, Gumurdulu Y, Ozer B, Tuncer I, Boyacioglu S. Subepithelial basement membrane thickness in patients with normal colonic mucosal appearance in colonoscopy: Results from southern Turkey. *World J Gastroenterol* 2004; 10(7): 1056-1058 <http://www.wjgnet.com/1007-9327/10/1056.asp>

INTRODUCTION

Lindstrom introduced the term “collagenous colitis” to describe a colon biopsy that showed hyalinized substance, known as a collagen band, between the transition zone of the subluminal basement membrane and the lamina propria^[1-8]. The English literature contains approximately 200 reports of this condition^[7]. Collagenous colitis is most often diagnosed in middle-aged women^[3,6-10]. In some patients this condition is associated with autoimmune diseases, such as diabetes mellitus, primary biliary cirrhosis, rheumatoid arthritis, and gluten-sensitive enteropathy^[3]. Some of the cases linked with histories of smoking, or antibiotic or non-steroidal anti-inflammatory drug (NSAID) ingestion^[1,3,6,7,9,11].

In healthy adults, the subepithelial basement membrane (SEBM) of the colon consists of collagen types I and IV, laminin, and fibronectin. The thickness of this layer varies from 0 to 7 µm^[3,5-7,12], and is slightly greater in the settings of hyperplastic polyps, colonic diverticulum, and congenital megacolon^[3,6]. In this study, we investigated SEBM thickness in biopsies from five different colonic sites in patients from the southern Anatolia region of Turkey. One of our aims was to determine the normal limits of SEBM thickness in this region in order to more accurately diagnose collagenous colitis in the population. Another objective was to investigate into links between SEBM thickness and age, and sex.

MATERIALS AND METHODS

The study included 100 patients who were admitted to our gastroenterology clinic with non-specific symptoms, such as chronic constipation, diarrhea, and abdominal distension and discomfort. Only two individuals had experienced short episodes of diarrhea. All the participants gave their informed consent for diagnostic colonoscopy. The protocol was carried out in accordance with the Helsinki Declaration as revised in 1989.

Each individual underwent colonoscopy and biopsies were collected from five different regions of the colon: the cecum, the ascending, transverse, and descending colon, and the rectum. Two biopsies were obtained from each segment. The specimens were fixed in 40 g/L neutral buffered formaldehyde, embedded in paraffin, and stained with hematoxylin-eosin, and slides were examined under the light microscope. Each slide was assessed for type of inflammation, intensity of inflammatory cells, superficial epithelial damage, cryptitis, and crypt abscesses. The finding of few lymphocytes, plasma cells, eosinophils, macrophages and scattered mast cells in lamina propria is considered to be normal in histopathological examination. Taken such a scene as normal (grade 0), intensity of inflammatory cells was graded on a three-tier scale. The predominant cell type (lymphocyte, eosinophil, or neutrophil) in the inflammatory infiltrate was also noted.

All the specimens were also histochemically prepared with periodic acid-Schiff (PAS), Masson's trichrome, and crystal violet stains. A calibrated eyepiece was used to measure SEBM thickness on the sections stained with Masson's trichrome at ×400 magnification. On every slide, we measured the thickest

part of the SEBM in non-tangential areas of tissue section that were distant from the crypts. The SEBM thickness for each segment in each patient was recorded. Also, for each patient, two of the same biopsied regions were randomly selected and the average SEBM thickness for these two sites was recorded. PAS stain was used to demonstrate intestinal parasites and fungi, and crystal violet was used to reveal the presence of amyloid. Differences among SEBM thickness in the different colon regions, and relationships between SEBM thickness and age, and sex were statistically evaluated. The data of SEBM thickness are reported as medians (ranges). Comparisons between median values of SEBM thickness belonging to each colon segment were performed using Mann-Whitney *U* test. The relationships between SEBM thickness and demographic parameters (age and sex), and SEBM thickness and intensity of inflammation were tested with Spearman's correlation. *P* values <0.05 were considered statistically significant.

RESULTS

The mean age in the study group was 50.0±13.3 yr (range, 18-82 yr). Of the 100 patients, 34 were men and 66 were women. In 93 of the cases, the mucosa appeared normal on colonoscopy. Of the 7 cases with abnormal findings, 3 showed mildly hyperemic mucosa, 2 exhibited colonic diverticula, 1 had a polyp, and 1 had a superficial ulcer. In the biopsy specimens, eosinophils were as numerous as lymphocytes in the inflammatory infiltrates. The cecum and rectum showed the largest amounts of infiltrate. In most cases, the inflammatory infiltrate in the rectal biopsies contained lymphocytes, plasmocytes, and neutrophils. None of the specimens showed amyloid deposition, intraepithelial lymphocytosis, epithelial vacuolization, desquamation, mucin loss, pseudostratification, or focal neutrophilic cryptitis.

The range and median SEBM thickness in each of the five colon segments are summarized in Table 1. The median SEBM thickness for the separate segments differed. The largest thickness was observed in rectal mucosa. The difference between rectum and transverse colon did not reach statistical significance, but there was a trend towards greater thickness in rectum. Cecum and ascending colon showed similar SEBM thickness. SEBM thickness was not correlated with patients' age or sex, but was positively correlated with intensity of inflammatory cells in each colon segment (Table 2). The thickness measured for each case ranged from 3-20 µm (Figure 1). In 1 of the 2 individuals with colonic diverticula, the SEBM in the descending colon and rectum was greater than 10 µm thick. In the 1 patient who had a polyp, the SEBM thickness in the rectum was 12 µm. In 2 cases, SEBM thickness was 15-20 µm in all segments of the colon. Both these individuals (a 50-year-old male and a 69-year-old woman) had long histories of chronic constipation and intermittent ingestion of NSAIDs. The colon biopsies in these 2 cases showed mild eosinophil infiltration.

Table 1 The median values of SEBM thickness in various colon segments

Colon segment	SEBM thickness (µm)	
	Median	Range
Cecum	5 ^a	3-12
Ascending colon	5 ^b	3-20
Transverse colon	8 ^a	3-20
Descending colon	8 ^{bad}	3-20
Rectum	10 ^d	3-20

*: NS, ^b*P*=0.001, ^a: SEBM was thicker in transverse colon compared to descending colon *P*=0.04, ^d*P*<0.001, ^e*P*=0.07.

Table 2 The Spearman's correlation coefficients for the relationship between SEBM thickness and severity of inflammation in various colon segments

Colon segment	Correlation coefficient (r)	<i>P</i>
Cecum	0.499	<0.0001
Ascending colon	0.642	<0.0001
Transverse colon	0.699	<0.0001
Descending colon	0.620	<0.0001
Rectum	0.553	<0.0001

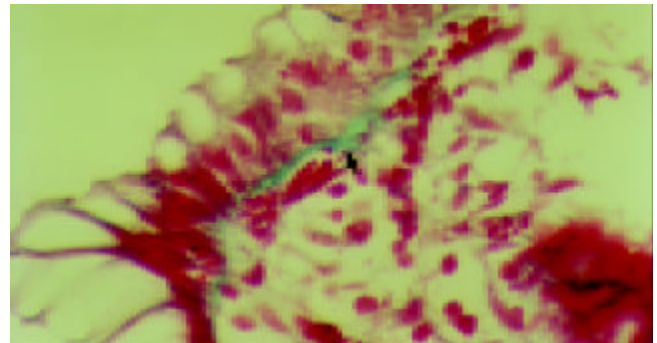


Figure 1 Photomicrograph of colonic mucosa showing normal SEBM (3-4 µm) just beneath the surface epithelium (Masson's trichrome x400).

DISCUSSION

The main histopathological criteria for collagenous colitis include the characteristic findings of a thick, continuous, hypocellular, eosinophilic, linear fibrous band beneath the surface epithelium, as well as intraepithelial lymphocytosis, epithelial vacuolization, and desquamation^[1,3,5-7,11]. One of the difficulties in diagnosing collagenous colitis is that different sources cite different SEBM thickness as one of the main criteria for diagnosis^[9]. Thus, sampling error is a probable cause of under diagnosis in collagenous colitis. Some investigators consider thickness >10 µm to be diagnostic, whereas others use >15 µm, and still others >30 µm^[3,5-7,11]. The SEBM thickness documented in cases of collagenous colitis in the English literature range from 11.5 to 60 µm^[6,13-18]. In a study of 564 patients conducted in 1982, the authors identified >10 µm in thickness as abnormal^[14]. In a series of 33 patients with collagenous colitis, Tanaka *et al*^[9] observed that 82% exhibited >10 µm in SEBM thickness in at least one area of the left colon. The rectum appeared normal in 72% of these cases, and only three patients showed a collagen band in the cecum. Tanaka *et al* used <7 µm as the criterion for normal SEBM thickness, and identified mucosal inflammation and SEBM thickness >10 µm as diagnostic criteria for collagenous colitis^[9].

SEBM thickness in the healthy population in the various studies in the literature ranges from 0 µm to 7 µm^[3,6,15]. In some of these investigations, estimates of SEBM thickness in the general population were derived from autopsy series^[6,14]. In a series of 457 patients that included adenocarcinoma, polyp, and megacolon cases as well as autopsy cases, Gledhill and Cole were only able to determine SEBM thickness in 190 of the subjects (6). In this group, SEBM thickness was <10 µm in 171 cases, between 10-15 µm in 12 cases, and >15 µm in 7 cases. Six of the 7 patients with collagen band thickness >15 µm and 6 of the 12 patients with thickness between 10-15 µm had diarrhea. The maximum SEBM thickness recorded by Gledhill and Cole was 80 µm, and the average in the 190 patients was 22.5 µm. Consistent with our study, the authors found that SEBM thickness >10 µm was associated with non-specific colitis, colonic diverticula, and epithelial polyp; however, they

presented no data related to inflammation^[6]. All the cases in our study exhibited SEBM, that is, no 0 μm values were recorded. The lowest value of SEBM thickness we observed was 3 μm , and the intensity of inflammation predominant in the tissue section with SEBM thickness of 3 μm was 0-1. Gledhill and Cole found that SEBM thickness was not correlated with age or sex^[6], similar to our results.

Our aims in this study were to determine the normal limits of SEBM thickness in the southern Anatolia region of Turkey, and to investigate for possible links between SEBM thickness and age, and sex. Studies of collagenous colitis patients in Europe and the United States have revealed substantially different SEBM thickness in these geographic regions. The nutritional habits of people in south and southeast Anatolia differ from those in Europe and the United States. The main nutritional sources in southern Turkey are animal protein and wheat products. The prevalence of parasitic infection, and particularly amebiasis, is very high in this area. In one study of 35 172 patients with diarrhea who were from south and southeast Anatolia, 26.4% had amebiasis (19). The same authors investigated infectious diseases transmitted by drinking water in a study that was conducted between 1994 and 1995 in southern Turkey. The results showed 7 281 new amebiasis cases during this 1-yr period, and revealed a rise in incidence of up to 41% during the summer^[20]. In our study, histological examination revealed colonic amebiasis in only 3 of 100 cases. In these 3 patients, rectal SEBM thickness ranged from 10-12 μm and the rectal biopsies all showed an eosinophil-rich inflammatory response.

Patients with collagenous colitis show different SEBM thickness in different segments of the colon. Most studies have shown that this collagenous layer is thicker in the distal colon than in the proximal regions^[3,5-7,11]. Research has also revealed that patients with collagen deposition of at least 15- μm in thickness in more than 30% of multiple colon biopsies eventually develop the clinical syndrome^[1,3]. In our study, the SEBM was thickest in the rectum, followed by the transverse colon, descending colon, ascending colon, and cecum, respectively. The same sequence did not apply to intensity of inflammation, *i.e.*, cecum was the second site exhibiting relatively higher count of inflammatory cell after rectum compared to other sites. This discordance may be explained by the absence of morphometric analysis, which could give more specific result about the count of inflammatory cells than routine light microscopic evaluation. Inflammatory response, parasitic infection such as amebiasis, and nutritional factors are all elements that potentially contribute to increased basement membrane thickness. Two of our patients with SEBM thickness between 12-15 μm in any colonic segment exhibited polyp and colonic diverticula, respectively. In 2 other cases with 15-20 μm SEBM thickness, there was a history of NSAID treatment but no history of diarrhea. The colon biopsies from the latter 2 patients showed moderate inflammatory response with eosinophils predominant in the infiltrate.

In summary, of the five colon segments studied in this patient group from southern Turkey, SEBM was thickest in the rectum. Our results indicate that, in this population, SEBM thickness is not correlated with age or sex, but is positively correlated with intensity of inflammation. This study provides more evidence that SEBM thickness varies according to geographic region, and that these differences may be culture-related. The findings also suggest that measuring SEBM thickness at one segment of the colon is inadequate and may

be misleading. The mean SEBM thickness for the separate colon segments differ, similar to established characteristics of collagenous colitis. The histopathological diagnosis of collagenous colitis should be made by measuring collagen band thickness in at least 3 or more non-tangential areas that are distant from the crypts. In addition to collagen band thickness, diagnosis of this condition must be based on characteristic clinical and histologic findings. The latter include superficial desquamation, intraepithelial lymphocytosis, and epithelial vacuolization.

REFERENCES

- 1 **Fenoglio-Preiser CM**, Noffsinger AE, Stemmermann GN. Non-neoplastic colon disease. In: *Gastrointestinal Pathology*. 2nd ed, Lippincott-Raven, Philadelphia 1999: 153-236
- 2 **Bohr J**, Olesen M, Tysk C, Jarnerot G. Collagenous and lymphocytic colitis: a clinical and histopathological review. *Can J Gastroenterol* 2000; **14**: 943-947
- 3 **Dogusoy G**. Mikroskopik kolit. *Endoskopi* 2001; **12**: 61-67
- 4 **Carpenter HA**, Tremaine WJ, Batts KP, Czaja A. Sequential histologic evaluations in collagenous colitis. *Dig Dis Sci* 1992; **37**: 1903-1909
- 5 **Bohr J**. A review of collagenous colitis. *Scand J Gastroenterol* 1998; **33**: 2-9
- 6 **Gledhill A**, Cole FM. Significance of basement membrane thickening in the human colon. *Gut* 1984; **25**: 1085-1088
- 7 **Halaby IA**, Rantis PC, Vernava AM, Longo WE. Collagenous colitis, pathogenesis and management. *Dis Colon Rectum* 1996; **39**: 573-578
- 8 **Tremanine WJ**. Diagnosing collagenous colitis: does it make a difference? *Eur J Gastroenterol Hepatol* 1999; **11**: 477-479
- 9 **Tanaka M**, Mazzoleni G, Riddell RH. Distribution of collagenous colitis. Utility of flexible sigmoidoscopy. *Gut* 1992; **33**: 65-70
- 10 **Cammarota G**, Pignataro F, Cuoco L. EUS in the diagnosis of collagenous colitis. *Gastrointest Endosc* 2001; **54**: 113-115
- 11 **Offner FA**, Jao RV, Lewin KJ, Havelec L, Weinstein WM. Collagenous colitis: a study of the distribution of morphological abnormalities and their histological detection. *Hum Pathol* 1999; **30**: 451-457
- 12 **Jessurun J**, Yardley JH, Lee ED, Vendrell DD, Schiller LR, Fordtran JS. Microscopic colitis and collagenous colitis: different names for the same condition? *Gastroenterology* 1986; **91**: 1583-1584
- 13 **Bogomoletz WV**, Adnet JJ, Birembaut P, Feydy P, Dupont P. Collagenous colitis: an unrecognized entity. *Gut* 1980; **21**: 164-168
- 14 **Van den Oord JJ**, Geboes K, Desmet V. Collagenous colitis: an abnormal collagen table? Two new cases and a review of the literature. *Am J Gastroenterol* 1982; **77**: 377-381
- 15 **Schiller LR**. Pathophysiology and treatment of microscopic colitis syndrome. *Lancet* 2000; **355**: 1198-1199
- 16 **Loffeld RJ**, Balk AT. Subepithelial collagen thickening in the colon: report on a series of 23 patients. *Digestion* 1998; **59**: 715-719
- 17 **Lee E**, Schiller LR, Vendrell DD, Santa CA, Fordtran JS. Subepithelial thickness in colon specimens from patients with microscopic colitis and collagenous colitis. *Gastroenterology* 1992; **103**: 1790-1796
- 18 **Jessurun J**, Yardley JH, Giardiello FM, Hamilton SR, Bayless TM. Collagenous colitis: a clinicopathologic study of 15 cases. *Human Pathol* 1987; **18**: 839-848
- 19 **Demirhindi H**, Akbaba M, Bahcebeci T, Karaomerlioglu A, Yalcin E. Situation of intestinal amebiasis among diarrheal diseases in Adana region, Cukurova, Turkey. Fifth International Conference on Travel Medicine. March 24-27, 1997. *Geneva, Switzerland*
- 20 **Bahcebeci T**, Demirhindi H, Akbaba M, Piskin A, Cegil K. Health and quality of drinking water in Adana city centre, Turkey. International Conference on Health, Environment and Development. October 14-17, 1996. Alexandria, Egypt

Irritable bowel syndrome consulters in Zhejiang province: The symptoms pattern, predominant bowel habit subgroups and quality of life

Jian-Min Si, Liang-Jing Wang, Shu-Jie Chen, Lei-Min Sun, Ning Dai

Jian-Min Si, Liang-Jing Wang, Shu-Jie Chen, Lei-Min Sun, Ning Dai, Department of Gastroenterology, Sir Run Run Shaw Hospital, Zhejiang University School of Medicine, Hangzhou 310016, Zhejiang Province, China

Correspondence to: Dr. Jian-Min Si, Department of Gastroenterology, Sir Run Run Shaw Hospital, Zhejiang University School of Medicine, 3 Qingchun Donglu, Hangzhou 310016, Zhejiang Province, China. sijm@163.net

Telephone: +86-571-87217002 **Fax:** +86-571-87217044

Received: 2003-06-26 **Accepted:** 2003-09-18

Abstract

AIM: To investigate the pattern of symptoms, predominant bowel habits and quality of life (QOL) by the Chinese version of the SF-36 in irritable bowel syndrome (IBS) consulters in Zhejiang province.

METHODS: From January 2001 to January 2002, 662 Roma II criteria-positive IBS patients were enrolled by gastroenterologists in 10 hospitals from Digestive Disease Center of Zhejiang (DDCZ). Patients were classified into constipation predominant IBS (IBS-C), diarrhea predominant IBS (IBS-D) and alternating constipation and diarrhea IBS (IBS-A) according to the predominant bowel habits. All patients were evaluated for the demographic checklists, IBS bowel symptoms, extra-colonic symptoms, and QOL by Chinese version of the SF-36 questionnaire.

RESULTS: (1) Besides abdominal pain, the predominant colonic symptoms were in order of altered stool form, abnormalities of stool passage, abdominal distension and passage of mucus in IBS patients. Also, IBS subjects reported generalized body discomfort and psychosocial problems including dyspeptic symptoms, poor appetite, heartburn, headache, back pain, difficulty with urination, fatigue, anxiety and depression. (2) IBS-C and IBS-A are more common among female patients, whereas male patients experienced more cases of IBS-D. In regards to the IBS symptoms, there were significant differences among IBS subgroups. Abdominal pain (frequency ≥ 2 days per week and duration ≥ 1 hour per day) was frequent in IBS-A patients ($P=0.010$ and 0.027 , respectively), IBS-D patients more frequently experienced the passage of mucus, dyspeptic symptoms and anxiety ($P=0.000$, 0.014 and 0.015 , respectively). (3) IBS patients experienced significant impairment in QOL, decrements in QOL were most pronounced in vitality, general health, mental health, and bodily pain. Compared with the general population (adjusted for gender and age), IBS patients scored significantly lower on all SF-scales ($P<0.001$), except for physical function scale ($P=0.149$). (4) QOL was impaired in all subgroups, particularly in scales of vitality, general health and mental health. Compared with IBS-D, QOL in IBS-C scored significantly lower on physical function, role physical, general health, role emotional, and mental health scales ($P=0.037$, 0.040 , 0.039 , 0.005 and 0.026 , respectively).

CONCLUSION: Besides colonic symptoms, IBS could cause generalized body discomfort and psychosocial problems. The IBS subgroups based on predominant bowel habits are helpful to identify clinical distinction of the IBS. QOL is significantly impaired in IBS patients. The Chinese version of the SF-36 health survey scales may be a useful measurement of IBS patients.

Si JM, Wang LJ, Chen SJ, Sun LM, Dai N. Irritable bowel syndrome consulters in Zhejiang province: The symptoms pattern, predominant bowel habit subgroups and quality of life. *World J Gastroenterol* 2004; 10(7): 1059-1064

<http://www.wjgnet.com/1007-9327/10/1059.asp>

INTRODUCTION

Irritable bowel syndrome (IBS) comprises a group of functional bowel disorders, in which abdominal pain or discomfort is associated with defecation or a change in bowel habits, and with features of disordered defecation^[1]. In developed countries, IBS is the most frequent reason for referrals to gastroenterologists, and the diagnosis of IBS has been noted in up to 4-30% of the general population in Western Europe and North America^[2-6]. A stratified randomized study in China reported that the prevalence of IBS in Beijing is 7.26% according to Manning criteria^[7]. However, there were no large-scale studies to evaluate IBS patients who consulted physicians in China.

On clinical grounds, it has been proposed that patients with IBS can be further subdivided into those who have either predominant constipation or diarrhea or an alternating bowel pattern. Differences between these subgroups have been observed regarding viscerosensory processing^[8,9] and autonomic function^[10-12]. But clinical relevance of IBS subgroups by predominant bowel habits was not so well covered in the literature.

IBS patients could manifest gastrointestinal disorders and be accompanied with psychosocial problems. The QOL consists of all aspects of patients' disorders and can evaluate the health status in detail. Although IBS is not a life-threatening condition, for most patients it is a chronic recurrent illness that is often accompanied by severe impairment in QOL. Generic QOL measures, such as SF-36 health survey, are designed to evaluate aspects of function status and well-being applicable to a population in general, which is also a well-standardized questionnaire for assessing the QOL of IBS^[6,13-16]. As we known, there were no prior studies that evaluated the QOL by the Chinese version of SF-36 in IBS patients.

In the present study, we aimed at evaluating the pattern of symptoms and QOL of the IBS-consulters in Zhejiang, in particular with respect to different IBS subgroups.

MATERIALS AND METHODS

Subjects

From January 2001 to January 2002, 662 consecutive Roma II

criteria positive IBS patients were enrolled by gastroenterologists from 10 hospitals in urban, suburban, island, and rural areas of Digestive Disease Center in Zhejiang (DDCZ). Patients were classified into three subgroups according to the following criteria^[6,17,18]: (1) Constipation- predominant IBS (IBS-C) indicated of patients who had at least two of the four symptoms 3 months, such as straining, hard or lumpy stools, incomplete evacuation 25% of the time, and/or two or less bowel movements per week, and no concurrent diarrhea symptoms as defined below; (2) Diarrhea-predominant IBS (IBS-D) was diagnosed by the presence of loose/watery stools >75% of the time, three or more diarrhea in a week, in the absence of constipation symptoms; and (3) Patients with mixed patterns of both constipation and diarrhea were classified as alternating-IBS (IBS-A). Patients with organic diseases related to IBS bowel symptoms were excluded. All patients completed the demographic checklists, symptom questionnaire, and SF-36 questionnaire.

Demographic checklists

Patients completed 5 demographic questions regarding their age, gender, profession, marital status and the level of education. The demographic data of general population in Zhejiang province were provided by Demographic Center of Zhejiang Province.

Symptom Questionnaire (SQ)

The SQ was divided into symptoms compatible with IBS and extra-colonic symptoms.

Symptoms compatible with IBS This symptom category included the following symptoms in the prior year (referred to Roma II symptom criteria): (1) the duration of abdominal pain per day (none, <1 h, 1-8 h, >8 h); (2) the frequency of abdominal pain per week (none, <2 d, 2-5 d, >5 d); (3) the frequency of altered stool forms including lumpy/hard or loose/ watery stool (none, <25%, 25-75%, >75%); (4) the frequency of altered stool passage pattern including staining, urgency, and feeling of incomplete evacuation (none, <25%, 25-75%, >75%); (5) the frequency of passage of mucus (none, <25%, 25-75%, >75%); and (6) the frequency of bloating or abdominal distension (none, <25%, 25-75%, >75%).

Extra-colonic symptoms Patients were asked if they experienced dyspeptic symptoms, poor appetite, or heartburn. In addition, patients were asked if they had any back pain, headache, difficulty in urination, fatigue, depression, or anxiety.

Health status SF-36 questionnaire

The validated SF-36 in Chinese version was provided by professor Li Lu in Social and Demographic Department in Zhejiang University. The SF-36 included 8 multi-item dimensions: physical function, role-physical (functional limitations due to physical health problem), bodily pain (limitation due to body pain), general health, vitality (energy/fatigue), social function, role emotional (functional limitations due to emotional problems), and mental health (psychological distress and psychological well-being). The SF-36 scored from 0 to 100, with higher scores indicating better QOL.

We compared the QOL of patients with IBS with previously published SF-36 data of Zhejiang general population ($n=1\ 972$).

All subjects were evaluated after giving informed consent by Zhejiang University School of medicine.

Statistical analysis

All of the statistical analyses were conducted using the SPSS 10.0 statistical software passage. Prevalence of symptoms was expressed in percentages. Comparisons between different IBS subgroups patients were performed using χ^2 test for categorical

data and t test or ANOVA test for continuous data. $P<0.05$ was considered significant.

RESULTS

Demographic characteristics

The mean age of 662 subjects was 44.78 ± 13.71 years, with 52.9% of the sample being woman. The majority of the subjects were in the age of 25-50 years (68.4%). Further information detailing the marital status, education level, and profession are provided in Table 1. Compared with the general population in Zhejiang, IBS were more common in the intellectuals and cadres ($P<0.001$), the young adulthood (25-50 years, $P<0.001$), and in females ($P<0.05$).

Table 1 The basic characteristics of IBS consulters

Characteristics	IBS sample ($n=662$)
Age (yr, %)	44.78±13.71
<20	1.5
20-29	9.5
30-39	30.4
40-49	25.8
50-59	17
60-69	10.5
70-79	5
>80	0.3
Gender ($n, \%$)	
Male	312 (47.1)
Female	350 (52.9)
Marital status ($n, \%$)	
Never married	51 (7.7)
Married	585 (88.4)
Widow	19 (2.8)
Divorced or separated	7 (1.1)
Education level ($n, \%$)	
Illiterate	87 (13.1)
Primary school	129 (19.5)
Junior middle school	184 (27.7)
Senior middle school	155 (23.5)
College or graduated	107 (16.2)
Profession ($n, \%$)	
Peasants	211 (31.8)
Workers	75 (11.3)
Cadres	62 (9.4)
Intellectuals	58 (8.7)
Merchants	105 (15.9)
Soldiers	57 (8.6)
Student	20 (3.0)
Retired and jobless	74 (11.3)

Prevalence of symptoms

The frequency of symptoms were in order of altered stool form (79.1%), abnormalities of stool passage (67.9%), abdominal pain duration ≥ 1 h/d (67.7%), abdominal distension (63.2%), abdominal pain frequency ≥ 2 d/wk (57.5%) and passage of mucus (49.8%) in IBS patients. A few IBS subjects reported having extra-colonic symptoms including fatigue (72.7%), dyspeptic symptoms (64.1%), anxiety (54.2%), depression (44.1%), poor appetite (38.2%), headache (29.0%), back pain (26.1%), heartburn (25.0%), and difficulty with urination (11.0%).

Abdominal pain duration ≥ 1 h/d was reported more common among female IBS than male patients (61.1% vs 53.7%, $P < 0.05$). Women also more frequently reported headache and poor appetite (both $P < 0.05$). More male patients reported difficulty in urination ($P < 0.05$). The data are shown in Table 2.

Table 2 Symptoms characteristics of IBS by gender

Symptoms (%)	Male (n=305)	Female (n=311)	P
IBS compatible symptoms			
Abdominal pain ≥ 1 hour/day	53.7	61.1	0.039
Abdominal pain ≥ 2 days/week	67.2	68.2	0.434
Altered stool form	80.0	78.1	0.312
Altered stool passage	66.8	68.8	0.325
Abdominal distension	60.7	65.6	0.118
Passage of mucus	51.1	48.2	0.260
Extra-colonic symptoms			
Dyspeptic symptoms	63.1	65.3	0.319
Poor appetite	33.6	43.0	0.011
Heartburn	28.4	21.3	0.066
Headache	24.1	33.6	0.024
Back pain	24.4	27.5	0.426
Difficulty in urination	15.6	6.2	0.000
Anxiety	51.0	57.1	0.200
Depression	40.2	47.7	0.114
Fatigue	72.0	73.7	0.897

Prevalence of IBS subgroups

Patients consisted of IBS-C (20.0%), IBS-D (47.7%), and IBS-A (32.3%) according to the predominant bowel habits. The IBS-C and IBS-A patients were composed mainly of women, which were 64.2% and 56.9%, respectively. But in the IBS-D,

more subjects (56.8%) were male. The distribution of IBS compatible symptoms and extra-colonic symptoms among the IBS subgroups are summarized in Table 3. Abdominal pain (frequency ≥ 2 days per week and duration ≥ 1 hour per day) consisted of 64.9% and 75.9% respectively in IBS-A patients ($P < 0.05$), while there was 58.1% of IBS-D patients with the passage of mucus ($P < 0.05$). Compared with other two subgroups of IBS, IBS-D patients more frequently experienced of dyspeptic symptoms (70.2%) and anxiety (62.0%) ($P < 0.05$).

Table 3 Symptoms in the IBS subgroups

Symptoms (%, n)	IBS-C (n=108)	IBS-D (n=258)	IBS-A (n=174)
Gender^b			
Male	38 (35.8)	147 (56.8)	75 (43.1)
Female	69 (64.2)	111 (43.2)	99 (56.9)
Age (yr)	44.2 \pm 13.1	45.8 \pm 13.7	44.6 \pm 14.2
Abdominal pain frequency ≥ 2 d/wk duration ≥ 1 h/d ^a	51 (47.2)	152 (58.9)	113 (64.9)
Abdominal pain	62 (57.4)	171 (66.3)	132 (75.9)
Abnormal stool form	84 (77.8)	218 (84.5)	133 (76.4)
Abnormal stool passage	75 (69.4)	179 (69.4)	121 (69.5)
Abdominal distension	65 (60.2)	157 (60.9)	118 (67.8)
Passage stool mucus ^a	34 (31.5)	150 (58.1)	87 (50.0)
Dyspeptic symptoms ^b	181 (70.2)	108 (62.0)	
Heartburn	25 (23.1)	59 (22.9)	45 (25.9)
Difficulty in urination	16 (14.8)	23 (8.9)	15 (8.6)
Depression	50 (46.3)	107 (41.5)	77 (44.3)
Fatigue	68 (62.9)	202 (78.3)	125 (71.8)
Anxiety ^b	51 (47.2)	160 (62.0)	88 (50.6)

^a $P < 0.05$, ^b $P < 0.001$ between the three subgroups.

Table 4 The SF-36 scales score in IBS versus general population (Normative) by gender

Scale (mean \pm SD)	Male			Female			IBS sample
	IBS	Norm	P	IBS	Norm	P	
PF	83.6 (20.1)	84.4 (18.6)	0.478	78.3 (19.2)	79.9 (20.7)	0.179	81.1 (19.8)
RP	60.9 (51.8)	82.4 (32.6)	0.000	50.0 (51.3)	79.9 (34.5)	0.000	55.7 (51.7)
BP	53.5 (18.6)	83.0 (19.0)	0.000	47.6 (20.4)	79.9 (21.8)	0.000	50.9 (19.8)
GH	43.4 (17.3)	58.0 (19.9)	0.000	38.2 (19.7)	55.2 (20.4)	0.000	41.0 (18.6)
VT	40.9 (19.8)	53.3 (20.9)	0.000	34.4 (18.5)	50.1 (20.7)	0.000	37.9 (19.5)
SF	67.2 (18.2)	83.1 (17.5)	0.000	62.9 (18.7)	82.9 (18.1)	0.000	65.3 (18.6)
RE	65.5 (56.1)	84.3 (32.3)	0.000	53.2 (43.8)	84.5 (32.5)	0.000	59.7 (50.9)
MH	50.4 (20.6)	60.3 (23.0)	0.000	44.0 (23.9)	59.1 (22.4)	0.000	47.4 (22.4)

Table 5 The SF-36 scales score in IBS versus general population (Normative) by age

Scale (mean \pm SD)	<44 yr			45-64 yr			≥ 65 yr		
	IBS	Norm	P	IBS	Norm	P	IBS	Norm	P
PF	85.5 (18.3)	86.0 (18.0)	0.599	81.2 (19.5)	82.0 (17.4)	0.359	67.6 (20.7)	68.5 (24.5)	0.747
RP	64.1 (57.7)	85.3 (29.0)	0.000	55.9 (51.8)	80.4 (34.3)	0.000	30.5 (37.4)	68.3 (42.8)	0.000
BP	53.4 (19.7)	85.0 (17.8)	0.000	51.1 (19.7)	78.4 (21.3)	0.000	46.0 (16.3)	75.3 (23.6)	0.000
GH	44.5 (18.0)	60.0 (19.8)	0.000	41.1 (18.6)	54.0 (19.4)	0.000	34.6 (14.9)	50.3 (20.9)	0.000
VT	40.6 (19.5)	53.3 (20.3)	0.000	37.9 (19.3)	51.2 (21.1)	0.000	25.8 (16.2)	48.4 (22.1)	0.000
SF	68.0 (18.1)	84.2 (16.9)	0.000	65.4 (18.5)	82.8 (17.6)	0.000	59.8 (18.0)	79.3 (20.9)	0.000
RE	61.7 (40.8)	85.3 (30.5)	0.000	59.7 (51.0)	85.1 (32.2)	0.000	55.0 (45.7)	79.5 (38.8)	0.059
MH	49.2 (18.0)	57.9 (21.4)	0.000	47.5 (22.4)	61.3 (23.5)	0.000	47.8 (18.2)	62.4 (25.1)	0.000

The SF-36 questionnaires

For IBS patients, the lowest mean scale scores were 37.9 in vitality and 41.0 in general health. The bodily pain and role emotional scales scores were also quite low (47.4 and 50.9, respectively). Compared with the general population (adjusted for gender), the IBS patients scored significantly lower on 7 SF-scales ($P<0.001$), with the exception of physical function scale. Adjusting for age, the decrement of scale score in IBS patients (≤ 65 years) are most pronounced in 7 categories of SF-36 except the physical function scale, while patients >65 years scored significantly lower on vitality, general health, bodily pain, social function and role emotional scales ($P<0.001$), as shown in Table 4 and Table 5.

QOL was impaired in all subgroups. The QOL in three subgroups are pronounced impaired in vitality, general health and mental health. Among different subgroups, IBS-C had poor QOL. Compared with IBS-D, QOL in IBS-C scored significantly lower on physical function, role physical, general health, role emotional and mental health scales ($P<0.05$). Compared with IBS-A, the 6 scales of QOL in IBS-C were more impaired, but there was no significant difference ($P>0.05$). As shown in Figure 1 and Table 6.

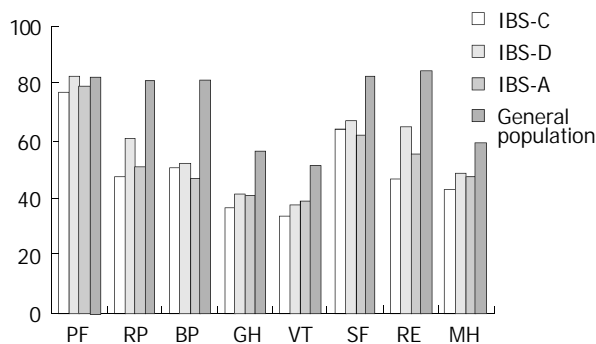


Figure 1 SF-36 scale score in different IBS subgroups compared with general population.

Table 6 SF-36 scale scores (mean±SD) among different IBS subgroups

SF-36	IBS-C	IBS-D	IBS-A	General population	P
PF	77.4 (22.1)	82.2 (17.6)	79.7 (20.7)	82.2 (19.8)	0.104
RP	47.1 (39.2)	61.3 (41.6)	50.9 (43.4)	81.2 (33.6)	0.043
BP	50.7 (20.9)	52.3 (19.8)	47.2 (19.8)	81.5 (20.5)	0.048
GH	36.9 (17.6)	41.7 (19.6)	40.5 (17.9)	56.7 (20.2)	0.110
VT	33.8 (19.0)	37.8 (19.3)	39.0 (20.0)	52.0 (20.9)	0.127
SF	63.9 (20.5)	66.9 (17.5)	62.0 (18.8)	83.0 (17.8)	0.032
RE	46.6 (44.4)	65.3 (38.7)	55.6 (43.1)	84.4 (32.4)	0.080
MH	42.6 (30.9)	48.7 (18.0)	47.9 (18.7)	59.7 (22.7)	0.061

DISCUSSION

IBS is important because it is associated with considerable morbidity, cost and poor QOL. IBS patients who consulted physicians (IBS-consulters) got more severe IBS symptoms^[19] and higher psychological discomfort^[20] compared to the non-consulters. Studies have reported that IBS-consulters had poor QOL than the non-consulters^[21]. Therefore, more and more studies were focused on evaluating the IBS-consulters patients. The data obtained in our study represents the reality of IBS-consulters in general population in Zhejiang province.

We demonstrated that male to female ratio was 1:1.21. Compared with the general population, IBS are more common among people between the age of 25 to 50 years (68.4% vs 51.9%,

$P<0.01$), and between the intellectuals and cadres ($P<0.001$). A few studies have shown IBS is more prevalent in women than in men^[3,6,7]. The majority of the subjects being the intellectuals and in the age of 18-40 years (51.6%) was also observed in recent study in Beijing^[7]. In the present study, we found that the most frequent symptom was altered stool form (79.1%), in order of abnormalities of stool passage (67.9%), abdominal pain (67.7%), abdominal distension (63.2%) and passage of mucus (49.8%) in IBS patients. IBS could reflect a wide range of symptoms, and abdominal pain was not the essential symptom. Although only colonic symptoms are used in the Manning or Rome criteria for the diagnosis of IBS, noncolonic symptoms arising elsewhere in the gastrointestinal tract or viscerosensory symptoms are common in IBS. It was considered that a large proportion of IBS patients complain of functional disorders of obscure origin, such as headache, low back pain, dysuria, depression, sleeping disorders, anxiety, and attention fatigue^[22-25]. Our study showed that IBS patients commonly presented with fatigue (72.7%), dyspeptic symptoms (64.1%), anxiety (54.2%), depression (44.1%), headache (29.0%), back pain (26.1%), heartburn (25.0%), and difficulty in urination (11.0%). In addition, an increased prevalence of extra-colonic symptoms, including headache and poor appetite were seen in female IBS patients.

IBS could be subdivided into IBS-C, IBS-D and IBS-A according to the predominant bowel habits. We found IBS-D (48.3%) to be the predominant habits, in order of IBS-A (32.7%) and IBS-C (19.0%). Lembo *et al*^[26] using Rome I diagnostic criteria, who suggested the IBS-A in 49%, IBS-D in 33%, and IBS-C in 18%. Another study found that the IBS-A in 38%, IBS-C in 37%, and IBS-D in 25% by Rome II criteria^[27]. The different prevalence may be due to the bias of sample of population or diagnostic criteria. We postulate that subjects with different bowel habits have different pathophysiologic conditions and therefore will differ with respect to their clinical characteristics, and designed to evaluate the gender distribution and symptoms as well as QOL among all subgroups. Results demonstrated that females had higher proportion of IBS-C and IBS-A, while there was a trend towards a higher proportion of being IBS-D in male patients. The data was consistent with recent studies of IBS in Europe and U.S.A.^[8,17]. Several physiological factors may play a role in these gender-related differences in self-reported bowel habits, including difference in central autonomic control, enteric nervous system physiology, and smooth muscle physiology^[28]. The subgroups had significant difference in IBS predominant bowel symptoms according to Roma-II criteria and extra-colonic symptoms. Abdominal pain (frequency ≥ 2 days per week and duration ≥ 1 hours per day) consisted of 64.9% and 75.9%, respectively in IBS-A patients, which was discriminates among the subgroups. It is of note that IBS-A patients were affected more by abdominal pain than were those with other subgroups. Mearin *et al*^[27] also reported that abdominal discomfort/pain were greater in the IBS-A subgroup than in the other two IBS subgroups, whereas IBS-D patients more frequently experienced of passage of mucus (58.1%), dyspeptic symptoms and anxiety ($P<0.05$). Conversely, another study showed that IBS-C patients accompanied with more higher severity of upper gastrointestinal symptoms and higher severity of lower gastrointestinal bloating than IBS-D patients, suggested that it may be related to different gastrointestinal transit or central processing of vagal-mediated afferent signals^[8]. We found that all three subgroups had impaired QOL. QOL scale score was similar in IBS-D and IBS-A, but lower in IBS-C. Compared with IBS-D patients, QOL in IBS-C scored significantly lower on physical function, role physical, general health, role emotional and mental health scales ($P<0.05$). There was a trend of decreasing of these 6 scales of QOL, but no

significant difference between IBS-C and IBS-A ($P>0.05$). Schmulson *et al*^[8] also observed that IBS-C more commonly reported impairment in sleep, appetite and sexual function, but there were no difference in SF-36 scores in different subgroups. Another investigation by Mearin *et al*^[27] indicated that QOL was affected similarly in all IBS subtypes. These results were contradicted with each other. So it was critically necessary to apply for universal criteria for the subgroups of IBS. In our present study, there were different gender distribution, clinical symptoms and QOL among the three IBS subgroups. This suggests that subdividing IBS in three groups based on bowel habits may identify clinically distinct entities, but needs to be evaluated in a more detailed study.

There is increasing recognition that what matters to most patients with chronic illness is how well they are able to function and how they feel about their daily life. Therefore, it is essential to understand the impact of IBS on patients' ability to function and well-being. The medical Outcome Study Short Form (SF-36) is a well-standardized questionnaire for assessing quality of life. The Chinese version of the SF-36 health survey scale has achieved conceptual equivalence and satisfied the psychometric scaling assumptions well enough to warrant as a standardized survey in China^[29]. As we have known, this is the first study to compare the QOL of patients with IBS and the general population in China by Chinese version of the SF-36. The present study showed that IBS patients have significantly impaired QOL, with the most pronounced decrements in vitality (energy/fatigue), general health, mental health, and bodily pain, furthermore, when compared with the general population in Zhejiang (adjusting for the age and gender distribution), IBS patients also scored significantly lower QOL on 7 SF-scales ($P<0.001$), with the exception of physical function scale. It is consistent with the study^[16,30] that QOL is low in patients with IBS, dimensions affected are particularly energy/fatigue, role limitation, physical pain and health perception. Gralnek *et al*^[30] reported that as compared with the U.S. general population (adjusted to the age and gender characteristics of IBS sample), the IBS patients scored significantly lower on each of the 8 SF-36 scales. Another study in European also showed that all aspects of QOL were adversely affected in IBS patients living in the UK and the United States^[31]. On the other hand, recent studies in Hong kong^[32,33] showed that only vitality score was lower in men with IBS, and the mental health score was significantly lower in women with IBS, compared with normal control. Our results confirm the findings that IBS had abroad and significant impact on a person's QOL, in addition to the disease activity and symptoms impacts. We postulate that the different results of QOL in studies are due to the cultural or health status perception differences between Eastern and Western countries. Generic QOL questionnaire SF-36, combined with IBS-specific QOL questionnaire will allow a clear understanding of link between IBS and QOL.

In conclusion, the present study offers insight into IBS-consulters patients in Zhejiang. Measurement of QOL in IBS can potentially help both medical decisions makers and policy planners allocated medical resources for treatment of patients.

REFERENCES

- 1 **Thompson WG**, Longstreth G, Drossman DA, Heaten K, Irvine EJ, Mulfer Lissner S. Functional bowel disorders and functional abdominal pain. WE (editors). Rome II. The Functional Gastrointestinal Disorders, 2nd edition. *Mclean, Virginia: Degnon Associates* 2000: 361-432
- 2 **Barbezat G**, Poulton R, Milne B, Howell S, Fawcett JP, Talley N. Prevalence and correlates of irritable bowel symptoms in a New Zealand birth cohort. *N Z Med J* 2002; **115**: U220
- 3 **Bommelaer G**, Dorval E, Denis P, Czernichow P, Frexinos J, Pelc A, Slama A, El Hasnaoui A. Prevalence of irritable bowel syndrome in the French population according to the Rome I criteria. *Gastroenterol Clin Biol* 2002; **26**: 1118-1123
- 4 **Saito YA**, Schoenfeld P, Locke GR 3rd. The epidemiology of irritable bowel syndrome in North America: a systematic review. *Am J Gastroenterol* 2002; **97**: 1910-1915
- 5 **Jones R**, Lydeard S. Irritable bowel syndrome in the general population. *BMJ* 1992; **304**: 87-90
- 6 **Masud MA**, Hasan M, Khan AK. Irritable bowel syndrome in a rural community in Bangladesh: prevalence, symptoms pattern, and health care seeking behavior. *Am J Gastroenterol* 2001; **96**: 1547-1552
- 7 **Pan G**, Lu S, Ke M, Han S, Guo H, Fang X. Epidemiologic study of the irritable bowel syndrome in Beijing: stratified randomized study by cluster sampling. *Chin Med J* 2000; **113**: 35-39
- 8 **Schmulson M**, Lee OY, Chang L, Naliboff B, Mayer EA. Symptom differences in moderate to severe IBS patients based on predominant bowel habit. *Am J Gastroenterol* 1999; **94**: 2929-2935
- 9 **Simren M**, Abrahamsson H, Bjornsson ES. An exaggerated sensory component of the gastrocolonic response in patients with irritable bowel syndrome. *Gut* 2001; **48**: 20-27
- 10 **Aggarwal A**, Cutts TF, Abell TL, Cardoso S, Familoni B, Bremer J, Karas J. Predominant symptoms in irritable bowel syndrome correlate with specific autonomic nervous system abnormalities. *Gastroenterology* 1994; **106**: 945-950
- 11 **Cole SJ**, Duncan HD, Claydon AH, Austin D, Bowling TE, Silk DB. Distal colonic motor activity in four subgroups of patients with irritable bowel syndrome. *Dig Dis Sci* 2002; **47**: 345-355
- 12 **Heitkemper M**, Jarrett M, Cain KC, Burr R, Levy RL, Feld A, Hertig V. Autonomic nervous system function in women with irritable bowel syndrome. *Dig Dis Sci* 2001; **46**: 1276-1284
- 13 **Weinryb RM**, Osterberg E, Blomquist L, Hultcrantz R, Krakau I, Asberg M. Psychological factors in irritable bowel syndrome: a population-based study of patients, non-patients and controls. *Scand J Gastroenterol* 2003; **38**: 503-510
- 14 **Creed F**, Ratcliffe J, Fernandez L, Tomenson B, Palmer S, Rigby C, Guthrie E, Read N, Thompson D. Health-related quality of life and health care costs in severe, refractory irritable bowel syndrome. *Ann Intern Med* 2001; **134**(9 Pt 2): 860-868
- 15 **Frank L**, Kleinman L, Rentz A, Ciesla G, Kim JJ, Zacker C. Health-related quality of life associated with irritable bowel syndrome: comparison with other chronic diseases. *Clin Ther* 2002; **24**: 675-689
- 16 **Whitehead WE**, Burnett CK, Cook EW 3rd, Taub E. Impact of irritable bowel syndrome on quality of life. *Dig Dis Sci* 1996; **41**: 2248-2253
- 17 **Simren M**, Abrahamsson H, Svedlund J, Bjornsson ES. Quality of life in patients with irritable bowel syndrome seen in referral centers versus primary care: the impact of gender and predominant bowel pattern. *Scand J Gastroenterol* 2001; **36**: 545-552
- 18 **Guthrie E**, Creed F, Fernandes L, Ratcliffe J, Van Der Jagt J, Martin J, Howlett S, Read N, Barlow J, Thompson D, Tomenson B. Cluster analysis of symptoms and health seeking behaviour differentiates subgroups of patients with severe irritable bowel syndrome. *Gut* 2003; **52**: 1616-1622
- 19 **Osterberg E**, Blomquist L, Krakau I, Weinryb RM, Asberg M, Hultcrantz R. A population study on irritable bowel syndrome and mental health. *Scand J Gastroenterol* 2000; **35**: 264-268
- 20 **Herschbach P**, Henrich G, von Rad M. Psychological factors in functional gastrointestinal disorders: characteristics of the disorder or of the illness behavior? *Psychosom Med* 1999; **61**: 148-153
- 21 **Li FX**, Patten SB, Hilsden RJ, Sutherland LR. Irritable bowel syndrome and health-related quality of life: a population-based study in Calgary, Alberta. *Can J Gastroenterol* 2003; **17**: 259-263
- 22 **Maxton DG**, Morris J, Whorwell PJ. More accurate diagnosis of irritable bowel syndrome by the use of 'non-colonic' symptomatology. *Gut* 1991; **32**: 784-786
- 23 **Huerta I**, Bonder A, Lopez L, Ocampo MA, Schmulson M. Differences in the stress symptoms rating scale in Spanish between

- patients with irritable bowel syndrome (IBS) and healthy controls. *Rev Gastroenterol Mex* 2002; **67**: 161-165
- 24 **Portincasa P**, Moschetta A, Baldassarre G, Altomare DF, Palasciano G. Pan-enteric dysmotility, impaired quality of life and alexithymia in a large group of patients meeting ROME II criteria for irritable bowel syndrome. *World J Gastroenterol* 2003; **9**: 2293-2299
- 25 **Wiklund IK**, Fullerton S, Hawkey CJ, Jones RH, Longstreth GF, Mayer EA, Peacock RA, Wilson IK, Naesdal J. An irritable bowel syndrome-specific symptom questionnaire: development and validation. *Scand J Gastroenterol* 2003; **38**: 947-954
- 26 **Lembo T**, Naliboff B, Munakata J, Fullerton S, Saba L, Tung S, Schmulson M, Mayer EA. Symptoms and visceral perception in patients with pain-predominant irritable bowel syndrome. *Am J Gastroenterol* 1999; **94**: 1320-1326
- 27 **Mearin F**, Balboa A, Badia X, Baro E, Caldwell E, Cucala M, Diaz-Rubio M, Fueyo A, Ponce J, Roset M, Talley NJ. Irritable bowel syndrome subtypes according to bowel habit: revisiting the alternating subtype. *Eur J Gastroenterol Hepatol* 2003; **15**: 165-172
- 28 **Lee OY**, Mayer EA, Schmulson M, Chang L, Naliboff B. Gender-related differences in IBS symptoms. *Am J Gastroenterol* 2001; **96**: 2184-2193
- 29 **Li L**, Wang HM, Shen Y. Development and psychometrics test of a Chinese version of the SF-36 health survey scales. *Zhonghua Yufang Yixue Zazhi* 2002; **36**: 109-113
- 30 **Gralnek IM**, Hays RD, Kilbourne A, Naliboff B, Mayer EA. The impact of irritable bowel syndrome on health-related quality of life. *Gastroenterology* 2000; **119**: 654-660
- 31 **Hahn BA**, Yan S, Strassels S. Impact of irritable bowel syndrome on quality of life and resource use in the United States and United Kingdom. *Digestion* 1999; **60**: 77-81
- 32 **Kwan AC**, Hu WH, Chan YK, Yeung YW, Lai TS, Yuen H. Prevalence of irritable bowel syndrome in Hong Kong. *J Gastroenterol Hepatol* 2002; **17**: 1180-1186
- 33 **Lau EM**, Chan FK, Ziea ET, Chan CS, Wu JC, Sung JJ. Epidemiology of irritable bowel syndrome in Chinese. *Dig Dis Sci* 2002; **47**: 2621-2624

Edited by Gupta MK **Proofread by** Xu FM

Barrett's esophagus and its correlation with gastroesophageal reflux in Chinese

Jun Zhang, Xiao-Li Chen, Kang-Min Wang, Xiao-Dan Guo, Ai-Li Zuo, Jun Gong

Jun Zhang, Jun Gong, Xiao-Dan Guo, Ai-Li Zuo, Section of Gastroenterology, Department of Medicine, Second Hospital of Xi'an Jiaotong University, Xi'an 710004, China

Xiao-Li Chen, Kang-Min Wang, Department of Pathology, Second Hospital of Xi'an Jiaotong University, Xi'an 710004, China

Correspondence to: Dr. Jun Zhang, Department of Gastroenterology, Second Hospital of Xi'an Jiaotong University, Xi'an 710004, Shaanxi Province, China. jun3z@163.com

Telephone: +86-29-7678009

Received: 2003-08-11 **Accepted:** 2003-09-18

Abstract

AIM: To study the prevalence of Barrett's esophagus in Chinese and its correlation with gastroesophageal reflux.

METHODS: This study was carried out in a large prospective series of 391 patients who had undergone upper endoscopy. The patients were divided into 3 groups according to the position of squamocolumnar junction (SCJ). Reflux esophagitis (RE) and its degree were recorded. Intestinal metaplasia (IM) in biopsy specimen was typed according to histochemistry and HE and alcian blue (pH2.5) staining separately. Results correlating with clinical, endoscopic, and pathological data were analysed.

RESULTS: The prevalence of IM endoscopically appearing Long-segment Barrett's Esophagus (LSBE) was 26.53%, Short-segment Barrett's Esophagus (SSBE) was 33.85% and gastroesophageal junction (GEJ) was 34.00%. IM increased with age of above 40 years old and no difference was found between male and female. Twelve were diagnosed as dysplasia (7 low-grade, 5 high-grade), 16 were diagnosed as cardiac adenocarcinoma and 1 as esophageal adenocarcinoma. The more far away the SCJ moved upward above GEJ, the higher the prevalence and the more severe the RE were.

CONCLUSION: There was no difference of the prevalence of IM in different places of SCJ, and IM increased with age of above 40 years old. It is important to pay attention to dysplasia in the distal esophagus and gastro-esophageal junction, and adenocarcinoma is more common in cardia than in esophagus. BE is a consequence of gastroesophageal reflux disease.

Zhang J, Chen XL, Wang KM, Guo XD, Zuo AL, Gong J. Barrett's esophagus and its correlation with gastroesophageal reflux in Chinese. *World J Gastroenterol* 2004; 10(7): 1065-1068
<http://www.wjgnet.com/1007-9327/10/1065.asp>

INTRODUCTION

Adenocarcinoma of the esophagus and gastro-esophageal junction (GEJ) is increasing, while the distal gastric cancer has been falling in the past two decades in North America, Europe, Japan and China. In China, the incidence of adenocarcinoma at

GEJ is increasing more obviously^[1-3].

Adenocarcinomas at the distal esophagus and GEJ differ from those in the rest of the stomach^[4]. They share epidemiological characteristics with and often originate from segments of Barrett's esophagus (BE). It is therefore proposed that both of them be called "esophagocardia adenocarcinoma"^[5]. It has been well defined that Barrett's esophagus is a premalignant condition for esophageal adenocarcinoma and most adenocarcinomas at GEJ^[6,7].

In early studies, BE was defined as the presence of specialized IM in a columnar-lined mucosa encompassing more than 3 cm proximal to GEJ or a LSBE(long-segment Barrett's esophagus)^[8]. Any columnar-lined mucosa found less than 3 cm above the GEJ was thought to be a normal variant. However studies in the past years indicate that there is a spectrum of involvement that includes the distal 3 cm of esophagus or a SSBE (short-segment Barrett's esophagus)^[9,10].

Although the cause of BE has not been defined finally, it is considered that BE has a strong correlation with chronic GERD (gastro-esophageal reflux disease)^[11]. Ten to twelve percent of patients with BE would receive endoscopy because of refluxing symptoms. Great attention has been paid to the studies of BE by overseas scholars. With the rapid development of China, the western food has become popular and fat persons are increasing, so is the GERD. But few studies on BE have been reported about the correlation between BE and GERD in Chinese. We performed a prospective study in order to determine the prevalence of BE in patients and to evaluate the correlation between BE and gastroesophageal reflux.

MATERIALS AND METHODS

Patients

Consecutive patients undergoing gastroscopy at our hospital from August 1, 2000 to August 30, 2001 were enrolled. Exclusion criteria were history of gastro-esophageal surgery and contraindication to performing biopsies. In each case, the following data were obtained: age, sex, and past medical history of ulcer, gastro-esophageal reflux symptoms (either heartburn or acid regurgitation), drug therapy, and past history of surgery.

The study was approved by the ethics committee of our hospital and all patients gave written informed consent prior to inclusion.

Endoscopic definition and biopsy

Endoscopy was performed by the same expert in a standard procedure, with visualization of the esophagus, stomach and duodenum. The appearance of SCJ was carefully studied in prograde view and after retroversion in the stomach. The position of GEJ was the boundary of tubular esophagus turning into stomach. According to the distance from GEJ to SCJ, the extent of the columnar lining, patients were divided into three groups^[12]: Group A, 98 patients, whose SCJ was at least 3 cm above GEJ, suggesting a LSBE; Group B, 127 patients, whose SCJ was less than 3 cm above GEJ, suggesting SSBE; Group C, 150 patients, whose SCJ and GEJ were at nearly same level. Endoscopic esophagitis was graded into Grade I as mucosal

hyperaemia, Grade II as non-circumferential mucosal breaks or erosions, Grade III as circumferential erosion or ulcer. Fifteen patients with cardiac adenocarcinoma and one patient with esophageal adenocarcinoma were excluded.

Standard four-quadrant biopsies were performed distal to the SCJ. Separate target biopsies were also taken from any suspicious erosions, nodules or ulcers. Four to six pieces of biopsy specimens were taken from each patient.

Biopsy specimens were fixed in 40 g/L buffered formaldehyde, embedded in paraffin wax, serially sectioned, and then stained with hematoxylin and eosin. BE was defined as the presence of distended, barrel-shaped goblet cells, indicative of intestinal metaplasia^[6,13,14](Figure 1). BE was confirmed by further sectioning and staining the biopsies with alcian blue (pH2.5). Each section was reviewed by two experienced gastrointestinal pathologists respectively.

Statistical analysis

Statistical analyses were performed using the SPSS9.0 analysis system. The χ^2 or Fisher's exact test was used when appropriate. $P < 0.05$ was considered statistically significant.

RESULTS

These patients consisted of 211 males and 180 females with a mean age of 52.41 yr (range 20-82 yr). Reflux was found in 149 cases, pain at superior belly in 89 cases, dysphagia in 26 cases, nausea and vomiting in 18 cases, melena in 13 cases and emaciation in 5 cases.

Clinic features of study population

There were 103 patients with RE (39 grade I, 35 grade II and 29 grade III), 69 with Barrett's esophagus (26 LSBE, 43 SSBE), 51 with IM at GEJ, 12 cases with dysplasia [7 low-grade dysplasia, LGD (Figure 2A,B); 5 high-grade dysplasia, HGD (Figure 2C)], 17 with adenocarcinoma at the gastro-esophageal junction and 1 with adenocarcinoma of esophagus. The age was positively related to the progress from RE→BE→LGD→HGD→adenocarcinoma (Table 1).

Table 1 Clinical features of study population

	Number	Average age(yr)	Male:Female
Total	391	52.41	211:180
RE I	39	52.12	26:13
II	35	53.67	26:9
III	29	55.56	24:5
IM at GEJ	51	54.37	39:12
SSBE	43	54.71	34:9
LSBE	26	58.66	20:6
LGD	7	59.57	5:2
HGD	5	62.00	3:2
Cardiac adenocarcinoma	15	62.64	13:2

LGD: Low grade dysplasia, HGD: High grade dysplasia, IM: Intestinal metaplasia.

Prevalence of IM and dysplasia at different SCJ

There were no significant differences in incidence of IM between three groups and between male and female of each group (Table 2).

Association of age and sex with the incidence of IM in different groups

In this study, IM was not found in patients under 30 years old.

However, it increased in patients over 30 years old and gradually reached the peak over 40 years old. There were no significant differences of the incidence of IM between males and females in different age groups ($P > 0.05$)(Table 2).

Relation between RE and different position of SCJ

Comparing the incidence and degree of RE with the different position of SCJ, the positive correlation was found. The longer the SCJ moved upward above GEJ, the higher the prevalence and the more severe the RE were (Table 3).

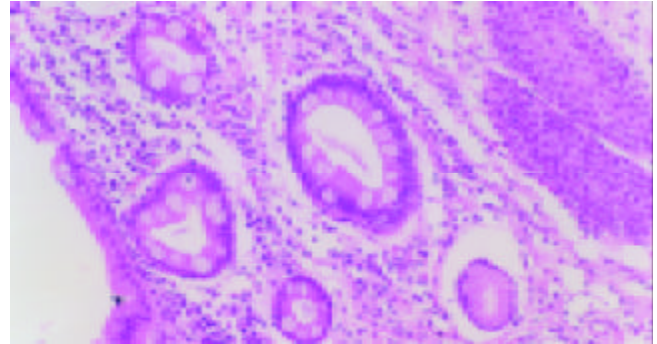


Figure 1 Goblet cells with HE stain (10×10).

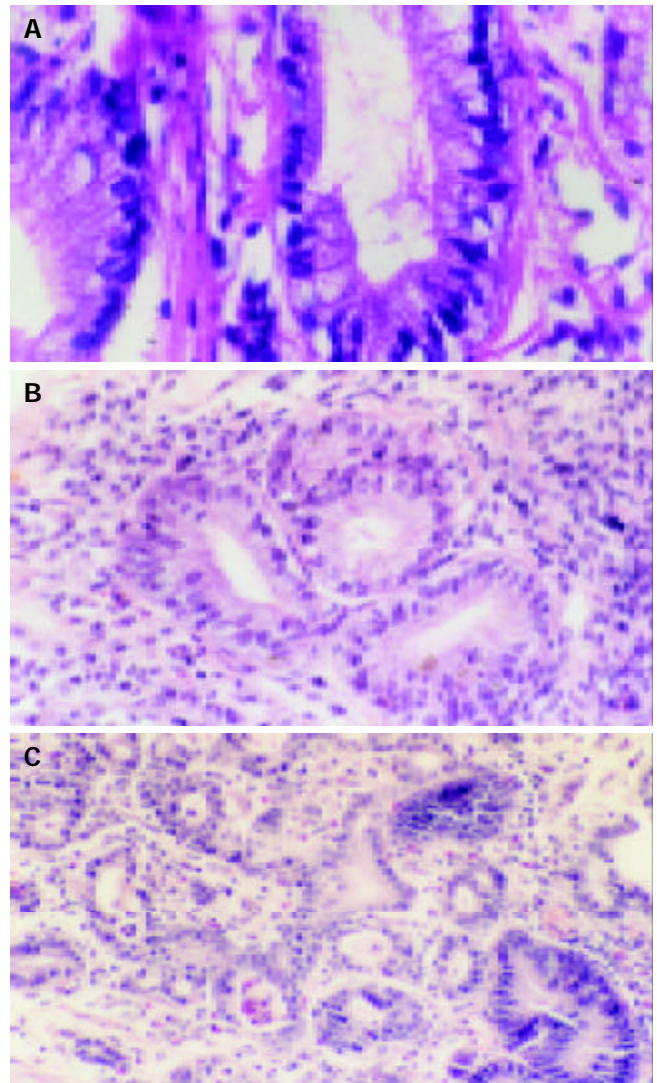


Figure 2 A: Barrett's esophagus with LGD (10×40), B: Barrett's esophagus with HGD (10×10), C: Barrett's esophagus with HGD and carcinogenesis (top left corner) (10×10).

Table 2 Prevalence of IM and dysplasia at different SCJ positions

Position of SCJ	Number (male/female)	Age(yr)	IM (male/female)	Incidence of IM (%)	Dysplasia	
					LGD	HGD
Group A	98 (61/37)	58.66	26 (20/6)	26.53	2	1
Group B	127 (63/64)	55.05	43 (25/18)	33.85	1	2
Group C	150 (71/79)	54.37	51 (19/32)	34.00	4	2
Total	375 (195/180)		120 (64/56)	32.00	7	5

The incidence between groups and between male and female of each group was compared by χ^2 test and $P > 0.05$.

Table 3 Different SCJ positions and RE

Position of SCJ	Number	RE I (%)	RE II (%)	RE III (%)	Total of RE (%)
Group A	98	13(13.26)	19(19.39)	24(24.48)	56(57.14)
Group B	127	17(13.38)	10(7.87)	2 (1.57)	29(22.83)
Group C	150	9 (6.00)	6 (4.00)	3 (2.00)	18(12.00)
The total	375	39(10.40)	35(9.33)	29(7.33)	103(27.46)

Analysis by trend χ^2 test, the incidence and degree of RE and the position of SCJ in groups C, B and A had a positive correlation. $P < 0.05$.

DISCUSSION

The point emphasized in original definition of Barrett's esophagus was the length replaced by columnar epithelium of normal squamous mucosa. However, the length is not vital in new definition of Barrett's esophagus, in which what is important is the presence of IM relating to adenocarcinoma^[15]. Researches in recent years have implicated the correlation between carcinoma of gastric cardia and Barrett's esophagus as well as IM at GEJ^[16,17]. Some researches discovered that about 35-40% carcinomas of gastric cardia were related with Barrett's esophagus, even some advanced esophageal adenocarcinomas at GEJ^[18,19]. These findings at least illuminate some correlation. The relationship between Barrett's esophagus and esophageal adenocarcinoma has been confirmed. Whether cardiac carcinoma is a consequence of IM is unclear.

The study population comprised 391 patients who underwent endoscopy. There were 103 patients with RE (39 grade I, 35 grade II and 29 grade III), 120 with Barrett's esophagus (26 LSBE, 43 SSBE), 51 with IM at GEJ, 12 with dysplasia (LGD 7 cases, HGD 5 cases), 15 with carcinoma of gastric cardia. More lesions were found in males than in females. Furthermore, pathologic changes from RE→Barrett's esophagus→dysplasia→canceration were related with increased age of patients.

According to the position of SCJ, the patients were divided into 3 groups in this study. The incidence of LSBE in group A was 26.53% (26/98), and the incidence of SSBE in group B was 33.85% (43/127) and IM in group C was 34.00% (51/150). These results were different from those of other scholars. Dias Percira^[20] discovered that the incidence of SSBE in Portuguese was 61.3% and the incidence of IM at GEJ was 25%. The incidence of IM at GEJ in Euramerican varied from 5% to 36%^[21,22]. Spechler^[23] found that the incidence of LSBE was 65.38%, far higher than that in our study. The high incidence of LSBE was directly related to esophageal adenocarcinoma. Nakamura *et al.*^[24] found that the incidence of IM at GEJ was 28% in Japanese, which was close to our result. Of course, the exact position of GEJ is very difficult to locate under gastroscop, even with surgical specimens. The generally accepted view is that the position of GEJ is the boundary of tubular esophagus turning into stomach. Moreover, the number of biopsy specimens also works on the detection rate of IM. The more the number of biopsy specimens are, the higher the detection rate of IM is. The numbers of biopsy specimens are directly related to the identification of Barrett's esophagus, however there are still no criteria as to how many biopsy specimens should be taken from one patient. Many scholars have suggested that more specimens should be taken in suspect

lesions and one piece of specimen should be taken at least every 2 cm respectively from each quadrant. Paull *et al.*^[25] found that IM was usually distributed in the proximal mucosa of lesion adjacent to squamocolumnar junction (SCJ). Specimens adjacent to SCJ are helpful to increase the detection rate of IM. In this study, at least one piece of specimen was taken respectively from each quadrant of distal columnar mucosa adjacent to SCJ and more specimens were taken if there were questionable lesions. So, 4-6 biopsies were taken from each patient. For biopsy specimens, the goblet cell secreting acidic mucus could be dyed blue by AB (pH2.5) staining, which was beneficial to the diagnosis of IM^[26].

Increasing researches considered that IM at GEJ had two origins, SSBE and IM of gastric cardia^[27]. Whether it is necessary to study SSBE and IM at GEJ separately or whether they are the same lesion is unknown. Besides, there are no exact definitions of IM at distal part of esophagus and at gastric cardia. Researches in recent years showed that the development of IM at GEJ might be related with infection of *H pylori*^[28]. The infection of *H pylori* in China is common, therefore, it is necessary to do more investigations.

In this research, IM was not found in patients younger than 30 years old. The incidence of IM increased with the age and reached the peak at the age of 50-70 yr, but the incidence of IM had no significant differences between males and females in different age groups and at different SCJ positions ($P > 0.05$). It was reported that attacks of Barrett's esophagus were seldom found in children and young people, but it would increase with the age. It will take about 20 yr to develop from Barrett's esophagus to esophageal adenocarcinoma^[29].

Researches showed that Barrett's esophagus was a precancerous lesion of esophageal adenocarcinoma and gastric cardia carcinoma. Pathologic researches discovered that canceration of Barrett's esophagus would undergo a pathologic process from SIM→LGD→HGD→carcinoma *in situ*→advanced adenocarcinoma. Some researches discovered that it took 1.5-10 yr to develop into adenocarcinoma from HGD^[30,31]. A few patients would remain at the stage of HGD for many years. Part of patients would develop into adenocarcinoma from IM in 3-10 years^[30,32]. Seven patients with LGD and 5 with HGD were diagnosed in this study and the follow-up for the patients with dysplasia should be strengthened. The patients with HGD should be followed up every 1-3 mo and multipoint biopsy should be taken to avoid delaying the diagnosis of tumors. We diagnosed 15 cases of cardiac adenocarcinoma and 1 case of esophageal adenocarcinoma, which showed that adenocarcinoma of cardia was more common than that of esophagus in China.

It is recognized by most scholars that RE leads to Barrett's esophagus. In our study (Table 3), the incidence of RE in group A (57.14%) was higher than that in group B (22.83%) and was higher in group B than in group C (12.00%). Furthermore, the incidence of RE III was also far higher in group A (24.48%) than in group B (1.57%). Dias found that the occurrence of RE in group of SSBE was higher than that in group of GEJ, which was similar to our conclusion^[20]. We examined the incidence and degree of RE as well as the SCJ position in groups C, B, A and found that they had a positive correlation ($P < 0.05$), that is, the longer the SCJ moved upward above GEJ, the higher the prevalence and the more severe of RE were. The result in this study conformed to the viewpoint of most researchers that the squamous epithelium of lower esophagus was replaced by columnar epithelium and then developed into intestinal metaplasia. There is no exact conclusion about whether IM at GEJ has relation to RE or not.

In a word, it is important to pay attention to the diagnosis of dysplasia in the distal esophagus and esophagogastric junctions. Cardia adenocarcinoma is more common than that of esophagus. BE is a consequence of gastroesophageal reflux disease.

REFERENCES

- 1 **Devesa SS**, Blot WJ, Fraumeni JF Jr. Changing patterns in the incidence of esophageal and gastric carcinoma in the United States. *Cancer* 1998; **83**: 2049-2053
- 2 **Blot WJ**, Devesa SS, Kneller RW, Fraumeni JF Jr. Rising incidence of adenocarcinoma of the esophagus and gastric cardia. *JAMA* 1991; **265**: 1287-1289
- 3 **Zhou Q**, Wang LD. Biologic characteristic of adenocarcinoma at GEJ. *Shijie Huaren Xiaohua Zazhi* 1998; **6**: 636-637
- 4 **Ruol A**, Parenti A, Zaninotto G, Merigliano S, Costantini M, Cagol M, Alfieri R, Bonavina L, Peracchia A, Ancona E. Intestinal metaplasia is the probable common precursor of adenocarcinoma in Barrett esophagus and adenocarcinoma of the gastric cardia. *Cancer* 2000; **88**: 2520-2528
- 5 **Rabinovitch PS**, Reid BJ, Haggitt RC, Norwood TH, Rubin CE. Progression to cancer in Barrett's esophagus is associated with genomic instability. *Lab Invest* 1989; **60**: 65-71
- 6 **Weston AP**, Krmpotich PT, Cherian R, Dixon A, Topalovski M. Prospective evaluation of intestinal metaplasia and dysplasia within the cardia of patients with Barrett's esophagus. *Dig Dis Sci* 1997; **42**: 597-602
- 7 **Cameron AJ**, Lomboy CT, Pera M, Carpenter HA. Adenocarcinoma of the esophagogastric junction and Barrett's esophagus. *Gastroenterology* 1995; **109**: 1541-1546
- 8 **Iacone C**, DeMeester TR, Little AG, Skinner DB. Barrett's esophagus. Functional assessment, proposed pathogenesis, and surgical therapy. *Arch Surg* 1983; **118**: 543-549
- 9 **Pera M**. Trends in incidence and prevalence of specialized intestinal metaplasia, Barrett's esophagus, and adenocarcinoma of the gastroesophageal junction. *World J Surg* 2003; **27**: 999-1008
- 10 **Weston AP**, Krmpotich P, Makdisi WF, Cherian R, Dixon A, McGregor DH, Banerjee SK. Short segment Barrett's esophagus: clinical and histological features, associated endoscopic findings, and association with gastric intestinal metaplasia. *Am J Gastroenterol* 1996; **91**: 981-986
- 11 **Hirota WK**, Loughney TM, Lazas DJ, Maydonovitch CL, Rholl V, Wong RK. Specialized intestinal metaplasia, dysplasia, and cancer of the esophagus and esophagogastric junction: prevalence and clinical data. *Gastroenterology* 1999; **116**: 277-285
- 12 **Spechler SJ**. Columnar-lined esophagus. Definitions. *Chest Surg Clin N Am* 2002; **12**: 1-13
- 13 **Menke-Pluymers MB**, Hop WC, Dees J, van Blankenstein M, Tilanus HW. Risk factors for the development of an adenocarcinoma in columnar-lined (Barrett) esophagus. The Rotterdam esophageal tumor study group. *Cancer* 1993; **72**: 1155-1158
- 14 **Rajan E**, Burgart LJ, Gostout CJ. Endoscopic and histologic diagnosis of Barrett esophagus. *Mayo Clin Proc* 2001; **76**: 217-225
- 15 **Sampliner RE**. Practice guidelines on the diagnosis, surveillance, and therapy of Barrett's esophagus. The Practice Parameters Committee of the American College of Gastroenterology. *Am J Gastroenterol* 1998; **93**: 1028-1032
- 16 **Zaninotto G**, Avellini C, Barbazza R, Baruchello G, Battaglia G, Benedetti E, Bernardi A, Boccu C, Bonoldi E, Bottona E, Bozzola L, Canizzaro R, Canzonieri V, Caroli A, Carta A, Colonna A, Costa-Biedo F, Dal Bo N, De Bastiani R, De Bernardin M, De Bernardinis F, De Pretis G, Di Mario F, Doglioni C, Donisi PM, Franceschi M, Furlanetto A, Germana B, Grassi SA, Macor V, Marcon V, Marin R, Meggiato T, Melina V, Menghi A, Milan R, Militello C, Molena D, Monica F, Murer B, Nisi E, Olivieri P, Orzes N, Parenti A, Paternello E, Penelli N, Pilotto A, Pisciole F, Pozzato F, Ronzani G, Rugge M, Saggiaro A, Stracca-Pansa V, Togni R, Valiante F, Vianello F. Prevalence of intestinal metaplasia in the distal oesophagus, oesophagogastric junction and gastric cardia in symptomatic patients in north-east Italy: a prospective, descriptive survey. The Italian Ulcer Study Group "GISU". *Dig Liver Dis* 2001; **33**: 316-321
- 17 **Hamilton SR**, Smith RR, Cameron JL. Prevalence and characteristics of Barrett esophagus in patients with adenocarcinoma of the esophagus or esophagogastric junction. *Hum Pathol* 1988; **19**: 942-948
- 18 **Rotterdam H**. Pathology of the gastric cardia. *Verh Dtsch Ges Pathol* 1999; **83**: 37-42
- 19 **Clark GW**, Smyrk TC, Burdiles P, Hoeft SF, Peters JH, Kiyabu M, Hinder RA, Bremner CG, DeMeester TR. Is Barrett's metaplasia the source of adenocarcinomas of the cardia? *Arch Surg* 1994; **129**: 609-614
- 20 **Pereira AD**, Suspiro A, Chaves P, Saraiva A, Gloria L, de Almeida JC, Leitao CN, Soares J, Mira FC. Short segments of Barrett's epithelium and intestinal metaplasia in normal appearing oesophagogastric junctions: the same or two different entities? *Gut* 1998; **42**: 659-662
- 21 **Voutilainen M**, Farkkila M, Juhola M, Nuorva K, Mauranen K, Mantynen T, Kunnamo I, Mecklin JP, Sipponen P. Specialized columnar epithelium of the esophagogastric junction: prevalence and associations. The Central Finland Endoscopy Study Group. *Am J Gastroenterol* 1999; **94**: 913-918
- 22 **Hirota WK**, Loughney TM, Lazas DJ, Maydonovitch CL, Rholl V, Wong RK. Specialized intestinal metaplasia, dysplasia, and cancer of the esophagus and esophagogastric junction: prevalence and clinical data. *Gastroenterology* 1999; **116**: 277-285
- 23 **Spechler SJ**, Zeroogian JM, Antonioli DA, Wang HH, Goyal RK. Prevalence of metaplasia at the gastro-oesophageal junction. *Lancet* 1994; **344**: 1533-1536
- 24 **Nakamura M**, Kawano T, Endo M, Iwai T. Intestinal metaplasia at the esophagogastric junction in Japanese patients without clinical Barrett's esophagus. *Am J Gastroenterol* 1999; **94**: 3145-3149
- 25 **Paull A**, Trier JS, Dalton MD, Camp RC, Loeb P, Goyal RK. The histologic spectrum of Barrett's esophagus. *N Engl J Med* 1976; **295**: 476-480
- 26 **Fireman Z**, Wagner G, Weissman J, Kopelman Y, Wagner Y, Groissman G, Sternberg A. Prevalence of short-segment Barrett's epithelium. *Dig Liver Dis* 2001; **33**: 322-325
- 27 **Sharma P**, Weston AP, Morales T, Topalovski M, Mayo MS, Sampliner RE. Relative risk of dysplasia for patients with intestinal metaplasia in the distal oesophagus and in the gastric cardia. *Gut* 2000; **46**: 9-13
- 28 **Hackelsberger A**, Gunther T, Schultze V, Manes G, Dominguez-Munoz JE, Roessner A, Malfertheiner P. Intestinal metaplasia at the gastro-oesophageal junction: *Helicobacter pylori* gastritis or gastro-oesophageal reflux disease? *Gut* 1998; **43**: 17-21
- 29 **Cameron AJ**. Epidemiologic Studies and the development of Barrett's esophagus. *Endoscopy* 1993; **25**: 635-636
- 30 **Hameeteman W**, Tytgat GN, Houthoff HJ, van den Tweel JG. Barrett's esophagus: development of dysplasia and adenocarcinoma. *Gastroenterology* 1989; **96**: 1249-1256
- 31 **Schnell TG**, Sontag SJ, Chejfec G, Aranha G, Metz A, O'Connell S, Seidel UJ, Sonnenberg A. Long-term nonsurgical management of Barrett's esophagus with high-grade dysplasia. *Gastroenterology* 2001; **120**: 1607-1619
- 32 **Sharma P**, Morales TG, Bhattacharyya A, Garewal HS, Sampliner RE. Dysplasia in short-segment Barrett's esophagus: a prospective 3-year follow-up. *Am J Gastroenterol* 1997; **92**: 2012-2016

NOD2 3020insC frameshift mutation is not associated with inflammatory bowel disease in Chinese patients of Han nationality

Qiu-Sha Guo, Bing Xia, Yi Jiang, Yan Qü, Jing Li

Qiu-Sha Guo, Bing Xia, Yi Jiang, Yan Qü, Jing Li, Department of Internal Medicine, Zhongnan Hospital, Wuhan University, Wuhan 430071, Hubei Province, China

Supported by the National Natural Science Foundation of China, No. 30370638

Correspondence to: Professor Bing Xia, MD, PhD, Department of Internal Medicine, Zhongnan Hospital, Medical School of Wuhan University, Wuhan, Hubei Province, China. bingxia@public.wh.hb.cn
Telephone: +86-27-67813247

Received: 2003-10-27 **Accepted:** 2003-12-16

Abstract

AIM: An insertion mutation at nucleotide 3020 (3020insC) in the Caspase recruitment domain gene (CARD15), originally reported as NOD2, is strongly associated with Crohn's disease. The C-insertion mutation at nucleotide 3020 (3020inC) in the leucine-rich repeat (LRR) region results in a frameshift in the 10th LRR followed by a premature stop codon. This truncation mutation is responsible for the inability to activate nuclear factor (NF)- κ B in response to bacterial lipopolysaccharide (LPS). The present study aimed to genotype NOD2/CARD15 gene 3020insC frameshift mutation in Chinese patients with inflammatory bowel disease.

METHODS: We genotyped an insertion polymorphism affecting the leucine-rich region of the protein product by the allele specific PCR in 74 unrelated patients with ulcerative colitis of Han nationality in Hubei Province of China, 15 patients with Crohn's disease and 172 healthy individuals.

RESULTS: No significant differences were found in the genotype and allele frequencies of the C-insertion mutation of NOD2 gene among patients with Crohn's disease and ulcerative colitis and healthy controls.

CONCLUSION: NOD2 gene 3020insC frameshift mutation is not a major contributor to the susceptibility to both Crohn's disease and ulcerative colitis in Chinese Han patients.

Guo QS, Xia B, Jiang Y, Qü Y, Li J. NOD2 3020insC frameshift mutation is not associated with inflammatory bowel disease in Chinese patients of Han nationality. *World J Gastroenterol* 2004; 10(7): 1069-1071
<http://www.wjgnet.com/1007-9327/10/1069.asp>

INTRODUCTION

Inflammatory bowel disease (IBD) is a chronic intestinal inflammatory disorder that is clinically classified into Crohn's disease (CD), ulcerative colitis (UC) and indeterminate colitis. IBD is characterized by a dysregulated mucosal immune response and its pathogenesis has not been fully illustrated, but several epidemiological and genetic studies have suggested that IBD is predisposed by certain environmental and genetic

factors^[1-3]. IBD1 was the first susceptible locus linked to Crohn's disease. Utilizing genome-wide linkage studies among families with multiple affected members, Hugot *et al.*^[1] mapped the IBD1 gene to the proximal region of the long arm of chromosome 16 (16q12) in the white population. In Jewish families, the IBD1 locus was demonstrated to be significantly associated with CD^[4], but not with ulcerative colitis. Hugot *et al.*^[5] identified nucleotide oligomerisation domain (NOD2) as the IBD1 gene through routine positional cloning methods, the same finding was also reported in several other studies^[6,7]. NOD2, a member of the NOD1/APAF1 gene family, comprises an amino-terminal effector domain, a nucleotide-binding domain and leucine-rich repeats (LRRs)^[8]. Recently, NOD2 has been known as Caspase activating recruitment domain (CARD) 15. NOD2/CARD molecule is expressed exclusively in monocytes and activates NF- κ B through the interaction with its N-terminal CARDs^[8]. As studies have shown that the signaling by tumor necrosis factor (TNF) and activation by nuclear factor (NF)- κ B play a key role in IBD, NOD2 mutation may lead to the variation of NF- κ B activation. Three mutations (R702W, G908R, 1007fs, respectively at SNP8, 12, and 13) have been identified in NOD2/CARD15, which were shown to be independently associated with CD. One of the mutations predisposing to CD is 1007fs, the C-insertion mutation at nucleotide 3020 (3020inC) in the leucine-rich repeat region, results in a frameshift in the 10th LRR followed by a premature stop codon. This truncation mutation may result in the inability to activate NF- κ B in response to bacterial lipopolysaccharides (LPS). Therefore, NOD2 is considered to play a role in the pathogenesis of CD.

Studies by Japanese and Hongkong researchers, however, have failed to identify the insertion mutation both in patients and in control subjects^[9,10]. Greek has shown that NOD2 is not significant in the pathogenesis of CD^[11]. These studies support that CD possesses genetic heterogeneity among different populations. In this present study, we genotyped the 3020insC mutation of NOD2 gene in CD and UC in Chinese subjects of Han nationality in Hubei Province, to identify the susceptible gene for Chinese.

MATERIALS AND METHODS

Patients

A total of 15 unrelated patients with CD and 74 patients with UC were included in this study. As a control group 174 healthy individuals were also recruited from medical staff and students in Zhongnan Hospital of Wuhan University, as well as from healthy volunteers in Wuhan city. The diagnosis of either UC or CD was established and verified by clinical, radiological, endoscopic and histological examinations in accordance with the criteria by Lennard-Johns^[12]. All the subjects included in this study were unrelated Chinese of Han nationality in Hubei Province. This study protocol was approved by the Ethic Committee of Medical School of Wuhan University.

Methods

DNA was isolated from peripheral blood leukocytes by conventional proteinase K digestion and phenol/chloroform

extraction methods. Allele-specific PCR was employed to detect the 3020insC mutation of NOD2 gene^[6] and to generate a nonspecific 533-bp product, along with a 319-bp fragment (wild type) and/or a 214-bp fragment (3020inC). The primers used for PCR are listed in Table 1. PCR was performed in a reaction system in a volume of 25 μ L containing sense and antisense primers (each in a volume of 0.5 μ L at the concentration of 20 pmol/ μ L), wild-type sense and 3020insC antisense primer respectively (each in a volume of 0.25 μ L at the concentration of 20 pmol/ μ L), 2.5 μ L of 10 \times buffer, 0.5 μ L of 10 mmol/L dNTPs, 1 μ L of template DNA, 0.5 μ L of AmpliTaq DNA polymerase (MBI Fermentas), and 19 μ L of ddH₂O. Amplification was carried out with a Perkin-Elmer thermocycler. The cycling was performed with an initial denaturation for 5 min at 94 $^{\circ}$ C, followed by 35 cycles at 94 $^{\circ}$ C for 45 s, at 59 $^{\circ}$ C for 45 s, at 72 $^{\circ}$ C for 45 s with a final extension at 72 $^{\circ}$ C for 7 min. The PCR products were identified by electrophoresis in non-denaturing polyacrylamide gels containing 8% acrylamide-bisacrylamide (29:1), 0.5 \times Tris-borate-EDTA (TBE), 100 g/L ammonium persulfate, and TEMED at 150 V for 1.5 h. The gels were then subjected to silver staining. The PCR products used for sequencing analyses were purified and analyzed using an ABI377 automated sequencer (Applied Biosystems, USA). DNA samples for genotype control analysis were kindly provided by the Laboratory of Immunogenetics of Free University of Amsterdam, Netherlands.

Table 1 Primers used for multiplex PCR

Primer	Sequence
Sense primer	5' -CTGAGCCTTTGTTGATGAGC-3'
Antisense primer	5' -TCTTCAACCACATCCCCATT-3'
Wild-type sense primer	5' -CAGAAGCCCTCCTGCAGGCCCT-3'
3020insC antisense primer	5' -CGCGTGCATTCTTTCATGGGGC-3'

Statistical analysis

Statistical analysis was performed with SPSS 11.5 software package. The data were analyzed by χ^2 test or Fisher's exact test. A *P* value less than 0.05 was considered statistically significant. The confidential intervals (CI) for the odds ratios (OR) were calculated by Woolf formula.

RESULTS

The results of the genotypes and allele frequencies of the 3020insC mutation in CD and UC patients and in ethnically matched Chinese healthy controls are shown in Table 2. Two heterozygotes of the mutation in UC patients and one in CD patients were identified, whereas only one heterozygote mutation was found in healthy controls. No significant associations were noted in genotypes and allele frequencies of the 3020insC mutation in UC (*P*=0.2165) or CD (*P*=0.1542) in comparison with the healthy controls. The NOD2 3020insC mutation was not associated with CD or UC in Hubei Han population.

Table 2 3020insC mutation in healthy controls and ulcerative colitis and Crohn's disease in Chinese Han population

Genome	Healthy controls (n=172)	Ulcerative colitis (n=74)	Crohn's disease (n=15)
Wild type	171	72	14
Heterozygote	1	2	1
3020insC mutation homozygote	0	0	0
Wild type allele frequency	99.7%	98.7%	96.7%
Mutative allele frequency	0.3%	1.3%	3.3%

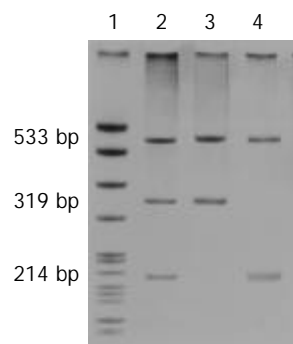


Figure 1 Identification of frameshift NOD2 mutation in Chinese population by allele specific PCR. Multiplex PCR was used to generate a nonspecific 533-bp and allele-specific amplified products, a 319-bp fragment (wild type) and a 214-bp fragment (C-insertion type). Lane 1: pBR322 DNA/*Msp*I markers; Lane 2: Heterozygous for 3020insC; Lane 3: Wild-type control; Lane 4: Homozygote for 3020insC. Numbers on the left are the lengths of the fragments.

DISCUSSION

In this study, we did not find any evidence suggestive of the association of NOD2 frameshift mutations with CD or UC. The allele frequency of 3020insC mutation was slightly increased in CD and UC patients when compared with the healthy controls, but there were no statistically significant differences among these three groups. After the initial report of the associations between mutations in the NOD2 gene and susceptibility to CD^[5,6], a German and British study^[7] soon found evidence to show that the insertion mutation in the NOD2 gene was responsible for a substantially increased susceptibility to CD but not to UC. Other studies have suggested that attributive risks of the 3020insC mutation of NOD2 differ in different ethnic nationalities and countries. A large-scale study in Japanese failed to identify the insertion mutation both in patients and in controls^[9], the same result was also reported by Leong *et al.*^[10] in Chinese population in Hong Kong. A study in a Cretan showed that NOD2/CARD15 was not significant in the pathogenesis of CD^[11]. All these data and the results of this study demonstrate that CD has genetic heterogeneity among different nationalities.

NOD2 was recently identified as a susceptible gene of CD in most Western countries, which provided an opportunity to study the relationship between NOD2 gene and innate immunity in CD. NOD2 was located in the peak region of linkage on chromosome 16q12 and a member of the NOD1/APAF1 gene family^[8], expressed primarily in monocytes and functioned to activate NF- κ B in response to LPS stimulation^[13,14]. 3020insC, which resulted in a frameshift mutation at the second nucleotide of codon 1007, a Leu1007 \rightarrow Pro substitution in the tenth LRR and followed by a premature stop codon, encoded a truncated NOD2 protein and led to a weakened innate immune response in CD^[8]. In our study we did not find any statistically significant association between the 3020insC mutation and CD. Other mechanisms of CD involving the susceptible gene and innate immunity have been suggested in Chinese Han nationality in Hubei Province.

REFERENCES

- 1 **Hugot JP**, Laurent-Puig P, Gower-Rousseau C, Olson JM, Lee JC, Beaugerie L, Naom I, Dupas JL, Van Gossum A, Orholm M, Bonaiti-Pellie C, Weissenbach J, Mathew CG, Lennard-Jones JE, Cortot A, Colombel JF, Thomas G. Mapping of a susceptibility locus for Crohn's disease on chromosome 16. *Nature* 1996; **379**: 821-823

- 2 **Cavanaugh J.** International collaboration provides convincing linkage replication in complex disease through analysis of a large pooled data set: Crohn disease and chromosome 16. *Am J Hum Genet* 2001; **68**: 1165-1171
- 3 **Curran ME,** Lau KF, Hampe J, Schreiber S, Bridger S, Macpherson AJ, Cardon LR, Sakul H, Harris TJ, Stokkers P, Van Deventer SJ, Mirza M, Raedler A, Kruis W, Meckler U, Theuer D, Herrmann T, Gionchetti P, Lee J, Mathew C, Lennard-Jones J. Genetic analysis of inflammatory bowel disease in a large European cohort supports linkage to chromosomes 12 and 16. *Gastroenterology* 1998; **115**: 1066-1071
- 4 **Akolkar PN,** Gulwani-Akolkar B, Lin XY, Zhou Z, Daly M, Katz S, Levine J, Present D, Gelb B, Desnick R, Mayer L, Silver J. The IBD1 locus for susceptibility to Crohn's disease has a greater impact in Ashkenazi Jews with early onset disease. *Am J Gastroenterol* 2001; **96**: 1127-1132
- 5 **Hugot JP,** Chamaillard M, Zouali H, Lesage S, Cezard JP, Belaiche J, Almer S, Tysk C, O' Morain CA, Gassull M, Binder V, Finkel Y, Cortot A, Modigliani R, Laurent-Puig P, Gower-Rousseau C, Macry J, Colombel JF, Sahbatou M, Thomas G. Association of NOD2 leucine-rich repeat variants with susceptibility to Crohn's disease. *Nature* 2001; **411**: 599-603
- 6 **Ogura Y,** Bonen DK, Inohara N, Nicolae DL, Chen FF, Ramos R, Britton H, Moran T, Karaliuskas R, Duerr RH, Achkar JP, Brant SR, Bayless TM, Kirschner BS, Hanauer SB, Nunez G, Cho JH. A frameshift mutation in NOD2 associated with susceptibility to Crohn's disease. *Nature* 2001; **411**: 603-606
- 7 **Hampe J,** Cuthbert A, Croucher PJ, Mirza MM, Mascheretti S, Fisher S, Frenzel H, King K, Hasselmeyer A, MacPherson AJ, Bridger S, van Deventer S, Forbes A, Nikolaus S, Lennard-Jones JE, Foelsch UR, Krawczak M, Lewis C, Schreiber S, Mathew CG. Association between insertion mutation in NOD2 gene and Crohn's disease in German and British populations. *Lancet* 2001; **357**: 1925-1928
- 8 **Ogura Y,** Inohara N, Benito A, Chen FF, Yamaoka S, Nunez G. Nod2, a Nod1/Apaf-1 family member that is restricted to monocytes and activates NF-kappaB. *J Biol Chem* 2001; **276**: 4812-4818
- 9 **Yamazaki K,** Takazoe M, Tanaka T, Kazumori T, Nakamura Y. Absence of mutation in the NOD2/CARD15 gene among 483 Japanese patients with Crohn's disease. *J Hum Genet* 2002; **47**: 469-472
- 10 **Leong RW,** Armuzzi A, Ahmad T, Wong ML, Tse P, Jewell DP, Sung JJ. NOD2/CARD15 gene polymorphisms and Crohn's disease in the Chinese population. *Aliment Pharmacol Ther* 2003; **17**: 1465-1470
- 11 **Roussomoustakaki M,** Koutroubakis I, Vardas EM, Dimoulios P, Kouroumalis EA, Baritaki S, Koutsoudakis G, Krambovitis E. NOD2 insertion mutation in a Cretan Crohn's disease population. *Gastroenterology* 2003; **124**: 272-273
- 12 **Lennard-Jones JE.** Classification of inflammatory bowel disease. *Scand J Gastroenterol Suppl* 1989; **170**: 2-6
- 13 **Neurath MF,** Pettersson S, Meyer zum Buschenfelde KH, Strober W. Local administration of antisense phosphorothioate oligonucleotides to the p65 subunit of NF-kappa B abrogates established experimental colitis in mice. *Nat Med* 1996; **2**: 998-1004
- 14 **Schreiber S,** Nikolaus S, Hampe J. Activation of nuclear factor kappa B inflammatory bowel disease. *Gut* 1998; **42**: 477-484

Edited by Chen WW and Wang XL **Proofread by** Xu FM

Therapeutic effects of endoscopic variceal ligation combined with partial splenic embolization for portal hypertension

Rui-Yun Xu, Bo Liu, Nan Lin

Rui-Yun Xu, Bo Liu, Nan Lin, Department of General Surgery, The Third Affiliated Hospital, Sun-Yet-San University, Guangzhou 510630, Guangdong Province, China

Correspondence to: Dr. Rui-Yun Xu, Department of General Surgery, The Third Affiliated Hospital, Sun-Yet-San University, Guangzhou 510630, Guangdong Province, China. xuruiyun@yahoo.com

Telephone: +86-20-87536260

Received: 2003-09-09 **Accepted:** 2003-10-27

Abstract

AIM: To evaluate the feasibility of a new strategy of endoscopic variceal ligation combined with partial splenic embolization (EVL-PSE) for patients with cirrhosis and portal hypertension.

METHODS: From May 1999 to May 2002, 41 cases with cirrhosis and portal hypertension underwent EVL-PSE. Hemodynamics of the main portal vein (MPV), the left gastric vein (LGV) and azygos vein, including maximum velocity, flow rate and vein diameter, were assessed by Doppler ultrasonography.

RESULTS: One case died from pulmonary artery embolism. One case complicated with splenic abscess was successfully managed by laparotomy. The esophageal varices and hypersplenism were well controlled after EVL-PSE in other patients. After EVL-PSE, the flow rate and velocity of MPV was significantly reduced ($P < 0.05$), as well as the flow rate of the LGV and azygos vein. During the follow-up, no recurrent bleeding was found.

CONCLUSION: Being more convenient and less invasive, EVL-PSE is hopeful to be a proper intervention strategy for portal hypertensive patients with impaired hepatic function or those intolerant to shunting or devascularization surgery.

Xu RY, Liu B, Lin N. Therapeutic effects of endoscopic variceal ligation combined with partial splenic embolization for portal hypertension. *World J Gastroenterol* 2004; 10(7): 1072-1074
<http://www.wjgnet.com/1007-9327/10/1072.asp>

INTRODUCTION

Recently, various non-surgical and less invasive treatments for liver cirrhosis and portal hypertension have been developed and accepted world-wide. However, these more up-to-date methods have their drawbacks, respectively. We introduced a new strategy combining endoscopic variceal ligation with partial splenic embolization (EVL-PSE) and examined its therapeutic features. The present study was thus designed to determine, in a controlled and prospective manner, whether this intervention would decrease the risk of variceal bleeding and improve the hypersplenism in cirrhotic patients effectively. In the meantime, we investigated the portal hemodynamic changes before and 1 week after EVL-PSE by Color Doppler Flow Imaging (CDFI).

MATERIALS AND METHODS

Patients

Between May 1999 and May 2002, 41 patients with portal hypertension underwent EVL-PSE in the Third Hospital Affiliated to Sun-Yet-San University, China. Data of the patients and control subjects are given in Table 1. Hepatitis induced cirrhosis was the main cause of portal hypertension. Functional hepatic reserve was classified according to the Pugh-modified Childs' scales. All patients met the following criteria: (1) history of at least once upper gastrointestinal hemorrhage; (2) varices of size III or IV; (3) without other diseases (e.g. cancer) decreasing one's life expectancy.

All patients in the EVL-PSE group had hypersplenism of various degrees and 15 cases presented with active variceal bleeding seen directly by endoscopy at admission. After a thorough clinical and physical examination, 40 volunteers without obvious defect in cardiovascular or digestive system were studied as control group.

Table 1 Clinical characteristics of cirrhotic patients and control subjects

	EVL-PSE group (n=41)	Control group (n=40)
Sex:male/female	32/9	29/11
Age:mean,range(years)	43,34-67	37,18-68
Childs' class:A/B/C	5/26/10	0
Etiology		
Viral hepatitis	37	0
Primary biliary cirrhosis	1	0
Schistosomiasis	4	0
Virix grading (III/IV)	14/26	
Red color sign	15	0

Procedures of EVL-PSE

(1) The procedure of EVL has been described in detail elsewhere^[1-6]. Ligation was performed at 1 to 5 cm above the gastroesophageal junction with 6 to 12 ligation sites per individual. EVL was repeated biweekly until all esophageal varices were ligated. (2) PSE was performed about 1 week after successful hemostasis by first EVL. (3) The PSE procedures: Selective splenic arterial cannulation and angiography were accomplished with a Seldinger's puncture of femoral artery^[7] to evaluate the mass of the spleen and its vascular supply. The catheter reached the far end of the splenic artery as possible, through which granules of Gelfoam (1-2 mm³) soaked in certain antibody were injected so as to make the peripheral branches embolized. According to the area differences judged from the angiography before and after PSE as well as the CT results, we estimated the infarction size. In our study, 30-60% of the spleen parenchyma were infarcted. (4) Antibiotics were used as routine systemically and locally before and after the operation. Intestinal preparations were done just like a colonic operation. (5) We measured hemodynamic parameters of the main portal vein (MPV), left gastric vein(LGV) and azygos vein, including maximum velocity, flow direction and vein diameter by Color Doppler ultrasonography (Philip SD 800, Holland), with a 2.0-7.5MHZ convex array transducer.

Scanning was performed with patients in a supine position and the portal vein and left gastric vein were visualized via a transabdominal way while imaging of the azygos vein was through suprasternal fossa. The blood flow velocity was calculated from Doppler spectral traces of 4-6 s with 1 to 10 mm sampling volume adjusted according to the respiration and the mean values were calculated as the mean blood flow velocity. To avoid equipment and operator variability, all examinations were performed using the same equipment by the same ultrasonogist.

Statistical analysis

Analyses were performed by using SPSS10.0 statistical packages. The results are presented as mean±SD and were considered to be significant if *P*<0.05. The data analyses before and 1 week after EVL-PSE of portal hypertensive patients were made using the paired *t*-test. Analysis of variance was used to verify differences between groups.

RESULTS

Efficacy of EVL-PSE on varices occlusion and bleeding control

EVL-PSE was performed successfully in all 41 cases. A total of 128 EVLs were done, with a mean of 3.1 (2-5) EVLs per patient. All esophageal varices were occluded. Nine cases with active variceal bleeding underwent successful emergent EVL. One patient suffered a recurrent bleeding 11 d after the initial intervention and received a repeated EVL with perfect result. No recurrent bleeding was observed in the other 40 cases during hospitalization, and no case presented with another hemorrhagic event during 2-24 mo follow-up (mean 9.9 mo).

Changes of laboratory parameters after EVL-PSE

The effect on blood routine examination is shown in Table 2, where a significant increment was observed both for leukocytes and thrombocytes 1 and 2 weeks after EVL-PSE. The changes of the hemoglobin contents throughout the operation was of no statistical significance.

Table 2 Changes of laboratory parameters after EVL-PSE

	Hemoglobin (g/L)	WBC (×10 ⁹ /L)	Platelet (×10 ⁹ /L)
Before EVL-PSE	104±14	2.9±0.6	55±11
1 wk after EVL-PSE	117±12	7.4±1.5 ^a	102±18 ^a
2 wk after EVL-PSE	119±16	6.1±1.2 ^a	120±24 ^a

^a*P*<0.05 vs before EVL-PSE.

Table 3 Comparison of hemodynamics between cirrhotic patients before EVL-PSE and control group

	Diameter (mm)		Blood flow velocity (cm/s)		Blood flow rate (L/min)	
	Controls	PSE-EVL group	Controls	PSE-EVL group	Controls	PSE-EVL group
Portal vein (n=37)	11.82±1.69	15.51±1.71 ^a	20.19±2.21	15.10±2.78 ^a	1.15±0.20	0.98±0.20 ^a
LGV (n=36)	3.72±0.79	6.33±1.49 ^a	7.72±1.88	15.71±3.63 ^a	0.06±0.03	0.45±0.19 ^a
Azygos vein (n=36)	6.00±1.09	10.08±1.17 ^a	16.03±3.01	29.22±6.72 ^a	0.34±0.04	1.20±0.35 ^a

^a*P*<0.05 vs control group.

Table 4 Comparison of hemodynamics 1 wk before and after EVL-PSE in cirrhotic patients

	Diameter (mm)		Blood flow velocity (cm/s)		Blood flow rate (L/min)	
	Before EVL-PSE	After EVL-PSE	Before EVL-PSE	After EVL-PSE	Before EVL-PSE	After EVL-PSE
Portal vein (n=40)	15.51±1.71	16.2±1.43 ¹	15.10±2.78	13.92±2.74 ^a	0.98±0.20	0.72±0.15 ^b
LGV(n=35)	6.33±1.49	7.41±1.81	15.71±3.63	12.11±2.79	0.45±0.19	0.44±0.19
Azygos vein (n=37)	10.08±1.17	7.12±1.22	29.22±6.72	20.11±5.01	1.20±0.35	0.68±0.23

¹*P*>0.05, ^a*P*<0.05, ^b*P*<0.01.

Gross and pathologic changes of spleens

Forty cases showed significantly smaller spleens after PSE, and the shrinkage degree correlated well with the infarcted area. One patient underwent splenectomy 2 wkafter PSE. Grossly the spleen presented with grey regions of segmental infarction, and microscopic examination suggested degeneration and necrosis of the splenic parenchyma with proliferation of surrounding fibrous tissue.

Adverse effects and complications

The majority of patients had EVL-related mild angina and/or retrosternal pain, which usually palliated spontaneously 3-5 d later without any special management. Forty cases had different degrees of fever and pain in left upper quadrant. The fever was usually around 38 °C and lasted 3-7 d with an exception of 28 d. One patient had splenic abscess and recovered after operation. Another case died 2 d after PSE due to pulmonary arterial embolism.

Color doppler ultrasound changes

Comparisons of Doppler parameters before EVL-PSE between the cirrhotic patients and controls are listed in Table 3. Significant differences were found in blood flow, blood flow rate and diameters of the main portal vein (MPV), left gastric vein (LGV) and azygos vein between the two groups. Table 4 presents the effects of EVL-PSE on the collateral branches of main portal vein and azygos vein. The diameters of MPV before and after the operation showed no difference, while the blood flow and blood flow rate decreased significantly, as well as the blood flow-rates of LGV and azygos vein.

DISCUSSION

What is the therapeutic strategy for portal hypertension? As medical doctors, we have been working on it assiduously. Poor hepatic function and impaired tolerance to the operation make it very important and of great clinical significance to explore an optimal strategy both effectively and the least invasively for portal hypertensive patients.

EVL is the widely accepted treatment for the bleeding of esophageal varices because of its definite efficacy, more convenience and safety and minor invasiveness. it, however, had a much longer course of treatment and the rate of recurrent hemorrhagic events in the short term was as high as 15-36%, especially before the varices were completely occluded^[8-10]. EVL alone had no effect on hypersplenism, either. PSE is a new interventional radiological method for the treatment of hypersplenism secondary to portal hypertension. Generally,

30-40% of splenic infarction by PSE could improve hypersplenism, and 50-60% would affect favourably the portal pressure^[7]. We discovered that the hypertrophic spleen would shrink more or less when the infarcted area reached 30-60%, with a significant increase of white blood cells and platelets in the peripheral blood ($P<0.05$), which suggested that PSE could improve the hypersplenism effectively. Former study demonstrated similar results. The content of hemoglobin changed little during PSE, because it was correlated much closely with the patients' bleeding history and the amount of transfusion.

The current study revealed no changes of the diameters ($P>0.05$) of MPV as well as its significantly lower blood flow velocity and decreased blood flow rate ($P<0.05$) after EVL-PSE. Traditional opinions held that portal blood flow after splenectomy or devascularization procedures would not decrease even would increase, while more up-to-date researches discovered that portal blood flow decreased as a result of devascularization, similar to that of decompressive shunts surgery^[11-13]. We found the similar results to a further degree, that is, the diameter of MPV after PSE showed no difference, the portal blood flow decreased significantly, however. Some held the opinion that the increased blood flow in portal hypertension come mainly from the splenic vein. PSE decreased the reflux of splenic vein, therefore, the blood flow of MPV decreased as well as its pressure. EVL-PSE decreased the blood flow and pressure of MPV equivalent to the conjoint effects of splenectomy and devascularization. The hemodynamic changes of MPV may be not quite the same because of individual difference, from which some scholars concluded that interventional therapy should be based on the patients' hemodynamic conditions individually. We found in the portal hypertension group enlarged LGVs and hepatofugal blood flow in the pre-operation examination, which both indicated the patency of the esophagocardiac collateral circulation. LGV dilated and its blood flow decreased after EVL-PSE, which probably were results of the increased blood flow of the mucosa in the fundus and gastric body after repeated ligation. The gastric mucosa might be damaged more severely as a consequence. We should go further to identify its long-term effects. The diameter and blood flow velocity were strikingly higher in portal hypertension patients than controls before EVL-PSE ($P<0.01$). Some studies reported the same conclusions. They considered that measurement of the azygos blood flow was of importance for the patients' treatment and prognosis^[14]. Main branches of the portosystemic collateral circulation being cut-off, the diameter and blood flow-rate of azygos vein decreased significantly after EVL-PSE ($P<0.01$). However, they were still higher than that of the controls, indicating that other shunts for the superior vena cava, such as the periesophageal veins and abdominal wall veins accounted for the flow of azygos vein to a great extent.

Except for an ectopic embolism resulting from inappropriate operation, the main complications in our study were PSE-related pain in left upper quadrant and mild to moderate fever, which could be relieved by a small dose of NSAID such as mezolol, etc. satisfactorily. Splenic abscess was diagnosed 2 wk after EVL-PSE in one case, and the patient whose spleen parenchyma was infarcted very much (about 70%) was recovered and discharged after splenectomy. Infarcted area more than 60% would induce more complications. Strengthened antibiotic use together with intestinal preparation and especially, perfect operation were the key points for a favorable result with less complications.

The esophageal varices were completely obliterated by EVL-PSE in 40 patients, with an average of 3.1 EVLs per patient. No case except one suffered recurrent bleeding during hospitalization and follow-up. In contrast, the obliteration rate

of esophageal varices was 80-91% by EVL alone, with an average of 4 EVLs per patient, and with a recurrent bleeding rate as high as 15-17.1%^[11]. EVL-PSE was superior to EVL alone. The underlying mechanism might be that PSE could decrease the blood flow of MPV, and the consequent pressure lowering of portal vein made varices less viable to recur.

Conclusively, EVL-PSE was effective in the treatment of esophageal variceal hemorrhage and hypersplenism secondary to portal hypertension, and it could also decrease the total EVLs needed to make the varices occluded and the rate of short-term recurrent bleeding. The reduction of blood flow of MPV lowered the risk of recurrent bleeding after EVL. Being very convenient and little invasive, EVL-PSE is probably the first choice of intervention at strategy for portal hypertensive patients with impaired hepatic function or those intolerant to shunting or devascularization surgery.

REFERENCES

- 1 **Liu XY**, Huang FZ, Long GH, Nie WP, Chen DJ, Liu R, Zhang YD. Endoscopic variceal ligation- summary experience of four years. *Zhongguo Neijing Zazhi* 1995; **1**: 3-5
- 2 **Wong T**, Pereira SP, McNair A, Harrison PM. A prospective, randomized comparison of the ease and safety of variceal ligation using a multi-band vs a conventional ligation device. *Endoscopy* 2000; **32**: 931-934
- 3 **Elli C**, May A, Wurster H. The first reusable multiple-band ligator for endoscopic hemostasis of variceal bleeding, nonvariceal bleeding and mucosal resection. *Endoscopy* 1999; **31**: 738-740
- 4 **Harada T**, Yoshida T, Shigemitsu T, Takeo Y, Tada M, Okita K. Therapeutic results of endoscopic variceal ligation for acute bleeding of oesophageal and gastric varices. *Gastroenterol Hepatol* 1999; **50**: 768-774
- 5 **Brenna E**, Flaaten B, Waldum HL, Myrvold HE. Treatment of esophageal varices with banding ligation. *Tidsskr Nor Laegeforen* 2000; **120**: 2626-2629
- 6 **Hata Y**, Hamada E, Takahashi M, Ota S, Ogura K, Shiina S, Okamoto M, Okudaira T, Teratani T, Maeda S, Koike Y, Sato S, Obi S, Tanaka T, Kawabe T, Shiratori Y, Kawase T, Nomura M, Omata M. Endoscopic variceal ligation is a sufficient procedure for the treatment of oesophageal varices in patients with hepatitis C liver cirrhosis: comparison with injection sclerotherapy. *J Gastroenterol Hepatol* 1999; **14**: 236-240
- 7 **Numata S**, Akagi K, Sakino I, Ogata H, Kawadoko T, Suzuki N, Nomiya K, Tsuji H, Fujishima M. Partial splenic embolization for the treatment of liver cirrhosis with hypersplenism: assessment of clinical response and liver function. *Nippon Shokakibyo Gakkai Zasshi* 1997; **94**: 526-531
- 8 **Lay CS**, Tsai YT, Teg CY, Shyu WS, Guo WS, Wu KL, Lo KJ. Endoscopic variceal ligation in prophylaxis of first variceal bleeding in cirrhotic patients with high-risk esophageal varices. *Hepatology* 1997; **25**: 1346-1350
- 9 **Bohnacker S**, Sriram PV, Soehendra N. The role of endoscopic therapy in the treatment of bleeding varices. *Baillieres Best Pract Res Clin Gastroenterol* 2000; **14**: 477-494
- 10 **De BK**, Ghoshal UC, Das T, Santra A, Biswas PK. Endoscopic variceal ligation for primary prophylaxis of oesophageal variceal bleed: preliminary report of a randomized controlled trial. *J Gastroenterol Hepatol* 1999; **14**: 220-224
- 11 **Huang YT**, Wang WM. Change and clinical significance of portal hemodynamics. *Puwai Linchuang* 1995; **10**: 294-297
- 12 **Sugano S**, Yamamoto K, Takamura N, Momiya K, Watanabe M, Ishii K. Azygos venous blood flow while fasting, postprandially, and after endoscopic variceal ligation, measured by magnetic resonance imaging. *J Gastroenterol* 1999; **34**: 310-314
- 13 **Li R**, Wen Y, Liu M, Li S. Use of color Doppler esophageal ultrasonography for assessing hemodynamics of the lower esophageal veins before and after endoscopic esophageal variceal ligation. *Hunan Yike Daxue Xuebao* 1999; **24**: 50-52
- 14 **Matsumoto A**, Hamamoto N, Ohnishi A, Miyoshi H, Sugi K, Kojima H, Kayazawa M, Morikawa H, Hirata I, Katsu K. Left gastric vein hemodynamics and variceal recurrence in patients undergoing prophylactic endoscopic ligation of high-risk esophageal varices. *Gastrointest Endosc* 1999; **50**: 768-774

New mutation points in 23S rRNA gene associated with *Helicobacter pylori* resistance to clarithromycin in northeast China

Qing Hao, Yan Li, Zhi-Jie Zhang, Yong Liu, Hong Gao

Qing Hao, Yan Li, Department of Gastroenterology, the 2nd Affiliated Hospital, China Medical University, Shenyang 110004, Liaoning Province, China

Zhi-Jie Zhang, Yong Liu, Clinical Center of Microbiology, the 2nd Affiliated Hospital, China Medical University, Shenyang 110004, Liaoning Province, China

Hong Gao, The Major Health Ministry Lab For Congenital Malformation, China Medical University, Shenyang 110004, Liaoning Province, China

Correspondence to: Dr. Yan Li, Department of Gastroenterology, the 2nd Affiliated Hospital, China Medical University, Shenyang 110004, Liaoning Province, China. liyan1@medmail.com.cn

Telephone: +86-24-83956416 **Fax:** +86-24-83250146

Received: 2003-10-20 **Accepted:** 2003-12-16

Abstract

AIM: To investigate the resistance rate of *Helicobacter pylori* (*H. pylori*) to clarithromycin, metronidazole, amoxicillin and tetracycline to guide clinical practice, and to study the mechanism of *H. pylori* resistant to clarithromycin.

METHODS: Thirty *H. pylori* strains were isolated from the mucosa of peptic ulcer, gastric tumor and chronic gastritis patients, then the minimal inhibitory concentration (MIC) to clarithromycin, metronidazole, amoxicillin and tetracycline was evaluated by E-test method. The sequence analysis of PCR fragments was conducted in 23S rRNA gene of *H. pylori* resistant to clarithromycin to get the resistance mechanism of the bacteria.

RESULTS: Among 30 *H. pylori* strains, 7 cases were resistant to clarithromycin, 12 to metronidazole, 2 to tetracycline and no strain was found to be resistant to amoxicillin. The resistance rates were 23.3%, 40%, 6.7% and 0%, respectively. Three new mutation points were found to be related to the clarithromycin resistance in *H. pylori* isolates, which were G2224A, C2245T and T2289C.

CONCLUSION: In northeast China, *H. pylori* shows high resistance to metronidazole, while sensitive to amoxicillin. The mechanism of resistance to clarithromycin may be related to the mutation of G2224A, C2245T and T2289C in the 23S rRNA gene.

Hao Q, Li Y, Zhang ZJ, Liu Y, Gao H. New mutation points in 23S rRNA gene associated with *Helicobacter pylori* resistance to clarithromycin in northeast China. *World J Gastroenterol* 2004; 10(7): 1075-1077

<http://www.wjgnet.com/1007-9327/10/1075.asp>

INTRODUCTION

H. pylori plays an important role in the pathogenesis of many digestive diseases. The recurrence of peptic ulcer and the development of the gastric cancer are also due to *H. pylori* infection^[1,2]. In the different eradication therapy regimen including PPI and multiple antibiotics, cases of eradication

failure due to resistance of *H. pylori* to antibiotics have been reported keeping increasing. The resistance mechanism of *H. pylori* in the former studies showed the mutation from A to G in 2 143 and 2 144 position of 23S rRNA gene. But in our study we found other three new mutation points in 23S rRNA gene related to the *H. pylori* resistance to clarithromycin.

MATERIALS AND METHODS

H. pylori strain

In the endoscopic examination of the patients with digestive symptoms, we collected such patients with peptic ulcer, chronic gastritis and gastric carcinoma as our subjects. Firstly, one piece of gastric antra mucosa biopsy specimen was obtained from the patients for the purpose of rapid urease enzyme test. Then two pieces of antra mucosa biopsy specimens were obtained from the same patient with *H. pylori* infection diagnosed by the positive rapid urease enzyme test. The biopsy specimens were cut up in sterile plate and then cultured on the Columbia agar base with 100 mL/L no-fiber fresh rabbit blood and 3 mg/L bacitracin at 37 °C for 3-5 d under microaerobic conditions (50 mL/L O₂, 100 mL/L CO₂, 850 mL/L N₂). The organisms were identified as *H. pylori* by Gram stain morphology, colony morphology and positive urease, catalase and oxidase activities. The typical bacteria were subcultured to obtain the pure *H. pylori* isolates.

Antibiotics susceptibility test

The pure *H. pylori* suspension of 1 McFrand unit was prepared with sterile 9 g/L sodium chloride, and spread onto the Mueller-Hinton agar base with 100 mL/L fresh rabbit blood. The minimal inhibitory concentration (MIC) of *H. pylori* to different antibiotics was evaluated with E-test strips. Strains were considered resistant to clarithromycin, metronidazole, amoxicillin and tetracycline if the MIC was ≥ 8 μ g/mL, 8 μ g/mL, 2 μ g/mL and 8 μ g/mL respectively.

Resistance mechanism analysis

Three clarithromycin resistant *H. pylori* isolates and one sensitive *H. pylori* isolate were chosen, that is, No.13 (MIC 8 mg/L), No. 17(MIC 64 mg/L), No.22 (MIC>256 mg/L) and No.33 (MIC 0.125 mg/L). The DNA was extracted from the bacteria with the phenol-chloroform extraction method. We designed primers according to the 23S rRNA gene sequence reported by Hiratsuka (GeneBank accession number U27270). The primers were synthesized by Shanghai Sangon corporation and the sequences were as follows: forward primer: 5' -CTG CAT GAA TGG CGT AAC GAG-3' (complementary to 23S rRNA gene sequence from 2 047 to 2 067); and reverse primer: 5' -GAG CGA CCG CCC CGA TCA AAC-3' (complementary to 23S rRNA gene sequence from 2 327 to 2 347), which will generate a 301 bp product. PCR amplification reaction mixture (20 μ L) contained 13.8 μ L double distilled H₂O, 2.5 μ L 10 \times PCR buffer, 2 μ L dNTPs (2.5 mmol/L), 0.2 μ L Ex-Taq polymerase (5u/ μ L), 1.5 μ L primer (1:5 \times) and 0.5 μ L DNA sample. PCR cycle conditions were 32 cycles of 94 °C for 40 s, 61.5 °C for 1 min, 72 °C for 1 min after 94 °C for 4 min once at

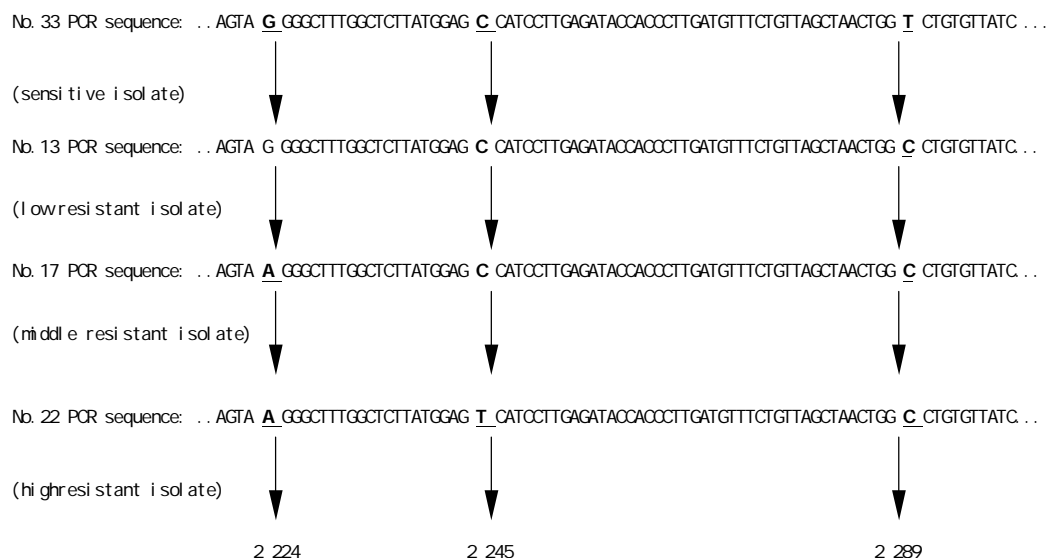


Figure 1 Mutations of 23S rRNA gene in *H pylori* resistant to clarithromycin.

first, then followed by a final extension step at 72 °C for 7 min. The purification of PCR products was observed by electrophoresis on an 80 g/L polyacrylamide gel. Then PCR products were sent to Sangon Corporation to conduct the sequence analysis. The amplified 23s rRNA gene sequence of resistant *H pylori* was compared to that of sensitive ones in order to find out the difference between them.

RESULTS

There were 7 cases among 30 *H pylori* isolates resistant to clarithromycin (MICs were from 8 mg/L to 256 mg/L), 12 cases of the isolates was resistant to metronidazole (MICs were from 24 mg/L to 256 mg/L), 2 cases resistant to tetracycline (MICs were 16 mg/L and 32 mg/L) and no case resistant to amoxicillin. The resistance rates to the above 4 different antibiotics were 23.3%, 40%, 6.7% and 0%, respectively.

No.33 *H pylori* isolate was sensitive to clarithromycin, while No.13, No.17, and No.22 isolates were all resistant to clarithromycin. Point mutations appeared at three positions of the intended DNA fragments of clarithromycin resistant *H pylori* 23s rRNA gene. In comparison with the sequence of sensitive *H pylori*, No.13 resistant isolate with MIC 8 mg/L had one point mutation from T to C at 2289 (T2289C), No.17 isolate with MIC 64 mg/L had two point mutations which were G to A at 2 224 position (G2224A) and T to C at 2 289 position (T2289C), and No.22 isolate with the highest MIC >256 mg/L had three point mutations, and these were mutations from G to A at 2 224 position (G2224A), from C to T at 2 245 position (C2245T) and the mutation from T to C at 2 289 position (T2289C). With the increasing resistance of *H pylori* to clarithromycin, the number of point mutation were increased (Figure 1).

DISCUSSION

The prevalence of *H pylori* infection is about one-half of the world's population^[3], and still higher in the developing countries and low socio-economic populations^[4-6]. It has been demonstrated that *H pylori* is an important etiologic factor of digestive diseases. *H pylori* infection is also correlated with cardio-cerebrovascular and pulmonary disease^[7-10]. So eradication of *H pylori* becomes very important in the cure of the above diseases, especially peptic ulcer. But recently, cases of eradication failure become more and more due to the resistance of *H pylori* to antibiotics in the triple regimens.

Tsuneoka *et al*^[11] reported that *H pylori* strains from 19 cases (82.6%) out of 23 of failed eradication therapy became resistant to clarithromycin. Reports have shown that about 3-14%^[12-14] of *H pylori* isolates are resistant to clarithromycin, 12-44%^[13-16] are resistant to metronidazole. But no *H pylori* was found primary resistant to amoxicillin. The study showed that tetracycline resistance rate was ranging from 0 to 11%^[13,16,17].

In our study, we isolated 30 *H pylori* strains from patients of peptic ulcer, chronic gastritis and gastric carcinoma and determined their MICs to clarithromycin, metronidazole, amoxicillin and tetracycline by E-test, respectively. Results showed a higher clarithromycin resistance than that in Europe (23.3%, 7/30). It is acknowledged that resistant clarithromycin *H pylori* strains become predominant because of antibiotics selective pressure. Clarithromycin frequently appearing in *H pylori* eradication therapy regimens led to the increasing of clarithromycin resistance. While in China, especially in northeast China, clarithromycin is rarely applied in clinic. How did the high resistance to clarithromycin generate? Is it associated with the extensive application of the other macrolide agents, such as erythromycin, azithromycin, and so on? Dose cross-resistance to macrolide exist among *H pylori* strains? Midolo and Saika *et al*^[18,19] have demonstrated the existence of this phenomenon. But no study on this aspect has been done in China. The high resistance to clarithromycin should be considered in selecting *H pylori* eradication therapy regimen.

Metronidazole has been extensively used to treat anaerobic and parasitic infections for a long time, especially in the developing countries. It has been demonstrated that previous exposure of *H pylori* to metronidazole *in vivo* results in the emergence of resistant strains. Metronidazole resistant rate was reported ranging from 12 to 44%, similar to that in this study (40%). But it was also reported that metronidazole resistance as determined by E-test was significantly higher than that determined by agar dilution. Houben *et al*^[20] found whether resistant to metronidazole could not affect the therapy outcome of OMC (omeprazole, metronidazole, clarithromycin) regimen. While in another study^[21], it showed that the eradication rates were higher than the sensitive rates compared with resistant strains.

Almost all the studies *in vitro* showed high susceptibility of *H pylori* to amoxicillin. This study had the same results. In 30 isolates *H pylori* strains, only 1 strain's MIC to amoxicillin was 4 µg/mL, and other MICs were all very low, between <0.016-0.75 µg/mL. The influence of gastric acid on bactericidal effects was little against amoxicillin compared with macrolide.

Furthermore, its activity *in vivo* is considerably enhanced when given concomitantly with proton pump inhibitors (PPI)^[22]. So amoxicillin is still a selection of optimal drugs for the eradication of *H pylori*. Tetracycline is seldom applied in clinical practice at present. So studies on it were also rare. Perhaps due to less application, tetracycline resistance was very low, similar to this study. It was reported that the effect of the combination of macrolide agents with tetracycline was favorable^[23].

The mechanism of *H pylori* resistance to clarithromycin was demonstrated to be associated with the mutation of A2143G or A2144G in 23S rRNA gene^[24]. Some other mutation points were also reported after that, such as A2142C, A2143C, A2143T, A2115C and G2141^[25]. Fontana^[26] found that T2717C mutation was related to the *H pylori* resistance. It was known that the genetic character of *H pylori* in the different area was different^[27,28], so did the genetic character of resistance *H pylori* strains^[29]. Using gene segment analysis directly to determine the mutation position has still not been reported in China yet. We found in our study that the number of mutation points increased with the MIC of the resistant strains. The higher MIC is, the more mutation points are. This result has not been reported in other studies. The further investigation is still required to demonstrate the geographic differences existing in *H pylori* from different countries.

REFERENCES

- Walsh JH, Peterson WL. The treatment of *Helicobacter pylori* infection in the management of peptic ulcer disease. *N Engl J Med* 1995; **333**: 984-991
- Wang RT, Wang T, Chen K, Wang JY, Zhang JP, Lin SR, Zhu YM, Zhang WM, Cao YX, Zhu CW, Yu H, Cong YJ, Zheng S, Wu BQ. *Helicobacter pylori* infection and gastric cancer: evidence from a retrospective cohort study and nested case-control study in China. *World J Gastroenterol* 2002; **8**: 1103-1107
- Dunn BE, Cohen H, Blaster MJ. *Helicobacter pylori*. *Clin Microbiol Rev* 1997; **10**: 720-741
- Bener A, Uduman SA, Ameen A, Alwash R, Pasha MA, Usmani MA, Al-Naili SR, Amiri KM. Prevalence of *Helicobacter pylori* infection among low socio-economic workers. *J Commun Dis* 2002; **34**: 179-184
- Wang KJ, Wang RT. Meta-analysis on the epidemiology of *Helicobacter pylori* infection in China. *Zhonghua Liuxing Bingxue Zazhi* 2003; **24**: 443-446
- Strnad M, Presecki V, Babus V, Turek S, Dominis M, Kalenic S, Hebrang A, Katicic M. Epidemiology of *Helicobacter pylori* infection. *Lijec Vjesn* 2002; **124**(Suppl): 5-9
- Mendall MA, Goggin PM, Molineaux N, Levy J, Toosy T, Strachan D, Camm AJ, Northfield TC. Relation of *Helicobacter pylori* infection and coronary heart disease. *Br Heart J* 1994; **71**: 437-439
- Pasceri V, Cammarota G, Patti G, Cuoco L, Gasbarrini A, Grillo RL, Fedeli G, Gasbarrini G, Maseri A. Association of virulent *Helicobacter pylori* strains with ischemic heart disease. *Circulation* 1998; **97**: 1675-1679
- Markus HS, Mendall MA. *Helicobacter pylori* infection: a risk factor for ischaemic cerebrovascular disease and carotid atheroma. *J Neurol Neurosurg Psychiatry* 1998; **64**: 104-107
- Roussos A, Philippou N, Gourgoulis KI. *Helicobacter pylori* infection and respiratory diseases: a review. *World J Gastroenterol* 2003; **9**: 5-8
- Tsuneoka H, Takaba M, Nagatomi Y, Mori K, Matsumoto T, Honda T. Sensitivity of *Helicobacter pylori* to amoxicillin and clarithromycin with special reference to eradication therapy. *Kansenshogaku Zasshi* 1998; **72**: 335-341
- Franzin L, Pennazio M, Cabodi D, Paolo Rossini F, Giannini P. Clarithromycin and amoxicillin susceptibility of *Helicobacter pylori* strains isolated from adult patients with gastric or duodenal ulcer in Italy. *Curr Microbiol* 2000; **40**: 96-100
- Taylor DE, Jiang Q, Fedorak RN. Antibiotic susceptibilities of *H pylori* strains isolated in the Province of Alberta. *Can J Gastroenterol* 1998; **12**: 295-298
- Savarino V, Zentilin P, Pivari M, Bisso G, Raffaella Mele M, Bilardi C, Borro P, Dulbecco P, Tessieri L, Mansi C, Borgonovo G, De Salvo L, Vigneri S. The impact of antibiotic resistance on the efficacy of three 7-day regimens against *Helicobacter pylori*. *Aliment Pharmacol Ther* 2000; **14**: 893-900
- Osato MS, Reddy R, Reddy SG, Penland RL, Graham DY. Comparison of the Etest and the NCCLS-approved agar dilution method to detect metronidazole and clarithromycin resistant *H pylori*. *Int J Antimicrob Agents* 2001; **17**: 39-44
- Ani AE, Malu AO, Onah JA, Queiroz DM, Kirschner G, Rocha GA. Antimicrobial susceptibility test of *Helicobacter pylori* isolated from Jos, Nigeria. *Trans R Soc Trop Med Hyg* 1999; **93**: 659-661
- Vasquez A, Valdez Y, Gilman RH, McDonald JJ, Westblom TU, Berg D, Mayta H, Gutierrez V. Metronidazole and clarithromycin resistance in *Helicobacter pylori* determined by measuring MICs of antimicrobial agents in color indicator egg yolk agar in a miniwell format. *J Clin Microbiol* 1996; **34**: 1232-1234
- Saika T, Kobayashi I, Fujioka T, Nasu M, Okamoto R, Inoue M. A mechanism of clarithromycin resistance in *Helicobacter pylori*. *Kansenshogaku Zasshi* 1998; **72**: 918-923
- Midolo PD, Bell JM, Lambert JR, Turnidge JD, Grayson ML. Antimicrobial resistance testing of *Helicobacter pylori*: a comparison of Etest and disk diffusion methods. *Pathology* 1997; **29**: 411-414
- Houben MH, Hensen EF, Rauws EA, Hulst RW, Hoff BW, Ende AV, Kate FJ, Tytgat GN. Randomized trial of omeprazole and clarithromycin combined with either metronidazole or amoxicillin in patients with metronidazole-resistant or-susceptible *Helicobacter pylori* strains. *Aliment Pharmacol Ther* 1999; **13**: 883-889
- Moayyedi P, Ragunathan PL, Mapstone N, Axon AT, Tompkins DS. Relevance of antibiotic sensitivities in predicting failure of omeprazole, clarithromycin, and tinidazole to eradicate *Helicobacter pylori*. *J Gastroenterol* 1998; **33**(Suppl): 62-65
- Hirschl AM, Rotter ML. Amoxicillin for the treatment of *Helicobacter pylori* infection. *J Gastroenterol* 1996; **31**(Suppl): 44-47
- Bamba H, Kondo Y, Wong RM, Sekine S, Matsuzaki F. Minimum inhibitory concentration of various single agents and the effect of their combinations against *Helicobacter pylori*, as estimated by a fast and simple *in vitro* assay method. *Am J Gastroenterol* 1997; **92**: 659-662
- Stone GG, Shortridge D, Flamm RK, Versalovic J, Beyer J, Idler K, Zulawinski L, Tanaka SK. Identification of a 23S rRNA gene mutation in clarithromycin-resistance *Helicobacter pylori*. *Helicobacter* 1996; **1**: 227-228
- Van Doorn LJ, Debets-Ossenkopp YJ, Marais A, Sanna R, Megraud F, Kusters JG, Quint WG. Rapid detection, by PCR and reverse hybridization, of mutations in the *Helicobacter pylori* 23S rRNA gene, associated with macrolide resistance. *Antimicrob Agents Chemother* 1999; **43**: 1779-1782
- Fontana C, Favaro M, Minelli S, Criscuolo AA, Pietroiusti A, Galante A, Favalli C. New site of modification of 23S rRNA association with clarithromycin resistance of *Helicobacter pylori* clinical isolates. *Antimicrob Agents Chemother* 2002; **46**: 3765-3769
- Mukhopadhyay AK, Kersulyte D, Jeony JY, Datta S, Ito Y, Chowdhury A, Chowdhury S, Santra A, Bhattacharya SK, Azuma T, Nair GB, Berg DE. Distinctiveness of genotypes of *Helicobacter pylori* in Calcutta, India. *J Bacteriol* 2000; **182**: 3219-3227
- Yu FJ, Wu DC, Ku CH, Lu CY, Su YC, Lee YC, Lin SR, Liu CS, Jan CM, Wang WM. Diagnosis of *Helicobacter pylori* infection by stool antigen test in southern Taiwan. *Kaohsiung J Med Sci* 2001; **17**: 344-350
- Meyer JM, Silliman NP, Wang W, Siepmann NY, Sugg JE, Morris D, Zhang J, Bhattacharyya H, King EC, Hopkins RJ. Risk factors for *Helicobacter pylori* resistance in the United States: the surveillance of *H pylori* antimicrobial resistance partnership (SHARP) study, 1993-1999. *Ann Intern Med* 2002; **136**: 13-24

Curse of schistosomiasis on Egyptian liver

Abdel-Rahman El-Zayadi

Abdel-Rahman El-Zayadi, Tropical Medicine Department, Ain Shams University and Cairo Liver Center, 5, El-Gergawy St, Dokki, Giza, Egypt

Correspondence to: Abdel-Rahman El-Zayadi, M.D., Professor of Hepatology and Gastroenterology, Tropical Medicine Department, Ain Shams University and Cairo Liver Center, 5, El-Gergawy St, Dokki, Giza, Egypt. clcz@tedata.net.eg

Telephone: +20-27603002 **Fax:** +20-27481900

Received: 2004-03-06 **Accepted:** 2004-03-20

El-Zayadi AR. Curse of schistosomiasis on Egyptian liver. *World J Gastroenterol* 2004; 10(8): 1079-1081

<http://www.wjgnet.com/1007-9327/10/1079.asp>

INTRODUCTION

Schistosomiasis is a chronic parasitic disease caused by a trematode blood fluke of the genus *Schistosoma* that belongs to the schistosomatidae family. The ancient Egyptians contracted the disease more than 4 000 years ago. It was recognized through haematuria, the main sign of urinary bilharziasis was recorded in the Kahun papyrus 1900 B.C. as "â-a-â" disease^[1].

One of the milestone events in the history of bilharziasis occurred in 1851, Theodor Bilharz, a German physician working at Cairo Medical School, saw the fluke in the mesenteric veins of post-mortem of an Egyptian boy^[2,3], then described two types of ova, one with a terminal spine, and the other with a lateral spine, which he considered to be the mature and immature ova, respectively, produced by the female worms of the same species^[2].

The controversy was finally settled by Leiper (1915-1918), when he demonstrated the presence of two species of *Bilharzia* that were different with regard to the morphology of the adult worms, the type of ova, the molluscan intermediate host, and the human habitat (*i.e.* the urogenital versus the intestinal tract)^[4].

Another milestone was the introduction by McDonagh (1918), of antimony as an antibilharzial agent, and the popularization of the drug by Christopherson (1918) in Egypt^[5,6].

In the life cycle, the adult worms live in terminal venules of the bowel (*S. mansoni*, *S. japonicum*) or bladder (*S. haematobium*). When eggs passed in feces or urine reach fresh water, a larval form is released that subsequently infects snails, the intermediate host. After development, infective larvae (cercariae) leave the snails, enter water, and infect exposed persons through the skin or mucous membranes. After penetration, the cercariae become "schistosomula" that reach the portal circulation in the liver, where they rapidly mature. After a few weeks, adult worms pair, mate, and migrate mainly to terminal venules of specific veins, where females deposit their eggs. By means of lytic secretions, some eggs reach the lumen of the bowel or bladder and are passed with feces or urine. Others are retained in the bowel or bladder wall, while still others are carried in the circulation to the liver, lung, and (less often) to other tissues.

PATHOGENESIS

Schistosomiasis is characterized by the formation of inflammatory granulomas around deposited parasite eggs^[7].

Granuloma formation is a cell-mediated immune response that is dependent on CD4⁺ T cells sensitized to schistosomal egg antigens^[8,9]. This T cell-mediated granulomatous response gets to the peak between 8 and 10 wk after exposure in mice. This acute stage granuloma is characterized by dense cellularity and maximum cytokine production^[7,10,11]. As the infection progresses into the chronic stage (16-20 wk postinfection), cytokine production and cellularity decrease while the fibrotic components of the immunopathologic process increase^[7,10,11]. Thus the end result of host responses to schistosome eggs in the liver is advanced portal fibrosis with dense deposits of collagens in greatly expanded portal tracts.

Hepatosplenic schistosomiasis (HSS)

Schistosomal involvement of the liver is an excellent model of the study of immunologic liver injury, fibrosis and hemodynamic disturbances in the absence of parenchymal injury^[12]. It may occur with all species of human schistosomiasis but is especially severe with *S. mansoni* and *S. japonicum*, both in acute and chronic phases of the disease^[13].

HSS is a chronic liver disease characterized by granulomatous reaction, portal fibrosis, pre-sinusoidal portal hypertension, splenomegaly, hypersplenism, esophageal varices and haemorrhage^[14]. The relative risk to develop hepatosplenomegaly in persons infected with *S. mansoni* have been reported in correlation with HLA-A1 and B5^[15].

In advanced HSS, there is excess collagen deposition, mainly in the portal tract and Disse's space with obstruction of sinusoidal fenestration, resulting in fibrosis and capillarization of sinusoids^[16]. According to whether the larger or small portal tract is mainly involved, Hashem^[17] classified schistosomal hepatic fibrosis into coarse (first described by Symmers in 1903)^[18] and fine types.

The term schistosomal cirrhosis is no longer used, as nodular regeneration and diffuse distortion of hepatic lobular architecture are not the features of hepatic schistosomiasis. The parenchyma between fibrotic areas is typically well preserved, correlating with the maintenance of nearly normal hepatic function, one of the clinical hallmarks of HSS^[19].

Diagnostic procedures include demonstration of ova in stool or in rectal snip, ultrasonography of the liver which reveals characteristic periportal fibrosis and sometimes distention of portal and splenic veins exceeding 12 or 10 mm width respectively, upper GI endoscopy which demonstrates esophageal and/or fundal varices and finally liver biopsy which shows Symmer's or pipe-stem fibrosis.

Concomitant infections with schistosomiasis

Several authors reported a higher frequency of chronic hepatitis B or C in patients with hepatosplenic schistosomiasis than in normal control subjects^[20-23]. A statistical correlation between previous parenteral therapy for schistosomiasis and the presence of HBsAg and HCV-Ab were reported in many studies^[23-26]. It was also proposed that these patients had an impaired immune response that enhanced their susceptibility to becoming chronic carriers^[27]. Concomitant infection with both schistosomiasis and hepatitis B or C causes more severe liver disease than infection with schistosomiasis alone^[28]. The prognosis for this group of patients was worse than that

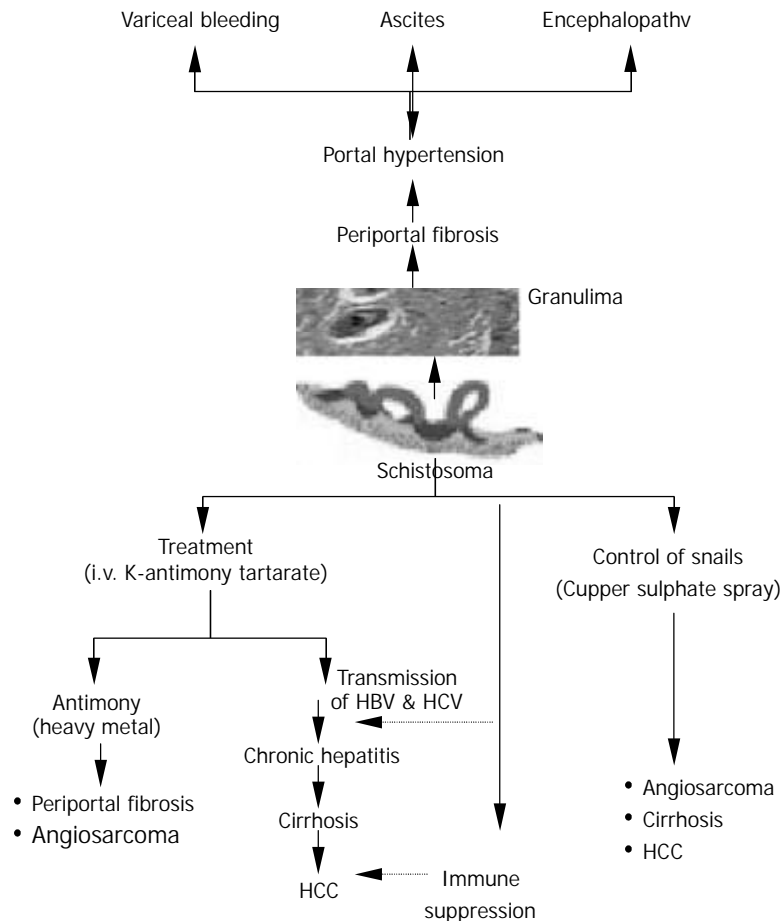


Figure 1 Impact of pathogenic mechanisms, therapeutic and control measures of schistosomiasis on the liver (El-Zayadi, 1998).

observed by either schistosomiasis or chronic hepatitis B or C as isolated problems^[29].

Depressed immunity may also account for chronic salmonellosis infection that often complicates advanced hepatosplenic schistosomiasis. There are prolonged fever and positive blood culture lasting for months and raised level of transaminases as a manifestation of non-specific hepatitis. It can only be cured by both antibacterial and antischistosomal agents^[30].

Curse of schistosomiasis on Egyptian liver

The curse of schistosomiasis on the liver involves both direct offensive effect as well as indirect effect of both intravenous therapy and molluscicides used for combating the snail intermediate hosts. The direct effect is represented by ova deposition in the portal tributaries with granuloma formation, which is replaced overtime by periportal fibrosis and hepatosplenomegaly. Subsequently, portal hypertension may result in the development of esophageal varices and variceal bleeding. Ascites and hepatic coma are the end-stage findings. The indirect effect is represented by both transmission of hepatitis B and hepatitis C through improperly sterilized glass syringes^[31] used at that time. In the meantime schistosomiasis induced immune suppression could result in increased persistence of viraemia following acute infection of both hepatitis B and C^[32]. This could partially explain the increased prevalence of HCV in Egypt. El-Zayadi *et al.*, 1986^[33] pointed out that the hepatotoxic effect of K antimony tartarate (tartar emetic) was a heavy metal like arsenic used as therapy in the development of portal fibrosis and angiosarcoma. Furthermore, the spray of copper sulphate in canals to combat the snail intermediate hosts has been proved to have a hepatotoxic effect

which was incriminated in the pathogenesis of angiosarcoma, hepatocellular carcinoma and cirrhosis^[34]. (Figure 1).

Recently, this gloomy picture has been dramatically changed with adoption of effective control measures and the use of oral therapy for schistosomiasis. In the meantime, the use of disposable syringes has reduced the risk of transmission of HBV and HCV.

REFERENCES

- 1 **Badr M.** Detection of bladder cancer. In: El-Bolkany, Chu Ed. Bladder cancer. *Al-Ahram Press* 1981: 1
- 2 **Bilharz T.** Fernere Beobachtungen über das die Pfortader des Menschen bewohnende *Distomum haematobium* und sein Verhältnis zu gewissen pathologischen Bildungen. *Z wiss Zool* 1852; **4**: 72
- 3 **Bilharz T.** Em Beitrag zur Helminthographia humana nebst Bemerkungen von Prof. C. Th. V. Siebold. *Z wiss Zool* 1852; **4**: 72
- 4 **Leiper R.** Report on the results of the Bilharzia mission to Egypt. *J Roy Army Med Corps* 1918; **30**: 235
- 5 **McDonagh J.** Antimony in bilharzia. *Lancet* 1918; **11**: 371
- 6 **Christopherson J.** Intravenous injection of antimonium tartaratum in bilharziosis. *Brit Med J* 1918; **2**: 652
- 7 **Boros DL.** Immunopathology of *Schistosoma mansoni* infection. *Clin Microbiol Rev* 1989; **2**: 250
- 8 **Mathew RC, Boros DL.** Anti-L3T4 antibody treatment suppresses hepatic granuloma formation and abrogates antigen-induced interleukin-2 production in *Schistosoma mansoni* infection. *Infect Immun* 1986; **54**: 820
- 9 **Iacomini J, Ricklan DE, Stadecker MJ.** T cells expressing the gamma delta T cell receptor are not required for egg granuloma formation in schistosomiasis. *Eur J Immunol* 1995; **25**: 884
- 10 **Boros DL, Pelley RP, Warren KS.** Spontaneous modulation of granulomatous hypersensitivity in schistosomiasis mansoni. *J*

- Immunol* 1975; **114**: 1437
- 11 **Doughty BL**, Phillips SM. Delayed hypersensitivity granuloma formation and modulation around *Schistosoma mansoni* eggs in vitro II. Regulatory T cell subsets. *J Immunol* 1982; **128**: 37
 - 12 **Dunn MA**, Kamel R. Hepatic Schistosomiasis. *Hepatology* 1981; **6**: 653-661
 - 13 **El-Rooby A**. Management of hepatic Schistosomiasis. *Semin Liver Dis* 1985; **3**: 263-276
 - 14 **Zimmon DS**, Kessler RE. Effect of portal venous blood flow diversion on portal pressure. *J Clin Invest* 1980; **65**: 1388-1397
 - 15 **Salam EA**, Ishaac S, Mahmoud AA. Histocompatibility-linked susceptibility for hepatosplenomegaly in Human schistosomiasis mansoni. *J Immunol* 1979; **123**: 1829-1831
 - 16 **Grimand JA**, Borojevic R. Chronic human Schistosomiasis mansoni. Pathology of the Disse's space. *Lab Invest* 1977; **19**: 77
 - 17 **Hashem M**. The etiology and pathogenesis of the endemic form of hepatosplenomegaly, "Egyptian splenomegaly". *J Egypt Med Assoc* 1947: 30-48
 - 18 **Symmers WSTC**. Note on a new form of liver cirrhosis due to the presence of ova of *Bilharzia haematobium*. *J Pathol Bacteriol* 1904; **9**: 237-239
 - 19 **Nash TE**, Cheever AW, Ottesen EA, Cook JA. Schistosome infection in humans: perspectives and recent findings. *Ann Intern Med* 1982; **97**: 740-754
 - 20 **Lyra LG**, Reboucas G, Andrade ZA. Hepatitis B surface antigen carrier state in hepatosplenic schistosomiasis. *Gastroenterology* 1976; **71**: 641-645
 - 21 **Zakaria S**, El Rasiky E, El-Kalouby A. Prevalence of HBsAg in schistosomiasis: B-Frequency in various stages of schistosomiasis. *Egypt J Bilhariz* 1979; **6**: 11-19
 - 22 **El-Badrawy N**, El-Rooby A, Hunter S. Association of HBsAg with hepatosplenic schistosomiasis. II- A clinico-pathological study of HBsAg and Anti-HBs in serum. *J Egypt Med Assoc* 1983; **66**: 571-582
 - 23 **Habib M**, Mohamed MK, Abdel-Aziz F, Magder LS, Abdel-Hamid M, Gamil F, Madkour S, Mikhail NN, Anwar W, Strickland GT, Fix AD, Sallam I. Hepatitis C virus infection in a community in the Nile Delta: Risk factors for seropositivity. *Hepatology* 2001; **33**: 248-253
 - 24 **Hyams KC**, Mansour MM, Massoud A, Dunn MA. Parenteral antischistosomal therapy: A potential risk factor for hepatitis B infection. *J Med Virol* 1987; **23**: 109-114
 - 25 **El-Zayadi A**, Massoud A, El-Fekhfakh E, Massoud M. Prevalence of hepatitis B surface antigen among urinary schistosomal patients receiving frequent parenteral antischistosomal therapy. *J Egypt Soc Parasitol* 1984; **14**: 61-64
 - 26 **Al-Arabi MA**, Hyams KC, Mahgoub M, Al-Hag AA, El-Ghorab N. Non-A, non-B hepatitis in Omdurman, Sudan. *J Med Virol* 1987; **21**: 217-222
 - 27 **Ganem D**. Persistent infection of humans with hepatitis B virus: mechanisms and consequences. *Rev Inf Dis* 1982; **4**: 1026-1047
 - 28 **Bassily S**, Dunn MA, Farid Z, Kilpatrick MD, El-Masry NA, Kamel LA, El-Alamy M, Murphy BL. Chronic hepatitis B in patients with *Schistosoma mansoni*. *J Trop Med Hyg* 1983; **86**: 67-71
 - 29 **Theilmann L**, Nour El Din SM, Seitz HK, Kommerell B, Gmelin K. Prevalence of antibodies to hepatitis C virus in sera from Egyptian patients with schistosomiasis. *Gastroenterol* 1990; **98**: A 640
 - 30 **Bassily S**, Farid Z, Hassan A. Prolonged Salmonella bacteremia in Egyptian farmers. *J Egypt Med Assoc* 1974; **57**: 490-497
 - 31 **Madwar MA**, El-Tahawy M, Strickland GT. The relationship between uncomplicated schistosomiasis and hepatitis B infection. *Trans R Soc Trop Med Hyg* 1989; **83**: 233-236
 - 32 **Ghaffar YA**, Fattah SA, Kamel M, Badr RM, Mahomed FF, Strickland GT. The impact of endemic schistosomiasis on acute viral hepatitis. *Am J Trop Med Hyg* 1991; **45**: 743-750
 - 33 **El-Zayadi A**, Khalil A, El-Samny N, Hamza MR, Selim O. Hepatic angiosarcoma among Egyptian farmers exposed to pesticides. *Hepatogastroenterology* 1986; **33**: 148-150
 - 34 **Pimentel JC**, Menezes AP. Liver disease in vineyard sprayers. *Gastroenterology* 1977; **77**: 275

Edited by Xu XQ and Wang XL Proofread by Xu FM

Hypoxia-inducible factor-1 in tumour angiogenesis

Yong-Hong Shi, Wei-Gang Fang

Yong-Hong Shi, Department of Pathology, Inner Mongolian Medical College, Department of Pathology, Health Science Center, Peking University 100083, Beijing, China

Wei-Gang Fang, Department of Pathology, Health Science Center, Peking University 100083, Beijing, China

Supported by Key Project of Science and Technology from Committee of Beijing Science and Technology (H020920030390)

Correspondence to: Professor Wei-Gang Fang, Department of Pathology, Peking University Health Science Center, 38 Xueyuan Road, Beijing 100083, China. wgfang@bjmu.edu.cn

Telephone: +86-10-82802599 **Fax:** +86-10-62015547

Received: 2003-09-06 **Accepted:** 2003-11-06

Abstract

Hypoxia-inducible factor-1 (HIF-1), composed of HIF- α and HIF- β subunits, is a heterodimeric transcriptional activator. In response to hypoxia, stimulation of growth factors, and activation of oncogenes as well as carcinogens, HIF-1 α is overexpressed and/or activated and targets those genes which are required for angiogenesis, metabolic adaptation to low oxygen and promotes survival. HIF-1 is critical for both physiological and pathological processes. Several dozens of putative direct HIF-1 target genes have been identified on the basis of one or more *cis*-acting hypoxia-response elements that contain an HIF-1 binding site. A variety of regulators including growth factors, genetic alterations, stress activators, and some carcinogens have been documented for regulation of HIF-1 in which several signaling pathways are involved depending on the stimuli and cell types. Activation of HIF-1 in combination with activated signaling pathways and regulators is implicated in tumour progression and prognosis. This review presents a summary of the structure and function of HIF-1 α , and correlation among specific regulators and their signaling pathways.

Shi YH, Fang WG. Hypoxia-inducible factor-1 in tumour angiogenesis. *World J Gastroenterol* 2004; 10(8): 1082-1087
<http://www.wjgnet.com/1007-9327/10/1082.asp>

INTRODUCTION

Angiogenesis is the development of new blood vessels from an existing vascular network. It is mostly related to pathological processes (wound healing, cardiac ischemia, diabetic retinopathy, and tumour growth and metastasis). Usually a developing tumour does not reach a threshold size of around 1-2 mm³ as lack of oxygen and nutrients and accumulation of waste products. Blood vessels in tumour are usually disorganized and lack of structural integrity and prone to collapse, which result in areas of inadequate perfusion and transient hypoxia.

However, in order for a macroscopic tumour to grow, adequate oxygen delivery must be effected via tumour angiogenesis that results from an increased synthesis of angiogenic factors and a decreased synthesis of anti-angiogenic factors. The metabolic adaptation of tumour cells to reduced oxygen availability by increasing glucose transport and glycolysis and shift the balance between pro- and anti-apoptotic factors to promote survival are also important consequences

in response to hypoxia. In this regard, HIF-1, induced by many factors is mainly implicated in tumour angiogenesis. This review mainly sets out to summarize the regulators of HIF-1 α and signaling pathways involved based on its structure and function.

HYPOXIA AND HIF-1

Hypoxia is one of the major drivers to tumour progression as hypoxic areas form in human tumours when the growth of tumour cells in a given area outstrips local neovascularization, thereby creating areas of inadequate perfusion. Although several transcriptional factors have been reported to be involved in the response to hypoxic stress such as AP-1, NF- κ B and HIF-1, HIF-1 is the most potent inducer of the expression of genes such as those encoding for glycolytic enzymes, VEGF and erythropoietin^[1-3].

HIF- α subunit exists as at least three isoforms, HIF-1 α , HIF-2 α and HIF-3 α . HIF-1 α and HIF-2 α can form heterodimers with HIF- β . Although HIF- β subunits are constitutive nuclear proteins, both HIF-1 α and HIF-2 α subunits are strongly induced by hypoxia in a similar manner. HIF-1 α is up-regulated in hypoxic tumour cells and activates the transcription of target genes by binding to *cis*-acting enhancers, hypoxic responsive element (HRE) close to the promoters of these genes with a result of tumour cellular adaptation to hypoxia and tumour angiogenesis, and promotion of further growth of the primary tumour. Studies have shown HIF-1 α to be over-expressed by both tumour cells and such stromal cells as macrophages in many forms of human malignancy^[4,5].

STRUCTURE OF HIF

Both of the two subunits of HIF belong to a family of bHLH-PAS. Interactions between HLH-PAS domains from the two subunits mediate their dimerization, and individual basic regions of the two subunits then make contact with their corresponding DNA sequences, namely HRE. Specific interactions between three amino acids (Ser22, Ala25, Arg30) of the HIF-1 subunit and DNA bases were identified^[6]. However, a major contribution towards the structure of HIF is attributed to a structure-function analysis of HIF-1 α , which has revealed: (1) The N-terminal half of the molecule (amino acids 1-390) containing the bHLH-PAS domain was required for dimerization and DNA binding^[7]. (2) The domains in C-terminal were required for hypoxia-induced nuclear localization, protein stabilization and transactivation^[8]. Further study suggested that amino acids 401-603 of HIF-1 α constituted an oxygen-dependent degradation domain (ODD), as presence or absence of this region had significant effects on the protein stability under non-hypoxia conditions^[9]. (3) There are two nuclear location signals (NLS) located within N-terminal (amino acids 17-33) and C-terminal (amino acids 718-721) respectively. However, only the one within C-terminal was responsible for inducible nuclear accumulation of HIF-1 α ^[10]. (4) HIF-1 α has been found to contain two transactivation domains (TAD) at the C-terminal (amino acids 531-575 and 786-826)^[8]. The transcriptional activation domains were separated by an amino acid sequence (amino acids 575-786) that inhibits transactivation (Figure 1)^[8].

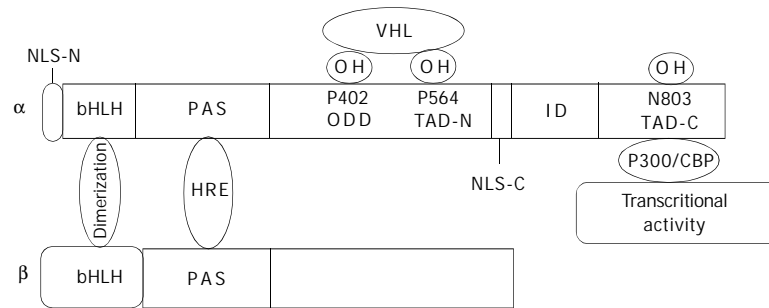


Figure 1 Molecular structure of HIF-1 α and HIF-1 β . bHLH domain mediates dimerization of the two subunits. PAS domain is responsible for DNA binding. Proline residues of 402 and 564 at ODD domain are hydroxylated by proline hydroxylase and recognized by VHL and then targeted to the ubiquitin proteasome pathway. Asn803 at the C-terminal transactivation domain (TAD-C) is hydroxylated by FIH-1 (factor inhibiting HIF-1) with a result of inhibition of HIF-1 α interaction with co-activator p300 and consequently inhibits transcriptional activity. The nuclear location signal at C-terminal functions in HIF-1 α translocation into nuclei.

REGULATION OF HIF-1

The first regulator of HIF-1 is oxygen. HIF-1 α appears to be the HIF-1 subunit regulated by hypoxia. The oxygen sensors in the HIF-1 α pathway are two kinds of oxygen dependent hydroxylases. One is prolyl hydroxylase which could hydroxylate the proline residues 402 and 564 at the oxygen dependent domain (ODD) of HIF-1 in the presence of oxygen and iron with a result of HIF- α degradation^[11]. The other is hydroxylation of Asn803 at the C-terminal transactivation domain (TAD-C) by FIH-1, which could inhibit the interaction of HIF-1 α with co-activator p300 with a subsequent inhibition of HIF-1 α transactivity^[12]. Chan *et al* employed a novel hydroxylation-specific antibody to detect hydroxylated HIF-1 α and their study further confirmed the hydroxylation of proline 564 at ODD of HIF-1 α under normoxia^[13].

Oncogene comes as the second regulator. Many oncogenes have effects on HIF-1 α . Among them, some function in regulation of HIF-1 α protein stability or degradation, others play roles in several activated signaling pathways. Tumour suppressor genes as p53 and von Hippel-Lindau (VHL) influence the levels and functions of HIF-1. The wild type (wt) form of p53 protein was involved in inhibiting HIF-1 activity by targeting the HIF-1 α subunit for Mdm2-mediated ubiquitination and proteasomal degradation^[14], and in inducing inhibitors of angiogenesis such as thrombospondin-1^[15], while loss of wt p53 (by gene deletion or mutation) could enhance HIF-1 α accumulation in hypoxia, and augment HIF-1 dependent expression of VEGF in tumour cells^[16]. The pVHL gene product could also regulate the stability of HIF- α for oxygen-dependent proteolysis^[17]. In the presence of oxygen, pVHL could bind to and target prolyl hydroxylated HIF- α subunits to the ubiquitin proteasome pathway^[18]. This process involved interaction between conserved sub-sequences within the oxygen-dependent degradation domains of HIF- α subunits and the β -domain of pVHL, with pVHL acting as the recognition element of a multicomponent E3 ubiquitin ligase^[19]. Furthermore, in VHL-deficient cells, Pro-564 in HIF-1 α had a detectable amount of hydroxylation following transition to hypoxia, indicating that the post-translational modification is not reversible^[13]. In addition, inactivation of other tumour suppressors such as PTEN which is an antagonist of PI-3K signaling could function by removing phosphate at the 3rd position of phosphatidylinositol biphosphate and triphosphate. Loss of the tumour suppressor function of PETN would augment HIF-1 mediated gene expression^[20] and restoration of PTEN could inhibit the expression of HIF-1 α ^[21]. Amplification of Akt1 and Akt2 is quite common in human tumours which express a high level of HIF-1 α . While activation of a variety of oncogenes and growth signaling pathways can induce the HIF system in non-hypoxic cells or amplify the response to hypoxia. Indeed, introduction of v-Src or RasV12 oncogenes resulted in

stabilization of normoxic HIF-1 α ^[17] and loss of hydroxylated-Pro-564 demonstrated that oncogenes induced stabilization of HIF-1 α signals by inhibiting prolyl hydroxylation^[13].

The third regulator is a battery of growth factors and cytokines from stromal and parenchymal cells such as EGF^[22], transforming growth factor- α ^[23], insulin-like growth factors 1 and 2^[24], heregulin^[25], and interleukin-1 β ^[26] via autocrine and paracrine pathways. These regulators not only induce the expression of HIF-1 α protein, HIF-1 DNA binding activity and transactivity, but also make HIF-1 target gene expression under normoxia or hypoxia. In addition, some of the growth factors are HIF-1 target genes such as IGF-2, IGF-BP1, 2 and 3, and TGF- α as well as VEGF, which make HIF-1 contribute to autocrine-signaling pathways.

The fourth one is a group of reactive oxygen species (ROS) resulting from carcinogens such as Vanadate^[27] and Cr (VI)^[28] or stimulation of cytokines such as angiotensin^[29] and TNF α ^[30]. However, it seems controversial when it comes to the production of ROS under hypoxia and their individual role in regulation of HIF-1 α . Some studies have provided experimental evidence in supporting the hypothesis that ROS generated from mitochondria increased under hypoxia and is required for HIF-1 activity and transcription of its downstream target genes^[31,32]. An alternative model proposed that hypoxia resulted in decreased production of ROS due to nicotinamide adenine dinucleotide phosphate (NADPH) oxidases^[33]. It is well known that ROS plays an important role in carcinogenesis induced by a variety of carcinogens. This was exemplified by Cr(VI) complex^[28], which could induce HIF-1 α activation and stabilization via ROS including O₂⁻, H₂O₂, and OH^[28], suggesting that HIF-1 α may play its role in carcinogenesis.

HIF-2 α , a homologue of HIF-1 α initially described as endothelium and fetus specific and named endothelial PAS protein-1/HIF-related factor/HIF-like factor, has also been cloned and shown to form a transcriptionally active complex with ARNT by transient transfection assay^[34]. Structurally and functionally HIF-2 α is highly similar to HIF-1 α , yet exhibits more restricted tissue-specific expression.

It has been shown that HIF-3 α also exhibits conservation with HIF-1 α and HIF-2 α in HLH and PAS domains, but does not possess a hypoxia-inducible domain^[35] and might function primarily as an inhibitor of HIF-1 α ^[36].

SIGNALING PATHWAYS INVOLVED IN REGULATION OF HIF-1 α

HIF-1 is a phosphorylated protein and its phosphorylation is involved in HIF-1 α subunit expression and/or stabilization as well as in the regulation of HIF-1 transcriptional activity. Three signaling pathways involved in the regulation of HIF-1 α have been reported to date.

The PI-3k pathway has been mainly and frequently implicated in regulation of HIF-1 α protein expression and stability^[26], although it was also involved in regulation of HIF-1 α transcription in a couple of studies^[37]. PI-3K is activated by ligation of a variety of growth factors to their cognate receptor tyrosine kinases with a subsequent phosphorylation and activation of its downstream signaling pathways such as a serine-threonine protein kinase Akt (protein kinase B) and FRAP (FBKP-12 rapamycin associated protein, also known as mammalian target of rapamycin) pathway.

Akt is also activated by hypoxia, yet its mechanism is still not clear. Activated Akt initiates two different pathways in regulation of HIF-1 α . The function of these two pathways appears to show consistent impact on HIF-1 α activation. In this regard, phospho-Akt either inhibits the function of GSK, a downstream target of Akt, via phosphorylation with a result of increased HIF-1 α stability under hypoxia in a time dependent manner^[22] or protein synthesis^[38,39], or activates FRAP pathway resulting in an increased HIF-1 α synthesis^[40].

A recent study performed by Sodhi showed that there was a potential consensus site in the oxygen-dependent degradation domain of HIF-1 α for GSK3 β and that this site could play a role in the regulation of HIF-1 α protein stability, highlighting the effect of PI-3K/Akt/GSK pathway on HIF-1 α ^[41]. It was further confirmed by co-transfection of an HIF-1 reporter plasmid either with the p85 or with the Akt dominant negative vector that the disruption of the PI-3K/Akt pathway impaired the activation of HIF-1 as well as VEGF gene transcription in hypoxic NIH3T3R cells^[20]. Besides, in a renal cancer cell line mutant for VHL, HIF-1 α was constitutively stabilized, and the PI-3K inhibitor still down-regulated HIF-1 α expression, suggesting a novel pathway for HIF-1 α protein regulation independent of VHL^[17]. HIF-1 α expression induced by EGF and insulin or loss of function of PTEN through PI-3K pathway^[20,22,42] provided an additional evidence.

In contrast, an alternative study showed that although serum stimulation could induced a slight accumulation of HIF-1 α protein in a PI-3K/Akt pathway dependent fashion, hypoxia induced much higher levels of HIF-1 α protein and HIF-1 DNA binding activity independent of PI-3K and mTOR activity and high levels of Akt signaling could modestly increase HIF-1 α protein, but this increase did not affect HIF-1 target gene expression. Besides the effects of constitutively active Akt on HIF-1 were cell type specific, drawing a conclusion that PI-3K/Akt pathway was not exclusive for hypoxic induction of HIF-1 subunits or activity, and constitutively active Akt was not itself sufficient to induce HIF activity^[43], suggesting that the involvement of PI-3K/Akt pathway in regulation of HIF-1 α is a much more complicated process which not only exhibits a cell type- and stimulus type- dependency, but also may have a cross talk with other unknown signaling pathways.

The Raf-1/MEK1/ERK pathway appears mainly to regulate HIF-1 transactivation and DNA binding activity and the C-terminal domain of the protein, was demonstrated to be directly phosphorylated by ERK1 by an *in vitro* kinase assay^[44]. Although HIF-1 α phosphorylation was not required for HIF-TAD/p300 interaction, MAPK was required for the transactivation activity of HIF-1 α . Furthermore, inhibition of MAPK could disrupt the HIF-p300 interaction and suppress the transactivation activity of p300^[45] and overexpression of MEK1, an upstream ERK activator, could stimulate the transactivation of both p300 and HIF-1 α ^[45]. Reporter gene assays and EMSA experiments *in vitro* have demonstrated that the MEK1 inhibitor PD98059 or ERK dominant negative mutants together with an HIF-1 reporter gene were able to block the transcriptional activity of HIF-1 without affecting its DNA binding activity^[28,44,46].

Mammalian cells respond to a variety of noxious stimuli such as chemicals, radiation, osmotic shock, and hypoxia by induction of stress activated protein kinases (SAPKs/JNK). Among them, both of p38 and JNK1 play critical roles in responding to cellular stress and promoting cell growth and survival. JNK1 and p38 are also serine/threonine protein kinases that phosphorylate nuclear transcriptional factors which regulate target genes in response to cellular stress. It has been shown that JNK1 and p38 were activated by hypoxia and involved in induction of HIF-1 α expression^[47]. Additional evidence indicated that HIF-1 α phosphorylation by p38 could be involved in inhibition of the inhibitory domain located within the C-terminal region of HIF-1 α ^[48]. Another study showed that p38 signaling mediated HIF-1 α and VEGF induction by Cr (VI) in DU145 human prostate carcinoma cells^[28].

In addition, a calmodulin dominant negative mutant and W7, a calmodulin antagonist, as well as BAPTA, an intracellular calcium chelator, inhibited hypoxia-induced HIF-1 activation. A MEKK1 (a kinase upstream of JNK) dominant negative mutant had no effect. Moreover, BAPTA, calmidazolium, a calmodulin antagonist and PD98059 inhibited VEGF secretion in hypoxic HepG2 cells. These results indicate that elevated calcium in hypoxia could participate in HIF-1 activation, suggesting that calcium and calmodulin act on the upstream of ERK in the hypoxia signal transduction pathway^[28].

One study in T47D cell indicated PI-3K/Akt was not activated under hypoxic condition^[17]. While our study in the same cell line showed that ERK1/2 was not activated by hypoxia either. However, bFGF activated PI-3K/Akt, ERK1/2 and p38 pathways both under normoxia and hypoxia. Under hypoxia, bFGF synergized with hypoxia in regulation of HIF-1 α protein expression and transactivation. While under normoxia, bFGF increased HIF-1 α protein synthesis and transactivation depending on PI-3K/Akt and ERK1/2 pathways respectively. p38 pathway had no effect on HIF-1 α and VEGF. Our result further confirmed the role of PI-3K/Akt and ERK1/2 in regulation of HIF-1 α was induced by growth factors and that activation of PI-3K/Akt and ERK1/2 by hypoxia was not a universal phenomenon (Figure 2).

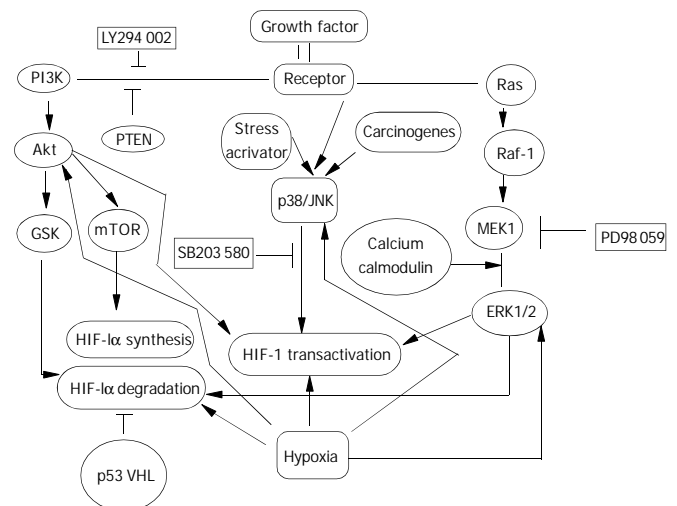


Figure 2 Signal transduction pathway in HIF-1 α regulation. Oncogenes, growth factors and hypoxia have been documented to regulate HIF-1 α protein and increase its transactivity. PI-3K/Akt, Raf-1/MEK1/ERK1/2 and p38/JNK pathways were activated in response to oncogenes, growth factors and stress activators such as hypoxia, and carcinogens to different extent in a cell type- and stimulus type-specific manner. GSK and mTOR were two target events of Akt and could contribute to decreasing HIF-1 α degradation and increasing HIF-1 α protein synthesis. Activated ERK1/2 could mainly up-regulate

HIF-1 α transcriptional activity. Calcium and Calmodulin could act on HIF-1 α indirectly as upstream events of ERK1/2. While the effect of p38/JNK pathway on HIF-1 α is controversial depending on stimulus and cell type. Some oncoproteins themselves are inter-events of those signal pathways. Amplification of p110, a subunit of PI-3K, Akt and loss of PTEN could contribute to activation of PI-3K pathway, while mutation of RAS and amplified Raf-1 and ERK1/2 could activate the extracellular-signal regulated kinase (ERK1/2). In addition, mutation of p53 and loss of VHL could decrease HIF-1 α degradation, although the signal pathways involved are poorly understood.

HIF-1 α , ANGIOGENESIS AND TUMOUR PROGNOSIS

HIF-1 has been taken as a key factor in regulation of VEGF and VEGFR and other angiogenic factors. Immunohistochemical analysis of human tumour biopsies revealed that dramatic overexpression of HIF-1 α was seen in common cancers^[49] and associated with tumour VEGF expression and vascularization^[50,51]. Constitutively expressed VEGF increased the number of new capillaries around hepatic sinuses^[52]. HIF-1 activity has also been manipulated in human cancer cell lines. Expression of VEGF, xenograft growth and angiogenesis were markedly increased in HCT116 colon cancer cells transfected with an expression vector encoding HIF-1 α ^[53]. In addition, emerging evidence has suggested that loss or gain of HIF-1 activity is negatively and positively correlated respectively with tumour growth and angiogenesis^[50,54-56].

VEGF overexpression in several tumours has been correlated with high vascularity, lymph node metastasis, and liver metastasis, and a poorer prognosis than VEGF-negative tumours^[57,58] and a direct relationship between angiogenesis and metastasis in a large and diverse array of other tumours, including melanomas, gliomas, cancers of the lung, bladder and prostate, and many others^[59,60] was established. Many reports have shown that intratumoural microvessel density (IMD) is a significant and independent prognostic indicator in human breast cancer.

In a study of ovarian cancer, HIF-1 α expression was correlated with apoptosis in most tumours. Besides, according to the identification of a *cis*-acting hypoxia-response element containing an HIF-1 binding site, a variety of proteins targeted by HIF-1 were involved in tumour cell proliferation, survival, adhesion and mobility, implicating the role of HIF-1 in these processes. A correlation of a reduced inducibility of HIF-1 α and HIF-2 α and an increased survival of the breast cancer cell lines under hypoxia was reported^[61].

In addition, HIF-1 α overexpression in combination with deficiency or mutation of tumour suppressor genes such as VHL, p53 and PTEN, and amplification of oncogenes (Akt, Ras, ERK1/2) was frequently seen in human cancer and these genetic alterations have been associated with tumour growth, invasion and metastasis. Clinically, a high level of HIF-1 α expression had an association with a decreased overall survival and a disease-free survival in lymph-node-negative breast cancer^[62] and an increased mortality in early stage cervical carcinoma^[63] and lymph-node-negative breast cancer^[50]. Furthermore, HIF-1 α overexpression was associated with treatment failure and/or mortality in nasopharyngeal squamous cell cancer^[64], suggesting a potential role of HIF-1 α in tumour prognosis. Finally, the findings that HER-2/*neu* immunoactivity and gene amplification, VEGF expression, and Ki-67 expression were correlated strongly with HIF-1 α positivity in lymph node negative breast carcinoma^[62] provided a further evidence. All data above support a hypothesis that the presence of hypoxia in a tumour reflects a poor prognosis^[65].

SUMMARY

HIF-1 activation is regulated through different mechanisms from

HIF-1 α subunit stabilization^[18,46], phosphorylation^[44], modification of redox conditions to interaction with coactivators^[45,66] involving several signal transduction pathways including PI-3K, MAPK (ERK1/2) and p38 pathways. However, it appears that these mechanisms and signaling pathways can be cell-type specific and stimulus-specific. Hypoxia, oncogenes and a variety of growth factors and cytokines increase HIF-1 α stability and/or synthesis and transactivation to initiate tumour angiogenesis, metabolic adaptation to hypoxic situation and promote cell survival or anti-apoptosis^[67,68] resulting from a consequence of more than sixty putative direct HIF-1 target gene expressions. Taken together, HIF-1 is activated in tumour and plays a critical role in initiation of tumour angiogenesis, tumour growth, progression and metastasis.

The crucial role of HIF-1 in tumour angiogenesis has sparked scientists and clinical researchers to try their best to understand the whole diagram of HIF-1 so as to find out novel approaches to inhibit HIF-1 overexpression. Indeed, the combination of anti-angiogenic agent and inhibitor of HIF-1 might be particularly efficacious, as the angiogenesis inhibitor would cut off the tumour's blood supply and HIF-1 inhibitor would reduce the ability of tumour adaptation to hypoxia and suppress the proliferation and promote apoptosis. Screens for small-molecule inhibitors of HIF-1 are underway and several agents that inhibit HIF-1, angiogenesis and xenograft growth have been identified. Full understanding of the regulators, and signal transduction pathways of HIF-1 and its interaction with other proteins is beneficial to the seeking of novel strategies to cure tumour and other angiogenic diseases.

REFERENCES

- 1 **Semenza GL**, Jiang BH, Leung SW, Passantino R, Concordet JP, Maire P, Giallongo A. Hypoxia response elements in the aldolase A, enolase 1, and lactate dehydrogenase A gene promoters contain essential binding sites for hypoxia-inducible factor 1. *J Biol Chem* 1996; **271**: 32529-32537
- 2 **Semenza GL**. HIF-1: mediator of physiological and pathophysiological responses to hypoxia. *J Appl Physiol* 2000; **88**: 1474-1480
- 3 **Ryan HE**, Lo J, Johnson RS. HIF-1 alpha is required for solid tumor formation and embryonic vascularization. *Embo J* 1998; **17**: 3005-3015
- 4 **Burke B**, Tang N, Corke KP, Tazzyman D, Ameri K, Wells M, Lewis CE. Expression of HIF-1 alpha by human macrophages: implications for the use of macrophages in hypoxia-regulated cancer gene therapy. *J Pathol* 2002; **196**: 204-212
- 5 **Lewis JS**, Landers RJ, Underwood JC, Harris AL, Lewis CE. Expression of vascular endothelial growth factor by macrophages is up-regulated in poorly vascularized areas of breast carcinomas. *J Pathol* 2000; **192**: 150-158
- 6 **Michel G**, Minet E, Ernest I, Roland I, Durant F, Remacle J, Michiels C. A model for the complex between the hypoxia-inducible factor-1 (HIF-1) and its consensus DNA sequence. *J Biomol Struct Dyn* 2000; **18**: 169-179
- 7 **Jiang BH**, Rue E, Wang GL, Roe R, Semenza GL. Dimerization, DNA binding, and transactivation properties of hypoxia-inducible factor 1. *J Biol Chem* 1996; **271**: 17771-17778
- 8 **Jiang BH**, Zheng JZ, Leung SW, Roe R, Semenza GL. Transactivation and inhibitory domains of hypoxia-inducible factor 1 alpha. Modulation of transcriptional activity by oxygen tension. *J Biol Chem* 1997; **272**: 19253-19260
- 9 **Huang LE**, Gu J, Schau M, Bunn HF. Regulation of hypoxia-inducible factor 1 alpha is mediated by an O-2-dependent degradation domain via the ubiquitin-proteasome pathway. *Proc Natl Acad Sci U S A* 1998; **95**: 7987-7992
- 10 **Vandromme M**, GauthierRouviere C, Lamb N, Fernandez A. Regulation of transcription factor localization: Fine-tuning of gene expression. *Trends Biochem Sci* 1996; **21**: 59-64
- 11 **Bruick RK**, McKnight SL. A conserved family of prolyl-4-hydroxylases that modify HIF. *Science* 2001; **294**: 1337-1340
- 12 **Lando D**, Peet DJ, Whelan DA, Gorman JJ, Whitelaw ML. Aspar-

- agine hydroxylation of the HIF transactivation domain a hypoxic switch. *Science* 2002; **295**: 858-861
- 13 **Chan DA**, Sutphin PD, Denko NC, Giaccia AJ. Role of prolyl hydroxylation in oncogenically stabilized hypoxia-inducible factor-1alpha. *J Biol Chem* 2002; **277**: 40112-40117
- 14 **Perkins GR**, Marshall CJ, Collins MKL. The role of MAP kinase in interleukin-3 stimulation of proliferation. *Blood* 1996; **87**: 3669-3675
- 15 **Dameron KM**, Volpert OV, Tainsky MA, Bouck N. Control of angiogenesis in fibroblasts by P53 regulation of thrombospondin-1. *Science* 1994; **265**: 1582-1584
- 16 **Bouvet M**, Ellis LM, Nishizaki M, Fujiwara T, Liu WB, Bucana CD, Fang B, Lee JJ, Roth JA. Adenovirus-mediated wild-type p53 gene transfer down-regulates vascular endothelial growth factor expression and inhibits angiogenesis in human colon cancer. *Cancer Res* 1998; **58**: 2288-2292
- 17 **Blancher C**, Moore JW, Robertson N, Harris AL. Effects of ras and von Hippel-Lindau (VHL) gene mutations on hypoxia-inducible factor (HIF)-1 alpha, HIF-2 alpha, and vascular endothelial growth factor expression and their regulation by the phosphatidylinositol 3'-kinase/Akt signaling pathway. *Cancer Res* 2001; **61**: 7349-7355
- 18 **Maxwell PH**, Wiesener MS, Chang GW, Clifford SC, Vaux EC, Cockman ME, Wykoff CC, Pugh CW, Maher ER, Ratcliffe PJ. The tumour suppressor protein VHL targets hypoxia-inducible factors for oxygen-dependent proteolysis. *Nature* 1999; **399**: 271-275
- 19 **Tanimoto K**, Makino Y, Pereira T, Poellinger L. Mechanism of regulation of the hypoxia-inducible factor-1 alpha by the von Hippel-Lindau tumor suppressor protein. *Embo J* 2000; **19**: 4298-4309
- 20 **Zundel W**, Schindler C, Haas-Kogan D, Koong A, Kaper F, Chen E, Gottchalk AR, Ryan HE, Johnson RS, Jefferson AB, Stokoe D, Giaccia AJ. Loss of PTEN facilitates HIF-1-mediated gene expression. *Genes Dev* 2000; **14**: 391-396
- 21 **Jiang BH**, Jiang GQ, Zheng JZ, Lu ZM, Hunter T, Vogt PK. Phosphatidylinositol 3-kinase signaling controls levels of hypoxia-inducible factor. *Cell Growth Differ* 2001; **12**: 363-369
- 22 **Zhong H**, Chiles K, Feldser D, Laughner E, Hanrahan C, Georgescu MM, Simons JW, Semenza GL. Modulation of hypoxia-inducible factor 1 alpha expression by the epidermal growth factor/phosphatidylinositol 3-kinase/PTEN/AKT/FRAP pathway in human prostate cancer cells: Implications for tumor angiogenesis and therapeutics. *Cancer Res* 2000; **60**: 1541-1545
- 23 **Krishnamachary B**, Berg-Dixon S, Kelly B, Agani F, Feldser D, Ferreira G, Iyer N, LaRush J, Pak B, Taghavi P, Semenza GL. Regulation of colon carcinoma cell invasion by hypoxia-inducible factor 1. *Cancer Res* 2003; **63**: 1138-1143
- 24 **Treins C**, Giorgetti-Peraldi S, Murdaca J, Semenza GL, Van Obberghen E. Insulin stimulates hypoxia-inducible factor 1 through a phosphatidylinositol 3-kinase/target of rapamycin-dependent signaling pathway. *J Biol Chem* 2002; **277**: 27975-27981
- 25 **Laughner E**, Taghavi P, Chiles K, Mahon PC, Semenza GL. HER2 (neu) signaling increases the rate of hypoxia-inducible factor 1 alpha (HIF-1 alpha) synthesis: Novel mechanism for HIF-1-mediated vascular endothelial growth factor expression. *Mol Cell Biol* 2001; **21**: 3995-4004
- 26 **Stiehl DP**, Jelkmann W, Wenger RH, Hellwig-Burgel T. Normoxic induction of the hypoxia-inducible factor 1alpha by insulin and interleukin-1beta involves the phosphatidylinositol 3-kinase pathway. *FEBS Lett* 2002; **512**: 157-162
- 27 **Gao N**, Ding M, Zheng JZ, Shi X, Jiang BH. Vanadate-induced expression of hypoxia-inducible factor 1 alpha and vascular endothelial growth factor through phosphatidylinositol 3-kinase/Akt pathway and reactive oxygen species. *J Biol Chem* 2002; **277**: 31963-31971
- 28 **Gao N**, Jiang BH, Corum L, Roberts JR, Antonini J, Zheng JZ, Flynn DC, Castranova V, Shi XI. p38 Signaling-mediated hypoxia-inducible factor 1alpha and vascular endothelial growth factor induction by Cr(VI) in DU145 human prostate carcinoma cells. *J Biol Chem* 2002; **277**: 45041-45048
- 29 **Richard DE**, Berra E, Pouyssegur J. Nonhypoxic pathway mediates the induction of hypoxia-inducible factor 1alpha in vascular smooth muscle cells. *J Biol Chem* 2000; **275**: 26765-26771
- 30 **Haddad JJ**, Land SC. A non-hypoxic, ROS-sensitive pathway mediates TNF-alpha-dependent regulation of HIF-1alpha. *FEBS Lett* 2001; **505**: 269-274
- 31 **Chandel NS**, McClintock DS, Feliciano CE, Wood TM, Melendez JA, Rodriguez AM, Schumacker PT. Reactive oxygen species generated at mitochondrial complex III stabilize hypoxia-inducible factor-1 alpha during hypoxia - A mechanism of O-2 sensing. *J Biol Chem* 2000; **275**: 25130-25138
- 32 **Chandel NS**, Maltepe E, Goldwasser E, Mathieu CE, Simon MC, Schumacker PT. Mitochondrial reactive oxygen species trigger hypoxia-induced transcription. *Proc Natl Acad Sci U S A* 1998; **95**: 11715-11720
- 33 **Ehleben W**, Bolling B, Merten E, Porwol T, Strohmaier AR, Acker H. Cytochromes and oxygen radicals as putative members of the oxygen sensing pathway. *Respir Physiol* 1998; **114**: 25-36
- 34 **Hogenesch JB**, Chan WK, Jackiw VH, Brown RC, Gu YZ, Pray-Grant M, Perdew GH, Bradfield CA. Characterization of a subset of the basic-helix-loop-helix-PAS superfamily that interacts with components of the dioxin signaling pathway. *J Biol Chem* 1997; **272**: 8581-8593
- 35 **Gu YZ**, Moran SM, Hogenesch JB, Wartman L, Bradfield CA. Molecular characterization and chromosomal localization of a third alpha-class hypoxia inducible factor subunit, HIF3alpha. *Gene Expr* 1998; **7**: 205-213
- 36 **Makino Y**, Kanopka A, Wilson WJ, Tanaka H, Poellinger L. Inhibitory PAS domain protein (IPAS) is a hypoxia-inducible splicing variant of the hypoxia-inducible factor-3alpha locus. *J Biol Chem* 2002; **277**: 32405-32408
- 37 **Burroughs KD**, Oh J, Barrett JC, DiAugustine RP. Phosphatidylinositol 3-kinase and mek1/2 are necessary for insulin-like growth factor-I-induced vascular endothelial growth factor synthesis in prostate epithelial cells: a role for hypoxia-inducible factor-1? *Mol Cancer Res* 2003; **1**: 312-322
- 38 **Welsh GI**, Miller CM, Loughlin AJ, Price NT, Proud CG. Regulation of eukaryotic initiation factor eIF2B: glycogen synthase kinase-3 phosphorylates a conserved serine which undergoes dephosphorylation in response to insulin. *FEBS Lett* 1998; **421**: 125-130
- 39 **Mottet D**, Dumont V, Deccache Y, Demazy C, Ninane N, Raes M, Michiels C. Regulation of hypoxia-inducible factor-1alpha protein level during hypoxic conditions by the phosphatidylinositol 3-kinase/Akt/ glycogen synthase kinase 3beta pathway in HepG2 cells. *J Biol Chem* 2003; **278**: 31277-31285
- 40 **Takata M**, Ogawa W, Kitamura T, Hino Y, Kuroda S, Kotani K, Klip A, Gingras AC, Sonenberg N, Kasuga M. Requirement for Akt (protein kinase B) in insulin-induced activation of glycogen synthase and phosphorylation of 4E-BP1 (PHAS-1). *J Biol Chem* 1999; **274**: 20611-20618
- 41 **Sodhi A**, Montaner S, Miyazaki H, Gutkind JS. MAPK and Akt act cooperatively but independently on hypoxia inducible factor-1 alpha in rasV12 upregulation of VEGF. *Biochem Biophys Res Commun* 2001; **287**: 292-300
- 42 **Feldser D**, Agani F, Iyer NV, Pak B, Ferreira G, Semenza GL. Reciprocal positive regulation of hypoxia-inducible factor 1 alpha and insulin-like growth factor 2. *Cancer Res* 1999; **59**: 3915-3918
- 43 **Arsham AM**, Plas DR, Thompson CB, Simon MC. Phosphatidylinositol 3-kinase/Akt signaling is neither required for hypoxic stabilization of HIF-1 alpha nor sufficient for HIF-1-dependent target gene transcription. *J Biol Chem* 2002; **277**: 15162-15170
- 44 **Minet E**, Arnould T, Michel G, Roland I, Mottet D, Raes M, Remacle J, Michiels C. ERK activation upon hypoxia: involvement in HIF-1 activation. *FEBS Lett* 2000; **468**: 53-58
- 45 **Sang N**, Bohensky J, Leshchinsky I, Srinivas V, Caro J. MAPK signaling up-regulates the activity of hypoxia-inducible factors by its effects on p300. *J Biol Chem* 2003; **278**: 14013-14019
- 46 **Salceda S**, Caro J. Hypoxia-inducible factor 1 alpha (HIF-1 alpha) protein is rapidly degraded by the ubiquitin-proteasome system under normoxic conditions - Its stabilization by hypoxia depends on redox-induced changes. *J Biol Chem* 1997; **272**: 22642-22647
- 47 **Shemirani B**, Crowe DL. Hypoxic induction of HIF-1alpha and VEGF expression in head and neck squamous cell carcinoma lines is mediated by stress activated protein kinases. *Oral Oncol* 2002; **38**: 251-257
- 48 **Sodhi A**, Montaner S, Patel V, Zohar M, Bais C, Mesri EA, Gutkind JS. The Kaposi's sarcoma-associated herpes virus G protein-coupled receptor up-regulates vascular endothelial growth factor expression and secretion through mitogen-activated protein

- kinase and p38 pathways acting on hypoxia-inducible factor 1alpha. *Cancer Res* 2000; **60**: 4873-4880
- 49 **Talks KL**, Turley H, Gatter KC, Maxwell PH, Pugh CW, Ratcliffe PJ, Harris AL. The expression and distribution of the hypoxia-inducible factors HIF-1 alpha and HIF-2 alpha in normal human tissues, cancers, and tumor-associated macrophages. *Am J Pathol* 2000; **157**: 411-421
- 50 **Bos R**, Zhong H, Hanrahan CF, Mommers EC, Semenza GL, Pinedo HM, Abeloff MD, Simons JW, van Diest PJ, van der Wall E. Levels of hypoxia-inducible factor-1 alpha during breast carcinogenesis. *J Natl Cancer Inst* 2001; **93**: 309-314
- 51 **Giatromanolaki A**, Koukourakis MI, Sivridis E, Turley H, Talks K, Pezzella F, Gatter KC, Harris AL. Relation of hypoxia inducible factor 1 alpha and 2 alpha in operable non-small cell lung cancer to angiogenic/molecular profile of tumours and survival. *Br J Cancer* 2001; **85**: 881-890
- 52 **Shi BM**, Wang XY, Mu QL, Wu TH, Liu HJ, Yang Z. Angiogenesis effect on rat liver after administration of expression vector encoding vascular endothelial growth factor D. *World J Gastroenterol* 2003; **9**: 312-315
- 53 **Ravi R**, Mookerjee B, Bhujwall ZM, Sutter CH, Artemov D, Zeng Q, Dillehay LE, Madan A, Semenza GL, Bedi A. Regulation of tumor angiogenesis by p53-induced degradation of hypoxia-inducible factor 1 alpha. *Genes Dev* 2000; **14**: 34-44
- 54 **Rak J**, Mitsuhashi Y, Sheehan C, Tamir A, Vilorio-Petit A, Filmus J, Mansour SJ, Ahn NG, Kerbel RS. Oncogenes and tumor angiogenesis: Differential modes of vascular endothelial growth factor up-regulation in ras- transformed epithelial cells and fibroblasts. *Cancer Res* 2000; **60**: 490-498
- 55 **Cormier-Regard S**, Nguyen SV, Claycomb WC. Adrenomedullin gene expression is developmentally regulated and induced by hypoxia in rat ventricular cardiac myocytes. *J Biol Chem* 1998; **273**: 17787-17792
- 56 **Mukhopadhyay CK**, Mazumder B, Fox PL. Role of hypoxia-inducible factor-1 in transcriptional activation of ceruloplasmin by iron deficiency. *J Biol Chem* 2000; **275**: 21048-21054
- 57 **Toi M**, Hoshina S, Takayangi T, Tominaga T. Association of vascular endothelial growth-factor expression with tumor angiogenesis and with early relapse in primary breast-cancer. *Jpn Cancer Res* 1994; **85**: 1045-1049
- 58 **Maeda K**, Chung YS, Ogawa Y, Takatsuka S, Kang SM, Ogawa M, Sawada T, Sowa M. Prognostic value of vascular endothelial growth factor expression in gastric carcinoma. *Cancer* 1996; **77**: 858-863
- 59 **Bochner BH**, Cote RJ, Weidner N, Groshen S, Chen SC, Skinner DG, Nichols PW. Angiogenesis in bladder-cancer-relationship between microvessel density and tumor prognosis. *J Natl Cancer Inst* 1995; **87**: 1603-1612
- 60 **Jaeger TM**, Weidner N, Chew K, Moore DH, Kerschmann RL, Waldman FM, Carroll PR. Tumor angiogenesis correlates with lymph-node metastases in invasive bladder-cancer. *J Urol* 1995; **154**: 69-71
- 61 **Blancher C**, Moore JW, Talks KL, Houlbrook S, Harris AL. Relationship of hypoxia-inducible factor (HIF)-1 alpha and HIF-2 alpha expression to vascular endothelial growth factor induction and hypoxia survival in human breast cancer cell lines. *Cancer Res* 2000; **60**: 7106-7113
- 62 **Bos R**, van der Greijer AE, Shvarts A, Meijer S, Pinedo HM, Semenza GL, van Diest PJ, van der Wall E. Levels of hypoxia-inducible factor-1alpha independently predict prognosis in patients with lymph node negative breast carcinoma. *Cancer* 2003; **97**: 1573-1581
- 63 **Birner P**, Schindl M, Obermair A, Breitenecker G, Oberhuber G. Expression of hypoxia-inducible factor 1alpha in epithelial ovarian tumors: its impact on prognosis and on response to chemotherapy. *Clin Cancer Res* 2001; **7**: 1661-1668
- 64 **Aebbersold DM**, Burri P, Beer KT, Laissue J, Djonov V, Greiner RH, Semenza GL. Expression of hypoxia-inducible factor-1alpha: a novel predictive and prognostic parameter in the radiotherapy of oropharyngeal cancer. *Cancer Res* 2001; **61**: 2911-2916
- 65 **Hockel M**, Vaupel P. Tumor hypoxia: definitions and current clinical, biologic, and molecular aspects. *J Natl Cancer Inst* 2001; **93**: 266-276
- 66 **Kallio PJ**, Okamoto K, Brien S, Carrero P, Makino Y, Tanaka H, Poellinger L. Signal transduction in hypoxic cells: inducible nuclear translocation and recruitment of the CBP/p300 coactivator by the hypoxia-inducible factor-1alpha. *EMBO J* 1998; **17**: 6573-6586
- 67 **Lin Z**, Weinberg JM, Malhotra R, Merritt SE, Holzman LB, Brosius FC. GLUT-1 reduces hypoxia-induced apoptosis and JNK pathway activation. *Am J Physiol Endocrinol Metab* 2000; **278**: E958-E966
- 68 **Minet E**, Michel G, Remacle J, Michiels C. Role of HIF-1 as a transcription factor involved in embryonic development, cancer progression and apoptosis (review). *Int J Mol Med* 2000; **5**: 253-259

Edited by Zhu LH and Wang XL. Proofread by Xu FM

Expression patterns of esophageal cancer deregulated genes in C57BL/6J mouse embryogenesis

Jian Zhang, Fu-Lu Gao, Hui-Ying Zhi, Ai-Ping Luo, Fang Ding, Min Wu, Zhi-Hua Liu

Jian Zhang, Hui-Ying Zhi, Ai-Ping Luo, Fang Ding, Min Wu, Zhi-Hua Liu, National Laboratory of Molecular Oncology, Cancer Institute, Chinese Academy of Medical Sciences and Peking Union Medical College, Beijing 100021, China

Jian Zhang, Hebei Normal University, Shijiazhuang 050016, Hebei Province, China

Fu-Lu Gao, Chengde Medical College, Chengde 067000, Hebei Province, China

Supported by China Key Program on Basic Research, No. G1998051021, Chinese Hi-tech R&D program, No. 2001AA231041, and Beijing Biomedical R&D Innovation Program, No. H020220020310

Correspondence to: Professor, Zhi-Hua Liu, Ph.D, National Laboratory of Molecular Oncology, Cancer Institute, Chinese Academy of Medical Sciences and Peking Union Medical College, Beijing 100021, China. liuzh@pubem.cicams.ac.cn

Telephone: +86-10-67723789 **Fax:** +86-10-67723789

Received: 2003-09-23 **Accepted:** 2004-01-12

Abstract

AIM: To investigate the expression patterns of esophageal squamous cell cancer deregulated genes in mid to late stages of C57BL/6J mouse embryogenesis, and the correlation between these genes in embryonic development and tumorigenesis of esophageal squamous cell cancer.

METHODS: Reverse northern screening was performed to examine the expression patterns of esophageal cancer deregulated genes in C57BL/6J mouse embryogenesis. To confirm the gene expression patterns, semi-quantitative reverse transcriptase-polymerase chain reaction (RT-PCR) was carried out for 3 of the randomly picked differentially expressed genes.

RESULTS: Within these esophageal cancer deregulated genes, 4 patterns of expression were observed at 3 stages embryonic d 11.5 (E11.5), embryonic d 13.5 (E13.5) and postnatal d1 (P1). (1) Up-regulation during the E11.5 period, down-regulation during the E13.5 and P1 period (up-down-down), the 10 up-regulated genes during the E11.5 period could be classified into 6 known genes and 4 unknown genes. The known genes included differentiation related genes (S100A8), immunity related gene (IGL), translation and transcription regulation genes (RPL15, EEF1A1), cytoskeletal protein (TUBA1), cysteine protease inhibitor (cystatin B). (2) Up-regulation during the E13.5 and P1 period (down-up-up), such as the SPRR2A which was down-regulated at E11.5. (3) Down-regulation during the E11.5 and E13.5 period (down-down-up), such as RHCG and keratin 4. (4) Fluctuating expression, down initially, up at E13.5, and then down again (down-up-down). EMP1 belonged to such a gene, which was highly expressed at E13.5.

CONCLUSION: The results will be helpful for understanding the function of esophageal squamous cell carcinoma (ESCC) deregulated genes in embryonic development and tumorigenesis. S100A8 and S100A9 may play different roles in early embryonic development. IGL may be an

oncofetal protein, and EMP1 relates with neurogenesis at E13.5. The genes identified pertinent to embryonic development may serve as candidate susceptibility genes for inherited esophageal cancer disorders as well as for various heritable disorders of embryonic development.

Zhang J, Gao FL, Zhi HY, Luo AP, Ding F, Wu M, Liu ZH. Expression patterns of esophageal cancer deregulated genes in C57BL/6J mouse embryogenesis. *World J Gastroenterol* 2004; 10(8): 1088-1092

<http://www.wjgnet.com/1007-9327/10/1088.asp>

INTRODUCTION

Esophageal cancer is one of the most lethal malignancies in the world. It exists in 2 main pathological types, esophageal squamous cell carcinoma (ESCC) and esophageal adenocarcinoma (EADC). ESCC is the predominant histological subtype of esophageal cancer and characterized by high mortality rate and regional variation in incidence in China^[1]. Due to the relatively late stage of diagnosis and poor treatment, its five-year survival rate remains below 10%^[2]. The development of better treatment modalities and better diagnostic and preventive approaches requires a understanding of the molecular mechanisms of the complex process of esophageal tumorigenesis.

Tumor development involves up-regulation and down-regulation of many genes. The study of these genes is important to understand the complex biological events that take place during the malignant transformation of normal tissues. cDNA microarray technology allows simultaneous determination of the expression level of thousands of genes^[3]. Up to date, by using the cDNA array technology, we have identified many genes differentially expressed in esophageal cancer, which potentially play key roles in the malignant behavior of esophagus^[4,5]. Investigation into the biological function of these genes could be helpful to understand the molecular mechanisms in tumorigenesis of ESCC.

Mouse is an ideal model system for studying the molecular mechanisms underlying the pathogenesis of human cancer. The generation of transgenic and gene-knockout mice has been instrument in determining the role of major determinants in this process, such as oncogenes and tumor-suppressor genes. In addition, mice at different development levels also provide a useful model for functional study of the genes. Understanding the temporal and spatial expression of a gene in embryogenesis will be useful for further analysis of its function in cancer^[6,7]. Here, the expression patterns of some ESCC deregulated genes in 3 embryonic stages were analyzed using reverse northern screening. Selected genes were further confirmed by RT-PCR assays. As a result, we found that genes with specific developmental functions were expressed at specific developmental stages. These genes cover a broad spectrum of cell biology processes including cell growth, differentiation, matrix metabolism, immunity response, and would be of significance to understanding the tumorigenesis of esophagus.

MATERIALS AND METHODS

Animal and tissue specimens

Time-mated C57BL/6J mice were obtained from Animal Institute, Chinese Academy of Medical Sciences. Mice were obtained from in-house breeding programs and maintained on a 12:12-h light-dark cycle and provided standard laboratory food and water. All manipulations of mice were done in accordance with policies of the Institute Animal Care and Use Committee. Timed mating was set up between adult wild-type mice. Females were inspected for plugs on the following day to ensure their successful mating. The day of plug detection was considered as E0.5. Embryo was dissected from pregnant mouse at the age of embryonic d 11.5 (E11.5), 13.5 (E13.5), and postnatal d 1 (P1). Three samples per time point were analyzed for statistical significance. The tissues were immediately frozen in liquid nitrogen until analysis.

Total RNA extraction

Total RNA was extracted from frozen tissues by using TRIzol™ reagent following the protocols of the manufacturer (GIBCO/BRL, New York, USA). The quality of RNA was confirmed on a formaldehyde agarose gel, and concentration was determined by reading the absorbance at 260/280 nm.

cDNA fragment acquisition

Plasmids of interested clones were selected from esophageal cDNA libraries and used as PCR templates. The primers used were T3 (AAT TAA CCC TCA CTA AAG GG) and T7 (GTA ATA CGA CTC ACT ATA GGC C). The average length of cDNA fragments was about 1 kb. The homology of these genes between human and mice was more than 50%.

Reverse northern screening

PCR fragments corresponding to 90 distinct clones were diluted in 0.5 mol/L NaOH and 1.5 mol/L NaCl and 0.2 mL (approximately 40 ng) of every slim was transferred onto duplicate nylon membranes (HyBond-N, Amersham Pharmacia Biotech, Arlington Heights, IL). The filter membranes were neutralized with 1.5 mol/L NaCl and 0.5 mol/L Tris-HCl (pH 7.5) for 5 min, dried at 80 °C for 60 min in the oven. cDNAs corresponding to the housekeeping gene β -actin and glyceraldehyde-3-phosphate dehydrogenase (GAPDH) were used as internal controls.

To generate the probes, ³²P-labeled cDNA was synthesized from RNA derived from mice of different embryonic period. mRNA was incubated with random hexamers (Promega Corp.) for 5 min at 65 °C, chilled on ice for at least 1 min, and added to a solution containing 50 U superscript IIRT in 20 mmol/L Tris-

HCl (pH 8.4); 5 mmol/L MgCl₂; 0.5 mmol/L each of deoxy (d)-ATP, dTTP, and dGTP, 5 mmol/L dCTP; and 50 mCi [³²P] dCTP in a final volume of 20 μ L. After 50 min of incubation at 42 °C, followed by incubation at 70 °C for 15 min, parental mRNA was removed from the cDNA synthesis reaction by addition of RNase H and incubation for 20 min at 37 °C. Unincorporated nucleotides were removed by gel filtration on Sephadex G-25 preloaded spin columns (Amersham Pharmacia Biotech, Uppsala, Sweden). The probe was denatured at 90 °C for 5 min before added to the hybridization solution.

The filter membranes were washed in 6 \times SSC and pre-hybridized for 5 h at 68 °C in a buffer containing 6 \times SSC, 2 \times Denhardt's (1 g/L each of Ficoll 400, polyvinylpyrrolidone, and BSA), 1 g/LSDS, and 0.1 g/L denatured salmon sperm DNA. Hybridization was carried out for 18 h at 68 °C using ³²P-labeled cDNA probes added in fresh prehybridization buffer. After the hybridization, the filters were washed (2 \times SSC and 1 g/L SDS), then exposed to X-ray film at -70 °C overnight with an intensifying screen^[8]. The images were scanned by Fluor-S MultiImager (Bio-Rad, California, USA) and the original intensity of every specific slim was quantitated with the software Multi-Analyst (Bio-Rad, California, USA). To avoid misinterpretation of the results possibly due to variation in the hybridization, any filter was normalized using 2 housekeeping genes, and a normalization coefficient calculated for each comparison was used to correct the signal intensities. The differential expression was considered as significant when the ratio of the signal from the same spot on different membranes was greater than 2.0.

Semi-quantitative RT-PCR

Total RNA was extracted by the method described above. Five micrograms total RNA of each sample was used to synthesize the first strand cDNA with SuperScript preamplification system for first strand cDNA synthesis kit (GIBCO/BRL, New York, USA). Then 1 μ L RT product was used as the template to amplify specific fragments. PCR reaction conditions were optimized individually for each gene studied, and the cycle number for PCR was adjusted so that the reactions fell within the linear range of product amplification. The expression of housekeeping gene GAPDH, was used as an internal control. The RT-PCR reaction product was analyzed by electrophoresis on a 15 g/L agarose gel. Electrophoresis images were scanned by Fluor-S MultiImager (Bio-Rad, California, USA) and the original intensity of every specific band was quantitated with the software Multi-Analyst (Bio-Rad, California, USA). Data were compared after being normalized by the intensity of GAPDH. The sequences of PCR primers and cycle number are listed in Table 1.

Table 1 Primers used for semi-quantitative RT-PCR and conditions of PCR reaction

Gene	Dir	Primer sequences (5' -3')	Product size	Anne (°C)*	PCR cycles
S100A8	F	TGA CAA TGC CGT CTG AAC TG	271	60.4	28
	R	TCC TTG TGG CTG TCT TTG TG			
S100A9	F	CAG CAT AAC CAC CAT CAT CG	310	60.1	28
	R	TTA CTT CCC ACA GCC TTT GC			
EMP-1	F	AGT GCA AGC CTT CAT GAT CC	599	60.0	28
	R	TCC GAT CTG GGT CTC CAT AC			
CSTB	F	GTC CCA GCT TGA ATC GAA AG	208	59.9	28
	R	ATC GTG CCT TTC TTT GTT GG			
GAPDH	F	ACCACAGTCCATGCCATCAC	452	According to target gene	
	R	TCCACCACCCTGTTGCTGTA			

*F, forward; R, reverse; Dir, direction; Anne, annealing temperature.

RESULTS

Reverse northern data

The expression of esophageal cancer deregulated genes during C57BL/6J mouse embryogenesis showed a clear difference. As shown in Figure 1, no signals were visible in the negative control spots, indicating that the hybridization was highly specific. The housekeeping gene density was similar, indicating that the results were credible.

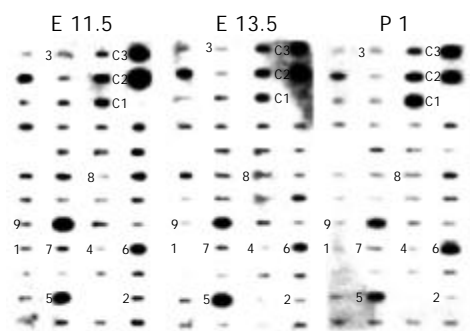


Figure 1 Representatives of esophageal cancer deregulated genes expressed in C57BL/6J mouse embryogenesis by reverse northern screening. Three filters were hybridized with ³²P-labeled cDNA probe from E11.5, E13.5 and P1 period. β -actin and GAPDH were used as controls. c1, negative control; c2, β -actin; c3, GAPDH; 1, S100A8; 2, IGL; 3, RPL15; 4, CSTB; 5, SPRR2A; 6, RHCG; 7, keratin 4; 8, EMP1; 9, S100A9.

By reverse northern screening, the results showed that the expression patterns of these genes were diverse and complex (Table 2). Four patterns of expression were seen at the 3 stages of E11.5, E13.5 and P1. (1) Up-regulation during the E11.5 period, down at E13.5 and P1 (up-down-down), the 10 up-regulated genes could be classed into 6 known genes and 4 unknown genes. The known genes included differentiation related genes (S100A8), immunity related gene (IGL), translation and transcription regulation genes (RPL15, EEF1A1), cytoskeleton protein (TUBA1), cysteine protease inhibitor (cystatin B). (2) Up-regulation during the E13.5 and postnatal d 1 period (down-up-up), such as the SPRR2A which was down-regulated at E11.5. (3) Down-regulation during the E11.5 and E13.5 period (down-down-up), such as RHCG and keratin 4.

Table 2 Expression pattern of esophageal cancer deregulated genes during C57BL/6J mouse development

Gene name	Unigene	E11.5	E13.5	P1	Expression pattern	Change in ESCC
S100A8	Hs.100000	0.12	0.06	0.05	up-down-down	down
IGL	Hs.181125	0.22	0.09	0.08	up-down-down	up
RPL15	Hs.74267	0.23	0.08	0.07	up-down-down	down
EEF1A1	Hs.181165	3.50	0.72	0.43	up-down-down	down
TUBA1	Hs.75318	9.06	1.13	0.54	up-down-down	down
cystatin B	Hs. 695	0.19	0.05	0.07	up-down-down	down
ASN 120	Hs.239758	5.04	0.99	1.00	up-down-down	down
ASN 141	Hs.15087	2.56	0.74	0.79	up-down-down	down
ASN 409	Hs.238513	2.86	0.3	0.34	up-down-down	down
ASN 109	Hs.154390	2.52	0.61	0.59	up-down-down	down
SPRR2A	Hs.355542	0.24	0.48	0.67	down-up-up	down
RHCG	Hs.279682	0.19	0.11	0.78	down-down-up	down
keratin 4	Hs.3235	0.08	0.05	0.35	down-down-up	down
EMP1	Hs.79368	0.16	0.32	0.16	down-up-down	down

IGL, immunoglobulin lambda locus; RPL15, ribosomal protein L15; EEF1A1, eukaryotic translation elongation factor 1 alpha1; TUBA1, tubulin alpha1 (testis specific); ASN, automated sequencing number; SPRR2A, small proline-rich protein 2A; RHCG, Rh type C glycoprotein; EMP1, epithelial membrane protein 1.

(4) Fluctuating expression, down initially, up at E13.5, and then down again (down-up-down), such as EMP1, which was highly expressed at E13.5.

Confirmation by RT-PCR

Three genes (S100A8, EMP-1, CSTB) with notable difference, as well as S100A9 were selected randomly for further confirmation by RT-PCR. As a result, the expression of these genes was consistent with the reverse Northern blot results (Figure 2). It indicated that the results of reverse Northern blot analysis were reliable.

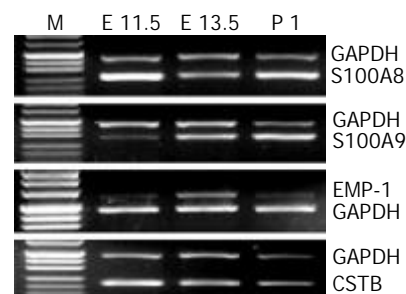


Figure 2 Expression patterns of several genes confirmed by multiplex semi-quantitative RT-PCR. All RT-PCR products were analyzed by electrophoresis on 15 g/L agarose gel. The expression of GAPDH was used as internal control and the size of GAPDH gene amplification was 452 bp.

DISCUSSION

Cancer and development are conceptually related. The normal embryonic development process might display many of the properties associated with tumor development and progression, such as rapid proliferation, migration of cells and formation of new blood vessels^[9]. Tumor formation in many cases results from the aberrant expression of a developmental program. Events in the tumor have their normal regulatory counterparts in the embryonic development. Thus, research into the molecular change involved in development is important not only for understanding of embryogenesis, but also for understanding and managing cancer. In this study, using the C57BL/6J mouse as a model system, we investigated the expression pattern of esophageal cancer deregulated genes

during 3 stages of embryogenesis. Esophageal cancer deregulated genes showed several kinds of expression pattern during embryogenesis, which provided useful information on the tumorigenesis of esophageal cancer.

During embryonic development of mice, genes exhibit complex patterns of spatial and temporal expression and direct organ development in a variety of ways. Differentially expressed genes in embryogenesis implicated that they might play important roles in development. Cancer cells resemble embryonic cells morphologically and share some characteristics with each other, such as rapid proliferation, reduced differentiation, and increased motility. The same intercellular signals that control proliferation and differentiation in development can control tumor development. These common signals are the focus of our study. In the present study, many esophageal cancer deregulated genes showed differential expression during mice embryonic development. These genes covered a broad spectrum of biologic functions including cell proliferation (RPL15)^[10,11], differentiation (S100A8^[5], SPRR2A^[12]), immune response (IGL)^[13], cytoskeletal protein (TUBA1)^[14] migration (cystatin B)^[15], *etc.* These findings provided further clues to the possible function of these deregulated genes and the tumorigenesis of ESCC.

The transition from cell proliferation to differentiation in embryonic development is under strict regulation. Cancer has been called a “developmental disorder”^[16] because it involves a disruption of the normal developmental program for cells, in terms of both differentiation and proliferation. Esophageal cancer is always characterized by uncontrolled proliferation of epithelial cells and failure to differentiate to the normal phenotype. The genes controlling proliferation and differentiation and their transition are very important. In ESCC, S100A8 and S100A9 are both significantly down-regulated and contribute to tumor progression but their function is not fully understood. It has been reported that S100A8 and S100A9 can form a heterodimer and co-express in neutrophils, monocytes, and some secretory epithelia^[17-19]. However, in this study, we found that the expression patterns of 2 members of S100 genes were not completely parallel during the process of embryogenesis. The expression of S100A8 was significantly higher at E11.5 than that of S100A9, but in the periods of E13.5 and P1 the 2 genes' expression patterns were similar. Previous studies have shown that S100A8 mRNA expressed without S100A9 mRNA within fetal cells infiltrating the decidua in the vicinity of the ectoplacental cone between 6.5 and 8.5 d postcoitum^[20]. Targeted disruption of the S100A8 gene caused rapid and synchronous embryo resorption by d 9.5 of development in homozygous null embryos, but the S100A9-deficient mice were viable, fertile, and generally healthy^[21]. These findings, together with the literature, suggest that S100A8 and S100A9 may play different roles in the embryonic development and process of ESCC.

The proliferative changes in cancer cells are usually accompanied with other changes in cellular activities, including reversion to a less differentiated, more developmentally primitive state. Genes expressed in embryogenesis, down-regulated with tissue maturation and re-expressed in cancer, are designated as oncofetal genes, many of which are used as tumor markers. In this study, we found that IGL was abundantly expressed at E11.5 of fetal life and down-regulated subsequently. Meanwhile, multiple myeloma (MM) related to immunoglobulin (Ig) types and light chain subtypes^[22], research proved that kappa and lambda type immunoglobulin light chains could increase the percentage of viable polymorphonuclear leucocytes by inhibiting apoptosis in a concentration-dependent manner^[23]. These findings, indicate that IGL may be an oncofetal protein, but the mechanism of IGL overexpression in ESCC is not clear. Its potential usage as a marker of early recurrence

and in gene therapy needs to be further studied. Structural gene is also important in embryogenesis and tumorigenesis. TUBA1 had the largest expression change of all the genes at E11.5, 6.7-fold. As we know^[14], microtubules are composed of tubulin alpha and beta. They participate in a large number of intracellular events including cell division, intracellular transport and secretion, axonal transport, and maintenance of cell morphology. The diminution of interphase cytoplasmic microtubules in tumor cells was probably due to the deficiency of microtubule organizing function in interphase tumor cells^[24].

Gene expression in specific phase implicates its specific function in that period. In our study, we found that epithelial membrane protein 1 (EMP1) was characteristically expressed at E13.5. It has been found EMP1 is a member of the PMP22 (peripheral myelin protein 22) family^[25,26]. It was expressed in most tissues of the adult mouse, with highest levels in the gastrointestinal tract and lung^[27]. High-level expression of EMP1 was associated with differentiation and growth arrest in squamous cells and the haematopoietic system^[28]. At the molecular level, EMP1 was thought to be involved in the regulation of the cell cycle, cell-cell recognition, and cell death^[29]. At E13.5, high EMP1 expression was found in the initial fiber tracts of the developing cerebellum^[30]. In the second stage of embryonic brain development (E13 to E16), the neuroepithelium remained active, but was coupled with the differentiation of neurons. Hence, the observed increased expression of EMP1 at E13.5 during the second stage of prenatal brain development, is related with the potential function of this molecule during neurogenesis. Whether the absence of EMP1 at P1 and E11.5 is due to down-regulation of expression in maturing cells or EMP1 expression is restricted to some embryonic tissue remains to be elucidated.

In summary, the results from the present study can contribute to our understanding of the function of deregulated genes in ESCC, which are important in both embryonic development and tumorigenesis. These genes identified in the special developmental stage of mice may play some roles in the control of growth, terminal differentiation and may have physiologic or pathological importance during normal development process and the development of ESCC. Finally, the genes identified pertinent to embryonic development may serve as candidate susceptibility genes for inherited esophageal cancer disorders as well as various heritable disorders of embryonic development. Further study is required for the precise relationship between the altered genes and the pathogenesis of esophageal squamous cell cancer and embryonic development.

REFERENCES

- 1 **Offner FA.** Etiology, molecular biology and pathology of squamous cell carcinoma of the esophagus. *Pathologie* 2000; **21**: 349-357
- 2 **Gamliel Z.** Incidence, epidemiology, and etiology of esophageal cancer. *Chest Surg Clin N Am* 2000; **10**: 441-450
- 3 **Selaru FM,** Zou T, Xu Y, Shustova V, Yin J, Mori Y, Sato F, Wang S, Oлару A, Shibata D, Greenwald BD, Krasna MJ, Abraham JM, Meltzer SJ. Global gene expression profiling in Barrett's esophagus and esophageal cancer: a comparative analysis using cDNA microarrays. *Oncogene* 2002; **21**: 475-478
- 4 **Lu J,** Liu Z, Xiong M, Wang Q, Wang X, Yang G, Zhao L, Qiu Z, Zhou C, Wu M. Gene expression profile changes in initiation and progression of squamous cell carcinoma of esophagus. *Int J Cancer* 2001; **91**: 288-294
- 5 **Zhi H,** Zhang J, Hu G, Lu J, Wang X, Zhou C, Wu M, Liu Z. The deregulation of arachidonic acid metabolism-related genes in human esophageal squamous cell carcinoma. *Int J Cancer* 2003; **106**: 327-333
- 6 **Maretto S,** Cordenonsi M, Dupont S, Braghetta P, Broccoli V, Hassan AB, Volpin D, Bressan GM, Piccolo S. Mapping Wnt/ β -catenin signaling during mouse development and in colorectal tumors. *Proc Natl Acad Sci U S A* 2003; **100**: 3299-3304

- 7 **Bonner AE**, Lemon WJ, You M. Gene expression signatures identify novel regulatory pathways during murine lung development: implications for lung tumorigenesis. *J Med Genet* 2003; **40**: 408-417
- 8 **Tollet-Egnell P**, Flores-Morales A, Odeberg J, Lundberg J, Norstedt G. Differential cloning of growth hormone-regulated hepatic transcripts in the aged rat. *Endocrinology* 2000; **141**: 910-921
- 9 **Wiseman BS**, Werb Z. Stromal effects on mammary gland development and breast cancer. *Science* 2002; **296**: 1046-1049
- 10 **Wang Q**, Yang C, Zhou J, Wang X, Wu M, Liu Z. Cloning and characterization of full-length human ribosomal protein L15 cDNA which was overexpressed in esophageal cancer. *Gene* 2001; **263**: 205-209
- 11 **Lee HS**, Mun JH, Kim SG. Characterization of cDNAs encoding cytoplasmic ribosomal protein L15 and L27a in petunia (*Petunia hybrida*): primary structures and coordinate expression. *Gene* 1999; **226**: 155-163
- 12 **Brembeck FH**, Opitz OG, Libermann TA, Rustgi AK. Dual function of the epithelial specific ets transcription factor, ELF3, in modulating differentiation. *Oncogene* 2000; **19**: 1941-1949
- 13 **Yang S**, Wang M, You W. Co-expression of immunoglobulin light chain kappa and lambda in gastric carcinoma cell. *Zhonghua Zhongliu Zazhi* 2002; **24**: 465-466
- 14 **Banerjee A**. Coordination of posttranslational modifications of bovine brain alpha-tubulin. Polyglycylation of delta2 tubulin. *J Biol Chem* 2002; **277**: 46140-46144
- 15 **Shiraishi T**, Mori M, Tanaka S, Sugimachi K, Akiyoshi T. Identification of cystatin B in human esophageal carcinoma, using differential displays in which the gene expression is related to lymph-node metastasis. *Int J Cancer* 1998; **79**: 175-178
- 16 **Dean M**. Cancer as a complex developmental disorder—nineteenth Cornelius P. Rhoads Memorial Award Lecture. *Cancer Res* 1998; **58**: 5633-5636
- 17 **Hessian PA**, Edgeworth J, Hogg N. MRP-8 and MRP-14, two abundant Ca(2+)-binding proteins of neutrophils and monocytes. *J Leukocyte Biol* 1993; **53**: 197-204
- 18 **Edgeworth J**, Gorman M, Bennett R, Freemont P, Hogg N. Identification of p8,14 as a highly abundant heterodimeric calcium binding protein complex of myeloid cells. *J Biol Chem* 1991; **266**: 7706-7713
- 19 **Siegenthaler G**, Roulin K, Chatellard-Gruaz D, Hotz R, Saurat JH, Hellman U, Hagens GA. A heterocomplex formed by the calcium-binding proteins MRP8 (S100A8) and MRP14 (S100A9) binds unsaturated fatty acids with high affinity. *J Biol Chem* 1997; **272**: 9371-9377
- 20 **Passey RJ**, Williams E, Lichanska AM, Wells C, Hu S, Geczy CL, Little MH, Hume DA. A null mutation in the inflammation-associated S100 protein S100A8 causes early resorption of the mouse embryo. *J Immunol* 1999; **163**: 2209-2216
- 21 **Manitz MP**, Horst B, Seeliger S, Strey A, Skryabin BV, Gunzer M, Frings W, Schonlau F, Roth J, Sorg C, Nacken W. Loss of S100A9 (MRP14) results in reduced interleukin-8-induced CD11b surface expression, a polarized microfilament system, and diminished responsiveness to chemoattractants *in vitro*. *Mol Cell Biol* 2003; **23**: 1034-1043
- 22 **Magrangeas F**, Nasser V, Avet-Loiseau H, Loriod B, Decaux O, Granjeaud S, Bertucci F, Birnbaum D, Nguyen C, Harousseau JL, Bataille R, Houlgatte R, Minvielle S. Gene expression profiling of multiple myeloma reveals molecular portraits in relation to the pathogenesis of the disease. *Blood* 2003; **101**: 4998-5006
- 23 **Cohen G**, Rudnicki M, Deicher R, Horl WH. Immunoglobulin light chains modulate polymorphonuclear leucocyte apoptosis. *Eur J Clin Invest* 2003; **33**: 669-676
- 24 **Lin ZX**, Wang DS, Lei SJ, Wang KR. Immunofluorescent studies on microtubules of normal and malignant human esophageal cells. *Sci Sin* 1986; **29**: 289-294
- 25 **Marvin KW**, Fujimoto W, Jetten AM. Identification and characterization of a novel squamous cell-associated gene related to PMP22. *J Biol Chem* 1995; **270**: 28910-28916
- 26 **Taylor V**, Welcher AA, Program AE, Suter U. Epithelial membrane protein-1, peripheral myelin protein 22, and lens membrane protein 20 define a novel gene family. *J Biol Chem* 1995; **270**: 28824-28833
- 27 **Lobsiger CS**, Magyar JP, Taylor V, Wulf P, Welcher AA, Program AE, Suter U. Identification and characterization of a cDNA and the structural gene encoding the mouse epithelial membrane protein-1. *Genomics* 1996; **36**: 379-387
- 28 **Ruegg CL**, Wu HY, Fagnoni FF, Engleman EG, Laus R. B4B, a novel growth-arrest gene, is expressed by a subset of progenitor/pre-B lymphocytes negative for cytoplasmic mu-chain. *J Immunol* 1996; **157**: 72-80
- 29 **Jetten AM**, Suter U. The peripheral myelin protein 22 and epithelial membrane protein family. *Prog Nucleic Acid Res Mol Biol* 2000; **64**: 97-129
- 30 **Wulf P**, Suter U. Embryonic expression of epithelial membrane protein 1 in early neurons. *Brain Res Dev Brain Res* 1999; **116**: 169-180

Edited by Zhu LH and Wang XL Proofread by Xu FM

Loss of myeloid-related proteins 8 and myeloid-related proteins 14 expression in human esophageal squamous cell carcinoma correlates with poor differentiation

Jian-Ping Kong, Fang Ding, Chuan-Nong Zhou, Xiu-Qin Wang, Xiao-Ping Miao, Min Wu, Zhi-Hua Liu

Jian-Ping Kong, Fang Ding, Chuan-Nong Zhou, Xiu-Qin Wang, Min Wu, Zhi-Hua Liu, National Laboratory of Molecular Oncology, Cancer Institute, Chinese Academy of Medical Sciences and Peking Union Medical College, Beijing 100021, China

Xiao-Ping Miao, Department of Etiology and Carcinogenesis, Cancer Institute, Chinese Academy of Medical Sciences and Peking Union Medical College, Beijing 100021, China

Supported by China Key Program on Basic Research, No.G1998051021, the Chinese Hi-tech R&D Program, No.2001AA231041, and National Science Foundation of China, No.30170519

Correspondence to: Dr. Zhi-Hua Liu, National Laboratory of Molecular Oncology, Cancer Institute, Chinese Academy of Medical Sciences and Peking Union Medical College, Beijing 100021, China. liuzh@pubem.cicams.ac.cn

Telephone: +86-10-67723789 **Fax:** +86-10-67723789

Received: 2003-10-20 **Accepted:** 2004-01-12

Abstract

AIM: To study the expression of myeloid-related proteins (MRP)8 and myeloid-related proteins(MRP)14 in human esophageal squamous cell carcinoma and to investigate if there was any correlation between MRP8 and MRP14 expression level and histopathological grade in these tumors.

METHODS: In this study, 65 cases of advanced esophageal squamous cell carcinoma were assessed for MRP8 and MRP14 expression using immunohistochemistry. Statistical analysis was performed for the comparison of MRP8 and MRP14 expression in normal and tumor tissues, and their relationship with clinicopathological features.

RESULTS: Reduced or absent expression of MRP8 and MRP14 was observed in esophageal squamous cell carcinoma, with a significant difference between tumor tissues and normal tissues ($P < 0.01$ and $P < 0.01$ for MRP8 and MRP14, respectively). Poorly differentiated tumors presented a greater decrease than well and moderately differentiated tumors, with a correlation between their protein level and histopathological grading ($P < 0.001$ and $P < 0.001$, respectively). However, no significant association was found between MRP8 and MRP14 expression and age or gender ($P > 0.05$).

CONCLUSION: These findings suggest that the decreased expression of MRP8 and MRP14 might play an important role in the pathogenesis of human esophageal squamous cell carcinoma, being particularly associated with poor differentiation of tumor cells.

Kong JP, Ding F, Zhou CN, Wang XQ, Miao XP, Wu M, Liu ZH. Loss of myeloid-related proteins 8 and myeloid-related proteins 14 expression in human esophageal squamous cell carcinoma correlates with poor differentiation. *World J Gastroenterol* 2004; 10(8): 1093-1097

<http://www.wjgnet.com/1007-9327/10/1093.asp>

INTRODUCTION

Human esophageal squamous cell cancer (ESCC) is one of the most frequent cancers with a predominant distribution in North China, where the mortality rate ranks second^[1]. A wide variety of biological events and mechanisms appear to have roles in the development and progression of ESCC^[2-4]. Deregulation of differentiation is another hallmark of multi-step carcinogenesis^[5]. Recent studies have demonstrated that the disruption of normal squamous cell differentiation may be one of the mechanisms for esophageal cancer development^[6]. In consequence, the defect in the pathway of terminal differentiation is clearly one of the most important abnormalities in esophageal carcinogenesis. In the majority of ESCCs some differentiation-associated mechanisms must be involved to explain the early events leading to the induction of the neoplastic phenotype.

Human esophageal mucosa is lined by a stratified squamous epithelium and its differentiation is a multistep and highly heterogeneous process requiring activation and deactivation of multiple and specific genes^[7,8]. Therefore it is worthwhile to investigate the tissue-specific molecules involved in the process of differentiation during esophagus tumorigenesis. Systematic approaches using microarray-based global transcriptome analysis might provide a powerful alternative with an unprecedented view scope in monitoring gene expression levels^[9]. By analyzing our cDNA microarray data, we have recently identified MRP8 and MRP14 as two down-regulated and differentiation-associated genes in a significant proportion of ESCCs^[10,11].

Myeloid-related protein 8 (MRP8; S100A8) and MRP14 (S100A9) are two calcium-binding proteins belonging to the S100 family^[12]. These proteins expressed during myeloid differentiation, are abundant in granulocytes and monocytes, and form a heterodimeric complex calprotectin in a Ca^{2+} -dependent manner^[13,14]. MRP8 and MRP14 also show a wide range of possible intracellular as well as extracellular functions. They have been shown to inhibit casein kinases I and II, to interact with cytoskeletal components to exert antimicrobial properties, especially against *Candida albicans*, to be involved in transcellular eicosanoid metabolism and to exhibit growth inhibitory activities against murine bone marrow cells, macrophages, and mitogen-stimulated lymphocytes^[15]. Typically, MRP8 and MRP14 are known to be differentially expressed at sites of acute and chronic inflammation^[16-19]. However, there is sparse information regarding the deregulation of MRP8 and/or MRP14 in several human common malignancies^[20-28]. And little is known about the possibility of abnormal expression of MRP8 and MRP14 in ESCC.

In this study, we investigated the expression of MRP8 and MRP14 immunohistochemically in a set of human esophageal squamous cell carcinoma tissues. We also evaluated the relationship between their expression level and clinicopathological features. Our data suggest that their down-regulation is an important event during ESCC progression, and may be involved in the dedifferentiation of neoplastic cells.

MATERIALS AND METHODS

Tissue samples

Sixty-five specimens of ESCC and adjacent normal mucosa were taken from patients who had not received radiotherapy or chemotherapy before surgery. Fresh samples were dissected manually to remove mixed connective tissues and stored in liquid nitrogen immediately after operation at the Cancer Hospital of Chinese Academy of Medical Sciences and Peking Union Medical College. The clinicopathological characteristics were evaluated by two senior pathologists according to the criteria of the WHO classification (1990).

Antibodies

Following antibodies were used in this study: anti-MRP8 and anti-MRP14 polyclonal antibodies (C-19, Santa Cruz Biotechnology Inc. Santa Cruz, CA). These antibodies were provided as goat polyclonal antibody against MRP8 and MRP14, respectively (Santa Cruz, CA) and were characterized extensively by Western blotting and enzyme-linked immunosorbent assays.

Immunohistochemical analysis

For immunohistochemical analysis, 5 μ m thick sections were cut from formalin-fixed paraffin-embedded tissue blocks, deparaffinized, rehydrated, dripped in 30 mL/L hydrogen peroxide solution for 15 min. Before staining, antigen retrieval was performed by heating the specimens in a microwave oven for 20 min in citrate buffer (pH 8.0). Then excess protein was blocked using normal rabbit serum for 30 min at room temperature. Goat anti-MRP8 polyclonal antibody and goat anti-MRP14 antibody were respectively applied to the sections at a 1:150 dilution, and sections were then incubated overnight at 4 °C. A streptavidinbiotin peroxidase detection system (Zymed Laboratories Inc. Francisco, USA) was used according to the manufacturer's instructions. 3,3'-diaminobenzidine was used as the chromogen and hematoxylin was used as the counterstain. Primary antibody was replaced by non-immune serum (Zymed Laboratories Inc. Francisco, USA) in the case of negative control^[29]. All slides were examined and scored independently

by two senior pathologists who were blinded to the pathological and clinical data, and a consensus was obtained between them.

Statistical analysis

The relationship of patients' demographic features, such as age and gender, to MRP8 and MRP14 expression was examined with the Fisher's exact test. The Chi-square test was used for the comparison of MRP8 and MRP14 expression levels between ESCC and the adjacent normal esophageal mucosa, and among different histopathological grades, including well, moderately and poorly differentiated ESCC. All data were analyzed using SigmaStat software (Jandel Scientific, San Rafael, CA, USA). Differences were considered statistically significant when *P*-values were less than 0.05.

RESULTS

Patients and tumor characteristics

In this study, we investigated 65 esophageal squamous cell carcinoma patients comprising 46 males and 19 females. The mean age of patients was 57.7 years and the median age was 57 years (between 38 and 75). Tumors were graded according to the World Health Organization classification: 30 tumors were well differentiated, 23 were moderately differentiated, and 12 were poorly differentiated.

MRP8 and MRP14 expression in ESCCs and matched normal esophageal mucosa

To verify the down-regulation of MRP8 and MRP14 in ESCC, we performed an immunohistochemical analysis on 65 advanced esophageal cancer specimens. In matched non-neoplastic esophageal epithelium, staining for both MRP8 and MRP14 started in the deepest suprabasal cells and increased in intensity toward the superficial layers. Staining was most pronounced in apical, more differentiated epithelial layers, but no staining was observed in columnar epithelial cells in the stratum basale (Figures 1A and 2A). Prominent MRP8 and MRP14 expression was also observed in monocytes and granulocytes. Of the 65 ESCC cases analyzed, MRP8 and MRP14 immunostaining was

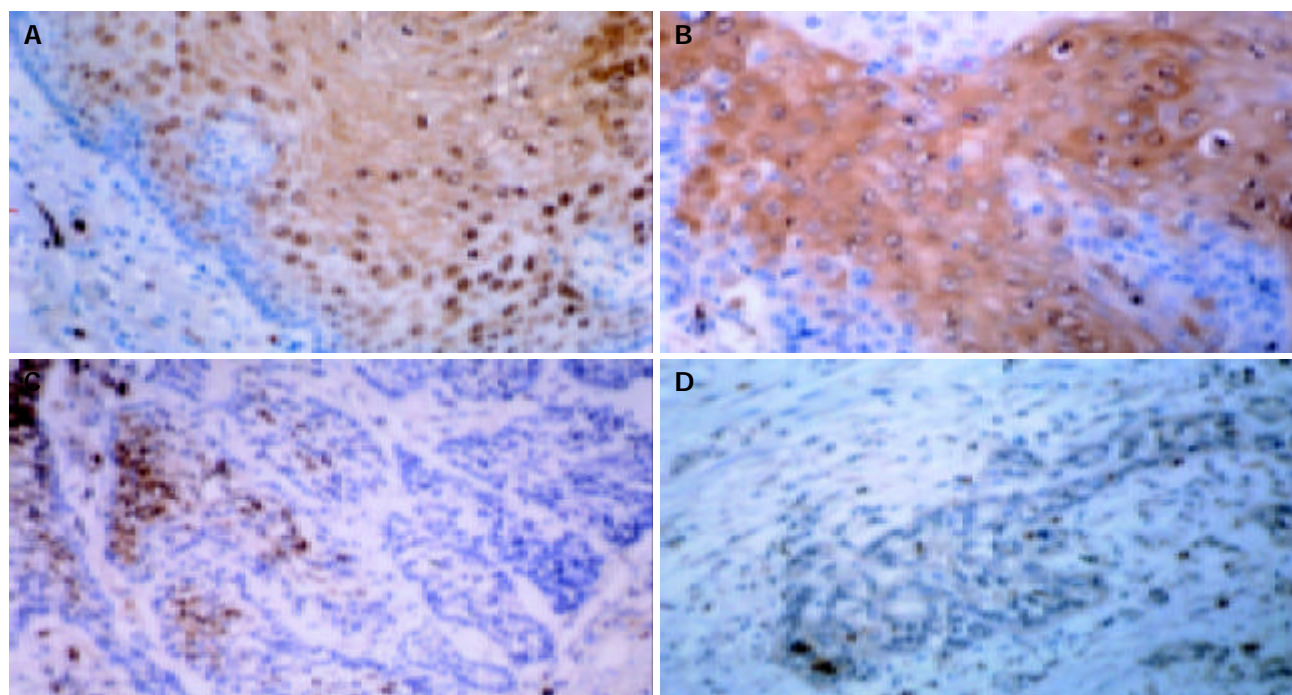


Figure 1 Immunohistochemistry for MRP8 in esophageal carcinoma tissues and normal epithelia (original magnification: $\times 400$). A: MRP8 expression in suprabasal layers of normal esophageal epithelium. B: MRP8 staining in well differentiated carcinoma. C: MRP8 staining in moderately differentiated carcinoma. D: MRP8 staining in poorly differentiated carcinoma.

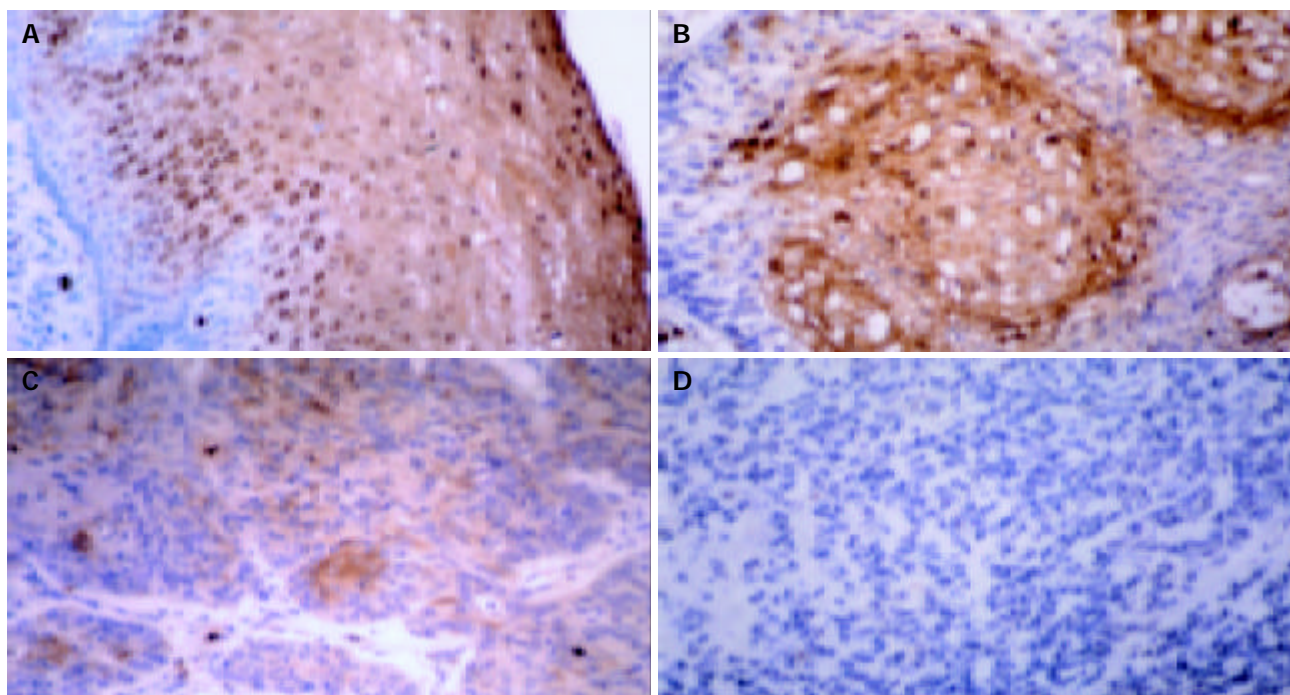


Figure 2 Immunohistochemistry of MRP14 in normal esophageal epithelium (A) and well (B), moderately (C) and poorly differentiated (D) carcinoma tissues. Normal esophageal epithelium showed strongly positive staining for MRP14. However, its staining in poorly differentiated carcinoma was significantly weaker than that in well and moderately differentiated carcinomas. Granulocytes and monocytes were also positively stained in all the sections. Original magnification: $\times 400$.

significantly reduced compared to the adjacent benign epithelia. The majority of tumors showed focal positive immunostaining in certain well differentiated areas, and undetectable in other less differentiated sections. In well differentiated carcinomas, the staining for MRP8 and MRP14 was positive in keratinized areas at the center of tumor foci, but decreased or undetectable in the marginal areas. However, in moderately and poorly differentiated carcinomas, the staining was sparsely weak or sporadic only in the well or moderately differentiated regions, whereas in other areas it was completely undetectable. The immunostaining was frequently heterogeneous even within one specimen, both in terms of percentage of positive cells and staining intensity (Figures 1B-D and 2B-D). The staining for MRP8 and MRP14 was predominant in the cytoplasm of benign cells and accumulated more in the nuclei of malignant cells. In surrounding stroma clear MRP8- and MRP14-positive monocytes and granulocytes could also be observed.

Relationship between MRP8 and MRP14 expression and clinicopathological characteristics in ESCCs

We further examined the relationship between MRP8 and MRP14 expression and clinicopathological findings in SCCs of the esophagus. Table 1 compares the expression of MRP8 and MRP14 in ESCC and matched non-neoplastic esophageal tissues. MRP8 was positive in 61(93.8%) of 65 normal mucosae detected and in 49(75.4%) of 65 ESCCs. MRP14 was found in all the normal mucosae detected and in 54(83.1%) of 65 ESCCs. Among ESCC cases, grade 0 staining, which means lack of expression in tumor tissues, was recorded in 24.6% for MRP8 and 16.9% for MRP14 of ESCC. In total, 9.2% and 13.8% of ESCC cases had grade 1+ for MRP8 and MRP14, respectively. Percentage of moderate staining for MRP8 and MRP14 was 44.6% (MRP8) and 32.3% (MRP14). And 21.5% and 36.9% of cases showed strong staining for MRP8 and MRP14. In comparison with ESCC tissue, the matched non-neoplastic esophageal tissue showed 44.6% (29 of 65) and 92.3% (60 of 65) strong staining for MRP8 and MRP14, respectively. These results indicated a significant reduction of

MRP8 and MRP14 expression in malignant *versus* benign tissue (MRP8: $P < 0.01$, MRP14: $P < 0.01$).

Table 1 Summary of immunohistochemical analysis of MRP8 and MRP14 in esophageal epithelium and tumors. (Fisher's exact test)

Expression Level ¹	MRP8			MRP14		
	Normal (%)	Tumors (%)	P-value	Normal (%)	Tumors (%)	P-value
3+	29(44.6)	14(21.5)	$<0.01^b$	60(92.3)	24(36.9)	$<0.01^d$
2+	32(49.2)	29(44.6)		3(4.6)	21(32.3)	
1+	0(0)	6(9.2)		0(0)	9(13.8)	
0	4(6.2)	16(24.6)		2(3.1)	11(16.9)	

¹3+, $\geq 50\%$; 2+, $\geq 5\%$ and $<50\%$; 1+, $<5\%$; 0, negative; ^b $P < 0.01$ vs normal tissues; ^d $P < 0.01$ vs normal tissues.

Table 2 Relationship between MRP8 and MRP14 immunoreactivity and clinicopathologic factors. (Chi-square Fisher exact test)

	Case Number (n)	MRP8 (+)	P value	MRP14 (+)	P value
Age (yr)					
≤57	35	25	NS	27	NS
>57	30	21		25	
Gender					
Male	46	34	NS	37	NS
Female	19	11		13	
Differentiation					
Well	30	29	$<0.001^b$	30	$<0.001^b$
Moderately	23	16		20	
Poorly	12	4		4	

^b $P < 0.001$ between MRP8 and MRP14 expression and histological grade, respectively.

In addition, we examined the correlation between MRP8 and MRP14 expression and clinicopathological features, and the

results are summarized in Table 2. According to clinicopathological grade, 65 primary ESCCs were classified into three groups: well moderately and poorly differentiated ESCC, respectively. To determine whether the altered expression of MRP8 and MRP14 had additional implications for poor differentiation, we performed Chi-square test in the three groups of ESCCs. There was a significant difference in the expression levels of MRP8 and MRP14 among different differentiation grades, being higher in the well differentiated tumors than in moderately and poorly differentiated tumors (MRP8: $P < 0.001$; MRP14: $P < 0.001$). However, their expression did not correlate with the other parameters such as age and gender ($P > 0.05$).

DISCUSSION

Squamous cell differentiation required the coordinated activation and repression of genes specific to the differentiation constitutes, and disruption of this program accompanied neoplasia^[30]. A better understanding of the factors and mechanisms regulating differentiation and of their disturbance in carcinogenesis would offer new possibilities to design novel tumor therapeutic strategies in the field of differentiation therapy^[5]. According to our cDNA microarray analysis, *MRP8* and *MRP14* were two genes in the down-regulated and differentiation-associated gene cluster, and their genetic alterations might contribute to esophageal tumorigenesis^[10,11]. However, information is limited regarding the possible biological significance of the altered expression of MRP8 and MRP14 during ESCC development. In this study, we revealed frequent loss of MRP8 and MRP14 expression in the majority of ESCCs and a significant correlation between MRP8 and MRP14 expression and clinicopathological parameters of ESCC.

MRP8 and MRP14 were preferentially expressed in the normal esophageal epithelia and lowly expressed in ESCCs. Previous reports have subsequently shown that the deregulation of MRP8 and/or MRP14 was associated with several common human malignancies, including carcinomas of the skin, stomach, colon, nasopharynx, lung, liver and anus, and follicular lymphoma as well^[20-28]. Therefore, our results further suggest that reduced expression of MRP8 and MRP14 in ESCC cells, but not in normal cells, plays an important role in esophageal carcinogenesis. It is interesting to note that MRP8 and MRP14 staining was decreased in poorly and moderately differentiated ESCCs when compared with well-differentiated ESCCs. These data suggest that loss of MRP8 and MRP14 expression in ESCC generally occurs along with worsening esophageal epithelial differentiation in histological grade. Identification of the grade of tumor malignancy would facilitate treatment strategies and provide important information for predicting the prognosis^[31]. To our knowledge, this is the first report on the relationship between MRP8 and MRP14 expression and histopathological grade of ESCC.

Although the fundamental role of MRP8 and MRP14 in myeloid differentiation and keratinocyte hyperproliferation is well established^[32,33], the detailed molecular processes that lead to down-regulation of MRP8 and MRP14 in esophageal epithelium during de-differentiation processes remain to be elucidated. Accumulation of MRP8 and MRP14 may play an important role in maintaining the differentiated status of well-differentiated ESCC, and preventing less differentiated ESCC. It is noteworthy that MRP14 expression level has a positive correlation with the differentiation degree of carcinomas derived from glandular cells, such as hepatocellular carcinoma, cholangiocellular carcinoma and pulmonary adenocarcinoma. In poorly differentiated adenocarcinoma (AC) cases, immunoreactivity of MRP8 and MRP14 was significantly higher than that in the moderately and well differentiated AC cases^[24,26]. These differences might reflect the different pathways or mechanisms that MRP8 and MRP14 were

involved in tumorigenesis of different cell origin.

The identification of MRP8 and MRP14 in esophageal epithelial cells may facilitate the elucidation of molecular mechanism of esophageal carcinogenesis. In normal human esophageal epithelia, MRP8 and MRP14 were expressed in regions containing differentiated cells but not in regions containing actively dividing cells, suggesting that MRP8 and MRP14 may be upregulated in the cellular differentiation status. Indeed, MRP8 and MRP14 were expressed in a tissue/cell-specific and differentiation-dependent manner, especially in the differentiation of monomyelocytes and keratinocytes^[34]. Warner-Bartnicki *et al* have reported that the expression of MRP8 and MRP14 was upregulated during mycophenolic acid and $1\alpha, 25$ -dihydroxyvitamin D_3 -mediated differentiation of HL-60 leukemia cells^[35]. Similarly, terminal differentiation of various epithelial cells was also linked to their constitutive expression^[17]. Consistent with these notions, our observation of their spatial and temporal distribution in esophageal epithelium also supported that MRP8 and MRP14 might collaboratively act to maintain differentiated progeny, playing a growth-suppressive and differentiation-associated role^[36]. Based on these findings, we would propose that MRP8 and MRP14 may be closely associated with the early events in the terminal differentiation of human normal esophageal epithelial cells and the epithelial expression of these proteins is thought to require a certain state of proliferation and/or differentiation.

The *MRP8* and *MRP14* genes, together with other 11 *S100* genes and epidermal differentiation complex (EDC) genes, have been mapped to human chromosome 1q21, which is structurally conserved during evolution. This region has revealed a most remarkable density of genes that fulfill important functions in terminal differentiation of the human epidermis^[37]. Among those genes, the expression of *S100A2*, *S100A4*, *S100A12*, *SPRR3*, *TGM-3* and other genes has also been identified to be altered in ESCCs^[38-42]. Within this chromosomal region, a number of abnormalities such as deletions, rearrangements or translocations were considered to be associated with neoplasia^[43,44]. Thus, 1q21 may be a region of the structural and numerical aberration involved in esophageal carcinogenesis and progression. Furthermore, the clustered organization has posed the question whether each gene is regulated by its own elements or by possible superior locus control elements as suggested for the EDC genes^[45].

In summary, reduced expression of MRP8 and MRP14 was observed in a majority of ESCCs, suggesting that their down-regulation is a common event in esophageal carcinogenesis and progression. In addition, there was a significant correlation between MRP8 and MRP14 expression and clinicopathological parameters involved in differentiation of ESCC. Poorly differentiated carcinomas showed markedly reduced expression than well and moderately differentiated carcinomas. Thus we conclude that MRP8 and MRP14 may play a significant role in the dedifferentiation process of esophageal neoplastic cells. Whether MRP8 and MRP14 expression is an important predictor for histological grade needs to be confirmed by clinical follow-up studies.

REFERENCES

- 1 **Zhang W**, Bailey-Wilson JE, Li W, Wang X, Zhang C, Mao X, Liu Z, Zhou C, Wu M. Segregation analysis of esophageal cancer in a moderately high-incidence area of northern China. *Am J Hum Genet* 2000; **67**: 110-119
- 2 **Huang Y**, Meltzer SJ, Yin J, Tong Y, Chang EH, Srivastava S, McDaniel T, Boynton RF, Zou ZQ. Altered messenger RNA and unique mutational profiles of p53 and Rb in human esophageal carcinomas. *Cancer Res* 1993; **53**: 1889-1894
- 3 **Mandard AM**, Hainaut P, Hollstein M. Genetic steps in the development of squamous cell carcinoma of the esophagus. *Mutat*

- Res* 2000; **462**: 335-342
- 4 **Wang HT**, Kong JP, Ding F, Wang XQ, Wang MK, Liu LX, Wu M, Liu ZH. Analysis of gene expression profile induced by EMP-1 in esophageal cancer cells using cDNA microarray. *World J Gastroenterol* 2003; **9**: 392-398
 - 5 **Fusenig NE**, Breitkreutz D, Boukamp P, Tomakidi P, Stark HJ. Differentiation and tumor progression. *Recent Results Cancer Res* 1995; **139**: 1-19
 - 6 **Kadowaki Y**, Fujiwara T, Fukazawa T, Shao J, Yasuda T, Itoshima T, Kagawa S, Hudson LG, Roth JA, Tanaka N. Induction of differentiation-dependent apoptosis in human esophageal squamous cell carcinoma by adenovirus-mediated p21^{ras} gene transfer. *Clin Cancer Res* 1999; **5**: 4233-4241
 - 7 **Lam AK**. Molecular biology of esophageal squamous cell carcinoma. *Crit Rev Oncol Hematol* 2000; **33**: 71-90
 - 8 **Sato N**, Hitomi J. S100P expression in human esophageal epithelial cells: Human esophageal epithelial cells sequentially produce different S100 proteins in the process of differentiation. *Anat Rec* 2002; **267**: 60-69
 - 9 **Lakhani SR**, Ashworth A. Microarray and histopathological analysis of tumours: the future and the past? *Nat Rev Cancer* 2001; **1**: 151-157
 - 10 **Lu J**, Liu Z, Xiong M, Wang Q, Wang X, Yang G, Zhao L, Qiu Z, Zhou C, Wu M. Gene expression profile changes in initiation and progression of squamous cell carcinoma of esophagus. *Int J Cancer* 2001; **91**: 288-294
 - 11 **Zhi H**, Zhang J, Hu G, Lu J, Wang X, Zhou C, Wu M, Liu Z. The deregulation of arachidonic acid metabolism-related genes in human esophageal squamous cell carcinoma. *Int J Cancer* 2003; **106**: 327-333
 - 12 **Hunter MJ**, Chazin WJ. High level expression and dimer characterization of the S100 EF-hand proteins, migration inhibitory factor-related proteins 8 and 14. *J Biol Chem* 1998; **273**: 12427-12435
 - 13 **Donato R**. S100: a multigenic family of calcium-modulated proteins of the EF-hand type with intracellular and extracellular functional roles. *Int J Biochem Cell Biol* 2001; **33**: 637-668
 - 14 **Heizmann CW**, Fritz G, Schafer BW. S100 proteins: structure, functions and pathology. *Front Biosci* 2002; **7**: d1356-1368
 - 15 **Kerkhoff C**, Klempt M, Sorg C. Novel insights into structure and function of MRP8 (S100A8) and MRP14 (S100A9). *Biochim Biophys Acta* 1998; **1448**: 200-211
 - 16 **Seeliger S**, Vogl T, Engels IH, Schroder JM, Sorg C, Sunderkotter C, Roth J. Expression of calcium-binding proteins MRP8 and MRP14 in inflammatory muscle diseases. *Am J Pathol* 2003; **163**: 947-956
 - 17 **Ross KF**, Herzberg MC. Calprotectin expression by gingival epithelial cells. *Infect Immun* 2001; **69**: 3248-3254
 - 18 **Bhardwaj RS**, Zotz C, Zwadlo-Klarwasser G, Roth J, Goebeler M, Mahnke K, Falk M, Meinardus-Hager G, Sorg C. The calcium-binding proteins MRP8 and MRP14 form a membrane-associated heterodimer in a subset of monocytes/macrophages present in acute but absent in chronic inflammatory lesions. *Eur J Immunol* 1992; **22**: 1891-1897
 - 19 **Frosch M**, Strey A, Vogl T, Wulffraat NM, Kuis W, Sunderkotter C, Harms E, Sorg C, Roth J. Myeloid-related proteins 8 and 14 are specifically secreted during interaction of phagocytes and activated endothelium and are useful markers for monitoring disease activity in pauciarticular-onset juvenile rheumatoid arthritis. *Arthritis Rheum* 2000; **43**: 628-637
 - 20 **Gebhardt C**, Breitenbach U, Tuckermann JP, Dittrich BT, Richter KH, Angel P. Calgranulins S100A8 and S100A9 are negatively regulated by glucocorticoids in a c-Fos-dependent manner and overexpressed throughout skin carcinogenesis. *Oncogene* 2002; **21**: 4266-4276
 - 21 **El-Rifai W**, Moskaluk CA, Abdrabbo MK, Harper J, Yoshida C, Riggins GJ, Frierson HF Jr, Powell SM. Gastric cancers overexpress S100A calcium-binding proteins. *Cancer Res* 2002; **62**: 6823-6826
 - 22 **Stulik J**, Osterreicher J, Koupilova K, Knizek, Macela A, Bures J, Jandik P, Langr F, Dedic K, Jungblut PR. The analysis of S100A9 and S100A8 expression in matched sets of macroscopically normal colon mucosa and colorectal carcinoma: the S100A9 and S100A8 positive cells underlie and invade tumor mass. *Electrophoresis* 1999; **20**: 1047-1054
 - 23 **Fung LF**, Lo AK, Yuen PW, Liu Y, Wang XH, Tsao SW. Differential gene expression in nasopharyngeal carcinoma cells. *Life Sci* 2000; **67**: 923-936
 - 24 **Arai K**, Teratani T, Nozawa R, Yamada T. Immunohistochemical investigation of S100A9 expression in pulmonary adenocarcinoma: S100A9 expression is associated with tumor differentiation. *Oncol Rep* 2001; **8**: 591-596
 - 25 **Hellmann GM**, Fields WR, Doolittle DJ. Gene expression profiling of cultured human bronchial epithelial and lung carcinoma cells. *Toxicol Sci* 2001; **61**: 154-163
 - 26 **Arai K**, Yamada T, Nozawa R. Immunohistochemical investigation of migration inhibitory factor-related protein (MRP)-14 expression in hepatocellular carcinoma. *Med Oncol* 2000; **17**: 183-188
 - 27 **Zucchini C**, Biolchi A, Strippoli P, Solmi R, Rosati G, Del Governatore M, Milano E, Ugolini G, Salfi N, Farina A, Caira A, Zanotti S, Carinci P, Valvassori L. Expression profile of epidermal differentiation complex genes in normal and anal cancer cells. *Int J Oncol* 2001; **9**: 1133-1141
 - 28 **Husson H**, Carideo EG, Neuberger D, Schultze J, Munoz O, Marks PW, Donovan JW, Chillemi AC, O'Connell P, Freedman AS. Gene expression profiling of follicular lymphoma and normal germinal center B cells using cDNA arrays. *Blood* 2002; **99**: 282-289
 - 29 **Hu H**, Xia SH, Li AD, Xu X, Cai Y, Han YL, Wei F, Chen BS, Huang XP, Han YS, Zhang JW, Zhang X, Wu M, Wang MR. Elevated expression of p63 protein in human esophageal squamous cell carcinomas. *Int J Cancer* 2002; **102**: 580-583
 - 30 **Jones SJ**, Dicker AJ, Dahler AL, Saunders NA. E2F as a regulator of keratinocyte proliferation: implications for skin tumor development. *J Invest Dermatol* 1997; **109**: 187-193
 - 31 **Sarbia M**, Gabbert HE. Modern pathology: prognostic parameters in squamous cell carcinoma of the esophagus. *Recent Results Cancer Res* 2000; **155**: 15-27
 - 32 **Van Roozendaal KE**, Darling D, Farzaneh F. DMSO and retinoic acid induce HL-60 differentiation by different but converging pathways. *Exp Cell Res* 1990; **90**: 137-140
 - 33 **Wilkinson MM**, Busuttill A, Haywrd C, Brock DJ, Dorin JR, Van Heyningen V. Expression pattern of two related cystic fibrosis-associated calcium-binding proteins in normal and abnormal tissues. *J Cell Sci* 1988; **91**(Pt 2): 221-230
 - 34 **Donato R**. Intracellular and extracellular roles of S100 proteins. *Microsc Res Tech* 2003; **60**: 540-551
 - 35 **Warner-Bartnicki AL**, Murao S, Collart FR, Huberman E. Regulated expression of MRP8 and MRP14 genes in human promyelocytic leukemic HL-60 cells treated with the differentiation-inducing agents mycophenolic acid and 1 α ,25-dihydroxyvitamin D₃. *Exp Cell Res* 1993; **204**: 241-246
 - 36 **Seery JP**. Stem cells of the oesophageal epithelium. *J Cell Sci* 2002; **115**(Pt 9): 1783-1789
 - 37 **Mischke D**, Korge BP, Marenholz I, Volz A, Ziegler A. Genes encoding structural proteins of epidermal cornification and S100 calcium-binding proteins form a gene complex ("epidermal differentiation complex") on human chromosome 1q21. *J Invest Dermatol* 1996; **106**: 989-992
 - 38 **Kyriazanos ID**, Tachibana M, Dhar DK, Shibakita M, Ono T, Kohno H, Nagasue N. Expression and prognostic significance of S100A2 protein in squamous cell carcinoma of the esophagus. *Oncol Rep* 2002; **9**: 503-510
 - 39 **Ninomiya I**, Ohta T, Fushida S, Endo Y, Hashimoto T, Yagi M, Fujimura T, Nishimura G, Tani T, Shimizu K, Yonemura Y, Heizmann CW, Schafer BW, Sasaki T, Miwa K. Increased expression of S100A4 and its prognostic significance in esophageal squamous cell carcinoma. *Int J Oncol* 2001; **18**: 715-720
 - 40 **Hitomi J**, Kimura T, Kusumi E, Nakagawa S, Kuwabara S, Hatakeyama K, Yamaguchi K. Novel S100 proteins in human esophageal epithelial cells: CAAF1 expression is associated with cell growth arrest. *Arch Histol Cytol* 1998; **6**: 163-178
 - 41 **Chen BS**, Wang MR, Cai Y, Xu X, Xu ZX, Han YL, Wu M. Decreased expression of *SPRR3* in Chinese human oesophageal cancer. *Carcinogenesis* 2000; **21**: 2147-2150
 - 42 **Chen BS**, Wang MR, Xu X, Cai Y, Xu ZX, Han YL, Wu M. Transglutaminase-3, an esophageal cancer-related gene. *Int J Cancer* 2000; **88**: 862-865
 - 43 **Schafer BW**, Heizmann CW. The S100 family of EF-hand calcium-binding proteins: functions and pathology. *Trends Biochem Sci* 1996; **21**: 134-140
 - 44 **Ridinger K**, Ilg EC, Niggli FK, Heizmann CW, Schafer BW. Clustered organization of S100 genes in human and mouse. *Biochim Biophys Acta* 1998; **1448**: 254-263
 - 45 **Elder JT**, Zhao X. Evidence for local control of gene expression in the epidermal differentiation complex. *Exp Dermatol* 2002; **11**: 406-412

Comparison of conformal and intensity-modulated techniques for simultaneous integrated boost radiotherapy of upper esophageal carcinoma

Wei-Hua Fu, Lu-Hua Wang, Zong-Mei Zhou, Jian-Rong Dai, Yi-Min Hu, Lu-Jun Zhao

Wei-Hua Fu, Lu-Hua Wang, Zong-Mei Zhou, Jian-Rong Dai, Yi-Min Hu, Lu-Jun Zhao, Department of Radiation Oncology, Cancer Institute (Hospital), Peking Union Medical College, Chinese Academy of Medical Sciences, Beijing 10021, China

Correspondence to: Lu-Hua Wang, Department of Radiation Oncology, PO Box 2258, Beijing 100021, China. wlhwq@yahoo.com
Fax: +86-10-67706153

Received: 2003-08-05 **Accepted:** 2003-10-12

Abstract

AIM: To compare intensity-modulated radiotherapy (IMRT) with conformal radiotherapy (CRT) by investigating the dose profiles of primary tumors, electively treated regions, and the doses to organs at risk.

METHODS: CRT and IMRT plans were designed for five patients with upper esophageal carcinoma. For each patient, target volumes for primary lesions (67.2 Gy) and electively treated regions (50.4 Gy) were predefined. An experienced planner manually designed one CRT plan. Four IMRT plans were generated with the same dose-volume constraints, but with different beam arrangements. Indices including dose distributions, dose volume histograms (DVHs) and conformity index were compared.

RESULTS: The plans with three intensity-modulated beams were discarded because the doses to spinal cord were larger than the tolerable dose 45Gy, and the dose on areas near the skin was up to 50Gy. When the number of intensity beams increased to five, IMRT plans were better than CRT plans in terms of the dose conformity and homogeneity of targets and the dose to OARs. The dose distributions changed little when the beam number increased from five to seven and nine.

CONCLUSION: IMRT is superior to CRT for the treatment of upper esophageal carcinoma with simultaneous integrated boost (SIB). Five equispaced coplanar intensity-modulated beams can produce desirable dose distributions. The primary tumor can get higher equivalent dose by SIB technique. The SIB-IMRT technique shortens the total treatment time, and is an easier, more efficient, and perhaps a less error-prone way in delivering IMRT.

Fu WH, Wang LH, Zhou ZM, Dai JR, Hu YM, Zhao LJ. Comparison of conformal and intensity-modulated techniques for simultaneous integrated boost radiotherapy of upper esophageal carcinoma. *World J Gastroenterol* 2004; 10(8): 1098-1102
<http://www.wjgnet.com/1007-9327/10/1098.asp>

INTRODUCTION

Esophageal carcinoma is one of the most common cancers in

china. Surgery and radiotherapy have always been the main treatment methods^[1-4]. Chen *et al*^[5] reported that the 5-year survival rate by radiation alone was comparable to that by surgery for patients with operable upper third lesions. Therefore, for diseases located in the upper esophageal region, including cervical and upper thoracic esophagus, radiotherapy is an efficient treatment selection. To give a higher radiation dose of between 60 Gy and 70 Gy to primary tumors and approximately 45 Gy to 50 Gy to electively irradiated lymph nodal regions is necessary for tumor local control. Spinal cord restricts the dose escalation of tumor and may affect the outcome of radiotherapy with conventional techniques, because it is close to cervical and upper thoracic esophagus and its endurance dose is less than 45 Gy. Lung is another dose limit factor in radiotherapy of esophageal cancer. Conformal radiotherapy (CRT) can reduce the irradiation volume of lung. But intensity-modulated radiotherapy (IMRT) is capable of producing more highly conformal dose distribution to a target and steeper dose gradients around the target edges than CRT. This capability makes it possible to give a high dose to the target volume while sparing adjacent normal tissues. Studies have shown benefits of IMRT in the treatment of head-and-neck^[6-13] and other cancers^[14-20].

The conventional technique for esophageal cancer is to use initial anterior-posterior large field arrangement followed by multi-field technique to boost the primary tumor with field size reduction. The large-field plan and boost plan are created independently. This makes it difficult to determine how the two plans affect each other. Tissues irradiated during the large-field phase receive unwanted additional dose during the boost phase from the beams irradiating the gross tumor. If simultaneous integrated boost (SIB) approach is applied, different dose requirements to the primary tumor and the elective regions can receive different doses within one fraction, and only one plan is needed for the entire course of treatment. Therefore, SIB-IMRT technique can overcome the drawbacks of conventional technique. Further more, it may shorten the treatment course by integrating the boost. The advantages of SIB-IMRT have been demonstrated for head-and-neck and prostate cancers^[21-24].

The purpose of our study was to evaluate SIB-IMRT technique for upper esophageal carcinoma and to compare the effect of SIB-IMRT with SIB-CRT. We analyzed the dose distributions of primary tumor and electively treated regions and the doses to lung and spinal cord, and investigated the influence of the number of intensity-modulated beams to the dose distributions.

MATERIALS AND METHODS

Patients were immobilized in supine position. Planning CT scans were performed at 5 mm slice thickness using a dedicated helical CT scanner (Siemens, Somatom Plus 4). The entire lungs were scanned for further plan evaluation. CT images were transferred to the inverse treatment planning system (MDS Nordion, Helax-TMS 6.1) through network (Siemens,

Lantis). Two target volumes, CTV1 and CTV2, were outlined on each set of the CT images. CTV1 included the gross tumor volume (GTV) with a margin of 3 cm in superior and inferior directions and 0.5 cm to 1.5 cm in other directions. CTV2 included correlated lymphatic drainage regions and extended to cricothyroid membrane. Margins of 0.5 cm were added to the CTVs in all directions to generate the planning target volumes (PTVs). The length of PTV1s ranged from 10.5 cm to 14.5 cm, and that of PTV2s ranged from 13 cm to 17 cm. The volume of PTV1s ranged from 167 cm³ to 251 cm³, and that of PTV2s ranged from 234 cm³ to 590 cm³ (note: PTV1 was surrounded by PTV2. The volume of PTV2 did not include the volume of corresponding PTV1). The patients were numbered in increasing orders with the size of PTV1. The spinal cord and lung were also contoured on the images.

The goal of the treatment was to deliver a prescribed dose of 67.2 Gy to at least 95% of PTV1 in 2.4 Gy fractions, and 50.4 Gy to at least 95% of PTV2 in 1.8 Gy fractions. The maximum dose to the spinal cord was 45 Gy. For the lungs, V_{20Gy} (the volume of the lung received more than 20 Gy) should be less than 25% of lung volume and V_{30Gy} (the volume of the lung received more than 30 Gy) should be less than 20% of lung.

One CRT plan and four IMRT plans were designed for each patient. Beam energy was 6MV X-ray. An experienced planner designed the beam arrangements of CRT plan by using trial and error method. The beam number and directions were manually adjusted to avoid the spinal cord and spare lung, and the beam weights were selected in order to maximize PTVs dose homogeneity. The beam number, directions, wedges and shape were different for these five patients because these parameters were set according to the position and shape of the targets. For example, the CRT plan of patient 1 used eight conformal beams from seven directions (*i.e.* 0°, 45°, 80°, 150°, 225°, 280° and 300°), and that of patient 3 used six conformal beams from five directions (*i.e.* 0°, 70°, 150°, 210° and 305°). Two beams, the large one covering PTV2, and the small one covering PTV1 could be in one beam direction. The beam arrangements of IMRT plans were same for these five patients by using three, five, seven and nine equispaced non-opposed coplanar beams in 360° beginning with 0°, respectively. The gantry angles for each beam arrangement are listed in Table 1. The beams would be delivered in a “step and shoot” mode with multileaf collimators. Delivery sequences were generated under the condition that the number of segments should be no more than 15 for each beam and the intensity levels were 10. The same dose-volume constraints were used for all the plannings during inverse optimization.

Table 1 Beam arrangement of IMRT plans

Number of beams	Gantry angles
3	0°, 120°, 240°
5	0°, 72°, 144°, 216°, 288°
7	0°, 52°, 103°, 154°, 206°, 257°, 308°
9	0°, 40°, 80°, 120°, 160°, 200°, 240°, 280°, 320°

For the purpose of comparison, all plans were normalized to make 95% of PTV1 receive the prescribed dose of 67.2 Gy. The following parameters of these plans in each patient were compared, isodose distributions, DVHs, conformity indices (*CI*), mean dose, standard deviation (*SD*) and D_{95} (lowest dose encompassing 95% of the target) for PTVs, maximum dose for spinal cord, V_{20Gy} , V_{30Gy} and mean dose for lungs.

The equation for calculating conformity index is as follows^[9,25]:

$$CI = \frac{V_{T.ref}}{V_T} \times \frac{V_{T.ref}}{V_{ref}} \quad (1)$$

where V_T is the target volume, $V_{T.ref}$ is the target volume covered by the reference isodose line, V_{ref} is the total volume covered by the reference isodose line. The value of *CI* is between zero and one. A *CI* of one represents the ideal situation that the target volume coincides exactly with the treatment volume, a *CI* of zero represents a plan in which there is no overlap between the two volumes. The reference dose was 67.2 Gy for PTV1 and 50.4 Gy for PTV2.

RESULTS

Isodose distributions

Since the plans of these patients had similar results of dose distributions in terms of target volume coverage and OARs sparing, only the isodose distributions and DVHs of patient 3 having the median PTV1 were presented. Figure 1 shows the isodose distributions on axial images for CRT and IMRT plans. PTV1 and PTV2 are shown as white lines. PTV1 was inside PTV2. The isodose lines were displayed on an absolute dose scale, the isodose levels of 67.2 Gy, 50.4 Gy, and 20 Gy were shown. All plans showed similar prescribed dose coverages of PTV1 and PTV2. However, the dose distributions outside the targets were different. For the IMRT plan with three beams, high isodose lines covered more normal tissues, the cervical spinal cord received more than 45 Gy. Some areas near the skin received a dose as high as 50 Gy. The dose to spinal cord exceeded the endurance dose for four of the five patients (*i.e.*

Table 2 Results for CRT and IMRT in five upper esophageal cancer patients(mean±SD)

Structure	Parameter	CRT	3F IMRT	5F IMRT	7F IMRT	9F IMRT
PTV1	Mean dose (Gy)	73.0±3.0	74.9±3.8	74.2±2.3	73.9±2.0	74.1±1.5
	SD (%)	6.3±3.7	6.7±2.7	6.0±2.0	5.7±2.1	6.0±1.7
	D_{95} (Gy)	67.2±0.0	67.2±0.0	67.2±0.0	67.2±0.0	67.2±0.0
	<i>CI</i>	0.47±0.16	0.59±0.18	0.70±0.04	0.74±0.06	0.75±0.07
PTV2	Mean dose (Gy)	65.3±4.4	60.0±2.3	59.3±1.4	58.4±1.8	58.4±2.0
	SD (%)	11.6±3.8	9.2±1.8	8.8±1.5	8.5±1.9	8.6±1.8
	D_{95} (Gy)	52.4±3.3	51.2±2.8	50.8±3.4	50.5±3.3	51.2±2.9
	<i>CI</i>	0.52±0.08	0.46±0.11	0.64±0.06	0.67±0.07	0.68±0.08
Lung	Mean dose (Gy)	12.4±1.7	11.1±1.2	10.8±1.3	10.7±1.3	10.9±1.2
	V_{20} (%)	24.7±2.8	22.1±1.7	22.4±0.7	23.2±1.6	23.8±1.7
	V_{30} (%)	18.6±2.9	15.1±1.6	15.0±1.9	13.5±2.2	13.5±3.2
Spinal cord	Maximum dose (Gy)	40.9±2.7	56.9±7.2	43.9±1.0	43.3±0.8	42.0±1.5

patient 2 to patient 5). Therefore, three beam IMRT plan was unacceptable. For the CRT plan, high isodose lines covered more normal tissues, indicating that the dose distributions of the 5, 7, and 9 beam IMRT plans were more conformal than CRT plan.

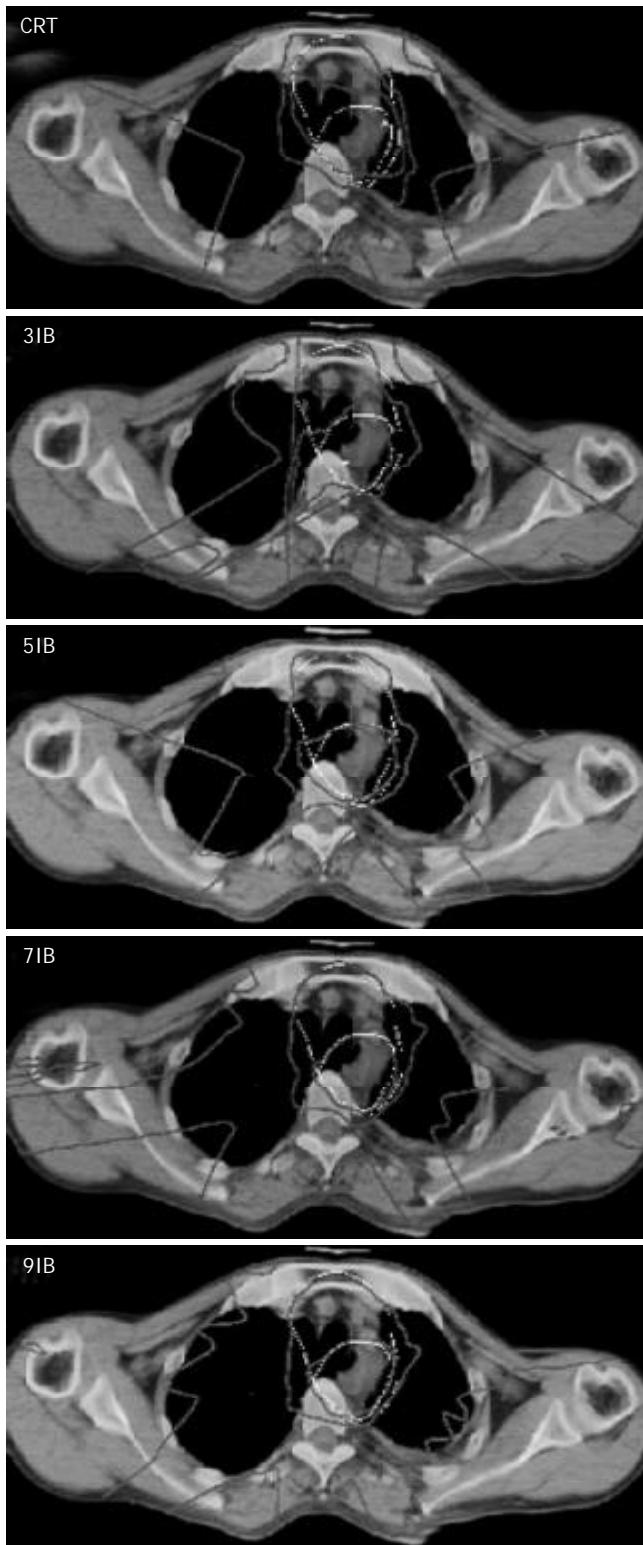


Figure 1 Isodose distributions on axial images for CRT and IMRT plans of patient 3. The white lines represent PTV1 and PTV2. PTV1 was inside PTV2. The isodose levels of 67.2 Gy, 50.4 Gy and 20 Gy were shown. IB stands for intensity-modulated beam.

Targets

DVHs of CRT and IMRT plans for PTV1 and PTV2 of patient 3 are shown in Figures 2A and 2B. The mean results for these

five patients are listed in Table 2. Three beam IMRT plan was presented to show the influence of the number of intensity-modulated beams. The targets' dose homogeneity and conformity of CRT plan were much worse than those of IMRT plans with the beam number no less than five. DVHs were similar to IMRT plans, and the indices did not show any obvious difference as the beam number increased from five to seven and nine. The conformity was improved as the number of intensity-modulated beams increased, but the improvement was marginal when beam number was over five.

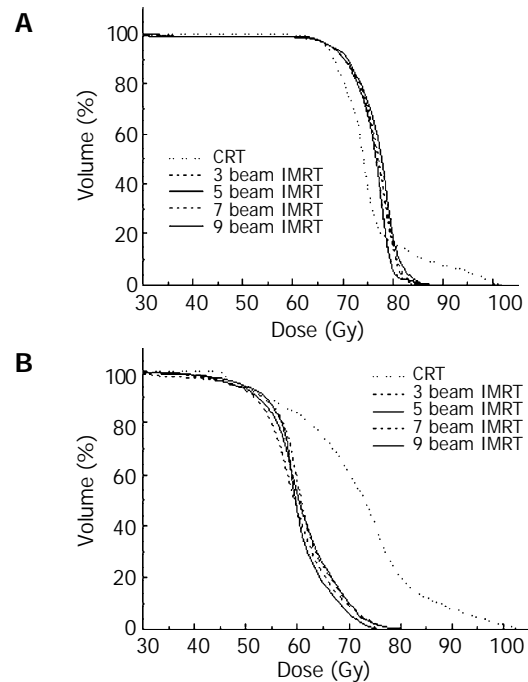


Figure 2 DVHs of PTVs for CRT and IMRT plans of patient 3. (A), PTV1; (B), PTV2.

OARs

The mean results of OARs for these five patients are listed in Table 2. The three beam IMRT plans were unacceptable as their doses to spinal cord were larger than the tolerable dose 45 Gy. The results in five, seven, and nine beam IMRT plans were similar and better than those of CRT plan in terms of sparing lung. The mean doses of lung for the five, seven, and nine beam IMRT plans were almost identical.

DISCUSSION

The cervical and upper thoracic esophageal regions are characterized by variation of body thickness, the distance of esophagus to the body surface, and the closeness of the target to the spinal cord. Acceptable SIB-IMRT plans were superior to SIB-CRT plans in treating tumors in these regions. The dose homogeneity of PTV2 improved, the volume of higher dose outside the primary tumor decreased, the dose conformity improved. The difference between SIB-CRT plans and SIB-IMRT plans was due to that SIB-CRT did not compensate for the variations of body thickness and depth of esophagus. It was difficult to protect the spinal cord while keeping the dose uniformity in the target volume with SIB-CRT plans. In addition, the benefit of CRT plan depended greatly upon the planner's experiences, and many trials were required to figure out the beam directions and weights. On the other hand, the planner only arranged the beam directions (Table 1) and set the dose-volume constraints in designing IMRT plan. The other work was done by the inverse treatment planning system.

Therefore, it took less time to design an IMRT plan than to adjust a CRT plan.

The ideal number of beams in an IMRT plan has not been decided. Generally, a larger number of beams would provide more parameters to adjust and, therefore a greater flexibility to achieve a desired dose distribution. However, the more the number of beams was used, the more the effort was required for planning, quality assurance, dosimetric verification and treatment. Practically, it was desirable to reduce the number of beams to as few as possible without compromising the quality of the treatment. Soderstrom and Brahme^[26,27] concluded that fewer intensity-modulated beams were needed than uniform beams to achieve the same or even better results, perhaps as few as three beams were sufficient in most cases provided beam angles were optimized. Mohan and Ling^[27,28] believed that the ideal minimum number of beams would depend upon a variety of geometrical and biological factors and the desired target dose level to achieve an adequate local control. Studies^[8,11,22,29] showed that the beams less than ten were enough for most clinical requirements. Thus, the number of beams used in our study was less than 10. Pirzkall *et al*^[30] concluded that the ideal number of beams was influenced by the photon energy for deeply seated targets.

From the results of this study, the plan with three equispaced coplanar intensity-modulated beams could not meet the requirement of OARs and its high dose conformity was worse than those with more beams. It might be due to the fact that the beam directions were not optimized. Five equispaced coplanar intensity-modulated beams were sufficient to get an adequate high dose coverage and a dose homogeneity for both targets of upper esophageal cancer. There was no obvious improvement in target dose homogeneity, conformity and the dose to OARs with more than five beams. Therefore we believed that for SIB-IMRT of upper esophageal carcinoma, five beams were sufficient to deliver a satisfactory dose distribution and further increase of the number of beams would complicate the treatment without significant improvement of dose distribution.

In addition, concomitant boost treatment may offer some radiobiological advantage in terms of a lower dose per fraction to normal tissues while delivering a higher dose per fraction to the targets. In this study, the dose per fraction to PTV1 and PTV2 was 2.4 Gy and 1.8 Gy, respectively. To compare with the conventional fractionation (2 Gy/f), we calculated the normalized total dose (NTD)^[22,23] that was the biological equivalent dose given in 2 Gy/f by linear-quadratic (LQ) model^[31]. The NTD for PTV1 and PTV2 was about 70 Gy and 49 Gy, respectively. Therefore, the primary tumor could get a higher dose with SIB treatment while the elective regions had an adequate dose. It was beneficial to tumor local control.

In conclusion, for SIB treatment of upper esophageal carcinoma, IMRT is better than CRT in terms of the target volume coverage, OARs sparing and time cost in treatment planning process. Five equispaced coplanar intensity-modulated beams produce desirable dose distributions. The SIB-IMRT technique not only shortens the total treatment time but also is an easier, more efficient, and perhaps a less error-prone way of delivering IMRT. Primary tumor can get a higher equivalent dose by SIB. The effect of SIB-IMRT is currently under clinical trial in our hospital.

REFERENCES

- Xiao ZF**. Esophageal carcinoma. In: Yin WB, Gu XZ, eds. 3rded. Radiation oncology. Beijing: Peking union medical college press 2002: 598-622
- Wang SJ**, Wen DG, Zhang J, Man X, Liu H. Intensify standardized therapy for esophageal and stomach cancer in tumor hospitals. *World J Gastroenterol* 2001; **7**: 80-82
- Xiao ZF**, Yang ZY, Zhou ZM, Yin WB, Gu XZ. Radiotherapy of double primary esophageal carcinoma. *World J Gastroenterol* 2000; **6**: 145-146
- Chen DF**. External radiotherapy in combination with brachytherapy in the treatment of 121 cases of esophageal cancer. *Shijie Huaren Xiaohua Zazhi* 1998; **6**: 127
- Chen DF**, Yang ZY, Yin WB. Radiotherapy of 180 cases of operable esophageal carcinoma. *China Natl J New Gastroenterol* 1997; **3**: 123-126
- Huang D**, Xia P, Akazawa P, Akazawa C, Quivey JM, Verhey LJ, Kaplan M, Lee N. Comparison of treatment plans using intensity-modulated radiotherapy and three-dimensional conformal radiotherapy for paranasal sinus carcinoma. *Int J Radiat Oncol Biol Phys* 2003; **56**: 158-168
- Lee N**, Xia P, Quivey JM, Sultanem K, Poon I, Akazawa C, Akazawa P, Weinberg V, Fu KK. Intensity-modulated radiotherapy in the treatment of nasopharyngeal carcinoma: an update of the UCSF experience. *Int J Radiat Oncol Biol Phys* 2002; **53**: 12-22
- Hsiung CY**, Yorke ED, Chui CS, Hunt MA, Ling CC, Huang EY, Wang CJ, Chen HC, Yeh SA, Hsu HC, Amols HI. Intensity-modulated radiotherapy versus conventional three-dimensional conformal radiotherapy for boost or salvage treatment of nasopharyngeal carcinoma. *Int J Radiat Oncol Biol Phys* 2002; **53**: 638-647
- Bragg CM**, Conway J, Robinson MH. The role of intensity-modulated radiotherapy in the treatment of parotid tumors. *Int J Radiat Oncol Biol Phys* 2002; **52**: 729-738
- Adams EJ**, Nutting CM, Convery DJ, Cosgrove VP, Henk JM, Dearnaley DP, Webb S. Potential role of intensity-modulated radiotherapy in the treatment of tumors of the maxillary sinus. *Int J Radiat Oncol Biol Phys* 2001; **51**: 579-588
- Hunt MA**, Zelefsky MJ, Wolden S, Chui CS, LoSasso T, Rosenzweig K, Chong L, Spirou SV, Fromme L, Lumley M, Amols HA, Ling CC, Leibel SA. Treatment planning and delivery of intensity-modulated radiotherapy for primary nasopharynx cancer. *Int J Radiat Oncol Biol Phys* 2001; **49**: 623-632
- Xia P**, Fu KK, Wong GW, Akazawa C, Verhey LJ. Comparison of treatment plans involving intensity-modulated radiotherapy for nasopharyngeal carcinoma. *Int J Radiat Oncol Biol Phys* 2000; **48**: 329-337
- Posner MD**, Quivey JM, Akazawa PF, Xia P, Akazawa C, Verhey LJ. Dose optimization for the treatment of anaplastic thyroid carcinoma: a comparison of treatment planning techniques. *Int J Radiat Oncol Biol Phys* 2000; **48**: 475-483
- De Meerleer GO**, Vakaet LA, De Gerssem WR, De Wagter C, De Naeyer B, De Neve W. Radiotherapy of prostate cancer with or without intensity modulated beams: a planning comparison. *Int J Radiat Oncol Biol Phys* 2000; **47**: 639-648
- Zelefsky MJ**, Fuks Z, Happersett L, Lee HJ, Ling CC, Burman CM, Hunt M, Wolfe T, Venkatraman ES, Jackson A, Skwarchuk M, Leibel SA. Clinical experience with intensity modulated radiation therapy (IMRT) in prostate cancer. *Radiother Oncol* 2000; **55**: 241-249
- Ling CC**, Burman C, Chui CS, Kutcher GJ, Leibel SA, LoSasso T, Mohan R, Bortfeld T, Reinstein L, Spirou S, Wang XH, Wu Q, Zelefsky M, Fuks Z. Conformal radiation treatment of prostate cancer using inversely-planned intensity-modulated photon beams produced with dynamic multileaf collimation. *Int J Radiat Oncol Biol Phys* 1996; **35**: 721-730
- Pirzkall A**, Carol M, Lohr F, Hoss A, Wannenmacher M, Debus J. Comparison of intensity-modulated radiotherapy with conventional conformal radiotherapy for complex-shaped tumors. *Int J Radiat Oncol Biol Phys* 2000; **48**: 1371-1380
- Evans PM**, Donovan EM, Partridge M, Childs PJ, Convery DJ, Eagle S, Hansen VN, Suter BL, Yarnold JR. The delivery of intensity modulated radiotherapy to the breast using multiple static fields. *Radiother Oncol* 2000; **57**: 79-89
- Hong L**, Hunt M, Chui C, Spirou S, Forster K, Lee H, Yahalom J, Kutcher GJ, McCormick B. Intensity-modulated tangential beam irradiation of the intact breast. *Int J Radiat Oncol Biol Phys* 1999; **44**: 1155-1164
- Cardinale RM**, Benedict SH, Wu Q, Zwicker RD, Gaballa HE,

- Mohan R. A comparison of three stereotactic radiotherapy techniques: ARCS vs. noncoplanar fixed field fields vs. intensity modulation. *Int J Radiat Oncol Biol Phys* 1998; **42**: 431-436
- 21 **Bos LJ**, Damen EMF, de Boer RW, Mijnheer BJ, McShan DL, Fraass BA, Kessler ML, Lebeaque JV. Reduction of rectal dose by integration of the boost in the large-field treatment plan for prostate irradiation. *Int J Radiat Oncol Biol Phys* 2002; **52**: 254-265
- 22 **Wu Q**, Manning M, Schmidt-Ullrich R, Mohan R. The potential for sparing of parotids and escalation of biologically effective dose with intensity-modulated radiation treatments of head and neck cancers: A treatment design study. *Int J Radiat Oncol Biol Phys* 2000; **46**: 195-205
- 23 **Mohan R**, Wu Q, Manning M, Schmidt-Ullrich R. Radiobiological considerations in the design of fractionation strategies for intensity modulated radiation therapy of head and neck cancers. *Int J Radiat Oncol Biol Phys* 2000; **46**: 619-630
- 24 **Butler EB**, Teh BS, Grant WH 3rd, Uhl BM, Kuppersmith RB, Chiu JK, Donovan DT, Woo SY. SMART (simultaneous modulated accelerated radiation therapy) boost: a new accelerated fractionation schedule for the treatment of head and neck cancer with intensity modulated radiotherapy. *Int J Radiat Oncol Biol Phys* 1999; **45**: 21-32
- 25 **van't Riet A**, MaK ACA, Moerland MA, Elders LH, van der Zee W. A conformation number to quantify the degree of conformality in brachytherapy and external beam irradiation: application to the prostate. *Int J Radiat Oncol Biol Phys* 1997; **37**: 731-736
- 26 **Söderström S**, Brahme A. Which is the most suitable number of photon beam portals in coplanar radiation therapy? *Int J Radiat Oncol Biol Phys* 1995; **33**: 151-159
- 27 **Söderström S**, Brahme A. Small is beautiful-and often enough: In response to the editorial by Mohan and Ling. *Int J Radiat Oncol Biol Phys* 1996; **34**: 757-759
- 28 **Mohan R**, Ling CC. When becometh less more? (editorial). *Int J Radiat Oncol Biol Phys* 1995; **33**: 235-237
- 29 **Stein J**, Mohan R, Wang XH, Bortfeld T, Wu Q, Preiser K, Ling CC, Schlegel W. Number and orientations of beams in intensity-modulated radiation treatments. *Med Phys* 1997; **24**: 149-160
- 30 **Pirzkall A**, Carol MP, Pickett B, Xia P, Roach M 3rd, Verhey LJ. The effect of beam energy and number of fields on photon-based IMRT for deep-seated targets. *Int J Radiat Oncol Biol Phys* 2002; **53**: 434-442
- 31 **Tai P**, Van Dyk J, Yu E, Battista J, Schmid M, Stitt L, Tonita J, Coad T. Radiation treatment for cervical esophagus: patterns of practice study in Canada, 1996. *Int J Radiat Oncol Biol Phys* 2000; **47**: 703-712

Edited by Ren SY and Wang XL Proofread by Xu FM

Clinicopathologic features of surgically resected primary gastric lymphoma

Seong-Ho Kong, Min-A Kim, Do-Joong Park, Hyuk-Joon Lee, Hye-Seung Lee, Chul-Woo Kim, Han-Kwang Yang, Dae-Seog Heo, Kuhn-Uk Lee, Kuk-Jin Choe

Seong-Ho Kong, Do-Joong Park, Hyuk-Joon Lee, Han-Kwang Yang, Kuhn-Uk Lee, Kuk-Jin Choe, Department of Surgery, Seoul National University College of Medicine, Seoul, Korea
Min-A Kim, Hye-Seung Lee, Chul-Woo Kim, Department of Pathology, Seoul National University College of Medicine, Seoul, Korea
Do-Joong Park, Hyuk-Joon Lee, Han-Kwang Yang, Dae-Seog Heo, Cancer Research Institute, Seoul National University College of Medicine, Seoul, Korea
Chul-Woo Kim, Tumor Immunity Medical Research Center and Cancer Research Institute, Seoul National University College of Medicine, Seoul, Korea
Dae-Seog Heo, Department of Internal Medicine, Seoul National University College of Medicine, Seoul, Korea
Correspondence to: Han-Kwang Yang, MD., Department of Surgery and Cancer Research Institute, Seoul National University College of Medicine, 28 Yongon-dong, Chongno-gu, Seoul, 110-744, Korea. hkyang@plaza.snu.ac.kr
Telephone: +82-2-760-3797 **Fax:** +82-2-3672-0047
Received: 2003-09-09 **Accepted:** 2003-12-30

Abstract

AIM: To analyze the clinicopathologic characteristics of surgically resected gastric lymphoma patients.

METHODS: We retrospectively analyzed 57 surgically resected gastric lymphoma patients, dividing them into 2 subgroups: Low grade MALToma (the LG group), High grade MALToma and Diffuse large B cell lymphoma (the HG group).

RESULTS: The numbers of patients were: 20 in the LG group, 37 in the HG group. The diagnostic rate of gastroscopy was 34.8% at primary diagnosis and 50% including differential diagnoses. The positive rates of *H pylori* were similar between the 2 groups (68% vs 77%). Multiple lesions were found in 19.3%. The proportion of mucosal and submucosal lesions was 80.0%(16/20) in the LG group, and 24.3%(9/37) in the HG group ($P<0.001$). Lymph node invasion rates were 10.5%(2/19) in the LG group and 44.1%(15/34) in the HG group ($P=0.031$). The numbers of recurred patients were none in the LG group, and 8 in the HG group. By univariate analysis, group ($P=0.024$) and TNM stage (stage I, II vs stages III, IV, $P=0.002$) were found to be the significant risk factors. There was a tendency of higher recurrence rate in the subtotal gastrectomy group than in the total gastrectomy group ($P=0.50$).

CONCLUSION: The HG groups had a more advanced stage and a higher recurrence rate than the LG group. Although there was no difference between subtotal and total gastrectomies, more careful assessments of multiplicities and radical resections with lymph node dissections seem to be needed because of multiplicity and LN invasion even in LG group.

Kong SH, Kim MA, Park DJ, Lee HJ, Lee HS, Kim CW, Yang HK, Heo DS, Lee KU, Choe KJ. Clinicopathologic features of surgically

resected primary gastric lymphoma. *World J Gastroenterol* 2004; 10(8): 1103-1109
<http://www.wjgnet.com/1007-9327/10/1103.asp>

INTRODUCTION

Because primary gastric lymphoma has a tendency to be localized in the stomach for a long time, surgical resection remains an important treatment modality^[1-3]. *Helicobacter pylori* has been proposed to be an important cause of the formation of mucosa associated lymphoid tissue (MALT) and the development of subsequent lymphoma. About 80% of low grade MALT lymphomas were found to be cured by *H pylori* eradication alone, and there are some reports in which high grade MALT lymphoma was also cured in this manner^[4]. Recently, lymphoma related with MALT was classified as 'extra nodal marginal zone B cell lymphoma of mucosa-associated lymphoid tissue (MALT lymphoma)' by WHO^[5]. According to the report of Isaacson *et al.*^[6] in 1983, gastric lymphoma may be divided into low grade MALT lymphoma, high grade MALT lymphoma, and diffuse large B cell lymphoma. The aim of this study was to analyze the clinicopathologic characteristics of surgically resected gastric lymphoma patients according to the postoperative histopathologic grades.

MATERIALS AND METHODS

We enrolled 57 gastric lymphoma patients who had undergone operations at Seoul National University Hospital from January 1995 to July 2002.

Primary gastric lymphoma was often divided into 3 categories: low grade MALT lymphoma, high grade MALT lymphoma, and diffuse large B cell lymphoma. Low grade MALT lymphoma was diagnosed when the classic features of MALT lymphoma were evident. The classic features were lymphoid atypical cells and destruction of mucosal walls (lymphoepithelial lesion), and the presence of centrocyte-like cells, lymphoid follicles, monocyte-like B-cells, lymphoplasmic cell, centroblast-like cells, and Dutcher bodies^[7,8]. When these cells became larger and crowded, and the features of low grade MALT lymphoma were seen partly, such cases were classified as high grade MALT lymphoma. When portions of low grade MALT lymphoma were absent, they were classified as diffuse large B cell lymphoma. (Figure 1) But, it was often difficult to differentiate diffuse large B cell lymphoma from high grade MALT lymphoma because the histopathologic sections from postoperative specimens sometimes did not include the portions of the classic features of low grade MALT lymphoma which were present partly.

We divided the patients into 2 groups according to the post-operative pathologic reports, namely the LG group (low grade MALT lymphoma) and the HG group (high grade MALT lymphoma and diffuse large B cell lymphoma).

Sex, age, operative method, postoperative stage, number of lesions, and recurrence were reviewed retrospectively using

medical records and phone-call surveillance. For postoperative staging, both the TNM staging system for gastric adenocarcinoma and the Musshoff staging system (modified Ann-Arbor stages) were used (Table 1).

Clinicopathologic data were compared using the chi-square test and Fisher's exact test. Survival rates were calculated using the Kaplan-Meier method and analyzed using the log-rank test. *P*-values of less than 0.05 were considered statistically significant.

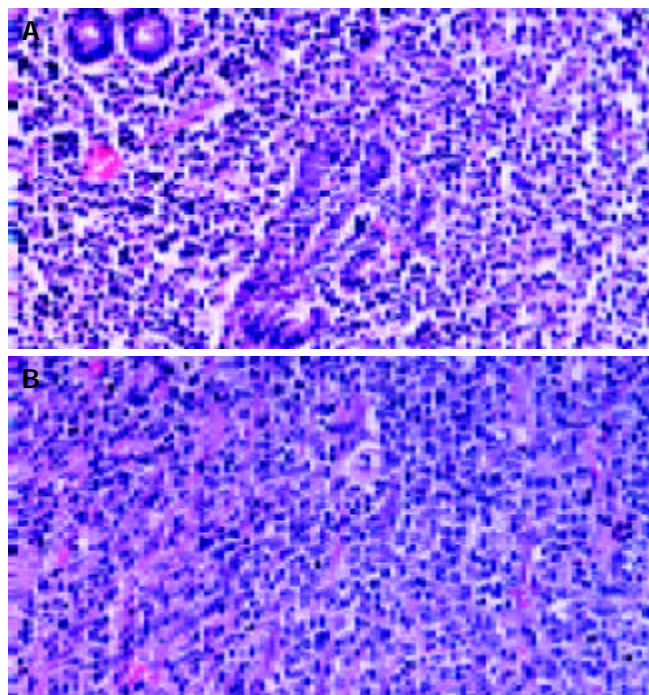


Figure 1 A: Low grade MALT lymphoma. Microphotograph showing proliferation of heterogeneous small B-cells, including marginal zone (centrocyte-like) cells, cells resembling monocytoid cells, small lymphocytes, and scattered immunoblast and centroblast-like cells. In epithelial tissue, neoplastic cells typically infiltrated the epithelium, forming lymphoepithelial lesions. B: Diffuse large B cell lymphoma. Microphotograph showing proliferation of large B lymphoid cells in a diffuse pattern. Tumor cells have a large and pleomorphic appearance with prominent nucleoli.

Table 1 Musshoff's modified Ann-Arbor stage

Stage	Definition
Ie	Involvement of a single extralymphatic organ or site ¹
Ie1	Involvement of mucosa or submucosa
Ie2	Involvement of more than submucosa
Ile	Involvement of two or more lymph node regions on the same side of the diaphragm with localized involvement of an extralymphatic organ and site ^{1,2}
Ile1	Involvement of regional lymph nodes
Ile2	Involvement of other lymph nodes beyond regional area
IIIe	Localized involvement of a single extralymphatic organ or site with involvement of lymph node regions on both sides of the diaphragm (IIIe) or involvement of the spleen (IIIe+s) or both (IIIe+s) ^{1,2}
IVe	Involvement of extranodal site(s) beyond that designated as "e" more than one extranodal deposit at any location, any involvement of liver or bone marrow ^{1,2}
E	localized, solitary involvement of extralymphatic tissue, excluding liver and bone marrow
1	Direct spread of a lymphoma into adjacent tissues or organs does not influence stage. Multifocal involvement of a single extralymphatic organ is classified as stage IE and not stage IV. Involvement of two or more segments of the gastrointestinal tract, isolated and not in continuity, is classified as stage IV (disseminated involvement of one or more extralymphatic organs).
2	The definitions of regional lymph nodes for individual sites of extranodal lymphomas are identical to the definitions of regional lymph nodes for individual sites of gastrointestinal carcinomas. For example, the regional lymph nodes for a primary gastric lymphoma are the perigastric nodes along the lesser and greater curvatures and the nodes located along the left gastric, common hepatic, splenic, and celiac arteries.

RESULTS

Clinical characteristics

The numbers of patients of the LG group and the HG group were 20(35.1%) and 37(64.9%), respectively. One patient had a synchronous gastric adenocarcinoma and low grade MALT lymphoma.

The male to female ratio was 1.11:1 (30:27) without any significant difference between the groups.

The mean age of the patients in the LG group was 52.6 years, and was 57.7 years in the HG group. There was no significant difference between the 2 groups. (*P*>0.05) (Table 2).

Table 2 Age and sex distribution of patients

	LG group	HG group	Total	<i>P</i> -value
<i>n</i> (%)	20 ¹ (35.1)	37 (64.9)	57	
Age (±SD)	52.6 (±11.4)	57.7 (±13.9)	55.9 (±13.2)	n.s.
Sex	10:10	20:17	30:27	n.s.
(M:F)	(1:1)	(1.18:1)	(1.11:1)	

LG group: patients with low grade MALT lymphoma, HG group: patients with high grade MALT lymphoma or diffuse large B cell lymphoma. ¹In 1 case: associated with AGC.

Table 3 Presenting symptoms and duration

Symptom	<i>n</i> (%)
Epigastric pain, discomfort	39 (68.4)
Gastrointestinal bleeding	9 (15.8)
Weight loss	9 (15.8)
Indigestion	7 (12.3)
Nausea/vomiting	4 (7.0)
Anorexia	4 (7.0)
Diarrhea	2 (3.5)
Others	3 (5.3)
No Symptom	6 (10.5)
Histopathology	Duration of symptom
LG group	11.9±24.9
HG group	5.2±9.0
Total	7.6±16.7 mo
<i>P</i> =n.s.	

Symptoms

Epigastric pain and discomfort were the most common symptoms. The duration of the symptoms of the LG group had a tendency to be longer than that of the HG group, but it was not statistically significant. Among B symptoms specific in lymphoma, only weight loss was found in 9 patients (15.8%), but fever and night sweats were not found. Moreover, the reason of weight loss was obscure, *i.e.*, as to whether it was a part of the B symptoms or a result of the gastrointestinal symptoms (Table 3).

Results of preoperative examination

Forty-six patients were enrolled whose records of preoperative gastroscopic findings were available. The accuracy of the primary diagnosis of lymphoma by preoperative gastroscopy was 34.8% (16/46), and the overall diagnosis rate including differential diagnosis was 50% (23/46) (Table 4).

There were 2 cases of adenocarcinoma in the preoperative pathologic reports. One was misdiagnosed as a adenocarcinoma and later diagnosed as a diffuse large B cell lymphoma postoperatively, and the other was a case of synchronous adenocarcinoma and lymphoma. The accuracy of histological grading of lymphoma with preoperative biopsy was 87.0% (40/46) as compared with the postoperative pathologic reports (Table 5).

To identify relationships with *H pylori*, a pathologic examination with or without a CLO test was used in 38 cases, the serology test (*H pylori* IgG) in 1 case, and both methods in 3 cases.

In our series, 73.8% (31/42) were related with *H pylori*. According to the groups, the positive rate of *H pylori* was 68.8% (11/16) in the LG group and 76.9% (20/26) in the HG group. There was no significant difference between the 2 groups.

Of the patients diagnosed as low grade MALT lymphoma, 5 patients took the regimen for *H pylori* eradication. Four patients had surgical resection later because of remnant lymphoma at follow-up gastroscopy, and 1 patient underwent the operation because of transformation to a higher grade.

Table 4 Preoperative endoscopic findings and diagnosis accuracy

	LG group (%)	HG group (%)	Total (%)
Lymphoma	6 (37.5)	10 (33.3)	16 (34.8)
AGC	4 (25.0)	17 (56.7)	21 (45.7)
EGC	5 (31.3)	2 (6.7)	7 (15.2)
Benign ulcer	1 (6.3)	1 (3.3)	2 (4.3)
Total	16 (100)	30 (100)	46 (100)
Dx. Rate	Lymphoma/total (%)		
Primary Dx	6/16 (37.5)	10/30 (33.3)	16/46 (34.8)
D/Dx	8/16 (50.0)	15/30 (50.0)	23/46 (50.0)

Dx: Diagnosis, D/Dx: Differential diagnosis.

Table 5 Comparison between gastroscopic biopsy and postoperative histopathology

Preop. \ Postop.	LG group (%)	HG group (%)	Total (%)
LG group	15 (78.9)	4 (21.1)	19 (100.0)
HG group	2 (7.4)	25 (92.6)	8 (100.0)
Total	17	29	46

Methods and results of operations

Subtotal gastrectomy was performed in 35 patients (61.4%), and total gastrectomy in 22 patients (39.6%), with no significant difference among the groups. Of these 22 patients, 7 also underwent splenectomy (Table 6).

In all groups, the lower third was the most common lymphoma

location, which occurred in 45.6% (26/57). If the patients with additional lesions in the upper or middle third were included, totally 54.4% (31/57) of patients had lesions in the lower third of the stomach. There was no significant difference between the groups (Table 7).

We used both staging systems, namely TNM stages and Musshoff stages (modified Ann-Arbor stages). Regardless of the staging system, patients in the LG group had more proportions of early lesions than those in HG group (Tables 8-9).

Table 6 Operation methods

	LG group (%)	HG group (%)	Total (%)
Subtotal gastrectomy	10 (50.0)	21 (56.8)	30 (52.6)
Other partial gastrectomy	2 (10.0)	3 (8.1)	5 (8.8)
Total gastrectomy	8 (40.0)	14 (37.8)	22 (38.6)
TG	7 (35.0)	8 (21.6)	15 (26.3)
TG + splenectomy	1 (5.0)	6 (16.2)	7 (12.3)
Total	20 (100)	37 (100)	57 (100)

P=n.s., TG: total gastrectomy.

Table 7 Location of lesions

	LG group (%)	HG group (%)	Total (%)
Lower 1/3	7 (35.0)	19 (51.4)	26 (45.6)
Middle 1/3	8 (40.0)	10 (27.0)	18 (31.6)
Upper 1/3	3 (15.0)	5 (13.5)	8 (14.0)
Lower + middle	2 (10.0)	2 (5.4)	4 (7.0)
Lower + upper	0 (0.0)	1 (2.7)	1 (1.8)
Total	20 (100)	37 (100)	57 (100)

Table 8 TNM stage

Stage	LG group (%)	HG group (%)	Total (%)
Ia (+ no residual)	15 (78.9)	7 (18.9)	22 (39.3)
Ib	3 (15.8)	12 (32.4)	15 (26.8)
II	0 (0.0)	11 (29.7)	11 (19.6)
IIIa	0 (0.0)	6 (16.2)	6 (10.7)
IV	1 (5.3)	1 (2.7)	2 (3.6)
Total	19 ¹ (100)	37 (100)	56 (100)

¹The information on the LN status of one patient (mucosal lesion) was not available among 20 low grade MALT lymphoma patients.

Table 9 Musshoff stage

Stage	LG group (%)	HG group (%)	Total (%)
Ie1 (+ no residual)	15 (78.9)	7 (18.9)	22 (39.3)
Ie2	2 (10.5)	15 (40.5)	17 (30.4)
Iie1	1 (5.3)	14 (37.8)	15 (26.8)
Iie2	1 (5.3)	1 (2.7)	2 (3.6)
Total	19 ¹ (100)	37 (100)	56 (100)

¹The information on the LN status of one patient (mucosal lesion) was not available among 20 low grade MALT lymphoma patients.

In the LG group, mucosal and submucosal lesions accounted for 80.0% (16/20), lesions invading into proper muscles accounted for 15.0% (3/20). In the HG group, the proportion of lesions within the submucosa was 24.3% (9/37), lesions in proper muscles and subserosal spaces were 62.2% (23/37), and lesions invading serosa were 8.1% (3/37).

In the HG group, one patient had the lesion invading the colon and pancreas, and one patient had a lymphoma directly invading the spleen and pancreas.

The LG group had a lower proportion of LN metastasis than the HG group. The number of patients who had regional LN invasion was 2 of 19 (10.5%, 1 submucosal lesion, 1 proper muscle lesion) in the LG group and 15 of 34(44.1%) in the HG group.

Multiple lesions were found in 11 patients (19.3%) according to the postoperative pathologic reports. In 2 cases, no lymphoma lesion was found in the postoperative specimens, one had a diffuse large B cell lymphoma which received preoperative chemotherapy (COPBLAM #6), and the other was diagnosed as low grade MALT lymphoma preoperatively who did not receive any special therapy before operation. There was no difference in the proportions of multiple lesions among the subgroups. In 11 patients with multiple lesions, 6 had subtotal gastrectomy, and the other 5 had total gastrectomy (Table 10).

Table 10 Number of lesions

Number	LG group (%)	HG group (%)	Total (%)
None or single	17 (85.0)	29 (83.3)	46 (80.7)
0	1 (5.0)	1 (2.7)	2 (3.5)
1	16 (80.0)	28 (75.7)	44 (77.2)
Multiple	3 (15.0)	8 (21.6)	11 (19.3)
2	1 (5.0)	7 (18.9)	8 (14.0)
6	0 (0.0)	1 (2.7)	1 (1.8)
Diffuse	2 (10.0)	0 (0.0)	2 (3.5)
Total	20 (100)	37 (100)	57 (100)

$P=n.s.$

Postoperative radiotherapy was indicated to those with remnant lesions in their resection margins. Two patients in the LG group and one in the HG group underwent radiotherapy, and remained alive at postoperative 13.5 mo, 66.3 mo, and 66.4 mo, respectively, without evidence of recurrence. Postoperative chemotherapy was applied to one patient with low grade MALT lymphoma invading the proper muscles and the regional LN. Twenty-four patients out of 32 patients (75.0%) in the HG group had postoperative chemotherapy. According to the Musshoff stage, only 1 patient of 19 stage Ie1 patients had postoperative chemotherapy. Ten of 15 stage Ie2 patients and 14 of 15 stage Iie patients received chemotherapy. In most cases, CHOP regimen (cyclophosphamide, doxorubicin, vincristine, prednisolone) was used.

Table 11 Characteristics of patients whose disease recurred

Sex/age	Op.	Loc.	Size(cm)	N	T	LN	Musshoff stage	Site of recurrence	DFS (mo)	Survival	OS (mo)
F/80	ST	LB	6x3	1	PM	8/26	Iie2	abdominal LN	0.4	Dead ¹	10.1
M/34	T	MB	8x2.5	1	PM	12/21	Iie1	abdominal LN, bone marrow	6.6	Dead	9.1
M/34	ST	MB	2.2x3	1	SS	0/60	Ie2	remnant stomach	7.6	Alive	57.2
F/59	ST	LB	4x3.5	1	SM	0/19	Ie1	paraaortic LN	10.4	Alive	13.4
M/85	ST	MB & LB	4x3	2	PM	0/64	Ie2	chest	18.2	Dead ²	42.0
F/55	T	HB	13x10	1	colon, pancreas	0/11	Ie2	abdominal LN	26.3	Dead	37.4
M/67	ST	LB	10x8	1	SS	16/53	Iie1	cervical LN	26.8	Dead ³	31.6
M/70	ST	MB	3x2	2	SM	5/19	Iie1	unknown ³	70.4	Dead	70.6

1.5x0.8

Op. : operation method, (ST: subtotal gastrectomy, T: total gastrectomy), Loc: location (LB: lower body, MB: midbody, HB: high body), T: T-stage (SM: submucosa, PM: proper muscle, SS: subserosa), LN: lymph nodes(positive nodes/resected nodes), DFS: disease free survival, OS: overall survival, ¹: pneumonia, ²: medullary infarct, ³: diagnosed in other hospital. Recurred site is uncertain.

Recurrence and risk factors

Patients were followed up for a mean 75.8 mo. Eight cases had recurrence, no patient in the LG group and 8 patients (21.6%) in the HG group (Table 11).

The locations of the recurrence were the remnant stomach in 1 case, and the intraabdominal lymph nodes in 4 cases. In the other case, the location was presumed to be the intraabdominal area. One case had a recurred lesion in the thorax, and another case in the neck.

Six of 8 patients with recurred diseases died. One died of pneumonia during chemotherapy for a recurred lymphoma, and another died of brain infarct of unknown etiology. The other 4 patients died of recurred disease progression.

Grades ($P=0.024$), TNM stages (stages I, II vs stages III, IV, $P=0.002$) were found to be risk factors by univariate analysis. Otherwise, age, sex, size of lesion, depth of invasion, lymph node metastasis, and the presence of multiple lesions, were all unrelated to recurrence (Figures 2, 3). Patients with Musshoff stage Iie lymphoma showed a tendency of lower 5 years disease-free survival rate than those with stage Ie lymphoma (87.1% vs 76.1%, $P=0.139$), but it was not significant. None of stage Ie patients in LG group had recurrence, but 4 of stage Ie HG group patients had recurrence (5-year disease-free survival rate 100% vs 77.9%, $P=0.080$).

The recurrence rate in the subtotal gastrectomy group (17.1%, 6/35) was slightly higher than that in the total gastrectomy group (9.1%, 2/22). In the HG group, the recurrence rate was 28.6%(6/21) in those with subtotal gastrectomy and 15.4%(2/13) in those with total gastrectomy. But it was not significant ($P=0.50$).

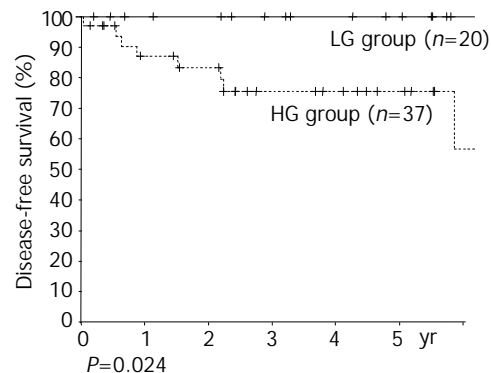


Figure 2 Disease free survival curve according to histopathology (LG group : low grade MALT lymphoma, HG group : high grade MALT lymphoma and diffuse large B cell lymphoma).

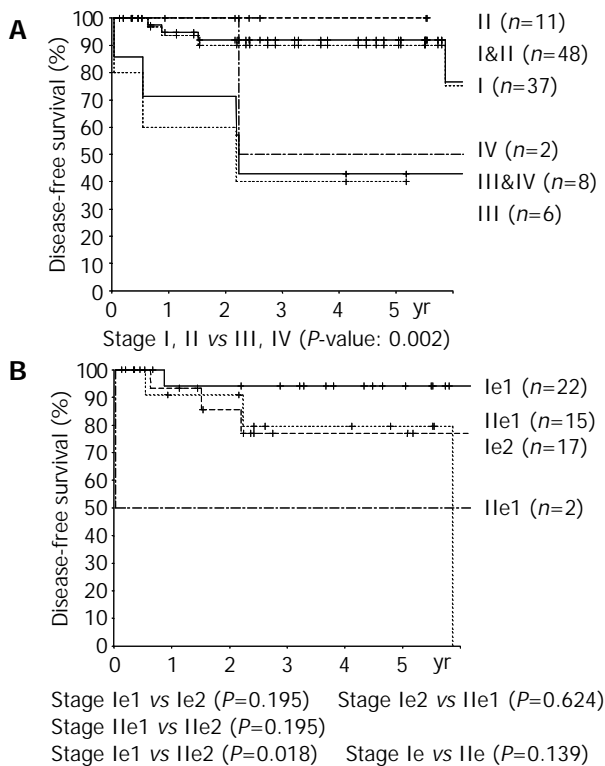


Figure 3 A: Disease free survival curves according to TNM stage, B: Disease free survival curves according to Musshoff stage.

DISCUSSION

The stomach is the most common intraabdominal organ for extralymphatic lymphoma in the abdominal cavity, about 20% of extralymphatic lymphomas occur in the stomach. Normally, the stomach has no lymphatic tissue in the mucosa or submucosa. The formation of MALT has been known to be related with *H pylori* and some autoimmune diseases^[9,10]. In our study, the proportion of patients with evidences of *H pylori* was 73.8% overall, and 68.8% in the low grade MALT lymphoma group. This result corresponded with the results of Paik *et al.*^[11] in Korea, but the figures were slightly lower than the 70-90% obtained elsewhere^[12]. The ratio of males to females was 1.11:1. Compared to other results in which the male to female ratios were 1.7:1-2:1, our result showed a higher proportion of female patients.

Some genetic abnormalities such as t(11:18)(q21:q21) have been discovered to be related with the process of MALT lymphoma formation by *H pylori*. t(11:18) existed in about 18-50% of MALT lymphomas. Liu *et al.*^[13] reported that low grade MALT lymphoma with t(11:18) was more resistant to *H pylori* eradication regimens. Remstein *et al.*^[14] reported that low grade MALT lymphoma without t(11:18) tended to have t(1:14) or to show aneuploidy. Moreover, abnormal manifestations of bcl-6, some trisomies (including trisomy 3), abnormality of P53, and hypermethylation of P15 or P16 are also thought to be related to the formation of MALT lymphoma. Thus, there might be several pathways to the formation of MALT lymphoma^[15].

Cabras *et al.*^[16] advocated multiple pathways to high grade transformation. The time taken for high grade transformation was estimated at about 10 years by Yoshino *et al.*^[17], which was not definite with our study. On the other hand, there were 4 cases in our study who had been diagnosed as low grade MALT lymphoma by preoperative gastroscopy, and they were diagnosed as higher grade lymphoma after *H pylori* eradication or surgery. So, there is a possibility that high grade transformations were observed within a few months.

We could spare the time and cost of attempting to eradicate *H pylori*, if we knew the characteristics of the group whose

diseases were resistant to *H pylori* eradication therapies and tended to transform to higher grades. Currently, t(11:18), *H pylori* with Cag A(+), invasion deeper than the submucosal layer by endoscopic ultrasonography, and lymph node metastasis have been reported to be risk factors of resistance^[18]. However, in our series, all 5 patients whose lymphoma invaded the submucosal layer without lymph node metastasis failed *H pylori* eradication and underwent operation, demonstrating the need for further studies on the risk factors involved.

Misdiagnoses could be made in patients with higher grade MALT lymphoma or diffuse large B cell lymphoma once diagnosed as low grade MALT lymphoma preoperatively. Strecker *et al.*^[19] reported that the accurate diagnostic rate with grade differentiation was 73% even in the large medical institutes because of the limitations of the small, partial biopsy samples produced by gastroscopic procedures. In our study also, 87% showed the same diagnosis and the same grade before and after operation.

Likewise, among the 19 patients once diagnosed as diffuse large B cell lymphoma preoperatively, 4(21.1%) were diagnosed as high grade MALT lymphoma because the portions of the classic features of low grade MALT lymphoma were found postoperatively. Even more, the histopathologic sections from postoperative specimens could miss the portions of the classic features of low grade MALT lymphoma which were present partly, too. This is the reason why we categorized both diffuse large B cell lymphoma and high grade MALT lymphoma patients into one group.

Eck *et al.*^[20] proposed complementary serology testing to confirm the relationship with *H pylori*, because positive results by serologic tests are obtained even in *H pylori*-negative patients by gastroscopic biopsy. We checked 4 cases in which serology testing was performed. Three patients were also positive by biopsy, but one patient had a positive serologic result despite a negative finding by gastroscopic biopsy.

Recently, some have suggested non-operative methods such as *H pylori* eradication, chemotherapy, or radiotherapy as the primary therapeutic strategies instead of surgery^[21,22]. Whereas in our study only 3 patients with remnant tumor in the resection margin undertook radiotherapy, Schechter *et al.*^[23] reported the complete resolution of 17 cases of MALT lymphomas in stages I and II with radiotherapy. The German multicenter study GIT NHL 01/92 in 2001 reported no significant difference in the survival or recurrence rates between 79 patients who had surgery alone or surgery with adjuvant chemotherapy and 106 patients who had chemotherapy alone^[24].

Investigators who suggested that chemotherapy was the primary strategy believed that there was no difference in the survival rates of surgical resection and chemotherapy, and that those who did not receive radical resection showed significant lower survival rates, and that chemotherapy can reduce the size of a lesion and make the surgery easier, even when it failed to effect a complete cure.

On the other hand, surgical resection as the primary therapy allowed the accurate staging of the lymphoma. Besides, in those patients with serious complications such as perforation and bleeding, surgical procedure became more difficult due to the fragile gastric wall, and the higher risk of postoperative complications. Moreover, peritoneal seeding could theoretically occur via the perforated gastric wall^[1-3,25].

We found that the proportion of patients with multiple lesions was 19.3%. In addition, cases in which the MALT lymphoma had spread along the mucosal layer to the esophagus or the duodenum were also reported. In the *H pylori* infected stomach, it is well known that gastric mucosa other than MALT lymphoma lesions, may have B cell monoclonality. Even after *H pylori* eradication therapy, it has been reported that about 50% of patients had B cell monoclonality in their gastric mucosa

[26,27]. It is not certain that this B cell monoclonality reflects the presence of a remnant or pre-malignant lesion. But if B cell monoclonality is a true pre-malignant lesion, we would rather perform total gastrectomy to completely remove possible malignant lesions.

In the clinical setting, some debates exist about the results of subtotal and total gastrectomies. Kodera *et al.*^[28] showed that there was no difference in the survival rates of 45 patients with subtotal gastrectomy and 37 patients with total gastrectomy among 82 patients with primary gastric lymphoma in stages I and II. Similar results were reported by Rodriguez-Sanjuan *et al.*^[29], and by Colucci *et al.*^[30]. Bozer *et al.*^[31] reported better survival rates in 13 patients with stages I and II primary gastric lymphoma who received total gastrectomy than in 24 patients who underwent subtotal gastrectomy. However, they mentioned the possibility of more complete lymph node dissection in the total gastrectomy group.

In the past, concurrent splenectomy and multiple lymph node biopsies were recommended for staging. But, the local spreading characteristics of primary gastric lymphoma make the splenectomy unnecessary if the spleen is not invaded. These characteristics sometimes make it reasonable to use the TNM staging systems instead of Ann-Arbor staging. There are some controversies on the necessity of multiple intraoperative lymph node biopsy. Chang *et al.*^[32] reported that about 40% of low grade lymphomas limited within the submucosal layer had lymph node metastasis. Our series also had 2 low grade lymphoma patients with lymph node metastasis, and 2 of HG group who had no lymph node metastasis (stage Ie) recurred in the intraabdominal lymph nodes. Only 1 patient among those with recurred diseases had recurred lesions in the remnant stomach, and the majority of them had their recurred lesions in lymph nodes. So, wide lymph node dissection must be performed, and additional biopsy for suspicious lymph nodes is recommended.

Therefore, subtotal gastrectomy can be performed safely with sufficient lymph node dissection, but sufficient preoperative searching for multiple lesions by gastroscopy or endoscopic ultrasonography is required, and close postoperative follow-up should be emphasized.

We could not find a definite relationship between the stages and the disease-free-survival rate, because of the small size of the objectives and a high proportion of recurred patients with lymph node negative lymphoma. One of them having a 13 cm×10 cm lymphoma directly invading colon and pancreas was classified as Musshoff stage Ie, and contributed to a high proportion of stage Ie patients in all recurred ones. All the recurred patients in stage-Ie were of HG group and none of LG group had recurred, even though it showed no significant differences. Most of them underwent sufficient lymph node dissection (D2), and the number of dissected lymph nodes was 64, 60, 19, 11, respectively. It implies that high grade lymphoma is more aggressive and has a greater possibility of systemic features than low grade lymphoma, even in early stage.

In conclusion, the majority of patients with low grade MALT lymphoma had early stage disease, which is curable by surgery only. The proportions of advanced diseases that need additional chemotherapy, and the proportions of recurred patients were lower in the LG group than in the HG group. The risk factors of recurrence were pathologic grade and TNM stage. Among the patients with recurred lymphoma, the number of patients who had subtotal gastrectomy was somewhat greater than the number of patients who had total gastrectomy, even though it was not significant. The existence of multiple lesions or lymph node metastasis even in low grade MALT lymphoma emphasizes the need for more thorough preoperative diagnosis, radical surgical resection with lymph node dissection, and careful postoperative follow-up.

REFERENCES

- 1 **Vaillant JC**, Ruskone-Fourmestreaux A, Aegerter P, Gayet B, Rambaud JC, Valleur P, Parc R. Management and long-term results of surgery for localized gastric lymphomas. *Am J Surg* 2000; **179**: 216-222
- 2 **Bartlett DL**, Karpeh MS Jr, Filippa DA, Brennan MF. Long-term follow-up after curative surgery for early gastric lymphoma. *Ann Surg* 1996; **223**: 53-62
- 3 **Salvagno L**, Soraru M, Busetto M, Puccetti C, Sava C, Endrizzi L, Giusto M, Aversa S, Chiarion Sileni V, Polico R, Bianco A, Rupolo M, Nitti D, Doglioni C, Lise M. Gastric non-Hodgkin's lymphoma: analysis of 252 patients from a multicenter study. *Tumori* 1999; **85**: 113-121
- 4 **Morgner A**, Miehle S, Stolte M, Neubauer A, Alpen B, Thiede C, Klann H, Hierlmeier FX, Ell C, Ehninger G, Bayerdorffer E. Development of early gastric cancer 4 and 5 years after complete remission of *Helicobacter pylori* associated gastric low-grade marginal zone B-cell lymphoma of MALT type. *World J Gastroenterol* 2001; **7**: 248-253
- 5 **Harris NL**, Jaffe ES, Diebold J, Flandrin G, Muller-Hermelink HK, Vardiman J, Lister TA, Bloomfield CD. The World Health Organization classification of neoplasms of the hematopoietic and lymphoid tissues: report of the Clinical Advisory Committee meeting—Airlie House, Virginia, November, 1997. *Hematol J* 2000; **1**: 53-66
- 6 **Isaacson P**, Wright DH. Malignant lymphoma of mucosa-associated lymphoid tissue. A distinctive type of B-cell lymphoma. *Cancer* 1983; **52**: 1410-1416
- 7 **Cheng H**, Wang J, Zhang CS, Yan PS, Zhang XH, Hu PZ, Ma FC. Clinicopathologic study of mucosa-associated lymphoid tissue lymphoma in gastroscopic biopsy. *World J Gastroenterol* 2003; **9**: 1270-1272
- 8 **Zhou Q**, Xu TR, Fan QH, Zhen ZX. Clinicopathologic study of primary intestinal B cell malignant lymphoma. *World J Gastroenterol* 1999; **5**: 538-540
- 9 **Xue FB**, Xu YY, Wan Y, Pan BR, Ren J, Fan DM. Association of *H pylori* infection with gastric carcinoma: a Meta analysis. *World J Gastroenterol* 2001; **7**: 801-804
- 10 **Stolte M**, Bayerdorffer E, Morgner A, Alpen B, Wundisch T, Thiede C, Neubauer A. *Helicobacter* and gastric MALT lymphoma. *Gut* 2002; **50**(Suppl 3): III19-24
- 11 **Paik KY**, Noh JH, Heo JS, Sohn TS, Choi SH, Joh JW, Kim S, Kim YI. Clinical analysis of MALT lymphoma in the stomach. *J Korean Surg Soc* 2002; **62**: 468-471
- 12 **Nakamura S**, Yao T, Aoyagi K, Lida M, Fujishima M, Tsuneyoshi M. *Helicobacter pylori* and primary gastric lymphoma. A histopathologic and immunohistochemical analysis of 237 patients. *Cancer* 1997; **79**: 3-11
- 13 **Liu H**, Ruskone-Fourmestreaux A, De Jong D, Pileri S, Thiede C, Lavergne A, Boot H, Caletti G, Wundisch T, Molina T, Taal BG, Elena S, Thomas T, Zinzani PL, Neubauer A, Stolte M, Hamoudi RA, Dogan A, Isaacson PG, Du MQ. T(11;18) is a marker for all stage gastric MALT lymphomas that will not respond to *H pylori* eradication. *Gastroenterology* 2002; **122**: 1286-1294
- 14 **Remstein ED**, Kurtin PJ, James CD, Wang XY, Meyer RG, Dewald GW. Mucosa-associated lymphoid tissue lymphomas with t(11;18)(q21;q21) and mucosa-associated lymphoid tissue lymphomas with aneuploidy develop along different pathogenetic pathways. *Am J Pathol* 2002; **161**: 63-71
- 15 **Du MQ**, Isaacson PG. Gastric MALT lymphoma: from aetiology to treatment. *Lancet Oncol* 2002; **3**: 97-104
- 16 **Cabras AD**, Weirich G, Fend F, Nahrig J, Bordi C, Hofler H, Werner M. Oligoclonality of a "composite" gastric diffuse large B-cell lymphoma with area of marginal zone B-cell lymphoma of the mucosa-associated lymphoid tissue type. *Virchows Arch* 2002; **440**: 209-214
- 17 **Yoshino T**, Omonishi K, Kobayashi K, Mannami T, Okada H, Mizuno M, Yamadori I, Kondo E, Akagi T. Clinicopathological features of gastric mucosa associated lymphoid tissue (MALT) lymphomas: high grade transformation and comparison with diffuse large B cell lymphomas without MALT lymphoma features. *J Clin Pathol* 2000; **53**: 187-190
- 18 **Ruskone-Fourmestreaux A**, Lavergne A, Aegerter PH, Megraud F, Palazzo L, de Mascarel A. Predictive factors of regression of

- gastric MALT lymphoma after anti-*Helicobacter pylori* treatment. *Gut* 2001; **48**: 290-292
- 19 **Strecker P**, Eck M, Greiner A, Kolve M, Schmausser B, Marx A, Fischbach W, Fellbaum C, Muller-Hermelink HK. Diagnostic value of stomach biopsy in comparison with surgical specimen in gastric B-cell lymphoma of the MALT type. *Pathologie* 1998; **19**: 209-213
- 20 **Eck M**, Greiner A, Schmausser B, Eck H, Kolve M, Fischbach W, Strecker P, Muller-Hermelink HK. Evaluation of *Helicobacter pylori* in gastric MALT-type lymphoma: difference between histologic and serologic diagnosis. *Mod Pathol* 1999; **12**: 1148-1151
- 21 **Tondini C**, Balzarotti M, Santoro A, Zanini M, Fornier M, Giardini R, Di Felice G, Bozzetti F, Bonadonna G. Initial chemotherapy for primary resectable large-cell lymphoma of the stomach. *Ann Oncol* 1997; **8**: 497-499
- 22 **Thieblemont C**, Dumontet C, Bouafia F, Hequet O, Arnaud P, Espinouse D, Felman P, Berger F, Salles G, Coiffier B. Outcome in relation to treatment modalities in 48 patients with localized gastric MALT lymphoma: a retrospective study of patients treated during 1976-2001. *Leuk Lymphoma* 2003; **44**: 257-262
- 23 **Schechter NR**, Portlock CS, Yahalom J. Treatment of mucosa-associated lymphoid tissue lymphoma of the stomach with radiation alone. *J Clin Oncol* 1998; **16**: 1916-1921
- 24 **Koch P**, del Valle F, Berdel WE, Willich NA, Reers B, Hiddemann W, Grothaus-Pinke B, Reinartz G, Brockmann J, Temmesfeld A, Schmitz R, Rube C, Probst A, Jaenke G, Bodenstern H, Junker A, Pott C, Schultze J, Heinecke A, Parwaresch R, Tiemann M. German Multicenter Study Group. Primary Gastrointestinal Non-Hodgkin's Lymphoma: II. Combined surgical and conservative or conservative management only in localized gastric lymphoma-Results of the Prospective German Multicenter Study GIT NHL 01/92. *J Clin Oncol* 2001; **19**: 3874-3883
- 25 **Kodera Y**, Yamamura Y, Nakamura S, Shimizu Y, Torii A, Hirai T, Yasui K, Morimoto T, Kato T, Kito T. The role of radical gastrectomy with systematic lymphadenectomy for the diagnosis and treatment of primary gastric lymphoma. *Ann Surg* 1998; **227**: 45-50
- 26 **Alpen B**, Thiede C, Wundisch T, Bayerdorffer E, Stolte M, Neubauer A. Molecular diagnostics in low-grade gastric marginal zone B-cell lymphoma of mucosa-associated lymphoid tissue type after *Helicobacter pylori* eradication therapy. *Clin Lymphoma* 2001; **2**: 103-108
- 27 **Thiede C**, Wundisch T, Alpen B, Neubauer B, Morgner A, Schmitz M, Ehninger G, Stolte M, Bayerdorffer E, Neubauer A. German MALT Lymphoma Study Group. Long-term persistence of monoclonal B cells after cure of *Helicobacter pylori* infection and complete histologic remission in gastric mucosa-associated lymphoid tissue B-cell lymphoma. *J Clin Oncol* 2001; **19**: 1600-1609
- 28 **Kodera Y**, Nakamura S, Yamamura Y, Shimizu Y, Torii A, Hirai T, Yasui K, Morimoto T, Kato T. Primary gastric B cell Lymphoma: audit of 82 cases treated with surgery and classified according to the concept of mucosa-associated lymphoid tissue lymphoma. *World J Surg* 2000; **24**: 857-862
- 29 **Rodriguez-Sanjuan JC**, Alvarez-Canas C, Casado F, Garcia-Castrillo L, Casanova D, Val-Bernal F, Naranjo A. Results and prognostic factors in stage I(E)-II(E) primary gastric lymphoma after gastrectomy. *J Am Coll Surg* 1999; **188**: 296-303
- 30 **Colucci G**, Naglieri E, Maiello E, Marzullo F, Caruso ML, Leo S, Pellicchia A, Cramarossa A, Timurian A, Prete F. Role of prognostic factors in the therapeutic strategy of primary gastric non Hodgkin's lymphomas. *Clin Ter* 1998; **149**: 25-30
- 31 **Bozer M**, Eroglu A, Ünal E, Eryavuz Y, Kocaoglu K, Demirci S. Survival after curative resection for stage IE and IIE primary gastric lymphoma. *Hepatogastroenterol* 2001; **48**: 1202-1205
- 32 **Chang DK**, Chin YJ, Kim JS, Jung HC, Kim CW, Song IS, Kim CY. Lymph node involvement rate in low-grade gastric mucosa-associated lymphoid tissue lymphoma-too high to be neglected. *Hepatogastroenterol* 1999; **46**: 2694-2700

Edited by Wang XL and Xu FM

c-Jun N-terminal kinase is required for vitamin E succinate-induced apoptosis in human gastric cancer cells

Kun Wu, Yan Zhao, Gui-Chang Li, Wei-Ping Yu

Kun Wu, Yan Zhao, Gui-Chang Li, Department of Nutrition and Food Hygiene, Public Health School, Harbin Medical University, Harbin 150001, Heilongjiang Province, China

Wei-Ping Yu, Genetics Institute, Texas University of USA, Austin, USA

Supported by National Natural Science Foundation of China, No. 39870662

Correspondence to: Professor Kun Wu, Department of Nutrition and Food Hygiene, Public Health School, Harbin Medical University, Harbin 150001, Heilongjiang Province, China. wukun@public.hr.hl.cn

Telephone: +86-451-3648665

Received: 2003-06-06 **Accepted:** 2003-07-30

Abstract

AIM: To investigate the roles of c-Jun N-terminal kinase (JNK) signaling pathway in vitamin E succinate-induced apoptosis in human gastric cancer SGC-7901 cells.

METHODS: Human gastric cancer cell lines (SGC-7901) were treated with vitamin E succinate (VES) at 5, 10, 20 mg/L. Succinic acid and vitamin E were used as vehicle controls and condition medium only as an untreated (UT) control. Apoptosis was observed by 4', 6-diamidino-2'-phenylindole dihydrochloride (DAPI) staining for morphological changes and by DNA fragmentation for biochemical alterations. Western blot analysis was applied to measure the expression of JNK and phosphorylated JNK. After the cells were transiently transfected with dominant negative mutant of JNK (DN-JNK) followed by treatment of VES, the expression of JNK and c-Jun protein was determined.

RESULTS: The apoptotic changes were observed after VES treatment by DNA fragmentation. DNA ladder in the 20 mg/L VES group was more clearly seen than that in 10 mg/L VES group and was not detected following treatment of UT control, succinate and vitamin E. VES at 5, 10 and 20 mg/L increased the expression of p-JNK by 2.5-, 2.8- and 4.2-fold, respectively. VES induced the phosphorylation of JNK beginning at 1.5 h and produced a sustained increase for 24 h with the peak level at 12 h. Transient transfection of DN-JNK blocked VES-triggered apoptosis by 52%. DN-JNK significantly increased the level of JNK, while decreasing the expression of VES-induced c-Jun protein.

CONCLUSION: VES-induced apoptosis in human gastric cancer SGC-7901 cells involves JNK signaling pathway via c-Jun and its downstream transcription factor.

Wu K, Zhao Y, Li GC, Yu WP. c-Jun N-terminal kinase is required for vitamin E succinate-induced apoptosis in human gastric cancer cells. *World J Gastroenterol* 2004; 10(8): 1110-1114 <http://www.wjgnet.com/1007-9327/10/1110.asp>

INTRODUCTION

Vitamin E is characterized as a fat-soluble membrane antioxidant^[1-3]. RRR- α -tocopheryl succinate (vitamin E succinate, VES), a

derivative of natural vitamin E, does not possess antioxidant properties unless succinate group is hydrolyzed by specific ester hydrolase. VES has been shown to be a potent growth inhibitor of a variety of malignant cell types *in vitro* and *in vivo*, including avian lymphoid cells^[4], murine B16 melanoma cells^[5] and EL4 T lymphoma cells^[6,7], human monoblastic leukemia cells^[8], prostate^[9,10], breast^[11-13] and gastric cancer cells^[14,15]. VES has also been shown to suppress tumorigenesis in hamster buccal pouch^[16], mouse forestomach^[17] and mammary gland^[18]. These antitumor effects seem to be selective for tumor cells since VES treatment is not toxic to normal cell lines^[11,19].

The molecular basis or mechanism for the growth inhibition activity of VES remains unclear, but it could be attributed to G1 cell cycle blockage^[11,20], DNA synthesis arrest^[4,7,21], increased expression of biologically active transforming growth factor- β s (TGF- β s) and their type II cell surface receptors^[4,22], the induction of differentiation^[23,24] and apoptosis^[21,25,26]. VES is a potent inducer of apoptosis in human gastric cancer cells and it appears that at least two signaling pathways to trigger apoptosis may be involved. One of the previous studies in our laboratory have demonstrated that VES activates biologically active TGF- β and then TGF- β increases the kinase activity of c-Jun N-terminal kinase (JNK) followed by phosphorylation of c-Jun, and finally activated c-Jun triggers apoptosis in human gastric cancer cells^[27]. The other shows that one of the death receptors, Fas plays an important role in VES-induced apoptosis, in that Fas activates Caspase-8 leading to a proteolytic cascade of Caspases through FADD^[28].

It is well established that apoptosis or programmed cell death plays a pivotal role in the development and homeostasis of metazons by eliminating superfluous or unwanted cells^[29-35]. Signals in response to stimulus-induced apoptosis or cellular stress affect the activity of transcription factors via several distant signal transduction pathways^[36-38]. It is becoming clear that members of mitogen-activated protein kinase (MAPK) family have been shown to mediate almost all the cellular processes from gene expression to cell death^[39-42]. In this study, we chose human gastric cancer cell line SGC-7901 as a model for VES-induced apoptosis. The roles of JNK, a member of MAPK family, were determined to further investigate the mechanism of VES-mediated growth inhibition of human gastric cancer cells.

MATERIALS AND METHODS

Materials

VES was purchased from Sigma Co. Ltd. RPMI 1 640 media, L₁POFECTAMINE PLUSTM reagent and prestained protein marker were purchased from Gibco BRL, 4', 6-diamidino-2'-phenylindole dihydrochloride (DAPI) from Roche Diagnostics Co. Proteinase K from Merck Co. JNK and GAPDH rabbit polyclonal antibodies, dominant negative mutant construct of JNK were gifts from Dr. Bob G Sanders and Dr. Kimberly Kline (University of Texas, Austin, USA). Phospho-JNK mouse monoclonal and c-Jun (H79) rabbit polyclonal antibody were from Santa Cruz Biotechnologies.

Methods

Cell culture Human gastric cancer cell line SGC-7901 was maintained in RPMI 1 640 medium supplemented with 100 mL/L fetal calf serum (FCS), 100 kU/L penicillin, 100 mg/L streptomycin and 2 mmol/L L-glutamine under 50 mL/L CO₂ in a humidified incubator at 37 °C. SGC-7901 cells were incubated for different periods in the presence of VES at 5, 10 and 20 mg/L (VES was dissolved in absolute ethanol and diluted in RPMI 1 640 complete condition medium correspondingly to a final concentration of VES and 1 mL/L ethanol). Both succinic acid and vitamin E dissolved in ethanol were used as vehicle controls and condition medium only was used as an untreated (UT) control.

DAPI staining and apoptotic evaluation Cells were treated with VES at 20 mg/L for 48 h, then harvested, washed with PBS and stained with 2 mg/L DAPI in 1 000 mL/L methanol for 30 min at 37 °C. Cells were viewed using a fluorescence microscope with ultraviolet (UV) excitation at 300-500 nm. Cells with nuclei containing clearly condensed chromatin or cells with fragmented nuclei were scored as apoptotic.

DNA fragmentation assay DNA fragmentation was determined by extraction of DNA followed by electrophoresis. In brief, cells were collected in an Eppendorf tube and washed twice with PBS. Cells were incubated for 1 h at 37 °C in 0.5 mL of extraction buffer containing 10 mmol/L Tris·Cl (pH 8.0), 0.1 mol/L EDTA, 20 mg/L trypsin and 5 g/L SDS. The mixture was reincubated with 20 g/L proteinase K for 3 h at 50 °C. An equal volume of buffer saturated phenol was added and the extracted DNA was collected by centrifugation at 5 000 r/min for 15 min at room temperature. DNA was precipitated by the addition of sodium acetate and absolute ethanol. DNA was dissolved in TE buffer and electrophoresed in 10 g/L agarose gel containing ethidium bromide and photographed under UV light.

Western blot analysis SGC-7901 cells treated with VES were harvested, washed with PBS and lysed in lysis buffer (150 mmol/L NaCl, 1 mL/L NP-40, 5 mg/L sodium deoxycholate, 1 g/L SDS, 50 mmol/L Tris (pH 7.4), 1 mmol/L DTT, 0.5 mmol/L Na₃VO₄, 10 mmol/L phenylmethylsulfonyl fluoride (PMSF), 10 mg/L trypsin, 10 mg/L aprotinin and 5 mg/L leupeptin). Following the centrifugation of 12 000 g for 30 min at 4 °C, the amount of protein in the supernatant was determined using Biorad DC protein assay. Equal amounts of protein were separated on 100 g/L SDS-PAGE and transferred to different nitrocellulose filters (Gibco BRL, USA) overnight. Blocked with 50 g/L defatty milk, the individual filters were initially incubated with JNK, or with c-Jun, or with GAPDH rabbit polyclonal antibodies, or with phospho-JNK monoclonal antibody and then all were incubated again with horseradish peroxidase-conjugated IgG. Afterwards DAB was added to develop the filters.

Transient transfection SGC-7901 cells were washed twice with serum-free medium without antibiotics and incubated for 3 h in 2 mL of serum-free medium containing 30 µL of LIPOFECT-AMINE reagent and 2 µg of dominant negative JNK or JNK vector. After 3 h, the cells were treated with VES.

RESULTS

VES induced apoptosis in SGC-7901 cells

SGC-7901 cells were cultured for 48 h and collected, and DNA was extracted. Gel electrophoresis of DNA extracted from cells after exposure to UT control, succinate, vitamin E and VES is shown in Figure 1. Fragmentation of chromosomal DNA characterized as a DNA ladder was observed following exposure to VES at 10 and 20 mg/L. DNA ladder in 20 mg/L VES group was more clearly seen than that in 10 mg/L VES group. However, DNA ladder was not detected following treatment of UT control, succinate and vitamin E. These results suggested that VES induced human gastric cancer SGC-7901 cells to undergo apoptosis.

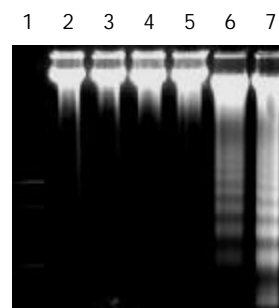


Figure 1 VES induced apoptosis by DNA fragmentation in SGC-7901 cells. Lane 1: Molecular weight marker; Lane 2: UT control; Lane 3: succinate; Lane 4: vitamin E; Lane 5: VES at 5 mg/L; Lane 6: VES at 10 mg/L; Lane 7: VES at 20 mg/L.

Effects of VES at different doses on phosphorylation of JNK

The expression of phospho-JNK (p-JNK) and JNK1/2 in the whole-cell lysates from UT control, succinate, vitamin E and VES-treated cells for 24 h was determined using Western blot analysis. The results revealed that VES increased the expression of p-JNK in an obvious dose-effect relationship. The levels of p-JNK protein in VES-stimulated cells at 5, 10 and 20 mg/L were increased by 2.5-, 2.8- and 4.2-fold over those in UT control-treated cells, respectively (Figure 2A, top panel; Figure 2B). The expression of JNK1/2 among different groups was not significantly different (Figure 2A, bottom panel; Figure 2B).

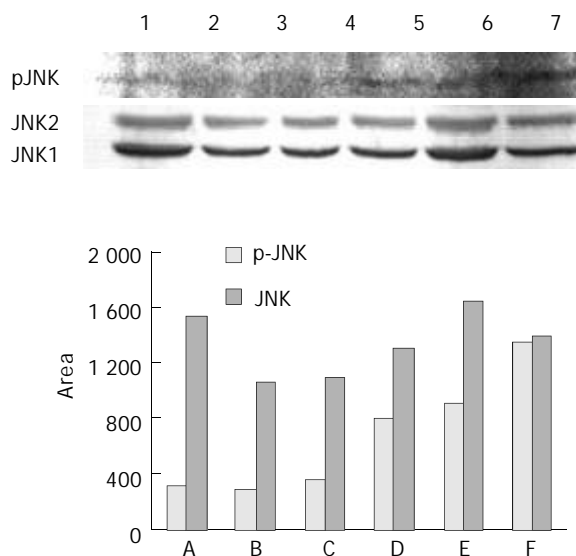


Figure 2 Expression of p-JNK and JNK in SGC-7901 cells following treatment of VES for 24 h. Lane 1: molecular weight marker; Lane 2: UT control; Lane 3: succinate; Lane 4: vitamin E; Lane 5: VES at 5 mg/L; Lane 6: VES at 10 mg/L; Lane 7: VES at 20 mg/L.

Effects of VES at different time points on phosphorylation of JNK

Since VES elevated the levels of p-JNK, we investigated whether VES might regulate the expression of p-JNK for 1.5, 3, 6, 12 and 24 h. VES at 20 mg/L induced a prolonged p-JNK expression starting at 1.5 h, peaking at 12 h and returning to the UT control level at 24 h after treatment (Figure 3A, top panel; Figure 3B). The levels of JNK1/2 were not increased by VES (Figure 3A, bottom panel; Figure 3B).

Effects of blockage of JNK on VES-mediated apoptosis

To further address the role of JNK signaling in VES-mediated apoptosis, studies were conducted to determine the effects of specific blockage of JNK with dominant negative mutants. SGC-

7901 cells were transiently transfected with an expression construct containing dominant negative JNK (DN-JNK, pcDNA3-Flag-JNK, tyrosine 185 and threonine 183 required for phosphorylation activity were replaced with alanine and phenylalanine, respectively), followed by treatment of VES at 20 mg/L. For DAPI staining, SGC-7901 cells were transfected with DN-JNK and then treated with VES for 48 h. Then the cells were collected and stained with DAPI and photographed under a fluorescence microscope. DN-JNK reduced VES-induced apoptosis by 52% compared with the apoptotic rate in empty vector control cells (Figures 4A, 4B). In addition, DN-JNK significantly increased the levels of JNK by 18-fold (Figure 5, top panel), while decreasing the expression of c-Jun to a barely detectable level compared with those in the empty vector cells (Figure 5, middle panel). GAPDH protein levels served to verify lane loads (Figure 5, bottom panel).

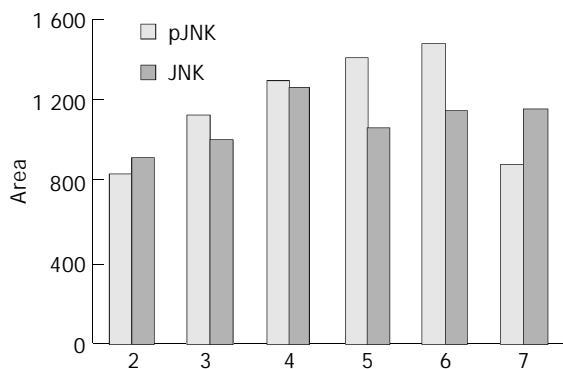
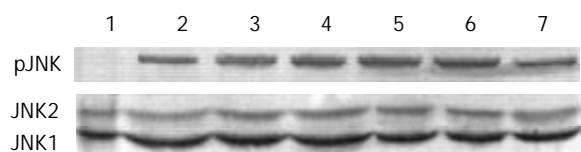


Figure 3 Expression of p-JNK and JNK in SGC-7901 cells following treatment of VES at 20 mg/L at different time points. Lane 1: molecular weight marker; Lane 2: UT control; Lanes 3-7: 20 mg/L VES treatment for 1.5, 3, 6, 12, 24 h.

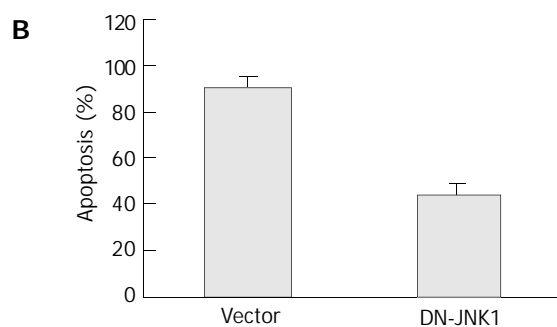
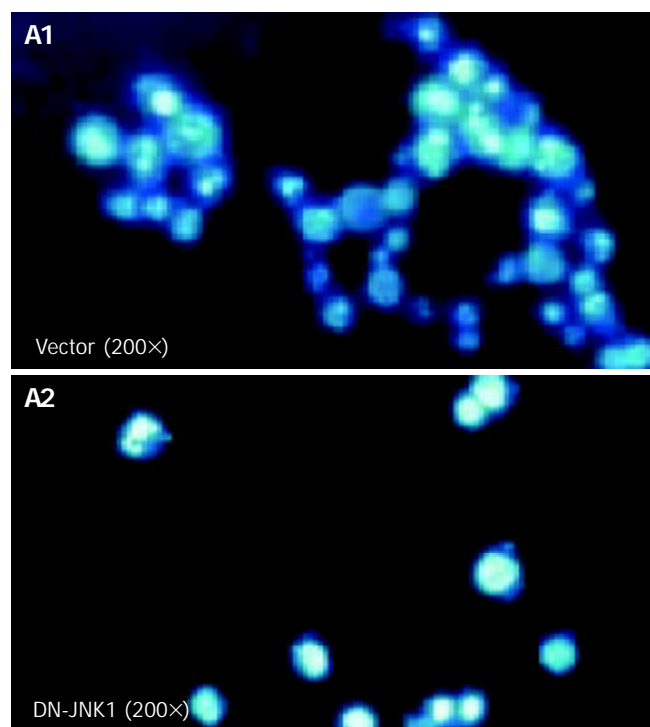


Figure 4 Effect of DN-JNK on VES-induced apoptosis. A: SGC-7901 cells were stained with DAPI; B: The apoptotic rate.

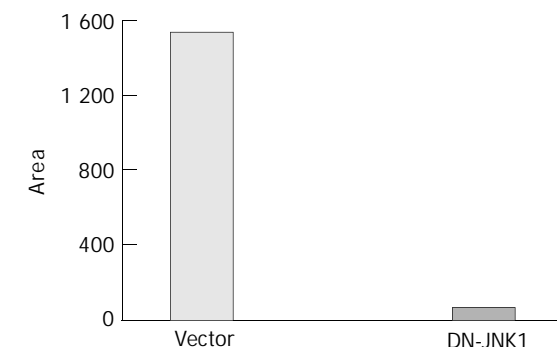
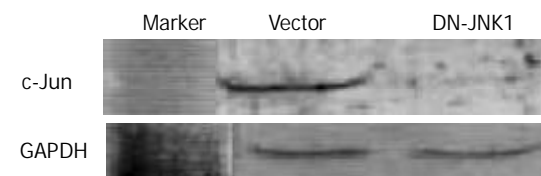
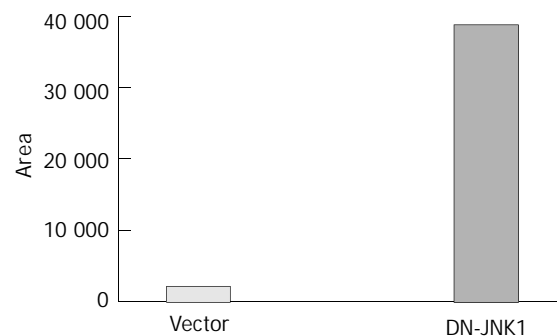
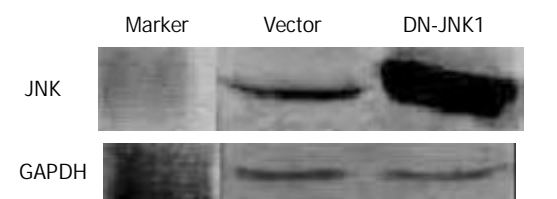


Figure 5 Effect of DN-JNK on expression of JNK and c-Jun when DN-JNK was transfected into SGC-7901 cells following treatment of VES for 24 h.

DISCUSSION

Apoptosis has been found to be an active and physiological process characterized by a series of morphological and biochemical alterations, including condensation of cytoplasm, loss of plasma membrane microvilli, fragmentation of nucleus and extensive degradation of chromosomal DNA into oligomers of 180 bp by endonuclease^[43,44]. Characteristic DNA ladder can

be seen on agarose gel by electrophoresis. In this study, evident DNA ladder appeared in VES-treated SGC-7901 cells, especially at 20 mg/L VES. Therefore, VES can induce SGC-7901 cells to undergo apoptosis.

MAPKs are serine-threonine protein kinases that could be activated by diverse stimuli ranging from cytokines, growth factors, neurotransmitters, hormones, cellular stress and cell adherence^[45-47]. MAPKs are evolutionarily conserved from yeast to human. MAPK activity is regulated through a three-tiered cascade composed of a MAPK kinase kinase (MKKK), a MAPK kinase (MKK/MEK) and a MAPK. Activated MAPKs could phosphorylate corresponding substrates, the majority of which are transcription factors^[48]. Mammalian MAPKs can be subdivided into five groups, namely extracellular signal-regulated kinase (ERK) 1/2, c-Jun amino-terminal kinase (JNK), p38, ERK3/4 and ERK5.

JNK, also known as stress-activated protein kinase (SAPK), is phosphorylated by MKK4/7 activated by various MKKKs. Activated JNK in turn could phosphorylate transcription factors, c-Jun and ATF-2, which are components of the dimeric activating protein (AP)-1^[49-51]. Here, we determined the expression of phospho-JNK and JNK in VES-stimulated SGC-7901 cells. The data showed that VES obviously increased the expression of p-JNK with a dose-effect relationship. The p-JNK levels were also elevated for a prolonged period after VES-treatment. VES induced activation of JNK beginning at 1.5 h after VES treatment and produced a sustain increase for 24 h with peak level at 12 h. The duration of JNK activation is critical in determining cell fate. Persistent activation of JNK has been shown to induce apoptosis. Thus, our results indicated a key role of JNK in VES-mediated apoptosis of human gastric cancer cells.

c-Jun transcription factor, a major target of JNK, belongs to an immediate early gene and could be rapidly and transiently induced in response to multiple extracellular stimuli^[52-54]. Its expression can form homodimers or associate with other transcription factor partner, including members of Jun, Fos and ATF-2, to form heterodimeric complexes. Its activation through phosphorylation by JNK has been implicated in a variety of processes including embryonic developments, cellular transformation and initiation of apoptosis in response to various stresses^[55-59]. JNK could phosphorylate c-Jun on serines 63 and 73 at the NH₂-terminal activating sites. This results in increased stability of c-Jun and an increase in its transactivation potential and DNA binding affinity. Our previous studies showed that VES upregulated the expression of c-jun mRNA and protein in SGC-7901 cells^[60]. In this study, transient transfection of dominant negative mutants of JNK (DN-JNK) blocked VES-triggered apoptosis by 52%. In addition, DN-JNK significantly increased the level of JNK, while decreased the expression of VES-induced c-Jun protein, indicating that JNK plays an important role in the regulation of c-Jun upstream.

Taken together, JNK is phosphorylated and activated in VES-induced apoptosis. JNK regulates the expression of c-Jun, a downstream transcription factor. All the data suggest that JNK plays a critical role in VES-induced apoptosis in human gastric cancer SGC-7901 cells. MAPK pathways are involved in a variety of responses affecting cell fate, such as cell proliferation and differentiation, adaptation to environment stress and apoptosis. None of the MAPK pathways including JNK is acting alone in cellular response, they are integrated with many other metabolic changes in the cells. Therefore, additional studies should provide insights into the interactions and significance among MAPK pathways.

ACKNOWLEDGMENTS

We are grateful to Dr. Bob G Sanders and Dr. Kimberly Kline,

University of Texas, Austin, USA, for giving us JNK and GAPDH antibodies and DN-JNK construct. We also thank Dr. Edgar J Love, University of Calgary, Canada, for critical reading of the manuscript.

REFERENCES

- 1 **Wang YF**, Li QF, Wang H, Mao Q, Wu CQ. Effects of vitamin E on experimental hepatic fibrosis in rats. *Huaren Xiaohua Zazhi* 1998; **6**: 207-209
- 2 **Jiang ZS**, Gao Y. Biological feature of matrix metalloproteinase and its action in metastasis of liver cancer. *Shijie Huaren Xiaohua Zazhi* 2000; **8**:1403-1404
- 3 **Tso P**, Lee T, DeMichele SJ. Randomized structured triglycerides increase lymphatic absorption of tocopherol and retinol compared with the equivalent physical mixture in a rat model of fat malabsorption. *J Nutr* 2001; **131**: 2157-2163
- 4 **Simmons-Menchaca M**, Qian M, Yu W, Sanders BG, Kline K. RRR- α -Tocopheryl succinate inhibits DNA synthesis and enhances the production and secretion of biologically active transforming growth factor- β by avian retrovirus-transformed lymphoid cells. *Nutr Cancer* 1995; **24**: 171-185
- 5 **Ottino P**, Duncan JR. Effect of α -tocopheryl succinate on free radical and lipid peroxidation levels in BL6 melanoma cells. *Free Radical Biol Med* 1997; **22**: 1145-1151
- 6 **Yu W**, Sanders BG, Kline K. Modulation of murine EL-4 thymic lymphoma cell proliferation and cytokine production by Vitamin E succinate. *Nutr Cancer* 1996; **25**: 137-149
- 7 **Yu W**, Sanders BG, Kline K. RRR- α -tocopheryl succinate inhibits EL4 thymic lymphoma cell growth by inducing apoptosis and DNA synthesis arrest. *Nutr Cancer* 1997; **27**: 92-101
- 8 **Fariss MW**, Fortuna MB, Everett CK, Smith JD, Trent DF, Djuric Z. The selective antiproliferative effects of α -tocopheryl hemisuccinate and cholesteryl hemisuccinate on murine leukemia cells result from the action of the intact compounds. *Cancer Res* 1994; **54**: 3346-3351
- 9 **Israel K**, Sanders BG, Kline K. RRR- α -Tocopheryl Succinate inhibits the proliferation of human prostatic tumor cells with defective cell cycle /differentiation pathways. *Nutr Cancer* 1995; **24**: 161-169
- 10 **Zhang Y**, Ni J, Messing EM, Chang E, Yang CR, Yeh S. Vitamin E succinate inhibits the function of androgen receptor and the expression of prostate-specific antigen in prostate cancer cells. *Proc Natl Acad Sci U S A* 2002; **99**: 7408-7413
- 11 **Kline K**, Yu W, Sanders BG. Vitamin E: mechanisms of action as tumor cell growth inhibitors. *Cancer and Nutrition*. K.N. Prasad and W.C. Cole (Eds). *IOS Press* 1998:37-53
- 12 **Turley JM**, Ruscetti FW, Kim SJ, Fu T, Gou FV, Rirchenall-Roberts MC. Vitamin E succinate inhibits proliferation of BT-20 human breast cancer cells:increased binding of cyclin A negatively regulates E2F transactivation activity. *Cancer Res* 1997; **57**: 2668-2675
- 13 **Kline K**, Yu W, Sanders BG. Vitamin E: mechanisms of action as tumor cell growth inhibitors. *J Nutr* 2001; **131**: 161S-163S
- 14 **Liu BH**, Wu K, Zhao DY. Inhibition of human gastric carcinoma cell growth by vitamin E succinate. *Weisheng Yanjiu* 2000; **29**: 172-174
- 15 **Wu K**, Guo J, Dan YJ, Liu BH. The effects of vitamin E succinate on apoptosis in human gastric cancer. *Weisheng Dulixue Zazhi* 1999; **13**: 84-90
- 16 **Schwartz J**, Shklar G. The selective cytotoxic effect of carotenoids and α -tocopherol on human cancer cell lines *in vitro*. *J Oral Maxillofac Surg* 1992; **50**: 367-373
- 17 **Wu K**, Shan YJ, Zhao Y, Yu JW, Liu BH. Inhibitory effects of RRR- α -tocopheryl succinate on bezo(a)pyrene (B(a)P)-induced forestomach carcinogenesis in female mice. *World J Gastroenterol* 2001; **7**: 60-65
- 18 **Malafa MP**, Neitzel LT. Vitamin E succinate promotes breast cancer tumor dormancy. *J Surg Res* 2000; **93**: 163-170
- 19 **Neuzil J**, Weber T, Gellert N, Weber C. Selective cancer cell killing by alpha-tocopheryl succinate. *Br J Cancer* 2000; **84**: 87-89
- 20 **Kline K**, Yu W, Zhao B, Israel K, Charpentier A, Simmons-Menchaca M, Sanders BG. Vitamin E Succinate: Mechanisms of action as tumor cell growth inhibitor. In: *Nutrients in Cancer*

- Prevention and Treatment*. Prasad KN, Santamaria L and Williams RM (eds). Totowa, NY: Humana 1995: 39-56
- 21 **Wu K**, Zhao Y, Liu BH, Li Y, Liu F, Guo J, Yu W. RRR- α -tocopheryl succinate inhibits human gastric cancer SGC-7901 cell growth by inducing apoptosis and DNA synthesis arrest. *World J Gastroenterol* 2002; **8**: 26-30
- 22 **Ariazi EA**, Satomi Y, Ellis MJ, Haag JD, Shi W, Sattler CA, Gould MN. Activation of the transforming growth factor beta signaling pathway and induction of cytostasis and apoptosis in mammary carcinomas treated with the anticancer agent perillyl alcohol. *Cancer Res* 1999; **59**: 1917-1928
- 23 **Kim SJ**, Bang OS, Lee YS, Kang SS. Production of inducible nitric oxide is required for monocytic differentiation of U937 cells induced by vitamin E-succinate. *J Cell Sci* 1998; **111**: 435-441
- 24 **You H**, Yu W, Sanders BG, Kline K. RRR- α -tocopheryl succinate induces MDA-MB-435 and MCF-7 human breast cancer cells to undergo differentiation. *Cell Growth Differ* 2001; **12**: 471-480
- 25 **Yu W**, Israel K, Liao QY, Aldaz CM, Sanders BG, Kline K. Vitamin E succinate (VES) induces Fas sensitivity in human breast cancer cells: role for M_r 43 000 Fas in VES-triggered apoptosis. *Cancer Res* 1999; **59**: 953-961
- 26 **Neuzil J**, Weber T, Schroder A, Lu M, Ostermann G, Gellert N, Mayne GC, Olejnicka B, Negre-Salvayre A, Sticha M, Coffey RJ, Weber C. Induction of cancer cell apoptosis by alpha-tocopheryl succinate: molecular pathways and structural requirements. *FASEB J* 2001; **15**: 403-415
- 27 **Wu K**, Liu BH, Zhao DY, Zhao Y. Effect of vitamin E succinate on the expression of TGF- β 1, c-Jun and JNK1 in human gastric cancer SGC-7901 cells. *World J Gastroenterol* 2001; **7**: 83-87
- 28 **Wu K**, Li Y, Zhao Y, Shan YJ, Xia W, Yu WP, Zhao L. Roles of Fas signaling pathway in vitamin E succinate-induced apoptosis in human gastric cancer SGC-7901 cells. *World J Gastroenterol* 2002; **8**: 982-986
- 29 **Liu HF**, Liu WW, Fang DC. Effect of combined anti Fas mAb and IFN- γ on the induction of apoptosis in human gastric carcinoma cell line SGC-7901. *Shijie Huaren Xiaohua Zazhi* 2000; **8**: 1361-1364
- 30 **Yang JQ**, Yang LY, Zhu HC. Mitomycin C induced apoptosis of human hepatoma cell. *Shijie Huaren Xiaohua Zazhi* 2001; **9**: 268-272
- 31 **Sun ZX**, Ma QW, Zhao TD, Wei YL, Wang GS, Li JS. Apoptosis induced by norcantharidin in human tumor cells. *World J Gastroenterol* 2000; **6**: 263-265
- 32 **Peng ZH**, Xing TH, Qiu GQ, Tang HM. Relationship between Fas/FasL expression and apoptosis of colon adenocarcinoma cell lines. *World J Gastroenterol* 2001; **7**: 88-92
- 33 **Xu AG**, Li SG, Liu JH, Gan AH. Function of apoptosis and expression of the proteins Bcl-2, p53 and C-myc in the development of gastric cancer. *World J Gastroenterol* 2001; **7**: 403-406
- 34 **Zhao Y**, Wu K. Cell death molecule Fas/CD95 and apoptosis. *Aibian Jibian Tubian* 2001; **13**: 55-58
- 35 **Yan J**, Xu YH. Tributyrin inhibits human gastric cancer SGC-7901 cell growth by inducing apoptosis and DNA synthesis arrest. *World J Gastroenterol* 2003; **9**: 660-664
- 36 **Shen YF**, Zhuang H, Shen JW, Chen SB. Cell apoptosis and neoplasms. *Shijie Huaren Xiaohua Zazhi* 1999; **7**: 267-268
- 37 **Liang WJ**, Zhang WD. Signal conducting mechanism of tumor necrosis factor inducing apoptosis. *Shijie Huaren Xiaohua Zazhi* 2000; **8**: 329-331
- 38 **Sun BH**, Zhao XP, Wang BJ, Yang DL, Hao LJ. FADD and TRADD expression and apoptosis in primary hepatocellular carcinoma. *World J Gastroenterol* 2000; **6**: 223-227
- 39 **Wu K**, Zhao Y, Yu WP. Study on apoptosis. *Guowai Yixue Yichuanxue Fence* 2001; **24**: 134-138
- 40 **Xiong LJ**, Zhu JF, Luo DD, Zen LL, Cai SQ. Effects of pentoxifylline on the hepatic content of TGF-beta1 and collagen in Schistosomiasis japonica mice with liver fibrosis. *World J Gastroenterol* 2003; **9**: 152-154
- 41 **Chang L**, Karin M. Mammalian MAP kinase signalling cascades. *Nature* 2001; **410**: 37-40
- 42 **Bhalla US**, Ram PT, Iyengar R. MAP kinase phosphatase as a locus of flexibility in a mitogen-activated protein kinase signaling network. *Science* 2002; **297**: 1018-1023
- 43 **Ashkenazi A**, Dixit VM. Apoptosis control by death and decoy receptors. *Curr Opin Cell Biol* 1999; **11**: 255-260
- 44 **Tao HQ**, Zou SC. Effect of preoperative regional artery chemotherapy on proliferation and apoptosis of gastric carcinoma cells. *World J Gastroenterol* 2002; **8**: 451-454
- 45 **Pearson G**, Robinson F, Beers Gibson T, Xu BE, Karandikar M, Berman K, Cobb MH. Mitogen-activated protein (MAP) kinase pathways: regulation and physiological functions. *Endocr Rev* 2001; **22**: 153-183
- 46 **Johnson GL**, Lapadat R. Mitogen-activated protein kinase pathways mediated by ERK, JNK, and p38 protein kinases. *Science* 2002; **298**: 1911-1912
- 47 **Cowan KJ**, Storey KB. Mitogen-activated protein kinases: new signaling pathways functioning in cellular responses to environmental stress. *J Exp Biol* 2003; **206**: 1107-1115
- 48 **Widmann C**, Gibson S, Jarpe MB, Johnson GL. Mitogen-activated protein kinase: conservation of a three-kinase module from yeast to human. *Physiol Rev* 1999; **79**: 143-180
- 49 **Lei K**, Davis RJ. JNK phosphorylation of Bim-related members of the Bcl2 family induces Bax-dependent apoptosis. *Proc Natl Acad Sci U S A* 2003; **100**: 2432-2437
- 50 **Clerk A**, Kemp TJ, Harrison JG, Mullen AJ, Barton PJR, Sugden PH. Up-regulation of c-jun mRNA in cardiac myocytes requires the extracellular signal-regulated kinase cascade, but c-Jun N-terminal kinases are required for efficient up-regulation of c-Jun protein. *Biochem J* 2002; **368**: 101-110
- 51 **Mauro A**, Ciccarelli C, De Cesaris P, Scoglio A, Bouché M, Molinaro M, Aquino A, Zani BM. PKC α -mediated ERK, JNK and p38 activation regulates the myogenic program in human rhabdomyosarcoma cells. *J Cell Sci* 2002; **115**: 3587-3599
- 52 **Feng DY**, Zheng H, Tan Y, Cheng RX. Effect of phosphorylation of MAPK and Stat3 and expression of c-fos and c-jun proteins on hepatocarcinogenesis and their clinical significance. *World J Gastroenterol* 2001; **7**: 33-36
- 53 **Zhu YH**, Hu DR, Nie QH, Liu GD, Tan ZX. Study on activation and c-fos, c-jun expression of *in vitro* cultured human hepatic stellate cells. *Shijie Huaren Xiaohua Zazhi* 2000; **8**: 299-302
- 54 **Yuen MF**, Wu PC, Lai VCH, Lau JYN, Lai CL. Expression of c-Myc, c-Fos, and c-jun in hepatocellular carcinoma. *Cancer* 2001; **91**: 106-112
- 55 **Schroeter H**, Spencer JPE, Rice-Evans C, Williams RJ. Flavonoids protect neurons from oxidized low-density-lipoprotein-induced apoptosis involving c-Jun N-terminal kinase (JNK), c-Jun and caspase-3. *Biochem J* 2001; **358**: 547-557
- 56 **Jiang LX**, Fu XB, Sun TZ, Yang YH, Gu XM. Relationship between oncogene c-jun activation and fibroblast growth factor receptor expression of ischemia reperfusion intestine in rats. *Shijie Huaren Xiaohua Zazhi* 1999; **7**: 498-500
- 57 **Fan M**, Goodwin ME, Birrer MJ, Chambers TC. The c-Jun NH₂-terminal protein kinase/AP-1 pathway is required for efficient apoptosis induced by vinblastine. *Cancer Res* 2001; **61**: 4450-4458
- 58 **Lei K**, Nimmual A, Zong WX, Kennedy NJ, Flavell RA, Thompson CB, Bar-Sagi D, Davis RJ. The Bax subfamily of Bcl2-related proteins is essential for apoptotic signal transduction by c-Jun NH₂-terminal kinase. *Mol Cell Biol* 2002; **22**: 4929-4942
- 59 **Qi X**, Pramanik R, Wang J, Schultz RM, Maitra RK, Han J, DeLuca HF, Chen G. The p38 and JNK pathways cooperate to trans-activate vitamin D receptor via c-Jun/AP-1 and sensitize human breast cancer cells to vitamin D₃-induced growth inhibition. *J Biol Chem* 2002; **277**: 25884-25892
- 60 **Zhao Y**, Wu K, Xia W, Shan YJ, Wu LJ, Yu WP. The effects of vitamin E succinate on the expression of c-jun gene and protein in human gastric cancer SGC-7901 cells. *World J Gastroenterol* 2002; **8**: 782-786

C-reactive protein, procalcitonin, interleukin-6, vascular endothelial growth factor and oxidative metabolites in diagnosis of infection and staging in patients with gastric cancer

Nevin Ilhan, Necip Ilhan, Yavuz Ilhan, Handan Akbulut, Mehmet Küçüküsu

Nevin Ilhan, Necip Ilhan, Mehmet Küçüküsu, Department of Biochemistry and Clinical Biochemistry, Firat University Firat Medical Centre, 23119, Elazig, Turkey

Yavuz Ilhan, Department of General Surgery, Firat University Firat Medical Centre, 23119, Elazig, Turkey

Handan Akbulut, Division of Immunology, Firat University Firat Medical Centre, 23119, Elazig, Turkey

Correspondence to: Dr. Nevin Ilhan, Firat Universitesi, Firat Tıp Merkezi, Biyokimya ve Klinik Biyokimya AD, 23119, Elazig, Turkey. drmilhan@yahoo.com

Telephone: +90-424-2333555-2147 **Fax:** +90-424-2388660

Received: 2003-06-04 **Accepted:** 2003-10-12

Abstract

AIM: The current study was to determine the serum/plasma levels of VEGF, IL-6, malondialdehyde (MDA), nitric oxide (NO), PCT and CRP in gastric carcinoma and correlation with the stages of the disease and accompanying infection.

METHODS: We examined the levels of serum VEGF, IL-6, PCT, CRP and plasma MDA, NO in 42 preoperative gastric cancer patients and 23 healthy subjects. There were infection anamneses that had no definite origin in 19 cancer patients.

RESULTS: The VEGF levels (mean±SD; pg/mL) were 478.05±178.29 and 473.85±131.24 in gastric cancer patients with and without infection, respectively, and these values were not significantly different ($P>0.05$). The levels of VEGF, CRP, PCT, IL-6, MDA and NO in cancer patients were significantly higher than those in healthy controls and the levels of CRP, PCT, IL-6, MDA and NO were statistically increased in infection group when compared with non-infection group ($P<0.001$).

CONCLUSION: Although serum VEGF concentrations were increased in gastric cancer, this increase might not be related to infection. CRP, PCT, IL-6, MDA and NO have obvious drawbacks in the diagnosis of infections in cancer patients. These markers may not help to identify infections in the primary evaluation of cancer patients and hence to avoid unnecessary antibiotic treatments as well as hospitalization. According to the results of this study, IL-6, MDA, NO and especially VEGF can be used as useful parameters to diagnose and grade gastric cancer.

Ilhan N, Ilhan N, Ilhan Y, Akbulut H, Küçüküsu M. C-reactive protein, procalcitonin, interleukin-6, vascular endothelial growth factor and oxidative metabolites in diagnosis of infection and staging in patients with gastric cancer. *World J Gastroenterol* 2004; 10(8): 1115-1120

<http://www.wjgnet.com/1007-9327/10/1115.asp>

INTRODUCTION

Adenocarcinoma of the stomach (ACS) is the second most

common cancer worldwide. Efforts directing at prevention, early detection and intensive therapy have been effectively proved early diagnosis saves lives. There are 2 distinct biological and etiologic subtypes of ACS: epidemic-intestinal type and endemic-diffuse-infiltrative type. Diet and environment are important factors for the epidemic form of ACS, which is associated with chronic atrophic gastritis and intestinal metaplasia of gastric mucosa. Genetic instability, inactivation of tumour suppressor genes, whereas activation of oncogenes, expression of growth factors, cytokines and angiogenic factors promote tumour progression and invasion^[1-5].

Angiogenesis in tumours, as well as in a number of physiological (vasculogenesis, wound repair, *etc.*) and pathological (diabetic retinopathy, macular degeneration, rheumatoid arthritis, cancers and psoriasis) conditions, is induced by a number of factors, of which the most prevalent and only endothelium-specific one is vascular endothelial growth factor VEGF, also referred to as vascular permeability factor^[6-9]. VEGF is a potent angiogenic mediator described in a wide variety of tumours, and it stimulates angiogenesis and increases vascular permeability^[10]. It has been reported to be synthesized and secreted by gastro-intestinal tract adenocarcinomas. Recent studies have revealed a relationship between the increased expression of VEGF and tumour growth, distant metastasis, and the poor prognosis of patients with gastric carcinoma^[11-13]. Experimentally, hypoxia and ischemia are known to induce angiogenesis in various cultured tumour cells by increasing VEGF^[14-17]. Increased risk of malignancy is associated with chronic inflammation caused by chemical and physical agents^[18], and autoimmune and inflammatory reactions of uncertain etiology^[19]. Gastric cancer is a global health problem. Several factors are suspected to play a role in gastric carcinogenesis, including effects of diet, exogenous chemicals, intragastric synthesis of carcinogens, genetic factors, infectious agents and pathological conditions in the stomach (such as gastritis). Studies have shown that high intake of smoked, salted and nitrated foods and carbohydrates and low intake of fruits, vegetables and milk significantly increase the risk for gastric cancer^[20,21]. Dietary factors, such as consumption of salted and nitrated food, are believed to be primarily responsible for the high incidence and mortality rates of gastric cancer in Turkey. Clinical and epidemiological studies have suggested a link between gastric cancer and concurrent or previous infection with a bacterium or virus. *Helicobacter pylori* (*H pylori*) is believed to play a role in about 60% of gastric cancer cases. Gastric carcinogenesis is a typical infection and inflammation-associated pathological alteration in which *H pylori* plays a critical role. Current knowledge of the detailed mechanisms underlying the interplay between biological modulators and lesions induced by *H pylori* is still incomplete^[22]. Immune response to *H pylori* involves a complex network of inflammatory mediators including chemokines [*e.g.* interleukin (IL)-8], pro-inflammatory cytokines (*e.g.* IL-1, IL-6, tumor necrosis factor α) and immunosuppressive peptides (*e.g.* IL-10)^[23]. It is believed that chronic infection with *H pylori* leads to alterations of the cell cycle, including increased epithelial

cell replication, increased rate of cell death (apoptosis) and production of oxidants. For instance, reactive oxygen species (ROS) could be elevated and cause oxidative DNA lesions in gastric epithelial cells during *H pylori*-elicited inflammation^[24]. This, in combination with depletion of antioxidant defenses, may predispose to carcinogenesis by increasing the likelihood of DNA mutagenesis. Accumulation of mutations may then lead to metaplasia, dysplasia and gastric cancer. The level of oxidative DNA lesions was significantly higher in patients with chronic atrophic gastritis or gastric cancer than in normal gastric tissues, indicating that a progressive accumulation of oxidative DNA lesions could play a major role in gastric carcinogenesis^[24-28]. Lipid peroxidation is initiated by free-radical attack of membrane lipids, generating large amounts of reactive products such as malondialdehyde (MDA), which have been implicated in tumour initiation and promotion.

Cytokines have been proposed to play an important role in *H pylori*-associated gastric inflammation and carcinogenesis, but the exact mechanism remains unclear. Several studies have indicated that infection with *H pylori* induced the expression and production of various cytokines in gastric mucosa, epithelial cells, or macrophages^[29,30]. IL-6, but not other cytokines, has recently been reported to be induced by *H pylori* infection in gastric epithelial cells^[31]. In addition, IL-6 has a strong activity in stimulating the growth of human gastric cancer cell lines. These findings suggest that IL-6 may have a potential role in the pathogenesis of gastric cancer^[32].

Recognized interactions and cytokine pathways mediated by surrounding stromal cells and between stromal cells and tumour play important roles in gastric carcinogenesis. VEGF and IL-6 are associated with the disease status of gastric carcinoma^[33]. However, their relationship remains unclear. IL-6 produced in malignant tumours and inflammatory tissues has a stimulatory effect on tumour growth and a direct angiogenic activity^[34]. Reactive oxygen species (ROS) and certain inflammatory cytokines always elevate during the human carcinogenic process. However, the biological significance of the interplay between ROS and inflammatory cytokines remains elusive. IL-6 is a pleotropic cytokine capable of not only inducing growth and differentiation but also modulating cellular apoptosis in many cell types^[35-37].

In normal gastric mucosa, nitric oxide (NO) inhibits acid secretion, stimulates mucus and bicarbonate secretions, elevates mucosal blood flow and accelerates the healing of ulcers^[38,39]. In some tumour tissues, NO has been found to enhance tumour angiogenesis and to induce vasodilatation, thus accelerating tumour growth^[40]. NO may differentially affect tumour progression depending on the levels and timing of release. NO can also decrease adhesion molecule expression, increase vascular permeability and angiogenesis^[41]. In addition to causing the initial mutagenic event leading to disease, NO has also been implicated, seemingly paradoxically, both in tumour reduction/prevention and in tumour promotion.

Chronic infection and inflammation have long been recognized as risk factors for a variety of human cancers. Procalcitonin (PCT), a 116 amino acid propeptide of calcitonin, has been proposed as a new diagnostic marker of severe infections. PCT is presumably synthesized in tissues other than thyroid C-cells, which are the source of calcitonin (CT) in normal physiology. At the same time, PCT is excreted by numerous cancers and might well be a useful biological marker for the follow-up of productive tumours. Enhanced production of calcitonin-like peptides was also seen in patients with different malignancies^[42,43]. Another infection marker, C-reactive protein (CRP), is most widely used as a marker of ongoing infection in clinical practice. The use of CRP values to diagnose infection in cancer patients was often difficult, because the underlying malignancy also induced CRP

production in hepatocytes^[42,44,45]. Infections in cancer patients are milder than sepsis, and they are often associated with tumour necrosis and obstructions. Although the underlying cancer seems to disturb PCT and CRP, there may be quantitative differences and these markers did not help to identify infections and stage of cancer.

In this study, we investigated the circulating levels of VEGF and IL-6 which are markers directly related with tumour, and MDA and NO which are oxidative stress markers, and determined the correlation between these markers and infection markers (PCT and CRP) in cancer patients with abdominal pain, vomiting, malnutrition, weight loss, and increasing tendency of infection.

MATERIALS AND METHODS

Materials

Forty-two gastric cancer patients admitted to Firat University Hospital between 2001 and 2002 were included in the study. Serum VEGF, IL-6, PCT, CRP and plasma MDA, NO (nitrite/nitrate) levels were measured in 42 patients with gastric cancer, and 23 healthy subjects. The patients aged 46-78 years (average age 62). Nineteen were men, and 23 were women. Characteristics and demographic data of the study population are shown in Table 1. None of the patients received chemotherapy or radiation therapy before surgery. Each patient underwent the following procedures: chest radiography, stomach imaging (ultrasound or CT scan), endoscopy, other organ computed tomography (CT) scan, mammography, breast ultrasound, clinical diagnosis and hematological and biochemical profiles. The clinicopathological parameters were studied for prognostic values including age, tumour size, histological type, lymph node involvement, vascular involvement, distant metastasis, and serosal invasion. The pathologic diagnosis and classification were made according to the Union Internationale Contre le Cancer (UICC) TNM clinical classification for gastric cancer^[46]. The histological diagnosis was based on morphological examination of hematoxylin and eosin-stained, routinely processed specimens. Tumour resection was carried out in all the patients (including 42 preoperative patients who subsequently underwent surgical resection for cure, and 4 patients with inoperable tumours). The control group consisted of 23 healthy controls (male: 11, female: 12, median age: 61 years (38-82 years)). ‘Healthy’ was defined as being free from diabetes mellitus, arteriosclerosis and acute illness and without hospitalization for any illness during the previous 2 years.

Table 1 Characteristics of studied populations and demographic data

	No. of subjects	Median age (yr) (interquartile range)	Sex (M/F)
Healthy control	23	61 (38-82)	11/12
Gastric cancer	42	62 (46-76)	19/23
Histologic type			
Adeno carcinoma	34	61 (46-76)	18/16
Signet-ring cell carcinoma	4	51 (48-62)	3/1
Mucinous carcinoma	4	56 (51-58)	1/3
Stage			
I	12	60 (46-74)	7/5
II	16	56 (51-64)	8/8
III	10	65 (62-72)	4/6
IV ¹	4	70 (68-76)	2/2

M, male; F, female. ¹Distant metastatic sites: peritoneal (2), hepatic (1), multiple sites (1).

Peripheral venous blood samples were collected in routine biochemical test tubes for VEGF, IL-6, PCT and CRP analysis and in EDTA.K3 tubes for MDA and NO (nitrite/nitrate) determination. Plasma and serum tubes were centrifuged at 3 500 r/min for 10 min at 4 °C. The serum and plasma were separated and stored at -70 °C until further processing.

Methods

Serum VEGF levels were determined by a quantitative sandwich enzyme immunoassay technique (Quantikine R&D Systems, Minneapolis, Minn.) according to the manufacturer’s instructions. The system used a solid phase monoclonal antibody and an enzyme-linked polyclonal antibody rose against recombinant human VEGF. For each analysis 100 µL of serum was used. All the analyses and calibrations were performed in duplicate. The calibrations on each microtiter plate included recombinant human VEGF standards. Results were calculated from a standard curve generated by a four-parameter logistic curve-fit and expressed in pg/mL. The coefficient of variation of interassay determinations reported by the manufacturer varied from 6.2% to 8.8% when the VEGF concentrations ranged between 50 and 1 000 pg/mL. Human IL-6 levels were determined by enzyme linked immunosorbent assay (ELISA) kits (Bender MedSystems, MedSystems Diagnostics, Vienna, Austria) according to the manufacturer’s guidelines.

Measurement of plasma MDA levels, MDA, the end product of lipid peroxidation, reacted with tiobarbutiric acid (TBA) to produce a fluorescence product, which was measured spectrophotometrically. Thus, plasma MDA levels were measured as an index of lipid peroxidation according to the TBA spectrophotometric method that was modified from the methods of Satoh and Yagi^[47]. 1, 1, 3, 3, tetraetoxyp propane was used as standard, and plasma MDA levels were expressed as nanomoles per milliliter.

The measurement of plasma NO was difficult because this radical was poorly soluble in water and had a short half-life in

tissue (10-60 s), but its half-life might be as long as 4 min in the presence of oxygen. For these reasons, the determination of NO itself was difficult and required the handling of radioisotopes. In spite of this, the end products, nitrate and nitrite, were preferentially used in clinical biochemistry. Nitrite, a stable end-product of NO, was measured in plasma by using the spectrophotometric Greiss reaction^[48]. One thousand µL experimental samples of deproteinised plasma was reacted with 500 µL N-naphthylethylenediamine, 10 g/L sulfanilamide for 45 min at room temperature and analyzed by spectrophotometry at 545 nm. Concentrations were determined by comparison with sodium nitrite. The lower limit of detection was 0.2 µmol/L.

The concentration of CRP in serum was determined by turbidimetric assay using Alfawassermann kits. Leukocyte counts were determined using a Beckman Coulter cell counter (Coulter Corporation, Miami, USA). Serum PCT concentrations were measured by immunoluminometric assay using Brahms kits, according to the manufacturer’s protocol (LumiTest; Brahms Diagnostica, Berlin, Germany). PCT levels were found to be <0.08 ng/mL in plasma from 23 healthy controls.

Statistical analysis was carried out using the Statistical Package for the Social Sciences (SPSS). The results were expressed as mean±SE. Mann–Whitney *U*-test and Pearson’s rank correlation test were used to compare levels of parameters among the patients. A *P* value <0.05 was considered statistically significant. Variables found to be significant at a level of *P*<0.05 were considered eligible for multivariate regression analysis.

RESULTS

Our findings on the assessed parameters in gastric cancer and healthy control subjects, and the differences between these parameters in infection and non-infection groups of cancer patients are shown in Table 2. Mean serum/plasma levels of IL-6, NO*, MDA, CRP and VEGF in patients with gastric cancer were significantly higher than those in the healthy

Table 2 Mean levels of VEGF, IL-6, PCT, CRP, MDA and NO in controls, cancer patients and in infection and non-infection groups of cancer patients

	Control (n=23)	Gastric cancer (n=42)	<i>P</i> value	Non-infection group (n=23)	Infection group (n=19)	<i>P</i> value
VEGF (pg/mL)	51.26±30.04	489.28±172.91 ^b	<0.000	462.84±165.46	521.28±180.72	NS
IL-6 (pg/mL)	1.41±0.34	4.68±2.00 ^b	<0.000	3.47±0.77	6.15±2.07 ^d	<0.000
PCT (ng/mL)	0.15±0.065	0.59±0.29 ^b	<0.000	0.42±0.19	0.79±0.27 ^d	<0.000
CRP (mg/L)	15.30±11.28	78.21±43.36 ^b	<0.000	57.83±16.45	102.89±52.71 ^d	<0.002
MDA(nmol/mL)	4.37±2.99	11.42±3.22 ^b	<0.000	9.85±2.12	13.32±3.35 ^d	<0.001
NO (µmol/L)	37.97±6.35	49.32±9.07 ^b	<0.000	45.79±9.16	53.59±7.06 ^d	<0.004

^b*P*<0.000 vs control, ^d*P*<0.005 vs non-infection group, NS: not significant.

Table 3 Mean serum levels of VEGF, IL-6, PCT, CRP, MDA and NO in different stages of cancer patients

	Stage I (n=12)	Stage II (n=16)	Stage III (n=10)	Stage IV (n=4)
VEGF (pg/mL)	331.92±106.45	471.85±113.57 ^b	580.87±94.64 ^{d,g}	802.14±128.57 ^{d,l,h}
IL-6 (pg/mL)	5.05±2.89	4.16±1.28	4.03±0.81	7.33±1.13 ^f
PCT (ng/mL)	0.63±0.37	0.56±0.32	0.57±0.23	0.67±0.22
CRP (mg/L)	82.08±61.92	77.75±38.21	62.50±21.41	107.75±30.27 ^e
MDA (nmol/mL)	8.99±2.39	11.25±2.66 ^a	12.34±2.03 ^b	17.07±2.06 ^{d,n,f}
NO (µmol/L)	41.11±6.36	48.34±7.06 ^a	54.84±3.82 ^{d,g}	64.16±3.72 ^{d,l,f}

^b*P*<0.005, ^a*P*<0.05, ^d*P*<0.000 vs stage I., ^l*P*<0.000, ⁿ*P*<0.001, ^g*P*<0.05 vs stage II., ^f*P*<0.001, ^e*P*<0.05 vs stage III.

Table 4 Pearson’s rank correlation coefficients between each two of serum/plasma MDA, NO, VEGF and IL-6 levels in gastric cancer patients

MDA-NO	MDA-VEGF	MDA-IL-6	VEGF-IL-6	VEGF-NO	IL-6-NO
<i>r</i> =0.674 <i>P</i> <0.000	<i>r</i> =0.556 <i>P</i> <0.000	<i>r</i> =0.434 <i>P</i> <0.004	<i>r</i> =0.192 <i>PVNS</i>	<i>r</i> =0.535 <i>P</i> <0.000	<i>r</i> =0.534 <i>P</i> <0.000

NS.: not significant.

controls. Serum VEGF levels in patients with gastric cancer were fairly higher than those in healthy controls, although it was not statistically significant compared between gastric cancer patients with and without infections.

As seen in Table 3, as the stage of the disease increased, slightly differences were observed in the levels of PCT and CRP. There were no differences in PCT levels among the 4 stages, whereas there was a statistically significant difference in CRP levels between stage 4 and stage 3 ($P < 0.001$). There was a statistically significant correlation between PCT and CRP in gastric cancer patients with or without infection ($r = 0.463$, $P < 0.02$, Figure 1). IL-6 levels were significantly increased in stage 4 compared with stage 2 and stage 3. Levels of MDA and NO, the markers of oxidative stress, were increased in line with the stage of cancer. However, we had some problems in evaluation of the results in different cancer stage groups because of the small number of patients in stage 4 group. CRP, PCT, IL-6, NO and MDA levels were significantly higher in the cancer group with infection than in gastric cancer group without infection ($P < 0.0001$). When the cancer group was classified based on their stages, VEGF levels were proportionally increased with the stage of cancer and there were statistically significant differences between the groups. Of the nineteen cancer patients with infection, 4 were in stage 1, 4 in stage 2, 6 in stage 3 and 5 in stage 4. Consequently, there was no significant difference among the stages of cancer patients with infection. Statistically significant correlations were determined in gastric cancer patients between each two of MDA, NO, VEGF, IL-6, except for the correlation between VEGF and IL-6 ($P > 0.05$) (Table 4).

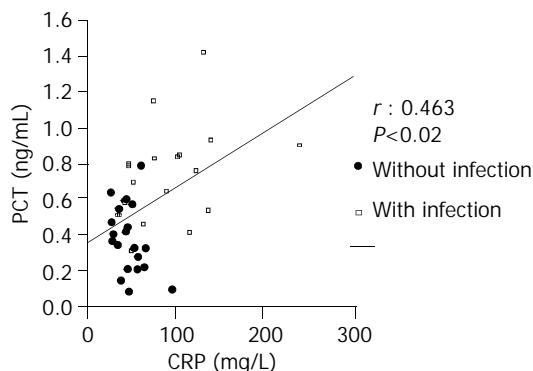


Figure 1 Correlations between serum PCT and CRP in gastric cancer group with and without infection.

DISCUSSION

Angiogenesis was required for tumour growth and progression and it was involved in metastasis^[6,8]. The process could result from an imbalance between positive and negative angiogenic regulators released by both tumour cells and host cells^[49]. Tumour vascularisation correlated directly with the prognosis of cancer patients in many carcinomas^[1-4]. Gastric cancer is a major malignant disease. The development in new diagnostic techniques and mass screening have led to increased detection rates of patients with early-stage gastric cancer. However, even after curative resection of early gastric cancer, there are still various types of recurrences, and residual occult disease and distant micro metastasis. Gastric adenocarcinoma is associated with a high incidence of serosal invasion, direct invasion into the neighboring organs, peritoneal dissemination, lymph node metastasis, and liver metastasis. These lesions have led to a low resection rate and a poor prognosis, however a curative operation should be attempted to improve the 5-year survival rate^[50]. Increased serum levels of VEGF in patients with various types of cancer and the relationship between tumour

development and these VEGF levels have been determined. In our study, we investigated the circulating levels of VEGF in gastric cancer patients as well as in healthy controls using a specific ELISA and found a statistically significant increase in VEGF levels directly proportional to the stage of cancer ($P < 0.001$). Significantly higher VEGF levels were found in cancer patients than in healthy controls, but the increased VEGF levels were not related to infection ($P > 0.05$). We concluded that VEGF was an important marker related with cancer.

IL-6 may play a role in tumour-related angiogenesis by inducing tumour cell proliferation and VEGF expression in tumour cells^[51-54]. In the present study, plasma levels of IL-6 were significantly elevated in advanced gastric cancer patients. This result could be explained by IL-6 production in tumour cells and by inflammatory cytokines produced by stromal cells, which stimulated IL-6 production in various cells^[52,53]. Serum IL-6 levels were significantly increased in cancer patients with infection than in those without infection ($P < 0.001$). It has been reported to be an independent prognostic factor by multivariate analysis in patients with metastatic disease^[55], and this result was confirmed by the present study, which found that plasma IL-6 was a predictor of metastasis and infection in patients with gastric cancer. Serum IL-6 levels in gastric carcinoma patients seemed to increase in a stage-related manner.

Infections are associated with elevated malondialdehyde in gastric mucosa which is a lipid peroxidation product. The infection of gastric mucosa stimulates influx of polymorphonuclear leukocytes, leading to the generation of reactive oxygen and nitrogen species. Cell membranes, rich in polyunsaturated fatty acids, are readily attacked by these compounds, producing fatty acid radicals and lipid hydroperoxides, which can decompose in complex ways, yielding species that are more radical and a wide range of compounds, notably aldehydes. Of these, MDA and 4-hydroxynonenal were most common^[24,28,56]. MDA formed by the breakdown of prostaglandin endoperoxides^[56], is a strongly genotoxic carbonyl compound that can react directly with DNA to produce a variety of adducts. Hypoxia generally takes place in tumours because of the increased oxygen requirement of proliferative cells and the increased tissue oncotic pressure. Hypoxia also induces VEGF and enhances lipid peroxidation and angiogenic potential of tumour cells. In our study, levels of MDA, the end product of lipid peroxidation, were higher both in patients with gastric cancer compared to healthy controls and in patients with infection compared to cancer patients without infection ($P < 0.000$, $P < 0.001$, respectively). Plasma MDA levels were also evaluated significantly when metastasis and invasion to other tissues occurred ($P < 0.001$).

VEGF stimulates NO production by endothelial cells *in vitro* and *in vivo*. To date, experiments examining the role of NO in cancer initiation and progression showed that NO played a complex role. NO could be involved in initiating diseases by damaging DNA^[39-41] and additionally, a much larger amount of NO released by cells in response to cytokines and endotoxins was synthesized by the inducible form of NOS and could mediate some of the cytotoxic and cytostatic effects of the immune system^[57]. NO could also have a protective role. It was essential for the tumoricidal activity of immune cells^[41,58-60]. Conversely, NO has been shown to have tumour-promoting effects^[60]. In this study, we demonstrated that plasma NO levels were increased in patients with gastric cancer. In cancer patients, NO levels were significantly higher in infection group than in non-infection group and were higher in stage 4 compared with stages 1 and 2.

PCT was a specific marker of infection and CRP an acute-phase reactant that serves as a pattern recognition molecule in the innate immune system^[42]. CRP has been traditionally thought as a bystander marker of vascular inflammation, which

did not play a direct role in the inflammatory process. However, recent evidences suggest that CRP may contribute directly to the proinflammatory state. CRP could stimulate monocyte release from inflammatory cytokines such as IL-1b, IL-6, and TNF- α and might directly act as a proinflammatory stimulus to phagocytic cells^[44,45,61]. PCT and CRP levels were significantly increased in cancer patients with infection compared to gastric cancer patients without infection and were significantly higher in all gastric cancer groups compared to control group ($P < 0.0001$). There was no statistically significant difference in PCT and CRP levels between different stages of cancer. PCT is an important determinant used in the diagnostic evaluation of fever and infections. Increased PCT levels in gastric cancer patients with infection can be used as a useful parameter for pre-diagnosis and follow-up. Therefore, CRP and PCT are two important markers for the diagnosis of infection in patients with cancer rather than for the diagnosis of cancer.

This study demonstrated that the plasma/serum levels of VEGF, IL-6, MDA and NO in patients with stage IV cancer were significantly higher than those in patients with stages I and II/III cancer, and that increased plasma levels of IL-6, MDA, NO and especially VEGF, might be useful in identifying metastatic gastric cancer patients, thus allowing more effective treatment strategies to be implemented. Moreover, our results support the existence of interactions between angiogenesis and the inflammatory system, which contributes to tumour metastasis and progression.

In conclusion, levels of MDA, IL-6, NO and especially VEGF can be used as important parameters for clinical diagnosis and follow up of cancer cases. CRP is a useful marker in the diagnosis of infections that frequently occur in cancer cases.

REFERENCES

- 1 **Wu CW**, Li AF, Chi CW, Huang CJ, Huang CL, Lui WY, Lin WC. Arg tyrosine kinase expression in human gastric adenocarcinoma is associated with vessel invasion. *Anticancer Res* 2003; **23**: 205-210
- 2 **Zivny J**, Wang TC, Yantiss R, Kim KH, Houghton J. Role of therapy or monitoring in preventing progression to gastric cancer. *J Clin Gastroenterol* 2003; **36**: 50-60
- 3 **Shukla NK**, Deo SV, Asthana S, Raina V, Dronamaraju SS. Neoadjuvant chemotherapy in advanced gastric cancer: results of a pilot study. *Trop Gastroenterol* 2002; **23**: 94-96
- 4 **Chatelain D**, de Lajarte-Thirouard AS, Tiret E, Flejou JF. Adenocarcinoma of the upper esophagus arising in heterotopic gastric mucosa: common pathogenesis with Barrett's adenocarcinoma? *Virchows Arch* 2002; **441**: 406-411
- 5 **Ohno S**, Fujii T, Ueda S, Nakamoto T, Kinugasa S, Yoshimura H, Tachibana M, Kubota H, Kumar Dhar D, Nagasue N. Predictive factors and timing for liver recurrence after curative resection of gastric carcinoma. *Am J Surg* 2003; **185**: 258-263
- 6 **Folkman J**. Seminars in Medicine of the Beth Israel Hospital, Boston. Clinical applications of research on angiogenesis. *New Engl J Med* 1995; **333**: 1757-1763
- 7 **Koch AE**, Harlow LA, Haines GK, Amento EP, Unemori EN, Wong WL, Pope RM, Ferrara N. Vascular endothelial growth factor. A cytokine modulating endothelial function in rheumatoid arthritis. *J Immunol* 1994; **152**: 4149-4156
- 8 **Dvorak HF**, Detmar M, Claffey KP, Nagy JA, van de Water L, Senger DR. Vascular permeability factor/vascular endothelial growth factor: An important mediator of angiogenesis in malignancy and inflammation. *Int Arch Allergy Immunol* 1995; **107**: 233-235
- 9 **Aiello LP**, Avery RL, Arrigg PG, Keyt BA, Jampel HD, Shah ST, Pasquale LR, Thieme H, Iwamoto MA, Park JE, Nguyen HV, Aiello LM, Ferrara N, King GL. Vascular endothelial growth factor in ocular fluid of patients with diabetic retinopathy and other retinal disorders. *N Engl J Med* 1994; **331**: 1480-1487
- 10 **Senger DR**, Brown LF, Claffey KP, Dvorak HF. Vascular permeability factor, tumor angiogenesis and stroma generation. *Invasion Metastasis* 1994; **14**: 385-394
- 11 **Yonemura Y**, Endo Y, Fujita H, Fushida S, Ninomiya I, Bandou E, Taniguchi K, Miwa K, Ohoyama S, Sugiyama K, Sasaki T. Role of vascular endothelial growth factor C expression in the development of lymph node metastasis in gastric cancer. *Clin Cancer Res* 1999; **5**: 1823-1829
- 12 **Maehara Y**, Kabashima A, Koga T, Tokunaga E, Takeuchi H, Kakeji Y, Sugimachi K. Vascular invasion and potential for tumor angiogenesis and metastasis in gastric carcinoma. *Surgery* 2000; **128**: 408-416
- 13 **Ikeguchi M**, Oka S, Saito H, Kondo A, Tsujitani S, Maeta M, Kaibara N. The expression of vascular endothelial growth factor and proliferative activity of cancer cells in gastric cancer. *Langenbeck's Arch Surg* 1999; **334**: 264-270
- 14 **Ferrara N**, Davis Smyth T. The biology of vascular endothelial growth factor. *Endocr Rev* 1997; **18**: 4-25
- 15 **Shweiki D**, Itin A, Soffer D, Keshet E. Vascular endothelial growth factor induced by hypoxia may mediate hypoxia-initiated angiogenesis. *Nature* 1992; **359**: 843-845
- 16 **Nomura M**, Yamagishi S, Harada S, Hayashi Y, Yamashita T, Yamashita J, Yamamoto H. Possible participation of autocrine and paracrine vascular endothelial growth factor in hypoxia-induced proliferation of endothelial cells and pericytes. *J Biol Chem* 1995; **270**: 28316-28324
- 17 **Waltenberger J**, Mayer U, Pentz S, Hombach V. Functional upregulation of the vascular endothelial growth factor receptor KDR by hypoxia. *Circulation* 1996; **94**: 1647-1652
- 18 **Gulumian M**. The role of oxidative stress in diseases caused by mineral dusts and fibres: current status and future of prophylaxis and treatment. *Mol Cell Biochem* 1999; **196**: 69-77
- 19 **Ekbom A**, Helmick C, Zack M, Adami HO. Ulcerative colitis and colorectal cancer. *N Engl J Med* 1990; **323**: 1228-1233
- 20 **Howson CP**, Hiyama T, Wynder EL. The decline in gastric cancer: epidemiology of an unplanned triumph. *Epidemiol Rev* 1986; **8**: 1-27
- 21 **Kramer BS**, Johnson KA. Other gastrointestinal cancers: stomach, liver. In: Greenwald P, Kramer BS, Weed DL, eds. Cancer Prevention and Control. New York: Marcel Dekker 1995: 673-694
- 22 **O'Connor F**, Buckley M, O'Morain C. *Helicobacter pylori*: the cancer link. *J R Soc Med* 1996; **88**: 674-678
- 23 **Bodger K**, Crabtree JE. *Helicobacter pylori* and gastric inflammation. *Br Med Bull* 1998; **54**: 139-150
- 24 **Lin MT**, Juan CY, Chang KJ, Chen WJ, Kuo ML. IL-6 inhibits apoptosis and retains oxidative DNA lesions in human gastric cancer AGS cells through up-regulation of anti-apoptotic gene mcl-1. *Carcinogenesis* 2001; **22**: 1947-1953
- 25 **Cahill RJ**, Kilgallen C, Beattie S, Hamilton H, O'Morain C. Gastric epithelial cell kinetics in the progression from normal mucosa to gastric carcinoma. *Gut* 1996; **38**: 177-181
- 26 **Blaser MJ**, Parsonnet J. Parasitism by the 'slow' bacterium *Helicobacter pylori* leads to altered gastric homeostasis and neoplasia. *J Clin Invest* 1994; **94**: 4-8
- 27 **Forman D**. *Helicobacter pylori* infection and cancer. *Br Med Bull* 1998; **54**: 71-78
- 28 **Correa P**, Miller MJ. Carcinogenesis, apoptosis and cell proliferation. *Br Med Bull* 1998; **54**: 151-162
- 29 **Arii K**, Tanimura H, Iwahashi M, Tsunoda T, Tani M, Noguchi K, Mizobata S, Hotta T, Nakamori M, Yamaue H. Neutrophil functions and cytokine production in patients with gastric cancer. *Hepatogastroenterology* 2000; **47**: 291-297
- 30 **Rossi G**, Fortuna D, Pancotto L, Renzoni G, Taccini E, Ghiara P, Rappuoli R, Giudice G. Immunohistochemical study of lymphocyte populations infiltrating the gastric mucosa of beagle dogs experimentally infected with *Helicobacter pylori*. *Infect Immun* 2000; **68**: 4769-4772
- 31 **Tanahashi T**, Kita M, Kodama T, Yamaoka Y, Sawai N, Ohno T, Mitsufuji S, Wei YP, Kashima K, Imanishi J. Cytokine expression and production by purified *Helicobacter pylori* urease in human gastric epithelial cells. *Infect Immun* 2000; **68**: 664-671
- 32 **Ito R**, Yasui W, Kuniyasu H, Yokozaki H, Tahara E. Expression of interleukin6 and its effect on the cell growth of gastric carcinoma cell lines. *Jpn J Cancer Res* 1997; **88**: 953-958
- 33 **Kabir S**, Daar GA. Serum levels of interleukin1, interleukin6 and tumour necrosis factor alpha in patients with gastric carcinoma.

- Cancer Lett* 1995; **95**: 207-212
- 34 **Kim HK**, Song KS, Park YS, Kang YH, Lee YJ, Lee KR, Kim HK, Ryu KW, Bae JM, Kim S. Elevated levels of circulating platelet microparticles, VEGF, IL6 and RANTES in patients with gastric cancer: possible role of a metastasis predictor. *European J Cancer* 2003; **39**: 184-191
- 35 **Parsonnet J**, Friedman GD, Vandersteen DP, Chang Y, Vogelstein JH, Orentreich N, Sibley RK. *Helicobacter pylori* infection and the risk of gastric carcinoma. *N Engl J Med* 1991; **325**: 1127-1131
- 36 **Hahm KB**, Lee KJ, Choi SY, Kim JH, Cho SW, Yim H, Park SJ, Chung MH. Possibility of chemoprevention by the eradication of *Helicobacter pylori*: oxidative DNA damage and apoptosis in *H pylori* infection. *Am J Gastroenterol* 1997; **92**: 1853-1857
- 37 **Farinati F**, Cardin R, Degan P, Rugge M, Mario FD, Bonvicini P, Naccarato R. Oxidative DNA damage accumulation in gastric carcinogenesis. *Gut* 1998; **42**: 351-356
- 38 **Brozozowski T**, Konturek SJ, Sliwowski Z, Drozdowicz D, Zaczec M, Kedra D. Role of Larginine, a substrate for nitric oxidesynthase, in gastroprotection and ulcer healing. *J Gastroenterol* 1997; **32**: 442-452
- 39 **Kato S**, Kitamura M, Korolkiewicz RP, Takeuchi K. Role of nitric oxide in regulation of gastric acid secretion in rats: effects of NO donors and synthase inhibitor. *Br J Pharmacol* 1998; **123**: 839-846
- 40 **Thomsen LL**, Miles DW. Role of nitric oxide in tumor progression: lessons from human tumours. *Cancer Metastasis Rev* 1998; **17**: 107-118
- 41 **Wink DA**, Vodovotz Y, Laval J, Laval F, Dewhirst MW, Mitchell JB. The multifaceted roles of nitric oxide in cancer. *Carcinogenesis* 1998; **19**: 711-721
- 42 **Kallio R**, Surcel HM, Bloigu A, Syrjala H. Creactive protein, procalcitonin and interleukin8 in the primary diagnosis of infections in cancer patients. *Eur J Cancer* 2000; **36**: 889-894
- 43 **Karzai W**, Oberhoffer M, MeierHellmann A, Reinhart K. Procalcitonin – a new indicator of the systemic response to severe infection. *Infection* 1997; **25**: 329-334
- 44 **Gabay C**, Kusner I. Acute phase protein and other systemic responses to inflammation. *N Engl J Med* 1999; **6**: 448-454
- 45 **Weinstein PS**, Skinner M, Sipe JD, Lokich JJ, Zamcheck N, Cohen AS. Acute phase proteins or tumour markers: the role of SAA, SAP, CRP and CEA as indicators of metastases in broad spectrum neoplastic diseases. *Scand J Immunol* 1984; **19**: 193-198
- 46 **Sobin LH**, Wittekind CH. TNM Classification of Malignant Tumours, 5th ed. International Union Against Cancer. In: *Wittekind CH, ed. New York: Wiley-Liss* 1997: 59-62
- 47 **Yagi K**. Assay of blood plasma or serum. *Met Enzymol* 1984; **105**: 328-331
- 48 **Green LC**, Wagner DA, Glogowski J, Skipper PL, Wishnok JS, Tannenbaum SR. Analysis of nitrate, nitrite and [¹⁵N] nitrate in biological fluids. *Anal Biochem* 1982; **126**: 131-138
- 49 **Rak J**, Filmus J, Finkenzeller G, Grugel S, Marme´ D, Kerbel RS. Oncogenes as inducers of tumor angiogenesis. *Cancer Metastasis Rev* 1995; **14**: 263-277
- 50 **Watanabe A**, Maehara Y, Okuyama T, Kakeji Y, Korenaga D, Sugimachi K. Gastric carcinoma with pyloric stenosis. *Surgery* 1998; **12**: 330-334
- 51 **Wu CW**, Wang SR, Chao MF, Wu TC. Serum Interleukin6 levels reflect disease status of gastric cancer. *Am J Gastroentrol* 1996; **91**: 1417-1422
- 52 **Balkwill F**, Mantovani A. Inflammation and cancer: back to Virchow? *Lancet* 2001; **357**: 539-545
- 53 **Salgado R**, Vermeulen PB, Benoy I, Weyjens R, Huget P, Van Marck E, Dirix LY. Platelet number and interleukin6 correlate with VEGF but not with bFGF serum levels of advanced cancer patients. *Br J Cancer* 1999; **80**: 892-897
- 54 **Salgado R**, Benoy I, Weytjens R, Vermeulen PB, Dirix LY. Serum vascular endothelial growth factor load and interleukin-6 in cancer patients– reply. *Br J Cancer* 2000; **82**: 1896
- 55 **Zhang GJ**, Adachi I. Serum interleukin6 levels correlate to tumor progression and prognosis in metastatic breast carcinoma. *Anticancer Res* 1999; **19**: 1427-1432
- 56 **Everett SM**, Singh R, Leuratti C, White KL, Neville P, Greenwood D, Marnett LJ, Schorah CJ, Forman D, Shuker D, Axon AT. A Levels of Malondialdehyde-Deoxyguanosine in the Gastric mucosa: relationship with lipid peroxidation, ascorbic acid, and *Helicobacter pylori*. *Cancer Epidemiol Biomarkers Prev* 2001; **10**: 369-376
- 57 **Assreuy J**, Cunha FQ, Liew FY, Moncada S. Feedback inhibition of nitric oxide synthase activity by nitric oxide. *Br J Pharmacol* 1993; **108**: 833-837
- 58 **DeRojas-Walker T**, Tamir S, Ji H, Wishnok JS, Tannenbaum SR. Nitric oxide induces oxidative damage in addition to deamination in macrophage DNA. *Chem Res Toxicol* 1995; **8**: 473-477
- 59 **Xiao L**, Eneroth PH, Qureshi GA. Nitric oxide synthase pathway may mediate human natural killer cell cytotoxicity. *Scand J Immunol* 1995; **42**: 505-511
- 60 **Mordan LJ**, Brunett TS, Zhang LX, Tom J, Cooney RV. Inhibitors of endogenous nitrogen oxide formation block the promotion of neoplastic transformation in C3H 10T1/2 fibroblasts. *Carcinogenesis* 1993; **14**: 1555-1559
- 61 **Ballou SP**, Lozanski G. Induction of inflammatory cytokine release from cultured human monocytes by Creactive protein. *Cytokine* 1992; **4**: 361-368

Edited by Wang XL Proofread by Xu FM

Survivin antisense oligodeoxynucleotide inhibits growth of gastric cancer cells

Jian-Hui Yang, Yi-Chu Zhang, Hui-Qing Qian

Jian-Hui Yang, Department of Oncological Surgery, Shidong Hospital, 200090, Shanghai, China

Yi-Chu Zhang, Department of General Surgery, Xinhua Hospital Affiliated to Shanghai Second Medical University, Shanghai 200092, China

Hui-Qing Qian, Department of Surgical Laboratory, Xinhua Hospital Affiliated to Shanghai Second Medical University, Shanghai 200092, China

Supported by Shanghai Key Research Project Grant in Medical Science Development (99ZD003)

Correspondence to: Dr. Jian-Hui Yang, Department of Oncological Surgery, Shidong Hospital, Ningguo Road 236, Shanghai 20090, China. yangjianhuicn@sohu.com

Telephone: +86-21-65433031-3204 **Fax:** +86-21-65111710

Received: 2003-03-04 **Accepted:** 2003-04-09

Abstract

AIM: To investigate the effect of transfected survivin antisense oligonucleotide (ASODN) on proliferation and apoptosis of gastric cancer cells.

METHODS: The authors designed ASODNs targeting different regions of survivin mRNA, including surviving ASODN1, ASODN2 and ASODN3. ASODNs were transfected into gastric cancer cell line SGC 7901, cell growth was detected by MTT assay. Cells exposed to the potent oligonucleotide were also examined for apoptosis induction by FCM and fluorescence microscopy. Semiquantitative RT-PCR and Western blot examinations were carried for expression of survivin mRNA and protein.

RESULTS: ASODN3 caused a statistically significant reduction of cell viability to 60.6% ($\pm 2.9\%$) ($P < 0.01$), while ASODN1 and ASODN2 had no such changes ($P > 0.05$). The cell growth was also significantly inhibited by ASODN3, compared with reversal and scrambled sequence. A significant loss of survivin mRNA was presented in ASODN3 treated cells and this was not seen in treatment with sense ODN or scramble ODN. Protein level was significantly decreased 48 h after survivin ASODN transfected by approximately 2-fold decrease compared with untreated controls. However, ASODN3 did not induce significant apoptosis response until 48 h after transfection ($P > 0.05$).

CONCLUSION: ASODN3, which targets translation initiation part, can be identified as a most potent antisense compound. Survivin ASODN3 may provide a novel approach to therapy of gastric cancer.

Yang JH, Zhang YC, Qian HQ. Survivin antisense oligodeoxynucleotide inhibits growth of gastric cancer cells. *World J Gastroenterol* 2004; 10(8): 1121-1124

<http://www.wjgnet.com/1007-9327/10/1121.asp>

INTRODUCTION

Disordered regulatory apoptosis plays an important role in

tumorigenesis^[1]. Several proteins that inhibit apoptosis have been identified, such as some members of bcl-2, HSP and IAP (inhibition of apoptosis). IAP gene family controls a downstream step in cell death by suppressing the activity of Caspases, the executors of cell death programs^[2]. Survivin is a newly identified gene in IAP family, and it is characterized by a unique structure with a single, baculovirus IAP repeat and no zinc-binding domain known as Ring finger^[3]. Its another characteristic is that it expresses in most human cancers but is essentially absent in normal tissues, which makes it an exciting potential therapeutic target in cancer treatment^[4].

Gastric cancer is one of the leading causes of cancer deaths in China, and it still has poor prognosis in spite of some progresses in treatment. It has been demonstrated from immunohistochemical analysis that about 34.5% of gastric cancers overexpress survivin, and are significantly associated with reduced apoptosis compared with survivin negative tumors^[5]. Recently, manipulating apoptosis gene by antisense oligodeoxynucleotide (ASOND) might provide new therapeutic strategies in treating human diseases^[6]. ASODN is a single-strand DNA which is complementary to specific regions of mRNA and capable of inhibiting the antiapoptotic gene, and it is noticeable that ASOND holds great promise as a pharmaceutical agent. Therefore, we investigated whether growth inhibition and induced apoptosis of gastric cancer cell line SGC7901 could be achieved by targeting survivin with ASODN.

MATERIALS AND METHODS

Cell culture

SGC7901 was maintained in RPMI 1640 and supplemented with 100 mL/L calf serum at 37 °C in humidified atmosphere containing 50 mL/L CO₂.

Immunohistochemistry

Cells were plated in 60 mm tissue culture dishes containing coverglasses overnight. The coverglasses were washed in phosphate-buffered saline (PBS), fixed for 30 min in 70 mL/L ethanol, washed twice in PBS. Quenching of the endogenous peroxidase activity was obtained by treatment with 0.3 mL/L H₂O₂ in methanol. The sections were blocked with 10 mL/L goat serum in PBS and incubated with 3 µg anti-survivin polyclonal antibody (gift from Dr. Katsuya Shiraki, First Department of Internal Medicine, Mie University School of Medicine, Tsu, Japan) at 4 °C overnight, then incubated with HRP-conjugated antibody for 30 min at room temperature. After three washes of 5 min in PBS, they were developed in a substrate solution of horseradish peroxidase. Negative control omitting survivin antibody was also performed to confirm the absence of non-specific reactions. Expression of survivin was classified into three levels: (-) no or weak staining, (+) less than 50% positive nuclei staining, and (++) greater than 50% positive nuclei staining of the total nuclei.

Oligodeoxynucleotide

ASODN1 and ASODN2 were designed by a computer program and could theoretically access survivin mRNA. ASODN3 was complementary to the initiation codon and 5 downstream

codons, and could empirically access survivin mRNA as shown in Table 1. In addition, the scramble sequence of survivin ASODN3 was as follows: 5' - GGACCA CGCTATCAGCCG-3', and reverse antisense (sense): 5' - ATG GGT GCC CCG ACG TTG-3'. Phosphothioalate oligodexynucleotides were synthesized using an applied biosystems 3 900 DNA synthesizer (Shenggong, Shanghai, China). After the synthesis, ODNs were purified by use of high-pressure liquid chromatography system, dissolved with PBS, and frozen in aliquots at -20 °C until use.

Table 1 Sequence of ASODNS and their target site

Name	Sequence	Position
ASODN1	5' - GTT CTT GGA TGT AGA GAT GC-3'	102-121
ASODN2	5' - GCT TCT TGA CAG AAA GGA A-3'	305-323
ASODN3	5' - CAA CGT CGG GGC ACC CAT-3'	50-67

Transfection

According to the manufacture's instructions, ODNs were delivered into cells in the form of complexes with Lipofection reagents (GIBCO, MD).

Measurement of cell growth

In vitro growth inhibitory effects of ODNs on SGC7901 were assessed by MTT assay performed according to the previously described protocol^[7] with a slight modification. Two × 10⁴ cells were seeded in each well of 96-well micrometer plates and allowed to attach overnight. The cells were then treated with 400 nmol/L ODN-Lipofection complex for 24 h and incubated for another 48 h. Subsequently, 20 μL of MTT (5 g/L, Sigma) in PBS was added to each well, followed by incubation for 4 h at 37 °C. Formazan crystals were dissolved in DMSO. Absorbance was determined with an enzyme-linked immunosorbent assay reader (model 318, Shanghai, China) at 540 nm. Each assay was performed nine times. The controls received medium alone. The results were expressed as mean ± SE of controls with no ODN.

Reverse transcriptase-PCR (RT-PCR) analysis of survivin mRNA

Total RNA was extracted from SGC7901 cells by modification of guanidium-thiocyanate acid phenol method^[8] and quantified based on the measured absorbance at 260 nm. cDNA was synthesized using 2 μg of RNA, 10⁶ U/L reverse transcriptase (GIBCO, Inc), 0.5 g/L Oligod T, in a total volume of 20 μL. Reaction was performed at 42 °C for 60 min, and terminated by heating at 99 °C for 5 min. The sequences of oligodexynucleotides primers for RT-PCR were as follows: survivin-S 5' -ATG GGT GCC CCG ACG TTG CC-3', survivin-A 5' -GCA GCT CCG GCC AGA GGC CT-3', β-actin-S 5' -GGC GGC ACC ACC TGT ACC CT-3' and β-actin-A 5' -AGG GGC CGG ACT CGT CATA CT-3', respectively. For amplification of cDNA, 2 μL cDNA product was subjected to PCR-based technique using 2.5 U of Taq DNA Polymerase, 1 μL each of forward and reverse primers, and 200 μmol/L each of dNTPs. PCR consisted of 35 cycles at 94 °C for 1 min, at 62 °C for 1 min and at 72 °C for 1 min followed by a final extension at 72 °C for 5 min.

Western blot analysis

Cells were washed in ice-cold PBS and lysed in a buffer using standard methods. After centrifugation at 10 000 g for 10 min, the supernatants were stored at -70 °C. Lysate equalized for protein content was separated in 150 g/L SDS-PAGE and transferred onto a PVDF membrane. The membranes were blocked for 1 h at room temperature in 10 g/L BSA, and incubated overnight at 4 °C with survivin antibody, followed by incubation with sheep anti-rabbit second antibody conjugated to horseradish peroxidase (Dako, Denmark) for 120 min. Finally

the membranes were developed with DAB and incubated until color developed sufficiently.

Measurement of apoptosis by flow cytometry and staining with Hchst 33342

In preparation of flow cytometry (FCM), SGC 7901 cells were centrifuged 72 h after transfection. The cells were washed with PBS, and fixed in 70 mL/L cold ethanol. Samples were treated with RNase (10 g/L), resuspended and stained with 10 g/L propidium iodide. After 30 min at room temperature in the dark, the cells were analyzed using a FCM scan flow cytometer. Apoptotic cells appeared in the cell cycle distribution as cells with DNA contents less than G₁ cells, and the percentage of apoptotic cells was calculated. In other experiments, transduced cells were cultivated for 24 h at 37 °C and assayed for nuclei staining. Both attached cells and detached cells were collected and resuspended. One drop of cell suspension was added to one drop of Hoechst 33 342 solution (10 mg/L in PBS), mixed gently on a slide, and immediately examined with Olympus fluorescence microscopy. Blue fluorescent condensed nuclei were interpreted as the number of apoptotic cells. Viable cells were interpreted as cells which exhibited green, diffusely stained intact nuclei. Cell ghosts with weak staining were not included in the cell count.

Statistical analysis

The data were expressed as mean ± SE. The results were analyzed by ANOVA test. *P* < 0.05 was considered statistically significant.

RESULTS

Expression of survivin in SGC7901

We examined the expression of survivin gene in SGC-7901 using immunohistochemistry. Expression of survivin was observed primarily in cytoplasm, and mild staining in nuclei (data not shown).

Cell proliferation assay

As shown in Figure 1, ASODN3 caused a statistically significant reduction of cell viability to 60.6 ± 2.9% (*P* < 0.01), while ASODN1 and ASODN2 had not such changes (*P* > 0.05). We also investigated whether growth inhibition was changed by control sequences including reversal antisense (*i.e.* sense) and scrambled sequence with the same composition. As shown in Figure 2, neither had any changes in activity (*P* > 0.05).

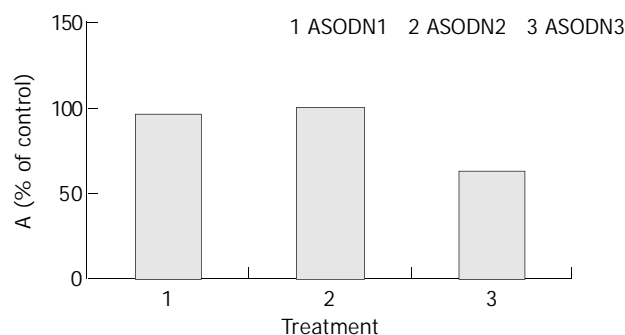


Figure 1 Cytotoxic effect of ASODN targeting different regions of survivin mRNA. Cells were cultured in plastic 96-well plates and quantitated using MTT assay as described in "Materials and Methods."

Induction of apoptosis by antisense oligodexynucleotide

Cells exposed to the oligonucleotides were examined for

apoptosis induction by FCM and fluorescence microscopy. As shown in Table 2, positive control 5-FU significantly induced apoptotic response, about $6.12 \pm 3.25\%$ for 24 h ($P < 0.01$) and $11.35 \pm 1.50\%$ for 48 h ($P < 0.01$). However, ASODN3 did not induce any significant apoptotic response until 48 h after transfection ($P > 0.05$). Fluorescence microscopy also did not show any increase of condensed nuclei (data not shown).

Table 2 Apoptosis rates of each group 24 and 48 h after transfection ($n=4$)

	24 h (%)	48 h (%)
Untreated	1.98 ± 0.40	3.74 ± 0.19
survivin ASODN	2.27 ± 0.48	4.57 ± 0.61
5-FU	6.12 ± 3.25	11.35 ± 1.50

Changes of survivin mRNA expression after transfection

As shown in Figure 3, a significant loss of survivin mRNA was detected in antisense treated cells and this was not seen in either sense ODN treated or scramble ODN treated cells.

Changes of survivin protein expression after transfection

We aimed to investigate whether survivin ASODN could downregulate survivin protein in SGC7901, and further determined whether it was in sequence-specific way. Figure 4 shows a typical change of survivin protein expression. Protein level was significantly decreased 48 h after survivin ASODN transfection (by approximately 2-fold decrease compared with untreated control), whereas either sense ODN treated or scramble ODN treated cells did not modulate survivin expression levels. To sum up, these results provided strong evidence of sequence specific mechanism of survivin ASODN.

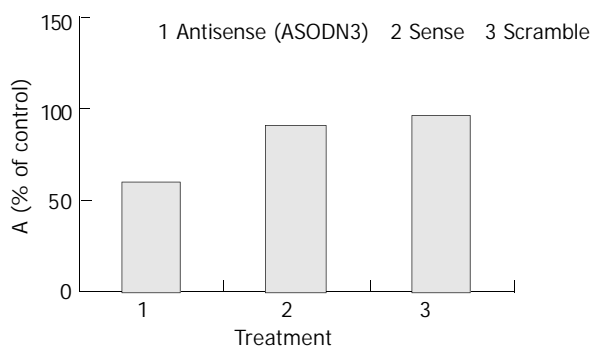


Figure 2 Cytotoxic effect of ASODN3 and control sequences.

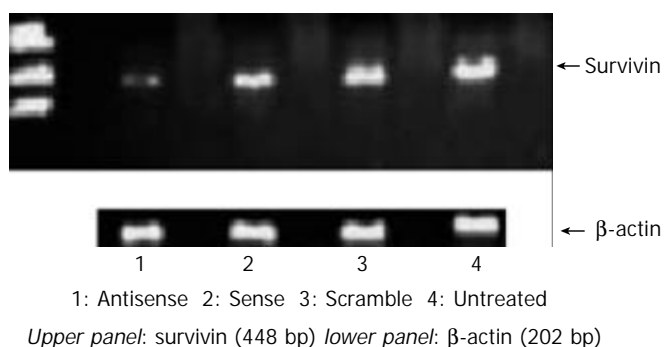


Figure 3 Survivin and β -actin (loading control) mRNA expression following incubation with antisense, sense, scramble and no ODN control. It shows ethidium bromide staining of conventional agarose gel electrophoresis after amplification.

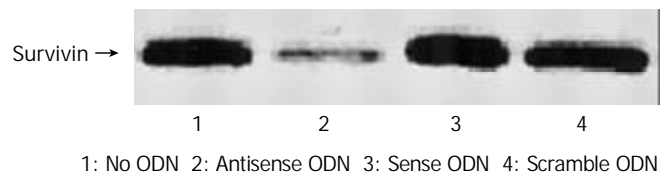


Figure 4 Survivin protein expression following incubation with survivin, antisense, sense, scramble and no ODN control. Strong decrease of survivin protein could be detected in the ASODN group.

DISCUSSION

ASODN represents a useful experimental approach for manipulating gene expression, and recently some antisense compounds have shown anticancer efficacy in numerous preclinical studies^[9-12]. Survivin was detectable in most types of cancer, and its presence was associated with a poor prognosis in many malignant tumors^[13-16]. In this study, we chose survivin as the molecular target and designed ASODN to observe its influence on growth and apoptosis of gastric cancer cell line SGC7901. An immunohistochemical study showed that SGC7901 could positively express survivin, prior to ASODN transfection.

Then, it should be considered to design an optimal site for antisense blocking, which is the key factor of antisense research. Previous researches showed not all areas of a mRNA molecular were amenable to antisense hybridization. Therefore, among the possible ASODNs against a given target nucleic acid, only a small number of sequences seemed to give rise to satisfactorily strong inhibition of target gene expression. The reason is unclear and probably involves mRNA secondary structure. Therefore, computer program was used to design ASODN, but sometimes its usefulness was elusive^[17]. On the other hand, empirically, ASODN targeting AUG starting site was most frequently used in antisense experiments^[18], such as bcl-2 ASODN application in various cancer cell lines^[19-23]. So far we still could not predict accurately the secondary structure of mRNA, and it is rather difficult to predict which is the best ASODN sequence unless through some screening experiments. In our experiment, ASODN1 and ASODN2 were designed by computer program and selected as candidate sequences. ASODN3 targeting the translation initiation codon region, was selected as another candidate sequence to screen the most potent sequence.

Survivin could regulate G2/M phase of the cell cycle by associating it with mitotic spindle microtubules^[24,25], and its expression was positively correlated with proliferation of hepatic^[26] and pancreatic^[27] carcinoma cells. Therefore, we tried to determine which sequence was potent by observing cell growth as previous studies^[7,28,29]. As a result, ASODN3 was able to suppress cell viability of approximate 40% decrease of the number of viable cells ($P < 0.01$), while ASODN1 and ASODN2 did not affect cell viability significantly ($P > 0.05$). On the other hand, the most widely recognized mechanism of ASODN involved RNase H mediated destruction of the target mRNA. Therefore, we also performed RT-PCR and Western blot to confirm the occurrence of antisense effect of ASODN3. As shown in Figures 3 and 4, ASODN3 caused a reduction in the mRNA and protein level 48 h after transduction. However, two different controls for ASODN3 did not modulate survivin mRNA and protein expression levels. Therefore, further evidences for sequence-specific antisense effect of ASODN3 were provided. The exact mechanism of ASODN3 is still unknown, and we suspect that the translation initiation codon region of survivin mRNA is probably a single strand.

In the present study, we identified that ASODN3 had a

potent sequence to inhibit cell growth, then we detected apoptosis by FCM and nuclei staining when survivin ASOND3 was transfected. However, it demonstrated that transfecting survivin ASODN solely was not sufficient to trigger apoptosis, indicating that decrease of cell viability was not due to apoptosis. Our results were different from the report by Olie RA^[30]. It seemed plausible that the effects of ASODN varied depending on the expression profile of treated cells. It was also probably due to the complexity of apoptotic pathway in which other antiapoptotic genes might play more important roles in gastric cancer cell line SGC-7901.

In conclusion, ASODN3 can inhibit the growth of gastric cancer cell line but can not induce apoptosis by itself. From a clinical standpoint, anti-cancer therapy still relies heavily on cytotoxic agents, in spite of some advances in identifying molecular target by ASODN treatment^[31]. So, it is meaningful to investigate further whether ASODN targeting survivin can enhance the sensitivity of chemotherapeutic drugs by decreasing apoptosis thresholds.

ACKNOWLEDGMENTS

We are grateful to Dr. Katsuya Shiraki (First Department of Internal Medicine, Mie University School of Medicine, Tsu, Japan) for providing anti-survivin antibody.

REFERENCES

- 1 **Reed JC**. Dysregulation of apoptosis in cancer. *J Clin Oncol* 1999; **17**: 2941-2953
- 2 **Deveraux QL**, Reed JC. IAP family proteins-suppressors of apoptosis. *Genes Dev* 1999; **13**: 239-252
- 3 **Ambrosini G**, Adida C, Altieri DC. A novel anti-apoptosis gene, survivin, expressed in cancer and lymphoma. *Nat Med* 1997; **3**: 917-921
- 4 **Altieri DC**, Marchisio PC, Marchisio C. Survivin apoptosis: an interloper between cell death and cell proliferation in cancer. *Lab Invest* 1999; **79**: 1327-1333
- 5 **Lu CD**, Altieri DC, Tanigawa N. Expression of a novel antiapoptosis gene, survivin, correlated with tumor cell apoptosis and p53 accumulation in gastric carcinomas. *Cancer Res* 1998; **58**: 1808-1812
- 6 **Nicholson DW**. From bench to clinic with apoptosis-based therapeutic agents. *Nature* 2000; **407**: 810-816
- 7 **Ziegler A**, Luedke GH, Fabbro D, Altmann KH, Stahel RA, Zangemeister-Wittke U. Induction of apoptosis in small-cell lung cancer cells by an antisense oligodeoxynucleotide targeting the Bcl-2 coding sequence. *J Natl Cancer Inst* 1997; **89**:1027-1036
- 8 **Chomczynski P**, Sacchi N. Single-step method of RNA isolation by acid guanidinium thiocyanate-phenol-chloroform extraction. *Anal Biochem* 1987; **162**: 156-159
- 9 **Yuen AR**, Sikic BI. Clinical studies of antisense therapy in cancer. *Front Biosci* 2000; **5**: D588-593
- 10 **Jansen B**, Wacheck V, Heere-Ress E, Schlagbauer-Wadl H, Hoeller C, Lucas T, Hoermann M, Hollenstein U, Wolff K, Pehamberger H. Chemosensitisation of malignant melanoma by BCL2 antisense therapy. *Lancet* 2000; **356**: 1728-1733
- 11 **Chi KN**, Gleave ME, Klasa R, Murray N, Bryce C, Lopes de Menezes DE, D' Aloisio S, Tolcher AW. A phase I dose-finding study of combined treatment with an antisense Bcl-2 oligonucleotide (Genasense) and mitoxantrone in patients with metastatic hormone-refractory prostate cancer. *Clin Cancer Res* 2001; **7**: 3920-3927
- 12 **Rudin CM**, Otterson GA, Mauer AM, Villalona-Calero MA, Tomek R, Prange B, George CM, Szeto L, Vokes EE. pilot trial of G3139, a bcl-2 antisense oligonucleotide, and paclitaxel in patients with chemorefractory small-cell lung cancer. *Ann Oncol* 2002; **13**: 539-545
- 13 **Ikehara M**, Oshita F, Kameda Y, Ito H, Ohgane N, Suzuki R, Saito H, Yamada K, Noda K, Mitsuda A. Expression of survivin correlated with vessel invasion is a marker of poor prognosis in small adenocarcinoma of the lung. *Oncol Rep* 2002; **9**: 835-838
- 14 **Dong Y**, Sui L, Watanabe Y, Sugimoto K, Tokuda M. Survivin expression in laryngeal squamous cell carcinomas and its prognostic implications. *Anticancer Res* 2002; **22**: 2377-2383
- 15 **Takai N**, Miyazaki T, Nishida M, Nasu K, Miyakawa I. Expression of survivin is associated with malignant potential in epithelial ovarian carcinoma. *Int J Mol Med* 2002; **10**: 211-216
- 16 **Takai N**, Miyazaki T, Nishida M, Nasu K, Miyakawa I. Survivin expression correlates with clinical stage, histological grade, invasive behavior and survival rate in endometrial carcinoma. *Cancer Lett* 2002; **184**: 105-116
- 17 **Reed JC**. Promise and problems of Bcl-2 antisense therapy. *J Natl Cancer Inst* 1997; **89**: 988-990
- 18 **Cotter FE**. Antisense therapy for lymphomas. *Hematol Oncol* 1997; **15**: 3-11
- 19 **Lopes D**, Mayer LD. Pharmacokinetics of Bcl-2 antisense oligonucleotide (G3139) combined with doxorubicin in SCID mice bearing human breast cancer solid tumor xenografts. *Cancer Chemother Pharmacol* 2002; **49**: 57-68
- 20 **Duggan BJ**, Maxwell P, Kelly JD, Canning P, Anderson NH, Keane PF, Johnston SR, Williamson KE. The effect of antisense Bcl-2 oligonucleotides on Bcl-2 protein expression and apoptosis in human bladder transitional cell carcinoma. *J Urol* 2001; **166**: 1098-1105
- 21 **Wacheck V**, Heere-Ress E, Halaschek-Wiener J, Lucas T, Meyer H, Eichler HG, Jansen B. Bcl-2 antisense oligonucleotides chemosensitize human gastric cancer in a SCID mouse xenotransplantation model. *J Mol Med* 2001; **79**: 587-593
- 22 **Hu Q**, Bally MB, Madden TD. Subcellular trafficking of antisense oligonucleotides and down-regulation of bcl-2 gene expression in human melanoma cells using a fusogenic liposome delivery system. *Nucleic Acids Res* 2002; **30**: 3632-3641
- 23 **van de Donk NW**, Kamphuis MM, van Dijk M, Borst HP, Bloem AC, Lokhorst HM. Chemosensitization of myeloma plasma cells by an antisense-mediated downregulation of Bcl-2 protein. *Leukemia* 2003; **17**: 211-219
- 24 **Ambrosini G**, Adida C, Sirugo G, Altieri DC. Induction of apoptosis and inhibition of cell proliferation by survivin gene targeting. *J Biol Chem* 1998; **273**: 11177-11182
- 25 **Yamamoto T**, Tanigawa N. The role of survivin as a new target of diagnosis and treatment in human cancer. *Med Electron Microsc* 2001; **34**: 207-212
- 26 **Ito T**, Shiraki K, Sugimoto K, Yamanaka T, Fujikawa K, Ito M. Survivin promotes cell proliferation in human hepatocellular carcinoma. *Hepatology* 2000; **31**: 1080-1085
- 27 **Sarela AI**, Verbeke CS, Ramsdale J, Davies CL, Markham AF, Guillou PJ. Expression of survivin, a novel inhibitor of apoptosis and cell cycle regulatory protein, in pancreatic adenocarcinoma. *Br J Cancer* 2002; **86**: 886-892
- 28 **Shankar SL**, Mani S, O' Guin KN, Kandimalla ER, Agrawal S, Shafit-Zagardo B. Survivin inhibition induces human neural tumor cell death through caspase-independent and- dependent pathways. *J Neurochem* 2001; **79**: 426-436
- 29 **Chen J**, Wu W, Tahir SK, Kroeger PE, Rosenberg SH, Cowsert LM, Bennett F, Krajewski S, Krajewska M, Welsh K, Reed JC, Ng SC. Down-regulation of survivin by antisense oligonucleotides increases apoptosis, inhibits cytokinesis and anchorage-independent growth. *Neoplasia* 2000; **2**: 235-241
- 30 **Olie RA**, Simoes-Wust AP, Baumann B, Leech SH, Fabbro D, Stahel RA. A novel antisense oligonucleotide targeting survivin expression induces apoptosis and sensitizes lung cancer cells to chemotherapy. *Cancer Res* 2000; **60**: 2805-2809
- 31 **Narayanan R**. Harnessing the power of antisense technology for combination chemotherapy. *J Natl Cancer Inst* 1997; **89**: 107-108

Expression of p21^{WAF1} and p53 and polymorphism of p21^{WAF1} gene in gastric carcinoma

Hai-Long Xie, Qi Su, Xiu-Sheng He, Xiao-Qiu Liang, Jian-Guo Zhou, Yin Song, Yi-Qin Li

Hai-Long Xie, Qi Su, Xiu-Sheng He, Xiao-Qiu Liang, Jian-Guo Zhou, Yin Song, Yi-Qin Li, Institute of Oncology, Nanhua University, Hengyang 421001, Hunan Province, China

Supported by the Key Programs during the 8th 5-Year Plan Period, the Bureau of Health, Hunan Province, China, No.9301

Correspondence to: Dr. Qi Su, Institute of Oncology, Nanhua University, Changsheng Xilu, Hengyang 421001, Hunan Province, China. suqi1@hotmail.com

Telephone: +86-734-8281547 **Fax:** +86-734-8281547

Received: 2003-08-26 **Accepted:** 2003-10-12

Abstract

AIM: To investigate the relationship between expression of p21^{WAF1} and p53 gene, and to evaluate the deletion and polymorphism of p21^{WAF1} gene in gastric carcinoma (GC).

METHODS: Expression of p21 and p53 proteins, and deletion and polymorphism of p21 gene in GC were examined by streptavidin-peroxidase conjugated method (SP) and polymerase chain reaction-restriction fragment length polymorphism (PCR-RFLP) respectively.

RESULTS: The expression of p21 and p53 was found in 100% (20/20) and 0% (0/20) of normal gastric mucosae (NGM), 92.5% (37/40) and 15.0% (6/40) of dysplasia (DP) and 39.8% (43/108) and 56.5% (61/108) of GC, respectively. The positive rate of p21 in GC was lower than that in NGM and DP ($P < 0.05$), while the positive rate of p53 in GC was higher than that in NGM and DP ($P < 0.05$). p21 and p53 were significantly expressed in 63.3% (19/30) and 36.7% (11/30), 35.0% (14/40) and 77.5% (31/40), 26.7% (4/15) and 80.0% (12/15), 30.8% (4/13) and 30.8% (4/13), and 20.0% (2/10) and 30.0% (3/10) of well-differentiated, poorly-differentiated, undifferentiated carcinomas, mucoid carcinomas and signet ring cell carcinomas. The expression of p21 in well-differentiated carcinomas was significantly higher than that in poorly-differentiated, un-differentiated, mucoid carcinomas and signet ring cell carcinomas ($P < 0.05$). Contrarily, The expression of p53 was increased from well-differentiated to poorly-differentiated and un-differentiated carcinomas ($P < 0.05$). The expression of p21 and p53 in paired primary and metastatic GC (35.3% and 70.6%) was different from non-metastatic GC (62.5% and 42.5%) markedly ($P < 0.05$). The expression of p21 in invasive superficial muscle (60.0%) was higher than that in invasive deep muscle or total layer (35.2%) ($P < 0.05$) and was higher in TNM stages I (60.0%) and II (56.2%) than in stages III (27.9%) and IV (22.2%) ($P < 0.05$), whereas the expression of p53 did not correlate to invasion depth or TNM staging ($P > 0.05$). The exoression patterns of p53+/p21-, and of p53-/p21+ were found in 5.0% and 82.5% of DP. There was a significant correlation between expression of p21 and p53 ($P < 0.05$). But there was no significant correlation between expression of both in GC ($P > 0.05$). There was no deletion in exon 2 of p21 gene in 30 cases of GC and 45 cases of non-GC, but polymorphism of p21 gene at exon 2 was found in 26.7% (8/30) of GC and 8.9% (4/45) of non-

GC, a significant difference was found between GC and non-GC ($P < 0.05$). There was no significant relation between p21 expression of polymorphism (37.5%, 3/8) and non-polymorphism (45.5%, 10/22) in GC ($P > 0.05$).

CONCLUSION: The loss of p21 protein and abnormal expression of p53 are related to carcinogenesis, differentiation and metastasis of GC. The expression of p21 is related to invasion and clinical staging in GC intimately. The expression of p21 protein depends on p53 protein largely in NGM and DP, but not in GC. No deletion of p21 gene in exon 2 can be found in GC. The polymorphism of p21 gene might be involved in gastric carcinogenesis. There is no significant association between polymorphism of p21 gene and expression of p21 protein.

Xie HL, Su Q, He XS, Liang XQ, Zhou JG, Song Y, Li YQ. Expression of p21^{WAF1} and p53 and polymorphism of p21^{WAF1} gene in gastric carcinoma. *World J Gastroenterol* 2004; 10 (8): 1125-1131

<http://www.wjgnet.com/1007-9327/10/1125.asp>

INTRODUCTION

Previous studies have shown that tumor suppressor genes play an important role in the progression of solid tumors. p21^{WAF1} is a recently identified gene. It encodes a nuclear protein of 21 ku, which inhibits cyclin-dependent kinase activity^[1-3]. p21 protein has been reported to work as critical downstream effectors of p53 and a potential inhibitor of cyclin-dependent kinases. Thus, p21^{WAF1} gene is thought to play a central role in tumor suppression^[4-9]. Alterations of p21 expression have been observed in a wide variety of human carcinomas by immunohistochemistry^[10-15]. GC is common in China^[16-27]. But the relationship between p21 and p53 proteins expression and prognosis of GC is unclear.

In this study, expression of p21 and p53 proteins was detected by streptavidin- peroxidase conjugated method (SP). PCR and PCR-RFLP methods were used to analyze the deletion and polymorphism of p21^{WAF1} gene in GC. The correlation between the expression of p21^{WAF1} gene and carcinogenesis, differentiation, invasion and metastases, and the deletion and gene polymorphism of exon 2 in p21^{WAF1} gene in GC were investigated.

MATERIALS AND METHODS

Materials

One hundred and eight cases of GC and 20 cases of normal gastric mucosa (NGM) and 40 cases of dysplasia (DP) with gastric ulcer at the First Affiliated Hospital of Nanhua University, between April 1990 and December 1997 were used for this study, including 30 cases of well-differentiated, 40 cases of poorly-differentiated, 15 cases of undifferentiated GC, 13 cases of signet ring cell carcinoma and 10 cases of mucoid carcinoma. Eighty-one cases were men and 27 cases women, with a mean age of 58 years at diagnosis. Sixty-eight cases had lymph node metastasis and 40 cases had no lymph node metastasis.

Fifteen cases were stage I, 32 cases stage II, 43 cases stage III and 18 cases stage IV according to TNM staging. None of them had received any therapy before surgery. Freshly resected specimens including carcinoma, pericarcinoma tissues and normal mucosas located far from carcinoma, were cut into 2-4 blocks under sterile conditions. Each block was 1.5 mm×1.5 mm×1.0 mm and stored at -80 °C for PCR and PCR-RFLP analysis. The rest tissues were fixed in 100 mL/L neutral formalin, dehydrated, cleaned and paraffin-embedded. All paraffin embedded tissues were cut into 5 μm thick sequential slices and mounted onto glass slides previously processed by polylys.

Methods

Reagents and instruments Moues anti-human p21^{WAF1} and p53 monoclonal antibody, SP kit and DAB were all purchased from Maxim Company, USA. Protease K (Merk, USA), ALW261 agar gel, propylene acrylamide, N-N-sulmethyl bipropylene acrylamide, ammonium persulfate, xylene nitrile, and bromophenol blue were purchased from Shanghai Sangon Company. PCR primers were synthesized by Shanghai Sangon. Primer sequences of p21^{WAF1} gene at exon 2, Sense: 5' - CCGGATCCGGCGCCATGTCAGAACCGGC-3', antisense: 5' - CCAGACAGGTCAGCCCTTGG-3'. The amplification fragment length was 536 bp, and 309 bp. Primer sequences of β-actin served as an internal control, Sense: 5' -TCCGTGGAGAAGAGC TACGA-3', antisense: 5' -GTACTTGCGCTCAG-AAGGAG-3'. The amplification fragment length was 309 bp.

SP immunohistochemical staining All immunohistochemical analyses were performed on routinely processed, formalin-fixed, paraffin-embedded tissues using SP. Briefly, sections were dewaxed, rehydrated endogenous peroxidase was blocked, first antibody was added, then antibody bridge and enzyme labeled SP were added, colorized by DAB, stained by hematoxylin, dehydrated, cleaned and paraffin-embedded, observed under a microscope. According to Seta' standard with a slight modification^[15], nuclei were considered positive when they showed a distinct brown color in the absence of background staining. A breast carcinoma with known positive immunostaining for p21 served as a positive control. Positive and negative control slides were included within each batch of slides. (+) indicates the cells were stained weakly or the number of stained cells was less than 25%, (++) indicates the cells were stained moderately or the stained cells were covered about 26-50%, (+++) indicates the cells were stained strongly or the number of stained cells was more than 50%.

Genomic DNA extraction High molecular weight DNA was isolated from tumors by standard protease K digestion and phenol-chloroform extraction. Frozen tissue of 0.5 g was put into liquid nitrogen and powdered immediately, 10×buffer (10 mmol/L Tris-HCl pH 8.0, 0.1 mol/L EDTA pH 8.0, 5 g/L SDS) was added and spanned in 37 °C water for 1 h at the same time. Protase K was added to the mixture at a final concentration of 100 mg/L in 50 °C water for 3 h and protease K was readjusted as possible reaction. After the mixture was lysed completely, 20 mg/L RNase reacted in 37 °C water for 1 h. Then saturated phenol was put together and bugged slightly for 10 min, centrifuged and extracted. The supernant was transferred to a cleaned plastic tube, saturated phenol was processed 3 times. 1/10 volume 3 mol/L NaAc and 2-2.5 times cold ethyl were added, DNA was precipitated by centrifugation. Ethyl was removed, DNA was washed by 700 mL/L ethyl, and centrifuged 3 times, dried, resolved with TE, A₂₆₀/A₂₈₀: 1.8-1.9, and stored at 0 °C for use.

PCR amplification PCR was performed in 100 μL reactive volume containing 0.5 μg DNA template, 200 μmol/L each of dCTP, DATP, dGTP, dTTP, 0.25 μmol/L primer, PCR buffer (Tris-HCl 10 mmol/L, pH 8.3, MgCl₂ 1.5 μmol/L, KCl 50 mmol/L, gelatin 100 mg/L) pre-denatured at 95 °C for 5 min and 1.5 μL of Taq DNA polymerase and 75 μL of mineral oil were added. These

samples were subjected to 30 cycles: at 95 °C for 1 min, at 68 °C for 1 min, at 72 °C for 1 min, and a final extension at 72 °C for 5 min. Five μL of PCR product and appropriate bromophenol blue were added to the sample point container and electrophoresed on 20 g/L agarose gel containing 0.5 mg/L ethidium bromide at a tank with 0.5×TBE liquid of electrophoresis, then they were observed and photographed with ultraviolet radiography.

PCR-RFLP A 50 μL PCR product was purified by ethanol, dissolved in 17 μL sterilized water, mixed with 2 μL 10×buffer and Alw261 2u, digested at 37 °C for 3 h. A 10 μL of the digested product and 10 μL loading buffer were added to the gel containing 80 g/L polypropylene acrylamide. Then it was vertically electrophoresed at 100 V for 4 h and gel was stained with silver in the following order: fixed in 100 mL/L alcohol for 10 min, oxidized in 100 g/L nitric acid for 3 min, washed in drip for 1 min with double distilled water, stained in 12 mmol/L silver nitric acid for 20 min, washed in drip for 1 min with double distilled water, colored in 0.028 mol/L anhydrous sodium carbonate and 0.19 g/L formaldehyde, ended by adding 100 mL/L glacial acetic acid, washed in drip with double distilled water and photographed.

Statistical analysis Statistical analysis was performed using Chi-square test and analysis of variance. A *P* value less than 0.05 was considered statistically significant.

RESULTS

Expression of p21^{WAF1} and p53 protein in gastric carcinoma

The positive expression rate of p21 and p53 protein was 100% (20/20) and 0% (0/20) in NGM, 92.5% (37/40) and 15.0% (6/40) in DP and 39.8% (43/108) and 56.5% (61/108) in GC, respectively (Figure 1) (Table 1). p21 expression could only be seen in mucosal epithelial and adenoepithelial cells in NGM, no staining in matrix fibrocytes, lymphocytes and smooth myocytes was observed. The positive rate of p21 in GC was lower than that in NGM and DP (*P*<0.05), and positive expression of p53 in GC was higher than that in NGM and DP (*P*<0.05). But there was no significant difference between NGM and DP (*P*>0.05). Among the 108 cases of GC, the positive rate of p21 and p53 proteins was 63.3% (19/30) and 36.7% (11/30), 35.0% (14/40) and 77.5% (31/40), 26.7% (4/15) and 80.0% (12/15), 30.8% (4/13) and 30.8% (4/13), and 20.0% (2/10) and 30.0% (30.0/100) in well-differentiated, poorly-differentiated, undifferentiated GC, mucoid carcinomas and signet ring cell carcinomas. The positive rate of p21 in well-differentiated GC was significantly higher than that in poorly-differentiated, undifferentiated, mucoid carcinomas and signet ring cell carcinomas (*P*<0.05). Contrarily, the expression of p53 was increased from well-differentiated to poorly-differentiated and undifferentiated GC (*P*<0.05). The positive rate of p21 and p53 in paired primary and lymph node metastatic GC (35.3% and 70.6%) was significantly different from that in non-metastasis carcinomas (62.5% and 42.5%) (*P*<0.05). The expression of p21 in invaded superficial muscle (60.0%) was higher than that in invaded deep muscle or total layer (35.2%) (*P*<0.05), and was higher in TNM stages I (60.0%) and II (56.2%) than that in stages III (27.9%) and IV (22.2%) (*P*<0.05). Whereas the expression of p53 did not correlate with invasion depth and TNM stages (*P*>0.05). There was no association between age and sex and expression of p21 and p53 (*P*>0.05) (Table 2).

Relationship between expression of p21^{WAF1} and p53

Five percent cases had p53 positivity and p21 negativity simultaneously, whereas 82.5% cases had p53 negativity and p21 positivity simultaneously in 40 cases of DP. There was a significant correlation between expression of p21 and p53 proteins (*P*<0.05). Meanwhile, 32.4% of p21 negativity and p53 positivity and 15.7% of p21 positivity and loss of p53 protein were detected in GC, but there was no significant correlation between expression of p21 and p53 proteins in GC (*P*>0.05) (Table 3).

Table 1 Expression of p21 and p53 proteins in normal gastric mucosa, dysplasia and gastric carcinoma

Tissue type	Cases number	p21				p53					
		Negativity (%)	Positivity (%)			Negativity (%)	Positivity (%)				
			+	++	+++		total	+	++	+++	total
NGM	20	0 (0)	6	7	7	20 (100)	20 (100)	0	0	0	0 (0)
DP	40	3 (7.5)	8	11	18	37 (92.5)	34 (85.0)	1	3	2	6 (15.0)
GC	108	65 (60.2)	9	14	20	43 (39.8)	47 (43.5)	17	19	25	61 (56.5)

NGM: normal gastric mucosa; DP: dysplasia; GC: gastric carcinoma.

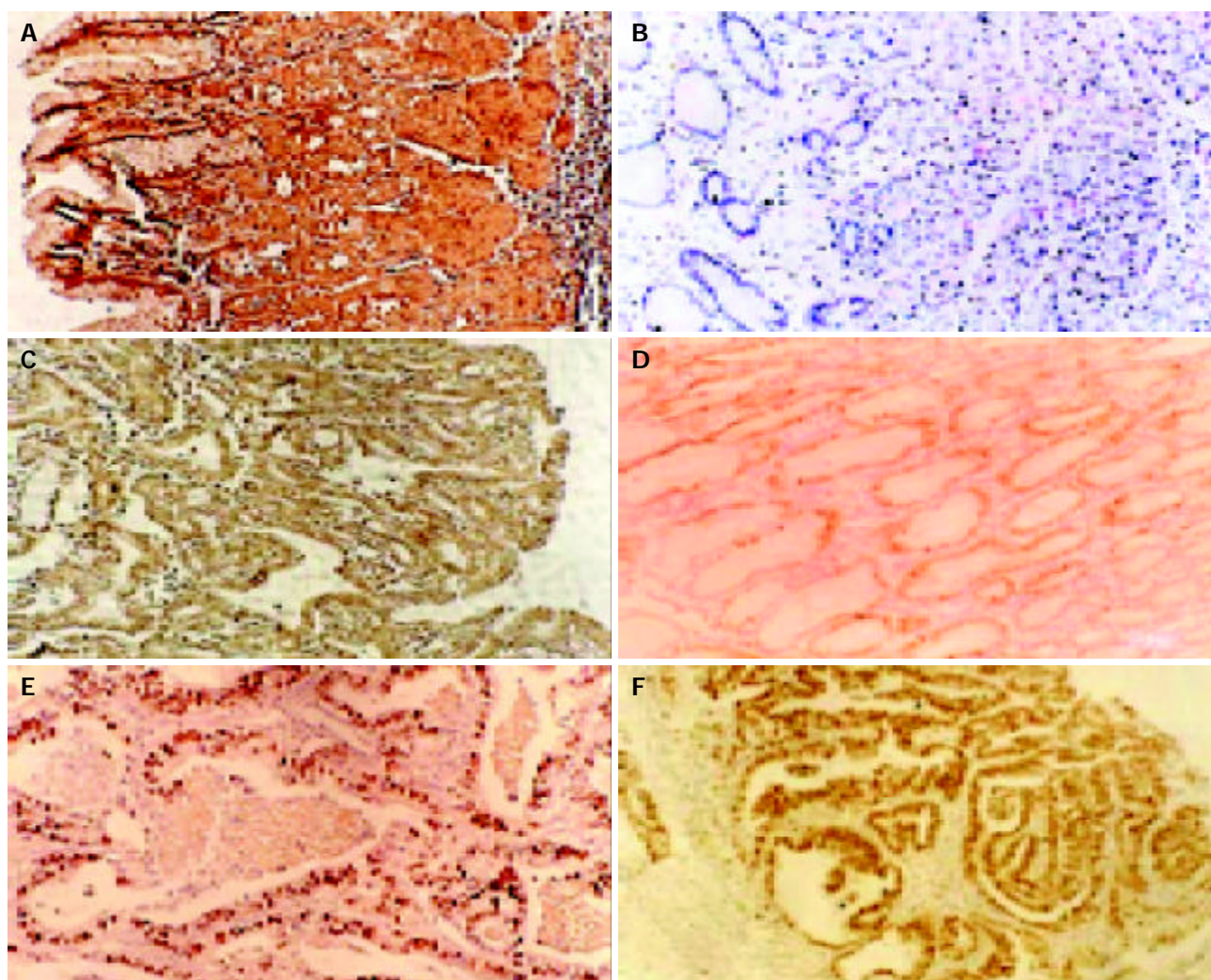


Figure 1 The results of immunohistochemical staining. A: p21 (left) and p53 (right) in NGM. $\times 100$, B: p21 (left) and p53 (right) in DP. $\times 100$, C: p21 (left $\times 200$) and p53 (right $\times 100$) in GC.

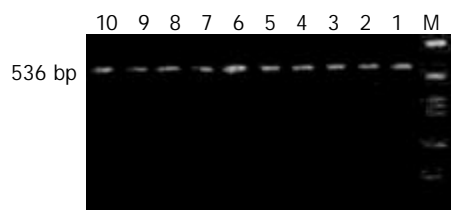


Figure 2 PCR amplified products at exon 2 of p21^{WAF1} gene. Lines 2, 4, 6, 8, 10: GC. Lines 1, 3, 5, 7, 9: tumor adjacent tissue. M: PCR marker.

Deletion and polymorphism of p21^{WAF1} gene at exon 2 in gastric carcinoma

PCR amplification showed target products in all GC and NGM.

All experiments were performed three times. The results were identical (Figure 2). The 536-bp PCR amplified fragment at exon 2 of p21 gene was digested with the ALW261 restriction enzyme. Digestion of the wild type allele produced DNA fragments with a length of 124, 174, and 238 bp. The C→A polymorphism created an extra enzyme recognition site, resulting in ALW261 digested fragments of 76, 98, 124, and 238 bp in length^[28] (Figure 3). There was no deletion at exon 2 of p21 gene in 30 cases of GC and 45 cases of non-GC, but polymorphism of p21 gene at exon 2 was found in 26.7% (8/30) of GC and 8.9% (4/45) of non-GC. A significant difference was found between GC and non-GC ($P < 0.05$). There was no significant relation between p21 expression of polymorphism (37.5%, 3/8) and non-polymorphism (45.5%, 10/22) in GC ($P > 0.05$).

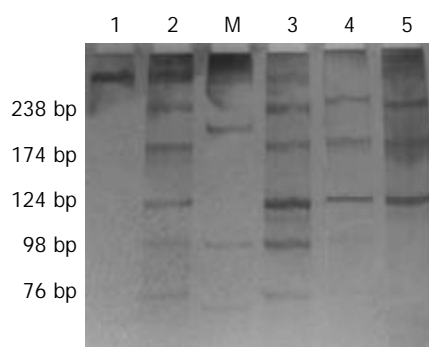


Figure 3 RFLP analysis of exon 2 of p21^{WAF1} gene and ALW261 digestion analysis of codon 31. Digestion of a 536 bp polymerase chain reaction fragment containing wild type exon 2 yielded fragments of 124, 174, and 238 bp in length (lanes 2, 3). The C→A polymerase polymorphism created an extra recognition site resulting in DNA fragments of 76, 98, 124, 174, and 238 bp in the heterozygote 9 (Lanes 4, 5). M: PCR marker. Lane 1: undigested fragment.

Table 2 Association of p21 and p53 expression with clinicopathologic parameters in gastric carcinoma

Parameters	Cases (n)	p21 positivity (%)	p53 positivity (%)
Age			
≤50	43	18 (41.9)	25 (58.1)
51-59	37	15 (40.5)	20 (54.1)
≥60	28	10 (35.7)	16 (57.1)
Sex			
Male	81	32 (39.5)	43 (53.1)
Female	27	11 (40.7)	18 (66.7)
Grade			
Well-differentiated	30	19 (63.3)	11 (36.7)
Poorly-differentiated	40	14 (35.0)	31 (77.5)
Undifferentiated	15	4 (26.7)	12 (80.0)
Mucoid	13	4 (30.8)	4 (30.8)
Signet ring cell	10	2 (20.0)	3 (30.0)
Invasion depth			
Superficial muscle	20	12 (60.0)	11 (55.0)
Total layer	88	31 (35.2)	50 (56.8)
Lymph node metastasis			
Absence	40	25 (62.5)	17 (42.5)
Presence	68	24 (35.3)	48 (70.6)
TNM stage			
I	15	9 (60.0)	7 (46.7)
II	32	18 (56.2)	17 (53.1)
III	43	12 (27.9)	26 (60.5)
IV	18	4 (22.2)	11 (61.1)

Table 3 Relationship between expression of p21 and p53 in gastric carcinoma and dysplasia

p21	p53		
	Positive (%)	Negative (%)	Total (%)
Dysplasia			
Positive	4 (10.0)	33 (82.5)	37 (92.5)
Negative	2 (5.0)	1 (2.5)	3 (7.5)
Total	6 (15.0)	34 (85.0)	40 (100)
Gastric carcinoma			
Positive	26 (24.1)	17 (15.7)	43 (39.8)
Negative	35 (32.4)	30 (27.8)	65 (60.2)
Total	61 (56.5)	47 (43.5)	108 (100)

DISCUSSION

p21^{WAF1} gene is localized at chromosome 6p21.2. It could play an important role in the regulation of cell cycle transitions in normal cells, inhibit several cyclin/CDK complexes and block cell cycle progression^[1-3]. Moreover, expression of p21 protein could be induced by p53. p21 protein is an important tumor suppressor and has been proposed as a tumor suppressor gene and a potential mediator of p53-associated tumorigenesis^[4-9]. However, unlike p53-deficient mice, p21-deficient mice could undergo normal development with no exhibition early tumorigenesis. On the other hand, it has been shown that p21 expression could be mediated through p53-independent pathways. Even in the presence of p53 alterations, p21 expression could be maintained. p21 might represent an independent marker of tumor behaviors^[29].

It was reported that p21 expression was limited to foveola epithelial cells. p53 expression was confined to only a few regenerative epithelial cells of the mucous neck region in NGM. Increased p21 expression was limited to surface DP epithelium and weak p53 expression was in full thickness of DP epithelium^[30]. It was found p53 was stained negatively, while p21 was stained positively in each NGM^[34]. In regard to expression of p21 and p53 in GC, Seo *et al.*^[4], Okuyama *et al.*^[7], Baldus *et al.*^[33], Oya *et al.*^[36], Kaye *et al.*^[37] and Xiangming *et al.*^[64] separately demonstrated various expression levels of 63.7% and 33.3%, 42.6% and 37.9%, 58% and 45%, 75% and 40%, 75% and 40%, and 90.2% and 28.9%. However, Zolota *et al.*^[31], Liu *et al.*^[32], Ogawa *et al.*^[35] and Gomyo *et al.*^[43] observed that the positive rates of p21 and p53 were 32% and 51%, 40.5% and 42.1%, 37.2% and 50%, 32% and 65%, respectively. Our study showed that expression of p21 and p53 was found in 100% (20/20) and 0% (0/20) of NGM, 92.5% (37/40) and 15.0% (6/40) of DP and 39.8% (43/108) and 56.5% (61/108) of GC, respectively. p21 expression could only be seen in mucosal epithelial and adenoepithelial cells in NGM. Expression of p21 and p53 in GC was remarkably different from that in DP and NGM ($P < 0.05$). The results indicated that gastric carcinogenesis was probably related to the loss of p21 expression and mutation of p53. This finding is consistent with other reports^[7,31,34,35,38,45]. It was found that the expression rate of p53 was 0% in LGAs, 9% in HGAs, 39% in IMCs and 43% in SMCs, and expression of p21 was present in 100% of LGAs, 74% of HGAs, 46% of IMCs and 4% of SMCs. Whereas p53+/p21- lesions were observed in 0% of LGAs, 4% of HGAs, 11% of IMCs and 26% of SMCs^[36].

Clinicopathologic and prognostic significances of p21 and p53 expression have been reported in various carcinomas^[10-15,48-52]. In GC, expression of p21 correlated with advanced stage, lymph node metastasis and survival^[4,6,32-34]. Univariate and multivariate survival analyses revealed that clinicopathological stage and expression status of p21 were independent prognostic factors^[34]. But it was also reported that expression of p21 was not associated with clinicopathological features^[64]. Expression of p53 correlated with depth of tumor invasion^[4], lymph node metastasis^[33] and poor prognosis^[32]. However, no significant correlation could be observed between the status of p53 expression and survival^[4]. Multivariate survival analysis revealed that TNM stage and lymph node state were independent prognostic factors^[32]. In multivariate survival analyses, neither p21 nor p53 emerged as an independent prognostic factor^[33]. There was no apparent correlation between the expression of p21 and p53 and tumor stage, depth of invasion or lymphnode metastases^[31]. There were significant differences in the incidence of p53 expression, the loss of p21 expression, and the 5-year survival rate between Pen-A type and Super type in early GC^[8]. Stratification of the carcinomas according to histological grade and growth pattern did not result in significant differences in p53 and p21 expression^[38].

The present study found that the positive rate of p21 expression was 63.3% in well-differentiated carcinomas, which was significantly higher than that in poorly-differentiated (35.0%), undifferentiated GC (26.7%), mucoid carcinomas (30.8%) and signet ring cell carcinomas (20.0%) ($P<0.05$). Contrarily, expression of p53 was increased from well-differentiated (36.7%) to poorly-differentiated (77.5%) and undifferentiated GC (80.0%) ($P<0.05$). The positive rate of p21 and p53 in paired primary and metastatic GC (35.3% and 70.6%) was markedly different from that in non-metastasis GC (62.5% and 42.5%) ($P<0.05$). The expression of p21 in invaded superficial muscle (60.0%) was higher than that in invaded deep muscle or total layer (35.2%) ($P<0.05$). The expression of p21 in TNM stages I (60.0%) and II (56.2%) was higher than that in stages III (27.9%) and IV (22.2%) ($P<0.05$). Whereas the expression of p53 did not correlate with invasion depth and TNM stage ($P>0.05$). Our results indicated that loss of p21 expression and mutation of p53 were related to carcinogenesis, differentiation and metastasis, and loss of p21 expression was related intimately to invasion depth and TNM stage. It was suggested that combined examination of p21 and p53 expression was a reliable prognostic marker for GC.

Many investigations showed that the mutation of p53 gene was common in various human carcinomas. Mutated p53 can act as a dominant oncogene. The immunoreactivity of p53 protein is a general indicator of tumors with altered p53 function. p21 performs a part of p53 function through the induction of p21 by wild type p53. However, p21 could be transcriptionally induced by wild type but not mutated p53^[14,54]. It was found that p21 gene expression level was high in wild type p53 human breast cancer cells, but low in mutated p53 human breast cancer cells, indicating p21 gene expression at mRNA and protein levels are associated with p53 phenotype^[55]. However, the expression of p21 protein was suppressed in neoplastic tissues with and without p53 gene alterations^[56]. Western blot analysis revealed increased expression of p21 protein after infection with AxCA-p53 in all the cell lines. It was suggested that the apoptotic pathway dominated the growth arrest pathway after infection with AxCA-p53^[40]. The level of p21 mRNA was very low or undetectable in all cell lines containing mutated p53 gene. But cell lines with wild-type p53 gene could express, it and the level of p21 mRNA was high in 8 GC cell lines^[45]. Qian *et al.* used Northern and Western blot to analyze the expression of p21 and found that p21 mRNA was expressed in 2 cases of 15 p53+ and all of the p53- cases, indicating inactivation of p53 was closely related with the unexpression of p21 mRNA in GC^[47]. However, some investigators believed p21 protein expression was unrelated with p53 protein expression^[4,35,37,39]. Accumulation of mutated p53 protein might suppress the expression of p21 protein in GC, and cancer cells with overexpression of p53 might have a high proliferative activity^[5]. Combined analysis of p21 and p53 showed that p21+/p53- GC displayed less aggressive characteristics, better survival and no recurrence after curative resection than other groups of GC^[4,7,35,41,64]. Evaluation of expressions of p53 and p21 might aid in predicting clinical prognosis for surgical treatment in GC^[7,32,35,38,41]. The p21 expression of non-neoplastic mucosae was most likely related to cell senescence and/or terminal differentiation. Moreover, p53-independent induction of p21 expression apparently occurred in a considerable proportion of early GC. It was suggested that defects downstream of p21 might cause this apparent discrepancy^[39]. In our studies, 5.0% cases were p53+/p21-, 82.5% cases were p53-/p21+ in totally 40 cases of DP. There was a significant correlation between expression of p21 and p53 ($P<0.05$). Meanwhile, 15.7% of p53-/p21+, 32.4% of p53+/p21-, 24.1% of p53+/p21+ and 27.8% of p53-/p21- were detected in GC, respectively. There was no significant correlation between p21 and P53 protein expression.

These findings suggested that p21 protein was expressed mostly in a p53-independent manner and in some other factors, such as platelet-derived growth factor (PDGF)^[57].

Alterations in the integrity of human p21 gene were rare events in human tumors^[58,59,61]. Mutation of p21 gene has not been detected^[6]. The promoter of p21 gene was not methylated in GC^[63]. However, recent reports have demonstrated an association of p21 gene polymorphisms with many carcinomas^[28,60,61]. No abnormal bands of p21 gene were found in all of samples or cell lines, but three major variants at exons 2 and 3 of the gene were found to be consistent with the existence of two different DNA polymorphisms. Sequence analysis of the amplified products producing these three variants at each exon from normal DNAs confirmed the presence of polymorphisms in p21 gene. Mutation within the coding portion of p21 gene was undetectable in a large series of human tumors, many of which had a normal p53 gene. This suggested that p21 alterations were generally caused indirectly by p53 mutation rather than by intragenic mutation of p21 itself^[58]. Two polymorphisms have previously been characterized in p21 gene: a C→A transversion at codon 31 (ser→arg) and a C→T transition at 20 nucleotides downstream from the 3' end of exon 3^[28]. The two polymorphisms were found in 18 of 96 tumor samples lacking p53 alterations (18.8%). Nine of 54 prostate adenocarcinoma samples (16.7%) contained both p21 variants, whereas 9 of 42 squamous cell carcinomas of the head and neck (21.4%) displayed both polymorphisms. Of the 110 controls examined, 10 (9.1%) had both alterations. Both p21 polymorphisms occurred in all samples examined and there was no indication of mutation in the coding region of p21 gene^[28]. We analysed the deletion of p21 gene at exon 2 with PCR and PCR-RFLP methods. No deletion of p21 gene was found in GC. The result suggested deletion at exon 2 of p21 gene was not the cause of loss expression of p21 gene. The induction of p21 was mediated by posttranscriptional mechanisms^[62]. The polymorphism of p21 gene at exon 2 was found in 26.7% (8/30) of GC and 8.9% (4/45) of non-GC. A significant difference was found between GC and non-GC ($P<0.05$). The results in this study indicated that the polymorphism of p21 gene might be involved in gastric carcinogenesis. But There was no significant relation between p21 expression of polymorphism (37.5%, 3/8) and non-polymorphism (45.5%, 10/22) in GC ($P>0.05$). Its mechanism is still unclear. It was found that p21 gene was activated only by histone deacetylase inhibitors, suggesting that formation of the inactive chromatins through histone deacetylation seems to be a general mechanism for inactivation of p21 gene in GC cells^[63].

REFERENCES

- 1 **el-Deiry WS**, Tokino T, Velculescu VE, Levy DB, Parsons R, Trent JM, Lin D, Mercer WE, Kinzler KW, Vogelstein B. WAF, A potential mediator of P53 tumor suppression. *Cell* 1993; **75**: 817-824
- 2 **Waga S**, Hannon GJ, Beach D, Stillman B. The P21WAF1 inhibitor of cyclin-dependent kinases controls DNA replication by interaction with PCNA. *Nature* 1994; **369**: 574-578
- 3 **Sherr CJ**. Carcinoma cell cycles. *Science* 1996; **274**: 1672-1677
- 4 **Seo YH**, Joo YE, Choi SK, Rew JS, Park CS, Kim SJ. Prognostic significance of p21 and p53 expression in gastric cancer. *Korean J Intern Med* 2003; **18**: 98-103
- 5 **Ikeguchi M**, Saito H, Kondo A, Tsujitani S, Maeta M, Kaibara N. Mutated p53 protein expression and proliferative activity in advanced gastric cancer. *Hepatogastroenterology* 1999; **46**: 2648-2653
- 6 **Park YE**, Choi KC, Choi YH. p21 expression and mutation in gastric carcinoma: analysis by immunohistochemistry and PCR-SSCP. *J Korean Med Sci* 1998; **13**: 507-512
- 7 **Okuyama T**, Maehara Y, Kabashima A, Takahashi I, Kakeji Y, Sugimachi K. Combined evaluation of expressions of p53 and

- p21 proteins as prognostic factors for patients with gastric carcinom. *Oncology* 2002; **63**: 353-361
- 8 **Noda H**, Maehara Y, Irie K, Kakeji Y, Yonemura T, Sugimachi K. Growth pattern and expressions of cell cycle regulator proteins p53 and p21WAF1/CIP1 in early gastric carcinoma. *Cancer* 2001; **92**: 1828-1835
- 9 **Tahara E**. Molecular biology of gastric cancer. *World J Surg* 1995; **19**: 484-490
- 10 **Ueno H**, Hirai T, Nishimoto N, Hihara J, Inoue H, Yoshida K, Yamashita Y, Toge T, Tsubota N. Prediction of lymph node metastasis by p53, p21 (Waf1), and PCNA expression in esophageal cancer patients. *J Exp Clin Cancer Res* 2003; **22**: 239-245
- 11 **Xie X**, Clausen OP, Boysen M. Prognostic significance of p21WAF1/CIP1 expression in tongue squamous cell carcinomas. *Arch Otolaryngol Head Neck Surg* 2002; **128**: 897-902
- 12 **Yen-Ping Kuo M**, Huang JS, Kok SH, Kuo YS, Chiang CP. Prognostic role of p21WAF1 expression in areca quid chewing and smoking-associated oral squamous cell carcinoma in Taiwan. *J Oral Pathol Med* 2002; **31**: 16-22
- 13 **Amatya VJ**, Takeshima Y, Sugiyama K, Kurisu K, Nishisaka T, Fukuhara T, Inai K. Immunohistochemical study of Ki-67 (MIB-1), p53 protein, p21WAF1, and p27KIP1 expression in benign, atypical, and anaplastic meningiomas. *Hum Pathol* 2001; **32**: 970-975
- 14 **Holm R**, Skovlund E, Skomedal H, Florenes VA, Tanum G. Reduced expression of p21WAF1 is an indicator of malignant behaviour in anal carcinomas. *Histopathology* 2001; **39**: 43-49
- 15 **Seta T**, Imazeki F, Yokosuka O, Saisho H, Suzuki T, Koide Y, Isono K. Expression of P53 and P21 WAF1 proteins in gastric and esophageal carcinomas comparison with mutations of P53 gene. *Dig Dis Sci* 1998; **43**: 279-289
- 16 **Parkin DM**. Global carcinoma statistics in the year 2000. *Lancet Oncol* 2001; **2**: 533-543
- 17 **Zheng ZH**, Xun XJ, Qiu GR, Liu YH, Wang MX, Sun KL. E-cadherin gene mutation in precarcinomaous condition, early and advanced stage of gastric carcinoma. *Shijie Huaren Xiaohua Zazhi* 2002; **10**: 153-156
- 18 **Cheng SD**, Wu YL, Zhang YP, Qiao MM, Guo QS. Abnormal drug accumulation in multidrug resistant gastric carcinoma cells. *Shijie Huaren Xiaohua Zazhi* 2001; **9**: 131-134
- 19 **Chen GY**, Wang DR. The expression and clinical significance of CD44v in human gastric cancers. *World J Gastroenterol* 2000; **6**: 125-127
- 20 **Wang RQ**, Fang DC, Liu WW. MUC2 gene expression in gastric cancer and preneoplastic lesion tissues. *Shijie Huaren Xiaohua Zazhi* 2000; **8**: 285-288
- 21 **Guo YQ**, Zhu ZH, Li JF. Flow cytometric analysis of apoptosis and proliferation in gastric cancer and precancerous lesion. *Shijie Huaren Xiaohua Zazhi* 2000; **8**: 983-987
- 22 **Chen SY**, Wang JY, Ji Y, Zhang XD, Zhu CW. Effects of *Helicobacter pylori* and protein kinase C on gene mutation in gastric carcinoma and precarcinomaous lesions. *Shijie Huaren Xiaohua Zazhi* 2001; **9**: 302-307
- 23 **Xu AG**, Li SG, Liu JH, Gan AH. Function of apoptosis and expression of the proteins Bcl-2, p53 and C-myc in the development of gastric cancer. *World J Gastroenterol* 2001; **7**: 403-406
- 24 **Wu K**, Zhao Y, Liu BH, Li Y, Liu F, Guo J, Yu WP. RRR- α -tocopheryl succinate inhibits human gastric cancer SGC-7901 cell growth by inducing apoptosis and DNA synthesis arrest. *World J Gastroenterol* 2002; **8**: 26-30
- 25 **He XS**, Su Q, Chen ZC, He XT, Long ZF, Ling H, Zhang LR. Expression, deletion and mutation of p16 gene in gastric cancer. *World J Gastroenterol* 2001; **7**: 515-521
- 26 **Sun XD**, Mu R, Zhou YS, Dai XD, Qiao YL, Zhang SV, Huangfu XM, Sun J, Li LD, Lu FZ. 1990-1992 mortality of stomach carcinoma in China. *Zhongguo Zhongliu Zazhi* 2002; **24**: 4-8
- 27 **Yang L**, Kuang LG, Zheng HC, Li JY, Wu DY, Zhang SM, Xin Y. PTEN encoding product: a marker for tumorigenesis and progression of gastric carcinoma. *World J Gastroenterol* 2003; **9**: 35-39
- 28 **Facher EA**, Becich MJ, Deka A, Law JC. Association between human carcinoma and two polymorphism, occurring together in the P21Waf1/Cip1 cyclin-dependent kinase inhibitor gene. *Cancer* 1997; **79**: 2424-2429
- 29 **Deng C**, Zhang P, Harper JW, Elledge SJ, Leder P. Mice lacking p21^{CIP1/WAF1} undergo normal development, but are defective in G1 checkpoint control. *Cell* 1995; **82**: 675-684
- 30 **Cho JH**, Kim WH. Altered topographic expression of 21WAF1/CIP1/SDI1, bcl2 and p53 during gastric carcinogenesis. *Pathol Res Pract* 1998; **194**: 309-317
- 31 **Zolota V**, Batistatou A, Tsamandas AC, Iliopoulos G, Scopa CD, Bonikos DS. Immuno-histochemical expression of TGF-beta1, p21WAF1, p53, Ki67, and angiogenesis in gastric carcinomas: a clinicopathologic study. *Int J Gastrointest Cancer* 2002; **32**: 83-89
- 32 **Liu XP**, Kawauchi S, Oga A, Suehiro Y, Tsushimi K, Tsushimi M, Sasaki K. Combined examination of p27(Kip1), p21(Waf1/Cip1) and p53 expression allows precise estimation of prognosis in patients with gastric carcinoma. *Histopathology* 2001; **39**: 603-610
- 33 **Baldus SE**, Schneider PM, Monig SP, Zirbes TK, Fromm S, Meyer W, Glossmann J, Schuler S, Thiele J, Holscher AH, Dienes HP. p21/waf1/cip1 in gastric cancer: associations with histopathological subtypes, lymphonodal metastasis, prognosis and p53 status. *Scand J Gastroenterol* 2001; **36**: 975-980
- 34 **Liu XP**, Tsushimi K, Tsushimi M, Kawauchi S, Oga A, Furuya T, Sasaki K. Expression of p21(WAF1/CIP1) and p53 proteins in gastric carcinoma: its relationships with cell proliferation activity and prognosis. *Cancer Lett* 2001; **170**: 183-189
- 35 **Ogawa M**, Onoda N, Maeda K, Kato Y, Nakata B, Kang SM, Sowa M, Hirakawa K. A combination analysis of p53 and p21 in gastric carcinoma as a strong indicator for prognosis. *Int J Mol Med* 2001; **7**: 479-483
- 36 **Oya M**, Yao T, Tsuneyoshi M. Expressions of cell-cycle regulatory gene products in conventional gastric adenomas: possible immunohistochemical markers of malignant transformation. *Hum Pathol* 2000; **31**: 279-287
- 37 **Kaye PV**, Radebold K, Isaacs S, Dent DM. Expression of p53 and p21waf1/cip1 in gastric carcinoma: lack of inter-relationship or correlation with prognosis. *Eur J Surg Oncol* 2000; **26**: 39-43
- 38 **Huang J**, Gan J. Relationship between expression of tumor suppressor protein p21 and p53 and cell proliferation in the gastric carcinoma. *Hunan Yike Daxue Xuebao* 1998; **23**: 441-443
- 39 **Craanen ME**, Blok P, Offerhaus GJ, Meijer GA, Dekker W, Kuipers EJ, Meuwissen SG. p21(Waf1/Cip1) expression and the p53/MDM2 feedback loop in gastric carcinogenesis. *J Pathol* 1999; **189**: 481-486
- 40 **Tatebe S**, Matsuura T, Endo K, Teramachi K, Nakamura T, Sato K, Ito H. A denovirus-mediated transfer of wild-type p53 gene results in apoptosis or growth arrest in human cultured gastric carcinoma cells. *Int J Oncol* 1999; **15**: 229-235
- 41 **Ikeguchi M**, Saito H, Katano K, Tsujitani S, Maeta M, Kaibara N. Expression of p53 and p21 are independent prognostic factors in patients with serosal invasion by gastric carcinoma. *Dig Dis Sci* 1998; **43**: 964-970
- 42 **Ikeguchi M**, Saito H, Katano K, Gomyo Y, Tsujitani S, Maeta M, Kaibara N. Relationship between the long-term effects of intraperitoneal chemotherapy and the expression of p53 and p21 in patients with gastric carcinoma at stage IIIa and stage IIIb. *Int Surg* 1997; **82**: 170-174
- 43 **Gomyo Y**, Ikeda M, Osaki M, Tatebe S, Tsujitani S, Ikeguchi M, Kaibara N, Ito H. Expression of p21 (waf1/cip1/sdi1), but not p53 protein, is a factor in the survival of patients with advanced gastric carcinoma. *Cancer* 1997; **79**: 2067-2072
- 44 **Ogawa M**, Maeda K, Onoda N, Chung YS, Sowa M. Loss of p21WAF1/CIP1 expression correlates with disease progression in gastric carcinoma. *Br J Cancer* 1997; **75**: 1617-1620
- 45 **Akama Y**, Yasui W, Kuniyasu H, Yokozaki H, Akagi M, Tahara H, Ishikawa T, Tahara E. Genetic status and expression of the cyclin-dependent kinase inhibitors in human gastric carcinoma cell lines. *Jpn J Cancer Res* 1996; **87**: 824-830
- 46 **Akagi M**, Yasui W, Akama Y, Yokozaki H, Tahara H, Haruma K, Kajiyama G, Tahara E. Inhibition of cell growth by transforming growth factor beta 1 is associated with p53-independent induction of p21 in gastric carcinoma cells. *Jpn J Cancer Res* 1996; **87**: 377-384

- 47 **Qian LP**, Lin GJ. Relationship of WAF1 and p53 in human gastric carcinomas. *Shanghai Yike Daxue Xuebao* 1998; **25**: 416-418
- 48 **Esposito V**, Baldi A, De Luca A, Groger AM, Loda M, Giordano GG, Caputi M, Baldi F, Pagano M, Giordano A. Prognostic role of the cyclin-dependent kinase inhibitor p27 in non-small cell lung cancer. *Cancer Res* 1997; **57**: 3381-3385
- 49 **Loda M**, Cukor B, Tam SW, Lavin P, Fiorentino M, Draetta GF, Jessup JM, Pagano M. Increased proteasome-dependent degradation of the cyclin-dependent kinase inhibitor p27 in aggressive colorectal carcinomas. *Nat Med* 1997; **3**: 231-233
- 50 **Catzavelos C**, Bhattacharya N, Ung YC, Wilson JA, Roncari L, Sandhu C, Shaw P, Yeger H, Morava-Protzner I, Kapusta L, Franssen E, Pritchard KI, Slingerland JM. Decreased levels of the cell-cycle inhibitor p27^{Kip1} protein: prognostic implications in primary breast carcinoma. *Nat Med* 1997; **3**: 227-230
- 51 **Porter PL**, Malone KE, Heagerty PJ, Alexander GM, Gatti LA, Firpo EJ, Daling JR, Roberts JM. Expression of cell-cycle regulators p27 and cyclin E, alone and in combination, correlate with survival in young breast carcinoma patients. *Nat Med* 1997; **3**: 222-225
- 52 **Tsihlias J**, Kapusta LR, DeBoer G, Morava-Protzner I, Zbieranowski I, Bhattacharya N, Catzavelos GC, Klotz LH, Slingerland JM. Loss of cyclin-dependent kinase inhibitor p27^{Kip1} is a novel prognostic factor in localized human prostate adenocarcinoma. *Cancer Res* 1998; **58**: 542-548
- 53 **Noda H**, Maehara Y, Irie K, Kakeji Y, Yonemura T, Sugimachi K. Growth pattern and expressions of cell cycle regulator proteins p53 and p21WAF1/CIP1 in early gastric carcinoma. *Cancer* 2001; **92**: 1828-1835
- 54 **Somasundaram K**, Zhang H, Zeng YX, Houvras Y, Peng Y, Zhang H, Wu GS, Licht JD, Weber BL, El-Deiry WS. Arrest of the cell cycle by the tumor-suppressor BRCA1 requires the CDK-inhibitor P21WAF1. *Nature* 1997; **389**: 187-190
- 55 **Jiang M**, Shao Z, Wu J. WAF1/CIP1/p21 gene in wild type p53 and mutant p53 human breast cancer cell lines in relation to its cytobiological features. *Zhonghua Zhongliu Zazhi* 1998; **20**: 181-184
- 56 **Yook JL**, kin J. Expression of p21WAF1/CIP1 is unrelated to p53 tumour suppressor gene status in oral squamous cell carcinomas. *Oral Oncol* 1998; **34**: 198-203
- 57 **Liu Y**, Martindale JL, Gorospe M, Holbrook NJ. Regulation of p21WAF1/CIP1 expression through mitogen-activated protein kinase signaling pathway. *Cancer Res* 1996; **56**: 31
- 58 **Shiohara M**, El-Deiry WS, Wada M, Nakamaki T, Takeuchi S, Yang R, Chen DL, Vogelstein B, Koeffler HP. Absence of WAF1 mutations in a variety of human malignancies. *Blood* 1994; **84**: 3781-3784
- 59 **Akama Y**, Yasui W, Kuniyasu H, Yokozaki H, Akagi M, Tahara H, Ishikawa T, Tahara E. No point mutations but codon 31 polymorphism and decreased expressed of the P21WAF1 gene in human gastric carcinomas. *Mol Cell Differen* 1996; **4**: 187-198
- 60 **Powell BL**, van Staveren IL, Roosken P, Grieu F, Berns EM, Iacopetta B. Associations between common polymorphisms in TP53 and p21WAF1/Cip1 and phenotypic features of breast cancer. *Carcinogenesis* 2002; **23**: 311-315
- 61 **Mousses S**, Ozcelik H, Lee PD, Malkin D, Bull SB, Andrulis IL. Two variants of the CIP1/WAF1 gene occur together and are associated with human cancer. *Hum Mol Genet* 1995; **4**: 1089-1092
- 62 **Schmidt-Grimminger DC**, Wu X, Jian Y, Broker TR, Chow LT. Post-transcriptional induction of p21cip1 protein in condy-lomata and dysplasias is inversely related to human papillomavirus activities. *Am J Pathol* 1998; **152**: 1015-1024
- 63 **Shin JY**, Kim HS, Park J, Park JB, Lee JY. Mechanism for inactivation of the KIP family cyclin-dependent kinase inhibitor genes in gastric cancer cells. *Cancer Res* 2000; **60**: 262-265
- 64 **Xiangming C**, Hokita S, Natsugoe S, Tanabe G, Baba M, Takao S, Kuroshima K, Aikou T. p21 expression is a prognostic factor in patients with p53-negative gastric cancer. *Cancer Lett* 2000; **148**: 181-188

Edited by Zhu LH and Wang XL Proofread by Xu FM

In vitro effects of recombinant human growth hormone on growth of human gastric cancer cell line BGC823 cells

Jia-Yong Chen, Dao-Ming Liang, Ping Gan, Yi Zhang, Jie Lin

Jia-Yong Chen, Dao-Ming Liang, Ping Gan, Yi Zhang, Jie Lin, Department of General Surgery of the Second Affiliated Hospital, Kunming Medical College, Kunming 650101, Yunnan Province, China

Correspondence to: Dr. Jia-Yong Chen, Department of General Surgery of the Second Affiliated Hospital, Kunming Medical College, Kunming 650101, Yunnan Province, China. chenjiayong776@hotmail.com

Telephone: +86-871-5352825 **Fax:** +86-871-5352087

Received: 2002-08-10 **Accepted:** 2003-11-12

Abstract

AIM: To study the effects of recombinant human growth hormone (rhGH) on growth of human gastric cancer cell line *in vitro*.

METHODS: Experiment was divided into control group, rhGH group, oxaliplatin (L-OHP) group and rhGH+L-OHP group. Cell inhibitory rate, cell cycle, cell proliferation index (PI) and DNA inhibitory rate of human gastric cancer line BGC823, at different concentrations of rhGH treatment were studied by cell culture, MTT assay and flow cytometry.

RESULTS: The distinctly accelerated effects of rhGH on multiplication of BGC823 cell line were not found *in vitro*. There was no statistical significance between rhGH group and control group, or between rhGH+L-OHP group and L-OHP group ($P>0.05$). The cell growth curve did not rise. Cell inhibitory rate and cells arrested in G₀-G₁ phase were obviously increased. Meanwhile, cells in S phase and PI were distinctly decreased and DNA inhibitory rate was obviously increased in rhGH+L-OHP group in comparison with control group and rhGH group, respectively ($P<0.01$). Cell inhibitory rate showed an increasing trend and PI showed a decreasing trend in rhGH+L-OHP group compared with L-OHP group.

CONCLUSION: *In vitro* rhGH does not accelerate the multiplication of human gastric cancer cells. It may increase the therapeutic efficacy when it is used in combination with anticancer drugs.

Chen JY, Liang DM, Gan P, Zhang Y, Lin J. *In vitro* effects of recombinant human growth hormone on growth of human gastric cancer cell line BGC823 cells. *World J Gastroenterol* 2004; 10(8): 1132-1136

<http://www.wjgnet.com/1007-9327/10/1132.asp>

INTRODUCTION

Human growth hormone (rhGH) promotes protein synthesis and lipid mobilization and accelerates nitrogen balance. It is extensively applied in clinic for the adjustment of metabolic state in patients with severe trauma, burn or major operations. It was reported that recombinant human growth hormone (rhGH) was also applied in postoperative patients with tumor, but it is controversial whether rhGH accelerates the growth of

tumor cells. In the present study we investigated the effects of rhGH on human gastric cancer cell line BGC823 *in vitro*, in order to clarify whether rhGH could be applied in postoperative patients with gastric cancer.

MATERIALS AND METHODS

Materials

Human gastric cancer cell line BGC823 was supplied by the cell bank of Shanghai Cell Biology Institute of Chinese Academy of Sciences. rhGH (Saizen) was supplied by Serono (Switzerland), one IU equals to 0.33 mg and the final concentration of rhGH was 50 ng/mL, 100 ng/mL, 200 ng/mL and 400 ng/mL respectively. Oxaliplatin (L-OHP) was selected as an anti-cancer drug supplied by Henrui Medical Company, Jiangsu, China, and its final concentration was 4 µg/ml. The main instruments were ELISA (EL340) and flow cytometer (EPICXU).

Methods

Experiment was divided into 4 groups: control group (I), anti-cancer drug group (II), rhGH group (III) and rhGH+anti-cancer drug group (IV) (Table 1).

Table 1 Experimental groups and concentrations of drugs

Groups	Names and concentrations of drugs
I	RPMI1640
II	L-OHP 4 µg/mL
III _a	rhGH 50 ng/mL
III _b	rhGH 100 ng/mL
III _c	rhGH 200 ng/mL
III _d	rhGH 400 ng/mL
IV _a	rhGH 50 ng/mL + L-OHP 4 µg/mL
IV _b	rhGH 100 ng/mL + L-OHP 4 µg/mL
IV _c	rhGH 200 ng/mL + L-OHP 4 µg/mL
IV _d	rhGH 400 ng/mL + L-OHP 4 µg/mL

BGC823 cells were placed in the medium containing 100 mL calf serum and RPMI1640, incubated at 37 °C in an atmosphere containing 50 mL CO₂ and 950 mL air. At logarithmic growth, the cells were digested by trypsin. Then the activity of the cells was examined (Via=99%) and the cells were counted in a hemocytometer using trypan blue exclusion. The density of single cell suspension was adjusted to 1×10⁵/mL for use.

Single-cell suspension was added into a 96-well plate and 90 µL suspension was added to each well and there were 4 duplicate wells in each group. When the cells completely adhered to the wall of the well 4 h later, 10 µL test drugs was added into the wells (In rhGH+L-OHP group, the ratio of the volume of both drugs was 1:1). The cells were cultured for 1, 2, 3 and 4 d, respectively, at 37 °C in an atmosphere containing 50 mL CO₂ and 950 mL air. In addition, the cells were cultured as above for 48 h to examine cell inhibitory rates. A 10 µL

MTT (5 mg/mL) was added to each well 4 h prior to the ending of experiment. When the experiment ended, 100 μ L triplicate liquid [100 g/L SDS-50 mL/L iso-butyl alcohol-0.012 mL/L HCL] was added into each well. Absorbent value of each well was examined at the wavelengths 570 nm and 630 nm by ELISA 12 h later.

A 10 mL cell suspension was placed and incubated in each well of 6-well plates and there were 3 duplicate wells in each group. When the cells completely adhered to the wall of wells 4 h later, the test drugs were added into each well as shown in Table 2.

Table 2 Scheme of drugs in each group

Group	I	II	III _a	III _b	III _c	III _d	IV _a	IV _b	IV _c	IV _d
L-OHP (μ L)	/	50	/	/	/	/	50.0	50	50	50
rhGH (μ L)	/	/	12.5	25	50	100	12.5	25	50	100
RPMI1640 (μ L)	150	100	137.5	125	100	50	87.5	75	50	/

The cells were gathered after cultured for 48 h and washed with PBS. After fixed with 700 mL/L alcohol, the cells were kept at 4 °C overnight, then stained with fluorescence. Finally the cell cycle was examined at the wavelength 488 nm. Barlogie cell cycle assay was used^[1].

Statistical analysis

Data were expressed as mean \pm SD and analyzed by variance analysis and *q* test. Statistical significance was considered at $P \leq 0.05$.

RESULTS

MTT colorimetric analysis

The inhibitory rate on gastric cancer cells was significantly higher in L-OHP group and rhGH+L-OHP group, compared with control group and rhGH group ($P < 0.01$). The inhibitory rate was also higher in rhGH+L-OHP group than in L-OHP group, though the difference had no statistical significance ($P > 0.05$). Between control group and rhGH group, the inhibitory rate did not change regularly with increase of the drug's dose (Table 3).

Table 3 Effects of rhGH and L-OHP on BGC823 cells ($n=4$, mean \pm SD)

Groups	OD values	Survival rate (%)	Inhibitory rate (%)
I	0.863 \pm 0.172	100.00	0
II	0.425 \pm 0.086 ^b	49.25 ^b	50.75 ^b
III _a	0.947 \pm 0.142	109.73	-9.73
III _b	0.894 \pm 0.220	103.59	-3.59
III _c	0.848 \pm 0.346	98.26	1.74
III _d	0.844 \pm 0.196	97.79	2.21
IV _a	0.338 \pm 0.240 ^b	39.17 ^b	60.83 ^b
IV _b	0.318 \pm 0.038 ^b	36.85 ^b	63.15 ^b
IV _c	0.318 \pm 0.018 ^b	36.85 ^b	63.15 ^b
IV _d	0.306 \pm 0.200 ^b	35.46 ^b	64.54 ^b

^b $P < 0.01$ vs control group or rhGH group.

Cell growth curve

Cell growth curve shows no obvious change between rhGH group and control group or between rhGH+L-OHP group and L-OHP group (Figures 1-2).

But it dropped sharply when rhGH+L-OHP and L-OHP groups were compared with the control group.

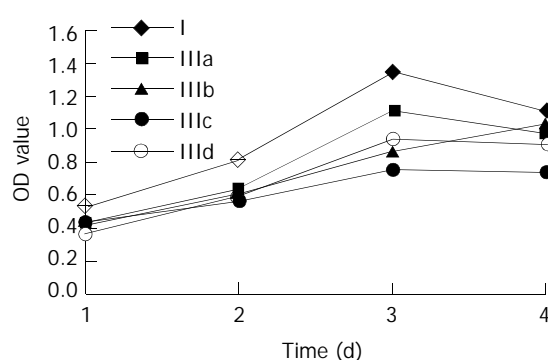


Figure 1 BGC823 cell growth curve.

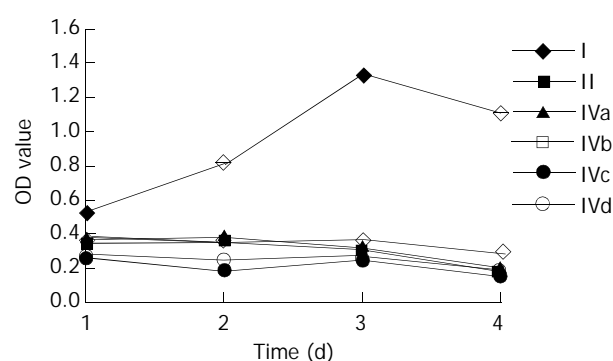


Figure 2 BGC823 cell growth curve.

Cell cycle

Cell cycle was obviously changed in L-OHP group and rhGH+L-OHP group. The number of cells in G_0 - G_1 phase was obviously more in L-OHP group and rhGH+L-OHP group than in control group or rhGH group ($P < 0.01$), but there was no significant difference in control group and rhGH group or in L-OHP group and rhGH+L-OHP group ($P > 0.05$). The cells in S phase were fewer in L-OHP group and rhGH+L-OHP group than in control group and rhGH group ($P < 0.01$), but there was no statistical significance between rhGH group and control group. The cells in G_2 -M phase were significantly fewer in L-OHP group and rhGH+L-OHP group than those in control group or rhGH group ($P < 0.01$). There was no statistical significance between L-OHP group and rhGH+L-OHP group or between control group and rhGH group. Further more, in S or G_2 -M phase the cell number had no regular change in rhGH+L-OHP group (Table 4) (Figures 3-5).

Table 4 Percentages of BGC823 cells in various phases of cell cycle ($n=3$, mean \pm SD)

Group	G_0 - G_1 (%)	S (%)	G_2 -M(%)
I	47.75 \pm 0.78	36.95 \pm 0.49	15.25 \pm 0.21
II	83.85 \pm 1.77 ^b	7.85 \pm 0.64 ^b	8.30 \pm 1.13 ^b
III _a	53.03 \pm 4.31	32.17 \pm 7.47	14.73 \pm 3.40
III _b	52.33 \pm 4.55	32.63 \pm 6.19	14.73 \pm 1.88
III _c	52.33 \pm 4.94	33.50 \pm 8.17	14.17 \pm 3.29
III _d	51.27 \pm 5.94	33.67 \pm 8.89	15.07 \pm 3.07
IV _a	85.07 \pm 2.62 ^b	6.67 \pm 3.88 ^b	8.00 \pm 1.82 ^b
IV _b	86.47 \pm 2.07 ^b	5.47 \pm 1.88 ^b	7.77 \pm 0.40 ^b
IV _c	85.53 \pm 0.47 ^b	7.87 \pm 4.99 ^b	6.37 \pm 5.61 ^b
IV _d	86.13 \pm 2.87 ^b	4.20 \pm 1.61 ^b	9.67 \pm 1.27 ^b

^b $P < 0.01$ vs control group or rhGH group.

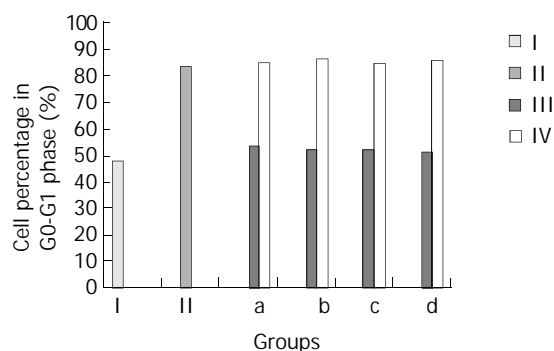


Figure 3 Percentages of cells in G0-G1 phase (%).

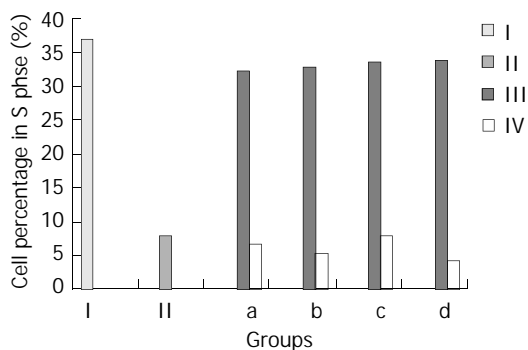


Figure 4 Percentage of cells in S phase (%).

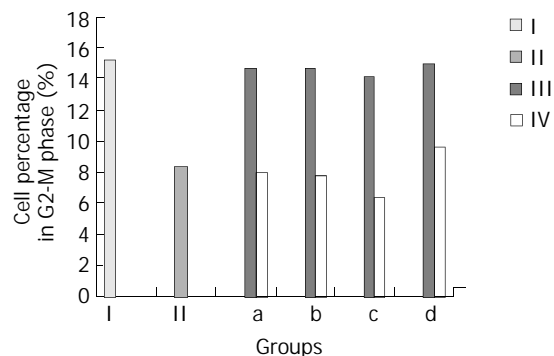


Figure 5 Percentage of cell in G2-M phase (%).

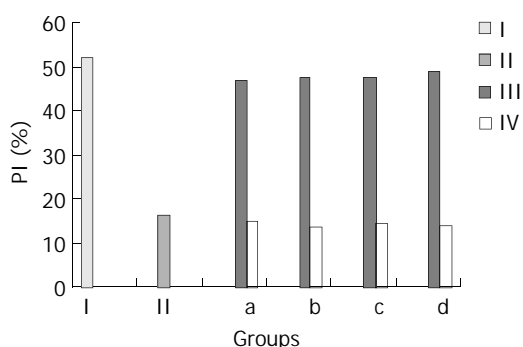


Figure 6 Cell PI (%).

Proliferation Index (PI)

PI was obviously reduced in L-OHP group compared with rhGH group or control group ($P < 0.01$), but there was no statistical significance between rhGH+L-OHP group and L-OHP group, or between rhGH group and control group ($P > 0.05$). PI showed a decreasing trend in rhGH+L-OHP group compared with L-OHP group (Table 5, Figure 6).

Table 5 Proliferation index in each group ($n=3$, mean \pm SD)

Group	PI
I	52.25 \pm 0.78
II	16.15 \pm 1.77 ^b
III _a	46.97 \pm 4.31
III _b	47.67 \pm 4.55
III _c	47.67 \pm 4.94
III _d	48.73 \pm 5.94
IV _a	14.93 \pm 2.62 ^b
IV _b	13.53 \pm 2.07 ^b
IV _c	14.47 \pm 0.47 ^b
IV _d	13.87 \pm 2.87 ^b

^b $P < 0.01$ vs control group or rhGH group.

DNA inhibitory rate

DNA inhibitory rate was obviously increased in rhGH+L-OHP group (group IV) compared with rhGH group (group III) ($P < 0.01$) (Table 6, Figure 7).

Table 6 DNA inhibitory rate in rhGH group and rhGH+L-OHP group ($n=3$, mean \pm SD)

Group	DNA inhibitory rate (%)
III _a	111.1 \pm 9.4
IV _a	178.1 \pm 6.8
III _b	109.5 \pm 9.8
IV _b	181.0 \pm 4.0
III _c	109.5 \pm 10.5
IV _c	178.2 \pm 1.9
III _d	107.2 \pm 12.4
IV _d	180.3 \pm 7.6

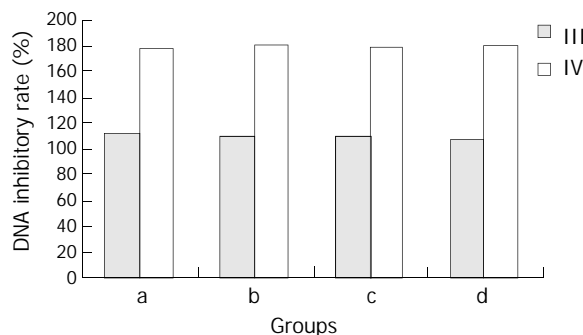


Figure 7 DNA inhibitory rate.

DISCUSSION

L-OHP is a new platinum compound that has the similar effects to cisplatin and carboplatin. The main mechanism of L-OHP is that it makes DNA broken by inserting platinum atom between two neighboring guanines or between guanine and adenosine in DNA, thus, DNA can not replicate or transcript. It is not a cell circle-specific anticancer drug. We determined its concentration *in vitro*, by referring to the maximal concentration in human plasma when the drug was used in pharmacological doses, and according to Limburg and Heckman formula. On the basis of this concentration, we devised the concentration gradient, and found the IC₅₀ that L-OHP affected BGC823 cells was 4 μ g/mL by sifting experiment of anti-cancer drugs *in vitro*. The majority of data reported that the concentration of rhGH *in vitro* was 50 ng/mL or 100 ng/mL^[2]. Qi *et al*^[3,4] devised the super-high concentration of 200 ng/mL according to its clinical

application. In addition, Estrov *et al*^[5] suggested that rhGH could accelerate human leukemia cell proliferation at high concentrations (250-300 ng/mL), so we proposed this concentration. The duration of the drug treatment was 48 h according to the double proliferation time of BGC823 cells.

rhGH is secreted by pituitary gland, it can reverse many nutritional and metabolic abnormalities associated with severe catabolic states. It has been shown that rhGH can promote protein synthesis, improve nitrogen balance, accelerate wound healing^[6-11], maintain host immune function and alleviate postoperative fatigue syndrome (POF)^[12]. GH has become available for clinical use. It was reported that rhGH enhanced positive nitrogen balance in metabolic recuperation of postoperative patients with malignant tumor^[13,14]. But it is still controversial whether rhGH should be used in postoperative tumor patients since hGH promotes the proliferation of normal cells, as well as tumor cells. Estrov *et al*^[5] reported rhGH could increase the risk of human leukemia and solid tumor at a high concentration. Ogilvy-Stuart *et al*^[15] thought rhGH was associated with the increasing risk for tumor, especially for colonic cancer, when it was used at a high concentration in patients with tumor. Akaza *et al*^[16] found rhGH promoted carcinogenesis of chemically induced rat urinary bladder cancer. Ng *et al*^[17] reported GH could increase the proportion of aneuploid cells in tumor-bearing rats. Some other studies showed that rhGH enhanced tumor growth^[18-20]. However, Harrison^[21] reported that rhGH did not prompt human pancreatic carcinoma growth. Tacke *et al*^[22] thought that postoperative treatment with rhGH in a short term led to a faster recovery of the immune function, increased the activity of NK cells, helped clear away potential cancer cells, and inhibited the recurrence of tumor. Fiebig *et al*^[23,24] also reported *in vitro* and *in vivo* rhGH did not promote tumor cells to proliferate. Bartlett *et al*^[25] suggested GH inhibited tumor growth in protein-starved animals. Still, some other studies reported that rhGH did not increase tumor growth^[26,27].

In the present study, the effects of rhGH on gastric tumor cells *in vitro* were investigated. The results showed that there was no apparent tumor growth stimulation. There were no distinct differences in survival rate, inhibitory rate, the number of cells in G₀-G₁ phase, S and G₂-M phase, PI and cell growth curve between rhGH group and control group or between rhGH+L-OHP group and L-OHP group ($P>0.05$). The results coincided with other clinical reports^[26] and showed that it did not increase gastric cancer cell growth *in vitro* after rhGH was administered. In addition, the cell percentage in proliferation phase (S and G₂-M phase) was not obviously different between rhGH+L-OHP group and L-OHP group ($P>0.05$), demonstrating that rhGH did not stimulate tumor cell proliferation. The cell inhibitory rate was distinctly increased, the cell percentage of S and G₂-M phase and PI was decreased ($P<0.05$) and the cell growth curve was apparently dropped between rhGH+L-OHP group and control group, and between rhGH+L-OHP group and rhGH group. The cell inhibitory rate showed an increasing trend and PI showed a decreasing trend in rhGH+L-OHP group compared with L-OHP group ($P>0.05$). These results indicated rhGH could enhance L-OHP effect on tumor cells. It provides support for the practice that tumor patients should be treated by metabolic recuperation after operation or that in advanced cancer and inoperative patients the cachexia was improved, or in chemotherapeutic patients the adverse effect was alleviated by use of rhGH.

The mechanism of rhGH underlying tumor cell proliferation is unknown. Some reports showed GH could indirectly stimulate tumor cell proliferation by combining with IGF-1 receptors on the surface of tumor cells^[28-32], but others showed that rhGH did not promote liver cancer cell proliferation because of reduced IGF-1 receptor expression^[33,34]. Wennbo *et al*^[35] found

that the activation of prolactin receptors but not mammary tumor induced by growth hormone receptors in transgenic mice. The exact mechanism of rhGH underlying gastrointestinal tumor cell proliferation is still unknown.

In conclusion rhGH does not promote gastric cancer cell proliferation and fission, on the contrary, it can enhance anti-cancer effects of drugs on gastric cancer cells *in vitro*.

REFERENCES

- 1 **Barlogie B**, Drewinko B, Schumann J, Freireich EJ. Pulse cytophotometric analysis of cell cycle perturbation with bleomycin *in vitro*. *Cancer Res* 1976; **36**: 1182-1187
- 2 **Yoshimura Y**, Iwashita M, Karube M, Oda T, Akiba M, Shiokawa S, Ando M, Yoshinaga A, Nakamura Y. Growth hormone stimulates follicular development by stimulating ovarian production of insulin-like growth factor-1. *Endocrinology* 1994; **135**: 887-894
- 3 **Qi XP**, Li JS, Chen C. Effect of human growth hormone on cell cycle kinetics in Lovo and LS-174-T cells. *Nanjing Daxue Xuebao* 2000; **36**: 598-602
- 4 **Qi XP**, Li JS, Chen C. Effect of human growth hormone on cell cycle kinetics in colonic cancer cells. *Changnei Yu Changwai Yinyang* 2001; **8**: 8-10
- 5 **Estrov Z**, Meir R, Barak Y, Zaizov R, Zadik Z. Human growth hormone and insulin-like growth factor-1 enhance the proliferation of human leukemic blasts. *J Clin Oncol* 1991; **9**: 394-399
- 6 **Raff T**, Germann G. Growth hormone in surgery-an assessment of current knowledge. *Chirurg* 1997; **69**: 995-1003
- 7 **Ma EL**. Changes of protein turnover in perioperative patients and effect of recombinant human growth hormone. *Zhonghua Waike Zazhi* 1992; **30**: 631-634
- 8 **Tacke J**, Bolder U, Lohlein D. Improved cumulated nitrogen balance after administration of recombinant human growth hormone in patients undergoing gastrointestinal surgery. *Infusionsther Transfusionsmed* 1994; **21**: 24-29
- 9 **Gu Y**, Wu ZH. The anabolic effects of recombinant human growth hormone and glutamine on parenterally fed, short bowel rats. *World J Gastroenterol* 2002; **8**: 752-757
- 10 **Chen HD**, Xie JL, Lai W. The effect of combined treatment of recombinant human growth hormone and insulin-like growth factor-1 on wound healing and protein catabolism in burned rats. *Zhongguo Xiufu Chongjian Waike Zazhi* 1999; **13**: 386-389
- 11 **Agis-Torres A**, Lopez-Oliva ME, Unzaga MT, Munoz-Martinez E. Body growth and substrate partitioning for fat and protein gain in weaned BALB/c mice treated with growth hormone. *Comp Biochem Physiol A Mol Integr Physiol* 2002; **132**: 247-256
- 12 **Mao Z**, Chen R, Zhao L. Effect of recombinant human growth hormone on postoperative fatigue syndrome in patients after cardiac operations. *Zhonghua Yixue Zazhi* 2002; **82**: 762-765
- 13 **Chen JY**, Zhang J, Tan J, Gan P, Sun M, Chen XZ. Evaluation of human growth hormone on gastric and gastric cancer patients after surgery. *Zhongguo Puwai Jichu Yu Linchuang Zazhi* 1999; **6**: 365-367
- 14 **Guerrero JA**, Capitan JM, Rosell J, Ruiz ME, Garcia E, Garcia-Carriazo M, Maldonado MJ, Vara Thorbeck R. Effect of growth hormone and parenteral nutrition on the catabolic phase following major digestive surgery. *Rev Esp Enferm Dig* 1992; **81**: 379-382
- 15 **Ogilvy-Stuart AL**, Ryder WD, Gattamaneni HR, Clayton PE, Shalet SM. Growth hormone and tumor recurrence. *BMJ* 1992; **304**: 1601-1605
- 16 **Akaza H**, Matsuki K, Matsushima H, Koiso K, Aso Y. Stimulatory effects of growth hormone on rat bladder carcinogenesis. *Cancer* 1991; **68**: 2418-2421
- 17 **Ng EH**, Rock CS, Lazarus D, Staiano-Coico L, Fischer E, Moldawer LL, Lowry SF. Impact of exogenous growth hormone on host preservation and tumor cell-cycle distribution in a rat sarcoma mode. *J Surg Res* 1991; **51**: 99-105
- 18 **Shalet SM**, Brennan BM, Reddingius RE. Growth hormone therapy and malignancy. *Horm Res* 1997; **48** (Suppl 4): 29-32
- 19 **Espat J**, Chamberlain RS, Sklar C, Blumgart LH. Hepatic adenoma associated with recombinant human growth hormone therapy in a patient with Turner's syndrome. *Dig Surg* 2000; **17**: 640-643
- 20 **Watanabe S**, Kobayashi Y. Exogenous hormones and human cancer. *Jpn J Clin Oncol* 1993; **23**: 1-13

- 21 **Harrison LE**, Blumberg D, Berman R, Ng B, Hochwald S, Brennan MF, Burt M. Effect of human growth hormone on human pancreatic carcinoma growth, protein and cell cycle kinetic. *J Surg Res* 1996; **61**: 317-322
- 22 **Tacke J**, Bolder U, Herrmann A, Berger G, Jauch KW. Long-term risk of gastrointestinal tumor recurrence after postoperative treatment with recombinant human growth hormone. *JPEN* 2000; **24**: 140-144
- 23 **Fiebig HH**, Dengler W, Hendriks HR. No evidence of tumor growth stimulation in human tumors *in vitro* following treatment with recombinant human growth hormone. *Anticancer Drugs* 2000; **11**: 659-664
- 24 **Fiebig HH**, Dengler WA, Drees M, Ruhanu T. Human growth hormone is able to reduce tumor induced cachexia in a human tumor xenograft model without tumor stimulation. In: Sagesse G, Stanhope R, eds. Recent advances on growth and growth hormone therapy. *London Freund* 1995; **2**: 239-251
- 25 **Bartlett DLT**, Stein P, Torosian MH, Philadelphia PA, Camden NJ. Effect of growth hormone and protein intake on tumor growth and host cachexia. *Surgery* 1995; **117**: 260-267
- 26 **Beentjes JA**, van Gorkom BA, Sluiter WJ, de Vries EG, Kleibeuker JH, Dullaart RP. One year growth hormone replacement therapy does not alter colonic epithelial cell proliferation in growth hormone deficient adults. *Clin Endocrinol* 2000; **52**: 457-462
- 27 **Blethen SL**, Allen DB, Graves D, August G, Moshang T, Rosenfeld R. Safety of recombinant deoxyribonucleic acid-derived growth hormone: The National Cooperative Growth Study experience. *J Clin Endocrinol Metab* 1996; **81**: 1704-1710
- 28 **Rapaport R**, Silis IN, Green L, Barrett P, Labus J, Skuza KA, Chartoff A, Goode L, Stene M, Petersen BH. Detection of human growth hormone receptor on IM cells and peripheral blood mononuclear cell subset by flow cytometry: Correlation with growth hormone-binding protein levels. *J Clin Endocrinol Metab* 1995; **2612-2619**
- 29 **Lincoln DT**, Kaiser HE, Raju GP, Waters MJ. Growth hormone and colorectal carcinoma: localization of receptor. *In Vivo* 2000; **14**: 41-49
- 30 **Nagano M**, Chastre E, Choquet A, Bara J, Gespach C, Kelly PA. Expression of prolactin and growth hormone receptor genes and their isoforms in the gastrointestinal tract. *Am J Physiol* 1995; **268** (3 Pt 1): G431-G442
- 31 **Chopin L**, Veveris-Lowe T, Philipps A, Herington A. Co-expression of GH and GHR isoforms in prostate cancer cell lines. *Growth Horm IGF Res* 2002; **12**: 126
- 32 **Amit T**, Hacham H, Daily O, Hertz P, Barkey RJ, Hochberg Z. The Hep G2 cell line in the study of growth hormone receptor/binding protein. *Mol Cell Endocrinol* 1994; **101**: 29-36
- 33 **Blanck A**, Assefaw-Redda Y, Eriksson LC, Gustafsson JA, Ekvarn S, Hallstrom IP. Growth hormone administration after treatment in the resistant hepatocyte model does not affect progression of rat liver carcinogenesis. *Cancer Lett* 1994; **79**: 193-198
- 34 **Levinovitz A**, Husman B, Eriksson LC, Norstedt G, Andersson G. Decreases expression of growth hormone receptor and growth hormone binding protein in rat liver nodules. *Mol Carcinog* 1990; **3**: 157-164
- 35 **Wennbo H**, Gebre-Medhin M, Gritli-Linde A, Ohlsson C, Isaksson OGP, Törnell J. Activation of the prolactin receptor but not the growth hormone receptor is important for induction of mammary tumor in transgenic mice. *J Clin Invest* 1997; **100**: 2744-2751

Edited by Zhu LH and Wang XL Proofread by Xu FM

Rapid progression of hepatocellular carcinoma after Radiofrequency Ablation

Andrea Ruzzenente, Giovanni de Manzoni, Matteo Molfetta, Silvia Pachera, Bruno Genco, Matteo Donataccio, Alfredo Guglielmi

Andrea Ruzzenente, Giovanni de Manzoni, Matteo Molfetta, Silvia Pachera, Bruno Genco, Matteo Donataccio, Alfredo Guglielmi, First Department of General Surgery, Verona University Medical School, Ospedale Maggiore Borgo Trento, Piazzale Stefani 1, 37126 Verona, Italy

Correspondence to: Dr Andrea Ruzzenente, First Department of General Surgery, Verona University Medical School, Ospedale Maggiore Borgo Trento, Piazzale Stefani 1, 37126 Verona, Italy. aruzzen@tin.it

Telephone: +39-45-807 2484 **Fax** +39-45-807 2484

Received: 2003-11-22 **Accepted:** 2003-12-24

Abstract

AIM: To report the results of radiofrequency ablation (RFA) of hepatocellular carcinoma (HCC) in cirrhotic patients and to describe the treatment related complications (mainly the rapid intrahepatic neoplastic progression).

METHODS: Eighty-seven consecutive cirrhotic patients with 104 HCC (mean diameter 3.9 cm, 1.3 SD) were submitted to RFA between January 1998 and June 2003. In all cases RFA was performed with percutaneous approach under ultrasound guidance using expandable electrode needles. Treatment efficacy (necrosis and recurrence) was estimated with dual phase computed tomography (CT) and alpha-fetoprotein (AFP) level.

RESULTS: Complete necrosis rate after single or multiple treatment was 100%, 87.7% and 57.1% in HCC smaller than 3 cm, between 3 and 5 cm and larger than 5 cm respectively ($P=0.02$). Seventeen lesions of 88 (19.3%) developed local recurrence after complete necrosis during a mean follow up of 19.2 mo. There were no treatment-related deaths in 130 procedures and major complications occurred in 8 patients (6.1%). In 4 patients, although complete local necrosis was achieved, we observed rapid intrahepatic neoplastic progression after treatment. Risk factors for rapid neoplastic progression were high preoperative AFP values and location of the tumor near segmental portal branches.

CONCLUSION: RFA is an effective treatment for hepatocellular carcinoma smaller than 5 cm with complete necrosis in more than 80% of lesions. Patients with elevated AFP levels and tumors located near the main portal branch are at risk for rapid neoplastic progression after RFA. Further studies are necessary to evaluate the incidence and pathogenesis of this underestimated complication.

Ruzzenente A, de Manzoni G, Molfetta M, Pachera S, Genco B, Donataccio M, Guglielmi A. Rapid progression of hepatocellular carcinoma after Radiofrequency Ablation. *World J Gastroenterol* 2004; 10(8): 1137-1140

<http://www.wjgnet.com/1007-9327/10/1137.asp>

INTRODUCTION

Hepatocellular carcinoma (HCC) is one of the most frequent

solid tumors with a worldwide incidence between 250 000 and 1 000 000 new cases per year^[1,2].

Surgical therapies could be applied only in 10-20% of patients^[3,4]. Liver resection is applicable in a small portion of patients because of advanced neoplastic stage or severity of liver diseases. Liver transplantation is available only in a small number of patients for shortage of donors^[5].

The majority of patients, ineligible for surgical therapies, can be submitted to local ablative therapies like percutaneous ethanol injection (PEI) and radiofrequency ablation (RFA). These local ablative therapies were considered to be radical in small HCCs^[6].

RFA showed good control of tumors with necrosis in more than 90% of HCC smaller than 5 cm^[7-10]. In HCC larger than 5 cm results were unsatisfactory with complete necrosis in less than 30%^[11].

Frequency of major complications related to the procedure was low, ranging from 5% to 15%^[12,13]. Self-limiting intraperitoneal bleeding, liver abscess and right pleural effusions have been the most frequently reported complications^[7,14].

Tumor seeding along the needle tract was also described but its incidence ranging from 0.6% to 12%, has been a matter of debate^[15-18].

Rapid intrahepatic neoplastic progression after treatment was described in literature only in 1 case report after transcatheter arterial chemoembolization (TACE) and RFA^[19].

To our knowledge no authors described this complication after RFA treatment.

The aim of this study was to describe the treatment related complications (mainly the rapid intrahepatic neoplastic progression) and the response rate of RFA of HCC in cirrhosis.

MATERIALS AND METHODS

From January 1st, 1998 to June 1st, 2003 patients submitted to RFA at the 1st Department of Surgery of Verona University Medical School were included in this study. Before treatment a detailed description of procedure was provided to patients and written informed consent was obtained from all cases. HCC was diagnosed on the basis of radiological criteria (2 coincident imaging techniques) or combined criteria [1 imaging technique associated with elevated alpha-fetoprotein (AFP) levels] according to Barcelona EASL Conference^[6]. Fine needle biopsy was performed only in cases of uncertain diagnosis^[6]. Before undergoing the procedure, patients underwent baseline clinical and laboratory evaluation of hepatic function, coagulation profile, blood cells and platelet count, hepatitis B and C virus serology and serum AFP level. Severity of cirrhosis was classified according to Child-Pugh classification and CLIP score^[20,21]. Patients eligible for RFA with Child-Pugh B cirrhosis and/or multinodular tumors, and small number of patients with Child-Pugh A cirrhosis and single potentially resectable tumor were included in the study.

Exclusion criteria from study were extra-hepatic metastasis, more than 4 nodules, tumor diameter >7 cm, Child-Pugh C cirrhosis, severe ascites, severe coagulopathy (platelets count < 40 000/mm³ and PT >1.5 INR) if not corrected with medical therapy and fresh-frozen plasma.

Antibiotic prophylaxis was administered in all patients before treatment. All patients were treated in operating room under general anesthesia. Treatment was conducted in all patients with percutaneous approach under ultrasound guidance using a radiofrequency generator (RITA medical system model 500 and 1 500, Mountain View, CA) through an expandable electrode needle as previously described^[22]. Blood count and liver function tests were performed 12 and 24 h after RFA.

All patients were discharged after 1 d, unless complications necessitated a longer hospitalization.

Treatment results were estimated by dual-phase computed tomography (CT) and AFP level performed 30 d after the procedure. CT and serum AFP were performed every 3 mo for the first year and then every 6 mo.

At dual phase, CT complete necrosis was defined as the absence of pathologic enhancement within or at the periphery of the treated HCC after at least 2 consecutive CT examinations.

Incomplete necrosis or local recurrences of HCC detected during follow up were retreated with RFA or PEI.

Statistical analysis

Data were collected prospectively and analyzed with statistical software (SPSS inc., Chicago, IL). Comparisons between different categories were carried out with contingency tables, and significance was determined by χ^2 . For all comparisons, significance was set at 0.05.

RESULTS

From January 1st, 1998 to June 1st, 2003, 87 patients with 104 HCCs and liver cirrhosis were submitted to RFA. Mean age was 67.9 years (range 41-88 years). Patient characteristics are described in Table 1. The mean follow up time was 19.2 mo. After the first treatment complete necrosis was achieved in 76 of 104 HCCs (73.1%). In 28 HCCs with incomplete necrosis RFA was repeated. After multiple treatments (range 2-4) 12 of 28 HCCs, with incomplete necrosis were completely ablated. Complete necrosis was achieved in HCC smaller than 3 cm, between 3 cm and 5 cm and bigger than 5 cm in 100%, 87.7% and 57.1%, respectively ($P=0.02$). The elevated AFP level before treatment was decreased to normal levels after complete necrosis. During the follow up 17 of 88 HCCs (19.3%) with complete necrosis showed local recurrence and 30 of 87 patients (34.4%) developed new intrahepatic tumors.

Treatment related complications

In 87 patients, 130 procedures were performed and treatment related complications occurred in 22 cases (16.9%) (Table 2). Minor complications occurred in 13 cases: fever $>38^\circ\text{C}$ and moderate pain for 5-6 d in 10 cases, right pleural effusions in 2 cases, cutaneous burn in the insertion site of the needle in 1 case. Major complications were observed in 8 patients: rapid tumor intrahepatic progression in 4 cases, bacterial endocarditis in 1 case, needle track seeding in 1 case, intraperitoneal bleeding in 1 case, hepatic decompensation in 1 case. All treatment related complications were managed with medical therapy. No treatment related mortality was observed.

Table 1 Characteristics of 87 cirrhotic HCC patients treated with RFA

Characteristic	n	(%)
Gender		
Male	71	81.6
Female	16	18.4
Etiology of cirrhosis		
HCV related	46	52.9
HBV related	11	12.6
HBV+HCV	3	3.4
Alcoholic	24	27.7
Other causes	3	3.4
Child-Pugh classification		
A	48	55.2
B	39	44.8
C	0	0
CLIP score		
0	25	28.7
1	42	48.3
2	19	21.8
4	1	1.2
Number of lesions		
Single	53	60.9
Multiple	34	39.1
Morphology of HCC		
Infiltrating	18	17.3
Noninfiltrating	86	82.7
Alfa-fetoprotein level		
<200 kU/L	79	90.8
≥ 200 kU/L	8	9.1

Table 2 Treatment-related complications occurred in 130 procedure

	Events n (%)
Minor complications	13 (10)
Fever ($>38^\circ\text{C}$) and moderate pain (5-6 d)	10 (7.7)
Right pleural effusion	2 (1.5)
Cutaneous burn	1 (0.8)
Major complications	8 (6.1)
Rapid tumor progression	4 (2.9)
Bacterial endocarditis	1 (0.8)
Neoplastic seeding	1 (0.8)
Peritoneal bleeding	1 (0.8)
Hepatic decompensation	1 (0.8)

Rapid tumor progression

After treatment, CT examination showed tumor complete necrosis with a wide neoplastic spread to the adjacent liver segments (Figure 1). After 30 d, AFP values showed a rapid increase in 3 of 4 patients, from a pretreatment value of 119 kU/L, 560 kU/L and 1 313 kU/L to 4 997 kU/L, 2 500 kU/L

Table 3 Characteristics of four patients with rapid tumor progression after RFA

Gender, age, etiology	Tumor size (cm)	Location	Differentiation
1. Male, 66 yr, alcohol	3.5	V segment	Poor
2. Male, 75 yr, HCV	3.8	VI segment	Poor
3. Male, 59 yr, HBV, HCV	4.5	VII segment	Poor
3. Male, 62 yr, HBV	4.5	IV segment	Moderate

^a: ≤ 1 cm from main or segmental portal branches.

and 5 282 kU/L, respectively. In the fourth patient, the baseline AFP value of 69 kU/L did not increase. Characteristics of patients and tumors are described in Table 3. We analyzed 10 variables in order to identify the risk factors for rapid tumor progression. The high AFP level and location of the tumor near the primary or secondary portal vein branches were more representative variables (Table 4). During the follow up 2 patients died after 2 and 3 mo for tumor progression, two patients were alive after 11 and 7 mo and they were submitted to transcatheter arterial chemoembolization (TACE).

Table 4 Risk factors for rapid tumor progression in 87 patients

Variables	No tumor progression (83)	Tumor progression (4)	P value
Child-Pugh class			
A/B	45/38	3/1	0.41
CLIP score			
0/1/2/4	25/40/17/1	0/2/2/0	0.43
Number lesions			
Single/multiple	50/33	2/2	0.68
AFP value			
<200/≥200 kU/L	77/6	2/2	0.04
Tumor size			
<3 cm/3-5 cm/5-7 cm	10/59/14	0/4/0	0.45
Tumor morphology			
Infiltrating/noninfiltrating	15/68	1/3	0.72
Portal vein thrombosis			
No/main portal branch/sectorial	71/1/3	3/0/1	0.17
Tumor location			
Peripheral/near main portal	60/23	1/3	0.04
Treatment			
Duration RFA (min)	27.7±13.7	25.6±7.5	0.40
Number insertions	2.0±1.3	1.7±0.9	0.33

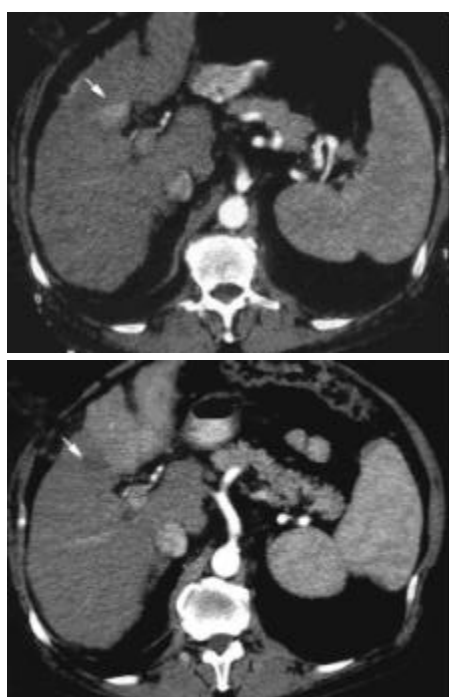


Figure 1 Contrast-enhancement arterial phase computed tomography (CT) scans before treatment (upper image) and 30 d after treatment (lower image). Tumor shows local necrosis (arrow) and rapid progression of the tumor in the left lobe with pathologic enhancement at CT.

DISCUSSION

More than 80% of patients with HCC could not be submitted to surgical treatment due to advanced tumor stage and poor hepatic function^[3,4]. In selected patients ablative treatments could achieve good results, which were similar to those of surgical resection in small HCCs^[23,24]. RFA could achieve complete necrosis in 90% of lesions smaller than 5 cm^[7-10,22]. In our study local recurrence occurred in 19.3% of tumors with complete necrosis and it was related to tumor size. There were no local recurrences during the follow up for HCCs smaller than 3 cm. In early clinical results RFA showed low incidence of major complications (5-15%)^[12,13,25]. Most frequent complications reported in literature were: capsular necrosis, intraperitoneal hemorrhage (usually self-limiting), subcapsular hematoma, cholecystitis, hepatic abscesses^[7,14].

Needle track seeding after RFA was reported with low incidence (0.6-2.8%), but in a recent study in 32 patients Llovet *et al* reported an incidence of 12%^[15-18]. The authors identified that tumors with poor differentiation, subcapsular location and high AFP levels were at risk for needle track seeding^[15].

Another complication recently observed was the rapid tumor progression after local treatment^[19]. This complication after RFA was described in only one case report in a patient who was previously submitted to TACE. In our experience 4 patients (4.5%) showed rapid intrahepatic spread of HCC after RFA without extrahepatic metastasis. To our knowledge this is the first report that describes this type of complication after RFA.

Seki *et al*, in their case report, suggested that aggressive biological behavior of the tumor might be involved in tumor progression^[19]. Moreover the author suggested that neoplastic cell spreading might have been promoted by TACE with selection of highly malignant cells with low adhesive potential after partial necrosis.

Our paper describes the occurrence of rapid neoplastic spread after RFA and we have identified the possible risk factors for this complication. Assessment of tumor and patients characteristics showed that high AFP level and location of tumor near the portal vein branches were associated with this complication. Moreover 3 of 4 patients had a poor differentiation of the tumor.

In our opinion, mechanisms involved in the pathogenesis of neoplastic progression may be the following. a) Tumors with vascular invasion are characterized by elevated intratumoral pressure^[26]. RFA during energy application may increase intratumoral pressure and favor intravascular spread of the tumor. b) Hooks delivering in “umbrella type” expandable needles may promote migration of neoplastic cells into portal vein branches. c) Creation of arterovenous fistula was reported after RFA^[12, 27]. This alteration of hepatic vascularization may promote migration of neoplastic cells into portal vein circulation.

Definitive conclusions cannot be drawn because this complication is probably still underestimated. In our opinion, tumors with a high AFP level, location near the main portal branches and poor differentiation should be carefully evaluated before RFA treatment.

REFERENCES

- 1 **Simonetti RG**, Liberati A, Angiolini C, Pagliaro L. Treatment of hepatocellular carcinoma: a systematic review of randomized controlled trials. *Ann Oncol* 1997; **8**: 117-136
- 2 **Schafer DF**, Sorrell MF. Hepatocellular carcinoma. *Lancet* 1999; **353**: 1253-1257
- 3 **Farinati F**, Rinaldi M, Gianni S, Naccarato R. How should patients with hepatocellular carcinoma be staged? Validation of a new prognostic system. *Cancer* 2000; **89**: 2266-2273
- 4 **Llovet JM**, Bustamante J, Castells A, Vilana R, Ayuso Mdel C, Sala M, Bru C, Rodes J, Bruix J. Natural history of untreated non-

- surgical hepatocellular carcinoma: rationale for the design and evaluation of therapeutic trials. *Hepatology* 1999; **29**: 62-67
- 5 **Bruix J**, Llovet JM. Prognostic prediction and treatment strategy in hepatocellular carcinoma. *Hepatology* 2002; **35**: 519-524
- 6 **Bruix J**, Sherman M, Llovet JM, Beaugrand M, Lencioni R, Burroughs AK, Christensen E, Pagliaro L, Colombo M, Rodes J. EASL Panel of Experts on HCC. Clinical management of hepatocellular carcinoma. Conclusions of the Barcelona-2000 EASL conference. European Association for the Study of the Liver. *J Hepatol* 2001; **35**: 421-430
- 7 **Curley SA**, Izzo F, Ellis LM, Nicolas Vauthey J, Vallone P. Radiofrequency ablation of hepatocellular cancer in 110 patients with cirrhosis. *Ann Surg* 2000; **232**: 381-391
- 8 **Gazelle GS**, Goldberg SN, Solbiati L, Livraghi T. Tumor ablation with radio-frequency energy. *Radiology* 2000; **217**: 633-646
- 9 **Giovannini M**, Moutardier V, Danisi C, Bories E, Pesenti C, Del pero JR. Treatment of Hepatocellular Carcinoma Using Percutaneous Radiofrequency Thermoablation: Results and Outcomes in 56 Patients. *J Gastrointest Surg* 2003; **7**: 791-796
- 10 **Shibata T**, Iimuro Y, Yamamoto Y, Maetani Y, Ametani F, Itoh K, Konishi J. Small hepatocellular carcinoma: comparison of radio-frequency ablation and percutaneous microwave coagulation therapy. *Radiology* 2002; **223**: 331-337
- 11 **Livraghi T**, Goldberg SN, Lazzaroni S. Hepatocellular carcinoma: radio-frequency ablation of medium and large lesions. *Radiology* 2000; **214**: 761-778
- 12 **Mulier S**, Mulier P, Ni Y, Miao Y, Dupas B, Marchal G, De Wever I, Michel L. Complications of radiofrequency coagulation of liver tumours. *Br J Surg* 2002; **89**: 1206-1222
- 13 **de Baere T**, Risse O, Kuoch V, Dromain C, Sengel C, Smayra T, Gamal El Din M, Letoublon C, Elias D. Adverse events during radiofrequency treatment of 582 hepatic tumors. *Am J Roentgenol* 2003; **181**: 695-700
- 14 **McGahan JP**, Dodd GD 3rd. Radiofrequency ablation of the liver: current status. *Am J Roentgenol* 2001; **176**: 3-16
- 15 **Llovet JM**, Vilana R, Bru C, Bianchi L, Salmeron JM, Boix L, Ganau S, Sala M, Pages M, Ayuso C, Sole M, Rodes J, Bruix J. Barcelona Clinic Liver Cancer (BCLC) Group. Increased risk of tumor seeding after percutaneous radiofrequency ablation for single hepatocellular carcinoma. *Hepatology* 2001; **33**: 1124-1129
- 16 **Bolondi L**, Gaiani S, Celli N, Piscaglia F. Tumor dissemination after radiofrequency ablation of hepatocellular carcinoma. *Hepatology* 2001; **34**: 608
- 17 **de Sio I**, Castellano L, De Girolamo V, di Santolo SS, Marone A, Del Vecchio Blanco C, Marone G. Tumor dissemination after radiofrequency ablation of hepatocellular carcinoma. *Hepatology* 2001; **34**: 609-610
- 18 **Goldberg SN**, Solbiati L. Tumor dissemination after radiofrequency ablation of hepatocellular carcinoma. *Hepatology* 2001; **34**: 609
- 19 **Seki T**, Tamai T, Ikeda K. Rapid progression of hepatocellular carcinoma after transcatheter arterial chemoembolization and percutaneous radiofrequency ablation in the primary tumour region. *Eur J Gastroenterol Hepatol* 2001; **13**: 291-294
- 20 **Pugh RN**, Murray-Lyon IM, Dawson JL, Pietroni MC, Williams R. Transection of the oesophagus for bleeding oesophageal varices. *Br J Surg* 1973; **60**: 646-649
- 21 **The Cancer of the Liver Italian Program (CLIP) investigators**. A new prognostic system for hepatocellular carcinoma: a retrospective study of 435 patients. *Hepatology* 1998; **28**: 751-755
- 22 **Guglielmi A**, Ruzzenente A, Battocchia A, Tonon A, Fracastoro G, Cordiano C. Radiofrequency ablation of hepatocellular carcinoma in cirrhotic patients. *Hepatogastroenterology* 2003; **50**: 480-484
- 23 **Vivarelli M**, Guglielmi A, Ruzzenente A, Cucchetti A, Bellusci R, Cordiano C, Cavallari A. Surgical resection versus percutaneous radiofrequency ablation in the treatment of hepatocellular carcinoma on cirrhotic liver. Accept for publication: *Annals of Surgery*
- 24 **Arii S**, Yamaoka Y, Futagawa S, Inoue K, Kobayashi K, Kojiro M, Makuuchi M, Nakamura Y, Okita K, Yamada R. Results of surgical and nonsurgical treatment for small-sized hepatocellular carcinomas: a retrospective and nationwide survey in Japan. The Liver Cancer Study Group of Japan. *Hepatology* 2000; **32**: 1224-1229
- 25 **Jiang HC**, Liu LX, Piao DX, Xu J, Zheng M, Zhu AL, Qi SY, Zhang WH, Wu LF. Clinical short-term results of radiofrequency ablation in liver cancers. *World J Gastroenterol* 2002; **8**: 624-630
- 26 **Tanaka T**, Yamanaka N, Oriyama T, Furukawa K, Okamoto E. Factors regulating tumor pressure in hepatocellular carcinoma and implications for tumor spread. *Hepatology* 1997; **26**: 283-287
- 27 **Catalano O**, Esposito M, Nunziata A, Siani A. Multiphase helical CT findings after percutaneous ablation procedures for hepatocellular carcinoma. *Abdom Imaging* 2000; **25**: 607-614

Edited by Wang XL and Xu FM

Significant correlation between expression level of HSP gp96 and progression of hepatitis B virus induced diseases

Xiao-Dong Zhu, Cheng-Lin Li, Zhen-Wei Lang, George F Gao, Po Tien

Xiao-Dong Zhu, Po Tien, Department of Molecular Virology, Institute of Microbiology, Chinese Academy of Sciences, Beijing 100080, China

Cheng-Lin Li, Zhen-Wei Lang, Department of Pathology, Beijing You' an Hospital, Beijing 100054, China

George F Gao, Nuffield Department of Clinical Medicine, John Radcliffe Hospital, University of Oxford, Headington, Oxford OX3 9DU, United Kingdom

Supported by the Major State Basic Research Development Program of China (Program 973) (Grant No. 2001CB510001)

Correspondence to: Professor Po Tien, Department of Molecular Virology, Institute of Microbiology, Chinese Academy of Sciences, Zhongguancun Beiyitiao, Beijing 100080, China. tienpo@sun.im.ac.cn

Telephone: +86-10-62554247 **Fax:** +86-10-62622101

Received: 2003-08-23 **Accepted:** 2003-10-12

Abstract

AIM: Gp96, also known as Grp94, is a member of heat shock protein (HSP) family and binds repertoires of peptides thereof eliciting peptide-specific T cell immune responses. It predominantly locates inside the endoplasmic reticulum (ER) with some cell surface expression in certain cancerous cells. Previous studies have shown that gp96 expression level was up-regulated in tumor cells, including hepatocellular carcinoma (HCC). However, relationship between the extent of gp96 expression and disease progression especially HBV-induced chronic infection, cirrhosis and hepatocellular carcinoma, has not been addressed before. As primary HCC can be induced and progressed from chronic hepatitis B virus (HBV) infection and HBV-induced cirrhosis, we designed an immunohistochemical experiment to test the correlation between gp96 expression level and HBV-induced disease progression, from chronic HBV infection, cirrhosis to HCC.

METHODS: We chose liver samples from different patients of hepatitis B virus induced diseases, including chronic hepatitis B (77 patients), cirrhosis (27 patients) and primary HCC (30 patients), to test the expression level of gp96 in different affected groups. Formalin-fixed, and paraffin-embedded liver tissues taken from these patients were immuno-stained by using an anti-gp96 monoclonal antibody for the expression level of gp96 protein in the sections. In addition, Western blotting of whole cell lysates derived from established human embryonic liver cell lines and several human HCC cell lines (Huh7, HepG2, SSMC-7721) was compared with the expression of gp96.

RESULTS: We found that the extent of elevated gp96 expression was significantly correlated with the disease progression, and was the highest in HCC patients, lowest in chronic HBV infection and was that of the cirrhosis in the middle.

CONCLUSION: Increased expression of gp96 might be used as a diagnostic or prognostic bio-marker for the HBV infection and HBV-induced diseases.

Zhu XD, Li CL, Lang ZW, Gao GF, Tien P. Significant correlation between expression level of HSP gp96 and progression of hepatitis B virus induced diseases. *World J Gastroenterol* 2004; 10(8): 1141-1145

<http://www.wjgnet.com/1007-9327/10/1141.asp>

INTRODUCTION

Heat shock protein (HSP) is a highly conserved group of cellular proteins and is up-expressed under hostile micro-environments, such as heat, hypoxia, acidosis, glucose deprivation, neoplasia and virus infection^[1-3]. It functions mainly as molecular chaperones to facilitate protein folding, allowing the exposed cells to adapt to gradual alterations in micro-environments and to survive. Recent studies have shown that expression of HSPs in cancerous cells is up-regulated in general but down-regulated in some cases^[4,5]. These have been used in some cases as disease-prognostic markers^[6-9]. However the molecular basis for over- or lower- expressions of HSPs in tumors is not completely understood. Based on their regulatory roles in cell apoptosis, HSPs have been divided into two groups: pro-apoptotic or anti-apoptotic HSPs^[10,11], e.g., HSP27 and HSP70 are anti-apoptotic, whereas HSP10 and HSP60 are pro-apoptotic^[10]. As such HSPs regulate cell apoptosis thereof, they modulate tumorigenicity and carcinogenesis.

Gp96 is a member of HSPs and shows anti-apoptotic effect in some tumor cells^[12]. It also activates both innate and adaptive immunity and currently is being tested extensively as an autologous therapeutic vaccine for tumors^[13-16]. Therefore it is a special member of the HSP family as a "Swiss-army knife" with multiple functions, both in immunity and tumorigenicity or carcinogenesis^[14,16]. We previously reported the identification of an HBV-specific HLA class I specific peptide bound to gp96 in HCC patients^[17,18], indicating its possible roles in immunity of HBV-induced HCC patients. At the same time, a Japanese group showed that gp96 expression level in HCC patients increased^[19] and implied its effect on tumorigenicity.

It is estimated that 350-400 million people worldwide are persistently infected with HBV and some of these persistent infected patients develop into cirrhosis or HCC in later stage^[20,21]. Therefore HBV is believed as one of the most successful human pathogens. Elucidation of the detailed pathogenesis mechanism of HBV infection, cirrhosis and HBV-induced HCC will shed light on virus-host interactions and ultimately lead to some prophylactic or therapeutic methods for the disease.

One previous report indicated that gp96 expression in HCC cells was highly up-regulated^[19]. However relationship between the extent of gp96 expression and disease progression, especially HBV-induced chronic infection, cirrhosis and HCC, has not been addressed before. Therefore we addressed this problem in the current study and the results showed that there existed a significant correlation between the expression level of gp96 and the disease progression in HBV-induced diseases. The results imply that gp96 might act as an anti-apoptotic factor in HBV-induced disease progression, thus facilitating the tumorigenicity.

MATERIALS AND METHODS

Human liver tissue samples

Seventy-two patients with chronic hepatitis B, 27 patients with liver cirrhosis and 30 patients with HCC were enrolled in this study. The patients were hospitalized in You-An Hospital, Beijing, China, between January 1998 and August 2002. All patients studied were infected with HBV examined with ELISA and were HBeAg positive in serum. The final diagnoses were confirmed by histological evaluation of the liver specimens. Sixteen control normal liver tissues were obtained from patients who underwent gastrectomy with all serological HBV-viral markers tested negative. None of the patients received irradiation or chemotherapy at the time of surgery. The liver specimens from patients with chronic hepatitis were obtained by needle biopsy and primary HCC and adjacent non-tumorous liver tissues were obtained by autopsy. All liver specimens were stained with hematoxylin and eosin and also with Masson's trichrome as well as Gordon Sweet's silver method for reticulin to confirm the histological diagnosis. In order to perform immunohistochemical study, liver specimens were fixed in 20% formalin and embedded in paraffin and cut into 5 μ m thick sections. All these manipulations were approved by the Institutional Bioethics Committee and informed consent was given by all patients and participants.

Cell lines and cell culture

Three established human HCC cell lines (Huh7, HepG2 and SSMC 7721) obtained from Cell Bank of Chinese Academy of Sciences and a human embryonic liver (HEL) cell line from Cell Bank of Peking Union Medical College were subjected to this study. HepG2, Huh7 and SSMC 7721 cells were grown in DMEM medium (Life Technologies, Inc) supplemented with 2 mmol/L L-glutamine and 100 mL/L fetal bovine serum (FBS). HEL cells were grown in DMEM medium containing 200 mL/L FBS. Cells were incubated at 37 °C under 50 mL/L CO₂ in a humidified atmosphere and media were changed on alternate days.

Immunohistochemistry

Formalin-fixed, paraffin-embedded liver specimens were deparaffinized in 3 times of xylene change (5 min each) followed by 2 changes in 100 mL/L ethanol. Immunohistochemistry for gp96 was performed using the avidin-biotin-peroxidase complex method (ABC immunostaining method). Endogenous peroxidase activity was blocked with a 15 min incubation in 3 mL/L methanol hydrogen peroxide. For gp96 antigen processing, sections were rehydrated and treated with 0.1 mmol/L citrate solution at 92 °C for 10 min. After 3 times of phosphate-buffered saline (PBS) change, sections were treated with normal goat serum for 20 min to block non-specific bindings. Then, a rat-derived monoclonal antibody (McAb) against gp96 (1:400 dilution; Neomarkers, USA) was added to the sections and incubated at 4 °C overnight. On the next day, both sets of tissue sections were rinsed with PBS 3 times (5 min each), then incubated with biotinylated goat anti-rat immunoglobulin (1:150 dilution; Goldenbridge Co.) at 37 °C for 20 min. After three times of PBS change, sections were soaked in streptavidin-biotinylated peroxidase complex at 37 °C for 20 min. Rinsed with PBS 3 times, the sections were finally incubated with diaminobenzidine-hydrogen peroxide to visualize the reaction products.

Immunoblotting

Whole cell lysate without trypsin treatment was prepared from culture cells using CCR5 lysis buffer (Promega, USA). After centrifugation, aliquots of each cell extracts containing an equal amount (15 μ g) was resolved by 100 g/L SDS-PAGE and electrophoretically transferred onto a nitrocellulose membrane.

Blots were probed with the anti-gp96 MAb (Neomarkers, USA). To verify that an equal amount of proteins was loaded onto the stocking gel, actin expression was simultaneously estimated in each example as the internal marker by Western blotting using anti-actin monoclonal antibody (Santa Cruz, USA). Protein concentration in the supernatants was measured using the Bradford assay (Bio-Rad laboratories Ltd, UK).

Gp96 expression and statistical analysis

For each tissue section, staining was assessed as negative, weakly positive or only focally positive (low-level expression), or strongly positive (high-level expression) and scored as 0, 1 and 2, respectively. When the stained cells accounted for $\geq 30\%$ of the total, the tissue was evaluated as strongly positive (grade 2). If the frequency of stained cells was $\leq 5\%$, the tissue was evaluated as negative (grade 0). The samples, with 5-30% of stained cells, were classified as weakly positive (grade 1).

Statistical significance of the data was analyzed using the chi-square test and set at $P < 0.05$.

RESULTS

Distribution of gp96 in normal, chronic hepatitis B, cirrhosis and HCC liver tissues

By using the ABC immunostaining method, we examined the presence of HSP gp96 in human liver parenchyma (Figure 1). Characteristically, HCC cells and normal hepatocytes were stained and the expressed styles could be diffusely cytoplasmic. In hepatitis liver tissues, the positive hepatocytes were often localized in periportal areas when the positive immunostaining was weak or few (Figure 1B). When more positive cells were stained, they often diffusely localized in the liver lobule. Moreover, the positive hepatocytes were markedly increased in regenerative liver cells. Cytoplasmic gp96 staining was significantly higher in HCC cells than in adjacent non-tumor liver cells (Figure 1G). In addition, nuclear staining for gp96 was also detected in a small number of HCC cells (Figure 1F), but not found in non-tumorous liver cells or cells derived from hepatitis, cirrhosis. This was consistent with the observation that gp96 localized in the nuclear envelope^[22]. Therefore the nuclear staining most likely reflected the outer nuclear membrane staining. It was observed that gp96 was detected not only in HCC cells and hepatocytes, but also expressed in lymphocytes (Figure 1H). Meanwhile, we observed specimens expressing gp96 in HCC with many leukocytes infiltrating tumour cells (Figure 1H). As a negative control, the second goat anti-rabbit antibody without prestaining of gp96 specific monoclonal antibody did not give any significant background staining, confirming the McAb specificity to gp96.

Table 1 Statistics of gp96 expression

Diagnosis	No	Negative	Weak	Strong	P-value ¹
CON	16	14	2	0	
CH	77	29	41	7	<0.01
LC	27	4	11	12	<0.01
HCC	30	0	9	21	<0.01

CON: control normal liver tissue; CH: chronic hepatitis; LC: liver cirrhosis; HCC: hepatocellular carcinoma. ¹Significance relative to control tissues.

Relations between histological findings and gp96 expression

To understand the association between intensity of gp96 staining and histological stages of chronic hepatitis, cirrhosis and primary HCC, semi-quantitative assessment of the gp96 expression level was performed according to the above criteria.

Typical staining grades (0, 1, 2) of the gp96 expression are shown in Figure 1 (1A, 1B and 1E respectively). As shown in Table 1, various staining patterns were observed for the gp96 expression. Of the specimens from 77 chronic hepatitis B and 27 liver cirrhosis, 62.3% and 85% were positive respectively. In 30 HCC tissues gp96 expression was positive (100%). These findings were statistically significant ($P < 0.01$) with respect to the control normal tissues. As shown in Figure 2, the expression level of gp96 was indeed correlated positively with their corresponding histological stages, and was the highest in HCC patients, lowest in chronic HBV infection and that of the cirrhosis was in the middle. However, there was no significant association between gp96 expression and patient ages, gender or other clinic-

pathologic characteristics (data not shown) in this study.

Expression of gp96 in several HCC cell lines

We examined the gp96 expression by Western blot in three HCC cell lines available (Huh7, HepG2 and SSMC-7721) with variable phenotypes and a human embryonic liver cell line (HEL) established by Cell Bank of Peking Union Medical College. As expected, gp96 expression was observed in all three HCC cell lines. However, in HEL cell line, there was no visible band in the immunoblot of crude materials (Figure 3). Furthermore, immunocytochemistry analysis also showed gp96 protein expression in SSMC-7721 cells but did not in HEL cells (Figure 4).

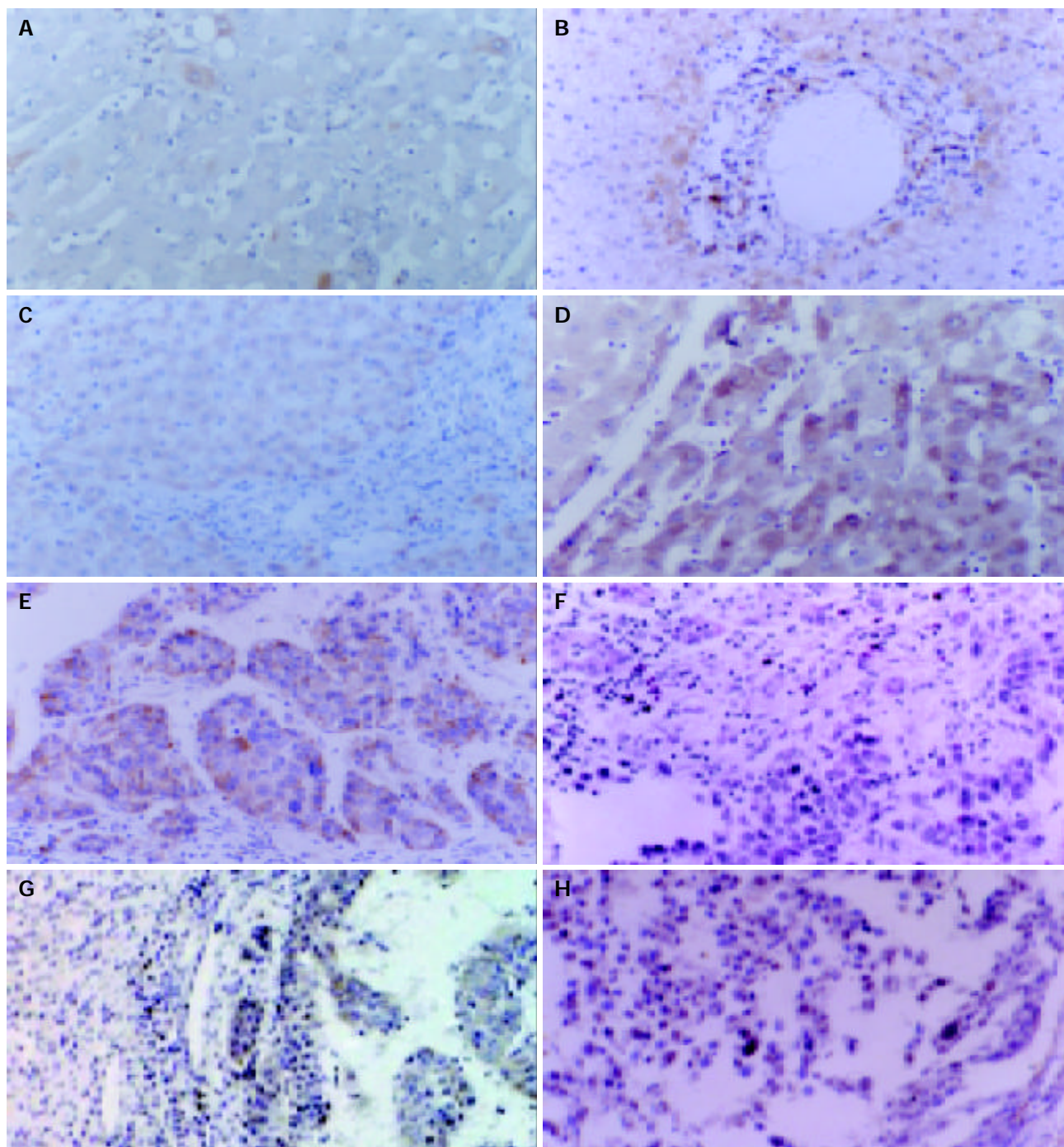


Figure 1 Sections of immunoperoxidase staining for gp96 in chronic hepatitis liver, liver cirrhosis and HCC. Several representative liver tissues with A: gp96 negative in chronic hepatitis, B: gp96 weakly positive in chronic hepatitis, C: gp96 strongly positive in chronic hepatitis, D: gp96 strongly detected in liver cirrhosis, E: gp96 strongly positive in HCC, F: gp96 positive in the nuclear and cytoplasmic staining, G: Cytoplasmic gp96 staining significantly higher in HCC cells than in adjacent non-tumorous liver cells, and H: gp96 expression in HCC accompanied by lymphocyte infiltration (indicated by arrow).

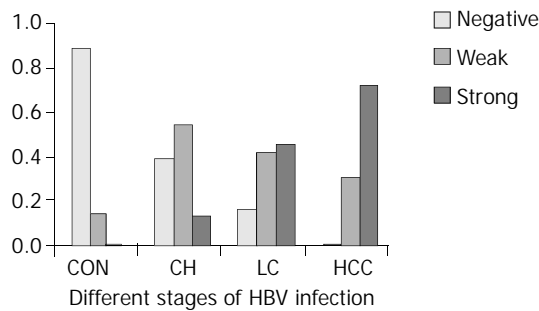


Figure 2 Correlation of gp96 expression and the progression of hepatitis B virus induced diseases. For the definition of gp96 staining density (negative, weak and strong), please see Materials and Methods. X-axis, different stages of HBV infection; Y axis, the percentage of classified samples numbers in total numbers of each group samples. CON: control normal liver tissue; CH: chronic hepatitis; LC: liver cirrhosis; HCC: hepatocellular carcinoma.

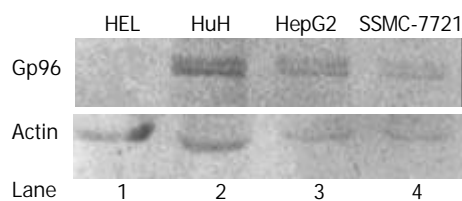


Figure 3 Western blotting analysis of gp96 expression in HCC cell lines and human embryonic liver cells (HEL). Clearly shown in the figure are high-level expression of gp96 in the HCC cell lines but not in HEL. Actin expression level was used as SDS-PAGE loading control.

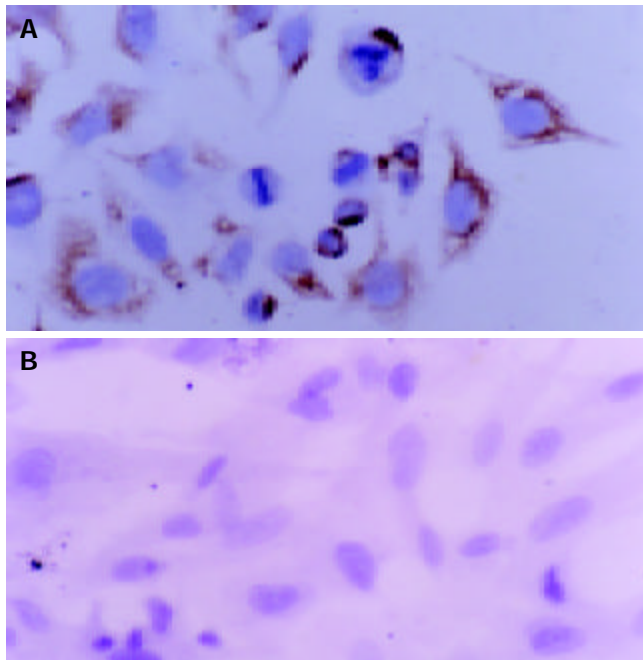


Figure 4 Immunocytochemical analysis of gp96 in HCC cell line SSMC-7721 (A) and HEL (B). High-level expression of gp96 was seen in SSMC-7721, but not in HEL.

DISCUSSION

In this study, the relationship between expression level of gp96 in liver tissues and the progression of HBV-induced diseases was quantitatively analyzed. It was clearly shown that there was a significant correlation. Gp96 expression increased as the HBV-induced disease progressed from chronic hepatitis to cirrhosis, then HCC. Elevated gp96 expression in tumour

cells, including HCC (not quantitatively) and human colorectal cancers, was reported earlier^[19,23], but its role in tumorigenicity is not clear. As the longevity of cirrhosis and HCC cells was observed compared to normal hepatocytes, it is plausible to propose that gp96 up-expression in these tumorous cells is closely related to the cell survival, thereof possibly preventing cell apoptosis. Some reports showed that gp96 might be a member of anti-apoptotic HSPs^[12]. Our current observation seems to support this notion. However, it is not clear yet if the gp96 up-expression in cirrhosis or HCC is the cause or the outcome of the disease progression. This needs to be addressed in future studies.

This obvious correlation has also raised another possibility, *i.e.*, whether evaluation of gp96 expression level can be used as a prognostic marker of HBV-induced diseases. HBV infection is a serious problem worldwide, especially in China. A substantial number of HBV carriers develop into cirrhosis and HCC, but the mechanism underlying the different outcomes among patients is not clear. There is an urgent need for identification of molecular biomarkers for the evaluation of HBV-carriers' prognostic factors. Although some studies suggested that HBxAg could be used as a pathological prognostic factor in the progression of HBV-induced diseases, the expression patterns were often contradictory^[24-26]. The expression level of other HSPs has been recognized as diagnostic or prognostic markers in certain tumours^[6-9,27-31]. Nonetheless, use of gp96 expression in this purpose has not been addressed before. Gp96 was constitutively expressed at very low levels in ER of a variety of normal cell types^[23] but the expression was dramatically enhanced by stressful conditions. Our data (Figure 4) are consistent with the previous observations as we did not detect any gp96 expression in HEL cell line but easily seen in HCC cell lines. Our results, combined with the earlier observation^[19], suggested that immunohistochemical detection of increased gp96 expression in liver tissues was associated with an increased risk of HBV chronic infection development into cirrhosis or HCC. In other words, increased expression of gp96 in liver tissues might be a valuable diagnostic or prognostic marker for chronic HBV-infection patients though further work needs to be done for a conclusive implication.

Gp96 is not an oncofetal protein as HEL cells showed negative staining in this study. Gp96 expression was not associated with cell differentiation stages either but with cell malignancy. This finding was correlated with the data from tissue specimens in which enhanced expression occurred in tumor tissues rather than in (even neighbouring) normal tissues. The role of gp96 in HCC tumorigenicity is not clear, but some studies have suggested that high-level expression of gp96 could contribute to tumorigenicity of other tumours^[23,32,33]. Gp96 expression was also reported to increase the immunity to tumours^[34-38]. At least the complex preparation of gp96 and bound-peptides has been being successfully used as autologous tumour vaccines^[13-16]. Our data however did not indicate a positive correlation of gp96 up-expression and host immunity against HBV-induced diseases as the high-level expression was associated with a worse clinical outcome. Why does not high expression level of gp96 in HCC or chronic HBV infection confer protection immunity on HCC or HBV-induced diseases? It is a complicated scenario. As to the other edge of the "Swiss-army-knife", the protection of gp96 against tumours was believed that gp96 could act as a chaperone to facilitate MHC class I peptide loading, therefore increasing the tumour peptides presented by MHC class I^[16,39]. Because of the down-regulation of MHC class I on tumorous cell surfaces, cytotoxic T cells (CTL) were in general in a low density in chronic HBV infection or HCC^[40], but exogenously introduced gp96-peptide complexes would help class I peptide loading through the up-taking of this complex by gp96 receptors on the cell surfaces, *e.g.* CD91^[16]. Through this way CTL response could be induced and the

cellular tumour immunity was provoked. The high expression level of gp96 in cirrhosis and HCC was complicated by other factors because their effects could confer immunity on HCC.

In conclusion, there is a positive correlation between HSP gp96 expression in liver tissues and HBV-induced disease progression. Its mechanism and possible application in HBV-infection patients should be further studied.

ACKNOWLEDGEMENT

We thank Professor Xue-Tao Cao, the principal scientist of 973 Program for his support. We are grateful to Dr. Catherine Zhang for her critical reading of the manuscript.

REFERENCES

- Lindquist S**, Craig EA. The heat-shock proteins. *Annu Rev Genet* 1988; **22**: 631-677
- Morimoto RI**. Cells in stress: transcriptional activation of heat shock genes. *Science* 1993; **259**: 1409-1410
- Schlesinger MJ**. Heat shock proteins. *J Biol Chem* 1990; **265**: 12111-12114
- Ciocca DR**, Adams DJ, Edwards DP, Bjerkke RJ, McGuire WL. Distribution of an estrogen-induced protein with a molecular weight of 24 000 in normal and malignant human tissues and cells. *Cancer Res* 1983; **43**: 1204-1210
- Ferrarini M**, Heltai S, Zocchi MR, Rugarli C. Unusual expression and localization of heat-shock proteins in human tumor cells. *Int J Cancer* 1992; **51**: 613-619
- Ciocca DR**, Vargas-Roig LM. Hsp27 as a prognostic and predictive factor in cancer. *Prog Mol Subcell Biol* 2002; **28**: 205-218
- Kawanishi K**, Shiozaki H, Doki Y, Sakita I, Inoue M, Yano M, Tsujinaka T, Shamma A, Monden M. Prognostic significance of heat shock proteins 27 and 70 in patients with squamous cell carcinoma of the esophagus. *Cancer* 1999; **85**: 1649-1657
- Chuma M**, Sakamoto M, Yamazaki K, Ohta T, Ohki M, Asaka M, Hirohashi S. Expression profiling in multistage hepatocarcinogenesis: identification of HSP70 as a molecular marker of early hepatocellular carcinoma. *Hepatology* 2003; **37**: 198-207
- Nakajima M**, Kuwano H, Miyazaki T, Masuda N, Kato H. Significant correlation between expression of heat shock proteins 27, 70 and lymphocyte infiltration in esophageal squamous cell carcinoma. *Cancer Lett* 2002; **178**: 99-106
- Garrido C**, Gurbuxani S, Ravagnan L, Kroemer G. Heat shock proteins: endogenous modulators of apoptotic cell death. *Biochem Biophys Res Commun* 2001; **286**: 433-442
- Parcellier A**, Gurbuxani S, Schmitt E, Solary E, Garrido C. Heat shock proteins, cellular chaperones that modulate mitochondrial cell death pathways. *Biochem Biophys Res Commun* 2003; **304**: 505-512
- Reddy RK**, Lu J, Lee AS. The endoplasmic reticulum chaperone glycoprotein GRP94 with Ca(2+)-binding and antiapoptotic properties is a novel proteolytic target of calpain during etoposide-induced apoptosis. *J Biol Chem* 1999; **274**: 28476-28483
- Li Z**. Priming of T cells by heat shock protein-peptide complexes as the basis of tumor vaccines. *Semin Immunol* 1997; **9**: 315-322
- Srivastava PK**, Amato RJ. Heat shock proteins: the 'Swiss Army Knife' vaccines against cancers and infectious agents. *Vaccine* 2001; **19**: 2590-2597
- Srivastava P**. Interaction of heat shock proteins with peptides and antigen presenting cells: chaperoning of the innate and adaptive immune responses. *Annu Rev Immunol* 2002; **20**: 395-425
- Srivastava P**. Roles of heat-shock proteins in innate and adaptive immunity. *Nat Rev Immunol* 2002; **2**: 185-194
- Meng SD**, Gao T, Gao GF, Tien P. HBV-specific peptide associated with heat-shock protein gp96. *Lancet* 2001; **357**: 528-529
- Meng SD**, Song J, Rao Z, Tien P, Gao GF. Three-step purification of gp96 from human liver tumor tissues suitable for isolation of gp96-bound peptides. *J Immunol Methods* 2002; **264**: 29-35
- Tanaka K**, Kondoh N, Shuda M, Matsubara O, Imazeki N, Ryo A, Wakatsuki T, Hada A, Goseki N, Igari T, Hatsuse K, Aihara T, Horiuchi S, Yamamoto N, Yamamoto M. Enhanced expression of mRNAs of antisecretory factor-1, gp96, DAD1 and CDC34 in hepatocellular carcinomas. *Biochim Biophys Acta* 2001; **1536**: 1-12
- Okuda K**. Hepatocellular carcinoma: recent progress. *Hepatology* 1992; **15**: 948-963
- Yu AS**, Keeffe EB. Management of hepatocellular carcinoma. *Rev Gastroenterol Disord* 2003; **3**: 8-24
- Altmeyer A**, Maki RG, Feldweg AM, Heike M, Protopopov VP, Masur SK, Srivastava PK. Tumor-specific cell surface expression of the-KDEL containing, endoplasmic reticular heat shock protein gp96. *Int J Cancer* 1996; **69**: 340-349
- Heike M**, Frenzel C, Meier D, Galle PR. Expression of stress protein gp96, a tumor rejection antigen, in human colorectal cancer. *Int J Cancer* 2000; **86**: 489-493
- Pal J**, Somogyi C, Szmolenszky AA, Szekeres G, Sipos J, Hegedus G, Martzinovits I, Molnar J, Nemeth P. Immunohistochemical assessment and prognostic value of hepatitis B virus X protein in chronic hepatitis and primary hepatocellular carcinomas using anti-HBxAg monoclonal antibody. *Pathol Oncol Res* 2001; **7**: 178-184
- Zhu M**, London WT, Duan LX, Feitelson MA. The value of hepatitis B x antigen as a prognostic marker in the development of hepatocellular carcinoma. *Int J Cancer* 1993; **55**: 571-576
- Wang WL**, London WT, Feitelson MA. Hepatitis B x antigen in hepatitis B virus carrier patients with liver cancer. *Cancer Res* 1991; **51**: 4971-4977
- Mese H**, Sasaki A, Nakayama S, Yoshioka N, Yoshihama Y, Kishimoto K, Matsumura T. Prognostic significance of heat shock protein 27 (HSP27) in patients with oral squamous cell carcinoma. *Oncol Rep* 2002; **9**: 341-344
- Cornford PA**, Dodson AR, Parsons KF, Desmond AD, Woolfenden A, Fordham M, Neoptolemos JP, Ke Y, Foster CS. Heat shock protein expression independently predicts clinical outcome in prostate cancer. *Cancer Res* 2000; **60**: 7099-7105
- Uozaki H**, Ishida T, Kakiuchi C, Horiuchi H, Gotoh T, Iijima T, Imamura T, Machinami R. Expression of heat shock proteins in osteosarcoma and its relationship to prognosis. *Pathol Res Pract* 2000; **196**: 665-673
- Shamma A**, Doki Y, Tsujinaka T, Shiozaki H, Inoue M, Yano M, Kawanishi K, Monden M. Loss of p27(KIP1) expression predicts poor prognosis in patients with esophageal squamous cell carcinoma. *Oncology* 2000; **58**: 152-158
- Vargas-Roig LM**, Fanelli MA, Lopez LA, Gago FE, Tello O, Aznar JC, Ciocca DR. Heat shock proteins and cell proliferation in human breast cancer biopsy samples. *Cancer Detect Prev* 1997; **21**: 441-451
- Menoret A**, Chandawarkar RY, Srivastava PK. Natural autoantibodies against heat-shock proteins hsp70 and gp96: implications for immunotherapy using heat-shock proteins. *Immunology* 2000; **101**: 364-370
- Menoret A**, Meflah K, Le Pendu J. Expression of the 100-kda glucose-regulated protein (GRP100/endoplasmic) is associated with tumorigenicity in a model of rat colon adenocarcinoma. *Int J Cancer* 1994; **56**: 400-405
- Randow F**, Seed B. Endoplasmic reticulum chaperone gp96 is required for innate immunity but not cell viability. *Nat Cell Biol* 2001; **3**: 891-896
- Singh-Jasuja H**, Scherer HU, Hilf N, Arnold-Schild D, Rammensee HG, Toes RE, Schild H. The heat shock protein gp96 induces maturation of dendritic cells and down-regulation of its receptor. *Eur J Immunol* 2000; **30**: 2211-2215
- Binder RJ**, Anderson KM, Basu S, Srivastava PK. Cutting edge: heat shock protein gp96 induces maturation and migration of CD11c+ cells *in vivo*. *J Immunol* 2000; **165**: 6029-6035
- Blachere NE**, Li Z, Chandawarkar RY, Suto R, Jaikaria NS, Basu S, Udono H, Srivastava PK. Heat shock protein-peptide complexes, reconstituted *in vitro*, elicit peptide-specific cytotoxic T lymphocyte response and tumor immunity. *J Exp Med* 1997; **186**: 1315-1322
- Santin AD**, Hermonat PL, Ravaggi A, Chiriva-Internati M, Hiserodt JC, Batchu RB, Pecorelli S, Parham GP. The effects of irradiation on the expression of a tumour rejection antigen (heat shock protein gp96) in human cervical cancer. *Int J Radiat Biol* 1998; **73**: 699-704
- Li Z**, Menoret A, Srivastava P. Roles of heat-shock proteins in antigen presentation and cross-presentation. *Curr Opin Immunol* 2002; **14**: 45-51
- Webster G**, Bertolotti A. Quantity and quality of virus-specific CD8 cell response: relevance to the design of a therapeutic vaccine for chronic HBV infection. *Mol Immunol* 2001; **38**: 467-473

Autologous cytokine-induced killer cell therapy in clinical trial phase I is safe in patients with primary hepatocellular carcinoma

Ming Shi, Bing Zhang, Zi-Rong Tang, Zhou-Yun Lei, Hui-Fen Wang, Yong-Yi Feng, Zhen-Ping Fan, Dong-Ping Xu, Fu-Sheng Wang

Ming Shi, Bing Zhang, Zi-Rong Tang, Zhou-Yun Lei, Hui-Fen Wang, Yong-Yi Feng, Zhen-Ping Fan, Dong-Ping Xu, Fu-Sheng Wang, Division of Biological Engineering, Institute of Infectious Diseases, 302 Hospital of PLA, Beijing 100039, China
Correspondence to: Dr. Fu-Sheng Wang, Research Center of Biotherapy, Beijing Institute of Infectious Diseases, 302 Hospital of PLA, Beijing 100039, China. fswang@public.bat.net.cn
Telephone: +86-10-66933332 **Fax:** +86-10-63831870
Received: 2003-08-23 **Accepted:** 2003-10-22

Abstract

AIM: To investigate the influence of autologous cytokine-induced killer (CIK) cells on the phenotypes of CIK effector cells, peripheral T lymphocyte subsets and dendritic cell subsets in patients with primary hepatocellular carcinoma (HCC).

METHODS: Peripheral blood mononuclear cells (PBMC) were collected by a blood cell separator from 13 patients with HCC, then expanded by priming them with interferon-gamma (IFN- γ) followed by monoclonal antibody (mAb) against CD3 and interleukin-2 (IL-2) the next day. The phenotypic patterns of CIK cells were characterized by flow cytometry on d 0, 4, 7, 10, 13 and 15 of incubation, respectively. Then, 5 mL of venous blood was obtained from HCC patients before or 8-10 d after CIK cells were transfused into patients to assess the influence of CIK cells on the percentages of effector cells, and proportions of DC1 or DC2 in peripheral blood by flow cytometry.

RESULTS: After two weeks of *in vitro* incubation, the percentages of CD3⁺CD8⁺, CD3⁺CD56⁺, and CD25⁺ cells increased significantly from 33.5 \pm 10.1%, 7.7 \pm 2.8%, and 12.3 \pm 4.5% to 36.6 \pm 9.0% (P <0.05), 18.9 \pm 6.9% (P <0.01), and 16.4 \pm 5.9% (P <0.05), respectively. However, the percentages of CD3⁺CD4⁺ and NK cells had no significant difference. The percentages of CD3⁺ and CD3⁺CD8⁺ cells were kept at high levels during the whole incubation period, but those of CD25⁺, and CD3⁺CD56⁺ cells began to decrease on d 7 and 13, respectively. The proportions of type I dendritic cell (DC1) and type II dendritic cell (DC2) subsets increased from 0.59 \pm 0.23% and 0.26 \pm 0.12% before CIK cell therapy to 0.85 \pm 0.27% and 0.43 \pm 0.19% (all P <0.01) after CIK cell transfusion, respectively. The symptoms and characteristics of HCC patients were relieved without major side effects.

CONCLUSION: Our results indicated that autologous CIK cells can efficiently improve the immunological status in HCC patients, and may provide a potent approach for HCC patients as the adoptive immunotherapy.

Shi M, Zhang B, Tang ZR, Lei ZY, Wang HF, Feng YY, Fan ZP, Xu DP, Wang FS. Autologous cytokine-induced killer cell therapy in clinical trial phase I is safe in patients with primary hepatocellular carcinoma. *World J Gastroenterol* 2004; 10 (8): 1146-1151

<http://www.wjgnet.com/1007-9327/10/1146.asp>

INTRODUCTION

Primary hepatocellular carcinoma (HCC) represents one of the most lethal neoplasms worldwide with a particularly high prevalence in China^[1]. Chronic viral hepatitis patients, especially hepatitis B or C patients, often fall victims to liver cirrhosis and subsequent HCC^[2,3]. The high percentage of chronicity may be due to the active combative mechanisms of the virus. In cirrhotic patients, the incidence of HCC annually has been reported to be between 2% and 7%. These findings indicate that prevention and early treatment of liver cancer, especially HCC, are an urgent and important issue.

HCC patients are often found to have functional deficiency in host adaptive immunity response and innate immunity response^[4]. Current therapeutic regimens including surgery, chemotherapy and radiotherapy for HCC often have very limited efficacy, and tumors tend to relapse or metastasize easily. Combination therapy becomes the most important means for treating HCC patients. Antitumor immunity is mainly dependent on cellular immune response. Therefore, cellular immunity dysfunction is one of the reasons why tumors are incurable, and easy to relapse or metastasize. Cytokine-induced killer (CIK) cells are shown to be a heterogeneous population, and the major population expresses both the T cell marker CD3 and the NK cell marker CD56, and is termed NKT cells. Cells with this phenotype are rare (1% to 5%) in natural peripheral blood mononuclear cells (PBMC)^[5]. CD3⁺CD56⁺ cells are able to expand nearly 1 000-fold when they are cultured with a cytokine cocktail comprising interferon- γ (IFN- γ), interleukin-2 (IL-2), mAbs against CD3, and interleukin-1 α (IL-1 α), and have a characteristic which is more effective in the treatment of tumors with a non-major histocompatibility complex (MHC)-restricted mechanism, and a most effective project^[6]. We have previously reported that CIK cells could suppress the growth of tumor cells *in vitro* when HCC cells were transplanted in mice^[7-10].

Dendritic cells (DCs) are specialized antigen-presenting cells (APC) in the immune system. They are critical for exerting T cell mediated immune responses, activating naïve T cells, and playing a critical role in innate immune response and adaptive immune response^[11]. DCs capture tumor-associated antigens (TAA) efficiently in peripheral tissues, transport these TAA from peripheral sites to primary and secondary lymphoid organs, express high levels of MHC I and MHC II molecules that present the processed TAA epitope specific T cells, express high levels of costimulatory CD80 and CD86 which are required to activate naïve and memory T cells, and synthesize important immunomodulatory mediators such as, IL-12, IFN- α , tumor necrosis factor (TNF)- α . DC contains at least two major distinct subsets, DC1 or DC2, which have mutually exclusive phenotypes and functions. DC1 is APC, and DC2 has been identified as the principal producer of IFN- α , a key cytokine involved in clearance of viral infections. They play a critical role in antiviral or antitumor immune response^[12,13]. We have recently reported that CIK cells could suppress the growth of HCC cells in animals or *ex vivo* effectively. In this study, we investigated the alterations of peripheral T lymphocyte subsets

and DC subsets in HCC patients for initial evaluation of autologous CIK therapy efficacy.

MATERIALS AND METHODS

Subjects

Thirteen patients (12 males and 1 female), mean age 46.8 ± 7.3 (range, 30-53) years, with confirmed diagnosis of HCC were recruited based on biochemical analysis and imaging examinations, such as ultrasonography, computed tomography and angiography. The general clinical data of HCC patients are summarized in Table 1. All cases were patients with hepatocirrhosis with more than 20 years of chronic HBV infection. After written informed consent was obtained from each patient, the patients with HCC began to receive CIK cell therapy protocol, which was approved by the Department of Health of Chinese PLA.

Reagents

Serum-free AIM-V medium was purchased from Invitrogen Corporation (GIBCO, USA). Recombinant human IL-2 (rhIL-2) was purchased from Beijing Red United Cross Pharmaceutical Co., LTD (China). Anti-CD3Ab was purchased from CIMAB (Cuba). Recombinant human IFN- γ (rh IFN- γ) was obtained from Shanghai Clonbiotech Co., LTD (China). Human albumin was obtained from Brief Introduction To Sino-Foreign Joint Venture, Harbin Sequel Bio-Engineering Medicine Co., LTD (China).

Isolation and culture of CIK cells

By using a blood cell separator (Spectra v 6.1, Cobe, USA), $(2-4) \times 10^9$ PBMC cells from each patient were obtained in a total volume of 50-60 mL. Cellular concentration was adjusted to 2×10^6 /mL in fresh serum-free AIM-V medium, and incubated at 37 °C in a humidified atmosphere of 50 mL/L CO₂ in the Lifecell tissue culture flask (Nexell Therapeutics Inc., USA). To generate CIK cells, 2 000 U/mL rhIFN- γ was added on the initial day. After 24 h of incubation, 50 ng/mL mAb against CD3, and 1 000 U/mL rhIL-2 were added. Fresh IL-2 and fresh AIM-V media were replenished every 3 d. On d 0, 4, 7, 10, 13, and 15, cell densities were determined, and the phenotypes were identified by flow cytometry (Becton Dickinson, USA), respectively. Cells were transfused back into HCC patients on days 10, 13, 15, respectively.

Surface marker analysis of CIK cells in cultured or peripheral blood

Incubated CIK cells were collected, washed, and stained with mouse against human CD3 and CD25 (mAbs) coupled to FITC respectively, and mAbs against CD4, CD8, CD16, CD19, and

CD56 coupled to PE (Becton Dickinson, San Jose, CA). Non-specific binding was determined using irrelevant mouse immunoglobulin isotypes IgG1-FITC, IgG2-FITC and IgG1 RD. Cells were incubated with Abs for 30 min at 4 °C. Excess Ab was removed and the stained cells were washed and analyzed or sorted by flow cytometry.

Analysis of DC subsets or CIK effector cells in peripheral blood

Five millilitre venous blood was obtained from each subject before and after CIK cell transfusion, respectively, to analyze DC subsets or effector cell phenotypes by flow cytometry. Briefly, blood cells were incubated with a lineage (lin) cocktail (anti-CD3, CD4, CD16, CD19, CD20, CD56) conjugated with FITC, PE-conjugated anti-CD11c or -CD123, PerCP-conjugated anti-HLA-DR for 30 min, then treated with FACS lysing solution for less than 10 min, washed by PBS, fixed with 2% paraformaldehyde for 20 min at 4 °C, and analyzed by flow cytometry^[14]. Other blood cells were used as described in cultured CIK cells to analyze the phenotypes of effector cells in peripheral blood.

Preparation and transfusion of CIK cell supernatants

Incubated CIK cells were transfused back into HCC patients via vein 3 times on days 10, 13 and 15, respectively. One-third of all CIK cells each time were collected by centrifugation for 20 min at 1 500 r/min, and washed twice in saline water (containing 5 g/L human albumin and IL-2 at 100 U/mL). About $(3-5) \times 10^9$ cells were resuspended in the same solution with 400-500 mL, then transfused back into patients intravenously.

Statistical analysis

The results were expressed as mean \pm SD. Results were analyzed by using SPSS software, and experiments were designed by self-pair. $P < 0.05$ was considered statistically significant.

RESULTS

Phenotypes of CIK cells in various culture time

The percentages of all effector cells varied over time *in vitro* incubation. The percentage of CD3⁺ T cells increased slowly, and kept a high level for a long time during the incubation period. The percentage of CD3⁺CD4⁺ decreased slightly, but that of CD3⁺CD8⁺ rose gradually. The percentage of CD3⁺CD56⁺ remarkably increased after incubation, and reached a maximum level on day 13, then gradually decreased during the further generations. The percentage of CD25⁺ increased rapidly after harvest, and reached a peak level on d 7, and then decreased rapidly (Figures 1 and 2).

Table 1 Clinical data of 13 hepatocellular carcinoma (HCC) patients

	Male/ Female	Age (yr)	HBV history	HCC stage	HBV viral load (copies DNA/mL)	ALT (U/L)	AFP (μ g/L)	TP (g/L)
1	M	32	10	Advanced	$<10^4$	34	>800	56
2	M	50	20	Advanced	5.02×10^6	40	31.9	65
3	F	52	12	Early	3.07×10^6	28	21.4	66
4	M	50	18	Advanced	1.69×10^5	150	60.6	63
5	M	49	15	Advanced	3.48×10^5	50	>1000	71
6	M	49	26	Advanced	2.02×10^6	35	121.9	73
7	M	45	10	Advanced	2.55×10^6	31	897.9	73
8	M	49	12	Advanced	3.44×10^5	98	<20	58
9	M	49	14	Advanced	1.66×10^5	78	139.6	84
10	M	51	15	Advanced	1.77×10^6	68	950	67
11	M	50	12	Advanced	$<10^4$	37	>1000	56
12	M	30	8	Early	1.26×10^7	50	>1210	68
13	M	53	14	Advanced	9.63×10^5	66	785.2	60

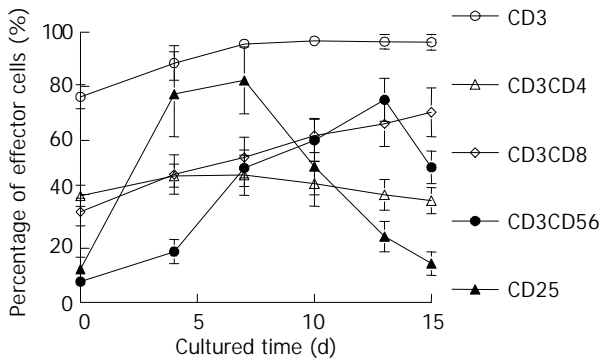


Figure 1 Dynamic analysis of CIK cellular phenotypes by flow cytometry.

Lymphocyte phenotype analysis before or after CIK cell transfusion

Before and 10 d after CIK cell transfusion, PBMCs were obtained from the same patient and analyzed for phenotypes by flow cytometry. Ten days after CIK cell transfusion, the proportions of CD3⁺CD8⁺, CD3⁺CD56⁺ and CD25⁺ in peripheral blood increased significantly from 33.5%, 7.7% and 12.3% to 36.6% (*P*<0.05), 18.9% (*P*<0.01) and 16.4% (*P*<0.05), respectively.

However, the proportions of CD3⁺CD4⁺ or NK cells declined slightly, and there were no significant differences before and after CIK cell transfusion (Figure 3). The longest observation time for patients was 108 d after CIK cell transfusion, others were 20-90 d, and the percentage of lymphocyte subpopulations was the same 8-10 d after CIK cell transfusion, and had no significant difference. Therefore, the proportions of effector cells in peripheral blood might last for more than 108 d. All the patients were under follow-up observation.

Analysis of DC subset proportion before or after CIK cell transfusion

The frequencies of DC1 and DC2 increased from 0.59% and 0.26% before CIK cell transfusion to 0.85% and 0.43% after CIK cell transfusion, respectively, and had a significant difference (*P*<0.01). Therefore, CIK cell treatment could enhance the proportions of DC1 and DC1 in peripheral blood in HCC patients (Figure 4).

HBV viral load analysis before and after CIK cell transfusion

Before CIK cell therapy, the average HBV viral load in HCC patients was 1.85×10⁶ copies of DNA/mL. After CIK cell transfusion, the average viral load was decreased to 8.75×10⁵ copies of DNA/mL in one month, 1.44×10⁵ copies of DNA/mL in 2 mo, and 1.41×10⁵ copies of DNA/mL in 3 mo (Figure 5).

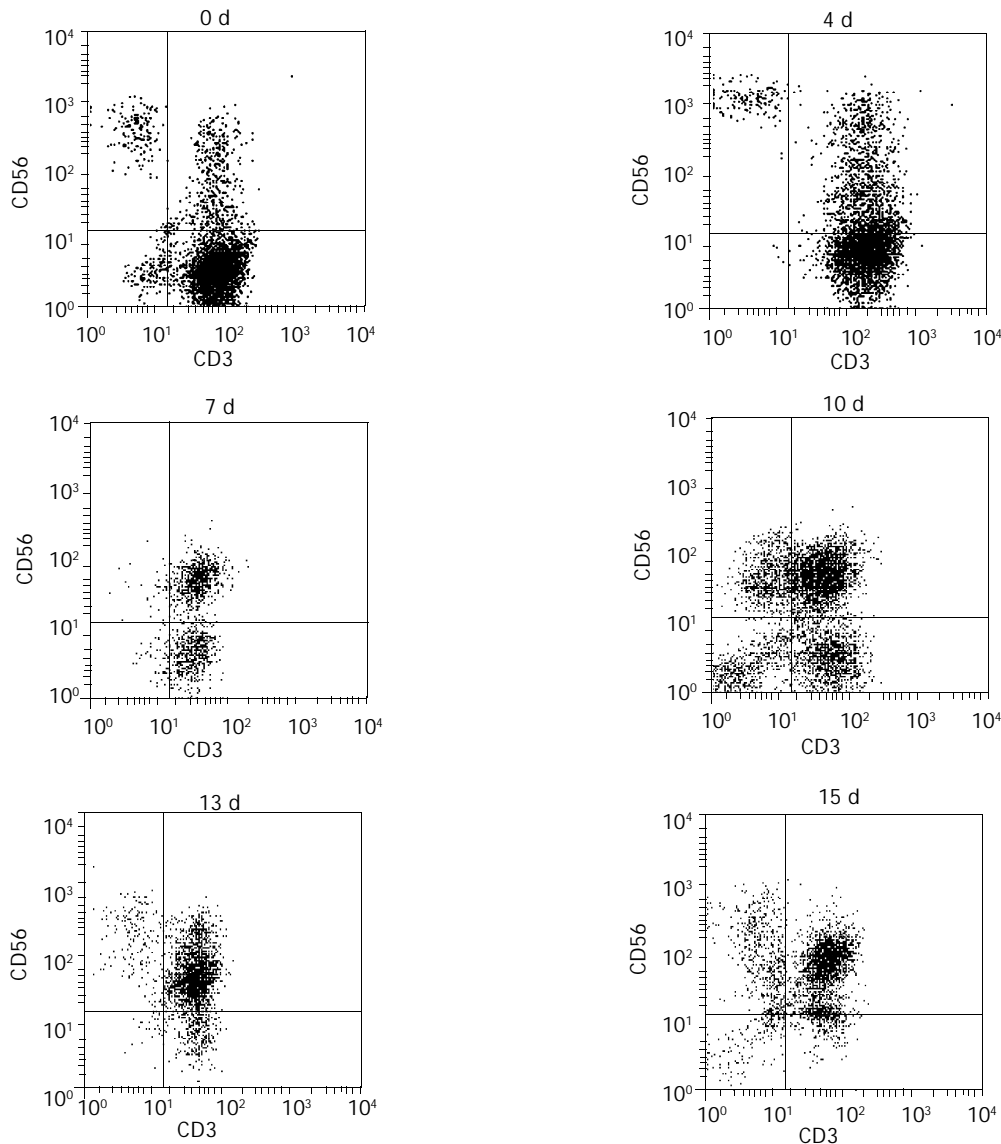


Figure 2 Phenotypic analysis of CD3⁺CD56⁺ cells in cultured cells by flow cytometry in various culture time.

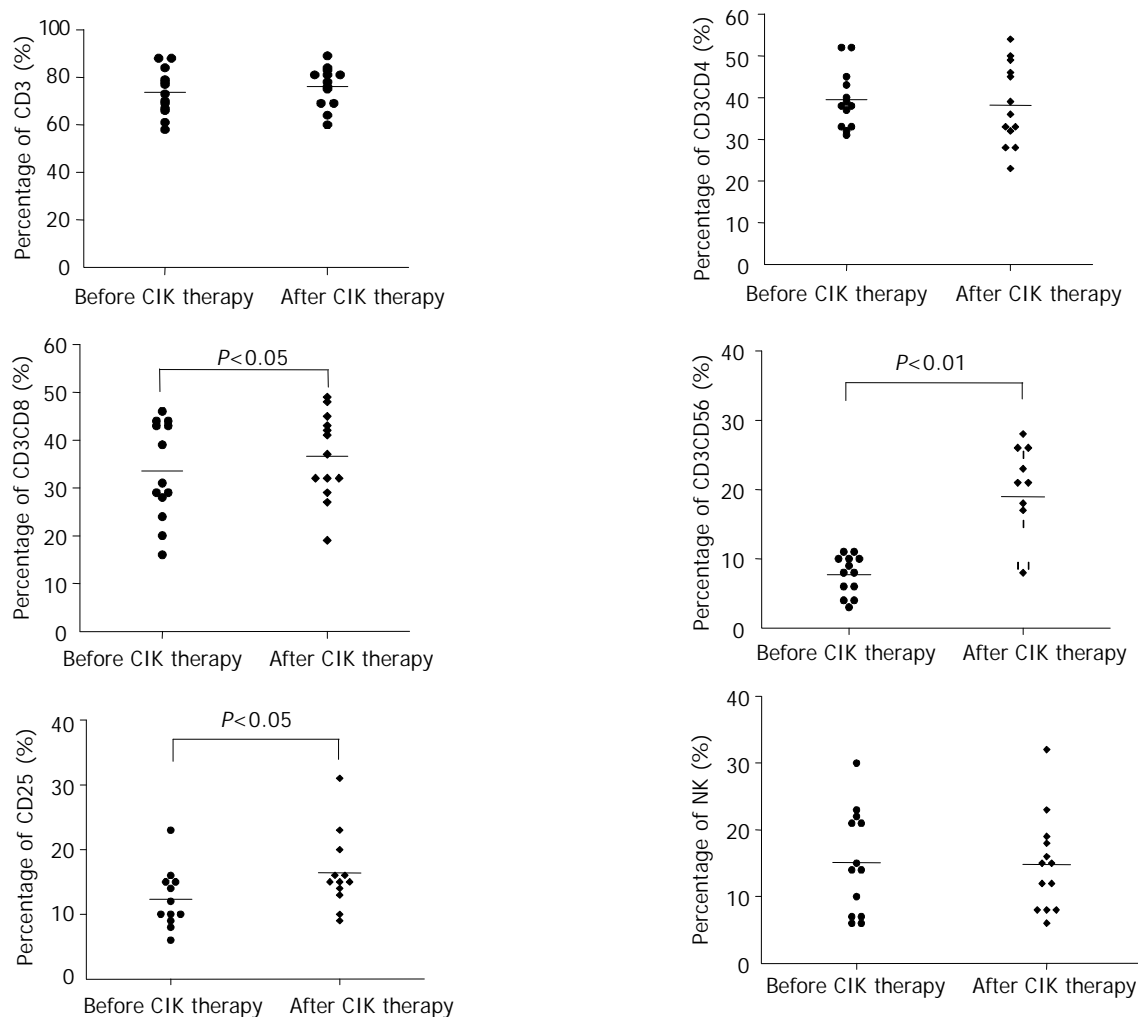


Figure 3 Percentages of lymphocyte subsets in peripheral blood of HCC patients before and after CIK cell therapy.

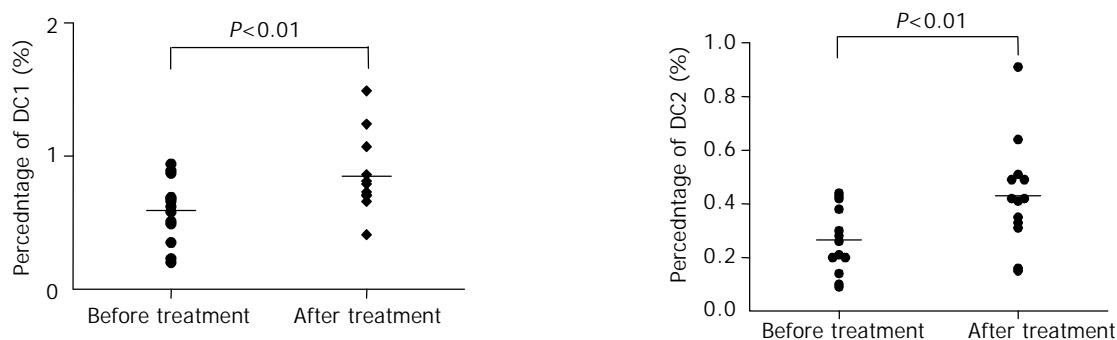


Figure 4 Proportions of DCs in HCC patient peripheral blood before and after CIK cell transfusion.

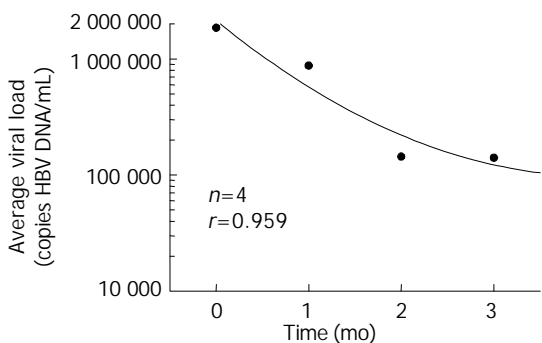


Figure 5 Average HBV viral load in HCC patient serum before and after CIK cell transfusion.

CIK cell therapy efficacy

After autologous CIK cell therapy, ameliorated symptoms, increased appetite, improved sleep and gained body weight were observed in most patients. The growth of tumors in all patients became slow down, the tumor volume was decreased in 3 patients. Most patients developed a fever 6 h after transfusion, and the body temperature was 37.5-40 °C, which could last for 6-8 h. Most fever patients recovered without any treatment. No side effects on liver and kidney were found. Therefore, the autologous CIK cell treatment was a safe and efficacious approach.

DISCUSSION

Heterogenous CIK cells could be generated from PBMC with

stimulation of multiple cytokines. The major marker of CIK cells was CD3⁺CD56⁺, termed NKT cells. It was thought that CIK cells which kill the tumor were non-MHC-restricted, but recently, NKT cells exerting efficient MHC- and non-MHC-restricted cytotoxicity against autologous tumor targets have been reported^[15]. One reason why tumors are difficult to cure is that tumor escapes the host immune monitor. The human immune system against the tumor is mainly dependent on the cellular immunity. The host immune response in HCC patients was significantly suppressed. The cell number and cytotoxicity are necessary for efficient immunotherapy of tumors. Autologous CIK cell immunotherapy is the most efficient approach of neoplasms. Our present study indicated that autologous CIK cell transfusion was safe and efficient to cure liver neoplasms.

In healthy condition, cells with phenotype of CD3⁺CD56⁺ were about 1-5% in peripheral blood^[5]. CD3⁺CD56⁺ cells could expand nearly 10-fold or even more than 100-fold under cytokine cocktail condition, and the cytotoxicity was greatly improved. The percentage of CD3⁺CD8⁺, CD3⁺CD56⁺ and CD25⁺ before CIK cell transfusion increased from 33.5%, 7.7%, 12.3% to 36.6%, 18.9%, and 16.4% after CIK cell transfusion in peripheral blood, respectively. The level of CD3⁺CD8⁺ could be kept as long as 100 d *in vivo*.

HBV chronic infection is the major pathogen of primary liver carcinoma. HCC patients had some immunity dysfunctions, including innate and adaptive immune responses^[4]. The study showed that the number of DCs was decreased or DCs displayed low function^[2,16,17]. DCs are considered unique APCs for their highly efficient capability of priming naïve T cells via direct cell-cell interactions and cytokine production, stimulating the propagation of naïve T cells, and playing a critical role in innate and adaptive immunity. They have been considered as one of the most potent regulators of the immunological mechanism^[18-20]. DC1 is of myeloid origin and could express CD11c, induce Th1 type of T cell differentiation and immunity. On the other hand, DC2 is of lymphoid origin and could express CD123, induce Th2 type of T cell differentiation and was involved in the induction of immunogenic tolerance^[21-23]. HBV patients exhibited a significant decrease in proportion of freshly isolated pDC1 to pDC2, and *ex vivo* generated DC1 function was impaired^[24]. DCs function was also suppressed in patients with HCC with hepatitis B and C virus infections^[25]. Decreased function of DCs might allow the development of tumor or the tumor itself might suppress the function of DCs^[26,27]. Our results showed that the proportions of DC1 and DC2 in the peripheral blood in HCC patients increased from 0.59% and 0.26% to 0.85% and 0.43% ($P < 0.01$) respectively after treatment with CIK cells. The reason was that some cytokines released by CIK cells, type I IFN for example, could promote the propagation or differentiation of DCs, enhancing the host immune response. Type I IFN can modulate DC activation/maturation and cytokine production in different ways depending on the experimental model and culture condition. The propagation of DC1 and DC2 could induce CTL against the tumor by producing more cytokines, and maintain the activity of CIK cells to kill the tumor efficiently^[28,29]. The studies showed that interaction between dendritic cells and CIK cells could lead to activation of both populations^[30]. This may provide a new approach in adoptive immunotherapy against tumors. Our data showed that HBV viral load decreased 3 mo after CIK cell therapy. The alpha-fetoprotein (AFP) in 6 cases significantly decreased. Serum alanine aminotransferase (sALT) decreased in 9 cases while enhanced in 2 cases. These results indicated that CIK cells played an essential role in anti-virus and anti-tumor treatment and improved the liver function. Our results also showed that CIK cell treatment efficacy was better when applied in combination with surgery or chemotherapy. For advanced HCC patients or those who were unfit for surgery or chemotherapy,

autologous CIK cell treatment could ameliorate symptoms, enhance quality of life and prolong the lives of patients.

In conclusion, autologous CIK therapy may greatly improve host immune responses. Therefore, CIK cells may have a major impact on immunotherapeutic protocols for patients with liver cancer.

REFERENCES

- 1 **Tang ZY**. Hepatocellular carcinoma-cause, treatment and metastasis. *World J Gastroenterol* 2001; **7**: 445-454
- 2 **Nakamoto Y**, Guidotti LG, Kuhlen CV, Fowler P, Chisari FV. Immune pathogenesis of hepatocellular carcinoma. *J Exp Med* 1998; **188**: 341-350
- 3 **Davis GL**. Hepatitis C, In Schiff ER, Sorrell MF, Maddrey WC. eds. Schiff's Diseases of the Liver, 8th ed, Lippincott-Raven Publishers, Philadelphia 1999: 793-836
- 4 **Ladhams A**, Schmidt C, Sing G, Butterworth L, Fielding G, Tesar P, Strong R, Leggett B, Powell L, Maddern G, Ellem K, Cooksley G. Treatment of non-resectable hepatocellular carcinoma with autologous tumor-pulsed dendritic cells. *J Gastroenterol Hepatol* 2002; **17**: 889-896
- 5 **Lu PH**, Negrin RS. A novel population of expanded human CD3⁺CD56⁺ cells derived from T cells with potent *in vivo* anti-tumor activity in mice with potent severe combined immunodeficiency. *J Immunol* 1994; **153**: 1687-1696
- 6 **Schmidt-Wolf IGH**, Lefterova P, Johnston V, Huhn D, Blume KG, Negrin RS. Propagation of T cells with NK cell marker. *Br J Haematol* 1994; **87**: 453-458
- 7 **Shi M**, Lei ZY, Wang FS, Zhang B, Li WL, Liu JC. Human cytokine-induced killer cells inhibit the growth of hepatocellular carcinoma cells transplanted in nude mice. *Zhongguo Zhongliu Shengwu Zhiliao Zazhi* 2002; **9**: 179-182
- 8 **Wang FS**, Liu MX, Zhang B, Shi M, Lei ZY, Sun WB, Du QY, Chen JM. Antitumor activities of human autologous cytokine-induced killer (CIK) cells against hepatocellular carcinoma cells *in vitro* and *in vivo*. *World J Gastroenterol* 2002; **8**: 464-468
- 9 **Du QY**, Liu MX, Wang FS. The effect of CIK against hepatocellular carcinoma cells *in vivo* or *ex vivo*. *Zhongguo Aizheng Zazhi* 2001; **11**: 325-327
- 10 **Du QY**, Wang FS, Xu DP, Liu H, Lei ZY, Liu MX, Wang YD, Cheng JM, Wu ZZ. Cytotoxic effects of CIK against hepatocellular carcinoma cells *in vitro*. *Shijie Huaren Xiaohua Zazhi* 2000; **8**: 863-866
- 11 **Banchereau J**, Briere F, Caux C, Davoust J, Lebecque S, Liu YJ, Pulendran B, Palucka K. Immunobiology of dendritic cells. *Annu Rev Immunol* 2000; **18**: 767-811
- 12 **Kunitani H**, Shimizu Y, Murata H, Higuchi K, Watanabe A. Phenotypic analysis of circulating and intrahepatic dendritic cell subsets in patients with chronic liver diseases. *J Hepatol* 2002; **36**: 734-741
- 13 **Hiasa Y**, Akbar SM, Abe M, Michitaka K, Horiike N, Onji M. Dendritic cell subtypes in autoimmune liver diseases; decreased expression of HLA DR and CD123 on type 2 dendritic cells. *Hepatol Res* 2002; **22**: 241-249
- 14 **Willmann K**, Dunne JF. A flow cytometric immune function assay for human peripheral blood dendritic cells. *J Leukoc Biol* 2000; **67**: 536-544
- 15 **Baxevanis CN**, Gritzapis AD, Tsitsilonis OE, Katsoulas HL, Papamichail M. HER-2/neu-derived peptide epitopes are also recognized by cytotoxic CD3(+)/CD56(+) (natural killer T) lymphocytes. *Int J Cancer* 2002; **98**: 864-872
- 16 **Xing LH**, Wang FS, Liu MX, Zhu CL, Lei ZY, Wang HF, Zhang B, Jin L. Property and implication of dendritic cells from peripheral blood monocytes in patients with persistent hepatitis B virus infection. *Zhonghua Chuanranbing Zazhi* 2001; **19**: 348-351
- 17 **Akbar SM**, Horiike N, Onji M, Hino O. Dendritic cells and chronic hepatitis virus carriers. *Intervirology* 2001; **44**: 199-208
- 18 **Lee WC**, Wang HC, Jeng LB, Chiang YJ, Lia CR, Huang PF, Chen MF, Qian S, Lu L. Effective treatment of small murine hepatocellular carcinoma by dendritic cells. *Hepatology* 2001; **34**: 896-905
- 19 **Friedl J**, Stift A, Paolini P, Roth E, Steger GG, Mader R, Jakesz R,

- Gnant MF. Tumor antigen pulsed dendritic cells enhance the cytolytic activity of tumor infiltrating lymphocytes in human hepatocellular cancer. *Cancer Biother Radiopharm* 2000; **15**: 477-486
- 20 **Liu YJ**, Kadowaki N, Risoan MC, Soumelis V. T cell activation and polarization by DC1 and DC2. *Curr Top Microbiol Immunol* 2000; **251**: 149-159
- 21 **Gilliet M**, Liu YJ. Human plasmacytoid-derived dendritic cells and the induction of T-regulatory cells. *Hum Immunol* 2002; **63**: 1149-1155
- 22 **Blom B**, Ligthart SJ, Schotte R, Spits H. Developmental origin of pre-DC2. *Hum Immunol* 2002; **63**: 1072-1080
- 23 **Risoan MC**, Soumelis V, Kadowaki N, Grouard G, Briere F, de Waal Malefyt R, Liu YJ. Reciprocal control of T helper cell and dendritic cell differentiation. *Science* 1999; **283**: 1183-1186
- 24 **Beckebaum S**, Cicinnati VR, Dworacki G, Muller-Berghaus J, Stolz D, Harnaha J, Whiteside TL, Thomson AW, Lu L, Fung JJ, Bonham CA. Reduction in the circulating pDC1/pDC2 ratio and impaired function of *ex vivo*-generated DC1 in chronic hepatitis B infection. *Clin Immunol* 2002; **104**: 138-150
- 25 **Kakumu S**, Ito S, Ishikawa T, Mita Y, Tagaya T, Fukuzawa Y, Yoshioka K. Decreased function of peripheral blood dendritic cells in patients with hepatocellular carcinoma with hepatitis B and C virus infection. *J Gastroenterol Hepatol* 2000; **15**: 431-436
- 26 **Chen S**, Akbar SM, Tanimoto K, Ninomiya T, Iuchi H, Michitaka K, Horiike N, Onji M. Absence of CD83-positive mature and activated dendritic cells at cancer nodules from patients with hepatocellular carcinoma: relevance to hepatocarcinogenesis. *Cancer Lett* 2000; **148**: 49-57
- 27 **Ninomiya T**, Akbar SM, Masumoto T, Horiike N, Onji M. Dendritic cells with immature phenotype and defective function in the peripheral blood from patients with hepatocellular carcinoma. *J Hepatol* 1999; **31**: 323-331
- 28 **Marten A**, Renoth S, von Lilienfeld-Toal M, Buttgerit P, Schakowski F, Glasmacher A, Sauerbruch T, Schmidt-Wolf IG. Enhanced lytic activity of cytokine-induced killer cells against multiple myeloma cells after co-culture with idiotype-pulsed dendritic cells. *Haematologica* 2001; **86**: 1029-1037
- 29 **Ziske C**, Marten A, Schottker B, Buttgerit P, Schakowski F, Gorschluter M, von Rucker A, Scheffold C, Chao N, Sauerbruch T, Schmidt-Wolf IG. Resistance of pancreatic carcinoma cells is reversed by coculturing NK-like T cells with dendritic cells pulsed with tumor-derived RNA and CA 19-9. *Mol Ther* 2001; **3**: 54-60
- 30 **Marten A**, Ziske C, Schottker B, Renoth S, Weineck S, Buttgerit P, Schakowski F, von Rucker A, Sauerbruch T, Schmidt-Wolf IG. Interactions between dendritic cells and cytokine-induced killer cells lead to an activation of both populations. *J Immunother* 2001; **24**: 502-510

Edited by Wang XL and Zhao M Proofread by Xu FM

Assessment of hepatocellular carcinoma vascularity before and after transcatheter arterial chemoembolization by using first pass perfusion weighted MR imaging

Jun-Gong Zhao, Gan-Sheng Feng, Xiang-Quan Kong, Xin Li, Ming-Hua Li, Ying-Sheng Cheng

Jun-Gong Zhao, Ming-Hua Li, Ying-Sheng Cheng, Department of Radiology, Sixth Affiliated Hospital of Shanghai Jiaotong University, Shanghai 200233, China

Gan-Sheng Feng, Xiang-Quan Kong, Xin Li, Department of Radiology, Union Hospital, Tongji Medical College, Huazhong University of Science and Technology, Wuhan 430022, Hubei Province, China

Correspondence to: Dr. Jun -Gong Zhao, Department of Radiology, Sixth Affiliated Hospital of Shanghai Jiaotong University, Shanghai 200233, China. zhaojun_gong@sohu.com

Telephone: +86-21-64369181 **Fax:** +86-21-64701361

Received: 2003-10-24 **Accepted:** 2004-12-29

Abstract

AIM: To assess the vascularity of hepatocellular carcinoma (HCC) before and after transcatheter arterial chemoembolization (TACE) with the quantitative parameters obtained by first pass perfusion weighted MR imaging (FP-MRI).

METHODS: Seventeen consecutive patients with one to three lesions in liver underwent FP-MRI before treatment. FP-MRI was also performed one, three, six, nine months, and one year after TACE. The baseline signal intensity (S0) of pre-TACE and one month after TACE was analyzed, the vascularity of HCC assessed by steepest slope of the signal intensity versus time curves (SS) was blindly correlated with their DSA feature and clinical outcome.

RESULT: No significant difference was found on baseline signal intensity (S0) between pre-TACE and one month after TACE ($F=0.309$, $P=0.583$). The SS (mean, 32% per second) of lesion one month after TACE was lower than that of pre-TACE (mean, 69% per second), but with no statistical significance ($F=3.067$, $P=0.092$). When local recurrence occurred, the time intensity curves became steeper. The vascularity of HCC before and after TACE graded by SS closely correlated with that by DSA ($K=0.453$, $P<0.05$).

CONCLUSION: FP-MRI is a useful criterion for selecting effective interventional treatment for patients with HCC in their initial treatment and during follow up.

Zhao JG, Feng GS, Kong XQ, Li X, Li MH, Cheng YS. Assessment of hepatocellular carcinoma vascularity before and after transcatheter arterial chemoembolization by using first pass perfusion weighted MR imaging. *World J Gastroenterol* 2004; 10(8): 1152-1156

<http://www.wjgnet.com/1007-9327/10/1152.asp>

INTRODUCTION

Transcatheter arterial chemoembolization (TACE) has been applied as an effective therapy to improve the survival rate in unresectable hepatocellular carcinoma (HCC) and to decrease the recurrence of resected HCC^[1,2]. The efficacy of TACE usually

depends on the vascularity (arterial blood supply) of HCC, that is, when HCC with hypervascularity, TACE is effective, otherwise, the efficacy of TACE is poor^[3,4], other ablation methods such as percutaneous radiofrequency and percutaneous ethanol injection are needed^[5-8]. Furthermore, since TACE is difficult to kill the entire tumor cells at one time, and it is generally used repeatedly or in combination with other ablation modalities. So it is essential to evaluate the tumor vascularity and its distribution before TACE and during follow up. Angiography is the golden standard to evaluate the tumor vascularity, but it is an invasive technique and is therefore not suitable for routine follow up. Generally, computed tomographic (CT) images could be considered as a routine modality to judge the efficacy of TACE depending upon the homogeneous and completely deposition of lipiodol within the lesion, but previous results indicated that even in lipiodol retention area there were viable tumor cells^[9]. So it is difficult to access the viability and necrosis of the tumor correctly depending upon the deposition of lipiodol. On the other hand, viable tumors could be enhanced on CT contrast scanning^[10,11], but the enhancement area within the lesions could also be affected by artifacts of the high concentrations of lipiodol, which could somewhat disturb the evaluation of vascularity during follow up. Although power Doppler ultrasonography was used to assess tumor vascularity, the detected velocities in the tumor were too slow to be detected, there were too many blooming artifacts associated with micro-bubble injection as well as artifacts resulted from respiration, and the duration of enhancement was short. So vascularity of tumors can not be evaluated in detail by power Doppler US^[12,13].

T1 weighted FP-MRI with excellent temporal resolution (more than one imaging per second) has been used to assess tumor angiogenesis of uterine cervical carcinoma, and has a good correlation with microvessel density (MVD)^[14]. The purpose of this study was to monitor the angiogenesis of HCC before and after TACE by FP-MRI compared with angiography and patient outcome, and to find out its feasibility and value in assessing vascularity of HCC.

MATERIALS AND METHODS

Between December 2000 and March 2002, patients with HCC included in this study fulfilled the following criteria, namely three or less HCC nodules and no portal thrombosis or extrahepatic metastasis. Seventeen patients (15 males, 2 females) were enrolled in this study. The age was 31-69 years, mean 48.5 years. The diagnosis of HCC was confirmed by fine needle biopsy.

Digital subtraction angiography (DSA) was performed through the celiac or hepatic artery, HCC were classified into the following 3 groups on the basis of vascularity by two angiographers independently who had no information on the current study: Grade A, tumors with more vascularity than nontumorous hepatic parenchyma; Grade B, tumors with vascularity similar to that of nontumorous hepatic parenchyma; and Grade C, tumors with less vascularity than Grade B tumors.

TACE was performed by injection of 8-10 mg mitomycin C mixed 30-50 mg doxorubicin and 10 mL of lipiodol (Guerbet,

Roissy, France) in either the right or left segmental branch of hepatic artery. Embolization was subsequently completed with gelform powder and a small amount of contrast medium under fluoroscopic guidance.

Before TACE and one, three, six, nine months, and one year after first TACE, patients with HCC underwent MR imaging by using a 1.5 T system (Magnetom Vision, Siemens Medical Systems) with a phased array coil, including T1WI (TR=525 ms, TE= 14 ms), T2WI (TR=4.4 ms, TE=90 ms) and FP-MRI scanning. T1WI and T2WI were used to identify the satisfactory plan and section for perfusion study. For the FP-MRI, a strong T1-weighted, turbo-FLASH sequence was used with a high temporal resolution of 1.196 s per section, two axial or coronal images (TR=3.3 ms, TE=1.4 ms, TI=300 ms) were acquired sequentially with 65 repetitions. At the end of the 4th acquisition, a total dose of 0.1 mmol/kg body mass of gadopentetate dimeglumine (Bellona, Beijing, China) was administered intravenously; 10 mL of saline was immediately flushed to ensure completely delivery of the entire dose of gadopentetate dimeglumine.

To quantitative analysis of FP-MRI, four circular region of interesting (ROI) were drawn, signal intensity time curve was obtained over ROI, the baseline signal intensity (S0) of pre-TACE and one month after TACE (that is, the signal on FP-MRI without gadopentetate dimeglumine) and the steepest slope of the curve (SS) were calculated according to previous method^[14]. When the nodules were similar to that of nontumorous hepatic parenchyma, they were classified into group II, while the nodules had larger or smaller SS than those of nontumorous hepatic parenchyma, and they were classified into group I or group III respectively.

All data were expressed as mean±SD, comparison was made by ANOVA, and the correlation between SS and DSA was assessed by Kappa statistic analysis. Significance was accepted when $P < 0.05$.

RESULTS

Lesion signal intensity characteristics before and after TACE
MR studies were performed 53 times in 17 patients, twenty-nine lesions were evaluated, the mean size of which was 6 cm (range, 2-16 cm). Almost all the lesions assessed before TACE were hypo- to isointense relative to the surrounding liver parenchyma on T1-weighted images, and the most portion of tumors was iso- to hyperintense relative to the surrounding liver parenchyma on T2-weighted images, and the heterogeneous signal intensity was observed when liquefied necrosis or fat degeneration occurred. All the lesions demonstrated inhomogeneous enhancement on the FP-MRI. One month after TACE, all the lesions also demonstrated hypo- to isointense relative to the surrounding liver parenchyma on T1-weighted images. The signal intensity became higher on T2-weighted images compared to that of pre-TACE. No significant difference was found on S0 between pre-TACE and one month after TACE ($F=0.309, P=0.583$) (Table 1), only rim enhancement was found on FP-MRI in all the patients.

Quantitative analysis of HCC angiogenesis before and after TACE

Time intensity curves derived from ROIs drawn in the most-enhancing portion of the tumor before TACE showed different enhancement patterns: Type A (10 cases, 59%) showed a rapid initial increase in signal intensity followed by a plateau, representing hypervascularity. Type B (7cases, 41%), however, showed a slow initial increase in signal intensity followed by a plateau, indicating mild hypervascularity or hypovascularity of the tumor (Figure 1). The SS (mean, 40%) in three patients with arteriportal shunting associated with HCC was lower than the mean value of total patients (mean, 69% per second).

After TACE, Time intensity curves drawn in the rim-

enhancing portion of the tumor showed less steep (mean SS, 32% per second), and its central area demonstrated a horizontal line. No significant difference was found on SS obtained in rim-enhancing portion of the lesions between pre-TACE and post-TACE ($F=3.067, P=0.092$) (Table 1). When local recurrence occurred (2 cases), Time intensity curves became steeper than the previous ones (Figure 2). There was a good correlation between SS and DSA in assessment of the vascularity of HCC ($K=0.453, P<0.05$) (Table 2).

Table 1 SS (% per second) and S0 of HCC before and after TACE

	cases	mean	minimum	maximum	F	P
SS						
Pre-TACE	17	69	37	101	3.067	0.092
After-TACE	15	32	11	52		
S0						
Pre-TACE	17	14.04	6.76	21.32	0.309	0.583
After-TACE	15	16.94	9.72	24.12		

Table 2 Relationship of DSA and SS in assessment of vascularity

DSA ¹	SS		
	I	II	III
A	7	2	1
B	2	8	0
C	5	0	3

¹ $K=0.453, P<0.05$ vs SS.

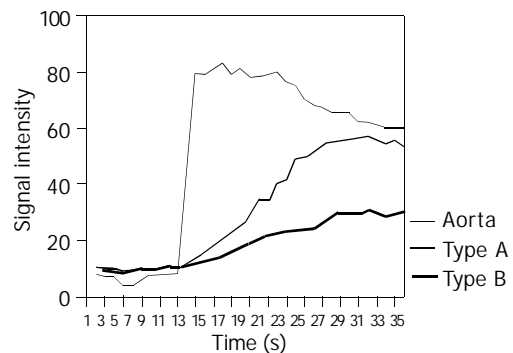
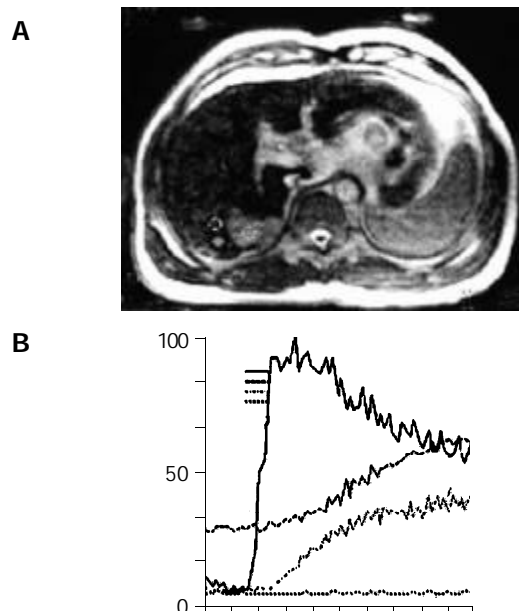


Figure 1 Signal intensity time curves of HCC in different groups before TACE. Type A represents hypervascularity, type B shows mild hypervascularity or hypovascularity of the tumor.



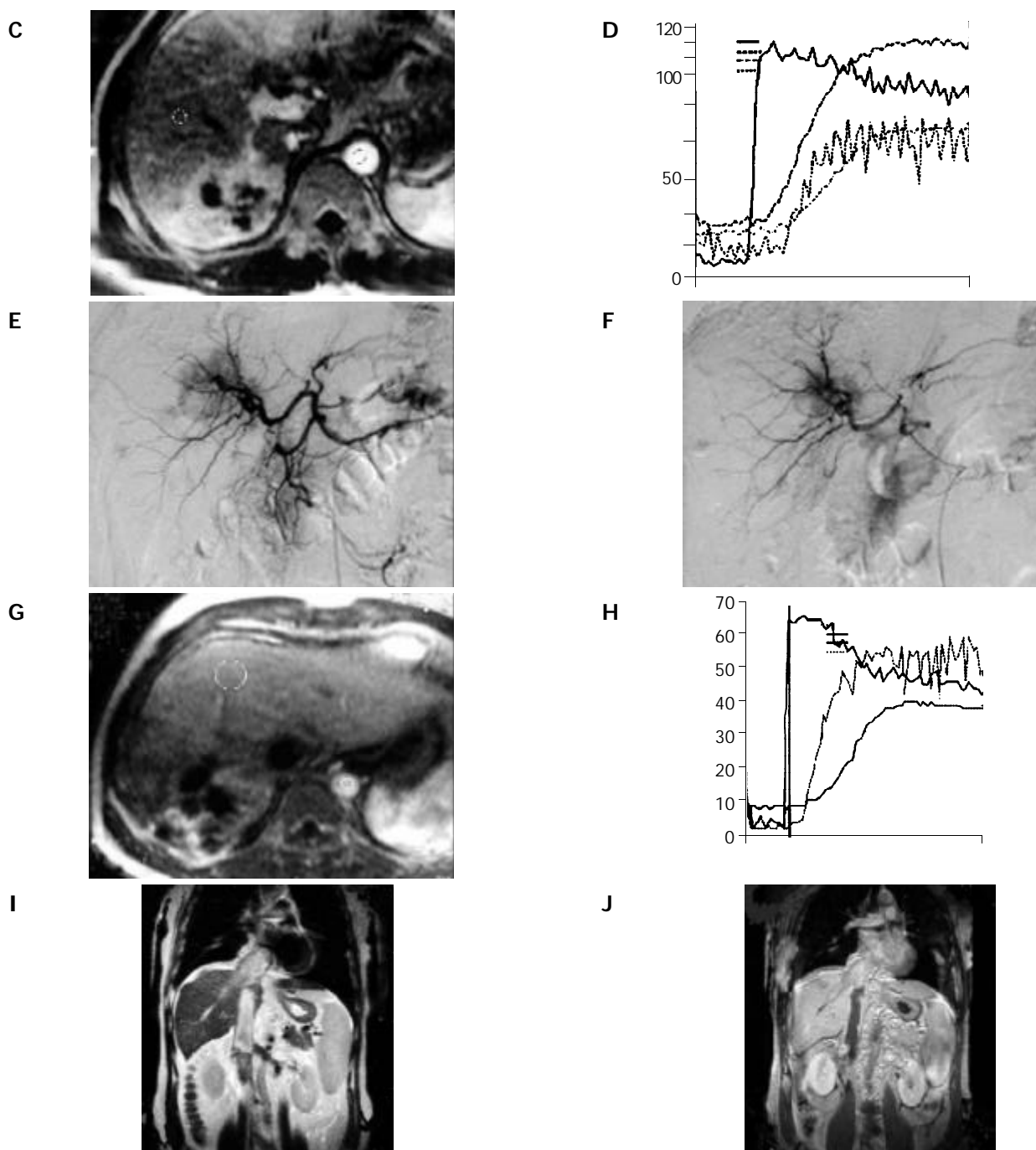


Figure 2 HCC before and after TACE. (A-B) FP-MRI and the signal intensity time curve derived from ROIs before TACE. (C-D) FP-MRI and the signal intensity time curve one month after TACE, the signal intensity time curve became steeper than that pre-TACE, indicating the remaining arterial blood supply of the lesion after TACE. (E) DSA before TACE and (F) DSA after TACE confirmed the FP-MRI finding. (G-H) one year after TACE, the lesion became larger and the signal intensity time curve became much steeper than that one month after TACE, suggesting the recurrence of the tumor. (I-J) T2 weighted image and enhanced T1 weighted image showing embolus in inferior vena cava and atrium dextrum.

DISCUSSION

Dynamic MR imaging with prior administration of gadopentetate dimeglumine has been used in a few studies to evaluate tumor angiogenesis^[15-18]. Gadopentetate dimeglumine is rapidly distributed in the extra-vascular space during the signal acquisition, so the relative changes in signal intensity on dynamic MR imaging are not only correlated with MVD itself but also with perfusion rate, micro-vessel permeability, and the size of extra-cellular leakage space as well. Which of these pathophysiological mechanisms in HCC is the major contribution to the differences in the contrast media uptake is not clear. Because of high temporal resolution, FP-MRI can monitor the contrast medium first passing the microvessels,

the relative changes of signal intensity is significantly associated with MVD, and has been used to assess tumor angiogenesis^[14]. T1 weighted FP-MRI or T2* weighted FP-MRI may be obtained depending upon the different sequences used^[14,19,20].

The time intensity curves derived from T1 weighted FP-MRI of HCC before TACE showed a rapid initial increase in signal intensity followed by a plateau corresponding to hypervascularity, while the time intensity curves showed a slow initial increase in signal intensity followed by a plateau representing mild hypervascularity or hypovascularity. Our study showed that there was a good correlation between SS derived from T1 weighted FP-MRI and DSA in assessment of

the vascularity of HCC. The different vascularity of HCC was due to its differentiation and size^[4,21,22], which resulted in different uptake and deposition of lipiodol. HCC with hypervascularity often has homogeneous deposition of lipiodol, and leads to complete necrosis of tumor and a better prognosis. When HCC with hypovascularity it shows incomplete necrosis because of poor deposition of lipiodol and only other ablation techniques are effective. Otherwise, unnecessary repeated TACE may be offset by worsening liver function in patients with cirrhosis, so it is important to identify the angiogenesis of HCC before TACE.

After TACE, the center of the lesion demonstrated no vascularity. Although the time intensity curves drawn in the rim-enhancing portion of the tumor was less steep than before, no significant difference was found on SS of the lesions pre-TACE and post-TACE. This result indicated that vascularity existed even after TACE. The vascularity after TACE was mainly due to collateral blood supply after TACE^[24,25]. Meanwhile, the expression of vascular endothelial growth factor (VEGF) of cancerous cells could be enhanced by TACE which might play an important role in reestablishing of blood supply to tumor after TACE^[23]. In this study, the incomplete embolization (because of larger lesions, mean size, 6 cm. complete embolization is at the expense of liver function) might contribute to the remains of arterial blood supply. The arterial blood supply after TACE could offer nutrition and oxygen to the remaining viable tumor cells, resulting in partial or incomplete necrosis of the tumor, recurrence would occur sooner or later. When HCC recurred, the time intensity curves became steep again, and the SS increased (Figure 2). The angiogenesis after TACE is a challenge to TACE. Up to now, TNP-470, cyanoacrylate, Plcg-mitomycin-microsphere and bletilla have been shown to improve the therapeutic results^[26-30]. On the other hand, how to correctly access the angiogenesis after TACE during follow up remains to be studied. The study presented here offers a noninvasive modality to evaluate the angiogenesis after TACE without artifact.

Our result also showed that there was no significant difference in the baseline signal intensity on FP-MRI pre-TACE and one month after TACE, indicating that the retention of lipiodol within the lesion did not influence the assessment of tumor vascularity after TACE. We encountered two patients with HCC who were treated with TACE in combination with percutaneous ethanol injection. Six months after the therapy, the patients were suspected of recurrence because of their increase of alpha-fetoprotein, although the lesion had high signal intensity on FP-MRI before administration of gadopentetate dimeglumine, the time intensity curves demonstrated the vascularity of the original lesion and intrahepatic metastatic lesions, which were confirmed by DSA.

The potential pitfall of the evaluation of HCC vascularity by using FP-MRI is that the arterioportal shunting (APS) coexists with HCC. APS breaks the equilibrium of normal dual blood supply to the liver tissue and affects the blood flow in tumors, the enhancement of tumors might be changed depending on the degree and location of the shunting^[31-33]. Large HCC might be enhanced poorly, and the vascularity might be underestimated because of the limited amount of contrast material passed through the tumor bed. The SS in three patients with APS associated with HCC (mean, 40% per second) was lower than the mean value of the patients (mean, 69% per second). Nevertheless, when the APS coexisted with HCC, the vascularity of HCC evaluated by using FP-MRI should be with caution, only when the shunting disappeared after embolization, was the vascularity of HCC assessed correctly.

The discrepancy between SS and DSA in assessment of the HCC vascularity derived from T1 weighted FP-MRI was within group III and group I. When SS showed hypervascularity

in five lesions, DSA demonstrated hypovascularity. SS showed hypovascularity in two lesions, DSA, however, demonstrated hypervascularity. The differences between these two techniques were due to the pattern of contrast media administered. The contrast media were administered through I.V. before MRI performance and through hepatic artery during DSA. As a result, the extrahepatic blood supply could not be revealed by DSA during arterial phase. This is the limitation of DSA in evaluation of HCC vascularity. On the other hand, the two sections of axial or coronal MR imaging not correlating with DSA point by point might contribute to their difference.

In summery, T1 weighted FP-MRI has been proved to be practical and noninvasive in assessment of the vascularity, and provides semi-quantitative criteria for the selection of patients to be treated with TACE or other ablation in their initial therapy and during follow up.

REFERENCES

- 1 **Sun HC**, Tang ZY. Preventive treatments for recurrence after curative resection of hepatocellular carcinoma-A literature review of randomized control trials. *World J Gastroenterol* 2003; **9**: 635-640
- 2 **Ernst O**, Sergent G, Mizrahi D, Delemazure O, Paris JC, L' Hermine C. Treatment of hepatocellular carcinoma by transcatheter arterial chemoembolization: comparison of planned periodic chemoembolization and chemoembolization based on tumor response. *Am J Roentgenol* 1999; **172**: 59-64
- 3 **Llado L**, Virgili J, Figueras J, Valls C, Dominguez J, Rafecas A, Torras J, Fabregat J, Guardiola J, Jaurrieta E. A prognostic index of the survival of patients with unresectable hepatocellular carcinoma after transcatheter arterial chemoembolization. *Cancer* 2000; **88**: 50-57
- 4 **Yamashita Y**, Matsukawa T, Arakawa A, Hatanaka Y, Urata J, Takahashi M. US-guided liver biopsy: predicting the effect of interventional treatment of hepatocellular carcinoma. *Radiology* 1995; **196**: 799-804
- 5 **Yamasaki T**, Kurokawa F, Shirahashi H, Kusano N, Hironaka K, Okita K. Percutaneous radiofrequency ablation therapy for patients with hepatocellular carcinoma during occlusion of hepatic blood flow. Comparison with standard percutaneous radiofrequency ablation therapy. *Cancer* 2002; **95**: 2353-2360
- 6 **Guo WJ**, Yu EX, Liu LM, Li J, Chen Z, Lin JH, Meng ZQ, Feng Y. Comparison between chemoembolization combined with radiotherapy and chemoembolization alone for large hepatocellular carcinoma. *World J Gastroenterol* 2003; **9**: 1697-1701
- 7 **Pacella CM**, Bizzarri G, Cecconi P, Caspani B, Magnolfi F, Bianchini A, Anelli V, Pacella S, Rossi Z. Hepatocellular carcinoma: long-term results of combined treatment with laser thermal ablation and transcatheter arterial chemoembolization. *Radiology* 2001; **219**: 669-678
- 8 **Tanaka K**, Nakamura S, Numata K, Kondo M, Morita K, Kitamura T, Saito S, Kiba T, Okazaki H, Sekihara H. The long term efficacy of combined transcatheter arterial embolization and percutaneous ethanol injection in the treatment of patients with large hepatocellular carcinoma and cirrhosis. *Cancer* 1998; **82**: 78-85
- 9 **Ito K**, Honjo K, Fujita T, Matsui M, Awaya H, Matsumoto T, Matsunaga N, Nakanishi T. Therapeutic efficacy of transcatheter arterial chemoembolization for hepatocellular carcinoma: MRI and pathology. *J Comput Assist Tomogr* 1995; **19**: 198-203
- 10 **Kim HC**, Kim AY, Han JK, Chung JW, Lee JY, Park JH, Choi BI. Hepatic arterial and portal venous phase helical CT in patients treated with transcatheter arterial chemoembolization for hepatocellular carcinoma: added value of unenhanced images. *Radiology* 2002; **225**: 773-780
- 11 **Tan LL**, Li YB, Chen DJ, Li SX, Jiang JD, Li ZM. Helical dual-phase CT scan in evaluating blood supply of primary hepatocellular carcinoma after transcatheter hepatic artery chemoembolization with lipiodol. *Zhonghua Zhongliu Zazhi* 2003; **25**: 82-84
- 12 **Choi D**, Lim HK, Kim SH, Lee WJ, Jang HJ, Lee JY, Paik SW,

- Koh KC, Lee JH. Hepatocellular carcinoma treated with percutaneous radio-frequency ablation: usefulness of power Doppler US with a microbubble contrast agent in evaluating therapeutic response-preliminary results. *Radiology* 2000; **217**: 558-563
- 13 **Du WH**, Yan WX, Wang X, Xiong XQ, Zhou Y, Li T. Vascularity of hepatic VX2 tumors of rabbits: assessment with conventional power Doppler US and contrast enhanced harmonic power Doppler US. *World J Gastroenterol* 2003; **9**: 258-261
- 14 **Hawighorst H**, Knapstein PG, Knopp MV, Weikel W, Brix G, Zuna I, Schonberg SO, Essig M, Vaupel P, van Kaick G. Uterine cervical carcinoma: comparison of standard and pharmacokinetic analysis of time-intensity curves for assessment of tumor angiogenesis and patient survival. *Cancer Res* 1998; **58**: 3598-3602
- 15 **Kubota K**, Hisa N, Nishikawa T, Fujiwara Y, Murata Y, Itoh S, Yoshida D, Yoshida S. Evaluation of hepatocellular carcinoma after treatment with transcatheter arterial chemoembolization: comparison of Lipiodol-CT, power Doppler sonography, and dynamic MRI. *Abdom Imaging* 2001; **26**: 184-190
- 16 **Yan FH**, Zhou KR, Cheng JM, Wang JH, Yan ZP, Da RR, Fan J, Ji Y. Role and limitation of FMPSGR dynamic contrast scanning in the follow-up of patients with hepatocellular carcinoma treated by TACE. *World J Gastroenterol* 2002; **8**: 658-662
- 17 **Fujita T**, Honjo K, Ito K, Takano K, Koike S, Okazaki H, Matsumoto T, Matsunaga N. Dynamic MR follow-up of small hepatocellular carcinoma after percutaneous ethanol injection therapy. *J Comput Assist Tomogr* 1998; **22**: 379-386
- 18 **Kuszyk BS**, Boitnott JK, Choti MA, Bluemke DA, Sheth S, Magee CA, Horton KM, Eng J, Fishman EK. Local tumor recurrence following hepatic cryoablation: radiologic-histopathologic correlation in a rabbit model. *Radiology* 2000; **217**: 477-486
- 19 **Ichikawa T**, Haradome H, Hachiya J, Nitatori T, Araki T. Perfusion-weighted MR imaging in the upper abdomen: preliminary clinical experience in 61 patients. *Am J Roentgenol* 1997; **169**: 1061-1066
- 20 **Ichikawa T**, Haradome H, Hachiya J, Nitatori T, Araki T. Characterization of hepatic lesions by perfusion-weighted MR imaging with an echoplanar sequence. *Am J Roentgenol* 1998; **170**: 1029-1034
- 21 **Ichikawa T**, Arbab AS, Araki T, Touyama K, Haradome H, Hachiya J, Yamaguchi M, Kumagai H, Aoki S. Perfusion MR imaging with a superparamagnetic iron oxide using T2-weighted and susceptibility-sensitive echoplanar sequences: evaluation of tumor vascularity in hepatocellular carcinoma. *Am J Roentgenol* 1999; **173**: 207-213
- 22 **Hayashi M**, Matsui O, Ueda K, Kawamori Y, Kadoya M, Yoshikawa J, Gabata T, Takashima T, Nonomura A, Nakanuma Y. Correlation between the blood supply and grade of malignancy of hepatocellular nodules associated with liver cirrhosis: evaluation by CT during intraarterial injection of contrast medium. *Am J Roentgenol* 1999; **172**: 969-976
- 23 **Shao G**, Wang J, Zhou K, Yan Z. Intratumoral microvessel density and expression of vascular endothelial growth factor in hepatocellular carcinoma after chemoembolization. *Zhonghua Ganzangbing Zazhi* 2002; **10**: 170-173
- 24 **Tancredi T**, McCuskey PA, Kan Z, Wallace S. Changes in rat liver microcirculation after experimental hepatic arterial embolization: comparison of different embolic agents. *Radiology* 1999; **211**: 177-181
- 25 **Won JY**, Lee do Y, Lee JT, Park SI, Kim MJ, Yoo HS, Suh SH, Park SJ. Supplemental transcatheter arterial chemoembolization through a collateral omental artery: treatment for hepatocellular carcinoma. *Cardiovasc Intervent Radiol* 2003; **26**: 136-140
- 26 **Lund EL**, Bastholm L, Kristjansen PE. Therapeutic synergy of TNP-470 and ionizing radiation: effects on tumor growth, vessel morphology, and angiogenesis in human glioblastoma multiforme xenografts. *Clin Cancer Res* 2000; **6**: 971-978
- 27 **Mugitani T**, Taniguchi H, Takada A, Yamaguchi A, Masuyama M, Hoshima M, Takahashi T. TNP-470 inhibits collateralization to complement the anti-tumor effect of hepatic artery ligation. *Br J Cancer* 1998; **77**: 638-642
- 28 **Qian J**, Truebenbach J, Graepler F, Pereira P, Huppert P, Eul T, Wiemann G, Claussen C. Application of poly-lactide-co-glycolide-microspheres in the transarterial chemoembolization in an animal model of hepatocellular carcinoma. *World J Gastroenterol* 2003; **9**: 94-98
- 29 **Loewe C**, Cejna M, Schoder M, Thurnher MM, Lammer J, Thurnher SA. Arterial embolization of unresectable hepatocellular carcinoma with use of cyanoacrylate and lipiodol. *J Vasc Interv Radiol* 2002; **13**: 61-69
- 30 **Feng GS**, Li X, Zheng CS, Zhou CK, Liu X, Wu HP. Mechanism of inhibition of tumor angiogenesis by Bletilla colloid: an experimental study. *Zhonghua Yixue Zazhi* 2003; **83**: 412-416
- 31 **Chen JH**, Chai JW, Huang CL, Hung HC, Shen WC, Lee SK. Proximal arterioportal shunting associated with hepatocellular carcinoma: features revealed by dynamic helical CT. *Am J Roentgenol* 1999; **172**: 403-407
- 32 **Lane MJ**, Jeffrey RB Jr, Katz DS. Spontaneous intrahepatic vascular shunts. *Am J Roentgenol* 2000; **174**: 125-131
- 33 **Choi D**, Choo SW, Lim JH, Lee SJ, Do YS, Choo IW. Opacification of the intrahepatic portal veins during CT hepatic arteriography. *J Comput Assist Tomogr* 2001; **25**: 218-224

Edited by Wang XL and Xu FM

Comparison of hydrocolonic sonography accuracy in preoperative staging between colon and rectal cancer

Hye Won Chung, Jae Bock Chung, Seung Woo Park, Si Young Song, Jin Kyung Kang, Chan Il Park

Hye Won Chung, Jae Bock Chung, Seung Woo Park, Si Young Song, Jin Kyung Kang, Department of Internal Medicine, Yonsei University College of Medicine, Seoul, South Korea

Chan Il Park, Department of Pathology, Yonsei University College of Medicine, Seoul, South Korea

Correspondence to: Jae Bock Chung, M.D. Department of Internal Medicine, Yonsei University College of Medicine, C.P.O Box 8044, Seoul, 120-752, South Korea. jbchung@yumc.yonsei.ac.kr

Telephone: +82-2-361-5427 **Fax:** +82-2-393-6884

Received: 2003-08-02 **Accepted:** 2003-09-13

Abstract

AIM: To compare the accuracy of hydrocolonic sonography (HUS) in determining the depth of invasion (T stage) in colon and rectal cancer.

METHODS: A total of 1 000-2 000 mL of saline was instilled per rectum using a system for barium enemas, and then ultrasonography was conducted by a SSA-270A (Toshiba Co, Japan) sonolayer unit with a 3.75 MHz for 17 patients with colon cancer and 13 patients with rectal cancer before operation. After operation, T stage in HUS was compared with postoperative histological findings.

RESULTS: Overall, the accuracy of T stage was 70%. It was 88% in colon cancer and 46% in rectal cancer. In evaluating nodal state, the accuracy of HUS was low in both colon (71%) and rectal cancers (46%) compared with conventional CT or MRI. The overall accuracy of N staging was 60%.

CONCLUSION: HUS is valuable to evaluate the depth of invasion in colon cancer, but is less valuable in rectal cancer. Because HUS is low-cost, noninvasive, and readily available at any place, this technique seems to be useful to determine the preoperative staging in colon cancer, but not in rectal cancer.

Chung HW, Chung JB, Park SW, Song SY, Kang JK, Park CI. Comparison of hydrocolonic sonography accuracy in preoperative staging between colon and rectal cancer. *World J Gastroenterol* 2004; 10(8): 1157-1161

<http://www.wjgnet.com/1007-9327/10/1157.asp>

INTRODUCTION

It is well recognized that the prognosis of colorectal cancer is very closely related to TNM stage^[1,2]. In general, computed tomography (CT) or magnetic resonance imaging (MRI) has been widely used for the clinical staging before surgery. These modalities have shown a comparatively high accuracy, especially in evaluating N and M stages. But these modalities have shown some limitation in the depth of invasion^[3-5]. Thus, to overcome this limitation, endoscopic ultrasonography (EUS) was developed, and has recently been widely performed^[5-11]. However, this modality requires endoluminal access and

expensive equipments available only at large medical institutes. Therefore, its application is limited.

Conventional ultrasonography (US) is a simple and safe method, most widely used for screening and diagnosis of abdominal diseases. But, it has limitations to evaluate the endoluminal surface and the depth of invasion of bowel wall^[11,12], because of the inability of sonic waves to penetrate air. Over the last years, sonographic evaluation of gastrointestinal (GI) tract has been improved by the instillation of water into the endoluminal area. This procedure is called hydro-sonography (HUS), which allows us to visualize the endoluminal lesion and the depth of invasion of bowel wall in stomach or colon^[13-23]. Because HUS is low-cost, non-invasive, and readily available in small medical institutes, it would be an acceptable modality for preoperative staging of colorectal cancer especially in evaluating the depth of invasion. The purpose of this prospective study was to compare the accuracy of HUS in T and N staging between colon and rectal cancer.

MATERIALS AND METHODS

Seventeen patients with colon cancer and 13 patients with rectal cancer, who visited Severance Hospital from 1997 to 2002, were enrolled. In all the cases, a barium enema was performed for detection of other lesions, and a colonoscopy with biopsy for histological confirmation was done as much as possible. They all underwent HUS before operation. Surgery was performed within 7 d after HUS, and we compared the histological stage with the preoperative stage by HUS. All the patients gave their written informed consent before treatment, and the study protocol was approved by the Ethical Committee for the Clinical Research of Institutional Review Board of Yonsei Medical Center in Korea.

For the preparation of bowel before HUS, all the patients took an oral laxative, magnesium sulfate 30 mg (Magrol 250 cc), and received two enemas using warm saline-soapy water suspension on the previous day of the examination. They did not eat anything overnight, and were given pre-medication, scopolamine-N-butyl bromide, 20 mg, intramuscularly just before examination for relaxation of the bowel and suppression of the sense of urgency for defecation. Eighteen Fr-Foley catheters were inserted through the anus and fixed to anal sphincter by ballooning. A total of 1 000-2 000 mL of warm saline water was instilled per rectum using a system, that was usually used for barium enemas (Pneumocolon; Barnes-Hind Barium Products) until the bowel wall was fully distended, and continuous sonography of the large intestine was conducted for adequate filling of water into the colon and rectum (Figure 1A). On occasion, the patients changed their position for optimal sonographic plane. We used a SSA-270A (Toshiba co, Japan) sonolayer unit with a 3.75 MHz convex type transducer, and lower frequency beams for proper penetration. The diagnosis of lesions was based on the sonographic evidence mentioned by Limberg^[16]. The main criteria for malignancy were as follows: irregular thickening of the bowel wall with visible destruction of layer boundaries, infiltration into adjacent structures. The main criteria for enlarged regional lymph nodes were as follows: ≥ 5 mm round hypoechoic mass to be delineated definitive

tumor margin around primary lesion because there were no accurate sonographic parameters to distinguish benign lymph node hyperplasia from malignant infiltration^[9]. The first hyperechoic layer adjacent to the lumen corresponded to mucus, the second hypoechoic layer to the muscularis mucosa (MM), the third hyperechoic layer to the submucosa (SM), the fourth hypoechoic layer to the muscularis propria (PM), the fifth echogenic layer to serosa and the peri-colic fat tissues. The integration of mucus and MM layer was defined as mucosa layer (M)^[16]. Normal images of colorectal wall architecture at each site were demonstrated in Figures 1B-F. A tumor was classified as T1 when the mass was confined to mucosal and submucosal layer of colon, as T2 when confined to the muscularis propria, as T3 when the tumor penetrated through muscularis propria layer (subserosa) and extended to the serosal layer (including pericolic fat infiltration), and as T4 when the tumor extended to the adjacent organs^[24]. Additionally, we compared HUS with abdominal pelvic CT in accuracy. Statistical analysis was performed with nonparametric paired *t*-test, Mann-Whitney test. A two tailed *P* value less than 0.05 was considered statistically significant.

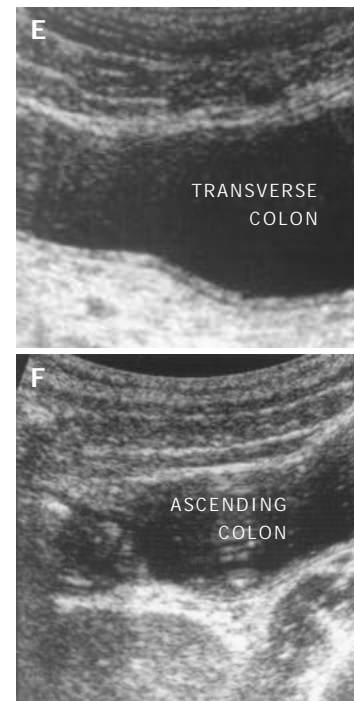
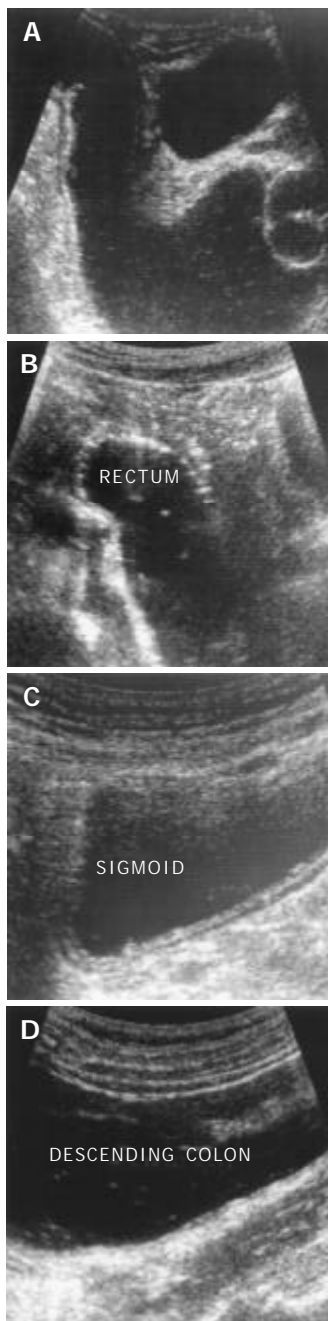


Figure 1 Normal images of five-layered colorectal wall architectures at each site. A: Distended rectum by instilling 1 000-2 000 mL warm saline inserted with a balloon catheter, B: rectum, C: sigmoid colon, D: descending colon, E: transverse colon, F: ascending colon. The first hyperechoic layer and the 2nd hypoechoic lesion were mucosa, the 3rd hyperechoic layer was submucosa, the 4th hypoechoic lesion was muscularis propria, and the 5th outer echogenic layer was serosa (from inner to outer of the lumen).

RESULTS

Patient characteristics

The clinicopathological characteristics of the thirty patients are demonstrated in Table 1. There were no significant differences between colon and rectal cancer ($P>0.05$).

Table 1 Characteristics of the patients ($n=30$)

	Colon cancer ($n=17$)	Rectal cancer ($n=13$)	<i>P</i> value
Sex			NS
Male	9	7	
Female	8	6	
Age			NS
Median (range)	52 (37-68)	56 (43-75)	
Size			NS
Mean (range)	5.76 (3-9)	5.8 (3-9)	
Time intervals to operation day			NS
Median (range)	4 (3-7)	5 (3-9)	
Failure to passage of colonoscopy	7	1	NS
Shape			NS
Polypoid	4	3	
Ulcerative	2	2	
Ulcerofungating	4	4	
Ulceroinfiltrative	7	4	
Site			
Rectum	-	13	
Sigmoid colon	4	-	
Descending colon	1	-	
Transverse colon	6	-	
Ascending colon	6	-	

($P=0.05$, Mann-Whitney test), NS: no significance.

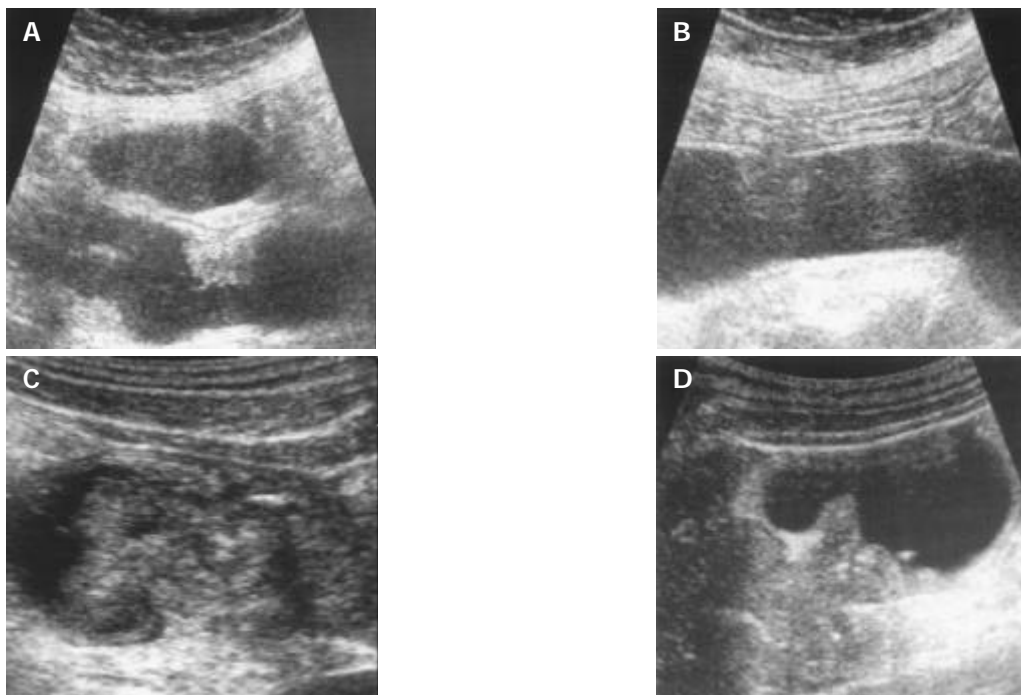


Figure 2 Images of HUS corresponding with their histological stage A: A round mass originated from submucosal (SM) layer in the descending colon, its histological stage was SM (T1). B: A round mass with deformed PM layer in transverse colon, its histological stage was PM (T2). C: A large endoluminal polypoid mass penetrating the wall and extending to pericolic fat layer. HUS judged stage was T3, its histological stage was T3. D: A carcinoma with serosal infiltration extending into pericolic adjacent tissue in descending colon. HUS judged stage was T4, its histological stage was T4.

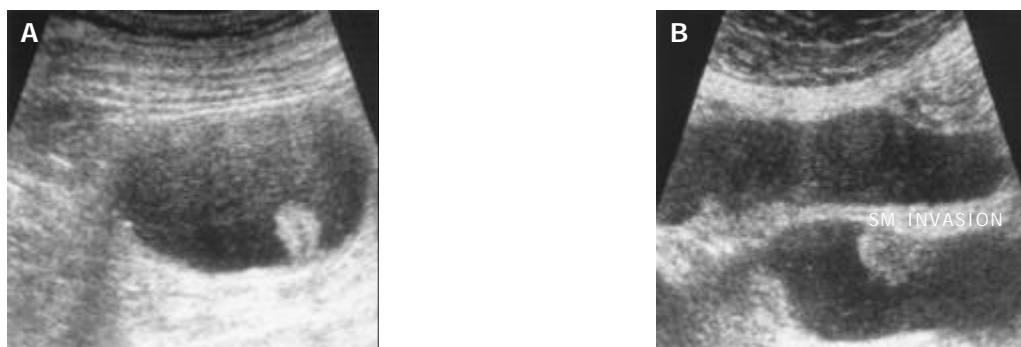


Figure 3 Images of HUS not corresponding with their histological stage. A: Sigmoid colon cancer; HUS judged as PM cancer (T2), but histology revealed pericolic fat infiltrated by tumor cells (T3). B: Transverse colon cancer; HUS judged as PM cancer (T2), but histology revealed intact PM layer and tumor cells infiltrated only SM layer (T1).

Detection for lesions

All the patients completed all the procedures successfully. Because we had acquired some information about the tumor location and shape before HUS by colonoscopy or barium enema, and the patients changed their position for optimal sonographic plane, no lesions were missed even though the tumor was located in the posterior wall opposite to the transducer, or a site adjacent to the loops of small bowel or flexure.

Depth of invasion and T stage

HUS made a correct staging in 21 of the 30 colorectal cancers. Figure 2 demonstrates the preoperative HUS imaging corresponding to the postoperative histological staging, and Figure 3 demonstrates the discordant staging. The overall accuracy of HUS was 70%.

The accuracy of staging by HUS was favorable in colon cancer (88%), especially when the lesions were located in the descending or ascending colon and their depth was confined to pericolic fat infiltration (93%) (Table 2). When the lesions were located in the sigmoid, transverse colon, and its flexure

and confined to the mucosal layer, the accuracy was relatively lower. Underestimated cases were relatively smaller than 2 cm and ulceroinfiltrating shaped masses, and overestimated cases were larger than 3 cm and fungating mass. But the differences were not statistically significant. In rectal cancer, however, the accuracy was unfavorable (46.1%) compared with colon cancer, at any site or of any shape (Table 2, $P = 0.038$). Table 3 demonstrates the accuracy of CT in staging of depth of invasion in colon and rectal cancers.

Nodal stage and N stage

The overall accuracy of HUS for N staging in colorectal cancer was 60%. The sensitivity and specificity were 55% and 67%, respectively. It showed 71% accuracy in colon cancer and 46% accuracy in rectal cancer, respectively. The accuracy of N staging by HUS was relatively lower than that by conventional CT or MRI in both colon and rectal cancers. In addition, the accuracy of N staging was affected by the size of the node. There was no statistically significant difference in the accuracy of N staging by HUS between colon and rectal cancers although

it was higher in colon cancer than in rectal cancer (Table 4). Table 5 demonstrates the accuracy of CT in staging of lymph node metastasis in colon and rectal cancers.

Table 2 Comparison of hydrocolonic sonography accuracy in depth of invasion between colon and rectal cancers ($P=0.038$)

Pathologic Diagnosis	Colon cancer				Accuracy (%)	Rectal cancer				Accuracy (%)
	T1	T2	T3	T4		T1	T2	T3	T4	
T1	1				1/1 (100)	1				0/1 (0.0)
T2	1				0/1 (0.0)	2	1			2/3 (66.7)
T3		1	14		14/15 (93)	3	4	1		4/8 (50.0)
T4					0/0			1		1/1 (100)
Total	2	1	14		15/17 (88)	5	6	2		6/13 (46.2)

Table 3 Comparison of the accuracy of CT in depth of invasion ($P=0.048$)

Pathologic Diagnosis	Colon cancer				Accuracy (%)	Rectal cancer				Accuracy (%)
	T1	T2	T3	T4		T1	T2	T3	T4	
T1		1			0/1 (0.0)	1				0/1 (0.0)
T2		1			1/1 (100)	1	2			1/3 (33.3)
T3		4	10	1	10/15 (66.7)	1	5	2		5/8 (62.5)
T4			0	0	0/0 (0.0)			1		0/1 (0.0)
Total	0	6	10	1	11/17 (64.7)	2	9	2		6/13 (46.2)

($P=0.05$, Mann-Whitney test).

Table 4 Comparison of the accuracy of hydrocolonic sonography in lymph node metastasis between colon and rectal cancers ($P=0.183$)

Pathologic Diagnosis	Colon cancer		Rectal cancer	
	n (-)	n (+)	n (-)	n (+)
N (-)	8	1	4	5
N (+)	4	4	2	2
Total	12	5	6	7
Accuracy (%)	12/17 (70.6)		6/13 (46.2)	

Table 5 Comparison of the accuracy of CT in lymph node metastasis ($P=0.275$)

Pathologic Diagnosis	Colon cancer		Rectal cancer	
	n (-)	n (+)	n (-)	n (+)
N (-)	8	1	5	4
N (+)	3	5	2	2
Total	12	5	7	6
Accuracy (%)	13/17 (76.5)		7/13 (53.8)	

($P=0.05$, Mann-Whitney test), N (-): lymph node negative, N (+): lymph node positive.

DISCUSSION

Over the last years, sonographic evaluation of gastrointestinal (GI) tract has been improved by the instillation of water into the endoluminal area, named as HUS^[13-24]. Allowing the sonographic differentiation of five layers of the colon wall, theoretically HUS was able to predict stage of colorectal cancer with a high sensitivity, specificity, and predictive value^[16,18,22,23]. HUS also could diagnose a variety of colonic endoluminal lesions including polyp, inflammatory bowel disease, etc. with a high accuracy^[14,15]. According to some reports, the accuracy of HUS was close to that of EUS in depth of invasion in colon cancer

(79-92%)^[22]. However, the accuracy of HUS in rectal cancer was poor^[22]. In the present study, we compared the accuracy of HUS in local staging between colon and rectal cancers, and observed under what condition the accuracy of HUS was relatively higher.

The accuracy of T staging by HUS was favorable in colon cancer (88%), especially when the lesions were located in the descending and ascending colon and their depth was confined to pericolic fat infiltration (93%). The result was similar to previous studies by Dux *et al.*^[22]. The lower accuracy of HUS in T staging of rectal cancer was assumed to be caused by anatomical obstacle, that is, pubic symphysis, and incomplete removal of bowel gas^[22]. Although the patient's position was changed to head-up or down position to avoid these obstacles, the limitation still occurred. In N staging, the accuracy of HUS was unfavorable in both colon and rectal cancers. The reasons might be that there were no accurate sonographic parameters to distinguish benign hyperplastic lymph node from malignant infiltration, and the nodes far away from the probe (N3) could not be traced sufficiently, and lymph node metastasis could occur without size enlargement^[9,10]. However, in our study, the accuracy of N staging was affected by the size of the node.

Sigmoidoscopy has been widely accepted as an outpatient diagnostic procedure for colorectal cancer. But, in reality, 40% of colonic tumors occurred outside the sigmoid^[25]. So, colonoscopy is required in order to detect the right side lesion. But incomplete studies were infrequent due to various reasons, such as lumen obstruction, poor preparation of the bowel, and anatomical problems, etc.^[26]. Under such circumstances, a barium enema may be performed for detection of the right side or upper side lesion except for obstructive diseases. But it can not evaluate the depth of invasion. Besides, EUS cannot be always performed because it requires endoluminal access. Thus, HUS may be preferred.

Although we detected all lesions, some were difficult to detect and evaluate, such as the lesions in patients with obesity, located in the flexure and adjacent to the small bowel, with their size less than 2 cm.

In conclusion, HUS is valuable in evaluating the depth of invasion (T) of colon cancer at any site and of any shape. However it has limitations in rectal cancer. Because HUS is low-cost, noninvasive, and readily available at any place, this technique seems to be useful in local staging of colon cancer especially in cases where colonoscopy and EUS can not be performed.

REFERENCES

- Rao AR, Kagan AR, Chan DM, Gilbert HA, Nussbaum H, Hintz BL. Patterns of recurrence following curative resection alone for adenocarcinoma of rectum and retrosigmoid colon. *Cancer* 1981; **48**: 1492-1495
- Sobin LH, Fleming ID. TNM Classification of Malignant Tumors, fifth edition (1997). Union Internationale Contre le Cancer and the American Joint Committee on Cancer. *Cancer* 1997; **80**: 1803-1804
- Gofieri R, Giampalma E, Leo P, Colecchia A, Selli S, Poggidi G, Gandolfi L, Gozzetti G, Trebbi F, Russo A. Comparison of magnetic resonance (0, 5 T), computed tomography, and endorectal ultrasonography in the preoperative staging of neoplasms of the rectum-sigma. Correlation with surgical and anatomopathologic findings. *Radiologia Medica* 1993; **85**: 773-783
- Thoeni RF. Colorectal cancer. Radiologic staging. *Radiol Clin North Am* 1997; **35**: 457-485
- Elmas N, Killi RM, Sever A. Colorectal carcinoma: radiological diagnosis and staging. *Eur J Radiol* 2002; **42**: 206-223
- Tio TL, Cohen P, Coene PP, udding J, den Hartog Jager FC, Tytgat GN. Endosonography and computed tomography of esophageal carcinoma: preoperative classification compared to the new (1987) TNM system. *Gastroenterology* 1989; **96**: 1478-1486

- 7 **Bhutani MS**, Nadella P. Utility of an upper echoendoscope for endoscopic ultrasonography of malignant and benign conditions of the sigmoid/left colon and the rectum. *Am J Gastroenterol* 2001; **96**: 3318-3322
- 8 **Hunerbein M**, Totkas S, Ghadimi BM, Schlag PM. Preoperative evaluation of colorectal neoplasms by colonoscopic miniprobe ultrasonography. *Ann Surg* 2000; **232**: 46-50
- 9 **Tio TL**, Coene PP, van Delden OM, Tytgat GN. Colorectal carcinoma: preoperative TNM classification with endosonography. *Radiology* 1991; **179**: 165-170
- 10 **Snady H**, Merrick MA. Improving the treatment of colorectal cancer: the role of EUS. *Cancer Invest* 1998; **16**: 572-581
- 11 **Schwerk W**, Braun B, Dombrowski H. Real-time ultrasound examination in the diagnosis of gastrointestinal tumors. *J Clin Ultrasound* 1979; **7**: 425-431
- 12 **Sianesi M**, Rossi A, Miselli A, Farinon AM. Ultrasonic detection of colonic carcinoma in emergency. *Dis Colon Rectum* 1984; **27**: 168-171
- 13 **Segura JM**, Olveira A, Conde P, Erdozain JC, Suarez J. Hydrogastric sonography in the preoperative staging of gastric cancer. *J Clin Ultrasound* 1999; **27**: 499-504
- 14 **Kan JH**, Fines BP, Funaki B. Conventional and hydrocolonic US of the appendix with CT correlation performed by on-call radiology residents. *Acad Radiol* 2001; **8**: 1208-1214
- 15 **Elewaut AE**, Afschrift M. Hydrocolonic sonography: a novel screening method for the detection of colon disease? *Bildgebung* 1995; **62**: 230-234
- 16 **Limberg B**. Diagnosis and Staging of colonic tumors by conventional abdominal sonography as compared with hydrocolonic sonography. *N Engl J Med* 1992; **327**: 65-69
- 17 **Archer BD**. Diagnosis of colonic tumors by hydrocolonic sonography. *N Engl J Med* 1992; **327**: 1459
- 18 **Hernandez-Socorro CR**, Guerra C, Hernandez-Romero J, Rey A, Lopez-Facal P, Alvares-Santullano V. Colorectal carcinomas: diagnosis and preoperative staging by hydrocolonic sonography. *Surgery* 1995; **117**: 609-615
- 19 **Pochaczewsky R**. Diagnosis of colonic tumors by hydrocolonic sonography. *N Engl J Med* 1992; **327**: 1459-1460
- 20 **Chui DW**, Gooding GA, McQuaid KR, Griswold V, Grendell JH. Hydrocolonic ultrasonography in the detection of colonic polyps and tumors. *N Engl J Med* 1994; **331**: 1685-1688
- 21 **Limberg B**. Hydrocolonic ultrasonography. *N Engl J Med* 1995; **332**: 1581-1582
- 22 **Dux M**, Roeren T, Kuntz C, Richter GM, Kauffmann GW. TNM staging of gastrointestinal tumors by hydrosonography: results of a histopathologically controlled study in 60 patients. *Abdom Imaging* 1997; **22**: 24-34
- 23 **Dixit R**, Chowdhury V, Kumar N. Hydrocolonic sonography in the evaluation of colonic lesions. *Abdom Imaging* 1999; **24**: 497-505
- 24 **Hermanek P**, Sobin LH, eds. TNM classification of malignant tumours, 4th ed, 2nd rev. Berlin: Springer, 1992: 45-55
- 25 **Rosato FE**, Marks G. Changing site distribution patterns of colorectal cancer at Thomas Jefferson University Hospital. *Dis Colon Rectum* 1981; **24**: 93-95
- 26 **Limberg B**. Hydrocolonic sonography - potentials and limitations of ultrasonographic diagnosis of colon diseases. *Z Gastroenterol* 2001; **39**: 1007-1015

Edited by Zhu LH and Wang XL Proofread by Xu FM

In vitro antitumor immune response induced by fusion of dendritic cells and colon cancer cells

Feng Xu, Ying-Jiang Ye, Shan Wang

Feng Xu, Ying-Jiang Ye, Shan Wang, Division of Surgical Oncology and Division of Gastrointestinal Surgery, People's Hospital, Peking University, 100044 Beijing, China

Supported by Technology Foundation of Ministry of Education, China

Correspondence to: Professor Shan Wang, Tutor of Doctoral Students, Division of Surgical Oncology and Division of Gastrointestinal Surgery, People's Hospital, Peking University, Beijing 100044, China. bronson_xu@yahoo.com.cn

Telephone: +86-10-68792772 **Fax:** +86-10-68792779

Received: 2003-10-08 **Accepted:** 2003-12-06

Abstract

AIM: The prevention of recurrence of colon cancer (CC) after operation is very important for improvement of the prognosis of CC patients, especially those with micro-metastasis. The generation of fused cells between dendritic cells (DCs) and tumor cells maybe an effective approach for tumor antigen presentation in immunotherapy. In this study, we fused human colon cancer SW480 cells and human peripheral blood - derived DCs to induce an antitumor activity against human CC.

METHODS: CC SW480 cells and human peripheral blood - derived DCs were fused with 500 mL/L polyethylene glycol (PEG).

RESULTS: The specific T cell responses activated by fusion cells (FCs), were observed. About 100 mL/L to 160 mL/L of the PEG-treated non-adherent cells with fluorescences were considered to be dendritomas that highly expressed the key molecules for antigen presentation in our five cases. *In vitro* studies showed that fusions effectively activated CD8⁺ T lymphocytes to secrete interferon- γ . The early apoptotic ratio of the colon cancer SW480 cells was higher than that of controls, which was affected by cytotoxic T lymphocytes (CTLs) stimulated by dendritomas.

CONCLUSION: The data indicate that fusion of tumor cells with DCs is an attractive strategy to induce tumor rejection.

Xu F, Ye YJ, Wang S. *In vitro* antitumor immune response induced by fusion of dendritic cells and colon cancer cells. *World J Gastroenterol* 2004; 10(8): 1162-1166

<http://www.wjgnet.com/1007-9327/10/1162.asp>

INTRODUCTION

Colon cancer (CC) is one of the most common malignancies in the Western world. As diet custom has changed these years, the number of cases is increasing in the Eastern world. Although surgical resection is the first choice worldwide, an effective approach for the treatment of CC patients with metastasis and cancer recurrence postoperation has not yet been found.

Dendritic cells (DCs) are potent antigen-presenting cells (APCs) which are the prime naive T cells and initiate a prime

immune response^[1,2]. Various DC-based strategies, such as DCs pulsed with tumor-associated peptides or proteins, viral transduction of DCs with tumor-specific genes or transfection with liposomal DNA or RNA, have been developed to introduce tumor specific antigens into DCs and thereby to generate cytotoxic T lymphocyte (CTL) responses against malignant cells^[3-9]. However, few tumor-specific antigens have been identified, and their immunogenicity is uncertain in most malignant tumors.

An attractive approach to the enhancement of antitumor activity is to generate the fusions between tumor cells and DCs^[10]. Multiple tumor antigens, including those unidentified yet, are processed endogenously and presented to T lymphocytes by the MHC class I and II pathways in the context of costimulatory signals^[11]. Some inspiring results have been reported *in vitro* and *in vivo* except that of human colon cancer due to the difficulty in isolating the tumor antigens from tumor tissues and the facility contaminated for primary culture^[12-16].

In this study, we fused human colon cancer SW480 cells and human peripheral blood - derived DCs to induce an antitumor activity against human CC, because they shared some common antigens between cells from tissue and cell line SW480.

MATERIALS AND METHODS

Colon cancer cell culture

Human SW480 colon cancer cells (ATCC#CCL-228) were grown in RPMI medium 1640 supplemented with 100 mL/L heat-inactivated FCS.

Preparation of DCs and CD8⁺ T cells

Peripheral blood mononuclear cells (PBMC) were isolated from patients with CC by Ficoll-Hypaque density-gradient centrifugation. The pure CD14⁺ PBMC and CD8⁺ T lymphocytes were isolated by MACS magnetic microbeads (Miltenyi, Germany) respectively according to the manufacturer's directions. CD14 PBMC were cultured for 1 wk in RPMI medium 1640/10% human serum containing 1 000 U/mL granulocyte-macrophage colony-stimulating factor (GM-CSF) and 1 000 U/mL IL-4. CD8⁺ T lymphocytes were cultured in RPMI medium 1640/10% human serum containing 20 u/mL IL-2.

Fluorescent staining and fusion

Tumor cells and DCs were stained red and green, respectively, using PKH26-GL and PKH67-GL kits (Sigma) according to the manufacture's directions. The tumor cells were irradiated at a dose of 30Gy before staining. Human DCs and tumor cells were fused together by mixing the two types at a ratio of 3:1 in a 15-mL conical centrifuge tube. One milliliter of 500 mL/L polyethylene glycol (PEG) (Sigma) was added to the cells by drops for 1 min. Nine milliliters of serum-free RPMI medium 1640 was added to the mixture for 10 min. The cells were pelleted by centrifugation at 500 g for 5 min. The supernatant was removed and the cells were resuspended in 5 mL complete DC medium and plated in a T25 flask that was incubated at 37 °C in 50 mL/L carbon dioxide.

DCs and fusions assays

Fusion efficacy was evaluated by fluorescence microscopic analysis and flow cytometry analysis using Facsort (Becton Dickinson). DCs were washed with PBS and incubated with murine antibodies HLA-DR-APC, CD80-PE, CD86-FITC (PharMingen) for 15 min at 4 °C. Fusions were washed with PBS and incubated with murine antibody HLA-DR-APC for 15 min at 4 °C. Samples were then washed, fixed with 10 g/L paraformaldehyde, and subjected to flow cytometry analysis.

Scanning electron microscopy observation

Cells were fixed with 12 g/L glutaraldehyde in 0.1 mol/L PBS (pH7.4). Fixed cells were coated with 1 g/L poly-L-lysine, dehydrated in ascending concentrations of ethanol, treated with isoamyl acetate, and critical-point dried with liquid CO₂. Specimens were coated with vacuum-evaporated, iron-spattered gold and observed with a S-2250N scanning electron microscope (HITACHI).

Cytotoxic T lymphocyte generation

Dendritomas obtained by using 500 mL/L PEG were mixed with CD8⁺ T lymphocytes at a ratio of 1:10. CD8⁺ cells to be used were pelleted by centrifugation at 500 g for 5 min and resuspended in 1 mL medium containing RPMI-1640, 10% human serum, 5 ng/mL IL-12, and 20 U/mL IL-2. The mixture was incubated at 37 °C in 50 mL/L carbon dioxide for 8 d. As controls, homologous DCs were mixed with CD8⁺ T cells at the same ratio.

Interferon- γ assay

Each day CTL-generating cultures were refed. The supernatants of cultures were harvested and frozen at -20 °C. Interferon- γ (IFN- γ) assay was performed on the supernatants by a commercially available ELISA kit (R&D). Each assay was

performed according to the manufacturer's instructions. The lower detection limit was 4 pg/mL. All samples and standards were run in triplicate.

Cytotoxic T lymphocyte assay

To determine whether dendritomas stimulated a tumor cell-specific CTL response, cytotoxicity assay was performed using the cultured tumor cells as target cells. CTL effector cells and tumor cells were mixed in a 24-well tissue culture plate with a round-bottom at the concentration of 100:1 effectors-to-target cells. The mixtures were incubated at 37 °C in 50 mL carbon dioxide for 2 d. Tumor apoptosis was measured using an Annexin V-FITC/PI kit (Clontech) by FACS analysis after the mixtures were cultured for 24 h and 48 h respectively. The tumor cells were detached and incubated with Annexin V-FITC for 30 min at 4 °C after the unattached CTLs were removed by magnetic microbeads. The samples were washed 3 times with PBS and measured by FACS analysis. To determine whether the lysis was tumor cell-specific, mammary cancer cells SK-BR-3 (ATCC#HTB-30) and ovarian cancer cells SK-OV-3 (ATCC#HTB-77) were used as target cells in similar cytotoxicity assay.

RESULTS

Fusion identification and fusion efficacy assay

On scanning electron microscopy, SW480 cells had short processes on a plain cell surface and DCs had long dendritic processes. Dendritomas were formed by fusions of the dendritic cells with CC cells (Figure 1). Fusion efficacy was about 16%. It was assessed by the analysis of fusions of SW480 cells stained with red fluorescent dye and DCs stained with green fluorescent dye using a fluorescent microscope (Figure 2) and flow cytometry respectively (Figure 3C).

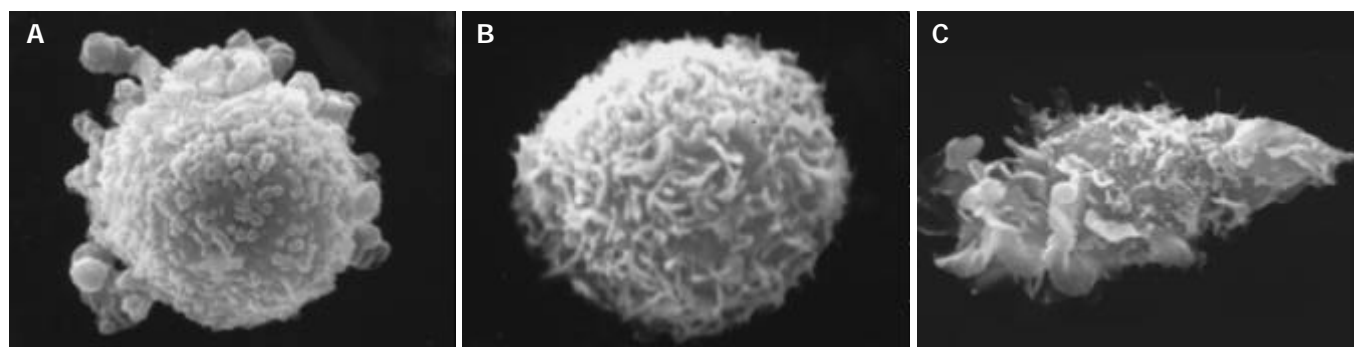


Figure 1 A: Scanning electron micrographs of DC. B: Scanning electron micrographs of SW480 cell. C: Scanning electron micrographs of larg nonadherent cell, possibly a DC/SW480 fusion cell after treatment with 50%PEG.

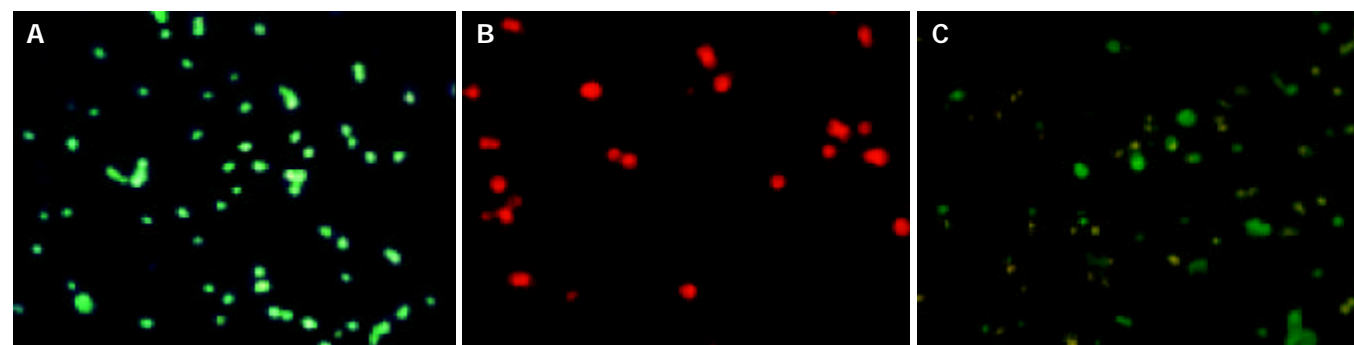


Figure 2 A: Fluorescent green staining of dendritic cells from peripheral blood mononuclear cells of patients using PKH67-GL. B: Fluorescent red staining of colon cancer cells SW480 using PKH26-GL. C: Fusion between PKH stained dendritic cells and tumor cells treated with PEG.

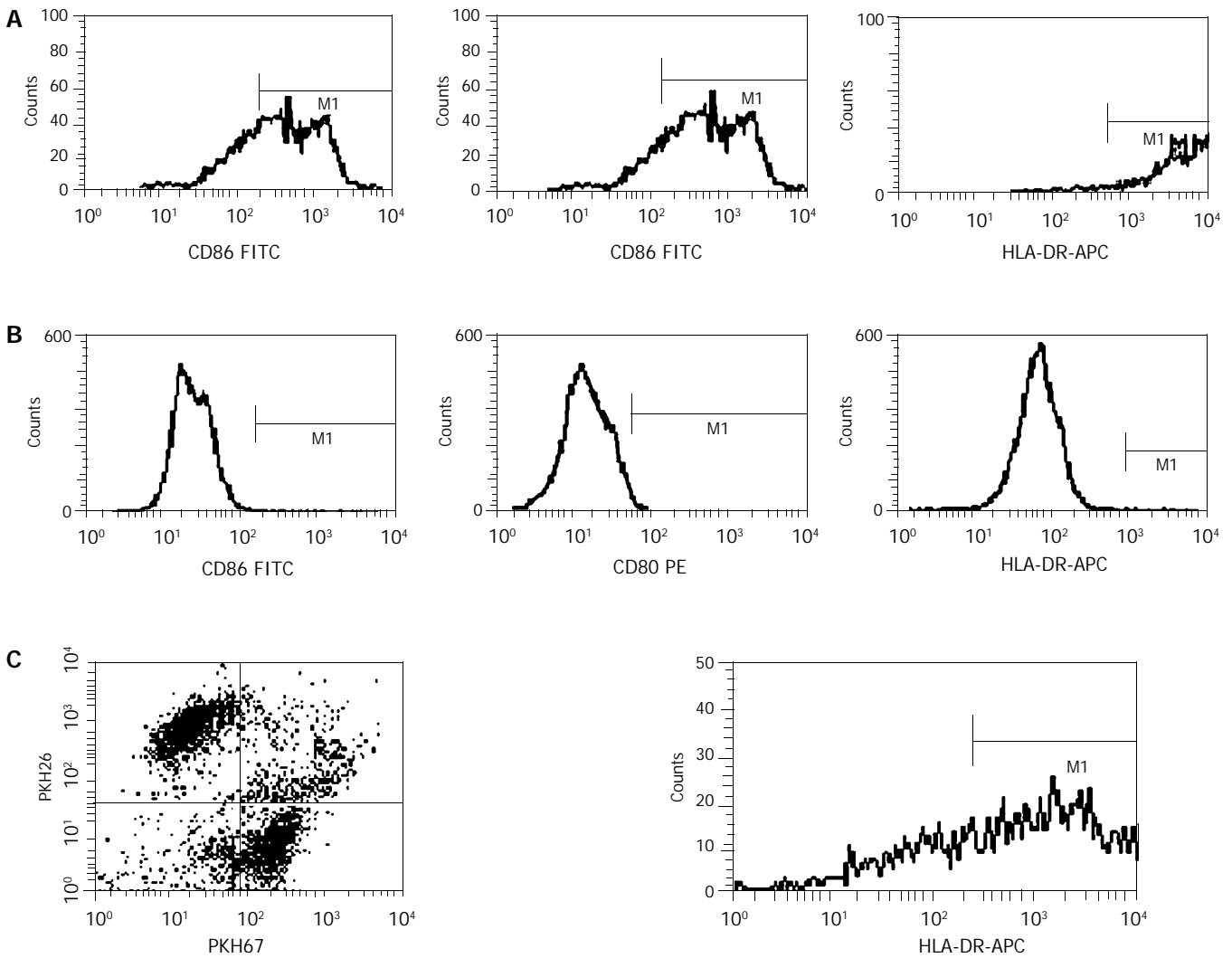


Figure 3 A: High expression of CD86, CD80 and HLA-DR by Dendritic cells, B: No expression of CD 86, CD80 and HLA-DR by SW480 cells, C: High expression of major molecule HLA-DR of DCs by dendritomas gated by dual red and fluorescent cells.

Characteristics of fusions of DCs and CC cells

To determine whether human DCs could be used in the generation of heterokaryons with tumor cells, DCs from PBMC of CC patients were prepared. Flow cytometry demonstrated that DCs highly expressed CD80, CD86 and HLA-DR, but SW480 cells did not. Dendritomas, which showed dual red and green fluorescence, highly expressed the major molecules HLA-DR of DCs (Figure 3).

Tumor cell-specific cytotoxic T lymphocytes stimulated by dendritomas

To determine whether dendritomas effectively presented tumor antigens to effective cells, CD8⁺ T lymphocytes were purified from autologous peripheral blood and cocultured with dendritomas at a ratio of 10:1. Trypan blue exclusion test showed that, 6 d after the stimulation, CTLs were activated to proliferate and the number of T cells increased (from 1.2×10⁷ to 1.8×10⁷). After activation, CTLs secreted high levels of IFN-γ, and the secretion of this cytokine induced by dendritomas was higher than that of controls (Figure 4).

Tumor cell apoptosis

To investigate whether the CTLs induced by dendritomas, had a tumor-specific response, CTLs and tumor cells were mixed in a 24-well tissue culture plate with a round-bottom at the concentration of 100:1 effectors-to-target cells. Tumor apoptosis was measured using an AnnexinV-FITC/PI kit by

FACS analysis after the mixtures were cultured for 24 h and 48 h respectively. The result indicated that the lysis was autologous tumor specific (Figure 5). The early apoptotic ratio of colon cancer SW480 cells was higher than that of controls, which was affected by cytotoxic T lymphocytes (CTL) that activated by dendritomas after co-cultured for 24 h. Although there were no differences in the apoptotic ratios of tumor cells after co-cultured for 48 h, the necrotic fragments of colon cancer were higher than those of controls.

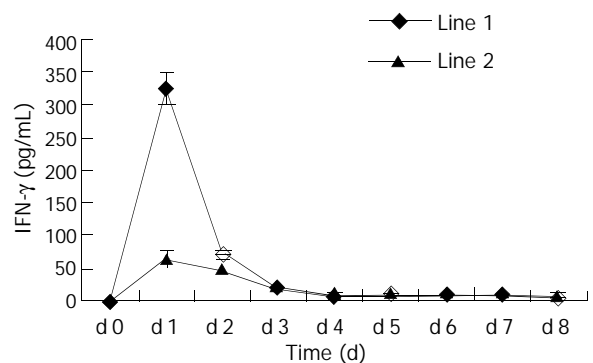


Figure 4 Interferon-γ expression by CTLs. Lane 1 represents IFN-γ expression by CD8⁺ T cells primed with dendritomas. Lane 2 represents IFN-γ expression by CD8⁺ T cells primed with DCs.

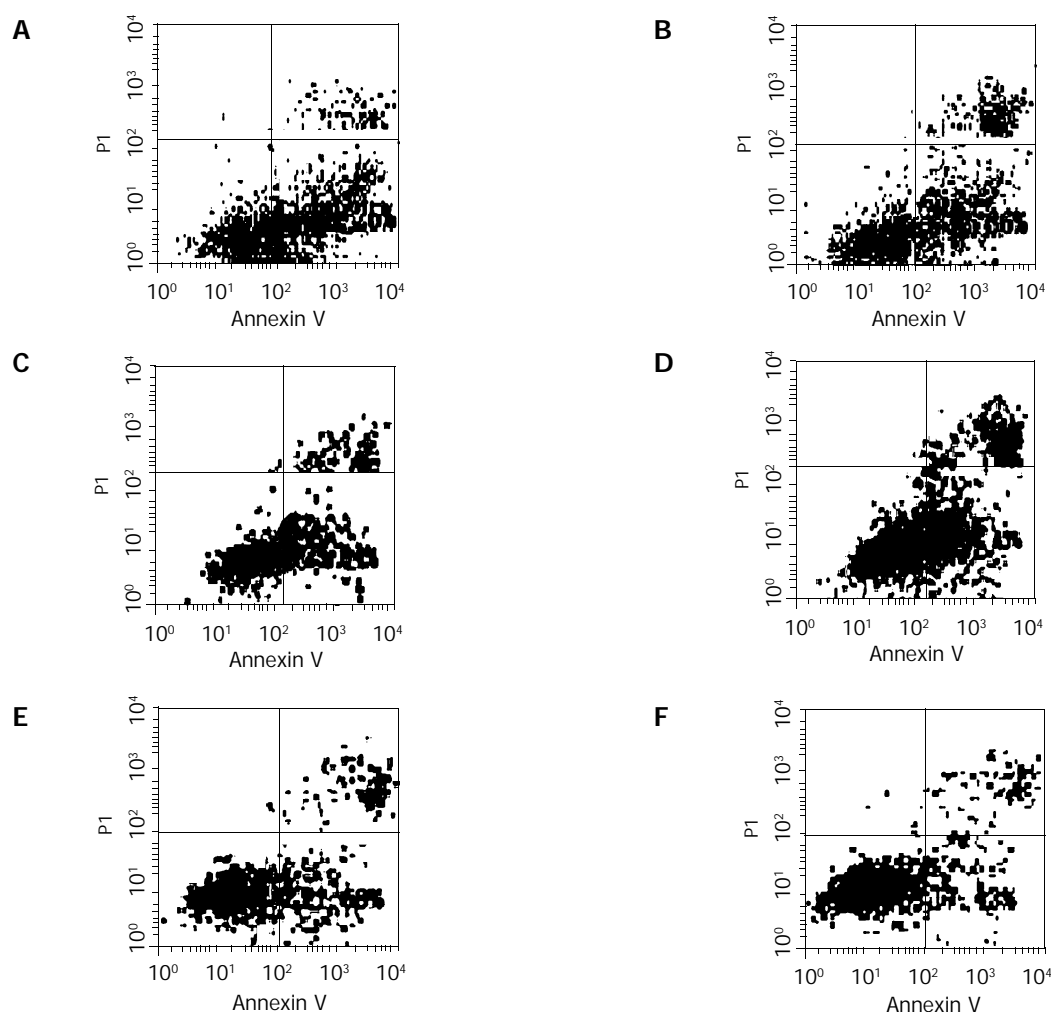


Figure 5 Early apoptosis (single Annexin V positive) of tumor cells measured by flow cytometry. The apoptotic ratios of SW480 cells affected by CTL induced dendritomas or physical mixture of SW480 cells and DCs without PEG, were about 38.25%(A) and 32.36% respectively (B). The apoptotic ratios of SK-BR-3 cells affected by CTL same as that in SW480, were about 25.64% (C) and 17.43%(D) respectively. The apoptotic ratios in SK-OV-3 were about 21.68% (E) and 17.43%(F).

DISCUSSION

Dendritic cells are professional antigen-presenting cells that play a vital role in stimulating immune responses. Not only can they activate naïve CD4⁺ T helper cells, but they also stimulate unprimed CD8⁺ cytotoxic T lymphocytes^[11,17,18]. Many studies have shown that DCs, when effectively loaded with or expressing tumor antigens, can activate antitumor immune responses through cellular and humoral actions^[19]. However, for those tumors whose tumor antigens have not been identified, especially for primary tumors from patients, fusion between DCs and tumor cells presented a promising alternative strategy. Because the process of isolating cells from primary tissues in gastrointestinal tumor was time-consuming and prone to contamination, these considerations have limited the clinical application of this approach. In this study, an attempt was made to fuse DCs with human colon cancer SW480 cells to induce a colon cancer-specific antitumor immune response, because there were some common antigens between primary tumor cells and homogenous cell line.

It is important to determine the fusion efficacy of DCs and tumor cells by treatment with PEG. Two-color FACS analysis showed that approximately 100 mL/L to 160 mL of PEG-treated non-adherent cells were positive for both PKH67-GL (DCs were fluorescently stained) and PKH26-GL (SW480 cells were fluorescently stained) in our 5 separate CC patients, which highly expressed the MHC of DCs for antigen presentation (Figure 3C). These results were consistent with those of the

landmark kidney cancer trial^[20]. It is conceivable, therefore, that the fusions are able to present tumor antigen (s) to naïve T cells by means of DC capability. Although exceptionally high fusion efficiencies sometimes have been reported using PEG, such reports might reflect an overlying optimistic interpretation of fluorescence-activated cell sorting data or nonrepresentative experiments^[21]. Because fusions could generate not only tumor-DC hybrids but also tumor-tumor hybrids, DCs and tumor cells were fused at a ratio of 3:1 to decrease the tumor-tumor hybrids. Two types of aliphatic fluorescent dyes, PKH-67GL and PKH-26GL, have been widely used to label viable cells for *in vitro* and *in vivo* cell tracking^[22,23]. In addition, researches have shown that there were no significant effects of the two dyes on cell viability, growth, or function^[24,25].

To determine whether dendritomas effectively presented tumor antigens to immune cells and activated T lymphocytes, CD8⁺ T cells were isolated, and *in vitro* stimulation was performed. Then IFN- γ , a well-known marker of T-cell activation, was measured. Results showed that the secretion of CTLs activated by dendritomas was higher than that of controls after stimulation. Fusion hybrid vaccines might be more effective than other DC-based strategies because of superior antigen presentation^[26]. Although DCs have a constant capacity of processing exogenous antigens to achieve a major histocompatibility complex class II-restricted antigen presentation, the major histocompatibility complex I-restricted antigen presentation is often difficult to demonstrate

when DCs are pulsed with complex protein antigens rather than with synthetic 8- or 9-mer peptides. Tumor-DC fusion potentially confers not only DC functionality but also a continuing source of endogenous tumor antigens for major histocompatibility complex class I presentation^[21].

In the early stages of apoptosis, which occurs at the cell surface, one of these plasma membrane alterations is the translocation of phosphatidylserine (PS) from the inner side of the plasma membrane to the outer layer, by which PS becomes exposed at the external surface of the cell. Annexin V is a Ca²⁺ dependent phospholipid-binding protein with high affinity for PS. Hence this protein can be used as a sensitive probe for PS exposure upon the cell membrane. So Annexin V assay offers the possibility of detecting early phases of apoptosis before the loss of cell membrane integrity and permits measurements of the kinetic of apoptotic death in relation to the cell cycle. More extensive FCM allows discrimination between different cell subpopulations that may or may not be involved in the apoptotic process. In comparison with the traditional tests, Annexin V assay was sensitive and easy to perform^[27]. To determine whether CTLs could lyse tumor cells, CTLs were harvested and apoptosis assay was performed using tumor cells as target cells. To confirm that the CTL activity was tumor cells specific, mammary cancer cells SK-BR-3 and ovarian cancer cells SK-OV-3 were used as target controls, in addition to colon cancer cells. The results indicated that the lysis was tumor cell specific (Figure 5). Similar results were obtained in the 5 cases.

Several preclinical studies have shown that vaccines consisting of such hybrids can provide effective active immunization against animal tumors and specific *in vitro* sensitization of human T cells to relevant tumor antigens^[10,11]. Furthermore, in contrast to other vaccine strategies, the tumor-DC fusion strategy has already been met with resounding clinical success when applied to the treatment of patients with advanced renal cancer^[20]. Immunization with fusions of DCs and human colon cancer cells may be a promising method for the prevention and treatment of micrometastasis and recurrence after operation of CC.

ACKNOWLEDGEMENTS

We thank Dr. Xiang-Bai Chen (Univ. Pittsburgh, USA) for critically reading the manuscript. This work was supported by Technology Foundation of the Ministry of Education (China).

REFERENCES

- 1 **Steinman RM.** The dendritic cells system and its role in immunogenicity. *Annu Rev Immunol* 1991; **9**: 271-296
- 2 **Banchereau J, Steinman RM.** Dendritic cells and the control of immunity. *Nature* 1998; **392**: 245-252
- 3 **Gong J, Chen L, Chen D, Kashiwaba M, Manome Y, Tanaka T, Kufe D.** Induction of antigen-specific antitumor immunity with adenovirus-transduced dendritic cells. *Gene Ther* 1997; **4**: 1023-1028
- 4 **Specht JM, Wang G, Do MT, Lam JS, Royal RE, Reeves ME, Rosenberg SA, Hwu P.** Dendritic cells retrovirally transduced with a model antigen gene are therapeutically effective against established pulmonary metastases. *J Exp Med* 1997; **186**: 1213-1221
- 5 **Boczkowski D, Nair SK, Snyder D, Gilboa E.** Dendritic cells pulsed with RNA are potent antigen-presenting cells *in vitro* and *in vivo*. *J Exp Med* 1996; **184**: 465-472
- 6 **Condon C, Watkins SC, Celluzzi CM, Thompson K, Falo LD Jr.** DNA-based immunization by *in vivo* transfection of dendritic cells. *Nat Med* 1996; **2**: 1122-1128
- 7 **Song W, Kong HL, Carpenter H, Torii H, Granstein R, Rafii S, Moore MA, Crystal RG.** Dendritic cells genetically modified with an adenovirus vector encoding the cDNA for a model antigen induce protective and therapeutic antitumor immunity. *J Exp Med* 1997; **186**: 1247-1256
- 8 **Ribas A, Butterfield LH, McBride WH, Jilani SM, Bui LA, Vollmer CM, Lau R, Dissette VB, Hu B, Chen AY, Glaspy JA, Economou JS.** Genetic immunization for the melanoma antigen MART-1/Melan-A using recombinant adenovirus-transduced murine dendritic cells. *Cancer Res* 1997; **57**: 2865-2869
- 9 **Song ES, Lee V, Surh CD, Lynn A, Brumm D, Jolly DJ, Warner JF, Chada S.** Antigen presentation in retroviral vector-mediated gene transfer *in vivo*. *Proc Natl Acad Sci U S A* 1997; **94**: 1943-1948
- 10 **Gong J, Chen D, Kashiwaba M, Kufe D.** Induction of antitumor activity by immunization with fusions of dendritic and carcinoma cells. *Nat Med* 1997; **3**: 558-561
- 11 **Gong J, Avigan D, Chen D, Wu Z, Koido S, Kashiwaba M, Kufe D.** Activation of antitumor cytotoxic T lymphocytes by fusions of human dendritic cells and breast carcinoma cells. *Proc Natl Acad Sci U S A* 2000; **97**: 2715-2718
- 12 **Wang J, Saffold S, Cao X, Krauss J, Chen W.** Eliciting T cell immunity against poorly immunogenic tumors by immunization with dendritic cell-tumor fusion vaccines. *J Immunol* 1998; **161**: 5516-5524
- 13 **Zhang J, Zhang JK, Zhuo SH, Chen HB.** Effect of a cancer vaccine prepared by fusions of hepatocarcinoma cells with dendritic cells. *World J Gastroenterol* 2001; **7**: 690-694
- 14 **Homma S, Toda G, Gong J, Kufe D, Ohno T.** Preventive antitumor activity against hepatocellular carcinoma (HCC) induced by immunization with fusions of dendritic cells and HCC cells in mice. *J Gastroenterol* 2001; **36**: 764-771
- 15 **Zhang JK, Li J, Zhang J, Chen HB, Chen SB.** Antitumor immunopreventive and immunotherapeutic effect in mice induced by hybrid vaccine of dendritic cells and hepatocarcinoma *in vivo*. *World J Gastroenterol* 2003; **9**: 479-484
- 16 **Kikuchi T, Akasaki Y, Irie M, Homma S, Abe T, Ohno T.** Results of a phase I clinical trial of vaccination of glioma patients with fusions of dendritic and glioma cells. *Cancer Immunol Immunother* 2001; **50**: 337-344
- 17 **Mehta-Damani A, Markowicz S, Engleman E.** Generation of antigen-specific CD8+ CTLs from naive precursors. *J Immunol* 1994; **153**: 996-1003
- 18 **Porgador A, Gilboa E.** Bone marrow-generated dendritic cells pulsed with a class I-restricted peptide are potent inducers of cytotoxic T lymphocytes. *J Exp Med* 1995; **182**: 255-260
- 19 **Shurin M.** Dendritic cells presenting tumor antigen. *Cancer Immunol Immunother* 1996; **43**: 158-164
- 20 **Kugler A, Stuhler G, Walden P, Zoller G, Zobywalski A, Brossart P, Trefzer U, Ullrich S, Muller CA, Becker V, Gross AJ, Hemmerlein B, Kanz L, Muller GA, Ringert RH.** Regression of human metastatic renal cell carcinoma after vaccination with tumor cell-dendritic cell hybrids. *Nat Med* 2000; **6**: 332-336
- 21 **Shu S, Cohen P.** Tumor-dendritic cell fusion technology and immunotherapy strategies. *J Immunother* 2001; **24**: 99-100
- 22 **Horan PK, Slezak SE.** Stable cell membrane labelling. *Nature* 1989; **340**: 167-168
- 23 **Horan PK, Melnicoff MJ, Jensen BD, Slezak SE.** Fluorescent cell labeling for *in vivo* and *in vitro* cell tracking. *Methods Cell Biol* 1990; **33**: 469-490
- 24 **Michelson AD, Barnard MR, Hechtman HB, MacGregor H, Connolly RJ, Loscalzo J, Valeri CR.** *In vivo* tracking of platelets: circulating degranulated platelets rapidly lose surface P-selectin but continue to circulate and function. *Proc Natl Acad Sci U S A* 1996; **93**: 11877-11882
- 25 **Oh DJ, Lee GM, Francis K, Palsson BO.** Phototoxicity of the fluorescent membrane dyes PKH2 and PKH26 on the human hematopoietic KG 1a progenitor cell line. *Cytometry* 1999; **36**: 312-318
- 26 **Hart I, Colaco C.** Immunotherapy. Fusion induces tumour rejection. *Nature* 1997; **338**: 626-627
- 27 **Vermes I, Haanen C, Steffens-Nakken H, Reutelingsperger C.** A novel assay for apoptosis. Flow cytometric detection of phosphatidylserine expression on early apoptotic cells using fluorescein labelled Annexin V. *J Immunol Methods* 1995; **184**: 39-51

Laparoscopic versus conventional open resection of rectal carcinoma: A clinical comparative study

Wen-Xi Wu, Yao-Min Sun, Yi-Bin Hua, Li-Zong Shen

Wen-Xi Wu, Yao-Min Sun, Yi-Bin Hua, Li-Zong Shen, Department of Gastrointestinal Surgery, the First Affiliated Hospital of Nanjing Medical University, Nanjing 210029, Jiangsu Province, China
Supported by Jiangsu Province Educational Foundation
Correspondence to: Dr. Wen-Xi Wu, Department of Surgery, the First Affiliated Hospital of Nanjing Medical University, Nanjing 210029, Jiangsu Province, China. wuwenxi@yahoo.com
Telephone: +86-25-3718836-6863 **Fax:** +86-25-6863798
Received: 2003-06-05 **Accepted:** 2003-08-25

Abstract

AIM: To evaluate the feasibility of laparoscopic resection of rectal carcinoma and to compare the short-term outcome of laparoscopic procedure with conventional open surgery for rectal cancer.

METHODS: Thirty-eight patients with rectal cancer were included in a prospective non-randomized study. The patients were assigned to laparoscopic ($n=18$) or open ($n=18$) colorectal resection. Case selection, surgical technique, and clinical and pathological results were reviewed.

RESULTS: The operative time was longer in laparoscopic resection group (LAP) than in open resection group (189 ± 18 min vs 146 ± 22 min, $P<0.05$). Intraoperative blood loss and postoperative complications were less in LAP resection group than in open resection group. An earlier return of bowel motility was observed after laparoscopic surgery. The overall postoperative morbidity was 5.6% in the LAP resection group and 27.8% in open resection group ($P<0.05$). No anastomotic leakage was found in both groups. The pathologic examination showed that the length of the resected specimen, the mean number of harvested lymph nodes in laparoscopic resection group were comparable to those in open resection group.

CONCLUSION: Laparoscopic total mesorectal excision (TME) for rectal cancer is a feasible but technically demanding procedure. The present study demonstrates the safety of the procedure, while oncologic results are comparable to the open surgery, with a favorable short-term outcome.

Wu WX, Sun YM, Hua YB, Shen LZ. Laparoscopic versus conventional open resection of rectal carcinoma: A clinical comparative study. *World J Gastroenterol* 2004; 10(8): 1167-1170

<http://www.wjgnet.com/1007-9327/10/1167.asp>

INTRODUCTION

Since the first series of successful laparoscopic colon resections reported in 1991^[1,2], the laparoscopic techniques for colorectal diseases have been accepted widely^[3]. Although generally accepted for the treatment of benign diseases of the colon and rectum, the role of laparoscopic technique in cancer surgery remains controversial. Early reports of trocar site and

wound recurrences of malignancies after laparoscopic procedures led to concerns over possible increased recurrences and the risk of peritoneal seeding from the pneumoperitoneum^[4-6]. The ability to adhere to oncologic principles during laparoscopic surgical resection and the implications for long-term survival were also questioned.

The technical approach can significantly affect the outcome in colorectal cancer patients. The key principles including *en bloc* resection with removal of corresponding lymphatics, no-touch technique^[7], and total mesorectal excision (TME) are often recommended in open surgery for colorectal cancer^[8]. These oncologic principles are as important in laparoscopic surgery as in open surgery.

We presented our preliminary collected data on laparoscopic surgery for rectal carcinoma versus open resection in our university hospital to assess the safety and feasibility of laparoscopic resection of rectum with total mesorectal excision technique.

MATERIALS AND METHODS

Patients

Thirty-six patients (16 women, 20 men) undergoing anterior recto-sigmoidal and abdominoperineal resections for rectal carcinoma between April 2002 and May 2003 at the 1st Affiliated Hospital of Nanjing Medical University (Nanjing, Jiangsu, China) were entered into a database. Pre- and post-operative care was standardized for both laparoscopic and open resection groups. Preoperative assessment included physical examination, liver function and carcinoembryonic antigen (CEA) tests, liver ultrasonography, and colonoscopy with biopsy. Patients who had intestinal obstruction, emergency surgery, adjacent organ invasion diagnosed preoperatively, and history of colon surgery were excluded for laparoscopic operation.

In laparoscopic resection group eighteen patients (9 women and 9 men) undergoing laparoscopic operation for rectal carcinoma were reviewed. Inclusion in the laparoscopic or conventional treatment group was not randomized. All patients were operated on by 2 groups of surgeons, 1 group of surgeons who had experiences in advanced laparoscopic techniques used a laparoscopic approach, and the other group of surgeons performed conventional resections.

The patients were treated with mechanical and antibiotic bowel preparation preoperatively. Surgery was done under general anesthesia. All patients received antibiotics intravenously at the time of induction in the operating room.

Methods

Patients were placed in the modified lithotomy position to facilitate either transanal stapled anastomosis or peritoneal resection. All patients had an indwelling urinary catheter. For the laparoscopic resection group the pneumoperitoneum was established with an intra-abdominal pressure of 15 mmHg.

The laparoscope was sited at the umbilicus, 4 trocars were inserted. In brief, two 5-mm ports were placed in the right and left upper quadrants and a 10-mm trocar for the left iliac fossa. A further 12-mm trocar was inserted in the right iliac fossa for the endoscopic stapling device. Mobilization and dissection of sigmoid colon and rectum were achieved by using ultrasonic

scissors. The following procedures were required: left colon mobilization (including the splenic flexure if necessary), identification of the left ureter, and intracorporeal ligation of the inferior mesenteric vessels with clips or stapling devices. Rectum and mesorectum were mobilized through the avascular plane between the intact mesorectum anteriorly and Waldeyer's fascia posteriorly by sharp dissection and extended down to the level of the levator muscle. The ureters, hypogastric nerve, and pelvic parasympathetic plexus were protected. After intracorporeal transection of the distal bowel with *endolinesal staplers*, the bowel was drawn out through a left lower quadrant incision under wound protection and divided with appropriate proximal clearance. The proximal anvil was placed extra corporeally, and anastomosis was performed by double stapling technique.

For abdominoperineal resection, laparoscopic procedures were followed by perineal resection in the standard fashion. A terminal colostomy was created at the left lower abdomen port site. With the help of the perineal surgeon, the rectum and the whole mesorectum were fully mobilized and the specimen was retrieved through the perineum wound. The perineum wound was closed primarily with placement of a drain connected to a low-pressure suction, in the pelvic cavity.

In the conventional surgery group open procedures were performed according to the surgeon's established technique, conforming to standard rules for rectal cancer.

Outcomes

Characteristics of the patients, operative variables, and short-term outcomes were analyzed. The patient information including age, gender, premorbid conditions, and previous surgery was reviewed. Operative variables, and short-term outcomes including time to resumption of oral intake, first day to flatus, and duration of hospitalization were analyzed as clinical parameters for study. Pathology reports were reviewed to obtain lymph node harvest data, length of specimen, distance from the closest margin, and margin status. Intra- or post-operative complications were reviewed, and all results were compared with those of conventional rectal resections in the open group.

Statistical analysis

Statistical analysis was performed with Student's *t*-test and χ^2 test. Results are expressed as mean \pm SD. A *P* value less than 0.05 was considered statistically significant.

RESULTS

The patients' characteristics in laparoscopic or open resection group are summarized in Table 1. The two groups were comparable in terms of age, sex, American Society of Anesthesia score (ASA score), pathologic stage and type of resection.

The mean operating time was significantly longer in LAP resection group than in open resection group. The amount of operative blood loss was lower in LAP resection group than in conventional surgery group (Table 2). No patients needed conversion to open surgery in laparoscopic resection group. However, rectum injury was found in two cases with low anterior resection after colon-rectum anastomosis. This was managed by laparoscopic suture closure and pelvic drainage for one week without further sequela. In one patient with heavy smoking history, significantly increased PaCO₂ was found after two hours' pneumoperitoneum during the operation, and the patient recovered after deflation of pneumoperitoneum and hyperventilation for a short period of 20 min (Table 3).

Post-operative complications were more frequent in the open resection group than in LAP resection group (5.6% vs 27.8%; *P*<0.05).

The passage of flatus occurred earlier in laparoscopic resection group, and oral intake could be started earlier in the

LAP resection group (*P*<0.05). Mean postoperative stay was shorter in LAP resection group than in open resection group, but the difference was not significant.

Table 1 Characteristics of patients in two groups

	LAP resection group (n=18)	Open resection group (n=18)	Difference (P value)
Age (Years)	52.4 \pm 7.9	54.1 \pm 6.8	NS
Male/Female	9:9	10:8	NS
ASAP score	2.4 \pm 0.2	2.5 \pm 0.3	NS
Operations			
LAR	11	12	NS
APR	7	6	NS
Duke's stage			
A	3	3	NS
B	9	7	NS
C	6	8	NS

NS: no statistical significance.

Table 2 Operative details for two groups

	LAP resection group (n=18)	Open resection group (n=18)	Difference (P value)
Operative time (min)	189 \pm 18	146 \pm 22	<0.05
Estimated blood loss (mL)	136 \pm 21	357 \pm 34	<0.01
Passing flatus (h)	43 \pm 5	78 \pm 12	<0.05
Oral intake (h)	58 \pm 9	89 \pm 13	<0.05
Hospital stay (d)	7.8 \pm 1.5	9.1 \pm 3.3	NS

Table 3 Complications of surgery for rectal carcinoma

Complication	Number of patients		P value
	LAP (n=18)	Open (n=18)	
Intraoperative			
Bleeding	0	2	NS
Rectum injury	2	1	NS
Increased PaCO ₂	1	0	NS
Postoperative			
Wound infection	0	1	NS
Urinary retention	1	2	NS
Prolonged ileum (>4d)	0	2	NS
Morbidity (%)	5.6	27.8	<0.05

Table 4 Pathology data in laparoscopic and open resection groups

	LAP resection group (n=18)	Open resection group (n=18)	Difference (P value)
Lymph nodes harvest	7.8 \pm 1.7	8.2 \pm 2.3	NS
Specimen length (cm)			
LAR	19.4 \pm 3.2	21.2 \pm 2.9	NS
APR	27.3 \pm 4.1	25.8 \pm 3.0	NS
Distal resection margin (cm)			
LAR	4.3 \pm 1.1	4.6 \pm 1.6	NS
Surgical margins	clear	clear	

To assess the adequacy of oncological resection, several parameters were examined from pathology reports. Evaluation of the resected specimens is summarized in Table 4. The mean number of lymph nodes removed in LAP or open resection group was 7.8 \pm 1.7 (range, 4-13) and 8.2 \pm 2.3 (range, 3-15), respectively. No significant difference was found between the 2 groups. The average lengths of removed specimens with the two surgical procedures were also comparable. Tumor distances from the closest margin were similar too for the two procedures, and were adequate from an oncological standpoint of view. Histological examination revealed that proximal and distal margins were free of tumor in all surgical specimens in both groups.

DISCUSSION

Laparoscopic techniques for colonic resection were described in 1991^[1,2], only 4 years after the introduction of laparoscopic cholecystectomy. Compared with conventional open surgery, laparoscopic surgery could offer a faster recovery, minimized postoperative ileums and pain, a shorter stay in hospital and a quicker return to normal activity^[9,10]. However, the better appearance was secondary in importance compared with recurrence and survival. Port site metastasis and lack of long-term data in oncological outcome for patients with laparoscopic resection of colorectal cancer are controversial issues.

The main controversies have centered on the oncologic adequacy of laparoscopic resection in comparison with classic open surgery^[11]. During laparoscopic resection, the colon and rectum can be mobilized by retraction of the bowel, using endoscopic graspers such as Bablocks, and the peritoneal attachments divided, using ultrasonic or electrocautery scissors. Our experiences show that the rectum can be excised with an intact mesorectal facial envelope all the way down to the level of the pelvic floor. The magnified views obtained deep in the pelvis at laparoscopy may facilitate accurate mesorectal dissection and vegetable nerve protection. Radical *en bloc* excision of the rectum and mesorectum, by low anterior resection or abdomino - perineal, has been the standard treatment for advanced rectal carcinoma^[12,13].

Concerning with port-site recurrence, numerous experimental studies have been published since 1991. They have analyzed the possible role of pneumoperitoneum and carbon dioxide^[14-20], the pathophysiology of minimally invasive techniques on tumor response and immunity^[21,22]. In laparoscopic procedure, the tumor was removed through small incisions^[23] in the abdominal wall or perineal, and this maneuver may theoretically lead to a risk of tumor contamination. To avoid port-site metastasis, Balli *et al.*^[24] described a routine to follow in colorectal cancer resection: fixation of trocars to the abdominal wall, high vascular ligation, isolation of specimens before extraction from the abdominal cavity, and intraperitoneal and trocar site irrigation with a tumoricidal solution. With improved incision protection techniques, the reported port-site recurrence rate dropped rapidly. Zmora^[25] reported a port-site recurrence rate of 1% in a review of 1737 patients undergone laparoscopic colorectal resection for malignancy. Ramos *et al.*^[26] reported abdominal wall metastases in only 3 of 208 patients with a minimum follow-up period of 1 year. All recurrences were in patients with Duke's C-stage carcinoma, and 2 of the 3 were found to have diffuse peritoneal carcinomatosis at the initial surgery. The port-site metastasis has not been a significant issue in the presence of adequate training and laparoscopic skills^[27,28].

Moreover, laparoscopic surgery for rectal carcinoma should concern about the safety of the procedure, especially in low anterior resections for lower rectal carcinoma. The anastomotic leak rate reported in a larger series of laparoscopic anterior resection was consistently less than 10%, which was comparable to that of conventional open anterior resection^[29,30]. In our present study, no anastomotic leak was found in laparoscopic resection group. However, the risks existed, especially in anterior resections for lower rectal carcinoma. For prevention of leakage, colorectal anastomosis must be tension-free and has a good blood supply. It was our routine to check the anastomosis for leaks in every case for laparoscopic low anterior resection. The pelvis was irrigated and filled with saline and the anastomosis was immersed. Then the rectum was insufflated with air, using a bulb syringe, for observing air bubbles. Pelvic drains were placed during all low anterior, abdominal perineal resections. Some authors have recommended protective ileostomy, and it might be used for low anterior resection in patients with borderline vascular status, malnutrition or neoadjuvant radiotherapy.

The stage I tumors (Duke's A) do not invade beyond the muscularis propria and have no lymph node metastasis. For this reason, stage I tumors have been considered to be the best indication for laparoscopic colectomy, with a very low rate of conversion to laparotomy (0-1%)^[31], no port-site metastasis and no deaths were reported at long-term follow-up^[32]. Adachi *et al.*^[33] found that the mean size of stage I tumors was 2.86 cm and that most tumors <2 cm in size were free of both serosal invasion and lymph node metastasis. In such situations, because of the inability to palpate colonic tumors during laparoscopy, tumor localization must be precisely identified before resection is undertaken. On-table colonoscopy at the time of surgery not only leads to prolonged operative time, but also makes further laparoscopic dissection impossible because of colonic distension. It is very helpful to use X-ray imaging at the time of preoperative colonoscopic examination to site small lesions accurately.

The rate of conversion to laparotomy ranged from 1.45% to 48% in literatures with a mean conversion rate of 15%^[34,35]. Reasons for conversion to open surgery are difficulty to provide exposure or to identify anatomy because of the larger tumor size and relatively smaller pelvis. Abdominal obesity or presence of adhesions from previous surgery may compound this difficulty. The fixity of the tumor or invasion to adjacent organs at laparoscopy needed to convert to a formal laparotomy in order to complete the planned procedure^[35,36]. The preoperative patient evaluation and surgeon's experience are important predictive factors as confirmed in our study.

Laparoscopic colorectal surgery invariably takes longer time than a corresponding open procedure. Again, operating time is reduced with increased laparoscopic experience. Our study also confirmed the low rate of postoperative complications after minimally invasive procedures. Postoperative ileum, urinary retention, and wound infections occurred less frequently than that in the open resection group. These advantages have also been confirmed by many authors^[37,38].

Repeated evidences have indicated that a laparoscopic approach in colorectal cancer has several advantages including a shorter hospital stay, less pain, a better appearance and decreased postoperative analgesia requirements. In fact, laparoscopic surgery has been found to be associated with significantly decreased intraoperative blood loss and postoperative complications as well^[39,40]. Furthermore, theoretic advantages of less physiologic trauma and immunologic suppression have recently received more attention in the literatures^[38,41]. A less intensive inflammatory response has also been demonstrated after laparoscopic surgery compared with conventional open surgery. The results of the present study showed that laparoscopic approaches to rectal carcinoma did not compromise early postoperative recovery.

Advanced rectal tumors accounted for 83.3% of the cases in our study. However, no long-term follow-up has been available at this time. Cammpault^[42] reported a 5-year survival rate of 60.7% in colorectal cancer patients with laparoscopic resection, with no difference compared with the open resection (62.5%). Recently, Franklin *et al.* reported the results of laparoscopic colectomy in 50 consecutive patients with stage III colorectal cancer, which was performed at a single hospital. The overall survival rates at 3 and 5 years were 54.5% and 38.5%, respectively, and the cancer-adjusted survival rates were 60.8% and 49%^[43].

For low rectal lesions laparoscopy-assisted abdominoperineal resection (28.6% in our series) also allowed earlier postoperative recovery, with an equivalent tumor clearance, morbidity, mortality, disease-free interval, and duration of survival^[10].

To date, all reported comparative nonrandomized studies and randomized studies have shown no difference in recurrence and survival rates with laparoscopic versus open colorectal resection, and a lower overall morbidity with laparoscopic procedure^[10].

In conclusion, our results suggest that laparoscopic resection for rectal cancer can be performed safely and without compromising oncological principles. There are definitely perioperative advantages with laparoscopic surgery.

REFERENCES

- Cooperman AM**, Katz V, Zimmon D, Botero G. Laparoscopic colon resection: a case report. *J Laparoendosc Surg* 1991; **1**: 221-224
- Saclarides TJ**, Ko ST, Airan M, Dillon C, Franklin J. Laparoscopic removal of a large colonic lipoma. Report of a case. *Dis Colon Rectum* 1991; **34**: 1027-1029
- Hartley JM**, Monson JR. The role of laparoscopy in the multimodality treatment of colorectal cancer. *Surg Clin North Am* 2002; **82**: 1019-1033
- Ciocco WC**, Schwartzman A, Golub RW. Abdominal wall recurrence after laparoscopic colectomy for colon cancer. *Surgery* 1994; **116**: 842-846
- Wexner SD**, Cohen SM. Port site metastases after laparoscopic colo-rectal surgery for cure of malignancy. *Br J Surg* 1995; **82**: 295-298
- Lacy AM**, Delgado S, Garcia-Valdecasas JC, Castells A, Pique JM, Grande L, Fuster J, Targarona EM, Pera M, Visa J. Port site metastases and recurrence after laparoscopic colectomy. A randomized trial. *Surg Endosc* 1998; **12**: 1039-1042
- Slanetz CA Jr**. Effect of no touch isolation on survival and recurrence in curative resections for colorectal cancer. *Ann Surg Oncol* 1998; **5**: 390-398
- Heald RJ**, Husband EM, Ryal RD. The mesorectum in rectal cancer surgery- the clue to pelvic recurrence? *Br J Surg* 1982; **69**: 613-616
- Monson JR**, Darzi A, Carey PD, Guillou PJ. Prospective evaluation of laparoscopic -assisted colectomy in an unselected group of patients. *Lancet* 1992; **340**: 831-833
- Yamamoto S**, Watanabe M, Hasegawa H, Kitajima M. Prospective evaluation of laparoscopic surgery for rectosigmoidal and rectal carcinoma. *Dis Colon Rectum* 2002; **45**: 1648-1654
- Baker RP**, White EE, Titu L, Duthie GS, Lee PW, Monson JR. Does laparoscopic abdominoperineal resection of the rectum compromise long-term survival? *Dis Colon Rectum* 2002; **45**: 1481-1485
- Reis Neto JA**, Quilici FA, Cordeiro F, Reis JA Jr, Kagohara O, Simoes Neto J. Laparoscopic total mesorectum excision. *JSL* 2002; **6**: 163-167
- Morino M**, Parini U, Giraudo G, Salval M, Brachet Contul R, Garrone C. Laparoscopic total mesorectal excision: a consecutive series of 100 patients. *Ann Surg* 2003; **237**: 335-342
- Scheidbach H**, Schneider C, Konradt J, Barlehner E, Kohler L, Wittekind CH, Kockerling F. Laparoscopic abdominoperineal resection and anterior resection with curative intent for carcinoma of the rectum. *Surg Endosc* 2002; **16**: 7-13
- Nelson H**. Laparoscopic colectomy for colon cancer -- a trail update. *Swiss Surg* 2001; **7**: 248-251
- Lujan HJ**, Plasencia G, Jacobs M, Viamonte M 3rd, Haetmann RF. Long-term survival after laparoscopic colon resection for cancer: complete five-year follow-up. *Dis Colon Rectum* 2002; **45**: 491-501
- Wexner SD**, Sands DR. What's new in colon and rectal surgery. *J Am Coll Surg* 2003; **196**: 95-103
- Chung CC**, Ha JP, Tsang WW, Li MK. Laparoscopic-assisted total mesorectal excision and colonic J pouch reconstruction in the treatment of rectal cancer. *Surg Endosc* 2001; **15**: 1098-1101
- Ishida H**, Murata N, Idezuki Y. Increased insufflation pressure enhances the development of liver metastasis in a mouse laparoscopy model. *World J Surg* 2001; **25**: 1537-1541
- Tomita H**, Marcello PW, Milsom JW, Gramlich TL, Fazio VW. CO2 pneumoperitoneum does not enhance tumor growth and metastasis: study of a rat cecal wall inoculation model. *Dis Colon Rectum* 2001; **44**: 1297-1301
- Basu A**, Wexner SD, Bergamaschi R. Validity of current experimental evidence on laparoscopic surgery for colorectal cancer. *Surg Endosc* 2003; **17**: 179
- Mehiggn BJ**, Hartley JE, Drew PJ, Saleh A, Dore PC, Lee PW, Monson JR. Changes in T cell subsets, interleukin-6 and C-reactive protein after laparoscopic and open colorectal resection for malignancy. *Surg Endosc* 2001; **15**: 1289-1293
- Hackert T**, Uhl W, Buchler MW. Specimen retrieval in laparoscopic colon surgery. *Dig Surg* 2002; **19**: 502-506
- Balli JE**, Franklin ME, Almeda JA, Glass JL, Diaz JA, Reymond M. How to prevent port - site metastases in laparoscopic colorectal surgery. *Surg Endosc* 2000; **14**: 1034-1036
- Zmora O**, Gervaz P, Wexner SD. Trocar site recurrence in laparoscopic surgery for colorectal cancer. *Surg Endosc* 2001; **15**: 788-793
- Ramos JM**, Gupta S, Anthone GJ, Ortega AE, Simons AJ, Beart RW Jr. Laparoscopy and colon cancer. Is the port site at risk? A preliminary report. *Arch Surg* 1994; **129**: 897-899
- Hazebroek EJ**. COLOR: a randomized clinical trail comparing laparoscopic and open resection for colon cancer. *Surg Endosc* 2002; **16**: 949-953
- Lumley J**, Stitz R, Stevenson A, Fielding G, Luck A. Laparoscopic colorectal surgery for cancer: intermediate to long-term outcomes. *Dis Colon Rectum* 2002; **45**: 867-872
- Pera M**, Delgado S, Garcia-Valdecasas JC, Pera M, Castells A, Pique JM, Bombuy E, Lacy AM. The management of leaking rectal anastomoses by minimally invasive techniques. *Surg Endosc* 2002; **16**: 603-606
- Scheidbach H**, Schneider C, Huegel O, Barlehner E, Konradt K, Wittekind C, Kockerling F. Laparoscopic sigmoid resection for cancer: curative resection and preliminary medium-term results. *Dis Colon Rectum* 2002; **45**: 1641-1647
- Kakisako K**, Sato K, Adachi Y, Shiraishi N, Miyahara M, Kitano S. Laparoscopic colectomy for Dukes A colon cancer. *Surg Laparosc Endosc Percutan Tech* 2000; **10**: 66-70
- Franklin ME Jr**, Rosenthal D, Abrego-Medina D, Dorman JP, Glass JL, Norem R, Diaz A. Prospective comparison of open vs laparoscopic colon surgery for carcinoma. Five -year results. *Dis Colon Rectum* 1996; **39**(10 Suppl): S35-46
- Adachi Y**, Sato K, Shiraishi N, Kakisako K, Tanimura H, Kitano S. Tumor size of colorectal cancer: indication for laparoscopic surgery. *Surg Laparosc Endosc* 1998; **8**: 269-272
- Yong L**, Deane M, Monson JR, Darzi A. Systematic review of laparoscopic surgery for colorectal malignancy. *Surg Endosc* 2001; **15**: 1431-1439
- Gervaz P**, Pikarsky A, Utech M, Secic M, Efron J, Belin B, Jain A, Wexner S. Converted laparoscopic colorectal surgery. *Surg Endosc* 2001; **15**: 827-832
- Baker RP**, White EE, Titu L, Duthie GS, Lee PW, Monson JR. Does laparoscopic abdominoperineal resection of the rectum compromise long-term survival? *Dis Colon Rectum* 2002; **45**: 1481-1485
- Weeks JC**, Nelson H, Gellber S, Sargent D, Schroeder G. Short-term quality-of -life outcomes following laparoscopic-assisted colectomy vs open colectomy for colon cancer: a randomized trail. *JAMA* 2002; **287**: 321-328
- Wu FP**, Sietses C, von Blomberg BM, van Leeuwen PA, Meijer S, Cuesta MA. Systemic and peritoneal inflammatory response after laparoscopic or conventional colon resection in cancer patients: a prospective, randomized trial. *Dis Colon Rectum* 2003; **46**: 147-155
- Hasegawa H**, Kabeshima Y, Watanabe M, Yamamoto S, Kitajima M. Randomized controlled trial of laparoscopic versus open colectomy for advanced colorectal cancer. *Surg Endosc* 2003; **17**: 636-640
- Lacy AM**, Garcia-Valdecasas JC, Delgado S, Castells A, Taura P, Pique JM, Visa J. Laparoscopic colectomy versus open colectomy for treatment of non-metastatic colon cancer: a radomised trail. *Lancet* 2002; **29**: 2224-2229
- Allendorf JD**, Bessler M, Whelan RL, Trokel M, Laird DA, Terry MB, Treat MR. Better preservation of immune function after laparoscopic -assisted vs open bowel resection in a murine model. *Dis Colon Rectum* 1996; **39**(10 Suppl): S67-72
- Champault GG**, Barrat C, Raselli R, Elizalde A, Catheline JM. Laparoscopic versus open surgery for colorectal carcinoma: a prospective clinical trail involving 157 cases with a mean follow-up of 5 years. *Surg Laparosc Endosc Percutan Tech* 2002; **12**: 88-95
- Franklin ME**, Kazantsev GB, Abrego D, Diaz-E JA, Balli J, Glass JL. Laparoscopic surgery for stage III colon cancer: Long-term follow - up. *Surg Endosc* 2000; **1**: 612-616

Effects of autoantibodies against β_1 -adrenoceptor in hepatitis virus myocarditis on action potential and L-type Ca^{2+} currents

Kun Liu, Yu-Hua Liao, Zhao-Hui Wang, Shu-Li Li, Ming Wang, Ling-Lan Zeng, Ming Tang

Kun Liu, Yu-Hua Liao, Zhao-Hui Wang, Ming Wang, Department of Cardiology, Institute of Cardiology, Union Hospital, Tongji Medical College of Huazhong University of Science and Technology, Wuhan 430022, Hubei Province, China

Shu-Li Li, Ling-Lan Zeng, Department of Infectious Diseases, Union Hospital, Tongji Medical College of Huazhong University of Science and Technology, Wuhan 430022, Hubei Province, China

Ming Tang, Department of Physiology, Tongji Medical College of Huazhong University of Science and Technology, Wuhan 430030, Hubei Province, China

Supported by the National Natural Science Foundation of China, NO.39970306

Correspondence to: Professor Yu-Hua Liao, Department of Cardiology, Institute of Cardiology, Union Hospital, Tongji Medical College of Huazhong University of Science and Technology, Wuhan 430022, Hubei Province, China. liaoyh27@hotmail.com

Telephone: +86-27-85726376

Received: 2003-11-12 **Accepted:** 2003-12-16

Abstract

AIM: To investigate the effects of autoantibodies against β_1 -adrenoceptor in hepatitis virus myocarditis on action potential and L-type Ca^{2+} currents.

METHODS: Fifteen samples of autoantibodies against β_1 -adrenoceptor positive sera of patients with hepatitis virus myocarditis were obtained and IgGs were purified by octanoic acid extraction. Binding of autoantibodies against β_1 -adrenoceptor to guinea pig cardiac myocytes was examined by immunofluorescence. Using the patch clamp technique, the effects on the action potential and $I_{\text{Ca-L}}$ of guinea pig cardiac myocytes caused by autoantibodies against β_1 -adrenoceptor in the absence and presence of metoprolol were investigated. Cell toxicity was examined by observing cell morphology and permeability of cardiac myocytes to trypan blue.

RESULTS: The specific binding of autoantibodies against β_1 -adrenoceptor to guinea pig cardiomyocytes was observed. Autoantibodies against β_1 -adrenoceptor diluted at 1:80 prolonged APD₂₀, APD₅₀ and APD₉₀ by 39.2%, 29.1% and 15.2% respectively, and only by 7.2%, 5.3% and 4.1% correspondingly in the presence of 1 $\mu\text{mol/L}$ metoprolol. Autoantibodies against β_1 -adrenoceptor diluted at 1:80, 1:100 and 1:120 significantly increased the $I_{\text{Ca-L}}$ peak current amplitude at 0 mV by 55.87 \pm 4.39%, 46.33 \pm 5.01% and 29.29 \pm 4.97% in a concentration-dependent manner. In contrast, after blocking of β_1 -adrenoceptors (1 $\mu\text{mol/L}$ metoprolol), autoantibodies against β_1 -adrenoceptor diluted at 1:80 induced a slight increase of $I_{\text{Ca-L}}$ peak amplitude only by 6.81 \pm 1.61%. A large number of cardiac myocytes exposed to high concentrations of autoantibodies against β_1 -adrenoceptor (1:80 and 1:100) were turned into rounded cells highly permeable to trypan blue.

CONCLUSION: Autoantibodies against β_1 -adrenoceptor may result in arrhythmias and/or impairment of myocardiums in HVM, which would be mediated by the enhancement of $I_{\text{Ca-L}}$.

Liu K, Liao YH, Wang ZH, Li SL, Wang M, Zeng LL, Tang M. Effects of autoantibodies against β_1 -adrenoceptor in hepatitis virus myocarditis on action potential and L-type Ca^{2+} currents. *World J Gastroenterol* 2004; 10(8): 1171-1175

<http://www.wjgnet.com/1007-9327/10/1171.asp>

INTRODUCTION

Viral hepatitis remains a worldwide public health problem^[1-4] and is reported by the Chinese Ministry of Public Health as an infectious disease with the highest morbidity and mortality in China. Many complications are considered to be involved in viral hepatitis^[5-17]. Hepatitis virus myocarditis (HVM) as a consequence of hepatitis virus infection, secondary to Coxsackie virus myocarditis in morbidity in hepatitis virus predominated areas of China, displays severe cardiac manifestations in addition to liver impairment^[18]. It was recently found that some cases of severe fulminant hepatitis virus myocarditis were accompanied by arrhythmias and/or cardiac injury. These cases were screened with a high prevalence of circulating autoantibodies against β_1 -adrenoceptor (anti- β_1 -receptor autoantibodies)^[18], which have been recognized in idiopathic dilated cardiomyopathy (DCM) and Chagas' cardiomyopathy^[19,20]. Using the patch clamp technique, we examined the effects of anti- β_1 -receptor autoantibodies from patients with HVM on the electrophysiological properties of cardiomyocytes so as to find the possible clinical significance of the autoantibodies.

MATERIALS AND METHODS

Samples collection

A peptide was synthesized according to the sequence of β_1 -adrenoceptor^[21]: H-W-W-R-A-E-S-D-E-A-R-R-C-Y-N-D-P-K-C-C-D-F-V-T-N-R and was used as an antigen in ELISA as described by our laboratory^[22] for screening of anti- β_1 -receptor autoantibodies in serum samples of patients diagnosed as HVM according to the Chinese diagnostic criteria for adult acute myocarditis approved in 1999^[23]. Fifteen serum samples were selected.

Antibody purification

As described by Seddik *et al.*^[24], IgGs in anti- β_1 -receptor autoantibodies-positive sera of patients with HVM were purified by octanoic acid extraction. The purity of IgGs was over 90%.

Cell preparation

Guinea pig ventricular myocytes were isolated essentially as described by Heubach *et al.*^[25] with a modification. An adult guinea pig weighing 200-300 g was anesthetized with sodium pentobarbitone (30 mg/kg i.p.), and the trachea was cannulated for artificial respiration. The chest was opened, and the aorta was cannulated *in situ*. The heart was dissected and retrograde perfused on a Langendorff perfusion system at 37 °C. It was perfused first with Tyrode's solution for about 1 min at a

hydrostatic pressure of 70 cm, second with nominally Ca^{2+} -free Tyrode's solution for 3 min, and subsequently with 0.25 g/L collagenase type I, 0.20 g/L protease type XIV and 0.25 g/L bovine serum albumin for about 5 min. Finally the heart was washed with KB solution for 4 min and the ventricles were cut and teased into pieces in KB solution. All the solutions were bubbled with 1 000 mL/L oxygen. The dissociated cells were then kept in KB solution at room temperature for at least 1 h before the experiment.

Antibody binding

The binding of anti- β_1 -receptor autoantibodies was examined by immunofluorescence. The isolated guinea pig cardiac myocytes were fixed by acetone at 4 °C. The fixed cells were washed three times with cold PBS, incubated with anti- β_1 -receptors autoantibody-positive or negative sera which were absorbed by the above peptide sequence (1:10) overnight at 4 °C, and then washed 3 times in cold PBS, followed by incubation with goat anti-human IgG labeled with FITC (1:90) for 1 h at 37 °C. After rinsed with PBS, the slides were mounted with cover slips for fluoscopy.

Electrophysiology

Cardiac myocytes were placed in Tyrode's solution and the Ca^{2+} resistant cells adhered to the coverslips of the recording chamber were selected for electrophysiological recording. Action potential and $I_{\text{Ca-L}}$ were recorded using the whole-cell configuration of the patch-clamp technique. The cells were held in current-clamp mode or voltage-clamp mode using an Axopatch 200-A amplifier (Axon Instruments, USA). Action potential was elicited by constant current pulses of 1nA amplitude and a 6ms duration at a rate of 0.2 Hz.

In voltage-clamp experiments, the holding potential was set at -80 mV. Na^+ and T-type Ca^{2+} channels were inactivated by applying a 100-ms prepulse to -40 mV immediately before each test pulse. The time course of changes in Ca^{2+} conductance was monitored by applying a 300-ms test pulse to 0 mV once every 5 seconds. For analysis of I-V relationship, after a 100-ms voltage step to -40 mV, 300-ms depolarizing voltage steps from -40 mV to +60 mV in 10 mV increments were used to elicit currents. Data were acquired and analyzed using the ISO2 (MFK, Germany) analysis software package.

Cell toxicity

Cell toxicity was examined by observing cell morphology and the permeability of cardiac myocytes to 20 g/L trypan blue. The live cardiac myocytes were rod-shaped and excluded trypan blue, whereas the dead cells were rounded and permeable to trypan blue.

Reagents

Tyrode's solution contained (mmol/L) NaCl 135, KCl 5.4, MgCl_2 1.0, NaH_2PO_4 0.33, CaCl_2 1.8, HEPES 10 and glucose 10 (pH adjusted to 7.4 with NaOH). KB solution contained (mmol/L) MgCl_2 5, KCl 40, KH_2PO_4 20, Taurine 20, Glutamic acid 50, EGTA 0.5, HEPES 10, glucose 10 (pH adjusted to 7.4 with KOH). All the chemicals for the electrophysiological experiment, enzymes and octanoic acid were purchased from Sigma Aldrich Company, USA. Metoprolol was a generous gift from AstraZeneca Company, USA. Goat anti-human IgG labeled with FITC was purchased from Wuhan Yafa Biotech Corp, China.

Statistical analysis

Data were expressed as mean \pm SEM and analysed using Student's *t* test. $P < 0.05$ was considered statistically significant.

RESULTS

Specific binding of anti- β_1 -receptors autoantibodies to cardiac myocytes

Green fluorescence in rod-shaped cardiac myocytes only in slides incubated with anti- β_1 -receptor autoantibodies-positive sera suggested the specific binding of anti- β_1 -receptor autoantibodies to cardiac myocytes.

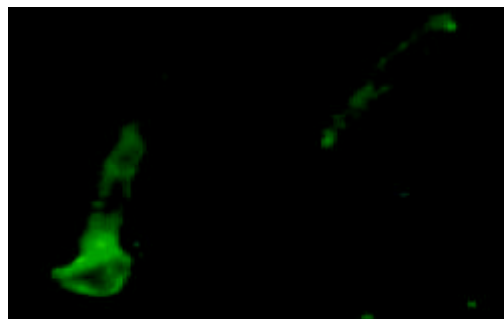


Figure 1 Specific binding of anti- β_1 -receptor autoantibodies to guinea pig cardiac myocytes. Rod-shaped cardiac myocytes were stained by immunofluorescence (second IgG labeled with FITC), suggesting the specific binding of anti- β_1 -receptor autoantibodies to cardiac myocytes.

Effects of anti- β_1 -receptor autoantibodies on action potential in cardiac myocytes in the absence and presence of metoprolol

The effects of anti- β_1 -receptor autoantibodies on action potential properties were tested in isolated cardiac myocytes in a current clamp mode of the patch clamp technique. After 5 min with stable action potentials, the antibodies diluted at 1:80 was superfused. The action potential duration (APD) was assessed as a duration to 20%, 50% and 90% repolarization (APD_{20} , APD_{50} and APD_{90} , respectively). Anti- β_1 -receptor autoantibodies diluted at 1:80 prolonged the APD in all phases of repolarization, and the increase averaged 39.2%, 29.1% and 15.2% for APD_{20} , APD_{50} and APD_{90} vs control. Thus the plateau was markedly prolonged (Figure 2 and Table 1).

Table 1 Effects of anti- β_1 -receptor autoantibodies diluted at 1:80 on action potential phases ($n=6$)

	Control	Anti- β_1 -receptor autoantibodies
APD_{20} (mV)	67.3 \pm 1.8	93.7 \pm 3.6 ^b
APD_{50} (mV)	148.8 \pm 5.4	192.1 \pm 6.7 ^b
APD_{90} (mV)	195.6 \pm 8.2	225.3 \pm 11.5 ^b

^b $P < 0.01$ vs control.

Whereas exposure of cells to anti- β_1 -receptor autoantibodies diluted at 1:80 in the presence of 1 $\mu\text{mol/L}$ metoprolol resulted in a slight prolongation of the APD. As in Table 2 shown, the increase averaged only 7.2%, 5.3% and 4.1% for APD_{20} , APD_{50} and APD_{90} vs control ($P < 0.01$ vs anti- β_1 -receptor autoantibodies diluted at 1:80).

Table 2 Effects of anti- β_1 -receptor autoantibodies diluted at 1:80 on action potential phases in the presence of 1 $\mu\text{mol/L}$ metoprolol ($n=6$)

	Control	Anti- β_1 -receptor autoantibodies and metoprolol
APD_{20} (mV)	65.8 \pm 1.1	70.5 \pm 2.3
APD_{50} (mV)	147.2 \pm 4.6	155.0 \pm 6.3
APD_{90} (mV)	196.2 \pm 5.1	204.3 \pm 9.4

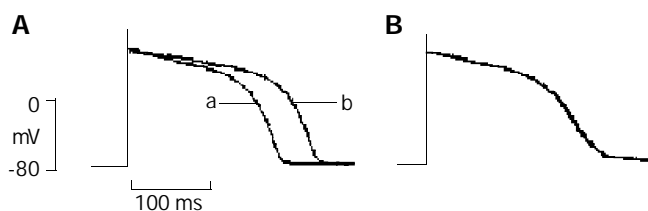


Figure 2 AP recordings before and after superfusion with anti- β_1 -receptor diluted at 1:80 in the absence and presence of 1 $\mu\text{mol/L}$ metoprolol. A: effect of anti- β_1 -receptor diluted an 1:80 on AP. ^arepresents AP before superfusion with 1:80 anti- β_1 -receptor autoantibodies, ^brepresents AP after superfusion with 1:80 anti- β_1 -receptor autoantibodies. B: no marked changes of AP after superfusion with 1:80 anti- β_1 -receptor autoantibodies in the presence of 1 $\mu\text{mol/L}$ metoprolol.

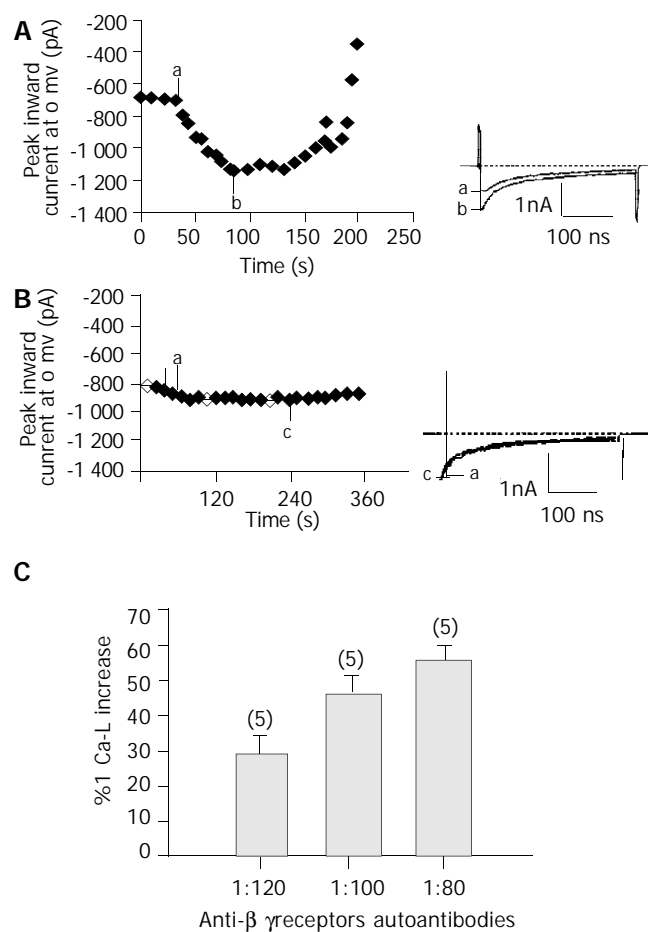


Figure 3 Effects of anti- β_1 -receptor autoantibodies on peak current amplitude of I_{Ca-L} in the absence and presence of 1 $\mu\text{mol/L}$ metoprolol. A and B (left): time-course changes of peak current amplitude of I_{Ca-L} before and after superfusion with anti- β_1 -receptor autoantibodies diluted at 1:80 (A) or in the presence of 1 $\mu\text{mol/L}$ metoprolol (B). A and B (right): traces of I_{Ca-L} before and after superfusion with anti- β_1 -receptor autoantibodies diluted at 1:80 (A) or before and after superfusion with anti- β_1 -receptor autoantibodies diluted an 1:80 in the presence of 1 $\mu\text{mol/L}$ metoprolol (B). ^arepresents the maximal peak current amplitude of I_{Ca-L} before superfusion with anti- β_1 -receptor autoantibodies diluted at 1:80, ^brepresents the maximal peak current amplitude of I_{Ca-L} after superfusion with anti- β_1 -receptor autoantibodies diluted an 1:80, ^crepresents the maximal peak current amplitude of I_{Ca-L} after superfusion with anti- β_1 -receptor autoantibodies diluted at 1:80 in the presence of 1 $\mu\text{mol/L}$ metoprolol. C: concentration dependence of anti- β_1 -receptor autoantibodies. The numbers in brackets indicate the number of cells studied at each concentration.

Effects of anti- β_1 -receptor autoantibodies on I_{Ca-L} channels in the absence and presence of metoprolol

As described above, anti- β_1 -receptor autoantibodies markedly prolonged the plateau, suggesting the antibodies might enhance I_{Ca-L} . We investigated the effect in the voltage clamp mode. Basal I_{Ca-L} was recorded 5–6 min after the cell membrane rupture, when I_{Ca-L} was stable. Exposure of cells to anti- β_1 -receptors diluted at 1:80 led to a significant increase of the amplitude of I_{Ca-L} , as the time course of changes (Figure 3 A left) and the current traces of I_{Ca-L} (Figure 3 A right) illustrated. The enhancement of I_{Ca-L} was rapid, and generally 20–30 s were sufficient for the full effect of the antibodies to take place. The rapid run-down of I_{Ca-L} followed after around 1 min. In light microscopy, the clamped cells were observed contracting and deteriorating. Beyond this dilution, the potentiating effect of the antibodies on I_{Ca-L} was too large to make effective voltage control. In 5 cells, anti- β_1 -receptor autoantibodies diluted at 1:80 caused an increase of $55.87 \pm 4.39\%$ in the basal current ($P < 0.01$ vs control), and the enhancement of I_{Ca-L} was in a concentration-dependent manner (Figure 3C).

I_{Ca-L} was recorded longer in cells exposed to anti- β_1 -receptor autoantibodies diluted at 1:80 in the presence of 1 $\mu\text{mol/L}$ metoprolol than that in the absence of metoprolol, with a slight increase of $6.81 \pm 1.61\%$ ($P < 0.01$ vs anti- β_1 -receptor autoantibodies diluted at 1:80) (Figure 3B).

We also investigated the current-voltage (*I-V*) relationship by addition of anti- β_1 -receptor autoantibodies in the absence and presence of metoprolol. Without shifting the *I-V* relationship, the antibodies caused a marked increase of current densities of I_{Ca-L} , whereas in the presence of 1 $\mu\text{mol/L}$ metoprolol, a slight increase was found at positive and negative potentials (Figure 4).

Overall, these results indicated that anti- β_1 -receptor autoantibodies could enhance I_{Ca-L} as agonists for β_1 -adrenoceptors.

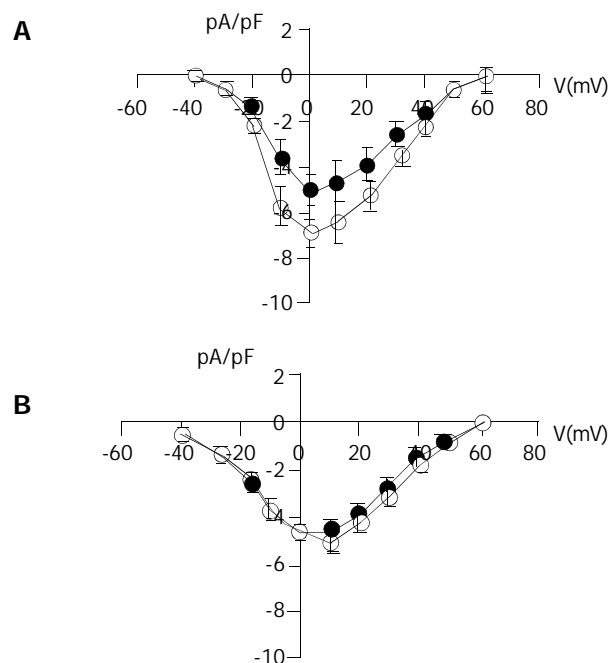


Figure 4 Effects of anti- β_1 -receptor autoantibodies diluted at 1:100 on current-voltage (*I-V*) relationships normalized to cell membrane capacitance measured in 5 cells (mean \pm SEM) during voltage steps from -40 to $+60$ mV in the absence (A) and presence of 1 $\mu\text{mol/L}$ metoprolol (B).

Cell toxicity effect

A large number of cardiac myocytes were exposed to high

concentrations (1:80 and 1:100) of anti- β_1 -receptor autoantibodies. Approximately over 90% rod-shaped cells with regular striation excluding trypan blue were turned into rounded cells highly permeable to the dye within 2 min (Figure 5).

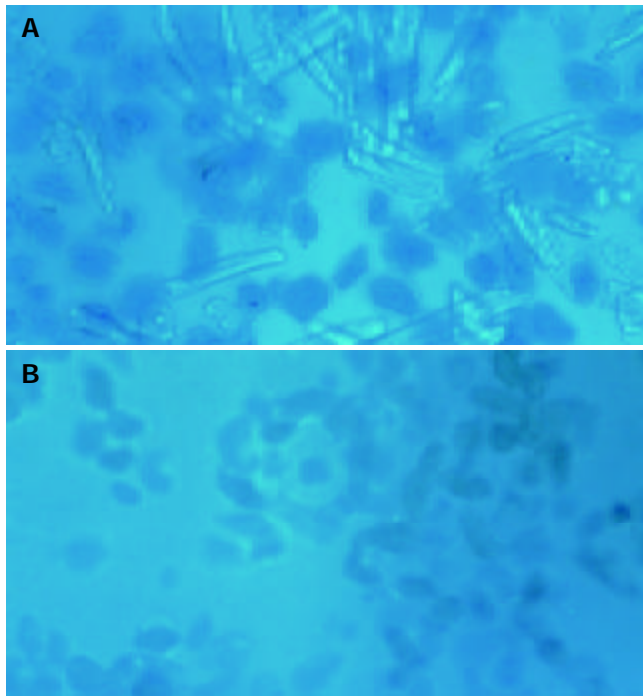


Figure 5 Cell toxicity effect of cardiac myocytes exposed to high concentrations of anti- β_1 -receptors autoantibodies. A: rod-shaped cells excluding trypan blue. B: rounded cells permeable to trypan blue.

DISCUSSION

It was documented that there was a high homology between mouse hepatitis virus and β_1 -adrenoceptors^[26]. Therefore, autoimmune response directed against β_1 -adrenoceptors can be initiated by cross reaction between these two molecules. In our clinical investigation, we found that the positive rate of hepatic virus antibodies and anti- β_1 -receptor autoantibodies was highly consistent in patients with HVM^[18]. Photomicrographs of guinea pig cardiac myocytes treated with anti- β_1 -receptor autoantibodies before and after absorbed by the peptide sequence of β_1 -adrenoceptor epitope and subsequently a fluorescently-tagged second antibody revealed the specific binding of autoantibodies in HVM to cardiac myocytes.

In heart diseases, interaction between catecholamine and β_1 -receptors could result in various arrhythmias especially tachycardia and was the main cause of sudden death^[27-29]. Based on our study, anti- β_1 -receptor autoantibodies in HVM, as isoprenaline-like agonists for β_1 -adrenoceptors were able to prolong the plateau of APD and enhance the Ca^{2+} permeability of cardiac myocytes via L-type Ca^{2+} channel, which triggers early after depolarization (EAD).

Ca^{2+} disorder was considered to be associated with myocarditis and cardiomyopathy^[30]. It was reported anti- β_1 -receptor autoantibodies in DCM could display a positive chronotropic effect on cultured neonatal rat ventricular cells without desensitization, thus increasing the metabolic pressure of myocardial cells^[31], which was further demonstrated to be mediated by $I_{\text{Ca-L}}$ ^[32]. The time-course changes of $I_{\text{Ca-L}}$ in the presence of anti- β_1 -receptor autoantibodies in HVM might reflect the process of the impairment of cardiac myocytes. About one minute after reaching the maximal peak value within 20-30s, $I_{\text{Ca-L}}$ was observed running down and accompanied by

the clamped cells contracting and deteriorating in the presence of anti- β_1 -receptor autoantibodies diluted at 1:80. Whereas $I_{\text{Ca-L}}$ was recorded longer in cells exposed to anti- β_1 -receptor autoantibodies diluted at 1:80 in the presence of 1 $\mu\text{mol/L}$ metoprolol. Furthermore, cell toxicity was observed by cell morphology and the permeability of cells to trypan blue. Rod-shaped cardiac myocytes exposed to high concentrations (1:80 and 1:100) of the antibodies were turned into rounded cells highly permeable to trypan blue. The overall influx of $I_{\text{Ca-L}}$ caused by anti- β_1 -receptor autoantibodies in HVM triggered electrophysiological and biochemical changes of cardiac myocytes and β_1 -adrenoceptor blocker (metoprolol) could inhibit these effects. These results may in fact contribute to the proper explanation of the findings in our clinical investigation. The clinical investigation indicated that myocardial injury of patients with positive anti- β_1 -receptor autoantibodies was more severe than that of patients with negative anti- β_1 -receptor autoantibodies. Some arrhythmias such as sinus tachycardia or ventricular arrhythmias were associated with anti- β_1 -receptor autoantibodies. These patients benefited from the use of β_1 -adrenoceptor blocker^[18].

In conclusion, autoantibodies against β_1 -adrenoceptors can result in arrhythmias and/or the impairment of myocardiums in HVM, which would be mediated by the enhancement of $I_{\text{Ca-L}}$. As a basic research, our investigation would help to give early diagnosis by examining the presence of autoantibodies against β_1 -adrenoceptor and beneficial treatment by properly utilizing selective β_1 -adrenoceptor blocker for hepatitis virus myocarditis.

REFERENCES

- 1 **Fleming J.** Current treatments for hepatitis. *J Infus Nurs* 2002; **25**: 379-382
- 2 **Torbenson M, Thomas DL.** Occult hepatitis B. *Lancet Infect Dis* 2002; **2**: 479-486
- 3 **Lok AS.** Hepatitis B infection: Pathogenesis and management. *J Hepatol* 2000; **32**(Suppl 1): 89-97
- 4 **Mazumdar TN.** Management of chronic hepatitis B infection: an update. *J Indian Med Assoc* 2001; **99**: 306-308
- 5 **Wisnom C, Siegel MA.** Advances in the diagnosis and management of human viral hepatitis. *Dent Clin North Am* 2003; **47**: 431-447
- 6 **Blendis L, Lurie Y, Oren R.** Occult HBV infection—both hidden and mysterious. *Gastroenterology* 2003; **125**: 1903-1905
- 7 **Matsumori A.** Symposium on clinical aspects in hepatitis virus infection. 5 Clinical practice of hepatitis: myocardial diseases, nephritis, and vasculitis associated with hepatitis virus. *Intern Med* 2001; **40**: 182-184
- 8 **Matsumori A.** Myocardial, renal, and vascular lesions caused by hepatitis viruses. *Nippon Naika Gakkai Zasshi* 2000; **89**: 1854-1859
- 9 **Watanabe H, Ono T, Muso E, Matsumori A, Sasayama S.** Hepatitis C virus infection manifesting as tubulointerstitial nephritis, cardiomyopathy, and hepatitis. *Am J Med* 2000; **109**: 176-177
- 10 **Jenny-Avital ER.** HCV-coinfection is associated with diabetes and CD4 decline. *AIDS Clin Care* 2003; **15**: 103-108
- 11 **de Leeuw N, Melchers WJ, Balk AH, de Jonge N, Galama JM.** Study on microbial persistence in end-stage idiopathic dilated cardiomyopathy. *Clin Infect Dis* 1999; **29**: 522-525
- 12 **Matsumori A.** Hepatitis C virus and cardiomyopathy. *Intern Med* 2001; **40**: 78-79
- 13 **Teragaki M, Nishiguchi S, Takeuchi K, Yoshiyama M, Akioka K, Yoshikawa J.** Prevalence of hepatitis C virus infection among patients with hypertrophic cardiomyopathy. *Heart Vessels* 2003; **18**: 167-170
- 14 **Naruse TK, Inoko H.** HLA and hepatitis C virus positive cardiomyopathy. *Nippon Rinsho* 2000; **58**: 212-217
- 15 **Sato Y, Takatsu Y, Yamada T, Kataoka K, Taniguchi R, Mimura R, Sasayama S, Matsumori A.** Interferon treatment for dilated cardiomyopathy and striated myopathy associated with hepatitis C virus infection based on serial measurements of serum concentrations of cardiac troponin T. *Jpn Circ J* 2000; **64**: 321-324

- 16 **Fagioli S**, Minniti F, Pevere S, Farinati F, Burra P, Livi U, Naccarato R, Chiaramonte M. HBV and HCV infections in heart transplant recipients. *J Heart Lung Transplant* 2001; **20**: 718-724
- 17 **Lunel F**, Cadranet JF, Rosenheim M, Dorent R, Di-Martino V, Payan C, Fretz C, Ghossein JJ, Bernard B, Dumont B, Perrin M, Gandjbachkh I, Huraux JM, Stuyver L, Opolon P. Hepatitis virus infections in heart transplant recipients: epidemiology, natural history, characteristics, and impact on survival. *Gastroenterology* 2000; **119**: 1064-1074
- 18 **Wang ZH**, Liao YH, Fu M. The frequency of occurrence of autoantibodies against beta1-adrenoceptors and its clinical relevance in patients with hepatitis virus myocarditis. *Autoimmunity* 2001; **34**: 241-245
- 19 **Wallukat G**, Nissen E, Morwinski R, Muller J. Autoantibodies against the beta- and muscarinic receptors in cardiomyopathy. *Herz* 2000; **25**: 261-266
- 20 **Mahler E**, Sepulveda P, Jeannequin O, Liegeard P, Gounon P, Wallukat G, Eftekhari P, Levin MJ, Hoebeke J, Hontebeyrie M. A monoclonal antibody against the immunodominant epitope of the ribosomal P2beta protein of *Trypanosoma cruzi* interacts with the human beta 1-adrenergic receptor. *Eur J Immunol* 2001; **31**: 2210-2216
- 21 **Mobini R**, Fu M, Wallukat G, Magnusson Y, Hjalmarson A, Hoebeke J. A monoclonal antibody directed against an autoimmune epitope on the human beta1-adrenergic receptor recognized in idiopathic dilated cardiomyopathy. *Hybridoma* 2000; **19**: 135-142
- 22 **Yuan HT**, Liao YH, Wang Z, Dong JH, Cao LS, Wang ZH, Wang JP, Fu ML. Prevention of myosin-induced autoimmune myocarditis in mice by anti-L3T4 monoclonal antibody. *Can J Physiol Pharmacol* 2003; **81**: 84-88
- 23 **National symposium on myocarditis and cardiomyopathy in Zhenjiang**. The referent standard in diagnosing adult acute viral myocarditis. *Zhonghua Xinxueguanbing Zazhi* 1999; **27**: 405-407
- 24 **Seddik SS**, Malak GA, Helmy MH. Improved purification and yield of the Egyptian snake *Cerastes cerastes* antitoxin by the use of caprylic acid. *J Nat Toxins* 2002; **11**: 323-328
- 25 **Heubach JF**, Kohler A, Wettwer E, Ravens U. T-Type and tetrodotoxin-sensitive Ca(2+) currents coexist in guinea pig ventricular myocytes and are both blocked by mibefradil. *Circ Res* 2000; **86**: 628-635
- 26 **Magnusson Y**, Hjalmarson A, Hoebeke J. β_1 -adrenoceptor autoimmunity in cardiomyopathy. *Int J Cardiol* 1996; **54**: 137-141
- 27 **Sumitomo N**, Harada K, Nagashima M, Yasuda T, Nakamura Y, Aragaki Y, Saito A, Kurosaki K, Jouo K, Koujiro M, Konishi S, Matsuoka S, Oono T, Hayakawa S, Miura M, Ushinohama H, Shibata T, Niimura I. Catecholaminergic polymorphic ventricular tachycardia: electrocardiographic characteristics and optimal therapeutic strategies to prevent sudden death. *Heart* 2003; **89**: 66-70
- 28 **Priori SG**, Napolitano C, Memmi M, Colombi B, Drago F, Gasparini M, DeSimone L, Coltorti F, Bloise R, Keegan R, Cruz Filho FE, Vignati G, Benatar A, DeLogu A. Clinical and molecular characterization of patients with catecholaminergic polymorphic ventricular tachycardia. *Circulation* 2002; **106**: 69-74
- 29 **Steinberg SF**, Alcott S, Pak E, Hu D, Protas L, Moise NS, Robinson RB, Rosen MR. Beta(1)-Receptors increase cAMP and induce abnormal Ca(i) cycling in the German shepherd sudden death model. *Am J Physiol Heart Circ Physiol* 2002; **282**: H1181-1188
- 30 **Rossner KL**, Freese KJ. Bupivacaine inhibition of L-type calcium current in ventricular cardiomyocytes of hamster. *Anesthesiology* 1997; **87**: 926-934
- 31 **Magnusson Y**, Wallukat G, Waagstein F, Hjalmarson A, Hoebeke J. Autoimmunity in idiopathic dilated cardiomyopathy. Characterization of antibodies against the beta 1-adrenoceptor with positive chronotropic effect. *Circulation* 1994; **89**: 2760-2767
- 32 **Christ T**, Wettwer E, Dobrev D, Adolph E, Knaut M, Wallukat G, Ravens U. Autoantibodies against the beta1 adrenoceptor from patients with dilated cardiomyopathy prolong action potential duration and enhance contractility in isolated cardiomyocytes. *J Mol Cell Cardiol* 2001; **33**: 1515-1525

Edited by Xu FM and Wang XL

Inhibitory effect of oxymatrine on serum hepatitis B virus DNA in HBV transgenic mice

Lun-Gen Lu, Min-De Zeng, Yi-Min Mao, Jing-Yuan Fang, Yu-Lin Song, Zhao-Hui Shen, Ai-Ping Cao

Lun-Gen Lu, Min-De Zeng, Yi-Min Mao, Jing-Yuan Fang, Yu-Lin Song, Zhao-Hui Shen, Ai-Ping Cao, Shanghai Institute of Digestive Disease, Renji Hospital, Shanghai Second Medical University, Shanghai 200001, China

Supported by the Key Project of Shanghai Medical Development Foundation, (No: 99ZDI001) and grants from 1999 Youth Liver Diseases Foundation of Chinese Liver Diseases Association

Correspondence to: Lun-Gen Lu, MD, Shanghai Institute of Digestive Disease, Renji Hospital, Shanghai Second Medical University, Shanghai 200001, China. lulungen@online.sh.cn

Telephone: +86-21-33070834 Fax: +86-21-63364118

Received: 2003-08-23 **Accepted:** 2003-10-07

Abstract

AIM: To study the inhibitory effect of oxymatrine on serum hepatitis B virus (HBV) DNA in HBV transgenic mice.

METHODS: HBV transgenic mice model was established by microinjection, and identified by HBV DNA integration and replication. Transgenic mice with replicating HBV were divided into 3 groups, and injected with normal saline (group A, $n=9$), 50 mg/kg (group B, $n=8$) and 100 mg/kg (group C, $n=9$) oxymatrine intraperitoneally once a day for 30 d, respectively. Quantitation of serum HBV DNA in HBV transgenic mice was performed by competitive polymerase chain reaction (PCR) in combination with DNA hybridization quantitative detection technique before and after treatment.

RESULTS: Compared with pre-treatment, the serum HBV DNA in group A ($F=1.04$, $P=0.9612$) and group B ($F=1.13$, $P=0.8739$) had no changes after treatment. However, in group C serum HBV DNA was significantly decreased ($F=13.97$, $P=0.0012$). The serum HBV DNA after treatment was lower in group C than in groups B and A ($F=8.65$, $P=0.0068$; $F=12.35$, $P=0.0018$; respectively). The serum HBV DNA after treatment was lower in group B than in group A, but there was no statistical significance ($F=1.43$, $P=0.652$).

CONCLUSION: Oxymatrine has inhibitory effects on serum HBV DNA in HBV transgenic mice.

Lu LG, Zeng MD, Mao YM, Fang JY, Song YL, Shen ZH, Cao AP. Inhibitory effect of oxymatrine on serum hepatitis B virus DNA in HBV transgenic mice. *World J Gastroenterol* 2004; 10(8): 1176-1179

<http://www.wjgnet.com/1007-9327/10/1176.asp>

INTRODUCTION

Hepatitis B virus (HBV) infection is a major cause of chronic hepatitis, cirrhosis, and hepatocellular cancer and accounts for 1 million deaths annually. Information on the virus load and the replicative activity of HBV is of paramount importance in the management of patients with chronic HBV infection, because of recent advances in medications which can effectively

suppress HBV replication by using nucleoside analogues, interferon and other drugs^[1-8]. Serological parameters include the levels of hepatitis B e antigen (HBeAg), DNA polymerase, HBV DNA measured by qualitative methods such as PCR or semi-quantitative dot blot hybridization, and HBV DNA quantitation by solution hybridization. The direct and quantitative nature of HBV DNA quantitation by solution hybridization makes it a useful clinical test to monitor serially the efficacy of antiviral therapy^[9-15].

The aim of chronic hepatitis B treatment is to control infectivity, eradicate the virus and prevent the development of cirrhosis. However, permanent loss of HBeAg and HBV DNA is unusual and HBsAg persistently presents. For many years, alpha interferon was the only approved therapy for chronic HBV infection in most countries around the world. Interferon is effective in only 30-40% patients. It must be given by injection and is frequently associated with fever and flu-like symptoms^[1-3]. Recently, lamivudine was approved for the treatment of chronic HBV infection in many regions of the world^[1]. Although convenient and well-tolerated, lamivudine's efficacy is similar to that of interferon and prolonged administration of lamivudine is associated with development of resistance^[6]. New agents, such as adefovir dipivoxil, offer promising effects when used either alone or in combination with lamivudine in the treatment of individuals who are 'treatment naïve' or have developed lamivudine resistance^[3,6]. Up to now, there is no specific therapy available for chronic hepatitis B. Therefore, the search continues for more efficacious treatments.

Many basic and clinical studies have revealed that oxymatrine has anti-hepatitis B virus effect, but the mechanism is unclear^[16-20]. The hosts of HBV are very scarce, and *ex vivo* culture of HBV is very difficult, thus limiting the study on HBV and its related diseases. Since 1985, a variety of HBV transgenic mice have come out in succession, providing a new approach to study the mechanism and treatment methods of HBV and its related diseases^[21-26]. Serum HBV DNA in transgenic mice was quantitated by competitive polymerase chain reaction (PCR) in combination with DNA hybridization technique in this study to assess the anti-HBV effect of oxymatrine, and to provide an important experimental basis for its clinical application.

MATERIALS AND METHODS

Plasmid P1.0 HBV was donated by Professor Xiang-Fu Wu (Institute of Biochemistry, Chinese Academy of Sciences). The complete genome (3.2 kb) of adr-type HBV was cloned at the *BamHI* site in PUC18 vector. ICR mice aged 8 wk were bought from Animal Center of Yangzhou University, raised in deparated animal rooms. Transgenic HBV mice obtained from Dr. Cheng Yong (Yangzhou University, Jiangsu Province) were used.

Detection of HBV integration in transgenic mice

Genomic DNA was extracted from the tails of HBV transgenic mice (about 1.0-1.5 cm) at age of 4 wk^[25]. The sequences of PCR primers were 5' -AGAGTCTAGACTCGTGGTGGACTT-3' and 5' -TACGAACCACTGAACAAATGGCAC-3'. The amplified segment was in the region of 470 bp HBc DNA. PCR reaction mixture containing 5 μ L 10 \times buffer (0.5 mol/L KCl, 0.1 mol/L

Tris-HCl pH8.3, 0.015 mol/L MgCl₂, 0.1 g/L glutin), 35 µL sterilized water, 5 µL 2 mmol/L dNTP, and 2 mL primers 1 and 2, was heated for 10 min at 95 °C to denature DNA. A 1 µL of Taq DNA polymerase was added to the mixture, which was overlaid with 50 µL of light mineral oil. The amplification reaction was run for 35 cycles as follows: denaturing at 93 °C for 60 s, annealing at 60 °C for 45 s, and extension at 72 °C for 1 min. A 5 µL amplification product was loaded into agarose gel for electrophoresis.

Identification of HBV expression in transgenic mice

The experimental procedures followed the instructions in the kit of Amplicor HBV monitor (Roche Diagnostic Systems, Inc.). Blood from positive HBV transgenic mice was collected and the serum was separated. Internal control was added to standard and samples. PCR was performed on HBV DNA extracted from serum. The sequences of primers were 5'-GTTGCCCGTTTGTCTCTAC-3', and 5'-biotin-GATGATGTGGTATTGGGGGC-3'. The reaction mixture was heated for 5 min at 94 °C to denature DNA, then amplification was carried out 30 cycles: denaturing at 94 °C for 30 s, annealing at 57 °C for 30 s, and extension at 72 °C for 45 s, plus a final extension at 72 °C for 5 min. The amplification product was separated by agarose gel electrophoresis, identified and quantitated by hybridization.

Quantitation by enzyme linked hybridization in microwell plate

The experiments were performed according to the instructions of the Amplicor HBV monitor kit.

The common probe (MXH2) was diluted with binding buffer. The sequence of the probe was 3'-AGCGTCCAGTCGTCGTTACAC-5' (500 nmol/L). A 50 µL of the diluted probe was added to each well in two DNA microwell plates and incubated at 37 °C for 2 h.

Pre-hybridization

The solution in the well was discarded, 50 µL wild segment capture probe diluted by 1× hybridization solution was added to each well of one plate. The sequence of the probe was 5' -TCGCAGGTCAGCAGCATGTGACATCAACTACCAGCACG-3' (500 nmol/L). Fifty µL mutation primer diluted by 1× hybridization solution was added to each well of the other plate. The sequence of the probe was 5' -GTTGCCCGTTTGTCTCTACATCACAAAGATCTACGTCGACGCAGGACCATGCAAGACCT-3' (500 nmol/L). The plate was incubated at 55 °C for 60 min, and then the solution was discarded. The plate was dried and washed twice with solution I.

Hybridization

The PCR products were diluted 10 times with distilled water, heated for 5 min at 100 °C to denature the DNA, then placed on ice immediately. One volume 2× hybridization solution was added to the product and 50 µL was added to the well. They were incubated at 48 °C for 60 min. The wells were washed three times with solution I at 48 °C for 3 min each. The solution was discarded and the plate was dried.

Signal assay

A 50 µL 1:1 000 diluted streptavidin-ALP complex was added to each well and incubated at 37 °C for 20 min. They were then washed four times for 4 min at 37 °C with solution II, dried, and

stained with the substrate (p-nitrophenol-sodium phosphate). Absorbance was read at 405 nm after 2 h.

Effect of oxymatrine on HBV transgenic mice

Twenty-six transgenic mice aged 8-12 wk (either sexes) were divided into 3 groups, and injected with normal saline (group A, *n*=9), 50 mg/kg (group B, *n*=8) and 100 mg/kg (group C, *n*=9) oxymatrine intraperitoneally once a day for 30 d, respectively. Serum HBV DNA in HBV transgenic mice was detected by competitive polymerase chain reaction (PCR) in combination with DNA hybridization quantitative detection technique before and after treatment.

Statistical analysis

All the data were analyzed by SAS software. ANOVA was used to evaluate the significance of the quantity of serum HBV DNA. *P*<0.05 was considered statistically significant.

RESULTS

HBV DNA integration and replication in transgenic mice

Among the 396 transgenic mice, 137 had HBV DNA integration (34.59%), and 26 had HBV replication in serum (6.56%).

The results of HBV DNA quantitation in transgenic mice before and after oxymatrine treatment are summarized in Table 1.

The results showed that there was no significant difference in HBV DNA quantity before treatment among the three groups. Compared with before treatment, there was no change in HBV DNA quantity in group A (*F*=1.04, *P*=0.9612). HBV DNA quantity was decreased in group B (*F*=1.13, *P*=0.8739), and was significantly decreased in group C (*F*=13.97, *P*=0.0012) after treatment. The level of HBV DNA was significantly lower in group C than in groups A (*F*=12.35, *P*=0.0018) and B (*F*=8.65, *P*=0.0068). HBV DNA quantity of group B after treatment was lower than that of group A, but there was no statistical difference (*F*=1.43, *P*=0.652).

DISCUSSION

With the advent of embryo microinjection technology, it was clear that many questions related to HBV infection might be directly examined by introduction of a partial or complete copy of HBV genome into transgenic mice. Several lines of HBV-transgenic mice have been prepared by introducing either the full HBV genome, or a partial or selected portion of HBV genome into an inbred strain of mice. The successful establishment of HBV-transgenic mice model and the expression of HBV gene products have shown that mice might be a host for the expression of HBV-related products. The characteristics of HBV infection in HBV transgenic mice have shown its potential utility as a model for study of anti-HBV drugs^[22-24,27-35]. HBV transgenic mice were generated by microinjection, our results revealed that HBV genome was integrated in the genome of mice and expressed effectively. It proved that we could obtain mice bearing complete HBV genomes. In the 396 transgenic mice, 137 had HBV DNA integration (34.59%), and 26 had HBV replication in serum (6.56%). The existence of HBV DNA in serum demonstrated that there was HBV gene replication in mice^[28,30,34,35].

Table 1 Results of HBV DNA quantitation in transgenic mice before and after oxymatrine treatment (fg/mL) (*n*, mean±SD)

Group	Group A		Group B		Group C	
Pre-treatment	9	10 933.33±5 591.06	8	12 762.5±4 891.96	9	10 164.44±5 842.93
Post-treatment	9	10 864.44±5 492.81	8	5 898.375±4 597.09	9	2 426.33±1 563.12 ^{b,d}

^b*P*<0.01 vs before treatment, ^d*P*<0.01 (vs after treatment in groups A and B).

Anti-HBV therapy of hepatitis B is still a difficult problem. Even the generally known drugs such as α -IFN and lamivudine have limitations such as low rate of HBV negativity, high price, side effects and virus variation. So it has become urgent to find new and effective anti-HBV drugs^[1-3]. Oxymatrine has been found to be a kind of alkaloid extracted from a Chinese herb *Sophora alopecuroides* L.^[20,36]. Basic and clinical researches have shown that oxymatrine has the following pharmacological effects: antiviral, protecting hepatocytes, antihepatic fibrosis, and immune regulation^[37-41]. In particular, its inhibitory effect on hepatitis B virus (HBV) has attracted wide attention in recent years. Oxymatrine has been proven to have distinct anti-virus effects in the treatment of chronic hepatitis B (CHB)^[16-20].

In vivo experiment indicated that oxymatrine could inhibit HBsAg and HBeAg secretion from HBV DNA transfected cell strain 2.2.15. In a certain range, with increased concentration and reaction time, the inhibitory rate increased gradually. Given the same concentration and reaction time, the inhibitory rate on HBsAg appeared to be higher than that on HBeAg^[42]. In an *in vivo* study on transgenic mice, the mice were injected intraperitoneally with 100 mg/kg, 200 mg/kg and 300 mg/kg oxymatrine everyday for 30 d. The amount of HBsAg and HBeAg decreased significantly compared with control group, and there was no difference among the treatment groups^[19,42]. A clinical research suggested that when oxymatrine was applied to treat chronic hepatitis B, the normalization rates of serum ALT and TB, and the negative conversion rates of serum HBsAg and HBV DNA were similar to those with alpha interferon^[42].

The amount of HBV DNA reflected the level of HBV replication directly. In this study we observed the effect of oxymatrine (50 mg/kg, 100 mg/kg) on HBV transgenic mice, and oxymatrine in both concentrations could inhibit the replication of HBV DNA. The results indicate that oxymatrine has inhibitory effects on the *in vivo* replication of HBV DNA. We still need to further explore how oxymatrine inhibits HBV DNA replication.

ACKNOWLEDGMENTS

We thank Professor Yong Cheng from Pasturag and Veterinary Institute, Yangzhou University, Jiangsu, Professor Gen-Shun Qian and Professor Shu-Guang Wan from Cancer Institute of Shanghai, Professor XiaoHui Miao and Dr. Wen-Sheng Chen from Changzheng Hospital of Shanghai, for the support and help in the experiment.

REFERENCES

- 1 **Malik AH**, Lee WM. Chronic hepatitis B virus infection: treatment strategies for the next millennium. *Ann Intern Med* 2000; **132**: 723-731
- 2 **Perrillo RP**. How will we use the new antiviral agents for hepatitis B? *Curr Gastroenterol Rep* 2002; **4**: 63-71
- 3 **Mutimer D**. Hepatitis B virus infection: resistance to antiviral agents. *J Clin Virol* 2001; **21**: 239-242
- 4 **Demirturk N**, Usluer G, Ozgunes I, Colak H, Kartal ED, Dincer S. Comparison of different treatment combinations for chronic hepatitis B infection. *J Chemother* 2002; **14**: 285-289
- 5 **Lau GK**. Hepatitis B infection in China. *Clin Liver Dis* 2001; **5**: 361-379
- 6 **Staschke KA**, Colacino JM. Drug discovery and development of antiviral agents for the treatment of chronic hepatitis B virus infection. *Prog Drug Res* 2001; Spec No: 111-183
- 7 **Yao N**, Hong Z, Lau JY. Application of structural biology tools in the study of viral hepatitis and the design of antiviral therapy. *Gastroenterology* 2002; **123**: 1350-1363
- 8 **Torresi J**, Locarnini S. Antiviral chemotherapy for the treatment of hepatitis B virus infections. *Gastroenterology* 2000; **118** (2 Suppl 1): S83-S103
- 9 **Weinberger KM**, Wiedenmann E, Bohm S, Jilg W. Sensitive and accurate quantitation of hepatitis B virus DNA using a

- kinetic fluorescence detection system (TaqMan PCR). *J Virol Methods* 2000; **85**: 75-82
- 10 **Noborg U**, Gusdal A, Pisa EK, Hedrum A, Lindh M. Automated quantitative analysis of hepatitis B virus DNA by using the Cobas Amplicor HBV monitor test. *J Clin Microbiol* 1999; **37**: 2793-2797
- 11 **Poljak M**, Marin IJ, Seme K, Brinovec V, Maticic M, Meglic-Volkar J, Lesnicar G, Vince A. Second-generation Hybrid capture test and Amplicor monitor test generate highly correlated hepatitis B virus DNA levels. *J Virol Methods* 2001; **97**: 165-169
- 12 **Marin IJ**, Poljak M, Seme K, Meglic-Volkar J, Maticic M, Lesnicar G, Brinovec V. Comparative evaluation of semiautomated COBAS AMPLICOR hepatitis B virus (HBV) monitor test and manual microwell plate-based AMPLICOR HBV MONITOR test. *J Clin Microbiol* 2001; **39**: 758-761
- 13 **Chan HL**, Leung NW, Lau TC, Wong ML, Sung JJ. Comparison of three different sensitive assays for hepatitis B virus DNA in monitoring of responses to antiviral therapy. *J Clin Microbiol* 2000; **38**: 3205-3208
- 14 **Lopez VA**, Bourne EJ, Lutz MW, Condreay LD. Assessment of the COBAS Amplicor HBV Monitor Test for quantitation of serum hepatitis B virus DNA levels. *J Clin Microbiol* 2002; **40**: 1972-1976
- 15 **Paraskevis D**, Haida C, Tassopoulos N, Raptopoulou M, Tsantoulas D, Papachristou H, Sypsa V, Hatzakis A. Development and assessment of a novel real-time PCR assay for quantitation of HBV DNA. *J Virol Methods* 2002; **103**: 201-212
- 16 **Chen YX**, Mao BY, Jiang JH. Relationship between serum load of HBV-DNA and therapeutic effect of oxymatrine in patients with chronic hepatitis B. *Zhongguo Zhongxiyi Jiehe Zazhi* 2002; **22**: 335-336
- 17 **Dong Y**, Xi H, Yu Y, Wang Q, Jiang K, Li L. Effects of oxymatrine on the serum levels of T helper cell 1 and 2 cytokines and the expression of the S gene in hepatitis B virus S gene transgenic mice: a study on the anti-hepatitis B virus mechanism of oxymatrine. *J Gastroenterol Hepatol* 2002; **17**: 1299-1306
- 18 **Yu YY**, Wang QH, Zhu LM, Zhang QB, Xu DZ, Guo YB, Wang CQ, Guo SH, Zhou XQ, Zhang LX. A clinical research on oxymatrine for the treatment of chronic hepatitis B. *Zhonghua Ganzhangbing Zazhi* 2002; **10**: 280-281
- 19 **Chen XS**, Wang GJ, Cai X, Yu HY, Hu YP. Inhibition of hepatitis B virus by oxymatrine *in vivo*. *World J Gastroenterol* 2001; **7**: 49-52
- 20 **Wang BE**. Treatment of chronic liver diseases with traditional Chinese medicine. *J Gastroenterol Hepatol* 2000; **15**(Suppl): E67-E70
- 21 **Singh M**, Kumar V. Transgenic mouse models of hepatitis B virus-associated hepatocellular carcinoma. *Rev Med Virol* 2003; **13**: 243-253
- 22 **Araki K**, Miyazaki J, Hino O, Tomita N, Chisaka O, Matsubara K, Yamamura K. Expression and replication of hepatitis B virus genome in transgenic mice. *Proc Natl Acad Sci U S A* 1989; **86**: 207-211
- 23 **Chisari FV**, Pinkert CA, Milich DR, Filippi P, McLachlan A, Palmiter RD, Brinster RL. A transgenic mouse model of the chronic hepatitis B surface antigen carrier state. *Science* 1985; **230**: 1157-1160
- 24 **Choo KB**, Liew LN, Chong KY, Lu RH, Cheng WT. Transgenome transcription and replication in the liver and extrahepatic tissues of a human hepatitis B virus transgenic mouse. *Virology* 1991; **182**: 785-792
- 25 **Zhu HZ**, Cheng GX, Chen JQ, Kuang SY, Cheng Y, Zhang XL, Li HD, Xu SF, Shi JQ, Qian GS, Gu JR. Preliminary study on the production of transgenic mice harboring hepatitis B virus X gene. *World J Gastroenterol* 1998; **4**: 536-539
- 26 **Akbar SK**, Onji M. Hepatitis B virus (HBV)-transgenic mice as an investigative tool to study immunopathology during HBV infection. *Int J Exp Pathol* 1998; **79**: 279-291
- 27 **Guidotti LG**, Morris A, Mendez H, Koch R, Silverman RH, Williams BR, Chisari FV. Interferon-regulated pathways that control hepatitis B virus replication in transgenic mice. *J Virol* 2002; **76**: 2617-2621
- 28 **Morrey JD**, Korba BE, Sidwell RW. Transgenic mice as a chemotherapeutic model for hepatitis B virus infection. *Antivir Ther* 1998; **3**(Suppl 3): 59-68

- 29 **Julander JG**, Sidwell RW, Morrey JD. Characterizing antiviral activity of adefovir dipivoxil in transgenic mice expressing hepatitis B virus. *Antiviral Res* 2002; **55**: 27-40
- 30 **Weber O**, Schlemmer KH, Hartmann E, Hagelschuer I, Paessens A, Graef E, Deres K, Goldmann S, Niewoehner U, Stoltefuss J, Haebich D, Ruebsamen-Waigmann H, Wohlfeil S. Inhibition of human hepatitis B virus (HBV) by a novel non-nucleosidic compound in a transgenic mouse model. *Antiviral Res* 2002; **54**: 69-78
- 31 **Hu YP**, Hu WJ, Zheng WC, Li JX, Dai DS, Wang XM, Zhang SZ, Yu HY, Sun W, Hao GR. Establishment of transgenic mouse harboring hepatitis B virus (adr subtype) genomes. *World J Gastroenterol* 2001; **7**: 111-114
- 32 **Larkin J**, Clayton MM, Liu J, Feitelson MA. Chronic ethanol consumption stimulates hepatitis B virus gene expression and replication in transgenic mice. *Hepatology* 2001; **34** (4 Pt 1): 792-797
- 33 **Xu Z**, Yen TS, Wu L, Madden CR, Tan W, Slagle BL, Ou JH. Enhancement of hepatitis B virus replication by its X protein in transgenic mice. *J Virol* 2002; **76**: 2579-2584
- 34 **Larkin J**, Clayton M, Sun B, Perchonock CE, Morgan JL, Siracusa LD, Michaels FH, Feitelson MA. Hepatitis B virus transgenic mouse model of chronic liver disease. *Nat Med* 1999; **5**: 907-912
- 35 **Kajino K**, Kamiya N, Yuasa S, Takahara T, Sakurai J, Yamamura K, Hino O. Evaluation of anti-hepatitis B virus (HBV) drugs using the HBV transgenic mouse: application of the semiquantitative polymerase chain reaction (PCR) for serum HBV DNA to monitor the drug efficacy. *Biochem Biophys Res Commun* 1997; **241**: 43-48
- 36 **Yamazaki M**. The pharmacological studies on matrine and oxymatrine. *Yakugaku Zasshi* 2000; **120**: 1025-1033
- 37 **Li J**, Li C, Zeng M. Preliminary study on therapeutic effect of oxymatrine in treating patients with chronic hepatitis C. *Zhongguo Zhongxiyi Jiehe Zazhi* 1998; **18**: 227-229
- 38 **Chen Y**, Li J, Zeng M, Lu L, Qu D, Mao Y, Fan Z, Hua J. The inhibitory effect of oxymatrine on hepatitis C virus *in vitro*. *Zhonghua Ganzangbing Zazhi* 2001; **9**(Suppl): 12-14
- 39 **Yang W**, Zeng M, Fan Z, Mao Y, Song Y, Jia Y, Lu L, Chen CW, Peng YS, Zhu HY. Prophylactic and therapeutic effect of oxymatrine on D-galactosamine-induced rat liver fibrosis. *Zhonghua Ganzangbing Zazhi* 2002; **10**: 193-196
- 40 **Xiang X**, Wang G, Cai X, Li Y. Effect of oxymatrine on murine fulminant hepatitis and hepatocyte apoptosis. *Chin Med J* 2002; **115**: 593-596
- 41 **Liu J**, Manheimer E, Tsutani K, Gluud C. Medicinal herbs for hepatitis C virus infection: a Cochrane hepatobiliary systematic review of randomized trials. *Am J Gastroenterol* 2003; **98**: 538-544
- 42 **Zeng Z**, Wang GJ, Si CW. Basic and clinical study of oxymatrine on HBV infection. *J Gastroenterol Hepatol* 1999; **14** (Suppl): A295-A297

Edited by Bo XN and Wang XL **Proofread by** Xu FM

Impact of *Helicobacter pylori* infection on histological changes in non-erosive reflux disease

Anthie Gatopoulou, Konstantinos Mimidis, Alexandra Giatromanolaki, Alexandros Polichronidis, Nikolaos Lirantzopoulos, Efthimios Sivridis, George Minopoulos

Anthie Gatopoulou, Konstantinos Mimidis, George Minopoulos, Endoscopy Unit, Democritus University of Thrace, Alexandroupolis, Greece

Konstantinos Mimidis, First Department of Internal Medicine, Democritus University of Thrace, Alexandroupolis, Greece

Efthimios Sivridis, Alexandra Giatromanolaki, Department of Pathology, Democritus University of Thrace, Alexandroupolis, Greece

Alexandros Polichronidis, Second Department of Surgery, Democritus University of Thrace, Alexandroupolis, Greece

Nikolaos Lirantzopoulos, George Minopoulos, First Department of Surgery, Democritus University of Thrace, Alexandroupolis, Greece

Correspondence to: Konstantinos Mimidis MD, Gastroenterologist, Lecturer in Internal Medicine, Chrisostomou Smirnis 8, 68100 Alexandroupolis, Greece. kmimidis@otenet.gr

Telephone: +3-2551074090 **Fax:** +3-2551030450

Received: 2003-09-15 **Accepted:** 2003-11-06

Gatopoulou A, Mimidis K, Giatromanolaki A, Polichronidis A, Lirantzopoulos N, Sivridis E, Minopoulos G. Impact of *Helicobacter pylori* infection on histological changes in non-erosive reflux disease. *World J Gastroenterol* 2004; 10(8): 1180-1182

<http://www.wjgnet.com/1007-9327/10/1180.asp>

INTRODUCTION

Helicobacter pylori (*H pylori*) is a prevalent pathogenetic factor associated with ulceration, dyspepsia, and adenocarcinoma^[1,2]. The role of *H pylori* in gastroesophageal reflux disease (GORD) has only recently received attention, with the evidence for an association between *H pylori* and GORD remaining uncertain^[3]. Diminution of peptic ulcer disease and adenocarcinoma of the distal stomach have paralleled the decreasing prevalence of *H pylori* infections in the developed world. At the same time, there has been an increase in GORD, Barrett's esophagus, and adenocarcinoma of the distal esophagus and proximal stomach, suggesting that *H pylori* protects against these esophageal diseases^[4,5].

Adequate assessment of reflux esophagitis has proved difficult to be assessed by endoscopy only, as the endoscopic appearance of the esophageal mucosa may be normal despite the presence of reflux symptoms^[6,7]. Non-erosive gastroesophageal reflux disease (NERD) is the most common diagnosis in patients with reflux symptoms when organic diseases such as ulcers, esophageal erosions, and carcinomas, have been excluded by esophagogastroduodenoscopy^[8].

Histological abnormalities have been described in GORD^[6,8-11], and hence it seems reasonable to diagnose non-erosive reflux disease by simple esophageal biopsies during endoscopy. These mild histological findings are mainly basal zone thickening, elongated papillae, alterations in intracellular glycogen content, infiltration with neutrophils, eosinophils and T-lymphocytes, and submucosal blood vessel dilatation^[6,8,9]. However, the available data on the diagnostic value of these histological criteria are contradictory^[9]. This study therefore evaluated prospectively the histological findings and the impact of *H pylori* infection in a group of symptomatic patients with erosive and non-erosive reflux disease.

MATERIALS AND METHODS

Patients

Fifty patients (29 men, 21 women; mean age 49.9 years) were evaluated prospectively in our endoscopic unit for symptoms compatible with GORD, namely heartburn, acid regurgitation, and/or epigastric pain. A standardized questionnaire was completed for each patient during an interview with an experienced gastroenterologist. Demographic details of the GORD patients were recorded, including age, sex, smoking and drinking habits, tea and coffee consumption, and concurrent medical conditions including hypertension and diabetes mellitus. None of the patients included in this study had a

Abstract

AIM: The evidence for an association between *Helicobacter pylori* (*H pylori*) and gastroesophageal reflux disease, either in non-erosive (NERD) or erosive esophagitis (ERD) remains uncertain. The available data on the histological changes in NERD and the effect on *H pylori* infection on them are elusive. The aim of this study therefore was to prospectively evaluate the histological findings and the impact of *H pylori* infection on a group of symptomatic patients with NERD.

METHODS: Fifty consecutive patients were prospectively evaluated for symptoms compatible with GORD. In all cases, routine endoscopy and lugol directed biopsies were performed and assessed histologically in a blinded manner.

RESULTS: The overall prevalence of *H pylori* infection was 70%. Twenty-nine patients out of 50 (58%) were NERD patients. No statistical significance was observed between the *H pylori* status and NERD. The remaining 21 (42%) were diagnosed as follows: 13 (26%), 6 (12%), 2(4%) with esophagitis grade A, B and C respectively. A statistically significant correlation was observed between the *H pylori*+ and esophagitis grade A, as well as between *H pylori*- and grade B. Biopsies from 2 patients were not included because of insufficient materials. Histologically, a basal zone hyperplasia was found in 47 (97.91%) patients, alterations of glycogen content in 47 (97.91%), papillae elongation in 33 (68.75%), blood vessels dilatation in 35(72.91%), chronic inflammation in 21 (43.75%), infiltration with eosinophils, neutrophils and T-lymphocytes in 4 (8.33%), 6 (12.5%) and 39 (81.25%) respectively. No correlation was observed between the *H pylori* status and the histological parameters studied either in NERD or GERD.

CONCLUSION: Histological assessment can not differentiate symptomatic patients with erosive versus non-erosive reflux disease. Moreover, *H pylori* infection may not act as an important factor in patients with NERD.

current or past history of peptic ulcer disease, previous gastric surgery or anti-*Helicobacter* therapy, or use of proton pump inhibitors, NSAIDs, steroids, or tetracycline during the past 4 wk. Ethics approval was obtained from the Ethics Committee of the University Hospital of Alexandroupolis, and patients gave their informed signed consent for biopsy specimens to be taken.

Methods

A routine endoscopy was performed by the same endoscopist on all patients using an (GIF-Q145) Olympus flexible endoscope. The distance between the esophagogastric junction and the incisor teeth was recorded. Reflux esophagitis was graded in accordance with the Los Angeles classification^[12]. *H pylori* status was determined by the rapid urease test and histological examination of biopsies taken from the antrum and the corpus^[13,14].

At least 4 biopsy specimens were taken 3 cm above the lower esophageal sphincter with Olympus biopsy forceps in a cross-fashion manner. In order to improve endoscopic visualization and provide biopsy orientation, 20 mL of 20 mg/L potassium iodine's solution (Lugol) was applied through a "spray" catheter^[15-17]. To obtain sufficient material and to ensure an almost vertical pinch biopsy specimen, the opened forceps were withdrawn towards the tip of the scope, which was bent towards maximally, and hence the forceps were pressed vertically against the esophageal wall. Specimens were fixed in 40 g/L formaldehyde^[8]. When all sections had been selected they were assessed histologically in a blinded manner (without endoscopic or clinical information). A standardized report completed by the histopathologist comprised an evaluation of the following histological parameters: basal zone hyperplasia, papillary length, dilatation of intraepithelial blood vessels, and semiquantitative cellular infiltration with T-lymphocytes, neutrophils, eosinophils. Alterations of glycogen content, erosion, ulceration and chronic inflammation were also assessed^[6,8-11].

Statistical analysis

Statistical analysis was performed using SPSS (version 11.0 for Windows) on data from all 50 patients. The analysis was based on demographic characteristics, such as age, sex, and presence of *H pylori* infection, as well as endoscopic and histological findings. Differences in the distribution of the variables of interest between subgroups of patients were examined by Pearson chi-square test or Fisher's exact test (the latter when small frequencies were present). Comparison between proportions in 2 independent groups was performed with the z-test statistic. *P*-values less than 0.05 were considered significant.

RESULTS

The relationship between endoscopic findings and the presence (*H pylori*+) or absence (*H pylori*-) of *H pylori* infection is shown in Figure 1.

The overall prevalence of *H pylori*+ was 70% (35 out of 50 patients). A normal appearance of esophageal mucosa (non-

erosive esophagitis) was observed in 29 out of 50 (58%) patients. No statistical significance was observed between *H pylori*+ and NERD patients [*H pylori*+ in 20 out of 35 (57.1%) vs *H pylori*- in 9 out of 15 (60%) patients *P*>0.05]. The remaining 21 (42%) patients with erosive esophagitis were diagnosed as follows: 13 (26%), 6 (12%) and 2 (4%) with esophagitis grades A, B and C respectively. None of the patients in our series suffered from esophagitis grade D. A statistically significant correlation was observed between the *H pylori*+ and esophagitis grade A [*H pylori*+ in 11 out of 35 (31.4%) vs *H pylori*- in 2 out of 15 (13.3%) patients, *P*<0.05]. Similarly, a statistical difference was observed in the group of patients with esophagitis grade B [*H pylori*+ in 2 out of 35 (5.7%) vs *H pylori*- in 4 out of 15 (26.7%) patients, *P*<0.05].

Figure 2 summarizes the distribution of patients according to biopsy findings and the existence of *H pylori*. Biopsies from 2 patients were not included because of insufficient materials. No difference was observed between the 2 variables of interest. As expected, the majority of patients examined (46 of 48, 95.8%) were diagnosed histologically as having esophagitis, despite the esophageal mucosa appearing normal under endoscopy.

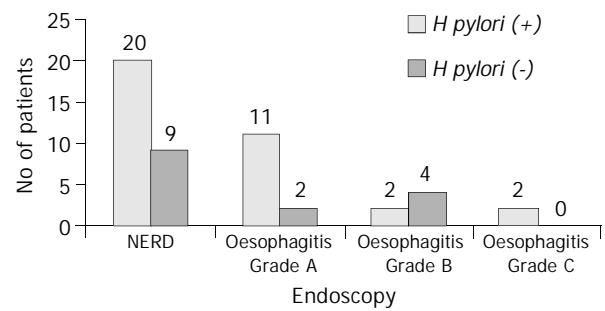


Figure 1 Findings at endoscopy. Note: *H pylori* (+): *Helicobacter pylori* positive patients; *H pylori* (-): *Helicobacter pylori* negative patients.

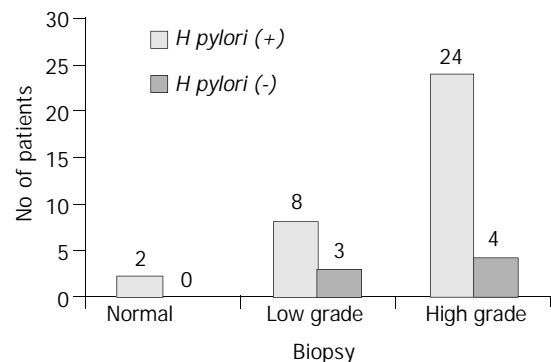


Figure 2 Findings at biopsy. *H pylori* (+): *Helicobacter pylori* positive patients, *H pylori* (-): *Helicobacter pylori* negative patients.

Table 1 Correlation of *H pylori* infection with the histological parameters esophagitis in NERD and GERD

Histological parameters	Total (n) of patients	NERD		ERD		<i>P</i>
		Patients (n) (%)	<i>H pylori</i> (+) (%)	Patients (n) (%)	<i>H pylori</i> (+) (%)	
Basal zone hyperplasia	47	28 (59.6)	19 (67.9)	19 (40.4)	14 (73.7)	0.462
Loss of glycogen	47	28 (59.6)	19 (67.9)	19 (40.4)	14 (73.7)	0.462
Papillae elongation	33	18 (54.4)	11 (61.1)	15 (45.6)	11 (73.3)	0.357
Blood vessels dilatation	35	20 (57.1)	15 (75.0)	15 (42.9)	12 (80.0)	0.527
Oesinophils infiltration	4	2 (50.0)	1 (50.0)	2 (50.0)	2 (100.0)	0.500
Neutrophils infiltration	6	2 (33.3)	1 (50.0)	4 (66.7)	3 (75.0)	0.600
T-lymphocytes infiltration	39	24 (61.5)	17 (70.8)	15 (38.5)	11 (73.3)	0.582
Chronic inflammation	21	13 (61.9)	10 (76.9)	8 (38.1)	5 (62.5)	0.410

Finally, Table 1 outlines the histological parameters of esophagitis with the presence or absence of erosions during endoscopy. We focused on patients with *H pylori* infection. No statistically significant difference was observed between *H pylori* (+) patients with erosive (ERD) and non-erosive esophagitis (NERD) for any of the histological parameters examined (*P* values refer to the numbers in italics).

DISCUSSION

This study investigated the impact of *H pylori* infection on the histological changes of non-erosive esophagitis. Our study was performed prospectively in a series of 50 patients with reflux symptoms. Esophageal erosions were found during endoscopy in 21 of these patients. The overall prevalence of *H pylori*+ was 70% (erosive: 15/21, 71.5%; non-erosive: 20/29, 68.9%). As expected, histological changes were noted in the majority of biopsies (95.8%) despite a normal appearance of esophageal mucosa under endoscopy in half of the cases.

In the group of patients with erosive esophagitis, *H pylori*+ was correlated with grade A esophagitis, whereas *H pylori*- was correlated with grade B disease. This probably indicates that *H pylori*- is a risk factor for ERD and aggravates the endoscopic appearance. This finding of a close association between *H pylori*+ and less serious endoscopic findings is consistent with other studies^[14,18-21]. Some studies have found an inverse relation between *H pylori* and esophagitis, once *H pylori* has been eradicated^[22,23]. In our series no patient had previously received eradication therapy. Furthermore, we confirmed previous findings that *H pylori* infection was not associated with positive or negative esophagitis findings in biopsies^[24,25].

In the second group of patients (those with non-erosive esophagitis), no correlation was observed between the *H pylori*+ and the histological parameters studied. Little is known about the relationship between *H pylori* infection and the histological variables in non-erosive esophagitis. The fact that there appears to be no correlation between the *H pylori*+ and any of the aforementioned mild changes probably implies that these are provoked by mechanisms other than *H pylori* infection^[26,27] (perhaps acid or bile reflux).

In conclusion, *H pylori* probably plays a statistically unimportant role in the histological changes seen in patients with non-erosive reflux disease, since similar histological alterations were detected in biopsies of both erosive and non-erosive esophagitis. Further research is required to identify other pathogenetic factors responsible for the histological parameters found in this group of patients.

REFERENCES

- 1 **Marshall BJ**, Warren JR. Unidentified curved bacilli in the stomach of patients with gastritis and peptic ulceration. *Lancet* 1984; **1**: 1311-1315
- 2 **Forman D**, Newell DG, Fullerton F, Yarnell JW, Stacey AR, Wald N, Sitas F. Association between infection with *Helicobacter pylori* and risk of gastric cancer: evidence from a prospective investigation. *BMJ* 1991; **302**: 1302-1305
- 3 **Raghunath A**, Hungin AP, Wooff D, Childs S. Prevalence of *Helicobacter pylori* in patients with gastroesophageal reflux disease: systematic review. *BMJ* 2003; **326**: 737-739
- 4 **El-Serag HB**, Sonnenberg A. Opposing time trends of peptic ulcer and reflux disease. *Gut* 1998; **43**: 327-333
- 5 **Pera M**, Cameron AJ, Trastek VF, Carpenter HA, Zinsmeister AR. Increasing incidence of adenocarcinoma of the esophagus and esophagogastric junction. *Gastroenterology* 1993; **104**: 510-513
- 6 **Riddell RH**. What mucosal biopsies have to offer. *Aliment Pharmacol Ther* 1997; **11**(Suppl 2): 19-25
- 7 **Wilkinson SP**. The limits of endoscopy in the diagnosis of oesophagitis, gastritis and duodenitis. *Aliment Pharmacol Ther* 1997; **11**(Suppl 2): 13-17
- 8 **Schindlbeck NE**, Wiebecke B, Klauser AG, Voderholzer WA, Muller-Lissner SA. Diagnostic value of histology in non-erosive gastroesophageal reflux disease. *Gut* 1996; **39**: 151-154
- 9 **Riddell RH**. The biopsy diagnosis of gastroesophageal reflux disease, Barrett oesophagus and sequelae of therapy. *Am J Surg Pathol* 1996; **20**: 31-51
- 10 **Richter JE**, Castell DO. Gastroesophageal reflux: pathogenesis, diagnosis and therapy. *Ann Intern Med* 1982; **97**: 93-103
- 11 **Frierson HF**. Histology in the diagnosis of reflux esophagitis. *Gastroenterol Clin North Am* 1990; **19**: 631-644
- 12 **Dent J**, Brun J, Fendrick AM, Fennerty MB, Janssens J, Kahrilas PJ, Lauritsen K, Reynolds JC, Shaw M, Talley NJ. An evidence-based appraisal of reflux disease management-The Genval Workshop Report. *Gut* 1999; **44**(Suppl 2): S1-16
- 13 **Unge P**. Assessment and significance of *Helicobacter pylori* infection. *Aliment Pharmacol Ther* 1997; **11**(Suppl 2): 33-39
- 14 **Wu JC**, Sung JJ, Chan FK, Ching JY, Ng AC, Go MY, Wong SK, Ng EK, Chung SC. *Helicobacter pylori* infection is associated with milder gastro-oesophageal reflux disease. *Aliment Pharmacol Ther* 2000; **14**: 427-432
- 15 **Rajan E**, Burgart JL, Gostout JC. Endoscopic and histologic diagnosis of Barrett esophagus. *Mayo Clin Proc* 2001; **76**: 217-225
- 16 **Tincani AJ**, Brandalise N, Altmani A, Scanavini RC, Valerio JB, Lage HT, Molina G, Martins AS. Diagnosis of superficial esophageal cancer and dysplasia using endoscopic screening with 2% Lugol dye solution in patients with head and neck cancer. *Head Neck* 2000; **22**: 170-174
- 17 **Canto MI**. Vital staining in Barrett's esophagus. *Gastrointest Endosc* 1999; **49**: 12-16
- 18 **Manes G**, Pieramico O, Uomo G, Mosca S, de Nucci C, Balzano A. Relationship of sliding hiatus hernia to gastroesophageal reflux disease: a possible role for *Helicobacter pylori* infection? *Dig Dis Sci* 2003; **48**: 303-307
- 19 **Vicari JJ**, Peek RM, Falk GM, Goldblum JR, Easley KA, Schnell J, Perez-Perez GI, Halter SA, Rice TW, Blaser MJ, Richter JE. The seroprevalence of CagA positive *Helicobacter pylori* strains in the spectrum of gastroesophageal reflux disease. *Gastroenterology* 1998; **115**: 50-57
- 20 **Haruma K**, Hamada H, Mihara M, Kamada T, Yoshira M, Sumii K, Kajiyama G, Kawanishi M. Negative association between *Helicobacter pylori* infection and reflux esophagitis in older patients, case control study in Japan. *Helicobacter* 2000; **5**: 24-29
- 21 **Manes G**, Mosca S, Laccetti M, Lioniello M, Balzano A. *Helicobacter pylori* infection, pattern of gastritis and symptoms in erosive and non-erosive gastroesophageal reflux disease. *Scand J Gastroenterol* 1999; **34**: 658-662
- 22 **Sharma P**. *Helicobacter pylori*: a debated factor in gastroesophageal reflux disease. *Dig Dis* 2000; **19**: 127-133
- 23 **Labenz J**, Blum AL, Bayerdorffer E, Meining A, Stolte M, Borsch G. Curing *Helicobacter Pylori* infection in patients with duodenal ulcer may provoke reflux esophagitis. *Gastroenterology* 1997; **112**: 1442-1447
- 24 **Villani L**, Trespi E, Fiocca R, Broglia F, Colla C, Luinetti O, Tinelli C, Solcia E. Analysis of gastroduodenitis and oesophagitis in relation to dyspeptic/ reflux symptoms. *Digestion* 1998; **59**: 91-101
- 25 **Pilotto A**, Franceschi M, Leandro G, Rasso M, Bozzola L, Valerio G, Di Mario F. Influence of *Helicobacter pylori* infection on severity of oesophagitis and response to therapy in the elderly. *Dig Liver Dis* 2002; **34**: 328-331
- 26 **Quigley EM**. New developments in the pathophysiology of gastro-oesophageal reflux disease (GERD): implications for patient management. *Aliment Pharmacol Ther* 2003; **17**: 43-51
- 27 **Pace F**, Porro GB. Gastroesophageal reflux and *Helicobacter pylori*: a review. *World J Gastroenterol* 2000; **6**: 311-314

Construction of prokaryotic expression system of 2 148-bp fragment from *cagA* gene and detection of *cagA* gene, CagA protein in *Helicobacter pylori* isolates and its antibody in sera of patients

Jie Yan, Yuan Wang, Shi-He Shao, Ya-Fei Mao, Hua-Wen Li, Yi-Hui Luo

Jie Yan, Ya-Fei Mao, Hua-Wen Li, Yi-Hui Luo, Department of Medical Microbiology and Parasitology, Medical College, Zhejiang University, Hangzhou 310031, Zhejiang Province, China

Yuan Wang, Shi-He Shao, Faculty of Laboratory Medicine, Northern University, Jilin 132001, Jilin Province, China

Supported by the Outstanding Young Teacher Fund of Education Ministry of China and the General Research Plan of Zhejiang Provincial Science and Technology Commission, No. 001110438

Correspondence to: Jie Yan, Department of Medical Microbiology and Parasitology, Medical College, Zhejiang University, Hangzhou 310031, Zhejiang Province, China. yanchen@mail.hz.zj.cn

Telephone: +86-571-87217385 **Fax:** +86-571-87217044

Received: 2003-10-24 **Accepted:** 2003-12-16

Abstract

AIM: To construct a prokaryotic expression system of a *Helicobacter pylori* (*H pylori*) *cagA* gene fragment and establish enzyme-linked immunosorbent assays (ELISA) for detecting CagA and its antibody, so as to understand the manner in which the infection of CagA-expressing *H pylori* (CagA⁺ *H pylori*) isolates cause diseases.

METHODS: *H pylori* strains in gastric biopsy specimens from 156 patients with positive results in rapid urease test were isolated. PCR was used to detect the frequency of *cagA* gene in the 109 *H pylori* isolates and to amplify a 2 148-bp fragment (*cagA1*) of *cagA* gene from a clinical strain Y06. A prokaryotic expression system of *cagA1* gene was constructed, and the expression of the target recombinant protein (rCagA1) was examined by SDS-PAGE. Western blotting and immunodiffusion assay were employed to determine the immunoreactivity and antigenicity of rCagA1, respectively. Two ELISAs were established to detect CagA expression in 109 *H pylori* isolates and the presence of CagA antibody in the corresponding patients' sera, and the correlations between infection with CagA⁺ *H pylori* and gastritis as well as peptic ulcer were analyzed.

RESULTS: Of all the clinical specimens obtained, 80.8% (126/156) were found to have *H pylori* isolates and 97.2% of the isolates (106/109) were positive for *cagA* gene. In comparison with the reported data, the cloned *cagA1* fragment possessed 94.83% and 93.30% homologies with the nucleotide and putative amino acid sequences, respectively. The output of rCagA1 produced by the constructed recombinant prokaryotic expression system was approximately 30% of the total bacterial protein. rCagA1 was able to bind to the commercial antibody against the whole-cells of *H pylori* and to induce the immunized rabbits to produce antibody with an immunodiffusion titer of 1:4. A proportion as high as 92.6% of the *H pylori* isolates (101/109) expressed CagA and 88.1% of the patients' serum samples (96/109) were CagA antibody-positive. The percentage of

CagA⁺ *H pylori* strains (97.9%) isolated from the biopsy specimens of peptic ulcer appeared to be higher than that from gastritis (88.5%), but the difference was not statistically significant ($\chi^2=3.48$, $P>0.05$).

CONCLUSION: rCagA1 produced by the prokaryotic expression system constructed in this study possesses good immunoreactivity and antigenicity, and the established ELISAs can be used to detect CagA of *H pylori* and its antibody. *H pylori* isolates show high frequencies of *cagA* gene and CagA expression, but the infections by CagA⁺ *H pylori* strains are not the most decisive factors to cause gastric diseases.

Yan J, Wang Y, Shao SH, Mao YF, Li HW, Luo YH. Construction of prokaryotic expression system of 2 148-bp fragment from *cagA* gene and detection of *cagA* gene, CagA protein in *Helicobacter pylori* isolates and its antibody in sera of patients. *World J Gastroenterol* 2004; 10(8): 1183-1190

<http://www.wjgnet.com/1007-9327/10/1183.asp>

INTRODUCTION

In China, gastritis and peptic ulcer are the most prevalent gastric diseases, and gastric cancer remains one of the most devastating malignant tumors with the highest morbidity^[1-20]. *Helicobacter pylori* (*H pylori*) has been recognized as a human-specific gastric pathogen that colonizes in the stomach of at least half of the world's populations^[21, 22]. Most infected individuals are asymptomatic, whereas in some cases, the infection causes acute, chronic gastritis or peptic ulceration, and plays an important role in the development of peptic ulcer and gastric adenocarcinoma, mucosa-associated lymphoid tissue (MALT) lymphoma and primary gastric non-Hodgkin's lymphoma^[23-28].

So far, no evidence for the toxicity of the protein (CagA) expressed by cytotoxin-associated gene A (*cagA*) of *H pylori* has been presented^[29, 30]. However, previous studies demonstrated that CagA was closely associated with the pathogenicity of *H pylori* and severity of *H pylori*-related diseases^[29-32]. Many epidemiological data indicated that the positive rate of *cagA* gene was significantly higher in the *H pylori* strains isolated from patients with peptic ulcer than in those with gastritis^[33]. Patients infected with *cagA*⁺ *H pylori* had a higher risk of developing gastric cancers than those infected with *cagA*⁻ strains^[34, 35]. Approximately 60% to 70% of *H pylori* strains isolated from European and North American populations carried *cagA* gene^[36-38], whereas over 90% of the isolates from Asia-Pacific populations were *cagA* gene-positive^[39-42]. Strong antigenicity of CagA usually induces antibody in patients with *cagA*⁺ *H pylori* infection and this antibody has been considered as a possible specific clinical indicator of *H pylori* infection^[43-45]. However, the data are scarce concerning the correlations between the presence of *cagA*, CagA expression and antibody production, CagA⁺ *H pylori* infection and types

of the resultant gastric diseases.

In the present study, a recombinant expression plasmid containing a relatively conserved *H pylori cagA* gene fragment 2 148 bp in length (*cagA1*) was constructed. *H pylori* strains in gastric biopsy specimens from patients with gastritis or peptic ulcer were isolated. The frequencies of *cagA* gene and expressions of *H pylori* isolates and CagA antibody in patients' sera were investigated. Furthermore, the correlations among CagA⁺ *H pylori* infection and types of the resulted gastric diseases were also analyzed for the purpose of understanding the pathogenic effect of CagA and the potential of CagA antibody detection in clinical diagnosis of *H pylori* infection.

MATERIALS AND METHODS

Materials

A typical *H pylori* strain named Y06 isolated clinically was used to amplify *cagA1* fragment. Primers for PCR amplification were synthesized by BioAsia (Shanghai, China). *Taq*-plus high fidelity PCR kit and restriction endonucleases were purchased from TaKaRa (Dalian, China). T-A cloning kit and sequencing service were provided by BBST (Shanghai, China). Plasmid *pET32a* as the expression vector and *E.coli* BL21DE3 as the host cell were purchased from Novagen (Novagen, Madison, USA). Rabbit antiserum against the whole cell of *H pylori*, HRP-labeling sheep antisera against rabbit IgG and human IgG were purchased from DAKO (Glostrup, Denmark) and Jackson ImmunoResearch (West Grove, USA), respectively. Agents used for isolation and identification of *H pylori* were purchased from BioMérieux (Marcy l'Étoile, France).

Gastric biopsy specimens with positive urease for *H pylori* isolation and serum samples for CagA antibody detection were collected from 156 patients in 4 hospitals in Hangzhou during Nov. 2001 to Feb. 2003. None of the patients had received nonsteroidal anti-inflammatory drugs, antacids or antibiotics within two weeks prior to the study. From the 156 patients, 126 biopsy specimens of *H pylori* isolates were obtained and 109 of the isolates survived after -70 °C storage. In the 109 patients (including 76 males and 33 females, with a mean age of 40.2 years), 61 patients suffered from chronic gastritis (41 chronic superficial gastritis, 10 chronic active gastritis, 10 chronic atrophy gastritis), and 48 had gastroduodenal ulcer (12 gastric ulcer, 30 duodenal ulcer, 6 gastric and duodenal ulcer).

Methods

Isolation and identification of *H pylori* Each of the biopsy specimen was homogenized with a tissue grinder and then inoculated on Columbia agar plates supplemented with 80 mL/L sheep blood, 5 g/L cyclodextrin, 5 mg/L trimethoprim, 10 mg/L vancomycin, 2.5 mg/L amphotericin B and 2 500 U/L cefsulodin. The plates were incubated at 37 °C under microaerobic conditions (50 mL/L O₂, 100mL/L CO₂ and 850 mL/L N₂) for 3 to 5 d. A bacterial isolate was identified as *H pylori* according to typical Gram staining morphology, positive results of biochemical tests for urease and oxidase, and slide agglutination with the commercial rabbit antibody against whole cell of the bacterium.

Preparation of DNA template Genomic DNA from each of the *H pylori* strains was extracted by conventional phenol-chloroform method and DNase-free RNase treatment. Concentration and purity of the DNA preparations were determined by ultraviolet spectrophotometry^[46].

Polymerase Chain reaction The primers were designed to amplify *cagA1* fragment from *H pylori* strain Y06 *cagA* gene based on the published data in GenBank. The sequence of sense primer with an endonuclease site of *EcoR* V was 5' -GCCGAT ATCATGATCAATAATCTTCAAGTAGC-3' , and that of the antisense primer with an endonuclease site of *XhoI* was 5' -

CGGCTCGAGTTATGAAAT CCATTCTGGATTG-3' . The total volume per PCR was 100 μL, containing 2.5 mol/L each of the dNTP, 250 nmol/L each of the two primers, 15 mol/L MgCl₂, 3.0 U *Taq*-plus polymerase, 100 ng DNA template and 1×PCR buffer (pH 8.3). The parameters for PCR were at 94 °C for 5 min, ×1; at 94 °C for 30 s, at 50 °C for 30 s, at 72 °C for 120 s, ×10; at 94 °C for 30 s, at 50 °C for 30 s, at 72 °C for 130 s (additional 10 s for each of the following cycles), ×20; at 72 °C for 10 min, ×1.

To increase the positive detection rate of *cagA* gene, two sets of primers derived from different regions of *cagA* gene were applied in PCR. The sequences of F1/B1 primers were 5' -GATAACAGGCAAGCTTTTGAGG-3' (sense), 5' -CTGCAAAAGATTGTTTGGCAGA-3' (antisense)^[31]. The sequences of D008/R008 primers were 5' -ATAATGCTAAAT TAGACAACCTTGAGCG-3' (sense), 5' -TTAGAATAATCAA CAAACATCACGCCA-3' (antisense)^[36]. Except for the primers and DNA templates, all the other reagents and reaction volumes used in PCR for *cagA* detection were the same as in *cagA1* amplification. The parameters for the two PCRs were at 94 °C for 5 min, ×1; at 94 °C for 30 s, at 55 °C for 1 min, at 72 °C for 90 s, ×35; at 72 °C for 7 min, ×1.

The results of PCR were observed under UV light after electrophoresis on 1.5% agarose gel pre-stained with ethidium bromide. The expected sizes of *cagA1* amplification fragment and the two target amplification fragments for *cagA* gene detection were 2 172 bp (including ATG, TAA, and a 18-bp sequence containing endonuclease sites and protective nucleotide residuals), 349 bp and 298 bp, respectively.

Cloning and sequencing The *cagA1* amplification fragment was cloned into plasmid vector *pUCm-T* (*pUCm-T-cagA1*) by using the T-A cloning kit according to the manufacturer's instructions. The recombinant plasmid was amplified in *E.coli* DH5α and then extracted by Sambrook's method^[46]. A professional company (BBST) was responsible for nucleotide sequence analysis of the inserted fragment. Two plasmids *pUCm-T-cagA1* and *pET32a* were extracted from two different strains of *E.coli* DH5α after amplification in LB medium and then digested with *EcoRV* and *XhoI*, respectively^[46]. The fragments *cagA1* and *pET32a* were recovered and ligated. The recombinant expression vector *pET32a-cagA1* was transformed into *E.coli* BL21DE3, and the expression system designated as *pET32a-cagA1-E.coli* BL21DE3. The *cagA1* fragment inserted in *pET32a* was sequenced again.

Expression and identification of target recombinant protein *pET32a-cagA1-E.coli* BL21DE3 was rotatively cultured in LB medium at 37 °C under induction with isopropylthio-β-D-galactoside (IPTG) at different concentrations of 1.0, 0.5 and 0.1 mmol/L, respectively. The supernatant and precipitate of the culture after incubation were separated by centrifugation and then the bacterial pellets were ultrasonically fragmented (300 V, 5 s×3). SDS-PAGE was used to measure the molecular mass and output of the target recombinant protein (rCagA1). Ni-NTA affinity chromatography was applied to collect rCagA1. The commercial rabbit antiserum against whole-cell *H pylori* and HRP-labeling sheep antiserum against rabbit IgG were used as the first and second antibodies to determine the immunoreactivity of rCagA1 by Western blotting, respectively. Rabbits were immunized with rCagA1 to prepare antisera. Immunodiffusion assay was performed to determine the antigenicity of rCagA1.

Enzyme-linked immunosorbent assay (ELISA) By using rCagA1 as the coating antigen at the concentration of 20 μg/mL, with the serum sample (1:400 dilution) from a patient as the first antibody and HRP-labeling sheep antibody against human IgG (1:4 000 dilution) as the second antibody, CagA antibody in the sera of the 126 *H pylori*-infected patients was detected. The result of ELISA for a patient's serum sample was

considered positive if the value of optical density at 490 nm (OD₄₉₀) exceeded the mean plus 3 standard deviations of 6 different negative serum samples^[47]. CagA expression in *H pylori* isolates was examined using ultrasonic supernatant of each of the *H pylori* isolates (50 µg/mL) as the coating antigen, self-prepared rabbit anti-rCagA1 serum (1:800 dilution) as the first antibody and HRP-labeling sheep antibody against rabbit IgG (1:3 000 dilution) as the second antibody. The result of ELISA for a *H pylori* ultrasonic supernatant sample was considered positive if its OD₄₉₀ value was over the mean plus 3 standard deviations of 6 separated *E.coli* DH5α ultrasonic supernatant samples at the same protein concentration^[47].

Analysis of correlation among *cagA* gene, CagA and its antibody and *H pylori*-related diseases According to the clinical data and the obtained results, the correlations among infection with *H pylori* carrying *cagA* gene and expressing CagA isolated from the patients' gastric biopsy specimens, and the type and severity of gastric diseases in the same patient were analyzed.

Statistical analysis

The nucleotide and putative amino acid sequences of the cloned *cagA1* fragment were compared for homologies with the published corresponding sequences (GenBank accession No. AB015416). χ^2 test was applied to analyze the clinical data, PCR results for *cagA* detection and ELISA results for CagA detection.

RESULTS

Positivity rate of *H pylori* in clinical isolates

In the 156 gastric biopsy specimens with positive urease, *H pylori* was detectable in 126 specimens, with a positivity rate of 80.8%.

```
(1) 61  ///TTTATCAATAATCTTCAAGTAGCTTTTCTCAAAGTTGATAACGCTGTCGCTTCATAC
(2) 61  ATG.....T.....

(1)121 GATCCTGATCAAAAATCAATCGTTGATAAGAACGATAGGGATAACAGGCAAGCTTTTGAA
(2)121 .....C.....T.....

(1)181 GGAATCTCGCAATTAAGGGAAGAATACTCCAATAAAGCGATCAAAAATCCTACCAAAAAG
(2)181 .....

(1)241 AATCAATATTTTCAGACTTTATCAATAAGAGCAATGATTTAATCAACAAAGACAATCTC
(2)241 .....G.....

(1)301 ATTGATGTAGATTCTCCACAAAGAGCTTTTCAGAAATTTGGGGATCAGCGTTACCGAATT
(2)301 .....A...G.....T..GA.....AC.....

(1)361 TTCACAAGTTGGGTGTCCCATCAAACGATCCGTCTAAAATCAACACCCGATCGATCCGA
(2)361 .....

(1)421 AATTTTATGGAAAATATCATAACAACCCCTATCCCTGATGATAAAGAGAAAGCGGAGTTT
(2)421 .....C....A....A.....

(1)481 TTGAAATCTGCCAAACAATCTTTTGCAGGAATCATTATAGGGAATCAAATCCGAACGGAT
(2)481 .....

(1)541 CAAAATTCATGGGCGTGTGTTGATGAGTCCTTGAAAGAAAGGCAAGAAGCAGAAAAAAT
(2)541 .....G.....A..T.....

(1)601 GGAGAGCCTACTGGTGGGGATTGGTTGGATATTTTCTCTCATTATATTTGACAAAAAA
(2)601 .....T.A.....G....A....G..

(1)661 CAATCTTTCGATGTCAAAGAAACAATCAATCAAGAACCAGTTCCCATGTCCAACCAGAT
(2)661 .....CT.....G.....

(1)721 TTAGCCACTACCACCACGACATACAAGGCTTACCGCCTGAAGCTAGAGATTTACTTGAT
(2)721 A.....C.....T....G....G.....

(1)781 GAAAGGGGTAATTTTCTAAATCACTCTTGGCGATATGAAATGTTAGATGTTGAGGGA
(2)781 .....C
```

PCR results

Using the primer pairs F1/B1 and D008/R008 respectively, 82.6% and 78.9% of the tested *H pylori* isolates (90/109) were positive for *cagA* gene, and the total *cagA* gene positivity rate was 97.2% (106/109). The target amplification products of *cagA1* from *H pylori* strain Y06 and two fragments for *cagA* gene detection from the isolates are shown in Figure 1.

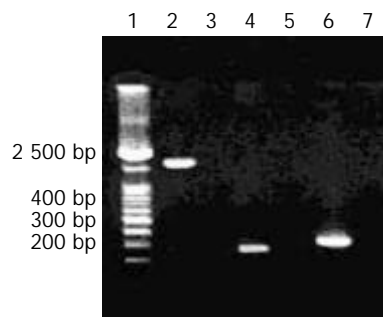


Figure 1 Target amplification fragments of *cagA* gene amplified from *H pylori* isolates with different primers. Lane 1: 100 bp DNA marker; Lanes 2, 4 and 6: Target amplification fragments by using *cagA1*, F1/B1 and D008/R008 primers, respectively; Lanes 3, 5 and 7: Blank controls.

Nucleotide sequence analysis

The nucleotide sequences of *cagA1* fragment in *pUCm-T-cagA1* and *pET32a-cagA1* were completely the same. The nucleotide and putative amino acid sequences of the cloned *cagA1* fragment showed 94.83% (Figure 2) and 93.30% (Figure 3) homologies with the published sequences from *H pylori* strain NCTC11637 (GenBank accession No.: AB015416), respectively.

(1)841 GTCGCTGACATTGATCCCAATTACAAGTTCAATCAATTATTGATTCACAATAACGCTCTG
(2)841C.....T.....

(1)901 TCTTCTGTGTTAATGGGGAGTCATAATGGCATAGAACCTGAAAAAGTTTCATTGTTGTAT
(2)901A.....

(1)961 GGGGGCAATGGTGGTCCTGGAGCTAGGCATGATTGGAACGCCACCGTTGGTTATAAAGAC
(2)961 .C.....TT.....C.A...C.....A..

(1)1021 CAACAAGGCAGCAATGTGGCTACAATAATTAATGTGCATATGAAAAACGGCAGTGGCTTA
(2)1021GA.....C.C.....

(1)1081 GTCATAGCAGGTGGTGAGAAAGGGATTAACAACCCTAGCTTTTATCTCTATAAAGAAGAC
(2)1081T.....C.....

(1)1141 CAACTCACAGGCTCACAAACGAGCATTAAAGTCAAGAAGAGATCCAAAACAAAATAGATTTTC
(2)1141G.....G.....

(1)1201 ATGGAATTTCTTGCACAAAATAATGCTAAATTAGACAACCTTGAGCAAGAAAGAGAAGGAA
(2)1201C.....G.....A...

(1)1261 AAATTCCGAACTGAGATTAAGATTTCCAAAAGACTCTAAGGCTTATTTAGACGCCCTA
(2)1261A..A.....G.....T.....

(1)1321 GGGAAATGATCGTATTGCTTTTGTCTAAAAAAGACACAAAACATTCAGCTTTAATTACT
(2)1321C.....C.....

(1)1381 GAGTTTGGTAATGGGGATTTGAGCTACACTCTCAAAGATTATGGGAAAAAAGCAGATAAA
(2)1381G.....G.....

(1)1441 GCTTTAGATAGGGAGAAAAATGTTACTCTTCAAGGTAGCCTAAAACATGATGGCGTGATG
(2)1441G.....A.....A.....

(1)1501 TTTGTCAATTATTCCAATTTCAAATACACCAACGCTTCCAAGAGTCTGATAAGGGCGTG
(2)1501T.....T.....C.....T...

(1)1561 GGCGTTACGAATGGCGTTTCGCATTTAGAAGTAGGCTTAAACAAGGTAGCTATCTTTAAT
(2)1561A.....C.....C.C.....G.....G.....

(1)1621 TTGCCTGATTTAATAATCTCGCTATCACTAGTTACGTAAGGCGGAATTTAGAGGATAAA
(2)1621T.....A.....

(1)1681 CTAACCACTAAAGGATTGTCCCAACAAGAAGCTAATAAGCTTATCAAAGATTTTTTGAGC
(2)1681 ...GT...G.....T.....

(1)1741 AGCAACAAAGAATTGGTTGGAAAACTTTAAACTTCAATAAAGCTGTAGCTGACGCTAAA
(2)1741G.....T.....

(1)1801 AACACAGGCAATTATGATGAAGTGAAAAAGCTCAGAAAGATCTTGAAAAATCTCTAAGG
(2)1801C.....

(1)1861 AAACGAGAGCATTAGAGAAAGAAGTAGAGAAAAAATTGGAGAGCAAAAGCGGAAACAAA
(2)1861C.....

(1)1921 AATAAAATGGAAGCAAAGCTCAAGCTAACAGCCAAAAGATGAGATTTTTGCGTTGATC
(2)1921G.....A.....

(1)1981 AATAAAGAGGCTAATAGAGACGCAAGAGCAATCGCTTACGCTCAGAATCTTAAAGGCATC
(2)1981G.....T.....

(1)2041 AAAAGGGAATTGTCTGATAAATTGAAAATGTCAACAAGAATTTGAAAGACTTTGATAAA
(2)2041AA.....G.....AG....

(1)2101 TCTTTTGTGATGAATTCAAAATGGCAAAAATAAGGATTTAGCAAGGCAGAAGAAACACTA
(2)2101T.....G...

(1)2161 AAAGCCCTTAAAGGTTTCGGTGAAAGATTTAGGTATCAATCCAGAATGGATTCA
(2)2161C.....A.....TAA

Figure 2 Comparison of nucleotide sequence homology of *cagA1* fragments between different *H pylori* strains. (1): Corresponding nucleotide sequence of *cagA1* fragment from *H pylori* strain NCTC11637. (2): Sequencing result of *cagA1* fragment from *H pylori* strain Y06. “///” indicates the deletion mutation of the nucleotide residuals. Underlined is the position of the primers.

```

(1) 1 INNLOVAFKVDNAVASYDPDQKSIVDKNDRDNRQAFEGISQLREEYSNKAIAKNPTKKNQ
(2) 1 .....P.....D.....

(1) 61 YSDFINKSNLDLINKDNLIDVESSTKSFQKFGDQRYRIFTSWVSHQNDPSKINTRSIRNF
(2) 61 .....IG...R.....T.....

(1) 121 MENIIQPPILDDKEKAEFLKSAQSFAGIIIGNQIRTDQKFMGVFDES�KERQEAENGE
(2) 121 .....P.....F.....

(1) 181 PTGGDWLDIFLSFIDKQSSDVKEAINQEPVPHVQPDIAATTTTIDIOGLPPEARDLLDER
(2) 181 .....V.N.E.....H.....S.....

(1) 241 GNFSKFTLGDMEMLDVEGVADIDPNYKFNQLLIHNNALSSVLMGSHNGIEPEKVSLLYGG
(2) 241 .....D.....A.....

(1) 301 NGGPGARHDWNATVGYKDOQGNVATIINVHMKNKSGSLVIAGGEKGINNPSFYLYKEDQL
(2) 301 ...F..K.....N...D...L.....

(1) 361 TGSQRALSQEEIQNKIDFMEFLAQNNAKLDNLSEKEKEKFRTEIKDFQKDSKAYLDALGN
(2) 361 .....R.....QN..E.....

(1) 421 DRIAFVSKKDTKHSALITEFGNGDLSYTLKDYGKKADKALDREKNVTLOGSLKHGDMFMV
(2) 421 .....P.....K.....R....E.....N.....

(1) 481 DYSNFKYTNASKNPNKGVGVTNGVSHLEVGFNKVAIFNLPDLNNLAITSFVRRNLEDKLT
(2) 481 N.....S.D.....DA..S..V.....N..V

(1) 541 TKGLSPQEANKLIKDFLSSNKELVGKTLNFNKAVADAKNTGNYDEVKKAQKDLEKSLRKR
(2) 541 .E...L.....A.....

(1) 601 EHLEKEVEKKLESKSGNKNMEAKAQANSQKDEIFALINKEANRDARAIAYAQNKGIKR
(2) 601 .....K.....S.....

(1) 661 ELSDKLENVNKNLKDFFKSFDEFKNGKKNKDFSKAEETLKALKGSVKDLGINPEWIS
(2) 661 .....KI..D....S.....

```

Figure 3 Comparison of putative amino acid sequence homology of *cagA1* fragment between different *H pylori* strains. (1): Corresponding putative amino acid sequence of *cagA1* fragment from *H pylori* strain NCTC11637. (2): Putative amino acid sequence of *cagA1* fragment from *H pylori* strain Y06. Underlined is the position of the primers.

Expression of target recombinant protein

IPTG at concentrations of 1.0, 0.5 and 0.1 mmol/L could efficiently induce the expression of rCagA1, which was detected mainly in the ultrasonic precipitate with an output of approximately 30% of the total bacterial proteins (Figure 4).

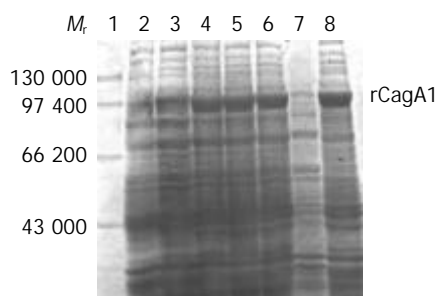


Figure 4 rCagA1 expression by *pET32a-cagA1-E.coli* BL21DE3 induced with IPTG. Lane 1: Protein marker; Lane 2: Blank control; Lane 3: Non-induced; Lanes 4-6: induced with 0.1, 0.5 and 1.0 mmol/L IPTG, respectively; Lanes 7 and 8: Bacterial supernatant and precipitate induced with 0.5 mmol/L IPTG, respectively.

Immunoreactivity and antigenicity of rCagA1

The commercial rabbit antibody against whole-cell *H pylori* could bind to rCagA1 as confirmed by Western blotting

(Figure 5). Immunodiffusion assay demonstrated a titer of 1:4 between rCagA1 and rabbit anti-rCagA1 serum.

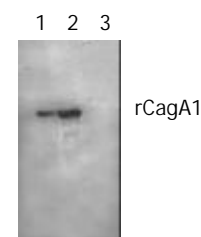


Figure 5 Western blotting of binding between rCagA1 and commercial rabbit antiserum against whole-cell *H pylori*. Lanes 1 and 2: 20 μ L and 40 μ L of rCagA1 extract, respectively; Lane 3: Blank control.

ELISA results

The mean A_{490} values (mean \pm SD) of the 6 negative serum samples was 0.37 ± 0.03 in the detection of specific antibodies in sera of patients, and the positive reference value of 0.46 was consequently derived. According to the reference value, 88.1% (96/109) of the tested patients' serum samples were positive for the rCagA1 antibodies with an A_{490} value ranging from 0.56 to 1.05 (Table 1). From the mean A_{490} values of the 5 negative bacterial controls (0.27 ± 0.09) in the detection of CagA1 in *H pylori* isolates, the positive reference value of 0.54 was

derived. According to the reference value, the epitope of rCagA1 with an A_{490} value ranging from 0.55% to 0.9792.6% (101/109) was detected in the tested *H pylori* isolates (Table 1).

Table 1 Detection of CagA expression in *H pylori* isolates and CagA antibody in infected patients' sera

Tested indicator	Tested cases	Positive cases	Negative cases	Positivity rate (%)
CagA gene	109	106	3	97.2
CagA protein	109	101	8	92.6
Anti-CagA	109	96	13	88.1

Correlation between CagA and gastric diseases

A high rate of 97.9% of *H pylori* isolated from the peptic ulcer specimens (47/48) and 88.5% from the gastritis specimens (54/61) was positive for CagA expression, showing no statistically significant difference between the two positive rates ($\chi^2=3.48$, $P>0.05$). Of the 8 *H pylori* strains in which CagA expression failed to be detected, 1, 1 and 6 strains were isolated from the biopsy specimens of gastric ulcer, chronic active gastritis and chronic superficial gastritis, respectively, and this distribution did not show any statistically significant difference, either ($\chi^2=1.23$, $P>0.05$).

DISCUSSION

CagA expressed by *H pylori* was demonstrated to induce cellular skeleton rearrangement and interleukin (IL)-8 secretion in gastric epithelial cells^[31,32]. IL-8, recognized as an inflammatory cytokine, could cause inflammation by inducing gathering of neutrophilic cells^[48,49]. Infection with *cagA*⁺ *H pylori* may elevate the risks of atrophic gastritis, intestinal metaplasia and gastric adenocarcinoma^[34,50,51], and CagA is therefore considered as the most important pathogenic factor of *H pylori*.

CagA gene had a single copy located at the terminal end of region I in *cag* pathogenic island (CPI)^[31,52], and was prone to mutation, especially in the 3' -end by insertion of different numbers of repeated sequences, resulting in the great variation in its length ranging from 3 444 to 5 925 bp in different isolates^[36,37]. According to the analysis of 37 *cagA* gene sequences from GenBank, a fragment with approximate 65 bp starting from the 5' -end of *cagA* gene of different *H pylori* isolates also exhibited frequent mutations such as replacement, insertion and deletion, etc. Therefore, a relatively conserved fragment of 2 148 bp from the 67th to 2 214th bp at 5' -end of *cagA* gene was selected for cloning, which was provisionally named as *cagA1*. In this study, homologies of the nucleotide and amino acid sequences of the cloned *cagA1* fragment reached 94.83% and 93.30% respectively in comparison with the reported sequences in GenBank (accession No.AB015416). High output of rCagA1, approximately 30% of the total bacterial protein, expressed by the constructed recombinant prokaryotic expression system *pET32a-cagA1-E.coli* BL21DE3 was confirmed by SDS-PAGE. rCagA1 could be recognized by a commercial antibody against whole-cell *H pylori* and was able to induce rabbit to produce high-titer antibodies, indicating that rCagA1 with good immunoreactivity and antigenicity can be used in ELISA as a qualified antigen for detecting CagA antibody and for preparing animal antiserum to detect CagA.

Yang *et al* reported that all the *cagA*⁺ *H pylori* isolates were capable of expressing CagA^[41]. However, we found that 5 strains of *cagA*⁺ *H pylori* (7.3%) failed to exhibit the expression. Considering the highly likely mutation in *cagA* genes from different *H pylori* isolates, this non-expression of CagA was probably due to sequence mutation or abnormal transcription

and translation^[36,37]. In the present study, 88.1% of the serum samples from the *H pylori*-infected patients (96/109) were positive for CagA antibody, and the positive rate was only slightly lower than those of *cagA* gene (97.2%) and CagA (92.6%) of the isolates, suggesting that CagA possesses strong antigenicity and usually induces detectable specific antibody in *cagA*⁺ *H pylori*-infected patients. However, we found in this study that 11.9% of the serum samples were negative for CagA antibody (13/109), including 3 cases (2.8%) of *cagA*⁻ *H pylori* infection, 5(4.6%) of *cagA*⁺ *H pylori* infection and 5(4.6%) of CagA⁺ *H pylori* infection. In addition, previously published data and our results suggest that over 90% of the *H pylori* isolates from Asia-Pacific areas were *cagA* gene-positive^[39-42], whereas 60% to 70% of the *H pylori* isolates from European and North American areas were positive^[36-38], indicating that the presence of CagA antibody could be used as a reference indicator with only a small risk of error for detecting *H pylori* infection in individuals from Asia-Pacific areas, but not for those from European or North American areas. It should be noted that the positive rate of *cagA* gene in the *H pylori* isolates in this study was as low as 78.9% to 82.6%, as detected using a single pair of primers F1/B1 or D008/R008, indicating that using multiple pairs of primers in PCR may increase the positive rate for *cagA* gene detection.

Covacci *et al* and Figueiredo *et al* reported that *cagA*⁺ *H pylori* infection could usually cause serious gastric diseases^[37,38]. For example, 90% of *H pylori* isolates from peptic ulcer patients were *cagA* gene-positive, while only 50% to 60% of the isolates from superficial gastritis were positive. However, the reports from Asia-Pacific areas did not show a definite correlation between *cagA*⁺ *H pylori* infection and severity of the diseases^[39-42]. Although *cagA*⁺ *H pylori* was isolated from chronic gastritis patients at a higher rate (97.9%) than from peptic ulcer patients (88.5%), the difference was not statistically significant ($\chi^2=3.48$, $P>0.05$), probably due to the high rate of *cagA* gene-carrying *H pylori* (97.2%) and a relative small population tested in this study.

ACKNOWLEDGEMENTS

We are grateful to the four hospitals in Hangzhou that provided gastric biopsy specimens for this study, and helped us to complete this research.

REFERENCES

- Zhang Z, Yuan Y, Gao H, Dong M, Wang L, Gong YH. Apoptosis, proliferation and *p53* gene expression of *H pylori* associated gastric epithelial lesions. *World J Gastroenterol* 2001; **7**: 779-782
- Lu XL, Qian KD, Tang XQ, Zhu YL, Du Q. Detection of *H pylori* DNA in gastric epithelial cells by *in situ* hybridization. *World J Gastroenterol* 2002; **8**: 305-307
- Yao YL, Xu B, Song YG, Zhang WD. Overexpression of cyclin E in Mongolian gerbil with *Helicobacter pylori*-induced gastric precancerosis. *World J Gastroenterol* 2002; **8**: 60-63
- Guo DL, Dong M, Wang L, Sun LP, Yuan Y. Expression of gastric cancer-associated MG7 antigen in gastric cancer, precancerous lesions and *H pylori*-associated gastric diseases. *World J Gastroenterol* 2002; **8**: 1009-1013
- Xia HHX. Association between *Helicobacter pylori* and gastric cancer: current knowledge and future research. *World J Gastroenterol* 1998; **4**: 93-96
- Tu SP, Zhong J, Tan JH, Jiang XH, Qiao MM, Wu YX, Jiang SH. Induction of apoptosis by arsenic trioxide and hydroxy camptothecin in gastric cancer cells *in vitro*. *World J Gastroenterol* 2000; **6**: 532-539
- Cai L, Yu SZ, Zhang ZF. *Helicobacter pylori* infection and risk of gastric cancer in Changle County, Fujian Province, China. *World J Gastroenterol* 2000; **6**: 374-376

- 8 **Xu AG**, Li SG, Liu JH, Gan AH. Function of apoptosis and expression of the proteins *Bcl-2*, *p53* and *C-myc* in the development of gastric cancer. *World J Gastroenterol* 2001; **7**: 403-406
- 9 **Wang X**, Lan M, Shi YQ, Lu J, Zhong YX, Wu HP, Zai HH, Ding J, Wu KC, Pan BR, Jin JP, Fan DM. Differential display of vincristine-resistance-related gene in gastric cancer SGC7901 cells. *World J Gastroenterol* 2002; **8**: 54-59
- 10 **Liu JR**, Li BX, Chen BQ, Han XH, Xue YB, Yang YM, Zheng YM, Liu RH. Effect of cis-9, trans-11-conjugated linoleic acid on cell cycle of gastric adenocarcinoma cell line (SGC-7901). *World J Gastroenterol* 2002; **8**: 224-229
- 11 **Niu WX**, Qin XY, Liu H, Wang CP. Clinicopathological analysis of patients with gastric cancer in 1200 cases. *World J Gastroenterol* 2001; **7**: 281-284
- 12 **Fang DC**, Yang SM, Zhou XD, Wang DX, Luo YH. Telomere erosion is independent of microsatellite instability but related to loss of heterozygosity in gastric cancer. *World J Gastroenterol* 2001; **7**: 522-526
- 13 **Morgner A**, Miehle S, Stolte M, Neubauer A, Alpen B, Thiede C, Klann H, Hierlmeier FX, Ell C, Ehninger G, Bayerdorffer E. Development of early gastric cancer 4 and 5 years after complete remission of *Helicobacter pylori*-associated gastric low-grade marginal zone B-cell lymphoma of MALT type. *World J Gastroenterol* 2001; **7**: 248-253
- 14 **Deng DJ**. Progress of gastric cancer etiology: n-nitrosamides in the 1990s. *World J Gastroenterol* 2000; **6**: 613-618
- 15 **Liu ZM**, Shou NH, Jiang XH. Expression of lung resistance protein in patients with gastric carcinoma and its clinical significance. *World J Gastroenterol* 2000; **6**: 433-434
- 16 **Cai L**, Yu SZ, Ye WM, Yi YN. Fish sauce and gastric cancer: an ecological study in Fujian Province, China. *World J Gastroenterol* 2000; **6**: 671-675
- 17 **Xue FB**, Xu YY, Wan Y, Pan BR, Ren J, Fan DM. Association of *H pylori* infection with gastric carcinoma: a Meta analysis. *World J Gastroenterol* 2001; **7**: 801-804
- 18 **Wang RT**, Wang T, Chen K, Wang JY, Zhang JP, Lin SR, Zhu YM, Zhang WM, Cao YX, Zhu CW, Yu H, Cong YJ, Zheng S, Wu BQ. *Helicobacter pylori* infection and gastric cancer: evidence from a retrospective cohort study and nested case-control study in China. *World J Gastroenterol* 2002; **8**: 1103-1107
- 19 **Liu DH**, Zhang XY, Fan DM, Huang YX, Zhang JS, Huang WQ, Zhang YQ, Huang QS, Ma WY, Chai YB, Jin M. Expression of vascular endothelial growth factor and its role in oncogenesis of human gastric carcinoma. *World J Gastroenterol* 2001; **7**: 500-505
- 20 **Cao WX**, Ou JM, Fei XF, Zhu ZG, Yin HR, Yan M, Lin YZ. Methionine-dependence and combination chemotherapy on human gastric cancer cells *in vitro*. *World J Gastroenterol* 2002; **8**: 230-232
- 21 **Michetti P**, Kreiss C, Kotloff K, Porta N, Blano JL, Bachmann D, Herranz M, Saldinger PF, Cortesey-Theulaz I, Losonsky G, Nichols R, Simon J, Stolte M, Acherman S, Monath TP, Blum AL. Oral immunization with urease and *Escherichia coli* heat-labile enterotoxin is safe and immunogenic in *Helicobacter pylori*-infected adults. *Gastroenterology* 1999; **116**: 804-812
- 22 **Rollan A**, Giancaspero R, Fuster F, Acevedo C, Figueroa C, Hola K, Schulz M, Duarte I. The long-term reinfection rate and the course of duodenal ulcer disease after eradication of *Helicobacter pylori* in a developing country. *Am J Gastroenterol* 2000; **95**: 50-56
- 23 **Suganuma M**, Kurusu M, Okabe S, Sueoka N, Yoshida M, Wakatsuki Y, Fujiki H. *Helicobacter pylori* membrane protein 1: a new carcinogenic factor of *Helicobacter pylori*. *Cancer Res* 2001; **61**: 6356-6359
- 24 **Nakamura S**, Matsumoto T, Suekane H, Takeshita M, Hizawa K, Kawasaki M, Yao T, Tsuneyoshi M, Iida M, Fujishima M. Predictive value of endoscopic ultrasonography for regression of gastric low grade and high grade MALT lymphomas after eradication of *Helicobacter pylori*. *Gut* 2001; **48**: 454-460
- 25 **Uemura N**, Okamoto S, Yamamoto S, Matsumura N, Yamaguchi S, Yamakido M, Taniyama K, Sasaki N, Schlemper RJ. *Helicobacter pylori* infection and the development of gastric cancer. *N Engl J Med* 2001; **345**: 8298-8332
- 26 **Morgner A**, Miehle S, Fischbach W, Schmitt W, Muller-Hermelink H, Greiner A, Thiede C, Schetelig J, Neubauer A, Stolte M, Ehninger G, Bayerdorffer E. Complete remission of primary high-grade B-cell gastric lymphoma after cure of *Helicobacter pylori* infection. *J Clin Oncol* 2001; **19**: 2041-2048
- 27 **Kate V**, Ananthakrishnan N, Badrinath S. Effect of *Helicobacter pylori* eradication on the ulcer recurrence rate after simple closure of perforated duodenal ulcer: retrospective and prospective randomized controlled studies. *Br J Surg* 2001; **88**: 1054-1058
- 28 **Gao HJ**, Yu LZ, Bai JF, Peng YS, Sun G, Zhao HL, Miu K, Lü XZ, Zhang XY, Zhao ZQ. Multiple genetic alterations and behavior of cellular biology in gastric cancer and other gastric mucosal lesions: *H pylori* infection, histological types and staging. *World J Gastroenterol* 2000; **6**: 848-854
- 29 **Atherton JC**, Cao P, Peek RM Jr, Tummuru MK, Blaser MJ, Cover TL. Mosaicism in vacuolating cytotoxin alleles of *Helicobacter pylori*. Association of specific vacA types with cytotoxin production and peptic ulceration. *J Biol Chem* 1995; **270**: 17771-17777
- 30 **Stein M**, Rappuoli R, Covacci A. Tyrosine phosphorylation of the *Helicobacter pylori* CagA antigen after *cag*-driven host cell translocation. *Proc Natl Acad Sci U S A* 2000; **97**: 1263-1268
- 31 **Censini S**, Lange C, Xiang Z, Crabtree JE, Ghiara P, Borodovsky M, Rappuoli R, Covacci A. *cag*, a pathogenicity island of *Helicobacter pylori*, encodes type I-specific and disease-associated virulence factors. *Proc Natl Acad Sci U S A* 1996; **93**: 14648-14653
- 32 **Nogueira C**, Figueiredo C, Carneiro F, Gomes AT, Barreira R, Figueira P, Salgado C, Belo L, Peixoto A, Bravo JC, Bravo LE, Realpe JL, Plaisier AP, Quint WG, Ruiz B, Correa P, van Doorn LJ. *Helicobacter pylori* genotypes may determine gastric histopathology. *Am J Pathol* 2001; **158**: 647-654
- 33 **Peek RM Jr**, Moss SF, Tham KT, Perez-Perez GI, Wang S, Miller GG, Atherton JC, Holt PR, Blaser MJ. *Helicobacter pylori cagA+* strains and dissociation of gastric epithelial cell proliferation from apoptosis. *J Natl Cancer Inst* 1997; **89**: 863-868
- 34 **Blaser MJ**, Perez-Perez GI, Kleanthous H, Cover TL, Peek RM, Chyou PH, Stemmermann GN, Nomura A. Infection with *Helicobacter pylori* strains possessing *cagA* is associated with an increased risk of developing adenocarcinoma of the stomach. *Cancer Res* 1995; **55**: 2111-2115
- 35 **Parsonnet J**, Friedman GD, Orentreich N, Vogelstein H. Risk for gastric cancer in people with CagA positive or CagA negative *Helicobacter pylori* infection. *Gut* 1997; **40**: 297-301
- 36 **Tummuru MK**, Cover TL, Blaser MJ. Cloning and expression of a high-molecular-mass major antigen of *Helicobacter pylori*: evidence of linkage to cytotoxin production. *Infect Immun* 1993; **61**: 1799-1809
- 37 **Covacci A**, Censini S, Bugnoli M, Petracca R, Burroni D, Macchia G, Massone A, Papini E, Xiang Z, Figura N. Molecular characterization of the 128-kDa immunodominant antigen of *Helicobacter pylori* associated with cytotoxicity and duodenal ulcer. *Proc Natl Acad Sci U S A* 1993; **90**: 5791-5795
- 38 **Figueiredo C**, van Doorn LJ, Nogueira C, Soares JM, Pinho C, Figueira P, Quint WG, Carneiro F. *Helicobacter pylori* genotypes are associated with clinical outcome in Portuguese patients and show a high prevalence of infections with multiple strains. *Scand J Gastroenterol* 2001; **36**: 128-135
- 39 **Ito Y**, Azuma T, Ito S, Miyaji H, Hirai M, Yamazaki Y, Sato F, Kato T, Kohli Y, Kuriyama M. Analysis and typing of the *vacA* gene from *cagA*-positive strains of *Helicobacter pylori* isolated in Japan. *J Clin Microbiol* 1997; **35**: 1710-1714
- 40 **Park SM**, Park J, Kim JG, Yoo BC. Relevance of *vacA* genotypes of *Helicobacter pylori* to *cagA* status and its clinical outcome. *Korean J Intern Med* 2001; **16**: 8-13
- 41 **Yang H**, Wu SV, Pichuanes S, Song M, Wang J, Zhou D, Xu Z, Quan S, Polito A, Walsh JH. High prevalence of *cagA*-positive strains in *Helicobacter pylori*-infected, healthy, young Chinese adult. *J Gastroenterol Hepatol* 1999; **14**: 476-480
- 42 **Park SM**, Park J, Kim JG, Cho HD, Cho JH, Lee DH, Cha YJ. Infection with *Helicobacter pylori* expressing the *cagA* gene is not associated with an increased risk of developing peptic ulcer diseases in Korean patients. *Scand J Gastroenterol* 1998; **33**: 923-927
- 43 **Chmiela M**, Wisniewska M, Bak-Romaniszyn L, Rechcinski T,

- Planeta-Malecka I, Bielanski W, Konturek SJ, Plonka M, Klink M, Rudnicka W. Serological differentiation of *Helicobacter pylori* CagA(+) and CagA(-) infections. *Arch Immunol Ther Exp* 2003; **51**: 131-136
- 44 **Park CY**, Kwak M, Gutierrez O, Graham DY, Yamaoka Y. Comparison of genotyping *Helicobacter pylori* directly from biopsy specimens and genotyping from bacterial cultures. *J Clin Microbiol* 2003; **41**: 3336-3338
- 45 **Tomasini ML**, Zanussi S, Sozzi M, Tedeschi R, Basaglia G, De Paoli P. Heterogeneity of *cag* genotypes in *Helicobacter pylori* isolates from human biopsy specimens. *Clin Microbiol* 2003; **41**: 976-980
- 46 **Sambrook J**, Fritsch EF, Maniatis T. Molecular Cloning, A Laboratory Manual, 2nd edition. *New York: Cold Spring Harbor Laboratory Press* 1989: 1.21-1.52, 2.60-2.80, 7.3-7.35, 9.14-9.22
- 47 **Chen Y**, Wang J, Shi L. *In vitro* study of the biological activities and immunogenicity of recombinant adhesion of *Helicobacter pylori* rHpaA. *Zhonghua Yixue Zazhi* 2001; **81**: 276-279
- 48 **Scholte GH**, van Doorn LJ, Cats A, Bloemena E, Lindeman J, Quint WG, Meuwissen SG, Kuipers EJ. Genotyping of *Helicobacter pylori* in paraffin-embedded gastric biopsy specimens: relation to histological parameters and effects on therapy. *Am J Gastroenterol* 2002; **97**: 1687-1695
- 49 **Kim JM**, Kim JS, Jung HC, Oh YK, Kim N, Song IS. Inhibition of *Helicobacter pylori*-induced nuclear factor-kappa B activation and interleukin-8 gene expression by ecabet sodium in gastric epithelial cells. *Helicobacter* 2003; **8**: 542-553
- 50 **Machado JC**, Figueiredo C, Canedo P, Pharoah P, Carvalho R, Nabais S, Castro Alves C, Campos ML, Van Doorn LJ, Caldas C, Seruca R, Carneiro F, Sobrinho-Simoes M. A proinflammatory genetic profile increases the risk for chronic atrophic gastritis and gastric carcinoma. *Gastroenterology* 2003; **125**: 364-371
- 51 **Beales IL**, Crabtree JE, Scunes D, Covacci A, Calam J. Antibodies to CagA protein are associated with gastric atrophy in *Helicobacter pylori* infection. *Eur J Gastroenterol Hepatol* 1996; **8**: 645-649
- 52 **Hoshino FB**, Katayama K, Watanabe K, Takahashi S, Uchimura H, Ando T. Heterogeneity found in the *cagA* gene of *Helicobacter pylori* from Japanese and non-Japanese isolate. *J Gastroenterol* 2000; **35**: 890-897

Edited by Chen WW and Wang XL Proofread by Xu FM

Adeno-associated virus mediated endostatin gene therapy in combination with topoisomerase inhibitor effectively controls liver tumor in mouse model

Sung Yi Hong, Myun Hee Lee, Kyung Sup Kim, Hyun Cheol Jung, Jae Kyung Roh, Woo Jin Hyung,
Sung Hoon Noh, Seung Ho Choi

Sung Yi Hong, Myun Hee Lee, Woo Jin Hyung, Sung Hoon Noh, Seung Ho Choi, Department of Surgery, Yonsei University College of Medicine, Seoul, Korea

Kyung Sup Kim, Institute of Genetic Science, Department of Biochemistry and Molecular Biology, Yonsei University College of Medicine, Seoul, Korea

Hyun Cheol Jung, Jae Kyung Roh, Oncology, Internal Medicine, Cancer Metastasis Research Center, Yonsei University College of Medicine

Supported by a faculty research grant of Yonsei University College of Medicine for 2002, No. 2002-06

Correspondence to: Dr Seung Ho Choi, Department of Surgery, Yonsei University College of Medicine, Youngdong PO Box 1217, Seoul, Korea. choish@yumc.yonsei.ac.kr

Telephone: +82-2-3497-3375 **Fax:** +82-2-3462-5994

Received: 2003-09-23 **Accepted:** 2003-12-01

Abstract

AIM: rAAV mediated endostatin gene therapy has been examined as a new method for treating cancer. However, a sustained and high protein delivery is required to achieve the desired therapeutic effects. We evaluated the impact of topoisomerase inhibitors in rAAV delivered endostatin gene therapy in a liver tumor model.

METHODS: rAAV containing endostatin expression cassettes were transduced into hepatoma cell lines. To test whether the topoisomerase inhibitor pretreatment increased the expression of endostatin, Western blotting and ELISA were performed. The biologic activity of endostatin was confirmed by endothelial cell proliferation and tube formation assays. The anti-tumor effects of the rAAV-endostatin vector combined with a topoisomerase inhibitor, etoposide, were evaluated in a mouse liver tumor model.

RESULTS: Topoisomerase inhibitors, including camptothecin and etoposide, were found to increase the endostatin expression level *in vitro*. The over-expressed endostatin, as a result of pretreatment with a topoisomerase inhibitor, was also biologically active. In animal experiments, the combined therapy of topoisomerase inhibitor, etoposide with the rAAV-endostatin vector had the best tumor-suppressive effect and tumor foci were barely observed in livers of the treated mice. Pretreatment with an etoposide increased the level of endostatin in the liver and serum of rAAV-endostatin treated mice. Finally, the mice treated with rAAV-endostatin in combination with etoposide showed the longest survival among the experimental models.

CONCLUSION: rAAV delivered endostatin gene therapy in combination with a topoisomerase inhibitor pretreatment is an effective modality for anticancer gene therapy.

Hong SY, Lee MH, Kim KS, Jung HC, Roh JK, Hyung WJ, Noh

SH, Choi SH. Adeno-associated virus mediated endostatin gene therapy in combination with topoisomerase inhibitor effectively controls liver tumor in mouse model. *World J Gastroenterol* 2004; 10(8): 1191-1197

<http://www.wjgnet.com/1007-9327/10/1191.asp>

INTRODUCTION

Antiangiogenic therapy for cancer has emerged as an exciting new therapeutic modality because tumors are angiogenesis-dependent during growth and metastasis^[1-6]. One of the most potent endogenous angiogenic inhibitors, endostatin, has been reported to inhibit endothelial proliferation and regression of solid tumors^[7-10]. Although endostatin induces and sustains the dormancy of tumor growth, large quantities of proteins are needed for prolonged periods^[9]. Moreover, besides being difficult to be purified, endostatin has a short half-life *in vivo*. In order to circumvent the obstacle presented by the pharmacokinetics of endostatin, delivery of the gene cassettes encoding endostatin has been attempted^[11-19].

Recombinant adeno-associated virus (rAAV) vector is a good candidate for antiangiogenesis-based cancer gene therapy^[20]. rAAV vector is derived from a nonpathogenic parvovirus that is capable of integrating into the host DNA, which allows the long-term expression. In addition, removal of the viral coding sequences minimizes immunogenicity. The rAAV vector has a broad host tropism and transduces in dividing and non-dividing cells. The liver is an important target for gene therapy, because of its large size, its protein synthesizing capacity and because it is easily accessible to vectors. Although the rAAV is a promising vector for liver-directed gene therapy, its potential for therapeutic use has been limited due to its inefficient transduction into the liver^[21,22]. In order to achieve high serum levels of endostatin with a stable expression, the transduction of non-dividing cell populations is essential in liver-directed gene therapy. Some topoisomerase inhibitors, such as etoposide or camptothecin, increase the transduction efficiency of the rAAV in non-dividing cells as well as in dividing cells^[23-25].

Therefore, this study investigated the potential of a rAAV vector-mediated endostatin gene therapy in combination with topoisomerase inhibitor in a liver tumor model. This paper demonstrates that a topoisomerase inhibitor in a rAAV delivered endostatin gene therapy enhances the antiangiogenic effects, and that this method has the potential to be used as a new strategy for cancer gene therapy.

MATERIALS AND METHODS

Cells culture

Hepa1c1c7 mouse hepatoma cell line (ATCC CRL 2026), S-180 murine sarcoma cell line (ATCC CCL-8) and 293-EBNA cells (transformed human embryonic kidney, ATCC R620-07) were grown in DMEM (Gibco BRL, Grand Island, NY) with 100 mL/L

heat inactivated (30 min at 56 °C) fetal bovine serum, 2 mmol/L L-glutamine, 100 units/mL penicillin, and 100 mg/mL streptomycin at 37 °C in 50 mL/LCO₂. The 293-EBNA cell line was maintained in medium containing geneticin (G418, 250 µg/mL; Gibco BRL). Human umbilical vein endothelial cells (HUVEC) were isolated from the human umbilical vein (Institutional review board approved protocol with informed consent) using a collagenase type I (Sigma, St. Louis, MO) perfusion. The cells were then grown on gelatin-coated tissue culture plates in M199 medium (Sigma) supplemented with 100 ng/mL heparin (Gibco BRL), 200 mL/L FBS, 100 mg/mL streptomycin, 100 U/mL penicillin, 3 ng/mL bFGF (Upstate, Waltham, MA).

rAAV vector construction and production

pEndoSTHB vector was kindly provided by Dr K.K. Tanabe (Harvard Medical School, Boston, MA), which contained murine endostatin cDNA downstream of murine Ig κ-chain signal peptide and upstream of a *c-myc* epitope^[26]. This plasmid was modified by site-directed mutagenesis (oligonucleotide primer 1: ACC-TCT-TTC-TCC-AAG-TAA-TGA-CTC-CAG-TGT-GGT-GGA, oligonucleotide primer 2: TCC-ACC-ACA-CTG-GAG-TCA-TTA-CTT-GGA-GAA-AGA-GGT), which mutated the sequence upstream of the *c-myc* epitope into stop codons to remove *c-myc* tag^[27]. AAV-helper free system (Stratagene, La Jolla, CA) was used to produce rAAV. *SaI* – *XhoI* fragment from modified pEndoSTHB was subcloned into the pCMV-MCS vector (Stratagene). Once this expression construct was verified, the *NotI* fragment, containing the expression cassette of endostatin, was cloned into the pAAV-LacZ viral expression vector (Stratagene). The parental vector rAAV-LacZ was used as control. pAAV-endostatin containing the cytomegalovirus (CMV) promoter with a murine Ig κ-chain signal peptide was flanked by cDNA of murine endostatin. The rAAV vectors were produced using a standard triple-plasmid transfection method, and purified by a heparin sulfate column separation^[28]. Briefly, the recombinant expression plasmid was co-transfected into 293-EBNA cells with pHelper (Stratagene) and pAAV-RC (Stratagene), which supply all the trans-acting factors required for AAV replication and packaging in 293-EBNA cells. rAAV stocks were subjected to 3 rounds of freezing and thawing. After cell debris was removed by centrifugation, the stocks were filtered using a low protein binding 5 µm syringe filter (Millipore, Bedford, MA), followed by a 0.8 µm syringe filter and subsequently by heparin agarose column (Sigma) separation. The viruses were finally concentrated in a millipore concentrator (100-ku cut off) and titrated by taking the average of three quantitative real time PCR using a LightCycler-FastStart DNA Master SYBR Green system (Roche Molecular Biochemicals, Mannheim, Germany) (forward primer: GGC-TAG-CCA-CCA-TGG-AGA-CAG-ACA, reverse primer: ACA-CTG-GAG-TCA-TTA-CTT-GGA-GAA, 10 min pre-incubation at 94 °C followed by 50 cycles at 94 °C for 15 s, at 60 °C for 5 s and at 72 °C for 10 s in a 7 700 Q-PCR machine, Applied Biosystems, Foster City, California).

Treatment with topoisomerase inhibitors

Stock solutions of etoposide (10 mmol/L) (Laboratories Lilly France, Fegersheim, France) and camptothecin (10 mmol/L) (Yakult Honsha, Tokyo, Japan) were stored at -20 °C and diluted into HBSS (Hanks' balanced salt solution, Gibco BRL) for use in experiments. Hepa1c1c7 cells were pretreated with either 3 µmol/L of etoposide or 10 µmol/L of camptothecin for 6 h, and then washed twice with L-DMEM (20 g/LFBS, 2 mmol/L L-glutamine in DMEM) prior to the rAAV addition. The vector was then added for transduction, and the plates were swirled gently at 30 min intervals during an incubation of 2 h. H-DMEM (180 g/LFBS, 2 mmol/L L-glutamine) was then added to each

plate, and incubation was continued for 48 h at 37 °C.

Western blot analysis

Western blot was performed on the protein from conditioned medium of rAAV transduced Hepa1c1c7 cells. The conditioned medium was concentrated in a Microcon YM-10 (millipore) and subjected to electrophoresis under reducing conditions on a 40-120 g/L NuPAGE gel (Invitrogen, San Diego, CA). The proteins obtained were transferred onto a nitrocellulose membrane (Invitrogen) and incubated overnight in 50 g/L nonfat milk in PBS at 4 °C. After three 10-min washes in 19 g/L nonfat milk, 1 g/L Tween 20 in PBS, the membranes were incubated in monoclonal goat anti-mouse endostatin antibodies (R&D Systems, Minneapolis, MN) diluted 1:500. After washing, the membranes were incubated in horseradish peroxidase-conjugated donkey anti-goat immunoglobulin (Santa Cruz Biotechnology, Santa Cruz, CA) diluted 1:4 000 and the proteins were detected using an ECL plus kit (Amersham Pharmacia Biotechnology, Uppsala, Sweden).

Endostatin enzyme immunoassay

Endostatin levels in the conditioned medium of cultured cells or in the mouse serum were determined using a mouse endostatin immunoassay kit (Chemicon International, Temecula, CA, USA).

Endothelial cell proliferation assay

HUVECs were plated on 5×10^3 in 96-well gelatin-coated plates and allowed to attach in complete medium for 4 h. The medium was then replaced by the conditioned medium, where the endostatin concentration was measured by an ELISA assay. After 1 h, an equal volume of $2 \times$ complete medium was added, and the number of cells was quantified by a colorimetric MTT assay on the indicated days. The test was performed in triplicate.

Endothelial cell tube formation assay

Twenty-four well plates were coated with 50 µL of Matrigel (BD Biosciences, Bedford, MA) in an ice bath and then incubated at 37 °C for 1 h. HUVECs at a density of 5×10^4 cells in each well were seeded and cultured in the conditioned media. After 18-h incubation, the plates were photographed. All tests were performed in triplicate.

In vivo tumor model

Animal experiments were carried out in accordance with the policies of Animal Research Committee of the Yonsei University College of Medicine. Twenty-five 8-wk-old female ICR mice (Charles River Laboratories, Wilmington, MA) were randomly divided into 5 equal groups, namely no treatment and rAAV-LacZ treatment alone as the control, treated with rAAV-LacZ in combination with etoposide pretreatment, treated with rAAV-endostatin alone, and treated with rAAV-endostatin in combination with etoposide pretreatment. In the pretreatment group, etoposide (40 mg/kg) in 200 µL HBSS was administered 3 times for a week by an intraperitoneal injection beginning 7 d before rAAV injection. Hepatic tumors were induced by directly injecting 5×10^6 S-180 murine sarcoma cells into the liver. Simultaneously, 500 µL of rAAV-mEndostatin (1.5×10^{12} viral particles) was injected into the spleen in the endostatin treatment groups in order to deliver viral particles into the liver. The mice were sacrificed 7 d after tumor cell injections by a halothane overdose to examine hepatic tumors. The tumor volume (TV) was determined using the following formula: $TV = (\text{Length} \times \text{width}^2) / 2$. In order to evaluate the long-term survival, the experiment was repeated and the mice were followed up for 2 mo. The survival time was defined from the day of tumor injection to death. The mice that were alive at the end of the follow-up period were estimated as the censored observation.

Localization of endostatin expression in liver

The livers were harvested and 5 μm -thick sections of the formalin-fixed, paraffin-embedded specimens were deparaffinized in xylene and heated in a citrate buffer for 10 min. Endogenous peroxidase activity was blocked by incubation with 10 mL/L H_2O_2 and 10 g/L Triton X-100. Goat anti-mouse antibodies were applied at a dilution of 1:60 overnight at 4 $^\circ\text{C}$. Biotinylated rabbit anti-goat antibodies (Vector, Burlingame, CA) were then applied for 1 h at room temperature at a 1:200 dilution. After incubation with streptavidin conjugated to horseradish peroxidase, a substrate containing chromogen, 3,3'-diaminobenzidine tetrahydrochloride, was added and the slides were counterstained with hematoxylin. All the slides were air-dried and kept in dark at 4 $^\circ\text{C}$ until evaluated.

Microvessel density (MVD) assessment

In order to analyze hepatic tumor microvessels, tissue sections (5 μm) of formalin-fixed, paraffin-embedded specimens were evaluated using rat anti-mouse CD34 antibodies (1:50; RAM34; Pharmingen, San Diego, CA) as the primary antibody and biotinylated rabbit anti-rat antibodies (Vector, Burlingame, CA) as the secondary antibody. After incubation of the tissue with streptavidin conjugated to horseradish peroxidase, the reactions were visualized by a substrate containing chromogen, 3,3'-diaminobenzidine tetrahydrochloride. The slides were counterstained with hematoxylin. At least 5 thin slices were made from each tumor and used for MVD assessment. MVD was estimated by counting the number of CD34-positive vessels in the tumor area, which was representative of the highest MVD at $\times 200$ magnification. The counts were typically made in 3-5 hot spots, and the highest MVD was used to characterize the tumor.

Statistical analysis

The data were expressed as mean \pm SD. Student's *t* test was used to analyze the statistical differences in endostatin levels in the conditioned medium of cultured cells or in mouse serum, endothelial cell proliferation, tumor size, or microvessel assessment among the groups. The Kaplan and Meier method was used to calculate the survival rate in the *in vivo* experiment and the survival differences between the groups were evaluated using the log-rank test. A $P < 0.05$ was considered statistically significant.

RESULTS

Increased *in vitro* expression of endostatin molecules on rAAV-endostatin transduced hepatoma cells by pretreatment with topoisomerase inhibitors

Hepa1c1c7 mouse hepatoma cells in the 10 cm plate were incubated with either rAAV-endostatin or rAAV-LacZ vectors (1×10^4 viral particles/cell) for 48 h. In the pretreatment group, etoposide (3 $\mu\text{mol/L}$) or camptothecin (10 $\mu\text{mol/L}$) was administered 6 h prior to transduction. Conditioned media were concentrated 10 times and used in both Western blotting and ELISA. The *in vitro* expression of endostatin was detected by Western blot analysis. The recombinant endostatin was visualized in the supernatant of Hepa1c1c7 cells transduced with rAAV-endostatin, but not in the supernatant of Hepa1c1c7 transduced with rAAV-LacZ. The endostatin expression level was enhanced as a result of the pretreatment with either etoposide or camptothecin (Figure 1A). ELISA was performed to quantify the expression level. Hepa1c1c7 cells transduced with rAAV-endostatin expressed endostatin (19.0 \pm 3.0 ng/mL) compared with the vector control (0.3 \pm 0.3 ng/mL) and mock control (0.3 \pm 0.2 ng/mL), and topoisomerase inhibitors enhanced significantly the endostatin expression level ($P < 0.05$) (Figure

1B). In the range of concentrations used in this study, etoposide or camptothecin had little effect on Hepa1c1c7 cell growth (data not shown). Etoposide increased the endostatin expression level more than camptothecin (43.3 \pm 5.1 vs 30.7 \pm 5.7 ng/mL, $P < 0.05$). Consequently, etoposide was chosen as a combination therapy in the *in vivo* experiment.

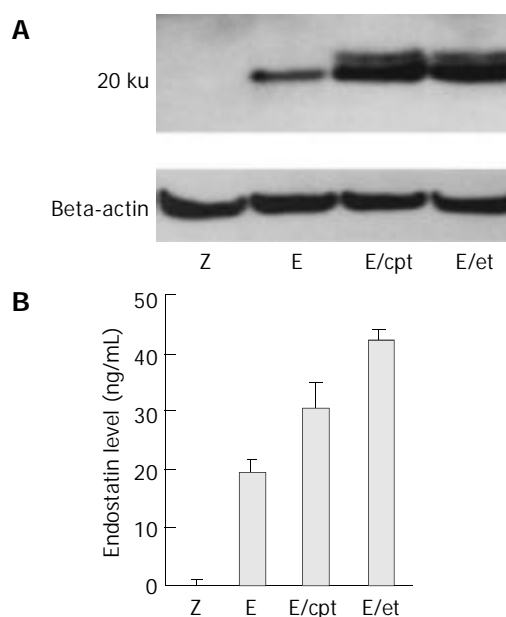


Figure 1 Effects of topoisomerase inhibitors on rAAV mediated endostatin expression level. Hepa1c1c7 mouse hepatoma cells were transduced with 1×10^4 particles/cell of rAAV-endostatin or rAAV-LacZ. In pretreatment group, etoposide (3 $\mu\text{mol/L}$) or camptothecin (10 $\mu\text{mol/L}$) was administered 6 h before transduction. Forty-eight hours later, the expression of endostatin was determined. A: Analysis of protein expression by NuPAGE electrophoresis, B: Concentration of endostatin measured by ELISA ($P < 0.05$, rAAV-endostatin in combination with pretreatment groups versus other groups). Z: rAAV-LacZ without pretreatment, E: rAAV-endostatin without pretreatment, E/et: rAAV-endostatin pretreated with etoposide, E/cpt: rAAV-endostatin pretreated with camptothecin.

In vitro biological activities of endostatin produced by rAAV vectors and pretreatment with topoisomerase inhibitors

As expected, the conditioned media from Hepa1c1c7 cells transduced with the control rAAV-LacZ vector did not influence either endothelial cell proliferation or tube formation compared to the conditioned media from the non-treated control (data not shown). Etoposide and camptothecin had a minor effect on the growth of HUVECs, and recombinant endostatin actively reduced endothelial cell growth. However, the conditioned media from rAAV-endostatin combined with etoposide group showed very strong inhibition (Figure 2A). Similarly, the recombinant endostatin suppressed tube formation of endothelial cells, and the rAAV-endostatin combined with etoposide group had the highest effect (Figure 2B).

Synergic effect of rAAV-endostatin with topoisomerase inhibitors in a mouse liver tumor model

Hepatic tumors were formed by injecting S-180 murine sarcoma cells directly into the predetermined site of the liver, and rAAV-Lac-Z treatment mice had similar hepatic tumors compared to non-treated mice (170.0 \pm 38.6 and 159.7 \pm 27.7 mm^3 , respectively). rAAV-LacZ in combination with etoposide and rAAV-endostatin reduced hepatic tumor burden (52.0 \pm 9.4 and 9.3 \pm 4.5 mm^3 , respectively) ($P < 0.05$, treated group vs non-treated or rAAV-Lac-Z treatment group). Interestingly, tumor nodules were barely

observed in the rAAV-endostatin plus etoposide group (Figure 3). Serum endostatin was hardly shown in non-treatment group (30.4 ± 20.8 ng/mL), rAAV-LacZ treatment alone (34.2 ± 21.4 ng/mL) and rAAV-LacZ plus etoposide groups (25.8 ± 19.9 ng/mL), although rAAV-endostatin induced detectable serum endostatin level (191.1 ± 54.7 ng/mL, $P < 0.05$, rAAV-endostatin group vs control groups). In contrast, rAAV-endostatin plus etoposide induced the highest endostatin level (321.5 ± 54.3 ng/mL, $P < 0.05$, rAAV-endostatin plus etoposide group vs other groups) (Figure 4). The *in vivo* expression of endostatin was detected immunohistochemically. Staining with anti-endostatin antibodies revealed positive cells in vessels of the liver sections from the rAAV-endostatin treatment group, whereas the control sections were negative, and a dramatic increase was observed in rAAV-endostatin plus etoposide treatment mice (Figure 5). Moreover, endostatin was stained in hepatocytes of rAAV-endostatin plus etoposide treatment mice. The microvessel densities in tumor were estimated by CD34 staining, which were found to be decreased in the rAAV treatment group (19.3 ± 4.5 , $P < 0.05$, rAAV treatment group vs control groups) compared with the mock control (97.7 ± 15.2) and the vector control (105.2 ± 17.6). As expected, the rAAV-endostatin plus etoposide treatment mice had the lowest microvessel density (7.6 ± 1.5) (Table 1). All the non-treated or rAAV-lacZ treated mice died within 30 d. rAAV-LacZ plus etoposide treatment barely affected the survival and rAAV-endostatin extended the survival time. However, the rAAV-endostatin plus etoposide treatment mice had the longest survival (Figure 6). In addition, significant endostatin expressions were detected in the surviving mice of rAAV-endostatin plus etoposide treatment group even after 2 mo (data not shown).

Table 1 Microvessel assessment of S-180 murine sarcoma tumors

Group	Microvessel density
No treatment	97.7 ± 15.2
rAAV-LacZ alone	105.2 ± 17.6
rAAV-LacZ plus etoposide	52.0 ± 9.4
rAAV-endostatin alone	19.3 ± 4.5
rAAV-endostatin plus etoposide	7.6 ± 1.5^a

The microvessel density was measured with a light microscope in the tumor representative of the highest microvessel density at magnification $\times 200$ ("hot spot"). ^a $P < 0.05$, rAAV-endostatin plus etoposide group against other groups.

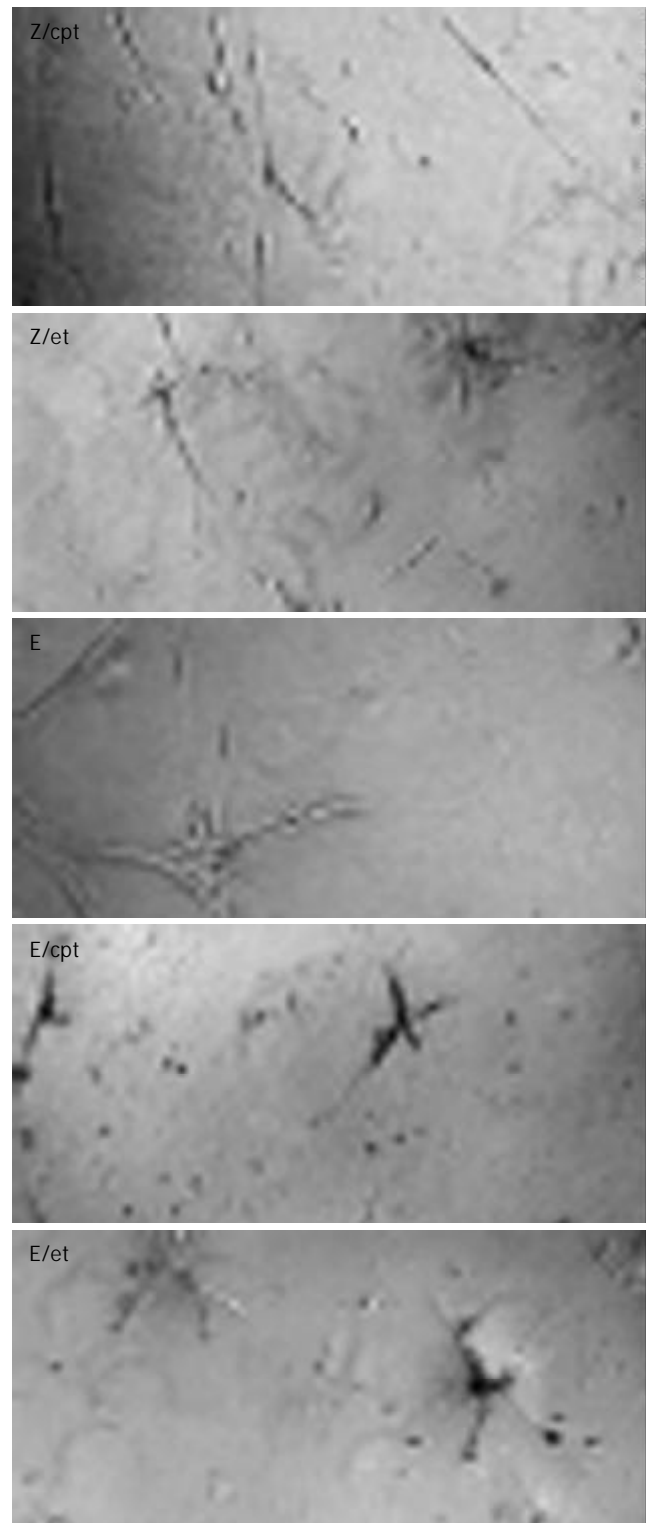
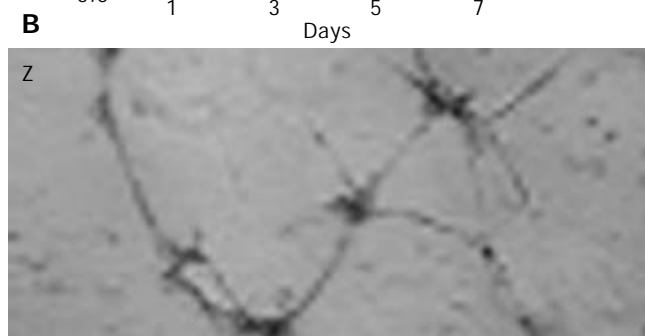
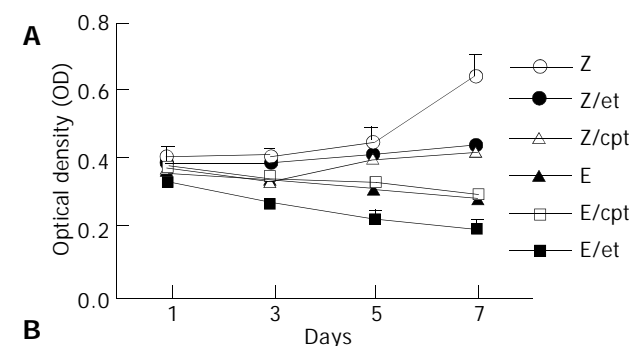


Figure 2 *In vitro* biological activities of expressed endostatin. A: 5×10^3 HUVECs in a 96-well were cultured in the conditioned media from Hepa1c1c7 mouse hepatoma cells without pretreatment (Z), those from the cells pretreated with etoposide (Z/et) or camptothecin (Z/cpt), those from the rAAV-endostatin transduced cells without pretreatment (E), those from rAAV-endostatin transduced cells pretreated with etoposide (E/et) or camptothecin (E/cpt). The number of cells was then calculated by a MTT assay. Each value represents mean \pm SD of 3 independent experiments ($P < 0.05$, rAAV-endostatin in combination with pretreatment groups versus other groups). B: Impact on tube formation of endothelial cells. HUVECs were seeded into 24-well plates coated with Matrigel at a density of 5×10^4 cells in each well and cultured in the conditioned media. After 18 h incubation, the level of cell growth and differentiation was observed. All tests were performed in triplicate.

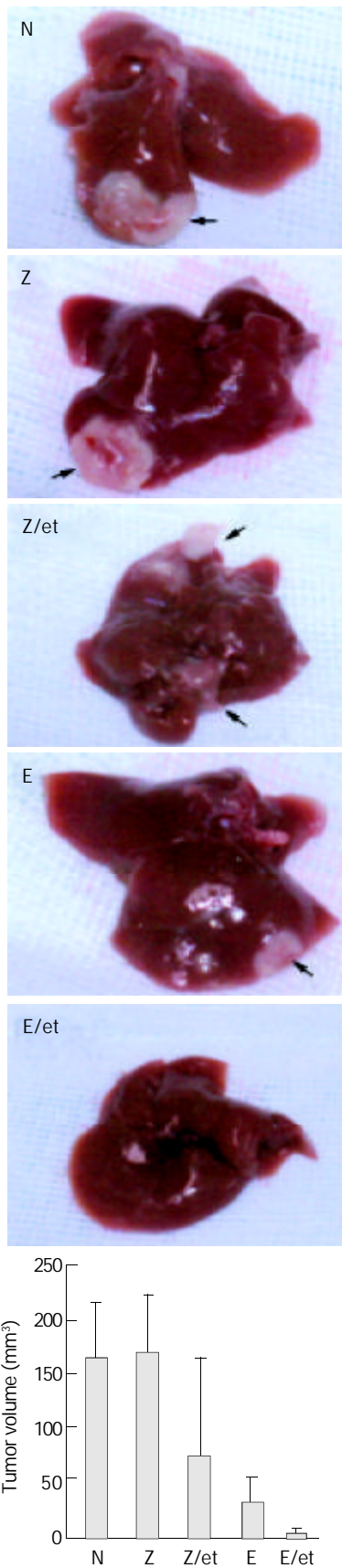


Figure 3 Effect of rAAV-endostatin in combination with etoposide on murine sarcoma bearing mice. Twenty five mice bearing S-180 murine sarcoma cells were randomly divided into 5 groups, namely no treatment, rAAV-LacZ alone, rAAV-LacZ plus etoposide pretreatment, rAAV-endostatin alone, and rAAV-endostatin plus etoposide pretreatment. In the pretreatment group, etoposide (40 mg/kg) was administered 3 times for one week by an intraperitoneal injection beginning 7 d prior to rAAV injection, and 1.5×10^{12} viral particles of rAAV-

endostatin vector were injected into the spleen simultaneously with tumor cell inoculation (5×10^6 S-180 cells) into the liver. The tumor volume was determined 7 d after injecting murine sarcoma cells ($P < 0.05$, rAAV plus etoposide group versus other groups). $Tumor\ volume = (Length \times width^2) / 2$.

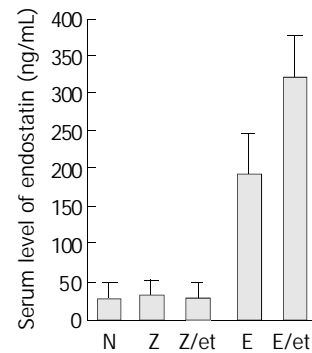


Figure 4 Mouse endostatin levels determined in sera of mice inoculated with murine sarcoma cells. S-180 murine sarcoma cells were inoculated into liver. Seven days later, ELISA determined the endostatin concentration and the results were expressed as mean \pm SD of 5 animals ($P < 0.05$, rAAV-endostatin plus etoposide group versus other groups).

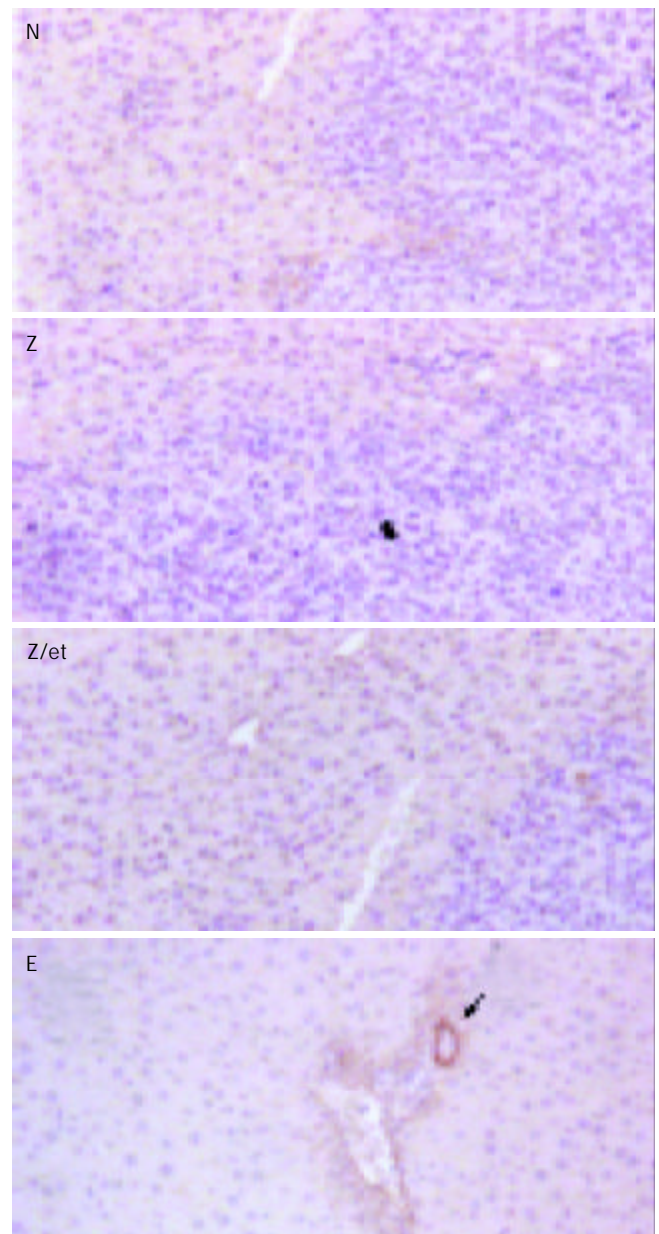




Figure 5 Detection of endostatin in livers of tumor-bearing mice. Hepatic tumors were induced by injecting murine sarcoma cells into the liver. After 7 d, the livers were harvested from the mice of different groups and analyzed by immunohistochemical staining for endostatin. Livers without treatment, rAAV-LacZ alone and rAAV-LacZ plus etoposide pretreatment did not express endostatin. The vessels of livers treated with rAAV-endostatin were stained with anti-endostatin antibodies and a significant increase was observed in the rAAV-endostatin plus etoposide treatment group (arrow). Endostatin was also detected in hepatocytes of the rAAV-endostatin plus etoposide treatment group (arrow head).

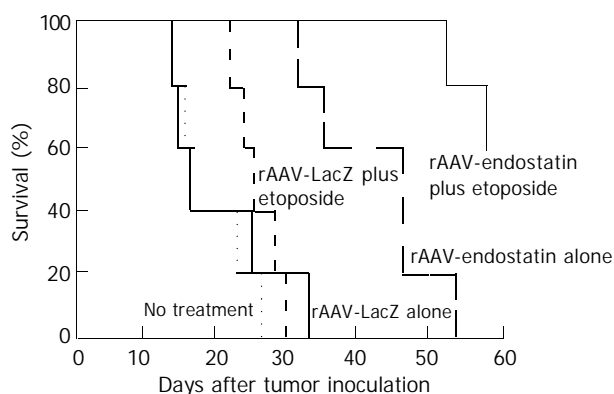


Figure 6 Survival time of sarcoma-bearing mice. Twenty-five mice were randomly divided into 5 groups: no treatment, rAAV-LacZ alone, rAAV-LacZ plus etoposide, rAAV-endostatin alone, or rAAV-endostatin plus etoposide. The tumor-bearing mice treated with rAAV-endostatin in combination with etoposide had a significantly longer survival than those in other groups ($P < 0.05$).

DISCUSSION

The transduction of non-dividing cell populations is an attractive goal of gene therapy, especially in terms of antiangiogenesis against cancer. rAAV vectors could transfer a foreign gene into non-dividing cells, but the gene transfer efficiency was too low^[29]. The transduction of non-dividing cells by AAV vectors was increased by DNA-damaging agents, such as γ and UV-irradiation and cisplatin, which were toxic to normal cells at the concentrations needed to increase transduction^[30]. In contrast, pretreatment with topoisomerase inhibitors increased AAV vector mediated transduction of non-dividing cells with a lower cytotoxicity^[23]. It was found in this study that topoisomerase inhibitors in rAAV mediated endostatin gene therapy increased endostatin expression level. Etoposide more effectively enhanced the expression of target molecules than camptothecin. This rAAV-endostatin plus etoposide treatment induced anti-angiogenic effects to a significantly larger extent than rAAV treatment only, and endostatin expression levels were found to correlate well with the antiangiogenic effects.

rAAV with a CMV promoter used in this study, proved stable and strongly expressed endostatin. Etoposide could irreversibly

inhibit CMV replication and suppress viral DNA and late viral-protein synthesis^[31]. It is unclear whether or not etoposide inhibits the function of CMV promoter. This study did not evaluate the effect of etoposide on CMV promoter. However, topoisomerase inhibitor increased the overall endostatin expression level.

This study examined the *in vivo* antitumor effects of combined therapy with rAAV-endostatin and etoposide. In this mouse model of a hepatic tumor, etoposide had little antitumor effect, and rAAV-endostatin alone was insufficient to control a hepatic tumor. However, the combined modality significantly enhanced the tumor response. Interestingly, endostatin expression was immunohistochemically detected in hepatocytes and was significantly increased around vessels in the liver of the rAAV-endostatin plus etoposide treatment group compared with those of the rAAV-endostatin alone group. The topoisomerase inhibitor increased the transduction efficiency of AAV in both S-phase and non S-phase cells, and hepatocytes were much more efficiently transduced than other cells^[24]. Overall, rAAV-endostatin in combination with etoposide increased the endostatin expression level in hepatocytes of mice, and induced sufficient control in the hepatic tumor model. One potential obstacle to the clinical application of rAAV-mediated anti-angiogenesis gene therapy is that it maintains high levels of the target molecules over a long-term. rAAV vector-mediated cancer gene therapy protocols combined with topoisomerase inhibitor pretreatment might be a solution to this problem.

ACKNOWLEDGMENTS

The authors thank Dr Woo Ik Yang in the Department of Pathology for his technical assistance.

REFERENCES

- 1 Guo XL, Lin GJ, Zhao H, Gao Y, Qian LP, Xu SR, Fu LN, Xu Q, Wang JJ. Inhibitory effects of docetaxel on expression of VEGF, bFGF and MMPs of LS174T cell. *World J Gastroenterol* 2003; **9**: 1995-1998
- 2 Gupta MK, Qin RY. Mechanism and its regulation of tumor-induced angiogenesis. *World J Gastroenterol* 2003; **9**: 1144-1155
- 3 Daly ME, Makris A, Reed M, Lewis CE. Hemostatic regulators of tumor angiogenesis: a source of antiangiogenic agents for cancer treatment? *J Natl Cancer Inst* 2003; **95**: 1660-1673
- 4 Folkman J. Role of angiogenesis in tumour growth and metastasis. *Semin Oncol* 2002; **29**(6 Suppl 16): 15-18
- 5 Folkman J. Angiogenesis inhibitors: a new class of drugs. *Cancer Biol Ther* 2003; **2**(4 Suppl): S127-133
- 6 Kiselev SM, Lutsenko SV, Severin SE, Severin ES. Tumor angiogenesis inhibitors. *Biochemistry* 2003; **68**: 497-513
- 7 Boehm T, Folkman J, Browder T, O'Reilly MS. Antiangiogenic therapy of experimental cancer does not induce acquired drug resistance. *Nature* 1997; **390**: 404-407
- 8 Li X, Fu GF, Fan YR, Shi CF, Liu XJ, Xu GX, Wang JJ. Potent inhibition of angiogenesis and liver tumor growth by administration of an aerosol containing a transferrin-liposome-endostatin complex. *World J Gastroenterol* 2003; **9**: 262-266
- 9 O'Reilly MS, Boehm T, Shing Y, Fukai N, Vasios G, Lane WS, Flynn E, Birkhead JR, Olsen BR, Folkman J. Endostatin: an endogenous inhibitor of angiogenesis and tumour growth. *Cell* 1997; **88**: 277-285
- 10 Wang X, Liu FK, Li X, Li JS, Xu GX. Retrovirus-mediated gene transfer of human endostatin inhibits growth of human liver carcinoma cells SMMC7721 in nude mice. *World J Gastroenterol* 2002; **8**: 1045-1049
- 11 Blezinger P, Wang J, Gondo M, Quezada A, Mehrens D, French M, Singhal A, Sullivan S, Rolland A, Ralston R, Min W. Systemic inhibition of tumor growth and tumor metastases by intramuscular administration of the endostatin gene. *Nat Biotechnol* 1999; **17**: 343-348
- 12 Chen QR, Kumar D, Stass SA, Mixson AJ. Liposomes complexed

- to plasmids encoding angiostatin and endostatin inhibit breast cancer in nude mice. *Cancer Res* 1999; **59**: 3308-3312
- 13 **Ding I**, Sun JZ, Fenton B, Liu WM, Kimsely P, Okunieff P, Min W. Intratumoral administration of endostatin plasmid inhibits vascular growth and perfusion in MCa-4 murine mammary carcinomas. *Cancer Res* 2001; **61**: 526-531
- 14 **Feldman AL**, Alexander HR, Hewitt SM, Lorang D, Thiruvathukal CE, Turner EM, Libutti SK. Effect of retroviral endostatin gene transfer on subcutaneous and intraperitoneal growth of murine tumors. *J Natl Cancer Inst* 2001; **93**: 1014-1020
- 15 **Langer JC**, Klotman ME, Hanss B, Tulchin N, Bruggeman LA, Klotman PE, Lipkowitz MS. Adeno-associated virus gene transfer into renal cells: potential for *in vivo* gene delivery. *Exp Nephrol* 1998; **6**: 189-194
- 16 **Li S**, Zhang X, Xia X, Zhou L, Breau R, Suen J, Hanna E. Intramuscular electroporation delivery of IFN- α gene therapy for inhibition of tumor growth located at a distant site. *Gene Ther* 2001; **8**: 400-407
- 17 **Nakashima Y**, Yano M, Kobayashi Y, Moriyama S, Sasaki H, Toyama T, Yamashita H, Fukai I, Iwase H, Yamakawa Y, Fujii Y. Endostatin gene therapy on murine lung metastases model utilizing cationic vector-mediated intravenous gene delivery. *Gene Ther* 2003; **10**: 123-130
- 18 **Nguyen JT**, Wu P, Clouse ME, Hlatky L, Terwilliger EF. Adeno-associated virus-mediated delivery of antiangiogenic factors as an antitumor strategy. *Cancer Res* 1998; **58**: 5673-5677
- 19 **Wang X**, Liu FK, Li X, Li JS, Xu GX. Inhibitory effect of endostatin expressed by human liver carcinoma SMMC7721 on endothelial cell proliferation *in vitro*. *World J Gastroenterol* 2002; **8**: 253-257
- 20 **Muzyczka N**. Use of adeno-associated virus as a general transduction vector for mammalian cells. *Curr Top Microbiol Immunol* 1992; **158**: 97-129
- 21 **Xiao W**, Berta SC, Lu MM, Moscioni AD, Tazelaar J, Wilson JM. Adeno-associated virus as a vector for liver-directed gene therapy. *J Virol* 1998; **72**: 10222-10226
- 22 **High K**. AAV-mediated gene transfer for hemophilia. *Genet Med* 2002; **4**(6 Suppl): 56S-61S
- 23 **Russell DW**, Alexander IE, Miller AD. DNA synthesis and topoisomerase inhibitors increase transduction by adeno-associated virus vectors. *Proc Natl Acad Sci U S A* 1995; **92**: 5719-5723
- 24 **Koeberl DD**, Alexander IE, Halbert CL, Russell DW, Miller AD. Persistent expression of human clotting factor IX from mouse liver after intravenous injection of adeno-associated virus vectors. *Proc Natl Acad Sci U S A* 1997; **94**: 1426-1431
- 25 **Peng D**, Qian C, Sun Y, Barajas MA, Prieto J. Transduction of hepatocellular carcinoma (HCC) using recombinant adeno-associated virus (rAAV): *in vitro* and *in vivo* effects of genotoxic agents. *J Hepatol* 2000; **32**: 975-985
- 26 **Yoon SS**, Eto H, Lin CM, Nakamura H, Pawlik TM, Song SU, Tanabe KK. Mouse endostatin inhibits the formation of lung and liver metastases. *Cancer Res* 1999; **59**: 6251-6256
- 27 **Weiner MP**, Costa GL, Schoettlin W, Cline J, Mathur E, Bauer JC. Site-directed mutagenesis of double-stranded DNA by the polymerase chain reaction. *Gene* 1994; **151**: 119-123
- 28 **Matsushita T**, Elliger S, Elliger C, Podsakoff G, Villarreal L, Kurtzman GJ, Iwaki Y, Colosi P. Adeno-associated virus vectors can be efficiently produced without helper virus. *Gene Ther* 1998; **5**: 938-945
- 29 **Russell DW**, Miller AD, Alexander IE. Adeno-associated virus vectors preferentially transduce cells in S phase. *Proc Natl Acad Sci U S A* 1994; **91**: 8915-8919
- 30 **Alexander IE**, Russell DW, Miller AD. DNA-damaging agents greatly increase the transduction of nondividing cells by adeno-associated virus vectors. *J Virol* 1994; **68**: 8282-8287
- 31 **Huang ES**, Benson JD, Huong SM, Wilson B, van der Horst C. Irreversible inhibition of human cytomegalovirus replication by topoisomerase II inhibitor, etoposide: a new strategy for the treatment of human cytomegalovirus infection. *Antiviral Res* 1992; **17**: 17-32

Edited by Xu JY and Wang XL Proofread by Xu FM

The protective mechanism of Yisheng Injection against hepatic ischemia reperfusion injury in mice

Feng Cheng, You-Ping Li, Jing-Qiu Cheng, Li Feng, Sheng-Fu Li

Feng Cheng, You-Ping Li, Jing-Qiu Cheng, Li Feng, Sheng-Fu Li, Laboratory of Transplant Engineering and Immunology, West China Hospital, Sichuan University, 37 Guoxue Xiang, Chengdu 610041, Sichuan Province, China

Supported by the National Natural Science Foundation of China, No. 30271676

Co-correspondents: You-Ping Li and Jing-Qiu Cheng

Correspondence to: Professor You-Ping Li, Key Laboratory of Transplant Engineering and Immunology of Health Ministry of China, West China Hospital, Sichuan University, 37 Guoxue Xiang, Chengdu 610041, Sichuan Province, China. yzmylab@hotmail.com

Telephone: +86-28-85422075 **Fax:** +86-28-85423458

Received: 2003-11-04 **Accepted:** 2003-12-16

Abstract

AIM: Hepatic ischemia/reperfusion injury may cause acute inflammatory, significant organ damage or dysfunction, and remains an important problem for liver transplantation. Our previous *in vivo* and *in vitro* studies demonstrated that Yisheng injection (YS), a traditional Chinese medicine, had protective effect on ischemia/reperfusion injury. In this study, we examined whether YS had protective effect for hepatic ischemia/reperfusion injury and explored its protective mechanism.

METHODS: Hepatic warm ischemia/reperfusion was induced in mice. YS at different doses (5, 10, 20 mg/kg) was injected intraperitoneally 24 h and 1 h before ischemia and a third dose was injected intravenously just before reperfusion. The hepatocellular injury, oxidative stress, neutrophil recruitment, proinflammatory mediators and adhesion molecules associated with hepatic ischemia/reperfusion injury were assayed by enzyme-linked immunosorbent assay (ELISA), immunohistochemical assay and reverse transcription polymerase chain reaction (RT-PCR).

RESULTS: Undergoing 90 min of ischemia and 6 h of reperfusion caused dramatical injuries in mouse livers. Administration of YS at doses of 5, 10 and 20 mg/kg effectively reduced serum levels of alanine aminotransferase (ALT), aspartate aminotransferase (AST) and lactate dehydrogenase (LDH), from $3\ 670\pm 463$ U/L, $2\ 362\pm 323$ U/L and $12\ 752\pm 1\ 455$ U/L in I/R group to $1\ 172\pm 257$ U/L, 845 ± 193 U/L and $2\ 866\pm 427$ U/L in YS (20 mg/kg) treated group, respectively ($P<0.01$). The liver myeloperoxidase (MPO) and malondialdehyde (MDA) contents were decreased from 1.1 ± 0.2 (U/mg protein) and 9.1 ± 0.7 (nmol/mg protein) in I/R group to 0.4 ± 0.1 (U/mg protein) and 5.5 ± 0.9 (nmol/mg protein) in YS (20 mg/kg) treated group, respectively ($P<0.01$). Moreover, the serum levels of tumor necrosis factor- α (TNF- α) were reduced from 55 ± 9.9 (pg/mL) in I/R group to 16 ± 4.2 (pg/mL) ($P<0.01$). Furthermore, the over-expressions of TNF- α and intercellular adhesion molecule-1 (ICAM-1) were suppressed by YS treatment in a dose-dependent manner.

CONCLUSION: YS attenuates hepatic warm ischemia/

reperfusion injury by reducing oxidative stress and suppressing the over-expression of proinflammatory mediators and adhesion molecules.

Cheng F, Li YP, Cheng JQ, Feng L, Li SF. The protective mechanism of Yisheng Injection against hepatic ischemia reperfusion injury in mice. *World J Gastroenterol* 2004; 10(8): 1198-1203

<http://www.wjgnet.com/1007-9327/10/1198.asp>

INTRODUCTION

Clinical and experimental evidences suggest that an initial insult to organ allografts may influence both early and late functional survival. This injury may be either immunologic or antigen independent^[1].

Hepatic ischemia/reperfusion injury is an important nonimmunologic factor and remains a significant problem and limitation of liver transplantation and may result in liver failure, remote organ failure, and even death^[2,3].

During the initial phase of hepatic ischemia-reperfusion injury, Kupffer cells are activated and release reactive oxygen species (ROS)^[4] and proinflammatory cytokines^[5], especially tumor necrosis factor- α (TNF- α)^[6,7]. The enhanced production of TNF- α plays an important role in the initiation of a cascade of events that causes significant liver injury mediated by neutrophils. One of the main functions of TNF- α is to up-regulate the expression of adhesion molecules, especially intercellular adhesion molecule-1 (ICAM-1), and then mediate the recruitment of neutrophils into the liver resulting in further hepatic injury^[8,9].

Ischemia-reperfusion injury becomes significant through rapid up-regulation and surface expression of adhesion molecules, and activation of circulating host leukocytes and their binding to the vascular endothelium^[10]. In addition, the insult from ischemia/reperfusion surrounding engraftment may trigger alloresponsiveness in the host, making it potentially more prone to rejection^[11]. Furthermore, the initial acute rejection injury predisposes to chronic graft dysfunction early injuries may also affect later events. For this reason, the protection of liver against ischemia-reperfusion injury (IRI) remains one of the major nonimmunologic problems of liver transplantation^[12].

Our previous studies demonstrate that Yisheng injection (YS), a herbal preparation developed from traditional Chinese medicine, can effectively protect endothelial cells against hypoxia/reoxygenation injury^[13,14]; decrease the blood viscosity in hypostasis rats^[15]; attenuate the sclerosis of transplanted abdominal aorta in rats by reducing the generation of free radicals and down-regulating the expression of TGF- β ^[16]; protect isolated testes against cold preservation/reperfusion injury through reducing lipid peroxidation, calcium supercharge and damage to mitochondrial function^[17]; and protect kidney against ischemia/reperfusion injury in pigs by reducing serum levels of TNF- α (unpublished results). In this study, we examined whether YS had protective effect for hepatic ischemia/reperfusion injury and explored its protective mechanism.

MATERIALS AND METHODS

Yisheng injection

Yisheng injection (YS, 20 mg/mL) was provided by Chengdu Huayi Drug Co (Chengdu, China). Its effective ingredients are alkaloids extracted from *Corydalis thalictrifolia* Franch. and *Schnabelia oligophylla* Hand.-Mazz. In this study, YS was diluted with sterile saline.

Animals

Male C57BL/6 mice weighing 22 to 25 g were purchased from Vital River Co, Beijing, China. All mice were provided with standard laboratory chow and water and housed in accordance with institutional animal care policies.

Experimental design

The mice were randomly assigned into five experimental groups as follows: (1) sham operation group, (2) I/R group (treated with saline), (3) small-dose (5 mg/kg of YS) treated group, (4) middle-dose (10 mg/kg of YS) treated group, (5) large-dose (20 mg/kg of YS) treated group.

The model of partial hepatic ischemia and reperfusion was performed with published method^[18]. Briefly, 24 h and 1 h before the induction of ischemia, the mice received intraperitoneally two times either sterile saline or YS (5, 10 or 20 mg/kg). They were anesthetized with sodium pentobarbital (60 mg/kg intraperitoneally), then a midline laparotomy was performed and an atraumatic clip was used to interrupt the arterial and the portal venous blood supply to the left lob of the liver. After 90 min of partial hepatic ischemia, the mice again received either sterile saline or YS (5, 10 or 20 mg/kg) via the lateral tail vein, and the clip was removed initiating hepatic reperfusion. Sham control mice underwent the same protocol, but without vascular occlusion. Abdomen was sutured by two layers with 4.0 suture.

In order to determine the proper reperfusion time point, we assayed the alanine transaminase (ALT) levels in the blood samples obtained at different time points of 2, 4, 6, 10 and 24 h of reperfusion following 90 min of ischemia, and found that the blood ALT level reached the peak at the end of 6 h of reperfusion (data not shown). So the time point of 6 h of reperfusion was chosen in this study. Mice were killed after 6 h of reperfusion following 90 min of ischemia, and liver tissue (from the ischemic lob) and blood samples were taken for analysis.

Blood assay

Blood was obtained at the time of sacrifice. The plasma concentrations of alanine aminotransferase (ALT), aspartate aminotransferase (AST) and lactate dehydrogenase (LDH) were measured in a clinical laboratory as markers of hepatic damage. The serum levels of TNF- α were determined by using an ELISA Kit (Jingmei Biotech Co, Shengzheng, China) according to the manufacturers' instructions.

Liver edema

The extent of liver edema was measured by tissue wet-to-dry weight ratios. After dissection, liver samples were weighed and then placed in a drying oven at 55 °C until a constant weight was obtained^[18]. In this determination, liver edema was represented by an increase in the wet-to-dry weight ratios.

Myeloperoxidase, superoxide dismutase and malondialdehyde assay

Liver samples were homogenized in 100 mmol/L Tris-HCl buffer and centrifuged at 10 000 g for 20 min, and then liver myeloperoxidase (MPO), superoxide dismutase (SOD) and malondialdehyde (MDA) contents were assayed by using assay kits (Jiancheng Biotech Ltd, Nanjing, China), and the protein contents were assayed by using assay kits (Bio-Rad, USA)

according to the manufacturers' instructions.

Immunohistochemical assay

Tissue samples were fixed in 40 mg/L buffered formaldehyde and embedded in paraffin. For immunohistologic analysis, 5 μ m sections of paraffin-embedded liver tissues were cut, and stained with primary anti-mouse mAbs against TNF- α (diluted, 1:500, Santa Cruz Biotech Co, Santa Cruz, CA) or ICAM-1 (diluted, 1:400, Santa Cruz Biotech Co, Santa Cruz, CA). After incubation, the sections were incubated with peroxidase-conjugated goat anti-mouse IgG. The bound peroxidase was detected using 3,3'-diaminobenzidine.

Reverse transcription-polymerase chain reaction

Total RNA was extracted from liver tissue using SV Total RNA Isolation System (Promega Co, Madison, WI, USA), according to the manufacturer's instructions, and was quantified by UV spectrophotometer. RNA (1 μ g) was reverse transcribed and amplified using TaKaRa One-Step RT-PCR Kit (TaKaRa Biotech Co, Dalian, China) at following RT-PCR conditions: 50 °C for 30 min; 30 cycles at 95 °C for 1 min, 59 °C for 90 s, and 72 °C for 2 min. Primers used in PCR reactions were as follows^[18]: TNF- α sense (5' -AGCCCACGTAGCAAACCACCAA-3') and antisense (5' -ACACCCATTCCCTTCACAGAGCAAT-3'), to give a 446-bp product; ICAM-1 sense (5' -TGGAAGTGCACGTGCTGTAT-3') and antisense (5' -ACCATTCTGTTC AAAAGCAG-3'), to give a 513-bp product; and β -actin sense (5' -CTGAAGTACCCATTGAACATGGC-3') and antisense (5' -CAGAGCAGTAATCTCCTTCTGCAT-3'), to give a 672-bp product. PCR products were stained with SYBR green dye, electrophoresed in a 20 g/L agarose gel, and photographed. Digital photographs were assessed with image-analysis software (Image-Pro Plus System, Media Cybernetics Co, USA) and mRNA expressions were evaluated by the band intensity ratios of TNF- α and ICAM-1 to β -actin and presented as percentage of β -actin.

Statistical analysis

All data were expressed as mean \pm SD. Statistical analysis was performed by analysis of variance (ANOVA), and Student's *t* test was used to compare individual group means. *P* values less than 0.05 were considered statistically significant.

RESULTS

YS suppressed hepatic injury

Hepatic injury was assessed by measuring serum levels of ALT, AST and LDH. Undergoing 90 min of hepatic ischemia and 6 h of reperfusion caused dramatical increases in serum ALT levels compared with sham controls, from 157 \pm 60 U/L to 3670 \pm 463 U/L (Figure 1A). Administration of YS at a dose of either 5, 10 or 20 mg/kg reduced the serum ALT levels by about 6.6%, 51.6% and 68.1% respectively, and YS at middle and large doses (10 and 20 mg/kg) showed significant effects (Figure 1A). Measurement of AST and LDH values reflected similar differences among the groups (Figure 1A, B), further demonstrating the dose-dependent protective effects of YS.

YS suppressed hepatic neutrophil recruitment and liver edema

Hepatic neutrophil recruitment was determined by liver MPO content and liver edema was determined by tissue wet-to-dry weight ratio. Hepatic ischemia and 6 h of reperfusion caused marked increases in liver MPO content compared with sham controls (Figure 2A). In the presence of YS (5, 10, 20 mg/kg), liver MPO content was significantly reduced by about 49.1%, 52.7% and 63.6% respectively (Figure 2A). In addition, administration of YS also reduced the liver edema in a dose-dependent manner (Figure 2B).

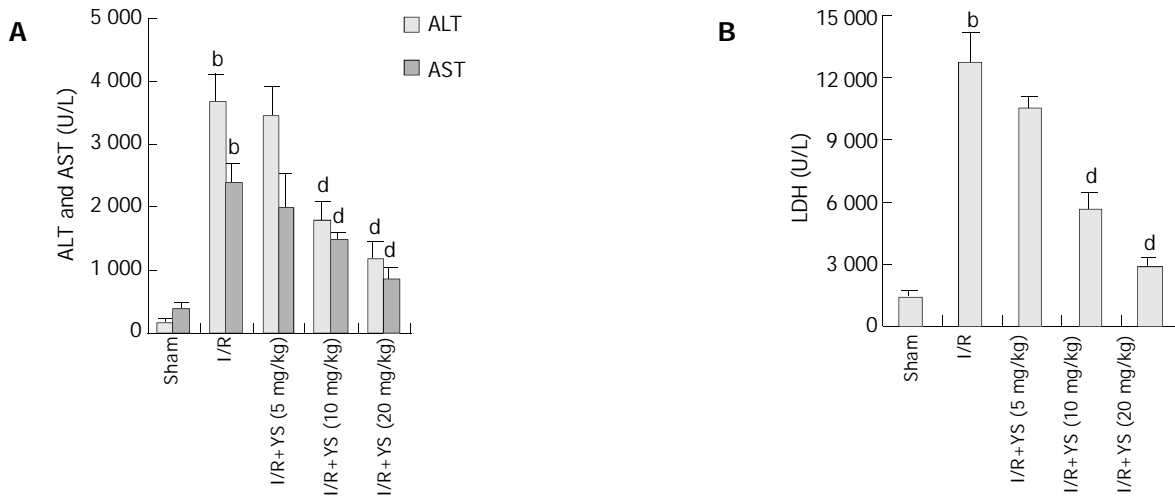


Figure 1 Effects of YS on hepatocellular injury induced by hepatic ischemia and reperfusion. After 90 min of ischemia and 6 h of reperfusion, serum levels of ALT, AST (A) and LDH (B) were determined. YS at different doses (5, 10, 20 mg/kg) was injected intraperitoneally 24 h and 1 h before ischemia and a third dose was injected intravenously just before reperfusion. For all groups, *n*=8. ^b*P*<0.01 compared with sham group; ^a*P*<0.01 compared with I/R group.

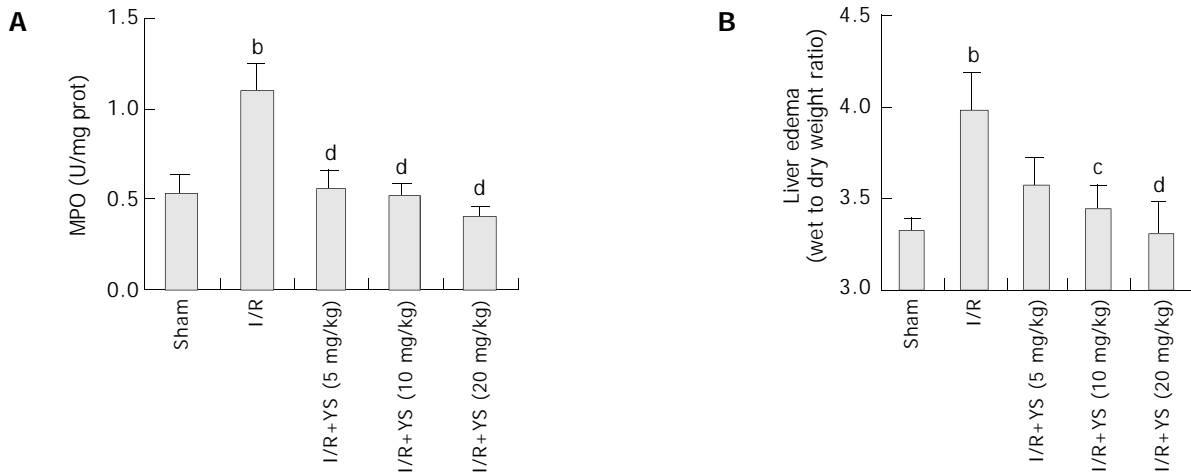


Figure 2 Effects of YS on neutrophil recruitment (A) and liver edema (B) induced by 90 min of ischemia and 6 h of reperfusion. MPO contents in liver tissues were analyzed as the index of neutrophil recruitment. Liver edema was determined by tissue wet-to-dry weight ratio. YS at different doses (5, 10, 20 mg/kg) was injected intraperitoneally 24 h and 1 h before ischemia and a third dose was injected intravenously just before reperfusion. For all groups, *n*=8. ^b*P*<0.01 compared with sham group; ^c*P*<0.05, ^a*P*<0.01 compared with I/R group.

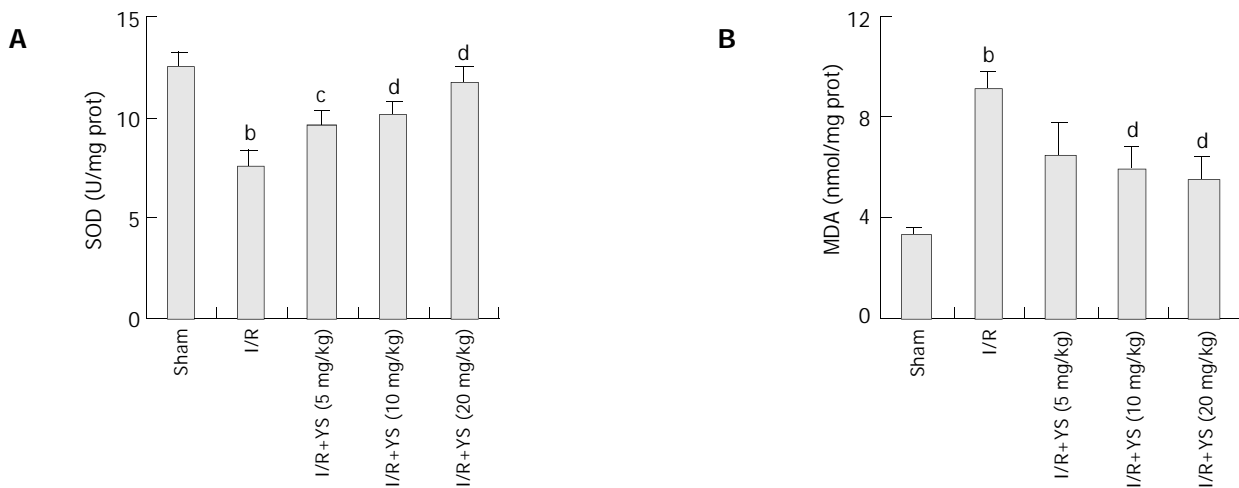


Figure 3 Effects of YS on SOD (A) and MDA (B) levels in liver tissues. After 90 min of ischemia and 6 h of reperfusion, liver tissues were homogenized and assayed for SOD and MDA levels as the index of hepatic oxidative stress. YS with different dose (5, 10, 20 mg/kg) was injected intraperitoneally 24 h and 1 h before ischemia and a third dose was injected intravenously just before reperfusion. For all groups, *n*=8. ^b*P*<0.01 compared with sham group; ^c*P*<0.05, ^a*P*<0.01 compared with I/R group.

YS reduced oxidative stress

Hepatic ischemia and 6 h of reperfusion caused marked decrease in liver SOD activity (Figure 3A) and resulted in remarkable increases in liver MDA content compared with sham controls (Figure 3B). In the presence of YS at doses of 5, 10 and 20 mg/kg, the liver SOD activities were elevated by about 26.6%, 33.6% and 54.8% respectively, and liver MDA content reduced by 28.6%, 35.2% and 39.6% respectively, both in a dose-dependent manner.

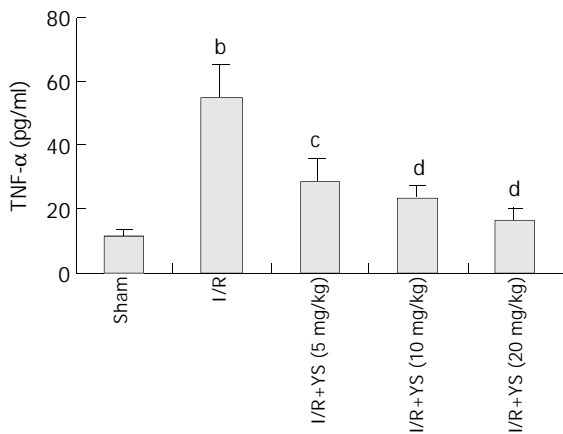


Figure 4 Effects of YS on serum levels of TNF- α analyzed by enzyme-linked immunosorbent assay. Mice were subjected to 90 min of ischemia and 6 h of reperfusion. Saline or YS with different dose (5, 10, 20 mg/kg) was injected intraperitoneally 24 h and 1 h before ischemia and a third dose was injected intravenously just before reperfusion. For all groups, $n=8$. ^b $P<0.01$ compared with sham group; ^c $P<0.05$, ^d $P<0.01$ compared with I/R group.

YS reduced TNF- α in serum and ICAM-1 on liver tissues

Hepatic ischemia and 6 h of reperfusion markedly increased the levels of TNF- α in sera (Figure 4). Administration of YS at different doses of 5, 10 and 20 mg/kg significantly reduced the serum levels of TNF- α by about 48.2%, 57.3% and 70.9% respectively (Figure 4). The over-expressions of TNF- α and ICAM-1 on liver tissues after I/R were demonstrated by immunohistochemical assay (Figure 5A, B; Figure 6A, B). In the presence of YS (20 mg/kg), hepatic ischemia/reperfusion-induced increases in TNF- α and ICAM-1 expression were dramatically suppressed (Figure 5C; Figure 6C).

YS reduced hepatic mRNA expression of TNF- α and ICAM-1

To determine the expressions of proinflammatory mediators and adhesion molecules, mRNA transcripts for TNF- α and ICAM-1 were assessed. RNA extracts from livers undergoing 90 min of ischemia and 6 h of reperfusion were analyzed by reverse transcription PCR. Furthermore, the band intensity ratios of TNF- α and ICAM-1 to β -actin were evaluated and presented as percentage of β -actin, and were compared among sham, I/R and YS-treated groups. Hepatic ischemia and reperfusion remarkably increased mRNA expression of TNF- α (Figure 7A) and ICAM-1 (Figure 7B), respectively. Administration of YS at doses of 5, 10 and 20 mg/kg significantly abrogated hepatic ischemia/reperfusion-induced increases in TNF- α and ICAM-1 mRNA expression (Figure 7A, B). The comparison of band intensity ratios of TNF- α and ICAM-1 to β -actin in sham, I/R and YS-treated groups demonstrated that YS treatment at doses of 5, 10 and 20 mg/kg effectively suppressed the evaluation of TNF- α and ICAM-1 mRNA expression in a dose-dependent manner (Figure 7C, D).

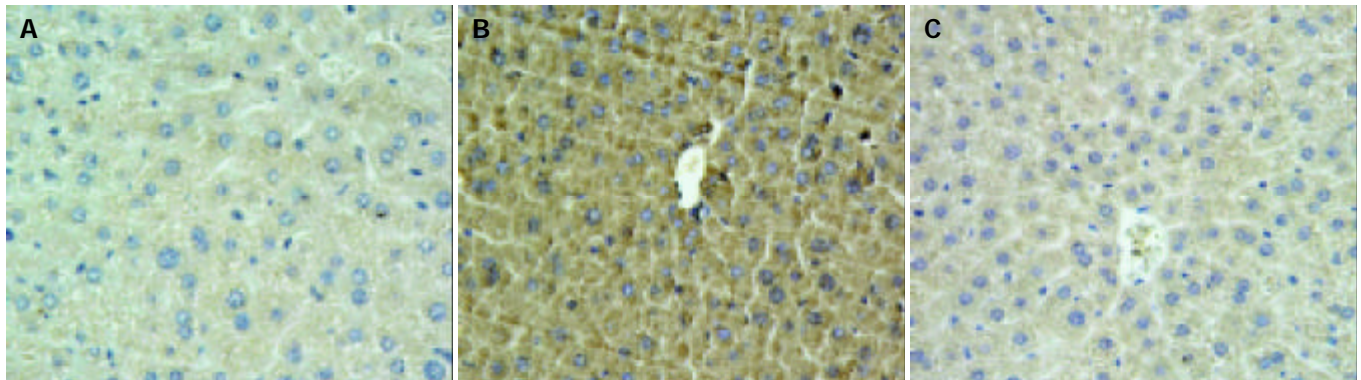


Figure 5 Immunohistochemical assay of TNF- α on liver tissue. Compared with sham control (A), the expression of TNF- α was highly up-regulated by 90 min of ischemia and 6 h of reperfusion (B), and the up-regulation of TNF- α expression was markedly inhibited by YS (20 mg/kg) (C). Original magnification: $\times 400$.

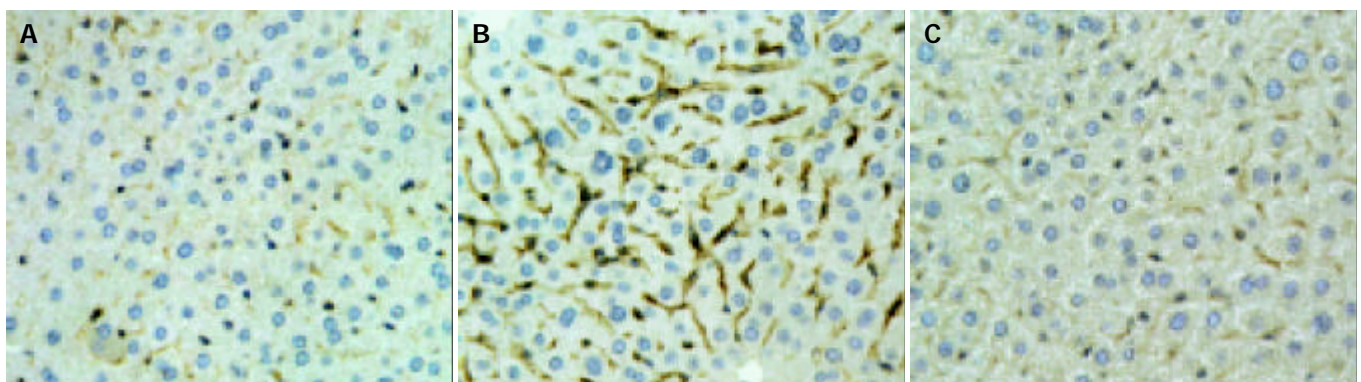


Figure 6 Immunohistochemical assay of ICAM-1 on liver tissue. Compared with sham control (A), the expression of ICAM-1 was highly up-regulated by 90 min of ischemia and 6 h of reperfusion (B), and the increase of ICAM-1 expression was dramatically inhibited by YS (20 mg/kg) (C). Original magnification: $\times 400$.

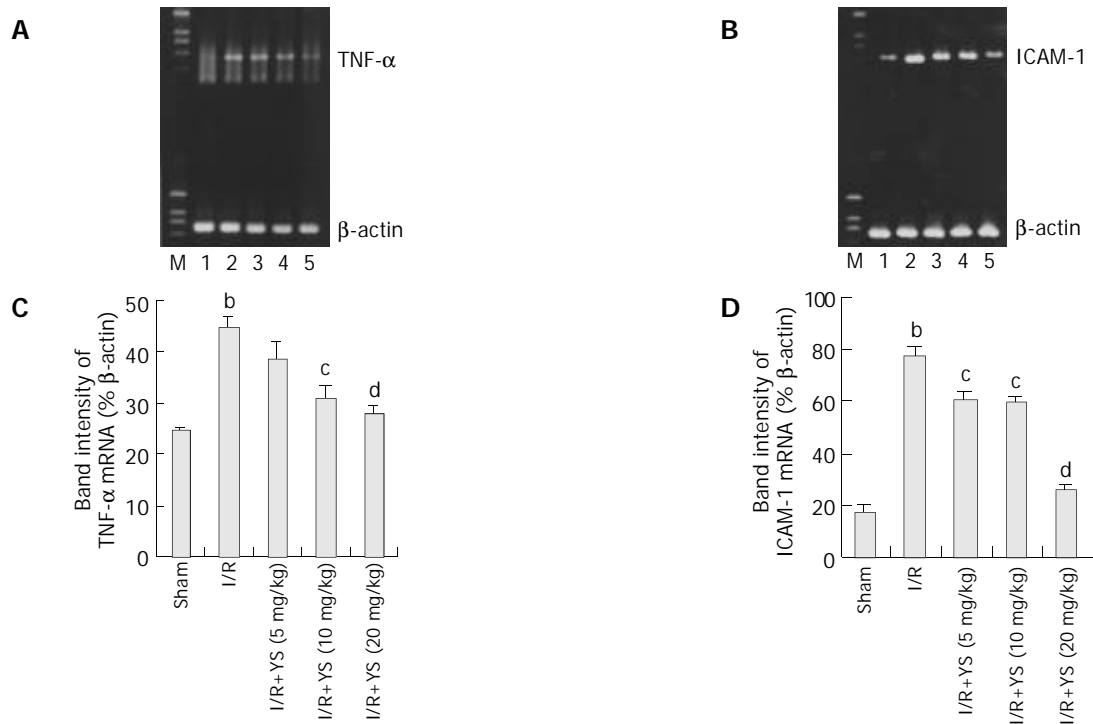


Figure 7 RT-PCR analysis of TNF- α (A) and ICAM-1 (B) mRNA expression in the liver tissues. β -actin was used as control. Mice were subjected to 90 min of ischemia and 6 h of reperfusion. Saline or YS with different dose (5, 10, 20 mg/kg) was injected intraperitoneally 24 h and 1 h before ischemia and a third dose was injected intravenously just before reperfusion. Liver RNA extracts were analyzed by reverse transcription PCR and stained with SYBR green dye. M: marker; L_{ain} 1: sham control; L_{ain} 2: I/R group; L_{ain} 3-5: 5, 10 and 20 mg/kg of YS treated groups. The band intensities of TNF- α (C) and ICAM-1 (D) in sham, I/R and YS-treated groups were compared. One representative experiment from three performed is shown. ^b $P < 0.01$ compared with sham group; ^c $P < 0.05$, ^a $P < 0.01$ compared with I/R group.

DISCUSSION

Ischemia-reperfusion (I/R) is an unavoidable process in liver transplantation. A major disadvantage of this event is an acute inflammatory response that may cause significant organ damage or dysfunction. Inflammatory organ injury is a primary concern after liver transplantation^[18]. Previous studies have identified many of the mediators involved in the pathogenesis of hepatic ischemia/reperfusion injury^[4-8]. Among them, ROS, TNF- α , ICAM-1 and neutrophil are central to this process^[6,19].

After warm ischemia, ROS produced at the moment of reperfusion activated and promoted the adhesion of leukocytes to microvascular endothelium^[20]. Previous studies suggest that free radicals formed during reperfusion are involved in the mechanism of graft failure following liver transplantation in the rat^[21]. Moreover, oxidative stress is found to have sustained for a long time after clinical liver transplantation^[22], and linked with primary graft nonfunction^[23]. Furthermore, studies of lung^[24] and renal^[25] transplant recipients have suggested that oxidative stress may predispose grafts to acute and chronic rejection. On the other hand, treatment of ROS-scavenging enzymes, such as SOD, can prevent the large increase in MPO activity (an index of tissue neutrophil count) associated with ischemia-reperfusion^[26], reduce hepatic oxidative stress, and effectively protect liver against ischemia-reperfusion injury and transplanted liver failure^[27,28].

Results in this study showed that treatment of YS at different doses of 5, 10 and 20 mg/kg elevated the liver SOD activities and reduced the hepatic MDA contents in a dose-dependent manner (Figure 3A, B), demonstrating YS' effects to reduce the oxidative stress caused by hepatic warm ischemia/reperfusion and attenuate subsequent organ damages (Figure 1A,B).

TNF- α produced by activated Kupffer cells is thought to play a central role in the initial phase of ischemia/reperfusion injury^[7]. Previous studies have showed that TNF- α caused overexpression of adhesion molecules on both endothelial cells and leukocytes^[29];

had multiple effects on neutrophil activity, including increased ROS generation^[30]; increased neutrophil aggregation and adhesion to endothelial cells^[31]; and resulted in hepatocyte necrosis^[32] or apoptosis^[33,34]. On the other hand, recent studies have demonstrated that neutralization with specific monoclonal antibodies against TNF- α before ischemia induction can ameliorate apoptosis and attenuate postischemic hepatic injury^[35].

Administration of YS significantly reduced the serum levels of TNF- α (Figure 4) and the TNF- α expression on liver tissues (Figure 5), and this effect was confirmed by RT-PCR analysis on TNF- α mRNA in liver tissues (Figure 7A, C). This means YS treatment can effectively reduce the release of TNF- α through suppressing the overexpression of TNF- α mRNA caused by hepatic ischemia/reperfusion, and attenuate subsequent insult events mediated by overexpression of TNF- α , such as up-regulation of adhesion molecules and neutrophil recruitment.

Normally, ICAM-1 is weakly expressed on portal and hepatic endothelium, but in acute rejection and ischemia/reperfusion there is over-expression of ICAM-1 on bile ducts, endothelium, and perivascular hepatocytes^[19,20]. ICAM-1 is found to be a potent specific indicator of rejection and may be useful in predicting which patient will progress to irreversible rejection^[19].

It has been found that TNF- α can directly up-regulate the expression of ICAM-1 in both lung and liver after hepatic ischemia/reperfusion injury^[7], and the over-expression of ICAM-1 may result in the adhesion and transmigration of neutrophils from the vascular lumen into tissue parenchyma^[36], ultimately leading to tissue injury and organ dysfunction^[18]. Furthermore, blockade of TNF- α decreases hepatic expression of the adhesion molecule ICAM-1 as well as liver neutrophil recruitment^[7].

Treatment with YS effectively suppressed the overexpression of ICAM-1 on liver tissue (Figure 6) and abrogated hepatic ischemia/reperfusion-induced increase in ICAM-1 mRNA expression (Figure 7B). As a result, the neutrophil recruitment

was effectively reduced by YS treatment (Figure 2A) and the liver edema was attenuated as well (Figure 2B).

In summary, YS treatment significantly reduced the oxidative stress, the overexpression of TNF- α and ICAM-1, and the neutrophil recruitment associated with hepatic ischemia/reperfusion, and finally effectively protected liver against ischemia/reperfusion injury. This drug would be a useful tool for preventing liver dysfunction or failure caused by hepatic ischemia/reperfusion injury in liver surgery and liver transplantation.

ACKNOWLEDGEMENTS

The authors thank Xia Qing-Jie, Yang Lai-Hong and Zhang Fa-Qiang for assistance with the illustrations.

REFERENCES

- Tullius SG**, Tilney NL. Both alloantigen-dependent and-independent factors influence chronic allograft rejection. *Transplantation* 1995; **59**: 313-318
- Liu DL**, Jeppsson B, Hakansson CH, Odselius R. Multiple-system organ damage resulting from prolonged hepatic inflow interruption. *Arch Surg* 1996; **131**: 442-447
- Gonzalez FX**, Rimola A, Grande L, Antolin M, Garcia-Valdecasas JC, Fuster J, Lacy AM, Cugat E, Visa J, Rodes J. Predictive factors of early postoperative graft function in human liver transplantation. *Hepatology* 1994; **20**: 565-573
- Jaeschke H**, Farhood A. Neutrophil and Kupffer cell-induced oxidant stress and ischemia-reperfusion injury in rat liver. *Am J Physiol* 1991; **260**(3 Pt 1): G355-G362
- Jiang Y**, Gu XP, Qiu YD, Sun XM, Chen LL, Zhang LH, Ding YT. Ischemic preconditioning decreases C-X-C chemokine expression and neutrophil accumulation early after liver transplantation in rats. *World J Gastroenterol* 2003; **9**: 2025-2029
- Colletti LM**, Remick DG, Burtch GD, Kunkel SL, Strieter RM, Campbell DA Jr. Role of tumor necrosis factor- α in the pathophysiologic alternations after hepatic ischemia/reperfusion injury in the rat. *J Clin Invest* 1990; **85**: 1936-1943
- Colletti LM**, Cortis A, Lukacs N, Kunkel SL, Green M, Strieter RM. Tumor necrosis factor up-regulates intercellular adhesion molecule 1, which is important in the neutrophil-dependent lung and liver injury associated with hepatic ischemia and reperfusion in the rat. *Shock* 1998; **10**: 182-191
- Farhood A**, McGuire GM, Manning AM, Miyasaka M, Smith CW, Jaeschke H. Intercellular adhesion molecule 1 (ICAM-1) expression and its role in neutrophil-induced ischemia-reperfusion injury in rat liver. *J Leukoc Biol* 1995; **57**: 368-374
- Gong JP**, Wu CX, Liu CA, Li SW, Shi YJ, Li XH, Peng Y. Liver sinusoidal endothelial cell injury by neutrophils in rats with acute obstructive cholangitis. *World J Gastroenterol* 2002; **8**: 342-345
- Tilney NL**, Guttman RD. Effects of initial ischemia/reperfusion injury on the transplanted kidney. *Transplantation* 1997; **64**: 945-947
- Shoskes DA**, Parfrey NA, Halloran PF. Increased major histocompatibility complex antigen expression in unilateral ischemic acute tubular necrosis in the mouse. *Transplantation* 1990; **49**: 201-207
- Clavien PA**, Harvey PRC, Strasberg SM. Preservation and reperfusion injuries in liver allografts. An overview and synthesis of current studies. *Transplantation* 1992; **53**: 957-978
- Li SF**, Jiang HM, Li YP, Wu DR, Zhang L, Zhang L, Cheng JQ. A study on the protective mechanism of Yisheng injection against the anoxia-reoxygenation injury to endothelial cells. *Huaxi Yike Daxue Xuebao* 2002; **33**: 215-219
- Jiang HM**, Li SF, Li YP. Influence of anoxia/reoxygenation on immunofunction of endothelial cells and effect of intervention with yisheng injection on it. *Zhongguo Zhongxiyi Jiehe Zazhi* 2003; **23**: 451-454
- Yang HR**, Chen JY, Cai SH, Li YP, Tang Q, Liu YB. Effects of YMB injection on hemorheology in rats. *Huaxi Yike Daxue Xuebao* 2000; **31**: 230-232
- Bu H**, Chen WG, Liu YB, Wu DR, Cheng JQ, Wang L. Experimental study on the protective effect of Yisheng injection on the sclerosis of transplanted abdominal aorta. *Huaxi Yiaoxue Zazhi* 2000; **15**: 185-188
- Jiang HM**, Li M, Li YP. Experimental study on isolated testes with ischemia/reperfusion injury. *Zhongguo Xiufu Chongjian Waike Zazhi* 2001; **15**: 377-381
- Yoshidome H**, Kato A, Edwards MJ, Lentsch AB. Interleukin-10 suppresses hepatic ischemia/reperfusion injury in mice: implications of a central role for nuclear factor κ B. *Hepatology* 1999; **30**: 203-208
- Adams DH**, Hubscher SG, Shaw J, Rothlein R, Neuberger JM. Intercellular adhesion molecule 1 on liver allografts during rejection. *Lancet* 1989; **2**: 1122-1125
- Granger DN**, Benoit JN, Suzuki M, Grisham MB. Leukocyte adherence to venular endothelium during ischemia-reperfusion. *Am J Physiol* 1989; **257**(5 Pt 1): G683-G688
- Henry DC**, Wenshi G, Sadayuki N, John JL, Ronald PM, Ronald GT. Evidence that free radicals are involved in graft failure following orthotopic liver transplantation in the rat-an electron paramagnetic resonance spin trapping study. *Transplantation* 1992; **54**: 199-204
- Burke A**, FitzGerald GA, Lucey MR. A prospective analysis of oxidative stress and liver transplantation. *Transplantation* 2002; **74**: 217-221
- Atalla SL**, Toledo-Pereyra LH, MacKenzie GH, Cederna JP. Influence of oxygen-derived free radical scavengers on ischemic livers. *Transplantation* 1985; **40**: 584-590
- Shiraishi T**, Kuroiwa A, Shirakusa T, Kawahara K, Yoneda S, Kitano K, Okabayashi K, Iwasaki A. Free radical-mediated tissue injury in acute lung allograft rejection and the effect of superoxide dismutase. *Ann Thorac Surg* 1997; **64**: 821-825
- Crishol JP**, Maggi MF, Vela C, Descomps B, Mourad G. Lipid metabolism and oxidative stress in renal transplantation: implications for chronic rejection. *Transplant Proc* 1996; **28**: 2820-2821
- Grisham MB**, Hernandez LA, Granger DN. Xanthine oxidase and neutrophil infiltration in intestinal ischemia. *Am J Physiol* 1986; **251**(4 Pt 1): G567-G574
- Wheeler MD**, Katuna M, Smutney OM, Froh M, Dikalova A, Mason RP, Samulski RJ, Thurman RG. Comparison of the effect of adenoviral delivery of three superoxide dismutase genes against hepatic ischemia-reperfusion injury. *Human Gene Therapy* 2001; **12**: 2167-2177
- Lehmann TG**, Wheeler MD, Froh M, Schwabe RF, Bunzendahl H, Samulski RJ, Lemasters JJ, Brenner DA, Thurman RG. Effects of three superoxide dismutase genes delivered with an adenovirus on graft function after transplantation of fatty livers in the rat. *Transplantation* 2003; **76**: 28-37
- Issekutz TB**. Effects of six different cytokines on lymphocyte adherence to microvascular endothelium and *in vivo* lymphocyte migration in the rat. *J Immunol* 1990; **144**: 2140-2146
- Tsujimoto M**, Yokota S, Vilcek J, Weissmann G. Tumor necrosis factor provokes superoxide anion generation from neutrophils. *Biochem Biophys Res Commun* 1986; **137**: 1094-1100
- Meyer JD**, Yurt RW, Duhane R, Hesse DG, Tracey KJ, Fong YM, Verma M, Shires GT, Dineen P, Lowry SF. Tumor necrosis factor-enhanced leukotriene B₄ generation and chemotaxis in human neutrophils. *Arch Surg* 1988; **123**: 1454-1458
- Yu YY**, Si CW, Tian XL, He Q, Xue HP. Effect of cytokines on liver necrosis. *World J Gastroenterol* 1998; **4**: 311-313
- Zang GQ**, Zhou XQ, Yu H, Xie Q, Zhao GM, Wang B, Guo Q, Xiang YQ, Liao D. Effect of hepatocyte apoptosis induced by TNF- α on acute severe hepatitis in mouse models. *World J Gastroenterol* 2000; **6**: 688-692
- Streetz K**, Leifeld L, Grundmann D, Ramakers J, Eckert K, Spengler U, Brenner D, Manns M, Trautwein C. Tumor necrosis factor in the pathogenesis of human and murine fulminant hepatic failure. *Gastroenterology* 2000; **119**: 446-460
- Ben-Ari Z**, Hochhauser E, Burstein I, Papo O, Kaganovsky E, Krasnov T, Vamichkim A, Vidne BA. Role of anti-tumor necrosis factor- α in ischemia/reperfusion injury in isolated rat liver in a blood-free environment. *Transplantation* 2002; **73**: 1875-1880
- Yadav SS**, Howell DN, Gao W, Steeber D, Harland RC, Clavien PA. L-selectin and ICAM-1 mediate reperfusion injury and neutrophil adhesion in the warm ischemic mouse liver. *Am J Physiol* 1998; **275**: G1341-G1352

CT biliary cystoscopy of gallbladder polyps

Ming-Wu Lou, Wei-Dong Hu, Yi Fan, Jin-Hua Chen, Zhan-Sen E, Guang-Fu Yang

Ming-Wu Lou, Wei-Dong Hu, Yi Fan, Jin-Hua Chen, Zhan-Sen E, Guang-Fu Yang, Department of Radiology, Longgang Central Hospital of Shenzhen City, Shenzhen 518116, Guangdong Province, China
Supported by the Scientific Bureau of Shenzhen City, No. 200006012
Correspondence to: Dr. Ming-Wu Lou, Department of Radiology, Longgang Central Hospital of Shenzhen City, Shenzhen 518116, Guangdong Province, China. mingwulou@sina.com
Telephone: +86-755-84809409 **Fax:** +86-755-84802448
Received: 2003-08-06 **Accepted:** 2003-10-07

Abstract

AIM: CT virtual endoscopy has been used in the study of various organs of body including the biliary tract, however, CT virtual endoscopy in diagnosis of gallbladder polyps has not yet been reported. This study was to evaluate the diagnostic value of CT virtual endoscopy in polyps of the gallbladder.

METHODS: Thirty-two cases of gallbladder polyps were examined by CT virtual endoscopy, ultrasound, CT scan with oral biliary contrast separately and confirmed by operation and pathology. CT biliary cystoscopic findings were analyzed and compared with those of ultrasound and CT scan with oral biliary contrast, and evaluated in comparison with operative and pathologic findings in all cases.

RESULTS: The detection rate of gallbladder polyps was 93.8%(90/96), 96.9%(93/96) and 79.2%(76/96) for CT cystoscopy, ultrasound and CT scan with oral contrast, respectively. CT biliary cystoscopy corresponded well with ultrasound as well as pathology in demonstrating the location, size and configuration of polyps. CT endoscopy was superior to ultrasound in viewing the polyps in a more precise way, 3 dimensionally from any angle in space, and showing the surface in details. CT biliary cystoscopy was also superior to CT scan with oral biliary contrast in terms of observation of the base of polyps for the presence of a pedicle, detection rates as well as image quality. The smallest polyp detected by CT biliary cystoscopy was measured 1.5 mm×2.2 mm×2.5 mm.

CONCLUSION: CT biliary cystoscopy is a non-invasive and accurate technique for diagnosis and management of gallbladder polyps.

Lou MW, Hu WD, Fan Y, Chen JH, E ZS, Yang GF. CT biliary cystoscopy of gallbladder polyps. *World J Gastroenterol* 2004; 10(8): 1204-1207

<http://www.wjgnet.com/1007-9327/10/1204.asp>

INTRODUCTION

Since Klein *et al.*^[1] in 1993 reported the computed tomographic cholangiography using spiral scanning and 3D image processing, many lesions of the biliary tract have been studied^[2-14]. In 1994 CT virtual endoscopy (CTVE) was introduced, its application in obtaining organ images has been described extensively^[15-28]. However, we have not seen any report concerning CTVE in the

diagnosis of polyps of the gallbladder. In the current paper we reported the CTVE findings of gallbladder polyps in 32 patients.

MATERIALS AND METHODS

From January 1999 to the present study, 32 patients with gallbladder polyps confirmed by operation and pathology underwent CT biliary cystoscopy (CT virtual endoscopy of the gallbladder, CTVEGB). There were 18 males and 14 females (age range, 28-47 years, mean age, 35.8 years). Eight patients had vague pain in the right upper abdomen, 4 patients had colicky pain, and the remaining 20 patients were asymptomatic. All patients had normal serum bilirubin and alkaline phosphatase levels. On the day of CTVEGB, abdominal ultrasonographic studies were done for all patients.

The CT scanner was Somatom plus 4 power helical CT (Siemens, Germany) with a Virtuoso workstation (WS). The sonographic equipment was color Doppler ultrasound HDL 5 000 (ATL USA). Sixteen hours prior to CT study, each patient took 4.5 g of iopanoic acids orally and the gastrointestinal tract was properly prepared. CT scanning parameters were: 120 kV, 200-220 mA, slice thickness 2-3 mm, pitch 1-1.2 or 1.5-2.0; image reconstruction interval: 0.8-1.2 mm or 1.5-2.0 mm, FOV 214-263 mm; scan time 25-32 s, scan speed 0.75 s per 360° revolution.

Image post processing was done by Dr. Hu. The reconstructed image was transferred to virtuoso WS. "Fly" software was used to obtain 3D stereo image of the gallbladder and surrounding structures, then virtual endoscopic image of the gallbladder was proceeded simply by double click on the mouse, threshold value was adjusted so that the normal gallbladder mucosa was displayed clearly (Figure 1). The threshold value ranged from -178-251HU. Color encoding was performed using green color (color of the bile). Endoscopy was carried out from any viewpoint in the gallbladder with varying views, size, speed and angle, and detailed scrutiny was performed. It took 1 h to complete CTVEGB. All axial source CT images were interpreted as spiral CT with oral biliary contrast (OCCT) and 3D stereo images using fly software as CTVEGB, which were done by two radiologists, who were unaware of the clinical and ultrasonographic information. Another two radiologists did ultrasonographic study. All radiologists worked together in evaluating the number, size, configuration, location, surface and base of polyps of the gallbladder. A professional statistician performed all statistical analyses by using a commercially available statistical software package (SAS Institute, Cary, Nc). The results of CTVEGB, OCCT, ultrasound and pathology were compared with each other by means of the chi-square test.

RESULTS

On OCCT, the gallbladder was clearly visualized in 32 cases. The 3D stereo view clearly displayed the gallbladder and its surrounding structures such as the liver, ribs and spine on maximum intensity projection (MIP) protocol. CTVEGB images were obtained from all patients. No procedure-related adverse reaction was observed in all 32 cases.

Correlation of CTVEGB with ultrasound

The 3D image, CTVEGB image (Figure 1A) and axial source

image could be displayed simultaneously on Virtuoso WS. CTVEGB could be manipulated flexibly from multiple views and various angles so that the location, size, configuration, surface and base of the polyps could be clearly shown better on CTVEGB than on ultrasound images. Among the 32 cases with gallbladder polyps, the detection rate of polyps was 96.9(93/96) by ultrasound and 93.8%(90/96) by CTVEGB. Comparison of ultrasound and CTVEGB with operative and pathologic findings is shown in Table 1. The smallest polyp detected by CTVEGB measured 1.5 mm×2.2 mm×2.5 mm (Figure 1B). One polyp with cauliflower appearance (Figure 1C) and another butterfly-like one were detected by CTVEGB, which were in accordance with ultrasound (Figure 1D) and operative findings. Pathologically both were confirmed to be inflammatory polyps of the gallbladder (Figure 1E).

Comparison between CTVEGB and OCCT

On OCCT, the gallbladder filled with contrast medium was well visualized, the polyps appeared as filling defects of various sizes and numbers. Among the 96 polyps, OCCT detected 76 while CTVEGB detected 90, the detection rate was 79.2% and 93.8% respectively. The correlation with operative and pathologic findings is shown in Table 2. CTVEGB missed 3

polyps with a diameter <3 mm, while OCCT missed 20 polyps with a diameter <5 mm. The difference was statistically significant ($P<0.01$, $\alpha=0.05$).

CTVEGB and pathological classification

The incidence of polyps was related to the pathologic type. Of the 90 polyps detected by CTVEGB, 60 were cholesterol polyps, in which 12(20%) were single cholesterol polyps (Figure 1B) and 48(80%) were multiple cholesterol polyps (Figure 1D). Among the 30 inflammatory polyps, 15(50%) were single polyps (Figure 1F) and 15 were multiple types (Figure 1C). The size of gallbladder polyps was related to pathologic types. Among the 90 polyps detected by CTVEGB, 60 were cholesterol polyps, in which 38(63%) had the greatest diameter ≤ 5 mm, 22 (37%) had a diameter of 5-10 mm and 0(0%) had a diameter of ≥ 10 mm. There were 30 inflammatory polyps, 10(33%) were ≤ 5 mm, 8(27%) were 5-10 mm and 12(40%) were ≥ 10 mm. The configuration of polyps was related to pathologic types. Among the 60 cholesterol polyps, 52(87%) had a spherical configuration, 7(11%) were papillary and 1(2%) irregular in outline. Of the 30 inflammatory polyps, 23(77%) were spherical and 7(23%) were irregular and none was papillary in form. The location of gallbladder polyps was

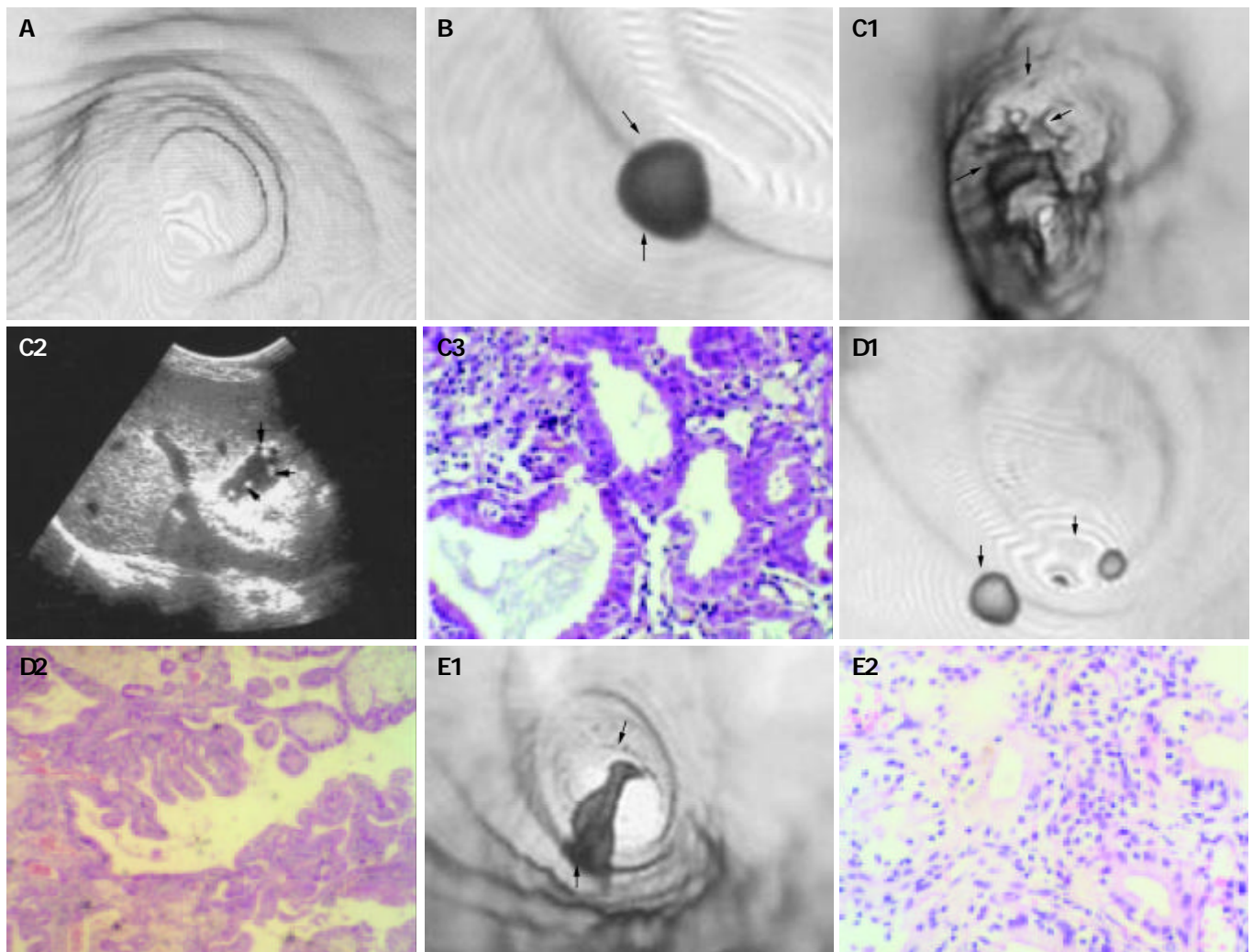


Figure 1 CTVEGB detection of gallbladder polyps. A: Surface detail of gallbladder displayed by CTVEGB in a 47-year old normal man. B: Smallest single cholesterol polyp (arrow head) detected by CTVEGB in a 28-year-old man. C: Multiple gallbladder polyps in a 30-year-old man. (1) Multiple polyps of cauliflower appearance and small polyps (arrow head). (2) Color ultrasonography found multiple polyps of cauliflower appearance and small polyps (arrow head). (3) Multiple polyps were inflammatory polyps on pathology (HE×20). D: Multiple cholesterol gallbladder polyps in a 30-year-old woman. Two cholesterol polyps (arrow head) were proved by pathology (HE×20). E: Single inflammatory gallbladder polyps in a 29-year-old woman. An irregular inflammatory polyp was proved by pathology (HE×20).

Table 1 Comparison of ultrasound and CTVEGB in 96 gallbladder polyps

Modality	Polyps (n)	Diameter (mm)			Location (n)			Configuration (n)					Base (n) peduncle	
		<5	5-10	10-	Neck	Body	Base	Spherical	Papillary	Irregular	Butterfly	Cauliflower	(-)	(+)
Pathology	96	54	30	12	24	64	8	81	7	6	1	1	58	38
Ultrasound	93	51	30	12	24	61	8	78	7	6	1	1	55	38
CTVEGB	90	48	30	12	24	58	8	75	7	6	1	1	52	38
χ^2	0.466	0.485			0.478			0.471					0.482	
P value	>0.05	>0.05			>0.05			>0.05					>0.05	

1. No statistical significance ($P>0.05$, $\alpha=0.05$) between ultrasound and CTVEGB findings; 2. CTVEGB is abbreviation of CT virtual endoscopy of the gall bladder.

Table 2 Comparison of OCCT and CTVEGB in 96 gallbladder polyps

Modality	Polyps	Diameter (mm)			Location (n)			Configuration (n)					Base (n) peduncle	
		<5	5-10	10-	Neck	Body	Base	Spherical	Papillary	Irregular	Butterfly	Cauliflower	(-)	(+)
Pathology	96	54	30	12	24	64	8	81	7	6	1	1	58	38
OCCT	76	34	30	12	24	44	8	61	7	6	1	1	52	24
CTVEGB	90	48	30	12	24	58	8	75	7	6	1	1	52	38
χ^2	7.518	8.561			8.157			7.743					14.797	
P value	<0.01	<0.01			<0.01			<0.01					<0.01	

1. Statistical difference between ultrasound and CTVEGB findings ($P<0.01$, $\alpha=0.05$); 2. CTVEGB is abbreviation of CT virtual endoscopy of the gall bladder; 3. OCCT is abbreviation of spiral CT with oral biliary contrast.

related to pathologic types. Of the cholesterol polyps, 40(67%) were located in the body of gallbladder, 19(31%) in the neck and 1(2%) in the base. Of the 30 inflammatory polyps, 18(60%) were located in the body of gallbladder, 5(17%) in the neck and 7(23%) in the base. The presence or absence of a pedicle was related to pathologic type. There were 36(60%) cholesterol polyps with a pedicle and 24(40%) devoid of a pedicle. Two (7%) inflammatory polyps were pedunculated and 28(93%) not.

DISCUSSION

A lot of techniques have been developed for studying the biliary tract. Ultrasonography, the technique of choice for studying the gallbladder, is of limited value in the evaluation of polyps of gallbladder, depending on the operator's skill. Intravenous cholangiography is a safe technique, but does not adequately opacify the polyps of gallbladder. Conventional computed tomography (CT) is inadequate for detection of low-density lesions of the gallbladder. ERCP and PTC can provide excellent delineation of biliary anatomy and pathology, but both are invasive and associated with risks and complications. MR cholangiography is a popular noninvasive technique and has been shown to be both sensitive to and specific for visualization of various conditions of the biliary tract. Although it is safe, the technique is contraindicated in patients with aneurysm clips or cardiac pacemakers. In addition, MR cholangiography may not be suitable for patients with claustrophobia or those with multiple metallic clips, which may cause artifacts. There are few alternatives to the invasive techniques, and additional noninvasive techniques are in demand.

Spiral CT allows imaging of a volume of tissue during a single breath-hold. Axial CT data could be reconstructed into two-dimensional multi-planar or three-dimensional (3D) volume-rendered images using workstations and image-rendering software^[1]. This CT technology combined with the administration of IV cholangiographic contrast agents could produce diagnostic images of the biliary tract^[2-7,9,10,14], and has been used for diagnosis of obstructive biliary disease, choledochocoele, choledocholithiasis and aberrance bile ducts. The main limitation of this technique is that the rate of allergic reactions and renal or hepatic toxicity (or both) are relatively

high due to by these contrast agents.

Oral cholangiographic contrast agents are a potential alternative to IV contrast agents. Unlike the later, these contrast agents had few side effects, such as diarrhea, loose stools, nausea and stinging on urination^[8]. Because the patients ingested 6 g iopanoic acid before CT examination^[8,11,13], the contrast agents were decreased to 4.5 g iopanoic acid. No side effect was found in our study. CT cholangiography was used to assess choledoch variants and describe choledocholithiasis^[8,11,13]. To our knowledge, there have been few studies or reports in which IV cholangiographic contrast agents were used to diagnose gallbladder polyps^[10]. It has not yet been established whether these oral contrast agents can reliably demonstrate gallbladder polyps on CTVEGB.

Some factors could influence the image quality of CTVEGB, which is important for precise diagnostic information. Usually 16 h after oral administration of 4.5 g iopanoic acid, CTVEGB could yield the image of gallbladder with a good quality. With a dose of 3.0 g, visualization of the gallbladder would be inadequate. Inadequate control of respiratory motion has adverse impact on image quality, resulting in failure to detect small lesions or ragged distortion of large lesions. Optimal image quality is achieved by single breath hold. Higher reconstruction rates such as 0.8-1.2 mm are more helpful in displaying minute lesions and the details. Higher pitch (1.5-2.0) may produce artifact-mimicking polyps or miss small lesions. Pitch 1.0-1.2 is a good choice. FOV is related to the displayed area of the surrounding structures but not to observation of the polyps. However, adequate FOV can clearly demonstrate the stereo relation of gallbladder and surrounding structures. The threshold value seriously affects effective observation of polyps. Variation of the threshold value leads to marked change in visualization of the size and appearance of polyps, therefore selecting appropriate threshold value is critical to avoid image distortion. Generally, a threshold value is selected so that the normal gallbladder mucosa is shown clearly.

Based on our clinical experience in diagnosing gallbladder polyps by CTVEGB, TVEGB can clearly display the normal anatomy of the interior of gallbladder. CTVEGB can clearly show the size, configuration, location, surface and base of gallbladder polyps in accordance with color ultrasound,

operative and pathologic findings. The smallest polyp reported in this article was 1.5 mm×2.2 mm×2.5 mm. Localization of the polyps was accurate. Good depiction of polyp configuration could be obtained. In this series 12 polyps with irregular appearance were proved to be inflammatory in nature with adhesions. Detailed observation of the base of polyps to confirm the presence of a pedicle by CTVEGB was possible by viewing from different angles and in this respect, CTVEGB was superior to color ultrasound. Among the 96 polyps, CTVEGB missed 6 polyps with the diameter less than 3 mm. Color ultrasound missed 3 polyps because of adhesion with surrounding tissues. The difference, however, was not statistically significant ($P>0.05$). The correspondence was good. OCTT, being a safe, simple and efficient method^[1-7], is capable of detecting biliary calculus, tumor, anomaly and dilatation of the biliary tract and protruding lesions with a bigger size. However, limited by the concentration of contrast medium, small polypous lesions are easily obscured and thus escaping detection by OCCT. In this series, 20 polyps with a diameter less than 5 mm were missed. OCCT is also inferior to CTVEGB in terms of observation of the base of polyps for the presence of a pedicle, detection rate as well as image quality.

In comparison of the findings of CTVEGB with pathological changes, in cholesterol polyps, multiple polyps were far more frequently seen than single polyps (80% vs 20%). While in inflammatory polyps, the incidence was 50% for each, indicating that most cholesterol polyps were multiple, while single polyp and multiple ones were equally common in inflammatory polyps. Among the cholesterol polyps, 63% were ≤ 5 mm, 37% were between 5-10 mm, none was ≥ 10 mm. While in inflammatory polyps, 33% were ≤ 5 mm, 27% was between 5-10 mm, 40% were ≥ 10 mm, indicating that smaller polyps (≤ 5 mm) were common in cholesterol polyps and bigger ones (≥ 10 mm) were common in inflammatory polyps. Among cholesterol polyps, spherical type was most common (87%), followed by papillary type (11%), then irregular type (2%). For inflammatory polyps, 77% were spherical type, 23% irregular type. There was no papillary inflammatory polyp in this series. For cholesterol polyps, 67% occurred in the body of gallbladder, 31% in the neck and 2% in the base. Whereas for inflammatory polyps, they were 60%, 23% and 17% in the body, base and neck respectively. Cholesterol polyps usually occurred in the body and neck of the gallbladder, while for inflammatory polyps usually in the body and base. Sixty percent of the cholesterol polyps were pedunculated and 40% were devoid of a pedicle. Most of the inflammatory polyps (93%) were non-pedunculated.

REFERENCES

- Klein HM**, Wein B, Truong S, Pfingsten FP, Gunther RW. Computed tomographic cholangiography using spiral scanning and 3D image processing. *Br J Radiol* 1993; **66**: 762-767
- Van Beers BE**, Lacrosse M, Trigaux JP, de Canniere L, De Ronde T, Pringot J. Noninvasive imaging of the biliary tree before or after laparoscopic cholecystectomy: use of three-dimensional spiral CT cholangiography. *Am J Roentgenol* 1994; **162**: 1331-1335
- Fleischmann D**, Ringl H, Schofl R, Potzi R, Kontrus M, Henk C, Bankier AA, Kettenbach J, Mostbeck GH. Three-dimensional spiral CT cholangiography in patients with suspected obstructive biliary disease: comparison with endoscopic retrograde cholangiography. *Radiology* 1996; **198**: 861-868
- Galeon M**, Deprez P, Van Beers BE, Pringot J. Spiral CT cholangiography of choledochocoele. *J Comput Assist Tomogr* 1996; **20**: 814-815
- Stockberger SM**, Sherman S, Kopecky KK. Helical CT cholangiography. *Abdom Imaging* 1996; **21**: 98-104
- Nascimento S**, Murray W, Wilson P. Computed tomography intravenous cholangiography. *Australas Radiol* 1997; **41**: 253-261
- Kwon AH**, Uetsuji S, Ogura T, Kamiyama Y. Spiral computed tomography scanning after intravenous infusion cholangiography for biliary duct anomalies. *Am J Surg* 1997; **174**: 396-402
- Chopra S**, Chintapalli KN, Ramakrishna K, Rhim H, Dodd GD 3rd. Helical CT cholangiography with oral cholecystography contrast material. *Radiology* 2000; **214**: 596-601
- Takahashi M**, Saida Y, Itai Y, Gunji N, Orii K, Watanabe Y. Re-evaluation of spiral CT cholangiography: basic consideration and reliability for detecting choledocholithiasis in 80 patients. *J Comput Assist Tomogr* 2000; **24**: 859-865
- Hirao K**, Miyazaki A, Fujimoto T, Isomoto I, Hayashi K. Evaluation of aberrant bile ducts before laparoscopic cholecystectomy: helical CT cholangiography versus MR cholangiography. *Am J Roentgenol* 2000; **175**: 713-720
- Soto JA**, Alvarez O, Múnera F, Velez SM, Valencia J, Ramirez N. Diagnosing bile duct stones: comparison of unenhanced helical CT oral contrast-enhanced CT, cholangiography, and MR cholangiography. *Am J Roentgenol* 2000; **175**: 1127-1134
- Breen DJ**, Nicholson A. The clinical utility of spiral CT cholangiography. *Clin Radiol* 2000; **55**: 733-739
- Caouli EM**, Paulson EK, Heyneman LE, Branch MS, Eubanks WS, Nelson RC. Helical CT cholangiography with three-dimensional volume rendering using an oral biliary contrast agent: feasibility of a novel technique. *Am J Roentgenol* 2000; **174**: 487-492
- Cabada Giadas T**, Sarria Octavio de Toledo L, Martinez-Berganza Asensio MT, Cozcolluela Cabrejas R, Alberdi Ibanez I, Alvarez Lopez A, Garcia-Asensio S. Helical CT cholangiography in the evaluation of the biliary tract: application to the diagnosis of choledocholithiasis. *Abdom Imaging* 2002; **27**: 61-70
- Sun CH**, Li ZP, Yan F, Yu SP, Xu DS, Xie HB, Lin PZ. CT virtual endoscopy of intravenous cystography: experimental study and clinical application. *Zhonghua Fangshexue Zazhi* 2003; **37**: 537-541
- Wang D**, Zhang WS, Xiong MH, Xu JX, Yu M, Xu CY. CT virtual endoscopy of the auditory ossicular chain and its preliminary clinical application. *Zhonghua Fangshexue Zazhi* 2000; **34**: 459-461
- Han P**. CT virtual endoscopy: a study of the capability to display the structures and abnormalities in nasal cavity. *Zhonghua Fangshexue Zazhi* 1999; **33**: 7-11
- Xiao Y**, Tian JM, Wang PJ, Zuo CJ, Wang MJ, Cui HW, Zeng H, Lu TZ, Xue H, Fan YL. Clinical application of CT virtual endoscopy in the diagnosis of aortic diseases. *Zhonghua Fangshexue Zazhi* 2000; **34**: 540-542
- Wang D**, Zhang WS, Xiong MH, Xu JX. CT virtual endoscopy of the larynx and hypo pharynx and its preliminary clinical application. *Zhonghua Fangshexue Zazhi* 2000; **34**: 548-550
- Hu CA**, Hao JM, Qian ZB. Preliminary clinical experience of spiral CT virtual colonoscopy for detection of colorectal polyps. *Zhonghua Fangshexue Zazhi* 2000; **34**: 313-315
- Tan LL**, Li YB, Li SX, Jiang JD, Liang TJ, Liu K. Application of SCTA and CTVE in diagnosing aortic dissection. *Zhongguo Linchuangyixue Yingxiang Zazhi* 2002; **13**: 190-202
- Chen F**, Zheng KE, Liu WH, Ju SH, Xu QZ. Evaluation of image quality of CT virtual endoscopy. *Zhonghua Fangshexue Zazhi* 2000; **34**: 765-769
- Zhang LQ**, Zhang J, Zhong GC. Application of CT virtual endoscopy to diseases of digestive system. *Shiyong Yiji Zazhi* 2002; **9**: 33-34
- Xie BJ**, Zheng XH, Li KX, Wan JH, Wu ZY. Anatomy structures of nasal cavity and paranasal sinus on virtual endoscopy and coronal image. *Linchuang Erbihouke Zazhi* 2001; **15**: 483-485
- Xu XJ**, Huang G, Gou Q, Ren XS. Clinical applications of multislice helix CT virtual gastroscopy and three-dimensional imaging in gastric tumors. *Shiyong Fangshexue Zazhi* 2002; **18**: 475-478
- Ding GQ**, Li XD, Yu DM, Zhang QW, Rui XF, Zhang DH, Li GH. Clinical applications of virtual endoscopy based on spiral CT scan in bladder neoplasm. *Linchang Chaoshengxue Zazhi* 2002; **17**: 656-658
- Liewald F, Lang G, Fleiter T, Sokiranski R, Halter G, Orend KH. Comparison of virtual and fiberoptic bronchoscopy. *Thorac Cardiovasc Surg* 1998; **46**: 361-364
- Han P**, Pirsig W, Ilgen F, Gorich J, Sokiranski R. Virtual endoscopy of the nasal cavity in comparison with fiberoptic endoscopy. *Eur Arch Otorhinolaryngol* 2000; **257**: 578-583

Hepatic progenitor cells in human liver cirrhosis: Immunohistochemical, electron microscopic and immunofluorescence confocal microscopic findings

Jia-Cheng Xiao, Xiao-Long Jin, Peter Ruck, Anne Adam, Edwin Kaiserling

Jia-Cheng Xiao, Xiao-Long Jin, Department of Pathology, Ruijin Hospital, Shanghai 2nd Medical University, Shanghai 200025, China
Peter Ruck, Anne Adam, Edwin Kaiserling, Institute of Pathology, University of Tübingen, 72076 Tübingen, Germany
Supported by the National Natural Science Foundation of China, No. 39870772; the Educational Committee Foundation of Shanghai, China, No. 98BJ03; the Fortune-Programm of the University of Tübingen, Germany, F.1462016

Correspondence to: Dr. Jia-Cheng Xiao, Department of Pathology, Ruijin Hospital, Shanghai 2nd Medical University, Shanghai 200025, China. jcxiao@public4.sta.net.cn

Telephone: +86-21-64370045-662233

Received: 2003-09-06 **Accepted:** 2003-10-12

Abstract

AIM: To investigate whether hepatic progenitor cells (HPC), that reveal the features of oval cells in rodents and small epithelial cells (SEC) in certain human liver disease, were also found in human liver cirrhosis (HLC).

METHODS: Surgical liver specimens from 20 cases of hepatitis B virus-positive HLC (15 cases containing hepatocellular carcinoma) were investigated by light microscopic immunohistochemistry (LM-IHC). Among them specimens from 15 cases were investigated by electron microscopy (EM) and those from 5 cases by immunofluorescence confocal laser scanning microscopy (ICLSM). Antibodies against cytokeratin 7 and albumin were used and single and/or double labelling were performed respectively.

RESULTS: LM-IHC showed that at the margins of regenerating nodules and in the fibrous septae, a small number of cells in the proliferating bile ductules were positive for CK7 and albumin. At the EM level these HPC were morphologically similar to the SEC described previously, and also similar to the oval cells seen in experimental hepatocarcinogenesis. They were characterized by their small size, oval shape, a high nucleus/cytoplasm ratio, a low organelle content in cytoplasm, and existence of tonofilaments and intercellular junctions. ICLSM revealed that HPC expressed both cytokeratin 7 and albumin.

CONCLUSION: HPC with ultrastructural and immunophenotypical features of oval cells, *i.e.*, hepatic stem cell-like cells as noted in other liver diseases, were found in HLC. These findings further support the hypothesis that bipotent hepatic stem cells, that may give rise to biliary epithelial cells and hepatocytes, exist in human livers.

Xiao JC, Jin XL, Ruck P, Adam A, Kaiserling E. Hepatic progenitor cells in human liver cirrhosis: Immunohistochemical, electron microscopic and immunofluorescence confocal microscopic findings. *World J Gastroenterol* 2004; 10(8): 1208-1211
<http://www.wjgnet.com/1007-9327/10/1208.asp>

INTRODUCTION

In rodents, administration of hepatocarcinogens could lead to proliferation of oval cells that are capable of differentiating towards both hepatocytes and bile duct epithelium. These oval cells are thought to be hepatic progenitor cells or stem cells^[1-4]. In contrast to the situation in rodents, it is still controversial, however, whether hepatic progenitor cells also exist in human livers. Recently, we described a population of cells with the morphological and immunophenotypical features of oval cells in hepatoblastoma (HB) that we termed small epithelial cells (SEC)^[5-6]. In further studies we also observed similar cells in livers of patients with hepatocellular carcinoma (HCC)^[7], extrahepatic biliary atresia (EBA)^[8] and HLC^[9].

SEC reveal certain morphological features, such as a small size, a high nucleus to cytoplasm ratio, intercellular junctions and tonofilaments. Under immunoelectron microscopy, SEC were found to express both cytokeratin 7 (a marker of biliary differentiation), and albumin (a marker of hepatocytic differentiation)^[5-9]. Thus SEC exhibit morphological and immunophenotypical features of oval cells in rodents. This study was undertaken to further verify that SEC did occur in hepatitis B virus (HBV)-positive HLC and that such cells played a key role in the pathogenesis of the disease. The findings further support the hypothesis of the existence of human hepatic stem cells.

MATERIALS AND METHODS

Fifteen surgical specimens of cirrhotic liver tissue adjacent to HCC were investigated. All patients were HBV-positive. As controls, 5 specimens of HBV-positive cirrhotic liver tissue from patients without liver tumour and 5 specimens of normal liver tissue were investigated.

For routine histological and immunohistological investigation, the tissue was fixed in 40 g/L buffered formaldehyde and embedded in paraffin. Immunohistochemical investigations were performed on all specimens using an undiluted monoclonal mouse antibody against cytokeratin 7 and a polyclonal antibody against albumin (both from DAKO, Glostrup, Denmark) diluted 1:1 000. Single labelling with each antibody separately, and double labelling using both antibodies on the same section, were carried out.

For conventional transmission electron-microscopic (TEM) investigation, the tissue was fixed in 40 g/L glutaraldehyde in 0.1 mol/L phosphate buffer (pH 7.3). TEM investigations as described elsewhere^[5-9] were performed on 10 cases of HLC with associated HCC. In order to distinguish labelling of the 2 antigens (cytokeratin 7 and albumin) in the double labelling procedure, goat anti-mouse IgG, goat anti-rabbit IgG as secondary antibodies and DAB (brown), NBT (green) as chromogen were used respectively.

For ICLSM investigation the specimens from 5 cases of HLC with associated HCC, 2 cases without HCC and 2 specimens of normal liver tissue were fixed in 40 g/L buffered formaldehyde and embedded in paraffin for immunohistochemical investigations.

Paraffined sections were prepared for immunofluorescent labelling. Briefly, primary antibodies against cytokeratin 7 (undiluted) and albumin (1:1 000 diluted in phosphate-buffered saline with 5 g/L bovine serum albumin and 1 g/L gelatine) and secondary antibodies (goat anti-mouse IgG and goat anti-rabbit IgG) conjugated with FITC or Cy3 (Sigma) were used. Double labelling using both antibodies on the same section was performed. Primary antibodies and secondary antibodies were incubated for 1 h at room temperature. Nuclear staining was carried out with DAPI (Sigma) in PBS. Slides were stored at 4 °C and analysed within 24 h. As a control, the primary antibody was omitted.

Immunofluorescence was observed with Zeiss LSM 510 (Zeiss; Jena, Germany). We used an argon laser at 488 nm in combination with a helium neon laser at 543 nm to excite the green (CK7) and red (albumin) fluorochromes simultaneously. Emitted fluorescence was detected with a 505-530 nm bandpass filter for the green signal, a 560 nm longpass filter for the red signal and 633 nm filter for the blue signal.

RESULTS

In all the investigated cases of HLC, micronodular and/or macronodular cirrhosis was a basic morphologic feature. In fibrous septae, proliferating bile ductules and lymphocytic infiltrates were found at a varying extent. Hepatic progenitor cells (HPC) with a histological picture morphologically similar to oval cells of rodents were found in all cases studied (Figure 1). HPC were numerous in proliferating bile ductules or noted as discretely scattered cells at the edge of regenerating nodules and in fibrous septae (Figure 1). The number of HPC varied from 2 to 10 in 40 high power fields. Their number was larger in cases exhibiting signs of active regeneration, but no differences were seen between cases with and without associated HCC. HPC, however, were not observed in normal livers. Immunohistochemical investigations showed that HPC could express both cytokeratin 7 and albumin (Figures 2-4). In the normal liver, hepatocytes were immunoreactive for albumin and biliary epithelial cells for cytokeratin 7. No double staining of albumin and cytokeratin 7 could be found in hepatocytes or biliary epithelial cells in normal livers.

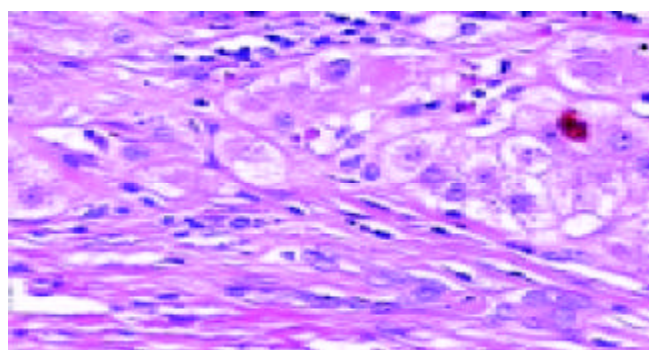


Figure 1 HLC. Several proliferating bile ductules are seen at the edge of a regenerating nodule. There is a dense, mostly lymphocytic inflammatory infiltrate. Haematoxylin and eosin $\times 200$.

At electron microscopic level, a very small number of cells with ultrastructural features typical of the SEC found in HB^[5,6], EBA^[8] and HCC^[7] were noted in all cases of HLC. As noted by light microscopy, HPC were mainly located in ductules that were composed of 2-8 cells, and they were also seen in the fibrous septae and at the periphery of nodules. They were characterized by their small size (8 to 18 μm), oval shape, scanty cytoplasm with a high nucleus/cytoplasm ratio, tonofilament bundles, tight junctions or desmosome-like junctions, and an

oval, electron-dense nucleus in which heterochromatin was seen as small clumps dispersed in the nucleoplasm with peripheral condensation. Junctions were found both between HPC and hepatocytes and between HPC and epithelial cells of small bile ductules (Figures 5 and 6).

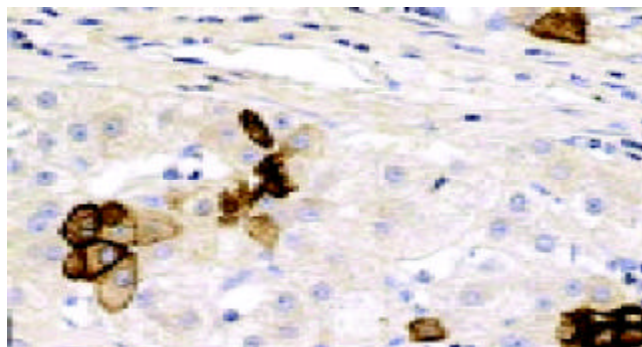


Figure 2 HLC. Immunohistochemical staining shows that cells of proliferated bile ductules are strongly positive for CK7. Anti-CK7, $\times 200$.

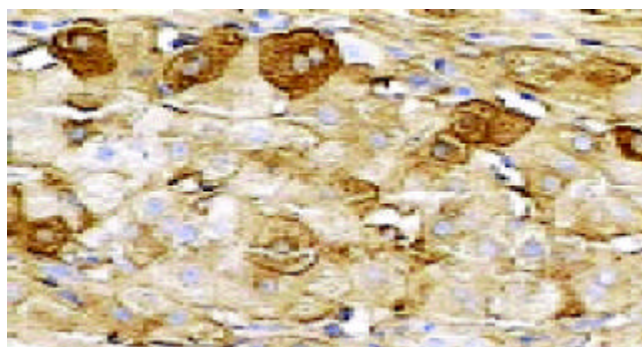


Figure 3 HLC. Some small hepatic progenitor cells, immunoreactive with albumin are seen at the edge of regenerated nodule. Anti-albumin $\times 200$.



Figure 4 HLC. Double labelling immunohistochemistry shows that cells of proliferated bile ductules are positive for CK7 (brown), hepatocytes are positive for albumin (green) and a few HPC are stained with both CK7 and albumin (brown-green). Anti-albumin and CK7, $\times 200$.

The number of organelles in HPC varied. Some contained numerous free ribosomes, and others contained free ribosomes and rough endoplasmic reticulum. As in EBA and hepatoblastoma^[8], HPC with ultrastructural features of differentiation towards biliary epithelial cells or hepatocytes were also found in HLC. These differentiated cells were mainly located in proliferating bile ductules. HPC with signs of biliary differentiation contained a higher number of tonofilament bundles than undifferentiated HPC and sometimes exhibited small surface microvilli and

formed bile canaliculi with neighboring hepatocytes^[9]. Some HPC were partly surrounded by a basement membrane. HPC with signs of hepatocytic differentiation exhibited more cytoplasm, more mitochondria and fewer tonofilament bundles than undifferentiated HLC. Intercellular junctions between HPC and adjacent biliary epithelial cells were noted not only in undifferentiated HLC but also in HLC with signs of biliary and hepatocytic differentiation (Figures 5 and 6).

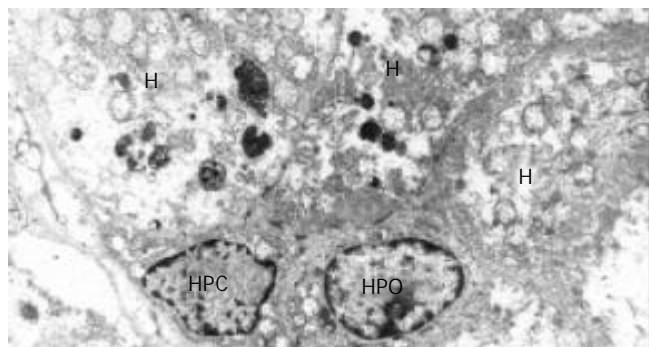


Figure 5 HLC. Under electron microscopy, two HPC characterized by small size (approximately 10 μm), oval shape, and high nucleo/cytoplasm ratio, are seen. They are adjacent to hepatocytes (H) on one side and to HPC on the other side. $\times 5\ 000$.

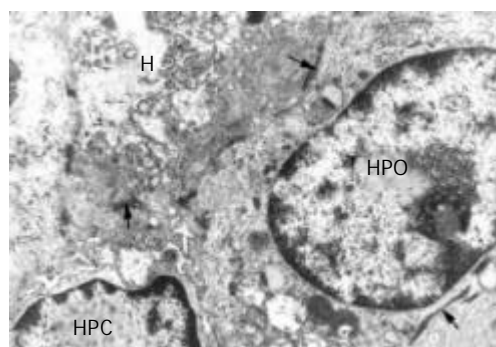


Figure 6 HLC. At higher magnification, cytoplasm of HPC is seen to contain tonofilaments (thin arrow) and intercellular junctions (thick arrows) between HPC and hepatocytes. $\times 16\ 000$.

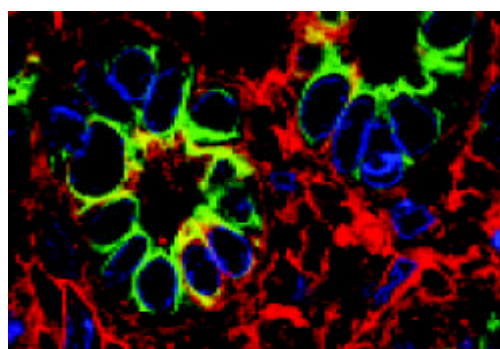


Figure 7 HLC. Immunofluorescence confocal laser scanning microscopy (ICLSM) indicates at edge of regenerating nodules, proliferating bile ductules in which not only bile epithelial cells (anti CK7, green), but also HPC (anti CK7 and albumin, orange) are noted. $\times 1\ 800$.

ICLSM investigation revealed labelling of HPC for both cyokeratin 7 and albumin. HPC with double labelling of both cyokeratin 7 and albumin were observed, as noted under light microscopy, at margins of regenerating nodules, in fibrous septae, and especially in proliferating bile ductules

that were composed of 2-8 cells. Although we could not see the accurate location of a labelling for cyokeratin 7 (as seen with immunoelectron microscopy, this was associated mainly with tonofilament bundles) and for albumin (this was cytoplasmic and diffuse), but the double labelling in HPC was rarely noted from this method. Some HPC (with signs of biliary differentiation) exhibited a stronger labelling for cyokeratin 7 and a weaker labelling for albumin. In comparison, those cells with signs of hepatocytic differentiation exhibited a stronger labelling for albumin and a weaker labelling for cyokeratin 7 (Figures 7 and 8).

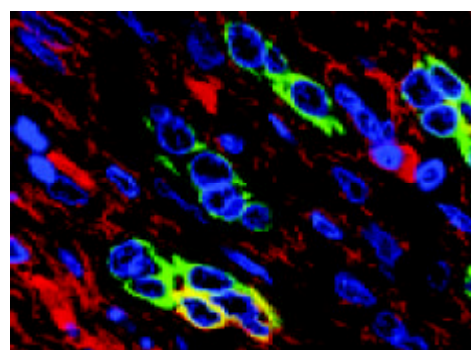


Figure 8 HLC. Immunofluorescence confocal laser scanning microscopy (ICLSM) shows that two proliferating bile ductules are composed only of bile epithelial cells (anti CK7, green), but one proliferating bile ductule contains HPC (anti CK7 and albumin, orange). $\times 1\ 000$.

DISCUSSION

In rodents, administration of hepatocarcinogens could lead to proliferation of oval cells, which are characterized by certain morphological features, such as a small size, an oval shape and a high nucleus/cytoplasm ratio^[1-4]. These cells express both biliary and hepatocytic markers, and are able to differentiate into biliary epithelial cells and hepatocytes. It has been widely accepted that oval cells represent hepatic stem cells in rodent livers, or are at least closely related to them^[2].

Whether bipotent hepatic stem cells that give rise to both biliary epithelial cells and hepatocytes exist in human livers, however, is still a matter of controversy^[2]. Cells with the morphologic features of oval cells in rodents have been recently, described in various liver diseases^[11-13]. In previous studies we demonstrated that cells with the morphological and immunophenotypical features of oval cells of rodents, that we termed SEC, existed in human livers under pathological conditions such as in HB^[5,6], HCC^[7], EBA^[8] and HLC^[9] but not in normal livers^[5-9]. In this study, we further demonstrated with immunohistochemistry, ICLSM and electron microscopic technique, that HPC did occur in HLC due to HBV infection in cases with and without associated HCC.

As in HB, HCC and EBA, HPC in HLC exhibit several important features that closely resemble those of oval cells of rodents. (1) They are often characterized by an oval shape and an oval nucleus, a high nucleus/cytoplasm ratio and a small size with 8-18 μm average diameter. (2) The ultrastructural features of HPC closely resemble those of oval cells as described in rodents^[10], *i.e.*, HPC represent desmosome-like or tight junctions, tonofilaments, microvillous interdigitations and basement membrane. (3) They exhibit corresponding immunophenotypes to oval cells as shown by immunohistochemistry and ICLSM. These cells are verified to express both albumin (a marker of hepatocytic differentiation) and cyokeratin 7 (in the liver a marker of biliary differentiation). (4) A positive correlation exists between the number of HPC

and the activity of cirrhosis. (5) HPC are located in bile ductules that contain 2-8 cells.

On the basis of our findings in HLC, as described in HB, EBA and HCC, it seems likely that HPC represent potential bipotent stem cells in human livers that by definition, give rise to biliary epithelial cells and hepatocytes.

There is a likeness of HLC to other liver diseases in that an association exists between the activity or severity of cirrhosis and the number of HPC. This has led us to advance the hypothesis that oval cell proliferation might not be disease-specific but occurs in response to progressive liver injury and fibrosis.

HPC mainly occurred in proliferating bile ductules that were found both in experimental animal models^[2] and in various human neoplastic and non-neoplastic liver diseases^[11-14]. As to the origin of proliferating ductules, the hypothesis of proliferation of pre-existing bile duct epithelium or a metaplasia of periportal hepatocytes has been reported^[2,3,15]. However, there is now increasing evidence that, at least in some cases, proliferating bile ductules arose directly from hepatic progenitor cells not only in rodents^[1-4], but also in various human liver diseases^[11-14]. This study indicated again that oval-like cells did appear in proliferating bile ductules in human livers and that these ductules might indeed arise from proliferation and differentiation of hepatic progenitor cells.

HPC have been recently demonstrated only in pathological liver specimens but not in normal livers. It can rationally be speculated that as in rodent livers, the activation and proliferation of putative stem cell pool in human livers took place only if the replicative capacity of hepatocytes was severely impaired after some endogenous or exogenous toxic injury or stimuli^[10,13,16]. Several studies indicated that HPC activation in rodent livers was regulated by or associated with various factors, such as tumour necrosis factor- α (TNF- α), transforming factor- α (TGF- α), epidermal growth factor (EGF), hepatocyte growth factor (HGF), *etc.*^[10,13,16]. Some non-hepatocytes such as Kupffer cells and Ito cells have also been reported to participate in HPC activation^[3]. These findings await to be verified in human liver diseases.

In conclusion, HLC caused by HBV-infection contain HPC. The findings further support the hypothesis that human hepatic progenitor cells may play a role in the course of liver diseases.

REFERENCES

- 1 **Dabeva MD**, Petkov PM, Sandhu J, Oren R, Laconi E, Hurston E, Shafritz DA. Proliferation and differentiation of fetal liver epithelial progenitor cells after transplantation into adult rat liver. *Am J Pathol* 2000; **156**: 2017-2031
- 2 **Forbes S**, Vig P, Poulson R, Thomas H, Alison M. Hepatic stem cells. *J Pathol* 2002; **197**: 510-518
- 3 **Yin L**, Lynch D, Ilic Z, Sell S. Proliferation and differentiation of ductular progenitor cells and littoral cells during the regeneration of the rat liver to CCl₄/2-AAF injury. *Histol Histopathol* 2002; **17**: 65-81
- 4 **Braun KM**, Thompson AW, Sandgren EP. Hepatic microenvironment affects oval cell localization in albumin-urokinase-type plasminogen activator transgenic mice. *Am J Pathol* 2003; **162**: 195-202
- 5 **Ruck P**, Xiao JC, Kaiserling E. Small epithelial cells and the histogenesis of hepatoblastoma. Electron microscopic, immunoelectron microscopic, and immunohistochemical findings. *Am J Pathol* 1996; **148**: 321-329
- 6 **Ruck P**, Xiao JC. Stem-like cells in hepatoblastoma. *Med Pediatr Oncol* 2002; **39**: 504-507
- 7 **Xiao JC**, Ruck P, Kaiserling E. Small epithelial cells in extrahepatic biliary atresia: electron microscopic and immunoelectron microscopic findings suggest a close relationship to liver progenitor cells. *Histopathology* 1999; **35**: 454-460
- 8 **Xiao JC**, Ruck P, Kaiserling E. Zur Bedeutung der kleinen epithelialen Zellen beim hepatozellulären Karzinom. Immunohistochemische, elektronenmikroskopische und immunoelektronenmikroskopische Befunde. *Verh Dtsch Ges Pathol* 1996; **80**: 407
- 9 **Xiao JC**, Ruck P, Adam A, Wang TX, Kaiserling E. Small epithelial cells in human liver cirrhosis exhibit features of hepatic stem-like cells: immunohistochemical, electron microscopic and immunoelectron microscopic findings. *Histopathology* 2003; **42**: 141-149
- 10 **Kiss A**, Schnur J, Szabo Z, Nagy P. Immunohistochemical analysis of atypical ductular reaction in the human liver, with special emphasis on the presence of growth factors and their receptors. *Liver* 2001; **21**: 237-246
- 11 **Van Den Heuvel MC**, Slooff MJ, Visser L, Muller M, De Jong KP, Poppema S, Gouw AS. Expression of anti-OV6 antibody and anti-N-CAM antibody along the biliary line of normal and diseased human livers. *Hepatology* 2001; **33**: 1387-1393
- 12 **Tan J**, Hytioglou P, Wiczorek R, Park YN, Thung SN, Arias B, Theise ND. Immunohistochemical evidence for hepatic progenitor cells in liver diseases. *Liver* 2002; **22**: 365-373
- 13 **Libbrecht L**, Roskams T. Hepatic progenitor cells in human liver diseases. *Semin Cell Dev Biol* 2002; **13**: 389-396
- 14 **Crosby HA**, Kelly DA, Strain AJ. Human hepatic stem-like cells isolated using c-kit or CD34 can differentiate into biliary epithelium. *Gastroenterology* 2001; **120**: 534-544
- 15 **Zhang Y**, Bai XF, Huang CX. Hepatic stem cells: existence and origin. *World J Gastroenterol* 2003; **9**: 201-204
- 16 **Lowes KN**, Croager EJ, Olynyk JK, Abraham LJ, Yeoh GC. Oval cell-mediated liver regeneration: Role of cytokines and growth factors. *J Gastroenterol Hepatol* 2003; **18**: 4-12

Edited by Lu HM and Wang XL **Proofread by** Xu FM

Comparison of treatment outcomes between biliary plastic stent placements with and without endoscopic sphincterotomy for inoperable malignant common bile duct obstruction

Pietro Di Giorgio, Leonardo De Luca

Pietro Di Giorgio, Leonardo De Luca, Department of Gastroenterology, Pellegrini Hospital, Napoli, Italy

Correspondence to: Pietro Di Giorgio v. M. Turchi 31, 80132 Napoli, Italy. digiorgiop@hotmail.com

Telephone: +339-81-7648324 **Fax:** +339-81-2543382

Received: 2003-12-10 **Accepted:** 2004-01-09

Abstract

AIM: Considerable controversy surrounds the adoption of endoscopic sphincterotomy (ES) to facilitate the placement of 10F plastic stents (PS) and to reduce the risk of pancreatitis. The aim of the study was to assess the possible advantages of ES before PS placement.

METHODS: From 3/1996 to 6/2001, 172 consecutive patients, who underwent placement of a single 10F polyethylene stent for inoperable malignant strictures of the common bile duct, were randomly assigned to 2 groups. In group A (96 patients), a ES was performed before PS placement. In Group B, 96 patients had PS directly. Early complications (within 30 d) and late effects (from 30 d to stent replacement) were assessed. Patency interval was defined as the period between PS placement and obstruction or death. The success of stent replacement in the 2 groups was evaluated.

RESULTS: Stent insertion was successful in 95.8%(92/96) of the pts in group A and in 93.7%(90/96) of the patients in group B ($P>0.05$). Early complications were more frequent in patients who underwent ES (6.5% vs 4.4%) but the data were not significant ($P>0.05$). In group A pancreatitis developed in two patients and bleeding in three; whereas pancreatitis occurred in 2 patients in group B. Complications were managed conservatively. No procedure related mortality occurred. All late complications were acute cholangitis due to stent occlusion. We performed a stent replacement in 87 patients that was successful in 84 cases without differences between groups.

CONCLUSION: Sphincterotomy does not seem to be necessary for placement of 10F-PS in patients with malignant common bile duct obstruction.

Di Giorgio P, De Luca L. Comparison of treatment outcomes between biliary plastic stent placements with and without endoscopic sphincterotomy for inoperable malignant common bile duct obstruction. *World J Gastroenterol* 2004; 10(8): 1212-1214

<http://www.wjgnet.com/1007-9327/10/1212.asp>

INTRODUCTION

Endoscopic insertion of biliary stents is the preferred method of palliation for inoperable malignant biliary obstruction^[1-3]. It

efficiently relieves jaundice and improve quality of life in patients with malignant obstructive biliary disease. The endoscopic approach is more cost-effective than the operative approach.

The use of plastic stents (PS) is nowadays recommended in patients with poor prognosis (less than 5-6 mo)^[4-6]. Initial endoscopic placement of a metal stent is a cost-saving strategy only in patients expected to survive longer than six months.

Controversy exists regarding the use of endoscopic sphincterotomy (ES) before placing 10F stents. Endoscopists who preferred to perform ES pointed out that it was easier to place stents and substitute. Also ES would decrease also post-procedure pancreatitis. Antagonist to ES aim to eliminate risks of complications due to ES. The purpose of this study was to evaluate the potential advantages for ES before PS placement.

MATERIALS AND METHODS

From March 1996 to June 2001 172 consecutive patients who underwent placement of a single 10F polyethylene stent (Cotton Leung biliary stent) for inoperable malignant stricture of the common bile duct, were randomly assigned to two groups (Table 1). In group A (96 patients) an ES was performed before PS was placed.

Group B (96 patients) received PS placement without ES.

The following patients were excluded namely those who had already had ES, precut papillotomy or stent placements, those with previous Billroth II resection and, also, those suffering from coagulopathy. Those with ampullary tumours were not included, either.

The diagnosis and poor prognosis of the patients were established by various imaging methods (US, EUS, TAC, MRC) and on the basis of age.

Patients were randomised by using sealed opaque envelopes. Randomisation was done only after diagnostic cholangiography had been performed.

This study reviewed and approved by the ethics committee of our hospital, was carried out in accordance with the Helsinki Declaration as revised in 1989. All patients were included after they had given their written informed consent on ethics committee forms.

All patients underwent operative endoscopic retrograde cholangiopancreatography (ERCP) with a duodenoscope (JF 140 Olympus) performed by 2 experienced endoscopists. A standard 0.035-inch guidewire to perform deep cannulation of the biliary tree and to pass through the strictures.

Occasionally a hydrophilic guidewire was used. In every patient we also aimed to visualize the pancreatic duct.

The success the technique was evaluated as a correct placement of the stent with good drainage of bile from the bile duct into the duodenum as visualized endoscopically. Early complications (occurring within 30 d) and late effects (from 30 d to stent replacement or death) were assessed. Complications of papillotomy were considered according to the criteria of Cotton^[7] Stents were not replaced routinely and patients were treated if occlusion of the stent or cholangitis

developed.

Occlusion was considered in patients with jaundice.

Patency interval was defined as the period between PS placement and obstruction.

Analysis of data was performed with the statistical package SPSS/PC version 4.0 (M.J. Norusis Chicago, Ill). Rate differences were tested by using the χ^2 analysis with Yates' correction and Fisher's exact test, when appropriate. The Mann whitney *U* test was used to compare median values of variables between the two groups. Values of $P < 0.05$ were regarded as statistically significant.

RESULTS

Patient characteristics did not differ between groups (Table 1). A histological diagnosis was obtained in 104 patients (54.1%) using biliary brushing and biopsies, and FNA-US. In the other cases we presume diagnosis using morphologic criteria.

A similar mean stents length among groups indicated a similar localization of biliary strictures.

Results of endoscopic treatment are shown in Table 2. The mean follow up time was 115±95 d (mean±SD).

Table 1 Patients characteristics

	Group A With ES	Group B w/o ES	Total
Patients	96	96	192
Median Age (±SD)	72±6	75±6	73±7
Gender (M/F)	51/35	47/39	98/74
Bilirubine (mg/dL)	13.5	11.9	12.7
Stent length(cm)	6.78	6.76	6.79
Visualization of pancreatic duct	77	79	156
Pancreatic cancer	64 (66.6 %)	67 (69.8 %)	131 (68.2%)
Cholangiocarcinoma	31 (32.3 %)	28 (29.1 %)	59 (30.7 %)
Metastatic lymph nodes	1 (1.1%)	1 (1.1%)	2 (1.1 %)

Table 2 Endoscopic technique results

	Group A With ES (%)	Group B w/o ES (%)	<i>P</i>
Successful stent insertion	92/96 (95.8)	90/96 (93.7)	0.745
Early complications	6/92 (6.5)	4/90 (4.4)	0.772
Pancreatitis	2/92 (2.2)	2/90 (2.2)	0.629
Bleeding	3/92 (3.7)	0/90	0.252
Clogging	1/92 (1.2)	2/90	0.985
Procedure related mortality	0	0	
Late complications	16/92 (17.4)	15/90 (16.6)	0.946
Migration	3/92 (3.2)	3/90 (3.3)	0.698

Four cases of pancreatitis were treated successfully with conservative therapy.

In all the 3 cases bleeding stopped after papillar needle infiltration with adrenaline solution.

In three cases we have early clogging of the prostheses and we performed an urgent stent replacement. No procedure related mortality occurred. In 6 cases (6.5%) stents migrated proximally. 86 patients died before stent occlusion (8 during the first month but non related to endoscopic therapy). Nine patients did not come for follow-up after the first period of 30 d.

Late complications in all cases were acute cholangitis due to stent occlusion.

Eighty-seven patients (47.8%) needed a stent replacement which was successful in 95.4% of the cases (Table 3).

Table 3 Stents replacement

	Group A with ES	Group B w/o ES	<i>P</i>
Patients (<i>n</i>)	41	46	
Successful stent replacement	39/41	45/46	0.919
Patency (median±SD)	109±15	110±18	0.765

DISCUSSION

Our data showed no differences between two groups in regard to success of stent insertion, incidence of early and late complications and patency. Our data were similar to those of literature^[8-9] limited to common bile duct obstructions.

In a retrospective study, Margulies^[10] considered the effect of sphincterotomy on acute and chronic complications of 10F stent therapy in 130 patients. The incidence of acute complications was higher in patients undergoing sphincterotomy 8.3% vs 1.2% ($P=0.04$). A gastrointestinal bleeding was seen in 3 cases (6.2%) in whom ES was performed. There were no inclusive criteria reported in this study, therefore we do not know whether patients with coagulopathy were considered.

In our experience the incidence of bleeding was lower. We had three cases of bleeding in the ES group (3.1%) which were treated successfully with endoscopic therapy.

Coagulopathy has been found to be an independent risk factor for hemorrhage after ES^[11] and its incidence increases in cholestasis^[12,13].

In a retrospective study, Tarnasky^[14], found that the rate of pancreatitis following transpapillary stenting without ES increased in patients with a proximal biliary stenosis because this kind of lesion worked as a fulcrum leading to a distal deflection of the stent and a consequential compression of the pancreatic orifice. Patients with proximal biliary strictures were at significantly increased risk for postprocedure pancreatitis (4 of 24) versus those with distal or no stricture (0 of 59) ($P=0.006$).

In our study the incidence of pancreatitis was not significantly different between the two groups (Group with ES: 2/92, Group without ES 2/90), probably because our patients did not have proximal stenosis.

Johanson^[15] examined multiple risk factors associated with stent migration such as stent diameter and length. In his study the odds ratio of proximal migration in patients with ES was 3.9, and 0.3 in patients without ES.

The association between sphincterotomy and proximal migration was not statistically significant, but the authors concluded if ES was not performed the risk of proximal migration might decrease.

Lahoti^[16] examined retrospectively 2 993 procedures for insertion of biliary or pancreatic duct stents. Thirty-three proximally migrated duct stents and twenty-six proximally migrated pancreatic duct stents were identified. All patients except one had a sphincterotomy.

Margulies^[10], on the other hand, found an increased incidence of migration in patients who had stents placed without ES. Stent migration was seen in 8.5% of patients in the no ES group.

In our experience, the incidence of proximal or distal migration was not so high and we didn't find differences between the groups.

Stent replacement was possible in 97.8% (45/46) of the patients who had not undergone ES, probably owing to the persistent dilation of the papilla caused by the presence of the stent.

In conclusion, according to our prospective study, placement of a 10 F biliary stent for common bile duct stenosis without ES is safe and has the same success rate of the ES technique.

No ES can avoid the risk of perforation and bleeding. ES must not be performed in patients with coagulation problems which are frequent in patients with cholestasis due to neoplastic biliary obstruction. If we consider long term complications of sphincterotomy whose range was 5.8-24%^[17-18] ES should not be performed in patients with non neoplastic pathology (bile leaks, non malignant strictures). We did not find any difference in stent replacement between patients with ES and those without.

REFERENCES

- 1 **Smith AC**, Dowsett JF, Russell RC, Hatfield AR, Cotton PB. Randomised trial of endoscopic stenting versus surgical by-pass in malignant low bile duct obstruction. *Lancet* 1994; **344**: 1655-1660
- 2 **Andersen JR**, Sorensen SM, Kruse A, Rokkjaer M, Matzen P. Randomised trial of endoscopic endoprotheses versus operative bypass in malignant obstructive jaundice. *Gut* 1989; **30**: 1132-1135
- 3 **Ballinger AB**, Mc Hugh M, Catnach SM, Alstead EM, Clark ML. Symptom relief and quality of life after stenting for malignant bile duct obstruction. *Gut* 1994; **35**: 467-470
- 4 **Prat F**, Chapat O, Ducot B, Poncon T, Pelletier G, Fritsch J, Choury AD, Buffet C. A randomized trial of endoscopic drainage methods for inoperable malignant strictures of the common bile duct. *Gastrointest Endosc* 1998; **47**: 1-7
- 5 **Prat F**, Chapat O, Ducot B, Poncon T, Fritsch J, Choury AD, Pelletier G, Buffet C. Predictive factors for survival of patients with inoperable malignant distal biliary strictures: a practical management guideline. *Gut* 1998; **42**: 76-80
- 6 **Arguedas MR**, Heudebert GH, Stinnett AA, Wilcox CM. Biliary stents in malignant obstructive jaundice due to pancreatic carcinoma: a cost-effectiveness analysis. *Am J Gastroenterol* 2002; **97**: 898-904
- 7 **Cotton PB**, Lehman G, Vennes J, Geenen JE, Russell RC, Meyers WC, Liguory C, Nickl N. Endoscopic sphincterotomy complications and their management: an attempt at consensus. *Gastrointest Endosc* 1991; **37**: 383-393
- 8 **Huibregtse K**, Tytgat GN. Palliative treatment of obstructive jaundice by transpapillary introduction of a large bore bile duct endoprotheses. *Gut* 1982; **23**: 371-375
- 9 **Siegel JH**, Snady H. The significance of endoscopically placed prostheses in the management of (biliary) obstruction due to carcinoma of the pancreas: results of non operative decompression in 227 patients. *Am J Gastroenterol* 1986; **81**: 634-641
- 10 **Margulies C**, Sampaio Siqueira E, Silverman WB, Lin XS, Martin JA, Rabinovitz M, Slivka A. The effect of endoscopic sphincterotomy on acute and chronic complications of biliary endoprotheses. *Gastrointest Endosc* 1999; **49**: 716-719
- 11 **Rabenstein T**, Schneider HT, Bulling D, Nicklas M, Katalinic A, Hahn EG, Martus P, Ell C. Analysis of the risk factors associated with endoscopic sphincterotomy techniques. *Endoscopy* 2000; **32**: 10-19
- 12 **Jorgensen B**, Fischer E, Ingeberg S, Hollaender N, Ring-Larsen H, Henriksen JH. Decreased blood platelet volume and count in patients with liver disease. *Scand J Gastroenterol* 1984; **19**: 492-499
- 13 **Kelly DA**, Summerfield JA. Hemostasis in liver disease. *Semin Liv Dis* 1987; **7**: 182-188
- 14 **Tarnasky PR**, Cunningham JT, Hawes RH, Hoffman BJ, Uflacker R, Vujic I, Cotton PB. Transpapillary stenting of proximal biliary strictures: does biliary Sphincterotomy reduce the risk of postprocedure pancreatitis? *Gastrointest Endosc* 1997; **45**: 46-51
- 15 **Johanson JF**, Schmalz MJ, Geenen JE. Incidence and risk factors for biliary and pancreatic stent migration. *Gastrointest Endosc* 1992; **38**: 341-346
- 16 **Lahoti S**, Catalano M, Geenen J, Schmalz MJ. Endoscopic retrieval of proximal migrated biliary and pancreatic stents: experience of a large referral center. *Gastrointest Endosc* 1998; **47**: 486-491
- 17 **Prat F**, Malak NA, Pelletier G, Buffet C, Fritsch J, Choury AD, Altman C, Liguory C, Etienne JP. Biliary symptoms and complications more than 8 years after endoscopic sphincterotomy for choledocholithiasis. *Gastroenterology* 1996; **110**: 894-899
- 18 **Bergman JJ**, van der Mey S, Rauws EA, Tijssen JG, Gouma DJ, Tytgat GN, Huibregtse K. Long-term follow-up after endoscopic sphincterotomy for bile duct stones in patients younger than 60 years of age. *Gastrointest Endosc* 1996; **44**: 643-649

Edited by Wang XL Proofread by Xu FM

Albendazole versus metronidazole treatment of adult giardiasis: An open randomized clinical study

Oguz Karabay, Ali Tamer, Huseyin Gunduz, Derya Kayas, Huseyin Arinc, Harika Celebi

Oguz Karabay, Ali Tamer, Huseyin Gunduz, Huseyin Arinc, Harika Celebi, Infectious Disease and Internal Medicine Department, Medical Faculty, Izzet Baysal Universty, Golkoy Kampusu/Bolu /Turkey
Derya Kayas, Internal Medicine Department Duzce, Social Security Hospital, Turkey

Correspondence to: Assist Professor Oguz Karabay, MD. Izzet Baysal Medical Faculty Infectious Disease Unit. Golkoy Kampusu/Bolu /Turkey. drkarabay@yahoo.com

Telephone: +903742534656 **Fax:** +903742534559

Received: 2003-10-08 **Accepted:** 2003-12-24

Abstract

AIM: To investigate the efficacy and tolerability of albendazole and metranidazole treatment in giardiasis.

METHODS: The open comparative randomized trial was carried out prospectively from December 1999 to July 2001 in Duzce City of Turkey. The diagnosis was based on the presence of signs and symptoms compatible with giardiasis including a positive stool examination of giardia cysts or trophozoite. Metranidazole group consisted of 29 patients and was given metranidazole 500 mg, three times a day for 5 d and albendazole group was consisted of 28 patients and was given albendazole 400 mg/d for 5 d.

RESULTS: There were no significant differences in demographical and therapeutical effects and patient's compliance between both groups. But side effects were seen more in metranidazole group than in albendazole group.

CONCLUSION: Albendazole is as effective as metranidazole in adults' giardiasis. Albendazole has less side effect potentials than metranidazole in the treatment of giardiasis.

Karabay O, Tamer A, Gunduz H, Kayas D, Arinc H, Celebi H. Albendazole versus metronidazole treatment of adult giardiasis: An open randomized clinical study. *World J Gastroenterol* 2004; 10(8): 1215-1217

<http://www.wjgnet.com/1007-9327/10/1215.asp>

INTRODUCTION

Giardia intestinalis is a protozoan parasite in the small intestine that causes extensive morbidity worldwide. Giardiasis is a hyperendemic disease in households lacking municipal sewer and water in the developing countries^[1]. The life cycle of *G. intestinalis* has 2 forms: the trophozoite and the cyst. As few as 10 cysts may establish infection^[2,3]. Giardiasis is currently treated with metronidazole, tinidazole and quinacrine^[3]. The adverse effects and treatment failures to some of the currently recommended drugs (particularly 5-nitroimidazoles) for giardia infection have given rise to the need for alternative anti giardial agents. Albendazole is an important alternative drug for treatment of giardiasis. *In vitro* Albendazole inhibits the growth of trophozoites of *G. intestinalis* and their adhesion to cultured intestinal epithelial cells and disturbs the activity of microtubules

and microribbons in the trophozoite's adhesive disk. The results of giardiasis treatment with albendazole have been confused. A lot of trials were carried out for giardiasis treatment with albendazole in pediatric groups. Albendazole was found to be effective for pediatric giardiasis patients. Albendazole at a dose of 400 mg per day for 5 d, cured 97 percent of infections in children in Bangladesh^[4]. A few studies were about the effects of albendazole on adult intestinal giardiasis. It was ineffective in a study of adult travelers returning from tropical areas^[3,5]. In this study we aimed to investigate effect of albendazol on adult giardiasis compared with metronidazole treatment.

MATERIALS AND METHODS

Subjects

Adults with diarrhea at the outpatient clinic of the Department of Infectious Diseases of Social Security Hospital in Duzce/Turkey were screened for enrollment in the study. After informed consent was obtained, a detailed medical history was taken from each patient and physical examination was performed. For the demonstration of trophozoites or cysts in the stool, 3 stool samples were obtained. Patients with diarrhea and *G. intestinalis* cysts or trophozoites in a sample were eligible for enrollment in the study. Diarrhea was defined as more than 4 times of unformed stools per day. Giardia cysts were identified in fresh faecal material by direct faecal microscopic examination. A stool culture was carried out to identify bacterial causes of diarrhea. Patients with a positive coproculture for bacterial causes of diarrhea were excluded from analysis. All patients had a clinical response, recorded on d 7, 15, and a parasitological response recorded on the basis of examination of 2 stool samples between d 7 and 15 after initiation of treatment.

Study medication

Patients were randomized to receive albendazole 400 mg/d for 5 d or metronidazole 500 mg thrice daily for 5 d.

Treatment methods

Of the original 67 (38 female and 29 male) patients who were selected, 57 (24 males and 33 females) completed this study in the follow-up period (Figure 1). Twenty-nine patients who received metronidazole (Falgy1®) 500 mg 3 times daily for 5 d. Twenty-eight patients received albendazole (Andazol®) 400 mg /d for 5 d.

Assessment of compliance

All patients were investigated for compliance to treatment, and one of the following requirements should be fulfilled in order to define a case as noncompliance to treatment, namely, failure to attend the controls, not use one or a few of the medicines at the instructed dose and the duration, not use the drug without taking the consent of the doctor.

Ethics

The study protocol was approved by the locally ethics committee. All patients were informed and agreed to participate in the study.

Table 1 Demographical and clinical findings of treatment groups (mean±SD)

Parameter	Metranidazol Group (n=29)	Albendazol Group (n=28)	P
Female /Male	18/11	15/13	#
Age (yr)	38±14	41±12	#
Hemoglobin	13.2±1.5	12.7±1.5	#
Leukocyte count	7 996±2 668	8 225±3 016	#
Faecal examination positive for cysts or trophozoits on d 7	0	0	NA
Faecal examination positive for cysts or trophozoits on d 15	0	1	NA
Metal taste	9	0	NA
Anorexia +/-	18	2	0.0001
Abdominal pain	3	1	#
After starting treatment healing of symptoms (h)	83±39	80±28	#
Advers effects other than anorexia	8	6	#
Non-compliance to treatment	7	5	#

#: $P>0.05$, NA: Not applicable.

Statistical analysis

Gender, age, mean hemoglobin concentration and leukocyte counts were compared between the 2 groups using non-parametric test (Mann-Whitney U test). Difference between the 2 groups was analyzed using chi-square test. We used Epi-info 6.0 (Centers for Disease Control, Atlanta) to perform the analysis and considered $P<0.05$ as statistically significant.

Criteria for exclusion

Patients receiving or having received antiparasitic drugs during the 10-d prior to commencing the study, patients with fever, pregnant women, mothers who were breast feeding, patients with known hypersensitivity to either albendazole or metronidazole, patients for whom any of the treatments used in the study were contraindicated.

one patient in of albendazole group was found to be positive for giardia cyst, while none of the patients in metranidazole group was positive for giardia cyst. Abdominal pain was found in 3 patients of metronidazole group and 1 patient of albendazole group ($P>0.05$). Vomiting was seen in 1 patient of metronidazole group and none in albendazole group. Noncompliance to treatment was found in 7 patients of metronidazole group and in 5 patients in albendazole group ($P>0.05$). Anorexia was found in 18 patients of metronidazole group and in 2 patients of albendazole group ($P<0.001$). Metal taste was determined in nine patients of metronidazole group and none in albendazole group. Records associated with other (headache, abdominal pain, dazedness) adverse effects except anorexia and metal taste were not found to be significantly different between the 2 groups ($P>0.05$).

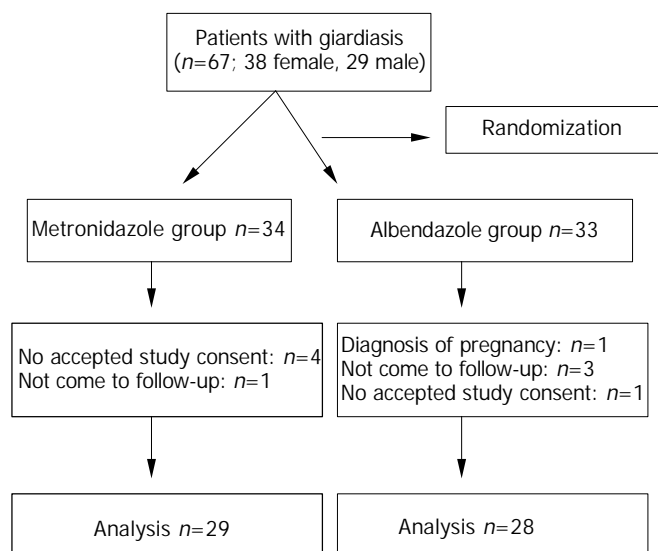


Figure 1 Flow chart of patients studied.

RESULTS

The clinical and demographic findings in the albendazole group and metronidazole group are presented in Table 1.

No positive giardia cyst was found in the stool samples of both albendazole and metronidazole groups on d 7. But on d 15

DISCUSSION

Infections with parasitic helminths and protozoa are important causes of morbidity and mortality worldwide. The protozoan parasite *Giardia intestinalis* (synonyms: *Giardia duodenalis* and *Giardia lamblia*) is recognized as a major cause of diarrheal illness in humans and livestock. It is one of the most important non-viral infectious agents causing diarrheal illness, the infection may be asymptomatic or present with a variety of symptoms such as diarrhea, weight loss, abdominal cramps and failure to thrive. *G.intestinalis* may attach to small bowel wall but not invade it. Trophozoites may be encysted and shed in faeces for future ingestion by other hosts. Whereas the organism can cause diarrhea and abdominal pain. Some people experienced only a mild self-limiting illness, while others developed a chronic illness lasting for several months. Furthermore, people might be infected without any symptoms, and it has even been suggested that some people could benefit from their carrier state^[6,7].

Although *Giardia* infections resolve spontaneously in 85% of patients within 6 wk, all patients with symptomatic giardiasis should be treated. Metronidazole and quinacrine are the first-line treatment options and are more than 90% effective. Tinidazole, furazolidone, paromomycin, mebendazole, and albendazole have been used as alternative anti-giardial drugs^[8]. Cedillo-Rivera *et al.*^[9] investigated the susceptibility of a strain of *Giardia lamblia* to benzimidazole carbamates, 5-nitroimidazoles, nitrofurans and other drugs. They found that albendazole was the most active compound among the 5-nitroimidazoles tested, ornidazole was the most effective, and

tinidazole, metronidazole, secnidazole were less active.

Various reports have published the effect of albendazole on giardiasis. Albendazole was found to be very effective on giardiasis^[10]. Misra *et al.*^[10] studied the effect of albendazole and metranidazole on giardiasis in 64 children aged 2-12 years. They concluded that albendazole was proved as effective as metronidazole in the treatment of giardia infection in children with the absence of anorexia. Similarly, another study found albendazole at dose of 400 mg /d for 5 d cured 97% of infections in children in Bangladesh^[4]. But, Escobedo *et al.* investigated in a comparative trial. One hundred and sixty-five Cuban children with confirmed giardiasis were randomized to receive albendazole (400 mg/d for 5 d), chloroquine (10 mg/kg twice daily for 5 d) or tinidazole (50 mg/kg, as a single dose). They found that tinidazole and chloroquine appeared equally effective, curing 91% and 86% of the children treated, respectively, and were significantly better than albendazole, which only cured 62% of the children^[11].

In this study we investigated the effect of albendazole and metronidazole on symptomatic adult giardiasis. We did not find any significant difference in demographical properties (gender, age), mean hemoglobins, and mean leukocytes between the 2 groups. Giardia cysts were not found in faecal examination both groups on d 7. But on d 15 after starting treatment, one patient was found to be positive for giardia in albendazole group and none in metronidazole group. We thought that this patient might be reinfected. After starting treatment, 9 patients complained of metal taste in metronidazole group and no patient in albendazole group. Anorexia was found in 18 patients of metronidazole group but only 2 patients complained of anorexia in albendazole group ($P < 0.01$). In terms of adverse effects, albendazole was found superior to metronidazole. Patients' compliance was found to be similar in both groups ($P > 0.05$). We thought that it might be due to a short treatment period (five days). Similarly, Chan Del Pino *et al.*^[12] investigated the efficacy and tolerance of albendazole compared with metranidazole, furazolidone, tinidazole and secnidazole in the treatment of giardiasis in 79 children. They concluded that albendazole was as effective as metronidazole, furazolidone, tinidazole and secnidazole, but faster in eradicating *Giardia lamblia* in children and had a better tolerance than metranidazole, furazolidone and tinidazole.

The drug resistance was not an important problem for giardiasis^[13-15]. In our country cost of both drugs is similarly. We thought that both drugs can be used in the treatment of giardiasis, because according to our results albendazole is as effective as metronidazole in adult's giardiasis and albendazole treatment has also less side effects than metronidazole.

ACKNOWLEDGEMENTS

The authors would like to thank Dr. Gurhan Konakci (Chief Manager of Social Security Duzce Hospital) for providing his help.

REFERENCES

- 1 **Redlinger T**, Corella-Barud V, Graham J, Galindo A, Avitia R, Cardenas V. Hyperendemic Cryptosporidium and Giardia in households lacking municipal sewer and water on the United States-Mexico border. *Am J Trop Med Hyg* 2002; **66**: 794-798
- 2 **Gardner TB**, Hill DR. Treatment of giardiasis. *Clin Microbiol Rev* 2001; **14**: 114-128
- 3 **Liu LX**, Weller PF. Antiparasitic drugs. *N Engl J Med* 1996; **334**: 1178-1184
- 4 **Hall A**, Nahar Q. Albendazole as a treatment for infections with Giardia duodenalis in children in Bangladesh. *Trans R Soc Trop Med Hyg* 1993; **87**: 84-86
- 5 **Kollaritsch H**, Jeschko E, Wiedermann G. Albendazole is highly effective against cutaneous larva migrans but not against Giardia infection: results of an open pilot trial in travellers returning from the tropics. *Trans R Soc Trop Med Hyg* 1993; **87**: 689
- 6 **Vesny CJ**, Peterson WL. The management of Giardiasis. *Aliment Pharmacol Ther* 1999; **13**: 843-850
- 7 **Homan WL**, Mank TG. Human giardiasis: genotype linked differences in clinical symptomatology. *Int J Parasitol* 2001; **31**: 822-826
- 8 **Tessier JL**, Davies G. Giardiasis. *Primary Care Update for OB/GYNs* 1999; **6**: 8-11
- 9 **Cedillo-Rivera R**, Munoz O. *In-vitro* susceptibility of Giardia lamblia to albendazole, mebendazole and other chemotherapeutic agents. *J Med Microbiol* 1992; **37**: 221-224
- 10 **Misra PK**, Kumar A, Agarwal V, Jagota SC. A comparative clinical trial of albendazole versus metronidazole in children with giardiasis. *Indian Pediatr* 1995; **32**: 779-782
- 11 **Escobedo AA**, Nunez FA, Moreira I, Vega E, Pareja A, Almirall P. Comparison of chloroquine, albendazole and tinidazole in the treatment of children with giardiasis. *Ann Trop Med Parasitol* 2003; **97**: 367-371
- 12 **Chan Del Pino M**, Cueva Cornejo L, Troyes Rivera L. Comparative study of albendazole versus nitrofurans and nitroimidazoles in the treatment of giardiasis in children. *Rev Gastroenterol Peru* 1999; **19**: 95-108
- 13 **Cruz A**, Sousa MI, Azeredo Z, Leite E, Figueiredo De Sousa JC, Cabral M. Isolation, excystation and axenization of Giardia lamblia isolates: *in vitro* susceptibility to metronidazole and albendazole. *J Antimicrob Chemother* 2003; **51**: 1017-1020
- 14 **Wright JM**, Dunn LA, Upcroft P, Upcroft JA. Efficacy of anti-giardial drugs. *Expert Opin Drug Sa* 2003; **2**: 529-541
- 15 **Ali SA**, Hill DR. Giardia intestinalis. *Curr Opin Infect Dis* 2003; **16**: 453-460

Edited by Wang XL and Xu FM

Effects of hemoperfusion adsorption and/or plasma exchange in treatment of severe viral hepatitis: A comparative study

Nian-Hai He, Ying-Jie Wang, Ze-Wen Wang, Jun Liu, Jia-Jia Li, Guo-Dong Liu, Yu-Ming Wang

Nian-Hai He, Ying-Jie Wang, Ze-Wen Wang, Jun Liu, Jia-Jia Li, Guo-Dong Liu, Yu-Ming Wang, Research Institute of Infectious Disease, Southwest Hospital, Third Military Medical University, Chongqing 400038, China

Supported by the National Natural Science Foundation of China, No.30027001

Correspondence to: Dr. Ying-Jie Wang, Research Institute of Infectious Disease, Southwest Hospital, Third Military Medical University, 29 Gaotanyan Zhengjie, Chongqing 400038, China. wangyj103@263.net

Telephone: +86-23-68754475-8062 **Fax:** +86-23-65334998

Received: 2003-09-15 **Accepted:** 2003-12-08

Abstract

AIM: Non-bioartificial liver has been applied to clinic for quite a long time, but the reported efficacy has been very different. The aim of this study was to compare the efficacy and safety of hemoperfusion adsorption, plasma exchange and plasma exchange plus hemoperfusion adsorption in treatment of severe viral hepatitis.

METHODS: Seventy-five patients with severe viral hepatitis were treated with hemoperfusion adsorption therapy (24 cases), plasma exchange therapy (17 cases) and plasma exchange plus hemoperfusion adsorption therapy (34 cases). The data of liver function, renal function, blood routine test, prothrombin time (PT) and prothrombin activity (PTa) pre- and post-therapy were analyzed.

RESULTS: Clinical symptoms of patients improved after treatment. The levels of aminotransferase, total bilirubin, direct bilirubin decreased significantly after 3 therapies ($P < 0.05$ or $P < 0.01$). PT, the level of total serum protein decreased significantly and PTa increased significantly after plasma exchange therapy and plasma exchange plus hemoperfusion adsorption therapy ($P < 0.05$ or $P < 0.01$). The side effects were few and mild in all patients.

CONCLUSION: Three therapies were effective in the treatment of severe viral hepatitis. Plasma exchange therapy and plasma exchange plus hemoperfusion adsorption therapy are better than hemoperfusion adsorption therapy.

He NH, Wang YJ, Wang ZW, Liu J, Li JJ, Liu GD, Wang YM. Effects of hemoperfusion adsorption and/or plasma exchange in treatment of severe viral hepatitis: A comparative study. *World J Gastroenterol* 2004; 10(8): 1218-1221
<http://www.wjgnet.com/1007-9327/10/1218.asp>

INTRODUCTION

The treatment of severe viral hepatitis is always intractable in clinic. The previous non-bioartificial liver has widely been applied to clinic treatment^[1-16], but its reported efficacy is various. In order to make an objective evaluation and comparison of the effects of non-bioartificial liver in the treatment of severe viral hepatitis, we chose three therapies of hemoperfusion

adsorption, plasma exchange and plasma exchange plus hemoperfusion adsorption and compared their efficacy and safety.

MATERIALS AND METHODS

Materials

Sixty-four males and 11 females aged from 23 to 66 (41.3 on average) years with severe viral hepatitis were hospitalized in our section from January 1998 to February 2002. The diagnosis of 75 patients meeting the criteria for severe viral hepatitis established in National Viral Hepatitis Symposium^[17], was all severe chronic hepatitis. The conditions of 75 patients were 4 at the early stage, 31 at the middle stage, 40 at the late stage of liver failure. Among them, there were 56 with simple hepatitis B virus (HBV) infection, 8 with HBV combined with hepatitis D virus (HDV) infection, 3 with HBV combined with hepatitis A virus (HAV) infection, 1 with HBV combined with hepatitis E virus (HEV) infection, 2 with hepatitis C virus (HCV) infection and 5 with all hepatitis virus markers negative. Before treatment, 41 had occurred hepatoencephalopathy, 9 hepatorenal syndrome, 20 spontaneous peritonitis, 5 septic shock and 3 gastrointestinal hemorrhage. Seventy-five patients were divided into 3 groups, respectively receiving hemoperfusion adsorption therapy (24 cases), plasma exchange therapy (17 cases) and plasma exchange plus hemoperfusion adsorption therapy (34 cases). There was no significant difference between three groups in clinical classification, pathogen, complications and clinical data of liver function, renal function, blood routine tests, PT, PTa ($P > 0.05$).

Methods

Hemoperfusion adsorption therapy In the computer-controlled system of Type HSZ2000 artificial liver device, we chose the program of hemoperfusion adsorption therapy. The blood was pumped out of the body with the flow velocity of 60-80 mL/min and into a new type of activated charcoal column for adsorption and then backed into the body with 100 mL saline through deferens. Meanwhile, the same quantity of protamine was infused to neutralize heparin so that coagulation time (CT) could become normalized. Each patient received hemoperfusion adsorption for 1 to 4 times and all patients received 52 times in total, averaging 2.2 times per person.

Plasma exchange therapy In the computer-controlled system of Type HSZ2000 artificial liver device, we chose the program of plasma exchange therapy. The blood was pumped out of the body with the flow velocity of 60-80 mL/min and into a plasma exchange filter to discard the plasma and then mixed up with fresh frozen plasma (FFP) with flow velocity of 30-50 mL/min to be reperfused back into the body with 50 mL 200 g/L albumin solution and 100 mL saline through deferens. The balance of output and input should be controlled closely. Meanwhile, the same quantity of protamine was infused to neutralize heparin so that coagulation time (CT) could get normalized. Each patient received plasma exchange for 1 to 4 times and all patients received 36 times in total, averaging 2.1 times per person.

Plasma exchange plus hemoperfusion adsorption therapy In the computer-controlled system of Type HSZ2000 artificial liver

device, we chose the program of plasma exchange plus hemoperfusion adsorption therapy. The blood was pumped out of the body with the flow velocity of 60-80 mL/min and into a plasma exchange filter to discard the plasma and then through activated charcoal column for adsorption and then mixed up with fresh frozen plasma (FFP) with flow velocity of 30-50 mL/min to be reperfused back into the body with 50 mL 200 g/L albumin solution and 100 mL saline through deferens. The balance of output and input should be controlled closely. Meanwhile, the same quantity of protamine was infused to neutralize heparin so that coagulation time (CT) could get normalized. Each patient received plasma exchange plus hemoperfusion adsorption from 1 to 4 times and all patients received 65 times in total, averaging 1.91 times per person. This process could last for one and a half to three hours and the exchanged plasma volume was up to 2 500-3 000 mL.

Experimental tests The blood samples were collected before and after each treatment to check the liver function, renal function, PT and for blood routine test.

Clinical therapeutic efficacy The standard to evaluate the clinical curative effect refers to the references^[18,19].

Statistical analysis

All data were shown as mean±SD. *t* test was used to compare the data before and after treatment.

RESULTS

The effect of hemoperfusion adsorption therapy

Liver function improved significantly after treatment (Table 1). The levels of alanine aminotransferase (ALT), aspartate aminotransferase (AST), total bilirubin (TB) and direct bilirubin (DB) were decreased significantly ($P<0.05$ or 0.01). Total serum protein (TSP) level was decreased but not significantly ($P>0.05$). Coagulation function improved after treatment. Prothrombin time decreased from 24.4 s to 21.31 s ($t=1.268$, $P>0.1$) and prothrombin activity was increased from 28.61% to 33.14% ($t=1.216$, $P>0.1$), but no significant difference was presented on statistical analysis.

Table 1 Comparison of liver function between pre- and post-therapy of hemoperfusion adsorption

	Pre-therapy	Post-therapy	<i>t</i>	<i>P</i>
ALT (IU/L)	80.3±52.9	40.4±15.2	2.628	<0.01
AST (IU/L)	123.6±57.8	79.9±42.6	2.249	<0.05
TB (μmol/L)	619.0±193.9	403.3±132.7	3.376	<0.01
DB (μmol/L)	345.1±125.4	233.6±94.9	2.622	<0.01
TSP (g/L)	63.9±8.8	57.9±8.7	1.359	>0.05

ALT: alanine aminotransferase, AST: aspartate aminotransferase, TB: total bilirubin, DB: direct bilirubin, TSP: total serum proteins.

The effect of plasma exchange therapy

Liver function improved greatly after treatment (Table 2). The levels of ALT, AST, TB, DB and TSP were decreased and significant difference was presented ($P<0.05$ or 0.01). Coagulation function improved greatly after plasma exchange. Prothrombin time decreased from 29.46 s to 23.74 s ($t=1.713$, $P<0.05$) and prothrombin activity was increased from 23.73% to 32.15% ($t=2.338$, $P<0.05$). Both showed significant differences on statistical analysis.

The effect of plasma exchange plus hemoperfusion adsorption therapy

Liver function improved immensely after treatment (Table 3).

The levels of ALT, AST, TB, DB and TSP were decreased and significant difference was presented ($P<0.05$ or 0.01). Coagulation function improved greatly. Prothrombin time decreased from 28.0 s to 22.9 s ($P<0.05$) and prothrombin activity was increased from 25.8% to 30.9% ($P<0.05$). Both showed significant differences on statistical analysis.

Table 2 Comparison of liver function pre- and post-therapy of plasma exchange

	Pre-therapy	Post-therapy	<i>t</i>	<i>P</i>
ALT (IU/L)	122.8±115.5	70.8±86.8	2.040	<0.05
AST (IU/L)	147.7±106.6	95.3±81.6	2.214	<0.05
TB (μmol/L)	488.3±189.9	300.6±135.9	4.596	<0.01
DB (μmol/L)	244.4±100.0	153.7±73.6	4.152	<0.01
TSP (g/L)	65.1±9.2	57.7±9.8	3.168	<0.01

Table 3 Comparison of liver function pre- and post-therapy of plasma exchange plus hemoperfusion adsorption

	Pre-therapy	Post-therapy	<i>t</i>	<i>P</i>
ALT (IU/L)	109.45±102.06	61.52±74.19	2.594	<0.02
AST (IU/L)	140.16±94.71	90.59±72.32	2.844	<0.01
TB (μmol/L)	528.75±200.57	332.16±142.91	5.459	<0.01
DB (μmol/L)	275.37±118.01	178.00±88.68	4.523	<0.01
TSP (g/L)	64.70±9.0	57.70±9.5	3.312	<0.01

The data of renal function and blood routine test pre- and post-therapy

Renal electrolytes showed no obvious changes and the levels of urea nitrogen and creatinine were shown no significant difference pre- and post-therapy ($P>0.01$ or 0.05).

There was no significant difference in the levels of white blood cells (WBC), red blood cells (RBC), hemoglobin (Hgb) and platelet (PLT) pre- and post-therapy ($P>0.01$ or 0.05).

Side effects

In the group with hemoperfusion adsorption therapy, 2 patients had side effects twice, skin itch and rash once, pyrogen reaction once. In the group with plasma exchange therapy, 3 patients experienced side effects 3 times, skin itch and rash once, hemolytic reaction once and transfusion reaction once. In the group with plasma exchange plus hemoperfusion adsorption therapy, 10 patients had side effects thirteen times, skin itch and rash once, numbed face and 4 limbs 4 times, blood pressure fluctuation once and hypothermia once, hemolytic reaction once, transfusion reaction once, pyrogen reaction once. All side effects were relieved after treatment and had no influence on the whole therapeutic process.

DISCUSSION

It has been proven that hemoperfusion adsorption plays a role in removal of bilirubin and intermediate molecular substances. Previously owing to the poor technique of activated charcoal filter, there were obvious side effects in application of hemoperfusion adsorption therapy. Especially some severe side effects such as serious hemorrhage following platelet destruction and hemolysis following erythrocyte destruction once made the clinical application and basic research of artificial liver support system home and abroad go to a standstill for a long period of time. In the past few years, because the advance of technique of activated charcoal filter and the particles of charcoal became smaller and their surface was processed, the chance of platelet destruction and erythrocyte destruction was

much less when the blood flowed through activated charcoal filter, biocompatibility of activated charcoal improved^[20]. Therefore, the therapy of hemoperfusion adsorption has again been applied to clinic to treat the liver failure patients^[21-23]. That 24 patients had an improvement in clinical symptoms temporarily and in liver function indicates hemoperfusion adsorption therapy has a temporary supportive effect on liver failure caused by severe viral hepatitis.

The mechanism of severe viral hepatitis is the cooperation of immunopathological lesion caused by hepatitis virus and the secondary lesion of liver cells that results from the great deal of cytokine such as tumor necrosis factor- α (TNF- α), interleukin-1 β (IL1- β), interleukin-10(IL10) released by intrahepatic and extrahepatic mononuclear macrophages due to the enteroendotoxemia following the impairment of hepatic barrier function. In this process, the secondary lesion plays an important role^[24-28]. Cytokine can induce hepatocyte apoptosis^[29]. Cytokine and endotoxin removal can relieve hepatic lesion, reduce leucocyte emigration and platelet aggregation and maintain the intracellular stabilization so as to delay or reverse the disease process and improve the prognosis.

Hemoperfusion adsorption therapy can eliminate endotoxin and cytokine nonspecifically and play an important role in supporting treatment of liver failure^[30].

Plasma exchange separated and discarded plasma of liver failure patients to remove the toxic substances (especially those binding with proteins) and compensated with normal fresh frozen plasma to supplement some essential substances such as coagulation factors, albumin, immunoglobulin so as to ameliorate the microenvironment of liver and accelerate the liver regeneration and the liver function recovery^[31,32]. The therapeutic effects of 17 acute liver failure patients who received plasma exchange therapy were similar to those reported abroad^[32,33], but quite different from those reported home^[22]. This may be related to the severity of the patients in our series who are all in the intermediate or late stages of liver failure caused by severe chronic hepatitis^[18,19] and in addition, the times of plasma exchange should be taken into consideration. Though the prognosis of patients receiving plasma exchange therapy did not live up to our expectation, the clinical symptoms of patients after treatment showed temporary relief and liver function and coagulation function improved obviously. So plasma exchange therapy has temporary supportive effects on liver failure caused by severe viral hepatitis.

Plasma exchange plus hemoperfusion adsorption therapy is a combination of plasma exchange and hemoperfusion adsorption, so it is more beneficial to the liver microenvironmental amelioration and liver regeneration and recovery of liver function. The therapeutic effects of 34 patients receiving plasma exchange plus hemoperfusion adsorption therapy showed coincidence with those receiving plasma exchange plus hemoperfusion adsorption therapy abroad^[33,34]. That the patients' clinical symptoms after treatment showed temporary relief and liver function and coagulation function improved obviously indicates this therapy has temporary supportive effects on liver failure caused by severe viral hepatitis.

In comparison among three groups pre- and post-therapy, the coagulation function amelioration and plasma protein decrease by plasma exchange therapy and plasma exchange plus hemoperfusion adsorption therapy were more obvious than those by hemoperfusion adsorption therapy.

The main advantages of hemoperfusion adsorption therapy are low cost and less protein loss. Theoretically, plasma exchange therapy is a relatively complete liver substitutive therapy and its effects have been proven, but a large supply of plasma, high cost, and easy infection of blood-transmitted diseases fail them and plasma exchange deprives patients of

hepatocyte growth substances. Consequently it may do harm to liver regeneration and long-term therapeutic effects. The concentrations of plasma proteins will decrease if plasma is not compensated enough after a great loss.

Through the liver failure rat model which received total blood exchange, Eguchi^[35] found that the hepatocyte regeneration was suppressed. In the fresh frozen plasma for exchange, there are a great deal of citrates which can increase the incidence of side effects after infused into the body and can do harm to hepatocyte energy metabolism and hepatocyte regeneration. How to advance various therapies and combine them with bioartificial liver support system in order to get good effects and reduce the side effects await further study^[36-41].

REFERENCES

- 1 **Chamuleau RA**. Artificial liver support in the third millennium. *Artif Cells Blood Substit Immobil Biotechnol* 2003; **31**: 117-126
- 2 **Chamuleau RA**. Bioartificial liver support anno 2001. *Metab Brain Dis* 2002; **17**: 485-491
- 3 **Kjaergard LL**, Liu J, Als-Nielsen B, Gluud C. Artificial and bioartificial support systems for acute and acute-on-chronic liver failure: a systematic review. *JAMA* 2003; **289**: 217-222
- 4 **Liu J**, Kjaergard LL, Als-Nielsen B, Gluud C. Artificial and bioartificial support systems for liver failure: a Cochrane Hepato-Biliary Group Protocol. *Liver* 2002; **22**: 433-438
- 5 **He J**, Xu TM, Zhou GP, Wang YZ, Pan TJ, Chen GC. Influence of plasma exchange on serum cytokines in severe viral hepatitis patients [Article in Chinese]. *Zhongguo Weizhongbing Jijiu Yixue* 2003; **15**: 106-108
- 6 **Kapoor D**, Williams R, Jalan R. MARS: a new treatment for hepatorenal failure. Molecular adsorbent and recirculating system. *Gastroenterology* 2000; **119**: 1799-1800
- 7 **Ellis AJ**, Hughes RD, Nicholl D, Langley PG, Wendon JA, O'Grady JG, Williams R. Temporary extracorporeal liver support for severe acute alcoholic hepatitis using the BioLogic-DT. *Int J Artif Organs* 1999; **22**: 27-34
- 8 **Fellidin M**, Friman S, Backman L, Siewert-Delle A, Henriksson BA, Larsson B, Olausson M. Treatment with the molecular adsorbent recirculating system in patients with acute liver failure. *Transplant Proc* 2003; **35**: 822-823
- 9 **Mitzner S**, Look J, Peszynski P, Klammt S, Majcher-Peszynska J, Gramowski A, Stange J, Schmidt R. Improvement in central nervous system functions during treatment of liver failure with albumin dialysis MARS—a review of clinical, biochemical, and electrophysiological data. *Metab Brain Dis* 2002; **17**: 463-475
- 10 **Kapoor D**. Molecular adsorbent recirculating system: Albumin dialysis-based extracorporeal liver assist device. *J Gastroenterol Hepatol* 2002; **17**(Suppl): S280-S286
- 11 **Mullhaupt B**, Kullak-Ublick GA, Ambuhl P, Maggiorini M, Stocker R, Kadry Z, Clavien PA, Renner EL. First clinical experience with Molecular Adsorbent Recirculating System (MARS) in six patients with severe acute on chronic liver failure. *Liver* 2002; **22**(Suppl): S59-62
- 12 **Schachschal G**, Morgera S, Kupferling S, Neumayer HH, Lochs H, Schmidt HH. Emerging indications for MARS dialysis. *Liver* 2002; **22**(Suppl): 63-68
- 13 **Chen S**, Zhang L, Shi Y, Yang X, Wang M. Molecular Adsorbent Recirculating System: clinical experience in patients with liver failure based on hepatitis B in China. *Liver* 2002; **22**(Suppl 2): 48-51
- 14 **Peszynski P**, Klammt S, Peters E, Mitzner S, Stange J, Schmidt R. Albumin dialysis: single pass vs recirculation (MARS). *Liver* 2002; **22**(Suppl 2): S40-42
- 15 **Wang X**, Zhou X, Miao J, Fan D. Clinical application of molecular adsorbent recirculating system-artificial liver support system. *Zhonghua Ganzangbing Zazhi* 2002; **10**: 232-234
- 16 **Zhou X**, Wang X, Yang Y, Zhao L, Miao J, Ding J, Fan D. Clinical research of patients with acute or chronic hepatic failure treated with molecular adsorbent recirculating system. *Zhonghua Ganzangbing Zazhi* 2002; **10**: 213-215
- 17 **Chinese Medical Association Society of Infectious Diseases**. The preventive project of viral hepatitis. *Zhonghua Ganzangbing Zazhi* 2000; **8**: 324-329

- 18 **Wang YJ**, Wang YM, He NH, Liu J, Niu RZ, Li MD. Preliminary study on a hybrid bioartificial liver support system in the treatment of severe chronic hepatitis. *Zhonghua Chuanranbing Zazhi* 2002; **20**: 14-16
- 19 **Chinese Medical Association Society of Infectious Diseases**. Therapeutic indicators, standard and technic guidance of artificial liver support system. *Zhonghua Chuanranbing Zazhi* 2002; **20**: 254-258
- 20 **Kramer L**, Gendo A, Madl C, Ferrara I, Funk G, Schenk P, Sunder-Plassmann G, Horl WH. Biocompatibility of a cuprophane charcoal-based detoxification device in cirrhotic patients with hepatic encephalopathy. *Am J Kidney Dis* 2000; **36**: 1193-1200
- 21 **Chen YK**. The recent development of physical artificial liver in the treatment of liver failure. *Zhongguo Weizhongbing Jijiu Yixue* 2002; **14**: 240-242
- 22 **He JQ**, Chen CY, Deng JT, Qi HX, Zhang XQ, Chen JQ. The clinical study of artificial liver in the treatment of severe hepatitis. *Zhongguo Weizhongbing Jijiu Yixue* 2000; **12**: 105-108
- 23 **Di Campli C**, Zileri Dal Verme L, Andrisani MC, Armuzzi A, Candelli M, Gaspari R, Gasbarrini A. Advances in extracorporeal detoxification by MARS dialysis in patients with liver failure. *Curr Med Chem* 2003; **10**: 341-348
- 24 **Dominguez Fernandez E**, Flohe S, Siemers F, Nau M, Schade FU. Endotoxin tolerance in rats: influence on LPS-induced changes in excretory liver function. *Inflamm Res* 2002; **51**: 500-505
- 25 **Chu CJ**, Chen CT, Wang SS, Lee FY, Chang FY, Lin HC, Wu SL, Lu RH, Chan CC, Huang HC, Lee SD. Hepatic encephalopathy in rats with thioacetamide-induced fulminant hepatic failure: role of endotoxin and tumor necrosis factor-alpha. *Zhonghua Yixue Zazhi* 2001; **64**: 321-330
- 26 **Shito M**, Balis UJ, Tompkins RG, Yarmush ML, Toner M. A fulminant hepatic failure model in the rat: involvement of interleukin-1beta and tumor necrosis factor-alpha. *Dig Dis Sci* 2001; **46**: 1700-1708
- 27 **Nagaki M**, Iwai H, Naiki T, Ohnishi H, Muto Y, Moriwaki H. High levels of serum interleukin-10 and tumor necrosis factor-alpha are associated with fatality in fulminant hepatitis. *J Infect Dis* 2000; **182**: 1103-1108
- 28 **Streetz K**, Leifeld L, Grundmann D, Ramakers J, Eckert K, Spengler U, Brenner D, Manns M, Trautwein C. Tumor necrosis factor alpha in the pathogenesis of human and murine fulminant hepatic failure. *Gastroenterology* 2000; **119**: 446-460
- 29 **Nakae H**, Narita K, Endo S. Soluble Fas and soluble Fas ligand levels in patients with acute hepatic failure. *J Crit Care* 2001; **16**: 59-63
- 30 **Nakae H**, Asanuma Y, Tajimi K. Cytokine removal by plasma exchange with continuous hemodiafiltration in critically ill patients. *Ther Apher* 2002; **6**: 419-424
- 31 **Nakae H**, Yonekawa T, Narita K, Endo S. Are proinflammatory cytokine concentrations reduced by plasma exchange in patients with severe acute hepatic failure? *Res Commun Mol Pathol Pharmacol* 2001; **109**: 65-72
- 32 **Nakamura T**, Ushiyama C, Suzuki S, Shimada N, Ebihara I, Suzuki M, Takahashi T, Koide H. Effect of plasma exchange on serum tissue inhibitor of metalloproteinase 1 and cytokine concentrations in patients with fulminant hepatitis. *Blood Purif* 2000; **18**: 50-54
- 33 **Iwai H**, Nagaki M, Naito T, Ishiki Y, Murakami N, Sugihara J, Muto Y, Moriwaki H. Removal of endotoxin and cytokines by plasma exchange in patients with acute hepatic failure. *Crit Care Med* 1998; **26**: 873-876
- 34 **Nakae H**, Yonekawa C, Wada H, Asanuma Y, Sato T, Tanaka H. Effectiveness of combining plasma exchange and continuous hemodiafiltration (combined modality therapy in a parallel circuit) in the treatment of patients with acute hepatic failure. *Ther Apher* 2001; **5**: 471-475
- 35 **Eguchi S**, Sugiyama N, Kawazoe Y, Kawashita Y, Fujioka H, Furui J, Kanematsu T. Total blood exchange suppresses the early stage of liver regeneration following partial hepatectomy in rats. *Artif Organs* 1998; **22**: 847-853
- 36 **Ho DW**, Fan ST, To J, Woo YH, Zhang Z, Lau C, Wong J. Selective plasma filtration for treatment of fulminant hepatic failure induced by D-galactosamine in a pig model. *Gut* 2002; **50**: 869-876
- 37 **Xue YL**, Zhao SF, Luo Y, Li XJ, Duan ZP, Chen XP, Li WG, Huang XQ, Li YL, Cui X, Zhong DG, Zhang ZY, Huang ZQ. TECA hybrid artificial liver support system in treatment of acute liver failure. *World J Gastroenterol* 2001; **7**: 826-829
- 38 **Xue YL**, Zhao SF, Zhang ZY, Wang YF, Li XJ, Huang XQ, Luo Y, Huang YC, Liu CG. Effects of a bioartificial liver support system on acetaminophen induced acute liver failure canines. *World J Gastroenterol* 1999; **5**: 308-311
- 39 **Jia ZS**, Xie YM, Yin GW, Di JR, Guo WP, Huang CX, Bai XF. Successful rescuing a pregnant woman with severe hepatitis E infection and postpartum massive hemorrhage. *World J Gastroenterol* 2003; **9**: 631-632
- 40 **Wang YJ**, Li MD, Wang YM, Nie QH, Chen GZ. Experimental study of bioartificial liver with cultured human liver cells. *World J Gastroenterol* 1999; **5**: 135-137
- 41 **Zhu XF**, Chen GH, He XS, Lu MQ, Wang GD, Cai CJ, Yang Y, Huang JF. Liver transplantation and artificial liver support in fulminant hepatic failure. *World J Gastroenterol* 2001; **7**: 566-568

Therapeutic polypeptides based on HBcAg₁₈₋₂₇ CTL epitope can induce antigen-specific CD8⁺ CTL-mediated cytotoxicity in HLA-A2 transgenic mice

Tong-Dong Shi, Yu-Zhang Wu, Zheng-Cai Jia, Wei Zhou, Li-Yun Zou

Tong-Dong Shi, Yu-Zhang Wu, Zheng-Cai Jia, Wei Zhou, Li-Yun Zou, Institute of Immunology, Third Military Medical University, Chongqing 400038, China

Supported by the National Natural Science Foundation of China, No.30271189, and the National 973 Project, No.2001CB510001

Co-correspondents: Tong-Dong Shi and Yu-Zhang Wu

Correspondence to: Dr. Tong-Dong Shi, Institute of Immunology, Third Military Medical University, 30 Gaotanyan Street, Chongqing 400038, China. tdshih@yahoo.com.cn

Telephone: +86-23-68752236-801 **Fax:** +86-23-68752789

Received: 2003-09-23 **Accepted:** 2003-12-16

Abstract

AIM: To explore how to trigger an HLA-I-restricted CD8⁺ T cell response to exogenously synthesized polypeptides *in vivo*.

METHODS: Three mimetic therapeutic polypeptides based on the immunodominant CTL epitope of HBcAg, the B- epitope of HBV PreS₂ region and a common T helper sequence of tetanus toxoid were designed and synthesized with Merrifield's solid-phase peptide synthesis method. Their immunological properties of inducing T_{H1} polarization, CD8⁺ HBV-specific CTL expansion and CD8⁺ T cell mediated cytotoxicity were investigated in HLA-A2 transgenic mice.

RESULTS: Results demonstrated that the mimetic polypeptides comprised of the immunodominant CTL, B-, and T helper epitopes could trigger specifically and effectively vigorous CD8⁺ HBV-specific CTL-mediated cytotoxicity and T_{H1} polarization of T cells in HLA-A2 transgenic mice.

CONCLUSION: A designed universal T helper plus B- epitopes with short and flexible linkers could dramatically improve the immunogenicity of CTL epitopes *in vivo*. And that the mimetic therapeutic peptides based on the reasonable match of the above CTL, B- and T helper epitopes could be a promising therapeutic peptide vaccine candidate against HBV infection.

Shi TD, Wu YZ, Jia ZC, Zhou W, Zou LY. Therapeutic polypeptides based on HBcAg₁₈₋₂₇ CTL epitope can induce antigen-specific CD8⁺ CTL-mediated cytotoxicity in HLA-A2 transgenic mice. *World J Gastroenterol* 2004; 10(8): 1222-1226
<http://www.wjgnet.com/1007-9327/10/1222.asp>

INTRODUCTION

At present, the commercial vaccines against HBV infection are mainly based on humoral responses which can prevent the virus infection, but can rarely interrupt the intracellular infection or lead to the infected cell clearance. As in other infections with noncytopathic viruses, an MHC class I-restricted cytotoxic T lymphocytes (CTLs) response to endogenous HBV antigens is believed to be the major determinant for infected

cell clearance, and HBV-specific CTL-mediated cytotoxicity plays the key role in controlling HBV infection and in the clearance of infected cells^[1-8].

Natural HBV antigens contain generally inappropriate epitopes which could elicit T_{H1}/T_{H2} disequilibrium, immune deviation or immune deficiency, and the conserved amino acid sequences might also interfere with intercellular communication. Thereby some viruses may evade the immune defence and present consistently in hepatocytes, and result in chronic hepatitis, liver cirrhosis, and even hepatocellular carcinoma^[9-19]. Thus new generations of therapeutic vaccines should induce CTL responses different from that induced by natural virus infection, and at the same time hold the specificity of HBV antigens. According to reports in recent years, effective protection relies on the appropriate match of a set of epitopes^[19,20]. Thus, natural antigens should be redesigned or modified on the basis of immunodominant epitopes.

In this study, we chose the immunodominant CTL epitope of HBcAg and the B cell epitope of HBV PreS₂ region, and introduced them into the common T helper epitope of tetanus toxoid to strengthen the Th response. Three mimetic peptides based on the above epitopes were initially designed and synthesized, and their immunological functions of inducing T_{H1} polarization, CD8⁺ HBV-specific CTL expansion and CD8⁺ HBV-specific CTL-mediated cytotoxicity were investigated in HLA-A2 transgenic mice. We aimed to explore how to trigger an HLA-I-restricted CD8⁺ T cell response to exogenously synthesized polypeptides *in vivo*, and to find a rational strategy of stimulating the HBV specific CTL response *in vivo* and to break to some extent the immune tolerance to HBV antigens.

MATERIALS AND METHODS

Materials

Inbred male and female HLA-A2 transgenic mice (H-2K^b) aging 6-8 wk were purchased from Jackson Laboratory, USA. Amino acids used for peptide synthesis were purchased from PE & ACT companies. Na₂⁵¹GrO₄ for target cell labeling in standard ⁵¹Gr release assay was from New England Nuclear (NENTM), Boston, USA. There were also materials used in this study as the following: RPMI1640 medium (Gibco), fetal calf serum (FCS) (HyClone), chimeric HLA-A2K^b tetramer kit (ProImmune, UK) and murine IFN-γ ELISpot kit (Diaclone, France).

Methods

Preparation of mimetic therapeutic polypeptides The immunodominant B- and CTL epitopes of HBV pre-S2 and HBcAg were identified on the basis of the HLA-A2.1 binding motifs^[21]. Mimetic polypeptides were calculated and sieved using computerized molecular design methods. Peptide1 was determined as the immunodominant HBcAg₁₈₋₂₇ CTL epitope peptide (FLPSDFFPSV), to the N-termini of which linked the common T helper sequence of tetanus toxoid with a linker of "-Gly-Gly-Gly-" as peptide2 (QYIKANSKFIGITE GGG FLPSDFFPSV). The common T helper epitope of tetanus

toxoid and the Pre-S2 B-epitope were linked to the N- and C-termini of the HBcAg₁₈₋₂₇ sequence respectively with the linker of “-Ala-Ala-Ala-” and “-Gly-Gly-Gly-” as peptide3 (QYKANSKFIGITEAAAFPSDFVGGDPRVRGLYFPA). Melanoma associated MART-1₂₇₋₃₅ CTL epitope peptide (AAGIGILTV) was used as irrelevant control.

The above peptide antigens were synthesized with the Merrifield's solid-phase peptide synthesis method (PE431A synthesizer), purified by RP-HPLC (WATERS 600) and analyzed by MS/MS (API 2000). All peptides with a purity over 95% were dissolved in DMSO with the concentration of 10 mg/mL and preserved at -70 °C.

Immunization of mice Mimetic polypeptides in DMSO were diluted with 0.02 mol/L, pH 7.2 phosphate buffered saline (PBS) and emulsified respectively with complete Freund's adjuvants (CFA) and incomplete Freund's adjuvants (IFA). HLA-A2 transgenic mice were separated into 5 groups with 3 in each. The mice were injected subcutaneously in the 2 flanks and in the hind footpads first with peptide1, 2, 3 and then irrelevant control peptide in CFA at 500 µg/kg dosage respectively. Two weeks later, the mice were immunized weekly with the same antigens at IFA in 250 µg/kg dosage for 4 times. The mice injected with PBS alone were used as negative controls.

Two weeks after the last time of immunization, the mice were killed, the splenocytes were separated and suspended in RPMI1640 medium supplemented with 100 mL/L FCS and used as fresh samples^[19].

T_{H1} polarization assay For the assay of T_{H1} polarization induced by mimetic peptides, mouse IFN-γ ELISPOT kit was used. Briefly^[19,22], 96-well PVDF membrane-bottomed plates were coated with capture anti-mouse IFN-γ mAb at 4 °C overnight. Fresh splenocytes were added to triplicated wells at 5×10³/well in the presence of 10 µg/mL relative mimetic antigens and the plates were incubated for 15 h at 37 °C in 50 mL/L CO₂. At the end of incubation, cells were washed off and a second biotinylated anti-IFN-γ mAb was added, followed by streptavidin-alkaline phosphatase conjugate and substrates. After the plates were washed with tap water and dried overnight, spots were counted under a stereomicroscope. The number of T_{H1} polarized cells (peptide-specific CD8⁺ T cells), expressed as IFN-γ secreting cells (ISC)/10⁶ lymphocytes, was calculated after subtracting negative control values. Results of samples were considered as positive if above the mean by three standard deviations and with a cut off of 50 ISC/10⁶ lymphocytes above mean background.

Cytotoxicity assay Peptide-specific CTL lines were primed as follows: The fresh splenocytes were plated at a concentration of 2×10⁵/mL in 24-well microplates (2 mL/well) in PRMI1640 medium supplemented with 100 mL/L FCS and 30 U/mL murine IL-2 and in the presence of 10 µg/mL corresponding mimetic peptides respectively, with an exception of the lymphocytes from negative controls which were just cultivated in medium supplemented with 100 mL/L FCS and 30 U/mL murine IL-2. Five days after stimulation, cells were harvested, and used as fresh effectors.

CTL-mediated cytotoxicity was detected by a standard 4 h ⁵¹Cr release assay^[18,19,23,24]. P815 cells were used as targets and preincubated with HBcAg₁₈₋₂₇ peptide 2 h before use. The 1×10⁶ target cells were labeled with 3.7×10⁶ Bq Na₂⁵¹CrO₄ in 0.8 mL RPMI1640 medium supplemented with 150 mL/L FCS for 60 min at 37 °C, and then washed 3 times before the addition of effectors. Various concentrations of effector cells were mixed with 1×10⁴ targets at effector/target (E/T) ratios of 12.5, 25, 50 and 100 in 200 µL of culture medium in 96-well V-bottomed microplate in triplicates. The microplate was centrifuged for 3 min at 500 r/min, and then incubated for 4 h at 37 °C in 50 mL/L CO₂. After the incubation terminated, 100 µL/well

of supernatants was harvested and counted on a γ-counter. Percentage of target cell specific lysis was determined as: [(average sample counts - average spontaneous counts)/(average maximum counts - average spontaneous counts)] ×100%. Maximum and spontaneous counts were measured using supernatants from wells receiving 1 mol/L HCl or culture medium alone, respectively. In all experiments, spontaneous counts should be less than 30% of maximum counts. CTL responses were considered positive if exceeded the mean of specific lysis caused by irrelevant mimetic antigen (MART-1₂₇₋₃₅) by 3 standard deviations and by 10%.

HBcAg₁₈₋₂₇ specific CD8⁺ CTL detection

Chimeric HLA-A2K^b tetramer binding kit was used to quantify the HBcAg₁₈₋₂₇-specific CD8⁺ T cells^[24-26]. A part of the fresh splenocytes separated from mice killed were washed with PBS, counted, suspended in PBS and separated equally into different tubes in 1.0 mL of each. The cells were stained with 25 ng/µL of tetramers for 20 min at 37 °C, and then washed and stained with anti-mouse CD8 mAb for 20 min at room temperature. All samples were collected, washed twice, dissolved into 300 µL of PBS and FACS-sorted on a FACstar (Beckton-Dicknson) with Cell Quest software. Results were expressed as percentages of tetramer-binding cells in the murine CD8⁺ T cell population. A total of 5×10⁵ events were acquired in each analysis. Results were considered as positive for tetramer-binding cells when above the mean caused by irrelevant mimetic antigen (MART-1₂₇₋₃₅) and above 0.1% CD8⁺ T cells.

Statistical analysis

All data were expressed as mean±SD. Statistical analysis was performed using a two-tailed Student's *t* test.

RESULTS

T_{H1} polarization induced by mimetic peptides

When the immunization terminated, the mice were killed and the spleen lymphocytes were used for T_{H1} polarization assay with an IFN-γ ELISPOT method. Spots of IFN-γ secreting cells generated could be observed in each of the mimetic peptides immunized groups. The negative control values of peptide-specific CD8⁺ T cells were on average 250±138 ISC/10⁶ lymphocytes. The most vigorous peptide-specific CD8⁺ T cells magnification was produced in peptide3 immunized mice with approximately 8 050±1 233.8 ISC/10⁶ lymphocytes generated. In peptide1 and 2 immunization groups, the peptide-specific CD8⁺ T cells induced were 1 150±236.7 and 1 367±231 ISC/10⁶ lymphocytes respectively. And also 1 135±312 ISC/10⁶ lymphocytes were generated in MART-1₂₇₋₃₅ CTL epitope peptide immunized mice (Table 1).

Cytotoxicity assay

When the mice were killed, the fresh splenocytes were separated and peptide-specific CTL lines were generated *ex vivo*. The CTL-mediated cytotoxicity induced was tested by standard 4 h ⁵¹Cr release assay against HBcAg₁₈₋₂₇ peptide preincubated P815 targets. Data demonstrated that all the three mimetic polypeptides based on HBcAg₁₈₋₂₇ CTL epitope could induce positive HBV-specific CTL response, among which peptide3 induced the most vigorous CTL activity, and as high as (55.3±10.1)% targets lysis was observed at E/T=100. The percentages of targets lysed in peptide1 and 2 immunization groups were dramatically lower than in peptide 3 group (*P*<0.01) and showed statistically no difference between. The spleen lymphocytes from irrelevant peptide control and negative control mice showed no specific target cell lysis activity (Table 2).

Table 1 T_{H1} polarization assay with an IFN- γ ELISPOT method. (mean \pm SD, n=18)

	Peptide1	Peptide2	Peptide3	MART-1 ₂₇₋₃₅	Negative controls
ISC/10 ⁶ lymphocytes	1 150 \pm 236.7 ^d	1 367 \pm 231 ^d	8 050 \pm 1 233.8 ^{db}	1 135 \pm 312	250 \pm 138

^dP<0.01 vs negative control; ^bP<0.01 vs peptide1 and 2 groups.

Table 2 Percentages of specific targets lysis by effector CTLs induced with different peptide antigens (mean \pm SD, n=18)

E/T ratios	Percentage of specific cell lysis (%)				
	Peptide1 ^d	Peptide2	Peptide3	MART-1 ₂₇₋₃₅	Negative controls
12.5	18.5 \pm 4.3 ^d	21.1 \pm 6.3 ^d	33.7 \pm 7.2 ^{db}	3.7 \pm 0.7	5.5 \pm 0.9
25	22.9 \pm 5.7 ^d	28.5 \pm 6.6 ^d	40.5 \pm 8.9 ^{db}	6.3 \pm 0.9	4.4 \pm 0.9
50	29.3 \pm 7.0 ^d	30.5 \pm 8.8 ^d	50.3 \pm 11.3 ^{db}	7.1 \pm 1.1	7.7 \pm 1.2
100	32.6 \pm 10.1 ^d	33.1 \pm 8.2 ^d	55.3 \pm 10.1 ^{db}	8.4 \pm 1.3	9.2 \pm 1.3

^dP<0.01 vs negative control; ^bP<0.01 vs peptide1 and 2 groups.

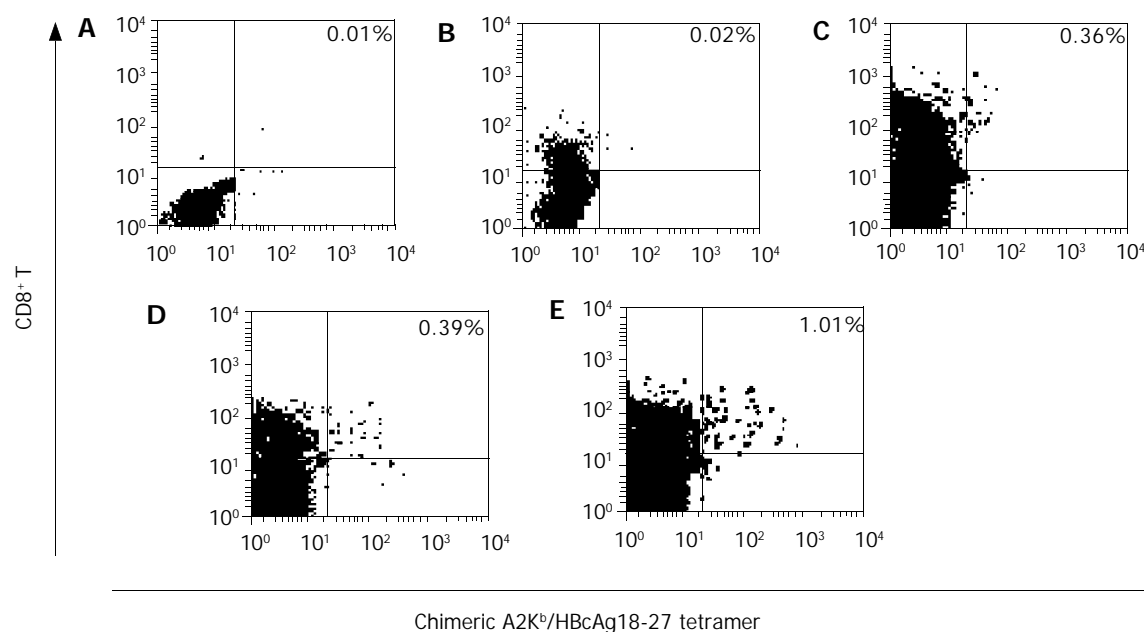


Figure 1 Detection of the HBcAg₁₈₋₂₇-specific CD8⁺ T cells produced with chimeric A2K^b/HBcAg₁₈₋₂₇ tetramer-binding assay. A: murine splenocytes from negative control mice, B: murine splenocytes from MART-1₂₇₋₃₅ irrelevant peptide immunized mice, C: murine splenocytes from peptide1 immunized mice, D: murine splenocytes from peptide2 immunized mice, E: murine splenocytes from peptide3 immunized mice.

HBcAg₁₈₋₂₇-specific CD8⁺ CTL detection

After the immunization terminated, the HBcAg₁₈₋₂₇-specific CD8⁺ T cells induced *in vivo* were quantified using chimeric A2K^b/HBcAg₁₈₋₂₇ tetramer-binding assay. No HBcAg₁₈₋₂₇-positive CD8⁺ T cells could be detected in the spleen lymphocytes from the negative control mice and the mice immunized with MART-1₂₇₋₃₉ peptide, and the tetramer staining was lower than background (0.02%). In splenocytes from the mice immunized with peptide1, 2 and 3, the frequencies of A2K^b/HBcAg₁₈₋₂₇ CD8 positive T cells were respectively 0.36% (3 600/10⁶ lymphocytes), 0.39% (3 900/10⁶ lymphocytes), and 1.01% (10 100/10⁶ lymphocytes). It showed no statistical difference between the effects induced by peptide1 and peptide2, and the immunogenicity of them was dramatically weaker than that of peptide3 (Figure 1).

DISCUSSION

HBV-specific CD8⁺ cytotoxic T cells play a critical role in viral clearance. Low HBV-specific CTL responses in chronic HBV infection may favor the persistence of virus, whereas

stimulation and expansion of HBV-specific CTL activity may assist elimination of HBV infection^[1-8]. Natural HBV antigens contain some inappropriate epitopes and conserved amino acid sequences which might induce inappropriate immune responses and result in hepatic pathology and lesions. Hence new generations of therapeutic vaccines should be designed on the basis of immunodominant epitopes which could induce CTL responses different from that induced by natural virus infection, and at the same time hold the specificity of HBV antigens. As in other infections with noncytopathic viruses, helper T cells control the intensity of CD8⁺ T-cell responses and helper T-cell responses might be compromised in chronic carriers of HBV^[27-32]. In this paper, we chose the immunodominant B cell epitope of HBV PreS₂ region and the CTL epitope of HBcAg, and introduced them into the common T helper epitope of tetanus toxoid to strengthen the Th response. Three mimetic peptides based on the above epitopes were initially designed and synthesized, and their immunological properties of inducing T_{H1} polarization, CD8⁺ T-cell expansion and CTL-mediated cytotoxicity were primarily investigated in HLA-A2 transgenic mice.

After immunization, the mice were killed and the splenocytes were separated, a direct tetramer-binding assay was used to detect the frequencies of HBcAg₁₈₋₂₇-specific CD8⁺ T cells, the results varied according to the peptides used. The highest frequency was from peptide3 immunized mice splenocytes. No statistical difference was observed between the frequencies of HBcAg₁₈₋₂₇-specific CD8⁺ T cells augmented in peptide1 and peptide2 mice groups, which indicated that the immunogenicity of short CTL epitope peptides *in vivo* could not be improved dramatically simply by introduction of a universal T helper epitope, and that by our reasonable match of the above immunodominant CTL, B-, T helper epitopes and linkers, the immunogenicity of HBcAg₁₈₋₂₇ CTL epitope of inducing HBV-specific CD8⁺ T cell expansion *in vivo* was dramatically improved.

The tetramer-binding assay detects only the number of T cells with an appropriate TCR but not their function^[24,33], so a chromium release assay and IFN- γ ELISpot assay were used to detect the immune functions of the mimetic antigens designed. And a highly significant correlation was found between the frequencies of HBcAg₁₈₋₂₇-specific CD8⁺ T cells and the functions of responding splenocytes from the mice. The three mimetic polypeptides designed could induce T_{H1} polarization of spleen lymphocytes and generate cytotoxicity in mice, among which peptide3 with the immunodominant B-, CTL and T helper epitopes was the most potent, peptide 1 and 2 could also produce the above immune functions but not as efficiently. After introducing T helper epitope into HBcAg₁₈₋₂₇, the CD8⁺ CTL frequency was not remarkably improved, and cytotoxic activity remained low, suggesting that the help provided by this conformation was not sufficient to drive proliferation of CTL, and their differentiation into mature killer cells. The comparatively higher immunogenicity of peptide3 might rely on its molecular structure: the introduction of T helper and B-epitopes, the design of short linkers “Ala-Ala-Ala” and “Gly-Gly-Gly”, and the reasonable match. The designed linker was proved to be highly flexible and might act as “hinges”. We surmise that the peptide be recognized by MHC-I and II restricted molecules, and be presented to CD4⁺ T cells and CD8⁺ T cells, and ultimately T helper and Tc cells be activated and functioned interactively. It indicated that introducing short and flexible “hinges” and “Th+B” epitopes into short CTL epitope peptides might dramatically improve the peptide’s immunogenicity and the ability of being presented to APCs *in vivo*. The results also demonstrated that designed peptide3 was highly immunogenic and HBV-specific *in vivo*, and might be a potential candidate for the therapeutic vaccine designed against hepatitis B.

Little knowledge is known so far on the molecular mechanisms of the *in vitro* and *in vivo* functions of the peptides^[33-38]. In our opinion, *in vivo* induction of cytotoxic activity relies on the efficient presentation by APCs, and the crucial point is how to improve the antigenicity of short peptides so to meet the needs for efficient antigen presentation *in vivo*. Thus to redesign or modify the linear short peptides on the basis of immunodominant epitopes, change their molecular properties to meet the needs of antigen presentation, and stimulate the direct recognition of the peptides by T_H/Tc cells may be a promising approach to this problem.

REFERENCES

- 1 **Stober D**, Trobonjaca Z, Reimann J, Schirmbeck R. Dendritic cells pulsed with exogenous hepatitis B surface antigen particles efficiently present epitopes to MHC class I-restricted cytotoxic T cells. *Eur J Immunol* 2002; **32**: 1099-1108
- 2 **Wei J**, Wang YQ, Lu ZM, Li GD, Wang Y, Zhang ZC. Detection of anti-preS1 antibodies for recovery of hepatitis B patients by immunoassay. *World J Gastroenterol* 2002; **8**: 276-281
- 3 **Storni T**, Lechner F, Erdmann I, Bachi T, Jegerlehner A, Dumrese T, Kundig TM, Ruedl C, Bachmann MF. Critical role for activation of antigen-presenting cells in priming of cytotoxic T cell responses after vaccination with virus-like particles. *J Immunol* 2002; **168**: 2880-2886
- 4 **Wan Y**, Wu Y, Bian J, Wang XZ, Zhou W, Jia ZC, Tan Y, Zhou L. Induction of hepatitis B virus-specific cytotoxic T lymphocytes response *in vivo* by filamentous phage display vaccine. *Vaccine* 2001; **19**: 2918-2923
- 5 **Bocher WO**, Dekel B, Schwerin W, Geissler M, Hoffmann S, Rohwer A, Arditti F, Cooper A, Bernhard H, Berrebi A, Rose-John S, Shaul Y, Galle PR, Lohr HF, Reisner Y. Induction of strong hepatitis B virus (HBV) specific T helper cell and cytotoxic T lymphocyte responses by therapeutic vaccination in the trimera mouse model of chronic HBV infection. *Eur J Immunol* 2001; **31**: 2071-2079
- 6 **Blackman MA**, Rouse BT, Chisari FV, Woodland DL. Viral immunology: challenges associated with the progression from bench to clinic. *Trends Immunol* 2002; **23**: 565-567
- 7 **Huang J**, Cai MY, Wei DP. HLA class I expression in primary hepatocellular carcinoma. *World J Gastroenterol* 2002; **8**: 654-657
- 8 **Thimme R**, Wieland S, Steiger C, Ghayeb J, Reimann KA, Purcell RH, Chisari FV. CD8(+) T cells mediate viral clearance and disease pathogenesis during acute hepatitis B virus infection. *J Virol* 2003; **77**: 68-76
- 9 **Rabe C**, Pilz T, Klostermann C, Berna M, Schild HH, Sauerbruch T, Caselmann WH. Clinical characteristics and outcome of a cohort of 101 patients with hepatocellular carcinoma. *World J Gastroenterol* 2001; **7**: 208-215
- 10 **Kessler JH**, Beekman NJ, Bres-Vloemans SA, Verdijk P, van Veelen PA, Kloosterman-Joosten AM, Vissers DC, ten Bosch GJ, Kester MG, Sijts A, Wouter Drijfhout J, Ossendorp F, Offringa R, Melief CJ. Efficient identification of novel HLA-A*0201-presented cytotoxic T lymphocyte epitopes in the widely expressed tumor antigen PRAME by proteasome-mediated digestion analysis. *J Exp Med* 2001; **193**: 73-88
- 11 **Ma CH**, Sun WS, Tian PK, Gao LF, Liu SX, Wang XY, Zhang LN, Cao YL, Han LH, Liang XH. A novel HBV antisense RNA gene delivery system targeting hepatocellular carcinoma. *World J Gastroenterol* 2003; **9**: 463-467
- 12 **Sette AD**, Dseroff C, Sidney J, Alexander J, Chesnut RW, Kakimi K, Guidotti LG, Chisari FV. Overcoming T cell tolerance to the hepatitis B virus surface in hepatitis B virus-transgenic mice. *J Immunol* 2001; **166**: 1389-1397
- 13 **Engler OB**, Dai WJ, Sette A, Hunziker IP, Reichen J, Pichler WJ, Cerny A. Peptide vaccines against hepatitis B virus: from animal model to human studies. *Mol Immunol* 2001; **38**: 457-465
- 14 **Kakimi K**, Isogawa M, Chung J, Sette A, Chisari FV. Immunogenicity and tolerogenicity of hepatitis B virus structural and nonstructural proteins: implications for immunotherapy of persistent viral infections. *J Virol* 2002; **76**: 8609-8620
- 15 **Thimme R**, Oldach D, Chang KM, Steiger C, Ray SC, Chisari FV. Determinants of viral clearance and persistence during acute hepatitis C virus infection. *J Exp Med* 2001; **194**: 1395-1406
- 16 **Kurts C**, Miller JF, Subramaniam RM, Carbone FR, Heath WR. Major histocompatibility complex class I-restricted cross-presentation is biased towards high dose antigens and those released during cellular destruction. *J Exp Med* 1998; **188**: 409-414
- 17 **Wiesmuller KH**, Bessler WG, Jung G. Solid phase peptide synthesis of lipopeptide vaccines eliciting epitope-specific B-, T-helper and T-killer cell response. *Int J Pept Protein Res* 1992; **40**: 255-260
- 18 **Zhou HC**, Xu DZ, Wand XP, Zhang JX, Huang Y, Yan YP, Zhu Y, Jin BQ. Identification of the epitopes on HCV core protein recognized by HLA-A2 restricted cytotoxic T lymphocytes. *World J Gastroenterol* 2001; **7**: 583-586
- 19 **Guan XJ**, Guan XJ, Wu YZ, Jia ZC, Shi TD, Tang Y. Construction and characterization of an experimental ISCOMS-based hepatitis B polypeptide vaccine. *World J Gastroenterol* 2002; **8**: 294-297
- 20 **Chaiken IM**, Williams WV. Identifying structure-function relationships in four-helix bundle cytokines: towards de novo mimetics design. *Trends Biotechnol* 1996; **14**: 369-375
- 21 **Livingston BD**, Crimi C, Fikes J, Chesnut RW, Sidney J, Sette

- A. Immunization with the HBV core 18-27 epitope elicits CTL responses in humans expressing different HLA-A2 supertype molecules. *Hum Immunol* 1999; **60**: 1013-1017
- 22 **Sun Y**, Iglesias E, Samri A, Kamkamidze G, Decoville T, Carcelain G, Autran B. A systematic comparison of methods to measure HIV-1 specific CD8 T cells. *J Immunol Methods* 2003; **272**: 23-34
- 23 **Wang FS**, Liu MX, Zhang B, Shi M, Lei ZY, Sun WB, Du QY, Chen JM. Antitumor activities of human autologous cytokine-induced killer (CIK) cells against hepatocellular carcinoma cells *in vitro* and *in vivo*. *World J Gastroenterol* 2002; **8**: 464-468
- 24 **Cederbrant K**, Marcusson-Stahl M, Condevaux F, Descotes J. NK-cell activity in immunotoxicity drug evaluation. *Toxicology* 2003; **185**: 241-250
- 25 **Choi EM**, Palmowski M, Chen J, Cerundolo V. The use of chimeric A2K(b) tetramers to monitor HLA A2 immune responses in HLA A2 transgenic mice. *J Immunol Methods* 2002; **268**: 35-41
- 26 **Kuzushima K**, Hayashi N, Kudoh A, Akatsuka Y, Tsujimura K, Morishima Y, Tsurumi T. Tetramer-assisted identification and characterization of epitopes recognized by HLA A*2402-restricted Epstein-Barr virus-specific CD8⁺ T cells. *Blood* 2003; **101**: 1460-1468
- 27 **Livingston BD**, Alexander J, Crimi C, Oseroff C, Celis E, Daly K, Guidotti LG, Chisari FV, Fikes J, Chesnut RW, Sette A. Altered helper T lymphocyte function associated with chronic hepatitis B virus infection and its role in response to therapeutic vaccination in humans. *J Immunol* 1999; **162**: 3088-3095
- 28 **Stebbing J**, Patterson S, Gotch F. New insights into the immunology and evolution of HIV. *Cell Res* 2003; **13**: 1-7
- 29 **Wu GH**, Zhang YW, Wu ZH. Modulation of postoperative immune and inflammatory response by immune-enhancing enteral diet in gastrointestinal cancer patients. *World J Gastroenterol* 2001; **7**: 357-362
- 30 **Zhu F**, Eckels DD. Functionally distinct helper T-cell epitopes of HCV and their role in modulation of NS3-specific, CD8⁺/tetramer positive CTL. *Hum Immunol* 2002; **63**: 710-718
- 31 **Carcelain G**, Tubiana R, Samri A, Calvez V, Delaugerre C, Agut H, Katlama C, Autran B. Transient mobilization of human immunodeficiency virus (HIV)-specific CD4 T-helper cells fails to control virus rebounds during intermittent antiretroviral therapy in chronic HIV type 1 infection. *J Virol* 2001; **75**: 234-241
- 32 **Ciavarra RP**, Greene AR, Horeth DR, Buherer K, van-Rooijen N, Tedeschi B. Antigen processing of vesicular stomatitis virus *in situ*. Interdigitating dendritic cells present viral antigens independent of marginal dendritic cells but fail to prime CD4⁽⁺⁾ and CD8⁽⁺⁾ T cells. *Immunology* 2000; **101**: 512-520
- 33 **Maini MK**, Boni C, Lee CK, Larrubia JR, Reignat S, Ogg GS, King AS, Herberg J, Gilson R, Alias A, Williams R, Vergani D, Naoumov NV, Ferrari C, Bertolotti A. The role of virus-specific CD8(+) cells in liver damage and viral control during persistent hepatitis B virus infection. *J Exp Med* 2000; **191**: 1269-1280
- 34 **Li LS**, Qu RY, Wang W, Guo H. Significance of changes of gastrointestinal peptides in blood and ileum of experimental spleen deficiency rats. *World J Gastroenterol* 2003; **9**: 553-556
- 35 **Li MS**, Li PF, He SP, Du GG, Li G. The promoting molecular mechanism of alpha-fetoprotein on the growth of human hepatoma Bel7402 cell line. *World J Gastroenterol* 2002; **8**: 469-475
- 36 **Billich A**. Thymosin alpha1. SciClone Pharmaceuticals. *Curr Opin Investig Drugs* 2002; **3**: 698-707
- 37 **Gripone P**, Rumin S, Urban S, Le Seyec J, Glaise D, Canine J, Guyomard C, Lucas J, Trepo C, Guguen-Guillouzo C. Infection of a human hepatoma cell line by hepatitis B virus. *Proc Natl Acad Sci U S A* 2002; **99**: 15655-15660
- 38 **Li D**, Takyar ST, Lott WB, Gowans EJ. Amino acids 1-20 of the hepatitis C virus (HCV) core protein specifically inhibit HCV IRES-dependent translation in HepG2 cells, and inhibit both HCV IRES- and cap-dependent translation in HuH7 and CV-1 cells. *J Gen Virol* 2003; **84**: 815-825

Edited by Zhu LH and Xu FM

Gastro-electric dysrhythm and lack of gastric interstitial cells of cajal

Qing-Lin Long, Dian-Chun Fang, Hong-Tao Shi, Yuan-Hui Luo

Qing-Lin Long, Dian-Chun Fang, Hong-Tao Shi, Yuan-Hui Luo, Gastroenterology Research Center, South-west Hospital, Third Military Medical University, Chongqing 40038, China

Correspondence to: Dr Dian-Chun Fang, Gastroenterology Research Center, South-west Hospital, Third Military Medical University, Chongqing, 40038, China. fangdianchun@hotmail.com

Telephone: +86-23-68754124

Received: 2003-09-06 **Accepted:** 2003-10-07

Abstract

AIM: The pathophysiology underlying gastrointestinal complications of long-standing diabetes is poorly understood. Recent evidence suggests an important role of interstitial cells of cajal in controlling gastrointestinal motility. The aim of this study was to clarify the changes of ultrastructural characteristics of interstitial cells of cajal in stomach of diabetic gastro-electric dysrhythmic rats.

METHODS: Rats were randomly divided into diabetic group and control group, the model of diabetic rats was established by peritoneally injection of streptozotocin. Electrogastrograms were recorded and interstitial cells of cajal in antrum were observed by electrictelescopy after diabetic model rat was established for 3 mo.

RESULTS: In the rats of diabetic group, the gastro-electric dysrhythmia was increased compared with control group, the abnormal rhythm index and the coefficient of variation of slow wave frequency were significantly higher than those of normal rats. The number of the gap junctions of interstitial cells of cajal in antrum of diabetic rats was significantly decreased, and the remaining structures were damaged. The organelles were also damaged, and vacuoles were formed.

CONCLUSION: It is possible that changes in ultrastructural characteristics of interstitial cells of cajal in stomach are one of the mechanisms underlying gastro-electric dysrhythm in diabetic rats.

Long QL, Fang DC, Shi HT, Luo YH. Gastro-electric dysrhythm and lack of gastric interstitial cells of cajal. *World J Gastroenterol* 2004; 10(8): 1227-1230

<http://www.wjgnet.com/1007-9327/10/1227.asp>

INTRODUCTION

Gastric motility abnormality occurs in up to 30- 50% of patients with long-standing diabetes. Symptoms of diabetic gastropathy can range from mild dyspepsia to recurrent vomiting and abdominal pain and may progress to irreversible end-stage gastric failure known as gastroparesis. Gastroparesis seriously affects quality of life. There is deterioration in glycemic control and incapacitating symptoms such as malnutrition, water and electrolyte imbalance, and aspiration may occur. However, the pathophysiology of diabetic gastropathy and gastroparesis,

including impaired fundic and pyloric relaxation and impaired electrical pacemaking, is still not delineated^[1-2]. It is generally considered that diabetic gastropathy and gastroparesis may be due to visceral autonomic neuropathy, hyperglucose and smooth muscle degeneration.

Interstitial cells of cajal (ICCs) are a unique class of cells dispersed in gastrointestinal tracts of mammals. In the region of gastric corpus and antrum, multipolar interstitial cells of cajal form two dimensional networks, and have been mistaken for neurons, glial cells, smooth muscle cells, macrophages and fibroblasts. In fact they are mesenchymal in origin. As interstitial cells of cajal develop, they assume major gastrointestinal motility. Interstitial cells of cajal are the pacemaker cells responsible both for initiating slow wave activity in gastrointestinal muscles and for active propagation of electrical slow wave. These cells also mediate motor inputs from the enteric nervous system.

Studies have also suggested that many gastrointestinal motor disorders have changes of number and/or structure of interstitial cells of cajal^[3-9]. In this study, we established the model of diabetic rats by peritoneal injection of streptozotocin, and intended to investigate the reason of gastric-electrical dysrhythmias by recording the gastric electrical activity and characterizing the ultrastructural features of interstitial cells of cajal in the antrum.

MATERIALS AND METHODS

Animals

Fifty 2-mo-old healthy Wistar rats (weighing 100-160 g) of either sex were obtained from Animal Center of Third Military Medical University and were divided randomly into control group ($n=20$) and diabetic group ($n=30$). After fasted overnight, diabetic group rats were injected intraperitoneally with streptozotocin (60 mg/kg) and control group rats were injected intraperitoneally with saline. Blood glucose concentration, weight, appetite and urine volume were measured every two weeks. In this test, diabetic group animals were considered as diabetic if blood glucose levels exceeded 16.9 mmol/L and were eliminated if blood glucose levels remained <16.9 mmol/L.

Gastric-electrical activity recorded

Gastric-electrical activities of control and diabetic group rats were recorded after 3 mo. After fasted over 12 h, rats were operated under anaesthesia with 3% soluble pentobarbitone (30 mg/kg) intraperitoneally. A pair of stainless platinum wires was implanted in deep muscular plexus of antrum. The wires were arranged in an arching line along the greater curvature about 0.5 cm apart from pylorus. The distance between electrodes was about 0.3 cm apart. The electrodes were affixed to the serosa by nonabsorbable sutures in the seromuscular layer of stomach. Teflon-insulated wires were brought out from nape through the anterior abdominal wall percutaneously. After surgery, the rats were transferred to a recovery cage for a week. After fasted overnight, rats underwent anaesthesia with 3% soluble pentobarbitone (30 mg/kg) intraperitoneally. Wires were connected with a gastro-electrical activity amplifier, and recorded parameters were adjusted. All recorded signals were

displayed and simultaneously recorded on computer. Gastric-electrical activity recorded lasting for 60 min. All recorded signals were analyzed by computer. In this study, the frequency of normal rat gastric slow wave was $4.41 \pm 0.91/\text{min}$ and its normal range was 2.63-6.19/min. Gastric slow wave was defined as bradygastria if its frequency was lower than 2.63/min and had a duration of longer than 1 min and form of slow wave was ruled and rhythm was in good order. Gastric slow wave was defined as tachygastria if its frequency was greater than 6.19/min and had a duration of longer than 1 min and form of slow wave was ruled and rhythm was in good order. Gastric slow wave was defined as dysrhythmias if its form of slow wave was not ruled and rhythm was in bad order and had a duration of longer than 1 min.

Morphological studies

After gastric-electrical activity was recorded, the abdomen was opened immediately and antrum was removed (antrum was cut apart 0.5 cm from pylorus) and fixed containing 3% glutaraldehyde and 4% paraformaldehyde. The specimens were rinsed twice in 0.2 mol/L saccharum-phosphate buffer and post-fixed in 10 g/L osmium tetroxide for 2 h at 4 °C. The specimens were then rinsed in distilled water, block-stained with saturated uranyl acetate solution for 3 h, dehydrated in a grade series of acetone and embedded in epoxy resin 618. Ultrathin sections were cut and double-stained with uranyl acetate and lead citromalic for observation under JEOL-2000EX electron microscope.

Statistical analysis

Values in the text were expressed as mean \pm SE. Statistically significant differences were tested using an analysis of variance. A *P* value <0.05 was taken as statistically significant.

RESULTS

Gastric-electrical activity

Slowform of normal rats was regular (Figure 1), the mean frequency of control rats was 4.41 ± 0.91 cpm (range: 2.63-6.19 cpm), the abnormal rhythm index was $18.00 \pm 4.96\%$ and the coefficient of variation of slow wave frequency was $10.00 \pm 6.46\%$. Compared with normal rats, diabetic rats had less chance of normal rhythm, the mean frequency was 4.03 ± 1.23 cpm (range: 1.62-6.44 cpm), its slowform was irregular (Figure 2). The abnormal rhythm index was $30.62 \pm 7.38\%$ and the coefficient of variation of slow wave frequency was $23.50 \pm 2.98\%$. Both of them were significantly higher than those of normal rats (*P*<0.01).

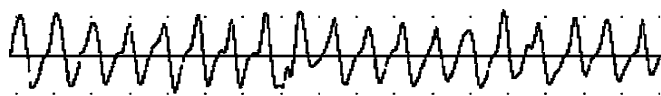


Figure 1 Electrogastrogram of normal rats.

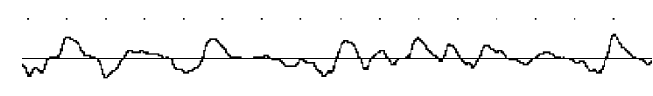


Figure 2 Electrogastrogram of diabetic rats.

Ultrastructural features of interstitial cells of cajal in rat antrum

In the normal rat antrum (Figure 3), interstitial cells of cajal were located within the circular muscle layer (ICC-CM) and in the myenteric region (ICC-AP) and were in closely associated with small nerve bundles. These cells were interconnected with each other and neighboring smooth muscle cells via a number of

large gap junctions. Interstitial cells of cajal in rat stomach were characterized by abundant mitochondria. Numerous caveolae were observed on cell membranes. The nucle were big and irregular, heterochromatins were often observed on the nuclear membrane and its strucure was clear. Their cytoplasm was usually less, and one or more processes were observed. Intermediate filaments, golgi apparatus, rough (RER) and smooth (RER) endoplasmic reticulum were abundant. Variation in the ultrastructural features of the intestinal cells of cajal in different regions was also observed. ICC-CM was characterized by dense cytoplasm, no basal lamina could be clearly identified. ICC-AP was characterized by numerous caveolae and a distinct basal lamina. In the antrum of diabetic rats (Figure 4), interstitial cells of cajal were fewer. The number of the gap junctions between interstitial cells of cajal and neuron cells, between interstitial cells of cajal and smooth muscle cells, and between themselves were decreased significantly. The remaining structures of those gap junctions were also damaged. Basal lamina was discontinuous and not distinct, some were apart from cell membrane and formed cavum. The organelles-mitochondria and ribosome, for example, were also significantly decreased. Mitochondria were swollen, vacuoles and cytoplasm were dissolved, vacuole and myelin figures were formed. Endoplasmic reticulum was dilated, cytoplasm was dissolving, vacuoles were formed and distributed along plasma membrane, perinuclear space was broadened.

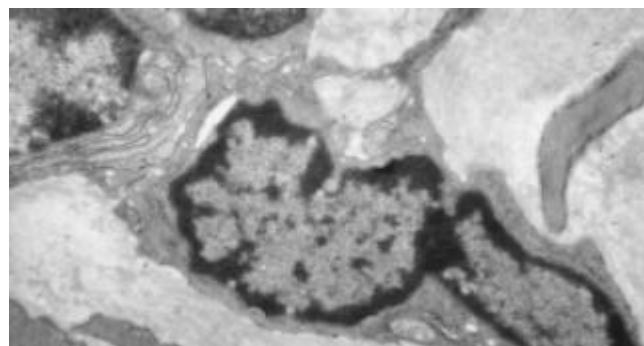


Figure 3 Interstitial cells of cajal of stomach in normal rats.

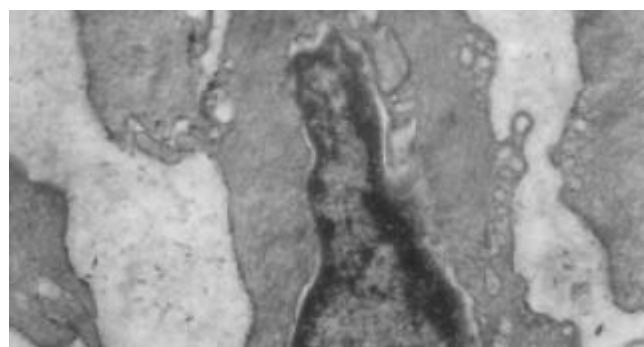


Figure 4 Interstitial cells of cajal of stomach in diabetic rats.

DISCUSSION

Despite reports of diabetic gastroparesis without autonomic neuropath, this disease, and, particularly, impaired electrical pacemaking, are usually considered to be the result of systemic and/or enteric neuropathies. Recent studies in spontaneously diabetic BioBreeding/Worcester rats and in streptozotocin-diabetic rats have demonstrated decreased nitric oxide synthase expression and reduced nitrenergic motor inputs to the stomach, as well as impaired intracellular signaling in response to excitatory neurotransmitters in gastric smooth muscle. Clearly,

these defects may contribute to the many abnormal features of diabetic gastropathy. However, it is unclear how impaired neural inputs (especially impaired inhibitory inputs) or impaired smooth muscle response to cholinergic stimulation could result in the loss of slow-wave activity, which has been observed in both humans and animals with diabetes.

Interstitial cells of Cajal were originally described in the gut more than hundred years ago by Ramón y Cajal^[5]. He characterized “interstitial neurons” as “primitive accessory components that perhaps modify smooth muscle contraction, subject themselves to regulation from principal neurones”. Cajal provided us with detailed pictures of methylene blue-stained networks of interstitial cells of cajal, which were described as spindle shaped or stellate cells with long, ramified cell processes and large, oval, nuclei with sparse perinuclear cytoplasm, and intercalated between autonomic nerve endings and smooth muscle cells. Interstitial cells of cajal were found within discrete locations within the *tunica muscularis* throughout the gastrointestinal tract and classified into five types according to different locations, *i.e.*, ICC-AP (Auerbach’s myenteric plexus) located between the circular and longitudinal muscle layers, ICC-DMP (deep muscular plexus) located between the inner thin and outer thick sublayers of the circular smooth muscle, ICC-SMP (submuscular plexus) located at the submucosal border, ICC-CM located within the outer thick circular muscle layer; and ICC-LM located within the longitudinal muscle layer.

Many studies have indicated that each organ manifests a unique pattern of distribution of interstitial cells of cajal. In the stomach of rats, we observed interstitial cells of cajal located in close association with small nerve bundles within the circular muscle layer (ICC-CM) and in the myenteric region (ICC-AP), no interstitial cells of cajal were found at the most inner region of the circular muscle layer, submucosal border and deep muscular plexus.

Though there are a large number of methods for identification of interstitial cells of cajal, such as methylene blue staining, zinc-iodide osmic acid (ZIO)-staining and immunohistochemistry using antibodies against kit protein. The “gold-standard” for identification of interstitial cells of cajal is still a combination of structural features in transmission electron microscopy. Although some structural variations have been described to be between species and between various regions of the gastrointestinal tract, the Interstitial cells of cajal ultrastructure are characterized by a combination of the following features: numerously large and often elongated mitochondrial profiles, large bundles of intermediate filaments, absence of thick filaments, presence of surface caveoli variably developed basal lamina, synapse-like contacts between Interstitial cells of cajal and tertiary nerve bundles, well-developed smooth endoplasmic reticulum and often also rough endoplasmic reticulum, close apposition or gap junction contact with smooth muscle cells.

Interstitial cells of cajal have ultrastructural distinction from fibroblasts or smooth muscle cells. Some interstitial cells of cajal may have muscle-like ultrastructural features, such as a basal lamina, caveolae, subsurface cistern and gap junctions. For this reason, some interstitial cells of cajal have been considered as modified or specialized smooth muscle cells. However, the interstitial cells of cajal do not contain the well-organized contractile apparatus characteristic of muscle cells. Some interstitial cells of cajal may have an appearance similar to fibroblasts and lack clear muscle-like features. However, even in these cases, they are distinguishable from fibroblast-like cells by a combination of features including a characteristic electron density of cytoplasm, large gap junctions, abundant intermediate filaments, numerous mitochondria, well-developed SER and flattened cisterns of RER. Furthermore, a great number

of collagen fibers often distribute around fibroblast cells.

Morphological observations have led to a number of hypotheses on the possible physiological roles of interstitial cells of cajal^[10-18]. (1) These cells may be the source of slow electrical waves in gastrointestinal tract. (2) They participate in conduction of electrical currents, and (3) They mediate neural signals between enteric nerves and muscles. These hypotheses have been tested by experiments. (1) Slow electrical waves in gastrointestinal muscle strips were absent when interstitial cells of cajal were removed by dissection or lesioned by cytotoxic chemicals. (2) Electrophysiological experiments on isolate cells confirmed that interstitial cells of cajal could generate rhythmic electrical activity and also respond to messenger molecules known to be released from enteric nerves. (3) In Ws/Ws mutant rats, or in mice treated with antibody against the protein c-kit, slow wave activity was impaired. (4) Slow wave passively decayed as a function of distance from the pacemaker appeared. (5) After removal of interstitial cells of cajal, smooth muscle cells continued to be excitable, but in the absence of interstitial cells of cajal, smooth muscle produced action potentials rather than slow wave-like activity. Studies have also suggested that many diseases of gastrointestinal motor disorders have changes in number and/or structure of Interstitial cells of cajal^[3-9]. In infants with hypertrophic pyloric stenosis, there was a significant decrease in the number of interstitial cells of cajal, this decrease was prominent in the ICC-AP. In some patients with pseudo-obstruction, there was a marked decrease in the number of interstitial cells of cajal. Constipation was a very prevalent motility problem, but its underlying mechanisms were obscure. Studies found that the volume of interstitial cells of cajal in the colon of patients with slow transit constipation was significantly decreased compared with normal controls.

Normal gastric emptying requires the proper function of the gastric electrical pacemaker system. Gastroparesis has been associated with electrical abnormalities, and deviations from normal slow-wave rhythm (dysrhythmias) have been reported to result in delayed gastric emptying. In this study, we established the model of diabetic rats by peritoneally injection of streptozotocin, and recorded the gastro-electrical activity after 3 mo. We discovered that in the rats of diabetic group, the gastro-electric dysrhythmia was increased compared with control group, the number of interstitial cells of cajal in antrum of diabetic rats was significantly decreased and the number of the gap junctions of interstitial cells of cajal also was significantly decreased, and the remaining structures were damaged. The organelles-mitochondria and ribosome, for example, were also significantly decreased. Mitochondria were swollen, myelin figures were formed. Endoplasmic reticulum was dilated, cytoplasm was dissolved, vacuoles were formed and distributed along plasma membrane, perinuclear space broadened. This shows that degeneration of interstitial cells of cajal is responsible for gastro-electrical dysrhythmias of diabetic rats, the identification of abnormalities in interstitial cells of cajal in diabetic gastro-electric dysrhythm offers a potential future therapy.

REFERENCES

- 1 **Qi HB**, Luo JY, Dai XG, Wang XQ. A study on motility in patients with diabetic gastroparesis. *Clin J New Gastroenterol* 1999; **5**: 661-662
- 2 **Quigley EMM**. The evaluation of gastrointestinal function in diabetic patients. *World J Gastroenterol* 1999; **5**: 277-282
- 3 **Long QL**, Fang DC. Function of interstitial cells of cajal in gastrointestinal tract. *Shijie Huaren Xiaohua Zazhi* 2002; **10**: 352-355
- 4 **Huizinga JD**, Berezin I, Sircar K, Hewlett B, Donnelly G, Bercik P, Ross C, Algoufi T, Fitzgerald P, Der T, Riddell RH, Collins SM, Jacobson K. Development of interstitial cells of Cajal in a

- full-term infant without an enteric nervous system. *Gastroenterology* 2001; **120**: 561-567
- 5 **He CL**, Soffer EE, Ferris CD, Walsh RM, Szurszewski JH, Farrugia G. Loss of interstitial cells of cajal and inhibitory innervation in insulin-dependent diabetes. *Gastroenterology* 2001; **121**: 427-434
- 6 **Der T**, Bercik P, Donnelly G, Jackson T, Berezin I, Collins SM, Huizinga JD. Interstitial cells of cajal and inflammation-induced motor dysfunction in the mouse small intestine. *Gastroenterology* 2000; **119**: 1590-1599
- 7 **He CL**, Burgart L, Wang L, Pemberton J, Young-Fadok T, Szurszewski J, Farrugia G. Decreased interstitial cell of cajal volume in patients with slow-transit constipation. *Gastroenterology* 2000; **118**: 14-21
- 8 **Hudson N**, Mayhew I, Pearson G. A reduction in interstitial cells of Cajal in horses with equine dysautonomia (grass sickness). *Auton Neurosci* 2001; **92**: 37-44
- 9 **Sandgren K**, Larsson LT, Ekblad E. Widespread changes in neurotransmitter expression and number of enteric neurons and interstitial cells of cajal in lethal spotted mice: an explanation for persisting dysmotility after operation for Hirschsprung's disease? *Dig Dis Sci* 2002; **47**: 1049-1064
- 10 **Komuro T**, Seki K, Horiguchi K. Ultrastructural characterization of the interstitial cells of Cajal. *Arch Histol Cytol* 1999; **62**: 295-316
- 11 **Koh SD**, Kim TW, Yan JY, Glasgow NJ, Ward SM, Sanders KM. Regulation of pacemaker currents in interstitial cells of Cajal from murine small intestine by cyclic nucleotides. *J Physiol* 2000; **527**(Pt1): 149-162
- 12 **Ordög T**, Takayama I, Cheung WKT, Ward SM, Sanders KM. Remodeling of networks of interstitial cells of Cajal in a murine model of diabetic gastroparesis. *Diabetes* 2000; **49**: 1731-1739
- 13 **Dickens EJ**, Edwards FR, Hirst GD. Selective knockout of intramuscular interstitial cells reveals their role in the generation of slow waves in mouse stomach. *J Physiol* 2001; **531**(Pt3): 827-833
- 14 **Daniel EE**, Thomas J, Ramnarain M, Bowes TJ, Jury J. Do gap junctions couple interstitial cells of Cajal pacing and neurotransmission to gastrointestinal smooth muscle? *Neurogastroenterol Motil* 2001; **13**: 297-307
- 15 **Salmhofer H**, Neuhuber WL, Ruth P, Huber A, Russwurm M, Allescher HD. Pivotal role of the interstitial cells of Cajal in the nitric oxide signaling pathway of rat small intestine. Morphological evidence. *Cell Tissue Res* 2001; **305**: 331-340
- 16 **Horiguchi K**, Sanders KM, Ward SM. Enteric motor neurons form synaptic-like junctions with interstitial cells of Cajal in the canine gastric antrum. *Cell Tissue Res* 2003; **311**: 299-313
- 17 **Jain D**, Moussa K, Tandon M, Culpepper-Morgan J, Proctor DD. Role of interstitial cells of Cajal in motility disorders of the bowel. *Am J Gastroenterol* 2003; **98**: 618-624
- 18 **Suzuki H**, Ward SM, Bayguinov YR, Edwards FR, Hirst GD. Involvement of intramuscular interstitial cells in nitregeric inhibition in the mouse gastric antrum. *J Physiol* 2003; **546**(Pt3): 751-763

Edited by Hu DK and Wang XL Proofread by Xu FM

Accurate diagnosis is essential for amebiasis

Levent Doganci, Mehmet Tanyuksel, Tumay Doganci

Levent Doganci, Department of Microbiology and Clinical Microbiology, Gulhane Military Medical Academy, 06018 Etlik/Ankara, Turkey

Mehmet Tanyuksel, Division of Medical Parasitology, Department of Microbiology and Clinical Microbiology, Gulhane Military Medical Academy, 06018 Etlik/Ankara, Turkey

Tumay Doganci, Department of Pediatric Gastroenterology, Social Security Hospital for Children, 06610 Diskapi/Ankara, Turkey

Correspondence to: Dr. Levent Doganci, Department of Clinical Microbiology and Clinical Microbiology, GATA, 06018 Etlik, Ankara, Turkey. levdog@gata.edu.tr

Telephone: +90-312-304 3401 **Fax:** +90-312-304 3402

Received: 2003-12-10 **Accepted:** 2004-01-05

Doganci L, Tanyuksel M, Doganci T. Accurate diagnosis is essential for amebiasis. *World J Gastroenterol* 2004; 10(8): 1231
<http://www.wjgnet.com/1007-9327/10/1231.asp>

Amebiasis is one of the three most common causes of death from parasitic disease, and *Entamoeba histolytica* is the most widely distributed parasites in the world. Particularly, *Entamoeba histolytica* infection in the developing countries is a significant health problem in amebiasis-endemic areas with a significant impact on infant mortality^[1]. In recent years a world wide increase in the number of patients with amebiasis has refocused attention on this important infection. On the other hand, improving the quality of parasitological methods and widespread use of accurate techniques have improved our knowledge about the disease.

We read with interest the publication by Ustun *et al.*^[2] and would like to comment on both the differentiation of *E. histolytica/Entamoeba dispar* and therapeutic approach to amebiasis in inflammatory bowel disease (IBD) cases. We strongly agree that IBD sometimes can co-exist with amebiasis. This infrequent phenomenon may also arise from inaccurate diagnosis, however before the specific anti-inflammatory treatment initiation for IBD, empirical anti-amebic treatment is usually suggested in the hyper-endemic regions. We think that those prevalences (54% and 69%) from other Turkish studies reported on the discussion section seem to be very high, and suggest the possibility of overdiagnosis. The current data given on subjects with IBD and controls clearly showed that the disease not only diminishing in Turkey but also accurate diagnosis of amebiasis with permanent staining technique maximized obtaining more valid results, as authors stated in their articles.

We also would like to note another recent article about climatic pattern of amebiasis in Turkey, published by Erdem *et al.*^[3], in a similar point of view for the accuracy of the diagnosis. Single microscopic examination is not a recommended diagnostic tool for accurate diagnosis of luminal amebiasis. Microscopy (also not clear in the article^[3] whether permanently stained smears such as trichrome staining was used or not) is one of the most difficult and insensitive techniques to interpret. In some cases, false positive results might be due to identification of human white blood cells as amoebae^[4-6]. Also, it did not allow to differentiate *E. histolytica* from *E. dispar* by using only trichrome staining method because both had similar morphological features as stated^[2]. Numerous studies have demonstrated the insufficiencies of microscopic examination in the diagnosis of *E. histolytica*^[4]. After the re-classification

of *Entamoeba* genus, it is essentially important to distinguish the 2 morphologically identical but biologically and immunogenetically different species: *E. histolytica* and *E. dispar*^[1,7,8]. In addition to this, *E. dispar* is the more prevalent strain than *E. histolytica* all over the world. Morphologically, the presence of ingested red blood cells in trophozoites is not adequate for the diagnosis of *E. histolytica* since Haque *et al.*^[9] have demonstrated that some *E. dispar* trophozoites might also contain ingested erythrocytes. So that, microscopy had a low sensitivity and could easily mislead the clinicians. At present, among the traditional and conventional approaches to the diagnosis of amebic colitis and liver abscess, serological testing remains an important instrument. In addition to this, for a decade there has been a reliable stool antigen detection using ELISA, which has a very high sensitivity and a good clinical correlation. Another important point to remember, if there is a high prevalence of intestinal amebiasis in a certain geographical area, then it should have been a large number of cases with extra-intestinal involvement and a high prevalence rate of specific antibody. So far, these indirect indicators have a very low percentage in Turkey.

The diagnosis and treatment of IBS in patients without appropriate diagnosis of intestinal amebiasis are a great challenge. The clinical presentations are very similar, and inaccurate laboratory methods could be misleading and even endoscopic examination might not solve the diagnostic dilemma. It is more realistic to start empirical anti-amebic treatment, preferably with metronidazol derivatives despite the fact that it would postpone the treatment for IBD as stated in classical medical literature.

In summary, since microscopy is neither sufficiently sensitive nor specific for the diagnosis of *E. histolytica* infection, it is essential to perform an antigen detection using ELISA^[9] or PCR analyses for accurate the diagnosis of intraluminal amebiasis to provide a more reliable comment on the epidemiological pattern and clinical impact of the disease.

REFERENCES

- 1 **Anonymous.** Amoebiasis. *Wkly Epidemiol Rec* 1997; **72**: 97-99
- 2 **Ustun S, Dagci H, Aksoy U, Guruz Y, Ersoz G.** Prevalence of amebiasis in inflammatory bowel disease in Turkey. *World J Gastroenterol* 2003; **9**: 1834-1835
- 3 **Erdem H, Kilic S, Cinar E, Pahsa A.** Symptomatic intestinal amoebiasis and climatic parameters. *Scand J Infect Dis* 2003; **35**: 186-188
- 4 **Tanyuksel M, Petri WA Jr.** Laboratory diagnosis of amebiasis. *Clin Microbiol Rev* 2003; **16**: 713-729
- 5 **Garcia LS, Bruckner DA.** *Diagnostic Medical Parasitology*, 3rd ed., Washington, DC: ASM 1997: 14-17
- 6 **Doganci L, Tanyuksel M, Gun H.** Overdiagnosis of intestinal amoebiasis in Turkey. *Lancet* 1997; **350**: 670
- 7 **Diamond LS, Clark CG.** A redescription of *Entamoeba histolytica* Schaudinn, 1903 (Emended Walker, 1911) separating it from *Entamoeba dispar* Brumpt, 1925. *J Eukaryot Microbiol* 1993; **40**: 340-344
- 8 **Tannich E, Horstmann RD, Knobloch J, Arnold HH.** Genomic DNA differences between pathogenic and nonpathogenic *Entamoeba histolytica*. *Proc Natl Acad Sci U S A* 1989; **86**: 5118-5122
- 9 **Haque R, Neville LM, Hahn P, Petri WA Jr.** Rapid diagnosis of *Entamoeba* infection by using *Entamoeba* and *Entamoeba histolytica* stool antigen detection kits. *J Clin Microbiol* 1995; **33**: 2558-2561